

Physics Abstracts

PAMPHLET BOX

Science Abstracts Series A
July-December 1973

Subject Index part B

U.I.C.C.
OCT 7 - 1974
LIBRARY



inspec
The Institution of Electrical Engineers

CONTENTS

Title page

i

Subject index

S1741

SIX-MONTHLY INDEXES TO SCIENCE ABSTRACTS

Cumulative indexes to Science Abstracts are published twice a year covering the period January-June and July-December. They comprise author and subject indexes and some specialised or 'small' indexes. For Physics Abstracts and Electrical & Electronics Abstracts the Author Index and Subject Index are published as separate volumes. In this case the Small Indexes are included in the Author Index volume.

Author index

This lists in alphabetical order all authors of papers abstracted in the abstracts journal during the six months covered by the index, together with the title of the paper. Where there are co-authors of a paper the title of the paper is given only under the name of the first author. The serial number of the paper in the abstracts journal is in the form 3-12345, ie 1973—abstract no. 12345.

'Small' indexes

These are specialised indexes which allow the user to find quickly particular types of information which might be difficult to find using the subject or author indexes.

Bibliography index

In this index reference is made to articles which contain a significant list of references or bibliography on the subjects listed.

Book index

This gives details of books received and abstracted by the abstracts journal.

Patent and Report indexes

These give details of those reports or patents which have been abstracted in the abstracts journal during the past six months.

Conference index

This index lists conferences for which published proceedings have been received and abstracted. Reference is given to the individual papers and their serial numbers in the abstracts journal.

Subject index

The Subject index provides an alphabetical subject key to the articles included in the abstracts journal. Some general guidance on its use is given below:

1. Look in the index for the name of the specific subject in which you are interested. In most cases this name will be a heading in the index and you will find relevant articles listed under it.
2. Occasionally you will be directed from the subject heading chosen to a different heading under which the relevant or additional articles are listed.
3. If you do not find the subject heading you first choose, try a more general heading.
4. Each entry under the heading relates to an article appearing in the abstracts journal and gives the serial number of that article in the journal preceded by the last digit of the current year, eg 3-12345: ie Abstract number 12345 in the abstracts journal for 1973.

Physics Abstracts

Volume 76, part 2 July-December 1973

Subject Index part B



inspec
The Institution of Electrical Engineers

Physics Abstracts is published twice monthly by the Institution of Electrical Engineers. Twice-yearly subject and author indexes covering the period January-June and July-December are included in the subscription. Printed by Unwin Brothers Limited, Old Woking, Surrey, England. Second class postage paid in New York, NY 10001, USA.

© 1974: THE INSTITUTION OF ELECTRICAL ENGINEERS

mass transfer continued

- liquid-liquid, conc. meas. near interface, microinterferometric technique 3-62380
- local mass transfer between a sphere and a liquid (*French*) 3-40755
- local mass transfer sensor to estimate the turbulence characteristics of the near-water layer of an air flow 3-57024
- lung, mathematical model of mass transport due to gaseous diffusion 3-51427
- metal, liquid, isothermal mass transfer, for diffusion coating prod. on Armo Fe (*Russian*) 3-80332
- metal poor stars, mass loss in stellar wind for fast rotation 3-77060
- molecular diffusion influence on mass transfer between turbulent liquids 3-40705
- multicomponent mass transfer in turbulent flow 3-60530
- multicomponent systems with movable phase interfaces, theory, solidification 3-62615
- 2-naphthol in water, mass transfer coeffs., fixed bed, cylindrical and oval-shaped pellets 3-79047
- neutron star accretion at the Galactic centre, upper limit of X-ray wavelength 3-42231
- non-zero contact angle meniscus evaporation, fluid flow in interline region 3-57733
- nonlinear heat and mass transfer problems, electric simulation 3-77917
- O₂ transfer to fermentations, effect of pressure 3-66696
- optical microscopy, application to electrochemical studies, review 3-66198
- oscillations effect on heat and mass transfer from sphere to medium, electrochemical study 3-80555
- particle fluid mass transfer, multiparticle system 3-63759
- planetary atmospheres, solar wind interaction rel. to ionization and mass loss 3-65783
- plasma, current-carrying, anomalous heating and momentum transfer, ion-reson. broadening influence 3-52524
- plasma electrodynamic acceleration, relaxation processes 3-60634
- polymer dilute soln. non-Newtonian flow, mass transfer with rotating disc 3-71816
- polymer dilute solutions, mass transfer 3-57827
- porous catalyst, heat and mass transfer, nonlinear boundary value problem solution 3-42911
- porous materials, absorbents expt. (*German*) 3-50800
- reacting species with temp. dependent reaction constant, combined heat and mass transfer 3-65065
- rotating disc in non-Newtonian fluid, mass transfer peculiarities 3-46386
- rotating fluid, mass transfer from base of an agitated cylindrical tank 3-57748
- rotating fluid, mass transfer from stationary disc to a fluid in Bode-wadt flow 3-57747
- sintering, stress induced diffusional transport, material continuity requirements 3-69332
- sintering, stress induced diffusional transport, material continuity requirements 3-69333
- skeleton-liquid-vapour-air-ice, transpiration cooling, unsteady conditions, eqns. 3-63642
- spherical bubble and its surrounding fluid, mass transfer (*German*) 3-40754
- stars, density gradient inversions in stellar envelopes rel. to mass loss 3-45085
- stars, T Tauri-type, mass loss through stellar wind 3-77061
- steady symmetric flow past elliptical cylinders 3-78947
- surface tension induced interfacial convection rel. to mass transfer rate 3-78940
- thermosphere, mag. storm characts. 3-51096
- turbulence, free stream, stagnation flow enhancement, heat and mass transfer 3-78933
- turbulent boundary layers, Van Driest damping parameter with mass transfer 3-43555
- turbulent pipe flow, heat and mass transfer in electrochemical reactions 3-57848
- two phase flow, heat transfer, expt. study 3-40708
- two-phase particulate systems, low Peclet number mass or heat transfer 3-79024
- unified theory of stationary transfers in industrial physics appl. to fluid flow 3-71844
- viscoelastic fluid flow past flat plate, heat and mass transfer 3-78945
- water stream, effect of rainfall on free surface on velocity (*German*) 3-40733
- water transport of cohesionless, fine graded, flaked sediment 3-80705
- X-ray binaries, self excited mass flow 3-81127
- CO₂ absorption in water in gas-liquid annular flow 3-63752
- Ge, film growth, iodide method, through flow system, diffusive 3-76144
- K₂SO₄ multiparticle crystal growth rates in vertical cones 3-47352
- N₂O₄ → 2NO₂ → 2NO + O₂ in turbulent flow, heat and mass transfer (*Russian*) 3-76447
- N₂O₄ reactive dissociating boundary layer flow, numerical calc. of heat and mass transfer, film model approx. 3-40758
- N₂O₄ reactive dissociating boundary layer flow, simplified calc. of heat- and mass-transfer 3-40759
- Na droplet, combustion model for LMFBR accident analysis 3-46076
- O transport in lower thermosphere rel. to hemispheric imbalance 3-51100

master equation see transport processes

materials

- see also individual materials, e.g. ceramics
- bitumens, industrial, optical spectra as means of identification (*Russian*) 3-64687
- constructional, brittle fracture criteria (*Russian*) 3-58774
- high cristobalite, structure determ. as function of temp. 3-61338
- mathematical approach, heterogeneous systems 3-64768
- polydisperse cohesive comps., cross-linked, theoret. principles of strength 3-76391
- processing, glow discharge electron beam applic. 3-59909
- science, mathematical framework, solved problems, book 3-56601

materials handling

- see also fluidised beds; grinding; transportation; winding (process)
- fissile metal, criticality study 3-43315
- nuclear fuel, safety criteria, supporting critical lattice data for both U and Pu bearing fuel 3-67405
- nuclear fuel, spent, Yankee Atomic Electric Co. shipping experience 3-67576
- nuclear reactor handling machine for Loviisa I 3-57574
- radioactive, handling and radiation protection, french standards (*French*) 3-66060
- radioactive, package licensing and analytical techniques of evaluation 3-67413
- ³H, radiation protection (*French*) 3-59458

materials testing

- see also acoustic applications; electron beam applications; laser beam applications; mechanical testing; nondestructive testing; semiconductor materials testing; ultrasonic applications
- ablative materials, laser activated model surface recession compensator system 3-59908
- abrasive wear specimen testing apparatus (*Russian*) 3-61239
- accelerated tests, statistical anal. of accuracy of Locati method, fatigue damage, rel. to 'stairs' method 3-53296
- activation volume determination, transient creep, internal friction meas. 3-50804
- Alclad sheet, 2024-T3, load sequences effect on crack propag. under random and program loading 3-65046
- alloy, low-cycle fatigue unit for cryogenic temps. 3-65056
- alternating bend testing, amplitude of deformation, meas. and control, resonant type e.m. machines 3-55913
- binary and quasibinary mixture, composition checking, accuracy, X-ray and γ-ray methods 3-69428
- boiler drums, non-steady operating conditions, life testing, varying tension, high temp. and pressure 3-50808
- brittle materials, apparatus for recording acoustic signals from cracks 3-42519
- brittle materials, impact tests, fracture toughness and absorbed energy release 3-58779
- calliper device to run load programs, probe force on specimen (*German*) 3-80513
- caprolon, self-heating and thermal fatigue during cyclic compression 3-61220
- ceramic, dynamic modulus technique 3-70262
- ceramic, elastic moduli and mech. Q of small specimens, resonant beam technique 3-70263
- ceramic, for high temp. e.m. windows, thermal cycling effects on struct. and props. 3-76280
- ceramic, fracture energy eval. using notched beam test 3-72934
- ceramic, impact testing, impacting pendulum initial energy effect on measured impact energy 3-76393
- ceramic, oxide, failure cracks development testing (*Russian*) 3-80426
- ceramic, thermal shock test rig 3-76394
- ceramic article, evaluation of conventional methods (*Polish*) 3-76407
- ceramic casting, equipment for determ. physical and mechanical props., heat treatment, pouring 3-50809
- ceramic specimens, miniature, high temp. tensile test 3-72961
- ceramics, microwave applications 3-47491
- clay, triaxial compression test, effects of specimen height and strain rate 3-69422
- coil and cold-rolled steel, using Lamb waves 3-41832
- composite, C fibre reinforced, interlaminar shear strength under impact conditions 3-55860
- composite, C fibre reinforced plastics, shear damage effects on torsional behaviour 3-55856
- composite, unidirectional, in-plane shear stress/strain response 3-55924
- Comsteel En 25, fracture toughness 3-64896
- concrete, cellular, compressive strength meas. 3-44699
- concrete, nine-gauges device, meas. inside elements 3-65055
- concrete, nonreinforced, triaxial testing 3-65049
- concrete, prestressed, reinforcement strength and position, non-destructive X-ray test, strain meas. (*German*) 3-69418
- concrete, resonant vibration freq. determ. method 3-73664
- concrete, resonant vibration frequency, acoustic impact technique 3-69408
- concrete beam, flexure loading rig; high temp. furnace combination, thermal expansion obs. 3-47496
- contact fatigue, flat specimens, running-in test method 3-50811
- crack detect. of steel sheet by acoustic emission 3-69411
- crack tip stress intensity factor, Mode I, determ. by holographic interferometry 3-73108
- creep, miniaturized uniaxial machine for remote applications 3-47530
- cryostat, reloading device, tensile testing at 20 K 3-51558
- cyclic elastic-plastic deformation, methods of anal. kinetic characteristics, fatigue damage, crack development 3-55910
- cyclic oxidation testing and data interpret. 3-73096
- cyclic strength tests, long-term, methodical features 3-42513
- device, volume stressed state, to 300C, effect of pressure, force and bending 3-50813
- dimensioning and strength calcs., conf., Budapest, Hungary (Oct. 1971) 3-69429
- dynamic photoelasticity, dual-beam polariscope and framing camera 3-73112
- electrical and electronic engineering, electron microscope use (*Rumanian*) 3-48573
- electrostatic copy paper, automatic system 3-66729
- endurance limit, accelerated determ. method 3-58785
- epoxy resins, impregnation of superconducting magnet windings 3-58786
- fatigue, alternating load testing, choice of number of steps in programme, stress below fatigue limit 3-55911
- fatigue and corrosion fatigue testing apparatus for large-size shaft specimens (*Russian*) 3-58776
- fatigue testing, low-cycle, compression-tension, in gaseous media, elevated temp. apparatus (*Russian*) 3-61240
- fatigue testing, low-cycle, in corrosive medium, apparatus (*Russian*) 3-58775

materials testing continued

fatigue testing under symmetrical tension-compression conditions, type VEDS-200A vibrostand use 3-65057
 fibreglass, fatigue strength, cyclic strength under shear loading, stress weakening by notches or steps 3-53297
 flat structure stress meas. using optical method (*French*) 3-59551
 four-ball machine, reduced machine time, lengthy friction path, wear of steel balls, effect of lubricating oils 3-53307
 glass fibre reinforced materials, interferometric detection of fracture noise (*German*) 3-70316
 graphite, tension-compression tests, strength in a plane stressed condition 3-53298
 graphite, work of fracture and fracture toughness 3-55926
 graphite antifriction materials, wear and friction properties, influence of adsorption 3-50810
 graphite ATJ, ablation at high temp. 3-44672
 graphite moderator, methane diffusion rel. to manufacture conditions (*German*) 3-71272
 hardness, microhardness, testing up to 1800 C, design of machine 3-53301
 hardness, testing from 20 to 1600 C, design of machine 3-53302
 heat pipes, bench and thermal vacuum testing 3-51548
 hot torsion test, plotting of flow curves, effect of specimen dimensions on slope (*German*) 3-73098
 hot torsion tests for solid and tubular specimens, specimen geometry effect 3-55925
 impact, development of stands, impact loading, intermediate crank and rotating crank 3-53305
 infrasonic meas. of elastic consts. and damping in flexure using Balanced Resonator 3-48348
 internal friction, meas. methods, survey 3-50802
 long time strength testing and equivalent damageability hypothesis 3-44705
 long-duration slow-cycle testing, thyristor servo drive unit 3-73106
 magnetic carrier type composites, short-time strength and deformability at high temps. 3-47463
 metal, fatigue strength, loading freq. depend. 3-44629
 metal, hot torsion testing for flow stress determ. 3-76416
 metal, thermal and structural stresses, electrical heating, const. length 3-73105
 metal and alloy shear props., high strain rates 3-58787
 metal coatings, wear resistance from electrical resistance 3-73103
 metal dynamic fracture under biaxial strain, exploding-wire expt. 3-73109
 metal fatigue damage, automatic information processing 3-80516
 metal pairs in mutual compression, zone of contact prop. testing apparatus (*Russian*) 3-58777
 metals, fatigue crack initiation, study by electrical resistance measurements 3-76396
 micro-indentation method and apparatus for studies in temp. zone near brittle failure (*Russian*) 3-80514
 Nimonic 90 and 108, tensile and compressive creep behaviour interpret. 3-58667
 nonferrous metals, energy dissipation in h.f. fatigue tests 3-58694
 nonmetallic materials, mech. props. testing apparatus for -80 to +300°C 3-65058
 nuclear fuel cladding tube, standard defect machining for test applic. (*Japanese*) 3-63132
 nuclear fuel element, automatic system, X-ray scanning (*German*) 3-80512
 nuclear pressure vessels, acoustic emission monitoring, proof tests 3-65062
 nuclear reactor fuel, post irradiation examination 3-43313
 plasma coatings, device for shear testing 3-53835
 plate, dynamic bending problems, extended reflective moire method 3-73110
 PMMA, fatigue crack retardation and closure 3-76381
 polymer, glassy, impact test, model exam. 3-58778
 polymer, u.s. anisotropy meas. and mech. props. 3-53308
 polymer films, impact testing technique 3-50807
 polymer materials at cryogenic temp. 3-58726
 polymeric materials, time marker for long term strength and instant of rupture 3-53834
 polymers, deformability, wide temp. range, device for plotting thermomechanical curves, constant load, continuous heating 3-55915
 polymers, mechanical, electrical and thermal properties 3-41829
 porcelain enamel adherence to steel, u.s. determ., nondestructive eval. 3-73097
 porous materials, compressive strength meas., appl. to cellular concretes 3-44699
 pulsed reactor fuel, dye penetrant, u.s. reflection, X-radiography, immersion density methods 3-67559
 quantities employed and relationship to basic SI units (*Hungarian*) 3-44703
 quartz-phenolic composite, quasistatic uniaxial strain and Hugoniot tests compared 3-73111
 recording device, two-coordinate stress/strain measurement applic. 3-76406
 refractories, thermally loaded, deformed state studies 3-44636
 sand, triaxial compression test, effects of specimen height and strain rate 3-69422
 scaling heat resistance meas. method for metallic materials (*Polish*) 3-50719
 semiconductor impurity and contact materials, electron beam microanalysis (*German*) 3-48646
 sheet material fatigue testing apparatus for cyclical extension conditions 3-80518
 sheet materials, relaxation stress testing device, thermocouple indicator, 300 to 1000C 3-53300
 slow crack growth test method 3-65048
 steam generators, nondestructive testing, tube to tube sheet welded joints 3-65060
 steel, austenitic stainless, irradi., with Ti and B additions, high-temp. deform. and fracture 3-63188
 steel, automatic device, heat resistance, distortion due to temp. fluctuation 3-42531
 steel, balls, rupture testing, ultracentrifuge, rotating mag. field, stress at centre of ball, residual deformation 3-53304
 steel, boiler tube billets, n.s. inspection, flow detection quality of tubes rel. to macrodefects 3-53303

materials testing continued

steel, Brinell hardness testing, difficult to reach areas, polystyrene replica 3-50806
 steel, case hardening depth, detn. using ultrasonics (*French*) 3-58790
 steel, constrained disc burst tests, elastic-plastic analysis 3-50822
 steel, Cr-Mo-V, low-alloy, creep rupture tests, effect of carbide repartition (*German*) 3-69255
 steel, creep rupture behaviour, 500-700°C, Rajakovic method (*German*) 3-47397
 steel, creep tests, supporting effect of bending specimens, 400-500°C (*German*) 3-69421
 steel, cyclic nonisothermal elastoplastic loading, diagram represent. 3-69431
 steel, energy dissipation in h.f. fatigue tests 3-58694
 steel, fatigue bending tests, stress gradient as cause of scale effect in brittle fracture 3-58782
 steel, fatigue crack propag. vel., depend. on degree of rarefaction of air, apparatus design (*Russian*) 3-80510
 steel, fatigue tests, low cycle fracture resist. in stress conc. zones, high temp. 3-69435
 steel, heat treated, inspection by electromagnetic comparator (*German*) 3-69417
 steel, high strength, creep rupture tests, effect of interruption in mechanical stress (*German*) 3-69253
 steel, high-strength, test method for transient stress conditions characterized at elevated temps. 3-69432
 steel, low-C, effect of interruptions in loading on mech. props. 3-55916
 steel, low-C, high strain fatigue tests, weld effects 3-69317
 steel, maraging, low cycle fatigue props., hydrostatic press. effect 3-80519
 steel, microhardness indentations method, plastic flow irregularity 3-76399
 steel, NiCrMo-V, mechanical hysteresis loop, Fortran program for low cycle fatigue test data processing (*Japanese*) 3-55799
 steel, repeated impact tension loading, strength, elongation (*German*) 3-76395
 steel, Si-Mn type, comparative evaluation of performance 3-55917
 steel, stainless, austenitic, stress corrosion cracking, electrochemical testing method by separating crack anode from cathode 3-47492
 steel, stainless, instantaneous strain, proof stress, creep rupture testing 3-47437
 steel, stress relaxation tests, bending, tension, time factor effect 3-50803
 steel, structural, creep tests, rel. to rectangular plates dimensioning 3-69438
 steel, structural, prefatigue influence on transition temp. (*German*) 3-69420
 steel, structural, tests for localized heating effects determ. 3-69436
 steel, thermoplastic shear and fracture during high-velocity sliding in rocket-sled testing 3-50748
 steel, welded, crack formation and propagation behaviour under fluctuating stress 3-72911
 steel, welded joints, fatigue strength at high temp. and low cycle loading 3-44706
 steel bar reinforcement, deformation, fatigue strength, spot welding effect (*German*) 3-44638
 steel cylinder, wire-wrapped, fracture resistance 3-50825
 steel plate, Charpy-V impact props., stat. analysis 3-50824
 steel plates and strips, simple u.s. testing equipment for defect indication efficiency of 100% (*German*) 3-47520
 steel plates with oblique hole, corner shape effect on elastic stress and strain conc. 3-50823
 steel pressure vessels, thick-walled, fracture mechanics aspects 3-76409
 steels, structural, low cycle fatigue effect on brittle fracture characteristics (*German*) 3-47523
 stepped specimens, fatigue strengths 3-55919
 strain curve relations in static and cyclical loading 3-80380
 stress corrosion crack testing using potentiostatic dynamic strain technique 3-61247
 stress corrosion cracking susceptibility test procedure 3-69402
 structural components, failure prevention 3-73095
 tensile specimen, necking during creep at const. load and ambient temp. (*German*) 3-65051
 tensile testing, light-weight grips for rod specimen 3-44702
 tensile testing machine extension for axial load and torque action, low temp. 3-58784
 tension-compression test fixture, for Bauschinger effect detn. 3-69407
 thermal fatigue crack, length meas., geometry, elec. potential distrib. method 3-55912
 thermal fatigue testing and method at subzero temp. 3-55918
 thermal fatigue testing of materials subjected to complex stressing 3-58783
 thin films, setting up of initial stresses, relaxation testing, corrosive media 3-53299
 tool materials, durability testing, vertical compression moulding, casting machine 3-53306
 torsion testing machine, for programmed simulation of hot working 3-53836
 u.s., information transfer approach 3-44701
 u.s., solids, hidden defects, shape and size determination, analytical method 3-73677
 u.s. contact testing, thickness of liquid couplant layer effect and other variables 3-61241
 u.s. pulse echo meas. of elastic consts. of slender specimens 3-48347
 variable-stress creep predictions, influence of scatter 3-41831
 vibration loading criterion 3-80517
 Weisemberg rheogoniometer for dynamic properties (*French*) 3-47493
 Zircaloy cladding, high temp. testing for use as thermocouple sheath in PWR 3-47431
 Al alloy, 2024-T3, fatigue crack delay and arrest due to single-peak tensile overloads 3-58789
 Al alloy, 7075-T6, high cycle fatigue crack growth detection using acoustic emission 3-76412

materials testing continued

- Al alloy, creep under variable uniaxial tensile loading, strain accumulation and rupture 3-69405
- Al alloy RR58, biaxial cyclic high-strain fatigue 3-73107
- Al alloy sheet, grade AMg6BM, loading freq. and directional anisotropy effect on fatigue strength 3-58678
- Al alloy sheet in symmetrical bending, circular hole effects on fatigue resist. 3-47423
- Al alloys, fracture strength under static and cyclic loads comparison 3-47424
- Al alloys, mechanical hysteresis loop, Fortran program for low cycle fatigue test data processing (*Japanese*) 3-55799
- Al-Cu-Mg alloy, high temp. fracture toughness test method 3-69433
- alloys, acoustic investigation of intercrystalline corrosion 3-69249
- Au-Cd, martensitic phase transformation, acoustic emission, e.m. detection 3-47498
- Be, fracture toughness eval. of hot pressed and forged specimens 3-50815
- Be, fracture toughness of hot pressed block and metal sheets 3-50814
- Be, fracture toughness props. of S-200 grade specimens 3-50816
- C fibres, securing technique at high temp. 3-55920
- Co-Cr alloys, low-ductility dental casting, elongation meas. and interpret. 3-69403
- Cu, fatigue crack propag. under superimposed sinusoidal loading (*Japanese*) 3-41735
- Cu plastic tensile deformation resistance, effect of grain size and deformation rate 3-69303
- Fe castings, pipe, strength gradient, transverse bending of ring sector 3-50805
- NaCl, scratch method for evaluation of X-ray effects 3-76398
- Ni alloy, energy dissipation in h.f. fatigue tests 3-58695
- Ni alloys, abrasion resistance, hot H_2SO_4 and HCl soln., method of assessment during friction 3-55914
- Si_3N_4 , hot-pressed, low cycle fatigue 3-76287
- Ti alloy, energy dissipation in h.f. fatigue tests 3-58695
- Ti alloys, fatigue resistance under asymmetrical cyclic loading, struct. effect 3-44635
- Ti alloys, fracture strength under static and cyclic loads comparison 3-47424
- TiO_2 , trace element spectrochemical analysis (*Polish*) 3-73955
- U, high purity, high temp. plastic flow in α , β and γ phases 3-41772
- U alloys, under conditions of rapid fission heating 3-47531
- U-Mo(10 wt.%) alloy, stress corrosion cracking, acoustic emission (*French*) 3-69404
- U-Nb(Ti) alloys, fracture toughness and mode correl. with microstruct. 3-76414
- Zn-Al alloys, acoustic investigation of intercrystalline corrosion 3-69249
- ZrO_2 , trace element spectrochemical analysis (*Polish*) 3-73955

mathematical analysis

- see also *approximation theory; Bessel functions; calculus; eigenvalues and eigenfunctions; Fourier analysis; integral equations; numerical analysis; series (mathematics)*
- causality calculations in the time domain for determ. optical constants from reflectance 3-80000
- chromatography, normalization techniques 3-66417
- finite cylinder, effectiveness factor 3-62405
- Hamiltonian system, constants of motion and degeneration 3-62393
- mass spectra, intensity distrib. along charge-exchange continua, mag. sector spectrometers 3-56975
- meteorological patterns, classification, Southern California 3-76752
- nonlinear heat conduction problems 3-61961

mathematical logic see formal logic

mathematical programming

- see also *dynamic programming; linear programming; nonlinear programming*
- Dubovitskii-Milyutin method, optimization theory 3-74019
- numerical optimisation, in lower bound plastic analysis of circular orthotropic plate 3-48731
- simplex-grid, fusibility diagram 3-72177

mathematics

- see also *algebra; combinatorial mathematics; convergence; digital arithmetic; equations; formal logic; functions; geometry; mathematical analysis; number theory; probability; statistics; topology*
- bibliography No.25 of unclassified documents published by AWRE 3-73627
- gamma-ray scatt., slab transmission and reflection functions, recurrence relations 3-60335
- Lagrangians, degenerate, canonical formalism 3-45627
- teaching, outlook in education, curriculum 3-66111
- teaching in secondary schools, links between science and mathematics 3-59515

matrices see matrix algebra

matrix algebra

- asymptotic property of elastic structures, use of matrices in design 3-74023
- atmospheric temperature, covariance matrices, means of atmospheric Planck function profiles, satellite meas. 3-44959
- beams and frames, elastica problems, matrix displacement solns. 3-45647
- Cauchy matrix system for non-autonomous differential eqns., asymptotic stability by Lyapunov method (*Russian*) 3-62417
- concavity of two functions of positive matrix from Herglotz functions 3-48697
- conformal transformation matrix for fields 3-43054
- conical shells, elastically constrained and stiffened, buckling anal., hydrostatic pressure, collocation method 3-45641
- convergence, sequence of operators in C_p 3-73981
- Conway-Dirac-Eddington matrices, applic. of quaternions to Lorentz transformations 3-77874
- crystal dynamical matrix, evaluation of local modes and Green's function for interstitials 3-64126
- crystal growth, transfer matrix method appl. 3-68178
- decay density matrix of mixed scalar-vector-tensor boson systems 3-45863

matrix algebra continued

- density matrix eqn., coupled coherent and incoherent exciton motion on linear chain 3-64310
- eigenproblems, application of Lanczos algorithm, extension from shell model to continuum states 3-67228
- eigenvalues of matrix pencil $A + \mu B$ obtained by algebraic invariants and combinatorial analysis 3-70513
- elastic plate resting on Winkler foundation, natural freqs. of transverse vibrs. 3-70670
- electromagnetics, stability of matrix equations 3-77932
- e.m. field problems considering symmetric conducting bodies, characteristic modes 3-77931
- factorisation modification, report 3-59733
- function minimization, Davidson-Fletcher Powell method modification 3-62391
- g-matrix of Zeeman spin Hamiltonian, diagonalization for low symmetry transition ions 3-64450
- general matrix, derivatives of eigensolutions calc. 3-77763
- Hamiltonian, torsional fine structure, rotational spectra, two-top molecules (*German*) 3-75053
- Hermite's (real symmetric) pair, eigenvalue detn. using successive approx. method (*German*) 3-48696
- independence of local algebras, connection between Neumann algebras and their commutation 3-73984
- instrument lag analysis, by fast Fourier transform and matrix inversion techniques 3-45407
- Lorentz group, finite and infinite dimensional representations 3-77766
- Lowdin orthogonalization and square root of positive self-adjoint matrix 3-60407
- Mathieu equations, matrix solutions 3-45626
- matrix stability, initial boundary value, parabolic eqn. 3-73991
- Meissner eqn. soln. appl. to geometrically nonlinear deformations of toroidal shells (*Russian*) 3-66551
- molecular orbitals calc., diagonal, nondiagonal matrix elements 3-78672
- molecular vibration phenomena, mean-square amplitude, relations, temp. depend. 3-63411
- multimode reactor kinetics eqns. new soln. method by matrix inversion 3-54524
- neutron transport two-dimensional calcs. using response matrix technique 3-46055
- non-self adjoint systems, derivatives of eigenvalues and eigenvectors 3-42740
- nonlinear parameters, least squares estimation, matrix evaluation 3-40155
- nonsemisimple matrices, perturbation series for eigenvalues and eigenvectors 3-40084
- normal matrices with entries from an arbitrary field of characteristic $\neq 2$ 3-66483
- nuclear reaction theory, general integro-differential eqn. for transition matrix, potential scattering 3-60138
- nuclear reactor space-time kinetics, fully implicit matrix decomposition 3-46064
- off shell T matrices for triplet states soln., symmetry properties 3-60088
- operator element calc. for harmonic oscillator dynamical group construction 3-77868
- optimal design of geodetic nets 3-76557
- permutation group in hyperspherical formalism, matrix elements and recurrence relation 3-57482
- perturbation theory, degenerate state, diagrams, perturbation expansions, eigenfunctions, secular matrix elements (*Russian*) 3-48768
- polarisation, Jones matrix, Mueller matrix, Pauli's spin matrices, Poincare sphere 3-66763
- rarefied gas, thermal conduction analog 3-67943
- reflection matrices, two-dimensional, reduction of numerical errors, neutron transport 3-62399
- representations, boosting matrix elements for reduction (*ian*) 3-77767
- sixteen-vertex model, transfer matrix 3-62611
- SO(n) class I irreducible representations, matrix elements 3-54062
- spin $1/2$ wave eqn., explicit representations for hierarchy of algebras 3-78090
- stiffness matrix for a beam with an axial force 3-42766
- SU_3 Lie algebra, matrix representation, Clebsch-Gordan coeffs. 3-62783
- transfer matrix technique, appl. to two-dimens. model of planar channeling 3-52653
- transformation of complex skew symmetric matrix into real normal form, Bloch-Messiah theorem 3-67219
- two-dimensional incompressible potential flow around multicomponent airfoils 3-46424
- Vlasov operator, continuum eigenfunctions and dispersion function relation 3-66481

Matteucci effect see magnetoelectric effects; magnetomechanical effects

maximum principle

- see also *dynamic programming*
- nuclear reactor, boron controlled, optimal xenon shutdown 3-74642
- Pontryagin, proof of equivalence relations in burn-up optimization problem 3-63130

maxmin technique see optimisation

Maxwell-Boltzmann distribution see statistical mechanics

Maxwell effect see flow birefringence

Maxwell equations see electromagnetism

mean free path, carrier see carrier mean free path

measurement

- see also *specific measurements, e.g. frequency measurement*
- see also *recording; units (measurement)*
- borehole parameters, electronic methods (*Rumanian*) 3-44944
- conference, Boulder, Colo., USA, (June 1972) 3-48329
- e.m. transition rate, nuclear spectroscopy study with Van de Graaff generator (*French*) 3-59619
- instrumentation, modular format 3-45529
- magnetic materials under incremental magnetisation, properties (*Rumanian*) 3-55386
- measurement process performance and assurance programmers 3-48331

measurement continued

- measurement science programme, CAL Poly. 3-48330
statistical analysis of fluctuations, applications (*German*) 3-48337

measurement errors

- aerosol particle size, distrib., statistics 3-65030
aerosol size distribution, effect on integrating nephelometer accuracy 3-47836
airborne temp. data, correction method for sensor response time 3-47837
binary and quasibinary mixture, composition checking, accuracy, X-ray and γ -ray methods 3-69428
Bragg angles misalignment effect in zero-layer Weissenberg X-ray photographs 3-49798
chronopotentiometry, improved, use of potentiostat and capacity-current addition device 3-73950
corneal refractive index rel. to thickness and pachometric meas. errors 3-70123
device, stabilising emission spectrum, reduction of meas. error, spark-arc discharge generator 3-73754
electrically conducting materials, thermophysical prop. meas. apparatus, measurement errors 3-53855
e.m. wave measurements from satellites, evaluation of experimental errors 3-80862
flow turbulence characteristics determ. by flow visualisation meth., estimation of the accuracy 3-54053
fluctuating processes, choice of sensor integration time in measurements 3-59177
foil thickness measurement, by X-ray transmission, error sources 3-61987
fringe measurement, meas. time and coherence depend. 3-66230
geodesy, deflections of vertical and undulations rel. to accuracies of gravity anomalies 3-61291
glass temperature, thermocouple and spectral methods 3-66169
holographic interferometry 3-dimens. displacement meas., errors 3-39939
Langmuir probes, contaminated surface and reliability of electron temp. meas. 3-57940
laser distance meas. system comparing phase of modulating signal 3-51960
liquid systems, capacitance meas., frequency changes, heterodyne wavemeter, errors 3-48470
luminescence decay time meas. errors caused by photomultiplier saturation 3-73898
magnetograph, Crimean Observatory, effect of systematic errors on total vector (*Russian*) 3-77185
magnetograph plane-parallel plate errors 3-51406
maximum values of stationary random process using discrete methods (*Russian*) 3-53824
m.o.s. structure, CV doping profile obs., correction for interface state errors 3-55338
multiscale system, maximum likelihood estimation 3-70259
oceanographic vane current direction sensor, errors from frictional coupling 3-80869
optical instruments, nonsymmetrical aberrations, coma, lateral colour, analysis 3-53896
plasma diagnostics, interferometric method, accuracy when optical components become heated 3-63877
plasma probe, due to inadequate reference electrode 3-63874
quantisation of information, estimation, classical theory of joint events (*French*) 3-73659
RATAN-600, radiotelescope, distortion of reflecting surface, thermal effect, radial errors (*Russian*) 3-81233
radiometrics, error elimination 3-77375
rear-surface current meter obs., errors rel. to wave motion 3-44966
refractive index, solid and liquid homogeneous isotropic materials, anal. of systematic errors (*Czech*) 3-53880
retarding potential analyzers, errors due to grid plane potential nonuniformities 3-53993
retention times, gas chromatographic, systematic meas. errors 3-66430
semiconductor film, on transparent substrate, optical density detn. 3-75958
semiconductor mobility, Hall effect obs., sample geometry effects 3-55261
spectrophotometry, precision theory, reading error, electrical noise 3-62320
spike-interval sequence correlation estimates, effect of meas. errors 3-59534
systematic, detection (*Russian*) 3-53825
Universal Time determ., effect of right-ascension errors in stellar positions 3-77032
vapour-liquid equilibrium, overall area tests for thermodynamic consistency, effect of random error 3-58119
video-densitometric vascular flowrate measurement 3-59686
X-ray photoelectron spectroscopy, binding energy, surface charge errors, external standards 3-72777

measurement standards

- see also temperature scales
4 π radioactive sources on electrosprayed ion exchange resin, for standardization 3-56927
acoustic noise meas. methods, standardisation (*French*) 3-62001
air quality measurements, Environmental Protection Agency, reference methods 3-53562
ambiguities in the use of unit names 3-42510
ampere, standard, kept at NPL, change during 1972 3-61982
automation engineering in industrial processes, trends and views (*German*) 3-48332
beam-foil, light source as absolute intensity standard, near i.r. to vacuum u.v. and X-ray region 3-77503
capacitor, ring, rectangular with no insulating gaps, capacitance calc. 3-56697
contact profilometer calibration, roughness standard production and evaluation (*Slovak*) 3-66128
dosimetric standards (*French*) 3-66315
electrical, background described 3-77378
electronic standard meter, for precision meas. with watt-hour meters (*French*) 3-51512
e.m.f. comparison of standard cells 3-56610
far u.v. NBS detector standard 3-51507

measurement standards continued

- flow measuring equipment, Molch tester-volumetric standard (*German*) 3-59541
force standard machines, elastic proving devices 3-53826
frequency, clockface estimation accuracy by normal regression theory (*Japanese*) 3-66130
gamma-ray standards, National Bureau of Standards, gamma-ray meas. techniques 3-62303
Josephson junction transducer 3-48474
light velocity measurement techniques over last 300 years, and to form metre standard (*Norwegian*) 3-70261
metre, in terms of light velocity (*Norwegian*) 3-70261
paramagnetic salt temperature scale, NBS-acoustic scale, IPTS-68, relationship 3-61980
photoelectron spectroscopy, binding energy meas., surface charge errors, external standards 3-72777
powder standard specimens, by vacuum evaporation 3-55906
radioastronomical, four regions for 21 cm standards 3-56460
reference voltage source comprising operational amplifiers 3-45411
rontgen absolute determination, magnetic field pressure ionization chamber construction (*German*) 3-48274
rontgen absolute determination, X-ray source construction and testing (*German*) 3-45326
spectral irradiance measurement, interlaboratory comparison 3-66126
time scale clamping and frequency collation, using v.l.f. radiowave propagation 3-51510
tungsten halogen incandescent lamps, spectral irradi. standards, 300-1200 nm 3-39920
of USSR and GDR, comparative meas. with McLeod gauge (*German*) 3-45409
volt, methods for absolute determination (*Hungarian*) 3-73663
v.u.v. wavelength standards 3-39936
X-ray photoelectron spectroscopy, binding energy, surface charge errors, Au and C use 3-72777
CO₂ laser light, absolute frequency meas. of R(12) transition at 9.3 microns 3-61981
¹²C¹⁶O, absolute wavenumbers of 2 \leftarrow 0 vibr. rot. band, near i.r. standards 3-56611
H arcs for vacuum u.v. radiometry 3-51549
He-Ne 633 nm frequency stabilized laser, wavelength values 3-48452
HgCo(SCN)₄, mag. susceptibility temp. depend. to 5K 3-52952
NbC electron microprobe reference materials 3-40078
²²⁶Ra, unit of mass 3-51509
W, monochromatic emissivity, 1200-2600K 3-69352

measurement systems

- ASCORECORD 3 DP coordinate measuring instrument, development 3-48154
electrical measurement standards background described 3-77378
electronic instruments, conference, Paris, France, 12-18 April (1973) 3-53745

geophysics applic. 3-76861**Hall effect, magnetic field measurement, temperature compensation and current stabilisation 3-51664****h.f. loss instrument, analysis and applic. (*Japanese*) 3-70325****interdisciplinary nature of transducers 3-48355****laser radiation measurement device (*Russian*) 3-73797****layered lunar/earth surfaces, measurement of electrical parameters, bibliography 3-45241****mass spectrometer and electron spectrometer, computer control, for meas. of metastable atoms and molecules (*French*) 3-51737****multiscale, maximum likelihood estimation 3-70259****musical acoustics, adaptation of frequency analyser type 2107 to automated 1/12 octave spectrum analysis 3-56579****photoelectric methods, for ultra low light intensity meas. 3-45575****measurement theory****absolute radiometry, instrumental theory (*French*) 3-45438****basic concepts, formulation (*German*) 3-59535****education in measurement engineering, status and outlook (*German*) 3-59537****engineering aspects of further education in signal/system/information theory (*German*) 3-59536****errors in maximum values of stationary random process using discrete methods (*Russian*) 3-53824****historical background, present situation and future aims, of measurement engineering (*German*) 3-61977****ionospheric probe meas. theory for lower ionosphere 3-53554****quantisation of information, estimation, classical theory of joint events (*French*) 3-73659****quantum, concepts of state preparation and determination 3-74088****simultaneous of several observables, postulational framework 3-74087****spectrophotometry, precision theory, reading error, electrical noise 3-62320****Stochastic-ergodic measuring methods (*German*) 3-70258****mechanical birefringence****see also photoelasticity****acoustic in solids, analogy with optical birefringence (*French*) 3-43830****1-4-diaminopiperazine polymers and metal chelates, dynamic mechanical, thermal electrical and tensile props. 3-80462****PMMA, biaxial orientation birefringence, rel. to degree of deformation 3-71682****polymers, amorphous, biaxial orientation, macromol. orientation distrib. function, rel. to birefringence 3-71682****GaP, stress induced, dispersion 3-64623****LiNbO₃, single cryst., residual-stress relax. effect 3-72596****mechanical engineering****ball motion in ball bearing, digital simulation method 3-48711****internal energy dissipation simulation in elastoplastic connections using analogue computers 3-57096****laser beam applications 3-40294****mechanical hysteresis loop, Fortran program for low cycle fatigue test data processing (*Japanese*) 3-55799****mechanical hysteresis loop, Fortran programs for stress-strain relationships (*Japanese*) 3-54090**

mechanical engineering continued

structures, dynamics and materials, conf., Williamsburg, USA (Mar 1973) 3-59749

mechanical impact *see impact***mechanical organs** *see artificial organs***mechanical oscillations**

acoustic nonlinear oscillations in pipes 3-51478
 air bubble in gel, volume pulsation by sonic excitation 3-42480
 airfoil, unsteady aerodynamics 3-57791
 axisymmetric plate with stabilised rotation, gyroscopic bound oscillation (*Russian*) 3-62525
 beam, hollow, smallest-weight, forced oscillations, parameter determ. (*Russian*) 3-62537
 beams in forced oscillation, determ. of two frequency transients (*Russian*) 3-62528
 bifurcation and stability of stabilising motions of complex mechanical systems (*Russian*) 3-66511
 body with fluid, eqns. of perturbed motion for large angles deviation of surface normal from axis (*Russian*) 3-70655
 Brownian oscillator with viscous after-effect, correl. functions, asymptotic form (*Russian*) 3-42897
 Chladni's figures, circular metal plates, normal mode frequency determination, empirical equations 3-59496
 constrained system, constraints and potential slowly varying, approx. formulae (*Italian*) 3-77839
 constrained system, slowly varying, approx. formulae, double pendulum (*Italian*) 3-77840
 cylinder, composite, torsional vibrations 3-62519
 cylinder, thick-walled, containing compressible liquid, mutually coupled elastic-acoustic waves (*Russian*) 3-62538
 cylinder, thin flexible, towed in viscous fluid 3-42811
 cylindrical shells of variable thickness and lumped-type enclosures of masses, natural oscillations (*Russian*) 3-40140
 damped system, linear eigenvalue problem 3-70540
 damping of impact action, effects of nonlinearity of anti shock damper (*Russian*) 3-74083
 deflectional-torsional, of multi-disc rotor, soln. of quasilinear differential eqns. (*Russian*) 3-42817
 digital incremental oscillator-analyzer system, for vibration testing, inherent limitations 3-61949
 earth's core, density perturbations, due to hydromagnetic oscillations 3-76594
 Earth's inner core, oscillations rel. to geomagnetic field generation 3-50924
 elastic, of liquid-filled tank, synthesis of optimal longitudinal travel control (*Russian*) 3-59773
 elastic bodies, nonhomogeneous, integration of eqn. using Ritz variational method 3-42802
 elastic cylindrical shell, liquid-filled, forced oscillations numerical analysis (*Russian*) 3-42816
 elastic natural and forced oscillations, calculated from boundary problem for integro-differential eqns. (*Russian*) 3-62521
 elastic nonlinear nonautonomous systems with variable parameters, random oscillations (*Russian*) 3-77844
 elastic-plastic, oscillator, plastic dissipation, a priori bounds 3-66565
 falling body, natural mode of oscillation of vortex (*Russian*) 3-62440
 forced, of cylindrical shells with gas-pressure fluctuations, variable stress analysis (*Russian*) 3-62535
 free oscillations of laterally inhomogeneous Earth, quasi-degenerate multiplet coupling 3-44754
 gas, nonviscous, small self-oscillations in gravitational field, completeness problem (*Russian*) 3-67952
 gyroscope, cardan suspension elastic deformation, effect on nutational oscillation frequency (*Russian*) 3-59742
 half-subharmonic oscillations, harmonic balance method study 3-42813
 impedance, point, impulse type excited extensional waveline, technique and procedure (*German*) 3-70219
 in-plane vibration of continuous curved beams, determ. of frequencies 3-74068
 infrasonic resonances, of passenger cars on motorways, narrow-band analysis 3-61948
 interaction of self oscillations, nonlinear friction and coordinate coupling interaction (*Russian*) 3-74074
 longitudinal, of nonlinear systems with disturbances propagating in their length (*Russian*) 3-66582
 machinery vibration, isolation and absorption 3-48295
 magnetospheric tail, plasma sheet oscillations, effect of magnetic field inhomogeneity 3-53536
 membranes, circular, in nonlinear elastic base, double frequency regime of natural oscillations (*Russian*) 3-62527
 MHD system, uniformly rot., variational principle and virial theorem 3-57821
 non-linear systems, step function excitation 3-59770
 nonlinear of analytic autonomous system, third-order normal forms 3-70676
 nonlinear recurrent formulae for calc. of normalising transformations and normal forms (*Russian*) 3-66580
 nonlinear system, condition for periodic oscillations (*Russian*) 3-62526
 one-degree of freedom system with nonlinear viscoelastic suspension, stability of equilibrium point (*Polish*) 3-70680
 one-degree-of-freedom system with jump-like variable mass, probabilistic problems (*Polish*) 3-66590
 oscillogyro, dynamics 3-66135
 pendulum with biaxial swing, systematic errors (*Russian*) 3-74077
 piles in water, vortex excitation 3-60545
 plane layer, dynamic coupled thermoelastic problem, dynamic perturbation, oscillating load (*Russian*) 3-70582
 plastic shell, three-layer, free oscillation, boundary conditions, Bubnov-Galerkin method, effect of angle of layer anisotropy (*Russian*) 3-70632
 porous materials, elastic matrix, acoustic wave induced, motion and continuity equations 3-59507
 prismatic shells filled with fluid, free oscillations 3-75236
 punch, adhesion to visco-elastic medium surface, axially-symmetric contact problem (*Russian*) 3-77848
 rectangular vessel with fluid, vertical periodic motions 3-67953

mechanical oscillations continued

relaxation self-oscillation in systems with friction (*Russian*) 3-57050
 rod, hollow, response to transient impulse 3-42810
 rotating body with viscous fluid in cavity, stability (*Russian*) 3-62536
 sandwich beams of unsymmetrical structure, free transverse vibrations, natural frequencies calc. 3-70639
 self-oscillation with friction, existence and stability (*Russian*) 3-57051
 single-index stereomechanical oscillator determ. using mechanical analogy in class of Lagrange's eqns. (*Polish*) 3-66594
 small, of heavy solid body around fixed point, existence of linear integrals (*Russian*) 3-66581
 solar 5-minute oscillations, near u.v. obs. of phase lags 3-80943
 solid body containing cavity completely filled with two immiscible fluids, motion (*Russian*) 3-66579
 solid body rotating, partially filled with viscous liquid, oscillation frequency determ. (*Russian*) 3-70658
 stamp, dynamic contact problem for isotropic semi-space, strain of longitudinal shear (*Russian*) 3-62467
 stars, oscillations and stability of rotating masses with magnetic fields 3-47986
 stellar oscillatory secular modes rel. to main-sequence stars and He-burning shells 3-51324
 string, with distributed point masses, analytical soln. based on corresponding functions (*Russian*) 3-42757
 suspended flexible line, small oscillations, power series solns. 3-70672
 testing apparatus for material characts. study under transverse and torsional oscillations 3-65059
 third-order non-linear systems, transient response 3-62524
 torsional oscillating sphere induced flow of a rotating viscous incompressible fluid 3-63671
 torsional proper frequencies of system with homogeneous centre and two fly wheels, anal. of Biot's method (*Italian*) 3-77832
 torsionally oscillating disc, induction of MHD flow 3-75258
 transverse, of heavy chain, use of transforms with orthogonal polynomial kernels 3-48698
 trifilar pendulum, inherent errors in measurement of moment of inertia 3-39845
 turbulent boundary-layer wall pressure spectrum, low-wavenumber region study 3-42466
 underwater bubbles, energy loss mechanism in oscillations 3-42481
 unsteady subsonic compressible flow around oscillating finite thickness wing 3-57789
 weakly coupled, oscillators behaviour near equilib. position (*Russian*) 3-74075
 wings with thickness, oscillating, unsteady transonic aerodynamics 3-57790
 He-Ne laser frequency stability 3-66815
 Ni, magnetoelastic oscillations, nonlinear, in torsional pendulum with Ni tube spring (*German*) 3-44304
 Ni rod, torsional spring element, magnetomech. amplification and generation of mech. vibrs. (*German*) 3-58408

mechanical permeability
see also diffusion in solids
 alkali silicate glasses, helium migration behaviour 3-75631
 borosilicate glass, of He, alkali oxide effects 3-44677
 glass, of He gas 3-72226
 glass ribbon composite, fabrication and characteriz. 3-76348
 steel, He permeability (*German*) 3-72887
 steel, of hydrogen, structure influence (*Russian*) 3-80254
 Fe, soft, He permeability (*German*) 3-72887
 Mo, of hydrogen, in mono- and polycrystals. (*Russian*) 3-58144
 Na₂O-K₂O-SiO₂ system glasses, He migration behaviour 3-75632
 W, of hydrogen, in mono- and polycrystals. (*Russian*) 3-58144

mechanical properties of liquids
 films, meas. of breakdown times 3-60835
 shear elasticity at various shear angles, rel. to supermolecular struct. 3-40948

mechanical properties of solids *see mechanical properties of substances*

mechanical properties of substances
see also anelasticity; bending; brittleness; deformation; elastic constants; elastic relaxation; elasticity; elasto-optical effects; fatigue; fracture; hardness; internal stresses; mechanical permeability; mechanical properties of liquids; mechanical strength; photoelasticity; photoplasticity; piezo-optical effects; plasticity; rupture; slip; stress/strain relations; tribology
 β -Al₂O₃ conductive ceramics for Na-S battery 3-80417
 alloy, two-phase, microstructure and properties, quantitative relationship 3-61140
 ceramic, thermoplastically produced, ion-phase exchange, hardening 3-76317
 cubic crystals, exponentially attractive and repulsive interatomic potential function applic. 3-68303
 epoxy resin, cured, filled with mica flake, dynamic 3-69379
 epoxy resin systems of reduced viscosity, gamma-irradiated, mechanical properties 3-50786
 epoxy resins, diamine-cured, dynamic 3-69378
 glassy polymers, book 3-46591
 glassy polymers, structure, packing density, free volume concepts, mech. behaviour 3-46592
 glycidyl amine resin systems of reduced viscosity, gamma-irradiated, mechanical properties 3-50786
 partially molten rock analogues, extensional wave velocity meas. technique 3-65204
 polymer, cracking and crazing, under tension, laser diffraction obs. 3-52667
 polymer, mech. relax., bundle model test (*German*) 3-60672
 sodium silicate glasses, effect of iron oxides on characterization 3-76378
 steel, stainless, determined in high-speed extension (*Russian*) 3-53250
 steel sheet, with 4.5-7.7%Si, mag. and mech. props. (*Japanese*) 3-41787
 teflon, aq. suspension 3-65026
 B, single crystal, characterization 3-44552

mechanical properties of substances continued

- Ni-B alloy, electroless plated 3-44301
 Si, surface props. rel. to planar technology 3-69179
 Ti alloys, determined in high-speed extension (*Russian*) 3-53250
 γ -U-Mo, pulsed reactor fuel, mechanical props. 3-63206
- mechanical strength**
see also compressive strength; rupture; shear strength; tensile strength
 adhesive bond strength, nondestructive vibrational meas., honeycomb sandwich panels 3-47513
 alkali halide, polycryst., fusion casting, mech. and opt. props. 3-76254
 alloy, two-phase, microstructure and properties, quantitative relationship 3-61140
 anisotropic stretched ring, elastic and strength props. analysis 3-80487
 Asbotextolit sheet exposed to high temps. on load-bearing zone surface, mech. failure 3-47472
 brittle materials, heat resist. problems and rupture 3-58702
 brittle materials, impact tests, fracture toughness and absorbed energy release 3-58779
 brittle prismatic bars weakened by round internal cracks 3-80379
 capron, electron irradi. rate and deform. rate effect (*Russian*) 3-80467
 cellulose, gamma-irradiated, changes in strength, heat of wetting, during storage 3-73059
 ceramic, effects of microstruct. and internal stress 3-76244
 ceramic, microcrack propag., long-term isotherms and isotherms after quenching (*German*) 3-44644
 ceramic spherical shells, load-bearing capacity under external press. 3-64977
 ceramic structures, photoelastic methods approach to stress investigation (*German*) 3-44645
 ceramics, time and temp. dependence, reinforcement of materials by filaments, strength-controlling structure 3-50756
 composite, fibre reinforced, transverse strength 3-73029
 composite, reinforced, strengthening, use of internal stresses 3-73022
 composite beam elastoplastic deformation, models 3-80456
 composite beam elastoplastic deformation, quasihomogeneity problem 3-80457
 cyanoacrylate IS 12, bond strength expts. for photoelasticity sandwich technique 3-48351
 cylinder subjected to transverse flexure, tangential stresses and testing of strength 3-59760
 cylindrical shells, effect of dynamic pre-loading on supporting power (*Russian*) 3-42785
 cylindrical specimen with ringcrack applic. to strength determ. in material with brittle fracture (*Russian*) 3-41760
 epoxy resins, impregnation of superconducting magnet windings 3-58786
 fast reactor, Na cooled, structural design criteria 3-67507
 fibre reinforced materials, effect of interlaminar stiffness and strength, plane stress 3-73023
 four-section equipment for creep and long-term strength testing in deep cooling conditions 3-47527
 glass, borosilicate, strengthening, dynamic hydrothermal treatment of surface 3-44673
 glass, crystallized, Al-containing, microstruct. rel. to mech. strength (*Japanese*) 3-44684
 glass, organic, endurance under cyclic elastoplastic deform., liq. media influence (*Russian*) 3-80465
 glass, rel. to surface microstructure 3-44674
 glass, strength correl. with glassy microsphere size and conc. 3-55884
 glass, torsional strength under hydrostatic pressure 3-65021
 glass ceramics, isothermal heat treatment effects 3-55835
 glass fibre, etched; structure and strength (*Russian*) 3-53280
 glass fibre reinforced polyester, impact strength 3-64980
 glass laminate, effect of porosity on strength 3-64987
 glass reinforced plastic and components, effect of proton-electron rad. on strength 3-61207
 glass reinforced plastics, effect of dynamic loading on mech. props. 3-50776
 glass ribbon composite, isotropy of strength 3-76349
 glass sheet with defect surface, temp. variation of strength in air and vacuum 3-47473
 glass-crystalline materials, cast, rupture character 3-47475
 glass-reinforced plastics, winding, change in degree of anisotropy, elastic and strength props. 3-73024
 glasses, time and temp. dependence, reinforcement of materials by filaments, strength-controlling structures 3-50756
 glassy polymers, toughening by rubber reinforcement, review 3-47481
 graphite, metal-impregnated, fracture resist. 3-76345
 graphite, reactor, neutron irradiation effect, 400°C (*German*) 3-71275
 halide laser windows, press forged, mech. props., grain size and alloying depend. 3-73786
 impact testing machine design description, 1.5 to 300 K range 3-55921
 jade, toughness 3-73195
 laminates, free edge model for catastrophic delamination 3-69369
 lenses, ophthalmic, strengthening, chemical ion exchange, evaluation 3-73740
 magnetic carrier type composites, short-time strength and deformability at high temps. 3-47463
 mathematical introduction, solved problems, book contrib. 3-58082
 metal, b.c.c., neutron irradi. damage effect on mech. props. 3-79380
 metal, ideal strength, Morse potentials use and limitations 3-58061
 neutron irradiation softening and effect of interstitials 3-79343
 nuclear fuel element, spherical, neutron irradiation and corrosion effect (*German*) 3-71265
 polycarbonate, bisphenol-A, short range intermol. ordering role in impact props. 3-80473
 polycarbonate, Charpy notched impact strength, A and B forms comparison 3-80474
 polydisperse cohesive comps., cross-linked, theoret. principles of strength 3-76391

mechanical strength continued

- polyethylene, linear, low-temp. toughness below glass transition 3-49852
 polymer, change of strength in process of orientation 3-71685
 polymer, glassy, impact test, model exam. 3-58778
 polymer, multiphase mixtures, pair additivity principle 3-73042
 polymer, oriented, theoretical strength from intermolecular interaction and finite chain length 3-57698
 polymer, reinforced with three dimensional woven multilayer glass fabric, deformation and strength characteristics 3-58712
 polymer, static fatigue, activator evaluation 3-61217
 polymer films, impact testing technique 3-50807
 polymer fracture mechanics, review 3-76364
 polyurethane, fracture toughness and impact strength, Dugdale model 3-80472
 polyurethane type plastic foams, cellular structure, mechanical props., model anal. 3-73090
 porcelain, sintered and with added calcined kaolin (*German*) 3-55833
 pyrocatechin-formaldehyde resins, structural changes during heat treatment, i.r. spectra (*Russian*) 3-63604
 quartz glass, fused, hydrolytic surface defects and high-strength state 3-72274
 refractories, brittle, thermal stress resist. caused by anisotropic behaviour of grains in polycryst. matrix (*German*) 3-61187
 refractory, fireclay, rel. to thermal shock behaviour 3-80414
 refractory, thermal shock damage resistance depend. 3-80404
 refractory concretes, calcium aluminate bonded, thermal shock testing 3-80405
 refractory oxide fibre eval. for high temp. rigidized insulation applic. 3-76276
 rubber reinforced plastics, transition magnitudes and impact improvement 3-50783
 sapphire disks, synthetic, biaxial flexural strength 3-73788
 sedimentary rocks, electrical resistivity and strength dependence on changes of pore pressure 3-65163
 shells, thin metallic under transverse loading, literature review (*Russian*) 3-76220
 soda-lime glass, polymeric coating effects on bend strength 3-76265
 steel, A19 alloy, Be, Ti and Zr additions effect (*Russian*) 3-72850
 steel, austenite thermal stabilization kinetics 3-50728
 steel, carbon-manganese and as-rolled mild, silicon and nitrogen influence on impact properties 3-68332
 steel, computerized time-temp. parametric analysis of stress-rupture data 3-50746
 steel, corrosion fatigue strength in sea water, cathodic polarization influence (*Russian*) 3-80316
 steel, Cr-Ni type, austenite struct. and strength changes during ageing (*Russian*) 3-80277
 steel, crack development resist. and yield stress, temp.-rate relationships (*Russian*) 3-58651
 steel, endurance at normal and low temps., effect of surface finish and surface treatment method 3-44634
 steel, etching medium comp. influence (*Russian*) 3-61164
 steel, eutectoid-composition, finely spheroidized, thermal mech. treatments influence on mech. props. 3-53258
 steel, ferrite-class, substructure and its effects on mech. behaviour (*Russian*) 3-53225
 steel, hardened, microstruct. of breaks and fracture toughness (*Russian*) 3-41716
 steel, heat resistant low-alloy CrMoWV type, Ti and Zr effects on long-term plasticity 3-69323
 steel, heat treated to different strength levels, adsorptional relief of failure (*Russian*) 3-58650
 steel, heat treatment, relaxation strength relations 3-55801
 steel, high-speed, welded blanks, struct. and props. after annealing 3-55814
 steel, low-C electromelted, comp. and complex deoxidizing effects (*Russian*) 3-58647
 steel, martensitic Ni-Cr-Mo-Co, toughness and strength characteriz. 3-64915
 steel, Ni-Cr-Mo, medium-C type, impact toughness of martensite and bainite 3-61180
 steel, plastic deformation and ageing effects (*Russian*) 3-69265
 steel, reactor structure, strain-rate influence, meas. equipment 3-67537
 steel, Si-Mn type, comparative evaluation of performance 3-55917
 steel, stainless, martensite reversion to austenite, strengthening effect 3-80214
 steel, stainless, Type 316, mech. and struct. props. for LMFBF cladding, rupture 3-47394
 steel, strengthening mechanism, high-temp. thermomech. treatment (*Russian*) 3-80309
 steel, technical cohesive strength determ. from internal energy 3-44627
 steel, with rare earth additions, brittle fracture susceptibility rel. to state of grain boundaries (*Russian*) 3-72894
 steel bar reinforcement, deformation, fatigue strength, spot welding effect (*German*) 3-44638
 steel disc reinforced polycarbonate, strength improvement 3-80440
 steel joints, high-strength, with low-strength weldment 3-69295
 steel plate, Charpy-V impact props., stat. analysis 3-50824
 steel plate, notched, stressed state, thickness depend. 3-80362
 steel with 9% Ni, low temperature notch toughness (*Japanese*) 3-41770
 steel/Cu bimetallic discs, stressed state characteriz. 3-44633
 stiffened panels containing fatigue cracks, residual strength characts. 3-64894
 time-dependent strength and failure, eqn. development 3-65020
 ultimate state criteria, role of structure parameters 3-58675
 variant construction 3-60768
 welded components, weak joint, viscous strength, effect of mech. inhomogeneity (*Russian*) 3-41792
 yield strength gradient depend. of crack propag. rates 3-76228
 Al, technical cohesive strength determ. from internal energy 3-44627
 Al coatings on steel, technique description 3-55802
 Al-Al₂O₃ alloys, ball-milled, room and elevated temp. props. 3-44613

mechanical strength continued

- Al-Mg-Si 6061 alloy, mechanical props. after very rapid heating 3-47405
- Al-Zn alloys, axisymm. extrusion, activation enthalpy and material consts. depend., relation to recrystn., substruct., mech. props. 3-47403
- Al-Zn-Mg alloys, axisymm. extrusion, activation enthalpy and material consts. depend., relation to recrystn., substruct., mech. props. 3-47403
- Al₂O₃, high integrity body design using chem.-mineralogical phase anal. 3-76274
- Al₂O₃, hot-pressed, annealing effect 3-72935
- Al₂O₃/transition metal carbide composites, sintering parameters correl. with mech. props. 3-73002
- B/epoxy prepreg tape, prestressing effects on composite strength props. 3-69375
- B₂C, B/C ratio depend. 3-80403
- C foams, syntactic, review 3-80443
- CaB₆, hot pressing and characteriz. 3-69347
- Cu, technical cohesive strength determ. from internal energy 3-44627
- Cu/Mo composite, stress deformation state, microhardness obs. 3-80369
- Fe, Armco, brittle fracture susceptibility rel. to state of grain boundaries (*Russian*) 3-72894
- Fe castings, pipe, strength gradient, transverse bending of ring sector 3-50805
- Fe-Cr-Ti alloys, titanium effects 3-69283
- Fe-Mo solid solns., low temp. strength, alloy softening, scavenging of interstitials 3-64921
- Fe-Ni-Al alloy, nitriding, hardness, struct. (*German*) 3-76193
- KCl, hot worked, strength and deformation behaviour 3-76252
- Li₂O-SiO₂ glasses crystallized after ion exchange below T_g, characteriz. 3-76266
- Mg sintered composites, cladding material of U fuel elements, mechanical properties, creep and rupture (*Czech*) 3-67556
- MgAl₂O₄, transparent shaped mat., fabrication and props. 3-72967
- MgTiO₃, hot-pressed, grain size effects 3-69339
- Mo, deformed, struct. stability and mech. characteriz. under prolonged influences of temp. and stress 3-44630
- Mo, u.s. vibr. effects (*Russian*) 3-69207
- Na₂O-CaO-SiO₂ glass rods, thermal stress resist., abrasion effect 3-76328
- Na₂O-SiO₂ glasses, strength characteriz. 3-76267
- Nb-W-Mo-Ti-Zr-C alloy, quenching, multicomponent solid soln. formation, ageing, carbide precipitation 3-76176
- Nb-W-Mo-Zr, aged carbide phase distrib., mech. strength, hardening (*Russian*) 3-41721
- Ni, technical cohesive strength determ. from internal energy 3-44627
- Ni composite, W(Mo) wire reinforced, diffusion, carbide layer formation, recrystallisation rel. to weakening (*Russian*) 3-53272
- Ni₃Al-Ni₃Nb eutectic, directionally solidified, characteriz. (*Russian*) 3-44605
- Pb-Ca-Sn alloys, battery grid mat., grain struct., mech. props., corrosion 3-41724
- α -Pu, room temp. bend strength 3-54540
- Se, amorphous, crystn. role 3-76366
- SiC, hot-pressed, fabrication and strength characteriz. 3-76295
- SiC, pyrolytic coatings of fuel particles, strength characteriz. 3-43311
- SiC, vol., area and temp. depend. 3-76285
- SiC refractories, bonded, room temp. to 1200°C, characteriz. 3-76288
- SiC/B, hot-pressed, correl. with grain struct. 3-76297
- SiC and composites, characteriz. for turbine applics. 3-76281
- Si₃N₄, hot pressing, high temp. flexure strength rel. to impurities, 1375°C 3-76305
- Si₃N₄, vol., area and temp. depend. 3-76285
- Si₃N₄/W, fibre reinforced, strength characteriz. for high temp. applics. 3-76352
- Si₃N₄-SiC composite system, microstruct. effect on strength 3-76296
- Si₃N₄ and composites, characteriz. for turbine applics. 3-76281
- SiO₂, fused, W fibre reinforced composite, hot pressing 3-76360
- Ti alloys, fracture, micromechanisms, hydrogen influence (*Russian*) 3-80322
- UO₂ bars, thermally shocked, crack healing, isothermal annealing effect 3-74727
- W:Be doped filament, secondary β -W, formation (*Hungarian*) 3-72986
- W-Ni-Fe composite, reinforced with W wire fibres 3-69370

mechanical testing

- see also *dynamic testing; hardness testing; mechanical variables measurement*
- abrasive wear specimen testing apparatus (*Russian*) 3-61239
- boiler drums, non-steady operating conditions, life testing, varying tension, high temp. and pressure 3-50808
- brittle materials, apparatus for recording acoustic signals from cracks 3-42519
- brittle materials, impact tests, fracture toughness and absorbed energy release 3-58779
- ceramic casting, equipment for determ. physical and mechanical props., heat treatment, pouring 3-50809
- circular plate, stiffness and critical load determ. from a simple bending test 3-80508
- clay, triaxial compression test, effects of specimen height and strain rate 3-69422
- composite, C fibre reinforced, interlaminar shear strength under impact conditions 3-55860
- composite, C fibre reinforced plastics, shear damage effects on torsional behaviour 3-55856
- composite, unidirectional, in-plane shear stress/strain response 3-55924
- compression jig, microstrain, macrostrain regions 3-76405
- concrete, nonreinforced, triaxial testing 3-65049
- contact fatigue, flat specimens, running-in test method 3-50811
- corrosion fatigue testing, environmental and superimposed wave effects (*Japanese*) 3-41830

mechanical testing continued

- creep testing machines, development and performance parameters 3-69437
- cryostat, reloading device, tensile testing at 20 K 3-51558
- cryostat for studying optical absorption under uniaxial stress 3-39899
- design props. of materials test method 3-50817
- device, volume stressed state, to 300C, effect of pressure, force and bending 3-50813
- dimensioning and strength calcs., conf., Budapest, Hungary (Oct. 1971) 3-69429
- four-ball machine, reduced machine time, lengthy friction path, wear of steel balls, effect of lubricating oils 3-53307
- four-section equipment for creep and long-term strength testing in deep cooling conditions 3-47527
- graphite, tension-compression tests, strength in a plane stressed condition 3-53298
- graphite antifriction materials, wear and friction properties, influence of adsorption 3-50810
- heat pipes, bench and thermal vacuum testing 3-51548
- hot torsion test, plotting of flow curves, effect of specimen dimensions on slope (*German*) 3-73098
- hot torsion tests for solid and tubular specimens, specimen geometry effect 3-55925
- impact testing machine design description, 1.5 to 300 K range 3-55921
- long time strength testing and equivalent damageability hypothesis 3-44705
- low interaction tension torsion load cell 3-66145
- magnetic carrier type composites, short-time strength and deformability at high temps. 3-47463
- metal, hot torsion testing for flow stress determ. 3-76416
- metal, thermal and structural stresses, electrical heating, const. length 3-73105
- metal coatings, wear resistance from electrical resistance 3-73103
- metal pairs in mutual compression, zone of contact prop. testing apparatus (*Russian*) 3-58777
- metal specimens, apparatus for measuring and recording elec. resist. 3-45535
- micro-indentation method and apparatus for studies in temp. zone near brittle failure (*Russian*) 3-80514
- multiposition test machine for high temp. testing in vacuum and gaseous media (*Russian*) 3-80511
- NT Nairit vulcanizates, deformed, crystallisation and melting, dilatometric method 3-73051
- nondestructive, basic metallurgy 3-53295
- nonmetallic materials, mech. props. testing apparatus for -80 to +300°C 3-65058
- plastic isotropic materials, math. model of damage accumulation 3-64936
- plate, perforated, with square and triangular penetration patterns, effective elastic consts. for bending 3-50821
- pneumatic creep testing machine (*German*) 3-65053
- cis-1, 4-polybutadiene vulcanizates, crystallisation and melting, dilatometric method 3-73051
- polymer, glassy, impact test, model exam. 3-58778
- polymer films, impact testing technique 3-50807
- polymers, deformability, wide temp. range, device for plotting thermomechanical curves, constant load, continuous heating 3-55915
- porcelain, sintered and with added calcined kaolin (*German*) 3-55833
- porous materials, compressive strength meas. 3-44699
- ring method of testing, correl. between high-temp. bending and tension stress relax. 3-69430
- rupture machine attachment for testing samples in biaxial stressed state at low temps. 3-47529
- sand, triaxial compression test, effects of specimen height and strain rate 3-69422
- scaling heat resistance meas. method for metallic materials (*Polish*) 3-50719
- sheet materials, relaxation stress testing device, thermocouple indicator, 300 to 1000C 3-53300
- small-sized precision rupture machine 3-76404
- steel, constrained disc burst tests, elastic-plastic analysis 3-50822
- steel, Cr-Mo-V, low-alloy, creep rupture tests, effect of carbide repartition (*German*) 3-69255
- steel, creep tests, supporting effect of bending specimens, 400-500°C (*German*) 3-69421
- steel, fatigue crack propag. vel., depend. on degree of rarefaction of air, apparatus design (*Russian*) 3-80510
- steel, high strength, creep rupture tests, effect of interruption in mechanical stress (*German*) 3-69253
- steel, high-strength, test method for transient stress conditions characteriz. at elevated temps. 3-69432
- steel, persistence of asperities in indentation experiments 3-72125
- steel, Si-Mn comparative evaluation 3-55917
- steel, stress relaxation tests, bending, tension, time factor effect 3-50803
- steel, structural, creep tests, rel. to rectangular plates dimensioning 3-69438
- steel cylinder, wire-wrapped, fracture resistance 3-50825
- steel plate, Charpy-V impact props., stat. analysis 3-50824
- steel plates with oblique hole, corner shape effect on elastic stress and strain conc. 3-50823
- steel pressure vessels, thick-walled, fracture mechanics aspects 3-76409
- tensile specimen, necking during creep at const. load and ambient temp. (*German*) 3-65051
- tensile testing, light-weight grips for rod specimen 3-44702
- tensile testing machine extension for axial load and torque action, low temp. 3-58784
- tensile testing small local deviations, influence in specimen diameter on conventional strain at maximum load in tensile test (*German*) 3-47524
- thin films, setting up of initial stresses, relaxation testing, corrosive media 3-53299
- tool materials, durability testing, vertical compression moulding, casting machine 3-53306
- tubular specimens, thin-walled, three-dimens. stress, testing device 3-73102

mechanical testing continued

- X-ray and γ -ray dosimetric methods (*French*) 3-66315
 Al-Cu-Mg alloy, high temp. fracture toughness test method 3-69433
 Co-Cr alloys, low-ductility dental casting, elongation meas. and interpret. 3-69403
 Fe castings, pipe, strength gradient, transverse bending of ring sector 3-50805
 U alloys, thermomech. testing under conditions of rapid fission heating 3-47531

mechanical variables control

- this heading is restricted to those variables which are not covered by other specific headings. See also, for example, force control; thickness control; velocity control; vibration control
 elastic deformation, anisotropic, single crystal, method for creation and control of deformation, uniform compression 3-73668

mechanical variables measurement

- this heading is restricted to those variables which are not covered by other specific headings. See also, for example, force measurement; thickness measurement; velocity measurement; vibration measurement

- ASCORECORD 3 DP coordinate measuring instrument, development 3-48154
 bathymetry effect, coastal upwelling, subsurface motion, induced jet 3-47673
 bubble size distributions, gas/solid fluidized layers, capacitive probe (*German*) 3-45617
 conference, Paris, France, 12-18 April (1973) 3-56619
 creep meas. using helically coiled springs, Bingham flow 3-45422
 cross section, limiting state, unhinged reinforced concrete arch, parabolic-shaped axis (*Russian*) 3-70268
 deformation quantitative meas. using holography 3-45414
 dimensional metrology, interdisciplinary nature of transducers 3-48355
 dimensional metrology, laser based systems 3-48357
 dynamic plasticity under combined stresses, medium rate tension-torsion machine 3-48354
 dynamic tensile failure in liquids new technique 3-39852
 elastic constants, dynamical determination by means of electromechanically excited resonators 3-51533
 fibre optics applic. 3-48362
 friction, static coeff. for spheres and cylinders 3-53843
 fringe method for meas. of deformations, vibr., contour lines and differences of objects 3-59550
 glassy polymers, use of Rheoribron for meas. of dynamic moduli 3-42515
 holographic interferometry for creep and failure studies 3-66149
 impedance, point, impulse type excited extensional waveline, technique and procedure (*German*) 3-70219
 inhomogeneous films, determination of distribution of material 3-45421
 internal friction, low-frequency installation, meas. frequency of torsional vibrations, electronic circuit 3-73669
 linear motion accuracy, interferometric method using diffraction grating 3-66131
 metal, plastic deformation investigation using exoelectron emission 3-48585
 nuclear fuel pins, neutron radiography, electronic image analyser, dimensional meas. 3-46148
 optical microscopy, application to electrochemical studies, review 3-66198
 partial arcs, best fit reference line method 3-61990
 radial mode coupling factors, piezoelectric ceramics, large variation in Poisson's ratio 3-45416
 small movement and vibrations, by laser photography 3-48361
 Tilttable Optical Circular Table, 320 S, VEB Carl Zeiss JENA 3-51599
 universal nuclear radiation meter, for industrial applic. (*German*) 3-48517
 viscoelastic properties, u.s. freqs., method for high viscosity liqs. 3-61993

mechanical waves see elastic waves**mechanics**

- see also bending; celestial mechanics; classical mechanics; damping; density; dynamics; fluid mechanics; intermolecular mechanics; kinematics; momentum; statics; statistical mechanics; wave mechanics

- averaged lagrangians containing higher derivatives 3-57043
 elastic discretized bodies, conservation laws and eqns. of motion 3-54083
 equivalent Lagrangians and quantization 3-48763
 generalized, extension to higher-order negative and positive derivatives 3-57046
 related integral theorem in phase space, Poisson's theorem generalization on constants of motion 3-51776
 tensor analysis on fundamental principles 3-42759

mechanics of fluids see fluid mechanics**medical effects of radiation see biological effects of radiation****medical electronics see biomedical electronics****medical information processing**

- chemico-clinical laboratory SILAB system (*Italian*) 3-48686
 evoked potential audiometry, clinical applic., special purpose computer for (*Hungarian*) 3-73575

medical sciences see medicine**medicine**

- see also biomedical engineering; cardiology; health hazards; patient diagnosis; patient monitoring; patient treatment; physiology
¹³¹I Hippurian renogram, computer-aided statistical analysis 3-56533

- bibliography No.25 of unclassified documents published by AWRE 3-73627

- data rel. to e.e.g. 3-59439
 health phys. conf. Miami Beach, USA (1973) 3-77246
 inverse problems solns., use of perturbation methods 3-54064
 isotope applications to diagnosis and therapy 3-66042
 lungs and other organs, ferromagnetic contamination 3-59438
 neutron radiotherapy, using accelerators 3-59443
 nuclear, in India, review 3-45317
 nuclear, proceedings of American Association of Physicists, Chicago, USA, 30 Nov-1 Dec, 1972 3-61914

medicine continued

- nuclear, tomography applic. 3-70147
 nuclear medicine, gamma-ray camera control, NUMES 2 system (*Italian*) 3-48598
 osteoporosis, methods of in-vivo measurement, review 3-66406
 physics course for pre-medical students 3-70228
 pre-medical physics course, nerve conduction 3-77350
 proton accelerators of USSR, medical uses for treatment of malignant tumours 3-59440
 proton radiation therapy, prospects 3-59444
 radiographic computer image enhancement 3-66040
 radionuclides, applications 3-45315
 radiotherapy using π^- from racetrack microtron 3-59445
 tomographic imaging in nuclear medicine, Conference, USA, 15-16 Sept. (1972) 3-70146
 ultrasonic, diagnostic and therapeutic applications, tolerance range of dosage (*German*) 3-77249
 white corpuscles automatic analyser, Larc, using dedicated microcomputer (*French*) 3-66396
 X-ray hypotonic duodenography 3-56540
 X-ray lymphography and supplementary procedures 3-56541
 X-ray renal arteriography 3-56542
⁶⁷Ga, production by deuteron bombardment of Zn for medical applications 3-59448

Meissner effect see superconductivity**melting****see also zone melting and refining**

- Adler transition, hard sphere system, derivation, equation of state, simplified theory 3-49980
 binary fused salt systems, polarisation power parameter 3-72178
 chain system technique for heat transfer 3-78944
 communal entropy, Monte Carlo estimation 3-45743
 crystal, three dimens. f.c.c., Lennard Jones model, mol. dynamics study 3-49972
 earth upper mantle model at high press. under water-saturated and water-undersaturated conditions 3-47620
 entropy constant determ. rel. to first-order transition theory 3-72183
 glass batch, time-temperature history, interface heat transfer (*German*) 3-44675
 glass form., new oxide, laser spin melting and free fall cooling 3-68168
 Hall effect measurement, melts, precision cell 3-42610
 hard sphere system (*German*) 3-62628
 Haverø meteorite, interpretation of obs. 3-45070
 heaped materials, preheating theory (*German*) 3-76189
 heat conduction for melting plate with ablation, solution of inverse problem (*Russian*) 3-66708
 heteropolymer, random two-component one-dimens. Ising model 3-63572
 high-press. melting, appl. to Earth core-mantle boundary 3-76614
 ice, shock-compression data 3-43865
 ice, superheated, compression fracture, internal melt figure nucleation 3-43868
 ice block, Stefan problem soln., zero degrees (*French*) 3-79474
 laser irradiation appl. (*Rumanian*) 3-62732
 Lindemann law, lattice dynamics approach 3-52687
 liquid structure, interatomic repulsion influence 3-55077
 LMFBR fuel subassemblies, determ. of wrapper-can meltthrough using THTB code 3-46079
 lunar melting and differentiation, chemical evidence 3-73459
 magmas, contemporaneous basaltic and rhyolitic, formation hypothesis, fractional melting 3-44761
 mathematical modelling methods, for solving problems (*Russian*) 3-53202
 metal, by electron beam, mechanisms (*Russian*) 3-53261
 metal and alloy, conf., Tokyo, Japan (Sept. 1972) 3-49820
 metals, change in volume, comparison with rare gases 3-49975
 metals, high pressures, maximum in curve due to repulsive potential softness 3-49977
 metals, molecular crystals, ideal three phase model 3-49974
 metals, simple, theories, hole formation, disorder, Gibbs free energy, variational techniques, Lindemann's law 3-49973
 miscible alloys, strain energy effect 3-72832
 muscovite, melting relations to 30 kbar in system $KAlSi_3O_8-Al_2O_3-H_2O$ 3-47612
 NT Nairit vulcanizates, deformed dilatometric method 3-73051
 nonmetallic crystals, electron processes 3-75609
 nuclear reactor fuel, exptl. and theoretical study, in-pile and out-of-pile techniques (*German*) 3-67470
 nuclear reactor fuel, LMFBR power temp. accident axial molten-fuel motion model 3-74731
 partial, during tempering, determ. by u.s. methods 3-53251
 poly(caproamide), salted 3-52410
 cis-1,4-polybutadiene vulcanisates, dilatometric method 3-73051
 polyethylene, struct. changes during annealing and fusion (*Russian*) 3-80498
 polyethylene single crystals, melting and morphology 3-67884
 refractory oxides, oxide compounds, h.f. heating, melting 3-72979
 rock melt during underground nuclear explosions, shock wave energy deposition 3-58875
 sandstone partial melting during frictional sliding in triaxial expt. 3-76628
 semi-infinite solid with temp. depend. thermal props., phase change problem soln. 3-64155
 semiconductors, cubic, Debye temperatures and Lindemann-Gilvayr melting law 3-75587
 E. Sidlaw Hills, Perth., melting relations of calc. alkaline lavas 3-53386
 simulated melting instability waves near stagnation region in hypersonic flow 3-46463
 small cluster of atoms, theory 3-46699
 snow melting rate, altitude depend. rel. to atm. temp. vertical profiles (*Japanese*) 3-56162
 statistical mechanics, melting curve maxima and solid-solid transitions, high pressure, two species model 3-49976
 steel, low-C, effects of melting processes, microstructures, season and annealing on sliding wear behaviour 3-41754
 steel ShKh15, ingots, electron beam effects (*Russian*) 3-72924
 theory based on lattice instability, comment 3-43866

melting continued

- theory based on lattice instability including liquid state 3-43867
thin film, by laser beam, one dimensional heat flow calc. 3-75691
upper mantle, partial melting and cond. anomalies 3-56045
Ag, magnetic susceptibility around melting point 3-58368
Ag-Cu, eutectic alloy, freezing and melting at very slow rates 3-53203
Al alloy, type D16, partial melting during tempering, determ. by u.s. methods 3-53251
Ar, relative volume change rel. to entropy 3-68391
Au, magnetic susceptibility around melting point 3-58368
BaO-ZrO₂-Al₂O₃ fusibility diagram 3-72177
Bi₂Se₃, density meas. from melting point to 1201°C 3-79401
Bi₂Te₃, density meas. from melting point to 1169°C 3-79401
Cu, magnetic susceptibility around melting point 3-58368
Fe, cost, contact melting, ferrite-graphite boundaries, laser light pulse effects (*Russian*) 3-41768
Fe, solid/molten transition point, surface free energy, temp. dependence, 0 to 2000 K (*German*) 3-72823
Fe at earth core-mantle boundary, significant structure theory 3-41900
Ga, photostimulated exoelectron emission rel. to melting, freezing chars. 3-58583
Ga thin films, transition temperature, thickness dependence, low-temp. condensed 3-50094
³He solid, effect of magnetic field on melting curve 3-55121
InAs, impurity distrib. under flux radioactive isotope method 3-75626
KCl-LiCl-FeCl₃, KCl-LiCl-AlCl₃, immiscible systems, diagrams of melting, thermography (*Russian*) 3-52691
Mg-Cd alloys, influence of melting on mag. props. (*Russian*) 3-68763
Na, relative volume change rel. to entropy 3-68391
PbBr₂-NaBr-CdBr₂, diagram of melting, thermodynamic calc. (*Russian*) 3-49967
Sb₂Se₃, density meas. from melting point to 1139°C 3-79401
Sb₂Te₃, density meas. from melting point to 1172°C 3-79401
UO₂, melted in air, He, rate of fission product release (*Japanese*) 3-74726
UO₂-cladding composite body, heat conduction with simultaneous solidification and melting 3-54548
ZrC and ZrC-B alloys, arc melting and homogenization 3-80430
- melting point**
acetone, press. depend. 3-79476
eutectics, use as secondary temp. standard above 2327K (*French*) 3-51550
i.r. spectra of solids, melting point, 20 to 120C, improved procedure 3-77359
metal, monovalent, elec. cond. change, rel. to struct. factor (*Russian*) 3-79664
metal, rel. to ratio of thermal cond. to viscosity in liq. phase (*Russian*) 3-44057
metals, polymorphic transitions A3→A2 or A1→A2, temp./melting pt. relationship 3-43877
polyethylene, tensile deformation effect 3-80483
polyethylene terephthalate fibre, effect of thermal treatment on thermomechanical props. (*Russian*) 3-80496
rare earth phosphides, cryst. chemistry and phys. props., review 3-64018
slag, liquid, evaporation rate as function of melting point, discharge current (*Russian*) 3-70488
Al, impurity-vacancy binding energy, core radius, Debye and melting temps., relations 3-52622
Bi-Pb(Sn) binary alloy, effect of ternary additions on positron annihilation, m.p. effects 3-68279
Cu, elec. cond. change, rel. to struct. factor (*Russian*) 3-79664
Fe, solid/molten transition point, surface free energy, temp. dependence, 0 to 2000 K (*German*) 3-72823
Fe₃C, rel. to reaction between graphite and liquid 3-69192
Ga creep of single crystals, near melting pt. (*Russian*) 3-44600
Lu, high purity, physical and metallurgical properties 3-63981
MgF₂-CaF₂ mixtures, evaporated films for PbTe t.f.t.s 3-79779
MnGa₂S₄ phases 3-79316
Mo, international practical temperature scale, secondary fixed point determ. 3-73661
Nb, pulse heating method, normal spectral emittance and electrical resistivity meas. 3-45449
Se, hexagonal and liquid in 298 to 1000 K range, enthalpy and temperature of fusion measurement 3-68416
ZrO₂-Zr_{1.5}La_{0.5}O₇, eutectics, use as secondary temp. standard above 2327K (*French*) 3-51550

membranes

- see also osmosis
artificial, phosphoinositide-protein, conductance, CaCl₂ conc. depend. 3-69487
artificial lipid-protein, potential at KCl/NaCl solution interface, Ca²⁺ effect 3-69486
bilayer with protein outside, X-ray diffraction pattern 3-48176
biochemical, with enzymes, modelling/simulation/identification and optimal control 3-53738
biological, double fixed charge solution-membrane ion partition effects and membrane potentials 3-56488
biological, ionic transport, Onsager's dipole chain model 3-56489
biological and erythrocyte, mechanical deformability 3-48174
biological cell membranes, ionic partition between surface and bulk water in silica gel, biological model 3-56491
biological free radicals in aq. environments, e.p.r. line shape calc. 3-47603
biological membrane pores, kinetics of diffusion and convection, computer simulation 3-56490
biomembranes, surface charge, evidence from K kinetics as function of external divalent cation concentration 3-65986
cat ear basilar membrane, vibrs. meas. by Mossbauer effect (*German*) 3-51426
cell-membrane resistance meas. using oscillator (*German*) 3-42271
cells, ellipsoidal, electrical potential differences, action potential 3-77203
cellular, double fixed charge, i.f. dielectric dispersion 3-56487
cellulose acetate, ultrathin and thick membranes, p.m.r. studies 'free' and restricted water 3-54770

membranes continued

- chlorophyll containing bileaflet membranes, electron transport 3-56483
circular, in nonlinear elastic base, double frequency regime of natural oscillations (*Russian*) 3-62527
clay minerals dielectric membrane polarisation (*German*) 3-73256
conductance, model system, steady state and time dependent electrical props., classical ion-membrane molecule interactions 3-81262
dehydration of hydrated ions in ionic diffusion 3-73136
diffusion-controlled evaporation through membranes, anomalous behaviour 3-46706
displacement determ., membrane stretched over surface with constant curvature (*Italian*) 3-48713
displacements, due to moving steady pressure distribution, steady state solution 3-77340
elastic, boundary value problem 3-74020
electrically induced carrier transport systems, potential difference analysis 3-53320
electrolytes, transportation across porous membranes, sorption-diffusion model (*Russian*) 3-55988
electroosmotic transport, conc. depend., uni-univalent electrolytes 3-61259
ellipsometry of membrane-like systems, review 3-77427
entropy changes associated with nerve impulses 3-45263
filters for atmospheric ice nuclei meas. 3-47839
fluid/membrane/fluid, Brillouin scattering from thermally excited wave 3-48171
glass electrode membranes, Li conc. profile and cation mobilities, determ. by ion sputtering 3-69471
glass membrane potentials, heterogeneous-site, solid state theory 3-69484
Helmholtz equation, isoperimetric norm bounds solutions 3-70677
homogeneous swollen, hydraulic permeability rel. to diffusion 3-54773
homogeneous swollen films, binary diffusivities 3-80574
humidity in membrane-filter ice nucleus chamber, comments on numerical estimates 3-47840
inflated circular cylindrical rubber membranes, bending rigidity 3-47466
ion exchange, design of electrochem. cell for study 3-51659
ion exchange, elec. cond. determ., effect of temp., resistance meas. 3-51658
jets, biological low Reynolds number with quiescent outer bathing solution, mixing 3-51428
lamellar potassium oleate-D₂O membrane bilayers, n.m.r. free induction decay, spin echoes 3-45258
leak-testing apparatus vacuum tightness, selective membrane for mass spectrometric monitoring 3-73716
lipid, bimolecular, elec. capacitance (*Czech*) 3-73573
lipid spherical bilayers, surface tension and contact angle meas. method 3-42693
lipid-cytochrome c membrane, X-ray diffraction structure determ. 3-48177
liquid flow over simple membranous surface, hydrodynamic stability (*Russian*) 3-63690
living cell, semipermeable properties, role of polarised water and of lipids, theory 3-81263
locust, adult female, rheological props. of extensible intersegmental membrane 3-42272
loudspeaker membranes, holographic vibration analysis 3-51881
low-impedance capillary electrode for large axon membrane potential recording 3-56994
multilayered membrane-type systems containing fluid layers, structure determ. methods 3-65984
multiwave shell, un-split model, forces (*Russian*) 3-42818
nitrocellulose, intracavity tuning element for dye laser 3-54227
osmotic, for H₂ partial press. meas. 3-48397
peripheral glomerular basement membrane, thickness distrib., statistical anal. 3-56484
permeability meas. 3-58813
pH oscillations, computer simulation in autocatalytic first order reactions 3-73167
polyethylene, surface morphological changes determ. using electron microscopy 3-80576
red blood cell membranes, strain energy function 3-48175
red cell, elastic modulus measurement, fluid mechanical technique, results 3-81261
resting potential, denervated muscle, mice 3-56494
shallow spherical membrane finite deflection, numerical soln. 3-62454
toroidal, nonlinear, inflated by const. normal press., axially symmetric deformation 3-70584
vibration analysis by optical spatial filtering method 3-42478
Z-pinch, noncylindrical, matching discharge circuit with membrane movement, neutron density, two dimensional snow plough model (*Russian*) 3-57950
C membranes, microporous, isothermal and thermo-osmotic gas adsorption 3-80575
K channel, nerve membrane, single ion electrodiffusion process 3-45259
- memories** see digital storage
memory devices see storage devices
mendelevium
ionisation energy calc. 3-60376
mendelevium compounds
No entries
mercury (metal)
adsorption of cyclohexane, interfacial tensions of pendant Hg drops 3-45420
adsorption of octadecane, actadecyl alcohol, octadecyl amine, stearic acid, interfacial tension meas. 3-50075
adsorption on Au, Auger spectroscopy 3-72255
adsorption on W, field emission obs., work function determ. 3-80145
arc cathode films, emission modes, visible appearance, surface dependence, dynamic field emission model 3-40816
atom, (²¹⁰Po) state, collision-induced banded emission obs. at 335 and 485 nm by phase shift, mechanism 3-60379

mercury (metal) continued

- atom, branching ratios, $2D_{5/2}$; $2D_{3/2}$ ratios meas. by photoelectron spectroscopy 3-71393
- atom, electron impact excitation, effective cross section determ. 3-74869
- atom, low energy electron scatt., ang. depend. of reson. struct. 3-60384
- atom, photoioniz. cross sections for states split by spin-orbit coupling 3-67684
- atom, spin polarisation, elastically scattered electrons (*Russian*) 3-49417
- atomic absorption, air-acetylene flames, effect of standard Hg(II) soln. 3-48639
- atomic electron struct. distortion due to high-intensity laser field 3-74772
- atoms, behind shock waves, ionisation and excitaton by electron impact 3-74853
- atoms of ^{198}Hg and ^{199}Hg , collisional transfer of orientation, double reson. obs. 3-52281
- calorimetric and vibrational studies, specific heat meas. 3-52706
- countercurrent flow with water packed columns, holdup flooding and pressure drop 3-60567
- detection by thin film resistance instrument 3-42712
- discharge, external electrodes, l.f. breakdown 3-75428
- discharge, Hg-N₂, nitrogen ionization as a function of N pressure 3-60650
- drops, charged, in aqueous electrolyte soln., theory of electrophoresis 3-59610
- electrode, stationary, a.c. and differential pulse polarograms, effect of potential sweep rate on peak height 3-53318
- electronic density of states in liquid 3-79604
- emulsion, with dispersed conducting phases (*French*) 3-80502
- flow in rotating mag. field (*Russian*) 3-79021
- fluid, supercritical region, meta-insulator transition, electronic structure, alloy analogy, numerical calculation 3-50143
- fluid, thermoelectric power, 600 to 1650C, 0 to 2 kbar, metal-dielectric transition, density of states 3-50194
- fluorescence, fine struct. emission spectrum, ($A^3O-u \rightarrow X^1\Sigma_g^+$) and ($A^3L_u \rightarrow X^1\Sigma_g^+$) transitions 3-54713
- gas bubble shape, size and movement (*German*) 3-75261
- harmonic generation, second, nonlinear optical properties, liquid and solid, transition region 3-48954
- interface with solids, interfacial and adhesion energy meas. by SEM 3-75659
- ion laser, with He buffer gas, CW emission at 6150 Å, excitation mechanism 3-45793
- laser, stability of oscill. freq. at 1.53 μ 3-45798
- liquid, electronic density of states calc. by Green's function methods 3-50108
- liquid, electronic props., high pressure effect on n.m.r., Hall effect and resist. 3-50173
- liquid, Lorenz number, Kohlrausch meas. method 3-75737
- liquid, pair interaction pot. calcs. 3-49838
- liquid, surface tension determ., drop-weight technique application 3-43928
- liquid, thermal cond., Lorenz no. (*German*) 3-50170
- liquid, thermal conductivity, Lorenz number, electrical conductivity, Kohlrausch method, Wiedemann Franz law 3-50181
- liquid, thermal diffusivity meas., high temp., laser flash technique 3-45448
- liquid-vapour system, molecular exchange 3-49983
- manometer outlet trap combination of cyclone separator and fibrous filter 3-62036
- metastable atoms, sensitization of fluoresc. of diatomic free radicals 3-60484
- MHD heat transfer from hot film probes in Hg 3-46393
- mixing in skull type crucible in alternating mag. field (*Russian*) 3-79014
- muonic atom, test for vacuum polarisation correction to 5-4 transitions (*German*) 3-52302
- nuclear targets, for heavy ion beams 3-51684
- photoelectric emission, freq. depend. 3-55726
- photoemission of solid and liquid, density of states (*German*) 3-50647
- photosensitization band fluorescence spectra in 6^3P_1 state 3-50842
- plasma, wave propagation in an ion sheath, effect on immersed antenna (*French*) 3-49712
- plasma ion density fluctuations meas. by optical absorption method 3-75422
- porometry, applic. to fibre porosity determ. 3-69400
- resonances in electron impact, energies and width 3-52288
- Santa Barbara Basin, conc. in marine sediments 3-61325
- spectrochemical analysis by atomic absorption and emission using 184.9 nm line 3-54049
- structure, energy-scanning X-ray diff. study 3-40831
- thermotransport in liq. Na 3-64197
- vapour in binary mixtures, electrodeless glow discharges, 3884 Å band emission, comment 3-49463
- wetted Al, reactions with liquid water 3-58812
- Ar-Hg discharge, capacitive, parameters investigation (*German*) 3-68105
- Ar-Hg plasma, hard excitation of feedback controlled instabilities 3-79124
- Hg atom, spin polarisation, elastically scattered electrons (*Russian*) 3-49417
- Hg sensitized fluorescence of metal vapours, excitation processes 3-71414
- Hg/SnI₂ arcs, absorpt., emission and temp. meas. 3-54887
- Hg-Ar low press. discharge, ion components, mass spectrometric analysis 3-79197
- Hg-SiO₂-Si inhomogeneities, scanning Hg probe meas. 3-72406
- Hg + Na vapour mixture, translational energy transfer collisions between metastable and admixed atoms, excitation function study 3-78537
- Hg + Na + N₂, collisional excitation transfer and quenching 3-78519
- Hg⁺ $\lambda=6150$ Å line intensity, when excited by electron beam 3-52287
- Hg₂, 550 nm emission band due to $3^2_u \rightarrow 3^0_u$ collision-induced transition 3-60444

mercury (metal) continued

- Hg²⁺, electronic polarisability in HgI₂ 3-72567
- Hg(3P) photosensitization of paraffins, energy transfer mechanism 3-50844
- Hg(3P_1) collisionally, induced production from Mg(1P_1) 3-54598
- ^{199}Hg , forbidden 2655.6 Å ($6^1S_0-6^3P_0$) line polarisation rate (*French*) 3-46179
- ^{199}Hg harmonically bound ground state ions, high resolution magnetic hyperfine resonance 3-49403
- ^{199}Hg vapour, optically oriented, mag. field depend. of nucl. relax. rate, adsorption energy eval. 3-67676
- Hg(3P_0) photosensitized decomposition of propane 3-50843
- Hg($6^3P_{0/2}$) + Hg($6^3P_{0/2}$) \rightarrow Hg⁺⁺ + Hg(6^1S_0), metastable atom collision, excitation, ionisation, cross section 3-46209
- InP:Hg, acceptor impurity, elec. and photoluminesc. props. 3-41581
- Kr:Hg trapped atoms, triplet splitting of 1P state 3-64695
- Ne-Hg, Ne-Xe-Hg mixtures, d.c. discharge, cataphoretic segregation effects 3-57959
- X-ray absorption spectra, 20 to 120 Å, excitation of 4f and 5s subshells 3-78448
- Mercury (planet)**
- atmosphere-solar wind interaction, determ. of atm. density 3-61686
- atmospheric density determ. from solar wind interaction 3-69885
- brightness temp., 21-cm. radio interferometer obs., effects of background confusion sources 3-56329
- brightness temp. meas. at 8.6 mm and 3.1 mm 3-47922
- orientation and shape determ. 3-56349
- perihelion precession, Whitehead's 3-space 3-76948
- perihelion advance, calc. using classical-relativistic mechanics of interacting point particles 3-59923
- satellite loss, effect of solar tidal friction 3-69837
- surface radiative transfer, effects of scattering and thermal conduction 3-61684
- mercury alloys**
- see also mercury compounds
- liquid, electronic props., high pressure effect on n.m.r., Hall effect and resist. 3-50173
- liquid, electronic transport properties, depend., composition isotherms 3-50174
- liquid, pseudopotential form factor, resistivity, anomalous thermopower, experimental determination 3-50104
- liquid, thermoelectric power, electrical resistivity, pressure dependence up to 5000 bar 3-50192
- Ca-Hg system, phase diagram 3-60785
- CdHg₂, calorimetric and vibrational studies, specific heat meas. 3-52706
- Hg-Cd-Te, thin film spectrophotometric chemical analysis, precision and accuracy, statistical analysis 3-51758
- Hg-Ga, liq., cluster fm. role in thermoelec. power and elec. resist. 3-50191
- Hg-In, liq., thermal cond., Lorenz no. (*German*) 3-50170
- Hg-In, liquid, Lorenz number, Kohlrausch meas. method 3-75737
- Hg-In liquid, thermal conductivity, Lorenz number, electrical conductivity, Kohlrausch method, Wiedemann Franz law 3-50181
- In-Hg liquid, sound velocity, anomalies 3-49936
- LiHg₃, calorimetric and vibrational studies, specific heat meas. 3-52706
- Mg-In system, thermodynamic props. of solid phases 3-58139
- Na-Hg, liquid, nuclear magnetic relaxation rate of ^{23}Na spin, temp. depend. 3-47160
- mercury compounds**
- see also mercury alloys
- dialkyl mercury, magneto-optical conformational analysis (*French*) 3-54609
- α -HgS, cinnabar, birefringence indices (*French*) 3-53080
- methylmercury compounds, concentration and distribution in estuarine sediments 3-73410
- organometallic, Fourier transform n.m.r. spectroscopy 3-75893
- Cd_{0.2}Hg_{0.8}Te, transmission spectra and elec. transport props. (*Russian*) 3-80021
- Cd,Hg_{1-x}Te alloys, hydrostatic pressure effects on conductivity and phase transitions 3-72386
- Cd,Hg_{1-x}Te film, elec. props. and cryst. struct., temp. depend. (*Russian*) 3-72359
- Cd,Hg_{1-x}Te mixed crystals, $x \leq 0.25$, energy gap, intrinsic electron concentration, effective mass, mobility, composition 3-52784
- Cd,Hg_{1-x}Te solid solutions, nonequilibrium carrier lifetimes, photocond., photoelectromag. effect 3-72369
- Cd,Hg_{1-x}Te thin film, preparation, deposition of HgTe onto CdTe, isothermal conditions, new method 3-53189
- Cu₂HgI₄, thermochromic, cryst. growth and refl. 3-61047
- (Hg₂)₃(AsO₄)₂, crystal structure 3-63989
- HgBi₂S₄, synthesis and cryst. struct. 3-60711
- HgBr, molecular cryst., phonon spectrum, Raman spectra and low freq. far i.r. obs. 3-76009
- HgBr₂, excited state force consts. calc. from bond charge model 3-52334
- HgBr₂, far i.r. reflectivity meas., polar optic phonons study 3-55571
- Hg_{1-x}Cd_xTe, electron radiation damage, annealing, conductivity, mobility, photoluminescence, photovoltaic response 3-54982
- Hg_{1-x}Cd_xTe, phonon spectra and scatt., thermoelec. power and thermal cond. obs. 3-60809
- Hg_{1-x}Cd_xTe($x=0.212$), n-type, magnetophonon effect, 50 to 130 K 3-46860
- HgCl free radicals, sensitized fluoresc. by Hg(6^3P_0) metastables 3-60484
- HgCl₂, ^{35}Cl n.q.r., Zeeman effect 3-44349
- HgCl₂, excited state force consts. calc. from bond charge model 3-52334
- HgCl₂ solution, dipole moment, temp. depend., 8.5-50°C 3-79976
- Hg₂Cl₂, for i.r. reflectivity meas., polar optic phonons study 3-55571
- HgCo(SCN)₄, mag. susceptibility temp. depend. to 5K 3-52952
- HgCr₂Se₄, paramagnetic resonance study 3-79909
- HgCr₂(Se₂S_{1-x})₄, struct. X-ray obs. 3-52615
- HgG, Hund's coupling case 3-67785
- HgH, long range interatomic potential determ. from quasi-bound vibrational levels 3-43385

mercury compounds continued

- HgH free radicals, sensitized fluoresc. by Hg(6^3P_0) metastables 3-60484
 HgI₂, effect of temperature and pressure on electrical conductance in molten state 3-72360
 HgI₂, high density excitons, biexciton annihilation, emission obs. 3-52806
 HgI₂ high resolution X-ray spectrometers 3-66382
 Hg(II) complex, HgX₂ (X=Cl, Br, I) in tri-n-butylphosphate soln., vibrational spectra 3-75034
 Hg(II) solutions, effect on atomic absorption of Hg, acetylene-air flames 3-48639
 Hg₂(NO₃)₂·2H₂O, H₂O molecule orientation from proton mag. resonance obs. 3-60992
 HgO, orthorhombic and rhombohedral, local cryst. field effects, phosphoresc. (French) 3-44452
 Hg₂P₂X₂ (X=Cl, Br), crystal structure and electrical props. 3-40883
 HgPbO₃, high-press. preparation, characterisation and structure 3-40872
 α -HgS, cinnabar, phonon freq. calc. 3-58096
 α -HgS, cinnabar, Raman scattering by phonons 3-58508
 HgS, luminescence spectra (French) 3-69098
 HgSe, conduction band structure from i.r. spectra 3-53112
 HgSe, effect of reactor irradiation on electrophysical props. HgTe solid solns. 3-64071
 HgSe, electron effective mass, Faraday effect obs. 3-75967
 HgSe, lattice thermal cond., depression due to phonon reson. scatt. between 4 and 30K 3-41058
 HgSe, photoemission and density of valence states 3-69138
 HgSe-HgS solid soln., conduction band structure from i.r. spectra 3-53112
 HgTd, band structure, fundamental reflectivity spectra (Polish) 3-41132
 HgTe, band structure, electro-, thermo- and piezoreflectance obs. 3-55635
 HgTe, effect of reactor irradiation on electrophysical props., HgSe solid solns. 3-64071
 HgTe, photoemission and density of valence states 3-69138
 HgTe, semiconductor material, electrolytic synthesis 3-69168
 HgTe, small bandgap semiconductor, band structure and optical properties 3-58211
 HgTe, thermoreflectance expt., example of i.r. laser modulation spectroscopy 3-55597
 HgTe growth, crystal platelets, from Hg solution, growth mechanism, physical properties, growth methods 3-53190
 HgTe-Mn, inverse susceptibility-temp. curves, paramagnetic Curie temps. and magnetic carrier effective number 3-64483
 HgTiO₃, high-press. preparation, characterisation and structure 3-40872
 Hg₂Zn_{1-x}Cr₂Se₄, i.r. absorpt. spectra due to lattice vibrations 3-80035
 KHgBr₃·H₂O, and KHgI₃·H₂O, polarised Raman and i.r. spectra, 10 to 4000 cm⁻¹, Urey-Bradley-Shimanouchi force field (French) 3-47258

mercury lamps *see mercury vapour lamps***mercury vapour lamps**

No entries

mesic and muonic atoms

- see also mesic and muonic molecules; muonium*
 charged particle-hydrogen like atom high energy rearrangement collisions, exotic atom formation 3-78526
 kaonic, formed by K⁻ absorption in liquid D₂, cascade time meas. 3-46218
 kaonic determ. of K-nucleus optical potential from KN scattering amplitude 3-54344
 mesic, self-consistency of vacuum polarisation (German) 3-52304
 mesic three-body system with Coulomb interaction, slow collisions, soln. of Schrodinger eqn. 3-70697
 muon-nucleus system, effects of Y₄ deformation on transition matrix elements 3-52129
 muonic, anomalous muon-nucleon interaction effects on fine and hyperfine splitting, nuclear radii 3-57615
 muonic, Breit eqn. analysis of recoil corrections to energy levels, μ -²⁰⁸Pb system 3-67719
 muonic, hyperfine structure, e.m. interaction of nucleus with charged particle 3-52065
 muonic, magnetic hyperfine structure, determ. of nuclear magnetic moments 3-45931
 muonic, test of vacuum polarisation and meas. of hyperfine interaction (German) 3-52302
 muonic, X-ray transition energies rel. to nuclear charge distrib. of ²⁰⁸Pb 3-71038
 muonic, X-ray transition data, reln. to muon mass value 3-67169
 muonic and pionic, X-ray transitions, determ. of nuclear quadrupole moment from quadrupole splitting 3-49096
 muonic atom, 2p→1s transition energy discrepancies, possibility of scalar, mass dependent, lepton-hadron interaction 3-57514
 muonic-atom, electron-nucleus scattering measurements, comparison of radii 3-57513
 noble muonic atoms, electron paramag., spin-orbit interaction effects 3-46217
 particles and antiparticles, baryon number variables for description of system 3-40436
 quartz, polarised μ^+ anomalous precession, study via asymm. decay 3-52305
 scalar coupling constant, Dirac equation 3-77870
 water and H₂O₂ aqueous solutions, chem. reactions, rel. to μ^- depolarization 3-41853
 X-ray radiation rates, nuclear motion correction 3-78647
 $p\mu + H^+ \rightarrow He\mu + p$ muon capture collision cross sections 3-49427
 Au, muonic, nucl. excitation (French) 3-54603
 Bi, muonic with polarised ²⁰⁹Bi nucleus, magnetic hyperfine structure, anomalous g-factor 3-46216
²⁰⁹Bi, muonic, determ. of magnetic hyperfine structure using polarised target 3-46008
 D, muonic, calc. of contributions to Lamb shift 3-52303
 H₂ + SF₆, muonic F and S X-ray intensities 3-67718
 He, muonic, formation (German) 3-49426
 He- μ^- transfer to Ar, unsuccessful search 3-67720

mesic and muonic atoms continued

- ¹¹⁵In muonic atoms, magnetization distrib. of single-particle states and 2⁺ rotational states 3-49209
¹⁷⁵Lu, muonic, quadrupole splitting in X-ray spectra, determ. of nuclear quadrupole moment 3-49133
¹⁷⁵Lu, muonic, spectroscopic quadrupole moment determ. and quadrupole h.f. splitting in pionic ¹⁷⁵Lu 3-49075
¹⁷⁵Lu μ , quadrupole splitting of X-ray transitions, determ. of nuclear quadrupole moment 3-49096
¹⁷⁵Lu pionic atom, search for strong interaction quadrupole effect 3-49134
¹⁹⁰Os, ¹⁹²Os muonic atoms, magnetization distrib. of single-particle states and 2⁺ rotational states 3-49209
¹⁹²Os, effects on γ -instability on muonic X-rays 3-60112
 Pb, limit for hypothetical scalar muon hadron interaction constant (Russian) 3-60394
 Pb isotopes, nucl. polarization and muonic X-ray spectrum 3-63351
²⁰⁸Pb, muonic, monopole polarisation of 1s_{1/2} level, study using Hartree-Fock methods 3-78234
²⁰⁸Pb, muonic, nuclear monopole polarisation calc. using Hartree-Fock eqns. 3-67172
 SF₆, muonic F and S X-ray intensities 3-67718
 Si, polarised μ^+ anomalous precession, study via asymm. decay 3-52305
²⁰³Tl, ²⁰⁵Tl muonic atoms, magnetization distrib. of single-particle states and 2⁺ rotational states 3-49209
²³⁵U, muonic quadrupole splitting in X-ray spectra, determ. of nuclear quadrupole moment 3-49133
²³⁵U μ , quadrupole splitting of X-ray transitions, determ. of nuclear quadrupole moment 3-49096

mesic and muonic molecules*see also mesic and muonic atoms*

No entries

mesomorphic state *see liquid crystals***meson absorption***see also nuclear reactions and scattering due to mesons*

- K⁻, in liquid D₂, cascade time meas. 3-46218
 π , in ³He, two nucleon model, ratio for nnp to nd production rates 3-78304

meson-baryon interactions*see also kaon-baryon interactions; pion-baryon interactions*

- meson + nucleon → meson + nucleon, nucleon polarisation effects, high energy predictions 3-74443
 $\eta N \rightarrow \eta N$ integral cross section of interaction in region of S₁₁N*(1535) resonance (Russian) 3-67100
 $\eta N \rightarrow \pi N$, integral cross section of interaction in region of S₁₁N*(1535) resonance (Russian) 3-67100
 ηN total cross section determ. from η photoproduction on nuclei at 2 GeV 3-49010
 $\omega N_1 \rightarrow \pi N_2$, vector meson dominance and Ball's invariant amplitudes 3-67084
 $\rho N_1 \rightarrow \pi N_2$, vector meson dominance and Ball's invariant amplitudes 3-67084

meson-baryon scattering*see also kaon-baryon scattering; pion-baryon scattering*

- σ -term, BBS coupling constants 3-67107
 D/F ratios of helicity flip and non-flip amplitudes 3-45889
 elastic, mass and width of broad resonances, amplitude parametrization 3-62862
 elastic polarisation and real part of nonflip amplitude 3-74431
 exchange degeneracy, baryon, crossing invariant solution and reggeon F/D ratios 3-78156
 symmetry breaking and triangular representation of chiral SU(3) 3-60001
 total cross-sections, Barger-Rubin reln. and comparison with exptl. data 3-52054
 urbarion rearrangement amplitudes in forward and backward regions, reln. to duality 3-74387
 p polarised targets, frozen spin, 50 mK, meson spectrometer 3-77612

meson capture*see also nuclear reactions and scattering due to mesons*

- K⁻-nuclear scattering lengths, current algebra, real part calc., sum rules 3-78183
 KN → $\Lambda(\Sigma)e^+e^-$, electron pair production, cross section calc. in Born approximation (Russian) 3-54346
 π^- capture by ⁶Li, photon spectra obs., 60-150 MeV 3-52207
¹⁴N, absorption of stopped π^- with ⁶Li emission, obs. using photoemulsion chamber, reaction channel branching (Russian) 3-67374
¹⁶O capture of stopped π^- with emission of ⁶Li, obs. using photoemulsion chambers, determ. reaction branchings (Russian) 3-67375

meson decay*see also kaon decay; meson hadronic decay; meson leptonic decay; pion decay*

- e.m., simple model description using vector dominance, SU₃ symmetry, ω - η , η - η' mixing 3-59966
 mixed scalar-vector-tensor boson systems, analysis of decay density matrix 3-57470
 resonances, SU₃ predictions, exact reduced-vertex symmetry 3-51986
 vector and pseudoscalar, asymptotic nonet-symmetry model, similarity with quark model 3-43104
 vector mesons, one photon exchange approximation, lepton polarisation 3-78145
 A₁ production in π -p interaction at 4.45 GeV/c, maximum decay 3-62890
 $\chi^0 \rightarrow \gamma\gamma$, obs. in π -p interactions at 3.8, 6, 8 and 12 GeV/c 3-78210
 $\eta(\eta') \rightarrow \gamma\gamma$, SU(2) ⊗ U(1) gauge theories of generalised σ model 3-57346
 $\eta \rightarrow \gamma\gamma$, obs. in π -p interactions at 3.8, 6, 8 and 12 GeV/c 3-78210
 f → $\gamma\gamma$, width, reln. to cross sections for photoproduction 3-40345
 $\omega(\rho) \rightarrow \pi\pi$, anomalous magnetic moments, strong interaction coupling consts. 3-59959
 $\rho(1710)$, decay modes study at 8 and 18.5 GeV/c in π -p interaction 3-43148

meson detection and measurement

- photoproduction process recording, pions, equipment, results 3-66312

meson detection and measurement continued

streamer chamber, description and optimum operational mode 3-77669

K, high-energy, multilayer proportional counter identification 3-73866

π , by scintillation counter, organic liquid, energy deposition and fluctuations 3-73869

π , high-energy, multilayer proportional counter identification 3-73866

meson effects

see also nuclear reactions and scattering due to mesons

$^2\text{H}(\gamma, n)p$, 22.2 MeV, corrections due to mesonic currents 3-71096

meson field theory

see also nuclear forces

σ model, renormalisation procedure 3-62764

chiral $\text{SU}(2) \times \text{SU}(2)$ invariant field theory for massless pions, mechanical analogue, complete solns. 3-48990

chiral symmetry breaking in quasikinet part of meson phenomenological Lagrangian, holonomy group 3-54289

Curzon field, generalised, soln. of Einstein eqns. in coupled e.m. and zero-mass scalar meson field 3-48976

f-meson, strong gravity field, effect on structure of baryons and hadrons 3-70890

few-body problem in nonrelativistic field theory 3-67224

gauge model for pion mass and ρ' vector boson, current algebraic treatment 3-70864

gauge model for pion mass and ρ' vector boson 3-70862

generalized nonlinear Lagrangian for pseudoscalar and scalar mesons 3-66932

Goldstone, neutral gauge fields, spontaneous symmetry breaking (Russian) 3-59927

Hamiltonian density for asymptotic scalar, pseudoscalar, fields with explicit, spontaneous, chiral symmetry breaking 3-59935

heavy vector mesons, spontaneously broken gauge theories, uniqueness 3-45848

high energy behaviour and gauge symmetry, Yang-Mills structure in vector meson theories 3-70861

Lee model, solutions for single V-particle state function and N- θ scattering matrix 3-66936

massless bosons, chiral self-interaction, Feynman rules 3-78080

meson field interac. with heavy source, SCF approximation 3-54268

nonlinear quark theory of fields of spin $s=2$ (Russian) 3-43119

pionic, and renormalization of axial coupling constant in nuclei 3-52150

pseudoscalar scattering, Yang-Mills fields 3-78170

sigma model, corrections to the axial anomaly 3-74403

skew-symmetric field quantisation, A_1 and ρ mesons from violation of local Lorentz invariance 3-48986

spontaneously broken gauge theory, gauge transformations of propagation 3-74310

tree diagram scattering amplitudes, gauge theory, vector mesons 3-78085

vector meson mass renormalisation, shadow-state theory, Feynman diagram techniques 3-59916

vector mesons, interacting, ξ -limiting process and additive

$\delta L(\sim i\partial^2(0))$ term 3-59921

vector mesons, interaction with quarks, tensor current divergence principle 3-70886

Yukawa potential, large coupling expansions for eigenenergies and Regge trajectories 3-74326

zero mass, scalar, coupled electromagnetic fields, interpretation of solutions, singular behaviour 3-57134

$\pi N A$ interaction, covariant derivation of characteristic surfaces, causality 3-51975

meson hadronic decay

see also kaon hadronic decay

$\Delta I=1/2$ rule in chiral current-mixing gauge theories 3-62807

f(1268) in model of pion excitation 3-74386

g(1680) in model of pion excitation 3-74386

nonlinear chiral Lagrangian model, exact field algebra 3-57326

octet dominance 3-45869

resonances, pionic decay, PCAC and Melosh transformation between constituent and current quarks 3-49021

vector meson \rightarrow pseudoscalar meson + photon, decay rates 3-62920

widths, from new form of universality based on ur-citon schemes 3-66962

A_1 , production in π^+ -nuclei coherent interactions, meas. of

$(A_1 \rightarrow \rho^+ \pi^0)/(A_1 \rightarrow \rho^0 \pi^+)$ branching ratio 3-74440

A_2^- mass spectra from $\eta\pi$ decay channel and missing mass analysis in $\pi^- p \rightarrow X^- p$ 3-57434

$B \rightarrow \pi\omega$, helicity states, spin and parity detn. 3-43144

$\eta \rightarrow \pi^+ \pi^-$, sought, not found 3-57328

$\eta \rightarrow \pi^+ \pi^- \gamma$, branching ratio $(\eta \rightarrow \pi^+ \pi^- \gamma)/(\eta \rightarrow \pi^+ \pi^- \pi^0)$, limit of rate 3-57328

$\eta \rightarrow \pi^+ \pi^- \gamma$, Dalitz plot distributions, ρ dominance of final state 3-57327

$\eta \rightarrow \pi^+ \pi^- \gamma$, decay rate calc. with finite dispersion relations 3-43091

$\eta \rightarrow \pi^+ \pi^- \pi^0$, branching ratio $(\eta \rightarrow \pi^+ \pi^- \gamma)/(\eta \rightarrow \pi^+ \pi^- \pi^0)$, limit of rate 3-57328

$\eta \rightarrow \pi^+ \pi^- \pi^0$, Dalitz plot distributions, ρ dominance of final state 3-57327

$\eta \rightarrow \pi^+ \pi^- \pi^0 \gamma$, sought, not found 3-57328

$\eta \rightarrow \pi\pi\pi$, chiral $\text{SU}(2) \times \text{SU}(2)$ symmetry, $\pi\pi$ scattering 3-45870

$\eta \rightarrow \pi\pi\pi$, reln. to Adler anomalies in pion electrodynamics 3-52001

$\eta \rightarrow \pi\pi\pi$, $\text{SU}(2)$ chiral breaking, calc. of decay rate 3-66975

$\eta \rightarrow \pi\pi\pi$, soft-meson current algebra technique, (8,8) symmetry breaking 3-74356

$\eta \rightarrow \pi\pi\pi$ as test of chiral symmetry breaking 3-43090

$\eta \rightarrow \pi\pi\pi$ decay rate, symmetry breaking models for η/η' sigma term 3-74333

$\eta \rightarrow \pi^+ \pi^- \gamma$ and $\eta' \rightarrow \pi^+ \pi^- \gamma$, from study of $K^- p$ interactions at 2.885 GeV/c 3-60041

η' (958) possible anisotropies in the production and decay correlations 3-54357

$f^0(1260)$, search for four-pion decay mode in 7.87 GeV/c $\pi^+ d$ interactions 3-54359

$f^0 \rightarrow \pi^+ \pi^+ \pi^- \pi^-$ obs. 3-60059

meson hadronic decay continued

$F_{35}(1877) \rightarrow \Delta\pi$, f-wave dominance, evidence for 70, L=2 baryon multiplet 3-57469

ω , phase of ρ - ω mixing parameter from unitarity relation 3-78230

$\phi \rightarrow \pi\pi$, appl. of ρ - ϕ e.m. mixing parameter 3-49005

ρ , phase of ρ - ω mixing parameter from unitarity relation 3-78230

meson interactions

see also kaon interactions; meson-baryon interactions; meson capture; meson-meson interactions; nuclear reactions and scattering due to mesons; pion interactions

charge exchange reactions in Regge-cut Van Hove model 3-57436

field theory with heavy source, SCF approximation 3-54268

inclusive, quark-model relns., exptl. check 3-40403

nonlinear quark theory of fields of spin $s=2$ (Russian) 3-43119

Odorico's bootstrap of pseudoscalar mesons 3-54326

pseudoscalar, nonleptonic decays and sub-hadronic interaction 3-62808

Regge trajectory, maximum behaviour of infinity 3-70955

symmetric group and meson Born amplitudes 3-54347

$\pi V \rightarrow \pi V$, kinematics, gauge invariance and helicity conservation 3-54318

meson leptonic decay

see also kaon leptonic decay

time, variation with velocity in interaction interpretation of special relativity theory 3-74130

vector meson, unitary-singlet contrib. to hadronic e.m. current 3-43083

vector meson decays into lepton pairs, deviation from e- μ universality 3-45885

$\pi \rightarrow \mu\nu$, coupling const. calc. from strong gravity theory 3-40331

$\pi^0 \rightarrow e^+ e^-$, reasons for experimentally search continuation, unitarity limit (Russian) 3-66968

$V \rightarrow ee$, decay rate calc. in algebraic model of hadrons, symmetry breaking relations 3-57347

meson magnetic moment

vector meson with anomalous mag. and quadrupole elec. moments in central field (Russian) 3-62828

W^\pm intermediate boson, dipole and electric quadrupole moments, helicity 3-59960

meson mass

B meson, from π -d interactions 7 GeV/c 3-60042

neutral scalar meson, from $K^+ \rightarrow \pi^+ e^+ e^-$ and $K^- \rightarrow \pi^- \mu^+ \mu^-$ decay probabilities (Russian) 3-74354

pseudoscalar, hybrid formula derivation for e.m. mass differences 3-67012

renormalisation, vector meson, shadow-state theory, Feynman diagram techniques 3-59916

spectra, determ. in relativistic quark model 3-67052

spectrum, linear dependence on isospin (Russian) 3-43124

0, mass, width and cross-section near threshold in π - π reaction 3-70975

B meson, prodn. and decay props. from $\pi^+ p$ reaction at 11 GeV/c 3-43144

η , near threshold in $\pi^- p \rightarrow$ missing mass + η 3-70975

K^0 , meas. using final state of $\pi^+ p$ interaction at 4 GeV/c 3-74476

$K^+ - K^0$ mass differences, bootstrap model of kaon (Russian) 3-70947

ω , near threshold in $\pi^- p \rightarrow$ missing mass + η 3-70975

π , gauge model, current algebraic treatment 3-70864

π , gauge model realising pseudo-Goldstone idea 3-70862

ρ meson, in bootstrapping calculation of linearly rising ρ Regge trajectory 3-74345

ρ' vector boson in gauge model realising pseudo-Goldstone idea for pion 3-70862

X^0 (958), near threshold in $\pi^- p \rightarrow$ missing mass + η 3-70975

meson-meson interactions

see also pion-pion interactions

nonlinear bootstrap in dual resonance model 3-59997

meson-meson scattering

see also pion-pion scattering

amplitudes consistent with current algebra constraints, four-point Green functions 3-57417

production mechanisms, inclusion in meson state studies 3-70984

pseudoscalar-pseudoscalar, Veneziano model consistent with partial conservation of octet and singlet axial-vector currents 3-62855

Regge eikonal representation for scattering amplitude containing virtual Veneziano blocks 3-62860

$\eta\pi \rightarrow \eta'\pi$, symmetry breaking models for η/η' sigma terms 3-74333

KK, Veneziano model accounting for Regge trajectories 3-62854

$K\pi$, low energy, general features from physical region method, dispersion relation 3-78188

$K\pi$, study using Argonne Effective Mass Spectrometer 3-70988

$K\pi$ inelastic final states and resonance parameter determ. from partial wave analysis of 2-3 body reactions 3-70982

$K\pi$ scattering study using $k^+ p$ reaction at 13 GeV, SLAC expt. 3-70989

$K\pi$ system with mass below 1 GeV produced in $K^+ p \rightarrow \Delta^+ + K^+ \pi^-$ reaction, partial wave analysis 3-70978

$K^- \pi^-$, elastic scattering cross section measured in $K^- p \rightarrow K^- \pi^- \Delta^{++}$ at 14.3 GeV/c 3-57423

$K^+ \pi^+$, elastic cross section, obs. in $K^+ p \rightarrow K^+ \pi^- \Delta^{++}$, 3-13 GeV/c 3-40398

$\pi\pi$, chiral $\text{SU}(2) \times \text{SU}(2)$ symmetry 3-45870

πK , low energy, chiral $\text{SU}(2) \times \text{SU}(2)$ symmetry, amplitudes consistent with unitarity and crossing 3-57420

meson photoproduction

non-diffractive production of resonances, peripheral cross sections 3-52014

phase-shift analysis and multipion production model, proton-neutron structure function difference 3-67037

pion, process recording, equipment, results 3-66312

point spinless pair, by two photons 3-52010

polarisation theorems for all spin-J boson exchanges 3-52013

pseudoscalar, coupling constants for cross-channel exchanges, determ. from sum rules 3-40324

pseudoscalar and vector meson production in high energy region, dual parton model 3-74372

vector meson prod. by polarized photons at 2.8, 4.7 and 9.3 GeV 3-54310

meson photoproduction continued

- vector-meson electroprod. at high virtual-photon four-momentum
3-52009
- η , on nuclear targets, 2 GeV, determ. of η N interaction total cross-section
3-49010
- η mesons on Be, C, Al, Cu, Ag, Pb, at 2 GeV, cross section meas.
3-78311
- f, lifetime, differential and total cross sections 3-40345
- $\rho \rightarrow \pi^- + \text{anything}$, 7.5 GeV, linearly polarised photon beam
3-67040
- $\rho \rightarrow \pi^0 \rho$ (ps), 3.4 GeV, linearly polarised photons, meas. asymmetry
of reaction 3-67036
- $\rho \rightarrow \pi^0 d$, corrections for multiple scattering, total and differential cross
sections (*Russian*) 3-70922
- $\rho \rightarrow W^+ v$, energy spectrum of total cross section (*Russian*)
3-49008
- $\rho N \rightarrow \eta N$, dual B_3 model with fixed and Regge poles 3-57351
- $\rho N \rightarrow K \Lambda$, dual B_3 model with fixed and Regge poles 3-57351
- $\rho N \rightarrow K \Sigma$, dual B_3 model with fixed and Regge poles 3-57351
- $\rho N \rightarrow N \pi$, Reggeized higher symmetry model, vector-meson dominance
test 3-78167
- $\rho N \rightarrow \omega N$, high energy region, dual parton model 3-74372
- $\rho N \rightarrow \pi^\pm + X$, 7.5 GeV, struct. functions, γp comparison 3-78144
- $\rho N \rightarrow \pi d$ threshold effect on ρN coupling of $P_{11}(1470)$, quark model
and exptl. data (*Spanish*) 3-67031
- $\rho N \rightarrow \pi^+ n$, 500-900 MeV, differential cross sections, search for resonance
production 3-40347
- $\rho N \rightarrow \pi^+ n$, differential cross section, 500-900 MeV 3-57349
- $\rho N \rightarrow \pi N$, dual B_3 model with fixed and Regge poles 3-57351
- $\rho N \rightarrow \pi N$, $E_\gamma < 450$ MeV, multichannel dispersion theory 3-62838
- $\rho N \rightarrow \pi N$, high energy region, dual parton model 3-74372
- $\rho N \rightarrow \rho^0 + X$, 7.5 GeV, vector dominance model 3-78144
- $\rho N \rightarrow \rho N$, high energy region, dual parton model 3-74372
- $\rho \rightarrow \eta p$, < 2.24 GeV, direct channel isobar model, electromagnetic
widths of resonance states 3-57357
- $\rho \rightarrow \eta p$ s-channel analysis in model of higher baryon couplings
3-43107
- $\rho \rightarrow K^+ \Lambda$, amplitude analysis 3-71008
- $\rho \rightarrow \omega p$, unnatural parity contribs., pion exchange 3-67017
- $\rho \rightarrow \rho^0 \rho$, 0.4 to 2.2 GeV backward prod., differential cross section
3-78133
- $\rho \rightarrow \rho^+ \pi^-$, $\rho^0 \pi^0$, cross-sect. meas., $E_\gamma = 600$ to 900 MeV
3-49015
- $\rho \rightarrow \rho p$, scaling and new kinematic variable n^2 3-57450
- $\rho \rightarrow \pi^- X^+$ inclusive reaction mediated by ρ meson production pion
spectrum study 3-74375
- $\rho \rightarrow \pi^0 p$, 4 GeV, target asymmetry 3-70919
- $\rho \rightarrow \pi^0 p$, dip region, amplitude constraints, dual absorption model
3-57352
- $\rho \rightarrow \pi^+ n$, 0.4-1.8 GeV, backward anal., differential cross sections
3-78135
- $\rho \rightarrow \pi^+ n$, numerical study of phase of backward amplitude 3-57355
- $\rho \rightarrow \pi^+ \pi^- p$, 4.1-6.2 GeV, longitudinal phase space analysis, one pion
exchange and dual models 3-57362
- $\rho \rightarrow \pi^\pm + X$, 7.5 GeV, struct. functions, γn comparison 3-78144
- $\rho \rightarrow \pi^0 p$, differential cross section in range 350-1175 MeV 3-62831
- $\rho \rightarrow \rho^0 p$ amplitude structure in Pomeran exchange reaction and s-channel
helicity nonconservation 3-74406
- $\rho \rightarrow \rho p$, scaling and new kinematic variable n^2 3-57450
- K^* , Regge model from kaon and exchange degenerate $K^*(892)$ -
 $K^{**}(1420)$ trajectories 3-40348
- π , evaluation of resonance-saturated dispersion relations for all charge
states 3-62832
- π , high-energy, dual relativistic quark model, scaling limits 3-74381
- π , test of amplitude signs predicted by transformation from current to
constituent quarks 3-78138
- π production using, PCAC constants, form factors 3-78143
- π^- photoproduction from ^{11}B 3-43234
- π^-/π^+ asym., prod. on nucleons by 16 GeV polarised photons
3-45878
- π^0 , 1000 to 1800 MeV, recoil proton polarisation, summary fits
3-59978
- π^0 , application of PCAC anomalies in quark-vector gluon model
3-67020
- π^0 , cross section calc. using two-body composite baryon model
3-74368
- π^0 , on deuterons. differential cross section, wave functions influence
3-70918
- π^+ , from ^{16}O , study using different dynamical amplitudes, particle-
hole correlations 3-54461
- π^+ , from ^{27}Al and ^{51}V 3-60159
- π^+ , from ^3He in first π -N resonance region, impulse approx., cross
section 3-67300
- π^\pm , 1-5 GeV, model (*Russian*) 3-67027
- π^\pm , from ^{12}C with excitation of analogue states 3-49240
- π^\pm , photo- and electroproduction on nuclei at high energies (*Rus-*
sian) 3-54462
- π^+ photoproduction and T_+ versus T_- analogue states in $N > Z$ nuclei
3-57508
- ρ , in γN scattering, extended hadronic structure of photon 3-57363
- $^{16}\text{O}(\gamma, \pi^+)^{16}\text{N}$, effect of Woods-Saxon wave functions on cross sections
for charged-pion photoproduction 3-63034

meson production

- see also kaon production; meson photoproduction; pion production
- B meson, from π -d interactions 7 GeV/c, mass, width 3-60042
- electroproduction, Primakov's effect (*Russian*) 3-67026
- higher resonance production in quark model, configuration mixing
3-67053
- mechanisms, inclusion in meson state studies 3-70984
- nonstrange mesons, diffractive production, harmonic-oscillator quark
model 3-57370
- pseudoscalar, in νN reactions in region of strong transmitted impulses,
Bornovsky model (*Russian*) 3-74357
- quarks and meson production at very high momentum 3-66965
- quasinuclear, via pole mechanism, spin effects (*Russian*) 3-40377
- resonances, in Reggeon-particle scattering, test of duality in baryon-
antibaryon amplitudes 3-49026
- resonances, non-diffractive production, peripheral cross sections for
photoproduction and hadron interactions 3-52014
- rising Regge trajectories and multiple production 3-52025

meson production continued

- S-matrix theory, high-energy nucleon-nucleon interactions, unitary
eikonal formalism 3-78203
- vector mesons, exchange degenerate Regge pole approach, pomeron
exchange component 3-57431
- A_2^- , missing mass analysis at 6.0 GeV/c in $\pi^- p \rightarrow X^- p$ 3-57434
- $B(1235)$, production on nuclei by 11.7 GeV/c π^+ induced reactions
3-40397
- $e^+e^- \rightarrow \text{resonance} + \text{anything}$, low, high energy, study of reactions,
resonances decaying into two charged mesons 3-59968
- ep, electroproduction of $\rho^0, \omega, 19.5$ GeV 3-67039
- η , from K-p interactions, 2.885 GeV/c, decay study 3-60041
- η' (958) possible anisotropies in the production and decay correlations
3-54357
- f^0 in $\pi^+ d$ interactions at 4 GeV/c, Estabrooks-Martin analysis
3-71014
- f^0 production in $\pi^- p$ two-prong events at 4.45 GeV/c 3-49056
- $\nu \mu N \rightarrow \text{meson} + \text{baryon} + \mu^-$ selection rules 3-66980
- $\nu^- \mu N \rightarrow \text{meson} + \text{baryon} + \mu^+$, selection rules 3-66980
- $pd \rightarrow ^3\text{He} + \text{missing mass. } \omega, \rho^0, \eta$ cross section meas., 5 GeV
3-78199
- $\pi^- p \rightarrow \chi^0(\rightarrow \gamma\gamma)n$, production cross sections at 3.8, 6, 8 and 12
GeV/c 3-78210
- $\pi^- p \rightarrow \eta(\rightarrow \gamma\gamma)n$, production cross sections at 3.8, 6, 8 and 12 GeV/c
3-78210
- $\pi^\pm p \rightarrow \rho N$, 6 GeV/c, differential cross sections, density matrix elements,
simple model proposed 3-67129
- ρ , in $\pi^- p \rightarrow \rho N$ interaction at 2.3 GeV/c, structure in momentum transfer
distrib. 3-71010
- $\rho(1710)$, production on nuclei by 11.7 GeV/c, π^+ induced reactions
3-40397
- ρ^0, ρ^- production in $\pi^- p$ two-prong events at 4.45 GeV/c 3-49056
- ρ^0 in $\pi^+ d$ interactions at 4 GeV/c, Estabrooks-Martin analysis
3-71014
- W scalar meson, leptonic production at super-high energies (*Rus-*
sian) 3-40336
- meson reactions** see meson interactions
- meson resonances**
see also omega mesons; phi mesons; rho mesons
- B meson, from π -d interactions 7 GeV/c 3-60042
- baryon-Reggeized antibaryon elastic scatt., dual props. from meson
resons. backward prod. data 3-57466
- classification schemes, coupling 3-52023
- diffractive excitation, phenomenological model 3-67096
- dispersion theoretical model of low energy particle resonance scatter-
ing amplitude 3-74342
- dual fermion emission vertex, missing gauge conditions 3-62858
- exotic, existence in inclusive reactions 3-60054
- exotic states in baryon-antibaryon system, exptl. tests, new sum rule
3-43145
- $f(1268)$ in model of pion excitation 3-74386
- f-meson, strong gravity field, effect on structure of baryons and
hadrons 3-70890
- $g(1680)$ in model of pion excitation 3-74386
- gauge-theory tree graphs, high-energy behaviour and massive vector
meson prod. 3-54273
- hadron interaction, threshold enhancements, resonance-dominance picture
3-62867
- heavy vector mesons, spontaneously broken gauge theories, unique-
ness 3-45848
- higher resonance production in quark model, configuration mixing
3-67053
- inclusive vector-meson production, at small t in dual resonance model
3-43164
- inclusive vector-meson production in dual resonance model 3-43161
- mass and width of broad resonance in meson-nucleon scattering,
amplitude parametrization 3-62862
- mixed scalar-vector-tensor boson systems, analysis of decay density
matrix 3-57470
- neutral vector meson exchange is $e^+e^- \rightarrow \mu^+\mu^-$ in gauge theories compar-
ison with radiative corrections 3-67015
- non-diffractive production, peripheral cross sections for photoproduc-
tion and hadron interactions 3-52014
- nonstrange mesons, diffractive production, harmonic-oscillator quark
model 3-57370
- pionic decay, PCAC and Melosh transformation between constituent
and current quarks 3-49021
- pionic decays, current-constituent quarks, $SU(6)_w$ 3-78152
- production, in Reggeon-particle scattering, test of duality in baryon-
antibaryon amplitudes 3-49026
- production in $\pi^+ p$ interactions to five and six body final states at 8
GeV/c (*Rumanian*) 3-49058
- production in two-body reaction, new relations from inclusive finite
mass sum rules 3-45920
- production mechanisms, inclusion in meson state studies 3-70984
- quark model and hadron spectra 3-59984
- quasi two-body e^+e^- annihilation into reson. states 3-70924
- Reggeized higher symmetry model, test of vector-meson dominance
model 3-78167
- scalar meson nonet, determ. of mixing angle, F/F + D ratio and coupl-
ing constant 3-60060
- skew-symmetric field quantisation, A_1 and ρ mesons from violation of
local Lorentz invariance 3-48986
- $SL(3, C)$ UIRs, mass formulas for resonance towers 3-62861
- spectrum, input to single particle exchange amplitudes, localisability,
renormalisation 3-78171
- strong and e.m. decays, SU_3 predictions, exact reduced-vertex sym-
metry 3-51986
- tensor meson exchange amplitudes, absorption model, effective rescat-
tering 3-67082
- trajectories, total decay width 3-60005
- tree diagram scattering amplitudes, gauge theory, vector mesons
3-78085
- two-body scattering, high-mass exotic resonances and plane consis-
tency 3-78175
- unitarity and resonances of arbitrarily large spin 3-60003
- unstable-particle theory and spectral function interpret. 3-45844
- vector, decay, asymptotic nonet-symmetry model, similarity with
quark model 3-43104
- vector meson \rightarrow pseudoscalar meson + photon, decay rates 3-62920

meson resonances continued

- vector meson decay into lepton pairs, deviation from $e\text{-}\mu$ universality, urbaryon model 3-74371
- vector meson decays into lepton pairs, deviation from $e\text{-}\mu$ universality 3-45885
- vector meson dominance, contributions to neutron-proton mass difference 3-59957
- vector meson dominance, relativistic quark model, e.m. props. 3-70925
- vector meson dominance and mass dependence of Ball's invariant amplitudes 3-67084
- vector meson dominance effects on parton cluster models, partonic content of virtual photon 3-67032
- vector meson dominance in description of neutral meson e.m. decay 3-59966
- vector meson dominance model, generalised for high energy electron-proton inelastic scattering 3-43111
- vector meson leptonic decays, unitary-singlet contrib. to hadronic e.m. current 3-43083
- vector meson mass renormalisation, shadow-state theory, Feynman diagram techniques 3-59916
- vector meson production in inelastic lepton scattering, analysis 3-78145
- vector meson with anomalous mag. and quadrupole elec. moments in central field (Russian) 3-62828
- vector mesons, heavy, Veneziano-type representations of form factors and couplings 3-67007
- vector mesons, interacting, ξ -limiting process and additive $\delta L(\sim i\delta^2(0))$ term 3-59921
- vector mesons, interaction with quarks, tensor current divergence principle 3-70886
- vector-meson dominance hypothesis and quark model for hadron photoproduction (Russian) 3-59975
- vector-meson mixing and broken nonet symmetry 3-57306
- A_1 , production in $\pi\text{-}$ nuclei coherent interactions, meas. of $(A_1 \rightarrow \rho^+ \pi^0)/(A_1 \rightarrow \rho^0 \pi^+)$ branching ratio 3-74440
- A_1 production in $\pi\text{-}p$ interaction at 4.45 GeV/c, maximum decay 3-62890
- A_1^{++} , doubly charged, in $\pi^+p \rightarrow \rho^0 p$ and $\pi^-p \rightarrow \rho^- p$ reactions, existence of true A_1 resonance 3-57401
- A_2 , calc. from pseudoscalar meson scattering model with Yang-Mills fields 3-78170
- A_2 exchange absorptive in $\pi^-p \rightarrow \pi^- \pi^+ n$ at 17.2 GeV/c 3-60039
- A_2 exchange amplitude in $\pi^-p \rightarrow \eta n$ and $K^-p \rightarrow \eta \Lambda(\Sigma)$ reactions 3-52046
- A_2 form, from πN interaction experiments, discussion (Slovak) 3-62888
- A_2 production in $\pi\text{-}$ interactions with quasifree neutrons of light nuclei (Russian) 3-40515
- A_2 -exchange and polarization effects in analysis of $\pi\pi$ scattering 3-70987
- A_2^- , missing mass analysis at 6.0 GeV/c in $\pi^-p \rightarrow X^- p$ 3-57434
- B , prodn. and decay props. from $\pi^\pm p$ reaction at 11 GeV/c 3-43144
- $B(1235)$, production on nuclei by 11.7 GeV/c π^\pm induced reactions 3-40397
- B^- production in $\pi^-p \rightarrow \rho^0 \pi$ at 9.1 GeV/c, spin-parity analysis 3-78200
- χ^0 , produced in $K^0 p \rightarrow \chi^0 p$, evidence for non-existence (Russian) 3-78110
- χ^0 , search in dimuon decays of K^0 3-78108
- $D_{15}^0(1652)$ in π photoproduction, evaluation of resonance-saturated dispersion relations for all charge states 3-62832
- δ , calc. from pseudoscalar meson scattering model with Yang-Mills fields 3-78170
- $e^+e^- \rightarrow f^0 + \text{anything}$, low, high energy, $f \rightarrow \pi^+ \pi^-$, $f' \rightarrow K^+ K^-$, study of reactions 3-59968
- η cross-section, width and S-wave production in $\pi\text{-}p$ interaction 3-70975
- η^0 , produced by $K^+p \rightarrow \text{four or five bodies}$ at 2.11 to 2.72 GeV/c, cross section 3-78204
- $\eta \rightarrow \eta\pi\pi$ decay rate, symmetry breaking models for η' sigma term 3-74333
- η' (958) possible anisotropies in the production and decay correlations 3-54357
- $\eta\eta'$ mixing hypothesis, description of e.m. decay of neutral mesons, width of η' 3-59966
- f , lifetime, differential and total cross sections for photoproduction 3-40345
- f production, obs. by phase-shift analysis of elastic $\pi\pi$ scattering, 600-1900 MeV 3-70983
- f resonance parameter determ. in π phase shift analysis of $\pi^-p \rightarrow \pi^- \pi^+ n$ reaction 3-70979
- F_0 , calc. from pseudoscalar meson scattering model with Yang-Mills fields 3-78170
- f_0 production in $\pi\text{-}p$ two-prong events at 4.45 GeV/c 3-49056
- f_0 production in $\pi^+ d$ interactions at 4 GeV/c, Estabrooks-Martin analysis 3-71014
- $f_0 \rightarrow \pi^+ \pi^- \pi^0$ obs. 3-60059
- $F_{35}(1877) \rightarrow \Delta\pi$, f-wave dominance, evidence for 70, L=2 baryon multiplet 3-57469
- $F_{37}(1940)$ in π photoproduction, evaluation of resonance-saturated dispersion relations for all charge states 3-62832
- f' , calc. from pseudoscalar meson scattering model with Yang-Mills fields 3-78170
- g production, obs. by phase-shift analysis of elastic $\pi\pi$ scattering 600-1900 MeV 3-70983
- $\gamma p \rightarrow \eta p$, <2.24 GeV, direct channel isobar model, electromagnetic widths of resonance states 3-57357
- $\gamma p \rightarrow V p$ vector meson prod. by polarized photons at 2.8, 4.7 and 9.3 GeV 3-54310
- K^* (892) production in threshold region using K^-p reaction, ang. distrib. 3-78182
- K^* , calc. from pseudoscalar meson scattering model with Yang-Mills fields 3-78170
- K^* , existence in low energy $K\pi$ scattering, dispersive method study 3-78188
- $K^*(1420)$, $K^*(890)$, masses and widths, obs. in $K^+p \rightarrow K^+ \pi^- \Delta^{++}$, 3-13 GeV/c 3-40398
- $K^*(888)$, $K^*(888)$ production on nucleons, isoscalar exchange contribs. 3-57431

meson resonances continued

- $K^*(890)$, production in $KN \rightarrow K^*N$ reaction 3-62891
- $K^*(892)$, produced by $K^+p \rightarrow \text{four or five bodies}$ at 2.11 to 2.72 GeV/c, cross section 3-78204
- $K^*(892)\text{-}K^*(1420)$ trajectories, kaon and exchange degenerate, in Regge model of K^+ photoproduction 3-40348
- K^{*0} (1420) decay and distribution using additive quark model, spin-parity assignment 3-62886
- $K^-d \rightarrow K^0 \pi^- d$, 5.5 GeV/c, \bar{K}^{*-} (890), \bar{K}^{*-} (1420), production mechanisms, decay angular distributions, model comparison 3-57447
- $K\text{-}p$ interactions, 8.25 GeV/c, cross sections for common final states and prominent resonances 3-60038
- $K\pi$ inelastic final states and resonance parameter determ. from partial wave analysis of 2 \rightarrow 3 body reactions 3-70982
- $K\pi$ scattering study using $K^\pm p$ reaction at 13 GeV, SLAC expt. 3-70989
- $K\pi$ system with mass below 1 GeV produced in $K^+p \rightarrow \Delta^+ K^+ \pi^-$ reaction, partial wave analysis 3-70978
- $K\pi\pi$ system, production and decay properties in K^+n and K^+p interactions, 4.6 GeV/c 3-57442
- $K\pi\pi$ system in $K^+p \rightarrow K\pi\pi n$ reactions at 14.3 GeV/c, Q-production 3-67136
- $K^+ \pi^+ \pi^-$, coherent production on nuclei at 10, 13 and 16 GeV/c (German) 3-52208
- κ , calc. from pseudoscalar meson scattering model with Yang-Mills fields 3-78170
- κ , mass and decay contact from generalised nonlinear Lagrangian for pseudoscalar and scalar mesons 3-66932
- $P_{11}(1430)$ in π photoproduction, evaluation of resonance-saturated dispersion relations for all charge states 3-62832
- pp annihilations in T-region, analysis of resonance production 3-78209
- pp scattering, diffraction and production of uncorrelated pairs of resonances in high-multiplicity reactions 3-52051
- $\pi N \rightarrow$ vector meson + Δ baryon, dipole coupling model 3-74442
- $\pi\pi$, S^* resonance, consistency with Roy's equations, resolution of up-down ambiguity 3-57419
- $\pi V \rightarrow \pi V$, kinematics, gauge invariance and helicity conservation 3-54318
- Q , production in $KN \rightarrow K^*N$ reaction 3-62891
- σ , calc. from pseudoscalar meson scattering model with Yang-Mills fields 3-78170
- $V \rightarrow ee$, decay rate calc. in algebraic model of hadrons, symmetry breaking relations 3-57347
- $X^0(960)$, Regge trajectory, exchange spin effect on elastic pp high-energy scattering (Russian) 3-78194
- X^0 cross section, width and S-wave production in $\pi\text{-}p$ interaction 3-70975
- Z_0^* , 1700 MeV/c², prediction from KN, KN scattering long range forces 3-78186
- meson scattering**
see also kaon scattering; meson-baryon scattering; meson-meson scattering; nuclear reactions and scattering due to mesons; pion scattering
meson-baryon scatt. and baryon resonances, partial wave analysis 3-45907
pseudoscalar, model based on coupling through massive Yang-Mills fields 3-78170
- meson spin and parity**
isospin, reln. to mass spectrum (Russian) 3-43124
isospin 2π phase shifts from $\pi^-p \rightarrow \pi^+ \pi^- n$ at 12.5 GeV/c 3-70994
mixed scalar-vector-tensor boson systems, analysis of decay density matrix 3-57470
quasinuclear meson production via pole mechanism, spin effects (Russian) 3-40377
 B meson, prodn. and decay props. from $\pi^\pm p$ reaction at 11 GeV/c 3-43144
 B^- , produced in $\pi^-p \rightarrow \rho^0 \pi$ at 9.1 GeV/c 3-78200
 η' , from K^-p interactions at 2.885 GeV/c, matrix element analysis 3-60041
 η' (958) possible anisotropies in the production and decay correlations 3-54357
 K^{*0} produced in $K^+p \rightarrow K^{*0} \Delta^{++}$ reaction, test of assignments, quark model 3-62886
 ω photoproduction, unnatural parity contribs., pion exchange 3-67017
 π spin states, excitation model 3-74386
 $\pi\text{-}C \rightarrow \pi^+ \pi^- \pi^- C^*$ (4.44) at 6.0 GeV/c, mass distrib. and spin-parity analysis of 3π system 3-67138
 $\pi\pi\pi$, coherent production by π^- on nuclei, 9 and 15.1 GeV/c, spin-parity analysis 3-49052
 ρ production in $\gamma p \rightarrow \pi^+ \pi^- \pi^+ p$ at 9-18 GeV, spin-parity analysis 3-57365
 $X^0(960)$, Regge trajectory, exchange spin effect on elastic pp high-energy scattering (Russian) 3-78194
- mesonic atoms** see mesic and muonic atoms
- mesonic molecules** see mesic and muonic molecules
- mesons**
see also cosmic ray mesons; kaons; mesic and muonic atoms; mesic and muonic molecules; meson resonances; pions
baryon-antibaryon bootstrap model of meson spectrum 3-57373
bootstrap model, complete, of quarks, mesons, baryons, Yukawa coupling and SU(3) symmetry 3-70946
current quark content, Melosh transformation 3-67051
 $J^P = 1^{++}$, formation of an ideal nonet using asymptotic SU(3) and chiral SU(3) \times SU(3) charge algebra 3-70954
multiperipheral model of meson and baryon multiplicities 3-54332
pseudoscalar, charged, 1.44 to 9.0 GeV², determ. of time-like e.m. form factors 3-70913
pseudoscalar, non-analytic terms in Gell-Mann-Okubo reln., symmetry breaking models 3-40369
scalar, pole model, parity violating hyperon decay, $NN\pi$ vertices 3-62809
scalar and pseudoscalar in broken nonlinear chiral SU(3) \times SU(3) dynamics (Russian) 3-66944
 U_3 symmetry between baryons and mesons 3-57305
 $\pi^-p \rightarrow X^-p$, cross sections of S, T and U mesons, 25 GeV/c 3-57452

mesosphere

- Aladdin II, results and achievements for mesosphere and lower thermosphere 3-69608
 Armadale district, N.S.W., classification temp. and precipitation vars. 3-76753
 chemistry and dynamics 3-61499
 circulation and thermal structure of stratosphere, lower mesosphere during seasonal transitions 3-59102
 cosmic ray intensity, comparison with altitude, diurnal and latitude dependences of ionic concentrations (*Russian*) 3-65596
 disturbance time-dependence rel. to impulsive source of NO 3-69609
 equatorial, solar activity effects on temp. 3-59130
 gravity wave-mean flow interactions, general circulation, turbulence 3-65406
 mesopause scatt. layer altitude over summer poles 3-65344
 mesospheric and stratospheric temps. remote sensing by microwave radiometry 3-56260
 model, photochemical including ionospheric processes 3-65412
 neutral constituents from PCA ion composition meas. 3-65417
 noctilucent clouds, Polish obs. in 1971 3-73360
 ozone in stratosphere and mesosphere, perturbations 3-59103
 stratospheric mixing at 25-50 km 3-53479
 structure variable, density, pressure, temperature, up to 90 km, extrapolation technique from soundings 3-59133
 temp. meas. of lower mesosphere from changes in satellite radiances 3-51027
 temp. response to geomagnetic activity var. 3-65377
 C compounds, photochemical model with vertical transport 3-73316
 CO and methane vertical distrib., model 3-73315
 H atomic concentrations rel. to OH emissions 3-51026
 N relative concentrations in stratosphere and mesosphere, one-dimensional model 3-69593
 O₃ concentrations in mesosphere and lower thermosphere at sunset, rocket obs. 3-51099

metal castings *see* castings**metal corrosion** *see* corrosion**metal-insulator boundaries**

- see also metal-insulator-metal structures*
 charge injection, storage, and transport, review 3-46832
 current-voltage characteristics, allowing for thermionic field emission of electrons (*Russian*) 3-44145
 dielectric diode, analogue simulation of one carrier injection (*Russian*) 3-75746
 electron and exciton states of dielec. 3-72396
 film-substrate interface, charge effects 3-50269
 surface excitons and phonons in presence of charge transfer 3-55335
 tunnel current in normal metals, effect of lattice oscill. 3-50280
 Ag-SiO superlattices, switching effect 3-72400
 NaCl/Pt interface, charging and discharging currents 3-79769
 SiO₂-Al(V)(Cr)(Mo), heterogeneous reactions and C-V characs. 3-72405
 SiO₂-metal, chem. reactions and C-V characs. 3-72404

metal-insulator-metal devices

- Au-Al₂O₃-Au diode, series resist. and series capacitance, time depend. (*French*) 3-64415

metal-insulator-metal structures

- charge relay transport under carrier injection conditions 3-60923
 disordered dielectric film between metal electrodes, electron tunnelling probability 3-46903
 ferroelectric material, pyroelectric effect (*Russian*) 3-72577
 metal-ZnS-metal, h.f. sputtered, capacity and loss tangent obs. (*French*) 3-58474
 one carrier injection, analogue simulation (*Russian*) 3-75746
 oxide thickness depend. of conduction mechanisms rel. to diode statistical characs. (*Russian*) 3-46906
 point junctions, nonlinearity mechanism of volt-ampere characs. 3-75794
 potential barrier parameters, two temp. method of determ. (*Russian*) 3-50279
 stearic acid film between metal electrodes, elec. props. 3-41273
 strain modulation electron tunnelling, metal band edge effects 3-55344
 surface conductivity of insulator 3-68708
 tunnel junction, dispersion relation, effects of barrier shape and WKB approx. 3-46905
 Al/tetracene/Au sandwich cell, rectification space-charge-limited conduction, photoelectric props. 3-46904
 Al-Al₂O₃-Al system, anodic oxidized, voltage depend. of capacitance (*Czech*) 3-72410
 Al-Al₂O₃-Al thin films, diode characs., high field effects 3-72409
 Al-LiF-Au, electron emission in vacuum and voltage-controlled neg. resist. 3-75795
 Al-oxide-Ag tunnel diode, Kondo effect rel. to 3d transition metal atomic layer at interface 3-55343
 Al-oxide-Al tunnel diodes, Kondo effect rel. to 3d transition metal atomic layer at interface 3-55343
 Al-SiO-Au, current-voltage characs., Poole-Frenkel effect (*French*) 3-72411
 Al-SiO-Au, internal photocurrent (*French*) 3-41274
 Au-NaCl-TiO₂-Ti, stable tunnelling 3-79776
 Au-SiO₂-Au thin film devices hot electron attenuation in oxide layer 3-41272
 In-CdS-In, relay mechanism of current flow 3-60924
 SiO, breakdown strength using different cathode metals, avalanche theory 3-46907
 SiO₂, time dependent breakdown due to Na ions 3-52911
 Ta-Ta₂O₅-ZnS:Tb³⁺-Au, films electroluminescent, electron injection via electron tunnelling mechanism 3-50626
 Ta-Ta₂O₅-ZnS:Tb³⁺-SiO₂-Au films, electroluminescent, electron injection via electron tunnelling mechanism 3-50626
 TiO₂, amorphous thin film, d.c. and a.c. construction 3-75798

metal-insulator-semiconductor devices

- see also field effect transistors*
 consumer IC's, ion implantation applic. 3-44542
 digital display system, gamma dosimeter, beta-gamma ratemeter 3-77282

metal-insulator-semiconductor devices continued

- local drive-in diffusion sources, Silox process, parasitic channel prevention applic. 3-58607
 m.n.o.s. memory, trap centres, thermally stimulated current meas. 3-79774
 m.n.o.s. structure utilisation in (opto)electronic devices (*Russian*) 3-44155
 m.o.s., fabrication, Si slice evaluation, use of Sirtl etch 3-41673
 m.o.s., n-channel, charge carrier mobility distrib. obs. (*Russian*) 3-52909
 m.o.s. capacitor, nonequilibrium current meas. of generation-recombination props. 3-44089
 m.o.s. devices, impact ionization current 3-64411
 m.o.s.f.e.t., gate capacity, analysis taking charge mobility changes into account (*Russian*) 3-52910
 n and p-channel Si gate technologies, comparison 3-58608
 Si-SiO₂ interface, nonavalanche injection of hot carriers 3-46895
- metal-insulator-semiconductor structures**
 electroluminescence in metal-insulator-luminor structure, space-charge-limited injection from insulator 3-50272
 flat band voltage meter 3-48465
 h.f. space charge capacitance, theory 3-44156
 inversion layer quantisation, exptl. verification, temp. range 25-75 K 3-55339
 metal-Al₂O₃(-SiO₂)-Si, C-V characteristics, effects of bias application 3-52901
 m.i.s.i.m., dynamic current switching regime (*Russian*) 3-44153
 m.n.o.s., charge exchange, log time depend. 3-64412
 m.n.o.s., discharge at low and zero gate voltages 3-46899
 m.n.o.s., discharge mechanisms at applied voltages and elevated temps. 3-55342
 m.n.o.s., ellipsometry of multilayered dielectrics 3-69174
 m.n.o.s., field effect mobility, effect of dielectric charge at oxide-nitride interface 3-55340
 m.n.o.s., polarization props. (*Russian*) 3-44152
 m.n.o.s., utilisation in (opto)electronic devices (*Russian*) 3-44155
 m.n.o.s. memory capacitors, back tunnelling, direct obs. method 3-60917
 m.n.o.s. system electronic processes, transitions between types of C-V, I-V and G-V characteristics 3-52902
 m.o.s., bulk lifetime detn. from capacitance and current obs. 3-55341
 m.o.s., C-V characs., determ. of energy spectrum of surface states for Si-SiO₂ interface 3-58321
 m.o.s., channel conductance in weak inversion 3-50274
 m.o.s., chemical reactions, voltage-capacitance characs., thermal instability 3-72404
 m.o.s., current instability rel. to surface barrier instability 3-44157
 m.o.s., CV doping profile obs., correction for interface state errors 3-55338
 m.o.s., defect exam. by scanning electron microscopy 3-68146
 m.o.s., elec. characs., photoelectric obs., theoretical analysis (*Russian*) 3-72408
 m.o.s., image forces and behaviour of mobile positive ions in SiO₂ 3-41267
 M.O.S., interface-state density determination in presence of statistical fluctuations of surface potential 3-68704
 m.o.s., ion beam degradation of C-V characs., inert ambient annealing 3-60919
 m.o.s., near surface impurity density distrib., CV charac. obs. 3-64408
 m.o.s., on (111), (100) n-Si, elec. props., influence of HCl in thermal oxidation 3-79771
 m.o.s., oxide implanted impurity, thermal redistrib. in Si 3-64793
 m.o.s., possible activation of mobile particles on oxide free surface 3-46900
 m.o.s., surface charge density, defects (*Slovak*) 3-46894
 m.o.s., surface treatment, effective impurity charge density in surface states 3-64410
 M.O.S., with nonstationary depletion layer, photoeffects, rel. to ionising radiation detection (*Russian*) 3-52905
 m.o.s. capacitance, oscillatory bias depend. 3-60920
 m.o.s. capacitor, collection inversion charge, minority carrier recombination, heavily doped layers 3-41202
 m.o.s. capacitor, determ. of lifetime from thermal generation and optical injection 3-79775
 m.o.s. capacitor, effects of nonuniform doping on generation lifetime meas. 3-79770
 m.o.s. device modelling by computer, surface state density peaks, Gray-Brown studies 3-50270
 m.o.s. system, C-V curve shift after cooling to 77 K due to charge trapping 3-46898
 m.o.s. systems, heterogeneous reactions, deposition conditions, heat treatment 3-72405
 m.o.s.t., surface inversion layer scatt. parameter determ. method 3-64407
 m.o.s.t. structure in a.c. mag. field, Hall effect study 3-60918
 parallel conductance, theoretical expression (*French*) 3-64413
 quantization effects in semiconductor inversion and accumulation layers 3-64414
 Schottky barrier, potential barrier transparency coefficient (*Russian*) 3-52907
 Schottky barrier diode, VI characs. allowing for tunnelling through space charge region (*Russian*) 3-52908
 surface conductivity of insulator 3-68708
 surface electron states, d.c. obs. under non steady-state conditions 3-46901
 surface-state density measurement by surface photovoltage method 3-52903
 technological review 3-50278
 X-rays from electron beam evaporation, effect (*Japanese*) 3-50273
 Al-Al₂O₃-SiO₂-Si, interface charge, traps due to oxygen vacancies 3-68705
 Al-AlN-Si, prep. by reactive evaporation, elec. props. (*Russian*) 3-52906
 Al-SiO₂-Si, KV electron energy dissipation in depth 3-72110
 Al₂O₃-GaAsP, IV, CV characs., and radiation effects 3-50277
 Al₂O₃-Si, IV, CV characs., and radiation effects 3-50277
 GaAs minority carrier diffusion length, obs. 3-64354

metal-insulator-semiconductor structures continued

- n-GaAs-Si₃N₄, energy spectrum of states at boundary (*Russian*) 3-50271
 GaAsP m.i.s. capacitor, fabrication by thermal oxidation 3-64789
 GaP native oxide, elec. props. obs. rel. to device passivation 3-41271
 Hg-SiO₂-Si, capacitance, cond. meas., scanning Hg probe, inhomogeneity 3-72406
 Mo/Au-SiO₂-Si, low-temp. treatment at 300 to 400 C, H₂ ambient, change of threshold voltage meas. 3-55337
 Si based, transient behaviour and recombination processes, review (*Hungarian*) 3-68707
 Si polycrystalline gate, enhanced B diffusion through oxide from B₂O₃ source 3-58606
 Si surface layer, carrier mobility, importance of phonon scattering 3-64409
 Si surface mobility, effect of charge inhomogeneities 3-41270
 Si-SiO₂, three layer interface model, electrical, struct. and thermal props. (*Russian*) 3-72407
 Si-SiO₂-Au, interface state occupancy, incremental conductance freq. depend. obs. 3-58323
 SiO₂ film, on Si, field enhancement dielec. breakdown, effect of mobile Na⁺ ions 3-79982
 SiO₂ film properties, effects of bombardment by Ar ions in r.f. plasma (*Russian*) 3-68706
 SiO₂ films, memory performance of m.o.s. transistors prepared by SiH₄-H₂O system 3-46896
 SiO₂ films, plasma oxidized dielectric strength and interface-state density 3-44154
 TiO₂-Si, insulating layer evaluation 3-50276
 W/Au-SiO₂-Si, low temp. treatment at 300 to 400 C, H₂ ambient, change of threshold voltage meas. 3-55337

metal-insulator transition

see also *electrical conductivity transitions*

- alkali metals, supercritical monovalent fluids, electronic structure 3-50142
 antiferromagnet, itinerant, model calcs. 3-64471
 conductor, N-shaped current-voltage charact. 3-75786
 current carriers density discontinuous change 3-72326
 diamond, metallic transition due to press., 77-600 K 3-52880
 diamond, transition to metallic state under press., semi-empirical LCAO band struct. calc. 3-72329
 disordered system, and short range order effects on electronic props. 3-46807
 electronically induced crystallographic transition, dynamic theory 3-49994
 exciton transitions, role of anisotropy in model 3-60858
 excitonic transition in doped anisotropic semimetal 3-75724
 fluid metals, conductivity, thermoelectric power, volume expansion effects, super- and sub-critical temps. 3-50179
 Hubbard model, Lifshits instability, stationary point approximation for functional integral 3-46806
 inhomogeneous liquid metals, conductivity, Hall coefficient, percolation aspects, numerical calculations 3-50141
 interband and intraband impurity scattering effect 3-75713
 magnetite, self-consistent calc. of Verwey ordering 3-58222
 metal-ammonia solns., metal-nonmetal transition, transport props. anal. 3-44126
 metallic monatomic chain localisation of conduction electrons at low temperature (*German*) 3-50163
 narrow band system, correlation effects rel. to magnetic and metal-insulator transitions 3-64975
 polymer with conjugated bonds, Mott semiconductor, one-dimensional theory 3-75715
 quasi-one-dimensional band conductor, Kohn anomaly 3-52801
 rare earth monochalcogenides, pressure induced semiconductor-metal transition 3-44031
 semiconductor, Mott transition, rel. to melting point 3-75609
 semiconductor-metal transition induced by electrostatic image forces 3-44029
 superconducting transition temp., effect of phase transition 3-50289
 transition metal chalcogenides, conf., Geneva, Switzerland (Apr 1973) 3-40897
 transition metal chalcogenides, semiconduction behaviour (*French*) 3-46847
 TTF-TCNQ, thermopower phenomena, 10-300K 3-64387
 Ag₂S(Se) semiconductor-metal transition, i.r. reflectivity obs. (*German*) 3-50571
 Bi, excitonic phase transition under strong mag. fields down to 1.06 K, u.s. attenuation 3-72327
 Bi_{1-x}Sb_x, semicond., pressure induced gapless state, galvanomag. props. 3-75714
 C, pyrolytic, negative magnetoresist., semicond.-metal transition (*German*) 3-72387
 Ca, self-consistent band calc. under high press., metal-semimetal transition 3-68538
 Ge, doped, metal to nonmetal transition in shallow donor states 3-55217
 Hg, fluid thermoelectric power, 600 to 1650C, 0 to 2 kbar, metal-dielectric transition, density of states 3-50194
 Hg fluid, supercritical region, electronic structure, alloy analogy, numerical calculation 3-50143
 K₂Pt(CN)₄Br_{0.3}·3H₂O, anisotropic Seebeck effects, temp. dependence, reln. to metal-insulator transition (*German*) 3-50184
 K₂Pt(CN)₄Br_{0.3}·3H₂O, n.m.r. obs. of low temp. insulating phase in one-dimensional conductor 3-55489
 K₂Pt(CN)₄Br_{0.3}·3H₂O, Pt Mossbauer meas. as test for metal-insulator transition with localisation of conduction electrons (*German*) 3-50492
 La₂CuO₄, metallic props. from 120 to 1000 K rel. to K₂NiF₄ structure 3-41241
 La₂NiO₄, metallic props. above 500 K rel. to K₂NiF₄ structure 3-41241
 MoS₂, layer type structure, electronic props. of two dimensional solids 3-50133
 Mo₂V_{1-x}O₂ whiskers, comp. depend. 3-60907
 NbSe₂, layer type structure, electronic props. of two dimensional solids 3-50133
 Nd₂CuO₄, semicond. props. from 120 to 1000 K rel. to K₂NiF₄ structure 3-41241

metal-insulator transition continued

- Nd₂NiO₄, metallic props. above 500 K rel. to K₂NiF₄ structure 3-41241
 Ni-S(Se)(As)(Sb) systems, d-electron considerations (*French*) 3-46804
 NiS, band structure calc. using simplified linear-combination-of-muffin-tin-orbitals method 3-58213
 NiS, metal-nonmetal transition investigation using Mossbauer effect of ⁵⁷Fe 3-53049
 NiS:⁵⁷Fe, metal-nonmetal transition, Mossbauer effect 3-41152
 NiS:⁵⁷Fe paramagnetic metal-antiferromagnetic nonmetal transition, Mossbauer study 3-44357
 NiS₂, (Ni_{1-x}Cu_x)S₂, (Ni_{1-x}Co_x)S₂, band structure, insulator-metal transition, weak ferromagnetism 3-41144
 Ni_{1-x}S:⁵⁷Fe, metal-nonmetal transition, Mossbauer effect, 4.2 to 300K 3-44030
 NiS_{2-x}Se_x, metal-semicond. phase diagram, resist., susceptibility and calorimetric meas. 3-72328
 Pr binary chalcogenides, mag. props., metal-insulator transition, superconductivity 3-41326
 Si, doped, metal to nonmetal transition in shallow donor states 3-55217
 Sm₂CuO₄, semicond. props. from 120 to 1000 K rel. to K₂NiF₄ structure 3-41241
 SmS:Gd, temp.-induced explosive first-order electronic phase transition 3-64297
 Sr, self-consistent band calc. under high press., metal-semimetal transition 3-68538
 Ti₂O₃, anomalies in specific heat meas. near transition 3-43882
 Ti₂O₃, elastic const. through transition, u.s. wave meas. 3-43821
 Tm binary chalcogenides, mag. props., metal-insulator transition, superconductivity 3-41326
 V_{1-x}Nb_xO₂, (0 ≤ x ≤ 0.33), vapour phase prep. and characteriz. of single crystals. (*French*) 3-72802
 VO₂ single crystal, heat capacity meas. above and below metal-semicond. transition 3-41025
 V₂O_{2n-1}, mag. props. and Mossbauer effect obs. 3-44028
 V₂O₃, ⁵¹V n.m.r., temp. depend. up to 1000K 3-68861
 V₂O₃:Cr, strongly correlated electrons in narrow band, impurity effects 3-55195
 V₂O₄, new monoclinic phases, temp. rel. to cryst. chem. 3-63979
 V₂O_{2n-1}, Magneli phases, and mag. transitions, review 3-46805
 ZrS₂, layer type structure, electronic props. of two dimensional solids
- devices**
- devices**
- metal-oxide-semiconductor field effect transistors** see *field effect transistors*
- metal-oxide semiconductor structures** see *metal-insulator-semiconductor structures*
- metal-semiconductor boundaries** see *semiconductor-metal boundaries*
- metal theory**
- see also *crystal electron states; electron gas*
- adiabatic perturbation theory 3-55237
 alkali metal, electron density state calc. (*Russian*) 3-79613
 alkali metals, effects of impurities on electron-phonon scattering time anisotropy 3-79450
 alkali metals, elec. resist. and thermopower, phonon drag effect 3-46681
 alkali metals, electrical resistivity, temp. variation 3-68586
 alkali metals, many-body effects on effective pseudo-potential 3-60853
 alloy Flinn operator, generalised appl. to multi-component systems, rel. to configurational Hamiltonian 3-79461
 alloys, binary, disordered, electronic structure using diagrammatic approach tight binding approximation 3-43982
 alloys, cluster approximations in electron spectrum 3-68535
 alloys, disordered, density of states, continued fraction technique, off-diagonal disorder 3-43981
 alloys, disordered, with clustering, electronic density of states, neighbourhood truncation scheme 3-68532
 Anderson model of localized moment, effect of orbital degeneracy 3-55392
 anisotropic metals, correlation energy 3-41114
 antiferromagnetic metal, magnetoresist. due to electron-spin scatt. at low temp. 3-58251
 Auger effect, dynamic theory, plasmon-electron interaction (*French*) 3-80138
 bound states, due to pair of interacting mag. impurities 3-64481
 bulk moduli and pseudopotential perturbation theory 3-46657
 charge density oscillation parameters calc. at impurity 3-64302
 conduction electron spin resonance saturation theory for thin samples 3-64553
 conduction e.s.r., microwave cavity size effects 3-47146
 cyclotron resonance line shapes, metal with non-ellipsoidal Fermi surfaces 3-79618
 cyclotron resonance on non-extremal orbits 3-58202
 deformation potentials under shear 3-55193
 diamagnetic metal, observability of nuclear orientation n.m.r. on paramag. impurity 3-47155
 dielectric const. structural depend., free electron calcs. 3-68536
 dilute alloy, screening, magnetic props., moving impurity (*French*) 3-72330
 disordered alloys, random transfer integrals 3-75719
 displaced charge sum rule for lattice relaxation 3-43838
 Doppler-shifted spin resonance in electron fluid 3-50387
 effective interionic pair potentials (*German*) 3-63972
 electric polarisability, small metal particles, Coulomb interaction of conduction electrons 3-46777
 electrical resistivity, interference effects between electron-phonon and electron-impurity scatt. at low temp. 3-79668
 electromigration, driving forces, pseudopotential based theory 3-41047
 electron correlation coeff. calc. at metallic densities 3-43971
 electron Fermi liquid, collisionless relax. of magnetization 3-68531
 electron gas, De Gennes correlation function method, appl. 3-46776
 electron gas, dielectric function calcs. at metallic density of electrons 3-50103
 electron gas, force on moving ion, semiclassical approx. 3-68530

metal theory continued

- electron gas model, study of lattice dynamic props. 3-79438
 electron mean free path, spatial variation near surface 3-41251
 electron mean free path temperature depend. in r.f. size effect, model 3-55251
 electron states in liquid and solid alloys, review 3-50122
 electron wind anisotropy, Fermi surface geom. and electron scatt. mechanism depend. (*Russian*) 3-79648
 electron-electron correlations, self-consistent Green's function (*Russian*) 3-68526
 electron-electron correlations, self-consistent Green's function (*Russian*) 3-68527
 electron-hole gas, average energy and pair correlation functions 3-68528
 electron-phonon interaction and characteristics of metal electron 3-75703
 e.m. excitation of sound, geometric reson., Fermi surface deform. pot. tensor 3-41126
 energy spectrum approx. calc. 3-64278
 Fermi energy, depend. on atomic number 3-68542
 ferromagnetic metals with p-type conductivity, spin wave interaction with e.m. waves 3-50550
 ferromagnetism, itinerant, correlation effect on electron self energy 3-64468
 film, normal and supercond. state, anomalous skin effect 3-44102
 films on metal substrate, theory of proximity effect for nonsuperconducting state 3-79670
 galvanomagnetic coefficients, inequalities 3-75731
 h.c.p., phonon dispersion 3-49953
 impure, electron-phonon interaction phenomena 3-68356
 interionic potentials, simple metals, interatomic force constants, elastic constants 3-68193
 linear chain of orbits coupled by magnetic breakdown, oscillatory magnetocond. 3-46789
 liquid, electronic density of states calc. by Green's function methods 3-50108
 liquid, electronic structure in tight-binding approx. 3-50109
 liquid, entropy of fusion determ. from partition function, Wigner-Seitz cell method 3-79501
 liquid, experimental clues to electronic structure, review 3-50106
 liquid, one body potentials for independent particle theory of resist. 3-64276
 liquid metal, electronic structure in tight-binding approx., single-site theory 3-43984
 liquid metals, magnetic susceptibility calc. 3-72449
 liquid metals, self-diffusion coeffs. calc. 3-55095
 liquid metals and alloys, tight-binding model, electronic density of states 3-79605
 local model pseudopotential optimization (*Russian*) 3-63977
 localised spin, next divergent terms for singlet ground state 3-64442
 magnetic alloys, dilute, u.s. attenuation, s-d interaction model 3-79823
 magnetic metal plasma minimum determ. using Boltzmann's transport and Maxwell's eqns. 3-47237
 magnetic nonlinearity of current dependence on electric field, caused by intrinsic field 3-50190
 magnetoacoustic resonance, under mag. breakdown conditions 3-58207
 magnetoresistance of polycrystals with open Fermi surface 3-50218
 melting, change in volume, comparison with rare gases 3-49975
 melting, high pressures, maximum in curve due to repulsive potential softness 3-49977
 melting, ideal three phase model, molecular crystals 3-49974
 melting, simple metals, theories, hole formation, disorder, Gibbs free energy, variational techniques, Lindemann's law 3-49973
 metal magnetic surface levels, resonance width 3-50260
 metal-vacuum interface, image charge, surface plasmon contrib. 3-41246
 multi-electron system, weakly delocalized, conditions of applicability of Heisenberg model (*Russian*) 3-50321
 model, M_2 crit. point, screening-enhanced optical absorpt. spectrum 3-41505
 monovalent, elec. cond., melting pt. phenomena, rel. to struct. factor (*Russian*) 3-79664
 monovalent, work function, and surface double layer potentials, from network model 3-41252
 muffin-tin orbitals approach to mol. energy levels calc. 3-78674
 multi-ion interaction in metals, asymptotically exact form 3-72301
 multiplet hole theory, core electron binding energies, transition metal ions, X-ray photoelectrons spectra 3-52794
 multivalent, interband optical absorpt. phenomena (*Russian*) 3-68963
 noble metal, generalized magnetic pseudopotential 3-44195
 non-transition metals, estimate of energies by pseudopotential method 3-60682
 one-dimensional system, application of renormalisation group technique to phase transition 3-64136
 one-dimensional systems, phase transition, renormalization group approach 3-60927
 optical spectra of core electrons in metals with incomplete shell 3-72668
 optical spectra of core electrons in metals with incomplete shell, overall line shapes 3-72669
 optoelectric effect in quantizing mag. fields 3-58297
 ordinary cyclotron electron waves, spectra 3-58208
 Peierls transition, fluctuation effects 3-58107
 phase coherent galvanomag. effects and mag. breakdown, Pippard network model approach 3-50189
 plasmon excitation, acoustic, in metal with overlapping d-, s-bands 3-58234
 positron behaviour, in metal with voids, vacancies and surfaces 3-46808
 pseudopotential, general model, appl. to positive ions 3-67635
 pseudopotential calcs., electronic exchange and correlation effects, equilib. lattice constants and bulk properties 3-46780
 pseudopotential in mag. field (*Russian*) 3-72310
 pure metal, elec. cond. at low temp., electron-electron collisions effects 3-55233
 rare earth metal, heavy, itinerant and localised states, comment on orthogonality 3-79623

metal theory continued

- rare earth metals, excitation of 4d electrons by high energy electron beam inelastic scattering 3-64280
 rare earth metals, localization of 5d electrons, calc. 3-79639
 Rayleigh wave absorption, in mag. fields, calc. 3-55453
 screened uniform charge model, orthogonality effects 3-55181
 self-consistent screening in simple cubic metal 3-43974
 simple, binding energy, compressibility, pseudopot. calcs. 3-54941
 singlet ground state of localized d-electrons coupled with cond. electrons 3-58220
 solid solution, dilute, number of electrons bound to implanted impurity atom 3-64304
 superconducting transitions, softening phenomena (*Russian*) 3-72415
 superplasticity and surface tension at phase transition, fluctuation model 3-49924
 surface, current noise with time-dependent impurity scatt. 3-50250
 surface, elec. field screening, tunnelling currents 3-50650
 surface, sum rule for electronic scatt. phase shifts 3-50256
 surface energy, correlation effects 3-58316
 surface energy, plasmon contrib. 3-58315
 surface energy, surface charge influence 3-55330
 surface energy at metal-metal interface, analytical model of electron density 3-55331
 surface energy calc. from work function and electron config. data 3-64393
 surface response to static and moving point charges and polarisable charge distrib. 3-58312
 surface-plasmon dispersion relation calc. using variational principle 3-55324
 thin film, field depend. of resist. 3-68590
 threshold phenomena in metals with open Fermi surfaces 3-50120
 transition metal, electron-phonon coupling calc., band structure parameters 3-79441
 transition metal alloy, chemist's view 3-41309
 transition metal alloy, pseudo potential band calc., review 3-41320
 transition metal alloys, binary, electronic density of states, superposition model 3-79602
 transition metal magnetism, effect of electron correlation on orbital interactions 3-72442
 transition metal solid solns., electronic heat capacity, alternative to rigid band model 3-79497
 transition metals, collective excitation phenomena (*Russian*) 3-68571
 transition metals, electron-phonon mass enhancement factor 3-68543
 transition metals, generalized surface states existence 3-64392
 transport equation for sound absorpt., rigorously solvable model 3-72385
 two-band model, magnetic props. 3-55407
 u.s. propagation, in quantized mag. field, effect of intense e.m. wave 3-60851
 vacancy-impurity interactions, theory using pseudopot. method 3-64030
 Van der Waals forces, nonlocal conductivity systems, external polarisation, calc. 3-70772
 void formation, lower and upper irradiation temp. limits 3-68242
 X-ray edge, freq. depend. phase shifts 3-72769
 Al, dielectric function effect on pseudopotential calcs. of electronic properties 3-44058
 Al, relax. and formation energy of $(1/2, 1/2, 1/2)$ interstitial defect, pseudopotential calc. 3-54956
 Ca, f.c.c.-b.c.c. phase transition rel. to s-d hybridisation 3-58128
 Cd, Gantmakher-Kaner effect and dopplers 3-64286
 Co, electronic structure calc. using theoretical model for charge density of 3d electrons 3-46972
 Cr, Compton profile for 3d electrons, Fermi momenta of transition metals 3-52781
 Cr, state-depend. potentials calcs. 3-79615
 Cs, liquid, model for electron collapse based on anomalous density variations with pressure 3-79606
 Cu, convergence properties of APW wavefunctions and matrix elements 3-55178
 Eu, antiferromagnet, model of Fermi surface 3-68760
 Fe, electronic structure calc. using theoretical model for charge density of 3d electrons 3-46972
 Gd, convergence properties of APW wavefunctions and matrix elements 3-55178
 Hg, liquid, electronic density of states calc. by Green's function methods 3-50108
 Hg, liquid, pressure effect on electronic props., nearly free electron and pseudogap models 3-50173
 In, liquid, electron structure, photoemission meas. 3-50107
 K, Compton profile, influence of electron correlation and crystal structure 3-75544
 K, momentum wave functions of APW, Compton profile calcs. 3-79616
 Li, alternant MO method, first-order density matrix and Fermi surface shape 3-60849
 Li, alternant MO method, total electronic energy 3-60850
 Li, Compton profile, influence of electron correlation and crystal structure 3-75544
 Li, electron density states calc. (*Russian*) 3-79613
 Li, Fermi surface, alternant MO method 3-64271
 Li, Fermi surface distortion, de Haas-van Alphen oscill. of mag. susceptibility 3-79620
 Li, momentum wave functions of APW, Compton profile calcs. 3-79616
 Na, Compton profile, influence of electron correlation and crystal structure 3-75544
 Na, momentum wave functions of APW, Compton profile calcs. 3-79616
 Nd, energy levels of Nd^{3+} ion in cryst. elec. field 3-64444
 Ni, electronic structure calc. using theoretical model for charge density of 3d electrons 3-46972
 Sn, liquid, electron structure, photoemission meas. 3-50107
 Sr, f.c.c.-b.c.c. phase transition rel. to s-d hybridisation 3-58128
 V, Compton profile, Fermi surfaces, KKR method calcs. 3-79617
 V, magnetization and total energy, as function of lattice const. 3-68757

metal theory continued

- V, state-depend. potentials calcs. 3-79615
- ZnAg phonon resistivity 3-79669
- ZnAl phonon resistivity 3-79669

metal vapor lamps *see metal vapour lamps***metal vapour lamps**

- see also mercury vapour lamps*
- quartz halide lamps, visible spectra (*German*) 3-48425

metallic thin films

- alloy, laser beam evaporated for elemental analysis 3-54044
- anomalous skin effect, normal and supercond. state, theory 3-44102
- charge transport parameters for metals with cubic symmetry, size effects 3-55242
- coatings, wear resistance from electrical resistance 3-73103
- conducting solid particles, ideally polarised, thin diffuse, electrophoresis 3-73074
- continuous, obs. thermoelec. power and temp. coeff. of resistance 3-75797
- deposition from electrical explosion, effect of discharge circuit parameters (*Russian*) 3-53174
- deposition rate determ. device description 3-53868
- detectability limit, electron microprobe 3-72295
- electrical resistance, electrical field dependence 3-68590
- electromigration mechanisms 3-75633
- electron photoejection and thermionic emission, cyclotron resonance spectra 3-72503
- electronic polarisability 3-50511
- e.m. interaction force between metallic grain and elec. image in substrate (*French*) 3-79586
- film-dielectric interface, thermal phonon radiation 3-55133
- f.m.r., bolometric detection (*Rumanian*) 3-64536
- getter sputtering device, static mode, low impurity const. 3-76128
- granular, i.r. permittivity, rel. to calc. of intergranular forces of coalescence (*French*) 3-64268
- heating capacities at liquid He-3 temps., microcalorimetry meas. 3-55091
- Incoloy 901, glaze oxide layers, structure and mechanism of formation during high temp. wear 3-64254
- information storage using laser beam, characts. of film arrays 3-74209
- i.r. internal reflectance spectrometry, surface chemical reactions and adsorption obs. 3-73164
- laser beam micromachining, thermal analysis 3-40298
- laser radiation, heating regime, steady and transient temp. field calcs. (*Russian*) 3-40277
- laser radiation damage, 10 μ m hole formation (*Russian*) 3-69110
- laser resonator film selector, separation of CO₂ rotational lines 3-45799
- mechanical vibrs. excited by relativistic charged particles 3-52641
- metal-insulator interface, charge effects 3-50269
- Mo thin films, laser-induced anisotropic thermoelectric voltages 3-60867
- Nimonic 75, C263 and 108, glaze oxide layers, structure and mechanism of formation during high temp. wear 3-64254
- noble metal thin film, transmission in vis. and near u.v. spectra regions (*French*) 3-76112
- optical and magneto-optical effects 3-69109
- optical constants, by reflectance, inhomogeneities obs. 3-64617
- optical properties of electrically insulating granular metal films 3-47332
- paramagnetic, spin-wave reson., surface pinning 3-72524
- permalloy, electrolytically deposited, inner effective field due to bidirectional rotation 3-41379
- Permalloy, vacuum-deposited, macrostresses, mol. beam angle of incidence and condensation rate depend. (*Russian*) 3-79587
- phonon emission, asymptotic distrib. of eigenvalues for wave eqn. and boundary effects 3-49947
- phonon generation by Joule heating 3-55040
- phonon radiation and electron-phonon interaction 3-55039
- piezoelectric, semi-infinite, coated with conducting thin film, effect of time-dependent heat flow on disturbances 3-74073
- plasma deposited metallic films, thermal conductivity calc. 3-60863
- plasma sprayed particles, blowholes 3-43968
- plastic deform., fatigue phenomena under boundary friction 3-41109
- polycrystalline, temp. coeff. of resist. thickness depend., exact and approximate eqns. 3-79778
- proximity effect for normal metal on normal substrate 3-79670
- quantitative adhesion test apparatus and method for vacuum deposited thin films 3-50818
- rare earth metal, cond. electron m.f.p. and conc. 3-79679
- resistance, temp. coeff., grain boundary effects 3-52823
- resistivity negative temperature coefficient relation 3-52912
- superconducting, internal friction and electrical resistance measurement, cryostat apparatus 3-48385
- tantalum-titanium alloy, preparation 3-64416
- vapour condensation on single cryst. surfaces, combined LEED, Auger electron and flash desorption spectroscopy 3-79562
- X-ray anal., Monte Carlo techniques in SEM 3-71989
- Ag, (111) and (100) single crystals., photoemission anisotropy obs. 3-64763
- Ag, aggregated thin film, anomalous opt. absorpt. 3-76110
- Ag, condensation in vacuum, development of oriented cryst. growth 3-52763
- Ag, crystallographic orientation, effect of Ar ion bombardment 3-55170
- Ag, damping of mech. vibr. (*Russian*) 3-72859
- Ag, He⁺ ion passage, coherent Coulomb excitation 3-40587
- Ag, iodination in α -AgI region 3-55172
- Ag, O chemisorption, effect on elec. resist. 3-41094
- Ag, reaction with I vapour in the β -AgI region 3-55171
- Ag, strain coeff. of resist., calc. 3-52813
- Ag, thermal cond., emissivity and elec. resist., 300-900 K 3-62018
- Ag, ultrahigh vacuum deposited on cold substrate, reverse recovery process interpret. 3-64263
- Ag, vacuum-deposited, internal friction peak due to stacking faults (*Russian*) 3-72284
- Ag adsorption, of O₂, kinetics, sticking probabilities, slow and fast adsorption, surface stoichiometry 3-46755

metallic thin films continued

- Ag developed grains, optical constants calc., filamentary thickness 3-47224
- Ag epitaxial growth on annealed Cu film 3-41108
- Ag film, effects of residual gas during deposition on optical props. 3-80001
- Ag nonradiative surface plasmons roughness induced decay, emitted radiation polarisation 3-46811
- Ag-Cr thin film mixtures, optical constants 3-80002
- Ag-Cu (50 at.%) amorphous thin film, structure (*German*) 3-58192
- Ag-Pd alloy, prep. and optical props. (*French*) 3-41527
- Al, absorption spectra of vapour quenched film deposited on another film 3-58572
- Al, current noise meas., constriction detect., sensitivity 3-68709
- Al, effects of energy losses on electron diff. intensities 3-43737
- Al, electromigration-stimulated motion of liquid alloy defect 3-41044
- Al, epitaxial, surface plasmons, LEED obs. 3-50257
- Al, evaporated, ohmic contacts for CdS epitaxial layer 3-52900
- Al, hot electron attenuation using m.i.m.s. tunnel triodes 3-79777
- Al, monoenergetic electron beam absorption 3-70264
- Al, phase transform on ion bombard., electron diff. obs. 3-72195
- Al, thermal cond., emissivity and elec. resist., 300-900 K 3-62018
- Al, transmission, reflection and absorption of electron beams, 10 to 35 keV, 1 to 3 A/cm², obs. 3-68284
- Al, ultrapure, optical parameters, effect of vacuum deposition conditions 3-50533
- Al alloys, with very large grains, electromigration and diffusion 3-41055
- Al films, work function meas. on (100), (110), and (111) surfaces 3-72393
- Al foil surfaces, ESCA studies rel. to oxide film thickness 3-61105
- Al reflectance coatings, LiF-protected, use in u.v. space optics 3-81252
- Al surface plasmon dispersion from LEED 3-50258
- Al thin films, energy spectra of transmitted electrons 3-49812
- Al vacuum condensed, growth and orientation rel. to residual air press. 3-46769
- Al₂O₃, ion implantation, complex cermet formation 3-72112
- Al-Cu, precipitation and solid soln. effects on electromigration 3-43958
- AlTa, r.f. cosputtered, X-ray analysis, resistivity and t.c.r. obs. 3-50096
- Au, arbitrarily oriented, protonogram indexing (*Russian*) 3-63922
- Au, Auger spectroscopy of submonolayer deposits on Si(III) surfaces 3-44510
- Au, condensation in vacuum, development of oriented cryst. growth 3-52763
- Au, conduction electron scatt., surface impurities (*French*) 3-79675
- Au, d-band position and width, low temp. thermomodulation meas. 3-55632
- Au, dechannelling from 2-MeV He⁺ damage 3-52656
- Au, discontinuous, aging, humidity effects, gauge factor and temp. coeff. of resistance measurement 3-58248
- Au, dislocation loop and void damage after He ion irradi., TEM obs. 3-60733
- Au, epitaxial, orientation, proton diff. determ. 3-75449
- Au, formation by vacuum evaporation on IV-VI semiconductors 3-61109
- Au, growth on KCl substrate, migrating crystallites, coalescence kinetics 3-68520
- Au, on diamond substrate, thermal phonon radiation power and temp. 3-41072
- Au, piezo, thermo and electroreflectance spectra, comparative props. 3-55631
- Au, quenched, Hall effect, annealing behaviour (*German*) 3-72349
- Au on NaCl (001) substrate, recrystallisation, electron microscopy and diffraction obs. 3-72293
- Au on NaCl (001) substrate, recrystallisation, X-ray measurements of strains 3-72294
- Au single crystal, proton scattering 3-49912
- Au thin film vacuum deposition on quartz, piezoelectric vibrations determ. of superficial mass (*French*) 3-59661
- Au-Cr alloy, structure and electrical conductivity of cosputtered films 3-43963
- Au-Ni, thin film couple, diffusion studied by optical reflectivity technique 3-79528
- Au-Ta, sputtered, struct. and thermal stability 3-64837
- Au on quartz, thermal phonon radiation into substrate 3-55043
- Be thin films, energy spectra of transmitted electrons 3-49812
- Bi, vacuum deposited, nucleus shape obs. 3-79595
- Bi cross sectional structure, electron microscopy analysis (*Japanese*) 3-50093
- Bi films from 180 to 40000 Å, meas. of electrical props. 3-41243
- Ca, elec. field effect on photoelec. efficiency, work function 3-64760
- Cd-Se spectrophotometric chemical analysis, precision and accuracy, statistical analysis 3-51758
- α -Ce, strongly disordered, resist., 1.5-300 K 3-68593
- Co, caesiated, photoelectron spin polarization, photon energy depend. 3-50643
- Co, n.m.r., magnetostriction effect on temp. depend. 3-75889
- Co-Ni alloy, Hall effect, cond., effective magnetiz. (*Russian*) 3-58249
- Co(P) and Co thin films, microstructure rel. to mag. props. 3-41106
- Cr, electrical conductivity, mean free path and conduction electron density determ. (*French*) 3-41277
- Cr, vacuum-deposited, constitution and struct. (*Russian*) 3-72283
- Cr film cathode, pulsed field emission at high current density 3-69143
- Cr thin films, recrystallisation during aging (*Russian*) 3-60845
- Cr-Ni, evaporated, structural and electrical props. as function of He, N₂, O₂ partial pressures 3-58247
- Cu, condensation in vacuum, development of oriented cryst. growth 3-52763
- Cu, damping of mech. vibr. (*Russian*) 3-72859
- Cu, monolayer, electronic props., Green's function method calc. 3-50254

metallic thin films continued

- Cu, on diamond substrate, thermal phonon radiation power and temp. 3-41072
- Cu, reaction with I₂ vapour 3-64261
- Cu, struct. effects on far u.v. spectra (*French*) 3-76111
- Cu, surface plasma oscillations 3-44133
- Cu, transmission, reflection and absorption of electron beams, 10 to 35 keV, 1 to 3 A/cm², obs. 3-68284
- Cu (111) growth on NaCl film in ultrahigh vacuum, and subsequent annealing 3-41108
- Cu alloys, props. and laws of structure formation of vacuum deposited films (*Russian*) 3-72285
- Cu anode foil, hardening of electrodeposits by ultrasound, scanning electron microscope study 3-61172
- Cu evaporated films, photoelectric and optical studies (*French*) 3-58301
- Cu polycrystalline foils of varying thickness, 50 keV electron scattering 3-69125
- Cu sputtering by protons, 33 to 150 keV, contribution of backscattered ions 3-80128
- Cu thin film vacuum deposition on quartz, piezoelectric vibrations determ. of superficial mass (*French*) 3-59661
- Cu:Fe Kondo effect, low temperature resistance obs. 3-68769
- Cu-based alloys, vapour deposited films, alloying additions effect on characts. for microelectronics (*Russian*) 3-53248
- Er, f.c.c. phase, vapour deposited, elec. conductivity 3-68587
- Er, non linear vol. expansion on He⁺ implantation 3-68301
- Er, surface oxide thickness determination by Auger spectroscopy and ion bombardment 3-45555
- deuterated Er film electrodes, vacuum arc ion source 3-56929
- Fe, amorphous, electron diffraction study of local atomic arrangement 3-79591
- Fe, epitaxial layer on Au, interfacial dislocations and residual elastic constraint (*French*) 3-46763
- Fe, oblique incidence, mag. anisotropy, substrate temp. depend. 3-47083
- α -Fe, phase transform on ion bombard., electron diffr. obs. 3-72195
- Fe film on Mg (001) surface, LEED-Auger electron spectroscopy study (*Japanese*) 3-48564
- Fe-Al alloy, lattice parameters, X-ray diffr. obs. (*Russian*) 3-60844
- Fe-Au epitaxial system, interfacial dislocations and coherence, electron diffraction studies (*French*) 3-41104
- Fe-Co alloy, Hall effect, cond., effective magnetiz. (*Russian*) 3-58249
- Fe-Co alloy, vacuum-deposited, macrostresses, mol. beam angle of incidence and condensation rate depend. (*Russian*) 3-79587
- Fe-Ni alloy, Hall effect, cond., effective magnetiz. (*Russian*) 3-58249
- Fe-Ni-Co alloys, n.m.r., magnetostriction effect on temp. depend. 3-75889
- Ga, amorphous electron diffr. obs., atomic struct. 3-68525
- Ga phase transitions, temperatures, thickness dependence low-temp. condensed 3-50094
- Gd, new f.c.c. phase, identification and oxidation characts. 3-79589
- Hg-Cd-Te spectrophotometric chemical analysis, precision and accuracy, statistical analysis 3-51758
- In on quartz, thermal phonon radiation into substrate 3-55043
- Ir thin film preparation, for transmission electron microscopy by electropolishing 3-48575
- LaB₆ thin films, electrical and optical props. 3-41596
- Li, anomalies in optical properties 3-50531
- Mg, quench-condensed, absence of superconductivity above 0.35 K 3-46918
- MnBi, on glass substrate, holographic readout efficiency determ. 3-77537
- MnBi, prep. conditions rel. to grain size 3-79584
- MnBi, single cryst. platelet, vacuum deposited mag. props., Kerr effects obs. 3-50427
- MnBi Faraday rotation, saturation wavelength dependence, absorpt. coeff., 500 to 1200 nm, protective layer 3-53087
- MnBi film growth from double layers, magneto-optical investigation 3-41107
- Mo films, phase composition and structure, mol. beam deposition 3-79592
- Ni, ⁸⁵Kr labelled adsorption of H₂, radiorelease, 273 K 3-43939
- Ni, adsorption of CO, multireflection i.r. spectra at room temp. and low pressure 3-68497
- Ni, amorphous, electron diffraction study of local atomic arrangement 3-79591
- Ni, chem. precipitated, struct. and effect on cylindrical mag. film props. (*Russian*) 3-60843
- Ni, deposition on cathode sputtering in pulsed discharge 3-61111
- Ni, electrodeposited dispersion-hardened electron micrographic exam. of thin films 3-61142
- Ni, electron microscope study of stretching and magnetisation (*German*) 3-72291
- Ni, meas. of CO differential heats of adsorp., surface coverage depend. (*German*) 3-80578
- Ni, Ni-Cu alloy, films, transformation into β -hydrides 3-80577
- Ni, on diamond substrate, thermal phonon radiation power and temp. 3-41072
- Ni, on Fe-Si alloy, influence on domain phase volume and magnetostriction (*Russian*) 3-44260
- Ni, on Si, thermal energy emission to liquid He 3-72246
- Ni, refl., 2-3 eV 3-52780
- Ni alloys, glaze oxide layers, structure and mechanism of formation during wear at high temp. 3-64254
- Ni films, H₂ adsorption coefficients and binding energy calc. (*German*) 3-79570
- Ni-Cr alloy, transmission reflection and absorption of electron beams, 10 to 35 keV, 1 to 3 A/cm², obs. 3-68284
- Ni-Fe, alloy magnetoresistance, influence of sample geometry 3-46829
- Ni-Fe, electrodeposited on Cu, uniaxial anisotropy, comp. depend. 3-64514
- Ni-Fe, mag. anisotropy, deuteron irradiation effect 3-79863
- Ni-Fe alloy, Neel wall and cross-tie wall stability 3-47093
- Ni-Fe-Mn alloy, mag. and galvanomag. props. 3-52830

metallic thin films continued

- Ni-SiO₂ film, granular metal, hopping cond., temp. depend. 3-52839
- Pb, friction theory, spherical contact, lubrication 3-75566
- Pb, monoenergetic electron beam absorption 3-70264
- Pb, on diamond substrate, thermal phonon radiation power and temp. 3-41072
- Pb, quenched, Hall effect, annealing behaviour (*German*) 3-72349
- Pb based alloys, order and annealing, phonon spectrum from electron tunnelling and resistance studies 3-41110
- Pb polycrystalline foils of varying thickness, 50 keV electron scattering 3-69125
- Pd, on Au substrate, misfit dislocation generation 3-64259
- Pd₃Mn thin films, antiphase domain boundaries 3-41739
- Pt, chemical vapour deposition for semiconductor devices 3-44547
- Pt film, sputtered in Ar discharge, optical and mass spectrometric analysis 3-43961
- Pt film, sputtered in Ar/N₂ discharge, optical and mass spectrometric analysis 3-43962
- Rb, granular thin films, surface plasma oscill., light absorption (*French*) 3-55702
- Rh, plastic foil, electrodeposition, addition of H₂O₂ soln. to electrolyte 3-76461
- Ru evaporated thin films, reflectivity and optical constants, in v.u.v. from 300 to 2000 Å 3-80069
- SbNa₂K, Cs photocathode, optical and photoelectric props. detn. (*French*) 3-41612
- Se, cond. electron m.f.p. and conc. 3-79679
- Se, amorphous and crystalline thin films, volume plasmon energies, dependence on density 3-41221
- α -Sn and β -Sn thin films, volume plasmon energies, dependence on density 3-41221
- Sn on quartz, thermal phonon radiation into substrate 3-55043
- Ta, Ar, O, N ion bombardment effect on resistance 3-58054
- Ta, epitaxial, on sapphire, prep. and struct. 3-52762
- Ta, Nb overlay, superconducting quantum galvanometer 3-70324
- Ta, phase composition and texture analysis by energy dispersive X-ray analysis 3-45566
- Ta, secondary ion emission, microanalysis 3-62321
- Ta, self-restoring autocathode, pulsed X-ray tube 3-73912
- Ta, sputtered, factors controlling struct. 3-41111
- Ta, sputtered, resistivity, Ar pressure effects 3-41276
- β -Ta, X-ray diffraction study, lattice constants determ., structural model 3-43966
- Ta film, sputtered in Ar discharge, optical and mass spectrometric analysis 3-43961
- Ta film, sputtered in Ar/N₂ discharge, optical and mass spectrometric analysis 3-43962
- β -Ta r.f. sputtered, resistivity, impurity, residual stresses, structure 3-52766
- Tb, photoelectron spectrum, struct. effects 3-61106
- Tb-Tl films, simple cubic structure 3-52768
- Tl, Hz diffusion coefficient, change in resistance meas. 3-51657
- Ti, single and polycrystal thin films, volume plasmon energies, dependence on density 3-41221
- Ti work function, Au and Ag substrates, ultra-high vacuum deposition 3-44130
- Ti:O, ion implantation, cermets structure 3-72112
- Tl, quenched, Hall effect, annealing behaviour (*German*) 3-72349
- V, vacuum-deposited, constitution and struct. (*Russian*) 3-72283
- W, chem. vapour deposition kinetics, 6-60 Torr, 500-870°C 3-41628
- W, deposited by r.f. sputtering, microstructure growth, resistivity and stresses 3-43959
- W, vacuum deposited, dislocation struct. changes due to thermal cycling (*Russian*) 3-53245
- W films, phase composition and structure, mol. beam deposition 3-79592
- W thin films, laser-induced anisotropic thermoelectric voltages 3-60867
- W/PtSi/Si system, kinetics of WSi₂ formation, rel. to IC metallisation 3-64787
- Y, cond. electron m.f.p. and conc. 3-79679
- Yb, elec. resistivity thickness depend., 200-850 Å 3-75796
- Zn, quenched, Hall effect, annealing behaviour (*German*) 3-72349
- Zn, u.h.v. deposited on Ge surfaces, obs. using mass spectrometric molecular beam method 3-61110
- ZnMn, dilute alloy, dilute film alloy, Kondo resist. down to 0.35 K, lattice defect influence 3-52820

metallisation

- see also electrodeposition*
- continuous vacuum process, computer data collection and processing (*French*) 3-51570
- deposition of polycrystalline Si and Al layers, heat-treating cycle, shallow diffused transistors 3-41661
- IC, electromigration mechanisms 3-75633
- Al, defect screening by current noise meas. 3-68709
- Al-Cu, for semiconductor devices, electromigration 3-64214
- Al₂O₃/metal composites, metallized, deposition processes and characterization. 3-76278
- Au-Ni, diffusion studies rel. to reliability 3-79528
- IC, electromigration and metallisation lifetimes 3-43891
- W/PtSi/Si system, kinetics of WSi₂ formation, rel. to IC production 3-64787
- Zn, thin film deposition on surface of Ge single crystals 3-61110

metallising *see* metallisation**metallization *see* metallisation****metallo-organic compounds *see* organometallic compounds****metallography**

- see also electron microscopy*
- alloy couples for duplex tubes, compatibility studies at high temp. 3-69278
- alloys, coarse-grained, X-ray studies, effect of turning, reciprocating and swinging motion 3-52558
- automatic plotting of reciprocal lattice zones 3-80270
- bend contour problem in electron metallography 3-44589
- β -brass, Widmanstätten precipitates morphology 3-47378
- β -brass binary and ternary alloys, embrittlement by liq. metals and aqueous ammonia 3-80343

metallography continued

- camera, NEOPHOT 2, applications 3-47495
 direct-replica prep. from steel fatigue specimen 3-46581
 dislocation arrays, planar and cellular, slip behaviour (*German, English*) 3-69241
 dislocation arrays as examples of small-angle boundaries (*German, English*) 3-61158
 dislocation contrast (*German, English*) 3-54914
 electron, microstruct. anal., bright field images, struct. factor, strain contrast 3-76181
 electron, systematic microstructural anal., thickness fringes, grain boundary contrast 3-47390
 electron microscope exam. method using replica made after thermal etching (*German*) 3-58632
 electron microscope microanalysis applics. (*German*) 3-69230
 electron microscopy, 1 MeV, in situ obs. of precip. and recrystn. 3-50704
 electron microscopy, h.v., appl. to low temp. radiation damage studies 3-49905
 electron microscopy, h.v., conf., Manchester, England, (Sept. 1972) 3-48576
 electron microscopy, h.v., state-of-the-art 3-49807
 field-ion atom-probe analysis applics. in iron and steel 3-76170
 grain boundary sliding meas., internal markers 3-47381
 grain orientation of polycrystals, determ. using thermal corrosion phenomenon (*French*) 3-61147
 grain structure examination method, plastically deformed and annealed metals and alloys 3-53226
 III-V semiconductors, thermal decomp. by laser beam 3-73152
 indirect orientation factor, microstructural constituents 3-47386
 inverse pole figure studies, random samples use 3-47380
 martensite, ferrous, tempered, iron microscopic study, effects of carbon content, lattice strain 3-58630
 metal lattice research, minicomputer applics. 3-80266
 metal/graphite alloys, spinulite appearance correl. by optical and electron microscopy 3-64840
 metals, h.c.p., foil thickness meas. using intersecting slip traces 3-47372
 microreflection applics. of microscope-photometer 3-47379
 Nimonic 80A, grain boundary cavitation, room temp. pre-strain effects, h.v. electron microscope obs. 3-50701
 optical alignment method for small specimens 3-61150
 phase analysis, methodology (*German, English*) 3-69202
 phase analysis methodology in technical alloys 3-76179
 point defects, field-ion image interpretation 3-75527
 Pseudo-Kikuchi patterns in SEM, surface oxides effect 3-80269
 rare earth metal perovskite carbides and borides, preparation, X-ray and metallographic studies 3-40907
 rare earth-group VIII metal systems, 7:3 phases, metallographic and X-ray obs. 3-79274
 recrystallisation texture prediction (*Russian*) 3-72848
 rolling texture determination, combination of inverse polar and direct figures 3-53227
 SEM, chip formation in metal machining dynamic viewing 3-58610
 SEM and TEM, area correlation techniques 3-59671
 s.e.m. stage, for obs. of chip formation in metal cutting 3-41691
 site, crystallite size determ., small-angle scattering of polarised light from continuous-wave gas laser 3-55834
 slip plane interaction with subgrain boundary, double refr. pattern obs. (*Russian*) 3-55779
 specimen prep. by powder separation technique 3-42556
 steel, A19 alloy, Be, Ti and Zr additions effect on struct. and mech. props. (*Russian*) 3-72850
 steel, archive samples exam. 3-80258
 steel, austenitic, containing Si on Ti, phase characteriz. 3-69222
 steel, austenitic stainless, a.c. electroetching for metallographic differentiation of δ -ferrite (*German, English*) 3-64866
 steel, borided, magnetic powder method 3-80281
 steel, cementite dissolution, in situ obs., h.v. electron microscopy 3-50706
 steel, Cr and Cr-Ni, as supplement to corrosion tests 3-47387
 steel, Cu-bearing, isothermal internal friction technique applic. to precip. 3-80268
 steel, Fe-Mn-C type, isothermal transform. induced struct. and props. 3-69224
 steel, ferrite, vanadium carbide precip. phenomena 3-69225
 steel, ferritic stainless, 475°C embrittlement phenomena 3-64914
 steel, high-alloy Cr and Cr-Mn, metallographic studies as supplement to short-time corrosion tests 3-44623
 steel, high-strength 4340M, grain refinement effect on microstruct. and mech. props. 3-64854
 steel, ledeburitic, carbide distrib. charact. by stereometric analysis (*German, English*) 3-53235
 steel, low-alloy pressure vessel, correlation between microstructure and electron fractography 3-47389
 steel, low-C, aging, structural changes electron microscope studies 3-47388
 steel, low-C vanadium, controlled-rolled and continuously cooled, microstruct. obs. by TEM 3-80259
 steel, maraging, struct. evolution under high speed cumulative thermal cycling (*French*) 3-80267
 steel, microalloyed structural, metallographic investigations by phase diagrams (*German*) 3-80202
 steel, nonmetallic inclusions, effect of sectioning errors on microscopic determ. 3-69229
 steel, rare-earth inoculated, contact microradiography obs. 3-61146
 steel, stainless, nitrided, phase identification 3-64838
 steel, thermoplastic shear and fracture during high-velocity sliding in rocket-sled testing 3-50748
 steel, wrought, inclusions, quant. impurity indices 3-50693
 surface oriented struct. form. under laser beam action 3-41786
 texture determ., neutron diffraction method, applic. to cold-rolled Zr sheets 3-64847
 thinning and dissolving out techniques (*German, English*) 3-64865
 transition metal perovskite carbides and borides, preparation, X-ray and metallographic studies 3-40907
 TV metallographic analyser, vol. percentage, specific interface, size distrib. 3-51584
 X-ray microanalyzer applics. (*Czech*) 3-55770

metallography continued

- Ag alloys, cold-worked, Voigt profile analysis for particle size and strain determ. 3-61141
 Al, Pseudo-Kikuchi patterns in SEM, surface oxides effect 3-80269
 Al alloys, intermetallic cpd. determ. 3-44588
 Al-Cu-Li-Mn-Cd alloy, complex phase behaviour 3-55761
 Al-Cu (3 wt.%) alloy, strain fields at Guinier-Preston zones, lattice resolution meas. 3-41705
 Al-Mg alloys, morphology of stress corrosion cracks and crack branching 3-80265
 Al-Mg-Li 01420 alloy with Zr, plate exam. 3-55783
 Al-Mg(11 wt.%) alloys, microstruct. and corrosion resist. after long-time natural ageing (*Russian*) 3-80249
 Al-Zn (28at%) alloy, discontinuous precip., h.v. electron microscope in situ obs. 3-50708
 Al-Zn-Mg-Cu-Cr alloy, as-cast, ingot processing effects on subgrain struct. 3-80264
 Cd, recrystallized during hot deform., orientation of grain boundaries 3-80262
 Co alloys, chem. and electrolytic polishing, etching 3-76180
 Co-Fe (8 wt.%) alloy single crystals, twin-slip, twin-twin and slip-twin interactions 3-40930
 Co-Fe alloys, stacking fault energy, conc. and temp. depend. 3-41706
 Co-Si eutectic alloy, struct. and mag. props. of phases 3-80201
 Cr bronze, rolling texture determ., X-ray diffraction technique, combination of inverse polar figure and direct figure 3-53227
 Cr-Rh alloy, system, constitution diagram obs. 3-69193
 Cu, dislocation struct. change during thermal cycling (*Russian*) 3-72900
 Cu, recrystn. and recovery after heavy rolling, h.v. electron microscope obs. 3-50702
 Cu alloys, cold-worked, Voigt profile analysis for particle size and strain determ. 3-61141
 Cu single crystals, fatigue crack tip region obs. by TEM 3-64852
 Cu-Fe alloy single crystals, containing γ -Fe precipitates work hardening phenomena 3-80226
 Cu-Ni alloys, mag. permeability correl. with microstruct. 3-75856
 Cu-P alloy, recrystn. and recovery after heavy rolling, h.v. electron microscope obs. 3-50702
 α -Fe, 1 MeV electron irradi. in electron microscope at 550°C dislocation loop geometry 3-49982
 Fe, cast, malleable high-sulphur, graphitization obs. 3-50736
 Fe, dislocation structure change during deform., hydrogen influence (*Russian*) 3-80253
 Fe, rolled, annealed twins, orientation, texture angle calc. 3-50694
 Fe-Al(40 at.%) alloy, ordered, slip systems, shear stress induced (*French*) 3-53212
 Fe-B alloy, magnetic powder method 3-80281
 Fe-Ni alloys, phase transforms., diffusion role, potentiokinetic obs. (*French*) 3-47362
 Fe-Pt alloys, martensite transform. near Fe₃Pt comp., austenite ordering effect 3-64822
 Fe-Pt alloys, martensite transform. near Fe₃Pt comp., austenite ordering effect 3-69201
 Fe-Si, shock loaded, struct. changes during heating (*Russian*) 3-80248
 Fe-Si (12.1 at.%) alloy, strains at antiphase boundaries (*Russian*) 3-72851
 GaAs, structural changes due to laser irradiation (*Russian*) 3-72771
 InP thin films on substrates, struct. anal. 3-72286
 Mg, compressed along c-axis, twinning deform. 3-80263
 Mo thin foils, in situ deform., 800 keV electron microscopy 3-50703
 Nb₃Sn, supercond., shock wave synthesis, phase form. obs. 3-69328
 Ni, pack-aluminizing, boundary conditions for diffusion 3-64964
 Ni, void nucleation, h.v. electron microscopy 3-49906
 Ni sulphides in Ni-base superalloys, crystal structure and morphology 3-40864
 Ni-Al(36 at.%) alloy, martensite struct. and behaviour (*Russian*) 3-80250
 Pb-Ca alloys, precip. behaviour during room-temp. ageing (*German*) 3-55790
 Ta, nitriding, struct. changes, h.v. electron microscopy, in situ obs. 3-50707
 Ta, surface-carburized, carbide precip. phenomena (*French*) 3-61153
 Ta/Li high temp. heat pipes, corrosion mechanism 3-40543
 Ti alloys, fracture, micromechanisms, hydrogen influence (*Russian*) 3-80322
 Ti-Cr alloys, aged, decomp. processes prior to omega phase detection 3-61148
 U adjusted, void nucleation behaviour 3-63192
 γ -U-Mo, fast burst reactor fuel, deformation and fracture behaviour 3-63207
 U-Nb alloys, niobium segregation phenomena 3-61149
 WC-Co compound powder, plasma spraying on hard metals, phases study (*German*) 3-50752
 Yb-Pd system, phase diagram determ. 3-64151
 ZnAl eutectoid alloy, in situ superplasticity expts., 1 MV electron microscope 3-50705
 Zr alloy corrosion film thinning for transmission electron microscopy (*German, English*) 3-61157
- metallurgical industries**
 ore sintering, numerical simulation 3-41794
 slags, simultaneous viscosity and elec. cond. meas. vibration viscosity meter 3-48467
- metallurgy**
 see also ageing; heat treatment; metalworking; powder metallurgy
 Auger electron spectroscopy in SEM 3-55707
 carbides, free enthalpy of formation, temp. depend. calc. method (*French*) 3-61127
 differential reflectometer applic. to materials research in corrosion, ordering and alloying 3-64812
 dimensioning and strength calcs., conf., Budapest, Hungary (Oct. 1971) 3-69429
 ion implantation and ion bombardment 3-64769
 probe testing and eval. for sampling molten iron and steel (*German*) 3-76190

metallurgy continued

- stored energy of cold work, book 3-44642
vacuum treatment of molten matte and white metal 3-64949

metalorganic compounds *see organometallic compounds***metals**

- see also actinides; alkali metals; alkaline earth metals; aluminium; bimetals; cadmium; ferromagnetic metals; indium; lead; mercury (metal); noble metals; rare earth metals; thallium; transition metals*
acoustic standing wave reson., e.m. excited, in high mag. field 3-58410
acoustic wave excitation by fast charged particles and gamma rays 3-75550
adsorption of inert gases, physisorption interaction energies prediction 3-64242
aggregated systems, optical props., plasma resonances 3-68948
aging effects, phenomenological theory 3-64951
amorphous, temp. depend. of electrical resistivity 3-46828
anisotropic, creep rates determ. 3-76219
anisotropic metal, bulge test and simple tension test data 3-68311
anisotropic metals, bulge caused by rolling 3-69271
atomic absorption spectroscopic methods, techniques and results, conf., London, England (Nov 1972) 3-48636
Bauschinger effect on surface layer under various loads, microfluidity area (*Russian*) 3-55754
b.c.c., defect kinetics during annealing, computer anal. 3-79345
b.c.c., defects, conf. Gaithersburg, USA, (Aug., 1973) 3-79367
b.c.c., dilatation centre and split dislocations elastic interaction 3-43790
b.c.c., electron microscope image contrast effects on anal. of dislocations 3-79361
b.c.c., low temp. neutron irradi. effects annealing recovery depend. 3-79381
b.c.c., neutron irradi., defect clusters rel. to impurity atoms 3-79334
b.c.c., neutron irradiation damage effect on mechanical properties 3-79380
b.c.c., neutron irradiation softening and effect of interstitials 3-79343
b.c.c., struct. factor changes near ductile/brittle transition (*Russian*) 3-55753
b.c.c. lattice, atomic config. of screw dislocations 3-40925
b.c.c. neutron irradi. effect on tensile props. 3-79386
b.c.c. neutron irradi. temp. effect on hardness 3-79387
Benioff zones, metallogenic belts and angle of dip 3-69524
binding energies in cubic metal surfaces 3-60681
brittleness, influence of intercrystallite internal absorpt. of impurities, liquid metal embrittlement (*Russian*) 3-69217
charge transport parameters for thin films with cubic symmetry, size effects 3-55242
composite, fibre reinforced, bonding and compatibility at dividing boundary (*Russian*) 3-53273
in concrete, corrosion, electrochemical behaviour (*French*) 3-69372
corrosion testing in electrolytes, active, passive states 3-76198
creep behaviour, basic mechanisms, review 3-46667
crystallisation, surface inactive impurity effects (*German*) 3-75489
cubic, grain boundary dislocations, Burgers vectors 3-55785
cyclic deformation at high temps., math. interpret. 3-69311
deformation at high-speed, delay of yield and hardening, model 3-76222
deformational hardening uniaxial creep (*Russian*) 3-41765
deposits, location using plate tectonics 3-76597
desorption of ions, mass spectrometric determination 3-48558
diffusion characts. of boundary and volume components of flow of diffusing hydrogen (*Russian*) 3-41041
diffusion of oxygen out of metal, flash desorption conditions 3-72271
diffusional creep inhibition by second phase particles 3-46668
diffusional saturation, external surface displacement (*Russian*) 3-58177
dislocation arrays, planar and cellular, slip behaviour (*German, English*) 3-69241
Doppler-broadened annihilation radiation 3-68541
dynamic fracture under biaxial strain, exploding-wire expt. 3-73109
dynamic plasticity, macroscopic and microscopic aspects, review 3-49923
elastic deformation of polycryst., grain slenderness effects on deform. mode 3-54992
electrocrysts., atom model, impedance plane display 3-73138
electrodeposition, three dimensional nucleation during potentiostatic pulse, simulation 3-69466
electron bombarded, light emission 3-76099
electron potential emission yield, theory 3-69117
erosion by water-jet impact, transient stress distrib. 3-72903
e.s.r., simple derivation of Bloch equations including anisotropy fields 3-60985
evaporation by intense laser radiation, liquid-vapour transition model 3-61102
evaporation by laser radiation, gas-dynamic struct. of plasma flare 3-75400
extrusion, material behaviour influence on force requirements and velocity (*German*) 3-41795
failure process in complex stress state, mechanism 3-58689
fatigue damage, automatic information processing 3-80516
fatigue damage process, temp. depend. 3-69315
fatigue strength, loading freq. depend. 3-44629
fatigue testing, low-cycle, compression-tension, in gaseous media, elevated temp. apparatus (*Russian*) 3-61240
f.c.c., 3 wave scatt. in electron diff. 3-71992
f.c.c., Debye-Waller factors, temp. variation, calc. using modified non-central force model 3-43858
f.c.c., diffusion of hydrogen isotopes, coeffs. calc. (*Russian*) 3-52720
f.c.c., self-diffusion, influence of isolated dislocations 3-79530
f.c.c. and b.c.c. lattices, rate relationships of dynamic yield pt. 3-43824
field ion microscopy, computer program for modelling ion images of spherical pores 3-80286
fluid, conductivity, thermoelectric power, volume expansion effects, super- and sub-critical temps., metal-insulator transition 3-50179

metals continued

- fracture mechanics methods applic. to fatigue life prediction 3-64892
fracture parameters, pair interaction influence (*Russian*) 3-72891
frictional forces deform. characts. generation under influence of surface-active lubricants (*Russian*) 3-58079
group IV to VIII, friction-hardened surfaces, microhardness obs. (*Russian*) 3-80329
hard, with gas covered surfaces, anomalously large adhesion coeff. 3-47419
h.c.p., foil thickness meas. using intersecting slip traces 3-47372
heat of solution, elements into, isodromic temp. control 3-70281
heat resistance estimation method for variable temp. conditions (*Russian*) 3-80425
heavy, energy loss of 2.0-MeV ⁴He ions, meas. 3-40944
ideal strength, Morse potentials use and limitations 3-58061
impurity effect on host atom diffusion, Ashcroft model pot. 3-50029
inelastic reflection of electrons, coeff., rel. to angle of incidence (*Russian*) 3-80125
internal friction, intrinsic amplitude depend. damping and modulus defect calc. method 3-64113
internal stresses, produced by dislocations, in cross rolled cylindrical specimen 3-69302
irradiated, growth, swelling and termination of voids with high temp. high dosage 3-79336
irradiated, void nucleation kinetics, impurity effects 3-64072
irradiation system and expt. techniques for metal ion injection into metals 3-59635
laser beam irradi., mech. deform. and disruption (*Russian*) 3-40958
laser crater production in planar fully developed evaporation of target 3-53163
laser-heated surface, energy of emitted electrons 3-80146
lasing of vapour caused by action of high power electron beam on metal target 3-48891
lattice distortion due to gas interstitials in b.c.c. metals 3-64029
load-elongation curves of pure b.c.c. structure at low temp. 3-72118
Lorenz ratios of technically important metals and alloys 3-55246
low temperature behaviour, Debye temp., energy role (*Russian*) 3-79498
lunar matter fragment, morphology 3-65808
magnetic glass, review 3-46977
magnetoelectric effects, determ. from torque in rotating mag. field, specimen dimension and shape effects 3-41174
mass spectrometer for analysis, Mattauch-Hertzog type, detection system, appls. (*Hungarian*) 3-77714
melting by electron beam, mechanisms (*Russian*) 3-53261
metal/metal interface, differential modulus effects on mech. behaviour 3-40921
monatomic, entropy of melting 3-72183
Mossbauer absorption spectra of implanted ⁵⁷Fe at room temperature 3-68903
neutron irradi., dislocation loop nucleation 3-40938
neutron irradi. creep during void form. 3-40939
neutron irradiated, role of depleted zones 3-52644
n.m.r. and mag. susceptibility correlation 3-64573
nonferrous, energy dissipation in h.f. fatigue tests 3-58694
organic coatings on metals, electrostatic fluidised bed technique, limitations 3-66720
oxidation rate const. maximum value w.r.t. temp. 3-65085
paramagnetic transition, magnetostriction obs. rel. to electron gas vol. expansion 3-50339
particles, combustion and burning, technique for laser study (*Russian*) 3-43042
particles dispersed in insulating medium, electrical conductivity model 3-44100
penetration by metal jet, high speed X-ray flash photography (*Russian*) 3-69263
phonon damping, acoustic, in cubic metal, electron-phonon induced linewidths 3-58100
photoemission, laser multiphon phenomena 3-76121
photoemission, two photon photocurrent calc., multiple beam illum. 3-72782
photoionisation and photoelectron spectroscopy of vapour and compounds 3-40577
photon emission induced by fast H⁺, He⁺ ion impact 3-61097
plastic anisotropy, Lankford calc. (*French*) 3-72912
plastic deformation degree assessment in crater with ball imprint, etch pit method 3-64938
plastic deformation investigation using exoelectron emission 3-48585
plastic flow, direct study by X-ray motion picture filming 3-76402
plastic flow stress determ. by hot torsion testing 3-76416
plastic isotropic materials, math. model of damage accumulation 3-64936
plastic strain meas. by strain-gauge methods under uniaxial stress condition 3-73100
polycrystalline surfaces, sputtering with high energetic inert gas ions, mean velocity of ejected particles 3-47341
polymorphic, transitions A3→A2 or A1→A2, temp./melting pt. relationship 3-43877
positron lifetime and lineshape factor, strongly deformed metals, influence of dislocations 3-52805
powders r.f. echoes in n.m.r. 3-79923
pulsed heating vaporization, mass spectroscopy, ion yield optimization 3-70455
quench hardening, isothermal recovery 3-64920
Rayleigh sound waves, electron absorpt. in parallel mag. field 3-49939
recrystallisation texture prediction (*Russian*) 3-72848
residual stress meas. and analysis using u.s. techniques 3-53839
ring wave production in metallic surfaces in laser radiation zone (*Russian*) 3-69111
secondary ion emission rel. to electronic structure 3-61096
shock compressibility, high vel. impact, explosive leading (*Russian*) 3-66573
short specimens above 1000°C, thermal conductivity, electrical conductivity and emissivity determ. method 3-77563
short-time stress/strain characteristic, temp. depend., thermally activated models 3-69309

metals continued

- single crystals, f.c.c., tensile behaviour, theoretical model (*French*) 3-64089
- sintered materials, refractory props., elec. resist. (*Polish*) 3-44665
- spin relaxation, longit., retardation effects, dynamical impurity susceptibility 3-68827
- sputtering coeff., sputtering saturation model and trapped amounts for metal ion injection into metal 3-61083
- sputtering in oxidizing atmosphere, model 3-64758
- strain energy function, finite elastic vol. change 3-40949
- stress analysis of composite bars with oblique boundaries, photoelastic, and interferometric obs. 3-44671
- stress corrosion, quantitative criterion (*Russian*) 3-41095
- stress distrib., magnetoelastic method 3-76397
- stress state around nonmetallic inclusion, microthermal e.m.f. meas. (*Russian*) 3-61137
- stress wave propagation, obeying the constitutive eqn. of the Johnson-Gilman type 3-64088
- stresses, thermal and structural, electrical heating, const. length 3-73105
- structural, catalytic poisoning and stress corrosion cracking control 3-64889
- superplastic state, electron emission during transition 3-60763
- surface, He beam scattering, Debye-Waller factor applic. 3-69113
- surface, possibility of field emission with Q-switched laser pulse 3-64766
- surface, trapping of gas atoms, sticking coeffs. 3-75676
- surface oriented struct. form. under laser beam action 3-41786
- surface topography, damage-induced, during particle bombardment 3-80134
- surfaces, Auger neutralisation of highly charged ions 3-69126
- surfaces, gas sorption at low pressures 3-75673
- surfaces, LEED studies on planes nonparallel with the surface 3-68471
- tensile creep at elevated temps., hydrostatic stress effect, X-ray obs. (*Japanese*) 3-40830
- thermal expansion, atomistic expression 3-41033
- thermodynamic props., expt. meas. techniques, review (*German*) 3-42539
- thermodynamic props., exptl. methods, review (*German*) 3-53200
- thermoelectric power, isotopic scatt. influences 3-52829
- thermogalvanic corrosion elements, irregular thermal loading 3-73104
- thin film, appl. to i.r. internal reflection spectrometry 3-73164
- thin plate, temp. depend. of elec. conductivity theory 3-58244
- time-dependent strength and failure, eqn. development 3-65020
- trace analysis in particulate pollutants by emission spectroscopy, review 3-45332
- transverse surface waves on piezoelectric material with metallic layer 3-41073
- type II superconductor phase transition rel. to plastic properties 3-55355
- u.s. excitation by charged particle beams 3-55034
- vacancies, obs. by quenching method under pressure up to 100 kbar 3-77417
- vacancy formation entropy, evaluation from positron annihilation data 3-46640
- vapour condensation on single cryst. surfaces, combined LEED, Auger electron and flash desorption spectroscopy 3-79562
- vapour reactions with halogens, chemilum. and photolum. of products 3-76421
- void formation under fast neutron irradiation, dislocation vibration as cure 3-40941
- in water, preconcentration using electrodeposition, X-ray fluorescence analysis 3-66423
- wear, delamination theory 3-72129
- X-ray crystallography, equation selection for correction of primary extinction 3-79209
- X-ray fluorescence analysis, sample preparation 3-62336
- yield surface shape, offset influence, different loading paths, slip theory model anal. 3-72889
- B content analysis by activation and absorption method 3-66458
- H, eqn. of state and phase equil., astron. appl. 3-42163
- H prod. in planets, correlation of theory and expt. 3-40684
- H-He mixtures under high press., appl. to giant planet interiors 3-42161

metalworking

- see also bending; cold working*
- steel, wear resistance, electrospray surface alloying effect 3-50739
- steel, white layers formed during treatment, characteriz. (*Russian*) 3-80330
- two-dimensional finite deformations, noncoaxiality implications 3-64965
- Fe-B-C hard facing alloy characteriz. 3-50740

metamagnetism

- domain structure, in region of transition 3-41346
- Heisenberg spin system on f.c.c. lattice with second neighbour interaction magnetisation process 3-72433
- Ising model displaying tricritical behaviour, ferromag. planes with antiferromag. coupling, high temp. series study 3-55397
- transitions, domain structure, mag. susceptibility and magnetostriction 3-68784
- DyAl garnet, tricritical point scaling test 3-60967
- ErAu, metamag. props., susceptibility and magnetization studies 3-47039
- FeCl₂, mag. field effects on optical spectrum, antiferromag.-ferromag. transition 3-41528
- FeCl₂, metamag. props. near tricritical point, ferromag.-antiferromag. transition, susceptibility, anisotropy calcs. 3-47026
- FeCl₂·2H₂O, metamag. systems, bound magnon-phonon pair coupling calc. 3-52984
- FeCl₂·2H₂O, antiferromag., ferrimag. and ferromag. phases, with applied mag. field 3-58383
- Fe₂P, magnetiz. evolution, Mossbauer obs. (*French*) 3-47191
- HoAu, metamag. props., susceptibility and magnetization studies 3-47039
- α-(Ni_{1-x}Zn_x)(OH)₂, metamag. props. with low threshold field, mag. viscosity 3-79826

meteor trails *see meteors***meteorites**

- see also meteors; micrometeorites*
- ages of eight recently fallen meteorites 3-61744
- Allende, Ca-Al rich inclusions, evidence for liquid origin 3-61749
- Allende, major element chemical variables among chondrules and white aggregate 3-59321
- Allende, rare-earth elements in matrix, inclusions, and chondrules 3-61741
- Allende meteorite, crystal structure and optical props., Ti³⁺ fassaite 3-45052
- Antarctic, chemical comp. and rare gas content of Yamato meteorites 3-56362
- Apollo 11-16 results, review 3-45046
- asteroid belt origin due to secular perturbations 3-56368
- astrobles, two Brazilian structures 3-61748
- Bruderheim, complex index of refraction, 1.1 to 5.2 μm 3-81013
- Bruderheim, olivine-hypersthene chondrite, photometric and polarimetric properties 3-59318
- Brundheim, complex refractive index between 1.1 and 5.2 μm 3-59325
- Canyon Diablo metallic spheroids rel. to breakup of Canyon Diablo meteorite 3-51307
- carbonaceous, D/H ratio rel. to D abundance in early solar system 3-47874
- carbonaceous chondrite, thermomag. anal. thermally unstable constituent decomposes to magnetite 3-81014
- carbonaceous chondrites, Xe isotope composition rel. to solar wind 3-61743
- chondrites, carbonaceous, heavy element abundances 3-73425
- chondrites, isotopic Pb ages determ. 3-61739
- chondrites, Tenham area, Queensland, Australia 3-56366
- chondrites with peculiar rare-earth patterns 3-81008
- chondrules, analogy with impact-generated spherules on Moon and Earth 3-65853
- conference, Chicago (1972) 3-56365
- cosmic ray bombardment, rel. to solar system history 3-77027
- cosmic ray tracks, calc. for surface exposure 3-44971
- explosive shock experiments at 500 and 1000 kbar. (*Russian*) 3-81009
- Gosnells iron, fragment of Mount Dooling octahedrite 3-47973
- Havero, ³⁷Ar, ³⁹Ar and ³H radioactivity meas. 3-45066
- Havero, chemical comp. compared with other ureilites 3-45065
- Havero, different forms of carbon 3-45064
- Havero, highly refl. and opaque components of mineral content 3-45067
- Havero, morphologies of Fe crystals 3-45063
- Havero ureilite, anal. of cosmogenic radionuclides 3-45062
- Havero ureilite, evidence for recrystallization and partial reduction 3-45070
- Havero ureilite, microscopic anal. 3-45061
- Havero ureilite, petrographic obs. 3-45071
- Havero ureilite elemental abundances 3-45068
- Havero ureilite, chemical anal. 3-45069
- impact craters, lab. simulation for interpreting direct research data 3-59316
- impact debris, comparison of lunar and terrestrial crater spherules 3-65803
- impacts on Moon and Earth, flux determ. 3-47968
- inert-gas-rich, volatile element content 3-59323
- iron meteorites, Widmanstätten Figure formation, evolution meteorite parent bodies 3-73470
- Juvinas achondrite, evidence of extinct nuclide ¹⁴⁶Sm 3-47966
- Keyes chondrite, depth variation of cosmogenic inert gases 3-51309
- Khor Temiki aubrite, evidence for solar flare rare gases 3-61668
- KREEP fragment containing niobian rutile 3-45057
- Lafayette, nakhlite meteorite, thermal history by ⁴⁰Ar-³⁹Ar method 3-56360
- Lunar Crater, impact-generated silicate spherules 3-65853
- Lunar lake, India, impact crater in basalt, shocked fragments discovery 3-59320
- magnetic remanence of tektites 3-61750
- Nakhlite, thermal history by ⁴⁰Ar-³⁹Ar method 3-56360
- Ness County, fall dates 3-45053
- niobian rutile found in Apollo 14 KREEP fragment 3-45057
- nuclide prod. rate by galactic cosmic rays 3-73467
- oceanographic impact, range of effects 3-59326
- Orgueil, magnetite, ¹²⁹I/¹²⁹Xe dating 3-77025
- Oro Grande chondrite and lithic inclusion, anal. 3-45059
- parent bodies, thermal model 3-53628
- pyroxenes, anisotropy of absorption bands, comparison with lunar and terrestrial pyroxenes 3-65795
- Ransom, discovery map and microscopic exam. 3-45060
- richerite, meteoritic amphibole 3-81006
- Seminole, anal. showing black olivine-bronzite or H4 group chondrite 3-45056
- Sikhote-Alin, radiation age 3-51310
- spectral reflectivities of 22 ordinary chondrites rel. to 36 asteroids 3-61740
- spectral reflectivity, class distinction 3-59324
- stream, forces acting on asteroid moving across stream 3-42186
- tektite ablation, calculations 3-61745
- tektites, element spatial distrib. determ. 3-51308
- tektites, Georgia, fission track ages and stratigraphic occurrence 3-69510
- tektites, thermal annealing of latent damage trails 3-61359
- Tunguska meteorite event, black hole of substellar mass as explanation 3-69751
- Washougal howardite, mineralogy and element abundances 3-45055
- Yilmia enstatite chondrite, mineralogy and petrology 3-45054
- B abundance theory 3-61624
- ²⁴⁸Cm in early Solar System from primitive meteorites 3-76963
- Fe meteorite corrosion, potentiostatic study 3-45058
- ⁵⁷Fe Mossbauer investigation of tektites 3-59322
- ²⁰⁷Pb/²⁰⁶Pb ratio, radiometric ages 3-77026
- ²⁰⁷Pb-²⁰⁶Pb isochron and age of 16 chondrites and one achondrite 3-61742

meteoroids

- see also meteorites; meteors*
- Apollo window meteoroid detection expt. 3-59328
- comet dust influxes into earth's atm., times and location 3-59125

meteoroids continued

- flux measurement, 1970 Geminid meteor shower 3-77183
- forces generated by stream moving rel. to planet or asteroid 3-69906
- interaction with lower thermosphere rel. to motion and processes 3-65854
- lunar fragmental surface material, production by meteoroid impact 3-47947
- lunar impact data, seismic meas. 3-61723
- micrometeoroid simulation, MHD compression of coaxial plasma accelerator flow 3-40810
- spacecraft hull puncturing by meteoric impact 3-59315
- spatial density, estimation from penetration and piezoelec. sensors, correction for angle of incidence 3-59317

meteorological instruments

- see also anemometers; barometers; hygrometers; ionospheric measuring apparatus
- automatic measuring buoy (Italian) 3-59198
- filters and impactors for collecting stratospheric particulate matter, relative efficiencies 3-76905
- f.m.-c.w. and optical radar, simultaneous obs. and forecasting applications 3-42085
- lightning detector, photoelectric, all-sky 3-59185
- marine proton magnetometer, APM-1, automated, selection of optimum sensor, meteorological tests (Russian) 3-47841
- NIMBUS-5, elec. scanning microwave radiometer 3-56175
- NIMBUS-5 microwave spectrometer experiment results 3-59067
- NOAA-2 environmental satellite for atmos. research 3-56258
- radar, civil aircraft, meteorological perturbations, ground mapping (French) 3-51194
- radiosonde recorder, calibration, multi-pulse generator 3-80857
- satellite instrum., modern improvements (Russian) 3-47826
- snowline mapping with NOAA-2 environmental satellite 3-56174
- superpressure balloons as isentropic/isopycnic tracers 3-53559
- weather Doppler radar, possibility of increased velocity capability and reduced range ambiguities 3-76904

meteorological optics see atmospheric optics**meteorology**

- see also climatology; wind
- 48-hour forecast 500 mb troughs and ridges, comparison of British and American model errors 3-47760
- air flow obs. in pine forest 3-73336
- air temperature ground inversions, near ground over India, effect of air pollution 3-80743
- Alicante, origin of dust which fell on 1972, 6 Feb. (Spanish) 3-56165
- Arabian Sea monsoon activity rel. to beat low over W. Pakistan 3-65323
- atmospheric circulation patterns, representation by a set of Tschebyscheff orthogonal polynomials, rel. to weather 3-80856
- atmospheric dynamics and circulation numerical simulation 3-51071
- Australia, monthly mean wind patterns at 40000 feet 3-59055
- Barcelona, anal. of solar radiation meas. (Spanish) 3-56166
- barotropic instability and predictability difference energy spectra 3-44890
- barotropic instability Rossby wave motion β effect, vorticity equation 3-44892
- barotropic model, divergent, prognosis of 500 mb surface 3-80741
- barotropic vorticity equation, lateral boundary conditions 3-44891
- British Isles, temperature changes rel. to weather type 3-44901
- Canadian Meteorological Centre, precipitation forecasts 3-47845
- cloud cover forecasts, six layer NMC PE model 3-76763
- cloud height and extinction coeff. meas. by new lidar 3-76912
- condensation determ. in dynamical weather model using Newton-Raphson procedure 3-47846
- cropped surfaces, Southern Ontario, equilib., pot. and actual evaporation 3-76757
- cyclonic disturbances, Indian region, trends and quasi-biennial oscillation 3-80742
- data acquisition employing remote-controlled radar systems 3-42059
- data centralization, Eole expt. (Italian) 3-61605
- Dee weather radar project, area precip. meas. 3-73404
- disturbed airflow over mountains, aircraft measurements 3-44910
- drop impactions rel. to number of precip. size drops 3-51053
- drought, Tamil Nadu, India, Subtropical Jet Stream System, anomalous upper level flow patterns 3-80737
- dry cold fronts, microstructure 3-76758
- Europe, exceptional weather events during 1972, review 3-73337
- evaporation, rel. to meteorological factors, correl. techniques 3-80739
- extended range predictability of 12-day weather patterns 3-65366
- extratropical cyclone parameters from Nimbus 2 HRIR meas. 3-65359
- Florida state, simultaneous obs. of tornado, waterspout and funnel cloud 3-73333
- f.m.-c.w. radar atmospheric sounding, new developments and applications 3-65519
- forecasting, repetition of weather sequences, circulation patterns 3-80770
- forecasting, skill and probability scores 3-47757
- forecasting of premonsoon thunderstorm/duststorm activity over Delhi region 3-65523
- freezing nuclei concentration, membrane filter method (German) 3-47842
- GARP rel. to numerical modelling and weather prediction 3-51072
- general circulation model, mathematical eqns. 3-69590
- geostrophic and mesoscale forcing, 32-km. moist primitive equation model 3-47733
- Global Circulation Model, error accumulation with updating experiments 3-76902
- grapel, conical, mechanism of origin, rain and hail formation 3-44889
- hail suppression experiments, effect of hailswath structure 3-51021
- Hawaii, proportion of volatile aerosols 3-51052
- historical weather patterns (1493-1860), large scale 3-76915
- hurricane Agnes, development shaped by ocean-atmosphere interactions during antecedent months 3-65388
- hurricane prediction 3-80864
- hydrologic decision strategies, minimax vs. expected value criteria 3-59062

meteorology continued

- hydrometeorological phenomena, periodicity, Furich's autocorrelation method (German) 3-76845
- ice crystal growth habits 3-61468
- India, 700-mb, 5-day mean contours and 5-day rainfall anomaly during July 3-65325
- India, evaporation data 3-47724
- India, extreme wind speeds in gusts 3-65330
- India, fluctuations in seasonal temp. oscillations 3-65324
- India, mean precipitable water vapour and rainfall liability index 3-51014
- Indian west coast rainfall during 1969 SW monsoon 3-80728
- instability of 2 level quasi-geostrophic waves in horizontal shear, seasonal var. and latitudinal distribution 3-73325
- i.r. stereoscopic line scanning from meteorological satellites 3-51177
- lidar applications 3-51196
- lidar for air monitoring and meteorology 3-51195
- lightning as acoustic source to determine near-storm atmospheric parameters 3-59184
- logarithmic wind profile in planetary boundary layers rel. to micrometeorology 3-47735
- long range forecasts, assessment method 3-51070
- long-range weather forecasting rel. to sea surface temp. anomalies 3-41977
- long-range weather forecasting using circulation analogues, 4-year experiment 3-47762
- mamma formation, obs. of hailstorm, time-lapse photography, radar meas. 3-80772
- Manchester Airport, diurnal variation 3-73334
- marine weather extremes, temp., rel. humidity, wind speed, visibility, salinity and upper air temp. 3-53496
- Marsta micro-meteorological field project, temp. and humidity profiles 3-73282
- maximum/minimum surface temp. automatic prediction, use of model output statistics 3-59194
- mesometeorology using NOAA satellites very high resolution radiometer 3-59192
- mesoscale forecasts, high pressure systems from satellite imagery 3-59110
- microseisms generation, hydrometeorological conditions 3-61345
- Nagpur, India, forecasting heavy rainfall during SW monsoon 3-80726
- New South Wales, relief influence on local temp. 3-80769
- night min. temp. forecasts at Wyton using embedded thermometers 3-65531
- Nimbus 4 SIRS temp. data, four-dimensional assimilation experiments 3-65357
- Nimbus-5, description of equipment and expts. 3-41873
- North Pacific, microbaroms azimuth rel. to severe weather systems 3-61485
- North Pacific Experiment, oceanic processes rel. to weather phenomena 3-44903
- numerical forecasting, boundary error reduction (German) 3-59172
- numerical simulation of cloud seeding experiments in selected Australian areas 3-65362
- numerical weather prediction, derivation of atmospheric balance eqns. for irreversible processes (German) 3-73284
- numerical weather prediction, limitations of hydrostatic system 3-59115
- numerical weather prediction over sphere, comparison of grids and difference approx. 3-51047
- objective analysis, review 3-80731
- objective analysis scheme, atmospheric wind field, spectral analyses 3-76860
- ocean upper mixed layer, time-dependent model, meteorological influences 3-65271
- orographic effect on wind and rain distribution around mountain gap 3-65327
- pattern classification, Southern California, by discriminant analysis 3-76752
- photodiode for weather forecasting in meteorological satellite 3-51197
- pine forest, estimated and measured roughness parameters 3-51051
- plan position indicator photographs, probability of encountering weather-echo near Gan 3-73401
- planetary boundary layer eqns., revision of Estoque and Bhummalkar method 3-73283
- Polar Experiment, review 3-56155
- Poona, district, India, rainfall over 1955-64 period 3-80725
- precipitation data anal., family of distribts. 3-51048
- probability score, vector partition 3-76907
- Puerto Rican marine atm., chemistry of aerosols, cloud droplets and rain 3-51035
- pulsed Doppler weather radar, storm wind velocity isotach displays 3-76911
- quality control of data 3-59092
- radar shower records, vertical motion of patterns 3-51055
- radio broadcasts, outline of information 3-73335
- rain drop spectra for 5 different climates, comparison (German) 3-47763
- rain patterns in cyclonic systems, frontal zones and convective storms, NIMBUS-5 obs. 3-56175
- rain-gauge on mast-top, performance during field test 3-44960
- rainbow and glory, vector theory of scattering 3-73287
- rainfall patterns over US from Nimbus 5 radiation data 3-59112
- Sahara, radiometric obs. (Spring 1967) (German) 3-69584
- satellite meteorology and picture interpretation, review 3-80734
- satellite obs. of fog and stratus behaviour rel. to short-range forecasting techniques 3-59111
- satellite pictures of cyclonic disturbances over Bay of Bengal and Arabian Sea 3-80735
- by satellites, legal aspects (French) 3-69737
- satellites, operational (Dutch) 3-59179
- SATIN station, problems in telemetry (French) 3-47828
- Scottish Highlands, changing pattern of snow distrib. 3-80771
- ship obs. accuracy and mesometeorological meas. in tropics (Russian) 3-47774
- simultaneous f.m.-c.w. and optical radar obs. 3-42085
- snow and pack-ice areas in fall rel. to insolation income 3-59099

meteorology continued

- snow hydrology, Western Himalayas, satellite pictures 3-80740
 solar corpuscular radiation, effect of variations on weather 3-80767
 solar radiation changes and effect on weather 3-80972
 Somali Current at 2°S, response to 1971 SW monsoon 3-53443
 Southeast Asia, weather and equatorial waves during summer monsoon 3-51049
 southwest monsoon period, India, 1971, rainfall and floods, Ganga Basin 3-80736
 St. Louis heat island, empirical model rel. to meteorological conditions 3-51044
 statistical freq. distrib. to predict floods, droughts and rainfall 3-56172
 statistical properties of precipitation patterns, space and time autocorrelation functions 3-65361
 storm and depression track prediction using computer oriented technique 3-80733
 summer maximum temp. at Nagpur, objective forecasting method 3-80854
 Sungei Buloh, Selangor, wet and dry spells persistence 3-76772
 sunshine, rel. to cloudiness over India, regression anal. 3-80745
 surface wind automated prediction, use of model output statistics 3-59193
 temperature field at 20 km altitude, Nimbus III obs. (Italian) 3-61604
 terrestrial environment monitoring from space, conference (Rome, March-April 1973) 3-50871
 thunderstorms, Delhi State, method of forecasting rel. to meteorological parameters 3-80855
 tornado, waterspout and funnel cloud, simultaneous obs. 3-73333
 tornado at Diamond Harbour, India on 21 March 1969, general description 3-80727
 transformed coordinate primitive equation atmospheric models, truncation error 3-47734
 tropical cyclone motion, statistical predictability 3-47747
 tropical cyclones of Western North Pacific Ocean, rapid intensification and low-latitude weakening 3-47749
 tropical storms and typhoons, speed after recurvature in N.W. Pacific Ocean 3-65360
 tropical storms/depressions movement forecasting for India, computer technique 3-65326
 troposphere over India, seasonal changes in pressure gradient, wind circulation and rainfall 3-80747
 trough development, 300-mb, rel. to geomag. storms 3-44846
 trough development rel. to geomag. storms, winter, Gulf of Alaska 3-69596
 truncated NWP models, energy consistency 3-47722
 typhoon soundings compared with hurricane soundings 3-47748
 typhoons crossing Philippines, changes in characters. 3-47750
 upper-air relative humidity rel. to cloud cover 3-59057
 urban meteorology, selected topics 3-47715
 water vapour absorption of solar radiation meas., shortwave absorptivity rel. to water path 3-44895
 waterdrops collision vel. rel. to delay time before coalescence 3-53477
 weather forecasting, by computers 3-44908
 weather forecasting, Euler equations, manifolds diffeomorphic to two dim. sphere, initial problem 3-63617
 weather forecasting, initial value problem for Euler eqns. on two dim. sphere 3-63616
 weather forecasting, long term, chances and prospects 3-73403
 weather forecasts in tabulated and worded form by computer interpretation of forecast charts 3-51050
 weather patterns, loss of information due to finite sample volume in radar-measured reflectivity 3-76761
 weather prediction models, boundary conditions 3-65316
 weather radar, remote data acquisition and processing 3-42059
 White Sands Missile Range, apparent 7-day period in visibility 3-51041
 wind velocity determ. from billow clouds, satellite obs. 3-59093

meteors

- see also meteorites; meteoroids*
 ablation theory departure effects on meteor shower flux determ. 3-56364
 acoustics, effects of atmospheric temperature and wind structure 3-61751
 η Aquarid shower, magnitudes, trail lengths, directions 3-81010
 bright fireballs, spectral radiation model 3-77017
 detection, optimum processing (Russian) 3-77021
 element abundance determ. by spectroscopy 3-65852
 frequency distribution function, according to age and lifetime, astronomical phenomena 3-76951
 Geminids 1959-1969, radar observation, overdense echoes 3-77015
 Giacobinid shower 1972, radio obs. 3-61746
 Giacobinids 1972, crepuscular meas. (French) 3-81007
 hyperbolic hypothesis, development rel. to cometary theory 3-45073
 ionospheric LF radio absorpt. events during major meteor shower 3-61524
 Leonid shower, caused by ejection of matter at perihelion of comet Tempel-Tuttle (Russian) 3-73473
 meteor wind data, solar semidiurnal component (Japanese) 3-56367
 Perseids, Comet P/Swift-Tuttle (1862 III) orbit redeterm. 3-77011
 Perseids, variations in distribution and physical properties 3-81002
 radiometric information optimum processing (Russian) 3-77020
 showers rel. to interaction with upper atmosphere to form dust cloud 3-65854
 signal processing automatic machine (Russian) 3-77023
 streams of meteors rel. to short-period comets 3-42185
 β Taurids shower, metallic ion abundances, mass spectrometry 3-77024
 trails, appl. to theory of atmospheric turbulent structure 3-65347
 trails, variation of colour index, photometric analysis 3-77016
 trails drift optimum processing (Russian) 3-77022
 trains, computational study of diffusion using self-consistent model for space charge electric field 3-77019

metering

- see also ammeters; electrometers; frequency meters; galvanometers; level meters; ohmmeters; phase meters; Q-meters; standing wave meters; volt-ampere meters; voltmeters; watt-hour meters; wattmeters*
 electric field, rotating probe induced charge obs. for precision measurement 3-45536
 laser pulse energy meter, digital 3-70283
 plasma density and temperature, direct display using Langmuir probe 3-68092
 universal nuclear radiation meter, for industrial measurement techniques (German) 3-48517

meters *see* metering**metrology *see* measurement****metrosils *see* varistors****MHD *see* magnetohydrodynamics****mica**

- anneal, crystal struct. 3-80596
 Auger, LEED obs. for depth analysis of cleaved mica surfaces 3-60830
 biotite crystals, variation of chemical composition for different ages or growth periods 3-65141
 electrical structure of matching cleavage surfaces 3-52889
 electron microscopy, mica disc, support for particulate specimens 3-54015
 epitaxial growth of Ti, crystallography and interfacial dislocations 3-55168
 fission-track aging 3-44779
 flake, filler in cured epoxy resin, dynamic mech. props. of filled specimen 3-69379
 fluorophlogopite, crystal struct. 3-80596
 intermolecular attractive forces, separations down to contact point 3-52406
 loss tangent and permittivity, 3-36.8 GHz (Russian) 3-50512
 muscovite, anisotropy of thermal expansion, electron diffr. obs. (Russian) 3-49877
 muscovite, epitaxy of Cd films 3-72279
 muscovite, e.s.r. spectra of Fe³⁺ 3-44322
 muscovite, growth spirals and screw dislocations, origin by electron microscopy replica techniques (French) 3-68265
 muscovite, melting relations to 30 kbar in system KAlSi₃O₈-Al₂O₃-H₂O 3-47612
 muscovite, pre-nucleated with silver crystal layers, deposition of Cd (German) 3-72280
 muscovite, surface tracks (S tracks) from external source of fissile nuclei 3-56945
 phlogopite, growth spirals and screw dislocations, origin by electron microscopy replica techniques (French) 3-68265
 radiation detector, scatt. recoil nuclei tracks, process 3-66327
 salt-mica, folding and microfabric development in experimentally deformed specimens 3-76605
 salt-mica, wet, folding at low strain rate 3-76606
 substrate, calcium stearate monolayers and multilayers 3-64108
 substrates, epitaxial growth of Cu, conditions, substrate temp., deposition rate, surface conditions, structure 3-44527
 track detectors, coincidence spectroscopy of fission fragments 3-48542
 Ba-mica/Al₂O₃ composites characteriz. 3-76342

Micelle systems *see* colloids**microanalysis**

- see also electron probe analysis*
 alloy, microprobe analysis, mean atomic no. calc. (German) 3-45589
 ceramic surfaces, ion scatt., Auger effect, secondary ion mass anal. 3-80418
 chemisorption/gas-surface fluorescence, Ta microanal., industrial effluent soln. 3-48657
 electron microscopy, metallurgy, mineralogy, biology, thin specimens, recent developments 3-66357
 extractive concentration, anal. of microquantities of elements, review 3-48647
 granite dust, microchem. determ. of quartz by size selective methods on membrane filters 3-54047
 ion scattering spectrometry, surface composition analysis 3-40041
 isotope abundance meas. with gas chromatography-mass spectrometer 3-40066
 mammalian tissue, ultrathin frozen dried sections, elemental composition, transmission electron microscopy, X-ray microanal. 3-56476
 metallographic appls. of electron microscope microanalysis (German) 3-69230
 organic compounds, decomposition, parallel determ. of N, C and H, semiautomatic app., purification of O₂ 3-48651
 polymeric insulation, chemical treeing, X-ray microprobe analysis 3-50516
 quantitative organic ultramicro elementary analysis, developments 3-48667
 reyerite, hydrated Ca-silicate, anal. 3-50885
 scanning electron microscopy, rough surfaces, coatings, thin sections 3-66469
 thin films and fine structure, Monte Carlo techniques in SEM 3-71989
 Ag⁺ concentration in biological samples, neutron activation analysis of trace amounts 3-62359
 Si₃, commercial microconstituent phases, rapid identification procedure 3-42732
 Ta film, secondary ion emission, surface and bulk analysis 3-62321
 UO₂/PuO₂ fuel elements, radiation effects anal. using electron micro-probe (German) 3-71311
 ZrC creep testing variation in C distrib., laser microanalyser 3-72977

microcalorimeters *see* calorimeters**microchemical analysis *see* microanalysis****microcircuits *see* integrated circuits****microcopying *see* microphotography****microelectrodes**

- impedance testing using swept frequency technique 3-42687
 intracellular, voltage clamping, short cardiac Purkinje fibres 3-66403

- microelectrodes** continued
 low-impedance capillary electrode for large axon membrane potential recording 3-56994
 low-impedance W microelectrode for recording from sensory ganglia 3-56993
 neuron activity recording, electronic control by fractions of a micron 3-62309
 photoengraved, for extracellular single-unit recording 3-45262
- microelectronics** *see integrated circuits*
- microfarad meters** *see capacitance measurement*
- microfiche** *see microforms*
- microfilm** *see microforms*
- microfilming** *see microphotography*
- microforms**
 equivalent projection density meas. of silver and vesicular films 3-39966
 micro-densitometer design and construction 3-39967
 Microfilm Duplicator, DOKUMATOR, VEB Carl Zeiss JENA, expose and development of diazo film 3-51642
 transmission density meas. of photographic layer in microfilming 3-39965
- microhardness** *see hardness*
- micromanometers** *see manometers*
- micrometeorites**
 cosmic dust trace element distribution in deep sea core 3-51005
 linear accelerator, for simulated micrometeorites 3-42629
 microtektite space absorption as cause of Pleistocene glaciation 3-59327
 microtektites, analogy with impact-generated spherules on Moon and Earth 3-65853
 microtektites of N. American strewnfield in Caribbean Sea sediment core 3-56361
 planetary capture mechanism 3-65628
- micrometeoroids** *see meteoroids*
- micrometers** *see micrometry*
- micrometry**
see also strain gauges; thickness measurement
 capacitance micrometers, design and applications 3-45419
 hole diameter inspection, design of perfectometer optical probes 3-53841
 hole diameter measurement, perfectometer for calibration of ring and slip gauges 3-53840
 length measurement, Moire fringe multiplication applic. 3-48441
 pneumatic micrometer for use in vacuum 3-59567
- microphones**
 polymer film, three layer capacitive, induced piezoelectricity by charge injection 3-68931
- microphonics** *see microphones*
- microphotography**
see also microforms
 liquid crystals, field induced nematic cholesteric relax. obs., transient 3-68151
 Microfilm Duplicator, DOKUMATOR, VEB Carl Zeiss JENA, expose and development of diazo film 3-51642
- microphotometers** *see densitometry; photometers*
- microprobe analysis, electron** *see electron probe analysis*
- micropulsations**
 auroral emission intensity pulsations assoc. with Pi 2 micropulsations 3-41907
 auroral oval micropulsations at sub-auroral zone station 3-65251
 conductivity anomalies, effect of induced mag. fields 3-44928
 English Channel region, effect of subterranean cond. anomalies 3-58922
 English Channel region, local conductivity anomalies in mag. fields 3-58921
 generation with large ground-based current loop 3-61430
 IPDP events assoc. with cosmic noise absorpt. during proton aurora substorms 3-61412
 latitude dependence of individual events, plasmopause and ground-based u.l.f. data 3-61426
 magnetic fields, effect of subterranean cond. anomalies 3-58922
 magnetic variometers array for micropulsation activity recording 3-50976
 magnetospheric micropulsations rel. to h.f. turbulence during substorms 3-61557
 MHD wave frequency and amplitude variations 3-69676
 Northern lights study with aid of TV and computer 3-42004
 Pc1 type, numerical soln. of coupled differential eqns. for ionospheric wave guide 3-73349
 Pc1 type (pearls) physical conditions in magnetosphere during excitation 3-69679
 Pc2,3, magnetosonic resonator in magnetosphere 3-80813
 Pc2,4 pulsations characts., interplanetary mag. field effects 3-41918
 Pc4 stable pulsations at conjugate points and at network of station 3-41911
 Pc1 fine structure, experimental evidence 3-53430
 Pc1 fine structure, theoretical interpretation 3-56125
 PC-4 and -5, general theory and origins 3-61434
 PC-4 and -5, solution of coupled equations using dipole field 3-61435
 Pc1 micropulsation polarisation, obs. at low-latitude sites 3-61403
 PDP synchronous development rel. to asymmetry of ring current during mag. storms 3-41919
 period changes after sudden negative impulses 3-53434
 Periodically structured Pc1 micropulsations during the recovery phase of intense magnetic storms 3-80665
 periods of pulsations rel. to size of magnetosphere and magnetopause distance 3-61433
 Pi2, freq. spectra and polarisation meas. 3-41928
 Pi2, obs. rel. to generation theories 3-41929
 Pi2 occurrence and source, rel. to solar activity 3-41930
 Pi2 pulsation spectra along meridional profile 3-56106
 Pi2 pulsations, time dependence of amplitude and frequency of MHD wave 3-69544
 Pi1 and 2 rel. to auroral pulsations 3-56110
- micropulsations** continued
 Pi 2 events and geomagnetic bays, geomagnetic time dependence 3-44847
 Pi 2 harmonic frequency content, spectral analysis of Earth current records 3-65248
 Pi 3-4 and Pi 1-2 rel. to equatorial electrojet, Chad and Central Africa obs. (French) 3-41925
 pulsations of diminishing period rel. to motion of magnetospheric plasma inhomogeneities 3-80660
 research from January 1969 to July 1972, review 3-41924
 statistical model as random temporal process 3-56104
 transverse pulsations in equatorial plane at synchronous altitude 3-61431
 u.l.f. waves associated with micropulsation substorm at synchronous orbit 3-61432
 Pi2 micropulsation parameters rel. to auroral zone processes 3-56105
- microrecording** *see microphotography*
- microreduction** *see microphotography*
- microscopes**
see also field emission microscopes
 Axiomat by Zeiss, modular design for microscopy, photomicrography and microphotometry, description 3-73730
 contact, in reflected light, and illum. of biological specimens 3-66193
 field depth enhancement and three-dimensional capability 3-77425
 focusing, speed, accuracy, modern mechanisms 3-53888
 heating, attachment for differential thermal anal., high-temp. technique, 1600 C, course of reaction in furnaces 3-53856
 high-speed three axis servoed microscope stage with digital control 3-48614
 holographic microscope, coherent noise elimination 3-45499
 image contrast, with synchronous scanning of object by point or raster field diaphragms 3-62053
 incident light illuminator, measuring microscope, VEB Carl Zeiss JENA antireflection coating 3-51586
 interference, incident-light, double-refracting, with variable wavefront shear 3-62048
 interference microscope, analysis of surface roughness (German) 3-66140
 i.r., with scanning device, for absolute temperature measurement of small surface areas (German) 3-59561
 light-sectioning attachment, shop measuring microscope BK 70 x 50, VEB Carl Zeiss JENA, surface and thickness meas. 3-51585
 measuring, profile inspection of paraboloidal aspherical surfaces using contact interferometer 3-66208
 objectives, with long working distance (Czech) 3-62046
 optical, Abbe's theory and further developments (German) 3-53879
 phase, Polanret variable densiphase 3-56659
 photoelectric, for length meas., accuracy comparisons (Slovak) 3-48409
 photoelectric, rotating plane-parallel plate, treatment of output (Czech) 3-51589
 polarising, device for obs. of 'opaque' minerals with transmitted i.r. light 3-42555
 refractometer, microscopic, VEB Carl Zeiss JENA, refractive index meas., biology, medicine, technical products 3-51587
 scanning, using synchrotron radiation of CEA 3-56850
 scanning and conventional transmission microscope equiv., reciprocity theory 3-77727
 scanning microscope photometer, with programmed control (German) 3-73748
 stereomicroscope, for photointerpretation, square wave response 3-73744
 straining stage design description 3-62082
 TV metallographic analyser, vol. percentage, specific interface, size distrib. 3-51584
 two-mirror aplanatic objective, reflecting surfaces profiles, determination (Russian) 3-59574
 X-ray, high-temp., internal structure, metallurgy 3-48592
 X-ray, scanning, using synchrotron radiation, 3-42684
- microscopy**
see also electron microscopy; ion microscopy
 Auger, scanning, in molecular beam epitaxy of GaAs and GaP 3-40040
 cermetes, oxides, colour contrast layer formation, gas etching technique, microscope obs. (German, English) 3-69240
 cholesterol derivatives, obs. of blue phase in amorphous-cholesteric transition 3-72000
 cholesteryl myristate, mesophase transitions, light scatt. and microscopic obs., cholesteric morphology 3-52571
 cholesteryl myristate, mesophase transitions, light scatt. and microscopic obs., spherulite growth kinetics 3-52572
 coals preparation of flexible thin sections, for macro- and micro-exam. 3-59152
 colour contrast layer formation in gas-ion-reaction chamber under electron irradi., microscope obs. (German, English) 3-69239
 composite materials, colour contrast layer formation, gas etching technique, microscope obs. (German, English) 3-69240
 dark field imaging system, two-point resolution under partially coherent illumination 3-54206
 diamond, optical, X-ray study of growth, struct., props. (Japanese) 3-72069
 electrochemical studies, review 3-66198
 electrochemistry, optical techniques, book 3-66195
 fluorescence and focused laser microscopy, biomedical applic. 3-73924
 fluorescence of specimens, polarisation study, interf.-type beamsplitter 3-62063
 image formation, coherence conditions influence (German) 3-42981
 infrared television microscopy studies, resolution, processed semiconductor materials 3-41664
 interference microscopic small lateral size meas. 3-45472
 kymography with intravital microscope (German) 3-51757
 laser, interference fringe microscopy, applic. to electric contacts 3-56671
 latex suspension, ordered structure obs. by metallurgical microscope 3-76385

microscopy continued

- linear phase technique 3-66176
- magnetic domain obs., dry Bitter technique (*German, English*) 3-51665
- metal, colour contrast layer formation, gas etching technique, microscope obs. (*German, English*) 3-69240
- metallography applics. of microref. 3-47379
- microtome sections, number and diameter of isodiametric spherical particles 3-57004
- nematocysts, interference microscopic determ. of refractive index (*German*) 3-54028
- optical alignment method for small specimens 3-61150
- oxides, colour contrast layer formation, gas etching technique, microscope obs. (*German, English*) 3-69240
- particle characterisation, use of Quantimet 720 for image processing 3-73731
- particle counting, slide preparation for 3-42668
- particle size analysis of polydisperse systems 3-42677
- phase objects, two-point resolution with partially coherent light illumination 3-54205
- polarising microscope, reflection images of small crystals of alkali halides 3-68947
- polymeric insulation, discharge treeing, optical obs. 3-50516
- rocks preparation of flexible thin sections, for macro- and micro-exam. 3-59152
- specimen cell for studying oriented liq. crystals 3-57974
- specimen prep. by powder separation technique 3-42556
- synaptic vesicles, measurement and estimation of true diameter 3-57005
- thin transparent coatings on particulates, eval. by focal plane screening technique 3-55908
- tracking 3 dimens. microscope specimens, automatic focusing algorithm 3-56990
- ultramicroscope, continuous-flow, coagulation mechanism 3-65029
- C blacks, paracrystalline distortions, optical diffraction obs. applying electron optics considerations 3-63954
- Si, commercial microconstituent phases, rapid identification procedure 3-42732

microtest *see microforms***microtomes** *see laboratory apparatus and techniques***microtrons**

- racetrack, for π^- production for radiotherapy 3-59445
- variable energy racetrack microtron, 4.5 to 18 MeV, Univ. of Western Ontario 3-56749

microwave acoustic devices *see acoustic microwave devices***microwave amplifiers**

- see also masers; parametric amplifiers*
- quantum paramagnetic amplifier, i.f. direct generation (*Russian*) 3-45818

microwave antenna arrays

- planar waveguides with projecting dielectric plates, diffraction 3-42960

microwave antennas

- see also waveguide antennas*
- plasma electron density, antenna admittance determ. 3-79167

microwave detectors

- microwave holography, concealed weapon detection using phase only information 3-66259
- radioastronomy, low-temp. bolometer heterodyne receiver, Kitt Peak Arizona, description 3-65971

microwave devices

- see also acoustic microwave devices; Gunn devices; IMPATT devices; masers; solid-state microwave devices; strip lines; waveguide components; waveguides*
- 120 MHz r.f. cavity, coupling to 700 A, 6 MeV electron pulsed beam 3-57274
- mesospheric and stratospheric temps. remote sensing by microwave radiometry 3-56260
- radiometer, S-band, use in sea surface temperature meas. 3-76920
- strain measurement, radiation environments 3-66147
- temperature measurement of nuclear reactor coolants by frequency shift caused by expansion of resonant cavity 3-70282

microwave filters

- polarising, unidirectionally conducting screen applic. 3-57193
- total power filter spectrometer for radioastronomy 3-59176

microwave generation

- see also microwave oscillators*
- decimetre wave, for medical therapy applic., 460 MHz, 100 W generator 3-53746
- intermittent, through electron beam-plasma interaction 3-43664
- Josephson junction, resonator connected, electrodynamic props. in Aslamazov-Larkin model 3-75817
- ribbon-filament tunnel superconducting contacts, matching with free space 3-68739

microwave heaters *see radiofrequency heating***microwave heating** *see radiofrequency heating***microwave links**

- attenuation due to water vapour, slant path estimation 3-56167
- crosstalk, scattering by oblate raindrops, 19.3 and 34.8 GHz, calculations 3-61473
- e.m. wave attenuation in rain, at 37 to 110 GHz 3-77949
- radiowave propagation through rain at 17.7 to 19.7 GHz (*Norwegian*) 3-61481
- rain attenuation at 7 to 8 GHz 3-51017
- rain attenuation meas. at millimetre waves over short paths 3-41964

microwave measurement

- ceramics, nondestructive testing, process control 3-47491
- dielectric dispersion, data acquisition, for low loss liquids 3-42602
- dielectric materials, permittivity and $\tan \delta$, 100-1000 MHz band (*Polish*) 3-73804
- e.m. wave attenuation in rain, at 37 to 110 GHz 3-77949
- ferrites, in millimetre region (*German*) 3-58431
- frequency counter, 10 Hz to 18 GHz, automatic 3-45524
- ionospheric scintillation at 4 and 6 GHz near geomagnetic equator, obs. 3-56193
- i.r. frequency synthesis using stabilised HCN laser 3-45832

microwave measurement continued

- liquids, complex permittivity, 5 to 40 GHz, theoretical analysis of reflected power method 3-73810
- low-loss nonresonant circuit, elec. field distrib. meas. (*Polish*) 3-42939
- passive microwave imaging, resolution limits 3-51179
- permittivity of liq. with high microwave losses, X-band interferometric apparatus modifications (*French*) 3-59608
- plasma, shock-heated, electron temp. determ. from microwave meas. 3-63880
- plasma density distribution meas. using an open barrel-shaped cavity 3-49760
- plasma diagnostics using open microwave resonators (*Rumanian*) 3-46556
- polystyrene particles in aqueous suspension, dielectric properties at microwave frequencies 3-44692
- radar cross section multiple resonance meas. for remote sensing of complex permittivity 3-47196
- radome boresight error meas., tower alignment system 3-45831
- reflection diagnostic method for plasma column in waveguide, analysis 3-43684
- reverberation meas. by sampling technique (*German*) 3-54195
- sea slope spectrum meas. by two-frequency microwave radar 3-42089
- semiconductor, K anisotropy factor meas. of Si and Ge (*French*) 3-60884
- semiconductor diode barrier capacitance, IED-30 meter 3-73806
- spectral analysis, discrete Fourier transform applic. 3-77577
- stellarator, plasma density determ. using open microwave resonator 3-52531
- tropospheric long-distance propagation above 1000 MHz (*German*) 3-76785
- water content measurement applic. (*Polish*) 3-57023
- YIG films on Gd-Ga-garnet substrates, ferromagnetic resonance linewidth at 2 to 8 GHz 3-79917

microwave oscillators

- see also Gunn oscillators; parametric oscillators; tunnel diode oscillators*
- decimetre wave, 460 MHz, 100 W, max. power, for medical therapy applic. 3-53746
- frequency lock system, digital design and performance 3-77578
- Gunn diode, coherence, under impact ionisation conditions 3-75749
- IMPATT diode, source for microwave e.p.r. 3-39979
- total power filter spectrometer 3-59176
- GaAs $n^+ - n - n^+$ transferred electron diode, continuous multilayer epitaxial growth 3-41688

microwave region *see microwaves***microwave spectra**

- see also molecular rotation; molecular vibration*
- acetaldehyde, collision broadening of rot. lines by O_2 3-67834
- amino acetonitrile, structure, bond angles, dipole moment 3-63485
- benzene solutions of binary mixtures of phenol, pyridines, benzaldehyde 3-80585
- benzophenone, microwave-optical double resonance, $n\pi^*$ triplet states 3-80121
- benzvalene, six isotopic species 3-78814
- carbon difluoride, centrifugal distortion anal. force field and dipole moments 3-78820
- chlorocyclohexane, equatorial, microwave rot. spectra anal. 3-78811
- 4-chloronortricyclene, ^{35}Cl nuclear quadrupole coupling constant 3-71567
- 2-chlorothiophene, microwave spectra, quadrupole coupling and rotational constants 3-43463
- crystal slightly doped with paramag. ions, X-band guided wave rot. and ellipticity, obs. (*French*) 3-50632
- cyanocyclobutane, dipole moment, quadrupole coupling consts., and conformation study 3-40634
- cyanocyclobutane, rot. spectrum, assignments, ring conformation 3-63484
- cyclohexene sulphide, 26.5-40 GHz, rotational consts. 3-43459
- cyclopent-3-enone, out-of-plane ring modes from far i.r., Raman and microwave spectra, pot. function 3-60467
- cyclopent-3-enone, ring planarity, r_s -structure and dipole moment 3-60466
- cyclopentadienone, dipole moment, life time 3-78813
- cyclopropanone, isotopic species, substitutional structure 3-63482
- 6-deuterofulvene, μ -wave spectrum, methylene group struct. 3-49477
- diatomic, transitions between fine structure components, reln. to radiation from stars 3-40604
- difluoromethane, hyperfine struct. meas. by beam maser spectroscopy 3-46303
- dimethyl cyanamide, struct., dipole moment, i.f. vibrs. 3-60464
- dimethylaminodifluorophosphine 3-49476
- dimethylsilane, rotational spectrum, validity of Hamiltonian for torsional fine structure (*German*) 3-75053
- 3,6-dioxabicyclo[3.1.0]hexane, dipole moment, conformation 3-63486
- discrete Fourier transforms, use in detailed microwave spectral analysis 3-77577
- Dutch Atomic and Molecular Physics Study Group investigations (*Dutch*) 3-49455
- elastomers, meas. of dielectric birefringence following stretching with mm waves (*French*) 3-58467
- ethanol, submillimetre refraction spectrum 3-69108
- ethylene oxide lines, collision broadening by quadrupolar mol. CO_2 3-52397
- formaldehyde, microwave collision diameters in rot. spectrum 3-67858
- formimide, gas phase conformation props. of amide bond 3-63483
- furan, rot. transitions, h.f.s. 3-54701
- glycolaldehydes, microwave spectra, substitution struct., intramolecular hydrogen bond and dipole moment 3-54703
- 6-hydroxy-2-formylfulvene, H-bonding, molecular symmetry 3-54698
- hydroxyacetonitrile, microwave spectroscopy, rotational isomerism, barriers to internal rotation 3-49479
- linear molecules, microwave spectra of l-doubling, centrifugal distortion effects 3-52374

microwave spectra continued

- methane, ground vibronic state, rot. transitions 3-75052
 methane, i.r.-r.f. double reson. study of pure rot. Q-branch transition 3-63405
 methane selenol, μ -wave spectrum, internal rot. barrier, struct. and dipole moment meas. 3-54700
 methyl chloroformate, internal rot. barrier, mol. structure 3-75050
 methylamine, obs. laboratory freq. list 3-43458
 methylamine chloride, internal rot. and inversion doubling 3-67829
 methylaminoethane, rot.-inversion spectrum analysis 3-63491
 3-methylene oxetane, μ -wave spectrum, mol. Zeeman effect, mag. susceptibility anisotropy, quadrupole moment meas. 3-52372
 methylenimine, microwave spectra, molecular constants 3-75051
 monochloroamine, rotation-inversion transitions in microwave spectrum, inversion barrier of amine group 3-40639
 NGC 7538, H 94 α recombination line obs. 3-70038
 nitroethylene, isotopic species, ground and excited vibrational states 3-78812
 2-nitrophenol, microwave spectrum, struct. of hydrogen bond 3-40638
 non-polar liquids, dielec. absorpt. in microwave and far infrared region 3-80120
 3-oxetanone, μ -wave spectrum, mol. Zeeman effect, mag. susceptibility anisotropy, quadrupole moments meas. 3-52372
 phenol-OD, microwave and i.r. transitions analysis by rot.-internal rot. theory 3-63490
 piezoelectric crystals, X-band echo 3-72576
 porphyrin, free base, Shpol'skii-matrix lowest triplet states obs. from microwave induced fluoresc. changes 3-76050
 trans-propylene imine, centrifugal distortion effects 3-60463
 cis-propyleneimine, ^{14}N quadrupole coupling consts. 3-63489
 propynal, millimetre wave spectrum, ground vibr. state 3-78816
 pyrene, zero-field, rotational constants determ. 3-63481
 pyrrole, beam maser spectroscopy, obs. of rotational transitions, nitrogen hyperfine parameters 3-78826
 rhodamine 6G, ESR triplet state meas. Ar ion laser irradiation 3-78028
 semiconductor plasma, microwave emission, hydromag. turbulence theory (French) 3-68656
 student laboratory of microwave spectra and molecular structure 3-66102
 tellurophene, rot. consts., low J lines, struct. 3-67826
 2-thiophenolaldehyde, gas, identification of O-S trans rotamer 3-63365
 trifluoroethylene, microwave moments and rotational constants 3-43461
 trimethylamine, mol. A_2 torsional frequency by computer aided microwave anal. 3-78821
 trimethylamine-borane, struct., dipole moment, rot. consts. 3-60465
 trimethylchlorosilane, nuclear quadrupole coupling and rotational const. determ. from microwave spectra (German) 3-60468
 2,8,9-trioxadadamantane, microwave spectrum 3-40636
 tropone, zero-field, rotational constants determ. 3-63481
 o-xylene, methyl rot. barrier, methyl conform. and dipole moment 3-67832
 Al I, quadrupole hyperfine structure, coupling constants (German) 3-57661
 AlBr, quadrupole h.f.s. of rot. transition (German) 3-57662
 AlCl, h.f.s. of rot. transition (German) 3-57662
 Ar-HCl, struct. determ. from microwave and r.f. spectra 3-75049
 ArHCl complex, structure determ. by mol. beam electric resonance spectroscopy 3-78824
 BaO, microwave optical double resonance obs. using c.w. dye laser 3-78039
 BaO microwave optical double resonance spectra 3-75063
 BrCN, pressure broadened line widths in microwave region 3-67837
 BrF₃, J₈₋₉ transition meas. 3-63492
 CH₄, rotational transitions in $v_3=1$ excited state, i.r. microwave double resonance method 3-52373
 CHO radical, obs. of K doubling transitions in rotational states, hyperfine interaction 3-78827
 COS, dipole moment function determ. 3-78768
 D₂¹⁷O and D₂¹⁸O, hyperfine struct. 3-78818
 (D₂O)₂, obs. by mol. beam electric resonance method 3-78825
 F₂CS, rot. consts., dipole moment 3-67827
 n-GaSb, magneto-microwave reflection, Voigt config., theoretical 3-72599
 GeO, rotational mag. moment meas. by molecular beam electric resonance spectra 3-78727
 HCO nonlinear free radical, Zeeman effect, microwave spectra theory and analysis 3-46306
 H₂CO, collision-induced transitions, velocity depend., obs. by triple resonance method 3-52384
 HNO and DNO, rot. consts., coupling consts., moments 3-63488
 H₂O pure rotation spectrum, approximate mean absorption coefficient 3-67833
 (H₂O)₂, obs. by mol. beam electric resonance method 3-78825
 H₃PBH₃, dipole moment, internal rotation barrier, staggered conformation, Stark splitting 3-54699
 HSiF₃, excited vibr. states, structure, force field models 3-63487
 IF, rotational spectrum, hyperfine structure analysis (German) 3-78822
 InSb, generation-recombination noise and microwave emission 3-44082
 InSb plasma, possibility of acoustic amplification and microwave radiation 3-68677
 KCl/adsorbed methyl chloride, microwave absorpt. 3-72265
 KI, quadrupole hyperfine structure meas. obs. in vibrational state (German) 3-57660
 NCN₃, anal. four nuclear quadrupole problem 3-78819
 NCO, Renner-Teller effect and vibronically induced bands in electronic spectrum 3-75048
 NH₃, inversion spectrum, collision broadening and shifting 3-67838
 NH₃, rot. energy transfer, direct obs. by time-resolved i.r.-microwave double reson. 3-78886
 NH₃, transient nutation effect obs. 3-49478
 NH₃ microwave absorption lineshift by non resonant i.r. laser radiation (French) 3-54702

microwave spectra continued

- NH₃ time-resolved, transient nutation signals, collision relaxation rates, Stark modulation 3-63539
 NO₂, microwave optical double resonance lines 3-78835
 N₂O₃, N quadrupole hyperfine splitting 3-46305
 NaCl/adsorbed methyl chloride, microwave absorpt. 3-72265
 NbSe₂, microwave absorption, critical fluctuations 3-41302
 O₂, X³ Σ_g^- state, resolution of discrepancies 3-78736
 O₂ atmospheric spectrum rel. to attenuation and phase dispersion 3-49480
 O₃, ¹⁸O substituted, rotational consts. 3-78782
 OCS, isotopically enriched, ground state and vibr. excited 3-67830
 OCS time-resolved, transient nutation signals, collision relaxation rates, Stark modulation 3-63539
 OH radical, spectra of excited rotational states 3-78853
 SF radical, microwave spectra 3-40637
 SF₂Cl, rot. spectrum, K-type splitting (French) 3-57659
 S₂O, centrifugal distortion consts., determ. 3-67828
 SO³Cl₂, nuclear quadrupole coupling constants 3-78839
 SiF₂, excited vibr. states, equil. struct., pot. function, Coriolis reson. 3-67831
 TeF₃Cl isotopic species, rot. consts. 3-46304

microwave spectrometers

- apparatus for determ. of mol. rotational relaxation rates by saturation time depend. meas. 3-48422
 e.s.r. video-spectrometer with crystal resonator, for operation at wide range of pressures and temp. 3-51666
 total power filter spectrometer for radioastronomy 3-59176
 CO₂ i.r. region, high resolution frequency measuring techniques, laser transitions 3-48420

microwave tubes

- see also *electron-wave tubes*
 Faraday cage, multiple diffusive reflection, linear Fredholm eqn. soln. 3-51965
 one-sided secondary electron resonance discharge in lattice-type fields in 3 cm band, experimental investigation 3-63913

microwaves

- electrodynamics, boundary-value problem solving by variational methods 3-66742
 electron beam, enhanced microwave emission due to transverse energy 3-68093
 electron beam passage through foils 3-71902
 emission from theta-pinch 3-79076
 gases, pulsed breakdown with low degree of preionisation 3-57956
 hamsters, Chinese, effect of 2450 MHz microwaves on x-ray radiation response 3-66058
 heterogeneous, plane, uniform e.m. waves, appl. (French) 3-66748
 hologram, numerical reconstruction of image 3-73776
 holography, concealed weapon detection using phase only information 3-66259
 imaging with enhanced resolution 3-42978
 interactions with low energy electrons, numerical soln. of eqns. of motion 3-50438
 laser flash evaporated metallized film, microwave passage and current 3-70852
 parallel planar array of dielectric cylinders, iterative focusing 3-42955
 plasma, fluctuating, microwave signal modulation, parameters determ. 3-75420
 plasma emission, heating, instability (Russian) 3-71919
 plasma emission during heating by intense electron beam 3-75403
 plasma fast electrons production at electron cyclotron frequency harmonics 3-75404
 plasma microwave absorption near singular points 3-75294
 plasmas, off resonance microwave created 3-57928
 plasmas, stochastic reflection, Walsh spectral analysis 3-75301
 radiation dosimetry, energy measuring thermocouples and thermistors, interaction with microwave field 3-70187
 refractive index fluctuations in atmospheric boundary layer 3-65307
 scattering in plasma-beam discharge 3-68096
 spectroscopic source excitation, radiation danger 3-66061
 student laboratory experiments on e.s.r. cyclotron resonance and electron density of a plasma 3-56603
 Ta superconducting thin films, nonlinear microwave props. 3-50304

Mie theory see *electromagnetic wave scattering***Milky Way** see *the Galaxy***milliammeters** see *ammeters***m.i.m. devices** see *metal-insulator-metal devices***m.i.m. structures** see *metal-insulator-metal structures***mineral oil industry** see *petroleum industry***mineralogy** see *minerals***minerals**

- see also *asbestos; garnets; mica; quartz; ruby*
 aconite, high temperature crystal chemistry 3-73189
 alkali feldspar, non linear variation of cell parameters with composition 3-80598
 alkaline rocks from Vermont, petrology, Mesozoic alkaline magmatism 3-76522
 almandine-garnet, shock wave Hugoniot data 3-50913
 alunite ore, powder, attachment to URS-50IM system, X-ray diffractometer, alunite content determ. 3-48593
 amblygonite-montebasite, F-content and physical properties 3-44775
 anisotropic andradite, zoned garnet, from Crested Butte, Colorado 3-80591
 annite, crystal structure from three-dimensional X-ray data 3-65220
 anorthite, tetrahedral bond length variations 3-50883
 anorthite 410 to 830°C, crystal structure 3-76498
 Apollo 17 results, conference, USA (1973) 3-65817
 Apollo 17 samples, mineralogy and geochemistry of opaque and non-opaque phase 3-65847
 Archean rocks, sedimentary deposition of subaerial alluvial fan, sedimentary environment interpretation 3-65132
 Atlantic deep-sea long-core samples, analysis 3-73227
 barite, plastic deform. rel. to longit. u.s. propag. vel. 3-46663

minerals continued

- basalt powder, multidomain, pseudo-single domain moments, low field t.r.m. meas. 3-58866
 basaltic class I titanomagnetites, $\text{Fe}^{3+}/\text{Fe}^{2+}$ ratios from Mossbauer spectroscopy 3-61305
 Benioff zones, metallogenic belts and angle of dip 3-69524
 berlinite, high-low inversion up to 6 kbar, differential thermal analysis 3-73200
 biotite crystals, variation of chemical composition for different ages or growth periods 3-65141
 Birch's law, exponential representation for minerals and rocks 3-65203
 Birch's Law, power law representation 3-73209
 boracite $\text{Mg}_2\text{ClB}_2\text{O}_{13}$ crystal structure refinement above transition point 3-73193
 borates, bond-valence summation, Zachariasen's method 3-60680
 braggite, crystal structure, Patterson methods 3-56008
 Calcic and alkali amphiboles from the Golden Horn Batholith, North Cascades, Washington 3-80594
 cavanisite, dimorphous Ca-V-silicate mineral from Oregon 3-50875
 cavansite, orthorhombic and layer-silicate structure 3-50876
 Chalcophyllite, simulated X-ray powder pattern data 3-73198
 chalcopyrite, CuFeS_2 , mag. transitions, 1 atmos.-20 kbar, Mossbauer obs., geophysics 3-41344
 chalcopyrite, mag. transitions at 5-16 kbar, geophysical significance 3-58865
 chondrites, Yilmia enstatite, mineralogy and petrology 3-45054
 chromian aluminian magnetite, Rh alloys, Pt nugget composition, Alaska 3-44763
 chromian titanomagnetite, Snake River Plain basalt, electron microprobe anal. 3-80588
 clay, crystal phase, water adsorption in intersheet space, review (Polish) 3-44832
 clinopyroxene, lattice deform. depend. on chem. substitution and temp. 3-80592
 conductive ore deposit prospecting, time-domain electromagnetic measurements 3-73374
 cordierite lava, St. Helena, S. Atlantic 3-80586
 Croteau rocks, Grenville Front, Labrador, polar wander and tectonic implications from palaeomagnetic data 3-76657
 crystal field effects in mantle minerals 3-44819
 datolite, refinement of crystal struct. 3-80599
 deposits, location using plate tectonics 3-76597
 Devonian palagonite tuff, zeolite facies, metamorphism in Silurian-Devonian fold belt 3-76527
 dickite, hydroxyl group orientation 3-50882
 diopside, high temperature crystal chemistry 3-73189
 East Pacific, equatorial, anal. of ferrimanganous sediments 3-65142
 eitelite, $\text{Na}_2\text{Mg}(\text{CO}_3)_2$, crystal structure, X-ray crystallography 3-44766
 elbaite, n.m.r. studies, ^1H , ^7Li , ^{11}B , ^{23}Na and ^{27}Al , crystal structure 3-44768
 electrical surveys, buried current electrodes, anal. models for interpretation appl. to mineralisation 3-80842
 enstatite, 2200-27000 cm^{-1} polarised spectra at room and liquid He temps. 3-50880
 enstatite, anisotropic electrical conductivity rel. to pressure and temperature 3-50905
 enstatite, high pressure break-down 3-44823
 epidote structure, $\text{Ca}_2\text{Al}_2\text{Si}_2\text{Fe}_{0.84}\text{Si}_3\text{O}_{13}\text{H}$, X-ray studies, Fe substitution 3-44767
 β eucryptite crystal structure rel. to temperature 3-73192
 eudialyte, crystal structure determination 3-79323
 feldspar, neutron diff. refinement of ordered orthoclase structure 3-50884
 feldspars, dating using thermoluminescence, fading effects 3-76572
 feldspars, K-rich monoclinic, crystal structures, T-O bond length variation 3-44771
 ferrian copiapite from California, crystal structure, thermal and chemical data 3-44777
 ferroan gahnite from quartz-biotite-almandine schist, Wind River mountains, Wyoming 3-80589
 ferrihypersthene single crystal up to 850°C, orthopyroxene structure 3-76497
 ferromagnetic, temp. of formation determ. from normal magnetisation curves 3-61300
 ferromanganese deposits, i.r. microanalysis for deducing formation history 3-61365
 ferromanganous sediments in equatorial East Pacific 3-65142
 fluor-tremolite, effect on crystal struct. and bonding of F substitution in hydroxy tremolite 3-80595
 fosterite, crystal structure at 20, 300, 600 and 900°C 3-76496
 Foyers plutonic complex, Invernesshire, palaeomagnetism, direction of magnetisation 3-41905
 galena, effects of atmospheric moisture on electrical resistivity 3-53399
 garnet in anorthosite-charnockite suite, bias and precision in electron probe microanalysis 3-76523
 Gaspe Peninsula, Quebec, aeromagnetic data applied to mining exploration 3-58938
 gaylussite, thermal properties by simultaneous thermal analysis 3-73196
 gem deposit of Pailin, Cambodia, fission track age rel. to recent tectonics 3-53421
 geochemistry, neutron activation analysis 3-65512
 glass, elastic constant, u.s. velocity meas. as a function of pressure 3-80650
 goethite formation on Mars 3-59273
 hanksite, $\text{Na}_2\text{K}(\text{CO}_3)_2(\text{SO}_4)_2\text{Cl}$ crystal 3-73201
 Haverro meteorite, different forms of carbon 3-45064
 Haverro meteorite, highly refl. and opaque components of mineral content 3-45067
 Haverro meteorite, petrographic obs. 3-45071
 hedenbergite, high temperature crystal chemistry 3-73189
 hedenbergite-ferrosilite pyroxene, synthetic, Mossbauer resonance spectroscopy of iron 3-80593
 hematite to goethite, surface weathering study using SEM 3-73199
 high pressure phases, from Hugoniot data 3-76539
 high pressure phases from Hugoniot data 3-65216
 high-pressure phases of mantle minerals elasticity data 3-65209

minerals continued

- horthonolite, crystal structure at 20, 300, 600 and 900°C 3-76496
 horthonolite, lunar, high temperature crystal chemistry 3-77000
 howieite, crystal structure from X-ray diffraction results, silicate structure 3-58844
 induced current distribution, conductive two-layer spherical body, interpretation of data over ore deposits 3-80657
 iron ore, Great Krivoy Rog, gravimetric data (Russian) 3-65501
 jadeite, high temperature crystal chemistry 3-73189
 jadeite, toughness 3-73195
 jadeite in omphacite pyroxene, activity-composition relation, theory 3-56028
 jamborite, new Ni hydroxide from northern Apennines, Italy 3-80590
 K partitioning between silicates and sulphide melts rel. to composition of primitive Earth core 3-41899
 kaolinite, hydroxyl group orientation 3-50882
 kernite from Tincalayu mine at Salta, Argentina 3-44776
 Kirkland Lake, Ontario, Archean mafic volcanics, palaeomagnetic and petrologic correlations 3-58969
 Lac St. Jean anorthosite and associated rocks, Rb-Sr ages and petrologic studies 3-65136
 lepidocrocite-hematite thermal transformation, and magnetisation behaviour 3-65240
 lepidolite, hydrothermal, anal. deposition from Ojo Caliente hot spring, Yellowstone National Park 3-80597
 liebenbergite structure, composition and properties 3-76499
 limonite formation on Mars 3-59273
 lunar, 2-4 mm soil fragments from 5 Apollo 17 sites 3-65837
 lunar, geochemical aspects of soil, basalts and breccia 3-65838
 lunar anorthositic rocks, natural exoemission, recrystallisation, deform. history 3-77007
 lunar basalt, large coarse grained and predominantly basalt particles (Apollo 17) 3-65829
 lunar basalt fragments pyroxene relations, Apollo 17 sample from Station 5 3-65825
 lunar deep drill core, Apollo 17, major and trace elements 3-65830
 lunar fading of induced thermoluminescence 3-69902
 Lunar fines, surface reduction by H_2 , relevance to solar wind effects 3-42179
 lunar fragment laden contact metamorphosed magnesian hornfels (Apollo 17) 3-65821
 lunar glass and cinder formation 3-65819
 lunar ilmenite basalt (Apollo 17 sample 75055) 3-65833
 lunar metal fragment, morphology 3-65808
 lunar opaque samples (Apollo 17) 3-65828
 lunar volcanic glass, orange and black, Apollo 17 sample 74220 from Shorty crater 3-65835
 maghemite, magnetic viscosity and quadrature susceptibility in single-domain assemblies 3-53394
 magma genesis, effect of dissolved metal oxides on SiO_2 content of minerals, shift of liquidus boundaries 3-80653
 magnesium spinel:Cr population determ. of metastable level (Russian) 3-50149
 magnetite, e.m. and magnetic system for aerial search for high-grade magnetic taconites (French) 3-47801
 magnetite, magnetic state after low temperature treatment 3-65239
 magnetite, magnetic viscosity and quadrature susceptibility in single-domain assemblies 3-53394
 magnetite, superparamagnetic and single-domain threshold sizes 3-53400
 magnetite ore tonnage from aerial e.m. survey 3-47800
 magnetite powder, multidomain, pseudo-single domain moments, low field t.r.m. meas. 3-58866
 magnetites, palaeointensity studies by Thellier technique 3-58972
 magnetomineralogical alteration trends, interpretation of magnetic anomaly patterns and contrast profiling 3-58933
 mantle, compressional and shear velocity profiles from Fe^{2+} and Mg^{2+} distributions 3-73229
 marble, Egyptian, neutron cross sections, nuclear reactor shielding material, evaluation 3-67625
 margarite, upper stability in presence of quartz 3-41885
 marine heavy-mineral deposits, prospecting off East African coast, Valdivia research ship voyage (German, English) 3-65276
 marine Mn nodules, microlaminations, scanning electron microscopy obs. 3-61446
 Matachewan dike swarm, Rb-Sr dating, evaluation of method 3-65137
 maucherite, $\text{Ni}_{11}\text{As}_8$, crystal structure, X-ray diffraction studies 3-44765
 McArthur Pb-Zn-Ag deposits, determ. of $^{34}\text{S}/^{32}\text{S}$ ratios 3-65176
 meionite, cryst. struct. determ. 3-68219
 metallic ore deposits rel. to continental drift 3-41883
 metamorphic rocks, mineral weight percentages using principle of constituent analysis 3-53381
 metamorphic rocks, schistosity and penetrative mineral lineation giving palaeostain directions 3-76518
 metamorphic rocks, variation in composition of muscovite and biotite, near Bancroft, Ontario 3-65135
 metamorphic rocks, variation in composition of plagioclase and epidote from Bancroft, Ontario 3-65134
 metavariscite, $\text{AlPO}_4 \cdot 2\text{H}_2\text{O}$, cryst. struct. 3-79290
 mica-type minerals, relative stabilities of polytypes 3-80643
 mimetite, force const. anal. 3-40992
 minasragrite, crystal structure and chemical anal. 3-50887
 mineral-groundmass partition coefficients for Ti rel. to Rb. in volcanic rocks 3-56030
 mullite fibre, fine diameter, characteriz. for high temp. use 3-76275
 muscovite plus quartz, high temp. stability, hydrothermal studies, nucleation mechanism 3-44770
 muscovite-calcite-quartz assemblage, stability 3-73197
 myrmekites from Haast-Schists, New Zealand 3-44778
 N. Atlantic and Caribbean oceanic rocks magnetic properties 3-73217
 N. Atlantic oceanic rocks, compressional wave velocities as a function of pressure 3-73218
 nacrite, hydroxyl group orientation 3-50882
 natrolite single crystal, high-temperature X-ray study 3-73191

minerals continued

- natural remanent magnetism, relationship to mineral constituents of intrusive rocks 3-58970
 nenadkevichite, mineral, Saint Hilaire Canada, crystalline structure (*French*) 3-61288
 nepheline syenite, mineralogical comp., computer calcs. 3-77739
 nephrite, toughness 3-73195
 normative, proportions in granitic rocks, calc. method 3-76510
 Oka carbonatite complex, X-ray fluorescence anal. of Sc abundance 3-80587
 Oligocene East Sooke gabbro, palaeomagnetism in Vancouver Island 3-73245
 olivine, 200-45000 cm⁻¹ polarisation spectra at room and liquid He temps. 3-50881
 olivine, dislocation 3-76561
 olivine, dislocation climb kinetic 3-65185
 olivine, elastic properties of germanate analogues 3-58847
 olivine, mantle derived, dislocation substruct., etching obs. 3-65184
 olivine and orthopyroxene, partition of Mn and Mg, experimental study 3-44818
 omphacite, order-disorder transforms. 3-50888
 opacities of transparent minerals rel. to temp. and wavelength 3-65217
 opaque, polarising-microscope obs. with transmitted i.r. light 3-42555
 open hearth smelting slag, Cu content, effect of ladle parameter, regression analysis 3-44607
 ore body, in uniform INPUT field, effect of magnetic permeability 3-76668
 ore deposit locations from gas anomalies in soil or air 3-59170
 ore trends, potential prospects, Earth Resources Technology Satellite, earth imaging 3-80852
 orthoclase, shock-induced phase change 3-50927
 orthopyroxene, combined transmission electron microscopy and microprobe analysis 3-44769
 orthopyroxene and olivine, partition of Mn and Mg, experimental study 3-44818
 orthopyroxenes, defect microstruct., dislocation substruct. 3-65186
 oxidic solids, ligand field spectra of CuO₄ Jahn-Teller distorted tetrahedra (*German*) 3-61052
 parkerite (Ni₃Bi₂S₂), crystal structure determ. 3-50878
 pegmatite deposits, in South Africa rel. to sources of nuclear fuel 3-58914
 pentagonite, dimorphous Ca-V-silicate mineral from Oregon 3-50875
 pentagonite, orthorhombic and layer-silicate structure 3-50876
 periclase, optical absorption spectra at high shock pressure 3-76858
 perovskites, A₂BWO₆ (A=Ca, Sr, Ba; B=Mg, Ca, Cd, Sr, Ba), luminescence of WO₆ (*Russian*) 3-41558
 petrographic analysis by sonic method 3-69728
 petroleum-gas saturation factor determ. from gas logging data (*Russian*) 3-47821
 phlogopite, crystal structure from three-dimensional X-ray data 3-65220
 plagioclase, high pressure stability, spinel gabbro xenoliths, Kerguelen Archipelago 3-44772
 plagioclase, shock effects, refractive index and birefringence obs. 3-61367
 poikilo-macrospherulitic feldspar, crystallization in Rhum peridotite 3-41894
 porphyry type deposits, apatite fission-track dating 3-65133
 powders, cold compaction, time-depend. deform. 3-47489
 principal alteration products from action of seawater on primary basalts 3-65131
 proustite, parametric freq. upconverter, background light 3-51944
 pyrite, effects of atmospheric moisture on electrical resistivity 3-53399
 pyrites, temp. depend. of Hall coefft. and elec. cond. between -150 and 500°C 3-69506
 pyromorphite, force const. anal. 3-40992
 pyroxene, Allende meteorite, crystal structure and optical props. 3-45052
 pyroxene shock effects, refractive index and birefringence obs. 3-61367
 pyroxenes, absorption band anisotropy in lunar, meteoritic and terrestrial samples 3-65795
 pyroxenes from lunar basalt 12021, augite-pigeonite miscibility gap 3-77001
 pyrrhotite, Fe₇S₈, mag. transitions, 1 atm. -20 kbar, Mossbauer obs., geophysics 3-41344
 pyrrhotite, mag. transitions at 5-16 kbar, geophysical significance 3-58865
 pyrrhotite, magnetic phase relations 3-58837
 pyrrhotite, reflectivity and angle of apparent rotation meas., comparison with troilite 3-50879
 pyrrhotite, shock compression expts. and possible S content of Earth's core 3-44798
 pyrrhotite, shock compression rel. to S content of Earth's core 3-65215
 quartz, deformation lamellae in ion thinned foils 3-69522
 quartz, i.f. electrical impedance parameters 3-53389
 quartz grains in folded sandstone beams, microfractures 3-76610
 quartz-stishovite shock induced transition, X-ray and optical obs. 3-76560
 radiometry, use of Cf²⁵² as detector (*Rumanian*) 3-51171
 reyerite, locality, formula and proposed structure 3-50885
 richerite, meteoritic amphibole 3-81006
 rivadavite, crystal structure, symbolic addition method 3-75508
 rock salt, behaviour under particle irradiation from high level nuclear waste (*German*) 3-53420
 rutile, single crystal, dielectric relaxation and effect of residual polarisation from 20 to 140°C (*Russian*) 3-61019
 rutile GeO₂, determ. of elastic constants 3-50926
 salt-mica, folding and microfabric development in experimentally deformed specimens 3-76605
 salt-mica, wet, folding at low strain rate 3-76606
 sapphire, Hall density, Hall mobility, temp. dependence 3-64361
 scapolite, Na and Cl rich, refined struct. 3-47610

minerals continued

- Seal rocks, Grenville Front, Labrador, polar wander and tectonic implications from palaeomagnetic data 3-76657
 Seldovia, Alaska, tectonic significance of blueschists mineral ages 3-50936
 silicate, stability, under approx. Venusian surface conditions 3-45037
 silicate spheres of radius 0.05-1 μ, extinction and scattering of 0.2-50 μ light rel. to interstellar dust 3-42249
 silicate structures, direct imaging of lattices by electron microscopy 3-63938
 silicates, extrinsic diffusion 3-69530
 silicates, liquid immiscibility, study of synthetic compositions, possible factor in rock formation 3-73226
 silicoborate garrelsites, crystal structure determination 3-73225
 sillimanites from volcanic inclusions and metamorphic rocks, comp. 3-50889
 spinel, elastic properties of germanate analogues 3-58847
 spinel, pressure dependence of single-crystal elastic constants and anharmonic props. 3-53408
 spodumene, high temperature crystal chemistry 3-73189
 stishovite, compression, isentropic bulk modulus 3-41876
 stishovite, thermal expansion coeffs. from X-ray diffraction study 3-65210
 sulphide minerals, pressure effects on optical transmission 3-64690
 superheavy elements in natural and proton-irradiated materials 3-60231
 talc-organosilicon oil mixtures, acoustic contact material, u.s. investigations of polymers 3-73678
 tetrahydrite, comp. variation and polymorphism in Cu-Sb-S system below 400°C 3-50877
 thermal and elastic moduli of rocks and crystals, holographic interferometric technique 3-61398
 thermodynamic stability diagrams of clay minerals in aqueous solution 3-41889
 tinalconite, crystal structure 3-50886
 titanian chromite, Snake River Plain basalt, electron microprobe anal. 3-80588
 titanian-chromian spinel series, Ti-poor chromite to Cr-poor titanomagnetite, layer formation, eastern Bushveld Complex 3-44762
 titanomagnetite, cation distrib. temp. depend., Mossbauer study 3-58868
 titanomagnetite, natural and synthetic, rotational hysteresis characts. with oxidation 3-58867
 titanomagnetite, ultrafine intergrowths effect on remanent magnetism 3-56095
 todorokite Mn deposit in median valley of Mid-Atlantic Ridge, hydrothermal mechanism 3-56091
 tourmaline, n.m.r. studies, ¹H, ⁷Li, ¹¹B, ²³Na and ²⁷Al, crystal structure 3-44768
 tremolite, crystal chemistry at high temperature 3-73190
 tremolite isograd near Marble Lake Ontario 3-65140
 trevorite, isotropic elastic properties rel. to spinel region of Earth's mantle 3-44817
 trioctahedral mica, fluorophlogopite and annite, crystal struct. 3-80596
 troilite, reflectivity and angle of apparent rotation meas., comparison with pyrrhotite 3-50879
 Turam interpretation, electromagnetic response of 2 dimensional inhomogeneities, dissipative half-space 3-76534
 turbidites, geometry and facies organisation 3-76520
 underground ore deposits, optical processing of aeromag. maps 3-80848
 ureyite, high temperature crystal chemistry 3-73189
 vanadinite, force const. anal. 3-40992
 verplanckite, cryst. struct., open framework 3-68218
 Wilkinson Basin, chemical, mineralogical and geotechnical analyses of clay cores 3-73260
 wollastonite (CaSiO₃) polytypism and stacking disorder 3-68277
 wood opal, structure comparison with high-tridymite 3-73194
 X-radiometric analyzer for light elements (*Russian*) 3-73393
 zeolite: Cu²⁺, e.s.r. study 3-53019
 zeolite, sedimentary, Mexico, X-ray diffraction and electron microscope studies 3-44774
 zeolite adsorbates, reln. between intracrystalline and self-diffusion, kinetic approach (*German*) 3-64244
 zeolites, A- and Y-types, mobility of benzene-1 from proton spin relax. (*German*) 3-64245
 zeolites, Ni-exchanged, dehydration effects on magnetic props. 3-44740
 zircon morphology crystallogenic indicator 3-52592
 zircons from early Precambrian Godthaab District Amitsoq Gneisses, radioactive dating 3-47619
 B oxyanion, Mulliken bond overlap population calc., rel. to bond lengths and angles 3-78692
 Be oxyanion, Mulliken bond overlap population calc., rel. to bond lengths and angles 3-78692
 Ca₂Al₂(Fe_{0.8}Si_{0.2})O₁₃H, epidote structure, X-ray studies, Fe substitution 3-44767
 Cu porphyry mineralization, complex electrical resistivity spectra 3-50907
 Cu-Ni ores Pt, Rh and Pd determ., X-ray spectrometry, segregation 3-48659
 Cu-Pb ores, determ. of Pb content by X-ray spectrometry (*Russian*) 3-73392
 (Fe, Ni)₂Si₁₁, eclogite nodules, kimberlite pipe, South Africa, phase equilib. 3-44764
 Fe content determ., appl. of correlation theory models (*Rumanian*) 3-51170
 Fe ore lenses in Malmberget region rel. to crustal stress distrib. stability 3-44802
 Fe ores, instrumental activation analysis, with short lived isotopes and accurate dead-time correction 3-45583
 Fe ores and mixtures, X-ray fluorescent determ. of Si and Al, rel. error calc. 3-48655
 Fe-containing minerals, crystal structure and mag. props. during chemical transforms. 3-61297
 Fe-Mn nodules, from Black sea, Mossbauer study 3-53461
 FeS₂ mineral samples, Mossbauer quantitative analysis of Fe²⁺/Fe³⁺ ratios 3-53040

minerals continued

- Fe₂SiO₄ (spinel and fayalite) disproportionation at pressures and temperatures of Earth's mantle 3-41898
 β -(Mg, Fe)₂SiO₄, elastic properties of germanate analogues 3-58847
 Mg_{0.81}Fe_{0.19}Ca_{0.03}Si₂O₆, orthopyroxene, combined transmission electron microscopy and microprobe analysis 3-44769
 MgO deformable shell model and geophysical applications 3-65208
 Mn freshwater deposits, accretion rates for ferromanganese nodules 3-47634
 Mn ore nodule deposits, survey of prospecting and exploration methods (*German, English*) 3-61324
 Mo isotope ratios, natural var. in single and separate Mo mineral deposits 3-65222
 NaAlO₂-SiO₂-H₂O, phase equilibria, Gibbs energy of formation 3-44773
 Na₂Mg(CO₃)₂, etelite, crystal structure, X-ray crystallography 3-44766
 Nb determ. in small quantities, X-ray fluorescence spectroscopic method 3-56253
 Ni₁₁As₈, maucherite, crystal structure, X-ray diffraction studies 3-44765
 Ni₂SiO₄-enthalpy of olivine-spinel transition by solution calorimetry at 713°C 3-76532
 Pb ores from NE Washington, isotopic compositions 3-56024
 Pb-Ba minerals, X-ray radiometric fluorescence anal., ¹⁰⁹Cd radioisotope source 3-48660
 Sn production, precipitation and separation of single phases, metallurgical products 3-50671
 Ta determ. in small quantities, X-ray fluorescence spectroscopic method 3-56253
 Ti³⁺ fassaite, Allende meteorite, crystal structure and optical props. 3-45052
 U content, in minerals induced fission track technique geochronology appl. 3-44831
 U-Th ores, gamma spectral borehole logging methods of registration (*Russian*) 3-73394
 U-Th ores, spectral assay using scintillation counters, influence of resolution (*Russian*) 3-73390
 UTeO₅, synthetic schmitterite, space group, cell consts. (*French*) 3-46610

mines (coal) see mining**mines (mineral) see mining****minicomputers**

- see also electronic calculators*
 automatic peak analysis, for spectroscopy, applic. 3-48421
 computer aided-instruction, chem. education, economics of use of minicomputers 3-73655
 control systems, particle-accelerators, decentralisation, advantages 3-56792
 electron probe system with GEPAC 30-2E minicomputer 3-42717
 experimental physics applications, software and peripherals 3-66394
 Harvard minicorrelator for radioastronomy 3-48146
 metal lattice research applics. 3-80266
 operating system for coupling to molecular beam expts. 3-78909
 Synchrotron Radiation Facility at Daresbury, CAMAC system for computer control of spectrometry 3-39990
 vibration control and analysis system, minicomputer based, high performance 3-70270

minimisation

- see also minimum principle*
 function, numerical methods 3-66501
 Krylov-Kolmogorov dynamic entropy minimization in nonequilibrium steady state 3-74180
 nuclear reactor, fast test, minimization of double-release problem in gas-tagged core 3-67427
 nuclear reactors, liquid metal fast breeder, transient effects 3-67506
 polypeptide energy, partial energies, cubic subdivision 3-75163
 thermal conductivity nonlinear least squares determ. technique 3-62627

minimization see minimisation**minimum principle**

- nonlinear boundary value problem in heat diffusion, variational soln. and error bound 3-48822
 plastic structures at finite deformation 3-51793

mining

- detection hazardous conditions, seismometry applic. 3-50902
 dosimeter, for Rn dosimetry in mines 3-53549
 electromagnetic transient response, wire loop in homogeneous conducting sphere, application to rescue 3-76867
 Elliot Lake area, rock stress before mining, studies on pillars, roofs, abutments 3-76514
 excavations in near-surface single-seam, two-dimensional computer analysis 3-44933
 gradiometric survey prospecting network, optimal dimensions (*Russian*) 3-65498
 U miner exposure, dosimetry, ²¹⁰Pb blood concentration, evaluation 3-70182

minimax technique see optimisation**minor planets see asteroids****minority carriers**

- generation-recombination meas., using m.o.s. struct. nonequilibrium current 3-44089
 lifetime, steady-state recombination conditions 3-44090
 lifetime measurement photoconductive decay time obs. 3-50243
 m.o.s. capacitor, collection inversion charge, minority carrier recombination, heavily doped layers 3-41202
 m.o.s. structures, Si based transient behaviour and recombination processes, review (*Hungarian*) 3-68707
 p-n junction, neutral region carrier conc. detn. using quasi Fermi levels 3-52892
 p-n-p semiconductor negative resistance origination by minority carrier injection (*Czech*) 3-55277
 semiconductor, acoustoelec. plasma transport and recombination delay 3-55312
 semiconductor, direct gap, cathodolum., excess minority carrier density 3-72761
 Si, epitaxial growth, p-n junctions, minority carrier lifetime, thyristor 3-41256

minority carriers continued

- GaAs diffusion lengths, measuring methods comparison 3-64354
 GaP:N, epitaxial layers, minority carrier lifetime, luminesc. efficiency green i.e.d. 3-41585
 p-GaSb-InSb mixed crystals minority carrier magnetophonon resonance 3-64356
 p-Ge, plastically deformed, photoelec. effects and minority carrier lifetime 3-58279
 n-Ge, surface lifetime degradation under low energy electron bombardment 3-44091
 Ge p-n-p structure, effective lifetime, effect on O conc. (*Russian*) 3-52896
 p-Ge:Ga, In, annealing of p-induced defects, impurity depend., minority carrier lifetime 3-79709
 p-InSb, minority carrier magnetophonon resonance 3-64356
 InSb, p-n junction, diffusion length, scanning electron microscopy 3-68695
 n-InSb, u.s. amplification, effect of minority carriers 3-46880
 Si, lifetime meas. at low injection intensities (*German*) 3-50219
 Si, single crystal films, vapour deposition, effect of minority carrier lifetime, epitaxy, autoping 3-41656
 n-Si, surface lifetime degradation under low energy electron bombardment 3-44091
 Si solar cell junctions, surface photovoltage obs. 3-41226
 ZnO:Li, photo-induced persistent internal quadrupole moment 3-46876

mirages see atmospheric optics; light refraction**mirrors**

- see also magnetic mirrors*
 aberrations, plate diagram, off-axis systems, Ebert and Czerny-Turner spectrographs 3-39911
 Anglo-Australian telescope, pairs of spherical mirrors for prime-focus correction 3-51412
 astronomical telescope, mirror aluminizers, description 3-77188
 calorimeter, for mirror absorpt. meas. of laser radiation 3-73680
 compound-mirror open resonator 3-53877
 dielectric multilayer light intensity distrib. 3-62050
 electron mirrors, axially symmetric, design 3-48967
 electrostatic objective of electron microscope, electrode geometry 3-62292
 equivalent triple mirrors with non-coplanar normal axes (*Russian*) 3-48407
 holographic testing (*German*) 3-45480
 interference, filters, multilayer, location of transmission extrema in terms of stationary points, manufacture 3-53897
 interferometers with parabolic optics, hyperbolic optics and with a thick confocal system, aberrations 3-77505
 laser, periodic multilayer dielectric system of ZnS and MgF₂, normal incidence, design formulae and graphs 3-45505
 laser, properties at non-normal incidence 3-62158
 laser, using common commercial glass 3-73651
 lightweight, elastic deform. under different support conditions 3-42548
 low absorbance optical interference coatings, design and meas. 3-77438
 microscope two-mirror objective, reflecting surfaces profiles, determination (*Russian*) 3-59574
 multiplier, adjustment for sensitivity in autocollimation method 3-62070
 nonideality calculation, laser theory, imperfectly reflecting surface (*Russian*) 3-66793
 optical resonators with annular 'slot' mirrors, field distrib. and freq. approximation 3-70831
 parabolic telescope mirrors, three-lens prime focus corrector 3-56459
 reflector surface of 6m. mm-wave telescope (*Japanese*) 3-70083
 resonator, ring, oppositely travelling waves, backward diff. scatt. by mirrors 3-48931
 spherical, obliquely illuminated, diffraction integral expansion in caustic region 3-77953
 spherical, spherical aberration, correction by plane parallel plate 3-53895
 spherical, wide angle, e.m. field structure in focal region 3-77944
 stereometry with mirror stereoscope facilitated by interpreter's table 3-53935
 telescope, three mirror anastigmatic design 3-77432
 three-mirror optical delay line 3-66191
 variable profile antenna, aberrations of main mirror, scanning the antenna pattern by shifts of the primary feed (*Russian*) 3-81226
 Al, mirror cast substrates, dimensional stability rel. to microstruct. 3-39897
 Cu mirror surfaces, for high power i.r. lasers, polishing and coating techniques 3-62153
 Rh films, evaporated, reflectance, transmittance, optical constants, effect of surface dielectric films 3-66203

m.i.s. devices see metal-insulator-semiconductor devices**m.i.s. structures see metal-insulator-semiconductor structures****miscibility see solubility****missiles**

No entries

mistakes see errors**mixed conductivity**

- Ag ion conductors, review 3-61260
 Ag₂Te, polymorphism obs. 3-68406
 Cu complex, N-alkyl-hexamethylenetetramine-Cu(I), superionic cond. 3-79521
 Cu_{2-x}S, rel. to phase transformations 3-68407
 Ho₂O₃, quasi-stoichiometric, electronic cond. mechanism (*French*) 3-79746
 K₁₁Ta₉Nb_{1-x}O₃Sn_{0.001}, flux-grown (*Japanese*) 3-41490

mixers (circuits)

- see also frequency converters; radio receivers*
 frequency, electron-cavity interactions, quantum theory 3-62726
 Josephson junctions, mixing and parametric effects, analogue computer simulation 3-41303
 seismic fan filters, mixers, comparison of use (*Russian*) 3-76889

mixing

- see also dissolving; heat of mixing; solubility; solutions
- angular momentum mixing, turbulence and secondary circulations 3-78957
- N Atlantic, fallout tritium and mixing in main thermocline 3-59034
- cavitation, stopped-flow devices, problems 3-73971
- chemical reactions micromixing, general environmental model 3-41834
- continuous flow systems, nonideal mixing, specific gravity differences effect 3-73170
- convective, of Keystone stack plumes 3-69565
- cumulus cloud convection parameterisation by lateral mixing and compensating subsidence 3-65338
- deep convective, in N.W. Mediterranean, preceding hydrographic conditions 3-65255
- lava-water dynamic mixing effects 3-61331
- liquid alloys, II binaries, immiscibility, miscibility syndrome concept 3-50000
- liquid mixing by large gas bubbles in bubble columns 3-63748
- liquid-liquid equilibrium data correlations, properties of NRTL equation 3-46713
- LMFBA, use of saturated liquid Na properties in fuel-coolant interaction analysis 3-46157
- LMFBR, 7-pin wire-wrap mixing expts., directional flow sweeping 3-46121
- LMFBR, local molten fuel-coolant interaction, pressure pulse on subassembly wall 3-46073
- LMFBR, mixing model for temp. distrib. in wire-wrap fuel assembly 3-46120
- LMFBR, voided-core disassembly, fuel-coolant interactions 3-46075
- LMFBR disassembly calcs. fuel-coolant interaction and differential motion effects 3-46074
- LMFBR fuel assemblies, dynamic expts. for heat transfer and mixing studies 3-46113
- micromixing in continuous flow system, 2 environment model rel. to accumulator model 3-63788
- non-Newtonian fluids, representation by two physical parameters (German) 3-54795
- particles, radioactive tracer techniques, collimator efficiency calc. 3-48340
- particles, tube mixer, radioactive tracer technique 3-48339
- polymerisation, radiation nonuniformly initiated, mixing effect 3-57689
- reactor molten fuel-coolant interactions, role of nucleation in vapor explosions 3-46077
- sand particles sieved to different sizes, ^{60}Co activated, study of binary system in tube mixer 3-44695
- solid particles mixing in a motionless mixer, stochastic approach 3-58814
- stratospheric mixing at 25-50 km 3-53479
- turbulent jet mixing at high supersonic speeds 3-54814
- Cu-Fe powder mixtures, degree of mixing (German) 3-47439
- Hg mixing in skull type crucible in alternating mag. field (Russian) 3-79014
- Li-Na liquid, immiscibility, heat of mixing at miscible temp. 3-49999
- Ne + H₂, liq., deviation from ideal mixing, exptl. obs. 3-49965

mixing, heat of see heat of mixing**mixing circuits** see mixers (circuits)**mixtures**

- see also mixing; solutions
- air-oil, horizontal stratified two-phase flow, pipes, flow patterns 3-71809
- alkali carbonate molten binary mixtures for fuel cells, elec. cond. 3-69462
- amide-water systems, deviations from ideal behaviour of mixtures 3-53356
- athermal and nonathermal, equilibrium association constants calc., effect of conc. constant, soln. composition (Russian) 3-50863
- binary, Flory's theory, crit. press. estimation 3-53349
- binary, mean field theory corrections 3-44182
- binary, quantal and classical, space-time correlation functions determ. 3-74152
- binary, with internal relax., light scatt. 3-80013
- binary and quasibinary, composition checking, accuracy, X-ray and γ -ray methods 3-69428
- binary fluids, λ line thermodynamics, specific heat limits and divergence 3-62636
- binary fluids, critical acoustic attenuation 3-60513
- binary gas mixtures, entropy and transport coefficients calc. (German) 3-40694
- binary gas mixtures, heat conduction between concentric cylinders 3-49525
- binary gas mixtures, mass transfer 3-67942
- binary gaseous diffusion coefficients, prediction and correlation 3-75177
- binary solvent, and benzophenone, effect on electronic spectral intensities 3-46264
- binary systems, isobaric vapour-liquid equilibrium data, prediction method 3-72186
- binary vapour mixtures of immiscible liquids, laminar gravity flow film, condensation 3-43566
- binary vapour-gaseous mixture, condensation-evaporation kinetics (French) 3-46391
- carbon tetrachloride-cyclohexane system, thermogravitational thermal diffusion, end effects 3-41037
- cholesteryl alkanoate liquid crystal, pure, and binary mixtures, structure effect on transition thermodynamics 3-52573
- complex gaseous mixtures, with He, calculation method for analysis using spectral line intensities (Russian) 3-48680
- critical binary mixture, possible violation of two-parameter universality 3-51843
- critical properties prediction methods 3-76488
- cumene-tetraline, chemiluminescence spectra, co-oxidation 3-41846
- 1,3-dioxolane-water mixtures, u.s. velocity rel. to water shell stabilization hypothesis 3-65125
- dry solids, random and non-random mixtures, stat. props., variance of sample comp. 3-55907

mixtures continued

- film boiling of saturated binary mixtures 3-64161
- flow of liquids with polymer admixture, applicability of viscoelastic hypothesis (Russian) 3-63771
- fluid dynamics, conservation laws, theory and numerical methods 3-49531
- gas, multicomponent diffusion in porous media 3-40750
- gas mixtures, cylindrically confined, explosive, model for the ignition, numerical soln. 3-46456
- gas-liquid, horizontal two-phase flow, local frictional drag meas., electrodiffusional method (Russian) 3-57028
- gas-liquid mixtures, swirl flow heat transfer in a vertical tube fitted with twisted-tapes 3-52437
- gas/solid mixtures, acoustic velocity and critical flow state calc. (German) 3-67965
- gases, binary, capillaries, diffusional barometric effect, diffusional friction coeff. (Russian) 3-57800
- interaction second virial coeffs., direct meas. technique 3-59659
- liquid, infinite dilution diffusion coefficients 3-76489
- liquid, perturbation theory and excess props. 3-43744
- liquid-gas mixtures, solubility investig. using perturbation theory 3-53357
- liquids, theoretical treatment by means of equilibrium models (German) 3-44746
- mean spherical model for mixture exhibiting phase separation 3-54183
- multicomponent liquid-liquid equilibrium, Renon's and Black's activity equations 3-58130
- nematic and cholesteric mesophase, helical inversion, circular dichroism meas. (German) 3-43754
- nitroethane-3-methylpentane mixture, shear dependence of the viscosity in the critical region 3-41039
- oil-water, immiscible liquids, laminar and turbulent transitional flow, stratified channel flow 3-67963
- organic liquid mixtures steady state of gravitational thermal diffusion columns (French) 3-41035
- polar liquids, thermodynamic properties, extension of partition function to mixtures using Scott's two fluid theory 3-65123
- polyacrylamide admixture effect on turbulent flow of water in flat rough tubes (Russian) 3-63770
- polymer, multiphase props., pair additivity principle 3-73042
- polystyrene-cyclohexane, mixture shear dependence of the viscosity in the critical region 3-41039
- simple liquid mixtures, Percus-Yevick theory evaluation 3-52708
- ternary liquid mixtures adsorption on solids 3-76486
- turbulent flows, concentration probabilities distribution and alternation (Russian) 3-54800
- two-phase, friction during turbulent flow in smooth tubes and channels 3-43627
- water and heavy water mixture, volume viscosity and struct. u.s. study 3-50020
- weak solutions in theory of mixtures for isotropic incompress. elastic solids (German) 3-54079
- CO₂/N₂ mixtures, vibrational transition rates by acoustical method 3-40667
- CO₂-air mixture composition determ. by differential fluidic amplifier (Slovak) 3-57012
- Cu-Fe powder mixtures, degree of mixing (German) 3-47439
- H-He system, thermodynamic props. at high press., astron. appl. 3-42161
- HD-He mixtures spin-lattice relaxation 3-46326
- HD-inert gas mixtures, viscomagnetic effect 3-52421
- He-methane system, phase equilibria at high press., appl. to Jupiter and Saturn 3-42162
- N₂-inert gas mixtures, viscomagnetic effect 3-52421
- Ne + H₂, liq., eqn. of state, exptl. obs. 3-49965

mm waves see microwaves**MO calculations** see molecular orbitals calculations**mobile antennas**

- in ionosphere, impedance and large signal excitation 3-59173

modelling see modelling**modelling**

- see also brain models; identification; physiological models; semiconductor device models; simulation
- acoustic field, electrical modelling, array of incoherent sources, theory 3-59484
- Aerts model, interface states 3-55332
- anti-pollution device design optimisation 3-48275
- arterial peripheral system (Italian) 3-61895
- atmosphere, mathematical, vorticity equation, non-divergent, barotropic, spectral form, approximate analytical solutions 3-76728
- atmospheres, aerothermodynamic calc., temp. at mandatory pressures, statistical determ. 3-53495
- atmospheric, mean temperature structure, effect of large scale eddies 3-76730
- biological systems employing radioanalysis incorporating computer recording (Italian) 3-54035
- biological transducers, using delta function trains 3-56497
- biophysical, evaluation of Bessel functions 3-51420
- calibration of multispectral scanner for Skylab 3-77461
- chromatography column, theoretical plate, nonlinear isotherm, computer calc. 3-70465
- climate theory, general circulation model, numerical expts. 3-59096
- climatic, effect of unknown parameters 3-56169
- constant temp. thermoanemometer, for transfer function and dynamic properties study (Russian) 3-42737
- crystalliser mathematical models of steady-state operation 3-72796
- deep-sea disposal of radioactive waste, safety evaluation models 3-70192
- earthquake, structure model, micromorphic continuum, focal region props., deformation of microstructure 3-44824
- EBR-II Hydraulic Test Facility, flow-modelling expts. 3-46115
- EBR-II hydraulic test facility, flow-modelling studies for homogeneous core loading 3-46117
- ecosystem modelling for Lake George NY 3-47714
- electrical, for soln. of impact problems (Russian) 3-45659
- electrical modelling, transient thermal cond. cast basalt stone (Russian) 3-41057
- electro-telluric field, rotation, electrolytic model tank 3-44947

modelling continued

- electrofluidic convertor, linear static model 3-77757
electron beams and ion beams current by automatic equipment (*Russian*) 3-57280
e.m. devices, static fields, infinite-band model for approx. analysis (*Russian*) 3-74188
e.m. modelling of deep sheet-like ore bodies for e.m. prospecting by combined loop version of transient pulse induction method 3-47799
extragalactic radio sources, ram pressure confinement models, relativistic motion, plasma cloud 3-48059
fast reactor subassembly accidents, pressure generation by water impact upon molten aluminium 3-67529
field ion images of spherical pores in metals, computer program 3-80286
field ion microscopy computer modelling of atomic positions on surface of acicular b.c.c. crystals 3-79203
fusion reactors, plasma behaviour prediction, computer models (*Dutch*) 3-74740
galactic cosmic ray interaction with interplanetary shock waves 3-76937
Galactic disc continuum radio structure, model based on density wave theory 3-77140
gas atomisation of liquids 3-65032
gaseous nebulae, low density, computer modelling, anal. of obs. data 3-48135
geoelectrics and hydrology multilayer analogs, boundary value problems soln. 3-56244
geologic units, analysis of magnetic anomalies Keweenaw volcanic rocks, Lake Superior 3-59159
geological structures, finite element model, fracture, boundary forces 3-41875
geomagnetic anomalous variation, Central Gulf of California 3-76662
geomagnetic anomalous variation, Northern Gulf of California 3-76661
geomagnetic micropulsation measurement, conductivity anomalies, effect of induced mag. fields 3-44928
Global Atmospheric Research Programme rel. to numerical modelling and weather prediction 3-51072
Global Circulation Model, updating experiments, error accumulation 3-76902
global cloud model for Earth-viewing missions simulation 3-47832
green flash at sunset and sunrise model, observations in Alaska 3-44907
of ground-water flow in an unconfined aquifer 3-56277
hologram, lens system, demonstration of holographic techniques 3-66244
hologram, lens system model 3-77984
hydrothermal system modelling, finite element approach 3-59212
hypothetical core disruption accident, mech. energy yield, energy dissipation mechanism 3-74675
hysteresis, e.m. field in hollow a.c. excited ferromagnetic cylinder (*Russian*) 3-45754
igneous rocks, unequal co-axial dipole pair model for data analysis 3-58955
infiltration, homogeneous soil, steady rain 3-56052
insolation, seasonal variation of atmosphere circulation statistical-dynamical model 3-44881
instantaneous plate tectonics, numerical modelling 3-56077
interaction process, production cross section determination for pp interactions (*Russian*) 3-60046
interstellar polarisation, simulation, frozen hydrocarbon matrices, para and nonparamag. porphyrins 3-48125
i.r. radiative fluxes, dusty atmosphere, appl. to Rajasthan Desert atmosphere, India 3-44885
irregular surfaces, mathematical modelling rel. to fine-structure topography 3-51775
isotherms, congruence, thermodynamic and math. consequences, heuristic method for modelling ΔG 3-72267
Kelvin wave generation, near shore thermocline, Lake Michigan 3-47674
kinetic modelling of aeration basins for wastewater treatment 3-45334
linear conceptual catchment models, time variance, rainfall rel. to runoff 3-56242
LMFBR, partially blocked subassembly, local boiling 3-67523
lung, mathematical model of mass transport due to gaseous diffusion 3-51427
magnetic model equations, magnetochemical parameters 3-58933
magnetotelluric study, western Canadian sedimentary basin, tensor analysis, numerical model 3-44853
mammalian cells, model of generation time distrib. including effects of growth temperature 3-59413
Markovian random process, nuclear reactor, number of neutrons, precursor nuclei and fuel temp. (*French*) 3-49309
Martian planetary boundary layer, sloping terrain, temp. and wind oscillations 3-45036
mathematical, inversion dynamics, above convective boundary layer 3-76732
mathematical, pulsed ultrasonic flowmeter output, velocity profiles in man 3-73928
mathematical, response analysis of polyvinylfluoride pyroelectric detectors 3-77393
mathematical, sintering process for UO_2 (*German*) 3-71323
mathematical, sinusoidally excited coupled circuits, Galerkin Urabe method (*French*) 3-70514
mathematical methods for solving solidification problems (*Russian*) 3-53202
mathematics teaching, optimisation 3-66112
metal, flow-modelling expts. 3-46115
molecular structures, computer modelling with versatile interactive graphics display system 3-52306
molecules, stereoscopic film of rotating models 3-61976
myelinated neuron, hybrid computer simulation of action potential generation and transmission 3-53740
N-dimensional surface modelling using weighting function 3-58855
neutron transport problems, application of Phase Space Time Evolution method using computer model 3-46053

modelling continued

- non-Newtonian fluids, laminar flow, viscous flow prediction, conduits, packed beds, porous media fluid models 3-71730
nonlinear viscoelastic materials, modelling, identification and prediction using Volterra integral eqn. 3-45646
nuclear fuel-sodium interaction, kinetic energy and pressure estimation 3-67531
nuclear molten fuel-sodium interaction, modelling 3-67532
nuclear reactor, CO_2 cooled, model of fission decay product deposition on coolant surfaces (*German*) 3-67496
nuclear reactor, reactivity determ., process control, analogue model (*Czech*) 3-60259
numerical, Benard convection in rotating fluid, three dimension study 3-75196
numerical, hailstone aerodynamics 3-76740
numerical dynamo models of earth's magnetic field, large magnetic Reynold's numbers 3-76663
optoelectronic, local detectors of visual analyser (*Russian*) 3-70129
permanent magnets, magnetic field distribution (*Russian*) 3-45756
photogrammetric mapping, stereophotograph space model 3-53936
Pluto, rotational axis orientation, model 3-47904
Poisson clustering model for statistical characteristics of microearthquakes 3-76546
polymerisation, mass, in heterogeneous systems (*German*) 3-65012
prebreakdown discharges, stream model (*Czech*) 3-43700
pulmonary mechanics mathematical model, alveolar surface contrib. 3-51421
radial flow passage, wakes and eddies, flow model 3-75208
reversibility of mathematical models, stochastic and deterministic models 3-40083
rotating stratified fluid, β plane, length scales, model, appl. to ocean circulation 3-46427
saccadic eye movements, generation of muscle force 3-53744
single cochlear nerve fibres, model for discharge activity 3-42299
speech recognition, adaptation model 3-81270
stratosphere, ozone and temperature changes, effect of water vapour and nitrogen oxides 3-76741
temperature changes in rivers, math. model 3-44969
thermal behaviour of automatic precision titration calorimeter 3-48365
thermonuclear fusion reactor, conceptual, modelling and optimisation 3-60322
transmittance models of inhomogeneous atmospheres 3-76903
transport processes in hydrologic system 3-59214
turbulent wall boundary layers using effective viscosity model 3-43560
type II superconductors, mag. hysteresis 3-52914
underground water, simulation of flow (*Russian*) 3-63620
unsteady radial flow, unconfined aquifer, pumped well 3-46489
 H_2 , inflammation and combustion, numerical anal. of kinetic models, delay time meas., effect of H_2O vapour (*Russian*) 3-47541
Si, cooperative diffusions of B and P, mathematical model 3-68433
Si material process, rel. to IC and device parameter control 3-41668

models see modelling

moderation (neutron) see neutron moderation

moderators

- see also beryllium; graphite; heavy water; nuclear reactors
adhesive matrix material, production and radiation behaviour (*German*) 3-71270
electrolytic disgregation, irradiated and non-irradiated, head-end step for reprocessing HTGR fuels 3-71283
graphite, calc. of expansion for low concentration of vacancies (*Spanish*) 3-64070
graphite, conference, Baden-Baden, Germany (June 1972) (*German*) 3-73034
graphite, gas cooled reactor, methane diffusion testing, rel. to manufacture (*German*) 3-71272
graphite, gasification reaction with CO_2 -based mixtures, irradiation effect (*German*) 3-71274
graphite, low temp. irradiation, dimensional changes (*German*) 3-71262
graphite, mechanical strength rel. to neutron irradiation, $400^\circ C$ (*German*) 3-71275
graphite, neutron irradi., thermal annealing effect on Young's modulus 3-67554
graphite, neutron irradiation, creep, press. loading, $500-800^\circ C$ (*German*) 3-71264
graphite, neutron irradiation, dimensional instability, density changes (*German*) 3-71256
graphite, neutron irradiation, high temp., thermal expansion (*German*) 3-71257
graphite, neutron irradiation, shrinkage, dimensional changes (*German*) 3-71261
graphite, neutron slowing down times, effect of anisotropy 3-74634
graphite, neutron wave propagation in finite assemblies multigroup diffusion approach 3-74626
graphite, oxidation in damp atmosphere, mech. strength, tensile stress effect (*German*) 3-71271
graphite, pyrolytic, irradiation, defect struct., $1000-1500^\circ C$ (*German*) 3-71253
graphite, radiation damage, vacancies, interstitials, X-ray obs. (*German*) 3-71255
graphite, radiation effects in reln. to role in fusion reactors 3-60331
graphite, reaction with H_2 , $600-1150^\circ C$, 1-40 atms. (*German*) 3-71246
graphite, reactor, neutron irradiation, tensile stress expansion (*German*) 3-71263
graphite, release procedure of fission Xe produced by β -decay of precursor ^{133}I at $1000^\circ C$ 3-71278
graphite, temp. discontinuities, effective thermal neutron temp., spatial variation, weighted residuals method 3-40527
graphite block, radiolytic oxidation in $CH_4-CH-CO_2$ mixture, diffusion effects (*German*) 3-71273
graphite coating for fuel particles, resin binder, rheology, press. effect (*German*) 3-71267
graphite for high temp. reactors (mechanical and thermal props.) (*German*) 3-71259
graphite from gilsonite coke, radiation behaviour, dimensional stability, thermal cond. (*German*) 3-71260

moderators continued

- graphite in reactor radiation field, absorbed dose meas. using isothermal calorimeter system 3-63137
 graphite matrix material and pyrocarbon in HTR fuel elements, microporosity (*German*) 3-71319
 graphite matrix material in HTR fuel elements, microporosity meas. (*German*) 3-71319
 graphite powder, high temp. reactor fuel pressings, struct., grain size distrib., radiation effects (*German*) 3-71268
 graphite reactor material, radiation damage, vacancies, 600-1400°C (*German*) 3-71254
 graphite-UC, compacted neutron target (*German*) 3-71258
 HTR cores, design with prismatic fuel elements 3-67457
 iron numerical soln. of time-dependent neutron slowing down in infinite media 3-60246
 lead, neutron slowing down times, effect of anisotropy 3-74634
 light water, temp. discontinuities, effective thermal neutron temp., spatial variation, weighted residuals method 3-40527
 matrix, microporosity, annealing and neutron irradiation effects (*German*) 3-71252
 noncrystalline, neutron thermalisation 3-49299
 pressed matrix for high temp. reactor fuel elements, dimensional stability rel. to neutron flux and irradiation temp. (*German*) 3-71269
 propene-pyrocarbon layers, structural changes under thermal treatment and neutron irradiation (*German*) 3-67600
 pure, in the two-zone convention, rel. to computation of group parameters in resonance region (*German*) 3-67390
 pyrocarbon, in HTR fuel elements, microporosity meas. using X-ray scattering (*German*) 3-71319
 pyrolytic-graphite fuel cans, U contamination, HTGR fuel elements (*German*) 3-67590
 water, age of ^{252}Cf fission neutrons, meas. by In resonance obs. 3-71297
 water, leak rate through steel, diffusion process theory (*German*) 3-71315
 water, light numerical soln. of time-dependent neutron slowing down in infinite media 3-60246
 water, neutron slowing down times, effect of anisotropy 3-74634
 water-beryllium square lattice, pulsed neutron expts., one-group diffusion model 3-71144
 BeO, thermal neutron wave meas. at h.f. 3-60281
 D₂O, critical levels, expts. in advanced thermal reactor 3-71190
 LiH, fabrication, cold, hot pressing, casting, properties, physical, mechanical, chemical, nuclear 3-60286
 U/graphite system, neutron wave interference phenomena 3-60276

modes, laser *see laser modes***modes, lattice vibrations** *see lattice dynamics***modular circuits** *see modules***modulation**

- see also amplitude modulation; demodulation; modulation spectroscopy; modulators; optical modulation; pulse modulation; Schwarz-Hora effect*
 electron beam modulation by laser beam 3-43052
 electron beam quantum modulation, on refl. from plane e.m. wave in medium 3-51968
 Kapitza-Dirac effect, electron beam scattering by laser 3-74298
 third order elastic constants of solids, modulation of sound by sound 3-77314
 Cds, microwave transmission, by acoustoelectric domains 3-68678

modulation factor *see modulation***modulation index** *see modulation***modulation spectroscopy**

- see also electroreflectance; magnetorefectance; piezoreflectance; thermoreflectance*
 acoustic phonon spectrometer, using optical modulation methods, mag. circular dichroism detect. 3-53847
 alloy, dilute, screening charges and impurity interactions, differential modulation obs. 3-55222
 angular reflectance method for optical const. meas. 3-53911
 anthracene, cryst., exciton band structure, thermoabsorpt. obs. 3-55230
 using beam-foil light source 3-53910
 birefringent materials, band gap determ. by refl. meas. with polarization modulation 3-68549
 conference, Tucson USA (1972) 3-55564
 crystals complex dielectric function, generalised expression 3-50557
 dielectric function derivative spectra at Van Hove singularities, temp., wavelength modulation 3-55543
 differential reflectometer applic. to materials research in corrosion, ordering and alloying 3-64812
 electric field modulation, new directions 3-55621
 electrochemical appl. 3-55967
 electronic division method 3-42569
 ellipsometer, for study of film optical props., surface dynamics 3-53885
 ellipsometry, appl. to electrode-electrolyte interface study 3-53886
 interference phenomena 3-53909
 ionic crystals, electromodulation, localised excitations, electron-phonon coupling 3-55566
 using laser i.r. beam, thermoreflectance expt. 3-55597
 low resolution i.r. derivative spectrometry for source concentration monitoring 3-73609
 m.i.m. diode, strain modulation electron tunnelling, metal band edge effects 3-55344
 modulation excitation spectrophotometry lens 3-66222
 molecular beams, velocity distrib., space modulation of radiofrequency field, shift of Zeeman pattern, devices (*French*) 3-49507
 organic compounds, adsorbed layers on Pt electrode, electrochemical aspects 3-55965
 photoemission, appl. to Au 3-55724
 piezomodulation, review 3-55643
 rare earth iron garnet films, epitaxial, wavelength, derivative absorption and reflectance spectra 3-55570
 semiconductor, elec. field profile determ. by electroabsorpt. 3-55645
 semiconductor, final-state interactions, excitons effect, electroabsorpt. 3-55637

modulation spectroscopy continued

- semiconductor, I-III-VI₂, band gap determ. by refl. meas. with polarization modulation 3-68549
 semiconductor, II-IV-V₂, for band structure obs., review 3-55205
 semiconductor, under uniaxial stress, review 3-55642
 wavelength, for exciton lines and interf. fringes 3-55626
 wavelength modulation in solids, spectrometer construction 3-55624
 wavelength modulation spectrometer, 2000-8000 Å 3-45485
 Au, s-p band photoemission data 3-55724
 Au film, d-band position and width, low temp. thermomodulation meas. 3-55632
 Au-GaP, Schottky barrier, wavelength modulated photovoltage spectra 3-55618
 BiI₃, electroabsorpt. of excitons, high field regime 3-55639
 CaF₂:Eu²⁺, study of Stark effect in zero-phonon spectra of local centres 3-55665
 Ca₃(PO₄)₂:F:Eu³⁺, study of Stark effect in zero-phonon spectra of local centres 3-55665
 CdGeAs₂, electroabsorp., band edge obs. 3-64686
 CdS, light and electron beam modulated reflectance, A, B exciton lines 3-55634
 CsI(Br), vacuum u.v. wavelength modulation spectrum 3-55625
 Cu-Ga(Ge), dilute alloy, screening charges and impurity interactions, differential modulation obs. 3-55222
 Cu-Zn(Al)(Ni), compositional modulation, absorpt. peaks rel. to band structure 3-55633
 CuCl, modulated excitonic spectra in elec. field 3-55638
 CuGaS₂, wavelength modulated absorpt., refl. spectra, excitonic structure and band gap shift 3-55636
 Cu₂O, modulated excitonic absorpt. in mag. or parallel elec. and mag. fields 3-55617
 Cu₂O, modulated excitonic spectra in elec. field 3-55638
 GaS, wavelength modulation spectra at 5K, 77K, 300K 3-55568
 GaSe, wavelength modulation spectra at 5K, 77K, 300K 3-55568
 Ge, amorphous film, cond. band, secondary emission and photoemission modulation spectra 3-55188
 KI, exciton level prediction 3-55229
 KTaO₃, wavelength-modulated spectrum, temp. variation of band gap 3-55569
 LiF, study of Stark effect in zero-phonon spectra of local N_i colour centres 3-55665
 LuFeO₃, wavelength modulated reflectivity, crystal field transitions obs. 3-47281
 MoS₂, anisotropic, band structure investigation 3-55567
 NH₃, rot. energy transfer, direct obs. by time-resolved i.r.-microwave double reson. 3-78886
 Ni, passive electrode, modulated reflectance measurement, surface layer structure 3-55964
 PbI₂, electroabsorpt. of excitons, high field regime 3-55639
 RbI, exciton level prediction 3-55229
 SbSI, wavelength modulation spectrum rel. to band structure 3-55625
 Se, anisotropic, band structure investigation 3-55567
 Se, trigonal, α -monoclinic, electroabsorpt. of excitons, high field regime 3-55639
 Si, derivative spectrum of indirect exciton absorpt., anal. 3-47290
 SrTiO₃, wavelength-modulated spectrum, temp. variation of band gap 3-55569
 TiBr, electroabsorpt. of excitons, high field regime 3-55639
 YIG, wavelength modulated reflectivity, crystal field transitions obs. 3-47281
 YIG:Ga substituted, wavelength modulated reflectivity, crystal field transitions obs. 3-47281
 ZnGeP₂, wavelength modulation spectrum rel. to band structure 3-55625

modulators

- see also modulation*
 intracavity, patent 3-62756
 for linear accelerator, solid-state line-type, for 10% duty factor 3-56949

modules

- automatic measuring instrumentation 3-45529

modulus, Young's *see Young's modulus***Moire fringes** *see light interference***moistening** *see wetting***moisture**

- see also humidity; mechanical permeability*
 flow through porous media, moisture movement, under partially saturated conditions 3-60581
 in gases at low pressure, absolute determ. (*Russian*) 3-42734
 granular materials, effect of moistening and dem moistening, influence of porosity (*German*) 3-47488
 nuclear reactor fuel element damage, reln. to manufacturing methods (*German*) 3-67610
 nuclear reactor fuel element defects due to local hydration, examination of KRB BWR (*German*) 3-67611
 Cu electrode, alternatively polarised, moisture effects (*Polish*) 3-58802

moisture content *see moisture***moisture measurement**

- in gas streams, nonexplosionproof piezoelectric analyser 3-59720
 microdetermination, organic and inorganic chemicals, review of techniques 3-77742
 microwave methods (*Poish*) 3-57023
 moving source neutron moisture gauge 3-66472
 Nimbus 4 THIR 6.7 μ obs. rel. to regional and global moisture analysis 3-51057
 paper, infrared absorption method 3-62338
 Sahara, radiometric obs. (Spring 1967) (*German*) 3-69584

molar volume *see density***molecular beams**

- see also particle velocity analysis*
 alkali atom-dimer exchange reactions, semi-empirical pot. energy surfaces 3-63541
 alkali halide optical spectra interpretation with aid of molecular beam scattering data 3-54667
 aromatic and heterocyclic molecules, reactions with F atoms, energy distrib. in reaction complex 3-73124

molecular beams continued

- butene isomers, reactions with F, unimol. decomp. of long-lived complex 3-73121
- computer-controlled expts., operating system 3-78909
- cross beam expt., differential elastic cross section, intensity and resolving power 3-78910
- detector, based on charged particle oscillator 3-77617
- diatomic molecules scattering from solid surface, classical model 3-72772
- dienes, reactions with F, unimol. decomp. of long-lived complexes 3-73122
- electric resonance spectroscopy for nucl. elec. hexadecapole moment determ. of ^{115}In 3-43176
- III-V semiconductor thin films, molecular beam epitaxy 3-72812
- impulsive tridimensional interaction with solid surface model in free molecular flow 3-57802
- inert gas pairs, differential elastic scatt. cross sections, intermol. pots. 3-71656
- interactions with solid surfaces 3-57801
- ion and metastable detection, S/N ratios 3-40046
- maser, nucl. spin analogue with cavities in series 3-62682
- maser oscillator, Zeeman mol. beam, nonlinear effects 3-78005
- mass-spectrometric identification of paramagnetic component, focusing of radicals 3-80545
- metastable state lifetimes, time-of-flight measurement technique 3-75151
- methyl chloride, ^{35}Cl and ^{37}Cl quadrupole coupling determ. with mol. beam maser spectrometer 3-49475
- olefins, reactions with F, unimol. decomp. of long-lived complexes 3-73122
- perdeuterobenzene, reaction with F, ang. depend. and recoil-energy spectrum of products 3-73123
- polyatomic free radical reaction ang. distrib. obs. 3-55933
- product state distribution analysis 3-65070
- pyrrole, beam maser spectroscopy, obs. of rotational transitions, nitrogen hyperfine parameters 3-78826
- residence time of K on W meas. 3-60839
- rotatable cryogenic target, for use with molecular beams 3-62031
- scattered by surface, veloc. distrib. (French) 3-56656
- slotted disc velocity selector, stabilized motor speed control system 3-54007
- surface scattering studies using versatile systems 3-39893
- Van der Waals complexes of inert gases with atoms and molecules, review of beam studies 3-78912
- velocity analysis using time-of-flight method with PDP-11 multiscaling interface 3-78908
- velocity distribution, by three-band selector 3-51739
- velocity distribution measurement, space modulation of radiofrequency field, shift of Zeeman pattern, devices (French) 3-49507
- ArHCl complex, structure determ. by mol. beam electric resonance spectroscopy 3-78824
- CO^+ , photofluoresc. by electron impact, relative oscillator strength for $\text{B}^2\Sigma$ state form. 3-46327
- CO_2 , condensation in free jet expansion, cluster growth 3-71652
- CO_2 , dimer form., condensation in free jet expansion 3-71651
- Cl, elementary interactions obs. 3-78907
- $\text{ClF}_3 + \text{D} \rightarrow \text{DF} + \text{ClF}_2$, found at high relative kinetic energies 3-60492
- $\text{ClF}_3 + \text{H} \rightarrow \text{ClF}_2 + \text{HF}$, evidence for occurrence at mean collision energies of 10 kcal/mole 3-60492
- $\text{ClF}_3 + \text{H} \rightarrow \text{HF} + \text{ClF}_2$, evidence for occurrence at mean collision energies of 10 kcal/mole 3-60492
- $\text{ClF}_3 + \text{H} \rightarrow 2\text{F} + \text{HF} + \text{Cl}$, evidence for occurrence at mean collision energies of 10 kcal/mole 3-60492
- CsCl , electron scattering, total cross section 3-75109
- CsF , electron scattering, total cross section 3-75109
- $\text{CsI} + \text{Xe} \rightarrow \text{Cs}^+ + \text{I}^- + \text{Xe}$, collisional dissociation dynamics 3-76449
- D_2 , mol.-mol. elastic scatt., crossed beam expts., central-field pots. 3-54753
- H_2 , anisotropic total collision cross-section 3-71614
- H_2 , elementary interactions obs. 3-78907
- H_2 and D_2 , scattering off other molecules by central field potentials in crossed beams 3-71660
- H_2 mol.-mol. elastic scatt., crossed beam expts., central-field pots. 3-54753
- H_2 supersonic nozzle beam, production of clusters 3-63562
- $\text{H}_2 + \text{D}_2$ exchange, mol.-beam study on low- and high-Miller-index Pt single cryst. surfaces 3-47599
- $\text{H}_2 + \text{NH}_3$, scattering with crossed beams 3-71653
- $\text{H}_2^+ + \text{He} \rightarrow \text{H} + \text{HeH}^+$, reaction kinetics 3-75144
- He reflection, study of reactions of oxygen and CO with polycrystalline tantalum, chemisorption (French) 3-44742
- $\text{He}^+ + \text{O}_2 \rightarrow \text{He} + \text{O} + \text{O}^+$, dissociative charge transfer, chemical dynamics 3-76450
- I_2 , absorpt. of He-Ne laser radiation, freq. stabilisation at 0.633μ 3-62707
- I_2 , continuous spectra assignment by photofragment spectroscopy, C state obs. 3-63535
- I_2 , high-resolution spectroscopy using laser-mol.-beam technique 3-40643
- KI, electron scattering, total cross section 3-75109
- NH_3 , h.f.s. lines of $J=3$, $K=3$ transition, central components separation (French) 3-43520
- NH_3 , maser meas. of relax. cross sections 3-54754
- $\text{NO}_2 + \text{Cs} \rightarrow \text{NO}_2^- + \text{Cs}^+$, relative cross section, energy depend. for NO_2 electron affinity meas. 3-49505
- O_2 , elementary interactions obs. 3-78907
- $\text{SF}_6 + \text{Li} \rightarrow \text{LiF} + \text{SF}$ LiF_2 vibrational energy and electric resonance spectra 3-43522
- TiF, electron scattering, total cross section 3-75109

molecular biophysics

- biological pattern formulation, morphogenesis 3-48166
- cylindrical polyelectrolytes, force balances 3-59411
- DNA, irradiation effects, physico-chemical structure, biological function (German) 3-70093
- DNA, rat liver mitochondria, precursor incorporation 3-56549
- erythrocytes, fixed, u.s. absorption through macromolecular interaction 3-45255

molecular biophysics continued

- Fresnel zone plate imaging, high resolution by spatially coded source 3-73598
- genetic alterations, X-ray induced ad-38 mutants, *Neurospora crassa*, revertibility 3-48262
- glycine, X-ray radical yield 3-66047
- heavy meromyosin ATPase, calorimetric study 3-48163
- hemoproteins, stereochem. of porphyrin and electronic struct. 3-46359
- heparin adsorption, by crosslinked polymer 3-56473
- human serum transferrin, changes in physical parameters due to irradiation 3-66053
- imaging with incoherent holography 3-73599
- intracellular Na in human erythrocytes and frog muscle, n.m.r. studied 3-48165
- lipid bilayers, e.p.r. spectra of spin labels 3-73571
- lymphocytes of rat spleen, intranuclear birefringence during chromatin activation reaction 3-56472
- membrane conductance, model system, steady state and time dependent electrical props., classical ion-membrane molecule interactions 3-81262
- membranes, free radicals in aq. environments, e.p.r. line shape calc. 3-47603
- n.m.r. spectroscopy, basic concepts, methods (German) 3-54029
- one-dimensional harmonic model of biomolecules 3-48164
- organic molecules in action, book 3-73572
- polyadenylic acid, polarography and electrode process 3-65981
- prebiological synthesis 3-73570
- RNA, sunlight formation of cyclobutane type pyrimidine dimers 3-56550
- spin labelling in e.s.r. spectra 3-44316
- TMV-RNA, inactivation by u.v. radiation in sunlight 3-59454
- Fe ion, in deoxyhemoglobin and deoxymyoglobin, rel. to oxygen binding mechanism 3-42269
- p-fluorophenylalanine labelled ^{18}F , for pancreas/liver scanning in rats 3-42370
- molecular bonds**
- see also bonds (chemical); hydrogen bonds
- (XYZ)P.S molecules, electronic nature of P-S bond (French) 3-49438
- amidoximes, valence vibr. bands of NH_2 , ND_2 and NHD groups, NH bonds inequivalence (French) 3-52365
- amino acetonitrile, microwave spectra, bond angles, dipole moment 3-63485
- aromatic triple bond molecules, description of radiative triplet props. 3-67841
- carboranes, multi-centre bonding, ab initio and semi-empirical MO study 3-63391
- 1-chloro-2,4-dinitrobenzene, n.q.r. study, C-Cl bond characts. determ. 3-43480
- p-chlorostyrene, rot. band contour analysis of O_0^0 bands of $\text{A}^1\text{A}' - \text{X}^1\text{A}'$ systems 3-63446
- Compton profile and bond energies additivity 3-63392
- cyanine dyes, relation between degree of conjugation and elec. conductivity (French) 3-50208
- dialkylaminophosphines, σ bond character of P-N bond, depending on substituent (French) 3-49439
- diatomic hybrids, correlation of bonding energy with internuclear distances, prediction of dissociation energies 3-54734
- ethylene ligands, torsional potential determ. from inelastic neutron scattering 3-54656
- ethylenes, substituted, electronegativity effect on bond lengths 3-67728
- fluorophosphate anions, n.m.r., P-P bond obs. 3-54721
- p-fluorostyrene, rot. band contour analysis of O_0^0 bands of $\text{A}^1\text{A}' - \text{X}^1\text{A}'$ systems 3-63446
- formaldehyde, hypothetical, C=N bond theory 3-71523
- guanidine(III) aquo-carbonatolanthanidates, hydrogen bonds, i.r. absorpt. (French) 3-40620
- hydrogen-bonded complexes, effect of temperature on ν_s band 3-46247
- hydrogen-bonded complexes, origin of temperature sensitivity of ν_s band 3-46248
- inert gas halides, many-body interaction effects on stability 3-57629
- inert gas matrix, distortion of isolated ionic mol. 3-74995
- methane, valence electron binding energies and momentum space wave functions 3-74945
- methanol, OH stretch, 3430 to 3940 cm^{-1} , torsional level transitions 3-78780
- N-methyl-d $_3$ -P,P,P-trimethylphosphine imide, vibr. spectra, P-N bond struct. 3-75024
- 2-nitrophenol, microwave spectrum, struct. of hydrogen bond 3-40638
- Pauling's bond enthalpy equation, orbital bases 3-74933
- polymer, π -conjugated heterocyclic, bond alternation 3-75164
- polymethine chains, alternating binding angles, max. overlap principle (German) 3-63571
- polystyrene, intramolecular cross linking, meas. of dimensions 3-78915
- polystyrene, intramolecular cross linking, synthesis and chemical characterisation 3-78913
- polystyrene, intramolecular crosslinked molecules, dimensions in soln. 3-78914
- quinoline, hydrogen bonding effect on absorpt. spectra (Russian) 3-54658
- radicals, CC bond lengths from e.p.r. 3-63367
- regular molecular assembly, structure, ring forming ellipse 3-63352
- tefluorophene, lengths, angles based on known data 3-67826
- tetracyanoethylene, radical anion salts, reson. Raman spectra and bond strengths 3-43446
- N,P,P,P-tetramethylphosphine imide, vibr. spectra, struct. of P-N bond 3-75024
- N,P,P,P-tetramethylphosphine imide and N-methyl-d $_3$ analogue, vibr. spectra analysis 3-78795
- thiomethyl group, C-S-C stretching modes, Raman spectra 3-67809
- triphenylcarbonium derivatives absolute fluorescence yields and bond order change during electronic transition (German) 3-57665
- triple bond aromatic mols., radiative triplet props. 3-67841
- valence-bond wavefunctions and population analyses 3-78665

molecular bonds continued

- vinylous amides, hindered rotation, N-C bond, chemical shift, coupling constants 3-5768
 Watson-Crick H bonding in adenosyl-3', 5'-uridine phosphate 3-40688
 AgBr, epitaxial attachment of dye aggregates to surface, ligand bonds red shift, benzothiazolocarboyanine 3-53342
 Au intermetallics, bond energies 3-54730
 BeH₂, valence-bond wavefunction 3-78665
 Ce(NO₃)₃ aqueous solutions, ligand numbers 3-44407
 Co(CO)₃NO, potential constns. backbonding, from vibrational spectra of six isotopic species 3-43442
 Cr(CO)₅L, L=ligand, direct evaluation of π -bonding 3-71556
 GeH₄, multiple-scatt. $\chi\alpha$ calcs. 3-54629
 NH₃.H₂O, SCF MO LCGO studies on hydrogen bonding 3-54648
 (NO)₂, dimer, bond lengths and angles, ab initio calcs. 3-74912
 N₂O₃, N-N bonding data from microwave spectrum 3-46305
 Pd complex, cyclic olefin, vibr. spectra obs. 3-78726
 Pt complex, cyclic olefin, vibr. spectra obs. 3-78726
 SiH₄, multiple-scatt. $\chi\alpha$ calcs. 3-54629
 SiH₃N₃, (p \rightarrow d) π -bonding in Si-N bond 3-43419
 (SiH₃)₃N (p \rightarrow d) π -bonding in Si-N bond 3-43419
 SiH₃NCO, (p \rightarrow d) π -bonding in Si-N bond 3-43419
 SnL₄, chemical bond structure interpreted by ¹¹⁹Sn Mossbauer transitions and n.q.r. 3-68889

molecular collision processes

- see also intermolecular mechanics; molecular electron scattering; molecular energy transfer collisions
 acetaldehyde, collision broadening of rot. lines by O₂ 3-67834
 acetaldehyde collisional deactivation by trans-butene-2 and isobutane, temp., pressure and excitation effect on photoluminescence 3-46313
 adiabatic-state expansion, translational factors in eikonal approx., effect on channel couplings 3-46198
 air, transport coeffs., calc. of distrib. functions, collision integrals, elec. cond. 3000 to 25000 K, 0.1 to 100 atm. (Russian) 3-57705
 alkali atom + Br₂ reaction cross-sections 3-73132
 alkali atom-dimer exchange reactions, semi-empirical pot. energy surfaces 3-63541
 alkali atoms, glory scattering from small molecules 3-71476
 anthracene, vibrational relaxation in triplet state 3-46312
 aromatic compounds fluoresc. state, heavy-atom collisional quenching, empirical law 3-52382
 atmospheric negative ions, collisional detachment of electrons 3-46212
 atom + diatom inelastic small-angle scattering, semiclassical calc. of rotational transitions 3-71638
 atom-diatom inelastic collisions at low energies, averaged adiabatic potentials 3-71482
 atom-molecule, eikonal expansion for excitation, dissociation and rearrangement 3-62570
 atom-molecule, model potential method calculation applications 3-74832
 atom-molecule, modified correspondence principle for strongly coupled states 3-51808
 atom-molecule rearrangement collisions, eikonal approximation in theory 3-76455
 atomic inner shell ionisation by heavy charge particles, perturbed stationary state theory 3-43359
 benzene vapour, thermal energy ion condensation reactions 3-41837
 biacetyl, electronic and vibrational relaxation, ground state molecules collisions 3-40649
 binary mixtures, viscomagnetic effect 3-52421
 classical approach to semi-classical scattering theory 3-71613
 classical trajectory eqns. in two-state approx., limits of applicability 3-78503
 conference, Beograd, Yugoslavia (July 1973) 3-71396
 conference, Beograd, Yugoslavia (July 1973) 3-71402
 correlated Gaussian wavefunctions use for chem. energies calc. for small systems 3-54621
 cross beam expt., differential elastic cross section, intensity and resolving power 3-78910
 depolarized Rayleigh line, non-Lorentzian shape and tensor polarization correl. function 3-78828
 diatomic molecule in collision with solid surface 3-72773
 diatomic molecules, formal and approximate evaluations of collision integrals 3-52404
 differential elastic scattering cross sections uniform semiclassical approximation, evaluation of the accuracy 3-46352
 1,1-difluoroethylene mass spectra, ion-molecule reactions 3-43506
 difluoromethane, hyperfine struct. meas. by beam maser spectroscopy 3-46303
 dissociation, collision induced, statistical theory 3-40661
 Doppler broadening effect on collision cross section functions, review 3-60485
 double perturbation theory for interacting systems 3-57676
 drift tubes, transport equation for ions 3-43535
 elastic non spherical scattering of molecules with rotational degrees of freedom, symmetry conditions 3-75101
 e.p.r. linewidths, gas-phase, and intermol. pots., theory 3-71367
 ethylene oxide lines, collision broadening by quadrupolar mol. CO₂ 3-52397
 exchange interaction, dependence on vibrational coordinates, asymptotic calc. 3-67697
 Feynman diagrams for perturbation theory, computer generation 3-70876
 fluoroethylene and ethylene mixture, ion-molecule reactions, mass spectra 3-43508
 formaldehyde, microwave collision diameters in rot. spectrum 3-67858
 halogen + alkali atom, differential cross sections from trajectory calcs. 3-67692
 homogeneous stationary gas, reacting, distrib. function calc., comparison of Boltzmann's law and Enskog's methods 3-71611
 hydrocarbons, C₃-unsaturated, ion-molecule reaction obs. by photoioniz. mass spectrometer 3-55932
 hydrogen halides, rotational relax in inert gas 3-49500
 indistinguishable mols., total cross sections expressions, extended distorted-wave treatment 3-46339

molecular collision processes continued

- inelastic and rearrangement scatt. processes, variation-perturbation treatment 3-62569
 inelastic impact parameter methods with effective potentials 3-40677
 inert gas pairs, differential elastic scatt. cross sections, intermol. pots. 3-71656
 ion-molecule collisions in radioactive sources, nucl. reson. fluoresc. obs. 3-63009
 light atoms and molecules K-shell X-ray emission and ionisation cross sections by H⁺, H₂⁺ and He⁺ impact 3-46334
 liquid, far infrared spectra, interpret. in terms of collision distrib. 3-80058
 liquid, l.f. depolarised light scatt., mol. motion 3-80052
 liquid spectroscopic props., method of mol. dynamics simulation 3-80051
 methane + Ar⁺, elastic differential cross section 3-75142
 methanes, deuterated, rare gas collision induced dissoci. (French) 3-71635
 methyl alcohol, ion-polar mol. collision theory, reaction kinetic energy depend. 3-46338
 multiphoton radiative collisions, in e.m. fields 3-78490
 p-2,5-phenyl-oxazolyl-benzene, fluorescence quenching by nitrobenzene (German) 3-43474
 polyatomic mols., rot. and vibr. excitation, quantum mech. scatt. theory 3-46346
 polyatomic mols., rot. and vibr. excitation, restricted distorted wave approx. 3-46347
 pressure fluctuations of molecular gas on wall, formulae 3-67893
 quantum theory of molecular scattering 3-63563
 quenching of metastable H atoms 3-78529
 Rayleigh scattering in liquids, binary collision model 3-80017
 reaction path bifurcation model 3-61249
 rearrangement collisions, exponential approximation 3-71612
 resonant gaseous medium, effect on laser pulse deformation (Russian) 3-45826
 rotational excitation scattering parameters, radial asymptotic expansions 3-40150
 semiclassical optical model 3-63545
 slow excited mols., calc. of collision cross section, resonance defect effect 3-49423
 solid surface diatomic molecules scattering, classical model 3-72772
 spectral line broadening, rare equation description, generating operator 3-63493
 symmetric top mols. and ions, close cross sections 3-46340
 symmetry-adapted perturbation expansions using unitary transforms. 3-62559
 tetrafluoroethylene, mass spectra, thermal ion-molecule reactions by ion cyclotron resonance 3-43507
 three-body exchange reactions, selection and quasi-selection rules 3-63543
 total collision cross section calc., multipole interaction in high energy approx. 3-54757
 trifluoroethylene, mass spectra, thermal ion-molecule reactions by ion cyclotron resonance 3-43507
 vinyl, substituted compound, u.s. relax. of conformational equilibria 3-54615
 Ar L-shell fluorescence yield charge-state dependence study by H⁺, H₂⁺ and He impact 3-49420
 Br₂ + H, rate constns. determ., classical trajectory calcs. 3-41844
 CH₄ + Li scatt., absolute total cross sections meas. 3-43362
 C₂N₂, far i.r. collision induced absorption in compressed gas, comparison with liquid phase absorption 3-60458
 CO, 147 nm Xe-sensitized fluoresc., phase shift obs. 3-46308
 CO, quenching by collisions with He, Ne, Ar, H₂ and D₂ 3-43519
 CO charge exchange reaction with O⁺ 3-40678
 CO lineshifts and widths calc. due to inert gas broadening of vibration-rotation lines 3-54707
 CO + K scattering cross section meas. 3-60496
 CO + Li scatt., absolute total cross sections meas. 3-43362
 CO₂, condensation in free jet expansion, cluster growth 3-71652
 CO₂, dimer form., condensation in free jet expansion 3-71651
 CO₂, rotational line overlap due to collision broadening in laser transitions 3-62699
 CO₂/N₂ mixtures, vibrational transition rates by acoustical method 3-40667
 CO₂ + Li scatt., absolute total cross sections meas. 3-43362
 CO⁺ (A²IT) formation from He(2S) interaction with COS⁺, H₂CO⁺, HCOOH⁺ and (HCO)₂⁺ 3-54736
 COCl + Xe ion-mol. reaction, XeCl⁺ form. in gas phase 3-52396
 Cl + HI \rightarrow HCl + I, isotope and mass weighting effects 3-55935
 Cl₂ dephasing collisions with He or Ar₂ or Cl₂, during laser light transmission through Cl₂, Cl₂-He and Cl₂-Ar gas mixtures 3-43030
 ClF₃ + D \rightarrow ClF₂ + DF, found at high relative kinetic energies 3-60492
 ClF₃ + H \rightarrow Cl + 2F + HF, evidence for occurrence at energies of 10 kcal/mole 3-60492
 ClF₃ + H \rightarrow HF + ClF₂, evidence for occurrence at energies of 10 kcal/mole 3-60492
 ClF₃ + H \rightarrow HF + F + ClF, evidence for occurrence at energies of 10 kcal/mole 3-60492
 Cs + methane, collisional excitation transfer rates, rotational effects 3-78516
 D + Cl₂ \rightarrow DCl + Cl, isotope and mass weighting effects 3-55935
 D₂ collisions with D atoms, gas phase recombination 3-40663
 D₂ mol.-mol. elastic scatt., crossed beam expts., central-field pots. 3-54753
 D₂ + Li scatt., absolute total cross sections meas. 3-43362
 D₂ + LiF solid surface, diffr. phenomena, close coupling formalism 3-76114
 F-He-F₂ system, gas-phase e.p.r. linewidths and intermol. pots. 3-71368
 F + D₂ \rightarrow DF + D, vibrational energy distributions, temp. depend. 3-55934
 F + H₂ \rightarrow FH + H collinear reaction, large quantum effects 3-44710
 F + H₂ \rightarrow HF + H, vibrational energy distributions, temp. depend. 3-55934
 GeH₂⁺ ion-molecule collisions with GeH₄ 3-52398

molecular collision processes continued

- H collisions with Ar, Kr, Xe, CO, CO₂ and methane in energy range 80-2000 eV, H⁻ production 3-46211
 H + Cl₂ → HCl + Cl, isotope and mass weighting effects 3-55935
 H + H₂, correlated Gaussian wavefunctions use for chem. energies calc. 3-54621
 H + H₂ → H₂ + H, distorted wave approximation 3-47533
 H⁺ with diatomic molecules, rotational excitation in low-energy collisions 3-71650
 H₂, anisotropic total collision cross-section 3-71614
 H₂, collision-induced fund. band in H₂-He and H₂-Ne mixtures 3-63540
 H₂, para, at room temperature, heat conductivity, Szentfelen-Beenaker effect, quantum mechanical calc. 3-52418
 H₂ and D₂, scattering off other molecules by central field potentials in crossed beams 3-71660
 H₂ collisions with H atoms, gas phase recombination 3-40663
 H₂ collisions with H(2³S) metastable atoms, chemiionisation 3-78902
 H₂ collisions with He and Ne, spin-lattice relaxation, anisotropic part of intermolecular potential 3-40683
 H₂ in Ar, liq. mixture, roto-translational spectrum of H₂ and intercollisional interference 3-80057
 H₂ with (001) face of LiF 3-72773
 H₂ + CL → H + HCl, force field and tunnelling effects, kinetic-isotope effects 3-50833
 H₂ + H, isotopic collinear reactions, exact quantum mech. reaction probabilities and rate consts. 3-55937
 H₂ + H, planar reactive scatt., semiclassical studies 3-55936
 H₂ + H collinear exchange reaction, role of direct and resonant processes 3-60491
 H₂ + H collinear reactive system, semiclassical collision theory 3-43510
 H₂ + H = H + H + H, thermal dissociation and recombination 3-43501
 H₂ + Li⁺, vibr. excitation, rot. effect 3-57675
 H₂ + LiF solid surface, diff. phenomena, close coupling formalism 3-76114
 H₂ + O⁺, reactive scatt. at relative energies below 15 eV, dynamics study 3-49414
 H₂⁺ and H₃⁺ collisions with H₂, D₂, N₂ and Ar, fast excited H atoms formation 3-43375
 H₂⁺ + He, product ion peaks near centroid scatt. mechanisms 3-40671
 HB + Ne⁺, charge transfer collisions, atomic metastables prod. 3-54593
 HBr + H, rate consts. determ., classical trajectory calcs. 3-41844
 H₂CO, collision-induced transitions, velocity depend., obs. by triple resonance method 3-52384
 HCl, absorpt. line broadening by gases, fund. band, temp. depend. 3-63544
 HCl lineshifts and widths due to inert gas broadening of vibration rotation lines 3-43467
 HCl lineshifts and widths calc., due to inert gas broadening of vibration-rotation lines 3-54706
 HCl + Ne⁺, charge transfer collisions, atomic metastables prod. 3-54593
 HD-He mixtures spin-lattice relaxation 3-46326
 HD + He, vibr. inelastic scatt., sudden approx. 3-40669
 HF + N₂, vibr. relax., kinetics 3-54748
 He⁺, He(2¹S) and He(2³S) charge transfer collisions with HCl and HBr 3-43523
 He⁺ charge exchange collisions with CO₂, optical study 3-43524
 He⁺ ion beams, charge neutralisation in collisions with Ar, H₂N₂, O₂, NO, CO, CO₂, methane, ethylene and acetylene 3-43369
 He⁺ + O₂ → He + O + O⁺, dissociative charge transfer, chemical dynamics 3-76450
 Hg + Na + N₂, collisional excitation transfer and quenching 3-78519
 Hg₂, 550 nm emission band due to ²Σ_u → ³Σ_u collision-induced transition 3-60444
 H₂mol.-mol. elastic scatt., crossed beam expts., central-field pots. 3-54753
 K + I₂, Monte Carlo simulation at superthermal energies 3-71615
 Li₂ + F → Li + LF, pot. energy surface, ab initio electronic struct. calcs. 3-47549
 LiF, He ion bombardment, inelastic collision probability (Russian) 3-68475
 Mg vapour, foreign gas quenching of resonance fluoresc. 3-60369
 N₂, paramag., H atom spin exchange cross-section, temp. range 310-390K 3-57612
 N₂, vibr. deactivation probability on collision with glass surface 3-46337
 N₂, vibrationally excited, charge transfer collisions with Ne⁺ 3-43370
 N₂ afterglows, Na atom emission, excitation process and Doppler temp. 3-46174
 N₂ collisions with He in afterglow, Penning reaction 3-52403
 N₂ dissolved in liquids, vibr. Raman bands, collisional narrowing effect 3-75019
 N₂ molecules in nozzle, anharmonic vibrational relaxation 3-54737
 N₂ + K scattering cross section meas. 3-60496
 N₂ + Li scatt., absolute total cross sections meas. 3-43362
 N₂ + O⁺, product ion peaks near centroid scatt. mechanisms 3-40671
 N₃⁺ production in N⁺ + N₂ collisions (German) 3-49498
 NH₃, beam maser meas. of relax. cross sections 3-54754
 NH₃-NH₃ relaxation rates, time-resolved microwave spectroscopy 3-63539
 NO, anisotropy of total collision cross section with Ar, Kr, Xe, glory struct. 3-78868
 NO, deviation from Lorentzian shape in the wings of collision broadened i.r. absorption lines 3-43466
 NO, ultrasonic dispersion, temp. depend., 423 to 500 K 3-40670
 NO collisions with carbon tetrachloride, CO₂, CS₂, N₂O, N₂, Ar, Kr, Xe, and trifluoromethane, orientational anisotropy in total collision cross section 3-46355
 NO + O₂ → NO₂ + O₂, O₂(¹Δ_g) and O₂(¹Σ_g⁺) possible production 3-47572
 NO⁺ charge exchange reactions with inert gases 3-43521

molecular collision processes continued

- NO₂, paramag., H atom spin exchange cross-section, temp. range 310-390K 3-57612
 N₂O₄ = 2NO₂ with Ar, N₂ and CO₂ diluents, heat cond. at 25°C 3-50834
 Na atoms, optically orientated, disorientation in collisions with saturated hydrocarbons (German) 3-43381
 Na fluorescence in Hg-Na-N₂ mixture, collisional quenching by N₂ 3-54571
 O atoms in metastable ³S₀ state, quenching rates 3-43380
 O⁺ + N₂ → NO⁺ + N, low energy study 3-40668
 O₂, paramag., H atom spin exchange cross-section, temp. range 310-390K 3-57612
 O₂ glow discharge, metastable level deactivation processes 3-52546
 O₂ vibrational relaxation in presence of atomic O 3-54738
 O₂ + O₂ interactions, absolute total scatt. cross sections meas. 3-71394
 O₃ charge transfer reactions with O⁻, O₂⁻, OH⁻, NO₂⁻, F⁻, Cl⁻, CO₃⁻ 3-46349
 OCS-Ar relaxation rates, time-resolved microwave spectroscopy 3-63539
 OCS-He relaxation rates, time-resolved microwave spectroscopy 3-63539
 OCS-OCS relaxation rates, time-resolved microwave spectroscopy 3-63539
 O₂(a¹Δ_g), collisional quenching studied by time-resolved absorption spectroscopy in vac. u.v. 3-46269
 PCl₃ excitation of P atoms, collisional quenching, kinetics rel. to ionisation potential, atomic spectroscopy 3-49415
 PbS, He ion bombardment, inelastic collision probability (Russian) 3-68475
 SF₆, coherent pulse transmission, reorientational collisions effects 3-51954
 SF₆ + Li scatt., absolute total cross sections meas. 3-43362
 SO₂, linewidth parameters for ΔJ = 1, 0 ≤ J ≤ 43 rotational transitions 3-43464
 SiH₄, endothermic ion-mol. reactions 3-40666
 T + H₂, T + D₂, and R + HD exchange collisions in 10 eV range, prediction of spectator stripping dynamics 3-76453
 TI halides, polar dissociation and reactive ionisation by inert gas collisions 3-76448
 TlBr, collision induced dissociative ion pair formation by Xe and Kr atoms, absolute cross sections 3-46353
 TlBr, collision induced dissociative ion pair formation by Xe and Kr atoms, threshold behaviour 3-46354
 TlCl, collision induced dissociative ion pair formation by Xe and Kr atoms, absolute cross sections 3-46353
 TlCl, collision induced dissociative ion pair formation by Xe and Kr atoms, threshold behaviour 3-46354
 TlI, collision induced dissociative ion pair formation by Xe and Kr atoms, absolute cross sections 3-46353
 TlI, collision induced dissociative ion pair formation by Xe and Kr atoms, threshold behaviour 3-46354
- molecular configurations and dimensions**
see also inorganic molecule configurations and dimensions; isomerism; macromolecular configurations and dimensions; molecular bonds; organic molecule configurations and dimensions
 atomic Cartesian coordinate calculation, COOR/1130 computer program, undergraduate students 3-48328
 bond lengths, angles, from ground state rotational constants 3-78652
 chain, moments of end-to-end vector, persistence and distrib. 3-67731
 computer modelling of molecular structures with versatile interactive graphics display system 3-52306
 computer program, in Fortran, for interatomic distance and angle calcs. (Czech) 3-54604
 computer study, automatic control system for models of molecular systems (ACSM MS) 3-74932
 conference, Columbus, USA (June 1973) 3-78722
 conformational study, equipment for meas. dihedral angles on models 3-77374
 coordination theory applic. to crystallography, Pfeiffer's contrib. 3-53816
 electron diffraction data, error estimation in determination of parameters 3-54910
 electron microscopy, computer generated image, effects of deconvolution 3-66349
 gas phase electron diffraction, three-atom scatt., general treatment 3-49431
 gas-phase electron diffraction meas., affect of atomic scattering amplitudes, partial wave calcs. 3-78661
 geometries and force constants calc. from CNDO wavefunctions by the force method 3-43396
 geometry changes, valence orbital behaviour and intermolec. separation 3-60418
 interesting walks and equivalence in graphs 3-62592
 large molecules calc., N⁴ depend. 3-67732
 Lewis acid-base complexes, theoret. analysis (French) 3-63355
 long chain formation in superstrong magnetic fields as compared with diatomic molecules and separate atoms 3-67723
 matrix trapped ionic mol., geometrical config. changes 3-74930
 maximum overlap criterion approach 3-78651
 planar correlation, Lennard-Jones potential, mol. struct. 3-71718
 prediction, VSEPR rules or teaching device, criticism, alternative procedure 3-53815
 regular molecular assembly, structure, ring forming ellipse 3-63352
 rotation, threefold barrier, equivalence of V₆ to torsional flexing 3-74972
 stereochemical invariance law for flexible molecules, combinatorial theory 3-53313
 student laboratory of microwave spectra and molecular structure 3-66102
 supermetric props. of mol. structs. 3-71494
 triatomic molecule, linear, computer appl. to calc. of pot. energy function 3-78710
- molecular dissociation**
see also heat of dissociation; molecular dissociation energies
 acetaldehyde predissociation, photoluminescence, temp., pressure and excitation wavelength effect 3-46313

molecular dissociation continued

- acetonitrile, photodissociation in vacuum u.v. meas. of yield curves and thermochemical parameters 3-75093
- acetylene, electron impact, rotational and vibrational energy level distrib., luminesc. 3-75127
- acetylene, molecular and dissociative photoionisation, hot bands obs. ethynyl ion heat of formation 3-75092
- acetylene nitrile, photodissociation in vacuum u.v. meas. of yield curves and thermochemical parameters 3-75093
- air hypersonic nozzle flow with high initial dissociation levels 3-43642
- atom-molecule collision induced, inverse theory for three-body recombination processes 3-78903
- atom-molecule collisions, eikonal expansion for excitation, dissociation and rearrangement 3-62570
- benzene photoionisation thresholds, quasi-equilib. theory 3-57674
- butene isomer complexes with fluorine, unimol. decomp. 3-73121
- carbon tetrafluoride, dissociative electron detachment processes 3-46343
- chemically reactive flow, producing laminar boundary layer, atomic recombination rate determ. by heat-transfer meas. 3-46498
- collision induced dissociation, statistical theory 3-40661
- cyclobutanol, fragmentation mechanism, mass spectra 3-75090
- diatom molecule dissociation in fast atoms or ions energy transfer collisions 3-49424
- diatom molecules dissociation, rotational states limited numbers effect 3-71630
- diene complexes with fluorine, unimol. decomp. 3-73122
- ethylene, electron impact, rotational and vibrational energy level distrib., luminesc. 3-75127
- ethylene and C₂D₆ threshold electron-photoion coincidence mass spectrometric study 3-43499
- formaldehyde, fluorescence decay of single vibronic levels, unimolecular dissociation 3-41864
- formaldehyde, sensitized decomposition to formyl radical, e.s.r. and electronic spectra 3-47577
- gases, reacting Coulomb H₂, quantum-statistical-mechanical formulation dissoc. as a consequence 3-71698
- heteronuclear diatomic mols., perturbation theory in closed form for multiphoton processes 3-71517
- homopolar diatomic multiphoton processes, time dependent, Born-Oppenheimer approx. 3-71516
- methane, electron impact, dissociative excitation, cross section meas. 3-75119
- methane + methyl cation, ion-molecule crossed beam reaction, short-lived intermediate, scrambling, kinetic model 3-73119
- methanes, deuterated, rare gas collision induced dissoc. (*French*) 3-71635
- methanol and methanol-d, ionisation and dissociation by electron impact 3-43496
- naphthols and naphtholate anions, calc. of pK_a* from shifts of fluorescence spectra 3-54714
- olefin complexes with fluorine, unimol. decomp. 3-73122
- perdeuterobenzene, reaction with F, ang. depend. and recoil-energy spectrum of products 3-73123
- positive column thermal contraction by dissociative recombination 3-75443
- Proton energy degradation in water vapor 3-71637
- radical, transient effects in time resolved ESR 3-80536
- solar and stellar atmospheres, BCA photospheric model, dissociation equilibrium 3-76970
- solid surface, of diatomic mols., rate eqns., Auger intensities 3-68494
- threshold in mol. absorpt., continuity discussion 3-46331
- trideuteromethanol ionisation and dissociation by electron impact 3-43496
- two-atomic molecules and ions, energy transfer to nuclei 3-75124
- AlAuC₂, dissociation energies, mass spectrometric determ. 3-52392
- AlC₂, dissociation energies, mass spectrometric determ. 3-52392
- Al₂C₂, dissociation energies, mass spectrometric determ. 3-52392
- BeH₂, symmetric dissociation, valence-bond calc. 3-78859
- CH⁺ dissociative and dielectronic recombination rates rel. to interstellar CH⁺ and CH densities 3-70033
- CH⁺ dissociative recombination rel. to models of interstellar clouds 3-70032
- CO, dissociative ionisation by electron impact, angular and kinetic energy distrib. of fragment ions 3-78870
- CO, ionisation and fragmentation by 5-45 keV Ne⁺, Na⁺ ions and Ne atoms 3-78898
- CO, on Pt, cross sections, role of primary and secondary electrons 3-55152
- CO⁺ collision-induced dissociation near threshold, energy dependence of cross-section 3-76451
- CO₂, electron impact, metastable dissoc. fragments, angular distrib. 3-75121
- CO₂, electron impact dissociative attachment, deconvolution of vibrational excitation structure 3-78878
- CO₂, rel. to anomalous transient behaviour of sealed CO₂ laser 3-62698
- CO₂ dissociation behind reflected shock waves 3-46332
- CO₂ photodissoc., CO and O excitation cross sections 3-44736
- CO₂ photodissociation, O(¹S) production at the 1216-Å Lyman-α line 3-40660
- CO₂-N₂-He laser discharges, plasma chemistry 3-43654
- CS₂⁺ metastable transitions leading to S⁺ + CS and CS⁺ + S under electron impact on CS₂ 3-78858
- Cl₂ bond strength, dissociation, student teaching 3-48320
- CsI + Xe → Cs⁺ + I⁻ + Xe, collisional 3-76449
- D₂⁺ collisional dissociation with D₂ and Ne, cross section 3-75141
- DCl, formation of negative ions by dissociative attachment 3-78866
- F₂, dissoc. rates in shock waves, density gradient meas. from 1400 to 2600 K 3-46330
- F₂O, photoionisation mass spectrometry 3-63533
- H₂, dissociative ionisation by electron impact, H⁺ production 3-75104
- H₂, dissociative ionisation by electron impact, angular and kinetic energy distrib. of fragment ions 3-78870
- H₂, electron impact, evidence for new dissociation channels 3-54743

molecular dissociation continued

- H₂, electron impact induced dissoc. to n=3 levels of atomic hydrogen 3-60363
- H₂, ion pair production in collision with Ne and Xe 3-78904
- H₂, ionisation and fragmentation by 5-45 keV Ne⁺, Na⁺ ions and Ne atoms 3-78898
- o-H₂, matrix treatment of dissociation rotation-vibration relaxation times 3-67857
- H₂, vibr.-vibr. pumping, induced dissoc. at 300 K 3-54747
- H₂ dissociation by u.v. photons rel. to heating of interstellar clouds 3-42240
- H₂ dissociation transition, stimulated emission cross section 3-40652
- H₂ + D₂, mol.-beam study on low-and high-miller-index Pt single cryst. surfaces 3-47599
- H₂ + H = H + H + H, thermal dissociation and recombination 3-43501
- H₂⁺, electron impact, dissoc. recomb. process, autoioniz. states calc. 3-75098
- H₂⁺ and H₃⁺ collisional dissociation with H₂, D₂, N₂ and Ar, fast excited H atoms formation 3-43375
- H₂⁺ and H₃⁺ collisional dissoc. on mol. targets, excited H atom form. 3-54749
- H₂⁺ collisional dissociation with H₂, cross section 3-75141
- HCl, formation of negative ions by dissociative attachment 3-78866
- HCl⁺ and DCl⁺, predissoc. in Å²Σ⁺ states 3-52393
- H₂O, electron impact, dissociative excitation processes, spectroscopic investigations 3-75114
- H₂O, electron impact, dissociative excitation, cross section meas. 3-75119
- H₂O, electron impact, dissociative excitations, emission cross sections, absolute meas. 3-75120
- H₂O, HDO, D₂O isotope effects in H⁻, D⁻ form. by dissoc. attachment (*French*) 3-49496
- H₂O, ionisation and dissociation by electron impact 3-43495
- H₂S, HDS, D₂S isotope effects in H⁻, D⁻ form. by dissoc. attachment (*French*) 3-49496
- H₂S, ionisation and dissociation by electron impact 3-43495
- He⁺ + O₂ → He + O + O⁺, dissociative charge transfer, chemical dynamics 3-76450
- HeH⁺, electron impact, Harris-type elliptic orbitals 3-75108
- HeH⁺, electron impact dissoc., Harris-type elliptic orbitals 3-75108
- I⁻, photodetachment from CsI, obs. of autodetaching state 3-57607
- I₂, continuous spectra assignment by photofragment spectroscopy, C state obs. 3-63535
- I₂, photodissociation by 5310 Å radiation, recomb. rate in inert gases obs. 3-54733
- I₂ photodissoc. laser, apparent late-time gain 3-62693
- I₂ photodissociation laser, kinetics of generation spectrum 3-62708
- methane, and ionization by electron impact 3-54742
- methane and CD₄, threshold electron-photoion coincidence mass spectrometric study 3-43499
- N₂, dissociative ionisation by electron impact, production of N⁺ and N₂⁺ 3-75105
- N₂, dissociative ionisation by electron impact, angular and kinetic energy distrib. of fragment ions 3-78870
- N₂, dissociative ionisation by electron impact 3-78871
- N₂, electron impact, dissociative excitation, extreme vacuum u.v. spectra 3-75117
- N₂, electron impact, excitation of N₂+C state, predissoc., isotope study, ²⁹N₂ and ³⁰N₂ 3-75115
- N₂, ionisation and fragmentation by 5-45 keV Ne⁺, Na⁺ ions and Ne atoms 3-78898
- N₂, negative glow discharge (*German*) 3-79196
- N₂⁺ → N⁺ + N, unimolecular dissociation, translational spectroscopy 3-75095
- NF₃ = NF₂ + F, spectrophotometric meas., behind shock wave in Ar 3-75094
- NH₃, and ionisation by electron impact 3-54741
- NH₃, catalytic decomposition on W (100), (110) and (111) cryst. faces 3-55987
- NH₃, electron impact, dissociative excitation, cross section meas. 3-75119
- NH₃ decomposition in h.f. discharge, excitation products obs. (*Russian*) 3-63538
- NH₄ClO₄, vacuum sublimation 3-55080
- NO, electron impact, dissociative excitation processes, spectroscopic investigations 3-75114
- NO, electron impact, radiation spectrum 2000 to 9000 Å 3-75128
- NO⁺ + e → N⁺ + O^{*} low-energy dissociative recombination rates, temperature dependence, theory 3-78881
- N₂O, dissociative excitation and ionisation excitation with synchrotron radiation 3-43504
- N₂O photodissociation, O(¹S) production at the 1216-Å Lyman-α line 3-40660
- N₂O unimolecular decomposition, N₂ quenching of O(¹D) 3-75137
- N₂O-N₂ mixture, in expanding supersonic jet, rapid cooling, dissociation reactions (*Russian*) 3-57872
- N₂O₄ = 2NO₂, with diluents, heat cond. at 25°C 3-50834
- N₂, electron impact, dissociative excitation, extreme vacuum u.v. spectra 3-75117
- O₂, gas discharge plasma, electron impact excitation and dissoc., effective cross section determ. 3-74871
- O₂, ionisation and fragmentation by 5-45 keV Ne⁺, Na⁺ ions and Ne atoms 3-78898
- O₂ atmospheric, photodissociation, solar u.v. flux variations 3-80756
- O₂ dissociation in r.f. discharge 3-57952
- O₂ glow discharge, metastable level deactivation processes 3-52546
- O₂ interaction with Ag surface sensors, degree of dissociation meas. (*Russian*) 3-66461
- O₂ photodissociation, O(¹S) production at the 1216-Å Lyman-α line 3-40660
- O₂⁺ dissociative recombination rel. to O(¹S) excitation in pulsating aurora 3-80785
- O₃ photodissociation, O(¹S) production at the 1216-Å Lyman-α line 3-40660
- P₂, equilibrium dissociation, mass spectroscopic investigation 3-46329
- PH₃, and ionisation by electron impact 3-54741

molecular dissociation continued

- Sb₂, Sb₃ and Sb₄, equilibrium dissociation, mass spectroscopic investigation 3-46329
 SBP, equilibrium dissociation, mass spectroscopic investigation 3-46329
 SBP₃, equilibrium dissociation, mass spectroscopic investigation 3-46329
 SiF₄, CO₂-laser induced dissociation 3-52391
 SiF₄, dissociative electron detachment processes 3-46343
 SiH₄, and ionization by electron impact 3-54742
 TI halides, polar dissociation and reactive ionisation by inert gas collisions 3-76448
 TIBr, collision induced dissociative ion pair formation by Xe and Kr atoms, absolute cross sections 3-46353
 TIBr, collision induced dissociative ion pair formation by Xe and Kr atoms, threshold behaviour 3-46354
 TICl, collision induced dissociative ion pair formation by Xe and Kr atoms, absolute cross sections 3-46353
 TICl, collision induced dissociative ion pair formation by Xe and Kr atoms, threshold behaviour 3-46354
 TII, collision induced dissociative ion pair formation by Xe and Kr atoms, absolute cross sections 3-46353
 TII, collision induced dissociative ion pair formation by Xe and Kr atoms, threshold behaviour 3-46354

molecular dissociation energies

- correlated Gaussian wavefunctions use for chem. energies calc. for small systems 3-54621
 diatomic hybrids, correlation of bonding energy with internuclear distances 3-54734
 diatomic mols., fundamental stretching vibration frequencies variation, relation to dissociation energies 3-49453
 heptafluoro-n-propyl cyanide, ionisation by electron impact, low energy 3-57679
 hydrocarbons, MOA calculations of CH stretching frequencies and dissociation energies 3-43429
 hydrocarbons, optimized extended Huckel method calc. 3-52313
 organic compound CH stretching frequencies, bond lengths and dissociation energies 3-46229
 pentafluoroethyl cyanide, ionisation by electron impact, low energy 3-57679
 pyrazoline compounds, molecular association in binary solvents, calcs. from temp. changes in absorption spectra (Russian) 3-80542
 AlAu, mass spectra obs. 3-54730
 AlO and Al₂O, isomol. gaseous equil. studies 3-43494
 AlS, H.H. and Lipincott three-parameter potential functions 3-78862
 BaCl, BaCl₂, spectrophotometric determ. 3-49493
 BaO, determ. in CO/N₂O flames 3-76425
 BaOH, BaOHCl, spectrophotometric determ. 3-49493
 BeH, long range interatomic potential and dissociation energies determ. from quasi-bound levels 3-43385
 CaCl, CaCl₂, spectrophotometric determ. 3-49493
 CaO, determ. in CO/N₂O flames 3-76425
 CaOH, CaOHCl, spectrophotometric determ. 3-49493
 CeO₂, dissoci. energy utilizing heats of reaction meas. 3-55929
 Ce₂O₂, dissoci. energy utilizing heats of reaction meas. 3-55929
 D₂, variational treatment, full electronic Hamiltonian 3-67748
 D₂, dissociation energy and heat of formation 3-53312
 EuAg, dissociation energy and heat of formation 3-53312
 F₂, anomalous prop. 3-67680
 F₂, dissociative ionization and dissociation energy, calc. of curves 3-49494
 H₂, variational treatment, full electronic Hamiltonian 3-67748
 H₂ and H₃, correlated Gaussian wavefunctions use for chem. energies calc. 3-54621
 HD⁺ vibrational energy spacings, dissoci. energy, theory 3-63402
 HgH, long range interatomic potential and dissociation energies determ. from quasi-bound levels 3-43385
¹²⁷I₂, analysis of B³I₀₀-X¹Σ_g⁺ system 3-60429
 NH₂⁺ + H₂ = H⁺ + NH₃⁺, rate consts. and D⁰₀(NH₂-H) derivation 3-55931
 NO₂ ionisation potential, 9.62 to 9.25 eV assoc. mass spectrometer 3-71604
 Ne₂, determ. from vacuum u.v. spectra using Rydberg-Klein-Rees method 3-67865
 O₂ vacuum u.v. absorption, spectra in solid Ar, Kr and N₂ matrices 3-53130
 S₂, H.H. and Lipincott three-parameter potential functions 3-78862
 SF₃ reactions with C, mass spectra studies 3-55938
 SO, H.H. potential functions 3-78862
 Sb₃ existence evidence, high temp. mass spectrometric study 3-43498
 SiC + GdP + C system, atomisation energies of gaseous mols. produced, mass spectrometry 3-75096
 SrO, determ. in CO/N₂O flames 3-76425
 VN thermodynamic props., effusion mass-spectrometric study 3-44662
 WF₆, negative ion formation by electron impact, bond dissociation energies 3-43497
 XeCl⁻ form. in gas phase from ion-mol. reaction 3-52396
- molecular electron correlations**
 azomethanes, nonradiative transitions and properties of lower triplet state, SCF-MO and CI calc. 3-63504
 basis set, new, for SCF and configuration interaction calcs. 3-71506
 bivariational solns., transcorrelated method 3-49383
 trans-butadiene, low lying π-electron states, configuration interaction calc. 3-74958
 Casimir-Polder separation theorem for second-order Coulomb energies 3-43408
 conjugated systems, application of RPA theory to excited states 3-52328
 (2,2)p-cyclophane and related compounds, electronic structure 3-78734
 p-difluorobenzene, electronic struct. and geom., CNDO-CI calcs. for ground and excited states 3-60423
 ensemble-representable reduced density matrices suggested by Xα transition state 3-78401
 ethyl cation, C₂H⁺, classical and non-classical struct. approach 3-74911

molecular electron correlations continued

- excited state CI studies, reduced partitioning procedure 3-74953
 finite electronic systems, Brueckner-Hartree-Fock method 3-43405
 free radicals, org., electronic struct., geometry change and substitution effects using INDO/CI formalism 3-63387
 group-function expansions of correlated wave functions 3-57627
 Hartree-Fock method, spin-extended, second-order density matrix spin components 3-60405
 intramolecular, mol. interactions at finite temps., unified treatment 3-75158
 ionic states obs. by high energy photoelectron spectroscopy, configuration interaction calc. of valence orbital relaxation 3-46335
 many-body perturbation methods applic. in discrete orbital basis 3-46233
 many-electron theory, cluster-function development 3-74778
 methane, semi-empirical effective pair correl. parameters and correl. energies 3-54624
 methylene, spin dipole-dipole parameters, ab initio calcs. 3-74939
 monofluorobenzene, electronic struct. and geom., CNDO-CI calcs. for ground and excited states 3-60423
 multiconfigurational zeroth-order wavefunctions iterative perturbation calculations of ground and excited state energies 3-49436
 naphthalenes, monosubstituted, electronic absorpt. spectra interpret. by config. analysis 3-67754
 nitrate esters, lower electronic states, CNDO config. interaction calcs. 3-49435
 nitromethane, lower electronic states, CNDO config. interaction calcs. 3-49435
 nuclei acid bases, in-plane electronic spectra using all valence electron MO-CI calcs 3-63386
 organic chain molecules, effective electron-electron interaction 3-75801
 perturbation calcs. for 1s2p, 1s²2p and 1s²2s states using Dalgarno interchange theorem and U function 3-71505
 pi-electron, collective motion model 3-74962
 singlet-triplet and triplet-triplet spectra, closed and restricted open shell semiempirical methods, configuration interaction 3-52342
 spectra, rel. to correlation effects in pi electron system 3-71534
 spin-correlation problems, unrestricted and spin extended Hartree-Fock theories 3-74956
 three-electron model system, correlation effects, natural spin orbital formalism, Hartree-Fock method 3-74955
 vibrational-rotational spectra electronic-nuclear interaction effect 3-63428
 vinyl cation, C₂H₃⁺, classical and non-classical struct. approach 3-74911
 [H₂O]₂⁺, correl. effects on energy curves for proton transfer 3-60412
 BH, semi-empirical effective pair correl. parameters and correl. energies 3-54624
 BH₃, equilibrium geometry and harmonic force consts., ab initio calc. including electron correlation 3-54657
 BH₃ dimerization and associated delocalization energy 3-57628
 BeAr, atomic contraction coefficients., valence shell correlation, LCAO-MO-SCF calc. using Gaussian basis functions 3-43410
 BeH₂, ground state, nonorthogonal configuration interaction 3-40591
 BeNe, atomic contraction coefficients., valence shell correlation, LCAO-MO-SCF calc. using Gaussian basis functions 3-43410
 CH, semi-empirical effective pair correl. parameters and correl. energies 3-54624
 CH, valence excited states, potential curves, ab initio CI calc. 3-71512
 CO₂, low-lying electronic states assignments 3-54630
 F₂, F₂⁺, F₂⁺, pot. energy curves and spectroscopic consts. calcs. 3-71496
 F₂ molecule, SF-CI calculations for ground and some excited states (German) 3-43406
 H₂, correlated Gaussian wavefunctions 3-60410
 H₂, electron capture and CI effect 3-71608
 H₂, electron scatt., first Born approx. 3-75102
 H₃⁺, correlated Gaussian wavefunctions 3-60410
 HF, semi-empirical effective pair correl. parameters and correl. energies 3-54624
 HNO₃, lower electronic states, CNDO config. interaction calcs. 3-49435
 H₂O, electronic excitation energies, ab initio calc., CI method and RPA applies. 3-74940
 HeH₃⁺, stability study using polarised Gaussian orbitals and VBCI wave functions 3-74954
 Li⁺/H₂ system, pot. hypersurface calc. including electron correl. 3-54756
 N₂, electron scatt., first Born approx. 3-75102
 N₂, semi-empirical effective pair correl. parameters and correl. energies 3-54624
 N₂⁺, config. interaction calcs. of low-lying quartet states 3-60413
 NF and NF⁺, pot. energy curves and spectroscopic consts. calcs. 3-71496
 NF and NF⁺, configuration interaction studies 3-40593
 NH, semi-empirical effective pair correl. parameters and correl. energies 3-54624
 NH₃-H₂O, LCAO calcs. for H bond energy (French) 3-71502
 NO₂, low-lying doublet states, SCF and CI calcs. 3-40592
 NO₂ ion, lower electronic states, CNDO config. interaction calcs. 3-49435
 NO₃ ion, lower electronic states, CNDO config. interaction calcs. 3-49435
 OD, A²Σ⁺ state, dipole moment and hyperfine consts. by SCF and configuration interaction calc. 3-40606
 OH, semi-empirical effective pair correl. parameters and correl. energies 3-54624
 PO valence shell states, spin-orbit coupling consts. variation with internuclear distance, CI calc. 3-71514
- molecular electron scattering**
 see also electron ionisation
 acetylene, dissoci., rotational and vibrational energy level distrib., luminesc. 3-75127
 angular distributions in resonance scattering 3-75131

molecular electron scattering continued

- carbon tetrafluoride, dissociative electron detachment processes 3-46343
- conference, Beograd, Yugoslavia (July 1973) 3-71396
- conference, Beograd, Yugoslavia (July 1973) 3-71402
- effective collision frequency of electrons in gases 3-49648
- elastic and inelastic, 0-50 eV, in reln. to space travel, upper atmosphere, sun, review (*Dutch*) 3-63317
- electron-impact ionisation pots., determ. incorporating Maxwellian inhomogeneity effects 3-46344
- ethane, excitation, emission spectra 3-75122
- ethylene, dissoci., rotational and vibrational energy level distrib., luminesc. 3-75127
- ethylene, excitation, emission spectra 3-75122
- ethylene and C₂D₆, threshold electron-photoion coincidence mass spectrometric study 3-43499
- freon, electron attachment cross sections in energy range up to 10 eV 3-78880
- by harmonic oscillator, electron-molecular collisions 3-71618
- high energy charged particle ionisation collisions, Bethe theory, photoabsorption data 3-75100
- hydrocarbons, excitation, Balmer β radiation, cross section meas. 3-75123
- inelastic, many body theory 3-71417
- inelastic scattering, adiabatic limit and nonadiabatic effects in second order transition pot. 3-74850
- inelastic scattering, generalised optical pot., many-body theory 3-74849
- inelastic thresholds and associated cusps determ. by new technique 3-78547
- ionization, energy loss and momentum transfer 3-40584
- methane, electron impact, dissociative excitation, cross section meas. 3-75119
- methane, excitation, emission spectra 3-75122
- methane, ion-molecule reactions with H₂O, H₂S and NH₃, resonant cyclotron ejection 3-73118
- methane, valence electron binding energies and momentum space wave functions 3-74945
- methane and CD₄, threshold electron-photoion coincidence mass spectrometric study 3-43499
- methanol and methanol-d, ionisation and dissociation by electron impact 3-43496
- polar molecule, scattering of charged particle by the field of a finite dipole 3-75125
- polar molecules, slow electron scattering 3-46342
- quasielastic electron knock-out, evidence of electronic struct. 3-74873
- spectroscopy electron scatt., review 3-60380
- trideuteromethanol, ionisation and dissociation by electron impact 3-43496
- two-atomic molecular and ions, dissoci. by energy transfer to nuclei 3-75124
- vibrational excitation cross sections calc. methods, comparison 3-46345
- water vapour, energy distrib. of secondary electrons released by fast electrons 3-80561
- B trihalides, ion-molecule reactions of B⁺ 3-75107
- CO, dissociative ionisation, angular and kinetic energy distrib. of fragment ions 3-78870
- CO, excitation, cross section and lifetime of metastable state 3-75118
- CO, excitation, differential cross section determ. 3-71620
- CO, in crossed beams, image intensifier study 3-78897
- CO, threshold excitation spectrum by electron impact 3-60483
- CO, vibr. level lifetimes of b³ Σ^+ state 3-52399
- CO resonances in electron impact, energies and configurations 3-52400
- CO⁺, photofluoresc. by electron impact, relative oscillator strength for B² Σ state form. 3-46327
- CO₂, dissociative attachment, deconvolution of vibrational excitation structure 3-78878
- CO₂, electron impact excitation and assignment of low-lying electronic states 3-71617
- CO₂, electron impact excitation, electron scattering spectra, assignment of low lying electronic states 3-75112
- CO₂, excitation, electron scattering spectra, assignment of low lying electronic states 3-75112
- CO₂, in crossed beams, image intensifier study 3-78897
- CO₂, metastable dissociation fragments, angular distrib. 3-75121
- CO₂-N₂-He laser discharge, plasma chemistry 3-43654
- CO₂⁺ excited ions, electron collisional deactivation 3-43511
- CS₂, metastable transitions leading to S⁺ + CS and CS⁺ + S 3-78858
- CsCl, thermal beams, electron scattering, total cross section 3-75109
- CsF, thermal beams, electron scattering, total cross section 3-75109
- H₂, (e,2e) reaction, momentum space wave function, electron binding energy 3-67861
- H₂, beam-beam scattering, scattered electron intensity, angular and energy loss dependence 3-74868
- H₂, Compton modified band obs. 3-54589
- H₂, cross-section of transitions between vibrational states in resonant scattering 3-78873
- H₂, differential cross section for elastic scatt. in first Born approx. 3-75103
- H₂, dissociative ionisation, angular and kinetic energy distrib. of fragment ions 3-78870
- H₂, dissociative ionisation by electron impact, H⁺ production 3-75104
- H₂, elastic scatt., Born approx. 3-46341
- H₂, electron impact induced dissoci. to n=3 levels of atomic hydrogen 3-60363
- H₂, first Born approx. 3-75102
- H₂, ioniz., electron impact, evidence for new dissociation channels 3-54743
- H₂, positron scatt., low energy, comparison of one and two centre formalisms 3-78879
- H₂, resonant rotational excitation 3-78872
- H₂, structures in ionisation near threshold 3-75130

molecular electron scattering continued

- H₂ resonances in electron impact, energies and configurations 3-52400
- H₂⁺, Bethe-Born theory of ionisation 3-78869
- H₂⁺, dissoci. recomb. process, autoioniz. states calc. 3-75098
- H₂O, dissociative excitations, emission cross sections, absolute meas. 3-75120
- H₂O, electron impact, dissociative excitation processes, spectroscopic investigations 3-75114
- H₂O, electron impact, dissociative excitation, cross section meas. 3-75119
- H₂O, ionisation and dissociation by electron impact 3-43495
- H₂O, ionisation at low energies 3-75129
- H₂S, ionisation and dissociation by electron impact 3-43495
- HeH⁺, dissociation, Harris-type elliptic orbitals 3-75108
- I₂, formation of I₂⁺ on electron impact, appearance pot. (*French*) 3-63534
- KI, thermal beams, electron scattering, total cross section 3-75109
- N₂, dissociative excitation, extreme vacuum u.v. spectra 3-75117
- N₂, dissociative ionisation, angular and kinetic energy distrib. of fragment ions 3-78870
- N₂, dissociative ionisation by electron impact, N⁺ and N₂⁺ production 3-75105
- N₂, electron impact excitation, lifetime and excitation function of the D³ Σ_u^+ state 3-75113
- N₂, electron-molecule collision freq. in crossed elec. and mag. fields 3-71970
- N₂, excitation, cross section of metastable A³ Σ_u^+ vibrational level 3-75116
- N₂, excitation, differential cross sections 3-75111
- N₂, excitation, lifetime and excitation function of the D³ Σ_u^+ state 3-75113
- N₂, excitation of N₂⁺ C state, predissoc., isotope study, ²⁹N₂ and ³⁰N₂ 3-75115
- N₂, first Born approx. 3-75102
- N₂, inelastic thresholds and associated cusps determ. by new technique 3-78547
- N₂, long range potential, depend. on internuclear distance 3-75126
- N₂, resonant excitation, cross-sections calc. 3-78875
- N₂, shape resonances in A- and B states 3-78876
- N₂, structures in appearance efficiency curve of N⁺ ions produced 3-78871
- N₂, electron impact excitation, contribution of the metastable E³ Σ_g^+ state to the population of the C³I_g state 3-43513
- N₂ gas, elastic, angular differential cross sections 3-71619
- N₂ resonances in electron impact, energies and configurations 3-52400
- N₂⁺ formation by electron impact of N₂ at 70 eV, cross section meas. 3-54740
- NH₃, electron impact, dissociative excitation, cross section meas. 3-75119
- NO, electron impact, dissociative excitation processes, spectroscopic investigations 3-75114
- NO, excitation and dissoci., radiation spectrum 2000 to 9000 Å 3-75128
- NO, negative ionic states in low-energy scattering 3-78874
- NO resonances in electron impact, energies and configurations 3-52400
- NO⁺ + e⁻ → N⁺ + O^{*} low-energy dissociative recombination rates, temperature dependence, theory 3-78881
- N₂O, excitation, K shell energy loss spectra 3-75110
- N₂O⁺ excited ions, electron collisional deactivation 3-43511
- O₂, dissociative excitation, extreme vacuum u.v. spectra 3-75117
- O₂, gas discharge plasma, electron impact excitation and dissoci., effective cross section determ. 3-74871
- O₂, negative ionic states in low-energy scattering 3-78874
- O₂, resonant vibr. excitation by slow electron impact 3-71616
- O₂, vibrational excitation, 4-15 eV 3-75106
- O₂ resonances in electron impact, energies and configurations 3-52400
- O₂⁺ dissociative recombination rel. to O(¹S) excitation in pulsating aurora 3-80785
- O₂⁺ first negative system and O and O⁺ multiplets, effective cross sections and excitation functions 3-43512
- SO₂, metastable transitions in SO₂⁺ spectra 3-78877
- Sb₃ existence evidence, high temp. mass spectrometric study 3-43498
- SiF₄, dissociative electron detachment processes 3-46343
- TiF, thermal beams, electron scattering, total cross section 3-75109
- WF₆, negative ion formation by electron impact 3-43497
- Xe₂, high pressure gas, vacuum u.v. emission excited by relativistic electron beam 3-52378

molecular electronic structure

- see also inorganic molecule electronic structure; molecular electron correlations; molecular metastable states; molecular orbitals; molecular polarisability
- asymmetric polyatomic molecules, rotational levels, rigid and nonrigid top models 3-60433
- Born-Oppenheimer approx. for wave functions and spectra, validity 3-63385
- Born-Oppenheimer method, powers expansion, orthogonal transformation, normal mols. (*Russian*) 3-49443
- Casimir-Polder separation theorem for second-order Coulomb energies 3-43408
- charge distrib., computer calcs. 3-54639
- closed shells, ionisation energy calculation 3-78676
- CNDO/2 charge density distrib. calc., monatomic overlap densities role 3-54622
- conference, Columbus, USA (June 1973) 3-78722
- crude adiabatic vibronic state wavefunctions and radiationless processes interpret. 3-43420
- diatomic, Π -state, collision induced rot. energy transfer 3-75139
- diatomic molecule, virial theorems, adiabatic representation 3-78670
- electron scattering spectroscopy, review 3-60380
- electrostatic potentials calc. from Poisson eqn. 3-54628
- energy levels, muffin-tin orbitals, using band theory of metals method 3-78674
- excited states, effect of perturbations, mol. orbital LCAO method 3-71498

molecular electronic structure continued

- excited triplet states, absolute sign of electron spin dipolar and nucl. quadrupole interactions 3-57667
 excited-state energies, constrained variation method 3-71511
 Feynman diagrams, for molecular ground states with closed electron shells 3-78691
 heteronuclear diatomic mols. closed form perturbation theory of, multiphoton transitions 3-71517
 heteropolar diatomic mols., multiphoton processes, Born-Oppenheimer approx. 3-67760
 induced electron current density props. of molecule under static uniform magnetic field 3-54636
 isoelectronic mols., first- and second-order props., continuous group L(1) approach 3-54650
 magnetic properties of molecules, influence of perturbations 3-57636
 many-electron theory, cluster-function development 3-74778
 momentum expectation values and total energies calc. from Compton scatt. data 3-63260
 multiphoton processes in homopolar diatomic Born-Oppenheimer approx. mols. 3-71516
 multipole moments, net, of Thomas-Fermi-Dirac and Thomas-Fermi electron densities 3-60415
 n.m.r. of ^{13}C applies. 3-67856
 non-orthogonal pair theory 3-67756
 one-electron properties calc. using coupled Hartree-Fock methods, computer program 3-67759
 photoionisation cross section dependence on photon energy 3-40578
 pi-electron, collective motion model 3-74962
 point charge model approach 3-54631
 polar molecules, symmetry of negative ions 3-60422
 polyatomic molecules and ions, genealogy in mol. spectroscopy 3-63432
 polyenes, optical absorpt. and emission spectra 3-71544
 quantum mechanics applic., for high school (*Hungarian*) 3-73633
 quasielastic electron knock-out, evidence of electronic struct. 3-74873
 quasimolecular terms at small distances, calc. using virial theorem 3-74906
 scattered-wave model, symmetrized form of secular eqn. 3-43409
 SCF theory, multiconfiguration, closed shell systems, model and Brillouin theorem 3-78675
 screened potential eqn. in RPA 3-57630
 small molecules, electron affinities theory 3-43411
 solvable electron network model development 3-50101
 tetrahedral hydrides, ground state energies and bond distances, stat. OCE calcs. (*German*) 3-67745
 Thomas-Fermi theory for $Z \rightarrow \infty$ 3-67636
 two-photon absorption in molecules, calcs. (*Russian*) 3-59899
 unrestricted Hartree-Fock calc., spin contamination 3-71510
 unrestricted Hartree-Fock perturbation theory 3-54623
 valence orbital behaviour during changes in intermolec. separation, united atom and CNDO/BW theories 3-60418
 vibronic and spin-orbit splitting in spectra, Jahn-Teller effect 3-67763
 vibronic intensity borrowing theory, Herzberg-Teller and Born-Oppenheimer coupling 3-40596

molecular energy levels see molecular electronic structure**molecular energy transfer collisions**

- acetone in solution, triplet state, charge transfer rel. to quenching by aromatic molecules 3-69474
 alkali atom + Br_2 reaction cross-sections 3-76454
 alkaline earth atoms + halogen molecule chemiluminescence rel. to electronic structure 3-78889
 aromatic hydrocarbons, quenching of triplet states in solution by O_2 3-61272
 aromatic hydrocarbons, quenching of triplet states in solution by O_2 3-61273
 atom + rigid symmetric top rotational excitation, distorted wave approx. 3-75135
 atom-diatom mol., product state distrib., vibr. temp. and rot. distrib. 3-65070
 atom-diatom molecule rotationally inelastic scattering with effective potentials 3-63558
 atom-molecule dissociation, inverse theory for three-body recombination processes 3-78903
 atom-polyatomic molecule, ITFITS model for vibration translation energy partitioning 3-75138
 biacetyl, vibr. relax. obs. by visible-i.r. double reson. technique 3-78885
 CO_2 , collisional relax. rate meas. from amplifier gain 3-71621
 computer-aided solutions to processes ion-pair formation and recombination 3-74889
 cycloheptatriene photoisomerisation 3-65096
 diatomic, Π -state, collision induced rot. energy transfer 3-75139
 diatomic free radicals, sensitized fluoresc. by $\text{Hg}(6^3\text{P}_0)$ metastables 3-60484
 diatomic molecule dissociation in fast atoms or ions energy transfer collisions 3-49424
 diatomic molecules dissociation, rotational states limited numbers effect 3-71630
 dioxane, PPO soln., radioluminesc. quenching mechanism 3-80085
 dissociation, two-atomic molecules and ions, energy transfer to nuclei 3-75124
 electron affinities from collisional electron detachment rates in non-thermal fields 3-74808
 electron emission, low-energy, in fast proton collisions 3-78899
 electron impact ionization, energy loss and momentum transfer 3-40584
 electron transfer between molecules in solution 3-80583
 electronic excitation, non-radiative transfer theory 3-78890
 fast ion penetration through gaseous media, electron capture and loss, average charge 3-78633
 fluoroethylene, ion-molecule reactions, mass spectra 3-75134
 formaldehyde, fluorescence decay of single vibronic levels 3-41864
 gaseous ion recombination, review 3-57678
 glyoxal vapour, excited at 4358 Å, collision induced intersystem crossing, photophysics 3-80566

molecular energy transfer collisions continued

- high energy, charged particle ionisation collisions, Bethe theory, photoabsorption data 3-75100
 inelastic collisions, rot. relax., transport and spectral props., kinetic theory 3-71622
 ion-dipole capture cross sections and rate coeffs., approx. and scaling laws 3-78884
 ion-molecule charge transfer trajectories computer animated films 3-75148
 ion-polar mol. collisions, momentum transfer and total scatt. cross sections, numerical calcs. 3-49506
 ionisation of highly excited atoms 3-78496
 ions, negative, with H atoms, associative-detachment reactions at thermal energy 3-49418
 isotope effects in ion-molecule reaction at < 10 eV (*Rumanian*) 3-67859
 K-shell excitation in heavy-ion collisions 3-78591
 ketones, aromatic, quenching of triplet state by O_2 in liq. soln. 3-76482
 ketones in solution, triplet state, charge transfer rel. to quenching by aromatic molecules 3-69474
 methane, temp. depend. of half widths of some self- and some foreign-gas-broadened lines 3-67836
 methane + methyl cation, ion-molecule crossed beam reaction, short-lived intermediate, scrambling, dissociation 3-73119
 methane charge transfer collisions with CO and CO_2 3-75133
 methane- CO_2 mixture, vibrational relaxation, u.s. velocity measurements 3-57680
 1-methylnaphthalene to substituted oxazoles and oxadiazoles, non-radiative, excimer mechanism (*Russian*) 3-63510
 near-resonant theory, cross section eval. 3-43514
 near-resonant vibration-rotation energy transfer 3-71642
 non-radiative, involving excimers (*Russian*) 3-63510
 nonadjacent vibrational transitions, interference between one- and two-quantum processes 3-71632
 optical model for exchange reactions 3-67862
 organic ions, double, triple ionisation pots. determ. collision-induced 3-63555
 string oscillator and atom, collinear collisions, quantum and classical treatments, comparison 3-40673
 perfluorocarbons, ion-molecule reactions, ion cyclotron resonance mass spectrometric obs. 3-52401
 polar diatom + atom scatt., rot. inelasticity, time depend. perturbation approach 3-71636
 polar diatom-atom scattering, rotational inelasticity, time-dependent perturbation theory 3-71645
 polyatomic mols. in excited states, vibr. relax. by inelastic collisions 3-60487
 polymethine dyes-aromatic hydrocarbons, triplet-triplet annihilation 3-69479
 resonance transfer of excitation energy, enhancement in channels 3-40675
 rhodamine dyes, conc. quenching of luminesc. in alcohol solns. 3-69075
 rhodamine dyes, from anthracene triplets, diffusion 3-69077
 rotational relaxation, spherical top gas molecules, collision equations, Bryan-Pidduck model 3-49499
 semiclassical theory, internal energy change of ion-pair, inelastic collisions with neutral atoms and molecules 3-63333
 small-energy transfer collisions dominated by long-range forces, theory, comment 3-46345
 sodium fluorescein in glycerol, Webers red edge effect 3-69078
 solution, fluoresc. quenching and nonradiative energy transfer 3-69060
 unsaturated hydrocarbon-H, change in hyperfine state of H atom 3-63347
 vibration \rightarrow vibration, review 3-57681
 vibrational, polyatomic mols., classical theory, exact approach (*German*) 3-63551
 vibrational, polyatomic mols., classical theory, higher order perturbation theory (*German*) 3-63552
 vibrational energy transfer, effect of straight path approximation and exchange forces 3-43515
 vibrational excitation, string-plucking model 3-49504
 vibrational relaxation rate meas. interpret. 3-54745
 vibrational to translational versus vibronic to translational energy transfer 3-40672
 vinyltrimethylsilane, charge transfer reactions with Ar, in r.f. discharge, mass spectrometric ion sampling 3-73941
 vinyltrimethylsilane ion-molecule reactions with Ar in discharge apparatus, ion sampling 3-73940
 Ar metastable atoms energy transfer reactions with SCS, SCO and SCCl_2 3-53310
 Ar + Cl_2 , X-rays from caramboles (double collision processes) 3-78595
 $\text{Ar}^+ + \text{N}_2$, differential inelastic scattering, 1-3 keV 3-75149
 $\text{Ar}^+ + \text{H}_2$, total cross sections for de-excitation of metastable Ar 3-78538
 $\text{Br}_2 + \text{Br}_2$, vibr. scatt., pot. well effect, SSH theory validity 3-49503
 CO, ionisation and fragmentation by 5-45 keV Ne^+ , Na^+ ions, and Ne atoms 3-78898
 CO, low temp., vibr. energy transfer rates in CO laser beam 3-74230
 CO, Ne gas mixture, vibration relax. rates, Landau-Teller model, i.r. spectra 3-75140
 CO, relaxation of vibrational levels studied by laser absorption 3-60488
 CO, vibr.-rot. transitions, rel. to pulsed chem. laser kinetics 3-74234
 CO, vibr.-translational relax. by foreign gases, localized heating 3-78887
 CO spectral line widths self-broadened and broadened by N_2 , O_2 , H_2 , HCl, NO and CO_2 (*French*) 3-67835
 CO symmetric and asymmetric charge transfer reactions with Kr expt. obs. 3-54594
 CO vibrational relaxation by O atoms 3-46348
 CO-additive mixtures, V \rightarrow V transfer rate measurement 3-78905
 CO- H_2 mixtures sound amplification from controlled excitation reactions 3-60495

molecular energy transfer collisions continued

- CO-SF₆, dipole-hexadecapole interaction, theory of linewidth broadening 3-67863
 CO + He⁺, optical emission from charge exchange products 3-78896
 CO + He⁺ in crossed beams, image intensifier study 3-78897
 CO + Ne, scatt., rot. inelasticity, time depend. perturbation approach 3-71636
 CO⁺ collision-induced dissociation near threshold, energy dependence of cross-section 3-76451
 CO⁺ + O₂, charge exchange in energy range 0.04 to 2 eV 3-71644
 CO₂, calc. of population relaxation for rotational levels 3-63559
 CO₂, relax. of 1090 lower laser level 3-74225
 CO₂ laser, Q-switched pulse duration, rot. relax. effect 3-66804
 CO₂ lasers, laser power and vibrational energy transfer 3-48885
 CO₂ upper laser level vibr. deactivation by ONF, COF₂ and O₂ 3-45790
 CO₂ vibrational relaxation in collisions with methane, tetradeuteriomethane and fluoromethane 3-54752
 CO₂/O₂ mixtures, vibr. relax. meas. 3-43516
 CO₂-methane mixture, vibrational relaxation, u.s. velocity measurements 3-57680
 CO₂ + He⁺, in crossed beams, image intensifier study 3-78897
 CO₂ + He⁺, optical emission from charge exchange products 3-78896
 CO₂ + O₂, charge exchange in energy range 0.04 to 2 eV 3-71644
 CO(A¹π), deactivation rel. to individual vib. levels 3-75150
 CO₂(001), vibrational relaxation by O₃, laser fluorescence technique 3-78888
 CO(³Π; v' = 0, 1, 2) quenching rate constants 3-43518
 CO(v = 1) + CO(v = 1) → CO(v = 0) + CO(v = 2), rate const. 3-45787
 CS, vibrational relaxation, Ar collisions, transition probabilities (*French*) 3-71633
 Cl + Cl₂, vibr. scatt., pot. well effect, SSH theory validity 3-49503
 ClF₃ + H → HF + Cl + 2F, kinetic study 3-73125
 Cs + RbCl, branching ratios, statistical approximation 3-75146
 CsI + Xe → Cs⁺ + I⁻ + Xe, reaction dynamics 3-76449
 D₂⁺ collisional dissociation with D₂ and Ne, cross section 3-75141
 D₂⁺ + N → ND⁺ + D, merged beam study, energy dependence of cross section 3-78900
 DF, vibrational relaxation, temp. depend. 3-75136
 DF-CO₂ mixtures, vibrational relaxation processes, temp. depend. 3-54751
 D₂O-D₂O, vib. to rot. energy transfer 3-52402
 F + aromatic (heterocyclic) molecules, energy distrib. in reaction complex 3-73124
 F + C₆D₆ → D + C₆D₅F, ang. depend. and recoil-energy spectrum of products 3-73123
 F + DF(v) → DF(v') + F vibr. relax. process, rate const., Monte Carlo calcs. 3-60486
 F + H₂ → FH + H collinear reaction, quantum, quasi-classical and semi-classical reaction probabilities 3-76457
 F + H₂ → HF + H, vibrational energy distributions, rotation effects 3-71627
 F + HF(v) → HF(v') + F vibr. relax. process, rate const., Monte Carlo calcs. 3-60486
 F + olefins (dienes), olefins, reactions with F, unimol. decomp. of long-lived complexes 3-73122
 H + H₂ collinear reaction, time delays, phase behaviour and resonances 3-76456
 H + H₂ → H₂ + H collinear reaction, streamlines of probability current density and tunnelling fractions 3-76458
 H⁺ + 2H₂ → H₃⁺ + H₂, rate coeff. meas. in drift tube mass spectrometer 3-78901
 H⁺ + 2H₂ → H₃⁺ + H₂ reaction rate coeff. meas. in drift tube mass spectrometer 3-75143
 H⁺ + D₂ → HD⁺ + D, semiclassical treatment of electronic transitions 3-75147
 H₂, 100 to 500 keV collisions with O⁻, O, O⁺, O⁺⁺, electron capture and loss cross sections 3-78632
 H₂, ionisation and fragmentation by 5-45 keV Ne⁺, Na⁺ ions, and Ne atoms 3-78898
 H₂, rotational, Raman linewidth measurement 3-67864
 H₂, vibr.-vibr. pumping, induced dissociation at 300 K 3-54747
 H₂ autoionisation meas. lifetimes discrepancy due to config. interaction effect in electron capture method 3-71608
 H₂ dissociation in collisions with Ne and Xe, ion pair production 3-78904
 H₂-He mixtures, quantum scattering theory of rotational relaxation and spectral line shape 3-46351
 H₂-rare gas mixtures, i.r. absorpt. quadrupole-induced transitions, diffusional narrowing 3-78882
 H₂ + alkali metal ions, L_α excitation cross sections, low energy 3-78892
 H₂ + Ar, at nonzero impact parameters, simultaneous vibr. and rot. transitions 3-75132
 H₂ + H collisions, processes altering charge state 3-40676
 H₂ + H₂, interference between one- and two-quantum excitation processes 3-71632
 H₂ + He collisions, electron loss cross section for fast non-metastable excited atoms 3-78625
 H₂ + P → H + H₂⁺, asymptotic cross section 3-63561
 H₂⁺ and H₃⁺ collisional dissociation on mol. targets, excited H atom form. 3-54749
 H₂⁺ collisional dissociation with H₂, cross section 3-75141
 H₂⁺ + He → HeH⁺ + H, study at low energies 3-60489
 H₃⁺ + D₂ → D₂H⁺ + H₂, energetics of proton transfer 3-75145
 HBr, vibrational relaxation in inert gases 3-60490
 HBr (V = 1) state, vibrational relaxation in methane, water, He and HD mixtures 3-71624
 HCl, vibrational relaxation in inert gases 3-60490
 HCl + Ne scatt., rot. inelasticity, time depend. perturbation approach 3-71636
 HF, V-V, V-R, and T transfer collisions, temp. depend. 3-40674
 HF, vibration to rotation energy transfer, dipole-dipole and hydrogen bond interactions 3-63557
 HF vibrational relaxation through collisions 3-54750
 HF vibrational relaxation in temp. range 600-2400 K, Ar and F collisions 3-71628

molecular energy transfer collisions continued

- HF + DF, vibr. relax., rate const. meas. by laser-excited fluoresc. method 3-49502
 HF + HCl, (HBr), (HI), vibr. relax., rate const. meas. by laser-excited fluoresc. method 3-49502
 HF(V = 1, 2), vibr. deactivation by hydrocarbon mols., rate const. 3-46350
 H₂⁺ + He → H + HeH⁺, reaction kinetics 3-75144
 H₂O-H₂O, vib. to rot. energy transfer 3-52402
 He-I₂ gas discharge, He⁺-I₂ charge transfer cross section meas. 3-63336
 He⁺ collisions with H₂ and N₂, electron transfer 3-78624
 He²⁺ collisions with H₂, N₂, O₂, formation of He⁺(2S) metastable ions 3-78623
 Hg(³P₁) collisionally induced production from Mg(¹P₁) 3-54598
 Hg6(³P₁) photosensitization band fluorescence spectra 3-50842
 I₂, excited atom quenching by O₂, opto-acoustic spectra obs. 3-78883
 I₂ excited state, with inert-gas atoms, classical trajectory calc. of vibr.-rot. energy transfer 3-71641
 I₂ molecules, excited by He-Ne laser, vibrational relaxation by collisions with He, Ne, Ar 3-60494
 I₂ + I₂, interference between one- and two-quantum excitation processes 3-71632
 KBr, vibr. excited, inelastic scatt. by Ar and CO₂ 3-54746
 Kr metastable atoms energy transfer reactions with SCS, SCO and SCCl₂ 3-53310
 Li + H₂, vibrational-rotational excitation, potential energy surface calc. 3-71639
 Li⁺ + H₂, classical Monte Carlo calc. for elastic and inelastic processes 3-71646
 Li⁺ + H₂, coupled-channel calc. for rotational excitation 3-71649
 Li⁺ + H₂, cross-sections for vibrational excitation 3-71648
 Li⁺ + H₂ elastic and inelastic collisions, coupled-channel calculations 3-71647
 N₂, collisions with fast He atoms, cross sections for loss of one and two electrons 3-78628
 N₂, E and F regions, vibration temp., energy loss mechanisms 3-80808
 N₂, ionisation and fragmentation by 5-45 keV Ne⁺, Na⁺ ions, and Ne atoms 3-78898
 N₂, Morse oscillator, collision transition probabilities and cross sections (*French*) 3-54744
 N₂, N₂⁺ excited products of NH₃ decomposition in h.f. discharge, collisional deactivation with H atoms (*Russian*) 3-63538
 N₂, vibrational relaxation by alkali atoms 3-71643
 N₂, vibrationally excited, chemi-ionisation of alkali atoms 3-78495
 N₂ collisional quenching of O(¹D), N₂ vibrational relaxation 3-75137
 N₂-alkali metal atom collision, electron-vibr. transitions 3-49413
 N₂ + H⁺, emission cross-sections for N₂⁺ (3914 Å) 3-78893
 N₂ + Ne⁺, emission cross-sections for N₂ 3914 Å and 3371 Å systems 3-78894
 N₂⁺ first negative 3914 Å band charge-transfer excitation by protons, photon-particle coincidence meas. 3-63560
 N₂⁺ with N₂ and NO, charge exchange energy range 0.04 to 2 eV 3-71644
 N₂⁺ + O → N₂ + O⁺, cross section meas., 1 eV to 500 eV 3-78635
 N₂⁺ + O → NO⁺ + N, cross section meas., 1 eV to 500 eV 3-78635
 N₂(B³Π_g) population by N₂(A³Σ_g⁺) during afterglow 3-71625
 NH₃, inversion spectrum, collision broadening and shifting 3-67838
 NH₃, rot. energy transfer, direct obs. by time-resolved i.r.-microwave double reson. 3-78886
 NH₃ ion-molecule reactions, relative rate constant 3-63556
 NH₃-SF₆, quadrupole-hexadecapole interaction, theory of linewidth broadening 3-67863
 NH₄-NH₄, vib. to rot. energy transfer 3-52402
 NO, monochromatically excited, energy transfer, vibrational relaxation, fluorescence 3-71623
 NO, vibrational energy transfer 3-71626
 NO + N → O + N₂, vibr. excited N₂ yield, Raman scatt. study 3-43517
 NO₂ + Cs → NO₂⁻ + Cs⁺, relative cross section, energy depend. for NO₂ electron affinity meas. 3-49505
 Na (3²P) doublet in flames, quenching by H₂ and O₂ collisions 3-52300
 NaLi rotational transitions, laser excited fluorescence 3-63553
 Ne + CO and Ne + HCl, rotational inelasticity, time-dependent perturbation theory 3-71645
 Ne₂ and Ne₂⁺, scattering and radiative processes in low-lying states, ab initio calc. 3-71640
 N₂(v = 0)-Cs(²P), quenching cross section of reson. excitation of Cs atom 3-49412
 O + CS₂ → SO + CS, reactive scattering in crossed beams 3-76452
 O + O₂, rate constants for charge transfer reactions, endothermic 3-63554
 O + O₂ → O + O₂ + e, electron affinities from collisional electron detachment rates in nonthermal fields 3-74808
 O₂, ionisation and fragmentation by 5-45 keV Ne⁺, Na⁺ ions, and Ne atoms 3-78898
 O₂ vibrational relaxation in an unsteady expansion wave 3-71629
 O₂ + H(H⁺), electronic excitation cross-sections 3-78895
 O₂ + O₂, vibr. scatt., pot. well effect, SSH theory validity 3-49503
 O₂ + O → O₂ + O⁻, cross section meas., 1 eV to 500 eV 3-78635
 O₂⁻ + Ar double charge transfer, translational energy spectrum of O₂⁻ ions 3-71634
 O₂⁻ + NO, charge exchange in energy range 0.04 to 2 eV 3-71644
 OCS, vibrational relaxation in inert gases 3-60490
 O(¹S) auroral green line excitation by N₂(A³Σ_g⁺) molecules energy transfer 3-41997
 P atoms in 3²DJ and 3²PJ states, kinetic study by atomic absorption spectroscopy 3-49397
 Rb(5²P_{3/2,1/2}) doublet, quenching and doublet mixing cross sections by N₂, O₂, H₂, H₂O 3-67694
 SF₆ + CO₂ total cross section meas., chemical accelerator 3-80544
 Te(⁵P₁), Te(⁵P₃), spin-orbit quenching by gases, rates, cross-sections 3-71371
 Xe₂, deexcitation rates meas. 3-71631

molecular excitation

- see also ionisation of molecules; molecular metastable states; molecular spectra; optical pumping
- acetaldehyde predissociation, photoluminescence, temp., pressure and excitation wavelength effect 3-46313
- acetone-ethylene system, intermolecular triplet transfer 3-69480
- afterglows theoretical and experimental review 3-68124
- alkali halides, impurity and intrinsic effects 3-68577
- allene, excited states, CNDO calc. using ligand geometries in transition metal complexes 3-60419
- aromatic hydrocarbons, quenching of triplet states in solution by O_2 3-61272
- aromatic hydrocarbons, quenching of triplet states in solution by O_2 3-61273
- aromatic hydrocarbons, quenching of triplet states in solution by NO and free radicals 3-61274
- aromatic molecules, effects of environment on excited states 3-60473
- atom-molecule collisions, eikonal expansion for excitation, dissociation and rearrangement 3-62570
- 7-azaindole, multiple excitation, biprotonic phototautomerism, hydrogen-bonded dimers, fluorescence 3-63548
- p-benzoquinone, ($-h_\alpha$ and $-d_\alpha$), fluoresc. obs., electronic struct. and dynamics 3-40648
- chemical reaction, selective control by laser 3-76483
- chlorophyll A, fluoresc. in polymer matrices, laser excitation 3-69074
- complex elemento-organic systems, effect of B, N on energy transfer 3-69084
- constrained variation method for excited-state energies 3-71511
- cyanine dyes, excited singlet-singlet absorption in solution 3-62739
- 1,3-cyclohexadiene, photochem. dimerisation, decay of light excited mols. 3-63549
- N,N-dialkyl-p-cyanoaniline, polar excimer fluorescence 3-54710
- diatomic, Π -state, collision induced rot. energy transfer 3-75139
- diatomic mol., resonances in electron impact 3-52400
- diatomic molecules, rotational excitation by low-energy H^+ collisions 3-71650
- dimethylcyclobutanone, laser-excited fluorescence, ultra-short-lived excited molecules 3-50841
- diphenylamine, in organic matrices at 77K role of solvent in delayed fluorescence by two photon excitation (French) 3-46314
- DNA, excited states, triplet quenching, photosensitisation 3-63588
- electron beam, variable sweep frequency, lifetimes 3-77495
- electron impact, vibr. excitation cross sections calc. methods, comparison 3-46345
- electronic, non-radiative transfer theory 3-78890
- ethane, electron impact, emission spectra 3-75122
- ethylene, electron impact, emission spectra 3-75122
- excited states of matter, symp., Lubbock, Texas, USA (Apr. 1971) 3-63547
- Feynman diagrams for perturbation theory, computer generation 3-70876
- formaldehyde, interstellar, 6 cm excitation temp. in dark dust clouds 3-70046
- formaldehyde, production and decay of excited states by photon impact 3-40665
- formaldehyde- h_2 and $-hd$, fluoresc. lifetime meas. $^1A_2 \rightarrow ^1A_1$ transition, N_2 laser 3-75057
- formaldehyde, theory of C=N bond 3-71523
- formyl radical in sensitized decomposition of formaldehyde 3-47577
- Hanle effect, irreducible tensor operators applic. (French) 3-71572
- hydrocarbons, electron impact, Balmer β radiation, cross section meas. 3-75123
- interference between one- and two-quantum processes in vibrational transitions in molecular collisions 3-71632
- interstellar methanol, E_1 - E_2 labelling of energy levels and anomalous excitation 3-81190
- ketones, aromatic, quenching of triplet state by O_2 in liq. soln. 3-76482
- light, temporal props., effect on decay curve 3-67845
- metalloporphyrins, energetics, triplet-triplet energy transfer 3-67847
- methane, electron impact, dissociative excitation, cross section meas. 3-75119
- methane, electron impact, emission spectra 3-75122
- methylene blue, photoquenching, depend. of quantum yield on pulse intensity and duration 3-67840
- naphthalene-anthracene sandwich pair, absorption and exciplex fluorescence spectra 3-47579
- naphthols and naphtholate anions, electronically excited states, calc. of pK_a from shifts of fluorescence spectra 3-54714
- α -naphthyl methacrylate and its copolymers with methyl methacrylate, excimeric and monomeric fluorescence 3-63579
- non-radiative energy transfer involving excimers (Russian) 3-63510
- O_2 π first negative system, effective cross sections and excitation functions 3-43512
- optical transitions to degenerate levels 3-60441
- optically detected electron spin locking and rotary echo trains in molecular excited states 3-43492
- photoquenching of large molecule depend. of quantum yield on pulse intensity and duration 3-67840
- phthalimide molecules, gas phase, lifetime of excited state under anti-Stokes excitation (Russian) 3-43469
- polyatomic mol. collision theory, rot. and vibr. excitation, quantum mech. treatment 3-46346
- polyatomic mol. collision theory, rot. and vibr. excitation, restricted distorted wave approx. 3-46347
- polyatomic molecules and ions, genealogy in mol. spectroscopy 3-63432
- polymethine dyes, intra-, intermolecular transforms. of electron energy 3-69479
- porphyrins, excited states, effects of metallic substitution 3-63550
- pyrene excimer, absorption spectrum by modulation excitation spectroscopy 3-46258
- pyrene single cryst., light absorpt., 4 to 300 K, ground-to-excimer, state absorpt. search 3-53150
- radiationless transitions of isolated mols., model approach 3-63505

molecular excitation continued

- resonance transfer of excitation energy, enhancement in channels 3-40675
- resonant laser pulses, N two-level molecule system, inversion, photon avalanches 3-74214
- rhodamine dyes, migration of excitation energy, lifetimes, conc. effect 3-69075
- sodium fluorescein in glycerol solution, Webers red edge effect 3-69078
- styrene, polymerisation effect, energy transfer, doping 3-69081
- tetraalkyl ammonium iodides, self-trapped exciton spectroscopy 3-69034
- toluene, thin films, fluorescence of benzyl radicals (Russian) 3-72701
- toluene in dilute solution, triplet yields 3-61065
- toluene solid solution, mechanism of singlet, triplet state formation 3-76467
- triplet states, absolute sign of electron spin dipolar and nucl. quadrupole interactions 3-57667
- vibrational excitation, string-plucking model 3-49504
- BBr, singlet-triplet transition, discharge spectroscopy (French) 3-67800
- BF, resonance fluorescence from A $^1\Pi$ states, vibronic transition probabilities 3-78838
- CH, valence excited states, potential curves 3-71512
- CH, valence excited states, props. 3-71513
- CN radical, multiconfiguration self-consistent field theory for excited states 3-46230
- CO, ($v=1$) and ($v=2$) states, vibr. excitation and relax. 3-45787
- CO, daytime emission of third positive bands, martian atmosphere 3-80990
- CO, electron impact, cross section and lifetime of metastable state 3-75118
- CO, electron impact, differential cross section determ. 3-71620
- CO, threshold excitation spectrum by electron impact 3-60483
- CO $^+$ fourth positive system, excitation by dissociative recombination of CO $^+$ ions 3-78860
- CO- H_2 mixtures sound amplification from controlled excitation reactions 3-60495
- CO $_2$, electron impact, electron scattering spectra, assignment of low lying electronic states 3-75112
- CO $_2$, electron impact, K shell energy loss spectra 3-75110
- CO $_2$, electron impact, metastable dissociation fragments, angular distrib. 3-75121
- CO $_2$, electron impact dissociative attachment, deconvolution of vibrational excitation structure 3-78878
- CO $_2$, electron impact excitation and assignment of low-lying electronic states 3-71617
- CO $_2$, excited CO $_2^+$ ion formation by vacuum u.v. radiation 3-40664
- CO $_2$, formation of excited mol. ions by photon impact cross section structures 3-78865
- CO $_2$ gas laser, electron excitation efficiency 3-43004
- CO $_2^+$, band strengths of, produced by photoionisation excitation of CO $_2$ 3-75059
- CO $_2^+$ 2890 Å band, photoionization excitation rel. to column excitation rates for planetary atmospheres 3-54732
- CO $_2^+$ excited ions, electron collisional deactivation 3-43511
- CO $^+$ (A $^1\Pi$) formation from He(2^3S) interaction with COS $^+$, H $_2$ CO $^+$, HCOOH $^+$ and (HCO) $_2^+$ 3-54736
- CO(A $^1\Pi$), deactivation rel. to individual vib. levels 3-75150
- CaF, thermal excitation using vacuum furnace, u.v. spectrum 3-54672
- CrS, thermal emission spectrum using vacuum furnace 3-54673
- Cs-inert gas atom pairs, excited mol. states 3-78470
- CSi, photodetachment cross section of I $^-$, obs. of autodetaching state 3-57607
- F $_2$, beam-foil lifetime meas. in vacuum u.v. 3-78747
- H $_2$, ($e,2e$) reaction, momentum space wave function, electron binding energy 3-67861
- H $_2$, coupled-channel calc. of rotational excitation by Li $^+$ collisions 3-71649
- H $_2$, cross sections for vibrational excitation by Li $^+$ impact 3-71648
- H $_2$, electron scatt., elastic, Born approx. 3-46341
- H $_2$, low energy, comparison of one and two centre formalisms 3-78879
- H $_2$, resonant rotational excitation by electron impact 3-78872
- H $_2$, vibr.-vibr. pumping, induced dissociation at 300 K 3-54747
- H $_2$ + Li $^+$ collisions, vibr. excitation, rot. effect 3-57675
- HBr, HCl, spectra of solid glass-like solns. with molecular anion admixture 3-64720
- H $_2O$, electron impact, dissociative excitation processes, spectroscopic investigations 3-75114
- H $_2O$, electron impact, dissociative excitation, cross section meas. 3-75119
- H $_2O$, electron impact, dissociative excitations, emission cross sections, absolute meas. 3-75120
- H $_2O$, Rydberg states, ionisation and excitation energies calc. 3-46268
- I $_2$, reson. Raman scatt., spectral var., excitation freq. depend. 3-40633
- I $_2$ molecules, excited by He-Ne laser, vibrational relaxation study, by collisions with He, Ne, Ar 3-60494
- Li + H $_2$, vibrational-rotational excitation, potential energy surface calc. 3-71639
- LiBr, LiCl, spectra of solid glass-like solns. with molecular anion admixture 3-64720
- MnS, thermal emission spectrum using vacuum furnace 3-54673
- N $_2$, by electron impact, shape resonances in A and B states 3-78876
- N $_2$, electron impact, cross section of metastable A $^3\Sigma_u^+$ vibrational level 3-75116
- N $_2$, electron impact, differential cross sections 3-75111
- N $_2$, electron impact, dissociative excitation, extreme vacuum u.v. spectra 3-75117
- N $_2$, electron impact, excitation of N $_2^+$ C state, predissoc., isotope study, $^{29}N_2$ and $^{30}N_2$ 3-75115
- N $_2$, electron impact, lifetime and excitation function of the D $^3\Sigma_u^+$ state 3-75113
- N $_2$, excited by Ne and Na ions, 0.3 to 2.0 MeV, fluoresc. efficiency 3-40644
- N $_2$, long range potential, depend. on internuclear distance 3-75126

molecular excitation continued

- N_2 , N_2^+ excited products of NH_3 decomposition in h.f. discharge, deactivation obs. (Russian) 3-63538
 N_2 , resonant excitation by low-energy electrons, cross-sections calc. 3-78875
 N_2 , vibr. excitation from $N+NO$ reaction, Raman scatt. study 3-43517
 N_2 , vibrationally excited, charge transfer collisions with Ne^+ 3-43370
 N_2 , vibrationally excited, chemi-ionisation of alkali atoms 3-78495
 N_2 electron impact excitation, contribution of the metastable $E^3\Sigma_g^+$ state to the population of the $C^3\Pi_u$ state 3-43513
 N_2+Ne^+ impact, emission cross-sections for N_2 3914 Å and 3371 Å systems 3-78894
 N_2^+ first negative 3914 Å band charge-transfer excitation by protons, photon-particle coincidence meas. 3-63560
 $N_2(B^3\Pi_g)$ population by $N_2(A^3\Sigma_u^+)$ during afterglow 3-71625
 $N_2(C^3\Pi_u; v'=0, 1)$, de-excitation in O_2+N_2 mixtures 3-49483
 NH_3 , electron impact, dissociative excitation, cross section meas. 3-75119
 NO , electron impact, dissociative excitation processes, spectroscopic investigations 3-75114
 NO , electron impact, radiation spectrum 2000 to 9000 Å 3-75128
 NO , monochromatically excited, energy transfer, vibrational relaxation, fluorescence 3-71623
 $NO+O_3 \rightarrow NO_2+O_2$, $O_2(^1\Delta_g)$ and $O_2(^1\Sigma_g^+)$ possible production 3-47572
 NO_2 , electronically excited, microwave optical double resonance 3-43479
 N_2O , dissociative excitation and ionisation excitation with synchrotron radiation 3-43504
 N_2O , electron impact, K shell energy loss spectra 3-75110
 N_2O , formation of excited mol. ions by photon impact, cross section structures 3-78865
 N_2O^+ excited ions, electron collisional deactivation 3-43511
 N_2 , fluorescence and zero-field level crossing spectroscopy of $C^2\Sigma^+$ state 3-78837
 NaK , laser excitation, obs. of molecular and atomic fluorescence spectra 3-40650
 Ne_2 and Ne_2^+ , scattering and radiative processes in low-lying states, ab initio calc. 3-71640
 Ne , vibrational excitation in low-energy electron impact, role of negative ionic states 3-78874
 O_2 , beam-foil lifetime meas. in vacuum u.v. 3-78747
 O_2 , cryst., absorpt. spectra, interaction effect 3-69022
 O_2 , electron impact, dissociative excitation, extreme vacuum u.v. spectra 3-75117
 O_2 , gas discharge plasma, electron impact excitation and dissociation, effective cross section determ. 3-74871
 O_2 , resonant vibr. excitation by slow electron impact 3-71616
 O_2 , vibrational excitation, 4-15 eV 3-75106
 O_2 , vibrational excitation in low-energy electron impact, role of negative ionic states 3-78874
 O_2 in upper atmosphere, production and decay of excited state in 50-100 km layer 3-69601
 $O_2+H(H^+)$ impact, electronic excitation cross-sections 3-78895
 O_2^+ dissociative recombination rel. to $O(^1S)$ excitation in pulsating aurora 3-80785
 O_3 , vibr. excitation using $O+O_2+O_2 \rightarrow O_3+O_2$ recomb. reaction 3-76477
 OH , excited, vibration-rotation bands, i.r. airglow, correl. of fluctuations 3-80789
 OH radical, microwave and magnetic resonance spectra of vibrationally excited states, Λ -doubling 3-78853
 $O_2(a^1\Delta_g)$, collisional quenching studied by time-resolved absorption spectroscopy in vac. u.v. 3-46269
 PN , resonance fluorescence from $A^1\Pi$ states, vibronic transition probabilities 3-78838
 S_2 , selectively excited, Hanle effect lifetime meas. 3-75062

molecular force constants

- 1,3,5,7-tetramethylsiladamtane (German) 3-43453
acetylene, two-centre calc. with Slater-type orbitals (Russian) 3-49444
alkali halide, rhombic dimer molecules 3-49428
alkali halide diatomic mol., pot. energy function 3-67769
alkali metal ozonides, $M^+O_3^-$ types, Ar matrix, reson. Raman spectrum 3-78808
alkali metal ozonides, matrix isolated, resonance Raman spectrum, vibrational analysis 3-71553
alkylsilanes, force consts. determ. 3-67776
amidoximes, valence vibr. bands of NH_2 , ND_2 and NHD groups, NH bonds inequivalence (French) 3-52365
amine- SO_2 complexes, force consts. for charact. vibrs., i.r. and Raman spectra 3-60461
benzene, vibrational spectrum theory 3-74987
bridged metal-metal bonded species, spectra 3-78796
5-bromotetrazole, single cryst., Raman active external phonon assignments, harmonic force const. calcs. 3-50573
centrifugal stretching constants, inequalities rigorous derivation 3-63414
2-chlorobutane, torsion force consts. and low-frequency bending assignments from i.r. and Raman spectra 3-71559
2-chloropropane, torsion force consts. and low-frequency bending assignments from i.r. and Raman spectra 3-71559
chloryl fluorides, Urey-Bradley force fields 3-67782
covalent crystals, valence force constants, least squares refinement 3-64122
cyclobutadiene (and deuterated), ground state potential energy surfaces, relevance to i.r. data 3-78662
cyclobutane, C-H bond length and stretching force const. CNDO/2 calc. 3-74925
cyclopropane, C-H bond length and stretching force const. CNDO/2 calc. 3-74925
determination from isotopic frequencies using parameter technique 3-43425
diatomic hydrides, rel. to deuteron quadrupole coupling consts. 3-78703
dichloropentane, torsion force consts., low frequency bending assignments from i.r. and Raman spectra 3-71559

molecular force constants continued

- empirical valence-force potentials, strain energies eval., use of constraints 3-60428
ethane, mol. force fields and isotopic rules determ. 3-54653
ethane, two-centre calc. with Slater-type orbitals (Russian) 3-49444
ethyl bromide and deuterated derivatives, normal coord. analysis of force fields 3-63407
ethyl fluoride, normal coordinate calcs. 3-75037
ethylene, harmonic force consts. determ. 3-60432
ethylene, two-centre calc. with Slater-type orbitals (Russian) 3-49444
extended Jacobian, determinant calc. 3-74978
geometries and force consts. calc. from CNDO wavefunctions by the force method 3-43396
Gillespie-Nyholm theory applied to force fields 3-63398
glyoxal and deuterated derivatives, vibrational constants 3-54662
Green's function approach and parametric study 3-60437
harmonic force consts. determ. using linear method of successive approx. 3-60432
hexafluoropropanol-2, vibr. freq., force field, mean amplitudes 3-63412
hydrocarbons with delocalized electronic systems, molecular mechanics method for bond order determ. 3-67729
kinematical evaluation 3-74969
mean-square amplitude matrix relations, theory temp. depend. 3-63411
metal-hexahalo species of group IV-VI, force constants and mean amplitudes of vibration calc. 3-60436
methane, from three term pot. energy function 3-72170
methanes, halogen-substituted, second virial coeffs. and force consts., recalculation 3-40600
methylene fluoride and methylene fluoride- d_2 , i.r. spectra assignment 3-78761
moniodomethyl radical, matrix i.r. spectra, bonding, force consts. 3-46276
one-electron properties calc. using coupled Hartree-Fock methods 3-67759
perhalyl fluorides, Urey-Bradley force field, calc. using i.r., Raman data 3-78713
planar XY_3 molecules, orbital valency force field, calc. in Cartesian co-ords. 3-63397
polyatomic molecular vibration, algorithm for formation of kinematic and force matrices (Russian) 3-78714
polyatomic mol., generalized valence force field determ. method (French) 3-54652
propene, quadratic force consts. estimation 3-74918
n-propyl fluoride, normal coordinate calcs. 3-75037
propynal, CNDO/2 calcs. 3-67755
spherical top mol., Raman band contour analyses and Coriolis consts. 3-67816
tetrachloroethylene, vibrational force fields, specific imposition of pots. parameters on nonbonded distances 3-71527
tetracyanomethane, i.r. spectra, vibrational assignment, normal coordinate analysis and thermodynamic functions 3-54684
thiourea and deuterium derivatives, vibr. spectrum calcs. 3-63415
transition metal anions, octahedral, quadratic pot. function 3-67771
trichloro-1,1,1 propanes, normal coord. calcs. and force consts. (French) 3-46250
trifluoromethyltrifluoroborate anion, Urey-Bradley force constant, vibration spectrum, i.r. and Raman spectra 3-57648
3,3,3-trifluoropropene, quadratic force consts. estimation 3-74918
urea and deuterium derivatives, vibr. spectrum calcs. 3-63415
 $ZrY_3(C_3)$, $ZrY_2(C_2)$, $ZrY(C)$ type molecules, high and low freq. separation method 3-74982
Ar, from three term pot. energy function 3-72170
 $As(CN)_3$ harmonic force fields, vibrational analysis 3-74977
 B_2F_4 , gaseous and cryst., Raman spectra, 25 to 1500 cm^{-1} , normal vibr. assignments and force consts. calc. 3-47250
 BH_3 , harmonic force consts. calc. ab initio including electron correlation 3-54657
 BH_3-NH_3 , BD_3-ND_3 , and BH_3-ND_3 , matrix isolated, i.r. spectra, force consts. calc. 3-40628
 BO_2 , excited state force consts. calc. from bond charge model 3-52334
 BO_2^- , in KCl and KBr, anharmonic force field calc. 3-43421
 BeH_2 , ground state nonorthogonal configuration interaction, force consts. calc. 3-40591
BrCN, vibrational anharmonicity, calc. using Anderson potential function 3-57644
 BrO_4^- Raman intensities and force constants 3-67822
 C_3 , excited state force consts. calc. from bond charge model 3-52334
 CN_2 , excited state force consts. calc. from bond charge model 3-52334
 CO_2^+ , excited state force consts. calc. from bond charge model 3-52334
ClCN, vibrational anharmonicity, calc. using Anderson potential function 3-57644
 ClO_2 , excited state force consts. calc. from bond charge model 3-52334
 ClO_4^- Raman intensities and force constants 3-67822
 $Co(CO)_3NO$, potential consts. from vibrational spectra of six isotopic species 3-43442
FCN, vibrational anharmonicity, calc. using Anderson potential 3-57644
 $FN^{14}O_2$ and $FN^{15}O_2$ molecules 3-52337
 $FeCl_4^-Br^-$, vibrational analysis 3-54655
 GaX_4^- , $X=Br, I$, orbital valence force field consts. and Coriolis coupling consts. calc. 3-49449
 Ge_2H_6 , Ge_2D_6 , mol. force fields and isotopic rules determ. 3-54653
 $H_2+Cl \rightarrow H+HCl$, force field and tunnelling effects, kinetic-isotope effects 3-50833
HCN AND DCN, anharmonic force field and equil. struct. 3-60430
HCP and DCP, anharmonic force field and equil. struct. 3-60430
HNSi, DNSi, HNGe and DNGe, valence form field calcs. 3-67767
 H_2O , excited state force consts. calc. from bond charge model 3-52334
 H_2O_2 , two-centre calc. with Slater-type orbitals (Russian) 3-49444

molecular force constants continued

- HSiF₃, excited vibr. states, microwave spectra, force field models 3-63487
- HfBr₄(Cl₄)(I₄), orbital valence force field consts. 3-67768
- HgBr₂, excited state force consts. calc. from bond charge model 3-52334
- HgCl₂, excited state force consts. calc. from bond charge model 3-52334
- I₂ reanalysis of spectroscopic data 3-63421
- ICN, vibrational anharmonicity, calc. using Anderson potential function 3-57644
- InBr₄⁻, orbital valence force field consts. and Coriolis coupling consts. calc. 3-49449
- Kr, from three term pot. energy function 3-72170
- Mg (II) complex, MgX₂nMe₂O, i.r. spectra, stretching consts. (French) 3-67824
- MgX₂²⁻, X=Cl, Br, I, intramolecular force fields 3-52333
- N₂H₄, two-centre calc. with Slater-type orbitals (Russian) 3-49444
- NbX₅ (X=Cl, F, Br) normal coordinate analysis and thermodynamic functions 3-54654
- O₃, general quartic force field calc. 3-46251
- O₂ potential function, second order anharmonic, force constants from zero order wave numbers (French) 3-43422
- PCN₃ harmonic force fields, vibrational analysis 3-74977
- PH₃, force constants and frequencies calc. 3-71528
- PO₄³⁻ Raman intensities and force constants 3-67822
- PbBr₄(Cl₄)(F₄)(I₄), orbital valence force field consts. 3-67768
- PbF₂, matrix isolated, i.r. spectra, valence force consts. 3-40630
- SO₂²⁻ Raman intensities and force constants 3-67822
- SOF₂, molecular force field 3-57639
- SO₂F₂, molecular force field 3-57639
- SeO₄²⁻ Raman intensities and force constants 3-67822
- Si₂H₆, Si₂D₆, mol. force fields and isotopic rules determ. 3-54653
- SnF₂, matrix isolated, i.r. spectra, valence force consts. 3-40630
- TaX₅ (X=Cl, F, Br) normal coordinate analysis and thermodynamic functions 3-54654
- TiBr₄(Cl₄)(F₄)(I₄), orbital valence force field consts. 3-67768
- TiX₄⁻, X=Cl, I, orbital valence force field consts. and Coriolis coupling consts. calc. 3-49449
- (UO₂Br₄)²⁻, progressive rigidity calc. 3-74985
- (UO₂Cl₄)²⁻, progressive rigidity calc. 3-74985
- (UO₂F₂)³⁻, progressive rigidity calc. 3-74985
- ZrBr₄(Cl₄)(F₄)(I₄), orbital valence force field consts. 3-67768

molecular force fields see **molecular force constants****molecular internal mechanics**

- see also **molecular electronic structure**
- acetaldehyde, internal rotation barriers rel. to localized charge distributions 3-54633
- alcohol vapour phase, infrared studies, self association 3-78770
- aldehydes, static and dynamical pot. surface distortions in ³A'(nπ*) states 3-63382
- alkali halide diatomic mols., pot. energy function 3-67769
- alkanes, halogenated, opt. mol. anisotropy in different media (French) 3-63424
- anthracene vapour, fluoresc. spectra, relax., Neporent diagrams 3-67846
- benzotrifluorides Fourier transform n.m.r., high pressure, ¹⁹F chemical shift 3-61003
- centrifugal distortion, asymmetric top mols., reduced Hamiltonian convergence 3-63425
- charge transfer and intermolecular interaction under optical excitation 3-71535
- complex, stability constants and dipole moments, determ. from permittivity meas. 3-65118
- convergent series expansions solutions, computer programming for algebraic (literal) operations 3-78709
- diacetyl, pure liq., active intramolecular motion in dielectric relax., spectral obs. 3-64602
- diatomic mol., kinetic and potential energy expectation values from vibrational energy levels 3-40598
- diatomic molecule, virial theorems, adiabatic representation 3-78670
- diatomic mols., RKR pots. and semiclassical centrifugal consts. 3-67779
- 1,2-difluoroimide, cis- and trans-, vibr. coupling effects an pot. functions 3-78702
- 1,2-difluoroethylene, cis- and trans-, vibr. coupling effects and pot. functions 3-78702
- α, ω diols, intramolecular hydrogen bonding, i.r. study 3-46293
- elastomer, chain rigidity from i.r. spectra (Russian) 3-71670
- formaldehyde, potential energy contribs. to energy function, geometry 3-71490
- formic acid, pot. energy surface curvature effect on kinetic isotope effects 3-76426
- formyl radical, potential energy, contribs. to energy function, geometry 3-71490
- heteronuclear diatomic mols. closed form perturbation theory of, multiphoton transitions 3-71517
- heteropolar diatomic, multiphoton processes, Born-Oppenheimer approx. 3-67760
- hexamethylbenzene, mode site splitting, Raman, far i.r. spectra 3-64134
- homopolar diatomic multiphoton processes, Born-Oppenheimer approx. 3-71516
- intramolecular vibrational energy transfer 3-43470
- 2',3'-isopropylideneadenosine, mol. interaction in soln., deuterium substitution effect on proton relax. times 3-75899
- Jahn-Teller effect, electron-vibr. interaction 3-67765
- linear XYZ molecules, anharmonic potential constants 3-63404
- methanol, hyperfine struct. in internal rotor molecules 3-78817
- methyl alcohol, internal rotation barriers rel. to localized charge distributions 3-54633
- methylamine, internal rotation barriers rel. to localized charge distributions 3-54633
- 3-methylpyridazine, n.m.r. and u.v. spectral changes due to intramol. transform. 3-75088
- molecular crystal, exciton spectra, Fermi-Davydov reson. 3-68998
- organic complex molecule, intramolecular relax. spectroscopic investigation 3-71536

molecular internal mechanics continued

- paraffins, ¹³C n.m.r., mag. shielding consts. calc. by Gaussian function 3-71593
- pentafluorophenol:n-Cl-aniline compound, Raman spectra, changes on polymorphic transition 3-72198
- perhalyl fluorides, Urey-Bradley force field, consts., pot. energy calcs. 3-78713
- poly-o-bromostyrene in benzene soln., high-resolution small-angle X-ray and light scatt. for mol. wt. determ. 3-67868
- polyatomic mols., potential energy function, unitary transformation operator for perturbation treatment of the Hamiltonian 3-40601
- polyatomic mols., transform. props. of centrifugal distortion consts. 3-63406
- propene, internal rotation barriers rel. to localized charge distributions 3-54633
- quasimolecular terms at small distances, calc. using virial theorem 3-74906
- rotation, threefold barrier, equivalence of V₆ to torsional flexing 3-74972
- strain energies eval., empirical valence-force pots., use of constraints 3-60428
- 1, 2, 4, 5-tetramethyl benzene, atom-atom pots., H atom coords. 3-72073
- triatomic molecule, linear, computer appl. to calc. of pot. energy function 3-78710
- triethylenediamine, UV absorpt. spectrum anal. of struct. 3-78740
- trifluoramine oxide, vibr. assignment and Urey-Bradley force field 3-40599
- triisopropyl phosphate and amine complex stability constant and dipole moment determ. from permittivity meas. 3-65118
- vinyllogous amides, hindered rotation, N-C bond, chemical shift, coupling constants 3-57668
- water, proton spin-lattice relaxation time meas., intramolecular and intermolecular relaxation processes 3-71577
- B₂H₆, Green's function anal. of vibr., coupling consts. 3-78697
- Ba(ClO₃)₂·H₂O(D₂O) i.r., Raman spectra, Davydov components, intramolecular modes 3-75973
- CO₂, pot. energy function, calc. and extrapolated results for ν₃ progression 3-78711
- CaF, potential energy curves and r-centroids 3-49448
- F₂, F₂⁺, F₂⁻, F₂²⁺, pot. energy curves and spectroscopic consts. 3-71496
- H₃, energy surfaces including valence bond config. interaction, extended diatomics study 3-54634
- HCl⁺, four isotopic combinations, RKR pots. calc. 3-78739
- HeH²⁺, ab initio calc. of potential energy curves in complex plane 3-74990
- LaO, astral radical, excited states, calc. of true potential energy curves, Rydberg-Klein-Rees method 3-78704
- Li₂ + F → Li + LiF, pot. energy, surface, ab initio electronic struct. calcs. 3-47549
- MgX₂²⁻, X=Cl, Br, I, intramolecular force fields 3-52333
- N₂⁺, config. interaction calcs. of low-lying quartet states 3-60413
- NF and NF⁻, pot. energy curves and spectroscopic consts. 3-71496
- NH₃, ND₃ and NT₃, Schrodinger eqn. analytical soln. for double minimum Morse pot., intramol. inversion 3-52332
- NbX₅ (X=Cl, F, Br) normal coordinate analysis and thermodynamic functions 3-54654
- TaX₅ (X=Cl, F, Br) normal coordinate analysis and thermodynamic functions 3-54654
- (XeH)⁺, pot. energy curves, LCAO-MO-SCF calcs. 3-74943

molecular libration

- alkali halides, librational and tunnelling levels of OH⁻ impurity 3-79453
- ethylene crystal, librational frequencies calc., Raman spectra 3-72608
- liquid, mol. dynamics obs. from i.r. absorpt. band profiles (French) 3-80018
- liquid, mol. motion, conf., Orsay, France, Jul. (1973) 3-64192
- trichloromethyl derivatives of P, CCl₃PCl₄ and (CCl₃)₂PCl₃, n.q.r. spectroscopy and mol. dynamics 3-75912
- D₂, solid, ordered phase, fund. Raman band, Q branch 3-80016
- DCl, solid, neutron diff. obs. 3-68380
- H₂, solid, ordered phase, fund. Raman band, Q branch 3-80016
- KCN, Raman and i.r. spectra, phase transition phenomena (French) 3-58509
- N₂, solid, β-α ordering transition, n.q.r. obs. 3-75590
- NH₄⁺ in ammonium salts, tunnelling study by proton magnetic resonance, reorientation and librations 3-44332

molecular mass see **molecular weight****molecular metastable states**

- beam-foil forbidden lines transition probabilities rel. to astronomical spectra 3-78430
- lifetimes, molecular beams, time-of-flight measurement technique 3-75151
- CO, electron impact excitation, cross section and lifetime of metastable state 3-75118
- CS₂⁺ metastable transitions leading to S⁺ + CS and CS⁺ + S under electron impact on CS₂ 3-78858
- H₂, produced in resonant electron scattering 3-78873
- He-H₂ mixtures, decaying plasmas, collision processes 3-63881
- Hg₂, fluoresc. fine struct. emission spectrum, (A³Σ_g⁺ → X¹Σ_g⁺) and (A³Π_g → X¹Σ_g⁺) transitions 3-54713
- N₂, electron impact excitation, cross section of metastable A³Σ_u⁺ vibrational level 3-75116
- N₂, r.f. spectra of metastable (A³Σ_u⁺) state, fine struct., mag. hyperfine struct., electric quadrupole consts. in 13 vibrational levels 3-40635
- N₂, secondary electron emission by metastable particle impact in ioniz. growth expts. 3-68116
- N₂, secondary electron emission by metastable particle impact in ioniz. growth expts. 3-68117
- N₂ electron impact excitation, contribution of the metastable E³Σ_g⁺ state to the population of the C³Π_u state 3-43513
- N₂(B³Π_g) population by N₂(A³Σ_u⁺) during afterglow 3-71625
- O₂ glow discharge, metastable level deactivation processes 3-52546
- SO₂, metastable transitions in SO₂⁻ spectra 3-78877

molecular moments

- alkali halides, diatomics, perturbation theory, ionic modes, dipole moment and interaction energy calc. 3-40682
- amino acetonitrile, microwave spectra, bond angles, dipole moment 3-63485
- anthronitrile, absorption and fluorescence spectra, solvent and pressure dependence, dipole moments determ. 3-41531
- aryldifluoromethyl ethers, dipole moments in benzene, calc. of moment μ_s from μ_n 3-71522
- aryldifluoromethylsulphides, dipole moments in benzene, calc. of moment μ_s from μ_n 3-71522
- aryldifluoromethylsulphones, dipole moments in benzene, calc. of moment μ_s from μ_n 3-71522
- aryldifluoromethylsulphoxides, dipole moments in benzene, calc. of moment μ_s from μ_n 3-71522
- azomethanes, nonradiative transitions and properties of lower triplet state, SCF-MO and CI calc. 3-63504
- azulene, benzophenone (naphthalene), impurity change of polarisability and dipole moment, $\pi\pi^*$ state 3-72662
- bicyclo(3.1.0).hexane analog, far i.r. spectra, dipole, mol. config. 3-63456
- chloroform intermol. complexes, spectroscopic and dielec. investig., comparison 3-74931
- β -chlorovinylketones, dipole moments, Pariser-Parr-Pople calc. 3-67733
- complex, stability constants and dipole moments, determ. from permittivity meas. 3-65118
- condensed matter, generalized Debye-Falkenhagen energy 3-79978
- cyanocyclobutane, μ -wave spectrum, dipole moment quadrupole coupling consts. and conformation study 3-40634
- cyanocyclobutane, dipole moment components, microwave spectra 3-63484
- cyclic molecules, quadrupole moments and diamag. susceptibilities calc. 3-63377
- cyclopent-3-enone, microwave spectra, ring polarity, r_s -structure and dipole moment 3-60466
- cyclopentadienone, microwave spectra, dipole moment, life time 3-78813
- cyclopropenone, elec. dipole and quadrupole moments, Stark and Zeeman effect obs. 3-63482
- dialkylaminophosphines, determination of electronic character of P-N bond from dipole moments (French) 3-49439
- diaryl disulphides, conformational props. calc. from dipole moments 3-43395
- diatomic, charge, 'hybrid parts, wavefunction calcs., polarisation 3-71500
- diatomic molecules, ions, MX^+ , dipole moments calcs. 3-78725
- diatomic mol., intensity theory, electronic transition moment variation 3-43436
- dimethyl cyanamide, dipole moment, microwave spectra 3-60464
- 1,2-dimethylindole, dipole moment changes determ. from Stokes shift temp. depend. 3-67839
- dimethylmercury solution dipole moment, temp. depend. 8.5-50°C 3-79976
- m-dinitrobenzenes, various substituents 3-74928
- 3,6-dioxabicyclo[3.1.0].hexane, microwave spectrum, dipole moment, conformation 3-63486
- dipole moments, classical and quantum mechanical representation equivalence 3-40597
- dipole moments determ. by Stark spectroscopy, environmental effects 3-63433
- dipole-dipole interaction in liquid, electronic spectra, luminescence 3-75970
- electric dipole moments from meas. in soln., ALGOL program 3-73180
- end-to-end vector of chain mol., persistence and distrib. 3-67731
- esters, elec. dipole moment at 1 MHz for mol. config. determ. 3-52350
- fluoroacetophenones, elec. dipole moments and conformations, o-, m- and p- 3-67724
- p-fluoroaniline, dipole moments determ., orientational Stark splitting obs. 3-63433
- fluorobenzenes, homosubstituted, all valence electron MO calcs. 3-67738
- glycolaldehydes, microwave spectra, substitution struct., intramolecular hydrogen bond and dipole moment 3-54703
- halobenzenes, π -orbitals, inductive and mesomeric effects 3-78690
- hydrocarbons, second moment of electronic charge distrib., additivity eqn. 3-74960
- indole, dipole moment changes determ. from Stokes shift temp. depend. 3-67839
- Jahn-Teller effect, electron-phonon interactions, F-centres 3-69039
- linear molecules, band moments and rot. autocorrel. functions for perpendicular transitions 3-63434
- linear molecules, microwave spectra of l-doubling, centrifugal distortion effects, dipole moments 3-52374
- liquid crystalline cholesteryl esters, odd even effect 3-63949
- maximum overlap criterion approach 3-78651
- methane, transition dipole moments for vibr.-rot. bands 3-67820
- methane selenol, μ -wave spectrum, internal rot. barrier, struct. and dipole moment meas. 3-54700
- methyl formate, methyl fluoroformate, INDO calcs. of dipole moment and conformation 3-63369
- methylaminoethane, rot.-inversion spectrum analysis 3-63491
- methylchloride, and isoelectronic series, SCF-MO calcs. 3-60409
- 3-methylene oxetane, μ -wave spectrum, mol. Zeeman effect, mag. susceptibility anisotropy, quadrupole moments meas. 3-52372
- methylenimine, microwave spectra, molecular constants 3-75051
- monohalide and monohydride molecules, rotational and hyperfine structure constants tables 3-49446
- multipole moments, net, of Thomas-Fermi-Dirac and Thomas-Fermi electron densities 3-60415
- 2-nitropropane, dipole moment determ. from dispersion of dielec. const. 3-55997
- non-polar liquids, dielec. absorpt. in microwave and far infrared region 3-80120
- non-polar liquids, far i.r. absorpt. 3-80056
- nuclei in mol., elec. dipole shielding tensors 3-43434
- organic EDA complexes in polar solvents excited state dipole moment from solvent shift 3-71537

molecular moments continued

- organic phosphates, dipole moments determ. 3-54637
- ovalbumin dipole moment, structure characteristics detn. by dielectric relaxation method (Rumanian) 3-43526
- 3-oxetanone, μ -wave spectrum, mol. Zeeman effect, mag. susceptibility anisotropy, quadrupole moments meas. 3-52372
- phenol complexes with pyridines, dipole moments and struct. 3-63358
- 3-phenylsulfonidone, solvent effect on spectrum, dipole moment determ. from first excited singlet state 3-47284
- point charge model approach 3-54631
- polycyano-compounds, solvent effect on u.v. spectra, dipole moments in excited singlet states (French) 3-63440
- polyphenylsiloxanes, dipole, mol. wt. depend. 3-64627
- propionic acid microwave meas. 3-63389
- propylene, dipole moment determ. 3-67750
- propynal, CNDO/2 calcs. 3-67755
- propynal, CNDO/2 calc., energy, electron distrib. dipole moment origin 3-63389
- pyrazine, ab initio MO wave functions 3-63372
- pyridine, ab initio MO wave functions 3-63372
- pyrone, quadrupole moments 3-63481
- ribonucleic acid dipole moment, structure characteristics detn. by dielectric relaxation method (Rumanian) 3-43526
- silyl pseudohalides, role of d functions in Si-N bond by stereochemistry, dipole moments and photoelectron spectra 3-43419
- Stark spectroscopy, molecular dipole moment determ., environmental effects 3-72600
- symmetric top rotor permanent electric dipole moment determ. from Stark effect 3-40155
- tellurophene, dipole, Stark shift meas. 3-67826
- ternary homonuclear systems, dipole moment 3-78664
- tetrabromomethane, far i.r. spectra and octopole moments 3-49466
- tetrafluoromethane, far i.r. spectra and octopole moments 3-49466
- 2-thiophenolaldehyde, gas, identification of O-S trans rotamer 3-63365
- 1,2,3-tribromopropane, dipole meas. in CCl_4 , C_6H_6 soln. 3-63465
- 1,2,3-trichloropropane, dipole meas. in CCl_4 , C_6H_6 soln. 3-63465
- trifluoroethylene, dipole, from microwave spectrum 3-43461
- trifluoromethylacetophenones, elec. dipole moments and conformations, o-, m- and p- 3-67724
- triisopropyl phosphate and amine complex stability constant and dipole moment determ. from permittivity meas. 3-65118
- trimethylamine-borane, dipole moment, microwave spectra 3-60465
- 2,8,9-trioxadadamantane, dipole moment 3-40636
- vinyl-fluoride, dipole moment determ. 3-67750
- o-xylene, microwave spectra, methyl rot. barrier, methyl conform. and dipole moment 3-67832
- o-xylyl, direction of transition moment, rotational constants 3-67794
- AlO, electric dipole transitions, band oscillator strengths 3-43433
- ArHCl complex, dipole moment axial component determ. by mol. beam electric resonance spectroscopy 3-78824
- BF₃, electronic struct. orbital energy, charge distrib., SCF calcs. 3-52320
- BeF₂, electronic struct. orbital energy, charge distrib., SCF calcs. 3-52320
- CF₂, electronic struct. orbital energy, charge distrib., SCF calcs. 3-52320
- CF₂, microwave spectra, centrifugal distortion anal. force field and dipole moment 3-78820
- CH, valence excited states, props. 3-71513
- CN, electric dipole moment of A²II state meas. by level anticrossing spectroscopy, Stark effect 3-75001
- C₂N₂, quadrupole moment, from far i.r. collision induced absorption in compressed gas 3-60458
- CO⁺, dipole moment, SCF calcs. 3-49437
- COS, dipole moment function determ. 3-78768
- ClF, dipole approx. effect on calc., Roothaan's nonempirical SCF MO LCAO method 3-78673
- ClF₃, dipole, approx. effect on calc., Roothaan's nonempirical SCF MO LCAO method 3-78673
- DCl, i.r. spectra, dipole moment function, vibration-rotation matrix elements determ. 3-52351
- DCl⁺, transition moment variation in A² Σ \rightarrow X²II transition rel. to HCl⁺ and HBr⁺ 3-78744
- D₂O dipole moment determ. from Stark meas. 3-75000
- F₂CS, microwave spectrum, structure and dipole moment 3-67827
- FCI, and isoelectronic series, SCF-MO calcs. 3-60409
- GeO, rotational mag. moment meas. by molecular beam electric resonance spectra 3-78727
- GeO magnetic susceptibility anisotropy, mol. g_r-factor, quadrupole moments (German) 3-71539
- H₂, energy and props. calc. using method of moments 3-43417
- H₂ isotopes, electric field gradient and magnetic spin-spin interactions 3-43438
- HBr⁺, transition moment variation in A² Σ \rightarrow X²II transition rel. to HCl⁺ and DCl⁺ 3-78744
- HCL⁺, transition moment variation in A² Σ \rightarrow X²II transition rel. to DCl⁺ and HBr⁺ 3-78744
- HCN, mag. susceptibility anisotropy, g-factor and mol. quadrupole moment 3-43435
- HCl, i.r. spectra, dipole moment function, vibration-rotation matrix elements determ. 3-52351
- HD, dipole moment, homopolar isotropically unsymmetric diatomic molecules, forbidden transitions 3-78708
- H₂D⁺, radio spectrum and dipole moment rel. to interstellar clouds 3-70031
- HDO dipole moment determ. from Stark meas. 3-75000
- HF, vibration to rotation energy transfer, dipole-dipole and hydrogen bond interactions 3-63557
- HNO and DNO, microwave spectra analysis 3-63488
- H₂O, rot. and centrifugal consts. calcs., appl. of energy moments method (Russian) 3-78701
- H₂O, rot. mag. moments calc. 3-60443
- H₂O dipole moment determ. from Stark meas. 3-75000
- H₂O₂⁺ system, coupling of proton motion with H bond stretching vibration, effect on dipole moment, polarisability, double min. potential surface 3-49457
- HOCl, and isoelectronic series, SCF-MO calcs. 3-60409

molecular moments continued

- H₃PBH₃, microwave spectra, dipole moment, internal rotation barrier, staggered conformation, Stark splitting 3-54699
 HgCl₂ solution, dipole moment, temp. depend. 8.5-50°C 3-79976
 LiH, dipole moment, MO calcs. 3-74935
 LiO, electric dipole transitions, band oscillator strengths 3-43433
 N₂ ground state, quadrupole moment and electric field gradient calcs. with generalised valence bond 3-78694
 NCN₃, microwave spectra, anal. four nuclear quadrupole problem 3-78819
 NF₂ electronic struct. orbital energy, charge distrib., SCF calcs. 3-52320
 NH₃, rot. mag. moments calc. 3-60443
 NH₂Cl, and isoelectronic series, SCF-MO calcs. 3-60409
 N₂O, far-i.r. absorpt. and quadrupole moment determ. 3-74999
 O₂, quadrupole moment determ. from collision broadened rot. line-widths of acetaldehyde 3-67834
 OD, A²Σ⁺ state, dipole moment and hyperfine consts. by SCF and configuration interaction calc. 3-40606
 OF₂, electronic struct. orbital energy, charge distrib., SCF calcs. 3-52320
 PbO magnetic susceptibility anisotropy, mol. g_J-factor, quadrupole moments (*German*) 3-71538
 PbO magnetic susceptibility anisotropy, mol. g_J-factor, quadrupole moments (*German*) 3-71539
 SF radical, microwave spectra, dipole moment calc. from Stark effect 3-40637
 SiO, rotational mag. moment meas. by molecular beam electric resonance spectra 3-78727
 SnO magnetic susceptibility anisotropy, mol. g_J-factor, quadrupole moments (*German*) 3-71538

molecular nuclear coupling

- acetylated glycopyranosyl chlorides, ³⁵Cl pure n.q.r., coupling const. and mol. conformation relation 3-49491
 acetylene, second-order props. calc. with virtual orbitals 3-54617
 aminophosphines, ¹⁵N-¹H coupling consts., bonding 3-71575
 benzenes, fluorinated, in liq. cryst. solvents, H-F and F-F nucl. mag. spin-spin coupling anisotropies 3-40655
 benzenes with side-chain interacting groups, substituent effects on proton spin-spin coupling 3-60478
 benzenium cation, CNDO/SP calc. of spin-spin coupling consts. 3-74936
 1-bromo-3,3,4-trifluorobutene-4, n.m.r. study, determ. of ¹⁹F, ¹³C, ¹H chemical shifts and coupling consts. 3-75072
 2-bromopyridine, n.m.r. of ¹³C, long-range ¹³C-¹H spin coupling consts. 3-43483
 butadiene-1,3, p.m.r., spin-spin coupling consts. 3-43484
 carbones and organotin derivatives, spin-spin coupling constants, J_{11b-1a}, J_{119m-CH3}, ¹H-¹¹⁹Sn n.m.r. method 3-78848
 chlorocyclohexane, equatorial, microwave rot. spectra anal. 3-78811
 4-chloronortricyclene, ³⁵Cl nuclear quadrupole coupling constant, microwave spectra 3-71567
 coumarin and methyl derivatives, σ and π electron contributions to long-range spin-spin coupling consts. 3-52387
 deuterium quadrupole coupling consts. calc. using core model approach 3-74937
 diatomic hydrides, deuterium quadrupole coupling consts., force consts. 3-78703
 diatomic spectra reduction to molecular constants, construction of RKR potentials 3-78706
 N,N'-dideuteroparachloroaniline, mag. dipole interact. in ND₂ group, ¹⁴N n.q.r. Zeeman effects 3-75910
 m-difluorobenzene, n.m.r. in nematic solvents, geom. and indirect F-F coupling anisotropy 3-60477
 1,1,1-difluoroethene, vibr. corrections of dipolar couplings 3-78700
 E⊗e system, singlet to doublet transition, lineshape calculation 3-43465
 ethane, second-order props. calc. with virtual orbitals 3-54617
 ethenes, fluorinated, in liq. cryst. solvents, H-F and F-F nucl. mag. spin-spin coupling anisotropies 3-40655
 ethyl compounds, uncoupled pulsed Fourier transform ¹³C n.m.r. obs. 3-75085
 ethylene, second-order props. calc. with virtual orbitals 3-54617
 fluoroacetones, n.m.r., H-F coupling, rot. isomerism 3-78843
 fluoroacetones, n.m.r. coupling consts. and rot. isomerism 3-46323
 fluorophosphate anions containing P-P bond, P-P coupling 3-54721
 free radicals, anisotropic hyperfine coupling constants 3-78844
 hydrocarbons, interpretation of C-H coupling consts. for directly bonded nuclei 3-75073
 trans-hydroxy-L-proline, proton NMR spectra, computer simulation, long range coupling constant, structural implications 3-75074
 INDO finite perturbation calcs. of spin-spin coupling consts. J_{hh}, J_{15nh}, J_{15p13c} 3-74952
 methane, second-order props. calc. with virtual orbitals 3-54617
 methanol, hyperfine struct. in internal rotor molecules, spin-spin interactions 3-78817
 methanol, uncoupled pulsed Fourier transform ¹³C n.m.r. obs. 3-75085
 methyl chloride, Cl quadrupole coupling, variation of strength with isotopic substitution 3-49475
 methyl chloroformate, ³⁵Cl quadrupole coupling consts. 3-75050
 methylaminoethane, rot.-inversion spectrum analysis 3-63491
 methylchloride, and isoelectronic series, SCF-MO calcs. 3-60409
 exo-methylene-cycloalkanes, ¹³C-¹³C coupling consts. and chem. shifts 3-75080
 methylfluoride, vibr. corrections of dipolar couplings 3-78700
 3-methylpyridazine, asymmetric signal of terminal ring CH₃ group, origin 3-75088
 monohalide and monohydride molecules, rotational and hyperfine structure constants tables 3-49446
 n.m.r., permanent magnet, chemically induced nuclear dynamic polarisation, nuclear and electron spin coupling 3-48324
 organic compounds, ¹³C continuous wave proton spin decoupling, virtual coupling 3-71574
 organic radicals, hyperfine coupling constants, π-electron mol. orbital calcs. 3-63383

molecular nuclear coupling continued

- organo(seleno,telluro)phosphorus cpds., ³¹P n.m.r. obs. of ³¹P-⁷⁷Se, ³¹P-¹²⁵Te spin-spin coupling consts. 3-75087
 organophosphorus cpds., spin coupling with ³¹P, exptl. determ. 3-75081
 organosilicon compounds, ¹J(¹³C-²⁹Si) spin-spin coupling consts. calc. by max. overlap approx. 3-75070
 phenolones (I and II)-Ni(AcAc)₂, dispersion of ¹H-(³¹P) heteronuclear chem.-exchange spin decoupling 3-75086
 cis-propyleneimine, ¹⁴N quadrupole coupling consts., microwave spectra 3-63489
 pyrazine, ab initio MO wave functions 3-63372
 pyridazine, pyrazole, pyridine, pyrrole, and thiazole, CNDO/2-INDO calc. of spin-spin coupling consts. 3-54722
 pyridinaldehydes, spin coupling consts., SCF INDO calcs. 3-60401
 pyridine, ab initio MO wave functions 3-63372
 pyridine, n.m.r. of ¹³C, long-range ¹³C-¹H spin coupling consts. 3-43483
 pyridine, uncoupled pulsed Fourier transform ¹³C n.m.r. obs. 3-75085
 pyridines, BEEM-π calcs. and ¹⁴N n.q.r. 3-63526
 pyridines, disubstituted, proton-proton coupling consts., additivity of substituent effects 3-60479
 pyrrole, ¹⁵N and ¹³C n.m.r., spin-spin coupling consts. 3-78846
 pyrrole, ¹⁵N enriched, natural abundance ¹³C n.m.r. obs. 3-75083
 pyrrole, beam maser spectroscopy, obs. of rotational transitions, nitrogen hyperfine parameters 3-78826
 thiophenes, ring proton-proton coupling consts., SCF INDO calcs. 3-60414
 tri-(3-bromo-2-thienyl) phosphine, off resonance proton decoupling, n.m.r. 3-75069
 trimethylchlorosilane, nuclear quadrupole coupling and rotational const. determ. from microwave spectra (*German*) 3-60468
 triphenylcarbonium derivatives, fluorescence correlation with bond order change as measure of coupling (*German*) 3-57665
 triphenylmethyl radical, ¹³C-E.S.R. coupling constants, π-radicals, hyperconjugation 3-78850
 vinyl cpds., indirect H-H and ¹³C-H spin-spin coupling consts., CNDO/2 calcs. (*German*) 3-63528
 vinyl-Pt complexes, coupling consts. Pt hybridisation 3-75065
 ArHCl complex, Cl quadrupole coupling const. determ. by mol. beam electric resonance spectroscopy 3-78824
 AuCl₃, n.q.r. of ³⁵Cl, spectral line asymmetry and spin echo envelope modulation 3-79942
 COF₂, spin-rotation interaction, ¹⁹F hyperfine struct., beam maser obs. 3-71573
¹³C-¹H spin-spin coupling over three bonds in simple molecules, INDO calc. 3-52388
 FCl, and isoelectronic series, SCF-MO calcs. 3-60409
 H₂O, in solid hydrates, correlations between free and H-bonded mols., ab initio calcs. 3-74991
 HOCl, and isoelectronic series, SCF-MO calcs. 3-60409
¹H-(³¹P) heteronuclear chemical exchange spin decoupling dispersion 3-75086
 NCN₃, microwave spectra, anal. four nuclear quadrupole problem 3-78819
 NH₃, elec. field gradient, core model approach 3-74937
 NH₂Cl, and isoelectronic series, SCF-MO calcs. 3-60409
 N₂O₃, N quadrupole hyperfine splitting 3-46305
 P halides, spin-spin coupling and chem. shift calcs. 3-71598
³¹P-⁷⁷Se in organophosphorus compounds, evidence of steric effects 3-46317
 SO³⁵Cl₂, quadrupole coupling consts. 3-78839
²⁹Si and ¹³C to magnetic nuclei, directly-bonded nucl. spin-spin coupling consts. 3-75077

molecular orbitals

- see also molecular orbitals calculations
 admixture coeffs. rel. to Raman scatt. 3-57624
 configuration interaction and valence bond theories, convergence 3-43401
 diatomic molecule, virial theorems, adiabatic representation 3-78670
 electronic momentum expectation values and total energies calc. from Compton scatt. data 3-63260
 electrostatic force theory, overlap effect, atomic dipole and exchange forces 3-52319
 energy localisation, first order scheme 3-43400
 ethylene sulphide, photoelectron spectrum obs. 3-54627
 fluoromethanol, localized MO, excited state geometry, gauche effect 3-74914
 formaldehyde, illustration of calculated orbitals 3-63375
 Hartree-Fock wavefunctions, converging closed shell, level shifting method 3-74776
 hydrocarbons, conjugated, graph theory applic. to topology depend. of π-electron parameters 3-46238
 inner-shell vacancy prod. mechanism during ion-atom collisions 3-67714
 many-body perturbation methods applic. in discrete orbital basis 3-46233
 monofluoroacetamide irradiated cryst., ELDOR of free radical, role of F p-orbital anisotropy 3-55972
 noble gases, solid, Mossbauer of dissolved Fe, nuclear quadrupole moment, electron densities, mol. orbits 3-41459
 nodal features, explanation of molecular geometry for inorganic AB_n(n=2-5) system 3-78658
 one-electron diatomic molecule, non-crossing rule for potential curves 3-71497
 prediction, VSEPR rules or teaching device, criticism, alternative procedure 3-53815
 quasienergy and quasienergetic states, strong monochromatic e.m. wave perturbation of atoms and mols. 3-74219
 relativistic effects, mol. integrals with Gaussian-type orbitals 3-57622
 SCF theory, multiconfiguration, closed shell systems, model and Brillouin theorem 3-78675
 SCF-LCAO-MO and SCF-Xα-SW approxs., comparison for ethane internal rot. barrier calcs. 3-40590
 Slater-type orbitals, two-centre calc., acetylene, ethane, ethylene, H₂O₂, N₂H₄ (*Russian*) 3-49444

molecular orbitals continued

- thiocarbonyl chloride, photoelectron spectra, ionisation potentials assigned to mol. orbitals 3-43502
 thiocarbonyl fluoride, photoelectron spectra, ionisation potentials assigned to mol. orbitals 3-43502
 Cr(CO)₅L, L = ligand, direct evaluation of π -bonding 3-71556
 Cu complexes, EPR spectra and covalent bonding in CuCl₄²⁻ and CuBr₄²⁻ ions 3-79901
 H₂, differential cross section for elastic scatt. in first Born approx. 3-75103
 H₂, intermediate states, calc. of cross-sections for dissociative recomb. and associative ionisation 3-75098
 H₂, quantum defect theory, vibr.-electron coupling, autoionisation 3-71607
 H₂⁺, ground state, improved James function 3-46239
 H_n⁺ clusters, geometry and binding energies 3-67741
 H₂, H₂⁺, ab initio calcs., review 3-57626
 HeH⁺, electron impact dissoci., Harris-type elliptic orbitals 3-75108
 LiH, LiH⁺, ab initio calcs., review 3-57626
 Mo (100) crystal face, excitation (French) 3-79563
 O₃⁻, CNDO-MO calculations 3-67735

molecular orbitals calculations

see also LCAO calculations; molecular electronic structure; self-consistent field methods

- π -electron, organic radicals, proton, N, f hyperfine coupling constants 3-63383
 ab initio, on small mols., review 3-57626
 ab initio and semi empirical, in interpretation of organic pseudohalides photoelectron spectra 3-43431
 ab initio and semi-empirical calc. of mol. struct. of propionaldehyde 3-74920
 ab initio calculations of $^1\Sigma^+$ state of BN 3-54641
 ab initio STO-3G calc. of barrier to internal rotation of PH₃BH₃ 3-46223
 acetonitrile-phenol complex, CNDO/2 calcs. of electronic struct. and configs. (French) 3-43390
 alkali halides, electronic struct. of dimer activator centres 3-68566
 alkali metals, diatomic mols., split-shell mol. orbital calcs. 3-43416
 alkyl derivs., straight chain, electron density distrib. 3-71525
 allene, excited states, CNDO calc. using ligand geometries in transition metal complexes 3-60419
 allyl radical, all-electron mol. orbital theory, symm. dilemma 3-43402
 aminodifluorophosphine, CNDO/2 approximation for conformational analysis (French) 3-63359
 approximate molecular orbital theory, balance and predictive capability 3-43399
 atomic collisions, close 3-71459
 attractive nonbonded interactions in organic molecules 3-63373
 azides, irradi., N₃ or N₃²⁻ radicals identification 3-61267
 benzenes, monosubstituted, ν_8 and ν_{19} vibr. i.r. band intensities, CNDO/2 calcs. 3-60456
 benzenes, multi-homosubstituted, variable electronegativity SCF-MO calcs. 3-67736
 benzenes, substituted, perturbation MO calc. of ionisation potentials, effects of induction and resonance 3-46333
 benzoic-acid, methyl derivatives, Pariser-Parr-Pople calc. with configuration interaction (French) 3-63379
 bicyclo [2,1,1] hexane, SCF-LCAO calcs. using optimised minimal set of Gaussian functions 3-67761
 biphenyl, triplet-triplet transition absorption spectrum 3-74946
 Brueckner (maximum overlap) soln. stability conditions in independent particle wave functions 3-67743
 camphor, ¹³C n.m.r. relax times 3-68881
 carbonyl group, 5-membered ring compounds, photoelectron spectroscopy, lone pair orbital ionisation potentials, INDO calcs. 3-54625
 carboranes, multi-centre bonding, ab initio and semi-empirical MO study 3-63391
 2-chlorotetrahydropyran, ab initio mol. wavefunction calc. 3-49491
 β -chlorovinylketones, Pariser-Parr-Pople calculations, conformational assignment 3-67733
 closed and restricted open shell semiempirical methods, configuration interaction of singlet-triplet and triplet-triplet spectra 3-52342
 closed shells, ionisation energy calculation 3-78676
 CNDO and extended Huckel calc. of SK₂ emission spectra of K₂S₂O₅ and KHSO₄ 3-47328
 CNDO computations of mol. ions emitted from light element targets 3-61086
 CNDO study of alternative mechanisms for cyclopropane isomerisation 3-47548
 CNDO wavefunctions calc. of mol. geometries and force consts. by the force method 3-43396
 CNDO/2, INDO and ab initio study of photoelectron spectra of organic pseudohalides 3-46256
 CNDO/2, ion electron structs., organic 3-60424
 CNDO/2 calc. of bond lengths and force consts. in cyclobutane and cyclopropane 3-74925
 CNDO/2 calc. of charge transfer props. of hydrogen bond 3-74961
 CNDO/2 calc. of K β X-ray emission spectra of S₈ and dibenzyl sulphide 3-52345
 CNDO/2 calc. of struct. of ethylene chlorine complex 3-54608
 CNDO/2 charge density distrib. calc., monatomic overlap densities role 3-54622
 CNDO/2-INDO calculations of spin-spin coupling consts. of pyridazine, pyrazole, pyridine, pyrrole, and thiazole 3-54722
 CNDO/2D wave functions, second moment of additivity eqn. for hydrocarbons 3-74960
 CNDO/SP calc. of g-tensors of free radicals 3-43491
 conjugated systems, application of RPA theory to excited states 3-52328
 correlated Gaussian wavefunctions use for chem. energies calc. for small systems 3-54621
 coumarin and methyl derivatives, σ and π electron contributions to long-range spin-spin coupling consts. 3-52387
 cyanine dyes, Huckel mol. orbital descriptions, contours approach 3-46232
 cyclic amides, opt. activity calcs. using INDO method 3-52322
 cyclic molecules, quadrupole moments and diamag. susceptibilities calc. 3-63377

molecular orbitals calculations continued

- cyclobutadiene (and deuterated), ground state potential energy surfaces, relevance to i.r. data 3-78662
 datolite, refinement of crystal struct. Huckel MO calc. 3-80599
 density localisation, heteronuclear diatomic and polyatomic 3-71501
 density matrix elements, first order, direct analytical calc. through third order 3-74779
 deutron quadrupole coupling consts. calc. using core model approach 3-74937
 diatomic, polarisation factors, 1s, 2s, 2p σ , 2p π 3-71500
 diatomic bound states, model calc. of avoided-crossing problem 3-78723
 diatomic mols., pot. curves calc. using decoupled Hartree-Fock methods 3-60408
 diethyl 5-bromouracil-1-malonate, C π \rightarrow π^* transition, assignment expr. verification and extended Huckel mol. orbital calc. 3-52324
 diethyl 5-nitrouracil-1-malonate, C π \rightarrow π^* transition, assignment expr. verification and extended Huckel mol. orbital calc. 3-52324
 diethyl uracil-1-malonate, C π \rightarrow π^* transition, assignment expr. verification and extended Huckel mol. orbital calc. 3-52324
 diethyl-5-methyluracil-1-malonate, C π \rightarrow π^* transition, assignment expr. verification and extended Huckel mol. orbital calc. 3-52324
 p-difluorobenzene, electronic struct. and geom., CNDO-CI calcs. for ground and excited states 3-60423
 dimethylaminodifluorophosphine, CNDO/2 approximation for conformational analysis (French) 3-63359
 2,4-dinitrotoluene, π , σ -electronic struct., conversion in ground state, CNDO/2 calcs. (Russian) 3-78678
 diphenylmethyl radical, stereochem., e.s.r. data interpret., INDO-MO calcs. 3-46228
 ethane, local bonding orbitals, FSGO model 3-71503
 ethyl radicals, ab initio calcs., mol. fragments 3-78668
 ethylcarbonium ion, nonempirical MO calcs. of energies rel. to geom. 3-63354
 ethylene triplet state, ab initio calcs., mol. fragments 3-78668
 ethylenes, monosubstituted, absolute i.r. intensities, CNDO/2 calc. 3-46243
 extended Huckel calc. of tautomerism of 4-methylumbelliferone 3-52309
 extended Huckel method, optimized for calc. ionisation potentials and dissociation energies of hydrocarbons 3-52313
 extended Huckel method calc. of coloured isomeric forms of spiropyran 3-74923
 extended Huckel theory determ. of energy gradients, application to cyclopentane 3-71489
 fluorobenzenes, homo-substituted, ground state electronic struct., extended Huckel MO calcs. 3-67737
 fluorobenzenes, homosubstituted, all valence electron MO calcs. 3-67738
 fluoromethanol, anomeric effect 3-60417
 1-fluorovinyl cations, geometrical study, INDO calc. 3-52325
 formic acid, ionic solvation, CNDO/2 calcs. on solvated univalent ions 3-53347
 free radicals, anisotropic hyperfine coupling constants 3-78844
 free radicals, organic, INDO method, geometry change and substitution effects on electronic structure 3-63387
 frontier molecular orbital theory, link between kinetics and bonding theory, elementary university chem. teaching 3-77355
 geminals with expanded bases, LiH 3-57635
 General SCF operator satisfying correct variational condition 3-71495
 Gillespie-Nyholm theory applied to force fields, points-on-a-sphere and extended Huckel analyses of trigonal bipyramids 3-63398
 heterocycles with divalent sulphur, resonance energy calcs. from thermodynamical data 3-67753
 homopolynucleotides, CNDO/2 and MINDO/2 energy band structs. 3-60498
 Huckel 4n + 2 rule for conjugated systems with large π -electron deficiency 3-78689
 Huckel method calc. of electronegativity and electron affinity 3-52330
 hydrides, group VI-VII, lone pair orbital energies 3-61966
 hydrocarbons, alternant, reson. energies calc. by semi-empirical method 3-67752
 hydrocarbons, MOA calculations of CH stretching frequencies and dissociation energies 3-43429
 hydroxymethylcarbonium ion, nonempirical MO calcs. of energies rel. to geom. 3-63354
 hydroxyacetoneitrile, barriers to internal rotation, group function and MO-LCAO-SCF computations 3-49432
 icosahedral irreducible tensors applics. 3-57623
 2,2'-iminobis(acetamidoxime) and its Ni(II) and Zn(II) complexes, INDO calculation 3-52331
 INDO, CNDO/2 calc. of torsional barriers of vinyl groups on cyclopropane rings 3-74924
 INDO, ion electron structs., organic 3-60424
 INDO calc. of nuclear spin-spin coupling over three bonds between ¹³C and ¹H in simple molecules 3-52388
 INDO finite perturbation calcs. of spin-spin coupling consts. J_{HH}, J_{15NH}, J_{15N13C} 3-74952
 integral evaluation, Gaussian atomic orbitals, general contraction 3-40595
 ionic crystals, impurity paramag. centre form. 3-68254
 ionisation potential, core electrons, Koopmans' theorem, molecular orbital calc., relaxation energies, effect on predicted chem. shift 3-49442
 large molecules calc., N⁴ depend. 3-67732
 local orbitals solns., systematic extensions 3-43404
 magnetic properties of molecules, influence of perturbations 3-57636
 matrix elements, diagonal, nondiagonal, equivalent orbitals 3-78672
 maximum overlap approximation calc. of spin-spin coupling consts. for organosilicons 3-75070
 maximum overlap criterion approach to geometries and moments 3-78651
 metallocenes, transition metal complexes, high energy photoelectron spectroscopy, binding energies, mol. orbital calc. 3-49441

molecular orbitals calculations continued

- methane, ground state energies and bond distances, stat. OCE calcs. (*German*) 3-67745
- methane, solid, cryst., band structure calc. in linear combination of mol. orbitals approx. 3-44013
- 2-methoxytetrahydropyran, anomeric effect 3-60417
- methyl anion, inversion pot. surface, HF represent., augmented basis set 3-74910
- methyl formate, methyl fluoromethoxy, INDO calcs. of dipole moment and conformation 3-63369
- methylchloride, and isoelectronic series, SCF-MO calcs. 3-60409
- methylene, spin dipole-dipole parameters, ab initio calcs. 3-74939
- methoxycarbonium ion trimer, geometry, CNDO/BW calc. 3-67726
- monofluorobenzene, electronic struct. and geom., CNDO-CI calcs. for ground and excited states 3-60423
- muffin-tin orbitals approach to energy levels calc. 3-78674
- Muller-Pritchard model, interpretation of C-H coupling consts. for directly bonded nuclei in hydrocarbons 3-75073
- naphthalenes, monosubstituted, electronic absorpt. spectra interpret. by config. analysis 3-67754
- natural orbitals calc. by perturbation theory, diagonalization of one-electron density matrix 3-74942
- NDDO calculations for hydrides 3-52312
- nitroalkanes, semi-empirical chem. shift calcs. 3-63521
- nitrobenzene, π -, σ -electronic struct., conversion in ground state, CNDO/2 calcs. (*Russian*) 3-78678
- o-nitrotoluene, π -, σ -electronic struct., conversion in ground state, CNDO/2 calcs. (*Russian*) 3-78678
- non-orthogonal pair theory of electronic structure 3-67756
- nuclei acid bases, in-plane electronic spectra using all valence electron MO-CI calcs. 3-63386
- olefins and radical cations, CNDO/2 calcs. of electronic props. 3-54649
- open shell systems, ab initio calcs., mol. fragments 3-78668
- optimization technique for Slater orbital exponents and SCF energy (*French*) 3-57621
- orbital correction method 3-43403
- organic radicals, spin density calc. by modified INDO and MZDO methods 3-46231
- Pariser-Parr-Pople calc. of π -electron densities in quinolines 3-74957
- Pariser-Parr-Pople calc. of π -electronic struct. of chromones 3-71507
- Pariser-Parr-Pople calc. of oscillator strengths of excited singlet states of conjugated hydrocarbons 3-52344
- Pariser-Parr-Pople calc. of singlet-triplet and triplet-triplet spectra of conjugated hydrocarbons 3-52343
- Pauling's bond enthalpy equation, orbital bases 3-74933
- PCILO, comparison with CNDO/2 calcs. 3-49434
- perturbation theory application to organic π systems, substituent induced ^{13}C chemical shifts 3-63374
- phenols, substituted, reactivity estimations by semiempirical MO-methods (*German*) 3-53314
- phenyl radical, hyperfine coupling, INDO calc., σ framework 3-52316
- planar mols., $d\pi$ orbitals contrib. in spin-orbit coupling 3-54643
- polymer, π -conjugated heterocyclic, bond alternation 3-75164
- polymer, simulated ab-initio mol. orbital method for band struct. 3-54767
- positron systems with H^- and other negative ions, SCF calculations 3-78648
- positron systems with negative ion and atoms, quasi-stationary states calc. 3-78649
- propargyl alcohol, barriers to internal rotation, group function anal., MO-LCAO-SCF computations 3-49432
- propionic acid, CNDO/2 calc. of electron struct. 3-63389
- propynal, CNDO/2 calc. of electronic struct. 3-63389
- propynal, CNDO/2 calcs. of electronic struct. 3-67755
- pyrazine, ab initio wave functions, mol. props. calc. 3-63372
- pyrazine cryst., triplet exciton Davydov splitting calc. 3-60862
- pyridinaldehydes, INDO calcs. of stereochem. and NMR parameters 3-60401
- pyridine, ab initio wave functions, mol. props. calc. 3-63372
- pyrimidine nucleosides, syn conformation stability, INDO method 3-63363
- SCF CNDO versus electrostatic calc. for protonation of organic three membered ring molecules 3-46234
- SCF MO approximate treatments, comparative study for hydrides 3-52312
- semi-empirical approximation, theory and appl. to homonuclear diatomic molecules 3-78663
- semiconductors, III-V and II-VI, nonlinear optical props., simple molecular orbital theory 3-48940
- simulated ab initio method, matrix element transfer 3-52311
- Slater orbital mol. integrals with numerical Fourier transform methods, exchange integrals 3-57619
- Slater-type orbitals, Gaussian approxs. criterion 3-60404
- spin-orbit coupling operator and CNDO approach in molecular spectroscopy 3-74950
- squaric acid and anion, Pariser-Parr calcs. 3-52360
- 4-substituted α -methylstyrenes and α -t-butylstyrenes, substituent effects, n.m.r. obs. and CNDO/2 calculations 3-52386
- 4-substituted styrenes, substituent effects, n.m.r. obs. and CNDO/2 calculations 3-52385
- symmetry-equivalent d-orbitals, Gaussian representations appl. to ammonia 3-67739
- thioformaldehyde, ab initio calcs. for ground and low-lying triplet states 3-52323
- thiophenes, ring proton-proton coupling consts., SCF INDO calcs. 3-60414
- toluene, π -, σ -electronic struct., conversion in ground state, CNDO/2 calcs. (*Russian*) 3-78678
- transition metal complexes, Fermi-contact term calc. from unrestricted Hartree-Fock MO method 3-74934
- triatomic inorganic radicals approx. molecular orbital calc. of anisotropic hyperfine interactions using INDO 3-60416
- trimethyl derivatives, $(\text{CH}_3)_3\text{M}$ ($\text{M} = \text{N}, \text{P}, \text{CH}, \text{SiH}$), conform. analysis, CNDO/2 calcs. 3-46222

molecular orbitals calculations continued

- 1,6,6a Si^{IV} -trithiapentalene oxygenated isologues, CNDO/2-SCF-MO calc., S...O interactions (*French*) 3-43412
- 1,6,6a Si^{IV} -trithiapentalene substituted oxygenated derivatives, CNDO/2 calc. of preferred conformations (*French*) 3-43413
- Tschischibabin (quinoid) type hydrocarbons, triplet state, Huckel calc. (*German*) 3-63511
- two-dimensional formamide network, CNDO/2 and MINDO/2 energy band structs. 3-54772
- uniform electron gas, total energy calc. 3-68529
- united atom and CNDO/BW theories, valence orbital behaviour during changes in intermolec. separation 3-60418
- unrestricted Hartree-Fock perturbation theory 3-54623
- valence bond study of TiF_3^+ 3-67757
- vinyl cpds., indirect H-H and ^{13}C -H spin-spin coupling consts., CNDO/2 calcs. (*German*) 3-63528
- vinyl radicals, 1-substituted, geometrical study, INDO calc. 3-52325
- vinyl radicals, ab initio calcs., mol. fragments 3-78668
- $\chi\alpha$ method comparison with ensemble average method 3-67646
- AlO , potential curves for ground and excited states, MCSCF study 3-78693
- As_2S_3 , mol. orbital investigation of electron energy states 3-58199
- As_2Se_3 , mol. orbital investigation of electron energy states 3-58199
- B complex, BF_3 -benzaldehyde, CNDO/2 calc. of electronic structure 3-52329
- BF_3 , ab initio bond length, polarity and atomic orbital calcs. 3-78653
- BF_3 -nitrogen base complexes, bonding, mol. orbital calc., photoelectron spectra 3-49440
- B_2F_4 , ab initio bond length, polarity and atomic orbital calcs. 3-78653
- BH_3 , equilibrium geometry and harmonic force consts., ab initio calc. including electron correlation 3-54657
- BH_3 dimerization and associated delocalization energy 3-57628
- BH_3NH_3 and perfluoroderivatives, Lewis acid-base complexes, optimized geometries, CNDO/2 calc. 3-43394
- CN, potential curves for ground and excited states, MCSCF study 3-78693
- CNDO/2 calc. of electronic struct. of some sulphur compounds (*French*) 3-54640
- CNDO/2 study of struct. and vibrational spectra of $\text{H}_2\text{O}\cdot\text{Cl}_2$ complex 3-54686
- CO_2 , semiempirical mol. orbital calc., reparametrisation, INDO 3 , barriers to internal rotation, bond angles and lengths 3-74948
- ^{13}C shielding consts., uncoupled Hartree-Fock calcs. using ab initio and NEMO wavefunctions 3-63376
- (CIHCl)- system, i.r., Raman activity of H bonds, theory (*German*) 3-71563
- Eu complex, $(\text{EuF}_6)^{4-}$, exchange splitting, spin densities, covalency, Hartree-Fock-Slater mol. orbital calcs. 3-50313
- F_2 , F_2^+ , F_2^- , F_2^{2+} , pot. energy curves and spectroscopic consts. calcs. 3-71496
- FCl, and isoelectronic series, SCF-MO calcs. 3-60409
- F_2O_2 and F_2S_2 , electronic structure and conformation (*French*) 3-43415
- F_2SO^- , bonding, CNDO MO calcs. (*German*) 3-74966
- Fe complex, tris(2,2'-bipyridyl)iron(II), SCF-MO PEEL calc. of electronic structure and excited states 3-63378
- Fe complex, tris(glyoxal-bis-N-methylimine)iron(II), SCF-MO PEEL calc. of electronic structure and excited states 3-63378
- GeH_4 , ground state energies and bond distances, stat. OCE calcs. (*German*) 3-67745
- GeH_4 , multiple-scatt. $\chi\alpha$ calcs. 3-54629
- H_2 , chemionisation in collisions with $\text{He}(2^3\text{S})$ metastable atoms, ab initio calc. 3-78902
- H_2 , complex orbitals in extended HF scheme 3-63370
- H_2 , correlated Gaussian wavefunctions use for chem. energies calc. 3-54621
- H_2 , correlated Gaussian wavefunctions 3-60410
- H_2 , electron scatt., first Born approx. 3-75102
- H_2 , ground state calcs. using H_2^+ -type elliptical basis orbitals 3-74941
- H_2 , Slater orbital exponents and SCF energy (*French*) 3-57621
- H_2 , solid, t-matrix calcs. for ground-state energies 3-72251
- H_2 autoionisation, energy depend. of $1/\Pi_+$ states on internuclear separation stabilization method 3-75099
- H_2^+ , exchange polarization energy, multipole struct. 3-75154
- H_2^+ , ground state calcs. using H_2^+ -type elliptical basis orbitals 3-74941
- H_3 , correlated Gaussian wavefunctions use for chem. energies calc. 3-54621
- H_3^+ , correlated Gaussian wavefunctions 3-60410
- H_3^+ , ground state calcs. using H_2^+ -type elliptical basis orbitals 3-74941
- HCO radical, hyperfine splitting consts., comparison of computation methods 3-57625
- HCl, solid, CNDO method, anal. H-bonding and charge transfer 3-74944
- $\text{H}_2\text{NO}\cdot$, HF hydrogen bonded radical, ab-initio study of stable configurations 3-43398
- $(\text{H}_2\text{NO}\cdot\cdot\text{H}_2\text{O})^-$, $\text{H}_2\text{NO}\cdot\cdot\text{H}_2\text{O}$, hydrogen bond energy 3-74965
- H_2O , natural orbitals calc. by perturbation theory, diagonalization of one-electron density matrix 3-74942
- H_2O bond orbital analysis of hydrogen bond 3-54618
- H_2O radicals trapped in aqueous solutions at 77K 3-55980
- H_2O^+ , minimum energy struct. and inversion barrier 3-74909
- H_2O_2^+ , solvation process, STO double zeta SCF wavefunctions 3-71504
- H_2O_2^+ , tunnelling in proton transfer between water mols. 3-78867
- HOCl, and isoelectronic series, SCF-MO calcs. 3-60409
- $\text{H}_2\text{PO}\cdot\text{BF}_3$, conformation and electronic structure, theoret. analysis, CNDO/2 method (*French*) 3-63355
- HS_2 radical, CNDO/2 calcs. of geometry 3-75003
- He_2^+ , LC wave function of Slater type AO, one electron model (*Russian*) 3-54620
- He_2^+ diatomic state, mol. autoioniz., rel. to single ioniz. of He by He^+ 3-52290
- He_2^{2+} , ground state calcs. using H_2^+ -type elliptical basis orbitals 3-74941

molecular orbitals calculations continued

- HeH⁺, ground state, semi-localized orbitals 3-60411
 HeH₃⁺, stability study using polarised Gaussian orbitals and VBCI wave functions 3-74954
³He, solid, t-matrix calcs. for ground-state energies 3-72251
 Li₂ + F → Li + LiF, pot. energy surface, ab initio electronic struct. calcs. 3-47549
 LiH, complex orbitals in extended HF scheme 3-63370
 MnO₄⁻ ion, ab initio SCF computation of ground and excited states 3-74938
 Mo complex, [Mo₂O₄Cl₄(H₂O)₂]²⁻, SCCC MO calculations of electronic structure 3-54651
 N₂, electron scatt., first Born approx. 3-75102
 N₂, generalised oscillator strength 3-74949
 N₂ ground state, generalized valence bond and configuration interaction calcs. 3-78694
 N₂⁺ low lying doublet states, generalized valence bond and configuration interaction calcs. 3-78695
 NF and NF⁻, pot. energy curves and spectroscopic consts. calcs. 3-71496
 NF₂ radical, ab initio unrestricted Hartree-Fock calculations 3-63394
 NH₃, calc. of properties using symmetry-equivalent d-orbitals, Gaussian representations 3-67739
 NH₃, elec. field gradient, core model approach 3-74937
 NH₂Cl, and isoelectronic series, SCF-MO calcs. 3-60409
 NH₃.H₂O, SCF MO LCGO studies on hydrogen bonding 3-54648
 NO₂⁻, semi-empirical chem. shift calcs. 3-63521
 NO₂⁺, semi-empirical chem. shift calcs. 3-63521
 NO₃⁻, semi-empirical chem. shift calcs. 3-63521
 Ne₂ and Ne₂⁺, scattering and radiative processes in low-lying states, ab initio calc. 3-71640
 Ni(CO)₄ and Ni(CN)₄²⁻ LCAO-MO-SCF contracted Gaussian, pi back-bonding analysis 3-67762
 O₂, natural orbitals calc. by perturbation theory, diagonalization of one-electron density matrix 3-74942
 O₃, non-empirical SCF studies of ring and open forms 3-78667
 O₃⁻ ion and related species, CNDO approximations 3-67735
 PH₃, PH₃⁺, PF₃ and PF₃⁺, geometry, SCF calculations 3-60399
 PbH₄, ground state energies and bond distances, stat. OCE calcs. (German) 3-67745
 SO₃²⁻ and SO₃F⁻ ions, sulphur K β X-ray emission spectra interpret. 3-52315
 SiH₄, ground state energies and bond distances, stat. OCE calcs. (German) 3-67745
 SiH₄, multiple-scatt. X α calcs. 3-54629
 SnH₄, ground state energies and bond distances, stat. OCE calcs. (German) 3-67745
 (XeH)⁺, pot. energy curves, LCAO-MO-SCF calcs. 3-74943
 XeOF₂, XeO₂F₂, and XeOF₄, Wolfsberg-Helmholz MO calc. of electronic and geometric structures 3-43414

molecular polarisability

- aqueous base solutions having i.r. absorption continua, very polarisable H-bonds 3-61285
 aromatic hydrocarbons, condensed, Stark effect 3-76012
 azulene, benzophenone (naphthalene), impurity change of polarisability and dipole moment, $\pi\pi^*$ state 3-72662
 chain molecules, thin cylinder model for Van der Waals forces 3-70773
 chloroform intermol. complexes, spectroscopic and dielec. investig., comparison 3-74931
 diatomic molecules, delta pot. function model approach 3-67770
 dipole-dipole interaction in liquid, electronic spectra, luminescence 3-75970
 double-photon scatt., by noncentro-symm. mols., anisotropy of non-linear polarisability 3-67792
 dynamic polarizability and oscillator strength, error bounds 3-43344
 hydrocarbons, conjugated, optical dipole polarisability calc. 3-43437
 icosahedral irreducible tensors applics. 3-57623
 in liquid state nonlinear third order polarisability, Kerr effect and Rayleigh scatt. obs. 3-40605
 modified Rayleigh-Schrodinger expsn., singlet state polarizabilities, conjugated mols. 3-74099
 2-nitropropane, deformation polarisation 3-55997
 phenylalanine, π -inductive effects rel. to π polarization effects 3-67747
 phenylalanine, π -inductive effects rel. to π polarization effects 3-67747
 phenylalkanes with polar or charged substituents, π -inductive effects rel. to π polarization effects 3-67747
 phenylglycine, π -inductive effects rel. to π polarization effects 3-67747
 Raman scattering efficiency depend., mol. crystals 3-72656
 Rayleigh light scattering theory, principle axes of tensor 3-62664
 symmetric top rotor, anisotropies calc. from Stark effect 3-40155
 tensor polarisability and related parameters 3-40569
 (ClHCl)⁻ system, nuclear motion, H bond energy calcs. (German) 3-71563
 H₂, polarisability depend. on internuclear distance 3-63435
 H₂ dynamic polarisability calc. by the distinguishable electron method 3-40594
 HCP, delta function model approach 3-67767
 HNC, HNSi and HNGe, delta function model approach 3-67767
 H₂O, coupled Hartree-Fock method calcs. of one-electron properties 3-71515
 H₂O₂⁺ system, coupling of proton motion with H bond stretching vibration, effect on dipole moment, polarisability, double min. potential surface 3-49457
 HOF, delta function model approach 3-67767
 NO₃⁺, vibr. freqs., correl. with cation polarising power and polarisability 3-49456

molecular quadrupole moments see molecular moments**molecular relaxation**

- see also dielectric phenomena
 n-alkanes, light scatt. spectrum 3-80053
 anthracene, vibrational relaxation in triplet state 3-46312
 benzene, in various solvents, orientational relax. rates, depolarised Rayleigh scatt. meas. 3-50574
 biacetyl, electronic and vibrational relaxation 3-40649

molecular relaxation continued

- biacetyl, vibr. relax. obs. by visible-i.r. double reson. technique 3-78885
 bromomethane, liquid, Raman spectroscopy, vibrational relaxation, mol. reorientation 3-75984
 Cole-Cole plot, angles of intersection rel. to dielec. relax. asymptotic behaviour 3-55523
 collisions, vibrational to translational versus vibronic to translational energy transfer 3-40672
 deuteriochloroform liquid, Raman spectroscopy, vibrational relaxation, mol. reorientation 3-75984
 p-N,N-dimethylamino-benzonitrile derivatives, two fluoresc. bands, solvent influence 3-76083
 dimethylchloride, isotopic dilution effect on i.r. absorpt. bandshape 3-54679
 fluoromethane, time resolved i.r.-microwave double resonance, rotational relaxation 3-71578
 gaseous molecular amplifiers, short-pulse, output energy relaxation losses 3-70809
 Green function treatment of decay theory 3-71571
 hydrogen halides, rotational relax in inert. gas 3-49500
 hydrogen-bonded systems, vib. and reorientational relax. 3-64669
 inelastic collisions, rot. relax., transport and spectral props., kinetic theory 3-71622
 interstellar masers, trapped i.r. lines and cross-relaxation 3-51393
 ionic states obs. by high energy photoelectron spectroscopy, configuration interaction calc. of valence orbital relaxation 3-46335
 ionisation potential, core electrons, Koopmans' theorem, molecular orbital calc., relaxation energies, effect on predicted chem. shift 3-49442
 isolated molecules, radiationless transitions 3-49482
 liquid, isotope effects on motions in classical limit 3-64194
 liquid, mol. motion, conf., Orsay, France, Jul. (1973) 3-64192
 liquid mixture, binary, light scattering 3-80013
 macromolecule, methyl group behaviour internal rotation and nonexponential nuclear relaxation 3-79936
 methane, deuterated, in inert liquids, rotational relaxation, i.r. spectra 3-78769
 methane-CO₂ gas mixture, vibrational relaxation, u.s. velocity measurements 3-57680
 nonequilibrium nozzle flows entropy of vibrationally relaxing diatomic gases 3-43633
 nuclear mag. relax. under hindered internal rot., time correl. functions 3-49492
 organic complex molecule, intramolecular relax. spectroscopic investig. 3-71536
 phthalimide derivatives in alcoholic soln., fluorescence relaxation of intermolecular interaction and spectral depend. of extinction time (Russian) 3-49487
 picosecond spectroscopy, review 3-57647
 polyatomic mols. in excited states, vibr. relax. by inelastic collisions 3-60487
 polyethylene, drawn, annealed, relaxation processes, effect on conformation and orientation factors (Russian) 3-47477
 rotational, spherical top gas molecules, collision equations, Bryan-Pidduck model 3-49499
 rotational relaxing gas flows geometry 3-78960
 sequential decay processes, interference effects 3-63502
 solute-solvent interactions determ. from dielectric relaxation data 3-53360
 toluene, in various solvents, orientational relax. rates, depolarised Rayleigh scatt. meas. 3-50574
 transition metal complexes, radiationless relaxation processes 3-43473
 transitions under influence of local interaction in stochastic motion 3-40180
 universal correlation failure, intermolecular processes, statistical method, absorption and luminescence spectra 3-76040
 vibrational relaxation rate meas. interpret. 3-54745
 vinyl, substituted compound, u.s. relax. of conformational equilibria 3-54615
 wave number dependence, relaxation time for longitudinal mode in simple liquids 3-63943
 p-xylene, in various solvents, orientational relax. rates, depolarised Rayleigh scatt. meas. 3-50574
 CO, (v=1) and (v=2) states, vibr. excitation and relax. 3-45787
 CO, low temp., vibr. energy transfer rates in CO laser beam 3-74230
 CO, Ne gas mixture, vibration relax. rates, Landau-Teller model, i.r. spectra 3-75140
 CO, relaxation of vibrational levels studied by laser absorption 3-60488
 CO, vibr.-translational relax. by foreign gases, localized heating 3-78887
 CO vibrational relaxation by O atoms 3-46348
 CO₂, rel. to effect of CO on population inversion in lasers 3-40249
 CO₂, relax. of 1090 lower laser level 3-74225
 CO₂, rot. relax effects in short pulse amplifier 3-66799
 CO₂, small signal gain in amplifier meas., 10⁰ to 02°0 rate 3-71621
 CO₂ amplifier system, rot. relax. effect, energy extraction 3-66800
 CO₂ laser, Q-switched pulse duration, rot. relax. effect 3-66804
 CO₂ lasers, laser power and vibrational energy transfer 3-48885
 CO₂ TEA laser, gain decay rates, vibr. relax. 3-40244
 CO₂ vibrational relaxation in collisions with methane, tetra-deuterio-methane and fluoromethane 3-54752
 CO₂/N₂ mixtures, vibrational transition rates by acoustical method 3-40667
 CO₂/O₂ mixtures, vibr. relax. meas. 3-43516
 CO₂-methane, gas mixture vibrational, u.s. velocity measurements 3-57680
 CO(A π), deactivation rel. to individual vib. levels 3-75150
 CO₂(001), vibrational relaxation by O₃, laser fluorescence technique 3-78888
 CS, vibrational relaxation, Ar collisions, transition probabilities (French) 3-71633
¹³C mag. resonance in investigation of mol. dynamics and structure 3-67856
 DF, vibrational relaxation, temp. depend. 3-75136

molecular relaxation continued

- DF-CO₂ mixtures, vibrational relaxation processes, temp. depend. 3-54751
 $F + DF(v) \rightarrow DF(v') + F$ vibr. relax. process, rate consts., Monte Carlo calcs. 3-60486
 $F + HF(v) \rightarrow HF(v') + F$ vibr. relax. process, rate consts., Monte Carlo calcs. 3-60486
H₂, compressed, Rayleigh-Brillouin scatt., rotational relax. 3-80032
o-H₂, matrix treatment of dissociation rotation-vibration relaxation times 3-7857
H₂-He mixtures, quantum scattering theory of rotational relaxation and spectral line shape 3-46351
HBr, vibrational relaxation in inert gases 3-60490
HBr (V=1) state, vibrational relaxation in methane, water, He and HD mixtures 3-71624
H₂CO, collision-induced transitions, velocity depend., obs. by triple resonance method 3-52384
HCl, vibrational relaxation in inert gases 3-60490
HF vibrational relaxation in temp. range 600-2400 K, Ar and F collisions 3-71628
HF + DF, vibr. relax., rate consts. meas. by laser-excited fluoresc. method 3-49502
HF + HCl, (HBr), (HI), vibr. relax., rate consts. meas. by laser-excited fluoresc. method 3-49502
HF + N₂, vibr. relax., kinetics 3-54748
I₂ molecules, excited by He-Ne laser, vibrational relaxation study 3-60494
⁶Li ¹⁹F, J=1→0 rotational transition, partial resolution 3-54704
N₂, vibr. deactivation probability on collision with glass surface 3-46337
N₂, vibr. relax. in luminesc. of solid nitrogen 3-44463
N₂, vibr. relax. using press. meas., shock tube study, comment 3-49501
N₂, vibrational relaxation by alkali atoms 3-71643
N₂ molecules in nozzle, anharmonic vibrational relaxation 3-54737
N₂ vibrational relaxation, quenching of O(D) 3-75137
N₂-N₂O mixture, expanding supersonic jet, rapid cooling, dissociation reactions (*Russian*) 3-57872
NH₃, beam maser meas. of relax. cross sections 3-54754
NH₃ microwave transient nutation measurement, Bloch eqns. for relaxation times 3-63539
NO, monochromatically excited, energy transfer, vibrational relaxation, fluorescence 3-71623
NO, Vibr. relax. time meas., 299 to 1000 K 3-43509
O₂ vibrational relaxation in presence of atomic O 3-54738
O₂ vibrational relaxation in an unsteady expansion wave 3-71629
OCS, vibrational relaxation in inert gases 3-60490
OCS microwave transient nutation measurement, Bloch eqns. for relaxation times 3-63539
UO₂ complex, uranyl β-diketonates, luminesc. spectra, relax. mechanism 3-72753

molecular reorientation

- acetone in soln., i.r. spectra obs. 3-64648
acetonitrile, liq., Raman bandshapes, diffusion consts. and activation energy 3-60661
acetylene, deuterated, plastic phase, n.m.r. 3-79246
n-alkyl ammonium chlorides wide line n.m.r. study of molecular motion 3-68852
anisotropic rotational diffusion equation, stochastic theory 3-79245
benzene, in various solvents, orientational relax. rates, depolarized Rayleigh scatt. meas. 3-50574
1-benzoyl-8-benzyl-naphthalene and 1-benzoylnaphthalene, viscosity-depend. phosphoresc. 3-76469
bisphenol-A uncured diglycidyl ether, pulsed n.m.r. study of molecular motion 3-58443
borazine, hexasubstituted crystals, p.m.r. obs. (*French*) 3-53026
bromomethane, liquid, Raman spectroscopy, mol. reorientation 3-75984
chloroform, liq., mol. reorient. at high press., n.m.r. relax. obs. 3-68871
cyclopropane molecules in cyclopropane clathrate deuterate 3-44346
deuteriochloroform liquid, Raman spectroscopy, mol. reorientation 3-75984
diethylamine, n.m.r. study 3-55497
diethylamine clathrate deuterate, n.m.r. study 3-55497
dinitrocarbanion reorientation in alkali salts, i.r. and u.v. spectra 3-69003
ether in chloroform soln., association and anisotropic mol. reorientation, n.m.r. obs. 3-68873
fluorobenzene-d₅, liq., mole. reorient. at high press., n.m.r. relax. obs. 3-68871
furan, condensed phases, i.r. spectral study 3-68996
hydrocarbons, liq., proton spin-lattice relax., press. depend. 3-41446
hydrogen-bonded systems, vib. and reorientational relax. 3-64669
iminoxyl radicals, ¹⁵N e.p.r. spectral linewidths, mol. reorientation effects 3-43486
liquid, from press. depend. Rayleigh scatt. 3-80055
liquid, mol. motion, conf., Orsay, France, Jul. (1973) 3-64192
liquid, Raman spectra line width and intensity temp. depend. 3-68994
liquid, reorientational motions at high press., n.m.r. relax. obs. 3-68871
liquid, simple, anisotropy in mol. reorientational motion 3-68995
liquid crystals, nematic, interfacial effects in magnetohydrostatic theory 3-43751
methane, solid, u.s. vel., lambda anomaly 3-55031
methyl chloride adsorbed on NaCl and KCl, potential barrier to orientation 3-72265
methyl iodide, and deuterated cpd., liq., reorientational motion temp. depend., Raman spectra obs. 3-64667
methyl iodide, liq., rot. diffusion, Raman and n.m.r. spin relax. obs. 3-75976
methyl iodide, liquid, mol. motions and interactions, temp. dependent Raman study 3-47248
methyl iodide, liquid, molecular vibration excitons, reorientation, Raman band profiles (*German*) 3-53113
methylbromide, mol. reorientation, Raman spectral obs. 3-64666

molecular reorientation continued

- molecular crystals, internal motions, phase transitions, n.q.r. spectra 3-75914
molecular crystals, nucl. mag. relax. rel. to random molecular reorientation 3-75895
neopentane plastic crystal, i.r. and Raman band shape analysis, mol. reorientation 3-75983
nondiffusional, stochastic theory, dielec., nucl. relax 3-79244
nuclear mag. relax. under hindered internal rot., time correl. times 3-49492
pivalic acid plastic crystal, Rayleigh scattering determ. of reorientational activation energy 3-44409
plastic crystal, p.m.r. obs., press. depend. 3-61005
Raman lineshapes analysis w.r.t. reorientational correl. functions 3-46274
Raman scattering efficiency, mol. crystals, theory 3-72656
spin density matrix, zero field 3-78712
tetrafluoromethane:CD₃H(CH₃D), solid, i.r. spectra 3-69002
toluene, in various solvents, orientational relax. rates, depolarized Rayleigh scatt. meas. 3-50574
trichlorodeuteromethane, mol. reorientation. Raman spectral obs. 3-64666
trichloromethyl derivatives of P, CCl₃PCL₄ and (CCl₃)₂PCL₃, n.q.r. spectroscopy and mol. dynamics 3-75912
tumbling system, low symmetry e.p.r., motionally averaged hyperfine structure and asymmetries 3-79896
Ar, liq. of H₂, rototranslational spectrum and intercollisional interference 3-80057
Ar:CD₃H (CH₃D), solid, i.r. spectra 3-69002
Co complex, [Co(NH₃)₄CO₃]₂SO₄, thermal motion of ammine groups, spin-lattice relax. obs. 3-50484
CsPF₆, reorientation motions and spin-rotation interaction 3-53033
CsSH in cubic phase, SH⁻ reorientation, neutron quasielastic scattering study 3-64597
H₂, solid, i.r. spectroscopic study, quantum diffusion 3-80015
H₂ collisions with He and Ne, scattering cross sections for molecular reorientation 3-40683
H₂ reorientation cross sections 3-75159
He:CD₃H(CH₃D), solid, i.r. spectra 3-69002
Kr:CD₃H(CH₃D), solid, i.r. spectra 3-69002
N₂:CD₃H(CH₃D), solid, i.r. spectra 3-69002
NH₄⁺ in ammonium salts, tunnelling study by proton magnetic resonance, reorientation and librations 3-44332
NH₄Cl, phase II, reorientational motion of NH₄⁺ ion, neutron scatt. obs. 3-68173
NH₄ClO₄, proton spin-lattice relax. obs. 3-44343
NH₄H₂AsO₄, l.f. hindered reorientation, n.m.r. obs., Curie pt. behavior, high temp. phase transition 3-61004
NaPF₆, reorientation motions and spin-rotation interaction 3-53033
O₂:CD₃H(CH₃D), solid, i.r. spectra 3-69002
RbSH in cubic phase, SH⁻ reorientation, neutron quasielastic scattering study 3-46597
SF₆, coherent pulse transmission, reorientational collision effects 3-51954
SF₆, liq., Raman obs. 3-68993

molecular rotation

- see also molecular spectra*
1,2-bis-(4-pyridyl) ethanes conformations of the rot. isomers, Raman and i.r. spectra 3-78772
acetaldehyde, collision broadening of rot. lines by O₂ 3-67834
acetaldehyde, internal rotation barriers rel. to localized charge distributions 3-54633
acetonitrile, liq., mol. reorientational motion, Raman bandshapes, diffusion consts. and activation energy 3-60661
acetonitrile-d₃, vibr.-rot. spectra analysis 3-63462
acetylene, electron impact dissociation, rotational and vibrational energy level distrib., luminesc. 3-75127
acrylic monomers, thermal relax. effect from hypersonic obs., mol. rot. of ester group about C-C bond 3-55990
alkyl mercaptans far i.r. spectra, torsional transitions 3-63457
aniline, mol. configuration determination, models for internal rotation, n.m.r. lanthanide shift studies 3-46226
anisotropic rotational diffusion equation, Markov process 3-79245
asymmetric polyatomic molecules, rotational levels, rigid and nonrigid top models 3-60433
atom + diatom inelastic small-angle scattering, semiclassical calc. of rotational transitions 3-71638
atom + rigid symmetric top rotational excitation, distorted wave approx. 3-75135
axially symmetric molecules, group C_{3v}, rot. line intensity in combination bands, rot. interaction 3-78781
azomethine-, azo-compounds and their protonated species, barriers to rotation and inversion 3-67727
benzene rotation mechanism near melting point 3-60435
benzotrifluorides Fourier transform n.m.r., high pressure, ¹⁹F chemical shift 3-61003
benzylcyanide, liq., mol. rot. at high press., n.m.r. relax. obs. 3-68871
tert-benzyl metal compounds, hindered rotation determ. by n.m.r. 3-63514
bicyclic alcohol, mol. configuration determination, models for internal rotation, n.m.r. lanthanide shift studies 3-46226
1-bromo-5-nitronaphthalene in benzene soln., relax. mechanism 3-68921
1,3-butadiene, conformers and internal rotation barriers, MO-SCF study 3-54607
butanol-2-(+), circular dichroism, comparison of theoretical and expt. results of rot. strengths 3-78746
t-butylamine clathrate deuterate, p.m.r. absorption and relaxation, study, isotropic molecular rotation 3-55492
t-butylamine p.m.r. absorption and relaxation study, isotropic molecular rotation 3-55492
t-butylchloride, self-diffusion coeff. and rot. correlation time determ. 3-68872
carbon difluoride, microwave spectra, centrifugal distortion anal. force field and dipole moments 3-78820
chemical reactions, product state distrib., vibr. temp. and rot. distrib. 3-65070
chlorocyclohexane, equatorial, microwave rot. spectra anal. 3-78811

molecular rotation continued

- chloroform crystalline, quadrupole relaxation of ^{35}Cl nucleus and effect on CCl_3 group mobility 3-75902
- p-chlorostyrene, rot. band contour analysis of O_0^0 bands of $\text{A}^1\text{A}'-\text{X}^1\text{A}'$ systems 3-63446
- chlorosubstituted hydrocarbons, i.r. spectra, intensities of characteristic bands of rotational isomers 3-78765
- 2-chlorothiophene, microwave spectra, quadrupole coupling and rotational constants 3-43463
- computer-calculated contours of vibronic bands in triplet-singlet transitions 3-78718
- cyanocyclobutane, microwave spectrum assignments 3-63484
- π -cyclobutadienyliron tricarbonyl, intramol. rot. obs. from nematic-phase n.m.r. 3-60481
- cyclohexene sulphide, microwave spectra 3-43459
- cyclopent-3-ene, microwave spectra, ring polarity, r_s -structure and dipole moment 3-60466
- cyclopentadienone, microwave spectra analysis and assignments 3-78813
- cyclopropane, vibr.-rot. Raman bands 3-63461
- diacetoneglucose, mol. configuration determination, models for internal rotation, n.m.r. lanthanide shift studies 3-46226
- diaryl disulphides, conformational props. calc. from dipole moments 3-43395
- diatomic, Π -state, collision induced rot. energy transfer 3-75139
- diatomic, spectral fine structure due to vibrational and rotational motion, astrophysics and atmospheric applications 3-40604
- diatomic and linear polyatomic molecules; rotational structure of spectra analysis by statistical and computer methods 3-63429
- diatomic electronic transition, rotational line intensities, theory 3-78717
- diatomic free radicals, sensitized fluoresc. by $\text{Hg}(6^3\text{P}_0)$ metastables 3-60484
- diatomic mol., Hund's coupling case, rot. energy and fine struct. of electronic states 3-63423
- diatomic mol., Hund's coupling case, rot. energy and fine struct. of electronic states 3-67785
- diatomic mol., resonances in electron impact 3-52400
- diatomic molecular wave functions and rotational line strengths calc. by RAM method including nuclear spin effect (French) 3-52339
- diatomic molecule, molecular constants determination, term value approach 3-78707
- diatomic molecules, RKR potentials, centrifugal distortion constants 3-78705
- diatomic molecules, rotation-vibration coupling, vibration intensities, closed form formulas 3-78698
- diatomic molecules, rotational excitation by low-energy H^+ collisions 3-71650
- diatomic molecules, vibr.-rot. spectra, intensity distrib., classical calc. 3-74984
- diatomic molecules dissociation, rotational states limited numbers effect 3-71630
- diatomic mols., pressure broadened spectral lines, intermolecular potential, nonrigidity influence 3-75157
- diatomic mols., RKR pots. and semiclassical centrifugal const. 3-67779
- diatomic spectra reduction to molecular constants, construction of RKR potentials 3-78706
- diatomic transitions, computer checking of rot. line intensity factors 3-63426
- dichloronaphthalenes in benzene soln., relax. mechanism 3-68921
- dimethyl cyanamide, barrier to internal rot. of methyl groups 3-60464
- dimethylacetylene cryst., phonon Raman spectra, mol. motions and phase transitions 3-55573
- dimethylacetylene substituted molecule, anal. of Hamiltonian, symmetry group and vibr. coords. 3-74975
- dimethylaminodifluorophosphine, rotational and distortion const. from microwave spectra 3-49476
- dimethylsilane, in torsional excited states, rotational spectra analysis (German) 3-43428
- dimethylsulphide, in torsional excited states, rotational spectra analysis (German) 3-43428
- 1,2-disubstituted ethanes, ab initio MO calc. of internal rotation 3-49451
- double-photon scatt., rotational, by noncentro-symm. mols., reversal ratios 3-67792
- ethane, internal barrier description, FSGO model 3-71503
- ethane, internal rot. barrier calcs., comparison between SCF-LCAO-MO and SCF-X α -SW approxs. 3-40590
- ethylcarbonium ion, nonempirical MO calcs. of energies rel. to geom. 3-63354
- ethylene, and similitudes, mols. symmetry effects in internal rotation 3-74974
- ethylene, electron impact dissoci., rotational and vibrational energy level distrib., luminesc. 3-75127
- ethylene oxide lines, collision broadening by quadrupolar mol. CO_2 3-52397
- eucarvone, protonated, Debye diffusion model 3-75076
- excitation scattering parameters, radial asymptotic expansions 3-40150
- ferrocene i.r. absorption spectra at low temp., phase transition, rotational barrier (French) 3-47260
- fluid, l.f. depolarized (VH) light, line shapes, coupling of rotational and translational motion 3-71533
- fluoroacetones, n.m.r. study and rotational isomerism 3-78843
- p-fluorostyrene, rot. band contour analysis of O_0^0 bands of $\text{A}^1\text{A}'-\text{X}^1\text{A}'$ systems 3-63446
- formaldehyde, factors for $2\nu_2$ band using i.r. spectra 3-63494
- formaldehyde, microwave collision diameters in rot. spectrum 3-67858
- uran, liquid, proton-spin relaxation and molecular motions 3-44344
- uran, liquid, reorientational phase, i.r. bandwidth, relax. 3-68996
- uran, rot. transitions, h.f.s. 3-54701
- ground state const. used in geometrical struct. determ. 3-78652
- halogenoalkanes in Ar matrices at 20K, i.r. spectra and molecular rotation 3-61037
- halopropanes, cryst. internal rot., isomerism, i.r., Raman spectra 3-72653

molecular rotation continued

- hexamethylenetetramine, proton and ^{14}N rotational correlation times in chloroform 3-75900
- homopolar isotopically unsymmetric diatomic molecules, forbidden transition, dipole moment of HD 3-78708
- hydrocarbon chains, correlation functions of internal motion 3-78847
- hydrocarbons, long chain viscous, nuclear spin-lattice relaxation, rotational motion mechanism 3-54769
- hydrogen halides, rotational relax in inert. gas 3-49500
- hydroxyacetone, barriers to internal rotation, group function anal., MO-LCAO-SCF computations 3-49432
- hydroxyacetone, microwave spectroscopy, rotational isomerism, barriers to internal rotation 3-49479
- hydroxymethylcarbonium ion, nonempirical MO calcs. of energies rel. to geom. 3-63354
- hyper-Raman spectra, pure rot. and vibr.-rot., selection rules 3-54693
- 2,2'-iminobis(acetamidoxime) and its Ni(II) and Zn(II) complexes, barrier to rotation 3-52331
- inert gas diatomic molecules, level spacings, calcs. 3-63400
- intermolecular interactions in condensed systems, induced i.r. spectra 3-72697
- internal rot. barriers determ., comment 3-49452
- ionic crystal impurity molecules, low temp. rotation in vibronic spectra 3-69041
- ionic crystal with impurity molecule, symmetry of electronic-vibrational-rotational transitions 3-69042
- isopropyl alcohol, far i.r. spectra, torsional transitions 3-63457
- linear molecules, band moments and rot. autocorrel. functions for perpendicular transitions 3-63434
- linear triatomic molecule, vibr.-rot. energy 3-63419
- linear triatomic molecule, vibrational-rotational levels calc. 3-46249
- liquid, mol. dynamics obs. from i.r. absorpt. band profiles (French) 3-80018
- liquid, mol. motion, conf., Orsay, France, Jul. (1973) 3-64192
- liquid, n.m.r. and neutron scatt. obs. 3-68875
- liquid spectroscopic props., method of mol. dynamics simulation 3-80051
- liquids, n.m.r., neutron spectroscopy 3-68877
- liquids, resonance line shapes for semi-integer spins, second order shifts by mol. rotation 3-41394
- macromolecules, methyl group behaviour, nonexponential nuclear relaxation 3-79936
- MBBA, correlation times by dielectric relaxation, i.r. line broadening and neutron scattering 3-68156
- methane: $\text{CD}_3\text{H}(\text{CH}_3\text{D})$, solid, i.r. spectra 3-69002
- methane, $^{12}\text{CH}_4$, ν_3 band, spectral parameters (French) 3-57653
- methane, $^{12}\text{CH}_4$, hyperfine splittings, F_1 , F_2 levels, ground vibr. state, calcs. 3-63401
- methane, analysis of the ν_4 band up to $J'=12$ 3-40632
- methane, deuterated, vibr.-rot. band ν_5 of 8 μm line (French) 3-57652
- methane, deuterated, in inert liquids, rotational relaxation, i.r. spectra 3-78769
- methane, hyperfine structure of vibration-rotation line, using laser saturated absorption 3-43456
- methane, in gaseous and liquid mixtures, i.r. band shapes and semiclassical rot. diffusion model 3-54681
- methane, J values determ. for $\nu_2 + \nu_3$ and $\nu_3 + \nu_4$ bands 3-40631
- methane, microwave spectrum, ground vibronic state, rot. transitions 3-75052
- methane, microwave-i.r. double resonance using 3.39 μ He-Ne laser line rotational transitions 3-43481
- methane, pure Q-branch transition, i.r.-r.f. double resonance 3-63405
- methane, solid, spin conversion, proton magnetisation, spin-lattice relaxation 3-75903
- methane, theory of absolute intensities for vibration-rotation transitions 3-67820
- methane selenol, μ -wave spectrum, internal rot. barrier, struct. and dipole moment meas. 3-54700
- methanol, hyperfine struct. in internal rotor molecules 3-78817
- methyl alcohol, internal rotation barriers rel. to localized charge distributions 3-54633
- methyl bromide, i.r. spectra, $2\nu_2$ band near 2600 cm^{-1} , rot. fine struct. 3-63454
- methyl chloroformate, internal rot. barrier, microwave spectrum 3-75050
- methyl fluoride, rot.-vibr. spectrum, 2000-2100 cm^{-1} 3-63463
- methyl iodide, Fermi and Coriolis resonances with $\nu_3 + \nu_6$ and ν_2 , ν_5 detailed analysis 3-71550
- methyl iodide, liq., rot. diffusion, Raman and n.m.r. spin relax. obs. 3-75976
- methyl iodide, liquid, mol. motions and interactions, temp. dependent Raman study 3-47248
- methyl iodide, Raman scattering, orientational motions 3-43445
- methyl iodide and CD_3I , liquid, Raman line-shapes, rotation and vibration analysis 3-41509
- methyl substituted aromatic radical ions, proton spin relax., CH_3 line-width 3-63517
- 2-methyl-butane and 2,3-dimethyl-butane, isomerism, Raman spectra 3-78793
- N-methyl-d $_3$ -P,P,P-trimethylphosphine imide, vibr. spectra, struct. of P-N bond 3-75024
- N-methyl-ethylidenimine isotopes, matrix and gas, i.r. spectra, 4000-200 cm^{-1} 3-78807
- methylamine, internal rotation barriers rel. to localized charge distributions 3-54633
- methylamine chloride, internal rot. and inversion doubling in microwave spectrum 3-67829
- methylaminoethane, rot.-inversion spectrum analysis 3-63491
- methylene fluoride-d $_2$, and methylene fluoride-d $_2$, i.r. spectra, force field 3-78761
- methylimine, microwave spectra, molecular constants 3-75051
- methylsilylchlorides, i.r. and Raman spectra, vibr. assignments and torsional barrier heights 3-54680
- monochloroamine, rotation-inversion transitions in microwave spectrum, inversion barrier of amine group 3-40639

molecular rotation continued

- monohalide and monohydride molecules, rotational and hyperfine structure constants tables 3-49446
 naphthalenes, substituted, electronic systems, rot. band contour anal. 3-57641
 near-resonant vibration-rotation energy transfer 3-71642
 neutron scattering obs. in solids and liq., review 3-68140
 neutron scattering studies, physico-chemical aspects, review 3-57645
 nitroethylene, isotopic species, ground and excited vibrational states 3-78812
 nitroethylene, torsion of nitro group, pot. parameters 3-63399
 nitromethane, rotational Zeeman effect (*German*) 3-43432
 nitrosomethane, SCF-LCAO-MO calculations on the rotational barrier 3-43391
 2,4,6-nonachloromesitylene, rotational isomerism, conformational energy, p.m.r. 3-67851
 n-nonadecane, rotor phase transition, inelastic neutron scattering study 3-49853
 nuclear mag. relax. under hindered internal rot., time correl. functions 3-49492
 nuclear spin-rotational relaxation, internal rot., rate eqn. 3-68880
 overall rotation interaction in rotation spectra (*German*) 3-60438
 PAA, correlation times by dielectric relaxation, i.r. line broadening and neutron scattering 3-68156
 pentachlorobenzene compounds, dielectric absorption, molecular rotation 3-72572
 2,4,6,8,10-pentamethylundecane crystalline and glassy films, i.r. spectra and rotational isomerism 3-47268
 phenol, molecular rotation study by neutron scattering and n.m.r. 3-52567
 phenol-OD, microwave and i.r. transitions analysis by rot.-internal rot. theory 3-63490
 phenyldichlorophosphine, rotational isomers 3-78659
 polar diatom-atom scattering, rotational inelasticity, time-dependent perturbation theory 3-71645
 poly(dimethyl siloxane), glass transition temperature meas. 3-79242
 polyatomic mol. collision theory, rot. and vibr. excitation, quantum mech. treatment 3-46346
 polyatomic mol. collision theory, rot. and vibr. excitation, restricted distorted wave approx. 3-46347
 polyatomic molecules, Coriolis coupling consts. transformation properties 3-60434
 polyatomic mols., potential energy function, unitary transformation operator for perturbation treatment of the Hamiltonian 3-40601
 polyatomic mols., transform. props. of centrifugal distortion consts. 3-63406
 polynucleotide chains, internal rot. barriers 3-46358
 polystyrene, intramolecular cross linking, radii of gyration meas. 3-78915
 polyvinylacetate, i.r. bands, temp. depend., 173 to 493 K, CH₃ rot. activation energy 3-46363
 potential curve calc. in zero approx. of generalised WKB method (*Russian*) 3-67766
 propane, in torsional excited states, rotational spectra analysis (*German*) 3-43428
 propargyl alcohol, barriers to internal rotation, group function anal., MO-LCAO-SCF computations 3-49432
 propene, internal rotation barriers rel. to localized charge distributions 3-54633
 trans-propylene imine, microwave spectra, centrifugal distortion effects 3-60463
 propynal, millimetre wave spectrum, ground vibr. state 3-78816
 propynal, rot. anal. of 0-0 band near 4145 Å 3-67793
 pyridine-4-d₁, near u.v. spectra, appl. of band contour anal. method 3-46307
 pyrrole, beam maser spectroscopy, obs. of rotational transitions, nitrogen hyperfine parameters 3-78826
 quinoline, liquid, rot.-vib. relax., Raman and i.r. spectral obs. 3-64670
 relaxation, spherical top gas molecules, collision equations, Bryan-Pidduck model 3-49499
 relaxation rates determ. by saturation time depend. meas. in microwave spectroscopy 3-48422
 rotational relaxation rates determ. by saturation time depend. meas. in microwave spectroscopy 3-48422
 sodium bromoacetate, and -d₂, vibr. spectra and structure 3-78798
 solid and fluid media, Rayleigh, Brillouin and Raman lines rel. to microscopic processes 3-80024
 spectral lines, halfwidth, intensity, determination, iterative solution of nonlinear least squares problem, method (*French*) 3-70310
 spectroscopy, automatic control system for models of molecular systems (ACSM MS) 3-74932
 symmetric molecule, rotational level splitting in the ground vibrational state 3-63417
 symmetric top mol., (± 1) quantum number label 3-67786
 symmetric top molecules, pure rotational Raman scattering 3-60454
 symmetric top molecules, three-photon scattering of laser light rotational line structure 3-60442
 telluraphene, microwave spectra, rot. consts., bonding 3-67826
 tetrahedral mols., sextic centrifugal distortion 3-63409
 tetrahedron hindered rotational energy levels in a tetrahedral crystal field 3-41145
 tetrahydrofuran clathrate hydrate, far i.r. absorption, rotational oscillations 3-80062
 1, 2, 4, 5-tetramethyl benzene, atom-atom pots., H atom coords. 3-72073
 N,P,P,P-tetramethylphosphine imide, vibr. spectra, struct. of P-N bond 3-75024
 thioamides, hindered rotation barriers, p.m.r. determ. 3-71529
 threefold barrier, equivalence of V₆ to torsional flexing 3-74972
 transition metal carbonyls in gas and liq. soln., vib.-rot. coupling effects on correlation functions 3-67825
 transport and spectral properties, kinetic theory, collision cross sections 3-71622
 triethylenediamine, UV absorpt. spectrum anal. of struct. 3-78740
 trifluoroethylene, assignment in ground and vibrationally excited states 3-43461
 trimethylamine, mol. A₂ torsional frequency by computer aided microwave anal. 3-78821

molecular rotation continued

- trimethylamine-borane, microwave spectra, rot. consts. 3-60465
 trimethylchlorosilane, nuclear quadrupole coupling and rotational const. determ. from microwave spectra (*German*) 3-60468
 trimethylsilyl cyanide and isocyanide, centrifugal distortion and rotational consts. 3-43462
 2,8,9-trioxadadamantane, microwave spectrum, vibrational satellites, rotational consts. 3-40636
 triphenylcarbonium derivatives, reduction of fluorescence yield by rotation (*German*) 3-57665
 1,1,2-trisubstituted ethanes, p.m.r. spectrum, theoretical appl. of coupling consts. depend. on internal rot. pot. function 3-46318
 trisubstituted methanes, ab initio MO calc. of conformations and stabilities 3-49429
 two-proton system with hindered rot., methyl group tunnelling, n.m.r. lineshapes 3-64562
 vibrational-rotational spectra electronic-nuclear interaction effect 3-63428
 o-xylene, microwave spectra, methyl rot. barrier, methyl conform. and dipole moment 3-67832
 o-xylyl, rotational contour analysis of electronic origin band in emission spectrum at 4683 Å 3-67794
 AlBr, quadrupole h.f.s. of rot. transition (*German*) 3-57662
 AlCl, hyperfine structure of rotational transition J=1→2 (*German*) 3-57662
 AlO, D₂Σ⁺-X₂Σ⁺ system, u.v. region, rotational and vibrational constants 3-60450
 AlO, fundamental vibration-rotation bands, relative spectral absorption coefficients 3-54683
 AlO, Morse oscill., r-centroids of 2Σ-X₂Σ⁺ bands 3-74986
 AlS radical, A₂Σ⁺-X₂Σ⁺ transition, emission spectrum (*French*) 3-6259
 Ar, liq. of H₂, rototranslational spectrum and intercollisional interference 3-80057
 ArHCl complex, rotational consts. determ. by mol. beam electric resonance spectroscopy 3-78824
 AsF, Hund's coupling case 3-67785
 AsO, emission spectra, rot. analysis 3-63439
 AsS, analysis of A²Π-X²Π band system 3-40613
 AuGa structure, incompletely resolved 0-0 band, isotope effect determination, visible spectrum (*French*) 3-43423
 B₂H₆, distortion const., Green's function anal. of vibr. 3-78697
¹⁰BH₃CO, mol. consts. of vibr.-rot. bands from i.r. study 3-78752
 Ba(ClO₃)₂.H₂O(D₂O), i.r. spectral mode assignment 3-75973
 BrF₃, rot. spectra, 70 and 140 GHz (*French*) 3-43460
 CF₃ compounds, -PH₂, -PD₂, -AsH₂, -AsD₂, vibr. spectra and normal coord. anal. (*German*) 3-46282
 CH, term values and molecular parameters for rotational and vibrational levels in visible and near u.v. region 3-75010
 CH⁺, term values and molecular parameters for rotational and vibrational levels in visible and near u.v. region 3-75010
 CH₄, microwave transition in v₃=1 excited state, i.r. microwave double resonance method 3-52373
 CHO radical, microwave spectrum, obs. of K doubling transition in rotational states, hyperfine interaction 3-78827
 CN mol. band system, solar temp. determ. 3-61669
 CO, absorpt. spectrum atlas, 1060-1900 Å 3-75007
 CO, diatomic mols. trapped in Ne matrix, absorpt. spectra, vibr. and rot. struct. 3-75011
 CO, pure and in Ar matrix, absolute i.r. absorption intensities, band shapes 3-80061
 CO, vibr.-rot. transitions, rel. to pulsed chem. laser kinetics 3-74234
 CO vibration-rotation LTE in late-type star model atmospheres 3-61761
 CO + Ne collisions, rot. inelasticity, time depend. perturbation approach 3-71636
 CO₂, calc. of population relaxation for rotational levels 3-63559
 CO₂, energy from transitions, time const., rot. relax. time 3-66799
 CO₂, Raman spectra, rotational const. determ. 3-49471
 CO₂, rotational line overlap due to collision broadening in laser transitions 3-62699
 CO₂, semiempirical mol. orbital calc., reparameterisation, INDO³, barriers to internal rotation, bond angles and lengths 3-74948
 CO₂ amplifier system, rot. relax. effect, energy extraction 3-66800
 CO₂ laser, pulse sharpening due to rotational level coupling 3-48876
 CO₂ laser, Q-switched pulse duration, rot. relax. effect 3-66804
 COF₂, ¹⁹F hyperfine struct., mag. shielding, beam maser spectra 3-71573
 CSe, emission spectrum meas., 3060-2680 Å, obs. of new band system, rotational analysis 3-78743
 C⁸⁰Se, emission spectrum analysis 3-60446
¹²C¹⁶O₂, rot. consts. from beats between Lamb dip stabilized lasers 3-63474
 Cs collisionally induced fine structure transition with Kr and methane, rotational effects 3-67695
 CsPF₆, reorientation motions and spin-rotation interaction 3-53033
 CsSh in cubic phase, SH⁻ reorientation, neutron quasielastic scattering study 3-46597
 CuBi, rotational analysis of A and B systems (*French*) 3-57642
 O-D₂, density-dependent phase transition and anisotropic interactions 3-75995
 D₂, Lyman and Werner bands, vacuum u.v. spectra, vibr. and rot. level anal. 3-40615
 DCl, dipole moment function, vibration-rotation matrix elements determ. 3-52351
 D₂¹⁷O and D₂¹⁸O, microwave spectra 3-78818
 N,N-dimethylamides, chalcogen replaced, hindered rot. about N-C amido band 3-52389
 F + DF(v) → DF(v') + F vibr. relax. process, rate consts., Monte Carlo calcs. 3-60486
 F + H₂ → HF + H, vibrational energy distributions, rotation effects 3-71627
 F + HF(v) → HF(v') + F vibr. relax. process, rate consts., Monte Carlo calcs. 3-60486
 F₂CS, rotational constants 3-67827
 FNO force consts. calc., use of vibration-rotational interactions and inertia defects 3-52337
 GeD₄, i.r. and Raman spectra, rovibrational consts. 3-63460

molecular rotation continued

- GeF, rotational structure in emission transitions of higher electronic states 3-78742
 GeH₄, forbidden rot. spectrum in ground vibronic state 3-67811
 GeH₄, pure rot. transitions, spectral meas. 3-43449
 GeO, Franck-Condon factors and r-centroids for (A-X) system 3-67797
 GeO, rotational mag. moment meas. by molecular beam electric resonance spectra 3-78727
 H₂, compressed, Rayleigh-Brillouin scatt., rotational relax. 3-80032
 H₂, coupled-channel calc. of rotational excitation by Li⁺ collisions 3-71649
 O-H₂, density dependent phase transition and anisotropic interactions 3-75995
 o-H₂, matrix treatment of dissociation rotation-vibration relaxation times 3-67857
 H₂, resonance collisions in energy transfer, Raman linewidth measurement 3-67864
 H₂, resonant rotational excitation by electron impact 3-78872
 o-H₂ molecular pairs, isolated, energy spectrum 3-46598
 H₂-He mixtures, quantum scattering theory of rotational relaxation and spectral line shape 3-46351
 H₂+Hr collisions at nonzero impact parameters, simultaneous vibr. and rot. transitions 3-75132
 H₂+Li⁺ collisions, vibr. excitation, rot. effect 3-57675
 HCN AND DCN, anharmonic force field and equil. struct. 3-60430
 HCP and DCP, anharmonic force field and equil. struct. 3-60430
 HCl, absorpt. line broadening by gases, fund. band, temp. depend. 3-63544
 HCl, dipole moment function, vibration-rotation matrix elements determ. 3-52351
 HCl gaseous mixtures with HBr and HI, low temp. absorpt. spectra (French) 3-78750
 HCl lineshifts and widths due to inert gas broadening of vibration-rotation lines 3-43467
 HCl+Ne collisions, rot. inelasticity, time dependent perturbation approach 3-71636
 HCl⁺, emission spectra of four isotopic combinations 3-78739
 H³⁵Cl, rot. consts. calc., optimum number and accuracy considerations 3-63416
 HF, V-V, V-R, and T energy transfer collisions, temp. depend. 3-40674
 HF, vibration to rotation energy transfer, dipole-dipole and hydrogen bond interactions 3-63557
 HNC, interstellar mol., determ. of props. 3-73549
 HNO and DNO, microwave spectra analysis 3-63488
 H₂O, Fourier transform spectrum, between 2930 and 4255 cm⁻¹ 3-78767
 H₂O, rot. and centrifugal consts. calcs., appl. of energy moments method (Russian) 3-78701
 H₂O, rot. mag. moments calc. 3-60443
 H₂O, rotational, distortion consts., spectral analysis deriv. 3-78715
 H₂O, rotational levels, rigid and nonrigid rot. models 3-60433
 H₂O and H₂O-trimethylamine complex, gas phase Raman spectra 3-78800
 H₂O molecule, IR vacuum spectra of vapour 3-78762
 H₂O pure rotation spectrum, approximate mean absorption coefficient 3-67833
 H₂O vapour transitions, tunable laser meas., 5 μm region 3-40622
 H₂¹⁶O, ν₂ band study, rotational levels 3-67823
 H₂¹⁶O, (000) and (020) states study, 2930 to 4255 cm⁻¹ region 3-78766
 H₂¹⁶O, high resolution i.r. spectra of ν₁+ν₂ and ν₂+ν₃ bands (French) 3-75025
 H₂O₂, pot. barriers calc. using SCF Xα SW method 3-46224
 H₃PBH₃, microwave spectra, dipole moment, internal rotation barrier, staggered conformation, Stark splitting 3-54699
 H₂S, rotational, distortion consts., spectral analysis deriv. 3-78715
 H₂, ab initio calc. of A¹Σ_g⁺←X¹Σ_g⁺ absorpt. spectrum 3-63445
 HgH, Hund's coupling case 3-67785
 I₂, rotational constants for highly excited vibrational levels 3-63421
 I₂ excited state collisions, classical trajectory calc. of vibr.-rot. energy transfer 3-71641
 IF, rotational spectrum, hyperfine structure analysis (German) 3-78822
¹²⁷I₂, analysis of B³Π₀←X¹Σ_g⁺ system 3-60429
 KNO₃, crystal, model for coupled rotation-displacement modes 3-79440
 Li+H₂, vibrational-rotational excitation, potential energy surface calc. 3-71639
 LiAlH₄, lib. motion, inelastic neutron scatt. obs. 3-60678
⁶Li ¹⁹F, J=1→0 rotational transition, partial resolution 3-54704
 LuH, electronic spectra, rotational analysis (French) 3-54659
 MgO, F¹Π-X¹Σ electronic transition 3-52361
 MgO, G¹Π-X¹Σ and G¹Π-A¹Π transitions assignment 3-71542
 N₂, diatomic mols. trapped in Ne matrix, absorpt. spectra, vibr. and rot. struct. 3-75011
 N₂, rot. structure blurring, perturbation of electronic transitions under foreign gas pressure 3-75012
 N₂, triplet states parameters calc. 3-60421
 N₂ Rydberg complexes band structures, rotational analysis 3-40616
 N₂-Ar solute-solvent systems, computer simulation of correl. functions, bandshapes and relax. times 3-64651
 N₂-Ar Van der Waals complex, i.r. absorption spectra, internal rotation 3-78805
 NCN₃, microwave spectra, anal. four nuclear quadrupole problem 3-78819
 NF and NF⁺, configuration interaction studies rotational and vibrational consts. calc. 3-40593
 NH₃, beam maser meas. of relax. cross sections 3-54754
 NH₃, optically pumped, obs. of submillimetre emission due to rotation-inversion transitions in ν₂ state 3-74232
 NH₃, pot. barriers calc. using SCF Xα SW method 3-46224
 NH₃, rot. energy transfer, direct obs. by time-resolved i.r.-microwave double reson. 3-78886
 NH₃, rot. mag. moments calc. 3-60443
 NH₃, rot. structure blurring, perturbation of electronic transitions under foreign gas pressure 3-75012

molecular rotation continued

- NH₃ in N₂ and Ar matrices, i.r. spectra 3-55589
 NH₄H₂PO₄, NH₄H₂AsO₄, (NH₄)₂H₂IO₆, NH₄ motion obs. by inelastic scattering of neutrons 3-79996
 NO, diatomic mols. trapped in Ne matrix, absorpt. spectra, vibr. and rot. struct. 3-75011
 NO, Doppler-limited i.r. mag. rot. spectrum, line shape 3-43448
 NO, fund. and first overtone bands obs. in NO-rare gas mixtures, 10000 psi 3-63444
 NO, rot. structure blurring, perturbation of electronic transitions under foreign gas pressure 3-75012
 NO laser, ²Δ←²Π near i.r. transition, rotational analysis of spectrum 3-66806
 NO₂, ²B₂←²A₁ transition, resonance fluorescence, rotational consts. 3-78783
 NSF, rot. analysis of ¹A'←¹A' band system 3-60447
 NaAlH₄, lib. motion, inelastic neutron scatt. obs. 3-60678
 NaLi collision-induced rotational transitions, laser excited fluorescence 3-63553
 NaPF₆, reorientation motions and spin-rotation interaction 3-53033
 O₂, X³Σ_g⁻ state, resolution of discrepancies 3-78736
 O₂-Ar Van der Waals complex, i.r. absorption spectra, internal rotation 3-78805
 O₂⁺, A₂Π_g←X₂Π_g second negative band system 3-78735
 O₃, ¹8O substituted, microwave spectra, rotational consts. 3-78782
 OCS, isotopically enriched, ground state and vibr. excited, microwave spectra 3-67830
 OCS, rot. structure blurring, perturbation of electronic transitions under foreign gas pressure 3-75012
 OD free radical, A²Σ⁺←X²Π_i electronic band system, rotational term values 3-78737
 OH, excited, vibration-rotation bands, i.r. airglow, correl. of fluctuations 3-80789
 OH (A²Σ←X²Π) rotational line strengths and energy level population in water vapour arc plasmas 3-43688
 OH in water vapour arc plasmas, rotational lines meas. 3-43687
 OH⁻, photodetachment spectra, rot. line strengths 3-40659
 OsO₄, rotational-vibr. spectra, narrow saturation resons. induced by CO₂ laser radiation 3-46279
 P₂ radical, electronic system bands analysis, π-π transition (French) 3-52353
 PH₃, ground state rot. consts., i.r. determ. 3-40626
 PH₃BH₃, barrier to internal rotation, electronic struct. 3-46223
 PrO, visible and IR spectra 3-75026
 RbSH in cubic phase, SH⁻ reorientation, neutron quasielastic scattering study 3-46597
 SF radical, microwave spectra, rotational consts. 3-40637
 SF₆Cl, rot. spectrum, K-type splitting (French) 3-57659
 SH, photodetachment spectra, rot. line strengths 3-40659
 SH(²Π_{3/2}) radical in two lowest rotational levels, gas phase e.p.r. spectra, proton hyperfine interactions 3-43490
 SO, Hund's coupling case 3-67785
 SO₂, ³B₁←¹A₁ band system, rotational analysis of (010), (100), and (110) bands 3-40611
 SO₂, linewidth parameters for ΔJ=1, 0≤J≤43 rotational transitions 3-43464
 S₂O, centrifugal distortion consts., microwave spectra analysis 3-67828
³²Se¹⁶O₂, ν₁+ν₂ combination band obs. 3-63453
 SeH⁻, photodetachment spectra, rot. line strengths 3-40659
 SiCl, rel. intensities of band spectra, vibrational overlap integral, calc. of Franck-Condon factors 3-78733
 SiF₂, microwave spectrum in excited vibr. states, equil. struct., pot. function, Coriolis reson. 3-67831
 SiO, rotational mag. moment meas. by molecular beam electric resonance spectra 3-78727
 SnCl radical, analysis of the a-X system (3400-3900 Å) (French) 3-49462
 SnCl radical, rotational anal., excited by Ar high tension discharge, B²Σ⁺←X²Π_i transition (French) 3-75006
 Srl, band system in 3350-3560 Å region 3-52362
 TeF₄Cl, rotational constants of isotopic species 3-46304
 YbH(D), Hund's coupling case 3-67785

molecular rotation in solids see nuclear magnetic resonance

molecular spectra

- see also macromolecular spectra; molecular electronic structure; molecular rotation; molecular vibration; molecular visible and ultraviolet spectra; spectra of inorganic molecules; spectra of organic molecules and substances
 asymmetric molecules, bandshape theory, dichroism, polarisation 3-72754
 axially symmetric molecules, group C_{3v}, rot. line intensity in combination bands 3-78781
 binary mixtures containing Hg vapour, electrodeless glow discharges, 3884 Å band emission, comment 3-49463
 Born-Oppenheimer approx. for wave functions and spectra, validity 3-63385
 computer simulation, electronic absorption spectra 3-49454
 conference, Columbus, USA (June 1973) 3-78722
 conference, Tallinn, USSR, May (1973) 3-67790
 continuous vibronic spectra, purely electronic transition energy calc. 3-63430
 correlation effects in pi electron system 3-71534
 data processing system, PUMSM 3-74996
 decay theory, Green function treatment 3-71571
 density matrix, irreducible decomp. for tensorial wave functions (Russian) 3-54399
 diatomic and linear polyatomic molecules; rotational structure of spectra analysis by statistical and computer methods 3-63429
 diatomic bound states, model calc. of avoided-crossing problem 3-78723
 diatomic molecular wave functions and rotational line strengths calc. by RAM method including nuclear spin effect (French) 3-52339
 diatomic molecules, empirical relation between spectroscopic consts. 3-78721
 diatomic mols., intensity theory, electronic transition moment variation 3-43436
 dipole-dipole interaction in liquid, electronic spectra, luminescence 3-75970

molecular spectra continued

- double-photon scatt., rotational, by noncentro-symm. mols., reversal ratios 3-67792
 Dutch Atomic and Molecular Physics Study Group investigations (*Dutch*) 3-49455
 E \otimes E system, singlet to doublet transition, lineshape calculation 3-43465
 electronic spectral oscillator strengths, solvent effects 3-40602
 ENDOR spectrum, coherence effects on line shape, Freed theory test (*German*) 3-57672
 e.p.r., mag. parameters of hyperfine struct. cepstrum transform. 3-63520
 ESCA, calc. by multiple-scatt.-X α method 3-40662
 Franck-Condon factors, interpolation formulae 3-67788
 frequency splittings, correlated data, least-squares analysis 3-67787
 furnace system, for high temp. obs. in vacuum u.v. 3-62104
 hydrogen-bonded systems, i.r. spectra, general theoretical model including Fermi reson. and vibr. modes coupling 3-52366
 inert gas matrix, distortion of isolated ionic mol. 3-74995
 intermolecular interaction and intramolecular charge transfer under optical excitation 3-71535
 intermolecular interactions in condensed systems, induced i.r. spectra 3-72697
 isolated molecules, radiative rates, energy depend. 3-78829
 lifetimes, use of high frequency electron beams 3-77495
 light-shift scattering, role of exchange for double well 3-63471
 linear molecules, band moments and rot. autocorrel. functions for perpendicular transitions 3-63434
 linear molecules, microwave spectra of l-doubling, centrifugal distortion effects 3-52374
 Lorenz-Lorentz eqn., generalised, applic. to absorbing solvent 3-74997
 molecular fluids, long range many mol. interactions, effect on absorpt. spectra 3-52405
 motion of molecules, neutron scattering studies, physico-chemical aspects, review 3-57645
 optical absorption, effect of mode-mode interaction in excited state, exact calculation of Franck-Condon factor 3-63447
 optical transitions to degenerate levels 3-60441
 oriented molecular films adsorbed within porous media, theory 3-60459
 pair perturbations in electronic spectra, exptl. data processing method (*French*) 3-52347
 polyatomic gases, absorption of synchrotron radiation 3-40614
 polyatomic molecules and ions, genealogy in mol. spectroscopy 3-63432
 polyenic molecules, vibr. absorpt. bands in electronic spectra, relative intensities calc. 3-63431
 r-centroids calc. 3-71531
 radiative and nonradiative transition probabilities, one-particle approximation formulae 3-67848
 rotational, automatic control system for models of molecular systems (ACSM MS) 3-74932
 spectral distrib. of absorption coeff. in vibr. spectra 3-74998
 spin-orbit coupling and mol. interaction with radiation field 3-52346
 spin-orbit coupling operator and CNDO approach 3-74950
 stellar, hot supergiants, molecular features around 1720 Å 3-69945
 symmetric top mol., (\pm l) quantum number label 3-67786
 symmetric top molecules, three-photon scattering of laser light rotational line structure 3-60442
 synchrotron radiation, meas. and techniques 3-39937
 synchrotron radiation as u.v. source, 10-1000 Å, spectroscopy applications, review 3-39930
 synchrotron radiation spectroscopy from 5 to 260 eV 3-40061
 triatomic molecules, influence of Renner effect on intensities of electronic-vibrational transitions 3-52348
 triplet-singlet transitions, vibronic bands, computer-calculated rot. contours 3-78718
 two-level systems, variational principle for weak stimulated absorpt. with energy minimizing fields 3-52341
 vibrational, semi-classical approach, regular and irregular spectra 3-66622
 vibrational frequencies tables 3-75039
 vibrational-rotational spectra electronic-nuclear interaction effect 3-63428
 weak absorption line detection, using glass:Nd laser 3-39933
 X-ray spectroscopy ESRIN-Bonn-Imperial College expt. with synchrotron radiation 3-40060

molecular structure (electronic) see *molecular electronic structure*
molecular structure (geometrical) see *molecular configurations and dimensions*

molecular vibration

- see also *Fermi resonance; molecular force constants; molecular spectra*
 (XYZ)P-S molecules, i.r. frequencies of P-S bonds (*French*) 3-49438
 1,1-difluoroethylene, Fermi resonances 3-75018
 n-hexane, low frequency mol. vibrations by neutron inelastic scattering 3-75577
 acenaphthene vinyl ethers, i.r. spectra, config., vib. (*Russian*) 3-63479
 acetaldoximes, normal coordinate calcs., normal vibrations, potential energy distributions (*German*) 3-74980
 acetaldoximes, normal vibrations, i.r. spectra (*German*) 3-74979
 acetic acid dimers, anharmonic couplings via Fermi reson. in strong coupling theory (*French*) 3-52336
 acetonitrile-d₃, vibr.-rot. spectra analysis 3-63462
 acetophenones, substituent effects on acetyl group config. rel. to carbonyl frequency 3-63353
 acetylene, electron impact dissoci., rotational and vibrational energy level distrib., luminesc. 3-75127
 acrolein, cis and trans, near u.v. absorption spectra, vibrational struct. 3-52352
 acrolein-d₁, near u.v. absorption spectra, vibrational struct. 3-52352
 in adsorbed mols. by fast moving dislocations 3-72273
 alcohols, liquid, detection of intermolecular coupling in Raman spectra 3-57657
 aldehydes, static and dynamical pot. surface distortions in $^3A''(n\pi^*)$ states 3-63382

molecular vibration continued

- aliphatic hydrocarbons, i.r. spectra, Davydov splitting, reson. 3-72654
 alkali halide:NH₄⁺, pressure var. of i.r. spectra 3-68363
 alkali halide, rhombic dimer molecules, thermodynamic functions and molecular parameters 3-49428
 alkali halide cryst., impurity mol. anion vibr. bands, temp. depend. of integral absorpt. 3-72695
 alkali metal chlorate monomers, matrix isolation study of modes, metal-chlorate vibration 3-78806
 alkali metal ozonide molecules, i.r. spectra, isotopic shifts, stretching modes 3-71552
 alkali metal ozonides, M⁺O₃⁻ types, Ar matrix, reson. Raman spectrum 3-78808
 alkali metal ozonides, matrix isolated, resonance Raman spectrum, vibrational analysis 3-71553
 n-alkyl fluorides, C-F stretching frequencies of rotational isomers 3-43426
 alkyl mercaptans far i.r. spectra, torsional transitions 3-63457
 amides, simple primary and secondary, identification and origin of N-H overtone and combination bands in near i.r. spectra 3-46291
 amidoximes, valence vibr. bands of NH₂, ND₂ and NHD groups, NH bonds inequivalence (*French*) 3-52365
 amine-SO₂ complexes, force consts. for charact. vibrs., i.r. and Raman spectra 3-60461
 6-aminopenicillic acid, i.r. vibrational spectrum, structural analysis (*Russian*) 3-78778
 anthracene, vibrational relaxation in triplet state 3-46312
 anthracene crystals, exciton fluoresc., relax. 3-66890
 aromatic, force const. determ. using Coulson-Longuet-Higgins formula (*Russian*) 3-63420
 aromatic hydrocarbons, mag. circular dichroism, vibronic coupling 3-74993
 asymmetric complexes, proton tunnelling effect on internal vibrs. 3-60427
 atom-polyatomic molecule collisions, ITFITS model for vibration translation energy partitioning 3-75138
 axially symmetric molecules, group C_{3v}, rot. line intensity in combination bands, vibr. interaction 3-78781
 azide and metalcarbonyl complexes, reson. Raman effect obs. (*German*) 3-78775
 azomethane, azomethane-d₆, Raman spectra and vibrational potential function 3-75017
 azulene, B-X(3500 Å) transition, medium-depend. effects, vibronic coupling, Fermi reson. 3-75002
 benzaldehyde, vibrations of $\bar{a}-\bar{x}$ system in free molecule 3-67843
 benzene, CH-stretching overtone spectrum analysis, phase coincidence problem 3-67777
 benzene, vibrational spectrum theory 3-74987
 benzenes, monosubstituted, ν_8 and ν_{19} vibrs., i.r. band intensities 3-60456
 benzodioxane-1,4, i.r. absorpt. bands temp. depend. in deform. vibrations region (*Russian*) 3-54694
 benzonitrile vibronic spectra, theoretical study 3-67783
 benzonitrile, vibrational analysis of the 2738 Å system 3-40610
 benzophenone-diphenylamine complex, form I, vibr. analysis of i.r. absorpt. spectrum (*French*) 3-57650
 1,4-benzoquinone, (and B0-d₄) single crystals 3-80045
 benzylpenicillin, i.r. vibrational spectrum, structural analysis (*Russian*) 3-78778
 biacetyl, electronic and vibrational relaxation 3-40649
 biacetyl, vibr. relax. obs. by visible-i.r. double reson. technique 3-78885
 bicyclo(3.1.0)hexane analogs, far i.r. spectra, ring puckering vibrs., mol. config. 3-63456
 bimolecular reactions, collinear, perturbation theory for vibrational transitions 3-73126
 biphenylene, Raman spectra, in-plane normal mode calc. and complete vib. assignment 3-61038
 bistrifluoromethyl sulphide, sulphoxide and disulphide, Raman spectra, normal modes vibr. assignments and depolarisation meas. 3-47274
 borine carbonyl, Green's function anal., mol. consts. 3-78696
 bridged metal-metal bonded species, spectra 3-78796
 m-bromoanisole, u.v. absorpt. spectra assignments 3-67799
 bromomethane, liquid, Raman spectroscopy, vibrational relaxation, mol. reorientation 3-75984
 bromophenols, isomeric, fundamental frequency assignment, effect of Br substitution 3-78758
 5-bromotetrazole, single cryst., Raman active external phonon assignments, harmonic force const. calcs. 3-50573
 bromoxylenes, vibrational spectra 3-46272
 3-butyne-2-one, i.r. and Raman spectra, vibrational assignment 3-71560
 carbamoylazides, and N-deuterated derivatives, i.r. and Raman spectra (*German*) 3-47271
 carbohydrates, i.r. spectra, config. depend. 3-72655
 carbon difluoride, microwave spectra, centrifugal distortion anal. force field and dipole moments 3-78820
 carbonyl group, C=O stretch region in vibr. spectrum 3-63410
 β -carotene and related compounds, Raman vibr. reson., in-plane vibr. model 3-78755
 centrifugal stretching constants, inequalities rigorous derivation 3-63414
 chemical reactions, product state distribs., vibr. temp. and rot. distribs. 3-65070
 chiral molecules, spectral anomalies, i.r. rotatory dispersion 3-71566
 2-chloroacrylonitrile, normal coordinate analysis 3-46252
 chlorobenzene, out-of-plane vibr. modes in ground and first excited singlet states 3-63408
 2-chlorobutane, torsion force consts. and low frequency bending assignments 3-71559
 chloroform, and deuterated analogue, Raman spectra and cryst. struct. at 77 K 3-50576
 chloromethanes, vacuum u.v. absorpt. spectra 3-52356
 N-chloropiperidine, vibrational analysis and conformation (*Russian*) 3-63476
 2-chloropropane, torsion force consts. and low-frequency bending assignments 3-71559

molecular vibration continued

- chlorosubstituted hydrocarbons, i.r. spectra, intensities of characteristic bonds of rotational isomers 3-78765
 chloryl fluorides, Urey-Bradley force fields 3-67782
 cinnoline in durene and naphthalene host cryst., electronic absorpt. spectra analysis 3-69028
 clathrates, far i.r. spectra, mol. crystals 3-72661
 collisions, nonadjacent vibrational transitions 3-71632
 collisions, vibrational to translational versus vibronic to translational energy transfer 3-40672
 complex hydrogen bonded cations, stretching and bending modes, vibrational spectra, proton potential 3-75031
 complex molecules, spectral distrib. of absorption coeff. in vibr. spectra 3-74998
 computer program for calcs. of mol. geometry and thermal vibs. in crystals (Czech) 3-54604
 continuous vibronic spectra, purely electronic transition energy calc. 3-63430
 coronene, luminescence and vibrational spectra 3-60460
 o-, m-cresols, i.r. absorption spectra, assignment of vibrational frequencies 3-78759
 crude adiabatic vibronic state wavefunctions and radiationless processes interpret. 3-43420
 cryptocyanine, forced Raman scattering 3-64655
 crystals, separation of internal and external vibrations, dynamical matrix, harmonic approximation 3-40991
 cyanmelluric acid salts, cyanmelluric ring charact. freq. in i.r. spectra (Russian) 3-71565
 cyanocyclobutane, microwave spectrum assignments 3-63484
 1,4-cyclohexadiene and 1,3-cyclohexadiene, ring-puckering vibs. 3-78790
 cyclohexene sulphide, microwave spectra 3-43459
 cyclopent-3-enone, out-of-plane ring modes from far i.r., Raman and microwave spectra, pot. function 3-60467
 cyclopentane, cryst., vibr. spectra, phase transition, 168 K 3-50565
 cyclopentanone, vibrational analysis, i.r. and Raman spectra 3-67812
 cyclopentene, i.r. and Raman spectra interpretation 3-54685
 cyclopropane, perpendicular bands in 3000 cm^{-1} region, Q-branches 3-67819
 cyclopropane, vibr.-rot. Raman bands 3-63461
 cyclopropane series ketones and thio ketones, position and intensity of i.r. bands (French) 3-46273
 cyclopropenone- d_0 (and - d_2), i.r. and Raman spectra 3-78785
 degeneracies in crystal field, splitting of bending modes of linear triatomic ions 3-55061
 N,N-deuterated propionamide, i.r. and Raman spectra, vibrational assignments 3-60452
 N,N-deuterated thiopropionamide, i.r. and Raman spectra, vibrational assignments 3-60452
 deuteriochloroform liquid, Raman spectroscopy, vibrational relaxation, mol. reorientation 3-75984
 diatomic, spectral fine structure due to vibrational and rotational motion, astrophysics and atmospheric applications 3-40604
 diatomic mol., kinetic and potential energy expectation values from vibrational energy levels 3-40598
 diatomic mol., resonances in electron impact 3-52400
 diatomic molecule, molecular constants determination, term value approach 3-78707
 diatomic molecules, mean vibr. amplitudes 3-67770
 diatomic molecules, rotation-vibration coupling, vibration intensities, closed form formulas 3-78698
 diatomic molecules, vibr.-rot. spectra, intensity distrib., classical calc. 3-74984
 diatomic molecules, visualization using desktop calculator 3-63565
 diatomic mols., fundamental stretching vibration frequencies variation 3-49453
 diatomic mols., RKR pots. and semiclassical centrifugal consts. 3-67779
 diatomic spectra reduction to molecular constants, construction of RKR potentials 3-78706
 dichloropentane, torsion force consts. and low frequency bending assignments 3-71559
 1,1-dicyanocyclopropane, liquid and vapour phase, vibrational spectrum 3-46287
 diethylamine, vibrational spectrum, absorption bands integrated intensities calc. 3-63469
 1,2-difluorodiimide, cis- and trans-, vibr. coupling effects and pot. functions 3-78702
 11,1-difluoroethene, vibr. corrections of dipolar couplings 3-78700
 1,2-difluoroethylene, cis- and trans-, vibr. coupling effects and pot. functions 3-78702
 2,3-dihydrofuran and 2,3-dihydrothiophene, ring-puckering vibs. 3-78790
 trans-1,4-diiodocyclohexane, vibrational analysis and conformation (Russian) 3-63476
 β -diketones, rare earth complexes, i.r. spectral band assignments 3-78751
 dimers, strong coupling and spectral consequences 3-78699
 dimethyl and diethyl-2,2-stanna-2 dithia-1,3-cyclopentanes, vibration assignments (French) 3-43454
 dimethyl cyanamide, i.f. vibs., microwave spectra 3-60464
 dimethylacetylene substituted molecule, anal. of Hamiltonian, symmetry group and vibr. coords. 3-74975
 dimethylchloride, isotopic dilution effect on i.r. absorpt. bandshape 3-54679
 3,3-dimethyldiazirine, i.r. and Raman spectra 3-78788
 1,4-dioxacyclohexadiene-2,5, far i.r. spectra, struct., ring bending modes 3-40624
 p-dioxane and H_2O_2 binary solutions, i.r. and Raman studies (French) 3-58512
 dioxolan, i.r. spectra, $\nu(\text{CH})$ vibs. of O-CH₂-O group (French) 3-46270
 diphenylpolyenes, conjugation and resonance Raman effect on Raman intensities 3-60423
 cis-1,4-ditertiarybutylcyclohexane, combined electron diffr., conform. energy and vibr. obs. 3-63357
 durene, methyl motions, vibr. exciton, temp. depend. 3-44042

molecular vibration continued

- electron impact, vibr. excitation cross sections calc. methods, comparison 3-46345
 energy transfer, vibrational relaxation rate meas. interpret. 3-54745
 energy transfer collisions effect of straight path approximation and exchange forces 3-43515
 e.p.r. spectra, $^2\text{E}_g$ state, second order reduction factors, Jahn-Teller effect 3-72507
 esters, mixed polyfluorinated, valency vibration absorption bands, carbonyl groups (Russian) 3-71530
 ethane, mol. force fields and isotopic rules determ. 3-54653
 ethanol, liquid, hydrogen bonded, association and assignment of OH overtones 3-75023
 ethyl chloroformate, vibrational spectra, rotational isomerism, normal coordinate analysis, mean amplitudes 3-54687
 ethyl cyanoformate, vibrational spectra, rotational isomerism, normal coordinate analysis, mean amplitudes 3-54687
 ethyl formate, vibrational spectra, rotational isomerism, normal coordinate analysis, mean amplitudes 3-54687
 ethylene, and similitudes, mols. symmetry effects in internal rotation 3-74974
 ethylene, electron impact dissoci., rotational and vibrational energy level distrib., luminesc. 3-75127
 ethylene ligands, torsional potential determ. from inelastic neutron scattering 3-54656
 ethylene oxide, Coriolis coupling coefficients, C-H stretching vibrations 3-49450
 ethylene oxide clathrate hydrate, stretching modes, ring breathing mode, i.r. spectra, 100K 3-54677
 ethylene oxide gas, C-H stretching and CH₂ wagging modes 3-54676
 ethylene oxide- d_4 , Coriolis coupling coefficients, C-H stretching vibrations 3-49450
 ethylene sulphide, Coriolis coupling coefficients, C-H stretching vibrations 3-49450
 ethylene sulphite and chlorophosphite, vibration and i.r. spectra, conforms. (Russian) 3-71492
 ethylenes, monosubstituted, absolute i.r. intensities, CNDO/2 calc. 3-46243
 ethylsulphates of yttrium and some rare earths, Raman spectra, H₂O mol. libration 3-50564
 ethynylbenzene vibronic spectra, theoretical study 3-67783
 excited state force consts. calc. from bond charge model 3-52334
 extended Jacobian, determinant calc. 3-74978
 f.c.c. and h.c.p. lattices, entropy, comparison of H theorem method with vibrational anal. 3-70768
 ferrocene vibrational study 3-67780
 fluid, i.f. depolarized (VH) light, line shapes, coupling of rotational and translational motion 3-71533
 1-fluoro-2, 4-dinitrobenzene, i.r. spectrum, 4000 to 250 cm^{-1} , vibr. assignments 3-49465
 4-fluoro-2-chlorotoluene vapour, near u.v. absorption spectrum, modes of vibration 3-46260
 force consts. determ. from isotopic frequencies using parameter representation 3-43425
 formaldehyde, fluorescence decay of single vibronic levels 3-41864
 formaldehyde- h_2 and - hd , fluoresc. lifetime meas. $^1\text{A}_2 \rightarrow ^1\text{A}_1$ transition, N₂ laser 3-75057
 formic acid, proton transfer barrier 3-63390
 formyl chloride, i.r. spectra, band assignments 3-78753
 four-membered ring organic molecules, ring puckering, substituent effects 3-78716
 fundamental frequencies, tables 3-74983
 2-furaldehyde and deuterio analog, vibr. spectra, band contours 3-67818
 furan, liquid, reorientational phase, i.r. bandwidth, relax. 3-68996
 Gillespie-Nyholm theory applied to force fields 3-63398
 glycerol single crystals, i.f. vibs. assignment, Raman spectra (French) 3-58497
 glyoxal- d_1 and glyoxal- d_2 5207 Å band system, vibrational assignment 3-54660
 H₂O being potential calc. 3-74971
 halide salts, C_{2v}, C_{3v}, symmetry group impurities, spectral props. 3-69043
 1-halo-3,3,3-trifluoropropynes, vibrational spectra 3-46296
 halogenhydrides, paramagnetic proton shielding, effect of vibration, interatomic distance (Russian) 3-49445
 halogenopyridines, vibrational spectra 3-46288
 2-halomethanes, intensity of valency vib. bands of C-Cl and C-Br bonds (Russian) 3-63478
 heteronuclear diatomic, vibr. freq. rel. to dissoci. energies 3-71517
 heteropolar diatomic mols., multiphoton processes, Born-Oppenheimer approx. 3-67760
 hexafluoro-2-propanol and deuterated analogues, solid, liquid and gaseous states, i.r. and Raman spectra 3-46286
 hexafluoroazomethane, fundamental frequencies 3-43452
 hexafluoropropanol-2, vibr. freq., force field, mean amplitudes 3-63412
 hexamethylbenzene single cryst., polarized Raman spectra, freqs. assignment 3-55572
 homopolar isotopically unsymmetric diatomic molecules, forbidden transition, dipole moment of HD 3-78708
 hydrocarbon, force field calcs. using CNDO/2 method 3-74951
 hydrocarbons, MOA calculations of CH stretching frequencies and dissociation energies 3-43429
 hydrogen-bonded complexes, effect of temperature on ν_s band 3-46247
 hydrogen-bonded complexes, origin of temperature sensitivity of ν_s band 3-46248
 hydrogen-bonded systems, vib. and reorientational relax. 3-64669
 hyper-Raman spectra, pure rot. and vibr.-rot., selection rules 3-54693
 inert gas diatomic molecules, level spacings, calcs. 3-63400
 inorganic complex salts, i.f. vibs., metal-ligand and complex ion-outer ion interactions 3-47246
 intensity borrowing theory, Herzberg-Teller and Born-Oppenheimer coupling 3-40596
 intermolecular interactions in condensed systems, induced i.r. spectra 3-72697

molecular vibration continued

- intramolecular vibrational energy transfer 3-43470
 iodobenzenes, o- and p-substituted, i.r. spectral band near 1000 cm⁻¹, substituent and solvent effects 3-46302
 ionic crystal impurity molecules, low temp. rotation in vibronic spectra 3-69041
 ionic crystal with impurity molecule, symmetry of electronic-vibrational-rotational transitions 3-69042
 isolated molecules, radiationless transitions 3-49482
 isopropyl alcohol far i.r. spectra, torsional transitions 3-63457
 isoquinoline vapour, electronic absorpt. spectrum assignments 3-67798
 isotope dynamic mixing and vibronic structure 3-74970
 IV-VI compounds, matrix isolation studies of i.r. spectra, laser-excited emission bands 3-78804
 Jahn-Teller systems, zero-phonon lines of singlet-multiplet transitions 3-68554
 ketones, polyfluorinated, valency vibration absorption bands, carbonyl groups (*Russian*) 3-71530
 lactams, conformational effects on N-H stretching frequencies, i.r. spectra 3-52408
 linear triatomic molecule, vib.-rot. energy 3-63419
 linear triatomic molecule, vibrational-rotational levels calc. 3-46249
 linear XYZ molecules, anharmonic potential constants 3-63404
 liquid, i.r. and Raman band profile analysis 3-64665
 liquid, mol. motion, conf., Orsay, France, Jul. (1973) 3-64192
 liquid, n.m.r. and neutron scatt. obs. 3-68875
 luminescence spectra, dichroism, polarisation theory, asymmetric mols. 3-72754
 matrix isolation technique investigated using ozone 3-60455
 2-mercaptoethanol, liq., vib. spectra and rot. isomerism 3-47245
 metal pyridine tetracyanonickelate complexes, i.r. and Raman spectra analysis 3-63467
 metal-hexahalo species of group IV-VI, force constants and mean amplitudes of vibration calc. 3-60436
 methane, ν_3 absorption band at 1.1 μ 3-71549
 methane, $^{12}\text{CH}_4$, ν_3 band, spectral parameters (*French*) 3-57653
 methane, $^{12}\text{CH}_4$, hyperfine splittings in rot. F₁, F₂ levels of ground vibr. state, calcs. 3-63401
 methane, ν_3 band of absorpt. spectrum from 2863-3132 cm⁻¹ (*French*) 3-49461
 methane, bideuterated, vibr.-rot. band ν_9 of 8 μ m line (*French*) 3-57652
 methane, CHD_2 , Fermi resonance effects in CH_3 and CD_3 stretching regions 3-57643
 methane, hyperfine structure of vibration-rotation line, using laser saturated absorption 3-43456
 methane, theory of absolute intensities for vibration-rotation transitions 3-67820
 methane-CO₂ mixture, vibrational relaxation, u.s. velocity measurements 3-57680
 methanes, halogen-substituted, second virial coeffs. and force consts. recalculation 3-40600
 methanol, liquid, hydrogen bonded, association and assignment of OH overtones 3-75023
 methanol, OH stretch, 3430 to 3940 cm⁻¹, torsional level transitions 3-78780
 methyl chloride-d₂, i.r. spectra analysis 3-63455
 methyl fluoride, rot.-vibr. spectrum, 2000-2100 cm⁻¹ 3-63463
 methyl fluoride, Stark effect of transitions of ν_3 band (*French*) 3-46271
 methyl iodide, liquid, collective excitation of mol. vibs., Raman spectra obs. 3-64668
 methyl iodide, liquid, molecular vibration excitons, Raman band profiles (*German*) 3-53113
 methyl iodide, Raman scattering, vibrational correlation 3-43444
 methyl iodide and CD₃I, liquid, Raman line-shapes, rotation and vibration analysis 3-41509
 2-methyl-1,3-dioxolane solid liquid gas, infrared, Raman spectra 3-54692
 N-methyl-d₃-P,P,P-trimethylphosphine imide, vibr. spectra, struct. of P-N bond 3-75024
 N-methyl-ethylidenimine isotopes, matrix and gas, i.r. spectra, 4000-200 cm⁻¹ 3-78807
 N-methylcarbamoylhalogens, i.r. and Raman spectra, 150 to 4000 cm⁻¹, vibr. assignments (*German*) 3-47270
 methylcyclopentane solid liquid gas, infrared, Raman spectra 3-54692
 methylene fluoride-d₂, and methylene fluoride-d₂, i.r. spectra, force field 3-78761
 methylfluoride, vibr. corrections of dipolar couplings 3-78700
 1,2-methylnaphthalene, vapour phase near u.v. absorpt. spectra assignments 3-67796
 N-methylpropionamide and N-deuterated N-methylpropionamide, normal coord. anal. 3-67774
 methylquinoline, 2-, 4-, 6-, 7-, 8-, in crystalline n-paraffins, quasi-linear phosphorescence spectra, vibrational 3-50609
 methylsilylchlorides, i.r. and Raman spectra, vibr. assignments and torsional barrier heights 3-54680
 methylsulphonyl fluoride, chloride, and bromide, normal coordinate analysis (*German*) 3-43424
 2-methyltetrahydrofuran solid liquid gas, infrared, Raman spectra 3-54692
 N-methylthiopropionamide, and N-deuterated analogue, i.r. and Raman spectra 3-49464
 molecular crystal, external, internal and semi-internal vibs., spectroscopic identification criteria 3-79442
 molecular crystal, Fermi-Davydov reson., exciton spectra 3-68998
 molecular crystal, reson. exchange, spectra, Fermi reson. 3-69000
 molecular crystals, transitions, optical activity, symm. depend. 3-72603
 molecular vibration levels under time dependent external pumping conditions 3-48895
 moniodomethyl radical, matrix i.r. spectra and bonding 3-46276
 multiphoton processes in homopolar diatomic Born-Oppenheimer approx. mols. 3-71516
 naphthalene, α -bromo- and β -chloro-, vibr. spectra and depolarisation ratio 3-52367
 naphthalene in p-dihalogenated benzene host crystals 3-80106

molecular vibration continued

- 1,6- and 1,8-naphthyridine, assignments of fundamental vibs. 3-63458
 near-resonant vibration-rotation energy transfer 3-71642
 neutron scattering obs. in solids and liqs., review 3-68140
 niobate ions in crystals, vibrational spectra 3-55602
 nitrophenols, isomeric, i.r. absorption spectra, vibrational assignments 3-78760
 nonequilibrium nozzle flows entropy of vibrationally relaxing diatomic gases 3-43633
 norbornadiene, vibrational spectra and assignments 3-72624
 norbornane, vibrational spectra and assignments 3-72624
 n-octane, low frequency mol. vibrations by neutron inelastic scattering 3-75577
 olefins, nonconjugated, consistent force field calc. 3-71526
 one-dimensional lattice with trapped oscillators, vibr.-translation coupling 3-57640
 optical absorption spectra, effect of mode-mode interaction in excited state, exact calculation of Franck-Condon factor 3-63447
 organic complex molecule, intramolecular relax. spectroscopic investigation 3-71536
 organic compound CH stretching frequencies, bond lengths and dissociation energies 3-46229
 organic disulphides Raman spectra, S-S and C-S stretching regions 3-54682
 organic molecule in solid solns., fluoresc. excitation bands narrowing, vibronic struct. 3-46311
 organometallic compounds, bonding, vibr. analysis 3-78797
 1,2,5-oxadiazole and deuterated species, vibrational spectra and fundamental frequencies 3-46299
 oxamides, mol. anal. phosphoresc. characts. 3-78833
 5-oxylbenzodioxane-1,4, i.r. absorpt. bands temp. depend. in deform. vibrations region (*Russian*) 3-54694
 2,4,6,8,10-pentamethylundecane crystalline and glassy films, i.r. spectra and rotational isomerism 3-47268
 n-pentane, solid, low frequency mol. vibrations by neutron inelastic scattering 3-75577
 perfluorocyclopentene, i.r. and Raman spectra interpretation 3-54685
 perturbation theory, first order, isotopic properties, Coriolis coupling 3-74989
 perylene, i.r. spectrum, out of plane vibrations 3-75040
 phenols, ortho substituted, torsional frequencies and conformational equilibria 3-52310
 phenoxymethylpenicillin, vibrational spectra, structural analysis (*Russian*) 3-78778
 phosphiran, normal modes, force field, barrier to inversion 3-75038
 polyacrylonitrile fibres, u.v. dichroism of C \equiv N valency vib. bands (*Russian*) 3-64689
 polyamides aliphatic, struct., lower freq. i.r. spectra (*German*) 3-71666
 polyatomic, algorithm for formation of kinematic and force matrices (*Russian*) 3-78714
 polyatomic mol. collision theory, rot. and vibr. excitation, quantum mech. treatment 3-46346
 polyatomic mol. collision theory, rot. and vibr. excitation, restricted distorted wave approx. 3-46347
 polyatomic mols., potential energy function, unitary transformation operator for perturbation treatment of the Hamiltonian 3-40601
 polyatomic mols., vibronic coupling in nonradiative transitions 3-60470
 polyatomic mols. in excited states, vibr. relax. by inelastic collisions 3-60487
 polyenic molecules, vibr. absorpt. bands in electronic spectra, relative intensities calc. 3-63431
 polyethylenepolyamines, effect of changes in conformation and units in chain on i.r. frequencies 3-54762
 poly-L-alanine, far-i.r. absorpt. spectra, 4-200 cm⁻¹, α -helix behaviour 3-78917
 polymer, of C=O groups, i.r. spectral obs., rel. to breakdown under load 3-58747
 polythreepptide films, Fermi resonance in i.r. spectra 3-75169
 porphyrins, mag. circular dichroism, vibronic coupling 3-74993
 potassium methyl xanthate-d₀ and -d₃, vibrational spectra and force constants (*German*) 3-46297
 potential barrier in external field, multiphoton ionisation 3-54735
 potential curve calc. in zero approx. of generalised WKB method (*Russian*) 3-67766
 1,2-propanedithiol, vibr. spectra and rot. isomerism 3-53093
 propionamide, i.r. and Raman spectra, vibrational assignments 3-60452
 propylene imine, i.r. and Raman spectra 3-78788
 propynal, millimetre wave spectrum, ground vibr. state 3-78816
 propyne-d₂, i.r. spectra analysis 3-63455
 protein, possibilities of low frequency vibrations revealing properties by conformation 3-60497
 PTFE, phase II and III, Raman spectra analysis 3-64643
 pyrene, emission-absorpt. asymmetry of S₁-S₀ transition, deuterium effect, vibronic coupling 3-54715
 pyridine, u.v. spectra, 3000 to 3400 Å, triplet-singlet absorpt., band assignments 3-49460
 pyridine N-oxides, far i.r. investigations and hydrogen bonding 3-46290
 pyridinium ion, in-plane vibrations calc. 3-74976
 pyrogermanates with linear bridge, vibr. spectra and isotopic shifts 3-46285
 pyrosilicates with linear bridge, vibr. spectra and isotopic shifts 3-46285
 quinoxaline, in durene and naphthalene host cryst., electronic absorpt. spectra analysis 3-69028
 quinoline, liquid, rot.-vib. relax., Raman and i.r. spectral obs. 3-64670
 quinoline-N-oxides and isoquinoline-N-oxides, i.r. behaviour of N-O group 3-54697
 Raman lineshapes analysis w.r.t. reorientational correl. functions 3-46274
 Raman scattering tensor, analytical expression development (*French*) 3-78748

molecular vibration continued

- rhodanine, dimeric structures, vibratory spectra calcs. (*Russian*) 3-75015
- rhodizionate anion, in soln. and salts, Raman spectra, intensity and depolarisation ratio 3-78801
- ruthenocene vibrational study 3-67780
- Schrodinger equation, radial, approx. analytical expression for soln. (*French*) 3-77858
- silacyclopentanes, vibr. analysis of i.r. and Raman spectra 3-63464
- silacyclobutane, (1-d), (1-d₂), silacyclopent-3-ene, ring-puckering 3-78789
- sodium anthranilate, i.r. spectra, metal-ligand stretching frequencies 3-54688
- sodium bromoacetate, and -d₂ spectra and structure 3-78798
- sodium bromoacetate and sodium bromoacetate-d₂, vibrational spectra and struct. 3-75987
- solid and fluid media, Rayleigh, Brillouin and Raman lines rel. to microscopic processes 3-80024
- spherical top mol.s., Raman band contour analyses and Coriolis consts. 3-67816
- stimulated Raman scattering, of phase modulated light pulses 3-62742
- symmetric molecule, rotational level splitting in the ground vibrational state 3-63417
- symmetric top mol., (± 1) quantum number label 3-67786
- symmetric top molecules, centrifugal stretching constants, upper and lower limits 3-63413
- symmetric top molecules, vibrational Zeeman effect 3-43427
- symmetric top mol.s., A₀ const. determ. from overtone bands 3-67778
- tartaric derivs., coordination cpds., external vib. freqs. of active and racemic forms, i.r. and Raman spectra 3-55581
- TCNE-benzene charge transfer complex, resonant Raman effect and charge distrib. 3-75977
- TCNQ complexes, high-conductivity, effect of vibronic interaction in i.r. spectra 3-72645
- 1,4-telluroxan in vapour, liquid, amorphous and crystalline state, vibrational spectra 3-46292
- tertiary amides, mean square and mean amplitudes for in-plane vibrations of various linkages 3-46246
- tertiary butanol, liquid, hydrogen bonded, association and assignment of OH overtones 3-75023
- tetra-allyl silane, vibrational spectra 3-46294
- tetra-allyl tin, vibrational spectra 3-46294
- tetrachloroethylene, vibrational force fields, specific imposition of pots. parameters on nonbounded distances 3-71527
- 1,1,2,2-tetrachlorotetrafluorocyclobutane and 1-chloro-2,2,3,3-tetrafluorocyclobutane 3-78787
- tetracyanoethylene, radical anion salts, reson. Raman spectra and bond strengths 3-43446
- tetracyanomethane, i.r. spectra, vibrational assignment, normal coordinate analysis and thermodynamic functions 3-54684
- 2, 3, 4, 5, tetrafluoroaniline, i.r. absorption spectrum, vibrational assignments 3-78757
- tetrafluoromethane, number density remote sensing in hypersonic flow using Raman scattering 3-71699
- tetrahalides of third, fourth and fifth group elements, mol. kinetic consts. calc. 3-49447
- tetrahedral mol.s., sextic centrifugal distortion 3-63409
- N,P,P,P-tetramethylphosphine imide, vibr. spectra, struct. of P-N bond 3-75024
- N,P,P,P-tetramethylphosphine imide and N-methyl-d₃ analogue, vibr. spectra analysis 3-78795
- 1,3,5,7-tetramethylsilaadamantane, vibrational assignment and force constants (*German*) 3-43453
- 1, 4, 5, 8-tetraoxanthraquinone, in octane matrix, fluoresc., electron-vibr. interactions 3-75060
- thiirane, sulphone, vibrational spectra 3-57655
- thioamides, mean square and mean amplitudes for in-plane vibrations of various linkages 3-46246
- thiocarbonyl chloride, photoelectron spectra, vibrational struct. 3-43502
- thiocarbonyl fluoride, photoelectron spectra, vibrational struct. 3-43502
- thiochlorides, vibrational spectra (*Russian*) 3-63477
- thiodiglycolic acid molecule thermal vibrations 3-67773
- thiomethyl group, C-S-C stretching, Raman spectra 3-67809
- thiophene, compliance constants, iterative consistency method 3-74981
- thiophosgene, 2780 angstroms absorpt. system, vibrational structure 3-63441
- thiopropionamide, i.r. and Raman spectra, vibrational assignments 3-60452
- thiourea and deuterium derivatives, vibr. spectrum calcs. 3-63415
- three-dimensional quartic oscillator, energy levels and matrix elements 3-74973
- time dependent external pumping conditions, distribution between levels 3-48895
- transition integrals, r-centroid approx. implications 3-46245
- transition metal anions, octahedral, mean vibr. amplitudes 3-67771
- transition metal carbonyls in gas and liq. soln., vib.-rot. coupling effects on correlation functions 3-67825
- transition metal complex, [M(1,8-naphthyridine)₄](ClO₄)₂; and K₄[M(oxalate)₄], i.f. i.r. obs. 3-78776
- transition metal complexes, ²E_g → ⁴A_{2g} transition, vibr. anal. 3-76061
- transition metal complexes, group IIIB and IVB, cis-1,2-dicyanoethylenedithiolate ion, electronic and vibrational spectra 3-57654
- transition metal diarsine complexes, containing high oxidation state metals, i.r. study 3-78774
- transition metal tungstates, i.r., Raman vibr. spectra assignments (*French*) 3-80020
- transition metal-DL-β-phenylalanine chelates, i.r. absorpt. spectra, normal coord. analysis 3-78771
- triatomic molecules, influence of Renner effect on intensities of electronic-vibrational transitions 3-52348
- triazoles, i.r. spectra and normal vibrations 3-71547
- 4-R-1,2,4-triazoline-3,5-diones, (R=H, CH₃, CH₂-CH₃, CH₂CH₂CH₂CH₃), vibrational structure 3-49459

molecular vibration continued

- 1,2,3-tribromopropane, vibr. spectra and conform. behaviour 3-63465
- trichloro-1,1,1 propanes, normal coord. calcs. and force consts. (*French*) 3-46250
- 1,1,1-trichloroethane, laser excited Raman bands and funds. 3-67814
- 1,2,3-trichloropropane, vibr. spectra and conform. behaviour 3-63465
- triethylenediamine, UV absorpt. spectrum anal. of struct. 3-78740
- trifluoramine oxide, vibr. assignment and Urey-Bradley force field 3-40599
- trifluoroethanol-trimethylamine vapour phase complex, effect of temperature on H bond ν , band 3-46247
- trifluoroethylamine, vibrational spectra 3-71558
- trifluoromethyltrifluoroborate anion, Urey-Bradley force constant, vibration spectrum, i.r. and Raman spectra 3-57648
- trimers, mag. circular dichroism, vibronic coupling 3-74993
- trimethylamine, mol. A₂ torsional frequency by computer aided microwave anal. 3-78821
- trimethylene chloroarsenite, heterocyclic, vibrational spectra and conformation 3-63472
- trimethylene chlorophosphite, heterocyclic, vibrational spectra and conformation 3-63472
- trimethylene oxide, far i.r. spectra, double minimum potential function 3-75022
- trimethylene oxide, p.m.r. spectra, ring puckering vibr., chem. shifts and spin-spin coupling meas. 3-54726
- trimethylene sulphide, deuterated analogues, ring puckering 3-78792
- trimethylene sulphide, p.m.r. spectra, ring puckering vibr., chem. shifts and spin-spin coupling meas. 3-54726
- 2,8,9-trioxadamantane, microwave spectrum, vibrational satellites, rotational consts. 3-40636
- tropolone, near u.v. absorpt. vibr. anal. 3-54671
- uranyl acetate, vibronic interaction, luminescence spectra 3-72748
- uranyl butyrate, vibronic interaction, luminescence spectra 3-72748
- uranyl propionate, vibronic interaction, luminescence spectra 3-72748
- urea and deuterium derivatives, vibr. spectrum calcs. 3-63415
- vibrational excitation, string-plucking model 3-49504
- vibrational frequencies tables 3-75039
- vibrational-rotational spectra electronic-nuclear interaction effect 3-63428
- vibronic and spin-orbit splitting in spectra, Jahn-Teller effect 3-67763
- water, heavy water, Raman spectra, effect of hydrogen bonding on intramolecular vibrations 3-80022
- water, Raman band shapes, depolarization ratio spectra 3-75020
- water vibrational spectra isolated in D₂ matrices 3-43443
- XY₂Z₂ molecules, mean vibr. amplitudes 3-67772
- XXY' molecules, isotope shift phenomena 3-67849
- Zeise's salt and related complexes, torsional potential for ethylene ligands 3-54656
- Al I, states obs., coupling constants calc. (*German*) 3-57661
- AlO, D₂Σ⁺ - X₂Σ⁺ system, u.v. region, rotational and vibrational constants 3-60450
- AlO, fundamental vibration-rotation bands, relative spectral absorption coefficients 3-54683
- AlS radical, A₂Σ⁺ - X₂Σ⁺ transition, emission spectrum (*French*) 3-46259
- As(CN)₃ harmonic force fields, vibrational analysis 3-74977
- BCl₂Br, BClBr₂, vibrational spectra 3-46298
- B₂F₄, gaseous and cryst., Raman spectra, 25 to 1500 cm⁻¹, normal vibr. assignments and intermol. force consts. calc. 3-47250
- BH₃, equilibrium geometry and harmonic force consts., ab initio calc. including electron correlation 3-54657
- BH₃-NH₃, BD₃-ND₃ and BH₃-ND₃, matrix isolated, i.r. spectra, force consts. calc. 3-40628
- B₂H₆, Green's function anal. of vibr., coupling consts. 3-78697
- BO-α system, r-centroids calc. 3-71531
- BO₂, excited state force consts. calc. from bond charge model 3-52334
- BO₂, laser-excited fluoresc., vibr. consts. in ground electronic state 3-43468
- BO₂⁻, in KCl and KBr, anharmonic force field calc. 3-43421
- B₂S₃ ring compounds, vibr. study 3-78784
- ¹⁰B₂H₆, ¹¹B₂H₆ and deuterated, Raman spectra, ring-puckering vibr. 3-78791
- ¹⁰BH₃CO, mol. consts. of vibr.-rot. bands from i.r. study 3-78752
- Ba(ClO₃)₂·H₂O(D₂O), i.r., Raman spectra, intramolecular and colattice modes 3-75973
- Ba(NO₃)₂ crystals, stimulated Raman scattering, combitones 3-66888
- Ba(NO₃)₂ mol. crystal spectra, influence of polarising effect of medium in region of internal vibr. 3-72647
- BeH, long range interatomic potential determ. from quasi-bound vibrational levels 3-43385
- BeH₂, ground state, nonorthogonal configuration interaction, vibration frequencies calc. from wave functions 3-40591
- Br₂ + Br₂, vibr. scatt., pot. well effect, SSH theory validity 3-49503
- BrCN, vibrational anharmonicity, calc. using Anderson potential function 3-57644
- n-butylacetylene, i.r. spectrum, Fermi resonance 3-44410
- C₃ molecule, thermodynamic functions, bending vibration potential 3-80580
- CF₃ compounds, -PH₂, -PD₂, -AsH₂, -AsD₂, vibr. spectra and normal coord. anal. (*German*) 3-46282
- CH, term values and molecular parameters for rotational and vibrational levels in visible and near u.v. region 3-75010
- CH⁺, term values and molecular parameters for rotational and vibrational levels in visible and near u.v. region 3-75010
- CH(halogen)₃, calc. of molecular Coriolis coupling constants 3-63418
- CN mol. band system, solar temp. determ. 3-61669
- CN₂, excited state force consts. calc. from bond charge model 3-52334
- CO, (v=1) and (v=2) states, vibr. excitation and relax. 3-45787
- CO, absorpt. spectrum atlas, 1060-1900 Å 3-75007

molecular vibration continued

- CO, diatomic mols. trapped in Ne matrix, absorpt. spectra, vibr. and rot. struct. 3-75011
- CO, low temp., vibr. energy transfer rates in CO laser beam 3-74230
- CO, Ne gas mixture, vibration relax. rates, Landau-Teller model, i.r. spectra 3-75140
- CO, pure and in Ar matrix, absolute i.r. absorption intensities, band shapes 3-80061
- CO, relaxation of vibrational levels studied by laser absorption 3-60488
- CO, vibr. level lifetimes of $b^3\Sigma^+$ state 3-52399
- CO, vibr.-rot. transitions, rel. to pulsed chem. laser kinetics 3-74234
- CO, vibr.-translational relax. by foreign gases, localized heating 3-78887
- CO, vibration level lifetimes, coincidence detection of scattered electron and emitted photon (*French*) 3-74806
- CO laser, vibrational temp. meas. 3-54222
- CO vibration-rotation LTE in late-type star model atmospheres 3-61761
- CO vibrational relaxation by O atoms 3-46348
- CO-additive mixtures, V→V energy transfer rate measurement 3-78905
- CO₂, electron impact dissociative attachment, deconvolution of vibrational excitation structure 3-78878
- CO₂, electron impact excitation and assignment of low-lying electronic states 3-71617
- CO₂, mixed mode contribs. to absorpt. at 10.6 μm 3-40619
- CO₂, pot. energy function, calc. and extrapolated results for ν_3 progression 3-78711
- CO₂, relax. of 1090 lower laser level 3-74225
- CO₂ lasers, laser power and vibrational energy transfer 3-48885
- CO₂ TEA laser, gain decay rates, vibr. relax. 3-40244
- CO₂ upper laser level vibr. deactivation by ONF, COF₂ and O₂ 3-45790
- CO₂ vibrational relaxation in collisions with methane, tetradeuteriomethane and fluoromethane 3-54752
- CO₂/N₂ mixtures, vibrational transition rates by acoustical method 3-40667
- CO₂/O₂ mixtures, vibr. relax. meas. 3-43516
- CO₂-methane mixture, vibrational relaxation, u.s. velocity measurements 3-57680
- C₂O₂, far i.r. and Raman spectra, potential function, low frequency bending mode 3-71548
- C₂O₂, Raman spectra, skeletal bending mode 3-78791
- CO(A π), deactivation rel. to individual vib. levels 3-75150
- CO₂⁺, excited state force consts. calc. from bond charge model 3-52334
- CS, vibrational relaxation, Ar collisions, transition probabilities (*French*) 3-71633
- CS₂, i.r. spectra, hot bands associated with vibr. transitions 3-67817
- CS₂, liquid, crystalline, fine structure of Raman spectra 3-75990
- CS₂, the $4\nu_2 + \nu_3$ band and general quartic force field 3-46289
- CS₂ crystals, Raman spectra, mol. modes assignments 3-61033
- CS₂ vibronic A-D bands 3-54661
- CS₂²⁻, CS₂Se²⁻, CS₂Se₂²⁻, vibrational spectra 3-46298
- Ca fluorapatite mol. crystal spectra, influence of polarising effect of medium in region of internal vibr. 3-72647
- CaF, potential energy curves and r-centroids 3-49448
- Cd(II) complex, CdX₂ (X=Cl, Br, I) in tri-n-butylphosphate soln., vibrational spectra 3-75034
- CdS:Ti²⁺, CdSe:Ti²⁺, Jahn-Teller struct. of absorpt. spectra 3-69035
- Cl + Cl₂, vibr. scatt., pot. well effect, SSH theory validity 3-49503
- ClCN, vibrational anharmonicity, calc. using Anderson potential function 3-57644
- ClO₂, excited state force consts. calc. from bond charge model 3-52334
- Co coordination cpds., external vib. freqs. of active and racemic forms, i.r. and Raman spectra 3-55581
- Co(CO)₂NO, potential consts. from vibrational spectra of six isotopic species 3-43442
- Co(II) complex, chelate of anthranilic acid, i.r. spectra, metal-ligand stretching frequencies 3-54688
- Cr(NH₃)₆³⁺ ion in non-cubic environments, $^2E \rightarrow ^4A$ transition 3-47283
- CrO₃Br- vibrational spectra, normal coordinate analysis rel. to MO₃Xⁿ⁻ (M=Cr, Mn, Tc, Re; X=F, Cl, Br, S; n=0,1) (*German*) 3-71557
- CrS, vibrational analysis 3-54673
- CuBi, rotational analysis of A and B systems (*French*) 3-57642
- Cu(II) complex, chelate of anthranilic acid, i.r. spectra, metal-ligand stretching frequencies 3-54688
- D₂, Lyman and Werner bands, vacuum u.v. spectra, vibr. and rot. level anal. 3-40615
- D₂, solid, ordered phase, fund. Raman band, Q branch 3-80016
- D₂, variational treatment, full electronic Hamiltonian 3-67748
- D₂⁺, vibr. energy level spacings 3-60431
- DBF₂, mean square vibr. amplitudes and thermodynamic functions 3-67775
- DCI, dipole moment function, vibration-rotation matrix elements determ. 3-52351
- DCI⁺, emission intensity of vibrational bands in A² $\Sigma \rightarrow X^2\Pi$ transition, rel. to HCl⁺ and HBr⁺ 3-78744
- DF, vibrational relaxation 3-54750
- DF, vibrational relaxation, temp. depend. 3-75136
- DF-CO₂ mixtures, vibrational relaxation processes, temp. depend. 3-54751
- D₂O₂, vibrational consts. calc. 3-52338
- Eu complexes, effect of line intensities in vibronic spectra 3-63506
- F + D₂ → DF + D, vibrational energy distributions, temp. depend. 3-55934
- F + DF(ν) → DF(ν') + F vibr. relax. process, rate consts., Monte Carlo calcs. 3-60486
- F + H₂ → HF + H, vibrational energy distributions, temp. depend. 3-55934
- F + H₂ → HF + H, vibrational energy distributions, rotation effects 3-71627

molecular vibration continued

- F + HF(ν) → HF(ν') + F vibr. relax. process, rate consts., Monte Carlo calcs. 3-60486
- FCN vibrational anharmonicity, calc. using Anderson potential function 3-57644
- F₂CS, B¹A₁ ← X¹A₁, $\pi^* \leftarrow \pi$ transition at 2000 Å, vibrational fine struct. 3-46265
- FNO force consts. calc., use of vibration-rotational interactions and inertia defects 3-52337
- FeCl₄-nBr_n⁻¹, vibrational analysis 3-54655
- GeD₄, i.r. and Raman spectra, rovibrational consts. 3-63460
- Ge₂H₆, Ge₂D₆, mol. force fields and isotopic rules determ. 3-54653
- GeO, Franck-Condon factors and r-centroids for (A-X) system 3-67797
- GeO, obs. of vibrational states in mol. beam electric resonance spectroscopy 3-78727
- H bond, i.r. spectra, general theoretical model including Fermi reson. and vibr. modes coupling 3-52366
- H₂, cross sections for vibrational excitation by Li⁺ impact 3-71648
- H₂, cross-section of transitions between vibrational states in resonant scattering of electrons 3-78873
- H₂, quantum defect theory, vibr.-electron coupling, autoionisation 3-71607
- H₂, solid, ordered phase, fund. Raman band, Q branch 3-80016
- H₂, variational treatment, full electronic Hamiltonian 3-67748
- H₂, vibr.-vibr. pumping, induced dissoci. at 300 K 3-54747
- H₂ and H₂⁺, vibr. energy level spacings 3-60431
- H₂ + Hr collisions at nonzero impact parameters, simultaneous vibr. and rot. transitions 3-75132
- H₂ + Li⁺ collisions, vibr. excitation, rot. effect 3-57675
- H₂⁺, electron charge difference density, vibr. motion effect 3-46240
- H₂⁺, nonadiabatic effects on lowest levels 3-63403
- HBF₂, mean square vibr. amplitudes and thermodynamic functions 3-67775
- HBr, vibrational relaxation in inert gases 3-60490
- HBr (V=1) state, vibrational relaxation in methane, water, He and HD mixtures 3-71624
- HBr gas, temp. depend. of vibration-to-vibration energy transfer 3-60493
- HBr⁺, emission intensity of vibrational bands in A² $\Sigma \rightarrow X^2\Pi$ transition, rel. to DCl⁺ and HCl⁺ 3-78744
- HCN and DCN, anharmonic force field and equil. struct. 3-60430
- HCP and DCP, anharmonic force field and equil. struct. 3-60430
- HCl, absorpt. line broadening by gases, fund. band, temp. depend. 3-63544
- HCl, dipole moment function, vibration-rotation matrix elements determ. 3-52351
- HCl, vibrational relaxation in inert gases 3-60490
- HCl gas, temp. depend. of vibration-to-vibration energy transfer 3-60493
- HCl gaseous mixtures with HBr and HI, low temp. absorpt. spectra (*French*) 3-78750
- HCl i.r. bands, amplification and displacement, depend. on hydrogen bond energy (*Russian*) 3-49473
- HCl lineshifts and widths due to inert gas broadening of vibration-rotation lines 3-43467
- HCl⁺, emission intensity of vibrational bands in A² $\Sigma \rightarrow X^2\Pi$ transition, rel. to DCl⁺ and HBr⁺ 3-78744
- HCl⁺, emission spectra of four isotopic combinations 3-78739
- HD + He, vibr. inelastic scatt., sudden approx. 3-40669
- HD⁺ theoretical adiabatic energy spacings, dissoci. energy 3-63402
- HDO, liquid Raman intensities of uncoupled OD oscillators 3-75979
- HDO in rare earth chloride soln., Raman spectra 3-75980
- HF, V-V, V-R, and T energy transfer collisions, temp. depend. 3-40674
- HF, vibration to rotation energy transfer, dipole-dipole and hydrogen bond interactions 3-63557
- HF, vibrational relaxation 3-54750
- HF vibrational relaxation in temp. range 600-2400 K, Ar and F collisions 3-71628
- HF + DF, vibr. relax., rate consts. meas. by laser-excited fluoresc. method 3-49502
- HF + HCl, (HBr), (HI), vibr. relax., rate consts. meas. by laser-excited fluoresc. method 3-49502
- HF + N₂, vibr. relax., kinetics 3-54748
- HF₂ in crystal field, splitting of bending modes 3-55061
- HF(V=1,2), vibr. deactivation by hydrocarbon mols., rate consts. 3-46350
- H₂O, centrifugal constants. calcs. for (000) vibratory state, appl. of energy moments method (*Russian*) 3-78701
- H₂O, coupled Hartree-Fock method calcs. of one-electron properties 3-71515
- H₂O, excited state force consts. calc. from bond charge model 3-52334
- H₂O, in solid hydrates, correlations between free H-bonded mols. ab initio calcs. 3-74991
- H₂O, near i.r. spectra, further anal. concerning vibr. assignments 3-43450
- H₂O, vibrational spectra, effect of intermolecular interactions, i.r. absorpt. intensity 3-63473
- H₂O and H₂O-trimethylamine complex, gas phase Raman spectra 3-78800
- H₂O molecule, IR vacuum spectra of vapour 3-78762
- H₂O + organic base, near i.r. struct. study and vibr. assignments 3-46275
- H₃O₂⁺ system, coupling of proton motion with H bond stretching vibration, effect on dipole moment, polarisability, double min. potential surface 3-49457
- HOF, DOF and H¹⁸OF, mean vibr. amplitudes 3-67767
- H₂O.Cl₂ complex, i.r. and CNDO/2 study 3-54686
- HS₂ radical, u.v. absorpt. spectrum and geometry 3-75003
- HSiF₃, microwave spectra, excited states, force field models 3-63487
- He₂, ab initio calc. of A¹ Σ_g^+ ← X¹ Σ_g^+ absorpt. spectrum 3-63445
- HeH₃⁺, stability study, estimation of vibrational frequencies 3-74954
- Hf(BH₄)₄:U(BH₄)₄, electronic absorpt., optical and e.p.r. spectra assignments 3-76033

molecular vibration continued

- HgBr₂, excited state force consts. calc. from bond charge model 3-52334
- HgCl₂, excited state force consts. calc. from bond charge model 3-52334
- HgH, long range interatomic potential determ. from quasi-bound vibrational levels 3-43385
- Hg(II) complex, HgX₂ (X=Cl, Br, I) in tri-n-butylphosphate soln., vibrational spectra 3-75034
- I₂, rotational constants for highly excited vibrational levels 3-63421
- I₂, visible emission spectra 3-78738
- I₂, excited state collisions, classical trajectory calc. of vibr.-rot. energy transfer 3-71641
- I₂ molecules, excited by He-Ne laser, vibrational relaxation study 3-60494
- ICN, vibrational anharmonicity, calc. using Anderson potential function 3-57644
- ¹²⁷I₂, long range potential in B³Π_g state 3-60429
- Ir coordination cpds., external vib. freqs. of active and racemic forms, i.r. and Raman spectra 3-55581
- KI, quadrupole hyperfine structure meas. obs. in vibrational state (German) 3-57660
- KNO₃, crystal, model for coupled rotation-displacement modes 3-79440
- LaAlO₃:Cr³⁺ crystals, electronic-vibrational spectrum, temp. var. 3-64721
- Li+H₂, vibrational-rotational excitation, potential energy surface calc. 3-71639
- LiF vibrational energy, production from Li+SF₆ mol. beams, electric resonance spectra 3-43522
- LiNO₃ solns. in liq. ammonia, vibr. spectra, solvent effects 3-55991
- Mg(II) complex, MgX₂·nMe₂O, i.r. spectra, stretching consts. (French) 3-67824
- Mg(H₂O)₂²⁺ salts, i.r. spectra, stretching vibrs. (French) 3-63466
- MgO, FII-XI² electronic transition 3-52361
- Mg₂SiO₄, isotopic species, i.r. and Raman spectra, vibr. studies and shift meas. 3-46284
- MgX₂⁻, X=Cl, Br, I, intramolecular force fields 3-52333
- Mn(II) complex, chelate of anthranilic acid, i.r. spectra, metal-ligand stretching frequencies 3-54688
- MnS, vibrational analysis 3-54673
- MoF₃, vibrational spectra 3-46278
- MoO₄²⁻, Raman, i.r. spectra of Na₂MoO₄, force constants, isotope shift 3-63450
- MoS₂²⁻, Raman, i.r. spectra of K₂MoS₄, Cs₂MoS₄, force constants, isotope shift 3-63450
- N₂, B³Π_g state vibrational levels, absolute populations determ. 3-75008
- N₂, diatomic mol. trapped in Ne matrix, absorpt. spectra, vibr. and rot. struct. 3-75011
- N₂, E and F regions, vibration temp., energy loss mechanisms 3-80808
- N₂, electron impact excitation, cross section of metastable A³Σ_u⁺ vibrational level 3-75116
- N₂, excited by electron impact, shape resonances in A and B states 3-78876
- N₂, kinetics, relaxation mechanisms, electronic quenching by N atoms 3-69072
- N₂, lifetime of D³Σ_u⁺ state 3-75005
- N₂, long range potential, depend. on internuclear distance 3-75126
- N₂, Morse oscillator, collision transition probabilities and cross sections (French) 3-54744
- N₂, resonant excitation by low-energy electrons, cross-sections calc. 3-78875
- N₂, triplet states parameters calc. 3-60421
- N₂, vibr. deactivation probability on collision with glass surface 3-46337
- N₂, vibr. excitation from N+NO reaction, Raman scatt. study 3-43517
- N₂, vibr. relax. in luminesc. of solid nitrogen 3-44463
- N₂, vibr. relax. using press. meas., shock tube study, comment 3-49501
- N₂, vibrational level lifetimes, coincidence detection of scattered electron and emitted photon (French) 3-74806
- N₂, vibrational relaxation by alkali atoms 3-71643
- N₂, vibrationally excited, chemi-ionisation of alkali atoms 3-78495
- N₂ dissolved in liquids, vibr. Raman bandshape, collisional narrowing effect 3-75019
- N₂ molecules in nozzle, anharmonic vibrational relaxation 3-54737
- N₂ r.f. spectrum of metastable (A³Σ_u⁺) state, fine struct., mag. hyperfine struct., electric quadrupole consts. for 13 vibrational levels 3-40635
- N₂ vibrational Raman spectra 3-49471
- N₂ vibrational relaxation, quenching of O(¹D) 3-75137
- N₂-Ar solute-solvent systems, computer simulation of correl. functions, bandshapes and relax. times 3-64651
- N₃⁻ in crystal field, splitting of bending modes 3-55061
- N₂Ar Van der Waals complex, i.r. absorption spectra, internal rotation 3-78805
- NCO, Renner-Teller effect and vibronically induced bands in electronic spectrum 3-75048
- NF and NF⁺, configuration interaction studies rotational and vibrational consts. calc. 3-40593
- NH₃, optically pumped, obs. of submillimetre emission due to rotation-inversion transitions in ν₂ state 3-74232
- NH₃, pot. consts. determ., floating one-centre wavefunction 3-74963
- NH₃, transient nutation effect in microwave transitions 3-49478
- NH₃ in N₂ and Ar matrices, i.r. spectra 3-55589
- NH₄NO₃ solns. in liq. ammonia, vibr. spectra, solvent effects 3-55991
- NO, diatomic mol. trapped in Ne matrix, absorpt. spectra, vibr. and rot. struct. 3-75011
- NO, excitation in low-energy electron impact, role of negative ionic states 3-78874
- NO, fund., and first overtone bands obs. in NO-rare gas mixtures, 10000 psi 3-63444
- NO, monochromatically excited, energy transfer, vibrational relaxation, fluorescence 3-71623
- NO, Vibr. relax. time meas., 299 to 1000 K 3-43509

molecular vibration continued

- NO, vibrational energy transfer 3-71626
- NO₂, flash photolysis, energy disequilibrium meas. 3-80568
- NO₂, vibr. struct. of ²B₁-²A₁ system 3-78729
- NO₃⁺, vibr. freqs., correl. with cation polarising power and polarisability 3-49456
- N₂O, discharge excited, vibr. luminesc., level populations (French) 3-52380
- NaClO₃ mol. crystal spectra, influence of polarising effect of medium in region of internal vibr. 3-72647
- NaO₂, Raman spectra, struct. changes at 230 and 201 K (German) 3-50569
- NbX₅ (X=Cl, F, Br) normal coordinate analysis and thermodynamic functions 3-54654
- Nd³⁺-2-hydroxy-3-naphthoic acid complex, i.r. spectra, vibr. modes 3-67815
- Ne⁺ charge transfer collisions with vibrationally excited N₂ 3-43370
- Ni(II) complex, chelate of anthranilic acid, i.r. spectra, metal ligand stretching frequencies 3-54688
- Ni(II) complex, ethyl xanthato, i.r. spectra assignments, normal coordinate analysis 3-54695
- Ni(II) complex, methyl xanthato, i.r. spectra assignments, normal coordinate analysis 3-54695
- α-O₂, at 1.3 K, bimol. series (Σ_g⁺→(ΔΔ) and (ΣΣ), absorpt. band fine struct. 3-44411
- O₂, electron impact, 4-15 eV 3-75106
- O₂, energy disequilibrium in flash photolysis of NO₂ 3-80568
- O₂, excitation in low-energy electron impact, role of negative ionic states 3-78874
- O₂, resonant vibr. excitation by slow electron impact 3-71616
- O₂, X³Σ_g⁻ state, resolution of discrepancies 3-78736
- O₂ in N₂ and CO condensed matrices, e.p.r., <10 K, torsional oscils. 3-43477
- O₂ in upper atmosphere, production and decay of excited state in 50-100 km layer 3-69601
- O₂ vacuum u.v. absorption, spectra in solid Ar, Kr and N₂ matrices 3-53130
- O₂ vibrational relaxation in presence of atomic O 3-54738
- O₂ vibrational relaxation in an unsteady expansion wave 3-71629
- O₂-Ar Van der Waals complex, i.r. absorption spectra, internal rotation 3-78805
- O₂+O₂, vibr. scatt., pot. well effect, SSH theory validity 3-49503
- O₂⁺, A₂Π_u-X²Π_g second negative band system 3-78735
- O₃, general quartic force field calc. 3-46251
- O₃, matrix isolated, i.r. spectra, vibr. freq. and force consts. 3-75044
- O₃, u.v. spectrum, features of photochemical interest 3-73155
- O₃, vibr. excitation using O+O₂+O₂→O₃+O₂ recomb. reaction 3-76477
- O₃ potential function, second order anharmonic, force constants obtained from zero order wave numbers (French) 3-43422
- OCS, isotopically enriched, ground state and vibr. excited, microwave spectra 3-67830
- OCS, vibrational relaxation in inert gases 3-60490
- OD, A²Σ⁺ state dipole moment and hyperfine consts. calc., vibrational motion 3-40606
- OH, excited, vibration-rotation bands, i.r. airglow, correl. of fluctuations 3-80789
- OH radical, microwave and magnetic resonance spectra of vibrationally excited states, A-doubling 3-78853
- OsO₄, rotational-vibr. spectra, narrow saturation resons. induced by CO₂ laser radiation 3-46279
- P₂ radical, electronic system bands analysis, π-π transition (French) 3-52353
- P(CN)₃, harmonic force fields, vibrational analysis 3-74977
- PF₃ and PF₃⁺, potential curves and barriers to inversion 3-60399
- PF₅, Gillespie-Nyholm calculations of force fields 3-63398
- PF₅, photoelectron spectrum, band assignments 3-78719
- P₂F₄, i.r. and Raman spectra, vibr. and mol. struct. 3-43457
- PH₃, force constants and frequencies calc. 3-71528
- PH₃ and PH₃⁺, potential curves and barriers to inversion 3-60399
- PN, resonance fluorescence from A¹Π states, vibronic transition probabilities 3-78838
- PS₃⁻, vibrational spectra 3-46298
- PbF₂, matrix isolated, i.r. spectra, valence force consts. 3-40630
- Pb(NO₃)₂ crystals, stimulated Raman scattering, combitones 3-66888
- Pb(NO₃)₂ mol. crystal spectra, influence of polarising effect of medium in region of internal vibr. 3-72647
- Pd complex, cyclic olefin, bonding vibr. spectra obs. 3-78726
- Pd complexes, Pd(PPh₃)₂X₂, Pd[P(PhO)₃]₂X₂, (X=Cl, Br), vibrational spectra 3-54689
- Pd(II) complexes, [X₂Pd(C₆H₅)₂], (X=Cl, Br), i.r. and Raman spectra, vibr. assignments 3-46300
- PrO, visible and IR spectra 3-75026
- Pt complex, cyclic olefin, bonding, vibr. spectra obs. 3-78726
- Pt(II) complexes, [X₂Pt(C₆H₅)₂], (X=Cl, Br), i.r. and Raman spectra, vibr. assignments 3-46300
- Rb-U complex fluorides, far i.r. absorption spectra 3-58499
- ReOF₄, vibrational spectra 3-72626
- Rh coordination cpds., external vib. freqs. of active and racemic forms, i.r. and Raman spectra 3-55581
- Rh⁺-complexes, ¹³C n.m.r., Rh-C coupling 3-63513
- α-S₈ crystals, Raman scatt. spectra, intermolecular vibratory terms splitting 3-72659
- SF₆⁻ square pyramidal ions, mean amplitudes of vibration calc. (German) 3-67781
- SF₆OOSF₆ in liquid phase, vibrational spectra 3-46295
- SH⁻ impurity in KBr(Cl)(I), h.p. effects on Raman scatt. 3-80019
- SO₂, 3400-3000 Å absorpt., vibr. analysis 3-67801
- SO₂, matrix isolated, i.r. spectra, vibr. freq. and force consts. 3-75044
- SO₂, u.v. spectrum in matrix isolation, vibr. struct. of 2348 Å system 3-63443
- SO₂, vibrational spectra, effect of intermolecular interactions, i.r. absorpt. intensity 3-63473
- SO₄²⁻, vibr. freq., environmental influence 3-75999
- S₂O₂, centrifugal distortion consts., microwave spectra analysis 3-67828

molecular vibration continued

- S_2O_2 , unstable, matrix isolated vibrational spectra, identification of new species 3-78803
 $^{32}S^{16}O_2$, $\nu_1 + \nu_2$ combination band obs. 3-63453
 SeF_6^- square pyramidal ions, mean amplitudes of vibration calc. (*German*) 3-67781
 SeO_2 , matrix isolated, i.r. spectra, vibr. freq. and force consts. 3-75044
 $SiCl_4$, rel. intensities of band spectra, vibrational overlap integral, calc. of Franck-Condon factors 3-78733
 SiF_2 , microwave spectrum in excited vibr. states, equil. struct., pot. function, Coriolis reson. 3-67831
 SiF_4 , bond length and vibr. amplitude by electron diff. 3-74915
 SiH_4 , ν_3 band, high resolution obs. (*French*) 3-54678
 Si_2H_6 , Si_2D_6 , mol. force fields and isotopic rules determ. 3-54653
 $SiH(\text{halogen})_3$, calc. of molecular Coriolis coupling constants 3-63418
 SiO , obs. of vibrational states in mol. beam electric resonance spectroscopy 3-78727
 SiO_2 , doping of films effect, electron delocalisation i.r. spectra 3-64646
 $SnCl$ radical, analysis of the α -X system (3400-3900 Å) (*French*) 3-49462
 SnF_2 , matrix isolated, i.r. spectra, valence force consts. 3-40630
 SnI_4 in soln., reson. Raman effects, stretching vibrs. enhancement 3-75013
 SrI , band spectrum in 6500-7200 Å region 3-63438
 SrI , band system in 3350-3560 Å region 3-52362
 TaF_5 , fund. vibr. modes, normal coord. anal. 3-52335
 TaX_5 (X=Cl, F, Br) normal coordinate analysis and thermodynamic functions 3-54654
 TeF_6^- square pyramidal ions, mean amplitudes of vibration calc. (*German*) 3-67781
 TeF_3Cl , Te-Cl wagging 3-46304
 TeO_2 , matrix isolated, i.r. spectra, vibr. freq. and force consts. 3-75044
 UO , UO_2 , UO_3 , i.r. spectra, 700 to 900 cm^{-1} , stretching modes study 3-40625
 UO_2Cl_2 , exciton-phonon interaction, luminesc., absorpt. 3-72751
 $UO_2(NO_3)_2$, exciton-phonon interaction, luminesc., absorpt. 3-72751
 UO_2SO_4 , electron-vibr. spectra, fine struct. 3-72752
 VCl_4 in soln., reson. Raman effects, stretching vibrs. enhancement 3-75013
 XY_3 type molecules, centrifugal distortion constants determ. 3-74988
 YF_2 , YF_3 , matrix isolated compounds, i.r. spectra, 40 to 800 cm^{-1} , freq. assignments 3-52370
 $Zn(II)$ complex, chelate of anthranilic acid, i.r. spectra, metal-ligand stretching frequencies 3-54688
 $Zn(II)$ complex, ZnX_2 (X=Cl, Br, I) in tri-n-butylphosphate soln., vibrational spectra 3-75034

molecular visible and ultraviolet spectra

- anthronitrile, absorption and fluorescence spectra, solvent and pressure dependence 3-41531
benzonitrile, vibrational analysis of the 2738 Å system 3-40610
cyclopentadienide anions, cyano-substituted, mag. circular dichroism, electronic transitions 3-40607
methane, fluoro-chloro derivatives, vacuum u.v. and photoelectron spectra, ionisation pots. 3-40617
3-phenylsindon, solvent effect on spectrum, dipole moment determ. from first excited singlet state 3-47284
phosphoric acid chloranhydrides, unsaturated, intramol. interactions (*Russian*) 3-40609
 AsS_3 , analysis of $A^{2\pi}X^{2\pi}$ band system 3-40613
AuGa rotation structure, incompletely resolved 0-0 band, isotope effect determination (*French*) 3-43423
 BX_3 , x=halogen, electronic absorpt., phosphorescence, singlet-triplet transitions 3-43439
 D_2 , Lyman and Werner bands, vacuum u.v. spectra, vibr. and rot. level anal. 3-40615
 DCl , vacuum u.v. absorption spectrum, analysis of autoionising Rydberg states 3-40618
 HCl , vacuum u.v. absorption spectrum, analysis of autoionising Rydberg states 3-40618
 H_2O , Rydberg states, ionisation and excitation energies calc. 3-46268
 I_2 , variable temp. photoelectron spectra, adiabatic ioniz. pot. 3-40658
 N_2 Rydberg complexes band structures, rotational analysis 3-40616
 NO_3^- , electronic absorpt., phosphorescence, singlet-triplet transitions 3-43439
 $(O_2)_2$, van der Waals molecule, i.r. and visible spectra 3-43447
 OH ($A^{2\Sigma} - X^{2\Pi}$) rotational line strengths and energy level population in water vapour arc plasmas 3-43688
 OH in water vapour arc plasmas, rotational lines meas. 3-43687
 SO_2 , $^3B_1 - A_1$ band system, rotational analysis of (010), (100), and (110) bands 3-40611
 SnI spectral bands between 215 and 250 nm 3-40612

molecular weight

- see also mass spectra; molecular weight determination
hydrocarbons, mol. formulae, calc. from mol. weight, functional analysis (*Rumanian*) 3-71484
ovalbumin, structure characteristics detn. by dielectric relaxation method (*Rumanian*) 3-43526
polydimethylvinylsiloxane, toluene solution, light scatt. obs., Zimm method (*Polish*) 3-57697
polyethylene, linear, effect of mol. wt. and crystallization conditions on dynamic mech. meas. (*Spanish*) 3-76368
polyethylene, linear, u.h. modulus, mod. weight effects on cold drawing, extended chain crystn. 3-50781
polyethylene solutions, Mark-Houwink relations 3-71680
polymer fracture surface energy, dependence on mol. wt., entanglement model 3-63595
polymer melts and solns., effect of mol. wt. and mol. wt. distrib. on viscoelastic props. 3-69384
polymer unperturbed chain dimensions from intrinsic viscosities determ. in good solvents 3-52407
polymers, molecular weights calculation 3-54760

molecular weight continued

- polymers, molecular wt. distribution determ. by temperature drop turbidimetry 3-57682
polymers, monodisperse, depend. of zero-shear viscosity on mol. wt. distrib. 3-57696
polystyrene solns. in toluene, monodisperse, refr. index increment, mol. wt. depend. 3-49516
polystyrene solutions, viscosity, effect of mol. weight, range of shear stresses, structure formation and orientation 3-71687
polyurethane block copolymers, segment size and polydispersity effect on props. 3-58759
polyvinyl acetate, self healing of cracks, molecular weight, and environment effects 3-58749
ribonucleic acid, structure characteristics detn. by dielectric relaxation method (*Rumanian*) 3-43526
SIS three block copolymer, cubic struct. characteriz. 3-50782
of stationary phase, effect on gas chromatographic data, activity coeff. 3-66429
of stationary phase, rel. to gas chromatography 3-62333
molecular weight determination
see also mass spectra
for computerized digital light scattering photometer 3-42714
coordination compounds, calc. using computer 3-62345
by low-angle laser light scattering from liquids 3-40293
poly-o-bromostyrene in benzene soln., high-resolution small-angle X-ray and light scatt. for mol. wt. determ. 3-67868
polymer, gel permeation chromatography, viscometry (*German*) 3-71662
polymer, mol. wt. and size by one conc. method in light scatt. 3-40687

molecules

- see also hydrogen neutral molecules; macromolecules; mesic and muonic molecules
interstellar, radioastronomic obs., discussion 3-45220
interstellar molecule formation in normal H I clouds 3-42238
interstellar shock waves and molecule formation 3-42239
polyatomic, Monte Carlo methods for calc. of multiple integrals (*Italian*) 3-40092
spherical tensors, ensemble averages 3-43493
Sun, molecular abundances from Zwaan's sunspot model 3-61662

Mollier diagrams see thermodynamic properties**molten metals** see liquid metals**molybdenum**

- adsorbed Ge, field emission study 3-64764
bamboo structure, rheological props. under flexural loads 3-47426
band structure, Fermi surface and spin-orbit interaction 3-58206
band structure calc., of cubic 4d Mo 3-72313
blistering under He ion bombard. 3-60749
cathode sputtering coeff., Ar, He and Xe discharges, role of ion capture (*Russian*) 3-69128
cathode sputtering rate meas. in inert gas glow discharge 3-54892
cathodic sputtering with Cs^+ , ang. dependence of energy spectra of ions 3-50639
chemical analysis, review 3-59695
chemisorption of O_2 , CO , H_2 , incidence reflectance studies 3-55157
creep rel. to long-term fracture 3-58677
deformed, struct. stability and mech. characteriz. under prolonged influences of temp. and stress 3-44630
desorption of K^+ , energy determ. 3-55153
diffusion of Fe, 1000-1350°C (*Japanese*) 3-72985
dislocation influence on neutron irradiation damage at 330K 3-68269
dislocation structure and mech. props., u.s. vibr. effects (*Russian*) 3-69207
ductile/brittle transition phenomena, struct. factor changes (*Russian*) 3-55753
elastic moduli meas. under hydrostatic press. by u.s. vel. method (*French*) 3-54994
electrical resistivity recovery stages III and IV, vacancy vs. interstitial migration 3-60722
electron beam heated, temp. distrib., mathematical analysis (*Russian*) 3-53262
electron beam welding of Ni and of Mo investigation of drop formation (*Russian*) 3-69327
electron diff. patterns of void and bubble arrays in irradi. Mo 3-52564
electron irradiated, displacement mechanisms, threshold energies 3-60742
energy loss of 2.0-MeV 4He ions, meas. 3-40944
evaporation rates in O_2 , air, water vapour from 1400 to 2300°C and 1.10⁻⁴ to 5.10⁻³ torr (*German*) 3-43871
FEM tip, microcrater form. on microparticle bombard. at limited field emission currents 3-44523
Fermi edge isochromat spectroscopic localization in conduction band 3-79624
Fermi surface determination using de Haas-van Alphen effect 3-58205
film growth, phase composition and structure, mol. beam deposition 3-79592
impure, temp. and strain rate influence on plasticity and stress/strain diagram appearance (*Russian*) 3-80344
internal friction, amplitude dependent, dislocation and stress effects 3-79429
internal friction of single crysts., temp. depend. (*Russian*) 3-43827
ion implantation and re-emission of He, temp. depend. 3-79394
isotope ratios, natural var. in single and separate Mo mineral deposits 3-65222
low temperature behaviour, Debye temp., energy role (*Russian*) 3-79498
matrix isolation spectra using triode sputtering source 3-61046
micro-yield region behaviour, stress/residual strain curves (*Russian*) 3-58648
m.p., international practical temperature scale, secondary fixed point determ. 3-73661
neutron irradi., internal friction and dynamic modulus relax. peaks due to stage I defects 3-54983
neutron irradi. temp. effect on hardness 3-79387
neutron irradiated, 650°C, damage struct. 3-46649

molybdenum continued

- neutron irradiated, irradi. temp. monitoring, void superlattice const. meas. 3-68291
 neutron irradiated, void formation, lower threshold temp. 3-68290
 neutron irradiation and plastic deformation, recovery model critical testing 3-79382
 paramagnetic susceptibility of single crystals, plastic strain influence (Russian) 3-79822
 particle, plasma sprayed, blowholes 3-43968
 permeability of hydrogen, in mono- and polycrystals. (Russian) 3-58144
 plasma coatings on Armco iron, form. kinetics and physicochem. props. (Russian) 3-80318
 polarisation charge measurement during ellipsometer evacuation 3-73727
 proton bombarded, electron emission, energy spectra 3-55716
 sintering, in organic binder, chemical stability in reducing atmosphere 3-69353
 slip line pattern and subsurface dislocation structure obs., electron microscope obs. 3-58036
 solubility in cementite steels (German) 3-76160
 surface, composition of two-dimensional oxide film 3-50082
 surface (100) crystal face, adsorption of gases, LEED study (French) 3-79563
 surface structure, anisotropic change during directional transport processes 3-55130
 surfaces, (100) and (110), heat of adsorption of Ba 3-55151
 tensile strength of single crystals, electron bombardment effect, cryst. orientation depend. (Russian) 3-61163
 thermal expansion at high temp. 3-69351
 thin films, laser-induced anisotropic thermoelectric voltages 3-60867
 thin foils, in situ deform., 800 keV electron microscopy 3-50703
 vacuum arc cathode, erosion and ionisation 3-57957
 wetting of Ag, hot-filament silver vapour source 3-39892
 wire, Ni-based composite material penetration, TiN barrier (Russian) 3-73012
 wire reinforced Ti composite, mech. props. 3-58719
 wire reinforcement of Ni, diffusion, carbide layer formation, recrystallisation rel. to weakening (Russian) 3-53272
 work function determ. near melting point using d.c. arc 3-69132
 X-ray emission, M_{α} , M_{β} , bands, wave functions of valence band electrons (Russian) 3-80117
 X-ray emission spectra 3-58569
 Cu/Mo composite, stress deformation state, microhardness obs. 3-80369
 Mo and W bearing seam, X-radiometric logging of boreholes (Russian) 3-73395
 Mo/Al fibre composites, deformation and fracture effect on brittle interfacial compounds 3-47457
 Mo/Au-SiO₂-Si, low-temp. treatment at 300 to 400 °C, H₂ ambient, change of threshold voltage meas. 3-55337
 Mo-Os system, interdiffusion coeff., electron microprobe study, polycrystalline couples 3-68442
 Mo-SiO₂ system, heterogeneous reactions, deposition conditions, heat treatment 3-72405
 Mo⁺ ion implanted in steel, friction changes 3-47410
⁹⁰Mo, dosimetry, mice, tissue distribution, excretion, effect of time 3-70186
 Mo(110) surface, cleaning procedures, low press. high temp. methods (Japanese) 3-50083
 SiO₂-Mo system, chem. reactions, C-V charact., thermal instability 3-72404
 ZrO₂/Mo, sintered cermet, elec. cond., 20-1700°C (German) 3-76308

molybdenum alloys

see also molybdenum compounds

- annealing, ZrO₂ form. on grain-, sub-boundaries and within grains (Russian) 3-76161
 as-cast, group VIII metals influence on struct. and props. (Russian) 3-55778
 cast, boundary strength increase by V microadditions 3-61177
 creep rel. to long-term fracture 3-58677
 electrothermal treatment, cold deformation 3-76216
 grain boundary precipitate constitution and conc., annealing influence (Russian) 3-44572
 low-alloy, plastic deform. degree influence on struct. and mech. props. (Russian) 3-58625
 Nimonic 108, grain boundary sliding and recrystn. during creep 3-58634
 Nimonic 90 and 108, tensile and compressive creep behaviour interpret. 3-58667
 Permalloy with Mo additions, Mossbauer effect of ⁵⁷Fe, annealing effects (Russian) 3-53038
 recrystallised, intercryst. fracture and carbide dissolution (Russian) 3-55777
 recrystallized, carbide segregation behaviour and effects (Russian) 3-55782
 recrystallized, ductile-brittle transition, group VIII element effects (Russian) 3-55776
 surface layer struct. rel. to recrystallization, X-ray analysis 3-76175
 Co-Ni-Mo-Cr, structural mechanisms of plastic deform. (French) 3-53211
 Cu-Mo composite, diffusion of Ni (Russian) 3-53222
 Fe-Mo, scale struct. (German) 3-76195
 Fe-Mo, yield stress and alloy softening, conc. depend. (Japanese) 3-41775
 Fe-Mo melt, N₂ diffusion addition effect (German) 3-47363
 Fe-Mo solid solns., low temp. strength, alloy softening, scavenging of interstitials 3-64921
 Fe-Mo(3.5 at.%) steady state creep, Ar atmosphere, microstructure, internal stress (Japanese) 3-72906
 Fe-Ni-Mo and Fe-Ni-Co-Mo martensites, hardening by tempering, comp. depend. (French) 3-44622
 Fe-Ni-Mo and Fe-Ni-Co-Mo maraging alloys, redistrib. of alloying elements during recovery (Russian) 3-80312
 Mn-Cu-Mo, Elinvar props. 3-64534
 Mo-Re alloy, analysis of lattice specific heat 3-58134
 Mo-C(Ta), stacking fault form. probability (Russian) 3-80275
 Mo-Cu-Ni, boundaries of single-phase side fields 3-80221

molybdenum alloys continued

- Mo-Ni system, phase diagram determ. using diffusion couples and equilibrated alloys 3-53209
 Mo-Permalloy/Cu core mag. composite wire characteriz. for memory applics. (Japanese) 3-50394
 Mo-Pt system, homogeneous domains of superconducting phases (French) 3-58329
 Mo-Re (35 at.%) interaction of twins with grain boundaries, substructures 3-41707
 Mo-Re-C, ageing, heat treatment, 1400-1800°C, hardness, microstructure 3-76174
 Mo-Re(34 at.%), α -phase precip. and flux pinning, electron microscope obs. and mag. hysteresis 3-50697
 Mo-Ti, (0.5 at.%)Ti, thermal cond. and elec. resist. meas. up to 1200K 3-52817
 Mo-Ti alloy, sputtering from Mo target, film structure and lattice parameters (Japanese) 3-64777
 Mo-Ti(0.5%), neutron irradi. temp. effect on hardness 3-79387
 Mo-Ti(0.5%) and Mo-Re(50%), neutron irradi. effect on tensile props. 3-79386
 Mo-Zr, grain coarsening during high temp. creep 3-64940
 MoBe₂₂, supercond. investig. (Russian) 3-46927
 MoNi₃, atomic struct. and microstruct., X-ray obs. (Russian) 3-79271
 Nb-Mo, anomalous behaviour during interdiffusion 3-72860
 Nb-W-Mo-Ti-Zr-C, quenching, ageing, carbide precipitation hardening 3-76176
 Ni-Fe-Mo, permeability-temp. curves, %Ni var. (German) 3-44275
 Ni-Fe-Mo-Ti-Nb for recording heads, mag. and mechanical props. 3-44265
 Ni-Mo, short-range order, comp. and heat treatment conditions depend. (Russian) 3-80207
 Ni-Mo, thermodynamic functions determ. by e.m.f. meas. using solid electrolyte (Japanese) 3-61124
 NiAl-Mo eutectic composites, directionally solidified, stability 3-69198
 δ -NiMo, domain struct, antiphase boundaries, inversion domains, permutation twins 3-60974
 Ni₃Mo, dissociated antiphase boundaries, electron microscope exam. 3-58636
 Ni₄Mo, plastic deform., twinning for ordered phase, slip in disordered phase 3-79408
 Ti-Mo-C-N system, boundary phase stability and crit. phenomena 3-80212
 β -Ti-Mo-Cr-Fe-Al, recrystallization, microstructure, texture 3-76178
 Ti-Mo-Zr-Sn, β_{m} , isothermal transforms. (French) 3-80203
 γ -U-Mo, fast burst reactor fuel, deformation and fracture behaviour 3-63207
 γ -U-Mo, pulsed reactor fuel, mechanical props. 3-63206
 U-Mo(10 wt. %), stress corrosion cracking, acoustic emission (French) 3-69404
 W-Mo, electrical resistivity and thermal conductivity 3-72972
 W-Mo alloy structure using field electron and field ion microscopes (German) 3-57972

molybdenum compounds

see also molybdenum alloys

- carbide precip. in steel during continuous cooling (French) 3-47416
 Gd₂(MoO₄)₃, domain wall motion during switching, ambient temperature to 160°C (German) 3-53070
 peroxo molybdates, i.r. spectra and structure 3-57656
 Bi₂O₃.3MoO₃ and Bi₂O₃.2MoO₃ crystal growth from molten salt soln. by 'pulling seed' method 3-72807
 Ga_{0.5}Mo₂S₄(Se₄) spinels, ferromag. semicond., characteriz. 3-72467
 Gd₂(MoO₄)₃, morphic piezoelectric and elastic coefficients (German) 3-53071
 MnS₂²⁻, Raman, i.r. spectra, force constants 3-63450
 Mo complex, [Mo₂O₄Cl₄(H₂O)₂]²⁻, SCCC MO calculations of electronic structure 3-54651
 Mo-S based ternary forms, superconductivity, comp. var. 3-68718
 Mo₂C, compound formation during sintering of Mo in organic binder 3-69353
 Mo(CO)₆, in gas and liq. soln., vib.-rot. coupling effects on correlation functions 3-67825
 MoF₅, vibrational spectra 3-46278
 MoF₆, Raman band contour analyses and Coriolis consts. 3-67816
 MoGe₂, X-ray emission spectra 3-58569
 MoN film, elec. and optical props., conducting neutral density filter applic. 3-64753
 MoO₂, compound formation during sintering of Mo in organic binder 3-69353
 MoO₂, Fermi surface obs., quantum Landau oscils. 3-75709
 MoO₃, polycryst., dielectric loss under simultaneous action of a.c. and d.c. fields 3-47207
 MoO₃ cpds., amorphous semicond., localized d¹ electron e.s.r. meas. 3-68847
 MoO₃ external standard for X-ray photoelectron spectroscopy 3-72777
 MoO₃.Li₂O melt, growth of Zr, Hf, Ti molybdates, struct. 3-75486
 MoO₄²⁻, mag. circular dichroism assignment of longest wavelength band 3-54663
 MoO₄²⁻, Raman, i.r. spectra, force constants 3-63450
 MoO₂Cl₂.H₂O, polycrystals, and stereochemistry 3-49874
 MoO₂Cl₂.H₂O, polypeptide struct. from non-space group extinctions 3-49873
 MoS₂, alkali metal intercalated, room temp. resistivity obs. 3-79691
 MoS₂, anisotropic, modulation spectroscopy obs., band structure 3-55567
 MoS₂, band structure 3-50126
 MoS₂, films, high resolution electron microscope obs. of extremely fine Au particles 3-49806
 MoS₂, lamellar lattice, heat capacity, thermodynamic props 3-41028
 MoS₂, layer type structure, electronic props. of two dimensional solids 3-50133
 MoS₂, mag. props., specimen purity and prep. method depend. (French) 3-64473

molybdenum compounds continued

- MoS₂, optical functions calculated from reflectivity data by Kramers-Kronig analysis 3-64618
 MoS₂, reflectivity in extreme u.v. range, band structure investigation 3-55609
 MoS₂, semiconductor, layer structure, mag. susceptibility, Van Vleck theory 3-41327
 MoS₂, single crystals, helical dislocations, transmission electron microscopy study 3-52630
 MoS₂ (Eu, Yb, Sr), intercalated layer type cpds., lattice parameters change, mag. ordering, Curie temp., supercond. 3-50371
 MoS₂, lattice vibrations, long-wavelength linear chain model, interlayer and intralayer force constants 3-40995
 MoS₂ lubricant, steel under hydrostatic pressing, plastic deform. (*Russian*) 3-72896
 MoS₂ photoemission, layer crystals, directional dependence, simple model 3-44519
 MoS₂:As, natural and synthetic, e.p.r. of As acceptors, g-values 3-50452
 MoS₂²⁻, mag. circular dichroism assignment of longest wavelength band 3-54663
 MoS₂(Se₂), lubricating action mechanism (*Russian*) 3-41798
 MoSe₂, i.r. absorpt. spectrum 3-47279
 MoSe₂, lamellar lattice, heat capacity, thermodynamic props. 3-41028
 MoTe₂, lamellar lattice, heat capacity, thermodynamic props. 3-41028
 MoTe₂, stacking fault energy calc. 3-68276
 Mo₂V_{1-x}O₂ whiskers, metal-semicond. transition phenomena, comp. depend. 3-60907
 rare earth molybdates, Ln₂(MoO₄)₃ and Ln₂MoO₆, structural and physical properties 3-64009
 V₂O₅:MoO₃ solid solutions, magnetic characteristics, 4.6-300K using Faraday-Curie balance 3-72459
 V₂O₅:MoO₃, physico-chemical props. 3-80582

moments (electric) see electric moments**moments (magnetic) see magnetic moments****moments (molecules) see molecular moments****momentum**

- see also angular momentum
 energy-momentum tensor, eigenvectors, Einstein-Maxwell theory 3-66663
 land and sea breezes, effects of turbulent transfer processes, numerical method 3-76680
 light diffraction by phase grating, momentum consideration 3-77964
 light wave momentum in a refracting medium 3-42957
 multiphoton excitation and ionis. rates, momentum-translation method, fallacy 3-78491
 ocean capillary waves, moving gust patterns, momentum exchange 3-47680
 photon beams, momentum transfer condition in diffr. effects 3-77956
 sea-air-interface, momentum and sensible heat fluxes meas. 3-47678
 solar pole-equator temp. differences, energetics and momentum balance 3-69823

monitoring

- see also patient monitoring; radiation monitoring
 air pollutants, automatic sampling and analysis, SO₂, NO₂, O₃, CO, hydrocarbons, suspended particles 3-53783
 air pollution, laser-radar system 3-66896
 animal activity-analysing system, infrared l.e.d.'s phototransistors, three arrays, computer analysis 3-73933
 atmosphere, monitoring of climatic parameters using spaceborne techniques 3-51073
 atmospheric pollution, computerised (*Japanese*) 3-66075
 beam position monitor, using precision thermistors 3-48501
 Earth environment monitoring using rockets 3-50874
 Earth strain monitoring using precise distance meas. 3-58853
 environmental monitoring from space for European demands 3-51075
 fatigue, strain multiplier applic. 3-59554
 geothermal spring water monitoring by neutron capture gamma rays using ²⁵²Cf 3-62360
 Gulf Stream surface features, satellite monitoring 3-59012
 high energy X-radiography, precision meas., dimensional change monitoring 3-45569
 in-reactor temperature monitor, indirect determ. of vapour pressure 3-67403
 intracranial pressure, using implantable pressure transducers 3-42685
 LMFBR, sodium cooled, water leaks into sodium 3-63148
 nuclear reactor fuel flow, for the SNR 300 (*German*) 3-67500
 nuclear reactor loose parts, monitoring system design, operating experience 3-74698
 oil pollution, remote sensing techniques 3-70194
 ozone, chemiluminescent monitors 3-77295
 personnel monitoring, film and thermoluminescent, comparison at high exposures, clinical results 3-77287
 production, U enrichment plant, computer controlled mass spectrometry system 3-70479
 river pollution (*Japanese*) 3-66076
 temperature, pyrometer, infra-red, selective absorption, waste gases from industrial furnaces 3-70284
 temperature, train wheels and jet engine rotors, i.r. pyrometer applic. 3-45435
 thin film reflectance and transmission, modulated beam photometer applic. 3-53901
 thoracic electrical impedance and regional ventilation of the lung, associated change, expt. 3-73931
 TV monitoring unit, for motion-picture filming (*Russian*) 3-51647
 URS-501M attachment, X-ray diffraction, material content, continuous monitoring 3-48593
 Zircaloy-2 pressure tubes, Hanford N reactor, monitoring, changes in material props., H content 3-67564

monitors see monitoring**monochromators**

- cleaning by action of O atoms 3-39909
 design, Cary principle applic. 3-66179

monochromators continued

- double vacuum, 800-2800 Å, toroidal concave diffraction gratings, fixed entrance and exit slits (*Russian*) 3-66225
 echelette type, apparatus function meas. in far i.r. using interference method 3-62127
 electron, for electron excitation function determ. 3-59910
 Grating Double Monochromator GDM 1000, VEB Carl Zeiss JENA, appl. to Raman and fluorescence spectroscopy 3-51610
 grazing incidence, synchrotron radiation focusing 3-39935
 high aperture ratio installation for phosphoresc. decay study 3-73725
 i.r. spectrometer, based on IKS-6 monochromator 3-51609
 large-aperture concave diffraction grating monochromator for wide wavelength region 3-62059
 middle u.v. spectrometer, Fabry-Perot interferometer, echelle monochromator 3-56464
 normal incidence, use with holographic concave gratings 3-39934
 photoconductivity spectra meas., automatic (*Russian*) 3-73752
 Seya Namioka monochromators in integrated optical system for vacuum u.v. 3-42550
 spectral contour of single spectral line or band, optimal recording conditions, second order system 3-53912
 spectral transmission function, effect on atomic absorption spectroscopy, continuous primary light source (*German*) 3-62108
 spectroscopic apparatus, review 3-56669
 SPM 2, optoelectronic mark device (*German*) 3-45470
 vacuum, holographic concave grating applic. 3-70313

monolayers**see also adsorbed layers**

- adsorption of gases on C block, specific surface area, heat of adsorption, student experiment 3-48327
 built-up, thickness meas. by multiple beam interferometry, comments 3-39851
 built-up, thickness meas. by multiple beam interferometry 3-39850
 calcium stearate, shear properties 3-64108
 charge monolayers, on insulating liquid interfaces, dynamics 3-75253
 isoenergetic substrates, adsorption isotherms, virial coeffs. of two dimensional gas 3-68381
 magnesium phthalocyanine, transition from aggregate to monomer state, spectral study 3-52753
 optical props. of sub-monolayer molecular films 3-47333
 refractive index profiles and thickness obs. using optical interference method 3-73766
 CaO, localised monolayer adsorpt. of spherically symmetric gases 3-43934
 He, lifetimes and binding energies, low temp. meas. by rapid-flash-desorption technique 3-64248
⁴He, two dimensional evaporation and substrate heterogeneity effects 3-55107
 MgO, localised monolayer adsorpt. of spherically symmetric gases 3-43934

monolithic integrated circuits**see also large scale integration**

- IC discriminator for neurological studies 3-42689
 Au-Ni metallisation, diffusion studies rel. to reliability 3-79528

monomers see molecules**Monte Carlo methods**

- annealing simulation of correlated point defects in f.c.c. metals 3-79531
 antiferromagnet, order-disorder transition in mag. field 3-68752
 astronomy, H-He mixture in giant planets, props. at high press. 3-42161
 atmospheric electron-photon shower, Monte Carlo calc. of fluctuations in Cherenkov radiation (*Russian*) 3-69773
 atmospheric optical communication through clouds, computer simulation of light pulse propagation 3-76700
 atmospheric scattering theory, Monte Carlo method for spherical atm. 3-73299
 boundary dose rates due to gamma rays at power reactor sites, Monte Carlo procedure 3-57591
 carrier mobility of Esaki superlattice 3-46830
 carrier transport calc., inelasticity of acoustic phonon scatt. 3-55256
 CASIM, shielding calc., for high energy accelerators 3-56772
 Cherenkov spectrometer for γ -astronomy, calc. of linearity and resolving capability (*Russian*) 3-65948
 cloud droplet coalescence, linearized kinetic eqn. numerical soln. (*Russian*) 3-69572
 cloud droplets coalescence, algorithm of numerical soln. of integral kinetics eqn. 3-73301
 communal entropy, Monte Carlo estimation 3-45743
 computer simulation of chain mols. 3-60400
 computer simulation of scaling eqn. of state of Heisenberg ferromagnet 3-44188
 continuous, Dirichlet problem soln. (*Italian*) 3-74003
 cosmic ray hadrons energies > 500 GeV, identification by rejection from intermediate radiation recorder (*Russian*) 3-69792
 cosmic ray jets, primary energies estimation, null correlation method 3-42101
 cosmic ray muon intensity at large rock, water depths, sea level spectrum (*Russian*) 3-80904
 cosmic ray nuclear cascade in atmosphere, Monte Carlo simulation including solar effects (*German*) 3-53582
 cosmic ray pion inelastic interactions with emulsion nuclei (Ag, Br, C, N, O) at 60 GeV, secondary particle calcs. (*Russian*) 3-69788
 criticality, of high burnup ²³⁹Pu, anal. of expts. 3-74729
 crystal ripening, stochastic model, computer simulation 3-63965
 diagnosis, chest X-ray, application of Monte Carlo method 3-73600
 diffusion correlation effects simulation in non-stoichiometric solids 3-52723
 dose, distributions calc. rel. to radiation therapy (*German*) 3-77269
 EAS, effect of boundaries of widely-extended detectors on determ. of axial coordinates and no. of particles in shower (*Russian*) 3-69769
 EAS fluctuations at sea level, primary protons, secondary particle spectra (*Russian*) 3-65603
 EAS simulation, rel. to electron component characteristics determ. 3-69776
 electron gas classical, integral equation solutions, comparison with Monte Carlo calc. 3-42881

Monte Carlo methods continued

- entropy estimation from Monte Carlo acceptance ratios, problems 3-70770
- fissile material storage, calcs. on double latching cell loadings 3-46156
- free molecular flow on concave surfaces, heat transfer and forces 3-46461
- frequency response of a dynamic system with statistical damping 3-42801
- gamma-ray buildup factors, including bremsstrahlung contribution, calc. 3-71336
- gamma-ray efficiency values for various source-to-detector geometries 3-62221
- gamma-ray scattered energy spectra, study of low energy components 3-57587
- hadronic cascades with new particle yield formation, Monte Carlo simulation 3-54349
- hard non-spherical molecule system, eqn. of state simulation 3-54161
- heavy-ion initiated nuclear-e.m. cascades, Monte Carlo calcs. 3-59234
- hydrocarbon chains, correlation functions of internal motion 3-78847
- hypersonic blunt body merged layer problem, numerical soln. of Navier-Stokes eqns. 3-52466
- intersection models for pipes carrying Pu nitrate solns., nuclear reactor criticality safety (*German*) 3-67543
- intranuclear cascade model of pion-emulsion nuclei scattering at high energies 3-67369
- irradiance reflectivity in and above ocean 3-59024
- Ising mag. system exhibiting tricritical points, Monte Carlo study 3-47025
- Ising model computer calcs. 3-50320
- isotropic incident flux in phantoms 3-48272
- Jupiter magnetosphere, energetic electron diffusion, synchrotron emission Monte-Carlo computer program 3-65787
- laser light nonlinear absorption, Monte Carlo treatment 3-59893
- liquid with noncentral forces, pair correl. function calc. 3-60659
- lunar regolith thickness distrib. determ. 3-47949
- molecular vibrational relax. process reaction rate calcs. 3-60486
- multiple integrals, calc. for polyatomic molecules (*Italian*) 3-40092
- muon scattering distribution 3-48514
- neutron cross-section perturbation determ. by correlated sampling using SAMCEP computer code 3-74636
- neutron detector with organic scintillator, operational effectiveness calc. using Monte Carlo program EFFI (*German*) 3-59645
- neutron elastic scattering simulation program 3-43142
- neutron flux determ., over extremely small volumes in criticality problems (*German*) 3-67388
- neutron multigroup calcs., probability table method 3-46056
- neutron resonance decay following capture, Monte Carlo simulation, resonance spin determ. 3-57519
- neutron spectra, energy and angular distributions calculations for ${}^7\text{Li}(p,n){}^7\text{Be}$ 3-59637
- neutron therapy facility, design using analogue Monte Carlo computer code 3-61922
- neutron transport calc., two dimensional 3-71148
- neutron transport during nuclear air burst, computer aided analysis 3-74621
- neutron transport in Fe, 10 keV-14 MeV spectra as function of mfp 3-67321
- neutron transport stationary problems, variance reduction techniques 3-74622
- neutron transport theory in boiling media 3-63107
- nonlinear absorption of laser radiation 3-74280
- nuclear cascades in rock, for primary hadron energies 3-3000 GeV, stopping pions, calcs. 3-44976
- nuclear reaction cross sections calc. 3-43252
- nuclear reactor reactivity due to cross-section perturbations, Monte-Carlo calcs. 3-49331
- optimisation method, modification to case when optimum soln. is at boundary of region (*Polish*) 3-66505
- phase-space integrals and asymptotic behaviour, numerical evaluation for high-energy collisions 3-43133
- photon wavelength selection, scattering process simulation, Monte Carlo programme, parallel computers 3-62433
- plasma simulation, radiation-induced 3-46560
- plasmas, radiation induced, using piecewise linearized predict-correct technique 3-75426
- plasticity, stochastic analysis 3-54108
- poly(glycine), short chains conformational statistics, chains with constrained ends, partition function 3-75162
- poly(L-alanine), short chains conformational statistics, chains with constrained ends, partition function 3-75162
- positive ion collection prediction, flat faced cylindrical probe 3-61601
- programs rel. to gamma and neutron fluxes and associated heating and damage (*German*) 3-67630
- proton injection into magnetic field, dispersal, reln. to solar particle flux variation (*Russian*) 3-65633
- radiotherapy 3-48251
- random substitutional alloy, onset of ferromagnetic order, computer simulation 3-47016
- reactor core calc. in three dimensional geometry (*German*) 3-74643
- reactor shield analysis, radiation transport 3-60341
- rectangular panels under subsonic and supersonic turbulence, generalised random forces 3-77798
- ring current proton precipitation, radiation production and energy dissipation in mid-latitudes 3-76818
- self-powered instantaneous neutron detector, sensitivity calcs. 3-51718
- SEM, calc. of electron scattering and secondary electron prod., Monte Carlo calc. 3-70432
- SEM, X-ray anal. of thin films and fine structure 3-71989
- shock wave reflection from thermally accommodating wall, molecular simulation Monte Carlo method 3-71788
- simulation of K + I₂ collisions at superthermal energies 3-71615
- simulation of nonmesonic decays of heavy hyperfragments 3-67250
- simulations, change in strong interaction characteristics at ultra-high energies 3-51234

Monte Carlo methods continued

- solar Lyman- α radiation transfer through plane-parallel atm. 3-53615
- solar proton events model including shock wave effects 3-42135
- solid, phonon transport simulation 3-68379
- source energy biasing optimisation 3-62432
- spheres with dipoles, Monte Carlo free energy with multistage sampling 3-74173
- stars, eqns. describing rotating gaseous medium 3-47865
- transferred electron dynamics, for LSA-like mode operation, simulation 3-55280
- transport of gamma-rays and electron, calcs. using Monte Carlo computer code 3-52235
- transport of neutrons and gamma-rays in carbon, calculational analysis 3-74638
- viscoplastic media hydrodynamics, time-dependent problems, Monte Carlo soln. method 3-71839
- water-like models, Monte Carlo studies of dielectric properties 3-68909
- wavelength coincidence statistics, appl. to stellar line identification 3-61800
- weighting methods for calculation of polymer configurations 3-67867
- X-ray absorbed disc 3-61927
- X-ray spectra, diagnostic energy range, scattered radiation 3-77290
- K⁻ decay properties, separation of events 3-66978
- Z⁻, emulsion nuclei capture, hyperfragment and cryptofragment prod. 3-74607
- Z⁻ capture in emulsion nuclei, Monte-Carlo simulation, determ. of Λ^0 trapping probability 3-52211
- Al-SiO₂-Si, KV electron energy dissipation in depth calc. 3-72110
- Au, Mott scattering 3-51688
- GaAs, with superlattice, calc. of electron drift velocity 3-68613
- H atom recombination, Monte-Carlo simulation 3-57614
- H₂, thermodynamic props. calc. using intermolecular potential 3-60508
- ³He, solid, calc. of ground-state energy, shell depend. correlation functions 3-68470
- ³He, solid, ground-state energy calcs. 3-46744
- KCl, molten, Pauling potential Monte Carlo computations 3-68150
- ¹⁶N γ -rays site-boundary dose calcs. for BWR nuclear plant, geometrical considerations 3-74755
- NaI well-type detectors, photopeak efficiency 3-40004
- Se, sputtered vitreous film, model of atomic arrangement 3-64264

moon

- see also lunar seismology; lunar structure
- 1 mm radiometry, cryogenic optical system 3-77180
- Al-Khwarizmi, basin on lunar far-side, Apollo mission data 3-73463
- albedo of disk, statistical distrib. 3-61721
- angular momentum loss of Earth-Moon system 3-53626
- anorthosite rocks, natural exoemission, recrystallisation, deform. history 3-77007
- Apollo 11 coarse fines, subsolidus reduction of residual ilmenite and early opaque crystallites 3-59291
- Apollo 12 lunar fines, alteration by H₂O vapour absorpt. 3-47946
- Apollo 12 soil samples, optical properties 3-51300
- Apollo 15, Ar in green glass spherule (15426), age and trapped gas 3-80999
- Apollo 15 breccia and soils, composition in green glasses 3-73460
- Apollo 15 green spherules, inferences from inert gas meas. 3-47957
- Apollo 15 soils, distribution of particle types according to selenological terrain 3-59289
- Apollo 15 soils and breccias, presence of primitive lunar basaltic comp. 3-47944
- Apollo 16 neutron stratigraphy, ¹⁵⁸Gd/¹⁵⁷Gd and ¹⁵⁰Sm/¹⁴⁹Sm ratios determ. 3-56351
- Apollo 16 rock, electron microprobe analysis of rust 3-59292
- Apollo 16 rocks, petrology and classification 3-53624
- Apollo 16 sample analysis, surface investigation 3-59290
- Apollo 17, dark mantling area nature and extent from earth-based meas. 3-61727
- Apollo 17, major and trace element chemistry of 30 samples 3-65842
- Apollo 17, traverse gravimeter results 3-61726
- Apollo 17 deep drill core, major and trace elements 3-65830
- Apollo 17 for u.v. spectrometer expt. 3-48157
- Apollo 17 material, isotopic ages 3-65845
- Apollo 17 orange soil and meteorite impact on liquid lava 3-56354
- Apollo 17 results, conference, USA (1973) 3-65817
- Apollo 17 rocks and soils, radionuclide conc. 3-61728
- Apollo 17 samples, mineralogy and geochemistry of opaque and non-opaque phase 3-65847
- Apollo 17 samples, preliminary examination 3-61725
- Apollo 17 site, electrical structure from r.f. interferometry 3-61890
- Apollo 17 sounding radar, surface obs. 3-61730
- Apollo data, review 3-51305
- Apollo lunar orbital mass spectrometer, absolute calibration 3-42257
- Apollo retroreflectors, selenocentric coordinates 3-56357
- Apollo-16 samples, evidence of volatile elements, suggesting outgassing 3-59281
- Apollo 11-16 results, review 3-45046
- Aristarchus crater ²²²Rn emanation, Apollo 15 obs. 3-45048
- artificial creation of stable lunar atmosphere rel. to gas addition rates 3-65810
- atmosphere, Apollo 17 far u.v. meas. 3-69905
- atmosphere, results from Apollo 17 miniature mass spectrometer 3-69904
- basalt, large coarse grained and predominantly basalt particles (Apollo 17) 3-65829
- basalt 12021, augite-pigeonite miscibility gap for pyroxenes 3-77001
- basalt 70035, Apollo 17, multistage cooling history 3-65843
- basalt fragments pyroxene relations, Apollo 17 sample from Station 5 3-65825
- basalts, Mare-like, KREEP-rich 3-61731
- black spots, reflectivity and radio backscatter comparison with surface structure and composition 3-77005
- breccias, lithification of Apollo 14 samples 3-47942

moon continued

- brightness temp. meas. at 8.6 mm and 3.1 mm 3-47922
 camera and lenses, used for lunar photography, modified Hasselblad 500 EL Data camera 3-70079
 capture by Earth, weak friction approx. and tidal evolution 3-80908
 capture origin, flyby encounter with earth, computer simulation model 3-59299
 carbide formation Fe silicates 3-65806
 centre of gravity-centre of figure offset 3-59282
 chemical composition of surface, expected γ -ray emission spectra 3-77004
 comet impact, evidence for Solar System origin 3-59254
 compositional mapping of surface, fluorescent X-ray, γ -ray, α -particle measurements 3-65804
 convection rel. to thermal history and instability growth 3-61715
 crater chronology in Hadley Rille-Apenine front and Cayley and Descartes formations 3-61729
 crater ejecta, model for distrib. and props. 3-59297
 craters, relationship for overall diameter and rim crest diameter 3-59296
 crust vol. structure determ. from seismic data 3-47953
 crystalline, rocks, ages, ion tracks and rare gases (Apollo 17) 3-65832
 dielectric and d.c. cond. of lunar samples 3-59305
 distance meas. using laser ranging instrument developed at Tokyo Astronomical Observatory (*Japanese*) 3-70087
 dust for u.v. reflectivity meas., Apollo 11, 12 and 14 samples 3-45041
 dynamical figure and density distrib. of interior 3-61722
 dynamics, use of Saros for orbit evolution study 3-47859
 eclipse, 1972 January 30, photoelectric obs. 3-45043
 eclipse 1971, 6 August, photoelectric and visual obs. 3-69897
 electromagnetic wave scattering, propag. parallel to diamagnetic cavity axis 3-65813
 electrostatic charging of lunar surface rel. to dust accumulation on far side 3-65353
 evolution, survey of astronomical, geochemical and geophysical data 3-47958
 exospheric ions, lunar acceleration 3-65814
 fines, fading of induced thermoluminescence 3-69902
 fines 74220, rare earth elements and Ba 3-65846
 formation from cluster of particles encircling Earth 3-47950
 Fra Mauro comp. glass, sintering and hot pressing 3-47942
 gaseous distrib. in Apollo 15 samples, implications 3-69901
 geochemical aspects of soil, basalts and breccia 3-65838
 geologic mapping, spectral types, charge transfer bands 3-59310
 geometrical figure approx. using harmonic anal. 3-59279
 ghost craters, formation during mare filling comparison with experimental craters deformed by isostatic filling 3-65801
 glass, Apollo 15 and 17, orange and green 3-65840
 glass spherules in Apollo sample 74220, origin 3-65844
 glasses, orange and green, props. rel. to mare basalts, model 3-65839
 granular aggregates, contribution of contact conductivity to thermal conductivity 3-73458
 gravity field representation by Lamé functions 3-61360
 grey appearance, solar wind effects 3-47952
 Hadley Apenine region, petrology of 2-4 mm soil fraction 3-47945
 Harold Urey, contrib. to lunar research 3-45398
 highlands, geochemistry of rocks 3-47959
 holocrystalline rocks from North Massif, petrology and genesis (Apollo 17 samples 76055 and 77135) 3-65850
 hortonolite, high temperature crystal chemistry 3-77000
 ilmenite basalt, Apollo 17 sample 70035, petrology 3-65851
 ilmenite basalt, Apollo 17 sample 75055, mineralogy and petrology 3-65833
 impact crater spherules, comparison with terrestrial impact debris 3-65803
 impact generated silicate spherules, analogy with meteoritic chondrules 3-65853
 induced magnetic fields, topology using asymmetric theory 3-65793
 induced magnetosphere, Apollo 12 and Explorer 35 experimental results 3-81000
 infrared remote sensing, compositional implications of Christiansen frequency maximums 3-73457
 interior composition, removal of CaO and Al₂O₃ content restraint 3-61717
 internal constitution and evolution 3-47962
 internal convection evidence from first-order topography 3-47930
 i.r. atlas charts of eclipsed moon 3-47951
 KREEP fragment containing niobian rutile 3-45057
 laser ranging for tectonic motions meas. 3-44936
 layered lunar/earth surfaces, measurement of electrical parameters, bibliography 3-45241
 libration, differential radio interferometry appl. 3-45249
 libration cloud, theoretical possibility in restricted three body problem 3-69803
 libration problem, observational eqns. in selenocentric horizontal system 3-73556
 limb-solar wind interaction, cool photoelectron effects 3-47891
 lunar, tides determ. anal. of methods 3-65504
 Lunar and Planetary Laboratory, and its telescopes review 3-70054
 Lunar fines, surface reduction by H₂, relevance to solar wind effects 3-42179
 lunar matter metal fragment, morphology 3-65808
 lunar origin rel. to mass ratio of Earth-Moon system 3-45045
 lunar sample, solar cosmic rays, alpha particle content past and present 3-51226
 lunisolar perturbations, computational method, effect on satellite motion 3-59247
 magnesium hornfels, fragment laden contact metamorphosed (Apollo 17) 3-65821
 magnetic dipole field 3-59301
 magnetic field, orbital mapping by Apollo 15 subsatellite 3-65796
 magnetic field intensity determ., thermal demagnetisation of breccias 3-47960
 magnetic field limb compressions 3-65811
 magnetic field meas. and contour map, remanent magnetization and large craters 3-42182

moon continued

- magnetic field perturbations at limb 3-65812
 magnetic fields, generation mechanism 3-47956
 magnetic monopoles, search in lunar materials with e.m. detector 3-67171
 magnetism, theory 3-59280
 magnetism rel. to history 3-51299
 magnetosphere, induction theory and model 3-51301
 mapping, effect of libration and other motions 3-47963
 Mare Humorum, spectral reflectivity meas. 3-56352
 Mare Imbrium lava flows, earth based radar response meas. 3-59308
 marginal zone charts errors, corrections to orbit inclination 3-59276
 megalithic lunar observatory, Ring of Brogar 3-65613
 melting and differentiation, chemical evidence 3-73459
 meteorite conference, Chicago (1972) 3-56365
 meteorite impacts, flux determ. 3-47968
 microstratigraphic chronology using mechanical erasure of particle tracks 3-69899
 monochromatic phase curves and albedos determ. from 0.35-1.0 μ and UVB obs. 3-45042
 night side, e.m. response to interplanetary magnetic field fluctuations 3-65791
 occultation of 139 Tauri, predicted position of Moon's centre found to be in error 3-65790
 occultations, photoelectric meas. of timings 3-61710
 opaque samples (Apollo 17) 3-65828
 orbit inclination, early history 3-76949
 orbit parameter calc. by computer, for students 3-56605
 orbit perturbation, post-Newtonian gravitational effects in lunar laser ranging 3-45047
 origin, weakness of tidal friction as energy sink in lunar capture 3-77006
 origin by backward extrapolation of dynamical properties 3-53622
 origin from solar nebula inside orbit of Mercury 3-65799
 particle track record of Luna 16 and 20 missions 3-47954
 permafrost simulation, dielectric relaxation, 100K 3-45050
 photoelectron layer above sunlit surface, simple models rel. to solar proton flux 3-61719
 photographs, lunar surface, Apollo 15, Itek optical-bar panoramic camera 3-65807
 photographs, lunar surface, Apollo 15, stereophotogrammetric reduction 3-65970
 pigeonite from lunar rock 12053, anti-phase domains from X-ray diffraction 3-65816
 polar wobble, 6-year effect on moonquakes 3-59298
 primary cosmic rays, altitude dependence and intensities near surface (*Russian*) 3-65576
 quasiperiodic orbits about translunar libration point, analysis 3-69896
 radar meas. by Apollos 14 and 15 3-69900
 range meas. using laser system 3-42177
 red spots, nature rel. to native radioactivity and pre-mare basalts 3-59307
 regolith thickness distrib. determ. using Monte Carlo method 3-47949
 rock luminescence, effect of u.v.-proton excitation 3-61718
 rock type identifications from small clasts and single mineral grains 3-65815
 rocks, magnetic props. rel. to lunar surface phenomena 3-59302
 rocks, nuclide prod. rate by galactic cosmic rays 3-73467
 selenodesy appl. of differential VLBI 3-56470
 selenodetic catalogues, systematic differences 3-59278
 selenodetic reference networks deformation due to rotation parameters errors 3-59277
 shape, elevations, Apollo 15 and 16 laser altimeter obs. 3-42183
 Shorty crater Apollo 17 sample 74220, orange soil analysis 3-65834
 Silver Spur, cross-hatching, hypersonic and supersonic turbulent gas flow 3-69903
 soil, Apollo 17 sample ¹⁸O/¹⁶O, ³⁰Si/²⁸Si, ¹³C/¹²C, D/H, H and C 3-65823
 soil, Apollo 17 samples, electrical and magnetic properties 3-65836
 soil, Apollo 17 samples analysis for halogens, P₂O₅, U, Li, Te 3-65831
 soil, lunar and terrestrial, elec. props. 3-59306
 soil, orange, glass particle composition in Apollo 17 sample 3-65827
 soil, orange, low oxidation states of Fe and Ti 3-65849
 soil, orange and grey samples, magnetic characteristics 3-65818
 soil, thermal history from ferromag. reson. 3-59304
 soil, unusual particles, from Apollo 16 expedition 3-59294
 soil, upper layer porosity from compaction parameter using opposition effect (*Russian*) 3-77003
 soil fragments from 5 Apollo 17 sites, 2-4 mm size 3-65837
 soil material, orange, viscous flow and crystallization (sample 74220) 3-65848
 soil sample, Apollo 17, C, S and inorganic gas abundances 3-65826
 soils, Apollo 17, morphology and chemistry of particles 3-65820
 soils, orange and grey Apollo 17 samples from Shorty crater 3-65841
 soils ages, ion tracks and rare gases (Apollo 17) 3-65832
 soils and breccias, mag. aftereffect 3-59283
 soils and rocks, Apollo 16 samples, magnetic props., mode of formation 3-59303
 solar flare of Aug. 1972, characterisation from lunar samples analyses 3-69842
 solar wind-Moon interaction, continuum fluid model 3-51276
 specific effective scatt. area in r.f. range 3-56312
 spherical astronomy for geological and geophysical obs. of Moon 3-51304
 stress differences determ., appl. of virial tensor 3-61720
 surface, comparison with Mars surface (*Hungarian*) 3-76989
 surface brightness temps., thermal cond. of upper 1.5 m of regolith 3-61713
 surface composition, remote optical analysis 3-65802
 surface gas sources, role of press. transient in detection and identification 3-51302
 surface microerosion rates, solar rare gases conc. 3-59312
 surface radiative transfer, effects of scattering and thermal conduction 3-61684

moon continued

- surface radioactivity, Apollo 15 and 16 γ -ray spectra 3-45049
 surface transient phenomena, three colour blink technique, image orthicon TV system 3-47943
 Taurus-Littrow, Apollo 17 soil samples in 1-2 mm size range, and their interpretation 3-65822
 Taurus-Littrow mare basalt and dark mantle soil 3-65824
 thermal evolution models, representing accretion, simulating differentiation and convection 3-65792
 thermal history models, mag. constraints 3-59287
 thermal ionosphere, electric potential in solar wind and magnetosheath 3-73456
 tidal oscill. in horizontal ionospheric drift at equator 3-53524
 translational-precessional motion in Earth-Sun gravitational field 3-76950
 vitrified cryst. rocks, simulated, characts. 3-59293
 volcanic glass and cinder formation 3-65819
 volcanic glass, orange and black, Apollo 17 sample 74220 from Shorty crater 3-65835
 water, possible sources and degassing from lunar interior 3-53623
 Watt's charts, systematic errors and effects on orbital elements (*Russian*) 3-77002
 xenoliths in Maar-type volcanoes and diatremes rel. to Moon, Mars and Venus 3-53403
⁴⁰Ar/³⁹Ar ages, spatial distribution in lunar breccia 14301, in situ meas. 3-61716
⁶⁰Co abundance at various depths 3-61712
 H depth distrib. in lunar materials 3-61711
 H in atmosphere, interpretation of Apollo 17 meas. 3-65809
 U-Pb systematics in lunar basalts, response to comment 3-53621
¹³¹Xe, high concentration in lunar rock, explanation by consideration of ¹³⁰Ba(n, γ) cross section 3-54482

moon structure see lunar structure**moonquakes** see lunar seismology**Morse potential**

- see also *intermolecular mechanics; kinetic theory*
 alkali halides, multiphonon i.r. absorpt. temp. depend. 3-64660
 anharmonic crystals, thermodynamic and dynamic properties (*Hungarian*) 3-75576
 calculation using programmable desktop machine, characts. of real functions 3-63565
 metal, ideal strength, Morse potentials use and limitations 3-58061
 molecule, heteropolar diatomic, multiphoton processes, pot. energy curves 3-67760
 molecule, homopolar diatomic multiphoton processes, pot. energy curves of excited electronic state 3-71516
 AIO molecule, Morse oscill., Franck-Condon factor calc. by generalised WKB approx. 3-74986
 Cu, point defect form. energy, use of pair pot. of atom interaction (*Russian*) 3-75522
 He₃, bound state existence, variational calc. 3-63566
 NH₃, ND₃ and NT₃, Schrodinger eqn. analytical soln. for double minimum Morse pot., intramol. inversion 3-52332
 PtC, Franck-Condon factors, r-centroids, α -averaging of Morse potential functions 3-78720
 PtO, Franck-Condon factors, r-centroids, α -averaging of Morse potential functions 3-78720

m.o.s. devices see metal-insulator-semiconductor devices**m.o.s. structures** see metal-insulator-semiconductor structures**m.o.s.f.e.t** see field effect transistors**Mossbauer effect**

- see also *gamma-ray absorption; nuclear excitation*
 accelerometers in Mossbauer spectroscopy 3-42683
 air radioactivity rel. to Fe concentration 3-65396
 alkali silicate glass, nucl. gamma res., struct., SO₂ treatment 3-68165
 asymmetry in spectra rel. to anisotropic diffusion in polycrystalline material 3-50500
 basaltic class I titanomagnetites, Fe³⁺/Fe²⁺ ratios from Mossbauer spectroscopy 3-61305
 biferricenium, biferricenylanium cations, ⁵⁷Fe Mossbauer spectra and intervalence transfer electronic absorpt. study 3-55507
 Brownian particles suspended in liquid, theory (*Russian*) 3-72559
 chalcopyrite, obs. of mag. transitions at 5-16 kbar, geophysical significance 3-58865
 coherent Coulomb excitation of Mossbauer transition in single cryst. 3-68897
 commutator, for const. velocity spectrometer 3-51751
 constant acceleration Mossbauer spectrometer (*Korean*) 3-70439
 crystals, Sn impurity optical characts. spectra, interactions 3-68565
 digital spectrometer, multichannel analyser controlled 3-70438
 electric field gradients at nuclei in charge perturbed lattices 3-47182
 ferric ions in Fe(NO₃)₃.9H₂O and frozen aqueous solns., mag. field depend. of spin-spin relax. time 3-75924
 ferrites, cubic, valencies of Mn and Fe ions, paramag. Mossbauer obs. 3-55510
 ferromagnetic crystal, magnetic anomalies 3-58462
 ferromagnetic dielec. with multidomains, Mossbauer study of u.s. generation by r.f. field 3-44307
 ferromagnets with impurities spin correlation functions of Mossbauer atom 3-75928
 frozen solutions, rel. to ion structure determ. 3-50506
 garnet-type antiferromagnetic substances 3-72558
 glass:Sn, Ga, second-order Doppler shift, superconductivity 3-75927
 hedenbergite-ferrosilite pyroxene, synthetic, Mossbauer resonance spectroscopy of iron 3-80593
 hortonolite, lunar, at high temperature 3-77000
 hyperfine interactions of trans-lead elements, review 3-68904
 hyperfine pattern, influence of high electrostatic fields 3-68900
 II-IV-V₂ semiconductors, effective charges of Fe impurity atoms from Mossbauer obs. 3-58456
 inelastic channels in presence of hyperfine splitting, suppression effect 3-68906
 Invar mag. anomalies 3-44354
 Jahn-Teller system, E-term, quadrupole splitting 3-75931
 laser using gamma quantum emission, two-stage excitation of nuclei by neutrons 3-74222
Mossbauer effect continued
 liquid crystals, spectroscopy, review 3-43747
 MⁿM^mF₆A (A=Rb, Cs, Tl; M=3d transition metal), modified pyrochlore 3-40880
 magnetic material, spin orientation, elec. field grad., Mossbauer-Faraday and mag. double refraction obs. 3-50496
 magnetic multilayer crystals, recoilless factor behaviour, Debye-Waller factor (*German*) 3-50493
 magnetic oxide, ⁵⁷Fe, hyperfine parameter analysis 3-50495
 mechanically chopped γ -rays, sideband intensities treatment 3-67257
 metal formate mixed crystals, cation position determ. (*German*) 3-79967
 metals:⁵⁷Fe, absorption spectra at room temperature 3-68903
 monocystal: impurity γ -radioactive nucleus, spectra, defection mechanism 3-79961
 Mossbauer effect, vibrational anisotropy for M1 or E1 γ resonance transitions 3-72549
 noble gases, solid, Mossbauer of dissolved Fe, nuclear quadrupole moment, electron densities, mol. orbits 3-41459
 nuclear excited-state moments meas., exptl. techniques 3-45933
 orbital double degenerate E-state, vibronic coupling effect on line shape, relaxation transitions 3-79960
 organic supercooled liquids, Mossbauer line broadening 3-68907
 organotin covalent compounds, vibr. modes from Mossbauer effect and Raman data 3-44355
 Permalloy with Mo additions, of ⁵⁷Fe, annealing effects (*Russian*) 3-53038
 point defects, resonance vibration modes, effect on recoilless fraction 3-75923
 polarisation of Mossbauer spectra, to determine reson. nuclei coords. 3-75450
 proportional counter for spectroscopy of steel by scattered electrons 3-66384
 pyrrhotite, obs. of mag. transitions at 5-16 kbar, geophysical significance 3-58865
 rare gas:⁵⁷Fe, frozen, hyperfine interactions obs. 3-41451
 scintillation resonance detector description 3-54020
 smectic ordered liq. cryst., ¹¹⁹Sn Mossbauer at 77K 3-55511
 spectrometer, interfacing with analysing system 3-70441
 spectrometer, Mossbauer, based on spectrometric section of diffractometer 3-51753
 spectrometer, using multichannel analyzer for time measurements 3-56987
 spectrometer, with ³He dilution refrigerator, for meas. down to 0.1 K 3-68895
 spectrometer recorder, multichannel pulse analyzer, const. vel. mode 3-73914
 spectrometers, interferometric calibration, problems and solutions 3-70437
 spin system, dependence of Mossbauer spectrum on degree of ordering 3-64588
 spin-ordered systems, Mossbauer freq. shift, second order Doppler shift 3-68898
 stainless steel, cold work meas., nondestructive methods 3-47504
 steel, ductile-brittle transition obs. 3-55815
 steel, industrial, mag. hyperfine field, isomer shift and quadrupole splitting (*Rumanian*) 3-47188
 steel, local mag. struct. of carbides formed during ϵ - χ - θ transforms (*Russian*) 3-79951
 steel, stainless, isomer shift, pressure depend. 3-72554
 steel, stainless, Mossbauer linewidth due to hyperfine interactions 3-47175
 ternary selenides, MFe₂Se₄, magnetic hyperfine field meas., 3d-electron delocalization (*French*) 3-72550
 time delayed expts., rel. to uncertainty principle interpretation 3-74096
 titanomagnetite, study of cation distrib. temp. depend. 3-58868
 tourmalines, crystallographic positions of Fe²⁺ determ. 3-72557
 transferrin, of ⁵⁷Fe, h.f.s., spectra analysis 3-63575
 transition metal tantalates, MeTaO₄, atomic and mol. ordering, mag. structure from 4.2 to 300K 3-79849
 vibration meas. of cat ear basilar membrane (*German*) 3-51426
 vibrational anisotropy for M1 or E1 γ resonance transitions 3-72549
 Weyl's gauge-invariant geometry exptl. test 3-42877
 ν resonant absorption, limits on elementary length 3-66979
¹³⁹La Mossbauer scatt. of 166 keV γ -rays 3-60119
 AgAlTe₂-AgGaTe₂-AgInTe₂, elec. field gradients at ¹²⁵Te, ¹²⁷I impurity nuclei 3-72555
 Al, anharmonic contributions to elastic and inelastic X-ray scattering at Bragg reflections 3-58091
 Al:⁵⁷Co, neutron irradiated and annealed, Mossbauer study of interstitial trapping 3-58454
 Al₂O₃, of ⁵⁷Fe, hyperfine pattern obs. 3-68900
 α -Al₂O₃-Fe₂O₃ solid solution 3-55513
 γ -AlOOH:Fe³⁺, magnetic hyperfine field obs. 3-50498
 Au-Yb dilute alloy, Mossbauer spectra, obs. on Kondo anomaly on relaxation rate 3-53050
¹⁹⁷Au γ -ray lifetime, linewidth meas., source in differing chemical environments 3-67260
 BaFeO₃, hexagonal, synthesis of 12 layer modification, Fe⁴⁺ isomer shift obs. 3-52612
 BaFeO₄, thermal decomposition products of BaFeO₄, magnetic props. 3-58451
 BaFe_{12-x-y-z}Zn_xTi_yMn_zO₁₉, ferrite, low temp. mag. props., 4.2-300 K 3-41331
 BaSnO₃:¹¹⁹Sn, selective modulation of recoilless γ -rays 3-55508
 Ba_{1-x}Sr_xFe_{12-x}Al₂O₁₉, substitution of Fe³⁺ by Al³⁺ 3-58452
 BaTiO₃, of ¹¹⁹Sn, probability, atomic vibr. anharmonicity 3-41454
 Be:⁵⁷Fe, clustering of Co along grain boundaries (*French*) 3-68902
 Bi₂FeO₆, antiferromagnetic, transition temp., magnetisation, quadrupole moments, Mossbauer obs. 3-79952
 Bi₂La_{1-x}FeO₃, sublattice magnetisations, Neel temps., superexchange isomer shift, elec. field splitting, Mossbauer obs. 3-50490
 Bi₂Ti₃FeO₂₇, ferroelec., mag. props. and Mossbauer effect 3-60961
 CaO-Fe₂O₃ system, antiferromagnetic properties, phase analysis (*German*) 3-47177
 Cd₂Nb_{2-2x}Sn_{2x}O_{7-2x}F_{2x}, solid soln. series, spectroscopic study of props. and phase transitions 3-79962

Mossbauer effect continued

- $\text{Cd}_3[\text{Fe}(\text{CN})_6]_2$, cubic ferricyanide, meas. down to 0.04 K, hyperfine structures 3-44351
- Co magnetically dead surface layers, Mossbauer obs. 3-68821
- Co metal, surface state of ferromagnet from Mossbauer spectra 3-72551
- Co_2MnSn , nuclear mag. moment determ. for ^{119}Sn 3-52075
- CoPt: ^{197}Au , thermal neutron radiation damage obs. 3-79958
- Co_2RuO_4 , of ^{99}Ru , nucl. quadrupole moments determ. 3-43170
- ^{57}Co Mossbauer source, Cu matrix 3-73916
- ^{61}Co , A_1 coefficient detn. by β - γ Mossbauer expt. during β -decay 3-40466
- $\text{Co}_3[\text{Fe}(\text{CN})_6]_2$, cubic ferricyanide, meas. down to 0.04 K, hyperfine structures 3-44351
- Cr: ^{57}Fe , obs. of mag. hyperfine interactions in 140 kOe external mag. fields 3-61011
- Cu, of ^{57}Fe 3-47181
- Cu:Fe Kondo system, Mossbauer effect meas. at high field and low temp. 3-58453
- Cu-Co solid solution, hydrostatic stress in coherent β Co particles, Mossbauer obs. 3-47376
- CuAlTe_2 - CuGaTe_2 - CuInTe_2 , elec. field gradients at ^{125}Te , ^{127}I impurity nuclei 3-72555
- $\text{Cu}_2\text{FeGeS}_4$, bariarite, antiferromagnet (French) 3-68894
- CuFeS_2 , chalcopyrite, mag. transitions, 1 atmos.-20 kbar, geophysics 3-41344
- $\text{Er}_x\text{Y}_{1-x}\text{Fe}_2$: ^{57}Fe , dipolar contributions to mag. hyperfine fields 3-79959
- EuAl_3 , hyperfine field contribs. 3-47187
- EuCu_2Si_2 , Mossbauer effect study of charge fluctuations between 4f level and conduction band 3-44359
- $\text{Eu}_x\text{Li}_{1-x}$ alloys, Mossbauer meas. of coexistence of superconductivity and magnetism 3-44164
- $\text{Eu}_x\text{La}_{1-x}\text{Al}_2$, hyperfine field contribs. 3-47187
- $\text{Eu}(\text{NH}_3)_6$, of ^{151}Eu , metallic nature and mag. order 3-47178
- $\text{Eu}_2\text{Ti}_2\text{O}_7$, quadrupole Mossbauer spectra of 103.2 keV γ -ray of ^{153}Eu , Goldanskii effect 3-53043
- $\text{Eu}_3\text{Ti}_2\text{O}_7$, ferrimag. ordering, exchange const. sublattice magnetisations, Mossbauer obs. 3-50378
- $\text{Eu}_x\text{Yb}_{1-x}\text{Al}(\text{Cu})_2$, hyperfine field contribs. 3-47187
- α -Fe, Mossbauer obs. of low temp. radiation damage 3-64587
- Fe, nuclear mag. moment determ. for ^{57}Fe 3-52075
- Fe, relax. time of magnetically generated r.f. phonons detn. 3-40985
- Fe, spectra of passive films in temperature range 4 K to 298 K 3-55512
- Fe based alloy, fitting of results in isomer shift electronic config. diagram 3-47186
- Fe complexes, tris(2,2'-bipyridyl)iron(II) and tris(glyoxal-bis-N-methylimine)iron(II) 3-63378
- Fe film, dead layers, Mossbauer obs. 3-60982
- Fe phosphate glasses, semiconducting, coordination states and magnetic structure determ. by Mossbauer spectroscopy 3-75922
- Fe-Al alloy, anomalous mag. props., mol. field theory, Mossbauer effect 3-46947
- Fe-Al-Ge alloy, lattice constant, hardness, conc. depend. 3-76159
- Fe-Be (23 at %) alloys, aged at 300°C, decomposition and ordering investigation 3-68901
- Fe-C martensite (1.86 wt.%C), study of aging by difference-spectra obs. 3-80197
- Fe-Co alloy, hyperfine fields at ^{119}Sn , Mossbauer obs. 3-47176
- Fe-Co: ^{119}Sn ferromagnetic alloys, magnetisation, 4.2 to 700 K, hyperfine interaction 3-41466
- Fe-graphite layered compounds, structural investigation 3-50503
- γ -Fe-Mn alloy, hyperfine fields at ^{119}Sn , Mossbauer obs. 3-47176
- γ -Fe-Mn alloys, internal mag. fields on ^{57}Fe , temp. depend. singularities (Russian) 3-44353
- Fe-Mn nodules, from Black sea, Mossbauer study 3-53461
- Fe-N, alloys and compounds, ^{57}Fe obs. of electronic states, tempering stages 3-79953
- Fe-N, solid solutions distribution of N atoms, ordered and disordered, hyperfine fields 3-53047
- Fe-N austenite, interstitial configs. (French) 3-53210
- Fe-Ni alloy, effect of annealing on mag. props. obs. 3-50497
- Fe-Ni alloys, effective field strength on ^{57}Fe from Mossbauer meas. 3-50504
- Fe-Ni: ^{119}Sn ferromagnetic alloys, magnetisation, 4.2 to 700 K, hyperfine interaction 3-41466
- Fe-Ni-Al alloys, induced change of Fe and Ni magnetic moments 3-50505
- Fe-Ni-Al alloys, of ^{57}Fe , spinodal decomp. obs. (Japanese) 3-61145
- Fe-Ni-Mn alloys, Invar-type, mag. behaviour (Russian) 3-68891
- Fe-Ni-Mo and Fe-Ni-Co-Mo maraging alloys, redistrib. of alloying elements during recovery (Russian) 3-80312
- Fe-Ni(31 at %) fine particles, superparamag. behaviour obs. 3-41378
- Fe-V(Cr), sigma phase, internal mag. field determ. by hyperfine broadening 3-58444
- Fe-W alloys, redistrib. of atoms on ageing (Russian) 3-53223
- $\text{Fe}_3^{2+}\text{Al}_2\text{Si}_2\text{O}_{12}$ cryst., elec. and mag. hyperfine interactions of ^{57}Fe nuclei near Neel point 3-75930
- Fe_2As spectroscopy, antiferro-paramagnetic transition Neel temperature, internal fields, quadrupole splittings 3-53042
- Fe_2As -transition metal arsenide solid solns., atomic ordering (French) 3-47192
- Fe_2As -transition metal arsenide solid solns., struct. and mag. ordering (French) 3-47193
- FeBO_3 , sublattice magnetisation, from hyperfine interaction, Mossbauer obs., exchange integral 3-41461
- FeC, mag. props. of χ and θ phases obs. 3-50502
- $\text{Fe}(\text{CO})_5$ in frozen organic solns., intermolecular interactions, Mossbauer obs. 3-79966
- FeCl_2 , under uniaxial stress, quadrupole interaction changes (French) 3-58460
- $\text{Fe}(\text{ClO}_4)_2 \cdot 6\text{H}_2\text{O}$ aqueous soln., frozen, Mossbauer effect and thermal analysis 3-41452
- $\text{Fe}(\text{ClO}_4)_2 \cdot 6\text{H}_2\text{O}$ aqueous soln., frozen, Mossbauer effect, thermal analysis 3-41453
- $\text{Fe}_{1-x}\text{Co}_x$ precipitated from Cu solid soln., spectra obs. 3-79964

Mossbauer effect continued

- $\text{Fe}_{1-x}(\text{Cr}_{0.5}\text{Ni}_{0.5})_x$, rel. to validity of rigid band model 3-44203
- FeF_3 , transferred mag. fields on $^{119}\text{Sn}^{4+}$ nucleus (French) 3-72553
- $\text{Fe}(\text{II})$ complex, dithiocyanatobis(2,2'-bipyridyl)iron(II), $^5T_2 \rightarrow ^1A_1$ transition, Debye-Waller factors, Mossbauer study 3-41343
- $\text{Fe}(\text{II})$ complexes, bis[2,4-bis(2-pyridyl)thiazole]Fe(II), Mossbauer spectra, $^5T_2 \rightarrow ^1A_1$ spin transition and residual paramagnetism 3-53037
- $\text{Fe}(\text{II})$ complexes with 4- and 4.7 substitutes 1.10-phenanthroline (German) 3-58446
- $\text{Fe}(\text{II})$ high-spin complex $(\text{N,N}'\text{-dicyclohexylthiourea})_6(\text{ClO}_4)_2$, orbital ground state reversal, Mossbauer obs. 3-75925
- $\text{Fe}(\text{III})$ complex, basic carboxylate, effect of asymmetric Hamiltonian 3-79955
- $\text{Fe}(\text{KSO}_4)_2 \cdot 6\text{H}_2\text{O}$, Mossbauer electric field gradient parameters 3-68893
- FeMeP , $\text{Me} = \text{Ni}, \text{Co}, \text{Mn}, \text{Cr}, \text{Zr}, \text{Nb}$ and Ta , site pref. of metal atoms 3-58447
- FeN , f.c.c., magnetic properties investigation 3-50499
- ^5FeN , and X-ray obs. of structure, nitrogen donor model 3-58449
- $\text{FeNH}_4(\text{SO}_4)_2 \cdot 12\text{H}_2\text{O}$, paramagnetic with pure dipole-dipole coupling, Mossbauer spectra, relaxation phenomena, spin wave model (German) 3-58463
- $\text{Fe}(\text{NO}_3)_3$ frozen solns., species identification 3-44352
- $\text{Fe}_{0.68}\text{Ni}_{0.32}$, Invar, hyperfine field and non-occal semi-microscopic mode (French) 3-44358
- Fe_{1-x}O , spectra interpretation 3-79965
- α - Fe_2O_3 , Mossbauer effect following $^{56}\text{Fe}(\text{d,p})^{57}\text{Fe}$ reaction 3-47190
- α - Fe_2O_3 , ultrafine particles, surface ions, mag. hyperfine and electric quadrupole splitting 3-61013
- α - Fe_2O_3 : ^{121}Sb , Sb^{5+} impurity parameters, hyperfine nuclear structure (French) 3-44362
- α - Fe_2O_3 :Sn, hematite, Morin transition temp., Sn^{4+} impurity effects, Mossbauer obs. 3-72472
- Fe_3O_4 , superparamagnetic behaviour of ultrafine particles, hyperfine spectrum 3-41465
- Fe_3O_4 , Zn, Ni and Cd substituted, elec. cond. and hyperfine interactions, band struct., Mossbauer obs. 3-46792
- Fe_3O_4 particles, magnetite, h.f. splitting, superparamag. behaviour (German) 3-50494
- FeOCl -pyridine complex, isomer shift and quadrupole splitting, mag. props. obs. 3-58450
- Fe_2P , magnetiz. evolution, metamag. behaviour (French) 3-47191
- Fe_2P , Mossbauer spectroscopy, vacancy distribution, mag. transition 3-41469
- Fe_2P -transition metal phosphide solid solns., atomic ordering (French) 3-47192
- FeS_2 mineral samples, Mossbauer quantitative analysis of $\text{Fe}^{2+}/\text{Fe}^{3+}$ ratios 3-53040
- Fe_2S_3 , pyrrhotite, mag. transitions, 1 atmos.-20 kbar, geophysics 3-41344
- FeSi alloys, Mossbauer study of ordering 3-44557
- FeSi_2 , quadrupole splitting, isomer shift, temp. depend. 3-55509
- Fe_3Sn , nuclear mag. moment determ. for ^{119}Sn 3-52075
- FeTi_2O_5 - Ti_2O_5 system, cryst. struct., ferrous ion site occupancy obs. 3-58020
- FeX ($\text{X} = \text{metaloid}$), hyperfine field at ^{57}Fe in interstitial and substitutional compounds 3-64589
- ^{57}Fe , chemical environment effects on lifetime of 14.4 keV state and Mossbauer meas., isomer shift calibration 3-62984
- ^{57}Fe Mossbauer investigation of tektites 3-59322
- α - $^{57}\text{Fe}_2\text{O}_3$, single cryst., energy anal. of diffracted reson. γ -rays 3-75929
- Gd compounds: ^{155}Gd , isomer shift, hyperfine fields and quadrupole splitting obs. 3-64584
- $\text{Gd}_3\text{Fe}_{3-x}\text{M}_x\text{O}_{12-x}\text{F}_x$, $\text{M} = 3\text{d}$ transition element, ion site occupation determ. (French) 3-79305
- Ge, magnetostriictively induced r.f. phonon time decay obs. 3-40986
- ^{178}Hf , ^{180}Hf , Mossbauer meas. of isomer shift and quadrupole moment ratios 3-49206
- $^{178}\text{Hf}/^{180}\text{Hf}$, ratio of quadrupole moments of 2^+ states 3-60086
- $\text{KAl}_3(\text{OH})_6(\text{SO}_4)_2 \cdot \text{Fe}^{3+}$, magnetic hyperfine field obs. 3-50498
- KCl:Sn, impurity centre investigations 3-41456
- $\text{K}_2\text{Pt}(\text{CN})_4\text{Br}_{0.30} \cdot 3\text{H}_2\text{O}$, one dimens. conductor, ^{195}Pt Mossbauer effect 3-53044
- $\text{K}_2\text{Pt}(\text{CN})_4\text{Br}_{0.3} \cdot 3\text{H}_2\text{O}$, Pt spectrum as test for metal-insulator transition with localisation of conduction electrons (German) 3-50492
- Kr gas-filled proportional counters, for ^{161}Dy (26 keV) Mossbauer studies 3-40036
- $\text{LaFe}_2\text{O}_{19}$, internal mag. field, isomer shift, quadrupole splitting, Curie temp. 3-58448
- $\text{Mg}_2\text{Mn}_{1-x}\text{Fe}_x\text{O}_4$ powders, phase composition, Mossbauer spectral studies 3-53041
- Mn-Zn, ferrites nonstoichiometric, magnetic sublattices, nuclear gamma ray resonance study 3-52981
- MnF_2 : Fe^{2+} , antiferromag. to paramag. transition, Mossbauer obs. 3-50360
- MnGaC , first order antiferromag.-ferromag. transition, carbon conc. depend. (French) 3-47049
- $(\text{NH}_4)_3\text{FeF}_6$, Mossbauer study of relax. phenomena 3-53045
- NH_4XCl_3 ($\text{X} = \text{Mn}, \text{Fe}, \text{Co}$), of ^{57}Fe , mag. and crystallographic transitions 3-79950
- NaCl emission spectra, deformation induced 3-53048
- NaCl:Sn, impurity centre investigations 3-41456
- Ni, hyperfine struct. of Mossbauer spectra, influence of paraprocesses near Curie temp. (Russian) 3-44215
- Ni ferrite, very fine grained, hot pressed, mag. props. obs. 3-50414
- Ni_2Al , Ga, mag. props. from Mossbauer meas. 3-79956
- $\text{Ni}_3\text{Al}(\text{Ga})$:Fe, meas. of giant moments in paramag. alloys, depend. on ferromag. crit. comp. 3-64585
- Ni_3Ga :Co, mag. props. from Mossbauer meas. 3-79956
- NiMn alloys, concentration depend. of Ni hyperfine fields 3-41458
- NiO : Sn^{4+} , impurity state determ. 3-72100
- NiPd, NiPt, alloys, concentration depend. of magnetic hyperfine fields 3-41457
- NiS , metal-nonmetal transition investigation using Mossbauer effect of ^{57}Fe 3-53049

Mossbauer effect continued

- NiS:⁵⁷Fe, metal-nonmetal transition, Mossbauer effect 3-41152
 NiS:⁵⁷Fe metal-nonmetal transition, paramagnetic-antiferromagnetic, susceptibility, thermoelectric power, conductivity, hyperfine field 3-44357
 Ni_{1-x}S:⁵⁷Fe; metal-nonmetal transition, Mossbauer effect, 4.2 to 300K 3-44030
 Ni_{0.65}Zn_{0.02}Fe_{0.33}O₄, Fe²⁺ distrib. in tetrahedral sites (*Russian*) 3-47189
 Ni_{1-x}Zn_xFe₂O₄, high field study 3-79963
 NpN, antiferromag., mag. props., hyperfine fields obs. 3-41348
 NpP, antiferromag. ordering at 130K in ferromag. sheets, neutron and Mossbauer obs. 3-72473
 NpPd₃(Sn₃(Ge₃)(Rh₃) compounds, hyperfine interactions, ²³⁷Np Mossbauer obs. 3-68905
 NpX, X=N, P, As, Sb, mag. props. obs. 3-41332
 Pb(Fe_{2/3}U_{1/3})O₃, crystallographic and mag. structure 3-72051
 Pb(Fe_{2/3}W_{1/3})O₃, crystallographic and mag. structure 3-72051
 PbTiO₃, of ¹¹⁹Sn, probability, atomic vibr. anharmonicity 3-41454
 PbZrO₃, of ¹¹⁹Sn, probability, atomic vibr. anharmonicity 3-41454
 PdEu, mag. props., ¹⁵¹Eu Mossbauer study 3-79954
 Pd₂MnSn, local mag. ordering of ⁵⁷Fe impurities 3-79832
 Pt:⁵⁷Fe, foil, evidence of impurity-host to host-host coupling const. variation 3-68896
 Pt₃Fe alloys, spectra, isomer shift, pressure depend. 3-72554
 PtMnSn, Mossbauer obs. of hyperfine field at ¹¹⁹Sn site 3-68899
 S, nuclear quadrupole interactions of ¹²⁵Te 3-50501
 Sb compounds, hyperfine interactions in intermetallic, ferromagnetic and ferroelectric compounds 3-44361
 Sb(CH₃)₂Br₂, Goldanskii-Karyagin effect, inconclusive 3-58455
 Se, nuclear quadrupole interactions of ¹²⁵Te 3-50501
 Si:⁵⁷Fe, spectra of 14.4 keV γ-rays at room temp. 3-47184
 Sm-Co intermetallic compounds, hyperfine interactions, ⁵⁷Fe Mossbauer study 3-61014
 Sn chalcogenides, radiation defects generated by (n,γ) reaction 3-72556
 Sn-S system, identification of Sn₃S₄, Sn₂S₃, spectra 3-72548
 Sn(CIO₄)₂·3H₂O, SnBu₄, SnBu₂Cl₂ and SnBu₂SO₄, absorption spectroscopy meas. of after-effects of ^{119m}Sn isomeric transition 3-55985
 SnL₄, chemical bond structure interpreted by ¹¹⁹Sn Mossbauer transitions and n.q.r. 3-68889
 Sn₂Nb₂(Ta₂)O₇, nonstoichiometric, Sn(II) and Sn(IV) valency states 3-50491
 Sn_{1-x}Sb_xO₂ system, electronic structure 3-68890
¹¹⁹Sn, Mossbauer meas. of magnetic moment of 23.8 keV state and hyperfine anomaly 3-49208
 SrFe_{2/3}Re_{1/3}O₃, ordered perovskite, semicond., ferrimag. props. below 475 K, Mossbauer obs. 3-79846
 Sr₂FeReO₆, ordered perovskite, metallic, ferrimag. props. below 419 K, Mossbauer obs. 3-79846
 Sr(Fe_{2/3}U_{1/3})O₃, crystallographic and mag. structure 3-72051
 SrTiO₃:Fe, photoconduct, obs. of valence states rel. to colour changes 3-58461
 SrTiO₃:Fe³⁺, overlap contribution to isomer shift calc. 3-64586
 TbFe_{1-x}Cr_xO₃, Mossbauer spectra fine struct., hyperfine field distrib. 3-58445
 Tb₂Y_{1-x}Fe₂:⁵⁷Fe, dipolar contributions to mag. hyperfine fields 3-79959
⁹⁹Tc, 140 keV level, nuclear parameters from spectra, 1.6-65 K 3-71077
 Te nuclear quadrupole interactions of ¹²⁵Te 3-50501
¹²⁵Te, resonance counter, design description 3-54019
 TmB₁₂:¹⁷⁰Yb, Debye-Waller factor, neutron irradiation (*French*) 3-72552
 Tm₂Fe₁₇, temp. depend. 4.2-350 K, mag. phase transition obs. 3-64495
 UTe hyperfine field, ordered magnetic moment by neutron diffraction, temp. depend., magnetic ordering 3-44356
 V_{0.2}O_{2-n}, mag. props. and metal-insulator transition 3-44028
¹⁸⁰W, Mossbauer determ. for 2⁺ state g-factor 3-60086
¹⁸⁰W/¹⁸²W, ratio of quadrupole moments of 2⁺ states 3-60086
 Y₂₋₈₋₂₂Ca_{0.222}Fe_{4-8-x}Sn_{0.2}V₂O₁₂, mag. fields on Sn⁴⁺ nuclei (*Russian*) 3-41467
 YFe₂, of ⁵⁷Fe, internal fields, quadrupole shifts, temp. depend. (*French*) 3-72547
 Y₂Fe₅₋₂M₂O₁₂₋₂F₂, M=3d transition element, ion site occupation determ. (*French*) 3-79305
 YFe_{0.8}Mn_{0.2}O₃, spin reorientation, Mossbauer and neutron diff. obs. 3-55434
 YIG, Ga-substituted, high homogeneity specification 3-41463
 YIG, Sn-substituted, quadrupole splitting and isomer shifts 3-41464
 Yb, even isotopes, γ-ray spectroscopic study, single-line Mossbauer absorption, Yb levels, deduced isomer shifts 3-60109
 YbB₆, of ¹⁷⁰Yb, Debye-Waller factor, neutron irradiation isotope shift (*French*) 3-72552
 ZnAl₂O₄:Fe³⁺, magnetic hyperfine field obs. 3-50498
 Zn_xNi_{1-x}Fe₂O₄, Yafet-Kittel canting angles, low-temp. Mossbauer obs. 3-47185
 ZnSiF₆·6H₂O, cryst. field splitting of Fe²⁺ ion 3-55506
 Zr-Nb (20 at wt. %), Mossbauer scatt. study of solid state phase transformations 3-55068

Mossbauer spectra see Mossbauer effect**motion** see dynamics**motion picture photography** see cinematography**motors, hydraulic** see hydraulic motors**movements, atmospheric** see atmospheric movements**moving-coil instruments**

pneumograph transducer based on small moving-coil loudspeaker 3-62306

moving coil microphones see microphones**μ-mesons** see muons**multichannel analysers** see pulse height analysers**multidimensional systems**

aerohydrodynamics, multidimensional problems, processing and analysis of computation results 3-49587

Faddeev's equations, transformation to unidimensional integro differential equations rel. to, multichannel band method (*Russian*) 3-62797

multiperipheral models see peripheral models**multiphase flow**

- ablate spheroidal particle assemblages, viscous flow at intermediate Reynolds numbers 3-63751
 aerosol particle, spherical, motion near walls 3-65037
 aggregated media oscillatory flow dispersion, effect of intra-aggregate diffusion 3-46487
 boiling refrigerants, pressure drop and convective heat transfer, three flow regions (*German*) 3-46385
 bubbles in infinite liquids, shapes and velocities, generalised graphical correlation 3-75263
 close packed cubic array of spheres near critical Reynolds number, flow pattern 3-40737
 fluidised bed, three phase flow (*German*) 3-46479
 fluidised beds, homogeneous to heterogeneous fluidisation transition, dynamic shock wave and velocity criteria (*German*) 3-46480
 gaseous suspension flow of solid and liq. particles with internal heating, radiative heat transfer 3-60576
 groundwater, functional coeffs., finite element analysis 3-46488
 liquid-liquid system, terminal velocity of falling drops, effect of heat transfer 3-75264
 non-Newtonian fluids, jet instability 3-67967
 particles in fluid, gravit. deposition in fibrous aerosol filters, theory, mechanisms 3-65034
 polyethylene oxide, viscoelastic flow, hole error meas. 3-67966
 pumped well, unconfined aquifer, unsteady radial flow, model 3-46489
 pumped well, water table drawdown, unconfined aquifer, unsteady radial flow 3-46490
 salinity profile, porous medium layer, effect on marginal stability, overabundance and thermal convection 3-47710
 sand, unsaturated stratified vertical column, water flow, effects of air and water pressure 3-46485
 supersonic heterogeneous, stoichiometric hydrogen-air mixture with suspended Al and Mg powders (*Russian*) 3-63768

multiple stars

see also binary stars

- Barnard's Star, planetary system rel. to proper motion obs. 3-59349
 BD + 66 degrees 34, triple system, astrometric anal. 3-51353
 binary and multiple systems of stars, book 3-51320
 eclipsing variables, natural motion of 122 stars (*Russian*) 3-61808
 O-type visual, absolute magnitudes and intrinsic colours 3-81080
 ι Orionis B, ³He content in atmosphere from coude spectrogram 3-81099
 β Persei, 5GHz obs. 3-61816
 space velocity, rel. to rotational velocity, field stars earlier than B6, double stars, cluster members 3-61796
 spectroscopic parameters for visual systems 3-51346
 trapezia, occurrence rel. to origin of runaway stars 3-51345
 W Ursae Majoris, possible triple 3-48050

multiplex transmission see multiplexing**multiplexers** see multiplexing equipment**multiplexing**

- see also frequency division multiplexing; time division multiplexing
 carrier freq. photography, multiplexing with extended broadband source 3-45775
 colour holography, using coded wavefronts 3-66243
 holographic recording by spatial frequency multiplexing, storage density improvement 3-59598
 holographic single-exposure multiplexing method, crosstalk elimination 3-45500
 Zircaloy tubing, u.s. inspection, wall thickness and ID meas., multiplexed instrumentation 3-47516

multiplexing equipment

- digital multiplexer, control system, Indiana Univ. cyclotron, control computer, description 3-56896
 f.m. seismic system with magnetic tape 3-80837

multiplier phototubes see photomultipliers**multipliers, electron** see electron multipliers**multivariable control systems**

- BWR, Halden, on-line computer method for neutron flux distrib. control 3-46066

multivariable systems

see also multivariable control systems

insect nervous visual system studies, white-noise identification techniques 3-45307

multivibrators

see also flip-flops

burst shaper, examination of hearing capability and echo location of dolphins 3-73935

muon capture

- see also nuclear reactions and scattering due to muons
 1p-shell nuclei, giant magnetic dipole analogue excitations 3-60126
 allowed transitions in 1p-shell nuclei, roles of weak hadron form factors 3-54437
 depolarization of stopped positive muons in liquids 3-68295
 matrix elements, reln. to invariant form factors by impulse approx. PCAC formulation 3-43216
 nuclear, configuration mixing and total capture rates in Primakoff closure approx. 3-67271
 nuclear absorption, nuclear reaction theory and improved factorization method 3-52151
 total capture rates, eval., sum-rule 3-74540
 (μ⁻, xnp), capture by nuclei with A=28-197, meas. of γ-ray energy and intensity 3-49243
 μ⁻, Fermi gas model, determ. of asymmetry parameter in terms of neutron energy 3-43217
 μ⁺e⁻ annihilation in e.m. field, ang. depend. of absorbed energy (*Russian*) 3-43224
 pμ + H²⁺ → Heμ + p muon capture collision cross sections 3-49427
 Ar, total nucl. capture rate meas. 3-46012
¹⁰B, partial transitions, gamma-neutrino correlation, dependence on structure and induced pseudoscalar coupling 3-63002
¹³⁸Ba, neutron emission, branching ratios 3-40463
²⁰⁹Bi, polarised, magnetic hyperfine structure in muonic atom, coupling consts. anomalous g-factor 3-46216
¹²C, low q² electron scattering from 15-109 MeV state, 35-55 MeV incident, conserved vector current test 3-60165

muon capture continued

- ^{40}Ca , radiative capture, high-energy and meas. of photon spectrum, induced pseudoscalar coupling const. 3-67274
 $^{40}\text{Ca}(\mu^-, \text{vnn})$, determ. of absolute capture probability by activation method (*Russian*) 3-40484
 ^{140}Ce , neutron emission, branching ratios 3-40463
 ^{142}Ce , neutron emission, branching ratios 3-40463
 He muonic atom formation (*German*) 3-49426
 $^6\text{Li}(\mu^-, \nu_e)^6\text{He}$, calc. of rates for semi-leptonic weak process using one-body densities determ. from e.m. data 3-49245
 ^{15}N partial transition, gamma-neutrino correlation, dependence on structure and induced pseudoscalar coupling 3-63002
 Ne, total nucl. capture rate meas. 3-46012
 ^{16}O , calc. of asymmetry in high energy neutron emission, transitions to ^{15}N levels 3-52149
 ^{16}O , exptl.-theoretical discrepancies, use of shape coexistence model 3-67269
 ^{16}O , partial muon capture rates leading to bound states of ^{16}N 3-60125
 ^{16}O , rate calc., effect of core-excitations and SU_4 symmetry 3-74543
 $^{32}\text{S}(\mu^-, \text{vnn})$, determ. of absolute capture probability by activation method (*Russian*) 3-40484
 ^{120}Sn , neutron emission, branching ratios 3-40463

muon decay

- renormalization of gauge theories 3-54296
 second order corrections in the unitary gauge, renormalisation of spontaneous symmetry breaking model 3-66925
 V-A theory spin, lifetime, mass, electrodynamics, decay, quantum number (*Hungarian*) 3-78232
 e^+e^- colliding beam expts., production and decay of single excited muon 3-59977
 $\mu \rightarrow e\nu$, electron-muon mass ratio, unified gauge theory, $\text{SU}(3) \times \text{SU}(3)$, $\text{SU}(4) \times \text{SU}(4)$ 3-78106
 $\mu \rightarrow e\nu$, probability assuming existence lepton nonconserving interaction

- $\mu^- \rightarrow e^- \nu_e \nu_\mu$, following $N^* \rightarrow N + \mu^- + e^-$, double β -decay via $\Delta Q = 2$ interactions 3-60130
 ν emission phenomenological model, muon parity conservation 3-78118

muon detection and measurement

- hodoscope, to determine direction of muon motion in cascade showers (*Russian*) 3-65611
 multiwire proportional counters external to bubble chamber, νp test of principle 3-77629
 streamer chamber for polarisation measurements 3-77668
 telescope for vertical muons, coupling function at 60 m water equivalent depth 3-48519

muon interactions

- see also muon capture; nuclear reactions and scattering due to muons
 μ n amplitude at threshold, polarizability contrib. calc. 3-78134
 μ n anomalous interactions, reln. to muonic atoms 3-57615
 μ n inelastic interactions at high energy, energy spectrum and angular distrib. 3-57369
 μp , 16 GeV inelastic scattering in hybrid bubble chamber, obs. of hadronic final states 3-70927
 $\mu^- Z \rightarrow \nu_\mu W^-$, differential cross section for scalar W-meson production at super-high energies (*Russian*) 3-40336
 Pb muonic atom, limit for hypothetical scalar muon hadron interaction constant (*Russian*) 3-60394

muon production

- neutrino and antineutrino high energy events 3-43093
 pair production by hadrons, quark parton model, proton and neutron structure function effects 3-78226
 quarks and muon pair production 3-66965
 scaling law derived using dilatation invariance 3-74337
 two-photon exchange production of lepton pairs in hadron-hadron collisions 3-67130
 $e^+e^- \rightarrow \mu^+\mu^-$, sign of muon charge asymmetry and models of unified e.m.-weak interactions (*Russian*) 3-67029
 $e^+e^- \rightarrow \mu^\pm(e^\pm)\nu_e\nu_\mu$, total cross sections (*Russian*) 3-59982
 e^+e^- colliding beam expts., production and decay of single excited muon 3-59977
 $e^+e^- \rightarrow \mu^+\mu^-$, weak boson effects in Weinberg's unified theory 3-66966
 $e^+e^- \rightarrow \mu^+\mu^-$ radiative corrections and neutral currents in unified gauge theories 3-67015
 $K_0^0 \rightarrow M^* \mu^+ \nu_\mu$, analysis of structure in $M_{\mu\nu}$ spectra 3-57319
 $K_1^0 \rightarrow \mu^+ \mu^-$, survey of possible explanations 3-62805
 $K_1^0 \rightarrow \chi^0 \nu \rightarrow \mu^+ \mu^- \gamma$, search for χ^0 using spark chamber magnetic spectrometer 3-78108
 $K_1^0 \rightarrow \mu^+ \mu^-$, obs. and branching ratio meas. 3-48997
 $K_1^0 \rightarrow \pi^- \mu^+ \nu_\mu$, muon polarisation meas. as time-reversal invariance expt. test 3-40334
 $\nu(Z) \rightarrow \nu \mu(Z)$, effects of neutral weak currents in charged lepton spectra 3-70906
 $pp \rightarrow \mu^+ \mu^-$ anything, multiperipheral theory 3-74468
 $pp \rightarrow \mu^+ \mu^- X$, spectral representation, scaling limit, light cone dominance 3-78222
 $W \rightarrow \mu \nu$ hadrons, single muon spectra in parton model 3-40396

muon scattering

- see also nuclear reactions and scattering due to muons
 distribution, by numerical integration and Monte Carlo methods 3-48514
 neutral currents and P-odd effects in deep inelastic μ scattering 3-74348

muonic atoms see mesic and muonic atoms**muonic molecules** see mesic and muonic molecules**muonium**

- atom-antiatom interactions 3-43389
 chemistry with radical form., implications of μ^+ depolarization mechanism in liquids 3-68295
 hyperfine interval, p recoil corrections 3-66998
 hyperfine structure interval at weak mag. fields, precision meas. 3-67721
 π - μ atom, study $2S_{1/2}-2P_{1/2}$ energy level shift and determ. of pion charge radius 3-66996

muons

- see also cosmic ray muons; mesic and muonic atoms
 anomalous magnetic moment, calculation of lower limit of masses of hypothetical charged particles 3-57341
 anomalous magnetic moment, W boson contrib. in Weinberg model 3-62825
 anomalous magnetic moment, Weinberg model, dispersion relations, U-gauge 3-78128
 beam dynamics in magnetised Fe 3-73840
 charge radius, fourth-order, contrib. to Lamb shift 3-49004
 electron-muon mass ratio, unified gauge theory, $\text{SU}(3) \times \text{SU}(3)$, $\text{SU}(4) \times \text{SU}(4)$ 3-78106
 hadron-shower calorimeter, for muon detection at high energies 3-40010
 low energy, experimental study (*French*) 3-60063
 magnetic moment, improved optical bounds for hadronic contrib. using Watson theorem 3-57345
 magnetic moment, optimal lower bound on quadratic functional integrals using Watson theorem 3-43103
 mass, comparison with pion-muon mass difference and muonic atom X-ray transition data 3-67169
 spin, lifetime, mass, electrodynamics, decay, quantum number (*Hungarian*) 3-78232
 e - μ mass difference, anomalous origin of masses 3-70907
 e - μ universality, reln. to urbarion model of vector meson decay into lepton pairs 3-74371
 μ^- , depolarization in water and H_2O_2 aqueous solutions 3-41853
 μ system, description from solutions of conformal invariant spinor equations 3-59915
 Y^+ , proposed positively charged heavy lepton, search 3-62817
 Fe, precession of μ^+ 3-43814
 Ni, precession of μ^+ through the Curie temp. 3-43814

muscovite see mica**music** see humanities**musical acoustics**

- brass instruments, growling effects 3-81352
 brass instruments, theory 3-77342
 cello, wolfnote investigation 3-81350
 cone woodwinds, register hole design 3-42485
 flute, headjoint cork posn., damping of higher modes 3-45379
 flute, mouth cavity resonance effects on frequency, experimental results 3-77336
 formant formation in musical sound (*German*) 3-51475
 low-pitched tones, quality and harshness 3-48303
 organ pipes and cavity resonators, comparison 3-45381
 pop music, hearing damage 3-73579
 singing and whistling range difference 3-51497
 tape recorded signals, adaptation of frequency analyser type 2107 to automated 1/12 octave spectrum analysis 3-56579
 tuning forks, plain, piezoelectric ceramic modified, measurement of constants, differential type filter 3-61950
 viola, tone quality, synthesized normal modes 3-45382
 violin resonances, electronic simulation 3-59499
 wind instrument tones, homomorphic analysis 3-48304
 woodwind instruments, theory 3-81351
 woodwinds, characterization by tone-hole cutoff freq. 3-45380

musical instruments

- brass, acoustic theory 3-77342
 brass instruments, growling effects 3-81352
 cello, wolfnote investigation 3-81350
 cone woodwinds, register hole design 3-42485
 electronic organ, operation 3-66092
 flute, headjoint cork posn., damping of higher modes 3-45379
 flute, mouth cavity resonance effects on frequency, experimental results 3-77336
 harpsichord soundboard and bridge, design and description 3-48305
 steel wire fatigue, cycles to failure and stress to failure Weibull distributions 3-41833
 viola, tone quality, synthesized normal modes 3-45382
 violin, acoustic vibrations, laser speckle interferometry, effects of clamping, formal model, main wood resonance 3-59497
 violin resonances, electronic simulation 3-59499
 violins, vibration modes by acoustical, optical, and musical methods 3-48302
 wind instrument tones, homomorphic analysis 3-48304
 woodwind instruments, theory 3-81351
 woodwinds, characterization by tone-hole cutoff freq. 3-45380

N-body problems

- see also celestial mechanics; many-body problems
 circular restricted three-body problem, global stability 3-69806
 elliptically-restricted 4-body problem rel. to orbits associated with Jupiter-Saturn system 3-42137
 Galilean satellites of Jupiter, dynamical motion (*French*) 3-42107
 generalised three-body problem, uniform circular movement of centres of inertia (*French*) 3-56298
 homographic motions of Newtonian point masses system, classification 3-51244
 libration cloud, theoretical possibility in restricted three body problem 3-69803
 N-body gravitation problem, integration scheme, near and distant stars 3-70726
 proto-star interaction in collapsing cluster, n-body integration 3-42224
 restricted 3-body problem, stability of periodic solutions 3-73429
 restricted 3-body problem rel. to Moon's translational-precessional motion 3-76950
 restricted three-body problem, doubly asymptotic orbits, transversality condition 3-69807
 restricted three-body problem, explicit 10th order solution 3-69809
 restricted three-body problem, families of periodic orbits 3-69805
 stellar cluster collisions, numerical study 3-48099
 three bodies, numerical stability of Lagrange eqns. (*Russian*) 3-77795
 three body, computer solution 3-56608
 three-body, restricted plane circular, partial soln. of Hamilton-Jacobi eqn. (*Russian*) 3-77793
 three-body problem, commensurable restricted, phase plane anal. 3-69804

N-body problems continued

- three-body problem, motion of oblate spheroids with common symmetry plane 3-51780
- two, anti-focal and eccentric anomalies (*Japanese*) 3-69810
- two-body problem, relation between true and eccentric anomalies 3-51250

N/D method

- Balazs method, bootstrap calc. of linearly rising ρ Regge trajectory 3-74345
- dispersion theoretical model of low energy particle resonance scattering amplitude 3-74342
- hyperon-nucleon scattering, anomalous thresholds, calcs. using analytic continuation and Cutcosky rule 3-57400
- potential scattering, criteria for validity of approximations 3-62792
- tautologies and optimization of eqns. 3-66950
- truncated, unitarized of Veneziano partial-wave amplitudes, sum rules for inelastic functions 3-67069
- $ev \rightarrow ev$, high-energy, N/D method analysis, intermediate weak boson effects 3-40329
- $\pi\pi$ scattering, low-energy, crossing symmetry calcs. of partial wave amplitudes current algebra type zeros 3-67114
- ρ meson properties, static $\pi\omega$ scattering 3-62921

natural gas technology

- floating drilling rigs, development of off-shore techniques (*German*) 3-65539

natural resources

- see also agriculture; dams; energy resources; mining; water supply
- aerial mapping of coastal wetland natural resources 3-53933
- Anacapa, California Channel Island, airborne and satellite remote sensing 3-51006
- Antarctica, resource potential, review 3-47614
- artesian well, unsteady drawout finite element method 3-56273
- dam, effect of severe frost, air and water temp., bending of the dam 3-73407
- data processing systems for Earth resources surveys, review 3-51174
- Earth Resources Technology Satellite, earth imaging systems, appl. to agriculture, marine and water resources 3-80851
- Earth Resources Technology Satellite, hydrological applications 3-80716
- Earth Resources Technology Satellite program, key technological challenges 3-51175
- ERTS multispectral scanning system for earth monitoring 3-44951
- fossil fuel burning and CO₂ rel. to atmospheric temperature increases 3-47720
- geothermal resources in Earth crust 3-56274
- groundwater hydrographs, barometrically conditioned fluctuations, elimination (*German*) 3-73276
- hydrologic decision strategies, minimax vs. expected value criteria 3-59062
- Israeli results from the ERTS-1 program Multi-Spectral Scanner obs. 3-50872
- linear conceptual catchment models, time variance, rainfall rel. to runoff 3-56242
- marine raw materials on sea bed and in seawater, in USSR (*German*) 3-61445
- oil and natural gas reserves rel. to continental drift 3-44794
- pegmatite deposits in South Africa rel. to sources of nuclear fuel 3-58914
- remote detection, balloon technology, geostationary balloons (*French*) 3-65503
- rivers, time variable waste input, dynamic water quality response, effect of longitudinal dispersion 3-56272
- satellite programmes for continuous remote sensing of land resources 3-51176
- Skylab A, synoptic survey of the Earth and solar disc 3-80849
- study, by satellites (*French*) 3-69727
- surveillance, processing techniques (*Italian*) 3-61594
- surveillance from space (*Italian*) 3-61593
- terrestrial environment monitoring from space, conference (Rome, March-April 1973) 3-50871
- Upper Colorado River, economic-hydrologic-air pollution model 3-59216

natural rubber see rubber**natural sciences**

- see also astronomy and astrophysics; biology; biophysics; chemistry; geology; mathematics; physics
- National Standard Reference Data System, critical evaluation of physical sciences data 3-48336

Navier-Stokes equations

- ablate spheroidal particle assemblages, viscous flow at intermediate Reynolds numbers 3-63751
- aerosol diffusio-phoresis of large particles, accounting for inertial terms in Navier-Stokes eqn. 3-49616
- analyticity of plane, steady state solutions 3-57707
- atmospheric large scale motion, appl. of finite difference approx. 3-61451
- axisymmetric flow of liquid (*Russian*) 3-63669
- Cauchy problem and quasi-periodic finite soln. using Navier-Stokes inequality (*French*) 3-59735
- coastline water, diffusion dispersive calc. 3-65269
- compressible, numerical experiments 3-49585
- Couette flow, time-dependent, rotational, numerical experiments 3-49564
- Couette turbulent flow, wall shear flow 3-60543
- Darcy's law, theoretical derivation using statistical approach 3-49617
- difference schemes for the solution, comparative study 3-49536
- discontinuous flows, special solns. 3-78931
- Euler equations, manifolds diffeomorphic to two dim. sphere, initial problem 3-63617
- Euler equations on two dim. sphere, proof of existence and uniqueness of initial value problem 3-63616
- evolution equation, proof of theorem (*Italian*) 3-71723
- flow in heated closed cavity, numerical soln. 3-57710
- flow past an impulsively started circular cylinder 3-57775
- flow patterns around heart valves, numerical method 3-53736
- fluid films, mechanically produced, hydrodynamic model of complex flow processes, boundary layer theory (*German*) 3-46499

Navier-Stokes equations continued

- with free boundaries, singularities at flow separation points 3-57871
- free surface flows, three-dimensional, in vicinity of submerged and exposed structures, numerical soln. 3-71732
- fully developed turbulence intermittency, as a consequence of the Navier-Stokes equations 3-43548
- helical coils, momentum transfer, alternating direction-implicit technique 3-78943
- helical turbulence and absolute equilibrium 3-57742
- hydrodynamic, distrib. of gas vels. round aerosol particle 3-63767
- hypersonic blunt body merged layer problem, numerical soln. of Navier-Stokes eqns. 3-52466
- incompressible fluid, flow between parallel plates, one in unsteady motion and the other at rest, Navier-Stokes equations calc. 3-78968
- incompressible three dimensional flow, nonregular soln. 3-71724
- inequality of evolution, theorem (*French*) 3-63614
- jet, laminar twisted submerged of viscous incompressible fluid, flow 3-54830
- jets, confined heterogeneous, laminar mixing, expt. obs. and theory 3-46497
- laminar supersonic flow over a two-dimensional compression corner, numerical solutions 3-49593
- MHD flow along infinite porous plate with constant suction 3-60566
- multi-level adaptive technique for fast numerical solution to boundary value problems 3-49535
- numerical soln. methods, review 3-49534
- periodically constricted tubes, steady state incompressible Newtonian flow, numerical soln. 3-57839
- rate of solution of horizontal surface of solid body in liquid, free convective cellular motion 3-46390
- reflecting oblique shock wave structure, numerical analysis 3-52472
- relativistic, cylindrically symm. solns. (*Italian*) 3-79040
- rotating viscous fluid, wave solution 3-75237
- secondary flow induced by double submerged jets 3-63668
- self-diffusion, Green-Kubo formulas and long tail of velocity autocorrelation function 3-54158
- space shuttle base region under reentry conditions, convection, numerical soln. by Telenin's method 3-52443
- spherically symmetric gas expansion into very low pressure, Navier Stokes equations soln. 3-52471
- stationary solutions of nonlinear problem, 3-dimens. system, rel. to viscous incompressible fluid (*Italian*) 3-49543
- steady flow in tube with circumferential wall cavity, numerical soln. 3-71774
- steady universal motions, constant vel. magnitude on Lamb surface 3-60528
- steady-state, finite difference methods 3-49537
- stratified fluid in rotating annulus, steady state, upwelling, numerical soln. 3-52447
- strong shock over a sharp leading edge, Navier-Stokes eqns., finite difference treatment 3-49598
- suspension, swirling laminar pipe flow 3-71823
- three dimensional film cooling slots effectiveness predictions 3-57729
- three-dimensional flows with recirculation, two calculation procedures 3-49538
- toroidal fully developed viscous flow in coiled circular pipes 3-57750
- transient three-dimensional fluid flow in the vicinity of large structures, numerical technique 3-52460
- tube flow, steady and developing, of vanishing Reynolds number, field descriptions 3-71733
- turbulence inertial range spectrum 3-67905
- turbulence theory, closure problems, review 3-78956
- turbulent transitions in convective flow 3-49563
- viscoelastic unsteady flow past infinite flat plate with variable suction 3-71760
- viscous flow past finite bodies, incompressible, two-dimensional, harmonic functionals rel. to Navier-Stokes equations 3-71772
- viscous fluid flow rel. to relax. time, Navier-Stokes eqns. generalisation (*Russian*) 3-63618
- viscous incompressible fluid, flow between parallel plates, one in unsteady motion and the other at rest, Navier-Stokes equations calc. 3-78968
- viscous incompressible fluid, flow between two parallel flat plates, one in uniform motion and the other at rest, uniform suction at stationary plate 3-78969
- viscous incompressible fluid, flow near an infinite porous flat plate, unsteady motion, uniform suction 3-78970
- water pulsatile laminar flow in distensible tubes, friction factors determ. 3-57805

navigation

- see also inertial navigation; laser beam applications; radar applications; radionavigation; sonar; tracking
- radar, civil aircraft, all weather landing aid (*French*) 3-51194
- by satellites, international aspects (*French*) 3-69745
- space, charts 3-77198
- spacecraft, application of Venus limb radiance, 600-700 cm⁻¹, calculations 3-73452
- spacecraft optical navigation technique, Marine nine 3-76999
- ultrastable atomic and molecular oscillators, applic. (*French*) 3-62679
- uniaxial gyro-stabilizer as angular velocity integrator, kinematic errors (*Russian*) 3-59545

nebulae

- see also galaxies; planetary nebulae
- A21, Medusa Nebula, interferometric obs. 3-53715
- Becklin-Neugebauer i.r. source in Orion Nebula, 3.45 μ circular polarization 3-69993
- Becklin-Neugebauer object in Orion Nebula, 10 μ linear polarization 3-69992
- Becklin-Neugebauer object in Orion Nebula, 2.2 and 3.5 μ polarization meas. 3-69991
- Carina nebula NGC 3372 obs. at 30 MHz 3-61871
- η Carinae, 100 μ obs. 3-45158

nebulae continued

- Cetus Arc nebulosity around Loop II, H α radial velocity meas. 3-59391
- Coalsack, search for flare-star spectra rel. to star formation 3-81208
- Crab, aperture synthesis of interstellar H I absorption 3-81106
- Crab, detection of pulsed high energy gamma rays 3-48074
- Crab, energy spectrum of relativistic electrons 3-70042
- Crab, longitudinal and transverse wave mode-mode coupling, energy conversion 3-75425
- Crab, production of magnetic fields, model rel. to obs. 3-48131
- Crab, pulsed high energy γ -rays coincident with optical pulses of Np0532 3-81128
- Crab, relativistic particle and magnetic field distributions, synchrotron radiation mechanism 3-77166
- Crab, synchrotron radiation, 912-90 Å, Zanstra's method (*Russian*) 3-77097
- Crab, weak Landau damping, heating of high energy electrons 3-73551
- Crab, X-ray studies of 1974-75 occultations 3-81210
- Crab filaments, emission line intensities rel. to elemental abundances 3-48132
- Crab Nebula, calc. of spectra of gaseous filaments 3-61873
- Crab Nebula, H and He atoms, ionisation and relative abundance (*Russian*) 3-45226
- Crab Nebula, origin of magnetic field and relativistic particles 3-44990
- Crab Nebula, second-order plasma interaction 3-61872
- Crab nebulae, radioastronomical obs., scanning the diagram of the variable profile antenna (*Russian*) 3-81248
- Cygnus Loop, X-ray spectrum 3-65940
- dark, search for 165 α and 166 α radio recombination lines 3-77163
- diffuse, shape of neutral hydrogen globules dependence on incident u.v. 3-77165
- DR 21(OH), NH $_3$ emission line obs. 3-56443
- exciting stars, UVB and spectral obs. of 45 objects (*French*) 3-53713
- expanding gas cloud, dynamical evolution 3-81206
- extensive phenomena at high galactic latitudes, H I regions, nebulosity and giant radio loops 3-42230
- galactic, 1 mm radiometry, cryogenic optical system 3-77180
- galactic, correlation study of C emission lines and OH absorpt. lines 3-48122
- galactic nebulae at $|b| > 20^\circ$, H β photometry 3-56452
- gaseous, low density, computer modelling, anal. of obs. data 3-48135
- Gum Nebula, interstellar measurements and assoc. with H II region 3-42246
- Gum Nebula, obs. below 20 MHz 3-51401
- IC 5070 (Pelican Nebula), variations in ratio of H α and [N II] lines 3-56453
- internal motions from AURA's Fabry-Perot interferometer observations 3-45252
- i.r. ground-based obs. at 34 microns 3-69994
- L1436, interstellar dust cloud, $^{12}\text{C}^{18}\text{O}$ emission rel. to formaldehyde lines 3-81188
- M17 (Omega nebula), flux density meas. at 0.955, 1.65 and 2.73 cm 3-45225
- M8, HCN radio emission from Hourglass region 3-51395
- M 42, photography with naturally-cooled emulsion at -35°C 3-65949
- Medusa (A21), interferometric obs. 3-53715
- NGC 2264, NH $_3$ emission line obs. 3-56443
- NGC 3372 (Carina Nebula), dynamical model 3-48134
- NGC 6445 (p-k 008 + 03 $^\circ$ 1), irregular ring nebula, spectrophotometric study 3-56451
- NGC 6618, (Omega nebula), flux density meas. at 0.955, 1.65 and 2.73 cm 3-45225
- NGC 7000 (North American Nebulae), variations in ratio of H α and [N II] lines 3-56453
- North American Nebula, variations in ratio of H α and [N II] lines 3-56453
- nova outburst, nebulosity, non-spherical struct., influence of white dwarf 3-69938
- Ophiuchi cloud, D/H ratio and D cosmic abundance 3-81199
- ρ Ophiuchi dark cloud, obs. of interstellar dust in cloud 3-51400
- Ophiuchus dark-cloud, 2 μ map, discovery of i.r. cluster 3-81209
- Orion, electrographic obs. of O II ratio 3-77164
- Orion, evolution of T Tauri stars 3-47999
- Orion, model rel. to protrusion of dense molecular cloud 3-70043
- Orion, models of internal dust distrib. 3-48133
- Orion Nebula, O underabundance meas. 3-56454
- Orion Nebula, obs. of high-n Balmer transitions 3-53714
- Orion Nebula, obs. of linear polarisation 3-73552
- Orion Nebula, OII brightness and HCHO radio emission rel. to globules 3-61865
- Orion Nebula, photometric obs. of BN i.r. source rel. to IRS 5 source 3-51369
- Orion Nebula, search for D92 α recombination line emission and D/H ratio 3-81107
- Pelican Nebula, variations in ratio of H α and [N II] lines 3-56453
- solar nebular hypothesis of Kant and Laplace 3-42123
- Wolf-Rayet stars, surrounding ring nebulae rel. to effective temperatures 3-81060
- Wolf-rayet stars with surrounding symmetrical nebulae 3-77078
- H II regions, i.r. nebular luminosity versus stellar luminosity in five regions 3-56449

Neel temperature

- see also *antiferromagnetism; ferrimagnetism*
- antiferromagnet, spin-1/2 anisotropic Heisenberg model 3-79815
- determination, using linear magnetoelastic effect 3-44202
- metal, magnetoresist. change 3-58251
- rare earth alloys, heavy, binary 3-68780
- rare earth insulator, superexchange interaction 3-72458
- semiconductor, antiferromagnetic, thermoelec. power near Neel temp., calc. 3-68655
- B $_2$ O $_3$ -BaO-Fe $_2$ O $_3$ glasses, magnetic susceptibility temperature dependence study, He-room temp. range 3-75834
- Ba $_2$ CoReO $_6$, 41 K, neutron diffr. obs. 3-47058

Neel temperature continued

- BaFeO $_2$, thermal decomposition products of BaFeO $_4$, Mossbauer obs. 3-58451
- Bi $_2$ Fe $_2$ O $_9$, antiferromagnetic, transition temp., magnetisation, quadrupole moments, Mossbauer obs. 3-79952
- Bi $_2$ La $_{1-x}$ FeO $_3$, sublattice magnetisations, Neel temps., superexchange isomer shift, elec. field splitting, Mossbauer obs. 3-50490
- CaO-Fe $_2$ O $_3$ system, antiferromagnetic properties, Mossbauer spectrometry (*German*) 3-47177
- CaV garnet: Zr, Ti substituted, mag. props. 3-47148
- Co-Mn-Fe alloy, mag. phase diagram, rel. to lattice parameters 3-50362
- CoCO $_3$, 18 K, electron excitation, Raman scatt. obs. 3-47243
- CoO, thermal cond. in range including Neel temp. 3-58379
- Cr, determ. from lattice const. temp. depend. X-ray meas. 3-68427
- Cr alloys, binary, Neel temp. determ. from resist. data 3-68785
- Cr-Fe alloy, transition to commensurate spin density wave state 3-41329
- Cr-Mn alloy, susceptibility max. rel. to itinerant antiferromag. coexistence with localised mag. moments 3-64487
- Cr-Ru alloy, depend. on Ru content, elec. resist. meas. 3-52819
- Cr-Si(1.37 at%), first order phase transition in mag. susceptibility 3-79837
- Cr $_2$ O $_3$, pressure induced T $_c$ shift, magnetoelectric determ. 3-75838
- Cr $_2$ O $_3$, rel. to off-diagonal magnetoelectric susceptibility 3-47002
- CsMnBr $_3$, 8.3 K, neutron diffr., mag. susceptibility and specific heat obs. 3-47060
- CsNiF $_3$, 2.7K, neutron diffr. obs. 3-44219
- Cu $_2$ FeGeS $_4$, birite, Mossbauer study (*French*) 3-68894
- Cu(IO $_3$) $_2$, α and γ -phases, cryst. struct., antiferromag. props. below 8.5 and 5 K 3-79306
- Dy, elec. resist. meas. near Neel temp., power law 3-46825
- Dy, mag. susceptibility anisotropy, second kind phase transition 3-72471
- Dy, resistivity meas., electron scatt. from spin fluctuations above Neel point 3-58245
- Eu, first order transition at 90.5K in applied mag. field 3-58384
- γ -Fe-Mn alloys, Mossbauer effect obs. of annealing effect (*Russian*) 3-44353
- Fe $_3^{2+}$ Al $_2$ Si $_2$ O $_{12}$ cryst., elec. and mag. hyperfine interactions near Neel point, Mossbauer obs. 3-75930
- Fe $_2$ As antiferro-paramagnetic transition, Mossbauer spectroscopy, internal fields, quadrupole splittings 3-53042
- FeCO $_3$, 35 K, electron excitation, Raman scatt. obs. 3-47243
- FeCl $_3$, phase transitions, neutron scatt. obs. 3-41341
- (FeF $_3$) $_{1-x}$ (KMnF $_3$), mixed system phase characteriz. 3-60965
- Fe $_2$ Ge $_2$ and monoclinic FeGe, Neel temp. behaviour (*French*) 3-44214
- Fe $_{65}$ (Ni $_{1-x}$ Mn $_x$) $_{35}$, Hall effect temp. depend. at Neel point 3-58250
- FeOCl-pyridine complex, Mossbauer effect obs. 3-58450
- ^3He , solid, three-body exchange effects 3-52745
- HoAg, 33 \pm 1 K, neutron diffr. obs. 3-47057
- HoPO $_4$, magnetic phase transition to antiferromagnetic state, susceptibility, magnetic moment, specific heat obs. 3-55428
- K $_2$ MnF $_4$, critical magnetic scattering, neutron diffraction measurements 3-72474
- LuFe garnet, magnetization near Neel temp. 3-55429
- MnB $_2$, neutron diffraction obs., 900 \pm 100 degrees C 3-47055
- MnO, magnetoelastic interaction, Neel temp., thermal expansion, uniaxial stress expts. 3-41390
- NiO, thermal cond. in range including Neel temp. 3-58379
- NiO powder, reduction, nucleation rate kinetics rel. to transition 3-55164
- NiO:Li, pressure sintered, Young's modulus and resistivity obs. 3-72466
- NiS: ^{57}Fe , metal-nonmetal transition, Mossbauer effect 3-41152
- NpN, magnetis. and resistivity obs. 3-41348
- PdEu, ^{151}Eu Mossbauer study 3-79954
- rare earth-gad compound, RAu $_2$, first order magnetic transition, susceptibility obs. 3-46999
- Rb $_2$ CoF $_4$, two-dimensional Ising antiferromagnet, neutron diffraction obs. of critical behaviour 3-75837
- RbMnBr $_3$, neutron diffr. and susceptibility obs. 3-47056
- RbMnBr $_4$.2H $_2$ O, magnetic phase diagram 3-50366
- RbMnF $_3$, antiferromag. reson. near Neel temp., u.s. wave coupling to antiferromag. spin waves (*French*) 3-41427
- Tb, magnetic susceptibility, temp. depend. 3-79829
- Tb-light rare earth alloys, neutron diffr. obs. 3-68790
- Tb $_{1-x}$ Y $_x$ Sb, sublattice magnetisation, exchange interaction, Neel temp. 3-68775
- ZnCr $_2$ Se $_4$, hydrostatic press. effects 3-58377

negative feedback see feedback

negative feedback control systems see closed loop systems

negative resistance

- n-p-i structure, temp. dependence of parameter spread (*Russian*) 3-44137
- semiconductor with impurity bands, negative magnetoresist. theory (*French*) 3-58281
- n-GaAs depletion layer amplification from negative differential mobility 3-41194
- n-InAs negative differential conductivity, instability, transverse magnetic field 3-52862
- negative resistance effects**
see also *Gunn effect*
- Josephson junction, parametric effect, demonstration 3-72428
- p-n-p semiconductor negative resistance origination by minority carrier injection (*Czech*) 3-55277
- p-n-p-n-p-structure, negative differential resistance, theoretical formulae (*Russian*) 3-50264
- p-n-p-n-p-structure, voltage-current characteristics calc. (*Russian*) 3-58319
- semiconductor, differential resist. controlled by photoinjection from metal contact 3-60881
- semiconductor, negative differential mobility, current instabilities in long samples 3-41201
- semiconductor, negative differential mobility rel. to power flow in Gunn effect 3-64345
- semiconductor, zero-gap, possibility of negative resist. effect, solid-state oscillator appl. 3-79698

negative resistance effects continued

- Al-LiF-Au electron emission in vacuum and voltage-controlled neg. resist. 3-75795
 As-S-Te-I glasses, inhomogeneous struct. depend. of I-V characts. (*Japanese*) 3-64391
 Bi_{1-x}GeO_{2-x}, carrier transport and current oscill. in relaxation semiconductor regime 3-44084
 C, pyrolytic, diamag. anisotropy, negative magnetic resist., temp. depend., 4.2-300K (*German*) 3-72445
 C, pyrolytic, negative magnetic resist., crystallization, semiconductor-metal transition, 1.5-300 K (*German*) 3-72387
 CdGeAs₂, glassy, S-type negative resist. (*Russian*) 3-64384
 p-CdTe, negative differential cond. and current oscill. 3-68636
 Cu:Fe films, magnetoresistance, Kondo effect 3-68769
 FeS₂, transverse magnetoresistance at 77 K and 4.2 K as function of magnetic field 3-52860
 n-Ga_{1-x}Al_xAs-p-GaAs, injection laser, double heterostruct., physical basis for negative resist. 3-78042
 n-GaAs, compensated, negative magnetoresist. obs. from 0.6 to 4.2 K 3-41207
 n-GaAs, doped, negative magnetoresist. rel. to shallow donor levels conc. 3-41210
 GaAs, neg. differential mobility, quasistatic analysis (*Polish*) 3-41192
 GaAs epitaxial film, high resist. layer 3-41225
 GaAs static negative resistance due to geometry effects, computer analysis 3-55283
 GaAs-Ti₂Co compensated semiconductor diode, IV characts. 3-58266
 GaAs(Cr), semi-insulating, donor-acceptor interaction effect on recombination and electrical instability 3-41156
 n-Ge, [110] mag. field induced below 20 to 30K 3-79699
 Ge, field enhanced recombination 3-55282
 p-Ge, rel. to saturation of current and step-like distrib. of field 3-46856
 n-Ge:Ni, illuminated, negative diff. resist. in presence of elec. domains and high surface recomb. rate 3-79708
 InP, velocity field characts., max. neg. differential mobility 3-55281
 InSb, Gunn effect in mag. field 3-58274
 n-InSb, hot electron magnetophonon reson. in longit. mag. fields, negative magnetoresist. 3-64358
 n-InSb, negative longit. magnetoresist. at 30K 3-64359
 n-InSb, reversal of sign of Hall coeff. in mag. freeze out regime 3-68653
 (La,Ce)Al₂, Kondo system, negative magnetoresist. 3-68770
 Pb-Bi alloy, supercond., negative differential resist. at high current densities 3-44165
 Se, liquid, current oscillations 3-68634
 Si, intervalley repopulation and negative differential mobility, 8K 3-46852
 Si:Al, compensated, p-i-n structure, negative resist. region with ambipolar drift mobility sign change 3-60915
 n-Si:Al, deep impurity levels, injection field effect, negative resist. region 3-64351
 Si:W, negative differential cond. in carrier capture by repulsive centres, double injection conditions 3-50216
 p-SiSb:Cu, film, negative magnetoresist., localised mag. states model 3-41209
 p-Te:Sb, impurity band cond. and negative magnetoresist., low temp. 3-44094
 n-ZnS-p-GaAs, heterojunctions, negative resistance at 77 to 293 K (*Russian*) 3-79761
 ZnTe-CdTe solid solutions, negative photocond., field depend. (*Russian*) 3-72383

negative temperature coefficient thermistors see thermistors

nematic phase see liquid crystals

neodymium

- absorption spectra, 1.13-4.42 eV, dispersion depend., quantum transitions (*Russian*) 3-80066
 crystal electric field, energy levels of Nd³⁺ ion 3-64444
 desorption from W, determination of kinetic characts. by temp. modulation method 3-50080
 glass: Nd³⁺ and glass:Nd³⁺ ceramics, fluorescence lifetimes 3-55677
 glass: Nd laser, high power, self-focusing damage 3-40262
 glass:Nd³⁺ Yb³⁺, segregation and energy transfer from Nd³⁺ to Yb³⁺ (*Russian*) 3-64735
 glass, phase separation effects on lasing parameters, absorpt., fluoresc. and damage threshold 3-54229
 glass laser, Nd³⁺ activated, apparatus for meas. of small nonactive absorption coefficients of the active elements (*Russian*) 3-48456
 ions, electric field, desorption from W (*Russian*) 3-68504
 laser, Nd³⁺:glass, parasitic oscills. calcs. with gain variation 3-74242
 laser Q factor electro-optical modulation, modulator components (*Russian*) 3-57230
 liquid, 1100-2100 K, thermal capacity, diffusivity and conductivity, simultaneous meas. 3-42543
 magnetic phase transitions, phenomenological approx. 3-64445
 magnetic phase transitions, phenomenological approx. 3-79808
 melt growth by crystn. 3-44537
 Nd-glass, high-power multi-laser system emitting picosecond pulses 3-66843
 thermal conductivity and Lorenz function, 2-45 K, rel. to magnetic transition 3-50165
 X-ray isotope shifts and variations of nuclear charge radii 3-67662
 X-ray photoemission spectra near Fermi energy 3-53168
 CaO.2Al₂O₃:Nd³⁺, e.p.r. and optical spectra rel. to ion site energy levels 3-44320
 CaS:Bi phosphors, effect of didymium ions on emission characteristics 3-47301
 CaWO₄:Nd³⁺, intermultiplet non-radiative transitions, three-phonon relax. 3-76045
 CaWO₄:Nd³⁺-LaNa(VO₄)₂:Nd³⁺ composite active medium, laser luminescence spectra 3-62720
 CaWO₄:Nd³⁺, paramag. spin-lattice relax., effect of odd normal vibrs. 3-58102
 Fe:Nd, transverse spin component, simple continuum model 3-41339

neodymium continued

- KY(WO₄)₂:Nd³⁺ crystal spectroscopic and generation study for laser 3-64691
 La₂Be₂O₇:Nd³⁺, absorption and luminescence spectra 3-44485
 LaCl₃:Pr³⁺, Nd³⁺, energy transfer between low-lying energy levels of Pr³⁺ and Nd³⁺ 3-53145
 Nd: glass laser, single freq., nonspiking free oscill. and Q-switched operation 3-45805
 Nd:glass, lasing action on ⁴F_{3/2}→⁴I_{9/2} transition in silicate and phosphate glasses 3-62721
 Nd:glass laser, CW, freq. tuning, mode locking 3-51930
 Nd:glass laser, GOS-301, design and components 3-70820
 Nd:glass laser, mode locked, improving reliability 3-62718
 Nd:glass laser, mode-locked, picosecond pulses, streak camera obs. 3-78041
 Nd:glass laser, mode-locked by saturable absorbers, spectral narrowing effect suppression 3-51932
 Nd:glass laser, recovery time of saturable absorbers for 1.06 μ mode-locking 3-59601
 Nd:glass laser action on ⁴F_{3/2}→⁴I_{13/2} transition manifold, lasing at 1.35 μm 3-45804
 Nd:glass laser slabs, face pumped, inversion spatial distrib. 3-40260
 Nd:glass laser system, overshoot inversion 3-66840
 Nd:glass mode locked laser, picosecond pulse development, output signal 3-48908
 Nd:YAG, fluorescence quenching rel. to use as laser material 3-48907
 Nd:YAG, stimulated emission cross section at 1061 microns 3-43017
 Nd:YAG c.w. laser with vortex stabilised lamp 3-45806
 Nd:YAG laser, pumping by miniature diode 3-66836
 Nd:YAG laser action on ⁴F_{3/2}→⁴I_{13/2} transition manifold, lasing at 1.35 μm 3-45804
 Nd:YAG laser, intracavity second harmonic generation using KNbO₃ 3-51948
 Nd:YAlO₄ laser action on ⁴F_{3/2}→⁴I_{13/2} transition manifold, lasing at 1.35 μm 3-45804
 Nd-glass, controllable single pulse laser 3-48910
 Nd-glass disk laser amplifier, design and operation 3-62717
 Nd-glass laser, angular divergence of beam using telescopic cavity 3-57233
 Nd³⁺, in CaWO₄ and YAG, epitaxial growth for thin film laser applic. 3-54230
 Nd³⁺, in YAG, energy level temp. shift, absorpt. and luminesc. spectra obs. 3-64727
 Nd³⁺, in YAG epitaxial film, laser oscillations obs. 3-51929
 Nd³⁺ impurity ionic crystals, excitation energy transfer (*Russian*) 3-41564
 Nd³⁺ in CaAl₂O₇, spectroscopic props. of stimulated radiation 3-72681
 Nd³⁺ in GaCl₃, struct. relax. effect on spectral props. 3-69036
 Nd³⁺ in garnet, crystal field theory, Stark splitting 3-72331
 Nd³⁺ in YAlO₃, Lu₃Al₅O₁₂, CaWO₄ and KY(WO₄)₂ crystals, stimulated emission investigation 3-43018
 Nd³⁺ ion excited state crystals, investigation of elementary cross-relaxation 3-64305
 Nd³⁺:LiLa(MoO₄)₂, investigation of stimulated emission 3-51934
 Nd³⁺:SrF₂-GdF₃, stimulated emission, 300K 3-72682
 Nd³⁺:YAG, Czochralski-grown, perfection and characts. for gems, lasers and substrates 3-76131
 Nd³⁺:YAG burst mode freq. doubled laser for high speed photography and holography application 3-43015
 Nd³⁺:YAG cryst., meas. of relax. time of laser transition 3-70821
 Nd³⁺:YAG laser, cavity dumped, instability due to time varying reflections 3-40263
 Nd³⁺: glass, relaxation rates meas. 3-51933
 PbMoO₄:Nd³⁺, cryst. Stark splitting, optical absorpt. and Zeeman spectra obs. 3-47297
 YAG:Nd, Lu, repetitively pulsed flashlamp-pumped laser material, thermal transient effects 3-62716
 YAG:Nd³⁺ single crystals, absorption bands (*Russian*) 3-69025
 YAG:Sc³⁺, Nd³⁺, solubility enhancement of Nd³⁺ by lattice expansion with Sc³⁺ 3-68415
 Y₃(Al_{1-x}Ga_x)₅O₁₂:Nd³⁺, spectroscopic study, non-random clustering of Nd with impurities 3-78040
 YAlO₃:Nd, Czochralski growth 3-69158
 YLAG:Nd³⁺, spectral props. and induced emission 3-53131

neodymium compounds

- acetate hydrates, cryst. growth and lattice parameters 3-60719
 ethylsulphate, Raman spectra 3-50564
 neodymium benzoyleacetate, u.v. diffuse reflectance spectra 3-47291
 2Nd₂O₃.xSb₂O₃, tetragonal and cubic cryst. structures, X-ray obs. 3-52603
 {Nd₂Yb₃}[Yb₂](Ga₃)O₁₂ garnet dodecahedral and octahedral site filling, structure factor calc. 3-40877
 Bi_{1-x}Nd_xFeO₃, solid solutions, intrinsic weak ferromagnetism 3-46998
 CaF₂:PrF₃(NdF₃, DyF₃, HoF₃, ErF₃, TmF₃), gamma-luminescence, phosphorescence, photoluminescences 3-53140
 CaF₂-NdF₃ system phase relations and characteriz. (*German*) 3-47443
 Nd³⁺-2-hydroxy-3-naphthoic acid complex, i.r. spectra, vibr. modes 3-67815
 NdB₄, ¹¹B Knight shift at the three different crystallographic sites 3-41439
 NdB₆ X-ray diff. anal., thermal props. 3-68423
 NdBO₃, flux growth of single crystals. 3-58595
 NdCo₂ thermal-decomposition, NdCo₂→NdCo₃+Nd, high temp. and vacuum 3-47558
 NdCrSe₃, mag. and elec. charact. 3-64497
 Nd₂CuO₄, semicond. props. from 120 to 1000 K rel. to K₂NiF₄ structure 3-41241
 NdF₃, far u.v. refl. spectra, 6-40 eV 3-58521
 NdFeO₃, magnetisation, spontaneous, susceptibilities, 2.2 to 725 K, spin orientations 3-52966
 NdM₂X_{2-x}, (M=Fe, Co, Ni, Ag), (X=Si, Ge), ferromag. Nd, Ce and diamag. M sublattices 3-64475
 NdMn₂O₈, mag. struct., neutron diff. (*French*) 3-44223

neodymium compounds continued

- Nd_2NiO_4 , metallic props. above 500 K rel. to K_2NiF_4 structure 3-41241
 $\text{NdO}_{1.5}\text{-CeO}_2$ $\text{MO}_{1.5}\text{-MO}_2$ (fluorite) type mixed oxide, phase relns. 3-64181
 Nd_2O_3 , single crystal, investigation on structural anisotropy (French) 3-64012
 Nd_2O_3 :glass ceramic, new laser host material 3-40265
 $\text{Nd}_2\text{O}_3\text{-POCl}_3\text{-SnCl}_4$ solutions Nd^{3+} luminescence, self-quenching 3-64713
 $\text{Nd}(\text{OH})_3$, exchange interactions rel. to ferromag. or antiferromag. low temp. ordering 3-47015
 $\text{Nd}(\text{OH})_2\text{Cl}$, cryst. struct. 3-49884
 $\text{A-Nd}_2\text{O}_3\text{-A-La}_2\text{O}_3$ and $\text{A-Nd}_2\text{O}_3\text{-C-Y}_2\text{O}_3$, investigation of the binary systems (French) 3-64152
 $\text{NdP}_2\text{O}_{14}$ fluorescence, energy transfer and level system rel. to laser use 3-50610
 $\text{NdP}_2\text{O}_{14}$ laser at 1.05 microns 3-48906
 Nd_5S_4 , magnetic ordering near 45K, temp. depend. of mag. moment 3-75860
 NdSBr crystal structure, X-ray diffraction study, rare earth sulfobromide isotopes (French) 3-60687
 NdTiNbO_6 , polycrystalline specimens, electrical conductivity, temperature dependence 3-75787
 $\text{Nd}(\text{benzoylacetate})_2^+$ complex in soln., spectral studies (Russian) 3-50559
 $\text{Sr}(\text{NO}_3)_2\text{-Nd}(\text{NO}_3)_3\text{-Na}_2\text{WO}_4\text{-H}_2\text{O}$ system, aqueous solutions, solid phase 3-76422
 U-Nd-O system, oxygen pot. meas. 3-72933

neon

- adsorption, isothermal and thermo-osmotic, by microporous C membranes 3-80575
 adsorption on Xe crystal, surface relaxation effects 3-46753
 atom, $2p_6\text{-}1s_5$, pulsed superradiant emission, coherence props., excitation conditions effect 3-51919
 atom, $2p^5\text{ }3p$ level lifetimes, Hanle effect meas. 3-78460
 atom, amplified spontaneous emission, high-gain transitions due to electric discharge 3-74805
 atom, Auger K-shell spectrum, effects of configuration interaction 3-78498
 atom, electron impact ionization cross section, 100-20000 eV, semiempirical calc. 3-78542
 atom, electron loss and capture by multiply charged ions, cross sections anomaly 3-52296
 atom, electron scatt., Compton modified band obs. 3-54589
 atom, electron scattering, elastic, 100, 150 and 200 eV 3-71427
 atom, electron scattering, elastic, 1.5-100 eV 3-71429
 atom, electron scattering, elastic, plane wave approximation 3-71426
 atom, fast charged particle scattering cross-section 3-67717
 atom, fast proton collisions, ionisation and unreliability of hydrogenic approximation 3-78589
 atom, fluorescence, K-shell, errors arising in statistical scaling procedure for defect config. 3-71385
 atom, ground state, correlated radial momentum distrib. and Compton profiles 3-46172
 atom, Hanle effect meas. of g-factors and polarizations of excited states 3-78461
 atom, $\text{K}\alpha$ X-ray transitions, oxygen-projectile charge state depend. 3-63308
 atom, lifetimes of levels, coincidence detection of scattered electron and emitted photon (French) 3-74806
 atom, photoionisation, $2s2p^63p(^1P^-)$ state, ang. distrib. and shape var. of resonance lines of photoelectrons 3-74819
 atom, photoionization cross sections, subshell, absolute, exptl. determ. 3-78481
 atom, positron total cross sections meas., 2-400 eV 3-60382
 atom, radial momentum distrib. and Compton profile determ. 3-54562
 atom, vacuum ultraviolet radiation, lifetime, pressure depend. 3-71373
 atom, X-ray emission, K-shell ionisation by H^+ and He^+ impact 3-78606
 atom collisions with Cs^+ , excitation cross sections 3-43372
 atom elastic scattering with He^+ 3-43378
 atom electron scattering, free-free absorption coefficients calc. 3-43371
 atom low energy charge-exchange excitation collisions with N^+ , O^+ , Na^+ , Mg^+ , radiation phase interference, optical polarisation 3-67715
 atomic levels, radiative lifetimes calc. 3-63291
 atomic quadrupole moments of excited states 3-71364
 atomic scattering from (111) plane of Ag crystal, velocity distribution meas. 3-47336
 atomic spectra, oscillator strengths calc. for resonance series $2p^6\text{-}2p^5ns$ 3-63290
 atoms, K X-ray fluores. spectrum 3-43351
 atoms, laser with external feedback, radiation props. (German) 3-48872
 atoms, total nucl. capture rates of muons 3-46012
 atoms bombardment of Ge, L-series X-ray spectra 3-43342
 atoms excitation in a glow discharge 3-60367
 Auger spectrum, K-shell, config. interaction effects 3-49408
 autoionising states line profiles in electroionisation curve 3-78474
 band struct., optical band gap, density of states, Hartree-Fock calcs. 3-52788
 beam-foil lifetime meas. in vacuum u.v. 3-78747
 collision of Ne ground-state atoms with Ar, Ar atom $2p$ level alignment destruction (French) 3-49425
 collisional de-excitation of I_2 molecules, fluorescence study 3-60494
 collisional deactivation of CO 3-43519
 collisions with $^3\text{He}^{2+}$, electron capture cross sections 3-78566
 collisions with D_2^+ , dissociation cross section 3-75141
 collisions with H_2 , spin-lattice relaxation, anisotropic part of intermolecular potential 3-40683
 collisions with H^+ , H_2^+ and He^+ , K-shell X-ray emission and ionisation cross sections 3-46334
 Compton profiles, incident X-ray energy dependence 3-54568

neon continued

- dimer, intermolecular potential energy function determ. from spectroscopic, equilibrium and transport data 3-67865
 discharge, external electrodes, i.f. breakdown 3-75428
 discharge emission identification by photoelectron spectroscopy 3-63894
 discharge with hollow cathode, mag. field effects (Russian) 3-57955
 electric breakdown in large gaps under conditions of preliminary ionization 3-63915
 electron detachment collisions with He and Ne, cross section calc. 3-74887
 electron energy loss spectra (French) 3-63311
 electron impact ioniz. cross sections and coeffs. 3-67701
 electron impact ionization, energy loss and momentum transfer 3-40584
 equation of state, reduced, for saturated liquid (Spanish) 3-43862
 frequency shift measurements in $3.39\text{ }\mu\text{m}$ transition with aid of CH_4 Lamb dip 3-78421
 gas, diffusion of K^+ , experimental variables and interaction potential depend. 3-40766
 gas mixtures with Kr and Xe, trace interdiffusion coefficients, temp. depend. 3-75181
 hyperfine structure of $3s_2$, level, level crossing meas. (French) 3-54576
 ionisation potential calc. 3-63305
 ionised, X-ray spectra with various targets 3-78446
 ions, 0.3 to 2.0 MeV, excitation of N, N_2 and air, fluoresc. efficiencies 3-40644
 isobaric heat capacity, adiabatic throttling effect, from 30 to 70 K 3-71707
 laser, higher order nonlinear effects, hexadecapole moment in $2p_4$ level 3-51915
 laser, with methane absorbing cell, mode competition in $3s_2\text{-}3p_4$ transition 3-74240
 liquid, thermodynamic parameters from m.p. to b.p. determ. by u.s. velocity 3-68420
 microwave discharge in strong mag. fields 3-75435
 migration in $\text{TiO}_2\text{-SiO}_2$ glass, activation energy, strain energy depend. 3-76330
 multi-configuration Hartree-Fock correlation study of $1s2s\text{ }^1S$ state 3-49382
 multipole polarisabilities, Van der Waals consts. 3-71365
 multipole polarisabilities and London dispersion forces between Ne and He atoms using double perturbation theory 3-40588
 plasma, decaying, doubly charged ion obs. 3-63810
 plasma, electrical conductivity calc. 3-79063
 plasma, electron velocity distribution function computation from probe data 3-49754
 plasma, luminescent, spectral line decay obs. (German) 3-68084
 plasma, mag. field effect on rot. (Russian) 3-71872
 plasma, weakly ionised, in external electric and magnetic field, electron kinetics (German) 3-71857
 polarisability and C(6) coefficient calc. from oscillator strength distribution 3-71363
 radiative mean life measurements, below 1000 Å 3-74797
 resonances in electron impact, energies and width 3-52288
 scattering of fast charged particles, total and ionisation cross-sections 3-78585
 shock-heated CO + Ne mixture, vibration relax. rates, Landau-Teller model, i.r. spectra 3-75140
 solid, Ar_2 , Kr_2 , Xe_2 mols, vacuum u.v. spectra 3-71546
 solid, Debye-Waller factor, mean-square nuclear displacements calc. 3-72154
 solid, isotopic mixtures, thermal conductivity measurements possibility of second sound propagation 3-55067
 solid, Ne_2 , interatomic pot. derived from solid-state data 3-68191
 solid-plastic deform. 3-58076
 test gas, absolute calibration of lunar orbital mass spectrometer 3-42257
 thermal conductivity, column method, 1000-1500K 3-75172
 thermal diffusion, state potentials 3-75171
 Ar ions in He, N_2 , Ne and Ar, nonmonotonic dependence of electron loss and capture cross sections on target atom nuclear charge 3-78629
 Ar + Ne, K X-ray prod. exponential projectile charge depend. 3-49422
 $\text{H}^+ + \text{Ne}$ slow inelastic collision cross-sections, formation of secondary ions 3-74898
 $\text{H}_2\text{-Ne}$ mixtures, collision-induced fund. band of H_2 3-63540
 He-Ne, c.w. laser, thermodiffusion effects rel. to beam intensity fluctuations 3-66816
 He-Ne, double-beam laser interferometer, for displacement meas. in angstrom range 3-61984
 He-Ne 633 nm laser, frequency stabilization by $^{127}\text{I}_2$ saturated absorption 3-48452
 He-Ne gas laser, freq. modulation (Russian) 3-66802
 He-Ne gas laser cavity, Brewster window, reflection and absorption losses, 6328 Å, calculations 3-66851
 He-Ne gas mixtures, K^+ ion reduced mobility, comparison with pure gases 3-46373
 He-Ne hollow cathode transverse discharge lasers 3-70803
 He-Ne internal mirror laser, freq. stabilisation, comments 3-51901
 He-Ne laser, 633 nm, stabilised to I hyperfine component, stability, reproducibility, absolute wavelength 3-51899
 He-Ne laser, absorp. by I_2 molecular beam, freq. stabilisation at $0.633\text{ }\mu\text{m}$ 3-62707
 He-Ne laser, current dependence of the $\text{Ne}3s_2$ level population 3-51907
 He-Ne laser, homogeneous broadening, $0.63\text{ }\mu\text{m}$ single mode, line parameters 3-40253
 He-Ne laser, influence of inhomogeneous h.f. electric field on parameters (Russian) 3-66803
 He-Ne laser, linear heterogeneity of amplification in active element (Russian) 3-78026
 He-Ne laser, methane stabilised at $3.39\text{ }\mu\text{m}$, ultimate stability 3-66814
 He-Ne laser, mode locking with Ne discharge cell, 6118 Å 3-48882
 He-Ne laser, optical frequency meter applic. 3-51639
 He-Ne laser, r.f. electric field effects on output 3-66819

neon continued

- He-Ne laser, region of strong interaction between modes, amplitude characteristics 3-48897
 He-Ne laser, stabilisation at 3.39 μ using sharp resonances in methane 3-62706
 He-Ne laser, TEM₁₀ gain, calc. 3-62695
 He-Ne laser, with nonlinear reson. absorpt., radiation rise time fluctuations 3-74235
 He-Ne laser frequency fluctuations due to mechanical vibrations 3-66815
 He-Ne mirror ended tube laser, light quasi-periodic noise 3-57224
 He-Ne mixtures, formation of NeHe⁺ ions, effect on electron-ion recombination coefficient 3-78643
 He-Ne ring laser, oppositely travelling waves polarised in different planes, generation 3-48932
 He-Ne stabilised lasers, relative freq. stabilities and modulation spectra (German) 3-51922
 He⁺ + Ne collisions at 0.3-3 keV, differential meas. of electron capture processes 3-74899
 Li⁺ + Ne slow inelastic collision cross-sections, formation of secondary ions 3-74898
 Na⁺ + Ne, absolute scattering cross-sections and interaction potential 3-71454
 Na⁺ + Ne collisions, low energy, strong polarization effects in optical radiation 3-63337
 Na⁺ + Ne collisions at 1.0-5.0 keV, differential cross-sections for electron transitions 3-74897
 Ne, Ne⁺, Ne²⁺, photoionization cross sections rel. to 2p subshell 3-78483
 Ne I, LS-term depend. of Slater integrals, single-config. approx. deviations 3-67641
 Ne I, parametric study of isotope shifts 3-67643
 Ne I isoelectronic sequence, Hartree-Fock calcs. for npⁿp config. terms, Slater integrals 3-63263
 Ne I isoelectronic sequence, theor. transition probabilities and energy levels 3-67633
 Ne I isoelectronic series, dipole polarizabilities from nf term values 3-78450
 Ne II, perturbations in 2pⁿs and 2pⁿd configurations, least squares fitting procedure 3-74792
 Ne IX line in solar corona, X-ray survey 3-65712
 Ne-Ar gas mixtures, K⁺ ion reduced mobility, comparison with pure gases 3-46373
 Ne-Ar glow discharge, current density and critical distance meas. 3-75444
 Ne-Ar nonideal, rarefied gases, molecular diffusion study 3-67897
 Ne-Ar Penning mixture, numerical simulation of transient d.c. breakdown 3-68115
 Ne-Hg, Ne-Xe-Hg mixtures, d.c. discharge, cataphoretic segregation effects 3-57959
 Ne-Li⁺ system, repulsive potential, determ. from inelastic scatt. cross sections 3-43384
 Ne-methyl chloride and Ne-methane gas mixtures, viscosity and non-polar-polar molecular interactions 3-60515
 Ne-Ne system, repulsive potential determ. from data for Li⁺-rare gas systems 3-43384
 Ne + Ar¹²⁻¹⁷⁺ fast collisions, exponential projectile charge dependence of Ar K and Ne K X-ray production 3-78601
 Ne + CO scattering, rotational inelasticity, time-dependent perturbation theory 3-71645
 Ne + CO(HCl) collisions, rot. inelasticity, time depend. perturbation approach 3-71636
 Ne + Cs⁺, slow collision, threshold behaviour of resonance lines 3-71466
 Ne + H₂, liq. mixtures, eqn. of state, exptl. obs. 3-49965
 Ne + H⁺ collisions at 100-600 keV, simultaneous meas. of X-rays and Auger electrons 3-78602
 Ne + HCl scattering rotational inelasticity, time-dependent perturbation theory 3-71645
 Ne + Li⁺ collisions, elastic and inelastic scatt. comparison with Fano-Lichten model 3-74884
 Ne + Ne interactions, absolute total scatt. cross sections meas. 3-71394
 Ne + Ne⁺ collisions at 50-600 keV, Auger spectra 3-78603
 Ne + O⁺, low-energy collisions, phase-interference effects 3-71465
 Ne⁺, ion implantation in LiNbO₃, effect on surface acoustic wave attenuation 3-52746
 Ne⁺ charge transfer collisions with vibrationally excited N₂ 3-43370
 Ne⁺ continuous operation lasers (German) 3-57223
 Ne⁺ inelastic excitation collisions with Ne, energy spectra 3-71450
 Ne⁺ ion bombardment of Zn and Cu single crystals, secondary electron emission, energy distribution 3-44512
 Ne⁺ + HBr, metastable prod. obs. 3-54593
 Ne⁺ + HCl, metastable prod. obs. 3-54593
 Ne⁺ + N₂ impact, emission cross-sections for N₂ 3914 Å and 3371 Å systems 3-78894
 Ne⁺ + Ne collisions, ion spectra interpret. 3-71449
 Ne⁺ + Ne collisions, K-shell electrons excitation, scaling law 3-71460
 Ne₂ and Ne₂⁺, scattering and radiative processes in low-lying states, ab initio calc. 3-71640
 Ne³⁺, photoionisation cross section calcs. 3-71383
²⁰Ne ions in Al foil, energy loss meas. from Doppler shifted γ -ray energies 3-46653
²⁰Ne + ²²Ne, thermal diffusion separation, effect of column misalignment 3-78928
 Ne⁺ + Ne collisions, saturated absorpt., collisional broadening study 3-46199
 Ne⁺(³P₂, ³P₀) + Ar \rightarrow Ne(¹S) + Ar⁺ + e, Penning ionisation process, low-energy cross section meas. by merging beam technique 3-78500
 Xe-Ne, ground state pot. energy curves, model 3-40589

neon compounds

- NeDCI Van der Waals complex, molecular beam studies 3-78912
 NeH⁺, ten-electron hydride, ground state calc., field form of perturbation theory 3-71521
 NeHCl Van der Waals complex, molecular beam studies 3-78912
 NeHe⁺ formation in Ne⁺ + Ne + He process in afterglow, effect on electron-ion recombination coeff. 3-78643

Neptune

- adiabatic temp. distrib. determ., comparison with core melting tem. 3-47928
 albedo, wavelength dependence from 0.3 to 1.1 μ photoelectric photometry 3-80982
 atmosphere, review 3-65780
 atmosphere dynamics rel. to planetary dynamics 3-47936
 gravitational field constraints on model of interior 3-47933
 interferometer obs. of 11.1 and 3.7 cm 3-56333
 interior processes model testing using atm. meas. 3-47934
 ionospheric physical and chemical processes 3-47937
 nonthermal radio emission 3-42154
 orbit residuals rel. to mass and position limits for hypothetical tenth planet 3-47929
 survey of present knowledge 3-45039
 H planet, high-pressure phenomena 3-42152

neptunium

- ionisation energy calc. 3-60376
²³⁷Np purification using Amberlite XE-270 exchange resin 3-67577
 Pu, electron-paramagnon electrical resistivity, high temp. behaviour 3-44062

neptunium compounds

- NpAs, mag. props., magnetis. and Mossbauer obs. 3-41332
 NpC, model for magnetic phase transitions 3-47035
 NpF₄-TlF, solid-liq. equilib. diag., phase identification (French) 3-60787
 NpN, antiferromag., neutron scatt., magnetis., and Mossbauer obs. 3-41348
 NpN, mag. props., magnetis. and Mossbauer effect obs. 3-41332
 NpP, antiferromag. ordering at 130K in ferromag. sheets, neutron and Mossbauer obs. 3-72473
 NpP, antiferromagnet, lattice parameters, low temp. X-ray study 3-52614
 NpP, mag. props., magnetis. and Mossbauer obs. 3-41332
 NpSb, mag. props., magnetis. and Mossbauer obs. 3-41332
 NpSe₃, Np₂Se₃, γ -Np₂Se₃, prep., thermal stability and X-ray charact. 3-54945

Nernst effect see magnetothermal effects

Nernst-Ettingshausen effect see magnetothermal effects

network theory see circuit theory

Neumann algebra see algebra

neural nets

- see also brain models
 bioelectric potentials in anisotropic ensembles of neuronal elements 3-45260
 entropy changes associated with nerve impulses 3-45263
 extracellular single-unit recording employing photoengraved microelectrodes 3-45262
 frog's visual analyser, information processing principles, model of novelty neurons (Russian) 3-48241
 human and animal visual analysers, neural network model (Russian) 3-48237
 human sensory receptors, some binary relationships (Russian) 3-48238
 neuron's firing pattern rel. to muscular length 3-51431
 neuron model, dendritic, steady-state, branch input resistance, attenuation, calculations 3-70099
 retinal nerve nets, interpretation of optical illusions by systems theory methods 3-45308

neuristor networks see neural nets

neuron models see neural nets

neurophysiology

- see also neural nets
 alert monkey, accommodative vergence, motor unit analysis 3-66008
 battery-powered implantable neuroelectric stimulator 3-48618
 cat retina, on-center neurons, receptive field periphery 3-66005
 compartmental model neuron, computer control 3-51430
 dendritic field analysis, projection method errors 3-45257
 digital thermal dolorimeter, for neurologic examination 3-48619
 e.e.g. signals, response to noise 3-53741
 eye head coordination, in monkeys, modelling 3-56515
 figure and ground, neurophysiological basis 3-81296
 flies, visual nervous system, development and applic. of white-noise modelling techniques 3-45307
 hearing, neural coding, tuning curves, two-tone inhibition, psycho-physical probe-tone experimental methods 3-77216
 hearing, precedence effects and auditory cells with long characteristic delays 3-77224
 kitten visual cortex, short-term stimulus-induced changes in connectivity 3-73585
 modelling, applicability of Fourier-Bessel expansions of evoked cortical potentials 3-59420
 neural inhibition, contrast effects, visual sensitivity 3-42351
 neuromuscular transmission, presynaptic and postsynaptic effects of Pb, frog expts. 3-45265
 neuron activity recording, electronic control of micro-electrode by fractions of a micron 3-62309
 peripheral auditory system, lateral inhibitory mechanism 3-77217
 peripheral nerve stimulation, for pain relief 3-48617
 pre-medical physics course, nerve conduction 3-77350
 rabbit, visual receptive-field characteristics of superior colliculus neurons after cortical lesions 3-77238
 spike-interval sequence correlation estimates, effect of meas. errors 3-59534
 stick insects, neuromuscular transmission, effect of glutamic acid 3-56495

neutrino interactions

- see also nuclear reactions and scattering due to neutrinos
 $\nu\bar{\nu}$, nonlocal quantum theory, ν e.m. form factor, four-fermion and W boson models (Russian) 3-59926
 beam expts. as probe of particle structure 3-74361
 cross section for production of heavy intermediate bosons and leptons, renormalizable theory (Russian) 3-59952
 elastic, asymptotic behaviour of total cross section, partial wave analysis 3-62815
 Goldstone neutrino interaction with e.m. field 3-52002
 Goldstone particle hypothesis, phenomenological Lagrangian for interaction description 3-66982

neutrino interactions continued

- hadron production without μ or e , neutral current behaviour 3-66984
 heavy lepton production, lower bound determ. 3-45872
 high energy neutrino and antineutrino events 3-43093
 high-energy, Adler and Gross-Llewellyn Smith sum rule testing 3-66987
 inclusive, high-energy, model based on three-triplet model of hadrons 3-43092
 inclusive current induced interactions, scaling behaviour due to light-cone singularities 3-40320
 massless particle total cross sections, Adler condition and high energy bounds 3-59942
 Mossbauer effect, limits on elementary length 3-66979
 motion in charged matter 3-66981
 neutrino production structure functions in deep inelastic region, $SU(6)_w$ on light cone 3-40319
 photon-neutrino weak coupling and self-consistent theory for weak interactions 3-45864
 primordial gas, role of electron-neutrino interaction 3-56310
 quarks and neutrino interactions 3-66965
 Salam-Weinberg model, weak interactions, interstellar energy loss rates 3-80919
 scaling consequences, bounds for E_μ/E_e , $Q^2/2ME_p$ effects of intermediate boson, heavy lepton 3-62819
 second-class currents in $\Delta(1236)$ production by neutrinos, tests 3-57331
 stability of originally massless lepton fields against spontaneous mass formation 3-70907
 $\gamma\nu$ weak interaction postulate, description of photon as $\nu\nu$ pair 3-62816
 N substructure probe, comparison with electron data 3-67047
 $\nu(\nu)N \rightarrow l^-(l^+) + \text{baryon} + \text{meson}$, Born model (Russian) 3-66988
 $\nu(\nu)N \rightarrow l^\pm X$, quark parton model, reln. between quark fragmentation and distribution functions 3-74380
 $\nu(Z) \rightarrow \nu\mu\mu(Z)$, effects of neutral weak currents in charged lepton spectra 3-70906
 $\nu_\mu + Z \rightarrow W^+ + \mu^- + Z$, intermediate boson mass, lower bound study 3-52064
 $\nu\mu N \rightarrow \text{meson} + \text{baryon} + \mu^-$, selection rules 3-66980
 $\nu\mu N \rightarrow \text{meson} + \text{baryon} + \mu^+$, selection rules 3-66980
 νN , deep inelastic, average inelasticity and average (momentum-transfer) 2 3-62814
 νN , high energy, higher-order corrections, phenomenology, sum rule 3-45868
 νN , π production, application of soft-pion techniques 3-57332
 νN inclusive scattering as probe of nucleon core structure 3-62813
 $\nu N \rightarrow \mu^- + \text{hadrons}$, 50, 145 GeV neutrino beam 3-59955
 $\nu N \rightarrow \mu^- + \text{hadrons}$, high energy inclusive reactions at CERN 3-66989
 $\nu n \rightarrow \mu^- p$, 0.7 GeV, axial vector mass determ. 3-70904
 $\nu N \rightarrow \mu^+ + \text{hadrons}$ high energy inclusive reactions at CERN 3-66989
 νN production processes parton model 3-62810
 νN pseudoscalar meson formation in region of strong transmitted impulses, Bornovsky model (Russian) 3-74357
 $\nu N \rightarrow Y^+ + \text{anything}$, search for heavy positively charged lepton Y^+ 3-62817
 $\nu_\mu N \rightarrow \mu^- + \text{hadrons}$, meas. of total cross sections as function of energy 3-66985
 $\nu_\mu n \rightarrow \mu^- p$, test of Weinberg model at CERN 3-66964
 $\nu_\mu N \rightarrow \mu^+ + \text{hadrons}$, meas. of total cross sections as function of energy 3-66985
 $\nu_\mu N \rightarrow \nu_\mu + \text{hadrons}$, calc. of semileptonic neutral currents assuming partons and Weinberg's renormalizable theory 3-70905
 $(\nu\nu)N \rightarrow \mu h X$ ($h = \pi, \rho, p$) integrated structure functions in generalised Bjorken limits 3-74383
 νp , bubble chamber detection, test of external muon identifier principle 3-77629
 $\nu p \rightarrow \mu^- \pi^+ p$, ~ 1 GeV/c, dominance by $\nu p \rightarrow \mu^- \Delta^{++}$ (1236), N- Δ axial current transition matrix elements, model predictions 3-57333
 $\nu p \rightarrow \mu^- \pi^+ p$, value of experimental study 3-70902
 $\nu p \rightarrow \mu^- + \text{hadrons}$, application of correspondence arguments 3-70937
 $\nu p \rightarrow \nu l^- + \text{hadrons}$, cross sections for $E_\nu = 50$ -1000 GeV (Russian) 3-40337
 $\nu p \rightarrow \nu n$ behaviour, Adler sum rule 3-43077
 $\nu_\mu p \rightarrow \mu^- \Delta^{++}$, test of Weinberg model at CERN 3-66964
 $\nu_\mu p \rightarrow \nu_\mu \Delta^+$, test of Weinberg model at CERN 3-66964
 $\nu_\mu p \rightarrow \nu_\mu \pi^+$, used in search for neutral weak currents, isovector or isotensor 3-62818
 $\nu Z \rightarrow Z \nu W^0$, differential cross section for scalar W-meson production at super-high energies (Russian) 3-40336
 π production on nuclear targets, test for neutral currents 3-43082
 H_2/D_2 track sensitive target, neutrino interaction studies in BEBC 3-77657

neutrino scattering

- see also *nuclear reactions and scattering due to neutrinos*
 deep inelastic, three triplet realisations of gauge models 3-43094
 gauge theories of weak interactions, sum rules for verification 3-74358
 inclusive π^\pm prod., quark-parton model, duality relation 3-78151
 longitudinal structure function, in deep-inelastic limit in canonical quark-gluon model 3-62847
 parton-model sum rules and positivity 3-54294
 radiative, lepton energy and angle dependence theorems 3-57334
 $e\nu \rightarrow e\nu$, high energy, N/D method analysis, intermediate weak boson effects 3-40329
 νB , deep inelastic, dual parton model description 3-70903
 νe , amplitude rel. to a generalisation of the Weinberg model of leptons 3-70892
 $\nu_e e \rightarrow \nu_e e$, explt. upper limit, implication for Filippov's theory 3-40328
 $\bar{\nu}_\mu e \rightarrow \bar{\nu}_\mu e$, Weinberg model test at CERN 3-66964
 $\nu_\mu e^- \rightarrow \nu_\mu e^-$, possible observation of event, Weinberg interpretation 3-66983
 νl , phenomenological model, muon parity conservation 3-78118
 νN , deep inelastic, finite-energy sum rules 3-40335
 νN , high energy, unified gauge theory, tests of scaling from total cross sections 3-74359
 νN , high-energy, at low q^2 , Adler test of PCAC 3-74360
 νN , inelastic, spin sum rules, light cone scaling 3-78116

neutrino scattering continued

- νN , inelastic structure-function relations from sum of direct-channel resonances 3-43109
 νN , spin-dependent, positivity inequalities from light-cone algebra of quark currents 3-40350
 νN deep inelastic scattering, parton model for cross-section x-dependence 3-78117
 νN high energy total cross section, unified gauge theory, tests of scaling 3-74359
 νN inelastic, spin sum rules, light cone scaling 3-78116
 $\nu N \rightarrow e^- + \text{hadrons}$, high energy meas., total cross sections, test muon conservation law 3-66986
 $\nu_e N \rightarrow e^+ + \text{hadrons}$, high energy, meas. total cross sections, test muon conservation law 3-66986
 $\nu\nu$ elastic, unsubtracted dispersion relation 3-59946
 $\nu\nu$ scattering, Yang-Mills field theory, gauge invariance, cancellation of divergences (Russian) 3-74322
 νp deep inelastic spin-dependent, determ. of sum rules in SU_4 bilocal algebra 3-62812
 $\nu_\mu p \rightarrow \nu_\mu p$, test of Weinberg model at CERN 3-66964

neutrinos

- see also *cosmic ray neutrinos*
 conformal invariance of mass condition for light-like particles, helicity 3-59918
 cosmological background ('sea') rel. to missing mass, space-time structure 3-80921
 discovery, experiments, review 3-74361
 electromagnetic radius, intermediate boson theory 3-54371
 e.m. form factor, nonlocal quantum theory, four-fermion and W boson models (Russian) 3-59926
 escape from Einstein's spherical cluster of gravitating masses 3-62585
 field, algebraic classification in general relativity 3-70719
 fields, space-times admitting two, Petrov type D classes 3-62584
 Goldstone particles, phenomenological Lagrangian for description of interactions 3-66982
 handedness, indefinite metric 3-62772
 handedness, lagrangians, mass and interaction 3-62773
 handedness, massless spin 1/2 eqn., symmetry properties 3-40309
 handedness, unusual group of external symmetries, quantisation of massless spin 1/2 eqn. 3-40310
 mass determ. from analysis of Curie plot of ^3H beta-decay 3-54441
 physics and astrophysical obs. 3-43167
 radiation field, combined neutrino-f-g variety field 3-48788
 review, shortcomings of different theories and hypothesis of weak interactions (Hungarian) 3-62811
 solar, fluctuation predictions, temperature variation of Earth's surface (Hungarian) 3-76973
 solar neutrino flux model and flux-cross-section product calc. 3-69832
 space-times admitting neutrino fields with zero energy and momentum 3-48975
 spectrum of neutrinos with different masses reln. to solar-neutrino expt. 3-42097
 superdense stars, effect of emission on evolution 3-80918
 $\nu\nu$ production by e pairs, weak boson effects in Weinberg's unified theory 3-66966
 ^8B source, positron decay, meas. annihilation γ -rays to determ. ^8B yield in $^6\text{Li}(^3\text{He}, n)^8\text{B}$ reaction 3-67351

neutron absorption

- see also *nuclear excitation; nuclear reactions and scattering due to neutrons*
 concrete, neutron penetration data, calc. of dose distrib. by moments method 3-74766
 control of boric acid concentration in coolant of PWR (German) 3-71326
 controlled fusion blankets and shields, perturbation theory for neutron and photon transport calcs. 3-74743
 graphite in reactor radiation field, absorbed dose meas. using isothermal calorimeter system 3-63137
 marble, Egyptian, cross-sections, nuclear reactor shielding material, evaluation 3-67625
 nuclear reactor, loss-of-target analysis, safety criteria 3-67421
 nuclear reactor, shield attenuation calc. 3-60342
 nuclear reactor fuel, structural materials, reactivity testing, quality control 3-63210
 resonance cross section in heterogeneous fast reactor for complicated geometries 3-74654
 slab transmission, reflection and finite reflector critical problems 3-60249
 slowing down in mixture of elements, semianalytical method for solving eqn. 3-52219
 thermal, in boiling media, calc. using approximate models and Monte Carlo techniques 3-63107
 tissue absorbed dose and dose equivalent for 3.5 GeV-1.0 TeV neutrons 3-52234
 (n, p) reactions, cross section meas. and applications to reactor physics and nucleosynthesis 3-74566
 Au, neutron absorption cross sections, 40 to 47 A neutrons 3-78333
 B, small concentrations determ. in metals using combined absorption and activation technique 3-70476
 B-Li concentration measurements, apparatus using neutron absorption and activation 3-42709
 $\text{BF}_3\text{-CO}_2$ gaseous mixtures, explt. thermal neutron flux distrib. 3-49303
 Co, neutron absorption cross sections, 4 to 47 A neutrons 3-78333

neutron angular distribution

- see also *neutron spectra*
 AGR heterogeneous core calcs., determ. of dipole extrapolation lengths 3-71168
 ENDF/B data, efficient representation in multigroup processing codes 3-71220
 fast angular flux spectrum in infinite carbon medium, moments method soln. 3-52220
 nuclear air burst, energy, space and time distrib. using Monte Carlo calcs. 3-74621
 reactor lattices, bare and D_2O reflected, space dependent neutron noise spectra rel. to detector efficiency 3-67399
 transport calcs., sensitivity to nonelastic angular distributions 3-60251

neutron angular distribution continued

- (p,n) charge exchange reactions, exact macroscopic charge independent analysis using optical model 3-67333
 from pp interactions, 19.1 and 10 GeV/c, comparison with theory (*Russian*) 3-60046
²⁷Al(p,n), angular distrib. for transitions to isobaric analogue states 3-63055
 Am-Be sources, neutron spectrum, effects of secondary interactions 3-77607
³⁸Ar(³He,n)⁴⁰Ca, excited J^π=0⁺ states in ⁴⁰Ca 3-74491
¹¹B(α,n)¹⁴N, E_α=12-15 MeV, cluster transfer 3-63070
⁹Be(α,n)¹²C, 4.5-5.85 MeV, meas. of neutron polarisation angular distrib., ¹³C states 3-62946
¹²C(n,n')¹²C, 13.9 MeV, angular correlation meas., 2⁺→0⁺ decay 3-78323
¹²C(n,n')¹²C, 1.98 MeV-4.64 MeV, phase shift and optical-model analysis 3-71106
¹²C(n,n')¹²C, 7-9 MeV, angular distrib. meas., comparison with optical model calcs. 3-63051
¹³C(α,n)¹⁶O, 2.075-2.43 MeV, neutron polarisation angular distrib., parity assignments of ¹⁷O 7.97-8.197 MeV states 3-67189
¹⁴C(d,n)¹⁵N, deuteron energies, 1.3 to 1.9 MeV, neutron polarisation ang. distrib. (*German*) 3-52197
⁵⁰Co, direct processes in 14.4 MeV inelastic neutron scattering (*Russian*) 3-40498
⁶⁵Cu(p,n)⁶⁵Zn, narrow reson. 148 eV above threshold 3-43248
 Fe(α,n) reactions, A=56, 57, precompound processes, 20 MeV, energy, angular distrib. of neutrons 3-60209
²H(n,n')²H, cross section and angular distrib. meas., 40-340 MeV (*Russian*) 3-74551
¹¹⁵In(α,n), 20 MeV, precompound processes, neutron energy and angular distrib. 3-60209
⁷Li(d,αn)⁴He, 1.0 MeV, α-n angular correlation meas., decay schemes 3-71120
²⁴Mg(³He,n)²⁶Si, 5.0 and 5.8 MeV, meas. of angular distrib. of neutron polarisation, DWBA analysis 3-67352
⁹³Nb, direct processes in 14.4 MeV inelastic neutron scattering (*Russian*) 3-40498
¹⁸O(p,n)¹⁸F, E_p=4.6 to 6.6 MeV, reson. investigation 3-54485
 Rb(n,n), natural targets, fast neutron scattering 3-43249
¹⁰³Rh(α,n), 20 MeV, precompound processes, neutron energy and angular distrib. 3-60209
 Sn(α,n) A=115-119, 124, 20 MeV, precompound processes, neutron energy and angular distrib. 3-60209
⁵¹V(p,n), angular distrib. for transitions to isobaric analogue states 3-63055
⁹⁰Zr, angular distrib. for transitions to isobaric analogue states 3-63055

neutron beam effects see *neutron effects***neutron detection and measurement**

- see also *dosimetry; neutron spectrometers*
 activation detector for neutron in high γ-ray flux field using neutron reactions 3-40006
 albedo-neutron dosimeter, thermal to fast, small, cheap 3-77285
 BD-9 integral discriminator, fast n scintillation counter, γ-radiation pulse elimination 3-70387
 calibration of neutron monitors for IGY programme, error analysis (*German*) 3-51694
 criticality neutron dosimeter, using ¹⁰³Rh(n,n')^{103m}Rh reaction 3-77273
 cylindrical counters, effect of field slugging in diffusion media, rel. to cosmic rays (*Russian*) 3-62243
 detector, 145 scintillator elements, on-line electroproduction experiment, calibration, performance 3-77636
 detector of fast time response 3-51704
 dosimeter based on fissioning isotopes 3-54553
 dosimetry, depth dose distributions, 14 MeV neutrons, experimental values, Monte Carlo calculations, comparison 3-77272
 fast neutron measuring channel and fission counter for analysis of transient reactor behaviour (*German*) 3-48518
 film density, by scintillator coincidence system 3-40033
 fission counter operation in LMFBR, effects of gas composition on gamma performance 3-45546
 fluence probes activation, Ge(Li) detector and automatic sample changer description 3-73862
 flux detector, electron current principle (*German*) 3-70395
 flux meas. using gamma compensated pulsed ionisation chamber 3-45547
 flux tilting expts. in asymmetrically poisoned demonstration-size fast reactor 3-49351
 HBWR, self-powered, neutron detectors, long-term test 3-52233
 ionisation chamber, parallel plate, for high intensity mixed neutron-gamma dose rate meas. 3-70393
 lead slowing down time spectrometer, fissile material assay, neutron slowing down studies 3-62267
 light water reactor rods, ²³⁵U content meas., Sb-Be neutron source 3-67558
 liquid scintillation system, for neutron studies with neutron-gamma discrimination 3-40014
 monitor for high-level flux-spectra-fluence characterization, prepn. and handling 3-46166
 nondestructive assay, nuclear waste, criticality problems and solutions 3-63248
 nuclear fuel assays, nondestructive testing, review 3-47502
 nuclear reactor, liquid-metal fast breeder, analytical study of source range monitoring system 3-67438
 nuclear reactor, power distribution in core, effect on external detectors (*German*) 3-71244
 nuclear reactor fuel elements, cask loading, inverse multiplication meas. in situ, criticality safety 3-63251
 nuclear track method, heavy particle discrimination, etching, counting (*German, English*) 3-62246
 organic scintillator, operational effectiveness calc. using Monte Carlo program EFF1 (*German*) 3-59645
 passive gamma neutron monitor, fissile content of waste and scrap, criticality safety 3-63254
 plastic scintillation Gd-loaded detector 3-40019
 population fluctuation, apparatus for meas., mean life time of neutrons (*French*) 3-49310

neutron detection and measurement continued

- position sensitive detectors and multi-counter arrays for neutron studies 3-56940
 pulsed neutron source techniques, criticality safety determination, reactivity of a reactor core 3-63231
 radiation monitoring of personnel, dosage standardisation independent of neutron energy 3-63241
 rock, thermalized neutron detection, time of establishment of equilibrium spectrum (*Russian*) 3-73391
 Rossi-α-expt., time interval of counter pulses meas., and computer simulation 3-66328
 scattering cross sections and gamma ray production, integral experiment method for sensitive test 3-49307
 scintillator, liquid organic, efficiency compared with DETEFT, OSS predictions 3-73865
 self-powered instantaneous detector, sensitivity calcs. using Monte Carlo method 3-51718
 small-angle elastic scattering cross-section meas., fast neutrons 3-74579
 spectra, flux meas. using nuclear track emulsions in artificial satellite of Cosmos series (*Russian*) 3-65608
 supermonitors using large counters of CHM-15 type, BF₃ gas with 80% B¹⁰ (*Russian*) 3-62236
 threshold detectors for neutron leakage spectra evaluation for dosimetry calcs. 3-59646
 time-of-flight spectrometer for fast neutrons, neutron-gamma discrimination (*German*) 3-59652
 track-etch radiography, alpha particles, protons, fast and thermal neutrons, polycarbonate plastics, cellulose nitrate 3-67627
 Z-pinch, noncylindrical, matching discharge circuit with membrane movement, neutron density, two dimensional snow plough model (*Russian*) 3-57950
 B, soluble poison meter, radiation monitoring 3-63253
 Gd, soluble poison meter, radiation monitoring 3-63253
⁴He gas detectors, ¹²⁴Sb-Be (γ,n) assay system, fissile content meas., small samples, fuel rods and solns. 3-67557
 MgO, fast neutron personnel dosimeter based on F-centre response 3-61925
¹⁴N(n,p)¹⁴C, use in neutron beam strength measurement 3-73864
 Pu monitoring, nondestructive assay, criticality prevention, scrap recovery 3-63249
 Rh neutron detector, flux and fluence, explicit solns. 3-42651
¹⁰³Rh(n,n')^{103m}Rh, thick foils, absolute counting of K X-rays 3-66316
 Si detectors, analytically determined response to polyenergetic beam 3-42650
neutron diffraction
 see also *neutron diffraction crystallography; neutron diffraction examination of materials*
 diffuse peaks intensities rel. to scatt. angle 3-49802
 elastic scattering of slow neutrons by standing e.m. wave, coherent scattering amplitude 3-62848
 thermal and zero-point oscill. interf. in neutron inelastic scatt., two phonon scatt. 3-68348
neutron diffraction crystallography
 see also *crystal atomic structure*
 backscattering diffractometer, Bragg refl. meas. from Si (*German*) 3-63933
 diffuse peaks intensities rel. to scatt. angle 3-49802
 Fermi surface investigation, neutron scatt. for Al₁₅ supercond. studies 3-46926
 ferroelectric, hydrogen bonded, coherent neutron scatt., at low temps., theory 3-55534
 ferroelectric, hydrogen bonded, coherent neutron scatt. at low temps., theory, tunnelling quasipin model 3-55535
 ferromagnet, spin-phonon interaction, effect on energy distrib. of one phonon neutron scatt. (*Russian*) 3-55437
 guide tube and diffractometer, for small angle scatt. of cold neutrons 3-43732
 inelastic neutron scattering, use of in-pile collimators 3-63930
 inelastic scattering, selection rules for chalcopyrite and famatinite structs. (*Russian*) 3-49948
 isotropic crystal containing random defect distrib., elastic X-ray and neutron scatt., static correl. functions (*German*) 3-52561
 isotropic systems, resolution in neutron crystal spectroscopy 3-52563
 liquid metals, structure, by time of flight diffr. 3-68149
 magnetic spiral structures, theory 3-47068
 molecular solids and liqs., tool for mol. motion obs., review 3-68140
 optimum scanning ratio obs. 3-63931
 perfect crystals, dynamical diffr. theory 3-54907
 Soller collimator, performance, figure of merit 3-52562
 spin density Patterson function from neutron diffr. data 3-52977
 texture determ., applic. to cold-rolled Zr sheets 3-64847
 time of flight high resolution diffractometer 3-46578
 vacuum furnace, for liquids and solids, up to 1100 K 3-43733
neutron diffraction examination of materials
 see also *neutron diffraction crystallography*
 alkyl ammonium tetrachloromanganate and deuterated analogues, cryst. and mag. transitions 3-47045
 aqueous solutions, long-wavelength limits of partial structure factors 3-54908
 aqueous solutions, struct. factors, multiple-pattern methods 3-60660
 complex structures, coherent inelastic scattering, phonon density of states 3-64123
 feldspar, neutron diffr. refinement of ordered orthoclase structure 3-50884
 ferroelectric, hydrogen bonded, coherent neutron scatt., at low temps., theory 3-55534
 ferroelectric, hydrogen bonded, coherent neutron scatt. at low temps., theory, tunnelling quasipin model 3-55535
 ferromagnet, dipole-dipole interaction role, in critical behaviour 3-47020
 ferromagnetic f.c.c., b.c.c., h.c.p. metals, selection rules for one-magnon inelastic scattering 3-55436
 n-hexane, solid, low frequency mol. vibrations by neutron inelastic scattering 3-75577
 liquid, mol. motion, n.m.r. and neutron scatt. obs. 3-68875
 liquid, molecular motion, random walk theory 3-68877

neutron diffraction examination of materials continued

- liquid crystal, nematic PAA, determ. of phase diagram 3-40847
 liquid crystals, homogeneously oriented nematic, cold neutron incoherent scattering 3-79225
 liquid metal, coherent and incoherent scatt., relation 3-49832
 liquid metal, paracrystalline distortions, cause 3-49830
 liquid metal and alloy, struct., review 3-49821
 liquid metal struct. and pair potentials, relation 3-49824
 local spin fluctuation system, neutron inelastic scatt. theory 3-55420
 magnetic structures, ordered, from unpolarised neutron diffr. data 3-52978
 magnetic susceptibility at 62 K, antiferromagnetic ordering 3-47066
 MBBA, rotational correlation times estimation 3-68156
 9-methyladenine.1-methylthymine complex, hydrogen bonding, struct. determ. by neutron diffraction 3-64022
 molecular fluids, ang. correl. effects 3-57979
 molecular motion studies, physico-chemical aspects, review 3-57645
 molecular solids and liqs., tool for mol. motion obs., review 3-68140
 n-nonadecane, rotator phase transition, inelastic neutron scattering study 3-49853
 n-octane, solid, low frequency mol. vibrations by neutron inelastic scattering 3-75577
 organic crystal, phonon dispersion and molecular rotation obs. (German) 3-60679
 PAA, rotational correlation times estimation 3-68156
 n-pentane, solid, low frequency mol. vibrations by neutron inelastic scattering 3-75577
 phenol, molecular rotation study by neutron scattering and n.m.r. 3-52567
 phonon measurement, three axis spectrometer, counting rate optimisation (German, English) 3-63932
 polypropylene oxide and deuterated derivative, dynamics, spin lattice relax. and neutron scatt. 3-67880
 rare earth compounds, Tm_2O_3 , ($T=Nd, Tb, Er$), sinusoidal and helical mag. structs. (French) 3-44223
 rare earth-Al-Fe(Co) alloys, ordering obs. 3-79273
 rare earth-aluminium intermetallics, Re-Al₂ type 3-50375
 silica glasses: TiO_2 , small angle neutron scattering for inhomogeneous structure obs. 3-68169
 spin translation groups, analysis and tabulation 3-79843
 steel, hardened, martensite atomic and mag. struct. 3-41742
 superconductor, A15 compound, neutron scatt. investigation of Fermi surface 3-46926
 superconductor, type II, magnetic field distrib., microscopic, of mixed state 3-72414
 ternary selenides, MFe_2Se_4 , magnetic moments rel. to 3d-electron delocalization (French) 3-72550
 tetramethylammonium manganese chloride, cation rotational motion 3-49855
 transition metal tantalates, $MeTaO_4$, atomic and mol. ordering, mag. structure from 4.2 to 300K 3-79849
 trifluoroacetic acid, crystal structure determ. 3-50572
 Zeise's salt and related complexes, determ. of torsional potential for ethylene ligands 3-54656
 $Ag_2H_3IO_6$, incoherent neutron scatt. and antiferroelec. modes 3-47222
 $Ag_4H_2O_{10}$, incoherent neutron scatt., assignment of vibrational modes 3-47222
 Al, liq., struct. factor determ. 3-63947
 Al-Mg alloys, Al-rich, preprecip. phenomena, Guinier-Preston zones (French) 3-80242
 Al-Mn dil. alloy, Kondo state, thermal neutron scatt. obs. (Hungarian) 3-55424
 Ar, at 85K, liquid struct. factor and radial distrib. function 3-46585
 AuMn alloys, antiferromagnetic ordering in t_2 phase, magnetic structure 3-47040
 Ba_2CoReO_6 , antiferromag. spiral struct. obs. 3-47058
 $BaAl_2Fe_2O_7$, ferrite cryst. struct. detn. 3-58022
 Ba_2MREO_6 , $M=Mn, Fe, Ni, Co$, solid-state synthesis and mag. props. 3-75829
 Br₂, liquid, high momentum transfer struct. factor, T-O-F neutron diffr. obs. 3-79224
 Ca_2Fe , anharmonic lattice vibrs., phonon-energy half width 3-52678
 Co-Fe asphericity of 3d electrons, concentration and temperature dependence, polarised neutron technique 3-41150
 Co-Fe single crystal, magnetic domain struct., polarised neutron obs. 3-72489
 Co-Ni asphericity of 3d electrons, concentration and temperature dependence, polarised neutron technique 3-41150
 Co-Ti-based Heusler alloys, mag. and chem. order 3-68791
 $(CoMn)_{1-x}Fe_x$, antiferromag. spin structure and atomic ordering obs. 3-58387
 Cr-Fe alloy, magnetic excitations in paramagnetic phase 3-41329
 $CrAs_{1-x}Sb_x$, mixed crystal, helimagnetism, mag. structure 3-41347
 CrSe, spin translation groups, umbrella arrangements 3-79843
 CsF, normal phonon dispersion, neutron coherent inelastic scatt. obs. 3-79445
 $Cs_2LiM(CN)_6$, ($M=Cr, Mn, Fe, Co$), cryst. struct. 3-79294
 $CsMnBr_3$, antiferromag., mag. ordering obs. 3-47060
 $CsNiF_3$, Neel temp. and three dimensional struct. obs. 3-44219
 $CsSH$, rot. dynamics and phase transitions, neutron scatt. investigation 3-40852
 $CsSH$ in cubic phase, SH- reorientation, neutron quasielastic scattering study 3-46597
 Cu, liq., collective excitations, neutron scatt. study 3-49833
 Cu, phonon distrib. function, slow neutron inelastic scatt. (Russian) 3-68354
 Cu-Mn alloy, antiferromag., short range order, temp. and heat treatment effects obs. 3-47059
 Cu-Sb liquid alloy, structure, combined neutron and X-ray diffraction obs. 3-52566
 CuF_2 , chemical and magnetic structure determ. (German) 3-50374
 $Co_0.5Mn_{0.5}Fe_2O_4$ cationic distrib., oxygen parameter, mag. moment 3-68224
 DCl, solid, obs. of mol. libration 3-68380
 $Er_{0.75}Lu_{0.25}$, mag. struct., transitions to c-axis longit. spin wave, antiferromag. conical structs. 3-79847

neutron diffraction examination of materials continued

- Eu, first order transition at 90.5K in applied mag. field, antiferromag. ordering 3-58384
 Fe, neutron magnetic disorder scatt. cross section for 3 at % impurities, temp. depend. 3-64506
 Fe, phonon distrib. function, slow neutron inelastic scatt. (Russian) 3-68353
 Fe, phonon distrib. function, slow neutron inelastic scatt., 24-874°C (Russian) 3-72151
 Fe-Ni, Invar, mag. diffuse scatt. of neutrons 3-68788
 Fe-Pt alloy, ordered equiatomic, mag. and atomic struct. (Russian) 3-68787
 Fe-Si single crystal, magnetic domain struct., polarised neutron obs. 3-72489
 $FeCl_3 \cdot 2H_2O$, antiferromag., ferrimag. and ferromag. phases, metamag. behaviour 3-58383
 FeCo alloy, ordered and disordered, mag. moment distrib. 3-47062
 Fe_2GeS_4 , mag. struct. (French) 3-47052
 Ga, liq., coherent and incoherent scatt., relation 3-49832
 Ga, liq., collective excitations, neutron scatt. study 3-49833
 Ga, liquid, coherent inelastic scatt. obs. of dynamic structure factor in supercooled state 3-49834
 $GaMn_3Co_{0.935}$, n.m.r. and neutron diffr., mag. struct. changes (French) 3-79924
 Ge, Laue diffraction, neutron Pendellosung fringe structure 3-43734
 Ge forbidden (222) neutron reflection, anharmonicity in nuclear motion 3-68352
 H gas, by neutron scatt. (German) 3-60504
 H-Ar liquid mixture, by neutron scatt. (German) 3-60504
 HCO_2 , energy loss neutron inelastic scattering spectra 3-60775
 $HCrO_2$, energy loss neutron inelastic scattering spectra 3-60775
 3He - 4He liquid mixtures, neutron inelastic scattering studies 3-60826
 4He , superfluid, inelastic neutron scatt. from free surface, ripplon spectrum 3-68463
 4He liquid, structure and excitations, review 3-58158
 Ho, rel. to theory of diffr. by mag. spiral structs. 3-47068
 HoAg, Neel temp. and mag. struct. obs. 3-47057
 $HoZn_2$, magnetocrystalline anisotropy, applied field effect on sinusoidal mag. structure 3-60972
 ^{165}Ho , neutron scatt. amplitude spin depend. part, obs. from 4.2-1.4 K (French) 3-50377
 KCl, Bragg reflection, integrated intensity measurements at room temp. 3-64128
 $KCuF_3$, one-dimens. antiferromagnet, intra-, interchain exchange interactions 3-68789
 K_2CuF_4 , two-dimens. ferromag., Heisenberg symm. 3-79845
 K_2MnF_4 , critical mag. scattering 3-72474
 $KNbO_3$, cubic-tetragonal-orthorhombic-rhombohedral ferroelectric transitions, profile refinement technique 3-64609
 $K_2Pt(CN)_4Br_{0.3} \cdot 3H_2O$, one-dimensional conductor, giant Kohn anomaly observation 3-43849
 Kr, short range triplet correlations, near critical point 3-75462
 Kr, solid, elastic const. data comparison from Brillouin and neutron scattering meas. 3-55033
 Kr solid, zero-sound elastic const., 114K, from phonon dispersion data 3-40952
 $LaAlO_3$, inelastic neutron scatt., soft phonon response function 3-55070
 $LiAlH_4$, lib. motion, inelastic neutron scatt. obs. 3-60678
 LiCl, aq. soln., neutron and X-ray diffr. struct. examination 3-43745
 $Li_{0.5}Fe_{0.5-x}Ga_{0.4}$, ferrite, crystal field constants and O parameter 3-79848
 $LiNO_2$, D-atom position determ. (German) 3-75501
 Lu, high purity, physical and metallurgical properties 3-63981
 $MgCr_2O_4$, off-centre displacement of Cr^{3+} ion 3-68228
 Mn-Fe-Ti-O spinel system, ion distrib. among lattice sites 3-75502
 MnB_2 , antiferromag. struct. and Neel temp. obs. 3-47055
 Mn_3CuN , mag. struct. and behaviour (French) 3-47048
 MnF_2 , antiferromag., transverse K-dependent susceptibility detn. 3-41333
 $Mn_{1-x}Fe_xAs$ phase, crystal structure, mag. props. 3-40901
 $Mn_{0.5}Fe_{0.5}Si_3$, at. and mag. struct. determ. 3-68792
 MnO powder method, magnetic form factor of Mn^{2+} experimental results and corrections, theoretical comparison 3-44221
 MnO antiferromagnet, low temperature, spin waves, neutron inelastic scatt. technique, dispersion relations 3-52982
 Mn_3SnC , mag. struct. and behaviour (French) 3-47048
 NH_4Cl , phase II, reorientational motion of NH_4^+ ions, neutron scatt. obs. 3-68173
 $NH_4H_2PO_4$, $NH_4H_2AsO_4$, $(NH_4)_2H_3IO_6$, antiferroelectric, NH_4 motion obs. 3-79996
 Na, liquid, inelastic scatt. obs. for dynamic structure factor calcs. 3-49835
 $NaAlH_4$, lib. motion, inelastic neutron scatt. obs. 3-60678
 NaSH, rot. dynamics and phase transitions, neutron scatt. investigation 3-40852
 Nb, superconducting, dirty, microscopic magnetic field distrib. 3-46923
 Nb, superconducting, misalignment of flux lines 3-64435
 $Nd(OH)_2Cl$, cryst. struct. 3-49884
 Ni, inelastic scatt. of slow neutrons, isotopic comp. effects (Russian) 3-40837
 Ni-Cu alloys, behaviour of localised moment of Ni 3-72475
 $Ni_{0.9}Cu_{0.1}Mn_{0.5}Sb_{0.5}$ atomic and magnetic-structure, X-ray and neutron diffraction, magnetometry, $0.05 \leq x \leq 0.4$ 3-49870
 $Ni_{0.86}Fe_{0.14}$ alloy, magnetic excitation peaks, spin waves 3-79857
 $NiFe_2 \cdot Al_2O_3$ ferrite, magnetic structure, crystallographic structure, influence of Al content, neutron diffraction examination 3-52980
 $Ni_3B_2O_{13}$, boracite, mag. struct. (German) 3-50376
 NiO, antiferromag.-paramag. transition, crit. behaviour of spontaneous magnetisation 3-58382
 $NiTiO_4$, solid solns. with $NiFe_2O_4$, Fe_2O_4 , cationic distrib. in spinel struct. 3-72454
 NpN, antiferromag., spin structure detn. 3-41348
 NpP, antiferromag. ordering at 130K in ferromag. sheets, neutron and Mossbauer obs. 3-72473

neutron diffraction examination of materials continued

- Pb, liquid, inelastic scatt. obs. for dynamic structure factor calcs. 3-49835
 5PbO.3GeO₂, ferroelec., struct. obs. 3-68226
 Pd-Ag alloy, localized modes of interstitial H, scatt. study 3-55063
¹⁴⁷Pm, mag. struct. 3-50373
 Rb, liq., coherent and incoherent scatt., relation 3-49832
 Rb, liq., collective excitations, neutron scatt. study 3-49833
 Rb₃CoF₄, two-dimensional Ising antiferromagnet, neutron diffraction obs. of critical behaviour 3-75837
 RbMnBr₃, antiferromag. struct. obs. 3-47056
 RbSH in cubic phase, SH⁻ reorientation, neutron quasielastic scattering study 3-46597
 Si, perfect single crystals, backscatt. obs. (German) 3-63933
 Si, rocking curve of vibrating single crystal, neutron diffraction 3-40836
 SiC, reaction-sintered, growth characs., polytype distrib., 6H₂ struct. absence 3-76299
 Sm, magnetic scatt. amplitudes, approx. ground states 3-50372
 Sn, liquid, structure analysis, time of flight neutron diff. obs. 3-68149
 SrTb₂Fe₂O₇, ferrite, cryst. struct. detn. 3-58022
 SrTiO₃, neutron scatt., microscopic theory for central peak 3-55060
 Tb-light rare earth alloys, mag. and cryst. struct. 3-68790
 TbZn₂, magnetocrystalline anisotropy, applied field effect on sinusoidal mag. structure 3-60972
 Th phonon spectrum, temp. dependence of Debye temp. 3-58092
 ThFe₁₇, magnetic structure determ. 3-47067
 Th(Fe_{1-x}Co_x)₅, magnetic structure determ. 3-47067
 Ti bonded with finely cryst. diamond particles, ω-Ti phase obs. (Russian) 3-73010
 TiNb₂O₇, powder neutron diffraction determ. of cation distribution 3-60713
 ortho-Ti₂Nb₁₀O₂₉, powder neutron diffraction determ. of cation distribution 3-60713
 Tm_{0.25}Y_{0.75}Al₂ crystal field spectroscopy, paramagnetic phase, energy distribution, field parameters 3-52955
 UCl₄, anhydrous, crystal structure obs. 3-68207
 UO₂Cl₂, structure from powder neutron diffraction 3-43768
 U₂P₄, mag. struct. determ. 3-68793
 UTe magnetic moment, hyperfine field by Mossbauer spectroscopy, temp. depend., magnetic ordering 3-44356
 V-Mn-Ga alloys, magnetic structure investigations, Curie temp. 3-47065
 VC_{0.75}, short-range ordered, diffuse scattering, neutron diffraction studies 3-40914
 V₂D, V₄D₃, crystal structure determ. between 5K and 425K structural transitions 3-46710
 Xe, solid, phonon frequency measurement by inelastic neutron scattering dispersion curves 3-64120
 XeO₂F₂, cryst. struct. and symmetry determ. by neutron diffraction 3-54946
 YFe_{0.8}Mn_{0.2}O₃, spin reorientation, Mossbauer and neutron diff. obs. 3-55434
 ZnGeN₂, ordering of Zn, Ge atoms (French) 3-79314
 ZnMn₃C, n.m.r. and neutron diff., mag. struct. changes (French) 3-79924
 ZnV₂O₄ spinel, magnetic structure investigation at 4.2 K and 293 K 3-60969
 Zr, cold-rolled sheets, texture determ. 3-64847
 ZrO₂, Sc₂O₃-stabilized, high temperature, phase equilibria studies 3-64150
 ZrSiO₄, anisotropic thermal expansion and compressibility, high temp. and high pressure X-ray diffraction, neutron diffraction 3-46721

neutron diffusion

- see also neutron flux
 asymptotic diffusion theory, analytic transient flow expression 3-54526
 bimodal criticality distributions in few group analysis 3-63108
 BWR, difference eqn. by semi-analytic method, coarse mesh model 3-71165
 BWR, two- and three-dimensional calcs. of superprompt critical excursion 3-46090
 criticality distrib. in group-collapsed neutron diffusion theory 3-49333
 criticality problem, optimum eigenvalue bounds 3-46051
 decay constant, effect of assembly shape in pulsed-neutron expts. multigroup eqn. soln. 3-63110
 depletion of system containing lumped poison, few-group diffusion theory versus many-group S_n approx. 3-49332
 EBR-II, experimental subassemblies, radial position, axial effects on nuclear props., diffusion theory code 3-71219
 EBR-II neutron shield system, diffusion and transport theory calcs. for deep penetration spectra 3-74687
 eigenvalue bounds, optimum, determ. using iterative method 3-67386
 energy dependent spatial mesh approximation, static few-group diffusion equations, coupling via scattering and fission 3-63118
 equation soln. using finite elements and finite differences methods 3-67389
 extrapolated endpoints in two-group theory 3-74627
 fast reactor SNEAK assemblies, exptl. and theoretical results for reactivity 3-71188
 fast reactor ZPR-6 assemblies, resistivity calcs. using Karlsruhe methods and data 3-71183
 fast reactors, analogy between thermal diffusion and continuous slowing down of neutrons 3-49334
 finite element analysis, nuclear reactor design, nuclear diffusion and transport calc. 3-63112
 finite element analysis, two-dimensional diffusion, effects of discontinuous props., smooth polynomials 3-63113
 finite element system in curvilinear co-ordinates 3-46048
 flux synthesis calculations, fast reactors, multidimensional diffusion theory problems 3-63115
 heterogeneous media, image pile theory and effective diffusion coefficients 3-63104
 heterogeneous non-multiplying plate assemblies, diffusion lengths determ. 3-60241
 infinite lattice fluxes, diffusion equation, cell homogenisation, rigorous treatment 3-71150

neutron diffusion continued

- in inhomogeneous atm., diffusion from distributed source 3-56265
 LMFBR demonstration plant benchmark control rod expts. 3-49350
 LMFBR Doppler coeffs., transport effects, comparison of diffusion and transport codes 3-49329
 LWR core simulator PRESTO, characteristics and performance 3-49364
 multidimensional kinetic problems, diffusion theory, state-of-art 3-71151
 multigroup approach to neutron wave propagation in finite graphite assemblies 3-74626
 multigroup diffusion coeffs., reactor design and analysis using transport theory calcs. 3-67387
 multigroup diffusion theory, energy-depend. buckling concept 3-60243
 multigroup theory for neutron wave propagation through subcritical assembly 3-71143
 multimode reactor kinetics eqns. new soln. method by matrix inversion 3-54524
 non-uniform reactor systems, rigorous diffusion model for cell homogenization 3-40526
 nuclear reactor fuel Interim Decay Storage Facility, upper Pu limit, transport and diffusion theory calc. 3-71298
 nuclear reactors, finite element analysis in space energy and time domains 3-74655
 one-dimensional eqn., analysis using CAIN computer code 3-71158
 one-group model, neutron burst decay in pulsed expts. in lattices 3-71144
 optimal source projection method 3-71152
 organic substances, thermal, static method used with plane source and Al container 3-63106
 radial coeffs. from perturbation flux distrib. in systems with anisotropies 3-49357
 reaction rate distrib. in ZPR-6 assembly 7, comparison of calcs. and meas. 3-71186
 slowing down of pulsed neutron, time- and space-depend. asymptotic behaviour 3-60242
 space-time diffn. theory, applic. of subcritical pulsed-neutron expts. 3-49324
 thermalization in H₂O-D₂O mixtures, 253-4K, pulsed neutrons and steady-state spectra 3-43268
 transport and diffusion theory comparison from calc. of minimum critical mass 3-46050
 uniform source half-space problem, extrapolated endpoint, Wiener-Hopf technique 3-43270
 wave propagation in multiplying media, reflector effect 3-74661
¹³⁴Cs, Peach Bottom HTGR D1305 fuel element, diffusion coeff., activity profile 3-74738
¹³⁷Cs, Peach Bottom HTGR D1305 fuel element, diffusion coeff., activity profile 3-74738
²⁴⁰Pu zoned critical expts., analysis in support of LWR-grade Pu utilization in FTR's 3-71187
⁸⁹Sr Peach Bottom HTGR D1305, fuel element, diffusion coeff., activity profile 3-74738
⁹⁰St, Peach Bottom HTGR D1305, fuel element, diffusion coeff., activity profile 3-74738
²³⁵U, crit. mass eval. using energy-depend. buckling concept. 3-60243
- neutron economy** see neutron flux
- neutron effects**
 see also nuclear reactions and scattering due to neutrons
 alloy, b.c.c., fast reactor neutron irradi., tensile props. 3-79386
 alloy, b.c.c., neutron irradi. temp. effect on hardness 3-79387
 alloy, irradi. creep during void form. 3-40939
 cathodes, irradi., high temp. emission characs., stability increase (Russian) 3-72785
 cellular response to fast neutrons 3-66052
 ceramic, point defect prod., detection and annealing 3-58052
 ceramic/metal bonded specimens, fast neutron irradi. induced swelling 3-78375
 cladding materials, void nucleation suppression by vacancy trapping mechanism 3-63200
 coated fuel particles in a HTR, transport behaviour and fission product profile determ. (German) 3-71320
 coated reactor fuel particles, rel. to life expectation in HTR (German) 3-71318
 controlled thermonuclear reactor radiation damage studies, neutron flux spectra 3-60253
 creep rates in fast reactor, eqn. predictions 3-43303
 creepage of nuclear fuels under neutron irradiation up to 1000°C (German) 3-71324
 damage and heating due to neutron and gamma fluxes, data library compilation (German) 3-67630
 α-Fe, irradi. defect annealing, computer anal. 3-79346
 ferromagnet, mag. moment reversal, switching vel., density 3-72476
 fissile materials, computerized nondestructive neutron interrogation technique for safeguards application 3-46072
 fusion reactor blanket design features, choice of constructional materials 3-67584
 fusion reactor blankets, calcs. of space dependent neutron and gamma heating rates 3-60328
 fusion-fission hybrids, subcritical thermal fission blanket, neutronic characteristics 3-60274
 GCFR rod irradiations, volatile fission product migration and plateout 3-46160
 graphite, calc. of expansion for low concentration of vacancies (Spanish) 3-64070
 graphite, creep, press. loading, 500-800°C (German) 3-71264
 graphite, dimensional instability, density changes (German) 3-71256
 graphite, irradi., thermal annealing effect on Young's modulus 3-67554
 graphite, low temp. irradiation, dimensional changes (German) 3-71262
 graphite, neutron activation analysis, impurity determ., gammaspectra 3-52638
 graphite, neutron irradiated, thermal cond. meas., 50 to 1000 C 3-46648

neutron effects continued

- graphite, pressure depend. of C-axis elastic parameters, effect of fast neutron irradiation 3-79404
- graphite, pyrolytic, defect struct., 1000-1500°C (*German*) 3-71253
- graphite, pyrolytic, g-factor anisotropy and e.p.r. linewidths, 300-4.2K, neutron irradi. effects (*French*) 3-47124
- graphite, pyrolytic (CAPG), elastic consts., press. depend., 0-7 kbar (*German*) 3-73037
- graphite, radiation damage, vacancies, interstitials, X-ray obs. (*German*) 3-71255
- graphite, radiation stability in high temp. reactors (*German*) 3-71259
- graphite, reactor, mechanical strength (*German*) 3-71275
- graphite, reactor, tensile stress expansion (*German*) 3-71263
- graphite, shrinkage, dimensional changes (*German*) 3-71261
- graphite, thermal expansion, high temp. (*German*) 3-71257
- graphite moderator, radiation effects in reln. to role in fusion reactors 3-60331
- graphite powder, high temp. reactor fuel pressings, struct., grain size distrib. (*German*) 3-71268
- graphite reactor material from gilsonite coke, dimensional stability, thermal cond. (*German*) 3-71260
- high-fast neutron doses, effect on graphite 3-67457
- high-temperature gas-cooled reactor fuels, performance at peak irradi. 3-63204
- laser using gamma quantum emission, two-stage excitation of nuclei by neutrons 3-74222
- Lung-equivalent material for fast neutron dose distribution studies 3-70138
- matrix materials, die-pressed, for HTR fuel elements, influence of manufacturing parameters (*German*) 3-67599
- metal, b.c.c., effect on tensile props. 3-79386
- metal, b.c.c., low temp. neutron irradi. effects, annealing recovery depend. 3-79381
- metal, b.c.c., neutron irradi. damage effect on mech. props. 3-79380
- metal, b.c.c. neutron irradi. temp. effect on hardness 3-79387
- metal, irradi., dislocation loop nucleation 3-40938
- metal, irradi., void nucleation kinetics, impurity effects 3-64072
- metal, irradi. creep during void form. 3-40939
- metal b.c.c., neutron irradi., defect clusters rel. to impurity atoms 3-79334
- metals, high-temp. void formation, dislocation vibration as cure 3-40941
- metals, neutron irradiated, role of depleted zones 3-52644
- microporosity meas. of graphite matrix material and pyrocarbon in HTR fuel elements (*German*) 3-71319
- mixed-oxide fuel elements, burnup measurement, EBR-II, ¹⁴⁸Nd analyses, comparison with neutronics calc. 3-67572
- monitor for high-level flux-spectra-fluence characterization, prep. and handling 3-46166
- mouse liver, effect of variations in LET and cell cycle on radiation hepatocarcinogenesis 3-66057
- Mylar, reactor irradi., on dielec. loss peaks, crystallinity 3-68923
- neutron irradiation softening and effect of interstitials 3-79343
- nuclear fuel element, spherical, mechanical strength (*German*) 3-71265
- nuclear reactor adhesive matrix material (*German*) 3-71270
- nuclear reactors, environmental atom implantation into solids by neutron collisions in reactors 3-60272
- nylon, reactor irradi., on dielec. loss peaks, crystallinity 3-68923
- oxide fuel pin irradiated in fast neutron flux, computer calc. of temp. and density profiles 3-67454
- oxide nuclear fuel, vacant space distribution analysis during irradiation (*German*) 3-71322
- perfluoromethylcyclohexane, dependence of radiolysis on dose, O₂ content, temp. and radiation type (*German*) 3-69481
- Permalloy, mag. texture influence on resist. to irradi. and temp. variations (*Russian*) 3-50406
- personnel albedo neutron dosimeter, TLND, response to neutrons of energy ≤ 400 MeV 3-52238
- pressed matrix, nuclear reactor fuel elements, dimensional stability (*German*) 3-71269
- propene-pyrocarbon layers, flat, structural changes, porosity meas. and crystal growth (*German*) 3-67600
- quartz, crystalline, colouration changes and position of absorption max, with dosage (*Russian*) 3-64702
- r.b.e. and o.e.r. values, neutron spectrum dependence 3-59453
- reactor fuel, faceted bubble transport kinetics 3-43295
- reactor graphite, radiation damage, vacancies 600-1400°C (*German*) 3-71254
- reactor matrix material, microporosity, annealing effect (*German*) 3-71252
- rocket solid propellant burning, effect of neutron irradi., safety analysis 3-49322
- space-time diffn. theory, applic. of subcritical pulsed-neutron expts. 3-49324
- stainless steel, austenitic, fracture surfaces, Auger spectroscopy 3-69248
- stainless steel, cold-worked, neutron irradiated, void formation, effect of irradiation temp. 3-68289
- stainless steel, fast neutron irradiated, fatigue crack propagation 3-6296
- stainless steel, reactor fuel, performance in Indian Point Unit No. 1, average burnup values 3-67569
- stainless steel, Young's modulus, effect of neutron irradiation-induced void formation 3-68310
- steel, ASTM A533-B, fatigue crack prop. behaviour 3-44611
- steel, austenitic, containing Nb, irradi. induced swelling, influence of quenching conditions (*French*) 3-40538
- steel, austenitic stainless, irradi., with Ti and B additions, high-temp. deform. and fracture 3-63188
- steel, embrittlement and annealing after irradiation, model based on Davidenkov criterion 3-72914
- steel, irradi. effect on elastic moduli 3-69272
- steel, stabilised, fast reactor fuel cans, influence of damage on performance (*German*) 3-71304
- steel, stainless, irradi. effect on elastic consts., ultrasonic technique 3-78386
- steel, stainless, stressed during irradi., microstruct. obs. 3-69245

neutron effects continued

- steel, stainless, Type 316, cold-worked Frank loop development, irradi. effects 3-44576
- steel, stainless, Type 316, irradi., stress-biased loop nucleation 3-67553
- steel, X18H10T, meas. of corrosion kinetics under n, γ -radiation in N₂O₄ 3-40546
- swelling, high temp., stress depend. 3-67548
- swine, 14 MeV neutrons, dosimetry and clinical response 3-53758
- total-body Ca determ. in humans by measuring ³⁷Ar in expired air after neutron irradiation 3-66025
- voiding ratios in 16 Cr-13 Ni-Nb stabilised steel at 350 to 550°C, fast neutron irradiation (*German*) 3-71303
- volume creep, non-conservative, under different stress states, discussion of original paper 3-61171
- Zircaloy-2 pressure tubes, Hanford N reactor, monitoring, changes in material props., H content 3-67564
- Al, irradi. void form., deform. influence and dislocation density depend. (*French*) 3-40940
- Al, pure, neutron irradi., He migration, effects of temp. and temp. gradients 3-64217
- Al:⁵⁷Co, neutron irradiated and annealed, Mossbauer study of interstitial trapping 3-58454
- Al₂O₃, fast neutron damage effects 3-78373
- α -Al₂O₃, reactor-irradi., F⁺-centres, e.s.r. obs. 3-41409
- Al₂O₃/Nb bonded components, stresses due to irradi. swelling of alumina 3-78374
- Al₂O₃-GaAsP m.i.s. structure, flatband voltage shift obs. 3-50277
- Al₂O₃-Si m.i.s. structure, flatband voltage obs. 3-50277
- BeO, irradi. sintered, He gas release and diffusion processes (*German*) 3-57568
- C, pyrolytic, coating (*German*) 3-71248
- C, pyrolytic, coating of fuel particles, anisotropy change, radiation damage (*German*) 3-71251
- C, pyrolytic, coating of nuclear fuel particles, structure, annealing effect (*German*) 3-71250
- C, pyrolytic, thermal cond. after fast neutron irradi., high-temp. reactor appl. 3-49367
- CO₂ quasistationary atmospheric press. laser, non-maintaining discharge controlled by neutron flux 3-70806
- ¹⁴C, sepn. from neutron-irradi. AlN by dry procedure 3-44739
- CaF₂, F-centre prod., absorpt. spectra, reactor irradi. 3-68252
- CeO₂, yttria-stabilized, fast neutron damage effects 3-78373
- CoPt, radiation damage, Mossbauer effect obs. on ¹⁹⁷Au 3-79958
- Cu, irradi. single crystals, slip phenomena 3-79377
- Cu, neutron irradi., fast vs thermal neutrons, defect production, elec. cond. monitoring 3-64073
- Cu, proton, neutron and fission neutron damage comparison 3-72105
- Cu-Ni alloys, void form. resist. 3-67547
- α -Fe, Mossbauer obs. of low temp. radiation damage 3-64587
- Fe, neutron irradi., fast vs thermal neutrons, defect production, elec. cond. monitoring 3-64073
- Fe, neutron-irradiated, mag. after-effect rel. to impurity-interstitial processes 3-44347
- Fe low temperature irradiation effects on deform. characts. 3-79376
- Fe-C alloys, irradi. defects influence on mag. after effects (*Russian*) 3-79872
- Fe₃Al, primary recoil atom spectra and damage cross-section 3-60747
- GaAs, fast neutron irradi., Franz-Keldysh effect 3-80009
- GaAs, on edge cathodolum., carrier lifetime 3-61079
- GaAs, on wavelength modulated and electroreflectance spectra 3-55629
- GaP:N, interstitial N defect form. on fast neutron or 2 MeV electron irradi. 3-46638
- Ga₂Te₃, unstable equilibrium and radiation defects 3-52645
- Ge, effect of neutron irradiation and B doping on X-ray diffraction 3-68286
- H₂ para to ortho conversion by gamma and neutron irradiation for nuclear propulsion 3-63154
- HgSe(Te), reactor irradi. solid solutions, electrophysical parameters 3-64071
- In₂Te₃, unstable equilibrium and radiation defects 3-52645
- KBr, stored energy meas. after 4.6K reactor irradi. 3-54984
- KCl, activation energy anal. after reactor irradiation 3-79378
- K₂SO₄, neutron irradiation effects on single crystals 3-79379
- LiF, macropore production due to thermal neutron and electron irradiation (*Russian*) 3-68288
- LiF crystal, F-like centre prod., e.p.r. obs. 3-79912
- LiNbO₃, neutron irradiation effects on single crystals 3-79379
- Mo, irradiation damage, influence of dislocations 3-68269
- Mo, neutron irradi., internal friction and dynamic modulus relax. peaks due to stage I defects 3-54983
- Mo, neutron irradiated, irradi. temp. monitoring, void superlattice const. meas. 3-68291
- Mo, neutron irradiated, void formation, lower threshold temp. 3-68290
- Mo, neutron irradiation and plastic deformation, recovery model critical testing 3-79382
- Mo, reactor irradi., 650°C, damage struct. 3-46649
- NaNO₃, neutron irradiation effects on single crystals 3-79379
- Nb, irradi. hardening, oxygen impurity effects, defect agglomeration 3-40937
- Nb, recovery after fast neutron irradiation at low temp. 3-68287
- Nb₃Sn, field, angular and defect dependence of critical current for $t \leq 4.2$ K 3-44168
- Ni, neutron irradi., fast vs thermal neutrons, defect production, elec. cond. monitoring 3-64073
- Ni₃Mn alloy, ordered, elec. resist. changes on fission fragment bombardment (*Russian*) 3-58242
- Pb_{0.95}Si_{0.05} (Zr_{0.53}, Ti_{0.47})O₃ + 3 wt.% PbO, ferroceramic, irradi. effects on mech. loss (*Russian*) 3-53065
- Pd, neutron irradi., fast vs thermal neutrons, defect production, elec. cond. monitoring 3-64073
- Si₃O₄, on adsorption of PO₄³⁻ ions 3-46756
- Si, carrier lifetime radiation const. rel. to neutron spectrum 3-44078
- Si, effect of neutron irradiation and B doping on X-ray diffraction 3-68286

neutron effects continued

- Si, p-n junctions characterisation of induced defects, thermally stimulated meas. capacitance and current 3-41257
 Si:Li, irradiated, spectra of Li-defect complexes 3-44434
 Si:P, slow neutron irradiation, uniform standard specimens, resistivity meas. accuracy check 3-47353
 SiC, irradi. induced defects, TEM specimen prep. by ion-bombardment thinning 3-57977
 SiC, pyrolytic, fuel particle coating, fast neutron damage simulation using h.v. electron beam 3-49368
 β -SiC, pyrolytic, irradi., thermal cond. 3-40539
 β -SiC, pyrolytic, irradi. induced void behaviour 3-63191
 SiC, Si-bonded, fission fragment irradi. effect on passive oxidation, 950°C 3-67551
 Sn chalcogenides, radiation defects generated by (n, γ) reaction 3-72556
 Su, diffuse scatt. by radiation prod. defects, meas. in anomalous transmission and near Bragg refl., comparison 3-43727
 Ti, annealed, irradi. effect on Bauschinger effect 3-64945
 Ti, neutron irradi., fast vs thermal neutrons, defect production, elec. cond. monitoring 3-64073
 Ti:⁴⁷Sc corrosion of Ti, radiometric study 3-42703
 Ti:Mn(W)(Cu)(Mo)(An), neutron activation anal. 3-42703
 (U, Pu)O₂ mixtures, exptl. examination after irradiation in HWR (*German*) 3-67614
 (U,Pu)O₂, LMFBR fuel rods, thermal and mech. eval. of oxide microstruct. 3-78381
 (U,Pu)O₂ fuel, irradi., O/M ratio effect on Pu redistrib. 3-46147
 (U,Pu)O₂ fuel rods, irradi., Pu and U diffusion 3-46143
 (U,Th)O₂ fuel particles, pyrolytic-graphite coated, creep deformation, 800-1200°C following irradiation (*German*) 3-71314
 U, alpha type, tear formation and growth in irradiated sample, effect of internal stress 3-63205
 UAl₃-Al micrographs showing structures in irradiated nuclear reactor fuel plates (*German*) 3-71321
 UAl₃-Al, micrographs showing structures in irradiated nuclear reactor fuel plates (*German*) 3-71321
 UC, fission-enhanced self-diffusion of uranium 3-71281
 UC, irradi., microprobe obs., precipitate distrib. (*German*) 3-57567
 UC-graphite compacted neutron target (*German*) 3-71258
 UC₂-ThC₂ spherules pyrolytic C encased, HTGR fuel element neutron irradiation (*German*) 3-71266
 UO₂, fission-enhanced self-diffusion of uranium 3-71281
 UO₂, in-reactor radiation induced creep behaviour 3-54543
 UO₂, irradi., morphology and growth rate of interlinked porosity 3-43306
 UO₂, surface fission tracks, replica electron microscopy obs. 3-63187
 UO₂, thermal-gradient migration of helium bubbles 3-67552
 UO₂, Zircaloy clad, fuel rods, fuel performance, hydride attack 3-67570
 UO₂ coated particles, exptl. determ. of effective resonance integral and Doppler effect in I/E neutron spectrum 3-43273
 UO₂ pellets, crack sintering rates meas. 3-46144
 UO₂-PuO₂ fuel pins, irradi., oxygen pot. gradient 3-63189
 UO₂-ThO₂-(Th,U)O₂ sol-gel-oxide, reactor fuel element manufacture and testing (*German*) 3-71266
 V, recovery after fast neutron irradiation at low temp. 3-68287
 V:O neutron irradi., and radiation anneal hardening, recovery and temp. depend. 3-79383
 V-Ti, and V interstitial alloys, neutron irradi., anneal hardening 3-79384
 V-Ti, neutron irradi. effect on high temp. mech. props. 3-79385
 W, neutron irradiated, irradi. temp. monitoring, void superlattice const. meas. 3-68291
 W, neutron irradiated, void formation, lower threshold temp. 3-68290
 Y₂O₃, zirconia-stabilized, fast neutron damage effects 3-78373
 Zr, irradi., resist. changes, recovery changes 3-69288
 Zr, irradi. at 24K, point defect creation and elimination (*French*) 3-52643
 Zr alloys, irradi., stress-relax. rel. to creep rates 3-40541
 Zr alloys, pressure tubes, creep, effect of neutron flux anisotropy rel. to stress directions 3-67565
 Zr and alloys, cold work and stress-relieving effect on irradi. growth behaviour 3-41773
 Zr₃Al₃, fast neutron irradi., disordering 3-49909
 ZrC irradiation effects, structure, properties 3-73016
 ZrO₂, yttria-stabilized, fast neutron damage effects 3-78373

neutron flux

- age calc., extended planar source expts., validity 3-74632
 AGR heterogeneous core calcs., determ. of dipole extrapolation lengths 3-71168
 angular, transport solutions for multilayer slab-cell systems 3-63120
 asymptotic diffusion theory, analytic transient flow expression 3-54526
 controlled thermonuclear reactor radiation damage studies, neutron flux spectra 3-60253
 critical reactors, variational estimates for integral parameters 3-74688
 criticality problems, use Monte Carlo methods to determ. mean flux over small volume (*German*) 3-67388
 density distortions, caused by cylindrical counters in diffusive media, rel. to cosmic rays (*Russian*) 3-62243
 detector, electron current principle (*German*) 3-70395
 diffusion coeffs. from perturbation flux distrib. in systems with anisotropies 3-49357
 diffusion eqn., one-dimensional, analysis using CAIN computer code 3-71158
 diffusion equation, cell homogenisation, rigorous treatment 3-71150
 distrib. in rectangular lattice cells, integral transport theory calcs. 3-60244
 distribution, and rod effectiveness rel. to evaluation of the critical expt. with Cesar II (*German*) 3-67488
 distribution rel. to cell system finiteness in axial direction 3-60252
 electron driven nuclear assembly, potential performance characteristics 3-48509
 fast angular flux spectrum in infinite carbon medium, moments method soln. 3-52220

neutron flux continued

- fast reactor core composition, systematic optimisation, integral reactor parameters, void reactivity 3-63226
 fast reactor transients, energy synthesis method, flux and bilinear flux few-group collapsing schemes 3-63116
 fast reactors, application of perturbation theory for calcs. of reactivity, Doppler effect (*Czech*) 3-74651
 FFTF pipe chase streaming expt. to validate analytical methods for neutron flux calc. 3-71222
 fissile sample Doppler effects, effect of local flux distortions 3-49360
 fission track method of measurement, standard U glasses 3-51726
 flux synthesis calculations, fast reactors, multidimensional diffusion theory problems 3-63115
 fusing plasma neutron diagnostics 3-63888
 monitor for high-level flux-spectra-fluence characterization, prep. and handling 3-46166
 multizone fast breeder reactors, criticality studies 3-52228
 noise, power reactor spatial coupling using coherence lengths concept (*German*) 3-67481
 noise analysis in a reactor with two weakly coupled asymmetric fission zones (*German*) 3-67482
 noise in boiling reactors, using Langevin analysis, of fluctuations arising from bubble aggregations 3-67391
 normalisation for large samples in neutron activation analysis 3-40074
 one-speed distrib. determ. using synthesis method of integral type and first flight collision probability 3-71141
 one-speed problems, exact transfer matrix formulation 3-60248
 probe activation measurement, Ge(Li) detector and automatic sample changer description 3-73862
 pulsed ionisation chamber, gamma compensated, for neutron flux and reactor power meas. 3-45547
 reaction rate distrib. in ZPR-6 assembly 7, comparison of calcs. and meas. 3-71186
 reactivity absolute, generalised source multiplication method 3-71213
 reactor expt. using Pu-enriched UO₂ fuel, booster effect on neutron density and reactivity 3-71226
 reactors, calc. using synthesis of multidimensional coarse and fine mesh calc. (*German*) 3-67466
 reflected reactors, core reactivity determ., area-ratio method 3-71205
 reproduction factors for ²³⁵U spheres, steel shells, immersed in UO₂ (NO₃)₂ solutions 3-63196
 scintillator coincidence system, for flux density measurements 3-40033
 slowing down of pulsed neutron, time- and space-depend. asymptotic behaviour 3-60242
 space, meas. rel. to atmospheric leakage and solar flux 3-69606
 thermal-neutron flux distrib. in BF₃-CO₂ gaseous mixtures 3-49303
 tilting expts. in asymmetrically poisoned demonstration-size fast reactor 3-49351
 total, angular, multigroup neutron transport in finite sphere, 3-63119
 ZPPB/FTR-2, calc. of neutron flux distrib. and neutron reaction rates 3-74686
 BeO, thermal neutron wave meas. at h.f. 3-60281
 D-T small mirror fusion device, 14 MeV neutron flux capabilities 3-63857
 Pu spherical metal assemblies, neutron importance, comparison of theory and expt. 3-71204
¹⁰³Rh(n,n')^{103m}Rh, thick foils, absolute counting of K X-rays 3-66316
 U thin foils, meas. of Doppler effect in thermal reactor up to 729°C 3-74679
 U/graphite system, neutron wave interference phenomena 3-60276
 Zr alloys, pressure tubes, creep, effect of neutron flux anisotropy rel. to stress directions 3-67565

neutron flux density see neutron flux**neutron interactions**

- see also nuclear reactions and scattering due to neutrons
 cross section compilation for proton and antiproton induced reactions 3-70973
 deep inelastic, proton-neutron structure function difference in resonance region 3-67037
 neutrino and antineutrino high energy events 3-43093
 in neutron stars, radial pulsations near onset of instability 3-61770
 s-process neutron capture time in stars from obs. 3-80910
 tissue containing H, C, N and O 3-45328
 total cross-sections, correlation between structures for p-p, p-p, p-n and K⁺-p interactions 3-45905
 en, possible expts. for an intersecting ring complex 3-66305
 en in the context of proposed storage ring systems 3-67048
 $\gamma n \rightarrow \pi^+ n$, 500-900 MeV, differential cross sections, search for resonance production 3-40347
 $\gamma n \rightarrow \pi^+ n$, photoproduction, differential cross section, 500-900 MeV 3-57349
 K⁻ $n \rightarrow \pi^- \Lambda$, pseudoscalar production line reversed reaction, amplitude analysis 3-71008
 K⁺ $n \rightarrow K^+ \pi^- p$, study of K π scattering using Argonne Effective Mass Spectrometer 3-70988
 K⁺ $n \rightarrow K^0 p$, 4.6 GeV, cross section meas., charge exchange 3-78207
 K⁺ $n \rightarrow K^0 p$, studied via reaction K⁺ $d \rightarrow K^0 p p$, 3.8 GeV/c, total, differential cross section, comparison with other data 3-60035
 K⁺ $n \rightarrow K^0 \pi^+ \pi^- p$, 4.6 GeV/c, cross-sections and (K $\pi\pi$) system production and decay properties 3-57442
 K⁺ $n \rightarrow K^+ \pi^- p$, strength of absorptive corrections to pion exchange Born term 3-49055
 K⁺ $n \rightarrow K^+ \pi^- \pi^0 p$, 4.6 GeV/c, cross-sections and (K $\pi\pi$) system production and decay properties 3-57442
 K⁺ $n \rightarrow K^+ \pi^+ \pi^- n$, 4.6 GeV/c, cross-sections and (K $\pi\pi$) system production and decay properties 3-57442
 K[±]n, 25-60 GeV total cross section calc., shadow corrections including inelastic screening (*Russian*) 3-67166
 μ pair production, quark parton model, proton and neutron structure function effects 3-78226
 μ n amplitude at threshold, polarizability contrib. calc. 3-78134

neutron interactions continued

- nd total cross sections, 0.7 to 3.6 GeV/c, n-n total cross section evaluation 3-60057
- ne amplitude at threshold, polarizability contrib. calc. 3-78134
- nn, secondary pion energies, approximation of experimental data (*Russian*) 3-62902
- np \rightarrow dy, circular polarisation of γ and weak P-odd NNp vertex (*Russian*) 3-40376
- np \rightarrow dy, γ circular polarisation, correction from divergent P-violating NNp vertex 3-78198
- np total cross section, 0.7 to 3.6 GeV/c, n-n total cross section evaluation 3-60057
- $\nu n \rightarrow \mu^- p$, 0.7 GeV, axial vector mass determ. 3-70904
- $\nu n \rightarrow \mu^- p$, test of Weinberg model at CERN 3-66964
- $\nu n N \rightarrow \nu n$ + hadrons, calc. of semileptonic neutral currents assuming partons and Weinberg's renormalizable theory 3-70905
- pn, 25-60 GeV total cross section calc., shadow corrections including inelastic screening (*Russian*) 3-67166
- pn annihilation and bound states 3-57399
- pn coherent generation of particles on emulsion nuclei at 200 GeV/c 3-74439
- pn inelastic collisions, 200 GeV/c, ang. characts. of secondary relativistic charged particles 3-78213
- pn \rightarrow NN π , 1.0 to 1.6 GeV/c, cross-section study 3-52053
- pn \rightarrow pp $\pi^+\pi^-\pi^-$, 28 GeV/c, statistical analysis of event-to-event fluctuations, evidence for strong clustering effects 3-74441
- pn \rightarrow $\pi^+\pi^-\pi^-$ annihilation at rest, two-variables expansions, analysis of Dalitz plot 3-57397
- pn \rightarrow $\pi\pi\pi$, Dalitz-plot distrib. explanation 3-57375
- π^-n , 40 GeV/c, charged-prong multiplicity distrib., scaling behaviour and local excitation model 3-43151
- π^-n , 40 GeV/c, γ quanta prod. 3-74428
- π^-n , multiple particle production at 40 GeV 3-52029
- $\pi^-n \rightarrow \pi^-\pi^+\pi^-n$, 3.9 GeV/c interactions on quasifree neutrons of light nuclei, resonance production (*Russian*) 3-40515
- $\pi^-n \rightarrow \rho^-p$, low-mass enhancement, doubled charged A_1^{--} and existence of true A_1 resonance 3-57401
- $\pi^+n \rightarrow K^0\Sigma^+$, Σ^+ polarization, 1.2 to 2.4 GeV/c 3-57437
- $\pi^+n \rightarrow \omega p$, 6.0 GeV/c differential cross section, spin density matrix elements, Regge exchange models 3-57435
- $\pi^+n \rightarrow \pi^+\pi^-p$, 6 GeV/c, study of $\pi\pi$ scattering in 0.6-1.42 GeV region, phase shift analysis 3-70991
- $\nu n N \rightarrow \nu n$ + hadrons, calc. of semileptonic neutral currents assuming partons and Weinberg's renormalizable theory 3-70905

neutron moderation

- elastic, in infinite homogeneous media, general theory 3-71145
- fast reactors, analogy between thermal diffusion and continuous slowing down of neutrons 3-49334
- flux, one-speed distrib. determ. using synthesis method of integral type 3-71141
- fusion reactor blanket design, theoretical and exptl. evaluation of neutron spectrum in graphite mock-up 3-60329
- graphite, radiation effects in reln. to role fusion reactors 3-60331
- graphite, temperature discontinuity, effective thermal neutron temp., spatial variation analysis, weighted residuals method 3-40527
- infinite homogeneous mixture, slowing down equation solution 3-78366
- infinite media, numerical soln. of time-dependent slowing down problems 3-60246
- light-water, temperature discontinuity, effective thermal neutron temp., spatial variation analysis, weighted residuals method 3-40527
- non-uniform reactor systems, rigorous diffusion model for cell homogenization 3-40526
- nuclear reactor space-time kinetics expts., delayed-neutron holdback, test of diffusion codes 3-49344
- pulse decay, influence of anisotropy on the critical buckling 3-74625
- pulses in noncrystalline moderators 3-49299
- slowing down of pulsed neutron, time- and space-depend. asymptotic behaviour 3-60242
- slowing-down times in H₂O, graphite, Pb, effect of anisotropy 3-74634
- space-dependent fast neutron spectra, calc. using SOPHIE and CICELY codes 3-63121
- subthermal neutron retardation by system of rot. plane neutron mirrors (*Russian*) 3-57549
- synthetic kernels for slowing down 3-46049
- thermal neutron howitzer, heavy metal addition to moderator 3-70369
- thermalization, as fluctuation of nonequilibrium steady state 3-78367
- water, slowing down spectrum calc. using Green's function 3-54521
- ²⁵²Cf, thermal neutron wave meas. at h.f. 3-60281
- ²⁵²Cf fission neutron age in water, meas. by In resonance obs. 3-71297
- ²³⁵U/graphite system, neutron wave interference phenomena 3-60276

neutron polarisation

- Compton scattering of off-shell photons on polarised nucleons, invariant amplitudes 3-67018
- polarimeter, for 3 MeV neutrons (*German*) 3-45549
- scattering of polarised neutrons on zero-spin nuclei, methods of polarisation measurement (*German*) 3-60156
- spin tagging by deuteron beam break up 3-67168
- ²H, neutron scatt., polarisation asymmetry, 35 MeV 3-74553
- NN interactions, polarisation structure at high energies, simple models 3-70969
- np charge exchange scattering from 2 to 12 GeV/c, polarisation parameter meas. 3-49049
- p-n polarisation role in models for atomic mass dependence of photo-nuclear giant resonance energy 3-74546
- pp \rightarrow nn charge exchange at 8 GeV/c, polarisation meas. 3-49050
- scattering, relation to differential cross section in baryon exchange, parity-doublet contributions 3-60025
- ⁹Be(α ,n)¹²C, 4.5-5.85 MeV, meas. of neutron polarisation angular distrib., ¹³C states 3-62946
- ¹²C(n, n), 2.1-4.7 MeV, total and elastic cross sections, phase shift analysis, analysing power 3-40489
- ¹²C(n,n), double scatt. technique, R-function anal., cross sections 3-78325

neutron polarisation continued

- ¹³C(α ,n)¹⁶O, 2.075-2.43 MeV, neutron polarisation angular distrib., parity assignments of ¹⁷O 7.97-8.197 MeV states 3-67189
- ¹⁴C(d, n)₀¹⁵N, deuteron energies, 1.3 to 1.9 MeV, neutron polarisation ang. distrib. (*German*) 3-52197
- ⁵⁹Co(n, γ)⁶⁰Co, with polarised neutron and nuclei, 0.065 eV, meas. of capture γ -rays 3-43245
- D(p,n)pp, breakup neutrons polarisation meas. at 21.5 MeV 3-52163
- ²H(d, n)³He reaction study below 1 MeV 3-40016
- ²H(d,n)³He, 330 keV, production reaction, small angle scattering by U, Pb and Cu 3-71109
- ²H(d,n)³He, polarised deuteron beam, 3.3-14.9 MeV, meas. of longitudinal polarization transfer at 0 degrees 3-57506
- ²H(γ ,n)p, enhancement of total and differential cross section 3-71096
- ²⁴Mg(³He,n)²⁶Si, 5.0 and 5.8 MeV, meas. of angular distrib. of neutron polarisation, DWBA analysis 3-67352

neutron production

- γ^5 theory, effect of nucleons in high energy collisions (*Russian*) 3-67132
- Al, by cosmic ray high energy muons, depth dependencies, electromagnetic interaction explanation (*Russian*) 3-61621
- deuteron breakup, monokinetic neutron beam up to 1.9 GeV/c, Saturne synchrotron Saclay France 3-77608
- deuteron electrodisintegration matrix element, reln. to neutron-proton phase shifts 3-70939
- dynamic characteristics, angular, momentum distribution, for pp interactions, 19.1 and 10 GeV/c (*Russian*) 3-60046
- fast reactor neutron spectrum generator, design and construction 3-52218
- intense beams, by ZGS injector-booster accelerator 3-48508
- lightning, effect on ¹⁴C ages in tree rings 3-76745
- lunar neutron prod. rate determ. by meas. of ⁶⁰Co conc. 3-61712
- nuclear reactor fuel, structural materials, reactivity testing, quality control 3-63210
- photoneutron spectra produced by electron bremsstrahlung on targets 3-57509
- Cd, by cosmic ray high energy muons, depth dependencies, electromagnetic interaction explanation (*Russian*) 3-61621
- Fe, by cosmic ray high energy muons, depth dependencies, electromagnetic interaction explanation (*Russian*) 3-61621
- ²⁵⁷Fm spontaneous fission, meas. of average number of prompt neutrons emitted 3-71138
- ³H(d,n)⁴He reaction in ion accelerators (*French*) 3-56917
- Pb, by cosmic ray high energy muons, depth dependencies, electromagnetic interaction explanation (*Russian*) 3-61621
- ²³⁸PuO₂, high purity, neutron yield 3-67628
- ²³⁹Pu fission neutron multiplicity and total gamma-ray energy 3-71137
- ThO₂-PuO₂ HTGR lattice, temp. dependence of infinite-medium neutron multiplication factor 3-49345

neutron-proton scattering

- bremsstrahlung, coplanar asymmetric, calc. at 130 MeV 3-74415
- bremsstrahlung calcs., cross sections, model depend. 3-40425
- bremsstrahlung obs. at 130 MeV, off-shell effects 3-74417
- bremsstrahlung study at 130, 200 MeV, non-coplanar effects 3-74416
- charge exchange forward spike, link with Goldberger-Treiman relation 3-67102
- charge exchange scattering from 2 to 12 GeV/c, polarisation parameter meas. 3-49049
- cross section compilation for proton and antiproton induced reactions 3-70973
- elastic, 10 to 26 GeV, deuteron form factor from Glauber theory (*Russian*) 3-57343
- elastic, 612 MeV, depolarization 3-40375
- elastic, near 50 MeV, phase-shift analysis 3-70972
- elastic scattering amplitude, 10-70 GeV slope parameter and real part determ. (*Russian*) 3-67122
- np \rightarrow pn, differential cross section, exchange degenerate Regge pole model 3-60033

neutron radiography

- see also nondestructive testing
- using accelerators 3-59443
- binary melts, obs. of unidirectional solidification with natural convection 3-72877
- heat pipes, high temp., Li mass transfer corrosion, neutron radiography 3-47499
- high speed, technique, image quality, scintillator screen, image intensifier, synchronisation features 3-45515
- nuclear fuel pins, electronic image analyser, dimensional meas. 3-46148
- r.b.e. and o.e.r. values, neutron spectrum dependence 3-59453
- reactor fuel specimens, dimensioning from thermal neutron radiographs 3-40545
- therapy facility, design using analogue Monte Carlo computer code 3-61922
- track-etch radiography, alpha particles, protons, fast and thermal neutrons, polycarbonate plastics, cellulose nitrate 3-67627
- ²⁵²Cf neutron radiography device, comparison of a multiplied and unmultiplied facility 3-63247

neutron reflection

- backscattering of fast neutrons from Al, Fe, Pb, 0.5-1.8 MeV, energy spectra 3-60250
- compact reactor reflector side regulation meas. and calcs. using ITR critical plant (*German*) 3-67474
- monoenergetic critical problem in anisotropic linear neutron scattering for slab bounded by infinite reflectors 3-67385
- reactor fuel in transit effect of reflection material on reactivity 3-63183
- slab transmission, reflection and finite reflector critical problems 3-60249
- SPR II, fast burst reactor, control and burst generation, nonfissile external reflector element 3-71212
- wave propagation in multiplying medium, reflector effect 3-74661

neutron scattering

- see also neutron flux; neutron-proton scattering; nuclear reactions and scattering due to neutrons
- anisotropic scattering effects in reflected fast critical assemblies 3-49328
- anisotropy, effect on slowing-down times in H_2O , graphite, Pb 3-74634
- benzene, cold neutron spectrum, data processing using cubic spline functions 3-57500
- benzene, verification of rotational frequency distribution calc. 3-60435
- classical elastic scattering probability function generalized to any arbitrary coordinate system 3-74631
- cross sections of polyphenyls and benzene near melting point, difference rel. to rotational mechanism 3-60435
- cross-section perturbation determ. by correlated sampling using SAM—CEP computer code 3-74636
- deep inelastic e-p and e-n cross sections comparison, 4.5-18 GeV 3-43114
- EBR II, anisotropic scattering calcs. for stainless steel reflector 3-46071
- elastic, by standing e.m. wave, coherent scattering amplitude 3-62848
- elastic, simulation computer program 3-43142
- elastic in graphite in nuclear reactor, rel. to calc. on effective resonance integral (German) 3-67587
- energy dependent spatial mesh approximation, static few-group diffusion equations, coupling via scattering and fission 3-63118
- fast-neutron spectra, efficient generation of high-order anisotropic elastic matrices 3-49330
- isotropic, flux distributions in rectangular lattice cells, using numerical techniques 3-60244
- monoenergetic critical problem for slab bounded by infinite reflectors 3-67385
- synthetic kernels for slowing down 3-46049
- thermal neutrons, high energy transfer, final states 3-68139
- thermal neutrons on inert gases, determ. of electron-neutron scattering length 3-70921
- transport problems, energy-dependent, in two adjacent media, singular eigenmode technique 3-74623
- transport theory, higher-order scattering anisotropy effects, variational calc. 3-54522
- two-group transport eqn. for linearly anisotropic scattering, critical slab soln. 3-49300
- two-neutron scattering length, effect of neutron electric polarizability 3-45978
- eN, inelastic structure-function relations from sum of direct-channel resonances 3-43109
- en scattering length as measured by thermal neutron scattering on inert gases, corrected value 3-70921
- K^+n elastic scattering, 0.64-1.51 GeV/c, meas. of differential cross sections 3-57412
- n-n scattering length and effective range from three-body calc. on $^2H(n,2n)^1H$ 3-78340
- nd, below deuteron break up threshold, quartet s phase shift, linear approximation (Russian) 3-60016
- nd, elastic scattering, Faddeev formalism, local potentials, comparison with separable potential model 3-62872
- nd, resonant group exam. and comparison with Faddeev's eqn., low energy (Russian) 3-43135
- nd scatt., SU(3) basis calc. of three-particle states 3-49037
- nd scattering, deuteron polarisation (German) 3-74410
- nn final-state interaction in $^2H(n,2n)p$, scattering length calc. 3-78336
- nn scattering length determ. from $^2H(n,p)nn$, exptl. requirements 3-71098
- nn scattering length determ. from $\pi^-d \rightarrow nnp$ final-state interaction 3-78181
- nn scattering length determ. from $^2H(n,np)n$ kinematically complete expt. 3-78338
- nn scattering length in $^2H(n,p)nn$ final state interaction, impulse approx. calc. 3-78339
- C, Monte Carlo calculational analysis of exptl. transport data 3-74638
- Ge(Li) detector, γ -ray intensity from Am-Be neutron source 3-70407
- $^7Li(p,n)^6Be$, scattering of keV neutrons, intarget assembly, angular distributions and energy spectra calculations 3-59637

neutron sources

- 14 MeV, intense, rotating target 3-56923
- anisotropy, effect on slowing-down times in H_2O , graphite, Pb 3-74634
- 'Apsara' reactor, 25 keV neutron beam, filtered 3-73855
- atmospheric and space 3-69606
- cavity, in graphite thermal columns of nuclear reactors, wall return neutron fluxes 3-57560
- cold, thermalization in H_2O - D_2O mixtures, 253-4K 3-43268
- designs of neutron generating tubes with hot cathode and ion source 3-42633
- electron driven nuclear assembly, potential performance characteristics 3-48509
- generator for liquid and gas flow meas. (German) 3-56915
- high-intensity, using deuteron bombardment of D, Li, Be and C 3-74596
- inhomogeneous atm., diffusion from distributed source 3-56265
- lunar soils, Apollo 16 lunar stratigraphy 3-56351
- moving source neutron moisture gauge 3-66472
- NG-150 generator, for activation analysis 3-53973
- SLOWPOKE, low-power cheap inherently safe laboratory reactor 3-70368
- standard neutron spectrum facility $\Sigma\Sigma$, calcs. with ENDF/B, comparison with expt. 3-49301
- thermal neutron howitzer, heavy metal addition to moderator 3-70369
- for total body neutron activation analysis, selection 3-77254
- ZGS injector-booster accelerator for intense neutron generator 3-48508
- Am-Be source, γ -ray response of Ge(Li) detector 3-70407
- Am-Be spectrum, angular distribution data, effects of secondary interactions 3-77607

neutron sources continued

- $^{13}C(\alpha,n)^{16}O$ reaction as source of polarised neutrons 3-67189
- ^{252}Cf , use in neutron activation analysis and radiography (Afrikaans) 3-62198
- ^{252}Cf applic. in industrial process control (German) 3-56916
- ^{252}Cf spontaneous fission neutrons, meas. of $^{235,238}U$ fission cross-sections 3-49294
- ^{252}Cf use in continuous monitoring of waterways 3-62358
- 2H -d and 3H -d reactions, absolute determ. of differential source strength (German) 3-59636
- $^3H(d,n)^4He$ reaction in ion accelerators (French) 3-56917
- Pu-Be, fabrication description for varying strengths and geometries 3-62213
- $^{238}PuO_2$, high purity, neutron yield 3-67628
- Sb-Be, light water reactor rods, ^{235}U content meas. 3-67558
- ^{124}Sb -Be (p,n) assay system, fissile content meas., 4He gas tube detectors 3-67557
- neutron spectra**
- see also neutron spectrometers
- angular, thermal, meas. in simulated BWR type box cells, rel. to results from integral transport program 3-63105
- annular core pulse reactor cavity, calc. and measurement 3-49326
- arbitrary neutron spectrum, reactor equivalence by multisource synthesis 3-60255
- backscattering of fast neutrons from Al, Fe, Pb, 0.5-1.8 MeV 3-60250
- controlled thermonuclear reactor radiation damage studies, neutron flux spectra 3-60253
- cosmic ray meas. using nuclear track emulsions, in artificial satellite of Cosmos series 200-400 km, 10 MeV (Russian) 3-65608
- cosmic rays, 0 to 2000 m, calc. energy using cadmium ratio (Russian) 3-65601
- delayed, rel. to non-destructive meas. of ^{235}U and ^{232}Th in high temp. spherical fuel elements (German) 3-67601
- delayed fission neutrons, energy distrib. meas. using 3He proportional counter 3-54515
- EBR-II, noise anal., time-dependent fluctuations, reactivity transfer function, neutron detector power spectra 3-71215
- EBR-II neutron shield system, diffusion and transport theory calcs. for deep penetration spectra 3-74687
- emission-time effects in pulsed Na assembly 3-49297
- fast, depleted U, anal. and interpretation, ENDF/B-III data 3-71154
- fast, efficient generation of high-order anisotropic elastic matrices 3-49330
- fast, measurement and analysis in Na, fast breeder reactor programme 3-71153
- fast angular flux spectrum in infinite carbon medium, moments method soln. 3-52220
- fast reactor neutron spectrum and criticality calcs., inclusion of $^{238}U(n, \gamma n')$ cross section 3-43282
- fast reactor neutron spectrum generator, design and construction 3-52218
- fast-neutron spectrum critical assemblies, effect of $^{238}U(n, \gamma n')$ reaction 3-43283
- fine-energy, due to resonance scattering effects in EBR reflector and structural subassembly regions 3-74628
- fissile detectors, for neutron spectrum measurement in L54 reactor 3-48528
- fusion neutron energies and spectra 3-40519
- fusion reactor blanket design, theoretical and exptl. evaluation of neutron spectrum in graphite mock-up 3-60329
- fusioning plasma neutron diagnostics 3-63888
- graphite, neutron fusion spectrum, reaction rates determ. 3-63100
- inclusive thermodynamical spectra of neutral particles 3-49060
- L54 reactor core centre, exptl. determ. of fast neutron spectrum, computer analysis 3-43274
- leakage, calc. for monoenergetic, fission and reactor sources and for various shields 3-49378
- LMFBR fuel pin, spectrum modification in ACPR for transient studies 3-46078
- many-resonance approx. for energy spectrum of fast reactors 3-43269
- miniature NE-213 detects for spectra meas. in core vicinity of fast critical assembly 3-70412
- monitor for high-level flux-spectra-fluence characterization, prepn. and handling 3-46166
- nuclear air burst, energy, space and time distrib. using Monte Carlo calcs. 3-74621
- nuclear reactor shield, H_2O and Fe, 25 keV to 1 MeV neutron spectral meas. 3-74752
- photon neutron spectra produced by electron bremsstrahlung on targets 3-57509
- plasma, laser produced, anomalous neutron generation 3-68039
- plasma, laser produced, neutron emission, collisionless electrostatic shock waves 3-75398
- plasmas, laser produced, neutron emission 3-40803
- prompt, from ^{235}U fission, re-fitting of previous data using computer program 3-74611
- reactor core calculations using Monte Carlo methods (German) 3-74643
- reactor lattices, bare and D_2O reflected, effects of detector placement on noise 3-67399
- resonances, even-even and odd-odd nuclei, particle-vibration model 3-78267
- scattering by nuclei, elastic and inelastic, techniques for measurement and processing of continuous spectra (German) 3-60193
- slowing down spectrum in water, calc. using Green's function 3-54521
- source spectra produced by 400 MeV electron in Cu, calcs. for soil, concrete, $FeTiO_3$, and iron shields 3-71342
- space, measurements rel. to atmospheric leakage and solar flux 3-69606
- space-dependent slowing down of fast neutron calc. using SOPHIE and CICELY codes 3-63121
- standard neutron spectrum facility $\Sigma\Sigma$, calcs. with ENDF/B, comparison with expt. 3-49301
- stochastic unfolding code for use with exptl. proton recoil data 3-51734
- tabular secondary energy distrib., interpolation 3-43226

neutron spectra continued

- thermal indexes, in D_2O moderated U and U-Pu fuel elements 3-74630
- thermal intensity, effect of field slugging caused by cylindrical counters in diffusion media (*Russian*) 3-62243
- thermal space-dependent, meas. in small Be assemblies 3-49298
- threshold detectors for neutron leakage spectra evaluation for dosimetry calcs. 3-59646
- wall return neutron fluxes for high- and intermediate-energy cavity neutron sources, numerical study 3-57560
- ZED-2 critical facility, ^{235}U booster rod expts., neutron spectrum parameters 3-49365
- (p, n) reaction on one neutron deficient nuclei, photoneutron mean energies, level density parameters 3-60080
- Am-Be sources, angular distributions data, effects of secondary interactions 3-77607
- ^{40}Ar photoneutron disintegration, 13-23 MeV 3-49238
- ^{64}As , $A=84$, 85, 86, produced in ^{235}U neutron induced fission, obs. of delayed neutron yield 3-43202
- ^{138}Ba , muon capture, neutron emission, branching ratios 3-40463
- $^{12}C(n, n)$ polarisation, energy meas. 3-78325
- $^{13}C(\alpha, n)^{16}O$, $E_\alpha=1.5$ MeV, total neutron yield, compound states in ^{17}O 3-40507
- ^{140}Ce , muon capture, neutron emission, branching ratios 3-40463
- ^{142}Ce , muon capture, neutron emission, branching ratios 3-40463
- ^{252}Cf , triple fission products, detection of 4He , 3He 3-78363
- ^{259}Cf , ternary fission, observation of 3He , neutron spectra 3-43261
- $^{65}Cu(p, n)^{65}Zn$, narrow reson. 148 eV above threshold 3-43248
- D_2O , fast neutron meas., 3He spectrometer 3-71157
- $^1H(d, 2p)n$, 12.6 MeV, two-dimensional coincidence spectra, p-n final state interaction 3-40477
- 2H bombardment of 2H , 7Li , 9Be and ^{12}C rel. to high intensity neutron sources 3-74596
- $^2H(p, n)2p$, spectra meas., 16-26 MeV, determ. of pp scattering length 3-78337
- $^2H(p, n)pp$, 16-26 MeV, neutron spectra meas., determ. of proton-proton final state interaction 3-71098
- $LiAlH_4$, M-H stretching freq. obs. from energy loss spectra 3-60678
- $^7Li(p, n)^7Be$ angular distributions, energy calculations using Monte Carlo method, target scattering effects 3-59637
- $^{94}Mo(p, n)^{94}Tc$, enhancement of neutron and gamma-ray yields at isobaric analogue resonances, ^{94}Tc excited states 3-67207
- $NaAlH_4$, M-H stretching freq. obs. from energy loss spectra 3-60678
- $NaNO_2$, transient phenomena of polarisation reversal, neutron time-of-flight method 3-72582
- ^{16}O , μ^- capture, calc. of asymmetry in high energy neutron emission, transitions to ^{15}N levels 3-52149
- $^{17}O(\alpha, n)^{20}Ne$, $E_\alpha=1.5$ MeV, total neutron yield, compound states in ^{21}Ne 3-40507
- $^{18}O(\alpha, n)^{21}Ne$, $E_\alpha=1.5$ MeV, total neutron yield, compound states in ^{22}Ne 3-40507
- Pb slowing-down-time spectrometer, neutron pulse width effects, time dependent neutron density 3-71156
- ^{239}Pu , fission, power, photon spectrum and neutron prodn., calc. by ORIGEN computer code 3-43284
- ^{239}Pu thermal fission, delayed neutron energy spectra meas. by proton-recoil proportional counter 3-49292
- ^{120}Sn , muon capture, neutron emission, branching ratios 3-40463
- Th, fast neutron meas., 3He spectrometer 3-71157
- $Th(NO_3)_4$, fast neutron meas., 3He spectrometer 3-71157
- Ti:Mn(W)(Cu)(Mo)(An), neutron activation anal. 3-42703
- U pile, exponential depleted, neutron spectrum meas., inelastic and capture cross-sections of ^{238}U , LMFBR assemblies 3-71155
- UO_2 coated particles, exptl. determ. of effective resonance integral and Doppler effect in I/E neutron spectrum 3-43273
- ^{233}U fission neutron spectra meas. 0.8-10 MeV 3-74618
- ^{233}U thermal fission, delayed neutron energy spectra meas. by proton-recoil proportional counter 3-49292
- ^{235}U , fission, power, photon spectrum and neutron prodn., calc. by ORIGEN computer code 3-43284
- ^{235}U thermal fission, delayed neutron energy spectra meas. by proton-recoil proportional counter 3-49292
- ^{238}U , discrepant cross sections in depleted block 3-49296

neutron spectrometers

- chopper, experimental determ. of transmission function 3-48551
- computer controlled triple axis neutron spectrometer, CAMAC instrumentation, FOCAL program 3-73883
- film density, by scintillator coincidence system 3-40033
- lead slowing down time spectrometer, fissile material assay, neutron slowing down studies 3-62267
- liquid scintillation, for cross-section measurements 3-51732
- miniature NE-213 detects for spectra meas. in core vicinity of fast critical assembly 3-70412
- multichannel pulse-height analyser for unfolding neutron spectra from proton recoil data 3-51734
- multisphere, response matrix calc. using discrete ordinates transport code 3-51733
- scattering by nuclei, elastic and inelastic, techniques for measurement and processing of continuous spectra (*German*) 3-60193
- solar neutron spectrometer for 10 to 50 MeV range (*German*) 3-62258
- stilbene crystal, organic scintillator, spectrometer line shape, experimental, Monte Carlo calculation 3-70408
- thermal neutron polarization analysis diffractometer 3-70413
- three axis, counting rate optimisation, phonon meas. (*German, English*) 3-63932
- time of flight, detection efficiency, tailored source spectra 3-62262
- time-of-flight, collection and processing of data from three spectrometers 3-62268
- time-of-flight, for fast neutrons, neutron-gamma discrimination (*German*) 3-59652
- time-of-flight, Harwell synchrocyclotron, total cross section of iron meas., 24-1000 keV 3-71117
- time-of-flight, resonance energy meas. for calibration 3-60174
- time-of-flight measurement with on-line computer for data logging (*German*) 3-59653
- triple-axis resolution function calc. 3-56971
- vacuum furnace, for liquids and solids, up to 1100 K 3-43733

neutron spectrometers continued

- p-recoil proportional counters, 25 keV to 1 MeV neutron spectra through reactor walls 3-74752
- 3He spectrometer, fast neutron meas., Th, D_2O , $Th(NO_3)_4$ 3-71157
- Pb slowing down time neutron spectrometer, fast reactor education 3-63161
- Pb slowing-down-time spectrometer, neutron pulse width effects, time dependent neutron density 3-71156
- neutron stars**
- see also pulsars*
- accreting, nuclear fusion forming X-ray source 3-81026
- accreting magnetic neutron star, radiation beaming rel. to X-ray pulsars 3-45083
- accretion at magnetic pole 3-81034
- accretion at the Galactic centre, upper limit at X-ray wavelengths 3-42231
- accretion model of X-ray sources, circumstellar matter 3-77128
- baryon relativistic effective mass, in superdense matter 3-66668
- bremsstrahlung spectrum, effect of Compton scattering 3-81047
- cold, solidification density, t-matrix calc. 3-42115
- cores, possibilities of pion condensation and nucleon crystallization 3-81033
- critical parameters rel. to gravitational collapse 3-69922
- crystallization density of cold dense neutron matter 3-51254
- equation of state of matter at supernuclear density 3-61631
- general-relativistic polytrops, stability and equation of state 3-69921
- gravit. collapse, T-p-abundance history 3-47866
- Hercules X-1, binary component, X-ray emission explained by gas accretion of neutron star 3-77130
- Hercules X-1, X-ray source, neutron star, mass meas. 3-45164
- hydrodynamic model for formation in carbon detonation supernova 3-81025
- Landau orbital ferromagnetism, temp. aspects 3-61764
- magnetosphere model, partial differential eqn. for rotating star in aligned magnetic field 3-69984
- massive close binary component, evolution and appl. to Cygnus X-3 3-53650
- MHD stability in white dwarfs and neutron stars, rel. to magnetic fields 3-42187
- Models for compact pulsing X-ray sources 3-81150
- nonequilibrium composition of shells and nuclear energy sources 3-61766
- nongeodesic radial accretion in Schwarzschild geometry 3-59250
- nuclear many-body theory calcs. of ground state configuration 3-51253
- physics course 3-77348
- pion condensation, electrically neutral, phase transitions 3-67248
- plasma turbulence, effect on spectra of scatt. by Langmuir oscill. 3-60611
- positron-annihilation radiation producing 473 keV feature 3-61759
- quakes rel. to model of solid planet and neutron stars 3-42168
- quasiradial pulsation freq. determ. using general relativity theory 3-53653
- rapidly rotating neutron stars 3-45091
- rotating, reaction to external torque, MHD theory of pulsar slowdown 3-69943
- rotating, stability and radial pulsation 3-61770
- rotating baryon config., internal structure 3-61639
- rotating magnetohydroelastic stars, variational principle for gravit. field eqns. 3-61632
- solid core and structure rel. to strongly interacting baryons 3-45089
- stellar evolution review 3-77038
- superconducting, intermediate state, proton energy gap 3-73475
- superdense cores, relativistic effective mass of nucleon in degenerate nucleon sea 3-73432
- supernovae envelope ejection rel. to rotational energy of neutron star 3-53652
- superposition of poloidal magnetic multipole fields (*German*) 3-69939
- surface superstrong magnetic fields, formation of long molecular chains 3-67723
- Vela pulsar, giant glitches rel. to neutronic quantum cryst. formation 3-56408
- X-ray astronomical observation, binary system component identification 3-61835
- π condensation in nuclear matter 3-54417
- neutron transport theory**
- see also neutron diffusion; neutron moderation*
- air-transport problem, one-dimensional, cross-section sensitivity analysis 3-74637
- asymptotic diffusion theory, analytic transient flow expression 3-54526
- atmospheric neutrons, production and propagation calcs. 3-59235
- Boltzmann eqn. solution using Monte Carlo methods rel. to reactor core calculations (*German*) 3-74643
- burst decay in pulsed expts. in lattices, one-group diffusion model 3-71144
- cell systems finiteness in axial direction rel. to flux distribution 3-60252
- chain reactions, subcritical assemblies, third order correlation function calc. (*German*) 3-71159
- collision probabilities in spheres with parabolic source distribution 3-63109
- compact reactors, rel. to calc. methods in spectra leakage and streaming (*German*) 3-67474
- computation of group parameters in the resonance regions using the program RESPU (*German*) 3-67390
- controlled fusion blankets and shields, perturbation theory for neutron and photon transport calcs. 3-74743
- coupled neutron-gamma transport in air, sensitivity analysis, total tissue dose 3-49306
- critical assemblies, effect of space-dependent fission matrices in transport calcs. 3-71221
- criticality problem, optimum eigenvalue bounds 3-46051
- cross sections, multiple reaction correction utilising limited multi-group, specially averaged theory rel. to ^{238}U 3-67320
- cross-section perturbation determ. by correlated sampling using SAM-CEP computer code 3-74636

neutron transport theory continued

- cross-section sensitivity analysis for discrete ordinates calcs., perturbation approach 3-74637
- diffusion and transport theory comparison from calc. of minimum critical mass 3-46050
- EBR-II, experimental subassemblies, radial position, axial effects on nuclear props., diffusion theory code 3-71219
- EBR-II neutron shield system, diffusion and transport theory calcs. for deep penetration spectra 3-74687
- eigenvalue bounds, optimisation using computational method 3-67386
- energy dependent spatial mesh approximation, static few-group diffusion equations, coupling via scattering and fission 3-63118
- energy-dependent, in two adjacent media, singular eigenmode technique 3-74623
- fast breeder techniques, application to fusion blanket design 3-60321
- fast multiplying system conditions for time eigenvalue existence of fund. mode 3-60239
- fast reactor calcs., eigenvalue and eigenvector problem (*Rumanian*) 3-49311
- fast reactor transients, energy synthesis method, flux and bilinear flux few-group collapsing schemes 3-63116
- fast-neutron spectra in Na, reln. to fast breeder reactor programme 3-71153
- finite element analysis, nuclear reactor design, nuclear diffusion and transport calc. 3-63112
- finite element calculations, variational principle, math. aspects 3-63111
- first flight escape probability for spherical shell with empty central region 3-60245
- flux distributions in rectangular lattice cells, mono energetic neutrons, isotropic scattering numerical methods 3-60244
- flux synthesis calculations, fast reactors, multidimensional diffusion theory problems 3-63115
- fusion reactor, reference theta pinch, discrete ordinates neutronic analysis 3-60326
- fusion reactor blanket design, theoretical and exptl. evaluation of neutron spectrum in graphite mock-up 3-60329
- geometry S_4 eqns. analytic soln. 3-52217
- graphite, moderator temp. discontinuity, effective thermal neutron temp., spatial variation, weighted residuals method 3-40527
- graphite, neutron fusion spectrum, reaction rates determ. 3-63100
- heterogeneous media, image pile theory and effective diffusion coefficients 3-63104
- higher-order scattering anisotropy effects, variational calc. 3-54522
- importance and fission density in spherical U metal assemblies 3-49302
- infinite lattice fluxes, diffusion equation, cell homogenisation, rigorous treatment 3-71150
- infinite medium field, time dependence produced by inversion of the Laplace transform of the time variable 3-60246
- integral eqns. asymptotic solns. with convolution kernel 3-48699
- integral transport program for arbitrary X-Y geometry systems, THER—MOGENE, expt. verification of results 3-63105
- kinetic eqn. soln. in cylindrical geometry using Jacoby polynomials (*Russian*) 3-74641
- light-wave, moderator temp. discontinuity, effective thermal neutron temp., spatial variation, weighted residuals method 3-40527
- LMFBR Doppler coeffs., transport effects, comparison of diffusion and transport codes 3-49329
- medium- and low-energy neutron cross section library, compilation 3-57526
- moderation, elastic, in infinite homogeneous media, general theory 3-71145
- monoenergetic eqn., Hilbert boundary value problem 3-46052
- monoenergetic integral eqn. singular eigenfunction soln. for finite radially reflected critical cylinders 3-71146
- monoenergetic time dependent neutron transport eqn. soln. by eigenfunction expansion for slab geometry 3-71142
- Monte Carlo calc. of neutron energy, space and time distrib. after nuclear air burst 3-74621
- Monte Carlo techniques, corrections to approximate models, rel. to boiling media 3-63107
- multidimensional kinetic problems, diffusion theory, state-of-art 3-71151
- multidirectional modal representation for angular density of one-speed eqn. 3-54525
- multigroup adjoint problem for heterogeneous reactor, formulation and solution 3-40528
- multigroup balance in finite sphere, Boltzmann equation 3-63119
- multigroup calcs., probability table method 3-46056
- multigroup diffusion coeffs., reactor design and analysis using transport 3-67387
- multigroup kinetics eqns., one-dimensional, quasistatic approx. and piecewise polynomials 3-46062
- multigroup reactivity calcs. and central worth discrepancy, fine-structure effects 3-74684
- multigroup S_n transport calcs. for hydrogenous media, truncation errors 3-74639
- multigroup transport cross sections, unified theory 3-49304
- multilayer slab cell systems, angular neutron flux 3-63120
- multimode reactor kinetics eqns. new soln. method by matrix inversion 3-54524
- multisphere spectrometer response matrix calc. using discrete ordinates transport code 3-51733
- noise, spatial correlation range in an infinite multiplying medium including effects of delayed neutrons 3-63128
- noise in boiling reactors, using Langevin analysis, of fluctuations arising from bubble aggregations 3-67391
- nuclear reactor fuel Interim Decay Storage Facility, upper Pu limit, transport and diffusion theory calc. 3-71298
- one-dimensional eqn., application of phase-space finite elements 3-60247
- one-speed model, exact time-dependent second spatial moment 3-43271
- one-speed problems, exact transfer matrix formulation 3-60248
- orthogonal adjointed flows rel. to reactivity disturbances using disturbance theory (*German*) 3-67475
- phase-space finite elements, two dims. transport calcs. 3-45733

neutron transport theory continued

- program, integral transport, for arbitrary X-Y geometry systems. 3-63103
- pulses in noncrystalline moderators 3-49299
- rational escape probability, analytical expression for factor A 3-60240
- reactivity feedback bowing, computer calcs. on optimisation of subassembly coolant flow rate 3-67449
- reactor shield weight optimization by perturbation method, computer program 3-74690
- reflection matrices, two-dimensional, reduction of numerical errors, neutron transport 3-62399
- resonance self-shielding factors, atom density interpolation used with ABBN cross sections 3-49327
- S_8 calcs., effects of photon emission anisotropy in air and sodium 3-49305
- second order discrete ordinate PL eqns. in multidimensional geometry 3-74629
- sensitivity of calcs. to nonelastic angular distributions 3-60251
- shielding, Fe(3 ft), stainless steel (1.5 ft), deep penetration cross-sections 3-74633
- slab transmission, reflection and finite reflector critical problems 3-60249
- source spectra produced by 400 MeV electron in Cu, calcs. for soil, concrete, FeTiO_3 , and iron shields 3-71342
- space- and time-dependent cross sections, application of Phase Space Time Evolution method 3-46053
- space-energy point transport, fast convergent method 3-63114
- stationary problems, variance reduction techniques in Monte Carlo solutions 3-74622
- synthesis method of integral type, first-flight collision probability calc. of one-speed flux distrib. 3-71141
- synthetic kernels for slowing down 3-46049
- thermal, field slaggings caused by cylindrical counters in diffusion media, distortions in flux density (*Russian*) 3-62243
- time dependence of second spatial moment calc. 3-71149
- two dimensional eqn. in X-Y geometry using finite element method 3-71147
- two-dimensional calc. using response matrix method 3-71148
- two-dimensional calcs. using response matrix technique 3-46055
- two-group transport eqn. for linearly anisotropic scattering, critical slab soln. 3-49300
- uniform source half-space problem, extrapolated endpoint, Wiener-Hopf technique 3-43270
- Walsh functions, approx. of transport equation 3-63117
- wave propagation in finite graphite assemblies, multigroup diffusion approach 3-74626
- wave propagation through subcritical assembly, multigroup diffusion theory 3-71143
- ZPPB/FTR-2, calc. of neutron flux distrib. and neutron reaction rates 3-74686
- C, Monte Carlo calculational analysis of exptl. transport data 3-74638
- Pu fuel, recycling, neutronics 3-57578

neutrons

- see also cosmic ray neutrons*
- 16 to 60 MeV neutron beams, dose rate measurements in phantoms 3-56559
- clinical linear electron accelerators, X-ray beams produced neutron dose measurements 3-53769
- dosimetry, at naval research laboratory cyclotron, USA 3-61926
- dosimetry and Kerma values in tissue-equivalent gases 3-53768
- effective orbital g-factor determ. from meas. on ^{206}Pb isomeric 12^+ state 3-49087
- electric dipole moment, improved upper limit 3-54308
- electric polarisability, effect on two-neutron scattering length 3-45978
- e.m. form factor determ. at squared four-momentum transfers up to 3 (GeV/c) 3-62823
- e.m. form factors, from ed quasielastic scattering 3-67041
- fast, determ. of enhancement factors for transition temp. in steel irradiation (*German*) 3-73113
- flux normalisation for large samples in neutron activation analysis 3-40074
- free neutron-electron bound state, non-zeroth order approx. 3-68569
- ionization chamber, operating characteristics 3-53975
- irradiation container with temp. control 3-51706
- magnetic moment of $i_{1/2}$ neutron in ^{207}Po , mesonic contrib. 3-49137
- mass difference, proton-neutron, contributions based on vector meson dominance 3-59957
- nuclear fission, neutron induced, obs. (*French*) 3-60228
- polarimeter, for 3 MeV neutrons (*German*) 3-45549
- radiographic imaging, with thin Gd converters 3-48566
- temperature measurement, rel. to temp. of medium, fission track detectors 3-48539
- thermal determ. of enhancement factors for transition temp. in steel irradiation (*German*) 3-73113
- time-of-flight spectrometer 3-51731
- n-p diff. in gauge theories of weak and e.m. interactions, cancellation of log. divergences 3-59964
- n-p mass difference, calc. from isospin gauge group models 3-59961
- n-p mass difference, cancellation of logarithmic divergences in unified theory of weak and e.m. interactions 3-70914
- np bremsstrahlung, one-pion-exchange-current contrib. 3-54396
- p-n mass difference, convergence of deep inelastic contribution to Cottingham formula 3-52005
- p-n mass difference, reln. to neutral weak currents, Weinberg's model 3-51997
- p-n mass difference in gauge theories of weak and e.m. interaction 3-74367

Newtonian fluids *see fluids***nickel**

- adsorption of O_2 , Auger electron spectroscopy, chemical shift and valence spectra 3-41090
- adsorption of O, CF₂O-BEBO calcs. 3-68501
- adsorption of stearic acid, contact angle rel. to surface coverage 3-43933
- adsorption of Te, LEED spectra determ. of atomic location 3-64240

nickel continued

- adsorption on W, surface self-diffusion of W, field electron microscope study 3-43940
annealed, recrystallisation centre growth rate, X-ray diffraction study 3-72861
atom, oscillator strength determ. (*Rumanian*) 3-63261
atomic absorption spectroscopy, trace metal determ., lubricating and crude oils, evaluation of carbon rod atomiser 3-70485
atomic forbidden lines transition probabilities, tables 3-74814
atoms, electronic structure and atomic magnetic moment calcs., new theoretical model 3-46972
Auger, reson., and autoionization processes with $\text{He}^+(2s)$, He^+ ions at Ni(100), (110) surface 3-47339
beam-foil lifetimes 3-78427
bombardment induced surface damage by Ar^+ , ion scatt., LEED 3-68292
cathode in glow discharge, D_2 diffusion 3-68131
cathode sputtering coeff., Ar, He and Xe discharges, role of ion capture (*Russian*) 3-69128
charge density distrib., form factor calcs. 3-64275
chemisorption bonding of $c(2 \times 2)$ chalcogen overlayers on (001) surface 3-60829
chemisorption of H_2 on (110) plane, obs. by flash desorpt. spectroscopy (*French*) 3-64249
coercive force change within single load cycle after cyclic push-pull deformation 3-60979
composite, W(Mo) wire reinforced, diffusion, carbide layer formation, recrystallisation rel. to weakening (*Russian*) 3-53272
composite materials, Ni-based, diffusion protection by TiN (*Russian*) 3-73012
creep rupture as cause of operational damage (*German, English*) 3-61174
crystal dislocations, sound absorpt., thermal effect (*Russian*) 3-72085
Debye-Waller factors, temp. variation, calc. using modified non-central force model 3-43858
deformation in high speed cutting, microstructure and hardness obs. (*Russian*) 3-80257
deformed in polyslip, structure-sensitive recovery 3-76172
degenerate narrow band, Pauli spin susceptibility and spin waves, Gutzwiller's variational method 3-55406
diffusion, of C, meas. difficulties 3-64210
diffusion, of hydrogen bulk and surface components (*Russian*) 3-79519
diffusion in Al-Al₃Ni, Cu-Mo and Cu-W composites (*Russian*) 3-53222
diffusivity and solubility of oxygen 3-41051
diffusivity of oxygen determ. by internal oxidation of dil. Ni-Be alloys 3-58147
diffusivity of oxygen determ. by internal oxidation of dil. Ni-Be alloys 3-58148
elastic bulk effect, during electron irradi. (*French*) 3-68283
elastic constants meas. by u.s. pulse echo method (*Japanese*) 3-50723
electrical resist. under pressure up to 60 kbar (*French*) 3-50164
electrode, passive, modulation spectroscopy, surface layer structure 3-55964
electrodeposited dispersion-hardened, electron micrographic exam. of thin films 3-61142
electrodeposits epitaxially grown on cube-textured Cu substrates, structure 3-75686
electron beam welding of Ni and of Mo investigation of drop formation (*Russian*) 3-69327
electron probe microanalysis, mass absorption coeffs. for CuLa line (*Japanese*) 3-57022
electron radiation damage, h.v. electron microscope study 3-49905
electron spin polarisation and d-band widths, magneto-optic Kerr effect meas. 3-50549
electron structure and s-d bond of atom 3-64283
electrotransport of ^{125}Sb (*French*) 3-41048
epitaxial growth from vapour phase 3-58594
etch pit shapes rel. to recrystn., orientation relationships (*French*) 3-44584
f.c.c., lattice dynamics, extended de Launay's model 3-55056
ferromagnet, magnetisation near surface, temp., spatial depend., band model 3-58363
ferromagnetic, hyperfine field on atomic nucleus 3-46953
ferromagnetic plates, Maxwell's eqns. for e.m. wave propag., refl. 3-72478
ferromagnetic resonance, in single crystal platelet, linewidth temp. depend. 3-41419
ferromagnetism and hyperfine fields, origin 3-41321
film, (100), magnetoelastic coeffs., ferromag. resonance obs. 3-47118
film, amorphous, local atomic arrangement, electron diff. obs. 3-79591
film, chem. precipitated, struct. and effect on cylindrical mag. film props. (*Russian*) 3-60843
film, electron microscope study of stretching and magnetisation (*German*) 3-72291
film, meas. of CO differential heats of adsorpt., surface coverage depend. (*German*) 3-80578
film, on Fe-Si alloy, influence on domain phase volume and magnetostriiction (*Russian*) 3-44260
film, planar Hall effect, anisotropy (*Russian*) 3-44060
film, pulse heated, Si substrate, thermal energy emission into liquid He 3-72246
film, transformation into β -hydrides 3-80577
film deposition on cathode sputtering in pulsed discharge 3-61111
films, adsorption of CO, multireflection i.r. spectra at room temp. and low pressure 3-68497
films, H_2 adsorption coefficients and binding energy calc. (*German*) 3-79570
films, oblique incidence anisotropy, contrib. of columnar grains 3-50392
fracture parameters, pair interaction influence (*Russian*) 3-72891
grain boundary energy 3-64057
grain boundary fracture mechanism (*Russian*) 3-61132
Hall effect, anisotropy meas. of magnetisation and Hall e.m.f. at temp. 80 to 600 K (*Russian*) 3-64322

nickel continued

- Hall effect and electrical resistance, temp. depend., 25-500°C (*Russian*) 3-44052
hardening by plastic deformation due to shock waves (*Russian*) 3-64898
indicator of extraterrestrial matter accretion on Earth 3-50870
ion beam K_α X-ray cross-sections, enhancement dependence on Z-number of target 3-78597
ion bombardment, swelling phenomena (*French*) 3-58053
ion bombardment, $^3\text{He}^+$, He distrib. profiles, $^3\text{He}(d,p)^4\text{He}$ reaction 3-63209
irradiated metal rel. to preparation of high activity ^{58}Co source 3-62205
Kapitza resistance obs. between 1 and 2K, dislocation effects 3-68458
Kerr magneto-optical effect, polar, single crystals, fields up to 100 Oe, visible spectrum, anomalous change 3-50551
Knoop microhardness analysis 3-61242
lattice dynamics, sp.ht., Debye-Waller factors 3-68343
LEED intensity profiles, surface states 3-50259
level lifetimes by beam-foil method, redetermination of solar abundance 3-78441
liquid, resistivity and thermopower, d resonance calc. 3-44059
low temperature behaviour, Debye temp., energy role (*Russian*) 3-79498
magnetic anisotropy, effect of band structure and shape of Fermi surface 3-50398
magnetic anisotropy, field depend., torque meas. 4.2-300K 3-47081
magnetic dynamic susceptibility, k-depend. exchange formalism 3-47000
magnetic films, (100) oriented, magneto-elastic anisotropy due to dislocations 3-79885
magnetisation, spontaneous, soln. rel. to equally coupled, i-d interaction ferromagnet 3-50327
magnetocaloric effect at Curie temp. 3-44212
magnetoelectric oscillations, nonlinear, in torsional pendulum with Ni tube spring (*German*) 3-44304
meteorite corrosion in neutral soln., depend. on Ni content 3-45058
Mossbauer spectra, hyperfine struct., influence of paraprocesses near Curie temp. (*Russian*) 3-44215
neutron irradiation, fast vs thermal neutrons, defect production, elec. cond. monitoring 3-64073
paramagnetic, electromigration of impurities, valence effect 3-75637
particle, plasma sprayed, blowholes 3-43968
permeation, diffusion and solubility of H_2 3-53238
photometric determination of Co in presence of Ni, thiouoluric acid complexes 3-48650
photon emission induced by fast H^+ , He^+ ion impact 3-61097
plasma coatings on Armco iron, form. kinetics and physicomech. props. (*Russian*) 3-80318
platelets, ferromagnetic resonances as function of orientation of sample at room temp. 3-44328
plating of ABS plastic, atm. exposure effect 3-73065
polycrystalline, magnetoelastic effect 3-79887
pore formation, on 40 keV Ni^+ ion irradi. of pure Ni 3-72106
positron annihilation in ferromag. Ni, band structure obs. 3-58361
powder, multiaxial, Wohlfarth-Kondorskii relation applicability (*Russian*) 3-60980
powders, highly dispersed, interdomain boundary obs., n.m.r. and f.m.r. absorption curves 3-75883
precession of μ^+ through the Curie temp. 3-43814
programme loading effect, influence of electron irradiation, yield point (*Russian*) 3-55008
proton impact, 15 keV, on Ni single cryst., energy distrib. for backscatt. 3-61100
radial distribution in Si cryst., radioactivation analysis, electrical measurements 3-72098
reflectance measurements, precision, 2 to 3 eV, fine structure, spin-orbit effects in exchange-split energy bands 3-52780
resistance element, linear temp. bridge design, math. approach 3-51543
rod, torsional spring element, magnetomech. amplification and generation of mech. vibrs. (*German*) 3-58408
sheet, (111) and (100) surfaces, effectiveness of cleaning techniques using auger electron spectroscopy 3-60841
slow neutron inelastic scattering, isotopic comp. effects (*Russian*) 3-40837
solubility and activity of carbon in pure crystals. (*Czech*) 3-55769
solubility of hydrogen, temp. depend. 3-41017
specific heat scaling functions comparison with Ising and Heisenberg models 3-50329
spin-orbit effects, precision reflectance 2-3 eV obs. 3-41525
splat quenching and production of amorphous Ni 3-80357
stripe domains, in single crystals, of intermediate thickness, micromag. struct., Lorentz microscopy 3-50417
substrate, deposition of Ag, model for Auger electron spectroscopy of layer growth systems 3-41605
substrate, implantation of ^{13}C and ^{18}F ions, range determ. (*German*) 3-49913
superparamagnetism of Ni fine particles, temp. and mag. field depend. 3-68819
surface, (100), atomic positions in $\text{C}(2 \times 2)$ oxygen struct., dynamical LEED obs. 3-64233
surface, (100), with $c(2 \times 2)$ S overlayers, struct., LEED obs. 3-68493
surface, polycryst., oblique Ar^+ bombardment in 1 keV range, sputtering yield, ion incident angle depend. (*German*) 3-47342
surface cleaning technique effectiveness, Auger obs. on (111), (100) and sheet 3-60841
surface electron states 3-50255
surface electronic properties, resonant d-level position 3-41245
surface magnetic properties, resonances and spin reversal 3-41392
surface phonons in $\text{C}(2 \times 2)$ layers on Ni(001), distinguishing of reconstructed and nonreconstructed layers 3-68492
surface structure rel. to high temp. creep deformation (*Japanese*) 3-76168
technical cohesive strength determ. from internal energy 3-44627

nickel continued

- thin film on diamond substrate, thermal phonon radiation power and temp. 3-41072
 thin films, ^{85}Kr labelled, adsorption of H_2 , radiorelease, 273 K 3-43939
 thoriated, impurity induced recrystn. 3-64849
 Tyablikov theory for Heisenberg spin 1/2 ferromagnet, comparison with experimental results 3-68749
 u.s. waves, 5 and 10 MHz, e.m. excitation 3-55452
 vacancy and dislocation conc., u.s. treatment effects (*Russian*) 3-41714
 void form. due to bombardment with 100 keV Ni^{2+} ions (*French*) 3-40942
 void nucleation, h.v. electron microscope studies 3-49906
 whisker, higher order elastic constants. deviations from Hooke's law 3-50097
 whiskers, mass production by reduction, effect of halide impurities 3-64269
 wire, excitation of torsional vibrs. 3-53008
 work hardened in tension, annealing twins role in primary recrystn. (*French*) 3-44585
 Au-Ni, thin film couple, diffusion studied by optical reflectivity technique 3-79528
 $\text{CdS}:\text{Cu}$, $\text{Ni}(\text{Fe})$, stimulated cond. at 77 K, $\text{Ni}(\text{Fe})$ impurities rel. to electron deep traps 3-41203
 Cu, sputtering and Ni ion injection, anomalous diffusion at room temp. and 77 K 3-61084
 $\text{Cu}:\text{Ni}(\text{Co})(\text{Fe})(\text{Cr})$, positron annihilation with impurity core electrons 3-64301
 p-GaAs:Mn, Co, Ni, Cr, transport props. rel. to deep impurity levels 3-41211
 n-Ge:Ni, illuminated, negative diff. resist. in presence of elec. domains and high surface recomb. rate 3-79708
 n-Ge:Ni, quasisurface cond. in strong elec. fields 3-75751
 Ge-Ni film, submm. wave detector, W-Ge-Ni point contacts (*Russian*) 3-73805
 LiCl-Ni X-ray photolum. and thermolum. (*Russian*) 3-69068
 $\text{MgO}:\text{Ni}^{2+}$, MCD spectra of $^3\text{A}_{2g} \rightarrow ^3\text{T}_{2g}$ band, zero-phonon lines and phonon sidebands 3-64642
 $\text{MgO}:\text{Ni}^{2+}$, optical transition study by circular magnetical dichroism (*French*) 3-41515
 NaCl:Ni, X-irradiated, stimulated processes 3-41592
 NaCl:Ni $^{++}$, position and energy of Ni^{++} ions (*German*) 3-58029
 Ni XIV, transition probability for forbidden line in solar spectra 3-42132
 Ni/ Al_2O_3 composite, components compatibility (*German*) 3-41811
 Ni/ Al_2O_3 whisker composite, compatibility limits 3-80441
 Ni/Cu interface, differential modulus effects on mech. behaviour 3-40921
 Ni-Co, ion pair exchange interaction in double nitrates 3-47011
 Ni-GaAs interface, energy structure, Schottky barrier height, Fermi level 3-60916
 Ni-glass-ceramic composite material, heat treatment, crystn. of dispersed glassy phase (*Russian*) 3-41799
 Ni-Mn, ion pair exchange interaction in double nitrates 3-47011
 Ni-SiO $_2$ film, granular metal, hopping cond., temp. depend. 3-52839
 Ni^{2+} , in KMgF_3 , K_2MgF_4 , KZnF_3 , K_2ZnF_4 , exchange interactions, e.s.r. and mag. suscept. obs. (*Japanese*) 3-50357
 Ni^{2+} , in RbMnF_3 , ^{19}F nuclear acoustic resonance obs. 3-41431
 $^{58}\text{Ni}^{+}$ ion bombardment of Ni, effect of beam scanning 3-64076
 Pd-Rh:Ni, spin fluctuation resist., 1.3-20 K 3-64480
 Si:Ni, short wavelength quenching of photocond. 3-50240
 Zn, sputtering and Ni-ion injection, anomalous diffusion at room temp. and 77 K 3-61084
 $\text{ZnS}:\text{Cu}, \text{Fe}(\text{Co}, \text{Ni})\text{O}$, rise, decay and temp. depend. of photocurrents 3-46867

nickel alloys

- see also nickel compounds; Permalloy
 abrasion resistance during friction, hot H_2SO_4 and HCl soln., wear, effect of hardness 3-55914
 Alnico, domain struct., magneto-optical and powder suspension studies (*Russian*) 3-44261
 Alnico V, domain struct. 3-79864
 Alnico-8 magnet alloy, zone melting conditions influence on mag. props. (*Japanese*) 3-50724
 cast, phase anal., microprobe anal., electron microscopy 3-76179
 fatigue crack growth meas. using pot. drop method 3-76415
 fatigue tests, h.f., energy dissipation 3-58695
 glaze oxide layers, structure and mechanism of formation during wear at high temp. 3-64254
 grain boundary energy, La and Ce additions effect (*Russian*) 3-80276
 heat resistant, tensile strength, statistical analysis 3-80375
 heat-resistant, deformability changes kinetics (*Russian*) 3-44602
 Incoloy 800, long-term sodium exposure effects on comp. and microstruct. 3-40555
 Incoloy 901, glaze oxide layers, structure and mechanism of formation during wear at high temp. 3-64254
 Inconel 718, thermal cond. and elec. resist. meas. up to 1200K 3-52817
 Inconel 718 sheet, time-depend. edge-notch sensitivity rel. to mech. and microstruct. characts. 3-64952
 Inconel 718 type alloys, morphology of precipitates and thermal stability 3-69232
 INVAR, cellular model of magnetism at finite temp. 3-52986
 Invar, ferromagnetic, thermodynamic properties calculations 3-52710
 Invar, spontaneous vol. magnetostriction, itinerant electron model 3-50433
 Invar, thermal contact conductance correlations in vacuo 3-47430
 Invar magnetic anomalies 3-44354
 Invar magnetic contribution to compressibility, from temp. depend. of elastic constants 3-61173
 liquid, Ostwald ripening of transition metal carbides (*German*) 3-41745
 low temp. resistivity meas. on dilute ferromagnetic alloys 3-75733
 magnetic disturbances spatial characts. 3-64507
 Nibcolloy, effect of additives on annealing textures 3-61136

nickel alloys continued

- Nimalloy, high mag. permeability, homogenizing treatment effect 3-64528
 Nimonic 108, grain boundary sliding and recrystn. during creep 3-58634
 Nimonic 75, C263, Nimonic 108, Incoloy 901, friction and wear in air at room temp. 3-64955
 Nimonic 75, C263 and 108, glaze oxide layers, structure and mechanism of formation during wear at high temp. 3-64254
 Nimonic 80A, grain boundary cavitation, room temp. pre-strain effects, h.v. electron microscope obs. 3-50701
 Nimonic 80A, secondary creep rate, 600°C, grain size effect 3-64924
 Nimonic 90 and 108, tensile and compressive creep behaviour interpreted. 3-58667
 Nimonic PE16, effect of isothermal aging on precipitate yield strength 3-58698
 pack-aluminizing, boundary conditions for diffusion 3-64964
 phase analysis, methodology (*German, English*) 3-69202
 quenched, critical voltage analysis of precipitation 3-61154
 with rare earth metals, magnetic structure and characteristics (*Rumanian*) 3-68816
 rare earth-Ni, 7:3 phases, cryst. struct. and mag. props. 3-79274
 rare earth-Ni, mag. and struct. props. (*Rumanian*) 3-63982
 superalloy, precip.-hardened, high temp. creep behaviour of single crystals. 3-64916
 superalloys, Ni sulphide formation, crystal structure and morphology 3-40864
 ternary, segregation of elements (*German*) 3-72881
 thoriated, impurity induced recrystn. 3-64849
 Ti-Ni reactor component bonding, phase form. and diffusion behaviour 3-57571
 Ticonal, critical temp. of mag. change pt., apparatus development 3-53956
 Ticonal, domain struct. features (*Russian*) 3-72487
 Ticonal alloy, $\alpha \rightarrow \alpha + \gamma$ transformation, rare earth additions effect 3-80220
 Udimet 700, hodographic prediction of cyclic creep 3-64961
 Udimet 700, inelastic high temp. materials behaviour prediction by strain-rate approach 3-64960
 u.s. treatment during vacuum arc melting, ingot struct. refinement, plasticity, corrosion-resistance (*Russian*) 3-53263
 ALNICO magnet alloys, spectrographic analysis 3-62339
 Al-Al $_3$ Ni aligned eutectic, tensile fracture behaviour at 293, 593, and 743 K 3-47408
 Al-Al $_3$ Ni composite, diffusion of Ni (*Russian*) 3-53222
 Al-Al $_3$ Ni eutectic composite, morphological factors affecting microstruct. coarsening 3-64858
 Al-Ni, Al-rich, rapidly quenched from vapour, metastable solid solubility 3-69247
 Al-Ni, surface struct. due to plane shock wave (*Russian*) 3-80306
 Al-Ni-Co high-titanium alloys, mag. props. characteriz. and Nb influence 3-44599
 ALNI, gas-free burning of metal mixtures and self-propagating high-temp. synthesis (*Russian*) 3-58699
 Co-Fe-Cr-Ni systems, magnetostriuctive delay line characts. (*Japanese*) 3-50436
 Co-Ni, 3d-electron asphericity conc. and temp. depend. 3-41150
 Co-Ni, Co-Ni-P film, annealing behaviour rel. to mag. props. 3-47111
 Co-Ni films, Hall effect, cond., effective magnetiz. (*Russian*) 3-58249
 Co-Ni system, binary phase diagram calc. 3-41701
 Co-Ni-Cr, precipitates formed by internal oxidation (*French*) 3-47384
 Co-Ni-Mo-Cr, structural mechanisms of plastic deform. (*French*) 3-53211
 Co-Ni-P ferromagnetic thin films, cylindrical symmetry, anisotropy field, film thickness and composition (*French*) 3-50431
 Co $_2$ V-Ni $_3$ V quasi-binary alloy, long range ordered structs. 3-55767
 Cr-Ni, composition dependence of shrinkage in sintering of systems charact. by eutectic constitution diagrams 3-80395
 Cr-Ni, eutectic Sn-Zn alloy effect on drilling (*Russian*) 3-76311
 Cr-Ni, oxidation, comp. depend. 3-58661
 Cr-Ni, stress relaxation resist. rel. to training loading, 850°C 3-80368
 Cr-Ni films, structural and electrical props. as function of He, N $_2$, O $_2$ partial pressures 3-58247
 Cr-Ni system, binary phase diagram calc. 3-41701
 Cu-Al-Ni, plane shock waves influence on martensitic transforms. (*Russian*) 3-72829
 Cu-Mn-Ni, manganin, impact loaded, piezoresistance coeff. nonlinearity 3-68930
 Cu-Ni, compositional modulation, absorpt. peaks rel. to band structure 3-55633
 Cu-Ni, dendritic solidification, microsegregation 3-69200
 Cu-Ni, dil., n.m.r. 3-53028
 Cu-Ni, electron lifetime and Dingle-Robinson temps. 3-44063
 Cu-Ni, interactions of impurity atoms with dislocations in dilute copper solutions (*Russian*) 3-72131
 Cu-Ni, mag. permeability correl. with microstruct. 3-75856
 Cu-Ni, nondestructive atomic studies, X-ray diffraction techniques 3-42681
 Cu-Ni, paramag. behaviour, influence of clustering 3-52957
 Cu-Ni, surface comp. changes due to Ar ion bombardment, Auger electron spectroscopy 3-44514
 Cu-Ni, surface struct. due to plane shock wave (*Russian*) 3-80306
 Cu-Ni, thermodynamic functions determ. by e.m.f. meas. using solid electrolyte (*Japanese*) 3-61124
 Cu-Ni, void form. resist. 3-67547
 Cu-Ni dendritic solidification, initial growth of dendrite structs. 3-69199
 Cu-Ni electron irradiation hardening at 78K and 300K 3-60743
 Cu-Ni multilayer system, u.s. vibrs. effect on pore form. and Kirkendall effect (*Russian*) 3-79518
 Cu-Ni-Co, precipitation phenomena, n.m.r. of ^{59}Co obs. 3-50473
 Cu-Ni-Cr, 2% Cr influence on struct. and mech. props. (*German*) 3-41780
 Cu-Ni-Mn high temp. spring material characteriz. 3-69203
 Cu-Ni-Zn, high strength microduplex, characteriz. 3-64911

nickel alloys continued

- CuNi:Fe, differential thermoelectric power, temp. depend. 3-79678
 CuNi-Sn directional solidification, melt vs. cryst. comp., ternary distrib. coeffs. (*German*) 3-55762
 Fe-(23 wt.%) Ni-(0.38 wt.%)C, martensite induced by plastic deformation, morphology and crystallography 3-44566
 Fe-Al-Al, Mossbauer effect of ^{57}Fe , spinodal decomp. obs. (*Japanese*) 3-61145
 Fe-Cr-Ni, deform., recovery and recrystn. of austenite 3-69285
 Fe-Cr-Ni, electron irradi., solute segregation to voids, transmission electron microscopy 3-64874
 Fe-Cr-Ni isothermal martensitic transform. (*Japanese*) 3-50681
 Fe-Cr-Ni systems, $\alpha + \gamma/\gamma$ phase boundary determ. (*Czech*) 3-55757
 Fe-Ni, austenite phase stabilization by cumulative thermal cycling (*French*) 3-41699
 Fe-Ni, austenite start temp., press. depend. 3-41694
 Fe-Ni, dispersion form. of carbides, nitrides (*French*) 3-53231
 Fe-Ni, effect of annealing on mag. props., Mossbauer obs. 3-50497
 Fe-Ni, form restoration process after bending, memory process 3-41784
 Fe-Ni, Invar, mag. diffuse scatt. of neutrons 3-68788
 Fe-Ni, Invar phenomena, plastic deform. and heat treatment effect (*Russian*) 3-58409
 Fe-Ni, Invar type, Ti addition effect on phys. props. (*Russian*) 3-79883
 Fe-Ni, Invar-type, magnetocryst. anisotropy, field depend. 3-68799
 Fe-Ni, isothermal and athermal transform., transform. induced hardening effects (*Russian*) 3-72826
 Fe-Ni, lattice parameter and magnetic moment, Invar effect origin 3-52965
 Fe-Ni, low temp. mech. props. characteriz. 3-50737
 Fe-Ni, martensitic transform. in pulsed mag. field (*Russian*) 3-44559
 Fe-Ni, phase transforms., diffusion role, potentiokinetic obs. (*French*) 3-47362
 Fe-Ni, polymorphic $\gamma \rightarrow \alpha$ transform kinetics (*Russian*) 3-69188
 Fe-Ni, quenching behaviour of delta ferrite (*French*) 3-44621
 Fe-Ni, scale struct. (*German*) 3-76195
 Fe-Ni, splat cooled, microstruct. and segregation 3-64841
 Fe-Ni, spontaneous and forced volume magnetostriction 3-68820
 Fe-Ni, struct. modifications during recovery of equil. by tempering subsequent to cooling 3-64930
 Fe-Ni, surface struct. due to plane shock wave (*Russian*) 3-80306
 Fe-Ni, susceptibility of paraprocess, temp. and comp. depend. (*Russian*) 3-72453
 Fe-Ni (31 at.%) fine particles, superparamag. behaviour, Mossbauer obs. 3-41378
 Fe-Ni (35-65 at.%) alloys, development (*German*) 3-64526
 Fe-Ni alloy, sample surface influence on thermomagnetic effects 3-50413
 γ -Fe-Ni alloys, ferromagnetic resonance 3-50471
 Fe-Ni and Fe-Ni-Cr, stacking fault energy, conc. depend., effect on martensitic transform. (*Russian*) 3-41715
 Fe-Ni atomic volumes calculation, atomic magnetic moment of Fe 3-43764
 Fe-Ni films, annealing effect on constitution and magnetoelectric parameter (*Russian*) 3-60984
 Fe-Ni films, cylindrical, surface roughness and thickness depend. of coercive force (*Russian*) 3-53003
 Fe-Ni films, equatorial Kerr effect in visible spectrum range (*Russian*) 3-61045
 Fe-Ni films, Hall effect, cond., effective magnetiz. (*Russian*) 3-58249
 Fe-Ni films, oxidation effects on mag. props. and constitution (*Russian*) 3-72481
 Fe-Ni Invars, additive effects on Curie pt. (*Russian*) 3-72461
 Fe-Ni liq. systems, stagnant, absorpt. rates of nitrogen, 1600°C 3-64808
 Fe-Ni melt, N_2 diffusion addition effect (*German*) 3-47363
 Fe-Ni powder, milling, specific surface, grain size distrib. rel. to surface active additive 3-80390
 Fe-Ni system, binary phase diagram calc. 3-41701
 Fe-Ni system, hydrogen diffusion coeff. at 25 and 58°C. 3-69226
 Fe-Ni: ^{119}Sn ferromagnetic, Mossbauer effect, magnetisation, 4.2 to 700 K, hyperfine interaction 3-41466
 Fe-Ni-Al, ferromag., adiabatic magnetn., giant negative magnetocaloric effect, temp. inversion 3-72348
 Fe-Ni-Al alloys, Mossbauer investigation, induced change of Fe and Ni magnetic moments 3-50505
 Fe-Ni-Al sheet, nitriding, hardening, struct., mech. props. (*German*) 3-76193
 Fe-Ni-C, martensite burst in deformed and thermally stabilized austenite 3-64826
 Fe-Ni-C, martensite form. during plastic deform. of metastable austenite 3-80209
 Fe-Ni-C martensite, interstitial ordering rel. to tetragonal struct. 3-64828
 Fe-Ni-Co, n.m.r., thin films, magnetostriction effect on temp. depend. 3-75889
 Fe-Ni-Co, reverse transform. struct. evolution characts. (*French*) 3-80204
 Fe-Ni-Co alloy, Invar, irreversible high field behaviour at low temps. 3-50435
 Fe-Ni-Co system phase characteriz. 3-64815
 Fe-Ni-Mn, Invar-type, Mossbauer obs. (*Russian*) 3-68891
 Fe-Ni-Mo and Fe-Ni-Co-Mo martensites, hardening by tempering, comp. depend. (*French*) 3-44622
 Fe-Ni-Mo and Fe-Ni-Co-Mo maraging alloys, redistrib. of alloying elements during recovery (*Russian*) 3-80312
 Fe-Ni-Ta, coherency strains influence on precipitate shape 3-69246
 Fe-Ni-Ti, continuous decomp. of γ -solid soln. (*Russian*) 3-58621
 Fe-Ni-W, struct. changes during ageing of martensite (*Russian*) 3-80247
 Fe-Ni-silica cermet, comp. depend. of mag. permeability and resistivity 3-50400
 Fe-Ni(31.15 wt.%) plastic deform. and thermal stabilization of austenite effect on martensite burst kinetics 3-41782

nickel alloys continued

- $\text{Fe}_2\text{Co}_7\text{Ni}_2$, saturation magnetisation, magnetic moment coherent potential approximation 3-50336
 $\text{Fe}_{1-x}(\text{Cr}_{0.5}\text{Ni}_{0.5})_x$, validity of rigid band model, expt. study 3-44203
 $\text{Fe}_{0.68}\text{Ni}_{0.32}$, Invar, hyperfine field and non-local semi-microscopic model, Mossbauer obs. (*French*) 3-44358
 $\text{Fe}_{65}(\text{Ni}_{1-x}\text{Mn}_x)_{35}$, Hall effect temp. depend. at Neel point 3-58250
 $\text{Fe}_2\text{Ni}_3\text{Mn}_2$, saturation magnetisation, magnetic moment coherent potential approximation 3-50336
 $\text{Gd}(\text{Al}_{1-x}\text{Ni}_x)_2$, Curie temp. meas. rel. to cond. electron number 3-58376
 $\text{LaCo}_5\text{Ni}_{5-x}$, mag. props. and lattice constants rel. to H_2 absorption 3-58380
 Mn-Ni, K X-ray absorp. edge obs. 3-64747
 Mn-Ni-Co nonmag. Elvina-type alloy characteriz. (*Japanese*) 3-44617
 Mo-Cu-Ni, boundaries of single-phase side fields 3-80221
 Mo-Ni system, phase diagram determ. using diffusion couples and equilibrated alloys 3-53209
 MoNi_3 , atomic struct. and microstruct., X-ray obs. (*Russian*) 3-79271
 N-W solid soln., interdiffusion coeffs., conc. depend., correl., with solidus line shape (*Russian*) 3-41712
 Ni/ ThO_2 interfacial and adhesion energy meas. by SEM 3-75659
 Ni-Al, ageing, spatial distrib. of second phase precipitates, correl. parameters (*Russian*) 3-44571
 Ni-Al, with large vol. contents of γ' -phase, plastic deform. mechanism (*Russian*) 3-61162
 Ni-Al cast superalloys, constitution and microstructure 3-50709
 Ni-Al(1.18 wt.%), substruct. misorientation changes during u.s. treatment and creep tests (*Russian*) 3-69212
 Ni-Al(36 at.%), martensite struct. and behaviour (*Russian*) 3-80250
 Ni-Al(36.8 at.%) martensite, cryst. struct. and internal twins 3-50718
 Ni-Au, density of states in valence band from X-ray photoelectron spectra 3-79601
 Ni-Au, quenched, elec. resist. meas., anomaly near ferromag. crit. comp. 3-68588
 Ni-B, electroless plating, mech. and magnetic props. 3-44301
 Ni-B alloys, grain boundary energy 3-64057
 Ni-B coating applic. to ceramic substrates by chem. reductive process 3-76235
 Ni-Be, dil., internal oxidation, rel. to oxygen diffusivity determ. in Ni 3-58147
 Ni-Be, dil., internal oxidation, rel. to oxygen diffusivity determ. in Ni 3-58148
 Ni-C ingot, unidirectionally solidified, periodic macrostructure 3-61159
 Ni-Co, dispersion-hardened, stacking fault energy effect on stress/strain curves 3-58670
 Ni-Co, Hall effect and elec. resist., 25-500°C (*Russian*) 3-44052
 Ni-Co, temp., magnetic induction and composition depend. on Hall and Nernst-Ettingshausen effects (*Russian*) 3-44061
 Ni-Co-W, struct. changes during ageing of martensite (*Russian*) 3-80247
 Ni-Cr, elec. resist. under pressure up to 60 kbar, comparison with pure Ni (*French*) 3-50164
 Ni-Cr, ionic transport, effective charge on Ni ions 3-55102
 Ni-Cr, liq., viscosity and elec. resist., 1300-1800°C (*Russian*) 3-50172
 Ni-Cr, superalloys, synthetic ash contact corrosion test, 1100°C (*Japanese*) 3-76200
 Ni-Cr alloys, surface hardening depth by metallographic method 3-53254
 Ni-Cr thin film, transmission, reflection and absorption of electron beams, 10 to 35 keV, 1 to 3 A/cm², obs. 3-68284
 Ni-Cr-Hf, fine HfO_2 dispersion prod. through internal oxidation 3-76187
 Ni-Cr(20 wt.%), sulphidation props., 700°C and low S press. 3-80337
 Ni-Cr(20 wt.%), with oxide dispersions, high temp. oxidation 3-76188
 Ni-Cr(30 wt.%) solid soln., electrotransfer of Cr ions (*Russian*) 3-68436
 Ni-Cr(49 wt.%), relation between superplasticity effects and extent of interphase boundary (*Russian*) 3-72895
 Ni-Cu, comparison of calculated magnetisation with published measurements 3-60945
 Ni-Cu, conc., local atomic environment effects 3-46945
 Ni-Cu, magnetomech. ratios, spin and orbital moments 3-47121
 Ni-Cu, Nordheim-Gorter plot of thermopower meas., Ni clusters 3-68598
 Ni-Cu alloys, behaviour of localised moment of Ni 3-72475
 Ni-Cu alloys, superparamagnetism 3-47053
 Ni-Cu system, activities of both components at 1400 K 3-64819
 Ni-Cu(3 wt.%) film, transformation into β -hydrides 3-80577
 Ni-Fe, effective field strength on ^{57}Fe from Mossbauer meas. 3-50504
 Ni-Fe, film, ferromag. resonance linewidth angle and thickness depend. 3-41420
 Ni-Fe, film, mag. anisotropy, deuteron irradiation effect 3-79863
 Ni-Fe, Invar type, substruct. effects on thermal expansion (*Russian*) 3-53224
 Ni-Fe, liquid viscosity, structure sensitivity, oscillator crucible method, liquidus to 1700 C, viscosity coefficient, activation energy 3-50022
 Ni-Fe, supercritical film, external stresses influence on stripe domains 3-72497
 Ni-Fe, transport props. at low temps., two band cond. model, density of states 3-55238
 Ni-Fe cylindrical films, magnetisation process in crossed alternating and steady magnetic fields 3-53002
 Ni-Fe film, electrodeposited on Cu, uniaxial anisotropy, comp. depend. 3-64514
 Ni-Fe film, Neel wall and cross-tie wall stability 3-47093
 Ni-Fe film strips, small magnetic reversal domain obs. 3-44291
 Ni-Fe magnetic films, (100) oriented, magneto-elastic anisotropy due to dislocations 3-79885

nickel alloys continued

- Ni-Fe thin films, electroless, structure and coercive force, agitation depend. 3-60848
- Ni-Fe thin films, magnetoresistance, influence of sample geometry 3-46829
- Ni-Fe-Mn film, mag. and galvanomag. props. 3-52830
- Ni-Fe-Mo, permeability-temp. curves, %Ni var. (German) 3-44275
- Ni-Fe-Mo-Ti-Nb for recording heads, mag. and mechanical props. 3-44265
- Ni-Fe-P thin film, electrodeposited, magnetic aging, mechanism 3-53006
- Ni-Fe(25 wt.%), opt. props., i.r. region obs. (Russian) 3-64664
- Ni-Fe(25 wt.%), spin rot. direction in Bloch walls, Lorentz microscopy modification (Russian) 3-41358
- Ni-Fe(40 wt.%) thermomag. effects, sample surface influence 3-47103
- Ni-Hf, thermo-e.m.f., temp. depend., 77-1300K (Russian) 3-72346
- Ni-Mn, elec. resist. under pressure up to 60 kbar, comparison with pure Ni (French) 3-50164
- Ni-Mn dilute alloys, band shifting resistivity 3-72342
- Ni-Mn-Fe, with exchange anisotropy, ordering influence on anisotropy and galvanomag. effect (Russian) 3-60971
- Ni-Mo, short-range order, comp. and heat treatment conditions depend. (Russian) 3-80207
- Ni-Mo, thermodynamic functions determ. by e.m.f. meas. using solid electrolyte (Japanese) 3-61124
- Ni-Pd, forced magnetostriction, temp. and comp. depend. 3-47120
- Ni-Pd, magnetocryst. anisotropy const., comp. depend. 3-47084
- Ni-Pt, mass-defect disordered alloy, phonon modes 3-64127
- Ni-Re, thermo-e.m.f., temp. depend., 77-1300K (Russian) 3-72346
- Ni-Rh, electronic density of states determ. 3-79603
- Ni-Rh, giant mag. moments critical behaviour near Curie point, magnetisation obs. 3-47031
- Ni-Ru, dilute, n.m.r. of host and impurity nuclei, hyperfine fields 3-64560
- Ni-Si, liq., short-range order, X-ray scatt. obs. (Russian) 3-41690
- Ni-Ta-Cr-Mn system dendritic duplex crystals, topography 3-41725
- Ni-transition metal, dil., electronic sp.ht., virtual bound levels model (French) 3-46715
- Ni-transition metal alloys, thermoelec. power and elec. resist. near Curie point 3-44213
- Ni-V, dil., ^{51}V n.m.r. line, environment effects near mag. transition critical conc. 3-64566
- Ni-W, thermo-e.m.f., temp. depend., 77-1300K (Russian) 3-72346
- Ni-Zn-Co, permivar hysteresis loop (Polish) 3-50432
- $\text{Ni}_3(\text{Al}, \text{W})$ single crystals, yield stress, dislocation rearrangements 3-80298
- NiAl, mag. susceptibility and electron transport props. 3-44053
- NiAl, steady-state creep and associated microstruct., stoichiometry deviations effects 3-58669
- NiAl single crystals, stoichiometric, steady-state creep, orientation depend. of deform. mode 3-64913
- NiAl-based ternary β Hume-Rothery phases, optical consts., rel. to valence electron conc. and defect struct. 3-68965
- NiAl-G(Mo) eutectic composites, directionally solidified, stability 3-69198
- Ni_3Al , low temp. specific heat obs. 3-44216
- Ni_3Al , ordering transition, TEM obs. 3-80198
- Ni_3Al single cryst. spring const. calc. 3-64805
- $\text{Ni}_3\text{Al:Fe}$, giant moments in paramag. alloys, depend. on ferromag. crit. comp., Mossbauer obs. 3-64585
- $\text{Ni}_3\text{Al:Fe}$, mag. props. from Mossbauer meas. 3-79956
- $\text{Ni}_3\text{Al-Ni}_3\text{Nb}$ eutectic, directionally solidified, microstruct. and mech. props. (Russian) 3-44605
- $\text{Ni}_3\text{Al}_{25-x}\text{Ga}_x$, $x=0$ and 10, mag. ordering, 2-50K 3-64504
- Ni_3As_8 , maucherite, crystal structure, X-ray diffraction studies 3-44765
- NiCo, spin wave stiffness constant, numerical calc. 3-75846
- NiCr, ThO_2 dispersed, high temp. stability and coarsening 3-64855
- NiCrCo, creep, defect behaviour, stress concentrator effects 3-69319
- NiCu alloy film, planar Hall effect, anisotropy (Russian) 3-44060
- $\text{Ni}_x\text{Cu}_{1-x}\text{MnSb}$ structure, atomic and magnetic, $0.05 \leq x \leq 0.4$, X-ray and neutron diffraction, magnetometry 3-49870
- NiFe film, evaporated, for mag. overlay cct., hysteretic props. 3-44232
- NiFe film, planar Hall effect, anisotropy (Russian) 3-44060
- NiFe spin wave stiffness constant, numerical calc. 3-75846
- $\text{Ni}_{0.86}\text{Fe}_{0.14}$, magnetic excitations, spin waves, inelastic neutron scattering 3-79857
- Ni_3Fe , atomic structure above critical ordering temp. 3-63980
- Ni_3Fe , heat capacity, exptl. data from 300 to 1670 K 3-79841
- Ni_3Fe , ordered structure in evaporated films, effect on mag. props. 3-41368
- Ni_3Fe and Ni_3FeCr , dislocation struct. at various strain hardening stages (Russian) 3-58626
- Ni_3Fe X-ray examination of structural state, mechanical properties, polycrystalline, degree of order, dislocations, slip lines 3-53233
- Ni_3Ga , deformed single cryst., nature of stacking faults, partial dislocations 3-79363
- Ni_3Ga , low temp. specific heat obs. 3-44216
- Ni_3Ga , paramag., magnetisation, susceptibility, $t < 80\text{K}$ 3-64476
- Ni_3Ga , paramag. props., Stoner-Edwards-Wohlfarth model 3-55415
- $\text{Ni}_3\text{Ga:Co}$, mag. props. from Mossbauer meas. 3-79956
- $\text{Ni}_3\text{Ga:Fe}$, giant moments in paramag. alloys, depend. on ferromag. crit. comp., Mossbauer obs. 3-64585
- $\text{Ni}_3\text{Ga:Fe}$, spatial distrib. of magnetisation around Fe impurities 3-64505
- NiMn, concentration depend. of Ni hyperfine field Mossbauer effect in ^{61}Ni 3-41458
- Ni_3Mn , ordered, elec. resist. changes on fission fragment bombardment (Russian) 3-58242
- Ni_3Mn , ordering effect on crit. shear stress magnitude (Russian) 3-44570
- $\delta\text{-NiMo}$, domain struct, antiphase boundaries, inversion domains, permutation twins 3-60974

nickel alloys continued

- Ni_3Mo , dissociated antiphase boundaries, electron microscope exam. 3-58636
- Ni_4Mo , plastic deform., twinning for ordered phase, slip in disordered phase 3-79408
- NiPd, concentration depend. of magnetic hyperfine fields, Mossbauer effect of ^{61}Ni 3-41457
- NiPt, concentration depend. of magnetic hyperfine fields, Mossbauer effect of ^{61}Ni 3-41457
- NiTiSb, Heusler type, cryst. structure and Pauli paramag. props. 3-58003
- Pd-Ni, absorption of H 3-55789
- Pd-Ni, Debye temp., temp. depend., sp. ht. study 3-72155
- Pd-Ni, localised spin fluctuations, comparison with Pd-Cr, Pt-Cr low temp. mag. props. 3-68768
- Pd-Ni-P, comp. depend. of glass transition temp. 3-68167
- Pt-Ni-P, comp. depend. of glass transition temp. 3-68167
- TiNi, twin and antiphase boundary formation, inhomogeneous shear mechanism, elec. resistivity anomaly 3-54972
- TiNi intermetallic, shape memory effect obs. (Russian) 3-80310
- W-Ni-Fe, ductility, fracture resistance rel. to microstructure (German) 3-80391
- W-Ni-Fe sintered composite, reinforcement with W wire fibres 3-69370
- WNi_3 , atomic struct. and microstruct., X-ray obs. (Russian) 3-79271
- nickel compounds**
see also nickel alloys
- $(35-x)\text{NiO} \cdot 8.2\text{ZnO} \cdot x\text{CoO} \cdot 57\text{Fe}_2\text{O}_3$, induced anisotropy in magnetic spectra, variation with amount of Co ions 3-47104
- ferrite, Ni^{2+} ions at tetrahedral sites, anisotropy contribs. 3-64512
- ferrite, superparamag. particles, struct. and mag. props rel. to milling 3-50425
- ferrite, very fine grained, hot pressed, mag. props. 3-50414
- formate, Mossbauer investigation of cation position in mixture with iron formate (German) 3-79967
- sulphides in Ni-base superalloys, crystal structure and morphology 3-40864
- $[\text{Ni}(\text{CN})_4]^{2-}$ X-irrad. complex in NaCl, e.p.r. obs. 3-64544
- $(\text{Co}, \text{Ni})\text{O}$, cation diffusion, semiconductivity and nonstoichiometry 3-41050
- CoO-NiO solid solns., interdiffusion coeffs., 1000-1600°C 3-55844
- Cu-Ni ores, Pt, Rh and Pd determ., X-ray spectrometry, segregation 3-48659
- (Fe, Ni) S_{11} , eclogite nodules, kimberlite pipe, South Africa, phase equilib. 3-44764
- Fe-Ni-S system, unit cell parameters of monosulphide, pentlandite and taenite phases 3-60707
- K(Mn, Ni)F₃, Heisenberg antiferromagnetic alloys, insulating coherent potential approximation 3-55395
- K₂(Mn, Ni)F₄, Heisenberg antiferromagnetic alloys, insulating coherent potential approximation 3-55395
- K(Ni, Zn)F₃, Heisenberg antiferromagnetic alloys, insulating coherent potential approximation 3-55395
- KNiF₃, crystal field and exchange parameters, decoupling transformation method 3-55208
- KNiF₃, lattice constants measurement, double-crystal diffractometry using white X-rays 3-52559
- KNiPO₄, antiferromagnetic, crystal structure, basis atoms coordinates and interatomic distances calc. 3-60715
- MnO, direct reflectance, thermorefectance, electroreflectance spectra interband gap determ. 3-55612
- MnO-NiO, crystal structure and electrical properties 3-75744
- $\text{Na}_2\text{Ni}_2\text{Si}_2\text{O}_{12}$, glasses on metal substrates, interfacial reactions and adherence 3-55882
- Ni complex, 1-10 phenanthroline, crystal electronic absorpt. spectrum anal. 3-80076
- Ni complex, 2,2'-iminobis(acetamidoxime) nickel (II), n.m.r. study of barrier to rotation 3-52331
- Ni complex, bis(O,O'-diethylthiophosphato)nickel(II) and related cpds., P atom-ligand bonding probe 3-52381
- Ni complex, bisquinoxaline-2,3-dithiol nickel, frequency dependence of conductivity and permittivity 3-72564
- Ni complex, hexapyridinenickel (II) nitrate, order-disorder transitions determ. from heat capacity 13-300 K (French) 3-49961
- Ni complex, $\text{Ni}(\text{HDTB})_2(\text{ClO}_4)_2 \cdot \text{EtOH}$, crystal and molecular structure, Patterson and Fourier methods, least squares calculations 3-60685
- Ni exchanged zeolites, structure determ. from magnetic props. 3-44740
- Ni-P films, annealing effect on struct., amorphous to cryst. change, precip. phenomena, mag. props. (Russian) 3-60843
- Ni-(Se)(As)(Sb) systems, phase diagrams, electronic struct. (French) 3-46804
- Ni-SiO₂, catalysts adsorption of H₂ or O₂, magnetic methods, strong and weak field, preferential fixation (French) 3-44741
- Ni-Zn chromite, cooperative Jahn-Teller transition, sound propagation effects nr. transition 3-46709
- Ni-Zn ferrite, hot pressed, prep. and props. for mag. head applic. 3-44264
- Ni(AcAc)₂-phospholenes (I and II), dispersion of ^1H -(^{31}P) heteronuc. chem.-exchange spin decoupling 3-75086
- NiAl, antiphase boundary energy by weak-beam technique of electron microscopy 3-60728
- NiAl_2O_4 spinel, equil. cation distrib., temp. depend. 3-55840
- $\text{NiAl}_2\text{O}_4\text{:CaO}$, sintered spinel, struct. rel. to CaO content (Polish) 3-44664
- NiBe, spin-lattice relax. and Knight shift of ^9Be (French) 3-41443
- $\text{Ni}(\text{CO})_4$, in gas and liq. soln., vib.-rot. coupling effects on correlation functions 3-67825
- $\text{Ni}(\text{CO})_4$ and $\text{Ni}(\text{CN})_4^{2-}$ LCAO-MO-SCF contracted Gaussian, pi back-bonding analysis 3-67762
- NiCl_2 , antiferromagnet, crit. e.p.r. spin dynamics, linewidth divergence behaviour 3-47136
- NiCl_2 , fundamental absorpt. spectra, broad and charge transfer bands 3-58524
- NiCl_2 -heavy water solns., struct. determ. by neutron diff. 3-60660
- NiCl_4^{2-} clusters, molecular orbital calcs., interatomic effects 3-68553

nickel compounds continued

- NiCl₂·6H₂O magnetic phase transition, antiferromagnetic-paramagnetic, antiferromagnetic spin-flop, a.c. magnetic susceptibility measurements 3-47043
- Ni_{0.92-1.0}Co_{0.08}Fe_{0.08}O₄, induced mag. anisotropy const., comp. depend. (*Russian*) 3-72483
- NiCoP film, electroless plated, for mag. overlay cct., hysteretic props. 3-44232
- NiF₂, antiferromag., freq. moments of mag. light scatt. 3-47242
- NiF₂, antiferromagnetic, spin wave spectra and magnon specific heat, magnetic field effects 3-47075
- NiF₂, linear magnetic birefringence, temp. derivative, magnetic specific heat 3-47227
- NiF₂²⁻, force consts. and mean vibr. amplitudes 3-67771
- NiF₆²⁻ and NiF₆⁴⁻, electronic spectra calc. by multiple scatt. method 3-52340
- NiF₆⁴⁻ clusters, molecular orbital calcs., interatomic effects 3-68553
- NiFe_{2-x}Al_xO₄ ferrite, magnetic structure, crystallographic structure, influence of Al content, neutron diffraction examination 3-52980
- NiFe_{0.6}Cr_{1.4}O₄, magnetostrictive and mag. props., cubic to tetragonal phase transition 3-75861
- NiFe₂O₄, CaO impurity influence on dielectric behaviour 3-53056
- NiFe₂O₄, solid soln. with Ni₂TiO₄, mag. props., cationic distrib. 3-72454
- NiFe₂O₄ polycrystalline film, highly stressed, ferromag. resonance obs. 3-41416
- Ni_{1-x}Fe_{2x/3}O₄ and Mg_{0.92-x}Ni_xFe_{2.08}O₄, induced mag. anisotropy const., comp. depend. (*Russian*) 3-72483
- NiFe₂Se₄, 3d-electron delocalization (*French*) 3-72550
- NiL₂²⁻ in (N(C₂H₅)₄)₂ ZnL₄, mag. circular dichroism spectrum, spin-orbit splitting, quenching 3-50601
- Ni₃IB₂O₁₃, boracite, mag. struct. (*German*) 3-50376
- Ni(II), solvation in HMPT, ³¹P and ¹³C heteronuclear pulsed n.m.r. obs. 3-75084
- Ni(II) anhydrous acetates, struct. 3-40908
- Ni(II) chelates, dimeric, mass spectra 3-60398
- Ni(II) complex, bis-isopropylsalicylaldiminato, single crystal, mag. anisotropy and susceptibility 3-72447
- Ni(II) complex, chelate of anthranilic acid, i.r. spectra, metal-ligand stretching frequencies 3-54688
- Ni(II) complex, ethyl xanthato, i.r. spectra assignments, normal coordinate analysis 3-54695
- Ni(II) complex, methyl xanthato, i.r. spectra assignments, normal coordinate analysis 3-54695
- Ni(II) complex, Ni(CH₃NHCH₂COO)₂·2H₂O, crystal and mol. struct. 3-79286
- Ni(II) complex, o-hydroxy-4-benzamidothio semicarbazide, distorted octahedral, visible absorption spectra 3-58517
- Ni(II) complex iminodiacetonickel(II), hygroscopic compound i.r. spectra, improved KBr pellet method 3-45491
- Ni(II) complex, Ni(N₂H₅)₂(SO₄)₂, susceptibility and sp. ht., applicability of Heisenberg linear chain model 3-47007
- Ni(IO₃)₂, cryst., mag. and nonlinear optical props. 3-52609
- Ni(IO₃)₂, prep. and characterisation, absorpt. from 35 to 33000 cm⁻¹ 3-53120
- Ni(IO₃)₂·2H₂O, paramag., cryst. struct. 3-75503
- Ni₂·6H₂O, cryst. structure and thermal expansion (*French*) 3-52611
- NiMn₂O₄, spinel structure, X-ray K-absorpt. edges of cations 3-44502
- NiMoS₄, cryst. structure obs. (*French*) 3-52607
- Ni₂N, film, electron state determ. by electron diffraction 3-79297
- Ni(NH₄)SO₄·6H₂O, precipitation from aqueous solns., 20-35°C 3-72795
- Ni(NH₄)₂(SO₄)₂·6H₂O, nucleation and precipitation from aqueous solution 3-52589
- Ni(NH₃)₆X₂ (X=Cl, Br, I, BF₄), i.r. line profile 3-72646
- NiO, adsorption of NO 3-41091
- NiO, antiferromag. props., symmetry of excitons, magnons, cryst. field splittings 3-64510
- NiO, antiferromag.-paramag. transition, crit. behaviour of spontaneous magnetisation 3-58382
- NiO, chem. transport, optimal growth range (*Russian*) 3-55733
- NiO, conc. depend. diffusion of Cr 3-64212
- NiO, exchange and superexchange parameters 3-41337
- NiO, mass spectrometry evaporated by electron beam 3-75097
- NiO, paramagnon symmetries and magnon dispersion relations 3-68796
- NiO, small particles, i.r. surface modes 3-41524
- NiO, thermal cond. in range including Neel temp. 3-58379
- NiO powder, reduction, nucleation rate, kinetics rel. to Neel transition 3-55164
- NiO surface, adsorption theory, structural and chemical defects (*Russian*) 3-79556
- NiO:Li, pressure sintered, Neel temp., Young's modulus and resistivity obs. 3-72466
- NiO:Sn⁴⁺, impurity state determ. by Mossbauer spectra 3-72100
- NiO-Al₂O₃ system, interdiffusion coeffs., vacancy conc. depend. 3-72222
- NiO-CaO solid soln., exsoln. kinetics and microstruct. development 3-72941
- NiO-CoO solid solns., defect struct. characteriz. 3-61192
- NiO-MgO single cryst. solid solns., comp. depend. of ⁶⁰Ni diffusion 3-72224
- Ni(OH)₂·Ni(NO₃)₂·2H₂O, structural investigation (*French*) 3-63990
- xNi(OH)₂·yNi(NO₃)₂·zH₂O, structural classification (*French*) 3-60696
- NiPS₃, preparation, crystal structure and magnetic properties 3-64003
- NiS, antiferromagnon dispersion function, coupling consts. 3-47072
- NiS, band structure calc. using simplified linear-combination-of-muffin-tin-orbitals method 3-58213
- NiS, metal-nonmetal transition investigation using Mossbauer effect of ⁵⁷Fe 3-53049
- NiS, thermal expansion and linear thermal expansion coeff., temp. depend. 3-46722
- NiS, valence band structure, X-ray photoelectron obs. of density of states 3-50124

nickel compounds continued

- NiS:⁵⁷Fe, metal-nonmetal transition, Mossbauer effect 3-41152
- NiS:⁵⁷Fe paramagnetic metal-antiferromagnetic nonmetal transition, Mossbauer study 3-44357
- NiS₂ (Ni_{1-x}Co_x)S₂ (Ni_{1-x}Co_x)S₂, band structure, insulator-metal transition, weak ferromagnetism 3-41144
- NiS₂, high-pressure effect on semiconductor-metal transition temp. 3-79751
- NiS₂, magnetic susceptibility, temp. depend., mag. transition at 31K 3-64496
- NiS₂, pyrite type, weak ferromag. T_c equiv. to antiferromag. M2-mode T_N, neutron diff. obs. 3-68783
- Ni_{1-x}S:⁵⁷Fe; metal-nonmetal transition, Mossbauer effect, 4.2 to 300K 3-44030
- NiSO₄·6H₂O and NiSO₄·6D₂O, vibrational spectra, frequency and temp. effects 3-44420
- α-NiSO₄·6H₂O e.p.r. measurements, single crystals, spin Hamiltonian parameters, direction cosines of crystalline field 3-50440
- NiSO₄·7H₂O, isomorphism, M²⁺·SO₄·7H₂O series, M=Mg, Zn, Ni, Fe, Co (*German*) 3-52613
- NiS_{2-x}Se_x, metal-semicond. phase diagram, resist., susceptibility and calorimetric meas. 3-72328
- NiSe, thermal expansion and linear thermal expansion coeff., temp. depend. 3-46722
- NiSe_{2-x} pyrites, prep. and elec. props. 3-60906
- NiSi, electron struct. determ. by X-ray electron and X-ray spectra (*Russian*) 3-58568
- NiSiF₆·6H₂O, zero-field splittings, e.p.r. thermometer applic. 3-44317
- Ni₂SiO₄-enthalpy of olivine-spinel transition by solution calorimetry at 713°C 3-76532
- NiSnCl₆·6H₂O and NiSnCl₆·6D₂O, vibrational spectra, frequency and temp. effects 3-44420
- (Ni_{1-x}T_x)B, electronic specific heat, transition metal impurities, density of states at Fermi level 3-41118
- NiTe, thermal expansion and linear thermal expansion coeff., temp. depend. 3-46722
- Ni₃Te₄, thermodynamic properties, from 298 to 950 K, order-disorder transition 3-68408
- Ni₂TiO₄, solid solns. with NiFe₂O₄, Fe₃O₄ mag. props., cationic distrib. 3-72454
- xNiTiO₃·(1-x)Fe₂O₃ rhombohedral solid soln., heat treatment influence on mag. and crystallographic props. (*French*) 3-44255
- NiTi₂(SO₄)₂·6H₂O, cross, spin-lattice relax., a.c. susceptibility meas. 3-79892
- Ni₃(VO₄)₂, n.m.r. spectra for ⁵¹V at room temp. 3-75890
- Ni₃V₂O₈, crystal struct. refinement 3-79292
- NiWO₄, absorption spectrum, effect of antiferromagnetic ordering 3-44413
- NiWO₄, antiferromag. reson. lines in far i.r. absorpt. spectrum 3-50469
- Ni₄X, complexes far-infrared spectra, (X=Cl, Br, I), pyridine and gamma-picoline, metal-ligand vibrations, isotope shifts 3-57649
- NiZn ferrite, superparamag. particles, struct. and mag. props. rel. to milling 3-50425
- Ni_{0.65}Zn_{0.05}Fe_{0.32}O₄, Fe²⁺ distrib. in tetrahedral sites, Mossbauer obs. (*Russian*) 3-47189
- Ni_{1-x}Zn_xFe₂O₄, high field Mossbauer study 3-79963
- (Ni_{1-x}Zn_x)₂(OH)₂ magnetic props. at 4.2 to 40 K and 50 to 45000 Oe, α, and β solids 3-79826
- Ni(110)-c(2×2)S surface, electron excited Auger spectrum, correlation with ion neutralization 3-44511
- night airglow** see *nightglow*
- night sky**
see also *nightglow*; *twilight*
brightness, in u.v. and visible, Kosmos 51 and 213 obs. in space (*Russian*) 3-44878
brightness in u.v. and visible kosmos 51 and 213 observations in space (*Russian*) 3-44877
He II x.u.v. radiation, sounding rocket obs. 3-51134
- nightglow**
continuum meas., diurnal and season variations 3-56184
diurnal variation at Dumka in relative intensity of 5577Å line 3-59129
geocoronal hydrogen, excitation of low luminosity Balmer emissions 3-76813
i.r. airglow structures, photographic parallax heights 3-53515
stellar component in B wavelength band 3-61794
twilight enhancement of 6300Å, 5577Å oxygen emission lines 3-65424
zenith intensity variations at El Leoncito Obs. 3-51088
HeII 304Å, HeI 584Å, intensity obs. at 180 km, altitude from rocket telescope system 3-65533
Na emission features, diurnal variations 3-47779
Na nightglow intensities in Europe-Africa sector diurnal, annual and solar cycle var. 3-51101
NaI, 5890/6Å, emission rate depend. on atm. structure and dynamics 3-65423
O I 6300 Å emission, average nighttime vertical profile 3-80778
O I forbidden red lines behaviour at Naini Tal 3-61492
O I permitted line emissions, excitation in tropical nightglow 3-53509
OH bands of Δv=2 sequence altitude distribution in the nightglow 3-56177
OH nightglow intensities in Europe-Africa sector, diurnal, annual and solar cycle var. 3-51101
OI 5577 Å laboratory emission, discharge expt. on oxygen and hydrogen gas mixture 3-57601
OI 6300 Å emission at low latitudes, Ogo 4 obs. in map-form 3-80782
- Nilsson's model** see *nuclear shell model*
- niobium**
anelastic relax. and internal friction after annealing in ultra high vacuum 3-43829
Auger spectroscopy investigation of reaction with O and N, reaction kinetics 3-55166
band structure, self-consistent APW calcs. at normal and reduced lattice spacings 3-43994
band structure calc., of cubic 4d Nb 3-72313

niobium continued

- bicrystal, growth by floating zone technique using Y-shaped seed from partially split single crystal 3-69160
 blister form. on He⁺, D⁺ bombard. of poly- and monocryst. Nb 3-60750
 blister formation, ⁴He⁺ ion implantation, orientation depend. 3-72111
 blistering due to D⁺ ions at 300 keV and above 3-40943
 blistering in He⁺ implanted (111) monocrystals 3-43812
 carburizing in glow discharge plasma 3-76217
 chemical analysis, review 3-59695
 cold deformed, short-term heat resist., gaseous medium influence (Russian) 3-80427
 creep-deformed, distribution of O₂, mass spectrographic exam., laser vapourisation (Russian) 3-41722
 cyclic deformation, enhanced strain aging, interstitial solute-moving dislocation interaction 3-50722
 defect influence on internal friction near normal-supercond. transition 3-52926
 defect structure of single crystals, deformed in rolling at 77K (Russian) 3-58627
 deformation mechanisms, 20-300K (French) 3-79409
 dehydrogenated, dislocation structures and mechanical props. determ. 3-80283
 deposition on Cr-Ni steel, nuclear reactor fuel cans, to form internal getter (German) 3-71306
 desorption of H₂ from Nb surface, spatial distrib. 3-55154
 diffusion of H and D 3-52725
 diffusion of hydrogen, anelastic obs. 3-79516
 dislocation loop, electron microscope image contrast, calc. 3-79361
 elastic moduli meas. under hydrostatic press. by u.s. vel. method (French) 3-54994
 elastoresistivity coeff. 3-58243
 electrical resist. from 77 to 293K, interstitial diffusion influence (French) 3-52818
 electronic struct. and density of states, empirical pseudopot. method calcs. 3-55192
 electrophysical props. of single crystals, high temp. heating influence (Russian) 3-41172
 fast-neutron cross sections, optical model, reln. to fusion reactor design 3-71113
 fusion reactor blanket, Li cooling, neutron and gamma heating rates 3-60328
 internal friction, i.f. obs. in normal and superconducting state (Russian) 3-46678
 ion implantation and re-emission of He, temp. depend. 3-79394
 ion implantation of Th, surface analysis by secondary emission mass spectroscopy (French) 3-40946
 ion irradiation by ⁴He⁺, bubble and blister formation 3-79393
 LEED investigation of reaction with O and N 3-55124
 magnetoacoustic oscillations, longitudinal and transverse waves, detection 3-52783
 mechanical properties, effects of interstitial solute additions 3-80340
 Meissner effect and stable trapping of fields 3-46940
 melting point, normal spectral emittance and electrical resistivity meas., pulse heating method 3-45449
 metal, b.c.c., lattice distortion due to gas interstitials 3-64029
 in minerals, determ., X-ray fluorescence spectroscopy 3-56253
 Nb, pure, surface superconductivity and pinning sites 3-55365
 neutron irradiation, hardening, oxygen impurity effects, defect agglomeration 3-40937
 neutron irradiation, temp. effect on hardness 3-79387
 oxidation investigation by static method of secondary ion mass spectrometry 3-75683
 plastic deform. at 2.17-300 K of high purity Nb single crystals (French) 3-55004
 precipitation in steel, strengthening obs. 3-64922
 preplastic deformation of single crystals, 4.2K, stress relax. obs. (French) 3-58066
 quenched, H-vacancy complex behaviour, internal friction obs. (Russian) 3-52671
 recovery after fast neutron irradiation at low temp. 3-68287
 solid and liquid, enthalpy meas. 3-72209
 solubility and diffusivity of H isotopes at high temps., reln. to CTR components 3-61161
 sputtering yields by D in keV range 3-60294
 superconducting, anomalous sp. ht., supercond. energy gap 3-46920
 superconducting, attenuation of transverse ultrasonic waves 3-72424
 superconducting, dirty, microscopic magnetic field distrib., neutron diffraction expts. 3-46923
 superconducting, fast particle irradiation effects 3-79395
 superconducting, Knight shift and nuclear spin relax. calc. 3-55356
 superconducting, misalignment of flux lines, neutron small-angle diffraction study 3-64435
 superconducting and normal states, temp. depend. of elastic consts. 3-68715
 superconducting cavities, attaining high fields, at SLAC 3-56722
 superconducting cavities, frozen-in flux, additional losses 3-56723
 superconducting cavity, electron loading 3-56721
 superconducting cavity beam deflectors 3-56863
 superconducting cylinder, permanent multipole mag. field storage, charged particle focussing 3-42631
 superconducting film, sputtered on metallic substrates, struct. and flux penetration 3-79788
 superconducting thin film quantum galvanometer, overlay on Ta 3-70324
 superconducting transition temperature, calc. of press. dependence 3-79789
 superconductor, pinning on point defects, statistical theory 3-68735
 superconductor, type II, vortex monocrystal creation and control (French) 3-50301
 superconductor, use as thermal insulations at low temp. 3-39882
 superpure, prep. of single crystals (Russian) 3-58349
 surface, interaction with O₂, high temperature (French) 3-79574
 surface, thin oxide film form., ellipsometric obs. (French) 3-46761

niobium continued

- tensile behaviour, 20 to 1000°C, interstitial effects (French) 3-80291
 thinning using twin-jet electropolishing unit, for transmission electron microscopy 3-50085
 u.s. absorption, purity depend. in normal, Meissner states, meas. and theory 3-64433
 work function determ. near melting point using d.c. arc 3-69132
 X-ray emission, Mv-, M_{2,3}-bands, wave functions of valence band electrons (Russian) 3-80117
 X-ray K absorption edge investigation for various Nb compounds 3-55697
 yield point temp. depend. rel. to dislocation pinning by oxygen interstitials (Russian) 3-72854
 Al₂O₃/Nb bonded components, stresses due to irradiation, swelling of alumina 3-78374
 CaF₂:Nb³⁺, e.s.r. and ENDOR studies 3-58425
 in α -Fe, internal friction peak phenomena due to Nb-N interaction 3-64871
 in Fe-Mn-C alloy, effect on crystal. (Russian) 3-44561
 He bubble formation and migration due to α -particle irradiation 3-52648
 Nb S-band superconducting cavity, with large beam tubes 3-56861
 Nb superconducting cavity, surface preparation techniques 3-56862
 Nb:O, N⁺ irradiation, effect of O impurity on void formation 3-79335
 Nb:W, Ta, impurity redistribution by electron beam float zone refining 3-44540
 Nb/Al₂O₃ composite, components compatibility (German) 3-41811
 Nb-H system, β -hydride phase, structure obs. by electron diffraction analysis 3-58637
 NbAl₂O₃ mixture type films, crit. current density, mixed state form., flux eddies, second crit. field (Russian) 3-68728
 O absorption, kinetics at low press. and high temp. (German) 3-43880
- niobium alloys**
see also niobium compounds
 Inconel 718 type alloys, morphology of precipitates and thermal stability 3-69232
 plastic deformation resistance, influence of small alloying additions (Russian) 3-72890
 surface blistering by He ions, effect on fusion reactor operation 3-60289
 CoNb intermetallics, orbital susceptibility and ⁵⁹Co Knight shift, d-electron motion (Russian) 3-52954
 Cu/Zr-Nb and Cu/Zr-Cu diffusion couple behaviour, intermediate phase props. (Japanese) 3-58612
 Cu-Nb, dilute, superconductivity, metallographic studies 3-75804
 Fe-Cr-Nb, precip. hardening phenomena 3-69281
 Nb-Al-Ge superconducting ribbon, resistive measurements 3-56696
 Nb-Al-Si alloy, at. absorption spectroscopy (French) 3-50678
 Nb-Al-Si alloy, isothermal sections at 1500°C and 1300°C, Nb(Si,Al)₂ phase behaviour (French) 3-50677
 Nb-Au phase diagram (German) 3-44565
 Nb-Mo, anomalous behaviour during interdiffusion 3-72860
 Nb-Ru system, martensitic transitions, temp. and conc. depend. (French) 3-58126
 Nb-Sn superconducting solenoid, 50 kG gas cooled, operated at 13 K 3-73700
 Nb-Ta(20 at.%), nitride precipitate morphology and struct. 3-64872
 Nb-Ti, ordered dislocation structure, hydrostatic pressure effects (Russian) 3-55788
 Nb-Ti, supercond., microstructure after cold deform., heat treatment 3-76182
 Nb-Ti, superconductors, welding, reduction of current degradation 3-41788
 Nb-Ti (64 at.%) superconducting wires, critical current density anisotropy 3-64428
 Nb-W-Mo-Ti-Zr-C, quenching, ageing, carbide precipitation hardening 3-76176
 Nb-W-Mo-Zr, aged, acbide phase distrib., electron microscope studies (Russian) 3-41721
 β -Nb-Zr, deform. temp. depend., slip, twinning and dislocations rel. to yield and fracture 3-52662
 Nb-Zr, interdiffusion, prolonged heating, X-ray microanal. (Russian) 3-69250
 Nb-Zr, solubility and diffusivity of H isotopes at high temps., reln. to CTR components 3-61161
 Nb-Zr, steady-state creep, Zr conc. depend. (Russian) 3-58642
 Nb-Zr (1 wt.%) alloy, sp. heat, electrical resistivity and hemispherical total emittance determination 3-64971
 Nb-Zr wire to Pb-Sn solder, blob junction, self-field effects on Josephson supercurrent 3-52934
 Nb-Zr-Ti, superconductors, welding, reduction of current degradation 3-41788
 Nb-Zr(1%), neutron irradiation effect on tensile props. 3-79386
 Nb-Zr(1%), neutron irradiation effect on hardness 3-79387
 Nb₃Al_{1-x}Be_x(B₂), superconducting critical temp., critical current density 3-50286
 Nb₃Al_{1-x}M_x, M = Be, B, Al5 struct., superconducting crit. temp. obs. 3-50297
 Nb₃Au_{1-x}Al₁₅ type phases, superconductivity, structure and magnetic susceptibility 3-58334
 Nb₃Sn, angular dependence of critical currents in transverse mag. field 3-41296
 Nb₃Sn, chemically deposited, longitudinal and transverse currents from 14.5 to 17.5K 3-44169
 Nb₃Sn, feasibility of nonphonon mechanism of superconductivity 3-41299
 Nb₃Sn, field, angular and defect dependence of critical current for $t \leq 4.2K$ 3-41168
 Nb₃Sn, fluxoid pinning on grain boundaries dependence on the mag. field direction 3-44166
 Nb₃Sn, phonon damping 3-49946
 Nb₃Sn, supercond., critical current density, temp. depend. 3-50298
 Nb₃Sn, supercond., cubic A-15 phase stabilization, a.c. heat capacity meas. 3-64422
 Nb₃Sn, supercond., shock wave synthesis from powder mixtures 3-69328
 Nb₃Sn multifilamentary composite wires, heat treatment effects on critical currents 3-60938

niobium alloys continued

- Nb₃Sn supercond. cylinder, permanent multipole mag. field storage, charged particle focussing 3-42631
 Nb₃Sn superconducting tapes, microprocessing by electron-beam microetching 3-56978
 Nb₃Sn superconducting tunnel junctions, effective phonon spectrum by electron tunnelling 3-68737
 Nb₃Sn-Pb(Sn), sputtered film supercond. junction, tunnel characts., energy gap values 3-75818
 Nb_{0.73}Ta_{0.27}, supercond., pot. difference, current depend., transverse mag. field (*French*) 3-55360
 (Nb_{1-x}Ta_x)Al_{1-y}Ge_y, A15 struct., superconducting crit. temp. obs. 3-50297
 (Nb_{1-x}Ta_x)₃Al_{1-y}Ge_y, superconducting critical temp., critical current density 3-50286
 NbTi, 40/60 wt.%, supercond., critical current density, temp. depend. 3-50298
 NbTi, filamentary superconducting composite, stability behaviour, flux jumps 3-50292
 NbTi, superconducting, fast particle irradiation effects 3-79395
 Nb₂X-A15 cpds., low temp. paramag. susceptibility and supercond. crit. temp. (*French*) 3-68724
 NbZr, superconducting, fast particle irradiation effects 3-79395
 Ni-Fe-Mo-Ti-Nb, for mag. recording heads, mag. and mech. props. 3-44265
 Ni₃Al-Ni₃Nb eutectic, directionally solidified, microstruct. and mech. props. (*Russian*) 3-44605
 Ta₇₀Nb₃₀, supercond. single cryst., magnetization and pinning 3-58344
 Ti-Nb(35 at. %), heat treatment effect on microstruct. and supercond. 3-79800
 U-Nb, fracture toughness and mode correl. with microstruct. 3-76414
 U-Nb, niobium segregation phenomena 3-61149
 U-Nb (4.5 wt. %), aged, stress corrosion cracking 3-69259
 U-Nb(4.5 wt. %), Al-coated, stress corrosion cracking 3-47411
 W-Nb, thermal expansion coeff., anomalous conc. depend. 3-72213
 Zr-Nb, carbide-oxide reaction prep. 3-72821
 Zr-Nb (19 wt. %), transform. and age hardening behaviour 3-47412
 Zr-Nb (20 at. wt. %), Mossbauer scatt. study of solid state phase transformations 3-55068
 Zr-Nb alloy preparation by carbide-oxide reaction, nuclear reactor use 3-60279
 Zr-Nb(2.5 wt. %), neutron irradiation growth behaviour, cold work and stress-relieving effect 3-41773

niobium compounds

see also niobium alloys

- niobate glass-ceramic, energy storage improvement by pressure crystallisation 3-75946
 niobate ions in crystals, vibrational spectra 3-55602
 oxides, stoichiometric variability in block structure and tunnel structures 3-40909
 X-ray K absorption edge of Nb 3-55697
 Cd₂Nb_{2-x}Sn_{2x}O_{7-2x}F_{2x}, Mossbauer study of props. and phase transitions 3-79962
 KNbO₃, intracavity second harmonic generation of YAlG/Nd laser 3-51948
 Nb-H systems 3-49993
 NbC, dispersion form. in stainless steel (*French*) 3-53231
 NbC, NbN, NbO, heat of formation calc. 3-43878
 NbC, sintered, galvanomag. props., 300 and 20.4 K (*Russian*) 3-50222
 NbC, X-ray determ. of Debye temp., thermal at. vibr. amplitude 3-72156
 NbC electron microprobe reference materials 3-40078
 NbC_{0.87}, single crystals, microhardness, temp. depend., room temp. through ductile-brittle transition 3-47446
 NbCl₅, molten, phase equilibrium, Raman spectra, 220-320°C (*German*) 3-52702
 NbH_{0.95}, positron annihilation, proton model 3-50131
 NbN, high supercond. transition temp. rel. to lattice instability 3-64421
 NbN, thin films, optical, elec. props., on fused silica surface 3-64755
 NbN film, reactively sputtered, supercond. critical current anisotropy 3-50299
 NbN superconducting films deposited by reactive sputtering, upper critical fields (*Japanese*) 3-68710
 Nb₁₂O₉, model of two interstitial metal and O atoms, electron microscope obs. 3-79337
 Nb₂O₅, reaction with Eu₂O₃, X-ray anal., lattice consts. determ. 3-75598
 Nb₂O₅, sputtering, surface binding energy, temp. depend., conversion to NbO 3-69119
 Nb₂O₅-CaO-SiO₂, new oxide glass, form. by laser spin melting and free fall cooling 3-68168
 NbS₂, band structure 3-50126
 Nb₁₄S₃, preparation, crystal structure determ. 3-40903
 NbSe₂, Ginzburg-Landau parameter anisotropy, penetration depths and coherent distances 3-55349
 NbSe₂, layer type structure, electronic props. of two dimensional solids 3-50133
 NbSe₂, lubricating action mechanism (*Russian*) 3-41798
 NbSe₂, microwave absorption, critical fluctuations 3-41302
 NbSe₂, optical functions calculated from reflectivity data by Kramers-Kronig analysis 3-64618
 NbSe₂, reflectivity in extreme u.v. range, band structure investigation 3-55609
 NbSe₂, supercond. transition temp., effect of 3d impurities 3-52922
 NbSe₂, temp. depend. of critical field ratio, supercond. meas. 3-68720
 NbSe₂ organic intercalation complexes, electron microscope examination 3-72039
 Nb₃Si, formation between 20 and 70 kbar and 1000-2000°C 3-58005
 Nb₃Sn, Meissner effect and stable trapping of fields 3-46940
 Nb(V) complex, characterisation, ¹⁹F, ¹H n.m.r. soln. study, isomer obs. (*French*) 3-53027
 NbX₅ (X=Cl, F, Br) normal coordinate analysis and thermodynamic functions 3-54654

niobium compounds continued

- Nb₂Zr₆O₁₇, crystal structure 3-58019
 Nb₂O₅:MgF₂ linear defects, extended, direct observation by high resolution electron microscopy 3-43805
 TiO₂.7Nb₂O₅, defect struct., high resolution electron microscope obs. 3-43804
 V_{1-x}Nb_xO₂, (0 ≤ x ≤ 0.33), vapour phase prep. and characteriz. of single crystals. (*French*) 3-72802
 β-ZrO₂.12Nb₂O₅, cryst. struct., high resolution electron microscope obs. 3-43777
- nitrogen**
- 3.9 GeV N ions, biophysical properties, dosimetry 3-56557
 3.9 GeV N ions, biophysical properties, microdosimetry 3-56558
 absorption and effusion in liquid Fe alloys (*German*) 3-76150
 absorption cross sections from 180 to 700 Å 3-67805
 absorption spectrum, N₂ diatomic mols. trapped in Ne matrix, vibr. and rot. structure 3-75011
 adsorbed on W, adsorption and desorption kinetics 3-79568
 adsorption, isothermal and thermo-osmotic, by microporous C membranes 3-80575
 adsorption, surface area meas. of colloidal crystalline materials 3-48343
 adsorption on metal oxides with preadsorbed NO 3-41091
 adsorption on Mo (100) face, LEED obs. (*French*) 3-79563
 afterglow, Lewis-Rayleigh type, group IA and IIB metal atom excitation 3-54575
 afterglows, Na atom emission, excitation process and Doppler temp. 3-46174
 arc, freely decaying, electrical conductance time consts. 3-71977
 arc, stable auroral red, vertical distrib. of mol. N₂ vibr. energy in thermosphere 3-69620
 aromatic molecules, effect on energy transfer processes 3-69084
 atmospheric, absorption spectra by N₂ and O₂ complexes near 4.3 μ (*Russian*) 3-73294
 atmospheric, oxinitride formation during melting of alumina, zirconia (*French*) 3-76335
 atmospheric conc. determ. by shock-layer radiometry during PAET entry-probe expt. 3-56187
 atmospheric relative concentrations in stratosphere and mesosphere, one-dimensional model 3-69593
 atom, absorption spectra, K shell excitation line breadth 3-63278
 atom, electron impact excitation, cross section meas. 3-40582
 atom, electron loss and capture by multiply charged ions, cross sections anomaly 3-52296
 atom, electronic corrols. role in X-ray and fast electron scatt. 3-52248
 atom, excitation state following dissociative recombination processes e + NO⁺ 3-78881
 atom, excited by Ne and Na ions, 0.3 to 2.0 MeV, fluoresce. efficiency 3-40644
 atom, ground state, single excitations in multiconfig. wavefunctions 3-71351
 atom, metastable autoionising 2s(2p)³3s⁴S_{5/2} state, detection 3-67689
 atom, multiconfiguration and polarized orbital close coupling calc., comparative study 3-71443
 atom, photoionisation cross section calc. 3-78484
 atom, SCF wavefunctions and energies for valence and excited states 3-74773
 atom electron scattering, free-free absorption coefficients calc. 3-43371
 atomic, oscillator strengths calc. based on analytic IPM model 3-74799
 atomic orbitals, SCF, Gaussian expansions, radial weighting effects 3-67649
 atoms and ions, electron scatt., config. interaction effects, cross sections 3-63328
 Auger spectroscopy of reaction with Nb (100) surface, reaction kinetics 3-55166
 aurora, rotational temp. meas. for N₂⁺, using rocketborne photometer 3-65534
 in auroras, vibr. population of B³π_g state, B¹ and W-state roles 3-69626
 beam-foil forbidden lines transition probabilities rel. to astronomical spectra 3-78430
 chemical shift calcs., n.m.r. 3-63521
 collision induced broadening of CO lines (*French*) 3-67835
 collision induced broadening of methane spectral lines, temp. depend. 3-67836
 collisional quenching of Na fluorescence 3-54571
 collisional quenching of O(¹D), N₂ vibrational relaxation 3-75137
 collisions with H⁺, H₂⁺, and H₃⁺, fast excited H atoms formation 3-43375
 collisions with H⁺, H₂⁺ and He⁺, K-shell X-ray emission and ionisation cross sections 3-46334
 collisions with He in afterglow, Penning reaction 3-52403
 collisions with NO, orientational anisotropy in total collision cross section 3-46355
 collisions with NO, vibrational energy transfer 3-71626
 complexes with 3d transition metals, electronic struct. calc., N₂ bonding 3-71518
 compressed, electrical strength, effect of electrode roughness 3-75446
 corona discharge in inhomogeneous field 3-49784
 dayglow N₂⁺ first negative band meas. at 3914 Å 3-51092
 dense fluid, hot electron injection, IV characts. density and appl. field depend. 3-71971
 desorption from K surface, activation energy, low temp. obs. (*German*) 3-43941
 diffusion in Fe alloy melt, 1500-1700°C, alloying elements effects (*German*) 3-47363
 diffusion in Fe-rich alloys, alloying element effects, thermodynamic factor (*German*) 3-47366
 diffusion in HD at 1 atm. and 300 K 3-78924
 diffusion processes, low density supersonic stream, electron beam techniques (*Russian*) 3-46462
 diluent effect on N₂O₄=2NO₂ system, heat cond. at 25°C 3-50834
 discharge, 100, 380 and 760 mmHg, formation time, transverse mag. field effects (*Russian*) 3-49776

nitrogen continued

- discharge, Hg-N₂, nitrogen ionization as a function of N pressure 3-60650
- discharges of large cross section at high overvoltage in homogeneous field 3-54888
- dissociative ionisation by electron impact, N⁺ and N²⁺ production 3-75105
- Einstein transition probability, for W³Δ_u ← B³Π_g system 3-40627
- electron impact excitation, contribution of the metastable E³Σ_g⁺ state to the population of the C³Π_u state 3-43513
- electron impact ionization, energy loss and momentum transfer 3-40584
- electron scattering, elastic, angular differential cross sections 3-71619
- electron-beam ionised, electrical conductivity 3-54839
- e.p.r. of O₂ impurity, effective zero-field splitting parameter calc. 3-50449
- equation of state, empirical pressure-explicit 3-63606
- equation of state, selection of functional form, least squares fitting 3-75593
- excitation transfer collisions with Rb, quenching and doublet mixing cross sections 3-67694
- expansion apparatus for measurement of Joule-Thomson effect 3-71708
- F1-region, atomic N ion density meas. 3-61546
- F₁-layer O/N₂ ratio, seasonal variation from vertical sounding data during solar activity minima 3-69660
- gas, electron swarm parameters, diffusion coeff., mobility, amplification coeff., Townsend ionisation coeff. 3-49526
- gas, pVT data and thermodynamic props. up to 1000°C and 5000 bar 3-49523
- gas, Rayleigh scatt., low-power He-Ne laser meas. 3-49388
- gas, transport and equilibrium props., utility of m-6-8 potential function 3-60512
- gas bubbling in water and aqueous solns., γ-radiolysis reln. to reactor cooling 3-71277
- gas mixture with Xe, trace interdiffusion coefficients, temp. depend. 3-75181
- Groombridge 1830, subdwarf, element abundance 3-56396
- intermolecular potential as effective cross section 3-71654
- intermolecular pots., empirical calc. from cryst. data 3-40681
- interstellar clouds, u.v. absorption spectra, ionisation of C, N and O, effects of X-ray flux 3-48129
- interstitial, effect on mech. props. of Nb and Ta 3-80340
- interstitial in Fe-V system, abnormal Snoek peak obs. 3-80229
- ion beam, highly stripped, Lyman X-rays 3-63279
- ion impact on Al, beam energy dependence of Al K_α X-ray satellite structure 3-78598
- ionization, secondary electron emission by metastable particle impact 3-68116
- ionization, secondary electron emission by metastable particle impact 3-68117
- ionosphere, E and F regions, vibration temp., energy loss mechanisms 3-80808
- isotopes, spectroscopic analysis (*Rumanian*) 3-62113
- kinetic theory collision cross sections, quadrupole-quadrupole interaction, DWBA 3-71697
- Knudsen molecular gas, effect of periodic variation of coeff. of heat transfer in mag. field 3-75174
- laser, for spark gap meas. (*German*) 3-59904
- laser, pulsed, longitudinal discharge, high specific power, 4.5 kW cm⁻³, pressure and voltage dependences 3-74227
- laser, short, high power, transversely excited, u.v. 3-51911
- laser, transverse discharge, 3371 Å, 300 kW, Blumlein power supply, use of ceramics, description 3-74228
- laser producing 120 kw u.v. pulses (*Japanese*) 3-48888
- LEED investigation of reaction with Nb (100) surface 3-55124
- liquid, bubble dynamics 3-43621
- liquid, heat pipe, thermal cond. meas., effect of power load and angle of inclination, axial temp. distrib. 3-53859
- liquid, intensification of dispersion by different pumping schemes (*Russian*) 3-74279
- liquid, spectroscopic props., method of mol. dynamics simulation 3-80051
- liquid density 3-58060
- matrix, NH₃ i.r. spectra 3-55589
- methane + N₂ + inert gases crystals, heats of fusion calc. 3-73171
- microdetermination in organic compounds, semiautomatic app., purification of O₂ 3-48651
- microliquefier of Hampson type (*Polish*) 3-48369
- molecular beam, condensation, granion vel. determ. (*French*) 3-78906
- molecular laser, high energy electron beam excited, superradiant laser action 3-54219
- molecule, atomic resonance radiation quenching of O(2¹D₂) in vacuum ultraviolet 3-71370
- molecule, crude adiabatic vibronic states 3-43420
- molecule, dissolved in liquids, vibr. Raman bandshape, collisional narrowing effect 3-75019
- molecule, electron impact, dissociative excitation, extreme vacuum u.v. spectra 3-75117
- molecule, electron impact, excitation of N₂+C state, predissoc., isotope study, ²⁰N₂ and ³⁰N₂ 3-75115
- molecule, electron impact excitation, cross section of metastable A³Σ_u⁺ vibrational level 3-75116
- molecule, electron impact excitation, differential cross sections 3-75111
- molecule, electron impact excitation, lifetime and excitation function of the D³Σ_u⁺ state 3-75113
- molecule, electron scatt., first Born approx. 3-75102
- molecule, ESCA spectra, calc. by multiple-scatt.-Xα method 3-40662
- molecule, excitation of B³Π_g state, glow discharge 3-75008
- molecule, excited by Ne and Na ions, 0.3 to 2.0 MeV, fluoresce. efficiency 3-40644
- molecule, generalised oscillator strength 3-74949
- molecule, ground state, generalized valence bond and configuration interaction calcs. 3-78694
- molecule, Morse oscillator, collision transition probabilities and cross sections (*French*) 3-54744

nitrogen continued

- molecule, photoabsorption coeffs. in 300-700 Å region 3-46262
- molecule, semi-empirical effective pair correl. parameters and correl. energies 3-54624
- molecule, triplet states parameters calc. 3-60421
- molecule, vibr. deactivation probability on collision with glass surface 3-46337
- molecule, vibr. excitation from N + NO reaction, Raman scatt. study 3-43517
- molecule, vibrational levels, lifetimes, coincidence detection of scattered electron and emitted photon (*French*) 3-74806
- molecule, vibrational relaxation by alkali atoms 3-71643
- molecule, vibrational spectra, lifetime of D³Σ_u⁺ state 3-75005
- molecule collisions with He⁺, single and double electron transfer cross sections 3-78624
- molecules, vibr. relax. using press. meas., shock tube study, comment 3-49501
- molecules in nozzle, anharmonic vibrational relaxation 3-54737
- negative flow discharge, number densities of neutral particles, mass spectrometry (*German*) 3-79196
- optical birefringence in α and β phases 3-55544
- Penning source, electron heating resonances, max. temperature rel. to mag. field 3-51685
- photoabsorpt. cross-section at He 584 Å line 3-49407
- photoabsorption coefficients from 400 to 650 Å using synchrotron radiation 3-40566
- photodissociation continuum determ., appl. to upper atm. emission 3-49497
- plasma, Debye type corrections influence on compressibility factor (*French*) 3-46510
- plasma, exact meas. of continuous emission 3-46555
- plasma, glow discharge, Langmuir probe study, electron density, electron energy distrib. (*Russian*) 3-57943
- plasma, isothermal, spectral determ. of temp. and electron conc. (*Russian*) 3-63890
- plasma, recombination rates meas. 3-43500
- plasma arc, convective arc model, limiting operating conditions (*Russian*) 3-40809
- plasmas, recombining, continuum emission 3-54835
- population of B³Π_g-state in glow discharge (*Russian*) 3-43345
- population of N₂(B³Π_g) by N₂(A³Σ_u⁺) during afterglow 3-71625
- o-positronium and free positron decay rates 3-74908
- pressure broadened spectral lines, intermolecular potential, nonrigidity influence 3-75157
- pressure virial analysis and Clausius-Mossotti function 3-60506
- pulsed microwave breakdown, with low degree of ionisation 3-57956
- Raman cross section, relative, short-pulse laser scatt. and photon counting obs. 3-57651
- Raman scattering, density effect, scattering polarisation, intensity, frequency shift, and line shape study 3-71551
- Raman scattering, induced, under cavity excitation, spectral width and line struct. 3-59895
- reaction with ethylene, emission spectra obs. 3-44718
- r.f. spectrum of metastable (3Σ_u⁺) state, fine struct., mag. hyperfine struct., electric quadrupole consts. for 13 vibrational levels 3-40635
- scattering cross section meas., K atomic beam attenuation 3-60496
- solid, kinetics, relaxation mechanisms, electronic quenching in luminesc. 3-69072
- solid, luminesc., vibr. relax. phenomena of N₂ mol. 3-44463
- solid matrix for H₂O.HCl complex, i.r. study 3-52369
- solubility in austenitic Cr-Ni steels, temp. and Cr content depend. (*German*) 3-47367
- solubility in Co and Co alloys, data survey 3-44567
- solubility in Fe alloys, central atoms model 3-80238
- solubility in pure Fe, temp. depend., α, δ and γ domains (*German*) 3-47367
- stars, main sequence, N₂ enrichment due to meridional circulation 3-69949
- stellar evolution, abundance variation, effect on horizontal branch models 3-77045
- thermal conductivity, Senftleben-Beenakker effect 3-71705
- thermal conductivity absolute meas. 3-71703
- thermal conductivity meas. using hot wire method, 0 to 150 C (*Russian*) 3-75175
- thermal conductivity measurement by transient hot wire method 3-71700
- thermomagnetic torque between 75 and 300 K 3-54787
- thermosphere, lower, quenching of vibrationally excited N₂ by O, temp. depend. 3-69621
- thermospheric N₂ density and temp., diurnal and semidiurnal var. from probe meas. 3-80784
- Townsend discharge, electron-molecule collision freq. in crossed elec. and mag. fields 3-71970
- unsaturated molecule threshold electron energy-loss spectra 3-67789
- in upper atmosphere, number densities measured during geomagnetic activity at high latitudes 3-61504
- vapour pressure, formulae, comparison, new rational method, new measurement technique 3-79480
- vibrational Raman spectra 3-49471
- vibrational temp., 001, of N₂ and CO₂, at 50 < z < 130 km., radiative transfer calc. 3-69623
- vibrationally excited, charge transfer collisions with Ne⁺ 3-43370
- viscomagnetic effect, temp. depend. 3-52420
- X-ray emission, K-shell ionisation by H⁺ and He⁺ impact 3-78606
- Σ_g⁺ state, correlation with unidentified 6895.5 Å and 8937.0 Å bands 3-74964
- Ar ions in He, N₂, Ne and Ar, nonmonotonic dependence of electron loss and capture cross sections on target atom nuclear charge 3-78629
- Ar/N₂ sputtering discharge for Pt and Ta films 3-43962
- Ar-N mixtures, fission counters, γ performance meas. 3-77626
- Ar⁺ + N₂, differential inelastic scattering, 1-3 keV 3-75149
- Cl₂, stellar nucleosynthesis 3-59337
- CO₂/N₂ mixtures, vibrational transition rates by acoustical method 3-40667
- CO₂-N₂ high-press. laser, elec. discharge excited, electron beam controlled, radiation power investigation 3-51906

nitrogen continued

- CO₂-N₂-He, near atmospheric in planar electrode geometry, laser gain characterisation 3-70804
 CO₂-N₂-He gasdynamic laser, power and gain calc., population inversion, adiabatic expansion through nozzle (*Russian*) 3-66824
 CO₂-N₂-He laser, stationary, amplification factor (*German*) 3-62700
 CO₂-N₂-He laser discharges, plasma chemistry 3-43654
 CO₂-N₂-He mixture, continuous generation at atmospheric pressure 3-57226
 Cr-Ni films, evaporated, structural and electrical props. as function of gas pressure 3-58247
 GaP:N, electrolum. at high excitation levels 3-76098
 GaP:N, interstitial N defect form. on fast neutron or 2 MeV electron irradi. 3-46638
 GaP:N, yellow electrolum. 3-80115
 GaP:N, Zeeman splitting of B-line at low mag. fields 3-50615
 H₂-N₂ gas mixtures, K⁺ ion reduced mobility, comparison with pure gases 3-46373
 HF+N₂, vibr. relax., kinetics 3-54748
 He-N₂ nonideal rarefied gases, molecular diffusion study 3-67897
 K⁺ in N₂, longitudinal-diffusion coefficient meas. at 293 K 3-43536
 N, ionisation potential calc. 3-63305
 N II multiplets, lightning spectra, relative line intensities 3-80764
 N+D₂⁺→D+ND⁺, merged beam study, energy dependence of cross section 3-78900
 N+NO→N₂+O, vibr. excited N₂ yield, Raman scatt. study 3-43517
 N+N+N→N₂+N recombination velocity const., low temp. non catalytic coatings (*Russian*) 3-63610
 N⁺, dissociative ionisation of N₂ by electron impact 3-75105
 N⁺ charge exchange collisions with inert gases, electron capture cross sections for ground and metastable states 3-78622
 N⁺ irradiation of Nb₂O, effect of O impurity on void formation 3-79335
 N⁺ low energy collisions with Ne atoms, radiation phase interference and optical polarisation effects 3-67715
 N⁺ metastable ions, destruction in collisions with inert gas atoms 3-78640
 N⁺+atoms (mols.), inelastic and superelastic scattering 3-78580
 N⁺+H→N+H⁺, calc. of thermal energy charge transfer cross section and rate constant, spin-forbidden ²II-²Σ transition 3-78636
 N₂ adsorption on chromia, aerol, aerosil, potential distrib. function from adsorption isotherms 3-75667
 N₂, Ar, methane ternary and binary systems, liquid-vapour equilibria at 112.00K, Gibbs free energy calc. 3-58120
 N₂, α→γ phase transition, Raman spectra, librational modes 3-72650
 N₂, coaxial laser, u.v. superradiant pulse width and peak power, operating conditions 3-78019
 N₂, deperturbation of Worley-Jenkins Rydberg series 3-49458
 N₂, dissociative ionisation by electron impact, angular and kinetic energy distrib. of fragment ions 3-78870
 N₂, electron scattering, inelastic thresholds 3-78547
 N₂, excited by electron impact, shape resonances in A and B states 3-78876
 N₂, ionisation and fragmentation by 5-45 keV Ne⁺, NA⁺ ions, and Ne atoms 3-78898
 N₂, low-energy electron emission in fast proton collisions 3-78899
 N₂, modification in calc. half-width of depolarised Rayleigh line 3-63436
 N₂, N₂⁺ excited products of NH₃ decomposition in h.f. discharge, deactivation obs. (*Russian*) 3-63538
 N₂, perturbation of electronic transitions under foreign gas pressure 3-75012
 N₂, resonances in electron impact, energies and configurations 3-52400
 N₂, resonant excitation by low-energy electrons, cross-sections calc. 3-78875
 N₂, solid, β-α ordering transition, pressure depend., n.q.r. obs. 3-75590
 N₂, solid, i.r., Raman spectra, theory, expt. 3-72660
 N₂, stimulated emission, 2000-3000 Å 3-78022
 N₂, structures in appearance efficiency curve of N⁺ ions produced by electron impact 3-78871
 N₂, vibrationally excited, chemi-ionisation of alkali atoms 3-78495
 N₂ crystal, N-containing, low temp. flashes and glows 3-72762
 N₂ first negative bands, electron fluorescence efficiencies, calculations 3-63509
 N₂ pulsed u.v. laser, stimulated emission phenomenon discussion 3-48902
 N₂ repetitively-pulsed high-power laser, design description 3-48453
 N₂ Rydberg complexes band structures 3-40616
 N₂ second positive 3160 Å emission in aurora, spatial separation from N₂⁺ first negative 3914 Å emission 3-51098
 N₂ second positive bands, electron fluorescence efficiencies, calculations 3-63509
 N₂ second positive system bands in dayglow, Kosmos-224 data 3-41983
 N₂ supersonic nozzle flow in high current arc, turbulence development 3-68008
 N₂ vibrational temp. in lower thermosphere, effect of O quenching 3-53512
 N₂:O₂ vacuum u.v. absorption spectra, vibrational analysis 3-53130
 N₂-alkali metal atom collision, electron-vibr. transitions 3-49413
 N₂-Ar solute-solvent systems, computer simulation of correl. functions, bandshapes and relax. times 3-64651
 N₂-Ar solutions, molecular thermodynamics in normal and critical regions 3-65121
 N₂-Ar-CH₄ system, vapour-liquid equilibrium (*French*) 3-64145
 N₂-CO₂ gas mixture, CO₂ frost formation in flow system 3-79486
 N₂-CO₂-He mixture, uniform field breakdown and transient glow formation 3-46572
 N₂-inert gas mixtures, viscomagnetic effect 3-52421
 N₂-methane, heats of mixing calc. by corresponding-states theory of mixtures 3-49524
 N₂-N₂O mixture, expanding supersonic jet, rapid cooling, dissociation reactions (*Russian*) 3-57872

nitrogen continued

- N₂+CO, diffusion and thermal diffusion coeffs., mag. field effects, model calcs. 3-54789
 N₂+H⁺ impact, emission cross-sections for N₂⁺ (3914Å) 3-78893
 N₂+Hg+Na, collisional excitation transfer and quenching 3-78519
 N₂+Li scatt., absolute total cross sections meas. 3-43362
 N₂+Ne⁺ impact, emission cross-sections for N₂ 3914 Å and 3371 Å systems 3-78894
 N₂+O₂ mixtures, N₂(C³Π_g; v'=0, 1) de-excitation, luminesc. study 3-49483
 N₂+O₂+H₂ flames, alkali metal atom collision process rates 3-80525
 N₂+O⁺, product ion peaks near centroid scatt. mechanisms 3-40671
 N₂+O⁺ to NO⁺+N, reaction rate coeff. for ionospheric F-region, drift tube meas. 3-69742
 N₂-molecular ions, electronic magnetic resonances 3-52390
 N₂⁺, config. interaction calcs. of low-lying quartet states 3-60413
 N₂⁺, dissociative ionisation of N₂ by electron impact 3-75105
 N₂⁺, emission cross-sections for 3914Å from H⁺ impact on N₂ 3-78893
 N₂⁺ 3914 Å daytime emission profiles during moderate solar activity, Kosmos-224 data 3-41984
 N₂⁺ 4278 Å band, photometric investigation of auroral emission 3-44913
 N₂⁺ first negative 3914 Å band charge-transfer excitation by protons, photon-particle coincidence meas. 3-63560
 N₂⁺ first negative 3914 Å emission in aurora, spatial separation from N₂ second positive 3160 Å emission 3-51098
 N₂⁺ first negative band meas. by shock-layer radiometry during Earth entry 3-56188
 N₂⁺ low lying doublet states, generalized valence bond and configuration interaction calcs. 3-78695
 N₂⁺ Meinel and O₂⁺ second negative bands, laser theory 3-74223
 N₂⁺→N⁺+N, unimolecular dissociation, translational spectroscopy 3-75095
 N₂⁺+N₂, charge exchange in energy range 0.04 to 2 eV 3-71644
 N₂⁺ formation by electron impact of N₂ at 70 eV, cross section meas. 3-54740
 N₃⁻ in crystal field, splitting of bending modes 3-55061
 N₃⁺, core description with small basis sets of SCF-MO-LCGO method (*German*) 3-52246
 N₃⁺ production in N⁺+N₂ collisions (*German*) 3-49498
 N₃⁺, collision with Ar, X-ray data calcs. 3-71452
 N₂O, use in adiabatic-compression installations, for obtaining high temp. gases 3-48378
¹⁵N mass spectrometer meas., high resolution, signal averaging method 3-66413
 NaK-N₂ two-phase flow in rectangular cross section channel with large aspect ratio, frictional pressure drop 3-71811
 N₂(v=0)-Cs(2P), quenching cross section of reson. excitation of Cs atom 3-49412
 O⁺+N₂→NO⁺+N, low energy study 3-40668
 Si, conc., solubility, and equilibrium distrib. coeff. of N₂ and O₂ 3-58046
 p-Si:N⁺(N₂⁺), lateral photovoltaic effect, reln. between dose and photovoltage 3-52872
 n-SiC:N, i.r. absorpt., role of free carriers 3-75996
 Ta, thin film resistors, ion bombardment effect on resistance 3-58054
 UC+N₂ reaction, graphitization of precipitating free carbon 3-47553
- nitrogen compounds**
see also ammonia; ammonium compounds
 azides, irradi., N₃ or N₃²⁻ radicals identification 3-61267
 hydride, influence of polarisation functions on molecular orbital hydrogenation energies 3-67744
 mesospheric disturbance, time-dependence rel. to impulsive source of NO 3-69609
 nitroethylene, torsion of nitro group, pot. parameters 3-63399
 NO⁺+O₃→NO₂⁺+O₂ laboratory expt. and ionospheric implications 3-51108
 organic radicals, hyperfine coupling constants, π-electron mol. orbital calcs. 3-63383
 oxides, reduction, rare earth manganites as catalysts with low ammonia yield 3-55943
 oxides in stratosphere, effect on ozone and temperature structure 3-76741
 Ba+ONCl→NO+BaCl, electronic states distrib. in products 3-80532
 CO/N₂O flames, alkaline earth oxides dissociation energies determ. 3-76425
 CO-N₂O flame, Na-catalyzed, l.p., vibr. disequil. 3-55928
 CO₂-N₂ gas laser, operating limits 3-57225
 Ca+ONCl→NO+CaCl, electronic states distrib. in products 3-80532
 Fe-N, solid solutions Mossbauer spectroscopy, distribution of N atoms, ordered and disordered, hyperfine fields 3-53047
 H+NF₂ system, chem. prod. of electronically excited states 3-58792
 H(D)+NO₂, isotope effect on reactive differential cross-section 3-73133
 HNO and DNO, microwave spectra analysis 3-63488
 N-Fe alloys, microstructure examination and production by sintering 3-55766
 N₂-Ar Van der Waals complex, i.r. absorption spectra, internal rotation 3-78805
 N₂-N₂O mixture, expanding supersonic jet, rapid cooling, dissociation reactions (*Russian*) 3-57872
 NCN₃, microwave spectra, anal. four nuclear quadrupole problem 3-78819
 NCO, Renner-Teller effect and vibronically induced bands in electronic spectrum 3-75048
 NF and NF⁺, pot. energy curves and spectroscopic consts. 3-71496
 NF and NF⁺, configuration interaction studies 3-40593
 NF₂, electronic struct., moments, orbital energy, charge distrib., SCF calcs. 3-52320
 NF₂ radical, ab initio unrestricted Hartree-Fock calculations of electronic structure 3-63394

nitrogen compounds continued

- NF_3 , dissociation rate meas., behind shock waves in Ar, spectrophotometric 3-75094
 NF_3 Knudsen molecular gas, effect of periodic variation of coeff. of heat transfer in mag. field 3-75174
 $\text{NF}_3 + \text{H}$ reactions in moderately fast flow system, e.s.r. and mass spectrometric studies 3-76430
 $\text{NF}_3 + \text{M}$ -donor transverse discharge HF chemical laser system 3-59859
 NH , semi-empirical effective pair correl. parameters and correl. energies 3-54624
 NH free radicals, sensitized fluoresc. by $\text{Hg}(6^3\text{P}_0)$ metastables 3-60484
 NH molecular lines and oscillator strengths in photosphere 3-69829
 NH_2 , absorpt. spectra, detection by intracavity dye laser technique 3-54666
 $\text{NH}_2^- + \text{H}_2 = \text{H}^- + \text{NHP}$, rate consts. and $\text{D}_0(\text{NH}_2\text{-H})$ derivation 3-55931
 NH_3 absorption coefficients in 2100-2250 Å region rel. to Jovian albedo 3-56330
 NH_3 in interstellar matter, excitation 3-45217
 NH_3 microwave transient nutation measurement, Bloch eqns. for relaxation times 3-63539
 NH_4^+ , ten-electron hydride, ground state calc., field form of perturbation theory 3-71521
 N_2H_4 , two centre calc., Slater type orbitals, vertical electronic transitions, bond distances, force constants (Russian) 3-49444
 NH_2Cl , and isoelectronic series, SCF-MO calcs. 3-60409
 NO , $a^4\Pi$ state, spin-forbidden lifetime, cooperative optical phenomena 3-54665
 NO , ATDL dispersion model for chemically reactive pollutants 3-76704
 NO , adsorption on metal oxides 3-41091
 NO , anisotropy of total collision cross section with Ar, Kr, Xe, glory struct. 3-78868
 NO , deviation from Lorentzian shape in the wings of collision broadened i.r. absorption lines 3-43466
 NO , diatomic mols. trapped in Ne matrix, absorpt. spectra, vibr. and rot. struct. 3-75011
 NO , Doppler-limited i.r. mag. rot. spectrum, line shape 3-43448
 NO , free radicals from organic compounds, mag. props. (French) 3-44745
 NO , fund. and first overtone bands obs. in NO-rare gas mixtures, 10000 psi 3-63444
 NO , molecule, electron impact, dissociative excitation processes, spectroscopic investigations 3-75114
 NO , molecule, electron impact excitation and dissociation, radiation spectrum 2000 to 9000 Å 3-75128
 NO , monochromatically excited, energy transfer, vibrational relaxation, fluorescence 3-71623
 NO , N_2O , mol. ESCA spectra, calc. by multiple-scatt.-Xα method 3-40662
 NO , NO_2 , atmospheric pollution, fluorescence detn. 3-70189
 NO , NO_2 , N_2O , i.r. spectra of air pollutants 3-53471
 NO , perturbation of electronic transitions under foreign gas pressure 3-75012
 NO , photoabsorpt. cross sections, 380-660 Å region 3-71606
 NO , r.f. excited, emission spectra from 200 to 600 nm 3-78815
 NO , relative Raman cross-section, from short pulse laser scatt. and photon counting obs. 3-57651
 NO , resonances in electron impact, energies and configurations 3-52400
 NO , stimulated emission, 2000-3000 Å 3-78022
 NO , stratospheric abundance, i.r. absorpt. spectra obs. (French) 3-61463
 NO , stratospheric vertical distrib. 3-73318
 NO , ultrasonic dispersion, temp. depend., 423 to 500 K 3-40670
 NO , Vibr. relax. time meas., 299 to 1000 K 3-43509
 NO , vibrational energy transfer 3-71626
 NO , vibrational excitation in low-energy electron impact, role of negative ionic states 3-78874
 NO , Zeeman effect, CO laser Q-switching applic. 3-66812
 NO absorption cross sections from 180 to 700 Å 3-67805
 NO and NO_2 air pollution in United Kingdom, survey of literature 3-41955
 NO and NO_2 emissions from stationary sources, monitoring, instrumental techniques 3-61933
 NO atmospheric density meas. during sunrise at Kauai, Hawaii 3-53503
 NO atmospheric u.v. fluorescence, satellite meas. rel. to diffusive transport model 3-80783
 NO collisions with carbon tetrachloride, CO_2 , CS_2 , N_2O , N_2 , Ar, Kr, Xe and trifluoromethane, orientational anisotropy in total collision cross section 3-46355
 NO concentrations in upper atmosphere from eclipse var. of ion concentrations 3-69610
 NO density in upper atmosphere, by fixed-grating Ebert u.v. spectrometer on Atmosphere Explorer 3-42077
 NO detection and comp. determ. in stratosphere (French) 3-51012
 NO detection in lower stratosphere 3-53490
 NO in situ meas. in stratosphere between 17 and 23 km 3-76775
 NO laser, $2\Delta-2\Pi$ near i.r. transition, rotational analysis of spectrum 3-66806
 NO paramagnetic molecule, H atom spin exchange cross-section, temp. range 310-390K 3-57612
 NO prod. in the stratosphere by N_2O oxidation 3-61450
 NO stratospheric production from past nuclear explosions, O_3 measurements 3-65348
 NO thermal conductivity, Senftleben-Beenakker effect 3-71705
 $\text{NO} + \text{O}_2 \rightarrow \text{NO}_2 + \text{O}_2$, $\text{O}_2(^1\Delta_g)$ and $\text{O}_2(^1\Sigma_g^+)$ possible production 3-47572
 NO^+ , valence states, spectroscopic consts. 3-63427
 NO^+ charge exchange reactions with inert gases 3-43521
 $\text{NO}^+ + e \rightarrow \text{N}^* + \text{O}^*$ low-energy dissociative recombination rates, temperature dependence, theory 3-78881
 NO_2 , $^2B_2-^2A_1$ transition, resonance fluorescence, rotational consts. 3-78783
 NO_2 , ATDL dispersion model for chemically reactive pollutants 3-76704
 NO_2 , air pollutant, automatic sampling and anal. 3-53783

nitrogen compounds continued

- NO_2 , electron affinity from $\text{Cs} + \text{NO}_2 \rightarrow \text{Cs}^+ + \text{NO}_2^-$ relative cross section, energy depend. meas. 3-49505
 NO_2 , electronically excited, microwave optical double resonance 3-43479
 NO_2 , flash photolysis, energy disequilibrium meas. 3-80568
 NO_2 , fluoresc., mag. quenching study, 0 to 15 kG 3-43471
 NO_2 , fluorescence, magnetic quenching 3-78836
 NO_2 , fluorescence excitation by CW dye laser 3-78834
 NO_2 , inelastic photon re-emission, air pollutants detect. 3-78832
 NO_2 , interaction with SnPb, alloy composition effect 3-68484
 NO_2 , low-lying doublet states, SCF and CI calcs. 3-40592
 NO_2 , microwave optical double resonance lines 3-78835
 NO_2 , separation of overlapping fluorescence and Raman lines 3-78756
 NO_2 , vibr. struct. of $^2B_1 \leftarrow ^2A_1$ system 3-78729
 $(\text{NO}_2)_2$ dimer, bond lengths and angles, ab initio calcs. 3-74912
 NO_2 ion, lower electronic states, CNDO config. interaction calcs. 3-49435
 NO_2 ionisation potential, 9.62 to 9.25 eV assoc. mass spectrometer 3-71604
 NO_2 paramagnetic molecule, H atom spin exchange cross-section, temp. range 310-390K 3-57612
 NO_2 , activated KBr and KI, opt. absorpt. at 300 K, 80 K and 4 K (Russian) 3-44432
 NO_2 , alkali halide crystal impurity centre 3-68361
 NO_2 , triplet state, e.s.r., phosphoresc., level crossing, in NaNO_2 3-72509
 NO_2^- and NO_3^- atmospheric negative ions, collisional detachment of electrons 3-46212
 NO_2^- charge transfer reactions with O_3 3-46349
 NO_2^- chemical shift for N, O, n.m.r. calcs. 3-63521
 NO_2^+ chemical shift for N, O, n.m.r. calcs. 3-63521
 NO_3 ion, lower electronic states, CNDO config. interaction calcs. 3-49435
 NO_3 ion effect on 18 Cr-8 Ni stainless steel, pitting and crevice corrosion (Japanese) 3-72907
 NO_3^- , activated KBr and KI, opt. absorpt. at 300 K, 80 K and 4 K (Russian) 3-44432
 NO_3^- , electronic structure, mol. orbitals, two atom differential overlap approx. 3-78688
 NO_3^- chemical shift, for N, O, n.m.r. calcs. 3-63521
 NO_3 emission, time integrated sampling, nitrate ion exchange analysis 3-70457
 N_2O , adsorption on Rh at room temp., sticking probability 3-68498
 N_2O , atmospheric vertical distrib., variation of i.r. solar spectrum with height 3-51022
 N_2O , broadening of i.r. absorption lines 3-49467
 N_2O , chem. reactions with metal vapours, chemilum. and photolum. of products 3-76421
 N_2O , discharge excited, vibr. luminesc., level populations (French) 3-52380
 N_2O , dissociative excitation and ionisation excitation with synchrotron radiation 3-43504
 N_2O , electric breakdown 3-63909
 N_2O , electron scavenging in γ radiolysis of propane and propylene 3-73145
 N_2O , far-i.r. absorpt. and quadrupole moment determ. 3-74999
 N_2O , formation of excited mol. ions by photon impact, cross section structures 3-78865
 N_2O , in air, quantitative determ. by gas chromatography using emissive He plasma detector 3-45611
 N_2O , molecule, electron excitation, K shell energy loss spectra 3-75110
 N_2O , pure chemical cw flame laser 3-54216
 N_2O , reaction with Na vapour, rate determ., chemiluminesc. obs., mechanism 3-80524
 N_2O absorption cross sections from 180 to 700 Å 3-67805
 N_2O crystals, i.r., Raman spectra, 2 phonon absorpt. 3-69001
 N_2O in plasma reaction channel, ion intensity meas. 3-79168
 N_2O laser, chemically pumped, optical gain and laser emission by flash photolysis of $\text{O}_3\text{-D}_2\text{-N}_2\text{O}$ 3-48873
 N_2O laser, self-mode locking, rotating mirror Q-switching 3-78015
 N_2O orientational anisotropy in total collision cross section 3-46355
 N_2O photodissociation, $\text{O}(^1\text{S})$ production at the 1216-Å Lyman- α line 3-40660
 N_2O unimolecular decomposition, N_2 quenching of $\text{O}(^1\text{D})$ 3-75137
 N_2O -acetylene gas shielded flame, Ba determination, atomic absorption spectrometry 3-48637
 N_2O^+ , geometries of \bar{X} and \bar{A} states, photoelectron spectra 3-63422
 N_2O^+ excited ions, electron collisional deactivation 3-43511
 N_2O_2 , microwave spectrum, N quadrupole hyperfine splitting 3-46305
 N_2O_4 , meas. of coeff. of conductivity, temp. up to 400 K, 120 and 160 bar, coaxial cylinder method 3-41872
 $\text{N}_2\text{O}_4 \rightarrow 2\text{NO}_2 + \text{O}_2$ reversible reaction in turbulent flow heat and mass transfer determ. (Russian) 3-76447
 N_2O_4 chemically reacting system, thermodynamic parameters, use in nuclear power stations (Czech) 3-44713
 N_2O_4 dissociated, intensification of heat transfer in tube with transverse ribbing (Russian) 3-76446
 N_2O_4 liquid, thermal data meas. rel. to liquid parahydrogen equation of state determ. (Russian) 3-75595
 N_2O_4 reactive dissociating boundary layer flow, numerical calc. of heat and mass transfer, film model approx. 3-40758
 N_2O_4 reactive dissociating boundary layer flow, simplified calc. of heat- and mass-transfer 3-40759
 $\text{N}_2\text{OH}^+ + \text{CO} \rightleftharpoons \text{COH}^+ + \text{N}_2\text{O}$, equilib. const. meas. at various temps. 3-55930
 $\text{N}_2\text{O}_4 = 2\text{NO}_2$, with diluents, heat cond. at 25°C 3-50834
 $(\text{NpCl}_2)_3$ orbital calcs., CNDO/2 approximation, geometrical studies 3-63364
 NS , fluorescence and zero-field level crossing spectroscopy of $\text{C}^{2\Sigma^+}$ state 3-78837
 NSF , rot. analysis of $^1\text{A}'-^1\text{A}'$ band system 3-60447
 NO_3^- , electronic absorption spectra, phosphorescence, singlet-triplet transitions 3-43439
 $(\text{NpF}_2)_3$ orbital calcs., CNDO/2 approximation, geometrical studies 3-63364

- nobelium**
ionisation energy calc. 3-60376
M-shell ionisation cross sections by collisions of simple heavy charged particles 3-43377
- nobelium compounds**
No entries
- noble gases** *see inert gases*
- noble metal alloys**
see also copper alloys; gold alloys; noble metal compounds; silver alloys
actinide (lanthanide)-noble metal phases, prep. and props. 3-46604
dilute, anisotropic electronic lifetime, Dingle temps. 3-64282
order dependence of electrical resistivity 3-64317
ordered, total electronic energy, pseudopotential method (Russian) 3-79614
Al-noble metal, valence bands, X-ray photoelectron obs. 3-64287
- noble metal compounds**
see also copper compounds; gold compounds; noble metal alloys; silver compounds
No entries
- noble metals**
see also copper; gold; silver
in alloy, ordered, total electronic energy, pseudopotential method (Russian) 3-79614
de Haas-van Alphen effect, impurity-induced strain influence 3-52782
electrical and thermal resist., temp. variation 3-55239
exchange corrections to fourth order crystal field parameter, rare-earth doped specimens 3-52800
Kondo type resistivity anomaly caused by 3d metal impurities 3-55423
liquid, interionic pair potentials using Born-Green eqn. 3-43746
magnetic pseudopotential, generalized expression 3-44195
piezo-thermoelectric effect, longitudinal, in polycrystalline wires 3-72347
plastically deformed, elec. resist. and thermo-e.m.f. meas. of recovery, defects contrib. (Russian) 3-79663
thin film, transmission in vis. and u.v. spectral regions (French) 3-76112
- noctilucent clouds** *see clouds*
- noise**
see also atmospheric; interference; random noise; shot noise; transit time noise; white noise
1/f noise theory 3-62603
Bevatron, r.f. noise effect on bunching 3-56828
cloud radio noise, mapping at 250 and 925 MHz 3-51040
coherent imaging system, suppression 3-66774
computer-generated holograms, low-noise recording methods 3-54201
corona on carrier channel differential-phase relay design 3-52541
ear signal detectability, internal noise masking 3-45301
electronic seismographs, noise in galvanometer substitute, inverse filter and negative feedback systems 3-76882
energy sources, high-level, offset device for suppression in low level detectors 3-62114
hydrodynamical, nuclear, reactor operation anal. on single channel and single phase flow model 3-74648
image intensifier, influence on visual detection thresholds 3-61900
intermodulation, Fresnel holograms 3-77986
jets, supersonic, noise reduction 3-52489
laser Doppler instrument for vibration measurement, S/N performance 3-66144
laser Doppler systems, analysis of S/N ratio 3-66265
magnetosphere, trapped e.m. radiation above plasma freq. 3-69691
magnetospheric electron concentrations from Ogo 3 lower hybrid resonance noise band 3-80819
magnetospheric VLF radio noise amplification by low-energy Cs-ion beam 3-69687
mechanical, nuclear, reactor operation anal. on single channel and single phase flow model 3-74648
metal surface, current noise with time-dependent impurity scatt. 3-50250
neutron, analysis in reactor with two weakly coupled asymmetric fission zones (German) 3-67482
neutron, resonance integral with interference scattering calc. 3-74624
neutron flux, power reactor spatial coupling using coherence lengths concept (German) 3-67481
neutron noise form CROCUS, analysis (French) 3-63180
neutron noise in nuclear reactor theory 3-63195
neutronic, spatial correlation range in an infinite multiplying medium including effects of delayed neutrons 3-63128
nuclear, reactor operation anal. on single channel and single phase flow model 3-74648
nuclear reactor, JMTR, application of on-line digital noise analysis to reactor diagnosis 3-71161
nuclear reactors, propagation of periodically modulated driving source 3-71164
optical Doppler radar, f.m. laser noise effects 3-40295
optical transfer for meas., noise effects 3-77455
photographic emulsions, film grain noise meas. by laser scatt. 3-77557
plasma, magnetised positive column, radial distribution and mean density 3-68085
plasma transport coefficients for an arbitrary fluctuation spectrum of particle velocity 3-49654
preamplifier noise in proportional counter measurements 3-56935
pyroelectric i.r. detector in evacuated tube, temp. distribution 3-51542
reactor, maximum value of coherence function 3-71162
S/N ratio in optical radar system, optimum filter 3-66772
Schottky barriers, unified theory of h.f. noise 3-44146
seismic, atmospheric deformation of the ground, prediction by convolving the microbarogram with transfer function 3-80838
seismic noise background in Alma-Ata and Tashkent 3-69504
seismographs, long period, noise suppression and stability 3-76883
semiconductor, hot electron noise calc. 3-41199
- noise continued**
soft X-ray appearance potential spectroscopy X-ray filtering for improved signal to noise ratio 3-73917
solar eclipse, 22nd Sept. 1968, structure of noise storm source (Russian) 3-45011
solar radio bursts, noise storm phenomena, polarised radiation from solar corona 3-75310
spectrophotometry, precision theory, reading error, electrical noise 3-62320
structural response to noise 3-59509
surface current noise, i.f., influence of surface recomb. 3-79752
synchronous counters with high noise-margin logic circuits (French) 3-45548
temperature signals, rel. to flow rate determ. in nuclear reactor with SNR geometry (German) 3-67490
thermal, nuclear, reactor operation anal. on single channel and single phase flow model 3-74648
two-stream mixing layer, turbulent correlation measurements 3-78936
variable profile antenna, RATAN-600 radiotelescope, calc. of noise temp., effect of field of scattering (Russian) 3-81228
Whistler mode hiss and soft electron fluxes in dayside-cusp ionosphere 3-69638
X-ray phosphor, noise equivalent absorption, rel. to integrated scintillation obs. 3-77733
He-Ne mirror ended tube laser, light quasi-periodic noise 3-57224
InSb, generation-recombination noise and microwave emission 3-44082
InSb, hot electron noise calc. 3-41199
Sn superconducting film bolometer, fluctuation effects 3-39883
W-emitters, K-covered, noise spectral densities, field emission flicker noise theories, diffusion induced 3-76122
- noise abatement**
see also acoustic wave absorption
airborne sound insulation, 'A' weighting curve, noise meas., white noise 3-53795
aircraft, community response to noise 3-42488
aircraft, suppression and control 3-42486
aircraft cockpit noise turbulent boundary layer induced 3-77341
aircraft engine jet density rel. to noise 3-61947
aircraft noise, house insulation 3-48296
audiometric programme 3-42474
box-girder type bridge structures, control of impact-excited noise 3-42467
control, gas turbine power plants, allowable levels, major sources, methods 3-73618
cylindrical ducts, higher-order modes, active control 3-42401
damage risk criteria, impulse noise 3-59434
detonation of, guns and shells, meteorological effects at 3.4 to 21.2 miles from source 3-76771
effective noise reduction, single number rating 3-56589
fan noise, reduction, annulus boundary layer removal 3-81346
finite difference methods rel. to acoustic noise in irregularly shaped rooms 3-61940
flow noise, steam piping in nuclear power plants, prediction and control 3-42482
flow of fluid over plate, noise reduction method 3-48299
high-speed trains, prediction of rail-wheel noise 3-51474
impact-induced noise in industry, measurement and control 3-42469
induction motors 3-42475
industrial environment, by double glazing 3-53796
jet aircraft, noise reduction 3-42487
jet airliner climb-out paths, min. effective noise calc. 3-77344
jet noise, moving frame analysis 3-45378
large panels, damping, loss factor meas., in situ 3-53794
lining, broadband, aircraft inlet, effect of wall shear layers 3-77335
neighbourhood noise, conference, London, England (1972) 3-56585
neighbourhood noise control, environmental noise level monitoring 3-56587
noise abatement zones, noise control 3-56588
noise abatement zones, review 3-56586
office equipment, reduction of impact noises 3-42468
outdoor noise transmission through walls and windows, theory 3-66088
power plant employee protection 3-42473
power plants, OSHA compliance plans 3-42472
power plants 3-42471
power-plant pump, design considerations for noise reduction 3-42476
pulp and paper industry 3-51481
sound measurement, for noise control, theory and practice 3-59555
spiral modes in lined ducts 3-81347
straight line source, acoustic barrier, scale model, Fresnel number 3-66091
straight line source, noise reduction by acoustic barrier (Japanese) 3-66094
transportation noise and vibration, human response 3-59435
World Trade Center, evaluation of noise control 3-56591
- noise control (acoustic)** *see noise abatement*
- noise control (interference)** *see interference suppression*
- noise elimination** *see interference suppression*
- noise measurement**
acoustic, in toll centre switching meas. 3-66089
acoustic, standardisation of methods (French) 3-62001
acoustic, test techniques, steady-state and pulse-train (transient) acoustic meas. 3-51538
acoustic noise amplitude statistical analyzer 3-45397
using correlator, development (Dutch) 3-77390
EBR-II, nuclear reactor, noise anal., time-dependent fluctuations, reactivity transfer function, neutron detector power spectra 3-71215
gas-discharge cell, noise characteristics determ. 3-63905
jet noise, moving frame analysis 3-45378
metal film, constriction detect. by current noise meas. 3-68709
nuclear reactor in-service monitoring, spectral and correlation anal. and resonance effects (German) 3-71230
sound level meter, statistical anal., motorway noise 3-53793
white noise, sound transmission, 'A' weighting curve 3-53795

nomenclature and symbols

see also units (measurement)

magnetostratigraphic nomenclature, terminology 3-76650
solid surface thermodynamics, symbols and nomenclature 3-52711

nomograms

see also graphs

earthquake magnitude data 3-61588
e.p.r. spectra, for spin exchange frequency determ. 3-58795
light scattering meas. of copolymer composition heterogeneity 3-63594
GaAs film, epitaxial, nomogram for conversion of Hall mobility to ion scatt. limited mobility 3-44158

nomographs see nomograms**non-Newtonian flow**

asymptotic Nusselt numbers, dissipative flow through ducts, heat transfer 3-40704
Bingham fluid, steady motion in curved annulus, streamlines 3-75279
Bingham solid behaviour in hydrodynamic lubrication 3-43638
Bingham solid behaviour in hydrodynamic lubrication 3-43639
carboxymethylcellulose soln., flow curve determ., rolling-ball viscometer 3-71688
convection, free and forced 3-71738
convective flow in pipes and channels 3-71745
Couette flow, viscoelastic, polymeric, stability prediction based on network rupture hypothesis, analysis 3-75277
elastico-viscous liquids, rectilinear flow, numerical solutions 3-71841
electrohydrodynamic flow in a pipe 3-43616
entrance flows of non-Newtonian fluids 3-52485
frictionally heated fluids, crit. parameters 3-63646
horizontal layers, onset of convection, stability (Russian) 3-43549
incompressible conducting liquid with power law, shear flow in time varying magnetic field (Russian) 3-60563
isothermal and nonisothermal laminar inelastic non-Newtonian tube entrance flow following a contraction 3-43543
laminar boundary layer, chain system technique for heat transfer 3-78944
liquid, rotational flow, interaction with stationary surface 3-40715
liquid droplet, suspended in linear shear field, bursting and deformation 3-79002
lunar orange soil, viscous flow (sample 74220) 3-65848
pipe flow heat transfer 3-57719
plastic melt, viscosity, molecular position change, temp. depend. (German) 3-65010
polar fluids, shearing flow, between two rotating coaxial cones 3-71843
polyethylene, non-Newtonian flow under conditions of an inhomogeneous temp. distribution 3-63593
polyacrylamide soln. flow curve determ., rolling-ball viscometer 3-71688
polyethylene melt, shear and elongational flow, stress-time data, network theory predictions 3-73062
polyethylene melt, viscoelastic flow through converging ducts, wall normal stresses, die swell behaviour 3-80459
polyethylene terephthalate, molten, departure from Newtonian behaviour 3-53285
polyisobutylene solutions, dynamic viscosity and elasticity, effect of steady-state flow 3-71686
polymer dilute soln. non-Newtonian flow, mass transfer with rotating disc 3-71816
polymer dilute solns. behaviour in inlet region of pipe 3-75267
polymer dilute solutions, mass transfer 3-57827
polymer flow between two rotating cylinders 3-40725
polymer melts, flow between coaxial cylinders under complex shear conditions 3-73048
polymer melts, shearing flow, anisotropy, second normal stress difference meas. 3-71842
polymer solutions, axial dispersion in porous media 3-57841
polymer sol., dil., frictional resist. of rotating disc 3-43628
polymeric solution extensional flow through small orifices 3-63790
polymers, molten, helical flow, cylindrical annulus, shear dependence of viscosity 3-73061
polypropylene melt, viscoelastic flow through converging ducts, wall normal stresses, die swell behaviour 3-80459
polystyrene, silas balloon filled, flow props. 3-69377
power law gas-liquid two phase annular flow, liquid film thickness 3-40738
power law Newtonian fluid, laminar boundary layer flow stability (Russian) 3-63680
power-law fluid flowing between parallel plates, heat transfer 3-57715
power-law fluids unsteady flow contributions 3-43556
rotating disc in non-Newtonian fluid, mass transfer peculiarities 3-46386
second grade Rivlin-Erickson magnetofluids, steady Hartmann flow and wave propagation 3-43618
second order fluid, laminar source flow, non-Newtonian parameter effects 3-49539
slow, two-dimensional, finite element analysis 3-57761
spiral motion of a cylinder in a non-Newtonian fluid 3-63672
stabilised flow, hydraulic resistances and heat emission 3-71743
strongly non-Newtonian fluids external flow over plate and circular cylinder, drag meas. 3-57768
suspension, rigid particle, subjected to const. vel. gradient flow, non-Newtonian viscosity correl. with Maxwell effect (French) 3-80501
synthetic lattices, rheology, influence of shear rate and temp. 3-69393
viscoelastic, in square cavity, comparison with Newtonian fluid (French) 3-79055
viscoelastic fluid, combined steady and oscillatory flows 3-71832
viscoelastic fluid flow past flat plate, heat and mass transfer 3-78945
viscous flow prediction, conduits, packed beds, porous media, fluid models 3-71730

non-Newtonian fluids

see also colloids; rheology

Bingham liquid, convective stability of vertical layer 3-60544

non-Newtonian fluids continued

convection heat transfer, free, in horizontal layer 3-63631
entrance flows 3-52485
free convection at a vertical plate with uniform flux condition 3-46411
heat and momentum transfer, viscous non-Newtonian fluids flowing through tubes 3-75200
jet instability, dispersion curves 3-67967
mixing, representation by two physical parameters (German) 3-54795
Ostwald-de Waele and Ellis fluids, hydrodynamic stability and natural convection, numerical soln. 3-57713
polymer flow between two rotating cylinders 3-40725
polymer fluid behaviour in elongational flow (Polish) 3-60501
polymer solutions, axial dispersion in porous media 3-57841
polymer solutions, internal viscosity models evaluation 3-53288
polymeric solution extensional flow through small orifices 3-63790
polymers, percolation expts. 3-71677
rotating disc in non-Newtonian fluid, mass transfer peculiarities 3-46386
second grade Rivlin-Erickson magnetofluids, steady Hartmann flow and wave propagation 3-43618
slide bearing performance under fluctuating speed using non-Newtonian viscoelasticity fluid lubricant 3-75565
strongly non-Newtonian fluids external flow over plate and circular cylinder, drag meas. 3-57768
suspension, rigid particle, subjected to const. vel. gradient flow, non-Newtonian viscosity correl. with Maxwell effect (French) 3-80501
thermal convection, rheological properties described by stress-relaxing Maxwell constitutive relations 3-67900
viscous flow prediction, conduits, packed beds, porous media, fluid model 3-71730
viscous liquid, power dissipation during motion, theorem for minimum (Italian) 3-43646

noncrystalline state structure
see also amorphous state; vitreous state
amorphous materials, electron micrographs theory 3-49809
amorphous polymers, X-ray diff. obs. 3-46593
borate glasses, structure theory 3-43757
dislocated random-network, dislocations and disjunctions 3-63955
Fortisan, variance anal. of X-ray profile line broadening 3-79241
glass fibre, etching effect on structure and strength (Russian) 3-53280
glass laminate, effect of porosity on strength 3-64987
glass-plastic, ageing and media effects on struct., X-ray shadow microscopy obs. (Russian) 3-41814
glassy polymers, book 3-46591
glassy polymers, structure, packing density, free volume concepts, mech. behaviour 3-46592
glassy polymers, thermodynamics 3-46718
metallic alloys, amorphous, model using dense random packings of equal and non-equal sized hard spheres 3-43755
plastic foam, effect of cellular struct. on mech. props. 3-65014
polyethylene, multiple transitions, glass temp., low-temp. toughness 3-63962
polyethylene, spherulites, twist model interpret., SEM obs. 3-57992
polyethylene, struct. changes during annealing and fusion (Russian) 3-80498
polyethylene terephthalate, amorphous state, annealing, change in supermolecular state 3-60667
polymer crystallisation, surface energy rel. to chain flexibility (Russian) 3-79243
polymers, amorphous, supermolecular structure model 3-60668
polymers, semi-crystalline, multiple transitions esp. double glass 3-63962
regular block copolymers, morphology 3-46594
silica glasses:TiO₂, small angle neutron scattering investigation 3-68169
Ag-Cu (50 at.%) amorphous thin film, structure (German) 3-58192
As-Se glasses, atomic radial distribution functions 3-57990
As₂S₃, amorphous, Raman and depolarisation spectra, struct. models 3-53105
As₂S₃, As₂Se₃, X-ray examination, ⁶⁰Co γ -radiation effects (Russian) 3-57991
As₂S₃, glassy, structure obs., γ -irrad. effects (Russian) 3-46647
As₂Te₂ film, amorphous, electron diff. exam. (Russian) 3-46772
Ba_{1-x}Th_xO_{3-2x}, 0 \leq x \leq 0.1, amorphous condensates, structure using electron diff. 3-75690
C, soft, partially graphitised, atomic layers mutual arrangement (French) 3-46620
C, vitreous, 1800°C processed, lattice struct. 3-60664
C black, paracrystalline distortions, optical diffraction obs. applying electron optics considerations 3-63954
C fibre, microstructural changes induced by plastic deformation at elevated temperatures 3-53286
C glassy, struct. analysis by X-ray Fourier transform technique 3-46590
C vitreous, interatomic bonds thermal transformation 3-40849
CaO-Al₂O₃-P₂O₅ glass, charge accumulation during electron irradi., influence of struct. (Russian) 3-43809
Gd-Co alloy thin films, amorphous, transmission electron microscopy and diffraction investigation 3-68523
Ge, amorphous, clathrate-like model 3-46785
Ge, amorphous, critical review of data and models 3-46589
Ge, amorphous, pressure effects on electronic and optical props. 3-43985
Ge, amorphous, short-range order, radial distrib. curves of density of atoms 3-60665
Ge, amorphous thin film, structure study by electron diff. 3-63937
Ge-Te, amorphous alloys, X-ray diffraction and density measurements, thermally induced changes 3-58259
Li-Si-O-N system, comp., silanol struct. characts. 3-75474
Si, amorphous, critical review of data and models 3-46589
Si-Al-O-N system, composition, silanol structure characts. 3-75474
Te-Ag(Au)(Cu) flow, amorphous, condensation, electron microscope obs. 3-75692
Te₆₀As₂₅Ge₁₅(Se)_x glass, physico-chem. props. (French) 3-60666

nondestructive testing

- see also crack detection
- acoustic emission, amplitude sorting 3-69425
- acoustic emission 3-45343
- adhesive bond strength, nondestructive vibrational meas., honeycomb sandwich panels 3-47513
- bars and billets surface defects by magnetic leakage methods 3-39976
- canning tubes employing u.s. technique 3-40544
- carbon fibre reinforced plastics skinned honeycomb, by holography 3-39947
- ceramics, microwave applications 3-47491
- cholesteric materials, industrial labs., medical clinics 3-71999
- computer appl. 3-69409
- concrete, holographic crack detection 3-69424
- concrete, prestressed, reinforcement strength and position, non-destructive X-ray test, strain meas. (German) 3-69418
- conference, Los Angeles, USA, (Mar. 1973) 3-47497
- cylinder, thick-walled, fatigue crack growth meas. and anal. technique 3-76413
- cylindrical work pieces with central bore-hole, u.s. wave attenuation (French) 3-69414
- eddy current heating, megahertz frequencies, O layers on Ti, fatigue crack detection 3-45531
- eddy current instruments, nondestructive inspection, performance specification 3-45530
- eddy current testing of irradiated fuel rods, location of surface irregularities 3-60261
- elastic plates and bars, integral equations for buckling loads 3-47494
- fissile materials, computerized nondestructive neutron interrogation technique for safeguards application 3-46072
- flaw size estimation study by u.s. scanning method with relative threshold 3-47521
- flying spot laser system, automatic fluorescent indication detection 3-47518
- future developments 3-44700
- gamma radiography industrial applications in South Africa (Afrikaans) 3-65064
- heat exchanger tubing, base line end in-service inspection u.s. testing 3-47506
- heat pipes, high temp., Li mass transfer corrosion, neutron radiography 3-47499
- high energy X-radiography, precision meas., dimensional change monitoring 3-45569
- Lamb wave u.s. bond inspection, airframe struct. 3-47512
- leakage-flux technique, magnetizing equipment characts. (German) 3-69415
- materials technology interaction 3-53293
- mechanical, basic metallurgy 3-53295
- metal, magnetoelastic method, stress distrib. across thickness 3-76397
- nuclear fuel assays, instrumentation, gamma-ray spectroscopy, neutron system, calorimetry, reviews 3-47502
- nuclear fuel element testing, X-ray scanning, automatic (German) 3-80512
- nuclear fuel fabrication and quality control 3-57553
- nuclear pressure vessels, acoustic emission monitoring, proof tests 3-65062
- nuclear reactor pressure vessel, proving tests evaluation (German) 3-73113
- nuclear reactors, LiNbO₃ piezoelec. transducer, u.s. inspection 3-65061
- nuclear research reactor pressure vessel, flaws in partial penetration welds (German) 3-71236
- optical component testing by interferometry, HeNe c.w. laser 3-77521
- porcelain enamel adherence to steel, u.s. determ. nondestructive eval. 3-73097
- proton scattering radiography 3-69423
- pulsed reactor fuel, dye penetrant, u.s. reflection, X-radiography, immersion density methods 3-67559
- quartz substrate, using one dimensional holography 3-77387
- radiographs, image enhancement of spatial frequency filtering, application to nondestructive testing 3-80509
- reactor fuel rod defects exam. (German) 3-67611
- reactor fuel specimens, dimensioning from thermal neutron radiographs 3-40545
- residual stress determination, metals, X-ray method, elastic constant 3-47501
- resonance method for mech. props. testing 3-73101
- room-temperature non indium metallic bond, tested by welding acoustic shear wave transducers to paratellurite 3-76230
- spatial frequency filtering of radiographs, optical Fourier transform enhancement 3-48594
- stainless steel, cold waste meas. 3-47504
- steam generators, tube to tube sheet welded joints 3-65060
- steel, case hardening depth, detn. using ultrasonics (French) 3-58790
- steel, heat treated, inspection by electromagnetic comparator (German) 3-69417
- steel plates and strips, simple u.s. testing equipment for defect indication efficiency of 100% (German) 3-47520
- steel pressure vessels in LWR, in-service examination 3-67456
- strain hardening transitions, nondestructive evaluation, acoustic emission monitoring 3-47508
- techniques survey, quantitative limits to capabilities 3-76410
- thermography, review 3-48364
- u.s., spectral analysis applies. 3-76411
- u.s., unconventional generation, reception and coupling of u.s. waves 3-53294
- u.s., use of nearfield and farfield terms (German) 3-69413
- u.s. anisotropy measurements and mechanical properties of polymers 3-53308
- u.s. contact testing, thickness of liquid couplant layer effect and other variables 3-61241
- u.s. generation, detection and coupling, unconventional methods (German) 3-50820
- u.s. probe sound field, automatic measurement installations (German) 3-69416

nondestructive testing continued

- u.s. testing facility, computer use for anal. routines, r.f. waveform, Fourier anal. 3-47515
- u.s. testing methods, information transfer approach 3-44701
- video tape, training programme 3-45402
- welded joints with artificial flaws, fatigue strength determ. by radiographic exam. (German) 3-69412
- welded steel pipe, u.s. variable angle transducer 3-47505
- wire rope, acoustic emission testing, tensile fatigue failure 3-47507
- Zircaloy tubing, u.s. inspection, wall thickness and ID meas., multiplexed instrumentation 3-47516
- Al alloy, 7075-T6, high cycle fatigue crack growth detection using acoustic emission 3-76412
- Al cladding, thickness meas., U fuel elements, gamma ray attenuation 3-47500
- Al-Al step-lap joint, adhesive bond strength 3-69410
- Au-Cd, martensitic phase transformation, acoustic emission, e.m. detection 3-47498
- B autoradiography applies. 3-66446
- B-Li concentration measurements, apparatus using neutron absorption and activation 3-42709
- SiC tubes, employing u.s. 3-43314
- Si₃N₄, hot-pressed, impurities and inclusions identification 3-76284
- U-Mo(10 wt.%) alloy, stress corrosion cracking, acoustic emission (French) 3-69404
- nonelectric final control devices**
- see also clutches; fluidic amplifiers
- precision hydromechanical displacement micropositioner 3-39860
- nonelectric sensing devices**
- air pollution, fuel-cell sensor 3-66073
- heat flow sensor, miniature, thermal cond. meas. 3-77396
- multispectral scanning system of Earth Resources Technology Satellite 3-44951
- nonequilibrium properties of superconductors**
- critical-velocity model 3-79797
- current density applied in type II supercond. section, crit. currents 3-55367
- dirty superconductor, Maki process, effect of elec. fields in excess electric current above transition pt. 3-75814
- e.m. wave absorption two-photon, Green's function solution, surface resistivity 3-50305
- film arrays of weakly coupled supercond. particles, model for crit. supercurrent 3-58342
- fluctuations, screening approx. in two dims. 3-64431
- harmonic generation process in gapless superconductors. 3-79806
- high-temperature superconductivity of nonequilibrium systems with repulsion 3-75813
- II, u.s. attenuation, Andreev scatt. 3-55370
- light fluctuation scatt. above critical temp. 3-55369
- multilayer system, superconducting thin films and Josephson barriers, critical current 3-58340
- pinning on point defects, statistical theory 3-79798
- small particles, superconducting fluctuations, pair breaking and nuclear relax. 3-60933
- spin-lattice relaxation, supercond. with electron transition, nonmag. impurity effects 3-58345
- surface superconductivity and pinning sites, expts. on Ta₉₂Nb₈, Ta₉₅Nb₅ and Nb 3-55365
- thermodynamic fluctuations, nuclear spin-lattice relaxation time, magnetic field enhancement 3-46930
- transition metal, nuclear spin relax., calc. 3-55356
- transition metal alloys, effect of localised spin fluctuations on transition point 3-52930
- two-band, interband electron scatt. influence on nucl. spin relax. time (Russian) 3-79799
- two-zone type, pure, dislocation retardation and weakening effect due to transition (Russian) 3-52928
- type II, attractive interaction between vortices at arbitrary temp. 3-68732
- type II superconductors, stability of critical states 3-50302
- type-II, critical current increase due to periodic distrib. of ferromag. particles 3-50295
- type-II, hard, calibration of hysteresis losses (Russian) 3-72422
- ultra-high field superconductors, electron-electron interactions (German) 3-72427
- voltage-current characts. of type II supercond. in transverse mag. field 3-55366
- vortex interaction with boundary between two superconductors 3-60935
- Al film, two-dims., order parameter fluctuations ang. depend. in mag. field 3-50296
- Cd, temp.-depend. peak in electronic attenuation of u.s. shear waves, rel. to Fermi surface geometry 3-79622
- Cd hexagonal crystals, u.s. study of supercond. state 3-72425
- CeRu₂Gd, local moment e.s.r. 3-44171
- HfV₂, acoustic wave velocity meas., lattice instabilities 3-79801
- In, pure and impure, nuclear spin-lattice relax. 3-46933
- In wire, destruction of type I supercond. by current 3-68730
- LaRu₂Gd, local moment e.s.r. 3-44171
- Mo-Re(34 at.%), α -phase precip. and flux pinning, electron microscope obs. and mag. hysteresis 3-50697
- Nb, point defect density fluctuations, pinning effect, statistical theory 3-68735
- Nb, superconducting, misalignment of flux lines, neutron small-angle diffraction study 3-64435
- Nb, type II, vortex monocystal creation and control (French) 3-50301
- Nb, u.s. absorpt., purity depend. in normal, Meissner states, meas. and theory 3-64433
- Nb₃Sn, angular dependence of critical currents in transverse mag. field 3-41296
- Nb₃Sn, fluxoid pinning on grain boundaries dependence on the mag. field direction 3-44166
- Nb₃Sn, phonon damping 3-49946
- Nb_{0.75}Ta_{0.25}, pot. difference, current depend., transverse mag. field (French) 3-55360
- Pb, dynamic intermediate state under influence of heat current 3-44167
- Pb and Pb-In alloys, surface impedance meas. (German) 3-52929

nonequilibrium properties of superconductors continued

- Pb film, mag. struct. of mixed state 3-52932
 Pb-In (50 at.%) alloy, force free mag. fields in superconductors 3-79804
 Pb-In(4 at.%) alloy, flow stress in normal and supercond. states, thermal cond. model approach 3-68727
 Re, high purity, transverse and longitudinal ultrasonic attenuation measurements of superconducting energy gap 3-58337
 Ta, type II, supercond.-normal transition by rectang. current pulse, flux flow and jump 3-68729
 Ta superconducting thin films, nonlinear microwave props. 3-50304
 Ta₇₀Nb₃₀, supercond. single cryst., magnetization and pinning 3-58344
 Ti-Nb(35 at.%) alloy, heat treatment effect, flux pinning 3-79800
 Ti wire, destruction of type I supercond. by current 3-68730
 V₃Ga composite wires, processing and superconducting props. 3-68726
 Zn hexagonal crystals, u.s. study of supercond. state 3-72425
 ZrV₂, acoustic wave velocity meas., lattice instabilities 3-79801

noneleptonic decays *see baryon hadronic decay; meson hadronic decay***nonlinear control systems**

- differential, stability and asymptotic stability of solutions, equivalent inner products method 3-73990

nonlinear differential equations

- aerodynamics of bodies in coning motion 3-46440
 autonomous system for motion of mechanical system, asymptotic stability of solns. (Polish) 3-66596
 boundary perturbation of cavity moving near rigid wall (Russian) 3-63729
 boundary problems, quasi-linearisation of soln. using iterative method, convergence (Russian) 3-70526
 boundary value problem for eqns. with specified implicit mode with retardation (Russian) 3-62414
 coupled, describing two mode gas laser, solns. 3-43005
 coupled elliptic, false transient method 3-75184
 deformed bubble motion in sparging layer (Russian) 3-63754
 dispersive waves, derivative-expansion method 3-77791
 eddy current distribution, in ferromag. cylinder, approx. soln. (German) 3-45746
 elastic nonlinear nonautonomous systems with variable parameters, random oscillations. (Russian) 3-77844
 elastically supported rigid disc with moving massive load, dynamic response 3-62457
 envelope-soliton solutions, exact 3-48806
 evolution eqns. of phys. significance, soln. using inverse scatt. method 3-51811
 fluid flow in heated closed cavity, numerical soln. 3-57710
 fourth order, modelling sinusoidally excited coupled electric circuit, subharmonic solutions (French) 3-70514
 Green's function soln. for nonlinear boundary conditions, appl. to strains in thin shells (Russian) 3-62412
 heat conduction, soln. for volume heat sources 3-66703
 hyperbolic, asymptotic properties of solns. to mixed problems (Polish) 3-70535
 hyperbolic, with partial derivatives, boundedness and stability of solns. (Polish) 3-66500
 iterative soln. of nonlinear system of eqns. in implicit form with partial differentials with delay 3-77779
 Jeffery-Hamel flow of dissipative plasma, similarity transformation 3-75302
 Karman, for stochastic process of nonlinear random vibrations of cylindrical shell (Polish) 3-66589
 Korteweg-de Vries, decay of continuous spectrum for solutions 3-73993
 modal, flexural vibration of beams, plates, rings, shells, Lagrange method 3-74057
 motion of system with nonlinear nonholonomic couplings of second order, Gauss principle (Russian) 3-42756
 N-soliton solutions for long waves in shallow-water and nonlinear lattices 3-48807
 non-Newtonian fluid flow, frictionally heated, crit. parameters 3-63646
 nonlinear boundary problems (Russian) 3-62404
 ore sintering furnace simulation, solution by repeated extrapolation 3-41794
 oscillatory chemical reactions, phase waves, diffusion equation 3-50826
 partial, gauge invariance and conservation laws 3-45853
 periodic second order, integration (Russian) 3-77784
 plane parallel unstable flow, numerical study of mildly non-linear partial differential equation 3-49545
 plate, rectangular, carrying concentrated mass, nonlinear vibrs. 3-74082
 population explosion, mathematical conditions 3-48704
 porous catalyst, heat and mass transfer, nonlinear boundary value problem solution 3-42911
 relativistic quasixchange group, integration of infinitesimal transformations 3-57312
 rod, twisted, contact stresses 3-70602
 scalar nonlinear wave equation for a cubic medium, stability of the fundamental mode (Russian) 3-66497
 stability and asymptotic stability of solutions, equivalent inner products method 3-73990
 stochastic systems, asymptotic expansion of solns. when parameter $\lambda \rightarrow \infty$ (Russian) 3-66493
 third order, global asymptotic stability 3-77776
 transformation of variables to normal form (Russian) 3-77785
 transport processes, formulation application variational principle 3-59829
 variable scale method of soln., appl. to mechanics problems, review (Polish) 3-66584
 vorticity equation, non-divergent, barotropic, spectral form. approximate analytical solutions 3-76728
 wave eqns., classical non linear relativistic, integration using Lie series 3-62765
 wave modulation, perturbation method, integro-partial differential eqns. 3-77864
 weak solutions of heat equations, methods (Japanese) 3-62422

nonlinear equations*see also nonlinear differential equations*

- human visual vibrational analyser model (Russian) 3-48243
 lumped network, exact N-soliton solution 3-48705
 lumped self-dual network, exact N-soliton soln. 3-48706
 viscoelastic fluid constitutive relation, critical test 3-66556

nonlinear network analysis

- eddy current loss analysis from Maxwell/Fredholm integral equation 3-40198
 lumped networks, lattice solitons, theoretical and experimental studies 3-66509
 N-soliton soln. of nonlinear lumped self-dual network eqns. 3-48706
 N-soliton solution of nonlinear lumped network eqn. 3-48705

nonlinear optics*see also Brillouin spectra; self-focusing*

- 3 photon scattering of light, isotropic medium, various pumping fields (Russian) 3-57254
 alkali metal, second harmonic generation, nonlinear polarisation 3-66873
 Amplification effect of backscattering by bodies placed in a medium with random inhomogeneities (Russian) 3-66871
 anthracene crystals, two-photon absorption 3-48944
 applied, book 3-43040
 atom, intense wave interactions anal. by hydrodynamical model 3-74126
 atomic interactions with e.m. fields, conf., Balatonfured, Hungary (Sept. 1972) 3-74770
 atomic scale, physical interpretation for teachers 3-70235
 atoms in e.m. field, velocity distrib. and nonlinear interference effects, effect of selective collisions 3-74275
 benzil, new meas. method for electro-optical consts. at h.f. 3-48404
 birefringent crystals, laser beam frequency mixing, applications, review 3-40288
 bremsstrahlung, two photon Compton scattering, stimulated, nonrelativistic cases 3-62749
 β -carotene, optical nonlinearities in conjugated systems 3-59888
 classical nonlinear active medium, coherence effect in spontaneous radiation, self-oscillation (Russian) 3-62753
 coherent Raman beat phenomenon analysis using coupled Maxwell-Schrodinger eqns. 3-62748
 compensation of effect of group retardation of waves by forced combination dispersion (Russian) 3-59900
 dense reson. medium, multiple photon echo, optical nutation 3-48941
 dichroism and optical anisotropy of media with oriented spins of free electrons 3-64632
 dielectric, anisotropic, microwave rel. to optical and electro-optical nonlinearities 3-43037
 dielectric and ferroelec. materials, and electro-optical props., review 3-43032
 dielectric fibre waveguide, picosecond nonlinear optical pulse transmission, anomalous dispersion 3-59885
 dispersion media, photon-echo spatial synchronism, distortion 3-62735
 double optical resonance, effects on gas laser (Russian) 3-70815
 elastic scattering of slow neutrons by standing e.m. wave, coherent scattering amplitude 3-62848
 e.m. field interactions with matter, book 3-74186
 excitons resonant interaction with intense coherent light 3-55231
 field fluctuations, random inhomogeneities, hybrid method (Russian) 3-66870
 filtering, logarithmic, nonlinear transforms. in coherent systems, half-tone screens 3-77445
 four-photon interaction in nonlinear medium of anisotropic molecules 3-74271
 Frenkel excitons, kinetic equations 3-66889
 frequency doublers for visible range, engineering design and optimization of parameters 3-70846
 n-GaAs drag effect in interband two photon transitions 3-44114
 gas conc. meas. by stimulated anti-Stokes scatt. 3-66438
 gases, contribution of collisions to multiphoton resonances 3-74817
 gases, stimulated Raman scatt., spatially bounded phase capture, anti-Stokes radiation 3-51951
 Gaussian laser beam stratification in cubic medium 3-62736
 glass: Nd laser, high power, self-focusing damage 3-40262
 glass, self-focusing ultrashort laser pulses 3-74273
 glass coated quartz nonlinear waveguide, second harmonic generation 3-59884
 Goos-Hanchen effect, longitudinal and transverse shifts associated with total internal reflection 3-59896
 guided-wave optics, coupled-mode theory 3-59890
 high quantum-efficiency i.r. up-conversion 3-66865
 holograms, nonlinearly recorded, of diffusely reflecting object, image contrast 3-62668
 III-V semiconductors, nonlinear interaction of e.m. and acoustic waves, hypersound generation 3-50542
 image conversion, resolving power, theory, expt. (Russian) 3-74268
 image conversion theory, Green's function method 3-62744
 induction and echo, influence of nonresonance states 3-57263
 internal SHG in laser, limitations for mode-locking enhancement 3-59876
 i.r. detector, operating on freq. conversion, noise 3-70850
 Kleinman forbidden nonlinear optical coeffs., magnitude and dispersion 3-59891
 KNbO₃, intracavity second harmonic generation of YAlG/Nd laser 3-51948
 Korteweg-de Vries eqn., initial discontinuity decay 3-45821
 large k-vector phonon generation by stimulated Raman scattering from picosecond pulses 3-55041
 laser harmonic generation, fifth picosecond, in multistage system 3-70849
 laser light nonlinear absorption, Monte Carlo treatment 3-59893
 laser pulse shaping, self-phase modulation in ruby, high power amplification, theory and experiment 3-48939
 laser radiation nonlinear absorpt., Monte Carlo treatment 3-74280
 laser resonator, exhibiting frequency dispersion, equation of motion 3-48934

nonlinear optics continued

- laser resonator Q-factor, switching by stimulated Mandelshtam Brillouin scatt. 3-70836
- leucosapphire, self-focusing ultrashort laser pulses 3-74273
- light waves four-photon forced dispersion during nonmonochromatic pumping (*Russian*) 3-48952
- liquid media, stimulated scattering and induced Bragg reflexion 3-66880
- liquid media stimulated scattering and induced Bragg reflection 3-66881
- lithium formate crystals, refractive indices measurement, 0.35 to 1.5 micron, Sellmeier relation 3-40285
- low-loss materials for waveguides, light-induced temp. rise 3-51949
- many interacting waves far from thermal equilibrium, statistics 3-43039
- master equation, strongly interacting systems 3-70794
- medium with nonlinearity saturation, stationary solns. of wave eqn. (*Russian*) 3-66869
- methane, induced Raman scatt. under cavity excitation, spectral width and line struct. 3-59895
- molecular crystal, absorp. band structure and origin of high nonlinear dielec. susceptibility 3-62740
- molecular crystals, theory of hyper-Raman effect 3-66891
- multiphoton absorption probability and incoherent and coherent pulses 3-57255
- multiphoton molecular light scattering by inhomogeneity of nonlinear polarisation 3-43036
- multiple and bi-soliton bound state solutions of sine-Gordon and related equations 3-57045
- nitroethane isooctane, critical liquid mixture, Mandelshtam-Brillouin spectra 3-80040
- nonlinear susceptibility tensor, permutation symmetry relation to photon number conservation laws in the dissipative media 3-57250
- one-dimensional superlattice, coherent phonon generation by optical mixing 3-41499
- optical waveguides, theory of SHG 3-59889
- optically transmitting materials, thermal lensing of laser beams, general formulation 3-57248
- organic crystals, second harmonic generation, mol. struct. 3-62738
- organic materials, powdered, optical second harmonic generation 3-57259
- parametric amplification, critical, oscillatory behaviour, time-dependent pump amplitude, phase 3-59894
- parametric four photon exchange effect, amplification and oscillation near pump field (*German*) 3-78056
- parametric light source inside laser resonator, phase fluctuations 3-74277
- parametric light sources, one and two resonators, transient processes 3-48948
- parametrically unstable nonlinear media, transient processes 3-40291
- phase matching, for parametric generation of far i.r., by periodic variation of nonlinear coeffs. 3-59892
- phase variation in coherent optical pulse propagation in two-level atoms medium 3-54244
- phase-matched second harmonic generation, efficiency 3-66884
- photoelastic interaction of optical and acoustic waves, absolute instability 3-70844
- photon echo polarisation, medium reaction on exciting light pulse 3-45822
- photon echoes, up-converted, or down-converted, generation in 3-level resonant medium 3-48942
- photon spin echo phenomena, transient and stationary regimes (*French*) 3-55482
- phthalocyanine solns., intersystem crossing probability calcs. 3-74281
- picosecond pumping, exptl. study of nonstationary nonlinear effects 3-78058
- plasma form. influence on freq. superbroadening in light filaments 3-66874
- polarizable particle interact. with e.m. waves, photon stim. scatt., two-photon drag (*French*) 3-66876
- polarization phenomena and nonlinear interference effects with allowance for collisions 3-40290
- ponderomotive forces in nonlinear media, laser beam interactions 3-45825
- proustite, difference freq. generation by mixing of dye lasers, 5.82-7.25 μm 3-57256
- proustite, parametric freq. upconverter, background light 3-51944
- quantum freq. converter, quantum theory, time depend. perturbation theory 3-66883
- quartz, self-focusing ultrashort laser pulses 3-74273
- quartz, third order susceptibility, absolute meas. from third harmonic generation 3-78064
- Rayleigh, and Raman scatt. nonlinear 3-74282
- refractive index temp. depend., meas. using thermal self-phase modulation 3-51595
- resonance radiation transfer, role of branching ratio 3-70762
- resonant 3 level system, photon echoes, anal. 3-78061
- resonant degenerate 3 level system, photon echoes, anal. 3-78062
- resonant gaseous medium, effect of particle collisions on laser pulse deformation (*Russian*) 3-45826
- resonant medium, two interacting laser beams 3-66863
- resonant Raman effect with damping 3-69006
- rhodamine 6G and benzophenone in soln., nonlinear absorpt., singlet-singlet energy transfer 3-78035
- ruby, self-induced transparency, temp.-depend phase memory 3-62747
- ruby radiation locked photon echoes, optical free induction 3-54243
- second harmonic frequency light generation in a Gaussian light 3-66868
- self-curving effect, two dimensional, time dependent 3-74267
- self-diffraction of emission caused by excited level absorpt. (*Russian*) 3-59898
- self-focused light beams, backward stimulated light scatt. and limiting diameters 3-62745
- self-focusing and self-trapping, existence and stability of eigenmodes 3-70840
- self-focusing parameter meas. using intrinsic optical damage 3-59583

nonlinear optics continued

- self-focusing waveguides, struct. of three-component vector fields 3-59897
- self-induced transparency, Maxwell-Bloch equation, N soliton solutions 3-62734
- semiconductor, laser beam propag. under two-photon resonance conditions 3-48950
- semiconductor glass, KS-type, temp. depend. of spectral region of decolonisation (*Russian*) 3-45827
- semiconductors, III-V and II-VI, nonlinear optical props., simple molecular orbital theory 3-48940
- semiconductors, laser beam self action 3-57262
- semiconductors, self-induced transparency by single-photon excitation by ultrashort light pulse 3-74270
- rel. to short light pulses (*Czech*) 3-70841
- single crystals, polarization and nonlinear optical props., theoretical anal. 3-54246
- solid, two-photon transitions near thresholds, electric field effect 3-80008
- solids, interaction mechanisms (*German*) 3-72592
- spectrograph using nonlinear controlled dispersion 3-59590
- spontaneous parametric scatt. in crystals, medium polarisation and elec. field effects (*Russian*) 3-66886
- spontaneous waveguide concentration of radiation in nonlinear medium, effectiveness, expt. study 3-57253
- stability of e.m. oscillations in media with cubic nonlinearity 3-66879
- stilbene powder, stimulated Raman scatt., energy and time charact., temp. effects 3-62751
- stimulated Compton scattering as radiation source, theoretical limits 3-40283
- stimulated emission without inversion, 2 photon emission 3-70842
- strontium formate, phase matched second harmonic generation and optical mixing 3-40281
- strontium formate dihydrate, phase matched second harmonic generation and optical mixing 3-40281
- sum-frequency e.m. generation in nonlinear film (*Russian*) 3-54247
- sum-frequency generation in nonlinear crystal, influence of inhomogeneities on image conversion 3-74276
- superconductors, two photon absorpt. 3-50305
- susceptibilities and parametric interactions, review 3-54248
- thermal lensing of laser beams in optically transmitting materials 3-66867
- thermal transient defocusing, intensity limitation and energy spreading in optical field 3-70848
- third optical harmonic with high conversion efficiency generation (*German*) 3-78057
- three photon process, absorpt. cross section and spin analysis 3-51952
- threshold values for scattering of light by light in vacuum free of field influences 3-70843
- transparency, self-induced, macroscopic theory 3-66877
- transparent solid dielectric, homogeneous, optically isotropic, transient self focusing of high power laser pulse 3-48949
- tunable difference freq. mixing at high repetition rates, 1.5-1.7 μm 3-45817
- two state system, non-resonant levels effect, Schrodinger eqn. representation, Stark shift 3-45782
- two-level atom system, polarisation effects, self-focusing (*Russian*) 3-57251
- two-level system, semiclassical theory of saturated absorpt. 3-62746
- two-photon absorption, giant, excitonic molecule, resonance, giant oscillator strength 3-40289
- two-photon absorption in molecules, calcs. (*Russian*) 3-59899
- two-photon photoionization absorpt. of optical, X-ray quanta 3-66878
- water, optical strength, effect of Cu^{2+} salt additives 3-57252
- water, stimulated short-wave radiation due to single freq. reson. of third-order nonlinear susceptibility 3-66882
- wave modulation, perturbation method, integro-partial differential eqns. 3-77864
- waveguide, index tuning of phase matched second harmonic generation 3-74265
- Ag_3AsS_3 , proustite, determ. of six photoelastic consts. by Bragg scatt. of laser light 3-75558
- Ag_3AsS_3 , proustite conversion of i.r. into visible, mutually perpendicular pumped signal beams, parameters, efficiency 3-40284
- Ag_3AsS_3 , parametric oscillator, singly resonant, tuned from 1.22 to 8.5 μm 3-40280
- Ar gas laser, continuous, population inversion, output (*French*) 3-48943
- BCl_2 , molecular gas, photon echo effect 3-62752
- BCl_3 resonantly absorbing gas, self-focusing of CO_2 laser radiation 3-51950
- $\text{Ba}_2\text{Ti}_2\text{Nb}_8\text{O}_{30}$, ferroelec. and optical props., room temp. to Curie temp. 3-72584
- $\text{BaY}_2\text{F}_8:\text{Yb},\text{Er}$, efficient i.r.-to-visible conversion by confinement of excitation energy 3-59887
- CO_2 , high power CO_2 laser beam absorption saturation effects 3-66854
- $\text{CaF}_2:\text{Er}^{3+}$, i.r. to visible upconversion, sequential pair process 3-54241
- $\text{Ca}(\text{IO}_3)_2 \cdot 6\text{H}_2\text{O}$, nonlinear coeffs. 3-46606
- CdIn_2S_4 , multi-quantum photoconductivity 3-60897
- CdS , external self-focusing of ruby laser beams (*Russian*) 3-40292
- CdS , thermal shift of laser wavelength during excitation pulse of electron beam 3-78044
- $\text{CdS}_{0.6}\text{Se}_{0.4}$ investigation of statistical props. of ultrashort light pulses by two-photon absorption 3-74274
- $\text{CdS}, \text{Se}_{1-x}$ single crystal., two-photon absorpt., comp. influence 3-70845
- Cs , four-photon reson. ionisation theory, quantum mech. method 3-49410
- Cs , multiphonon ionisation and absorpt. of ruby laser light (*French*) 3-46195
- CuBr , second order coefficient, absolute sign and magnitude 3-68953
- CuCl , reson. second harmonic generation in exciton region, freq. depend. 3-51956

nonlinear optics continued

- CuCl, second order coefficients, absolute sign and magnitude 3-68953
- CuGaSe, prep., struct., second harmonic generation, bandgap 3-61113
- CuGaS_{0.5}Se_{1.5}, prep., struct., second harmonic generation, bandgap 3-61113
- CuGaS_{1.5}Se_{0.5}, prep., struct., second harmonic generation band gap 3-61113
- CuI, second order coefficients, absolute sign and magnitude 3-68953
- α -Cu(IO₃)₂, second harmonic generation 3-79306
- D₂O broadband picosecond continuum and light gate, time resolution and characteristics 3-45820
- GaAs, two photon absorption, light pulse duration depend. 3-54242
- GaAs, two-photon absorption of Nd laser radiation 3-66864
- GaSe, second harmonic generation, nonlinear susceptibility coeff. (French) 3-54240
- Ge, nonlinear loss in 2.5 to 4 micron range 3-74264
- H, six-photon reson. ionisation theory, quantum mech. method 3-49410
- HF, delayed spontaneous emission, inhomogeneous broadening effects 3-45796
- α -HIO₃, spontaneous parametric emission and light scatt. by polaritons 3-48945
- H₂O broadband picosecond continuum and light gate, time resolution and characteristics 3-45820
- INPs, coeffs. characteriz., refr. indices, birefringence 3-80004
- In₂S₃, optical transitions involving different numbers of photons 3-74272
- InSb, degenerate, linear circular two photon dichroism 3-43033
- InSb, nonlinear polarisability dispersion, band struct. parameter 3-43038
- InSb, Raman spin flip tunable laser, high power pulsed operation 3-57257
- InSb, self focussing of e.m. beams, nonlocal effects 3-57249
- InSb, spontaneous spin-flip Raman line width, non reson. non linearity, 2K 3-57258
- InSb, tunable far i.r. generation by difference freq. mixing 3-54239
- InSb i.r. absorption, $\lambda = 10.6 \mu$, 92 to 151K, hole lifetimes, temperature, light intensity 3-51959
- KH₂PO₄, 90° phase matched, second harmonic generation in u.v. 3-51946
- KH₂PO₄, new meas. method for electro-optical consts. at h.f. 3-48404
- KH₂PO₄, noncollinear second harmonic generation 3-66875
- KH₂PO₄, Raman susceptibility, stimulated Raman effect 3-51953
- KH₂PO₄, second harmonic converter for Nd:glass laser 3-74245
- KH₂PO₄, vector synchronous interaction of light waves 3-62741
- KNbO₃, optical coeffs. at 1.06 μ , Marker fringe method 3-68954
- Li⁺ gas, harmonic power generation using nonlinear optical polarisabilities 3-57260
- LiIO₃, contours pattern due to second harmonic generation, using ruby laser 3-78066
- LiIO₃, new meas. method for electro-optical consts. at h.f. 3-48404
- LiIO₃, parametric and polariton light scatt. 3-51957
- LiInS₂, second harmonic generation of ternary semiconductor 3-45819
- LiNbO₃, birefringence changes on laser irradi., ellipsometric obs. 3-74266
- LiNbO₃, grown from stoichiometric melts, for nonlinear optical props. optimisation 3-44532
- LiNbO₃, i.r. optical parametric fluoresc. 3-43031
- LiNbO₃, parametric and polariton light scatt. 3-51957
- LiNbO₃, reduced, tunable for i.r. generation by difference freq. mixing using dye laser 3-51945
- LiNbO₃, second harmonic generation 3-48946
- LiNbO₃, temperature derivative of second harmonic generation 3-74278
- N₂, induced Raman scatt. under cavity excitation, spectral width and line struct. 3-59895
- N₂, liquid, intensification of dispersion by different pumping schemes (Russian) 3-74279
- NH₃ gas, self induced transparency with CO₂ laser pulses 3-66866
- NH₄H₂PO₄, vector synchronous interaction of light waves 3-62741
- (NH₄)₂h₂PO₄, second harmonic generation of Ar laser lines by 90° phase matching 3-51947
- NaNO₂, second harmonic generation, spontaneous polarization, temp. depend. 3-78060
- Ne laser, higher order nonlinear effects, hexadecapole moment in 2P₄ level 3-51915
- PbS₂O₆.4H₂O, cryst. symm. class 32, determ. from second harmonic generation 3-72061
- PrCl₃ quantum counter, direct i.r. image upconversion 3-57247
- Rb, vapour, adiabatic following and slow optical pulse propag. 3-45823
- Rb vapour, optical pulse self steepening with possible shock formation 3-57261
- SF₆, coherent pulse transmission, reorientational collisions effects 3-51954
- SF₆, liquid, stimulated Raman scatt. 3-70847
- SF₆, molecular gas, photon echo effect 3-62752
- SF₆ resonantly absorbing gas, self-focusing of CO₂ laser radiation 3-51950
- Si, indirect two-photon transitions at 1.06 μ m 3-40286
- Te, multi-photon absorption after laser irradiation, carrier generation 3-55284
- TeO₂, nonlinear susceptibility dispersion, 0.35-0.53 μ m 3-43034
- Xe harmonic power generation using nonlinear optical polarisabilities 3-57260
- ZnO, reson. second harmonic generation in exciton region, freq. depend. 3-51956

nonlinear programming

- see also *convex programming; quadratic programming*
- fast reactor, design optimisation system with nonlinear programming method 3-57555
- optimisation, holographic recording conditions, thin amplitude hologram, nonlinear programming method by computer (Russian) 3-77538

nonlinear programming continued

- PWR determ. of emergency core coding carryout rate correlation by nonlinear programming 3-46086
- shell, stiffened cylindrical, minimum weight optimisation using random search analysis (Russian) 3-62504
- nonlinear symmetries**
- SU_n × SU_n, chiral group, nonlinear realisation of symmetries and localisability 3-74338
- nonlinear systems**
- see also *nonlinear control systems*
- frog's visual analyser, information processing principles, model of novelty neurons (Russian) 3-48241
- insect nervous visual system studies, white-noise identification techniques 3-45307
- irreversible processes, nonlinear, system motion in thermodynamic theory 3-74174
- nuclear reactor, suboptimal control using low-order models 3-54528
- oscillatory mechanisms, dynamic interactions (Russian) 3-74061
- vibrating, with many degrees of freedom, normal coords. in principal resons. anal. (Polish) 3-59771
- nonparametric statistics**
- No entries
- nonpolar crystal lattice vibrations**
- anthraquinone single cryst., far-i.r. spectra, translational lattice vibrs., Fermi reson. 3-61034
- biphenylene, Raman spectra, in-plane normal mode calc. and complete vib. assignment 3-61038
- graphite, bulk and surface atoms, simple Born model, displacements, calculations (French) 3-40983
- H₂, self consistent equation of state 3-55052
- hexamethylbenzene single cryst., polarized Raman spectra, freqs. assignment 3-55572
- inorganic complex salts, l.f. vibrs., metal-ligand and complex ion-outer ion interactions 3-47246
- molecular and atomic thermal vibrs., computer calc. program (Czech) 3-54604
- naphthalene, anharmonicity of lattice vibr. and lifetime of optical phonons 3-72644
- naphthalene, arylethylene depend., spectrum phonon struct. 3-68357
- 1,5-naphthyridine in durene mixed cryst. spectra, isotope effect on localized phonons 3-58542
- n-paraffin crystals, Raman spectra 3-72641
- stilbene, anharmonicity of lattice vibr. and lifetime of optical phonons 3-72644
- tartaric derivatives, Raman and i.r. spectra external vibration frequencies of active and racemic forms 3-55581
- 2,4,6-triphenyltriazine, Raman active lattice spectrum, 300 and 30K 3-55578
- Au:V, lattice specific heat reduction due to V impurities 3-55065
- BaTiO₃, anharmonicity, Mossbauer obs. 3-41454
- CDTe, vibr. normal modes, freq. wave vector dispersion relations 3-52680
- Co coordination compounds, Raman and i.r. spectra external vibration frequencies of active and racemic forms 3-55581
- Cu₂O normal vibrations, group theoretical analysis 3-49944
- GaSe long-wavelength linear chain model, interlayer and intralayer force constants 3-40995
- hexamethylbenzene, phase transition at 116 K, phase III morphology, vib. spectra and absorpt. anisotropy 3-60794
- Ir coordination compounds, Raman and i.r. spectra external vibration frequencies of active and racemic forms 3-55581
- K₂Pt(CN)₄Br₃.30H₂O, one dimens. cond., Peierls distortion, Kohn anomaly 3-49900
- Li, lattice dynamics, phonon dispersion 3-55053
- Mo:Re alloy, analysis of lattice specific heat 3-58134
- MoS₂ long-wavelength linear chain model, interlayer and intralayer force constants 3-40995
- NaO₂, Raman spectra, struct. changes at 230 and 201 K (German) 3-50569
- PbTiO₃, anharmonicity, Mossbauer obs. 3-41454
- PbZrO₃, anharmonicity, Mossbauer obs. 3-41454
- Rh coordination compounds, Raman and i.r. spectra external vibration frequencies of active and racemic forms 3-55581
- ZnTe, vibr. normal modes, freq. wave vector dispersion relations 3-52680
- nonradiative transitions**
- acetone:rare earth ions, role of solvent 3-64717
- acetonitrile:rare earth ions, role of solvent 3-64717
- alcohol:rare earth ions, role of solvent 3-64717
- anthracene, position-dependent deuterium effects, triplet lifetime measurement 3-65100
- anthracene crystals, nonradiative destruction of triplet excitons by excess electrons 3-44451
- aromatic molecules in soln., fluoresc. quantum yields from highly excited states 3-78830
- azomethanes, nonradiative transitions and properties of lower triplet state 3-63504
- basis-independent matrix elements, intersystem crossing applic. 3-75055
- benzene, cryst., ¹B_{1u} ← ¹A_{1g} 0-0 transition obs. 3-76051
- benzene, deuteration effect on radiationless transition probability, multiphonon transitions approach (Russian) 3-80092
- cooperative, nonradiative multiphonon relaxation 3-72700
- DMSO:Eu³⁺ soln., radiative and radiationless processes 3-55683
- dye laser, internal conversion rate meas., second to first excited singlet state 3-78032
- electronic excitation in solid and gas phase 3-78890
- ethynyl-benzene and derivatives, absolute calc. radiationless decay of lowest triplet state 3-67842
- fergusonite type crystals doped with rare earth ions, virtual recharge 3-41506
- p-fluorobenzotrifluoride, fluoresc. quantum yields and decay times, rate consts. 3-63495
- p-fluorotoluene, fluoresc. quantum yields and decay times, rate consts. 3-63495
- glass, nonradiative relax. of excited UO₂ ions 3-72749
- glyoxal vapour, excited at 4358 Å, collision induced intersystem crossing, photophysics 3-80566

nonradiative transitions continued

- in impurity centres, theory, transition probabilities 3-76044
 impurity-phonon systems with static Jahn-Teller effect, multiphonon nonradiative relax. 3-41151
 intercombination transitions, spin-orbital perturbation (*Russian*) 3-68964
 internal quenching of fluoresc., compensation law 3-60471
 isolated molecules, excited states evolution, model approach 3-63505
 isolated molecules, radiationless transitions 3-49482
 liquid, obs. using picosecond pulses 3-72702
 liquid phase, singlet-singlet exchange reson. transfer of electronic excitation 3-76048
 many-electron atoms, non-stationary states, theory 3-78399
 metalloporphyrins, spin-orbit coupling and heavy atom effect on radiationless transitions 3-63498
 1-methylnaphthalene energy transfer to substituted oxazoles and oxadiazoles, excimer mechanism (*Russian*) 3-63510
 molecular electronic radiationless transitions, perturbations, interaction continua 3-67845
 naphthalene Franck-Condon factors, correl. function anal. T_1 - S_0 transitions 3-64709
 oxygen quenching of aromatic triplet states in solution 3-61272
 oxygen quenching of aromatic triplet states in solution 3-61273
 polyatomic mols., crude adiabatic vibronic state approach 3-43420
 polyatomic mols., effect on absorpt. lineshapes and fluoresc. decay curves 3-63501
 polyatomic mols., vibronic coupling 3-60470
 pyrene and derivatives, vapour-phase fluoresc. from second excited singlet state 3-67844
 quasi-stationary states in large mols., linewidth depend. 3-60469
 rate constant determ. at absolute zero 3-72601
 ruby, radiative and nonradiative transitions, temp. depend., emission quenching 3-41568
 scheelite type crystals doped with rare earth ions, virtual recharge 3-41506
 sequential decay processes, interference effects 3-63502
 solution, fluoresc. quenching and nonradiative energy transfer 3-69060
 transition metal complexes, radiationless relaxation processes 3-43473
 transition probabilities, one-particle approximation formulae 3-67848
 tunnel, in strong e.m. field 3-76046
 uranyl acetate, vibronic interaction, luminescence spectra 3-72748
 uranyl butyrate, vibronic interaction, luminescence spectra 3-72748
 uranyl propionate, vibronic interaction, luminescence spectra 3-72748
 $\text{CaF}_2:\text{Sm}^{2+}$, room temp. lifetime meas. 3-72708
 $\text{CaWO}_4:\text{Nd}^{3+}$ intermultiplet relax. 3-76045
 GaAs, laser excited, non radiative recombination of electrons and holes 3-79711
 GaAs double heterostructure laser, degradation due to nonradiative recomb. component 3-54235
 $\text{GdCl}_3 \cdot 6\text{H}_2\text{O}:\text{Dy}^{3+}$, Eu^{3+} , anharmonicity role, energy transfer, theory 3-76047
 $\text{HCl}(\text{Br}):\text{CN}^-$ aqueous solution, nonradiative transitions in luminesc. centres (*Russian*) 3-72717
 $\text{LaAlO}_3:\text{Eu}^{3+}$ radiative non-radiative decay (*French*) 3-72709
 $\text{POCl}_3:\text{SnCl}_4$ with Eu^{3+} ion, solvent effect 3-69055
 Pd complexes of ethiophyrin and mesoporphyrin, nonfluorescent, quantum yield for intermolecular conversion (*Russian*) 3-49488
 Rh(III) complex, halopentammine, radiative and radiationless decay processes 3-73158
 SO_2 isolated mols. excited within first allowed absorpt. band, non-radiative decay processes 3-54709
 $\text{Sr}_3(\text{PO}_4)_2:\text{Eu}^{2+}$, radiationless recombinations in surface layers (*Russian*) 3-50612
 Tb^{3+} in DMSO, radiative and nonradiative transitions rel. to energy transfer model 3-64732
 $\text{Y}_2\text{O}_3:\text{Eu}^{3+}$, Tb^{3+} , radiationless recombinations in surface layers (*Russian*) 3-50612

novae

- see also supernovae
 RX Andromedae, Z Camelopardalis type star, high-speed photometric obs. 3-65893
 SY Cancri, Z Camelopardalis type star, high-speed photometric obs. 3-65893
 cataclysmic variables, masses of white dwarf primaries 3-48017
 Cephei, 1971, photometry, light variations, estimation of photometric distance 3-81101
 Cephei 1971, light curve, early spectral changes 3-77102
 coronal line formation, time-depend. of intensities 3-61792
 explosive phase characts. (*Italian*) 3-59345
 AH Herculis, high-speed photometry of dwarf nova, light curve analysis 3-45116
 i.r. sources, dust shell models 3-51371
 light origin, luminosity, model 3-65870
 nebosity, nova outburst, non-spherical struct., influence of white dwarf 3-69938
 Nova Doradus 1971a in LMC, UBV obs. 3-56391
 outburst characteristics rel. to initial N abundance, hydrodynamic evolution 3-45088
 outburst interpretation rel. to thermal waves in stars 3-53649
 KT Persei, Z Camelopardalis type star, high-speed photometric obs. 3-65893
 pre-nova model, pulsational instability 3-47992
 Serpenti 1970, u.v. spectrophotometry 3-48040
 RR Telescopii, emission line spectrum during 1968 rel. to nova-like properties 3-42196
 thermal wave movement in non-uniform media 3-69919

novoids see novae**nozzles**

- air hypersonic nozzle flow with high initial dissociation levels 3-43642
 annular flow propagation in a cylindrical duct 3-57857
 coaxial axisymmetric supersonic, sonic line 3-57855
 condensing steam, flow through Laval nozzle, shock waves 3-71831

nozzles continued

- critical-flow, cylindrical; effect on air-flow of back-pressure, throat Reynolds number 3-71846
 diatomic gas flow, hypersonic, nonequilib., oscillatory (*Russian*) 3-63716
 dust-laden gas suspension, entropy losses in the flow in a nozzle 3-63773
 flows calc. using Pade fractions 3-57854
 free turbulent jet with constant amplitude transverse pressure gradients near nozzle exit, sinusoidal excitation 3-60590
 gas dynamic lasers, rapid expansion nozzles 3-45788
 gas in finite length nozzle, solns. for mixed subsonic and supersonic flows 3-46447
 gas/liquid reactive propeller with ballast-boosted traction (*Russian*) 3-63794
 gasdynamic laser, output-power-characteristics 3-48886
 hypersonic tunnel wall, upstream wall temps. effects, turbulent boundary layer profile meas. 3-57780
 jet, double concentric, nozzle conditions influence on main region characts. 3-54828
 jet, supersonic, escaping from nozzle into off-design modes, apparent mass investigation 3-60587
 jet density distribution rel. to nozzle shape (*Russian*) 3-63792
 jets, laminar, viscous, stability, influence of nozzle shape 3-79041
 Laval, supersonic wind tunnel application 3-51773
 Ludwig tubes, high performance, aerodynamics 3-63704
 magnetic, nonisothermal plasma flow 3-49670
 nonequilibrium nozzle flows entropy of vibrationally relaxing diatomic gases 3-43633
 plasma, magnetodynamic-arc thruster exhausts electron number density and temp., temporal characts. 3-46557
 plasma steady state ion acceleration in magnetic nozzle for 2-20 keV 3-54847
 plenum, rapidly filling unsteady flow processes 3-46453
 relativistic gas dynamics, shock wave and nozzle flow 3-49618
 residual and single drop formation, Lohstein vol. ratios 3-71807
 rocket exhaust plumes, effect of nozzle boundary layers 3-49620
 slot injection into a supersonic stream, expt. study 3-63700
 slowly varying, plane jet flows 3-79049
 sonic, low-density streams, high pressure drops, transition between continuous and rarefied flow, flow behind a Mach disc (*Russian*) 3-57873
 starting process in the nozzle of a nonreflected shock tunnel 3-46495
 steam spontaneous condensation in u.s. nozzles 3-52493
 supersonic jet flows, noise reduction comparison with sonic nozzle 3-43637
 supersonic mixing, for CO_2 gas dynamic laser 3-51633
 swirler resistance 3-54833
 three-dimensional liquid rocket nozzle admittances, expt. determ., combustion stability 3-46496
 transient exhaust plume interaction with a rarefied atmosphere 3-43643
 transonic laminar boundary layers with surface curvature, flow through nozzle throat 3-57769
 transonic nozzle flow with a parabolic temperature distribution 3-40752
 transonic nozzle flow with uniform gas properties 3-43634
 turbulent boundary layer flow, subsonic jet model (*Russian*) 3-63692
 turbulent nozzle wall boundary layer-shock wave interactions in rectangular channels 3-43572
 two phase nozzle processes, effect of initial parameters 3-49624
 two-phase flow, outflow into vacuum, equilib. flow, analysis (*Russian*) 3-63758
 uniflow gas/water jet impeller model tests (*Russian*) 3-63793
 CO_2 - N_2 -He gasdynamic laser, power and gain calc., population inversion, adiabatic expansion through nozzle (*Russian*) 3-66824
 N_2 molecules in nozzle, anharmonic vibrational relaxation 3-54737
 N_2 supersonic nozzle flow in high current arc, turbulence development 3-68008
 N_2 - N_2O mixture, expanding supersonic jet, rapid cooling, dissociation reactions (*Russian*) 3-57872
 ^{235}U enrichment in separation nozzle process, added light gases H_2 , He and D_2 comparison (*German*) 3-69493
 ^{235}U enrichment in separation nozzle process, entropy production mechanisms (*German*) 3-69494

NTC thermistors see thermistors**v (neutrino)** see neutrinos**nuclear acoustic resonance**

- pulsed and continuous excitation in spin 1 systems 3-58436
 spin-phonon interaction tensor determ. 3-75896
 Al, absorpt. and dispersion meas., 70 to 275 K 3-50478
 Al, by elec. quadrupole coupling (*French*) 3-55481
 Al, gradient-elastic tensor determ. 3-44331
 CsMnF_3 , temp. dependence of ^{55}Mn resonance 3-55487
 Cu, via coupling to mag. dipole moment 3-58440
 LiF, nuclear quadrupole spin-phonon coupling, u.s. wave propag. 3-75891
 $\text{NaCl}(\text{F})$, nuclear quadrupole spin-phonon coupling, u.s. wave propag. 3-75891
 NaClO_3 , cross relax., n.m.r. acoustic saturation obs. 3-68869
 NaClO_3 , n.m.r. u.s. saturation study on strain distrib. 3-68858
 RbMnF_3 , impurity doped, of ^{19}F 3-41431
 Ta, elastic constns. obs., anomalous line broadening 3-64080

nuclear alignment see nuclear polarisation**nuclear binding energy**

- see also nuclear forces
 bound-state properties of three and four nucleons with realistic NN-potential 3-49163
 Brueckner-Hartree-Fock approach, self-consistent treatment of Pauli operator 3-60104
 compressibility, in two body interaction 3-60068
 deformation dependence of total binding energy, collective model (*German*) 3-49170
 density-dependent effective interactions, effect on spherical nuclear calcs. 3-52108
 energy density formalism for description of bulk properties 3-43190

nuclear binding energy continued

- four-particle states for identical spin-zero particles with separable interaction (*Russian*) 3-40437
heavy and superheavy, properties of energy surfaces (*Russian*) 3-52067
hyperfine structure, nuclear structure effects 3-52066
hypernuclei up to ^{25}Mg , α -particle model, comparison with shell model, nuclear distortion 3-57488
light nuclei, kinetic energy, internucleon interaction, binding and excitation energies 3-40407
magic nuclei, collective excitation, variational calc. of binding energies and spectra (*Russian*) 3-71064
momentum transfer dependence, 280-600 MeV/c, quasielastic electron scattering ^6Li , ^4Li , ^9Be (*Russian*) 3-57515
nonlocal separable nucleon-nucleon interaction parameters approach 3-40424
nuclear matter, $^1\text{S}_0$ two-nucleon transition matrix parametrization 3-78235
one-pion exchange potential, nuclear matter trial wave function determ. 3-40422
penetrability through double-hump fission barriers, F-matrix calc. 3-52213
potential energy surface with inclusion of axial asymmetry 3-52069
rare earths, Hartree-Fock calc. of ground-state properties 3-78275
Saxon-Woods potential, computer program for s-state binding energy and wave functions 3-67289
single-nucleon knock-out mechanism for pion induced reactions at medium energies 3-63087
spherical nuclei, determ. using coherent non-local separable N-N interactions 3-74502
spin-orbit bound nuclei and asymptotic saturation 3-54372
square well potentials with varying repulsion, accuracy of unitary pole approx. 3-49160
Strutinsky smoothing and partition function approach 3-52114
temperature dependent nuclear binding energies rel. to nucleosynthesis in stars 3-42112
three-nucleon bound state, T-matrix perturbation theory 3-60065
three-nucleon bound state problems 3-49162
three-particle system, accuracy of Brueckner theory for light nuclei 3-57480
 $\Delta(1236)$ involved corrections, including exchange effects and realistic correlation functions 3-54416
 Δ resonance effect (*Russian*) 3-71037
 ^8Be effective kinetic energy four-body forces contribution to binding energy 3-49072
 $^{12}\text{C}_\Lambda$ hypernucleus, production in $^{12}\text{C}(\text{K}^-, \pi^-)$ reaction, spectroscopy 3-78278
 ^2H , determ. using coherent non-local separable N-N interactions 3-74502
 ^3H , calc. for Reid's soft-core nucleon-nucleon interaction 3-49073
 ^3H , determ. using coherent non-local separable N-N interactions 3-74502
 ^3H , effect of short-range part of nucleon nucleon interaction, low energy properties 3-62959
 ^3H , evidence for strong three-body force 3-78262
 ^3H , investigation of off-shell effects, various nucleon-nucleon potentials 3-71036
 ^3H , three-body calcs. 3-78260
 ^3H , three-body forces, various theories 3-78261
 $^3\text{H}^{1,2,3}$ state below break-up threshold, Gammel-Brueckner potential 3-52107
 ^3H hypernucleus, Λ -d scattering lengths, dependence on $\Lambda\Sigma$ coupling, perturbative treatment 3-62979
 $^3\text{He}^{1,2,3}$ state below break-up threshold, Gammel-Brueckner potential 3-52107
 ^4He , calc. of bound state energies using four body integral eqns. 3-71053
 ^4He , effective kinetic energy four-body forces contribution to binding energy 3-49072
 ^4He , soft core potentials, dependence of binding energy, nucleon density, form factors 3-45979
 ^6Li , multichannel three-body model approach 3-40408
 ^6Li , three body wave function, rel. to low lying states and electron scattering excitation 3-62944
 $^9\text{Li}_\Lambda$, production by K^- interaction in nuclear emulsion at 3.0 GeV/c 3-74520
Mn isotopes, calc. using Hartree-Fock-Bogoliubov method 3-67246
Mn isotopes, study using Hartree-Fock-Bogoliubov method 3-67246
 $^{143}\text{Nd}(n, \gamma)^{140}\text{Ce}$, hindrance factors for γ -ray transitions near neutron binding energy 3-49218
 ^{16}O , $^1\text{S}_0$ two-nucleon transition matrix parametrization 3-78235
 ^{16}O , calc. from off-energy-shell continuation of $^1\text{S}_0$ two-nucleon T matrix 3-78259
 ^{16}O , $^1\text{S}_0$ two-nucleon transition matrix parametrization 3-78235
 ^{16}O , calc. from off-energy-shell continuation of $^1\text{S}_0$ two-nucleon T matrix 3-78259
V isotopes study using Hartree-Fock-Bogoliubov method 3-67246

nuclear bombardment targets

- see also nuclear reactions and scattering
backings, for charged particle induced X-ray fluorescence analysis of biomedical specimens 3-51681
chamber, for capture reactions 3-42636
condensed hydrogen jet, target production, in vacuo 3-48503
dynamic loop target for in-cyclotron production of ^{18}F 3-39998
holder design, for cyclotron isotope production 3-39999
photoneutron spectra produced by electron bremsstrahlung on targets 3-57509
photoproduction of η meson on Be, C, Al, Cu, Ag, Pb, $E_\gamma=2$ GeV 3-49010
plexiglas track sensitive target in cryogenic bubble chamber, physics run 3-70402
proton, polarised, superconducting magnet, d.c., C-frame, Argonne USA, description 3-56926
rotating, intense 14 MeV neutron source 3-56923
rotating holder, for low melting point targets 3-51683
track sensitive, in bubble chamber, design loading analysis 3-70403
track sensitive, isotropic γ -detection 3-73876
track sensitive targets, geometrical construction of events 3-77656
track sensitive targets, review 3-77649

nuclear bombardment targets continued

- ^{11}B self-supporting, preparation method 3-77610
 ^{209}Bi , polarised by low temperature orientation, study of magnetic hfs in muonic atom 3-46008
 ^{13}C ion, implanted in Ni- and Ta-substrates, range determ. (*German*) 3-49913
 ^{13}C self-supporting, preparation method 3-77610
 ^{19}F ion, implanted in Ni- and Ta-substrates, range determ. (*German*) 3-49913
 H_2 , liquid, length meas., optical technique 3-51678
 H_2 , liquid Cerenkov radiation, use for localisation of interaction point along beam line and as reaction trigger, technique 3-77613
 H_2 , liquid universal design, case of alteration description 3-77604
 H_2 , liquid H_2 , polyethyleneterephthalate, Lawsonite film 3-48502
 H_2 , track sensitive targets, in Ne/ H_2 bubble chamber 3-77655
 H_2 internal jet target at NAL, study of $\text{pp} \rightarrow \text{pX}$ inclusive reaction, 40-260 GeV/c 3-71022
 H_2 liquid target, for high-energy physics experiments 3-53974
 H_2/D_2 track sensitive target, neutrino interaction studies in BEBC 3-77657
 $\text{H}_2(\text{D}_2)$, supersonic jet target, density profiles 3-56924
 ^3H for neutron production in ion accelerators (*French*) 3-56917
 Hg , for heavy ion beams 3-51684
T-Ti targets, optimum thickness for production of 14 MeV neutrons by 150 keV deuterons 3-51682
UC-graphite compacted neutron target (*German*) 3-71258
- nuclear branching and mixing ratios**
 ^{53}Mn , excited state obs. by $^{53}\text{Cr}(\text{p}, \text{n})$ reaction 3-67192
 $\text{A}=20$ to 52, isospin mixing from the effective nuclear interaction 3-71062
charge symmetric reactions $^{10}\text{B}(\text{d}, \text{p})^{11}\text{B}$, $^{10}\text{B}(\text{d}, \text{n})^{11}\text{C}$, branching ratios of cross sections 3-74599
compound statistical reactions, determ. isospin mixing fraction 3-71093
(γ, γ') reactions, M2-E1 mixing ratios, effect of overlapping resonances 3-63036
 ^{36}Ar γ -ray decay, $^{35}\text{Cl}(\text{p}, \gamma)^{36}\text{Ar}$, $\text{E}=0.8-2.6$ MeV, shell model calculation 3-71078
 ^{134}Ba , E0 contrs. in 2^+ to 2^+ transitions, directional correlation functions 3-62991
 ^{136}Ba , mixing ratios determ. from γ - γ correlation 3-40457
 ^{138}Ba , spins and mixing ratios from γ - γ directional correl. 3-78238
 ^{141}Ba , ^{141}La , absolute branching ratio detn. 3-54435
 ^{210}Bi , gamma decay of excited states populated in $^{209}\text{Bi}(\text{d}, \text{p})$ reaction, shell model interpretation 3-67259
 ^{40}Ca , double gamma decay phenomena 3-60117
 ^{110}Cd , E0 contrs. in 2^+ to 2^+ transitions, directional correlation functions 3-62991
 ^{35}Cl from $^{34}\text{S}(\text{p}, \gamma)^{35}\text{Cl}$, gamma ray transitions and lifetimes 3-43214
 ^{36}Cl pop. in $^{35}\text{Cl}(\text{d}, \text{p})^{36}\text{Cl}$ reaction, gamma-ray decay, meas. mean lives of states 3-67262
 ^{52}Cr , branching ratios of analogue states populated in $^{51}\text{V}(\text{p}, \gamma)$ reaction 3-78287
 ^{61}Cu , via $^{58}\text{Ni}(\text{He}, \text{p})$ reaction spectrometry 3-67261
 ^{150}Dy , α -decay branching ratios 3-54446
 ^{151}Dy , α -decay branching ratios 3-54446
 ^{160}Dy , determ. multipole ratio from directional angular correlations 3-67256
 ^{160}Dy , E0 contrs. in 2^+ to 2^+ transitions, directional correlation functions 3-62991
 ^{251}Fm , alpha decay, determ. multipolarities of prominent transitions and alpha branching 3-67281
 ^{70}Ga , γ -ray branching ratios following $^{70}\text{Zn}(\text{p}, \text{n})$ reaction 3-62931
 ^{131}I , branching ratio detn. 3-54436
 ^{82}Kr , E0 contrs. in 2^+ to 2^+ transitions, directional correlation functions 3-62991
 ^{175}Lu , E2/M1 mixing ratio of gamma ray transition 3-71082
 ^{24}Mg , branching ratio for γ transitions from 4.235 MeV level 3-40439
 ^{28}Mg , gamma-ray spectroscopy of low-lying levels populated in $^{26}\text{Mg}(\text{H}, \text{p})$ reaction 3-67258
 ^{26}Mg , multipole mixing ratios of transitions 3-60070
 ^{45}Ni , absorption of stopped π^- , with emission of ^8Li , determ. branching of reaction channels (*Russian*) 3-67374
 ^{17}N β -decay to unbound states of ^{17}O , branching ratio determ. 3-60121
 ^{23}Na from $^{12}\text{C}(^{12}\text{C}, \text{p})^{23}\text{Na}$, high spin states study, branching ratios 3-49185
 $^{23}\text{Na}(\text{p}, \gamma)^{24}\text{Mg}$, 3905 keV, lowest T=2 level, γ branching ratios 3-78285
 ^{24}Na , from $^{23}\text{Na}(\text{d}, \text{p})$, 2.5 and 2.8 MeV 3-63063
 ^{24}Na from $^{23}\text{Na}(\text{d}, \text{p})$, 2.45 MeV 3-62986
 ^{59}Ni , low-lying levels populated in $^{58}\text{Fe}(\alpha, \text{n})$ reaction 3-49213
 ^{16}O , stopped π^- capture with ^8Li emission determ. reaction branching (*Russian*) 3-67375
 ^{29}P , levels up to 4.76 MeV populated in $^{28}\text{Si}(\text{p}, \gamma)$ reaction 3-49144
 ^{32}P from $^{29}\text{Si}(\alpha, \text{p})$ $\text{E}_\alpha=10.65$ to 11.00 MeV, deduced levels 3-60108
 ^{33}P , populated via $^{31}\text{P}(\text{t}, \text{p})^{33}\text{P}$ reaction, low-lying states lifetime meas. and props. 3-54427
 ^{207}Pb , angular correlation studies 3-49219
 ^{147}Pr , 145 keV transition, penetration parameter, M1-E2 mixing ratio 3-78279
 ^{10}Rh , E2/M1 mixing ratio assignments from gamma ray anisotropy meas. 3-74534
 ^{30}S , DSAM, γ -decay, $^{28}\text{Si}(\text{He}, \text{n})$ reaction 3-78289
 ^{32}S , transitions from isobaric analogue resonances in $^{31}\text{P}(\text{p}, \gamma)$, $^{31}\text{P}(\text{p}, \text{p})$ and $^{31}\text{P}(\text{p}, \alpha)$ reactions (*French*) 3-78299
 $^{33}\text{S}(\text{p}, \gamma)^{34}\text{Cl}$, ^{34}Cl nuclear levels investigation 3-52102
 ^{46}Se , γ -decay of low-lying states 3-78282
 ^{88}Sr , mixing ratio for 898 keV transition (*German*) 3-60118
 ^{154}Tb , isomeric states, meas. with ^{154}Gd , gamma and beta decay following proton excitation 3-67263
 ^{149}Tb , α -decay branching ratios 3-54446
 ^{47}V , γ -decay of analogue resonances in $^{46}\text{Ti}(\text{p}, \gamma)$, mixing ratios (*German*) 3-78251
 ^{183}W , ^{184}W , mixing ratios of transitions following orientation meas. on $^{183,184}\text{Re}$ 3-60110
 ^{174}Yb pop. in $^{173}\text{Yb}(\text{n}, \gamma)$ reaction, gamma decay of excited $\text{K}=0$ rotational bands 3-74533

nuclear branching and mixing ratios continued⁶⁷Zn, γ - γ ang. correl. meas. of mixing ratios 3-62999**nuclear charge**

A=19 isobar asymmetry, due to Coulomb interaction determ. 3-67176

Brueckner-Hartree-Fock approach, self-consistent treatment of Pauli operator 3-60104

conjugate nuclei, magnetic moments analysis in framework of charge symmetry 3-45945

density dependent residual interaction calcs., effective charges and g-factors 3-49118

density errors detd. from electron scattering 3-54375

fission liquid-drop model, charge vibrs. 3-78360

form factor evaluation with intrinsic hyperspherical coordinate wave functions 3-67182

lanthanides produced by 24 GeV proton irradiation of tungsten, charge dispersion curves 3-40486

light nuclei, parameters of quadrupole, hexadecapole and 2⁶ pole deformation (*Russian*) 3-67183muon-nucleus system, effects of Y₄ deformation on transition matrix elements 3-52129penetration effect in theory of internal conversion, influence of nuclear charge distrib. (*Russian*) 3-74527

radial density, self consistent, and sum rules for charge from factors rel. to electron scattering 3-67314

radii, r.m. effect of non axial deformation in rotating heavy nuclei 3-67181

rare-earth nuclei, even, change of charge radii due to rotational transitions, cranking model 3-52130

screening effects on critical charge, calc. 3-54374

shape calc., nuclear and Coulomb, reduction of apparent discrepancies 3-60067

superheavy nuclei, non-existence of critical charge 3-43169

superheavy nuclei ²⁸⁰112 and ⁴⁰⁸168, charge and mass distrib. calc. by hyperspheric functions method (*Russian*) 3-74479

volumes detn. by optical pumping far from stability 3-45962

²⁰⁹Bi(e,e), 250 and 500 MeV, meas. of cross section, charge density and difference with ²⁰⁸Pb 3-52172¹⁴C, ground state charge distrib. determ. from elastic electron scattering 3-57512⁴⁰Ca, distribution from cross sections of elastic electron scattering, phase-shift code analysis 3-62927C(μ,μ)C, 190 MeV/c elastic scattering in low-momentum-transfer region, form factor and electron-muon universality 3-74565

Dy isotopes, variations in charge radii from X-ray isotope shift obs. 3-67662

⁵⁷Fe, calibration of isomer shift by lifetime meas. in different chemical environments (*German*) 3-49186⁵⁷Fe, change in charge radius between 14.4 keV and ground states, isomer shift calibration 3-62984³H, evidence for strong three-body forces 3-62955⁴He, charge form factor, self consistent centre of mass correction, Hartree-Fock method 3-62975⁴He charge form factor from normalization of p-³He and n-³He tails 3-49074¹⁸³Hg, variable collective inertia and mean square charge radius 3-62930¹⁹⁷Hg, variable collective inertia and mean square charge radius 3-62930⁴In, A=117, 130, 132-134, produced in ²³²Th neutron-induced fission, charge distrib. meas. 3-43260³⁹K, distribution from cross sections of elastic electron scattering, phase-shift code analysis 3-62927²⁴Mg, deformed distributions determ. from electron scattering within rotational model 3-62926¹⁶Mg, shell model calcs. 3-62951

Nd isotopes, variations in charge radii from X-ray isotope shift obs. 3-67662

²⁰Ne, deformed distributions determ. from electron scattering within rotational model 3-62926¹⁶O region, charge radii and polarisation effects 3-67179

Pb, elastic scattering of low-energy pions, charge radius determ. 3-71128

Pb isotopes, variations in charge radii from X-ray isotope shift obs. 3-67662

Pb region, effective E2 charges, particle-oscillating core coupling, polarisation 3-45924

²⁰⁸Pb, distrib. determ. from elastic electron scattering and muonic X-rays 3-71038²⁰⁸Pb(e,e), 250 and 500 MeV, meas. of cross section, charge density and difference with ²⁰⁹Bi 3-52172²¹⁰Po, effective charge of [zh₂^{9/2}]⁺ states 3-45925²⁴⁰Po, effective charge of proton h_{9/2} from lifetimes meas. (*French*) 3-45992¹²¹Sb, radii, sign and magnitude, determination using isomeric shift meas. in Sb alloys (*Russian*) 3-62929⁴⁴Sc, isospin mixing from the effective nuclear interaction 3-71062²⁸Si, deformed distributions determ. from electron scattering within rotational model 3-62926

Sm isotopes, variations in charge radii from X-ray isotope shift obs. 3-67662

¹¹⁹Sn, radii, sign and magnitude, determination using isomeric shift meas. in Sn alloys (*Russian*) 3-62929¹⁸¹Ta 482 keV transition, short-range correlations, effective charge, parity violation, polarisation 3-57490²³⁵U, ²³⁵U fission, thermal-neutron induced, fragment mass distrib., fine structure, charge distrib., structure, correlations 3-40518²³⁵U, fission by protons, charge dispersion of products in light-mass region 3-57544²³⁸U, interaction with 11.5 GeV protons, charge dispersion and recoil props. at A=131 3-40520²³⁸U, proton fission, charge dispersion of isotopes of Sb 3-57545

Yb isotopes, variations in charge radii from X-ray isotope shift obs. 3-67662

¹⁸²Yb, charge and mass distrib. calc. by hyperspheric functions method, reln. to superheavy nuclei (*Russian*) 3-74479⁶⁶Zn, Fermi distributions, effects of neutron subshell filling from cross section meas. of electron scattering (*Russian*) 3-67316⁶⁸Zn, Fermi distributions, effects of neutron subshell filling from cross section meas. of electron scattering (*Russian*) 3-67316**nuclear chemistry**

see also nuclear reactions and scattering

applications in art and archaeology, review 3-53809

element 115 (eka-Bi), prediction of props. from Bi 3-80571

hot atom reactions, steady state theory 3-41867

recoil hot atom systems collision distribution, inelastic processes effect 3-73161

teaching, applic. of stellar nucleosynthesis 3-61964

H^{82m}Br-CH₄ system, reaction of isomeric transition-activated ⁸²Br 3-65115

H* + methanethiol hot atom reactions 3-76485

T hot atom reactions with D₂, H₂ and methane, stochastic and analytical investigation 3-65114**nuclear cluster model**

Alaga model coupling of three particle (hole) valence-shell cluster to quadrupole vibrations 3-67238

alpha particle model, electron scatt. by 2s-1d shell nuclei (*Russian*) 3-78313

alpha-decay widths analysis for molecular viewpoints in light nuclei 3-60133

alpha-particle model, hypernuclei up to ²⁵Mg, comparison with shell model, nuclear distortion 3-57488

alpha-structure amplitudes for 1p shell 3-40434

bound state energy determ. of a three alpha-particle system, using Faddeev eqn's. 3-67243

DWBA analysis of Li induced single nucleon transfer reactions 3-60102

Iwamoto-Yamada cluster expansion, diagrammatic methods and renormalization 3-78271

Jastrow correls., variational approach 3-54414

linked-cluster theorem and Rayleigh-Schrodinger expansion in finite model spaces 3-45988

shell cluster coupling scheme, structure calcs. 3-74511

SO(5), irred. represent., projected basis in theory of 5-D quasi-spin 3-54413

three-body cluster, heating props., Jastrow correlation function 3-74517

triton exchange in reaction ⁷Li(α,α), 8.6-12.5 MeV and 17-22.5 MeV 3-63071

unified shell-cluster model analogous to LCAO-MO-SCF method, H.F. basis 3-43194

(n, α) reaction, A>90, α -emission by pre-equilibrium processes 3-60180⁹Be, α -clusters, studied via ⁹Be(p, α)⁸He, 35 to 160 MeV, Woods-Saxon wave function description 3-60179⁹Be, π^{\pm} total cross sections and π -⁹Be coupling constant, Glauber model 3-46043¹²C, multichannel three- α model, two-level internal structure 3-78272¹²C three-boson model, generator coordinate approach 3-62974¹²C(p,p)¹²C, high-energy, single particle description, cluster-like correlation effects 3-43247¹²C- α + ⁸Be, virtual decays, α -cluster wave functions 3-54412⁴He charge form factor from normalization of p-³He and n-³He tails 3-49074⁶Li, multichannel three-body model, binding energies of isospin states 3-40408⁶Li(d,d α)²H, quasi-free scattering at 52 MeV, determ. of α -cluster momentum distrib. 3-49273⁶Li(e,e), high-momentum-transfer, deformed cluster model 3-60166⁶Li(p,³He)⁴He, to determ. α + d, ³He + t, clustering in ⁶Li, two-mode finite-range analysis 3-60103⁶Li(p,pt), 590 MeV, cross-section meas., recoil momentum of three-nucleon residual system 3-74587²⁰Ne, α -widths based on ¹⁶O and α -cluster model 3-62943¹⁶O, effect of α -channel introduction on continuum structure, reln. to photoneuclear cross sections 3-45989¹⁶O, shell model calc. of α -transfer form factors and widths 3-45980¹⁶O(α,α)¹⁶O, vertex functions, forward alpha-particle scattering 3-60211¹⁶O- α + ¹²C, virtual decays, α -cluster wave functions 3-54412**nuclear collective model**

see also cranking model; nuclear liquid drop model

0⁺ excits. in even actinide nuclei, calcs. based on finite Fermi systems 3-45981¹²³Sb perturbation approach to particle-vibration coupling model 3-52115A=250-261, study of collective vibrational states of even-even nuclei in superfluidity model (*Russian*) 3-49140

Alaga, coupling of three particle (hole) valence-shell cluster to quadrupole vibrations 3-67238

algebraic-variational approach to collective motion theory for shell model with R(5) symmetry 3-62961

alpha-particle inelastic scattering in continuum, A=51-206, energy spectra, collective modes and optical model 3-67347

anomalous coupling states with spin I=j-1, e.m. properties 3-49104

asymmetric rotor, yrast states 3-54407

asymmetric rotor model, quadrupole moment for high spin rotational states 3-49114

asymmetric rotor with variable moment-of-inertia, extension to quasi-bands 3-43199

axially symmetric rotational and vibrational mode identification using polarised proton inelastic scattering 3-60101

backbending, rotation-alignment preferred to pairing-collapse model 3-71052

Belyaev-Zelevinski method for station as intrinsic nuclear excitation, extension 3-67242

Bohr-Mottelson, microscopic analogue, induced representations, wave function props. 3-78270

boson description of collective states, odd vibrational nuclei 3-54408

boson expansion technique for moments and related structure of vibrational and transitional nuclei 3-49102

boson variational approach, calc. of static moments and other anharmonic effects 3-49103

centre-of-mass motion, perturbation theory for projected states 3-42851

core excitation effects on ¹⁶O muon capture rate calcs. 3-74543

nuclear collective model continued

- core polarisation process in $^{54}\text{Fe}(p,p')$ to 2^+ state at 1.409 MeV 3-78237
- core polarization in ^{90}Zr , helion and triton inelastic scattering 3-78345
- Coriolis-coupling calc. of low-lying states of Ru, Pd and Cd isotopes 3-43180
- correlation model extension for continuum states of ^{12}C in giant dipole reson. region 3-43229
- coupling scheme based on particle-plus-rotor model for high angular momenta and intermediate deformation 3-45986
- deformation, search for normal oscillations in finite nuclei (*German*) 3-49170
- deformed nuclei, competition between Coriolis-anti-pairing and decoupled band hybridization 3-67241
- dense system energy calc. by variational method 3-40178
- E2 transitional energies and rotational energy formulae 3-49203
- energy density formalism for description of bulk properties 3-43190
- equilibrium nuclei deformation, calc. using one-particle infinite potentials (*Russian*) 3-57484
- even-even nuclei, quadrupole moments of excited states by reorientation effect in Coulomb excitation 3-54379
- even-even spherical nuclei, interaction between collective and quasi-particle excitations (*Russian*) 3-74514
- excitation of lowest collective states in $A=40, 90, 208$ nuclei, form factors (*Russian*) 3-67237
- excitation probability for low lying collective states, e.m. transition probabilities (*Russian*) 3-67288
- Fermi gas model calc. of magnetic moments caused by meson exchange 3-45928
- Fermi gas model for neutron emission in μ^- capture, asymmetry parameter 3-43217
- Fermi-gas, interpretation of quasielastic electron scattering on ^6Li , ^7Li , ^9Be , 1184 MeV (*Russian*) 3-57515
- finite in particular ellipsoidal deformation 3-60100
- fission mass asymmetry on dynamic process described by collective coordinate 3-60236
- fission-fragment anisotropies, for nuclei with double barrier, microscopic calcs. 3-63096
- fluctuation energies in shape fluctuation model and phenomenon of shrinkage 3-49176
- folded, for ^{24}Mg alpha-particle scattering at 104 MeV 3-60208
- function of inertia calc. for large-amplitude collective motion in Lipkin model 3-49175
- generalised, for inelastic electron scattering, ^{114}Cd , ^{64}Zn , ^{24}Mg examples 3-67239
- generator coord. method for nucl. bound states and reactions 3-52116
- governor model moment of inertia, correction 3-62970
- governor model of Trainor and Gupta, approx of deformed rotating nucleus, backbending 3-62971
- heavy and superheavy nuclei, calcs. of fission barriers 3-54520
- heavy and superheavy nuclei, spurious state contribs. in shape and stability calcs. 3-45926
- heavy nuclei, rotating, determ. of axial and non axial deformability 3-67181
- inertial mass parameter B determ. in adiabatic approx., superheavy and neutron-rich nuclei 3-62924
- intermediate mass region, Coriolis coupling calcs. 3-78252
- intermediate-coupling unified, ^{109}Ag negative parity states 3-71061
- isobaric analogue resonances, collective isovector monopole contrib. to spreading width 3-49229
- isoscalar transition densities, models and sum rules 3-40454
- level densities, influence of continuum on microscopic calcs. 3-67204
- M2 transitions, deformed nuclei of odd mass, pairing and coupling (*French*) 3-43204
- microscopic analysis of $^{39}\text{K}(d,d')$ inelastic scattering, 12.8 MeV 3-49267
- microscopic description of (p,p') scattering, role of collective imaginary form factor 3-60186
- microscopic wave functions of levels from inelastic α -particle scattering at 166 MeV 3-60182
- moment of inertia calcs. in presence of RPA correlations 3-49181
- moment of inertia parameter, derivation by method of moments 3-71045
- Nilsson orbits for nucleon in Woods-Saxon potential with deformation and coupled to core rotational states 3-71063
- non-rotational states, particle-particle and particle-hole interactions 3-67240
- nonadiabatic rotational, effect of Coriolis force on E1 transitions between bands 3-78290
- nucleons, paired, isospin degrees of freedom in collective motions 3-78269
- pairing correlations and simultaneous projection of particle number and angular momentum for $A=20-34$ 3-52118
- pairing correlations study in BCS theory and RPA, analogies with solid state physics 3-74513
- pairing-plus-quadrupole model, constrained-Hartree-Bogolyubov treatment, for high spin nuclei 3-45982
- pairing-vibrational 0^+ states in Pt isotopes, effect on quadrupole pairing strength 3-78256
- particle motion in guide potentials and the collective nuclear motion 3-43200
- particle number projection study with generator coord. method 3-45987
- particle plus rotor model, rel. to rotation of moderately deformed odd-A nuclei 3-62965
- particle-hole states in deformed and spherical nuclei, moment and energy distributions (*Russian*) 3-62967
- particle-vibration, nuclear spreading widths of ^{207}Pb and ^{209}Pb $(1/2)^+$ doorway resonances 3-74492
- particle-vibration model, neutron resonances in even-even, odd-odd nuclei 3-78267
- phonons, self-consistent random phase approximation amplitudes, many fermion model 3-78273
- quadrupole deformation, microscopic treatment of collective motion using group theory 3-49173
- quasi-particle excitation model, applicability near saddle point of fissionable nuclei (*Russian*) 3-40525

nuclear collective model continued

- quasi-rotational band description, transition nuclei 3-60075
- quasiparticle approx., treatment of pairing forces (*Rumanian*) 3-62973
- rare earth region deformed nuclei; rot. flow model for spectra 3-62969
- rare-earth rotating deformed nuclei, moments of inertia 3-49171
- resonance energies of nuclei considered as rigid bodies 3-57485
- review of e.m. transitions and moments 3-54433
- review of new facets of nuclear structure 3-78268
- rotating nuclei, finite temp. calc. of angular velocity and moments of inertia 3-49178
- rotation at high angular momenta, schematic two-level description 3-57483
- rotational anomaly and Hartree-Fock-Bogoliubov eqns. 3-49174
- rotational bands, Coriolis force interactions, differences in moments of inertia, nuclei with $173 \leq A \leq 189$ (*Russian*) 3-71039
- rotational bands as induced group representations 3-43197
- rotational energies, angular velocity expansion, application to doubly even nuclei $A=140-195$ 3-52117
- rotational energy expansion in powers of angular velocity of rotation, diagonalization of rotational Hamiltonian 3-62968
- rotational model rel. to deformations of ground bands in ^{20}Ne , ^{24}Mg and ^{28}Si 3-62926
- rotational motion, single j shell, quadrupole interaction, equivalence to Bohr's model 3-60096
- rotational spectra, coupling scheme 3-62966
- rotational theory number displacement degrees of freedom 3-54409
- semiphenomenological model, applic. to rot. spectra 3-60098
- semiphenomenological model, applic. to rot. spectra 3-60099
- shape isomers, spontaneously fissioning, properties of quadrupole vibrational states 3-45984
- Skyrme-Levinson, generalised, expression for moment of inertia, ground state energy 3-74515
- spherical to deformed transition in single-j shell, algebraic approach 3-54410
- static quadrupole moments of 2^+ states of even isotopes of Ca, Ti, Cr, Fe, Ni, Ba, Nd, Sm 3-49099
- statistical model for nucleon distrib. in nuclei, surface curvature and Coulomb field effects (*Russian*) 3-40433
- stretching model, generalized, for ground-state bands in even-even nuclei 3-40432
- Thomas-Fermi gas model for proton imaginary optical potential 3-52187
- two quasiparticle systems, effects of strong rotation-particle coupling on nuclear energy levels 3-62942
- unified, alternative formulation for non-adiabatic effects in spectra of deformed odd-A nuclei 3-40431
- uniform, shape of yrast line, pairing and spin distrib. effects 3-67205
- unipolar and quadrupolar vibrations, asymptotic frequencies, nuclei with large nucleon number (*Russian*) 3-71064
- variable moment of inertia, for high-spin states in rotational bands 3-67201
- variable moment of inertia, two-parameter description of rotational energies 3-74496
- variable moment of inertia model, extension to high spins 3-54411
- vibration model, collective state study of even single-closed-shell nuclei 3-63039
- (d,d') form factor, nucl. struct. depend. of phase 3-63067
- $^{27}\text{Al}(\gamma, \pi^+)^{27}\text{Mg}$, recoil range of ^{27}Mg , obs. and Fermi gas model calc. 3-60161
- ^{12}C , microscopic treatment of coupled monopole and quadrupole vibration using generator coordinate method 3-45985
- ^{12}C , photoneuclear reaction process in giant dipole reson. region in collective correl. model 3-52171
- Ca isotopes, quadrupole moments and coexistence of spherical and deformed bands 3-49095
- ^{40}Ca , microscopic treatment of coupled monopole and quadrupole vibration using generator coordinate method 3-45985
- ^{40}Ca region, pairing vibrations in theory of finite Fermi systems 3-49172
- ^{42}Ca , ^{44}Ca , quadrupole moments and coexistence, $B(E2)$ values, model comparison 3-52076
- ^{110}Cd , vibrational metal, agreement with exptl. M1/E2 mixing ratios 3-46009
- ^{159}Dy , spreading width of rotational doorway states 3-67203
- ^{54}Fe , ^{56}Fe , proton spin flip angular distributions at 12 MeV, collective model DWBA calculations 3-63048
- ^4He , microscopic treatment of coupled monopole and quadrupole vibration using generator coordinate method 3-45985
- La, odd-A isotopes, decoupled band description using angular momentum projection method for coherent phonon state 3-45983
- ^{171}Lu , ^{173}Lu , one-quasiparticle state equilibrium deformations, influence on E1 transition probabilities 3-49216
- ^{24}Mg , 60-90 MeV, deuteron scattering, optical model, coupled channel analysis, collective model features 3-43253
- ^{20}Ne , microscopic treatment of coupled monopole and quadrupole vibration using generator coordinate method 3-45985
- ^{58}Ni , alpha particle scattering, 139 MeV, inelastic cross sections using DWBA analysis 3-63076
- ^{16}O , microscopic treatment of coupled monopole and quadrupole vibration using generator coordinate method 3-45985
- ^{183}Os ground-state rotational band, back- and forwardbending, moment of inertia 3-74498
- Pb region, electric multipole moments and transition probabilities of single-particle states 3-43174
- Pb-region, magnetic moments of single particle states, calc. including mesonic exchange currents 3-52080
- ^{208}Pb , alpha particle scattering, 139 MeV, inelastic cross sections using DWBA analysis 3-63076
- ^{208}Pb , collective excitations study using 54 MeV inelastic proton scattering 3-63056
- ^{208}Pb , semi-empirical analysis magnetic moments of single-particle (hole) states assumed core, $B(M1)$ values 3-52081
- Pb(p,t), $A=208, 206, 204, 35$ MeV, two-neutron pick-up strengths, transition from single-particle to collective 3-60187
- ^{210}Po , collective state study with inelastic scattering of deuterons, protons, tritons 3-43183

nuclear collective model continued

- ¹¹⁹Sb perturbation approach to particle-vibration coupling model 3-52115
¹²¹Sb, perturbation approach to particle-vibration coupling model 3-52115
⁴⁵Sc, angular distrib. of γ -rays from (n, n' γ) reaction, support for collective description 3-74589
¹⁵⁰Sm, energy level calculations (*Russian*) 3-71066
 Sn isotopes, interaction between collective and quasiparticle excitations, energies, wave functions, B(E2) values (*Russian*) 3-74514
 Sr isotopes, shell model for rotation-like spectra 3-60085
 Te(p,p'), even-A isotopes obs. of strong L=5 transitions, 2⁺-pole collective motion 3-67326
⁴⁸Ti, ⁵⁰Ti, proton spin flip angular distributions at 12 MeV, collective model DWBA calculations 3-63048
¹⁷⁹W, three quasiparticle states populated in ¹⁷⁹Re decay, microscopic model (*Russian*) 3-52089
¹⁶⁸Yb, γ -band population by indirect (p,t) processes 3-46030

nuclear collective motion see *nuclear collective model*

nuclear coupling, molecular see *molecular nuclear coupling*

nuclear decay schemes see *radioactive decay schemes*

nuclear decay theory

- see also *alpha decay theory; beta decay theory; radioactivity*
 compound nuclei, wave packets and analysis of lifetime meas., non decaying probability 3-62015
 compound nucleus, involving analogue resonance, and not involving Hauser-Feshbach formula 3-67293
 decaying nuclear states, structure 3-52136
 deuteron emission from compound nucleus, resonance level width by expansion method 3-52157
 excited nuclei, statistical theory of decay, competition between fission and evaporation 3-43263
 exciton model, emission and formation probability of complex particles 3-60137
 gamma decay, phenomenological T-violating internucleon potential 3-62988
 heavy-ion reactions, sequential decay of light fragments 3-49282
 hyperfragments, heavy, nonmesonic decay, Monte Carlo simulation 3-67250
 isobaric analogue resonances, proton decay, multiple-particle mechanism (*Russian*) 3-52155
 isobaric-analogue states, spectra and angular distrib. of photoprotons (*Russian*) 3-57477
 muon capture, configuration mixing and total capture rates in Primakoff closure approx. 3-67271
 partial state densities from realistic single-particle states 3-49148
 perturbation of decay rates, review 3-54442
 potential barrier, two-bump penetration influence of fission potential on penetrance curve (*Russian*) 3-67223
 resonance levels, correlation between fission and reduced neutron widths 3-54512
 sequential decay processes, analysis of angular correlations 3-67284
 transuranium elements, ratio evaporative to fission width Γ_n/Γ_f , energy dependence (*Russian*) 3-57548
¹⁸¹Ta, interpretation of nucleon emission following proton bombardment at energies of tens of MeV 3-52182

nuclear deformation see *nuclear shape*

nuclear electric moment

- see also *molecular nuclear coupling*
 Alaga model coupling of three particle (hole) valence-shell cluster to quadrupole vibrations 3-67238
 density dependent residual interaction calcs., effective charges and g-factors 3-49118
 dipole sum rules, enhancement factor calc. 3-78240
 E2 static moments and E2, E4 transition moments determ. by Coulomb excitation 3-45935
 even-even nuclei, quadrupole moments of excited states by reorientation effect in Coulomb excitation 3-54379
 f_{7/2} shell nuclei, quadrupole moment, configuration mixing calcs. 3-49125
 light nuclei, Coulomb excitation, polarizability and static quadrupole moment 3-45936
 noble gases, solid, Mossbauer of dissolved Fe, nuclear quadrupole moment, electron densities, mol. orbits 3-41459
 photoeffect, electric dipole sum rule, retardation effect and relativistic correction 3-67310
 quadrupole, hexadecapole and 2⁶ pole, deformation parameters rel. to light nuclei deformation (*Russian*) 3-67183
 quadrupole, matrix elements, effect of non axial deformation in rotating heavy nuclei 3-67181
 quadrupole, shell model spectroscopy of f-p-shell nuclei with 42 ≤ A ≤ 44, core excitation effects 3-67236
 quadrupole moment, effect on hyperfine structure of atomic spectra 3-52066
 quadrupole moment, nonlocal separable nucleon-nucleon interaction parameters approach 3-40424
 quadrupole moment determ. from bound-muonic viewpoint 3-52129
 quadrupole moment determ. from hfs of X-ray transitions in muonic atoms 3-49096
 quadrupole moment for high spin rotational states, asymmetric rotor model 3-49114
 quadrupole moment of A=20-34 nuclei, Hartree-Bogolubov theory 3-52118
 quadrupole moments of first 2⁺ states of nuclei with A=48-116 from inelastic electron scattering 3-49100
 review of e.m. transitions and moments 3-54433
 Rutherford scattering deviations due to ground state quadrupole moment 3-52153
 short-lived high spin states, review of exptl. measurement techniques 3-45930
 static quadrupole, meas. by reorientation effect in Coulomb excitation 3-46038
 static quadrupole deformation, effect on strong interaction effective range (*Russian*) 3-57479
 static quadrupole moments of 2⁺ states of even isotopes of Ca, Ti, Cr, Fe, Ni, Ba, Nd, Sm 3-49099
 two-neutron-hole states in even N=80 nuclei, intermediate coupling model 3-67215

nuclear electric moment continued

- vibrational nuclei, configuration mixing, reduced transition probabilities and quadrupole moments 3-60084
¹⁰⁹Ag quadrupole moment, Coulomb excitation in ¹⁰⁹Ag(¹⁶O, ¹⁶O') and ¹⁰⁹Ag(α , α') 3-71040
²⁸Al, ²⁹Al, shell model calcs. using modified surface-delta-interaction Hamiltonian 3-49167
 Au, muonic, quadrupole moment (*French*) 3-54603
¹¹B, ¹²B, quadrupole moment calc. using Cohen Kurath wavefunctions 3-49128
¹²B, ¹³B, recoil polarisation through nuclear reaction into Mg crystal, quadrupole coupling, Q(¹²B) to Q(¹³B) ratio 3-49079
¹²B, recoil implanted in Ta following ¹¹B(d,p) reaction, n.m.r. meas., determ. of sign of eqQ 3-49078
¹²B β -decay, search for weak-electric moment 3-49224
¹³⁰Ba, quadrupole moments of first excited states, reorientation eff. meas. 3-49112
¹³⁴Ba, quadrupole moments of first excited states, reorientation eff. meas. 3-49112
¹³⁶Ba, quadrupole moments of first excited states, reorientation eff. Meas. 3-49112
⁹Be, inelastic electron scattering, electromagnetic properties, Nilsson model and experiment comparison 3-54386
⁹Be, quadrupole moment determ. 3-46169
¹¹C, quadrupole moment calc. using Cohen Kurath wavefunctions 3-49128
 Ca isotopes, quadrupole moments and coexistence of spherical and deformed bands 3-49095
⁴⁰Ca region, eff. of core excitation on B(E2) values 3-45965
⁴²Ca, ⁴⁴Ca, quadrupole moments and coexistence, B(E2) values, model comparison 3-52076
⁴²Ca E2 transition strength, ratio between B(E2) values for Coulomb excitation of 2⁺ states in ⁴⁶Ca and ⁴²Ca 3-49193
⁴⁶Ca E2 transition strength, ratio between B(E2) values for Coulomb excitation of 2⁺ states in ⁴⁶Ca and ⁴²Ca 3-49193
 Cd isotopes, quadrupole moment of 2⁺ state 3-49103
 Cd quadrupole interaction, pressure variation, PAC meas. 3-61012
¹¹¹Cd, electric quadrupole interaction for 247 keV level in In following ¹¹¹In decay, TDPAC meas. 3-45941
¹¹⁴Cd, quadrupole moment of 2₁⁺ state, calc. using boson expansion technique 3-49102
¹⁴⁰Ce, 2.083 MeV state populated in ¹⁴⁰La β^- decay, quadrupole moment determ. by TDPAC 3-49085
 Co isotopes, quadrupole moments, calc. using Hartree-Fock-Bogolubov method 3-67246
⁵⁰Cr, quadrupole deformation measurements of first excited states 3-49143
⁵²Cr, quadrupole deformation measurements of first excited states 3-49143
⁵³Cr, ground state static quadrupole moment from Coulomb excitation meas. 3-40410
⁵³Cr, static quadrupole moment determ. from reorientation effect in Coulomb excitation by ²²S 3-46038
⁵⁴Cr, quadrupole deformation measurements of first excited states 3-49143
 Dy, A=162, 164, Coulomb excitation, quadrupole and hexadecapole transition moments 3-49201
¹⁶⁴Dy, Coulomb excitation, meas. of hexadecapole transition moments and M(E2; 0 → 2) 3-49195
 Er, A=166, 168, 170, Coulomb excitation, quadrupole and hexadecapole transition moments 3-49201
¹⁶⁶Er, Coulomb excitation, meas. of hexadecapole transition moments and M(E2; 0 → 2) 3-49195
¹⁷⁶Er, static quadrupole moment determ. from reorientation effect in Coulomb excitation by ⁸¹Br 3-46038
¹⁷⁰Er, static quadrupole moment of first 2⁺ state by Coulomb excitation using ⁸¹Br 3-62935
¹⁹F, polarized, implantation in Zn single crystal, quadrupole interaction of 197 keV level 3-49081
²⁰F β^- -emitter, determ. of quadrupole moment from n.m.r. meas. on polarised nuclei in MgF₂ 3-45947
 Gd, A=158, 160, Coulomb excitation, quadrupole and hexadecapole transition moments 3-49201
¹⁵⁸Gd, Coulomb excitation, meas. of hexadecapole transition moments and M(E2; 0 → 2) 3-49195
^aGe, A=67, 69, 71, meas. of quadrupole interaction on 9/2 and 5/2 levels in Zn and Ga by TDPAD 3-45949
⁷¹Ge, quadrupole interaction of 9/2⁺ state in liquid Ga, relaxation time by γ -ray anisotropy meas. 3-49082
²H photoeffect, electric-quadrupole contrib. 3-67299
²H quadrupole moment determ. from nucleon-nucleon interaction 3-74501
¹⁷⁵Hf, nuclear alignment in Hf metal at 3 mk, meas. γ -ray anisotropies 3-71082
¹⁷⁸Hf, ¹⁸⁰Hf, Mossbauer meas. of isomer shift and quadrupole moment ratios 3-49206
¹⁷⁸Hf/¹⁸⁰Hf, ratio of quadrupole moments of 2⁺ states 3-60086
¹⁸⁰Hf, nuclear alignment in Hf metal at 3 mk, meas. γ -ray anisotropies 3-71082
¹⁸⁰Hf recoil implanted in single crystals, nucl. quadrupole precession, PAC obs. 3-41462
¹⁸⁶Hg, Yrast states up to 14⁺ stable quadrupole deformation 3-67200
¹⁶⁵Ho, quadrupole moment meas. by proton and alpha scattering from aligned target 3-45944
¹¹⁵In, hexadecapole moment, mol. beam elec. reson. spectroscopy 3-43176
¹¹⁵In, nuclear quadrupole interaction sign, obs. by β - γ directional corrs. in Cd metal 3-52079
¹⁹¹Ir, h.f.s. obs. of ⁴F_{9/2} atomic ground state, ABMR meas. 3-67191
¹⁹³Ir, h.f.s. obs. of ⁴F_{9/2} atomic ground state, ABMR meas. 3-67191
¹³³La, quadrupole moment of 535 keV state determ. by time-differential PAC meas. in La metal 3-52082
⁶Li, one-body densities for valence nucleons, determ. of wave-function parameters using e.m. data 3-49245
¹⁷⁵Lu, muonic, spectroscopic quadrupole moment determ. and quadrupole h.f. splitting in pionic ¹⁷⁵Lu 3-49075
¹⁷⁵Lu, spectroscopic quadrupole moment determ. from quadrupole splitting in muonic atoms 3-49133

nuclear electric moment continued

- ¹⁷⁵Lu μ , quadrupole splitting of X-ray transitions, determ. of nuclear quadrupole moment 3-49096
- ¹⁷⁵Lu pionic atom, search for strong interaction quadrupole effect 3-49134
- ²⁷Mg, ²⁸Mg, shell model calcs. using modified surface-delta-interaction Hamiltonian 3-49167
- Mn isotopes, quadrupole moments, calc. using Hartree-Fock-Bogoliubov method 3-67246
- ¹²N, quadrupole moment calc. using Cohen Kurath wavefunctions 3-49128
- ²³Na dipole strength obs. using ²²Ne(p, $\gamma_0 + \gamma_1$)²³Na reaction, dipole strength splitting 3-63054
- Pb region, effective E2 charges, particle-oscillating core coupling, polarisation 3-45924
- Pb region, quadrupole moments of single-particle states in finite Fermi system theory 3-43174
- ²⁰⁸Pb, Coulomb excitation with heavy ions, static quadrupole moment of 3- state from γ -ray meas. 3-49101
- ¹⁰⁵Pd, nucl. quadrupole moment from h.f.s. consts. 3-52261
- Pt even isotopes, A=180 to 190, effect of quadrupole-pairing interaction on J π =0⁺ vibrs. 3-78256
- ¹⁹⁴Pt, Coulomb excitation by ¹⁶O and ³²S, quadrupole moment of first 2⁺ state by reorientation precession technique 3-45942
- ⁸³Rb, quadrupole moments determ. by level crossing and ODR, h.f.s. consts. 3-40411
- ⁸⁴Rb, quadrupole moments determ. by level crossing and ODR, h.f.s. consts. 3-40411
- ⁸⁶Rb, quadrupole moments determ. by level crossing and ODR, h.f.s. consts. 3-40411
- Se, A=75, 77, 79, 81, 83, anomalous coupling states, calc. of nuclear moments 3-49115
- Sm, A=148, 150, 152, Coulomb excitation, determ. of static quadrupole moments of first excited states 3-49113
- Sm, A=152, 154, Coulomb excitation, quadrupole and hexadecapole transition moments 3-49201
- ¹⁴⁸Sm-¹⁵⁴Sm, transition from vibrational to deformed nucleus, boson expansion technique, quadrupole moments 3-49102
- ¹⁵⁰Sm, Coulomb excitation by ¹⁶O and ³²S, quadrupole moment of first 2⁺ state by reorientation precession technique 3-45942
- ¹⁵⁰Sm, quadrupole interaction on recoil through Sm, calc. of electric field gradient 3-45943
- ¹⁵⁰Sm, quadrupole moments calc. using phenomenological collective model (Russian) 3-71066
- ¹⁵²Sm, ¹⁵⁴Sm, Coulomb excitation, meas. of hexadecapole transition moments and M(E2; 0 \rightarrow 2) 3-49195
- ¹⁵²Sm, ¹⁵⁴Sm, Coulomb excitation of 2⁺ and 4⁺ levels, determ. of E4 moments 3-49202
- ¹¹⁵Sn, quadrupole interaction of 11/2⁻ state in liquid In, relaxation time by γ -ray anisotropy meas. 3-49082
- ¹⁸¹Ta, quadrupole moment of 482 keV state meas. by time differential PAC in Re metal 3-52078
- Te isotopes, quadrupole moment of 2⁺ state 3-49103
- ¹²⁴Te, quadrupole moment meas. by reorientation effect 3-49111
- ¹²⁵Te, nucl. quadrupole interactions in isoelectronic cryst. hosts of S, Se, and Te 3-50501
- ¹²⁶Te, quadrupole moment meas. by reorientation effect 3-49111
- ¹²⁸Te, quadrupole moment meas. by reorientation effect 3-49111
- ⁴⁹Ti, quadrupole moment determ. from obs. of transitions in K=3/2⁺ rotational band 3-74494
- ²³⁵U, spectroscopic quadrupole moment determ. from quadrupole splitting in muonic atoms 3-49133
- ²³⁵U μ , quadrupole splitting of X-ray transitions, determ. of nuclear quadrupole moment 3-49096
- V isotopes, quadrupole moments, calc. using Hartree-Fock-Bogoliubov method 3-67246
- W, A=182, 184, 186, Coulomb excitation with ¹⁶O, meas. of quadrupole interaction in Te crystal (German) 3-49187
- ¹⁸⁰W/¹⁸²W, ratio of quadrupole moments of 2⁺ states 3-60086
- ¹⁸⁶W recoil implanted in single crystals, nucl. quadrupole precession, PAC obs. 3-41462
- ¹⁷⁴Yb, Coulomb excitation, meas. of hexadecapole transition moments and M(E2; 0 \rightarrow 2) 3-49195

nuclear electromagnetic transitions see nuclear energy level transitions**nuclear electron capture**

- see also beta-decay; nuclear reactions and scattering due to electrons
- decay rates, perturbation, reviews 3-54442
- forbidden ratios, non-unique, use of nuclear matrix elements 3-78292
- stars, collapsing dense, effect of electron capture on temperature and chemical composition 3-65878
- ²¹⁰At, decay to levels in ²¹⁰Po, γ - γ delayed coincidence meas. 3-45925
- ⁷Be, branching ratios, determ. from ⁷Li(p,n)⁷Be 3-67266
- ⁷Be in BeO, effect of pressure on electron capture decay constant 3-63013
- ¹³⁴Ce \rightarrow ¹³⁴La, determ. of decay energies (Russian) 3-49223
- ³⁶Cl, meas. inner bremsstrahlung spectra at 600 to 1040 keV, determ. transition energy and form factor (Russian) 3-67279
- ⁵⁷Co decay, 122 keV, transition, E2/M1 mixing ratio determ. by orientation 3-46006
- ¹³²Cs, gamma activity, half-life 3-67268
- ¹⁴⁹Dy \rightarrow ¹⁴⁹Tb transition probability by electron capture (French) 3-63003
- ¹⁶⁰Er \rightarrow ¹⁶⁰Ho, determ. of decay energies (Russian) 3-49223
- ²⁵²Es, decay scheme 3-54443
- ⁷⁵Ge decay to ⁷⁵As, obs. of γ -ray spectrum 3-49210
- ¹¹¹In \rightarrow ¹¹¹Cd, decay, quadrupole interaction with electric field gradient in Cd, γ - γ angular correlation meas. 3-47183
- ¹⁰⁸In, decay scheme, spin and parity, j-j coupling model 3-63004
- ⁷⁶Kr \rightarrow ⁷⁶Br decay, study of ⁷⁶Br level scheme 3-49220
- ¹⁶⁹Lu \rightarrow ¹⁶⁹Yb, meas. of γ -ray, positron and conversion electron spectra, ¹⁶⁹Yb energy levels (Russian) 3-52090
- ⁹³Np decay, energies and rel. intensities for γ -ray transitions 3-54434
- ⁹³Np decay, energies and rel. intensities for γ -ray transitions 3-54434

nuclear electron capture continued

- ¹⁸²Os beta decay to ¹⁸²Re, gamma and internal conversion meas. 3-49227
- ²⁰⁶Po \rightarrow ²⁰⁶Bi, decay scheme revision from ²⁰⁶Bi 10.84 keV strong M1 transition obs. 3-52135
- ²³⁵Pu decay, half-life, level scheme, branching intensities 3-40462
- ¹⁰¹Rh \rightarrow ¹⁰¹Ru, determ. of lifetime of excited states in ¹⁰¹Ru (Russian) 3-78280
- ²⁰⁹Rn decay to levels in ²⁰⁹At, obs. of gamma rays and conversion electrons 3-74542
- ²¹⁰Rn \rightarrow ²¹⁰At, decay scheme and spin assignments 3-43223
- ⁷⁵Se decay, 285 keV γ line of ⁷⁵As, nucl. reson. fluoresc. obs. 3-63009
- ¹¹³Sn disintegration energy, error in P_i/P_k meas. due to presence of ^{119m}Sn 3-49226
- ⁹⁵Tc decay to levels in ⁹⁵Mo, spins and multipole mixing ratios 3-60070
- ²⁰⁴Tl, radiative capture of 1s electrons, internal bremsstrahlung measurement 3-54440
- ¹¹³Xe, β -delayed proton emission, energy spectrum 3-54438
- ⁸⁸Y, β -decay rate, Sr fluorescence yield 3-74544
- ⁶⁵Zn, branching ratios, determ. from ⁶⁵Cu(p,n)⁶⁵Zn 3-67266
- nuclear emulsions** see nuclear track emulsions
- nuclear energy** see nuclear power
- nuclear energy level lifetimes**
see also nuclear energy level transitions
- ⁵³Mn, excited state obs. by ⁵³Cr(p,n γ) reaction 3-67192
- Doppler γ -lines, lifetime determ. using maximum probability method (Russian) 3-71073
- Doppler shift attenuation meas. of γ -rays following Coulomb excitation (Russian) 3-71074
- ³⁵Ar, first excited state populated in ³²S(α ,n γ) 3-45996
- ³⁷Ar, 1612 keV level, populated via ³⁴S(α ,n)³⁷Ar reaction 3-45991
- ⁷²As, half-life of new isomeric state 215 keV populated in ⁷²Ge(p,n) reaction 3-45956
- ⁷⁷As, half-life of excited states populated in ⁷⁷Ge β -decay 3-60111
- ¹⁹⁷Au Mossbauer γ ray 3-67260
- ¹³⁶Ba, levels and transitions study 3-40457
- ²⁰⁴Bi, half-life of high spin isomeric state 3-49152
- ²¹⁰Bi, excited states populated in ²⁰⁹Bi(d,p γ) reaction, reduced matrix element calc. 3-67259
- ³⁹Ca excited states populated in ⁴⁰Ca(³He, α γ) reaction 3-43210
- ⁴¹Ca, γ transitions between high-spin states, heavy-ion induced reaction obs. 3-74530
- ³⁵Cl, first 7/2⁻ level populated in ³²S(α ,p) reaction, recoil distance method 3-78284
- ³⁵Cl from ³⁴S(p, γ)³⁵Cl, gamma ray transitions and lifetimes 3-43214
- ³⁵Cl pop. in ³⁵Cl(d,p)³⁵Cl reaction, meas. lifetimes using attenuated Doppler shift method 3-67262
- ³⁷Cl, first 7/2⁻ level populated in ³⁴S(α ,p) reaction, recoil distance method 3-78284
- ³⁸Cl, low lying states populated by (d,p) reaction meas. using attenuated-Doppler-shift 3-62989
- ⁴⁸Cr from ⁴⁰Ca(¹⁰B, pny), 19, 22.5, 25 MeV, γ -ray spectroscopy 3-62985
- ⁵⁰Cr, recoil-distance lifetime meas. for excited states 3-40448
- ⁶¹Cu, via ⁵⁸Ni(⁴He,p) γ reaction spectrometry 3-67261
- ⁶²Cu excited states, time differential perturbed ang. distrib. obs. 3-63000
- ⁶Dy, A=158, 160, 162 above 1.5 MeV, meas., model anal. 3-78250
- ¹⁶⁴Er, above 1.5 MeV, meas., model anal. 3-78250
- ¹⁸F, Doppler shift attenuation meas. 3-62996
- ²⁰F, Doppler shift attenuation meas. 3-62996
- ⁵⁵Fe mean life of excited states, recoil distance method (French) 3-43205
- ⁵⁷Fe, 14.4 keV state, chemical environment effect on lifetime, isomer shift determ. 3-62984
- ⁷⁰Ga, half-life of 879 keV level 3-62982
- Ge, nucl. lifetimes by blocking technique, computer simulation 3-40443
- ¹⁸⁴Hf, half-life meas., γ and β decay 3-60129
- ¹⁶⁵Ho, resonant scattering of gamma-rays, determ. of 94.69 keV level lifetime (Russian) 3-52168
- ³⁹K excited states populated in ³⁶Ar(α , p γ) reaction 3-43210
- ⁴⁰K, 2542 keV level mean lifetime 3-60116
- ⁴⁰K, low lying states populated by (d,p) reaction meas. using attenuated-Doppler-shift 3-62989
- ⁴¹K, γ transitions between high-spin states, heavy-ion induced reaction obs. 3-74530
- ²⁸Mg, gamma-ray spectroscopy of low-lying levels populated in ²⁶Mg(³H,p γ) reaction 3-67258
- ⁵⁰Mn pop. in ⁵⁰Cr(p,n)⁵⁰Mn, determ. separation energy of isomeric states from beta⁺ decay meas. 3-67212
- ⁹⁴Mo, 2953 keV state populated in ⁹²Zr(α ,nn) reaction 3-49084
- ¹⁴N from ¹²C(³He,p), E=5.54 MeV, Doppler shift attenuation (French) 3-67255
- ²³Na from ¹²C(¹²C, p γ)²³Na, high spin states study, branching ratios 3-49185
- ²⁴Na from ²³Na(d, p γ) 2.45 MeV 3-62986
- ⁹¹Nb, 17/2⁻ state populated in ⁸⁹Y(α ,nn) reaction, time-differential meas. 3-49194
- ⁵⁹Ni, low-lying levels populated in ⁵⁶Fe(α ,n) reaction 3-49213
- ⁶⁰Ni, DSA meas. of levels populated in ⁶⁰Ni(p, γ) reaction 3-52132
- ¹⁸⁰O, Doppler shift attenuation meas. 3-62996
- ¹⁹²Os, half-life of excited states populated in ¹⁹²Ir β -decay 3-60111
- ²⁹P, levels up to 4.76 MeV populated in ²⁸Si(p, γ) reaction 3-49144
- ³²P from ²⁹Si(α ,p γ) E α =10.65 to 11.00 MeV, deduced levels 3-60108
- ³³P, Doppler shift attenuation meas. 3-40446
- ³³P, populated via ³¹P(t, p γ)³³P reaction, low-lying states lifetime meas. and props. 3-54427
- ¹⁹⁴Pb isomeric state behaviour, γ - γ coincidence obs. 3-62992
- ¹⁹⁶Pb isomeric state behaviour, γ - γ coincidence obs. 3-62992
- ¹⁹⁸Pb isomeric state behaviour, γ - γ coincidence obs. 3-62992
- ²⁰⁰Pb isomeric state behaviour, γ - γ coincidence obs. 3-62992
- ²⁰⁹Pb, l-forbidden 11_{1/2}⁻ \rightarrow 2g_{3/2} M1 transitions 3-60114
- ²¹⁰Po, half-lives of 6⁺ and 4⁺ states 3-62998
- ¹⁰³Rh, γ - γ directional correl. obs. 3-62997

nuclear energy level lifetimes continued

- ⁹⁹Ru, excited states populated in ⁹⁹Rh decay (*Russian*) 3-78280
¹⁰¹Ru, excited states populated in ¹⁰¹Rh, ¹⁰¹Tc decay (*Russian*) 3-78280
³⁰Si, DSAM, γ -decay, ²⁸Si(³He,n) reaction 3-78289
³³S(p,p)³⁴Cl, ³⁴Cl nuclear levels investigation 3-52102
¹²²Sb, 1.8 μ s state magnetic moment, g factor determ. by stroboscopic method 3-67187
⁴⁵Sc, γ -decay of low-lying states 3-78282
¹¹⁴Sn, high spin isomeric state populated in ¹¹²Cd(α ,nn) reaction 3-45958
¹⁸¹Ta, half-life of 482 keV level 3-54419
⁹⁷Tc, half-life of excited states populated in ⁹⁷Ru β -decay 3-60111
⁹⁹Tc, 140 keV level, Mossbauer spectra giving $T_{1/2}$ 3-71077
¹³²Te, half-life meas. of levels populated in ¹³²Sb beta decay 3-49214
⁴⁶Ti, recoil-distance lifetime meas. for excited states 3-40448
²³⁹U compound nucleus formed in ²³⁸U + n reaction, 1.6-4.3 MeV (*Russian*) 3-40497
¹³¹Xe, populated from ¹³¹I, 341.2 and 404.8 keV level lifetime meas. (*German*) 3-52139
¹⁶⁸Yb, above 1.5 MeV, meas., model anal. 3-78250
⁹¹Zr, 15/2⁻ state populated in ⁸⁹Y(α ,nn) reaction, time-differential meas. 3-49194

nuclear energy level transitions

see also nuclear branching and mixing ratios

- 1p-shell nuclei, allowed muon capture transitions, roles of weak hadron form factors 3-54437
 1p-shell nuclei daughter states, low lying, distributions of allowed muon capture strengths 3-60126
 $42 \leq A \leq 44$, shell model spectroscopy of f-p-shell, calc. B(M1)'s and B(E2)'s for low lying states 3-67236
¹²³Sb reduced E2 transition probabilities, calc. from particle-vibration coupling model 3-52115
²⁸Si, search for 6⁻ analogue-antianalogue states as resonance in ²⁷Al(p,p), γ -ray decay 3-57476
 A=17-27, projected Hartree-Fock calcs. of spin-isospin matrix elements 3-49180
 A=19 isobar, M1 transition calc. in charge asymmetry determ. 3-67176
 A=19 nuclei, core-polarisation effects on E2 transitions 3-52134
 A=7 and 8 nuclei, shell model calculations, non-normal parity states 3-54403
 allowed β transitions, induced β - γ correl. of directions 3-78283
 anomalous coupling states with spin I=j-1, e.m. properties 3-49104
 B(E2) transition rates in non-rotational collective nuclear states and particle-particle, particle-hole interactions 3-67240
 B(E2) values of A=20-34 nuclei, Hartree-Bogolubov theory 3-52118
 compound nuclei, wave packets and analysis of lifetime meas., non-decaying probability 3-60115
 compound-nucleus reactions at high angular momentum, excitation functions and photon emission 3-63083
 decaying nuclear states, structure 3-52136
 density dependent residual interaction calcs., effective charges and g-factors 3-49118
 directional correlations of γ -radiations from states oriented by nuclear reactions or cryogenic methods 3-71079
 Doppler γ -lines, comparison of theory and expt. using maximum probability method (*Russian*) 3-71073
 Doppler shift attenuation, lifetimes of nuclear excited states 3-42625
 Doppler shift attenuation of γ -rays following Coulomb excitation, lifetime determ. (*Russian*) 3-71074
 Doppler shifts of γ -rays emitted from excited states of nuclei slowing down in Kr gas 3-66314
 Doppler-shifted γ -rays, nuclear lifetimes from line shapes 3-42621
 E0 transitions for levels with zero and nonzero spin, phenomenological model 3-54425
 E1, for study of β -transitions in neutron magic nuclei 3-71088
 E1 photoabsorption sum rule, reln. to orbital g-factor due to exchange currents 3-49119
 E2, E4 transition moments determ. by Coulomb excitation 3-45935
 E2 transition strengths in ²⁰Ne and ²⁴Mg determ. using variation after projection Hartree-Fock method 3-67245
 E2 transitional energies and rotational energy formulae 3-49203
 E2 transitions, effect of momentum fluctuation in theory of nonlocal nuclear forces 3-67220
 electron-nucleus showers, E \geq 10 GeV, cosmic ray muon contribution (*Russian*) 3-80903
 even-even deformed nuclei, E2 and E0 transitions from excited 0⁺ to ground state bands 3-49217
 even-even nuclei, quadrupole moments of excited states by reorientation effect in Coulomb excitation 3-54379
 excitation by electron transition, electromagnetic interaction between electron and nucleus 3-57507
 excitation by gamma rays of radioactive sources 3-67305
 excitation probability for low lying collective states, e.m. transition probabilities (*Russian*) 3-67288
 exotic atom level widths, nuclear motion correction to X-ray yields 3-78647
 fission fragments from neutron induced fission of ²³⁵U 3-46045
 gamma-ray spectra following keV neutron capture, data table 3-74580
 Green's function method, near Fermi level, one and two particle density matrices 3-78255
 ground state band, description using field theoretical methods of quantum many body theory 3-71065
 hypernuclei, A=4, spin dependence of Λ N interaction 3-71072
 isoscalar transition densities, models and sum rules 3-40454
 lifetime determ. by Doppler shift attenuation following neutron transfer reactions (*German*) 3-49188
 lifetimes of some odd-A deformed nuclei, determ. of effective g_r values 3-49110
 light nuclei, Coulomb excitation polarizability and static quadrupole moment 3-45936
 long-lived isomer spectroscopy, pulsed-beam expts., influence of time-windows on NMR-PAC line shapes 3-45995
 M2 transitions, deformed nuclei of odd mass, model (*French*) 3-43204
 nuclear energy level transitions continued
 mirror nuclei, M-1 transition probabilities and analogue β -decays 3-45953
 mirror pair, M1 transitions, spin-isospin distribution 3-45954
 Mossbauer effect, vibrational anisotropy for M1 or E1 γ resonance transitions 3-72549
 muon-nucleus system, Y_d deformation contrib. to transition matrix elements 3-52129
 N=82 nuclei, Z=51-59, pseudo LS coupling shell model study of energy levels and e.m. properties 3-49126
 nuclear reaction theory transition matrix, general formalism 3-60138
 off-shell transition matrix, coupled-channel approach 3-60136
 parity-violating nucleon one-meson exchange potentials in current-current quark model 3-48994
 parity-violation expts., exchange effects 3-40444
 penetration effect in theory of internal conversion, influence of nuclear charge distrib. (*Russian*) 3-74527
 rare earth region, excited 0⁺ states in two-nucleon transfer reactions (*Russian*) 3-52091
 rare-earth nuclei, even, change of charge radii due to rotational transitions, cranking model 3-52130
 reduced widths determ. using reaction of particle production on light nuclei (*Russian*) 3-40515
 relativistic corrections in nuclear-plus-e.m. Hamiltonian 3-62956
 renormalization of E0, M1 and E2 operators 3-49204
 resonance states, giant, scattering of 1p-1h state into 2p-2h state by high energy photon 3-71092
 resonant-particle production, coincidence meas. between decay products, spectroscopic tool 3-52156
 retardation across phase transition, superfluid to normal state, schematic two-level model of rotation at high angular momenta 3-57483
 review of e.m. transitions and moments 3-54433
 rotational, Coriolis mixing effect, E1 transition probability 3-78290
 single-level configurations, determ. of matrix elements of two-body M1 operator 3-49123
 spatial parity nonconservation effects in e.m. transitions including higher approxs. (*Russian*) 3-74529
 T invariance, angular γ correlation in 7.79 to 0.79 MeV cascade accompanying ³⁵Cl capture of slow polarised neutrons (*Russian*) 3-57492
 T-invariant angular correlations in pair conversion process in polarised nuclei (*Russian*) 3-52125
 two-neutron-hole states in even N=80 nuclei, spectra and transition probabilities 3-67215
 vibrational nuclei, configuration mixing, reduced transition probabilities and quadrupole moments 3-60084
 X-ray emission rel. to rarefied lower excitation levels in even-even nuclei near closed shells (*Russian*) 3-67173
¹³⁹La Mossbauer scatt. of 166 keV γ -rays 3-60119
¹⁰⁹Ag, intermediate coupling model 3-71061
²⁷Al, (p,n) isobaric analogue transitions, 22 to 40 MeV 3-63055
²⁷Al, resonance scattering of bremsstrahlung, low-lying level study 3-52094
²⁷Al from ²⁶Mg(¹⁶O,¹⁵N) at 42 MeV, spectroscopic factors, recoil effects 3-67367
²⁸Al, ²⁹Al, shell model calcs. using modified surface-delta-interaction Hamiltonian 3-49167
²⁸Al, γ -ray transitions from lowest T=2 states populated in ²⁶Mg(³He, p) 3-43211
 Ar isotopes A=39 to 42, E2 and M1 transition rates using extended model 3-62949
³⁵Ar, lifetime of first excited state populated in ³²S(α ,n γ) reaction 3-45996
³⁶Ar, ground-state transitions obs. in ⁴⁰Ca(d,⁶Li) reaction 3-78341
³⁶Ar levels, from ³⁵Cl(p,p), E=0.8-2.6 MeV, shell model calculation of odd parity levels 3-71078
³⁷Ar, 1612 keV level, mean lifetime meas. 3-45991
³⁸Ar, γ decay props. of 3⁻ states 3-45993
³⁸Ar ground-state transitions obs. in ⁴²Ca(d,⁶Li) reaction 3-78341
⁷²As, half-life of new isomeric level at 215 keV populated in ⁷²Ge(p,n) reaction 3-45956
⁷⁴As, levels populated in ⁷²Ge(³He, d) reaction at 17 MeV 3-43182
⁷⁵As, γ -transitions of excited states populated by electron capture from ⁷⁵Se 3-49210
⁷⁷As, meas. $T_{1/2}$ of excited states using delayed coincidence technique for ⁷⁷Ge β -decay 3-60111
²⁰⁹At, obs. of γ -rays and conversion electrons in decay of ²⁰⁹Rn 3-74542
 Au, muonic transitions (*French*) 3-54603
¹⁹³Au(183d) \rightarrow ¹⁹³Pt, decay schemes, ¹⁹³Pt excited states, spin and parity assignments 3-52137
¹⁹⁶Au, oriented, γ radiation anisotropy, n.m.r. 3-40453
¹⁹⁷Au, lifetime Mossbauer gamma ray, linewidth, meas., Au source in differing chemical environments 3-67260
¹⁹⁸Au, oriented, γ radiation anisotropy, n.m.r. 3-40453
¹⁹⁸Au isomeric 115.2 keV transition, γ -ray meas., multipolarities 3-43209
^{200m}Au, oriented, γ radiation anisotropy, n.m.r. 3-40453
¹⁰B muon capture, partial transitions, gamma-neutrino directional correlation 3-63002
¹¹B, resonance scattering of bremsstrahlung, low-lying level study 3-52094
¹³⁴Ba, E0 contrib. in 2⁺ to 2⁺ transitions, directional correlation functions 3-62991
¹³⁴Ba, obs. of γ -transitions in ¹³⁴La decay scheme (*Russian*) 3-52141
¹³⁴Ba, zero-phonon γ transition search 3-62993
¹³⁶Ba, levels and transitions study 3-40457
¹³⁷Ba, population by ¹³⁶Xe(α , 3n), meas. of γ -ray spectra, Doppler shift, half-lives 3-45974
¹³⁸Ba, population by ¹³⁶Xe(α , 2n), meas. of γ -ray spectra, Doppler shift, half-lives 3-45974
¹³⁸Ba, spins and mixing ratio from γ - γ directional correl. following ¹³⁸Cs decay 3-78238
⁹Be, inelastic electron scattering, electromagnetic properties, Nilsson model and experiment comparison 3-54386
²⁰⁴Bi, half-life of high spin isomeric state 3-49152
²⁰⁵Bi, fragmentation of proton levels from (³He,d) and (α ,t) reactions on ²⁰⁴Pb 3-63080

nuclear energy level transitions continued

- ²⁰⁷Bi, fragmentation of proton levels from (³He,d) and (α ,t) reactions on ²⁰⁶Pb 3-63080
- ²⁰⁷Bi decay, relative intensity and internal conversion coeff. meas. 3-52123
- ²⁰⁸Bi, lifetimes and M1 transitions, implications for configuration mixing calcs. 3-45998
- ²⁰⁹Bi, M1-, M2-, M4- transition rates calc. using linear response theory of finite Fermi systems 3-49129
- ²¹⁰Bi, gamma decay of excited states, populated in ²⁰⁹Bi(d,p γ) reaction, shell model interpretation 3-67259
- ⁷⁶Br, from ⁷⁶Kr decay level energies spins, parities and transition probabilities 3-49220
- ⁷⁹Br, E2 and M1 reduced transition probabilities, core excitation calc. 3-46005
- ⁷⁹Br, $\gamma\gamma$ directional correlations meas., spin and parity assignments (*German*) 3-40459
- ⁸¹Br, E2 and M1 reduced transition probabilities, core excitation calc. 3-46005
- ¹²C, $2^+ \rightarrow 0^+$ decay of first excited state, meas. in ¹²C(n,n' γ) reaction 3-78323
- ¹²C, decay of photo resonances, shell model analysis, cross sections and branching ratios 3-49239
- ¹²C, low- q^2 electron scattering from 15-109 MeV state, transition probability meas. 3-60165
- ¹²C, weak and e.m. processes, particle-hole model approach 3-40455
- ¹⁵C muon capture, partial transitions, gamma-neutrino directional correlation 3-63002
- Ca isotopes, quadrupole moments and coexistence of spherical and deformed bands 3-49095
- ³⁹Ca, lifetimes of excited states populated in ⁴⁰Ca(³He, α) reaction 3-43210
- ⁴⁰Ca, double gamma decay phenomena 3-60117
- ⁴⁰Ca, excited $J^\pi = 0^+$ states from ³⁸Ar(³He,n)⁴⁰Ca 3-74491
- ⁴⁰Ca excited states, up to 9 MeV, gamma branching ratios, lifetimes, excitation properties, structure groups (*French*) 3-43179
- ⁴⁰Ca region, eff. of core excitation on B(E2) values 3-45965
- ⁴⁰Ca(p,p') reaction, electric transition rates 3-43250
- ⁴¹Ca, γ transitions between high-spin states, heavy-ion induced reaction obs. 3-74530
- ⁴²Ca, ⁴⁴Ca, quadrupole moments and coexistence, B(E2) values, model comparison 3-52076
- ⁴²Ca E2 transition strength, ratio between B(E2) values for Coulomb excitation of 2^+ states in ⁴⁶Ca and ⁴²Ca 3-49193
- ⁴³Ca, isobaric analogue of lowest $3/2^-$ state, total M1 strength 3-67195
- ⁴⁶Ca E2 transition strength, ratio between B(E2) values for Coulomb excitation of 2^+ states in ⁴⁶Ca and ⁴²Ca 3-49193
- ⁴⁸Ca(p, γ)⁴⁹Sc, M1 transition strength from $3/2^-$ isobaric analogue state 3-54420
- ⁴⁸Ca(p, γ)⁴⁹Sc, spin-parity of ⁴⁹Sc levels from $3/2^-$ isobaric analogue state γ -decay 3-54377
- Cd even isotopes, B(E2; $0 \rightarrow 2$) values from ⁴He inelastic excitation probabilities 3-46036
- ¹⁰⁶Cd(α , α' γ), props. of $2'$ and $2''$ states, E=11.0 MeV 3-46003
- ¹¹⁸Cd, E0 contrib. in $2^+ \rightarrow 2^+$ transitions, directional correlation functions 3-62991
- ¹¹⁰Cd, from β -decay of ^{110m}Ag oriented in Fe and Ni, meas. of γ -ray anisotropies, M1/E2 mixing ratios 3-46009
- ¹¹⁰Cd, ground-state transitions obs. in ¹¹⁴Sn(d,⁶Li) reaction 3-78341
- ¹¹¹Cd, quadrupole interaction with electric field gradient in Cd, γ - γ angular correlation meas. 3-47183
- ¹¹²Cd(α , α' γ), props. of $2'$ and $2''$ states, E=11.0 MeV 3-46003
- ¹¹⁴Cd(α , α' γ), props. of $2'$ and $2''$ states, E=11.0 MeV 3-46003
- Ce even isotopes, A=130-138, in-beam electron conversion from γ -ray levels 3-67264
- ¹³⁷Ce lifetimes and γ -ray spectra from ¹³⁷Pr decay (*Russian*) 3-49222
- ¹⁴⁰Ce, 2.083 MeV state populated in ¹⁴⁰La β^- decay, quadrupole moment determ. by TDPAC 3-49085
- ¹⁴⁰Ce, ground state transitions to first 2^+ , 3^- and 4^+ states, reduced matrix elements (*German*) 3-46021
- ¹⁴⁰Ce, γ decay props. of 3^- states 3-45993
- ¹⁴²Ce, ground state transitions to first 2^+ , 3^- and 4^+ states, reduced matrix elements (*German*) 3-46021
- ²⁴⁷Cf, multipolarities of transitions from levels populated in ²⁵¹Fm α -decay 3-67281
- ²⁵²Cf spontaneous fission fragments, γ cascades 3-62994
- ³⁴Cl, from ³³S(p, γ)³⁴Cl, mean life and branching ratios of bound states 3-52102
- ³⁴Cl, lifetimes of levels populated in ³²S(³He,p) reaction at 9 MeV 3-49215
- ³⁵Cl, high-spin states obs. using ³²S(α , p) reaction, $\gamma\gamma$ coincidence, angular distrib., yield function meas. 3-74493
- ³⁵Cl, lifetime of first $7/2^-$ level meas. by recoil distance method in ³²S(α ,p) reaction 3-78284
- ³⁵Cl from ³⁴S(p, γ)³⁵Cl, gamma ray transitions and lifetimes 3-43214
- ³⁶Cl, pop. in ³⁵Cl(d,p) reaction, decay, meas. branching ratios, state lives, shell model configs. 3-67262
- ³⁷Cl, lifetime of first $7/2^-$ level meas. by recoil distance method in ³⁴S(α ,p) reaction 3-78284
- ³⁸Cl, e.m. transition rates, meas. lives of low lying states using attenuated-Doppler-shift method 3-62989
- Co isotopes, B(E2) values and single-particle spectra, calc. using Hartree-Fock-Bogoliubov method 3-67246
- ⁵⁶Co, ⁵⁷Co, effective M1 operators, shell model calcs. 3-49124
- ⁵⁶Co, γ -ray transitions props. from ⁵⁶Ni decay and ⁵⁶Fe(p, n) γ ⁵⁶Co 3-54426
- ⁵⁷Co decay, 122 keV, transition, E2/M1 mixing ratio determ. by orientation 3-46006
- ⁵⁸Co, spin assignments from (³He, p) and (³He, p γ) reactions on ⁵⁶Fe 3-54428
- ⁵⁹Co, mixing ratios from gamma-gamma angular corrs. 3-43213
- ⁶⁰Co, anisotropies and intensities of transitions in ⁵⁹Co(n, γ) with polarised neutrons and nuclei 3-43245
- ⁶⁰Co, spin determ. from meas. of γ -ray asymmetry in ⁵⁹Co(n, γ) reaction 3-60175
- ⁴⁸Cr, from ⁴⁰Ca(¹⁰B, pnp), 19, 22.5, 25 MeV, γ -ray spectroscopy 3-62985

nuclear energy level transitions continued

- ⁴⁹Cr, ⁵¹Cr, γ -transitions, study of spherical shell-model states of high angular momentum 3-40416
- ⁵⁰Cr, recoil-distance lifetime meas. for excited states 3-40448
- ⁵¹Cr, decay, relative intensity and internal conversion coeff. meas. 3-52123
- ⁵²Cr, ground-state transitions obs. in ⁵⁶Fe(d,⁶Li) reaction 3-78341
- ⁵³Cr, effective M1 operators, shell model calcs. 3-49124
- ⁵³Cr high-spin states populated in ⁵⁰Ti(α ,n) reaction decay properties 3-52096
- ¹³³Cs, internal conversion of 161- and 223-keV transitions (*German*) 3-74536
- ¹³³Cs Coulomb excitation, meas. of γ -ray energies, branching ratios, B(E2) values 3-52200
- ¹³⁷Cs, decay, relative intensity and internal conversion coeff. meas. 3-52123
- ¹⁴⁰Cs, β and γ activity obs. using ARIEL on line isotope separator, ground state spin assignment (*French*) 3-60123
- ⁶¹Cu, from ⁵⁸Ni(⁴He,p γ), directional-correlation and Doppler-shift lifetime meas. 3-67261
- ⁶¹Cu analogue states in ⁶⁰Ni(p, γ) reaction, decay schemes and branching ratios 3-46001
- ⁶²Cu excited states, time differential perturbed ang. distrib. obs. 3-63000
- ⁶⁴Cu, ⁶⁶Cu, lifetimes of isomeric 6^- states populated in (d,p) reactions, M2 transitions 3-45955
- ⁶⁴Cu, polarisation of deexcitation γ -rays following ⁶⁴Ni(p,n γ) reaction (*Russian*) 3-52126
- Dy, A=162, 164, Coulomb excitation, electric quadrupole and hexadecapole transition moments 3-49201
- ¹⁶²Dy, A=158, 160, 162, above 1.5 MeV, lifetime meas., probability anal. 3-78250
- ¹⁵⁴Dy from ¹⁴⁶Nd(¹²C,xn,p) reaction, high spin states, transition of ground rotational band 3-60217
- ¹⁵⁵Dy from ¹⁴⁶Nd(¹²C,xn,p) reaction, high spin states, stretched E2 transitions 3-60217
- ¹⁵⁶Dy, influence of rotation on moment of inertia of high-spin ground state members 3-52098
- ¹⁵⁸Dy, B(E2) values and collective gyromagnetic ratio as function of angular momentum 3-49097
- ¹⁵⁹Dy, rotational excitation properties 3-43212
- ¹⁶⁰Dy, determ. particle parameters of E2 transitions and multipole mixing ratios 3-67256
- ¹⁶⁰Dy, E0 contrib. in $2^+ \rightarrow 2^+$ transitions, directional correlation functions 3-62991
- ¹⁶⁰Dy, γ decay props. of 3^- states 3-45993
- ¹⁶¹Dy, Coulomb excitation of 43.8 keV state, Mossbauer effect study of transition 3-62990
- ¹⁶⁴Dy, Coulomb excitation, meas. of hexadecapole transition moments and M(E2; $0 \rightarrow 2$) 3-49195
- ¹⁰¹Eh, n.m.r., gamma ray anisotropy meas., spin and E2/M1 mixing ratio assignments 3-74534
- Er, A=166, 168, 170, Coulomb excitation, electric quadrupole and hexadecapole transition moments 3-49201
- ¹⁶⁸Er, influence of rotation on moment of inertia of high-spin ground state members 3-52098
- ¹⁶⁸Er, above 1.5 MeV, lifetime meas., probability anal. 3-78250
- ¹⁶⁸Er, Coulomb excitation, meas. of hexadecapole transition moments and M(E2; $0 \rightarrow 2$) 3-49195
- ¹⁶⁸Er, non-adiabatic effect on collective g-factors and K-forbidden M1 transitions 3-49098
- ¹⁶⁸Er γ cascade directional correl. after ¹⁶⁶Ho β^- decay in YES cryst. (*French*) 3-53039
- ¹⁶⁸Er hyperfine interaction in lanthanum and yttrium ethyl sulphates, γ - γ directional correl. (*French*) 3-47179
- ¹⁶⁸Er, γ -ray spectroscopy of levels populated in ¹⁶⁸Ho β -decay 3-67273
- ¹⁵¹Eu, ¹⁵³Eu, hyperfine anomaly between ground and excited states 3-49207
- ¹⁸F, lifetimes meas. by Doppler shift attenuation method 3-62996
- ¹⁹F, nuclear Zeeman splitting by anal. linear polarization 3-71081
- ¹⁹F, three particle structure, comparison with decay strengths from positive parity states 3-52113
- ²⁰F, γ -ray transitions, linear polarization meas. 3-40447
- ²⁰F, lifetimes meas. by Doppler shift attenuation method 3-62996
- ⁵³Fe, alignment of excited states meas. technique using anisotropy of emitted γ -rays 3-49080
- ⁵⁴Fe, ground-state transitions obs. in ⁵⁸Ni(d,⁶Li) reaction 3-78341
- ⁵⁵Fe from ⁵⁶Fe(d,t) reaction, low-lying levels study 3-74485
- ⁵⁵Fe mean life of 3 excited states, recoil distance method (*French*) 3-43205
- ⁵⁶Fe, effective M1 operators, shell model calcs. 3-49124
- ⁵⁶Fe, γ -rays from levels fed by ⁵⁶Mn β -decay (*French*) 3-78293
- ⁵⁷Fe, calibration of isomer shift by lifetime meas. in different chemical environments (*German*) 3-49186
- ⁵⁷Fe, chemical environment effects on lifetime of 14.4 keV state and Mossbauer meas., isomer shift calibration 3-62984
- ⁵⁷Fe, electron spin polarised, 14.4 keV transition, internal conversion coeffs. and conversion electron intensity 3-40442
- ⁵⁷Fe from ⁵⁶Fe(d,p)⁵⁷Fe, ground state doublet study 3-43215
- ⁶⁹Ga, obs. using photoexcitation, elastic and inelastic resonance decays at 7306, 6874 keV 3-62948
- ⁶⁹Ga, reson. fluoresc. obs., ground-state transition strengths 3-40450
- ⁷⁰Ga, placement of 188 keV transitions 3-62982
- ⁷⁰Ga from ⁷⁰Zn(p,n γ) reaction, 1.7-3.2 MeV, gamma-ray angular distrib. and branching ratios 3-62931
- ⁷¹Ga, reson. fluoresc. obs., ground-state transition strengths 3-40450
- Gd, A=158, 160, Coulomb excitation, electric quadrupole and hexadecapole transition moments 3-49201
- ¹⁴⁶Gd, energy level spectroscopic investigation, spin assignments and lifetime meas. 3-54429
- ¹⁴⁸Gd, energy level spectroscopic investigation, spin assignments and lifetime meas. 3-54429
- ¹⁵⁰Gd, energy level spectroscopic investigation, spin assignments and lifetime meas. 3-54429
- ¹⁵¹Gd spherical nucleus from ¹⁴⁹Sm(α ,2n)¹⁵¹Gd, $11^-/2$ [505] rotational band identification 3-74489
- ¹⁵³Gd, levels populated in ¹⁵³Gd(p,t) 3-52086

nuclear energy level transitions continued

- ¹⁵⁴Gd, 2⁺ and 4⁺ states, populated by ¹⁵⁴Eu beta decay, lifetime meas. 3-52128
- ¹⁵⁴Gd, gamma-decay of levels populated in ¹⁵⁴Tb isomeric state β decay 3-67263
- ¹⁵⁵Gd from ¹³⁷Gd(p,t) ¹⁵⁵Gd, energy level study 3-52086
- ¹⁵⁸Gd, Coulomb excitation, meas. of hexadecapole transition moments and M(E2; 0 \rightarrow 2) 3-49195
- Ge, nucl. lifetimes by blocking technique, computer simulation 3-40443
- ⁶⁵Ge, 31 transitions placed in level scheme 3-60131
- ⁶⁹Ge, level structure from de-excitation gamma ray obs. in ⁶⁹Ga(p, n)⁶⁹Ge reaction 3-54384
- ⁷¹Ge, from thermal neutron capture, E1 transitions (Russian) 3-71083
- ⁴He_A* excited states produced by K⁻ meson stopping in ^{6,7}Li, obs. of γ transitions 3-78277
- ⁴He_A*, excited states produced by K⁻ mesons stopping in ^{6,7}Li, obs. of γ -transitions 3-78277
- Hf even-even isotopes produced in (p, xn γ) reactions, de-excitation 3-49191
- ¹⁷³Hf levels populated in decay of ¹⁷³Ta 3-40421
- ¹⁷⁴Hf, ¹⁷⁶Hf isomeric states populated in (α , nn γ) reactions, g-factors and proton-neutron mixing ratios 3-45967
- ¹⁷⁷Hf, 249.7 keV level, half-life meas. 3-49198
- ¹⁷⁷Hf, mag. dipole moments, ground state h.f.s. 3-40412
- ¹⁷⁷Hf angular correlations meas. 3-62983
- ¹⁷⁸Hf, ¹⁸⁰Hf, Mossbauer meas. of isomer shift and quadrupole moment ratios 3-49206
- ¹⁷⁹Hf, mag. dipole moments, ground state h.f.s. 3-40412
- ¹⁸⁰Hf, parity mixing of 501 keV transition, backscatt. polarimeter meas. 3-67265
- ¹⁸⁴Hf, half-life meas., B and γ decay 3-60129
- Hg isomers, precision magnetic moment determ., hyperfine-structure anomalies, optical pumping expt. 3-62933
- ¹⁹⁸Hg, 412 keV pure E2 transition, K-shell conversion coefficient by beta-ray spectrometer 3-67253
- ²⁰⁰Hg decay scheme, spins and multiplicities 3-40453
- ^{199m}Hg, precision magnetic moment determ., hyperfine-structure anomalies, optical pumping expt. 3-62933
- ¹⁶⁵Ho, from ¹⁶⁵Ho(n,n' γ), relative intensities of γ lines (Russian) 3-71059
- ¹⁶⁵Ho, resonant scattering of gamma-rays, determ. of 94.69 keV level lifetime (Russian) 3-52168
- ¹²²I, M1 transitions, three low lying levels, half lives 3-54424
- ¹²⁷I Coulomb excitation, meas. of γ -ray energies, branching ratios and B(E2) values 3-52200
- ¹²⁹I, orientation study of excited states populated in decay of ^{129m}Te, ^{129m}Te 3-52131
- ¹²⁹I Coulomb excitation, meas. of γ -ray energies, branching ratios and B(E2) values 3-52200
- ¹²⁹I levels populated in ¹²⁹Te β -decay following ¹²⁸Te(n, γ) reaction 3-74537
- ¹¹⁵In, from ¹¹⁵Cd decay, meas. of B(E2) and B(M2) values, coexistence study 3-49197
- ¹¹⁵In, nuclear quadrupole interaction sign, obs. by β - γ directional corrs. in Cd metal 3-52079
- ¹¹⁵In muonic atoms, magnetization distrib. of single-particle states and 2⁺ rotational states 3-49209
- ¹⁸⁷Ir, probability of depopulation, determ. from ¹⁸⁷Pt decay scheme 3-71049
- ¹⁹¹Ir, low-lying level struct. and e.m. props. 3-62953
- ¹⁹²Ir decay, relative intensity and internal conversion coeff. meas. 3-52123
- ¹⁹²Ir \rightarrow ¹⁹²Pt, E0/E2 and E2/M1 multipole mixing amplitudes of γ -transitions, meas. 3-46002
- ¹⁹³Ir, low-lying level struct. and e.m. props. 3-62953
- ¹⁹⁵Ir(2.3h) \rightarrow ¹⁹⁵Pt, decay scheme, ¹⁹⁵Pt excited states, spin and parity assignments 3-52137
- ¹⁹⁵Ir(3.7h) \rightarrow ¹⁹⁵Pt, decay scheme, ¹⁹⁵Pt excited states, spin and parity assignments 3-52137
- ³⁶K, lifetimes of excited states populated in ³⁶Ar(α , pp) reaction 3-43210
- ⁴⁰K, e.m. decay scheme below 3.2 MeV excitation, γ -ray study using ³⁷Cl(α , n) and ⁴⁰Ar(p, n) reactions 3-43208
- ⁴⁰K, e.m. transition rates, meas. lives of low lying states using attenuated-Doppler-shift method 3-62989
- ⁴⁰K, lifetime of 2542 keV level 3-60116
- ⁴¹K, γ transitions between high-spin states, heavy-ion induced reaction obs. 3-74530
- Kr even isotopes, A=78-84, in-beam electron conversion from yrast levels 3-67264
- ⁸²Kr, E0 contrib. in 2⁺ to 2⁺ transitions, directional correlation functions 3-62991
- La neutron deficient isotopes, energy level obs., prolate deformation 3-45976
- ¹³¹La levels populated in ¹³¹Ca beta decay, Coriolis effects (French) 3-52148
- ¹³³La, quadrupole moment of 535 keV state determ. by time-differential PAC meas. in La metal 3-52082
- ¹⁴⁶La fragments from ²⁵²Cf spontaneous fission, γ cascades 3-62994
- ⁶Li, resonance scattering of bremsstrahlung, low-lying level study 3-52094
- ⁷¹Li, E1 polarisation, Coulomb excitation, ²⁰⁸Pb (⁷¹Li, ⁷¹Li' γ) 3-78288
- ¹⁶¹Lu, γ -ray transition, deduced energy levels 3-54423
- ¹⁶⁷Lu, ¹⁶⁹Lu, levels populated in ¹⁶⁷Hf and ¹⁶⁹Hf decay, Nilsson model assignments 3-52147
- ¹⁷¹Lu, ¹⁷³Lu, E1 transition probabilities calc. using equilibrium deformations of one-quasiparticle states 3-49216
- ¹⁷¹Lu, ¹⁷³Lu, high-spin rotational states populated in ¹⁶⁹Tm(d, 2n γ) and ¹⁷³Yb(d, 2n γ) reactions 3-60077
- ¹⁷¹Lu, isomeric E1 and M1 transitions, half-lives 3-54422
- ¹⁷¹Lu, rot. bands, stripping reaction studies 3-62939
- ¹⁷³Lu, isomeric E1 and M1 transitions, half-lives 3-54422
- ¹⁷⁵Lu, E2/M1 mixing ratio determ., from γ -ray anisotropy temp. dependence 3-71082
- ¹⁷⁵Lu pionic atom, search for strong interaction quadrupole effect 3-49134

nuclear energy level transitions continued

- ²⁴Mg, 4.235 MeV level, gamma transitions, branching ratio meas. 3-40439
- ²⁴Mg, gamma-decay of lowest T=2 state populated in ²³Na(p, γ) reaction, branching ratios 3-78285
- ²⁴Mg, shell model calcs. 3-62951
- ²⁵Mg γ -decay study 3-40458
- ²⁶Mg, B(E2) value of first excited state, inelastic electron scattering, Nilsson model comparison 3-57489
- ²⁶Mg excited states populated in ²⁶Na beta decay, γ -ray spectra 3-74541
- ²⁷Mg, ²⁸Mg, shell model calcs. using modified surface-delta-interaction Hamiltonian 3-49167
- ²⁸Mg, gamma-ray spectra of low lying levels, from Mg(³H, pp)²⁸Mg reaction 3-67258
- Mn isotopes, B(E2) values and single-particle spectra calc. using Hartree-Fock-Bogoliubov method 3-67246
- ⁵³Mn, excited state obs. by ⁵³Cr(p, n γ) reaction 3-67192
- ⁵³Mn, γ -emission from levels excited in ⁵³Cr(p, n) reaction at 6 MeV (Russian) 3-74526
- ⁵⁴Mn, ⁵⁵Mn, effective M1 operators, shell model calcs. 3-49124
- ⁵⁴Mn, polarisation of deexcitation γ -rays following ⁵⁴Cr(p, n γ) reaction (Russian) 3-52126
- ⁵⁵Mn, multi-channel study of fine structure of analogue state following ⁵⁴Cr proton induced reactions 3-52133
- ⁹¹Mo, de-excitation of high-spin states populated in α -particle induced reactions 3-78249
- ⁹³Mo, populated in ⁹²Mo(n, γ)⁹³Mo, γ spectra analysis 3-63058
- ⁹⁴Mo, 2953 keV state populated in ⁹²Zr(α , nn) reaction, time-differential PAC meas., lifetime determ. 3-49084
- ⁹⁵Mo, spins of levels, and multipole mixing ratios of transitions 3-60070
- ⁹⁷Mo, ⁹⁹Mo, transition scheme following ⁹⁶Mo(n, γ) and ⁹⁸Mo(n, γ) reactions (Russian) 3-52177
- ¹⁰⁵Mo fragments from ²⁵²Cf spontaneous fission, γ cascades 3-62994
- ^{93m}Mo 6.9 hr, mag. moment and spin determ. 3-62934
- ¹⁴N, decay of photo resonances, shell model analysis, cross sections and branching ratios 3-49239
- ¹⁴N, from ¹²C(³He, p) E=5.54 MeV, Doppler shift attenuation, deduced levels and half lives (French) 3-67255
- ¹⁴N, magnetic moment of 3-, 5.83 level, Blume-Scherer model of PAC in gas 3-49083
- ¹⁵N, level study using ¹⁴C(p, γ) reaction at low energy 3-49255
- ²³Na, angular distrib. of γ -rays emitted in decay of highly excited states, decay schemes (Russian) 3-74528
- ²³Na from ¹²C(¹²C, p)²³Na, high spin states study 3-49185
- ²⁴Na, from ²³Na(d, p) γ , 2.45 MeV 3-62986
- ²⁴Na, from ²³Na(d, p) γ , 2.5 and 2.8 MeV, deduced levels, branching ratios 3-63063
- ²⁴Na, γ -ray transitions from lowest T=2 states populated in ²²Ne(³He, p) reaction 3-43211
- ⁹¹Nb, lifetime and g-factor of 17/2- state populated in ⁸⁹Y(α , nn) reaction, time-diff. meas. 3-49194
- ⁹³Nb, product of ⁹⁰Zr(α , pp) γ , 14.77 MeV, γ -decay of low lying levels 3-57491
- ¹⁴²Nd(¹⁶O, ¹⁶O)¹⁴²Nd, 54-72 MeV, interference of Coulomb and nuclear excitation, B(E2) values and optical model 3-52201
- ¹⁴³Nd(n, γ)¹⁴⁰Ce, hindrance factors for γ -ray transitions near neutron binding energy 3-49218
- ¹⁴⁶Nd(n, γ)¹⁴⁷Nd, activation resonance integral meas., gamma spectra 3-54467
- ¹⁴⁷Nd \rightarrow ¹⁴⁷Pm, γ - γ directional correlation of seven cascades 3-49200
- ¹⁴⁸Nd(n, γ)¹⁴⁹Nd, activation resonance integral meas., gamma spectra 3-54467
- ¹⁵⁰Nd(n, γ)¹⁵¹Nd, activation resonance integral meas., gamma spectra 3-54467
- ²⁰Ne, B(E2) interband and intraband reduced transition probabilities, Tamm-Dancoff calc. 3-49156
- ²⁰Ne, mirror symmetry props. and Fermi decay strength to isobaric analog state from ²⁰Na β^+ decay obs. 3-60127
- ²²Ne(p, t)²⁰Ne, inelastic excitation effects, coupled-channel-Born-approx. analysis of allowed and forbidden transitions 3-67332
- ⁵⁸Ni, inelastic alpha-particle scattering, DWBA analysis of transition cross sections 3-63076
- ⁵⁸Ni(¹⁶O, ¹⁶O)⁵⁸Ni, 35-60 MeV, interference of Coulomb and nuclear excitation, B(E2) values and optical model 3-52201
- ⁵⁹Ni, M1 and E2 transition rates for low-lying levels, Kuo-Brown interaction 3-46004
- ⁵⁹Ni low-lying levels populated in ⁵⁶Fe(α , n), meas. of lifetimes, mixing, branching ratios 3-49213
- ⁶⁰Ni, lifetimes and decays of energy levels populated in ⁶⁰Ni(p, p' γ) and ⁵⁹Co(³He, d γ) reactions 3-52132
- ⁶⁰Ni(e, e'), quadrupole and giant dipole resonance excitation, form factors, characteristics (Russian) 3-71104
- ¹⁶O, 6.05 MeV 0⁺ state predicted by variational calc., B(E2) value in ¹⁸O(p, t) reaction 3-67177
- ¹⁶O, coexistence model for structure of giant dipole resonance, exptl. test 3-49230
- ¹⁶O, e.m. decays of the 1- levels at 12.44, 13.09 MeV (French) 3-49192
- ¹⁶O, even parity transitions, form factor calc., weak coupling model 3-60163
- ¹⁶O, excited odd-parity states in inelastic electron scattering, Brown-Green model 3-63040
- ¹⁶O, γ -ray spectra of levels excited by high energy proton bombardment (Russian) 3-40456
- ¹⁶O, transition moments in electron excitation of T-1 neg.-parity oscillations 3-46020
- ¹⁸O, lifetimes meas. by Doppler shift attenuation method 3-62996
- ¹⁸O, lowest monopole transitions, form factor calc., weak coupling model 3-60163
- ¹⁸O lifetimes and excitation energies from ¹⁸F(t, α) γ 3-54490
- ¹⁸²Os, γ -decay of high-spin states populated in ¹⁸²W(α , 8n) reaction, ground-state band obs. 3-74498
- ¹⁸⁴Os level structure from ¹⁸⁴Ir decay and ¹⁸⁵Re(p, 2n γ) reaction 3-62941
- ¹⁸⁹Os, populated by ¹⁸⁹Re decay, excited level scheme, spin and parity assignments 3-54432

nuclear energy level transitions continued

- ¹⁹⁰Os, ¹⁹²Os muonic, broadening of $2^+ \rightarrow 0^+$ transition, determ. of hyperfine splitting (*German*) 3-52302
- ¹⁹⁰Os, ¹⁹²Os muonic atoms, magnetization distrib. of single-particle states and 2^+ rotational states 3-49209
- ¹⁹²Os, effects on γ -instability on muonic X-rays 3-60112
- ¹⁹²Os, γ -ray level depopulation 3-40414
- ¹⁹²Os, meas. $T_{1/2}$ of excited states using delayed coincidence technique for ¹⁹²Ir β -decay 3-60111
- ²⁹P, lifetimes, branching ratios and multiple mixing ratios of levels populated in ²⁸Si(p,p) reaction 3-49144
- ³¹P from ³⁰Si(¹⁶O,¹⁵N) at 42 MeV, spectroscopic factors, recoil effects 3-67367
- ³³P, excited state ang. correl. studies, decay modes, multipole mixing ratios 3-40449
- ³³P, populated via ³⁷P(t, p)³³P reaction, low-lying states lifetime meas. and props. 3-54427
- ³³P lifetimes meas. by Doppler shift attenuation, spin-parity assignments 3-40446
- ²³¹Pa, product of ²³⁵Np α decay, α , β and γ transition probabilities, Coriolis interaction 3-57499
- Pb region, E2 and E3 transition probabilities for single particle states in finite Fermi system theory 3-43174
- Pb region, effective E2 charges, particle-oscillating core coupling, polarisation 3-45924
- ¹⁹⁴Pb isomeric state behaviour, γ - γ coincidence obs. 3-62992
- ¹⁹⁶Pb isomeric state behaviour, γ - γ coincidence obs. 3-62992
- ¹⁹⁸Pb isomeric state behaviour, γ - γ coincidence obs. 3-62992
- ²⁰⁰Pb isomeric state behaviour, γ - γ coincidence obs. 3-62992
- ²⁰⁵Pb, high spin three neutron hole states of configurations, containing the $i_{13/2}$ orbital 3-52100
- ²⁰⁶Pb, 120 μ s 2.2 MeV state perturbation γ -ray meas. on ²⁰⁶Bi oriented in Ni 3-78286
- ²⁰⁷Pb, ²⁰⁸Pb, magnetic moments of first excited states meas. by $\gamma\gamma$ -IPAC technique 3-45960
- ²⁰⁷Pb, ²⁰⁹Pb, M1-, M2-, M4-transition rates calc. using linear response theory of finite Fermi systems 3-49129
- ²⁰⁷Pb, angular correlation studies 3-49219
- ²⁰⁷Pb, E2 effective charge meas. from radioactive decay of polarised ²⁰⁷Bi 3-46008
- ²⁰⁸Pb, inelastic alpha-particle scattering, DWBA analysis of transitions cross sections 3-63076
- ²⁰⁸Pb, M2 transition at 7.51 MeV, RPA calc. with density dependent interaction 3-49153
- ²⁰⁸Pb, semi-empirical analysis magnetic moments of single-particle (hole) states assumed core, B(M1) values 3-52081
- ²⁰⁸Pb muonic atom, X-ray transition energies rel. to nuclear charge distrib. 3-71038
- ²⁰⁸Pb region, magnetic dipole transition rates 3-49205
- ²⁰⁸Pb region, probabilities, and magnetic multipole moments of single particle states 3-60071
- ²⁰⁸Pb region, single particle transitions, renormalization of E2 and M1 matrix elements 3-45999
- ²⁰⁸Pb(d,p)²⁰⁹Pb, diffraction model for extraction of spectroscopic factors 3-60140
- ²⁰⁹Pb, I-forbidden $1i_{11/2} \rightarrow 2g_{9/2}$ M1 transition, mean lifetime and B(M1) meas. 3-60114
- Pb(p,t), A=208, 206, 204, 35 MeV, two-neutron pick-up strengths, transition from single-particle to collective 3-60187
- Pd, Coulomb excitation in Pd-Fe target, transient magnetic field effects on recoil in Fe lattice, γ -ray meas. 3-49269
- ¹⁰⁸Pd, zero-phonon γ transition search 3-62993
- ¹⁴³Pm, effective M2 gamma transition moments 3-45997
- ¹⁴³Pm, from ¹⁴¹Pr(α , 2n γ), e.m. props. of low-lying levels, M2, E3 transition probabilities 3-67254
- ¹⁴³Pm, from ¹⁴⁸Nd(p,6n γ), e.m. props. of low-lying levels, M2, E3 transition probabilities 3-67254
- ¹⁴⁵Pm, effective M2 gamma transition moments 3-45997
- ¹⁴⁷Pm, decay scheme, Ge(Li)-Ge(Li) coincidence studies 3-45994
- ²⁰⁴Po, core polariz. eff. in $\pi h_{9/2}$ shell of 8^+ states and g-factors 3-45969
- ²⁰⁶Po core polariz. eff. in $\pi h_{9/2}$ shell of 8^+ states and g-factors 3-45969
- ²⁰⁶Po \rightarrow ²⁰⁶Bi, decay scheme revision from ²⁰⁶Bi 10.84 keV strong M1 transition obs. 3-52135
- ²¹⁰Po, B(E2) values of collective states, study with inelastic scattering of deuterons, protons, tritons 3-43183
- ²¹⁰Po, half-lives of 6^+ and 4^+ states, meas. by γ - γ delayed coincidence method 3-45925
- ²¹⁰Po, half-lives of 6^+ and 4^+ states 3-62998
- ²¹⁰Po core-excited state, magnetic moment determ. by time-differential spin-rotation meas. 3-45972
- ²¹⁰Po₂, $g(\pi h_{9/2}, J)$ difference for 6^+ and 8^+ states, DPAC^{9/2} meas. of lifetimes 3-45951
- ²¹¹Po, 1065 keV ($15/2^-$) state, meas. of lifetime 3-49092
- ²⁴⁰Po, effective charge of proton $h_{9/2}$ from lifetimes meas. (*French*) 3-45992
- ¹³⁴Pr \rightarrow ¹³⁴Ce, decay scheme for isomeric and ground state from γ -ray obs. 3-49184
- ¹³⁷Pr, lifetimes of levels populated in ¹³⁷Nd decay (*Russian*) 3-52140
- ¹⁴¹Pr, effective M2 gamma transition moments 3-45997
- ¹⁴⁷Pr, 145 keV transition penetration parameter, M1-E2 mixing ratio 3-78279
- ¹⁴⁸Pr, γ -ray energies and half-lives, Ge(Li) meas. in prodn. from ²³⁵U fission 3-43203
- ¹⁴⁹Pr, γ -ray energies and half-lives, Ge(Li) meas. in prodn. from ²³⁵U fission 3-43203
- α T, A=192, 194, 196, lifetimes, branching ratios, B(M1) and B(E2) values of 2^+ and 2^+_{rot} states 3-49196
- ¹⁹⁰Pt level scheme populated in ¹⁹⁰Au decay 3-67278
- ¹⁹²Pt, angular correlations of K- and L-conversion electrons (*Russian*) 3-71075
- ¹⁹²Pt, gamma decay, phenomenological T-violating internucleon potential 3-62988
- ¹⁹²Pt, γ -ray level depopulation 3-40414
- ¹⁹⁴Pt, spins, multipole mixing ratios of γ -transitions, E2 ratio comparison with theory 3-54385
- ²¹⁸Pu, B(E3) values for octupole states and new Nilsson orbitals, (d,t) and (d,d') reactions 3-43185

nuclear energy level transitions continued

- ⁸⁵Rb, ⁸⁷Rb, γ -ray transitions of Coulomb excited levels, B(E2) values structure determ. 3-40415
- ⁸⁵Rb, fast neutron scattering, (n,n), (n,n') and (n,n', γ) reactions 3-43249
- ⁸⁷Rb, fast neutron scattering, (n,n), (n,n') and (n,n', γ) reactions 3-43249
- ¹⁸²Re, from beta decay of ¹⁸²Os, gamma and internal conversion meas. 3-49227
- ¹⁸⁷Re, 134 keV transition, penetration effects 3-49190
- ¹⁰³Rh, γ - γ directional correl. obs. 3-62997
- Ru, Coulomb excitation in Ru-Fe target, transient magnetic field effects on recoil in Fe lattice, γ -ray meas. 3-49269
- ⁹³Ru, de-excitation of high-spin states populated in α -particle induced reactions 3-78249
- ⁹⁹Ru, excited state lifetime obtained from ⁹⁹Rh decay, γ -transition probability (*Russian*) 3-78280
- ¹⁰¹Ru, excited state lifetime obtained from ¹⁰¹Rh and ¹⁰¹Tc decay, γ -transition probability (*Russian*) 3-78280
- ¹⁰⁶Ru, low-lying levels associated with β^- decay of ¹⁰⁶Tc 3-62952
- ¹⁰⁸Ru, low-lying levels associated with β^- decay of ¹⁰⁸Tc 3-62952
- ¹⁰⁹Ru fragments from ²⁵²Cf spontaneous fission, γ cascades 3-62994
- ¹¹¹Ru fragments from ²⁵²Cf spontaneous fission, γ cascades 3-62994
- ³⁰S, low lying, γ -decay, ²⁸Si(³He,n) reaction, DSAM 3-78289
- ³²S, γ -decay scheme, from ³¹P(p,p) γ obs. 3-60190
- ³²S, isobaric analogue resonances study using ³¹P(p,p)³²S, ³¹P(p,p)³¹P, 2) 3-78299
- ³⁵S, from ³⁴S(d,p) reaction, excitation functions for transitions to lowest states Ericson fluctuation theory 3-67339
- ¹²¹Sb, elec. quadrupole reduced transition probabilities 3-54406
- ¹²¹Sb, reduced E2 transition probabilities, calc. from particle-vibration coupling model 3-52115
- ¹²¹Sb, reson. fluoresc. obs., scatt. widths 3-40451
- ¹²²Sb, first excited state populated by ¹²²Sn(p,n) reaction, stroboscope resonance determ. of magnetic moment 3-45959
- ¹²²Sb, magnetic moment of 1.8 μ s state g factor determ. by stroboscopic method 3-67187
- ¹²³Sb, reson. fluoresc. obs., scatt. widths 3-40451
- ¹²⁵Sb decay, weak transitions and accurate gamma intensities 3-54431
- ¹³⁰Sb excited states populated in β -decay of $\tilde{7}^-$ isomer and ground state of ¹³⁰Sn (*Russian*) 3-71085
- ⁴²Sc, alignment of excited states meas. technique using anisotropy of emitted γ -rays 3-49080
- ⁴⁴Sc, γ decay of low-lying states, lifetimes, ang. distrib. meas. 3-78282
- ⁴⁴Sc, proposed $K^\pi=0^-$ band 3-49145
- ⁴⁴Sc excited states populated by ⁴¹K(α ,n γ), decay modes and spin assignments, $K=0^-$ band 3-74495
- ⁴⁵Sc, γ -transitions, study of spherical shell-model states of high angular momentum 3-40416
- ⁴⁵Sc, $K=3/2^+$ rotational band study using ⁴²Ca + α reaction 3-74494
- ⁴⁵Sc, reson. fluoresc. obs., ground-state transition strengths 3-40450
- ⁴⁵Sc(n, n' γ) E=1.41 MeV, γ -ray angular distribution 3-74589
- ⁴⁹Sc negative-parity state lifetimes using ⁴⁸Ca(p,p)⁴⁸Sc reaction 3-40445
- Se, A=75, 77, 79, 81, 83, anomalous coupling states, calc. of nuclear moments 3-49115
- Se, A=77, 79, 81, from thermal neutron capture, E1 transitions (*Russian*) 3-71083
- Se even isotopes, A=72-78, in-beam electron conversion from yrast levels 3-67264
- ⁷⁵Se, gamma-transition scheme following ⁷⁴Se(n, γ) reaction (*Russian*) 3-52176
- ⁷⁸Se, γ -transitions following ⁷⁸Br \rightarrow ⁷⁸Se β decay, level structure 3-78247
- ⁷⁸Se transition scheme following ⁷⁷Se(n, γ) reaction (*Russian*) 3-49250
- ²⁸Si, decay scheme for levels populated in ²⁷Al(p,p) γ reactions (*French*) 3-49251
- ²⁹Si, angular correlation, γ -ray linear polarisation and lifetime meas. of high spin negative parity states 3-43171
- ²⁹Si, from ²⁸Mg(α , n γ) reaction, high-spin states using neutron time-of-flight spectrometer 3-52084
- ²⁹Si(α ,p)³²P $E_\alpha=10.65, 10.69, 11.00$ MeV, ³²P deduced levels, mixing and branching ratios yielding dipole and quadrupole transition strengths 3-60108
- Sm, A=148, 150, 152, yield of de-excitation γ -rays following Coulomb excitation, quadrupole moment determ. 3-49113
- Sm, A=152, 154, Coulomb excitation, electric quadrupole and hexadecapole transition moments 3-49201
- ¹⁴⁷Sm, obs. of new γ -transitions and new levels from ¹⁴⁷Eu decay (*Russian*) 3-74525
- ¹⁵⁰Sm, E0 and E2, phenomenological collective model calculations (*Russian*) 3-71066
- ¹⁵¹Sm levels populated in ¹⁵¹Pm decay 3-78244
- ¹⁵²Sm, ¹⁵⁴Sm, Coulomb excitation, meas. of hexadecapole transition moments and M(E2; 0 \rightarrow 2) 3-49195
- ¹⁵²Sm, ¹⁵⁴Sm, Coulomb excitation of 2^+ and 4^+ levels, determ. of E4 moments 3-49202
- ¹⁵²Sm, E4 matrix elements 3-63001
- ¹⁵⁴Sm, E4 matrix elements 3-63001
- ¹⁵⁴Sm, excited by (n, n' γ) reaction, γ -branching ratio meas., structure determ. 3-67196
- ¹⁵⁷Sm 8 min. nuclide, decay phenomena 3-62995
- ¹¹⁴Sn, high-spin isomeric state populated in ¹¹²Cd(α ,nn) reaction, lifetime and g-factor determ. 3-45958
- ¹¹⁷Sn, E3 and M4 transitions, conversion coefficient measurement, comparison with theory 3-54430
- ¹¹⁹Sn, gamma transitions between low-lying levels populated in ¹¹⁹In decay and ¹¹⁸Sn(n, γ) 3-49212
- ¹¹⁹Sn, Mossbauer meas. of magnetic moment of 23.8 keV state and hyperfine anomaly 3-49208
- ⁸³Sr, transitions between levels populated in ⁸³Ym.s decay 3-46007
- ⁸⁶Sr, population of 8^+ state by ⁸⁶Sr(p,pnn) reaction, time differential pattern of 627 keV gamma-ray 3-45957

nuclear energy level transitions continued

- ⁸⁸Sr, mixing of giant magnetic dipole state with 1^+ state at 3.49 MeV 3-60113
- ⁸⁸Sr, mixing ratio for 898 keV transition, ang. correl. meas. for 898-1836 keV cascade (*German*) 3-60118
- ⁸⁸Sr(¹⁶O, ¹⁶O)⁸⁸Sr, 45-60 MeV, interference of Coulomb and nuclear excitation, B(E2) values and optical model 3-52201
- ⁹⁰Sr, search for the first α -excited state, gamma transition intensities and spins of 1655, 1892 and 2207 KeV states 3-40440
- ¹⁷⁷Ta, isomeric E1 and M1 transitions, half-lives 3-54422
- ¹⁷⁷Ta, populated in ¹⁷⁷W decay, $\gamma\gamma$ coincidence meas. (*Russian*) 3-74521
- ¹⁸¹Ta, half-life of 482 keV level 3-54419
- ¹⁸¹Ta 482 keV transition, short-range correlations, effective charge, parity violation, polarisation 3-57490
- ¹⁸²Ta, gamma decay PAC meas. for g factor determ. of ¹⁸²W $K^\pi=2^-$ band 3-67184
- ¹⁶⁰Tb low energy transitions, multipolarities 3-43178
- ¹⁶¹Tb levels populated in ¹⁶¹Gd β^- decay 3-43219
- ⁹³Tc, de-excitation study of high spin states 3-78248
- ⁹⁴Tc, excited states, obs. of neutron and gamma-ray yields from ⁹⁴Mo(p,n)⁹⁴Tc reaction at isobaric analog. resonances 3-67207
- ⁹⁷Tc, $T_{1/2}$ of excited states using delayed coincidence technique for ⁹⁷Ru β -decay 3-60111
- ⁹⁹Tc, 140 keV γ -ray transition, Mossbauer resonance spectra 3-71077
- ⁹⁹Tc, directional correlation and multipole mixing 3-49199
- ¹⁰¹Tc levels populated in ¹⁰¹Mo decay, γ -ray spectra and internal conversion coeffs. (*Russian*) 3-49141
- Te even isotopes, A=114-126, in-beam electron conversion from yrast levels 3-67264
- Te neutron-rich even nuclei, systematics of E2 transition rates 3-49214
- ¹²⁵Te, 35.5 keV M1 transition line intensities, chemical effects 3-74531
- ¹²⁷Te, mag. mom. $\mu_{3/2}$ detn. by nuclear orientation meas. 3-45966
- ¹²⁷Te, mag. mom. $\mu_{3/2}$ detn. by nuclear orientation meas. 3-45966
- ¹³²Te, transition probability meas. of levels populated in ¹³²Sb β -decay, half-life determ. 3-49214
- ^{123m}Te, nuclear orientation detn. of mag. mom. 3-49106
- ^{125m}Te, nuclear orientation detn. of mag. mom. 3-49106
- ^{127m}Te, nuclear orientation detn. of mag. mom. 3-49106
- ^{129m}Te, nuclear orientation detn. of mag. mom. 3-49106
- Te(p,p'), even-A isotopes obs. of strong L=5 transitions, 2^+ -pole collective motion 3-67326
- ⁴⁴Ti from ⁴⁰Ca(α ,p)⁴⁴Ti, rotational bands obs. 3-74490
- ⁴⁵Ti, ⁴⁷Ti, p-transitions, study of spherical shell-model states of high angular momentum 3-40416
- ⁴⁵Ti, K=3/2⁺ rotational band study using ⁴²Ca + α reaction 3-74494
- ⁴⁶Ti, recoil-distance lifetime meas. for excited states 3-40448
- ⁴⁷Ti levels populated in ⁴⁷V β -decay, spin and parity assignments 3-52146
- ²⁰²Tl, 7⁺ isomeric state populated in ²⁰⁴Hg(p,nnn), γ -ray spectra, time-differential spin rotation 3-49086
- ²⁰³Tl, ²⁰³Tl muonic atoms, magnetization distrib. of single-particle states and 2⁺ rotational states 3-49209
- ²⁰⁷Tl, M1-, M2-, M4-transition rates calc. using linear response theory of finite Fermi systems 3-49129
- ¹⁶⁸Tm rot. band obs. in ¹⁶⁹Tm(d,t)¹⁶⁸Tm 3-63069
- ²³³U levels populated in ²³³Pa decay 3-74535
- ²³⁴U levels excited by (d,d') reaction, reduced transition probabilities 3-54388
- ²³⁶U, low lying excited states, following ²³⁵U(n, γ)²³⁶U reactions 3-67335
- ²³⁶U, measurements of low energy γ -rays following thermal neutron capture in ²³⁵U 3-63042
- ²³⁶U levels excited by (d,d') reaction, reduced transition probabilities 3-54388
- ²³⁸U, neutron induced reaction, γ ray spectra calcs. for E1, E2, M1, M2, transitions 3-67322
- ²³⁹U compound nucleus, lifetime meas. following formation in ²³⁸U + n reaction, 1.6-4.3 MeV (*Russian*) 3-40497
- V isotopes, B(E2) values and single-particle spectra calc. using Hartree-Fock-Bogoliubov method 3-67246
- ⁴⁷V decay study using ⁴⁷Ti(p,n) and ⁴⁰Ca(¹⁰B,2pn) reactions 3-49146
- ⁴⁸V, low-lying levels populated in ⁴⁰Ca(¹⁰B,pp) and ⁴⁰Ca(¹²C,pppn) reactions 3-49135
- ⁴⁹V, p-transitions, study of spherical shell-model states of high angular momentum 3-40416
- ⁵¹V, (p,n) isobaric analogue transitions, 22 to 40 MeV 3-63055
- ⁵¹V(p,n)⁵¹Cr, energy dependence of analogue transition, 16 to 26 MeV 3-63053
- W, A=182, 184, 186, angular correlation meas. of γ -transition following Coulomb excitation, quadrupole interaction in Te (*German*) 3-49187
- W even-even isotopes produced in (p,xny) reactions, de-excitation 3-49191
- ¹⁷⁹W levels populated in ¹⁷⁹Re decay, γ -ray spectra and γ - γ coincidence meas. (*Russian*) 3-52089
- ¹⁸¹W, Coriolis mixing effects in levels populated by ¹⁷⁹Hf(α , 2n) and ¹⁸⁰Hf(α , 3n) reactions 3-60079
- ¹⁸¹W, mixing ratios from nuclear orientation meas. on ¹⁸³Re, ¹⁸⁴Re 3-60110
- ¹⁸²W, mag. mom. of $K^\pi=2^-$ band, γ - γ correlation study 3-49109
- ¹⁸⁴W, mixing ratios from nuclear orientation meas. on ¹⁸³Re, ¹⁸⁴Re 3-60110
- ¹²⁵Xe, ¹²⁷Xe, γ - γ directional correlation at high gas densities (*German*) 3-49189
- ¹³¹Xe, populated from ¹³¹I decay, 341.2 and 404.8 keV level lifetime meas. (*German*) 3-52139
- ¹³²Xe, γ cascades, perturbed angular correlation meas. for g-factor, 668 keV state 3-78242
- ⁹⁵Y decay scheme, population of ⁹⁵Zr levels (*French*) 3-71087
- Yb, even isotopes, γ -ray spectroscopic study, single-line Mossbauer absorption, Yb levels, deduced isomer shifts 3-60109
- Yb even-even isotopes produced in (p,xny) reactions, de-excitation 3-49191
- ¹⁶⁸Yb, above 1.5 MeV, lifetime meas., probability anal. 3-78250

nuclear energy level transitions continued

- ¹⁷⁴Yb, Coulomb excitation, meas. of hexadecapole transition moments and M(E2; 0 \rightarrow 2) 3-49195
- ¹⁷⁴Yb gamma decay of excited K=0 rotational bands following pop. in ¹⁷³Yb(n, γ) reaction 3-74533
- ⁶⁷Zn, γ - γ ang. correl. meas. of mixing ratios 3-62999
- ⁶⁷Zn, from thermal neutron capture, energy levels and E1 transitions (*Russian*) 3-71083
- ⁸⁹Zr, de-excitation of high-spin states populated in α -particle induced reactions 3-78249
- ⁹⁰Zr, (p,n) isobaric analogue transitions, 22 to 40 MeV 3-63055
- ⁹¹Zr, lifetime and g-factor of 15/2⁻ state populated in ⁸⁸Sr(α ,n) reaction 3-49194
- nuclear energy levels**
see also isobaric analogue states; nuclear energy level transitions; nuclear excitation; nuclear shape; nuclear structure
- A=174-185, equilibrium deformations and structures of ground and excited states (*Russian*) 3-52088
- A=250-261, study of collective vibrational states of even-even nuclei in superfluidity model (*Russian*) 3-49140
- A=4 nuclei, compilation of data 3-43181
- A=7 and 8 nuclei, shell model calculations, non-normal parity states 3-54403
- actinide region, deformation energies and moments of inertia for isomeric states (*German*) 3-52071
- asymmetric fission, semi-classical level density theory, shell-effects 3-49290
- bound state energy spectrum of three structureless alpha particles with differing nuclear potentials 3-67243
- closed shell nuclei, ground state correlations, density-matrix formulation 3-74510
- deformation, axially symmetric or γ -unstable, from preferred nucleon shapes 3-60082
- deformation energy calcs. for heavy nuclei, microscopic approach using shell-correction parameters 3-67178
- deformed, competition between Coriolis-anti-pairing and decoupled band hybridization 3-67241
- deformed doubly even nuclei, density matrix approach to Inglis cranking model 3-71065
- deformed intrinsic state, ang. momentum distrib. and average temp. 3-71067
- deformed nuclei, energy level diagram, total nuclear energy and equilibrium deform. (*Rumanian*) 3-45977
- deformed nuclei spurious 1⁺ state, separation out from excited 1⁺ state 3-54383
- densities, influence of continuum on microscopic calcs. 3-67204
- density calculations and exptl. studies, review 3-54394
- doorway states, effect on spectrum statistics 3-60076
- doublet splitting in even A deformed nuclei between excited 2 quasi-particle states 3-57478
- even nuclei, ground-state rotational bands, two-nucleon transfer amplitudes 3-43189
- even-even spherical nuclei, interaction between collective and quasi-particle excitations (*Russian*) 3-74514
- even-even spherical nuclei, low-lying 2⁺ and 3⁻ states, harmonic and anharmonic approxs. (*Russian*) 3-71047
- excitation by electrons and hadrons at high energy 3-60162
- excitation spectra, low frequency, of even-even nuclei, systematic features near closed shell 3-67206
- excited states, magnetic moments determ. from muonic atom hyperfine structure 3-45931
- finite nuclei, single-hole strength distrib., second moment 3-52105
- fissile nuclei, shell and heating effects 3-78266
- fissile nuclei, partial widths of resonance levels, spin-dependent statistics 3-67376
- function of inertia calc. for large-amplitude collective motion in Lipkin model 3-49175
- governor model of Trainor and Gupta, approx of deformed rotating nucleus, backbending 3-62971
- Green's function method, transitions, one and two particle density matrices 3-78255
- ground state, realistic one-particle density matrix and single-particle description 3-52111
- ground state calculations, self consistent potential, rearrangement energies 3-71058
- ground state rotational band in shell model with R(5) symmetry, intrinsic state generation 3-62962
- ground state rotational spectra, back-bending effect from particle number projection 3-49177
- ground-state energy for vibrational deformed nuclei, generalised Skyrme-Levinson model 3-74515
- Hartree-Fock, constrained, calculations, 'inaccessible regions' 3-71069
- heavy and superheavy nuclei, spurious state contribs. in shape and stability calcs. 3-45926
- high-spin states in rotational bands, semiclassical description, variable moment of inertia 3-67201
- hypernuclei, A=4, spin dependence of ΛN interaction 3-71072
- intermediate mass region, Coriolis coupling calcs. 3-78252
- intermediate-state summations in effective shell model interaction, convergence rate 3-62964
- isospin impurities in low-lying and unbound states 3-54382
- Kuo interaction in untruncated shell-model calcs. in sd-shells, production of band shifts 3-67202
- light nuclei, obs. of S-wave levels near threshold for tensor-polarised deuteron reaction 3-49261
- light nuclei, quadrupole and hexadecapole deformations, Hartree-Fock approx. 3-49179
- light nuclei states, oscillator cluster parentage and supermultiplet expansion 3-52112
- low energy states, minimisation of energy variance for determinantal state and Hartree-Fock state 3-49150
- magic nuclei, collective excitation, variational calc. of binding energies and spectra (*Russian*) 3-71064
- microscopic wave functions of levels from inelastic α -particle scattering at 166 MeV 3-60182
- N=50 isotopes, interaction between collective and quasiparticle excitations, energies, wave functions, B(E2) values (*Russian*) 3-74514

nuclear energy levels continued

- N=82 isotopes, interaction between collective and quasiparticle excitations, energies, wave functions, $B(E2)$ values (*Russian*) 3-74514
- N=82 nuclei, Z=51-59, pseudo LS coupling shell model study of energy levels and e.m. properties 3-49126
- neutron-proton configuration effect on p -instability of deformation 3-49165
- Nilsson's deformed nuclei, mass formula 3-74478
- Nilsson orbits for nucleon in Woods-Saxon potential with deformation and coupled to core rotational states 3-71063
- odd-A nuclei, moderately deformed, solution particle plus rotor model 3-62965
- odd-odd nuclei with small inaxiality, calc. of energy spectrum of excited states (*Russian*) 3-52093
- one-neutron deficient nuclei, level density systematics from (α, n) reactions 3-60080
- optical model pot., imaginary part, ground state corrls. effect 3-52154
- orientation of spin system at low temps., orientation parameters 3-71080
- partial state densities from realistic single-particle states 3-49148
- quadrupole deformation, microscopic treatment of collective motion using group theory 3-49173
- quadrupole moment for high spin rotational states, asymmetric rotor model 3-49114
- quasi-ground band, effect of changes in potential energy surface on internal ratio 3-43184
- quasi-rotational bands, solvable model, transition nuclei 3-60075
- rare earth, calc. of ground state props. using Hartree-Fock calc. 3-78275
- rare earth deformed nuclei, change in mean square radius between ground and excited states 3-49132
- rare earth region, calc. of ground state deformation (*German*) 3-52087
- rare earth region, excited O^+ states in two-nucleon transfer reactions (*Russian*) 3-52091
- repulsion phenomenon, statistical measure 3-57474
- rotation energy expansion in powers of angular velocity of rotation using microscopic method 3-62968
- rotational band, description by single j shell model, quadrupole interaction, equivalence to Bohr's model 3-60096
- rotational band structure above phase transition, schematic two-level model of rotation at high angular momenta 3-57483
- rotational bands, Coriolis force interactions, differences in moments of inertia, nuclei with $173 \leq A \leq 189$ (*Russian*) 3-71039
- rotational bands as induced group representations 3-43197
- rotational energies, angular velocity expansion, application to doubly even nuclei $A=140-195$ 3-52117
- rotational excitations, extension of Belyaev-Zelevinski method 3-67242
- rotational ground band energies in even nuclei, two-parameter description, variable moment of inertia model 3-74496
- shape isomers, spontaneously fissioning, properties of quadrupole vibrational states 3-45984
- single particle states, $35 \leq A \leq 65$ 3-54387
- single-nucleon hole states produced in knock-out reactions, unbound character of core 3-63026
- spectra in the $1f_{7/2}$ shell for nuclei with $A=43-53$ 3-78245
- spherical nuclei, analysis of excited states using β -decay probability log ft values (*Russian*) 3-78291
- spin determ. using alpha-particle scatt. 3-63072
- structure calculation, density dependent interactions 3-54404
- Strutinsky smoothing and partition function approach 3-52114
- tensor vibrational or rotational states, inelastic lepton scatt. 3-78236
- three-particle spectrum, resonance interaction, studies at various mass ratios 3-60078
- two-neutron-hole states in even $N=80$ nuclei, intermediate-coupling model 3-67215
- vibrational nuclei, configuration mixing, reduced transition probabilities and quadrupole moments 3-60084
- yrast line, pairing and spin distrib. effects 3-67205
- n resonances, even-even and odd-odd nuclei, particle-vibration model 3-78267
- Ag odd isotopes, coupling of three particle (hole) valence-shell cluster to quadrupole vibrations 3-67238
- ^{109}Ag , intermediate coupling model 3-71061
- ^{109}Ag Coulomb excitation, meas. of quadrupole moments of first $3/2^-$ and $5/2^-$ states 3-71040
- ^{106m}Ag decay, gamma ray spectra and transition multipolarity 3-71076
- ^{26}Al , populated in $^{27}\text{Al}(^3\text{He}, \alpha)$ reaction, spectroscopic factors 3-67355
- ^{26}Al , levels and spectroscopic factors from $^{27}\text{Al}(p, d)$ reaction 3-52097
- ^{27}Al , resonance scattering of bremsstrahlung, low-lying level study 3-52094
- ^{28}Al , ^{29}Al , shell model calcs. using modified surface-delta-interaction Hamiltonian 3-49167
- ^{28}Al , excitation in $^{27}\text{Al}(d, p)$ reaction (*Russian*) 3-52189
- Ar isotopes, $A=39$ to 42 , low lying states, using $(\pi d3/2)^{-2}(\nu f7/2)^n$ model, $E2$, $M1$ transition rates 3-62949
- ^{35}Ar , populated in $^{36}\text{Ar}(^3\text{He}, \alpha)$, spectroscopic factors 3-67354
- ^{36}Ar , from $^{35}\text{Cl}(p, \gamma)$, $E=0.8-2.6$ MeV, shell model calculation of parity levels 3-71078
- ^{37}Ar , 1612 keV level, mean lifetime meas. 3-45991
- ^{69}As , population in decay of ^{69}Se isomeric states 3-43222
- ^{72}As , obs. of new isomeric level at 215 keV populated in $^{72}\text{Ge}(p, n)$ reaction 3-45956
- ^{74}As , levels populated in $^{73}\text{Ge}(^3\text{He}, d)$ reaction at 17 MeV 3-43182
- ^{75}As , magnetic moment of 265 keV level using integral method of perturbed angular correlation technique 3-49105
- ^{209}At , positive parity core excited states populated in electron capture decay of ^{209}Rn 3-74542
- ^{210}At levels populated in ^{210}Rn decay 3-43223
- ^{19}Au , $A=196, 198, 200$, magnetic moments of 12^- states, low-temp. orientation expts. 3-45952
- ^{10}B , deduced levels from $^9\text{Be}(p, p)^9\text{Be}$, 0.8 to 2.7 MeV 3-63047
- ^{10}B , verification of model representation of excited states using ^9Be -proton interactions (*Russian*) 3-74570

nuclear energy levels continued

- ^{11}B , resonance scattering of bremsstrahlung, low-lying level study 3-52094
- ^{11}B , spectroscopic factors of 6.76 MeV level deduced from DWBA analysis of $^{10}\text{B}(d, p)^{11}\text{B}$ 3-62938
- ^{14}B , low-lying level structure studied by $^{14}\text{C}(^7\text{Li}, ^7\text{Be})^{14}\text{B}$ 3-62925
- ^{130}Ba , quadrupole moments of first excited states, reorientation eff. meas. 3-49112
- ^{134}Ba , quadrupole moments of first excited states, reorientation eff. meas. 3-49112
- ^{136}Ba , levels and transitions study 3-40457
- ^{136}Ba , quadrupole moments of first excited states, reorientation eff. Meas. 3-49112
- ^{137}Ba , structure study using $^{136}\text{Xe}(\alpha, 3n)$ reaction 3-45974
- ^{138}Ba , structure study using $^{136}\text{Xe}(\alpha, 2n)$ reaction 3-45974
- ^{139}Ba levels populated in $^{138}\text{Ba}(d, p)$ reaction at 19 MeV 3-46033
- ^{140}Ba produced by ^{140}Cs beta-decay, tentative level scheme (*French*) 3-60123
- ^{8}Be , ground band levels, alpha-decay widths of model wave function calc. 3-60133
- ^{8}Be , second excited state obs. from $^7\text{Li}+d$ reaction 3-62954
- ^{8}Be level determ. from $^7\text{Li}(d, n_0)$ reaction with polarised 800 keV deuterons 3-60197
- ^{8}Be structure determ. from $^7\text{Li}(p, \gamma)^7\text{Li}$ 3-46025
- ^9Be , inelastic electron scattering, electromagnetic properties, Nilsson model and experiment comparison 3-54386
- ^9Be , structure determ. from proton scattering studies, 6-30 MeV 3-52184
- $^9\text{Be}(e, e')$, electroexcitation of levels in 14-18 MeV region 3-54465
- ^{204}Bi , high-spin isomeric state populated by heavy-ion and α -particle induced reactions 3-49152
- ^{205}Bi , fragmentation of proton levels from $(^3\text{He}, d)$ and (α, t) reactions on ^{204}Pb 3-63080
- ^{206}Bi , low-lying one-proton three-neutron-hole states 3-52135
- ^{206}Bi , fragmentation of proton levels from $(^3\text{He}, d)$ and (α, t) reactions on ^{206}Pb 3-63080
- ^{207}Bi , low lying levels, weak coupling structure 3-57523
- ^{21}Bi , $7/2^-$ first excited state, semi-realistic shell model calc. 3-78254
- ^{248}Bk , decay product of ^{252}Es by α decay 3-54443
- ^{249}Bk , ^{253}Es α -decay study 3-63017
- ^{250}Bk , ^{254}Es α -decay study 3-63017
- ^{250}Bk , from α -decay of ^{254m}Es 3-54444
- ^{76}Br , from ^{76}Kr decay level energies spins, parities and transition probabilities 3-49220
- ^{79}Br , $\gamma\gamma$ directional correlations meas., spin and parity assignments (*German*) 3-40459
- ^{83}Br excited levels populated in $^{83g} + ^m\text{Se}$ decay 3-63010
- ^{83}Br production from $^{80}\text{Se}(\alpha, p)^{83}\text{Br}$, energy levels study 3-52103
- ^{12}C , giant dipole states and excited dipole states in continuum approx., (γ, n) and (N, p) reaction 3-67193
- ^{12}C , ground-state rotational band study from ^{16}O α -transfer reactions 3-45980
- ^{12}C , multichannel three- α model, two-level internal structure 3-78272
- ^{12}C , single and mutual excitation of first excited state, elastic, inelastic scattering channels 3-60220
- $^{12}\text{C}_A$ hypernucleus, production in $^{12}\text{C}(K^-, \pi^-)$ reaction, spectroscopy 3-78278
- $^{12}\text{C}(p, d)^{11}\text{C}$, at 185 MeV, deep-lying hole states 3-52101
- ^{12}C , (d, p) reaction to unbound states, comparison with DWBA theory 3-54488
- ^{13}C , from $^{11}\text{B}(d, p_0)$, $E=1-4$ MeV, cross sections, giant dipole resonance region 3-67341
- ^{13}C , from $^{12}\text{C}(d, p)^{13}\text{C}$ and neutron scattering on ^{12}C , application of real Weinberg state method 3-57471
- ^{13}C , proton hole spectrum calc. in continuum shell model with residual interaction 3-54389
- ^{13}C from $^{12}\text{C}(p, \pi^+)$, $E=185$ MeV 3-67323
- ^{13}C highly excited states in $^9\text{Be}(\alpha, \alpha)^9\text{Be}$, spin-parity assignments 3-63075
- ^{13}C level parameters from $^{12}\text{C}(n, n)$ reaction 3-40489
- ^{13}C spectroscopic strengths from $^{12}\text{C}(\alpha, ^3\text{He})$ reaction 3-49270
- ^{13}C states, investigation via neutron polarisation in $^9\text{Be}(\alpha, n)^{12}\text{C}$ reaction 3-62946
- ^{14}C , ground state charge distrib. determ. from elastic electron scattering 3-57512
- ^{15}C populated in $^{14}\text{C}(d, p)^{15}\text{C}$ reaction, meas. proton spectra, excitation energies and level widths 3-67208
- Ca isotopes, quadrupole moments and coexistence of spherical and deformed bands 3-49095
- ^{40}Ca , excited $J^\pi=0^+$ states from $^{38}\text{Ar}(^3\text{He}, n)^{40}\text{Ca}$ 3-74491
- ^{40}Ca , low-lying level struct. from electron scatt. studies 3-40482
- ^{40}Ca excited states, up to 9 MeV, gamma branching ratios, lifetimes, excitation properties, structure groups (*French*) 3-43179
- ^{40}Ca region, pairing vibrations in theory of finite Fermi systems 3-49172
- $^{40}\text{Ca}(p, d)^{39}\text{Ca}$, at 185 MeV, deep-lying hole states 3-52101
- $^{40}\text{Ca}(p, p')^{40}\text{Ca}^*$, excitation of $f_{7/2}-d_{3/2}^{-1}$ states, effect of vector and tensor forces 3-67328
- ^{41}Ca , high spin states in $K=3/2^+$ and $K=3/2^-$ rotational bands 3-60072
- ^{42}Ca , $1d_{3/2}$ protons studied via $^{42}\text{Ca}(d, ^3\text{He})^{41}\text{K}$ reaction using DWBA anal. 3-74480
- ^{46}Ca , from $^{46}\text{Ca}(p, p')$, 16 MeV 3-54391
- ^{46}Ca , study up to 6.3 MeV excitation energy using $^{48}\text{Ca}(p, t)$ reaction 3-67211
- ^{48}Ca , $1f_{7/2}$ neutrons studied via $(^3\text{He}, \alpha_0)$, (d, t_0) and (p, d_0) reactions using DWBA anal. 3-74480
- Cd isotopes, odd-mass, Coriolis-coupling calc. of low-lying states 3-43180
- ^{105}Cd , multiparticle levels, decay scheme (*Russian*) 3-74487
- ^{107}Cd level scheme study through $^{107}\text{Ag}(p, n)$ and $^{106}\text{Cd}(d, p)$ reactions and ^{107}In decay 3-49154
- ^{112}Cd , ^{114}Cd 2^+ state excitation in (p, t) reactions, effect of inelastic scattering 3-46032
- ^{114}Cd , quadrupole moment of 2_1^+ state, calc. using boson expansion technique 3-49102
- ^{134}Ce excited states populated in ^{134}Pr decay 3-49184

nuclear energy levels continued

- ²⁴⁷Cf, from ²⁵¹Fm alpha decay, rotational band obs. and, Nilsson and single particle state assignments 3-67281
- ²⁵²Cf, decay product of ²⁵²Es by electron capture 3-54443
- ³⁴Cl from ³²S(p, γ)³⁴Cl, nuclear levels investigation 3-52102
- ³⁵Cl, from ³²S(α ,p)³⁵Cl reaction, meas. proton spectra, 20 MeV 3-62947
- ³⁵Cl, high-spin states obs. using ³²S(α , p) reaction, $\gamma\gamma$ coincidence, angular distrib., yield function meas. 3-74493
- ³⁶Cl, levels and spectroscopic factors from ³⁷Al(p,d) reaction 3-52097
- ⁶Co, A=243, 245, 247, review of Nilsson orbitals 3-40419
- ⁶Co, A=57, 59, 60, selective population of highly excited states by (α ,p) reaction 3-78346
- ⁵⁷Co, new energy levels found using ⁵⁷Fe(p,n)⁵⁷Co (German) 3-60196
- ⁴⁸Cr, from ⁴⁰Ca(¹⁰B, pnp), 19, 22.5, 25 MeV, γ -ray spectroscopy 3-62985
- ⁵⁰Cr, quadrupole deformation measurements of first excited states 3-49143
- ⁵¹Cr, angular momentum determ. for levels populated in ⁵⁰Cr(d,p) reaction (Russian) 3-52190
- ⁵²Cr, quadrupole deformation measurements of first excited states 3-49143
- ⁵³Cr, levels populated in ⁵²Cr(d,p) reaction at 10 MeV, polarised deuteron beam 3-49266
- ⁵³Cr high-spin states populated in ⁵⁰Ti(α ,n) reaction 3-52096
- ⁵³Cr, quadrupole deformation measurements of first excited states 3-49143
- ¹³⁷Cs, energy level scheme 3-40463
- ⁶¹Cu, ⁶⁴Cu, selective population of highly excited states by (α ,p) reaction 3-78346
- ⁶¹Cu structure determ. from ⁵⁸Ni(⁴He,p γ) reaction 3-67261
- Dy, A=158, 160, 162 pop. in Gd(α ,2n)Dy reaction, g factor meas. of high spin rotational states 3-67188
- Dy odd mass A=155-163, study by (³He, α) reaction 3-40420
- ¹⁶⁰Dy, A=158, 160, 162, struct. above 1.5 MeV, model anal. 3-78250
- ¹⁵⁵Dy, influence of rotation on moment of inertia of high-spin ground state members 3-52098
- ¹⁵⁹Dy, spreading width of rotational doorway states 3-67203
- ¹⁶¹Dy, Coulomb excitation of 43.8 keV state, Mossbauer effect study of transition 3-62990
- ¹⁶²Dy doublet splitting in even A deformed nuclei between excited 2 quasiparticle states 3-57478
- ¹⁵⁷Er, ¹⁵⁹Er, test of backbending models 3-71052
- ¹⁶⁰Er, influence of rotation on moment of inertia of high-spin ground state members 3-52098
- ¹⁶⁰Er, excited by electron bremsstrahlung, spin, parity, ground state transition widths 3-71057
- ¹⁶⁷Er (d, d') ¹⁶⁷Er, energy levels study 3-40413
- ¹⁶⁸Er, excited by electron bremsstrahlung, spin, parity, ground state transition widths 3-71057
- ¹⁶⁸Er, ground state, rotational bands, obs. by Ge(Li) spectroscopy of ¹⁶⁸Ho β -decay 3-67273
- ¹⁶⁸Er doublet splitting in even A deformed nuclei between excited 2 quasiparticle states 3-57478
- ¹⁷⁰Er, excited by electron bremsstrahlung, spin, parity, ground state transition widths 3-71057
- ¹⁵¹Eu, ¹⁵³Eu, hyperfine anomaly between ground and excited states 3-49207
- ¹⁷F, states from 3.8 and 4.8 MeV ¹⁵N(³He,n, γ)¹⁷F reaction 3-74603
- ¹⁹F, low-lying level struct. from electron scatt. studies 3-40482
- ¹⁹F, three particle structure, comparison with decay strengths from positive parity states 3-52113
- ¹⁹F from ¹⁶O(t, t) reaction, obs. resonances, levels of large triton partial width 3-60200
- ²⁰F β -emitter, determ. of quadrupole moment from n.m.r. meas. on polarised nuclei in MgF₂ 3-45947
- ⁵⁴Fe, 2+ state from ⁵⁴Fe(p,p'), differential cross section, spin-flip probability, asymmetry 3-78237
- ⁵⁵Fe, levels populated in ⁵⁴Fe(d,p) reaction at 10 MeV, polarised deuteron beam 3-49266
- ⁵⁵Fe from ⁵⁶Fe(d,t) reaction, low-lying levels study 3-74485
- ⁵⁶Fe, from neutron decay meas. in ⁵⁶Fe(p,n)⁵⁵Fe reaction 3-71101
- ⁵⁶Fe levels fed by ⁵⁶Mn β -decay (French) 3-78293
- ⁵⁶Fe(p,d)⁵⁵Fe, at 185 MeV, deep-lying hole states 3-52101
- ⁵⁶Fe, spin, parity assignment to doorway state resonance, from analysis of neutron scattering by ⁵⁶Fe 3-60177
- ⁵⁷Fe from ⁵⁶Fe(d,p)⁵⁷Fe, ground state doublet study 3-43215
- ²⁵⁰Fm, existence and assignments of isomer states, cross bombardment techniques 3-62950
- ²⁵¹Fm, alpha decay, single particle state assignment to ground level 3-67281
- Ga odd isotopes, coupling of three-particle (hole) valence-shell cluster to quadrupole vibrations 3-67238
- ⁶⁹Ga, obs. using photoexcitation, elastic and inelastic resonance decays at 7306, 6874 keV 3-62948
- ⁷⁰Ga from ⁷⁰Zn(p,n γ) reaction, 1.7-3.2 MeV, level 3-62931
- Gd even isotopes, A=150-158, population in (p,t) reaction, DWBA analysis 3-67336
- ¹⁵¹Gd spherical nucleus from ¹⁴⁹Sm(α ,2n)¹⁵¹Gd, 11-/2 [505] rotational band identification 3-74489
- ¹⁵³Gd, levels populated in ¹⁵³Gd(p,t) 3-52086
- ¹⁵³Gd from ¹⁵⁷Gd(p,t)¹⁵³Gd, energy level study 3-52086
- ⁶⁶Ge, A=67, 69, 71, meas. of quadrupole interaction on 9/2 and 5/2 levels in Zn and Ga by TDPAD 3-45949
- ⁶⁵Ge, ground state spin and parity 3-60131
- ⁶⁷Ge, magnetic moment of excited 9/2+ state by perturbed angular distrib. meas. on ⁶⁴Zn(α ,n) 3-45948
- ⁶⁹Ge, obs. from de-excitation gamma rays and conversion electrons in ⁶⁹Ga(p,n)⁶⁹Ge reaction 3-54384
- ⁷¹Ge, from thermal neutron capture (Russian) 3-71083
- ³He ^{1,2}+ state below break-up threshold, Gammel-Brueckner potential 3-52107
- ⁴He excited states, effects of Λ - Σ coupling 3-67252
- ⁴He ^{1,2}+He, hyperon + rigid 3N core model, effects of Λ - Σ coupling 3-67251
- ³He, search for excited states with p + ⁶Li reaction, 35-56 MeV 3-49138

nuclear energy levels continued

- ³He ^{1,2}+ state below break-up threshold, Gammel-Brueckner potential 3-52107
- ⁴He, 0+ state, model with separable potential 3-78263
- ⁴He, calc. of bound state energies using four body integral eqns. 3-71053
- ⁴He, ground state, variational techniques, pseudometric approach, separation of centre-of-mass contributions 3-60074
- ⁴He, T=O state study from ²H(d,p) and ²H(d,n) 3-46017
- ⁴He excited states obs. in ²H(α ,dt)¹H sequential reaction at 70 MeV 3-63032
- ⁵He, ground and first excited state obs. from ⁷Li + d reaction 3-62954
- ⁵He, level structure determ. using ²H + ³He system 3-74556
- ⁵He excited states obs. in ²H(α ,pd)³H sequential reaction at 70 MeV 3-63032
- ⁴He excited states, effects of Λ - Σ coupling 3-67252
- Hf odd-neutron nucleides, rotational band structure from Yb(α , xn) reactions, Nilsson model 3-40417
- ¹⁶⁶Hf, from ¹⁵⁰Sm(²⁰Ne,4n), E=93 MeV, deduced levels, feeding times by recoil-distance Doppler shift measurements 3-60215
- ¹⁶⁸Hf, ¹⁷⁰Hf from ^{152,154}Sm(²⁰Ne,4n), E=86 MeV, deduced levels, feeding times by recoil-distance Doppler shift measurements 3-60215
- ¹⁷³Hf levels populated in decay of ¹⁷³Ta 3-40421
- ¹⁷⁵Hf, energy levels, state wave functions from 12 MeV ¹⁷⁶Hf(d,t)¹⁷⁵Hf reaction 3-74497
- ¹⁷⁶Hf, spacing of ground-state levels 3-67174
- ¹⁷⁷Hf, ground state h.f.s. 3-40412
- ¹⁷⁸Hf from ¹⁷⁸Lu decay, spin-parity assignments 3-67276
- ¹⁷⁹Hf, ground state h.f.s. 3-40412
- Hg neutron deficient isotopes, self-consistent calc. of possible shape transition 3-67180
- ¹⁸⁶Hg, Yrast states up to 14+ stable quadrupole deformation 3-67200
- ¹⁹⁹Hg, g-factor of 208 keV 3/2- state, meas. by ion implantation perturbed angular correlation technique 3-45970
- ¹⁶⁵Ho, from ¹⁶⁵Ho(n,n' γ), comparison with pair correlation model (Russian) 3-71059
- ¹⁶⁵Ho, populated in decay of ^{165m}Sm β 3-43207
- I odd isotopes, coupling of three particle (hole) valence-shell cluster to quadrupole vibrations 3-67238
- ¹²⁵I, 188 keV excited state, g-factor calc. by perturbed ang. correl. method 3-78243
- ¹²⁹I, orientation study of excited states populated in decay of ^{129m}Te, ^{129m}Te 3-52131
- ¹³⁵I pop. in ¹³⁵Te beta decay, proton particle states determ. 3-71050
- In odd mass isotopes, excited quadrupole deformation, theory 3-49142
- ¹¹⁵In, deformed and spherical states, numerical calc. of coexistence problem 3-54393
- ¹¹⁵In, from ¹¹⁵Cd decay, study of coexistence 3-49197
- ¹²In muonic atoms, magnetization distrib. of single-particle states and 2+ rotational states 3-49209
- ¹¹⁹In, energy level scheme 3-40463
- ¹⁸⁴Ir, effects of strong rotation-particle coupling, for two-quasiparticle systems 3-62942
- ¹⁸⁶Ir effects of strong rotation-particle coupling, for two-quasiparticle systems 3-62942
- ¹⁸⁷Ir, spin, parity and probability of depopulating transition determ. from ¹⁸⁷Pt decay scheme 3-71049
- ¹⁸⁹Ir, low lying levels, core-excitation model approach 3-71046
- ¹⁹¹Ir, low lying levels, core-excitation model approach 3-71046
- ¹⁹¹Ir, low-lying level struct. and e.m. props. 3-62953
- ¹⁹³Ir, low lying levels, core-excitation model approach 3-71046
- ¹⁹³Ir, low-lying level struct. and e.m. props. 3-62953
- La, odd-A isotopes, decoupled bond description using angular momentum projection method for coherent phonon state 3-45983
- La neutron deficient isotopes, energy level obs., prolate deformation 3-45976
- ¹³¹La levels populated in ¹³¹Ca beta decay, Coriolis effects (French) 3-52148
- ¹³³La \rightarrow ¹³³Ba, excited levels meas. 3-57472
- ¹³⁹La, energy level scheme 3-40463
- ¹⁴¹La, energy level scheme 3-40463
- ⁵Li, level structure determ. using ²H + ³H system 3-74556
- ⁶Li, isospin mixing, asymmetry energy depend., ³H(³He,d)⁶He 3-78306
- ⁶Li, isospin mixing study by deuteron decay meas., Mott-Schwinger interaction 3-71043
- ⁶Li, low lying states, three body wave function analysis 3-62944
- ⁶Li, resonance scattering of bremsstrahlung, low-lying level study 3-52094
- ¹⁶⁴Lu, struct. above 1.5 MeV, model anal. 3-78250
- ¹⁶¹Lu, γ -ray transition, deduced energy levels 3-54423
- ¹⁶⁷Lu, ¹⁶⁹Lu, levels populated in ¹⁶⁷Hf and ¹⁶⁹Hf decay, Nilsson model assignments 3-52147
- ¹⁷¹Lu, ¹⁷³Lu, one-quasiparticle state equilibrium deformations, influence on E1 transition probabilities 3-49216
- ¹⁷¹Lu, high-spin rotational states and evidence for $\Delta K=2$ and $\Delta K=4$ mixings 3-60077
- ¹⁷¹Lu, rot. bands, stripping reaction studies 3-62939
- ¹⁷³Lu, high-spin rotational states and evidence for $\Delta K=2$ and $\Delta K=4$ mixings 3-60077
- ¹⁷⁶Lu, mixing of $K^\pi=3^-$ and 4- bands 3-67198
- ¹⁷⁸Lu, from ¹⁷⁵Yb decay, spin-parity assignments 3-67276
- ²⁴Mg, deformations of ground bands determ. from electron scattering and rotational model 3-62926
- ²⁴Mg, level schemes deduced using variation after projection Hartree-Fock method 3-67245
- ²⁴Mg, particle-hole nature for two lowest 3- states, direct reaction study 3-49151
- ²⁴Mg, shell model calcs. 3-62951
- ²⁴Mg(p,d)²³Mg, at 185 MeV, deep-lying hole states 3-52101
- ²⁷Mg, ²⁸Mg, shell model calcs. using modified surface-delta-interaction Hamiltonian 3-49167
- Mn odd isotopes, coupling of three-particle (hole) valence-shell cluster to quadrupole vibration 3-67238
- ⁵⁰Mn pop. in ⁵⁰Cr(p,n)⁵⁰Mn, determ. separation of isomeric levels from beta+ decay threshold energies 3-67212

nuclear energy levels continued

- ⁵³Mn, excited state obs. by ⁵³Cr(p,n_p) reaction 3-67192
⁵⁴Mn, levels up to 4.3 MeV excitation using spectroscopic method on ⁵⁶Fe(d,α) reaction 3-60201
⁹¹Mo, high spin states populated in α-particle induced reactions 3-78249
⁹⁴Mo from ⁹⁵Mo(p,d) reaction l-values and spectroscopic factors for low-lying states 3-63049
⁹⁶Mo from ⁹⁷Mo(p,d) reaction l-values and spectroscopic factors for low-lying states 3-63049
⁹⁸Mo, product of ¹⁰⁰Mo(p,t), 19 MeV, cross section measurements, search for excited rotational band, spin and parity assignments 3-54390
¹²¹N, apparent reaction dependence of width of first excited state in ¹²C(d,n)¹²¹N* reaction 3-62945
¹²¹N, f-wave decay of 8.9 MeV level, proton spin slip in ¹²C(p, p₁)¹²C 3-74590
¹²³N, obs. of new T=1/2 levels scattering of polarised protons on ¹²C (German) 3-49139
¹²³N from ¹²C(p, p₀) and ¹²C(p, p₁), high-energy levels study 3-52085
¹⁴N, 3-, 5.83 level excited in ¹²C(He,p) reaction, recoil into gas and Blume-Scherer model 3-49083
¹⁴N, deduced from ¹⁴C(d,d), optical model anal. 3-78343
¹⁴N level structure determ. from ¹⁰B(α,α')¹⁰B reaction excitation functions and α-particle decay 3-71055
¹⁴N(p,d)¹³N, at 185 MeV, deep-lying hole states 3-52101
¹⁵N, from ¹³C(d,p₀), E=1-4 MeV, cross sections, giant dipole resonance region 3-67341
¹⁵N, level study using ¹⁴C(p,p₀) reaction at low energy 3-49255
¹⁵N levels populated following muon capture by ¹⁶O 3-52149
¹⁵N non-normal parity states, shell model calc. 3-74482
²²Na pop in ¹⁰B(¹⁶O,α) reaction, selection of strong candidates for high spin members of bands 3-67364
²³Na from ¹²C(¹²C, p)²³Na, high spin states study 3-49185
²⁴Na, from ²³Na(d, p), 2.5 and 2.8 MeV, deduced levels, branching ratios 3-63063
²⁵Na, level scheme determ. using ²⁶Mg(d, τ) reaction, spectroscopic factors 3-52095
⁹³Nb, product of ⁹²Zr(α, p), 14.77 MeV, γ-decay of low lying levels 3-57491
¹⁴²Nd, N=82, levels populated in ¹⁴²Pr, ¹⁴²Pm β decays, spin and parity assignments 3-49155
¹⁴²Nd, neutron particle-hole states population in ¹⁴²Nd(p, p') and ¹⁴³Nd(d, t) 3-67325
²⁰Ne, assignments to high-spin negative parity states from angular correlation meas. 3-49136
²⁰Ne, α-widths and spectroscopic factors of ground-state band and first K=0- band 3-62943
²⁰Ne, deformations of ground bands determ. from electron scattering and rotational model 3-62926
²⁰Ne, excited states, Tamm-Dancoff calc. 3-49156
²⁰Ne, ground-state rotational band study from ¹⁶O α-transfer reactions 3-45980
²⁰Ne, K=0- band levels, alpha-decay widths of model wave functions calc. 3-60133
²⁰Ne, level schemes deduced using variation after projection Hartree-Fock method 3-67245
²⁰Ne generator coordinate method rel. to low lying nuclear states 3-60094
²⁰Ne(α, α')²⁰Ne, 104 MeV α-particle scatt., nucl. density distrib., size and shape 3-54498
²⁰Ne(α, α')²⁰Ne, 104 MeV α-particles, differential cross sections, anal. using deformed folding model 3-54498
²¹Ne, compound state obs. in total neutron yield from ¹⁷O(α, n)²⁰Ne 3-40507
²²Ne, compound state obs. in total neutron yield from ¹⁸O(α, n)²¹Ne 3-40507
Ni, highly excited levels, study by elastic and inelastic scattering of Fe capture gamma-rays 3-49241
Ni isotopes, energy spectra of normal parity states in shell model, effective-interaction calcs. 3-67210
⁵⁶Ni, effective interactions and 1f_{7/2} sub-shell closure in 2p-1f shell 3-49169
⁵⁹Ni level struct. from ⁵⁸Ni(d, p) at 8 MeV 3-45973
⁶⁰Ni, excitation energies by time-of-flight system 3-73884
⁶⁰Ni, from neutron decay meas. in ⁶⁰Ni(p, n)⁵⁹Ni reaction 3-71101
⁶⁰Ni, ground and excited states populated in Zn(d, ⁶Li) reaction 3-52195
⁶⁰Ni, proton configuration study using ⁵⁹Co(³He, d)_p reaction 3-52132
⁶²Ni, ground and excited states populated in Zn(d, ⁶Li) reaction 3-52195
⁶²Ni(¹²C, ¹¹B)⁶³Cu, j depend., finite-range calcs. 3-52203
⁶²Ni(¹⁶O, ¹³N)⁶³Cu, j depend., finite-range calcs. 3-52203
⁶⁹Ni, ground and excited states populated in Zn(d, ⁶Li) reaction 3-52195
²⁵⁴No, existence and assignments of isomer states, cross bombardment techniques 3-62950
O even isotopes, single-closed-shell, HF, HFB, BCS approximations 3-71070
¹⁴O excited states via ang. correl. obs. of ¹²C(³He, n)¹⁴O(p)¹³N at 12 MeV 3-40509
¹⁵O non-normal parity states, shell model calc. 3-74482
¹⁶O, 6.05 MeV 0+ state predicted by variational calc., B(E2) value in ¹⁸O(p, t) reaction 3-67177
¹⁶O, coexistence model for structure of giant dipole resonance, explt. test 3-49230
¹⁶O, negative parity T=0 states, SU(3) coupling in shell model calcs. 3-78253
¹⁶O non-normal parity states, shell model calc. 3-74482
¹⁶O structure determ. using interaction boson model 3-52099
¹⁶O(p, d)¹⁵O, at 185 MeV, deep-lying hole states 3-52101
¹⁷O, (d, p) reaction to unbound states, comparison with DWBA theory 3-54488
¹⁷O, compound state obs. in total neutron yield from ¹³C(α, n)¹⁶O 3-40507
¹⁷O, parities of 7.97 to 8.197 MeV states from meas. on ¹³C(α, n)¹⁶O reaction 3-67189
¹⁷O level structure, from neutron total cross sections 3-67209
¹⁷O unbound states populated in ¹⁷N β-decay 3-60121

nuclear energy levels continued

- Os, A=182, 184, 186 and 188, backbending and forking of yrast levels 3-71051
¹⁷⁸Os, from ¹⁵⁴Sm(²⁸Si, 4n), E=104 MeV, deduced levels, feeding times by recoil-distance Doppler shift measurements 3-60215
¹⁸²Os, ground state levels and γ-vibrational bands 3-67194
¹⁸³Os ground-state rotational band, back- and forwardbending, moment of inertia 3-74498
¹⁸⁴Os, ground state levels and γ-vibrational bands 3-67194
¹⁸⁴Os populated by ¹⁸⁴Ir decay and ¹⁸⁵Re(p, 2n_p) reaction 3-62941
¹⁸⁶Os, ground state levels and γ-vibrational bands 3-67194
¹⁸⁸Os, ground state levels and γ-vibrational bands 3-67194
¹⁸⁹Os, populated by ¹⁸⁹Re decay, excited level scheme, spin and parity assignments 3-54432
¹⁹⁰Os, ¹⁹²Os muonic atoms, magnetization distrib. of single-particle states and 2+ rotational states 3-49209
¹⁹²Os, γ-ray level depopulation 3-40414
²⁹P, levels up to 4.76 MeV populated in ²⁸Si(p, p) reaction 3-49144
³⁰P compound nucleus parameters from ²⁸Si(d, p)²⁹Si at 2-4.2 MeV 3-40503
³⁰P level characteriz. from proton scatt. on ²⁹Si at 2.5-3.4 MeV 3-60191
³²P, from ²⁹Si(α, p), E_α=10.65, 10.69, 11.00 MeV, deduced levels, mixing, branching ratios 3-60108
³²P, from ³¹P(d, p), E=10 MeV, angular distributions, deduced ln, spectroscopic factors 3-60198
³³P, level scheme, ang. correl. obs. 3-40449
²³¹Pa, product of ²³⁵Np α decay, α, β and γ transition probabilities, Coriolis interaction 3-57499
Pb, highly excited levels, study by elastic and inelastic scattering of Fe capture gamma-rays 3-49241
²⁰⁵Pb, high spin three neutron hole states of configurations, containing the i_{3/2} orbital 3-52100
²⁰⁷Pb, (1/2)⁺ doorway resonance, nuclear spreading width in particle-vibration model 3-74492
²⁰⁷Pb, neutron scatt. structure study, 13-17 MeV (Hungarian) 3-43239
²⁰⁸Pb, collective excitations study using 54 MeV inelastic proton scattering 3-63056
²⁰⁸Pb, inelastic electron scattering form factors of low-lying states, Migdal theory 3-49247
²⁰⁸Pb, RPA calcs. of low lying states, density dependent interaction 3-49153
²⁰⁹Pb, (1/2)⁺ doorway resonance, nuclear spreading width in particle-vibration model 3-74492
Pd, systematic behaviour of quasirotonal bands 3-67199
Pd isotopes, odd-mass, Coriolis-coupling calc. of low-lying states 3-43180
⁹⁸Pd, population of ground state band up to J=8 3-45975
¹⁰⁰Pd, ¹⁰²Pd, forking of ground state bands populated in heavy ion induced reactions 3-45975
¹⁰²Pd, level struct. using ⁹⁹Ru(α, n_p) reaction 3-40510
¹⁴³Pm, e.m. props. of low-lying levels, M2, E3 transition probabilities 3-67254
¹⁴⁷Pm, decay scheme, Ge(Li)-Ge(Li) coincidence studies 3-45994
¹⁵¹Pm, determ. from ¹⁵¹Nd decay 3-43220
¹⁵⁰Po, collective states, study with inelastic scattering of deuterons, protons, tritons 3-43183
²¹⁰Po, M1 core polarizabilities of 8+ and 6+ states, shell model calcs. 3-49117
²¹⁰Po₂, g(τh_{9/2}, J₂) difference for 6₁⁺ and 8₁⁺ states, DPAC^{9/2} meas. of lifetimes 3-45951
¹⁴¹Pr, γ-ray transition obs. in ¹⁴¹Nd decay scheme (Russian) 3-52092
¹⁴¹Pr magic nucleus, excitation of quasiproton states by ¹⁴¹Nd decay (Russian) 3-52092
Pt even isotopes, A=180 to 190, effect of quadrupole-pairing interaction on J_π=0⁺ vibr. 3-78256
¹⁹⁰Pt level scheme populated in ¹⁹⁰Au decay 3-67278
¹⁹²Pt, γ-ray level depopulation 3-40414
¹⁹⁴Pt, spins, multipole mixing ratios of γ-transitions, E2 ratio comparison with theory 3-54385
²³⁷Pu, A=237, 239, 241, review of Nilsson orbitals 3-40419
²³⁷Pu pop. in ²³⁸Pu(d, t) 12.1, 13.1 MeV obs. of five Nilsson orbitals 3-67197
²³⁸Pu, B(E3) values for octupole states and new Nilsson orbitals, (d, t) and (d, d') reactions 3-43185
²³⁹Pu, study by reactions ²³⁸Pu(d, p) and ²³⁹Pu(d, d') 3-40418
²³⁹Pu pop. in ²³⁸Pu(d, p) and ²³⁹Pu(d, d') 12.1, 13.1 MeV, obs. of Nilsson orbitals, K_π=1₂⁻ octupole band assignment 3-67197
⁸⁵Rb, ⁸⁷Rb, structure of levels from γ-transitions of Coulomb excited levels 3-40415
⁸⁵Rb, fast neutron scattering, energy level spectra of low lying levels 3-43249
⁸⁵Rb, produced in ⁸⁶Sr(³He, α)⁸⁵Rb, meas. α-particle spectra and ang. distrib. 3-71056
⁸⁷Rb, fast neutron scattering, energy level spectra of low lying levels 3-43249
¹⁰¹Rh, oriented, n.m.r., meas. gamma ray anisotropies and E2/M1 mixing ratios, proton states 3-74534
¹⁰³Rh, γ-γ directional correl. obs. 3-62997
Ru, isotopes, odd-mass, Coriolis-coupling calc. of low-lying states 3-43180
⁹³Ru, high spin states populated in α-particle induced reactions 3-78249
⁹⁴Ru, level structure up to 4 MeV excitation, study by ⁹⁶Ru(p, t) reaction 3-49147
¹⁰⁶Ru, low-lying levels associated with β- decay of ¹⁰⁶Tc 3-62952
¹⁰⁸Ru, low-lying levels associated with β- decay of ¹⁰⁸Tc 3-62952
⁹⁰S, low lying, γ-decay, ²⁸Si(³He, n) reaction, DSAM 3-78289
³¹S, 1₂⁺ and 3₂⁺ states excited in ³²S(p, d) reaction (Russian) 3-74569
³²S, first 3- levels excited by inelastic proton scattering (Russian) 3-74569
³²S, hexadecapole phonon states obs. using ³²S(p, p') 3-74583
³²S, lowest T=2 state characteriz. from ³¹P(p, p) 3-60190
³²S quadrupole and hexadecapole deformations, Hartree-Fock approx. 3-49179
³⁴S, 1₂⁺ and 3₂⁺ states excited in ³⁴S(p, d) reaction (Russian) 3-74569

nuclear energy levels continued

- ³³S, excitation in ³²S(d,p) reaction (*Russian*) 3-52189
³⁴S, first 3- levels excited by inelastic proton scattering (*Russian*) 3-74569
³⁴S from ³²S(t,p)³⁴S reaction, nature of (1f_{7/2})² states from distorted wave anal. 3-71054
Sb isotopes, possible 2p-1t configs. studied using Te(t,α) and Te(t,t) reactions (*Spanish*) 3-74484
¹¹⁷Sb, multiparticle levels, decay scheme (*Russian*) 3-74487
¹²²Sb, magnetic moment of 1.8 μs state g factor determ. by stroboscopic method 3-67187
¹³⁰Sb excited states populated in β-decay of 7- isomer and ground state of ¹³⁰Sn (*Russian*) 3-71085
¹³²Sb, proton-neutron-hole type states populated in decay of doubly magic ¹³²Sn (*Russian*) 3-74486
¹³²Sb, states with spin 4+ and parity 8-, β-decay (*Russian*) 3-74538
¹³³Sb pop. in ¹³³Sn β decay, proton particle states determ. 3-71050
⁴¹Sc, doorway state struct., ⁴⁰Ca inelastic proton scatt. 3-78319
⁴¹Sc produced in ⁴⁰Ca(³He,d₀)⁴¹Sc, 1f_{7/2} proton studied using DWBA anal. 3-74480
⁴²Sc, population in ⁴⁰Ca(α,d)⁴²Sc, 25.5 MeV, d ang. distrib. meas. 3-78246
⁴⁴Sc, determ. by γ decay study, spins, parities, struct. 3-78282
⁴⁴Sc, proposed K^π=0- band 3-49145
⁴⁴Sc excited states populated by ⁴¹K(α,np), decay modes and spin assignments, K^π=0- band 3-74495
⁴⁵Sc, K=3/2+ rotational band study using ⁴²Ca+α reaction 3-74494
Se, A=75, 77, 79, 81, 83, anomalous coupling states, calc. of nuclear moments 3-49115
Se, A=77, 79, 81, from thermal neutron capture (*Russian*) 3-71083
⁷⁸Se, level structure and γ-transitions following β+ decay of ⁷⁸Br 3-78247
²⁸Si, deformation from ¹⁶O+²⁸Si elastic and inelastic scattering, 33 to 38 MeV 3-63082
²⁸Si, deformations of ground bands determ. from electron scattering and rotational model 3-62926
²⁸Si, neutron elastic and inelastic backscattering at 14.2 MeV, time-of-flight spectroscopy, energy level obs. 3-74575
²⁸Si(p,d)²⁷Si, at 185 MeV, deep-lying hole states 3-52101
²⁸Si, 3.07, 3.62 and 4.08 MeV levels populated in ³¹P(d,α) reaction at E_d<4.0 MeV (*Russian*) 3-71118
²⁹Si, high spin negative parity states associated with oblate deformation, population in ²⁶Mg(α,n) 3-43171
²⁹Si, low-lying level struct. from ²⁸Si(d,p)²⁹Si at 2-4.2 MeV 3-40503
³⁰Si excitation energies in ²⁸Si(t,p)³⁰Si reaction 3-62940
Sm, A=150, 152, 154, 0.8-15 MeV, neutron total cross section differences, nuclear deformation effects 3-60188
¹⁴⁴Sm(p,p'), 9.3-11.0 MeV, analogue resonances, excited levels and low lying states 3-63046
¹⁴⁷Sm, obs. of new p-transitions and new levels from ¹⁴⁷Eu decay (*Russian*) 3-74525
¹⁴⁸Sm-¹⁵⁴Sm, transition from vibrational to deformed nucleus, boson expansion technique, quadrupole moments 3-49102
¹⁵⁰Sm, phenomenological collective model calculations (*Russian*) 3-71066
¹⁵¹Sm levels populated in ¹⁵¹Pm decay 3-78244
¹⁵¹Sm levels populated in (d,t), (d,p) and (³He,α) reactions 3-74594
¹⁵⁴Sm, excited by (n, n') reaction, determ. structure, spin and parity from γ-ray spectra 3-67196
Sn isotopes, interaction between collective and quasiparticle excitations, energies, wave functions, B(E2) values (*Russian*) 3-74514
Sn low-lying 2+ and 3- states, harmonic and anharmonic approxs. (*Russian*) 3-71047
Sn region, 11/2- states magnetic moment determ. using first-order core polarisation effects 3-67186
¹¹¹Sn, population in ¹¹²Sn(d,t) reaction, transfer angular momentum and spectroscopic factors 3-52104
¹¹³Sn, population in ¹¹²Sn(d,p) reaction, transfer angular momentum and spectroscopic factors 3-52104
¹¹⁴Sn, ¹¹⁶Sn 2+ state excitation in (p,t) reactions, effect of inelastic scattering 3-46032
¹¹⁹Sn, Mossbauer meas. of magnetic moment of 23.8 keV state and hyperfine anomaly 3-49208
¹²³Sn, population in ¹²²Sn(d,p) and ¹²⁴Sn(d,t) reaction, transfer angular momentum and spectroscopic factors 3-52104
¹²⁵Sn, pop. in (d,p) and (α,³He) reactions, neutron shell structure determ. 3-67213
¹³⁰Sn, excited two-neutron-hole states populated in ¹³⁰In decay (*Russian*) 3-71086
¹³⁰Sn, two-neutron-hole nucleus, excited states obs. in beta decay of ¹³⁰In 3-60081
¹³²Sn, doubly closed shell, population of first excited state in ¹³²In β-decay 3-49149
¹³²Sn, twice-magic, obs. of first excited state populated in ¹³²In beta decay (*Russian*) 3-71048
Sr isotopes, shell model for rotation-like spectra 3-60085
⁸⁷Sr levels, from ⁸³Ym.s. decay, spin-parity assignments 3-46007
⁸⁴Sr, populated in (p,t) reaction, low-lying excitations 3-54392
⁸⁶Sr, populated in (p,t) reaction, low-lying excitations 3-54392
⁸⁸Sr, mixing of giant magnetic dipole state with 1+ state at 3.49 MeV 3-60113
⁸⁸Sr(d,p)⁸⁹Sr, particle coupling to octupole state 3-46026
⁸⁸Sr(p,p')⁸⁸Sr, isobaric analogue resonances and particle coupling to octupole state 3-46026
¹⁷⁷Ta, populated in ¹⁷⁷W decay, γγ coincidence meas. (*Russian*) 3-74521
¹⁸⁴Ta, excited level struct., rel. to ¹⁸⁴Hf decay scheme 3-60129
¹⁶⁰Tb level scheme 3-43178
¹⁶¹Tb levels populated in ¹⁶¹Gd β- decay 3-43219
⁹³Tc, de-excitation study of high spin states 3-78248
¹⁰¹Tc, three particle and anomalous excited states populated in ¹⁰¹Mo decay (*Russian*) 3-49141
Te, A=128-120, 2+ state excitation in (p,t) reactions, effect of inelastic scattering 3-46032
Te low-lying 2+ and 3- states, harmonic and anharmonic approxs. (*Russian*) 3-71047
¹³²Te level scheme, from obs. of ¹³²Sb β-decay (*Russian*) 3-74538

nuclear energy levels continued

- ²³¹Th, ²³³Th, review of Nilsson orbitals 3-40419
⁴⁴Ti from ⁴⁰Ca(α,γ)⁴⁴Ti, rotational bands obs. 3-74490
⁴⁴Ti→⁴⁴Sc→⁴⁴Ca decay scheme (*Russian*) 3-52124
⁴⁵Ti, K=3/2+ rotational band study using ⁴²Ca+α reaction 3-74494
⁴⁷Ti levels populated in ⁴⁷V β-decay, spin and parity assignments 3-52146
⁵⁰Ti(p,p), high resolution cross section meas., 1.83-2.97 MeV 3-78324
²⁰³Tl, ²⁰⁵Tl muonic atoms, magnetization distrib. of single-particle states and 2+ rotational states 3-49209
¹⁶⁸Tm rot. band obs. in ¹⁶⁹Tm(d,t)¹⁶⁸Tm 3-63069
¹⁶⁹Tm, determ. of magnetic moments of 316, 379 keV excited states (*Japanese*) 3-74481
^eU, A=235, 237, 239, review of Nilsson orbitals 3-40419
²³³U levels populated in ²³³Pa decay 3-74535
²³⁴U, deduced from inelastic deuteron scattering 3-54388
²³⁵U, multilevel analysis of neutron capture and fission cross sections up to 60 eV 3-63094
²³⁶U, deduced from inelastic deuteron scattering 3-54388
²⁵⁶U, pop. in ²³⁵U(n,γ)²⁵⁶U reaction, γ-rays meas., spin of resonances 3-67335
^{234m}U, level scheme (*French*) 3-40465
⁴⁷V, low-lying levels populated in ⁴⁷Ti(p,n) and ⁴⁰Ca(¹⁰B,ppn) reactions 3-49146
⁴⁸V, low-lying level structure study using ⁵⁰Cr(d,α) reaction 3-57534
⁴⁸V, low-lying levels populated in ⁴⁰Ca(¹⁰B,pp) and ⁴⁰Ca(¹²C,ppnn) reactions 3-49135
⁵⁰V, low-lying level structure study using ⁵²Cr(d,α) reaction 3-57534
¹⁷⁹W, three quasiparticle states populated in ¹⁷⁹Re decay, microscopic model (*Russian*) 3-52089
¹⁸⁰W, spacing ground-state levels 3-67174
¹⁸¹W, excited states populated by ¹⁷⁹Hf(α, 2n) and ¹⁸⁰Hf(α, 3n) reactions, effects of Coriolis mixing 3-60079
¹⁸²W, from ¹⁸³W(d,t) and ¹⁸³W(³He,α), two quasiparticle states and collective excitations 3-57475
¹⁸²W, K^π=2- band study through g-factor meas. 3-67184
¹⁸²W, spacing of ground-state levels 3-67174
¹⁸⁴W, from ¹⁸²W(t, p), 20 MeV, deduced levels 3-63064
¹⁸⁴W, from ¹⁸³W(d,p), two quasiparticle states and collective excitations 3-57475
¹³⁰Xe, 0+ levels obs. using beta spectrum of ¹³⁰Cs (*Russian*) 3-67216
¹³⁰Xe, level structure determ. from beta-decay of ¹³⁰Im, ¹³⁰Ie and ¹³⁰Cs 3-67214
¹³²Xe, 668 keV state, perturbed angular correlation meas. for g-factor 3-78242
⁸⁷Y, populated in (p,t) reaction, low-lying excitations 3-54392
⁸⁸Y, two-hole multiplets from ⁸⁹Y(d,t) and ⁹⁰Zr(d,α) studies 3-54491
⁸⁹Y, 2p_{1/2} and 1g_{9/2} states pop in ⁸⁸Sr(¹⁶O, ¹⁵N)⁸⁹Y reaction, rel. to recoil effects 3-67363
⁹⁰Y, levels studied via ⁸⁹Y(p,p')⁸⁹Y*, shell model, conversion to analogue resonances 3-60176
Yb, even isotopes, γ-ray spectroscopic study, single-line Mossbauer absorption, Yb levels, deduced isomer shifts 3-60109
¹⁶⁸Yb, γ-band population by indirect (p,t) processes 3-46030
¹⁶⁸Yb, struct. above 1.5 MeV, model anal. 3-78250
¹⁶⁹Yb energy level scheme, study by ¹⁶⁹Lu decay obs. (*Russian*) 3-52090
¹⁷²Yb doublet splitting in even A deformed nuclei between excited 2 quasiparticle states 3-57478
¹⁷⁴Yb, pop. in ¹⁷³Yb(n,p) excited K=0 rotational bands 3-74533
⁶⁶Zn, selective population of highly excited states by (α,p) reaction 3-78346
⁶⁷Zn, magnetic moment of excited 9/2+ state by perturbed angular distrib. meas. on ⁶⁴Ni(α,n) 3-45948
⁶⁹Zn, from thermal neutron capture (*Russian*) 3-71083
⁸⁹Zr, high spin states populated in α-particle induced reactions 3-78249
⁹⁰Zr, excitation of levels by inelastic proton scattering at 40 MeV, distorted wave calcs. 3-63057
⁹¹Zr, levels populated in ⁹⁰Zr(d,p) reaction at 10 MeV, polarised deuteron beam 3-49266
⁹³Zr, neutron shell struct. from (d,p) and (α,³He) reactions 3-40504
⁹⁵Zr, excited levels population in ⁹⁵Y decay (*French*) 3-71087
⁹⁵Zr, neutron shell struct. from (d,p) and (α,³He) reactions 3-40504
⁹⁷Zr, neutron shell struct. from (d,p) and (α,³He) reactions 3-40504

nuclear engineering

- American Nuclear Society meeting, Chicago, USA, June 1973 3-63102
controlled thermonuclear fusion expts. and engineering aspects, conference, Austin, Texas, USA (Nov. 1972) 3-60295
design, computer aided instruction by conversational teaching programmes 3-62346
dosimetry, secondary standard, WHO Regional Reference Centres for, project implementation 3-54555
environmental radioactivity, International Reference Centre, activities 3-54554
European Nuclear Documentation Service, structure and features of system 3-74477
fast reactor, aseismic design, research and development in Japan 3-67511
fast reactor education, Pb slowing down time neutron spectrometer 3-63161
FTR power performance, analysis of engineering mockup critical expts. 3-49352
German, 4th nuclear program for 1973-76, overview (*German*) 3-43272
industrial and educational needs, role of the university 3-61957
Japanese industrial group's activities 3-63147
Japanese industries, Mitsubishi Group's activities 3-63146
Japanese industries, present state, overview 3-63140
practical reactor design, teaching at undergraduate level 3-61972
products, materials and services directory 3-39984
reactors, conference, Karlsruhe, Germany (April 1973) 3-67384

nuclear engineering continued

- review of future trends, cooperation between USSR and W. Germany 3-78365
- SNR-300, design of loop-concept reactor tank 3-40532
- standardization, responsibilities of industry and Atomic Energy Commission 3-67383
- standards, education 3-61959
- standards, information availability 3-74620
- standards, responsibilities of industry and Atomic Energy Commission 3-67382
- standards program, status 3-67381
- storage of fissile solutions, vessel design and analysis 3-63149
- turbulence theory, Navier-Stokes eqns. closure problems, review 3-78956

nuclear excitation

- see also isobaric analogue states; Mossbauer effect; nuclear energy level transitions; nuclear energy levels
- 0⁺ excit. in even actinide nuclei, calcs. based on finite Fermi systems 3-45981
- 1p-shell nuclei, giant magnetic dipole analogue excitations by allowed muon capture 3-60126
- collective states in A=40, 90, 208 nuclei, form factors (Russian) 3-67237
- Coulomb, determ. of E2 static moments and E2, E4 transition moments 3-45935
- Coulomb, Doppler shift attenuation of γ -rays lifetime determ. (Russian) 3-71074
- Coulomb, quantum mechanical coupled channel code for higher lying states 3-46014
- Coulomb, reorientation effect, meas. of static quadrupole moments 3-46038
- Coulomb excitation of short-lived states, magnetic moment meas. by recoil-into-gas method 3-45934
- Coulomb mixing intensity between T=T₀ isobaric analogue state and T=T₀-1 monopolar excitations (Russian) 3-74488
- deformation, finite and ellipsoidal, in collective model 3-60100
- electroexcitation form factors and fixed-polarity sum rules 3-49244
- electron transition process, virtual photon absorption, electromagnetic interaction 3-57507
- even-even nuclei, quadrupole moments of excited states by reorientation effect in Coulomb excitation 3-54379
- fissile nuclei, disappearance of shell effect on heating, 60-80 MeV 3-78266
- gamma ray excitation from radioactive sources 3-67305
- giant multipole resonant state of E2 character excited in various nuclei by ³He scatt. 3-60202
- giant resonance excitation of doubly closed shell nuclei, spin dependent effects 3-78297
- by high energy electrons, protons, pions, alpha particles, comparative analysis 3-60164
- inelastic proton scattering, 30 MeV, target excitations and optical potential 3-49256
- level excitation by electrons and hadrons at high energy 3-60162
- light nuclei, Coulomb excitation, polarizability and static quadrupole moment 3-45936
- light nuclei, kinetic energy, internucleon interaction, binding and excitation energies 3-40407
- magic nuclei, collective excitation, variational calc. of binding energies and spectra (Russian) 3-71064
- muon capture rates, excitation energy dependence 3-74540
- particles of near barrier energies, quasicalssical variant of the coupled-channel method (Russian) 3-67288
- quasi-particle excitation model, applicability near saddle point of fissionable nuclei (Russian) 3-40525
- rare-earth deformed nuclei, number-conserving treatment of the BCS-Tamm-Dancoff approximation 3-43191
- rotational, extension of Belyaev-Zelevinski method 3-67242
- spectra, low frequency, of even-even nuclei near closed shell 3-67206
- tensor degree of freedom spin depend., nucleon-lepton interaction 3-78236
- v-induced, weak and e.m. interactions, low energy cross sections (Russian) 3-63041
- ¹⁰⁹Ag Coulomb excitation, meas. of quadrupole moments of first 3/2⁻ and 5/2⁻ states 3-71040
- ³⁷Ar, average level width at excitation energies near 17 MeV studied in ³⁵Cl (d,p) ³⁶Cl 3-63062
- ²¹¹At, excitation functions and recoil ranges from ⁸⁴Kr-induced reactions on ²⁰⁹Bi 3-63084
- Au, muonic transitions (French) 3-54603
- ¹⁹⁷Au(d,pxn)¹⁹⁸-¹⁹⁹Au, 25-86 MeV, excitation function meas., equilibrium statistical and hybrid models 3-57532
- ¹⁹⁷Au(d,xn)¹⁹⁹-²⁰⁰Hg, 25-86 MeV, excitation function meas., equilibrium statistical and hybrid models 3-57532
- ¹²B analogue state, excitation during charged pion photoproduction from ¹²C 3-49240
- ²⁰⁹Bi, radiative proton capture cross sections, 10 to 50 MeV, excitation function 3-78318
- ⁷⁹Br, E2 and M1 reduced transition probabilities, core excitation calc. 3-46005
- ⁸¹Br, E2 and M1 reduced transition probabilities, core excitation calc. 3-46005
- ¹²C(n,n')¹²C* (4.44 MeV), neutron spin flip at 15.0 MeV, γ -ray coincidence meas. 3-60195
- ¹⁴C(¹²C,¹²C)¹⁴C elastic scatt., excitation functions near Coulomb barrier 3-49283
- ¹⁴C(¹²C, α)²²Ne, excitation functions near Coulomb barrier 3-49283
- ¹⁴C(¹²C,d)²⁴Na, excitation functions near Coulomb barrier 3-49283
- ¹⁴C(¹²C,t)²³Na, excitation functions near Coulomb barrier 3-49283
- ⁴⁰Ca, random phase approx. calc. of excitation energy of breathing modes 3-52119
- ⁴⁰Ca(p,p') reaction, excitation of lowest 3- and 5- levels 3-43250
- ⁴²Ca, ⁴⁶Ca, Coulomb excitation of 2⁺ states, ratio between B(E2) values 3-49193
- ⁴⁸Ca(¹⁴N, ¹³C)⁴⁹Sc, possible L-dependent angular distributions 3-54503
- Cd even isotopes, B(E2; 0 \rightarrow 2) values from ⁴He inelastic excitation probabilities 3-46036
- ¹⁰⁷Cd level scheme study through ¹⁰⁷Ag (p, η) and ¹⁰⁶Cd(d,pp) reactions and ¹⁰⁷In decay 3-49154

nuclear excitation continued

- ¹⁴⁰Ce(¹⁶O, ¹⁵N)¹⁴¹Pr, E=56 to 63 MeV, measure excitation functions, DWBA analysis 3-71127
- ¹⁴⁰Ce(¹⁸O, ¹⁷O)¹⁴¹Ce, E=56 to 61 MeV, measure excitation functions, DWBA analysis 3-71127
- ⁴⁸Cr prod. from reactions involving ⁵⁰Cr* compound-system, excitation functions 3-40512
- ⁵⁰Cr* compound-system, test of independence postulate in Bohr theory 3-40512
- ⁵³Cr, Coulomb excitation by ³²S, reorientation effect, static quadrupole moment determ. 3-46038
- ¹³³Cs(α , α'), Coulomb excitation, 6-11 MeV, meas. of de-excitation γ -rays 3-52200
- Dy, A=162, 164, Coulomb excitation, electric quadrupole and hexadecapole transition moments 3-49201
- ¹⁵⁹Dy, rotational excitation properties 3-43212
- ¹⁶¹Dy, Coulomb excitation of 43.8 keV state, Mossbauer effect study of transition 3-62990
- Er, A=166, 168, 170, Coulomb excitation, electric quadrupole and hexadecapole transition moments 3-49201
- ¹⁶⁷Er (d, d') ¹⁶⁷Er, energy levels study 3-40413
- ¹⁷⁰Er, Coulomb excitation by ⁸¹Br, reorientation effect, static quadrupole moment determ. 3-46038
- ¹⁷⁰Er, static quadrupole moment of first 2⁺ state by Coulomb excitation using ⁸¹Br 3-62935
- ⁵⁶Fe, Coulomb excitation by ¹⁶O, reorientation effect, energy dependence 3-46038
- ⁵⁷Fe from ⁵⁶Fe(d,p)⁵⁷Fe, ground state doublet study 3-43215
- Gd, A=158, 160, Coulomb excitation, electric quadrupole and hexadecapole transition moments 3-49201
- ³He, search for excited states with p + ⁶Li reaction, 35-56 MeV 3-49138
- ¹²¹I(α , α'), Coulomb excitation, 6-11 MeV, meas. of de-excitation γ -rays 3-52200
- ¹²⁹I(α , α'), Coulomb excitation, 6-11 MeV, meas. of de-excitation γ -rays 3-52200
- ³⁹K(d,d'), inelastic scattering, 12.8 MeV, microscopic analysis of 2.52 MeV state excitation 3-49267
- ⁶Li, electroexcitation form factors and fixed-polarity sum rules 3-49244
- ⁶Li(⁶Li, ⁶He)⁶Be, ang. distrib. and excitation functions 3-52202
- ⁶Li(⁶Li, ⁶Li*)(3.56), ang. distrib. and excitation functions 3-52202
- ⁷Li, Coulomb excitation, E1 polarisation, ²⁰⁸Pb(⁷Li,⁷Li') γ 3-78288
- ¹²N analogue state, excitation during charged pion photoproduction from ¹²C 3-49240
- ¹⁴N, optical model anal. of ¹⁴C(d,d), 4-10 MeV 3-78343
- ¹⁴²Nd, neutron particle-hole states population in ¹⁴²Nd(p,p') and ¹⁴³Nd(d,t) 3-67325
- ¹⁴²Nd(¹⁶O, ¹⁶O)¹⁴²Nd, 54-72 MeV, interference of Coulomb and nuclear excitation, B(E2) values and optical model 3-52201
- ²⁰Ne(α ,n)²³Ne, threshold to 31 MeV, evidence for boson-mode excitations 3-60214
- ²²Ne(p,t)²⁰Ne, inelastic excitation effects, coupled-channel-Born-approx. analysis of allowed and forbidden transitions 3-67332
- ⁵⁸Ni(¹⁶O, ¹⁶O)⁵⁸Ni, 35-60 MeV, interference of Coulomb and nuclear excitation, B(E2) values and optical model 3-52201
- ⁶⁰Ni(e,e'), quadrupole and giant dipole resonance excitation, form factors, characteristics (Russian) 3-71104
- ¹⁶O, random phase approx. calc. of excitation energy of breathing modes 3-52119
- ¹⁶O(α ,n)¹⁹Ne, threshold to 26 MeV, evidence for boson-mode excitations 3-60214
- ¹⁸O lifetimes and excitation energies from ¹⁹F(t, α) γ 3-54490
- ³⁰P compound nucleus parameters from ²⁸Si(d,p)²⁹Si at 2-4.2 MeV 3-40503
- Pb isotopes, rel. to muonic X-ray spectrum 3-63351
- ²⁰⁸Pb, Coulomb excitation with heavy ions, static quadrupole moment of 3⁻ state from γ -ray meas. 3-49101
- ²⁰⁸Pb, electroexcitation of giant resonances 3-43236
- ²⁰⁸Pb, nucl. response function, excitation props., numerical calc. method 3-52120
- ²⁰⁸Pb, RPA calcs. of excitation energies and probabilities of low lying states 3-49153
- ²⁰⁸Pb, random phase approx. calc. of excitation energy of breathing modes 3-52119
- Pd, Coulomb excitation in Pd-Fe target, transient magnetic field effects on recoil in Fe lattice, γ -ray meas. 3-49269
- ²³⁷Pu, relative excitations of spontaneous fission shape isomers 3-71136
- ²¹⁰Rn, excitation functions and recoil ranges from ⁸⁴Kr-induced reactions on ²⁰⁹Bi 3-63084
- ²¹¹Rn, excitation functions and recoil ranges from ⁸⁴Kr-induced reactions on ²⁰⁹Bi 3-63084
- Ru, Coulomb excitation in Ru-Fe target, transient magnetic field effects on recoil in Fe lattice, γ -ray meas. 3-49269
- ⁹⁶Ru, ¹⁶O irradiation, excitation function of α -emitters (Russian) 3-57497
- ³⁵S, from ³⁴S(d,p) reaction, excitation functions for transitions to lowest states Ericson fluctuation theory 3-67339
- ²⁸Si inelastic scattering of 25.25 MeV polarised protons, ground state rotational band excitation 3-52174
- Sm, A=148, 150, 152, Coulomb excitation, determ. of static quadrupole moments of first excited states 3-49113
- Sm, A=152, 154, Coulomb excitation, electric quadrupole and hexadecapole transition moments 3-49201
- ¹⁵²Sm, ¹⁵⁴Sm, Coulomb excitation of 2⁺ and 4⁺ levels, determ. of E4 moments 3-49202
- ¹²⁰Sn, random phase approx. calc. of excitation energy of breathing modes 3-52119
- ⁸⁸Sr(¹⁶O, ¹⁵N)⁸⁹Y, E=42.5 to 50 MeV, measure excitation functions, DWBA analysis 3-71127
- ⁸⁸Sr(¹⁶O, ¹⁶O)⁸⁸Sr, 45-60 MeV, interference of Coulomb and nuclear excitation, B(E2) values and optical model 3-52201
- ⁸⁸Sr(d,p)⁸⁹Sr, excitation function anomaly effects at neutron analogue channel threshold 3-40500
- ¹⁰⁹Te, delayed proton emission, excitation function, statistical model analysis, β -decay strength function (Russian) 3-57497
- ⁴⁸V prod. from reactions involving ⁵⁰Cr* compound-system, excitation functions 3-40512

nuclear excitation continued

- W, A = 182, 184, 186, Coulomb excitation with ^{16}O , meas. of quadrupole interaction in Te crystal (*German*) 3-49187
 ^{168}Yb , γ -band population by indirect (p,t) processes 3-46030
 ^{90}Zr , random phase approx. calc. of excitation energy of breathing modes 3-52119

nuclear explosions

see also *nuclear fission; weapons*

- air burst, neutron transport derived using Monte Carlo calcs. 3-74621
 Amchitka Island Test Site events, seismic surface waves rel. to source mechanism 3-53413
 atmospheric ionization and radar wave attenuation 3-54550
 atmospheric production from past nuclear explosions, O_3 measurements 3-65348
 BOXCAR, freq. domain response 3-58878
 CANNIKIN, close-in ground motion 3-50899
 CANNIKIN, ground deform. meas. 3-50900
 CANNIKIN, ground shock effects on shallow onshore waters 3-51209
 CANNIKIN, hydrological effects 3-51208
 CANNIKIN, long-period water-wave meas. 3-53439
 CANNIKIN, quasi-static mag. field changes 3-50962
 CANNIKIN, secular strain meas. in Aleutian Islands 3-50896
 CANNIKIN, seismic and tectonic related events 3-50893
 CANNIKIN, strain and tilt data 3-50898
 CANNIKIN, strain and tilt meas. 3-50897
 CANNIKIN, T-phase radiation, sofar hydrophone recordings 3-53401
 CANNIKIN, visible geological effects 3-50901
 CANNIKIN nuclear explosion, predicted and postshot geological and geophysical factors 3-50891
 CANNIKIN tectonic strain-release meas. from seismic surface waves 3-50894
 CANNIKIN underground nuclear explosion at Amchitka, seismic results 3-44837
 9th Chinese atmospheric nuclear test, Sr meas. in air and rain 3-53476
 decaying spherical shocks in solid, linear Q effects, finite difference calcs. 3-70648
 detection, large seismic arrays 3-65180
 earth core, velocity model, revised, travel times and amplitudes, earthquakes and underground nuclear explosions 3-80619
 ejecta distribution, row charge, mathematical/physical model 3-63239
 elapsed time estimation, activity of ^{95}Nb in radioactive fallout (*Japanese*) 3-57585
 energy release, pressure effects, comparison with chemical simulations 3-67620
 fast breeder reactor safety, critical excursion 3-67622
 fast reactor, core meltdown accident and vessel response, obs. 3-67621
 fast reactor structure, rapid energy release, mechanical effects, assessment 3-67536
 HANDLEY, multipole source model for strain-step field 3-56014
 Lightning induced by nuclear bursts 3-80757
 lower mantle shear wave travel times from nuclear explosions 3-58887
 microfission explosions, application to controlled release of thermo-nuclear energy 3-63233
 MILROW, close-in ground motion 3-50899
 MILROW, long-period water-wave meas. 3-53439
 MILROW, seismic and tectonic related events 3-50893
 neutron source for ^{249}Cf induced fission, cross section in 13 eV to 3 MeV range 3-78358
 PKIKP phases, amplitude meas., identification from nuclear explosions and earthquakes 3-80648
 S. Nevada, nuclear explosions and cavity collapses, radiation of Rayleigh wave energy 3-44785
 seismological discrimination between earthquakes and underground explosions 3-56021
 Semipalatinsk underground nuclear explosions, source parameters, P-wave spectra 3-44826
 spallation and generation of surface waves by underground explosion 3-53414
 underground, amplitude yield scaling, slope parameter 3-76505
 underground, rock melt, shock wave energy deposition 3-58875
 underground, seismic magnitudes estimation 3-56011
 underground, seismic moment, long-period radiation, value of explosive point source model 3-80609
 underground, thermal effects and possible uses 3-57586
 underground, Yucca Flat, seismic spectra 3-44780
 underground explosions, local seismic phenomena immediately after event 3-50933
 β -decay characteristics of hot particles (*Japanese*) 3-54551

nuclear field theory see *quantum field theory*

nuclear fission

- see also *fission counters; nuclear explosions; nuclear fission of uranium; nuclear fission products; nuclear reactors; photofission*
 actinide region, dynamics, cranking model calcs., role of reflection asymmetry in shape 3-49288
 asymmetric, semi-classical level density theory, shell-effects 3-49290
 asymmetry considerations, two-centre shell model generalization 3-43264
 Cm isotopes A = 244 to 250, barrier height meas., effects near and nature of N = 152 shell 3-71134
 critical assemblies, effect of space-dependent fission matrices in transport calcs. 3-71221
 double-hump barrier of Strutinsky type, penetrability 3-49285
 double-hump barriers, penetrability 3-74610
 energy dependent spatial mesh approximation, static few-group diffusion equations, coupling via scattering and fission 3-63118
 excited nuclei, statistical theory of decay, competition between fission and evaporation 3-43263
 fast fission factor calc. using Monte Carlo methods in reactor core calcs. (*German*) 3-74643
 Galaxy, r-process path termination in nuclear yield ratio dating 3-73437

nuclear fission continued

- glass fission-fragment tract detectors, angular characteristics 3-53985
 heavy and superheavy nuclei, binding energy and stability study (*Russian*) 3-52067
 heavy and superheavy nuclei, calcs. of fission barriers 3-54520
 heavy and superheavy nuclei, spurious state contribs. in shape and stability calcs. 3-45926
 in-core fission chambers, gas-loss compensation 3-71182
 laser induced, shock and compression by laser pulses enhanced by liq. layers on solid surfaces 3-57245
 light nuclei with ang. momenta near liquid-drop limit 3-63093
 liquid-drop model, charge vibrs. 3-78360
 LMFBR design, improvement of physical techniques and calculations 3-71195
 mass asymmetry as dynamic process described by collective coordinate 3-60236
 mass resolution, in fission-fragment double-kinetic-energy measurements 3-51670
 micro fission-fusion chain reactions, bootstrap mode coupling and critical mass reduction 3-54514
 micro-fission chain reactions, application to controlled release of thermonuclear energy 3-52215
 microcritical mass, by supercompression, for producing ultrastrong mag. fields and particle acceleration 3-54513
 multigroup neutron cross section adjustment by correlation method 3-43262
 neutron emission probabilities from delayed neutron precursors 3-67280
 neutron induced, obs. (*French*) 3-60228
 neutron reaction cross sections, multiple reaction correction 3-67320
 parity, spatial violation, through the two hump barrier 3-67379
 partial widths of resonance levels in fissile nuclei, spin-dependent statistics 3-67376
 penetrability through double-hump fission barriers, F-matrix calc. 3-52213
 potential barrier, two-bump penetration influence of fission potential on penetrance curve (*Russian*) 3-67223
 power plant calorimetrics, energy release in fission, isotopic composition of spent fuel 3-54529
 prompt neutrons, anal. using equilib. statistical model 3-43267
 quasi-particle excitation model, applicability near saddle point of fissionable nuclei (*Russian*) 3-40525
 r-process cycle times, rel. to astrophysical superheavy element synthesis 3-65620
 rate determ. rel. to reactor control by activation of Dy-Al-wires, power ratio of weakly coupled cores 3-63129
 reactor criticality safety, measurement requirements 3-67406
 resonance levels, correlation between fission and reduced neutron widths 3-54512
 review, potential energy surfaces of deformed heavy nuclei, two-centre shell model, superheavy nuclei (*Japanese*) 3-71133
 shape isomerism of fissioning nuclei 3-62928
 shape isomers, spontaneously fissioning, properties of quadrupole vibrational states 3-45984
 spontaneous, cranking model calc. of life-time (*German*) 3-49286
 stellar plasma, dense, fission barrier reduction, shell and surface symmetry effects and superheavy elements 3-69940
 storage of fissile solutions, vessel design and analysis 3-63149
 superheavy elements and actinides prod. by secondary reactions in W targets 3-60232
 ternary, in liquid drop model, determ. of saddlepoint energies 3-52214
 thermal neutron cross-section of fissionable elements in multilevel-multichannel formalism (*Rumanian*) 3-49291
 track dating applications in art and archaeology, review 3-53809
 transuranium elements, ratio evaporative to fission width Γ_n/Γ_f , energy dependence (*Russian*) 3-57548
 two-centre shell model with Lawrence family of liquid-drop shapes as equipotentials 3-49289
 ^{227}Ac , symmetric, asymmetric near fission threshold, direct reactions ^3He beam on ^{226}Ra target 3-60238
 ^{228}Ac , symmetric, asymmetric near fission threshold, direct reactions ^3He beam on ^{226}Ra target 3-60238
 Am, spontaneously fissioning isomer prod. in 14 MeV neutron reactions 3-71132
 ^{240}Am spontaneously fissionable isomer, decay, search for α -emission (*Russian*) 3-40470
 ^{241}Am , neutron induced, Kr and Xe yields 3-67378
 ^{242}Am , neutron induced, Kr and Xe yields 3-67378
 ^{242}Am spontaneously fissionable isomer, decay, search for α -emission (*Russian*) 3-40470
 ^{197}Au , induced by 70-200 MeV protons, cross section and angular anisotropy (*Russian*) 3-40523
 ^{209}Bi , 1 GeV proton bombardment, angular distribution of fragments, momentum transfer (*Russian*) 3-57547
 ^{209}Bi , induced by 1 GeV protons, angular correlations of mass and energy distrib. of fragments (*Russian*) 3-40524
 ^{249}Cf , neutron induced fission cross section using neutrons from underground nuclear explosion 3-78358
 ^{252}Cf , spontaneous, X-ray spectra at different kinetic energies of light fragments, mass yield fine structure (*Russian*) 3-40522
 ^{252}Cf , triple fission, angular, energy spectra of α particles and neutrons 3-78363
 ^{252}Cf spontaneous fission neutrons, meas. of $^{235,238}\text{U}$ fission cross-sections 3-49294
 ^{259}Cf , ternary fission, observation of ^3He , neutron spectra 3-43261
 ^{244}Cm , ^{246}Cm , spontaneous, prompt neutron multiplicity, dispersion 3-78364
 ^{246}Cm , coincident fragment energy meas. deduce pre neutron emission mass and total KE distrib. 3-71135
 $^{246}\text{Cm}(^{16}\text{O},\text{F})$, 102.5 MeV, fragment kinetic energy, comparison with static scission model and fission systematics predictions 3-74616
 ^{248}Cm , pot. energy calcs., asymmetry 3-43264
 ^{252}Fm , pot. energy calcs., asymmetry 3-43264
 ^{257}Fm spontaneous fission, meas. of average number of prompt neutrons emitted 3-71138
 ^{258}Fm , pot. energy calcs., asymmetry, symmetric fission preference 3-43264

nuclear fission continued

- ²⁶⁴Fm, pot. energy calcs., asymmetry, symmetric fission preference 3-43264
- Np, spontaneously fissioning isomer prod. in 14 MeV neutron reactions 3-71132
- ²³⁶Np, search for fissioning isomers in region of 60 μ s half-life 3-78357
- ²³⁷Np, neutron induced, Kr and Xe yields 3-67378
- ²³⁸Np, neutron induced, Kr and Xe yields 3-67378
- Pb, induced by 12.2 GeV protons, binary and ternary fission 3-52216
- ⁶Pb, A = 206-208, induced by 70-200 MeV protons, cross section and angular anisotropy (*Russian*) 3-40523
- ²⁰²Pb, pot. energy calcs., asymmetry, symmetric fission preference 3-43264
- ²¹⁰Po, pot. energy calcs., asymmetry, symmetric fission preference 3-43264
- Pt, induced by 12.2 GeV protons, binary and ternary fission 3-52216
- Pu, spontaneously fissioning isomer prod. in 14 MeV neutron reactions 3-71132
- ²³⁷Pu, spontaneous, relative excitations of the shape isomers 3-71136
- ²³⁸Pu, 18 eV to 3 MeV n-induced fission, resonance cross-sections 3-74613
- ²³⁹Pu, anomaly of fission reaction threshold from 1.5 to 7.5 MeV 3-52212
- ²³⁹Pu, composite nuclei, nucleon pairing effects, two lumped fission barrier 3-40521
- ²³⁹Pu, energy spectrum, angular distribution of ⁴He and ⁶He fission products 3-54517
- ²³⁹Pu, neutron induced, meas. of prompt ν -values in fast and thermalised fluxes 3-60229
- ²³⁹Pu, neutron-induced cross-section below 30 keV, high resolution meas. 3-60234
- ²³⁹Pu, partial widths of resonance levels in fissile nuclei, spin-dependent statistics 3-67376
- ²³⁹Pu, power, photon spectrum and neutron prodn., calc. by ORIGEN computer code 3-43284
- ²³⁹Pu, thermal, delayed neutron energy spectra meas. using gas-filled proton recoil proportional counters 3-49292
- ²³⁹Pu, thermal neutron capture, probability of formation of spontaneously fissionable isomer states (*Russian*) 3-71139
- ²³⁹Pu, thermal neutron induced, gamma rays of primary fission products 3-49287
- ²³⁹Pu, time spectrum of fission fragments, using pulsed cyclotron beam 3-51674
- ²³⁹Pu(n, f) in ZPR-6 assembly 7, comparison of calc. and meas. reaction rate distrib. and fission integrals 3-71186
- ²³⁹Pu(n, f), ternary to binary fission ratio meas., 0.02 to 50 eV 3-78361
- ²⁴⁰Pu, anomaly of fission reaction threshold from 1.5 to 7.5 MeV 3-52212
- ²⁴⁰Pu, shell structure and fission asymmetry, statistical model, fragment mass distributions 3-60235
- ²⁴⁰Pu zoned critical expts., analysis in support of LWR-grade Pu utilization in FTR's 3-71187
- ²⁴¹Pu fissile element cross section, influence on fast crit. assembly parameters 3-60277
- ²⁴¹Pu spontaneously fissionable isomer, decay, search for α -emission (*Russian*) 3-40470
- ²⁴¹Pu-²³⁵U fission cross-section ratio meas. for neutron energies 5 keV-1.2 MeV 3-60233
- ²⁴²Pu, anomaly of fission reaction threshold from 1.5 to 7.5 MeV 3-52212
- ²⁴²Pu, neutron resonance parameters from (n,n) and (n,p) reactions, calc. of fission widths 3-49258
- ²⁴²Pu, parameters of subthreshold fission structure from neutron total cross sections 3-63095
- ²⁴³Pu, composite nuclei, nucleon pairing effects, two lumped fission barrier 3-40521
- ¹⁸⁶Re, 1 GeV proton bombardment, angular distribution of fragments, momentum transfer (*Russian*) 3-57547
- Th, induced by 12.2 GeV protons, binary and ternary fission 3-52216
- Th, spontaneously fissioning isomer prod. in 14 MeV neutron reactions 3-71132
- ²³²Th, 1 GeV proton bombardment, angular distribution of fragments, momentum transfer (*Russian*) 3-57547
- ²³²Th, mass distrib. of fragments, excitation energy depend. 3-78266
- ²³²Th, meas. of integral fission cross section in ²³²Cf fission neutron spectrum 3-74619
- ²³²Th, neutron induced 14.8 MeV, charge distrib. meas. for ⁴In, two-mode fission hypothesis 3-43260
- ²³²Th(¹⁶O, F), 102.5 MeV, fragment kinetic energy, comparison with static scission model and fission systematics predictions 3-74616
- U alloys, thermomechanical testing under conditions of rapid fission heating 3-47531

nuclear fission of uranium

- axial fission rate distribution, effect of UO₂ insulator pellets, EBR-II 3-63167
- fission track technique, U content in minerals, geochronology appl. 3-44831
- fission-track aging, mica 3-44779
- neutron emission probabilities from delayed neutron precursors 3-67280
- neutron importance and fission density in spherical U metal assemblies 3-49302
- proton induced, 4.8 GeV, ¹⁴Be and ¹⁷B isotopes obs. 3-63092
- in rocks, neutron distrib. from spontaneous fission of U nuclei 3-61301
- spontaneously fissioning isomer prod. in 14 MeV neutron reactions 3-71132
- ternary, induced by high-energy protons, cross-sections for three-prong events 3-57546
- thermal neutron capture, probability of formation of spontaneously fissionable isomer states (*Russian*) 3-71139
- ²³³U, ²³⁵U, thermal-neutron induced, fragment mass distrib., fine structure, charge distrib., structure, correlations 3-40518

nuclear fission of uranium continued

- ²³³U, ²³⁵U fission, thermal-neutron induced, fragment mass distrib., fine structure, charge distrib., structure, correlations 3-40518
- ²³³U, by protons, charge dispersion of products in light-mass region 3-57544
- ²³³U, cumulative fission yield reviewed 3-71140
- ²³³U, low-energy neutron induced, resonance parameters and cross-sections 3-49293
- ²³³U, neutron spectra meas. 0.8-10 MeV 3-74618
- ²³³U, neutron-induced cross-sections below 30 keV, high resolution meas. 3-60234
- ²³³U, proton induced, 7 to 13 MeV, fragment mass and energy distributions, discussion of shell effects 3-54519
- ²³³U, thermal, delayed neutron energy spectra meas. using gas-filled proton recoil proportional counters 3-49292
- ²³³U, thermal neutrons, yield, mass, energy spectra 3-78362
- ²³⁵U, absolute determ. of cross-section for 964 keV neutrons 3-49295
- ²³⁵U, cross section and anisotropy for photofission 3-60230
- ²³⁵U, cross-section meas. for ²⁵²Cf spontaneous fission neutrons 3-49294
- ²³⁵U, cumulative fission yield reviewed 3-71140
- ²³⁵U, fission fragments prompt gamma energy from prompt neutron numbers, liquid-drop model calc. 3-54510
- ²³⁵U, low-energy neutron induced, resonance parameters and cross-sections 3-49293
- ²³⁵U, meas. neutron fission and capture cross sections at 8 eV to 10 keV 3-74612
- ²³⁵U, multilevel analysis of neutron capture and fission cross sections up to 60 eV 3-63094
- ²³⁵U, neutron induced, de-excitation of primary fission fragments 3-46045
- ²³⁵U, neutron induced, meas. of prompt ν -values in fast and thermalised fluxes 3-60229
- ²³⁵U, neutron irradi., fission fragment energy spectra on passage through gases (*Russian*) 3-57542
- ²³⁵U, neutron multiplicity measurement on resolved fission resonances 3-63091
- ²³⁵U, neutron-induced cross-sections below 30 keV, high resolution meas. 3-60234
- ²³⁵U, neutron-induced fission, spin determ. of resons. 3-74614
- ²³⁵U, power, photon spectrum and neutron prodn., calc. by ORIGEN computer code 3-43284
- ²³⁵U, prompt neutron spectra, data re-fitting using a computer program 3-74611
- ²³⁵U, proton induced, 7 to 13 MeV, fragment mass and energy distributions, discussion of shell effects 3-54519
- ²³⁵U, ternary fission in thermal and reson. neutron energy regions, alpha particle spectra 3-54511
- ²³⁵U, thermal, delayed neutron energy spectra meas. using gas-filled proton recoil proportional counters 3-49292
- ²³⁵U, thermal neutron induced, gamma rays of primary fission products 3-49287
- ²³⁵U, thermal neutrons, yield, mass, energy spectra 3-78362
- ²³⁵U, thermal-neutron induced, obs. of delayed neutrons from produced As isotopes 3-43202
- ²³⁵U and ²³³U, criticality research, fission process, Oak Ridge Critical Experiments Facility 3-63227
- ²³⁵U by thermal neutrons, β ray spectra 3-63101
- ²³⁵U cross section, meas. of (n,p) reaction cross section by activation method 3-74591
- ²³⁵U enriched cores, prompt and delayed modes rel. to spacial correction factor for reactivity of system 3-67400
- ²³⁵U partial widths of resonance levels in fissile nuclei, spin-dependent statistics 3-67376
- ²³⁵U ranges in all existing natural elements 3-58058
- ²³⁵U triple fission, thermal neutron induced, study of ⁸He decay (*Russian*) 3-40469
- ²³⁵U-²⁴¹Pu cross-section ratio meas. for neutron energies 5 keV-1.2 MeV 3-60233
- ²³⁵U(p, f), 5 to 8 MeV, cross-section from yield curve 3-78359
- ²³⁵U(n, F), thermal energy, α -particle polar emission 3-54516
- ²³⁵U(n, F) meas. delayed and prompt gamma ray energies using neutron detector and Ge(Li) crystal 3-67335
- ²³⁵U(n, f), spectroscopic meas. on neutron-rich products, on line meas. separation 3-49211
- ²³⁶U, photofission cross-sect. meas., threshold to 8 MeV 3-46046
- ²³⁶U, pot. energy calcs., asymmetry 3-43264
- ²³⁶U mass asymmetry as dynamic process described by collective coordinate 3-60236
- ²³⁷U, search for fissioning isomers in region of 60 μ s half-life 3-78357
- ²³⁸U, 1 GeV proton bombardment, angular distribution of fragments, momentum transfer (*Russian*) 3-57547
- ²³⁸U, 800 MeV photofission, meas. of peak-to-valley ratio 3-74617
- ²³⁸U, anomaly of fission reaction threshold from 1.5 to 7.5 MeV 3-52212
- ²³⁸U, cross-section meas. for ²⁵²Cf spontaneous fission neutrons 3-49294
- ²³⁸U, fast neutron induced reactions, γ ray production cross section, spectrum calcs. 3-67322
- ²³⁸U, induced by 1 GeV protons, angular correlations of mass and energy distrib. of fragments (*Russian*) 3-40524
- ²³⁸U, induced by 70-200 MeV protons, cross section and angular anisotropy (*Russian*) 3-40523
- ²³⁸U, interaction with 11.5 GeV protons, charge dispersion and recoil props. at A = 131 3-40520
- ²³⁸U, mass distrib. of fragments, excitation energy depend. 3-78266
- ²³⁸U, photofission, mass yield distrib., 25-40 MeV 3-67377
- ²³⁸U, proton fission, charge dispersion of isotopes of Sb 3-57545
- ²³⁸U, proton induced, 7 to 13 MeV, fragment mass and energy distributions, discussion of shell effects 3-54519
- ²³⁸U, spontaneous fission, high-energy γ -ray obs. 3-43265
- ²³⁸U, spontaneous fission and radio-chemical yield 3-57543
- ²³⁸U Doppler reactivity mapping in FFTF engineering mockup critical, calcs. and expts. 3-71191
- ²³⁸U electrofission, 70 MeV, meas. of fragment kinetic energy 3-43259
- ²³⁸U(p, f), 5 to 8 MeV, cross-section from yield curve 3-78359

nuclear fission of uranium continued

- ²³⁸U(n, f), in ZPR-6 assembly 7, comparison of calc. and meas. reaction rate distrib. and fission integrals 3-71186
²³⁸U(n, f), subthreshold fission obs. 3-54518
²³⁸U(p, f), 11.5 GeV, Xe isotopes yields cross sections and recoil props. 3-74615
^{236m}U spontaneously fissionable isomer, search in ²³⁵U(n, γ) reaction (*Russian*) 3-57530
 ZrU and ZrH₂U reactor fuel elements, release of Xe 3-63122

nuclear fission piles see nuclear reactors**nuclear fission products**

- AGR, fuel rating distribution determ. 3-43292
 anisotropies, for nuclei with double barrier, microscopic calcs. 3-63096
 calorimetric meas. and γ -ray spectra at various cooling times determination of burn-up 3-67541
 concentrations in reactor coolant determ. using sapphire radiation-monitoring loop in Pegasus reactor (*German*) 3-67464
 corrosion reactions on austenitic steel fuel element cladding (*German*) 3-71307
 decay heat, gamma-ray noise analysis (*Japanese*) 3-71167
 delayed neutrons, energy distrib. meas. using ³He proportional counter 3-54515
 electrostatic analyzer 3-54001
 fast reactor, calcs. for fission product poisoning, appl. to ²³⁸U-²³⁹Pu oxide-fuelled LMFBR 3-49356
 fast reactor, Na pool fire, sodium oxide and fission products, release functions 3-67540
 fixed-charge fragments, X-ray emission spectra, reln. to shell structure (*Russian*) 3-67173
 flow checking by input anal., correlation of fission gases, re-processing of fuels (*German*) 3-67602
 fragment identification, plastic nuclear track detectors 3-62247
 free gaseous, emission rate from HTR fuel specimens (*German*) 3-67596
 fuel reprocessing waste problems (*French*) 3-40547
 gas release, FFTF subassembly, potential for fuel failure propagation 3-71292
 gas release, pin-to-pin failure propagation, pressure pulse loading, buckling failure criterion 3-74732
 gas release rate, porous flow model, failed LMFBR fuel rods 3-71291
 gas release rates, impedance, local flow starvation, LMFBR subassembly 3-74676
 gases, rare, diffusion through fuel element cladding (*German*) 3-67393
 GCFR rod irradiations, volatile fission product migration and plateout 3-46160
 inert gases, external γ -ray emission rel. to, isopleths of dose following hypothetical reactor hazards 3-67623
 leakage, accidental, rates and amounts, water-cooled reactors 3-74749
 LMFBR, ²³⁹Pu fueled, post-shutdown fission product energy release calcs. 3-67441
 long life, separation from highly active waste solution by ion migration (*German*) 3-71346
 mass distribution meas. using time of flight and particle channelling technique 3-62266
 neutron age calc., extended planar source expts., validity 3-74632
 prompt neutrons, averaged number per ²³⁵U and ²³⁹Pu fission 3-60229
 quasi-particle excitation model, applicability near saddle point of fissionable nuclei (*Russian*) 3-40525
 radioactive gas release from mixed-oxide and metal fuel elements to cover gas in EBR-II, comparison 3-67578
 radioactive waste, LWR type, storage, design (*French*) 3-46133
 radionuclide meas. in marine samples near nuclear power stations 3-69557
 reactor coolant activity, and filter efficiency determ. using monitoring loop (*German*) 3-67465
 recovery by fluorination process using BrF₃ 3-43289
 relative concentration meas. to determ. burn-up in fast nuclear reactors, techniques review (*German*) 3-71240
 superheavy elements in natural and proton-irradiated materials 3-60231
 surface tracks in UO₂, replica electron microscopy obs. 3-63187
 X-ray spectra at different kinetic energies of light fragments, mass yield fine structure (*Russian*) 3-40522
 Ac isotopes, symmetric, asymmetric fission triple-humped mass distributions, fission barrier 3-60238
⁸¹As, A=84, 85, 86, produced in ²³⁵U neutron induced fission, obs. of delayed neutron yield 3-43202
¹⁷B, isotope obs. at limits of particle stability 3-63092
 Ba retention in coated particle fuels, SiC coating layer study 3-74723
¹⁴³Ba, half-life and γ -ray energy by direct meas. 3-78281
¹⁴⁴Ba, half-life and gamma-ray energy by direct meas. 3-78281
¹⁴Be isotope obs. at limits of particle stability 3-63092
²⁰⁹Bi, 1 GeV proton bombardment, angular distribution of fragments, momentum transfer (*Russian*) 3-57547
²⁰⁹Bi, induced by 1 GeV protons, angular correlations of mass and energy distrib. of fragments (*Russian*) 3-40524
²⁵²Cf, detection of ⁴He, ⁶He, α particle and neutron spectra 3-78363
²⁵²Cf, fission fragments prompt gamma energy from prompt neutron numbers, liquid-drop model calc. 3-54510
²⁵²Cf fission neutron age in water, meas. by In resonance obs. 3-71297
²⁵²Cf fission neutron spectrum, meas. of ²³²Th integral fission cross section 3-74619
²⁵²Cf fission vs. prompt γ -ray energy, fragment-mass ratios 3-43266
²⁵²Cf spontaneous fission fragments, γ cascades 3-62994
²⁴⁴Cm, ²⁴⁶Cm, spontaneous, prompt neutron multiplicity, dispersion 3-78364
²⁴⁶Cm, mass and kinetic energy distrib. determ., spontaneous fission 3-71135
 Cs, A=138 to 142, fission products, determ. beta-decay energies, end point energies and Q values 3-67277
 Cs, A=143-145, mass separated following ²³⁵U fission, gamma-ray energies 3-49211
 Cs, deposition on primary coolant surfaces of CO₂ cooled reactor, physical model (*German*) 3-67496
 Cs, transport behaviour of coated fuel particles with heavy burn-up in a HTR (*German*) 3-71320
 Gd poisoned BWR fuel element, local distribution from gamma-scanning method (*German*) 3-67613
⁴He, from thermal fission of ²³⁹Pu, energy spectrum, angular distribution 3-54517
⁶He, from thermal neutron fission of ²³⁹Pu, energy spectrum angular distribution 3-54517
 I, deposition on primary coolant surfaces of CO₂ cooled reactor, physical model (*German*) 3-67496
 I, stress corrosion effects in Zry-encased fuel rods in BWR and PWR (*German*) 3-67612
¹³¹I, radiochemical yield from ²³⁸U spontaneous fission 3-57543
¹¹⁰In, A=117, 130, 132-134, produced in ²³²Th neutron-induced fission, charge distrib. meas. 3-43260
 Kr, yield from neutron fission of ²³⁷Np, ²³⁸Np, ²⁴¹Am and ²⁴²Am 3-67378
 Kr gaseous products and daughters, β -decay energies for A=88-93 3-57496
⁹⁹Mo, radiochemical yield from ²³⁸U spontaneous fission 3-57543
 Pu, volatilization for reprocessing 3-54539
²³⁹Pu, cumulative fission yield reviewed 3-71140
²³⁹Pu, fission fragments prompt gamma energy from prompt neutron numbers, liquid-drop model calc. 3-54510
²³⁹Pu, neutron multiplicity and total gamma-ray energy 3-71137
²³⁹Pu, thermal neutron induced, gamma rays of primary fission products 3-49287
²⁴⁰Pu, calc. fragment mass distribution using a statistical model 3-60235
²⁴¹Pu, cumulative fission yield reviewed 3-71140
¹⁸⁶Re, 1 GeV proton bombardment, angular distribution of fragments, momentum transfer (*Russian*) 3-57547
 Sr, retention in coated particle fuels, SiC coating layer study 3-74723
 Sr, transport in graphite, concentration profiles, importance in helium-cooled HTRs (*German*) 3-71243
²³²Th, 1 GeV proton bombardment, angular distribution of fragments, momentum transfer (*Russian*) 3-57547
²³²Th, mass distrib., excitation energy depend. 3-78266
 U alloys, nuclear fuel, fission gas release, effect of vol. swelling, probabilistic model 3-63208
 U-Pu, nuclear fuel, fission gas release, effect of vol. swelling, probabilistic model 3-63208
 UF₆, partial pressure determ. from meas. of U radioactivity (*German*) 3-66462
 UO₂, melted in air, He, rate of fission product release (*Japanese*) 3-74726
²³³U, cumulative fission yield reviewed 3-71140
²³³U, fission by protons, charge dispersion of products in light-mass region 3-57544
²³³U, fission by thermal neutrons, yield, mass, energy spectra 3-78362
²³³U, fission fragments prompt gamma energy from prompt neutron numbers, liquid-drop model calc. 3-54510
²³³U, neutron spectra meas. 0.8-10 MeV 3-74618
²³³U, cumulative fission yield reviewed 3-71140
²³⁵U, fission by thermal neutrons, yield, mass, energy spectra 3-78362
²³⁵U, fission fragments prompt gamma energy from prompt neutron numbers, liquid-drop model calc. 3-54510
²³⁵U, neutron induced, de-excitation of primary fission fragments 3-46045
²³⁵U, neutron irradi., fission fragment energy spectra on passage through gases (*Russian*) 3-57542
²³⁵U, thermal neutron induced, gamma rays of primary fission products 3-49287
²³⁵U fragments, back-scatt. from thin metal films 3-61090
²³⁵U(n, f) yield, contributions of neutron multiplicity 3-63091
²³⁸U, 1 GeV proton bombardment, angular distribution of fragments, momentum transfer (*Russian*) 3-57547
²³⁸U, induced by 1 GeV protons, angular correlations of mass and energy distrib. of fragments (*Russian*) 3-40524
²³⁸U, interaction with 11.5 GeV protons, charge dispersion and recoil props. at A=131 3-40520
²³⁸U, mass distrib. of fragments, excitation energy depend. 3-78266
²³⁸U electrofission, 70 MeV, meas. of fragment kinetic energy 3-43259
 Xe, A=122 to 136 from ²³⁸U(p, f) at 11.5 GeV yields, cross sections and recoil props. 3-74615
 Xe, A=138 to 142, meas. beta-decay energies using a well-type plastic scintillator in coin. with Ge(Li) γ detector 3-67277
 Xe, azimuthal oscillations, effect of temp. coupling (*German*) 3-67494
 Xe, reactivity effects following power reductions in WWR-SM type reactors 3-67394
 Xe, yield from neutron fission of ²³⁷Np, ²³⁸Np, ²⁴¹Am, and ²⁴²Am 3-67378
 Xe in ZrU and ZrH₂U reactor fuel elements 3-63122
 Xe induced spatial oscillations in power reactor, control 3-57556
 Xe instabilities in large power reactor, optimal control (*German*) 3-67493
 Xe produced by β -decay of precursor ¹³¹I in graphite at 1000°C, release procedure 3-71278

nuclear fission products continued

- nuclear fission products see nuclear reactors**
- nuclear forces**
 see also meson field theory; nuclear binding energy
 1p-shell nuclei, giant magnetic dipole analogue excitations 3-60126
¹⁵O p-p potential, shape, phase shifts 3-78257
 A=19 isobar, charge asymmetry due to Coulomb interaction determ. 3-67176
 Brueckner-Hartree-Fock approach, self-consistent treatment of Pauli operator 3-60104
 central potentials, l-wave reduction to s-wave 3-60087
 computational approach to inverse problem in JWKB approximation, alpha-particle scattering 3-60143
 Coriolis-coupling calc. of low-lying states of Ru, Pd and Cd isotopes 3-43180

nuclear forces continued

- Coulomb displacement energy, phenomenology of shell effects 3-43193
- deformed nuclei, translation and rotation invariance conditions for Hamiltonian 3-67232
- density rearrangement effects, single-particle energies, removal and addition times 3-67226
- density-dependent effective interactions, effect on spherical nuclear calcs. 3-52108
- doubly odd self-conjugate nuclei, e.m. corrections in Coulomb displacement energies 3-49161
- effective interaction, density dependent, in structure calcs. 3-54404
- effective interaction of shell model, non-perturbative calc. using Padé approximants 3-67221
- effective interaction properties for simple 2×2 matrix 3-67222
- effective interactions in nuclei, generalization of algebraic approach 3-49159
- effective two-body interaction, truncation of configuration space in shell model 3-67233
- e.m. pot. between two finite size nucleons 3-43186
- exchange current, N^*_{33} -isobar and tensor force effects on magnetic moments 3-45927
- exchange magnetic moment, calc. of isoscalar part by p -exchange and OBE models 3-49121
- exciton model, emission and formation probability of complex particles 3-60137
- few particle problems, conference, Los Angeles, USA (28 Aug-1 Sep 1972) 3-74500
- four nucleons, interaction in even orbital momentum states, integral equations (Russian) 3-74507
- heavy nuclei, inhomogeneity of nucleon distrib. (Russian) 3-62958
- internuclear interaction, shell model calcs. 3-40407
- Jastrow-type Brueckner-Hartree-Fock calculation for finite nuclei, $A=4$ to 48 3-60106
- Kuo interaction in untruncated shell-model calcs. in sd-shells, production of band shifts 3-67202
- Lane's potential and eqns., isospin (Rumanian) 3-62957
- low-energy deuteron break up on heavy nuclei, neutron-nucleus interaction 3-54487
- matter, high-density, N-body forces 3-74519
- meson exchange, effect on magnetic moments 3-45928
- meson exchange in two nucleon interaction, Cohen approximation to scalar Bethe Salpeter eqn. 3-60089
- mirror nuclear, charge symmetry of force, magnetic moments and β -decay 3-45953
- multinucleon correlations and effective force, appl. of theory from few-nucleon systems (Russian) 3-71060
- multiparticle, $N=Z$, pi-meson spectrum, phase transition in nuclear matter 3-60105
- neutron matter with relativistic one-boson-exchange potential 3-40435
- neutron star matter at sub-nuclear densities, ground state configuration 3-51253
- neutron-proton bremsstrahlung, one-pion-exchange-current contrib. 3-54396
- non-local separable potential, positive energy bound states 3-43188
- non-rotational collective nuclear states, particle-particle and particle-hole interactions 3-67240
- nonlocal separable nucleon-nucleon interaction parameters 3-40424
- nonlocality effects, quantum-mechanical momentum fluctuation 3-67220
- nuclear interactions, effective from closed shell plus two spectra, isospin mixing 3-71062
- nucleon- Δ forces, effect of isospin assignment of Δ_{33} 3-67218
- nucleon-nucleus effective interaction, non local effects 3-60184
- nucleon-nucleus potential rel. to optical potentials for composite projectiles, adiabatic approximation 3-60142
- off energy shell T matrix, symmetry property 3-60088
- off-shell two-nucleon T matrix, singular-core interaction and one-pion exchange constraints 3-74499
- one-pion exchange potential, nuclear matter trial wave function determ. 3-40422
- pairing, theorem on transformation of complex skew symmetric matrix into real normal form 3-67219
- pairing forces, methods of treatment, quasiparticle approx. (Rumanian) 3-62973
- pairing plus multipole multipole force model for even-even spherical nuclei, quasiboson approx. (Russian) 3-74514
- pairing rel. to shell corrections to masses using Bogolyubov-Hartree-Fock approximation (Russian) 3-67175
- particles and antiparticles, baryon number variables for description of system 3-40436
- potential barrier, two-bump penetration influence of fission potential on penetrance curve (Russian) 3-67223
- potential scattering using nuclear reaction theory transition motion 3-60138
- potential summing using half shell t-matrix 3-74505
- quadrupole, two-nucleon transfer amplitudes in ground-state rotational bands of even nuclei 3-43189
- rank-one separable potential calcs of nuclear matter 3-49182
- realistic NN-potentials for three and four nucleon bound state problems 3-49163
- Reid's soft-core nucleon-nucleon interaction, calc. of triton binding energy 3-49073
- relativistic corrections in nucleon-plus-e.m. Hamiltonian 3-62956
- relativistic corrections to magnetic moment 3-49122
- relativistic quantum field theory, application of HF method, nuclear force problem 3-54259
- repulsive Bartlett potential, spin-dependent effects in giant resonance excitation of doubly-closed shell nuclei 3-78297
- repulsive core, limitations on short distance behaviour 3-67217
- S-wave interaction of nucleons 3-62977
- separable representation of two body interactions T matrix 3-60090
- separable-pair method for motion of many-body systems interacting through two-body forces 3-40423
- shape calc., nuclear and Coulomb, reduction of apparent discrepancies 3-60067
- shell model form factors with effective nucleon-nucleon interactions 3-49158

nuclear forces continued

- short range behaviour, information from high energy elastic and inelastic cross sections 3-70999
- short-range pairing, rel. to nuclear rotational Hamiltonian, expansion of nuclear rotational energy 3-62968
- spin $1/2$ particles, scattering by spin 1 particles, polarisation (German) 3-54335
- spin $1/2$ particles scattering by spin 1 particles, polarisation (German) 3-54334
- spin-orbit bound nuclei and asymptotic saturation 3-54372
- square well potentials with varying repulsion, accuracy of unitary pole approx. 3-49160
- strong interaction effective range, dynamic deformation explanation (Russian) 3-57479
- tensor polarisation in nucleon-deuteron scattering with two-term nonlocal separable potentials 3-54395
- three body final state reactions, invariant description 3-43150
- three nucleon, and 2S defects, Amado model predictions 3-67225
- three nucleon problem, backward $p+d$ elastic scattering below 1 GeV, energy dependence 3-52109
- three-body pion-mediated interactions, off-shell effects, binding energies and isobaric states 3-78261
- three-body problem, definition, triton binding energy calcs. 3-78260
- three-nucleon problem, independent Faddeev amplitudes 3-40427
- three-nucleon problem, independent Faddeev amplitudes 3-40428
- three-nucleon problem, separable expansions of t-matrix 3-49164
- three-particle bound state, sensitivity to equivalent interactions 3-78264
- three-particle spectrum, resonance interaction, studies at various mass ratios 3-60078
- three-particle system, accuracy of Brueckner theory for light nuclei 3-57480
- three-particle system interacting via two-particle and three-particle pots., scatt. amplitudes 3-40426
- triton exchange in reaction $^7\text{Li}(\alpha, \alpha)$, 8.6-12.5 MeV and 17-22.5 MeV 3-63071
- two-body scattering with separable potentials, polarisation 3-52110
- two-neutron scattering length, effect of neutron electric polarizability 3-45978
- two-nucleon boundary-condition-model interaction, modified, off-energy-shell T-matrix 3-43187
- two-nucleon nonlocal interaction, calc. of surface energy of nuclear matter 3-43201
- two-nucleon T matrix off energy shell, wave function models 3-78258
- two-nucleon transition matrix, 1S_0 partial wave, off-energy-shell continuation 3-78259
- wave function determ. for one nucleon on and one off shell, new theory 3-74504
- Yukawa potential, appl. of linked cluster decomposition of S-matrix 3-62779
- Yukawa potential, large coupling expansions for eigenenergies and Regge trajectories 3-74326
- $\Delta(1236)$ involved corrections, including exchange effects and realistic correlation functions 3-54416
- N-N, short range part, rel. to three nucleon system low energy properties 3-62959
- N-N effective range expansion parameters review 3-54397
- N-N interaction, coherent non local separable potentials in three body problems 3-74502
- N-N interaction, exchange part, effect on sum rule for electron-nucleus scattering (Russian) 3-40483
- N-N interaction, review of recent exptl. data 3-74501
- N-N interaction, with Yamaguchi form factors and separable potentials 3-74503
- N-N nonlocal core potentials, off-shell effects in triton binding energy calcs. 3-71036
- N-N potential, Reid, electric dipole sum rule and two body correlations 3-78240
- N-N potentials, are boson exchange, in many nucleon context 3-60091
- N-N potentials, study of off shell effects using p - p bremsstrahlung and $^2\text{H}(p,2p)n$ expts. 3-78335
- N-N spin-orbit potentials, reln. to deuteron magnetic moment 3-71044
- Nd backward scattering, elastic cross section, virtual states of trinucleon, Amado model 3-52165
- np bremsstrahlung at 130 MeV, asymmetric, nuclear potential 3-74415
- np bremsstrahlung calcs., cross sections, model depend. 3-40425
- p - p polarisation role in models for atomic mass dependence of photonuclear giant resonance energy 3-74546
- pp scattering, spin correlation parameters, 50 MeV 3-63030
- Ar isotopes, n - n , p - p , n - p interactions rel. to properties of low lying states, E2, M1 transition rates 3-62949
- ^8Be effective kinetic energy four-body forces contribution to binding energy 3-49072
- $^{12}\text{C}(\pi^+, NN)$, study of short range correlations, three-body partial wave analysis 3-60222
- Fe, nucleon partial inelasticity coeff. (Russian) 3-49157
- ^2H , breakup in heavy nuclei fields, 7-12 MeV 3-60204
- ^2H , nucleon induced exact breakup calc. using solution of three-particle Faddeev eqn. 3-60155
- $^2\text{H}(\text{H}, \text{dp})n$, breakup reaction, 14-36 MeV, modified plane wave impulse approximation theory 3-60154
- $^2\text{H}(n, 2n)^1\text{H}$ break-up process local two-nucleon S-wave potentials and separable Yamaguchi potential 3-60150
- ^3H , evidence for strong three-body forces 3-62955
- ^3H , evidence for strong three-body force 3-78262
- ^3H , magnetic moment, effect of meson-exchange currents 3-49120
- $^3\text{H}^{1,2+}$ state below break-up threshold, Gammel-Brueckner potential 3-52107
- ^3He , magnetic moment, effect of meson-exchange currents 3-49120
- $^3\text{He}^{1,2+}$ state below break-up threshold, Gammel-Brueckner potential 3-52107
- ^4He , effective kinetic energy four-body forces contribution to binding energy 3-49072
- ^4He , soft core potentials, dependence of binding energy, nucleon density, form factors 3-45979

nuclear forces continued

- $H^2(n,p)H^3$, cross section, meson-exchange corrections 3-54456
 6Li , three body wave function, rel. to low lying states and electron scattering excitation 3-62944
 ^{56}Ni , effective interactions and $1f_{7/2}$ sub-shell closure in $2p-1f$ shell 3-49169
 $^{16}O(p,d)^{15}O$, effect of short-range correlations due to repulsive core in N-N interaction 3-46024
 ^{208}Pb , RPA calcs. of low lying states, density dependent interaction 3-49153
 ^{209}Pb , imaginary optical potential for s-wave neutrons incident on ^{208}Pb 3-60141
 $t \rightarrow d + n$ vertex, coupling constant and form factor 3-52106

nuclear fusion

see also fusion reactors; nuclear explosions; thermonuclear reactions

- accreting neutron stars nuclear fusion forming X-ray source 3-81026
 breeding ratio cross-section sensitivity in fusion reactor blanket 3-63098
 British research, history and future prospects 3-49728
 controlled, applic. of high powered lasers 3-62685
 controlled expts., necessary conditions for steady-state operation 3-60625
 controlled fusion at Wisconsin University, education and research 3-63238
 controlled fusion research and education in USA universities 3-63237
 controlled fusion research in 17 countries 3-71329
 controlled thermonuclear fusion expts. and engineering aspects, conference, Austin, Texas, USA (Nov. 1972) 3-60295
 controlled thermonuclear reactor materials, automated method for calculating energy deposition 3-63097
 cybernetic methods of studying controlled fusion (Russian) 3-71923
 energy balance control in fusion plasma 3-57930
 energy sources, present state and future prospects (Croatian) 3-60292
 graphite, neutron fusion spectrum, reaction rates determ. 3-63100
 KMS laser fusion experiments 3-63099
 laser applications, energy production 3-62709
 laser beam applic. (French) 3-60291
 laser induced, present state and future prospects (German) 3-43316
 laser induced, shock and compression by laser pulses enhanced by liq. layers on solid surfaces 3-57245
 laser initiated, feasibility 3-78390
 laser irradiation appl. (Rumanian) 3-62732
 light nuclei with ang. momenta near liquid-drop limit 3-63093
 micro fission-fusion chain reactions, bootstrap mode coupling and critical mass reduction 3-54514
 multigroup kerma factors and partial cross sections library for fusion neutronics and photonics 3-63235
 neutron energies and spectra 3-40519
 plasma, inhomogeneous, parametric scatt. instabilities rel. to laser penetration 3-68052
 plasma, neutron diagnostics 3-63888
 plasma, two-temp., general eqns. for laser heating including fusion heat 3-60617
 plasma, two-temp., laser heating, in focus system, numerical analysis of averaged eqns., incl. fusion energy 3-75397
 plasma, two-temp., laser heating, numerical analysis, incl. recovered nuclear fusion energy 3-75396
 plasma, two-temperature, conductivity-laser heating including fusion energy 3-60616
 plasma atomic parameters for CTR research 3-79155
 plasma engineering, monograph 3-49632
 plasma focus, laser cumulative heating, thermonuclear fusion consideration 3-63854
 plasma fusion laser systems 3-68044
 plasma heating, laser concentric cumulation, heat of nuclear fusion consideration 3-63855
 reactor engineering in the nuclear engineering curriculum at Texas University 3-61956
 research using TOKAMAK type medium beta torus JFT-2 (Japanese) 3-60293
 review of expts. at Los Alamos Scientific Laboratory, theta pinches and Z pinches 3-60643
 target manufacture, solid hydrogen and deuterium 3-77414
 technology at Michigan university, educational and research activities 3-61955
 technology first year graduate course at Illinois University 3-61954
 thermonuclear, laser-induced, review 3-71330
 Tokamak turbulent heating, high electric field effect on design 3-60644
 ^{27}Al , ^{32}S induced reaction, fusion barrier meas. 3-46042
 ^{40}Ca , ^{32}S induced reaction, fusion barrier meas. 3-46042
 D solid target, laser light absorption, wavelength depend. 3-49731
 D-D plasma power balance calcs., equilibrium parameters 3-60620
 D-T plasma, laser compression, averaged equations allowing for fusion heat 3-68040
 D-T plasma, laser compression, averaged description 3-68041
 3He -d self-colliding mixture (migma), nonplasma nonthermal power source 3-74742
 ^{24}Mg , ^{32}S induced reaction, fusion barrier meas. 3-46042
 ^{58}Ni , ^{32}S induced reaction, fusion barrier meas. 3-46042
 U-D thermonuclear plasma, controlled fusion, obtained by composite macro-particle collisions 3-49733

nuclear fusion reactors see fusion reactors**nuclear induction** see nuclear magnetic resonance**nuclear instrumentation**

see also angular correlation techniques; beam handling equipment; counters; counting circuits; particle accelerators; particle track visualisation; radiation detectors

- ALICE flying spot digitizing system, application to spark chamber and oscilloscope data 3-40024
 bubble and spark chamber data analysis at CNAF 3-77701
 CAMAC module, for event recognition 3-40027
 collimator, coaxial circular aperture, for space radiation meas., optimum design 3-62231
 computer applications, small, system aspects 3-66299

nuclear instrumentation continued

- computer system, for multiparameter measurements 3-40030
 data acquisition systems, for heavy ion reactions 3-40028
 electrostatic analyzer, for separating fission fragments 3-54001
 fuel movement visualization using fast neutron hodoscope in 7 pin loss of flow simulation 3-67419
 gating circuits, two and four quadrant, crossed atomic beam experiments, electronics 3-62256
 high energy physics, conference, Frascati, Italy (1973) 3-77597
 in-core, self-powered neutron detectors in HBWR long-term test 3-52233
 linear scanistor, for processing graphical information 3-51727
 mass-selecting apparatus, for energy loss of fission fragments in gases 3-40002
 neutron irradiation container with temp. control 3-51706
 PEPR II system, at Oxford and Padova 3-77702
 power reactor systems, book 3-59617
 products, materials and services directory 3-39984
 pulse shaper, integrating discriminator, AND-NOT, AND-OR-NOT and power supply for time and amplitude analysis 3-53987
 random address reader, circuit description 3-62254
 reactor bubble emission, acoustic meas. (French) 3-66158
 sample changer, for automatic irradiation apparatus 3-39982
 scintillation counting equipment, review 3-62224
 standardisation, in Italy (Italian) 3-42620
 time-to-digital converter, for event recognition 3-40027
 United Kingdom programme 3-54531
 Ge-Li detector linked to calculator Multi-8 type, analysis in nuclear reactor (French) 3-66330

nuclear interactions see nuclear reactions and scattering**nuclear isomerism**

- see also nuclear energy levels; nuclear excitation
 ^{200}Pb isomeric state behaviour, γ - γ coincidence obs. 3-62992
 actinide region, deformation energies and moments of inertia for isomeric states (German) 3-52071
 cyclotron beam pulsing for transitions with small cross sections 3-51674
 shape isomers, fissioning nuclei 3-62928
 shape isomers, spontaneously fissioning, properties of quadrupole vibrational states 3-45984
 (n,p) reactions, activation cross sections and isomer ratios as a function of incident energy, statistical model calc. (German) 3-52173
 ^{222m}Ac product of ^{232}Th and 600 MeV protons, 62 sec. half life 3-54483
 Am, spontaneously fissioning isomer prod. in 14 MeV neutron reactions 3-71132
 ^{240}Am spontaneously fissionable isomer, decay, search for α -emission (Russian) 3-40470
 ^{242}Am spontaneously fissionable isomer, decay, search for α -emission (Russian) 3-40470
 $^{75}As(n,p)^{75m}As$ cross section for 14.8 MeV neutrons 3-63061
 ^{198}Au isomeric 115.2 keV transition, γ -ray meas., multipolarities 3-43209
 ^{197m}Au , from $^{197}Au(\gamma,\gamma')$, 100-800 MeV, measured half life, E_γ 3-67308
 ^{200m}Au , oriented, n.m.r., γ -ray anisotropy obs. 3-40453
 ^{204}Bi , high-spin isomeric state populated by heavy-ion and α -particle induced reactions 3-49152
 ^{208}Bi , 10 $^{-6}$, 0.88 ms isomeric state, nuclear magnetic resonance, g-factor meas. 3-71042
 ^{64}Cu , ^{66}Cu , magnetic moments and lifetimes of isomeric 6 $^{-}$ states 3-45955
 ^{57}Fe , calibration of isomer shift by lifetime meas. in different chemical environments (German) 3-49186
 ^{57}Fe , calibration of isomer shift from lifetime and Mossbauer meas. on 14.4 keV state 3-62984
 ^{250}Fm , existence and assignments of isomer states, cross bombardment techniques 3-62950
 ^{174}Hf , ^{176}Hf isomeric states populated in (α ,nnp) reactions, g-factors and proton-neutron mixing ratios 3-45967
 ^{178}Hf , ^{180}Hf , Mossbauer meas. of isomer shift and quadrupole moment ratios 3-49206
 $^{179}Hf(n,n_2)^{178m}Hf$ cross section for 14.8 MeV neutrons 3-63061
 $^{113}In(n,n_2)^{114m}In$ cross section for 14.8 MeV neutrons 3-63061
 ^{115m}In , from $^{115}In(\gamma,\gamma')$ 100-800 MeV, measured half life, E_γ 3-67308
 ^{161}Lu 7.3 ms isomer from $^{148}Sm(^{19}F,6n)$, γ -ray transition and energy levels 3-54423
 ^{171}Lu , isomeric E1 and M1 transitions, half-lives 3-54422
 ^{173}Lu , isomeric E1 and M1 transitions, half-lives 3-54422
 ^{50}Mn pop. in $^{50}Cr(p,n)^{50}Mn$, determ. separation of isomeric levels, threshold energy meas. 3-67212
 $^{96}Mo(p,n)^{96}Tc$ m.s., 10-65 MeV, production cross sections and isomer ratios of 4 $^{+}$ and 7 $^{+}$ states in ^{96}Tc 3-43240
 ^{93m}Mo 6.9 hr, mag. moment and spin determ. 3-62934
 ^{137}Nd , decay scheme study (Russian) 3-52140
 ^{254}No , existence and assignments of isomer states, cross bombardment techniques 3-62950
 Np, spontaneously fissioning isomer prod. in 14 MeV neutron reactions 3-71132
 ^{160}O , quadrupole deformed 6.05 MeV 0 $^{+}$ state 3-67177
 ^{194}Pb isomeric state behaviour, γ - γ coincidence obs. 3-62992
 ^{196}Pb isomeric state behaviour, γ - γ coincidence obs. 3-62992
 ^{198}Pb isomeric state behaviour, γ - γ coincidence obs. 3-62992
 Po, A=204-210, from Pb(3He , xn + γ) and Pb(α , xn + γ), stroboscopic resonance method, g-factors 3-71041
 $^{134}Pr \rightarrow ^{134}Ce$, decay scheme for isomeric and ground state from γ -ray obs. 3-49184
 Pu, spontaneously fissioning isomer prod. in 14 MeV neutron reactions 3-71132
 ^{237}Pu , spontaneous fission shape isomer, relative excitations 3-71136
 ^{239}Pu , thermal neutron capture, probability of formation of spontaneously fissionable isomer states (Russian) 3-71139
 ^{241}Pu spontaneously fissionable isomer, decay, search for α -emission (Russian) 3-40470
 ^{121}Sb , isomeric shift, meas. charge radius sign and magnitude (Russian) 3-62929
 ^{69}Se isomeric state decay behaviour, levels of ^{69}As 3-43222

nuclear isomerism continued

- ¹¹⁰Sn, isomeric shift, meas. charge radius sign and magnitude (*Russian*) 3-62929
¹²⁷Ta, isomeric E1 and M1 transitions, half-lives 3-54422
¹⁴⁷Tb, short-lived isomer behaviour 3-40464
¹⁴⁸Tb, short-lived isomer behaviour 3-40464
¹⁵⁴Tb, half lives and branching ratios of three isomeric states determ., spin assignments 3-67263
Th, spontaneously fissioning isomer prod. in 14 MeV neutron reactions 3-71132
U, spontaneously fissioning isomer prod. in 14 MeV neutron reactions 3-71132
²³⁵U, thermal neutron capture, probability of formation of spontaneously fissionable isomer states (*Russian*) 3-71139
^{235m}U, from ²³⁵U(n, γ), 60 keV, search, measured cross sections (*Russian*) 3-57530
⁸⁹Y(n, 2n)^{88m}Y cross section for 14.8 MeV neutrons 3-63061
^{89m}Y, from ⁸⁹Y(p, γ), 100-800 MeV, measured half life, E γ 3-67308
Yb, even isotopes, γ -ray spectroscopic study, single-line Mossbauer absorption, Yb levels, deduced isomer shifts 3-60109

nuclear liquid drop model

- broken symmetry systems, self-consistency conditions 3-59933
excited nuclei, statistical theory of decay, competition between fission and evaporation 3-43263
fissionable nuclei, Fermi-gas model for density of excited states 3-78266
fission, two-centre shell model with Lawrence family of liquid-drop shapes as equipotentials 3-49289
fission in stellar plasma, of heavy nuclides, shell and surface symmetry effects 3-69940
fission model, charge vibr. 3-78360
light nuclei with ang. momenta near liquid-drop limit, fission and fusion 3-63093
normalization of shell-model nuclei to liquid-drop model nuclei 3-62972
Strutinsky's averaging method of shell corrections for various potentials 3-49168
ternary fission, determ. of saddlepoint energies 3-52214
toroidal and spherical bubble nuclei, stability against breathing and sausage deformations 3-43198
⁴⁰Ca, nucl. breathing modes calc. 3-52119
²⁵²Cf, fission fragments prompt gamma energy from prompt neutron numbers, liquid-drop model calc. 3-54510
¹⁶⁰O, nucl. breathing modes calc. 3-52119
²⁰⁸Pb, nucl. breathing modes calc. 3-52119
²³⁹Pu, fission fragments prompt gamma energy from prompt neutron numbers, liquid-drop model calc. 3-54510
¹²⁰Sn, nucl. breathing modes calc. 3-52119
²³⁵U, fission fragments prompt gamma energy from prompt neutron numbers, liquid-drop model calc. 3-54510
⁹⁰Zr, nucl. breathing modes calc. 3-52119

nuclear magnetic moment

- see also gyromagnetic ratio; molecular nuclear coupling; nuclear magnetic resonance
A=17-27, projected Hartree-Fock calcs. of spin-isospin matrix elements 3-49180
A=70 mass region, compilation of magnetic moments of excited 9/2⁺ states 3-45948
anomalous coupling states with spin I=j-1, e.m. properties 3-49104
anomalous g_i factor, empirical deduction for nucleons 3-49094
compilation and evaluation of 'best-value' list, effects of environment of nucleus 3-45937
conjugate nuclei, analysis of magnetic and Gamow-Teller moments, one-body operator framework 3-45945
 $d_{3/2}$ nuclei, g factor determ. from configuration mixing, calc. of first-order effects 3-52072
deformed nuclei, calcs. using zeroth and second order wave functions 3-45968
deformed nuclei, magnetic moments in pseudo SU(3) model 3-49130
deformed nuclei around Ba, gyromag. ratios 3-43172
density dependent residual interaction calcs., effective charges and g-factors 3-49118
dipole operator, effects of core polarisation and mesonic exchange current 3-45946
effective g_s values for some odd-A deformed nuclei from lifetime meas. 3-49110
exchange current, N^{*}₃₃-isobar and tensor force effects 3-45927
exchange magnetic moment, calc. of isoscalar part by ρ -exchange and OBE models 3-49121
excited levels, time-integral angular correlation expts. using gaseous sources 3-49076
 $f_{7/2}$ shell nuclei, configuration mixing calcs. 3-49125
giant analogue excitations by allowed muon capture in 1p-shell nuclei 3-60126
hadron magnetic dipole moments, description 3-49003
high-spin isomeric states, mesonic anomaly in orbital g factors 3-45929
hyperfine structure of muonic atoms, determ. of nuclear magnetism distrib. and moments of excited states 3-45931
isomeric states, nuclear alignment meas. technique using anisotropy of emitted γ -rays 3-49080
meson exchange effects, pion theory and Fermi gas model 3-45928
mirror moments and effective g-factor for nucleon in nuclei 3-45953
mirror pair, spin-isospin distribution 3-45954
odd A nuclei with simple configuration, calc. using Kuo's effective interactions 3-49127
one spin species, n.m.r. absorption lineshape, high nuclear polarisations, paramag. impurities 3-60996
relativistic corrections, determ. from Dirac eqn. 3-43175
relativistic corrections 3-49122
review of e.m. transitions and moments 3-54433
shell model spectroscopy of f-p-shell nuclei with 42 \leq A \leq 44, core excitation effects 3-67236
short-lived high spin states, review of exptl. measurement techniques 3-45930
short-lived states, meas. by use of stopper in recoil-into-gas method, hyperfine interactions 3-45934

nuclear magnetic moment continued

- single-level configurations, determ. of matrix elements of two-body M1 operator 3-49123
three-nucleon bound state problems 3-49162
²⁸Al, ²⁹Al, shell model calcs. using modified surface-delta-interaction Hamiltonian 3-49167
⁷²As, of new isomeric level at 215 keV populated in ⁷²Ge(p,n) reaction 3-45956
⁷⁵As, of 265 keV level, using integral method of perturbed angular correlation technique 3-49105
²¹¹At, anomalous g_i-factor meas. by DPAD method 3-45961
²¹¹At, g-factor meas. of 21/2⁻ state by DPAD method 3-49093
AuIn₂ measurement, magnetometer, thermometry from 1.7 mK to 0.5K 3-73817
^aAu, A=196, 198, 200, magnetic moments of 12⁻ states, low-temp. orientation expts. 3-45952
¹⁹⁶Au, oriented, n.m.r. obs. 3-40453
¹⁹⁸Au, oriented, n.m.r. obs. 3-40453
^{200m}Au, oriented, n.m.r. obs. 3-40453
⁸B, recoil polarisation from ⁶Li(³He,n), n.m.r. meas. of β -decay asymmetry, magnetic moment determ. 3-49077
⁸B in Ta, n.m.r. detn. of mag. moment 3-45963
¹²B, from spin inversion by transverse pulse technique 3-49224
¹²B in Ta, n.m.r. detn. of mag. moment 3-45963
Bi radioactive isotopes, low temperature orientation in ferromagnetic BiMn, nuclear structure studies 3-46008
²⁰⁶Bi, 10⁻, 0.88 ms isomeric state, moments of pure shell model states from g-factor meas. 3-71042
²⁰⁹Bi, calc. of dipole and octupole moments using linear response theory of finite Fermi systems 3-49129
²⁰⁹Bi, polarised, magnetic hyperfine structure in muonic atom, coupling consts. anomalous g-factor 3-46216
⁴¹Ca, violation of additivity of Iff_{7/2} neutron moments 3-45964
⁴¹Ca deformed component inclusion 3-43173
⁴³Ca, n.m.r. obs. in aqueous calcium salt solns. 3-74483
⁵⁶Co, ⁵⁷Co, effective M1 operators, shell model calcs. 3-49124
⁵³Cr, effective M1 operators, shell model calcs. 3-49124
⁶²Cu excited states, time differential perturbed ang. distrib. obs. 3-63000
⁶⁴Cu, ⁶⁶Cu, isomeric 6⁻ states populated in (d,p) reactions, time differential obs. of Larmor precession 3-45955
¹⁶¹Dy, Coulomb excitation of 43.8 keV state, Mossbauer effect study of transition 3-62990
¹⁵¹Eu, hyperfine broadening of X-ray lines 3-49391
⁵⁶Fe, effective M1 operators, shell model calcs. 3-49124
⁵⁷Fe, from Mossbauer meas. 3-52075
⁶⁴Ge, of excited 9/2⁺ state by perturbed angular distrib. meas. on ⁶⁴Zn(α ,n) 3-45948
¹H, determ. of ratio of proton and deuteron moments 3-62936
¹H pseudo magnetic moments meas. method 3-67185
²H, change from spin-orbit potential in nucleon-nucleon interaction, various potentials 3-71044
²H, determ. of ratio of proton and deuteron moments 3-62936
¹H, effect of meson-exchange currents 3-49120
³H, magnetic moment, effect of meson-exchange currents 3-49120
³H, quark model study, nucleon and nuclear resonance effects 3-52073
³He, nucl. polarisation by optical pumping, apparatus development and relax. time meas. (*French*) 3-46185
³He, quark model study, nucleon and nuclear resonance effects 3-52073
¹⁷⁷Hf, dipole moments, ground state h.f.s. 3-40412
¹⁷⁹Hf, dipole moments, ground state h.f.s. 3-40412
Hg isomers, precision magnetic moment determ., hyperfine-structure anomalies, optical pumping expt. 3-62933
Hg isotopes, distribution of nuclear magnetisation 3-78241
^{199m}Hg, precision magnetic moment determ., hyperfine-structure anomalies, optical pumping expt. 3-62933
¹²⁵¹I, 188 keV excited state, g-factor calc. by perturbed ang. correl. method 3-78243
¹²⁵In muonic atoms, magnetization distrib. of single-particle states and 2⁺ rotational states 3-49209
¹⁹¹Ir, 171 keV level 3-40452
¹⁹¹Ir, low-lying level struct. and e.m. props. 3-62953
¹⁹³Ir, low-lying level struct. and e.m. props. 3-62953
K isotopes, g factor determ. from configuration mixing, calc. of first-order effects 3-52072
³K, spin and magnetic moment determ. from β -decay asymmetry following polarisation by optical pumping 3-45939
³K, deformed component inclusion 3-43173
⁶Li, one-body densities for valence nucleons, determ. of wave-function parameters using e.m. data 3-49245
⁶Li, dipole moment determ. from Knight shift and spin-lattice relax. meas. in metal foils 3-40409
²⁷Mg, ²⁸Mg, shell model calcs. using modified surface-delta-interaction Hamiltonian 3-49167
⁵⁴Mn, ⁵⁵Mn, effective M1 operators, shell model calcs. 3-49124
⁵⁵Mn in Cr-Mn antiferromagnetic alloys, n.m.r. 3-68857
^{93m}Mo 6.9 hr, ang. distrib. obs. 3-62934
¹⁴N, 3⁻, 5.83 level excited in ¹²C(³He,p) reaction, recoil into gas and Blume-Scherer model 3-49083
¹⁷O, Schmidt value reduction 3-43173
¹⁹⁰Os, ¹⁹²Os muonic atoms, magnetization distrib. of single-particle states and 2⁺ rotational states 3-49209
¹⁹³Os, ground state, orientation obs. 3-40452
²⁰⁷Pa, g-factor of 13/2⁺ state and mesonic contrib. to moment of i_{13/2} neutron 3-49137
Pb region, g-factors of high-spin shell model states, summary 3-45950
Pb-region single particle states, reaction matrix calc. including mesonic exchange currents 3-52080
²⁰⁶Pb, 12⁺ isomeric state populated in ²⁰⁴Hg(α ,n) reaction, neutron effective orbital g-factor 3-49087
²⁰⁷Pb, ²⁰⁸Pb, first excited states meas. by $\gamma\gamma$ -IPAC technique 3-45960
²⁰⁷Pb, ²⁰⁹Pb, calc. of dipole and octupole moments using linear response theory of finite Fermi systems 3-49129
²⁰⁸Pb, semi-empirical analysis magnetic moments of single-particle (hole) states assumed core, B(M1) values 3-52081
²⁰⁸Pb region, magnetic dipole transition rates 3-49205

nuclear magnetic moment continued

- ²⁰⁸Pb region, multipole, transition probabilities of single-particle states 3-60071
- ¹⁴³Pm, effective M2 gamma transition moments 3-45997
- ¹⁴⁵Pm, effective M2 gamma transition moments 3-45997
- Po isotopes, g-factors of $[\pi h^2]_8^+$ and $[(\pi h^2)_{9/2}]_{8(0)} \times \nu P_{1/2}^{-1}]_{17/2}^-$ states 3-71041
- ²⁰⁴Po, $[(\pi h^2)_{9/2}]_8^+$ states, meas. 3-49088
- ²⁰⁴Po, g-factor of 8^+ states, meas. by stroboscopic resonance method 3-49090
- ²⁰⁶Po, $[(\pi h^2)_{9/2}]_8^+$ states, meas. 3-49088
- ²⁰⁶Po, g-factor of 8^+ states, meas. by stroboscopic resonance method 3-49090
- ²⁰⁷Po, g-factor of $13/2^+$ neutron hole state, from ²⁰⁶Pb(α , 3n), E=38 MeV 3-49089
- ²⁰⁸Po, g-factor of 8^+ states, meas. by stroboscopic resonance method 3-49090
- ²⁰⁹Po, g-factor of $17/2^-$ state, meas. by stroboscopic resonance method 3-49090
- ²¹⁰Po, g-factor of 8^+ states, meas. by stroboscopic resonance method 3-49090
- ²¹⁰Po, M1 core polarizabilities of 8^+ and 6^+ states, shell model calcs. 3-49117
- ²¹⁰Po, mag. mom. meas. of core excited isomer of $]13^-$ by time-diff. spin-rot. method 3-49091
- ²¹⁰Po core-excited state, magnetic moment determ. by time-differential spin-rotation meas. 3-45972
- ²¹⁰Po₂, $g(\pi h^2)_{9/2}$ difference for 6_1^+ and 8_1^+ states, DPAC^{9/2} meas. of lifetimes 3-45951
- ¹⁴¹Pr, effective M2 gamma transition moments 3-45997
- RaE, determ. of configuration mixing ratios consistent with beta-decay and magnetic moment 3-52144
- ¹⁸³Re, meas. by nuc. orientation 3-49107
- ¹⁸³Re, orientation in Fe matrix, γ -ray anisotropy and magnetic hyperfine interaction 3-60110
- ¹⁸⁴Re, meas. by nuc. orientation 3-49107
- ¹⁸⁴Re, orientation in Fe matrix, γ -ray anisotropy and magnetic hyperfine interaction 3-60110
- ¹⁸⁴Re, meas. by nuc. orientation 3-49107
- ⁹⁹Ru, quadrupole moments ratio determ. by Mossbauer spectra 3-43170
- ³⁵S magnetic moment, n.m.r. obs. Larmor frequencies, chemical shift (German) 3-67190
- ¹²¹Sb, hyperfine broadening of X-ray lines 3-49391
- ¹²²Sb, $1.8 \mu\text{s}$ state, g factor determ. by stroboscopic method 3-67187
- ¹²²Sb, first excited state populated by ¹²²Sn(p,n) reaction, stroboscope resonance determ. of magnetic moment 3-45959
- ⁴¹Sc, recoil polarisation from ⁴⁰Ca(d,n), n.m.r. meas. of β -decay asymmetry, magnetic moment determ. 3-45938
- ⁴¹Sc in Ta, n.m.r. detn. of mag. moment 3-45963
- Se, A=75, 77, 79, 81, 83, anomalous coupling states, calc. of nuclear moments 3-49115
- Sn region, $11/2^-$ states, determ. from first-order core polarisation effects 3-67186
- ¹¹⁹Sn, from Mossbauer meas. on Co₂MnSn and Fe₃Sn 3-52075
- ¹¹⁹Sn, Mossbauer meas. of magnetic moment of 23.8 keV state and hyperfine anomaly 3-49208
- ⁸⁶Sr, g-factor of 8^+ state by time differential PAD method 3-54378
- ⁸⁶Sr, meas. on 8^+ state populated in ⁸⁸Sr(p,pnn) reaction 3-45957
- ⁸⁶Sr, mixing of giant magnetic dipole state with 1^+ state at 3.49 MeV 3-60113
- Te, odd mass isomers, study using nuclear orientation technique, γ -ray anisotropy meas. 3-60069
- ¹²⁷Te, $\mu_{3/2}$ detn. by nuclear orientation meas. 3-45966
- ¹²⁹Te, $\mu_{3/2}$ detn. by nuclear orientation meas. 3-45966
- ¹²³Te, nuclear orientation detn. of mag. mom. 3-49106
- ¹²⁵Te, nuclear orientation detn. of mag. mom. 3-49106
- ¹²⁵Te, nuclear orientation expt. at low temp., analysis in pairing-plus-quadrupole model 3-43177
- ¹²⁷Te, nuclear orientation detn. of mag. mom. 3-49106
- ¹²⁹Te, nuclear orientation detn. of mag. mom. 3-49106
- ²⁰³Tl, ²⁰⁵Tl muonic atoms, magnetization distrib. of single-particle states and 2^+ rotational states 3-49209
- ²⁰⁷Tl, calc. of dipole and octupole moments using linear response theory of finite Fermi systems 3-49129
- ¹⁶⁹Tm, moments of 316-, 379 keV excited states (Japanese) 3-74481
- ⁵¹V pseudo magnetic moments meas. method 3-67185
- ¹⁸²W, $K\pi=2^-$ band, γ - γ correlation study 3-49109
- ¹⁸⁷W, ground state, orientation obs. 3-40452
- ¹²⁹Xe, 40 keV level, time-integral angular correlation expts. using gaseous sources 3-49076
- ¹³³Xe, nuclear orientation expt. at low temp., analysis in pairing-plus-quadrupole model 3-43177
- ⁶⁷Zn, n.m.r. obs. in aq Zn(ClO₄)₂ soln. 3-79926
- ⁶⁷Zn, of excited $9/2^+$ state by perturbed angular distrib. meas. on ⁶⁴Ni(α ,n) 3-45948

nuclear magnetic resonance

- see also chemical shift; ENDOR; INDOR; knight shift; molecular nuclear coupling; nuclear acoustic resonance; nuclear quadrupole resonance; spin-lattice relaxation; spin-spin relaxation
- 2-[2'-pentaboran(9)yl]pentaborane(9), accidental degeneracy in ¹¹B n.m.r. spectrum, partially relaxed Fourier transform resolution 3-78840
- N-(diphenylmethylene)-aniline, determ. of dihedral angle of A ring 3-71486
- absorption lineshape, high polarisation, one spin species, paramag. impurities, M₁, M₂ 3-60996
- acetone, (CH₃)₂CO-(CD₃)₂CO mixture, determ. of ratio of proton and deuterium nuclear mag. moments 3-62936
- acetone, oriented, D spectra quadrupole coupling const. 3-64564
- acetone, partially deuterated, determ. of ratio of proton and deuterium nuclear mag. moments 3-62936
- acetylene, deuterated, plastic phase 3-79246
- alkali metal, radical anion soln., n.m.r. studies 3-44734
- alkali metal salts in propylene carbonate, of ²³Na, ionic solvation study 3-79931
- n-alkyl ammonium chlorides, wide line study of molecular motion 3-68852

nuclear magnetic resonance continued

- alkyl derivs., straight chain, electron density distrib. 3-71525
- 1-alkyl-3-aryltriazenes, tautomerism, n.m.r. spectroscopy 3-74929
- aminophosphines, ¹⁵N-¹H coupling consts., bonding 3-71575
- antiferromagnet, two-dimens., crit. exponents for n.m.r., e.p.r. line-widths 3-58418
- benzenes, fluorinated, in liq. cryst. solvents, H-F and F-F nucl. mag. spin-spin coupling anisotropies 3-40655
- benzil, position of phenyl rings 3-71486
- benzophenones, orthosubstituted, conformational preferences, ¹³C n.m.r., calc. torsional angles 3-49489
- benzotrifluorides Fourier transform, high pressure, ¹⁹F chemical shift, intermolecular, intramolecular effects 3-61003
- benzylcyanide, liq., mol. rot. at high press., n.m.r. relax. obs. 3-68871
- tert-benzyllic metal compounds, structure and hindered rotation determ. 3-63514
- biphenyl radical anions, ¹H and ²D n.m.r. studies 3-43488
- bis(cyclooctatetraene)iron, n.m.r. study, line-width and second moment rel. to temp. 3-50477
- bisphenol-A, diglycidyl ether, cured with methylenedianiline, pulsed n.m.r. studies, molecular motion 3-54771
- bisphenol-A uncured diglycidyl ether, pulsed n.m.r. study of molecular motion 3-58443
- Bloch equations and adiabatic rapid passage with radiation damping 3-68822
- borate glasses, ²³Na and ⁷Li n.m.r. studies (German) 3-72544
- 1-bromo-3,3,4-trifluorobutene-4, determ. of ¹⁹F, ¹³C and ¹H chemical shifts and coupling constants 3-75072
- 2-bromo-5-chlorothiophene, n.m.r. AB spectrum, use of compensating device for parasitic beat signal 3-77595
- 2-brompyridine, of ¹³C, long-range ¹³C-¹H spin coupling consts. 3-43483
- t-butylchloride, self-diffusion coeff. and rot. correlation time determ. 3-68872
- camphor, mol. dynamics, ¹³C n.m.r. relax. times 3-68881
- cancerous tissue, spin echo obs. 3-42366
- carboranes and organotin derivatives, ¹H-¹¹B heteronuclear magnetic double resonance spectra 3-78848
- chemical applications of ¹³C n.m.r. 3-54729
- chemically induced nuclear dynamic polarisation, nuclear and electron spin coupling, student experiment 3-48324
- chloroform, liq., mol. reorient. at high press., n.m.r. relax. obs. 3-68871
- coherence effects induced by aperiodic impulses (French) 3-52263
- coherence resonances, analog calcs., Bloch eqns. (French) 3-54573
- computer controlled digital freq. synthesizer for n.m.r. spectroscopy 3-77593
- computer simulation 3-78854
- conference, Athens, Georgia, USA, Oct. 1972 3-54719
- conformations, H and ¹³C n.m.r. spectroscopy 3-67875
- π -cyclobutadienyliron tricarbonyl, intramol. rot. obs. from nematic-phase n.m.r. 3-60481
- d.c. electromagnet, automatic n.m.r. control of flux density 3-48488
- deuterated acetamide, of D, spin mixing to give pure n.q.r. 3-63522
- dialkylaminophosphines, determination of electronic character of P-N bond (French) 3-49439
- diamagnetic crystals, line shape 3-75908
- diamagnetic metal, observability of nuclear orientation n.m.r. on paramag. impurity 3-47155
- 4,4'-dichlorobiphenyl oriented in nematic M.B.B.A., structure and conformation 3-67853
- m-difluorobenzene, in nematic solvents, geom. and indirect F-F coupling anisotropy 3-60477
- 1,2-difluoroethane in nematic solvents 3-43482
- dimethoxybenzene, ortho, meta and para, nuclear spin-lattice relaxation, cross correlation effects 3-55490
- 2,4-dimethoxypentane, ¹³C n.m.r. studies on stereochemical configurations 3-63577
- dimethyl sulphoxide, D spectra, quadrupole coupling consts. 3-64564
- dinucleotides, backbone conformation, ¹³P and ¹H fast Fourier transform n.m.r. spectroscopy 3-67850
- dipolar coupled spin system in rigid lattice, tetrahedral magic echo generation 3-72531
- dipolar operators, broadening effects interpret. 3-68823
- double resonance spectra of partially aligned systems, computer calculations 3-47171
- durene single crystals, ¹³C chem. shielding tensors using proton-enhanced n.m.r. 3-64580
- elastomer, rapidly rotated, line narrowing effect, monomer ratio and conform. struct. obs. 3-78916
- elbaite, n.m.r. studies, ¹H, ⁷Li, ¹¹B, ²³Na and ²⁷Al, crystal structure 3-44768
- electronic spin-spin interactions contrib., in dynamic nuclear polarisation, theory 3-79890
- enzyme-substrate transition states, conformational changes, ¹³C chemical shifts 3-71674
- epoxy resin, thermoplastic polymer mixture, mol. mobility 3-64578
- ethenes, fluorinated, in liq. cryst. solvents, H-F and F-F nucl. mag. spin-spin coupling anisotropies 3-40655
- ether in chloroform soln., association and anisotropic mol. reorientation, n.m.r. obs. 3-68873
- ethylene and vinyl acetate copolymers, partly crystalline, molecular mobility, dynamic meas. (German) 3-63589
- Fe-Ru alloy, dilute, n.m.r. of host and impurity nuclei, hyperfine fields 3-64560
- ferromagnetic film, decoupling of nuclear-electron modes at ferromag. resonance 3-41417
- ferromagnetic films, magnetostriction effect on temp. depend. 3-75889
- flip-flop sequence for restoring Zeeman order in laboratory reference frame 3-53029
- fluorenone radical anions, ¹H and ²D n.m.r. studies 3-43488
- fluoroacetones, rotational isomerism 3-78843
- fluoroacetones, coupling consts. and rot. isomerism 3-46323
- fluorobenzene-d₅, liq., mole. reorient. at high press., n.m.r. relax. obs. 3-68871
- fluorocyclopentenes, ¹⁹F chem. shift and (F,F) coupling 3-57669
- fluorophosphate anions containing P-P bond 3-54721

nuclear magnetic resonance continued

- Fourier analysis of high resolution spectra 3-66295
 Fourier spectroscopy, saturation effects 3-60997
 Fourier synthesised excitation, homonuclear decoupling, solvent line suppression application 3-72505
 Fourier transform, ^{117}Sn , ^{119}Sn spin-lattice relax. times 3-68884
 Fourier transform, pulsed, spin-lattice relax. times 3-68824
 Fourier transform, repetitive pulse, causality principle, absorpt., dispersion 3-64535
 Fourier transform methods, relaxation study 3-70334
 Fourier transform n.m.r., Varian XL-100, observation of nuclei other than ^1H and ^{13}C 3-77589
 Fourier transform n.m.r. spectroscopy 3-53957
 Fourier transform relationship between n.m.r. free induction decay and c.w. line shape, comment 3-60994
 Fourier transform relationship between n.m.r. free induction decay and c.w. lineshape, reply to comment 3-60995
 Fourier transform spectra, Wangness-Bloch-Redfield kinetic equation 3-68859
 Fourier transform spectrometer, computerised 3-66293
 Fourier transform/CW variable freq. spectroscopy on XL-100-15 3-77590
 free induction decay with radiation damping, general treatment 3-55479
 gas phase, review 3-60521
 gases self-diffusion, n.m.r. technique and pulsed spectrometer 3-66292
 ground state spin and moments of shortlived nuclei, measurement technique 3-45932
 hexamethylenetetramine, ^{14}N rotational correl. time in chloroform 3-75900
 holocyclopentanes, spectra, conformations, calcs. 3-63366
 hydrated systems, study using frequency dependence of relaxation processes 3-53960
 hydrocarbons, conformation and distortion, n.m.r. and i.r. spectra (*Russian*) 3-71491
 hydrocarbons adsorbed on zeolites, ^{13}C n.m.r. investigations (*German*) 3-47600
 hydroxyl protons, special spectral features 3-79928
 III-V semiconductors, n.m.r. obs. of stoichiometry deviations 3-44336
 imidazole derivatives and complexes, high resolution ^{13}C n.m.r. spectra 3-75892
 2,2'-iminobis(acetamidoxime) and its Ni(II) and Zn(II) complexes, barrier to rotation 3-52331
 intracellular Na in human erythrocytes and frog muscle, line intensities 3-48165
 intramolecular reorientation, time correl. functions 3-49492
 inversion of nuclear magnetization by π pulse, effect of inhomogeneity of external field (*Russian*) 3-42614
 lamellar potassium oleate- D_2O membrane bilayers, n.m.r. free induction decay, spin echoes 3-45258
 Licristal IV, nematic phase, diffusion coeff. anisotropy for small mols., n.m.r. technique meas. 3-52576
 LiF, gamma-irradiated, ^{19}F n.m.r. 3-79370
 line shape, motional narrowing, analysis 3-41436
 linear spectrum meas., statistical analysis 3-75867
 lineshapes, asymmetry due to nonrandom mag. field inhomogeneities 3-64563
 liquid, mol. motion, n.m.r. and neutron scatt. obs. 3-68875
 liquid, mol. motion effect on relax. 3-68883
 liquid, molecular motion, random walk theory 3-68877
 liquid, molecular motion obs., limitations 3-72214
 liquid, reorientational motions at high press., n.m.r. relax. obs. 3-68871
 liquid, simple, anisotropy in mol. reorientational motion 3-68995
 liquid, translational motion and intermol. relax. rate 3-68870
 liquid, transverse relaxation rates, measurement errors 3-79935
 liquid crystal, lyotropic, deuteron spectrum of ordered D_2O , mag. field gradient effect 3-47154
 liquid crystal, smectic-A to nematic transition, second order, orientational order 3-54925
 liquid crystals, spectroscopy, review 3-43747
 liquids, wall effects in nuclear relaxation 3-62188
 lithium stearate spin-lattice relaxation measurements, polycrystalline samples, room temp., Provotorov theory, Redfield theory 3-58437
 long-lived isomer spectroscopy, pulsed-beam expts., influence of time-windows on NMR-PAC line shapes 3-45995
 lyotropic liquid crystal, proton relaxation study of paraffinic chain motions 3-41445
 lyotropic nematic phases, complex ion struct. using n.m.r. technique 3-55484
 magnetic field gradient measurement by effect on n.m.r. free induction decay 3-53955
 magnetic field measurement applic., a.m. of magnetic field (*Hungarian*) 3-70331
 many-site exchange problems, line shape calculation, Kubo-Sack probability matrices 3-80540
 maser, nucl. spin analogue with cavities in series 3-62682
 measurement of unresolved couplings in first-order spectra 3-53958
 metallic powders, r.f. echoes 3-79923
 metalloenes, paramagnetic ^{13}C spin density distrib., pulse Fourier transform n.m.r. 3-75906
 methane, solid, spin conversion, proton magnetisation, spin-lattice relaxation 3-75903
 methanol, liquid, ^{13}C nuclear magnetic relaxation mechanism 3-44345
 methyl iodide, liq., rot. diffusion obs. 3-75976
 methylamines, liquid, self-diffusion coeffs., n.m.r. obs. 3-68874
 methylene chloride mixtures with toluene, benzene and xylenes, dielectric polarisation, n.m.r., u.v. and i.r. studies 3-58817
 exo-methylenecycloalkanes, ^{13}C - ^{13}C coupling consts. and chem. shifts 3-75080
 3-methylpyridazine, asymmetric signal of terminal ring CH_3 group, origin 3-75088
 millidegree thermometer, continuous wave, design, low temp. application 3-48388

nuclear magnetic resonance continued

- molecular conformational anal. by ^{13}C n.m.r., lanthanide shift reagents, T_1 meas. 3-67855
 molecular crystals, rel. to random molecular reorientation 3-75895
 molecular spherical tensors, ensemble averages 3-43493
 moment measurement, truncating errors in spectra 3-63523
 monocrystal: impurity γ -radioactive nucleus, spectra, defection mechanism 3-79961
 monosaccharides, amorphous spin-lattice relaxation time, temp. depend. 3-79940
 multiplet splittings, deception simplicity and virtual coupling 3-77592
 multipulse and Fourier transform expts., computer simulations using density matrix eqns. of motion 3-75868
 muscle water, proton mobilities 3-56486
 naphthalene mol. struct. determ. by n.m.r. in a nematic solvent 3-74919
 non-exponential decay, analysis 3-44333
 nucleotides, 2',3'-cyclic, ^{13}C and ^1H n.m.r. study of conformations 3-63570
 nucleotides, 3',5'-cyclic, ^{13}C n.m.r. spectra, conformation investigation 3-63569
 observation installation, weak signals, phase quantisation method 3-73821
 organic ammonium salts, ^{13}C and ^{14}N nuclear relax., using Fourier transform spectrometer 3-68882
 organic compounds, ^{13}C , continuous wave proton spin decoupling, virtual coupling 3-71574
 organic molecules, uncoupled pulsed Fourier transform ^{13}C n.m.r. spectra 3-75085
 organo(seleno,telluro)phosphorus cpds., ^{31}P n.m.r. obs. of ^{31}P - ^{77}Se , ^{31}P - ^{125}Te spin-spin coupling consts. 3-75087
 organometallic compounds, Fourier transform n.m.r. spectroscopy, spin-spin coupling consts. 3-75893
 organophosphorus compounds, asymmetric centres, Fourier transform spectroscopy 3-75894
 organosilicon compound, ^{29}Si , ^{13}C n.m.r. meas., substituent effect 3-72533
 orthosubstituted diphenyl sulphones, n.m.r. data and conformational preferences 3-54718
 3-oxypiperidone-4, stereochemical structure (*Russian*) 3-71493
 3-oxytetrahydrothiopyranone-4, stereochemical structure (*Russian*) 3-71493
 paraffins, ^{13}C n.m.r., mag. shielding consts. calc. by Gaussian function 3-71593
 parasitic beat signal, use of solid state compensating device 3-77595
 passive spin stabilizers, static, dynamical and statistical characteristics (*Russian*) 3-44337
 pentanes, 2,4-disubstituted, n.m.r. conformation analysis using local interaction model 3-71487
 perdeuteronitrobenzene dissolved in benzene and CCl_4 , elec. field induced dipolar alignment 3-64565
 phenanthrene radical anions, ^1H and ^2D n.m.r. studies 3-43488
 phenol, molecular rotation study by neutron scattering and n.m.r. 3-52567
 phospholenes (I and II)-Ni(AcAc), dispersion of ^1H -(^{31}P) heteronuclear chem.-exchange spin decoupling 3-75086
 phosphonium salts, ^{31}P n.m.r. obs., electron delocalization through P rel. to $\text{d}_\pi\text{-p}_\pi$ bonding 3-71597
 phytoene isomers, of ^{13}C , struct. obs. 3-46361
 PMMA, stereocomplex between isotactic and syndiotactic oligomers in soln., struct., n.m.r. obs. 3-75168
 polarisation, at saturation of allowed and forbidden resonances (*Russian*) 3-68855
 poly-L-alanine, optical rotation dispersion config. transforms. 3-63581
 poly-L-leucine, optical rotation dispersion, config. transforms. 3-63581
 polyacrylates and model compounds, ^{13}C n.m.r. 3-63576
 polyacrylic acid and model compounds, ^{13}C n.m.r. 3-63576
 polyalkenamers, n.m.r. and i.r. spectroscopy, structural unit determ. 3-54046
 polyalkyl vinyl ethers, ^{13}C n.m.r. studies on stereochemical configurations 3-63577
 polyethylene, molecular motion, line shape analysis (*German*) 3-61007
 polyethylene molecule, with fixed ends, rel. to struct. of partly crystallised substances (*German*) 3-60999
 polyethylene terephthalate, amorphous, n.m.r. expts. for nuclear relaxation, spin dynamics 3-75909
 polyisopropyl acrylate, ^{13}C n.m.r. 3-63576
 polymethyl acrylates and model compounds, ^{13}C n.m.r. 3-63576
 polymethyl vinyl ether, ^{13}C n.m.r. studies on stereochemical configurations 3-63577
 polypeptide in non-protonating solvents, helix-coil transition, n.m.r. obs. 3-67870
 polysodium acrylate and model compounds, ^{13}C n.m.r. 3-63576
 porous media containing NaCl soln., of ^{23}Na , relax. rates obs. 3-60993
 porphyrin and alkylsubstituted derivatives, ^{13}C Fourier transform spectroscopy 3-71601
 potassium caproate spin-lattice relaxation measurements, polycrystalline samples, room temp., Provotorov theory, Redfield theory 3-58437
 proton-enhanced, of dilute spins in solids, h.f. resolution 3-61010
 pulse Fourier transform ^{199}Hg n.m.r. spectroscopy 3-59615
 pulsed, for solid fat content determ. in partially crystallized fats 3-62190
 pulsed n.m.r. signals, one- and two-component, amplitude conversion analysing method 3-75870
 pulsed NMR spectrometer, interface to Varian 620/i computer 3-39981
 pyridine, of ^{13}C , long-range ^{13}C - ^1H spin coupling consts. 3-43483
 pyridine nucleotides, conformation, ^{13}P and ^1H fast Fourier transform n.m.r. spectroscopy 3-67850
 pyridine-bromine complex oriented in nematic phase, geometry 3-41432
 L-pyroglytamic acid, and conformations, and related compounds (*French*) 3-63519
 pyrrole, ^{15}N enriched, natural abundance ^{13}C n.m.r. obs. 3-75083

nuclear magnetic resonance continued

- pyrrole, of ^{15}N and ^{13}C , coupling consts. 3-78846
 quantitative meas., optimum experimental conditions 3-77591
 rare earth yttrium iron garnet, $\text{R}_{0.3}\text{Y}_{2.7}\text{Fe}_3\text{O}_{12}$: ^{57}Fe , spin echo method, domain wall motion 3-50475
 ribonucleic acid, transfer, ^{31}P and ^1H high resolution spectra, chemical shift 3-75167
 Rouse chain, transverse nucl. magnetisation dynamics, fluctuation effects 3-40690
 saccharides and polysaccharides, conformational analysis by n.m.r. (*Russian*) 3-63587
 self-diffusion coefficient, Fourier transform of spin echo, pulsed gradient 3-68868
 silicate glasses, ^{23}Na and ^7Li n.m.r. studies (*German*) 3-72544
 simulation, multipulse, Fourier transform, Bloch equations, effect on magnetisation vector 3-56708
 single coil service resonant circuit, for pulsed nuclear resonance 3-45540
 sodium hydrogen oxalate monohydrate, deuteron magnetic resonance, hydrogen bond studies 3-72529
 solid surface/adsorbed molecules, n.m.r. line shape and relaxation times (*Russian*) 3-55499
 solvation shell obs. using ^{13}C and ^{27}Al n.m.r. 3-71603
 solvation shell obs. using ^{13}C and ^{31}P heteronuclear pulsed n.m.r. 3-75084
 spectrometer, c.w., for H_1 field meas. using dynamic nuclear polarisation 3-45538
 spectrometer, two pulse experiments, interfaced minicomputer, techniques 3-73828
 spectrometry, scheme for self-correcting coherent phase errors 3-58414
 spectroscopy, computer for display and processing 3-66294
 spectroscopy, digital program controlled generator 3-66296
 spectroscopy, molecular biological research, basic concepts, methods (*German*) 3-54029
 spin echo, Fourier transform methods for relax. rates 3-64576
 spin echo observation techniques (*French*) 3-53012
 spin echo phenomena, transient and stationary regimes (*French*) 3-55482
 spin generator, for n.m.r. spectroscopy 3-56707
 spin-lattice relax. time meas. using repetitive sweep techniques 3-59616
 spin-lattice relaxation time, influence of cross relaxation effect 3-75071
 strontium formate dihydrate, deuterated, struct., deuteron mag. reson. study 3-64569
 4-substituted α -methylstyrenes and α -t-butylstyrenes, substituent effects 3-52386
 4-substituted styrenes, substituent effects 3-52385
 symmetrical spin system with arbitrary spin I, theory of n.m.r. spectra (*German*) 3-53031
 symmetrical spin systems with $I=Y_2$, theory of n.m.r. spectra (*German*) 3-53030
 o-terphenylphenols, Fourier transform ^{13}C n.m.r. spectra 3-71590
 1, 1, 1, 2-tetrachloro-2-methylpropane, solid, n.m.r. static and rotating frame relaxation 3-72538
 tetramethyltitanium/tetramethylaluminium, methyl group exchange, d.m.r. obs. 3-75089
 tetraphenylethylene, conformation of phenyl rings, using n.m.r. and Fraenkel relation 3-71485
 thermometers at very low temps., possible limitation 3-55480
 thermostat, 8 to 400 K temp. control 3-51551
 thulium ethyl sulphate, ^{169}Tm line width 3-64577
 thyatron switch, for pulsed apparatus 3-66290
 using time-sharing technique for signal amplification (*German*) 3-42612
 tourmaline minerals, n.m.r. studies, ^1H , ^7Li , ^{11}B , ^{23}Na and ^{27}Al , crystal structure 3-44768
 transition metal complexes, electron relax. time determ. by ^{13}C and ^{14}N n.m.r. 3-75078
 tri-(3-bromo-2-thienyl) phosphine, ^{13}C - ^{31}P coupling, off resonance proton decoupling 3-75069
 trichloroethylene in mixtures of HMPT and cyclohexane, ^{13}C and ^1H chemical shifts as function of conc. and temp. 3-75898
 tricyclic hydrocarbons, ^{13}C n.m.r. spectra for struct. determ. 3-75067
 2,4,6-trifluoronitrobenzene, ^1H , ^{19}F , and ^{14}N spectra, external field effects 3-68854
 two isotropically rotating molecules, magnetic dipolar interaction 3-46599
 two-cycle n.m.r. spectrometer based on spin echo effect, non-stationary analysis (*Russian*) 3-66291
 two-phase systems, mathematical processing of expt. data (*Russian*) 3-62189
 two-proton system with hindered rot., methyl group tunnelling, n.m.r. lineshapes 3-64562
 vinyl acetate and ethylene copolymers, partly crystalline, molecular mobility, dynamic meas. (*German*) 3-63589
 vinyl-Pt complexes, coupling consts. Pt hybridisation 3-75065
 water, self-diffusion meas. 3-68430
 yttrium ethyl sulphate: Dy, Yb, proton polarisation and relaxation, pulsed refrigerator optimal conditions 3-47161
 yttrium ethyl sulphate: Er, c.w. n.m.r. spectrometer for H_1 field meas. 3-45538
 zeolitic germanates, relaxation rel. to diffusion processes 3-55495
 Ag halides depolarization and beta-decay of ^{110}Ag , n.m.r. obs. 3-61006
 Ag-Gd, dilute, mag. susceptibility, n.m.r. and thermolec. power obs. of impurity state 3-68765
 $\text{Ag}_2\text{H}_3\text{O}_6$ quadrupole interaction of ^{127}I , phase transform. behaviour (*German*) 3-53034
 AgPF_6 , chemical shift in n.m.r. of ^{19}F 3-61002
 ^{110m}Ag oriented in Fe and Ni, meas. of hyperfine interactions by n.m.r., β -mixing 3-46009
 $\text{Al}(\text{BH}_4)_3$, correlated NMR-Raman spectra 3-72623
 $\text{Al}_{1-x}\text{Cu}_x$:Mn, liquid alloy, n.m.r. shifts and relaxation times, local moment formation 3-58438
 Ar, liq., self-diffusion meas. 3-68430
 $\text{As}(\text{C}_2\text{F}_5)_3$, i.r. and Raman spectra and ^{19}F n.m.r. 3-71561

nuclear magnetic resonance continued

- ^{196}Au , oriented, γ -ray anisotropy temp. depend., h.f.s., mag. moments, spins 3-40453
 ^{198}Au , oriented, γ -ray anisotropy temp. depend., h.f.s., mag. moments, spins 3-40453
 ^{200m}Au , oriented, γ -ray anisotropy temp. depend., h.f.s., mag. moments, spins 3-40453
 BH^-4 and BF^-4 ions, ^{10}B - ^{11}B primary isotope effect on boron nucl. shielding 3-46324
 B_2H_6 and B_2D_6 , ^{11}B , splittings resolution, line narrowing technique 3-57666
 ^8B , recoil polarisation from $^6\text{Li}(^2\text{He},n)$, n.m.r. meas. of β -decay asymmetry, magnetic moment determ. 3-49077
 ^8B in Ta, mag. moment detn. and eqQ sign assignment 3-45963
 ^{12}B in Ta, mag. moment detn. and eqQ sign assignment 3-45963
 $\text{BaFe}_{12}\text{O}_{19}$: ^{57}Fe domain walls, freq. shift in static mag. field 3-79929
 ^{206}Bi , 10-, 0.88 ms isomeric state, g-factor meas. using in-beam NMR-PAC 3-71042
 ^{13}C , peaks assignment by off-reson. irradi. of strongly coupled protons 3-43485
 ^{13}C , use of added Cr(III) in solutions in measurements 3-55496
 ^{13}C Eu-induced Fermi contact shifts 3-63516
 ^{13}C Fourier transform apparatus at 14.2 kG, probe for 20 mm spinning sample tubes 3-73827
 ^{13}C lanthanide-induced contact versus pseudocontact shifts 3-63515
 ^{13}C mag. resonance in investigation of mol. dynamics and structure 3-67856
 ^{13}C - ^1H , intermolecular Overhauser effect 3-43478
 CaF_2 spin-lattice relaxation measurements, polycrystalline samples, room temp., Provotorov theory, Redfield theory 3-58437
 CaF_2 : Yb^{3+} , near nuclei magnetic resonance 3-44334
 ^{43}Ca , aqueous solns. of CaBr_2 , CaCl_2 , $\text{Ca}(\text{NO}_3)_2$ 3-74483
 CdF_2 : ErF_3 , ^{19}F n.m.r. at 8 and 16 MHz 3-44329
 $^{111}\text{Cd}^+$, fund. level orientation by collisions with metastable He, h.f.s. const. (*French*) 3-78502
 $\text{Ce}_{1-x}\text{La}_x\text{Al}_3$ ($\text{R}=\text{Gd}, \text{Tb}, \text{Er}$), ^{27}Al spectra 3-41434
 Co , hexagonal, n.m.r. of ^{59}Co at domain wall, spin-lattice relax. 3-47162
 Co , pulsed, origin of single pulse echo 3-64561
 Co complex, $[\text{Co}(\text{NH}_3)_4\text{CO}_3]_2\text{SO}_4$, thermal motion of ammine groups, spin-lattice relax. obs. 3-50484
 Co_3B and Co_2B , pulsed nucl. ferromag. reson. of ^{59}Co , h.f.s. (*French*) 3-68853
 Co_2SiO_4 , of ^{29}Si , long range superexchange interactions via Co-O-Si-O-Co linkages 3-72530
 $\text{Co}_3(\text{VO}_4)_2$: ^{51}V , n.m.r. spectra at room temp. in freq. range 8.3-17.5 MHz 3-75890
 Cr-Mn antiferromagnetic alloys, internal field of ^{55}Mn and mag. moment 3-68857
 CrBr_3 , anisotropic ferromagnet, domain wall enhanced 3-50474
 CrBr_3 , ferromag., wall enhanced n.m.r. 3-72527
 $\text{Cr}(\text{III})$ doping of solutions for obtaining ^{13}C relaxation data 3-55496
 CrVO_4 : ^{51}V n.m.r. spectra at room temp. in freq. range 8.3-27.5 MHz 3-75890
 CsPF_6 , pulsed n.m.r., F spin-lattice relaxation 3-47159
 Cu-Co alloy, of ^{59}Co , precipitation phenomena obs. 3-50473
 Cu-Ni dilute alloy, 6-60 kG fields, liq. He temp. 3-53028
 Cu-Ni-Co alloy, of ^{59}Co , precipitation phenomena obs. 3-50473
 CuBr : ^{63}Cu , ^{65}Cu , ^{81}Br , spin-lattice relaxation time measurements from 78 K to 300 K 3-55493
 CuCl : ^{63}Cu , ^{65}Cu , ^{81}Br , spin-lattice relaxation time measurements from 78 K to 300 K 3-55493
 CuI : ^{63}Cu , ^{65}Cu , ^{81}Br , spin-lattice relaxation time measurements from 78 K to 300 K 3-55493
 CuMn alloy, of ^{63}Cu , near neighbour wipeout and satellites obs. 3-47152
 DyBe_{13} , susceptibility, mag. moment and ^9Be nuclear mag. relax. (*French*) 3-55427
 DyFeO_3 , ^{57}Fe n.m.r. in domain walls 3-72532
 ErFeO_3 , influence of ordering of Er^{3+} on Fe sublattices 3-50476
 $\text{Eu}_{1-x}\text{Gd}_x\text{Se}$, mag. hyperfine interactions rel. to cond. electron polarisation, n.m.r. obs. 3-64559
 ^{20}F β -emitter, determ. of quadrupole moment from n.m.r. meas. on polarised nuclei in MgF_2 3-45947
 Fe-V alloy, spin echo spectra of ^{51}V at 4.2 K 3-58435
 Fe_2P , ferromagnetic, n.m.r. study 3-41442
 Fe_2P , ferromag., wall enhanced n.m.r. 3-72527
 FeSi-CoSi solid soln., moment formation, itinerant ferromag., ^{59}Co n.m.r. 3-64494
 FeVO_4 : ^{51}V , n.m.r. spectra at room temp. in freq. range 8.3-17.5 MHz 3-75890
 Ga , ($n^2\text{P}^0$ - $n^2\text{D}_1$) resonance lines, collision broadening, cross-sections (*Russian*) 3-72770
 $\text{GaMn}_{0.935}\text{Co}_{0.065}$, n.m.r. and neutron diff., mag. struct. changes (*French*) 3-79924
 Gd , ferromagnetic, spectra of ^{155}Gd and ^{157}Gd at 4.2 K in zero external field 3-44330
 GdAl_2 , transferred mag. induced ^{27}Al quadrupole interaction obs. 3-41448
 GdBe_{13} , susceptibility, mag. moment and ^9Be nuclear mag. relax. (*French*) 3-55427
 $\text{Gd}_2\text{Co}_{17}$, spin echo obs., 77 K (*French*) 3-79933
 GdP , Heisenberg paramag., dynamics, pulsed n.m.r. obs. 3-41447
 GdX_2 , $\text{X}=\text{Al}, \text{Pt}, \text{Ir}, \text{Rh}$, cubic Laves phase, ferromagnetic, hyperfine fields 3-79927
 $(\text{GeF}_2)_n\text{GeF}_4$, broadline spectrum 3-55599
 H_2 , h.c.p., nuclear-longitudinal relax. time, 5.5 and 29 MHz 3-53036
 $\text{H}_2\text{O-D}_2\text{O}$ mixture, determ. of ratio of proton and deuteron nuclear mag. moments 3-62936
 ^1H - ^{31}P heteronuclear chemical exchange spin decoupling dispersion 3-75086
 ^3He , liq., spin diffusion near crit. pt. 3-50045
 ^3He , liquid, extraordinary, static nuclear magnetism 3-68465
 ^3He , potential parameters determ. from T_1 meas. 3-46215
 $^3\text{He A}$, microscopic theory of anomalous n.m.r. shift 3-58160
 Hg , liquid metal and alloys, effect of pressure up to 7 kbar 3-50173
 Hg isomers, precision magnetic moment determ., hyperfine-structure anomalies, optical pumping expt. 3-62933

nuclear magnetic resonance continued

- lineshapes in optical pumping expt. (French) 3-74004
²⁰³Hg, optically aligned, γ -radiation emission, anisotropy and time modulation 3-46000
^{199m}Hg, precision magnetic moment determ., hyperfine-structure anomalies, optical pumping expt. 3-62933
InI, ($n^2P_{1/2}$ - $n^2D_{3/2}$) resonance lines, collision broadening, cross-sections (Russian) 3-72770
¹⁹¹Ir, h.f.s. obs. of $^4F_{9/2}$ atomic ground state, ABMR meas. 3-67191
¹⁹³Ir, h.f.s. obs. of $^4F_{9/2}$ atomic ground state, ABMR meas. 3-67191
(K,NH₄)₂CuCl₄·2H₂O, 3-dimensional Heisenberg ferromagnet, magnetic interactions, n.m.r. obs. 3-60998
KCl:OH, double paraelectric n.m.r., relaxation times 3-68888
K₂CuF₄, two-dimens. ferromag., magnetisation, n.m.r. obs., 1.66-4.21K 3-58399
K₂NiF₄·¹⁹F, two-dimens. antiferromagnet, crit. exponents for n.m.r. linewidths 3-58418
KPF₆, chemical shift in n.m.r. of ¹⁹F 3-61002
KPF₆, pulsed n.m.r., F spin-lattice relaxation 3-47159
K₂P₂O₄F₂, investigation of P-P bond 3-54721
K₂Pt(CN)₄·Br_{0.3}·nH₂O quasi one-dimens. conductor, temp. depend. behaviour for ¹⁹⁵Pt reson. (German) 3-50482
Kr gas, spin-lattice relax. of ⁸³Kr, mechanism (German) 3-49395
LaP₂Gd, Heisenberg paramag., dynamics, pulsed n.m.r. obs. 3-41447
Li-A-zeolite, temp. depend. of absorption line width, arrangement and mobility of Li⁺ ions 3-44335
LiO₃, of ⁷Li, quadrupole interaction and dipole-dipole splitting (Russian) 3-41450
Li₂O-K₂O-TiO₂-SiO₂ glass system, spectra of ⁷Li, ion struct. 3-72528
⁷Li, nuclear magnetic spin relaxation by self-diffusion, T₁ρ as function of freq. (German) 3-47163
LuP₂Gd, Heisenberg paramag., dynamics, pulsed n.m.r. obs. 3-41447
p-methoxy-benzylidene-p'-n-butyl-aniline, diffusion coeff. for tetramethylsilane, n.m.r. technique meas. 3-52576
 γ -Mn alloy, antiferromag., small internal field, satellite signal indep. of impurity atom species 3-68856
 α -Mn alloys, antiferromag., ⁵⁵Mn n.m.r. 3-47153
MnF₂, ferromag., wall enhanced n.m.r. 3-72527
⁹³Mo 6.9 hr, mag. moment and spin determ. 3-62934
N₂-Ar solute-solvent systems, computer simulation of correl. functions, bandshapes and relax. times 3-64651
ND₄⁺ in crystals 3-54725
ND₄DSO₄, ferroelectric structure by deuteron mag. reson. 3-64569
NH₄Cl, N and Cl spin-lattice relaxation near λ -transition 3-55494
NH₃(D₂), liq., self-diffusion coeffs., spin-echo obs. 3-41036
NH₄H₂PO₄, NH₄H₂AsO₄, (NH₄)₂H₂SiO₆, deuteron, NH₄ motion obs. 3-79996
NH₄PF₆, chemical shift in n.m.r. of ¹⁹F 3-61002
NaCl single crystals, deformed, annealing, n.m.r. studies (Russian) 3-64093
Na(D₂H₁₋₂)₂(SeO₃)₂, spin-lattice relaxation time, ferroelectric transitions 3-79938
NaNH₄SeO₄·2H₂O, cryst. struct., n.m.r. obs. of H atoms 3-75516
Na₂O-B₂O₃-SiO₂ glass, ¹¹B, coordination struct. (German) 3-68162
NaPF₆, chemical shift in n.m.r. of ¹⁹F 3-61002
NaPF₆, pulsed n.m.r., F spin-lattice relaxation 3-47159
Na₃P₂O₇·F·12H₂O, investigation of P-P bond 3-54721
Nb(V) complex, characterisation, ¹⁹F, ¹H n.m.r. soln. study, isomer obs. (French) 3-53027
Ni powders, highly dispersed, n.m.r. absorption curves, interdomain boundary obs. 3-75883
Ni-Ru alloy, dilute, n.m.r. of host and impurity nuclei, hyperfine fields 3-64560
Ni-V alloy, dil., ⁵¹V n.m.r. line, environment effects near mag. transition critical conc. 3-64566
Ni(II), solvation in HMPT, ³¹P and ¹³C heteronuclear pulsed n.m.r. obs. 3-75084
Ni₃(VO₄)₂·⁵¹V, n.m.r. spectra at room temp. in freq. range 8.3-17.5 MHz 3-75890
PF₃ in nematic soln., ¹⁹F and ³¹P n.m.r. spectra, configuration and chemical shift 3-67854
³¹P, NMR study, glass-crystal phase transformation, P₂Se₃, CdGeP₂ semiconductors (Russian) 3-72197
³¹P-(¹H), ¹H-(³¹P) heteronuclear n.m.d.r., nonlinearities and nucl. Overhauser effect 3-75082
P(C₂F₅)₃, i.r. and Raman spectra and ¹⁹F n.m.r. 3-71561
²⁰⁷Pb, relax. mechanism in aq. Pb(ClO₄)₂ soln. 3-58442
Pd₂MnSb: ⁵⁵Mn: ¹²⁵Sb, spin echo method, magnitude and sign of hyperfine fields 3-50485
PuAl₂, of ²⁷Al, spin fluctuation effects in spin-lattice relax. 3-41441
RBe₁₃ intermetallic compounds, (R=La, Ce, Nd, Gd) magnetic properties, hyperfine interactions, spin dynamics 3-52969
Rb, rot. frame coherent resons. on fund. level of ⁸⁵Rb (French) 3-54574
Rb atoms, nutation echoes obtained by nonresonant oscill. field 3-78455
Rb polarisation, spin-exchange collisions with Cs, relaxation of electronic polarisation 3-54587
RbMnF₃, nonlinear effects in nuclear echo 3-64567
RbPF₆, pulsed n.m.r., F spin-lattice relaxation 3-47159
⁸⁵Rb, Larmor frequencies, n.m.r. obs. (German) 3-67190
¹⁰¹Rh, oriented, temp. dependence of gamma ray anisotropies meas., determ. E2/M1 mixing ratios 3-74534
Rh₂-complexes, ¹³C n.m.r., Rh-C coupling 3-63513
³³S magnetic moment, n.m.r. obs. Larmor frequencies, chemical shift (German) 3-67190
Sb(C₂F₅)₃, i.r. and Raman spectra and ¹⁹F n.m.r. 3-71561
⁴¹Sc, recoil polarisation from ⁴⁰Ca(d,n), n.m.r. meas. of β -decay asymmetry, magnetic moment determ. 3-45938
⁴¹Sc in Ta, mag. moment detn. and eqQ sign assignment 3-45963
Si compounds ²⁹Si Overhauser effect, T₁ meas. 3-68878
SiO₂ surface, porous and non-porous water adsorption 3-61000
SmSe and SmS_{1-x}Se_x, exchange-induced hyperfine fields at ⁷⁷Se 3-58439
TbBe₃, susceptibility, mag. moment and ⁸³Be nuclear mag. relax. (French) 3-55427
TiO₂:Cr³⁺, dynamic nuclear polarisation meas. of ¹⁷O spectrum, determ. of field gradient tensor (German) 3-50488
TlI, ($n^2P_{1/2}$ - $n^2D_{3/2}$) resonance lines, collision broadening, cross-sections (Russian) 3-72770
UAl₂, of ²⁷Al, spin fluctuation effects in spin-lattice relax. 3-41441
UF₆·2.5H₂O, position and mobility of H₂O 3-79925
V-Ru alloy, near equiatomic, electronic transition, ⁵¹V n.m.r. study 3-53032
V₃Ga_{1-x}Sn_x, density of states at Fermi level, supercond. transition temp. rel. to electronic struct., n.m.r. obs. 3-41289
VO²⁺ in dimethylformamide and dimethylacetamide solns., n.m.r., e.p.r. study of coordination 3-41433
V₂O₃-Cr₂O₃, antiferromag. state, n.m.r., hyperfine field, mag. moment, spin moment 3-55478
YCl₃·6H₂O:Yb, proton polarisation and relaxation, pulsed refrigerator optimal conditions 3-47161
Y₂Co₁₇, spin echo obs., 77 K (French) 3-79933
YFe₂, n.m.r. spin echo spectra of Y hyperfine fields 3-79922
Y₂Fe₁₇, n.m.r. spin echo spectra of Y hyperfine fields 3-79922
YFe₃, n.m.r. spin echo spectra of Y hyperfine fields 3-79922
Zn(ClO₄)₂ aqueous solution, mag. moment of ⁶⁷Zn and shielding of Zn ions by water 3-79926
Zn(II) complexes, organophosphoric anions, halogen and pseudohalogen perturbations (French) 3-75505
ZnMn₂C, n.m.r. and neutron diffr., mag. struct. changes (French) 3-79924
nuclear mass
fission mass asymmetry as dynamic process described by collective coordinate 3-60236
Nilsson's deformed nuclei, mass formula 3-74478
shell corrections in presence of pairing (Russian) 3-67175
superheavy nuclei ²⁸⁰112 and ⁴⁰⁸168, charge and mass distrib. calc. by hyperspheric function method (Russian) 3-74479
¹⁷⁴Hf, atomic mass determ. 3-67174
³¹Al, T₂=5/2 nuclide, mass and β decay 3-54373
³⁷Ar, isobaric mass quartets 3-60066
¹⁴B mass excess meas. using ¹⁴C(⁷Li, ⁷Be)¹⁴B, at 52 Mev 3

nuclear matter continued

- single-particle energies, effect of removal and addition times, density rearrangement 3-67226
- superheavy nuclei ²⁸⁰112 and ⁴⁰⁸168, charge and mass distrib. calc. by hyperspheric functions method (*Russian*) 3-74479
- at supernuclear densities, eqn. of state 3-61631
- surface energy of semi-infinite system, calc. using two nucleon nonlocal interaction 3-43201
- thermal properties and effective mass concept in schematic model 3-67249
- three-boson system of structureless alpha particles, bound state energy spectra 3-67243
- transparency increase to propagation of diffractively dissociated hadronic system 3-60135
- $\Delta(1236)$ involved corrections, including exchange effects and realistic correlation functions 3-54416
- N-N interaction, coherent non-local separable 3-74502
- N-N potentials, are boson exchange, in many nucleon context 3-60091
- π condensation in nucl. and neutron star matter, equilib. thermodynamic conditions 3-49183
- π condensation with ref. to neutron stars 3-54417
- ¹⁶O, A=16, 17, 18, 65 MeV elastic proton scattering, microscopic analysis, determ. of matter distrib. 3-40490

nuclear models

- see also *nuclear cluster model; nuclear collective model; nuclear reaction and scattering models; nuclear shell model*
- Amado model rel. to three nucleon systems and ³S defects 3-67225
- coexistence model, appl. to muon capture in ¹⁶O 3-67269
- deformed nuclei, magnetic moments in pseudo SU(3) model 3-49130
- hyperon + rigid 3N core, of $^4\Lambda\text{H} - ^4\Lambda\text{He}$, effects of Λ - Σ coupling 3-67251
- level density calculations and exptl. studies, review 3-54394
- matrix eigenproblems, application of Lanczos algorithm, extension from shell model to continuum states 3-67228
- pion-exchange, especially dispersion models, nucleon-nucleon interaction 3-74501
- random phase approx. study of E2 and E0 properties of excited 0⁺ states in even-even deformed nuclei 3-49217
- weak coupling model for ¹⁶O, ¹⁸O 3-60163
- ¹⁶O, coexistence model for structure of giant dipole resonance, exptl. test 3-49230

nuclear moment of inertia

- heading is late addition, see also *nuclear moments; nuclear spin and parity*
- A=20-34 nuclei, Hartree-Bogolubov theory for ground state rotational bands 3-52118
- collective approach, body-fixed coordinate system (*German*) 3-74516
- deformed doubly even nuclei, density matrix approach to Inglis cranking model 3-71065
- deformed rotating nuclei, backbending in simple stretching model 3-62971
- even-even nuclei, asym. shape and variable moment of inertia model 3-54380
- fission-fragment anisotropies for nuclei with double barrier, microscopic calcs. 3-63096
- governor model moment of inertia, correction 3-62970
- high-spin states in rotational bands, semiclassical description 3-67201
- quasi-rotational band description, transition nuclei 3-60075
- rigid body model, resonance energy determ. 3-57485
- rotational energy expansion in powers of angular velocity of rotation 3-62968
- rotational theory, number displacement degrees of freedom, effect on moment of inertia 3-54409
- variable moment of inertia model of rotational energies in even nuclei 3-74496
- vibrational deformed nuclei, Skyrme-Levinson model 3-74515
- Yoccoz formula derivation using classical statistical mechanics for deformed intrinsic nuclear state 3-71067
- ⁴⁰Ca, ⁴²Ca, quadrupole moments and coexistence, model comparison 3-52076
- ¹⁵⁶Dy, influence of nuclear rotation on moment of inertia 3-52098
- ¹⁶⁰Er, influence of nuclear rotation on moment of inertia 3-52098
- ¹⁸²Os ground-state rotational band, obs. of back- and forwardbending 3-74498

nuclear moments

- see also *nuclear electric moment; nuclear magnetic moment; nuclear moment of inertia*
- actinide region, deformation energies and moments of inertia for isomeric states (*German*) 3-52071
- conference on nuclear moments and structure, Osaka, Japan (September 1972) 3-45922
- configuration mixing effects, for 1f_{7/2} nuclei, isospin 3-49116
- cranking model calc. of moment of inertia using HFB theory with particle number projection, back-bending 3-49177
- deformed nuclei around Ba, ground state moments of inertia 3-43172
- e.m. interaction of nucleus with charged particle, interpretation of hyperfine interaction data 3-52065
- even-even nuclei, asym. shape and variable moment of inertia model 3-54380
- excited states, exptl. measurement techniques, scope and limitations 3-45933
- finite nuclei, single-hole strength distrib., second moment 3-52105
- fluctuation energies in shape fluctuation model and phenomenon of shrinkage 3-49176
- ground state meas. by nuclear resonance, atomic beam resonance and optical pumping, hyperfine anomalies 3-45932
- high spin nuclei, pairing-plus-quadrupole model, constrained-Hartree-Bogolyubov treatment, moments discontinuity study 3-45982
- inertia at high spin of deformed nuclei 3-52083
- inertia for vibrational deformed nuclei, generalised Skyrme-Levinson model 3-74515
- inertia parameter, derivation by method of moments 3-71045
- isovector monopole state and the escape width of double analogue resonances 3-45971

nuclear moments continued

- moment of inertia, rotational anomaly and Hartree-Fock-Bogoliubov eqns. 3-49174
 - moment of inertia calcs. in presence of RPA correlations 3-49181
 - multipole, Hartree-Fock calc. for rare earths 3-78275
 - multipole, interaction with anomalous magnetic moments of elastically scattering electrons (*Russian*) 3-74564
 - N=82 nuclei, Z=51-59, pseudo LS coupling shell model study of energy levels and e.m. properties 3-49126
 - rare earth deformed nuclei, difference in monopole moment for ground and excited states 3-49132
 - rare-earth rotating deformed nuclei, moments of inertia, collective models 3-49171
 - renormalization of E0, M1 and E2 operators 3-49204
 - rotating nuclei, finite temp. calc. of angular velocity and moments of inertia 3-49178
 - rotational bands, Coriolis force interactions, differences in moments of inertia, nuclei with 173 ≤ A ≤ 189 (*Russian*) 3-71039
 - spin moments detn. by optical pumping far from stability 3-45962
 - static, boson variational approach to collective motion 3-49103
 - static in ²⁰Ne and ²⁴Mg, determ. using variation after projection Hartree-Fock method 3-67245
 - ¹⁵⁶Dy, influence of rotation on moment of inertia of high-spin ground state members 3-52098
 - ¹⁵⁸Dy, moment of inertia dependence on angular momentum 3-49097
 - ¹⁶⁰Er, influence of rotation on moment of inertia of high-spin ground state members 3-52098
 - Hf, even-even isotopes, mean moments of inertia 3-49191
 - ¹⁹⁹Hg, g-factor of 208 keV 3/2⁺ state, meas. by ion implantation perturbed angular correlation technique 3-45970
 - ¹⁶⁰O, transition moments in electron excitation of T-1 neg.-parity oscillations 3-46020
 - ¹⁸³Os ground-state rotational band, back- and forwardbending, moment of inertia 3-74498
 - Pr binary chalcogenides, mag. props., metal-insulator transition, superconductivity 3-41326
 - Tm binary chalcogenides, mag. props., metal-insulator transition, superconductivity 3-41326
 - W, even-even isotopes, mean moments of inertia 3-49191
 - Yb, even-even isotopes, mean moments of inertia 3-49191
- nuclear muon capture** see *muon capture*
- nuclear optical model**
- alpha-particle inelastic scattering in continuum, A=51-206, energy spectra, collective modes and optical model 3-67347
 - coherent production of three pions on nuclei 9 to 15 GeV, total cross section determ. 3-67368
 - computational approach to inverse problem in JWKB approximation, alpha-particle scattering 3-60143
 - DWBA, modified, direct reactions on light nuclei, ¹¹B(³He,α)¹⁰B 3-60210
 - elastic nucleus-nucleus scattering, particle and hole transfer optical model and molecular approx. 3-49278
 - elastic scattering at 70 MeV, numerical accuracy of optical model calcs. 3-74601
 - electron quasielastic scattering comparison of short-range correlation and distortion effects 3-57511
 - excitation of nuclear levels by electrons and hadrons at high energy 3-60162
 - folded collective, for ²⁴Mg alpha-particle scattering at 104 MeV 3-60208
 - four-parameter, for elastic alpha-particle scattering on Ni, Co and Cu 3-67348
 - generalised potentials derived from systematic fast neutron elastic scattering study 3-74574
 - generator coordinate method for scattering, exact soln. 3-54452
 - heavy ion elastic scattering, semiclassical treatment 3-63085
 - heavy ion reactions, dynamical treatment of absorption 3-67362
 - heavy-ion reactions, low energy, repulsive cores in the optical potential, surface thickness determ. 3-67366
 - high-energy processes, optical concepts 3-48993
 - inelastic proton scattering, 30 MeV, target excitations and optical potential 3-49256
 - isobar-doorway model for pion-nucleus scattering 3-43258
 - leptodermous distributions, geometric properties 3-52070
 - meson-nucleus optical potentials, modified 3-60224
 - multiple scattering model, appl. to theory of optical potentials at high energies (*Russian*) 3-67292
 - neutron optical potentials, equivalent, in separable energy dependent approximation 3-71091
 - neutron-nucleus interaction in low energy deuteron break up on heavy-nuclei 3-54487
 - Nilsson orbits for nucleon in Woods-Saxon potential with deformation and coupled to core rotational states 3-71063
 - nucleon charge independent potential determ., appl. to (p,n) charge exchange reaction on ²⁰⁸Pb and ²⁰⁹Bi 3-67333
 - nucleon-nucleus optical model potential, imaginary part 3-54450
 - nucleon-nucleus optical potential definition using Low eqn. 3-71111
 - nucleon-nucleus potential, contrib. of pick-up reaction 3-78303
 - nucleon-nucleus potential rel. to optical potentials for composite projectiles, adiabatic approximation 3-60142
 - nucleon-nucleus potential spin-spin term, DWBA anal., spherical and tensor terms 3-67291
 - off-shell correction to high-energy optical potential, resonance region 3-63022
 - phenomenological model for rotational nuclei 3-57505
 - pion-nucleus optical potential, off-shell transition matrix, coupled-channel approach 3-60136
 - pion-nucleus scattering 3-74608
 - pion-nucleus scattering in (3,3) resonance region, many-body formulation 3-54509
 - potential, imaginary part, ground state corrls. effect 3-52154
 - potential, root mean square radius in ¹²C(π⁻, π⁻)¹²C scattering 3-78354
 - potential for scattering from system of finite-mass particles 3-54451
 - proton imaginary optical potential, (N-Z)/A dependence and Thomas-Fermi gas model 3-52187

nuclear optical model continued

- proton-nucleus scattering, energy dependence of real central optical potential 3-60185
 quasielastic reactions, isospin depend. 3-40474
 renormalization of axial coupling constant, reln. to pionic field, optical model 3-52150
 Saxon-Woods potential, computer program for s-state binding energy and wave functions 3-67289
 semiclassical, applic. to mol. collisions 3-63545
 α -particle inelastic scattering on nuclei with $A=12-208$, optical potentials 3-60182
 K-nucleus optical potential determ. from KN scattering amplitude, K-mesic atom 3-54344
 (n, γ) radiative capture, mass region $40 \leq A \leq 70$ 3-78334
 N-nucleus scattering, influence of exchange on optical potential, lowest order exchange processes 3-67290
 π -nucleus optical potential, non-overlapping potentials and Ericson-Ericson renormalization 3-57541
 π -nucleus optical potential, density expansion second order terms 3-63086
 π -nucleus optical potential with crossing theory 3-63089
 π -nucleus optical potentials, low-energy, local potentials 3-43257
 π -nucleus optical potentials, theoretic basis from multiple scattering 3-52206
 π -nucleus scattering, optical model, DAMIT computer code, calculation technique 3-78353
 π -nucleus scattering in 3,3 resonance region, exclusion principle effects 3-54508
 π -nucleus scattering near (3,3) resonance using dynamically modified optical potential 3-67370
 ^{10}B , (p, α), (p, n) and (p, p) reactions at low energies, optical model and Hauser-Feshbach analysis 3-57533
 ^{138}Ba (d, d), 19 MeV, determ. of optical model parameters 3-46033
 ^{138}Ba (p, p), 17 MeV, determ. of optical model parameters 3-46033
 ^9Be , (d, d) and (d, p) reactions at low energies, optical model and Hauser-Feshbach analysis 3-57533
 ^9Be elastic proton scattering, 13-30 MeV, spherical optical model analysis 3-52184
 ^{12}C , alpha-particle elastic and inelastic scattering at 139 MeV, optical model and DWBA analyses 3-49270
 ^{12}C (n, n) ^{12}C , 1.98 MeV-4.64 MeV, phase shift and optical-model analysis 3-71106
 ^{12}C (n, n) ^{12}C , 7-9 MeV, angular distrib. meas., comparison with optical model calcs. 3-63051
 ^{12}C (p, pp) ^{11}B , nucleon correl. effect, 1 GeV, distorted wave method 3-78330
 ^{13}C (π^+ , π^0) ^{13}N , optical model studies, comparison with exptl. cross sections, 30-90 MeV 3-60223
 ^{14}C , deuteron elastic scatt., 4-10 MeV, ang. distrib., spin, parity 3-78343
 ^{40}Ca , proton elastic scattering, coupling to pickup channels, contrib. to optical potential 3-46031
 ^{40}Ca (α , α'), 29 MeV, coupled-channel calcs., influence of J-dependent absorption on cross section 3-67353
 Fe, $A=54, 56, 58$, scattering of polarised 12.3 MeV deuterons, vector analysing power and cross sections 3-52194
 Gd, $A=154-160$, total neutron cross section meas., deformation effects, optical model (Russian) 3-52178
 (^4He , α) reactions on s-d shell nuclei, analysis using average ^3He and α optical potentials 3-49272
 ^3He elastic scattering, numerical accuracy, calcs., 70 MeV 3-74601
 ^3He elastic scattering at 217 MeV on ^6Li , ^9Be , ^{12}C , ^{28}Si , ^{40}Ca , ^{58}Ni , ^{89}Y , ^{20}Zr , ^{120}Sn , ^{208}Pb , optical potential 3-52199
 ^3He polarisation in elastic scattering from ^{27}Al and ^{28}Si , deduced parameters 3-67349
 ^4He (p, p) ^4He elastic scatt. at 1 GeV, precise single-scatt. optical pot. fit 3-46018
 ^7Li , ^7Li , elastic, inelastic scatt., on ^{12}C , ^{13}C , ^{16}O , ^{26}Mg , ^{28}Si 3-78349
 ^7Li (d, t) ^6Li , 12 MeV, ambiguities resolved by exchange mode spectroscopic factor examination 3-71122
 ^{24}Mg , 60-90 MeV, deuteron scattering, optical model and coupled channel analysis 3-43253
 ^{93}Nb , neutron total (0.25 to 0.5 MeV) and differential (1.8 to 4.0 MeV) scattering cross-sections, optical model, J^{π} values 3-78331
 Nd, $A=142-150$, total neutron cross section meas., deformation effects, optical model (Russian) 3-52178
 ^{142}Nd (^{16}O , ^{16}O) ^{142}Nd , 54-72 MeV, interference of Coulomb and nuclear excitation, B(E2) values and optical model 3-52201
 ^{20}Ne (d, d) ^{20}Ne , 11.6 MeV polarised deuterons vector analysing power, optical model, differential cross section 3-52193
 ^{22}Ne (d, d) ^{22}Ne , 11.6 MeV polarised deuterons vector analysing power, optical model, differential cross section 3-52193
 ^{58}Ni , alpha-particle scattering, 139 MeV, analysis elastic cross sections using Woods-Saxon potential 3-63076
 ^{58}Ni (^{16}O , ^{16}O) ^{58}Ni , 35-60 MeV, interference of Coulomb and nuclear excitation, B(E2) values and optical model 3-52201
 ^{60}Ni , neutron elastic and inelastic scatt. from 2 to 8.5 MeV, differential and total cross-sections calc. 3-57531
 ^{60}Ni , scattering of polarised 12.3 MeV deuterons, vector analysing power and cross sections 3-52194
 ^{60}Ni (^3He , ^3He) ^{60}Ni , energy depend. phenomena, $E=29.6-71.1$ MeV 3-60213
 ^{60}Ni (^3He , ^3He) ^{60}Ni , optical-model-family ambiguity, $E=29.6-71.1$ MeV 3-60212
 ^{60}Ni (d, p) ^{61}Ni , 10 MeV, vector analysing power, ang. distrib. meas., DWBA calcs. 3-78239
 $^{\circ}\text{O}$, $A=16, 17, 18, 65$ MeV elastic proton scattering, microscopic analysis, determ. of matter distrib. 3-40490
 ^{14}O (d, d) ^{14}O , 11.6 MeV polarised deuterons vector analysing power, optical model 3-52193
 ^{16}O (α , α), wave functions and reflection coeffs. deduced from optical model, $E=20.1$ MeV 3-43254
 ^{16}O (α , α') ^{16}O , 20.1 MeV, optical model analysis using independent geometries for real and imaginary potentials 3-67346
 ^{16}O (d, d) ^{16}O , 11.6 MeV polarised deuterons vector analysing power, optical model 3-52193
 ^{16}O (γ , π^+) ^{16}N , effect of Woods-Saxon wave functions on cross sections for charged-pion photoproduction 3-63034

nuclear optical model continued

- ^{16}O (p, d) ^{15}O , effect of short-range correlations due to repulsive core in N-N interaction 3-46024
 ^{16}O (π , π^-) ^{16}O , total and differential cross sections in 3-3 resonance region, optical potential calcs. 3-63090
 ^{208}Pb , alpha-particle scattering, 139 MeV, analysis elastic cross sections using Woods-Saxon potential 3-63076
 ^{208}Pb (d, d) 12.3 MeV, vector analysing power, differential cross section, deduced optical model parameters 3-60199
 ^{209}Pb , imaginary optical potential for s-wave neutrons incident on ^{208}Pb 3-60141
 Pb(π^+ , π^+)Pb, elastic differential cross section, comparison of theory and expt. 3-71128
 ^{32}S (p, p) ^{32}S , 5-6 MeV, meas. of excitation functions and angular distrib., optical model description of cross-section (Russian) 3-52180
 ^{28}Si (p, p) ^{28}Si , 5-6 MeV, meas. of excitation functions and angular distrib., optical model description of cross-section (Russian) 3-52180
 Si(n, n'), spin-flip probability and diff. cross section 3-54480
 Si(p, p)Si, 17-29 MeV, analysing powers and cross sections in ^{29}P giant resonance region, optical model analysis 3-67327
 Sm, $A=144-154$, total neutron cross section meas., deformation effects, optical model (Russian) 3-52178
 ^{120}Sn (d, d), (d, d), polarized, ang. distrib. of diff. cross-sect. and optical model calcs. 3-46035
 ^{88}Sr (^{16}O , ^{16}O) ^{88}Sr , 45-60 MeV, interference of Coulomb and nuclear excitation, B(E2) values and optical model 3-52201
 Te(t, t)Te, study of optical potential depth and Sb isotope structure (Spanish) 3-74484
 ^{89}Y , 60-90 MeV, deuteron scattering, optical model and coupled channel analysis 3-43253
 ^{90}Zr (d, d) scatt., spin depend. investigation, optical model pot. explanation 3-40499

nuclear orientation see *nuclear polarisation*

nuclear particle track visualisation see *particle track visualisation*

nuclear photoeffect see *nuclear reactions and scattering due to photons*

nuclear physics

see also *nuclear shape*

- annual review (1972), book 3-53808
 computer program, for data acquisition 3-51668
 data processing, use of cubic spline functions, computer program 3-57500
 electrons and photons, 150 MeV-600 MeV experimental study (French) 3-60063
 European Nuclear Documentation Service, structure and features of system 3-74477
 heavy-ion accelerator applications 3-51673
 interdisciplinary nuclear science at a liberal arts college 3-51487
 low energy, appl. to fund. interactions of elementary particles, book 3-78233
 in medicine, proceedings of American Association of Physicists, Chicago, USA, 30 Nov-1 Dec, 1972 3-61914
 products, materials and services directory 3-39984
 radiation, book 3-62922

nuclear polarisation

see also *magnetic double resonance*

- $A=19$ nuclei, core-polarisation effects on E2 transitions 3-52134
 alignment of excited states meas. by anisotropy of emitted γ -rays, magnetic moment determ. 3-49080
 asymmetric split-pair superconducting magnet, for nuclear polarization experiments 3-56969
 atomic ^{15}O ions, optical pumping charge-exchange method for nuclear spin orientation 3-67677
 beta decay in $N=82$ region, new confirmation of quenching of nuclear matrix elements 3-57495
 chemically induced, dynamic, decomposition of benzoyl peroxide, cycl-cohexyl percarbonate, perocetyl isopropyl carbonate, azo cpds., methyl radical 3-71579
 cluster constituents polarisation in unified shell-cluster model analogous to molecular orbitals 3-43194
 core polarisation effects on β -transitions for neutron magic nuclei 3-71088
 cyclohexane: nitroxide free radical, molecular self-diffusion, nuclear spin-lattice relaxation and dynamic polarisation 3-49854
 duren single crystals, ^{13}C chem. shielding tensors using proton-enhanced n.m.r. 3-64580
 dynamic, thermodynamics, phonons, electrons and impurities interaction (German) 3-79946
 dynamic polarisation by solid effect, equivalence of rate equation and diffusion theory for isotropic distributions 3-68887
 even-even nuclei, quadrupole moments of excited states by reorientation effect in Coulomb excitation 3-54379
 free radicals, chemically induced dynamic spin polarization, hydrodynamic effect 3-80537
 light nuclei, Coulomb excitation, polarizability and static quadrupole moment 3-45936
 magnetic moments, effects of core polarisation and mesonic exchange current 3-45946
 multispin systems with exchange interaction, quantum theory 3-75921
 n.m.r., permanent magnet, chemically induced nuclear dynamic polarisation, nuclear and electron spin coupling 3-48324
 nucleon-nucleus optical potential, spin-spin term, DWBA anal., spherical and tensor terms 3-67291
 orientation at low temps., orientation parameters 3-71080
 orientation at low temps., technique for excited-state moments meas. 3-45933
 orientation of states by nuclear reactions or cryogenic methods, directional correlations of emitted γ -radiation 3-71079
 proton-enhanced n.m.r. of dilute spins in solids, h.f. resolution 3-61010
 reorientation effect in Coulomb excitation, meas. of static quadrupole moments 3-46038
 at saturation of allowed and forbidden resonances (Russian) 3-68855
 semiconductors, spin-magneto-phonon resonance and nuclear d.c. polarisation 3-55455
 solid state effect, radiation dosimetry 3-40552

nuclear polarisation continued

- spin systems, n.m.r. absorption lineshape, paramag. impurities, solid effect 3-60996
- T-invariant angular correlations in pair conversion process in polarised nuclei (*Russian*) 3-52125
- yttrium ethyl sulphate: Dy, Yb, proton polarisation and relaxation, pulsed refrigerator optimal conditions 3-47161
- Ag halides depolarization and beta-decay of ^{110}Ag , n.m.r. obs. 3-61006
- ^{110m}Ag oriented in Fe and Ni, meas. of hyperfine interactions by n.m.r., β -mixing 3-46009
- Au, muonic transitions (*French*) 3-54603
- $^{\text{a}}\text{Au}$, A=196, 198, 200, magnetic moments of 12^- states, low-temp. orientation expts. 3-45952
- ^{196}Au , oriented, n.m.r., γ -ray anisotropy temp. depend., mag. moments, spins 3-40453
- ^{198}Au , oriented, n.m.r., γ -ray anisotropy temp. depend., mag. moments, spins 3-40453
- ^{200m}Au , oriented, n.m.r., γ -ray anisotropy temp. depend., mag. moments, spins 3-40453
- ^8B , recoil polarisation from $^6\text{Li}(^3\text{He},n)$, n.m.r. meas. of β -decay asymmetry, magnetic moment determ. 3-49077
- ^8B in Ta, magnetic moment determ. by n.m.r. and β -decay using polarisation reversal 3-45963
- ^{12}B , ^{13}B , recoil polarisation through nuclear reaction into Mg crystal, quadrupole coupling, $Q(^{12}\text{B})$ to $Q(^{13}\text{B})$ ratio 3-49079
- ^{12}B , alignment of ground state from γ -ray angular distrib. meas. of $^{11}\text{B}(d,p\gamma)$ reaction 3-49078
- ^{12}B β -decay, search for weak-electric moment 3-49224
- ^{130}Ba , quadrupole moments of first excited states, reorientation eff. meas. 3-49112
- ^{134}Ba , quadrupole moments of first excited states, reorientation eff. meas. 3-49112
- ^{136}Ba , quadrupole moments of first excited states, reorientation eff. Meas. 3-49112
- Bi radioactive isotopes, low temperature orientation in ferromagnetic BiMn , use in nuclear structure studies 3-46008
- ^{206}Bi in Ni, γ -ray distrib. meas., transition determ. of ^{206}Pb 3-78286
- ^{209}Bi , polarised, magnetic hyperfine structure in muonic atom, coupling consts. anomalous g-factor 3-46216
- $^{111}\text{Cd}^+$, fund. level orientation by collisions with metastable He, h.f.s. const. (*French*) 3-78502
- ^{57}Co decay, 122 keV, transition, E2/M1 mixing ratio determ. by orientation 3-46006
- ^{58}Co , oriented, accurate meas. of positron asymmetry 3-63005
- $^{58}\text{Co}(n, \gamma)^{59}\text{Co}$, with polarised neutron and nuclei, 0.065 eV, meas. of capture γ -rays 3-43245
- Cr^{3+} aquacomplex in viscous soln., intermediate effect between Overhauser and solid effects 3-75079
- ^{53}Cr , ground state static quadrupole moment from Coulomb excitation meas. 3-40410
- D, muonic, calc. of contributions to Lamb shift 3-52303
- ^{19}F , nuclear Zeeman splitting by anal. linear polarization 3-71081
- ^{19}F , polarized, implantation in Zn single crystal, quadrupole interaction of 197 keV level 3-49081
- ^{20}F , γ -ray transitions, linear polarization meas. 3-40447
- ^{20}F β -emitter, determ. of quadrupole moment from n.m.r. meas. on polarised nuclei in MgF_2 3-45947
- Fe, hyperfine field of ^{135}Xe , ^{131}Xe determ., lattice sites 3-72323
- ^3He , by optical pumping, apparatus development and relax. time meas. (*French*) 3-46185
- ^3He , by optical pumping, relax. time meas. at surfaces (*French*) 3-46186
- ^3He in elastic scattering from ^{27}Al and ^{28}Si nuclei, determ. optical model parameters 3-67349
- $^3\text{He}^{2+}$, nucl. polarisation feasibility by electron-transfer processes 3-51686
- ^{175}Hf , quadrupole alignment in Hf metal at 3 mK, meas. γ -ray anisotropies 3-71082
- ^{180}Hf , quadrupole alignment in Hf metal at 3 mK, meas. γ -ray anisotropies 3-71082
- Hg isomers, precision magnetic moment determ., hyperfine-structure anomalies, optical pumping expt. 3-62933
- ^{201}Hg , n.m.r. lineshape in optical pumping expt. (*French*) 3-74804
- ^{203}Hg , optically aligned, γ -radiation emission, anisotropy and time modulation 3-46000
- ^{199m}Hg , precision magnetic moment determ., hyperfine-structure anomalies, optical pumping expt. 3-62933
- ^{165}Ho , quadrupole moment meas. by proton and alpha scattering from aligned target 3-45944
- ^{129}I , orientation study of excited states populated in decay of ^{129}Te , ^{129m}Te 3-52131
- ^{36}K , polarisation by optical pumping method, β -decay asymmetry, determ. of spin and magnetic moment 3-45939
- ^7Li , Coulomb excitation, particle- γ coincidence technique 3-78288
- ^8Li , short lived, spin exchange polarisation and hyperfine splitting meas. 3-52138
- ^{90}Mo , directional correlations meas. for several gamma gamma cascades 3-60070
- Ni^{3+} aquacomplex in viscous soln., intermediate effect between Overhauser and solid effects 3-75079
- ^{16}O region, charge radii and polarisation effects 3-67179
- ^{17}O , n.m.r. in $\text{TiO}_2\text{:Cr}^{3+}$ by dynamic nuclear polarization method (*German*) 3-50488
- ^{185}Os decay, γ -ray ang. distrib., orientation obs. 3-40452
- ^{191}Os decay, γ -ray ang. distrib., orientation obs. 3-40452
- ^{193}Os decay, γ -ray ang. distrib., orientation obs. 3-40452
- Pb isotopes, rel. to muonic X-ray spectrum 3-63351
- Pb region, effective E2 charges, particle-oscillating core coupling, polarisation 3-45924
- ^{208}Pb , muonic, Hartree-Fock calc. of monopole polarisation 3-67172
- ^{208}Pb muonic, monopole polarisation of $1s_{1/2}$ level 3-78234
- ^{204}Po , core polariz. eff. in $\pi h_{9/2}$ shell of 8^+ states and g-factors 3-45969
- ^{206}Po , core polariz. eff. in $\pi h_{9/2}$ shell of 8^+ states and g-factors 3-45969
- ^{194}Pt , Coulomb excitation by ^{16}O and ^{32}S , quadrupole moment of first 2^+ state by reorientation precession technique 3-45942

nuclear polarisation continued

- ReAe, determ. of configuration mixing ratios consistent with beta-decay and magnetic moment 3-52144
- ^{183}Re from $\text{W}(d, xn)$, determ. magnetic hyperfine interaction from gamma ray anisotropies 3-60110
- ^{183}Re mag. mom. meas. by nuc. orientation 3-49107
- ^{184}Re from $\text{W}(d, xn)$, determ. magnetic hyperfine interaction from gamma ray anisotropies 3-60110
- ^{184}Re mag. mom. meas. by nuc. orientation 3-49107
- ^{184m}Re mag. mom. meas. by nuc. orientation 3-49107
- ^{41}Sc , recoil polarisation from $^{40}\text{Ca}(d,n)$, n.m.r. meas. of β -decay asymmetry, magnetic moment determ. 3-45938
- ^{41}Sc in Ta, magnetic moment determ. by n.m.r. and β -decay using polarisation reversal 3-45963
- ^{150}Sm , Coulomb excitation by ^{16}O and ^{32}S , quadrupole moment of first 2^+ state by reorientation precession technique 3-45942
- Sn region, first-order core polarisation effects, rel. to determ. of magnetic moments of $11/2^-$ states 3-67186
- ^{181}Ta 482 keV transition, short-range correlations, effective charge, parity violation, polarisation 3-57490
- Te, odd mass isomers, magnetic moment determ. by orientation technique 3-60069
- ^{124}Te , quadrupole moment meas. by reorientation effect 3-49111
- ^{126}Te , quadrupole moment meas. by reorientation effect 3-49111
- ^{127}Te , mag. mom. $\mu_{3/2}$ detn. by nuclear orientation meas. 3-45966
- ^{128}Te , quadrupole moment meas. by reorientation effect 3-49111
- ^{129}Te , mag. mom. $\mu_{3/2}$ detn. by nuclear orientation meas. 3-45966
- ^{123m}Te , nuclear orientation detn. of mag. mom. 3-49106
- ^{125m}Te , low temp. expt., magnetic moment meas. 3-43177
- ^{125m}Te , nuclear orientation detn. of mag. mom. 3-49106
- ^{127m}Te , nuclear orientation detn. of mag. mom. 3-49106
- ^{129m}Te , nuclear orientation detn. of mag. mom. 3-49106
- ^{187}W decay, γ -ray ang. distrib., orientation obs. 3-40452
- ^{133m}Xe , low temp. expt., magnetic moment meas. 3-43177
- $\text{YCl}_3 \cdot 6\text{H}_2\text{O}$: Yb, proton polarisation and relaxation, pulsed refrigerator optimal conditions 3-47161
- ^{175}Yb , orientation in Au and Ag, determ. from γ -ray anisotropy 3-47180
- ^{90}Zr , helion and triton inelastic scattering, shell-model analysis with core polarization effects 3-78345
- $^{90}\text{Zr}(d,p)^{91}\text{Zr}$, j-dependence of vector analysing power and cross section 3-46034

nuclear power

see also nuclear reactors

- burn-up optimization, proof of equivalence relations using Pontryagin method 3-63130
- BWR, development studies for increasing power level (*German*) 3-67497
- Canadian, annual report 3-71228
- controlled thermonuclear reactors, prospects for fusion power, review 3-52232
- FTR power performance, analysis of engineering mockup critical expts. 3-49352
- fuel financing, evolution of concept 3-67410
- fusion reactor, Princeton reference design model, optimisation of breeding blanket cooling design 3-60312
- fusion reactor as 1.8 gigawatt electric power plant 3-60303
- fusion reactors power-balance parameters for Q and ϵ as measures of performance 3-60309
- German, 4th nuclear program for 1973-76, overview (*German*) 3-43272
- HTR, direct cycle for electricity generation, selection of materials 3-67583
- industries in Japan, Mitsubishi Group's activities 3-63146
- Japanese, development and utilization policy 3-63141
- Japanese, public acceptance 3-63145
- Japanese Atomic Energy Research Institute, activities 3-63139
- Japanese industrial group's activities 3-63147
- Japanese industries, present state, overview 3-63140
- programme in U.K. 3-54530
- radiation standards in U.S., pollution control 3-43319
- reactor, excursion calcs. using Parajito Dynamics Code 3-46081
- thermonuclear plants, of Electricite de France, development (*German*) 3-67618
- United Kingdom, fissile material processing centres (*Dutch*) 3-71173
- United States, present status and future trends 3-67397
- waste self-burial, utilising decay heat to melt rock 3-67415
- weakly-coupled cores, power ratio meas., comparison of methods 3-63129
- world energy problems, nuclear solns., conference, Washington D.C., USA (Nov 1972) 3-46047
- $^{244}\text{Cm}_2\text{O}_3$, compatibility with refractory metal, fuel for radioisotopic applications 3-69363

nuclear power stations

see also nuclear reactors

- acoustic surveillance system, development and evaluation 3-66156
- American Nuclear Society meeting, Chicago, USA, June 1973 3-63102
- architectural engineering, codes and standards 3-63160
- Atucha, in service fuel element exchange, manipulating equipment tests (*German*) 3-71232
- boundary dose rates due to gamma rays at power reactor sites, Monte Carlo procedure 3-57591
- BWR, safety, stochastic decision making procedure 3-46084
- BWR, training simulator, computer controlled 3-52226
- BWR at Nine Mile Point, survey of radiation levels and shielding 3-71340
- BWR plant, ^{16}N site-boundary dose calcs., geometrical considerations 3-74755
- BWR system, study of radiation shielding in operational and shutdown conditions 3-71341
- BWRs at Dresden station, recent operating experience and startup 3-49317
- Canadian Nuclear Power Program, construction and operation of thermal power reactors 3-46098
- commission of plant at Wurgassen (*German*) 3-74717
- discharges, meas. of turbulent diffusivities 3-63163
- dosimetry, secondary standard, WHO Regional Reference Centres 3-54555

nuclear power stations continued

- Dragon reactor, irradiation facility, HTR fuel concepts and fuel element designs 3-67458
- fast reactor neutron spectrum generator, design and construction 3-52218
- French Nuclear Program, gas-graphite and water reactors 3-46099
- fuel element cans for, automatic inspection 3-57554
- fuel handling machine for Loviisa I 3-57574
- fusion reactor, radiological implications 3-42380
- GCFR demonstration plant, response to depressurization accidents, computer program analysis 3-46106
- GCFR plant using direct cycle, response to rapid loss of pressure due to duct rupture 3-46107
- German nuclear power programme, LWR construction and operation 3-46100
- Italian nuclear power program, thermal reactor construction and operating experience 3-46101
- Japanese nuclear power program, operation and construction experience 3-46102
- licensing, role of standards 3-63159
- Maine-Yankee Power Station, design, initial operation 3-74694
- maximum ground conc. of effluents, plume rise calc. 3-63245
- nuclear instrument and control technicians, basic elec. and electronics course 3-73645
- operating and startup procedures, Brunswick Steam Electric Plant, emergency and fuel handling procedures 3-73641
- operating experience, procedures and standards, conf., Myrtle Beach, South Carolina, USA (Aug 1973) 3-74691
- operating procedures, manual for plant safety 3-73639
- operating procedures, min. risk to health and safety 3-73638
- operating procedures, plant safety 3-73640
- operator training, present state and future trends 3-52221
- Oyster Creek Station, capability and operating experience 3-49315
- personnel, training 3-52222
- plant calorimetrics, isotopic composition of spent fuel, reln. to energy release in fission 3-54529
- preoperational testing of Fort St. Vrain Unit No.1 3-49314
- pressure vessel testing using ultrasonics, compensation from base material, surface and group differentials (German) 3-70276
- programme in U.K. 3-54530
- protective containment system, underground 3-77268
- PWR, radionuclide concs. in marine animals, monitoring sensitivity 3-74767
- PWR, startup and early operating experience at Palisades Plant 3-49316
- PWR, study of dynamics by fluctuation and pseudorandom input analyses 3-46123
- PWR of Rochester Gas and Electric Corporation R.E. Ginna, unit no.1, criticality and commercial operation 3-49319
- PWR performance and selected experiences of Connecticut Yankee and Millstone I 3-49318
- PWR protection system, effects of electrical underfrequency transients 3-46085
- PWR technology, progress, experience gained 3-74664
- Quad-Cities Station, operating experience 3-74693
- radiation monitoring, CEGB 3-53759
- radiation monitoring, environmental radioactivity, International Reference Centre, activities 3-54554
- radiation problems, safety 3-63144
- radiation protection standards (Dutch) 3-78392
- radiation stack monitor design for γ -ray exposure from Kr-Xe gaseous mixture 3-78394
- radioactive material build-up detection and control 3-74768
- radionuclide meas. in marine samples near nuclear power stations 3-69557
- reactor pressure vessel evaluation by irradiation response of steel to Pellini and NDT tests (German) 3-73113
- reactor shielding, advances, book 3-60337
- safety evaluation, design for pipe break outside of containment 3-67433
- safety-related occurrences, 1972 review 3-74700
- San Onofre I, evaluation of operating reactor hydraulic performance 3-67445
- seismic qualifications, Category I equipment, structures, systems and components 3-69537
- ship, seamen training 3-52224
- standardisation of nuclear instrumentation, in Italy (Italian) 3-42620
- standards, operating procedures, personnel, safe and reliable plant operation 3-73642
- standards hierarchy and interrelationships 3-67380
- steam generators, nondestructive testing, tube to tube sheet welded joints 3-65060
- THTR 300 MWe, acceptance procedure and technical safety (German) 3-71237
- training centre for operators, description 3-52223
- training simulator for Swedish utilities 3-52225
- water-cooled, routine monitoring system 3-74750
- γ -ray files, N-16 content 3-74747
- $^{60}\text{Co}/^{137}\text{Cs}$ content of coastal sediments near nuclear power station coolant discharge into seawater 3-69558

nuclear quadrupole moments *see nuclear electric moment***nuclear quadrupole resonance**

- acetylated glycopyranosyl chlorides, ^{35}Cl pure n.q.r., coupling const. and mol. conformation relation 3-49491
- ammonium hydrogen bis(chloroacetate), ^{35}Cl n.q.r., ferroelectric phase transition 3-79992
- antimony triphenyl-d₁₅, solid, deuteron quadrupole coupling at 77K 3-44348
- 1-chloro-2,4-dinitrobenzene, Zeeman effect 3-43480
- chloroform crystalline, quadrupole relaxation of ^{35}Cl nucleus and effect on CCl_3 group mobility 3-75902
- deuterated acetamide, of D, fine structure 3-63522
- 3,6-dichloropyridazine-d₂, solid, deuteron quadrupole coupling at 77K 3-44348
- $\text{N,N}'$ -dideuteroparachloroaniline, mag. dipole interact. in ND_2 group, ^{14}N n.q.r. Zeeman effects 3-75910
- double resonance experiment, sample transfer device 3-42615
- guanidium ion, ^{14}N study 3-79943

nuclear quadrupole resonance continued

- hedenbergite-ferrosilite pyroxene, synthetic, Mossbauer resonance spectroscopy of iron 3-80593
- hexamethylphosphoramide, pulsed ^{14}N n.q.r., use of multichannel accumulators 3-73829
- methylurea, ^{14}N n.q.r. at 77K and 296K 3-55500
- molecular crystals, motional averaging, zone centre contrib. 3-68885
- molecular crystals, spectral behaviour 3-75914
- multichannel accumulator applications, pulsed ^{14}N n.q.r. studies 3-73829
- organic compounds, polycryst., Zeeman ^{35}Cl n.q.r. spectra 3-75911
- pulse radiospectrometer, resolving power, effect of spectral width, passband of receivers 3-48487
- pyridines, BEEM- π calcs. and ^{14}N n.q.r. 3-63526
- Raman vibrational line shapes, reorientational correlation functions, appl. to nuclear quadrupole coupling constants 3-46274
- rare earth bromide hexahydrates, ^{79}Br and ^{81}Br n.q.r. 3-75913
- saturation theory, spin 3/2 nuclei in molecular crystal, nonequilibrium statistical operator 3-50486
- solids, T^4 dependence of n.q.r. frequencies 3-47165
- spectrometer, coherent pulse, freq. shift operation, apparatus 3-73824
- spectrometer system for lineshape determ. 3-48489
- trichloromethyl derivatives of P, CCl_3PCl_4 and $(\text{CCl}_3)_2\text{PCl}_3$, n.q.r. spectroscopy and mol. dynamics 3-75912
- Ag_2AsS_3 , proustite, n.q.r. spectrum and spin-lattice relax. time of ^{75}As , 300-4.2K (Russian) 3-79944
- Al, cond. electron charge density around Sc impurity 3-47168
- Al-Cr(Mn) alloy, dil., screening charge depression, 1.4K, field cycling double reson. study 3-47167
- AuCl_3 , of ^{35}Cl , spectral line asymmetry and spin echo envelope modulation 3-79942
- ^{12}B , ^{13}B , recoil polarisation through nuclear reaction into Mg crystal, quadrupole coupling, $Q(^{12}\text{B})$ to $Q(^{13}\text{B})$ ratio 3-49079
- ^{12}B , recoil implanted in Ta following $^{11}\text{B}(\text{d},\text{p})$ reaction, n.m.r. meas., determ. of sign of eqQ 3-49078
- $\text{BaI}_2 \cdot 2\text{H}_2\text{O}$, of ^{137}Ba , ^{135}Ba , quadrupole couplings, isomorphism 3-64579
- BiCl_3 , of ^{35}Cl , temp., pressure depend., volume effects 3-72545
- $\text{Br}_2\text{Sn-Mn}(\text{CO})_5$, of halogens, reson. freq. temp. depend. 3-47166
- CDI_2 , two-frequency spin echo 3-44350
- $\text{Cl}_3\text{Sn-Mn}(\text{CO})_5$, of halogens, reson. freq. temp. depend. 3-47166
- HgCl_2 , ^{35}Cl n.q.r., Zeeman effect 3-44349
- $\text{I}_3\text{Sn-Mn}(\text{CO})_5$, of halogens, reson. freq. temp. depend. 3-47166
- In, liquid, temp. depend. of Knight shift and nuclear spin relaxation rate, pseudopotential method 3-47169
- KClO_4 , formation and annealing of free radicals created by irradiation 3-61268
- K_2ReCl_6 110.9 K displacive phase transform., Zeeman n.q.r. meas. of order parameter 3-46712
- LiIO_3 , hexagonal and tetragonal, vibr. and ^{127}I n.q.r. spectra (Russian) 3-79945
- N_2 , solid, β - α ordering transition, pressure depend., n.q.r. obs. 3-75590
- $(\text{NH}_4)_2\text{PtBr}_6$, displacive phase transition ^{79}Br n.q.r. and spin-lattice relaxation time meas. 3-41449
- NaClO_4 , formation and annealing of free radicals created by irradiation 3-61268
- SbCl_3 , polycrystalline, Zeeman n.q.r. 3-61008
- SnI_4 , chemical bond structure interpreted by ^{119}Sn Mossbauer transitions and n.q.r. 3-68889
- $\text{YBr}_3 \cdot 6\text{H}_2\text{O}$, ^{79}Br and ^{81}Br n.q.r. 3-75913

nuclear radius *see nuclear size***nuclear reaction and scattering models**

- see also nuclear optical model*
- absorption model, two-nucleon, with range depend., short-range repulsion, for pion absorption in ^3He 3-78304
- Amado model and Watson-Migdal approach for neutron-neutron scattering length in $^2\text{H}(\text{n},2\text{n})\text{p}$ 3-78336
- Amado model of two-body processes in $^2\text{H}(\text{p},\text{pp})\text{n}$ reaction 3-71099
- Brown-Green model for ^{16}O , inelastic electron scattering, excited odd-parity states 3-63040
- cascade model, intra-nuclear, pion- and nucleon-nucleus inelastic scattering, >10 GeV 3-78314
- cascade model, resonance production, nuclear reaction mechanism, 3-5 GeV (Russian) 3-78295
- cascade-plus-evaporation model for 600 MeV proton interaction with complex nuclei 3-57528
- classical model, sub-Coulomb neutron transfer, vector analysing power, predictions for (d^+, p) , (d^+, t) reactions 3-60146
- coexistence model for $^{42}\text{Ca}(\text{p},^3\text{H})^{40}\text{Ca}$ reaction, cross section predictions 3-67329
- collective correlations for continuum states of ^{12}C in giant dipole reson. region 3-43229
- compound nucleus ^6Li , in $^3\text{H}(^6\text{He},\text{d})^4\text{He}$, isospin mixing 3-78306
- compound nucleus decay involving analogue resonance, energy dependence of excitation curves 3-67293
- compound nucleus statistical model, prediction of γ -ray angular distributions for $^{70}\text{Zn}(\text{p},\text{n})$ reaction 3-62931
- compound states, Coulomb mixing corrections neutron, escape from isobaric analogue resonance 3-78298
- coupled channel resonating group calculations, effect of imaginary potentials on spurious resonances 3-78296
- coupled channel separable potential model with off-shell transition matrix 3-60136
- coupled-channel analysis of heavy-ion scattering systems 3-60220
- coupled-channel Born approx. anal. of (p,t) excitation of unnatural parity final states from O^+ targets 3-78326
- coupled-channel calc. rel. to energy dependence of $^{51}\text{V}(\text{p},\text{n})^{51}\text{Cr}$ analogue transition 16 to 26 MeV 3-63053
- coupled-channel method, quasiclassical variation rel. to excitation by particles of near barrier energies (Russian) 3-67288
- coupled-channel-Born-approx. analysis of allowed and forbidden $^{22}\text{Ne}(\text{p},\text{t})^{20}\text{Ne}$ transitions 3-67332
- coupled-channels description of $^{88}\text{Sr}(^3\text{He},\text{t})^{88}\text{Y}$ to doublet states, multistep contribs. 3-67350
- diffraction model for extraction of spectroscopic factors from direct transfer reactions, accuracy 3-60140

nuclear reaction and scattering models continued

- diffraction model of deuteron stripping, effect of nuclear boundary spread and Coulomb interaction (*Russian*) 3-74548
- diffraction theory for polarisation of elastically scattering protons (*Russian*) 3-78328
- direct capture model, $^3\text{H}(^3\text{He},p)^6\text{Li}$ cross section, ~ 10 MeV 3-78308
- direct transfer, finite range approximation, recoil effects 3-78302
- doorway state, analysis of neutron scattering by ^{56}Fe 3-60177
- DWBA analysis of deuteron disintegration in nuclear field (*German*) 3-49263
- DWBA calcs. of local equivalent form factor, use of non-locality corrections 3-67287
- DWBA theory with charge exchange and isospin 3-57504
- electron scattering by 2s-1d shell nuclei α -particle model (*Russian*) 3-78313
- equilibrium statistical and hybrid models for $^{197}\text{Au}(d, xn)p$ excitation functions, 25-86 MeV 3-57532
- Ericson fluctuation theory for $^{34}\text{S}(d, p)^{35}\text{S}$ reaction 3-67339
- evaporation model, effect of ^6Li fragments on heavy product emission 3-78316
- evaporation model, Hagedorn-Macke, corrections (*Spanish*) 3-43228
- exciton model, emission and formation probability of complex particles 3-60137
- exciton model approach to pre-equil. decay 3-43230
- generator coord. method for nucl. bound states and reactions 3-52116
- Glauber model for π^\pm Be scattering, total cross sections 3-46043
- Hauser-Feshbach-Moldauer formalism, rel. to resonance interference effects in fast neutron reactions 3-71107
- heavy ion transfer reactions, model for angular distrib. including dynamic wave packet dispersion 3-49281
- heavy-ion interactions at high energy, Fermi gas cloud model 3-57539
- impulse approx., validity for $^2\text{H}(n, p)nn$ reaction at 14 MeV 3-78339
- intra-nuclear cascade, rel. to high energy inelastic, pion-heavy emulsion nuclei interactions 3-67369
- intranuclear cascade, rel. to proton bombardment of nuclei with $A=12$ to 209 at 30 to 60 MeV 3-74588
- knock-out, single-nucleon hole states, unbound character of core 3-63026
- light nuclei, possible relativistic effect in $(p, 2p)$ reaction 3-40485
- microscopic analysis of $^{39}\text{K}(d, d')$ inelastic scattering, 12.8 MeV 3-49267
- modified plane wave impulse approximation theory rel. to $^2\text{H}(^2\text{H}, dp)n$ reaction 3-60154
- nucleon radiative capture, complex coupling model 3-74585
- nucleon-nucleus scatt., off-shell effects 3-54453
- photodisintegration process, nuclear momentum distribution in nucleus rel. to $^4\text{He}(p, p)^3\text{H}$ reaction 3-67302
- pre-equilibrium, extended Griffin model, residual two-body matrix elements 3-63019
- pre-equilibrium nucleon emission model for proton bombardment of ^{181}Ta at tens of MeV energies 3-52182
- propagation of coherently produced systems through nuclei 3-63018
- R-matrix theories, two level, rel. to closely spaced resonance levels in a single channel 3-60145
- R-matrix theory, generalised rel. to $^{12}\text{C}+n$, low energy scattering 3-60183
- R-matrix theory description of off-shell resonances 3-63024
- R-matrix theory off-shell, description of resonances in $^{15}\text{N}(d, p)^{16}\text{N}(\text{unbound})$ 3-63065
- radial density, self consistent, and sum rules for charge from factors rel. to electron scattering 3-67314
- resonating group treatment of composite particle scattering, extension to heavy system 3-74602
- rotational model, coupled channels rel. to ^{28}Si nuclear deformation in $^{16}\text{O}+^{28}\text{Si}$, scattering 3-63082
- second-order effects in $(^3\text{He}, t)$ reaction 3-49271
- separable-potential model for nucleon-nucleus interaction 3-43243
- shell, background cross section and correlation between partial widths, relation 3-54454
- shell effects and neutron strength functions for elastic nucleon scattering 3-78321
- shell model, large basis, study of nucleon-transfer overlaps 3-67295
- shell model approach to the correlation between photon and particle widths 3-60144
- single-nucleon knock-out mechanism for pion induced reactions at medium energies 3-63087
- statistical model from theory of stationary irreversible processes 3-40476
- strong-absorption model for elastic, polarisation and inelastic proton scattering 3-52183
- sudden approx. for (p, d) reactions with high Q -values 3-74581
- three body scattering theory, Lippmann Schwinger equations, deuteron induced reactions 3-54447
- three body scattering theory, Lippmann Schwinger equations, complete continuity of projected kernel 3-54448
- three body scattering theory, Lippmann Schwinger equations 3-57503
- two-saddle point model for deuteron elastic scattering, polarisation effects study by steepest descent method (*Russian*) 3-74595
- (n, α) reaction, $A>90$, α -emission by pre-equilibrium processes 3-60180
- Nd background scattering, elastic cross section, virtual states of trinucleon, Amado model 3-52165
- $^{12}\text{C}(p, \pi^+)$, cross-section for π^+ production calc. in Jastrow model, comparison with IPM 3-49259
- ^{15}C continuum shell model calcs. 3-54401
- $^3\text{H}(p, p)^4\text{He}$, 156 MeV radiative capture, calc. of differential cross section in peripheral model 3-52164
- $^4\text{He}(\alpha, \alpha)^4\text{He}$, Regge representation including background term 3-52162
- $^{113}\text{In}(p, \alpha)^{112}\text{Cd}$, 14 MeV, combination of equilb., nonequilb. models to fit α spectrum data 3-78315
- $^{208}\text{Pb}(n, p)^{209}\text{Pb}$, 2.25 to 7.25 MeV, direct and compound nucleus contrib., modified Hauser-Feshbach theory 3-78332

nuclear reactions and scattering

- see also chemical effects of nuclear reactions and scattering; direct nuclear reactions and scattering; high-energy nuclear reactions and scattering; nuclear fission; nuclear fusion; nuclear reaction and scattering models; nuclear reactions and scattering due to alpha-particles; nuclear reactions and scattering due to cosmic rays; nuclear reactions and scattering due to deuterons; nuclear reactions and scattering due to electrons; nuclear reactions and scattering due to helium-3; nuclear reactions and scattering due to hyperons; nuclear reactions and scattering due to mesons; nuclear reactions and scattering due to muons; nuclear reactions and scattering due to neutrinos; nuclear reactions and scattering due to nucleons; nuclear reactions and scattering due to photons; nuclear reactions and scattering due to tritons; nuclear reactions and scattering involving few nucleon systems; nuclear resonance reactions and scattering; nuclear spallation; polarisation in nuclear reactions and scattering; statistical theory of nuclear reactions and scattering; thermonuclear reactions
- γ -ray absolute yields, considering cascade transitions 3-53977
- angular and energy distributions, calc. for reactions with 3 or more particles in final state (*Spanish*) 3-57501
- charged-particle, total cross section in terms of s wave interaction barrier 3-67361
- differential cross sections, extended geometry, incident particle continuum 3-62216
- diffraction dissociation of hadrons on nuclei, mass interference patterns 3-60135
- dispersion relations for elastic scatt. of charged particles from nuclei, low-energy 3-46015
- Doppler γ -lines, comparison of theory and expt. using maximum probability method (*Russian*) 3-71073
- DWBA analysis of deuteron disintegration in fields of heavier nuclei (*German*) 3-49264
- elementary particle interactions with nuclei, invariant form factors and impulse approx. 3-43216
- generator coordinate method for scattering, exact soln. 3-54452
- generator coordinates, real and purely imaginary for scattering problems 3-67283
- generator-coordinate amplitude, boundary conditions, solution to Hill-Wheeler equation 3-63020
- incoherent multiple-scattering effects in production of particles on nuclear targets 3-43227
- level density calculations and exptl. studies, review 3-54394
- multiparticle production models rel. to inclusive nucl. scatt. 3-62865
- optical concepts in high-energy physics 3-48993
- optical potential for scattering from system of finite-mass particles 3-54451
- orientation of states, directional correlations of emitted γ -radiation 3-71079
- rare earth region, excited O^+ states in two-nucleon transfer reactions (*Russian*) 3-52091
- relativistic corrections in nuclear-plus-e.m. Hamiltonian 3-62956
- rescattering series convergence, reln. to proton-deuteron scattering 3-63021
- Rutherford scattering deviations due to ground state quadrupole moment 3-52153
- sequential decay processes, analysis of angular correlations 3-67284
- Sun's surface, H and He isotopes in solar cosmic rays (*Russian*) 3-65565
- tabular secondary neutron and photon energy distribns., interpolation 3-43226
- three-nucleon scattering, ^2S state amplitudes in Amado model 3-67225
- three-particle final states, boundary conditions approach 3-67101
- three-particle reactions, angular distrib. analysis 3-40472
- threshold behaviour of three-particle scattering amplitude from gas approx. in many-body problem 3-67286
- threshold phenomena and their observation, S-matrix unitarity basis 3-67285
- transition matrix of reaction theory, potential scattering 3-60138
- triangular diagrams, pole singularity 3-57502
- two-body relativistic kinematics, computer calc. of transformation relations 3-71090
- two-nucleon transfer reaction cross sections, DWBA analysis, absolute normalization 3-40473
- unstable states, correspondence with resonances, potential scattering 3-42834
- ^{159}Dy , spreading width of rotational doorway states 3-67203
- nuclear reactions and scattering due to alpha-particles**
- $A=12$ -208, inelastic, 166 MeV, first collective levels, microscopic wave functions of nuclear levels 3-60182
- compound statistical reactions, test of independence hypothesis and isospin conservation 3-71093
- Coulomb excitation of Pd and Ru isotopes in Pd-Fe and Ru-Fe targets, recoil expts. 3-49269
- elastic scattering, high energy, theory of optical potential (*Russian*) 3-67292
- excitation at high energies, cross section comparison with electrons, protons, pions 3-60164
- inelastic scattering in continuum, $A=51$ -206, energy spectra, collective modes and optical model 3-67347
- large-angle scattering, exchange amplitude interpret., knock-on process 3-40508
- level spin determ. method using α -scatt. 3-63072
- propagation in photographic nuclei, calc. (*Russian*) 3-49274
- rare earth nuclei, Coulomb excitation, meas. of hexadecapole transition moments and $M(E2; 0 \rightarrow 2)$ 3-49195
- (α, xn) 25-62 MeV, excitation of yrast levels in Se, Kr, Te and Ce, in-beam electron conversion 3-67264
- $^{109}\text{Ag}(\alpha, \alpha')$, 8 MeV, quadrupole moments by Coulomb excitation 3-71040
- $^{36}\text{Ar}(\alpha, pp)^{39}\text{K}$, 7.30-10.45 MeV, determ. of lifetimes of excited states 3-43210
- $^{10}\text{B}(\alpha, 2\alpha)^6\text{Li}$, 24 MeV, angular distrib. of sequential decay process 3-40472
- $^{10}\text{B}(\alpha, \alpha)^{10}\text{B}$, 2.0-4.3 MeV, obs. of level structure in ^{14}N , excitation functions and α -particle decay 3-71055
- $^{11}\text{B}(\alpha, ^3\text{He})$, $E_\alpha=65$ MeV, α -transfer feasibility studies 3-63073
- $^{11}\text{B}(\alpha, n)^{14}\text{N}$, $E_\alpha=12$ -15 MeV, cluster transfer 3-63070

nuclear reactions and scattering due to alpha-particles continued

- Ba(α ,n)La, study of odd-A La isotopes, $A=131-139$ by particle spectroscopy 3-45976
- ⁹Be(α , α')⁹Be, 1.7-6.2 MeV, excitation functions and angular distrib., compound-nucleus theory, ¹³C states 3-63075
- ⁹Be(α ,n), neutron spectra of ²⁴Am-²⁵Be source 3-77607
- ⁹Be(α , α')¹²C, 4.5-5.85 MeV, meas. of neutron polarisation angular distrib., ¹³C states 3-62946
- ²⁰⁹Bi(α ,nn)²¹¹At, population of isomeric three proton state in ²¹¹At, anomalous of g-factor determ. 3-45961
- ²⁰⁹Bi(α ,nn)²¹¹At, population of 21/2⁻ state in ²¹¹At, g-factor determ. 3-49093
- ¹²C, elastic and inelastic scattering at 139 MeV, optical model and DWBA analyses 3-49270
- ¹²C(α ,³He)¹³C, 139 MeV, DWBA analysis, differential cross section, ¹³C spectroscopic strength 3-49270
- ¹²C(α ,⁴Be), $E_\alpha=65$ MeV, α -transfer feasibility studies 3-63073
- ¹²C(α , α'), 20-35 MeV, intermediate structure study in complete break-up process (Russian) 3-74600
- ¹²C(α , α')¹²C, 104 MeV, computational approach to inverse problem in JWKB approximation 3-60143
- ¹³C(α ,n)¹⁶O, $E_\alpha=1.5$ MeV, total neutron yield, compound states in ¹⁷O 3-40507
- ¹³C(α ,n)¹⁶O, 2.075-2.43 MeV, neutron polarisation angular distrib., parity assignments of ¹⁷O 7.97-8.197 MeV states 3-67189
- ⁴⁰Ca(α , α'), 29 MeV, coupled-channel calcs., influence of J-dependent absorption on cross section 3-67353
- ⁴⁰Ca(α , α')⁴⁰Ca, coupled-channel calcs., influence of J-dependent absorption on cross section 3-67353
- ⁴⁰Ca(α ,d)⁴²Sc, study of ⁴²Sc, 25.5 MeV, d ang. distrib. meas. 3-78246
- ⁴⁰Ca(α ,p)⁴¹Ti, rotational bands obs. 3-74490
- ⁴⁰Ca, ⁴⁰Ca, Coulomb excitation of 2⁺ states, ratio between B(E2) values 3-49193
- ⁴⁰Ca(α ,p(n)), 10.2-14.2 MeV, population of spherical shell-model states of high angular momentum in 1f_{7/2} nuclei 3-40416
- ⁴⁰Ca(α ,n)⁴²Ti, 10.2-14.2 MeV, study of K=3/2⁺ rotational band 3-74494
- ⁴⁰Ca(α ,p)⁴³Sc, 10.2-14.2 MeV, study of K=3/2⁺ rotational band 3-74494
- Cd even isotopes, interference between Coulomb and nuclear elastic and inelastic scattering 3-46036
- ¹⁰⁶Cd(α , α')¹⁰⁶Cd, props. of 2⁺ and 2⁺ states, $E=11.0$ MeV 3-46003
- ¹¹²Cd(α , α')¹¹²Cd, props. of 2⁺ and 2⁺ states, $E=11.0$ MeV 3-46003
- ¹¹²Cd(α ,nn)¹¹⁴Sn, 22 MeV, population of high spin isomeric states in ¹¹⁴Sn, g-factor determ. 3-45958
- ¹¹²Cd(α , α')¹¹²Cd, props. of 2⁺ and 2⁺ states, $E=11.0$ MeV 3-46003
- ⁷¹Cl(α ,n)⁷⁰K, study of e.m. decay scheme below 3.2 MeV excitation 3-43208
- Co(α , α'), 22 to 29 MeV interference maxima in backward excitation curve and angular distrib. 3-67348
- ⁵²Cr(α ,np)⁵⁵Fe, mean life measurement for excited states, 11 MeV incident energy, recoil distance method (French) 3-43205
- ¹³⁵Cs(α , α')¹³⁵Cs, Coulomb excitation, 6-11 MeV, meas. of de-excitation γ -rays 3-52200
- Cu(α , α'), 22 to 29 MeV interference maxima in backward excitation curve 3-67348
- ⁶³Cu(α ,p)⁶⁴Zn 3-78346
- ⁵⁶Dy(α ,nnnn)¹⁶⁰Er, 47-50 MeV, population of high-spin members of ground state rotational bands 3-52098
- ¹⁶⁰Dy(α ,n), high spin states in ¹⁵⁹Er 3-62937
- ¹⁶¹Dy, Coulomb excitation of 43.8 keV state, Mossbauer effect study of transition 3-62990
- ⁵F(α ,n), high resolution study around neutron threshold, resonance obs. 3-46037
- ¹⁹F(α ,p), high resolution study around neutron threshold, resonance obs. 3-46037
- ⁵⁶Fe(α ,p)⁵⁷Co, 23 MeV, selective population of highly excited states 3-78346
- ⁵⁶Fe(α ,n)⁵⁶Ni, 8.5 and 10.5 MeV, meas. of Doppler shift attenuations and recoil distance 3-49213
- ⁵⁶Fe(α ,p)⁵⁶Co 3-78346
- ⁵⁷Fe(α ,p)⁵⁶Co 3-78346
- Fe(α ,n) reactions, $A=56, 57$, precompound processes, 20 MeV, energy, angular distrib. of neutrons 3-60209
- Ga, time differential perturbed angular distrib. meas. of quadrupole interaction on Ge isomeric levels 3-45949
- ¹⁵⁴Gd(α ,He,xn)¹⁵²Dy, high angular momentum, excitation functions and photon emission, compound nucleus mechanism 3-63083
- ¹⁵⁴Gd(α ,2n)¹⁵²Dy, production and separation processes 3-57535
- ¹⁵⁴Gd(α ,nnnn)¹⁵²Dy, 47-50 MeV, population of high-spin members of ground state rotational bands 3-52098
- ¹⁵⁴Gd(α ,3n)¹⁵¹Dy, production and separation processes 3-57535
- ¹⁵⁴Gd(α ,n)¹⁵⁴Dy, production and separation processes 3-57535
- ¹⁵⁴Gd(α ,3n)¹⁵¹Dy, ¹⁵¹Dy rotational excitations properties 3-43212
- Gd(α ,2n)¹⁵²Dy, g factor meas. of high-spin rotational states in Dy with $A=158, 160, 162$ 3-67188
- H(α , α')n, differential cross section, off energy shell impulse approximation 3-54455
- H(α ,d)H, 70 MeV sequential reaction through ⁴He, obs. of excited states 3-63032
- H(α ,pd)H, 70 MeV sequential reaction through ⁴He, obs. of excited states 3-63032
- H(α ,t)³He, 82 MeV, multi-interaction, finite-range, two-mode DWBA analysis 3-67297
- He(α , α') bremsstrahlung meas. at 9.35 MeV, differential cross section determ. 3-74561
- He(α , α')He, Regge representation including background term 3-52162
- ¹⁷⁶Hf, ¹⁷⁶Hf isomeric states populated in (α ,nnp) reaction, g-factor and proton-neutron mixing ratios 3-45967
- H(α ,2n)¹⁸⁰W, 29-43 MeV, obs. of Coriolis mixing effects in ¹⁸⁰W 3-60079
- ¹⁸⁰Hf(α ,3n)¹⁸¹W, 29-43 MeV, obs. of Coriolis mixing effects in ¹⁸¹W 3-60079
- Hg(α ,2n)²⁰⁰Pb, 27 MeV, population of 12⁺ isomeric state in ²⁰⁰Pb, g-factor meas. 3-49087
- Hg(α ,3n)²⁰³Pb, high spin three neutron hole states of ²⁰³Pb 3-52100

nuclear reactions and scattering due to alpha-particles continued

- ¹⁶⁰Ho, quadrupole moment meas. by proton and alpha scattering from aligned target 3-45944
- ¹²⁷I(α , α')¹²⁷I, Coulomb-excitation, 6-11 MeV, meas. of de-excitation γ -rays 3-52200
- ¹²⁹I(α , α')¹²⁹I, Coulomb excitation, 6-11 MeV, meas. of de-excitation γ -rays 3-52200
- ¹¹⁵In(α ,n), 20 MeV, precompound processes, neutron energy and angular distrib. 3-60209
- ⁴¹K(α ,np)⁴⁴Sc, 10-14 MeV, γ -ray spectra, $\gamma\gamma$ -coincidences and yield function meas., ⁴⁴Sc excited states 3-74495
- ⁴¹K(α ,np)⁴⁴Sc, level scheme of ⁴⁴Sc, lifetime meas. ang. distrib. 3-78282
- Li(α , α'), elastic and inelastic, 8.6-12.5 MeV and 17-22.5 MeV, excitation functions, triton exchange 3-63071
- ¹⁷⁵Lu(α ,2n)¹⁷⁷Ta, 27 MeV, half lives of ¹⁷⁷Ta levels, comparison with Nilsson model, hindrance factors 3-54422
- ²⁴Mg, 104 MeV scattering analysis using a folded collective model 3-60208
- ²⁶Mg(α ,np)²⁹Si, product high-spin states obs. using neutron time-of-flight spectrometer 3-52084
- ²⁶Mg(α ,n)²⁹Si, population of high spin negative parity states in ²⁹Si associated with oblate deformation 3-43171
- ⁹²Mo(α ,p2n)⁹³Tc, 37-43 MeV, population of high spin states 3-78248
- ⁹²Mo(α ,3n)⁹⁵Tc, (α , α')⁹⁵Ru, population of high spin states, 37-43 MeV 3-78249
- ²⁰Ne(α , α')²⁰Ne, 104 MeV α -particles, differential cross sections, anal. using deformed folding model 3-54498
- ²⁰Ne(α ,n)²³Mg, threshold to 31 MeV, evidence for boson-mode excitations 3-60214
- ²¹Ne(α ,n)²⁴Mg, 1 to 5 MeV bombarding energies, total neutron yield 3-54497
- ²²Ne(α ,n)²⁵Mg, 1 to 5 MeV bombarding energies, total neutron yield 3-54497
- ⁵⁸Ni, elastic, inelastic, 139 MeV, elastic cross sections, potential well depth 3-63076
- ⁵⁸Ni(α ,He,p)⁶¹Cu, 9.7-12.2 MeV reaction spectrometry 3-67261
- ⁵⁸Ni(α ,p)⁶¹Cu 3-78346
- ⁶¹Ni(α ,p)⁶⁴Cu 3-78346
- ⁶⁴Ni(α ,n)⁶⁷Zn, perturbed angular distrib. meas. determ. of magnetic moment of excited 9/2⁺ state of ⁶⁷Zn 3-45948
- Ni(α , α'), 22 to 29 MeV interference maxima in backward excitation curve 3-67348
- ¹⁶O, forward elastic scattering, cluster model vertex functions 3-60211
- ¹⁶O- α scattering, extension of resonating group method to heavy system 3-74602
- ¹⁶O(α , α'), wave functions and reflection coeffs. deduced from optical model, $E=20.1$ MeV 3-43254
- ¹⁶O(α ,⁴Be), $E_\alpha=65$ MeV, α -transfer feasibility studies 3-63073
- ¹⁶O(α , α')¹⁶O, inelastic scatt. to 2⁻ state via nonlocal interaction 3-54466
- ¹⁶O(α , α')¹⁶O, 20.1 MeV, optical model analysis using independent geometries for real and imaginary potentials 3-67346
- ¹⁶O(α ,n)¹⁹Ne, threshold to 26 MeV, evidence for boson-mode excitations 3-60214
- ¹⁷O(α ,n)²⁰Ne, $E_\alpha=1.5$ MeV, total neutron yield, compound states in ²¹Ne 3-40507
- ¹⁸O(α ,n)²¹Ne, $E_\alpha=1.5$ MeV, total neutron yield, compound states in ²²Ne 3-40507
- ²⁰⁴Pb(α ,2n)²⁰⁶Po, mag. mom. meas. of [(π h_{9/2})²]⁸ states 3-49088
- ²⁰⁴Pb(α ,t)²⁰⁵Bi, fragmentation of proton levels of ²⁰⁵Bi 3-63080
- ²⁰⁵Pb(α ,nnn)²⁰⁷Po, population of 13/2⁺ state in ²⁰⁷Po, magnetic moment determ. 3-49089
- ²⁰⁵Pb(α ,t)²⁰⁷Bi, fragmentation of proton levels of ²⁰⁷Bi 3-63080
- ²⁰⁸Pb elastic and inelastic, 139 MeV, potential well ambiguity, elastic cross sections 3-63076
- ²⁰⁸Pb(α ,n)²¹¹Po, population of (15/2⁻) state in ²¹¹Po, lifetime and g-factor determ. 3-49092
- ²⁰⁸Pb(α ,nn)²¹⁰Po, population of core excited isomeric state in ²¹⁰Po, magnetic moment determ. 3-49091
- ²⁰⁸Pb(α ,2n)²¹⁰Po, population of core-excited isomeric state in ²¹⁰Po, time-differential spin-rotation meas. 3-45972
- ²⁰⁸Pb(α , α'), 90 MeV, cross section analysis, obs. of new giant resonance 3-63077
- Pb(α ,xn)Po, population of high-spin isomeric states in Po isotopes magnetic moment determ. 3-49090
- Pb(α ,xn+p), $E=25-29$ MeV, stroboscopic resonance method, g-factors for Po isotopes 3-71041
- ²⁰⁴Pn(α ,4n)²⁰⁴Po, mag. mom. meas. of [(π h_{9/2})²]⁸ states 3-49088
- ¹⁴¹Pr(α ,2n)¹⁴³Pm, e.m. props. of low-lying levels, M2, E3 transition probabilities 3-67254
- ¹⁹⁸Pt(¹B,nnnnn)²⁰⁴Bi, population of high-spin isomeric state in ²⁰⁴Bi 3-49152
- ¹⁰³Rh(α ,n), 20 MeV, precompound processes, neutron energy and angular distrib. 3-60209
- ⁹⁹Ru(α ,n)¹⁰²Pd, level struct. of ¹⁰²Pd 3-40510
- ³²S(α ,p)³⁵Cl, 12-16 MeV, study of high spin states in ³⁵Cl by $\gamma\gamma$ -coincidence, angular distrib., yield function meas. 3-74493
- ³²S(α ,np)³⁵Ar, lifetime of first excited state in ³⁵Ar 3-45996
- ³²S(α ,p)³⁵Cl, 11.2 MeV meas. of lifetime of first 7/2⁻ level in ³⁵Cl by recoil distance method 3-78284
- ³²S(α ,p)³⁵Cl, obs. states of ³⁵Cl from proton spectra meas. 20 MeV 3-62947
- ³⁴S(α ,n)³⁷Ar, population of 1612 keV level, mean lifetime meas. 3-45991
- ³⁴S(α ,p)³⁷Cl, 11.2 MeV, meas. of lifetime of first 7/2⁻ level in ³⁷Cl by recoil distance method 3-78284
- ⁸⁰Se(α ,p)⁸³Br, energy levels of ⁸³Br study 3-52103
- ²⁸Si(α ,n)²⁸Si, 104 MeV α -particles, differential cross sections, anal. using deformed folding model 3-54498
- ²⁸Si(α ,p)³²P, $E_\alpha=10.65, 10.69, 11.00$ MeV, $\gamma\gamma$ angular correlations, DSA lifetime measurements, ³²P deduced levels, mixing, branching ratios 3-60108
- ¹⁴⁹Sm(α ,2n)¹⁵¹Gd, 11-/2 [505] rotational band identification 3-74489
- ¹⁵²Sm, ¹⁵⁴Sm, Coulomb excitation of 2⁺ and 4⁺ levels, determ. of E4 moments 3-49202

nuclear reactions and scattering due to alpha-particles continued

- ¹²⁴Sn(α ,³He)¹²⁵Sn, meas. differential cross section at 65.7 MeV rel. to neutron shell structure determ. of ¹²⁵Sn 3-67213
 Sn(α ,n), A = 115-119, 124, 20 MeV, precompound processes, neutron energy and angular distrib. 3-60209
⁸⁸Sr(α ,3n γ), (α , α' n γ)⁸⁹Zr, population of high spin states, 37-43 MeV 3-78249
⁸⁸Sr(α ,n)⁹¹Zr, 16 MeV, population of high-spin states in ⁹¹Zr, time differential meas. 3-49194
¹⁸⁴Ta(α ,He,xn)¹⁸⁵-¹⁸⁶Re, high angular momentum, excitation functions and photon emission, compound nucleus mechanism 3-63083
⁴⁶Ti, ⁴⁸Ti, 10.2-14.2 MeV, population of spherical shell-model states of high angular momentum in 1f_{7/2} nuclei 3-40416
⁴⁶Ti, test of independence postulate in Bohr theory of compound-nucleus decay 3-40512
⁵⁰Ti(α ,n)⁵³Cr(p), 10.2-14.2 MeV, decay properties of high-spin states in ⁵³Cr 3-52096
¹⁶⁹Tm(α ,nnp)¹⁷¹Lu, 23-27 MeV, γ -ray obs, level scheme determ. 3-60077
¹⁶⁹Tm(α ,2n)¹⁷¹Lu, γ radiation and conversion electrons, rot. bands of ¹⁷¹Lu 3-62939
¹⁸²W(α ,2np)¹⁸⁴Os 30 MeV, ground state levels and gamma vibrational bands in ¹⁸⁴Os 3-67194
¹⁸⁴W(α ,2np)¹⁸⁶Os, 30 MeV, ground state levels and gamma vibrational bands in ¹⁸⁶Os 3-67194
¹⁸⁶W(α ,2np)¹⁸⁸Os, 30 MeV, ground state levels and gamma vibrational bands in ¹⁸⁸Os 3-67194
¹⁸⁶W(α ,8n)¹⁸²Os, 106 MeV, γ -decay to ground state rotational band in ¹⁸²Os 3-74498
¹³⁵Xe(α , 2n)¹³⁸Ba, 20-29 MeV, meas. of cross section, angular distrib., γ -ray spectra, level structure obs. 3-45974
¹³⁶Xe(α , 3n)¹³⁷Ba, 20-29 MeV, meas. of cross section, angular distrib., γ -ray spectra, level structure obs. 3-45974
⁸⁹Y(α ,nn)⁹¹Nb, 21 MeV, population of high-spin state in ⁹¹Nb, time differential meas. 3-49194
⁹Yb(α , xn), A = 171, 174, 176, x = 2, 3, 20-43 MeV, population of rotational bands in odd Hf nuclei 3-40417
 Yb(α ,t), rot. bands of ¹⁷¹Lu 3-62939
 Zn, time differential perturbed angular distrib. meas. of quadrupole-interaction on Ge isomeric levels 3-45949
⁶⁴Zn(α ,n)⁶⁷Ge, perturbed angular distrib. meas., determ. of magnetic moment of excited 9/2⁺ state of ⁶⁷Ge 3-45948
⁹⁰Zr(α ,3np), (α , α' n γ)⁹¹Mo, population of high spin states, 37-43 MeV 3-78249
⁹⁰Zr(α , α')⁹⁰Zr, 104 MeV, computational approach to inverse problem in JWKB approximation 3-60143
⁹⁰Zr(α ,p2np)⁹¹Nb, 37-43 MeV, population of high spin states 3-78248
⁹⁰Zr(α ,pp)⁹³Nb, 14.77 MeV, γ -decay of ⁹³Nb low lying levels 3-57491
⁹²Zr(α ,He), E = 65.7 MeV, neutron shell struct. of ⁹³Zr 3-40504
⁹²Zr(α ,nn)⁹⁴Mo, 24 MeV, population of 2953 keV state in ⁹⁴Mo, time-differential PAC meas. 3-49084
⁹⁴Zr(α ,He), E = 65.7 MeV, neutron shell struct. of ⁹⁵Zr 3-40504
⁹⁶Zr(α ,He), E = 65.7 MeV, neutron shell struct. of ⁹⁷Zr 3-40504

nuclear reactions and scattering due to cosmic rays

see also cosmic ray effects and interactions

- air nuclei, nucleon interaction at energies > 30 GeV, possible inelastic cross section behaviour (Russian) 3-42102
 air nuclei, nucleon interactions at mountain altitudes, 600-10000 GeV, integral energy spectrum (Russian) 3-69781
 air nuclei, proton interaction, increasing cross sections 3-67160
 atmospheric neutron production by proton interactions with air-nuclei 3-59235
 electron-nucleus showers, E \geq 10 GeV, cosmic ray muon contribution (Russian) 3-80903
 emulsion nuclei (Ag, Br, C, N, O), pion inelastic interactions at 60 GeV, Monte Carlo calcs. (Russian) 3-69788
 heavy-ion initiated nuclear-e.m. cascades, Monte Carlo calcs. 3-59234
 inclusive nucleon and pion production from proton-nucleus collisions, semiempirical model 3-57465
 inclusive particle-nucleus reactions at accelerator and cosmic-ray energies, prediction 3-57518
 inelastic collisions of pions and nucleons with nuclei \geq 10 GeV, intra-nuclear cascade model 3-78314
 interstellar gas interactions, cross-sections for high-energy proton interactions with targets with Z \leq 28 3-43237
 interstellar gas interactions, cross-sections for proton interactions with targets heavier than Ni 3-43238
 ionisation calorimeter study, above 10¹² eV, counting, observation 3-77615
 multiplicities from intra-nuclear cascading 10¹⁵ eV cosmic ray proton 3-74586
 nucleon-nucleon interactions in energy range 24-300 GeV, energy spectra of secondary nucleons (Russian) 3-69786
 secondary particles produced at interaction of multiply charged relativistic nuclei with emulsion nuclei (Russian) 3-65606
 total proton-nucleus cross-section and coherent processes in TeV region from cosmic-ray data 3-51237
 C, nucleon interactions at mountain altitudes, 600-10000 GeV, integral energy spectrum (Russian) 3-69781
 C, proton inelastic interactions, 10¹¹-10¹² eV, effective cross-section meas. on PROTON-4 satellite (Russian) 3-69787
 Fe, avalanches induced by charged and neutral particles, cascade curves (Russian) 3-65609
 Fe, nucleon interactions at mountain altitudes, 600-10000 GeV, integral energy spectrum (Russian) 3-69781
 Pb, nucleon interactions at mountain altitudes, 600-10000 GeV, integral energy spectrum (Russian) 3-69781
 Pb avalanches induced by charged and neutral particles, energy transferred to neutral pions (Russian) 3-65609

nuclear reactions and scattering due to deuterons

- antisymmetrization effects calc., practical procedure 3-67344
 break-up in heavy nuclear field above Coulomb barrier (German) 3-49265
 breakup, neutron beam production, monokinetic, up to 1.9 GeV/c, Saturne synchrotron Saclay France 3-77608
 diffraction model of deuteron stripping, effect of nuclear boundary spread and Coulomb interaction (Russian) 3-74548

nuclear reactions and scattering due to deuterons continued

- disintegration effects, choice of nucleon-nucleus potential in optical potential calcs. 3-60142
 disintegration in nuclear field, DWBA analysis (German) 3-49263
 elastic scattering, high energy, theory of optical potential (Russian) 3-67292
 elastic scattering, medium energy, polarisation effects on cross sections and spin tensors (Russian) 3-74595
 emulsion, interactions of 9.4 GeV/c deuterons, multiplicity and angular distrib. 3-52196
 light nuclei, obs. of S-wave levels near threshold using tensor-polarised deuterons 3-49261
 low-energy deuteron break up on heavy nuclei, neutron-nucleus interaction 3-54487
 nonadiabatic effects in high-energy scattering and effects due to deviations from geometrical optics (Russian) 3-67337
 one-neutron transfer reaction for ¹⁴N, ¹⁷O, ^{57,58}Ni, ^{206,207}Pb, ^{209,210}Pb, form factor calc. 3-43246
 stripping (d,p) reactions, reversibility, Born and DWBA calculations, one-dimensional model 3-60147
 three-body scattering theory, Lippmann Schwinger equations, deuteron induced reactions 3-54447
 (d,d') form factor, nucl. struct. depend. of phase 3-63067
 (d,p) and complementary (p,d) reactions, comparative treatment of spectroscopic factors 3-40502
 (d,p) sub-Coulomb stripping and analog-resonance results near closed shells 3-67342
 (d,p) reactions, compound nucleus contribs. to T₂₀ analysing power 3-67343
 (d,p) reactions, threshold effects in the proton spectrum 3-71121
 (d,t) reaction, 12 MeV, ²³⁸Pu energy level study 3-43185
 π production, energy, cross sections (Russian) 3-60206
 Al cross-section for stripping and dissociation at 2.7 GeV/c measurement 3-78344
²⁷Al(d, α)²⁵Mg, ²⁵Mg γ -decay study 3-40458
²⁷Al(d,p)²⁸Al, region from hyperbarrier to Coulomb stripping, obs. of ²⁸Al energy levels (Russian) 3-52189
³⁶Ar(d,p)³⁷Ar neutron reson. ³⁷Ar, DWBA anal. 3-54492
³⁸Ar(d,p)³⁹Ar, neutron reson. ³⁹Ar, DWBA anal. 3-54492
 Au, breakup of deuterons, 7-12 MeV, meas. angular correlation, breakup cross section 3-60204
 Au, deuteron disintegration in Coulomb field, energy and angular distrib. of products (Russian) 3-67340
¹⁹⁷Au(d,p), 100 MeV, diffraction model of deuteron stripping, effect of nuclear boundary spread and Coulomb interaction (Russian) 3-74548
¹⁹⁷Au(d,pxn)¹⁹⁸-²⁰⁰Au, 25-86 MeV, excitation function meas., equilibrium statistical and hybrid models 3-57532
¹⁹⁷Au(d,xn)¹⁹⁹-²⁰¹Hg, 25-86 MeV, excitation function meas., equilibrium statistical and hybrid models 3-57532
 Au(d,pn)Au, disintegration at 12 and 10.5 MeV, energy-angle correlations, DWBA analysis (German) 3-49264
¹⁰B(d,p)¹¹B, 0.67-2.32 MeV, DWBA analysis deduced spectroscopic factors of 6.76 MeV level of ¹¹B 3-62938
¹⁰B(d,n)¹¹C, low energy, branching ratios, isobaric analogue states 3-74599
¹⁰B(d,p)¹¹B, low energy, branching ratios, isobaric analogue states 3-74599
¹⁰B(d,t), j-dependence of triton angular distrib. (Russian) 3-52191
¹¹B(d,p)¹²C, E = 1-4 MeV, cross sections, ¹³C deduced resonances 3-67341
¹¹B(d,p)¹²B, polarised recoil of ¹²B into Mg crystal, quadrupole coupling 3-49079
¹¹B(d,p)¹²B, recoil implantation in Ta, n.m.r. meas., alignment and quadrupole spectrum determ. 3-49078
¹³⁸Ba(d,p), 19 MeV, determ. of optical model parameters 3-46033
¹³⁸Ba(d,p)¹³⁹Ba, 19 MeV, angular distrib. meas., determ. of orbital angular momentum transfer and spectroscopic factors 3-46033
 Be cross-section for stripping and dissociation at 2.7 GeV/c measurement 3-78344
⁹Be, 20 MeV, neutron yields and spectra, rel. to high intensity neutron sources 3-74596
⁹Be, (d,d) and (d,p) reactions at low energies, optical model and Hauser-Feshbach analysis 3-57533
⁹Be(d,p), 12.3 MeV, importance of D-state effects 3-54486
⁹Be(d,t), j-dependence of triton angular distrib. (Russian) 3-52191
¹⁰Be(d, α)⁹Li cross sections modification for half-life of ¹⁰Be 3-40505
¹⁰Be(d,p)¹¹Be cross sections modification for half-life of ¹⁰Be 3-40505
 Bi, deuteron disintegration in Coulomb field, energy and angular distrib. of products (Russian) 3-67340
²⁰⁹Bi(d,py) reaction, obs. gamma decay of ²¹⁰Bi excited states, shell model interpretation 3-67259
 C cross-section for stripping and dissociation at 2.7 GeV/c measurement 3-78344
¹²C, 20 MeV, neutron yields and spectra, rel. to high intensity neutron sources 3-74596
¹²C(α ,Li,d)¹⁵O, ¹⁶O(d, α +d)¹²C, angular correlations, plane-wave approx. (Russian) 3-78301
¹²C(d, α)¹¹B*, ³He continuous spectrum calculated, direct reaction mechanism 3-60207
¹²C(d,n)¹³N*, determ. of apparent reaction dependence of width of ¹³N first excited state 3-62945
¹²C(d,p), 12.3 MeV, importance of D-state effects 3-54486
¹²C(d,p), coupling const. determ. in peripheral models including form factor effects (Russian) 3-74598
¹²C(d,p), rel. to model independent anal. of stripping to unbound levels 3-67296
¹²C(d,p)¹³C, 9.3 to 15.0 MeV, comparison with DWBA theory, cross sections and resonance widths 3-54488
¹²C(d,p)¹³C, unbound levels in ¹³C, application of real Weinberg state method 3-57471
¹²C(d,py)¹³C, determ. of angular distrib. of protons near resonances by shape-studies of γ -ray lines 3-40501
¹³C(d, γ)¹⁵N, E = 1-4 MeV, cross sections, ¹⁵N deduced resonances 3-67341
¹³C(d,t), j-dependence of triton angular distrib. (Russian) 3-52191
¹⁴C elastic scatt., 4-10 MeV, ang. distrib. meas., reson., optical model anal. 3-78343

nuclear reactions and scattering due to deuterons continued

- ¹⁴C(d,n)¹⁵N, deuteron energies, 1.3 to 1.9 MeV, neutron polarisation ang. distrib. (*German*) 3-52197
- ¹⁴C(d,p) stripping form factors, continuum shell model for ¹⁵C 3-54401
- ¹⁴C(d,p)¹⁵C, analysis of ¹⁵C states, 12 to 14 MeV, excitation energies and level widths 3-67208
- ⁴⁰Ca, (d,p), 12.3 MeV, importance of D-state effects 3-54486
- ⁴⁰Ca(²He,d)⁴¹Sc, meas. differential cross section, use DWBA to study $1f_{7/2}$ proton in ⁴¹Sc 3-74480
- ⁴⁰Ca(d,Li), 28 MeV, cross-section, spectroscopic factors 3-78341
- ⁴⁰Ca(d,n)⁴¹Sc, recoil polarisation of ⁴¹Sc, n.m.r. meas. of β -decay asymmetry, magnetic moment determ. 3-45938
- ⁴⁰Ca(d,p)⁴¹Ca, high resolution study of weak transitions, high spin states of rotational bands in ⁴¹Ca 3-60072
- ⁴²Ca(d,³He)⁴⁴K, meas. differential cross sections, use DWBA to study $1d_{3/2}$ protons in ⁴²Ca 3-74480
- ⁴²Ca(d,Li), 28 MeV, cross-section, spectroscopic factors 3-78341
- ¹⁰⁶Cd(d,p) reaction, 12 MeV, nuclear structure study 3-67345
- ¹⁰⁶Cd(d,pp)¹⁰⁷Cd, ¹⁰⁷Cd level scheme study 3-49154
- ¹⁰⁶Cd(d,i) reaction, 16 MeV, nuclear structure study 3-67345
- ³⁵Cl(d,p)³⁶Cl, 1.68-2.5 MeV excitation functions and ang. distributions 3-63062
- ³⁵Cl(d,p)³⁶Cl, 3.5 MeV, gamma-ray decay ³⁶Cl, determ. branching ratios and mean lives of states 3-67262
- ³⁷Cl(d,p)³⁸Cl, meas. of e.m. transition rates in ³⁸Cl 3-62989
- ⁵⁰Cr(d, α)⁴⁸V, 15 MeV, excitation energies and angular distrib. meas. for ⁴⁸V levels 3-57534
- ⁵⁰Cr(d,p)⁵¹Cr, region from hyperbarrier to Coulomb stripping, spectroscopic study (*Russian*) 3-52190
- ⁵²Cr(d,p)⁵³Cr, deuteron D-state effects obs. 3-63066
- ⁵²Cr(d, α)⁵⁰V, 15 MeV, excitation energies and angular distrib. meas. for ⁴⁸V levels 3-57534
- ⁵²Cr(d,p)⁵³Cr, 10 MeV, tensor polarised deuteron beam, meas. of analysing powers and cross sections 3-49266
- Cu cross-section for stripping and dissociation at 2.7 GeV/c measurement 3-78344
- ⁶³Cu(d,p)⁶⁴Cu, 6.5 MeV, γ -ray spectroscopy study of ⁶⁴Cu 3-45955
- ⁶³Cu(d,p)⁶⁶Cu, 6.5 MeV, γ -ray spectroscopy study of ⁶⁶Cu 3-45955
- D₂ plasma, energy deposition of a fast deuteron 3-60614
- ¹⁶⁷Er(d,d')¹⁶⁷Er, energy levels study 3-40413
- ¹⁹F(d,p), 12.3 MeV, importance of D-state effects 3-54486
- ¹⁹F(d,³He)¹⁸O, analogue state, distorted wave theory extended to include charge exchange channel 3-60203
- ¹⁹F(d,t)¹⁸F, analogue state distorted wave theory extended to include charge exchange channel 3-60203
- Fe, A=54, 56, 58, scattering of polarised 12.3 MeV deuterons, vector analysing power and cross sections 3-52194
- ⁵⁴Fe(d,p)⁵⁵Fe, 10 MeV, tensor polarised deuteron beam, meas. of analysing powers and cross sections 3-49266
- ⁵⁴Fe(d,t)⁵⁵Fe, low-lying levels study 3-74485
- ⁵⁴Fe(d,Li), 28 MeV, cross-section, spectroscopic factors 3-78341
- ⁵⁴Fe(d, α) reaction, 12 MeV meas. alpha particle angular distribution, ⁵⁴Mn levels 3-60201
- ⁵⁶Fe(d,p)⁵⁷Fe, ground state doublet of ⁵⁷Fe study 3-43215
- ⁵⁶Fe(d,p)⁵⁷Fe, Mossbauer effect in α -Fe₂O₃ following reaction 3-47190
- ¹H(d,2p)n, 12.6 MeV, two-dimensional coincidence spectra, p-n final state interaction 3-40477
- ¹H(d,d')¹H scattering, 30 MeV, meas. of vector and tensor analysing power 3-49235
- ²H, 20 MeV, neutron yields and spectra, rel. to high intensity neutron sources 3-74596
- ²H, high energies, elastic scatt., d splitting and nucleon transfer, cross sections (*Russian*) 3-40383
- ²H-d and ³H-d reactions, absolute determ. of differential neutron source strength (*German*) 3-59636
- ²H + ³H, study by one-channel resonating-group method, phase shift and cross section determ. 3-74556
- ²H + ³He, study by one-channel resonating-group method, phase shift and cross section determ. 3-74556
- ²H(²H,dp)n, breakup reaction, 14-36 MeV, modified plane wave impulse approximation theory 3-60154
- ²H(d,n)³He, up to 1 MeV, polarization of neutrons 3-40016
- ²H(d,³He)n, liquid organic scintillator efficiency 3-73865
- ²H(d,d')²H, 3-11.5 MeV polarised deuterons, meas. of vector and tensor analysing powers (*German*) 3-49233
- ²H(d,n)³He, 3-11.5 MeV polarised deuterons, meas. of vector and tensor analysing powers (*German*) 3-49233
- ²H(d,n)³He, 330 keV, 3 MeV polarised neutron production 3-71109
- ²H(d,n)³He, polarised deuteron beam, 3.3-14.9 MeV, meas. of longitudinal polarization transfer at 0 degrees 3-57506
- ²H(d,n)³He, rel. diff. cross-sect. meas., 300 to 700 keV 3-46017
- ²H(d,p)³H, 3-11.5 MeV polarised deuterons, meas. of vector and tensor analysing powers (*German*) 3-49233
- ²H(d,p)³H, 6-15 MeV, meas. of polarisation transfer coeffs. at angle of 0° 3-74555
- ²H(d,p)³H, rel. diff. cross-sect. meas., 300 to 700 keV 3-46017
- ²H(d,pd)n, spatial localization effects 3-63033
- ³H target, 50 MeV, quasifree reaction mechanisms, absolute cross sections and correlation spectra 3-67303
- ³He(d,p)⁴He, He distrib. profiles in Ni, stainless steel, ³He⁺ ion bombardment 3-63209
- ³He(d,d')⁴He, 11.5 to 17 MeV, incident vector polarised ²H, meas. vector analysing power Γ_{11} 3-74552
- ¹⁷⁶Hf(d,t)¹⁷⁷Hf, 12 MeV, energy levels, state wave functions of ¹⁷⁷Hf 3-74497
- ³K(d,d'), inelastic scattering, 12.8 MeV, microscopic analysis of 2.52 MeV state excitation 3-49267
- ³K(d,p)⁴⁰K, meas. of e.m. transition rates in ⁴⁰K 3-62989
- ⁶Li(d, α)⁴He, 3-11.5 MeV, tensor analysing power and differential cross section meas. (*German*) 3-52188
- ⁶Li(d,d α)²H, quasi-free scattering at 52 MeV, determ. of α -cluster momentum distrib. 3-49273
- ⁷Li, 20 MeV, neutron yields and spectra, rel. to high intensity neutron sources 3-74596
- ⁷Li, states of ³He and ⁴Be obs. 3-62954
- ⁷Li(d, α n)⁴He, 1.0 MeV, α -n angular correlation meas., decay schemes 3-71120

nuclear reactions and scattering due to deuterons continued

- ⁷Li(d,n)⁸Be, polarised 800 keV deuterons, meas. of analysing powers and relative cross section 3-60197
- ⁷Li(d,n) $\alpha\alpha$, analysis of bidimensional spectra in relative coordinate system 3-52192
- ⁷Li(d,t)⁶Li, 12 MeV, neutron and α -particle transfer mechanisms study using DWBA formalism 3-71122
- ²⁴Mg, 60-90 MeV, deuteron scattering, optical model and coupled channel analysis 3-43253
- ²⁴Mg(d,pp)²⁵Mg, ²⁵Mg γ -decay study 3-40458
- ²⁵Mg(d,p), 12.3 MeV, importance of D-state effects 3-54486
- ²⁶Mg(d, γ)²⁵Na, 29 MeV, angular distrib. meas., ²⁵Na structure determ. 3-52095
- ⁹²Mo(d,n), DWBA anal. of analogue states, effect of fine structure 3-74547
- ¹⁴N(d,d)¹⁴N vector analyzing powers comparison with ¹⁴N(d,t)¹³N 3-74597
- ¹⁴N(d,t)¹³N vector analyzing powers comparison with ¹⁴N(d,d)¹⁴N 3-74597
- ¹⁵N(d,p)¹⁶N(unbound), off shell behaviour rel to R-matrix theory 3-63065
- ²³Na(d,pp)²⁴Na, 2.45 MeV, ²⁴Na deduced levels, γ -branching, lifetimes, spin restrictions 3-62986
- ²³Na(d,pp)²⁴Na, 2.5 and 2.8 MeV, ²⁴Na deduced levels, branching ratios 3-63063
- ¹⁴³Nd(d,t), neutron particle-hole states in ¹⁴²Nd 3-67325
- ²⁰Ne(d, α)¹⁸F, E_d =6-11 MeV, large isospin selection-rule violation 3-60205
- ²⁰Ne(d,d)²⁰Ne, 11.6 MeV polarised deuterons vector analysing power, optical model, differential cross section 3-52193
- ²²Ne(d,d)²²Ne, 11.6 MeV polarised deuterons vector analysing power, optical model, differential cross section 3-52193
- ⁵⁸Ni(d,p)⁵⁹Ni, 10 MeV, meas. of angular distrib. of vector analysing power and absolute cross section 3-52077
- ⁵⁸Ni(d,Li), 28 MeV, cross-section, spectroscopic factors 3-78341
- ⁵⁸Ni(d,p), 100 MeV, diffraction model of deuteron stripping, effect of nuclear boundary spread and Coulomb interaction (*Russian*) 3-74548
- ⁵⁸Ni(d,p)⁵⁹Ni, E_d =8 MeV, level struct. of ⁵⁹Ni 3-45973
- ⁶⁰Ni scattering of polarised 12.3 MeV deuterons, vector analysing power and cross sections 3-52194
- ⁶⁰Ni(d,p)⁶¹Ni, 10 MeV, vector analysing power, ang. distrib. meas., DWBA calcs. 3-78239
- ¹⁴O(d,d')¹⁴O, 11.6 MeV polarised deuterons vector analysing power, optical model 3-52193
- ¹⁶O, excitation functions and angular distrib. for elastic scattering, (d,p) and (d, α) reactions 0.98-1.97 MeV 3-43251
- ¹⁶O(d,p), 12.3 MeV, importance of D-state effects 3-54486
- ¹⁶O(d,d')¹⁶O, 11.6 MeV polarised deuterons vector analysing power, optical model 3-52193
- ¹⁶O(d,p), coupling const. determ. in peripheral models including form factor effects (*Russian*) 3-74598
- ¹⁶O(d,p)¹⁷O, 9.3 to 15.0 MeV, comparison with DWBA theory, cross sections and resonance widths 3-54488
- ³¹P(d, α)²⁸Si, E_d <4.0 MeV, reaction mechanism study from α -particle angular distrib., compound nucleus formation (*Russian*) 3-71118
- ³¹P(d,p)³²P, E_d =10 MeV, angular distributions, ³²P deduced ln, spectroscopic factors 3-60198
- Pb, breakup of deuterons, 7-12 MeV, meas. angular correlation, breakup cross section 3-60204
- Pb, deuteron disintegration in Coulomb field, energy and angular distrib. of products (*Russian*) 3-67340
- Pb cross-section for stripping and dissociation at 2.7 GeV/c measurement 3-78344
- ²⁰⁸Pb(d,p)²⁰⁹Zr, deuteron D-state effects obs. 3-63066
- ²⁰⁸Pb(d,p)²⁰⁹Pb, diffraction model for extraction of spectroscopic factors 3-60140
- ²⁰⁸Pb(d,p)²⁰⁹Pb, n transfer to unbound states, illustration of general formalism 3-67358
- ²⁰⁸Pb(d,d') 12.3 MeV, vector analysing power, differential cross section, deduced optical model parameters 3-60199
- ²⁰⁸Pb(d,p), 12.3 MeV, vector analysing power, differential cross section, ²⁰⁹Pb deduced levels, DWBA analysis 3-60199
- ²⁰⁸Pb(d,t), 12.3 MeV, vector analysing power, differential cross section, ²⁰⁷Pb deduced levels, DWBA analysis 3-60199
- Pb(d,pn)Pb, disintegration at 12 and 10.5 MeV, energy-angle correlations, DWBA analysis (*German*) 3-49264
- ²¹⁰Po(d,d'), 17.0 MeV, study of collective states 3-43183
- ²³⁸Pu(d,p)²³⁹Pu, 12 and 13 MeV, study of ²³⁹Pu energy levels 3-40418
- ²³⁸Pu(d,d') 12 and 13 MeV, energy level study 3-43185
- ²³⁸Pu(d,p)²³⁹Pu, 12.1, 13.1 MeV determ. energy levels in ²³⁷Pu 3-67197
- ²³⁸Pu(d,t)²³⁷Pu, 12.1, 13.1 MeV determ. energy levels in ²³⁷Pu 3-67197
- ²³⁹Pu(d,d') ²³⁹Pu, 12 and 13 MeV, study of ²³⁹Pu energy levels 3-40418
- ²³⁹Pu(d,d'), 12.1, 13.1 MeV, determ. of ²³⁹Pu energy levels, $K^\pi=1, 2^-$ octupole band assignment 3-67197
- ³²S(d,³He)³¹P vector analyzing powers comparison with ³²S(d,d)³²S 3-74597
- ³²S(d,d)³²S, vector analyzing powers comparison with ³²S(d,³He)³¹P 3-74597
- ³²S(d,p)³³S, region from hyperbarrier to Coulomb stripping, obs. of ³³S energy levels (*Russian*) 3-52189
- ³⁴S(d,p)³⁵S, excitation functions for transitions to lowest two excited states of ³⁵S Ericson fluctuation theory 3-67339
- ²⁸Si(d,p), 12.3 MeV importance of D-state effects 3-54486
- ²⁸Si(d,p)²⁹Si, E_d =2-4.2 MeV, reaction mechanism, ³⁰P compound nucleus parameters 3-40503
- ²⁹Si(d,p)³⁰Si, angular distrib. of proton groups, 10 MeV 3-62940
- ³⁰Si(d, α)²⁸Al, 4.850-5.825 MeV, reliability of statistical model predictions of relative cross sections 3-49262
- ³⁰Si(d,d)³⁰Si vector analyzing powers comparison with ³⁰Si(d,t)²⁹Si 3-74597
- ³⁰Si(d,p)³¹Si, low deuteron energies, proton angular distrib. comparison of direct and compound nucleus mechanisms (*Russian*) 3-71119
- ³⁰Si(d,t)²⁹Si vector analyzing powers comparison with ³⁰Si(d,d)³⁰Si 3-74597

nuclear reactions and scattering due to deuterons continued

- ¹⁵⁰Sm(d,p)¹⁵¹Sm, transfer 1 values ¹⁵¹Sm ground state, wave function 3-74594
¹⁵²Sm(d,t)¹⁵¹Sm, transfer 1 values ¹⁵¹Sm ground state, wave function 3-74594
¹¹²Sn(d,p) ¹¹³Sn, 12 MeV, study of ¹¹¹Sn energy levels 3-52104
¹¹²Sn(d,t) ¹¹¹Sn, 17 MeV, study of ¹¹¹Sn energy levels 3-52104
¹¹⁴Sn(d,Li), 36 MeV, cross-section, spectroscopic factors 3-78341
¹²⁰Sn(d,d),(d,d), polarized, ang. distrib. of diff. cross-sect. and optical model calcs. 3-46035
¹²²Sn(d,p) ¹²³Sn, 12 MeV, study of ¹²³Sn energy levels 3-52104
¹²⁴Sn(d,p) ¹²⁵Sn meas. differential cross section at 33.3 MeV rel. to neutron shell structure determ. of ¹²⁵Sn 3-67213
¹²⁴Sn(d,t) ¹²³Sn, 17 MeV, study of ¹²³Sn energy levels 3-52104
⁸⁸Sr(d,np)⁸⁸Sr, cross section meas. at 170° for 7.5 to 10.0 MeV deuterons 3-49268
⁸⁸Sr(d,p)⁸⁸Sr, anomaly effects at neutron analogue channel threshold 3-40500
⁸⁸Sr(d,p)⁸⁹Sr, particle coupling to octupole state 3-46026
¹²⁸Te(d,p)¹²⁸Te and complementary (p,d) reactions, comparative treatment of spectroscopic factors 3-40502
¹³⁶Te(d,³He)¹²⁵Sb, spectroscopic factors, theoretical and exptal. comparison 3-54406
¹⁶⁸Tm(d,t)¹⁶⁸Tm, E_α=17 MeV, rot. bands of ¹⁶⁸Tm 3-63069
²³⁴U(d,d'), 16 MeV, ²³⁴U energy levels 3-54388
²³⁶U(d,d'), 16 MeV, ²³⁶U energy levels 3-54388
¹⁸³W(d,p)¹⁸⁴W, 12.1 MeV, ¹⁸⁴W deduced levels, two quasiparticle configurations 3-57475
¹⁸³W(d,t)¹⁸²W, 12.1 MeV, ¹⁸²W deduced levels, two quasiparticle configurations 3-57475
⁸⁹Y, 60-90 MeV, deuteron scattering, optical model and coupled channel analysis 3-43253
⁸⁹Y(d,t)⁸⁸Y, product two-hole multiplets 3-54491
¹⁷¹Yb(d,2n)¹⁷¹Lu 13.5 MeV, ¹⁷¹Lu half lives deduced, comparison with Nilsson model, hindrance factors 3-54422
¹⁷³Yb(d,2n)¹⁷³Lu 13.5 MeV, ¹⁷³Lu half lives deduced, comparison with Nilsson model, hindrance factors 3-54422
¹⁷³Yb(d,nnp)¹⁷³Lu, 13.5 MeV, γ-ray obs., level scheme determ. 3-60077
⁶⁴Zn(d,⁶Li)⁶⁰Ni, 27.25 MeV, differential cross sections, Ni levels, DWBA analysis 3-52195
⁶⁶Zn(d,⁶Li)⁶²Ni, 27.25 MeV, differential cross sections, Ni levels, DWBA analysis 3-52195
⁶⁸Zn(d,⁶Li)⁶⁴Ni, 27.25 MeV, differential cross sections, Ni levels, DWBA analysis 3-52195
⁹⁰Zr(d,p)⁹¹Zr, deuteron D-state effects obs. 3-63066
⁹⁰Zr(d,α)⁸⁸Y, product two-hole multiplets 3-54491
⁹⁰Zr(d,d) scatt., spin depend. investigation 3-40499
⁹⁰Zr(d,p)⁹¹Ar, 10 MeV, tensor polarised deuteron beam, meas. of analysing powers and cross sections 3-49266
⁹⁰Zr(d,p)⁹¹Zr, j-dependence of vector analysing power and cross section 3-46034
⁹²Zr(d,p), E_α=33.3 MeV, neutron shell struct. of ⁹³Zr 3-40504
⁹⁴Zr(d,p), E_α=33.3 MeV, neutron shell struct. of ⁹⁵Zr 3-40504
⁹⁶Zr(d,p), E_α=33.3 MeV, neutron shell struct. of ⁹⁷Zr 3-40504

nuclear reactions and scattering due to electrons

- charge density errors detd. from electron scattering 3-54375
 elastic low-energy scattering, Coulomb distortion, approximants to form factors 3-78312
 elastic scattering, differential cross section, spirality correlations, anomalous magnetic moment interaction with multipole moment (*Russian*) 3-74564
 electroexcitation form factors and fixed-polarity sum rules 3-49244
 electron-nucleus bremsstrahlung at 300 keV, coincidence meas. (*German*) 3-71413
 electroproduction of charged π-mesons on nuclei at high energies (*Russian*) 3-54462
 e.m. interaction of nucleus with charged particle, interpretation of hyperfine interaction data 3-52065
 energy density formalism for description of bulk properties 3-43190
 excitation at high energies, cross section comparison with protons, pions, alpha particles 3-60164
 excitation of levels by high energy electrons 3-60162
 external bremsstrahlung due to ⁹⁰Sr-⁹⁰Y beta particles 3-67313
 form factors for ²⁰Ne and ²⁴Mg, determ. using variation after projection Hartree-Fock method 3-67245
 inelastic scattering, collective model description, ¹¹⁴Cd, ⁶⁴Zn, ²⁴Mg examples 3-67239
 inelastic scattering, determ. of static quadrupole moments of first 2+ states of nuclei with A=48-116 3-49100
 light nuclei, inelastic scatt., electron angular distrib., theory (*Russian*) 3-67315
 light nuclei, polarisation of emitted protons (*Russian*) 3-63038
 magnetic electron scattering, eikonal approx. 3-49246
 neutron source spectra produced by 400 MeV electrons in Cu, calcs. for soil, concrete, FeTiO₃, and iron shields 3-71342
 nucleon-nucleon correlation effects (*Czech*) 3-71103
 quasielastic scattering comparison of short-range correlation and distortion effects 3-57511
 radial density, self-consistent, sum rules for charge form factor 3-67314
 scattering, meas. to nuclear radii, comparison with muonic-atom meas. 3-57513
 scattering by 2s-1d shell nuclei, α-particle model (*Russian*) 3-78313
 sum rule, effect of exchange part of nucleon-nucleon interaction (*Russian*) 3-40483
 sum rules 3-49242
 superheavy nuclei, electron and positron scattering, non-existence of critical charge 3-43169
⁹Be(e, e), 1184 MeV, quasielastic scattering, shell and Fermi gas model interpretation (*Russian*) 3-57515
⁹Be(e,e'), electroexcitation of levels in 14-18 MeV region 3-54465
⁹Be(e,e') 66 to 106 MeV, comparison with Nilsson model 3-54386
⁸³Bi(e⁺, e⁺)⁸⁴Se, elastic scattering, 100 and 200 keV, differential cross sections 3-63037
²⁰⁹Bi, 500 MeV elastic magnetic electron scattering, eikonal approx. 3-49246
²⁰⁹Bi(e,e), 250 and 500 MeV, meas. of cross section, charge density and difference with ²⁰⁸Pb 3-52172

nuclear reactions and scattering due to electrons continued

- ¹²C, low q², from 15.109 MeV 1+ state, 35-55 MeV incident, conserved vector current test 3-60165
¹²C inelastic scatt., electron angular distrib., calc. compared with expt. (*Russian*) 3-67315
¹⁴C(e,e)¹⁴C, 374.6 MeV, cross-section meas., determ. of ground state charge distribution 3-57512
⁴⁰Ca, elastic, cross sections, phase-shift code analysis rel. to charge distribution 3-62927
⁴⁰Ca, inelastic scatt. form factors, low-lying level struct. 3-40482
⁴⁰Ca(e, e), determ. of equilibrium density of nucleons in nucleus (*Russian*) 3-40433
⁴⁰Ca(e,e'), 710 MeV, proton ang. distrib. 3-43235
 Ce, inelastic scatt. of 50 and 65 MeV electrons, giant resons. total and groundstate radiative widths (*German*) 3-46021
⁵²Cr(e,e'), E=209 MeV, study of collective states, comparison with microscopic vibrational model 3-63039
¹⁹F, elastic and inelastic scatt. form factors, low-lying level struct. 3-40482
⁵⁴Fe(e,e'), E=209 MeV, study of collective states, comparison with microscopic vibrational model 3-63039
³He, high-energy inelastic electron scattering, final state interaction effects on cross section (*Russian*) 3-52158
³He(e,e')²H, cross section, depend. on p-d relative motion energy 3-78310
 He(e,e), A=3, 4, evidence for hard core existence (*German*) 3-46016
³⁹K, elastic, cross sections, phase-shift code analysis rel. to charge distribution 3-62927
 La, inelastic scatt. of 50 and 65 MeV electrons, giant resons. total and groundstate radiative widths (*German*) 3-46021
⁶Li, elastic and inelastic magnetic electron scattering, determ. of one-body densities 3-49245
⁶Li, electroexcitation form factors and fixed-polarity sum rules 3-49244
⁶Li, form factor for excitation from ground state to second excited state, wave model calc. 3-62944
⁶Li(e, e), 1184 MeV, quasielastic scattering, shell and Fermi gas model interpretation (*Russian*) 3-57515
⁶Li(e,e), high-momentum-transfer, deformed cluster model 3-60166
⁶Li(e, e), 1184 MeV, quasielastic scattering, shell and Fermi gas model interpretation (*Russian*) 3-57515
²⁴Mg, deformed distributions determ. from electron scattering within rotational model 3-62926
²⁶Mg, B(E2) value of first excited state, Nilsson model comparison 3-57489
⁹⁰Mo(e,e'), E=209 MeV, study of collective states, comparison with microscopic vibrational model 3-63039
²⁰Ne, deformed distributions determ. from electron scattering within rotational model 3-62926
⁶⁰Ni(e,e'), quadrupole and giant dipole resonance excitation, form factors, characteristics (*Russian*) 3-71104
¹⁶O, Brown-Green model, inelastic electron scattering, excited odd-parity states 3-63040
¹⁶O, inelastic, even parity transitions, calc. form factors using weak coupling model 3-60163
¹⁶O, transition moments in electron excitation of T-1 neg.-parity oscillations 3-46020
¹⁸O, inelastic, calc. form factors for two lowest monopole transitions 3-60163
²⁰⁸Pb, electroexcitation of giant resonances 3-43236
²⁰⁸Pb, inelastic electron scattering form factors of low-lying states, Migdal theory 3-49247
²⁰⁸Pb(e,e), 250 and 500 MeV, meas. of cross section, charge density and difference with ²⁰⁹Bi 3-52172
²⁰⁸Pb(e,e)²⁰⁸Pb, nuclear charge distrib. determ., muonic X-rays 3-71038
 Pr, inelastic scatt. of 50 and 65 MeV electrons, giant resons. total and groundstate radiative widths (*German*) 3-46021
³⁴Se(e⁺, e⁺)³⁴Se, elastic scattering, 100 and 200 keV, differential cross sections 3-63037
²⁸Si, deformed distributions determ. from electron scattering within rotational model 3-62926
 Sn(e,e'), A=116, 120, 124, E=209 MeV, study of collective states, comparison with microscopic vibrational model 3-63039
⁵⁰Ti(e,e'), E=209 MeV, study of collective states, comparison with microscopic vibrational model 3-63039
²³⁸U, electrofission, 70 MeV, meas. of fragment kinetic energy 3-43259
⁶⁶Zn, elastic scattering, 225 MeV meas. cross sections rel. to Fermi charge distribution of nucleus (*Russian*) 3-67316
⁶⁸Zn, elastic and inelastic scattering, 225 MeV meas. cross sections rel. to Fermi charge distribution of nucleus (*Russian*) 3-67316
⁹⁰Zr(e,e'), E=209 MeV, study of collective states, comparison with microscopic vibrational model 3-63039

nuclear reactions and scattering due to gamma-rays see nuclear reactions and scattering due to photons**nuclear reactions and scattering due to helium-3**

- (³He,α) reaction, study of energy levels in odd mass Dy nuclei, A=155-163, 25.5 MeV 3-40420
 disintegration effects choice of nucleon-nucleus potential in optical potential calcs. 3-60142
 elastic scattering, high energy, theory of optical potential (*Russian*) 3-67292
 elastic scattering at 217 MeV on ⁶Li, ⁹Be, ¹²C, ²⁸Si, ⁴⁰Ca, ⁶⁸Ni, ⁸⁹Y, ⁹⁰Zr, ¹²⁰Sn, ²⁰⁸Pb, optical potential 3-52199
 elastic scattering at 70 MeV, numerical accuracy of optical model calcs. 3-74601
 giant multipole resonant state of E2 character excited in various nuclei 3-60202
 two-nucleon transfer reaction, finite range calculations 3-54495
²¹Al(³He, ³He)²¹Al, 21 MeV meas. polarisation of ³He, deduced optical model parameters 3-67349
²⁷Al(³He,α)²⁶Al, 18 MeV neutron pickup, angular distrib., ²⁶Al level structure 3-67355
³⁶Ar(³He,α)³⁵Ar, 18 MeV neutron pick-up, determ. of ³⁵Ar level structure 3-67354
³⁸Ar(³He,n)⁴⁰Ca, excited J^π=0+ states in ⁴⁰Ca 3-74491
⁴⁰Ar(³He, ³He), 28 MeV, anomalous backward angle scattering 3-54494

nuclear reactions and scattering due to helium-3 continued

- $^{19}\text{Au}(^3\text{He}, ^3\text{He}')$, cross section analysis, obs. of new giant resonance 3-63077
- $^{11}\text{B}(^3\text{He}, \alpha)^{10}\text{B}$, 8.0 to 12.0 MeV, coupled-channel Born approximation, direct reactions on light nuclei 3-60210
- $\text{Ba}(^3\text{He}, d)\text{La}$, study of odd-A La isotopes, $A=131-139$ by particle spectroscopy 3-45976
- $^9\text{Be}(^3\text{He}, n)^{11}\text{C}$, compound nucleus mechanism, forbidden J 3-52198
- $^9\text{Be}(^3\text{He}, n)^{11}\text{C}$, compound nucleus mechanism, forbidden J 3-52198
- $^9\text{Be}(^3\text{He}, p)^{11}\text{B}$, compound nucleus mechanism, forbidden J 3-52198
- $^9\text{Be}(^3\text{He}, p)^{11}\text{B}$, compound nucleus mechanism, forbidden J 3-52198
- $^{12}\text{C}(^3\text{He}, n)^{14}\text{O}(p)^{13}\text{N}$, $E=12$ MeV, ang. correl. meas., excited states of ^{14}O 3-40509
- $^{12}\text{C}(^3\text{He}, \alpha)^{11}\text{C}$, 42 MeV, multi-step processes, coupled-channel analysis 3-40506
- $^{12}\text{C}(^3\text{He}, p)^{14}\text{N}$, 15 MeV, magnetic moment of 3^- , 5.83 level meas. by recoil into gas method and Blume-Scherer model 3-49083
- $^{12}\text{C}(^3\text{He}, p)^{14}\text{N}$, 3-11 MeV, reaction mechanism study by use of p-p angular-correlation method 3-63074
- $^{12}\text{C}(^3\text{He}, p)^{14}\text{N}$, 7 to 17 MeV, meas. ang. distribution, total cross section, compound nuclear effects 3-63078
- $^{12}\text{C}(^3\text{He}, p)^{14}\text{N}$, differential cross section, form factor, calculated for various perturbation interactions 3-54495
- $^{12}\text{C}(^3\text{He}, p)^{14}\text{N}$, $E=5.54$ MeV, Doppler shift attenuation, ^{14}N deduced levels and half lives (French) 3-67255
- $^{13}\text{C}(^3\text{He}, ^3\text{He})^{13}\text{C}$, ang. distrib. of ^6He particles from two lowest states 3-54496
- $^{40}\text{Ca}(^3\text{He}, ^3\text{He})$, 28 MeV, anomalous backward angle scattering 3-54494
- $^{40}\text{Ca}(^3\text{He}, \alpha p)^{39}\text{Ca}$, 8.0-10.0 MeV, determ. of lifetimes of excited states 3-43210
- $^{40}\text{Ca}(^3\text{He}, ^6\text{He})^{37}\text{Ca}$, isobaric mass quartets of ^{37}Ca 3-60066
- $^{42}\text{Ca}(^3\text{He}, ^3\text{He})$, 28 MeV, anomalous backward angle scattering 3-54494
- $^{48}\text{Ca}(^3\text{He}, t)^{48}\text{Sc}$, 2nd order perturbation method with $(^3\text{He}-\alpha-t)$ process and DWBA 3-71123
- $^{59}\text{Co}(^3\text{He}, d)^{59}\text{Ni}$, 18 MeV, meas. of d^p coincidences, determ. of ^{60}Ni decay scheme 3-52132
- $^{19}\text{F}(^3\text{He}, \alpha)^{18}\text{O}$, excitation energies and lifetimes of ^{18}O states 3-54490
- $^{54}\text{Fe}(^3\text{He}, t)^{54}\text{Co}$, 24 MeV, differential cross sections, ang. distrib. 3-63079
- $^{56}\text{Fe}(^3\text{He}, p)^{56}\text{Co}$, product energy levels, spin assignments 3-54428
- $^{56}\text{Fe}(^3\text{He}, p)^{56}\text{Co}$, product energy levels, spin assignment 3-54428
- $^{74}\text{Ge}(^3\text{He}, d)^{74}\text{As}$, 17 MeV, level structure of ^{74}As 3-43182
- $^2\text{H}(^3\text{He}, ^3\text{H})$ p, effects of exchange, final-state interactions and distorted waves 3-52161
- $^2\text{H}(^3\text{He}, ^3\text{He})$ p, effects of exchange, final-state interactions and distorted waves 3-52161
- $^2\text{H}(^3\text{He}, p)^3\text{H}$, 50 MeV, quasifree reaction mechanisms, absolute cross sections and correlation spectra 3-67303
- ^3H target, 50 MeV, quasifree reaction mechanisms, absolute cross sections and correlation spectra 3-67303
- $^3\text{H}(^3\text{He}, d)^4\text{He}$, 291-800 keV, ^6Li levels, isospin violation, energy depend. 3-78306
- $^3\text{H}(^3\text{He}, p)^3\text{He}$, ~ 10 MeV, direct capture model for cross-section 3-78308
- $(^3\text{He}, ^3\text{He})$ reactions on s-d shell nuclei, analysis using average ^3He and α optical potentials 3-49272
- $(^3\text{He}, \alpha)$ reactions on s-d shell nuclei, analysis using average ^3He and α optical potentials 3-49272
- $(^3\text{He}, d)$ reactions, differential cross sections, ^3He -dp vertex functions 3-54489
- $(^3\text{He}, p)$ cross sections to 0^+ isobaric analogue pairs, ^{20}Ne to ^{56}Fe , 15 MeV 3-78342
- $^6\text{He}(^3\text{He}, ^3\text{He}')$ at 7.4 MeV, meas. bremsstrahlung, differential cross section determ. 3-74560
- $^{39}\text{K}(^3\text{He}, ^3\text{He})$, 28 MeV, anomalous backward angle scattering 3-54494
- $^{39}\text{K}(^3\text{He}, d)^{40}\text{Ca}$ 18 MeV incident energy, excited states study (French) 3-43179
- $^{41}\text{K}(^3\text{He}, ^3\text{He})$, 28 MeV, anomalous backward angle scattering 3-54494
- $^6\text{Li}(^3\text{He}, n)^8\text{B}$, meas. ^8B yield from its positron decay, rel. to neutrino detection 3-67351
- $^6\text{Li}(^3\text{He}, n)^8\text{B}$, recoil polarisation of ^8B , n.m.r. meas. of β -decay asymmetry, magnetic moment determ. 3-49077
- $^6\text{Li}(^3\text{He}, p)^8\text{Be}$, 17 MeV multi-interaction, finite-range, two-mode DWBA analysis 3-67297
- $^{24}\text{Mg}(^3\text{He}, ^6\text{He})^{21}\text{Mg}$, isobaric mass quartets of ^{21}Mg 3-60066
- $^{24}\text{Mg}(^3\text{He}, n)^{25}\text{Si}$, 5.0 and 5.8 MeV, meas. of angular distrib. of neutron polarisation, DWBA analysis 3-67352
- $^{26}\text{Mg}(^3\text{He}, p)^{26}\text{Al}$, 8-0 MeV, meas. of γ -ray transitions from lowest T=2 states 3-43211
- $^{92}\text{Mo}(^3\text{He}, d)^{93}\text{Tc}$, 30.2 MeV, stripping to analogue resons. using complex energy eigenstates 3-63081
- $^{19}\text{F}(^3\text{He}, n)^{17}\text{F}$, 3.8 and 4.8 MeV, investigation of ^{17}F states 3-74603
- $^{23}\text{Na}(^3\text{He}, d)^{24}\text{Mg}$, study of particle-hole nature of lowest 3^- states in ^{24}Mg 3-49151
- $^{22}\text{Ne}(^3\text{He}, p)^{24}\text{Na}$, 9.0 MeV, meas. of γ -ray transitions from lowest T=2 states 3-43211
- $\text{Ni}(^3\text{He}, t)\text{Cu}$, excitation of 2^+ analogues in Cu isotopes, DWBA analysis, second-order effects 3-49271
- $^{58}\text{Ni}(^3\text{He}, t)^{58}\text{Cu}$, 24 MeV, differential cross sections, ang. distrib. 3-63079
- $^{60}\text{Ni}(^3\text{He}, ^3\text{He})^{60}\text{Ni}$, optical-model-family ambiguity, $E=29.6-71.1$ MeV 3-60212
- $^{60}\text{Ni}(^3\text{He}, ^3\text{He})^{60}\text{Ni}$, optical model, energy depend. phenomena, $E=29.6-71.1$ MeV 3-60213
- $^{60}\text{Ni}(^3\text{He}, t)^{60}\text{Cu}$, 24 MeV, differential cross sections, ang. distrib. 3-63079
- $\text{Pb}(^3\text{He}, xn + \gamma)$, $E=28-30$ MeV, stroboscopic resonance method, g-factors for Po isotopes 3-71041
- $\text{Pb}(^3\text{He}, xn)\text{Po}$, population of high-spin isomeric states in Po isotopes, magnetic moment determ. 3-49090
- $^{204}\text{Pb}(^3\text{He}, d)^{205}\text{Bi}$, fragmentation of proton levels of ^{205}Bi 3-63080
- $^{206}\text{Pb}(^3\text{He}, d)^{207}\text{Bi}$, fragmentation of proton levels of ^{207}Bi 3-63080
- $^{208}\text{Pb}(^3\text{He}, ^3\text{He}')$, 75 MeV, cross section analysis, obs. of new giant resonance 3-63077

nuclear reactions and scattering due to helium-3 continued

- $^{32}\text{S}(^3\text{He}, p)^{34}\text{Cl}$, 9 MeV, p-p coincidence and Doppler-shift attenuation meas. 3-49215
- $^{125}\text{Sb}(^3\text{He}, d)^{126}\text{Sb}$, spectroscopic factors, theoretical and exptal. comparison 3-54406
- $^{28}\text{Si}(^3\text{He}, ^3\text{He})^{28}\text{Si}$, 21 MeV meas. polarisation of ^3He , deduced optical model parameters 3-67349
- $^{28}\text{Si}(^3\text{He}, n)$, γ -decay of ^{28}Si low lying levels, 7-10 MeV 3-78289
- $^{152}\text{Sm}(^3\text{He}, \alpha)^{151}\text{Sm}$, transfer l values ^{151}Sm ground state, wave function 3-74594
- $^{88}\text{Sr}(^3\text{He}, t)^{88}\text{Y}$ to doublet states, 23 MeV, coupled-channel study of multistep contribs. 3-67350
- $^{47}\text{Ti}(^3\text{He}, t)^{46}\text{V}$, 2nd order perturbation method with $(^3\text{He}-\alpha-t)$ process and DWBA 3-71123
- ^{47}Ti , test of independence postulate in Bohr theory of compound-nucleus decay 3-40512
- $^{48}\text{Ti}(^3\text{He}, t)^{48}\text{V}$, 2nd order perturbation method with $(^3\text{He}-\alpha-t)$ process and DWBA 3-71123
- $^{50}\text{Ti}(^3\text{He}, t)^{50}\text{V}$, 2nd order perturbation method with $(^3\text{He}-\alpha-t)$ process and DWBA 3-71123
- $^{183}\text{W}(^3\text{He}, \alpha)^{182}\text{W}$, 20.3 MeV, ^{182}W deduced levels, two quasiparticle configurations 3-57475
- $\text{Yb}(^3\text{He}, d)$, rot. bands of ^{171}Lu 3-62939
- ^{90}Zr , inelastic scattering, shell-model analysis with core polarization effects 3-78345
- $^{90}\text{Zr}(^3\text{He}, t)^{90}\text{Nb}$, 2nd order perturbation method with $(^3\text{He}-\alpha-t)$ process and DWBA 3-71123

nuclear reactions and scattering due to hyperons

Σ^- , emulsion nuclei capture, hyperfragment and crytofragment prod. Monte Carlo study 3-74607

nuclear reactions and scattering due to mesons

- capture, giant resonance excitation of doubly-closed shell nuclei, spin dependent effects 3-78297
- coherent production of $K^+\pi^+\pi^-$ on nuclei at 10, 13 and 16 GeV/c (German) 3-52208
- heavy nuclei, inelastic scattering of pions, ω -pole exchange, $3\pi\gamma$ coupling const. (Russian) 3-40517
- modified meson-nucleus optical potentials 3-60224
- pion-nucleus scattering in (3,3) resonance region, many-body formulation 3-54509
- propagation of coherently produced systems through nuclei, pion absorption and emission 3-63018
- K^- interactions in emulsion at 3 GeV/c, production of $^9\text{Li}_h$ hypernucleus 3-74520
- K^\pm , $A=9$ to 238, 6 to 60 GeV/c, meas. absorption cross section and determ. nuclear radii (Russian) 3-67338
- K^\pm , on complex nuclei, 6-60 GeV/c, absorpt. cross sections, nucleus radii 3-78352
- K_L - K_S regeneration from nuclei, transmission and diffraction 3-40332
- π^- , > 10 GeV, cascade-evaporative model analysis (Russian) 3-60194
- π^- , nuclear excitation at high energies, cross section comparison with electrons, protons, alpha particles 3-60164
- π elastic and resonance scattering in isobar-doorway model 3-43258
- π^- induced, three pion coherent production, 9 to 15 GeV, total cross section determ. 3-67368
- π^- induced, high energy inelastic on heavy emulsion nuclei, secondary particle characteristics analysis 3-67369
- π^- induced, low energy, intranuclear cascade studies, (3,3) isobar finite lifetime effects 3-67372
- π^- induced single-nucleon knock-out reaction at medium energy, mechanism study 3-63087
- π -nucleus inelastic scattering, ≥ 10 GeV, intra-nuclear cascade model 3-78314
- π -nucleus optical potential, non-overlapping potentials and Ericson-Ericson renormalization 3-57541
- π -nucleus optical potential, off-shell transition matrix, coupled-channel approach 3-60136
- π -nucleus optical potential, density expansion second order terms 3-63086
- π -nucleus optical potential with crossing theory 3-63089
- π -nucleus optical potentials, low-energy, local potentials 3-43257
- π -nucleus optical potentials, theoretic basis from multiple scattering 3-52206
- π -nucleus scattering, inner Coulomb corrections in semi classical model 3-78355
- π -nucleus scattering, optical model, DAMIT computer code, calculation technique 3-78353
- π -nucleus scattering, simple optical model 3-74608
- π -nucleus scattering in 3,3 resonance region, exclusion principle effects 3-54508
- π -nucleus scattering near (3,3) resonance using dynamically modified optical potential 3-67370
- π^- collisions with emulsion nuclei, 1.5 GeV, energy division 3-60226
- π^- inelastic interactions with light nuclei, multiplicity distrib. of charged particles (Russian) 3-40516
- π^- interactions, 9 and 15.1 GeV/c, spin-parity analysis of coherently produced $\pi^+\pi^-\pi^+$ 3-49052
- π^- - ^{132}Xe producing photons, 9 GeV, correlation between longit. and transverse momenta 3-78351
- π^+ -nuclei interactions, π coherent production at $\sim 10\text{GeV/c}$, 3π branching ratios 3-74440
- π^\pm , $A=9$ to 238, 6 to 60 GeV/c, meas. absorption cross section and determ. nuclear radii (Russian) 3-67338
- π^\pm , on complex nuclei, 6-60 GeV/c, absorpt. cross sections, nucleus radii 3-78352
- π^\pm ^4He , elastic scatt., e.m. pion radius 3-78305
- $\pi^+^3\text{He}$ scattering at 100 MeV, rel. to determ. of $\pi^+^3\text{He}^3\text{H}$ coupling constant (Russian) 3-67304
- π radiative capture, giant resonance excitation of doubly-closed shell nuclei, spin-dependent effects 3-78297
- Al, meas. of cross sections of π^- and π^+ at beam momentum 0.71-2.00 GeV/c 3-71130
- Al, π^- , π^+ reaction cross sections, 713 to 1447 MeV, deduced neutron density 3-54507
- $^{27}\text{Al}(\pi^-, \pi^- p)^{26}\text{Mg}^*$, mechanism at small momentum transfer 3-52210
- $^{27}\text{Al}(\pi^-, \pi^0)^{27}\text{Si}$, 100 MeV, activation cross section determ. 3-54506

nuclear reactions and scattering due to mesons continued

- ^9Be , induced 90-860 MeV total cross-section meas. π -nucleus coupling constant obtained 3-71131
- ^9Be , π^\pm total cross sections and π ^9Be coupling constant, Glauber model 3-46043
- ^9Be , total cross sections of π^\pm mesons, 90-860 MeV 3-74609
- $^9\text{Be}(\pi, \pi)^9\text{Be}$, 90-860 MeV, π -nucleus coupling constant determ. from π scatt. 3-63088
- $^{209}\text{Bi}(\pi^+, \pi^- + \text{xn})^{209-\text{z}}\text{At}$, cross section for formation of ^{207}At (Russian) 3-71129
- C, meas. of cross sections of π^- and π^+ at beam momentum 0.71-2.00 GeV/c 3-71130
- C, π^\pm reactions, 90-850 MeV, Coulomb effects in total cross-sections 3-60227
- C, total cross sections of π^\pm mesons, 90-860 MeV 3-74609
- $^{12}\text{C}(\text{K}^-, \pi^-)^{12}\text{C}_\Lambda$, hypernucleus spectroscopy 3-78278
- $^{12}\text{C}(\pi^-, \text{NN})$, study of short range correlations, three-body partial wave analysis 3-60222
- $^{12}\text{C}(\pi^-, \pi^-)^{12}\text{C}$, optical potential root mean square radius determ. 3-78354
- $^{12}\text{C}(\pi^+, \text{p})$, relativistic field theoretic description 3-46044
- $^{12}\text{C}(\pi^+, \pi^+ \text{ n} + \pi^+ \text{ p})$ at (3/2, 3/2) resonance, meas. absolute cross section 3-60225
- $^{12}\text{C}(\pi^+, \pi^+ \text{ p})^{11}\text{B}$, mechanism of single-nucleon knock-out process 3-63087
- $^{12}\text{C}(\pi^+, \pi^+ \text{ p})^{11}\text{B}$, $E_\pi = 130$ MeV, quasielastic scatt. cross sections analysis (French) 3-52209
- $^{12}\text{C}(\pi^\pm, \pi^\pm)$ type, isobar mechanism, high energy 3-78356
- $^{12}\text{C}(\pi^+, \pi^0)^{13}\text{N}$, optical model studies, comparison with exptl. cross sections, 30-90 MeV 3-60223
- $^{13}\text{C}(\pi^+, \pi^0)^{13}\text{N}$ single-charge exchange, total and differential cross section calc. 3-67371
- Λ production through $\text{n}(\text{K}^-, \pi^-)\Lambda^0$ reaction, with 500-800 MeV/c kaons 3-54418
- Ca, meas. of cross sections of π^- and π^+ at beam momentum 0.71-2.00 GeV/c 3-71130
- Ca, π^- , π^+ reaction cross sections, 584 to 1856 MeV, deduced neutron density 3-54507
- $\text{Cl}(\pi^-, \pi^+ \pi^+ \pi^+)$ reaction with quasifree neutrons in nucleus, 3.9 GeV/c, resonance production (Russian) 3-40515
- $\text{C}(\pi^-, \pi^+ \pi^+ \pi^+)$ reaction with quasifree neutron in nucleus, 3.9 GeV/c, resonance production (Russian) 3-40515
- C, π^- , π^+ reaction cross sections, 584 to 1856 MeV, deduced neutron density 3-54507
- Cu spallation, induced by π^+ and π^- at 65 MeV, radiochemical yield determ. 3-67373
- $^{19}\text{F}(\pi, \pi)^{18}\text{N}$, cross-section meas. at (3/2, 3/2) resonance 3-49284
- $\text{F}(\pi^-, \pi^+ \pi^+ \pi^+)$ reaction with quasifree neutrons in nucleus, 3.9 GeV/c, resonance production (Russian) 3-40515
- ^2H , pion-induced scattering in $\Delta(1236)$ energy region, three body problem 3-78177
- $^2\text{H}(\pi^+, \pi^+)^2\text{H}$ elastic scattering near 3-3 resonance, angular distrib., cross sections, 141-256 MeV 3-40379
- $^2\text{H}(\pi^\pm, \pi^\pm)$ type, isobar mechanism, high energy 3-78356
- ^4He , π scattering, ambiguities in phase-shift analysis 3-43232
- Λ production through $\text{n}(\text{K}^-, \pi^-)\Lambda^0$ reaction, with 500-800 MeV/c kaons 3-54418
- Ho, meas. of cross sections of π^- and π^+ at beam momentum 0.71-2.00 GeV/c 3-71130
- Ho, π^- , π^+ reaction cross sections, 713 to 1447 MeV, deduced neutron density 3-54507
- ^6Li , K^- induced reaction at 640 MeV/c, γ -spectra, $^4\text{He}_\Lambda^*$, $^4\text{He}_\Lambda^*$ production 3-78277
- ^6Li , total cross sections of π^\pm mesons, 90-860 MeV 3-74609
- $^6\text{Li}(\pi^-, \pi^- \text{ p})^5\text{He}$, $q < 170$ MeV/c, meas. of cross sections, angular and momentum distrib., reaction mechanisms (Russian) 3-40514
- $^6\text{Li}(\pi^-, \gamma)^5\text{He}$, capture reaction, 60-150 MeV mass-6 system obs. 3-52207
- $^6\text{Li}(\pi^-, \pi^- \text{ p})$, allowance for final nucleus instability in quasielastic knockout of protons 3-60172
- ^7Li , K^- induced reaction at 640 MeV/c, γ -spectra, $^4\text{He}_\Lambda^*$, $^4\text{He}_\Lambda^*$ production 3-78277
- ^7Li , induced 90-860 MeV total cross-section meas. π -nucleus coupling constant obtained 3-71131
- ^7Li , total cross sections of π^\pm mesons, 90-860 MeV 3-74609
- $^7\text{Li}(\pi, \pi)^7\text{Li}$, 90-860 MeV, π -nucleus coupling constant determ. from π scatt. 3-63088
- ^{14}N , absorption of stopped π^- , with ^8Li emission, obs. using photoemulsion chamber, reaction channel branching (Russian) 3-67374
- $^{14}\text{N}(\pi, \pi)^{13}\text{N}$, cross-section meas. at (3/2, 3/2) resonance 3-49284
- $^{14}\text{N}(\pi^+, \pi^0)^{14}\text{O}$ single-charge exchange, total and differential cross section calc. 3-67371
- Λ N production through $\text{n}(\text{K}^-, \pi^-)\Lambda^0$ reaction, with 500-800 MeV/c kaons 3-54418
- Ni, meas. of cross sections of π^- and π^+ at beam momentum 0.71-2.00 GeV/c 3-71130
- Ni, π^- , π^+ reaction cross sections, 584 to 1856 MeV, deduced neutron density 3-54507
- O, total cross sections of π^\pm mesons, 90-340 MeV 3-74609
- ^{16}O , pion scattering, giant resonance excitation of doubly-closed shell nuclei, spin dependent effects 3-78297
- ^{16}O capture of stopped π^- with emission of ^8Li , obs. using photoemulsion chambers, determ. reaction branchings (Russian) 3-67375
- $^{16}\text{O}(\pi^-, \pi^-)^{16}\text{O}$, total and differential cross sections in 3-3 resonance region, optical potential calcs. 3-63090
- Pb, meas. of cross sections of π^- and π^+ at beam momentum 0.71-2.00 GeV/c 3-71130
- Pb and ^{208}Pb , π^- , π^+ reaction cross sections, 584 to 1856 MeV and 713 to 1447 MeV, deduced neutron density 3-54507
- $\text{Pb}(\pi^\pm, \pi^\pm)\text{Pb}$, low-energy differential cross section meas. in region of large Coulomb nuclear interference, optical model 3-71128
- Sn, meas. of cross sections of π^- and π^+ at beam momentum 0.71-2.00 GeV/c 3-71130
- Sn and ^{120}Sn , 584 to 1856 MeV, π^- , π^+ reaction cross sections, 584 to 1856 MeV and 713 to 1447 MeV, deduced neutron density 3-54507

nuclear reactions and scattering due to muons

- absorption, nuclear reaction theory and improved factorization method 3-52151
- muonic X-rays, fissionable material assay 3-63201

nuclear reactions and scattering due to muons continued

- (μ^-, xnpp) , capture by nuclei with $A=28-197$, meas. of γ -ray energy and intensity 3-49243
- $^{40}\text{Ca}(\mu^-, \text{vnn})$, determ. of absolute capture probability by activation method (Russian) 3-40484
- $\text{C}(\mu, \mu)\text{C}$, 190 MeV/c elastic scattering in low-momentum-transfer region, form factor and electron-muon universality 3-74565
- $^{16}\text{O}(\mu^-, \text{n})^{15}\text{N}$, calc. of asymmetry in high energy neutron emission, transitions to ^{15}N levels 3-52149
- $\text{Pb}(\mu, \mu)\text{Pb}$, low-energy differential cross section meas., determ. of Pb change radius 3-71128
- $^{32}\text{S}(\mu^-, \text{vnn})$, determ. of absolute capture probability by activation method (Russian) 3-40484
- nuclear reactions and scattering due to neutrinos**
- excitation by weak and e.m. interactions, low energy cross sections (Russian) 3-63041
- giant resonance excitation of doubly-closed shell nuclei, spin-dependent effects 3-78297
- $^6\text{Li}(\nu_e, \text{e})^6\text{He}$, calc. of rates for semi-leptonic weak processes using one-body densities determ. from e.m. data 3-49245
- nuclear reactions and scattering due to neutrons**
- $A > 90$, (n, α) reactions, emission by pre-equilibrium processes, spectrum and excitation function 3-60180
- activation anal. of geological samples, elemental determs. 3-73957
- activation detector for neutron in high γ -ray flux field 3-40006
- backscattering of fast neutrons from Al, Fe, Pb, 0.5-1.8 MeV, energy spectra 3-60250
- cross section and resonance integrals from ETOT and ETOT, advances in processing ENDF/B III libraries 3-74682
- cross sections, multiple reaction correction, utilising transport theory, $E \geq 0.1$ MeV rel. to ^{238}U 3-67320
- cross-section data, use of computer-techniques in publication 3-46054
- cross-section measurements, using liquid scintillation spectrometer 3-51732
- cross-section sensitivity studies for ZPR-6 assembly 7 using VARI-ID variational program 3-74680
- cross-section sets, characterization of uncertainties 3-74681
- elastic, fast, systematic study rel. to derivation of generalised optical model potentials 3-74574
- elastic and inelastic scattering, techniques for measurement and processing of continuous spectra (German) 3-60193
- gamma-ray production cross-sections from 14.2 MeV neutron interactions with ^{23}Na , ^{24}Mg , ^{28}Si , ^{32}S , ^{48}Ti , ^{52}Cr , ^{56}Fe 3-54469
- gas jet recoil transport system, for radioactive products in neutron reactions 3-51671
- inelastic scattering, time-of-flight measurement with on-line computer for data logging (German) 3-59653
- integral transport program for arbitrary X-Y geometry systems, THER—MOGENE, expt. verification of results 3-63105
- integrated cross sections, exact Doppler broadening to higher temps. numerical method 3-74635
- inversely populated medium, multiple acceleration of neutrons 3-71112
- L54 reactor core centre, exptl. determ. of fast neutron spectrum, computer analysis 3-43274
- low energy scattering, separable potential construction using optical model 3-71091
- low-A nuclei, small-angle elastic scattering cross-section meas., fast neutrons 3-74579
- medium- and low-energy neutron cross section library, compilation 3-57526
- multigroup neutron cross section adjustment by correlation method 3-43262
- neutron-activation analysis, ^{16}N isotope rel. to O content 3-51764
- r-process cycle times, rel. to astrophysical superheavy element synthesis 3-65620
- radiative capture, Monte Carlo simulation of resonance decay, determ. of resonance spin 3-57519
- radiative capture cross sections for nuclei with $59 \leq A \leq 133$ 3-49252
- resonance energy meas. for calibration of time-of-flight spectrometer 3-60174
- resonance interference effects using Hauser-Feshbach-Moldauer formalism 3-71107
- resonance levels, correlation between fission and reduced neutron widths 3-54512
- scattering cross sections and gamma ray production, integral experiment method for sensitive test 3-49307
- scattering of polarised neutrons on zero-spin nuclei, methods of polarisation measurement (German) 3-60156
- standard neutron spectrum facility $\Sigma\Sigma$, calcs. with ENDF/B, comparison with expt. 3-49301
- structure investigation, conference, Gaussig, Germany (29 November-3 December 1971) 3-60064
- thermal neutron cross-section of fissionable elements in multilevel-multichannel formalism (Rumanian) 3-49291
- ^2H , neutron scatt., polarisation asymmetry, 35 MeV 3-74553
- (n, γ) , 5-300 keV neutron capture, data table of γ -ray spectra 3-74580
- (n, γ) radiative capture, $40 \leq A \leq 70$, optical model calcs. 3-78334
- $(\text{n}, 2\text{n})$, 14.78 MeV activation cross sections 3-74573
- (n, α) , 14.78 MeV activation cross sections 3-74573
- (n, α) cross sections, 14-15 MeV, obs., review 3-78329
- (n, p) pre-equilibrium reactions on medium and heavy nuclei, 20-30 MeV, fluctuations in statistical theory 3-40475
- nd quartet, solution methods, Faddeev theorem, Lagrange polynomials 3-78309
- ^{110}Ag , n capture in Ag halides, β -decay asymmetry and n.m.r. 3-61006
- $^{27}\text{Al}(\text{n}, \gamma)$, thermal neutrons, test of photon production data from ENDF/B-III material 1135 3-57527

nuclear reactions and scattering due to neutrons continued

- ²⁷Al(n,p)²⁶Mg energies <6 MeV, cross section meas. rel. to ²³⁵U fission using activation method 3-74591
- Al(n,n₀)Al, meas. differential cross sections at 14.8 MeV, Schwinger prediction 3-71108
- ²⁴⁰Am(n,2n), spontaneously fissioning isomer prod., E_n=14 MeV 3-71132
- ²⁴¹Am, thermal neutron capture cross sections and capture resonance integrals for ^{242m}Am, ^{242g}Am production 3-43242
- ²⁴²Am(n,p)^{242g}Am, gamma-ray spectra meas. and analysis 3-49248
- ²⁴²Am(n,2n), spontaneously fissioning isomer prod., E_n=14 MeV 3-71132
- ²⁴³Am(n,n'), spontaneously fissioning isomer prod., E_n=14 MeV 3-71132
- ⁷⁵As(n,2n)⁷⁴As cross-section meas. rel. to ⁶⁵Cu(n,2n)⁶⁴Cu, at 14.1 MeV 3-57517
- ⁷⁵As(n,p)^{75m}As cross section for 14.8 MeV neutrons 3-63061
- Au, neutron absorption cross sections, 4 to 47 A neutrons 3-78333
- ¹⁹⁷Au(n,p), E_n=14 MeV, proton spectra anal. 3-67319
- ¹⁰B(n,n₀)α used as standard cross section shape for ²³⁵U fission cross section meas. 3-74612
- ¹³⁰Ba(n,p)¹³¹Cs, g-factor, 133 keV excited state meas. by PAC method 3-49108
- ¹³⁰Ba(n,p)¹³¹Xe, 0.5 to 5000 eV, large epithermal resonances, explanation of ¹³¹Xe concentrations in lunar rocks 3-54482
- Be, anisotropic scattering eff. in reflected fast critical assemblies, calc. 3-49328
- ²⁰⁹Bi(n,2n)^{208m}Pb, isomeric cross section at 14.8 MeV 3-54468
- ²⁰⁹Bi(n,α), thermal neutron energies, cross sections determ. 3-43244
- Br, radiative capture of 14.1 MeV neutrons, prompt γ-ray spectra 3-40441
- ¹²C, elastic and inelastic scattering, 7-9 MeV, differential cross sections and angular distrib. 3-63051
- ¹²C, giant dipole states and excited dipole states in continuum approx., (γ,N) and (N,γ) reaction 3-67193
- ¹²C, microscopic description using generalised R-matrix theory 3-60183
- ¹²C, resonant, unbound levels in ¹³C, application of real Weinberg state method 3-57471
- ¹²C(n,n), 2.1-4.7 MeV, total and elastic cross sections, phase shift analysis, analysing power 3-40489
- ¹²C(n,n)¹²C*, (4.44 MeV), neutron spin flip at 15.0 MeV, γ-ray coincidence meas. 3-60195
- ¹²C(n,n')¹²C, 13.9 MeV, angular correlation meas., 2⁺→0⁺ decay 3-78323
- ¹²C(n,n), 2-5 MeV, absolute polarisation, cross sections using R-function theory anal. 3-78325
- ¹²C(n,n)¹²C, 1.98 MeV-4.64 MeV, phase shift and optical-model analysis 3-71106
- ¹²C(n,n)¹²C R-matrix theories, two level, rel. to closely spaced resonance levels in a single channel 3-60145
- ¹²C(α,n)¹⁷O, meas. of absolute neutron yields, 2-9 MeV 3-54493
- ¹³C cross sections, continuum shell model for ¹³C 3-54401
- Ca, fast neutron total cross sections, 5.0-8.5 MeV 3-60169
- ⁴⁰Ca, gamma-ray producing reactions, cross-section calcs. 3-57525
- Ce, neutron total cross section 1.0 to 2.0 MeV, optical model comparison 3-54474
- Ce, total neutron cross section fluctuations, 1-2 MeV, compound nucleus explanation 3-54475
- ²⁴⁹Cf, neutron induced fission cross section using neutrons from underground nuclear explosion 3-78358
- Cl, fast neutron total cross sections, 5.0-8.5 MeV 3-60169
- ³⁵Cl, 7.79 to 0.79 MeV cascade accompanying capture, T invariance in electromagnetic transitions (Russian) 3-57492
- ²⁴⁴Cm(n,f) spontaneous, fragment mass and kinetic energy distrib. determ. 3-71135
- Co, neutron absorption cross sections, 4 to 47 A neutrons 3-78333
- ⁵⁹Co, direct processes in 14.4 MeV inelastic neutron scattering (Russian) 3-40498
- ⁵⁹Co(n,γ)⁶⁰Co, polarised target and thermal neutrons, meas. of γ-ray asymmetry 3-60175
- ⁵⁹Co(n,γ)⁶⁰Co, with polarised neutrons and nuclei, 0.065 eV, meas. of capture γ-rays 3-43245
- Cu, radiative capture of 14.1 MeV neutrons, prompt γ-ray spectra 3-40441
- ⁶⁴Cu(n,n)⁶⁴Cu, 3 MeV polarised neutrons from ²H(d,n)³He, meas. differential cross sections and asymmetries 3-71109
- Cu(n,p), 14 MeV radiative capture, spectra and partial cross section meas. 3-60173
- ²⁵¹Es, thermal-neutron capture cross-sections and capture resonance integrals 3-57516
- ¹⁵²Eu(n,α), E_n=14 MeV, knock-on mechanism 3-63044
- ¹⁹F(n,n'), time-differential PAD obs. of magnetic interaction of 197 keV level with CaF₂ 3-46023
- Fe, elemental, meas. and evaluation of total cross section minima, 24-750 keV 3-54523
- Fe, gamma-ray production in range 0.8-20 MeV, cross-section meas. 3-43241
- Fe, total cross section meas., 24-1000 keV, using Harwell synchrotron time-of-flight spectrometer 3-71117
- Fe 14 MeV incident, 10 keV-14 MeV spectra, as function of mfp 3-67321
- ⁵⁶Fe capture, gamma ray yields from branching ratios and statistical analysis 3-74577
- ⁵⁶Fe(n,n'), 300-500 keV above threshold for excitation of 2⁺ levels, cross section energy dependence (Russian) 3-74571
- ⁵⁶Fe(n,n'), E=1.43 to 2.15 MeV, differential cross sections, spin, parity assignment to ⁵⁷Fe doorway state resonance 3-60177
- ⁵⁶Fe(n,n'), 0.8-9.0 MeV, cross section for gamma-ray production 3-52185
- ⁵⁶Fe(n,n'), E=1.43 to 2.15 MeV, differential cross sections, spin, parity assignment to ⁵⁷Fe doorway state resonance 3-60177
- ⁵⁶Fe(n,n'), E=1.43 to 2.15 MeV, differential cross sections, spin, parity assignment to ⁵⁷Fe doorway state resonance 3-60177
- ⁵⁶Fe(n,p)⁵⁶Mn, cross section used as standard for activation cross section meas. at 14.78 MeV 3-74573
- Fe(n,p)Mn, energies <6 MeV, cross section meas. rel. to ²³⁵U fission using activation method 3-74591

nuclear reactions and scattering due to neutrons continued

- ¹⁹F, radiative capture below 1500 keV, single-level resonance parameters 3-63052
- Gd, A=154-160, total neutron cross section meas., deformation effects, optical model (Russian) 3-52178
- Gd, neutron total cross section 1.0 to 2.0 MeV, optical model comparison 3-54474
- Gd, total neutron cross section fluctuations, 1-2 MeV, compound nucleus explanation 3-54475
- ¹⁵⁷Gd, nonstatistical effects in γ-ray spectra emitted in decays of neutronic resonances (Russian) 3-52181
- ⁷⁰Ge(n,p)⁷¹Ge, thermal energies, ⁷¹Ge energy levels (Russian) 3-71083
- ⁷¹Ge, thermal neutron capture, non accidental nature of anticorrelations (Russian) 3-57529
- ⁷³Ge, thermal neutron capture, non accidental nature of anticorrelations (Russian) 3-57529
- ¹H(n,n), ang. distrib., 24 and 27.2 MeV neutrons 3-40478
- ¹H(n,p), thermal radiative capture, meson exchange effects 3-60153
- ²H, low-energy neutron scattering, resonant group exam. and comparison with Fadeev's eqn. (Russian) 3-43135
- ²H-n three-particle scattering, Alt-Grassberger-Sandhas perturbation theory 3-49237
- ²H(n,2n)¹H break-up process local two-nucleon S-wave potentials and separable Yamaguchi potential 3-60150
- ²H(n,2n)¹H, three-body calc. of neutron-neutron scattering length and effective range 3-78340
- ²H(n,2n)p, 14.17 MeV, cross section and neutron-neutron scattering length calc. Amado model 3-78336
- ²H(n,n), scatt. amplitude exam. by Feynman diagram tech. 3-54457
- ²H(n,n)²H, cross section and angular distrib. meas., 40-340 MeV (Russian) 3-74551
- ²H(n,np)n, 130 MeV, kinematically complete expt., determ. of neutron-neutron scattering length 3-78338
- ²H(n,p)n, 14 MeV, spectra meas., validity of impulse approx. for nn scattering length 3-78339
- ³H(d,n)⁴He reaction in ion accelerators for neutron production (French) 3-56917
- ³H(n,p)nn, exptl. requirements for determ. of neutron-neutron scattering length 3-71098
- ⁴He(N,N)⁴He, comparison of ⁴He-⁴He-n and ⁴He-³H-p coupling constants, reln. to ⁴He structure (German) 3-49234
- ⁴He(n,n)⁴He, 0-21 MeV, energy dependent phase shift analysis, error matrices 3-60152
- ⁴He(n,n)⁴He, asymmetry meas. to deduce neutron polarisation in ²H(d,n)³He reaction 3-71109
- ⁴He(n,n)⁴He, energies <3 MeV, energy-dependent phase shift analysis, effective range parameters 3-60151
- ¹⁷⁷Hf(n,2n)^{178m} cross section for 14.8 MeV neutrons 3-63061
- ¹⁷⁷Hf, nonstatistical effects in γ-ray spectra emitted in decays of neutronic resonances (Russian) 3-52181
- ¹⁷⁷Hf(n,p)^{178m}Hf, half life of high-spin isomeric state in ¹⁷⁸Hf and capture production cross section 3-62987
- ¹⁸⁰Hf(n,α), thermal neutron energies, cross sections determ. 3-43244
- Hg, neutron total cross section, 1.0 to 2.0 MeV, optical model comparison 3-54474
- Hg, total neutron cross section fluctuations, 1-2 MeV, compound nucleus explanation 3-54475
- ¹⁹⁸Hg(n,n'), cross section near energy threshold, deviations from statistical model (Russian) 3-74568
- ²⁰⁰Hg(n,n'), cross section near energy threshold, deviations from statistical model (Russian) 3-74568
- ²⁰²Hg(n,n'), cross section near energy threshold, deviations from statistical model (Russian) 3-74568
- Hg(n,n)¹⁹⁹Hg, meas. differential cross sections at 14.8 MeV, Schwinger prediction 3-71108
- ²H(n,p)³H, cross section, meson-exchange corrections 3-54456
- Ho, neutron total cross section, 1.0 to 2.0 MeV, optical model comparison 3-54474
- Ho, total neutron cross section fluctuations, 1-2 MeV, compound nucleus explanation 3-54475
- ¹⁶⁵Ho(n,n'), ¹⁶⁵Ho excited levels, comparison with pair correlation model (Russian) 3-71059
- I, radiative capture of 14.1 MeV neutrons, prompt γ-ray spectra 3-40441
- In, radiative capture of 14.1 MeV neutrons, prompt γ-ray spectra 3-40441
- ¹¹⁵In(n,2n)^{114m}In cross section for 14.8 MeV neutrons 3-63061
- ¹¹⁵In(n,e)¹¹⁶In, conversion electron spectra, spin and parity assignments 3-71116
- ¹¹⁵In(n,p)¹¹⁶In, 150 to 630 keV, meas. neutron capture cross sections by activation technique 3-74572
- ¹¹⁶In from ¹¹⁵In(n,e)¹¹⁶In, conversion electron spectra, spin and parity assignments 3-71116
- In resonance energy, determ. of ²⁵²Cf fission neutron age in water 3-71297
- ¹⁹¹Ir(n,p)¹⁹²Ir, gamma-ray spectra meas. and analysis 3-49248
- ¹⁹¹Ir(n,p)¹⁹²Ir + ¹⁹⁴Ir, gamma-ray spectra meas. and analysis 3-49248
- K, fast neutron total cross sections, 5.0-8.5 MeV 3-60169
- La, neutron total cross section 1.0 to 2.0 MeV, optical model comparison 3-54474
- La, total neutron cross section fluctuations, 1-2 MeV, compound nucleus explanation 3-54475
- ⁶Li(n,t)⁴He, in French tritium production (French) 3-57550
- ⁷Li(n,n)⁷Li, design of tritium breeding blankets for fusion reactors 3-60327
- Mg, fast neutron total cross sections, 5.0-8.5 MeV 3-60169
- Mo, A=94, 96, 98, 100, thermal neutron capture, meas. of gamma-ray spectra (Russian) 3-52179
- ⁹²Mo, neutron reson. parameter 3-40495
- ⁹²Mo(n,p)⁹³Mo, γ spectra, giant reson., partial radiation widths, E1 and M1 transitions 3-63058
- ⁹⁶Mo(n,p)⁹⁷Mo, thermal neutrons, meas. of γ-ray spectra (Russian) 3-52177
- ⁹⁸Mo(n,p)⁹⁹Mo, thermal neutrons, meas. of γ-ray spectra (Russian) 3-52177
- ¹⁰⁰Mo(n,p)¹⁰¹Mo, thermal neutrons, meas. of γ-ray spectra (Russian) 3-52177
- ¹⁴N(n,p)¹⁴C, use in neutron beam strength measurement 3-73864

nuclear reactions and scattering due to neutrons continued

- ¹⁴N(n,x γ), 4.22-15.40 MeV, meas. of gamma-ray production cross section using Ge(Li) detector 3-74593
- ²³Na(n, γ), fast neutron cross-section of ²⁴Na (*Rumanian*) 3-63060
- Nb, fast-neutron cross sections, optical model, reln. to fusion reactor design 3-71113
- ⁹³Nb, direct processes in 14.4 MeV inelastic neutron scattering (*Russian*) 3-40498
- ⁹³Nb, neutron total (0.25 to 0.5 MeV) and differential (1.8 to 4.0 MeV) scattering cross-sections, optical model, J π values 3-78331
- ⁹³Nb(n, γ)⁹⁴Nb, E γ =30-100 eV, channel spin components of p-wave neutron widths 3-60192
- Nd, A=142-150, total neutron cross section meas., deformation effects, optical model (*Russian*) 3-52178
- ¹⁴³Nd(n, γ)¹⁴⁰Ce, hindrance factors for γ -ray transitions near neutron binding energy 3-49218
- ¹⁴⁶Nd(n, γ)¹⁴⁷Nd, activation resonance integral meas. 3-54467
- ¹⁴⁸Nd(n, γ)¹⁴⁹Nd, activation resonance integral meas. 3-54467
- ¹⁵⁰Nd(n, γ)¹⁵¹Nd, activation resonance integral meas. 3-54467
- ²²Ne(p,n), high resolution study around neutron threshold resonance obs. 3-46037
- ²²Ne(p,p, γ), high resolution study around neutron threshold resonance obs. 3-46037
- ⁵⁸Ni, activation cross-sections for 14.7 MeV neutrons 3-54470
- ⁵⁸Ni(n,p)⁵⁸Co energies <6 MeV, cross section meas. rel. to ²³⁵U fission using activation method 3-74591
- ⁶⁰Ni, activation cross-sections for 14.7 MeV neutrons 3-54470
- ⁶⁰Ni elastic and inelastic scatt. from 2 to 8.5 MeV, differential and total cross-sections calc. 3-57531
- ²³⁷Np(n, γ)²³⁸Np, gamma-ray spectra meas. and analysis 3-49248
- ¹⁶O, neutron total cross sections, 0.6-4.33 MeV, determ. of ¹⁷O level structure 3-67209
- ¹⁶O(n,n), separable-potential model approach 3-43243
- ¹⁶O(n,n)¹⁶O R-matrix theories, two level, rel. to closely spaced resonance levels in a single channel 3-60145
- ¹⁷O(n, α)¹⁴C, O determ. and distrib. in biological materials from α tracks 3-66457
- ³¹P(n, γ), 0.8-9.0 MeV, cross section for gamma-ray production 3-52185
- Pb, A=206-208, gamma-ray producing reactions, cross-section calcs. 3-57525
- ²⁰⁸Pb(n,2n)²⁰⁵Pb, isomeric cross section at 14.8 MeV 3-54468
- ²⁰⁸Pb(n, γ), s-wave doorway state in photon channel from capture cross section measurements 3-57524
- ²⁰⁸Pb(n,n), cross section near energy threshold, deviations from statistical model (*Russian*) 3-74568
- ²⁰⁷Pb, structure study, 13-17 MeV (*Hungarian*) 3-43239
- ²⁰⁷Pb(n,2n)²⁰⁶Pb, isomeric cross section at 14.8 MeV 3-54468
- ²⁰⁷Pb(n,n)²⁰⁷Pb, 3 MeV polarised neutrons from ²H(d,n)³He, meas. differential cross sections and asymmetries 3-71109
- ²⁰⁸Pb* produced in neutron resonance reaction, particle-vibration calc. 3-78267
- ²⁰⁸Pb(n,2n)²⁰⁷Pb, isomeric cross section at 14.8 MeV 3-54468
- ²⁰⁸Pb(n, α), thermal neutron energies, cross sections determ. 3-43244
- ²⁰⁸Pb(n, γ)²⁰⁹Pb, 2.25 to 7.25 MeV, direct and compound nucleus contrib., modified Hauser-Feshbach theory 3-78332
- ²⁰⁸Pb(n,n)²⁰⁸Pb, imaginary optical potential 3-60141
- ²⁰⁹Pb,n \rightarrow ²¹⁰Bi*, neutron resonance, particle-vibration calc. 3-78267
- Pb(n,n α)Pb, meas. differential cross sections at 14.8 MeV, Schwinger prediction 3-71108
- Pr, neutron total cross section 1.0 to 2.0 MeV, optical model comparison 3-54474
- Pr, total neutron cross section fluctuations, 1-2 MeV, compound nucleus explanation 3-54475
- ¹⁹⁸Pt(n,p)¹⁹⁸Ir, p-transition obs., ¹⁹⁸Ir half-life, existence evidence 3-63008
- ²³⁸Pu, 18 eV to 3 MeV n-induced fission, resonance cross-sections 3-74613
- ²³⁸Pu, γ -ray emission from neutron capture 3-74578
- ²³⁸Pu, anisotropic scattering eff. in reflected fast critical assemblies, calc. 3-49328
- ²³⁸Pu, multilevel effects in unresolved resonance region 3-71114
- ²³⁸Pu, thermal neutron capture, probability of formation of spontaneously fissionable isomer states (*Russian*) 3-71139
- ²³⁸Pu, total and elastic scatt. neutron cross sections 3-60170
- ²³⁹Pu(n,f), cross-sections below 30 keV, high resolution meas. 3-60234
- ²³⁹Pu(n,2n) and ²³⁹Pu(n,n), spontaneously fissioning isomer prod., E γ =14 MeV 3-71132
- ²³⁹Pu(n,f), ternary to binary fission ratio meas., 0.02 to 50 eV 3-78361
- ²⁴⁰Pu, anisotropic scattering eff. in reflected fast critical assemblies, calc. 3-49328
- ²⁴⁰Pu zoned critical expts., analysis in support of LWR-grade Pu utilization in FTR's 3-71187
- ²⁴¹Pu(n,2n) spontaneously fissioning isomer prod., E γ =14 MeV 3-71132
- ²⁴¹Pu:²³⁵U fission cross-section ratio meas. for neutron energies 5 keV-1.2 MeV 3-60233
- ²⁴¹Pu(n,f), cross-sections below 30 keV, high resolution meas. 3-60234
- ²⁴²Pu, total cross section, 600 eV-81 keV, subthreshold fission structure parameters 3-63095
- ²⁴²Pu(n, γ), 20-1300 eV, cross-section meas., determ. of resonance parameters 3-49258
- ²⁴²Pu(n,n), 20-1300 eV, cross-section meas., determ. of resonance parameters 3-49258
- ⁸⁵Rb, fast neutron scattering, (n,n), (n,n') and (n,n', γ) reactions 3-43249
- ⁸⁷Rb, fast neutron scattering, (n,n), (n,n') and (n,n', γ) reactions 3-43249
- ¹⁰³Rh(n,n')¹⁰³Rh, criticality neutron dosimeter 3-77273
- Sb(n, γ), 14 MeV radiative capture, spectra and partial cross section meas. 3-60173
- ⁴⁵Sc(n, γ) E=1.41 MEV, γ angular distribution, ⁴⁵Sc levels spin assignment 3-74589
- Se, radiative capture of 14.1 MeV neutrons, prompt γ -ray spectra 3-40441

nuclear reactions and scattering due to neutrons continued

- ⁷⁴Se(n, γ)⁷⁵Se, thermal neutrons, meas. of γ -ray spectrum (*Russian*) 3-52176
- ⁷⁶Se(n, γ)⁷⁷Se, thermal energies, ⁷⁷Se energy levels (*Russian*) 3-71083
- ⁷⁷Se(n, γ)⁷⁸Se, thermal neutron, gamma-ray spectrum meas. (*Russian*) 3-49250
- ⁷⁸Se(n, γ)⁷⁹Se, thermal energies, ⁷⁹Se energy levels (*Russian*) 3-71083
- ⁸⁰Se(n, γ)⁸¹Se, thermal energies, ⁸¹Se energy levels (*Russian*) 3-71083
- ⁸¹Se, thermal neutron capture, non accidental nature of anticorrelations (*Russian*) 3-57529
- ²⁸Si, elastic and inelastic backscattering at 14.2 MeV, time-of-flight spectroscopy, energy level obs. 3-74575
- Si(n,n'), spin-flip probability and diffl. cross section meas., E=7.44 MeV 3-54480
- Sm, A=144-154, total neutron cross section meas., deformation effects, optical model (*Russian*) 3-52178
- Sm, A=150, 152, 154, 0.8-15 MeV, neutron total cross section differences, nuclear deformation effects 3-60188
- ¹⁴⁷Sm, nonstatistical effects in γ -ray spectra emitted in decays of neutronic resonances (*Russian*) 3-52181
- ¹⁵⁴Sm(n,n' γ), 1.1 to 2.3 MeV, determ. energy level structure, spin and parity from γ -ray spectra 3-67196
- ¹¹⁸Sn(n, γ)¹¹⁹Sn, 46-5000 eV, obs. of gamma transitions between low-lying levels in ¹¹⁹Sn 3-49212
- Sn(n,n α)Sn, meas. differential cross sections at 14.8 MeV, Schwinger prediction 3-71108
- Ta, neutron total cross section, 1.0 to 2.0 MeV, optical model comparison 3-54474
- Ta, total neutron cross section fluctuations, 1-2 MeV, compound nucleus explanation 3-54475
- Ta(n,n α)Ta, meas. differential cross sections at 14.8 MeV, Schwinger prediction 3-71108
- ¹⁵⁹Tb(n, α), E γ =14 MeV, knock-on mechanism 3-63044
- ¹²⁸Te(n, γ)¹²⁹Te, gamma ray meas., decay schemes 3-74537
- ²³²Th, meas. of integral fission cross section in ²³²Cf fission neutron spectrum 3-74619
- ²³²Th contents determ. (*Japanese*) 3-59698
- ²³²Th(n, γ)²³³Th, gamma-ray spectra meas. and analysis 3-49248
- ⁴⁸Ti(n,n'), 300-500 keV above threshold for excitation of 2 $^{+}$ levels, cross section energy dependence (*Russian*) 3-74571
- ⁴⁸Ti(n,n'), 300-500 keV above threshold for excitation of 2 $^{+}$ levels, cross section energy dependence (*Russian*) 3-74571
- Ti(n,p)Sc energies <6 MeV, cross section meas. rel. to ²³⁵U fission using activation method 3-74591
- ²⁰³Tl(n,2n)²⁰²mTl, isomeric cross section at 14.8 MeV 3-54468
- ²⁰³Tl(n, α), thermal neutron energies, cross sections determ. 3-43244
- ²⁰⁵Tl(n,2n)²⁰⁴mTl, isomeric cross section at 14.8 MeV 3-54468
- ¹⁶⁹Tm(n, α), E γ =14 MeV, knock-on mechanism 3-63044
- ¹⁶⁹Tm(n, γ), resonance parameters and capture cross section from neutron time-of-flight meas. 3-49260
- ¹⁶⁹Tm(n, γ) background cross section and correlation between partial widths, relation 3-54454
- ²³⁵U, ²³⁵U fission by thermal neutrons, mass, energy spectra 3-78362
- ²³⁵U fission, low-energy neutron induced, resonance parameters and cross-sections 3-49293
- ²³⁵U(n,f), cross-sections below 30 keV, high resolution meas. 3-60234
- ²³⁵U, anisotropic scattering eff. in reflected fast critical assemblies, calc. 3-49328
- ²³⁵U, multilevel analysis of neutron capture and fission cross sections up to 60 eV 3-63094
- ²³⁵U, multilevel effect in unresolved resonance region 3-71114
- ²³⁵U, neutron-induced fission, spin determ. of resons. 3-74614
- ²³⁵U, thermal neutron capture, probability of formation of spontaneously fissionable isomer states (*Russian*) 3-71139
- ²³⁵U(n, γ), measurements of low energy γ -rays following thermal neutron capture 3-63042
- ²³⁵U capture and fission cross sections, 8 eV-10 keV 3-74612
- ²³⁵U enriched cores, prompt and delayed modes rel. to spacial correction factor for reactivity of system 3-67400
- ²³⁵U fission, absolute determ. of cross-section for 964 keV neutrons 3-49295
- ²³⁵U fission, cross-section meas. for ²³²Cf spontaneous fission neutrons 3-49294
- ²³⁵U fission, low-energy neutron induced, resonance parameters and cross-sections 3-49293
- ²³⁵U fission by thermal neutrons, β ray spectra 3-63101
- ²³⁵U(n, γ) ²³⁶mU, 60 keV, search for spontaneously fissionable ²³⁶mU measured cross sections (*Russian*) 3-57530
- ²³⁵U(n,f), cross-sections below 30 keV, high resolution meas. 3-60234
- ²³⁵U(n,f) neutron multiplicity measurement on resolved fission resonances 3-63091
- ²³⁵U(n, γ)²³⁶U, meas. capture gamma rays to determ. ²³⁶U level structure, and spin 3-67335
- ²³⁸U, 1.6-4.3 MeV neutron energy, meas. of ²³⁹U compound nucleus life time (*Russian*) 3-40497
- ²³⁸U, anisotropic scattering eff. in reflected fast critical assemblies, calc. 3-49328
- ²³⁸U, capture cross section for energies up to 100 keV, γ -ray meas. 3-74576
- ²³⁸U, γ ray spectra, calcs., for slow and fast neutron capture, rel. to reactor shielding 3-67322
- ²³⁸U, inelastic and capture cross-sections, neutron spectrum meas., LMFBR assemblies 3-71155
- ²³⁸U fission, cross-section meas. for ²³²Cf spontaneous fission neutrons 3-49294
- ²³⁸U(n,p) in ZPR-6 assembly 7, comparison of calc. and meas. reaction rate distrib. and fission integrals 3-71186
- ²³⁸U(n, γ n') cross-section in calcs. of fast reactor neutron spectrum and criticality 3-43282
- ²³⁸U(n, γ n') reaction, effect in fast-neutron spectrum critical assemblies 3-43283
- ²³⁸U(n, γ), evaluation of uncertainties in total radiation widths 3-74592

nuclear reactions and scattering due to neutrons continued

- $^{238}\text{U}(n,\gamma)^{239}\text{U}(n,f)$ reaction rate ratio determ. by foil activation analysis in critical facilities, Ge(Li) detectors 3-49347
 $^{238}\text{U}(n,\gamma)^{239}\text{U}$, 150 to 630 keV, meas. neutron capture cross sections by activation technique 3-74572
 $^{238}\text{U}(n,n_0)^{238}\text{U}$, meas. differential cross sections at 14.8 MeV, Schwinger prediction 3-71108
 $^{238}\text{U}(n,n)^{238}\text{U}$, 10.5-21.5 eV, data processing using cubic spline functions 3-57500
 $^{238}\text{U}(n,n)^{238}\text{U}$, 3 MeV polarised neutrons from $^2\text{H}(d,n)^3\text{He}$, meas. differential cross sections and asymmetries 3-71109
 ^{135}Xe , capture cross section measurement using mass separated ion implanted samples and gamma ray spectrometry 3-60171
 $^{\text{Y}}$, neutron total cross section 1.0 to 2.0 MeV, optical model comparison 3-54474
 $^{\text{Y}}$, total neutron cross section fluctuations, 1-2 MeV, compound nucleus explanation 3-54475
 $^{89}\text{Y}(n,n)^{89}\text{Y}$ 0.9 to 1.2 MeV, generalized R-matrix interpretation of total cross section 3-49254
 $^{173}\text{Yb}(n,p)^{174}\text{Yb}$, gamma decay of excited $K=0$ rotational bands in ^{174}Yb 3-74533
 $^{68}\text{Zn}(n,p)^{69}\text{Zn}$, thermal energies, ^{69}Zn energy levels (Russian) 3-71083
 ^{69}Zn , thermal neutron capture, non accidental nature of anticorrelations (Russian) 3-57529
 $^{\text{Zr}}$, neutron total cross section 1.0 to 2.0 MeV, optical model comparison 3-54474
 $^{\text{Zr}}$, total neutron cross section fluctuations, 1-2 MeV, compound nucleus explanation 3-54475
 ^{90}Zr , Zircaloy-2, total cross section meas., 0.4 to 2.4 MeV 3-60285
 $^{\text{Zr}}(n,\gamma)$, 14 MeV radiative capture, spectra and partial cross section meas. 3-60173

nuclear reactions and scattering due to nuclei of $Z > 2$

- $A=40-96$ nuclei, ^{16}O and ^{12}C induced reactions above Coulomb barrier, angular distrib. 3-49276
 complex nuclei, analysis of elastic scattering differential cross sections, strong interaction effective range (Russian) 3-57479
 compound-nucleus reactions, conserved isospin quantum number consequences 3-60148
 elastic nucleus-nucleus scattering, particle and hole transfer optical model and molecular approx. 3-49278
 elastic scattering, interference effects, semi-classical analysis (French) 3-78347
 elastic scattering, semiclassical treatment 3-63085
 fast ion interaction with nuclei use of Glauber theory formulae (Russian) 3-49274
 heavy ion collisions, autoionisation spectra of positrons produced in over critical field 3-67356
 heavy ion elastic scattering, rainbow interference effects 3-60218
 heavy ion excitation of short-lived high spin states, nuclear moments measurement techniques 3-45930
 heavy ion induced reaction populating states in ^{102}Pd and ^{100}Pd , obs. of forking 3-45975
 heavy ion reactions, dynamical treatment of absorption 3-67362
 heavy ion scattering, elastic and inelastic, interference effects 3-49280
 heavy ion transfer reactions, model for angular distrib. including dynamic wave packet dispersion 3-49281
 heavy-ion collisions, validity of classical estimates of dynamical Coulomb barrier 3-49279
 heavy-ion induced reactions, determ. of energy level lifetime by Doppler shift attenuation (German) 3-49188
 heavy-ion initiated nuclear-e.m. cascades, Monte Carlo calcs. 3-59234
 heavy-ion interactions at high energy, Fermi gas cloud model 3-57539
 heavy-ion reactions, sequential decay of light fragments 3-49282
 heavy-ion single-nucleon transfer reactions, recoil effects, DWBA and exptl. study 3-71125
 multinucleon transfer reactions, spectroscopic study 3-57538
 recoil effects, single nuclear transfer, j-dependence, energy dependence, angular momentum of residual nucleus 3-60216
 secondary particles produced at interaction of multiply charged relativistic nuclei with emulsion nuclei (Russian) 3-65606
 semi-classical description, dual basis for non-orthogonality of shell-model states 3-67359
 superheavy nuclei production, stability, fission review (Japanese) 3-71133
 superstrange nuclei, multiple prod. 3-62980
 transfer reactions, ^6Li , ^7Li on ^{12}C , ^{13}C , ^{16}O , ^{26}Mg , ^{28}Si , finite range DWBA calcs. 3-78349
 transfer reactions, DWBA, finite range, recoil, computer code calcs. 3-78348
 transfer reactions between heavy nuclei, Q-value dependence of cross section (German) 3-49275
 transuranium elements, ratio evaporative to fission width Γ_n/Γ_f , energy dependence (Russian) 3-57548
 two nucleon transfer between heavy ions, effect of indirect transitions and Q-dependence 3-54504
 two nucleon transfer reactions, DWBA formulation 3-57540
 two-nucleon transfer between heavy ions, reaction mechanism in semi-classical approx. 3-52204
 e^+ spontaneous production by Coulomb field of heavy nucleus 3-74604
 n transfer to unbound states, DWBA analysis, general formulation, (d,p) reaction special case 3-67358
 $^{109}\text{Ag}(^{16}\text{O},^{16}\text{O})^*$, 33 MeV, quadrupole moments by Coulomb excitation 3-71040
 ^{27}Al , ^{16}O compound reactions, γ transitions between high-spin states of ^{41}K and ^{41}Ca 3-74530
 ^{27}Al , ^{32}S induced reaction, fusion barrier meas. 3-46042
 $^{36}\text{Ar}(^{16}\text{O},^{12}\text{C})^{40}\text{Ca}$ 58 MeV incident energy, excited states study (French) 3-43179
 $^{36}\text{Ar}(^7\text{Li},t)^{40}\text{Ca}$ 28 MeV incident energy, excited states study (French) 3-43179
 ^{197}Au , irradiated by ^{40}Ar , ^{84}Kr , ^{136}Xe ions, product yields, mechanism 3-78350
 $^{197}\text{Au}(^{12}\text{C}$, light particles), $E=125$ MeV, study of emitted light particles and radioactive products 3-71126
- nuclear reactions and scattering due to nuclei of $Z > 2$ continued**
 $^{197}\text{Au}(^{16}\text{O}$, light particles), $E=135$ and 166 MeV, study of emitted light particles and radioactive products 3-71126
 $^{10}\text{B}(^{16}\text{O},\alpha)$, pop high spin states in ^{22}Na , meas. ang. distrib., obs. strong selectivity 3-67364
 $^{10}\text{B}(^{18}\text{O},2p)^{26}\text{Na}$, 42 MeV, ^{26}Na decay study, mass excess determ. 3-74541
 ^{11}B heavy-ion single-nucleon transfer reactions, recoil effects, DWBA and exptl. study 3-71125
 $^{11}\text{B}(^{18}\text{O},2p)^{27}\text{Na}$, 42 MeV, ^{27}Na beta decay study, mass excess determ. 3-74541
 ^{130}Ba , quadrupole moments of first excited states, reorientation eff. meas. 3-49112
 ^{134}Ba , quadrupole moments of first excited states, reorientation eff. meas. 3-49112
 ^{136}Ba , quadrupole moments of first excited states, reorientation eff. Meas. 3-49112
 $^{136}\text{Ba}(^{20}\text{Ne},xn)^{156-+}\text{Dy}$, high angular momentum, excitation functions and photon emission, compound nucleus mechanism 3-63083
 ^{209}Bi , ^{84}Kr -induced transfer reactions, excitation functions and recoil ranges of residual nuclei 3-63084
 ^{11}C heavy-ion single-nucleon transfer reactions, recoil effect, DWBA and exptl. study 3-71125
 ^{12}C on ^{12}C , 40-60 MeV inelastic scattering, single and mutual excitation strengths, coupled-channel analysis 3-60220
 $^{12}\text{C} + ^{12}\text{C}$, total reaction cross section meas., rel. to repulsive cores in the optical potential 3-67366
 $^{12}\text{C} + ^{16}\text{O}$, total reactions cross section meas., rel. to repulsive cores in the optical potential 3-67366
 $^{12}\text{C}(^{10}\text{B},^7\text{Be})^{15}\text{N}$ analog reactions at 100 MeV 3-54501
 $^{12}\text{C}(^{10}\text{B},^7\text{Li})^{15}\text{O}$ analog reactions at 100 MeV 3-54501
 $^{12}\text{C}(^{12}\text{C},\alpha)^{20}\text{Ne}$, low energy, rel. to carbon burning era of nucleosynthesis in stellar evolution 3-40511
 $^{12}\text{C}(^{12}\text{C},\alpha\alpha\gamma)^{16}\text{O}$, study of high-spin negative parity states in ^{20}Ne by $\alpha\alpha\gamma$ coincidence meas. 3-49136
 $^{12}\text{C}(^{12}\text{C},p)^{23}\text{Na}$, low energy, rel. to carbon burning era of nucleosynthesis in stellar evolution 3-40511
 $^{12}\text{C}(^{12}\text{C},pp)^{23}\text{Na}$, high spin states of ^{23}Na study 3-49185
 $^{12}\text{C}(^{12}\text{C},^{12}\text{C})^{12}\text{C}$, 10 to 37.6 MeV kinematical analysis, compound and direct model comparison 3-67360
 $^{12}\text{C}(^{14}\text{N},d)^{24}\text{Mg}$, product high spin states assignment 3-54381
 $^{12}\text{C}(^{16}\text{O},^{12}\text{C})^{16}\text{O}$, 65 and 80 MeV, ang. distrib. meas., strongly absorbing potential 3-60221
 $^{12}\text{C}(^{16}\text{O},^{16}\text{O})^{12}\text{C}$, 65 and 80 MeV, ang. distrib. meas., strongly absorbing potential 3-60221
 $^{12}\text{C}(^{16}\text{O},^{12}\text{O})^{16}\text{O}$, DWBA anal. of alpha transfer reaction 3-71124
 $^{12}\text{C}(^6\text{Li},\alpha)^{14}\text{N}$, 33 MeV, obs., DWBA approx. analysis 3-54502
 $^{12}\text{C}(^6\text{Li},d)^{16}\text{O}$, $^{16}\text{O}(d,\alpha+d)^{12}\text{C}$, angular correlations, plane-wave approx. (Russian) 3-78301
 $^{12}\text{C}(^7\text{Li},^6\text{Li})^{13}\text{C}$, cluster model DWBA analysis, n-d, n- τ cluster interaction 3-60102
 $^{13}\text{C}(^{13}\text{C},^{13}\text{C})^{13}\text{C}$, 14.0-27.5 MeV, meas. of angular distrib. and excitation functions, molecular wave function description 3-46039
 $^{13}\text{C}(^{16}\text{O},^{17}\text{O})^{12}\text{C}$, persistence of $^{12}\text{C} + ^{16}\text{O} \rightarrow ^{28}\text{Si}$ reson. 3-54500
 $^{13}\text{C}(^7\text{Li},p)^{19}\text{O}$, spins of low-lying states, $E=16$ MeV 3-54505
 $^{14}\text{C}(^{12}\text{C},^{12}\text{C})^{14}\text{C}$ elastic scatt., excitation functions near Coulomb barrier 3-49283
 $^{14}\text{C}(^{12}\text{C},\alpha)^{22}\text{Ne}$, excitation functions near Coulomb barrier 3-49283
 $^{14}\text{C}(^{12}\text{C},d)^{24}\text{Na}$, excitation functions near Coulomb barrier 3-49283
 $^{14}\text{C}(^{12}\text{C},t)^{23}\text{Na}$, excitation functions near Coulomb barrier 3-49283
 $^{14}\text{C}(^{16}\text{O},^{18}\text{O})^{12}\text{C}$, $E=20$ to 30 MeV, meas. ang. distrib., interference between α -particle and two-neutron transfer 3-67365
 $^{14}\text{C}(^7\text{Li},^7\text{Be})^{14}\text{B}$, 52 MeV, study of mass excess and low-lying level structure in ^{14}B 3-62925
 ^{40}Ca , ^{32}S induced reaction, fusion barrier meas. 3-46042
 $^{40}\text{Ca}(^{10}\text{B},pnp)^{48}\text{Cr}$, 19, 22.5, 25 MeV, γ -ray spectroscopy of ^{48}Cr 3-62985
 $^{40}\text{Ca}(^{10}\text{B},pp)^{48}\text{V}$, low-lying states study 3-49135
 $^{40}\text{Ca}(^{10}\text{B},ppn)^{40}\text{V}$, low-lying levels study 3-49146
 $^{40}\text{Ca}(^{12}\text{C},2p)^{50}\text{Cr}$, population of high-spin levels in residual nucleus 3-40448
 $^{40}\text{Ca}(^{12}\text{C},pppn)^{48}\text{V}$, low-lying states study 3-49135
 $^{40}\text{Ca}(^{16}\text{O},2pn)^{53}\text{Fe}$, alignment of ^{53}Fe excited states meas. by anisotropy of emitted γ -rays, magnetic moment determ. 3-49080
 $^{40}\text{Ca}(^{16}\text{O},^{12}\text{C})^{44}\text{Ti}$, DWBA anal. of alpha transfer reaction 3-71124
 $^{40}\text{Ca}(^6\text{Li},d)^{44}\text{Ti}$, DWBA anal. of alpha transfer reaction 3-71124
 $^{48}\text{Ca}(^{14}\text{N},^{13}\text{C})^{49}\text{Sc}$, possible L-dependent angular distributions 3-54503
 $^{48}\text{Ca}(^{14}\text{N},^{13}\text{C})^{49}\text{Sc}$, 40 MeV, ang. oscillations 3-74605
 $^{48}\text{Ca}(^{16}\text{O},^{14}\text{C})^{50}\text{Ti}$, DWBA analysis of ang. distrib. 3-57538
 ^{116}Cd , ^{84}Kr reactions, effective thresholds calc. 3-40513
 ^{140}Ce , ^{16}O induced one-proton, two-proton and α -transfer reactions, 63-66.5 MeV, cross section and transfer probability 3-49277
 $^{140}\text{Ce}(^{16}\text{O},^{15}\text{N})^{141}\text{Pr}$, $E=56$ to 63 MeV, measure excitation functions, DWBA analysis 3-71127
 $^{140}\text{Ce}(^{16}\text{O},xn)^{156-+}\text{Dy}$, high angular momentum, excitation functions and photon emission, compound nucleus mechanism 3-63083
 $^{140}\text{Ce}(^{18}\text{O},^{17}\text{O})^{141}\text{Ce}$, $E=56$ to 61 MeV, measure excitation functions, DWBA analysis 3-71127
 $^{246}\text{Cm}(^{16}\text{O},F)$, 102.5 MeV, fragment kinetic energy, comparison with static scission model and fission systematics predictions 3-74616
 $^{\text{Cr}}$, Coulomb excitation of first excited state by ^{32}S ions, quadrupole deformation meas. 3-49143
 ^{53}Cr , ground state static quadrupole moment from Coulomb excitation meas. 3-40410
 ^{164}Dy , ^{40}Ar reactions, effective thresholds calc. 3-40513
 ^{170}Er , static quadrupole moment of first 2^+ state by Coulomb excitation using ^{81}Br 3-62935
 $^{19}\text{F}(^{15}\text{N},^{15}\text{N})^{19}\text{F}$ scatt. at low energies and elastic transfer 3-52205
 $^{54}\text{Fe}(^{12}\text{C},^{11}\text{B})^{55}\text{Co}$, semiclassical anal. of results, j and Q depend. explanation 3-46041
 $^{54}\text{Fe}(^{14}\text{N},^{13}\text{C})^{55}\text{Co}$, semiclassical anal. of results, j and Q depend. explanation 3-46041
 $^{54}\text{Fe}(^{16}\text{O},^{12}\text{C})^{58}\text{Ni}$, DWBA analysis of ang. distrib. 3-57538
 $^{54}\text{Fe}(^{16}\text{O},^{15}\text{N})^{55}\text{Co}$, semiclassical anal. of results, j and Q depend. explanation 3-46041
 ^{72}Ge , ^{84}Kr reactions, effective thresholds calc. 3-40513
 ^{180}Hf , Coulomb excitation, quadrupole precession after recoil implantation in Hf crystals. 3-41462

nuclear reactions and scattering due to nuclei of $Z > 2$ continued

- ^6Li , ^7Li induced elastic scattering on ^{12}C , ^{13}C , ^{16}O , ^{26}Mg , ^{28}Si , 34, 36 MeV, meas. 3-78349
- ^6Li , ^7Li induced inelastic scattering on ^{12}C , ^{13}C , ^{16}O , ^{26}Mg , ^{28}Si , 34, 36 MeV, meas. 3-78349
- ^6Li (^6Li , ^6He) ^6Be , ang. distrib. and excitation functions 3-52202
- ^6Li (^6Li , $^6\text{Li}^*(3.56)$) $^6\text{Li}^*(3.56)$, ang. distrib. and excitation functions 3-52202
- ^{24}Mg , ^{19}F compound reactions, γ transitions between high-spin states of ^{41}K and ^{41}Ca 3-74530
- ^{24}Mg , ^{32}S induced reaction, fusion barrier meas. 3-46042
- ^{26}Mg , ^{18}O compound reactions, γ transitions between high-spin states of ^{41}K and ^{41}Ca 3-74530
- ^{26}Mg (^{16}O , ^{14}C), 45 and 60 MeV, abrupt change between smooth and oscillatory angular distrib. 3-57536
- ^{26}Mg (^{16}O , ^{15}N), 45 and 60 MeV, abrupt change between smooth and oscillatory angular distrib. 3-57536
- ^{26}Mg (^{16}O , ^{15}N) ^{27}Al , 42 MeV, determ. of spectroscopic factors using no recoil DWBA, rel. to recoil effects determ. 3-67367
- ^{26}Mg (^{18}O , ^{16}O) ^{28}Mg , two nucleon transfer reactions, DWBA formulation 3-57540
- ^{142}Nd , ^{16}O induced one-proton, two-proton and α -transfer reactions, 63-66.5 MeV, cross section and transfer probability 3-49277
- ^{142}Nd (^{16}O , ^{16}O) ^{142}Nd , 54-72 MeV, interference of Coulomb and nuclear excitation, B(E2) values and optical model 3-52201
- ^{142}Nd (^{40}Ar , xn) $^{182-x}\text{Pt}$, E < 300 MeV, excitation functions 3-54499
- ^{144}Nd (^{12}C , xn) $^{156-x}\text{Dy}$, high angular momentum, excitation functions and photon emission, compound nucleus mechanism 3-63083
- ^{144}Nd (^{16}O , 4n), high spin states in ^{156}Er 3-62937
- ^{146}Nd (^{12}C , xn, γ), high spin states in ^{155}Dy and ^{154}Dy 3-60217
- ^{146}Nd (^{18}O , nnnn) ^{160}Er , 72 MeV, population of high-spin members of ground state rotational bands 3-52098
- ^{148}Nd (^{16}O , nnnn) ^{160}Er , 70-76 MeV, population of high-spin members of ground state rotational bands 3-52098
- ^{60}Ni (^{18}O , ^{16}O) reactions, A=58, 60, 62, 64, anomalous and normal angular distributions 3-43256
- ^{58}Ni , ^{32}S induced reaction, fusion barrier meas. 3-46042
- ^{58}Ni (^{16}O , ^{16}O) ^{58}Ni , 35-60 MeV, interference of Coulomb and nuclear excitation, B(E2) values and optical model 3-52201
- ^{58}Ni (^6Li , ^6Li), break-up study, E=12 to 24 MeV 3-46040
- ^{58}Ni (^6Li , α (d)), break-up study, E=12 to 24 MeV 3-46040
- ^{58}Ni (^7Li , ^7Li), break-up study, E=12 to 24 MeV 3-46040
- ^{58}Ni (^7Li , α (t)), break-up study, E=12 to 24 MeV 3-46040
- ^{62}Ni (^{12}C , ^{11}B) ^{63}Cu , j depend., finite-range calcs. 3-52203
- ^{62}Ni (^{16}O , ^{13}N) ^{63}Cu , j depend., finite-range calcs. 3-52203
- ^{16}O - ^{16}O scattering, extension of resonating group method to heavy system 3-74602
- ^{16}O + ^{16}O , total reaction cross section meas., rel. to repulsive cores in the optical potential 3-67366
- ^{16}O (^{19}F , ^{19}F) ^{16}O scatt. at low energies and elastic transfer 3-52205
- ^{16}O (^6Li , t), excitation functions, direct nature of reaction 3-57537
- ^{18}O (^{13}C , p) ^{26}Na , 35 MeV, ^{26}Na beta decay study and mass excess determ. 3-74541
- ^{18}O (^{19}F , ^{19}F) ^{18}O scatt. at low energies and elastic transfer 3-52205
- ^{208}Pb , ^{11}B induced transfer reactions above Coulomb barrier, selective excitation of particle, hole states 3-60219
- ^{208}Pb , Coulomb excitation with heavy ions, static quadrupole moment of 3- state from γ -ray meas. 3-49101
- ^{208}Pb , single-proton transfer reactions induced by ^{12}C and ^{16}O ions, recoil effects evidence 3-43255
- ^{208}Pb (^7Li , ^7Li), study of E1 polarisation in ^7Li Coulomb excitation, 18-30 MeV 3-78288
- ^{194}Pt , Coulomb excitation by ^{16}O and ^{32}S , quadrupole moment of first 2^+ state by reorientation precession technique 3-45942
- ^{85}Rb , ^{87}Rb (Cl, Cl γ), 52-64 MeV Coulomb excitation, obs. of γ -transition to $^{85,87}\text{Rb}$ levels 3-40415
- ^{96}Ru , ^{16}O irradiation, excitation function of α -emitters (Russian) 3-57497
- ^{32}S , ^{18}O reaction, test of independence postulate in Bohr theory of compound-nucleus decay 3-40512
- ^{32}S (^{16}O , 2p) ^{46}Ti , population of high-spin levels in residual nucleus 3-40448
- ^{34}S , ^{16}O reaction, test of independence postulate in Bohr theory of compound-nucleus decay 3-40512
- ^{28}Si , ^{22}Ne reaction, test of independence postulate in Bohr theory of compound-nucleus decay 3-40512
- ^{28}Si + ^{16}O , deformation of ^{28}Si , from elastic and inelastic scattering, 33 to 38 MeV 3-63082
- ^{28}Si + ^{18}O , deformation of ^{28}Si , from elastic and inelastic scattering, 33 to 38 MeV 3-63082
- ^{28}Si (^{16}O , pn) ^{42}Sc , alignment of ^{42}Sc excited states meas. by anisotropy of emitted γ -rays, magnetic moment determ. 3-49080
- ^{28}Si (^{18}O , pny) ^{44}Sc , level scheme of ^{44}Sc , lifetime meas., ang. distrib. 3-78282
- ^{30}Si (^{16}O , ^{15}N) ^{31}P , 42 MeV, determ. of spectroscopic factors using no recoil DWBA, rel. to recoil effects determ. 3-67367
- ^{144}Sm , ^{147}Sm , bombardment with ^{20}Ne , production of new Hf isotope α emitters 3-63016
- ^{144}Sm , ^{16}O induced one-proton, two-proton and α -transfer reactions, 63-66.5 MeV, cross section and transfer probability 3-49277
- ^{144}Sm (^{24}Mg , xn) $^{162,163,164}\text{W}$, 110-204 MeV, α -decay of W isotopes, half lives 3-57498
- ^{144}Sm (^{40}Ar , pxn) $^{183-x}\text{Au}$, E < 300 MeV, excitation functions 3-54499
- ^{147}Sm (^{24}Mg , xn) $^{163,164}\text{W}$, 110-204 MeV, α -decay of W isotopes half lives 3-57498
- ^{148}Sm (^{19}F , 6n) ^{161}Lu , 105 to 145 MeV, γ -ray transition observed, ^{161}Lu levels deduced 3-54423
- ^{150}Sm , Coulomb excitation by ^{16}O and ^{32}S , quadrupole moment of first 2^+ state by reorientation precession technique 3-45942
- ^{150}Sm (^{20}Ne , 4n) ^{166}Hf , E=93 MeV, ^{166}Hf deduced levels, feeding times by recoil-distance Doppler shift measurements 3-60215
- ^{152}Sm (^{20}Ne , 4n) ^{168}Hf , E=86 MeV, ^{168}Hf deduced levels, feeding times by recoil-distance Doppler shift measurements 3-60215
- ^{154}Sm (^{20}Ne , 4n) ^{170}Hf , 86 MeV, feeding times for population of quasi-rotational bands in ^{170}Hf 3-60215
- ^{154}Sm (^{28}Si , 4n) ^{178}Os , E=104 MeV, ^{178}Os deduced levels, feeding times by recoil-distance Doppler shift measurements 3-60215
- $\text{Sn}(^{14}\text{N}, \text{xn})\text{La}$, study of odd-A La isotopes A=125-137 by in-beam γ -ray spectroscopy 3-45976

nuclear reactions and scattering due to nuclei of $Z > 2$ continued

- ^{118}Sn (^6Li , ^6Li), break-up study, E=12 to 24 MeV 3-46040
- ^{118}Sn (^6Li , α (d)) break-up study, E=12 to 24 MeV 3-46040
- ^{118}Sn (^7Li , ^7Li), break-up study, E=12 to 24 MeV 3-46040
- ^{118}Sn (^7Li , α (t)), break-up study, E=12 to 24 MeV 3-46040
- ^{88}Sr (^{16}O , ^{15}N) ^{89}Y , schematic study and evidence for recoil effects 3-67363
- ^{88}Sr (^{16}O , ^{15}N) ^{89}Y , E=42.5 to 50 MeV, measure excitation functions, DWBA analysis 3-71127
- ^{88}Sr (^{16}O , ^{16}O) ^{88}Sr , 45-60 MeV, interference of Coulomb and nuclear excitation, B(E2) values and optical model 3-52201
- ^{181}Ta , irradiated by ^{40}Ar , ^{84}Kr , ^{136}Xe ions, product yields, mechanism 3-78350
- ^{159}Tb , (^{40}Ar , xn) $^{199-x}\text{Bi}$, E < 300 MeV, excitation functions 3-54499
- ^{124}Te (^{16}O , ^{16}O), (^6He , ^6He), quadrupole moment meas. by reorientation effect 3-49111
- ^{126}Te (^{16}O , ^{16}O), (^6He , ^6He), quadrupole moment meas. by reorientation effect 3-49111
- ^{128}Te (^{16}O , ^{16}O), (^6He , ^6He), quadrupole moment meas. by reorientation effect 3-49111
- ^{232}Th (^{16}O , F), 102.5 MeV, fragment kinetic energy, comparison with static scission model and fission systematics predictions 3-74616
- ^{232}Th (^{22}Ne , X), 174 MeV, energy spectra of 58 light particles (X), Z=3-12, A=6-27 3-67357
- ^{203}Tl (α , nnn) ^{204}Bi , population of high-spin isomeric state in ^{204}Bi 3-49152
- ^{238}U , interaction barrier in heavy charged particle reactions 3-67361
- ^{238}U , irradiated by ^{40}Ar , ^{84}Kr , ^{136}Xe ions, product yields, mechanism 3-78350
- ^{186}W , Coulomb excitation, quadrupole precession after recoil implantation in Gd crystals. 3-41462
- ^{90}Zr (^{16}O , ^{12}C) ^{104}Mo , optimum Q-value near Coulomb barrier 3-74606
- ^{96}Zr (^{16}O , ^{12}C) ^{100}Mo , optimum Q-value near Coulomb barrier 3-74606
- ^{96}Zr (^{16}O , ^{14}O) ^{98}Mo , optimum Q-value near Coulomb barrier 3-74606

nuclear reactions and scattering due to nucleons

see also nuclear reactions and scattering due to neutrons; nuclear reactions and scattering due to protons

- air nuclei, cosmic ray interactions at mountain altitudes, 600-10000 GeV, integral energy spectrum (Russian) 3-69781
- cascade evaporative model analysis, > 10 GeV (Russian) 3-60194
- deuteron-nucleon elastic scattering at high energies, convergence of iterative diagram (Russian) 3-52159
- elastic scatt., off-shell effects 3-54453
- elastic scattering, shell effects and neutron strength functions 3-78321
- inelastic scattering, ≥ 10 GeV, intra-nuclear cascade model 3-78314
- inelastic scattering, shell model form factors with effective interaction 3-49158
- nucleon-nucleus effective interaction, non local effects 3-60184
- nucleon-nucleus optical potential definition using Low eqn. 3-71111
- odd-mass nuclei, scattering, spin-spin term of optical potential, DWBA analysis 3-67291
- radiative capture, complex coupling model 3-74585
- separable-potential model approach 3-43243
- shell model approach, S-matrix calculation, difference between optical model for slow neutron case (Russian) 3-71115
- Nd backward scattering, elastic cross section, virtual states of trinucleon, Amado model 3-52165
- C, cosmic ray interactions at mountain altitudes, 600-10000 GeV, integral energy spectrum (Russian) 3-69781
- ^{40}Ca (N,N) scattering influence of exchange on optical potential, lowest order exchange processes 3-67290
- Fe, cosmic ray interactions at mountain altitudes, 600-10000 GeV, integral energy spectrum (Russian) 3-69781
- ^2H , exact breakup calc. by soln. of three-particle Faddeev eqn. 3-60155
- ^2H breakup reaction, new set of kinematic variables 3-71095
- ^2H (N,N), Coulomb-modified dispersion relation, low-energy 3-49236
- ^{16}O (N,N) scattering, influence of exchange on optical potential, lowest order exchange processes 3-67290
- Pb, cosmic ray interactions at mountain altitudes, 600-10000 GeV, integral energy spectrum (Russian) 3-69781

nuclear reactions and scattering due to photons

- see also Compton effect; photodisintegration
- A=113 to 209, 15.1 MeV, incident plane polarised photons, spectra obs. 3-71102
- A=7 and 8 nuclei, shell model calculations, non-normal parity states, cross sections 3-54403
- activation detector for γ -rays under coexisting neutron field 3-40006
- cross section calculation, yield curve, modified Penfold-Leiss method, numerical computation (Russian) 3-67311
- elastic scattering by spin zero nuclei, low-frequency limit, cross-section calc. 3-54459
- electric dipole sum rule and two body correlations calc. 3-78240
- excitation by gamma rays of radioactive sources 3-67305
- Generalized dispersive photonuclear sum rule 3-67309
- giant resonance energy, role of proton-neutron polarisation in models for atomic mass dependence 3-74546
- giant resonance excitation of doubly-closed shell nuclei, spin dependent effects, charged pion photoproduction 3-78297
- giant resonances, damping in heavy and medium-heavy nuclei, thermalisation and cooling-off processes 3-71092
- using multifilament proportional counters 3-51702
- nucleon emission, short range correlation effects in (γ , p) and (γ , n) processes 3-67306
- Nucleus(γ , ppxn) ^{24}Na , $13 \leq Z_{\text{nucleus}} \leq 29$, yields for 100 MeV $\leq E_{\gamma, \text{max}} \leq 1000$ MeV 3-54464
- photoeffect, electric dipole sum rule, retardation effect and relativistic correction 3-67310
- photon difference data, effective decorrelation of errors 3-51711
- photonuclear spectra produced by electron bremsstrahlung on targets 3-57509

nuclear reactions and scattering due to photons continued

- photonuclear giant resonance data 3-57510
 photonuclear processes involving γ -bremsstrahlung, correlation effects and stability of inverse problem solns. (*Russian*) 3-52169
 photonuclear reaction with monochromatic photons (*French*) 3-60157
 photoproduction of charged π -mesons on nuclei at high energies (*Russian*) 3-54462
 sum rule calcs., momentum fluctuation in theory of nonlocal nuclear forces 3-67220
 total cross section at high energies, hadronic shadowing effects 3-60158
 total cross sections for γ -rays, 13 keV-17.6 MeV, comparison of expt. and theory 3-67307
 (γ , n) reaction on one neutron deficient nuclei, photoneutron mean energies, level density parameters 3-60080
 (γ , η), on Be, C, Al, Cu, Ag, Pb, $E_\gamma=2$ GeV, cross section meas. 3-78311
 (γ , γ'), M2-E1 mixing ratios, effect of overlapping reson. 3-63036
 π^+ photoproduction and T_+ versus T_- analogue states in $N > Z$ nuclei 3-57508
¹⁰⁷Ag, photo-proton emission, 80 to 260 MeV, from 400 MeV bremsstrahlung 3-74563
²⁷Al, photon-induced fragmentation by 1 GeV bremsstrahlung 3-60160
²⁷Al, resonance scattering of bremsstrahlung, low-lying level study 3-52094
²⁷Al(γ , 4p5n)¹⁸F, 0.3-1 GeV, meas. of photoproduction cross sections by activation analysis 3-40479
²⁷Al(γ , π^+)²⁷Mg, 250, 400, 800 MeV, mean range of recoil nuclei 3-60161
²⁷Al(γ , π^+)²⁷Mg, free-nucleon photopion prod. amplitude and shell model calcs. 3-60159
¹⁹⁷Au, photo-proton emission, 80 to 260 MeV, from 400 MeV bremsstrahlung 3-74563
¹⁹⁷Au(γ , γ')^{197m}Au, 100-800 MeV, yield curves, deduced cross sections, ^{197m}Au measured half life, E_γ 3-67308
⁸B photodisintegration in solar interior 3-65642
¹¹B, resonance scattering of bremsstrahlung, low-lying level study 3-52094
¹¹B(γ , π^-)¹¹C, theoretical photoproduction investigation 3-43234
¹²C, charged pion photoproduction with excitation of ¹²B, ¹²N analogue states 3-49240
¹²C, decay of photon resonances, shell model analysis, cross sections and branching ratios 3-49239
¹²C, giant dipole states and excited dipole states in continuum approx., (γ , N) and (γ , p) reaction 3-67193
¹²C, photonuclear reaction process in giant dipole reson. region in collective correl. model 3-52171
⁵⁰Cr(γ , n)⁴⁹Cr, 20.43 to 22.22 MeV, cross section by detection of ⁴⁹Cr positron activity 3-54460
⁶³Cu, photo-proton emission, 80 to 260 MeV, from 400 MeV bremsstrahlung 3-74563
¹⁹F(γ , xn) reaction, effective cross section meas. from threshold to 25 MeV 3-54463
⁵⁶Fe(γ , n) meas. absolute differential cross section near thresholds 3-71101
⁶⁹Ga, energy level obs. using photoexcitation, elastic and inelastic, resonance decays at 7306, 6874 keV 3-62948
³He, π^+ photoproduction in first π -N resonance region, impulse approx., cross section 3-67300
⁴He(γ , p)³H and ⁴He(γ , n)³He cross section ratio in giant resonance region, charge symmetry 3-52160
¹⁶⁵Ho, resonant scattering of gamma-rays, determ. of 94.69 keV level lifetime (*Russian*) 3-52168
¹¹⁵In(γ , γ')^{115m}In, 100-800 MeV, yield curves, deduced cross sections, ^{115m}In measured half life, E_γ 3-67308
⁶Li, resonance scattering of bremsstrahlung low-lying level study 3-52094
⁶Li(γ , p)⁵He at $E_\gamma=60$ MeV, meas. proton spectra, excitation of ($1p$)⁻¹, ($1s$)⁻¹ hole states 3-71100
⁷Li(γ , pt)³H, $E_\gamma \leq 27$ MeV, determ. integral reaction cross section from energy and momentum conservation (*Russian*) 3-67312
⁷Li(γ , p)⁶He, 60 MeV, proton spectra, excitation of residual hole states 3-71100
¹⁴N, decay of photon resonances, shell model analysis, cross sections and branching ratios 3-49239
 Ni, elastic and inelastic scattering of Fe capture gamma-rays, energy level study 3-49241
⁶⁰Ni photoabsorption, dynamic deformability, reln. to intermediate structure of giant resonance (*Russian*) 3-74562
⁶⁰Ni(γ , n), meas. absolute differential cross section near thresholds 3-71101
¹⁶O, effect of α -channel introduction on continuum structure, reln. to photonuclear cross sections 3-45989
¹⁶O(γ , π^+)¹⁵N, study using different dynamical amplitudes, particle-hole correlations 3-54461
¹⁶O(γ , π^+)¹⁶N, effect of Woods-Saxon wave functions on cross sections for charged-pion photoproduction 3-63034
 Pb, elastic and inelastic scattering of Fe capture gamma-rays, energy level study 3-49241
²⁰⁸Pb photoabsorption, dynamic deformability, reln. to intermediate structure of giant resonance (*Russian*) 3-74562
²⁰⁸Pb(γ , n) background cross section and correlation between partial widths, relation 3-54454
 Pb(γ , γ'), diff. cross sect. meas. 0.145 to 1.33 MeV 3-46019
³²S, photon-induced fragmentation by 1 GeV bremsstrahlung 3-60160
²⁹Si(γ , n) background cross section and correlation between partial widths, relation 3-54454
²³²Th, photoionisation cross-sect. meas., threshold to 8 MeV 3-46046
²³⁶U, photoionisation cross-sect. meas., threshold to 8 MeV 3-46046
²³⁸U, nucl. Raman effect, giant dipole reson. parameters 3-40480
⁵¹V(γ , π^+)⁵¹Ti, free-nucleon photopion prod. amplitude and shell model calcs. 3-60159
⁸⁹Y(γ , γ')^{89m}Y, 100-800 MeV, yield curves, deduced cross sections, ^{89m}Y measured half life, E_γ 3-67308
 Yb(γ , γ'), even isotopes, $E=76.5$ to 84.3 keV, single-line Mossbauer absorption, Yb levels, deduced isomer shifts 3-60109
⁶⁴Zn(γ , n)⁶³Zn cross section meas. from 20.4 to 21.9 MeV 3-52167

nuclear reactions and scattering due to photons continued

- ⁹⁰Zr photoabsorption, dynamic deformability, reln. to intermediate structure of giant resonance (*Russian*) 3-74562
nuclear reactions and scattering due to protons
 A=12 to 209, 30 to 60 MeV proton bombardment, complete H, and He particle spectra 3-74588
 absorption cross sections for 6-60 GeV/c protons and antiprotons on nuclei with A=9-238, radii determ. (*Russian*) 3-67338
 complex nuclei, 6-60 GeV/c, absorpt. cross sections, nucleus radii 3-78352
 compound statistical reactions, test of independence hypothesis and isospin conservation 3-71093
 compound-nucleus reactions, conserved isospin quantum number consequences 3-60148
 cosmic ray origin in reactions induced by fast protons in shell of supernova (*Russian*) 3-65618
 cross-sections for high-energy interactions with targets heavier than Ni, astrophysical appl. 3-43238
 cross-sections for high-energy reactions with targets with $Z \leq 28$, astrophysical appl. 3-43237
 elastic scattering, polarization, diff. theory (*Russian*) 3-78328
 electron pair production, nuclear collisions in emulsion by 200 GeV protons 3-71018
 excitation at high energies, cross section comparison with electrons, pions, alpha particles 3-60164
 fractional-parentage coeffs. determ. from inelastic proton scatt. through analog reson. 3-63059
 heavy nuclei, antiproton absorption study of neutron structure 3-60083
 imaginary optical potential, (N-Z)/A dependence and Thomas-Fermi gas model 3-52187
 inclusive nucleon and pion production from proton-nucleus collisions, semiempirical model 3-57465
 inelastic scattering, 30 MeV, target excitations and optical potential 3-49256
 inelastic scattering, polarisation effects, analysing capability reln. to reaction amplitude (*Russian*) 3-67318
 inelastic scattering of polarised protons, identification of collective modes 3-60101
 light nuclei, pion production by 600 MeV protons, forward cross section calc. 3-57520
 light nuclei, possible relativistic effect in (p , p) reaction 3-40485
 multiplicities from intra-nuclear cascading 10¹⁵ eV cosmic ray proton 3-74586
 one-neutron transfer reaction for ¹⁴Li, ¹⁷O, ⁵⁷⁻⁵⁸Ni, ^{206, 207}Pb, ^{209, 210}Pb, form factor calc. 3-43246
 optical potentials, phenomenological, energy, mass number dependence rel. to effective nuclear energy 3-60142
 production of short-lived neutron deficient nuclei in Tm to Hg region (*Russian*) 3-52142
 quasi-free scattering, determ. of spin-orbit coupling of nuclear protons 3-60073
 Rutherford scattering, indirect determ. of energy loss coeff. of protons channelled along $\langle 111 \rangle$ direction in silicon 3-64077
 strong-absorption model for elastic, polarisation and inelastic proton scattering 3-52183
 total proton-nucleus cross-section and coherent processes in TeV region from cosmic-ray data 3-51237
 two-neutron transfer cross sections, Monte Carlo calcs. 3-43252
⁶²Ni(p , p)⁶²Ni, isobaric analogue resonances, double-scattering techniques, polarisation study, 2.43-2.75 MeV 3-63045
 (p , d) and complementary (d , p) reactions, comparative treatment of spectroscopic factors 3-40502
 (p , n) pre-equilibrium reactions on medium and heavy nuclei, 20-30 MeV, fluctuations in statistical theory 3-40475
 pp scattering, spin correlation parameters, 50 MeV reln. to nuclear forces 3-63030
 π^+ production, two-body input cross sections corrections, nuclear effects, 740 MeV 3-67331
⁵⁵Mn(p , p)⁵⁵Mn, isobaric analog reson. obs. 3-67317
 Ag, 300 GeV, cross-section calc. 3-54477
 Ag, 5 GeV proton bombardment, energy spectra of fragments 3-40496
 Ag induced ^{6,7}Li emission, 25 GeV/c, effect of fragment on heavy product emission 3-78316
¹⁰⁷Ag(p , np)¹⁰⁷Cd, ¹⁰⁷Cd level scheme study 3-49154
 Al, 600 MeV proton bombardment, low-energy proton production, cascade + evaporation model 3-57528
²⁷Al (p , n), isobaric analogue transitions proton energy 22 to 40 MeV, meas. angular distribution 3-63055
²⁷Al(p , α)²⁴Mg, 2100-3100 keV, excitation function (*French*) 3-49251
²⁷Al(p , α)²⁴Mg, 0.633, 0.731, 0.937, 1.183 MeV, meas. of single crystal blocking effect, determ. of reaction time 3-52186
²⁷Al(p , d)²⁶Al, 19, 20 MeV, angular distrib. meas., determ. of spectroscopic factors and levels of ²⁶Al 3-52097
²⁷Al(p , γ), $E_p=1.9$ -3.1 MeV, γ radiations, reson. intensities (*French*) 3-78317
²⁷Al(p , γ)²⁸Si, 2100-3100 keV, excitation function (*French*) 3-49251
²⁷Al(p , γ)²⁸Si, search for 6⁻ analogue-antianalogue states and subsequent γ decay 3-57476
²⁷Al(p , γ)²⁷Al, 2100-3100 keV, excitation function (*French*) 3-49251
²⁷Al(p , γ)²⁷Al, energy dependence of real central optical potential, 25-1000 MeV 3-60185
³⁶Ar(p , n)³⁶K, 17 MeV, determ. of ³⁶K spin and magnetic moment from β -decay asymmetry 3-45939
⁴⁰Ar(p , n)⁴⁰K, gamma-ray angular distrib. and correlation in ⁴⁰K e.m. decay scheme 3-43208
⁴⁰Ar(p , p), 40 MeV polarised protons, asymmetry meas. at small angles 3-40487
 Au, 600 MeV proton bombardment, low-energy proton production, cascade + evaporation model 3-57528
 Au, (p , n) analogue transition, cross-section meas. 3-40491
¹⁹⁷Au fission, induced by 70-200 MeV protons, cross section and angular anisotropy (*Russian*) 3-40523
¹⁰B, (p , α), (p , n) and (p , p') reactions at low energies, optical model and Hauser-Feshbach analysis 3-57533

nuclear reactions and scattering due to protons continued

- ¹¹B(p, α), 2.0 and 2.65 MeV, α -particle coincidence spectra, calc. of resonant peak positions (*Russian*) 3-74567
- ¹⁸Ba(p, p), 17 MeV, determ. of optical model parameters 3-46033
- ¹⁸Be, high-energy proton interactions, Σ^- prod. 3-46029
- ⁹Be, 1.9 to 3 MeV interactions, verification of model representation of ¹⁰B excited states (*Russian*) 3-74570
- ⁹Be proton scattering, 6-30 MeV, differential cross section excitation functions and angular distributions 3-52184
- ⁹Be(p, α), 30-700 keV, meas. cross sections, R matrix compound nucleus model, ¹⁰B deduced resonance parameters 3-60181
- ⁹Be(p, d), 30-700 keV, cross section and angular distrib. meas., ¹⁰B resonance parameters 3-60181
- ⁹Be(p, p)⁹Be 0.8 to 2.7 MeV, analysing power, deduced phase shifts, ¹⁰B deduced levels 3-63047
- ⁹Be(p, α)⁶Li, 6 MeV multi-interaction, finite-range, two-mode DWBA analysis 3-67297
- ⁹Be(p, α)⁵He, 35 to 160 MeV, description using various wave functions, α -clusters for ⁹Be 3-60179
- ¹⁰Be(p, p)¹¹Be cross sections modification for half-life of ¹⁰Be 3-40505
- ²⁰⁷Bi(p, t)²⁰⁷Bi, 17.8 MeV, weak coupling structure in ²⁰⁷Bi 3-57523
- ²⁰⁷Bi, 1 GeV, angular distribution of fission fragments, momentum transfer (*Russian*) 3-57547
- ²⁰⁹Bi, (p, n) analogue transition, cross-section meas. 3-40491
- ²⁰⁹Bi, radiative proton capture cross sections, 10 to 50 MeV, excitation function 3-78318
- ²⁰⁹Bi fission, induced by 1 GeV protons, angular correlations of mass and energy distrib. of fragments (*Russian*) 3-40524
- ²⁰⁹Bi(p, 2n)²⁰⁸Po, cross section and recoil range 3-71105
- ²⁰⁹Bi(p, n)²⁰⁹Bi, quasielastic reaction, macroscopic charge-independent analysis and coupled Lane eqn. solution 3-67333
- ²⁰⁹Bi(p, n)²⁰⁹Po, cross section and recoil range 3-71105
- Br induced ⁶Li emission, 25 GeV/c, effect of fragment on heavy product emission 3-78316
- C, 600 MeV proton bombardment, low-energy proton production, cascade + evaporation model 3-57528
- C, cosmic ray inelastic interactions, 10¹¹-10¹² eV, effective cross-section meas. on PROTON-4 satellite (*Russian*) 3-69787
- C + p absorption study of neutron structure 3-60083
- ¹²C, elastic and inelastic scattering, 9.5-11.5 MeV, obs. of new T = 1/2 levels in ¹³N (*German*) 3-49139
- ¹²C, elastic and inelastic scattering of 1.04 GeV protons, angular distrib. meas. 3-57522
- ¹²C, giant dipole states and excited dipole states in continuum approx., (p, N) and (N, p) reaction 3-67193
- ¹²C(p, γ)¹³N, ¹³N high energy levels study 3-52085
- ¹²C(p, p)₁¹²C, proton spin flip in ¹³N 8.9 MeV level, f-wave decay 3-74590
- ¹²C(p, p₁), study of high-energy levels in ¹³N by obs. of de-excitation γ -rays 3-52085
- ¹²C(p, π^+)¹³C, T_p = 185 MeV, DWBA calcs., π prod. cross sections 3-40492
- ¹²C(p, 2p), separation energy spectra calc. in continuum shell model 3-54389
- ¹²C(p, d)¹¹C, at 185 MeV, deep-lying hole states 3-52101
- ¹²C(p, d)¹¹C high Q-value reaction, sudden approximation study 3-74581
- ¹²C(p, p)₁¹³N, apparent reaction dependence of width of ¹³N first excited state 3-62945
- ¹²C(p, p)₁¹²C, 1 GeV, differential cross section calc. using Glauber multiple scattering theory 3-57521
- ¹²C(p, p)₁¹²C, absolute polarization measured at 50° in range 2.0-4.5 MeV, use as polarimeter 3-63029
- ¹²C(p, p)₁¹²C, apparent reaction dependence of width of ¹³N first excited state 3-62945
- ¹²C(p, p)₁¹²C, energy dependence of real central optical potential, 25-1000 MeV 3-60185
- ¹²C(p, p)₁¹²C, first T = 3/2 resonance by time-of-flight system 3-73884
- ¹²C(p, p)₁¹²C, high-energy, single particle description, cluster-like correlation effects 3-43247
- ¹²C(p, pp)¹¹B, nucleon correl. effect, 1 GeV, distorted wave method 3-78330
- ¹²C(p, π^+), cross-section for π^+ production calc. in Jastrow model, comparison with IPM 3-49259
- ¹²C(p, π^+), relativistic field theoretic description 3-46044
- ¹²C(p, π^+)¹³C, E = 185 MeV, energy spectra, angular distribution, ¹³C deduced levels, comparison with one-nucleon model 3-67323
- ¹³C spallation by 150 and 600 MeV protons, production of ⁷Be, ⁹Be, and ¹⁰Be rel. to astrophysical conditions 3-54476
- ¹⁴C(p, γ)¹⁵N, cross section meas. 7.7-12.0 MeV, resonance structure and energy level determ. 3-49255
- ⁴⁰Ca, elastic scattering, coupling to pickup channels, contrib. to optical potential 3-46031
- ⁴⁰Ca, inelastic proton scatt., ⁴¹Sc doorway state struct. 3-78319
- ⁴⁰Ca(p, p' γ)⁴⁰Ca 12 MeV incident energy, excited states study (*French*) 3-43179
- ⁴⁰Ca(p, d)³⁹Ca, at 185 MeV, deep-lying hole states 3-52101
- ⁴⁰Ca(p, p'), 3.35 MeV state population through reson. in ⁴¹Sc compound nucleus 3-60117
- ⁴⁰Ca(p, p') reaction effective interactions 3-43250
- ⁴⁰Ca(p, p')⁴⁰Ca*, excitation of f_{7/2}-d_{3/2}⁻¹ states, effect of vector and tensor forces 3-67328
- ⁴⁰Ca(p, p)⁴⁰Ca, energy dependence of real central optical potential, 25-1000 MeV 3-60185
- ⁴²Ca(p, t)⁴⁰Ca, cross section predictions from coexistence model 3-67329
- ⁴⁴Ca(p, p)₁⁴⁵Sc, 1.24 to 1.27 MeV, determ. isobaric analogue of lowest 3/2⁻ state of ⁴⁵Ca 3-67195
- ⁴⁴Ca(p, p), rel. to isobaric analogue of lowest 3/2⁻ state of ⁴⁵Ca determ. 3-67195
- ⁴⁴Ca(p, n)₁⁴⁴Sc, level scheme of ⁴⁴Sc lifetime meas. ang. distrib. 3-78282
- ⁴⁶Ca(p, p')⁴⁶Ca, 16 MeV, ⁴⁶Ca level structure 3-54391
- ⁴⁶Ca(p, γ)⁴⁶Sc, M1 transition strength from 3/2⁻ isobaric analogue state 3-54420
- ⁴⁶Ca(p, γ)⁴⁶Sc, spin-parity of ⁴⁶Sc levels from 3/2⁻ isobaric analogue state γ -decay 3-54377
- ⁴⁸Ca(p, γ)⁴⁸Sc, negative-parity state lifetimes of ⁴⁸Sc 3-40445

nuclear reactions and scattering due to protons continued

- ⁴⁸Ca(p, t)⁴⁶Ca, 39 MeV high resolution study, obs. of new levels in ⁴⁶Ca 3-67211
- ⁴Cd(p, t)⁴-²Cd, Cd = 116 and 114, 52 MeV, excitation of 2⁺ states, effect of inelastic scattering processes 3-46032
- ¹⁴²Ce(p, 2p), high-energy excitation function, calc. 3-46027
- ³⁵Cl(p, γ)³⁶Ar, E = 0.8-2.6 MeV, ³⁶Ar deduced levels, shell model calculation of odd-parity levels 3-71078
- ³⁷Cl(p, d)³⁶Cl, 19, 20 MeV, angular distrib. meas., determ. of spectroscopic factors and levels of ³⁶Al 3-52097
- Co, 11.5, 200 and 300 GeV proton irradiation, spallation products cross section meas. 3-46028
- ⁵⁰Cr(p, n)⁵⁰Mn, obs. of isomeric states of ⁵⁰Mn, meas. threshold energies and beta⁺ decay modes 3-67212
- ⁵³Cr(p, n)⁵³Mn, 6 MeV, obs. of ⁵³Mn γ -transitions (*Russian*) 3-74526
- ⁵³Cr(p, n)₁⁵³Mn, excited states of ⁵³Mn 3-67192
- ⁵⁴Cr(p, γ)⁵⁴Mn, meas. of polarisation of deexciting gamma-rays (*Russian*) 3-52126
- ⁵⁴Cr(p, p), (p, p₁), (p, p₂), 1.98-2.02 MeV, multichannel study of ⁵⁵Mn isobaric analogue resonances 3-52133
- ⁵⁴Cr(p, p) and ⁵⁴Cr(p, α), conserved isospin quantum number consequences 3-60148
- ⁶³Cr(p, n)₁⁶³Zn, determ. of branching ratios of electron capture transitions 3-67266
- Cu, 600 MeV proton bombardment, low-energy proton production, cascade + evaporation model 3-57528
- Cu spallation at 205 MeV, radiochemical yield determ. 3-67373
- ⁶³Cu(p, 2n)⁶²Zn, 1.5-11.5 GeV, total cross sections 3-40493
- ⁶³Cu(p, n)⁶³Zn, 1.5-11.5 GeV, total cross sections 3-40493
- ⁶⁵Cu(p, n)₁⁶⁵Zn, narrow reson. 148 eV above threshold 3-43248
- ¹⁹F(p, p'₁)¹⁹F, core-polarisation effects, DWBA analysis 3-52134
- ⁵⁰Fe(p, d)⁵⁰Fe, at 185 MeV, deep-lying hole states 3-52101
- ⁵⁴Fe, ⁵⁶Fe, inelastic scattering, proton spin-flip at 12 MeV 3-63048
- ⁵⁴Fe(p, p)₁⁵⁴Fe, E_p = 19.6 MeV, study of 2⁺ state, limitations of collective model 3-78237
- ⁵⁶Fe(p, n)₁⁵⁶Co, γ -ray transition props. study in ⁵⁶Co 3-54426
- ⁵⁷Fe(p, 2p), high-energy excitation function, calc. 3-46027
- ⁵⁷Fe(p, n)₁⁵⁷Co, 4.9, 5.6 and 6.2 MeV, new levels found in ⁵⁷Co (*German*) 3-60196
- Ga, time differential perturbed angular distrib. meas. of quadrupole interaction on Ge isomeric levels 3-45949
- ⁶⁹Ga(p, n)⁶⁹Ge, ⁶⁹Ge level structure from de-excitation gamma ray obs. 3-54384
- Ga(p, n), liquid target, excitation of 9/2⁺ state in ⁷¹Ge, meas. of quadrupole interaction 3-49082
- ¹⁵⁴Gd, target, production of isomeric states, determ. branching ratios between states of ¹⁵⁴Tb 3-67263
- ¹⁵⁵Gd(p, t)₁¹⁵⁵Gd, energy level study 3-52086
- ¹⁵⁷Gd(p, t)₁¹⁵⁷Gd, energy level study 3-52086
- Gd(p, t), even isotopes, A = 152-160, 18 MeV, population of states in ¹⁵⁰-¹⁵⁸Gd 3-67336
- ⁷²Ge(p, n)₁⁷²As, study of ⁷²As energy spectrum, obs. of new isomeric level, 215 keV 3-45956
- ⁷⁴Ge(p, n)₁⁷⁴As, 3.5, 3.8 and 4.0 MeV, γ -ray angular distribution, ⁷⁴As deduced spins and parities 3-54472
- H⁺-H bremsstrahlung, 156 MeV differential cross sections, off shell effects 3-78335
- ¹H(p, p)₁¹H, absolute cross-section meas., 500-2000 keV (*German*) 3-49231
- ¹H(pp₁) at 4.21 MeV, relative cross sections determ., gas target 3-74558
- ²H(p, p'), ϵ = 20-50 MeV, total reaction cross sections 3-71094
- ²H(p, 2p) at 65 MeV, cross section meas., energy and target mass dependence 3-71097
- ²H(p, 2p), 156 MeV differential cross sections, off shell effects 3-78335
- ²H(p, n)2p, spectra meas., 16-26 MeV, determ. of pp scattering length 3-78337
- ²H(p, n)pp, 16-26 MeV, neutron spectra meas., determ. of proton-proton final state interaction 3-71098
- ²H(p, p)₁²H, backward elastic scattering below 1 GeV, energy dependence 3-52109
- ²H(p, pp)n, 30 MeV, obs. of prominent two-body processes, comparison with Amado model 3-71099
- ²H(p, pp)n, 30-100 MeV, rescattering series convergence 3-63021
- ²H(p, pp)n, 39.5 MeV cross section meas. over large volume of phase space, final state interaction effects 3-74557
- ²H(p, π)³H 340 to 670 MeV, study using Yao-Barry model 3-78307
- ³H, prodn. at high-energies from C and Si 3-54478
- ³H(p, γ)³He, 156 MeV radiative capture, calc. of differential cross section in peripheral model 3-52164
- ³H(p, n)₁³He, E_p = 156 MeV, multiple scatt. effects, Glauber approx. 3-43233
- ³H(p, p)₁³He, E_p = 156 MeV, multiple scatt. effects, Glauber approx. 3-43233
- ³He, prodn. at high-energies from C and Si 3-54478
- ³He(p, 2p) at 85 MeV, cross section meas., energy and target mass dependence 3-71097
- ³He(p, p)₁³He, E_p = 156 MeV, multiple scatt. effects, Glauber approx. 3-43233
- ³He, prodn. at high-energies from C and Si 3-54478
- ³He(p, 2p) at 100 MeV, cross section meas., energy and target mass dependence 3-71097
- ³He(p, d)₁³He, inelastic channels at medium incident energies 3-54479
- ³He(p, p'₁)³He, 22, 45 MeV, p- α bremsstrahlung and cross section meas. 3-74559
- ³He(p, p), Coulomb-modified dispersion relation, low-energy 3-49236
- ³He(p, p)₁³He, 0-23 MeV, energy dependent phase shift analysis, error matrices 3-60152
- ³He(p, p)₁³He, analysis by forward dispersion relations, determ. of pole residues and coupling consts. 3-49232
- ³He(p, p)₁³He, energies \leq 5 MeV, energy-dependent phase shift analysis, effective range parameters 3-60151
- ³He(p, p)₁³He elastic scatt. at 1 GeV, precise single-scatt. optical pot. fit 3-46018
- ²⁰⁴Hg(p, nnn)²⁰²Tl 28 MeV, population of 7⁺ isomeric state in ²⁰²Tl, g factor determ. 3-49086

nuclear reactions and scattering due to protons continued

- ¹⁶⁵Ho, quadrupole moment meas. by proton and alpha scattering from aligned target 3-45944
¹¹⁵In(p,α)¹¹²Cd, 14 MeV, or energy spectra, fit to reaction models 3-78315
 In(p,n), liquid target, excitation of 11/2⁻ state in ¹¹⁵Sn, meas. of quadrupole interaction 3-49082
³⁹K, effect of ground state correlations on imaginary part of optical-model potential 3-52154
³⁹K (p,p'), imaginary part of optical model potential 3-54450
³⁹K(p,n)³⁹Ca, 10 MeV, study of ³⁹Ca β-decay 3-67275
⁶Li, 35-56 MeV, search for excited states of ³He 3-49138
⁶Li(p,³He)⁴He, 12 to 16 MeV, meas. ³He, ⁴He angular distributions, determ. clustering in ⁶Li, two-mode finite-range analysis 3-60103
⁶Li(p,2p), allowance for final nucleus instability in quasielastic knockout of protons 3-60172
⁶Li(p,pd)⁴He, 50 MeV, test of polegraph with Treiman-Yang criterion 3-52175
⁶Li(p,pt), 590 MeV, cross-section meas., recoil momentum of three-nucleon residual system 3-74587
⁷Li(p,n)⁷Be, scattering of keV neutrons, intarget assembly, angular distributions and energy spectra calculations 3-59637
⁷Li(p,n)⁷Be determ. of branching ratios of electron capture transitions 3-67266
⁷Li(p,p)⁷Li, 0.4-2.5 MeV, polarisation and phase shift analysis, resonances and ⁸Be level structure 3-46025
¹⁷⁵Lu(p,xnp)¹⁷²Hf, x=2, 4, 6, A=174, 172, 170, compound nucleus reaction de-excitation 3-49191
²⁴Mg(p,d)²³Mg, at 185 MeV, deep-lying hole states 3-52101
²⁴Mg(p,p'), ²⁴Mg(p,d) strongly coupled, spinless nucleon model, pick-up reaction, deformation parameters 3-54473
²⁵Mg(p,2p), high-energy excitation function, calc. 3-46027
²⁵Mg(p,d)²³Mg, study of particle-hole nature of lowest 3⁻ states in ²⁴Mg 3-49151
⁵⁵Mn(p,γ)⁵⁶Fe, ⁵⁶Mn analogue states in ⁵⁶Fe compound nucleus 3-54421
⁵⁵Mn(p,n)⁵⁶Fe, ⁵⁶Mn analogue states in ⁵⁶Fe compound nucleus 3-54421
⁵⁵Mn(p,γ)⁵⁶Fe, isobaric analogue state of ⁵⁶Mn 0.211 MeV level 3-60168
⁵⁵Mn(p,p)⁵⁵Mn, isobaric analogue state of ⁵⁶Mn 0.211 MeV level 3-60168
⁵⁶Mn(p,γ)⁵⁶Fe, isobaric analog reson. obs. 3-67317
⁹²Mo(p,p'), 40 MeV, role of collective imaginary form factor in microscopic description 3-60186
⁹²Mo(p,p)⁹²Mo, 4.3 and 5.3 MeV, obs. of fine structure in analogue resonances, s1/2 and d5/2 states (German) 3-49249
⁹⁴Mo(p,n)⁹⁴Tc, obs. excited states ⁹⁴Tc, using neutron and gamma ray yields at isobaric analog. resonances 3-67207
⁹⁴Mo(p,n)⁹⁴Tc^{m,s}, isomer ratio comparison to ⁹⁶Mo(p,n)⁹⁶Tc^{m,s} 3-57473
⁹⁶Mo(p,d)⁹⁶Mo, angular distrib. of deuterons, 26 MeV 3-63049
⁹⁶Mo(p,n)⁹⁶Tc^{m,s}, 10-65 MeV, production cross sections and isomer ratios of 4⁺ and 7⁺ states in ⁹⁶Tc 3-43240
⁹⁷Mo(p,d)⁹⁶Mo, 26 MeV, deuteron angular distrib. 3-63049
¹⁰⁰Mo(p,t)⁹⁸Mo, 19 MeV, ⁹⁸Mo, cross section measurements, spin and parity assignments, search for excited rotational band 3-54390
¹⁴N, spallation, production of Li, Be, B isotopes, 17 to 42 MeV, meas. cross sections, astrophysical significance 3-67330
¹⁴N(p,d)¹³N, at 185 MeV, deep-lying hole states 3-52101
²³Na, population of highly excited states, e.m. transition probabilities (Russian) 3-74528
²³Na(p,γ)²⁴Mg, ²⁴Mg 4.235 MeV level, gamma transitions, branching ratio meas. 3-40439
²³Na(p,γ)²⁴Mg, 3905 keV, lowest T=2 level, γ branching ratios 3-78285
¹⁴²Nd(p,p'), neutron particle-hole states population on analog reson. 3-67325
¹⁴⁸Nd(p,6n)¹⁴³Pm, e.m. props. of low-lying levels, M2, E3 transition probabilities 3-67254
²²Ne(p,γ₀+γ₁)²³Na, rel. to electric dipole strength splitting in ²³Na, giant resonance region 3-63054
²²Ne(p,t)²⁰Ne, inelastic excitation effects, coupled-channel-Born-approx. analysis of allowed and forbidden transitions 3-67332
²²Ne(p,t)²⁰Ne 4.97 MeV 2⁻ transition, excitation of unnatural parity states from O⁺ targets 3-78326
 Ni, 600 MeV proton bombardment, low-energy proton production, cascade + evaporation model 3-57528
⁵⁸Ni, elastic and inelastic scattering of 1.04 GeV protons, angular distrib. meas. 3-57522
⁵⁸Ni, elastic and inelastic scatt. of 1 GeV protons, theory, comparison with expt. 3-78320
⁵⁸Ni(p,α)⁵⁵Co, Q value meas., mass discrepancies with 1971 tables 3-45923
⁵⁸Ni(p,p')⁵⁸Ni, E_p=60 MeV polarized protons, giant reson. excitation 3-74584
⁵⁸Ni(p,p)⁵⁸Ni, 1 GeV, differential cross section calc. using Glauber multiple scattering theory 3-57521
⁵⁸Ni(p,t)⁵⁶Ni, E_p=45 MeV, finite range effects by multipole expansion method 3-67294
⁶⁰Ni(p,p')⁶⁰Ni, 12 MeV, DSA meas. of lifetimes and decays of energy levels 3-52132
⁶⁰Ni(p,γ)⁶¹Cu, 1.5-1.9 MeV, obs. of analogue states in ⁶¹Cu 3-46001
⁶⁴Ni(p,n)⁶⁴Cu, meas. of polarisation of deexciting gamma-rays (Russian) 3-52126
 Ni(p,t), broken-pair approx. wave functions analysis 3-40494
 O, A=16, 17, 18, 65 MeV elastic scattering, microscopic analysis, determ. of matter distrib. 3-40490
¹⁶O excitation of levels by high energy protons, 1.0, 2.9, 6.3 GeV, γ-ray spectra (Russian) 3-40456
¹⁶O(p,³He), violation of isospin conservation, E_p=27 MeV 3-63050
¹⁶O(p,α)¹³N, 5.4 to 9.9 MeV, total cross sections by positron decay of ¹³N, reaction rate at 4×10⁹K 3-60178
¹⁶O(p,α)¹³N, total cross section, threshold to 7.7 MeV 3-63043
¹⁶O(p,d)¹⁵O, at 185 MeV, deep-lying hole states 3-52101
¹⁶O(p,d)¹⁵O, effect of short-range correlations due to repulsive core in N-N interaction 3-46024
¹⁶O(p,d)¹⁵O high Q-value reaction, sudden approximation study 3-74581

nuclear reactions and scattering due to protons continued

- ¹⁶O(p,p')¹⁶O, inelastic scatt. to 2⁻ state via nonlocal interaction 3-54466
¹⁶O(p,p)¹⁶O, energy dependence of real central optical potential, 25-1000 MeV 3-60185
¹⁶O(p,pp)¹⁵N, giant multipole resons. L=1,2 and 3, excitation 3-54484
¹⁶O(p,t), calc. B(E2) value and strength rel. to 6.05 MeV 0⁺ state in ¹⁶O 3-67177
¹⁶O(p,t), violation of isospin conservation, E_p=27 MeV 3-63050
¹⁷O(p,n)¹⁷F, 0-5 MeV, meas. total neutron yields, neutron production cross sections 3-60189
¹⁸O(p,n)¹⁸F, 0-4 MeV, meas. total neutron yields, neutron production cross sections 3-60189
¹⁸O(p,n)¹⁸F, E_p=4.6 to 6.6 MeV, reson. investigation 3-54485
³¹P, photoprotons in giant resonance region, (γ, p₀), (γ, p₁) reactions 3-54458
³¹P(γ, p₀)³⁰Si, photoprotons in giant resonance region, for ³¹P 3-54458
³¹P(p,α)²⁸Si, 1240-1600 keV, isobaric analogue reson. study of ³²S (French) 3-78299
³¹P(p,γ)³²S, 1240-1600 keV, isobaric analogue reson. study of ³²S (French) 3-78299
³¹P(p,γ)³²S, lowest T=2 state of ³²S characteriz. 3-60190
³¹P(p,p)³¹P, 1240-1600 keV, isobaric analogue reson. study of ³²S (French) 3-78299
 Pb, induced by 12.2 GeV protons, binary and ternary fission 3-52216
 Pb + p absorption study of neutron structure 3-60083
²⁰⁸Pb, A=206-208, fission, induced by 70-200 MeV protons, cross section and angular anisotropy (Russian) 3-40523
²⁰⁷Pb, elastic and inelastic scattering, 11.1-14.4 MeV, decay amplitudes of ²⁰⁸Pb(0⁺) analogue resonance 3-49253
²⁰⁸Pb, elastic and inelastic scattering of 1.04 GeV protons, angular distrib. meas. 3-57522
²⁰⁸Pb, elastic and inelastic scatt. of 1 GeV protons, theory comparison with expt. 3-78320
²⁰⁸Pb 11 MeV giant reson., quadrupole assignment 3-63025
²⁰⁸Pb(p,n)²⁰⁸Pb, quasielastic reaction, macroscopic charge-independent analysis and coupled Lane eqn. solution 3-67333
²⁰⁸Pb(p,p'), 54 MeV, study of collective excitations in ²⁰⁸Pb 3-63056
²⁰⁸Pb(p,p)²⁰⁸Pb, 1 GeV, differential cross section calc. using Glauber multiple scattering theory 3-57521
²⁰⁸Pb(p,p)²⁰⁸Pb, energy dependence of real central optical potential, 25-1000 MeV 3-60185
²⁰⁸Pb(p,t), differential cross section 3-74582
²⁰⁸Pb(p,t)²⁰⁸Pb, 17.8 MeV, relationship in structures of ²⁰⁷Bi and ²⁰⁶Pb, weak coupling structure in ²⁰⁷Bi 3-57523
 Pb(p,t), A=208, 206, 204, 35 MeV, two-neutron pick-up strengths, transition from single-particle to collective 3-60187
²¹⁰Po(p,p'), 17.8 MeV, study of collective states 3-43183
 Pt, induced by 12.2 GeV protons, binary and ternary fission 3-52216
¹⁸⁵Re(p,2n)¹⁸³Re, in-beam spectroscopy, ¹⁸⁴Os level structure 3-62941
¹⁸⁵Re(p,2n)¹⁸⁴Os, 14 MeV, ground state levels and gamma vibrational bands, in ¹⁸⁴Os 3-67194
¹⁸⁵Re(p,4n)¹⁸²Os, 37 MeV, ground state levels and gamma vibrational bands in ¹⁸²Os 3-67194
¹⁸⁶Re, 1 GeV, angular distribution of fission fragments, momentum transfer (Russian) 3-57547
¹⁸⁷Re(p,2n)¹⁸⁶Os, 14 MeV, ground state levels and gamma vibrational bands, in ¹⁸⁶Os 3-67194
¹⁸⁷Re(p,4n)¹⁸⁴Os, 37 MeV, ground state levels and gamma vibrational bands in ¹⁸⁴Os 3-67194
⁹⁶Ru(p,γ)⁹⁶Ru, 31.1 MeV, study of level structure up to 4 MeV excitation 3-49147
³²S(γ, p₀)³¹P, photoprotons in giant resonance region, for ³¹P 3-54458
³²S(p,d)³¹S, differential cross sections associated with excitation of 1₂⁺ and 3₂⁺ states (Russian) 3-74569
³²S(p,p'), differential cross sections and inelastic scattering asymmetry for first 3⁻ levels excitation (Russian) 3-74569
³²S(p,p'), polarized, scattering, differential cross sections 3-74583
³²S(p,γ)³²S, 5-6 MeV, meas. of excitation functions and angular distrib., optical model description of cross-section (Russian) 3-52180
³³S(p,γ)³⁴Cl, ³⁴Cl nuclear levels investigation 3-52102
³⁴S(p,d)³³S, differential cross sections associated with excitation of 1₂⁺ and 3₂⁺ states (Russian) 3-74569
³⁴S(p,γ)³⁵Cl, gamma ray transitions and lifetimes in ³⁵Cl 3-43214
³⁴S(p,p'), differential cross sections and inelastic scattering asymmetry for first 3⁻ levels excitation (Russian) 3-74569
⁴⁵Sc(p,p), 1.6 to 1.8 MeV, fit of analogue resonances in ⁴⁶Ti compound nucleus 3-63023
²⁸Si(p,d)²⁷Si, at 185 MeV, deep-lying hole states 3-52101
²⁸Si(p,γ)²⁹P, study of ²⁹P levels up to 4.76 MeV 3-49144
²⁸Si(p,γ)²⁹P indirect determ. of energy loss coeff. of protons channelled along <111> direction in silicon 3-64077
²⁸Si(p,p)²⁸Si, 25.25 MeV polarised protons, ground state rotational band excitation 3-52174
²⁸Si(p,p)²⁸Si, 5-6 MeV, meas. of excitation functions and angular distrib., optical model description of cross-section (Russian) 3-52180
²⁹Si, elastic and inelastic resons., E_p=2.5-3.4 MeV 3-60191
³⁰Si(p,2p), high-energy excitation function, calc. 3-46027
 Si(p,p)Si, 17-29 MeV, analysing powers and cross sections in ²⁹P giant resonance region, optical model analysis 3-67327
¹⁴⁴Sm(p,n)¹⁴⁴Sm, reaction on analogue resonances, 9.3-11.0 MeV, ¹⁴⁴Sm deduced levels 3-63046
¹⁴⁸Sm, ¹⁵²Sm inelastic scattering of polarised protons, identification of collective modes 3-60101
¹⁵⁴Sm(p,t)¹⁵²Sm, finite range DWBA calcs. 3-78327
⁵Sn(p,t)⁴-²Sn, A=118 and 116, 52 MeV, excitation of 2⁺ states, effect of inelastic scattering processes 3-46032
¹¹⁸Sn(p,2p), high-energy excitation function, calc. 3-46027
¹²²Sn(p,n)¹²²Sb 11 MeV, population of first excited state in ¹²²Sb, magnetic moment determ. by stroboscope method 3-45959
 Sn(p,p'), A=116, 120, 124, 40 MeV, role of collective imaginary form factor in microscopic description 3-60186

nuclear reactions and scattering due to protons continued

- ⁸⁶Sr(p,t)⁸⁴Sr, at 49.5 MeV proton energy, product low-lying excitations 3-54392
- ⁸⁸Sr isobaric analogue resonance, neutron escape, Coulomb mixing corrections 3-78298
- ⁸⁸Sr(p,p')⁸⁸Sr, isobaric analogue resonances and particle coupling to octupole state 3-46026
- ⁸⁸Sr(p,pnn)⁸⁶Sr, 51 MeV, population of 8⁺ state in ⁸⁶Sr 3-45957
- ⁸⁸Sr(p,t)⁸⁶Sr, at 49.5 MeV proton energy, product low-lying excitations 3-54392
- Ta + p absorption study of neutron structure 3-60083
- ¹⁸¹Ta, (p,n) analogue transition, cross-section meas. 3-40491
- ¹⁸¹Ta, interpretation of nucleon emission following proton bombardment at energies of tens of MeV 3-52182
- ¹⁸¹Ta(p,p3n) excitation function meas., pre-equilibrium nucleon emission model 3-52182
- ¹⁸¹Ta(p,xnp)^aW, x = 2, 4, A = 180, 178, compound nucleus reaction de-excitation 3-49191
- ^aTe(p,t)-^aTe, A = 130-122, 52 MeV, excitation of 2⁺ states, effect of inelastic scattering processes 3-46032
- ¹²⁸Te(p,d)¹²⁷Te and complementary (d,p) reactions, comparative treatment of spectroscopic factors 3-40502
- Te(p,p'), even-A isotopes obs. of strong L = 5 transitions, 2⁵-pole collective motion 3-67326
- Th, induced by 12.2 GeV protons, binary and ternary fission 3-52216
- ²³²Th, 1 GeV, angular distribution of fission fragments, momentum transfer (*Russian*) 3-57547
- ²³²Th, 600 MeV protons, production of 62 sec. ^{222m}Ac 3-54483
- Ti + p absorption study of neutron structure 3-60083
- ⁴⁶Ti(p,γ)⁴⁷V, level scheme of ⁴⁷V, reson., spin, parity (*German*) 3-78251
- ⁴⁷Ti(p,n)⁴⁷V, low-lying levels study 3-49146
- ⁴⁸Ti, ⁵⁰Ti, inelastic scattering, proton spin-flip at 12 MeV 3-63048
- ⁴⁸Ti(p,t)⁴⁶Ti, 51 MeV, angular momentum transfers, ⁴⁶Ti deduced levels, enhancement factors 3-54471
- ⁵⁰Ti(p,p), high resolution, cross section meas., spins, parities, widths, 1.83-2.97 MeV 3-78324
- ¹⁶⁹Tm(p,xnp)^aYb, x = 2, 4, A = 168, 166, compound nucleus reaction de-excitation 3-49191
- U, 24 GeV, protons, neutron-rich Na isotope prod., on-line mass-spectrometric meas. 3-52068
- U, 5 GeV, proton bombardment, energy spectra of fragments 3-40496
- U, ternary fission induced by high-energy protons, cross-sections for three-prong events 3-57546
- ²³⁸U, 1 GeV, angular distribution of fission fragments, momentum transfer (*Russian*) 3-57547
- ²³⁸U, fission and spallation, 11.5 GeV, Xe isotope cross sections and recoil properties 3-74615
- ²³⁸U, interaction with 11.5 GeV protons, charge dispersion and recoil props. at A = 131 3-40520
- ²³⁸U fission, induced by 1 GeV protons, angular correlations of mass and energy distrib. of fragments (*Russian*) 3-40524
- ²³⁸U fission, induced by 70-200 MeV protons, cross section and angular anisotropy (*Russian*) 3-40523
- ²⁵⁸U(p,Cu) reaction at 11.5 GeV, meas. cross section and recoil properties of Cu isotopes of A = 61, 64, 67 3-67334
- V, 3- and 29-GeV proton interaction, product radionuclide yields 3-54481
- V, 300 GeV proton irradiation, spallation products cross section meas. 3-46028
- ⁵¹V (p,n), isobaric analogue transitions proton energy 22 to 40 MeV, meas. angular distribution 3-63055
- ⁵¹V(p,p')⁵²Cr, isobaric analogue states, γ-decay props., 745-820 keV 3-78287
- ⁵¹V(p,n)⁵¹Cr, analogue transition, 16 to 26 MeV, energy dependence 3-63053
- W, 24 GeV irradiation, meas. of cumulative and independent yields of lanthanides 3-40486
- ¹⁸⁶W(p,p), high-energy excitation function, calc. 3-46027
- ⁸⁹Y(p,p')⁸⁹Y*, excitation functions, ⁹⁰Y levels calculated from shell model, conversion to analogue resonances 3-60176
- ⁸⁹Y(p,t)⁸⁷Y, at 49.5 MeV proton energy, product low-lying excitations 3-54392
- ¹⁷⁰Yb(p,t)¹⁶⁸Yb, indirect processes populating γ-band of ¹⁶⁸Yb 3-46030
- ¹⁷³Yb(p,n)¹⁷³Lu, γ-ray obs., level scheme determ. 3-60077
- ¹⁷⁶Yb(p,t)¹⁷⁴Yb, 16 MeV polarised protons, meas. of vector analysing power and differential cross section 3-49257
- Zn, time differential perturbed angular distrib. meas. of quadrupole interaction on Ge isomeric levels 3-45949
- ⁷⁰Zn(p,n)⁷⁰Ga, level structure of ⁷⁰Ga, proton bombardment energy 1.7-3.2 MeV 3-62931
- ⁷⁰Zn(p,n)⁷⁰Ga placement of 188 keV transition in ⁷⁰Ga 3-62982
- ⁹⁰Zr (p,n), isobaric analogue transitions proton energy 22 to 40 MeV, meas. angular distribution 3-63055
- ⁹⁰Zr(p,p')⁹⁰Zr*, 40 MeV, differential cross sections for excitation of ⁹⁰Zr levels, distorted wave calcs. 3-63057
- ⁹²Zr(p,p') 6.5 MeV, angular distribution of spin-flip probability, interference effect 3-67324

nuclear reactions and scattering due to tritons

- disintegration effects choice of nucleon-nucleus potential in optical potential calcs. 3-60142
- elastic scattering, high energy, theory of optical potential (*Russian*) 3-67292
- two-neutron transfer cross sections, Monte Carlo calcs. 3-43252
- (t,d) reactions at sub-Coulomb energies, t-dn vertex functions 3-54489
- (t,p), cross sections to 0⁺ isobaric analogue pairs, ²⁰Ne to ⁵⁶Fe, 15 MeV 3-78342
- ¹¹B(t,p)¹³B, polarised recoil of ¹³B into Mg crystal, quadrupole coupling 3-49079
- ⁹Be(t,Li*)⁶He, E_t = 23.5 MeV, supermultiplet symmetry 3-63068
- ⁹Be(t,Li)⁶He, E_t = 23.5 MeV, supermultiplet symmetry 3-63068
- ⁴⁰Ca(t,p)⁴²Ca, nuclear overlap, cross section prediction 3-67282
- ²⁶Mg(p,γ)²⁸Mg, 2.9 MeV, gamma-ray spectroscopy of low lying levels 3-67258
- Ni(t,p), broken-pair approx. wave functions analysis 3-40494

nuclear reactions and scattering due to tritons continued

- ¹⁶O(t,t), 1.4-3.7 MeV, ¹⁶F deduced levels from angular distrib. and excitation function meas. 3-60200
- ¹⁶O(t,p)¹⁸O, two-nucleon transfer form factor in tail region, large basis shell model approach 3-67295
- ³¹P(t,pp)³³P, product low-lying states lifetime meas. and props. 3-54427
- ³¹P(t,p)³³P, spins and decay modes of ³³P, ang. correl. studies 3-40449
- ²¹⁰Po(t,t'), 20.0 MeV, study of collective states 3-43183
- ³²Si(p,p)³⁴Si, distorted wave anal. rel. to (11/2)² states in ³⁴Si 3-71054
- ²⁸Si(t,p)³⁰Si, 6-12.1 MeV, excitation energies of levels in ³⁰Si, angular distrib. of proton groups 3-62940
- ⁸⁶Sr(³H,α)⁸⁵Rb, 15 MeV, meas. α-particle spectra, determ. levels ⁸⁵Rb 3-71056
- Te(t,α)Sb, study of captured proton wave function and Sb isotope structures (*Spanish*) 3-74484
- Te(t,t)Te, study of optical potential depth and Sb isotope structure (*Spanish*) 3-74484
- ¹⁸²W(t,p)¹⁸⁴W, 20 MeV, cross sections, angular distributions, ¹⁸⁴W deduced levels 3-63064
- ⁹⁰Zr, inelastic scattering, shell-model analysis with core polarization effects 3-78345
- nuclear reactions and scattering due to X-rays** see *nuclear reactions and scattering due to photons*
- nuclear reactions and scattering involving few nucleon systems**
i.e. with A ≤ 4
- deuteron disintegration in nuclear field, DWBA analysis (*German*) 3-49263
- deuteron-nucleon elastic scattering at high energies, convergence of iterative diagram (*Russian*) 3-52159
- elastic scattering of deuterons, medium energy, polarisation effects on cross sections and spin tensors (*Russian*) 3-74595
- few particle problems, conference, Los Angeles, USA (28 Aug-1 Sep 1972) 3-74500
- light nuclei, obs. of S-wave levels near threshold for tensor-polarised deuteron reaction 3-49261
- nucleon-nucleus effective interaction, non local effects 3-60184
- optical potentials, phenomenological, energy, mass number dependence rel. to effective nuclear energy 3-60142
- tensor polarisation in nucleon-deuteron scattering with two-term nonlocal separable potentials 3-54395
- three-body system, effective range approximation, energy spectrum 3-78300
- three-nucleon bound state problems 3-49162
- three-particle reaction, gaps in energy spectrum 3-60149
- d + ³He and p + α coupled channel resonating group calculations, effect of imaginary potentials on spurious resonances 3-78296
- ²H, neutron scatt., polarisation asymmetry, 35 MeV 3-74553
- Nd backward scattering, elastic cross section, virtual states of trinucleon, Amado model 3-52165
- nd quartet, solution methods, Faddeev theorem, Lagrange polynomials 3-78309
- pp scattering, spin correlation parameters, 50 MeV reln. to nuclear forces 3-63030
- DT plasma, fast α particle reactions 3-57925
- D(p,n)pp, breakup neutrons polarisation meas. at 21.5 MeV 3-52163
- ¹H-¹H bremsstrahlung, 156 MeV differential cross sections, off shell effects 3-78335
- ¹H(d,2pn), 12.6 MeV, two-dimensional coincidence spectra, p-n final state interaction 3-40477
- ¹H(d,d')¹H scattering, 30 MeV, meas. of vector and tensor analysing power 3-49235
- ¹H(n,n), ang. distrib., 24 and 27.2 MeV neutrons 3-40478
- ¹H(n,p), thermal radiative capture, meson exchange effects 3-60153
- ¹H(n,pn), 50 MeV, differential cross sections 3-63031
- ¹H(p,p)¹H, absolute cross-section meas., 500-2000 keV (*German*) 3-49231
- ¹H(pp') at 4.21 MeV, relative cross sections determ., gas target 3-74558
- ²H, ²H induced reaction at 20 MeV, meas. neutron spectra and yield 3-74596
- ²H, deuteron interactions at high energy (*Russian*) 3-40383
- ²H, low-energy neutron scattering, resonant group exam. and comparison with Faddeev's eqn. (*Russian*) 3-43135
- ²H, nucleon breakup reaction, new set of kinematic variables 3-71095
- ²H, nucleon induced exact breakup calc. by solution of three-particle Faddeev eqn. 3-60155
- ²H, pion induced near Δ(1236) resonance energy region 3-78177
- ²H-d and ³H-d reactions, absolute determ. of differential neutron source strength (*German*) 3-59636
- ²H-n three-particle scattering, Alt-Grassberger-Sandhas perturbation theory 3-49237
- ²H + ³H, study by one-channel resonating-group method, phase shift and cross section determ. 3-74556
- ²H + ³He, study by one-channel resonating-group method, phase shift and cross section determ. 3-74556
- ²H(²H,dp)n, breakup reaction, 14-36 MeV, modified plane wave impulse approximation theory 3-60154
- ²H(³He, ³H)p, effects of exchange, final-state interactions and distorted waves 3-52161
- ²H(³He, ³He)p, effects of exchange, final-state interactions and distorted waves 3-52161
- ²H(³He,p)p, quasifree reaction mechanisms, absolute cross sections, correlation spectra, pole diagrams 3-67303
- ²H(α,ap)n, differential cross section, off energy shell impulse approximation 3-54455
- ²H(α,d)¹H, 70 MeV sequential reaction through ⁴He, obs. of excited states 3-63032
- ²H(α,pd)²H, 70 MeV sequential reaction through ³He, obs. of excited states 3-63032
- ²H(d, ³He)n, liquid organic scintillator efficiency 3-73865
- ²H(d,d)³He, 3-11.5 MeV polarised deuterons, meas. of vector and tensor analysing powers (*German*) 3-49233
- ²H(d,n)³He, 3-11.5 MeV polarised deuterons, meas. of vector and tensor analysing powers (*German*) 3-49233
- ²H(d,n)³He, 330 keV, 3 MeV neutron production 3-71109

nuclear reactions and scattering involving few nucleon systems continued

- $^2\text{H}(\text{d},\text{n})^3\text{He}$, polarised deuteron beam, 3.3-14.9 MeV, meas. of longitudinal polarization transfer at 0 degrees 3-57506
 $^2\text{H}(\text{d},\text{n})^3\text{He}$, rel. diff. cross-sect. meas., 300 to 700 keV 3-46017
 $^2\text{H}(\text{d},\text{p})^3\text{H}$, 3-11.5 MeV polarised deuterons, meas. of vector and tensor analysing powers (German) 3-49233
 $^2\text{H}(\text{d},\text{p})^3\text{H}$, 6-15 MeV, meas. of polarisation transfer coeffs. at angle of 0° 3-74555
 $^2\text{H}(\text{d},\text{p})^3\text{H}$, rel. diff. cross-sect. meas., 300 to 700 keV 3-46017
 $^2\text{H}(\text{d},\text{pd})\text{n}$, spatial localization effects 3-63033
 $^2\text{H}(\text{q},\text{n})\text{p}$, calc. corrections due to mesonic currents, total and differential cross sections 3-71096
 $^2\text{H}(\text{n}, 2\text{n})^3\text{H}$ break-up process local two-nucleon S-wave potentials and separable Yamaguchi potential 3-60150
 $^2\text{H}(\text{n}, 2\text{p})^3\text{H}$, three-body calc. of neutron-neutron scattering length and effective range 3-78340
 $^2\text{H}(\text{n}, 2\text{n})\text{p}$, 14.17 MeV, cross section and neutron-neutron scattering length calc. Amado model 3-78336
 $^2\text{H}(\text{n}, \text{n})$, scatt. amplitude exam. by Feynman diagram tech. 3-54457
 $^2\text{H}(\text{n}, \text{n})^3\text{H}$, cross section and angular distrib. meas., 40-340 MeV (Russian) 3-74551
 $^2\text{H}(\text{n}, \text{np})\text{n}$, 130 MeV, kinematically complete expt., determ. of neutron-neutron scattering length 3-78338
 $^2\text{H}(\text{n}, \text{p})\text{nn}$, 14 MeV, spectra meas., validity of impulse approx. for nn scattering length 3-78339
 $^2\text{H}(\text{p}, \text{p}')$, $\epsilon=20$ -50 MeV, total reaction cross sections 3-71094
 $^2\text{H}(\text{p}, 2\text{p})$ at 65 MeV, cross section meas., energy and target mass dependence 3-71097
 $^2\text{H}(\text{p}, 2\text{p})\text{n}$, 156 MeV differential cross sections, off shell effects 3-78335
 $^2\text{H}(\text{p}, \text{n})2\text{p}$, spectra meas., 16-26 MeV, determ. of pp scattering length 3-78337
 $^2\text{H}(\text{p}, \text{n})\text{pp}$, 16-26 MeV, neutron spectra meas., determ. of proton-proton final state interaction 3-71098
 $^2\text{H}(\text{p}, \text{p})^3\text{H}$, backward elastic scattering below 1 GeV, energy dependence 3-52109
 $^2\text{H}(\text{p}, \text{pp})\text{n}$, 30 MeV, obs. of prominent two-body processes, comparison with Amado model 3-71099
 $^2\text{H}(\text{p}, \text{pp})\text{n}$, 30-100 MeV, rescattering series convergence 3-63021
 $^2\text{H}(\text{p}, \text{pp})\text{n}$, 39.5 MeV cross section meas. over large volume of phase space, final state interaction effects 3-74557
 $^2\text{H}(\text{p}, \pi)^3\text{H}$ 340 to 670 MeV, study using Yao-Barry model 3-78307
 $^2\text{H}(\pi^+, \pi^+)^3\text{H}$ elastic scattering near 3-3 resonance, angular distrib., cross sections, 141-256 MeV 3-40379
 $^3\text{H} + ^3\text{H}$, 35 MeV, quasifree reaction mechanisms, absolute cross sections, correlation spectra, pole diagrams 3-67303
 $^3\text{H} + ^3\text{He}$, 50 MeV, quasifree reaction mechanisms, absolute cross sections, correlation spectra, pole diagrams 3-67303
 $^3\text{H}(^3\text{He}, \text{d})^4\text{He}$, 291-800 keV, ^6Li levels, isospin violation, energy depend. 3-78306
 $^3\text{H}(^3\text{He}, \text{p})^4\text{Li}$, obs. of direct and resonant capture 3-78308
 $^3\text{H}(\text{d}, \text{n})^4\text{He}$ reaction in ion accelerators for neutron production (French) 3-56917
 $^3\text{H}(\text{p}, \text{p})^4\text{He}$, 156 MeV radiative capture, calc. of differential cross section in peripheral model 3-52164
 $^3\text{H}(\text{p}, \text{n})^3\text{He}$, $E_p=156$ MeV, multiple scatt. effects, Glauber approx. 3-43233
 $^3\text{H}(\text{p}, \text{p})^3\text{H}$, $E_p=156$ MeV, multiple scatt. effects, Glauber approx. 3-43233
 ^3He , high-energy inelastic electron scattering, final state interaction effects on cross section (Russian) 3-52158
 ^3He pion absorption, two-nucleon model, ratio for nnp to nd production rates 3-78304
 ^3He -d self-colliding mixture (migma), nonplasma nonthermal fusion power source 3-74742
 $^3\text{He}(\text{d}, \text{p})^4\text{He}$, ^3He distrib. profiles in Ni, stainless steel, $^3\text{He}^+$ ion bombardment 3-63209
 $^3\text{He}(\text{e}, \text{e}')^2\text{H}$, cross section, depend. on p-d relative motion energy 3-78310
 $^3\text{He}(\text{p}, \text{d})^4\text{H}$, differential cross-section meas., 11-65 MeV 3-74554
 $^3\text{He}(\text{p}, 2\text{p})$ at 85 MeV, cross section meas., energy and target mass dependence 3-71097
 $^3\text{He}(\text{p}, \text{p})^3\text{H}$, $E_p=156$ MeV, multiple scatt. effects, Glauber approx. 3-43233
 $^4\text{He}(^3\text{He}, ^3\text{He}')$ at 7.4 MeV, meas. bremsstrahlung, differential cross section determ. 3-74560
 $^4\text{He}(\text{N}, \text{N})^4\text{He}$, comparison of ^4He - ^3He -n and ^4He - ^3H -p coupling constants, reln. to ^4He structure (German) 3-49234
 $^4\text{He}(\alpha, \alpha')$ bremsstrahlung meas. at 9.35 MeV, differential cross section determ. 3-74561
 $^4\text{He}(\alpha, \alpha)^4\text{He}$, Regge representation including background term 3-52162
 $^4\text{He}(\text{d}, \text{d})^4\text{He}$, 11.5 to 17 MeV, incident vector polarised ^2H , meas. vector analysing power iT_{11} 3-74552
 $^4\text{He}(\text{n}, \text{n})^4\text{He}$, 0-21 MeV, energy dependent phase shift analysis, error matrices 3-60152
 $^4\text{He}(\text{n}, \text{n})^4\text{He}$, energies ≤ 3 MeV, energy-dependent phase shift analysis, effective range parameters 3-60151
 $^4\text{He}(\text{p}, 2\text{p})$ at 100 MeV, cross section meas., energy and target mass dependence 3-71097
 $^4\text{He}(\text{p}, \text{p}')^4\text{He}$, 22, 45 MeV, p- α bremsstrahlung and cross section meas. 3-74559
 $^4\text{He}(\text{p}, \text{p})$, Coulomb-modified dispersion relation, low-energy 3-49236
 $^4\text{He}(\text{p}, \text{p})^4\text{He}$, 0-23 MeV, energy dependent phase shift analysis, error matrices 3-60152
 $^4\text{He}(\text{p}, \text{p})^4\text{He}$, analysis by forward dispersion relations, determ. of pole residues and coupling consts. 3-49232
 $^4\text{He}(\text{p}, \text{p})^4\text{He}$, energies ≤ 5 MeV, energy-dependent phase shift analysis, effective range parameters 3-60151
 $^4\text{He}(\text{p}, \text{p})^4\text{He}$ elastic scatt. at 1 GeV, precise single-scatt. optical pot. fit 3-46018
 $\text{H}^2(\text{n}, \text{p})\text{H}^3$, cross section, meson-exchange corrections 3-54456
 $t=d+n$ vertex, coupling constant and form factor 3-52106

nuclear reactor fuel

- ATR, Japan critical expts. on cluster-type fuel lattices 3-71190
 AVR elements, computer simulation of burn-up (German) 3-71239
 AVR elements, post irradiation studies (German) 3-67593
 axial fuel shuffling, for HTGR 3-63162

nuclear reactor fuel continued

- axial molten-fuel motion model, LMFBR power-temp. accident, fuel melting, shutdown mechanism 3-74731
 buckling of natural and Pu enriched elements, meas. from cooling-channel temp. coeff. (German) 3-67588
 burn up meas., by determ. of relative concentrations of fission products (German) 3-71240
 burnout location on 16-rod 12-ft BWR bundle 3-67446
 burnout prediction method for BWR rod bundles, determ. of critical average steam quality 3-67447
 burnup determination, destructive measurement (Japanese) 3-71279
 burnup determination following irradiation using chemical and isotopic analysis 3-74704
 BWR, examination and tests of irradiated and non irradiated elements (German) 3-67610
 BWR, fuel rod defects, examination, effects of moisture content (German) 3-67611
 BWR, fuel rod defects due to fission iodine in Zry-4 encasing tubes (German) 3-67612
 BWR element with Gd poisoning, burn-up determ. from gamma scanning process (German) 3-67613
 BWR fuel assemblies containing Gd as burnable poison, burnup and transport codes 3-71203
 BWR fuel elements, transfer functions under boiling conditions 3-46126
 BWR fuels, performance 3-67570
 carbide pins, design and layout for high power breeder reactors (German) 3-67605
 cask, NFS-4 for spent fuel 3-67575
 centrifuge enrichment in U.K. 3-54545
 ceramic, fission gas release, kinetics rel. to operation of reactor cycles (German) 3-43305
 ceramic, use of V-base cladding materials, reactivity and compatibility studies 3-43288
 ceramic elements in sodium cooled FBR, venting device 3-71285
 cladding failure, flow channel blockage, core response 3-46087
 Clementine reactor, history of development 3-67562
 Clinton, Hanford and Brookhaven reactors history and development 3-63212
 coated particle, in HTGR, current research status (Japanese) 3-46134
 coated particle at the THTR 300 MWe power station, technical safety (German) 3-71237
 coated particles, loose, in packed beds, thermal conductivity under irradiation (German) 3-67542
 coated particles, stresses caused by neutron irradiation, life expectation in HTR (German) 3-71318
 coated particles with UO_2 kernels, amoeba effect, high temp. failure (German) 3-67550
 compact uranium zircon hydride core, meas. and calc. of importance functions (German) 3-67475
 core design of AEG boiling-water reactor using 8×8 fuel elements (German) 3-67476
 core layout and rod-bank characteristics during zero power operation (German) 3-67478
 criticality safety control for fuel facilities in Japan (Japanese) 3-43277
 decontamination of plutonia contaminated thermal reactor systems 3-57589
 defected rods, effect of friction on gas release rate 3-67428
 depletion of system containing lumped poison, few-group diffusion theory versus many-group S_n approx. 3-49332
 distribution, optimisation method based on linear programming rel. to fixed power reactor 3-74657
 Dragon reactor, irradiation facility, HTR fuel concepts and fuel element designs 3-67458
 drop rod reactivity profiles, loading effects, reactor kinetics, EBR-II 3-71218
 dye penetrant, u.s. reflection, X-radiography, immersion density methods 3-67559
 EBR-II, comparison of radioactive gas release from mixed-oxide and metal fuel element to cover gas 3-67578
 EBR-II operation evaluation with high burnup metal driver 3-49312
 eddy current testing of irradiated fuel rods, location of surface irregularities 3-60261
 electrically heated and simulated fuel bundles development 3-67526
 element components 3-54546
 element design for high-temp. gas cooled reactor, progress and projections 3-46149
 element for high temp. reactor, pressed matrix, dimensional stability rel. to neutron flux and irradiation temp. (German) 3-71269
 element length, percentage increase after seven years use (German) 3-74769
 element spacing in relation to thermal shock conditions in liquid Na coolant (German) 3-67586
 element stresses at discontinuities and interactions by finite elements in two dimensions 3-63125
 elements with etched surfaces, heat transfer and pressure loss in gas cooled reactors (German) 3-67489
 emission rate of free gaseous fission products from HTR fuel specimens (German) 3-67596
 enriched uranium, for Western Europe, forecasts (Italian) 3-63186
 enrichment plant, construction, experience (Dutch) 3-43286
 equation of state rel. to energy release from severe excursions in fast reactors 3-63181
 exchange, in service manipulating equipment tests (German) 3-71232
 exposed, criticality control parameters, critical mass calcs. using computer codes 3-46151
 faceted bubble transport kinetics 3-43295
 failed element identification, probabilistic method using a gas tag system 3-71170
 failed fuel behaviour, effects on reactor operation, obs. 3-67518
 failure location, computational technique 3-63225
 failure propagation, FFTF subassembly, fission gas release 3-71292
 fast, heat fuel assembly removal system failure (Russian) 3-67520
 fast, local fuel failure, simulation experiments 3-67521

nuclear reactor fuel continued

- fast, safety implications of fuel pin transient behaviour, obs. 3-67519
- fast, thermal interaction between liquid alumina and liquid sodium, obs. 3-67527
- fast breeder fuel element in sodium, flow and vibration behaviour (*German*) 3-63123
- fast flux test facility, fuel failure monitoring model 3-63168
- fast mixed-oxide fuelled prototype reactor, effects of partial load and flow control on power coeffs. 3-71163
- fast reactor disassembly, autocatalysis 3-60264
- fast reactors, selection of gas tag compositions for locating failed fuel elements 3-49361
- FBR elements, chemical analysis after high burn-up (*German*) 3-71307
- FBR elements, fissile isotope mixture determ. at various levels of burn up (*German*) 3-71312
- FBR fuel elements, larger diam. development, manufacture, processing and handling (*German*) 3-71309
- FFTF fuel assembly, duct pressure response anal., stainless steel, ANSYS computer code 3-71293
- FFTF-like pins having local overenrichment, TREAT Mk II loop expts. 3-46159
- finance, purchase of heat derived from nuclear fuel under heat supply contract 3-67409
- financing, evolution of concept 3-67410
- financing, review 3-67408
- financing alternatives, evolution 3-67573
- fissile materials, computerized nondestructive neutron interrogation technique for safeguards application 3-46072
- fissile metal, criticality study for handling and storage 3-43315
- fissile sample Doppler effects, effect of local flux distortions 3-49360
- fission gas pressure measurement by null-balance pressure sensor 3-70294
- fission gas release rates, impedance, local flow starvation, LMFBR subassembly 3-74676
- fission gases, rare, diffusion through fuel element cladding (*German*) 3-67393
- fission track registration technique, for estimation of ^{235}U in U samples 3-51722
- fluorinated bed coat, motion of solids 3-67580
- FTR, fuel pin enrichments and control rod loadings 3-71199
- FTR driver fuel assembly, prototypic, test in flowing sodium, final inspection 3-46122
- FTR fuel enrichment parameters 3-71193
- fuel element cans, automatic inspection 3-57554
- fuel element development program (*French*) 3-67544
- fuel-coolant interaction analysis, use of saturated liquid sodium properties 3-46157
- gamma scan system, enrichment, fuel column density uniformity, ^{235}U content meas. 3-66320
- GCFBR fuel elements, fuel-rod grid-spacer wear and fretting 3-67444
- GCFR and LMFBR fuel requirement similarities 3-74721
- GCFR rod irradiations, volatile fission product migration and plateout 3-46160
- general discussion article 3-60273
- handling machine for Lovisa I 3-57574
- handling procedures, Brunswick Steam Electric Plant 3-73641
- handling safety criteria, supporting critical lattice data for both U and Pu bearing fuel 3-67405
- heat transfer, forced convective, to superheated steam in rod bundles 3-63182
- heat transfer in fuel assemblies of reactors with liquid metal cooling 3-49308
- heavy water, lengthening of fuel pins during normal operation 3-46135
- heterogeneous fast reactor, fuel plates, neutron resonance cross section for complicated geometries 3-74654
- hexagonal arrays, determ. of pressure profiles across assemblies in fast reactors using thermal hydraulic anal. (*German*) 3-67589
- hexagonal fuel assembly response, LMFBR safety anal., internal pressures, effect of coolant STRAW dynamic finite element code 3-71294
- high-temperature gas-cooled reactor fuels, performance at peak irradiation 3-63204
- highly irradiated, reprocessing, waste problems (*French*) 3-40547
- history of development for EBR-I 3-67563
- HTGR, Peach Bottom Reactor, test bed for HTGR fuel element demonstration tests 3-74735
- HTR, coated particles with heavy burn-up, Cs transport mechanism determ. (*German*) 3-71320
- HTR cores, design with prismatic fuel elements 3-67457
- HTR elements, die-pressed matrix materials influence of manufacturing parameters on irradiation behaviour (*German*) 3-67599
- HTR elements, irradiation tests, meas. dimensional and density changes (*German*) 3-67592
- HTR fuel, evaluation of resonance absorption by Dragon method 3-67579
- HTR fuel bodies, quality assurance of free heavy metals 3-67581
- HTR fuel compacts, irradiated, corrosion experiments 3-67582
- HTR fuels, influence of grain structure on the effective resonance integral (*German*) 3-67587
- interaction with coolant during fast reactor disassembly accidents, evaluation 3-67533
- interaction with sodium, kinetic energy and pressure calc. 3-67531
- Interim Decay Storage Facility, upper Pu limit, transport and diffusion theory calc. 3-71298
- irradiated, burn-up determination, using heat output from radionuclides being formed by fission 3-67541
- irradiated, combustion rate meas. using adiabatic calorimeter (*French*) 3-73694
- irradiated, gamma scanning meas. for rating distribution determ. 3-43292
- isotopic meas. at reprocessing plants 3-63166
- Japanese activities Japanese development 3-63143
- Japanese industry, fuel cycle activities 3-63142
- LMFBR, criterion for free-contact fragmentation in molten-fuel-coolant interaction 3-46092

nuclear reactor fuel continued

- LMFBR, local molten fuel-coolant interaction, pressure pulse on subassembly wall 3-46073
- LMFBR, voided-core disassembly, fuel-coolant interactions 3-46075
- LMFBR disassembly calcs. fuel-coolant interaction and differential motion effects 3-46074
- LMFBR fuel rods, cladding mechanical interaction 3-63221
- LMFBR fuel rods, cladding strain considerations 3-63222
- LMFBR fuel rods, failed, fission gas release rate, porous flow model 3-71291
- LMFBR fuel subassemblies, determ. of wrapper-can meltthrough using THTB code 3-46079
- LMFBR fuel subassemblies, exptl. evaluation of fission-gas release under subsonic and near subsonic conditions 3-67429
- LMFBR fuel-coolant interaction, noncoherence and heat transfer cutoff, Na vapour 3-71289
- LMFBR pin, spectrum modification in ACPR for transient studies 3-46078
- loading patterns, charact., quantitative analysis 3-57552
- LWR, potential when fuelled with metallic thorium 3-67585
- Markovian random process, nuclear reactor, number of neutrons, precursor nuclei and fuel temp. (*French*) 3-49309
- melting, in fast reactors, exptl. and theoretical study, in-pile and out-of-pile techniques (*German*) 3-67470
- micro elements in fixed bed reactor, thermophysical characteristics anal. (*Russian*) 3-74703
- mixed core, TRIGA standard and TRIGA-FLIP fuels, performance testing 3-74737
- mixed-oxide fuel elements, burnup measurement, EBR-II, ^{148}Nd analyses, comparison with neutronics calc. 3-67572
- molten, interaction with sodium, modelling 3-67532
- molten fuel-coolant interaction, damage to reactor structures, model, REXCO-H code, containment anal. 3-71295
- molten fuel-coolant interaction, reduction of gas-expansion work, cold liquid, heat flow to liquid surfaces 3-71177
- molten fuel-coolant interactions, role of nucleation in vapor explosion 3-46077
- molten fuel/coolant dynamics, fast reactor overpower excursion, accident mitigation 3-71290
- movement visualization using fast neutron hodoscope in 7 pin loss of flow simulation 3-67419
- MTR type elements, temp.-time behaviour after FRG primary pump shutdown (*German*) 3-74644
- multipin in-pile expts., thermal-hydraulic analysis using COBRA III code 3-46129
- NDT during fabrication and quality control 3-57553
- neutron measurement in situ, cask loading, criticality safety 3-63251
- neutron radiography, electronic image analyser, dimensional meas. 3-46148
- neutron spectra, space-dependent fast, calc. using SOPHIE and CICELY codes 3-63121
- Nine Mile Point BWR, corrosion product deposits 3-63217
- noncubic storage arrays, water-sprinkled, computer calcs. of criticality safety 3-46155
- nondestructive testing, instrumentation, gamma-ray spectroscopy, neutron system, calorimetry, review 3-47502
- operating experience, procedures and standards, conf., Myrtle Beach, South Carolina, USA (Aug 1973) 3-74691
- oxide, vacant space distribution analysis during irradiation (*German*) 3-71322
- oxide elements, compatibility with their steel cladding, and corrosion inhibition 3-71308
- oxide elements, in-pile compatibility with austenitic steels, corrosion layer depth meas. (*German*) 3-71313
- oxide fuel columns, in-reactor transient heating conditions, simulation 3-63203
- oxide fuel pin irradiated in fast neutron flux, computer calc. of temp. and density profiles 3-67454
- performance and design, GE BWE, Oyster Creek, wet sipping procedures 3-67567
- pin deformation in Na-cooled FBR under transient loading, computer-aided anal. (*German*) 3-67604
- pin design and layout in FBR, anal. of stresses in casing tubes (*German*) 3-67603
- pin-to-pin failure propagation, pressure pulse loading, fission gas release, buckling failure criterion 3-74732
- poison rod insertion, coolant poisoning, fuel ejection, LMFBR, backup safety device, evaluation 3-74672
- power reactor fuel element evolution, development strategies 3-60280
- pressings containing graphite powder, radiation effects (*German*) 3-71268
- pressurised water reactors, Westinghouse, review of fuel designs 3-67566
- propene-pyrocabon layers, structural changes under thermal treatment and neutron irradiation (*German*) 3-67600
- Pu, reprocessing, value from throwaway cycle 3-57575
- Pu fuel technology, processing and fabrication technology 3-57576
- PWR fuel-element assembly, full scale mock-up, experimental obs. (*German*) 3-67462
- PWR fuels, performance and development. Babcock and Wilcox power plants 3-63213
- radioactive waste disposal, alternative storage areas 3-71338
- re-processing, input and possibilities of verification (*German*) 3-67602
- reactivity testing, reactor fuel and structural materials, quality control tests 3-63210
- reduced-size fuel bundle testing for use in gas-cooled fast reactors 3-46103
- refractory, factors affecting swelling at high temperatures 3-63198
- reprocessing, cryogenic approach to noble gas recovery 3-67414
- reprocessing, HTGR, electrolytic disgregation of irradiated and non-irradiated graphite 3-71283
- reprocessing and refabrication, treatment of radioactive waste, HTR, fuel cycle costs 3-71169
- reprocessing in U.K. 3-54544
- reprocessing solvents, determ. of hydroxamic acids by spectrophotometry 3-71225

nuclear reactor fuel continued

- H.B. Robinson Unit No.2, refuelling operations, maintenance, inspection and testing during shutdown 3-74734
- rod-bundle nuclear fuel elements, transient subchannel analysis, mathematical model 3-63153
- rod-drop experiments, subcriticality determ., inverse kinetics technique 3-71214
- rods, finite bundle, longitudinal laminar flow, asymmetric effects 3-60267
- rods, unbaffled, turbulent longitudinal flow, heat transfer 3-60268
- roughened rod cluster, pressure drop calc. for parallel flow of coolant in GCFR 3-74666
- shipping of spent fuel, Yankee Atomic Electric Co. experience 3-67576
- single phase flow model, noise source propagation, kinetic eqns. for neutrons, fuel and coolant temp. 3-71164
- slender rods in cylindrical duct, acoustically induced vibrs. 3-71174
- spacing, influence on contact wear and dynamic stresses in cladding 3-67398
- spent, and radioactive waste disposal, soln. 3-43294
- spent, isotopic composition, reln. to energy release in fission 3-54529
- spherical element, high temperature, non-destructive meas. of ^{235}U and ^{232}Th (German) 3-67601
- spherical elements, calc. cycle for charging calc. rel. to run-in phase of THTR-300 reactor (German) 3-67485
- spherical low enrichment elements, evaluation of critical expt. with Cesar II (German) 3-67488
- stainless steel, fragmentation, molten fuel-coolant interactions, Na coolant 3-74730
- stainless steel, performance in pressurized water reactor, Indian Point Unit No. 1 3-67569
- storage, accident prevention (German) 3-57563
- subassembly wrapper response to internal pressure, in fast reactor 3-46058
- temperature fluctuations, apparatus for meas., thermal power spectral densities (French) 3-49310
- testing, automatic X-ray scanning system (German) 3-80512
- testing and post irradiation examination 3-43313
- thermal conductivity, porosity depend. 3-40537
- thermoelastic stresses, fuel sheath deformed by cracked fuel pellet, FORTRAN program CHANTER 3-48730
- transport in packages influence of material used on reactivity 3-63183
- transport via sea, licensing, German Atomic Law (German) 3-63185
- TRIGA core management model 3-49370
- TRIGA fuel management, computer program using new data input language 3-49369
- U fuel element, analysis of effects of stat. fluctuations on structure (Czech) 3-43312
- uranium dichalcogenides, magnetic properties with composition close to UY_2 3-64485
- variable rod distribution rel. to thermohydraulic optimisation in fast neutron reactors (German) 3-67486
- ZPPR Assembly 2, heterogeneity effects in plate fuelled assembly for LMFBR design 3-74653
- (β - γ) chamber, for nuclide determination in off-gas samples 3-40012
- ^{134}Cs , Peach Bottom HTGR D1305 fuel element, diffusion coeff., activity profile 3-74738
- ^{137}Cs , Peach Bottom HTGR D1305 fuel element, diffusion coeff., activity profile 3-74738
- D-T, for mirror fusion reactor, 200 MWe, design study 3-60311
- D_2 , solid, evaporation in a fusion plasma 3-78389
- H, applic. (Dutch) 3-40534
- Na bonded (U,Pu)C fuel pins, endurance potential and safety 3-43293
- (Pu,U)O₂, early-in-life failures, release of fuel and fission products 3-63223
- (Pu,U)O₂ fuel rods, failed, effect of O₂ availability on expansion 3-63224
- Pu, comparison of clean and LWR-grade fuel for neutronics characteristics of FFTF core 3-49371
- Pu, mass spectroscopic determ. by isotope dilution method (Czech) 3-42708
- Pu, recycled, optimal use, PWR as example (German) 3-67598
- Pu, recycled, use in heavy water reactor, technical and economic feasibility (German) 3-71316
- Pu, recycling, neutronics 3-57578
- Pu, recycling in boiling water reactor, economic investigation (German) 3-67597
- Pu, reprocessing, polarographic determination of small quantities in solution (German) 3-71325
- Pu, subcritical fast reactor, reactivity meas., rod drop method 3-71208
- Pu, voloxidation for reprocessing 3-54539
- Pu content, calorimetric determ. prior to irradiation 3-71287
- Pu fuel technology, radiation exposure consideration in LWR fuel manufact. 3-57588
- Pu high-burnup solns., computer calcs. of critical parameter using two-isotope approx. 3-46153
- Pu indifference value of pressurized water reactors 3-67411
- Pu recovery by fluorination process using BrF_3 3-43289
- Pu recycle fuelled reactors, behaviour of transient Xe concentration as function of core Pu fraction 3-49340
- Pu recycling in LWR, Belgian programme, exptl. assessment of physics methods calcs. 3-49363
- Pu recycling in PWR, reliability assessment of CNEN neutronic codes 3-49362
- Pu spherical metal assemblies, neutron importance, comparison of theory and expt. 3-71204
- Pu zero-power reactor, LMFBR demonstration plant benchmark control rod expts. 3-49350
- Pu zero-power subcritical reactivity meas. using polarity coherence function technique 3-49346
- Pu-U nitrate solns., computer calcs. of criticality factors based on exptl. data 3-46152
- $\text{Pu}(\text{NO}_3)_4$ solutions, slab geometry, criticality experiments 3-63197
- PuO₂, criticality safety in LWR fuel fabrication 3-57577

nuclear reactor fuel continued

- PuO₂ aerosol, release during LMFBR large core disruptive accident, transfer to second containment, calc. models 3-71178
- PuO₂ sols, solvent extraction process, description 3-65039
- PuO₂-UO₂-polystyrene mixtures, LWR, 7.6 wt% Pu, criticality expts., computer calcs. 3-46154
- ^{238}Pu , 18 eV to 3 MeV n-induced fission, resonance cross-sections 3-74613
- ^{238}Pu , neutron capture cross-section, resonance parameters, γ -ray emission 3-74578
- ^{239}Pu , ^{241}Pu , use in existing power stations (German) 3-46163
- ^{239}Pu , fission, power, photon spectrum and neutron prodn., calc. by ORIGEN computer code 3-43284
- ^{239}Pu , high burnup, criticality expts. and effects of heavy element isotopes on reactivity 3-74729
- ^{239}Pu , neutron collision probabilities in spheres with parabolic source distribution 3-63109
- ^{239}Pu fast reactors, post-shutdown fission product energy release calcs. 3-67441
- ^{239}Pu fission, neutron induced, meas. of prompt ν -values in fast and thermalised fluxes 3-60229
- ^{239}Pu foil irradiation meas. in engineering mockup critical expts. for FTR 3-49352
- ^{240}Pu zoned critical expts., analysis in support of LWR-grade Pu utilization in FTR's 3-71187
- ^{241}Pu fissile element cross section, influence on fast crit. assembly parameters 3-60277
- ^{124}Sb -Be (γ ,n) assay system, fissile content meas., ^4He gas tube detectors 3-67557
- ^{89}Sr , Peach Bottom HTGR D1305 fuel element, diffusion coeff., activity profile 3-74738
- ^{90}Sr , Peach Bottom HTGR D1305 fuel element, diffusion coeff., activity profile 3-74738
- Th- ^{233}U gas core breeder, analysis of configurations for MHD power generation 3-67440
- ThO₂, thermal diffusivity meas., 900 to 2550 C, flash method (French) 3-47445
- ThO₂-PuO₂ HTGR lattice, temp. dependence of infinite-medium neutron multiplication factor 3-49345
- ThO₂-PuO₂ lattice temp. dependence of conversion ratio 3-71171
- (U, Pu)-Co-O system, thermal diffusion mechanisms 3-63232
- (U, Pu)C pellets manufacture by reactive sintering (German) 3-43302
- (U, Pu)O₂, heterogeneous mechanically mixed, finest fraction PuO₂, irradiated in HWR (German) 3-67614
- (U, Pu)O₂, homogeneously precipitated in finest fraction, irradiated in HWR (German) 3-67614
- (U, Pu)O₂, homogenised by melting in all fractions, exptl. examination of rods and capsules (German) 3-67614
- (U, Pu)O₂-x, oxygen redistrib. behaviour 3-43308
- (U,Ce)O₂ mixed oxide fuels, chem. anal. by redox method 3-66459
- (U,Pu)O₂ pellets, sintering variable effects on chem. and phys. characterization. 3-78379
- (U,Pu)O₂, brittle fracture behaviour 3-43309
- (U,Pu)O₂, cladding attack causes and control 3-78383
- (U,Pu)O₂, conservation eqns. governing porosity and actinide redistrib. 3-46145
- (U,Pu)O₂, fabrication, chem. process characterization. 3-78380
- (U,Pu)O₂, irradi., O/M ratio effect on PU redistrib. 3-46147
- (U,Pu)O₂, LMFBR fuel rods, thermal and mech. eval. of oxide microstruct. 3-78381
- (U,Pu)O₂ fuel pins, in-pile radial temp. profiles, simulation 3-46142
- (U,Pu)O₂ fuel pins, plutonium redistrib. considerations 3-46141
- (U,Pu)O₂ fuel rods, irradi., Pu and U diffusion 3-46143
- (U,Pu)O₂ mixed fuels, thermodynamic behaviour 3-57569
- (U,Pu)O₂ pellets, parametrically designed, atmospheric stability obs. 3-78382
- (U,Pu)O₂ pellets, quantification of processing parameter effects on chem. and phys. chars. 3-78378
- (U,Pu)O₂ solid solns., oxidation props., model interpret. 3-54542
- (U,Pu)O₂-x fuel pellets, creep at high stress 3-72950
- (U,Pu)O₂-x pellets, compressive creep, comp. depend. 3-74728
- (U,Th)O₂ fuel particles, pyrolytic-graphite coated, creep deformation, 800-1200°C following irradiation (German) 3-71314
- U, computer controlled mass spectrometry system for enrichment plant 3-70479
- U, cylindrical array, fast neutron meas., ^3He spectrometer 3-71157
- U, depleted, fast neutron spectra, anal. and interpretation, ENDF/B-III data 3-71154
- U, enriched, supply to European countries, future trends (French) 3-60288
- U, enrichment processes, review 3-71286
- U, irradi., Pu recovery using tertiary amine extractants, anal. methods 3-57583
- U, mass spectroscopic determ. by isotope dilution method (Czech) 3-42708
- U, meas. of Doppler effect in thin foils up to 729°C, comparison with theory 3-74679
- U, methods of rod fabrication for CP-3, history 3-67561
- U, natural vs. depleted, use in LMFBR 3-67574
- U, replacement of natural by ^{235}U enriched in heavy water reactors (German) 3-71317
- U, resources and production in United States, review 3-74722
- U, thermal neutron spectrum indexes in D₂O moderated fuel elements 3-74630
- U alloys, nuclear fuel, fission gas release, effect of vol. swelling, probabilistic model 3-63208
- U contamination in pyrolytic-graphite fuel cans using data from HTGR fuel elements (German) 3-67590
- U demand and growth of nuclear power, overview 3-43291
- U enrichment, potential of nozzle-separation technique (German) 3-71302
- U ore processing, techniques and prospects (French) 3-49366
- U oxides, macrodetermination of O₂ by graphite reduction method 3-66411
- U pile, exponential depleted, neutron spectrum meas., inelastic and capture cross-sections of ^{238}U , LMFBR assemblies 3-71155
- U plasma, emission coeff. meas., theory comparison for design calcs. 3-78385

nuclear reactor fuel continued

- U recovery by fluorination process using BrF_3 3-43289
 U rods, coupled cores, kinetics meas., ZED-2 reactor 3-71210
 U supply in West Germany, overview (*German*) 3-63184
 U-C system, thermal diffusion mechanisms 3-63232
 U-C-H system, thermal diffusion mechanisms 3-63232
 U-C-O system, thermal diffusion mechanisms 3-63232
 U-metal spherical assemblies, neutron importance and fission density 3-49302
 γ -U-Mo, fast burst reactor fuel, deformation and fracture behaviour 3-63207
 γ -U-Mo, pulsed reactor fuel, mechanical props. 3-63206
 U-Pu, nuclear fuel, fission gas release, effect of vol. swelling, probabilistic model 3-63208
 U-Pu, thermal neutron spectrum indexes in D_2O moderated fuel elements 3-74630
 U-Pu carbides, summary of development, properties and uses 3-63211
 (U/Th) O_2 pellets, industrial production, for use in HTGR (*German*) 3-67591
 UAl_x , in research reactors, advantages, disadvantages and operating experience 3-71296
 UAl_x -Al manufacture, properties and irradiation behaviour, plates in high flux reactors (*German*) 3-71321
 UC_2 , production using oxalate method for use in FBR (*German*) 3-67608
 UC_2 -Th C_2 spherules, pyrolytic C encased, HTGR elements, radiation testing (*German*) 3-71266
 UC_x compatibility with stainless steel bonded with sodium, carbon transfer kinetics 3-43307
 UF_3 , UF_4 molten fluoride solutions in graphite at 850K, equilibria of uranium carbides 3-43290
 UF_4 , production from UO_2 electrolyte reduction, pilot plant tests (*Spanish*) 3-76460
 U_3Na , production using oxalate method for use in FBR (*German*) 3-67608
 UO_2 , criticality safety in LWR fuel fabrication 3-57577
 UO_2 , fragmentation, molten fuel-coolant interactions, Na coolant 3-74730
 UO_2 , high temp. oxidation, effect of compaction, exposed area and initial composition 3-60275
 UO_2 , in-reactor radiation induced creep behaviour 3-54543
 UO_2 , insulator pellets, effect on axial ^{235}U fission rate distrib., EBR-II 3-63167
 UO_2 , irradi., morphology and growth rate of interlinked porosity 3-43306
 UO_2 , irradiated fuel element under accident conditions, obs. (*French*) 3-67616
 UO_2 , manufacture monitoring, development of in-line instruments (*German*) 3-67606
 UO_2 , melted in air, He, rate of fission product release (*Japanese*) 3-74726
 UO_2 , particles, TRISCO coated, thermochem. stability 3-78384
 UO_2 , pellets and vipac, thermal conductivity meas. 3-63220
 UO_2 , Pu-enriched in ZED-2 expt., booster effect on neutron density and reactivity 3-71226
 UO_2 , re-solution effects and fission gas swelling 3-43301
 UO_2 , sintered, compacting effects, mathematical model of sintering process (*German*) 3-71323
 UO_2 , slightly enriched, H.B. Robinson Unit No.2, Cycle 1 fuel performance 3-74733
 UO_2 , thermal diffusivity meas., 750 to 2700 C, flash method (*French*) 3-47445
 UO_2 , thermal-gradient migration of helium bubbles 3-67552
 UO_2 , Zircaloy clad, fuel performance 3-67570
 UO_2 , Zircaloy-4 clad, fuel performance, C-E, KWU pressurised water reactors 3-67571
 UO_2 bars, thermally shocked, crack healing, isothermal annealing effect 3-74727
 UO_2 coated particles, exptl. determ. of effective resonance integral and Doppler effect in I/E neutron spectrum 3-43273
 UO_2 fuel rods with Zr alloy cladding, manuf., present state in Germany (*German*) 3-43285
 UO_2 helices, γ -radiation effect on creep 3-57570
 UO_2 microsphere fabrication by hydrolysis from uranyl nitrate soln., controlled porosity 3-46146
 UO_2 particles in water, heat removal, simulation expt. for fast reactor fuel debris 3-46093
 UO_2 pellets, crack sintering rates meas. 3-46144
 UO_2 powders, microstruct. evolution during press. sintering 3-78377
 UO_2/PuO_2 elements, electron micro-probe anal. showing radiation induced changes (*German*) 3-71311
 UO_2 -cladding composite body, heat conduction with simultaneous solidification and melting 3-54548
 UO_2 -in-Zircaloy fuel assemblies, performance in CANDU reactors, Canada 3-67568
 UO_2 -Na interaction, demonstration by water-molten aluminium thermal interaction under impact conditions for pressures calc. 3-67530
 UO_2 -Na interactions, pressure pulses, estimates 3-67617
 UO_2 - PuO_2 , irradiated fuel element under accident conditions, obs. (*French*) 3-67616
 UO_2 - PuO_2 , creepage under neutron irradiation up to 1000°C (*German*) 3-71324
 UO_2 - PuO_2 , pellets and sol-gel, thermal conductivity meas. 3-63220
 UO_2 - PuO_2 , use in thermal reactors 3-57579
 UO_2 - PuO_2 fuel pins, irradi., oxygen pot. gradient 3-63189
 UO_2 - SiO_2 vitroceraic rods, Cu admission and distribution 3-57581
 UO_2 -Th O_2 -(Th, U) O_2 sol-gel-oxide, HTGR fuel element manufacture, neutron irradiation (*German*) 3-71266
 UO_2 -Zr, FBR fuel, oxygen pressures calc., model 3-40536
 $\text{UO}_2\text{ZrO}_2\text{CaO}$, fuel element for TREAT convertor 3-63219
 UO_{2+x} -MgO system, phase equilibrium using X-ray diffraction methods 3-74725
 $\text{U}_{0.75}\text{Pu}_{0.25}\text{O}_{2-x}$, equil. oxygen pot., conc. depend. 3-54541
 ^{233}U , re fabrication into particles, and production by a chemical precipitation process (*German*) 3-67607
 ^{233}U separation from thorium and thorium oxide, pilot plant at Trombay 3-71301

nuclear reactor fuel continued

- ^{235}U , heavy water reactors, light water infiltration reactivity effects Ames Laboratory Research Reactor, safety considerations 3-74737
 ^{235}U , neutron collision probabilities in spheres with parabolic source distribution 3-63109
 ^{235}U , with improved performance 3-52231
 ^{235}U booster rod expts. in ZED-2 critical facility, neutron spectrum parameters 3-49365
 ^{235}U content measurement, Sb-Be neutron source 3-67558
 ^{235}U enriched, spheres, immersed in UO_2 (NO_2) $_2$ solutions, mild or boron stainless steel shells, uncoupling effects 3-63196
 ^{235}U enrichment, gaseous diffusion plant, operation 3-74720
 ^{235}U fission, neutron induced, meas. of prompt ν -values in fast and thermalised fluxes 3-60229
 ^{238}U , Doppler reactivity, axial traverses, inverse kinetic techniques 3-71211
 ^{238}U , neutron spectrum meas. for discrepant cross sections in depleted block 3-49296
 ^{238}U Doppler reactivity mapping in FFTF engineering mockup critical calcs. and expts. 3-71191
 ^{238}U - ^{239}Pu oxide-fuelled LMFBR, calcs. of fission product poisoning 3-49356
 $^{238}\text{U}(n,\gamma)^{239}\text{U}$ reaction rate ratio determ. by foil activation analysis in critical facilities, Ge(Li) detectors 3-49347
 UO_2 - PuO_2 -fuel elements, irradiated, data evaluation, performance under high burn-up conditions (*German*) 3-71310
 ZrH $_2$ U fuel elements, release of fission product Xe 3-63122
 ZrU fuel elements, release of fission product Xe 3-63122
- nuclear reactor materials**
see also moderators; nuclear reactor fuel
 absorber rods, treatment for reactor with spherical elements using transport and diffusion programs (*German*) 3-67484
 advanced test reactor, coolant chemistry characterization 3-63211
 alloy, b.c.c., defects, conf. Gaithersburg, USA, (Aug., 1973) 3-79367
 alloy, b.c.c., neutron irradiation effect on tensile props. 3-79386
 burn-up optimization, proof of equivalence relations using Pontryagin method 3-63130
 BWR fuel cans, time and site dependent stress and deformation distribution anal. (*German*) 3-67609
 BWR structural materials electrochem. meas. of corrosion processes 3-71276
 canning tubes testing employing u.s. technique 3-40544
 cell composition and characteristic value of central cell reactivity worth, exptl. detn. 3-43287
 ceramic/metal bonded specimens, fast neutron irradiation induced swelling 3-78375
 ceramics, applic. of surface anal. to porosity study (*Czech*) 3-61237
 cladding in reactor pressure vessels, effect of crystal orientation in welded joints (*German*) 3-72929
 cladding materials, void nucleation suppression by vacancy trapping mechanism 3-63200
 compact reactors, reflector side regulation meas. and calcs. using ITT critical plant (*German*) 3-67474
 concrete stressed pressure vessels, for THTR, construction techniques and design criteria (*German*) 3-74712
 concrete vessels, prestressed, loading to failure, stress conditions 3-60271
 controlled thermonuclear reactor materials, automated method for calculating energy deposition 3-63097
 coolant, outlet pressure control in Mannheim power reactor, circulating system modification 3-67459
 coolant, supervision of activity by γ -spectrometry, computer evaluation (*German*) 3-71327
 coolant, thermo- and fluiddynamic behaviour calc. during normal and emergency shutdown (*German*) 3-67463
 coolant, variation of void fraction during exponential flow and power transients in BWR 3-74665
 coolant boiling in LMFBR and PWR, acoustical detection in 20-50 kHz range 3-46162
 coolant loss, fast reactors, design basis accidents, safety and containment provisions 3-71181
 coolant-slug-impact accident, fast reactor head cover, impulsive loading, nonlinear dynamic anal. 3-74673
 coolants, high-density, for controlled thermonuclear fusion reactor blankets 3-60314
 coolants in power reactors, dual-energy method for measuring void fractions 3-66476
 creep, miniaturized uniaxial machine for remote applications 3-47530
 creep of tubular specimens, air gauge for measurement 3-63138
 creep rates in fast reactor, eqn. predictions 3-43303
 criticality safety determination, pulsed neutron source techniques 3-63231
 design basis accidents, loss of coolant, emergency core cooling system, evolution of technology 3-74677
 displacement damage, h.v. electron microscopy study 3-49807
 double latching cell loadings in storage arrays 3-46156
 Dynamic Slug Impact Model, coolant-reactor vessel head impact, safety anal., MIMIC simulation 3-71176
 engineering test reactor, coolant chemistry characterization 3-63211
 environmental atom implantation into solids by neutron collisions in reactors 3-60272
 fast neutron irradiated, fatigue crack propagation 3-69296
 fast reactor core composition, systematic optimisation, void reactivity 3-63226
 α -Fe, irradiat. defect annealing, computer anal. 3-79346
 fuel specimens, dimensioning from thermal neutron radiographs 3-40545
 fuel-coolant interaction, hypothetical core disruptive accident, mech. energy yield, energy dissipation mechanism 3-74675
 fusion neutronics and photonics, multigroup kerma factors and partial cross sections library 3-63235
 fusion reactor, Princeton reference design model, optimisation of breeding blanket cooling design 3-60312
 fusion reactor blanket design features, choice of constructional materials 3-67584
 fusion reactor technology studies at ORNL 3-60320
 gamma-ray measurements, nuclear material accountability 3-62303

nuclear reactor materials continued

- gas-cooled, alternate-stud-type artificial roughness, meas. of heat transfer and friction coeffs. 3-46104
- graphite, pyrolytic, g-factor anisotropy and e.p.r. linewidths, 300-4.2K, neutron irradi. effects (*French*) 3-47124
- graphite, work of fracture and fracture toughness 3-55926
- graphite, Young's modulus, annealing and pre-stressing effect 3-41816
- graphite irradiation (*Dutch*) 3-57564
- graphite-UC, compacted neutron target (*German*) 3-71258
- HTR, direct cycle, selection of materials 3-67583
- HTR fuel particle coatings, stress calc., analytical model 3-63190
- Incoloy 800, long-term sodium exposure effects on comp. and microstruct. 3-40535
- instrumentation for UK nuc. prog. 3-54531
- lead slowing down time spectrometer, fissile material assay, neutron slowing down studies 3-62267
- Leidenfrost temp. calc. for liquid metals, cryogenics, hydrocarbons and water 3-64169
- liners for stressed concrete reactor pressure vessel, design questions (*German*) 3-74713
- liquid metal cooled reactors, heat transfer in fuel assemblies 3-49308
- liquid metal subchannel crossflow in LMFBR subassemblies with wire-wrap spacers 3-46111
- LMFBR, heat removal from beds of core-material debris in sodium 3-46093
- LMFBR, potential failure of hexcan wrapper due to thermal stresses from local nonuniform temp. distrib. 3-46108
- low energy excursions, reactor containment, implicit continuous Eulerian containment code 3-71175
- matrix, die-pressed for HTR fuel elements influence of manufacturing parameters on irradiation behaviour (*German*) 3-67599
- metal, b.c.c., defects, conf., Gaithersburg, USA, (Aug., 1973) 3-79367
- metal, b.c.c., low temp. neutron irradi. effects, annealing recovery depend. 3-79381
- metal, b.c.c., neutron irradi. effect on tensile props. 3-79386
- metal, irradi., void nucleation kinetics, impurity effects 3-64072
- metal, neutron irradi., dislocation loop nucleation 3-40938
- metal b.c.c., neutron irradi., defect clusters rel. to impurity atoms 3-79334
- metal oxides in water-cooled reactor, thermodynamics 3-57582
- metals, anisotropic, creep rates determ. 3-76219
- mixed-oxide fuel pin centreline temps., meas. to 2700°C 3-45453
- molten salt breeder, reactor, Raman spectra of Be_2F_7^- and more complex species 3-53091
- molten salts, solubility of BF_3 3-46140
- muonic X-rays, fissionable material assay 3-63201
- Na, in fast breeder reactor, obs. of fuel element behaviour (*German*) 3-63123
- neutron irradi. creep during void form. 3-40939
- neutron irradiation softening and effect of interstitials 3-79343
- nondestructive testing, conf., Los Angeles, USA, (Mar. 1973) 3-47497
- organic coolants, HB-40, toluene, dimethylphthalate, thermal conductivity 3-72236
- package licensing and analytical techniques of evaluation 3-67413
- for packaging and transport of radioactive material, effect on reactivity 3-63183
- point defect prod., detection and annealing on neutron irradi. 3-58052
- polyethylene, characteristics over long periods (*German*) 3-67595
- power station build-up of radioactive materials, detection and control 3-74768
- pressure vessels, acoustic emission monitoring, proof tests 3-65062
- pressure vessels for advanced gas-cooled reactor 3-54547
- processing centres in United Kingdom (*Dutch*) 3-71173
- reactor pressure vessels, acoustic emission flow monitor, computer controlled, real-time software operating system 3-47510
- reprocessing of fuel, cryogenic approach to noble gas recovery 3-67414
- reproduction and consumption rates calculation (*Rumanian*) 3-63151
- resonance self-shielding factors, atom density interpolation used with ABBN cross sections 3-49327
- sample work analysis, group collapsing effect in perturbation theory 3-60257
- SNR-300 fuel cans with integral spiral fluting, and geometrical meas. (*German*) 3-71305
- spherical fuel element, mechanical strength rel. to neutron irradiation and corrosion (*German*) 3-71265
- stainless steel, $^3\text{He}^+$ ion implant profiles, $^3\text{He}(d,p)^4\text{He}$ reaction 3-63209
- stainless steels, carburization-decarburization in Na environment 3-63215
- steel, acoustic emission, spectrum anal., deformation and crack propagation 3-47509
- steel, ASTM A533-B, fatigue crack propag. behaviour, temp. and neutron irradi. effect 3-44611
- steel, austenitic, containing Nb, neutron irradi. induced swelling, influence of quenching conditions (*French*) 3-40538
- steel, austenitic, fuel cans, in-pile compatibility with oxide fuel elements (*German*) 3-71313
- steel, austenitic, stainless, deformed Type 316, microstructural characterization as function of deformation 3-47393
- steel, austenitic stainless, α -irrad., recrystn. influence on high-temp. embrittlement 3-44614
- steel, austenitic stainless, chloride stress corrosion cracking, design of containment spray additive system 3-67425
- steel, austenitic stainless, cold working effect on helium embrittlement and creep rupture 3-44612
- steel, austenitic stainless, irradi., with Ti and B additions, high-temp. deform. and fracture 3-63188
- steel, austenitic stainless, long-term sodium exposure effects on comp. and microstruct. 3-40535
- steel, austenitic, fuel cladding in FBR, corrosion by Cs (*German*) 3-71307
- steel, benchmark expt. for neutron transport 3-74633

nuclear reactor materials continued

- steel, corrosion by Na and H_2O in nuclear reactor pressure vessels 3-74719
- steel, Cr-Mn type, effect of carbon addition on mech. props. 3-47432
- steel, embrittlement and annealing after neutron irradiation, model based on Davidenkov criterion 3-72914
- steel, fast reactor, void formation by ion bombardment 3-71284
- steel, helium-implanted stainless, elevated temp. fatigue characteristics in reln. to fusion reactors 3-61183
- steel, in LMFBR subassembly duct wall, thermal stress analysis for severe thermal loading 3-46161
- steel, low-C, boiling water reactors, critical concentration of O_2 and Cl (*German*) 3-67594
- steel, mild, dislocation loops generated by 1 MeV electron irradi., 550°C 3-76171
- steel, stabilised, voiding ratio meas. following irradiation by neutrons and C^{++} ions (*German*) 3-71303
- steel, stabilised fast reactor fuel cans, sodium corrosion tests (*German*) 3-71304
- steel, stainless, 20%Cr/25%Ni niobium stabilized, acetone heterogeneous decomposition, kinetics 3-71299
- steel, stainless, and Al/steel couples, decontamination soln. characterization and use 3-60283
- steel, stainless, bonded with sodium, compatibility with carbide fuel, carbon transfer kinetics 3-43307
- steel, stainless, corrosion by liquid sodium 3-43310
- steel, stainless, implanted He, effect on fatigue life, microstructural effects 3-64947
- steel, stainless, irradi. effect on elastic consts., ultrasonic technique 3-78386
- steel, stainless, nickel ion bombarded, gross swelling direct meas. 3-40540
- steel, stainless, reflector in experimental breeder reactor for use as irradiation facility 3-71196
- steel, stainless, stressed during irradi., microstruct. obs. 3-69245
- steel, stainless, Type 304, effect of exposed nonmetallic inclusions on corrosion resistance instigated, reactor environment 3-53240
- steel, stainless, Type 304, Ni ion bombardment, void swelling behaviour 3-46139
- steel, stainless, Type 304, shielded metal-arc weldments, props. 3-47435
- steel, stainless, Type 316, cold-worked Frank loop development, irradi. effects 3-44576
- steel, stainless, Type 316, helium re-emission and surface deform. during -170 to 700°C implantation 3-46651
- steel, stainless, Type 316, irradi., stress-biased loop nucleation 3-67553
- steel, stainless, Type 316, mech. and struct. props. for LMFBR cladding, rupture 3-47394
- steel, stainless, Type 316, proton irradi., void form and hydrogen effects 3-46138
- steel, stainless austenitic, void volume swelling rel. to grain size 3-64864
- steel, stainless austenitic, X-ray analysis of phases 3-47391
- steel, stainless fuel cladding, solid loaded irradiated, ductility 3-47433
- steel, UHB stainless 724LN, austenitic, improved creep strength mechanism 3-69324
- steel, weld metal, Type 316, struct. and props. 3-47434
- steel, X18H10T, meas. of corrosion kinetics under n, γ -radiation in N_2O_4 3-40546
- steel cladding, compatibility with oxide fuel elements, corrosion reactions 3-71308
- steel cladding- UO_2 composite body, heat conduction with simultaneous solidification and melting 3-54548
- steel fuel cans, Cr-Ni, internal coating of Nb getter layer, exptl. techniques (*German*) 3-71306
- steel pressure vessels, struct. stability characterization. 3-69322
- steel pressure vessels in LWR, in-service examination 3-67456
- steel reflector stainless in EBR-II, loading, startup, and initial operation 3-46130
- steel-reflected loading in EBR-II, reactivity feedback analysis 3-46131
- structural design guidelines for exptl. fast Na-cooled reactor JOYO 3-40530
- swelling, high temp., stress depend. 3-67548
- thermometer, ultrasonic, in-reactor fuel rod centreline high-temp. meas. 3-45454
- Ti-Ni alloy reactor component bonding, phase form. and diffusion behaviour 3-57571
- U fueled, C-Fe-moderated system, bimodal criticality distributions in few group neutron diffusion analysis 3-63108
- void growth termination in irradi. mats. 3-79336
- volume creep, non-conservative, under different stress states, discussion of original paper 3-61171
- waste self-burial, utilising decay heat to melt rock 3-67415
- water and aqueous solns., γ -radiolysis under N_2 gas bubbling 3-71277
- water-cooled, $\text{Co-H}_2\text{O}$ system thermodynamics at elevated temps. 3-47605
- water-cooled, $\text{Fe-H}_2\text{O}$ system thermodynamics at elevated temps. 3-44749
- Zircaloy, hydrogen supercharging during corrosion 3-44610
- Zircaloy, stress corrosion cracking behaviour in iodine vapour 3-43297
- Zircaloy cladding, high temp.-testing for use as thermocouple sheath in PWR 3-47431
- Zircaloy tubing, u.s. inspection, wall thickness and ID meas., multiplexed instrumentation 3-47516
- Zircaloy-2, accelerated oxidation, in steam at high pressure following heat treatment 3-71300
- Zircaloy-2, corrosion of oxide layer, subsurface pitting, stress cracks 3-80387
- Zircaloy-2, morphology of thick oxide films 3-43951
- Zircaloy-2, quenched, strain ageing behaviour 3-58665
- Zircaloy-2, stress corrosion cracking in neutral aqueous chloride solns., 25°C 3-69260
- Zircaloy-2 corrosion in flowing water and steam, 310-320°C (*Japanese*) 3-71280

nuclear reactor materials continued

- Zircaloy-2 oxide film, heat transfer characts. 3-60278
 Zircaloy-2 pressure tubes, Hanford N reactor, monitoring, changes in material props., H content 3-67564
 Zircaloy-4, β - α phase transform. 3-47361
 Zircaloy-4 spacers, vacuum soldering process (German) 3-72930
 Zircaloy-H system, hydride precip., resistometric obs. 3-64875
 Zr/steel rolled joints, hydriding and protection in reactors 3-57572
¹³³Ba diffusion into reactor-grade graphite 3-46150
 Ag-In-Cd control rods in PWR, test of CNEN neutronic codes 3-74683
 Al, ion irradi., partially-ordered void lattice obs. 3-46650
 Al, neutron irradi. void form., deform. influence and dislocation density depend. (French) 3-40940
 Al and Al/steel couples, decontamination soln. characteriz. and use 3-60283
 Al cladding, thickness meas., U fuel elements, gamma ray attenuation 3-47500
 Al-Al₂O₃ alloys, ball-milled, room and elevated temp. props. 3-44613
 Al₂O₃, fast neutron damage effects 3-78373
 Al₂O₃/B₄C ceramics, extraction-flame photometric determ. of boron 3-78376
 Al₂O₃/Nb bonded components, stresses due to irradi. swelling of alumina 3-78374
 B, in core, optimal Xe shutdowns 3-74642
 B₁₂C₂, void morphologies 3-71282
 B₄C mockup control rods for flux tilting expts. in asymmetrically poisoned fast reactor 3-49351
 BF₃-CO₂ gaseous mixtures, exptl. thermal neutron flux distrib. 3-49303
¹⁰B absorber loading in fast test reactor control rods 3-71199
 Be, anisotropic scattering eff. in reflected fast critical assemblies, calc. 3-49328
 Be, as beam-stop material in controlled thermonuclear reactor, neutron flux spectra 3-60253
 Be, small assemblies, space-dependent thermal neutron spectra 3-49298
 BeO, neutron irradi. sintered, He gas release and diffusion processes (German) 3-57568
 C, as beam-stop material in controlled thermonuclear reactor, neutron flux spectra 3-60253
 C, pyrolytic, coating choice, economic costs (German) 3-71247
 C, pyrolytic, coating for HTGR fuel particles, fluidised bed deposition, thermal expansion, 300-1100°C (German) 3-71249
 C, pyrolytic, coating of fuel particles, anisotropy change, radiation damage (German) 3-71251
 C, pyrolytic, coating of nuclear fuel particles, structure, annealing, and neutron irradiation effects (German) 3-71250
 C, pyrolytic, coatings for fuel particles, fabrication and performance 3-43300
 C, pyrolytic, high temp. reactor fuel coating, thermal cond. after fast neutron irradi. 3-49367
 C, pyrolytic coating, butane derivation, radiation damage resistance (German) 3-71248
 C activity in liquid Na, measurement by equilibration method 3-63199
 CeO₂, yttria-stabilized, fast neutron damage effects 3-78373
 Cu, irradi. with 500 keV Cu⁺ ions, void form. phenomena (French) 3-54986
 Cu, proton, neutron and fission neutron damage comparison 3-72105
 Cu-Mg alloys, liquid, thermodynamic props. determ. by vapour pressure meas. 3-72822
 Cu-Ni alloys, void form. resist. 3-67547
 D-T fusion, breeding ratio cross-section sensitivity in fusion reactor blanket 3-63098
 Fe, 2 in thick, with H₂O, neutron shielding, 25 keV to 1 MeV, spectrometer meas. 3-74752
 Fe, benchmark expt. for neutron transport 3-74633
 Fe-Ni system, hydrogen diffusion coeff. at 25 and 58°C 3-69226
 Gd poisoned rods in primary core design for boiling water reactor with graded enrichment (German) 3-67477
 Gd₂O₃, polycrystalline monoclinic, elastic moduli rel. to porosity 3-76326
 H₃BO₃, control of concentration in coolant of PWR (German) 3-71326
 H₂O, neutron shielding, 25 keV to 1 MeV, spectrometer meas. 3-74752
 He coolant in HTR, chemical reactions in primary circuit due to addition of H₂O, CO₂, H₂, CO, CH₄, N₂, NH₃, and CO₂ + N (German) 3-74718
 HfO₂, Y₂O₃ stabilized, thermal expansion 3-61195
 Li, in fusion reactor blanket, entry region effects of flow and pressure drop 3-60313
 Li liquid, coolant performance for low- β Tokamak D-T reactor 3-60315
 LiH, oxidation, LiOH reaction layer structure 3-43952
 Mg sintered composites, cladding material of U fuel elements, mechanical properties, creep and rupture (Czech) 3-67556
 Mo, He⁺ ion implantation and re-emission, temp. depend. 3-79394
 Mo, neutron irradi. temp. effect on hardness 3-79387
 Mo, neutron irradiation and plastic deformation, recovery model critical testing 3-79382
 Mo, reactor irradi., 650°C, damage struct. 3-46649
 Mo-Ti(0.5%), neutron irradi. temp. effect on hardness 3-79387
 N₂O₄ chemically reacting system, thermodynamic parameters, use in nuclear power stations (Czech) 3-44713
 Na, coolant, LMFBR fuel-coolant interaction, noncoherence and heat transfer cutoff 3-71289
 Na, expanding vaporized coolant, simulation of mech. energy release, reactor energy of source characterisation 3-74674
 Na, flow velocity through FFTF fuel assembly, meas. using eddy-current flowmeter 3-45621
 Na, flowing temp. correlation in a heated test section with SNR geometry (German) 3-67490
 Na, heat removal from LMFBR fuel assembly by natural circulation 3-46114
 Na, in LMFBR 19-rod fuel assembly, edge-channel swirl flow, analysis using ORRIBLE code 3-46110

nuclear reactor materials continued

- Na, in steam generators on test rigs, water leaks, monitoring 3-63148
 Na, initial explosion in direct heated channel, ejection vel. and residual film 3-60258
 Na, liq., thermotransport of Be and Hg 3-64197
 Na, liquid, temperature noise meas. in heat transfer expt. in four-rod bundle 3-67453
 Na, liquid, two-phase and subcooled, thermodynamic props., calc. molten fuel-coolant interactions, potential accidents 3-71288
 Na, liquid coolant, calc. of maximal voiding effects using computer program (German) 3-67472
 Na, liquid coolant, temperature measurement by microwave techniques 3-70282
 Na, liquid fires efficacy of aerosol suppressants and fast reactor containment (German) 3-67471
 Na, model for droplet combustion in LMFBR accident analysis 3-46076
 Na, molten fuel-coolant interactions, fragmentation of UO₂ and stainless steel 3-74730
 Na, nuclear reactor coolant, eddy current flowmeter, wet vs. dry performance 3-66477
 Na, primary coolant, meas. and anal. of fast neutron spectra, fast breeder reactor 3-71153
 Na, pulsed assembly, neutron emission-time effects 3-49297
 Na, removal of Cs, by activated charcoal, in thermal convection capsule 3-63216
 Na, saturated properties, use in LMFBR fuel-coolant interaction analysis 3-46157
 Na, technology, problems (French) 3-67545
 Na, technology (French) 3-67546
 Na, turbulent transport properties for thermal design of LMFBR cores 3-46112
 Na boiling caused by local blockages, exptl. study 3-46095
 Na coolant temperatures meas. following local primary circuit blockage (German) 3-67491
 Na liquid coolant, thermal shock conditions rel. to fuel-element spacing (German) 3-67586
 Na systems, C activity meas. 3-63214
 Na vapour, effect of noncondensables on condensation rate from single rising HCDA bubble 3-46158
 Na void effect in SNR-300, absorber system criticality switching (German) 3-67473
 Na voiding effect in LMFBR, test of calcs. by approximate DB² method 3-71200
 Na-void coeffs. in LMFBR, analysis from direct k-calcs. 3-71201
 Nb, blistering due to D⁺ ions at 300 keV and above 3-40943
 Nb, dislocation loop, electron microscope image contrast, calc. 3-79361
 Nb, fast-neutron cross sections, optical model, reln. to fusion reactor design 3-71113
 Nb, He bubble formation and migration due to α -particle irradiation 3-52648
 Nb, He⁺ ion implantation and re-emission, temp. depend. 3-79394
 Nb, ion irradiation by ⁴He⁺ bubble and blister formation 3-79393
 Nb, neutron irradi. temp. effect on hardness 3-79387
 Nb, neutron total and scattering cross sections in continuum region 3-78331
 Nb, recovery after fast neutron irradiation at low temp. 3-68287
 Nb, solubility and diffusivity of H isotopes at high temps., reln. to CTR components 3-61161
 Nb alloys, surface blistering by He ions, effect in fusion reactor operation 3-60289
 Nb sputtering yields by D in keV range 3-60294
 Nb₂O, N⁺ irradi. effect of O impurity on void formation 3-79335
 Nb-Zr, solubility and diffusivity of H isotopes at high temps., reln. to CTR components 3-61161
 Nb-Zr (1 wt.%) alloy, high temp. props. characteriz. 3-64971
 Nb-Zr(1%), neutron irradi. temp. effect on hardness 3-79387
 Nb₃Sn multifilamentary composite wires, heat treatment effects on critical currents 3-60938
 Ni, ³He⁺ ion implant profiles, ³He(d,p)⁴He reaction 3-63209
 Ni, irradi. with Ni⁺ ions, swelling phenomena (French) 3-58053
 Ni, void form. due to bombardment with 100 keV Ni²⁺ ions (French) 3-40942
²³⁷Np purification using Amberlite XE-270 exchange resin 3-67577
 Pu, α = β transforms, cinematic obs. 3-47359
 Pu, β - α and γ - α transforms., quenching obs. 3-47360
 Pu, criticality studies, Dow Rocky Flats Nuclear Safety Laboratory 3-63229
 α -Pu, room temp. bend strength 3-54540
 Pu, self-irradiation damage obs. by positron annihilation 3-63194
 Pu-U mixtures, criticality safety, effect of Gd, B-containing Raschig rings 3-63228
 PuWC_{1.75} ternary phase, cryst. struct. and comp. 3-44649
²³⁹Pu, anisotropic scattering eff. in reflected fast critical assemblies, calc. 3-49328
²³⁹Pu, nitrate solutions, criticality studies, effect of acid molarity and ²⁴⁰Pu content 3-63230
²³⁹Pu, total and elastic scatt. neutron cross sections 3-60170
²⁴⁰Pu, anisotropic scattering eff. in reflected fast critical assemblies, calc. 3-49328
 SiC, pyrolytic, Cs migration 3-43296
 SiC, pyrolytic, fuel particle coating, h.v. transmission electron microscope obs. 3-49368
 β -SiC, pyrolytic, irradi. induced void behaviour 3-63191
 β -SiC, pyrolytic, neutron-irrad., thermal cond. 3-40539
 SiC, pyrolytic coatings of fuel particles, strength characteriz. 3-43311
 SiC, Si-bonded, fission fragment irradi. effect on passive oxidation, 950°C 3-67551
 SiC coatings for fuel particles, fabrication and performance 3-43300
 SiC fuel coating layer, microstructural changes at high temp., study 3-74723
 SiC tubes testing using u.s. 3-43314
 Ta, proton irradi., void form and hydrogen effects 3-46138
 Ta/Li high temp. heat pipes, corrosion mechanism 3-40543
 Th, fast neutron meas. ³He spectrometer 3-71157
 Th, isolation from ores, history, atomic energy programme 3-67560
 Th nuclear pure samples Cr traces spectrochemical determ. 3-70493

nuclear reactor materials continued

- Th-²³³U gas core breeder, analysis of configurations for MHD power generation 3-67440
- ThC₂Ni_{1-x} formation in ThN, graphite carbothermic reaction 3-74724
- Th(NO₃)₄, fast neutron meas. ³He spectrometer 3-71157
- ThO₂ powders, phys. props. and influence on sinterability 3-80402
- ThO₂:Ca²⁺(Y³⁺), optical absorpt. and fluoresc. 3-55678
- (U,Th)O₂ solid solns., elec. cond., 800-1200°C 3-67549
- U, criticality studies, Dow Rocky Flats Nuclear Safety Laboratory 3-63229
- U, high purity, high temp. plastic flow in α , β and γ phases 3-41772
- U, isolation from ores, history, atomic energy programme 3-67560
- U, warm working effects on mech. and fabrication props. 3-72904
- U adjusted, void nucleation behaviour 3-63192
- U admixture, periodicity of equil. coeffs. of distribution (*Russian*) 3-60282
- U alloys, thermomechanical testing under conditions of rapid fission heating 3-47531
- U in acid media, electrochem. behaviour, influence of V, Cr and C additions (*French*) 3-47561
- U/graphite system, neutron wave interference phenomena 3-60276
- U-Mo(10 wt.%) alloy, stress corrosion cracking, acoustic emission (*French*) 3-69404
- U-Nb(4.5 wt.%) alloy, Al-coated, stress corrosion cracking 3-47411
- U-Pu-N ternary system, equil. assessments 3-46136
- U-Se and U-Se-C systems, solid-state relationships 3-43299
- U-Ti(7 wt.%) alloy, texture 3-69228
- UC, fission-enhanced self-diffusion of uranium 3-71281
- UC, irradi., microprobe obs., precipitate distrib. (*German*) 3-57567
- UC-US system UC-rich solid soln., prep. procedure 3-63193
- UC + N₂ reaction, graphitization of precipitating free carbon 3-47553
- UC_x, actinide diffusion, phase boundary behaviour, high temp. 3-43298
- UC_x, bainitic transforms., carbide phase nomenclature 3-55836
- UF₆, partial pressure determ. from meas. on U radioactivity (*German*) 3-66462
- UF₆ conversion to ceramic grade UO₂ powder 3-57580
- UF₆C₂, standard free energy of form. from e.m.f. meas. (*Japanese*) 3-61125
- UN_x ($x > 1.75$), preparation and X-ray investigation (*German*) 3-50759
- U₂N₃, nonstoichiometry, statistical model for anal. of thermodynamic props. 3-68190
- UO₂, ¹²⁴Sb-Be (γ ,n) assay system, fissile content meas., ⁴He gas tube detectors 3-67557
- UO₂, diffusional creep, limitation by interfacial processes 3-80400
- UO₂, elec. resist., grain boundary effects 3-44648
- UO₂, fission-enhanced self-diffusion of uranium 3-71281
- UO₂, hyperstoichiometric single crystals., deform. model 3-55849
- UO₂, porous stoichiometric and hyperstoichiometric, thermal cond., 670-1270 K 3-43304
- UO₂, stoichiometric, primary creep 3-72949
- UO₂, stoichiometric, surface and interfacial props. 3-46137
- UO₂, surface fission tracks, replica electron microscopy obs. 3-63187
- UO₂ and U₃O₈, thermal cond., 100 to 300 K, phonon mean free path 3-40542
- UO₂ microspheres, compressibility determ., microscopy, struct. depend. 3-80424
- UO₂ powders, thermal precip. from sols 3-67555
- UO₂ solid layer, penetration by liq. Na jet, theory 3-80342
- UO₂-Na vapours, mechanism of explosive interactions 3-60284
- UO₂-SiO₂ system melts, spinodal decomp. and primary crystn. 3-72984
- U₃O₈, high-temp. phase transition, 300-800°C 3-64972
- U_{0.79}Pu_{0.21}C_{1.02}, compressive creep and hot hardness 3-61188
- U_{0.9}Pu_{0.1}C-W system, phase diagram obs. 3-47451
- U₃Si, polycryst., lattice parameters, counter-diffractometer parameter determ. 3-41802
- U₃Si interpretation of corrosion product, phases after in-reactor defect tests 3-74739
- UWC₂, standard free energy of form. from e.m.f. meas. (*Japanese*) 3-61125
- ²³⁵U, criticality research, Oak Ridge Critical Experiments Facility 3-63227
- ²³⁵U, anisotropic scattering eff. in reflected fast critical assemblies, calc. 3-49328
- ²³⁵U, crit. mass eval. using energy-depend. buckling concept. 3-60243
- ²³⁵U, criticality research, Oak Ridge Critical Experiments Facility 3-63227
- ²³⁵U and ²³³U, nitrate solutions, criticality studies, effect of acid molarity and ²⁴⁰Pu content 3-63230
- ²³⁸U, anisotropic scattering eff. in reflected fast critical assemblies, calc. 3-49328
- V, He⁺ ion implantation and re-emission, temp. depend. 3-79394
- V, ion irradiation by He⁺ bubble and blister formation, 3-79393
- V, recovery after fast neutron irradiation at low temp. 3-68287
- V, solubility and diffusivity of H isotopes at high temps., reln. to CTR components 3-61161
- V alloys, surface blistering by He ions, effect in fusion reactor operation 3-60289
- V:O neutron irradi., and radiation anneal hardening, recovery and temp. depend. 3-79383
- V-20% Ti alloys, surface blistering by He ions, effect in fusion reactor operation 3-60289
- V-base cladding materials with ceramic fuels, reactivity and compatibility studies 3-43288
- V-Ti, neutron irradi. effect on high temp. mech. props. 3-79385
- V-Ti alloys, neutron irradi., anneal hardening 3-79384
- W, W⁺ irradi. field ion microscope study of point defect struct. 3-79392
- Xe, spatial control in reln. to load changes, assessment of overload operation 3-49313
- Y₂O₃, zirconia-stabilized, fast neutron damage effects 3-78373

nuclear reactor materials continued

- Zr, diffusion of oxygen, using ¹⁸O(p, α)¹⁵N reaction (*Russian*) 3-58142
- Zr, elastic parameters of single crystals., oxygen effects 3-76204
- α -Zr, h.c.p., electron diffraction patterns 3-49872
- Zr, neutron irradi., resist. changes, recovery changes 3-69288
- Zr, total neutron cross section meas. for Zircaloy-2, ⁹⁰Zr 3-60285
- Zr alloys, neutron irradi., stress-relax. rel. to creep rates 3-40541
- Zr alloys, pressure tubes, creep, effect of neutron flux anisotropy rel. to stress directions 3-67565
- Zr alloys in molten salts, 300-500°C, current-voltage characteristics and oxidation rate 3-72918
- Zr and alloys, cold work and stress-relieving effect on irradi. growth behaviour 3-41773
- Zr and alloys, void formation under irradiation in high-voltage electron microscope 3-78387
- Zr and Zircaloy-2, oxidized, wear in water, characteriz. 3-57573
- Zr single crystals., compression parallel to c-axis, 78-1100 K 3-46659
- Zr-Cr-Nb, effect of heat treatment on tensile strength and hardness 3-61165
- Zr-H system, hydride precip., resistometric obs. 3-64875
- Zr-Nb (19 wt.%) alloy, transform. and age hardening behaviour 3-47412
- Zr-Nb alloy preparation by carbide-oxide reaction, nuclear reactor use 3-60279
- Zr-Nb alloys, carbide-oxide reaction prep. 3-72821
- Zr-O(8.5 at.%), fracture surface behaviour 3-47375
- ZrC, neutron irradi. effects, struct. and props. 3-73016
- ZrO₂, yttria-stabilized, fast neutron damage effects 3-78373
- nuclear reactor moderators** *see moderators*
- nuclear reactor operation**
- acoustic surveillance system for pressure boundary monitoring and rupture prevention 3-66156
- Advanced Test Reactor, available operating time improvement, instrument, component and maintenance modifications, personnel training 3-74695
- blowdown, simulation of loss-of-coolant accident in BWR 3-78369
- boiling reactors, effects neutron noise, and Langevin analysis of fluctuation 3-67391
- Brunswick Nuclear Plant, operator training programme 3-73644
- buckling of natural and Pu enriched elements, meas. from cooling-channel temp. coeff. (*German*) 3-67588
- BWR, after-cooler concept, optimisation and safety requirements (*German*) 3-71235
- BWR, burnout location on 16-rod 12-ft length bundle 3-67446
- BWR, fuel element cans, operational behaviour (*German*) 3-71242
- BWR, opening characteristics of balanced relief and safety valve, and half opening time (*German*) 3-74708
- BWR, surface rewetting in emergency core cooling, mass carryover fraction data 3-74667
- BWR, training simulator, computer controlled 3-52226
- BWR flooding technique for loss of coolant (*Japanese*) 3-74650
- BWR rod bundles, burnout prediction method, determ. of critical average steam quality 3-67447
- BWR simulation, Swedish training centre 3-52225
- BWRs at Dresden station, recent operating experience and startup 3-49317
- candidate selection and training 3-73629
- component reliability, registration system and experience (*French*) 3-67515
- condensation meas. by relief valve blow-off (*German*) 3-74710
- control rod drive computer application, problems, apparatus and program (*German*) 3-74706
- control rod effectiveness calc. in zero power operation using computer programs (*German*) 3-67478
- coolant activity and composition and fission-product filter efficiency determ. using monitoring loop (*German*) 3-67465
- coolant crossflow induction in a flat channel by wall fins 3-74669
- core elements handling, testing facility and manipulation sequences 3-43279
- core power distrib. smoothing by fuzzy automaton using search technique of control rod pattern 3-71160
- critical expt. evaluation with Cesar II using spherical low-enrichment fuel elements (*German*) 3-67488
- decontamination of plutonia contaminated thermal reactor systems 3-57589
- design basis accidents, loss of coolant, emergency core cooling system, evolution of technology 3-74677
- Dynamic Slug Impact Model, coolant-reactor vessel head impact, safety anal., MIMIC simulation 3-71176
- EBR-II, burnup and fluence history calc. using discrete ordinate transport code 3-52230
- EBR-II, correlation of primary coolant pump performance data, reln. to power level uncertainty 3-67448
- EBR-II, drop rod reactivity profiles, loading effects, reactor kinetics 3-71218
- EBR-II, evaluation with high burnup metal driver fuel Mark II 3-49312
- EBR-II, loading, startup and initial operation with stainless-steel reflector 3-46130
- EBR-II, noise anal., time-dependent fluctuations, reactivity transfer function, neutron detector power spectra 3-71215
- EBR-II, reactivity feedback analysis in steel-reflected loading 3-46131
- EBR-II, run-to-run variations in power distrib. 3-57561
- EBR-II feedback transfer function comparison for rod-drop and rod-oscillator experiments 3-57559
- emergency shutdown thermal behaviour in a water-cooled reactor (*German*) 3-67461
- energy release from severe excursions in fast reactors, eqn. of state of reactor fuel 3-63181
- fast, burn up meas., by determ. of relative concentrations of fission products (*German*) 3-71240
- fast, Na ejection in transition regime power redistribution (*French*) 3-67524
- fast breeder, core accidents, mechanical effects 3-67534
- fast breeder, safety and reliability, conference, Karlsruhe, Germany (1972) 3-67501
- fast breeder, safety and reliability, design engineering 3-67502

nuclear reactor operation continued

- fast breeder reactor, vibration of fuel element in sodium (*German*) 3-63123
- fast mixed-oxide fueled prototype reactor, effects of partial load and flow control on power coeffs. 3-71163
- fast oxide reactor, operating experience 3-67516
- fast reactor, friction factor for gas flow from defected fuel rods 3-67428
- fast reactor fuel elements, theoretical and expt. studies of melting (*German*) 3-67470
- fast reactor head cover, impulsive loading, coolant-slug-impact accident, nonlinear dynamic anal. 3-74673
- fast reactors, design basis accidents, loss of coolant, safety and containment provisions 3-71181
- fast reactors, selection of gas tag compositions for locating failed fuel elements 3-49361
- FBR, fissile isotope mixture determ. at various levels of burn up in fuel elements (*German*) 3-71312
- FBR, steady and cyclic operation, stresses in encasing tubes from fuel rod distortion (*German*) 3-67603
- FFTF fuel assembly, duct pressure response anal., stainless steel, ANSYS computer code 3-71293
- FFTF subassembly, potential for fuel failure propagation, fission gas release 3-71292
- fission product concentration in reactor coolant determ. using sapphire radiation monitoring loop (*German*) 3-67464
- fission product decay heat, γ -ray noise analysis (*Japanese*) 3-71167
- flow oscillations in core channel and occurrence of critical heat flux, computer analysis 3-67424
- FRG, primary pump shutdown, temp.-time behaviour in MTR type fuel elements (*German*) 3-74644
- fuel exchange, in service manipulating equipment tests (*German*) 3-71232
- fuel rod failure effects, obs. 3-67518
- fusion D-T, thermal instability and control of inhomogeneous plasma 3-75393
- gas-graphite and PWR in French Nuclear Power Program 3-46099
- GCFCR fuel elements, fuel-rod grid-spacer wear and fretting 3-67444
- GCFCR demonstration plant, response to depressurization accidents, computer program analysis 3-46106
- GCFCR plant using direct cycle, response to rapid loss of pressure due to duct rupture 3-46107
- GCFCR pressure equalization system, irradiation results 3-63171
- general discussion article 3-60273
- heavy water reactors, light water infiltration reactivity effects, Ames Laboratory Research Reactor, safety considerations 3-74736
- high burn-up conditions, prediction of fuel element performance from data on UO_2 - PuO_2 elements (*German*) 3-71310
- high temperature reactor, high pressure He gas test loop, electric heating (*Japanese*) 3-71166
- high-temperature gas-cooled reactor fuels, performance at peak irradiation 3-63204
- HTG reactor, tritium release during normal running and fault condition 3-67455
- HTGR, pyrolytic-graphite coated (U,Th) O_2 fuel particles, creep deformation, operational limits (*German*) 3-71314
- HTGR, Xe azimuthal oscillations, effect of temp. coupling (*German*) 3-67494
- HTGR design basis accidents, primary cooling system, depressurization 3-74678
- HTGR fuel performance, Peach Bottom Reactor testing 3-74735
- HWR, ZED-2, kinetics meas., coupled cores, U metal rods, square lattice 3-71210
- HWR-PHW line, construction and operation, Canadian Nuclear Power Program 3-46098
- hydraulic performance of San Onofre I, in-core determ. of engineering factor on enthalpy rise 3-67445
- hypothetical core disruptive accident, mech. energy yield, energy dissipation mechanism 3-74675
- instructors, selection and development guidelines 3-73647
- JMTR, application of on-line digital noise analysis to reactor diagnosis 3-71161
- kinetic tests on reactors using a cross-correlations method with pseudostochastic reactivity modulation (*German*) 3-67483
- LMFBR, ^{239}Pu fueled, post-shutdown fission product energy release calcs. 3-67441
- LMFBR, backup safety device, evaluation, poison rod insertion, coolant poisoning 3-74672
- LMFBR, Na, expanding vaporized coolant, simulation of mech. energy release, reactor energy source characterisations 3-74674
- LMFBR, Na-cooled obs. of dynamic relations using computer techniques (*German*) 3-67495
- LMFBR, on-line reactivity computer for detection of anomalous behaviour 3-67436
- LMFBR, potential failure of hexcan wrapper due to thermal stresses from local nonuniform temp. distrib. 3-46108
- LMFBR, prevention of local fault propagation arising from local cooling disturbances 3-46096
- LMFBR, reactor physics problems 3-71194
- LMFBR, response of subassembly duct wall to severe thermal loading during coolant boiling 3-46161
- LMFBR, sodium cooled, water leaks into sodium, monitoring 3-63148
- LMFBR, subcritical reactivity meas., survey of techniques 3-71207
- LMFBR fuel rods, failed, fission gas release rate, porous flow model 3-71291
- LMFBR large core-disruptive accident, PuO_2 aerosol release, transfer to second containment, calc. models 3-71178
- LMFBR radial blanket assemblies, design considerations for full-load operating conditions 3-67426
- LMFBR safety analysis, hexagonal fuel assembly response, effect of coolant STRAW dynamic finite element code 3-71294
- LMFBR subassembly, local flow starvation, fission gas release 3-74676
- load follow, Xe spatial control problems 3-49313
- loose parts, monitoring system design, operating experience 3-74698

nuclear reactor operation continued

- loss-of-coolant accident, emergency provisions, computer simulation and exptl. programs 3-71172
- LWR, construction and operation experience in Germany 3-4610
- LWR, pulsed anal. using REACT two point kinetic code 3-74644
- LWR's, operation and construction experience in Japan 3-46102
- Maine Yankee reactor, damping of Xe oscillations 3-74699
- Maine-Yankee Power Station, design, initial operation 3-74694
- Mannheim power reactor, modifications to circulating system, outlet pressure control 3-67459
- mixed core, TRIGA standard and TRIGA-FLIP fuels, performance testing 3-74737
- molten fuel-coolant interaction, damage to reactor structures, model REXCO-H code, containment anal. 3-71295
- molten fuel-coolant interaction, reduction of gas-expansion work, co-liquid, heat flow to liquid surfaces 3-71177
- multidimensional kinetic problems, diffusion theory, state-of-art 3-71151
- neutron noise analysis in reactor with two weakly coupled asymmetric fission zones (*German*) 3-67482
- noise anal. on single channel and single phase flow model 3-74648
- operator on-site systems training, cold licence AEC exam. 3-73644
- operator requalification, on-site systems training 3-73643
- operator selection and training 3-73628
- operator training, in-plant production of black and white video tapes 3-73649
- operator training, use of simulators 3-73648
- outlet valve malfunction and failure in Wurgassen BWR circulating system (*German*) 3-67460
- oxide fuel columns, in-reactor transient heating conditions, simulation 3-63203
- Oyster Creek Station, capability and operating experience 3-49315
- Penn State TRIGA reactor, subcooled boiling 3-49320
- personnel, training 3-52222
- pin-to-pin failure propagation, pressure pulse loading, fission gas release, buckling failure criterion 3-74732
- post-dryout heat transfer 3-71229
- power distrib. in core, on-line calculational method 3-43276
- power plant calorimetrics, energy release in fission, isotopic composition of spent fuel 3-54529
- power pulse variances, periodically pulsed 1 MW fast reactor 3-74662
- power ratio determ. of weakly coupled cores, period reactivity meas. fission rate meas. using Dy-Al-wires 3-63129
- power reaction, control of spatial Xe-induced oscillations 3-57555
- power reactor, large, optimal control of xenon instabilities (*German*) 3-67493
- preoperational, cold and hot tests on power plant at Wurgassen (*German*) 3-74717
- preoperational testing of Fort St. Vrain Unit No.1 3-49314
- pressure field, local pulsed, at blow-down in condenser chamber of pressure reduction system (*German*) 3-74709
- pressure vessel fracture and safety analysis 3-63133
- procedures, Brunswick Steam Electric Plant, emergency and fuel handling procedures 3-73641
- procedures, manual for plant safety 3-73639
- procedures, min. risk to health and safety 3-73638
- procedures, Pilgrim Station, plant safety 3-73640
- procedures, standards, personnel, safe and reliable plant operation 3-73642
- procedures, standards and experiences, conf., Myrtle Beach, South Carolina, USA (Aug 1973) 3-74691
- propagation of pressure and density in two-component two-phase system 3-71812
- PULSTAR reactor, North Carolina State University, delivery and operation, Quality Assurance Programme 3-74697
- PWR, combustion behaviour and influence of site-dependent water densities (*German*) 3-67480
- PWR, control procedures for spatial Xe oscillation, computer simulations and tests 3-46132
- PWR, dynamic response characteristics, core, steam generators, frequency response functions 3-71217
- PWR, effect of irregularities on fuel consumption, statistical model 3-43278
- PWR, integrated, safety considerations for after heat removal (*German*) 3-71234
- PWR, loss-of-coolant accident, computer calcs. and blowdown expts 3-60266
- PWR, reliability assessment of CNEN neutronic codes for Pu recycling 3-49362
- PWR, startup and early operating experience at Palisades Plant 3-49316
- PWR, throughput meas. using heat surge method, development of apparatus (*German*) 3-70507
- PWR fuel element assembly full scale mock-up, meas. temperature and heat-transfer coeff. (*German*) 3-67462
- PWR of Rochester Gas and Electric Corporation R.E. Ginna, unit no.1, criticality and commercial operation 3-49319
- PWR performance and selected experiences of Connecticut Yankee and Millstone I 3-49318
- PWR pressure vessel breach during blow-down phase using computer simulation (*German*) 3-71238
- PWR pressure vessels calc. hydrodynamic loading using computer model (*German*) 3-67492
- PWR simulation, Swedish training centre 3-52225
- PWR technology, progress, experience gained 3-74664
- Quad-Cities Station, operating experience 3-74693
- re-processing of fuels, input anal. and possibilities of verification (*German*) 3-67602
- reactivity, dynamic determ., computer control appl. (*Czech*) 3-60259
- reactivity, excess, determ. by meas. of prompt neutron decay constants (*German*) 3-63124
- reactivity estimation, time varying, using method of nonlinear filtering 3-74656
- reactivity unit conversion, dep. on reactor operating conditions, effective delayed neutron fraction 3-74640
- research reactor, experience with UAl₃ fuel 3-71296
- H.B. Robinson Unit No.2, Cycle 1 fuel performance, slightly enriched UO_2 3-74733

nuclear reactor operation continued

- H.B. Robinson Unit No.2, operating experience 3-74692
 H.B. Robinson Unit No.2, refuelling operations, maintenance, inspection and testing during shutdown 3-74734
 safety during scram system trip, obs. (*Russian*) 3-67514
 self-regulated damped power oscillations of the Health Physics Research Reactor 3-49321
 shaft seals in pressurized water, endurance tests 3-57562
 ship, seamen training 3-52224
 shock losses within channel flow induced by discontinuities in cross sectional area 3-63126
 shutdown, coolant thermo- and fluiddynamic behaviour calc. (*German*) 3-67463
 shutdown, mathematical model for prediction of fuel plate temps. 3-71224
 sneak circuit analysis, detection of latent circuit paths, unplanned modes of operation 3-74701
 SNR 300, reventing and exventing, operational data on associated activity (*German*) 3-74715
 SNR-300, emergency cooling system, special requirements (*German*) 3-71233
 spent fuel transportation risks, improved model 3-63165
 SPR II, fast burst reactor, control and burst generation, nonfissile external reflector element 3-71212
 steam condenser chamber failure, cause and countermeasures (*German*) 3-74707
 subcritical fast reactor, reactivity meas., Pu fuel, rod drop method 3-71208
 subcritical reactivity, detn., by pulsed source method when die-away is not purely exponential 3-49325
 temp. correlation meas. in flowing Na in a heated test section with SNR geometry (*German*) 3-67490
 thermal power reactors, construction and operating experience in Italy 3-46101
 thermal reactor transients, calc., testing computational models, quasistatic method 3-71209
 training, present state and future trends 3-52221
 training centre for operators, description 3-52223
 transient behaviour analysis fast neutron measuring channel with fission counter (*German*) 3-48518
 water reactors, safety-related occurrences, 1972 review 3-74700
 ZPR-9, FFTF Engineering Mock up Core, ^{238}U , Doppler reactivity, axial traverses, inverse kinetic techniques 3-71211
 ^{16}N power control system at FMRB 3-71227
 Na, initial expulsion in direct heated channel, ejection vel. and residual film 3-60258
 Na, liquid fires efficacy of aerosol suppressants and fast reactor containment (*German*) 3-67471
 Na coolant temperatures meas. following local primary circuit blockage (*German*) 3-67491
 Na void effect in SNR-300, absorber system criticality switching (*German*) 3-67473
 Na-cooled fast reactive, ebullition onset in laminar and boundary-layer flow (*German*) 3-67469
 Pu recycle fuelled reactors, behaviour of transient Xe concentration as function of core Pu fraction 3-49340
 Pu-fuelled fast reactor, calc. of maximal Na voiding effects using computer program (*German*) 3-67472
 ^{241}Pu fissile element cross section, influence on fast crit. assembly parameters 3-60277

nuclear reactor theory

- absorber rods, treatment for reactor with spherical elements using transport and diffusion programs (*German*) 3-67484
 AGR heterogeneous core calcs., determ. of dipole extrapolation lengths 3-71168
 arbitrary neutron spectrum, reactor equivalence by multisource synthesis 3-60255
 asymptotic, influence of anisotropy on critical buckling in decay of neutron pulses 3-74625
 axial fuel shuffling, for HTGR 3-63162
 benchmark tests and comparisons using ENDF/B Version III data 3-49358
 buckling, axisymmetric of shallow spherical shells and using finite element method 3-74647
 burn-up optimization, proof of equivalence relations using Pontryagin method 3-63130
 BWR, AEG core design using 8×8 fuel elements (*German*) 3-67476
 BWR, difference eqn. for diffusion calculation by semi-analytic method, coarse mesh model 3-71165
 BWR, Halden, on-line computer method for neutron flux distrib. control 3-46066
 BWR, two- and three-dimensional calcs. of superprompt critical excursion 3-46090
 BWR, variation of void fraction during exponential flow and power transients 3-74665
 BWR, with graded enrichment, Gd-poisoned rods in primary core design (*German*) 3-67477
 BWR coolant system fault anal. using DYSYS-STANDARD a modular simulation program (*German*) 3-67468
 BWR core varying hydrogen-to-metal ratio, computer-aided criticality study, various temps. and void conditions 3-49335
 BWR fuel assemblies containing Gd as burnable poison, burnup and transport codes 3-71203
 central worth discrepancy, correlation study, computer analysis 3-49359
 coolant, thermo- and fluiddynamic behaviour calc. during normal and emergency shutdown (*German*) 3-67463
 coolant crossflow induction in a flat channel by wall fins 3-74669
 creep buckling, non linear with random temp. variations 3-74671
 critical assemblies, effect of space-dependent fission matrices in transport calcs. 3-71221
 critical assemblies, multicell heterogeneity and errors due to standard unit cell treatment 3-71189
 critical reactors, variational estimates for integral parameters 3-74688
 criticality distrib. in group-collapsed neutron diffusion theory 3-49333
 criticality problem, optimum eigenvalue bounds for diffusion and transport theory 3-46051

nuclear reactor theory continued

- criticality problems, use Monte Carlo methods to determ. mean flux over small volume (*German*) 3-67388
 depletion of system containing lumped poison, few-group diffusion theory versus many-group S_n approx. 3-49332
 design engineering, computer aided instruction by conversational teaching programmes 3-62346
 design problems, buckling instability in tubes under internal and external flow 3-67452
 design problems for loop insert in sodium fast reactor 3-67451
 EBR II, anisotropic scattering calcs. for stainless steel reflector 3-46071
 EBR-II, optimisation of subassembly coolant flow rates to minimize thermal bowing effects 3-67449
 EBR-II neutron shield system, diffusion and transport theory calcs. for deep penetration spectra 3-74687
 elementary critical condition, exact analytical soln., by age-diffusion theory 3-54534
 ENDF/B data testing, MC², SDX comparison 3-63178
 fast, heat fuel assembly removal system failure (*Russian*) 3-67520
 fast, Na ejection in transition regime power redistribution (*French*) 3-67524
 fast breeder ^{238}U - ^{239}Pu reactors optimisation, cooperative games 3-52227
 fast breeder techniques, application to fusion blanket design 3-60321
 fast flux test facility, activated corrosion product radiation levels 3-63169
 fast flux test facility, fuel failure monitoring model 3-63168
 fast multizoned monodimensional, a calculation algorithm (*Rumanian*) 3-63151
 fast reactor calcs., eigenvalue and eigenvector problem (*Rumanian*) 3-49311
 fast reactor neutron spectrum and criticality calcs., inclusion of $^{238}\text{U}(n, \gamma n')$ cross section 3-43282
 fast reactor resonance cross-sections, calc. in resolved and unresolved energy regions 3-74659
 fast reactor subassemblies, local blockages 3-67522
 fast reactor ZPR-6 assemblies, resistivity calcs. using Karlsruhe methods and data 3-71183
 fast reactors, analogy between thermal diffusion and continuous slowing down of neutrons 3-49334
 fast reactors, application of perturbation theory for calc. of reactivity, Doppler effect, void coeffs. (*Czech*) 3-74651
 fast-neutron spectra, efficient generation of high-order anisotropic elastic matrices 3-49330
 fast-neutron spectrum critical assemblies, effect of $^{238}\text{U}(n, \gamma n')$ reaction 3-43283
 fault tree analysis, new approach, effect on reliability and safety analysis 3-46068
 FFTF core, calc. of neutronics characteristics using clean and LWR-grade Pu fuel 3-49371
 finite element analysis, nuclear reactor design, nuclear diffusion and transport calc. 3-63112
 fissile sample Doppler effects, effect of local flux distortions 3-49360
 fixed bed reactive, thermophysical characteristics anal. (*Russian*) 3-74703
 fuel tube, temp. field, with special boundary conditions 3-54538
 functional and technique estimations of time decay const. due to perturbations in steady state system 3-74658
 fusion-fission breeder, future potential in reln. to fuel shortage 3-60302
 GCFR, pressure drop for parallel flow through a roughened rod cluster 3-74666
 general discussion article 3-60273
 heat flow shape factors for hollow, regular polygonal prisms, determ. 3-74670
 heat transfer, evaluation of lumped parameter techniques 3-54533
 heat transfer and pressure loss for fuel elements with etched surfaces (*German*) 3-67489
 heterodyne digital filtering technique, power spectral density, coherence function anal. 3-78368
 heterogeneous fast reactor, neutron resonance absorption in complicated geometries 3-74654
 HTGR, Xe azimuthal oscillations, effect of temp. coupling (*German*) 3-67494
 importance function calc. and meas. using a compact uranium-zircon hydride core (*German*) 3-67475
 kinetics eqns., three-dimensional space dependent, soln. by semi-implicit method 3-60263
 large power reactor, spatial effects in reactivity determ. 3-71185
 least squares methods, non-linear, parameter estimation 3-78370
 LMFBR, analysis of Na-void coeffs. from direct k-calcs. 3-71201
 LMFBR, partially blocked subassembly, local boiling, modelling 3-67523
 LMFBR, test of approximate DB² method for calc. of Na voiding effect 3-71200
 LMFBR, ZPR-6 assembly 7, comparison of calc. and meas. reaction rate distrib. and fission integrals 3-71186
 LMFBR Doppler coeffs., transport effects, comparison of diffusion and transport codes 3-49329
 LMFBR dynamics, improved reactivity table model using variational estimates 3-49339
 LWR, pulse operation anal. using REACT two point kinetic code 3-74646
 LWR core simulator PRESTO, characteristics and performance 3-49364
 Markovian random process, number of neutrons, precursor nuclei and fuel temp. (*French*) 3-49309
 MINX, multigroup interpretation of nuclear cross sections 3-63177
 molten fuel-sodium interaction, modelling 3-67532
 monoenergetic critical problem in anisotropic linear neutron scattering for slab bounded by infinite reflectors 3-67385
 MSR, application of Pourbaix diagrams to molten fluoride systems (*Spanish*) 3-74645
 multigroup cross sections, MC²-2/SDX capability 3-63176
 multigroup cross sections, shielding factor method 3-63175
 multigroup kinetics eqns., one-dimensional, quasistatic approx. and piecewise polynomials 3-46062

nuclear reactor theory continued

- multigroup reactivity calcs. and central worth discrepancy, fine-structure effects 3-74684
- multilevel effects in unresolved resonance region 3-71114
- multimode reactor kinetics eqns. new soln. method by matrix inversion 3-54524
- multizonal fast, game theory for initial breeding optimization (*Rumanian*) 3-63152
- neutron and gamma flux determ. using Monte Carlo programs rel. to damage and heating (*German*) 3-67630
- neutron angular distribution data ENDF/B, efficient representation in multigroup processing codes 3-71220
- neutron cross sections and resonance integrals from ETOG and ETOT, advances in processing ENDF/B III libraries 3-74682
- neutron cross-section sets, characterization of uncertainties 3-74681
- neutron diffusion, finite element analysis in space energy and time domains 3-74655
- neutron diffusion coeffs. from perturbation flux distrib. in systems with anisotropies 3-49357
- neutron diffusion design and analysis using transport theory calcs. coeffs. 3-67387
- neutron diffusion eqn., one-dimensional, analysis using CAIN computer code 3-71158
- neutron diffusion eqn. soln. using finite elements and finite differences methods 3-67389
- neutron energy release parameters, multigroup neutron reactions cross sections, from ENDF/B, MACK 3-63179
- neutron flux calc. using synthesis of multidimensional coarse and fine mesh calc. (*German*) 3-67466
- neutron flux distribution rel. to cell system finiteness in axial direction 3-60252
- neutron flux distributions in rectangular lattice cells, soln. using numerical techniques 3-60244
- neutron group parameters in resonance region computation using program RESPU (*German*) 3-67390
- neutron multigroup calcs., probability table method 3-46056
- neutron noise, spatial correlation range in an infinite multiplying medium including effects of delayed neutrons 3-63128
- neutron noise analysis in reactor with two weakly coupled asymmetric fission zones (*German*) 3-67482
- neutron noise form CROCUS, analysis (*French*) 3-63180
- neutron physical parameters, uncertainties in prediction for SNR 300 and large breeder reactors (*German*) 3-67487
- neutron transport, reactor core calcs. using Monte Carlo methods, in three dimensional geometry (*German*) 3-74643
- neutron transport theory in boiling media 3-63107
- neutron wave propagation, reflector effect, multiplying medium 3-74661
- noise, spatial coupling of power reactor using coherence-lengths concept (*German*) 3-67481
- noise anal. on single channel and single phase flow model 3-74648
- noise analysis, maximum value of coherence function 3-71162
- noise neutron 3-63195
- non-uniform reactor systems, rigorous diffusion model for cell homogenization 3-40526
- optimisation of material distrib. in cores, using linear programming in an iterative method 3-74657
- optimisation study of fast N₂O₄ cooled power reactor 3-40533
- power pulse variances, periodically pulsed 1 MW fast reactor 3-74662
- prompt feedback reactor, stability with changes in eigenvalue 3-43280
- PWR, combustion behaviour and influence of site-dependent water densities (*German*) 3-67480
- PWR, test of CNEN neutronic codes for Ag-In-Cd control rods 3-74683
- reactivity, dynamic determ., computer control appl. (*Czech*) 3-60259
- reactivity, time varying estimation using method of nonlinear filtering 3-74656
- reactivity absolute, generalised source multiplication method 3-71213
- reactivity change calcs., generalized perturbation method, second-order term evaluation 3-60265
- reactivity changes calcs. using higher order perturbation method 3-60262
- reactivity coeffs., central, discrepancy between meas. and calc. values 3-74660
- reactivity due to cross-section perturbations, Monte Carlo calcs. 3-49331
- reflected, core reactivity determ., area-ratio method 3-71205
- relativistic reactor processes, optimal estimation technique 3-74663
- resonance self-shielding factors, atom density interpolation used with ABBN cross sections 3-49327
- rods, finite bundle, longitudinal laminar flow, asymmetric effects 3-60267
- rods, un baffled, turbulent longitudinal flow, heat transfer 3-60268
- sample worth analysis, group collapsing effect in perturbation theory 3-60257
- secondary fast reactor optimisation, mathematical game 3-54535
- shield design, application of second-order perturbation theory to sensitivity studies 3-74689
- shield weight optimization by perturbation method, computer program 3-74690
- shutdown, mathematical model for prediction of fuel plate temps. 3-71224
- space-dependent kinetics calcs., improved temporal truncation error 3-46065
- space-time dependent eqns., reduction of computer time using source projection methods 3-46067
- space-time kinetics, fully implicit matrix decomposition 3-46064
- sparse-time kinetics and heat flow problems, new numerical method 3-46063
- spring colliding with rigid body, solid viscosities and dynamic behaviour 3-60270
- subcritical assemblies, third order correlation function calc. (*German*) 3-71159
- thermal analysis, treatment of uncertainties by expanded method of correlated temperatures 3-46070

nuclear reactor theory continued

- thermal reactor dynamics, two-dimensional, comparison of quasistatic and direct methods 3-46061
 - THTR-300 run-in phase, calc. cycle for charging calc. in reactor with spherical fuel elements (*German*) 3-67485
 - transient sub-channel analysis of rod-bundle fuel elements 3-63151
 - transport and diffusion theory comparison from calc. of minimum critical mass 3-46050
 - two-phase mixing for annular flow in simulated rod bundle geometries 3-43281
 - two-phase pressure losses calc. by evaluation of two phase friction in fluid flow 3-74668
 - variable rod distribution rel. to thermohydraulic optimisation in fast neutron reactors (*German*) 3-67486
 - wall return neutron fluxes for high- and intermediate-energy cavity neutron sources, numerical study 3-57560
 - weighted L₁ space, application to reactor theory eigenvalue problems 3-63131
 - zero power operation, for determ. reactivity and rod-bank characteristics (*German*) 3-67478
 - zero-power Pu reactor-3, demonstration reactor benchmark, calculations for subcriticality expts. 3-49355
 - ZPPB/FTR-2, calc. of neutron flux distrib. and neutron reaction rates 3-74686
 - ZPR 6 assembly 7, cross section sensitivity studies using VARI-III variational program 3-74680
 - Na-cooled fast reactive, ebullition onset in laminar and boundary-layer flow (*German*) 3-67469
 - Na-cooled fast reactor calcs. using BRUST program, economics-power optimisation (*German*) 3-67467
 - Pu spherical metal assemblies, neutron importance, comparison of theory and expt. 3-71204
 - UO₂, fission gas swelling, long range migration, low temp. 3-63174
 - UO₂-Na interaction, demonstration by water-molten aluminium thermal interaction under impact conditions for pressures calc. 3-67530
- nuclear reactors**
- see also fusion reactors; nuclear power stations; nuclear reactor materials; nuclear reactor operation; nuclear reactor theory
 - accidents, study by chemical simulation experiments 3-67535
 - Advanced Test Reactor, available operating time improvement, instrument, component and maintenance modifications, personnel training 3-74695
 - AGR, gamma scanning meas. on irradiated fuel, for rating distribution determ. 3-43292
 - AGR heterogeneous core calcs., determ. of dipole extrapolation lengths 3-71168
 - air pollution, filters, NMC type, particulate collection, nuclear reactor airborne radioactive products, evaluation 3-67624
 - American Nuclear Society meeting, Chicago, USA, June 1973 3-63102
 - Annular Core Pulse, spectrum modification for LMFBR fuel pin transient studies 3-46078
 - 'Apsara' reactor, 25 keV neutron beam, filtered 3-73855
 - architectural engineering, codes and standards 3-63160
 - ATR, Japan critical expts. on cluster-type fuel lattices 3-71190
 - Babcock and Wilcox Test Reactor, decommissioning procedure 3-74696
 - boiling water and pressurized water power reactors, background noise for acoustic emission 3-59500
 - boiling water pressure tube reactor, CIRENE plant, digital simulation for hydrodynamic processes and core heat-up 3-67396
 - breeder, fuel elements with improved performance 3-52231
 - breeder, high power, design and layout of carbide fuel pins using SATURN-1 program (*German*) 3-67605
 - bubble emission, acoustic meas., instrumentation (*French*) 3-66151
 - BWR, AEG-Telefunken, basic design features (*German*) 3-71241
 - BWR, after-cooler concept, optimisation and safety requirements (*German*) 3-71235
 - BWR, blowdown expts. simulating loss of coolant accidents, computer analysis 3-78369
 - BWR, corrosion effects on pressure vessels, comparison with Na-cooled reactors 3-74719
 - BWR, development studies for increasing power level (*German*) 3-67497
 - BWR, effects of moisture content, and formation of zirconium hydride on fuel element damage (*German*) 3-67610
 - BWR, fuel rod defects, examination, effects of moisture content (*German*) 3-67611
 - BWR, fuel rod defects due to fission iodine in Zry-4 encasing tubes (*German*) 3-67612
 - BWR, integral control rod predictions 3-67412
 - BWR, opening characteristics of balanced relief and safety valve, and half opening time (*German*) 3-74708
 - BWR, safety vessel and reactor building development (*German*) 3-74716
 - BWR, single pin expulsion and reentry test 3-67417
 - BWR, surface wetting in emergency core cooling, expts. 3-74666
 - BWR, time and site dependent stress and deformation distr. of fuel cans variable power conditions (*German*) 3-67609
 - BWR, training simulator, computer controlled 3-52226
 - BWR, use of carbon steel, critical concentration of O₂ and Cl (*German*) 3-67594
 - BWR, variation of void fraction during exponential flow and power transients 3-74665
 - BWR, various types of Pu recycling, economic investigation (*German*) 3-67597
 - BWR at Nine Mile Point, survey of radiation levels and shielding 3-71340
 - BWR fuel elements, transfer functions under boiling conditions 3-46126
 - BWR system, study of radiation shielding in operational and shutdown conditions 3-71341
 - CANDU (Canada deuterium uranium) reactors, economics 3-7470
 - chemonuclear, low temp. fissionochemical loop, design and operation features 3-74649
 - CIRENE H.W.R., comparison with L.W.R. future development 3-63136

nuclear reactors continued

- CIRENE pressure tube H.W.R., R and D, comparison with other systems 3-63135
- coaxial-flow, gaseous core, model of dynamic behaviour 3-78371
- compact, meas. and calcs. on reflector side regulation using ITR critical plant (German) 3-67474
- complex radiation field, absorbed dose of gamma rays and neutrons by graphite, isothermal calorimeter meas. 3-63137
- component design, material technology, problems (French) 3-67545
- compressor, diaphragm, as auxiliary equipment in nuclear engineering 3-54532
- constrained bolt behaviour, reactor plug subjected to dynamic load, obs. 3-67537
- containments, safety margins in pressure-temperature transients calc. 3-46091
- control, artificial intelligence approach, heuristic programming, learning theory 3-71216
- control rod guide tube repair, in pressure vessel of KAHL research reactor (German) 3-71236
- control rods, reactivity equivalent, multivariable meas. 3-60256
- core, fuel loading patterns, charact., quantitative analysis 3-57552
- criticality, experimental determ. 3-67404
- criticality accidents, CRAC expt. 3-67407
- criticality safety, measurement requirements 3-67406
- criticality safety at pipe intersections for Pu nitrate solns. (German) 3-67543
- criticality safety control for fuel facilities in Japan (Japanese) 3-43277
- damage to structures, molten fuel-coolant interaction, model, REXCO-H code, containment anal. 3-71295
- design, teaching, role of standards 3-61971
- design and licensing, using EMERALD-NORMAL 3-63164
- design basis accidents, emergency core cooling system, evolution of technology 3-74677
- design basis accidents, evaluation 3-71180
- development, summary of recent work on quantitative representation of the economics (German) 3-67498
- dismantling of Elk River Reactor, radioactive operations 3-71339
- dosimetry, internal exposure, nuclear power station primary steam heat maintenance, whole body counting, urinalysis 3-70183
- dosimetry, secondary standard, WHO Regional Reference Centres 3-54555
- dynamic response of primary containment, calc. using hydrodynamic elastic-plastic computer code 3-46080
- Dynamic Slug Impact Model, coolant-reactor vessel head impact, safety anal., MIMIC simulation 3-71176
- EBOR reactor vessel, fatigue cracks, acoustic emission response 3-46059
- EBR, resonance scattering effects in reflector and structural-subassembly regions 3-74628
- EBR-II, correlation of mechanical noise with neutron noise, subassembly vibration meas. 3-67450
- EBR-II, drop rod reactivity profiles, loading effects, reactor kinetics 3-71218
- EBR-II, experimental subassemblies, radial position, axial effects on nuclear props., diffusion theory code 3-71219
- EBR-II, noise anal., time-dependent fluctuations, reactivity transfer function, neutron detector power spectra 3-71215
- EBR-II, physics-oriented design considerations for role as irradiation facility 3-71196
- EBR-II, thermal mixing in outlet plenum, exptl. study using hydraulic test facility 3-67431
- EBR-II dosimetry meas. analysis, irradiation environment and spectrum 3-52229
- EBR-II feedback transfer function comparison for rod-drop and rod-oscillator experiments 3-57559
- EBR-II Hydraulic Test Facility, design, construction and commissioning 3-46116
- EBR-II Hydraulic Test Facility, flow-modelling expts. 3-46115
- EBR-II hydraulic test facility, flow-modelling studies for homogeneous core loading 3-46117
- EBR-II radial reflector, analysis of hypothetical inlet flow blockages 3-46094
- electromagnetic pumps and flowmeters, for liquid metal control 3-43275
- ENDF/B-III, depleted U, fast neutron spectra, anal. and interpretation, ENDF/B-III data 3-71154
- engineered safety features, design, probability, statistical risk 3-71179
- engineering, conference, Karlsruhe, Germany (April 1973) 3-67384
- experiments in ZED-2 with Pu-enriched UO_2 fuel, booster effect on neutron density and reactivity 3-71226
- fact, subassembly accidents, pressure generation by water impact upon molten aluminium, modelling 3-67529
- fast, aseismic design, research and development in Japan 3-67511
- fast, calcs. for fission product poisoning, appl. to ^{238}U - ^{239}Pu oxide-fuelled LMFBR 3-49356
- fast, containment design, UK practice 3-67513
- fast, containment systems, dynamic response calc. 3-67536
- fast, core design, safety and reliability 3-67503
- fast, core design, safety and reliability 3-67517
- fast, core meltdown accident and vessel response, obs. 3-67621
- fast, core safety, research studies and experiments 3-67526
- fast, demonstration size, asymmetrically poisoned, flux tilting studies 3-49351
- fast, design basis accidents, loss of coolant, safety and containment provisions 3-71181
- fast, energy release limiting, Doppler coeff. effectiveness, obs. 3-67539
- fast, fuel element safety and endurance potential 3-43293
- fast, local failure in core, theoretical study (Russian) 3-67520
- fast, local fuel failure, simulation experiments 3-67521
- fast, molten lead interaction with water, obs. 3-67528
- fast, Na cooled, heat removal systems, design 3-67504
- fast, Na cooled, irradiated full element under accident conditions, obs. (French) 3-67616
- fast, Na cooled, steam generators for, design 3-67505
- fast, Na cooled, structural design criteria 3-67507

nuclear reactors continued

- fast, Na ejection in transition regime power redistribution, calc. and obs. (French) 3-67524
- fast, Na pool fire, sodium oxide and fission products, release functions 3-67540
- fast, neutron energy spectrum, many resonance approx. 3-43269
- fast, neutron spectrum generator, design and construction 3-52218
- fast, optimisation of material distrib. in cores, using iterative method 3-74657
- fast, safety against local blockages, calc. 3-67522
- fast, sodium cooled, internal pressures, response of fuel subassembly wrapper 3-46058
- fast, thermal interaction between liquid alumina and liquid sodium, obs. 3-67527
- fast, UO_2 -Na interaction, demonstration by water-molten aluminium thermal interaction under impact conditions for pressures calc. 3-67530
- fast breeder, design data from standard neutron spectrum facility $\Sigma\Sigma$ 3-49301
- fast breeder, evaluation of parfait blanket concept 3-67439
- fast breeder, financing, legislation (Dutch) 3-57551
- fast breeder, Japanese development 3-63143
- fast breeder, safety, critical excursion 3-67622
- fast breeder critical facilities, foil activation analysis for meas. of $^{238}\text{U}(n,\gamma)/^{239}\text{Pu}(n,f)$ reaction rate ratio 3-49347
- fast flux test facility, plugging temp. indicator, analysis 3-63172
- fast Na-cooled exptl. reactors, JOYO, guidelines for structural design 3-40530
- fast neutron, influence of sodium technology (French) 3-67546
- fast reactor design optimisation system with nonlinear programming method 3-57555
- fast reactor disassembly, autocatalysis 3-60264
- fast reactor disassembly accidents, fuel-coolant interaction evaluation 3-67533
- fast reactor disassembly analysis, space-energy-dependent, safety 3-46083
- fast reactor head cover, impulsive loading, coolant-slug-impact accident, nonlinear dynamic anal. 3-74673
- fast reactor overpower excursion, molten fuel/coolant dynamics, accident mitigation 3-71290
- fast reactor physics in France, review 3-49353
- fast reactor physics program in Japan, review of current status 3-49337
- fast reactor physics program in USA, review 3-49338
- fast reactor physics progression Federal Republic of Germany, review 3-49336
- fast reactor SNEAK assemblies, exptl. and theoretical results for reactivity 3-71188
- fast safety assessment, Bethe-Tait approximation 3-67538
- fast-breeder development in Holland, financing of (Dutch) 3-46057
- FBR, production of phase pure heavy duty fuels by the oxalate method (German) 3-67608
- FBR, role of Cs in corrosion of austenitic steel cladding of fuel elements (German) 3-71307
- FBR, sodium cooled, venting device for ceramic fuel elements 3-71285
- FBR fuel elements, larger diam. development, manufacture, processing and handling (German) 3-71309
- FFTF engineering mockup, structural material Doppler effect meas. 3-71184
- FFTF engineering mockup critical, ^{238}U Doppler reactivity mapping, calcs. and expts. 3-71191
- FFTF pipe chase streaming expt. to validate analytical methods for neutron flux calc. 3-71222
- FFTF subassembly, potential for fuel failure propagation, fission gas release 3-71292
- fissile detectors, for neutron spectrum measurement in L54 reactor 3-48528
- fission, laser isotope separation application 3-63156
- fission gas pressure measurement by null-balance pressure sensor 3-70294
- fission gases, rare, diffusion through fuel element cladding (German) 3-67393
- fission products from breeder reaction, atmospheric distrib. and safety measures 3-40551
- fixed bed, thermophysical characteristics anal. (Russian) 3-74703
- floating power plants for offshore siting 3-60260
- FRG, primary pump shutdown, temp.-time behaviour in MTR type fuel elements (German) 3-74644
- FTR, analysis of high ^{240}Pu zoned critical expts. in support of LWR-grade Pu utilization 3-71187
- FTR, Doppler effect prediction from SEFOR expts. 3-71202
- FTR, fuel pin enrichments and control rod loadings 3-71199
- FTR design, physics aspects including fuel enrichment parameters 3-71193
- FTR gas tag system, minimization of double-release problem 3-67427
- FTR power performance, analysis of engineering mockup critical expts. 3-49352
- FTR/EMC shielding expts., analysis of thermoluminescent dosimeter irradiations 3-71223
- FTR/LMFBR fuel assembly simulation, meas. of bare rod subchannel flow rates 3-67442
- fuel cladding tube, standard defect machining for test applic. (Japanese) 3-63132
- fuel element spacing, influence on contact wear and dynamic stresses in cladding 3-67398
- fuel element withdrawal equipment (German) 3-71245
- fuel flow monitor for the SNR 300 (German) 3-67500
- fuel movement visualization using fast neutron hodoscope in 7 pin loss of flow simulation 3-67419
- fusion, D-T, thermal instability and control of inhomogeneous plasma 3-75393
- fusion-fission hybrids, subcritical thermal fission blanket, neutronic characteristics 3-60274
- gamma ray spectrometry (French) 3-66330
- gas core breeder, analysis of configurations for MHD power generation 3-67440

nuclear reactors continued

- gas-cooled, alternate-stud-type artificial roughness, meas. of heat transfer and friction coeffs. 3-46104
- gas-cooled, merit index for heat transfer 3-57557
- gas-cooled, merit index for heat transfer 3-57558
- gas-cooled, radiative heat transfer by solid suspension laminar flow with radiating fluid 3-40529
- gas-cooled fast reactor design studies in Federal Republic of Germany 3-46103
- GCFBR, physics design problems affecting performance and economics 3-71197
- GCFR, heat transfer and fluid flow problems 3-46105
- GCFR, pressure drop for parallel flow through a roughened rod cluster 3-74666
- GCFR, tests of enhanced heat transfer surfaces 3-67443
- HBWR, self-powered, neutron detectors, long-term test 3-52233
- heat transfer from core to coolers, calc. 3-67512
- heat transfer in four-pin bundle, temperature noise of liquid sodium 3-67453
- heat transfer in heat pipes and thermosyphons 3-63155
- heating channel void fraction meas. by gamma-ray attenuation technique, channelling corrections 3-46127
- heavy water, CIRENE prototype, design features and safety performance 3-63134
- heavy water, lengthening of fuel pins during normal operation 3-46135
- heavy water, light water infiltration reactivity effects, Ames Laboratory Research Reactor, safety considerations 3-74736
- heavy water, recycled Pu fuel, technical and economic feasibility (German) 3-71316
- high flux reactors, manufacture, properties and irradiation behaviour of UAl_3 -Al fuel element plates (German) 3-71321
- high power, fuel reprocessing, waste problems (French) 3-40547
- high temperature, AVR fuel elements, post-irradiation studies (German) 3-67593
- highflow, and research reactors, development and construction review (Russian) 3-74702
- HTGR, ^{235}U fuels refabrication and production by a chemical precipitation process (German) 3-67607
- HTGR, electrolytic disintegration of irradiated and non-irradiated graphite, fuel reprocessing 3-71283
- HTGR, industrial production considerations for manufacture of (U/Th) O_2 pellets (German) 3-67591
- HTGR, pyrolytic-graphite fuel cans, U contamination (German) 3-67590
- HTGR, use of coated particle fuels (Japanese) 3-46134
- HTGR and GCFR, evolution 3-74721
- HTGR core reactivity, pulsed neutron experiments, computer simulation 3-71206
- HTGR D1305, Peach Bottom, fuel element activity profiles, ^{89}Sr , ^{90}Sr , ^{134}Cs , ^{137}Cs 3-74738
- HTGR design basis accidents, primary cooling system, depressurisation 3-74678
- HTGR lattice, ThO_2 - PuO_2 fueled, temp. dependence of conversion ratio 3-71171
- HTR, ^{14}C production and environmental contamination 3-71335
- HTR, emission of radioactive iodine, A=129-135, accumulation in Federal German Republic (German) 3-67631
- HTR, emission rate of free gaseous fission products in fuel specimens (German) 3-67596
- HTR, fuel reprocessing and refabrication, treatment of radioactive waste 3-71169
- HTR, He cooled, chemical reactions in primary circuit (German) 3-74718
- HTR, helium-cooled, transport of strontium in graphite (German) 3-71243
- HTR, irradiation expts. in coated fuel particles to check Walther's stress model (German) 3-71318
- HTR, steam for methane reforming, pilot plant study (German) 3-69495
- HTR cores, design with prismatic fuel elements 3-67457
- HTR experimental plant, discharge of radioactive material (German) 3-67632
- HTR fuel, evaluation of resonance absorption by Dragon method 3-67579
- HTR fuel bodies, quality assurance of free heavy metals 3-67581
- HTR fuel compacts, irradiated, corrosion experiments 3-67582
- HWBR, coherence length meas. rel. to spatial coupling of power reactor noise (German) 3-67481
- HWR, emission of radioactive iodine, A=129-135, accumulation in Federal German Republic (German) 3-67631
- HWR, replacement of natural U by highly enriched ^{235}U fuel (German) 3-71317
- HWR, ZED-2, kinetics meas., coupled cores, U metal rods, square lattice 3-71210
- H.W.R. and L.W.R. comparison, future prospects of CIRENE reactor 3-63136
- hybrid fission-fusion, energy balance and particle conservation eqns., numerical solns. 3-67392
- in-core fission chambers, gas-loss compensation 3-71182
- instrumentation for UK nuc. prog. 3-54531
- instrumentation systems, book 3-59617
- irradiated steel, reaction products identification by electron probe microanalysis and gamma-ray spectrometry 3-66447
- JOYO, fast Na-cooled exptl. reactor, guidelines for structural design 3-40530
- L54 reactor core centre, exptl. determ. of fast neutron spectrum, computer analysis 3-43274
- laminar flow, fully developed, in finite rod bundles arbitrary arrangement 3-46124
- lattices, bare and D_2O reflected space dependent neutron noise spectra rel. to detector efficiency 3-67399
- licensing, role of standards 3-63159
- light water, radioactive waste disposal, soln. 3-43294
- light water systems, automated u.s. in-service inspection 3-47503
- liquid metal cooling, thermal inlet computation program (German) 3-54527
- liquid metal fast breeder, coolant system decontamination studies 3-63170

nuclear reactors continued

- LMFBA, use of saturated liquid Na properties in fuel-coolant interaction analysis 3-46157
- LMFBR, 300 MWe, prototype SNR 300, design features (German) 3-67509
- LMFBR, 7-pin wire-wrap mixing expts., directional flow sweeping 3-46121
- LMFBR, accidental conditions, obs. 3-67525
- LMFBR, analytical study of source range monitoring system 3-67438
- LMFBR, application of Pajarito Dynamics Code to power transient study 3-46082
- LMFBR, backup safety device, evaluation, poison rod insertion, coolant poisoning 3-74672
- LMFBR, criterion for free-contact fragmentation in molten-fuel-coolant interaction 3-46092
- LMFBR, economic utilization of U, natural vs. depleted 3-67574
- LMFBR, effect of noncondensibles on rate of Na vapour condensation from single rising HCDA bubble 3-46158
- LMFBR, exptl. obs. of Na boiling caused by local blockages 3-46095
- LMFBR, fuel pin transient behaviour, obs. 3-67519
- LMFBR, geometrical optimisation of core-blanket system, performance characteristics 3-49349
- LMFBR, heat transfer system design, safety 3-67508
- LMFBR, in-vessel fission counters, effect of gas composition on gamma performance 3-45546
- LMFBR, initial voiding characts.-estimation 3-67416
- LMFBR, interrelationships between core design, reactor physics and safety 3-71198
- LMFBR, local molten fuel-coolant interaction, pressure pulse on subassembly wall 3-46073
- LMFBR, loop failure threshold expt. 3-67418
- LMFBR, loss-of-flow accidents, in-pile simulations 3-67420
- LMFBR, meas. and anal. of fast neutron spectra in Na 3-71153
- LMFBR, mixing model for temp. distrib. in wire-wrap fuel assembly 3-46120
- LMFBR, Na-cooled, anal. of fuel pin deformation under transient loading using computer program (German) 3-67604
- LMFBR, operation with fuel rod failures 3-67518
- LMFBR, oxide-fueled, heat transfer from boiling pools with internal heat generation 3-46118
- LMFBR, partially blocked subassembly, local boiling, modelling 3-67523
- LMFBR, pressure profile across fuel element assemblies (German) 3-67589
- LMFBR, safety related experiments 3-67516
- LMFBR, simulation of mech. energy release, reactor energy source characterisation 3-74674
- LMFBR, subcritical reactivity meas., survey of techniques 3-71207
- LMFBR, system for protection against local core malfunction 3-46097
- LMFBR, thermal-hydraulic channel arrangement in rod bundle 3-67432
- LMFBR, transient effects, minimisation 3-67506
- LMFBR, uncontrolled energy releases 3-67534
- LMFBR, unprotected overpower transients, simplified model of pre-disassembly phase including fuel movement 3-60269
- LMFBR, voided-core disassembly, fuel-coolant interactions 3-46075
- LMFBR, ZPR-6 assembly 7, comparison of calc. and meas. reaction rate distrib. and fission integrals 3-71186
- LMFBR 19-rod fuel assembly, edge-channel swirl flow, analysis using ORRIBLE code 3-46110
- LMFBR accident analysis, model for Na droplet combustion 3-46076
- LMFBR assemblies, exponential depleted U pile, neutron spectrum meas. 3-71155
- LMFBR control rod assemblies, hydraulic and scram dynamics analysis 3-67430
- LMFBR core design, reactor physics problems 3-71194
- LMFBR cores, turbulent transport properties for thermal design 3-46112
- LMFBR demonstration plant, subcritical worth meas. of simulated control rod banks 3-49348
- LMFBR demonstration plant benchmark control rod expts. 3-49350
- LMFBR design, improvement of physical techniques and calculations 3-71195
- LMFBR design considerations, performance and safety, review 3-71192
- LMFBR design parameters, ^{238}U neutron capture cross section 3-74576
- LMFBR design using ZPPR Assembly 2 demonstration model 3-74653
- LMFBR disassembly calcs. fuel-coolant interaction and differential motion effects 3-46074
- LMFBR fuel assemblies, dynamic expts. for heat transfer and mixing studies 3-46113
- LMFBR fuel assembly, heat removal by Na natural circulation 3-46114
- LMFBR fuel subassemblies, determ. of wrapper-can meltdown using THTB code 3-46079
- LMFBR fuel subassemblies, exptl. evaluation of fission-gas release under subsonic and near subsonic conditions 3-67429
- LMFBR fuel subassembly with wire-wrap spacers, exptl. determ. of subchannel coolant crossflow 3-46111
- LMFBR large core-disruptive accident, PuO_2 aerosol release, transfer to second containment, calc. models 3-71178
- LMFBR power temp. accident, fuel melting, shutdown mechanism, axial molten-fuel motion model 3-74731
- LMFBR safety analysis, hexagonal fuel assembly response, effect of coolant STRAW dynamic finite element code 3-71294
- LMFBR subassembly, local flow starvation, fission gas release 3-74676
- loose parts, monitoring system design, operating experience 3-74698
- loss-of-target accident, safety criteria 3-67421
- low energy excursions, reactor containment, implicit continuous Eulerian containment code 3-71175

nuclear reactors continued

- LWR, automatic coolant activity monitor based on Ge(Li) detector 3-67629
- LWR, Belgian Pu recycle programme, exptl. assessment of physics methods calcs. 3-49363
- LWR, catalyst performance for post loss-of-coolant accident recombiner applications 3-67423
- LWR, emission of radioactive iodine, A=129-135, accumulation in Federal German Republic (*German*) 3-67631
- LWR, pulse operation anal. using REACT two point kinetic code 3-74646
- LWR, radioactive wastes, storage, design (*French*) 3-46133
- LWR, steel pressure vessels in-service examination 3-67456
- LWR technology, opportunities for university research 3-63157
- LWTR design for LWR development (*German*) 3-67499
- Maine Yankee reactor, damping of Xe oscillations 3-74699
- Maine-Yankee Power Station, design, initial operation 3-74694
- MFBR, emission of radioactive iodine, A=129-135, accumulation in Federal German Republic (*German*) 3-67631
- minimum total mass reactor, calc. 3-40531
- molten fuel-coolant interactions, role of nucleation in vapor explosion 3-46077
- MSR, application of Pourbaix diagrams to molten fluoride systems (*Spanish*) 3-74645
- multizone fast breeder reactors, criticality studies 3-52228
- neutron emission-time effects in pulsed Na assembly 3-49297
- neutron population, fuel temp., apparatus for fluctuation meas., mean life time of neutrons, heat transfer coeff. (*French*) 3-49310
- neutron spectra, thermal space-dependent, meas. in small Be assemblies 3-49298
- neutron spectra of annular core pulse reactor cavity, calc. and measurement 3-49326
- nuclear installation, airborne effluents, WEERIE program 3-77297
- offshore, hydrogen as pollution free fuel, feasibility (*Dutch*) 3-40534
- operating experience, procedures and standards, conf., Myrtle Beach, South Carolina, USA (Aug 1973) 3-74691
- operator training, present state and future trends 3-52221
- Peach Bottom Reactor, test bed for HTGR fuel element demonstration tests 3-74735
- period meas., digital instrument 3-60254
- personnel, training 3-52222
- pipe break loads, design of structural supports 3-67435
- pipe break outside of containment, plant design safety evaluation 3-67433
- pipe rupture, analysis of effects 3-67434
- post-accident spray systems, corrosion of steel containment, additive system requirements 3-67425
- power, steam generators safety against sodium-water reaction 3-67615
- power and neutron flux meas. using gamma compensated pulsed ionisation chamber 3-45547
- power distribution in core, effect on external detectors (*German*) 3-71244
- power excursion calcs. using Pajarito Dynamics Code, appl. to Godiva, Kiwi-TNT and Snaptran expts. 3-46081
- power plant operator training centre, description 3-52223
- power reactor fuel element evolution, development strategies 3-60280
- power reactor stability subject to stochastic macroscopic parameter variation 3-74652
- pressure tank system, reliability analysis, totally automated probabilistic approach 3-46069
- pressure tube CIRENE prototype, stresses and strains in static-elastic conditions of core support 3-67395
- pressure vessel, proving tests, evaluation (*German*) 3-73113
- pressure vessel, transient heat transfer for boiling water, thermal stresses 3-63127
- pressure vessels, acoustic emission monitoring, proof tests 3-65062
- pressurised water reactors, Westinghouse, review of fuel designs 3-67566
- pressurized water reactor, Pu indifference value 3-67411
- pressurized water reactor, radioactive waste, activity conc. calc., primary to secondary leakage 3-52239
- prestressed cast iron reactor pressure vessel, construction principles 3-60287
- products, materials and services directory 3-39984
- PULSTAR reactor, North Carolina State University, delivery and operation, Quality Assurance Programme 3-74697
- PWR, conceptual in-vessel design for containment of molten core 3-67422
- PWR, control of boron concentration in coolant (*German*) 3-71326
- PWR, coolant loss, containment rupture, resulting I doses (*German*) 3-71345
- PWR, core response during LOCA resulting from fuel cladding failure 3-46087
- PWR, defects in Zry-encased fuel rods due to volatile fission-products (*German*) 3-67612
- PWR, dynamic response characteristics, core, steam generators, frequency response functions 3-71217
- PWR, exptl. determ. of post-LOCA steam relief 3-46088
- PWR, exptl. verification of temp. distrib. in primary shield during power operation 3-54536
- PWR, integrated, safety considerations for after heat removal (*German*) 3-71234
- PWR, noise analysis for in-service monitoring (*German*) 3-71230
- PWR, optimal use of recycled Pu as fuel (*German*) 3-67598
- PWR, radionuclide concs. in marine animals, monitoring sensitivity 3-74767
- PWR, shielding design and analysis methods 3-74685
- PWR, Siemens, exptl. verification of design calcs. (*German*) 3-67479
- PWR, study of dynamics by fluctuation and pseudorandom input analyses 3-46123
- PWR, thermohydraulic stability of steam generators (*German*) 3-71231
- PWR, throughput meas. using heat surge method, development of apparatus (*German*) 3-70507
- PWR core, three-dimensional kinetic analysis of reactivity insertion, necessity of protection-grade circuits 3-46089

nuclear reactors continued

- PWR determ. of emergency core coding carryout rate correlation by nonlinear programming 3-46086
- PWR protection system, effects of electrical underfrequency transients 3-46085
- PWR thermal design, new thermal-hydraulic code THINC-IV 3-46125
- Quad-Cities Station, operating experience 3-74693
- radiation monitoring, environmental radioactivity, International Reference Centre, activities 3-54554
- radioactive waste, site for ground disposal, migration of multiple nuclides 3-78393
- reactivity, spatially independent, meas. in pulsed-neutron expts. 3-67400
- reactivity monitoring system based on nonlinear filtering technique 3-67437
- reactivity unit conversion, dep. on reactor operating conditions, effective delayed neutron fraction 3-74640
- H.B. Robinson Unit No.2, Cycle 1 fuel performance, slightly enriched UO_2 3-74733
- H.B. Robinson Unit No.2, operating experience 3-74692
- H.B. Robinson Unit No.2, refuelling operations, maintenance, inspection and testing during shutdown 3-74734
- rocket solid propellant burning, effect of neutron irradi., safety analysis 3-49322
- rod-drop experiments, subcriticality determ., inverse kinetics technique 3-71214
- safety, quality assurance and in-service inspection 3-67401
- safety, stochastic decision making procedure 3-46084
- SEFOR cold trap, flow regulation problems 3-63173
- SEFOR Core II, flow oscillation expts., study of reactivity feedback and dynamics 3-49341
- shield analysis, radiation interaction with matter 3-60339
- shield attenuation calc. 3-60342
- shield design 3-60343
- shield design 3-60344
- shield design 3-60345
- shield design 3-60346
- shielding, advances, book 3-60337
- shielding, radiation sources 3-60338
- shielding analysis, Boltzmann transport eqn., soln. 3-60340
- shielding employing magnetite and serpentine 3-60332
- Siemens training reactor, absolute power calibration, real time correlator-spectrum display system 3-62196
- single phase flow model, noise source propagation, kinetic eqns. for neutrons, fuel and coolant temp. 3-71164
- SLOWPOKE, low-power cheap inherently safe laboratory reactor 3-70368
- SNR 300, cavitation and oscillation tests on a single stage radial pump (*German*) 3-74714
- SNR 300, reventing and exventing, operational data on associated activity (*German*) 3-74715
- SNR-300, design of loop concept reactor tank 3-40532
- SNR-300, emergency cooling system, special requirements (*German*) 3-71233
- SNR-300 bowing coeff., calculational capabilities of SCHWOW code 3-46109
- space-time kinetics expts., delayed-neutron holdback, test of diffusion codes 3-49344
- SPR II, fast burst reactor, control and burst generation, nonfissile external reflector element 3-71212
- standards, preparation, ANS role 3-63158
- standards, training 3-61958
- standards hierarchy and interrelationships 3-67380
- steam generators, safety, experimental study (*German*) 3-67510
- subassembly interchannel mixing program for heat transfer in wire-wrapped pin bundle 3-46119
- subcritical thermal reactor systems, pulsed-neutron expts., space-time diffusion theory 3-49324
- suboptimal control using low-order models 3-54528
- thermal, advanced type, Japanese development 3-63143
- thermal breeders, review 3-54537
- THTR, stressed concrete reactor pressure vessel, concept and layout (*German*) 3-74711
- THTR concrete stressed pressure vessels, construction techniques and design criteria (*German*) 3-74712
- transient heating is fuel element, meas. with intrinsic thermocouple, dynamic behaviour 3-45444
- transient non-boiling forced-convection heat transfer, effect of wall heat capacity 3-46417
- transport processes, error characterisation of analytic methods 3-71328
- TRIGA, numerical soln. of Poisson's heat eqn. by computer using finite difference techniques 3-63150
- u.s. inspection, LiNbO_3 piezoelec. transducer 3-65061
- void fraction, diabatic local, meas. using hot-wire anemometer 3-46128
- voiding, coherent detection methods, exptl. study 3-49342
- vortex sheet, continuous, rel. to development of in line instruments for monitoring UO_2 manufacture (*German*) 3-67606
- Walter Reed Reactor dismantling and defueling project 3-49323
- waste self-burial, utilising decay heat to melt rock 3-67415
- water cooled, γ -spectrometry supervision of coolant activity (*German*) 3-71327
- water cooled, review of two-phase flow instabilities 3-60569
- water moderated, tritium leak rate through steel, diffusion process theory (*German*) 3-71315
- water pollution effects, aquatic environment 3-77298
- water reactors, safety-related occurrences, 1972 review 3-74700
- water-cooled, accidental fission product release, ratio and amounts 3-74749
- weakly coupled TRIGA-type cores, exptl. study of large amplitude transients 3-49343
- world energy problems, nuclear solns., conference, Washington D.C., USA (Nov 1972) 3-46047
- WWR-SM type, Xe reactivity effects following power reductions 3-67394
- ZED-2 critical facility, ^{235}U booster rod expts., neutron spectrum parameters 3-49365

nuclear reactors continued

- zero power transfer function measurement, reactivity oscillation technique (*Portuguese*) 3-46060
 zero-power plutonium demonstration reactor benchmark program, critical configurations 3-49354
 zero-power Pu reactor, subcritical reactivity meas. using polarity coherence function technique 3-49346
 ZPPR Assembly 2, heterogeneity effects, data for LMFBR design 3-74653
 ZPR-9, FFTF Engineering Mock up Core, ^{238}U , Doppler reactivity, axial traverses, inverse kinetic techniques 3-71211
 B controlled, optimal Xe shutdown, application of Pontryagin's optimum theory 3-74642
 CO_2 cooled, effect of deposition of fission decay products on primary coolant surfaces, physical model (*German*) 3-67496
 ^3H production, French facilities (*French*) 3-57550
 ThO_2 -PuO $_2$ HTGR lattice, temp. dependence of infinite-medium neutron multiplication factor 3-49345
 ^{235}U enriched cores, meas. kinetic distortion effect to obtain spatial correction factor for the reactivity of system 3-67400

nuclear resonance reactions and scattering

- A=113-209, 15.1 MeV scattering of plane-polarised photons, giant resonance excitation 3-71102
 background cross section and correlation between partial widths, relation, shell model 3-54454
 cascade model, resonance production, nuclear reaction mechanism, 3-5 GeV (*Russian*) 3-78295
 compound nucleus decay involving analogue resonance, energy dependence of excitation curves 3-67293
 coupled channel resonating group calculations, effect of imaginary potentials on spurious resonances 3-78296
 deuteron emission from compound nucleus, resonance level width by expansion method 3-52157
 distorted wave theory of analogue states extended to include charge exchange channel 3-60203
 fast reactor calculations, cross-section calc., resolved and unresolved energy regions 3-74659
 fast reactors, neutron energy spectrum, many resonance approx. 3-43269
 fissile nuclei, partial widths of resonance levels, spin-dependent statistics 3-67376
 fission, rel. to reduced neutron widths, fissionable nuclei resonance levels 3-54512
 fractional-parentage coeffs. determ. from inelastic proton scatt. through analog reson. 3-63059
 giant electric and mag., excitation in inelastic electron scattering (*Czech*) 3-71103
 giant multipole resonant state of E2 character excited in various nuclei by ^3He scatt. 3-60202
 giant resonance damping in heavy and medium-heavy nuclei, thermalisation and cooling-off processes 3-71092
 giant resonance excitation of doubly closed shell nuclei, spin dependent effects 3-78297
 inelastic proton scattering, 30 MeV, target excitations and optical potential 3-49256
 inelastic proton scattering, polarisation effects, analysing capability reln. to reaction amplitude (*Russian*) 3-67318
 light nuclei, obs. of S-wave levels near threshold for tensor-polarised deuteron reaction 3-49261
 neutron, resonance integral with interference scattering calc. 3-74624
 neutron resonance decay following capture, Monte Carlo simulation, resonance spin determ. 3-57519
 neutron resonance energy meas. for calibration of time-of-flight spectrometer 3-60174
 nucleon transfer reactions, effect of fine structure in analogue states 3-74547
 off-shell correction to high-energy optical potential, resonance region 3-63022
 off-shell resonances, generalization of Breit-Wigner formula rel. to R-matrix theory 3-63024
 photoneutron giant resonance data 3-57510
 photoneutron giant resonance energy, role of proton-neutron polarisation in models for atomic mass dependence 3-74546
 pion-nucleus scattering in (3,3) resonance region, many-body formulation 3-54509
 resonance scattering effects in reflector and structural-subassembly regions of an EBR 3-74628
 resonant-particle production, coincidence meas. between decay products, spectroscopic tool 3-52156
 resonating group treatment of composite particle scattering, extension to heavy system 3-74602
 shell model approach to the correlation between photon and particle widths of compound resonances 3-60144
 three-body system, effective range approximation, energy spectrum 3-78300
 transfer reactions between heavy nuclei, Q-value dependence of cross section (*German*) 3-49275
 (d,p) sub-Coulomb stripping and analog-resonance results near closed shells 3-67342
 (p,p'), M2-E1 mixing ratios, effect of overlapping resons. 3-63036
 (n, p), 5-300 keV neutron capture, data table of γ -ray spectra 3-74580
 n induced reactions, fast, resonance interference effects using Hauser-Feshbach-Moldauer formalism 3-71107
 $^{62}\text{Ni}(p,p)^{62}\text{Ni}$, isobaric analogue resonances, double-scattering techniques, polarisation study, 2.43-2.75 MeV 3-63045
 π elastic and resonance scattering in isobar-doorway model 3-43258
 π -induced, low energy, intranuclear cascade studies, (3,3) isobar finite lifetime effects 3-67372
 π -nucleus scattering in 3,3 resonance region, exclusion principle effects 3-54508
 π -nucleus scattering in (3,3) resonance region using dynamically modified optical potential 3-67370
 π^+ photoproduction and T_+ versus T_- analogue states in $N > Z$ nuclei 3-57508
 $^{55}\text{Mn}(p,p)^{55}\text{Mn}$, isobaric analog reson. obs. 3-67317
 ^{27}Al , resonance scattering of bremsstrahlung, low-lying level study 3-52094

nuclear resonance reactions and scattering continued

- $^{27}\text{Al}(p,\alpha)^{24}\text{Mg}$, 0.633, 0.731, 0.937, 1.183 MeV, meas. of single crystal blocking effect, determ. of reaction time 3-52186
 $^{27}\text{Al}(p,\gamma)$, $E_p = 1.9$ -3.1 MeV, γ radiations, reson. intensities (*French*) 3-78317
 $^{27}\text{Al}(p,\gamma)^{28}\text{Si}$, for twenty three resonances, 2100-3100 keV (*French*) 3-49251
 $^{27}\text{Al}(p,\gamma)^{28}\text{Si}$, search for 6 $^-$ analogue-antianalogue states and subsequent γ decay 3-57476
 ^{241}Am , thermal neutron capture cross sections and capture resonance integrals for ^{242m}Am , ^{242s}Am production 3-43242
 $^{36}\text{Ar}(d,p)^{37}\text{Ar}$ neutron reson. ^{37}Ar , DWBA anal. 3-54492
 $^{38}\text{Ar}(d,p)^{39}\text{Ar}$ neutron reson. ^{39}Ar , DWBA anal. 3-54492
 $^{197}\text{Au}(^3\text{He}, ^3\text{He}')$, cross section analysis, obs. of new giant resonance 3-63077
 $^{10}\text{B}(\alpha,\alpha)^{10}\text{B}$, 2.0-4.3 MeV, obs. of level structure in ^{10}N , excitation functions and α -particle decay 3-71055
 ^{11}B , resonance scattering of bremsstrahlung, low-lying level study 3-52094
 $^{11}\text{B}(d,\gamma)^{12}\text{C}$, $E = 1$ -4 MeV, cross sections, ^{13}C deduced resonances 3-67341
 $^{11}\text{B}(p,\alpha\alpha)$, 2.0 and 2.65 MeV, α -particle coincidence spectra, calc. of resonant peak positions (*Russian*) 3-74567
 $^9\text{Be}(\alpha,\alpha)^9\text{Be}$, 1.7-6.2 MeV, excitation functions and angular distrib., compound-nucleus theory, ^{13}C states 3-63075
 $^9\text{Be}(p,\alpha)$, 30-700 keV, meas. cross sections, R matrix compound nucleus model, ^{10}B deduced resonance parameters 3-60181
 $^9\text{Be}(p,d)$, 30-700 keV, cross section and angular distrib. meas., ^{10}B resonance parameters 3-60181
 ^{210}Bi , neutron resonance, particle-vibration calc. 3-78267
 ^{12}C , charged pion photoproduction with excitation of ^{12}B , ^{12}N analogue states 3-49240
 ^{12}C , decay of photo resonances, shell model analysis, cross sections and branching ratios 3-49239
 ^{12}C , giant dipole states and excited dipole states in continuum approx., (p,N) and (N,p) reaction 3-67193
 ^{12}C , photoneuclear reaction process in giant dipole reson. region in collective correl. model 3-52171
 ^{12}C continuum states in giant dipole reson. region, collective correl. 3-43229
 $^{12}\text{C} + ^{16}\text{O} \rightarrow ^{28}\text{Si}$ reson., persistence in $^{13}\text{C}(^{16}\text{O}, ^{17}\text{O})^{12}\text{C}$ 3-54500
 $^{12}\text{C}(^{12}\text{C}, \alpha)^{20}\text{Ne}$, low energy, intermediate reson. struct. 3-40511
 $^{12}\text{C}(^{12}\text{C}, p)^{23}\text{Na}$, low energy, intermediate reson. struct. 3-40511
 $^{12}\text{C}(d,p)$, to ^{13}C unbound states, comparison with DWBA theory 3-54488
 $^{12}\text{C}(d,p)^{13}\text{C}$, determ. of angular distrib. of protons near resonances by shape-studies of γ -ray lines 3-40501
 $^{12}\text{C}(n,n)^{12}\text{C}$ R-matrix theories, two level, rel. to closely spaced resonance levels in a single channel 3-60145
 $^{12}\text{C}(\pi^+, \pi^- n + \pi^+ p)$ at (3/2,3/2) resonance, meas. absolute cross section 3-60225
 ^{13}C , from $^{12}\text{C}(d,p)^{13}\text{C}$ and neutron scattering on ^{12}C , application of real Weinberg state method 3-57471
 $^{13}\text{C}(d,\gamma)^{14}\text{N}$, $E = 1$ -4 MeV, cross sections, ^{15}N deduced resonances 3-67341
 ^{14}C , deuteron elastic scatt., 4.5 MeV, optical model anal. 3-78343
 $^{14}\text{C}(p,\gamma)^{15}\text{N}$, cross section meas. 7.7-12.0 MeV, resonance structure and energy level determ. 3-49255
 ^{15}C continuum shell model calcs. 3-54401
 ^{40}Ca , inelastic proton scatt., ^{41}Sc doorway state struct. 3-78319
 $^{40}\text{Ca}(p,p)$, 3.35 MeV state population through reson. in ^{41}Sc compound nucleus 3-60117
 $^{44}\text{Ca}(p,\gamma)^{45}\text{Sc}$, 1.24 to 1.27 MeV, determ. isobaric analogue of lowest 3/2 $^-$ state of ^{45}Ca 3-67195
 $^{44}\text{Ca}(p,\gamma)^{44}\text{Ca}$, 1.24 to 1.27 MeV, determ. isobaric analogue of lowest 3/2 $^-$ state of ^{45}Ca 3-67195
 $^{48}\text{Ca}(p,\gamma)^{49}\text{Sc}$, M1 transition strength from 3/2 $^-$ isobaric analogue state 3-54420
 $^{48}\text{Ca}(p,\gamma)^{49}\text{Sc}$, spin-parity of ^{49}Sc levels from 3/2 $^-$ isobaric analogue state γ -decay 3-54377
 Ce, inelastic scatt. of 50 and 65 MeV electrons, giant resons. total and groundstate radiative widths (*German*) 3-46021
 $^{35}\text{Cl}(p,\gamma)^{36}\text{Ar}$, $E_p = 0.8$ -2.6 MeV, angular distributions of γ -ray transitions 3-71078
 $^{54}\text{Cr}(p,p)$, (p,p,p), (p,p), 1.98-2.02 MeV, multichannel study of ^{55}Mn isobaric analogue resonances 3-52133
 $^{65}\text{Cu}(p,n)^{65}\text{Zn}$, narrow reson. 148 eV above threshold 3-43248
 $^{19}\text{F}(\alpha,n)$, high resolution study near neutron threshold, resonance obs. 3-46037
 $^{19}\text{F}(\alpha,p)$, high resolution study near neutron threshold, resonance obs. 3-46037
 ^{56}Fe , intermediate structure in neutron scattering cross sections 3-60177
 $^{56}\text{Fe}(n,n)$ meas. absolute differential cross section near thresholds 3-71101
 ^{19}F , neutron radiative capture below 1500 keV, single-level resonance parameters 3-63052
 ^{69}Ga , energy level obs. using photoexcitation, elastic and inelastic, resonance decays at 7306, 6874 keV 3-62948
 ^{157}Gd , nonstatistical effects in γ -ray spectra emitted in decays of neutron resonances (*Russian*) 3-52181
 ^2H , pion induced near $\Delta(1236)$ resonance energy region 3-78177
 $^2\text{H} + ^3\text{H}$, study by one-channel resonating-group method, phase shift and cross section determ. 3-74556
 $^2\text{H} + ^3\text{He}$, study by one-channel resonating-group method, phase shift and cross section determ. 3-74556
 $^3\text{H}(^2\text{He},p)^6\text{Li}$, obs. of direct and resonant capture 3-78308
 ^3He , π^+ photoproduction in first π -N resonance region, impulse approx., cross section 3-67300
 $^4\text{He}(p,p)^3\text{H}$ and $^4\text{He}(p,n)^3\text{He}$ cross section ratio in giant resonance region, charge symmetry 3-52160
 ^{177}Hf , nonstatistical effects in γ -ray spectra emitted in decays of neutron resonances (*Russian*) 3-52181
 ^{165}Ho , resonant scattering of gamma-rays, determ. of 94.69 keV level lifetime (*Russian*) 3-52168
 In, neutron resonance energy, determ. of ^{252}Cf fission neutron age in water 3-71297
 La, inelastic scatt. of 50 and 65 MeV electrons, giant resons. total and groundstate radiative widths (*German*) 3-46021

nuclear resonance reactions and scattering continued

- ⁶Li, resonance scattering of bremsstrahlung, low-lying level study 3-52094
- ⁷Li(p,p)⁷Li, 0.4-2.5 MeV, polarisation and phase shift analysis, resonances and ⁸Be level structure 3-46025
- ⁵⁵Mn(p, γ)⁵⁶Fe, ⁵⁶Mn isobaric analogue states in ⁵⁶Fe compound nucleus 3-54421
- ⁵⁵Mn(p, n)⁵⁶Fe, ⁵⁶Mn isobaric analogue states in ⁵⁶Fe compound nucleus 3-54421
- ⁵⁵Mn(p, γ)⁵⁶Fe, isobaric analogue state of ⁵⁶Mn 0.211 MeV level 3-60168
- ⁵⁵Mn(p, γ)⁵⁶Fe, isobaric analog reson. obs. 3-67317
- ⁵⁵Mn(p, γ)⁵⁵Mn, isobaric analogue state of ⁵⁶Mn 0.211 MeV level 3-60168
- ⁹²Mo, neutron reson. parameter 3-40495
- ⁹²Mo(³He, d)⁹³Tc^a, 30.2 MeV, stripping to analogue resons. using complex energy eigenstates 3-63081
- ⁹²Mo(d, n), DWBA anal. of analogue states, effect of fine structure 3-74547
- ⁹²Mo(n, γ)⁹³Mo, γ spectra, giant reson., partial radiation widths, E1 and M1 transitions 3-63058
- ⁹²Mo(p, γ)⁹²Mo, 4.3 and 5.3 MeV, obs. of fine structure in analogue resonances, s1/2 and d5/2 states (*German*) 3-49249
- ⁹⁴Mo(p, n)⁹⁴Tc, obs. excited states ⁹⁴Tc, using neutron and gamma ray yields at isobaric analog. resonances 3-67207
- ¹⁴N, decay of photo resonances, shell model analysis, cross sections and branching ratios 3-49239
- ¹⁵N(d, p)¹⁶N(unbounded), off shell behaviour rel to R-matrix theory 3-63065
- ²³Na(p, γ)²⁴Mg, ²⁴Mg 4.235 MeV level, gamma transitions, branching ratio meas. 3-40439
- ²³Na(p, γ)²⁴Mg, 3905 keV, lowest T=2 level, γ branching ratios 3-78285
- ⁹³Nb(n, γ)⁹⁴Nb, E_g=30-100 eV, channel spin components of p-wave neutron widths 3-60192
- ¹⁴²Nd(p, p'), neutron particle-hole states population on analog reson. 3-67325
- ¹⁴⁶Nd(n, p)¹⁴⁷Nd, activation resonance integral meas. 3-54467
- ¹⁴⁸Nd(n, p)¹⁴⁹Nd, activation resonance integral meas. 3-54467
- ¹⁵⁰Nd(n, p)¹⁵¹Nd, activation resonance integral meas. 3-54467
- ²²Ne(p, $\gamma_0 + \gamma_1$)²³Na, rel. to electric dipole strength splitting in ²³Na, giant resonance region 3-63054
- ²²Ne(p, n), high resolution study near neutron threshold, resonance obs. 3-46037
- ²²Ne(p, γ), high resolution study near neutron threshold, resonance obs. 3-46037
- Ni, elastic and inelastic scattering of Fe capture gamma-rays, obs. of resonant levels 3-49241
- Ni(³He, t)Cu, excitation of 2⁺ analogues in Cu isotopes, DWBA analysis, second-order effects 3-49271
- ⁵⁸Ni(p, p')⁵⁸Ni, E_p=60 MeV polarized protons, giant reson. excitation 3-74584
- ⁶⁰Ni photoabsorption, dynamic deformability, reln. to intermediate structure of giant resonance (*Russian*) 3-74562
- ⁶⁰Ni(e, e'), quadrupole and giant dipole resonance excitation, form factors, characteristics (*Russian*) 3-71104
- ⁶⁰Ni(p, n), meas. absolute differential cross section near thresholds 3-71101
- ⁶⁰Ni(p, γ)⁶¹Cu, 1.5-1.9 MeV, obs. of analogue states in ⁶¹Cu 3-46001
- ¹⁶O, coexistence model for structure of giant dipole resonance, exptl. test 3-49230
- ¹⁶O(d, p) to ¹⁷O unbound states, comparison with DWBA theory 3-54488
- ¹⁶O(n, n)¹⁶O R-matrix theories, two level, rel. to closely spaced resonance levels in a single channel 3-60145
- ¹⁶O(p, pp)¹⁵N, giant multipole resons. L=1,2 and 3, excitation 3-54484
- ¹⁶O(π^- , π^-)¹⁶O, total and differential cross sections in 3-3 resonance region, optical potential calcs. 3-63090
- ¹⁶O(t, t), 1.4-3.7 MeV, analysed using Humblet-Rosenfield theory, ¹⁹F deduced levels 3-60200
- ¹⁸O(p, n)¹⁸F, E_p=4.6 to 6.6 MeV, reson. investigation 3-54485
- ³¹P, photoprotons in giant resonance region, (γ , p₀), (γ , p₁) reactions 3-54458
- ³¹P(γ , p₀)³⁰Si, photoprotons in giant resonance region, for ³¹P 3-54458
- ³¹P(p, α)²⁸Si, ³²S analogue reson. study, spin, parity, widths, 1240-1600 keV (*French*) 3-78299
- ³¹P(p, γ)³²S, lowest T=2 state of ³²S characteriz. 3-60190
- ³¹P(p, γ)³²S, strength determ., γ -ray schemes, spin, parity, 1240-1600 keV (*French*) 3-78299
- ³¹P(p, p)³¹P, proton orbital momenta, spin, parity, ³²S analogue reson., 1240-1600 keV (*French*) 3-78299
- Pb, elastic and inelastic scattering of Fe capture gamma-rays, obs. of resonant levels 3-49241
- Pb(³He, xn + γ), E=28-30 MeV, stroboscopic resonance method, g-factors for Po isotopes 3-71041
- ²⁰⁷Pb proton elastic and inelastic scattering, 11.1-14.4 MeV, decay amplitudes of ²⁰⁸Pb(0⁺) analogue resonance 3-49253
- ²⁰⁸Pb, electroexcitation of giant resonances 3-43236
- ²⁰⁸Pb, neutron resonance, particle-vibration calc. 3-78267
- ²⁰⁸Pb 11 MeV giant reson., quadrupole assignment 3-63025
- ²⁰⁸Pb photoabsorption, dynamic deformability, reln. to intermediate structure of giant resonance (*Russian*) 3-74562
- ²⁰⁸Pb(³He, ³He), 75 MeV, cross section analysis, obs. of new giant resonance 3-63077
- ²⁰⁸Pb(α , α'), 90 MeV, cross section analysis, obs. of new giant resonance 3-63077
- Pb(α , xn + γ), E=25-29 MeV, stroboscopic resonance method, g-factors for Po isotopes 3-71041
- Pr, inelastic scatt. of 50 and 65 MeV electrons, giant resons. total and groundstate radiative widths (*German*) 3-46021
- ²³⁸Pu, neutron capture cross-section, resonance parameters, γ -ray emission 3-74578
- ²³⁹Pu, multilevel effects in unresolved resonance region 3-71114
- ²³⁹Pu(n, f), ternary to binary fission ratio meas., 0.02 to 50 eV 3-78361
- ²⁴²Pu(n, γ), 20-1300 eV, cross-section meas., determ. of resonance parameters 3-49258

nuclear resonance reactions and scattering continued

- ²⁴²Pu(n, n), 20-1300 eV, cross-section meas., determ. of resonance parameters 3-49258
- ³²S(γ , p₀)³¹P, photoprotons in giant resonance region, for ³¹P 3-54458
- ³²S(p, γ)³⁴Cl, ³⁴Cl nuclear levels investigation 3-52102
- ³²S(p, γ)³²Cl, gamma ray transitions and lifetimes in ³²Cl 3-43214
- ⁴⁶Sc(p, p), 1.6 to 1.8 MeV, fit of analogue resonances in ⁴⁶Ti compound nucleus 3-63023
- ²⁸Si(p, γ)²⁹P, study of ²⁹P levels up to 4.76 MeV 3-49144
- ²⁹Si, elastic and inelastic proton scatt., E_p=2.5-3.4 MeV 3-60191
- Si(p, p)Si, 17-29 MeV, analysing powers and cross sections in ²⁹P giant resonance region, optical model analysis 3-67327
- ¹⁴⁴Sm(p, p'), reaction on analogue resonances, 9.3-11.0 MeV, ¹⁴⁴Sm deduced levels 3-63046
- ¹⁴⁷Sm, nonstatistical effects in γ -ray spectra emitted in decays of neutron resonances (*Russian*) 3-52181
- ⁸⁸Sr(d, np)⁸⁸Sr, cross section meas. at 170° for 7.5 to 10.0 MeV deuterons 3-49268
- ⁸⁹Sr, neutron escape from isobaric analogue resonance, proton induced Coulomb mixing corrections 3-78298
- ¹⁶⁹Tm(n, γ), resonance parameters and capture cross section from neutron time-of-flight meas. 3-49260
- ²³⁵U fission, low-energy neutron induced, resonance parameters and cross-sections 3-49293
- ²³⁵U, multilevel effects in unresolved resonance region 3-71114
- ²³⁵U, neutron-induced fission, spin determ. of resons. 3-74614
- ²³⁵U fission, low-energy neutron induced, resonance parameters and cross-sections 3-49293
- ²³⁵U(n, f) yield, contributions of neutron multiplicity 3-63091
- ²³⁵U(n, γ)²³⁶U, meas. capture gamma rays to determ. ²³⁶U level structure, and spin 3-67335
- ²³⁸U, nucl. Raman effect, giant dipole reson. parameters 3-40480
- ⁵¹V(γ , γ)⁵²Cr, isobaric analogue states, γ -decay props, 745-820 keV 3-78287
- ⁵¹V(p, n)⁵¹Cr, energy dependence of analogue transition, 16 to 26 MeV 3-63053
- ⁷¹V(p, γ)⁷²V, level scheme of ⁷²V, spin, parity (*German*) 3-78251
- ⁸⁹Y(n, n)⁸⁹Y 0.9 to 1.2 MeV, generalized R-matrix interpretation of total cross section 3-49254
- ⁸⁹Y(p, γ)⁸⁹Y*, continuum analysis of isobaric analogue resonances, shell model 3-60176
- ⁹²Zr photoabsorption, dynamic deformability, reln. to intermediate structure of giant resonance (*Russian*) 3-74562
- ⁹²Zr(p, p') 6.5 MeV, spin flip probability angular distribution on 3/2⁺ analogue resonance 3-67324

nuclear scattering see nuclear reactions and scattering

nuclear shape

- A=174-189, equilibrium deformations and structures of ground and excited states (*Russian*) 3-52088
- actinide region, deformation energies and moments of inertia for isomeric states (*German*) 3-52071
- Coulomb and nuclear meas. compared, reduction of discrepancies 3-60067
- deformation, axially-symmetric or gamma-unstable, from preferred nucleon shape 3-60082
- deformation, finite, in collective model 3-60100
- deformation γ -instability, effect of neutron-proton configuration 3-49165
- deformed nuclei of odd mass, M2 transitions, model (*French*) 3-43204
- deformed rotating nuclei, backbending in simple stretching model 3-62971
- even-even nuclei, asymm. shape and variable moment of inertia model 3-54380
- fission, two-centre shell model with Lawrence family of liquid-drop shapes as equipotential 3-49289
- fission dynamics in actinide region, role of reflection asymmetry in shape 3-49288
- fission mass asymmetry as dynamic process described by collective coordinate 3-60236
- fission-fragment anisotropies for nuclei with double barrier, microscopic calcs. 3-63096
- heavy and superheavy nuclei, spurious state contribs. in shape and stability calcs. 3-45926
- heavy nuclei, deformation energy curve calc. using microscopic method 3-67178
- intermediate deformation, coupling scheme based on particle-plus-rotator model 3-45986
- isomers, fissioning nuclei 3-62928
- light nuclei, deformation parameters (*Russian*) 3-67183
- light nuclei, quadrupole and hexadecapole deformation, Hartree-Fock approx. 3-49179
- muon-nucleus system, effect of Y₄ deformation on transition matrix elements 3-52129
- Nilsson's deformed nuclei, mass formula 3-74478
- odd-mass nuclei, deformed and spherical states, coexistence 3-54393
- penetrability through double-hump fission barriers, F-matrix calc. 3-52213
- potential energy surface with inclusion of axial symmetry 3-52069
- rare earth nuclei, deformed, change in mean square radius between ground and excited states 3-49132
- rare earth region, calcs. of ground state deformations (*German*) 3-52087
- rare-earth deformed nuclei, number-conserving treatment of the BCS-Tamm-Dancoff approximation 3-43191
- rare-earth rotating deformed nuclei, moments of inertia 3-49171
- rigid body model, resonance energy determ. 3-57485
- spontaneously fissioning shape isomers, properties of quadrupole vibrational 3-45984
- tensor degree of freedom 3-78236
- ⁹²Ba, A=130,134,136, rel. to quadrupole moment meas. by reorientation method 3-49112
- Hg neutron deficient isotopes, self consistent calcs. of possible shape transitions 3-67180
- ¹¹⁵In, deformed and spherical states, numerical calcs. of coexistence problem 3-54393
- La neutron-deficient isotopes, prolate deformation 3-45976

nuclear shape continued

- ⁶⁰Ni photoabsorption, dynamic deformability, reln. to intermediate structure of giant resonance (*Russian*) 3-74562
²⁰⁸Pb photoabsorption, dynamic deformability, reln. to intermediate structure of giant resonance (*Russian*) 3-74562
²⁸Si, deformation parameters determ. from ¹⁶O + ²⁸Si elastic and inelastic scattering 3-63082
²⁹Si, high spin negative parity states associated with oblate deformation 3-43171
⁹⁰Zr photoabsorption, dynamic deformability, reln. to intermediate structure of giant resonance (*Russian*) 3-74562

nuclear shell model

- 1f-2p nuclei, effective-interaction calc. on energy spectra, appl. to Ni isotopes 3-67210
 β -decay, matrix element calcs. single-particle model with Woods-Saxon potential (*Rumanian*) 3-43218
A=27-29 nuclei, calcs. using modified surface-delta-interaction Hamiltonian 3-49167
A=7 and 8 nuclei, non-normal parity states calculations, energy levels, E1 radiative widths, cross sections of photonuclear reactions 3-54403
A \leq 44, spectroscopy of f-p-shell, core-excitation effects 3-67236
Alaga model coupling of three particle (hole) valence-shell cluster to quadrupole vibrations 3-67238
algebraic-variational approach to collective motion theory for shell model with R(5) symmetry 3-62961
asymmetric fission, semi-classical level density theory, shell-effects 3-49290
beta decay, wave functions computed, compared with strengths of allowed Gamow-Teller beta decay 3-60122
bound-state model extension for continuum states of ¹²C in giant dipole reson. region 3-43229
closed shell nuclei, ground state correlations, density-matrix formulation 3-74510
cluster coupling scheme, structure calcs. 3-74511
configuration mixing effects on nuclear moments for 1f_{7/2} nuclei 3-49116
configuration space truncation, and nature of effective two-body interaction 3-67233
continuum calcs., multiple complex energy S-matrix poles 3-60095
core-excitation model, nuclear energy levels of ¹⁸⁹, ¹⁹¹, ¹⁹³Ir 3-71046
Coriolis-coupling calc. of low-lying states of Ru, Pd and Cd isotopes 3-43180
correlation between photon and particle widths of compound resonances 3-60144
Coulomb displacement energy, phenomenology of shell effects 3-43193
coupling schemes, seniority scheme, generalised seniority and rotational spectra 3-62966
decaying nuclear states, structure 3-52136
deformation energy calcs. for heavy nuclei, microscopic approach using shell-correction parameters 3-67178
deformed component inclusion and mag. moment corrections in ⁴¹Ca and ³⁹K 3-43173
deformed nuclei, translation and rotation invariance conditions for Hamiltonian 3-67232
deformed-harmonic oscillator, method of generating functions for matrix element calc. 3-74508
double-hump barrier of Strutinsky type, penetrability 3-49285
effective interaction, non-perturbative calc. using Padé approximants 3-67221
effective interaction properties for simple 2 \times 2 matrix 3-67222
effective M1 operator calcs. in nuclei with N=29 and 30, configuration mixing 3-49124
energy density formalism for description of bulk properties 3-43190
even-even nuclei, low frequency excitation spectra near closed shell, systematics 3-67206
excited fissionable nuclei, shell effect disappearance on heating 3-78266
f_{7/2} shell nuclei, magnetic and quadrupole moments, configuration mixing calcs. 3-49125
fission, two-centre model, asymmetry considerations 3-43264
fission, two-centre shell model with Lawrence family of liquid-drop shapes as equipotentials 3-49289
fission of U isotopes, proton induced, influence of nuclear shell effects on fragment mass and energy 3-54519
fixed-charge fragments, X-ray emission spectra, reln. to shell structure (*Russian*) 3-67173
form factors for nucleon inelastic scatt. with effective nucleon-nucleon interactions 3-49158
fractional parentage coefficients, j-j coupling, 7/2 or 9/2 shell 3-74509
Gamow-Teller β -strength functions, refinement in shell model approach 3-49225
generator coordinate method, optimal separation of centre-of-mass motion 3-74512
ground state calculations, self consistent potential, rearrangement energies 3-71058
ground state rotational band in shell model with R(5) symmetry, intrinsic state generation 3-62962
heavy and superheavy nuclei, spurious state contribs. in shape and stability calcs. 3-45926
hypernuclei up to ²³Mg, for comparison with alpha particle model, nuclear distortion 3-57488
independent particle, inadequacies in explaining ⁴He ground state 3-60074
intermediate coupling, ¹⁰⁹Ag negative parity states 3-71061
intermediate coupling model, RPA equations for 2-particle 1-hole states 3-54402
intermediate-coupling, for two-neutron-hole states in even N=80 nuclei 3-67215
intermediate-state summations in effective shell model interaction, convergence rate 3-62964
Kuo interaction in untruncated shell-model calcs. in sd-shells, production of band shifts 3-67202
large basis, study of nucleon-transfer overlaps 3-67295
light nuclei, electron angular distrib. in inelastic scattering (*Russian*) 3-67315
light nuclei, kinetic energy, internucleon interaction, binding and excitation energies 3-40407

nuclear shell model continued

- light nuclei states, oscillator cluster parentage and supermultiplet expansion 3-52112
M2 transitions, deformed nuclei of odd mass, pairing and coupling (*French*) 3-43204
magnetic moments of neutron-hole states from g-factor meas. of 10-isomeric state in ²⁰⁶Bi 3-71042
many-particle average of product of one-body operators, group theory, energy moments 3-60097
masses, corrections in presence of pairing forces, using Bogolyubov Hartree-Fock approx. (*Russian*) 3-67175
N=50 nuclei, generalized seniority scheme 3-43196
N=82 nuclei, Z=51-59, pseudo LS coupling shell model study of energy levels and e.m. properties 3-49126
neutron-proton configuration effect on ν -instability of deformation 3-49165
Nilsson, comparison with data on ²⁶Mg first excited state 3-57489
Nilsson, giant resonances in heavy and medium-heavy nuclei, 1p-1h dipole and quadrupole basis states determ. 3-71092
Nilsson, volume conservation interpretation, potential separation, deformation to radius relation 3-67234
Nilsson's deformed nuclei, mass formula 3-74478
Nilsson generalised model, deformed nuclear intrinsic states (*Rumanian*) 3-45977
Nilsson model, energy fluctuations 3-67235
Nilsson model analysis of half-lives of ¹⁷⁷Ta, ¹⁷¹Lu and ¹⁷³Lu 3-54422
Nilsson single particle, with Coriolis coupling between bands (3_2^+ , 4_{02}^+), (1_2^+ , 4_{00}^+) in ¹⁸⁷Ir nucleus 3-71049
Nilsson-state assignments to levels in ²⁴⁷Cf, and ²⁵¹Fm, in alpha-decay of ²⁵¹Fm 3-67281
non-normal parity states calc. in nuclei with A=16 and 15 3-74482
normalization of shell-model nuclei to liquid-drop model nuclei 3-62972
nuclear interactions, effective from closed shell plus two spectra, isospin mixing 3-71062
nucleon scattering, elastic, shell effects and neutron strength functions 3-78321
nucleon-nucleus elastic scattering, S-matrix calculation, difference between optical model for slow neutron case (*Russian*) 3-71115
off-shell resonances, generalization of Breit-Wigner formula rel. to R-matrix theory 3-63024
one particle, interpretation of quasielastic electron scattering on ⁶Li, ⁷Li, ⁹Be, 1184 MeV (*Russian*) 3-57515
orbital g-factors, effect of exchange currents 3-52074
pair correlation, calculation of ¹⁶⁵Ho levels, comparison with ¹⁶⁵Ho(n,n γ) results (*Russian*) 3-71059
partial state densities from realistic single-particle states 3-49148
particle plus rotor model, rel. to rotation of moderately deformed odd-A nuclei 3-62965
particle-hole model approach to weak and e.m. processes in ¹²C 3-40455
particle-hole states in deformed and spherical nuclei, degenerate Fermi gas model (*Russian*) 3-62967
photoproduction of positive pions from ²⁷Al and ⁵¹V 3-60159
photoprotons, decay of isobaric analogue states, spectra and angular distribution, analysis (*Russian*) 3-57477
potential energy surface with inclusion of axial asymmetry 3-52069
projection of N-nucleon component from zero-, two-, and four-quasi-particle state, ¹¹⁶Sn example 3-67230
proton particle states determ. from meas. of beta decay of ¹³³Sn and ¹³⁷Te 3-71050
reactions, background cross section and correlation between partial widths, relation 3-54454
realistic one-particle density matrix and single-particle description 3-52111
renormalization of operators S and τ S in nuclei with LS doubly closed shell \pm one nucleon 3-49166
review of e.m. transitions and moments 3-54433
reviews present status and suggests reasons for its success 3-67231
rotational band, description by single j shell model, quadrupole interaction, equivalence to Bohr's model 3-60096
separable-potential model for nucleon-nucleus interaction 3-43243
single-nucleon hole states produced in knock-out reactions, unbound character of core 3-63026
single-particle degrees of freedom, relationship to collective degrees of freedom (*Russian*) 3-67237
single-particle strengths in odd mass ²⁰⁸Pb region, Dyson eqn., quasi-particle concept 3-62963
spherical, spectra in the 1f_{7/2} shell for nuclei with A=43-53 3-78245
static quadrupole moments of 2+ states of even isotopes of Ca, Ti, Cr, Fe, Ni, Ba, Nd, Sm 3-49099
structure calculation, density dependent interactions 3-54404
Strutinsky's averaging method of shell corrections for various potentials 3-49168
Strutinsky's shell correction model with Woods Saxon potential for deformation energy calcs. (*German*) 3-52071
Strutinsky smoothing and partition function approach 3-52114
SU(3) coupling for negative parity states of ¹⁶O 3-78253
tensor degree of freedom spin depend., nucleon-lepton interaction 3-78236
toroidal and spherical bubble nuclei, stability against breathing and sausage deformations 3-43198
truncated space, single-particle description of nondegenerate finite-particle system 3-43195
two particle-two hole states, isospin splittings in TDA and RPA 3-43192
two quasiparticle systems, effects of strong rotation-particle coupling on nuclear energy levels 3-62942
two-centre, review of fission, superheavy nuclei (*Japanese*) 3-71133
unified shell-cluster model analogous to LCAO-MO-SCF method, H.F. basis 3-43194
²⁸Al, ²⁹Al, calcs. using modified surface-delta-interaction Hamiltonian 3-49167
Ar isotopes, A=39 to 42, low lying states, using $(\pi d3/2)^{-2}(\nu f7/2)^n$ model, E2, M1 transition rates 3-62949
³⁶Ar negative parity levels calculation 3-71078

nuclear shell model continued

- ⁹Be, inelastic electron scattering, electromagnetic properties, Nilsson model and experiment comparison 3-54386
- ²¹⁰Bi, gamma decay of excited states populated in ²⁰⁹Bi(d,p) reaction 3-67259
- ²¹¹Bi, 7/2⁻ first excited state, semi-realistic shell model calc. 3-78254
- ⁷⁹Br, E2 and M1 reduced transition probabilities, core excitation calc. 3-46005
- ⁸¹Br, E2 and M1 reduced transition probabilities, core excitation calc. 3-46005
- ¹²C, decay of photo resonances, shell model analysis, cross sections and branching ratios 3-49239
- ¹²C(p,p)¹²C, high-energy, single particle description, cluster-like correlation effects 3-43247
- ¹³C, proton hole spectrum calc. in continuum shell model with residual interaction 3-54389
- ¹³C continuum: shell model calculations 3-54401
- Ca, A=42-48, shell-model study using pairing-plus-surface-tensor interaction 3-54405
- ⁴⁰Ca realistic one-particle density matrix and single-particle description 3-52111
- ⁴²Ca, ⁴⁴Ca, quadrupole moments and coexistence, B(E2) values, model comparison 3-52076
- ³⁶Cl, gamma-ray decay, mean lives, branching ratios and radiative rates determ. 3-67262
- ³⁶Cl, negative parity levels calculation 3-71078
- ³⁸Cl, e.m. transition rates, meas. lives of low lying states using attenuated-Doppler-shift method 3-62989
- ⁴Ca, A=243, 245, 247, review of Nilsson orbitals 3-40419
- ¹⁹F, three particle structure, comparison with decay strengths from positive parity states 3-52113
- He(e,e), A=3, 4, evidence for hard core existence (*German*) 3-46016
- Hf odd-neutron nucleides, rotational band structure from Yb(α , xn) reactions, Nilsson model 3-40417
- ¹⁰⁸In, j-j coupling model for β^+ /electron capture decay, spin and parity 3-63004
- ⁴⁰K, e.m. transition rates, meas. lives of low lying states using attenuated-Doppler-shift method 3-62989
- ¹⁶⁷Lu, ¹⁶⁹Lu, levels populated in ¹⁶⁷Hf and ¹⁶⁹Hf decay, Nilsson model assignments 3-52147
- ²⁴Mg, particle-hole nature for two lowest 3- states, direct reaction study 3-49151
- ²⁴Mg, single-particle energies and effective charges 3-62951
- ²⁷Mg, ²⁸Mg, calcs. using modified surface-delta-interaction Hamiltonian 3-49167
- ¹⁴N, absorption of stopped π^- mesons with ⁸Li emission, nucleon cluster effects (*Russian*) 3-67374
- ¹⁴N, decay of photo resonances, shell model analysis, cross sections and branching ratios 3-49239
- ⁵⁶Ni, effective interactions and 1f_{7/2} sub-shell closure in 2p-1f shell 3-49169
- ¹⁶O, binding energy, from ¹⁵O two-nucleon transition matrix 3-78235
- ¹⁶O, effect of α -channel introduction on continuum structure, reln. to photonuclear cross sections 3-45989
- ¹⁶O, shell model calc. of α -transfer form factors and widths 3-45980
- ¹⁶O realistic one-particle density matrix and single-particle description 3-52111
- ¹⁶O structure determ. using interaction boson model 3-52099
- ¹⁶O, binding energy, from ¹⁵O two-nucleon transition matrix 3-78235
- Pb region, g-factors of high-spin shell model states, summary 3-45950
- ²⁰⁸Pb single-particle potentials, form factor calcs. for single-neutron transfer reactions 3-67298
- Pb(p,t), A=208, 206, 204, 35 MeV, two-neutron pick-up strengths, transition from single-particle to collective 3-60187
- ²¹⁰Po, M1 core polarizabilities of 8⁺ and 6⁺ states, shell model calcs. 3-49117
- ⁴Pu, A=237, 239, 241, review of Nilsson orbitals 3-40419
- ²⁴⁰Pu, fission asymmetry, disappearance of shell effects with increasing excitation energy 3-60235
- Sb, odd-A isotopes, two-particle-one-hole states 3-54406
- ¹²³Sb, g-factor calcs. including configuration mixing, comparison with expt. 3-45959
- ¹²³Sb beta decay, matrix element extraction and vector matrix element ratio 3-67270
- ¹²⁴Sb beta decay, matrix element extraction and vector matrix element ratio 3-67270
- ¹¹⁹Sn, configuration mixing calcs. of magnetic moment of 23.8 keV state and hyperfine anomaly 3-49208
- ¹²⁵Sn, neutron shell structure determ. by (d,p) and (α ,³He) reactions 3-67213
- Sr isotopes, shell model for rotation-like spectra 3-60085
- Th, A=218-220, α -decay energies and half lives meas., comparison with shell model theory 3-54445
- ²³¹Th, ²³³Th, review of Nilsson orbitals 3-40419
- ⁴U, A=235, 237, 239, review of Nilsson orbitals 3-40419
- ¹¹⁶Xe, Gamow-Teller β -strength functions, refinement in shell model approach 3-49225
- ⁹⁰Y, determination of levels from ⁸⁹Y(p,p')⁸⁹Y* 3-60176
- ⁹⁰Zr, helion and triton inelastic scattering, core polarization 3-78345

nuclear size

- charge radii of ²⁰Ne and ²⁴Mg determ. using variation after projection Hartree-Fock method 3-67245
- charge volumes detn. by optical pumping far from stability 3-45962
- complex nuclei radii, at wt. depend, from π^+ , K⁺, proton scatt. expts. 3-78352
- compressibility rel. to binding energy, mean kinetic energy, per particle, density power in two body interaction 3-60068
- deformability, axial and non axial, determ. in heavy rotating nuclei 3-67181
- diffraction model of deuteron stripping, effect of nuclear boundary spread and Coulomb interaction (*Russian*) 3-74548
- energy density formalism for description of bulk properties 3-43190
- even-even nuclei, asymm. shape and variable moment of inertia model 3-54380

nuclear size continued

- fluctuation energies in shape fluctuation model and phenomenon of shrinkage 3-49176
- hyperfine structure, nuclear structure effects 3-52066
- leptodermous distributions, geometric properties 3-52070
- matter radii anomalies from Coulomb displacement energies, DWBA calc. 3-74480
- muonic atom, effect of anomalous nuon-nucleon interaction on nuclear radius 3-57615
- muonic-atom, electron-nucleus scattering measurements, comparison of radii 3-57513
- odd-mass nuclei, deformed and spherical states, coexistence 3-54393
- radii determ. from absorption cross sections of π^+ , K⁺, p and p on nuclei with A=9 to 238 at 6 to 60 GeV/c (*Russian*) 3-67338
- radius, sensitivity of allowed β -decay, Z>40 3-40460
- radius charges due to inner Coulomb correction to pion nucleus scattering 3-78355
- rare earth deformed nuclei, change in mean square radius between ground and excited states 3-49132
- rare earth nuclei, neutron total cross section fluctuations, 1.0 to 2.0 MeV, compound nucleus explanation 3-54475
- rare-earth nuclei, even, change of charge radii due to rotational transitions, cranking model 3-52130
- shape calc., nuclear and Coulomb, reduction of apparent discrepancies 3-60067
- tensor deformation, degree of freedom, nucleon-lepton interaction 3-78236
- volume conservation in Nilsson model potential separation, deformation to radius relation 3-67234
- Al, π^+ reaction cross sections, 0.7-2.0 GeV/c, reln. to size 3-71130
- C, π^+ reaction cross sections, 0.7-2.0 GeV/c, reln. to size 3-71130
- ¹²C from ¹²C- π^- elastic scattering, root mean square radius of optical potential 3-78354
- Ca, π^+ reaction cross sections, 0.7-2.0 GeV/c, reln. to size 3-71130
- Ce, neutron total cross section, 1.0 to 2.0 MeV, optical model comparison 3-54474
- ⁵⁰Cr(p,n)⁴⁹Cr, 20.43 to 22.22 MeV, cross section by detection of ⁴⁹Cr positron activity 3-54460
- D, muonic, calc. of contributions to Lamb shift 3-52303
- Dy isotopes, variations in charge radii from X-ray isotope shift obs. 3-67662
- ¹⁶¹Dy, difference in radius between ground and 43.8 keV excited state, Mossbauer effect study 3-62990
- ⁵⁷Fe, calibration of isomer shift by lifetime meas. in different chemical environments (*German*) 3-49186
- ⁵⁷Fe, change in charge radius between 14.4 keV and ground states, isomer shift calibration 3-62984
- Gd, neutron total cross section, 1.0 to 2.0 MeV, optical model comparison 3-54474
- ⁴He equivalent radius determ. from π^- -⁴He scattering at 3.48 and 6.13 GeV/c (*Russian*) 3-67124
- Hg, neutron total cross section, 1.0 to 2.0 MeV, optical model comparison 3-54474
- Hg, neutron total cross section fluctuations, 1.0 to 2.0 MeV, compound nucleus explanation 3-54475
- ¹⁸³Hg, variable collective inertia and mean square charge radius 3-62930
- ¹⁸⁷Hg, variable collective inertia and mean square charge radius 3-62930
- Ho, neutron total cross section, 1.0 to 2.0 MeV, optical model comparison 3-54474
- Ho, π^+ reaction cross sections, 0.7-2.0 GeV/c, reln. to size 3-71130
- La, neutron total cross section, 1.0 to 2.0 MeV, optical model comparison 3-54474
- La, neutron total cross-section fluctuations, 1.0 to 2.0 MeV, compound nucleus explanation 3-54475
- ¹³⁹La Mossbauer scatt. of 166 keV γ -rays, mean square nuclear charge radius deduced 3-60119
- Nd isotopes, variations in charge radii from X-ray isotope shift obs. 3-67662
- Ni, π^+ reaction cross sections, 0.7-2.0 GeV/c, reln. to size 3-71130
- ¹⁰Mo muon capture, exptl.-theoretical discrepancies, use of size coexistence model 3-67269
- ¹⁶O region, charge radii and polarisation effects 3-67179
- Pb, change radius and neutron matter radius determ. from low-energy elastic scattering of pions and muons 3-71128
- Pb, π^+ reaction cross sections, 0.7-2.0 GeV/c, reln. to size 3-71130
- Pb isotopes, variations in charge radii from X-ray isotope shift obs. 3-67662
- Pr, neutron total cross section, 1.0 to 2.0 MeV, optical model comparison 3-54474
- ¹²¹Sb, charge radius, sign and magnitude determ. using isomeric shift meas. (*Russian*) 3-62929
- Sm isotopes, variations in charge radii from X-ray isotope shift obs. 3-67662
- Sn, π^+ reaction cross sections, 0.7-2.0 GeV/c, reln. to size 3-71130
- ¹¹⁹Sn, charge radius, sign and magnitude determ. using isomeric shift meas. (*Russian*) 3-62929
- Ta, neutron total cross section, 1.0 to 2.0 MeV, optical model comparison 3-54474
- Ta, neutron total cross section fluctuations, 1.0 to 2.0 MeV, compound nucleus explanation 3-54475
- ⁹⁹Tc, Mossbauer resonance spectra of 140 keV level, giving $\Delta\langle r^2 \rangle$ 3-71077
- Y, neutron total cross section, 1.0 to 2.0 MeV, optical model comparison 3-54474
- Y, neutron total cross section fluctuations, 1.0 to 2.0 MeV, compound nucleus explanation 3-54475
- Yb isotopes, variations in charge radii from X-ray isotope shift obs. 3-67662
- Zr, neutron total cross section, 1.0 to 2.0 MeV, optical model comparison 3-54474
- Zr, neutron total cross section fluctuations, 1.0 to 2.0 MeV, compound nucleus explanation 3-54475

nuclear spallation

- ²⁷Al, photon-induced fragmentation by 1 GeV bremsstrahlung 3-60160

nuclear spallation continued

- ¹³C spallation by 150 and 600 MeV protons, production of ⁷Be, ⁹Be, and ¹⁰Be rel. to astrophysical conditions 3-54476
 Co, 11.5, 200 and 300 GeV proton irradiation, cross sections meas. 3-46028
 Cu, induced by 65 MeV π^+ and π^- and by 205 MeV protons, radiochemical yield determ. 3-67373
 F prod. in interstellar matter, cosmic ray abundance 3-51216
¹⁴N, meas. cross section for production of Li, Be, and B isotopes, 17 to 42 MeV astrophysical significance 3-67330
³²S, photon-induced fragmentation by 1 GeV bremsstrahlung 3-60160
²³⁸U proton induced, 11.5 GeV, Xe isotope yields cross sections and recoil props. 3-74615
 V, 3- and 29-GeV proton interaction, product radionuclide yields 3-54481
 V, 300 GeV, proton irradiation, cross sections meas. 3-46028

nuclear spin and parity

- ¹⁷₂ nuclei, assignments to spherical shell-model states of high angular momentum 3-40416
⁵⁸Co, assignments from (³He, p) and (³He, pp) reactions on ⁵⁶Fe 3-54428
 A=4 nuclei, compilation of energy levels 3-43181
 A=7 and 8 nuclei, shell model calculations, non-normal parity states, cross sections of photonuclear reactions 3-54403
 anomalous coupling states with spin I=j-1, e.m. properties 3-49104
 compound-nucleus reactions, conserved isospin quantum number consequences 3-60148
 DWBA theory with charge exchange and isospin 3-57504
 giant resonance excitation of doubly closed shell nuclei, spin dependent effects 3-78297
 ground state spin meas. by nuclear resonance, atomic beam resonance and optical pumping, hyperfine anomalies 3-45932
 high-spin isomeric states, mesonic anomaly in orbital g factors from magnetic moment meas. 3-45929
 integral equations, four nucleons with spin and isospin (Russian) 3-74507
 isospin in nuclear potential, Lane's eqn. and approximation (Rumanian) 3-62957
 isospin centroids of residual nuclei from single-nucleon transfer in Ca, Ni and Zr regions 3-63028
 isospin conservation (German) 3-54376
 isospin depend. of optical model parameters for quasielastic reactions 3-40474
 isospin impurities, theory and study of low-lying and unbound states 3-54382
 log ft values for forbidden β transitions, rules for spin and parity assignments 3-62932
 method, using alpha-particle scatt. to determine level spin 3-63072
 mirror pair, spin-isospin distribution 3-45954
 neutron resonance spin determ. from Monte Carlo simulation of decay 3-57519
 nucleons, paired, isospin degrees of freedom in collective motions 3-78269
 orientation of spin system at low temps., orientation parameters 3-71080
 parity-violating transitions, nucleon-one-meson exchange potentials in current-current quark model 3-48994
 parity-violation expts., exchange effects 3-40444
 proton spin flip in ¹²C(p, p)¹²C, f-wave decay of ¹³N 8.9 MeV level 3-74590
 quadrupole moment for high spin rotational states, asymmetric rotor model 3-49114
 rotational theory number displacement degrees of freedom, even and odd parity orbitals 3-54409
 spin dependence of AN interaction in A=4 hypernuclei 3-71072
 spin flip probability angular distribution from ⁹²Zr(p, p'), 6.5 MeV, interference effect 3-67324
 spin moments detn. by optical pumping far from stability 3-45962
 spin-orbit coupling of nuclear protons, quasi-free scattering determ. 3-60073
 spin-spin term of nucleon-nucleus optical potential, DWBA analysis 3-67291
 tensor deformation, spin depend., nucleon-lepton interaction 3-78236
 two particle-two hole states, isospin splittings in TDA and RPA 3-43192
 unnatural parity final states, (p, t) excitation via multistep processes 3-78326
 yrast line, pairing and spin distrib. effects 3-67205
¹⁰⁹Ag negative parity states, intermediate coupling model 3-71061
²⁸Al, excitation in ²⁷Al(d, p) reaction (Russian) 3-52189
³⁶Ar levels, from ³⁵Cl(p, p), E=0.8-2.6 MeV, shell model calculation of odd parity levels 3-71078
⁷²As, assignment of new isomeric level at 215 keV populated in ⁷²Ge(p, n) reaction 3-45956
⁷⁴As, product of ⁷⁴Ge(p, np) at 3.5, 3.8, 4.0 MeV 3-54472
²⁰⁹At, assignments to levels populated in electron capture decay of ²⁰⁹Rn 3-74542
²¹⁰At levels populated in ²¹⁰Rn decay 3-43223
¹³³Ba, excited levels mass in β -decay of ¹³³La 3-57472
¹³⁸Ba, spins and mixing ratio from γ - γ directional correl. following ¹³⁸Cs decay 3-78238
¹³⁹Ba, assignments to levels populated in ¹³⁸Ba(d, p) reaction at 19 MeV 3-46033
⁹Be, compound nucleus produced in ⁷Li(d, α)⁹He reaction, 17.48 MeV excitation level 3-71120
⁹Be(³He, n)¹¹C, compound nucleus mechanism, forbidden J 3-52198
⁹Be(³He, np)¹¹C, compound nucleus mechanism, forbidden J 3-52198
⁹Be(³He, p)¹¹B, compound nucleus mechanism, forbidden J 3-52198
⁹Be(³He, pp)¹¹B, compound nucleus mechanism, forbidden J 3-52198
²⁰⁴Bi, high-spin isomeric state populated by heavy-ion and α -particle induced reactions 3-49152
²⁴⁸Bk, decay product of ²⁵²Es by α decay 3-54443
⁷⁶Br, from ⁷⁶Kr decay level energies spins, parities and transition probabilities 3-49220

nuclear spin and parity continued

- ⁷⁹Br, $\gamma\gamma$ directional correlations meas., spin and parity assignments (German) 3-40459
⁸³Br excited levels populated in ⁸³g + ^mSe decay 3-63010
⁸³Br production from ⁸⁰Se(α , p)⁸³Br, energy levels study 3-52103
¹³C highly excited states in ⁹Be(α , α')⁹Be, spin-parity assignments 3-63075
¹³C states, investigation via neutron polarisation in ⁹Be(α , n)¹²C reaction 3-62946
⁴¹Ca, high spin states in K=3/2⁺ and K=3/2⁻ rotational bands 3-60072
⁴⁸Ca, assignments to low lying states populated in ⁴⁸Ca(p, t) reactions 3-67211
⁴⁶Ca, from ⁴⁶Ca(p, p'), 16 MeV 3-54391
 Cd isotopes, odd-mass, Coriolis-coupling calc. of low-lying states 3-43180
¹⁰⁵Cd, assignments to levels populated in ¹⁰⁶Cd(d, t) reaction 3-67345
¹⁰⁷Cd, assignments to levels populated in ¹⁰⁶Cd(d, p) reaction 3-67345
¹⁰⁷Cd level scheme study through ¹⁰⁷Ag (p, n γ) and ¹⁰⁶Cd(d, p γ) reactions and ¹⁰⁷In decay 3-49154
¹⁴⁰Ce, 246.4 keV level, from γ - γ ang. correl. meas. 3-45993
³⁴Cl, assignments to levels populated in ³²S(³He, p) reaction at 9 MeV 3-49215
³⁵Cl, high-spin states obs. using ³²S(α , p) reaction, $\gamma\gamma$ coincidence, angular distrib., yield function meas. 3-74493
³⁶Cl, spin values of 0.788 and 1.598 MeV levels 3-63062
⁵⁴Co, assignments from (³He, t) reactions 3-63079
⁶⁰Co, spin determ. from meas. of γ -ray asymmetry in ⁵⁹Co(n, γ) reaction 3-60175
⁶⁰Co, spins of levels populated in ⁵⁹Co(n, γ) reaction 3-43245
⁴⁸Cr, from ⁴⁰Ca(¹⁰B, pnp), 19, 22.5, 25 MeV, γ -ray spectroscopy 3-62985
⁵³Cr high-spin states populated in ⁵⁰Ti(α , n) reaction 3-52096
¹³³Cs, spin assignment to 633 keV level populated by Coulomb excitation 3-52200
¹⁴⁰Cs, spin assignment (1-) far ground state level (French) 3-60123
⁸⁸Cu, assignments from (³He, t) reactions 3-63079
⁶⁰Cu, assignments from (³He, t) reactions 3-63079
⁶¹Cu, spin assignments to levels populated by ⁶⁰Ni(p, γ) reaction, analogue states 3-46001
 Dy, A=158, 160, 162 pop. in Gd(α , 2n)Dy reaction, g factor meas. of high spin rotational states 3-67188
¹⁵⁴Dy, high spin states, transitions of ground rotational band 3-60217
¹⁵³Dy, high spin states, E2 transitions between levels of strongly mixed positive-parity band 3-60217
¹⁵⁶Dy, influence of rotation on moment of inertia of high-spin ground state members 3-52098
¹⁵⁶Er, high-spin states population and backbending effect 3-62937
¹⁶⁰Er, influence of rotation on moment of inertia of high-spin ground state members 3-52098
¹⁶⁶Er, excited by electron bremsstrahlung 3-71057
¹⁶⁸Er, excited by electron bremsstrahlung 3-71057
¹⁶⁸Er, ground state, rotational bands, obs. by Ge(Li) spectroscopy of ¹⁶⁸Ho β -decay 3-67273
¹⁷⁰Er, excited by electron bremsstrahlung 3-71057
¹⁹F, three particle structure, comparison with decay strengths from positive parity states 3-52113
²⁰F, γ -ray transitions, linear polarization meas. 3-40447
⁵⁴Fe, ⁵⁶Fe, proton spin flip angular distributions at 12 MeV, collective model DWBA calculations 3-63048
⁵⁴Fe, 2+ state from ⁵⁴Fe(p, p'), differential cross section, spin-flip probability, asymmetry 3-78237
⁵⁷Fe, assignment to doorway state resonance, from analysis of neutron scattering by ⁵⁶Fe 3-60177
⁶⁹Ga, energy level study, parity of 7306 keV level determ. using Compton polarimeter 3-62948
⁷⁰Ga, spin assignments to levels populated in ⁷⁰Zn(p, n γ) reaction 3-62931
¹⁴⁶Gd, energy level spectroscopic investigation, spin assignments and lifetime meas. 3-54429
¹⁴⁸Gd, energy level spectroscopic investigation, nuclear assignments and lifetime meas. 3-54429
¹⁵⁰Gd, energy level spectroscopic investigation, spin assignments and lifetime meas. 3-54429
⁶⁵Ge ground state, to be 3/2- (5/2-) 3-60131
²H, spin-orbit potential in nucleon-nucleon interaction, change in magnetic moment 3-71044
¹⁸⁰Hf, parity mixing of 501 keV transition, backscatt. polarimeter meas. 3-67265
²⁰⁰Hg decay scheme, spins and multipolarities 3-40453
¹²⁹I, orientation study of excited states populated in decay of ¹²⁹gTe, ^{129m}Te 3-52131
¹²⁹I, spin assignment to 696 keV level populated by Coulomb excitation 3-52200
¹¹⁶In, assignments to levels populated in ¹¹⁵In(n, e) reaction 3-71116
¹⁰⁸In, β^- /electron capture decay, j-j coupling model 3-63004
¹⁸⁷Ir, excited levels, determ. from ¹⁸⁷Pt decay scheme 3-71049
³⁶K, spin and magnetic moment determ. from β -decay asymmetry following polarisation by optical pumping 3-45939
⁴⁰K, assignments to levels below 3.2 MeV excitation in ³⁷Cl(α , n) and ⁴⁰Ar(p, n) reactions 3-43208
¹³¹La levels populated in ¹³¹Ca beta decay, Coriolis effects (French) 3-52148
⁶Li, isospin mixing, asymmetry energy depend., ³H(³He, d)⁴He 3-78306
⁶Li, isospin mixing study by deuteron decay meas., Mott-Schwinger interaction 3-71043
⁸Li, short lived, spin exchange polarisation and hyperfine splitting meas. 3-52138
¹⁶⁷Lu, ¹⁶⁹Lu, levels populated in ¹⁶⁷Hf and ¹⁶⁹Hf decay, Nilsson model assignments 3-52147
¹⁷¹Lu, ¹⁷³Lu, high-spin rotational states, evidence for $\Delta K=2$ and $\Delta K=4$ mixings 3-60077
²⁴Mg, high spin states assignments, from ¹²C(¹⁴N, d)²⁴Mg reaction 3-54381
²⁸Mg, spin assignments to low-lying levels populated in ²⁶Mg(²H, p γ) reaction 3-67258

nuclear spin and parity continued

- ⁵³Mn, excited state obs. by ⁵³Cr(p,n γ) reaction 3-67192
⁵⁶Mn 0.211 MeV level isobaric analogue state 3-60168
⁹²Mo, neutron reson. parameter 3-40495
⁹⁵Mo, spins of levels, and multipole mixing ratios of transitions 3-60070
⁹⁸Mo, product of ¹⁰⁰Mo(p,t), 19 MeV cross section measurements, search for excited rotational band 3-54390
^{93m}Mo 6.9 hr, ang. distrib. obs. 3-62934
¹³N, obs. of new T=1/2 levels scattering of polarised protons on ¹²C (German) 3-49139
¹⁴N, assignments to levels populated in ¹⁰B(α,α')¹⁰B reaction 3-71055
¹⁴N, energy levels deduced from ¹⁴C(d,d), optical model anal. 3-78343
¹⁵N, non-normal parity states calc. 3-74482
²²Na pop in ¹⁰B(¹⁶O, α) reaction, selection of strong candidates for high spin members of bands 3-67364
²³Na, from ¹²C(¹²C, pp)²³Na, high spin states study 3-49185
²⁴Na, from ²³Na(d, p γ), 2.45 MeV 3-62986
²⁴Na, beta decay meas. for spin determ. 3-74541
⁹³Nb, neutron total (0.25 to 0.5 MeV) and differential (1.8 to 4.0 MeV) scattering cross-sections, optical model, J π values 3-78331
⁹³Nb, product of ⁹⁰Zr(α,γ), 14.77 MeV, γ -decay of low lying levels 3-57491
¹⁴²Nd, N=82, levels populated in ¹⁴²Pr, ¹⁴²Pm β decays, spin and parity assignments 3-49155
²⁰Ne, assignments to high-spin negative parity states from angular correlation meas. 3-49136
²⁰Ne(d, α)¹⁸F, E α =6-11 MeV, large isospin selection-rule violation 3-60205
Ni, spins of highly excited levels, study by elastic and inelastic scattering of Fe capture gamma-rays 3-49241
⁵⁹Ni, spin assignments to low lying levels populated in ⁵⁶Fe(α,γ) 3-49213
⁵⁹Ni, spin assignments to levels populated in ⁵⁸Ni(d, p) 3-52077
⁵⁹Ni level struct. from ⁵⁸Ni(d, p) at 8 MeV 3-45973
⁶⁰Ni, assignments to levels populated in ⁶⁰Ni(p, p γ) reaction 3-52132
⁶¹Ni, spin assignments to levels populated in ⁶⁰Ni(d, p) reaction at 10 MeV 3-78239
¹⁴⁰O excited states via ang. correl. obs. of ¹²C(³He, n)¹⁴⁰O(p)¹³N at 12 MeV 3-40509
¹⁵⁰O, non-normal parity states calc. 3-74482
¹⁶⁰O, even parity transitions, calc. form factors using weak coupling model 3-60163
¹⁶⁰O, excited odd-parity states in inelastic electron scattering, Brown-Green model 3-63040
¹⁶⁰O, negative parity T=0 states, SU(3) coupling in shell model calcs. 3-78253
¹⁶⁰O non-normal parity states calc. 3-74482
¹⁷⁰O, parities of 7.97 to 8.197 MeV states from meas. on ¹³C(α,γ)¹⁶⁰O reaction 3-67189
¹⁷⁰O level structure, from neutron total cross sections 3-67209
¹⁹⁰O, low-lying states spin from ¹³C(⁷Li, p) E=16 MeV 3-54505
¹⁸²Os, γ -decay of high-spin states populated in ¹⁸²W(α,γ) reaction, ground-state band obs. 3-74498
¹⁸⁹Os, populated by ¹⁸⁹Re decay, excited level scheme, spin and parity assignments 3-54432
²⁹P, assignments to levels up to 4.76 MeV populated in ²⁸Si(p, γ) reaction 3-49144
³⁰P compound nucleus parameters from ²⁸Si(d, p)²⁹Si at 2-4.2 MeV 3-40503
³⁰P level characteriz. from proton scatt. on ²⁹Si at 2.5-3.4 MeV 3-60191
³²P, from ²⁹Si(α,γ), E α =10.65, 10.69, 11.00 MeV, deduced levels, mixing, branching ratios 3-60108
³³P, excited state spins, ang. correl. obs. 3-40449
³³P, populated via ³⁷P(t, p)³³P reaction, low-lying states lifetime meas. and props. 3-54427
³³P lifetimes meas. by Doppler shift attenuation, spin-parity assignments 3-40446
Pb, spins of highly excited levels, study by elastic and inelastic scattering of Fe capture gamma-rays 3-49241
²⁰⁵Pb, high spin three neutron hole states of configurations, containing the i_{13/2} orbital 3-52100
Pd isotopes, odd-mass, Coriolis-coupling calc. of low-lying states 3-43180
¹⁰²Pd, level struct. using ⁹⁹Ru(α,γ) reaction 3-40510
¹⁵¹Pm, determ. from ¹⁵¹Nd decay 3-43220
²¹⁰Po, assignments to, collective states, study with inelastic scattering of deuterons, protons, tritons 3-43183
²¹⁰Po core-excited state, magnetic moment determ. by time-differential spin-rotation meas. 3-45972
Pt even isotopes, influence of quadrupole-pairing interaction on J π =0 $^{+}$ vibrations 3-78256
¹⁹⁰Pt level scheme populated in ¹⁹⁰Au decay 3-67278
¹⁹⁴Pt, spins, multipole mixing ratios of γ -transitions, E2 ratio comparison with theory 3-54385
¹⁹⁵Pt, excited states, spin and parity assignments from ¹⁹⁵Ir.s.m., ¹⁹⁵Au decay 3-52137
⁸⁵Rb, ⁸⁷Rb, assignments to levels populated in Coulomb excitation 3-40415
¹⁰¹Rh, oriented, n.m.r., hyperfine splitting and gamma ray anisotropy meas. 3-74534
Ru isotopes, odd-mass, Coriolis-coupling calc. of low-lying states 3-43180
⁹⁴Ru, level structure up to 4 MeV excitation, study by ⁹⁶Ru(p,t) reaction 3-49147
⁹⁵S, γ -decay, ²⁸Si(³He, n) reaction, 3676 keV state 3-78289
³²S, isobaric analogue resonances study using ³¹P(p, γ)³²S, ³¹P(p,p)³¹P, 2) 3-78299
³³S, excitation in ³²S(d,p) reaction (Russian) 3-52189
⁴⁴Sc, isospin mixing from the effective nuclear interaction 3-71062
⁴⁴Sc, level scheme, γ decay study deformed bands, shell model 3-78282
⁴⁴Sc, proposed K π =0 $^{-}$ band 3-49145
⁴⁴Sc excited states populated by ⁴¹K(α,γ), decay modes and spin assignments, K π =0 $^{-}$ band 3-74495

nuclear spin and parity continued

- ⁴⁵Sc, spin of 1238 keV level, from ⁴⁵Sc(n,n γ) E=1.41 MeV γ -ray angular distribution 3-74589
⁴⁹Sc, assignments to levels from γ -decay of isobaric analogue states 3-54377
⁴⁹Sc, spin assignment for 4493 keV state, low lying negative parity states calc. 3-40445
²⁹Si, from ²⁶Mg(α,γ) reaction, high-spin states using neutron time-of-flight spectrometer 3-52084
²⁹Si, high spin negative parity states associated with oblate deformation, population in ²⁶Mg(α,γ) 3-43171
³⁰Si, assignments to levels populated in ²⁸Si(t,p) and ²⁹Si(d,p) reactions 3-62940
⁴⁵Si, assignments to levels in K=3/2 $^{+}$ rotational band 3-74494
¹⁵¹Sm levels populated in ¹⁵¹Pm decay 3-78244
¹⁵⁴Sm excited by (n, n γ) reaction determ. energy level structure from γ -ray spectra 3-67196
¹¹⁴Sn, high-spin isomeric state populated in ¹¹²Cd(α,γ) reaction, lifetime and g-factor determ. 3-45958
¹²⁵Sn pop. in (d,p) and (α,γ) reactions, neutron shell structure determ., spin assignments 3-67213
¹³⁰Sn, assignments to excited states populated in ¹³⁰In β -decay 3-60081
⁸³Sr levels, from ⁸³Y.m.s. decay 3-46007
⁹⁰Sr, search for the first 0 $^{+}$ excited state, gamma transition intensities and spins of 1655, 1892 and 2207 KeV states 3-40440
¹⁸¹Ta 482 keV transition, short-range correlations, effective charge, parity violation, polarisation 3-57490
¹⁵⁴Tb, determ. branching ratios and half lives of the three isomeric states, spin assignments 3-67263
⁹⁴Tc, excited states, obs. of neutron and gamma-ray yields from ⁹⁴Mo(p,n)⁹⁴Tc reaction at isobaric analog. resonances 3-67207
⁴⁷Ti, assignments to levels in K=3/2 $^{+}$ rotational band 3-74494
⁴⁶Ti, levels up to 5.0 MeV, enhancement factors 3-54471
⁴⁷Ti levels populated in ⁴⁷V β -decay, spin and parity assignments 3-52146
⁴⁸Ti, ⁵⁰Ti, proton spin flip angular distributions at 12 MeV, collective model DWBA calculations 3-63048
⁵⁰Ti(p,p γ), high resolution cross section meas., 1.83-2.97 MeV 3-78324
²⁰²Tl, 7 $^{+}$ isomeric state populated in ²⁰⁴Hg(p,nnn), γ -ray spectra, time-differential spin rotation 3-49086
¹⁶⁸Tm rot. band obs. in ¹⁶⁹Tm(d,t)¹⁶⁸Tm 3-63069
²³³U, assignments to levels populated in ²³³Pa decay 3-74535
²³⁵U, neutron-induced fission, spin determ. of resons. 3-74614
²³⁶U, from (n, γ) reaction, measurements of low energy γ rays, 1383, 1342 KeV levels deduced 3-63042
²³⁶U, pop. in ²³⁵U(n, γ)²³⁶U reaction, γ -rays meas., spin of resonances 3-67335
⁴⁷V, assignments to levels populated in ⁴⁶Ti(p, γ) reaction from γ -decay of IAR (German) 3-78251
⁴⁷V, low-lying levels populated in ⁴⁷Ti(p,n) and ⁴⁰Ca(¹⁰B,ppn) reactions 3-49146
⁴⁸V, low-lying levels populated in ⁴⁰Ca(¹⁰B,pp) and ⁴⁰Ca(¹²C,pppn) reactions 3-49135
¹⁸³W, superhyperfine interaction with Fe³⁺ electron spin, e.s.r. at low concentrations 3-41404
¹³⁰Xe, 0 $^{+}$ levels obs. using beta spectrum of ¹³⁰Cs (Russian) 3-67216
⁹⁰Zr, based on data from ⁸⁹Y(p,p γ)⁸⁹Y* 3-60176
⁹⁰Zr(d,d) scatt., spin depend. investigation 3-40499
⁹²Zr(d,p)⁹¹Zr, j-dependence of vector analysing power and cross section 3-46034
- nuclear spin-lattice relaxation** see spin-lattice relaxation
nuclear spin-spin relaxation see spin-spin relaxation
nuclear structure
 see also nuclear energy levels; nuclear matter; nuclear models; nuclear theory
 1 GeV energy range, experimental study using high resolution spectrometer (French) 3-59620
 cluster coupling shell model scheme calcs. 3-74511
 conference on nuclear moments and structure, Osaka, Japan (September 1972) 3-45922
 density dependent interactions in structure calculations 3-54404
 electron-nuclear interaction, effects on hyperfine structure of atomic spectra 3-52066
 electrons and photons, 150 MeV-600 MeV experimental study (French) 3-60063
 e.m. interaction of nucleus with charged particle, interpretation of hyperfine interaction data 3-52065
 exchange current, N $^{*}_{33}$ -isobar and tensor force effects on magnetic moments 3-45927
 form factor study, matrix elements for interaction of nucleons with the core of nuclei (Russian) 3-67237
 Gaussian approximations use in calcs. on deformed nuclei 3-78265
 Hamiltonian for deformed nuclear intrinsic states, other representation and high deform. limit (Rumanian) 3-45977
 Hartree-Fock-Bogoliubov overlap states, calc. with group theory (German) 3-57486
 neutron investigation, conference, Gaussig, Germany (29 November-3 December 1971) 3-60064
 review of new facets, esp. of collective behaviour 3-78268
 spectroscopic study of heavy ion induced multinucleon transfer reactions 3-57538
 C, neutron halo deduced from p absorption 3-60083
¹²C, projected Hartree Fock calc. with realistic interaction 3-52121
²⁰Ne(α,α')²⁰Ne, 104 MeV α -particle scatt., nucl. density distrib., size and shape 3-54498
 Pb, neutron structure deduced from antiproton absorption 3-60083
²⁸Si(α,α')²⁸Si, 104 MeV α -particle scatt., nucl. density distrib., size and shape 3-54498
 Ta, neutron structure deduced from antiproton absorption 3-60083
 Ti, neutron structure deduced from antiproton absorption 3-60083
- nuclear theory**
 see also BCS theory; clebsch-gordan coefficients; nuclear structure
 A=17-27, projected Hartree-Fock calcs. of spin-isospin matrix elements 3-49180
 back-bending in rotational spectra, particle number projection, cranking model and HFB theory 3-49177

nuclear theory continued

- Brueckner-Hartree-Fock approach, self-consistent treatment of Pauli operator 3-60104
- bubble configurations of ^{36}Ar and ^{200}Hg , Hartree-Fock calc. 3-78274
- canonical SU_3 basis, unitary scheme density matrix (*Russian*) 3-54400
- centre-of-mass motion and angular momentum projection, rotational energies calc. 3-67247
- closed shell nuclei, ground state correlations, density-matrix formulation 3-74510
- Coulomb displacement energy, phenomenology of shell effects 3-43193
- Coulomb mixing intensity between $T=T_0$ isobaric analogue state and $T=T_0-1$ monopolar excitations (*Russian*) 3-74488
- coupling scheme based on particle-plus-rotor model for high angular momenta and intermediate deformation 3-45986
- deformation energy calcs. for heavy nuclei, microscopic approach using shell-correction parameters 3-67178
- deformed intrinsic state, ang. momentum distrib. and average temp. 3-71067
- deformed-harmonic oscillator, method of generating functions for matrix element calc. 3-74508
- density matrix, irreducible decomp. for tensorial wave functions (*Russian*) 3-54399
- density-dependent effective interactions, effect on spherical nuclear calcs. 3-52108
- distorted wave theory of analogue states extended to include charge exchange channel 3-60203
- effective interactions in nuclei, generalization of algebraic approach 3-49159
- electron bridge effect in calcs. of circular polarisation in γ transitions (*Russian*) 3-74529
- energy density formalism for description of bulk properties 3-43190
- even-even nuclei, low frequency excitation spectra near closed shell, systematic features 3-67206
- even-even nuclei, microscopic theory of two-phonon states 3-74518
- few-body problem in nonrelativistic field theory 3-67224
- finite nuclei, single-hole strength distrib., second moment 3-52105
- four-particle system, pole approximation in integral equations (*Russian*) 3-60092
- Gaussian approximations use in calcs. on deformed nuclei 3-78265
- generator coordinate method applied to ^{20}Ne 3-60094
- ground state calculations, self consistent potential, rearrangement energies 3-71058
- Hartree-Bogoliubov states, number and ang. momentum projection 3-71071
- Hartree-Fock calc., two-particle matrix element evaluation 3-67244
- Hartree-Fock projection before variation method, stability conditions and computational aspects 3-71068
- Hartree-Fock-Bogoliubov overlap states, calc. with group theory (*German*) 3-57486
- heavy nuclei, inhomogeneity of nucleon distrib. (*Russian*) 3-62958
- isoscalar factors of Clebsch-Gordan coeffs., for U_n semicanonical basis (*Russian*) 3-57481
- isovector δg_{mes} produced by Hamada-Johnstone potential, calcs. for light and Pb region nuclei 3-49131
- Iwamoto-Yamada cluster expansion, diagrammatic methods and renormalization 3-78271
- linked-cluster theorem and Rayleigh-Schrodinger expansion in finite model spaces 3-45988
- low energy states, minimisation of energy variance for determinantal state and Hartree-Fock state 3-49150
- many-body Hamiltonian, Brueckner theory applic. 3-40430
- matrix eigenproblems, application of Lanczos algorithm, extension from shell model to continuum states 3-67228
- maximum overlap orbitals, rearrangement terms, Euler Lagrange eqn. 3-62960
- mesonic effects in nuclei 3-49071
- moment of inertia calcs. in presence of RPA correlations 3-49181
- multinucleon correlations and effective force, appl. of theory from few-nucleon systems (*Russian*) 3-71060
- neutron star matter at sub-nuclear densities, ground state configuration 3-51253
- non-local separable potential, positive energy bound states 3-43188
- odd A nuclei with simple configuration, magnetic moment calc. using Kuo's effective interaction 3-49127
- odd-A nuclei, attenuation of Coriolis coupling, unified model 3-40431
- odd-odd nuclei with small inaxiality, calc. of energy spectrum of excited states (*Russian*) 3-52093
- off energy shell T matrix, symmetry property 3-60088
- off-energy-shell T-matrix in modified boundary-condition-model interaction 3-43187
- off-shell two-nucleon T matrix, singular-core interaction and one-pion exchange constraints 3-74499
- optimal separation of centre-of-mass motion, determ. of best internal wave function 3-74512
- orbital g-factor due to exchange currents, reln. to E1 sum rule 3-49119
- orbital g-factors, effect of exchange currents, shell model calcs. 3-52074
- pairing, theorem on transformation of complex skew symmetric matrix into real normal form 3-67219
- penetrability through double-hump fission barriers, F-matrix calc. 3-52213
- permutation group in hyperspherical formalism, matrix elements and recurrence relation 3-57482
- potential energy surface with inclusion of axial asymmetry 3-52069
- projection operators, product form and scheme for approximate projection 3-67229
- quadrupole deformation, microscopic treatment of collective motion using group theory 3-49173
- quasi-ground band, effect of changes in potential energy surface on internal ratio 3-43184
- random phase approximation, ^{180}Pt to ^{190}Pt even isotopes, quadrupole effect on $J^\pi=0^+$ vibrs. 3-78256
- random phase approximation, one and two particle density matrices 3-78255

nuclear theory continued

- random phase approximation, quasi-particle rel. to non-rotational collective nuclear states 3-67240
- rare-earth deformed nuclei, number-conserving treatment of the BCS-Tamm-Dancoff approximation 3-43191
- renormalization of operators S and τS in nuclei with LS doubly closed shell \pm one nucleon 3-49166
- resonance energies of nuclei considered as rigid bodies 3-57485
- resonating group method, kernel calc. in harmonic oscillator basis 3-74511
- rotating nuclei, finite temp. calc. of angular velocity and moments of inertia 3-49178
- rotational anomaly and Hartree-Fock-Bogoliubov eqns. 3-49174
- rotational bands as induced group representations 3-43197
- rotational theory number displacement degrees of freedom 3-54409
- scattering problems, use of generator coordinates 3-67283
- single-particle description of nondegenerate finite-particle system in truncated space 3-43195
- spectrum statistics, effect of doorway states 3-60076
- square well potentials with varying repulsion, accuracy of unitary pole approx. 3-49160
- Strutinsky's averaging method of shell corrections for various potentials 3-49168
- Strutinsky smoothing and partition function approach 3-52114
- symmetrical group, matrix elements and Clebsch-Gordan coeffs. of irreducible operators (*Russian*) 3-54398
- t matrix, utility of separable expansions, appl. to trinucleon system 3-74506
- three-body problem, K-harmonic method (*Russian*) 3-40429
- three-nucleon bound state problems 3-49162
- three-particle resonance wave function, variational expression for Gilbert Schmidt eigenvalues (*Russian*) 3-60093
- three-particle system, accuracy of Brueckner theory for light nuclei 3-57480
- three-particle system interacting via two-particle and three-particle pots., scatt. amplitudes 3-40426
- threshold phenomena and their observation, S-matrix unitarity basis 3-67285
- toroidal and spherical bubble nuclei, stability against breathing and sausage deformations 3-43198
- two particle-two hole states, isospin splittings in TDA and RPA 3-43192
- ^{208}Bi , lifetimes and M1 transitions, implications for configuration mixing calcs. 3-45998
- ^6Li one-body densities, reln. between e.m. and weak processes in nuclei 3-49245
- Pb-region, magnetic moments of single particle states, calc. including mesonic exchange currents 3-52080
- ^{208}Pb , inelastic electron scattering form factors of low-lying states, Migdal theory 3-49247
- ^{208}Pb , nucl. response function, excitation props., numerical calc. method 3-52120
- ^{208}Pb , RPA calcs. of low lying states, density dependent interaction 3-49153
- nuclear track emulsions**
- chambers, effect of electron divergence in air gaps on measurement of cascade energy (*Russian*) 3-62249
- coherent generation of particles by 200 GeV/c protons 3-74439
- controlled sensitivity by electric field, photoemulsion camera (*Russian*) 3-73871
- cosmic ray pion inelastic interactions with emulsion nuclei (Ag, Br, C, N, O) at 60 GeV, secondary particle calcs. (*Russian*) 3-69788
- cosmic rays, extraction of high-energy particle information from emulsion data 3-56295
- e.p.r. centres due to presence of tanning agent 3-62248
- grain density of tracks determ. from cavity lengths distrib. (*French*) 3-56941
- heavy nuclei, low-energy, track regression in plastic detectors and photoemulsion due to prolonged exposure (*Russian*) 3-66323
- neutron dosimetry, heavy particle discrimination, etching, counting (*German, English*) 3-62246
- neutron spectra, flux 10 MeV, in artificial satellite of Cosmos series, 200-400 km (*Russian*) 3-65608
- photodisintegration of emulsion nuclei, cross section determ. for 1-4.5 GeV bremsstrahlung (*Russian*) 3-40481
- proton collisions, 200 GeV, white star formation 3-74451
- proton interactions at 200 GeV, mean-free-path and charged multiplicity determ. 3-74452
- proton interactions at 200 GeV, multiplicity distrib., Castagnoli method 3-71025
- proton spectra, using artificial satellite of Cosmos series, 200-400 km, 8 BeV, radiation hazards (*Russian*) 3-65607
- proton track lengths, β -delayed proton emission from ^{113}Xe 3-54438
- sensitivity temp. depend., theoretical expression 3-66326
- π^- collisions with emulsion nuclei, 1.5 GeV, energy division 3-60226
- W emulsion nuclei, 200 GeV proton interactions 3-71024
- nucleation**
- see also crystal growth
- atomistic theory of nucleation rate 3-75695
- atoms, small face centred cubic cluster, 3 to 87 atoms, configuration free energy, atomistic calc. nucleation rate calc. 3-48824
- cholesteryl myristate, mesophase transitions, light scatt. and microscopic obs., spherulite growth kinetics 3-52572
- cholesteryl esters, mesomorphic, spherulite growth kinetics 3-52570
- cloud condensation, activation supersaturation meas., NaCl aerosol, particle size rel. to nucleation 3-44896
- cloud condensation nuclei, supersaturation spectrum, aerosol size distribution and composition 3-76737
- cloud seeding, computer model determ. of convective growth, comments 3-47833
- cloud seeding, fog dispersal, AgI-K₂SO₄ smokes, steady flow cloud chamber 3-80865
- condensation, boiling, homogeneous nucleation theory, corrections for nonideal gases 3-41011
- crystallisation mechanism, heterogeneous nucleation for epitaxial growth 3-40857
- crystallization centre formation in melts and solns., statistics of initial stage in formation (*German*) 3-53185

nucleation continued

- cupric iodates, crystal growth from gel and characterisation 3-80152
 dibutylphthalate aerosol nucleation by NaCl and AgCl 3-58770
 diphasic boiling fluids, thermics and heat exchanges (*French*) 3-43624
 dislocation loop nucleus size, expt. determ. from dimens. change meas. (*French*) 3-54968
 droplet nucleation from vapour, crit. supersaturation values 3-75613
 electrodeposition, three dimensional nucleation during potentiostatic pulse, simulation 3-69466
 ferroelectric switching, nucleation causing wall motion, appl. to barium titanate, triglycine sulphate 3-64612
 ferromagnetic plate, nucleation field calc., mag. anisotropy constant 3-75858
 film growth, coalescence kinetics of migrating crystallites 3-68520
 gas bubble, during crystallisation, review and theory 3-63967
 heterogeneous, and crystal growth, numerical simulation 3-63969
 n-hexane, superheated, nucleation, effect of elec. fields 3-49987
 homogeneous nucleation theory validity 3-79473
 ice, diffusional deposition on AgI, Lake Effect storms, snow crystal struct., Ag content 3-76768
 ice, radionuclide nucleation, supercooled H₂O drops 3-76769
 ice, two-dimensional phase changes and heterogeneous nucleation 3-49969
 ice by AgI, electric field effects 3-47739
 ice nucleation theory and line tension 3-49970
 kinetics for continuous agitated crystalliser design 3-72794
 liquid crystals, nematic-cholesteric relax., electric field induced 3-68151
 liquids, induced by electric field, bubble chamber design for study 3-77719
 marine air, Aitken and giant nuclei, salt conc., wind speed 3-47741
 mathematical framework, solved problems, book contrib. 3-57997
 mechanism at high adsorbate coverages 3-40856
 metal, supercooled melt, spontaneous crystn. kinetics (*Russian*) 3-58609
 metastable liquids and gases, theory of nucleation near crit. point 3-75656
 muscovite plus quartz, high temp. stability, hydrothermal studies, nucleation mechanism 3-44770
 polymer, theory of precipitation from supersaturated solutions 3-63590
 precipitation development, freezing nuclei derived from soil particles 3-76739
 reactor molten fuel-coolant interactions, role of nucleation in vapor explosions 3-46077
 refrigerant nucleate pool boiling heat transfer coeff. pressure dependence, obs. and calc. (*German*) 3-68393
 small cluster of atoms, melting, theory 3-46699
 snow crystals, ice nucleation, cloud seeding 3-73319
 T Tauri stars, grain formation in expanding envelopes 3-48001
 TCNQ crystal, nucleation kinetics of allotropic transformation 3-79488
 theory for analysis of results from shock tube study of condensation kinetics 3-79478
 thin film heterogeneous nucleation theory, application of cluster growth rates 3-43964
 thin film nucleation kinetics, additional processes 3-79596
 three dimensional layer growth by diffusion 3-52764
 water, relative threshold nucleation temps. for active nucleation catalysts 3-49971
 water vapour, homogeneous nucleation using diffusion cloud chamber 3-64164
 Ag, on NaCl: Ag₂SO₄ doped and undoped crystals, epitaxy, electron microscope examination, nucleation and growth processes 3-46768
 Ag, vapour deposition on amorphous C substrates 3-41632
 AgBr growth, formation kinetics, colloidal particles, temperature dependence 3-72021
 AgI as contact or sublimation nuclei, electron-microscopic study 3-64173
 AgI hydrosols, ice-nucleating properties, UV radiation 3-44897
 Au on KCl, spatial distrib., electrostatic defect interactions 3-72023
 Bi thin film, vacuum deposited, nucleus shape obs. 3-79595
 CO₂, condensation in free jet expansion, cluster growth 3-71652
 CO₂ molecules, sticking coeff. on solid H₂O 3-41093
 Ca₁₀(PO₄)₆(OH)₂, hydrothermal growth of single crystals, conditions for nucleation, nucleation and growth 3-69147
 CdS platelets, growth mechanism 3-43965
⁴He, hcp single crystal growth technique, c-axis orientation of 0 and 90°, computer simulation of nucleation 3-51554
 KBr soln., crystn. and nucleation, thermal effects, analysis method 3-43759
 Mo-Re(34 at. %), σ -phase precip. and flux pinning, electron microscope obs. and mag. hysteresis 3-50697
 Na, liquid, explosive vapour interaction following infection into molten UO₂ 3-60284
 NaCl aerosol, activation supersaturation meas., particle size rel. to nucleation 3-44896
 Na₂O-CaO-SiO₂ glass-forming system, nucleation and crystn. 3-72010
 Ni(NH₄)₂(SO₄)₂·6H₂O, rate obs. for agitated and non-agitated systems between 0 and 35°C 3-52589
 Pd, vapour deposition on amorphous C substrates 3-41632
 Si crystal growth, kinetics, O content, seed rotation 3-68175
 Ta film, sputtered, factors controlling struct. 3-41111
 W, condensation on its own surface 3-52752
 Zn film deposition on single crystal Ge surfaces 3-61110
 Zn silicate glass, alkali, nucleation and crystallization properties 3-75476
 ZnO film, prep. by cold plasma condensation, growth kinetics (*French*) 3-52772

nuclei see nucleus**nuclei with A ≤ 5**

- A=3, T-matrix perturbation theory in bound state 3-60065
 A=4 nuclei, compilation of energy levels 3-43181
 atomic nuclei, collision with H-like ions, ionisation cross-section, influence of structure of bound state (*Russian*) 3-67707
 bound-state properties of three and four nucleons with realistic NN-potential 3-49163

nuclei with A ≤ 5 continued

- four nucleons, interaction in even orbital momentum states, integral equations (*Russian*) 3-74507
 gas, nuclear spin-lattice relax. rel. to O₂ conc., at 23°C 3-54793
 hypernuclei, A=4, ΔN interaction spin dependence 3-71072
 tri-nucleon system exchange magnetic moment, calc. of isoscalar part by ρ -exchange and OBE models 3-49121
 trinucleon system from N-d backward elastic scattering, virtual states 3-52165
²D, n.m.r. in t-butylchloride, self-diffusion coeff. and rot. correlation time determ. 3-68872
²D n.m.r., cryst. structure obs. of NaNH₄SeO₄·2H₂O 3-75516
 D(p,n)p, breakup neutrons polarisation meas. at 21.5 MeV 3-52163
¹H, determ. of ratio of proton and deuteron nuclear mag. moments 3-62936
¹H, n.m.r. in t-butylchloride, self-diffusion coeff. and rot. correlation time determ. 3-68872
¹H, p.m.r. in 2,4,6-nonachloromesitylene, rotational isomerism, conformational energy 3-67851
¹H chem. shifts in fluoroacetones 3-46323
¹H fast Fourier transform n.m.r. spectroscopy of pyridine nucleotides, esp. dinucleotides, conformation 3-67850
¹H n.m.r., cryst. structure obs. of NaNH₄SeO₄·2H₂O 3-75516
¹H off resonance decoupling, ¹³C n.m.r. of tri(3-bromo-2-thienyl)phosphine 3-75069
¹H p.m.r. in 2,4,6-trifluoronitrobenzene, external electric field effects 3-68854
¹H p.m.r. in K₂Pt(CN)₄Br_{0.3}·nH₂O (*German*) 3-50482
¹H p.m.r. of butadiene-1,3 3-43484
¹H p.m.r. of cis and trans phytoene isomers 3-46361
¹H pseudo magnetic moments meas. method 3-67185
¹H-¹H, heteronuclear magnetic double resonance spectra, carboranes and organotin derivatives 3-78848
¹H-¹⁵N n.m.r. coupling consts. of aminophosphines, bonding 3-71575
¹H-¹H bremsstrahlung, 156 MeV differential cross sections, off shell effects 3-78335
¹H-(³¹P), ³¹P-(¹H) heteronuclear n.m.d.r., nonlinearities and nucl. Overhauser effect 3-75082
¹H-(³¹P) heteronuclear chemical exchange spin decoupling dispersion 3-75086
¹H(d,d)³H scattering, 30 MeV, meas. of vector and tensor analysing power 3-49235
¹H(n,n), ang. distrib., 24 and 27.2 MeV neutrons 3-40478
¹H(n,p), thermal radiative capture, meson exchange effects 3-60153
¹H(n,p), 50 MeV, differential cross sections 3-63031
¹H(p,p)¹H, absolute cross-section meas., 500-2000 keV (*German*) 3-49231
²H, breakup in heavy nuclei fields, 7-12 MeV 3-60204
²H, change in magnetic moment from spin-orbit potential in nucleon-nucleon interaction 3-71044
²H, d-induced reaction, neutron yields and spectra meas., rel. to high intensity neutron sources 3-74596
²H, determ. of ratio of proton and deuteron nuclear mag. moments 3-62936
²H, deuteron interactions at high energy (*Russian*) 3-40383
²H, disintegration effect on optical potential using adiabatic approximation, nucleon-nucleus potential 3-60142
²H, n.m.r. obs. of methyl group exchange in tetramethyltitanium and tetramethylaluminum 3-75089
²H, n.m.r. of ether in chloroform, association and anisotropic mol. reorientation 3-68873
²H, neutron scatt., polarization asymmetry, 35 MeV 3-74553
²H, nucleon breakup reaction, new set of kinematic variables 3-71095
²H, nucleon induced exact breakup calc. by solution of three-particle Faddeev eqn. 3-60155
²H, phase shifts, binding energy and quadrupole moment calc. using N-N interaction with Yamaguchi form factors 3-74503
²H binding energy determ. using coherent non-local separable N-N interactions 3-74502
²H decoupling, effect on n.m.r. spectrum of polypropylene-2-d₁ sulphide 3-63578
²H exchange magnetic moment, calc. of isoscalar part by ρ -exchange and OBE models 3-49121
²H n.m.r. in lyotropic liq. cryst., mag. field gradient 3-47154
²H n.q.r. in CH₃COND₂, fine structure 3-63522
²H photoeffect, electric-quadrupole contrib. 3-67299
²H-d and ³H-d reactions, absolute determ. of differential neutron source strength (*German*) 3-59636
²H + ³He, study by one-channel resonating group method, phase shift and differential cross section 3-74556
²H + ³He, study by one-channel resonating group method, phase shift and differential cross section 3-74556
²H(²H, d)p, breakup reaction, 14-36 MeV, modified plane wave impulse approximation theory 3-60154
²H(³He, ³H)p, effects of exchange, final-state interactions and distorted waves 3-52161
²H(³He, ³He)p, effects of exchange, final-state interactions and distorted waves 3-52161
²H(³He, p)t, quasifree reaction mechanisms, absolute cross sections, correlation spectra, pole diagrams 3-67303
²H(α , α p), differential cross section, off energy shell impulse approximation 3-54455
²H(α ,dt)¹H, 70 MeV sequential reaction through ⁴He, obs. of excited states 3-63032
²H(α ,pd)³H, 70 MeV sequential reaction through ³He, obs. of excited states 3-63032
²H(α ,t)³He, 82 MeV, multi-interaction, finite-range, two-mode DWBA analysis 3-67297
²H(d, ³He)n, liquid organic scintillator efficiency 3-73865
²H(d, n)³He, up to 1 MeV, polarization of neutrons 3-40016
²H(d,d)²H, 3-11.5 MeV polarised deuterons, meas. of vector and tensor analysing powers (*German*) 3-49233
²H(d,n)³He, 3-11.5 MeV polarised deuterons, meas. of vector and tensor analysing powers (*German*) 3-49233
²H(d,n)³He, 330 keV, 3 MeV polarised neutron production 3-71109
²H(d,n)³He, polarised deuteron beam, 3.3-14.9 MeV, meas. of longitudinal polarization transfer at 0 degrees 3-57506

nuclei with $A \leq 5$ continued

- $^2\text{H}(d,n)^3\text{He}$, rel. diff. cross-sect. meas., 300 to 700 keV 3-46017
 $^2\text{H}(d,p)^3\text{H}$, 3-11.5 MeV polarised deuterons, meas. of vector and tensor analysing powers (*German*) 3-49233
 $^2\text{H}(d,p)^3\text{H}$, 6-15 MeV, meas. of polarisation transfer coeffs. at angle of 0° 3-74555
 $^2\text{H}(d,p)^3\text{H}$, rel. diff. cross-sect. meas., 300 to 700 keV 3-46017
 $^2\text{H}(d,pd)n$, spatial localization effects 3-63033
 $^2\text{H}(p,n)p$, 22.2 MeV, calc. corrections due to mesonic currents, proton and neutron polarisation 3-71096
 $^2\text{H}(n,2n)^3\text{H}$ break-up process local two-nucleon S-wave potentials and separable Yamaguchi potential 3-60150
 $^2\text{H}(n,2n)^3\text{H}$, three-body calc. of neutron-neutron scattering length and effective range 3-78340
 $^2\text{H}(n,2n)p$, 14.17 MeV, cross section and neutron-neutron scattering length calc. Amado model 3-78336
 $^2\text{H}(n,n)$, scatt. amplitude exam. by Feynman diagram tech. 3-54457
 $^2\text{H}(n,n)^2\text{H}$, cross section and angular distrib. meas., 40-340 MeV (*Russian*) 3-74551
 $^2\text{H}(n,np)n$, 130 MeV, kinematically complete ext., determ. of neutron-neutron scattering length 3-78338
 $^2\text{H}(n,p)nn$, 14 MeV, spectra meas., validity of impulse approx. for nn scattering length 3-78339
 $^2\text{H}(p,2p)$ at 65 MeV cross section meas., energy and target mass dependence 3-71097
 $^2\text{H}(p,2p)n$, 156 MeV differential cross sections, off shell effects 3-78335
 $^2\text{H}(p,n)2p$, spectra meas., 16-26 MeV, determ. of pp scattering length 3-78337
 $^2\text{H}(p,n)pp$, 16-26 MeV, neutron spectra meas., determ. of proton-proton final state interaction 3-71098
 $^2\text{H}(p,pp)n$, 30 MeV, obs. of prominent two-body processes, comparison with Amado model 3-71099
 $^2\text{H}(p,pp)n$, 30-100 MeV, rescattering series convergence 3-63021
 $^2\text{H}(p,pp)n$, 39.5 MeV cross section meas. over large volume of phase space, final state interaction effects 3-74557
 $^2\text{H}(\pi^+\pi^-)$ type reaction, isobar mechanism, high energy 3-78356
 ^2H , binding energy calc. for Reid's soft-core nucleon-nucleon interaction 3-49073
 ^3H , β -decay, Curie plot analysis, determ. of neutrino mass. 3-54441
 ^3H , disintegration effect on optical potential using adiabatic approximation, nucleon-nucleus potential 3-60142
 ^3H , effect of short-range part of nucleon nucleon interaction, low energy properties 3-62959
 ^3H , evidence for strong three-body forces 3-62955
 ^3H , evidence for strong three-body force 3-78262
 ^3H , French production facilities (*French*) 3-57550
 ^3H , handling, radiation protection (*French*) 3-59458
 ^3H , liquid scintillation counter for radioactivity measurements 3-42649
 ^3H , magnetic moment, effect of meson-exchange currents 3-49120
 ^3H , natural gas, radiation dose calcs., hypothetical exposure 3-78395
 ^3H , profiles, meas. of accumulation on Jungfraujoch (*German*) 3-51210
 ^3H , supersmall quantity meas. by low-background installation using miniature proportional counters (*Russian*) 3-65403
 ^3H , three-body forces, various theories 3-78261
 $^3\text{H}^{1,2}$ state below break-up threshold, Gammel-Brueckner potential 3-52107
 ^3H binding energy, investigation of off-shell effects, various nucleon-nucleon potentials 3-71036
 ^3H binding energy, three-body calcs. 3-78260
 ^3H binding energy determ. using coherent non-local separable N-N interactions 3-74502
 ^3H concentration in North Pacific, liquid scintillation counting 3-69561
 ^3H in Haverro meteorite, radioactivity meas. 3-45066
 ^3H magnetic moment, quark model study, nucleon and nuclear resonance effects 3-52073
 $^3\text{H} + ^2\text{H}$, 35 MeV, quasifree reaction mechanisms, absolute cross sections, correlation spectra, pole diagrams 3-67303
 $^3\text{H} + ^3\text{He}$, 50 MeV, quasifree reaction mechanisms, absolute cross sections, correlation spectra, pole diagrams 3-67303
 $^3\text{H}(^3\text{He},d)^4\text{He}$, 291-800 keV, ^6Li levels, isospin violation, energy depend. 3-78306
 $^3\text{H}(^3\text{He},p)^6\text{Li}$, ~ 10 MeV, direct capture model for cross-section 3-78308
 $^3\text{H}(d,n)^4\text{He}$ reaction in ion accelerators for neutron production (*French*) 3-56917
 $^3\text{H}(n,p)nn$, exptl. requirements for determ. of neutron-neutron scattering length 3-71098
 $^3\text{H}(p,\gamma)^4\text{He}$, 156 MeV radiative capture, calc. of differential cross section in peripheral model 3-52164
 $^3\text{H}(n,p)^3\text{He}$, $E_p = 156$ MeV, multiple scatt. effects, Glauber approx. 3-43233
 $^3\text{H}(p,p)^3\text{H}$, $E_p = 156$ MeV, multiple scatt. effects, Glauber approx. 3-43233
 $^4\text{He}^*$, excited states produced by K^- mesons stopping in ^6Li , obs. of γ -transitions 3-78277
 ^4He , binding energy, Λ -d scattering lengths, dependence on $\Lambda\Sigma$ coupling, perturbative treatment 3-62979
 ^4He excited states, effects of $\Lambda\Sigma$ coupling 3-67252
 ^4He hyperon + rigid 3N core model, effects of $\Lambda\Sigma$ coupling 3-67251
 ^4He , disintegration effect on optical potential using adiabatic approximation, nucleon-nucleus potential 3-60142
 ^4He , from $^6\text{Li}(p,^3\text{He})^4\text{He}$, meas. angular distribution rel. to clustering in ^6Li 3-60103
 ^4He , high-energy inelastic electron scattering, final state interaction effects on cross section (*Russian*) 3-52158
 ^4He , liquid, continuous refrigerator, flow impedance construction 3-51553
 ^4He , magnetic moment, effect of meson-exchange currents 3-49120
 ^4He , ν decay, Mossbauer effect, limits on elementary length 3-66979
 ^4He , polarisation in elastic scattering from ^{27}Al and ^{28}Si , deduced optical model parameters 3-67349
 ^4He , production spectra in 30 to 60 MeV proton bombardment of nuclei with $A=12$ to 209 3-74588

nuclei with $A \leq 5$ continued

- ^4He , π^+ photoproduction in first π -N resonance region, impulse approx., cross section 3-67300
 ^4He , search for excited states with $p + ^6\text{Li}$ reaction, 35-56 MeV 3-49138
 $^4\text{He}^{1,2}$ state below break-up threshold, Gammel-Brueckner potential 3-52107
 ^4He average optical potential, appl. to $(^3\text{He}, \alpha)$ reaction on s-d shell nuclei 3-49272
 ^4He continuous spectrum associated with reaction $^{12}\text{C}(d, ^3\text{He})^{11}\text{B}$, direct reaction mechanism 3-60207
 ^4He photodisintegration, two-body, cross section calc. using ^3He and proton-deuteron wave functions 3-67301
 ^4He pion absorption, two-nucleon model, ratio for nnp to nd production rates 3-78304
 ^4He spectrometer, fast neutron meas., Th, D_2O , $\text{Th}(\text{NO}_3)_4$ 3-7115
 ^4He -He region, introduction into blanket of D-D fusion machine 3-60324
 $^4\text{He}^+$, ion bombardment, Ni, stainless steel, He distrib. profiles, $^4\text{He}(d,p)^4\text{He}$ reaction 3-63209
 $^4\text{He}^{2+}$, nucl. polarisation feasibility by electron-transfer processes 3-51686
 ^4He -d self-colliding mixture (migma), nonplasma nonthermal fusion power source 3-74742
 $^4\text{He} + ^3\text{H}$, reactions, 50 MeV, quasifree reaction mechanisms, absolute cross sections and correlation spectra 3-67303
 $^4\text{He}(e,e'p)^3\text{He}$, cross section, depend. on p-d relative motion energy 3-78310
 $^4\text{He}(p,d)^3\text{H}$, differential cross-section meas., 11-65 MeV 3-74554
 $^4\text{He}(p,2p)$ at 85 MeV cross section meas., energy and target mass dependence 3-71097
 $^4\text{He}(p,p)^4\text{He}$, $E_p = 156$ MeV, multiple scatt. effects, Glauber approx. 3-43233
 ^4He , calc. of bound state energies using four body integral eqns. 3-71053
 ^4He , charge form factor, self consistent centre of mass correction, Hartree-Fock method 3-62975
 ^4He , effective kinetic energy four-body forces contribution to binding energy 3-49072
 ^4He , electric-dipole sum rule and two-body correlations 3-78240
 ^4He , from thermal neutron fission of ^{239}Pu , energy spectrum, angular distribution 3-54517
 ^4He , ground state, variational techniques, pseudometric approach, separation of centre-of-mass contributions 3-60074
 ^4He , liquid, continuous refrigerator, flow impedance construction 3-51553
 ^4He , microscopic treatment of coupled monopole and quadrupole vibration using generator coordinate method 3-45985
 ^4He , model with separable potential, 0^+ state 3-78263
 ^4He , p elastic scatt. at 1 GeV, precise single-scatt. optical pot. fit 3-46018
 ^4He , pumping to 0.7 K, adsorption pump, cryostat design 3-48392
 ^4He , π scattering, ambiguities in phase-shift analysis 3-43232
 ^4He , soft core potentials, dependence of binding energy, nucleon density, form factors 3-45979
 ^4He , T=O state study from $^2\text{H}(d,p)$ and $^2\text{H}(d,n)$ 3-46017
 ^4He average optical potential, appl. to $(^3\text{He}, \alpha)$ reaction on s-d shell nuclei 3-49272
 ^4He charge form factor from normalization of p- ^3He and n- ^3He tails 3-49074
 ^4He equivalent radius determ. from π^- - ^4He scattering at 3.48 and 6.13 GeV/c (*Russian*) 3-67124
 ^4He excited states obs. in $^2\text{H}(\alpha,dt)^3\text{H}$ sequential reaction at 70 MeV 3-63032
 ^4He from $^6\text{Li}(p,^3\text{He})^4\text{He}$, meas. angular distribution rel. to clustering in ^6Li 3-60103
 ^4He gas detectors, $^{124}\text{Sb}-\text{Be}(p,n)$ assay system, fissile content meas., small samples, fuel rods and solns. 3-67557
 ^4He ground state binding energy calc. in totally symmetric wave function approx. (*Russian*) 3-40437
 ^4He magnetic moment, quark model study, nucleon and nuclear resonance effects 3-52073
 $^4\text{He}^*$, excited states produced by K^- mesons stopping in ^6Li , obs. of γ -transitions 3-78277
 $^4\text{He}-\pi^+$ elastic scatt., e.m. pion radius 3-78305
 $^4\text{He}(^3\text{He}, ^3\text{He})$ at 7.4 MeV, meas. bremsstrahlung, differential cross section determ. 3-74560
 $^4\text{He}(N,N)^4\text{He}$, comparison of $^4\text{He}-^3\text{He}$ -n and $^4\text{He}-^3\text{He}$ -p coupling constants, reln. to ^4He structure (*German*) 3-49234
 $^4\text{He}(\alpha,\alpha')$ bremsstrahlung meas. at 9.35 MeV, differential cross section determ. 3-74561
 $^4\text{He}(\alpha,\alpha')^4\text{He}$, Regge representation including background term 3-52162
 $^4\text{He}(d,d)^4\text{He}$, 11.5 to 17 MeV, incident vector polarised ^2H , meas. vector analysing power iT_{11} 3-74552
 $^4\text{He}(p,p)^4\text{He}$, 180 to 320 MeV, photon energies, meas. differential cross section, proton angular distribution 3-67302
 $^4\text{He}(p,p)^4\text{He}$ and $^4\text{He}(p,n)^3\text{He}$ cross section ratio in giant resonance region, charge symmetry 3-52160
 $^4\text{He}(n,n)^4\text{He}$, 0-21 MeV, energy dependent phase shift analysis, error matrices 3-60152
 $^4\text{He}(n,n)^4\text{He}$, asymmetry meas. to deduce neutron polarisation in $^2\text{H}(d,n)^3\text{He}$ reaction 3-71109
 $^4\text{He}(n,n)^4\text{He}$, energies ≤ 3 MeV, energy-dependent phase shift analysis, effective range parameters 3-60151
 $^4\text{He}(p,2p)$ at 100 MeV cross section meas., energy and target mass dependence 3-71097
 $^4\text{He}(p,d)^3\text{He}$, inelastic channels at medium incident energies 3-54479
 $^4\text{He}(p,p)^4\text{He}$, 22, 45 MeV, p- α bremsstrahlung and cross section meas. 3-74559
 $^4\text{He}(p,p)$, Coulomb-modified dispersion relation, low-energy 3-49236
 $^4\text{He}(p,p)^4\text{He}$, 0-23 MeV, energy dependent phase shift analysis, error matrices 3-60152
 $^4\text{He}(p,p)^4\text{He}$, analysis by forward dispersion relations, determ. of pole residues and coupling consts. 3-49232
 $^4\text{He}(p,p)^4\text{He}$, energies ≤ 5 MeV, energy-dependent phase shift analysis, effective range parameters 3-60151
 $^4\text{He}(p,\pi^+)$, 600 MeV, forward cross section calc. 3-57520

nuclei with $A \leq 5$ continued

- ^4He , fission product of ^{252}Cf , detection, yield 3-78363
 ^4He , ground and first excited state obs. from $^7\text{Li} + d$ reaction 3-62954
 ^4He , level structure determ. using $^2\text{H} + ^3\text{He}$ system 3-74556
 ^4He , obs. in ^{252}Cf ternary fission 3-43261
 ^4He excited states obs. in $^2\text{H}(\alpha, p)^3\text{H}$ sequential reactions at 70 MeV 3-63032
 ^4He , prod. through $n(K^-, \pi^-)A^0$ reaction, with 500-800 MeV/c kaons 3-54418
 ^4He excited states, effects of Λ - Σ coupling 3-67252
 $^4\text{He} - ^4\text{H}$ hyperon + rigid $3N$ core model, effects of Λ - Σ coupling 3-67251
 $\text{He}(e, e)$, $A=3, 4$, evidence for hard core existence (German) 3-46016
 $\text{H}^2(n, p)\text{H}^3$, cross section, meson-exchange corrections 3-54456
 ^4Li , four nucleon cluster, rel. to capture of π^- mesons in ^{16}O nuclei with ^8Li emission (Russian) 3-67375
 ^5Li , level structure determ. using $^2\text{H} + ^3\text{H}$ system 3-74556
 ^6Li , allowance for final nucleus instability in quasielastic knockout of protons 3-60172
 $t = d + n$ vertex, coupling constant and form factor 3-52106

nuclei with $6 \leq A \leq 19$

- $A=17-27$, projected Hartree-Fock calcs. of spin-isospin matrix elements 3-49180
 $A=19$ isobar, charge asymmetry due to Coulomb interaction determ. 3-67176
 $A=19$ nuclei, core-polarisation effects on E2 transitions 3-52134
 $A=7$ and 8 nuclei, shell model calculations, non-normal parity states, cross sections of photonuclear reactions 3-54403
light nuclei states, oscillator cluster parentage and supermultiplet expansion 3-52112
nuclear Zeeman splitting by anal. linear polarization 3-71081
 ^7Li , n.m.r. spectra of $\text{Li}_2\text{O-K}_2\text{O-TiO}_2\text{-SiO}_2$ glass, ion struct. 3-72528
 B , isotopes produced in ^{14}N spallation, meas. production cross section, 17 to 42 MeV astrophysical significance 3-67330
 ^8B , produced in $^6\text{Li}(^3\text{He}, n)^8\text{B}$, reaction, meas. yield from positron decay rel. to neutrino detection 3-67351
 ^8B , recoil polarisation from $^6\text{Li}(^3\text{He}, n)$, n.m.r. meas. of β -decay asymmetry, magnetic moment determ. 3-49077
 ^8B in Ta , n.m.r. detn. of mag. moment 3-45963
 ^8B photodisintegration in solar interior 3-65642
 ^{10}B , (p, α) , (p, n) and (p, p') reactions at low energies, optical model and Hauser-Feshbach analysis 3-57533
 ^{10}B , deduced levels from $^9\text{Be}(p, p)^9\text{Be}$, 0.8 to 2.7 MeV 3-63047
 ^{10}B , muon capture, partial transitions, gamma-neutrino correlation 3-63002
 ^{10}B , verification of model representation of excited states using ^9Be -proton interactions (Russian) 3-74570
 ^{10}B - ^{11}B primary isotope effect on boron nucl. shielding 3-46324
 $^{10}\text{B}(^4\text{He}, \alpha)$, pop high spin states in ^{23}Na , meas. ang. distrib., obs. strong selectivity 3-67364
 $^{10}\text{B}(\alpha, 2\alpha)^8\text{Li}$, 24 MeV, angular distrib. of sequential decay process 3-40472
 $^{10}\text{B}(\alpha, \alpha)^{10}\text{B}$, 2.0-4.3 MeV, obs. of level structure in ^{14}N , excitation functions and α -particle decay 3-71055
 $^{10}\text{B}(d, p)^{11}\text{B}$, 0.67-2.32 MeV, DWBA analysis deduced spectroscopic factors of 6.76 MeV level of ^{11}B 3-62938
 $^{10}\text{B}(d, n)^{11}\text{B}$, low energy branching ratios, isobaric analogue states 3-74599
 $^{10}\text{B}(d, p)^{11}\text{B}$, low energy, branching ratios, isobaric analogue states 3-74599
 $^{10}\text{B}(d, t)$, j-dependence of triton angular distrib. (Russian) 3-52191
 $^{10}\text{B}(n, \alpha)$ used as standard cross section shape for ^{235}U fission cross section meas. 3-74612
 ^{11}B , ^{12}B , quadrupole moment calc. using Cohen Kurath wavefunctions 3-49128
 ^{11}B , n.m.r. studies of tourmaline minerals especially elbaite crystal structure 3-44768
 ^{11}B , operation of d.n.m.r. spectrometer attachment 3-73825
 ^{11}B , resonance scattering of bremsstrahlung, low-lying level study 3-52094
 ^{11}B , spectroscopic factors of 6.76 MeV level deduced from DWBA analysis of $^{10}\text{B}(d, p)^{11}\text{B}$ 3-62938
 ^{11}B heavy-ion single-nucleon transfer reactions, recoil effects, DWBA and exptl. study 3-71125
 ^{11}B n.m.r. in 2-[2'-pentaboran(9)yl]pentaborane(9) 3-78840
 ^{11}B n.m.r. in B_2H_6 and B_3D_6 , splittings resolution, line narrowing technique 3-57666
 ^{11}B n.m.r. in $\text{Na}_2\text{O-B}_2\text{O}_3\text{-SiO}_2$ glass, coordination struct. (German) 3-68162
 ^{11}B production in $^9\text{Be}(^3\text{He}, pp)^{11}\text{B}$ and $^9\text{Be}(^3\text{He}, p)^{11}\text{B}$ reactions, compound nucleus mechanism, forbidden J 3-52198
 $^{11}\text{B-H}$, heteronuclear magnetic double resonance spectra, carboranes and organotin derivatives 3-78848
 $^{11}\text{B}^*$, highly excited nucleus, from $^{12}\text{C}(d, ^3\text{He})$, ^3He continuous spectrum calculated, direct reaction mechanism 3-60207
 $^{11}\text{B}(^3\text{He}, \alpha)^{10}\text{B}$, 8.0 to 12.0 MeV, coupled-channel Born approximation, direct reactions on light nuclei 3-60210
 $^{11}\text{B}(\alpha, ^8\text{Be})$, $E_\alpha=65$ MeV, α -transfer feasibility studies 3-63073
 $^{11}\text{B}(\alpha, n)^{14}\text{N}$, $E_\alpha=12-15$ MeV, cluster transfer 3-63070
 $^{11}\text{B}(d, p)^{12}\text{B}$, $E=1-4$ MeV, cross sections, ^{13}C deduced resonances 3-67341
 $^{11}\text{B}(d, p)^{12}\text{B}$, recoil implantation in Ta , n.m.r. meas., alignment and quadrupole spectrum determ. 3-49078
 $^{11}\text{B}(\gamma, \pi^-)^{11}\text{C}$, theoretical photoproduction investigation 3-43234
 $^{11}\text{B}(p, 3\alpha)$, 2.0 and 2.65 MeV, α -particle coincidence spectra, calc. of resonant peak positions (Russian) 3-74567
 ^{12}B , ^{13}B , recoil polarisation through nuclear reaction into Mg crystal, quadrupole coupling, $Q(^{12}\text{B})$ to $Q(^{13}\text{B})$ ratio 3-49079
 ^{12}B , recoil implanted in Ta following $^{11}\text{B}(d, p)$ reaction, n.m.r. meas., determ. of sign of eqQ 3-49078
 ^{12}B analogue state, excitation during charged pion photoproduction from ^{12}C 3-49240
 ^{12}B β -decay, search for weak-electric moment 3-49224
 ^{12}B in Ta , n.m.r. detn. of mag. moment 3-45963
 ^{12}B , mass excess and low lying level structure studied by $^{14}\text{C}(\text{Li}, ^7\text{Be})^{12}\text{B}$ 3-62925
 ^{13}B , isotope obs. at limits of particle stability 3-63092
- nuclei with $6 \leq A \leq 19$ continued
 Be , anisotropic scattering eff. in reflected fast critical assemblies, calc. 3-49328
 Be , high-energy proton interactions, Σ^- prod. 3-46029
 Be , isotopes produced in ^{14}N spallation, meas. production cross section, 17 to 42 MeV astrophysical significance 3-67330
 Be deuteron cross-section for stripping and dissociation, 2.7 GeV/c, measurement 3-78344
 ^7Be , branching ratios of electron capture transitions 3-67266
 ^7Be destruction in solar interior 3-53601
 ^7Be in BeO , effect of pressure on electron capture decay constant 3-63013
 ^7Be production in spallation of ^{13}C by 150 and 600 MeV protons rel. to astrophysical conditions 3-54476
 ^8Be , alpha-decay width analysis, ground band levels, model wave functions 3-60133
 ^8Be , η -meson photoproduction, 2 GeV, cross section meas. 3-78311
 ^8Be , second excited state obs. from $^7\text{Li} + d$ reaction 3-62954
 ^8Be , unified shell-cluster model based on molecular orbital method 3-43194
 ^8Be effective kinetic energy four-body forces contribution to binding energy 3-49072
 ^8Be level determ. from $^7\text{Li}(d, n\alpha)$ reaction with polarised 800 keV deuterons 3-60197
 ^8Be structure determ. from $^7\text{Li}(p, p)^7\text{Li}$ 3-46025
 ^9Be , ^2h induced reaction at 20 MeV, meas. neutron spectra and yield 3-74596
 ^9Be , 1.9 to 3 MeV proton interactions, verification of model representation of ^{10}B excited states (Russian) 3-74570
 ^9Be , (d, d) and (d, p) reactions at low energies, optical model and Hauser-Feshbach analysis 3-57533
 ^9Be , compound nucleus, produced in $^7\text{Li}(d, \alpha n)^4\text{He}$, spin, parity assignment 3-71120
 ^9Be , inelastic electron scattering, electromagnetic properties, Nilsson model and experiment comparison 3-54386
 ^9Be , nuclear mag. relax. in GdBe_{13} , TbBe_{13} and DyBe_{13} (French) 3-55427
 ^9Be , π induced 90-860 MeV total cross-section meas. π -nucleus coupling constant obtained 3-71131
 ^9Be , π^\pm total cross sections and π ^9Be coupling constant, Glauber model 3-46043
 ^9Be , quadrupole moment determ. 3-46169
 ^9Be , structure determ. from proton scattering studies, 6-30 MeV 3-52184
 ^9Be , total cross sections of π^\pm mesons, 90-860 MeV 3-74609
 ^9Be (d, p) , 12.3 MeV, importance of D-state effects 3-54486
 ^9Be production in spallation of ^{13}C by 150 and 600 MeV protons rel. to astrophysical conditions 3-54476
 $^9\text{Be} + \text{D}$, fast neutron dose rate 3-77288
 $^9\text{Be}(^3\text{He}, n)^{11}\text{C}$, compound nucleus mechanism, forbidden J 3-52198
 $^9\text{Be}(^3\text{He}, n)^{11}\text{C}$, compound nucleus mechanism, forbidden J 3-52198
 $^9\text{Be}(^3\text{He}, p)^{11}\text{B}$, compound nucleus mechanism, forbidden J 3-52198
 $^9\text{Be}(^3\text{He}, p)^{11}\text{B}$, compound nucleus mechanism, forbidden J 3-52198
 $^9\text{Be}(\alpha, \alpha)^9\text{Be}$, 1.7-6.2 MeV, excitation functions and angular distrib., compound-nucleus theory, ^{13}C states 3-63075
 $^9\text{Be}(\alpha, n)$, neutron spectra of $^{241}\text{Am-}^9\text{Be}$ source 3-77607
 $^9\text{Be}(\alpha, n)^{12}\text{C}$, 4.5-5.85 MeV, meas. of neutron polarisation angular distrib., ^{13}C states 3-62946
 $^9\text{Be}(d, t)$, j-dependence of triton angular distrib. (Russian) 3-52191
 $^9\text{Be}(e, e)$, 1184 MeV, quasielastic scattering, shell and Fermi gas model interpretation (Russian) 3-57515
 $^9\text{Be}(e, e)$, electroexcitation of levels in 14-18 MeV region 3-54465
 $^9\text{Be}(p, \alpha)$, 30-700 keV, meas. cross sections, R matrix compound nucleus model, ^{10}B deduced resonance parameters 3-60181
 $^9\text{Be}(p, d)$, 30-700 keV, cross section and angular distrib. meas., ^{10}B resonance parameters 3-60181
 $^9\text{Be}(p, p)^9\text{Be}$ 0.8 to 2.7 MeV, analysing power, deduced phase shifts, ^{10}B deduced levels 3-63047
 $^9\text{Be}(p, \alpha)^6\text{Li}$, 6 MeV multi-interaction, finite-range, two-mode DWBA analysis 3-67297
 $^9\text{Be}(p, \alpha)^6\text{He}$, 35 to 160 MeV, description using various wave functions, α -clusters for ^9Be 3-60179
 $^9\text{Be}(\pi, \pi)^9\text{Be}$, 90-860 MeV, π -nucleus coupling constant determ. from π scat. 3-63088
 $^9\text{Be}(t, ^6\text{Li})^9\text{Be}$, $E_t=23.5$ MeV, supermultiplet symmetry 3-63068
 $^9\text{Be}(t, ^6\text{Li})^9\text{Be}$, $E_t=23.5$ MeV, supermultiplet symmetry 3-63068
 ^{10}Be , resonance parameters from cross section meas. on $^9\text{Be}(p, \alpha)$, (d, p) reaction 3-60181
 ^{10}Be half-life, modification of cross sections for $^{10}\text{Be}(d, p)^{11}\text{Be}$, $^{10}\text{Be}(d, \alpha)^8\text{Li}$ and $^{10}\text{Be}(p, p)^{11}\text{B}$ 3-40505
 ^{10}Be production in spallation of ^{13}C by 150 and 600 MeV protons rel. to astrophysical conditions 3-54476
 $^{10}\text{Be}(d, \alpha)^8\text{Li}$ cross sections modification for half-life of ^{10}Be 3-40505
 $^{10}\text{Be}(d, p)^{11}\text{Be}$ cross sections modification for half-life of ^{10}Be 3-40505
 $^{10}\text{Be}(p, p)^{11}\text{Be}$ cross sections modification for half-life of ^{10}Be 3-40505
 ^{14}Be , isotope obs. at limits of particle stability 3-63092
 C , cosmic ray proton inelastic interactions, $10^{11}-10^{12}$ eV, effective cross-section meas. on PROTON-4 satellite (Russian) 3-69787
 C , hadron scattering, Regge-pole model analysis, factorization 3-67073
 C , neutron halo deduced from p absorption 3-60083
 C , nucleon cosmic ray interactions at mountain altitudes, 600-10000 GeV, integral energy spectrum (Russian) 3-69781
 C , π^- , π^+ reaction cross sections, 584 to 1856 MeV, deduced neutron density 3-54507
 C , π^\pm reactions, 90-850 MeV, Coulomb effects in total cross-sections 3-60227
 C , total cross sections of π^\pm mesons, 90-860 MeV 3-74609
 C , total neutron cross section meas. 0.4-2.4 MeV 3-60285
 C deuteron cross-section for stripping and dissociation, 2.7 GeV/c, measurement 3-78344
 ^{11}C , quadrupole moment calc. using Cohen Kurath wavefunctions 3-49128
 ^{11}C activity, conversion factors for dose and dose equivalent 3-77280

nuclei with $6 \leq A \leq 19$ continued

- ^{11}C heavy-ion single-nucleon transfer reactions, recoil effect, DWBA and exptl. study 3-71125
- ^{11}C production in $^9\text{Be}(^3\text{He}, n)^{11}\text{C}$ and $^9\text{Be}(^3\text{He}, n)^{11}\text{C}$ reactions, compound nucleus mechanism, forbidden J 3-52198
- ^{12}C , ^{13}C , elastic, inelastic scatt. of ^6Li , ^7Li , single nucleon transfer, meas. 3-78349
- ^{12}C , ^2H induced reaction at 20 MeV, meas. neutron spectra and yield 3-74596
- ^{12}C , alpha-particle elastic and inelastic scattering at 139 MeV, optical model and DWBA analyses 3-49270
- ^{12}C , calc. of quadrupole, hexadecapole and 2^6 pole deformation parameters (Russian) 3-67183
- ^{12}C , charged pion photoproduction with excitation of ^{12}B , ^{12}N analogue states 3-49240
- ^{12}C , decay of photo resonances, shell model analysis, cross section and branching ratios 3-49239
- ^{12}C , elastic and inelastic scattering of 1.04 GeV protons, angular distrib. meas. 3-57522
- ^{12}C , electron inelastic scatt., electron angular distrib., calc. compared with expt. (Russian) 3-67315
- ^{12}C , η -meson photoproduction, 2 GeV, cross section meas. 3-78311
- ^{12}C , giant dipole states and excited dipole states in continuum approx., (ν, N) and (N, ν) reaction 3-67193
- ^{12}C , ground-state rotational band study from ^{16}O α -decay 3-45980
- ^{12}C , J=0 states described by cluster model of three structureless alpha particles 3-67243
- ^{12}C , low energy neutron scattering, microscopic description using generalised R-matrix theory 3-60183
- ^{12}C , low q^2 electron scattering from 15-109 MeV state, 35-55 MeV incident, conserved vector current test 3-60165
- ^{12}C , microscopic treatment of coupled monopole and quadrupole vibration using generator coordinate method 3-45985
- ^{12}C , multichannel three- α model, two-level internal structure 3-78272
- ^{12}C , neutron elastic and inelastic scattering, 7-9 MeV, differential cross sections and angular distrib. 3-63051
- ^{12}C , neutron elastic resonant scattering, unbound levels in ^{13}C , application of real Weinberg state method 3-57471
- ^{12}C , photodisintegration, de-excitation gamma ray meas., interpretation 3-52166
- ^{12}C , photoneuclear reaction process in giant dipole reson. region in collective correl. model 3-52171
- ^{12}C , pion scattering in 3,3 resonance region, exclusion principle effects 3-54508
- ^{12}C , polarized proton scattering, 9.5-11.5 MeV, obs. of $T=1/2$ ^{13}N levels (German) 3-49139
- ^{12}C , projected Hartree Fock calc. with realistic interaction 3-52121
- ^{12}C , resonance fluorescence of 1^+ state at 15.1 MeV, production of polarised photons 3-71102
- ^{12}C , unified shell-cluster model based on molecular orbital method 3-43194
- ^{12}C , weak and e.m. processes, particle-hole model approach 3-40455
- ^{12}C (d,p), 12.3 MeV, importance of D-state effects 3-54486
- ^{12}C continuum states in giant dipole reson. region, collective correl. 3-43229
- ^{12}C on ^{12}C , 40-60 MeV inelastic scattering, single and mutual excitation strengths, coupled-channel analysis 3-60220
- ^{12}C three-boson model, generator coordinate approach 3-62974
- ^{12}C , hypernucleus, production in $^{12}\text{C}(K^-, \pi^-)$ reaction, spectroscopy 3-78278
- ^{12}C - ^{12}C reaction, excitation functions determ. from dynamical treatment of absorption 3-67362
- $^{12}\text{C} + ^{12}\text{C}$, total reaction cross section meas., rel. to repulsive cores in the optical potential 3-67366
- $^{12}\text{C} + ^{16}\text{O}$, total reaction cross section meas., rel. to repulsive cores in the optical potential 3-67366
- $^{12}\text{C} + ^{16}\text{O} \rightarrow ^{28}\text{Si}$ reson., persistence in $^{13}\text{C}(^{16}\text{O}, ^{17}\text{O})^{12}\text{C}$ 3-54500
- $^{12}\text{C}(^{10}\text{B}, ^7\text{Be})^{15}\text{N}$ analog reactions at 100 MeV 3-54501
- $^{12}\text{C}(^{10}\text{B}, ^7\text{Li})^{15}\text{O}$ analog reactions at 100 MeV 3-54501
- $^{12}\text{C}(^{12}\text{C}, \alpha)^{20}\text{Ne}$, low energy, rel. to carbon burning era of nucleosynthesis in stellar evolution 3-40511
- $^{12}\text{C}(^{12}\text{C}, p)^{23}\text{Na}$, low energy, rel. to carbon burning era of nucleosynthesis in stellar evolution 3-40511
- $^{12}\text{C}(^{12}\text{C}, p)^{23}\text{Na}$, high spin states of ^{23}Na study 3-49185
- $^{12}\text{C}(^{12}\text{C}, ^{12}\text{C})^{12}\text{C}$, 10 to 37.6 MeV kinematical analysis, compound and direct model comparison 3-67360
- $^{12}\text{C}(^{12}\text{C}, \alpha\alpha)^{16}\text{O}$, study of high-spin negative parity states in ^{20}Ne by α - γ coincidence meas. 3-49136
- $^{12}\text{C}(^{14}\text{N}, d)^{24}\text{Mg}$, product high spin states assignment 3-54381
- $^{12}\text{C}(^{16}\text{O}, ^{12}\text{C})^{16}\text{O}$, 65 and 80 MeV, ang. distrib. meas., strongly absorbing potential 3-60221
- $^{12}\text{C}(^{16}\text{O}, ^{16}\text{O})^{12}\text{C}$, 65 and 80 MeV, ang. distrib. meas., strongly absorbing potential 3-60221
- $^{12}\text{C}(^{16}\text{O}, ^{12}\text{C})^{16}\text{O}$, DWBA anal. of alpha transfer reaction 3-71124
- $^{12}\text{C}(^3\text{He}, n)^{14}\text{O}(p)^{13}\text{N}$, E=12 MeV, ang. correl. meas., excited states of ^{14}O 3-40509
- $^{12}\text{C}(^3\text{He}, \alpha)^{11}\text{C}$, 42 MeV, multi-step processes, coupled-channel analysis 3-40506
- $^{12}\text{C}(^3\text{He}, p)^{14}\text{N}$, 3-11 MeV, reaction mechanism study by use of p-p angular-correlation method 3-63074
- $^{12}\text{C}(^3\text{He}, p)^{14}\text{N}$, 7 to 17 MeV, meas. ang. distribution, total cross section, compound nuclear effects 3-63078
- $^{12}\text{C}(^3\text{He}, p)^{14}\text{N}$, differential cross section, form factor, calculated for various perturbation interactions 3-54495
- $^{12}\text{C}(^3\text{He}, p)^{14}\text{N}$, E=5.54 MeV, Doppler shift attenuation, ^{14}N deduced levels and half lives (French) 3-67255
- $^{12}\text{C}(^6\text{Li}, \alpha)^{14}\text{N}$, 33 MeV, obs., DWBA approx. analysis 3-54502
- $^{12}\text{C}(^6\text{Li}, d)^{16}\text{O}$, $^{16}\text{O}(d, \alpha + d)^{12}\text{C}$, angular correlations, plane-wave approx. (Russian) 3-78301
- $^{12}\text{C}(^6\text{Li}, ^6\text{Li})^{13}\text{C}$, cluster model DWBA analysis, n-d, n- τ cluster interaction 3-60102
- $^{12}\text{C}(\alpha, ^3\text{He})^{13}\text{C}$, 139 MeV, DWBA analysis, differential cross section, ^{13}C spectroscopic strength 3-49270
- $^{12}\text{C}(\alpha, ^3\text{He})$, $E_\alpha=65$ MeV, α -transfer feasibility studies 3-63073
- $^{12}\text{C}(\alpha, \alpha)$, 20-35 MeV, intermediate structure study in complete break-up process (Russian) 3-74600
- $^{12}\text{C}(\alpha, \alpha)^{12}\text{C}$, 104 MeV, computational approach to inverse problem in JWKB approximation 3-60143

nuclei with $6 \leq A \leq 19$ continued

- $^{12}\text{C}(d, ^3\text{He})^{11}\text{B}^*$, ^3He continuum spectrum calculated, direct reaction mechanism 3-60207
- $^{12}\text{C}(d, n)^{13}\text{N}^*$, determ. of apparent reaction dependence of width of ^{13}N first excited state 3-62945
- $^{12}\text{C}(d, p)$, coupling const. determ. in peripheral models including form factor effects (Russian) 3-74598
- $^{12}\text{C}(d, p)$, rel. to model independent anal. of stripping to unbound levels 3-67296
- $^{12}\text{C}(d, p)^{13}\text{C}$, 9.3 to 15.0 MeV, comparison with DWBA theory, cross sections and resonance widths 3-54488
- $^{12}\text{C}(d, p)^{13}\text{C}$, unbound levels in ^{13}C , application of real Weinberg state method 3-57471
- $^{12}\text{C}(d, p)^{13}\text{C}$, determ. of angular distrib. of protons near resonances by shape-studies of γ -ray lines 3-40501
- $^{12}\text{C}(n, n)$, 2.1-4.7 MeV, total and elastic cross sections, phase shift analysis, analysing power 3-40489
- $^{12}\text{C}(n, n)^{12}\text{C}^*$ (4.44 MeV), neutron spin flip at 15.0 MeV, γ -ray coincidence meas. 3-60195
- $^{12}\text{C}(n, n)^{12}\text{C}$, 13.9 MeV, angular correlation meas., $2^+ \rightarrow 0^+$ decay 3-78323
- $^{12}\text{C}(n, n)$, 2-5 MeV, absolute polarisation, cross sections using R-function theory anal. 3-78325
- $^{12}\text{C}(n, n)^{12}\text{C}$, 1.98 MeV-4.64 MeV, phase shift and optical-model analysis 3-71106
- $^{12}\text{C}(n, n)^{12}\text{C}$ R-matrix theories, two level, rel. to closely spaced resonance levels in a single channel 3-60145
- $^{12}\text{C}(p, \gamma)^{13}\text{N}$, ^{13}N high energy levels study 3-52085
- $^{12}\text{C}(p, p)^{12}\text{C}$, proton spin flip in ^{13}N 8.9 MeV level, f-wave decay 3-74590
- $^{12}\text{C}(p, p)$, study of high-energy levels in ^{13}N by obs. of de-excitation γ -rays 3-52085
- $^{12}\text{C}(p, \pi^+)^{13}\text{C}$, $T_p=185$ MeV, DWBA calcs., π prod. cross sections 3-40492
- $^{12}\text{C}(p, d)^{11}\text{C}$, at 185 MeV, deep-lying hole states 3-52101
- $^{12}\text{C}(p, d)^{11}\text{C}$ high Q-value reaction, sudden approximation study 3-74581
- $^{12}\text{C}(p, p)^{12}\text{C}$, 1 GeV, differential cross section calc. using Glauber multiple scattering theory 3-57521
- $^{12}\text{C}(p, p)^{12}\text{C}$, absolute polarization measured at 50° in range 2.0-4.5 MeV, use as polarimeter 3-63029
- $^{12}\text{C}(p, p)^{12}\text{C}$, energy dependence of real central optical potential, 25-1000 MeV 3-60185
- $^{12}\text{C}(p, p)^{12}\text{C}$, first $T=3/2$ resonance by time-of-flight system 3-73884
- $^{12}\text{C}(p, p)^{12}\text{C}$, high-energy, single particle description, cluster-like correlation effects 3-43247
- $^{12}\text{C}(p, pp)^{11}\text{B}$, nucleon correl. effect, 1 GeV, distorted wave method 3-78330
- $^{12}\text{C}(p, \pi^+)$, cross-section for π^+ production calc. in Jastrow model, comparison with IPM 3-49259
- $^{12}\text{C}(p, \pi^+)$, relativistic field theoretic description 3-46044
- $^{12}\text{C}(p, \pi^+)^{13}\text{C}$, $E=185$ MeV, energy spectra, angular distribution, ^{13}C deduced levels, comparison with one-nucleon model 3-67323
- $^{12}\text{C}(\pi^-, NN)$, study of short range correlations, three-body partial wave analysis 3-60222
- $^{12}\text{C}(\pi^-, \pi^-)^{12}\text{C}$, optical potential root mean square radius determ. 3-78354
- $^{12}\text{C}(\pi^+, p)$, relativistic field theoretic description 3-46044
- $^{12}\text{C}(\pi^+, \pi^+)^{12}\text{C}$ reaction at (3/2, 3/2) resonance, meas. absolute cross section 3-60225
- $^{12}\text{C}(\pi^+, \pi^+)^{11}\text{B}$, mechanism of single-nucleon knock-out process 3-63087
- $^{12}\text{C}(\pi^+, \pi^+)^{11}\text{B}$, $E_\pi=130$ MeV, quasielastic scatt. cross sections analysis (French) 3-52209
- $^{12}\text{C}(\pi^+, \pi^+)^{12}\text{C}$ type reaction, isobar mechanism, high energy 3-78356
- $^{12}\text{C} \rightarrow \alpha + ^8\text{Be}$, virtual decays, α -cluster wave functions 3-54412
- ^{13}C , (d,p) reaction to unbound states, comparison with DWBA theory, cross sections, resonance widths 3-54488
- ^{13}C , chem. shift, in polycyclic hydrocarbons 3-71588
- ^{13}C , chem. shift in organic isomers 3-71586
- ^{13}C , chemical shift, Fourier spectroscopy, $\text{Fe}(\text{CO})_5$ powder pattern 3-68864
- ^{13}C , directly-bonded nucl. spin-spin coupling consts. 3-75077
- ^{13}C , FT n.m.r. of chlorocyclohexane at low temp., conformational anal. 3-71582
- ^{13}C , f.t. n.m.r. spectra of alkylsubstituted derivatives 3-72537
- ^{13}C , Fourier transform n.m.r., spectroscopy of organometallic compounds 3-75893
- ^{13}C , from $^{13}\text{C}(d, p)$, $E=1-4$ MeV, cross sections, giant dipole resonance region 3-67341
- ^{13}C , high resolution n.m.r. spectra of imidazole derivatives and complexes 3-57892
- ^{13}C , n.m.r., Fourier transform, spin-lattice relax. time meas. 3-68824
- ^{13}C , n.m.r., methods and chem. appl. 3-54729
- ^{13}C , n.m.r. determ. of electron relax. time in transition metal complexes 3-75078
- ^{13}C , n.m.r. for protonated eucaryone, electronic distrib. 3-75076
- ^{13}C , n.m.r. in ^{15}N enriched pyrrole 3-75083
- ^{13}C , n.m.r. in 6-membered P-containing heterocycles 3-71591
- ^{13}C , n.m.r. in benzoylacetones 3-71592
- ^{13}C , n.m.r. in bicyclo[3.2.1]octane derivatives 3-71585
- ^{13}C , n.m.r. in bipyrindyls and their protonated forms 3-71594
- ^{13}C , n.m.r. in carbonyl-containing organic derivatives 3-71584
- ^{13}C , n.m.r. in o-terphenylphenols 3-71590
- ^{13}C , n.m.r. in organosilicon compound 3-72533
- ^{13}C , n.m.r. in paraffins 3-71593
- ^{13}C , n.m.r. in quinolizidine alkaloids 3-71587
- ^{13}C , n.m.r. of cyclohexanic derivatives, diamag. effect. 3-71583
- ^{13}C , n.m.r. of orthosubstituted benzophenones, conformational preferences, calc. torsional angles 3-49489
- ^{13}C , n.m.r. peaks assignment by off-reson. irradi. of strongly coupled protons 3-43485
- ^{13}C , n.m.r. relax times, camphor mol. dynamics 3-68881
- ^{13}C , n.m.r. spectra for tricyclic hydrocarbon struct. determ. 3-75067
- ^{13}C , n.m.r. spectra in diastereomeric compounds 3-71589
- ^{13}C , nuclear relax., dynamics, field gradients, ammonium salts 3-68882

nuclei with $6 \leq A \leq 19$ continued

- ^{13}C , proton hole spectrum calc. in continuum shell model with residual interaction 3-54389
- ^{13}C , substituent induced chemical shifts in organic π systems, perturbation theory appl. 3-63374
- ^{13}C and ^{27}Al heteronuclear n.m.r., solvation shell obs. 3-71603
- ^{13}C and ^{31}P heteronuclear pulsed n.m.r., solvation shell obs. on Ni(II) in HMPT 3-75084
- ^{13}C chem. shielding tensors using proton-enhanced n.m.r. in duren crystals. 3-64580
- ^{13}C Fourier transform apparatus at 14.2 kG, probe for 20 mm spinning sample tubes 3-73827
- ^{13}C from $^{12}\text{C}(\text{d},\text{p})^{13}\text{C}$ and neutron scattering on ^{12}C , unbound levels, application of real Weinberg state method 3-57471
- ^{13}C from $^{12}\text{C}(\text{p},\pi^+)$, $E=185$ MeV, deduced levels 3-67323
- ^{13}C highly excited states in $^9\text{Be}(\alpha,\alpha')^9\text{Be}$, spin-parity assignments 3-63075
- ^{13}C ion, implanted in Ni- and Ta-substrates, range determ. (German) 3-49913
- ^{13}C level parameters from $^{12}\text{C}(\text{n},\text{n})$ reaction 3-40489
- ^{13}C mag. resonance in investigation of mol. dynamics and structure 3-67856
- ^{13}C multiplet spectra, organic liqs., Fourier transform., cross-relax. effects 3-68879
- ^{13}C n.m.r., continuous wave proton spin decoupling, virtual coupling 3-71574
- ^{13}C n.m.r., suppression of nucl. Overhauser enhancement using chemical shift reagents 3-56709
- ^{13}C n.m.r. in poly(vinyl alcohol) 3-54764
- ^{13}C n.m.r. in pyrrrole 3-78846
- ^{13}C n.m.r. investigations of adsorbed hydrocarbons (German) 3-47600
- ^{13}C n.m.r. of alkanes, solvent effects 3-71580
- ^{13}C n.m.r. of cis and trans phytoene isomers 3-46361
- ^{13}C n.m.r. of ethylene-1-olefin copolymers 3-54763
- ^{13}C n.m.r. of symm. naphthyridines, electronic density 3-71581
- ^{13}C n.m.r. spectra, decoupled pulsed Fourier transform mode, obs. of simple organic cpds. 3-75085
- ^{13}C n.m.r. spectra in ferrocene, π -cyclopentadienyl derivatives 3-75897
- ^{13}C n.m.r. spectra of cholesterol, pyridine, uridine, solvent effects 3-63512
- ^{13}C n.m.r. spectroscopy of protein, mol. conformations 3-67875
- ^{13}C n.m.r. study in 1-bromo-3,3,4-trifluorobutene-4, determ. of chemical shifts and coupling consts. 3-75072
- ^{13}C nuclear magnetic relaxation mechanism in liquid methanol 3-44345
- ^{13}C shielding consts., uncoupled Hartree-Fock calcs. using ab initio and NEMO wavefunctions 3-63376
- ^{13}C spallation by 150 and 600 MeV protons, production of ^7Be , ^9Be , and ^{10}Be rel. to astrophysical conditions 3-54476
- ^{13}C spectral assignments, spin-lattice relax. times 3-67874
- ^{13}C spectroscopic strengths from $^{12}\text{C}(\alpha,\alpha')^4\text{He}$ reaction 3-49270
- ^{13}C spin density distrib. in paramag. metallocenes by pulse Fourier transform n.m.r. 3-75906
- ^{13}C spin-lattice relaxation measurements in solutions, use of added Cr(III) 3-55496
- ^{13}C states, investigation via neutron polarisation in $^9\text{Be}(\alpha,\text{n})^{12}\text{C}$ reaction 3-62946
- ^{13}C , ^{31}P coupling in tri-(3-bromo-2-thienyl) phosphine, off resonance proton decoupling, n.m.r. 3-75069
- $^{13}\text{C}(^{13}\text{C}, ^{13}\text{C})^{13}\text{C}$, 14.0-27.5 MeV, meas. of angular distrib. and excitation functions, molecular wave function description 3-46039
- $^{13}\text{C}(^{16}\text{O}, ^{17}\text{O})^{12}\text{C}$, persistence of $^{12}\text{C} + ^{16}\text{O} \rightarrow ^{28}\text{Si}$ reson. 3-54500
- $^{13}\text{C}(^3\text{He}, ^3\text{He})^{10}\text{C}$, ang. distrib. of ^4He particles from two lowest states 3-54496
- $^{13}\text{C}(^7\text{Li}, \text{p})^{10}\text{O}$, spins of low-lying states, $E=16$ MeV 3-54505
- $^{13}\text{C}(\alpha, \text{n})^{16}\text{O}$, $E_\alpha=1.5$ MeV, total neutron yield, compound states in ^{17}O 3-40500
- $^{13}\text{C}(\alpha, \text{n})^{16}\text{O}$, 2.075-2.43 MeV, neutron polarisation angular distrib., parity assignments of ^{17}O 7.97-8.197 MeV states 3-67189
- $^{13}\text{C}(\alpha, \text{n})^{17}\text{O}$, meas. of absolute neutron yields, 2.9 MeV 3-54493
- $^{13}\text{C}(\text{d}, \text{p})^{15}\text{N}$, $E=1.4$ MeV, cross sections, ^{15}N deduced resonances 3-67341
- $^{13}\text{C}(\text{d}, \text{t})$, j-dependence of triton angular distrib. (Russian) 3-52191
- $^{13}\text{C}(\pi^+, \pi^0)^{13}\text{N}$, optical model studies, comparison with exptl. cross sections, 30-90 MeV 3-60223
- $^{13}\text{C}(\pi^+, \pi^0)^{13}\text{N}$ single-charge exchange, total and differential cross section calc. 3-67371
- ^{13}C , cross sections for neutron reaction, continuum shell model for ^{15}C 3-54401
- ^{13}C , deuteron elastic scatt., 4-10 MeV, ang. distrib. meas., reson., optical model anal. 3-78343
- ^{13}C , ground state charge distrib. determ. from elastic electron scattering 3-57512
- ^{13}C , lifetime of 6.89 MeV state determ. by Doppler shift attenuation following heavy-ion excitation (German) 3-49188
- ^{13}C , production in HTR, environmental contamination 3-71335
- ^{13}C , radiometric method, thermodynamic activity meas., C in steel and alloys 3-54039
- ^{13}C , sepn. from neutron-irrad. AlN by dry procedure 3-44739
- ^{13}C beta-decay effects on org. mol. electronic struct. 3-80570
- ^{13}C -isoxazole, distrib. in adrenals, ovaries and breast carcinoma 3-56529
- $^{13}\text{C}(^{12}\text{C}, ^{12}\text{C})^{14}\text{C}$ elastic scatt., excitation functions near Coulomb barrier 3-49283
- $^{13}\text{C}(^{12}\text{C}, \alpha)^{22}\text{Ne}$, excitation functions near Coulomb barrier 3-49283
- $^{13}\text{C}(^{12}\text{C}, \text{d})^{24}\text{Na}$, excitation functions near Coulomb barrier 3-49283
- $^{13}\text{C}(^{12}\text{C}, \text{t})^{23}\text{Na}$, excitation functions near Coulomb barrier 3-49283
- $^{13}\text{C}(^{16}\text{O}, ^{18}\text{O})^{12}\text{C}$, $E=20$ to 30 MeV, meas. ang. distrib., interference between α -particle and two-neutron transfer 3-67365
- $^{13}\text{C}(^7\text{Li}, ^7\text{Be})^{14}\text{B}$, 52 MeV, study of mass excess and low-lying level structure in ^{14}B 3-62925
- $^{13}\text{C}(\text{d}, \text{n})^{15}\text{N}$, deuteron energies, 1.3 to 1.9 MeV, neutron polarisation ang. distrib. (German) 3-52197
- $^{13}\text{C}(\text{d}, \text{p})$ stripping form factors, continuum shell model for ^{15}C 3-54401
- $^{13}\text{C}(\text{p}, \text{p})^{15}\text{N}$, cross section meas. 7.7-12.0 MeV, resonance structure and energy level determ. 3-49255

nuclei with $6 \leq A \leq 19$ continued

- ^{15}C , transition to first excited level by ^{15}N , independent multipole amplitude analysis 3-63002
- ^{15}C continuum shell model calculations 3-54401
- ^{15}C states via $^{14}\text{C}(\text{d}, \text{p})^{15}\text{C}$ reaction meas. proton spectra, excitation energies and level widths 3-67208
- ^{15}C , prod. through $\text{n}(\text{K}^-, \pi^-)^{10}\text{A}^0$ reaction, with 500-800 MeV/c kaons 3-54418
- $\text{C}(\mu, \mu)\text{C}$, 190 MeV/c elastic scattering in low-momentum-transfer region, form factor and electron-muon universality 3-74565
- $\text{C}(\pi^-, \pi^-\pi^+\pi^-)$ reaction with quasifree neutrons in nucleus, 3.9 GeV/c, resonance production (Russian) 3-40515
- $\text{C}\pi^-\pi^+\pi^-\pi^-\text{C}^*(4.44)$ at 6.0 GeV/c 3-67138
- ^{17}F , states from 3.8 and 4.8 MeV $^{15}\text{N}(^3\text{He}, \text{n})^{17}\text{F}$ reaction. 3-74603
- ^{18}F , discrepancies between d, ^3He and d, t yields and distorted wave theory 3-60203
- ^{18}F , lifetimes meas. by Doppler shift attenuation method 3-62996
- ^{18}F , photoproduction from ^{27}Al , 0.3-1 GeV 3-40479
- ^{18}F isotope, in-cyclotron production by $^{18}\text{O}(\text{d}, \alpha)^{18}\text{F}$ on water 3-39998
- ^{19}F , chemical shift, charge den. distrib. in V complexes 3-75064
- ^{19}F , electron scatt. form factors, low-lying level structure. 3-40482
- ^{19}F , in trifluoromethyl radical, vinyl-Pt complexes, coupling consts. 3-75065
- ^{19}F , n.m.r. in 2,4,6-trifluoronitrobenzene, external electric field effects 3-68854
- ^{19}F , n.m.r. in $\text{CdF}_2:\text{ErF}_3$ at 8 and 16 MHz 3-44329
- ^{19}F , n.m.r. in fluorocyclopentenes 3-57669
- ^{19}F , n.m.r. in NaPF_6 , AgPF_6 , KPF_6 , NH_4PF_6 , chemical shift 3-61002
- ^{19}F , n.m.r. in $\text{UF}_4 \cdot 2.5\text{H}_2\text{O}$ 3-79925
- ^{19}F , nuclear acoustic resonance in impurity doped RbMnF_3 3-41431
- ^{19}F , polarized, implantation in Zn single crystal, quadrupole interaction of 197 keV level 3-49081
- ^{19}F , three particle structure, comparison with decay strengths from positive parity states 3-52113
- ^{19}F chem. shift anisotropy in 1,1-difluoroethene 3-49490
- ^{19}F chem. shift in rapidly rotated elastomers 3-78916
- ^{19}F chem. shifts in fluoroacetones 3-46323
- ^{19}F from $^{18}\text{O}(\text{t}, \text{t})$, 1.4-3.7 MeV, obs. resonances, deduced levels using Humbert-Rosenfeld theory 3-60200
- ^{19}F hyperfine structure in COF_2 , mag. shielding, beam maser spectra 3-71573
- ^{19}F ion, implanted in Ni- and Ta-substrates, range determ. (German) 3-49913
- ^{19}F magnetic resonance spectra of PF_3 in nematic soln. 3-67854
- ^{19}F n.m.r. in fluorophosphate anions containing P-P bond 3-54721
- ^{19}F n.m.r. in p -irradiated LiF 3-79370
- ^{19}F n.m.r. in substituted metallised acetylides 3-71561
- ^{19}F n.m.r. study in 1-bromo-3,3,4-trifluorobutene-4, determ. of chemical shifts and coupling consts. 3-75072
- $^{19}\text{F}(^{15}\text{N}, ^{15}\text{N})^{19}\text{F}$ scatt. at low energies and elastic transfer 3-52205
- $^{19}\text{F}(\alpha, \text{n})$, high resolution study around neutron threshold, resonance obs. 3-46037
- $^{19}\text{F}(\alpha, \text{p})$, high resolution study around neutron threshold, resonance obs. 3-46037
- $^{19}\text{F}(\text{d}, ^3\text{He})^{18}\text{O}$, analogue state, distorted wave theory extended to include charge exchange channel 3-60203
- $^{19}\text{F}(\text{d}, \text{p})$, 12.3 MeV, importance of D-state effects 3-54486
- $^{19}\text{F}(\text{d}, \text{t})^{18}\text{F}$, analogue state distorted wave theory extended to include charge exchange channel 3-60203
- $^{19}\text{F}(\text{p}, \text{xn})$ reaction, effective cross section meas. from threshold to 25 MeV 3-54463
- $^{19}\text{F}(\text{n}, \text{n}')$, time-differential PAD obs. of magnetic interaction of 197 keV level with CaF_2 3-46023
- $^{19}\text{F}(\text{p}, \text{p})^{19}\text{F}$, core-polarisation effects, DWBA analysis 3-52134
- $^{19}\text{F}(\pi, \pi)^{18}\text{N}$, cross-section meas. at (3/2, 3/2) resonance 3-49284
- $^{19}\text{F}(\text{t}, \alpha)^{18}\text{O}$, excitation energies and lifetimes of ^{18}O states 3-54490
- ^{19}F , neutron radiative capture below 1500 keV, single-level resonance parameters 3-63052
- $\text{F}(\pi^-, \pi^-\pi^+\pi^-)$ reaction with quasifree neutrons in nucleus, 3.9 GeV/c, resonance production (Russian) 3-40515
- ^3H , prodn. by high-energy proton from C and Si 3-54478
- ^3He , prodn. by high-energy proton from C and Si 3-54478
- ^4He , prodn. by high-energy proton from C and Si 3-54478
- ^5He , asymmetry of decay products about c.m. recoil direction, compound nucleus formation 3-71120
- ^6He , decay, fission product of ^{252}Cf , detection, yield 3-78363
- ^6He , from thermal neutron fission of ^{239}Pu , energy spectrum, angular distribution 3-54517
- ^8He decay, from triple fission of ^{235}U induced by neutrons, probability for $^8\text{He} \rightarrow ^8\text{Li} \rightarrow ^8\text{Be} + 2\alpha$ (Russian) 3-40469
- Li, isotopes produced in ^{14}N spallation, meas. production cross section, 17 to 42 MeV 3-67330
- ^6Li , ^7Li , Coulomb excitation, polarizabilities and static quadrupole moments 3-45936
- ^6Li , ^7Li , elastic, inelastic scatt. on ^{12}C , ^{13}C , ^{16}O , ^{26}Mg , ^{28}Si , single nucleon transfer 3-78349
- ^6Li , ^7Li cluster model structure, DWBA analysis of (^7Li , ^6Li) transfer reaction 3-60102
- ^6Li , electroexcitation form factors and fixed-polarity sum rules 3-49244
- ^6Li , excitation by electron scattering, calc. with three body wave function 3-62944
- ^6Li , isospin mixing study by deuteron decay meas., Mott-Schwinger interaction 3-71043
- ^6Li , K $^-$ induced reaction at 640 MeV/c, γ -spectra, $^4\text{H}_\alpha$, $^4\text{He}^*$ production 3-78277
- ^6Li , levels from $^3\text{H}(^3\text{He}, \text{d})^4\text{He}$, energy depend. isospin violation 3-78306
- ^6Li , multichannel three-body model, binding energies of isospin states 3-40408
- ^6Li , proton-induced reactions, 35-56 MeV, search for excited states of ^3He 3-49138
- ^6Li , resonance scattering of bremsstrahlung, low-lying level study 3-52094
- ^6Li , total cross sections of π^\pm mesons, 90-860 MeV 3-74609
- ^6Li levels, oscillator cluster parentage and supermultiplet expansion 3-52112

nuclei with $6 \leq A \leq 19$ continued

- ⁶Li one-body densities, reln. between e.m. and weak processes in nuclei 3-49245
- ⁶Li threshold photodisintegration, low-energy total cross section in sequential-decay model 3-63035
- ⁶Li(³He,n)⁸Be, meas. ⁸B yield from its positron decay, rel. to neutrino detection 3-67351
- ⁶Li(³He,p)⁸Be, 17 MeV, multi-interaction, finite-range, two-mode DWBA analysis 3-67297
- ⁶Li(⁶Li,⁶He)⁸Be, ang. distrib. and excitation functions 3-52202
- ⁶Li(⁶Li,⁶Li*(3.56))⁶Li*(3.56), ang. distrib. and excitation functions 3-52202
- ⁶Li(d, α)⁴He, 3-11.5 MeV, tensor analyzing power and differential cross section meas. (German) 3-52188
- ⁶Li(d, α)²H, quasi-free scattering at 52 MeV, determ. of α -cluster momentum distrib. 3-49273
- ⁶Li(e,e), 1184 MeV, quasielastic scattering, shell and Fermi gas model interpretation (Russian) 3-57515
- ⁶Li(e,e), high-momentum-transfer, deformed cluster model 3-60166
- ⁶Li(γ ,p)⁵He at E_p=60 MeV, meas. proton spectra, excitation of (1p)⁻¹, (1s)⁻¹ hole states 3-71100
- ⁶Li(γ ,³He)⁴He, 12-16 MeV, determ. clustering in ⁶Li using two-mode finite-range analysis 3-60103
- ⁶Li(p,pd)⁴He, 50 MeV, test of polegraph with Treiman-Yang criterion 3-52175
- ⁶Li(p,pt), 590 MeV, cross-section meas., recoil momentum of three-nucleon residual system 3-74587
- ⁶Li(π^- , π^- p)⁸Be, q < 170 MeV/c, meas. of cross sections, angular and momentum distrib., reaction mechanisms (Russian) 3-40514
- ⁶Li(π^- ,p)⁶He, capture reaction, 60-150 MeV mass-6 system obs. 3-52207
- ⁷Li, ²H induced reaction at 20 MeV, meas. neutron spectra and yield 3-74596
- ⁷Li, E1 polarisation, Coulomb excitation in ²⁰⁸Pb(⁷Li, ⁷Li γ) 3-78288
- ⁷Li, K⁻ induced reaction at 640 MeV/c, γ -spectra, ⁴He*, ⁴HeA* production 3-78277
- ⁷Li, n.m.r. in dehydrated Li-A-zeolite 3-44335
- ⁷Li, n.m.r. in Li₂O₃ (Russian) 3-41450
- ⁷Li, n.m.r. studies of tourmaline minerals especially elbaite crystal structure 3-44768
- ⁷Li, nuclear magnetic spin relaxation by self-diffusion, T₁ as function of freq. (German) 3-47163
- ⁷Li, nuclear quadrupole spin-phonon coupling in LiF crystals. 3-75891
- ⁷Li, π induced, 90-860 MeV total cross-section meas. π -nucleus coupling constant obtained 3-71131
- ⁷Li, states of ⁵He and ⁸Be obs. 3-62954
- ⁷Li, total cross sections of π^\pm mesons, 90-860 MeV 3-74609
- ⁷Li in borate and silicate glasses n.m.r. studies (German) 3-72544
- ⁷Li(α , α), elastic and inelastic, 8.6-12.5 MeV and 17-22.5 MeV, excitation functions, triton exchange 3-63071
- ⁷Li(d, α)⁴He, 1.0 MeV, α -n angular correlation meas., decay schemes 3-71120
- ⁷Li(d,n)⁸Be, polarised 800 keV deuterons, meas. of analysing powers and relative cross section 3-60197
- ⁷Li(d,n) α , analysis of bidimensional spectra in relative coordinate system 3-52192
- ⁷Li(d,t)⁶Li, 12 MeV, neutron and α -particle transfer mechanisms study using DWBA formalism 3-71122
- ⁷Li(e,e), 1184 MeV, quasielastic scattering, shell and Fermi gas model interpretation (Russian) 3-57515
- ⁷Li(γ ,pt)³He, E_p < 27 MeV, determ. integral reaction cross section from energy and momentum conservation (Russian) 3-67312
- ⁷Li(γ ,p)⁶He, 60 MeV, proton spectra, excitation of residual hole states 3-71100
- ⁷Li(n,nT)⁴He, design of tritium breeding blankets for fusion reactors 3-60327
- ⁷Li(p,n)⁷Be, scattering of keV neutrons, intarget assembly, angular distributions and energy spectra calculations 3-59637
- ⁷Li(p,p)⁷Li, 0.4-2.5 MeV, polarisation and phase shift analysis, resonances and ⁸Be level structure 3-46025
- ⁷Li(π , π)⁷Li, 90-860 MeV, π -nucleus coupling constant determ. from π scatt. 3-63088
- ⁸Li, emission following stopped π^- absorption in O nuclei, obs. using photoemulsion chambers (Russian) 3-67375
- ⁸Li, mag. dipole moment determ. from Knight shift and spin-lattice relax. meas. in metal foils 3-40409
- ⁸Li, short lived, spin exchange polarisation and hyperfine splitting meas. 3-52138
- ⁸Li emission, following π^- absorption in nitrogen nuclei, obs. using photoemulsion chamber (Russian) 3-67374
- ⁹LiA, production by K⁻ interactions in nuclear emulsion at 3.0 GeV/c, binding energy determ. 3-74520
- ¹²N, quadrupole moment calc. using Cohen Kurath wavefunctions 3-49128
- ¹²N analogue state, excitation during charged pion photoproduction from ¹²C 3-49240
- ¹²N, from ¹⁶O(p, α), 5.4 to 9.9 MeV, total cross sections by positron decay of ¹³N, reaction rate at 4 \times 10⁹K 3-60178
- ¹²N, obs. of new T=1/2 levels scattering of polarised protons on ¹²C (German) 3-49139
- ¹²N, proton spin flip, f-wave decay 8.9 MeV level 3-74590
- ¹²N from ¹²C(p, γ) and ¹²C(p,p'), high-energy levels study 3-52085
- ¹⁴N, ¹⁵N one-neutron transfer reaction, microscopic form factor 3-43246
- ¹⁴N, decay of photo resonances, shell model analysis, cross section and branching ratios 3-49239
- ¹⁴N, energy levels deduced from ¹⁴C(d,d), optical model anal. 3-78343
- ¹⁴N, from ¹²C(³He,p) E=5.54 MeV, Doppler shift attenuation, deduced levels and half lives (French) 3-67255
- ¹⁴N, Knight shift in Cs-NH₃ solution 3-73173
- ¹⁴N, magnetic moment of 3-, 5.83 level, Blume-Scherer model of PAC in gas 3-49083
- ¹⁴N, n.m.r. in 2,4,6-trifluoronitrobenzene, external electric field effects 3-68854
- ¹⁴N, n.m.r. in heterocyclics (French) 3-63518
- ¹⁴N, n.q.r. in hexamethylphosphoramide 3-73829
- ¹⁴N, n.q.r. in methylurea 3-55500

nuclei with $6 \leq A \leq 19$ continued

- ¹⁴N, n.q.r. Zeeman effect obs. of mag. dipole interac. in ND₂ group in N,N'-dideuteroparachloroaniline 3-75910
- ¹⁴N, nuclear relax., dynamics gradients, ammonium salts 3-68882
- ¹⁴N, operation of d.n.m.r. spectrometer attachment 3-73825
- ¹⁴N, spallation, production of Li, Be, B isotopes, 17 to 42 MeV, meas. cross sections, astrophysical significance 3-67330
- ¹⁴N, spin-lattice relax. in NH₄Cl near λ -transition 3-55494
- ¹⁴N, stopped π^- absorption with ⁸Li emission obs. using photo emulsion chambers, nucleon cluster effects (Russian) 3-67374
- ¹⁴N level structure determ. from ¹⁰B(α , α')¹⁰B reaction excitation functions and α -particle decay 3-71055
- ¹⁴N n.m.r. shifts in azoles 3-71599
- ¹⁴N n.q.r. in guanidinium ion 3-79943
- ¹⁴N n.q.r. in pyridines 3-63526
- ¹⁴N quadrupolar splitting determ. in phosphorescent quinoline, ENDOR in 3.601 GHz zero-field transition 3-46316
- ¹⁴N rotational correlation time of hexamethylenetetramine in chloroform 3-75900
- ¹⁴N(d,d)¹⁴N, 11.6 MeV polarised deuterons, vector analysing power, optical model analysis 3-52193
- ¹⁴N(d,d)¹⁴N vector analyzing, powers comparison with ¹⁴N(d,t)¹³N 3-74597
- ¹⁴N(n,p)¹⁴C, use in neutron beam strength measurement 3-73864
- ¹⁴N(n,xp), 4.22-15.40 MeV, meas. of gamma-ray production cross section using Ge(Li) detector 3-74593
- ¹⁴N(p,d)¹³N, at 185 MeV, deep-lying hole states 3-52101
- ¹⁴N(p, π^+), 600 MeV, forward cross section calc. 3-57520
- ¹⁴N(π , π)¹³N, cross-section meas. at (3/2, 3/2) resonance 3-49284
- ¹⁵N, e.p.r. spectral linewidths of iminoxyl radicals, mol. reorientation effects 3-43486
- ¹⁵N, from ¹³C(d, γ), E=1-4 MeV, cross sections, giant dipole resonance region 3-67341
- ¹⁵N, level study using ¹⁴C(p, γ) reaction at low energy 3-49255
- ¹⁵N, n.m.r. in pyrolyse 3-78846
- ¹⁵N, non-normal parity states calc. 3-74482
- ¹⁵N chemical shift in concentrated aqueous solns. of ammonium salts 3-68862
- ¹⁵N levels populated following muon capture by ¹⁶O 3-52149
- ¹⁵N muon capture, partial transitions, gamma-neutrino correlation 3-63002
- ¹⁵N n.m.r. in enriched glycine aqueous soln., chemical shift, relaxation, pH depend. 3-64570
- ¹⁵N n.m.r. spectroscopy, organic and inorganic mols. 3-71602
- ¹⁵N-H n.m.r. coupling consists. of aminophosphines, bonding 3-71575
- ¹⁵N(²He,n)¹⁷F, 3.8 and 4.8 MeV, investigation of ¹⁷F states 3-74603
- ¹⁶N, detection, rel. to O content, neutron activation anal. 3-51764
- ¹⁶N bound states from muon capture on ¹⁶O, rate meas. 3-60125
- ¹⁶N gamma-radiation in turbine building of boiling water reactor, shielding requirement 3-71341
- ¹⁶N γ -rays site-boundary dose calcs. for BWR nuclear plant, geometrical considerations 3-74755
- ¹⁶N resonances in reaction ¹⁵N(d,p) off shell behaviour rel to R-matrix theory 3-63065
- ¹⁷N, β -decay to unbound states of ¹⁷O, branching ratio determ. 3-60121
- ¹⁸N, prod. through n(K⁻, π^-) Λ^0 reaction, with 500-800 MeV/c kaons 3-54418
- O, fast neutron small-angle scattering, elastic cross-section meas. 3-74579
- O, total cross sections of π^\pm mesons, 90-340 MeV 3-74609
- O isotopes, single-closed shell, self-consistent calcs. 3-71070
- O¹⁷, chem. shift due to solvent-solute interactions in electrolyte solns. 3-71595
- ¹⁶O, A=16, 17, 18, 65 MeV elastic proton scattering, microscopic analysis, determ. of matter distrib. 3-40490
- ¹⁴O excited states via ang. correl. obs. of ¹²C(³He, n)¹⁴O(p)¹³N at 12 MeV 3-40509
- ¹⁵O, production with Van de Graaff acceleration 3-73833
- ¹⁵O non-normal parity states calc. 3-74482
- ¹⁶O, ¹⁵O two-nucleon transition matrix parametrization 3-78235
- ¹⁶O, 6.05 MeV O⁺ state predicted by variational calc., B(E2) value in ¹⁸O(p,t) reaction 3-67177
- ¹⁶O, Brown-Green model, inelastic electron scattering, excited odd-parity states 3-63040
- ¹⁶O, coexistence model for structure of giant dipole resonance, exptl. test 3-49230
- ¹⁶O, coupling const. determ. in peripheral models including form factor effects (Russian) 3-74598
- ¹⁶O, e.m. decays of the 1⁻ levels at 12.44, 13.09 MeV (French) 3-49192
- ¹⁶O, effect of α -channel introduction on continuum structure, reln. to photoneuclear cross sections 3-45989
- ¹⁶O, elastic, inelastic scatt. of ⁶Li, ⁷Li, single nucleon transfer, meas. 3-78349
- ¹⁶O, inelastic electron scattering and weak coupling model, calc. of form factors 3-60163
- ¹⁶O, microscopic treatment of coupled monopole and quadrupole vibration using generator coordinate method 3-45985
- ¹⁶O, muon capture, rate calc., effect of core-excitation and SU₄ symmetry 3-74543
- ¹⁶O, μ^- capture, calc. of asymmetry in high energy neutron emission, transitions to ¹⁵N levels 3-52149
- ¹⁶O, neutron total cross sections, 0.6-4.33 MeV, determ. of ¹⁷O level structure 3-67209
- ¹⁶O, nucl. breathing modes calc. 3-52119
- ¹⁶O, partial muon capture rates leading to bound states of ¹⁶N 3-60125
- ¹⁶O, photodisintegration, de-excitation gamma ray meas., interpretation 3-52166
- ¹⁶O, pion scattering, giant resonance excitation of doubly-closed shell nuclei, spin dependent effects 3-78297
- ¹⁶O, reactions induced by deuterons 0.98-1.97 MeV 3-43251
- ¹⁶O, SU(3) coupling for negative parity states in shell model calcs. 3-78253
- ¹⁶O, shell model calc. of α -transfer form factors and widths 3-45980
- ¹⁶O, transition moments in electron excitation of T-1 neg.-parity oscillations 3-46020
- ¹⁶O (d,p), 12.3 MeV, importance of D-state effects 3-54486

nuclei with $6 \leq A \leq 19$ continued

- ^{16}O binding energy, calc. from off-energy-shell continuation of ^{15}O two-nucleon T matrix 3-78259
- ^{16}O capture of stopped π^- with emission of ^8Li , obs. using photoemulsion chambers, determ. reaction branchings (*Russian*) 3-67375
- ^{16}O electric dipole sum rule and two body correlations calc. 3-78240
- ^{16}O excitation of levels by high energy protons, 1.0, 2.9, 6.3 GeV, γ -ray spectra (*Russian*) 3-40456
- ^{16}O muon capture, exptl.-theoretical discrepancies, use of size coexistence model 3-67269
- ^{16}O non-normal parity states calc. 3-74482
- ^{16}O realistic one-particle density matrix and single-particle description 3-52111
- ^{16}O region, charge radii and polarisation effects 3-67179
- ^{16}O structure determ. using interaction boson model 3-52099
- ^{16}O - ^{16}O scattering, extension of resonating group method to heavy system 3-74602
- ^{16}O - α scattering, extension of resonating group method to heavy system 3-74602
- $^{16}\text{O} + ^{16}\text{O}$, total reaction cross section meas., rel. to repulsive cores in the optical potential 3-67366
- $^{16}\text{O}(^{19}\text{F}, ^{15}\text{F})^{16}\text{O}$ scatt. at low energies and elastic transfer 3-52205
- $^{16}\text{O}(^7\text{Li}, t)$, excitation functions, direct nature of reaction 3-57537
- $^{16}\text{O}(N, N)$ scattering, influence of exchange on optical potential, lowest order exchange processes 3-67290
- $^{16}\text{O}(\alpha, \alpha)$, wave functions and reflection coeffs. deduced from optical model, $E = 20.1$ MeV 3-43254
- $^{16}\text{O}(\alpha, ^8\text{Be})$, $E_\alpha = 65$ MeV, α -transfer feasibility studies 3-63073
- $^{16}\text{O}(\alpha, \alpha')^{16}\text{O}$, inelastic scatt. to 2^- state via nonlocal interaction 3-54466
- $^{16}\text{O}(\alpha, \alpha')^{16}\text{O}$, 20.1 MeV, optical model analysis using independent geometries for real and imaginary potentials 3-67346
- $^{16}\text{O}(\alpha, \alpha')^{16}\text{O}$, forward scattering, cluster model vertex functions 3-60211
- $^{16}\text{O}(\alpha, n)^{15}\text{Ne}$, threshold to 26 MeV, evidence for boson-mode excitations 3-60214
- $^{16}\text{O}(d, d)^{16}\text{O}$, 11.6 MeV polarised deuterons, vector analysing power, optical model analysis 3-52193
- $^{16}\text{O}(d, p)^{17}\text{O}$, 9.3 to 15.0 MeV, comparison with DWBA theory, cross sections and resonance widths 3-54488
- $^{16}\text{O}(p, \pi^+)^{15}\text{N}$, study using different dynamical amplitudes, particle-hole correlations 3-54461
- $^{16}\text{O}(p, p)^{15}\text{N}$, bremsstrahlung and 50-80 MeV energies, cross-section meas. 3-52170
- $^{16}\text{O}(p, \pi^+)^{16}\text{N}$, effect of Woods-Saxon wave functions on cross sections for charged-pion photoproduction 3-63034
- $^{16}\text{O}(n, n)$, separable-potential model approach 3-43243
- $^{16}\text{O}(n, n)^{16}\text{O}$ R-matrix theories, two level, rel. to closely spaced resonance levels in a single channel 3-60145
- $^{16}\text{O}(p, ^3\text{He})$, violation of isospin conservation, $E_p = 27$ MeV 3-63050
- $^{16}\text{O}(p, \alpha)^{13}\text{N}$, 5.4 to 9.9 MeV, total cross sections by positron decay of ^{13}N , reaction rate at $4 \times 10^8 \text{ K}$ 3-60178
- $^{16}\text{O}(p, \alpha)^{13}\text{N}$, total cross section, threshold to 7.7 MeV 3-63043
- $^{16}\text{O}(p, d)^{15}\text{O}$, at 185 MeV, deep-lying hole states 3-52101
- $^{16}\text{O}(p, d)^{15}\text{O}$, effect of short-range correlations due to repulsive core in N-N interaction 3-46024
- $^{16}\text{O}(p, d)^{15}\text{O}$ high Q-value reaction, sudden approximation study 3-74581
- $^{16}\text{O}(p, p')^{16}\text{O}$, inelastic scatt. to 2^- state via nonlocal interaction 3-54466
- $^{16}\text{O}(p, p)^{16}\text{O}$, energy dependence of real central optical potential, 25-1000 MeV 3-60185
- $^{16}\text{O}(p, pp)^{15}\text{N}$, giant multipole resons. $L=1, 2$ and 3, excitation 3-54484
- $^{16}\text{O}(p, t)$, violation of isospin conservation, $E_p = 27$ MeV 3-63050
- $^{16}\text{O}(\pi^-, \pi^-)^{16}\text{O}$, total and differential cross sections in 3-3 resonance region, optical potential calcs. 3-63090
- $^{16}\text{O}(t, t)$, 1.4-3.7 MeV, ^{19}F deduced levels from angular distrib. and excitation function meas. 3-60200
- $^{16}\text{O}(t, p)^{16}\text{O}$, two-nucleon transfer form factor in tail region, large basis shell model approach 3-67295
- $^{16}\text{O} \rightarrow \alpha + ^{12}\text{C}$, virtual decays, α -cluster wave functions 3-54412
- ^{17}O , ^{18}O one-neutron transfer reaction, microscopic form factor 3-43246
- ^{17}O , (d, p) reaction to unbound states, comparison with DWBA theory, cross sections, resonance widths 3-54488
- ^{17}O , compound state obs. in total neutron yield from $^{13}\text{C}(\alpha, n)^{16}\text{O}$ 3-40507
- ^{17}O , ENDOR in MgO , F^+ centre obs. 3-68886
- ^{17}O , mag. moment, Schmidt value reduction 3-43173
- ^{17}O , n.m.r. in $\text{TiO}_2 \cdot \text{Cr}^{3+}$ by dynamic nuclear polarization method (*German*) 3-50488
- ^{17}O , parities of 7.97 to 8.197 MeV states from meas. on $^{13}\text{C}(\alpha, n)^{16}\text{O}$ reaction 3-67189
- ^{17}O level structure, from neutron total cross sections 3-67209
- ^{17}O tracer, alpha track O determ. in Al_2O_3 , citric acid 3-66457
- ^{17}O unbound states populated in ^{17}N β -decay 3-60121
- $^{17}\text{O}(\alpha, n)^{20}\text{Ne}$, $E_\alpha = 1.5$ MeV, total neutron yield, compound states in ^{21}Ne 3-40507
- $^{17}\text{O}(n, \alpha)^{14}\text{C}$, tracks for O determ. and distrib. in biological materials 3-66457
- $^{17}\text{O}(p, n)^{17}\text{F}$, 0.5 MeV, meas. total neutron yields, neutron production cross sections 3-60189
- ^{18}O , ^{15}O two-nucleon transition matrix parametrization 3-78235
- ^{18}O , discrepancies between d, ^3He and d,t yields and distorted wave theory 3-60203
- ^{18}O , inelastic electron scattering and weak coupling model, form factors for lowest monopole transitions 3-60163
- ^{18}O , intermediate-state summations in effective shell model interaction, convergence rate 3-62964
- ^{18}O , lifetimes meas. by Doppler shift attenuation method 3-62996
- ^{18}O binding energy, calc. from off-energy-shell continuation of ^{15}O two-nucleon T matrix 3-78259
- ^{18}O distribution, Atlantic Ocean, isotope formation of surface waters, distrib. of salinity (*Russian*) 3-47694
- ^{18}O lifetimes and excitation energies from $^{19}\text{F}(t, \alpha\gamma)$ 3-54490
- ^{18}O profiles, meas. of accumulation on Jungfrauoch (*German*) 3-51210
- $^{18}\text{O}(^{19}\text{F}, ^{19}\text{F})^{18}\text{O}$ scatt. at low energies and elastic transfer 3-52205

nuclei with $6 \leq A \leq 19$ continued

- $^{18}\text{O}(\alpha, n)^{21}\text{Ne}$, $E_\alpha = 1.5$ MeV, total neutron yield, compound states in ^{22}Ne 3-40507
- $^{18}\text{O}(p, n)^{18}\text{F}$, 0.4 MeV, meas. total neutron yields, neutron production cross sections 3-60189
- $^{18}\text{O}(p, n)^{18}\text{F}$, $E_p = 4.6$ to 6.6 MeV, reson. investigation 3-54485
- ^{19}O , low-lying states spin from $^{13}\text{C}(^7\text{Li}, p)$ $E = 16$ MeV 3-54505
- ^{19}P fast Fourier transform n.m.r. spectroscopy of pyridine nucleotides, esp. dinucleotides, conformation 3-67850
- ^{19}P magnetic resonance spectra of PF_3 in nematic soln. 3-67854
- $^{12}\text{X}(p, \pi^+)$, 600 MeV, forward cross section calc. 3-57520
- nuclei with $20 \leq A \leq 38$**
- ^{28}Si , search for 6^- analogue-antianalogue states as resonance in $^{27}\text{Al}(p, p)$, γ -ray decay 3-57476
- ^{28}Si , n.m.r. in organosilicon cpds. 3-71596
- ^{35}Cl , n.q.r. in ammonium hydrogen bis(chloroacetate) 3-79992
- $A = 17-27$, projected Hartree-Fock calcs. of spin-isospin matrix elements 3-49180
- $A = 20, 24$, isospin mixing from the effective nuclear interaction 3-71062
- $A = 20-34$, Hartree-Bogolubov calcs. of rotational energies, moments of inertia, pairing correlations, quadrupole moments, $B(E2)$ values 3-52118
- cosmic radiation of low energy, charge composition from stacked nuclear emulsions 3-53576
- isobaric analogue pairs, 0^+ , production in (t, p) and (^3He , p) reactions 3-78342
- Nucleus $(\gamma, \gamma p x n)^{24}\text{Na}$, $13 \leq Z_{\text{nucleus}} \leq 29$, yields for 100 MeV $\leq E_{\gamma, \text{max}} \leq 1000$ MeV 3-54464
- single particle states energies, $35 \leq A \leq 65$ 3-54387
- ^{29}Si , directly-bonded nucl. spin-spin coupling consts. 3-75077
- Al , fast neutron small-angle scattering, elastic cross-section meas. 3-74579
- Al , neutron production by cosmic ray high energy muons, depth dependency, e.m. interaction explanation (*Russian*) 3-61621
- Al , π^- , π^+ reaction cross sections, 713 to 1447 MeV, deduced neutron density 3-54507
- Al deuteron cross-section for stripping and dissociation, 2.7 GeV/c, measurement 3-78344
- ^{26}Al , levels and spectroscopic factors from $^{27}\text{Al}(p, d)$ reaction 3-52097
- ^{26}Al energy levels, populated in $^{27}\text{Al}(^3\text{He}, \alpha)$ reaction, spectroscopic factors 3-67355
- ^{26}Al Kuo interaction in untruncated shell-model calcs. in sd-shells, production of band shifts 3-67202
- ^{27}Al , ^{16}O compound reactions, γ transitions between high-spin states of ^{41}K and ^{41}Ca 3-74530
- ^{27}Al , ^{32}S induced reaction, fusion barrier meas. 3-46042
- ^{27}Al , η -meson photoproduction, 2 GeV, cross section meas. 3-78311
- ^{27}Al , Knight shift meas. (*Russian*) 3-47157
- ^{27}Al , n.m.r. in GdAl_2 , transferred mag. induced quadrupole interact. obs. 3-41448
- ^{27}Al , n.m.r. studies of tourmaline minerals especially elbaite crystal structure 3-44768
- ^{27}Al , nuclear spin-lattice relax. in UAl_2 and PuAl_2 , spin fluctuation effects 3-41441
- ^{27}Al , operation of d.n.m.r. spectrometer attachment 3-73825
- ^{27}Al , photon-induced fragmentation by 1 GeV bremsstrahlung 3-60160
- ^{27}Al , resonance scattering of bremsstrahlung, low-lying level study 3-52094
- $^{27}\text{Al}(p, n)$, isobaric analogue transitions, 22 to 40 MeV proton energy, meas. angular distributions 3-63055
- ^{27}Al and ^{13}C heteronuclear n.m.r., solvation shell obs. 3-71603
- ^{27}Al from $^{26}\text{Mg}(^{16}\text{O}, ^{15}\text{N})$ at 42 MeV, spectroscopic factors, recoil effects 3-67367
- ^{27}Al n.m.r., Fourier transform variable field expt. with internal ^2H lock 3-77589
- $^{27}\text{Al}(^3\text{He}, ^3\text{He})^{27}\text{Al}$, 21 MeV meas. polarisation of ^3He , deduced optical model parameters 3-67349
- $^{27}\text{Al}(^3\text{He}, \alpha)^{26}\text{Al}$, 18 MeV neutron pickup, angular distrib., ^{26}Al level structure 3-67355
- $^{27}\text{Al}(d, \alpha)^{25}\text{Mg}$, ^{25}Mg γ -decay study 3-40458
- $^{27}\text{Al}(d, p)^{28}\text{Al}$, region from hyperbarrier to Coulomb stripping, obs. of ^{28}Al energy levels (*Russian*) 3-52189
- $^{27}\text{Al}(p, p)^{27}\text{Al}$, 0.3-1 GeV, meas. of photoproduction cross sections by activation analysis 3-40479
- $^{27}\text{Al}(p, \pi^+)^{27}\text{Mg}$, 250, 400, 800 MeV, mean range of recoil nuclei 3-60161
- $^{27}\text{Al}(p, \pi^+)^{27}\text{Mg}$, free-nucleon photoprod. amplitude and shell model calcs. 3-60159
- $^{27}\text{Al}(n, p)$, thermal neutrons, test of photon production data from ENDF/B-III material 1135 3-57527
- $^{27}\text{Al}(n, n_0)^{27}\text{Al}$, 14.8 MeV, meas. differential cross sections, the Schwinger prediction 3-71108
- $^{27}\text{Al}(n, p)^{27}\text{Mg}$ energies < 6 MeV, cross section meas. rel. to ^{235}U fission using activation method 3-74591
- $^{27}\text{Al}(p, \alpha)^{24}\text{Mg}$, 2100-3100 keV, excitation function (*French*) 3-49251
- $^{27}\text{Al}(p, \alpha)^{24}\text{Mg}$, 0.633, 0.731, 0.937, 1.183 MeV, meas. of single crystal blocking effect, determ. of reaction time 3-52186
- $^{27}\text{Al}(p, d)^{26}\text{Al}$, 19, 20 MeV, angular distrib. meas., determ. of spectroscopic factors and levels of ^{26}Al 3-52097
- $^{27}\text{Al}(p, p)$, $E_p = 1.9-3.1$ MeV, γ radiations, reson. intensities (*French*) 3-78317
- $^{27}\text{Al}(p, p)^{28}\text{Si}$, 2100-3100 keV, excitation function (*French*) 3-49251
- $^{27}\text{Al}(p, p)^{28}\text{Si}$, search for 6^- analogue-antianalogue states and subsequent γ decay 3-57476
- $^{27}\text{Al}(p, p')^{27}\text{Al}$, 2100-3100 keV, excitation function (*French*) 3-49251
- $^{27}\text{Al}(p, p)^{27}\text{Al}$, energy dependence of real central optical potential, 25-1000 MeV 3-60185
- $^{27}\text{Al}(\pi^-, \pi^-)^{26}\text{Mg}^*$, mechanism at small momentum transfer 3-52210
- $^{27}\text{Al}(\pi^+, \pi^0)^{27}\text{Si}$, 100 MeV, activation cross section determ. 3-54506
- ^{28}Al , ^{29}Al , shell model calcs. using modified surface-delta-interaction Hamiltonian 3-49167
- ^{28}Al , excitation in $^{27}\text{Al}(d, p)$ reaction (*Russian*) 3-52189

nuclei with $20 \leq A \leq 38$ continued

- ²¹Al, γ -ray transitions from lowest $T=2$ states populated in ²⁶Mg (³He, p) 3-43211
- ²¹Al, $T_z=5/2$ nuclide, mass and β decay half-life 3-54373
- ²¹Al, bubble configuration determ. using Hartree Fock methods 3-78274
- ²⁵Ar, lifetime of first excited state populated in ³²S(α ,n γ) reaction 3-45996
- ²⁵Ar energy levels populated in ³⁶Ar(³He, α), spectroscopic factors 3-67354
- ²⁶Ar, calc. of quadrupole, hexadecapole, and ²⁶ pole deformation parameters (*Russian*) 3-67183
- ²⁶Ar, from ³⁵Cl(p, γ), $E=0.8-2.6$ MeV, deduced levels, shell model calculation of odd parity levels 3-71078
- ²⁶Ar(¹⁶O, ¹²C)⁴⁰Ca 58 MeV incident energy, excited states study (*French*) 3-43179
- ²⁶Ar(³He, α)³⁵Ar, 18 MeV neutron pick-up, determ. of ³⁵Ar level structure 3-67354
- ²⁶Ar(⁷Li, t)⁴⁰Ca 28 MeV incident energy, excited states study (*French*) 3-43179
- ²⁶Ar(d, p)³⁷Ar neutron reson. ³⁷Ar, DWBA anal. 3-54492
- ²⁶Ar(p,n)³⁶K, 17 MeV, determ. of ³⁶K spin and magnetic moment from β -decay asymmetry 3-45939
- ²⁷Ar, 1612 keV level, mean lifetime meas. 3-45991
- ²⁷Ar, average level width at excitation energies near 17 MeV studied in ³⁵Cl (d,p) ³⁶Cl 3-63062
- ²⁷Ar, half-life by gas proportional counters (*French*) 3-57493
- ²⁷Ar, isobaric mass quartets 3-60066
- ²⁷Ar activity variation in troposphere (*German*) 3-51013
- ²⁷Ar in Haverro meteorite, radioactivity meas. 3-45066
- ²⁷Ar supersmall quantity meas. by low-background installation using miniature proportional counters (*Russian*) 3-65403
- ²⁸Ar, γ decay props. of 3^- states 3-45993
- ²⁸Ar(³He,n)⁴⁰Ca, excited $J^\pi=0^+$ states in ⁴⁰Ca 3-74491
- ²⁸Ar(d, p)³⁹Ar, neutron reson. ³⁹Ar, DWBA anal. 3-54492
- ²⁷Ca, isobaric mass quartets 3-60066
- Cl, fast neutron total cross sections, 5.0-8.5 MeV 3-60169
- ²⁴Cl, lifetimes of levels populated in ³²S(²He, p) reaction at 9 MeV 3-49215
- ²⁴Cl from ³³S(p, γ)³⁴Cl, nuclear levels investigation 3-52102
- ³⁵Cl, ³⁷Cl, n.q.r. in trichloromethyl derivatives of P 3-75912
- ³⁵Cl, 7.79 to 0.79 MeV cascade accompanying capture of slow polarised neutrons, T invariance of angular γ correlation (*Russian*) 3-57492
- ³⁵Cl, energy level spectra meas. from ³²S(α ,p)³⁵Cl reaction, 20 MeV 3-62947
- ³⁵Cl, high-spin states obs. using ³²S(α , p) reaction, $\gamma\gamma$ coincidence, angular distrib., yield function meas. 3-74493
- ³⁵Cl, lifetime of first 7/2⁻ level meas. by recoil distance method in ³²S(α ,p) reaction 3-78284
- ³⁵Cl, n.m.r. in t-butylchloride, self-diffusion coeff. and rot. correlation time determ. 3-68872
- ³⁵Cl, n.m.r. of ether in chloroform, association and anisotropic mol. reorientation 3-68873
- ³⁵Cl, n.q.r. in BiCl₃ temp., pressure depend. 3-72545
- ³⁵Cl, n.q.r. in SbCl₃, Zeeman effect 3-61008
- ³⁵Cl, pure n.q.r. in acetylated glycopyranosyl chlorides, coupling const. and mol. conformation relation 3-49491
- ³⁵Cl, spin-lattice relax. in NH₄Cl near λ -transition 3-55494
- ³⁵Cl, Zeeman n.q.r. spectra in polycryst. organic cpds. 3-75911
- ³⁵Cl (d, p) ³⁶Cl, 1.68-2.5 MeV excitation functions and ang. distributions 3-63062
- ³⁵Cl and ³⁷Cl quadrupole coupling in methyl chloride, effect of isotopic substitution 3-49475
- ³⁵Cl from ³⁴S(p, γ)³⁵Cl, gamma ray transitions and lifetimes 3-43214
- ³⁵Cl n.q.r. in AuCl₃, spectral line asymmetry and spin echo envelope modulation 3-79942
- ³⁵Cl n.q.r. in HgCl₂, Zeeman effect 3-44349
- ³⁵Cl quadrupole coupling constant of 4-chloronortricyclene, microwave spectra 3-71567
- ³⁵Cl quadrupole coupling consts. of methyl chloroformate 3-75050
- ³⁵Cl(p, γ)³⁶Ar, $E=0.8-2.6$ MeV, ³⁶Ar deduced levels, shell model calculation of odd-parity levels 3-71078
- ³⁶Cl, inner bremsstrahlung rel. to electron capture, meas. spectrum in energy range 600 to 1040 keV (*Russian*) 3-67279
- ³⁶Cl, levels and spectroscopic factors from ³⁷Al(p,d) reaction 3-52097
- ³⁶Cl, pop. in ³⁵Cl(d,p) reaction, decay, meas. branching ratios, state lives, shell model configs. 3-67262
- ³⁶Cl, shell model calculation of negative parity levels 3-71078
- ³⁶Cl, spin values of 0.788 and 1.598 MeV levels 3-63062
- ³⁷Cl, lifetime of first 7/2⁻ level meas. by recoil distance method in ³⁴S(α ,p) reaction 3-78284
- ³⁷Cl, n.m.r., Larmor frequency 3-74483
- ³⁷Cl(α ,n)⁴⁰K, study of e.m. decay scheme below 3.2 MeV excitation 3-43208
- ³⁷Cl(p,d)³⁶Cl, 19, 20 MeV, angular distrib. meas., determ. of spectroscopic factors and levels of ³⁶Al 3-52097
- ³⁸Cl, e.m. transition rates, meas. lives of low lying states using attenuated-Doppler-shift method 3-62989
- Cl(π^- , $\pi^- \pi^+ \pi^-$) reaction with quasifree neutrons in nucleus, 3.9 GeV/c, resonance production (*Russian*) 3-40515
- ²⁰F, γ -ray transitions, linear polarization meas. 3-40447
- ²⁰F, lifetime of 6.89 MeV state determ. by Doppler shift attenuation following heavy-ion excitation (*German*) 3-49188
- ²⁰F, lifetimes meas. by Doppler shift attenuation method 3-62996
- ²⁰F β -emitter, determ. of quadrupole moment from n.m.r. meas. on polarised nuclei in MgF₂ 3-45947
- ²²F β decay 3-43221
- ¹H-(³¹P) heteronuclear chemical exchange spin decoupling dispersion 3-75086
- K isotopes, g factor determ. from configuration mixing, calc. of first-order effects 3-52072
- ³⁶K, polarisation by optical pumping method, β -decay asymmetry, determ. of spin and magnetic moment 3-45939
- ³⁷K, isobaric mass quartets 3-60066
- ⁴⁰K, total body in 1-12 month old infants, whole body counting, age and weight correlation 3-73594
- Mg, fast neutron total cross sections, 5.0-8.5 MeV 3-60169
- ²¹Mg, β^+ -delayed proton decay, half-life meas. 3-60128

nuclei with $20 \leq A \leq 38$ continued

- ²¹Mg, isobaric mass quartets 3-60066
- ²⁴Mg, ¹⁹F compound reactions, γ transitions between high-spin states of ⁴¹K and ⁴¹Ca 3-74530
- ²⁴Mg, ³²S induced reaction, fusion barrier meas. 3-46042
- ²⁴Mg, 4.235 MeV level, gamma transitions, branching ratio meas. 3-40439
- ²⁴Mg, 60-90 MeV, deuteron scattering, optical model and coupled channel analysis 3-43253
- ²⁴Mg, alpha particle scattering, 104 MeV inelastic, elastic, analysis using folded collective model 3-60208
- ²⁴Mg, calc. of quadrupole, hexadecapole and ²⁶ pole deformation parameters (*Russian*) 3-67183
- ²⁴Mg, deformations of ground bands determ. from electron scattering and rotational model 3-62926
- ²⁴Mg, electron scatt., α -particle model calc. (*Russian*) 3-78313
- ²⁴Mg, gamma-decay of lowest $T=2$ state populated in ²³Na(p, γ) reaction, branching ratios 3-78285
- ²⁴Mg, high spin states assignments, from ¹²C(¹⁴N,d)²⁴Mg reaction 3-54381
- ²⁴Mg, inelastic 14.2 MeV neutron interactions, gamma-ray production cross sections 3-54469
- ²⁴Mg, inelastic electron scattering, collective model description 3-67239
- ²⁴Mg, particle-hole nature for two lowest 3^- states, direct reaction study 3-49151
- ²⁴Mg, shell model calcs. 3-62951
- ²⁴Mg, structure studies in the variation after projection Hartree-Fock method 3-67245
- ²⁴Mg(³He,⁹He)²¹Mg, isobaric mass quartets of ²¹Mg 3-60066
- ²⁴Mg(³He,n)²⁶Si, 5.0 and 5.8 MeV, meas. of angular distrib. of neutron polarisation, DWBA analysis 3-67352
- ²⁴Mg(d,pp)²³Mg, ²³Mg γ -decay study 3-40458
- ²⁴Mg(p,d)²³Mg, at 185 MeV, deep-lying hole states 3-52101
- ²⁴Mg(p,p'), ²⁴Mg(p,d) strongly coupled, spinless nucleon model, deformation parameters 3-54473
- ²⁵Mg (d,p), 12.3 MeV, importance of D-state effects 3-54486
- ²⁵Mg γ -decay study 3-40458
- ²⁵Mg hyperfine confirmation of localised ground state model of V-centre in MgO 3-58429
- ²⁵Mg(p,2p), high-energy excitation function, calc. 3-46027
- ²⁶Mg, ¹⁸O compound reactions, γ transitions between high-spin states of ⁴¹K and ⁴¹Ca 3-74530
- ²⁶Mg, B(E2) value of first excited state, inelastic electron scattering, Nilsson model comparison 3-57489
- ²⁶Mg, elastic, inelastic scatt. of ⁶Li, ⁷Li, single nucleon transfer, meas. 3-78349
- ²⁶Mg(¹⁶O, ¹⁴C), 45 and 60 MeV, abrupt change between smooth and oscillatory angular distrib. 3-57536
- ²⁶Mg(¹⁶O, ¹⁵N), 45 and 60 MeV, abrupt change between smooth and oscillatory angular distrib. 3-57536
- ²⁶Mg(¹⁶O, ¹⁵N)²⁷Al, 42 MeV, determ. of spectroscopic factors using no recoil DWBA, rel. to recoil effects determ. 3-67367
- ²⁶Mg(¹⁸O, ¹⁶O)²⁸Mg, two nucleon transfer reactions, DWBA formulation 3-57540
- ²⁶Mg(³H,pp)²⁸Mg, 2.9 MeV, spectra of low lying levels in ²⁸Mg 3-67258
- ²⁶Mg(³He, p)²⁸Al, 8.0 MeV, meas. of γ -ray transitions from lowest $T=2$ states 3-43211
- ²⁶Mg(α , n)²⁸Si, product high-spin states obs. using neutron time-of-flight spectrometer 3-52084
- ²⁶Mg(α ,n)²⁹Si, population of high spin negative parity states in ²⁹Si associated with oblate deformation 3-43171
- ²⁶Mg(d, t)²⁵Na, 29 MeV, angular distrib. meas., ²⁵Na structure determ. 3-52095
- ²⁷Mg, ²⁸Mg, shell model calcs. using modified surface-delta-interaction Hamiltonian 3-49167
- ²⁸Mg, gamma-ray spectroscopy of low-lying levels using ²⁶Mg(³H,pp)²⁸Mg reaction 3-67258
- Na, neutron-rich isotopes, on-line mass-spectrometric meas. 3-52068
- ²⁰Na \rightarrow ²⁰Ne β^+ decay, mirror symmetry props. and Fermi decay strength to isobaric analog state 3-60127
- ²²Na, pressure dependence of self-diffusion in NaCl 3-58150
- ²²Na pop of high spin states in the reaction ¹⁰B(¹⁶O, α) 3-67364
- ²³Na, ²⁴Na Kuo interaction in truncated shell-model calcs. in sd-shells, production of band shifts 3-67202
- ²³Na, angular distrib. of γ -rays emitted in decay of highly excited states, decay schemes (*Russian*) 3-74528
- ²³Na, inelastic 14.2 MeV neutron interactions, gamma-ray production cross sections 3-54469
- ²³Na, n.m.r. relax. in porous media containing NaCl soln. 3-60993
- ²³Na, n.m.r. studies of tourmaline minerals especially elbaite crystal structure 3-44768
- ²³Na, nuclear quadrupole spin-phonon coupling in NaCl(F) crystals. 3-75891
- ²³Na dipole strength obs. using ²²Ne(p, γ_0 + γ_1)²³Na reaction, dipole strength splitting 3-63054
- ²³Na from ¹²C(¹²C, pp)²³Na, high spin states study 3-49185
- ²³Na in borate and silicate glasses n.m.r. studies (*German*) 3-72544
- ²³Na n.m.r., Fourier transform variable field expt. with internal ²H lock 3-77589
- ²³Na n.m.r. measurements, alkali metal salts in propylene carbonate 3-79931
- ²³Na(d, pp)²⁴Na, 2.45 MeV, ²⁴Na deduced levels, γ -branching, lifetimes, spin restrictions 3-62986
- ²³Na(d, pp)²⁴Na, 2.5 and 2.8 MeV, ²⁴Na deduced levels, branching ratios 3-63063
- ²³Na(p, γ)²⁴Mg, 4.235 MeV level, gamma transitions, branching ratio meas. 3-40439
- ²³Na(p, γ)²⁴Mg, 3905 keV, lowest $T=2$ level, γ branching ratios 3-78285
- ²⁴Na, effect of chemical combination on half life (*German*) 3-49221
- ²⁴Na, from ²³Na(d, pp), 2.45 MeV, deduced levels, γ -branching, lifetimes, spin restrictions 3-62986
- ²⁴Na, from ²³Na(d, pp), 2.5 and 2.8 MeV, deduced levels, branching ratios 3-63063
- ²⁴Na, γ -ray transitions from lowest $T=2$ states populated in ²²Ne(³He, p) reaction 3-43211
- ²⁴Na, photoprod. from nuclei with $13 \leq Z \leq 29$ 3-54464

nuclei with $20 \leq A \leq 38$ continued

- ²⁴Na radioactive source, nuclear excitation by gamma rays 3-67305
²⁴Na, level scheme determ. using ²⁶Mg(d, τ) reaction, spectroscopic factors 3-52095
²⁶Na, beta decay, mass excess and $T_{1/2}$ determ. 3-74541
²⁷Na beta decay, mass excess and $T_{1/2}$ determ. 3-74541
²⁴Na, excited by ²³Na (n, γ) reaction, fast neutron cross-section (Rumanian) 3-63060
²⁰Ne, assignments to high-spin negative parity states from angular correlation meas. 3-49136
²⁰Ne, α -widths based on ¹⁶O and α -cluster model 3-62943
²⁰Ne, calc. of quadrupole, hexadecapole and 2⁶ pole deformation parameters (Russian) 3-67183
²⁰Ne, deformations of ground bands determ. from electron scattering and rotational model 3-62926
²⁰Ne, electron scatt., α -particle model calc. (Russian) 3-78313
²⁰Ne, excited states, Tamm-Dancoff calc. 3-49156
²⁰Ne, generator coordinate method, rel. to low lying nuclear states 3-60094
²⁰Ne, ground-state rotational band study from ¹⁶O α -decay 3-45980
²⁰Ne, microscopic treatment of coupled monopole and quadrupole vibration using generator coordinate method 3-45985
²⁰Ne, mirror symmetry props. and Fermi decay strength to isobaric analog state from ²⁰Na β^+ decay obs. 3-60127
²⁰Ne, structure studies in the variation after projection Hartree-Fock method 3-67245
²⁰Ne alpha-decay width analysis, ground band levels, model wave functions 3-60133
²⁰Ne(α , γ)²⁰Ne, 104 MeV α -particles, differential cross sections, anal. using deformed folding model 3-54498
²⁰Ne(α , n)²³Mg, threshold to 31 MeV, evidence for boson-mode excitations 3-60214
²⁰Ne(d, α)¹⁸F, E_d = 6-11 MeV, large isospin selection-rule violation 3-60205
²⁰Ne(d, d)²⁰Ne, 11.6 MeV polarised deuterons, vector analysing power, optical model analysis 3-52193
²¹Ne, compound state obs. in total neutron yield from ¹⁷O(α , n)²⁰Ne 3-40507
²¹Ne(α , n)²⁴Mg, 1 to 5 MeV bombarding energies, total neutron yield 3-54497
²²Ne, compound state obs. in total neutron yield from ¹⁸O(α , n)²¹Ne 3-40507
²²Ne(α , p)²⁴Na, 9.0 MeV, meas. of γ -ray transitions from lowest T = 2 states 3-43211
²²Ne(α , n)²⁵Mg, 1 to 5 MeV bombarding energies, total neutron yield 3-54497
²²Ne(d, d)²²Ne, 11.6 MeV polarised deuterons, vector analysing power, optical model analysis 3-52193
²²Ne(γ , $\gamma_0 + \gamma_1$)²²Na, rel. to electric dipole strength splitting in ²³Na, giant resonance region 3-63054
²²Ne(p, n), high resolution study around neutron threshold, resonance obs. 3-46037
²²Ne(p, p, γ) high resolution study around neutron threshold resonance obs. 3-46037
²²Ne(p, t)²⁰Ne, inelastic excitation effects, coupled-channel-Born-approx. analysis of allowed and forbidden transitions 3-67332
²²Ne(p, t)²⁰Ne 4.97 MeV 2- transition, excitation of unnatural parity states from O⁺ targets 3-78326
²⁹P, levels up to 4.76 MeV populated in ²⁸Si(p, γ) reaction 3-49144
²⁹P giant resonance region, obs. of Si(p, p)Si scattering 3-67327
³⁰P compound nucleus parameters from ²⁸Si(d, p)²⁹Si at 2-4.2 MeV 3-40503
³⁰P level characteriz. from proton scatt. on ²⁹Si at 2.5-3.4 MeV 3-60191
³¹P, ferromagnetic Fe₂P, n.m.r. study 3-41442
³¹P, NMR study, glass-crystal phase transformation, P₂Se₃, CdGeP₂ semiconductors (Russian) 3-72197
³¹P, n.m.r. obs. of ³¹P-⁷⁷Se, ³¹P-¹²⁵Te spin-spin coupling consts. in organo(seleno, telluro)phosphorus cpds. 3-75087
³¹P, photoprotons in giant reson. region, (γ , p₀), (γ , p₁) reactions 3-54458
³¹P and ¹³C heteronuclear pulsed n.m.r., solvation shell obs. on Ni(II) in HMPT 3-75084
³¹P chemical shift, Fourier spectroscopy, Fe(CO)₅ powder pattern 3-68864
³¹P from ³⁰Si(¹⁶O, ¹⁵N) at 42 MeV, spectroscopic factors, recoil effects 3-67367
³¹P n.m.r. in fluorophosphate anions containing P-P bond 3-54721
³¹P n.m.r. in phosphonium salts 3-71597
³¹P n.m.r. shifts in cyclic phosphorus cpds. 3-71600
³¹P-¹³C coupling in tri-(3-bromo-2-thienyl) phosphine, off resonance proton decoupling, n.m.r. 3-75069
³¹P-(¹H), ¹H-(³¹P) heteronuclear n.m.d.r., nonlinearities and nucl. Overhauser effect 3-75082
³¹P(d, α)²⁹Si, E_d < 4.0 MeV, reaction mechanism study from α -particle angular distrib., compound nucleus formation (Russian) 3-71118
³¹P(d, p)³²P, E = 10 MeV, angular distributions, ³²P deduced ln, spectroscopic factors 3-60198
³¹P(γ , p₀)³⁰Si, photoprotons in giant reson. region, for ³¹P 3-54458
³¹P(n, γ), 0.8-9.0 MeV, cross section for gamma-ray production 3-52185
³¹P(p, γ)³²S, lowest T = 2 state of ³²S characteriz. 3-60190
³¹P(t, p)³³P, product low-lying states lifetime meas. and props. 3-54427
³¹P(t, p)³³P, spins and decay modes of ³³P, ang. correl. studies 3-40449
²²P, diagnosis of malignant conditions of the eye from Cherenkov radiation (Czech) 3-70136
²²P, from ²⁹Si(α , p), E_α = 10.65, 10.69, 11.00 MeV, deduced levels, mixing, branching ratios 3-60108
²²P, from ³¹P(d, p), E = 10 MeV, angular distributions, deduced ln, spectroscopic factors 3-60198
²²P, radiation effects on mosquito larvae 3-59457
²²P beta source, absorption of particles Cu, Ag, Sn and Pb foil targets 3-49376
³³P, excited state ang. correl. studies 3-40449
³³P, populated via ³¹P(t, p)³³P reaction, low-lying states lifetime meas. and props. 3-54427
³³P Kuo interaction in untruncated shell-model calcs. in sd-shells, production of band shifts 3-67202

nuclei with $20 \leq A \leq 38$ continued

- ³³P lifetimes meas. by Doppler shift attenuation, spin-parity assignments 3-40446
³⁴P, nucl. mass from β ray energy spectra meas. 3-54373
³⁰S, γ -decay, low lying levels, ²⁸Si(³He, n), DSAM lifetime meas. 3-78289
³¹S, 1_2^+ and 3_2^+ states excited in ³²S(p, d) reaction (Russian) 3-74569
³²S, ¹⁸O reaction, test of independence postulate in Bohr theory of compound-nucleus decay 3-40512
³²S, calc. of quadrupole, hexadecapole, and 2⁶ pole deformation parameters (Russian) 3-67183
³²S, electron scatt., α -particle model calc. (Russian) 3-78313
³²S, first 3- levels excited by inelastic proton scattering (Russian) 3-74569
³²S, inelastic 14.2 MeV neutron interactions, gamma-ray production cross sections 3-54469
³²S, isobaric analogue reson., γ -ray study using ³¹P(p, γ)³²S, ³¹P(p, p)³¹P, ³¹P(p, α)²⁸Si (French) 3-78299
³²S, lowest T = 2 state characteriz. from ³¹P(p, γ) 3-60190
³²S, photon-induced fragmentation by 1 GeV bremsstrahlung 3-60160
³²S quadrupole and hexadecapole deformations, Hartree-Fock approx. 3-49179
³²S(¹⁶O, 2p)⁴⁶Ti, population of high-spin levels in residual nucleus 3-40448
³²S(³He, p)³⁴Cl, 9 MeV, p- γ coincidence and Doppler-shift attenuation meas. 3-49215
³²S(α , p)³⁵Cl, 12-16 MeV, study of high spin states in ³⁵Cl by γ -coincidence, angular distrib., yield function meas. 3-74493
³²S(α , n)³⁵Ar, lifetime of first excited state in ³⁵Ar 3-45996
³²S(α , p)³⁵Cl, 11.2 MeV meas. of lifetime of first 7/2- level in ³⁵Cl by recoil distance method 3-78284
³²S(α , p)³⁵Cl, obs. states of ³⁵Cl from proton spectra meas., 20 MeV 3-62947
³²S(d, d)³²S vector analyzing powers comparison with ³²S(d, ³He)³¹P 3-74597
³²S(d, p)³³S, region from hyperbarrier to Coulomb stripping, obs. of ³³S energy levels (Russian) 3-52189
³²S(γ , p₀)³¹P, photoprotons in giant reson. region, for ³¹P 3-54458
³²S(μ^- , ν nn), determ. of absolute capture probability by activation method (Russian) 3-40484
³²S(p, p'), polarized scattering, hexadecapole phonon state 3-74583
³²S(p, p)³²S, 5-6 MeV, meas. of excitation functions and angular distrib., optical model description of cross-section (Russian) 3-52180
³²S(t, p)³⁴S, distorted wave anal. rel. to (1f_{7/2})² states in ³⁴S 3-71054
³²S, 1_2^+ and 3_2^+ states excited in ³⁴S(p, d) reaction (Russian) 3-74569
³³S, compound nucleus formation in ³¹P(d, α)²⁹Si reaction, E_d < 4.0 MeV (Russian) 3-71118
³³S, excitation in ³²S(d, p) reaction (Russian) 3-52189
³³S magnetic moment, n.m.r. obs. Larmor frequencies, chemical shift (German) 3-67190
³³S(p, γ)³⁴Cl, ³⁴Cl nuclear levels investigation 3-52102
³⁴S, ¹⁶O reaction, test of independence postulate in Bohr theory of compound-nucleus decay 3-40512
³⁴S, first 3- levels excited by inelastic proton scattering (Russian) 3-74569
³⁴S, from ³²S(t, p)³⁴S reaction, nature of (1f_{7/2})² states from distorted wave anal. 3-71054
³⁴S(α , n)³⁷Ar, population of 1612 keV level, mean lifetime meas. 3-45991
³⁴S(α , p)³⁷Cl, 11.2 MeV, meas. of lifetime of first 7/2- level in ³⁷Cl by recoil distance method 3-78284
³⁴S(d, p)³⁵S, excitation functions for transitions to lowest two excited states of ³⁵S Ericson fluctuation theory 3-67339
³⁴S(p, γ)³⁵Cl, gamma ray transitions and lifetimes in ³⁵Cl 3-43214
³⁴S, from ³⁴S(d, p) reaction, excitation functions for transitions to lowest two excited states, Ericson fluctuation theory 3-67339
³⁴Se(e⁺, e⁺)³⁴Se, elastic scattering, 100 and 200 keV, differential cross sections 3-63037
¹⁸Si (d, p), 12.3 MeV, importance of D-state effects 3-54486
²⁸Si, predictions from shell model calcs. for ²⁸Mg 3-62951
²⁸Si, ²²Ne reaction, test of independence postulate in Bohr theory of compound-nucleus decay 3-40512
²⁸Si, calc. of quadrupole, hexadecapole and 2⁶ pole deformation parameters (Russian) 3-67183
²⁸Si, deformations of ground bands determ. from electron scattering and rotational model 3-62926
²⁸Si, elastic, inelastic scatt. of ⁶Li, ⁷Li, single nucleon transfer, meas. 3-78349
²⁸Si, electron scatt., α -particle model calc. (Russian) 3-78313
²⁸Si, Hartree-Fock solutions, application of Skyrme-Levinson model 3-74515
²⁸Si, inelastic 14.2 MeV neutron interactions, gamma-ray production cross sections 3-54469
²⁸Si, neutron elastic and inelastic backscattering at 14.2 MeV, time-of-flight spectroscopy, energy level obs. 3-74575
²⁸Si, nuclear deformation from ¹⁶O + ²⁸Si elastic and inelastic scattering 3-63082
²⁸Si inelastic scattering of 25.25 MeV polarised protons, ground state rotational band excitation 3-52174
²⁸Si(¹⁶O, pn)⁴⁴Sc, level scheme of ⁴⁴Sc, lifetime meas., ang. distrib. 3-78282
²⁸Si(³He, ³He)²⁸Si, 21 MeV meas. polarisation of ³He, deduced optical model parameters 3-67349
²⁸Si(³He, n), γ -decay of ³⁰S low lying levels 3-78289
²⁸Si(α , α')²⁸Si, 104 MeV α -particles, differential cross sections, anal. using deformed folding model 3-54498
²⁸Si(d, p)²⁹Si, E_d = 2-4.2 MeV, reaction mechanism, ³⁰P compound nucleus parameters 3-40503
²⁸Si(p, d)²⁹Si, at 185 MeV, deep-lying hole states 3-52101
²⁸Si(p, γ)²⁹P, study of ²⁹P levels up to 4.76 MeV 3-49144
²⁸Si(p, γ)²⁹P indirect determ. of energy loss coeff. of protons channelled along (111) direction in silicon 3-64077
²⁸Si(p, p)²⁸Si, 5-6 MeV, meas. of excitation functions and angular distrib., optical model description of cross-section (Russian) 3-52180

nuclei with $20 \leq A \leq 38$ continued

- $^{28}\text{Si}(t,p)^{30}\text{Si}$, 6-12.1 MeV, excitation energies of levels in ^{30}Si , angular distrib. of proton groups 3-62940
 ^{29}Si , elastic and inelastic proton scatt., $E_p = 2.5\text{-}3.4$ MeV, reson. obs. 3-60191
 ^{29}Si , energy levels populated in $^{31}\text{P}(d,\alpha)$ reaction at $E_d < 4.0$ MeV (Russian) 3-71118
 ^{29}Si , from $^{26}\text{Mg}(\alpha, n\gamma)$ reaction, high-spin states using neutron time-of-flight spectrometer 3-52084
 ^{29}Si , high spin negative parity states associated with oblate deformation, population in $^{26}\text{Mg}(\alpha, n)$ 3-43171
 ^{29}Si , low-lying level struct. from $^{28}\text{Si}(d,p)^{29}\text{Si}$ at 2-4.2 MeV 3-40503
 ^{29}Si , n.m.r., in Co_2SiO_4 , long range superexchange interactions via Co-O-Si-O-Co linkages 3-72530
 ^{29}Si , n.m.r. in organosilicon compound 3-72533
 ^{29}Si , n.m.r. Overhauser effect, Ti meas. 3-68878
 ^{29}Si spin-lattice relaxation and Overhauser enhancement in organosilicon compounds 3-64574
 $^{29}\text{Si}(\alpha, p)^{32}\text{P}$, $E_\alpha = 10.65, 10.69, 11.00$ MeV, py angular correlations, DSA lifetime measurements, ^{32}P deduced levels, mixing, branching ratios 3-60108
 $^{29}\text{Si}(d,p)^{30}\text{Si}$, angular distrib. of proton groups, 10 MeV 3-62940
 $^{29}\text{Si}(p,n)$, background cross section and correlation between partial widths, relation 3-54454
 ^{30}Si , spin parity assignments to levels populated in $^{28}\text{Si}(t,p)$ and $^{29}\text{Si}(d,p)$ reactions 3-62940
 $^{30}\text{Si}(^{16}\text{O}, ^{15}\text{N})^{31}\text{P}$, 42 MeV, determ. of spectroscopic factors using no recoil DWBA, rel. to recoil effects determ. 3-67367
 $^{30}\text{Si}(d,\alpha)^{28}\text{Al}$, 4.850-5.825 MeV, reliability of statistical model predictions of relative cross sections 3-49262
 $^{30}\text{Si}(d,d)^{30}\text{Si}$ vector analyzing powers comparison with $^{30}\text{Si}(d,t)^{29}\text{Si}$ 3-74597
 $^{30}\text{Si}(d,p)^{31}\text{Si}$, low deuteron energies, proton angular distrib. comparison of direct and compound nucleus mechanisms (Russian) 3-71119
 $^{30}\text{Si}(p,2p)$, high-energy excitation function, calc. 3-46027
 $\text{Si}(n,n')$, spin-flip probability and diff. cross section meas., $E = 7.44$ MeV 3-54480
 $\text{Si}(p,p)\text{Si}$, 17-29 MeV, analysing powers and cross sections in ^{29}P giant resonance region, optical model analysis 3-67327
Ti, neutron halo deduced from p absorption 3-60083

nuclei with $39 \leq A \leq 58$

- 42 $\leq A \leq 44$, shell model spectroscopy of f-p-shell, core-excitation effects 3-67236
 $A = 39$ to 56, isobaric analogue pairs, 0^+ , production in (t,p) and ($^3\text{He}, p$) reactions 3-78342
 $A = 40\text{-}58$ even nuclei, ^{16}O and ^{12}C induced reactions above Coulomb barrier, angular distrib. 3-49276
 $A = 44$ to 52, isospin mixing from the effective nuclear interaction 3-71062
 $A = 48, 52$, quadrupole moments of first 2^+ states from inelastic electron scattering 3-49100
cosmic radiation of low energy, charge composition from stacked nuclear emulsions 3-53576
cosmic ray trans-Fe nuclei, change and energy spectra 3-56294
 $f_{7/2}$ shell nuclei, magnetic and quadrupole moments, configuration mixing calcs. 3-49125
neutron capture gamma-ray yields from branching ratios and statistical analysis 3-74577
Nucleus(γ, ypxn) ^{24}Na , $13 \leq Z_{\text{nucleus}} \leq 29$, yields for 100 MeV $\leq E_{\text{pmax}} \leq 1000$ MeV 3-54464
single particle states energies, $35 \leq A \leq 65$ 3-54387
static quadrupole moments of 2^+ states of even isotopes of Ca, Ti, Cr, Fe, Ni 3-49099
temperature dependent nuclear binding energies rel. to nucleosynthesis in stars 3-42112
(n, γ) radiative capture, optical model calc. 3-78334
 $^{55}\text{Mn}(p,p)^{55}\text{Mn}$, isobaric analog reson. obs. 3-67317
Ar, $A = 39$ to 42, properties using $(\tau d3/2)^2(p\tau f/2)^n$ model, and extended model, E2, M1 transition rates 3-62949
 $^{36}\text{Ar}(\alpha, p)^{39}\text{K}$, 7.30-10.45 MeV, determ. of lifetimes of excited states 3-43210
 ^{39}Ar in Haverro meteorite, radioactivity meas. 3-45066
 ^{39}Ar production from ^{40}Ar photoneutron disintegration, 13-23 MeV 3-49238
 ^{40}Ar ($^3\text{He}, ^3\text{He}$), 28 MeV, anomalous backward angle scattering 3-54494
 ^{40}Ar ions, irradiation of ^{181}Ta , ^{197}Au , ^{238}U , reaction products, mechanisms 3-78350
 ^{40}Ar photoneutron disintegration, 13-23 MeV 3-49238
 $^{40}\text{Ar}(p,n)^{40}\text{K}$, gamma-ray angular distrib. and correlations in ^{40}K e.m. decay scheme 3-43208
 $^{40}\text{Ar}(p,p)$, 40 MeV polarised protons, asymmetry meas. at small angles 3-40487
 ^{41}Ar , mobile detector, description 3-42645
Ca, $A = 42\text{-}48$, shell-model study using pairing-plus-surface-tensor interaction 3-54405
Ca, fast neutron total cross sections, 5.0-8.5 MeV 3-60169
Ca, π^- , π^+ reaction cross sections, 584 to 1856 MeV, deduced neutron density 3-54507
Ca $A = 40, 42, 48$, single nuclear transfer reactions 3-74480
Ca isotopes, quadrupole moments and coexistence of spherical and deformed bands 3-49095
Ca region targets, single-nucleon transfer reactions, isospin centroids 3-63028
 ^{39}Ca , lifetimes of excited states populated in $^{40}\text{Ca}(^3\text{He}, \alpha\gamma)$ reaction 3-43210
 ^{39}Ca β -decay, meas. of half-life, ft values, and Gamow-Teller matrix elements 3-67275
 ^{40}Ca , ^{32}S induced reaction, fusion barrier meas. 3-46042
 ^{40}Ca , charge distributions, elastic electron scattering cross sections, phase-shift code analysis 3-62927
 ^{40}Ca , double gamma decay phenomena 3-60117
 ^{40}Ca , electric-dipole sum rule and two-body correlations 3-78240
 ^{40}Ca , electron scatt. form factors, low-lying level struct. 3-40482
 ^{40}Ca , excited $J^\pi = 0^+$ states from $^{38}\text{Ar}(^3\text{He}, n)^{40}\text{Ca}$ 3-74491
 ^{40}Ca , inelastic proton scatt., ^{41}Sc doorway state struct. 3-78319
 ^{40}Ca , microscopic treatment of coupled monopole and quadrupole vibration using generator coordinate method 3-45985
nuclei with $39 \leq A \leq 58$ continued
 ^{40}Ca , neutron induced gamma-ray producing reactions, cross-section calcs. 3-57525
 ^{40}Ca , nucl. breathing modes calc. 3-52119
 ^{40}Ca , photodisintegration, de-excitation gamma ray meas., interpretation 3-52166
 ^{40}Ca , proton elastic scattering, coupling to pickup channels, contrib. to optical potential 3-46031
 ^{40}Ca , radiative muon capture, high-energy and meas. of photon spectrum, induced pseudoscalar coupling const. 3-67274
 ^{40}Ca ($^3\text{He}, ^3\text{He}$), 28 MeV, anomalous backward angle scattering 3-54494
 $^{40}\text{Ca}(d,p)$, 12.3 MeV, importance of D-state effects 3-54486
 ^{40}Ca excited states, up to 9 MeV, gamma branching ratios, lifetimes, excitation properties, structure groups (French) 3-43179
 ^{40}Ca realistic one-particle density matrix and single-particle description 3-52111
 ^{40}Ca region, eff. of core excitation on $B(E2)$ values 3-45965
 ^{40}Ca region, pairing vibrations in theory of finite Fermi systems 3-49172
 ^{40}Ca relationship between single particle and collective degrees of freedom (Russian) 3-67237
 $^{40}\text{Ca}(^{10}\text{B}, pnp)^{48}\text{Cr}$, 19, 22.5, 25 MeV, γ -ray spectroscopy of ^{48}Cr 3-62985
 $^{40}\text{Ca}(^{10}\text{B}, pp)^{48}\text{V}$, low-lying states study 3-49135
 $^{40}\text{Ca}(^{10}\text{B}, ppn)^{47}\text{V}$, low-lying levels study 3-49146
 $^{40}\text{Ca}(^{12}\text{C}, 2p)^{50}\text{Cr}$, population of high-spin levels in residual nucleus 3-40448
 $^{40}\text{Ca}(^{12}\text{C}, pppn)^{48}\text{V}$, low-lying states study 3-49135
 $^{40}\text{Ca}(^{16}\text{O}, ^{12}\text{C})^{44}\text{Ti}$, DWBA anal. of alpha transfer reaction 3-71124
 $^{40}\text{Ca}(^3\text{He}, \alpha\gamma)^{39}\text{Ca}$, 8.0-10.0 MeV, determ. of lifetimes of excited states 3-43210
 $^{40}\text{Ca}(^3\text{He}, ^6\text{He})^{37}\text{Ca}$, isobaric mass quartets of ^{37}Ca 3-60066
 $^{40}\text{Ca}(^6\text{Li}, d)^{44}\text{Ti}$, DWBA anal. of alpha transfer reaction 3-71124
 $^{40}\text{Ca}(N,N)$ scattering influence of exchange on optical potential, lowest order exchange processes 3-67290
 $^{40}\text{Ca}(\alpha, \alpha')$, 29 MeV, coupled-channel calcs., influence of J-dependent absorption on cross section 3-67353
 $^{40}\text{Ca}(\alpha, d)^{42}\text{Sc}$, study of ^{42}Sc , 25.5 MeV, d ang. distrib. meas. 3-78246
 $^{40}\text{Ca}(\alpha, p)^{44}\text{Ti}$, rotational bands obs. 3-74490
 $^{40}\text{Ca}(d, Li)$, 28 MeV, cross-section, spectroscopic factors 3-78341
 $^{40}\text{Ca}(d, p)^{41}\text{Ca}$, high resolution study of weak transitions, high spin states of rotational bands in ^{41}Ca 3-60072
 $^{40}\text{Ca}(e, e)$, determ. of equilibrium density of nucleons in nucleus (Russian) 3-40433
 $^{40}\text{Ca}(e, e'p)$, 710 MeV, proton ang. distrib. 3-43235
 $^{40}\text{Ca}(u^-, nn)$, determ. of absolute capture probability by activation method (Russian) 3-40484
 $^{40}\text{Ca}(p, p')^{40}\text{Ca}$ 12 MeV incident energy, excited states study (French) 3-43179
 $^{40}\text{Ca}(p, d)^{39}\text{Ca}$, at 185 MeV, deep-lying hole states 3-52101
 $^{40}\text{Ca}(p, p')^{41}\text{Sc}$, 3 MeV, study of ^{41}Sc β -decay, Q-value determ. 3-67275
 $^{40}\text{Ca}(p, p')$ reaction effective interactions 3-43250
 $^{40}\text{Ca}(p, p')^{40}\text{Ca}^*$, excitation of $f_{7/2}\text{-}d_{3/2}^{-1}$ states, effect of vector and tensor forces 3-67328
 $^{40}\text{Ca}(p, p)^{40}\text{Ca}$, energy dependence of real central optical potential, 25-1000 MeV 3-60185
 $^{40}\text{Ca}(t, p)^{42}\text{Ca}$, nuclear overlap, cross section prediction 3-67282
 ^{41}Ca , γ transitions between high-spin states, heavy-ion induced reaction obs. 3-74530
 ^{41}Ca , high spin states in $K = 3/2^+$ and $K = 3/2^-$ rotational bands 3-60072
 ^{41}Ca , mag. moment and deformed component 3-43173
 ^{41}Ca , violation of additivity of $I_{f_{7/2}}$ neutron moments 3-45964
 ^{42}Ca , ^{44}Ca , quadrupole moments and coexistence, $B(E2)$ values, model comparison 3-52076
 ^{42}Ca ($^3\text{He}, ^3\text{He}$), 28 MeV, anomalous backward angle scattering 3-54494
 ^{42}Ca E2 transition strength, ratio between $B(E2)$ values for Coulomb excitation of 2^+ states in ^{46}Ca and ^{42}Ca 3-49193
 $^{42}\text{Ca}(\alpha, n)^{45}\text{Ti}$, 10.2-14.2 MeV, study of $K = 3/2^+$ rotational band 3-74494
 $^{42}\text{Ca}(\alpha, p)^{45}\text{Si}$, 10.2-14.2 MeV, study of $K = 3/2^+$ rotational band 3-74494
 $^{42}\text{Ca}(d, Li)$, 28 MeV, cross-section, spectroscopic factors 3-78341
 $^{42}\text{Ca}(p, t)^{40}\text{Ca}$, cross section predictions from coexistence model 3-67329
 ^{43}Ca , n.m.r., Larmor frequency, magnetic moment, chemical shifts 3-74483
 $^{44}\text{Ca}(p, p)^{44}\text{Sc}$ rel. to isobaric analogue of lowest $3/2^-$ state of ^{45}Ca determ. 3-67195
 $^{44}\text{Ca}(p, p)^{44}\text{Ca}$ rel. to isobaric analogue of lowest $3/2^-$ state of ^{45}Ca determ. 3-67195
 $^{44}\text{Ca}(p, n\gamma)^{44}\text{Sc}$, level scheme of ^{44}Sc , lifetime meas., ang. distrib. 3-78282
 ^{45}Ca pop. in $^{44}\text{Ca}(p, p)$, (p, γ), determ. isobaric analogue of lowest $3/2^-$ state 3-67195
 ^{46}Ca , level study up to 6.3 MeV excitation energy using $^{48}\text{Ca}(p, t)$ reaction 3-67211
 ^{46}Ca E2 transition strength, ratio between $B(E2)$ values for Coulomb excitation of 2^+ states in ^{46}Ca and ^{42}Ca 3-49193
 $^{46}\text{Ca}(p, p)^{46}\text{Ca}$, 16 MeV, ^{46}Ca level structure 3-54391
 $^{46}\text{Ca}(^{14}\text{N}, ^{13}\text{C})^{49}\text{Sc}$, possible L-dependent angular distributions 3-54503
 $^{46}\text{Ca}(^{14}\text{N}, ^{13}\text{C})^{49}\text{Sc}$, 40 MeV, ang. oscillations 3-74605
 $^{46}\text{Ca}(^{16}\text{O}, ^{14}\text{C})^{50}\text{Ti}$, DWBA analysis of ang. distrib. 3-57538
 $^{46}\text{Ca}(^3\text{He}, t)^{48}\text{Sc}$, 2nd order perturbation method with ($^3\text{He}-\alpha$ -t) process and DWBA 3-71123
 $^{48}\text{Ca}(p, p)^{48}\text{Sc}$, M1 transition strength from $3/2^-$ isobaric analogue state 3-54420
 $^{48}\text{Ca}(p, p)^{48}\text{Sc}$, spin-parity of ^{49}Sc levels from $3/2^-$ isobaric analogue state γ -decay 3-54377
 $^{48}\text{Ca}(p, p)^{48}\text{Sc}$, negative-parity state lifetimes of ^{49}Sc 3-40445
 $^{48}\text{Ca}(p, t)^{46}\text{Ca}$, 39 MeV high resolution study, obs. of new levels in ^{46}Ca 3-67211
Co isotopes, study using Hartree-Fock-Bogoliubov method 3-67246
 ^{54}Co , assignments from ($^3\text{He}, t$) reactions 3-63079
 ^{54}Co , half-life meas. 3-40461

nuclei with $39 \leq A \leq 58$ continued

- ^{56}Co , ^{57}Co , effective M1 operators, shell model calcs. 3-49124
 ^{56}Co , γ -ray transitions props. from ^{56}Ni decay and $^{56}\text{Fe}(p, n)^{56}\text{Co}$ 3-54426
 ^{57}Co , in Al, interstitial atom trapping, Mossbauer meas. after neutron irradiation 3-58454
 ^{57}Co , new energy levels found using $^{57}\text{Fe}(p, n)^{57}\text{Co}$ (German) 3-60196
 ^{57}Co , radioactive precipitate, secondary electron emission 3-49228
 ^{57}Co , selective population of highly excited states by (α, p) reaction 3-78346
 ^{57}Co decay, 122 keV, transition, E2/M1 mixing ratio determ. by orientation 3-46006
 ^{58}Co , spin assignments from $(^3\text{He}, p)$ and $(^3\text{He}, pp)$ reactions on ^{56}Fe 3-54428
 ^{58}Co high activity source preparation from irradiated Ni 3-62205
 ^{58}Co energy spectra in $1f_{7/2}$ shell 3-78245
 ^{48}Cr from $^{40}\text{Ca}(^{10}\text{B}, pnp)$, 19, 22.5, 25 MeV, γ -ray spectroscopy 3-62985
 ^{48}Cr prod. from reactions involving $^{50}\text{Cr}^*$ compound-system, excitation functions 3-40512
 ^{48}Cr , ^{51}Cr , spherical shell-model states of high angular momentum, α -particle induced reactions 3-40416
 ^{50}Cr , quadrupole deformation measurements of first excited states 3-49143
 ^{50}Cr , recoil-distance lifetime meas. for excited states 3-40448
 $^{50}\text{Cr}^*$ compound-system, test of independence postulate in Bohr theory 3-40512
 $^{50}\text{Cr}(d, \alpha)^{48}\text{V}$, 15 MeV, excitation energies and angular distrib. meas. for ^{48}V levels 3-57534
 $^{50}\text{Cr}(d, p)^{51}\text{Cr}$, region from hyperbarrier to Coulomb stripping, spectroscopic study (Russian) 3-52190
 $^{50}\text{Cr}(p, n)^{49}\text{Cr}$, 20.43 to 22.22 MeV, cross section by detection of ^{49}Cr positron activity 3-54460
 ^{51}Cr , angular momentum determ. for levels populated in $^{50}\text{Cr}(d, p)$ reaction (Russian) 3-52190
 ^{51}Cr decay, relative intensity and internal conversion coeff. meas. 3-52123
 ^{52}Cr , inelastic 14.2 MeV neutron interactions, gamma-ray production cross sections 3-54469
 ^{52}Cr , quadrupole deformation measurements of first excited states 3-49143
 ^{52}Cr isobaric analogue states, γ -ray decay study, $^{51}\text{V}(p, p)^{52}\text{Cr}$ 3-78287
 $^{52}\text{Cr}(d, p)^{53}\text{Cr}$, deuteron D-state effects obs. 3-63066
 $^{52}\text{Cr}(d, \alpha)^{50}\text{V}$, 15 MeV, excitation energies and angular distrib. meas. for ^{48}V levels 3-57534
 $^{52}\text{Cr}(d, p)^{53}\text{Cr}$, 10 MeV, tensor polarised deuteron beam, meas. of analysing powers and cross sections 3-49266
 $^{52}\text{Cr}(e, e')$, $E=209$ MeV, study of collective states, comparison with microscopic vibrational model 3-63039
 ^{53}Cr , effective M1 operators, shell model calcs. 3-49124
 ^{53}Cr , ground state static quadrupole moment from Coulomb excitation meas. 3-40410
 ^{53}Cr , levels populated in $^{52}\text{Cr}(d, p)$ reaction at 10 MeV, polarised deuteron beam 3-49266
 ^{53}Cr , static quadrupole moment determ. from reorientation effect in Coulomb excitation by ^{25}S 3-46038
 ^{53}Cr high-spin states populated in $^{48}\text{Ti}(\alpha, n)$ reaction decay properties 3-52096
 $^{53}\text{Cr}(p, n)^{53}\text{Mn}$, 6 MeV, obs. of ^{53}Mn γ -transitions (Russian) 3-74526
 $^{53}\text{Cr}(p, n)^{53}\text{Mn}$, excited states of ^{53}Mn 3-67192
 ^{53}Cr , quadrupole deformation measurements of first excited states 3-49143
 $^{54}\text{Cr}(p, p)$, (p, pp) , (p, γ) , 1.98-2.02 MeV, multichannel study of ^{53}Mn isobaric analogue resonances 3-52133
 $^{54}\text{Cr}(p, p)$ and $^{54}\text{Cr}(p, \alpha)$, conserved isospin quantum number consequences 3-60148
 Cu , ^{57}Fe , pressure depend. of Mossbauer fraction and energy shift at 298K and 94K 3-41455
 ^{58}Cu , assignments from $(^3\text{He}, t)$ reactions 3-63079
 Fe , 14-MeV neutron bombardment, meas. and calcs. of neutron spectra 3-67321
 Fe , $A=54, 56, 58$, scattering of polarised 12.3 MeV deuterons, vector analysing power and cross sections 3-52194
 Fe , avalanches induced by charged and neutral cosmic ray particles (Russian) 3-65609
 Fe , elemental, meas. and evaluation of neutron total cross-section minima, 24-750 keV 3-54523
 Fe , fast neutron small-angle scattering, elastic cross-section meas. 3-74579
 Fe , hedenbergite-ferrosilite pyroxene, synthetic, Mossbauer resonance spectroscopy of iron 3-80593
 Fe , neutron induced gamma-ray production in range 0.8-20 MeV, cross-section meas. 3-43241
 Fe , neutron production by cosmic ray high energy muons, depth dependency, e.m. interaction explanation (Russian) 3-61621
 Fe , neutron total cross section meas., 24-1000 keV, using Harwell synchrocyclotron time-of-flight spectrometer 3-71117
 Fe , nucleon cosmic ray interactions at mountain altitudes, 600-10000 GeV, integral energy spectrum (Russian) 3-69781
 Fe , nucleon partial inelasticity coeff. (Russian) 3-49157
 ^{56}Fe , compound statistical reactions, test of independence hypothesis and isospin conservation 3-71093
 $^{56}\text{Fe}(p, d)^{55}\text{Fe}$, at 185 MeV, deep-lying hole states 3-52101
 ^{56}Fe , for hemopoietic marrow scanning 3-70137
 ^{56}Fe , Mossbauer effect in bis[2,4-bis(2-pyridyl)thiazole]Fe(II) complexes 3-53037
 ^{56}Fe , alignment of excited states meas. technique using anisotropy of emitted γ -rays 3-49080
 ^{56}Fe , ^{56}Fe , proton spin flip angular distributions at 12 MeV, collective model DWBA calculations 3-63048
 ^{56}Fe , isobaric analog reson. states population in (p, γ) and (p, p) reactions 3-67317
 $^{56}\text{Fe}(^{12}\text{C}, ^{11}\text{B})^{55}\text{Co}$, semiclassical anal. of results, j and Q depend. explanation 3-46041
 $^{56}\text{Fe}(^{14}\text{N}, ^{13}\text{C})^{55}\text{Co}$, semiclassical anal. of results, j and Q depend. explanation 3-46041
 $^{56}\text{Fe}(^{16}\text{O}, ^{12}\text{C})^{54}\text{Ni}$, DWBA analysis of ang. distrib. 3-57538

nuclei with $39 \leq A \leq 58$ continued

- $^{54}\text{Fe}(^{16}\text{O}, ^{15}\text{N})^{53}\text{Co}$, semiclassical anal. of results, j and Q depend. explanation 3-46041
 $^{54}\text{Fe}(^3\text{He}, t)^{54}\text{Co}$, 24 MeV, differential cross sections, ang. distrib. 3-63079
 $^{54}\text{Fe}(d, p)^{55}\text{Fe}$, 10 MeV, tensor polarised deuteron beam, meas. of analysing powers and cross sections 3-49266
 $^{54}\text{Fe}(e, e')$, $E=209$ MeV, study of collective states, comparison with microscopic vibrational model 3-63039
 $^{54}\text{Fe}(p, p)^{54}\text{Fe}$, $E_p=19.6$ MeV, study of 2^+ state, limitations of collective model 3-78237
 ^{55}Fe , levels populated in $^{54}\text{Fe}(d, p)$ reaction at 10 MeV, polarised deuteron beam 3-49266
 ^{55}Fe from $^{56}\text{Fe}(d, t)$ reaction, low-lying levels study 3-74485
 ^{55}Fe mean life of 3 excited states, recoil distance method (French) 3-43205
 ^{56}Fe , Coulomb excitation by ^{16}O , reorientation effect, energy dependence 3-46038
 ^{56}Fe , effective M1 operators, shell model calcs. 3-49124
 ^{56}Fe , γ -rays from levels fed by 56 Mn β -decay (French) 3-78293
 ^{56}Fe , inelastic 14.2 MeV neutron interactions, gamma-ray production cross sections 3-54469
 ^{56}Fe compound nucleus, ^{56}Mn isobaric analogue states, (p, γ) , (p, n) reactions obs. 3-54421
 $^{56}\text{Fe}(^3\text{He}, p)^{58}\text{Co}$, product energy levels, spin assignments 3-54428
 $^{56}\text{Fe}(^3\text{He}, pp)^{58}\text{Co}$, product energy levels, spin assignment 3-54428
 $^{56}\text{Fe}(\alpha, n)^{59}\text{Ni}$, 8.5 and 10.5 MeV, meas. of Doppler shift attenuation and recoil distance 3-49213
 $^{56}\text{Fe}(d, t)^{55}\text{Fe}$, low-lying levels study 3-74485
 $^{56}\text{Fe}(d, Li)$, 28 MeV, cross-section, spectroscopic factors 3-78341
 $^{56}\text{Fe}(d, \alpha)$ reaction, 12 MeV meas. alpha particle angular distribution, ^{54}Mn levels 3-60201
 $^{56}\text{Fe}(d, p)^{57}\text{Fe}$, ground state doublet of ^{57}Fe study 3-43215
 $^{56}\text{Fe}(d, p)^{57}\text{Fe}$, Mossbauer effect in $\alpha\text{-Fe}_2\text{O}_3$ following reaction 3-47190
 $^{56}\text{Fe}(p, n)$ meas. absolute differential cross section near thresholds 3-71101
 $^{56}\text{Fe}(n, n')$, 300-500 keV above threshold for excitation of 2^+ levels, cross section energy dependence (Russian) 3-74571
 $^{56}\text{Fe}(n, n')$, $E=1.43$ to 2.15 MeV, differential cross sections, spin, parity assignment to ^{57}Fe doorway state resonance 3-60177
 $^{56}\text{Fe}(n, p)$, 0.8-9.0 MeV, cross section for gamma-ray production 3-52185
 $^{56}\text{Fe}(n, p)$, $E=1.43$ to 2.15 MeV, differential cross sections, spin, parity assignment to ^{57}Fe doorway state resonance 3-60177
 $^{56}\text{Fe}(n, n)$, $E=1.43$ to 2.15 MeV, differential cross sections, spin, parity assignment to ^{57}Fe doorway state resonance 3-60177
 $^{56}\text{Fe}(p, n)^{56}\text{Mn}$, cross section used as standard for activation cross section meas. at 14.78 MeV 3-74573
 $^{56}\text{Fe}(p, n)^{56}\text{Co}$, γ -ray transition props. study in ^{56}Co 3-54426
 ^{57}Fe , calibration of isomer shift by lifetime meas. in different chemical environments (German) 3-49186
 ^{57}Fe , calibration of isomer shift using lifetime and Mossbauer meas. on 14.4 keV state 3-62984
 ^{57}Fe , electron spin polarised, 14.4 keV transition, internal conversion coeffs. and conversion electron intensity 3-40442
 ^{57}Fe , implanted in Si, Mossbauer spectra of 14.4 keV γ -rays at room temp. 3-47184
 ^{57}Fe , in $\text{Fe}_3\text{Al}_2\text{Si}_3\text{O}_{12}$ cryst., elec. and mag. hyperfine interactions, Mossbauer obs. 3-75930
 ^{57}Fe , in FeX (X=metaloid), hyperfine field in interstitial and substitutional compounds 3-64589
 ^{57}Fe , local mag. ordering of Fe impurities in Pd_2MnSn 3-79832
 ^{57}Fe , mag. moment, from Mossbauer meas. 3-52075
 ^{57}Fe , Mossbauer effect in Cu 3-47181
 ^{57}Fe , Mossbauer effect in frozen rare gas matrix, hyperfine interactions obs. 3-41451
 ^{57}Fe , Mossbauer effect in Fe-N 3-79953
 ^{57}Fe , Mossbauer effect in Sm-Co intermetallic cpds. 3-61014
 ^{57}Fe , Mossbauer spectra of biferricenium and biferricenylum cations, intervalence transfer study 3-55507
 ^{57}Fe , Mossbauer spectroscopy in magnetic oxides 3-50495
 ^{57}Fe , n.m.r. freq. shift in BaFe_2O_9 in static mag. field 3-79929
 ^{57}Fe , n.m.r. in DyFeO_3 domain walls 3-72532
 ^{57}Fe , n.m.r. in $\text{R}_0\text{Y}_2\text{Fe}_3\text{O}_{12}$ (R=rare earth) 3-50475
 ^{57}Fe , spin, parity assignment to doorway state resonance, from analysis of neutron scattering by ^{56}Fe 3-60177
 ^{57}Fe effective field strength in Fe-Ni alloys, Mossbauer meas. 3-50504
 ^{57}Fe from $^{56}\text{Fe}(d, p)^{57}\text{Fe}$, ground state doublet study 3-43215
 ^{57}Fe impurity in II-IV-V₂ semiconductors, effective charges from Mossbauer obs. 3-58456
 ^{57}Fe in ErFeO_3 , n.m.r. investigation of effect of ordering of Er^{3+} on Fe sublattices 3-50476
 ^{57}Fe in ferromagnetic Fe_2P , n.m.r. study 3-41442
 ^{57}Fe in garnet, hyperfine field obs. by ENDOR 3-64583
 ^{57}Fe in NiS, metal-nonmetal transition investigation using Mossbauer effect 3-53049
 ^{57}Fe Mossbauer effect in Fe-Ni-Al alloys (Japanese) 3-61145
 ^{57}Fe Mossbauer effect in $\gamma\text{-Fe-Mn}$ alloys (Russian) 3-44353
 ^{57}Fe Mossbauer effect in Invar-type Fe-Ni-Mn alloys (Russian) 3-68891
 ^{57}Fe Mossbauer effect in $\text{LaFe}_{12}\text{O}_{19}$ 3-58448
 ^{57}Fe Mossbauer effect in mag. multilayer crystals, recoilless factor behaviour (German) 3-50493
 ^{57}Fe Mossbauer effect in NH_4MnCl_3 , NH_4FeCl_3 and NH_4CoCl_3 3-79950
 ^{57}Fe Mossbauer effect in Permalloys with Mo additions (Russian) 3-53038
 ^{57}Fe Mossbauer effect in transferrin 3-63575
 ^{57}Fe Mossbauer effect in YFe_2 (French) 3-72547
 ^{57}Fe Mossbauer effect in $\text{ZnSiF}_6 \cdot 6\text{H}_2\text{O}$ 3-55506
 ^{57}Fe Mossbauer hyperfine pattern, influence of high electrostatic fields 3-68900
 ^{57}Fe Mossbauer investigation of tektites 3-59322
 $^{57}\text{Fe}(p, n)^{57}\text{Co}$, 4.9, 5.6 and 6.2 MeV, new levels found in ^{57}Co (German) 3-60196
 $\text{Fe}(\alpha, n)$ reactions, $A=56, 57$, precompound processes, 20 MeV, energy, angular distrib. of neutrons 3-60209

nuclei with $39 \leq A \leq 58$ continued

- Fe(n,p)Mn, energies <6 MeV, cross section meas. rel. to ^{235}U fission using activation method 3-74591
- K, fast neutron total cross sections, 5.0-8.5 MeV 3-60169
- K isotopes, g factor determ. from configuration mixing, calc. of first-order effects 3-52072
- ^{39}K , charge distributions, elastic electron scattering cross sections, phase-shift code analysis 3-62927
- ^{39}K , lifetimes of excited states populated in $^{36}\text{Ar}(\alpha, \text{pp})$ reaction 3-43210
- ^{39}K , mag. moment and deformed component 3-43173
- ^{39}K (^3He , ^3He), 28 MeV, anomalous backward angle scattering 3-54494
- $^{39}\text{K} + \text{p}$, effect of ground state correlations on imaginary part of optical-model potential 3-52154
- $^{39}\text{K}(^3\text{He}, \text{d})^{40}\text{Ca}$ 18 MeV incident energy, excited states study (French) 3-43179
- $^{39}\text{K}(\text{d}, \text{d}')$, inelastic scattering, 12.8 MeV, microscopic analysis of 2.52 MeV state excitation 3-49267
- $^{39}\text{K}(\text{p}, \text{n})^{39}\text{Ca}$, 10 MeV, study of ^{39}Ca β -decay 3-67275
- $^{39}\text{K}(\text{p}, \text{p}')$, imaginary part of optical model potential 3-54450
- ^{40}K , e.m. decay scheme below 3.2 MeV excitation, γ -ray study using $^{37}\text{Cl}(\alpha, \text{n})$ and $^{40}\text{Ar}(\text{p}, \text{n})$ reactions 3-43208
- ^{40}K , e.m. transition rates, meas. lives of low lying states using attenuated-Doppler-shift method 3-62989
- ^{40}K , lifetime of 2542 keV level 3-60116
- ^{41}K , γ transitions between high-spin states, heavy-ion induced reaction obs. 3-74530
- ^{41}K (^3He , ^3He), 28 MeV, anomalous backward angle scattering 3-54494
- $^{41}\text{K}(\alpha, \text{n})^{44}\text{Sc}$, 10-14 MeV, γ -ray spectra, $\gamma\gamma$ -coincidences and yield function meas., ^{44}Sc excited states 3-74495
- $^{41}\text{K}(\alpha, \text{n})^{44}\text{Sc}$, level scheme of ^{44}Sc , lifetime meas. ang. distrib. 3-78282
- Mn isotopes, study using Hartree-Fock-Bogoliubov method 3-67246
- Mn odd isotopes, coupling of three-particle (hole) valence-shell cluster to quadrupole vibrations 3-67238
- ^{50}Mn , half-life meas. 3-40461
- ^{50}Mn pop. in $^{50}\text{Cr}(\text{p}, \text{n})^{50}\text{Mn}$, determ. separation of isomeric levels from β^+ decay threshold energies 3-67212
- ^{53}Mn , excited state obs. by $^{53}\text{Cr}(\text{p}, \text{n})$ reaction 3-67192
- ^{53}Mn , γ -emission from levels excited in $^{53}\text{Cr}(\text{p}, \text{n})$ reaction at 6 MeV (Russian) 3-74526
- ^{54}Mn , ^{55}Mn , effective M1 operators, shell model calcs. 3-49124
- ^{54}Mn , diffusion coeffs. in Rhone sediments 3-56142
- ^{54}Mn , levels up to 4.3 MeV excitation using spectroscopic method on $^{56}\text{Fe}(\text{d}, \alpha)$ reaction 3-60201
- ^{55}Mn , multi-channel study of fine structure of analogue state following ^{54}Cr proton induced reactions 3-52133
- ^{55}Mn , n.m.r. in antiferromag. α -Mn alloys 3-47153
- ^{55}Mn , nuclear echo in RbMnF_3 3-64567
- ^{55}Mn compound nucleus behaviour in $^{54}\text{Cr}(\text{p}, \text{p})$ and $^{54}\text{Cr}(\text{p}, \alpha)$ reactions 3-60148
- ^{55}Mn internal field, n.m.r. of Cr-Mn antiferromagnetic alloys 3-68857
- ^{55}Mn nuclear acoustic resonance in CsMnF_3 , temp. dependence 3-55487
- $^{55}\text{Mn}(\text{p}, \text{p})^{56}\text{Fe}$, ^{56}Mn isobaric analogue states in ^{56}Fe compound nucleus 3-54421
- $^{55}\text{Mn}(\text{p}, \text{n})^{56}\text{Fe}$, ^{56}Mn isobaric analogue states in ^{56}Fe compound nucleus 3-54421
- $^{55}\text{Mn}(\text{p}, \text{p})^{56}\text{Fe}$, isobaric analogue state of ^{56}Mn 0.211 MeV level 3-60168
- $^{55}\text{Mn}(\text{p}, \text{p})^{55}\text{Mn}$, isobaric analogue state of ^{56}Mn 0.211 MeV level 3-60168
- ^{56}Mn , β -decay, feeding of ^{56}Fe energy levels (French) 3-78293
- ^{56}Mn 0.211 MeV level isobaric analogue state 3-60168
- $^{56}\text{Mn}(\text{p}, \text{p})^{56}\text{Fe}$, isobaric analog reson. obs. 3-67317
- Ni, even isotopes, appl. of particle number projection study with generator coord. method 3-45987
- Ni, π^+ , π^- reaction cross sections, 584 to 1856 MeV, deduced neutron density 3-54507
- Ni isotopes, application of self-consistent core-particle coupling method 3-54415
- Ni isotopes, energy spectra of normal parity states in shell model, effective-interaction calcs. 3-67210
- Ni isotopes, even, (p,t) and (t,p) reaction data analysis using broken-pair approx. 3-40494
- $\text{Ni}(^3\text{He}, \text{t})\text{Cu}$, excitation of 2^+ analogues in Cu isotopes, DWBA analysis, second-order effects 3-49271
- ^{56}Ni , ^{32}S induced reaction, fusion barrier meas. 3-46042
- ^{56}Ni , effective interactions and $1f_{7/2}$ sub-shell closure in $2p$ - $1f$ shell 3-49169
- ^{56}Ni decay, γ -ray transition props. study in ^{56}Co 3-54426
- ^{58}Ni , activation cross-sections for 14.7 MeV neutrons 3-54470
- ^{58}Ni , alpha-particle scattering, 139 MeV, analysis elastic cross sections using Woods-Saxon potential 3-63076
- ^{58}Ni , elastic and inelastic scattering of 1.04 GeV protons, angular distrib. meas. 3-57522
- ^{58}Ni , elastic and inelastic scatt. of 1 GeV protons, theory, comparison with expt. 3-78320
- $^{58}\text{Ni}^+$ ion bombardment of Ni, effect of beam scanning 3-64076
- $^{58}\text{Ni}(^{16}\text{O}, ^{16}\text{O})^{58}\text{Ni}$, 35-60 MeV, interference of Coulomb and nuclear excitation 3-52201
- $^{58}\text{Ni}(^{16}\text{O}, ^{16}\text{O})$ reactions, anomalous and normal angular distributions 3-43256
- $^{58}\text{Ni}(^3\text{He}, \text{t})^{58}\text{Cu}$, 24 MeV, differential cross sections, ang. distrib. 3-63079
- $^{58}\text{Ni}(^4\text{He}, \text{p})^{61}\text{Cu}$, 9.7-12.2 MeV reaction spectrometry 3-67261
- $^{58}\text{Ni}(^6\text{Li}, ^6\text{Li})$, break-up study, $E=12$ to 24 MeV 3-46040
- $^{58}\text{Ni}(^6\text{Li}, \alpha(\text{d}))$, break-up study, $E=12$ to 24 MeV 3-46040
- $^{58}\text{Ni}(^7\text{Li}, ^7\text{Li})$, break-up study, $E=12$ to 24 MeV 3-46040
- $^{58}\text{Ni}(\text{d}, \text{p})^{59}\text{Ni}$, 10 MeV, meas. of angular distrib. of vector analysing power and absolute cross section 3-52077
- $^{58}\text{Ni}(\text{d}, \text{Li})$, 28 MeV, cross-section, spectroscopic factors 3-78341
- $^{58}\text{Ni}(\text{d}, \text{p})$, 100 MeV, diffraction model, effect of nuclear boundary spread and Coulomb interaction (Russian) 3-74548
- $^{58}\text{Ni}(\text{d}, \text{p})^{59}\text{Ni}$, $E_d=8$ MeV, level struct. of ^{59}Ni 3-45973

nuclei with $39 \leq A \leq 58$ continued

- $^{58}\text{Ni}(\text{n}, \text{p})^{58}\text{Co}$ energies <6 MeV, cross section meas. rel. to ^{235}U fission using activation method 3-74591
- $^{58}\text{Ni}(\text{p}, \alpha)^{55}\text{Co}$, Q value meas., mass discrepancies with 1971 tables 3-45923
- $^{58}\text{Ni}(\text{p}, \text{p}')^{58}\text{Ni}$, $E_p=60$ MeV polarized protons, giant reson. excitation 3-74584
- $^{58}\text{Ni}(\text{p}, \text{p}')^{58}\text{Ni}$, 1 GeV, differential cross section calc. using Glauber multiple scattering theory 3-57521
- $^{58}\text{Ni}(\text{p}, \text{t})^{56}\text{Ni}$, $E_p=45$ MeV, finite range effects by multipole expansion method 3-67294
- $^{57,58}\text{Ni}$ one-neutron transfer reaction, microscopic form factor 3-43246
- ^{58}O , oriented, positron asymmetry meas. 474 keV, 0.013K, using semiconductor detector telescope 3-63005
- Pd_2MnSb : ^{55}Mn , n.m.r. study, magnitude and sign of hyperfine fields 3-50485
- ^{42}Pr radioactive source, nuclear excitation by gamma rays 3-67305
- ^{42}Sc , doorway state struct., ^{40}Ca inelastic proton scatt. 3-78319
- ^{41}Sc , recoil polarisation from $^{40}\text{Ca}(\text{d}, \text{n})$, n.m.r. meas. of β -decay asymmetry, magnetic moment determ. 3-45938
- ^{41}Sc β -decay, meas. of half-life, and ft values, and Gamow-Teller matrix elements 3-67275
- ^{41}Sc in Ta, n.m.r. detn. of mag. moment 3-45963
- ^{41}Sc produced in $^{40}\text{Ca}(^3\text{He}, \text{d})^{41}\text{Sc}$, $1f_{7/2}$ proton state studied using DWBA anal. 3-74480
- ^{42}Sc , alignment of excited states meas. technique using anisotropy of emitted γ -rays 3-49080
- ^{42}Sc , population in $^{40}\text{Ca}(\alpha, \text{d})^{42}\text{Sc}$, 25.5 MeV, d ang. distrib. meas. 3-78246
- ^{42}Sc , γ decay of low-lying states, lifetimes, ang. distrib. meas. 3-78282
- ^{44}Sc , isospin mixing from the effective nuclear interaction 3-71062
- ^{44}Sc , proposed $K^\pi=0^-$ band 3-49145
- ^{44}Sc excited states populated by $^{41}\text{K}(\alpha, \text{n})$, decay modes and spin assignments, $K=0^-$ band 3-74495
- ^{45}Sc , 8.113 and 8.130 MeV states as split isobaric analogue of lowest $3/2^-$ state of ^{45}Ca 3-67195
- ^{45}Sc , deduce levels forming split isobaric analogue of lowest $3/2^-$ state of ^{45}Ca 3-67195
- ^{45}Sc , $K=3/2^+$ rotational band study using $^{42}\text{Ca} + \alpha$ reaction 3-74494
- ^{45}Sc , spherical shell-model states of high angular momentum, α -particle induced reactions 3-40416
- ^{45}Sc , transition strengths, reson. fluores. obs. 3-40450
- $^{45}\text{Sc}(\text{n}, \text{n}') E=1.41$ MeV, γ angular distribution, ^{45}Sc levels spin assignment 3-74589
- $^{45}\text{Sc}(\text{p}, \text{p})$, 1.6 to 1.8 MeV, fit of analogue resonances in ^{46}Ti compound nucleus 3-63023
- ^{46}Sc energy spectra in $1f_{7/2}$ shell 3-78245
- ^{46}Sc radioactive source, nuclear excitation by gamma rays 3-67305
- ^{46}Sc , corrosion of Ti, radiometric study 3-42703
- ^{49}Sc , M1 transition strength from $3/2^-$ isobaric analogue state, $^{48}\text{Ca}(\text{p}, \text{p})^{49}\text{Sc}$ reaction 3-54420
- ^{49}Sc from $^{48}\text{Ca}(^{14}\text{N}, ^{13}\text{C})^{49}\text{Sc}$, possible L-dependent angular distributions 3-54503
- ^{49}Sc levels, spin-parity from $3/2^-$ isobaric analogue state γ -decay, $^{48}\text{Ca}(\text{p}, \text{p})^{49}\text{Sc}$ reaction 3-54377
- ^{49}Sc negative-parity state lifetimes using $^{48}\text{Ca}(\text{p}, \text{p})^{49}\text{Sc}$ reaction 3-40445
- $^{118}\text{Sn}(^6\text{Li}, \alpha(\text{d}))$ break-up study, $E=12$ to 24 MeV 3-46040
- ^{46}Ti from $^{40}\text{Ca}(\alpha, \text{p})^{46}\text{Ti}$, rotational bands obs. 3-74490
- $^{44}\text{Ti} \rightarrow ^{44}\text{Sc}$ α -Ca decay scheme (Russian) 3-52124
- ^{45}Ti , ^{47}Ti , spherical shell-model states of high angular momentum, α -particle induced reactions 3-40416
- ^{45}Ti , $K=3/2^+$ rotational band study using $^{42}\text{Ca} + \alpha$ reaction 3-74494
- ^{46}Ti , compound nucleus, fit of analogue resonances from $^{45}\text{Sc}(\text{p}, \text{p})$ reaction 1.6 to 1.8 MeV 3-63023
- ^{46}Ti , deduced levels, enhancement factors 3-54471
- ^{46}Ti , recoil-distance lifetime meas. for excited states 3-40448
- ^{46}Ti , test of independence postulate in Bohr theory of compound-nucleus decay 3-40512
- $^{46}\text{Ti}(^3\text{He}, \text{t})^{46}\text{V}$, 2nd order perturbation method with $(^3\text{He}-\alpha)$ process and DWBA 3-71123
- $^{46}\text{Ti}(\text{n}, \text{n}')$, 300-500 keV above threshold for excitation of 2^+ levels, cross section energy dependence (Russian) 3-74571
- $^{46}\text{Ti}(\text{p}, \text{p})^{47}\text{V}$, level scheme of ^{47}V , reson., spin, parity (German) 3-78251
- ^{47}Ti , test of independence postulate in Bohr theory of compound-nucleus decay 3-40512
- ^{47}Ti levels populated in ^{47}V β -decay, spin and parity assignments 3-52146
- $^{47}\text{Ti}(\text{p}, \text{n})^{47}\text{V}$, low-lying levels study 3-49146
- ^{48}Ti , ^{50}Ti , proton spin flip angular distributions at 12 MeV, collective model DWBA calculations 3-63048
- ^{48}Ti , inelastic 14.2 MeV neutron interactions, gamma-ray production cross sections 3-54469
- ^{48}Ti energy spectra in $1f_{7/2}$ shell 3-78245
- $^{48}\text{Ti}(^3\text{He}, \text{t})^{48}\text{V}$, 2nd order perturbation method with $(^3\text{He}-\alpha)$ process and DWBA 3-71123
- $^{48}\text{Ti}(\text{n}, \text{n}')$, 300-500 keV above threshold for excitation of 2^+ levels, cross section energy dependence (Russian) 3-74571
- $^{48}\text{Ti}(\text{p}, \text{t})^{46}\text{Ti}$, 51 MeV, angular momentum transfers, ^{46}Ti deduced levels, enhancement factors 3-54471
- $^{50}\text{Ti}(^3\text{He}, \text{t})^{50}\text{V}$, 2nd order perturbation method with $(^3\text{He}-\alpha)$ process and DWBA 3-71123
- $^{50}\text{Ti}(\alpha, \text{n})^{53}\text{Cr}(\text{p}, \text{p})$, 10.2-14.2 MeV, decay properties of high-spin states in ^{53}Cr 3-52096
- $^{50}\text{Ti}(\text{e}, \text{e})$, $E=209$ MeV, study of collective states, comparison with microscopic vibrational model 3-63039
- $^{50}\text{Ti}(\text{p}, \text{p})$, high resolution, cross section meas., spins, parities, widths, 1.83-2.97 MeV 3-78324
- $\text{Ti}(\text{n}, \text{p})\text{Sc}$ energies <6 MeV, cross section meas. rel. to ^{235}U fission using activation method 3-74591
- V, 3- and 29-GeV proton interaction, product radionuclide yields 3-54481
- V, 300 GeV proton irradiation, spallation products cross section meas. 3-46028
- V isotopes, study using Hartree-Fock-Bogoliubov method 3-67246

nuclei with $39 \leq A \leq 58$ continued

- ⁴⁶V, half-life meas. 3-40461
⁴⁷V, level scheme using ⁴⁶Ti(p, γ) reson., spin, parity (*German*) 3-78251
⁴⁷V, low-lying levels study by ⁴⁷Ti(p,n) and ⁴⁰Ca(¹⁰B,ppn) 3-49146
⁴⁷V energy spectra in 1f_{7/2} shell 3-78245
⁴⁷V \rightarrow ⁴⁷Ti β -decay, meas. of γ -ray spectra, half-life and log ft values 3-52146
⁴⁸V, low-lying level structure study using ⁵⁰Cr(d, α) reaction 3-57534
⁴⁸V, low-lying levels populated in ⁴⁰Ca(¹⁰B,pp) and ⁴⁰Ca(¹²C,pppn) reactions 3-49135
⁴⁸V prod. from reactions involving ⁵⁰Cr* compound-system, excitation functions 3-40512
⁴⁹V, spherical shell-model states of high angular momentum, α -particle induced reactions 3-40416
⁵⁰V, low-lying level structure study using ⁵²Cr(d, α) reaction 3-57534
⁵¹V, (p,n) isobaric analogue transitions, 22 to 40 MeV proton energy, meas. angular distributions 3-63055
⁵¹V, n.m.r. in near-equiatomic V-Ru alloy 3-53032
⁵¹V, n.m.r. in Ni-V dil. alloy 3-64566
⁵¹V, n.m.r. in V₂O₃ 3-68861
⁵¹V, n.m.r. spectra for FeVO₄, CrVO₄, Co₃(VO₄)₂, Ni₃(VO₄)₂ 3-75890
⁵¹V Knight shift in (V_{1-x}Cr_x)₂Ge ternary solid solns. (*Russian*) 3-52917
⁵¹V Knight shift in V₃(Si_{1-x}Ge_x) solid solns. (*Russian*) 3-58327
⁵¹V n.m.r., Fourier transform variable field expt. with internal ²H lock 3-77589
⁵¹V n.m.r. in Fe-V alloy at 4.2K 3-58435
⁵¹V pseudo magnetic moments meas. method 3-67185
⁵¹V(γ , π^+)⁵¹Ti, free-nucleon photopion prod. amplitude and shell model calcs. 3-60159
⁵¹V(p, γ)⁵²Cr, γ -ray decay study, ⁵²Cr isobaric analogue states 3-78287
⁵¹V(p,n)⁵¹Cr, analogue transition, 16 to 26 MeV, energy dependence 3-63053
⁹²Zr(d,p)⁹¹Zr, 10 MeV, tensor polarised deuteron beam, meas. of analysing powers and cross sections 3-49266

nuclei with $59 \leq A \leq 89$

- ⁶⁰Ge, magnetic moment of excited 9/2⁺ state by perturbed angular distrib. meas. on ⁶⁴Zn(α ,n) 3-45948
 $A=59-89$ even nuclei, ¹⁶O and ¹²C induced reactions above Coulomb barrier, angular distrib. 3-49276
 $A=60, 64, 70$, quadrupole moments of first 2⁺ states from inelastic electron scattering 3-49100
 $A=70$ mass region, compilation of magnetic moments of excited 9/2⁺ states 3-45948
Nucleus(γ , γ pxn)²⁴Na, 13 $\leq Z_{\text{nucleus}} \leq 29$, yields for 100 MeV $\leq E_{\text{max}} \leq 1000$ MeV 3-54464
radiative neutron capture cross sections for $59 \leq A \leq 87$ 3-49252
single particle states energies, $35 \leq A \leq 65$ 3-54387
temperature dependent nuclear binding energies rel. to nucleosynthesis in stars 3-42112
(n, γ) radiative capture, optical model calc. 3-78334
(n,p) reactions, activation cross sections and isomer ratios as a function of incident energy, statistical model calc. (*German*) 3-52173
⁶²Ni(p,p)⁶²Ni, isobaric analogue resonances, double-scattering techniques, polarisation study, 2.43-2.75 MeV 3-63045
⁷¹Ga, chem. shifts and linewidths for GaCl_{4-x} ions in acetonitrile soln. 3-72535
⁸⁴As, $A=84-86$, produced in ²³⁵U neutron induced fission, delayed-neutron meas., half-life determ. 3-43202
⁸⁴As levels population in decay of ⁸⁹Se isomeric states 3-43222
⁷²As, obs. of new isomeric level at 215 keV populated in ⁷²Ge(p,n) reaction 3-45956
⁷⁴As, deduced spins and parities, product of ⁷⁴Ge(p,n) γ 3-54472
⁷⁴As, levels populated in ⁷³Ge(³He,d) reaction at 17 MeV 3-43182
⁷⁵As, γ -transitions of excited states populated by electron capture from ⁷⁵Se 3-49210
⁷⁵As, magnetic moment of 265 keV level using integral method of perturbed angular correlation technique 3-49105
⁷⁵As, n.q.r. and spin lattice relax. time in proustite, 300-4.2K (*Russian*) 3-79944
⁷⁵As, 285 keV γ line after EC decay of ⁷⁵Se, nucl. reson. fluoresc. obs. 3-63009
⁷⁵As(n, $2n$)⁷⁴As cross-section meas. rel. to ⁶⁵Cu(n, $2n$)⁶⁴Cu, at 14.1 MeV 3-57517
⁷⁵As(n, γ)⁷⁵As, cross section for 14.8 MeV neutrons 3-63061
⁷⁵As, meas. T_{1/2} of excited states using delayed coincidence technique for ⁷⁷Ge β -decay 3-60111
⁸³Bi(e⁺, e⁺)⁸⁴Se, elastic scattering, 100 and 200 keV, differential cross sections 3-63037
Br induced ^{6,7}Li emission, 25 GeV/c, effect of fragment on heavy product emission 3-78316
⁸¹Br, $A=79, 81$ radiative capture of 14.1 MeV neutrons, prompt γ -ray spectra 3-40441
⁸¹Br position decay, isomeric states population in ⁸⁹Se 3-43222
⁷⁶Br, from ⁷⁶Kr decay level energies spins, parities and transition probabilities 3-49220
⁷⁸Br \rightarrow ⁷⁸Se β^+ decay, level structure determ. 3-78247
⁷⁸Br, ⁸¹Br, n.q.r. in rare earth and yttrium bromide hexahydrates 3-75913
⁷⁹Br, E2 and M1 reduced transition probabilities, core excitation calc. 3-46005
⁷⁹Br, $\gamma\gamma$ directional correlations meas., spin and parity assignments (*German*) 3-40459
⁷⁹Br n.m.r., Fourier transform variable field expt. with internal ²H lock 3-77589
⁷⁹Br n.q.r. meas. of displacive phase transition in (NH₄)₂PtBr₆ 3-41449
⁸¹Br, E2 and M1 reduced transition probabilities, core excitation calc. 3-46005
⁸¹Br, in cuprous halides, nuclear spin-lattice relaxation times, temp. depend. 3-55493
⁸²Br, isomeric transition-activated, reaction in H⁸²mBr-CH₄ 3-65115
⁸²Br excited levels populated in ⁸³Se α -Se decay 3-63010
⁸³Br production from ⁸⁰Se(α ,p)⁸³Br, energy levels study 3-52103

nuclei with $59 \leq A \leq 89$ continued

- Co, 11.5, 220 and 300 GeV proton irradiation, spallation products cross section meas. 3-46028
Co, neutron absorption cross sections, 4 to 47 A neutrons 3-78333
Co (α , α), 22 to 29 MeV interference maxima in backward excitation curve and angular distrib. 3-67348
⁵⁹Co, ⁶⁰Co, selective population of highly excited states by (α ,p) reaction 3-78346
⁵⁹Co, direct processes in 14.4 MeV inelastic neutron scattering (*Russian*) 3-40498
⁵⁹Co, mixing ratios from gamma-gamma angular correl. 3-43213
⁵⁹Co, n.m.r. in Cu-Co and Cu-Ni-Co alloys, precipitation phenomena obs. 3-50473
⁵⁹Co, n.m.r. in dil. liq. Sn-Co alloy 3-64572
⁵⁹Co, n.m.r. in FeSi-CoSi solid soln. 3-64494
⁵⁹Co Knight shift in Co-transition metal intermetallics (*Russian*) 3-52954
⁵⁹Co pulsed n.m.r. in Co₃B and Co₂B (*French*) 3-68853
⁵⁹Co(³He, d)⁶⁰Ni, 18 MeV, meas. of d γ coincidences, determ. of ⁶⁰Ni decay scheme 3-52132
⁵⁹Co(n, γ)⁶⁰Co, polarised target and thermal neutrons, meas. of γ -ray asymmetry 3-60175
⁵⁹Co(n, γ)⁶⁰Co, with polarised neutrons and nuclei, 0.065 eV, meas. of capture γ -rays 3-43245
⁶⁰Co, anisotropies and intensities of transitions in ⁵⁹Co(n, γ) with polarised neutrons and nuclei 3-43245
⁶⁰Co, diffusion coeffs. in Rhone sediments 3-56142
⁶⁰Co, γ -radiation, Kodak RM film latent image stability 3-77561
⁶⁰Co, spin determ. from meas. of γ -ray asymmetry in ⁵⁹Co(n, γ) reaction 3-60175
⁶⁰Co abundance in lunar samples 3-61712
⁶⁰Co gamma irradiation, human serum albumin, polymerisation, cross-linkages, sedimentation velocity technique 3-48264
⁶⁰Co post-mastectomy chest wall irradiation, dose per field 3-66068
⁶⁰Co radioactive source, nuclear excitation by gamma rays 3-67305
⁶⁰Co/¹³⁷Cs content of coastal sediments near nuclear power station coolant discharge into seawater 3-69558
⁶¹Co, A₁ coefficient detn. by β - γ Mossbauer expt. during β -decay 3-40466
⁵⁴Cr(p,n)⁵⁴Mn, meas. of polarisation of deexciting gamma-rays (*Russian*) 3-52126
Cu, $A=61, 64, 67$, cross section and recoil props. from ²³⁸U(p,Cu) at 11.5 GeV 3-67334
Cu, excitation of 2⁺ analogues in Ni(³He, t) reaction, second order effects 3-49271
Cu (α , α), 22 to 29 MeV interference maxima in backward excitation curve 3-67348
Cu deuteron cross-section for stripping and dissociation, 2.7 GeV/c, measurement 3-78344
Cu spallation, induced by 65 MeV π^+ and π^- and by 205 MeV protons, radiochemical yield determ. 3-67373
⁶⁴Cu, $A=63, 65$, radiative capture of 14.1 MeV neutrons, prompt γ -ray spectra 3-40441
⁶⁴Cu, assignments from (³He,t) reactions 3-63079
⁶⁴Cu, ⁶⁴Cu, selective population of highly excited states by (α ,p) reaction 3-78346
⁶⁴Cu, structure, directional-correlation and Doppler-shift lifetime meas. via ⁵⁸Ni(⁴He,pp) reaction 3-67261
⁶⁴Cu analogue states in ⁶⁰Ni(p, γ) reaction, decay stat schemes and branching ratios 3-46001
⁶²Cu excited states, lifetimes and mag. moments obs. 3-63000
⁶³Cu, compound statistical reactions, test of independence hypothesis and isospin conservation 3-71093
⁶³Cu, in cuprous halides, nuclear spin-lattice relaxation times, temp. depend. 3-55493
⁶³Cu, n.m.r. in CuMn alloy, near neighbour wipeout and satellites obs. 3-47152
⁶³Cu n.m.r., Fourier transform variable field expt. with internal ²H lock 3-77589
⁶³Cu(d,p)⁶⁴Cu, 6.5 MeV, γ -ray spectroscopy study of ⁶⁴Cu 3-45955
⁶³Cu(p, $2n$)⁶²Zn, 1.5-11.5 GeV, total cross sections 3-40493
⁶³Cu(p,n)⁶³Zn, 1.5-11.5 GeV, total cross sections 3-40493
⁶⁴Cu, ⁶⁶Cu, magnetic moments and lifetimes of isomeric 6⁺ states 3-45955
⁶⁴Cu, η -meson photoproduction, 2 GeV, cross section meas. 3-78311
⁶⁴Cu, polarisation of deexcitation γ -rays following ⁶⁴Ni(p,n) γ reaction (*Russian*) 3-52126
⁶⁴Cu(n,n)⁶⁴Cu, meas. differential cross section and asymmetries, incident polarised neutrons from ²H(d,n)³He 3-71109
⁶⁵Cu, in cuprous halides, nuclear spin-lattice relaxation times, temp. depend. 3-55493
⁶⁵Cu(d,p)⁶⁶Cu, 6.5 MeV, γ -ray spectroscopy study of ⁶⁶Cu 3-45955
⁶⁵Cu(p,n)⁶⁵Zn, narrow reson. 148 eV above threshold 3-43248
⁶⁹Cu, photo-protons emission, 80 to 260 MeV, from 400 MeV bremsstrahlung 3-74563
Cu(n, γ), 14 MeV radiative capture, spectra and partial cross section meas. 3-60173
⁵⁷Fe(p,2p), high-energy excitation function, calc. 3-46027
⁵⁷Fe diffusion in swaged W powder, autoradiography, 1300-1900°C (*Hungarian*) 3-72987
Ga odd isotopes, coupling of three-particle (hole) valence-shell cluster to quadrupole vibrations 3-67238
⁶⁷Ga, production by deuteron bombardment of Zn for medical applications 3-59448
⁶⁷Ga scanning, for localization of psos abscs 3-66022
⁶⁷Ga-citrate photscan, tumour location 3-48252
⁶⁹Ga, chem. shifts and linewidths for GaCl_{4-x} ions in acetonitrile soln. 3-72535
⁶⁹Ga, energy level obs. using photoexcitation, elastic and inelastic, resonance decays at 7306, 6874 keV 3-62948
⁶⁹Ga, transition strengths, reson. fluoresc. obs. 3-40450
⁶⁹Ga(p, n)⁶⁹Ge, ⁶⁹Ge level structure from de-excitation gamma ray obs. 3-54384
⁷⁰Ga, placement of 188 keV transitions 3-62982
⁷⁰Ga from ⁷⁰Zn(p,n) γ reaction, 1.7-3.2 MeV, level 3-62931
⁷¹Ga, transition strengths, reson. fluoresc. obs. 3-40450
Ge, nucl. lifetimes by blocking technique, computer simulation 3-40443

nuclei with $59 \leq A \leq 89$ continued

- ⁶⁴Ge, A=67, 69, 71, quadrupole interaction on isomeric levels in Zn and Ga following nuclear reaction 3-45949
- ⁶⁵Ge → ⁶⁵Ga, half life, γ -ray intensities, spin and parity of ground state 3-60131
- ⁶⁹Ge, level structure from de-excitation gamma ray obs. in ⁶⁹Ga(p, n)⁶⁹Ge reaction 3-54384
- ⁷⁰Ge(n, γ)⁷¹Ge, thermal energies, ⁷¹Ge energy levels (Russian) 3-71083
- ⁷¹Ge, quadrupole interaction of 9/2⁺ state in liquid Ga, relaxation time by γ -ray anisotropy meas. 3-49082
- ⁷¹Ge, thermal neutron capture, non accidental nature of anticorrelations (Russian) 3-57529
- ⁷¹Ge from thermal neutron capture, energy levels (Russian) 3-71083
- ⁷²Ge, ⁸⁴Kr reactions, effective thresholds calc. 3-40513
- ⁷²Ge(p, n)⁷²As, study of ⁷²As energy spectrum, obs. of new isomeric level, 215 keV 3-45956
- ⁷³Ge, thermal neutron capture, nonaccidental nature of anticorrelations (Russian) 3-57529
- ⁷³Ge(³He, d)⁷⁴As, 17 MeV, level structure of ⁷⁴As 3-43182
- ⁷⁴Ge(p, n γ), 3.5, 3.8 and 4.0 MeV, γ -ray angular distribution, ⁷⁴As deduced spins and parities 3-54472
- ⁷¹Ge → ⁷⁷As, delayed coincidence meas. of half-life of ⁷⁷As excited states 3-60111
- Kr even isotopes, A=78-84, in-beam electron conversion from yrast levels 3-67264
- ⁷²Kr, gamma decay, T_{1/2} determ., produced in ⁵⁸Ni(¹⁶O, 2n)⁷²Kr reaction 3-74532
- ⁷²Kr, new N=Z isotope, obs. of β -delayed γ -rays, determ. of decay scheme 3-46011
- ⁷³Kr, produced in ⁵⁸Ni(¹⁶O, n)⁷³Kr, gamma decay, T_{1/2} determ. 3-74532
- ⁷⁶Kr → ⁷⁶Br, decay props. and ⁷⁶Br level energies, spins, parities and transition probabilities 3-49220
- ⁸¹Kr radioactive isotope, formation in atmosphere, influence of cosmic ray intensity (Russian) 3-65322
- ⁸²Kr, E0 contrib. in 2⁺ to 2⁺ transitions, directional correlation functions 3-62991
- ⁸³Kr n.m.r. in Kr gas (German) 3-49395
- ⁸⁴Kr ions, irradiation of ¹⁸¹Ta, ¹⁹⁷Au, ²³⁸U, reaction products, mechanisms 3-78350
- ⁸⁵Kr, in natural gas, radiation dose calcs., hypothetical exposure 3-78395
- ⁸⁵Kr incorporation into Ni, Fe, Cu by film evaporation 3-39997
- ⁸⁵Kr leak testing technique 3-51562
- ⁸⁸Kr, β -decay energies, comparisons and predictions for other nuclei 3-57496
- ⁸⁹Kr, β -decay energies, comparisons and predictions for other nuclei 3-57496
- ⁵⁴Mn, polarisation of deexcitation γ -rays following ⁵⁴Cr(p, n γ) reaction (Russian) 3-52126
- Ni, elastic and inelastic scattering of Fe capture gamma-rays, energy level study 3-49241
- Ni, even isotopes, appl. of particle number projection study with generator coord. method 3-45987
- Ni (α , α), 22 to 29 MeV interference maxima in backward excitation curve 3-67348
- Ni isotopes, application of self-consistent core-particle coupling method 3-54415
- Ni isotopes, even, (p, t) and (t, p) reaction data analysis using broken-pair approx. 3-40494
- Ni region targets, single-nucleon transfer reactions, isospin centroids 3-63028
- ⁶¹Ni(¹⁸O, ¹⁶O) reactions, A=58, 60, 62, 64, anomalous and normal angular distributions 3-43256
- ⁵⁹Ni, M1 and E2 transition rates for low-lying levels, Kuo-Brown interaction 3-46004
- ⁵⁹Ni, spin assignments to levels populated in ⁵⁸Ni(d, p) 3-52077
- ⁵⁹Ni level struct. from ⁵⁸Ni(d, p) at 8 MeV 3-45973
- ⁵⁹Ni low lying levels populated in ⁵⁶Fe(α , n), meas. of lifetimes, mixing, branching ratios 3-49213
- ⁶⁰Ni, activation cross-sections for 14.7 MeV neutrons 3-54470
- ⁶⁰Ni, compound statistical reactions, test of independence hypothesis and isospin conservation 3-71093
- ⁶⁰Ni, excitation energies by time-of-flight system 3-73884
- ⁶⁰Ni, ground and excited states populated in Zn(d, ⁶Li) reaction 3-52195
- ⁶⁰Ni, lifetimes and decays of energy levels populated in ⁶⁰Ni(p, p' γ) and ⁵⁹Co(³He, d) γ reactions 3-52132
- ⁶⁰Ni, neutron elastic and inelastic scatt. from 2 to 8.5 MeV, differential and total cross-sections calc. 3-57531
- ⁶⁰Ni, scattering of polarised 12.3 MeV deuterons, vector analysing power and cross sections 3-52194
- ⁶⁰Ni photoabsorption, dynamic deformability, reln. to intermediate structure of giant resonance (Russian) 3-74562
- ⁶⁰Ni(³He, ³He)⁶⁰Ni, optical-model-family ambiguity, E=29.6-71.1 MeV 3-60212
- ⁶⁰Ni(³He, ³He)⁶⁰Ni, optical model, energy depend. phenomena, E=29.6-71.1 MeV 3-60213
- ⁶⁰Ni(³He, t)⁶⁰Cu, 24 MeV, differential cross sections, ang. distrib. 3-63079
- ⁶⁰Ni(d, p)⁶¹Ni, 10 MeV, vector analysing power, ang. distrib. meas., DWBA calcs. 3-78239
- ⁶⁰Ni(e, e'), quadrupole and giant dipole resonance excitation, form factors, characteristics (Russian) 3-71104
- ⁶⁰Ni(p, n), meas. absolute differential cross section near thresholds 3-71101
- ⁶⁰Ni(p, p' γ)⁶⁰Ni, 12 MeV, DSA meas. of lifetimes and decays of energy levels 3-52132
- ⁶⁰Ni(p, γ)⁶¹Cu, 1.5-1.9 MeV, obs. of analogue states in ⁶¹Cu 3-46001
- ⁶¹Ni, Mossbauer effect, concentration depend. of magnetic hyperfine fields 3-41457
- ⁶¹Ni, Mossbauer effect, concentration depend. of Ni hyperfine fields 3-41458
- ⁶¹Ni, ground and excited states populated in Zn(d, ⁶Li) reaction 3-52195
- ⁶²Ni(¹²C, ¹¹B)⁶³Cu, j depend., finite-range calcs. 3-52203
- ⁶²Ni(¹⁶O, ¹⁵N)⁶³Cu, j depend., finite-range calcs. 3-52203

nuclei with $59 \leq A \leq 89$ continued

- ⁶⁴Ni(α , n)⁶⁷Zn, perturbed angular distrib. meas., determ. of magnetic moment of excited 9/2⁺ state of ⁶⁷Zn 3-45948
- ⁶⁴Ni(p, n γ)⁶⁴Cu, meas. of polarisation of deexciting gamma-rays (Russian) 3-52126
- ⁶⁵Ni log ft values for forbidden β transitions, rules for spin and parity assignments 3-62932
- ⁶⁹Ni, ground and excited states populated in Zn(d, ⁶Li) reaction 3-52195
- ³¹P, spin coupling in organophosphorus cpds., explt. determ. 3-75081
- Pb, neutron structure deduced from antiproton absorption 3-60083
- ⁸³Rb, quadrupole moments determ. by level crossing and ODR, h.f.s. const. 3-40411
- ⁸⁴Rb, coronary blood flow assessment, critical review 3-56537
- ⁸⁴Rb, quadrupole moments determ. by level crossing and ODR, h.f.s. const. 3-40411
- ⁸⁵Rb, ⁸⁷Rb, γ -ray transitions of Coulomb excited levels, B(E2) values, structure determ. 3-40415
- ⁸⁵Rb, fast neutron scattering, (n, n), (n, n') and (n, n', γ) reactions 3-43249
- ⁸⁵Rb, Larmor frequencies, n.m.r. obs. (German) 3-67190
- ⁸⁵Rb ENDOR on ion pairs in soln. 3-78849
- ⁸⁵Rb n.m.r., rot. frame coherent resons. on fund. level (French) 3-54574
- ⁸⁵Rb produced in ⁸⁶Sr(³H, α)⁸⁵Rb, reaction, energy level determ. from α -particle spectra 3-71056
- ⁸⁶Rb, quadrupole moments determ. by level crossing and ODR, h.f.s. const. 3-40411
- ⁸⁶Rb extraction, blood flow changes, mouse tissue, X-irradiation appl. to clinical radiation therapy 3-48263
- ⁸⁷Rb, fast neutron scattering, (n, n), (n, n') and (n, n', γ) reactions 3-43249
- ⁸⁷Rb ENDOR on ion pairs in soln. 3-78849
- ⁸⁸Rb, β -decay energies, comparisons and predictions for other nuclei 3-57496
- Se, A=75, 77, 79, 81, 83, anomalous coupling states, calc. of nuclear moments 3-49115
- Se, A=77, 79, 81, from thermal neutron capture, energy levels (Russian) 3-71083
- Se even isotopes, A=72-78, in-beam electron conversion from yrast levels 3-67264
- ⁷⁴Se, A=74, 76, 77, 78, 80, 82, radiative capture of 14.1 MeV neutrons, prompt γ -ray spectra 3-40441
- ⁶⁹Se isomeric state decay behaviour, levels of ⁶⁹As 3-43222
- ⁷⁴Se(n, γ)⁷⁵Se, thermal neutrons, meas. of γ -ray spectrum (Russian) 3-52176
- ⁷⁵Se, gamma-transition scheme following ⁷⁴Se(n, γ) reaction (Russian) 3-52176
- ⁷⁵Se, γ -ray energies and relative intensities 3-43206
- ⁷⁵Se electron capture decay to ⁷⁵As, obs. of γ -ray spectrum 3-49210
- ⁷⁵Se electron capture decay, 285 keV γ line of ⁷⁵As, nucl. reson. fluoresc. obs. 3-63009
- ⁷⁵Se, exchange-induced hyperfine fields in SmSe and SmS_{1-x}Se_x 3-58439
- ⁷⁷Se, n.m.r. in 2-substituted selenophenes, substituent shifts 3-50481
- ⁷⁷Se(n, γ)⁷⁸Se, thermal neutron, gamma-ray spectrum meas. (Russian) 3-49250
- ⁷⁸Se, level structure and γ -transitions following β^+ decay of ⁷⁸Br 3-78247
- ⁷⁸Se transition scheme following ⁷⁷Se(n, γ) reaction (Russian) 3-49250
- ⁸⁰Se(α , p)⁸³Br, energy levels of ⁸³Br study 3-52103
- ⁸⁰Se, thermal neutron capture, nonaccidental nature of anticorrelations (Russian) 3-57529
- ⁸³g + ^mSe → ⁸³Br, β -branchings, ⁸³Br levels 3-63010
- Se(n, γ) A(target)=76, 78, 80, ⁷⁷Se, ⁷⁹Se, ⁸¹Se energy levels (Russian) 3-71083
- Sr fluorescence yield from ⁸⁸Y β -decay 3-74544
- Sr isotopes, shell model for rotation-like spectra 3-60085
- ⁸⁸Sr, isobaric analogue resonance, proton induced, neutron escape, Coulomb mixing corrections 3-78298
- ⁸³Sr levels, from ⁸³Y^{m.s.} decay, spin-parity assignments 3-46007
- ⁸⁴Sr, populated in (p, t) reaction, low-lying excitations 3-54392
- ⁸⁵Sr, diffusion coeffs. in Rhone sediments 3-56142
- ⁸⁶Sr, g-factor or 8⁺ state by time differential PAD method 3-54378
- ⁸⁶Sr, magnetic moment of 8⁺ state populated in ⁸⁸Sr(p, pnn) reaction 3-45957
- ⁸⁶Sr, populated in (p, t) reaction, low-lying excitations 3-54392
- ⁸⁶Sr(²H, α)⁸⁸Rb, 15 MeV, meas. α -particle spectra, determ. levels ⁸⁸Rb 3-71056
- ⁸⁶Sr(p, t)⁸⁶Sr, at 49.5 MeV proton energy, product low-lying excitations 3-54392
- ⁸⁸Sr, ang. correl. meas. for 898-1836 keV cascade, mixing ratio for 898 keV transition (German) 3-60118
- ⁸⁸Sr, mixing of giant magnetic dipole state with 1⁺ state at 3.49 MeV 3-60113
- ⁸⁸Sr (α , 3n γ), (α , α' n γ) reactions to populate ⁸⁹Zr, high spin states 3-78249
- ⁸⁸Sr(¹⁶O, ¹⁵N)⁸⁹Y, schematic study and evidence for recoil effects 3-67363
- ⁸⁸Sr(¹⁶O, ¹⁵N)⁸⁹Y, E=42.5 to 50 MeV, measure excitation functions, DWBA analysis 3-71127
- ⁸⁸Sr(¹⁶O, ¹⁶O)⁸⁸Sr, 45-60 MeV, interference of Coulomb and nuclear excitation 3-52201
- ⁸⁸Sr(²He, t)⁸⁸Y to doublet states, 23 MeV, coupled-channel study of multistep contribs. 3-67350
- ⁸⁸Sr(α , n)⁹¹Zr, 16 MeV, population of high-spin states in ⁹¹Zr, time differential meas. 3-49194
- ⁸⁸Sr(d, np)⁸⁸Sr, cross section meas. at 170° for 7.5 to 10.0 MeV deuterons 3-49268
- ⁸⁸Sr(d, p)⁸⁸Sr, anomaly effects at neutron analogue channel threshold 3-40500
- ⁸⁸Sr(d, p)⁸⁹Sr, particle coupling to octupole state 3-46026
- ⁸⁸Sr(p, p)⁸⁸Sr, isobaric analogue resonances and particle coupling to octupole state 3-46026
- ⁸⁸Sr(p, pnn)⁸⁶Sr, 51 MeV, population of 8⁺ state in ⁸⁶Sr 3-45957
- ⁸⁸Sr(p, t)⁸⁶Sr, at 49.5 MeV proton energy, product low-lying excitations 3-54392

nuclei with 59 ≤ A ≤ 89 continued

⁸⁹Sr, beta source, absorption of particles in Cu, Ag, Sn and Pb foil targets 3-49376
⁸⁹Sr, Peach Bottom HTGR D1305 fuel element, diffusion coeff., activity profile 3-74738
^{87m}Sr, combined lung-liver scan, preliminary expt. in animals 3-56536
Ta, neutron halo deduced from p absorption 3-60083
Y, neutron total cross section, 1.0 to 2.0 MeV, optical model comparison 3-54474
Y, neutron total cross section fluctuations, 1.0 to 2.0 MeV, compound nucleus explanation 3-54475
⁸³Y_{m,g} → ⁸³Sr, decay schemes and spin-parity assignments 3-46007
⁸⁷Y, populated in (p,t) reaction, low-lying excitations 3-54392
⁸⁸Y, two-hole multiplets from ⁸⁹Y(d,t) and ⁹⁰Zr(d,α) studies 3-54491
⁸⁸Y electron capture decay, Sr fluorescence yield 3-74544
⁸⁸Y → ⁸⁸Sr, a directional correlations meas. for 898-1836 keV cascade (German) 3-60118
⁸⁹Y, 2p_{1/2} and 1g_{9/2} states pop in ⁸⁸Sr(¹⁶O, ¹⁵N)⁸⁹Y reaction, rel. to recoil effects 3-67363
⁸⁹Y, 60-90 MeV, deuteron scattering, optical model and coupled channel analysis 3-43253
⁸⁹Y, from ⁸⁸Sr(¹⁶O, ¹⁵N), E=42.5 to 50 MeV, excitation functions, DWBA analysis 3-71127
⁸⁹Y, n.m.r. spin echo spectra of Y hyperfine fields in YFe₂, YFe₃ and Y₂Fe₁₇ 3-79922
⁸⁹Y(α,n)⁹¹Nb, 21 MeV, population of high-spin state in ⁹¹Nb, time differential meas. 3-49194
⁸⁹Y(d,t)⁸⁸Y, product two-hole multiplets 3-54491
⁸⁹Y(p,p')^{89m}Y, 100-800 MeV, yield curves, deduced cross sections, measured half life, E_p 3-67308
⁸⁹Y(n,n)^{83m1,2}Y, cross section for 14.8 MeV neutrons 3-63061
⁸⁹Y(n,n)⁸⁹Y 0.9 to 1.2 MeV, generalized R-matrix interpretation of total cross section 3-49254
⁸⁹Y(p,p')⁸⁹Y*, excitation functions, 2nd and 3rd excited states of ⁸⁹Y 3-60176
⁸⁹Y(p,t)⁸⁷Y, at 49.5 MeV proton energy, product low-lying excitations 3-54392
⁶²Zn production in ⁶⁴Zn(γ,n)⁶²Zn 20.4 to 21.9 MeV, positron activity meas. 3-52167
⁶²Zn, compound statistical reactions, test of independence hypothesis and isospin conservation 3-71093
⁶²Zn, inelastic electron scattering, collective model description 3-67239
⁶²Zn(α,n)⁶⁷Ge, perturbed angular distrib. meas., determ. of magnetic moment of excited 9/2⁺ state of ⁶⁷Ge 3-45948
⁶²Zn(d,⁶Li)⁶⁰Ni, 27.25 MeV, differential cross sections, Ni levels, DWBA analysis 3-52195
⁶²Zn(p,n)⁶³Zn cross section meas. from 20.4 to 21.9 MeV 3-52167
⁶²Zn, branching ratios of electron capture transitions 3-67266
⁶²Zn, diffusion coeffs. in Rhone sediments 3-56142
⁶²Zn, compound statistical reactions, test of independence hypothesis and isospin conservation 3-71093
⁶²Zn, elastic electron scattering, meas. cross sections rel. to nuclear Fermi charge distribution (Russian) 3-67316
⁶²Zn, selective population of highly excited states by (α,p) reaction 3-78346
⁶²Zn(d,⁶Li)⁶²Ni, 27.25 MeV, differential cross sections, Ni levels, DWBA analysis 3-52195
⁶²Zn, γ-γ ang. correl. meas. of mixing ratios 3-62999
⁶²Zn, mag. moment, n.m.r. obs. in aq. Zn(ClO₄)₂ soln. 3-79926
⁶²Zn, magnetic moment of excited 9/2⁺ state by perturbed angular distrib. meas. on ⁶⁴Ni(α,n) 3-45948
⁶²Zn, elastic and inelastic electron scattering, meas. cross sections rel. to nuclear Fermi charge distribution (Russian) 3-67316
⁶²Zn(d,⁶Li)⁶⁴Ni, 27.25 MeV, differential cross sections, Ni levels, DWBA analysis 3-52195
⁶²Zn(n,p)⁶⁹Zn, thermal energies, ⁶⁹Zn energy levels (Russian) 3-71083
⁶²Zn, from thermal neutron capture, energy levels (Russian) 3-71083
⁶²Zn thermal neutron capture, non accidental nature of anticorrelations (Russian) 3-57529
⁷⁰Zn(p,ny)⁷⁰Ga, level structure of ⁷⁰Ga, proton bombardment energy 1.7-3.2 MeV 3-62931
⁷⁰Zn(p,ny)⁷⁰Ga placement of 188 keV transition in ⁷⁰Ga 3-62982
⁸⁷Zr, high spin states, γ-ray spectra, populated in (α,3np), (α,α'ny) 3-78249

nuclei with 90 ≤ A ≤ 149

¹²³Sb perturbation approach to particle-vibration coupling model 3-52115
⁹⁰Zr relationship between single particle and collective degrees of freedom (Russian) 3-67237
A=110, 114, 116, quadrupole moments of first 2⁺ states from inelastic electron scattering 3-49100
A=90-96 even nuclei, ¹⁶O and ¹²C induced reactions above Coulomb barrier, angular distrib. 3-49276
beta decay in N=82 region, new confirmation of quenching of nuclear matrix elements 3-57495
doubly even nuclei, A>140, angular velocity expansions of rotational energies 3-52117
even N=80, two-neutron-hole states, intermediate coupling model 3-67215
lanthanides, cumulative and independent yields from 24 GeV proton irradiation of tungsten 3-40486
N=50 isotopes, interaction between collective and quasi-particle excitation, energies, wave functions, B(E2) values (Russian) 3-74514
N=50 nuclei, generalized seniority scheme 3-43196
N=82 nuclei, Z=51-59, pseudo LS coupling shell model study of energy levels and e.m. properties 3-49126
radiative neutron capture cross sections for 96 ≤ A ≤ 133 3-49252
rare earth region, calc. of ground state deformation (German) 3-52087
rare-earth deformed nuclei, number-conserving treatment of the BCS-Tamm-Dancoff approximation 3-43191
static quadrupole moments of 2⁺ states of even isotopes of Ba and Nd 3-49099
translational, quasi-rotational bands, solvable model 3-60075

nuclei with 90 ≤ A ≤ 149 continued

Z ≥ 60, nucl. energy spectrum near 1 GeV/amu, new cosmic ray source evidence 3-53581
(n,p) reactions, activation cross sections and isomer ratios as a function of incident energy, statistical model calc. (German) 3-52173
¹¹⁰Ag, n capture in Ag halides, β-decay asymmetry and n.m.r. 3-61006
⁹⁰(Sr+Y) extended radioactive source, influence of chemical and physical factors on electrolytic deposition rate 3-62212
Ag, 300 GeV p reactions cross-section calc. 3-54477
Ag, 5 GeV proton bombardment, energy spectra of fragments 3-40496
Ag induced ^{6,7}Li emission, 25 GeV/c, effect of fragment on heavy product emission 3-78316
Ag odd isotopes, coupling of three-particle (hole) valence-shell cluster to quadrupole vibrations 3-67238
¹⁰⁵Ag → ¹⁰⁵Pd, γ-ray and β-decay intensities (Russian) 3-74522
¹⁰⁷Ag, ¹⁰⁹Ag magnetic moments of short-lived states, hyperfine interaction, recoil into-gas method 3-45934
¹⁰⁷Ag, photo-proton emission, 80 to 260 MeV, from 400 MeV bremsstrahlung 3-74563
¹⁰⁷Ag(p,ny)¹⁰⁷Cd, ¹⁰⁷Cd level scheme study 3-49154
¹⁰⁸Ag, η-meson photoproduction, 2 GeV, cross section meas. 3-78311
¹⁰⁹Ag, quadrupole moments by Coulomb excitation in ¹⁰⁹Ag(¹⁶O, ¹⁶O') and ¹⁰⁹Ag(α,α') 3-71040
¹⁰⁹Ag negative parity states, intermediate coupling model 3-71061
¹¹¹Ag, fission product, meas. concentration in reactor coolant using sapphire radiation-monitoring loop (German) 3-67464
^{106m}Ag decay, gamma ray spectra and transition multipolarity 3-71076
^{108m}Ag, γ-ray energies and relative intensities 3-43206
^{110m}Ag, fission product, meas. concentration in reactor coolant using sapphire radiation-monitoring loop (German) 3-67464
^{110m}Ag oriented in Fe and Ni, meas. of hyperfine interactions by n.m.r., β-mixing 3-46009
¹¹⁹At isomer shift in Sn_{1-x}Sb_xO₂ system, Mossbauer spectra 3-68890
Ba(³He,d)La, study of odd-A La isotopes, A=131-139 by particle spectroscopy 3-45976
¹³⁰Ba, quadrupole moments of first excited states, reorientation eff. meas. 3-49112
¹³⁰Ba(n,p)¹³¹Cs, g-factor, 133 keV excited state meas. by PAC method 3-49108
¹³⁰Ba(n,p)¹³¹Xe, 0.5 to 5000 eV, large epithermal resonances, explanation of ¹³¹Xe concentrations in lunar rocks 3-54482
¹³³Ba, excited levels mass in β-decay of ¹³³La 3-57472
¹³³Ba, γ-ray energies and relative intensities 3-43206
¹³⁴Ba, E0 contrib. in 2⁺ to 2⁺ transitions, directional correlation functions 3-62991
¹³⁴Ba, obs. of γ-transitions in ¹³⁴La decay scheme (Russian) 3-52141
¹³⁴Ba, quadrupole moments of first excited states, reorientation eff. meas. 3-49112
¹³⁴Ba, zero-phonon γ transition search 3-62993
¹³⁵Ba, n.q.r., in Ba halide dihydrates 3-64579
¹³⁶Ba, levels and transitions study 3-40457
¹³⁶Ba, quadrupole moments of first excited states, reorientation eff. meas. 3-49112
¹³⁶Ba(²⁰Ne,xn)¹⁵⁶⁻¹⁵⁸Dy, high angular momentum, excitation functions and photon emission, compound nucleus mechanism 3-63083
¹³⁷Ba, n.q.r. in Ba halid dihydrates 3-64579
¹³⁷Ba, structure study using ¹³⁶Xe(α, 3n) reaction 3-45974
¹³⁸Ba, muon capture, neutron emission, branching ratios 3-40463
¹³⁸Ba, spins and mixing ratio from γ-γ directional correl. following ¹³⁸Cs decay 3-78238
¹³⁸Ba, structure study using ¹³⁶Xe(α, 2n) reaction 3-45974
¹³⁸Ba(d, p)¹³⁹Ba, 19 MeV, angular distrib. meas., determ. of orbital angular momentum transfer and spectroscopic factors 3-46033
¹³⁹Ba levels populated in ¹³⁸Ba(d, p) reaction at 19 MeV 3-46033
¹⁴⁰Ba, from ¹⁴⁰Cs beta-decay, tentative energy level scheme (French) 3-60123
¹⁴⁰Ba, meas. concentration in reactor coolant using sapphire radiation-monitoring loop (German) 3-67464
¹⁴¹Ba-¹⁴¹La, absolute branching ratio detn. 3-54435
¹⁴²Ba, half-life and γ-ray energy by direct meas. 3-78281
¹⁴⁴Ba, half-life and γ-ray energy by direct meas. 3-78281
Ba(α,t)La, study of odd-A La isotopes, A=131-139 by particle spectroscopy 3-45976
Cd, neutron production by cosmic ray high energy muons, depth dependency, e.m. interaction explanation (Russian) 3-61621
Cd even isotopes, interference between Coulomb or nuclear elastic and inelastic scattering of ⁴He 3-46036
Cd isotopes, odd-mass, Coriolis-coupling calc. of low-lying states 3-43180
Cd isotopes, quadrupole moment of 2⁺ state 3-49103
¹¹⁶Cd(p,t)¹¹⁶⁻¹¹⁸Cd, Cd=116 and 114, 52 MeV, excitation of 2⁺ states, effect of inelastic scattering processes 3-46032
¹⁰⁵Cd, multiparticle levels, decay scheme (Russian) 3-74487
¹⁰⁵Cd, spin-parity, assignments to levels populated in ¹⁰⁶Cd(d,t) reaction 3-67345
¹⁰⁵Cd(α,α'γγ), props. of 2' and 2'' states, E=11.0 MeV 3-46003
¹⁰⁶Cd(d,p) reaction, 12MeV, nuclear structure study 3-67345
¹⁰⁶Cd(d,py)¹⁰⁷Cd, ¹⁰⁷Cd level scheme study 3-49154
¹⁰⁶Cd(d,t) reaction, 16MeV, nuclear structure study 3-67345
¹⁰⁷Cd, level scheme study through ¹⁰⁷Ag(p,ny) and ¹⁰⁶Cd(d,py) reactions and ¹⁰⁷In decay 3-49154
¹⁰⁷Cd, spin-parity assignments to levels populated in ¹⁰⁶Cd(d,p) reaction 3-67345
¹⁰⁹Cd, X-ray radiometric fluorescence anal., Pb-Ba minerals 3-48660
¹¹⁰Cd, E0 contrib. in 2⁺ to 2⁺ transitions, directional correlation functions 3-62991
¹¹⁰Cd, from β-decay of ^{110m}Ag oriented in Fe and Ni, meas. of γ-ray anisotropies, M1/E2 mixing ratios 3-46009
¹¹¹Cd, electric quadrupole interaction for 247 keV level in In following ¹¹¹In decay, TDPA meas. 3-45941
¹¹¹Cd, quadrupole interaction with electric field gradient in Cd, γ-γ angular correlation meas. 3-47183
¹¹¹Cd excited quadrupole moment meas. 3-61012

nuclei with $90 \leq A \leq 149$ continued

- ¹¹¹Cd h.f.s. interactions in Dy, PAC obs. 3-41468
¹¹¹Cd in ferromag. rare earth metals, PAC obs. of mag. hyperfine field 3-64591
¹¹²Cd($\alpha, \alpha' \gamma$), props. of 2' and 2'' states, E=11.0 MeV 3-46003
¹¹²Cd(α, n)¹¹⁴Sn, 22 MeV, population of high spin isomeric states in ¹¹⁴Sn, g-factor determ. 3-45958
¹¹³Cd, chem. shifts of Cd salts and complexes in soln. 3-72534
¹¹⁴Cd, inelastic electron scattering, collective model description 3-67239
¹¹⁴Cd, quadrupole moment of 2⁺ state, calc. using boson expansion technique 3-49102
¹¹⁴Cd($\alpha, \alpha' \gamma$), props. of 2' and 2'' states, E=11.0 MeV 3-46003
¹¹⁵Cd \rightarrow ¹¹⁵In, product nuclear quadrupole interaction sign, obs. by β - γ directional corrls. in Cd metal 3-52079
¹¹⁶Cd, ⁸⁴Kr reactions, effective thresholds calc. 3-40513
^{111m}Cd in KNiF₃, KCOF₃ and RbMnF₃, perturbed angular correlation, supertransferred hyperfine interaction 3-44360
¹¹⁶Cd, inelastic, scatt. of 50 and 65 MeV electrons, giant resons. total and groundstate radiative widths (German) 3-46021
¹¹⁶Cd, neutron total cross section, 1.0 to 2.0 MeV, optical model comparison 3-54474
¹¹⁶Cd, neutron total cross section fluctuations, 1.0 to 2.0 MeV, compound nucleus explanation 3-54475
¹¹⁶Cd even isotopes, A=130-138, in-beam electron conversion from γ -ray levels 3-67264
¹³¹Ce \rightarrow ¹³¹La, determ. of partial level scheme for ¹³¹La (French) 3-52148
¹³⁴Ce excited states populated in ¹³⁴Pr decay 3-49184
¹³⁴Ce \rightarrow ¹³⁴La, determ. of decay energies (Russian) 3-49223
¹³⁷Ce lifetimes and γ -ray spectra from ¹³⁷Pr decay (Russian) 3-49222
¹⁴⁰Ce, ¹⁶O induced one-proton, two-proton and α -transfer reactions, 63-66.5 MeV, cross section and transfer probability 3-49277
¹⁴⁰Ce, 2.083 MeV state populated in ¹⁴⁰La β -decay, quadrupole moment determ. by TDPAC 3-49085
¹⁴⁰Ce, ground state transitions to first 2⁺, 3- and 4⁺ states, reduced matrix elements (German) 3-46021
¹⁴⁰Ce, γ decay props. of 3⁺ states 3-45993
¹⁴⁰Ce, muon capture, neutron emission, branching ratios 3-40463
¹⁴⁰Ce(¹⁶O, ¹⁵N)¹⁴¹Pr, E=56 to 63 MeV, measure excitation functions, DWBA analysis 3-71127
¹⁴⁰Ce(¹⁶O, xn)^{156-x}Dy, high angular momentum, excitation functions and photon emission, compound nucleus mechanism 3-63083
¹⁴⁰Ce(¹⁸O, ¹⁷O)¹⁴¹Ce, E=56 to 61 MeV, measure excitation functions, DWBA analysis 3-71127
¹⁴¹Ce, diffusion coeffs. in Rhone sediments 3-56142
¹⁴¹Ce, from ¹⁴⁰Ce(¹⁸O, ¹⁷O), E=56 to 61 MeV, excitation functions, DWBA analysis 3-71127
¹⁴¹Ce ¹⁴⁴Ce radioisotopic activity ratio obs. by γ spectrometry of rain-water 3-69581
¹⁴²Ce, ground state transitions to first 2⁺, 3- and 4⁺ states, reduced matrix elements (German) 3-46021
¹⁴²Ce, muon capture, neutron emission, branching ratios 3-40463
¹⁴²Ce(p, p₂), high-energy excitation function, calc. 3-46027
⁵⁸¹⁴⁰Ce₈₂, 328-487 keV cascade in La₂O₃, WO₃, ang. corrl. 3-68892
¹⁴²Cs, A=129, 131, radiation dose calculation to various organs 3-53776
¹⁴²Cs, A=138 to 142, fission products, determ. beta-decay energies, end point energies and Q values 3-67277
¹⁴²Cs, A=143-145, and beta decay products, gamma ray energies 3-49211
¹³⁰Cs, beta decay spectrum meas. rel. to quantum number assignment 0⁺ to levels in ¹³⁰Xe (Russian) 3-67216
¹³⁰Cs beta-decay to ¹³⁰Xe level structure determ. 3-67214
¹³¹Cs, g-factor 133 keV excited state meas. by PAC method 3-49108
¹³²Cs, gamma activity, half-life 3-67268
¹³²Cs, decay from ¹³³Xe, charge distrib. 3-60107
¹³³Cs, internal conversion of 161- and 223-keV transitions (German) 3-74536
¹³³Cs Coulomb excitation, meas. of γ -ray energies, branching ratios, B(E2) values 3-52200
¹³³Cs Knight shift, in Cs-NH₃ solution 3-73173
¹³³Cs, fission product, meas. concentration in reactor coolant using sapphire radiation-monitoring loop (German) 3-67464
¹³⁴Cs, half-life meas. by mass spectrometry over 9.8 yrs. 3-57494
¹³⁴Cs, Peach Bottom HTGR D1305 fuel element, diffusion coeff., activity profile 3-74738
¹³⁶Cs, beta decay to ¹³⁶Ba, ¹³⁶Ba levels and transitions study 3-40457
¹³⁷Cs, diffusion coeffs. in Rhone sediments 3-56142
¹³⁷Cs, energy level scheme 3-40463
¹³⁷Cs, fission product, meas. concentration in reactor coolant using sapphire radiation-monitoring loop (German) 3-67464
¹³⁷Cs, half-life meas. by mass spectrometry over 11 yrs. 3-57494
¹³⁷Cs, method of determ. in river sediments and soils, report 3-73398
¹³⁷Cs, Peach Bottom HTGR D1305 fuel element, diffusion coeff., activity profile 3-74738
¹³⁷Cs concentration in Japanese coastal sediments, obs. 3-69559
¹³⁷Cs concentration in Japanese coastal waters, obs. 3-69560
¹³⁷Cs concentration in Nishiyama soils, vegetables and human diets 3-69514
¹³⁷Cs concentration in volcanic ash paddy soil, obs. 3-69515
¹³⁷Cs content of soils in Niigata Prefecture, Japan 3-69513
¹³⁷Cs decay, relative intensity and internal conversion coeff. meas. 3-52123
¹³⁷Cs γ -ray backscatt. by finite barriers 3-60333
¹³⁷Cs internal conversion spectrum using electron-X-ray coincidence technique 3-40038
¹³⁷Cs/^{137m}Ba radioisotope generator system, separation of ^{137m}Ba, CuCo[Fe(CN)₆]₄ adsorbent 3-48505
¹³⁸Cs to levels in ¹³⁸Ba, spins and mixing ratios from γ - γ directional corrl. 3-78238
¹⁴⁰Cs, β and γ activity obs. using ARIEL on line isotope separator, ground state spin assignment (French) 3-60123
¹⁴⁹Dy \rightarrow ¹⁴⁹Tb transition probability by electron capture (French) 3-63003
¹⁰¹Eh, n.m.r., gamma ray anisotropy meas., spin and E2/M1 mixing ratio assignments 3-74534

nuclei with $90 \leq A \leq 149$ continued

- ¹⁴⁷Eu \rightarrow ¹⁴⁷Sm, obs. of new γ -transitions and new levels in ¹⁴⁷Sm (Russian) 3-74525
¹⁴⁶Gd, energy level spectroscopic investigation, spin assignments and lifetime meas. 3-54429
¹⁴⁶Gd, γ -ray spectra meas. with Ge(Li) spectrometer (Russian) 3-74524
¹⁴⁸Gd, energy level spectroscopic investigation, spin assignments and lifetime meas. 3-54429
¹⁴⁹Gd, γ -ray spectra meas. with Ge(Li) spectrometer (Russian) 3-74524
¹Odd isotopes, coupling of three-particle (hole) valence-shell cluster to quadrupole vibrations 3-67238
¹²¹, half lives of three low lying levels, M1 transitions 3-54424
¹²³I production for diagnosis 3-45316
¹²⁵I, 188 keV excited state, g-factor determ. by ang. corrl. method 3-78243
¹²⁷I, impurity nuclei, elec. field gradients in A/B^{III}Te₂ crystals, Mossbauer effect 3-72555
¹²⁷I, n.q.r. spectra of LiIO₃ (Russian) 3-79945
¹²⁷I, radiative capture of 14.1 MeV neutrons, prompt γ -ray spectra 3-40441
¹²⁷I Coulomb excitation, meas. of γ -ray energies, branching ratios, B(E2) values 3-52200
¹²⁷I in CdI₂, two-frequency spin echo 3-44350
¹²⁷I quadrupole interaction in Ag₂H₃IO₆ (German) 3-53034
¹²⁹I, orientation study of excited states populated in decay of ^{129m}Te, ^{129m}Te 3-52131
¹²⁹I Coulomb excitation, meas. of γ -ray energies, branching ratios, B(E2) values 3-52200
¹²⁹I from ¹²⁹Te beta decay, gamma ray meas., decay schemes 3-74537
¹³⁰I, beta-decay to ¹³⁰Xe, level structure determ. 3-67214
¹³¹I, branching ratio detn. 3-54436
¹³¹I, γ -ray energies and relative intensities 3-43206
¹³¹I meas. concentration in reactor coolant using sapphire radiation-monitoring loop (German) 3-67464
¹³¹I \rightarrow ¹³¹Xe, product 341.2 and 404.8 keV level lifetime meas. (German) 3-52139
¹³¹I, radiochemical yield from ²³⁸U spontaneous fission 3-57543
¹³¹I β -decay in irradiated graphite at 1000°C, release process for fission Xe 3-71278
¹³⁵I pop. in ¹³⁵Te beta decay, proton particle states determ. 3-71050
¹In odd mass isotopes, excited quadrupole deformation, theory 3-49142
¹In, A=115, 113, radiative capture of 14.1 MeV neutrons, prompt γ -ray spectra 3-40441
¹In, A=117, 130, 132-134, produced in ²³²Th neutron-induced fission, charge distrib. meas. 3-43260
¹⁰⁷In decay, ¹⁰⁷Cd level scheme study 3-49154
¹¹¹In, for hemopoietic marrow scanning 3-70137
¹¹¹In, quadrupole interaction with electric field gradient of ¹¹¹Cd in Cd 3-47183
¹¹⁵In, deformed and spherical states, numerical calc. of coexistence problem 3-54393
¹¹⁵In, elec. hexadecapole moment, mol. beam elec. reson. spectroscopy 3-43176
¹¹⁵In, from ¹¹⁵Cd decay, meas. of B(E2) and B(M2) values, coexistence study 3-49197
¹¹⁵In, nuclear quadrupole interaction sign, obs. by β - γ directional corrls. in Cd metal 3-52079
¹¹⁵In muonic atoms, magnetization distrib. of single particle states and 2⁺ rotational states 3-49209
¹¹⁵In(α, n), 20 MeV, precompound processes, neutron energy and angular distrib. 3-60209
¹¹⁵In(p, γ)^{115m}In, 100-800 MeV, yield curves, deduced cross sections, ^{115m}In measured half life E_γ 3-67308
¹¹⁵In(n, 2n)^{114m}In, cross section for 14.8 MeV neutrons 3-63061
¹¹⁵In(n, e)¹¹⁵In, conversion electron spectra, spin and parity assignments 3-71116
¹¹⁵In(n, γ)¹¹⁵In, 150 to 630 keV, meas. neutron capture cross sections by activation technique 3-74572
¹¹⁵In(p, α)¹¹²Cd, 14 MeV, α energy spectra, fit to reaction models 3-78315
¹¹⁹In, energy level scheme 3-40463
¹¹⁹In \rightarrow ¹¹⁹Sn, β -decay, obs. of gamma transitions between low-lying levels in ¹¹⁹Sn 3-49212
¹³⁰In β -decay, obs. of excited states in ¹³⁰Sn two-neutron-hole nucleus 3-60081
¹³⁰In \rightarrow ¹³⁰Sn decay, obs. of excited two-neutron-hole states in ¹³⁰Sn (Russian) 3-71086
¹³²In 1.2 s β -decay, population of first excited state in doubly closed shell ¹³²Sn 3-49149
¹³²In β -decay, population of first excited state in twice magic ¹³²Sn (Russian) 3-71048
^{108m}In, β^+ / electron capture decay, spin and parity, j-j coupling model 3-63004
⁹⁰Kr β -decay energies, comparisons and predictions for other nuclei 3-57496
⁹¹Kr, β -decay energies, comparisons and predictions for other nuclei 3-57496
⁹²Kr, β -decay energies, comparisons and predictions for other nuclei 3-57496
⁹³Kr, β -decay energies, comparisons and predictions for other nuclei 3-57496
¹La, inelastic scatt. of 50 and 65 MeV electrons, giant resons. total and groundstate radiative widths (German) 3-46021
¹La, neutron total cross section, 1.0 to 2.0 MeV, optical model comparison 3-54474
¹La, neutron total cross section fluctuations, 1.0 to 2.0 MeV, compound nucleus explanation 3-54475
¹La, odd-A isotopes, decoupled bond description using angular momentum projection method for coherent phonon state 3-45983
¹La neutron-deficient isotopes, prolate deformation 3-45976
¹³¹La levels populated in ¹³¹Ce beta decay, Coriolis effects (French) 3-52148
¹³³La, quadrupole moment of 535 keV state determ. by time-differential PAC meas. in La metal 3-52082
¹³³La \rightarrow ¹³³Ba, excited levels meas. 3-57472

nuclei with 90 ≤ A ≤ 149 continued

¹³⁴La → ¹³⁴Ba, obs. of β-spectra, conversion electron spectra, γ-rays and γγ coefficients (*Russian*) 3-52141
¹³⁹La, energy level scheme 3-40463
¹³⁹La Mossbauer scatt. of 166 keV γ-rays, mean square nuclear charge radius deduced 3-60119
¹⁴⁰La 3- → 4+ β decay, β-γ directional correl. obs. 3-67267
¹⁴⁰La β- decay in crystalline electric field gradient, determ. of ¹⁴⁰Ce quadrupole moment by TDPAC 3-49085
¹⁴¹La, energy level scheme 3-40463
¹⁴⁶La fragments from ²⁵²Cf spontaneous fission, γ cascades 3-62994
Mo, A = 94, 96, 98, 100, thermal neutron capture, meas. of gamma-ray spectra (*Russian*) 3-52179
⁹¹Mo, high spin states, γ-ray spectra, populated in (α,3nγ), (α,α'ny) 3-78249
⁹²Mo, neutron reson. parameter 3-40495
⁹²Mo (α,3nγ), (α,α'ny) reactions to populate ⁸⁹Zr, high spin states 3-78249
⁹²Mo (α,p2nγ) ⁹³Tc reaction to populate high spin states 3-78248
⁹²Mo(He,d)⁹³Tc, 30.2 MeV, stripping to analogue resons. using complex energy eigenstates 3-63081
⁹²Mo(d,n), DWBA anal. of analogue states, effect of fine structure 3-74547
⁹²Mo(e,e'), E = 209 MeV, study of collective states, comparison with microscopic vibrational model 3-63039
⁹²Mo(n,p)⁹³Mo, γ spectra, giant reson., partial radiation widths, E1 and M1 transitions 3-63058
⁹²Mo(p,p'), 40 MeV, role of collective imaginary form factor in microscopic description 3-60186
⁹²Mo(p,p)⁹²Mo, 4.3 and 5.3 MeV, obs. of fine structure in analogue resonances, s1/2 and d5/2 states (*German*) 3-49249
⁹³Mo, populated in ⁹²Mo(n,p)⁹³Mo, γ spectra analysis 3-63058
⁹³Mo, 2953 keV state populated in ⁹²Zr(α,nn) reaction, time-differential PAC meas., of g-factor 3-49084
⁹⁴Mo from ⁹²Mo(p,d) reaction l-values and spectroscopic factors for low-lying states 3-63049
⁹⁴Mo(p,n)⁹⁴Tc, obs. excited states ⁹⁴Tc, using neutron and gamma ray yields at isobaric analog. resonances 3-67207
⁹⁴Mo(p,n)⁹⁴Tc^{m.s.}, isomer ratio comparison to ⁹⁶Mo(p,n)⁹⁶Tc^{m.s.} 3-57473
⁹⁵Mo, spins of levels, and multipole mixing ratios of transitions 3-60070
⁹⁵Mo(p,d)⁹⁴Mo, angular distrib. of deuterons, 26 MeV 3-63049
⁹⁶Mo from ⁹⁷Mo(p,d) reaction l-values and spectroscopic factors for low-lying states 3-63049
⁹⁶Mo(n,p)⁹⁷Mo, thermal neutrons, meas. of γ-ray spectra (*Russian*) 3-52177
⁹⁶Mo(p,n)⁹⁶Tc^{m.s.}, 10-65 MeV, production cross sections and isomer ratios of 4+ and 7+ states in ⁹⁶Tc 3-43240
⁹⁷Mo, ⁹⁹Mo, transition scheme following ⁹⁶Mo(n,p) and ⁹⁸Mo(n,p) reactions (*Russian*) 3-52177
⁹⁷Mo(p,d)⁹⁶Mo, 26 MeV, deuteron angular distrib. 3-63049
⁹⁸Mo, product of ¹⁰⁰Mo(p,t), 19 MeV, cross section measurements, spin and parity assignments, search for excited rotational band 3-54390
⁹⁸Mo(n,p)⁹⁹Mo, thermal neutrons, meas. of γ-ray spectra (*Russian*) 3-52177
⁹⁹Mo radiochemical yield from ²³⁸U spontaneous fission 3-57543
¹⁰⁰Mo(n,p)¹⁰¹Mo, thermal neutrons, meas. of γ-ray spectra (*Russian*) 3-52177
¹⁰⁰Mo(p,t)⁹⁸Mo, 19 MeV, ⁹⁸Mo, cross section measurements, spin and parity assignments, search for excited rotational band 3-54390
¹⁰¹Mo → ¹⁰¹Tc, meas. of γ-ray spectra and internal conversion coeffs., ¹⁰¹Tc energy level scheme (*Russian*) 3-49141
¹⁰⁵Mo fragments from ²⁵²Cf spontaneous fission, γ cascades 3-62994
Nb, fast-neutron cross sections, optical model, reln. to fusion reactor design 3-71113
⁹¹Nb, high spin states, γ-ray spectra, populated in (α,p2nγ) reaction, 37-43 MeV 3-78248
⁹³Nb, direct processes in 14.4 MeV inelastic neutron scattering (*Russian*) 3-40498
⁹³Nb, neutron total (0.25 to 0.5 MeV) and differential (1.8 to 4.0 MeV) scattering cross-sections, optical model, J^π values 3-78331
⁹³Nb, product of ⁹⁰Zr(α,pp), 14.77 MeV, γ-decay of low lying levels 3-57491
⁹³Nb(n,p)⁹⁴Nb, E_n = 30-100 eV, channel spin components of p-wave neutron widths 3-60192
⁹³Nb, activity in radioactive fallout, nuclear explosions, elapsed time estimation (*Japanese*) 3-57585
⁹³Nb, lifetime and g-factor of 17/2- state populated in ⁸⁹Y(α,nn) reaction, time diff. meas. 3-49194
Nd, A = 142-150, total neutron cross section meas., deformation effects, optical model (*Russian*) 3-52178
Nd isotopes, X-ray isotope shifts and variations of charge radii 3-67662
¹³⁶Nd → ¹³⁶Pr decay scheme, obs. of new γ-ray transitions, multipolarity determ. (*Russian*) 3-71084
¹³⁷Nd → ¹³⁷Pr, from γ-ray, X-ray, conversion electron, β+ and γγ coincidence spectra (*Russian*) 3-52140
¹⁴¹Nd → ¹⁴¹Pr, obs. of γ-ray, X-ray, γγ-coincidence, conversion electron and positron spectra (*Russian*) 3-52092
¹⁴²Nd, ¹⁶⁰ induced one-proton, two-proton and α-transfer reactions, 63-66.5 MeV, cross sections and transfer probability 3-49277
¹⁴²Nd, N = 82, levels populated in ¹⁴²Pr, ¹⁴²Pm β decays, spin and parity assignments 3-49155
¹⁴²Nd, neutron particle-hole states population in ¹⁴²Nd(p,p') and ¹⁴²Nd(d,t) 3-67325
¹⁴²Nd(¹⁶O, ¹⁶O)¹⁴²Nd, 54-72 MeV, interference of Coulomb and nuclear excitation 3-52201
¹⁴²Nd(⁴⁰Ar, xn)¹⁸² → ¹⁸²Pt, E < 300 MeV, excitation functions 3-54499
¹⁴²Nd(p,p'), neutron particle-hole states population on analog reson. 3-67325
¹⁴³Nd, ¹⁴⁵Nd, neutron resonance spin determ. from Monte Carlo simulation of decay 3-57519
¹⁴³Nd(d,t), neutron particle-hole states in ¹⁴²Nd 3-67325
¹⁴³Nd(n,α)¹⁴⁰Ce, hindrance factors for γ-ray transitions near neutron binding energy 3-49218

nuclei with 90 ≤ A ≤ 149 continued

¹⁴⁴Nd(¹²C, xn)¹⁵⁶ → ¹⁵⁶Dy, high angular momentum, excitation functions and photon emission, compound nucleus mechanism 3-63083
¹⁴⁴Nd(¹⁶O, 4n), high spin states in ¹⁵⁶Er 3-62937
¹⁴⁶Nd(¹²C, xn, p), high spin states in ¹⁵⁵Dy and ¹⁵⁴Dy 3-60217
¹⁴⁶Nd(¹⁸O, nnnn)¹⁶⁰Er, 72 MeV, population of high-spin members of ground state rotational bands 3-52098
¹⁴⁶Nd(n,p)¹⁴⁷Nd, activation resonance integral meas. 3-54467
¹⁴⁷Nd production from ¹⁴⁶Nd(n,p)¹⁴⁷Nd, activation resonance integral meas. 3-54467
¹⁴⁷Nd → ¹⁴⁷Pm, γ-γ directional correlation of seven cascades 3-49200
¹⁴⁸Nd analysis, mixed-oxide fuel elements, burnup meas., comparison with neutronics calc. 3-67572
¹⁴⁸Nd(¹⁴O, nnnn)¹⁶⁰Er, 70-76 MeV, population of high-spin members of ground state rotational bands 3-52098
¹⁴⁸Nd(n,p)¹⁴⁹Nd, activation resonance integral meas. 3-54467
¹⁴⁸Nd(p,6n)¹⁴³Pm, e.m. props. of low-lying levels, M2, E3 transition probabilities 3-67254
¹⁴⁹Nd production from ¹⁴⁸Nd(n,p)¹⁴⁹Nd, activation resonance integral meas. 3-54467
⁵⁸Ni(⁶Li, ⁶Li), break-up study, E = 12 to 24 MeV 3-46040
Pd, Coulomb excitation in Pd-Fe target, transient magnetic field effects on recoil in Fe lattice, γ-ray meas. 3-49269
Pd, systematic behaviour of quasiroational bands 3-67199
Pd isotopes, odd-mass, Coriolis-coupling calc. of low-lying states 3-43180
Pd₂MnSb: ¹²³Sb, n.m.r. study, magnitude and sign of hyperfine fields 3-50485
⁹⁸Pd, population of ground state band up to J = 8 3-45975
¹⁰⁰Pd, ¹⁰²Pd, forking of ground state bands populated in heavy ion induced reactions 3-45975
¹⁰⁰Pd, two-parameter description of rotational energies 3-74496
¹⁰²Pd, level struct. using ⁹⁹Ru(α,n,γ) reaction 3-40510
¹⁰⁸Pd, zero-phonon γ transition search 3-62993
¹⁴²Pm → ¹⁴²Nd, β+ decay, obs. of ¹⁴²Nd levels 3-49155
¹⁴²Pm, e.m. props. of low-lying levels, M2, E3 transition probabilities 3-67254
¹⁴³Pm, effective M2 gamma transition moments 3-45997
¹⁴⁴Pm log ft values for forbidden β transitions, rules for spin and parity assignments 3-62932
¹⁴⁵Pm, effective M2 gamma transition moments 3-45997
¹⁴⁷Pm, decay scheme, Ge(Li)-Ge(Li) coincidence studies 3-45994
¹⁴⁷Pm/Al, ¹⁴⁷Pm/Ag, bremsstrahlung continuous spectra and characteristic radn., calc. (*Czech*) 3-60334
Pr, inelastic scatt. of 50 and 65 MeV electrons, giant resons. total and groundstate radiative widths (*German*) 3-46021
Pr, neutron total cross section, 1.0 to 2.0 MeV, optical model comparison 3-54474
Pr, neutron total cross section fluctuations, 1.0 to 2.0 MeV, compound nucleus explanation 3-54475
¹³⁴Pr → ¹³⁴Ce, decay scheme for isomeric and ground state from γ-ray obs. 3-49184
¹³⁶Pr → ¹³⁶Ce decay scheme, obs. of new γ-ray transitions, multipolarity determ. (*Russian*) 3-71084
¹³⁷Pr, lifetimes of levels populated in ¹³⁷Nd decay (*Russian*) 3-52140
¹³⁷Pr → ¹³⁷Ce, from γ-ray spectra, internal conversion electrons, positron emission, γ-γ coincidences and ¹³⁷Ce lifetimes (*Russian*) 3-49222
¹⁴¹Pr, effective M2 gamma transition moments 3-45997
¹⁴¹Pr, from ¹⁴⁰Ce (¹⁶O, ¹⁵N), E = 56 to 63 MeV, excitation functions, DWBA analysis 3-71127
¹⁴¹Pr magic nucleus, excitation of quasiproton states by ¹⁴¹Nd decay (*Russian*) 3-52092
¹⁴¹Pr(α, 2n)¹⁴³Pm, e.m. props. of low-lying levels, M2, E3 transition probabilities 3-67254
¹⁴²Pr → ¹⁴²Nd, β- decay, obs. of ¹⁴²Nd levels 3-49155
¹⁴³Pr, K-shell autoionization probability, β-decay 3-78294
¹⁴⁷Pr, 145 keV transition penetration parameter, M1-E2 mixing ratio 3-78279
¹⁴⁸Pr, γ-ray energies and half-lives, Ge(Li) meas. in prodn. from ²³⁵U fission 3-43203
¹⁴⁹Pr, γ-ray energies and half-lives, Ge(Li) meas. in prodn. from ²³⁵U fission 3-43203
⁹⁰Rb, β-decay energies, comparisons and predictions for other nuclei 3-57496
⁹¹Rb, β-decay energies, comparisons and predictions for other nuclei 3-57496
⁹²Rb, β-decay energies, comparisons and predictions for other nuclei 3-57496
⁹³Rb, β-decay energies, comparisons and predictions for other nuclei 3-57496
⁹⁹Rh population in ⁹⁹Tc disintegration 3-63006
¹⁰³Rh, γ-γ directional correl. obs. 3-62997
¹⁰³Rh magnetic moments of short-lived states, hyperfine interaction recoil-into-gas method 3-45934
¹⁰³Rh(α,n), 20 MeV, precompound processes, neutron energy and angular distrib. 3-60209
¹⁰³Rh(n,n')^{103m}Rh, thick foils, absolute counting of K X-rays 3-66316
¹⁰³Rh(n,n')^{103m}Rh, criticality neutron dosimeter 3-77273
^{103m}Rh, half-life determination 3-40438
Ru, Coulomb excitation in Ru-Fe target, transient magnetic field effects on recoil in Fe lattice, γ-ray meas. 3-49269
Ru isotopes, odd-mass, Coriolis-coupling calc. of low-lying states 3-43180
⁹³Ru, high spin states, γ-ray spectra, populated in (α,3nγ), (α,α'ny) 3-78249
⁹⁴Ru, level structure up to 4 MeV excitation, study by ⁹⁶Ru(p,t) reaction 3-49147
⁹⁶Ru, ¹⁶⁰ irradiation, excitation function of α-emitters (*Russian*) 3-57497
⁹⁶Ru(p,t)⁹⁴Ru, 31.1 MeV, study of level structure up to 4 MeV excitation 3-49147
⁹⁷Ru → ⁹⁷Tc, delayed coincidence meas. of half-life of ⁹⁷Tc excited states 3-60111
⁹⁹Ru, excited state lifetime obtained from ⁹⁹Rh decay, γ-transition probability (*Russian*) 3-78280
⁹⁹Ru, quadrupole moments ratio determ. by Mossbauer spectra 3-43170

nuclei with $90 \leq A \leq 149$ continued

- ⁹⁹Ru(α, n, γ) ¹⁰²Pd, level struct. of ¹⁰²Pd 3-40510
¹⁰¹Ru, excited state lifetime obtained from ¹⁰¹Rh and ¹⁰¹Tc decay, γ -transition probability (*Russian*) 3-78280
¹⁰³Ru: ¹⁰⁶Ru radioisotopic activity ratio obs. by γ spectrometry 3-69581
¹⁰⁶Ru complexes effect on coprecipitation yields from seawater, obs. 3-69556
¹⁰⁶Ru low-lying level obs. from β^- decay of ¹⁰⁶Tc 3-62952
¹⁰⁸Ru low-lying level obs. from β^- decay of ¹⁰⁸Tc 3-62952
¹⁰⁹Ru fragments from ²⁵²Cf spontaneous fission, γ cascades 3-62994
¹¹¹Ru fragments from ²⁵²Cf spontaneous fission, γ cascades 3-62994
¹⁴⁹Sa, spin analyser in thermal neutron polarization analysis diffractometer 3-70413
Sb, odd-A isotopes, two-particle-one-hole states 3-54406
Sb isotopes, possible 2p-1t configs. studied using Te(t, α) and Te(t, t) reactions (*Spanish*) 3-74484
¹¹⁷Sb, multiparticle levels, decay scheme (*Russian*) 3-74487
¹¹⁷Sb perturbation approach to particle-vibration coupling model 3-52115
¹²¹Sb, charge radius sign and magnitude determination (*Russian*) 3-62929
¹²¹Sb, elec. quadrupole reduced transition probabilities 3-54406
¹²¹Sb, hyperfine broadening of X-ray lines, reln. to magnetic moment 3-49391
¹²¹Sb, Mossbauer effect in Sb(CH₃)₂Br₂ 3-58455
¹²¹Sb, Mossbauer spectra in Sn_{1-x}Sb_xO₂ system 3-68890
¹²¹Sb, perturbation approach to particle-vibration coupling model 3-52115
¹²¹Sb, transition strengths, reson. fluoresc. obs. 3-40451
¹²²Sb, first excited state populated by ¹²²Sn(p, n) reaction, stroboscopic resonance determ. of magnetic moment 3-45959
¹²²Sb, magnetic moment of 1.8 μ s state g factor determ. by stroboscopic method 3-67187
¹²²Sb beta decay, extraction of matrix elements 3-67270
¹²³Sb, transition strengths, reson. fluoresc. obs. 3-40451
¹²⁴Sb beta decay, extraction of matrix elements 3-67270
¹²⁴Sb-Be (γ, n) assay system, fissile content meas., ⁴He gas tube detectors 3-67557
¹²⁴Sb(³He, d)¹²⁵Sb, spectroscopic factors, theoretical and exptl. comparison 3-54406
¹²⁵Sb decay, weak transitions and accurate gamma intensities 3-54431
¹³⁰Sb excited states populated in β^- decay of 7- isomer and ground state of ¹³⁰Sn (*Russian*) 3-71085
¹³²Sb, proton-neutron-hole type states populated in decay of doubly magic ¹³²Sn (*Russian*) 3-74486
¹³²Sb beta decay to levels in ¹³²Te, transition probabilities 3-49214
¹³²Sb \rightarrow ¹³²Te, β^- decay of two states with half-lives 3.4 and 4.9 mins. (*Russian*) 3-74538
¹³³Sb pop. in ¹³³Sn beta decay, proton particle states determ. 3-71050
Sb(n, γ), 14 MeV radiative capture, spectra and partial cross section meas. 3-60173
Sm, A=144-154, total neutron cross section meas., deformation effects, optical model (*Russian*) 3-52178
¹⁴⁴Sm, ¹⁴⁷Sm, bombardment with ²⁰Ne, production of new Hf isotope α emitters 3-63016
¹⁴⁴Sm, ¹⁶⁰ induced one-proton, two-proton and α -transfer reactions, 63-66.5 MeV, cross section and transfer probability 3-49277
¹⁴⁴Sm(²⁴Mg, xn)^{162,163,164}W, 110-204 MeV, α -decay of W isotopes, half lives 3-57498
¹⁴⁴Sm(⁴⁰Ar, pxn)^{183-x}Au, E<300 MeV, excitation functions 3-54499
¹⁴⁴Sm(p, p'), reaction on analogue resonances, 9.3-11.0 MeV, ¹⁴⁴Sm deduced levels 3-63046
¹⁴⁷Sm, nonstatistical effects in γ -ray spectra emitted in decays of neutronic resonances (*Russian*) 3-52181
¹⁴⁷Sm, obs. of new γ -transitions and new levels from ¹⁴⁷Eu decay (*Russian*) 3-74525
¹⁴⁷Sm(²⁴Mg, xn)^{163,164}W, 110-204 MeV, α -decay of W isotopes half lives 3-57498
¹⁴⁸Sm, Coulomb excitation, determ. of static quadrupole moments of first excited states 3-49113
¹⁴⁸Sm, inelastic scattering of polarised protons, identification of collective modes 3-60101
¹⁴⁸Sm-¹⁵⁴Sm, transition from vibrational to deformed nucleus, boson expansion technique, quadrupole moments 3-49102
¹⁴⁹Sm($\alpha, 2n$)¹⁵¹Gd, 11-²/2 [505] rotational band identification 3-74489
Sn, fast neutron small-angle scattering, elastic cross-section meas. 3-74579
Sn and ¹²⁰Sn, π^- , π^+ reaction cross sections, 584 to 1856 MeV and 713 to 1447 MeV, deduced neutron density 3-54507
Sn isotopes, interaction between collective and quasiparticle excitation, energies, wave functions, B(E2) values (*Russian*) 3-74514
Sn low-lying 2⁺ and 3⁺ states, harmonic and anharmonic approxs. (*Russian*) 3-71047
Sn(¹⁴N, xn)La, study of odd-A La isotopes A=125-137 by in-beam γ -ray spectroscopy 3-45976
^eSn(p, t)^{e-2}Sn, A=118 and 116, 52 MeV, excitation of 2⁺ states, effect of inelastic scattering processes 3-46032
¹¹¹Sn, energy levels, deuteron bombardment, magnetic spectrography in nuclear emulsions 3-52104
¹¹²Sn(d, p) ¹¹³Sn, 12 MeV, study of ¹²³Sn energy levels 3-52104
¹¹²Sn(d, t) ¹¹³Sn, 17 MeV, study of ¹²³Sn energy levels 3-52104
¹¹³Sn, electron capture disintegration energy, error in P_i/P_f meas. due to presence of ^{119m}Sn 3-49226
¹¹³Sn, energy levels deuteron bombardment, magnetic spectrography in nuclear emulsions 3-52104
¹¹³Sn, γ -ray energies and relative intensities 3-43206
¹¹³Sn, high spin isomeric state populated in ¹¹²Cd(α, nn) reaction, lifetime and g-factor determ. 3-45958
¹¹⁴Sn(d, Li), 36 MeV, cross-section, spectroscopic factors 3-78341
¹¹⁵Sn, quadrupole interaction of 11/2⁺ state in liquid In, relaxation time by γ -ray anisotropy meas. 3-49082
¹¹⁶Sn, projection of N-nucleon component from zero-, two-, and four-quasi-particle state 3-67230

nuclei with $90 \leq A \leq 149$ continued

- ¹¹⁷Sn, ¹¹⁹Sn, spin-lattice relaxation in organic compounds 3-68884
¹¹⁷Sn, E3 and M4 transitions, conversion coefficient measurement, comparison with theory 3-54430
¹¹⁸Sn, high spin isomeric state, time-differential PAC determ. of g-factor 3-45958
¹¹⁸Sn(⁶Li, ⁶Li), break-up study, E=12 to 24 MeV 3-46040
¹¹⁸Sn(⁶Li, α (d)) break-up study, E=12 to 24 MeV 3-46040
¹¹⁸Sn(n, γ)¹¹⁹Sn, 46-5000 eV, obs. of gamma transitions between low-lying levels in ¹¹⁹Sn 3-49212
¹¹⁸Sn(n, γ)¹¹⁹Sn, emission γ -reson. spectroscopy 3-72556
¹¹⁸Sn(p, 2p), high-energy excitation function, calc. 3-46027
¹¹⁹Sn, charge radius sign and magnitude determination (*Russian*) 3-62929
¹¹⁹Sn, gamma transitions between low-lying levels populated in ¹¹⁹In decay and ¹¹⁸Sn(n, γ) 3-49212
¹¹⁹Sn, in BaSnO₃ Mossbauer spectra, selective modulation of recoilless γ -rays 3-55508
¹¹⁹Sn, mag. hyperfine interaction in Fe-Ni and Fe-Co alloys, Mossbauer and magnetization obs. 3-41466
¹¹⁹Sn, mag. moment, from Mossbauer meas. on Co₂MnSn and Fe₃Sn 3-52075
¹¹⁹Sn, Mossbauer meas. of magnetic moment of 23.8 keV state and hyperfine anomaly 3-49208
¹¹⁹Sn, n.m.r. Knight shifts and spin-lattice relax. time in CeSn₂In_{3-x} alloy 3-50480
¹¹⁹Sn in smectic ordered liq. cryst., ¹¹⁹Sn Mossbauer at 77K 3-55511
¹¹⁹Sn region, magnetic moments of 11/2⁻ states determ. using first order core polarisation effects 3-67186
¹¹⁹Sn-¹H, n.m.r., carbonates and organotin derivatives 3-78848
¹¹⁹Sn⁺, Mossbauer effect in FeF₃ (*French*) 3-72553
¹¹⁹Sn(n, n₀)¹¹⁹Sn, 14.8 MeV, meas. differential cross sections, the Schwinger prediction 3-71108
¹²⁰Sn, muon capture, neutron emission, branching ratios 3-40463
¹²⁰Sn, nucl. breathing modes calc. 3-52119
¹²⁰Sn, spectrum of SnCl radical, rotational anal. excited by Ar high tension discharge, B₂ Σ^+ -X²I₁ transition (*French*) 3-75006
¹²⁰Sn(d, d), (d, d), polarized, ang. distrib. of diff. cross-sect. and optical model calcs. 3-46035
¹²²Sn(d, p) ¹²³Sn, 12 MeV, study of ¹²³Sn energy levels 3-52104
¹²²Sn(p, n)¹²²Sb 11 MeV, population of first excited state in ¹²²Sb, magnetic moment determ. by stroboscope method 3-45959
¹²³Sn, energy levels, deuteron bombardment, magnetic spectrography in nuclear emulsions 3-52104
¹²⁴Sn($\alpha, ^3$ He)¹²⁵Sn, meas. differential cross section at 65.7 MeV rel. to neutron shell structure determ. of ¹²⁵Sn 3-67213
¹²⁴Sn(d, p) ¹²⁵Sn meas. differential cross section at 33.3 MeV rel. to neutron shell structures determ. of ¹²⁵Sn 3-67213
¹²⁴Sn(d, t) ¹²⁵Sn, 17 MeV, study of ¹²³Sn energy levels 3-52104
¹²⁵Sn, pop. in (d, p) and ($\alpha, ^3$ He) reactions, neutron shell structure determ. 3-67213
¹³⁰Sn, β^- decay of 7- isomer and ground state to excited states in ¹³⁰Sb, obs. of γ -transitions (*Russian*) 3-71085
¹³⁰Sn, excited two-neutron-hole states populated in ¹³⁰In decay (*Russian*) 3-71086
¹³⁰Sn, two-neutron-hole nucleus, excited states obs. in beta decay of ¹³⁰In 3-60081
¹³²Sn, doubly closed shell, population of first excited state in ¹³²In β^- decay 3-49149
¹³²Sn, twice-magic, obs. of first excited state populated in ¹³²In beta decay (*Russian*) 3-71048
¹³²Sn \rightarrow ¹³²Sb decay scheme, obs. of proton-neutron-hole type states populated in ¹³²Sb (*Russian*) 3-74486
¹³³Sn, beta decay pop. levels in ¹³³Sb, T_{1/2} and proton particle states determ. 3-71050
^{117m}Sn, as bone-scanning agent, evaluation 3-53748
^{119m}Sn, emission γ -reson. spectroscopy 3-72556
^{119m}Sn isomeric transition after-effects in Sn cpds., Mossbauer obs. 3-55985
Sn(α, n) A=115-119, 124, 20 MeV, precompound processes, neutron energy and angular distrib. 3-60209
Sn(e, e'), A=116, 120, 124, E=209 MeV, study of collective states, comparison with microscopic vibrational model 3-63039
Sn(p, p'), A=116, 120, 124, 40 MeV, role of collective imaginary form factor in microscopic description 3-60186
⁹⁰Sr, method of determ. in river sediments and soils, report 3-73398
⁹⁰Sr, Peach Bottom HTGR D1305 fuel element, diffusion coeff., activity profile 3-74738
⁹⁰Sr, search for the first 0⁺ excited state, gamma transition intensities and spins of 1655, 1892 and 2207 KeV states 3-40440
⁹⁰Sr concentration in Japanese coastal waters, obs. 3-69560
⁹⁰Sr concentration in volcanic ash paddy soil, obs. 3-69515
⁹⁰Sr content of soils in Niigata Prefecture, Japan 3-69513
⁹⁰Sr-⁹⁰Y beta particles, external bremsstrahlung 3-67313
⁹⁰Sr + ⁹⁰Y, radiation effects on mosquito larvae 3-59457
⁹⁰Sr + ⁹⁰Y source in radiometer, sensitivity to distance of source from window (*Czech*) 3-42646
⁹²Sr, β^- decay energies, comparisons and predictions for other nuclei 3-57496
¹⁴⁷Tb, short-lived isomer behaviour 3-40464
¹⁴⁸Tb, short-lived isomer behaviour 3-40464
^{149m}Tb, product of ¹⁴¹Pr bombarded with ¹²C, α -decay branching ratios 3-54446
⁹³Tc, high spin states, γ -ray spectra populated in ($\alpha, p2n\gamma$) reaction, 37-43 MeV 3-78248
⁹³Tc^a isobaric analogue reons. from 30.2 MeV ⁹²Mo(³He, d)⁹³Tc^a ang. distrib. 3-63081
⁹⁵Tc decay to levels in ⁹⁵Mo, spins and multipole mixing ratios 3-60070
⁹⁶Tc π , production cross section and isomer ratios of 4⁺ and 7⁺ states from ⁹⁶Mo(p, n) reaction, 10-65 MeV 3-43240
⁹⁷Tc, T_{1/2} of excited states using delayed coincidence technique for ⁹⁷Ru β^- -decay 3-60111
⁹⁹Tc, directional correlation and multipole mixing of γ -transitions 3-49199
⁹⁹Tc, intravenous bolus injection, cranial scintiphotographic blood flow defects, cerebral vascular disease 3-73595
⁹⁹Tc, nuclear parameters of 140 keV Mossbauer level from spectroscopy, 1.6-65 K 3-71077

nuclei with $90 \leq A \leq 149$ continued

- ^{99}Tc labelled diphosphonate, uptake by bone lesions rel. to radiation therapy 3-73597
- $^{99}\text{Tc} \rightarrow ^{99}\text{Rh}$, low-intensity β^- transition obs. 3-63006
- ^{101}Tc , three particle and anomalous excited states populated in ^{101}Mo decay (Russian) 3-49141
- ^{106}Tc β^- decay, levels of ^{106}Ru 3-62952
- ^{108}Tc β^- decay, levels of ^{108}Ru 3-62952
- ^{109}Tc , fine structure meas. in delayed-proton spectra 3-46010
- ^{111}Tc , fine structure meas. in delayed-proton spectra 3-46010
- ^{99m}Tc , brain scans, tuberous sclerosis, vascularity 3-51461
- ^{99m}Tc pertechnetate, acquired cardiovascular disease, radionuclide angiocardigraphy 3-53756
- ^{99m}Tc pertechnetate, pericardial effusion, radionuclide angiocardigraphy 3-56539
- ^{99m}Tc -S colloid, lung uptake, heart and lung time-activity curves, reticuloendothelial mechanism 3-51459
- ^{99m}Tc -streptokinase, localisation of deep vein thrombosis, animal studies, appl. to man 3-48253
- $^{99m}\text{TcO}_4^-$, radionuclide cerebral angiograms, effect of injection volume 3-51460
- Te even isotopes, $A=114$ -126 in-beam electron conversion from yrast levels 3-67264
- Te isotopes, quadrupole moment of 2^+ state 3-49103
- Te low-lying 2^+ and 3^- states, harmonic and anharmonic approx. (Russian) 3-71047
- Te neutron-rich even nuclei, systematics of E2 transition rates 3-49214
- $^a\text{Te}(p,1)^{a-2}\text{Te}$, $A=130$ -122, 52 MeV, excitation of 2^+ states, effect of inelastic scattering processes 3-46032
- ^{109}Te , delayed proton emission, excitation function, statistical model analysis, β -decay strength function (Russian) 3-57497
- ^{109}Te delayed proton spectrum, fine structure, statistical fluctuations (Russian) 3-40467
- ^{111}Te delayed proton spectrum, fine structure, statistical fluctuations (Russian) 3-40467
- ^{124}Te , quadrupole moment meas. by reorientation effect 3-49111
- ^{125}Te , 35.5 keV M1 transition line intensities, chemical effects 3-74531
- ^{125}Te , elec. field gradients in $\text{A}^{100}\text{Te}_2$ crystals, Mossbauer effect 3-72555
- ^{125}Te , Mossbauer effect resonance counter, design description 3-54019
- ^{125}Te , nucl. quadrupole interactions in isoelectronic cryst. hosts of S, Se, and Te 3-50501
- ^{126}Te , quadrupole moment meas. by reorientation effect 3-49111
- $^{126}\text{Te}(d,^3\text{He})^{125}\text{Sb}$, spectroscopic factors, theoretical and exptl. comparison 3-54406
- ^{127}Te , mag. mom. $\mu_{3/2}$ detn. by nuclear orientation meas. 3-45966
- ^{128}Te , quadrupole moment meas. by reorientation effect 3-49111
- $^{128}\text{Te}(d,p)^{129}\text{Te}$ and complementary (p,d) reactions, comparative treatment of spectroscopic factors 3-40502
- $^{128}\text{Te}(n,\gamma)^{129}\text{Te}$, gamma ray meas., decay schemes 3-74537
- $^{128}\text{Te}(p,d)^{129}\text{Te}$ and complementary (d,p) reactions, comparative treatment of spectroscopic factors 3-40502
- ^{129}Te , mag. mom. $\mu_{3/2}$ detn. by nuclear orientation meas. 3-45966
- ^{129}Te from $^{128}\text{Te}(n,\gamma)^{129}\text{Te}$, gamma ray meas., decay schemes 3-74537
- $^{129}\text{Te}m_{\pi} \rightarrow ^{129}\text{I}$, meas. of γ -ray angular distrib., orientation study of ^{129}I excited states 3-52131
- ^{132}Te , transition probability meas. of levels populated in ^{132}Sb β -decay, half-life determ. 3-49214
- ^{132}Te energy level scheme, from obs. of ^{132}Sb β -decay (Russian) 3-74538
- ^{135}Te beta decay pop. levels in ^{135}I , $T_{1/2}$ and proton particle states determ. 3-71050
- ^{128m}Te , nuclear orientation detn. of mag. mom. 3-49106
- ^{128m}Te from $\text{Te}(n,\gamma)$, magnetic dipole moments study by nuclear orientation 3-60069
- ^{125m}Te , nuclear orientation detn. of mag. mom. 3-49106
- ^{125m}Te magnetic moment meas. in nuclear orientation expt., analysis in pairing-plus-quadrupole model 3-43177
- ^{127m}Te , nuclear orientation detn. of mag. mom. 3-49106
- ^{127m}Te from $\text{Te}(n,\gamma)$, magnetic dipole moments study by nuclear orientation 3-60069
- ^{129m}Te , nuclear orientation detn. of mag. mom. 3-49106
- ^{129m}Te from $\text{Te}(n,\gamma)$, magnetic dipole moments study by nuclear orientation 3-60069
- $\text{Te}(p,p')$, even-A isotopes obs. of strong $L=5$ transitions, 25-pole collective motion 3-67326
- $\text{Te}(t,\alpha)\text{Sb}$, study of captured proton wave function and Sb isotope structures (Spanish) 3-74484
- $\text{Te}(t,t)$, study of optical potential depth and Sb isotope structure (Spanish) 3-74484
- Xe, $A=138$ to 142, fission products, meas. beta-decay energies, and end point energies and Q values 3-67277
- Xe isotopes, produced in ^{238}U fission and spallation, proton induced cross section and recoil props. 3-74615
- Xe produced by β -decay of precursor ^{133}I in graphite at 1000°C , release procedure 3-71278
- ^{113}Xe , half life, β -delayed proton emission 3-54438
- ^{116}Xe , Gamow-Teller β -strength functions, refinement in shell model approach 3-49225
- ^{122}Xe , half-lives of ^{122}I excited levels 3-54424
- ^{124}Xe , two-parameter description of rotational energies 3-74496
- ^{125}Xe , ^{127}Xe , γ - γ directional correlation at high gas densities (German) 3-49189
- ^{129}Xe , g-factor of 40 keV level, time-integral angular correlation expts. using gaseous sources 3-49076
- ^{130}Xe , 0^+ levels, quantum number assignment through beta decay meas. of ^{130}Cs (Russian) 3-67216
- ^{130}Xe , level structure determ. from beta-decay of ^{130}I , ^{130}I and ^{130}Cs 3-67214
- ^{131}Xe , populated from ^{131}I decay, 341.2 and 404.8 keV level lifetime meas. (German) 3-52139
- ^{131}Xe product of $^{130}\text{Ba}(n,\gamma)$, large epithermal resonance explanation of high concentration in lunar rocks 3-54482
- ^{132}Xe , 668 keV state, perturbed angular correlation meas. for g-factor 3-78242

nuclei with $90 \leq A \leq 149$ continued

- ^{132}Xe - $\pi^- \rightarrow$ photons, 9 GeV, correlation between longit. and transverse momenta 3-78351
- ^{133}Xe , ^{131}Xe , hyperfine field at Fe lattice sites, nucl. orientation expts. 3-72323
- ^{133}Xe , coronary blood flow assessment, critical review 3-56537
- ^{133}Xe , decay to ^{133}Cs , charge distrib. 3-60107
- ^{133}Xe , measurement of neutron capture cross section by the activity depletion method 3-60171
- ^{136}Xe ions, irradiation of ^{181}Ta , ^{197}Au , ^{238}U , reaction products, mechanisms 3-78350
- $^{136}\text{Xe}(\alpha, 2n)^{138}\text{Ba}$, 20-29 MeV, meas. of cross section, angular distrib., γ -ray spectra, level structure obs. 3-45974
- $^{136}\text{Xe}(\alpha, 3n)^{137}\text{Ba}$, 20-29 MeV, meas. of cross section, angular distrib., γ -ray spectra, level structure obs. 3-45974
- ^{129m}Xe , half-life determ. 3-52127
- ^{133m}Xe magnetic moment meas. in nuclear orientation expt., analysis in pairing-plus-quadrupole model 3-43177
- ^{90}Y , levels studied via $^{89}\text{Y}(p,p')^{89}\text{Y}^*$, shell model, conversion to analogue resonances 3-60176
- ^{91}Y beta source, absorption of particles in Cu, Ag, Sn and Pb foil targets 3-49376
- $^{95}\text{Y} \rightarrow ^{95}\text{Zr}$, half-life, decay scheme, γ -ray meas. (French) 3-71087
- ^{90m}Y log ft values for forbidden β transitions, rules for spin and parity assignments 3-62932
- Zr, neutron total cross section, 1.0 to 2.0 MeV, optical model comparison 3-54474
- Zr, neutron total cross section fluctuations, 1.0 to 2.0 MeV, compound nucleus explanation 3-54475
- Zr region targets, single-nucleon transfer reactions, isospin centroids 3-63028
- ^{90}Zr , (p,n), isobaric analogue transitions, 22 to 40 MeV proton energy, meas. angular distributions 3-63055
- ^{90}Zr , excitation of levels by inelastic proton scattering at 40 MeV, distorted wave calcs. 3-63057
- ^{90}Zr , helion and triton inelastic scattering, shell-model analysis with core polarization effects 3-78345
- ^{90}Zr , nucl. breathing modes calc. 3-52119
- ^{90}Zr , spin, parity for analogue resonances based on $^{89}\text{Y}(p,p')^{89}\text{Y}^*$ 3-60176
- ^{90}Zr , Zircaloy-2, total neutron cross section meas., 0.4-2.4 MeV 3-60285
- $^{90}\text{Zr}(\alpha, 3n\gamma)$, ($\alpha, \alpha'n\gamma$) reactions to populate ^{89}Zr , high spin states 3-78249
- $^{90}\text{Zr}(\alpha, p2n)^{91}\text{Nb}$ reaction to populate high spin states 3-78248
- ^{90}Zr photoabsorption, dynamic deformability, reln. to intermediate structure of giant resonance (Russian) 3-74562
- $^{90}\text{Zr}(^{16}\text{O}, ^{12}\text{C})^{94}\text{Mo}$, optimum Q-value near Coulomb barrier 3-74606
- $^{90}\text{Zr}(^3\text{He}, t)^{90}\text{Nb}$, 2nd order perturbation method with ($^3\text{He}-\alpha$ -t) process and DWBA 3-71123
- $^{90}\text{Zr}(\alpha, \alpha')^{90}\text{Zr}$, 104 MeV, computational approach to inverse problem in JWKB approximation 3-60143
- $^{90}\text{Zr}(\alpha, p\gamma)^{93}\text{Nb}$, 14.77 MeV, γ -decay of ^{93}Nb low lying levels, 3-57491
- $^{90}\text{Zr}(d, p)^{91}\text{Zr}$, deuteron D-state effects obs. 3-63066
- $^{90}\text{Zr}(d, \alpha)^{88}\text{Y}$, product two-hole multiplets 3-54491
- $^{90}\text{Zr}(d, d)$ scatt., spin depend. investigation 3-40499
- $^{90}\text{Zr}(d, p)^{91}\text{Zr}$, 10 MeV, tensor polarised deuteron beam, meas. of analysing powers and cross sections 3-49266
- $^{90}\text{Zr}(d, p)^{91}\text{Zr}$, j-dependence of vector analysing power and cross section 3-46034
- $^{90}\text{Zr}(e, e')$, $E=209$ MeV, study of collective states, comparison with microscopic vibrational model 3-63039
- ^{91}Zr , levels populated in $^{90}\text{Zr}(d, p)$ reaction at 10 MeV, polarised deuteron beam 3-49266
- ^{91}Zr , lifetime and g-factor of $15/2^-$ state populated in $^{88}\text{Sr}(\alpha, n)$ reaction 3-49194
- $^{92}\text{Zr}(\alpha, ^3\text{He})$, $E=65.7$ MeV, neutron shell struct. of ^{92}Zr 3-40504
- $^{92}\text{Zr}(\alpha, n)^{94}\text{Mo}$, 24 MeV, population of 2953 keV state in ^{94}Mo , time-differential PAC meas. 3-49084
- $^{92}\text{Zr}(d, p)$, $E_d=33.3$ MeV, neutron shell ^{92}Zr 3-40504
- $^{92}\text{Zr}(p, p')^6.5$ MeV, angular distribution of spin-flip probability, interference effect 3-67324
- ^{93}Zr , neutron shell struct. from (d,p) and ($\alpha, ^3\text{He}$) reactions 3-40504
- $^{94}\text{Zr}(\alpha, ^3\text{He})$, $E=65.7$ MeV, neutron shell struct. of ^{94}Zr 3-40504
- $^{94}\text{Zr}(d, p)$, $E_d=33.3$ MeV, neutron shell struct. of ^{94}Zr 3-40504
- ^{95}Zr , neutron shell struct. from (d,p) and ($\alpha, ^3\text{He}$) reactions 3-40504
- ^{95}Zr populated in ^{95}Y decay, excited levels (French) 3-71087
- $^{96}\text{Zr}(^{16}\text{O}, ^{12}\text{C})^{100}\text{Mo}$, optimum Q-value near Coulomb barrier 3-74606
- $^{96}\text{Zr}(^{16}\text{O}, ^{14}\text{O})^{98}\text{Mo}$, optimum Q-value near Coulomb barrier 3-74606
- $^{96}\text{Zr}(\alpha, ^3\text{He})$, $E=65.7$ MeV, neutron shell struct. of ^{96}Zr 3-40504
- $^{96}\text{Zr}(d, p)$, $E_d=33.3$ MeV, neutron shell struct. of ^{96}Zr 3-40504
- ^{97}Zr , neutron shell struct. from (d,p) and ($\alpha, ^3\text{He}$) reactions 3-40504
- $\text{Zr}(n, \gamma)$, 14 MeV radiative capture, spectra and partial cross section meas. 3-60173

nuclei with $150 \leq A \leq 189$

- $A=173$ -189, rotational bands, Coriolis force interactions, differences in moments of inertia (Russian) 3-71039
- $A=174$ -185, equilibrium deformations and structures of ground and excited states (Russian) 3-52088
- doubly even nuclei, $A < 195$, angular velocity expansions of rotational energies 3-52117
- excited nuclei, statistical theory of decay, competition between fission and evaporation 3-43263
- lanthanides, cumulative and independent yields from 24 GeV proton irradiation of tungsten 3-40486
- odd-A deformed nuclei, effective g_r values 3-49110
- rare earth deformed nuclei, change in mean square radius between ground and excited states 3-49132
- rare earth nuclei, deformed heavy, nonschematic description of β -decay process 3-71089
- rare earth region, calc. of ground state deformation (German) 3-52087
- rare earth region, excited 0^+ states in two-nucleon transfer reactions (Russian) 3-52091
- rare earth region deformed nuclei; rot. flow model for spectra 3-62969

nuclei with $150 \leq A \leq 189$ continued

- rare earths, ground state intrinsic deformation props., determ. using Hartree-Fock approximation 3-78275
- rare-earth deformed nuclei, number-conserving treatment of the BCS-Tamm-Dancoff approximation 3-43191
- rare-earth nuclei, even, change of charge radii due to rotational transitions, cranking model 3-52130
- rare-earth rotating deformed nuclei, moments of inertia 3-49171
- static quadrupole moments of 2^+ states of even isotopes of Sm 3-49099
- $Z \geq 60$, nucl. energy spectrum near 1 GeV/amu, new cosmic ray source evidence 3-53581
- ^{177}Au , α -particle energy 3-54499
- ^{189}Bi , deduced half life and α -particle energy 3-54499
- Dy, A = 158, 160, 162 pop. in $\text{Gd}(\alpha, 2n)\text{Dy}$ reaction, g factor meas. of high spin rotational states 3-67188
- Dy, A = 162, 164, Coulomb excitation, quadrupole and hexadecapole transition moments 3-49201
- Dy, odd mass A = 155-163, level study by $(^3\text{He}, \alpha)$ 3-40420
- Dy isotopes, X-ray isotope shifts and variations in charge radii 3-67662
- ^{159}Dy , A = 158, 160, 162, lifetime, struct. of levels above 1.5 MeV, meas., anal. 3-78250
- ^{150}Dy , product of ^{141}Pr bombarded with ^{14}N , α -decay branching ratios 3-54446
- ^{151}Dy , product of ^{141}Pr bombarded with ^{14}N , α -decay branching ratios 3-54446
- ^{154}Dy from $^{146}\text{Nd}(^{12}\text{C}, \text{xn}, \gamma)$ reaction, high spin state, transition of ground rotational band 3-60217
- ^{155}Dy from $^{146}\text{Nd}(^{12}\text{C}, \text{xn}, \gamma)$ reaction, high spin states, stretched E2 transitions 3-60217
- ^{156}Dy , influence of rotation on moment of inertia of high-spin ground state members 3-52098
- ^{157}Dy , production by α bombard. of Gd 3-57535
- ^{157}Dy , angular momentum dependence of collective gyromagnetic ratio 3-49097
- ^{159}Dy , rotational excitation properties 3-43212
- ^{159}Dy , spreading width of rotational doorway states 3-67203
- ^{160}Dy , determ. particle parameters of E2 transitions and multipole mixing ratios 3-67256
- ^{160}Dy , E0 contrib. in $2^+ \rightarrow 2^+$ transitions, directional correlation functions 3-62991
- ^{160}Dy , γ decay props. of 3^- states 3-45993
- $^{160}\text{Dy}(\alpha, \text{nnnn})^{156}\text{Er}$, 47-50 MeV, population of high-spin members of ground state rotational bands 3-52098
- $^{160}\text{Dy}(\alpha, 8n)$, high spin states in ^{156}Er 3-62937
- ^{161}Dy , Coulomb excitation of 43.8 keV state, Mossbauer effect study of transition 3-62990
- ^{161}Dy in ferromagnetic TbAl_2 , internal fields and relaxation effects, perturbed angular correlation meas. 3-53046
- ^{162}Dy doublet splitting in even A deformed nuclei between excited 2 quasiparticle states 3-57478
- ^{164}Dy , ^{40}Ar reactions, effective thresholds calc. 3-40513
- ^{164}Dy , Coulomb excitation, meas. of hexadecapole transition moments and $M(E2; 0 \rightarrow 2)$ 3-49195
- ^{165m}Dy , decay to levels of ^{165}Ho 3-43207
- Er, A = 166, 168, 170, Coulomb excitation, quadrupole and hexadecapole transition moments 3-49201
- $^{153}\text{Er} \rightarrow ^{149}\text{Dy}$ α decay, electron capture obs. of ^{149}Dy (French) 3-63003
- ^{156}Er , high-spin states population and backbending effect 3-62937
- ^{157}Er , ^{159}Er , test of backbending models 3-71052
- ^{160}Er , influence of rotation on moment of inertia of high-spin ground state members 3-52098
- $^{160}\text{Er} \rightarrow ^{160}\text{Ho}$, determ. of decay energies (Russian) 3-49223
- ^{162}Er , two-parameter description of rotational energies 3-74496
- ^{166}Er , ^{168}Er , Coulomb excitation, meas. of hexadecapole transition moments and $M(E2; 0 \rightarrow 2)$ 3-49195
- ^{166}Er , $\gamma\gamma$ cascade directional correl. after $^{166}\text{Ho} \beta^-$ decay in YES cryst. (French) 3-53039
- ^{166}Er , non-adiabatic effect on collective g-factors and K-forbidden M1 transitions 3-49098
- ^{166}Er hyperfine interaction in lanthanum and yttrium ethyl sulphates, $\gamma\gamma$ directional correl. (French) 3-47179
- ^{167}Er (d, d') ^{167}Er , energy levels study 3-40413
- ^{168}Er , ground state, rotational bands, obs. by $\text{Ge}(\text{Li})$ spectroscopy of $^{168}\text{Ho} \beta$ -decay 3-67273
- ^{168}Er doublet splitting in even A deformed nuclei between excited 2 quasiparticle states 3-57478
- ^{170}Er , static quadrupole moment determ. from reorientation effect in Coulomb excitation by ^{81}Br 3-46038
- ^{170}Er , static quadrupole moment of first 2^+ state by Coulomb excitation using ^{81}Br 3-62935
- ^{151}Eu , ^{153}Eu , hyperfine anomaly between ground and excited states 3-49207
- ^{151}Eu , hyperfine broadening of X-ray lines, reln. to magnetic moment 3-49391
- ^{151}Eu , Mossbauer effect in PdEu 3-79954
- ^{151}Eu Mossbauer effect in $\text{Eu}(\text{NH}_3)_3$ 3-47178
- ^{152}Eu decay, cascading transitions, effect on registration of γ -quanta in total energy peaks (Russian) 3-70377
- ^{153}Eu , Mossbauer spectrum in $\text{Eu}_2\text{Ti}_2\text{O}_7$, Goldanskii effect 3-53043
- $^{153}\text{Eu}(n, \alpha)$, $E_\alpha = 14$ MeV, knock-on mechanism 3-63044
- $^{154}\text{Eu} \rightarrow ^{154}\text{Gd}$, population of 2^+ and 4^+ states, lifetime meas. 3-52128
- $^{155}\text{Eu} \rightarrow ^{155}\text{Gd}$, first-forbidden β decays, correction matrix element effects 3-63012
- $^{155}\text{Eu} \rightarrow ^{155}\text{Gd}$ decay, effects of microscopical theory of Coriolis forces 3-63011
- Gd, A = 154-160, total neutron cross section meas., deformation effects, optical model (Russian) 3-52178
- Gd, A = 158, 160, Coulomb excitation, quadrupole and hexadecapole transition moments 3-49201
- Gd, neutron total cross section, 1.0 to 2.0 MeV, optical model comparison 3-54474
- Gd, neutron total cross section fluctuations, 1.0 to 2.0 MeV, compound nucleus explanation 3-54475
- Gd even isotopes, A = 150-158, population in (p,t) reaction, DWBA analysis 3-67336

nuclei with $150 \leq A \leq 189$ continued

- ^{150}Gd , energy level spectroscopic investigation, spin assignments and lifetime meas. 3-54429
- ^{151}Gd spherical nucleus from $^{149}\text{Sm}(\alpha, 2n)^{151}\text{Gd}$, $11^-/2$ [505] rotational band identification 3-74489
- ^{152}Gd , two-parameter description of rotational energies 3-74496
- ^{154}Gd , 2^+ and 4^+ states, populated by ^{154}Eu beta decay, lifetime meas. 3-52128
- ^{154}Gd , gamma-decay of levels populated in ^{154}Tb isomeric state β decay 3-67263
- $^{154}\text{Gd}(^4\text{He}, \text{xn})^{158-160}\text{Dy}$, high angular momentum, excitation functions and photon emission, compound nucleus mechanism 3-63083
- ^{155}Gd , ^{157}Gd , n.m.r. spectra in ferromagnetic Gd metal at 4.2 K in zero external field 3-44330
- ^{155}Gd from $^{137}\text{Gd}(\text{p}, \text{t})^{155}\text{Gd}$, energy level study 3-52086
- $^{155}\text{Gd}^{3+}$ and $^{157}\text{Gd}^{3+}$, hyperfine interaction in $\text{Bi}_2\text{Mg}_3(\text{NO})_{12} \cdot 24\text{H}_2\text{O}$ ENDOR 3-79948
- $^{155}\text{Gd}(\alpha, 2n)^{157}\text{Dy}$, production and separation processes 3-57535
- $^{155}\text{Gd}(\text{p}, \text{t})^{155}\text{Gd}$, energy level study 3-52086
- $^{156}\text{Gd}(\alpha, \text{nnnn})^{156}\text{Dy}$, 47-50 MeV, population of high-spin members of ground state rotational bands 3-52098
- $^{156}\text{Gd}(\alpha, 3n)^{157}\text{Dy}$, production and separation processes 3-57535
- ^{157}Gd , nonstatistical effects in γ -ray spectra emitted in decays of neutron resonances (Russian) 3-52181
- $^{157}\text{Gd}(\alpha, n)^{158}\text{Dy}$, production and separation processes 3-57535
- $^{157}\text{Gd}(\text{p}, \text{t})^{155}\text{Gd}$, energy level study 3-52086
- ^{158}Gd , Coulomb excitation, meas. of hexadecapole transition moments and $M(E2; 0 \rightarrow 2)$ 3-49195
- $^{158}\text{Gd}(\alpha, 3n)^{159}\text{Dy}$, ^{151}Dy rotational excitations properties 3-43212
- $^{161}\text{Gd} \rightarrow ^{161}\text{Tb} \beta^-$ decay, γ -ray spectra, ^{161}Tb levels 3-43219
- $\text{Gd}(\alpha, 2n)\text{Dy}$, g factor meas. of high-spin rotational states in Dy with A = 158, 160, 162 3-67188
- Hf even-even isotopes produced in (p,xn γ) reactions, de-excitation 3-49191
- Hf odd-neutron nucleides, rotational band structure from $\text{Yb}(\alpha, \text{xn})$ reactions, Nilsson model 3-40417
- ^{159}Hf , new isotopes produced by ^{20}Ne bombardment of Sm, α emission 3-63016
- ^{160}Hf , new isotopes produced by ^{20}Ne bombardment of Sm, α emission 3-63016
- ^{161}Hf , new isotopes produced by ^{20}Ne bombardment of Sm, α emission 3-63016
- ^{166}Hf , from $^{150}\text{Sm}(^{20}\text{Ne}, 4n)$, E = 93 MeV, deduced levels, feeding times by recoil-distance Doppler shift measurements 3-60215
- $^{167}\text{Hf} \rightarrow ^{167}\text{Lu}$, 2.05 min, meas. of K/β^+ ratio, determs. of total decay energy, Nilsson model assignments 3-52147
- ^{168}Hf , ^{170}Hf from $^{152,154}\text{Sm}(^{20}\text{Ne}, 4n)$, E = 86 MeV, deduced levels, feeding times by recoil-distance Doppler shift measurements 3-60215
- $^{169}\text{Hf} \rightarrow ^{169}\text{Lu}$, 3.25 min, meas. of K/β^+ ratio, determs. of total decay energy, Nilsson model assignments 3-52147
- ^{170}Hf , two-parameter description of rotational energies 3-74496
- ^{172}Hf , half-life meas. 3-52143
- ^{173}Hf levels populated in decay of ^{173}Ta 3-40421
- ^{174}Hf , atomic mass determ. 3-67174
- ^{174}Hf , isomeric states meas. to study proton to neutron mixing ratios 3-45967
- ^{175}Hf , energy levels, state wave functions from 12 MeV $^{176}\text{Hf}(\text{d}, \text{t})^{175}\text{Hf}$ reaction 3-74497
- ^{175}Hf , quadrupole alignment in Hf metal at 3 mK, meas. γ -ray anisotropies 3-71082
- ^{176}Hf , isomeric states meas. to study proton to neutron mixing ratios 3-45967
- ^{176}Hf , spacing of ground-state levels 3-67174
- $^{176}\text{Hf}(\text{d}, \text{t})^{175}\text{Hf}$, 12 MeV, energy levels, state wave functions of ^{175}Hf 3-74497
- ^{177}Hf , 249.7 keV level, half-life meas. 3-49198
- ^{177}Hf , mag. dipole moments, ground state h.f.s. 3-40412
- ^{177}Hf , neutron resonance spin determ. from Monte Carlo simulation of decay 3-57519
- ^{177}Hf , nonstatistical effects in γ -ray spectra emitted in decays of neutron resonances (Russian) 3-52181
- ^{177}Hf angular correlations meas. 3-62983
- $^{177}\text{Hf}(n, \text{p})^{178m}\text{Hf}$, half life of high-spin isomeric state in ^{178}Hf and capture production cross section 3-62987
- ^{178}Hf , ^{180}Hf , Mossbauer meas. of isomer shift and quadrupole moment ratios 3-49206
- ^{178}Hf from ^{178}Lu decay, spin-parity assignments 3-67276
- ^{178}Hf high-spin isomeric state, half life and neutron capture production cross section 3-62987
- $^{178}\text{Hf}/^{180}\text{Hf}$, ratio of quadrupole moments of 2^+ states 3-60086
- ^{179}Hf , mag. dipole moments, ground state h.f.s. 3-40412
- $^{179}\text{Hf}(\alpha, 2n)^{181}\text{W}$, 29-43 MeV, obs. of Coriolis mixing effects in ^{181}W 3-60079
- $^{180}\text{Hf}(n, \alpha)$, thermal neutron energies, cross sections determ. 3-43244
- ^{184}Hf , half-life meas., B and γ decay 3-60129
- ^{177m}Hf , half-life meas. 3-63007
- $^{179m2}\text{Hf}$, half-life meas. 3-63007
- Hg neutron deficient isotopes, self-consistent calc. of possible shape transition 3-67180
- ^{185}Hg , variable collective inertia and mean square charge radius 3-62930
- ^{186}Hg , γ -ray spectra Yrast states up to 14^+ stable quadrupole deformation PAC obs. 3-41462
- $^{180}\text{Hf}(\alpha, 3n)^{181}\text{W}$, 29-43 MeV, obs. of Coriolis mixing effects in ^{181}W 3-60079
- $^{180}\text{Hf}(n, \alpha)$, thermal neutron energies, cross sections determ. 3-43244
- ^{184}Hf , half-life meas., B and γ decay 3-60129
- ^{177m}Hf , half-life meas. 3-63007
- $^{179m2}\text{Hf}$, half-life meas. 3-63007
- Hg neutron deficient isotopes, self-consistent calc. of possible shape transition 3-67180
- ^{185}Hg , variable collective inertia and mean square charge radius 3-62930
- ^{186}Hg , γ -ray spectra Yrast states up to 14^+ stable quadrupole deformation PAC obs. 3-41462
- $^{180}\text{Hf}(\alpha, 3n)^{181}\text{W}$, 29-43 MeV, obs. of Coriolis mixing effects in ^{181}W 3-60079
- $^{180}\text{Hf}(n, \alpha)$, thermal neutron energies, cross sections determ. 3-43244
- ^{184}Hf , half-life meas., B and γ decay 3-60129
- ^{177m}Hf , half-life meas. 3-63007
- $^{179m2}\text{Hf}$, half-life meas. 3-63007
- Hg neutron deficient isotopes, self-consistent calc. of possible shape transition 3-67180
- ^{185}Hg , variable collective inertia and mean square charge radius 3-62930
- ^{186}Hg , γ -ray spectra Yrast states up to 14^+ stable quadrupole deformation PAC obs. 3-41462
- $^{180}\text{Hf}(\alpha, 3n)^{181}\text{W}$, 29-43 MeV, obs. of Coriolis mixing effects in ^{181}W 3-60079
- $^{180}\text{Hf}(n, \alpha)$, thermal neutron energies, cross sections determ. 3-43244
- ^{184}Hf , half-life meas., B and γ decay 3-60129
- ^{177m}Hf , half-life meas. 3-63007
- $^{179m2}\text{Hf}$, half-life meas. 3-63007
- Hg neutron deficient isotopes, self-consistent calc. of possible shape transition 3-67180
- ^{185}Hg , variable collective inertia and mean square charge radius 3-62930
- ^{186}Hg , γ -ray spectra Yrast states up to 14^+ stable quadrupole deformation PAC obs. 3-41462
- $^{180}\text{Hf}(\alpha, 3n)^{181}\text{W}$, 29-43 MeV, obs. of Coriolis mixing effects in ^{181}W 3-60079
- $^{180}\text{Hf}(n, \alpha)$, thermal neutron energies, cross sections determ. 3-43244
- ^{184}Hf , half-life meas., B and γ decay 3-60129
- ^{177m}Hf , half-life meas. 3-63007
- $^{179m2}\text{Hf}$, half-life meas. 3-63007
- Hg neutron deficient isotopes, self-consistent calc. of possible shape transition 3-67180
- ^{185}Hg , variable collective inertia and mean square charge radius 3-62930
- ^{186}Hg , γ -ray spectra Yrast states up to 14^+ stable quadrupole deformation PAC obs. 3-41462
- $^{180}\text{Hf}(\alpha, 3n)^{181}\text{W}$, 29-43 MeV, obs. of Coriolis mixing effects in ^{181}W 3-60079
- $^{180}\text{Hf}(n, \alpha)$, thermal neutron energies, cross sections determ. 3-43244
- ^{184}Hf , half-life meas., B and γ decay 3-60129
- ^{177m}Hf , half-life meas. 3-63007
- $^{179m2}\text{Hf}$, half-life meas. 3-63007
- Hg neutron deficient isotopes, self-consistent calc. of possible shape transition 3-67180
- ^{185}Hg , variable collective inertia and mean square charge radius 3-62930
- ^{186}Hg , γ -ray spectra Yrast states up to 14^+ stable quadrupole deformation PAC obs. 3-41462
- $^{180}\text{Hf}(\alpha, 3n)^{181}\text{W}$, 29-43 MeV, obs. of Coriolis mixing effects in ^{181}W 3-60079
- $^{180}\text{Hf}(n, \alpha)$, thermal neutron energies, cross sections determ. 3-43244
- ^{184}Hf , half-life meas., B and γ decay 3-60129
- ^{177m}Hf , half-life meas. 3-63007
- $^{179m2}\text{Hf}$, half-life meas. 3-63007
- Hg neutron deficient isotopes, self-consistent calc. of possible shape transition 3-67180
- ^{185}Hg , variable collective inertia and mean square charge radius 3-62930
- ^{186}Hg , γ -ray spectra Yrast states up to 14^+ stable quadrupole deformation PAC obs. 3-41462
- $^{180}\text{Hf}(\alpha, 3n)^{181}\text{W}$, 29-43 MeV, obs. of Coriolis mixing effects in ^{181}W 3-60079
- $^{180}\text{Hf}(n, \alpha)$, thermal neutron energies, cross sections determ. 3-43244
- ^{184}Hf , half-life meas., B and γ decay 3-60129
- ^{177m}Hf , half-life meas. 3-63007
- $^{179m2}\text{Hf}$, half-life meas. 3-63007
- Hg neutron deficient isotopes, self-consistent calc. of possible shape transition 3-67180
- ^{185}Hg , variable collective inertia and mean square charge radius 3-62930
- ^{186}Hg , γ -ray spectra Yrast states up to 14^+ stable quadrupole deformation PAC obs. 3-41462
- $^{180}\text{Hf}(\alpha, 3n)^{181}\text{W}$, 29-43 MeV, obs. of Coriolis mixing effects in ^{181}W 3-60079
- $^{180}\text{Hf}(n, \alpha)$, thermal neutron energies, cross sections determ. 3-43244
- ^{184}Hf , half-life meas., B and γ decay 3-60129
- ^{177m}Hf , half-life meas. 3-63007
- $^{179m2}\text{Hf}$, half-life meas. 3-63007
- Hg neutron deficient isotopes, self-consistent calc. of possible shape transition 3-67180
- ^{185}Hg , variable collective inertia and mean square charge radius 3-62930
- ^{186}Hg , γ -ray spectra Yrast states up to 14^+ stable quadrupole deformation PAC obs. 3-41462
- $^{180}\text{Hf}(\alpha, 3n)^{181}\text{W}$, 29-43 MeV, obs. of Coriolis mixing effects in ^{181}W 3-60079
- $^{180}\text{Hf}(n, \alpha)$, thermal neutron energies, cross sections determ. 3-43244
- ^{184}Hf , half-life meas., B and γ decay 3-60129
- ^{177m}Hf , half-life meas. 3-63007
- $^{179m2}\text{Hf}$, half-life meas. 3-63007
- Hg neutron deficient isotopes, self-consistent calc. of possible shape transition 3-67180
- ^{185}Hg , variable collective inertia and mean square charge radius 3-62930
- ^{186}Hg , γ -ray spectra Yrast states up to 14^+ stable quadrupole deformation PAC obs. 3-41462
- $^{180}\text{Hf}(\alpha, 3n)^{181}\text{W}$, 29-43 MeV, obs. of Coriolis mixing effects in ^{181}W 3-60079
- $^{180}\text{Hf}(n, \alpha)$, thermal neutron energies, cross sections determ. 3-43244
- ^{184}Hf , half-life meas., B and γ decay 3-60129
- ^{177m}Hf , half-life meas. 3-63007
- $^{179m2}\text{Hf}$, half-life meas. 3-63007
- Hg neutron deficient isotopes, self-consistent calc. of possible shape transition 3-67180
- ^{185}Hg , variable collective inertia and mean square charge radius 3-62930
- ^{186}Hg , γ -ray spectra Yrast states up to 14^+ stable quadrupole deformation PAC obs. 3-41462
- $^{180}\text{Hf}(\alpha, 3n)^{181}\text{W}$, 29-43 MeV, obs. of Coriolis mixing effects in ^{181}W 3-60079
- $^{180}\text{Hf}(n, \alpha)$, thermal neutron energies, cross sections determ. 3-43244
- ^{184}Hf , half-life meas., B and γ decay 3-60129
- ^{177m}Hf , half-life meas. 3-63007
- $^{179m2}\text{Hf}$, half-life meas. 3-63007
- Hg neutron deficient isotopes, self-consistent calc. of possible shape transition 3-67180
- ^{185}Hg , variable collective inertia and mean square charge radius 3-62930
- ^{186}Hg , γ -ray spectra Yrast states up to 14^+ stable quadrupole deformation PAC obs. 3-41462
- $^{180}\text{Hf}(\alpha, 3n)^{181}\text{W}$, 29-43 MeV, obs. of Coriolis mixing effects in ^{181}W 3-60079
- $^{180}\text{Hf}(n, \alpha)$, thermal neutron energies, cross sections determ. 3-43244
- ^{184}Hf , half-life meas., B and γ decay 3-60129
- ^{177m}Hf , half-life meas. 3-63007
- $^{179m2}\text{Hf}$, half-life meas. 3-63007
- Hg neutron deficient isotopes, self-consistent calc. of possible shape transition 3-67180
- ^{185}Hg , variable collective inertia and mean square charge radius 3-62930
- ^{186}Hg , γ -ray spectra Yrast states up to 14^+ stable quadrupole deformation PAC obs. 3-41462
- $^{180}\text{Hf}(\alpha, 3n)^{181}\text{W}$, 29-43 MeV, obs. of Coriolis mixing effects in ^{181}W 3-60079
- $^{180}\text{Hf}(n, \alpha)$, thermal neutron energies, cross sections determ. 3-43244
- ^{184}Hf , half-life meas., B and γ decay 3-60129
- ^{177m}Hf , half-life meas. 3-63007
- $^{179m2}\text{Hf}$, half-life meas. 3-63007
- Hg neutron deficient isotopes, self-consistent calc. of possible shape transition 3-67180
- ^{185}Hg , variable collective inertia and mean square charge radius 3-62930
- ^{186}Hg , γ -ray spectra Yrast states up to 14^+ stable quadrupole deformation PAC obs. 3-41462
- $^{180}\text{Hf}(\alpha, 3n)^{181}\text{W}$, 29-43 MeV, obs. of Coriolis mixing effects in ^{181}W 3-60079
- $^{180}\text{Hf}(n, \alpha)$, thermal neutron energies, cross sections determ. 3-43244
- ^{184}Hf , half-life meas., B and γ decay 3-60129
- ^{177m}Hf , half-life meas. 3-63007
- $^{179m2}\text{Hf}$, half-life meas. 3-63007
- Hg neutron deficient isotopes, self-consistent calc. of possible shape transition 3-67180
- ^{185}Hg , variable collective inertia and mean square charge radius 3-62930
- ^{186}Hg , γ -ray spectra Yrast states up to 14^+ stable quadrupole deformation PAC obs. 3-41462
- $^{180}\text{Hf}(\alpha, 3n)^{181}\text{W}$, 29-43 MeV, obs. of Coriolis mixing effects in ^{181}W 3-60079
- $^{180}\text{Hf}(n, \alpha)$, thermal neutron energies, cross sections determ. 3-43244
- ^{184}Hf , half-life meas., B and γ decay 3-60129
- ^{177m}Hf , half-life meas. 3-63007
- $^{179m2}\text{Hf}$, half-life meas. 3-63007
- Hg neutron deficient isotopes, self-consistent calc. of possible shape transition 3-67180
- ^{185}Hg , variable collective inertia and mean square charge radius 3-62930
- ^{186}Hg , γ -ray spectra Yrast states up to 14^+ stable quadrupole deformation PAC obs. 3-41462
- $^{180}\text{Hf}(\alpha, 3n)^{181}\text{W}$, 29-43 MeV, obs. of Coriolis mixing effects in ^{181}W 3-60079
- $^{180}\text{Hf}(n, \alpha)$, thermal neutron energies, cross sections determ. 3-43244
- ^{184}Hf , half-life meas., B and γ decay 3-60129
- ^{177m}Hf , half-life meas. 3-63007
- $^{179m2}\text{Hf}$, half-life meas. 3-63007
- Hg neutron deficient isotopes, self-consistent calc. of possible shape transition 3-67180
- ^{185}Hg , variable collective inertia and mean square charge radius 3-62930
- ^{186}Hg , γ -ray spectra Yrast states up to 14^+ stable quadrupole deformation PAC obs. 3-41462
- $^{180}\text{Hf}(\alpha, 3n)^{181}\text{W}$, 29-43 MeV, obs. of Coriolis mixing effects in ^{181}W 3-60079
- $^{180}\text{Hf}(n, \alpha)$, thermal neutron energies, cross sections determ. 3-43244
- ^{184}Hf , half-life meas., B and γ decay 3-60129
- ^{177m}Hf , half-life meas. 3-63007
- $^{179m2}\text{Hf}$, half-life meas. 3-63007
- Hg neutron deficient isotopes, self-consistent calc. of possible shape transition 3-67180
- ^{185}Hg , variable collective inertia and mean square charge radius 3-62930
- ^{186}Hg , γ -ray spectra Yrast states up

nuclei with $150 \leq A \leq 189$ continued

- ^{160}Ho , π^- , π^+ reaction cross sections, 713 to 1447 MeV, deduced neutron density 3-54507
- ^{165}Ho , populated in decay of ^{165m}Dy 3-43207
- ^{165}Ho , quadrupole moment meas. by proton and alpha scattering from aligned target 3-45944
- ^{165}Ho , resonant scattering of gamma-rays, determ. of 94.69 keV level lifetime (*Russian*) 3-52168
- $^{165}\text{Ho}(n,n'\gamma)$, ^{165}Ho excited levels, comparison with pair correlation model (*Russian*) 3-71059
- ^{166}Ho β^- decay in YES cryst., ^{166}Er $\gamma\gamma$ cascade directional correl. (*French*) 3-53039
- $^{166}\text{Ho}^m$, as efficiency calibration standard for Ge(Li) detectors 3-48335
- ^{168}Ho , beta decay to levels in ^{168}Er , Ge(Li) spectroscopy, rotational band identification 3-67273
- ^{184}Ir , effects of strong rotation-particle coupling on energy levels of two-quasiparticle systems 3-62942
- ^{184}Ir decay to ^{184}Os , level structure 3-62941
- ^{185}Ir produced in ^{187}W decay, orientation studies, transition parameters 3-40452
- ^{187}Ir , effects of strong rotation-particle coupling on energy levels of two-quasiparticle systems 3-62942
- ^{187}Ir , nature of excited levels from ^{187}Pt decay scheme determ. 3-71049
- ^{189}Ir , low lying levels, core-excitation model approach 3-71046
- ^{191}Ir produced in ^{187}W decay, orientation studies, transition parameters 3-40452
- ^{193}Ir produced in ^{187}W decay, orientation studies, transition parameters 3-40452
- ^{164}Lu , lifetime, struct. of levels above 1.5 MeV, meas., anal. 3-78250
- ^{167}Lu , ^{169}Lu , levels populated in ^{167}Hf and ^{169}Hf decay, Nilsson model assignments 3-52147
- $^{169}\text{Lu} \rightarrow ^{169}\text{Yb}$, meas. of γ -ray, positron and conversion electron spectra, ^{169}Yb energy levels (*Russian*) 3-52090
- ^{171}Lu , ^{173}Lu , E1 transition probabilities calc. using equilibrium deformations of one-quasiparticle states 3-49216
- ^{171}Lu , high-spin rotational states and evidence for $\Delta K=2$ and $\Delta K=4$ mixings 3-60077
- ^{171}Lu , rot. bands, stripping reaction studies 3-62939
- ^{171}Lu levels, half lives deduced, comparison with Nilsson model, hindrance factors 3-54422
- ^{173}Lu , high-spin rotational states and evidence for $\Delta K=2$ and $\Delta K=4$ mixings 3-60077
- ^{173}Lu levels, half lives deduced, comparison with Nilsson model, hindrance factors 3-54422
- ^{175}Lu , E2/M1 mixing ratio determ., from γ -ray anisotropy temp. dependence 3-71082
- ^{175}Lu , muonic, spectroscopic quadrupole moment determ. and quadrupole h.f. splitting in pionic ^{175}Lu 3-49075
- ^{175}Lu , quadrupole moment determ. from quadrupole splitting in X-ray transitions of muonic atom 3-49096
- ^{175}Lu , spectroscopic quadrupole moment determ. from quadrupole splitting in muonic atoms 3-49133
- ^{175}Lu pionic atom, search for strong interaction quadrupole effect 3-49134
- $^{175}\text{Lu}(\alpha, 2n)^{177}\text{Ta}$, 27 MeV, half lives of ^{177}Ta levels, comparison with Nilsson model, hindrance factors 3-54422
- $^{175}\text{Lu}(p, n\gamma)^{176}\text{Hf}$, $x=2, 4, 6$, $A=174, 172, 170$, de-excitation, ground state rot. bands population 3-49191
- ^{176}Lu , mixing of $K^\pi=3^-$ and 4^- bands 3-67198
- ^{177}Lu decay to ^{177}Hf , angular correlations meas. 3-62983
- $^{177}\text{Lu} \rightarrow ^{177}\text{Hf}$ β -decay, meas. of half-life of 249.7 keV level in ^{177}Hf 3-49198
- ^{178}Lu , from ^{178}Yb decay and $^{176}\text{Yb}(t, n)$ reaction, half-life, β and γ energies and coincidences, log ft. values 3-67276
- ^{161m}Lu , from $^{148}\text{Sm}(^{19}\text{F}, 6n)$, energy levels, observed γ -ray transition 3-54423
- Nd , $A=142-150$, total neutron cross section meas., deformation effects, optical model (*Russian*) 3-52178
- $^{150}\text{Nd}(n, \gamma)^{151}\text{Nd}$, activation resonance integral meas. 3-54467
- ^{151}Nd , decay, level struct. determ. for ^{151}Pm 3-43220
- ^{151}Nd production from $^{150}\text{Nd}(n, \gamma)^{151}\text{Nd}$, activation resonance integral meas. 3-54467
- Os , $A=182, 184, 186$ and 188 , backbending and forking of yrast levels 3-71051
- ^{178}Os , from $^{154}\text{Sm}(^{28}\text{Si}, 4n)$, $E=104$ MeV, deduced levels, feeding times by recoil-distance Doppler shift measurements 3-60215
- ^{182}Os , ground state levels and γ -vibrational bands 3-67194
- ^{182}Os beta decay to ^{182}Re , gamma and internal conversion meas. 3-49227
- ^{183}Os ground-state rotational band, back- and forwardbending, moment of inertia 3-74498
- ^{184}Os , ground state levels and γ -vibrational bands 3-67194
- ^{184}Os level structure from ^{184}Ir decay and $^{185}\text{Re}(p, 2n\gamma)$ reaction 3-62941
- ^{185}Os decay, orientation obs., γ -ray ang. distrib. 3-40452
- ^{186}Os , ground state levels and γ -vibrational bands 3-67194
- ^{187}Os , ^{189}Os , neutron resonance spin determ. from Monte Carlo simulation of decay 3-57519
- ^{188}Os , ground state levels and γ -vibrational bands 3-67194
- ^{189}Os , populated by ^{189}Re decay, excited level scheme, spin and parity assignments 3-54432
- ^{191}Os decay, orientation obs., X-ray ang. distrib. 3-40452
- ^{193}Os decay, orientation obs., X-ray ang. distrib. 3-40452
- ^{151}Pm , level struct., determ. from ^{151}Nd decay 3-43220
- $^{151}\text{Pm} \rightarrow ^{151}\text{Sm}$, γ -ray spectra and level scheme 3-78244
- ^{173}Pt , α -particle energy 3-54499
- ^{180}Pt , effect of quadrupole pairing interaction on $J^\pi=0^+$ vibr. 3-78256
- ^{182}Pt , effect of quadrupole-pairing interaction on $J^\pi=0^+$ vibr. 3-78256
- ^{184}Pt , effect of quadrupole-pairing interaction on $J^\pi=0^+$ vibr. 3-78256
- ^{184}Pt , two-parameter description of rotational energies 3-74496
- ^{186}Pt , effect of quadrupole-pairing interaction on $J^\pi=0^+$ vibr. 3-78256
- ^{187}Pt , decay scheme determ., nature of excited levels in ^{187}Ir 3-71049

nuclei with $150 \leq A \leq 189$ continued

- ^{188}Pt , effect of quadrupole-pairing interaction on $J^\pi=0^+$ vibr. 3-78256
- $^{179}\text{Re} \rightarrow ^{179}\text{W}$, γ -ray spectra and γ - γ coincidence meas., study of three-quasiparticle states in ^{179}W (*Russian*) 3-52089
- ^{182}Re production from ^{182}Os beta-decay 3-49227
- ^{183}Re , orientation in Fe matrix, γ -ray anisotropy and magnetic hyperfine interaction 3-60110
- ^{183}Re mag. mom. meas. by nuc. orientation 3-49107
- ^{184}Re , orientation in Fe matrix, γ -ray anisotropy and magnetic hyperfine interaction 3-60110
- ^{184}Re mag. mom. meas. by nuc. orientation 3-49107
- $^{184}\text{Re} \rightarrow ^{184}\text{W}$, internal conversion electron spectrum, relative intensities of K- and γ -lines (*Russian*) 3-74523
- ^{185}Re , ^{187}Re , neutron resonance spin determ. from Monte Carlo simulation of decay 3-57519
- $^{185}\text{Re}(p, 2n\gamma)^{186}\text{Os}$, in-beam spectroscopy, ^{184}Os level structure 3-62941
- $^{185}\text{Re}(p, 2n\gamma)^{184}\text{Os}$, $^{185}\text{Re}(p, 4n\gamma)^{182}\text{Os}$, $E_p=14$ and 37 MeV, ^{184}Os and ^{182}Os levels characteriz. 3-67194
- ^{186}Re , 1 GeV proton bombardment, angular distribution of fission fragments, momentum transfer (*Russian*) 3-57547
- ^{187}Re , 134 keV transition, penetration effects 3-49190
- ^{187}Re in stars, enhanced β -decay rate rel. to recycling of r-process elements and age of Galaxy 3-42113
- ^{187}Re produced in ^{187}W decay, orientation studies, transition parameters 3-40452
- $^{187}\text{Re}(p, 2n\gamma)^{186}\text{Os}$, $^{187}\text{Re}(p, 4n\gamma)^{184}\text{Os}$, $E_p=14$ and 37 MeV, ^{186}Os and ^{184}Os levels characteriz. 3-67194
- $^{189}\text{Re} \rightarrow ^{189}\text{Os}$, product excited level scheme, spin and parity assignments 3-54432
- ^{184m}Re mag. mom. meas. by nuc. orientation 3-49107
- Sm , $A=144-154$, total neutron cross section meas., deformation effects, optical model (*Russian*) 3-52178
- Sm , $A=150, 152, 154, 0.8-15$ MeV, neutron total cross section differences, nuclear deformation effects 3-60188
- Sm , $A=152, 154$, Coulomb excitation, quadrupole and hexadecapole transition moments 3-49201
- Sm isotopes, X-ray isotope shifts and variations in charge radii 3-67662
- $^{148}\text{Sm}(^{19}\text{F}, 6n)^{161m}\text{Lu}$, 105 to 145 MeV, γ -ray transition observed, ^{161}Lu levels deduced 3-54423
- ^{150}Sm , ^{152}Sm , Coulomb excitation, determ. of static quadrupole moments of first excited states 3-49113
- ^{150}Sm , Coulomb excitation by ^{160}O and ^{32}S , quadrupole moment of first 2^+ state by reorientation precession technique 3-45942
- ^{150}Sm , energy level calculations in phenomenological collective model (*Russian*) 3-71066
- ^{150}Sm , quadrupole interaction on recoil through Sm , calc. of electric field gradient 3-45943
- $^{150}\text{Sm}(^{20}\text{Ne}, 4n)^{166}\text{Hf}$, $E=93$ MeV, ^{166}Hf deduced levels, feeding times by recoil-distance Doppler shift measurements 3-60215
- $^{150}\text{Sm}(d, p)^{151}\text{Sm}$, transfer 1 values, ^{151}Sm levels 3-74594
- ^{151}Sm levels populated in ^{151}Pm decay 3-78244
- ^{151}Sm levels populated in (d, t), (d, p) and ($^3\text{He}, \alpha$) reactions 3-74594
- ^{152}Sm , ^{154}Sm , Coulomb excitation, meas. of hexadecapole transition moments and $M(E2; 0 \rightarrow 2)$ 3-49195
- ^{152}Sm , ^{154}Sm , Coulomb excitation of 2^+ and 4^+ levels, determ. of E4 moments 3-49202
- ^{152}Sm , E4 matrix elements 3-63001
- ^{152}Sm , inelastic scattering of polarised protons, identification of collective modes 3-60101
- ^{152}Sm , two-parameter description of rotational energies 3-74496
- $^{152}\text{Sm}(^{20}\text{Ne}, 4n)^{168}\text{Hf}$, $E=86$ MeV, ^{168}Hf deduced levels, feeding times by recoil-distance Doppler shift measurements 3-60215
- $^{152}\text{Sm}(^3\text{He}, \alpha)^{151}\text{Sm}$, transfer 1 values, ^{151}Sm levels 3-74594
- $^{152}\text{Sm}(d, t)^{151}\text{Sm}$, transfer 1 values, ^{151}Sm levels 3-74594
- ^{154}Sm , deformed, transition from vibrational ^{148}Sm , boson expansion technique 3-49102
- ^{154}Sm , E4 matrix elements 3-63001
- $^{154}\text{Sm}(n, n'\gamma)$, 1.1 to 2.3 MeV, determ. energy level structure, spin and parity from γ -ray spectra 3-67196
- $^{154}\text{Sm}(^{20}\text{Ne}, 4n)^{170}\text{Hf}$, 86 MeV, feeding times for population of quasi-rotational bands in ^{170}Hf 3-60215
- $^{154}\text{Sm}(^{28}\text{Si}, 4n)^{178}\text{Os}$, $E=104$ MeV, ^{178}Os deduced levels, feeding times by recoil-distance Doppler shift measurements 3-60215
- $^{154}\text{Sm}(p, t)^{152}\text{Sm}$, finite range DWBA calcs. 3-78327
- ^{157}Sm 8 min. nuclide, decay phenomena 3-62995
- Ta , neutron total cross section, 1.0 to 2.0 MeV, optical model comparison 3-54474
- Ta , neutron total cross section fluctuations, 1.0 to 2.0 MeV, compound nucleus explanation 3-54475
- $^{151}\text{Ta}(p, n\gamma)^{150}\text{W}$, $x=2, 4$, $A=180, 178$, de-excitation, ground state rot. bands population 3-49191
- $^{173}\text{Ta} \rightarrow ^{173}\text{Hf}$ decay, energy levels of ^{173}Hf 3-40421
- ^{177}Ta , populated in ^{177}W decay, $\gamma\gamma$ coincidence meas. (*Russian*) 3-74521
- ^{177}Ta levels, half lives deduced, comparison with Nilsson model, hindrance factors 3-54422
- ^{181}Ta , (p, n) analogue transition, cross-section meas. 3-40491
- ^{181}Ta , half-life of 482 keV level 3-54419
- ^{181}Ta , interpretation of nucleon emission following proton bombardment at energies of tens of MeV 3-52182
- ^{181}Ta , irradiated by ^{40}Ar , ^{84}Kr , ^{136}Xe ions, product yields, mechanism 3-78350
- ^{181}Ta , PAC spectrum, in RbHfF_6 3-79957
- ^{181}Ta , quadrupole moment of 482 keV state meas. by time differential PAC in Re metal 3-52078
- ^{181}Ta 482 keV transition, short-range correlations, effective charge, parity violation, polarisation 3-57490
- ^{181}Ta in Hf , electric quadrupole interaction as function of annealing temp. 3-55505
- $^{181}\text{Ta}(^4\text{He}, xn)^{185-x}\text{Re}$, high angular momentum, excitation functions and photon emission, compound nucleus mechanism 3-63083
- $^{181}\text{Ta}(n, n_0)^{181}\text{Ta}$, 14.8 MeV, meas. differential cross sections, the Schwinger prediction 3-71108
- ^{182}Ta , PAC meas. on γ - γ cascades rel. to g-factor determ. of $K^\pi=2^-$ band in ^{182}W 3-67184
- ^{184}Ta , excited level struct., rel. to ^{184}Hf decay scheme 3-60129
- ^{154}Tb , determ. branching ratios and half lives of the three isomeric states, spin assignments 3-67263

nuclei with $150 \leq A \leq 189$ continued

- ¹⁵⁹Tb(⁴⁰Ar, xn)¹⁹⁹-²¹Bi, E < 300 MeV, excitation functions 3-54499
¹⁵⁹Tb(n, α), E_n = 14 MeV, knock-on mechanism 3-63044
¹⁶⁰Tb level scheme 3-43178
¹⁶¹Tb levels populated in ¹⁶¹Gd β⁻ decay 3-43219
 Tm to Hg short-lived neutron deficient nuclei, spectroscopic investigation of half-life (*Russian*) 3-52142
¹⁶⁸Tm rot. band obs. in ¹⁶⁹Tm(d, t)¹⁶⁸Tm 3-63069
¹⁶⁹Tm, determ. of magnetic moments of 316, 379 keV excited states (*Japanese*) 3-74481
¹⁶⁹Tm, n.m.r. in thulium ethyl sulphate 3-64577
¹⁶⁹Tm(α, 2n)¹⁷¹Lu, γ radiation and conversion electrons, rot. bands of ¹⁷¹Lu 3-62939
¹⁶⁹Tm(α, nnp)¹⁷¹Lu, 23.27 MeV, γ-ray obs., level scheme determ. 3-60077
¹⁶⁹Tm(d, t)¹⁶⁸Tm, E_d = 17 MeV, rot. bands of ¹⁶⁸Tm 3-63069
¹⁶⁹Tm(n, α), E_n = 14 MeV, knock-on mechanism 3-63044
¹⁶⁹Tm(n, p), background cross section and correlation between partial widths, relation 3-54454
¹⁶⁹Tm(n, p), resonance parameters and capture cross section from neutron time-of-flight meas. 3-49260
¹⁶⁹Tm(p, xnp)¹⁷¹Lu, X = 2, 4, A = 168, 166, de-excitation, ground state rot. bands population 3-49191
 W, 24 GeV proton irradiation, meas. of cumulative and independent yields of lanthanides 3-40486
 W, A = 182, 184, 186, Coulomb excitation with ¹⁶⁰O, meas. of quadrupole interaction in Te crystal (*German*) 3-49187
 W emulsion nuclei, 200 GeV proton interactions 3-71024
 W even-even isotopes produced in (p, xnp) reactions, de-excitation 3-49191
¹⁶²W from ¹⁴⁴Sm(²³Mg, 6n), α-decay 3-57498
¹⁶³W, from ¹⁴⁴Sm(²⁴Mg, 5n), and ¹⁴⁷Sm(²⁴Mg, 8n), α-decay, half lives 3-57498
¹⁶⁴W from ¹⁴⁴Sm(²⁴Mg, 4n) and ¹⁴⁷Sm(²⁴Mg, 7n), α-decay and half lives 3-57498
¹⁷⁷W → ¹⁷⁷Ta, γγ coincidence meas., determ. of ¹⁷⁷Ta level scheme (*Russian*) 3-74521
¹⁷⁹W, three quasiparticle states populated in ¹⁷⁹Re decay, microscopic model (*Russian*) 3-52089
¹⁸⁰W, atomic mass and spacing of ground-state levels 3-67174
¹⁸⁰W, Mossbauer determ. for 2⁺ state g-factor 3-60086
¹⁸⁰W/¹⁸²W, ratio of quadrupole moments of 2⁺ states 3-60086
¹⁸¹W, excited states populated by ¹⁷⁹Hf(α, 2n) and ¹⁸⁰Hf(α, 3n) reactions, effects of Coriolis mixing 3-60079
¹⁸²W, from ¹⁸³W(d, t) and ¹⁸³W(3He, α), two quasiparticle states and collective excitations 3-57475
¹⁸²W, g factor meas. rel. to study of K^π = 2⁻ band 3-67184
¹⁸²W, mag. mom. of K^π = 2⁻ band, γ-γ correlation study 3-49109
¹⁸²W, spacing of ground-state levels 3-67174
¹⁸²W(α, 2np)¹⁸⁴Os, E_α = 30 MeV, ¹⁸⁴Os levels characteriz. 3-67194
¹⁸²W(t, p)¹⁸⁴W, 20 MeV, cross sections, angular distributions, ¹⁸⁴W deduced levels 3-63064
¹⁸³W, mixing ratios from nuclear orientation meas. on ¹⁸³Re, ¹⁸⁴Re 3-60110
¹⁸³W(3He, α)¹⁸²W 20.3 MeV, ¹⁸²W two quasiparticle states and collective excitations 3-57475
¹⁸³W(d, p)¹⁸⁴W, 12.1 MeV, ¹⁸⁴W two quasiparticle states and collective excitations 3-57475
¹⁸³W(d, t)¹⁸²W, 12.1 MeV, ¹⁸²W two quasiparticle states and collective excitations 3-57475
¹⁸⁴W, from ¹⁸²W(t, p), 20 MeV, deduced levels 3-63064
¹⁸⁴W, from ¹⁸³W(d, p), two quasiparticle states and collective excitations 3-57475
¹⁸⁴W, mixing ratios from nuclear orientation meas. on ¹⁸³Re, ¹⁸⁴Re 3-60110
¹⁸⁴W(α, 2np)¹⁸⁶Os, E_α = 30 MeV, ¹⁸⁶Os levels characteriz. 3-67194
¹⁸⁵W diffusion in swaged W powder, autoradiography, 1300-1900°C (*Hungarian*) 3-72987
¹⁸⁶W recoil implanted in single crystals, nucl. quadrupole precession, PAC obs. 3-41462
¹⁸⁶W(α, 2np)¹⁸⁸Os, E_α = 30 MeV, ¹⁸⁸Os levels characteriz. 3-67194
¹⁸⁶W(α, 8n)¹⁸²Os, 106 MeV, γ-decay to ground state rotational band in ¹⁸²Os 3-74498
¹⁸⁶W(p, 2p), high-energy excitation function, calc. 3-46027
¹⁸⁷W decay, orientation obs., γ-ray ang. distrib. 3-40452
 Yb, even isotopes, γ-ray spectroscopic study, single-line Mossbauer absorption, Yb levels, deduced isomer shifts 3-60109
 Yb even-even isotopes produced in (p, xnp) reactions, de-excitation 3-49191
 Yb isotopes, X-ray isotope shifts and variations in charge radii 3-67662
 Yb(³He, d), rot. bands of ¹⁷¹Lu 3-62939
²Yb(α, xn), A = 171, 174, 176, x = 2, 3, 20-43 MeV, population of rotational bands in odd Hf nuclei 3-40417
¹⁶⁸Yb, γ-band population by indirect (p, t) processes 3-46030
¹⁶⁸Yb, lifetime, struct. of levels above 1.5 MeV, meas., anal. 3-78250
¹⁶⁹Yb energy level scheme, study by ¹⁶⁹Lu decay obs. (*Russian*) 3-52090
¹⁷⁰Yb in YbB₂, TmB₂, Mossbauer spectroscopy, Debye-Ealler factors (*French*) 3-72552
¹⁷¹Yb(d, 2n)¹⁷³Lu 13.5 MeV, ¹⁷³Lu half lives deduced, comparison with Nilsson model, hindrance factors 3-54422
¹⁷²Yb doublet splitting in even A deformed nuclei between excited 2 quasiparticle states 3-57478
¹⁷³Yb(d, nn)¹⁷³Lu, 13.5 MeV, γ-ray obs., level scheme determ. 3-60077
¹⁷³Yb(d, 2n)¹⁷³Lu 13.5 MeV, ¹⁷³Lu half lives deduced 3-54422
¹⁷³Yb(n, p)¹⁷⁴Yb, gamma decay of excited K = 0 rotational bands in ¹⁷⁴Yb 3-74533
¹⁷³Yb(p, np)¹⁷³Lu, γ-ray obs., level scheme determ. 3-60077
¹⁷⁴Yb, Coulomb excitation, meas. of hexadecapole transition moments and M(E2; 0 → 2) 3-49195
¹⁷⁴Yb pop. in ¹⁷³Yb(n, p) reaction, gamma decay of excited K = 0 rotational bands 3-74533
¹⁷⁵Yb, orientation in Au and Ag, determ. from γ-ray anisotropy 3-47180
¹⁷⁶Yb(p, t)¹⁷⁴Yb, 16 MeV polarised protons, meas. of vector analysing power and differential cross section 3-49257

nuclei with $150 \leq A \leq 189$ continued

- ¹⁷⁸Yb decay, β and γ energies and coincidences, log ft. values, deduced ¹⁷⁸Lu levels 3-67276
¹⁸²Yb, charge and mass distrib. calc. by hyperspheric functions method, reln. to superheavy nuclei (*Russian*) 3-74479
 Yb(α, t), rot. bands of ¹⁷¹Lu 3-62939
 nuclei with $190 \leq A \leq 219$
 excited nuclei, statistical theory of decay, competition between fission and evaporation 3-43263
 N = 82 isotopes, interaction between collective and quasi-particle excitation, energies, wave function, B(E2) values (*Russian*) 3-74514
 Z ≥ 60, nucl. energy spectrum near 1 GeV/amu, new cosmic ray source evidence 3-53581
²⁰⁷At, from ²⁰⁹Bi(π⁺, π⁻ + 2n), cross section (*Russian*) 3-71129
²⁰⁹At levels populated in electron capture decay of ²⁰⁹Rn, transition and spin assignments 3-74542
²¹⁰At, electron capture decay to levels in ²¹⁰Po, γ-γ delayed coincidence meas. 3-45925
²¹¹At, anomalous g-factor meas. by DPAD method 3-45961
²¹¹At, excitation functions and recoil ranges from ⁸⁴Kr-induced reactions on ²⁰⁹Bi 3-63084
²¹¹At, g-factor meas. of 21/2⁻ state by DPAD method 3-49093
²¹¹At, possible formation in π⁺ double charge exchange reactions with ²⁰⁹Bi (*Russian*) 3-71129
 Au, breakup of deuterons, 7-12 MeV, meas. angular correlations, breakup cross section 3-60204
 Au, deuteron disintegration in Coulomb field, energy and angular distrib. of products (*Russian*) 3-67340
 Au, neutron absorption cross sections, 4 to 47 A neutrons 3-78333
¹⁹⁰Au, A = 196, 198, 200, magnetic moments of 12⁻ states, low-temp. orientation expts. 3-45952
¹⁹⁰Au → ¹⁹⁰Pt decay scheme assignments 3-67278
¹⁹⁵Au(183d) → ¹⁹⁵Pt, decay schemes, ¹⁹⁵Pt excited states, spin and parity assignments 3-52137
¹⁹⁶Au, oriented, n.m.r., γ-ray anisotropy obs. 3-40453
¹⁹⁷Au, (p, n) analogue transition, cross-section meas. 3-40491
¹⁹⁷Au, irradiated by ⁴⁰Ar, ⁸⁴Kr, ¹³⁶Xe ions, product yields, mechanism 3-78350
¹⁹⁷Au, lifetime Mossbauer gamma ray, linewidth, meas., Au source in differing chemical environments 3-67260
¹⁹⁷Au, photo-proton emission, 80 to 260 MeV, from 400 MeV bremsstrahlung 3-74563
¹⁹⁷Au, thermal neutron radiation damage obs., Mossbauer effect 3-79958
¹⁹⁷Au fission induced by 70-200 MeV protons, cross section and angular anisotropy (*Russian*) 3-40523
¹⁹⁷Au(¹²C, light particles), E = 125 MeV, study of emitted light particles and radioactive products 3-71126
¹⁹⁷Au(¹⁶O, light particles), E = 135 and 166 MeV, study of emitted light particles and radioactive products 3-71126
¹⁹⁷Au(³He, ³He), cross section analysis, obs. of new giant resonance 3-63077
¹⁹⁷Au(d, p), 100 MeV, diffraction model, effect of nuclear boundary spread and Coulomb interaction (*Russian*) 3-74548
¹⁹⁷Au(d, p, xn)¹⁹⁸-²⁰⁰Au, 25-86 MeV, excitation function meas., equilibrium statistical and hybrid models 3-57532
¹⁹⁷Au(d, xn)¹⁹⁹-²⁰⁰Au, 25-86 MeV, excitation function meas., equilibrium statistical and hybrid models 3-57532
¹⁹⁷Au(γ, γ)^{197m}Au, 100-800 MeV, yield curves deduced cross sections, ^{197m}Au measured half life, E_γ 3-67308
¹⁹⁷Au(n, p), E_n = 14 MeV, proton spectra anal. 3-67319
¹⁹⁸Au, oriented, n.m.r., γ-ray anisotropy obs. 3-40453
¹⁹⁸Au isomeric 115.2 keV transition, γ-ray meas., multipolarities 3-43209
^{200m}Au, oriented, n.m.r., γ-ray anisotropy obs. 3-40453
 Au(d, pn)Au, disintegration at 12 and 10.5 MeV, energy-angle correlations, DWBA analysis (*German*) 3-49264
 Bi, deuteron disintegration in Coulomb field, energy and angular distrib. of products (*Russian*) 3-67340
 Bi, usefulness in predictions of element 115 (eka-Bi) props. 3-80571
 Bi radioactive isotopes, low temperature orientation in ferromagnetic BiMn, nuclear structure studies 3-46008
²⁰⁴Bi, high-spin isomeric state populated by heavy-ion and α-particle induced reactions 3-49152
²⁰⁵Bi, fragmentation of proton levels from (³He, d) and (α, t) reactions on ²⁰⁴Pb 3-63080
²⁰⁶Bi, 10⁻, 0.88 ms isomeric state, g-factor meas. rel. to magnetic moment of shell model states 3-71042
²⁰⁶Bi, γ-ray distrib. meas., oriented in Ni, transition determ. of ²⁰⁶Pb 3-78286
²⁰⁶Bi, low-lying one-proton three-neutron-hole states 3-52135
²⁰⁷Bi, fragmentation of proton levels from (³He, d) and (α, t) reactions on ²⁰⁶Pb 3-63080
²⁰⁷Bi, product of ²⁰⁹Bi(p, t), 17.8 MeV, weak coupling structure 3-57523
²⁰⁷Bi decay, relative intensity and internal conversion coeff. meas. 3-52123
²⁰⁸Bi, lifetimes and M1 transitions, implications for configuration mixing calcs. 3-45998
²⁰⁹Bi, ⁸⁴Kr-induced transfer reactions, excitation functions and recoil ranges of residual nuclei 3-63084
²⁰⁹Bi, 1 GeV proton bombardment, angular distribution of fission fragments, momentum transfer (*Russian*) 3-57547
²⁰⁹Bi, 500 MeV elastic magnetic electron scattering, eikonal approx. 3-49246
²⁰⁹Bi, (p, n) analogue transition, cross-section meas. 3-40491
²⁰⁹Bi, calc. of magnetic properties using linear response theory of finite Fermi systems 3-49129
²⁰⁹Bi, magnetic moment calc. using Kuo's effective interaction 3-49127
²⁰⁹Bi, polarised, magnetic hyperfine structure in muonic atom, coupling consts. anomalous g-factor 3-46216
²⁰⁹Bi, radiative proton capture cross sections, 10 to 50 MeV, exciton function 3-78318
²⁰⁹Bi, single-particle strengths using Dyson eqn. rel. to finite Fermi systems 3-62963
²⁰⁹Bi fission, induced by 1 GeV protons, angular correlations of mass and energy distrib. of fragments (*Russian*) 3-40524

nuclei with $190 \leq A \leq 219$ continued

²⁰⁹Bi(α , nn)²¹¹At, population of isomeric three proton state in ²¹¹At, anomalous of g-factor determ. 3-45961
²⁰⁹Bi(α , nn)²¹¹At, population of 21/2⁻ state in ²¹¹At, g-factor determ. 3-49093
²⁰⁹Bi(d, py) reaction, obs. gamma decay of ²¹⁰Bi excited states, shell model interpretation 3-67259
²⁰⁹Bi(e, e), 250 and 500 MeV, meas. of cross section, charge density and difference with ²⁰⁸Pb 3-52172
²⁰⁹Bi(n, 2n)^{208m}Pb, isomeric cross section at 14.8 MeV 3-54468
²⁰⁹Bi(n, α), thermal neutron energies, cross sections determ. 3-43244
²⁰⁹Bi(p, 2n)²⁰⁸Po, cross section and recoil range 3-71105
²⁰⁹Bi(p, n)²⁰⁹Bi, quasielastic reaction, macroscopic charge-independent anal. and coupled Lane eqn. soln. 3-67333
²⁰⁹Bi(p, n)²⁰⁹Po, cross section and recoil range 3-71105
²⁰⁹Bi(p, t)²⁰⁷Bi, E_p = 17.8 MeV, weak coupling structure in ²⁰⁷Bi. 3-57523
²⁰⁹Bi(π^+ , π^- + xn)^{209-*}At, cross section for formation of ²⁰⁷At (*Russian*) 3-71129
²¹⁰Bi, gamma decay of excited states, populated in ²⁰⁹Bi(d, py) reaction, shell model interpretation 3-67259
²¹⁰Bi, neutron resonances, particle-vibration calc., ²⁰⁹Pb intrinsic doorway 3-78267
²¹¹Bi, 7/2⁻ first excited state, semi-realistic shell model calc. 3-78254
¹⁹⁴Hf, half-life meas. 3-52143
Hg, muonic, test for vacuum polarisation correction to 5-4 transitions (*German*) 3-52302
Hg, neutron total cross section, 1.0 to 2.0 MeV, optical model comparison 3-54474
Hg, neutron total cross section fluctuations, 1.0 to 2.0 MeV, compound nucleus explanation 3-54475
Hg isomers, precision magnetic moment determ., hyperfine-structure anomalies, optical pumping expt. 3-62933
Hg isotopes, distribution of nuclear magnetisation 3-78241
Hg neutron deficient isotopes, self-consistent calc. of possible shape transition 3-67180
¹⁹⁸Hg, 412 keV pure E2 transition, K-shell conversion coefficient by beta-ray spectrometer 3-67253
¹⁹⁸Hg(n, n), cross section near energy threshold, deviations from statistical model (*Russian*) 3-74568
¹⁹⁹Hg, g-factor of 208 keV 3/2⁻ state, meas. by ion implantation perturbed angular correlation technique 3-45970
¹⁹⁹Hg n.m.r. spectroscopy, pulse Fourier transform technique 3-59615
²⁰⁰Hg bubble configuration determ. using Hartree Fock methods 3-78274
²⁰⁰Hg decay scheme, spins and multipolarities 3-40453
²⁰⁰Hg(n, n)²⁰⁰Hg, 14.8 MeV, meas. differential cross sections, the Schwinger prediction 3-71108
²⁰⁰Hg(n, n), cross section near energy threshold, deviations from statistical model (*Russian*) 3-74568
²⁰¹Hg, n.m.r. lineshape in optical pumping expt. (*French*) 3-74804
²⁰²Hg(n, n), cross section near energy threshold, deviations from statistical model (*Russian*) 3-74568
²⁰³Hg, optically aligned, γ -radiation emission, anisotropy and time modulation 3-46000
²⁰⁴Hg(α , 3n)²⁰⁵Pb, high spin three neutron hole states of ²⁰⁵Pb 3-52100
²⁰⁴Hg(p, nnn)²⁰²Tl, 28 MeV, population of 7⁺ isomeric state in ²⁰²Tl, g factor determ. 3-49086
^{199m}Hg, precision magnetic moment determ., hyperfine-structure anomalies, optical pumping expt. 3-62933
¹⁹¹Ir, h.f.s. obs. of ⁴F_{9/2} atomic ground state, ABMR meas. 3-67191
¹⁹¹Ir, low lying levels, core-excitation model approach 3-71046
¹⁹¹Ir, low-lying level struct. and e.m. props. 3-62953
¹⁹¹Ir(n, γ)¹⁹²Ir, gamma-ray spectra meas. and analysis 3-49248
¹⁹²Ir, electron capture and β^+ decay to ¹⁹²Os, β^- decay to ¹⁹²Pt levels 3-40414
¹⁹²Ir decay, relative intensity and internal conversion coeff. meas. 3-52123
¹⁹²Ir \rightarrow ¹⁹²Os, delayed coincidence meas. of half-life of ¹⁹²Os excited states 3-60111
¹⁹²Ir \rightarrow ¹⁹²Pt, E0/E2 and E2/M1 multipole mixing amplitudes of γ -transitions, meas. 3-46002
¹⁹³Ir, h.f.s. obs. of ⁴F_{9/2} atomic ground state, ABMR meas. 3-67191
¹⁹³Ir, low lying levels, core excitation model approach 3-71046
¹⁹³Ir, low-lying level struct. and e.m. props. 3-62953
¹⁹³Ir(2, 3h) \rightarrow ¹⁹⁵Pt, decay scheme, ¹⁹⁵Pt excited states, spin and parity assignments 3-52137
¹⁹⁵Ir(3, 7h) \rightarrow ¹⁹⁵Pt, decay scheme, ¹⁹⁵Pt excited states, spin and parity assignments 3-52137
¹⁹⁸Ir existence, evidence from γ -transition obs. on ¹⁹⁸Pt(n, p) 3-63008
Ir(n, γ)¹⁹²Ir + ¹⁹⁴Ir, gamma-ray spectra meas. and analysis 3-49248
¹⁹⁰Os, ¹⁹²Os muonic, broadening of 2⁻O⁺ transition, determ. of hyperfine splitting (*German*) 3-52302
¹⁹⁰Os, ¹⁹²Os muonic atoms, magnetization distrib. of single-particle states and 2⁺ rotational states 3-49209
¹⁹²Os, effects on γ -instability on muonic X-rays 3-60112
¹⁹²Os, energy level study 3-40414
¹⁹²Os, meas. T_{1/2} of excited states using delayed coincidence technique for ¹⁹²Ir β -decay 3-60111
²⁰⁸Pb(α , t)²⁰⁶Pb, E _{α} = 17.8 MeV, ²⁰⁷Bi struct. rel. to ²⁰⁶Pb 3-57523
Pb, A = 206-208, neutron induced gamma-ray producing reactions, cross-section calcs. 3-57525
Pb, avalanches induced by charged and neutral cosmic ray particles (*Russian*) 3-65609
Pb, breakup of deuterons, 7-12 MeV, meas. angular correlations, breakup cross section 3-60204
Pb, deuteron disintegration in Coulomb field, energy and angular distrib. of products (*Russian*) 3-67340
Pb, elastic and inelastic scattering of Fe capture gamma-rays, energy level study 3-49241
Pb, elastic scattering of low-energy pions and muons, determ. of charge radius and neutron matter radius 3-71128
Pb, fast neutron small-angle scattering, elastic cross-section meas. 3-74579

nuclei with $190 \leq A \leq 219$ continued

Pb, induced by 12.2 GeV protons, binary and ternary fission 3-52216
Pb, neutron production by cosmic ray high energy muons, depth dependency, e.m. interaction explanation (*Russian*) 3-61621
Pb, nucleon cosmic ray interactions at mountain altitudes, 600-10000 GeV, integral energy spectrum (*Russian*) 3-69781
Pb and ²⁰⁸Pb, π^- , π^+ reaction cross sections, 584 to 1856 MeV and 713 to 1447 MeV, deduced neutron density 3-54507
Pb deuteron cross-section for stripping and dissociation, 2.7 GeV/c, measurement 3-78344
Pb isotopes, nucl. polarization and muonic X-ray spectrum 3-63351
Pb isotopes, X-ray isotope shifts and variations of charge radii 3-67662
Pb muonic atom, limit for hypothetical scalar muon hadron interaction constant (*Russian*) 3-60394
Pb region, effective E2 charges, particle-oscillating core coupling, polarisation 3-45924
Pb region, electric multipole moments and transition probabilities of single-particle states 3-43174
Pb region, g-factors of high-spin shell model states, summary 3-45950
Pb-region, magnetic moments of single particle states, calc. including mesonic exchange currents 3-52080
Pb(³He, xn + γ), E = 28-30 MeV, stroboscopic resonance method, g-factors for Po isotopes 3-71041
²⁰⁸Pb A = 206-208, fission induced by 70-200 MeV protons, cross section and angular anisotropy (*Russian*) 3-40523
¹⁹⁴Pb isomeric state behaviour, γ - γ coincidence obs. 3-62992
¹⁹⁶Pb isomeric state behaviour, γ - γ coincidence obs. 3-62992
¹⁹⁸Pb isomeric state behaviour, γ - γ coincidence obs. 3-62992
²⁰⁰Pb isomeric state behaviour, γ - γ coincidence obs. 3-62992
²⁰²Pb, asymmetry in fission, symmetric fission preference 3-43264
²⁰⁴Pb(³He, d)²⁰⁵Bi, fragmentation of proton levels of ²⁰⁵Bi 3-63080
²⁰⁴Pb(α , 2n)²⁰⁶Po, mag. mom. meas. of [(π h_{9/2})²] π ⁺ states 3-49088
²⁰⁴Pb(α , t)²⁰⁵Bi, fragmentation of proton levels of ²⁰⁵Bi 3-63080
²⁰⁵Pb, high spin three neutron hole states of configurations, containing the 1i_{3/2} orbital 3-52100
²⁰⁶Pb, ²⁰⁷Pb, one-nucleon transfer reaction, microscopic form factor 3-43246
²⁰⁶Pb, 120 μ s 2.2 MeV state perturbation γ -ray meas. on ²⁰⁶Bi oriented in Ni 3-78286
²⁰⁶Pb, g-factor of 12⁺ isomeric state populated in ²⁰⁴Hg(α , 2n) reaction 3-49087
²⁰⁶Pb, product of ²⁰⁸Pb(p, t), 17.8 MeV, relationship to structure of ²⁰⁷Bi, weak coupling structure of ²⁰⁷Bi 3-57523
²⁰⁶Pb(³He, d)²⁰⁷Bi, fragmentation of proton levels of ²⁰⁷Bi 3-63080
²⁰⁶Pb(α , t)²⁰⁷Bi, fragmentation of proton levels of ²⁰⁷Bi 3-63080
²⁰⁶Pb(n, 2n)^{205m}Pb, isomeric cross section at 14.8 MeV 3-54468
²⁰⁶Pb(n, γ), s-wave doorway state in photon channel form capture cross section measurements 3-57524
²⁰⁸Pb(n, n), cross section near energy threshold, deviations from statistical model (*Russian*) 3-74568
²⁰⁷Pb, ²⁰⁸Pb, magnetic moments of first excited states meas. by $\gamma\gamma$ -IPAC technique 3-45960
²⁰⁷Pb, ²⁰⁸Pb, calc. of magnetic properties using linear response theory of finite Fermi systems 3-49129
²⁰⁷Pb, (1/2)⁺ doorway resonance, nuclear spreading width in particle-vibration model 3-74492
²⁰⁷Pb, angular correlation studies 3-49219
²⁰⁷Pb, E2 effective charge in $\nu f_{7/2}^{-1} - \nu f_{5/2}^{-1}$ transition, meas. using polarised Bi 3-46008
²⁰⁷Pb, η -meson photoproduction, 2 GeV, cross section meas. 3-78311
²⁰⁷Pb, from ²⁰⁸Pb(d⁺, t) 12.3 MeV, vector analysing power, differential cross section, ²⁰⁷Pb deduced levels, DWBA analysis 3-60199
²⁰⁷Pb, neutron scatt. structure study, 13-17 MeV (*Hungarian*) 3-43239
²⁰⁷Pb, single-particle strengths using Dyson eqn. rel. to finite Fermi systems 3-62963
²⁰⁷Pb, spin-rotation as dominant relax. mechanism in aq. Pb(ClO₄)₂ soln. 3-58442
²⁰⁷Pb proton elastic and inelastic scattering, 11.1-14.4 MeV, decay amplitudes of ²⁰⁸Pb(O⁺) analogue resonance 3-49253
²⁰⁷Pb(n, 2n)^{206m}Pb, isomeric cross section at 14.8 MeV 3-54468
²⁰⁷Pb(n, n)²⁰⁷Pb, 14.8 MeV, meas. differential cross sections, the Schwinger prediction 3-71108
²⁰⁷Pb(n, n)²⁰⁷Pb, meas. differential cross section and asymmetries, incident polarised neutrons from ²(d, n)³He 3-71109
²⁰⁸Pb, ¹¹B induced transfer reactions above Coulomb barrier, selective excitation of particle, hole states 3-60219
²⁰⁸Pb, alpha-particle scattering, 139 MeV, analysis elastic cross sections using Woods-Saxon potential 3-63076
²⁰⁸Pb, collective excitations study using 54 MeV inelastic proton scattering 3-63056
²⁰⁸Pb, Coulomb excitation with heavy ions, static quadrupole moment of 3⁻ state from γ -ray meas. 3-49101
²⁰⁸Pb, distrib. determ. from elastic electron scattering and muonic X-rays 3-71038
²⁰⁸Pb, elastic and inelastic scattering of 1.04 GeV protons, angular distrib. meas. 3-57522
²⁰⁸Pb, elastic and inelastic scatt. of 1 GeV protons, theory comparison with expt. 3-78320
²⁰⁸Pb, electroexcitation of giant resonances 3-43236
²⁰⁸Pb, inelastic electron scattering form factors of low-lying states, Migdal theory 3-49247
²⁰⁸Pb, muonic, Hartree-Fock study of monopole polarisation of 1s_{1/2} level 3-78234
²⁰⁸Pb, muonic, nuclear monopole polarisation calc. using Hartree-Fock eqns. 3-67172
²⁰⁸Pb, neutron resonances, particle-vibration calc., ²⁰⁹Pb intrinsic doorway 3-78267
²⁰⁸Pb, nucl. breathing modes calc. 3-52119
²⁰⁸Pb, nucl. response function, excitation props., numerical calc. method 3-52120
²⁰⁸Pb, RPA calcs. of low lying states, density dependent interaction 3-49153
²⁰⁸Pb, semi-empirical analysis magnetic moments of single-particle (hole) states assumed core, B(M1) values 3-52081

nuclei with $190 \leq A \leq 219$ continued

- ²⁰⁸Pb, single neutron transfer, sub-Coulomb, form factor calcs. and single-particle potentials 3-67298
- ²⁰⁸Pb, single particle energies, removal and addition times effects, comparison with experiment 3-67226
- ²⁰⁸Pb, single-proton transfer reactions induced by ¹²C and ¹⁶O ions, recoil effects evidence 3-43255
- ²⁰⁸Pb 11 MeV giant reson., quadrupole assignment 3-63025
- ²⁰⁸Pb photoabsorption, dynamic deformability, reln. to intermediate structure of giant resonance (Russian) 3-74562
- ²⁰⁸Pb region, high-spin isomeric states, mesonic anomaly in orbital g factors 3-45929
- ²⁰⁸Pb region, magnetic dipole transition rates 3-49205
- ²⁰⁸Pb region, magnetic multipole moments and transition probabilities of single-particle states 3-60071
- ²⁰⁸Pb region, single particle transitions, renormalization of E2 and M1 matrix elements 3-45999
- ²⁰⁸Pb relationship between single particle and collective degrees of freedom (Russian) 3-67237
- ²⁰⁸Pb- μ , recoil corrections to energy levels using Breit eqn. analysis 3-67719
- ²⁰⁸Pb(³He,³He'), 75 MeV, cross section analysis, obs. of new giant resonance 3-63077
- ²⁰⁸Pb(⁷Li,⁷Li'), study of E1 polarisation in ⁷Li Coulomb excitation, 18-30 MeV 3-78288
- ²⁰⁸Pb(0⁺) analogue resonance decay amplitudes from proton scattering on ²⁰⁷Pb 3-49253
- ²⁰⁸Pb(α ,2n)²¹⁰Po, population of core-excited isomeric state in ²¹⁰Po, time-differential spin-rotation meas. 3-45972
- ²⁰⁸Pb(α , α'), 90 MeV, cross section analysis, obs. of new giant resonance 3-63077
- ²⁰⁸Pb(d,p)²⁰⁹Zr, deuteron D-state effects obs. 3-63066
- ²⁰⁸Pb(d,p)²⁰⁹Pb, diffraction model for extraction of spectroscopic factors 3-60140
- ²⁰⁸Pb(d,p)²⁰⁹Pb, n transfer to unbound states, illustration of general formalism 3-67358
- ²⁰⁸Pb(d⁺,d) 12.3 MeV, vector analysing power, differential cross section, deduced optical model parameters 3-60199
- ²⁰⁸Pb(d⁺,p), 12.3 MeV, vector analysing power, differential cross section, ²⁰⁹Pb deduced levels, DWBA analysis 3-60199
- ²⁰⁸Pb(d⁺,t), 12.3 MeV, vector analysing power, differential cross section, ²⁰⁷Pb deduced levels, DWBA analysis 3-60199
- ²⁰⁸Pb(e,e), 250 and 500 MeV, meas. of cross section, charge density and difference with ²⁰⁹Bi 3-52172
- ²⁰⁸Pb(γ ,n), background cross section and correlation between partial widths, relation 3-54454
- ²⁰⁸Pb(n,2n)^{207m}Pb, isomeric cross section at 14.8 MeV 3-54468
- ²⁰⁸Pb(n, α), thermal neutron energies, cross sections determ. 3-43244
- ²⁰⁸Pb(n, γ)²⁰⁹Pb, 2.25 to 7.25 MeV, direct and compound nucleus contrib., modified Hauser-Feshbach theory 3-78332
- ²⁰⁸Pb(n,n)²⁰⁸Pb, imaginary optical potential 3-60141
- ²⁰⁸Pb(p,n)²⁰⁸Pb, quasielastic reaction, macroscopic charge-independent analysis, coupled Lane eqn. soln. 3-67333
- ²⁰⁸Pb(p,p)²⁰⁸Pb, 1 GeV, differential cross section calc. using Glauber multiple scattering theory 3-57521
- ²⁰⁸Pb(p,p)²⁰⁸Pb, energy dependence of real central optical potential, 25-1000 MeV 3-60185
- ²⁰⁸Pb(p,t), two step (p,d)-(d,t) mechanism 3-74582
- ²⁰⁹Pb, (1/2)⁺ doorway resonance, nuclear spreading width in particle-vibration model 3-74492
- ²⁰⁹Pb, from ²⁰⁸Pb(d⁺,p), 12.3 MeV, vector analysing power, differential cross section, ²⁰⁹Pb deduced levels, DWBA analysis 3-60199
- ²⁰⁹Pb, imaginary optical potential for s-wave neutrons incident on ²⁰⁸Pb 3-60141
- ²⁰⁹Pb, 1-forbidden $11_{1/2} \rightarrow 2g_{9/2}$ M1 transition, mean lifetime and B(M1) meas. 3-60114
- ²⁰⁹Pb, single-particle strengths using Dyson eqn. rel. to finite Fermi systems 3-62963
- Pb(α ,xn + γ), E=25-29 MeV, stroboscopic resonance method, g-factors for Po isotopes 3-71041
- Pb(d,pn)Pb, disintegration at 12 and 10.5 MeV, energy-angle correlations, DWBA analysis (German) 3-49264
- Pb(γ , γ), diff. cross sect. meas. 0.145 to 1.33 MeV 3-46019
- Pb(p,t), A=208, 206, 204, 35 MeV, two-neutron pick-up strengths, transition from single-particle to collective 3-60187
- ²⁰⁹Pn(α ,4n)²⁰⁴Po, mag. mom. meas. of ($\pi\hbar\omega_{3/2}$)²8⁺ states 3-49088
- Po, A=204-210, from Pb(³He,xn + γ) and Pb(α ,xn + γ), stroboscopic resonance method, g-factors 3-71041
- ²¹⁰Po, core polariz. eff. in $\pi\hbar\omega_{3/2}$ shell of 8⁺ states and g-factors 3-45969
- ²¹⁰Po, g-factor of 8⁺ states, meas. by stroboscopic resonance method 3-49090
- ²¹⁰Po [($\pi\hbar\omega_{3/2}$)²8⁺ states, meas. of mag. mom. 3-49088
- ²¹⁰Po, [($\pi\hbar\omega_{3/2}$)²8⁺ states, meas. of mag. mom. 3-49088
- ²¹⁰Po, core polariz. eff. in $\pi\hbar\omega_{3/2}$ shell of 8⁺ states and g-factors 3-45969
- ²¹⁰Po, g-factor of 8⁺ states, meas. by stroboscopic resonance method 3-49090
- ²¹⁰Po \rightarrow ²⁰⁶Bi, decay scheme revision from ²⁰⁶Bi 10.84 keV strong M1 transition obs. 3-52135
- ²¹⁰Po, g-factor of 13/2⁺ neutron hole state, from ²⁰⁶Pb(α ,3n), E=38 MeV 3-49089
- ²¹⁰Po, magnetic moment of 13/2⁺ state and mesonic contrib. to moment of $1_{13/2}$ neutron 3-49137
- ²⁰⁸Po, ²⁰⁹Po alpha-decay following ²⁰⁹Bi(p,n) and (p,2n) reaction 3-71105
- ²⁰⁸Po, g-factor of 8⁺ states, meas. by stroboscopic resonance method 3-49090
- ²⁰⁹Po, g-factor of 17/2⁻ state, meas. by stroboscopic resonance method 3-49090
- ²¹⁰Po, asymmetry in fission, symmetric fission preference 3-43264
- ²¹⁰Po, α energy, absolute determ. (French) 3-60132
- ²¹⁰Po, collective state study with inelastic scattering of deuterons, protons, tritons 3-43183
- ²¹⁰Po, core-excited state, magnetic moment determ. by time-differential spin-rotation meas. 3-45972
- ²¹⁰Po, g-factor of 8⁺ states, meas. by stroboscopic resonance method 3-49090

nuclei with $190 \leq A \leq 219$ continued

- ²¹⁰Po, half-lives of 6⁺ and 4⁺ states, meas. by γ - γ delayed coincidence method 3-45925
- ²¹⁰Po, half-lives of 6⁺ and 4⁺ states 3-62998
- ²¹⁰Po, M1 core polarizabilities of 8⁺ and 6⁺ states, shell model calcs. 3-49117
- ²¹⁰Po, mag. mom. meas. of core excited isomer of $]13^{-}$ by time-diff. spin-rot. method 3-49091
- ²¹⁰Po₂, g($\pi\hbar\omega_{3/2}$)² difference for 6₁⁺ and 8₁⁺ states, DPAC^{9/2} meas. of lifetimes 3-45951
- ²¹¹Po, 1065 keV (15/2⁻) state, meas. of lifetime and g-factor 3-49092
- Pt, induced by 12.2 GeV protons, binary and ternary fission 3-52216
- ^aPt, A=192, 194, 196, e.m. properties of 2⁺ and 2⁺ states 3-49196
- ¹⁹⁰Pt, effect of quadrupole-pairing interaction on J⁺=0⁺ vibrs. 3-78256
- ¹⁹⁰Pt level scheme populated in ¹⁹⁰Au decay 3-67278
- ¹⁹²Pt, angular correlations of K- and L-conversion electrons (Russian) 3-71075
- ¹⁹²Pt, energy level study 3-40414
- ¹⁹²Pt, gamma decay, phenomenological T-violating internucleon potential 3-62988
- ¹⁹⁴Pt, Coulomb excitation by ¹⁶O and ³²S, quadrupole moment of first 2⁺ state by reorientation precession technique 3-45942
- ¹⁹⁴Pt, spins, multipole mixing ratios of γ -transitions, E2 ratio comparison with theory 3-54385
- ¹⁹⁵Pt, coupling const. with proton in vinyl-Pt complexes 3-75065
- ¹⁹⁵Pt, excited states, spin and parity assignments from ¹⁹⁵Ir s.m., ¹⁹⁵Au decay 3-52137
- ¹⁹⁵Pt n.m.r. in K₂Pt(CN)₄Br_{0.3}·nH₂O (German) 3-50482
- ²¹¹Pt(¹¹B, nnnnn)²⁰⁴Bi, population of high-spin isomeric state in ²⁰⁴Bi 3-49152
- RaE, determ. of configuration mixing ratios consistent with beta-decay and magnetic moment 3-52144
- ²⁰⁹Rn, electron capture decay to levels in ²⁰⁹At, obs. of gamma rays and conversion electrons 3-74542
- ²¹⁰Rn, excitation functions and recoil ranges from ⁸⁴Kr-induced reactions on ²⁰⁹Bi 3-63084
- ²¹⁰Rn \rightarrow ²¹⁰At, electron capture decay 3-43223
- ²¹¹Rn, excitation functions and recoil ranges from ⁸⁴Kr-induced reactions on ²⁰⁹Bi 3-63084
- ²¹⁸Th, α -decay energies and half lives meas. 3-54445
- ²¹⁸Th α -decay, new isotope, determ. of decay energy, half-life, reduced α -particle width 3-60134
- ²¹⁹Th, α -decay energies and half lives meas. 3-54445
- ²²⁰Th, α -decay energies and half lives meas. 3-54445
- ²⁰²Tl, g-factor of 7⁺ isomeric state determ. by time-differential spin-rotation 3-49086
- ²⁰³Tl, ²⁰⁵Tl muonic atoms, magnetization distrib. of single particle states and 2⁺ rotational states 3-49209
- ²⁰³Tl, muonic, test for vacuum polarisation correction to 5-4 transitions (German) 3-52302
- ²⁰³Tl(α ,nnn)²⁰⁴Bi, population of high-spin isomeric state in ²⁰⁴Bi 3-49152
- ²⁰³Tl(n,2n)^{202m}gTl, isomeric cross section at 14.8 MeV 3-54468
- ²⁰³Tl(n, α), thermal neutron energies, cross sections determ. 3-43244
- ²⁰⁴Tl, radiative capture of 1s electrons, internal bremsstrahlung measurement 3-54440
- ²⁰⁵Tl(n,2n)^{204m}Tl, isomeric cross section at 14.8 MeV 3-54468
- ²⁰⁷Tl, calc. of magnetic properties using linear response theory of finite Fermi systems 3-49129
- ²⁰⁷Tl, single-particle strengths using Dyson eqn. rel. to finite Fermi systems 3-62963
- Tm to Hg short-lived neutron deficient nuclei, spectroscopic investigation of half-life (Russian) 3-52142

nuclei with $A \geq 220$

- A=250-261, study of collective vibrational states of even-even nuclei in superfluidity model (Russian) 3-49140
- actinide region, deformation energies and moments of inertia for isomeric states (German) 3-52071
- dosimeter calibration against primary ²⁴¹Am beams, connection methods (French) 3-56556
- element 115 (eka-Bi), prediction of props. from Bi 3-80571
- even actinide nuclei, 0⁺ excitations, calcs. based on finite Fermi systems 3-45981
- excited nuclei, statistical theory of decay, competition between fission and evaporation 3-43263
- fission dynamics in actinide region, role of reflection asymmetry in shape 3-49288
- heavy and superheavy, binding energy and stability study (Russian) 3-52067
- heavy and superheavy nuclei, calcs. of fission barriers 3-54520
- heavy isotopes, mass table construction 3-43322
- neutron multiplicity measurement on resolved fission resonances 3-63091
- neutron-rich nuclei $\leq Z \leq 104$, $172 \leq N \leq 194$ nuclear inertial mass parameter B determ. in adiabatic approx. 3-62924
- superheavy ²⁵⁷104 daughter X-ray identification 3-63015
- superheavy elements and actinides prod. by secondary reactions in W targets 3-60232
- superheavy elements in natural and proton-irradiated materials 3-60231
- superheavy nuclei 108 $\leq Z \leq 124$, $172 \leq N \leq 188$, nuclear inertial mass parameter B determ. in adiabatic approx. 3-62924
- superheavy nuclei ²⁸⁰112 and ⁴⁰⁸168, charge and mass distrib. calc. by hyperspheric functions method (Russian) 3-74479
- transuranium elements, ratio evaporative to fission width Γ_n/Γ_f , energy dependence (Russian) 3-57548
- Z \geq 60, nucl. energy spectrum near 1 GeV/amu, new cosmic ray source evidence 3-53581
- ²²⁷Ac, symmetric, asymmetric near fission threshold, direct reactions ³He beam on ²²⁶Ra target 3-60238
- ²²⁸Ac, symmetric, asymmetric near fission threshold, direct reactions ³He beam on ²²⁶Ra target 3-60238
- ²²⁸Ac 62 sec, product of ²³²Th and 600 MeV protons 3-54483
- Am, spontaneously fissioning isomer prod. in 14 MeV neutron reactions 3-71132

nuclei with $A \geq 220$ continued

- ²⁴⁰Am spontaneously fissionable isomer, decay, search for α -emission (*Russian*) 3-40470
- ²⁴¹Am, α -decay, electron pair prod. mechanism 3-40468
- ²⁴¹Am, effect on reactivity of ²³⁹Pu nitrate solutions, rel. to criticality expts. 3-74729
- ²⁴¹Am, γ -radiation, Kodak RM film latent image stability 3-77561
- ²⁴¹Am, neutron fission, Kr and Xe yields 3-67378
- ²⁴¹Am, thermal neutron capture cross sections and capture resonance integrals for ^{242m}Am, ^{242s}Am production 3-43242
- ²⁴¹Am polycrystalline source, perturbation of α - γ angular correlation 3-43225
- ²⁴¹Am-⁹Be neutron source, neutron spectrum meas. 3-77607
- ²⁴¹Am(n, γ)²⁴²Am, gamma-ray spectra meas. and analysis 3-49248
- ²⁴²Am, neutron fission, Kr and Xe yields 3-67378
- ²⁴²Am spontaneously fissionable isomer, decay, search for α -emission (*Russian*) 3-40470
- ²⁴⁸Bk, decay product of ²⁵²Es by α decay, deduced levels 3-54443
- ²⁴⁹Bk, energy levels, ²⁵³Es α -decay study 3-63017
- ²⁵⁰Bk, energy levels, ²⁵⁴Es α -decay study 3-63017
- ²⁵⁰Bk deduced energy levels, from α -decay of ²⁵⁴Es 3-54444
- Cf²⁵², use as detector in geophysical radiometry (*Rumanian*) 3-51171
- ²⁴⁷Cf produced in ²⁵¹Fm alpha decay, rotational band obs. and Nilsson state assignments 3-67281
- ²⁴⁸Cf, α -decay, total half-life obs., spontaneous fission half-life determ. 3-46013
- ²⁴⁹Cf, neutron induced fission cross section using neutrons from underground nuclear explosion 3-78358
- ²⁵²Cf, decay product of ²⁵²Es by electron capture, deduced levels 3-54443
- ²⁵²Cf, fission fragments prompt gamma energy from prompt neutron numbers, liquid-drop model calc. 3-54510
- ²⁵²Cf, triple fission, products, α -particle, neutron spectra 3-78363
- ²⁵²Cf, use in neutron activation analysis and radiography (*Afrikaans*) 3-62198
- ²⁵²Cf fission neutron age in water, meas. by In resonance obs. 3-71297
- ²⁵²Cf fission neutron spectrum, meas. of ²³²Th integral fission cross section 3-74619
- ²⁵²Cf fission vs. prompt γ -ray energy, fragment-mass ratios 3-43266
- ²⁵²Cf neutron radiography device, comparison of a multiplied and unmultiplied facility, 3-63247
- ²⁵²Cf spontaneous fission, fragment X-ray spectra and mass yield fine structure (*Russian*) 3-40522
- ²⁵²Cf spontaneous fission fragments, γ cascades 3-62994
- ²⁵²Cf spontaneous fission neutrons, meas. of ²³⁵,²³⁸U fission cross sections 3-49294
- ²⁵⁹Cf, ternary fission, observation of ³He, neutron spectra 3-43261
- Cm isotopes $A=244$ to 250 meas. of fission barrier heights, effects near and nature of $N=152$ shell 3-71134
- ²⁴Cm, $A=243$, 245, 247, review of Nilsson orbitals 3-40419
- ²⁴²Cm, radiolysis conditions, cation-exchange chromatography, high pressure system (*German*) 3-73163
- ²⁴²Cm from ²⁴¹Am neutron irradiation, α -particle source for surveyor, preparation 3-62208
- ²⁴⁴Cm, ²⁴⁶Cm, spontaneous fission, prompt neutron multiplicity, dispersion 3-78364
- ²⁴⁶Cm(¹⁶O,F), 102.5 MeV, fragment kinetic energy, comparison with static scission model and fission systematics predictions 3-74616
- ²⁴⁶Cm(n,f) spontaneous, fragment mass and kinetic energy distrib. determ. 3-71135
- ²⁴⁷Cm as short-lived r -process chronometer in nucleocosmochronological studies 3-51255
- ²⁴⁸Cm, asymmetry in fission 3-43264
- ²⁴⁸Cm in early Solar System from primitive meteorites 3-76963
- ²⁵²Es, decay scheme 3-54443
- ²⁵³Es, α -decay and ²⁴⁹Bk energy levels 3-63017
- ²⁵³Es, thermal-neutron capture cross-sections and capture resonance integrals 3-57516
- ²⁵⁴Es, α -decay and ²⁵⁰Bk energy levels 3-63017
- ^{254m}Es, α decay scheme, X-ray and γ -ray energies associated with β -decay 3-54444
- ²⁵⁰Fm, existence and assignments of isomer states, cross bombardment techniques 3-62950
- ²⁵¹Fm, α -decay scheme and branching determ., $1/2$ meas. from γ -ray decay 3-67281
- ²⁵²Fm, asymmetry in fission 3-43264
- ²⁵⁷Fm spontaneous fission, meas. of average number of prompt neutrons emitted 3-71138
- ²⁵⁸Fm, asymmetry in fission, symmetric fission preference 3-43264
- ²⁶⁴Fm, asymmetry in fission, symmetric fission preference 3-43264
- ²⁵⁴No, existence and assignments of isomer states, cross bombardment techniques 3-62950
- Np, spontaneously fissioning isomer prod. in 14 MeV neutron reactions 3-71132
- ²³⁵Np, decay schemes, energy level spacings, transition probabilities interpretation by strong Coriolis interaction 3-57499
- ²³⁶Np, search for fissioning isomers in region of 60 μ s half-life 3-78357
- ²³⁷Np, Mossbauer effect in NpPd₃(Sn₃)(Ge₃)(Rh₃) 3-68905
- ²³⁷Np, neutron fission, Kr and Xe yields 3-67378
- ²³⁷Np(n, γ)²³⁸Np, gamma-ray spectra meas. and analysis 3-49248
- ²³⁸Np, neutron fission, Kr and Xe yields 3-67378
- ⁹³²³⁸Np electron capture decay, energies and rel. intensities for γ -ray transitions 3-54434
- ⁹³²³⁸Np electron capture decay, energies and rel. intensities for γ -ray transitions 3-54434
- ²³¹Pa, product of ²³⁵Np α decay, α , β and γ transition probabilities, Coriolis interaction 3-57499
- ²³²Pa for ²³²Th analysis (*Japanese*) 3-59698
- ²³²Pa \rightarrow ²³³U, obs. using semiconductor detectors and coincidence techniques 3-74535
- ²³⁴Pa, isotope discovery and naming 3-51484
- ^{234m}Pa/UX₂, decay characteristics (*French*) 3-40465
- ²⁴⁰Po, effective charge of proton $h_{9/2}$ from lifetimes meas. (*French*) 3-45992

nuclei with $A \geq 220$ continued

- ²³⁸,²³⁹Pu, ²⁴¹Am sequential determ. in environmental samples 3-66451
- Pu, spontaneously fissioning isomer prod. in 14 MeV neutron reactions 3-71132
- ²⁴¹Pu, $A=237$, 239, 241, review of Nilsson orbitals 3-40419
- ²³⁹Pu decay, electron capture, half-life, level scheme, branching intensities 3-40462
- ²³⁹Pu, relative excitations of spontaneous fission shape isomers 3-71136
- ²³⁹Pu pop. in ²³⁸Pu(d,t) 12.1, 13.1 MeV obs. of five Nilsson orbitals 3-67197
- ²³⁸Pu, 18 eV to 3 MeV n-induced fission, resonance cross-sections 3-74613
- ²³⁸Pu, α -particle energy loss and range straggling in CH₄, CO₂, CF₄, CF₂Cl₂, SF₆, comparison with Payne-Titeica model (*Russian*) 3-59638
- ²³⁸Pu, B(E3) values for octupole states and new Nilsson orbitals, (d,t) and (d,d') reactions 3-43185
- ²³⁸Pu, neutron capture cross-section, resonance parameters, γ -ray emission 3-74578
- ²³⁸PuO₂, high purity, neutron yield 3-67628
- ²³⁸Pu(d, p)²³⁹Pu, 12 and 13 MeV, study of ²³⁹Pu energy levels 3-40418
- ²³⁹Pu, anisotropic scattering eff. in reflected fast critical assemblies, calc. 3-49328
- ²³⁹Pu, anomaly of fission reaction threshold from 1.5 to 7.5 MeV 3-52212
- ²³⁹Pu, composite nuclei, nucleon pairing effects, two lumped fission barrier 3-40521
- ²³⁹Pu, cumulative fission yield reviewed 3-71140
- ²³⁹Pu, energy levels, study by reactions ²³⁸Pu(d, p) and ²³⁹Pu(d, d') 3-40418
- ²³⁹Pu, fission, power, photon spectrum and neutron prodn., calc. by ORIGIN computer code 3-43284
- ²³⁹Pu, fission fragments prompt gamma energy from prompt neutron numbers, liquid-drop model calc. 3-54510
- ²³⁹Pu, fission track detection, neutron temperature, rel. to temp. of medium 3-48539
- ²³⁹Pu, high burnup fuel, criticality expts., KENO Monte Carlo code anal. 3-74729
- ²³⁹Pu, multilevel effects in unresolved resonance region 3-71114
- ²³⁹Pu, neutron collision probabilities in spheres with parabolic source distribution 3-63109
- ²³⁹Pu, nitrate solutions, criticality studies, effect of acid molarity and ²⁴⁰Pu content 3-63230
- ²³⁹Pu, thermal neutron capture, probability of formation of spontaneously fissionable isomer states (*Russian*) 3-71139
- ²³⁹Pu, thermal neutron fission, energy spectrum, angular distribution of ⁴He and ⁶He fission products 3-54517
- ²³⁹Pu, time spectrum of fission fragments using pulsed cyclotron beam 3-51674
- ²³⁹Pu, total and elastic scatt. neutron cross sections 3-60170
- ²³⁹Pu delayed fission neutrons, energy distrib. meas. using ³He proportional counter 3-54515
- ²³⁹Pu fast reactors, post-shutdown fission product energy release calcs. 3-67441
- ²³⁹Pu fission, neutron induced, meas. of prompt ν -values in fast and thermalised fluxes 3-60229
- ²³⁹Pu fission, neutron-induced cross-sections below 30 keV, high resolution meas. 3-60234
- ²³⁹Pu fission, thermal neutron induced, gamma rays of primary fission products 3-49287
- ²³⁹Pu fission neutron multiplicity and total gamma-ray energy 3-71137
- ²³⁹Pu foil irradiation meas. in engineering mockup critical expts. for FTR 3-49352
- ²³⁹Pu partial widths of resonance levels, spin-dependent statistics 3-67376
- ²³⁹Pu pop. in ²³⁸Pu(d,p) and ²³⁹Pu(d,d') 12.1, 13.1 MeV, obs of Nilsson orbitals, $K^{\pi}=1_{-2}^{-}$ octupole band assignment 3-67197
- ²³⁹Pu thermal fission, delayed neutron energy spectra meas. by proton-recoil proportional counter 3-49292
- ²³⁹Pu(n, f) in ZPR-6 assembly 7, comparison of calc. and meas. reaction rate distrib. and fission integrals 3-71186
- ²³⁹Pu(n,f), ternary to binary fission ratio meas., 0.02 to 50 eV 3-78361
- ²⁴⁰Pu, anisotropic scattering eff. in reflected fast critical assemblies, calc. 3-49328
- ²⁴⁰Pu, anomaly of fission reaction threshold from 1.5 to 7.5 MeV 3-52212
- ²⁴⁰Pu, effect on criticality safety of ²³⁹Pu, ²³⁵U and ²³³U 3-63230
- ²⁴⁰Pu, influence of double barrier on quadrupole absorption component 3-60237
- ²⁴⁰Pu, shell structure and fission asymmetry, statistical model, fragment mass distributions 3-60235
- ²⁴⁰Pu in clean and LWR-grade fuel, comparison of neutronics characteristics of FFTF core 3-49371
- ²⁴⁰Pu zoned critical expts., analysis in support of LWR-grade Pu utilization in FTR's 3-71187
- ²⁴¹Pu, cumulative fission yield reviewed 3-71140
- ²⁴¹Pu fissile element cross section, influence on fast crit. assembly parameters 3-60277
- ²⁴¹Pu fission, neutron-induced cross-sections below 30 keV, high resolution meas. 3-60234
- ²⁴¹Pu spontaneously fissionable isomer, decay, search for α -emission (*Russian*) 3-40470
- ²⁴¹Pu:²³⁵U fission cross-section ratio meas. for neutron energies 5 keV-1.2 MeV 3-60233
- ²⁴²Pu, anomaly of fission reaction threshold from 1.5 to 7.5 MeV 3-52212
- ²⁴²Pu, neutron resonance parameters from (n,n) and (n, γ) reactions, calc. of fission widths 3-49258
- ²⁴²Pu, neutron total cross section, 600 eV-81 keV, subthreshold fission structure parameters 3-63095
- ²⁴³Pu, composite nuclei, nucleon pairing effects, two lumped fission barrier 3-40521
- ²²⁴Ra decay, perturbed α - γ angular correlations 3-40471
- ²²⁶Ra, γ -radiation, kodak RM film latent image stability 3-77561
- ²²⁸Ra, mass unit measurement standard 3-51509

nuclei with $A \geq 220$ continued

- ²²⁶Ra target, direct reaction with ³He beam rel. to fission of Ac isotopes near fission threshold 3-60238
- Rn, daughter aerosols, closed vessel storage, mobility spectrum, time variation 3-62981
- ²²⁰Rn and ²²²Rn exhalation from surface soil layer 3-53478
- ²²⁰Rn daughter products, radioactivity measurement by plastic scintillators 3-40011
- ²²²Rn emanation from lunar crater Aristarchus, Apollo 15 α -spectra obs. 3-45048
- Th, induced by 12.2 GeV protons, binary and ternary fission 3-52216
- Th, spontaneously fissioning isomer prod. in 14 MeV neutron reactions 3-71132
- ²²⁸Th decay, perturbed α - γ angular correlations 3-40471
- ²³¹Th, ²³³Th, review of Nilsson orbitals 3-40419
- ²³¹Th, decay schemes, energy level spacings, transition probabilities interpretation by strong Coriolis interaction 3-57499
- ²³²Th, 1 GeV proton bombardment, angular distribution of fission fragments, momentum transfer (Russian) 3-57547
- ²³²Th, 600 MeV protons, production of 62 sec. ^{222m}Ac 3-54483
- ²³²Th, atomic mass meas. 3-43322
- ²³²Th, influence of double barrier on quadrupole absorption component 3-60237
- ²³²Th, meas. of integral fission cross section in ²³²Cf fission neutron spectrum 3-74619
- ²³²Th, neutron activation analysis (Japanese) 3-59698
- ²³²Th, non-destructive meas. in high temperature spherical reactor fuel elements (German) 3-67601
- ²³²Th, photofission, mass yield distrib., 25-40 MeV, γ -spectra 3-67377
- ²³²Th, photofission cross-sect. meas., threshold to 8 MeV 3-46046
- ²³²Th, shell effects, excitation energy, fission fragments mass distrib. 3-78266
- ²³²Th delayed fission neutrons, energy distrib. meas. using ³He proportional counter 3-54515
- ²³²Th fission, neutron induced 14.8 MeV, charge distrib. meas. for ⁴In, two-mode fission hypothesis 3-43260
- ²³²Th(¹⁶O,F), 102.5 MeV, fragment kinetic energy, comparison with static scission model and fission systematics predictions 3-74616
- ²³²Th(²²Ne,X), 174 MeV, energy spectra of 58 light particles (X), Z=3-12, A=6-27 3-67357
- ²³²Th(n, γ)²³³Th, gamma-ray spectra meas. and analysis 3-49248
- ²³²Th β^- decay, precision meas. of γ -ray energies 3-74539
- Tn daughters, lung dose as function of depth 3-42381
- U, 24 GeV proton interactions, neutron-rich Na isotope prod., on-line mass-spectrometric meas. 3-52068
- U, 5 GeV proton bombardment, energy spectra of fragments 3-40496
- U, A=233, 235, 238, delayed fission neutrons, energy distrib. meas. using ³He proportional counter 3-54515
- U, spontaneously fissioning isomer prod. in 14 MeV neutron reactions 3-71132
- U, ternary fission induced by high-energy protons, cross-sections for three-prong events 3-57546
- ^aU, A=235, 237, 239, review of Nilsson orbitals 3-40419
- ²³⁵U fission, thermal-neutron induced, fragment mass distrib., fine structure, charge distrib., structure, correlations 3-40518
- ²³⁵U, criticality research, Oak Ridge Critical Experiments Facility 3-63227
- ²³⁵U, cumulative fission yield reviewed 3-71140
- ²³⁵U fission by protons, charge dispersion of products in light-mass region 3-57544
- ²³⁵U, fission by thermal neutrons, yield, mass, energy spectra 3-78362
- ²³⁵U, fission fragments prompt gamma energy from prompt neutron numbers, liquid-drop model calc. 3-54510
- ²³⁵U, nitrate solutions, criticality studies, effect of acid molarity and ²⁴⁰Pu content 3-63230
- ²³⁵U, proton induced fission, 7 to 13 MeV, fragment mass and energy distributions, discussion of shell effects 3-54519
- ²³⁵U energy levels populated in ²³⁵Pa decay 3-74535
- ²³⁵U fission, low-energy neutron induced, resonance parameters and cross-sections 3-49293
- ²³⁵U fission, neutron-induced cross-sections below 30 keV, high resolution meas. 3-60234
- ²³⁵U fission neutron spectra meas. 0.8-10 MeV 3-74618
- ²³⁵U thermal fission, delayed neutron energy spectra meas. by proton-recoil proportional counter 3-49292
- ²³⁴U energy levels, deduced from inelastic deuteron scattering 3-54388
- ²³⁵U, atomic mass meas. 3-43322
- ²³⁵U, axial fission rate distrib., effect of UO₂ insulator pellets, EBR-II 3-63167
- ²³⁵U, crit. mass eval. using energy-depend. buckling concept. 3-60243
- ²³⁵U, criticality research, Oak Ridge Critical Experiments Facility 3-63227
- ²³⁵U, cross section and anisotropy for photofission 3-60230
- ²³⁵U, cumulative fission yield reviewed 3-71140
- ²³⁵U, fission, power, photon spectrum and neutron prodn., calc. by ORIGIN computer code 3-43284
- ²³⁵U, fission by thermal neutrons, yield, mass, energy spectra 3-78362
- ²³⁵U, fission fragments, back-scatt. from thin metal films 3-61090
- ²³⁵U, fission fragments prompt gamma energy from prompt neutron numbers, liquid-drop model calc. 3-54510
- ²³⁵U, fission track detection, neutron temperature, rel. to temp. of medium 3-48539
- ²³⁵U, heavy water reactors, light water infiltration reactivity effects, Ames Laboratory Research Reactor, safety considerations 3-74736
- ²³⁵U, meas. neutron fission and capture cross sections at 8 eV to 10 keV 3-74612
- ²³⁵U, multilevel analysis of neutron capture and fission cross sections up to 60 eV 3-63094
- ²³⁵U, multilevel effects in unresolved resonance region 3-71114
- ²³⁵U, neutron collision probabilities in spheres with parabolic source distribution 3-63109
- ²³⁵U, neutron irradi., fission fragment energy spectra on passage through gases (Russian) 3-57542

nuclei with $A \geq 220$ continued

- ²³⁵U, neutron-induced fission, spin determ. of reson. 3-74614
- ²³⁵U, nitrate solutions, criticality studies, effect of acid molarity and ²⁴⁰Pu content 3-63230
- ²³⁵U, non-destructive meas. in high temperature spherical reactor fuel elements (German) 3-67601
- ²³⁵U, nuclear excitation by electron transition, extended to isotope separation 3-57507
- ²³⁵U, proton induced fission, 7 to 13 MeV, fragment mass and energy distributions, discussion of shell effects 3-54519
- ²³⁵U, quadrupole moment determ. from quadrupole splitting in X-ray transitions of muonic atom 3-49096
- ²³⁵U, spectroscopic quadrupole moment determ. from quadrupole splitting in muonic atoms 3-49133
- ²³⁵U, ternary fission in thermal and reson. neutron energy regions, alpha particle spectra 3-54511
- ²³⁵U, thermal neutron capture, probability of formation of spontaneously fissionable isomer states (Russian) 3-71139
- ²³⁵U(n, γ), measurements of low energy γ -rays following thermal neutron capture 3-63042
- ²³⁵U anisotropic scattering eff. in reflected fast critical assemblies, calc. 3-49328
- ²³⁵U booster rod expts. in ZED-2 critical facility, neutron spectrum parameters 3-49365
- ²³⁵U content, nuclear fuel rod, gamma scan system 3-66320
- ²³⁵U content in U slab, determ. by source-sample fission coincidence and random driver 3-62232
- ²³⁵U content measurement, light water reactor rods, Sb-Be neutron source 3-67558
- ²³⁵U enriched cores, prompt and delayed modes rel. to spacial correction factor for reactivity of system 3-67400
- ²³⁵U fission, absolute determ. of cross-section for 964 keV neutrons 3-49295
- ²³⁵U fission, cross-section meas. for ²⁵²Cf spontaneous fission neutrons 3-49294
- ²³⁵U fission, low-energy neutron induced, resonance parameters and cross-sections 3-49293
- ²³⁵U fission, neutron induced, de-excitation of primary fission fragments 3-46045
- ²³⁵U fission, neutron induced, meas. of prompt ν -values in fast and thermalised fluxes 3-60229
- ²³⁵U fission, neutron-induced cross-sections below 30 keV, high resolution meas. 3-60234
- ²³⁵U fission, thermal neutron induced, gamma rays of primary fission products 3-49287
- ²³⁵U fission by thermal neutrons β ray spectra 3-63101
- ²³⁵U fission fragment range in all existing natural elements 3-58058
- ²³⁵U in U samples, estimation by fission track registration technique 3-51722
- ²³⁵U partial widths of resonance levels, spin-dependent statistics 3-67376
- ²³⁵U thermal fission, delayed neutron energy spectra meas. by proton-recoil proportional counter 3-49292
- ²³⁵U triple fission, thermal neutron induced, study of ⁸He decay (Russian) 3-40469
- ²³⁵U:²⁴¹Pu fission cross-section ratio meas. for neutron energies 5 keV-1.2 MeV 3-60233
- ²³⁵U ∞ source preparation and detecting system for decay rates 3-42635
- ²³⁵U(γ ,f), 5 to 8 MeV, cross-section from yield curve 3-78359
- ²³⁵U(n, γ)^{236m}U, 60 keV, search for spontaneously fissionable ^{236m}U measured cross sections (Russian) 3-57530
- ²³⁵U(n,f), thermal energy, α -particle polar emission 3-54516
- ²³⁵U(n, γ)²³⁶U, meas. γ -ray energies determ. ²³⁶U level schemes 3-67335
- ²³⁶U, asymmetry in fission 3-43264
- ²³⁶U, from (n, γ) reaction, measurements of low energy γ rays, 1383, 1342 KeV levels deduced 3-63042
- ²³⁶U, photofission cross-sect. meas., threshold to 8 MeV 3-46046
- ²³⁶U, pop. in ²³⁵U(n, γ)²³⁶U reaction determ. level scheme and transitions from meas. of γ -ray energies 3-67335
- ²³⁶U energy levels, deduced from inelastic deuteron scattering 3-54388
- ²³⁶U fission mass asymmetry as dynamic process described by collective coordinate 3-60236
- ²³⁷U, search for fissioning isomers in region of 60 μ s half-life 3-78357
- ²³⁸U, 1 GeV proton bombardment, angular distribution of fission fragments, momentum transfer (Russian) 3-57547
- ²³⁸U, 800 MeV photofission, meas. of peak-to-valley ratio 3-74617
- ²³⁸U, anisotropic scattering eff. in reflected fast critical assemblies, calc. 3-49328
- ²³⁸U, anomaly of fission reaction threshold from 1.5 to 7.5 MeV 3-52212
- ²³⁸U, atomic mass meas. 3-43322
- ²³⁸U, Doppler reactivity, axial traverses, inverse kinetic techniques 3-71211
- ²³⁸U, fission and spallation, 11.5 GeV, Xe isotope cross sections and recoil properties 3-74615
- ²³⁸U, γ ray spectra, calcs. for slow and fast neutron capture, rel. to reactor shielding 3-67322
- ²³⁸U, inelastic and capture cross-sections, neutron spectrum meas., LMFBR assemblies 3-71155
- ²³⁸U, interaction barrier in heavy charged particle reactions 3-67361
- ²³⁸U, interaction with 11.5 GeV protons, charge dispersion and recoil props. at A=131 3-40520
- ²³⁸U, irradiated by ⁴⁰Ar, ⁸⁴Kr, ¹³⁶Xe ions, product yields, mechanism 3-78350
- ²³⁸U, neutron capture cross section for energies up to 100 keV, γ -ray meas. 3-74576
- ²³⁸U, neutron reaction, 1.6-4.3 MeV, meas. of ²³⁹U compound nucleus life time (Russian) 3-40497
- ²³⁸U, neutron spectrum meas. for discrepant cross sections in depleted block 3-49296
- ²³⁸U, nucl. Raman effect, giant dipole reson. parameters 3-40480
- ²³⁸U, proton fission, charge dispersion of isotopes of Sb 3-57545
- ²³⁸U, proton induced fission, 7 to 13 MeV, fragment mass and energy distributions, discussion of shell effects 3-54519
- ²³⁸U, shell effects, excitation energy, fission fragments mass distrib. 3-78266

nuclei with $A \geq 220$ continued

- ^{238}U , spontaneous fission, high-energy γ -ray obs. 3-43265
- ^{238}U , spontaneous fission and radio-chemical yield 3-57543
- ^{238}U , two-parameter description of rotational energies 3-74496
- ^{238}U Doppler reactivity mapping in FFTF engineering mockup critical, calcs. and expts. 3-71191
- ^{238}U electrofission, 70 MeV, meas. of fragment kinetic energy 3-43259
- ^{238}U fission, cross-section meas. for ^{252}Cf spontaneous fission neutrons 3-49294
- ^{238}U fission, induced by 1 GeV protons, angular correlations of mass and energy distrib. of fragments (Russian) 3-40524
- ^{238}U fission induced by 70-200 MeV protons, cross section and angular anisotropy (Russian) 3-40523
- ^{238}U neutron cross sections, multiple reaction correction utilising transport theory 3-67320
- $^{238}\text{U}(\gamma, f)$, 5 to 8 MeV, cross-section from yield curve 3-78359
- $^{238}\text{U}(n, f)$, in ZPR-6 assembly 7, comparison of calc. and meas. reaction rate distrib. and fission integrals 3-71186
- $^{238}\text{U}(n, \gamma)$ in ZPR-6 assembly 7, comparison of calc. and meas. reaction rate distrib. and fission integrals 3-71186
- $^{238}\text{U}(n, \gamma)$ cross-section in calcs. of fast reactor neutron spectrum and criticality 3-43282
- $^{238}\text{U}(n, \gamma)$ reaction, effect in fast-neutron spectrum critical assemblies 3-43283
- $^{238}\text{U}(n, f)$, subthreshold fission obs. 3-54518
- $^{238}\text{U}(n, \gamma)$, evaluation of uncertainties in total radiation widths 3-74592
- $^{238}\text{U}(n, \gamma)/^{239}\text{U}(n, f)$ reaction rate ratio determ. by foil activation analysis in critical facilities, Ge(Li) detectors 3-49347
- $^{238}\text{U}(n, \gamma)/^{239}\text{U}$, 150 to 630 keV, meas. neutron capture cross sections by activation technique 3-74572
- $^{238}\text{U}(n, n_0)^{238}\text{U}$, 14.8 MeV, meas. differential cross sections, the Schwinger prediction 3-71108
- $^{238}\text{U}(n, n)^{238}\text{U}$, meas. differential cross section and asymmetries, incident polarised neutrons from $^2\text{H}(d, n)^3\text{He}$ 3-71109
- ^{238}U compound nucleus, lifetime meas. following formation in $^{238}\text{U} + n$ reaction, 1.6-4.3 MeV (Russian) 3-40497
- $^{238}\text{U}(p, \text{Cu})$ reaction at 11.5 GeV, meas. cross section and recoil properties of Cu isotopes of $A=61, 64, 67$ 3-67334
- ^{238}U , level scheme (French) 3-40465
- ^{236}mU , from $^{235}\text{U}(n, \gamma)$, 60 keV, search, measured cross sections (Russian) 3-57530

nucleic acids see macromolecules

nucleon interactions

- see also hyperon-nucleon interactions; kaon-nucleon interactions; neutron interactions; nucleon-nucleon interactions; pion-nucleon interactions; proton interactions
- electroproduction, lepton + nucleon \rightarrow lepton + hadron + hadronic debris, phenomenological discussion of processes 3-67044
- inclusive, quark-model relns., expl. check 3-40403
- lepton-nucleon deep inelastic, quark-parton model and nucleon charge symmetry 3-40355
- meson + nucleon \rightarrow meson + meson + nucleon, nucleon polarisation effects, high energy predictions 3-74443
- weak and e.m. interactions model 3-78105
- eN, inclusive, on H, D, Be, Al, Cu and Au targets 3-70926
- eN \rightarrow eN π , low energy, current algebra model with hard pions (Russian) 3-40361
- eN \rightarrow eN π ($h=\pi, \rho, \gamma$), integrated structure functions in generalised Bjorken limits 3-74383
- eN \rightarrow eN π , quark parton model, reln. between quark fragmentation and distribution functions 3-74380
- eN \rightarrow eN Δ , multipole (kinematic) analysis, invariant and scalar amplitudes (Russian) 3-54319
- eN π \rightarrow eN π + anything, deep inelastic one-particle inclusive process in parton model 3-52015
- $\eta\text{N} \rightarrow \eta\text{N}$, integral cross section of interaction in region of $\text{S}_{11}\text{N}^*(1535)$ resonance (Russian) 3-67100
- $\eta\text{N} \rightarrow \pi\text{N}$, integral cross section of interaction in region of $\text{S}_{11}\text{N}^*(1535)$ resonance (Russian) 3-67100
- ηN total cross section determ. from η photoproduction on nuclei at 2 GeV 3-49010
- γN , 16 GeV polarised photons, charged pion production asymmetries 3-45878
- $\gamma\text{N} \rightarrow \eta\text{N}$, dual B_3 model with fixed and Regge poles 3-57351
- $\gamma\text{N} \rightarrow \text{K}\Lambda$, dual B_3 model with fixed and Regge poles 3-57351
- $\gamma\text{N} \rightarrow \text{K}\Sigma$, dual B_3 model with fixed and Regge poles 3-57351
- $\gamma\text{N} \rightarrow \pi\Delta$ threshold effect on γN coupling of $\text{P}_{11}(1470)$, quark model and expl. data (Spanish) 3-67031
- $\gamma\text{N} \rightarrow \pi\text{N}$, dual B_3 model with fixed and Regge poles 3-57351
- $\gamma\text{N} \rightarrow \pi\text{N}$, $E_\gamma < 450$ MeV, multichannel dispersion theory 3-62838
- μN anomalous interactions, reln. to muonic atoms 3-57615
- μN inelastic interactions at high energy, energy spectrum and angular distrib. 3-57369
- $\mu^- \text{Z} \rightarrow \text{Z}\mu \text{W}_0^-$, differential cross section for scalar W-meson production at super-high energies (Russian) 3-40336
- Nd reactions in flight up to 50 GeV/c, cross section compilation 3-60018
- $\nu(\bar{\nu})\text{N} \rightarrow \text{L}^-(\text{L}^+) + \text{baryon} + \text{meson}$, Born model 3-66988 (Russian)
- $\nu\mu\text{N} \rightarrow \text{meson} + \text{baryon} + \mu^-$, selection rules 3-66980
- $\nu\mu\text{N} \rightarrow \text{meson} + \text{baryon} + \mu^+$, selection rules 3-66980
- νN , deep inelastic, average inelasticity and average (momentum-transfer) 2 3-62814
- νN , deep inelastic, finite-energy sum rules 3-40335
- νN , high energy, higher-order corrections, phenomenology, sum rule 3-45868
- $\bar{\nu}\text{N}$ inclusive scattering as probe of nucleon core structure 3-62813
- $\nu\text{N} \rightarrow \mu^- + \text{hadrons}$, 50, 145 GeV neutrino beam 3-59955
- $\nu\text{N} \rightarrow \mu^- + \text{hadrons}$, high energy inclusive reactions at CERN 3-66989
- $\nu\text{N} \rightarrow \mu^+ + \text{hadrons}$ high energy inclusive reactions at CERN 3-66989
- νN pseudoscalar meson formation in region of strong transmitted impulses, Bornovsky model (Russian) 3-74357
- $\nu\text{N} \rightarrow \text{Y}^+ + \text{anything}$, search for heavy positively charged lepton Y^+ 3-62817
- $\nu\mu\text{N} \rightarrow \mu^- + \text{hadrons}$, meas. of total cross sections as function of energy 3-66095

nucleon interactions continued

- $\nu\mu\text{N} \rightarrow \mu^+ + \text{hadrons}$, meas. of total cross sections as function of energy 3-66985
- $(\nu\mu)\text{N} \rightarrow \mu h\text{X}$ ($h=\pi, \rho, \gamma$) integrated structure functions in generalised Bjorken limits 3-74383
- $\nu\text{Z} \rightarrow \text{Z}\mu \text{W}_0^-$, differential cross section for scalar W-meson production at super-high energies (Russian) 3-40336
- $\omega\text{N}_1 \rightarrow \pi\text{N}_2$, vector meson dominance and mass dependence of Ball's invariant amplitudes 3-67084
- $\pi\text{N}\Delta$ interaction, covariant derivation of characteristic surfaces, causality 3-51975
- $\rho^0\text{N}_1 \rightarrow \pi\text{N}_2$, vector meson dominance and mass dependence of Ball's invariant amplitudes 3-67084
- nucleon-nucleon interactions**
 - see also proton-proton interactions
 - cascade evaporation model for nucleon-nucleon collisions at energies > 10 GeV (Russian) 3-60194
 - central pot. depend. on πd scattering length 3-78178
 - collective motions, paired nucleons, isospin degrees of freedom 3-78269
 - energy spectra of residual nucleons following nucleon-nuclear interactions, 24-300 GeV (Russian) 3-69786
 - high energy, W boson detection by lepton spectra anal. and quark parton model (Russian) 3-67062
 - incoherent nuclear production processes, cross sections 3-78322
 - inelastic at 200 GeV, multiperipheral model, comparison with cosmic ray data (Russian) 3-67133
 - low energy, potential model anal. using two pion exchange potential or scalar meson (720) 3-74408
 - meson exchange, Cohen approximation to scalar Bethe Salpeter eqn. 3-60089
 - meson production, S-matrix theory, high-energy, unitary eikonal formalism 3-78203
 - multiperipheral theory at high energies elastic and charge exchange amplitudes near $t=0$ (Russian) 3-67099
 - multiplicity distribution, simple geometric model 3-60015
 - nn, secondary pion energies, approximation of experimental data (Russian) 3-62902
 - nuclear interaction conference, Los Angeles, USA (28 Aug-1 Sep 1972) 3-74500
 - polarisation structure at high energies, simple models 3-70969
 - polarisation structure of reactions with four spin $1/2$ particles 3-74550
 - relativistic resonance propagator for $\pi\pi$ phase shift analysis 3-70993
 - NN, sum rule for production of doubly charged exotic meson resonances 3-43145
 - NN \rightarrow 2 pseudoscalar mesons, resonance ang. distributions 3-62885
 - NN \rightarrow (AK)N, 6 MeV/c charge-channel analysis without I-spin-exchange interference 3-78197
 - NN \rightarrow (EK)N, 6 MeV/c, charge-channel analysis without I-spin-exchange interference 3-78197
 - NN annihilation into pions, statistical model with new charge weight factor 3-67137
 - nn final-state interaction in $^2\text{H}(n, n)\text{p}$, scattering length calc. 3-78336
 - NN $\rightarrow \pi^\pm + \text{anything}$ at rest, soft-pion limits of inclusive pion distrib., test of PCAC 3-52056
 - NN $\rightarrow \pi\pi$, consistency conditions for helicity amplitudes 3-67103
 - NN reactions in flight up to 50 GeV/c, cross section compilation 3-60018
 - NN two body mesonic annihilations 3-70970
 - $n\text{p} \rightarrow \text{d}\gamma$, γ circular polarisation, correction from divergent P-violating NN π vertex 3-78198
 - pn, 25-60 GeV total cross section calc., shadow corrections including inelastic screening (Russian) 3-67166
 - pN, 70 GeV, unsuccessful search for heavy quasistable leptons 3-60022
 - pn 25-60 GeV total cross section calc., shadow corrections including inelastic screening (Russian) 3-67166
 - pN $\rightarrow \mu^+ \mu^- \text{hadrons}$, single muon spectra in parton model 3-40396
 - pN $\rightarrow \text{YN}$ low energies, one-pion exchange contribution to cross section (Russian) 3-60017
 - π exchange contributions, from πN phase shift analysis 3-67105
- nucleon-nucleon scattering**
 - see also neutron-proton scattering; proton-proton scattering
 - Bethe-Salpeter eqn., partial-wave analysis by computer 3-57394
 - correlation effects in electron scattering by nuclei (Czech) 3-71103
 - elastic, diffractive excitation of hadron resonances, phenomenological model 3-67096
 - inelastic at very high energies, bremsstrahlung model calcs. 3-67131
 - matrix Padé approximants, $^1\text{S}_0$ and $^3\text{P}_0$ partial waves 3-74413
 - multiplicity distribution systematics, isosinglet exchange 3-57443
 - potential model for hyperon-nucleon scattering, check 3-62874
 - scalar meson nonet, determ. of mixing angle, F/F + D ratio and coupling constant 3-60060
 - n-n scattering length and effective range from three-body calc. on $^2\text{H}(n, n)^3\text{H}$ 3-78340
 - NN \rightarrow NN, resonance ang. distributions 3-62885
 - nn scattering length determ. from $\pi^- \text{d} \rightarrow \text{nn}\pi$: final-state interaction 3-78181
 - nn scattering length determ. from $^2\text{H}(n, \text{np})\text{n}$ kinematically complete expt. 3-78338
 - nn scattering length in $^2\text{H}(n, \text{p})\text{nn}$ final state interaction, impulse approx. calc. 3-78339
- nucleon scattering**
 - see also hyperon-nucleon scattering; kaon-nucleon scattering; neutron scattering; nucleon-nucleon scattering; pion-nucleon scattering; proton scattering
 - Compton scattering forward spin-flip amplitude, Drell-Hearn-Gerasimov sum rule saturation 3-57311
 - Compton scattering of off-shell photons on polarised nucleons, invariant amplitudes 3-67018
 - deep inelastic, valence quark model of mixed symmetry and s-channel picture 3-62842
 - hadron-nucleon amplitudes, off-shell values, effect on hadron-nucleon amplitudes and exotic atoms 3-57541
 - inclusive 1^-N scattering at high-energy, tests for weak neutral current 3-57317

nucleon scattering continued

- nucleon Compton amplitudes, positivity restrictions 3-43106
- spin 1/2 particles, scattering by spin 1 particles, polarisation (*German*) 3-54335
- spin 1/2 particles scattering by spin 1 particles, polarisation (*German*) 3-54334
- cN, deep inelastic, scaling of individual channels, unified approach to resonances and partons 3-78140
- eN, deep inelastic, final state prediction using composite model of nucleon 3-78139
- En, deep inelastic, vector dominance and parton model anal. 3-74382
- eN, parton-model sum rules and positivity 3-54294
- eN, spin-dependent, positivity inequalities from light-cone algebra of quark currents 3-40350
- eN deep inelastic, scaling asymptotics in local quantum field theory 3-70869
- eN inelastic, in Bjorken-Paschos proton model 3-45883
- e-N inelastic scatt., comparison with photoabsorption in higher baryon coupling model 3-43115
- γ N, high energy, extended hadronic structure 3-57363
- γ N, reln. of isovector forward Compton amplitude to forward isospin even π N scattering amplitude with zero-mass pions 3-62834
- IN \rightarrow IN ν , lepton polarisation, one-photon approximation anal., decay 3-78145
- ν B, deep inelastic, dual parton model description 3-70903
- ν N, high-energy, at low q^2 , Adler test of PCAC 3-74360
- ν N, inelastic, spin sum rules, light cone scaling 3-78116
- ν N, inelastic structure-function relations from sum of direct-channel resonances 3-43109
- ν N, spin-dependent, positivity inequalities from light-cone algebra of quark currents 3-40350
- ν N deep inelastic scattering, parton model for cross-section x-dependence 3-78117
- ν N scalar scatt., Jost-Lehmann-Dyson representation and scaling 3-54315
- $\nu_e N \rightarrow e^- +$ hadrons, high energy, meas. total cross sections, test muon conservation law 3-66986
- $\nu_e N \rightarrow e^+ +$ hadrons, high energy, meas. total cross sections, test muon conservation law 3-66986

nucleons

- see also cosmic ray nucleons; neutrons; protons
- β -decay of bound nucleons in complex nuclei, differences from free nucleon decays 3-52145
- anomalous g_i factors for nucleons in nuclei, empirical deduction 3-49094
- core structure, antineutrino-nucleon inclusive scattering as probe 3-62813
- form factors, from dispersion model analysis of $\pi^- p \rightarrow e^+ e^- n$ (*Russian*) 3-59963
- form factors, scaling law from composite model of hadrons 3-70912
- parity-violating nucleon one-meson exchange potentials in current-current quark model 3-48994
- parton chain model, reln. to electroproduction 3-62829
- production, inclusive cross sections calc. in pionization region from PCAC 3-78220
- renormalisation const., rigorous upper bound, pion-nucleon coupling const., phase shifts 3-59989
- substructure studies using ν and e probes 3-67047

nucleus

- see also hypernuclei; nuclei with $A \leq 5$; nuclei with $6 \leq A \leq 19$; nuclei with $39 \leq A \leq 58$; nuclei with $59 \leq A \leq 89$; nuclei with $90 \leq A \leq 149$; nuclei with $150 \leq A \leq 189$; nuclei with $190 \leq A \leq 219$; nuclei with $A \geq 220$
- No entries

number theory

- see also digital arithmetic
- lattice sums evaluation in two and three dimensions 3-45730

numerical analysis

- see also approximation theory; difference equations; error analysis; finite element analysis; function approximation; function evaluation; functional analysis; functional equations; interpolation; iterative methods; Monte Carlo methods
- artesian well, unsteady drawout finite element method 3-56273
- atmospheric small-scale convection, numerical simulation 3-53493
- BCS approximation application to supercond. nuclei (*Rumanian*) 3-64425
- bonded connections, finite element analysis 3-41793
- circular orthotropic plate, lower bound plastic analysis 3-48731
- composite structure biaxially loaded longitudinally stiffened, elastic stability 3-59764
- crack analysis, collocation and finite elements 3-74036
- crack problem 3-40118
- cracks, finite element method for calc. of stress intensity factors 3-40126
- cracks, numerical soln. of integral equations 3-40125
- cracks in elastic bodies, finite element method soln. 3-40127
- cross-anisotropic deposits, settlement using isotropic theory 3-80600
- cylinder with internal aperture, determ. of non-stationary temperature field (*Russian*) 3-45662
- cylindrical shells with meridional cut, axisymmetric and antisymmetric potentials and deformations (*Russian*) 3-42783
- elastic contact problems, finite element method 3-66522
- elastic layer, transient disturbance by a buried spherical source 3-76864
- elastically constrained conical shells under hydrostatic press., buckling analysis by collocation method 3-59762
- elastoplastic plane medium, discretized model 3-40134
- elementary particle interactions, numerical study of ambiguities in phase-shift analysis 3-40406
- error-function, computing derivatives and integrals 3-66486
- finite element, accuracy for stress analysis of elastic plate with circular hole 3-40109
- finite element, of completely incompressible creeping flow 3-40105
- finite element, of stress intensity factors in cracked plates 3-40108
- finite element formulation of elastoviscoplastic constitutive relations, soln. of viscoplasticity 3-40098

numerical analysis continued

- flow viscous, in entrance region of parallel plates, numerical solution 3-46379
 - groundwater flow subject to time-varying recharge 3-73414
 - infinite series, numerical calc. including asymptotic props. 3-66489
 - lake Biwa-ko seiche, numerical experiments using nonlinear two dimensional model 3-76925
 - linearized functions, estimation of the error, and region of applicability (*Russian*) 3-70756
 - magnetotelluric response two dimensional sloping contact 3-76865
 - materials of heterogeneous systems 3-64768
 - Mathieu equations, matrix solutions 3-45626
 - meteorological data, objective analysis 3-80731
 - multiexponential decay curves, analysis by method of modulating functions (*French*) 3-49484
 - nonlinear pulsations of vibrationally unstable upper main sequence stars, direct numerical integrations 3-42189
 - nonlinear transformations, effect on computation of weak solns. 3-71731
 - nonuniform hereditary media, potentials and deformations (*Russian*) 3-42782
 - optimum finite-element idealizations, theorem 3-45650
 - Pade approximant applications including ϵ -algorithm 3-62427
 - paraboloid of resolution loaded at top by axial concentrated force, equilibrium (*Russian*) 3-62468
 - piezoelectric-semiconductor layered medium, acoustoelec. amplification of surface waves 3-68680
 - planar problems, stress intensity factors; approx. technique 3-74038
 - plane contact problem for linear deformation in presence of adhesion forces, Jacobian soln. (*Russian*) 3-42771
 - plasma confinement, toroidal, low-pressure axisymmetric stability analysis 3-46546
 - reflecting oblique shock wave structure 3-52472
 - resilient plane with round compression, influence of friction forces on stress distrib. (*Russian*) 3-45663
 - restricted three-body problem, families of periodic orbits 3-69805
 - rigid-body motions in curved finite elements, explicit addition 3-45683
 - seismogram integration giving true ground motion 3-76872
 - semiconductor four point probe measurements, correction devisors, cylindrical coordinates 3-68619
 - spherical shell, shallow, dynamic buckling 3-70660
 - stationary geothermal perturbation due to deep water rise (*French*) 3-42092
 - steel plate, anisotropic, notched, upper yield strength, stress-strain, finite element anal. (*Japanese*) 3-55798
 - telluric field over faulted basement 3-76593
 - thermoelastic stresses in expanding rectangle, appl. of extended source method and new numerical techniques 3-70586
 - thermoviscoplastic media, steady state wave propagation, dual variational principles 3-70647
 - three and four dimensional boundary layer theory, computational problems 3-49579
 - vibrations of flexible cables about static equilib. position (*Italian*) 3-40142
 - D-T inhomogeneous plasma, numerical analysis of thermal stability rel. to fuel injection 3-60619
- numerical methods**
- see also convergence of numerical methods; predictor-corrector methods
 - acoustic four-terminal transmission network, transmission loss by finite-element method 3-48289
 - aerohydrodynamics, multidimensional problems, processing and analysis of computation results 3-49587
 - aeromagnetic maps, source location technique 3-59160
 - airfoils, thick cambered, inviscid compressible flow through cascade 3-75226
 - anisotropic viscoelastic cylinder, centrifugal stresses analysis, numerical soln. 3-62453
 - atmospheric dynamics and circulation numerical simulation 3-51071
 - atmospheric spherical harmonics series summation, alternative algorithm 3-47758
 - atmospheric turbulence, quasi-geostrophic, numerical simulation 3-73324
 - averaged equations of concentric compression of plasmas by laser implosion of thin 'heavy' coating 3-57922
 - biological tracer data analysis, exponential components of response, calc. by numerical technique 3-70177
 - blast wave propagation problems, numerical solns. 3-52473
 - boundary layer equation, rel. to turbulent viscous fluid heat transfer and drag calc. (*Russian*) 3-52457
 - boundary layer flows, turbulent, non-reacting and equilibrium chemically reacting 3-52454
 - Bubnov-Galerkin method for bending stresses in inherently aging laminar on flexible base (*Russian*) 3-45677
 - Bubnov-Galerkin procedure wing panel behaviour in transitional region in gas flow (*Russian*) 3-46446
 - buckling under shear, diagonal stiffeners reinforcing clamped infinitely long plate, optimum distribution 3-57088
 - chemical kinetics, steady-state approx. in differential eqns. 3-44712
 - collocation method for determ. of difference eqns. for transverse vibrations of elastic bar (*German*) 3-42828
 - combined free and forced convective heat transfer and fluid flow in rotating curved rectangular tubes, numerical soln. 3-46404
 - computation, time-distance curves, dipping refractor, seismic waves 3-76535
 - conducting cylinder, e.m. fields and diffraction problems, integral eqn. soln. 3-51854
 - constant thermal diffusivity flows over in finite plane wall, soln. by Wiener-Hopf technique 3-46400
 - convection positive conservative second and higher order difference equations 3-49561
 - convergent series expansions solutions, computer programming for algebraic (literal) operations 3-78709
 - crack problems, asymptotic approximations 3-40121
 - cracks, edge and surface problems, soln. with alternating method 3-40122
 - cracks, two-dimensions, solution by conformal mapping technique 3-40119

numerical methods continued

- curve fitting, approximating function, best fit definition, subroutines 3-74008
- curved finite elements by the method of initial strains 3-42767
- dislocation loops, by weak-beam imaging 3-59668
- distribution, by numerical integration and Monte Carlo methods 3-48514
- elastic stress intensity factors computation, finite element methods eval. 3-48725
- electron diffusion equation, solution by finite difference mesh method 3-42638
- element stiffness matrices, strain energy content, weighted eigenvalue method 3-45638
- e.m. flowmeter, response to nonaxisymmetric rectilinear flows 3-66478
- e.m. theory, implementation of method of moments 3-48832
- e.m. wave scatt. by resistively loaded strips 3-40210
- e.m. wave scattering, noniterative soln. of integral eqns. 3-62544
- fine structure e.s.r. spectra, in strong crystal fields, spin Hamiltonian consts. determ. numerical solution 3-44312
- finite difference equations, determination of effect of singularities 3-40107
- finite element, for flow of viscoelastic materials (*Russian*) 3-45660
- finite element grids based on minimum pot. energy, optimization 3-48726
- finite elements for axisymmetric solids under arbitrary loadings with nodes on origin 3-48740
- flexural vibrations in orthotropic plates, natural freq. calc. 3-42809
- flow, unsaturated, through porous media, soln. of Richard's equation 3-57845
- flow around bodies, 2 dimens. (*Japanese*) 3-49544
- flow patterns around heart valves, numerical method 3-53736
- flows, steady, three-dimensional with recirculation, two calculation procedures 3-49538
- flows, unsteady two dimensional with free boundary 3-75185
- fluid dynamics numerical methods (conf. Paris, France, July 1972) 3-49533
- fluid mechanics, numerical methods, volume II, (Conf. Paris, France, July 1972) 3-78930
- fluid mechanics numerical methods, volume II, (Conf. Paris, France, July 1972) 3-49530
- forced convection with uniform heating in flow over a plate and fully developed flow in a tube, numerical soln. 3-46406
- gas mixtures, cylindrically confined, explosive, model for the ignition, numerical soln. 3-46456
- gaussian quadrature, solution of Planck's equation 3-77913
- geodesic generation in colour space, gradient algorithm development 3-81312
- geodesic inverse, numerical integration (*German*) 3-42058
- geometry S_4 eqns. analytic soln. 3-52217
- geophysical time function spectra recovery 3-42054
- gravitational thermal diffusion columns, steady state, numerical calc. (*French*) 3-41034
- grooved shafts in elastic bending, stress conc. factors calc. using point-matching technique 3-54098
- hard-sphere collision operator, eigenfunctions and spectrum, numerical soln. 3-40176
- heat conduction in solids with nonlinear boundary conditions, finite element method 3-45739
- Helmholtz equation with non-uniform boundary conditions, solution by finite difference approach 3-42387
- Hermite's (real symmetric) matrix pair, eigenvalue detn. using successive approx. method (*German*) 3-48696
- hydrocarbons, conjugated, optical dipole polarisability calc. 3-43437
- hypersonic and supersonic flowfields around slab delta wing, algorithm for three-dimensional method of characteristics 3-49580
- iceberg drift determ. from synoptic weather data 3-59201
- ideal compressible flow, conservative difference scheme, monotonicity 3-49588
- image reconstruction from microwave hologram 3-73776
- incompressible liquid flow in transverse mag. field, boundary layer eqn. soln. by characteristics method (*Russian*) 3-43607
- incremental technique, for plastic deformation of multilayer cylindrical shell with non-isothermal loading (*Russian*) 3-40133
- indentation, ring stamp problem, elastic half-space, exact solution, recurrent relationships (*Russian*) 3-70581
- indentation of plastic rigid halfspace by a smooth spherical stamp (*Russian*) 3-70623
- integral equation soln., rel. to neutron flux distributions in rectangular lattice cells 3-60244
- integration, generalized procedure for divergent integrals, numerical computation 3-45628
- integration and approx. analysis for forced oscillations of liquid-filled elastic cylindrical shell (*Russian*) 3-42816
- internal flows, three dimensional, viscous, computation 3-49630
- isothermal and nonisothermal laminar inelastic non-Newtonian tube entrance flow following a contraction 3-43543
- laminar combined convective flow over flat plates, numerical study 3-46403
- laser theory complex-values kernels, initial value method for integral operators 3-42997
- line radiative transport in nonhomogeneous media, improved separability approximation 3-42912
- linear induction motor end effect, numerical integration of thrust force integral equations 3-66719
- liquid drop oscillations, numerical method soln. 3-46465
- long wave eqn., limits of time stepping for numerical solutions 3-40701
- magnetohydrodynamic blast wave, planar and spherical 3-57895
- magnetotelluric study, western Canadian sedimentary basin, tensor analysis, numerical model 3-44853
- material and/or geometrically nonlinear structural analysis, evaluation of solution procedures 3-45673
- Maxwell's equations (*French*) 3-48831
- MHD streamline flow around circular cylinder, numerical study (*Russian*) 3-43615
- modal-type soln. for dynamic nonlinear response of cylindrical shells to asymmetric pressure loading 3-70554

numerical methods continued

- model of thermal radiation in dusty atmosphere 3-44885
- N-body gravitation problem, integration scheme, near and distant stars 3-70726
- natural convection boundary layer flow over horizontal and slightly inclined surfaces, stability, numerical integration 3-40722
- Navier-Stokes equations, compressible, numerical experiments 3-49585
- Navier-Stokes equations numerical soln. methods, review 3-49534
- Newton-Raphson method for determ. of condensation in dynamical weather model 3-47846
- nine-point Poisson operator, analytic inversion 3-42742
- non isothermal laminar flow of gases through cooled tubes, numerical solutions 3-46407
- nonlinear aerodynamics of bodies in coning motion 3-46440
- nonlinear waves, evolution in a dissipative medium with dispersion, numerical simulation (*Russian*) 3-68031
- nuclear reactor kinetics eqns., three-dimensional space dependent, soln. by semi-implicit method 3-60263
- oceanography, flow calculations in baroclinic ocean, numerical methods and results 3-73262
- orthotropic skew plates, postbuckling behaviour, numerical soln. 3-62491
- periodically constricted tubes, steady state incompressible Newtonian flow, numerical soln. 3-57839
- phase-space integrals and asymptotic behaviour, numerical evaluation for high-energy collisions 3-43133
- piston motion, dry friction, numerical anal. (*Russian*) 3-42761
- plane parallel unstable flow, numerical study of mildly non-linear partial differential equation 3-49545
- planetary atm. temp. structure determ. 3-47920
- planetary boundary layer eqns., revision of Estoque and Bhumralkar method 3-73283
- plasma h.f. instabilities in arbitrary configurations, numerical method 3-79150
- plastic flow in hot rolling, math. predictions, temp. distrib. effects 3-80339
- polyatomic molecules, potential energy, function vibrational Hamiltonian calc. 3-40601
- power density spectra calculation 3-42460
- probabilistic radiative transfer, mean number of scatterings, numerical soln. 3-42914
- radial asymptotic expansions for singular potentials, numerical integration 3-40149
- radiative transfer theory, angular quadrature perturbations, numerical solution 3-42913
- raindrop falling at terminal velocity in vertical electric field, stresses, numerical method 3-47766
- rapid flow past circular cylinders vortex method, numerical soln. 3-49567
- rarefied gas, thermal conduction analog 3-67943
- recalcitrant synchrotron integrals evaluation for case of guide fields comprising magnetic segments 3-57184
- relaxation spectrum, hybrid method 3-66557
- rimmed Cassegrain resonator, modes and losses, numerical iterative procedure 3-78053
- Ritz method for natural oscillations of variable-thickness cylindrical shells augmented by masses (*Russian*) 3-40140
- rotational excitation scattering parameters, radial asymptotic expansions, numerical integration 3-40150
- Runge-Kutta, end effects calc. in Faraday type MHD generators with nonequilibrium plasmas 3-46558
- scattering data, analytic continuation, necessity of nearly-best possible methods 3-62556
- Schrodinger eqn. finite difference boundary value method of soln., comparison with Cooley-Cashion-Zare method 3-42844
- self-avoiding random walk on triangular or honeycomb lattice, numerical study 3-40183
- semitransparent cylindrical medium solidification, heat conduction and radiation, integral method 3-46701
- separated shear layer, inviscid reattachment 3-49591
- shock tube interaction-region boundary layer, nonlinear problem 3-57794
- shooting method for soln. of eigenvalue problem of unsymmetric wrinkling of circular plates 3-74054
- Smith-Purcell radiation, from line charge moving parallel to reflection grating 3-42943
- solar spectra line inversion method 3-51333
- space shuffle flowfields computation using noncentred finite difference schemes 3-43569
- steady flow at Mach number one past wing airfoil, computational method 3-52463
- stochastic dynamic system with 3 degrees of freedom, numerical study by dimensional mapping 3-42748
- stress and strain calc. using finite element and dynamic relax. methods 3-47808
- structural dynamic analysis, condensation of finite element eigenproblems 3-45680
- TCNR methods, for nuclear reactor spare-time kinetics and heat flow problems 3-46063
- Telenin's method for soln. of convective heat transfer in space shuttle base region 3-52443
- three-body problem, commensurable restricted, phase plane anal. 3-69804
- torsion of prismatic bars, numerical soln. 3-48715
- transonic aerodynamic field around airfoils, numerical procedure for a free boundary-value problem in hodograph plane 3-49584
- transonic flow about wing-cylinder combinations and lifting swept wings, relaxation methods 3-49589
- transonic flow around airfoils, time dependent calc. 3-49592
- transonic flow around plane and axisymmetrical bodies, numerical approach 3-49590
- transonic flow past lifting wings 3-63708
- triatomic molecule, linear, computer appl. to calc. of pot. energy function 3-78710
- turbulent boundary layer, high order moments of Reynolds shear stress fluctuations calc. 3-46435
- turbulent boundary layer flow above a change in surface roughness, mixing lengths and energy eqn. models comparison 3-52461

numerical methods continued

- turbulent boundary layer shape after corner expansion, numerical calculation 3-57856
- turbulent shear flow near walls, mag. field influence, numerical soln. (*Russian*) 3-43603
- turbulent skin friction on a rotating disc, integral calc. 3-57721
- turbulent transitions in convective flow 3-49563
- two discrete vibrating systems synthesis using eigenvalue modification 3-42753
- unsteady and three-dimensional boundary layer flows 3-71761
- unsteady boundary layer, separation, numerical investigation 3-60550
- unsteady boundary layer equations when there are regions of backflow, numerical integration method 3-46434
- unsteady flow with shocks, computational methods 3-49596
- viscoplastic media hydrodynamics, time-dependent problems, Monte Carlo soln. method 3-71839
- viscous flow, incompressible fluid, rectangular cavities, finite-difference equations, behaviour of vortices 3-71755
- viscous three-dimensional flow between convergent travelling surfaces, modified Marker-and-Cell technique 3-75209
- water waves, vortex sheet representation of Laplace eqn. 3-43581
- weather forecasting, boundary error reduction (*German*) 3-59172

numerical methods, convergence *see convergence of numerical methods***nuvitors**

No entries

Nyquist noise *see thermal noise***occultations**

- Brinkmann's method for planetary atmosphere composition meas. using occultation curve spikes, critique 3-47912
- Crab nebula, X-ray studies, 1974-75 3-81210
- Europa, by IO, indication of polar cap 3-61690
- Galilean satellites by Sun and Earth during 1973-74 period 3-47908
- GX5-1, accurate position from lunar occultations, Copernicus satellite obs. 3-59367
- GX 3+1, by Moon, detection of gamma-ray spectral line by balloon borne FWHM instruments 3-77125
- Jovian satellite-satellite eclipses and occultations 3-47918
- R Leonis by Moon, angular diameter determ. from obs. during lunar occultations 3-77085
- lunar, photoelectric meas. of timings 3-61710
- lunar occultations of stars, photoelectric photometer with msec. integration time 3-45248
- Mars., analysis of Mariner 9 occultation data 3-61708
- Mars, Mariner 9 S band occultation meas. of atm. and topography 3-69868
- Mars, of Mariner 9, approx. to surface and atm. 3-69869
- moon, obs. effects of lunar motions 3-47963
- Ooty radioresources, lunar occultation obs. at 327 MHz of 6 objects with flat spectra 3-42206
- planetary atmosphere study by radio occultation of spacecraft 3-65968
- planetary atmosphere study by radio occultation of spacecraft, Pioneer and Mariner outer planet missions 3-65969
- SAO 76530, 4 August 1972, grazing occultation 3-65897
- β_1 Scorpii, by Jupiter, photometric obs. 3-45035
- 139 Tauri, by Moon, predicted positions of Moon's centre and star found to be in error 3-65790
- two-satellite microwave occultation system for terrestrial atmospheric pressure profile determ. 3-51187
- 2U 1700-37, X-ray source, obs. indicating possible binary system 3-48073

ocean water *see seawater***oceanography**

- see also liquid waves; seawater; tides*
- acoustic echo-sounding techniques and appl. to gravity-wave, turbulence and stability studies 3-65517
- acoustic pulse propagation, amplitude spectra 3-81339
- acoustic wave backscattering, ocean volume between Vancouver Island and Hawaii, spectral characteristics, depth ranging 3-77330
- acoustic wave backscattering, volume, Tasman Sea, Coral Sea, Indian Ocean, 2.5 to 16 kHz, characteristics, effects of fish 3-81340
- acoustic wave reverberation, diurnal variation in California current, 3 to 30 kHz, frequency dependence 3-77329
- acoustic wave scattering from surface, frequency smearing 3-42395
- adaptive measurements, computer methods (*Russian*) 3-51203
- adaptive meter, equations of dynamics, study of nonstationary hydrophysical elements (*Russian*) 3-80872
- S.W. Africa, anal. of phosphates in sediments 3-56144
- air-sea gas exchange, effect of air bubble solns. 3-50990
- air-sea interface, mechanics of dynamic roughness 3-59019
- air-water interface, evaporation and energy transfer, effect of wind and waves 3-47679
- airborne and satellite remote sensing of Anacapa Island natural resources 3-51006
- airborne radiative transfer from tropical sea, land surfaces, obs. and calcs. 3-59100
- airflow above natural waves, turbulence wave-related fluctuations 3-47740
- albedo of sea surface, comments on high values 3-47684
- ambient acoustics meas., free diving buoy 3-53569
- American Geophysical Union, conference (Washington, D.C., USA, 16-20 Apr 1973) 3-56004
- Antarctic Ocean, Ba conc. rel. to geochemistry of ^{226}Ra 3-65260
- Arabian Sea, quasi-stationary ocean currents 3-65282
- Arabian Sea, upwelling and upward mixing during s.w. monsoon season 3-50985
- Arctic Basin, obs. of ice shifts 3-65279
- Arctic Ocean, temp. microstructure anomalies 3-53452
- Arctic Ocean water, wintertime surface layer convection rel. to sea ice formation 3-44856
- Arctic sea ice rel. to maritime transport technology 3-80884
- Arctic Seas, dissipation of tidal energy (*Russian*) 3-73268
- North Atlantic, 1948-68 water temp. anomalies, long-period var. 3-41937
- North Atlantic, average monthly positions of oceanic fronts 3-41938
- N Atlantic, fallout tritium and mixing in main thermocline 3-59034
- oceanography** continued
- N Atlantic, longitudinal var. of aerosol radioactivity over N. Atlantic Ocean 3-80759
- SE Atlantic, O_2 minimum layer, structure and characteristics 3-41939
- E. Atlantic, obs. of variability in thermohaline staircase 3-53460
- Atlantic, tropical, discriminant statistical analysis of oceanological characteristics, probability estimates of formation of water masses (*Russian*) 3-80694
- Atlantic deep-sea long-core samples, analysis 3-73227
- Atlantic Ocean, dissolved O_2 , isotopic anal., mass spectrometry (*Russian*) 3-47695
- N. and W. Atlantic Ocean, in situ O meas. 3-53446
- Atlantic Ocean, isotopic formation of surface waters, distrib. of salinity and ^{18}O (*Russian*) 3-47694
- Atlantic Ocean temperature and salinity variations, survey over many years, mean square deviation calc. (*Russian*) 3-47699
- Atlantic tropical zone, distrib. and dynamics of dissolved mineral P, seasonal effects (*Russian*) 3-80701
- Atlantic tropical zone, transparency, attenuation coeff. rel. to density gradient, effect of plankton biomass (*Russian*) 3-47700
- Atlantis Fracture Zone, camera and pinger seabed observations 3-80680
- atmosphere and ocean interaction mechanism during a storm 3-76684
- atmospheric CO source 3-73312
- attenuance spectral method, determination of suspended inorganic substance, Baltic Sea (*German*) 3-76916
- automatic measuring buoy (*Italian*) 3-59198
- Bahama Islands, bathythermograph obs. rel. to Rossby waves 3-80688
- Baltic, heat exchange coeff. and turbulent thermal conductivity calc. (*German*) 3-65263
- Baltic Sea, long term oscill. in annual mean sea level during 1811-1970 period 3-47665
- baroclinic circulation, appl. of Schvets method 3-73266
- baroclinic instability, spatial growth, appl. to Gulf Stream 3-56150
- baroclinic instability in western boundary current, numerical model 3-44857
- baroclinic ocean, numerical methods and results of flow calculations 3-73262
- baroclinic vortex, two-layer fluid, instability, separate circulations 3-46426
- bathymetric, obs. during marine geophysical study off western India 3-53391
- bathythermographs, mechanical, reliability study 3-76921
- Bay of Biscay, relict and recent shelf deposits, lithology 3-41941
- Bay of Biscay, vertical structure of semi-diurnal tidal currents 3-53457
- beach profiles, Chedabucto Bay, Nova Scotia, effect of sediment removal 3-76679
- beaches and bays, effect of storm tides on motion and height of water 3-58990
- Beaufort Sea (S), warm water advection during Aug-Sept. 1971 period 3-53453
- Beaufort Sea ice, remote sensing during 1972, March 3-59025
- bioluminescence measurement, instrumentation and methods (*Russian*) 3-47702
- Biscay Seamount, bathymetric map rel. to morphology and origin 3-44865
- Black Sea, sorption of B and Si using granulated $\text{Zr}(\text{OH})_4$ (*Russian*) 3-80698
- Black Sea tsunami following Erzincan (1939 December 26) earthquake, tide-gauge data 3-47704
- bottom-sensing signal generator for use with STD systems 3-53563
- Bristol channel, circulation rel. to salinity and temp. distribution 3-65261
- bubble transport theory with application to the upper ocean 3-49612
- California coast, currents on continental shelf, multilayer hydrodynamical-numerical model 3-58991
- S. California shallow coastal water, temp. var., surface wave height and water motion 3-58989
- Cape Waters, South Africa, obs. of quasimonochromatic 0.05 Hz gravity waves 3-53459
- capillary wave modification by gravity waves 3-56152
- capillary wave spectrum, high-order analysis of reflected daylight 3-42090
- Caribbean deep sea core, late pleistocene, palaeoclimatic investigation, isotopic and faunal methods 3-76783
- Caribbean Sea, boron content and distrib., boron-chlorine ratio (*Russian*) 3-47692
- NE Caribbean Sea, tidal observations near amphidrome 3-59045
- circular basin, shoaling formula for spiral waves 3-50992
- circulation of homogeneous ocean, induced by continental slopes, wind stress 3-47670
- CLIMAP programme, study of climatic fluctuations through deep sea cores 3-76781
- cloud lines, anomalous, maritime condensation processes, effects of atmospheric trace constituents 3-58984
- coastal upwelling, β effect, wind-driven model, longshore and offshore flow 3-47671
- coastal upwelling, ocean circulation model, time-dependent winds 3-47672
- coastal upwelling, turbulent diffusion horizontal and vertical Prandtl numbers 3-47682
- coastal upwelling, wind-driven, effect of bathymetry subsurface motion, induced jet 3-47673
- coastal water optical properties airborne photometry 3-77477
- coastline waters, diffusion and dispersion 3-65269
- compact pack ice, one-dimensional collision model for drift 3-73409
- conical hot Pt film probes, limitations as flow sensors 3-51201
- continental shelf, Oregon, sealevel and current l.f. variations 3-47676
- continental shelf circulation, diagnostic model 3-56151
- continental shelf front dynamics, obs. and model 3-59016
- continental shelf model, seasonal density structure and circulation 3-59023
- continuously stratified ocean, upwelling and coastal jets 3-59015
- convective flow in ellipsoidal cavity 3-71741

oceanography continued

- corrosion in sea water, effects of depth of submergence, temp., salinity, pH, velocity of currents and conc. of dissolved gases (*Russian*) 3-80697
- 'Crab' remote-controlled underwater craft 3-69746
- cryogenic sensors, nuclear-precessional magnetometer, signal/noise ratio, liquids with high nuclear mag. susceptibility (*Russian*) 3-45457
- current calc., Pacific Ocean, wind and density nonuniformities, bottom topography, discharge of Antarctic circular current (*Russian*) 3-47697
- current measurements, Lake Superior, 1971, aerial photography and photogrammetry 3-47683
- current meter array, objective data anal. 3-59200
- current meter compasses, effects of non-linearities 3-53564
- current meters, review 3-69747
- current sensor, electromagnetic, heading error 3-76919
- current system, oscillations 3-80712
- currents, calc., South Pacific Ocean, level surface equation, differential approx. method (*Russian*) 3-47690
- currents, calc., wind stress, variable ocean depth (*Russian*) 3-47687
- currents, Cromwell and Lomonosov 3-73265
- currents, quasi-stationary, meas. technique 3-65282
- currents, surge and ebb, role of nonuniformity of wind, inertial effects, bottom topography (*Russian*) 3-80691
- currents, the regularity of reconstruction of a mesoscale turbulent structure (*Russian*) 3-80696
- currents, wind driven, Washington continental shelf, effect of surface current and wind direction 3-80721
- currents off the Equator, calc., density distrib. (*Russian*) 3-47685
- cyclonic rotary currents in N.Hemisphere, possible origin 3-41936
- data acquisition using sensors 3-42088
- data recording ocean depths, legal problems (*French*) 3-56263
- data transmission, telemetering buoys, computer M-220-M, radiochannel, subprogramme details (*Russian*) 3-47850
- deep ocean channels, response to wide band pulses 3-42440
- deep submersibles, glass-reinforced plastics under high pressure 3-69374
- deep water wave component growth and decay 3-47708
- deep-sea disposal of radioactive waste, safety evaluation models 3-70192
- deep-sea sediments, late pleistocene-holocene, spectral analysis, non-random fluctuations 3-76782
- deep-sea sediments, variations in intensity of magnetisation and inclination 3-59039
- Delaware Bay, dynamics of aquatic frontal systems 3-58988
- dense water formation, topographic effects, theoretical model 3-65256
- depth determ., errors of thermometric method 3-42086
- directional wave height spectra for 7 second ocean waves, synthetic aperture obs. 3-58982
- dynamics of free edgewaves on coastal upwelling frontal zones 3-59002
- Earth Resources Technology Satellite, appl. to oceanography and coastal zone processes 3-80717
- East Mediterranean, changes in isotopic comp. during Holocene 3-51000
- East Pacific Rise at 39°S, thermal environment 3-76618
- edge waves, field meas. of water currents close to shore 3-41934
- electric currents induced by fluid convection 3-73249
- energy balance and transport processes 3-59044
- energy containing oceanic eddies, waves and turbulence theoretical models 3-65254
- Epstein-type under-ocean duct, sound propagation using normal-mode approach 3-41948
- Equatorial Pacific, telecommunications 3-56146
- Equatorial Pacific core, oxygen isotope and palaeomagnetic stratigraphy 3-76693
- equatorial thermocline, eastward jet and westward current meas. and theory 3-80715
- equipment, Dillingham Corp. Hydro Products Division 3-53568
- filtration of spatial frequencies, effect of parameters of a slotted flat analyser (*Russian*) 3-80873
- finite-difference methods, shortcomings for oceanographic work 3-59006
- flat ocean, irradiance refl., radiative transfer eqn. 3-53438
- floating drilling rigs, development of off-shore techniques (*German*) 3-65539
- E Florida coast, unusual plume behaviour from ocean outfall 3-61444
- four-dimensional analysis, automated collection and processing of data (*Russian*) 3-47849
- frontal system in upwell regime, west of Cape Town 3-73275
- Galapagos Islands region, optical and hydrographic obs. of Cromwell Current 3-53454
- Galapagos spreading centre, faulting rel. to near-bottom soundings 3-65201
- gas exchange across air-water interface, transfer of O₂, CO₂ and water vapour 3-44855
- GATE, instrumentation and international cooperation 3-80880
- general oceanic turbulence equations study (*French*) 3-65268
- GEOSECS Atlantic cruise, light scattering and particulate matter results 3-58995
- GEOSECS first intercalibration station, temporal var. of excess-Rn profiles 3-58993
- GEOSECS meas. of excess-Rn in near bottom and surface Atlantic water 3-58994
- geotechnical var. meas. in place from small submersible 3-80868
- geothermal field, heating of cold-water intrusions 3-58981
- Gibraltar Strait, optical struct. of water masses (*Russian*) 3-80703
- global energy, time-depend. model eqn. of earth-atm.-ocean 3-47609
- global water exchange, mathematical theory 3-80765
- gravimeter, GMKP, tests at sea, effectiveness in the presence of icebergs (*Russian*) 3-73963
- gravity wave lines observed by NOAA satellites 3-58985
- Gulf of California, heat flow meas. rel. to sedimentation 3-53445
- Gulf of California, tidal patterns and energy balance 3-41935

oceanography continued

- Gulf of Maine, props. of sediments recovered with giant piston corer 3-58836
- Gulf of Mexico, D distribution 3-61442
- Gulf of Mexico, sources, sinks and concs. of light hydrocarbons 3-73273
- Gulf Stream, 49°30'W, current metering, section runs, XBT survey, STD 3-80679
- Gulf Stream, current meter array near 39°25'N, 49°54'W 3-59011
- Gulf Stream, dynamical structure of western boundary currents 3-58997
- Gulf Stream, meanders rel. to spatially growing waves 3-56150
- Gulf Stream, obs. of cyclonic eddy, STD meas. 3-59013
- Gulf Stream, variability of deep flow 3-59010
- Gulf Stream anticyclonic eddy, observed formation 3-65274
- Gulf Stream splitting, effect of topography on ocean currents 3-59008
- Gulf Stream surface features, satellite monitoring 3-59012
- heat and moisture fluxes, momentum above ocean, calc. 3-76726
- heat flux from sea meas. using 2-wavelength radiometer, divergence effects 3-51202
- heated discharge, coastal zones, effluent dynamics modelling 3-53462
- h.f. waves rel. to aerodynamic roughness and wind speed 3-61440
- horizontal turbulent diffusion coeffs. in littoral zone of Black Sea using aerial survey data 3-51004
- hydrophysical data, collection and processing, M-220M computer (*Russian*) 3-80871
- hydrophysical instruments, cylindrical sensors, spectral characteristics, design (*Russian*) 3-47848
- hydrophysical problem solution, selection of optimal set of operations, digital probability computing system (*Russian*) 3-80695
- Hydroplot/Hydrolog system, survey and data processing 3-53567
- ice age sea surface temps. compared with present temps. 3-76690
- iceberg drift determ. from synoptic weather data 3-59201
- iceberg mass meas. 3-59027
- icebergs, anal. of accompanying circulation features, forecast of 1973 iceberg season, Labrador and Newfoundland 3-80718
- icebergs, anal. of accompanying circulation features, forecast of 1973 iceberg season, Labrador and Newfoundland 3-80719
- illumination field under wavy surface, correlation function and power spectrum 3-73264
- Indian E. Coast, sea temp. variations 3-47667
- W Indian Ocean, equatorial undercurrent during SW monsoon 3-80690
- Indian Ocean, high-speed equatorial surface currents 3-76697
- Indian Ocean, square average free-air gravity anomalies (*German*) 3-73277
- inland seas, ocean coast, underwater ambient noise distrib. 3-77331
- instrument depth control techniques 3-65541
- instrumentation for Oceanic Monitoring, Assessment and Prediction program 3-80882
- instrumentation for polar studies 3-80881
- instrumentation for research 3-65537
- instrumentation prospects 3-80883
- internal gravity wave scattering by deep ocean fine-structure 3-61443
- internal wave breaking rel. to microstructure 3-65253
- internal wave dissipation, variable depth basin, effect of viscosity (*Russian*) 3-50997
- internal wave effects on depth of sound-scatt. layer 3-65284
- internal wave generation, travelling field of pressure, sea with a discontinuity layer (*Russian*) 3-80692
- internal wave meas., fine structure contamination 3-59204
- internal wave obs. using directional h.f. transducer 3-59038
- internal wave resonant generation 3-73270
- internal wave strain, temp. perturbations, vertical spectra 3-47677
- internal waves, stratified sea, effect of surface pressures, density variations (*Russian*) 3-47689
- intracoastal waterway, quality management model 3-58983
- Ionian Sea, shallow thermal structure during summer 1972 period 3-59030
- irradiance reflectivity in and above ocean 3-59024
- Israeli results from the ERTS-1 program Multi-Spectral Scanner obs. 3-50872
- Kakhovka reservoir, suspended sediment flow rate 3-76928
- Kelvin wave generation, near shore thermocline, Lake Michigan 3-47674
- lake, evaporation and cooling under unstable atmos. conditions 3-56149
- lake Biwa-ko seiche, numerical experiments using nonlinear two dimensional model 3-76925
- large-scale dynamics of open ocean, meas. of mean wind and drag coeff. 3-50995
- LIDAR deep sea meas. (*German*) 3-59199
- light scattering indicatrices, meas. and calc., Junge type particle size distrib. (*Russian*) 3-50998
- Liverpool Bay, residual drift near sea bed, obs. study 3-65262
- Lomonosov Current, characts. of thermohaline structure 3-65277
- Long Island Sound, dredge spoil disposal, biological, chem. and phys. studies 3-53782
- long period waves, influence of horizontal component of Earth's rotation 3-73261
- long waves in shallow triangular river channels 3-56153
- long waves on rotating ocean, generation rel. to wind stress distribution 3-65285
- long waves on surface of rotating sea due to travelling disturbances 3-50986
- long-period water-wave activity meas. assoc. with MILROW and CANNIKIN nuclear explosions 3-53439
- longshore energy flux, longshore flux and longshore sediment transport 3-59043
- Loop Current time series 3-59009
- M₂ tidal currents, structure in N.W. Atlantic 3-65259
- magnetic field induction in shelving oceans by external agencies rel. to geomagnetic field reversals 3-65229
- magnetostriuctive transducer for use underwater 3-53792
- mapping of temperature and salinity, effects of winds and tides 3-41944
- marine air, Aitken and giant nuclei, salt conc., wind speed 3-47741

oceanography continued

- marine exploration, computer control systems for real time data output 3-65494
- marine heavy-mineral deposits, prospecting off East African coast, Valdivia research ship voyage (*German, English*) 3-65276
- marine instrumentation, technical requirements rel. to failure 3-80877
- marine near-bottom magnetic anomalies rel. to field over last 5 m.y. 3-58932
- marine radioecological experiments, general recommendations for design 3-47847
- marine raw materials on sea bed and in seawater, in USSR (*German*) 3-61445
- marine research, unmanned remote control systems, Benthos-300 during apparatus (*German, English*) 3-65538
- marine sciences instrumentation symposium (Florida, 31 Jan.-2 Feb., 1973) 3-80876
- marine sediments, worldwide unconformities rel. to eustatic changes of sea level 3-56042
- mean shear effects on inertial-period currents frequency shift 3-59001
- mechanism of tsunami earthquakes 3-44816
- Mediterranean, anal. of longit. waves (*Spanish*) 3-56145
- N.W. Mediterranean, deep convective mixing preceding hydrographic conditions 3-65255
- Mediterranean, shallow water sound transmission data, decay laws 3-41950
- Mediterranean, velocity of outflow 3-76691
- Mediterranean, vertical winter circulation pattern 3-51003
- W Mediterranean magnetic anomaly pattern from 600 m aeromagnetic survey 3-56103
- meteorite impact, range of effects 3-59326
- methane concs. in marine environments 3-73274
- Mid-Atlantic Ridge, asymmetrical bathymetry rel. to fracture zones 3-58861
- Mid-Atlantic Ridge, deep-tow magnetic meas. of anomalies across axial valley 3-56141
- mid-ocean mesoscale modelling of flow patterns rel. to bottom topography 3-58996
- mixed layer, heating-cooling processes on diurnal scale 3-59032
- Mn nodules, microlaminations, scanning electron microscopy obs. 3-61446
- mobile hydrospace systems, general description of bionics (*German*) 3-61607
- modelling of geomagnetic var. in or near ocean using generalized image technique 3-59196
- moving gust patterns, 'Cat's paws', surface capillary waves 3-47680
- N. Atlantic deep-sea core V23-82, climatic record, past 130000 years 3-76784
- N. Sea, long term distribution 3-56154
- National Data Buoy Center, Sensor system development programs 3-80879
- naviface, cloud shadow effects 3-59020
- Nimbus-5, description of equipment and expts. 3-41873
- non-stationary processes, classification 3-47666
- nonexplosive submarine volcanism, sof ar obs. 3-76569
- North Atlantic, deglacial warming 3-76696
- North Atlantic, semiannual variability of system of currents (*Russian*) 3-80693
- North Atlantic storm microseisms, meas. at Oulu, Finland 3-61341
- North Pacific, large-scale sea surface temp. fluctuations 3-59029
- North Pacific Experiment, oceanic processes rel. to weather phenomena 3-44903
- North Pacific Ocean, atmospheric effects of sea surface temp. anomalies 3-41945
- North-east Pacific, seasonal variation of underwater noise 3-41933
- Northeast Atlantic post-Eemian palaeoceanography, core samples 3-41943
- Northern Hemisphere oceans, annual poleward energy transport 3-65270
- northwestern African margin, sea floor spreading from six geophysical profiles 3-73259
- objective analysis, automated collection and processing of data (*Russian*) 3-47849
- ocean beds, upper centimeters, gamma-density measuring device (*German*) 3-61608
- ocean engineering wave mechanics, book 3-56264
- ocean wave height meas. by two frequency radar interferometry 3-59197
- Ocean Weather Station 'P' obs., spectral anal. 3-59014
- ocean-bottom acoustic-transponder-array survey, nonclassical determ. of spatial coords. 3-44965
- offshore bars, mechanism for origin and corrosion 3-59041
- oil slick, viscous-gravity spreading 3-58979
- open bay, numerical study of steady-state circulation 3-61441
- optical images underwater transmission, Fourier techniques application to test linear-invariant hypothesis 3-45781
- W. Pacific, equatorial undercurrent, meas. and theories 3-58998
- Western Pacific, heat flow in marginal seas 3-76698
- Pacific, N.E., late pleistocene-holocene changes from radiolarian assemblages 3-76695
- Pacific, tropical S.E., cores, stratigraphic and palaeoclimatic analysis 3-76694
- NE Pacific, upper layer modification at Ocean Station Papa 3-61439
- NW Pacific Basin, new data on bottom relief 3-41942
- Pacific circulation and temp. distribution, two-level numerical model predictions 3-59005
- Pacific equatorial zone, bioluminesc., rel. between spatial distrib. and hydrological and hydrophysical parameters (*Russian*) 3-80702
- Pacific equatorial zone, currents, new circulation of water scheme (*Russian*) 3-47698
- Pacific Ocean, vertical sound velocity distrib. at great depths 3-42438
- Pacific Ocean sediment, Ra, Th and U isotopes in interstitial water 3-65267
- Pacific Ocean transition zone, distrib. of bottom relief and sea depth 3-47705

oceanography continued

- Pacific subarctic zone, warm intermediate layer, winter convection 3-80707
- particle sedimentation in thermocline 3-59031
- passive microwave radiometry, appl. to Earth resources surveys 3-51178
- phosphate-water isotopic temp. scale 3-61438
- photometer calibration rel. to air, directed light, attenuation coeff. meas., effect of salinity and temp. (*Russian*) 3-45483
- post glacial sea level changes from marine shell deposits in New Brunswick 3-73408
- pressure, waves in sea from linearised Navier-Stokes equations 3-80704
- pressure tolerant electronics, for deep ocean applications 3-53566
- Project FAMOUS, planning of Mid-Atlantic Ridge investigations 3-44863
- radar mapping of sea surface, centimetre radiowave scattering, analysis under different hydrometeorological conditions 3-65287
- radiant energy transfer, effect of multiple scatt. 3-59206
- radioactive pollution, dosimetric implications for man 3-77300
- radioactive pollution detection, γ -spectrometer probe 3-56261
- radiowave scattering by sea surface, at small slip angles (*Russian*) 3-44859
- rear-surface current meter obs., errors rel. to wave motion 3-44966
- Red Sea hot brine pool, geothermal convection 3-59036
- remote sensing of sea states using skywave radar 3-44967
- research vessel, model of the use of technical means in carrying out research, Markovian process (*Russian*) 3-80874
- rip current dynamics, model 3-53447
- Rockall channel, temp., density, chemical comp. annual cycles 3-80678
- rotating stratified fluid, β plane, length scales, model, appl. to ocean circulation 3-46427
- rough sea surface, slope probability characteristics of deep water waves (*Russian*) 3-73269
- salinity profile, porous medium layer, effect on marginal stability, overstability and thermal convection 3-47710
- salty hydrothermal soln., comp. rel. to oceanic chemical evolution 3-56143
- Samoan Passage, near-bottom thermocline 3-50999
- San Diego trough sediments, acoustic reflectivity, in situ meas. 3-61942
- sand ridges and waves on tidal sea shelves 3-47706
- Sargasso Sea, bottom pressure and temperatures 3-69563
- Sargasso Sea, sound speed measurements, eddy patterns 3-80681
- Sargasso Sea particles, two component Mie scattering model 3-76678
- sea ice, attenuation of swell 3-58974
- sea ice, bine content 3-80708
- sea ice, effect on reflectivity, spectral composition of solar radiation, Antarctica 3-80774
- sea ice, microwave signatures of 1st-year and multi-year ice 3-58975
- sea ice growler detection by radar, anomalous performance 3-76922
- sea ice imagery using airborne multifrequency side-looking radar 3-51200
- sea ice in polar regions, satellite obs. 3-59026
- sea ice probing with video pulse sequence 3-73406
- sea level variations, linear extrapolation using parametric model (*Russian*) 3-80685
- sea noise, energy spectral characteristics 3-77333
- Sea of Azov, diurnal variations of transparency, light pulse method (*Russian*) 3-69564
- Sea of Japan, shipborne geomagnetic survey, method used and results 3-50981
- sea slope spectrum meas. by two-frequency microwave radar 3-42089
- sea surface conditions, microwave radiometric obs. 3-50991
- sea surface temp., 1953-60, coherence of transpacific movements of anomalies 3-53458
- sea surface temp., improved radiometric meas. using polarizing radiometer (*French*) 3-51207
- sea surface temp. anomalies rel. to long-range weather forecasting 3-41977
- sea surface temp. chart prod. from satellite i.r. meas. 3-59028
- sea surface topography, soln. of geodetic boundary value problem 3-58854
- sea waves and drift current, wind maintained, energy expended 3-76683
- sea waves assoc. with microseism generation 3-61346
- sea waves rel. to microseisms, USSR data 3-61344
- sea-air interaction, thermodynamical model 3-69554
- sea-air interactions, dust and radon, sources and sinks 3-59077
- sea-air interface, energy balance changes rel. to cooling-water effects (*German*) 3-47703
- sea-air interface energy fluxes rel. to convective activity in tropical Atlantic Ocean 3-50987
- sea-air-interface, momentum and sensible heat fluxes meas. 3-47678
- seaquakes study 3-42447
- seasonal surface water temp. var. in World's Oceans 3-51002
- seawater sampling bottle-cuvette for investigating optical properties 3-42087
- sediment consolidation tests, water content determ. 3-73375
- sediment shear strength, vertical var. rel. to geotechnical properties 3-44864
- sedimental logic and stratigraphic patterns 3-59040
- seismic sounding, resolution assessment using reflected-wave method 3-47851
- seismic waves, pendulum system for study and recording 3-76852
- seven second ocean waves, directional spectra 3-59018
- shallow sea, nonlinear nonstationary wind circulation problem (*Russian*) 3-80687
- shallow water equation based fine mesh barotropic model, boundary conditions 3-65288
- shear layers in a rotating stratified fluid with bottom topography 3-44862
- shelf waves, continental shelf, dynamics of topographic Rossby waves 3-80720
- shelf waves of continuously stratified ocean 3-65289

oceanography continued

- sill fjords, stochastic process of deep water exchanges 3-65273
 slightly stratified ocean, evolution of inertial frequency oscillations 3-69555
 solid state oceanography current meter 3-56262
 Somali Current at 2°S, response to 1971 SW monsoon 3-53443
 sonar, development and uses of new device (*German*) 3-61606
 sound speed in open water, tables 3-44861
 sound velocity depth profile, ray theory, series expansions 3-70217
 South Pacific, long range sound propagation, effect of bottom topology 3-41946
 Southern Ocean, Indian sector, hydrological characts. of frontal zone 3-65283
 southern ocean, meas. of dissolved CO₂, methane and H₂ in surface seawater 3-53451
 spray drops content meas. in near sea layer of the atmosphere 3-76727
 standing wave region, emission of microseismic oscill. and infrasound 3-44791
 s.t.d., equipment and performance 3-80878
 STD data logging system, f.m. audio signals 3-80867
 stillborn marginal ocean in Caledonian orogenic belt of N.W. Norway 3-76584
 Strait of Gibraltar, turbidity meas. 3-59035
 straits and sills, model of two-layer rotating fluid flow 3-59004
 stratified, internal wave generation in tank expt. 3-63726
 stratified Taylor column 3-47669
 subarctic airborne survey, use of real-time satellite imagery 3-59203
 submarine longshore sand bar formation rel. to slowly var. Stokes waves 3-65265
 submarine volcanic eruptions rel. to fuel-coolant interactions 3-76576
 surf zone anal. using computer graphic projections 3-59021
 surface duct sound propagation, normal and virtual modes 3-48283
 surface gravity wave, explicit expression for wavelength 3-65275
 surface gravity waves, infrasound radiation into atmosphere (*Russian*) 3-80682
 surface pollution meas. by satellite (*Italian*) 3-61609
 surface slicks, i.r. characs., comparison between natural and oil slicks 3-69744
 surface sound backscattering strength at low frequency, relationship with gravity wave spectrum 3-42450
 surface temp. meas. in 12 μ window, water vapour absorp. meas. 3-59124
 surface temp. sensing from NOAA satellite scanning radiometer, atm. effects 3-50994
 surface temperature maxima rel. to global distribution of double cloud bands 3-65391
 surface temperature meas. by S-band radiometer 3-76920
 surface temperature measurement, using polarised i.r. radiometer (*French*) 3-65536
 surface water rate fields study (*Russian*) 3-47711
 surface waves, large-pass filtering paper strip-chart records 3-59202
 surface wind over upwelling area off coast near Pisco, Peru 3-41962
 surface-generated noise, envelope structure 3-42465
 surface-internal gravity wave interactions (*Russian*) 3-80683
 temperature field above sea determ. (*Russian*) 3-73267
 temperature salinity and pressure, ocean soundings correction using computer 3-65543
 Texas coast, subsidence rate determ. from tidal meas. 3-53450
 thermal wave propag. through sea floor sediment 3-50993
 thermocline, expt. studies 3-59037
 tidal bore, acoustic wave propagation 3-41949
 tidal estuaries, shoaling, influence of density stratification 3-76685
 tidal forces, simultaneous gravimeter obs. (*German*) 3-56147
 tidal stream residual flow, boundary conditions 3-65286
 todorokite Mn deposit in median valley of Mid-Atlantic Ridge, hydrothermal mechanism 3-56091
 towed hydrological measuring system, meas. of parameters of hydrological fields (*Russian*) 3-80870
 transparency intensity, attenuation coeff., effect of instrument movement, role of zoo- and phytoplankton (*French*) 3-47691
 transverse sand bar formation, model 3-53449
 tropical Atlantic, analysis of quasi-geostrophic waves rel. to observed eddies 3-59000
 tropical Atlantic, large scale anti cyclonic eddy velocity disturbance, detection by anchored buoy stations 3-73257
 Tropical Atlantic, water transparency rel. to temp., salinity, density and relative turbidity (*Russian*) 3-47693
 Tropical Atlantic hydrophysical polygon, temp., fluctuations 3-73272
 Tropical North Atlantic, vertical temperature structure (*Russian*) 3-80686
 Tropics, accuracy of meteorological ship obs. (*Russian*) 3-47774
 tsunami, ionospheric response rel. to prediction 3-69644
 tsunami, possible associated ionospheric disturbance 3-69643
 tsunami generation 3-58980
 tsunami model, generation and open-sea characts. 3-53440
 tsunami warning system using ionospheric technique 3-69748
 tsunamis generation and propagation in ocean of uniform depth 3-76689
 turbidity currents, parameters, methods of computing 3-80713
 turbidity currents associated with earthquakes, energy rel. to tsunamis 3-41940
 turbulence transition in shear layer between 2 streams of different salinities and speeds, lab. expt. 3-60531
 turbulent fields of velocity and temp., great depths, bottom currents, surface active layer (*Russian*) 3-47701
 turbulent flow rate, β -effect in ocean with rectangular boundary (*Russian*) 3-47712
 two layer ocean model rel. to eddies and waves 3-58999
 two-dimensional numerical tidal model with unequal grid-spacing 3-59007
 two-dimensional wave energy spectra 3-47709
 two-layer circulation model, density eqns. for upper layer (*Russian*) 3-80684
 two-layer fluid model, stability to nongeostrophic disturbances 3-47770

oceanography continued

- two-layer ocean, stationary wind driven circulation effect of bottom friction (*Russian*) 3-69553
 underwater laboratories, and their future (*German*) 3-65540
 underwater sound, surface duct propagation loss measurements, using explosive source 3-41947
 Unmanned Arctic Research Submersible System 3-44968
 upper active ocean layers, hurricane and typhoon effects at OWS Tango in Pacific 3-51001
 upper mixed layer, time-dependent model, meteorological influences 3-65271
 upwelling layers in steady, wind-driven stratified ocean 3-65272
 Ust-Kamchatsk, tsunami (*Russian*) 3-47713
 vane current direction sensor, errors from frictional coupling 3-80869
 velocity field, monochromatic wave 3-79006
 velocity shear fluctuations meas. 3-59033
 vertical circulations rel. to oceanic fronts in Atlantic and Pacific 3-50989
 viscous fluid unidimensional motion, nonlinear evolution equation 3-57808
 vortex formation over rippled beds by progressive waves 3-58992
 Wachapreague tidal inlet, response characts. 3-59042
 wake phenomenon, Pacific Equatorial Undercurrent, 1967, Spring 3-47681
 Waltair, Indian E. coast, tidal currents rel. to continental shelf shell zone 3-47668
 Walvis Ridge, structure of marginal termination 3-65197
 warming of lower troposphere by sea rel. to surface humidity mixing ratio 3-44900
 water masses, vertical boundaries, South Atlantic Ocean, T-S analysis 3-80706
 water-air interface, rate of Rn exchange rel. to that of O₂ and CO₂, film model 3-80722
 wave generation in rotating fluids by travelling forcing effects 3-79005
 wave height spectra meas., shipboard obs. 3-53448
 wave problem in finite depth ocean, Green's function 3-73263
 wave refraction, linear profile of descending bottom (*German*) 3-76917
 waveguides (oceanic) microseism propag. 3-61342
 waves, mean length of runs of high waves 3-50996
 wavy water surface slope rel. to orbital vel. of wind generated waves 3-73271
 West Indies, Canadian tropical research 3-56002
 western equatorial Pacific Ocean, heat flow measurements at plate boundary 3-73220
 western North Pacific, vertical profiles of temp., salinity, dissolved O₂, alkalinity and nutrients 3-73258
 Wilkinson Basin, chemical, mineralogical and geotechnical analyses of clay cores 3-73260
 wind induced tidal oscillations of sea and reservoir surfaces 3-76682
 wind waves, horizontal orbital velocity and acceleration spectra determ. (*Polish*) 3-44868
 wind waves, two-dimensional energy spectrum, calc. of direction of propagation of spectral components and angular width (*Russian*) 3-80699
 wind-driven currents in shallow lake or sea 3-76692
 wind-mixed layer, deepening rel. to model of mixing process 3-44858
 wind-roughened sea surface, elevation, slope and curvature spectra 3-59017
 Yamato Rise sedimentary layer structure from seismic reflection profiles 3-65280
 B, coprecipitation from the sea, using Fe(OH)₃, effect of pH, conc., quantity of coprecipitant (*Russian*) 3-80700
 CO and methane, atom. sources and sinks, conference (St. Petersburg, USA, 15-17 Aug. 1972) 3-73181
 Co₂, industrial, future content of atmosphere and oceans, computer calcs. 3-51065
 Fe-Mn nodules, from Black sea, Mossbauer study 3-53461
 Mn ore nodule deposits, survey of prospecting and exploration methods (*German, English*) 3-61324
 O₂ minimum layer in SE Atlantic, structure and characteristics 3-41939
 Sr content, spectroscopic determination, Sr-Cl ratio (*Russian*) 3-47696
- OCR** see optical character recognition
octet theory see SU₃ theory
ODMR see magnetic double resonance
ohmic contacts
 surface potential distrib. at high ohmic devices, electron gun meas. (*German*) 3-50251
 CdS crystals, soldering or diffusing pure In 3-77575
 CdS epitaxial layer, using evap. Al film 3-52900
 n-GaP, of Au-Ni, current and temp. depend., activation energy 3-46892
- ohmmeters**
 see also resistance measurement
 digital, uses p.w.m., designed for resistances of transducers for non-electrical quantities 3-70326
 internally calibrated, principles, diagram (*Spanish*) 3-66283
- oil technology**
 boreholes, electronic measurements and telemetering (*Rumanian*) 3-44944
 floating drilling rigs, deveopment of off-shore techniques (*German*) 3-65539
 spills, water pollution, cleanup using waste paper, technique 3-81330
- oiling (lubrication)** see lubrication
oils, insulating see insulating oils
omega mesons
 p - ω interference, isolation in π -N \rightarrow π - π +N interactions, 3-6 GeV/c 3-70988
 electroprod. at high virtual-photon four-momentum 3-52009
 photoproduction, unnatural parity contribs., pion exchange 3-67017
 photoproduction in high-energy region, dual parton model 3-74372

omega mesons continued

- $e^+e^- \rightarrow$ hadrons, duality relation between vector meson formation and scaling behaviour 3-70932
- $IN \rightarrow IN\omega$, lepton polarisation, one-photon approximation anal., decay 3-78145
- ω cross-section, width and S-wave production in π^-p interaction 3-70975
- $\omega \rightarrow \pi\gamma$, transition magnetic moments of hadrons, sidewise dispersion relations 3-59959
- ω^0 , produced by $K^+p \rightarrow$ four or five bodies at 2.11 to 2.72 GeV/c, cross section 3-78204
- $\omega N_1 \rightarrow \pi N_2$, vector meson dominance and mass dependence of Ball's invariant amplitudes 3-67084
- $\omega\rho$ mixing hypothesis, description of e.m. decay of neutral meson 3-59966
- $pd \rightarrow {}^3\text{He}\omega$, 5 GeV, cross section meas. 3-78199
- $pp \rightarrow \omega^0\pi^+\pi^-$, in T-region, 2.1-2.24 GeV 3-78209
- $\pi\omega$, scattering, static model, description of ρ meson properties 3-62921
- $\rho\omega$ interference in $\pi N \rightarrow \pi\pi N$ interaction at 3, 4 and 6 GeV/c 3-71013
- $\rho\omega$ mixing parameter phase from unitarity relation 3-78230

omegatrons see cyclotrons**on-off control**

- thermostat, electronic 3-51540

online operation

- see also process control
- Aberdeen section scanner for rectilinear, arc, transverse and longitudinal section scanning 3-42368
- blood analysis (Italian) 3-54032
- BWR, Halden, on-line computer method for neutron flux distrib. control 3-46066
- data acquisition system for Omega project at CERN 3-66333
- elementary particle interaction expt., description of on-line computer system 3-66322
- elementary particle physics data, acquisition by video tape recorder and computer 3-54023
- gas chromatography, industrial appl. 3-40077
- gas chromatography-mass spectrometer with on-line computer controlled multiple ion detection 3-40066
- gas chromatography-minicomputer system, peak area integration, biomedical appl. 3-70466
- gas chromatography/elemental reaction analyzer combination, stop-flow arrangement 3-70450
- LMFBR, reactivity computer for detection of anomalous behaviour 3-67436
- mass spectral data, high resolution, instrumental and numerical considerations for on-line interpretation 3-62328
- neutron time-of-flight measurement with on-line computer for data logging (German) 3-59653
- nuclear medicine, gamma-ray camera control, NUMES 2 system (Italian) 3-48598
- nuclear reactor, JMTR, application of on-line digital noise analysis to reactor diagnosis 3-71161
- nuclear track plates, automatic scanning device, on-line computer program 3-40025
- patients having implanted cardiac electrical stimulators (Italian) 3-54022
- plasma, on-line correlation measurements 3-57951
- radiotelescopes, on-line computer control, operation, hardware and architecture 3-70091
- respiratory functions (Italian) 3-54036
- solid state physics, computer appls. (Japanese) 3-71981
- spectrometer system, digital laser Raman, online control of data acquisition 3-62105
- spectrophotometer, computer controlled 3-66217
- voltammetry, reversible cyclic, data acquisition and analysis 3-70445

Onsager relations see thermodynamics**Onsager theory of dielectrics see dielectric properties of substances****opacimeters see turbidimetry****opalescence**

- see also critical opalescence
- No entries

OPDAR see optical radar**operating amplifiers see operational amplifiers****operating systems (computers)**

- for molecular beam expts. 3-78909

operational amplifiers

- automatic precision titration calorimeter, automation 3-45595
- automatic precision titration calorimeter, temp. meas. 3-45594
- for exposure meter for electron microscope 3-56691
- fast transmembrane potential recording buffer amplifier, input capacitance <0.01 pF 3-56997
- n.m.r., Varian HR-220, track-field sweep decoupling 3-73826
- reference voltage source 3-45411
- solid state hot wire anemometer feedback controller 3-47830

operations analysis see operations research**operations research**

- see also decision theory and analysis; game theory
- manuals of operation and their logics, operational statistics 3-74113

operator training see training**optic mode of crystals see lattice dynamics****optical aberrations see aberrations****optical activity see optical rotation****optical auroras see aurora****optical character recognition**

- complex filtering in reading machines, Fourier transform hologram method 3-48958

optical communication

- see also laser beam applications; optical links
- atmospheric, computer simulation of light pulse propagation through clouds 3-76700
- atmospheric light pulse propagation through clouds 3-76701
- binary laser system, photocount statistics rel. to atmospheric turbulence 3-57207
- coherent, of linear phased array radar signals 3-48856

optical communication continued

- detector, dynamic range limiting information capacity 3-48855
- dispersion in fibres and fibre lasers 3-48458
- GaAs injection lasers, mesa type, fabrication (German) 3-59907
- mean universal curve for optical angle of refraction 3-51077
- optics at Bell laboratories, optical communications, comments 3-40221
- optics at Bell laboratories, optical communications, reply to comments 3-40222
- photography, random-carrier, optical modulation techniques, theory and experimental results 3-66271
- pulse signal reflection, from moving mirror (Russian) 3-42973
- resolution limit, communication theory (German) 3-59848
- video and audio channel transmission on He-Ne laser beam (Spanish) 3-51962

optical communication equipment

see also optical waveguides

- dye laser amplifier, using rhodamine 6G flash lamp pumped 3-66828
- optics at Bell laboratories, optical communications, comments 3-40221
- optics at Bell laboratories, optical communications, reply to comments 3-40222
- p.c.m. repeater, using GaAs laser, error-rate obs. 3-66897
- six-channel t.d.m. telephone equipment using GaAs laser diode (Japanese) 3-59847
- three-mirror optical delay line 3-66191
- transmissometer, atmospheric attenuation measurements, automatic recording, 0.9 microns, mists and fogs 3-59178
- GaAs laser, transversely adjusted gap, for optical communication systems 3-48919

optical constants

see also light absorption; reflectivity; refractive index

- alkali halides, strain-optical constant ratios, u.s. determ. 3-80007
- alkanes, halogenated, opt. mol. anisotropy in different media (French) 3-63424
- n-alkanes, molecular optical anisotropy, depolarised Rayleigh scattering 3-49469
- angular reflectance modulation meas. method 3-53911
- aromatic polynitro compounds, electrochemical circulation cell, electrolysis, electronic absorption spectra, optical density meas. 3-45534
- benzene, solid, electron energy loss meas. 3-64622
- benzil, new meas. method for electro-optical consts. at h.f. 3-48404
- butadiene- α -methyl styrene, carbon black filled, i.r. spectra, multi-attenuated total internal reflection, optical constants (Russian) 3-47280
- calculation from reflectance data, causality calc. in time domain 3-80000
- condensed media refl. spectra, appl. of Kramers-Kronig relation for optical consts. calc. 3-44388
- dielectric function derivative spectra at Van Hove singularities, temp., wavelength modulation 3-55543
- electrophotographic layers, optical constants and structure properties, diffuse reflection spectra, binding material (Russian) 3-77559
- ellipsometer, new, principle, realisation and performance (French) 3-62047
- gas, compressed, virial coeffs., coeffs. of expansion of optical complex and refractometric virial coeffs., connection 3-49962
- generalized f-sum rules and superconvergent relations 3-53075
- hydrocarbon, solid, calc. from electron energy loss spectra, Kramers-Kronig transform. 3-79397
- interface measurements, ellipsometer design 3-73727
- i.r. reflection spectroscopy ATR methods for determ. (Polish) 3-48426
- Kramers-Kronig determ. method from attenuated reflection spectra 3-68957
- Kubo theory improvement for linear and local susceptibility (German) 3-68959
- metal layer, vacuum deposited, by reflectance, inhomogeneities obs. 3-64617
- Na solid and liquid, optical consts. depend. on aggregation and temp. for $\lambda=0.3$ to $2.5 \mu\text{m}$ (German) 3-72595
- nonlinear susceptibility and parametric interactions, review 3-54248
- pivalic acid plastic crystal, Brillouin and Rayleigh scattering determ. of phonon lifetimes, elastic and optical constants. 3-44409
- polyoxyethylene oligomers, molecular optical anisotropy, depolarised Rayleigh scattering 3-49469
- quartz, amorphous, optical characteristics in 1400-200 cm^{-1} region, calc. using Kramers-Kronig relations 3-53096
- rutile-structure oxides at high pressure, lattice dynamics rel. to elastic and optical props. 3-64125
- semiconductor film, on transparent substrate, optical density detn. 3-75958
- solids, measurement methods, review (French) 3-41494
- spectroscopy, reflection, of optically active materials 3-68950
- sub-monolayer molecular films, specular reflectance and ellipsometry equations 3-47333
- thin films, characterization theory 3-50534
- transparent dielectric, surface damage during short light pulse irradi. 3-48937
- transparent minerals, opacities rel. to temp. and wavelength 3-65217
- Ag, aggregated thin film, anomalous opt. absorpt. 3-76110
- Ag developed grains, optical constants calc., filamentary thickness 3-47224
- Ag film, effects of residual gas during deposition on optical props. 3-80001
- Ag-Cr thin films mixtures, complex dielectric constant 3-80002
- α -Ag₂S, i.r. and far i.r. spectra, Kramers-Kronig analysis 3-53108
- Ag₂S(Se), Kramers-Kronig analysis of i.r. reflectivity data (German) 3-50571
- Al, ultrathin thin films, effect of vacuum deposition conditions 3-50533
- Au, analysis for contribs. to dielectric const., Kramers-Kronig relation 3-64592
- BaTiO₃, imaginary dielec. function determ. from band structure and optical spectrum 3-44003
- Bi, electron energy loss meas. from 2 to 40 eV (German) 3-55542
- Bi film, determ. by ellipsometry 3-64621

optical constants continued

- CdCr₂Se₄, magnetic semicond., from reflectivity near Curie temp. 3-68955
- CdTe, 300-1100 nm (*Russian*) 3-47225
- Cs, pure thick layer in u.h.v., spectral range 250-630 nm (*French*) 3-41610
- Cs halides, strain, calc. using two ion polarisable shell model 3-47198
- CuBr, second order nonlinear optical coeffs., absolute sign and magnitude 3-68953
- CuCl, second order nonlinear optical coeffs., absolute sign and magnitude 3-68953
- CuI, second order nonlinear optical coeffs., absolute sign and magnitude 3-68953
- Dy, 1-20 μ m absorpt. spectra obs. (*Russian*) 3-44421
- EuO, Kramers-Kronig analysis of reflection at room temp., 0-14 eV, energy level determ. (*German*) 3-53117
- EuO, Kramers-Kronig relation, magnetic field modulated magnetorefractance 3-55614
- EuO(Gd), magnetorefractance, Kramers-Kronig analysis, optical consts. 3-50562
- EuS, Kramers-Kronig relation, magnetic field modulated magnetorefractance 3-55614
- EuS, magnetorefractance, Kramers-Kronig analysis, optical consts. 3-50562
- Fe-Ni alloy films, freq. depend. (*Russian*) 3-61045
- GaSe, determ. by ellipsometric methods 3-39901
- GaTe, layer compound, Kramers-Kronig relations, excitation photorefractance 3-55610
- GeO₂, amorphous, hexagonal and tetragonal, i.r. reflection spectra obs., 4000-200 cm⁻¹ region 3-64616
- GeTe, optical props. and energy gap from reflectance spectra 3-64685
- HgTe, 300-1100 nm (*Russian*) 3-47225
- InPSe₃, nonlinear optical coefficients 3-80004
- K, pure thick layers in u.h.v., spectral range 250-630 nm (*French*) 3-41610
- KH₂PO₄, new meas. method for electro-optical consts. at h.f. 3-48404
- KNbO₃, nonlinear coeffs., at 1.06 μ m, Marker fringe method 3-68954
- K₂Pt(CN)₄Br_{0.3}(H₂O) unidimensional metallic conductor, determ. by laser light reflection meas. (*German*) 3-50532
- K₂Pt(CN)₄Br_{0.3}·3H₂O, optical cond. and electron interaction 3-68958
- K₂WO₄, optical props. determ. from 0.1 to 38 eV 3-80072
- La, polarimetric obs., 1.13-4.42 eV, dispersion depend. (*Russian*) 3-80066
- LaB₆ thin films, computer determination, relation to electrical props. 3-41596
- LiF, cryst., optical dielec. function, self consistent field band struct. calc. 3-50535
- LiIO₃, new meas. method for electro-optical consts. at h.f. 3-48404
- ⁷LiF and natural LiF, i.r., calc. using shell model lattice dynamical data 3-41516
- MgAl₂O₄, transparent shaped mat., fabrication and props. 3-72967
- MgF₂ thin films, slightly absorbing, 1000 to 2000 Å (*French*) 3-41496
- (NH₄)₂SO₄ aq. soln., optical consts. from attenuated total refl. spectroscopy 3-53074
- Na, pure thick layers in u.h.v., spectral range 250-630 nm (*French*) 3-41610
- Na₂WO₄ optical props. determ. from 0.1 to 38 eV 3-80072
- Nd, polarimetric obs., 1.13-4.42 eV, dispersion depend. (*Russian*) 3-80066
- Ni-Fe(25 wt.%) alloy, i.r. region obs. (*Russian*) 3-64664
- NiAl-based ternary β Hume-Rothery phases, rel. to valence electron conc. and defect struct. 3-68965
- Pb halides, absorption spectra at 4.2 K and 78 K 3-44389
- PbBr₂ film, absorpt. spectra obs., energy range 3.5-11.0 eV 3-76017
- PbCl₂ film, absorpt. spectra obs., energy range 3.5-11.0 eV 3-76017
- (Pb_{0.92}La_{0.08})(Zr_{0.65}Ti_{0.35})_{0.98}O₃ ceramics characterization, porosity and grain size effects 3-55532
- Pd, 1-9 μ m spectral range obs. 3-75992
- Pr, polarimetric obs., 1.13-4.42 eV, dispersion depend. (*Russian*) 3-80066
- Rb, pure thick layer in u.h.v., spectral range 250-630 nm (*French*) 3-41610
- Rb halides, strain, calc. using two ion polarisable shell model 3-47198
- Rh, films, mirrors, evaporated, reflectance, transmittance, optical constants, effect of surface dielectric films 3-66203
- Ru evaporated thin films, in v.u.v. from 300 to 2000 Å 3-80069
- Sb₂S₃ monocrysts., and valent electron plasmonic oscill. freq. calcs., interband optical transitions (*Russian*) 3-55540
- Se-As(0-24 at.%As), determ. from fast electron energy losses, atomic arrangement 3-72288
- SrCl₂, determ. from i.r. reflection spectrum using Kramers-Kronig theory 3-49951
- SrTiO₃, Kramers-Kronig analysis, electroreflectance measurements 3-55613
- Ti, determination between 0.4 and 10 microns 3-72594

optical design techniques

- see also optical instruments
- apochromats, design from two and three different glasses 3-66210
- automatic lens design, quadratic model (*German*) 3-77471
- biocular viewing device, design procedure 3-45473
- cylindrical cell, use in multiple scatt. meas. 3-74206
- flat structure stress meas. (*French*) 3-59551
- Head-Up Display lens, appl. of biocular design procedure 3-77472
- i.r. variable focal length lens, range closure simulation 3-77456
- Japanese single lens camera, design and testing of lenses 3-77548
- laser Doppler velocimeter, turbulent flow obs. (*Russian*) 3-45508
- laser heterodyne receiver, 10.6 μ m 3-77541
- low absorbance optical interference coatings, design and meas. 3-77438
- nonpolarising reflector design 3-77437

optical design techniques continued

- optical multilayer interference filters, design, computer refining method 3-39907
- o.t.f. for lens performance 3-66207
- precision lenses, design manufacturing coordination 3-77451
- reflector, nonpolarizing 3-73733
- refracting surfaces, to produce specified irradiance distrib. 3-77466
- spherical mirror, spherical aberrations, correction by plane parallel plate 3-53895
- spherical surfaces, equivalent centred systems, ray tracing 3-48415
- two surface all reflecting Schmidt lens, correcting surface 3-77433
- CO₂ laser design procedure 3-74224
- Ge lens collimator, tilted component, for 8-12 μ m i.r. 3-77434
- optical detection of magnetic resonance** see magnetic double resonance
- optical dispersion**
- see also optical constants
- atmospheric, intensity fluctuations and angle of arrival of laser light determ. (*Russian*) 3-77972
- compensation of effect of group retardation of waves by forced combination dispersion (*Russian*) 3-59900
- corrugated dielectric waveguide, dispersion Brillouin diagram 3-51864
- corrugated dielectric waveguide dispersion, coupled mode analysis 3-51865
- dielectric fibre waveguide, picosecond nonlinear optical pulse transmission, anomalous dispersion 3-59885
- in fibres, dispersive characteristics 3-48458
- forced combination dispersion, pumping schemes for intensification in liquid nitrogen (*Russian*) 3-74279
- garnet, Czochralski-grown, perfection and charact. for gems, lasers and substrates 3-76131
- holograms, formation, optical properties by dispersion theory (*Russian*) 3-57209
- inhomogeneous media, derivation of diffraction theory 3-48851
- instrument for meas. of dispersion and absorpt. in vacuum u.v. 3-45468
- laser beam spread in turbulent atmosphere (*Japanese*) 3-41970
- laser resonator, exhibiting frequency dispersion, equation of motion 3-48934
- liquid crystals, pretransition phenomena just above clearing point 3-63950
- nonplanar fluid, vel. of light in critical region of polarisation 3-60523
- semiconductor, intraband light absorption, by free carrier interactions 3-50597
- spectrograph using nonlinear controlled dispersion 3-59590
- surface waves, at vacuum-complex dielec. const. medium interface, Brewster case (*German*) 3-77966
- triglycine sulphate crystals, influence of defects near the fundamental absorption edge 3-80081
- water, refr. index eval. using two-state theory 3-68951
- waveguide, pulse transmission rel. to dielec. dispersion 3-51855
- Ba(NO₃)₂·H₂O crystals, optical activity, absorpt. spectra and dispersion 3-76025
- CdS, exciton refl. spectra for oblique incidence of light, spatial dispersion effects 3-55646
- La, absorpt. spectra dispersion depend., 1.13-4.42 eV (*Russian*) 3-80066
- NaCl, film, surface optical vibrations, frustrated total internal reflection obs. 3-50063
- Nd, absorpt. spectra dispersion depend., 1.13-4.42 eV (*Russian*) 3-80066
- Pr, absorpt. spectra dispersion depend., 1.13-4.42 eV (*Russian*) 3-80066
- (SrCa)S₂O₆·4H₂O, mixed crystals, dispersion of optical activity 3-76026
- optical fibres** see fibre optics; optical waveguides
- optical films**
- antireflection coating, for far i.r. scatter filters 3-66181
- dielectric mirror coating, reflectance measurements using laser beam 3-66186
- dielectric multilayer mirror, light intensity distrib. 3-62050
- dielectric thin film on absorbing substrate, refl. conditions, laser material (*Polish*) 3-50593
- electro-optical coeff. sign determ., from interf. and electro-interf. comparison 3-73769
- ellipsometer, modulated, for study of film props. 3-53885
- glasses containing silver halides, thin film phase, reversible changes of optical density, phototropism 3-76108
- holographic grating coupler, for optical waveguide, perturbation analysis 3-66177
- liquid, optical waveguides, organic compounds, molecular excitation, techniques (*German*) 3-64752
- metal, vacuum deposited, optical consts. by reflectance, inhomogeneities obs. 3-64617
- multilayer film filters, fabrication, for thermal detectors 3-62010
- multilayer media, amplitude and transmittance 3-77959
- narrow band optical filters, thickness monitoring by turning method, absorpt. effects 3-51531
- noble metal, transmission in vis. and u.v. spectral regions (*French*) 3-76112
- optical coating of variable refr. index, prep. and props. 3-62093
- organic, principal index variation with wavelength (*French*) 3-80064
- polarising, metal, vacuum evaporation technique 3-77460
- polymer, low loss, with adjustable refr. index 3-53157
- polyurethane, light modes, refr. index, thickness, dispersion 3-47335
- quantitative adhesion test apparatus and method for vacuum deposited thin films 3-50818
- radiative props., substrate effect on absorpt., refl. and transmittance 3-64751
- reflectance, transmittance of evaporated films, apparatus for in situ meas. 3-77448
- refractive index and thickness from single angle refl. meas. 3-51594
- refractive index meas. methods, review 3-77462

optical films continued

- semiconductor, on transparent substrate, optical density detn. 3-75958
- transparent membrane, between phosphor and photosensitive material, modulation transfer function 3-66768
- vacuum deposited, diffusion pump oil photoluminesc. and light transmission rel. to contamination 3-69048
- Ag, aggregated thin film, anomalous opt. absorpt. 3-76110
- Ag surface film, coated with Al_2O_3 and Si, solar absorb., thermal emissivity prep. 3-56660
- As-S amorphous film, photographic effects, 77 and 293 K, interpretation 3-69015
- As_2S_3 , cryst., photo-induced shift of light transmission edge, structure changes 3-58525
- As_2S_3 , on LiNbO_3 substrate, acousto-optical light diffraction 3-68960
- As_2S_3 chalcogenide glass, antireflection coating 3-70306
- As_2S_3 -Ge glasses, amorphous film, absorpt. edge depend. on comp. 3-64701
- Au, d-band position and width, low temp. thermomodulation meas. 3-55632
- Au, piezo, thermo and electroreflectance spectra, comparative props. 3-55631
- Au-Se-SnO₂ system, amorphous optical memory obs., depend. on Se film thickness 3-50541
- CaF_2 , antireflection coating of As_2S_3 chalcogenide glass 3-70306
- CdS , epitaxial, optical and elec. props., rel. to suitability for use as transparent electrode 3-64330
- CrN, elec. and optical props., conducting neutral density filter applic. 3-64753
- Cu thin film, struct. effects on far u.v. spectra (French) 3-76111
- HfO_2 antireflection coatings on fluorite lenses 3-62068
- LiF , light modes, ref. index, thickness, dispersion 3-47335
- MgF_2 , antireflection coating of As_2S_3 chalcogenide glass 3-70306
- MgF_2 monolayer antireflection coating on glass, evaluation (Czech) 3-66189
- MgF_2 optical constants, slightly absorbing, 1000 to 2000 Å (French) 3-41496
- MnBi, prep. conditions rel. to grain size, magneto-optic memory appl. 3-79584
- MoN, elec. and optical props., conducting neutral density filter applic. 3-64753
- Na_3AlF_6 , cryolite on Cr, thickness and dispersion meas., ellipsometric method 3-62049
- PbBr_2 , optical constants, energy range 3.5-11.0 eV, absorp. spectra obs. 3-76017
- PbCl_2 , optical constants, energy range 3.5-11.0 eV, absorp. spectra obs. 3-76017
- Rh, mirrors, evaporated, reflectance, transmittance, optical constants, effect of surface dielectric films 3-66203
- Sb-Se, amorphous, evaporation, comp. depend. of optical and transport props. 3-68522
- Sb_2O_3 , refractive index, 300-4000 nm, rel. to microstructure 3-76113
- SiO_2 , antireflection coatings, moisture resistant, vac. evaporation 3-62074
- SiO_2 antireflection coatings on fluorite lenses 3-62068
- $\text{SiO}_2/\text{TiO}_2$ two-layer antireflection coating on glass, evaluation (Czech) 3-66189
- SnO_2 , antireflection coatings, moisture resistant, vac. evaporation 3-62074
- Ta_2O_5 , ellipsometric investigation of electro-optic and electrostrictive effects 3-80122
- TiO_2 antireflection coatings on fluorite lenses 3-62068
- WN, elec. and optical props., conducting neutral density filter applic. 3-64753
- YAG: Ho^{3+} , epitaxial, laser oscill. obs. 3-51929
- YAG: Nd^{3+} , epitaxial, laser oscill. obs. 3-51929
- $\text{Y}_3-\text{Bi}_2\text{Fe}_2\text{O}_{12}$ garnet film, Faraday rotation and optical absorpt. 3-53085
- ZnO , epitaxially grown, electro-optic and acousto-optic interactions 3-47228
- ZnS , on Sb, thickness and dispersion meas., ellipsometric method 3-62049
- $\text{ZnS}:\text{Er}^{3+}$, electrolum., impact excitation by hot electrons 3-80111
- $\text{ZnS}-\text{MgF}_2$ optical coating of variable refr. index, prep. and props. 3-62093
- ZrO_2 , antireflection coatings, moisture resistant, vac. evaporation 3-62074

optical filters

- see also light absorption; optical films
- 130-280 Å region 3-51750
- aeromagnetic maps, directional filtering with optical correlator 3-80848
- apodisation filters, for image formation (German) 3-56666
- broad-band versus narrow-band at absolute threshold for dark-adapted retina 3-51437
- broadband u.v. refl. filters for space applications, characts. 3-48139
- cathodoluminescence instrument, description (French) 3-69098
- coherent optical spatial filtering, applications 3-66174
- composite filters, echellette parameters in far i.r. region 3-62055
- contrast dielec. narrow-band interference filters, half-width 1 to 3 nm, optical props. 3-42577
- cyanine dyes, excited singlet-singlet absorption in solution 3-62739
- dye laser tuning by the use of Christiansen filters 3-39955
- Fabry-Perot passive cavity, matched filter detect. of mode-locked laser signals 3-74251
- far i.r. scatter filter, antireflection coating techniques 3-66181
- Fourier hologram filter, pattern recognition and size determ. of signals (French) 3-66770
- Fourier plane, real-time operation 3-77428
- glass, phosphate, for filters extracting 560-640 nm spectral range 3-70314
- glasses for colour grading and stage illumination, temp.-induced colour changes 3-77459
- guided-wave optics, coupled-mode theory 3-59890
- holographic, coherent lensless matched 3-77526
- holographic matched filters, analysis of information capacity 3-48854

optical filters continued

- interference, for broadband photometry in u.v., 1200-1900 Å, appl. in astronomy 3-77175
- interference, mirrors, multilayer, location of transmission extrema in terms of stationary points, manufacture 3-53897
- interference, multilayer film type, fabrication 3-62010
- interference filters, bandwidth narrowing caused by an increase in the phase dispersion of the multilayer mirrors 3-62126
- i.r., far, high-pass transmission, Yoshinaga type suitable materials, transmission properties 3-70302
- laser beam inertialess saturable filter 3-43029
- laser protective materials, selection and testing, filter measurements 3-73789
- liquid optical filter, tunable, with sharp cutoff 3-51576
- lowpass dielec. multilayer, extraction of Tschebysheff design data 3-62124
- Lyot filters, thickness of contrast elements 3-65973
- multilayer dielectric, realization on Mylar substrate (French) 3-53914
- multilayer interference filters, design, computer refining method 3-39907
- narrow band, solid Fabry-Perot etalon for space applic. 3-73764
- narrow band $\text{H}\alpha$ interference filter, ang. depend. of optical props. (French) 3-42256
- narrow band interference filters optical thickness control (French) 3-51603
- neutral density filters with nonlinear density profiles, prep. by vacuum evaporation 3-45477
- nonlinear transform, and logarithmic filtering in coherent optical systems 3-66771
- nonlinear transforms, logarithmic filtering in coherent systems, half-tone screens 3-77445
- organic dissolved filters for spectrum width restriction in giant pulse ruby laser (Russian) 3-70823
- polarisation, interference-type, thermo-optic compensation of wide-angle controllable stages 3-62135
- polyethylene echelette gratings, double-ruled, large-constant, for long wavelength i.r. region 3-62060
- polyethylene powder, spectral transmission, one component filter 3-62072
- radiographs, image enhancement of spatial frequency filtering, application to nondestructive testing 3-80509
- return-pass birefringent Fabry-Perot filters 3-51618
- ring laser with bleachable filter, time characts. 3-45814
- spatial, for IC mask tolerance measurement and defect detection 3-74285
- spatial filtering of thermal source to give coherent light 3-77958
- spatial filtering subtraction, appl. to thin film and IC mask inspection 3-62121
- spatial filtering system, for low contrast fingerprint image enhancement 3-66199
- spatial freq. with circular symm., realisation (French) 3-66205
- subtractive method of thin film interf. filter design 3-59591
- thin film narrow band optical filters, thickness monitoring by turning method, absorpt. effects 3-51531
- tinted lens for aviators and skiers, spectral transmission assessment 3-66182
- ultrasoft X-rays, 50-2000 Å, spatially inhomogeneous filters 3-45568
- Universal Birefringent Filter at Sacramento Peak Observatory 3-81217
- Al filters, unbacked, increase in transmittance on exposure to r.f. and d.c. discharges in O_2 3-77435
- CdSb , i.r. radiation filter 3-64619
- CrN film, conducting with negative t.c.r. 3-64753
- MoN film, conducting with negative t.c.r. 3-64753
- WN film, conducting with negative t.c.r. 3-64753

optical images

- Abbe's theory and holographic imaging (German) 3-54198
- Abbe sine condition and principles of image formation (German) 3-54203
- analysis, multiplex coding (French) 3-66781
- angular spectral analysis of $[\cos\alpha x]$, summation technique 3-77990
- apodisation, laser scanners, frequency response, optimisation, theory 3-66264
- apodisation filters, for image formation (German) 3-56666
- astronomical, effect of atmospheric temp. and vel. fields 3-61888
- astronomical spectrograph camera, effect of component separation on image quality 3-73562
- atmospheric degradation, role of turbulence 3-80754
- atmospheric limits, degradation of modulation transfer function 3-77992
- biocular design procedure, design of Head-Up Display lens and biocular eyepiece 3-77472
- coherent, noise suppression 3-66774
- coherent imagery of extended objects, second class of apodisation functions 3-77996
- coherent optical processor, degraded image restoration by composite grating 3-51573
- coherent optical processor, single step detection of blurred image 3-51574
- coherent optical systems, imaging, temporal analogy 3-45474
- colour image quality, correlation with perceived quality assessment 3-77991
- dark field imaging system, two-point resolution under partially coherent illumination 3-54206
- defocused image reconstruction 3-62676
- defocused optical system in partially space coherent illumination, imaging characts. 3-51883
- dye, rigid film, anisotropic image form. 3-73798
- edge spread function imaged by circular aperture 3-48863
- electro-optical devices applications 3-48411
- encoding, for identification security 3-66773
- evaluation, rel. to lenses, optical transfer function and figure of merit 3-73743
- evaluation techniques, physical parameters and numerical evaluation 3-54204
- focused, holographic interferometry, sensitivity and resolution 3-62149

optical images continued

- Fourier holography, wave-optical derivation of isoplanatism (*German*) 3-57215
 Fourier spectrometer, transforms, apodization 3-62140
 Fourier transform spectroscopy, apodisation and phase information 3-45495
 Fourier transforms, multidimens., image processing with finite scanning apertures 3-74208
 Fresnel zone plates, scaled, for coded aperture imaging 3-66391
 hologram, image quality, depend. on photographic emulsion layer, diff. efficiency 3-51879
 holograms of transparencies, image reconstruction with semiconductor laser 3-45777
 holographic, geometrical construction of primary and secondary images (*Czech*) 3-48445
 holographic, noise suppression, parametric, complex holograms 3-40226
 holographic, optimum exposure and storage times for spirochromenes of indoline series 3-42583
 holographic, superresolution, multiple superposition of image holograms with different carrier frequencies 3-40227
 holographic correction of aberrations caused by main-mirror deformation 3-62669
 holographic image speckle reduction by random spatial sampling of hologram aperture 3-51875
 holographic recording, by multimode laser radiation 3-62670
 holographic screen samplers, for reduction of speckle in image 3-77531
 holographic stereograms, anamorphic imagery, geometric optics calcs. 3-45774
 holographic storage media, thermoplastic-photoconductor ghost images 3-77982
 iconics problems, image matrix representation 3-51887
 incoherent image processing by generation of corrective motion blur (*German*) 3-51885
 information loss due to attenuation of signal by scattering or absorption across gap 3-48860
 intensity transmission linearity of imaging system, binary phase object for testing (*German*) 3-77993
 interferometric technique, for image recording and restoration degraded by aberrations 3-42574
 inversion theorem for finite Fourier transforms and number of degrees of freedom 3-51884
 kinoforms, computing method, image reconstruction error reduction 3-73773
 laser speckle patterns obs. through finite-size scanning apertures, first order prob. densities 3-62675
 lens, simple, image form., wave theory 3-77995
 line, autocollimation, relative divergence, use in focusing apparatus 3-62065
 linearity of imaging processes, intensity-transfer, test method (*German*) 3-51602
 low-light-level imaging, using negative-electron-affinity photocathodes 3-48372
 microscope, contrast, with synchronous scanning of object by point or raster field diaphragms 3-62053
 microscope, two-point resolution of phase objects illuminated with partially coherent light 3-54205
 microscopic image formation, coherence conditions influence (*German*) 3-42981
 motion degradation, space variant system analysis, two dimensional linear incoherent optical system 3-66769
 neutron imaging, with thin Gd convertors 3-48566
 nonlinear cryst., resolving power of image conversion (*Russian*) 3-74268
 nonlinear crystal, influence of inhomogeneities on image conversion by sum-freq. generation 3-74276
 ocean water, clear, imaging in backscatt. light, inhomogeneities effects 3-41932
 partial coherence evaluation, freq.-response control 3-70300
 partially coherent imaging, two-point resolution criteria, Rayleigh criterion 3-62674
 periodic objects under partially coherent illumination 3-42982
 photographic emulsions, modulation transfer function, meas. by image anal. method 3-51874
 photography, photogrammetric, depth of field and image scale of object 3-73802
 plane images, normalisation of rotation, interference effects (*Russian*) 3-48240
 planetary nebulae, recognition, colour photography, anomalous images, visual examination 3-81056
 radiographs, image enhancement of spatial frequency filtering, application to nondestructive testing 3-80509
 reconstruction from projections 3-77994
 red stars, recognition, colour photography, anomalous images, visual examination 3-81056
 reflective system, corrections for third-order aberrations to closed-form solutions 3-42979
 resolution limit, communication theory (*German*) 3-59848
 resolution of point sources of light, analysed by quantum detection theory 3-59850
 sheets of circular cone geometry, quantitative optical effects (*German*) 3-45765
 slit, autocollimation, nonflat reflecting surface, illum. distrib. calc. 3-62064
 slotted flat analyser, effect of parameters on filtration of spatial frequencies, formation of image using luminescent semiplane (*Russian*) 3-80873
 solar X-ray emitting spots, pinhole camera image (*German*) 3-80973
 spatial spectra of luminance field, scaling 3-62118
 stellar, removal of atmospheric turbulence 3-81254
 subtraction by polarisation-shifted periodic carrier 3-53882
 subtraction of images, dependence on illumination 3-77976
 surface wave lenses and focusing 3-45769
 synthesis by array systems, computer simulation 3-70786
 telescope, segmented mirror, synthetic aperture imagery, new processing method 3-77446
 television camera tubes and direct-view intensifiers for low-light-level imaging 3-48413

optical images continued

- transfer functions for partially coherent illumination 3-77725
 transforming system, radiation distrib., image formulas 3-51888
 two-dimensional image receptors, shape of testing target 3-62084
 underwater transmission, Fourier techniques application to test linear-invariant hypothesis 3-45781
 vision/optical aids interaction, image evaluation methods 3-70117
 Si technology impact, on low-light-level imaging 3-48373
- optical information processing**
 aeromagnetic maps, directional filtering with optical correlator 3-80848
 analogue optical computer, to obtain Laplacian average of input field 3-77979
 birefringent beam splitter, four-polarised-wave interf. device, appls. 3-77506
 coherent optical processing concepts 3-77974
 coherent optical processor, degraded image restoration by composite grating 3-51573
 coherent optical processor, single step detection of blurred image 3-51574
 coherent processor with optical feedback 3-77980
 contour generation, from stereo photography 3-77981
 data processing, lasers, holography data storage, systems, techniques, review 3-59849
 digital computer system, theory 3-77449
 earth science, diffraction anal., Fourier optics appl. 3-80847
 ferroelectric phase transitions, appl. to optical data recording (*French*) 3-75949
 fingerprint low contrast image, enhancement by spatial filtering 3-66199
 Fourier hologram filter, pattern recognition and size determ. of signals (*French*) 3-66770
 frequency offset use in incoherent optical data processing 3-62665
 hologram and kinoform memories, comparison of random and deterministic phase coding 3-73774
 holographic interferograms, automatic data reduction 3-73772
 holographic matched filters, analysis of information capacity 3-48854
 holographic system, maximum information capacity calc. 3-74213
 image motion, space variant system analysis, two dimensional linear incoherent optical system 3-66769
 image processing with finite scanning apertures, multidimens. Fourier transforms 3-74208
 image subtraction 3-77976
 incoherent, in real-time parallel system 3-77978
 information assessment methods 3-40219
 interface devices, review 3-77975
 laser beam storage, characts. of thin film metal arrays 3-74209
 leukocyte classification by coherent optical techniques 3-77738
 liquid crystal optical transparency, reduction of switching time 3-45779
 liquid crystal transparency for hologram recording 3-45778
 luminous point objects, determination of coordinates of group 3-70787
 microscope images, particle characterisation using Quantimet 720 3-73731
 nonlinear transform, and logarithmic filtering in coherent optical systems 3-66771
 parallel image processor, on-board spacecraft, design concepts 3-45475
 radar data, synthetic aperture, review 3-77977
 S/N ratio in optical radar system 3-66772
 scattering of radiation and information content 3-42975
 telescope, segmented mirror, synthetic aperture imagery, new processing method 3-77446
- optical instrument testing**
 aberrations, nonsymmetrical, coma, lateral colour, measurement errors in instruments, analysis 3-53896
 astronomical instrument manufacture, optical components, quality and testing 3-48153
 multispectral scanner for Skylab, use of model for calibration 3-77461
 o.t.f. for lens performance 3-66207
 plate diagram, mirror system aberrations, off-axis systems, Ebert and Czerny-Turner spectrographs 3-39911
 scales and reticles, optical instrument manufacture, classification in terms of material and manufacture 3-53899
- optical instruments**
 see also colorimeters; coronagraphs; diffractometers; holographic instruments; laser velocimeters; light interferometers; monochromators; optical prisms; photometers; polarimeters; refractometers
 acoustooptic light deflector, input characteristics 3-45471
 alignment holder, electro-optic crystal studies, high temperatures, rapid and accurate alignment 3-62083
 atmospheric particulate instrumentation by laser light scattering systems, design, performance parameters, results 3-56687
 beam and modulator-splitter, design, 2 jointly rotating elements 3-73729
 binocular viewing device, design procedure 3-45473
 cell, fluid studies from 78 to 350 K, upto 10 MNm⁻² pressures, description 3-62054
 circular dichroism study, ultrasonic modulator, recording 3-73726
 coherent optical processor, degraded image restoration by composite grating 3-51573
 coherent optical processor, single step detection of blurred image 3-51574
 cryostat for studying optical absorption under uniaxial stress 3-39899
 curve tracer, for pulsed laser diodes 3-39905
 diffusers, random phase, design and synthesis 3-66187
 electrochemistry, optical techniques, book 3-66195
 encoder plate measurements, by laser/calculator system 3-59600
 flames, mean turbulence visualization, optical spatial filtering method 3-56665
 fluorometer, high-speed image convertor, for obs. of dye soln. fluoresc. 3-76085
 Fresnel zone plates, micro-fabrication and characts. 3-51572
 infinitely narrow beam constants calc. 3-62052
 i.r. testing devices, pyrometers, displays, image convertors, new instruments in E. Europe, review (*German*) 3-73685

optical instruments continued

- light guides, plastics fibre application to optical instruments 3-51588
- light pipes, for SEM, electron detector, perspex with thin film coating 3-77722
- measurement of dispersion and absorpt. in vacuum u.v. 3-45468
- microapertures for use in adjustment, production methods 3-62069
- mirror multiplier, adjustment for increased sensitivity of autocollimation method 3-62070
- multiple bounce reflectometer, absolute accuracy improvement by systematic errors reduction 3-51571
- objective, three components, telecentric ray paths, design 3-62066
- Optical Society of America, conference, Rochester, USA (1973) 3-77431
- pancratic objectives, system for focusing at small distances 3-62073
- perfectometer, design for optical probing of hole dia. 3-53841
- perfectometer, for calibrating ring and slip gauges for internal hole dia. meas. 3-53840
- photographic material resolution, 440 to 2960 mm⁻¹, LIR 1 interference resolution measuring instrument, specifications, operation, design 3-53937
- planar optical phase element fabrication 3-53891
- pulsed isolator, based on Faraday cell 3-51583
- ratio reflectometer, pellicle beam splitter, wavelength depend. transmission 3-66180
- reflexicon, new two-stage axiconic reflector, laser and holographic appl. 3-62043
- reflectometer, high accuracy, evaluation for specular materials 3-73723
- reflector, nonpolarizing, design 3-73733
- reflectors for optical rangefinders with light modulation by polarisation 3-61995
- scales and reticles, optical instrument manufacture, classification in terms of material and manufacture 3-53899
- scanning system output, spatially periodic signal spectral struct. 3-42554
- scintillation counter with light guide, energy resolution 3-56937
- single-beam device for in situ meas., reflectance, transmittance of evaporated films 3-77448
- stack gases, continuous monitoring, optical instrumentation 3-61931
- stereometry with mirror stereoscope facilitated by interpreter's table 3-53935
- stereoscope, focal-plane lens type, vertical scale exaggeration in contour mapping 3-53884
- surface track counting instrument, for solid track detectors 3-53986
- three-mirror optical delay line 3-66191
- v.u.v. mounting design for synchrotron radiation 3-39994
- wedges used as light beam deflectors 3-62058
- White cell, modified, generation of square lattice of focal points 3-51575
- X-Y tape recorder, polar coordinate design, for recording small light sources (*German*) 3-45469
- H₂, liquid target, length meas., optical technique 3-51678

optical interferometers *see light interferometers***optical links**

- see also laser beam applications; optical communication equipment*
- atmospheric turbulence remote probing 3-76749
- fibre and integrated optics applications by Defense Department 3-74284
- space link, using CO₂ lasers (*German*) 3-54251
- CO₂ laser, for space communications 3-48901

optical masers *see lasers***optical materials**

- see also fibre optics; glass*
- alkali halide, polycryst., fusion casting, mech. and opt. props. 3-76254
- alkali halide, polycryst., i.r. laser window mat. develop. and charact. 3-73787
- astronomical instrument manufacture, optical components, quality and testing 3-48153
- cementing of large lenses, manufacturing problems, technique, optical cements 3-39913
- chemical vapour deposition production techniques 3-77470
- corundum plates, single-crystal, process for grinding and polishing 3-62088
- crystal containing inclusions, i.r. absorption theory and material failure 3-58487
- dielectric thin film on absorbing substrate, refl. conditions, laser material (*Polish*) 3-50593
- filters, far i.r., high-pass transmission, Yoshinaga type suitable materials, transmission properties 3-70302
- fluorite, antireflection coatings on lenses of 3-62068
- glass, polished optical, exoelectron emission, rel. to surface structure and stress 3-72784
- glass low loss, for fibre optics, prep. method 3-53892
- graded-index antireflection coatings 3-77436
- ground surfaces, holographic inspection in reflected light 3-66211
- halide laser windows, press forged, mech. props., grain size and alloying depend. 3-73786
- homogeneity, expt. determination of sensitivity of luminous point method 3-62086
- i.r. transmitting mat., hot pressing 3-76253
- i.r. transmitting mats., review 3-73785
- KRS5, new acousto-optical material of high performance (*French*) 3-68961
- KRS 5 crystal, thermal, photon depolarisation currents, light polarisation 3-68671
- laser windows, stress and temp. analysis for surface cooling or heating 3-70319
- low absorbance optical interference coatings, design and meas. 3-77438
- nitrobenzene, electric field behaviour rel. to Kerr cell 3-47229
- nonlinear, applications review 3-54248
- nonpolarising reflector design 3-77437
- nonuniform layer, boundary problem approx. soln. and interpolation formulas 3-42968
- optical coating of variable refr. index, prep. and props. 3-62093

optical materials continued

- Optical Society of America, conference, Rochester, USA (1973) 3-77431
- optical windows, surface correction for refr. index in homogeneity 3-51578
- optimum apodisers, influence of spherical aberration on performance 3-77440
- photochromic, thermochromic, electrically controlled optical storage 3-70789
- photochromic glasses, photographic and holographic charact. curves 3-48448
- proton dosage distrib. with depth, calc. 3-64075
- quartz, transmission and reflection spectra in vac. u.v. 3-69016
- quartz glass, experimental apparatus for determining emissivity, high temp. 3-70307
- sapphire disks, synthetic, biaxial flexural strength 3-73788
- self-focusing parameter meas. using intrinsic optical damage 3-59583
- spectroscopy, reflection, of optically active materials 3-68950
- surface finishing, applic. of ion bombardment of insulators 3-72775
- thermal lensing of laser beams in optically transmitting materials 3-57248
- titania-silica glasses, thermal expansion meas. by photoelectric and u.s. techniques 3-51593
- Al diffusers, spectrophotometric props. 3-48418
- Al reflectance coatings, LiF-protected, use in u.v. space optics 3-81252
- BaSO₄, depolarisation of diffusely reflected radiation (*German*) 3-66206
- Ba₂Sr_{1-x}Nb₂O₆, Ba₂NaNb₂O₁₅, single cryst. growth, refr. index homogeneity 3-50653
- CaCO₃, Iceland spar, single cryst. growth technique 3-50654
- CaF₂ window for H₂ lamp, effect of vac. u.v. on transmittance 3-62117
- Ca₂La₈(SiO₄)₆O₂, elastic and thermal props. 3-43819
- CaO, dense polycrystalline transparent, hot pressing fabrication 3-76329
- CdT₂, thermal annealing procedure for reduction of 10.6 μ optical losses 3-64802
- GaSe, optical constants, determ. by ellipsometric methods 3-39901
- HgBi₂S₄, synthesis and cryst. struct. 3-60711
- KCl, hot worked, strength and deformation behaviour 3-76252
- KCl, press forged, strengthening effects 3-45502
- KCl billet, crack free, constrained hot pressing technique 3-69362
- LaF₃, gas laser examination of optical defects 3-70303
- LiF single polished crystals, use in far u.v. optics 3-62090
- LiF window for H₂ lamp, effect of vac. u.v. on transmittance 3-62117
- α -LiIO₃ polar crystal, obs. of electro-optical twinning 3-72028
- LiNbO₃, grown from stoichiometric melts, for nonlinear optical props. optimisation 3-44532
- LiNbO₃ crystal, laser damage susceptibility rel. to growth and purity control 3-69358
- MgAl₂O₄, transparent shaped mat., fabrication and props. 3-72967
- NaCl, laser induced breakdown field strength, pulse duration depend. 3-51941
- Nd³⁺-2-hydroxy-3-naphthoic acid complex, i.r. spectra, vibr. modes 3-67815
- Pb₃(Ge₂Si₂)O₁₁, optically active ferroelec., Si conc. depend. of dielec. props. 3-61025
- YAlO₃, biaxial cryst., refr. indices 3-41492
- ZnS-MgF₂ optical coating of variable refr. index, prep. and props. 3-62093
- optical microscopes** *see microscopes*
- optical model (nuclear)** *see nuclear optical model*
- optical modulation**
- anharmonic diatomic lattices, time evolution of nonlinearly modulated waves 3-46687
- coherent optical processing of linear phased array radar signals 3-48856
- contrast vision (*Italian*) 3-56522
- demodulation of optically modulated electrons using extended interaction 3-51966
- diffraction grating, geometric description of optical phase modulation 3-54199
- Doppler radar, f.m. laser noise effects 3-40295
- electro-optic modulators, properties and applications 3-66266
- electro-optical modulator, temperature independent operation in ruby resonator (*Russian*) 3-66269
- electrooptic modulator comprising two coupled dielectric waveguides suitable for integrated optical circuit 3-59580
- fibre-optic components, modulation transfer functions, determ. from edge response curves 3-42974
- fly's-eye lenslets and photographic emulsion system, resolution and modulation transfer function 3-62164
- guided optical wave, bulk acoustic wave interaction 3-55545
- guided-wave optics, coupled-mode theory 3-59890
- laser, forced phase synchronism mode (*Russian*) 3-62687
- laser distance meas. system comparing phase of modulating signal 3-51960
- laser electro-optical modulation rel. to generation growth time instability obs. (*Russian*) 3-62689
- light beam modulator splitter, design, 2 jointly rotating elements 3-73729
- light modulator, Kerr cell, for laser with external spherical mirrors 3-73790
- magneto-optical effect detection, using electro-optic modulator 3-44397
- modulation transfer function visualisation by speckle pattern techniques 3-51856
- modulator, intracavity, patent 3-62756
- modulators, extinction ratio rel. to light absorption 3-62656
- m.t.f. analyser model FPK-1, description 3-59582
- MTF meas. in visible and i.r., interferometric technique for airborne expts. 3-51616
- MTF of form $\exp(-(\omega/\omega_c)^n)$, point spread functions, line spread functions, edge response functions 3-40220
- multichannel TV coupling modulation, wide bandwidth, low power consumption, CO₂ laser 3-40300

optical modulation continued

- noncritical optical heterodyning using two successive ultrasonic light modulators 3-51611
 nonlinear wave modulation, perturbation method, integro-partial differential eqns. 3-77864
 optical rangefinders, reflectors with light modulation by polarisation 3-61995
 phase-modulated light, detection by heterodyne method 3-62085
 Q-factor of solid state laser, modulator components (*Russian*) 3-57230
 sectoral modulator, for suppression of scattered light in recording of luminescence spectra 3-51608
 by successive u.s. waves, beat freq. spectra obs. 3-70783
 thermal medium, meas. of temp. fluctuations by light intensity modulation 3-73682
 transfer functions, scattering media, for target contrast indirect light 3-54200
 transfer functions, wide-angle camera lenses, new direct measurement method 3-53940
 t.w. laser phase modulator, using rectangular waveguide loaded with electro-optical material (*Korean*) 3-77544
 two-level system in interaction with linearly polarized e.m. field, energy spectrum 3-42983
 u.s., circular dichroism study 3-73726
 video and audio channel transmission on He-Ne laser beam (*Spanish*) 3-51962
 wavelength modulation spectrometer, 2000-8000 3-45485
 CdTe, recryst. layers, low voltage modulation of monochromatic light 3-41503
 n-GaAs, in elec. field, by nonequilibrium optical phonons 3-58491
 GaAs laser diode (*German*) 3-59875
 GaP p-n junction, He-Ne laser at near grazing incidence 3-40279
 GaP p-n junction, modulation of laser light, waveguide properties (*German*) 3-53079
 GaP p-n junction, phase modulation of He-Ne laser light by Pockels effect 3-53922
 LiNbO₃ ring laser, mode synchronisation, resonant modulation, ultra short light pulse excitation, 10⁻¹⁰ sec (*Russian*) 3-57235

optical modulators *see* modulators; optical modulation**optical prisms**

- dispersion, method for improving selection of prismatic dispersion prism and interferometers 3-74253
 doubly-refracting for s.h.f. waves, and utilization of TV equipment for demonstrations (*Russian*) 3-48323
 erecting system using two rectangular prisms 3-70301
 laser resonators, polarised, compound TIR prism, phase change compensation 3-39958
 Pellin-Broca prism, mounting for laser work, comment 3-51577
 Pellin-Broca prism mounting for laser work, reply to comments 3-51579

optical projectors

- automatic focusing device, CdS photocells in bridge circuit (*Japanese*) 3-53876
 Centering Projector-10, VEB Carl Zeiss JENA, positioning device, workpiece alignment 3-51600
 heat filter, absorpt, operating efficiency, rel. to interference and combination types 3-66194
 image-replicator, multiple-objective projection system 3-53938
 measuring, MP 320, microelectronics appl. 3-45514
 opaque system, improved luminous efficiency 3-62067
 sound track system for projector slides (*Spanish*) 3-42595

optical properties of substances

- see also* acousto-optical effects; birefringence; brightness; colour; dichroism; dielectric function; elasto-optical effects; electro-optical effects; magneto-optical effects; optical constants; optical rotation; photochromism; piezo-optical effects; pleochroism; reflectivity; thermo-optical effects
 aggregated metal system, plasma resonances 3-68948
 amorphous solids, photocrystallisation (*French*) 3-75624
 anisotropy of absorption bands in lunar, meteoritic and terrestrial pyroxenes 3-65795
 Apollo 12 soil samples 3-51300
 bentonite-water suspensions structure in shear flow, optical properties 3-50795
 Bruderheim meteorite, olivine-hypersthene chondrite, photometric and polarimetric properties 3-59318
 cellulose tributylate molecules, sedimentation constant, diffusion coeff., intrinsic viscosity, optical anisotropy effect of different solvents (*Russian*) 3-46368
 cholesteric liquid crystals 3-61026
 colour contrast layer formation, on metallographic specimens, gas etching technique, microscope obs. (*German, English*) 3-69240
 gas mixture, indeterminacy in heat transfer (*Russian*) 3-67933
 Gibraltar Strait, optical struct. of water masses (*Russian*) 3-80703
 liquid crystals, appl. 3-71999
 lunar silicate rock powders, darkening by solar wind sputtering 3-65797
 metallic thin films, optical and magneto-optical effects 3-69109
 seawater sampling bottle-cuvette for investigating optical properties 3-42087
 silicate spheres of radius 0.05-1 μ , extinction and scattering of 0.2-50 μ light rel. to interstellar dust 3-42249
 solids, linear effects (*German*) 3-72592
 terrestrial rocks and glasses, optical constants in 0.2-50 μ range 3-58830
 thin films, reflectance analogue computer determ. 3-45476
 transition metal nitrides, thin films 3-64755
 Al vapour, laser-produced, screening effect 3-52423
 Ba₂LiNb₃O₁₅ ferroelectric, 2nd harmonic generation of 1.06 μ m Nd:YAG laser radiation, nonlinear optical properties 3-51958
 CrN film, elec. and optical props., conducting neutral density filter applic. 3-64753
 Cu evaporated films, photoelectric and optical studies (*French*) 3-58301
 GaAs, related compounds, conference, Boulder, Colo., USA, Sept. (1972) 3-41678
 Ge, amorphous, rel. to electronic band structure and transport props. 3-72351
 Li, thin layers, anomalies 3-50531

optical properties of substances continued

- LiF, doped, effect of soluble impurity on resistance to destruction by light 3-66862
 MgF₂ monolayer antireflection coating on glass, evaluation (*Czech*) 3-66189
 MoN film, elec. and optical props., conducting neutral density filter applic. 3-64753
 Pr₆O₁₁ thin films, optical properties meas. by photometry and ellipsometry 3-53159
 Si, amorphous, rel. to electronic band structure and transport props. 3-72351
 SiO₂/TiO₂ two-layer antireflection coating on glass, evaluation (*Czech*) 3-66189
 WN film, conducting with negative t.c.r., elec. and optical props., conducting neutral density filter applic. 3-64753
 ZnS and cryolite contrast dielec. narrow-band interference filters, half-width 1 to 3 nm 3-42577
- optical pumping**
see also atomic excitation; lasers; molecular excitation
 alkali metal atoms, optically pumped, spin-exchange shift and narrowing of magnetic resonance lines 3-54580
 alkali metals, nuclear spin effect on D₂ optical pumping 3-54582
 anthracene crystals, exciton fluoresce. 3-66890
 atom, degenerate levels mixing by strong off-resonant fields, saturation effects 3-46187
 atom, Haroche type reson. obs. in double reson. expt. 3-67670
 atom, transverse optical pumping, saturation effect in r.f. spectroscopy 3-63288
 atomic ¹⁹F ions, optical pumping charge-exchange method for nuclear spin orientation 3-67677
 atomic beam, photoioniz. detection of upper level optical reson. (*French*) 3-57603
 Bloch-Siegert shift, analytical expressions 3-60366
 Bloch-Siegert shift, quantum calc. of higher order terms 3-60364
 Bloch-Siegert shift of coherence reson., higher order terms 3-60365
 Bloch-Siegert shift of r.f. reson., power series expansion 3-67667
 coherence resonances, analog calcs., Bloch eqns. (*French*) 3-54573
 coherence resonances in alignment-orientation coupling processes induced by electric field 3-49394
 cresyl violet-rhodamine 6G dye mixture, excitation transfer, gain spectra obs. 3-70818
 crystal pumped by periodic sequence of ultra short light pulses, excitation of second harmonic 3-48947
 discharge lamps, electrodeless, chopping in very short times, circuit and method 3-45507
 DTTC-methanol solution, gain as function of power, wavelength, time 3-70816
 dye laser, tunable range extension using third harmonic Nd:YAG pump 3-66829
 dye laser picosecond emission on transverse pumping 3-57229
 ethyl fluoride, gaseous, submillimetre laser lines by optical pumping 3-51916
 formaldehyde-h₂ and -hd, fluoresc. lifetime meas. ¹A₂-¹A₁ transition, N₂ laser 3-75057
 formic acid, gaseous, submillimetre laser lines by optical pumping 3-51916
 gas, double reson. theory for transitions between hyperfine levels 3-49402
 gas, ring laser, effect on stability of 3 mode oscillation 3-62704
 gas laser with pumping from internal light sources, radiation absorption probability (*Russian*) 3-48898
 glyoxal vapour, excited at 4358 μ , collision induced intersystem crossing, photophysics 3-80566
 ground state spin and moments of shortlived nuclei, measurement technique 3-45932
 Hanle effect applic. to small mag. field meas. 3-78457
 Hanle effect saturation by intense broad band laser radiation, comment 3-49400
 laser pumping, hollow Xe lamp, laser rods up to 45 mm diameter, design, laser tests 3-53921
 laser rod, transient temp. distrib. for single shot and repetitively pulsed operation 3-59866
 lattice vibrations, relax. and dynamic characts. resonance optical pumping effects 3-58101
 light waves four-photon forced dispersion during nonmonochromatic pumping (*Russian*) 3-48952
 magnesium spinel:Cr, population determ. of metastable level (*Russian*) 3-50149
 magnetisation evolution in two rotating r.f. fields, Bloch eqn. 3-49398
 methyl alcohol waveguide laser in far i.r., CO₂ laser pumping 3-66850
 methyl fluoride, gas laser, 30 kW peak, 496 micron characts., CO₂ TEA laser pumping 3-78020
 methyl fluoride, using CO₂ laser, intense superradiant emission at 496 μ m obs. 3-53127
 4-methylumbelliferone, laser action 3-76064
 N two-level molecules system, inversion, coherent luminescence 3-74214
 nuclear spin moments and charge volumes detn. 3-45962
 organic binary solutions, fast-electron beam pumping 3-40259
 parametric four photon exchange effect, amplification and oscillation near pump field (*German*) 3-78056
 photoionisation laser plasma, effect of Cs 3-66805
 planar resonator, laser operation at high pumping levels 3-45812
 polymethine dye lasers, flashlamp excited, i.r. emission, mode locking, tuning 3-45801
 pulsed laser action, charge transfer between positive ions and atoms or mols. 3-74223
 push pull ruby maser, inversion ratio 3-51895
 quantum freq. converter, quantum theory, time depend. perturbation theory 3-66883
 resonance radiation transfer, role of branching ratio 3-70762
 resonant 3 level system, photon echoes, coherent, nonlinear 3-78061
 resonant degenerate 3 level system, photon echoes, anal. 3-78062
 rhodamine 6 G, photochemical method for determ. of pumping light energy 3-62713
 rhodamine 6G, c.w. Ar⁺ pumped, tuning, open flowing passive absorber 3-66827

optical pumping continued

- rhodamine 6G laser, high average power, low distortion, using face pumped zigzag configuration 3-54225
- Rhodamine B dye laser light polarisation 3-78030
- ruby:Cr, population determ. of metastable level (*Russian*) 3-50149
- ruby, verification of Kramers-Kronig relations 3-48909
- ruby cylinders, polarisation properties 3-78000
- semiconductor, photoconducting, electron component of permittivity, external-pumping-induced change 3-58307
- semiconductor laser, electron beam pumping, using gas plasma gun 3-54232
- semiconductors, electron spin relax meas. 3-68845
- solid lasers, sensitized energy transfer and near i.r. operation, review 3-48917
- Stark effect, resonances, fluoresc. first harmonic, intensity, field freq. 3-71372
- threshold theory of laser generation in p-n junctions with exponential band tails 3-40270
- time dependent amplitude, phase, critical, oscillatory behaviour in parametric amplification 3-59894
- two-level system, photon statistics influence on Bloch-Siegert shift 3-52266
- two-level system interacting with one-mode quantized field, r.f. reson. phenomena 3-63289
- Ag₃AsS₃, proustite conversion of i.r. into visible, mutually perpendicular pumped signal beams, parameters, efficiency 3-40284
- Ar, stimulated emission in linear discharge, pulsed electron beam pumping 3-48890
- Ar stimulated emission, multiple photon pumping 3-66794
- Ba arc spectra, excited state absorpt. spectroscopy of levels pumped by dye lasers 3-63284
- BaO microwave optical double resonance spectra 3-75063
- ¹³⁷Ba⁺ ion-He(Ar) gas buffer collision, hyperfine pressure shifts, optical pumping obs. 3-67713
- CO, (v=1) and (v=2) states, vibr. excitation and relax. 3-45787
- CO, vibr.-translational relax. by foreign gases, localized heating 3-78887
- CO₂, medium pressure laser plasma, continuous uniform excitation, using controlled avalanche ionisation 3-51904
- CO₂ laser media, fast burst reactor, elec. sustainer 3-66797
- CO₂-N₂ high-pressure laser, elec. discharge excited, electron beam controlled, radiation power investigation 3-51906
- CaCO₃, stimulated Raman scatt., picosecond pumping, group retardation effects 3-78058
- Cd, Hanle effect in the case of impulse excitation of 6¹D₂ level 3-63293
- CdS, room temp. lasing using glow discharge excitation 3-66838
- CdS, spontaneous and stimulated luminescence excited by multiphoton optical pumping 3-58557
- CdS laser, electron-beam pumped, influence of mech. treatment of resonator 3-74249
- CdS laser, KGP-2, electron beam pumped 3-48922
- CdS,Se_{1-x} single cryst., nonlinear two-photon absorpt., comp. influence 3-70845
- CdSe parametric oscillator, pumped by HF laser 3-78059
- Cs atom, longitudinal and transverse resonance competition, expt. 3-67675
- ¹³³Cs vapour, pumping by injection laser radiation 3-48887
- Dy²⁺:CaF₂ pumped with short pulses, delay of stimulated emission 3-48913
- GaAs, electron beam pumped scanning laser 3-48927
- GaAs, waveguide laser, fundamental 0.11 micron corrugation feedback 3-78048
- GaAs laser, electron beam pumped, radiating mirror, divergence of output radiation 3-74248
- GaAs laser surface, corrugation feedback, fabrication, spectrum, pumping power 3-48918
- GaAs single cryst., laser threshold value reduction after 600 keV electron irradiation 3-72716
- Ge 709 meV luminescence, optical pumping threshold, new phenomena in exciton condensation 3-55319
- Ge luminescence following optical pumping, carrier density and binding energy of electron-hole liquid 3-58554
- H₂ dissociation transition, stimulated emission cross section 3-40652
- H₂CO, collision-induced transitions, velocity depend. 3-52384
- He-Ne laser, current dependence of the Ne3s₂ level population 3-51907
- He⁺ + rare gas atom collisions, vacuum u.v. emissions, optical excitation apparatus 3-71467
- ³He, nucl. polarisation by optical pumping, apparatus development and relax. time meas. (*French*) 3-46185
- ³He, nucl. polarization by optical pumping, relax. time meas. at surfaces (*French*) 3-46186
- Hg isomers, precision magnetic moment determ., hyperfine-structure anomalies, optical pumping expt. 3-62933
- ¹⁹⁹Hg harmonically bound ground state ions, high resolution magnetic hyperfine resonance 3-49403
- ¹⁹⁹Hg vapour, optically oriented, mag. field depend. of nucl. relax. rate, adsorption energy eval. 3-67676
- ²⁰¹Hg, n.m.r. lineshape in optical pumping expt. (*French*) 3-74804
- ²⁰³Hg, optically aligned, γ -radiation emission, anisotropy and time modulation 3-46000
- ^{199m}Hg, precision magnetic moment determ., hyperfine-structure anomalies, optical pumping expt. 3-62933
- LiIO₃, second harmonic generation, picosecond pumping, group retardation effects 3-78058
- ⁶Li, short lived, spin exchange polarisation and hyperfine splitting meas. 3-52138
- MnF₂, fluorescence spectrum, time for excitons to scatter across Brillouin zones 3-72713
- N₂, coaxial laser, u.v. superradiant pulse width and peak power, operating conditions 3-78019
- N₂, liquid, intensification of dispersion by different pumping schemes (*Russian*) 3-74279
- N₂ laser, high energy electron beam excited, superradiant laser action 3-54219
- NH₃, rot. energy transfer, direct obs. by time-resolved i.r.-microwave double reson. 3-78886
- NH₃ by CO₂ TEA laser, obs. of submillimetre emission 3-74232

optical pumping continued

- Na, D₂ reson. lines, power broadening by optical nutation, laser saturation spectra 3-67669
- Na, electron spin-exchange collision cross sections, temp. depend. 3-67705
- Na, thermal atomic beam, c.w. velocity selection by dye laser optical pumping 3-78463
- Nd:glass, laser emission as source for some laser 3-62721
- Nd:YAG c.w. laser with vortex stabilised lamp 3-45806
- Nd:YAG laser, pumping by miniature diode 3-66836
- Nd³⁺: glass, relaxation rates meas. 3-51933
- Ne, hyperfine structure of 3s₂ level, level crossing meas. (*French*) 3-54576
- O₃, submillimetre laser lines by optical pumping 3-51916
- O₂-D₂-N₂O chemical, gas laser, optical gain and laser emission from flash photolysis 3-48873
- O₂-D₂(H₂)-CO₂ chemical, gas laser, optical gain and laser emission from flash photolysis 3-48873
- Rb, electron spin-exchange collision cross sections, temp. depend. 3-67705
- Rb, rot. frame coherent resons. on fund. level of ⁸⁵Rb (*French*) 3-54574
- Rb atoms, nutation echoes obtained by nonresonant oscill. field 3-78455
- Rb beam, incoherent reson. fluoresc. from coherently excited state, neoclassical radiation theory test 3-63296
- Rb beam excited by short coherent optical pulse, incoherent reson. fluoresc. 3-63295
- Rb polarisation, spin-exchange collisions with Cs, relaxation of electronic polarisation 3-54587
- ⁸⁷Rb maser, light shift and light broadening 3-54209
- ⁸⁷Rb vapour, optically pumped, parametric frequency conversion of resonance radiation 3-43350
- SF₆, liquid, stimulated Raman scatt. 3-70847
- Sr⁺ in optically pumped ⁵P_{3/2} excited state, collisional depolarisation by inert gas atoms 3-46210
- Xe molecular laser, vacuum u.v. emission, electron beam excited 3-66808
- Xe stimulated emission, multiple photon pumping 3-66794
- YAG:Cr, population determ. of metastable level (*Russian*) 3-50149
- ZnS, spontaneous and stimulated luminescence excited by multiphoton optical pumping 3-58557
- optical quantum generators** see lasers
- optical radar**
see also laser beam applications
- aerosol scatt. obs. and balloon-borne conc. meas. in lower stratosphere 3-41981
- aerosol size distrib. remote meas., theory and appls. 3-45487
- atmospheric mountain lee waves, lidar obs. 3-47834
- clouds, backscatt., polarisation props. 3-53465
- deep sea meas. (*German*) 3-59199
- Doppler, f.m. laser noise effects 3-40295
- information processing, incoherent, applications 3-77978
- laser distance meas. system comparing phase of modulating signal 3-51960
- laser radar system, Langley Research Center, description 3-40301
- laser tracking system, detection relationships rel. to return signal fluctuations 3-53919
- Lidar techniques for atmospheric pollution studies 3-45331
- phase light rangefinder employing CO₂ laser 3-70853
- pollution detection, aerosol fluorescence implications for lidar detection 3-77294
- range curve aberration of hologram, synthetic aperture radar, corrections 3-77527
- S/N ratio in system 3-66772
- satellite ranging, Tokyo Astronomical Observatory 3-62755
- upper atmos., aerosol layers, laser radar obs. 3-56190
- water quality meas. with lidar polarimeter 3-42384
- wires and cables, laser refl. coeffs. at 10.6 μ m, wire avoidance system 3-51940
- optical resolving power**
see also optical instrument testing
- Cassegrain telescope, extending field of resolution 3-70060
- dark field imaging system, two-point resolution under partially coherent illumination 3-54206
- diffraction gratings, set of two 3-62061
- Doppler radar, f.m. laser noise effects 3-40295
- fly's-eye lenses and photographic emulsion system, resolution and modulation transfer function 3-62164
- holographic, superresolution, multiple superposition of image holograms with different carrier frequencies 3-40227
- holographic screen samplers, for reduction of speckle in image 3-77531
- image conversion using nonlinear optics, theory, expt. (*Russian*) 3-74268
- image tube, meas. by laser interferometer 3-56675
- interferometer, scanning Fabry-Perot, instrument functions 3-62130
- microscope, two-point resolution of phase objects illuminated with partially coherent light 3-54205
- microwave imaging with enhanced resolution 3-42978
- n.q.r. pulse radiospectrometer, resolving power, effect of spectral width, passband of receivers 3-48487
- partially coherent imaging, two-point resolution criteria, Rayleigh criterion 3-62674
- photographic materials, 440 to 2960 nm⁻¹, LIR 1 interference resolution measuring instrument, specifications, operation, design 3-53937
- point sources of light, resolution analysed by quantum detection theory 3-59850
- remote sounding methods, comparison 3-42084
- resolution limit, communication theory (*German*) 3-59848
- scanning electron microscope rel. to lens aberration, gun brightness, signal/noise ratio 3-70434
- SEM, high voltage, effect on 3-66381
- spherical lenses, obs., information and optical synthetic aperture 3-66907
- telescopes, visual resolution, effect of vibration, allowable angular oscillations 3-56467

optical rotation

- see also *Faraday effect*; *Kerr magneto-optical effect*
 butanol-2-(+), circular dichroism, comparison of theoretical and expt. results of rot. strengths 3-78746
 Chandrasekhar's formula, parameters determ. for dispersion (*Russian*) 3-50538
 chiral molecules, circular differential Raman spectra 3-78802
 chiral molecules, spectral anomalies, i.r. rotatory dispersion 3-71566
 chlorophyll-a, time depend., micellar detergent conc. depend. 3-72680
 cyclic amides, opt. activity calcs. using INDO method 3-52322
 dye dimer-DNA complex, induced optical activity, circular dichroism 3-63597
 electrodynamics of optically active media, boundary conditions 3-74207
 ellipsometer, new, principle, realisation and performance (*French*) 3-62047
 fluid, optically active, light scattering from fluctuations 3-51873
 α -haloketones, fluorine anomaly 3-63393
 liquid crystals, cholesteric, right-and left-handed, pitch and sample thickness depend. 3-41497
 liquid crystals, cholesteric, binary system, twofold helical inversion obs. from circular dichroism and optical rotatory power meas. (*German*) 3-52579
 methane derivative, CHFCIBr , calc. using polarisability theory 3-41493
 molecular crystals, vibr. transitions, symm. depend., spectra, theory 3-72603
 oriented molecules, theory, Kirkwoods formulation 3-75957
 polarisability theory 3-41493
 semiconductor with non-parabolic energy bands, hot electron Faraday rotation and birefr. 3-64630
 spectroscopy, reflection, of optically active materials 3-68950
 spontaneous generation of optical activity 3-73635
 transparent uniaxial media, rotatory power, gyroelec. and gyromag. contribs. (*French*) 3-77957
 UO_2^{2+} complexes, circular dichroism and interpretation of electronic spectra 3-76029
 $\text{Ba}(\text{NO}_3)_2 \cdot \text{H}_2\text{O}$ crystals, activity curves, absorpt. spectra and dispersion 3-76025
 $\text{Gd}_3\text{Fe}_5\text{O}_{12}$, Faraday effect, transition metal ion effects 3-50545
 n-Ge microwave Faraday rotation, conductivity variation, Verdet constant 3-53088
 α - LiIO_3 , growth mechanism and polarity determ., obs. of optical activity 3-72028
 Mn-Bi-Te magnetic film, readout diffraction efficiency of holographic storage 3-42976
 MnBi thin films, Faraday rotation, saturation wavelength dependence, absorpt. coeff., 500 to 1200 nm, protective layer 3-53087
 $(\text{SrCa})\text{S}_2\text{O}_6 \cdot 4\text{H}_2\text{O}$, mixed crystals, dispersion of optical activity 3-76026
 $\text{Y}_{3-x}\text{Bi}_x\text{Fe}_5\text{O}_{12}$ garnet film, Faraday rotation and optical absorpt. 3-53085
 YIG, critical props., reduced total magnetisation, Faraday rot. obs. 3-47030
 YIG, Faraday effect, spin wave obs. 3-47231
 α - $\text{Zn}(\text{H}_2\text{O})_6\text{SeO}_4 \cdot \text{Co}$, laevorotatory, cryst. struct. and absolute config. 3-40866

optical storage devices

- see also *holography*
 Holograms for archival storage 3-77539
 holographic coding plate memory 3-51625
 holographic memories with storage capacities beyond 10^8 bit (*German*) 3-51628
 holographic memory, high capacity optimisation of information characteristics 3-48859
 holographic random access memories, design relationships 3-51876
 holographic read-only memory, laboratory model (*German*) 3-51629
 holographic read-write memory, capacity enhancement by 3D storage 3-48444
 holographic readout efficiency of MnBi thin magnetic films 3-77537
 holographic storage media, thermoplastic-photoconductor ghost images 3-77982
 liquid crystal storage cells, light scatt. angular depend. 3-53084
 optimum sequential holographic data storage, linear optimisation 3-48857
 page composer for holographic data storage 3-42580
 KBr crystal, crystal lattice structure, optical information recording (*Czech*) 3-53129
 KCl, M_n centres, high density optical memory using dichroic absorpt. 3-44431
 KCl crystal, crystal lattice structure, optical information recording (*Czech*) 3-53129
 MnBi films, for magneto-optical memories 3-50546

optical stores

- see also *holography*
 associative magnetooptical store, using multiple longitudinal Kerr reflections 3-44398
 binary data, in paraphase code on phase holograms 3-62672
 electrophotosensitive material application 3-53917
 hologram and kinoform memories, comparison of random and deterministic phase coding 3-73774
 holographic, practical system 3-40224
 holographic, using binary photosensitive material, characs. calc. and computer simulation 3-45773
 holographic digital storage in thermoplastic-photoconductor devices 3-40229
 holographic digital storage system (*German*) 3-45497
 holographic recording by spatial frequency multiplexing, storage density improvement 3-59598
 information processing, incoherent, applications 3-77978
 kinoforms, computing method, image reconstruction error reduction 3-73773
 laser mass memory, vaporised regions on reflective metallic surface 3-40296
 liquid crystal optical transparency, reduction of switching time 3-45779

optical stores continued

- liquid crystal transparency for hologram recording 3-45778
 miniature quasi-Fourier holograms 3-43041
 read-write holographic memory, design/development and implementation 3-45834
 reversible holographic recording materials 3-70789
 Au-Se-SnO₂ system, amorphous optical memory obs., depend. on Se film thickness 3-50541
 Mn-Bi-Te magnetic film, holographic storage, diffraction efficiency 3-42976
 $\text{Y}_{3-x}\text{Gd}_x\text{Fe}_5\text{O}_{12}$ epitaxial films, garnets, magnetic anisotropy, temp. depend., optical memory applications 3-44303

optical systems

- acousto-optical bench, for light diffraction by u.s. wave obs. (*French*) 3-51539
 alignment, improvement in laser flare spot method 3-42552
 antenna tower alignment system for radome boresight error meas. 3-45831
 autocollimation, mirror multiplier adjustment, increased sensitivity 3-62070
 biocular eyepiece, appl. of biocular design procedure 3-77472
 coherent optical systems, imaging, temporal analogy 3-45474
 condensing scheme for intensifying v.u.v. from plasma 3-79172
 deflector using controlled total reflection at an interface (*Czech*) 3-62044
 equivalent triple mirrors with non-coplanar normal axes (*Russian*) 3-48407
 erecting system using two rectangular prisms 3-70301
 heterogeneous, plane, uniform e.m. waves, appl. (*French*) 3-66748
 high-pressure installation for optical investigations, liquid nitrogen temperatures, compressed gas, description 3-77429
 immersion detector, basic parameters meas. 3-62099
 integrated system with Seya Namioka monochromators for vacuum u.v. 3-42550
 i.r. optics, micromachining of components 3-77457
 isoplanatic optical system, point spread function, coherence growth 3-56663
 low-angle laser light scattering 3-40293
 multi-interface, flux monitoring 3-77961
 night-vision system, design considerations 3-48412
 oblique grid shadow graph for meas. of temperature distrib. in transparent fluid 3-39898
 Optical Soc. America meeting, Rochester, N.Y., USA(1973) 3-77430
 partial coherence evaluation, freq.-response control 3-70300
 photoelectric autocollimator, internal stray light 3-39906
 polarisation depend. intensity transmittance 3-42549
 polychromatic optical transmission function in canonical coordinates, for wave aberration and chromatism (*Russian*) 3-59841
 Ritchey-Cretien systems, concave aspheric surfaces, computer testing (*Russian*) 3-42558
 rotating high speed objects, exam. technique, non-stroboscopic system 3-48410
 sensor for tracing edge of work 3-66204
 spatial filtering, for low contrast fingerprint image enhancement 3-66199
 speed measurement, comparison of coherent/incoherent systems 3-73795
 vision/optical aids interaction, image evaluation methods 3-70117
 for wave slope and height meas., comparison with conventional wave height probes 3-62042

optical telescopes see *telescopes***optical television recording** see *telerecording***optical testing**

- see also *optical instrument testing*; *optical workshop techniques*
 aspheric surfaces, aberration testing by synthetic holograms and partial lens compensation 3-45479
 astronomical objective lenses, inspection method in transmitted light 3-70081
 component testing by interferometry, HeNe c.w. laser 3-77521
 contact lens power 3-48403
 fibres, unclad vitreous silica and soda-lime silicate glasses, spectral transmission losses, measurement 3-70304
 Fourier transform lens, wavefront investigation with fan trace interferometer 3-51597
 glass inhomogeneity determ. by interferometric method 3-77469
 ground surfaces, holographic inspection in reflected light 3-66211
 intensity comparison, sector disc method 3-39915
 Japanese single lens camera, design and testing of lenses 3-77548
 large aberrations evaluation using lateral-shear interferometry 3-77511
 laser, frequency stability, long term, measurement method, uncertainties (*German*) 3-73741
 Laser multiple-beam wave-front-testing interferometer 3-77513
 laser Twyman-Green wave-front testing interferometer, absolute calibration method 3-77514
 lens, testing for optimum performance 3-59585
 lens, with wavefront shearing interferometer using computer-aided analysis 3-66200
 lens surface shape inspection by multipass unequal-arm laser interferometer 3-39945
 lenses, review 3-77450
 linear motion accuracy, interferometric method using diffraction grating 3-66131
 linearity of imaging processes, intensity-transfer, test method (*German*) 3-51602
 mirrors, by synthetic holographic interferometry (*German*) 3-45480
 m.t.f. analyser model FPK-1, description 3-59582
 nondestructive optical contour mapping method 3-51516
 optical absorpt. precision meas. by calorimetric method 3-39908
 optical lens, testing or image evaluation, optical transfer function and figure of merit 3-73743
 optical transfer for meas., noise effects 3-77455
 optical windows, surface correction for refractive index inhomogeneity 3-77468
 parallel plates production testing with multipass scanning interferometer 3-77517

optical testing continued

- photographic lenses, modulation transfer for analysis, wavelength weighting 3-77549
- Polaroid Land lenses 3-77547
- Ritchey-Cretien systems, concave aspheric surfaces, computer testing (*Russian*) 3-42558
- Ronchi test, fringes sharpening 3-77467
- spherical surface inspection by interferometer 3-66209
- stereomicroscope, for photointerpretation, square wave response 3-73744
- stress corrosion cracking prediction by triboellipsometry 3-47420
- surface film thickness determ. by refl. meas. 3-45413
- tensors, optical transfer fn. evaluation 3-77454
- textile patterns, match acceptability decisions, colour difference formulas 3-45482
- thick walled glass cylinders, internal meas. 3-77458
- thin film windows, alphanone for meas. heat absorption by infrared method 3-73784
- two wavelength interferometry, static testing and extension to dynamic testing 3-66132
- two-dimensional image receptors, shape of testing target 3-62084
- visual acuity, optimal classification and presentation of optotypes, absolute determinations (*German*) 3-73582
- visual acuity testing of young children 3-70118
- LaF₃, gas laser examination of optical defects 3-70303
- Rh, films, mirrors, evaporated, reflectance, transmittance, optical constants, effect of surface dielectric films 3-66203

optical variables control

- emission spectrum, stabilising device, reduction of meas. error, spark-arc discharge generator 3-73754
- fluorescence intensity, liquid crystals 3-76073
- transparency of liquid crystals for hologram recording 3-45778
- wavelength of light in colorimetry, computer 3-62096
- X-ray determ. of stresses in thin films and substrates by automatic Bragg angle control 3-41669

optical variables measurement

- see also *colorimetry; densitometry; light velocity measurement; photometry; polarimetry; refractive index measurement; turbidimetry*
- angular reflectance modulation meas. method for optical consis. 3-53911
- birefringence in crystals, sensitive meas. method 3-50556
- circular dichroism installation, recording 3-73726
- contact lens power 3-48403
- crystal, low absorpt. coeff. meas., laser beam calorimetric method 3-68949
- dielectric mirror coating, reflectance measurements using laser beam 3-66186
- electro-optical coeff. sign determ., from interf. and electro-interf. comparison 3-73769
- ellipsometry, electrochem. studies, surfaces and surface films, review 3-66197
- equivalent projection density meas. of silver and vesicular films 3-39966
- fluorescent and incandescent lamps, spectral irradiance meas. interlaboratory comparison 3-66126
- glass, low absorpt. loss, meas. technique 3-53894
- glass bulk attenuation meas. using twin beam spectrophotometer 3-53907
- image tube resolution meas. by laser interferometer 3-56675
- instrument for meas. of dispersion and absorpt. in vacuum u.v. 3-45468
- intensity comparison, sector disc method 3-39915
- interface constants, ellipsometer design, construct. 3-73727
- laser, single pulse, coherence meas., interferometric method 3-66853
- laser backscatter detection and meas. method 3-42587
- laser pulses, peak height measurement system, design, operation 3-62160
- laser pulsewidth, picosecond, meas. using Kerr effect shutter 3-59603
- modulation-transfer functions, wide-angle camera lenses, new direct measurement method 3-53940
- optical absorpt. precision meas. by calorimetric method 3-39908
- optical density, liquids, using scanistor photoelectrocolorimeter 3-73728
- photographic material resolution, 440 to 2960 nm⁻¹, LIR 1 interference resolution measuring instrument, specifications, operation, design 3-53937
- phototubes, spectral sensitivity measurement, interlaboratory comparison 3-66218
- polarimeter using rotating birefringent plate compensator 3-59579
- power, in electro-optical systems 3-73745
- reflectance, transmittance of evaporated films, apparatus for in situ meas. 3-77448
- refractive power, in small regions, using position sensing photodiodes (*German*) 3-73742
- self-focusing parameter meas. using intrinsic optical damage 3-59583
- solids, exptl. methods, review (*French*) 3-41494
- transmission density, of photographic layer in microfilming 3-39965
- vision spectral sensitivity meas. by flicker threshold procedure 3-70132
- wave slope and height meas. technique, comparison with conventional wave height probes 3-62042
- SbNa₂K, Cs photocathode, optical and photoelectric props. detn. (*French*) 3-41612

optical waveguides

- bulk acoustic wave interaction, mode conversion, phase and amplitude modulation obs. 3-55545
- corrugated dielectric waveguide, dispersion Brillouin diagram 3-51864
- corrugated dielectric waveguide dispersion, coupled mode analysis 3-51865
- coupled-mode theory for guided wave optics 3-59890
- coupling, grating prod. by SEM 3-70298
- design for use with CO₂ lasers (*German*) 3-54251
- dielectric fibre waveguide, picosecond nonlinear optical pulse transmission, anomalous dispersion 3-59885

optical waveguides continued

- dispersive dielectric fibres, transmission of stationary nonlinear optical pulses 3-59886
- distributed-feedback, conditions for laser oscill. 3-51939
- dye laser amplifier, using rhodamine 6G flash lamp pumped 3-66828
- electrooptic light modulator 3-59580
- fibre, scattering losses in glasses, use of multicomponent materials 3-73736
- fibre radius, outer and inner to outer ratio, determ. using plane polarized laser beam 3-77504
- finite-aperture waveguide-laser resonators 3-59877
- functional junctions in integrated optics theory using methods of partial waves 3-51867
- fused silica, with transition element impurities, optical absorption characteristics 3-73739
- gain-induced modes in planar structures 3-62684
- glass, absorption losses due to trace transition metal impurities and u.v. absorpt. bands 3-53883
- glass, fused silica and quartz, light absorpt. at 1.06 μ 3-73732
- glass coated quartz nonlinear waveguide, second harmonic generation 3-59884
- glass fibre, concentration fluctuation scattering 3-73737
- glass fibre, low-loss, light scattering from composition fluctuations frozen in during cooling 3-75480
- glass fibres, intrinsic optical absorption 3-75971
- glass fibres, review of drawing techniques 3-73734
- harmonic generation, second, phase matched, index tuning 3-74265
- holographic instruments, refractor and reflector, microwave and optical wavelength range, use of dielec. waveguides 3-73777
- holographic thin film coupling resonances 3-77536
- holographic thin film grating coupler, perturbation analysis 3-66177
- laser, dye, prep. by diffusion 3-66831
- liquid core optical fibres, preform drawing technique 3-53893
- liquid crystal, low loss, electro-optic switching 3-44393
- liquid thin films, organic compounds, molecular excitation, techniques (*German*) 3-64752
- low loss glass prep., method 3-53892
- low-loss liquid-core fibre waveguide construction description 3-50787
- low-loss materials for waveguides, light-induced temp. rise 3-51949
- methyl alcohol waveguide laser in far i.r., CO₂ laser pumping 3-66850
- multimode glass optical fibres, preform drawing technique 3-53893
- optics at Bell laboratories, optical communications, comments 3-40221
- optics at Bell laboratories, optical communications, reply to comments 3-40222
- polarisation conversion, Goos-Haenchen shifts, ray optical analysis 3-51868
- polymer film, low loss, with adjustable refr. index 3-53157
- pulse transmission rel. to dielec. dispersion 3-51855
- resonator, optical, waveguide type oscillation modes 3-70835
- second harmonic generation, phase matching 3-48848
- second harmonic generation, theory 3-59889
- square-law medium, effect of n² term on modes 3-59845
- Substrate cleaning for integrated optical waveguides 3-79576
- thin film on piezoelectric substrate, diffraction of guided light by u.s. elastic waves (*French*) 3-40215
- transition radiation in dielectric plate, charged particle perpendicular to waveguide axis (*Russian*) 3-49902
- very low loss, preparation using fused silica-type glasses and unique vapour deposition method 3-73735
- vitroous silica uncled fibre, spectral loss meas. 3-53073
- waveguide laser mode patterns in near and far field, Fresnel and Fraunhofer field distrib. 3-40235
- CO₂ sealed-off laser waveguide 3-59861
- CaWO₄:Nd³⁺ waveguide laser, epitaxial growth 3-54230
- CdS, diffused Se, wave eqn. soln., TE, TM modes 3-66756
- GaAs, waveguide laser, optically pumped, fundamental 0.1 μ m corrugation feedback 3-78048
- GaAs diode laser, stripe geometry, light coupling into optical fibre with spherical end 3-43022
- GaAs epitaxial waveguide with corrugation feedback, laser oscill. 3-66844
- GaAs-Al_xGa_{1-x}As single crystal, 3D light guides, optical IC fabrication, molecular beam epitaxy, photolithography 3-48414
- GaP p-n junction, modulation of laser light, waveguide properties (*German*) 3-53079
- LiNbO₃ single crystal film growth 3-61023
- YAG:Nd³⁺ waveguide laser, epitaxial growth 3-54230
- ZnO film, epitaxially grown, electro-optic and acousto-optic interactions 3-47228
- ZnS or ZnSe heteroepitaxial film on GaAs, leaky wave propagation 3-41597

optical workshop techniques

- alignment holder, electro-optic crystal studies, high temperatures, rapid and accurate alignment 3-62083
- aspherical optical components manufacture by vacuum assisted press. shaping 3-39914
- cementing of large lenses, manufacturing problems, technique, optical cements 3-39913
- Centering Projector-10, VEB Carl Zeiss JENA, positioning device, workpiece alignment 3-51600
- chemical vapour deposition techniques for manufacture of large optics and optical replicas 3-77470
- collimation, multi-aperture technique 3-70305
- corundum plates, single-crystal, process for grinding and polishing 3-62088
- device holder, for luminescent diodes (*German*) 3-42557
- differential reflectometer, electronic divider 3-53890
- diffraction gratings, design and production methods 3-62081
- emissivity determ. at high temp. 3-70307
- Fine-Positioning Device FAE-4, VEB Carl Zeiss JENA, optical symmetry adjustment 3-51601
- glass grinding in type SnP machines, dynamometer 3-39862
- glass low loss, for fibre optics, prep. method 3-53892
- grinding machine, A02 continuous grinder, flat surfaces of glass components, design 3-53898

optical workshop techniques continued

- holograph table, vibration resistant, massive cast Fe slab 3-73779
- interference mirrors and filters, multilayer, location of transmission extrema in terms of stationary points, manufacture 3-53897
- ion polishing of glass 3-62087
- i.r. optics, micromachining of components 3-77457
- kinoforn fabrication, new method using pen and drum plotter with spatial filtering 3-66246
- large optical surfaces, automated production 3-77453
- lens centering method using collimator and autocollimator devices 3-62089
- lens design, nonlinear optimization, Grey's method 3-39910
- lens mountings 3-77452
- lenses, manufacture and testing 3-77450
- lenses, ophthalmic, strengthening, chemical ion exchange, evaluation 3-73740
- liquid core optical fibres, preform drawing technique 3-53893
- luminous point method, expt. determination of sensitivity 3-62086
- machine for fabricating axially symmetric concave aspheric 3-51598
- monochromator, cleaning by action of O atoms 3-39909
- motion trajectories of luminous objects, high-speed stereoscopic investigation 3-51520
- mounting optical component blanks, use of low-melting alloys 3-62092
- multimode glass optical fibres, preform drawing technique 3-53893
- narrow band interference filters optical thickness control (French) 3-51603
- neutral density filters with nonlinear density profiles, prep. by vacuum evaporation 3-45477
- phase-modulated light, detection by heterodyne method 3-62085
- planar optical phase element fabrication 3-53891
- precision lenses, design manufacturing coordination 3-77451
- production technology, book 3-42559
- profile inspection of planoidal aspherical surfaces, on measuring microscope using contact interferometer 3-66208
- reflectance attachment, for grain products 3-48603
- Ronchi test, fringes sharpening 3-77467
- scales and reticles, optical instrument manufacture, classification in terms of material and manufacture 3-53899
- silica glass, optical prop. modification by ion bombardment 3-59584
- spectacle glasses, automatic edge grinder, diamond discs, test results, advantages, problems (German) 3-66202
- surface equidistant shaping with lapping tool 3-39912
- thin films, specimen transfer devices, high vacuum, low temp. 3-53889
- Tilttable Optical Circular Table, 320 S, VEB Carl Zeiss JENA 3-51599
- zone melting, growth of single oxide crystals, light oven design, techniques (German) 3-64784
- BSO₄, depolarisation of diffusely reflected radiation (German) 3-66206
- GaAs-Al_xGa_{1-x}As waveguides, miniature 3D, optical IC fabrication, molecular beam epitaxy, photolithography 3-48414

optics

- see also aberrations; atmospheric optics; fibre optics; geometrical optics; integrated optics; mirrors; nonlinear optics; particle optics; physical optics; quantum optics*
- beam eigenfunctions, resonator modes, beam propagation, hermite gaussian functions of coupler argument 3-66759
- emission problem for electrical magnetic optically uniaxial media, Green's tensor function determ. (German) 3-62408
- light, colour and photography, teaching course for artists 3-51485

optimal control

- see also dynamic programming; game theory; maximum principle*
- active vibration suppression of system driven by external pulsed forces (Russian) 3-66575
- BWR, Halden, on-line computer method for neutron flux distrib. control 3-46066
- electrodeposition time optimal method with pulsating current 3-61262
- jet airliner climb-out paths, min. effective noise calc. 3-77344
- large systems, biochemical membranes with enzymes, modelling/simulation/identification and optimal control 3-53738
- longitudinal travel control of liquid-filled elastic tank (Russian) 3-59773
- nuclear reactor, reactivity estimation, Kalman filter with nonlinear feedback loop 3-74656
- reactors, Xe instabilities (German) 3-67493
- Stokes flow, optimum profiles 3-52495
- suboptimal, of nuclear reactor, using low-order models 3-54528

optimal systems

- hydrophysical problem solution, selection of optimal set of operations, digital probability computing system (Russian) 3-80695
- oceanography, objective and four-dimensional anal., automated collection and processing of data (Russian) 3-47849

optimisation

- see also minimisation*
- anti-pollution device design 3-48275
- beam chopper system for tandem accelerator, high-energy side, optimum dimensioning (German) 3-59634
- buckling under shear, diagonal stiffeners reinforcing clamped infinitely long plate, optimum distribution 3-57088
- burn-up problems in nuclear reactor, equivalence relations 3-63130
- circular orthotropic plate, lower bound plastic analysis, using mathematical programming 3-48731
- under constraints, application to collision amplitudes at asymptotic and finite energies 3-43166
- continuum mechanics, conference, Los Angeles, USA (August 1971) 3-74018
- damping of transient processes in mechanical systems (Polish) 3-66518
- design of geodetic nets 3-76557
- design of structures through variational principles 3-74045
- diffuse object holographic recording, when group of point sources present 3-62671
- disc, magnet coil, current density variation current distrib. optimisation (French) 3-48485
- Dubovitskii-Milyutin method 3-74019

optimisation continued

- e.m. impact systems (German) 3-40201
- energy transfer, between magnetic field and thin conducting plate 3-57179
- fast breeder ²³⁸U-²³⁹Pu reactors optimisation, cooperative games 3-52227
- fast reactor core composition, systematic optimisation, void reactivity 3-63226
- fast reactor design optimisation system with nonlinear programming method 3-57555
- fibre reinforced composite structures, minimum weight design 3-73015
- finite element grids based on minimum pot. energy 3-48726
- finite-element idealizations, theorem 3-45650
- fusion reactor, Princeton reference design model, optimisation of breeding blanket cooling design 3-60312
- galactic mass distribution models, optimisation by scaling 3-70012
- geodesy over sea, radar altimeter optimisation 3-44932
- gravitational antennas, shape optimisation 3-66678
- holographic memory, high capacity optimisation of information characteristics 3-48859
- holographic recording conditions, thin amplitude hologram, nonlinear programming method by computer (Russian) 3-77538
- iterative method rel. to material distrib. in fast nuclear reactor cores 3-74657
- lens design, nonlinear optimization, Grey's method 3-39910
- LMFBR, geometrical optimisation of core-blanket system, performance characteristics 3-49349
- mine gradiometric survey prospecting network, optimal dimensions (Russian) 3-65498
- modal sound attenuation in ducts in zero mean flow 3-49581
- model-building course, mathematics teaching 3-66112
- molecular bond lengths optimisation in all-valence electron SCF-MO calcs. 3-46227
- Monte Carlo source energy biasing optimisation 3-62432
- multi-cavity klystron system for ion bunching, optimisation computer program (German) 3-59911
- multicomponent liquid-liquid equilibrium, Renon's and Black's activity equations 3-58130
- multizonal fast, game theory for initial breeding optimization (Rumanian) 3-63152
- N/D equations, tautologies 3-66950
- nuclear power reactor, N₂O₄ cooled, optimisation study 3-40533
- nuclear reactor, EBR II, optimisation of subassembly coolant flow rates to minimize thermal bowing effects 3-67449
- nuclear reactor shield design 3-60344
- nuclear reactor shield weight, perturbation method, computer program 3-74690
- optimum sequential holographic data storage, linear optimisation 3-48857
- orbital variational trial functions, optimisation 3-40556
- radiometric information processing (Russian) 3-77020
- secondary fast reactor optimisation, mathematical game 3-54535
- shell, stiffened cylindrical, minimum weight optimisation using random search analysis (Russian) 3-62504
- Slater orbital exponents and SCF energy (French) 3-57621
- space telescope, optimum mirror support design, two-stage computer-oriented process 3-70092
- statistical methods, comparison, study of boundaries (Polish) 3-66505
- structures, dynamics and materials, conf., Williamsburg, USA (Mar 1973) 3-59749
- structures with buckling constraints, optimal design using iterative finite element method 3-45649
- surface runoff system, storm records, determ. of optimal kernels, computational technique 3-56243
- swirling fluid flow, reduction of independ. variables and optimization 3-57753
- thermodynamic, current leads, cooling, refrigerator min. power input calc. 3-48382
- thermohydraulic, fuel elements in fast neutron reactors, variable rod distribution (German) 3-67486
- thermonuclear fusion reactor, conceptual, modelling and optimisation 3-60322
- Tokamak fusion reactors, simplified parametric study 3-60642
- Tokamak reactor, design for optimum power 3-63236
- turbulence models, using logical search algorithm 3-49547
- V-groove and rectangular cavities, directional thermal emission optimisation 3-45443
- variable path cell, Q-switch attachment, Laser Mirospectral Analyzer, VEB Carl Zeiss, JENA, optimisation of anal. results 3-51766
- vibrating beam under axial compression, optimum design 3-40135
- He refrigerator cycle with cascade coupling of expansion engines, optimisation 3-62632

optimization *see optimisation***optimum control** *see optimal control***optoelectronic devices**

- see also photoelectric devices*
- colorimeter, for small colour difference meas. on continuously moving band 3-51604
- component sealing and connecting techniques (German) 3-50669
- crystal growth of photochromic and electrochromic materials 3-50656
- human visual receptive field, optic-electronic model of local detectors of visual analyser (Russian) 3-70129
- for interferometric ellipsometry 3-62139
- i.r. and optical imaging 3-48411
- m.n.o.s. structure utilisation (Russian) 3-44155
- solid-state devices, conference, Lancaster, England, 12-15 Sept. (1972) 3-55743
- spatial spectra of luminance field meas. scaling 3-62118
- CdS film, epitaxial, optical and elec. props., rel. to suitability for use as transparent electrode 3-64330
- GaAs, related compounds, conference, Boulder, Colo., USA, Sept. (1972) 3-41678

OR *see operations research*

orbital calculation methods

- see also *atomic orbitals; Hartree-Fock method; molecular orbitals calculations; self-consistent field methods*
 CNDO, electron population analysis problems 3-71353
 CNDO/2, calc. of conformation and electronic struct. of $\text{H}_3\text{PO}_4\cdot\text{BF}_3$ (French) 3-63355
 CNDO/2, force field calcs. and applic. to hydrocarbons and mol. crystals 3-74951
 crystal space orbitals, plane waves, computation 3-75495
 distinguishable electron method for atomic electronic struct. calc. 3-54559
 Earth satellite circular orbit determ. from obs. at unknown times 3-61630
 Hylleraas-type calcs. for Be ground state 3-67650
 INDO, opt. activity calcs. for simple cyclic amides 3-52322
 INDO and MZDO modified methods for spin density calculations 3-46231
 Kepler orbit determ. from mixed data 3-59245
 length and velocity formulas, comment, approx. oscillator-strength calcs. 3-71354
 local orbitals method, systematic extensions, solns. for solid-state and mol. cases 3-43404
 methane, valence electron binding energies and momentum space wave functions 3-74945
 multiconfiguration and polarized orbital close coupling calc., comparative study 3-71443
 open shell systems, ab initio calcs., mol. fragments 3-78668
 Pariser-Parr, applic. to squaric acid and anions 3-52360
 PCILO, comparison with CNDO/2 calcs. 3-49434
 PEEL semi-empirical SCF-MO method applied to electronic structure of Fe(II) complexes 3-63378
 polarized distorted wave, excitation of one electron systems by electron impact 3-71438
 SAMO method for polymers 3-54767
 sequence-adapted mol. tensors, algebraic methods and cryst. field theory applics. 3-57620
 Slater orbital mol. integrals with numerical Fourier transform methods, exchange integrals 3-57619
 student teaching paper comparison of HF and maximum overlap orbitals 3-70236
 variational trial functions, optimisation 3-40556
 wave functions for atomic orbitals of Na and Mg ground states 3-49380
 Be oscillator strengths, model potential calc. 3-78433
 He, nuclear charge expansion method, screening parameter, isoelectronic sequence 3-74782
 Li, isoelectronic sequence, transition probabilities, NCEM screening parameter 3-74783
 Mg oscillator strengths, model potential calc. 3-78433

orbitals, atomic see *atomic orbitals***orbitals, molecular** see *molecular orbitals***order-disorder changes** see *order-disorder transformations***order-disorder transformations**

- acenaphthylene, packing probabilities 3-60782
 adsorbed systems, quantum lattice gas model, ordering transitions 3-64243
 alloy, disordered, odd-order correls., quasibinary approx. 3-79463
 alloy, ordered, volatilisation, statistical theory (Russian) 3-69185
 alloy, radiation-induced disordering, model approach (Russian) 3-72831
 amorphous to crystalline, optically induced, characts. (French) 3-75624
 antiferromagnet, nearest neighbour triangular lattice, phase diagram in mag. field 3-68752
 in b.c.c. hard sphere lattice gas with second-neighbor exclusion 3-40186
 cuprous sulphides, energy band scheme and optical properties 3-68547
 differential reflectometer applic. to materials research problems 3-64812
 displacive phase transitions, theory 3-46692
 ice, relaxational proton ordering and glassy crystalline state, heat capacity meas. 3-64135
 Ising model, spin-1/2, in transverse field, basic theory 3-58113
 Ising model, spin-1/2, in transverse field, spectral functions and damping 3-58114
 magnetite, self-consistent calc. of Verwey ordering 3-58222
 MBBA, isotropic phase, optical-field-induced ordering 3-40846
 methane, solid deuterated, orientational order parameter 3-46694
 omphacite, electron microscope exam. 3-50888
 oversoftening, faintness indices for all zero wavenumber vibrational modes, ferroelectricity, ferroelasticity 3-49960
 Permalloy, electroplated thin film, isochronal annealing behaviour 3-79881
 phenanthrene molecules in solid solutions, spectroscopic manifestation of ordering 3-64656
 poly(dimethyl siloxane), glass transition temperature meas. 3-79242
 rodlike particles gas, phase transition 3-75589
 solid solution, multicomponent, clustering and ordering, fluctuations and kinetics 3-55751
 steel, electron bombarded, low-temp. reversible disorder-order phenomena and carbon redistrib. (Russian) 3-69187
 transition metal carbides, microhardness, temp. depend. 3-47446
 AgBr-CuBr mixed crystals., phase behaviour and lattice disorder, calorimetric obs. (German) 3-64184
 AgI, polycryst., thermal expansion change 3-75629
 AgIn, sp. ht., elec. resist., X-ray diffr. and mag. susceptibility obs. 3-64831
 Ar, atoms, small clusters, mol. dynamics study 3-43859
 As-Se-Pb, glass formation (Russian) 3-73069
 Au₃Cu alloys with Fe additions, atomic ordering influence on mag. props. (Russian) 3-68764
 Cd-Mg(Zn) alloys, h.c.p., pseudopotential study 3-69195
 CdGeP₂, semiconductor, glass-crystal phase transition, NMR of P³¹ (Russian) 3-72197
 Cr₂Te₄, from heat capacity and the thermodynamic props. obs., 298 to 950 K 3-68408
 CsSH, Raman scatt. study 3-55590
 Cu-Au, binary system, transform. theory, phase diagram calc. 3-44562

order-disorder transformations continued

- Cu-Au, binary system, transform. theory, calcs. for long and short range order parameters 3-44563
 Cu-Pd alloy, investigation of disordering processes (Russian) 3-69190
 CuPt alloy, crystallographic ordering mechanism and modified microstruct. 3-80215
 Fe-Al, single-, two-phase state transform., slow cooling and isothermal annealing 3-80216
 Fe-Co alloys, rates of ordering and antiphase domain coalescence during isothermal annealing 3-58614
 Fe-Ni-C martensite, interstitial ordering rel. to tetragonal struct. 3-64828
 Fe-Si alloy, annealing, elec. resist. (Japanese) 3-72837
 Fe₃Al, paramagnetic susceptibility as probe into atomic ordering 3-60957
 Fe₃Al, resistivity anomaly near order-disorder transition 3-55241
 Fe₃Al, transition rel. to elec. resist. and mag. susceptibility 3-47033
 FeCo, low temp sp.ht. of ordered and disordered systems, electronic and harmonic phonon contributions 3-64185
 Ge film, density of state changes at amorphous-cryst. transition, photoemission obs. 3-43987
 Ge-Se semiconductor glasses, mag. susceptibility, temp. dependence, glass-fusion transition (Russian) 3-72456
 o-H₂ effect of correlations on transition temp. calc. 3-72163
 Hf₂O, superstructure and transform. of interstitial O 3-58111
 KCN, Raman and i.r. spectra, phonon modes and librations obs. (French) 3-58509
 KCN, Raman scattering study 3-72648
 LiAlO₂:Mnⁿ⁺, effect of ordering on phosphorescence 3-55682
 LiFe₂O₈, defect struct. characteriz. 3-68275
 Li_{1/2}Fe_{3/2}O₄ spinel, expansion meas., differential thermal anal., substitution (French) 3-75591
 LiXVO₄, (X=Mg, Co, Ni, Cu, Zn), vibr. spectra obs. 3-52689
 N₂, solid, primitive cubic α to disordered hexagonal β , pressure depend., n.q.r. obs. 3-75590
 NH₄Br, specific heat anomaly near orientational phase transition 3-49995
 NH₄Br(Cl), lambda order-disorder transition, u.s. obs., mode-mode coupling theory 3-41000
 NH₄Cl, N and Cl spin-lattice relaxation near λ -transition 3-55494
 NH₄Cl, order-disorder phenomena, acoustic attenuation and dispersion 3-43860
 NH₄Cl, refr. index, near -30°C 3-68956
 NH₄Cl, u.s. attenuation temp. depend. anal. crit. of order-disorder lambda transition 3-72139
 NH₄Cl(I), u.v. reflectivity obs., ordered and disordered phases 3-80074
 NaNO₂, second harmonic generation for SRO obs. in paraelec. state 3-64613
 NaSH, Raman scatt. study 3-55590
 Ni complex, hexapyridinenickel (II) nitrate, determ. from heat capacity 73-300 K (French) 3-49961
 Ni₃Al alloy, ordering transition, TEM obs. 3-80198
 Ni₃Te₄, heat capacity and thermodynamic props. obs., 298-950 K 3-68408
 P₂Se₃, semiconductor, glass-crystal phase transition, NMR of P³¹ (Russian) 3-72197
 Pb based alloys, amorphous to crystalline state 3-41110
 Pu-Fe, (10 at.%Fe), eutectic, order-disorder and antiphase structure, heat capacity meas. 3-60799
 RbSH, Raman scatt. study 3-55590
 TlSb₃ films, amorphous to crystalline, effects on electrophysical props. (Russian) 3-79588
 U₃O₈, high-temp. phase transition, 300-800°C 3-64972
 V₆C₅, influence on elec. resist. meas. 3-44075
 V₆C₅, V₆C₇, rel. to vacancy ordering effects on thermodynamic props. 3-72973
 V₈C₇, influence on elec. resist. meas. 3-44075

ordinary ray see *birefringence***ores** see *minerals***organic acids** see *organic compounds***organic bonds** see *bonds (chemical)***organic compounds**

- see also *free radicals; macromolecules; organometallic compounds; plastics; polymers; Rochelle salt; waxes*
 1,2-bis-(4-pyridyl) ethanes conformations of the rot. isomers, Raman and i.r. spectra 3-78772
 2-[2'-pentaboran(9)yl]pentaborane(9), accidental degeneracy in ¹¹B n.m.r. spectrum, partially relaxed Fourier transform resolution 3-78840
 N-(diphenylmethylene)-aniline, determ. of dihedral angle of A ring 3-71486
 1,1-difluoroethylene, Fermi resonances 3-75018
 9,10-dibromanthracene, autoassociation in vitreous solutions, study by absorption spectra (French) 3-50591
 absorption spectrum of local centres, correl. functions, multiplet structure 3-64681
 acenaphthene, quasi-linear absorption and luminescence 3-72747
 acenaphthene radical, in n-pentane, multiplicity of the quasi-line fluoresc. spectrum 3-64716
 acenaphthene vinyl ethers, i.r. spectra, config., vib. (Russian) 3-63479
 acenaphthylene order and disorder rel. to packing probabilities 3-60782
 acetaldehyde, collision broadening of rot. lines by O₂ 3-67834
 acetaldehyde, internal rotation barriers rel. to localized charge distributions 3-54633
 acetaldehyde, photoluminescence, temperature, pressure, and and excitation wavelength effect 3-46313
 acetaldoximes, i.r. spectra, normal vibrations (German) 3-74979
 acetaldoximes, normal coordinate calcs., normal vibrations, potential energy distributions (German) 3-74980
 acetamide, solvent effects in hydrolysis reaction rate 3-69457
 acetamide PVA in solution, thermoelasticity, gels 3-63601
 acetalide, resonance freq. splittings of some vibrs. 3-75581
 acetates, determ. of dielectric relax. at microwave freq. 3-72569
 acetates in soln., dielec. dispersion characts. and dipole moments 3-68920

organic compounds continued

- acetic acid, cryst., hydrogen bond vibr., i.r. and Raman spectra obs. 3-72640
- acetic acid, HF and HNO_3 , controlled preferential etching, Si, doped epitaxial layer 3-61659
- acetic acid dimers, anharmonic couplings via Fermi reson. in strong coupling theory (*French*) 3-52336
- acetic acid- H_2O -carbon tetrachloride, coexistence curve shape near plait point 3-75600
- acetone: rare earth ions, role of solvent in processes of nonradiative energy transfer 3-64717
- acetone, αNPO excimer formation thermodynamic properties, solvent effect 3-80584
- acetone, liquid, mol. motion, depolarised Rayleigh scatt. obs. 3-79223
- acetone, liquid, reorientational motions from press. depend. Rayleigh scatt. 3-80055
- acetone, liquid-vapour equilib. with chloroform diethyl ether 3-64165
- acetone, oriented, n.m.r. spectra quadrupole coupling const. 3-64564
- acetone, pressure effect on melting point 3-79476
- acetone complexes with chlorophenol derivatives, hydrogen bond energies spectroscopic determ. (*Russian*) 3-49474
- acetone heterogeneous decomposition on 20% Cr/25%Ni niobium stabilised stainless steel, kinetics, deposit characterisation 3-71299
- acetone in soln., i.r. spectra obs. 3-64648
- acetone in solution, triplet state, charge transfer rel. to quenching by aromatic molecules 3-69474
- acetone in steel vessel, inhibition of carbon deposition by sulphur poisoning 3-73168
- acetone in uranine solutions, fluorescence light intensity, influence of degree of dispersion 3-41575
- acetone oxime- d_6 , hydrogen bonding, self-association, low temp. i.r. spectra 3-64640
- acetone-ethylene system, intermolecular triplet excitation transfer 3-69480
- acetonitrile: rare earth ions, role of solvent in processes of nonradiative energy transfer 3-64717
- acetonitrile, αNPO excimer formation, thermodynamic properties, solvent effect 3-80584
- acetonitrile, CH_3CN and CD_3CN , Raman spectra and phase transition, lattice modes 3-55588
- acetonitrile, liq., mol. reorientational motion, Raman bandshapes, diffusion consts. and activation energy 3-60661
- acetonitrile, liq. struct. determ. from X-ray scatt. (*German*) 3-63944
- acetonitrile, photodissociation and photoionisation in vacuum u.v., Rydberg states obs. 3-75093
- acetonitrile, solvent for aromatic molecules, effect on excited states 3-60473
- acetonitrile dipole-dipole molecular interaction with phosphonium salts, i.r. spectra obs. (*Russian*) 3-50850
- acetonitrile- d_3 , vibr.-rot. spectra analysis 3-63462
- acetonitrile-phenol complex, CNDO/2 calcs. of electronic struct. and configs. (*French*) 3-43390
- acetophenone, in alcoholic soln., triplet state, absorpt. spectra obs. (*Russian*) 3-80067
- acetophenone derivative, photosensitisation of DNA, excited states 3-63588
- acetophenone in soln., triplet-singlet energy transfer to 9,10-dibromoanthracene 3-76088
- acetophenones, substituent effects on acetyl group config. rel. to carbonyl frequency 3-63353
- acetoxybenzal p-phenetidine, nematic liquid crystal, p.m.r. 3-53025
- acetoxybenzal-p-aminoazobenzene nematic liq. cryst., proton mag. reson., degree of order 3-55485
- acetoxybenzal-p-anisidine nematic liq. cryst., proton mag. reson., degree of order 3-55485
- 4-acetylenaphthene, in paraffin matrices, phosphoresc. spectra, low temp. 3-72731
- acetylated glycopyranosyl chlorides, ^{35}Cl pure n.q.r., coupling const. and mol. conformation relation 3-49491
- acetylene, density localised mol. orbital calcs. 3-71501
- acetylene, deuterated, plastic phase, n.m.r. 3-79246
- acetylene, explosion decomposition, particle size of carbon black rel. to temp. (*Russian*) 3-47543
- acetylene, molecular and dissociative photoionisation, hot bands obs. ethynyl ion heat of formation 3-75092
- acetylene, molecule, electron impact dissociation, rotational and vibrational energy level distrib., luminesc. 3-75127
- acetylene, second-order press. calc. with virtual orbitals 3-54617
- acetylene, two centre calc., Slater type orbitals, vertical electronic transitions, bond distances, force constants (*Russian*) 3-49444
- acetylene, weak absorpt. line detection, using glass: Nd laser 3-39933
- acetylene + oxygen flames, reduced-pressure, spectroscopic obs. of methene and methyl radicals 3-47532
- acetylene glycerols, i.r. obs. of hydrogen bonds 3-75047
- acetylene in different liquid crystals, proton magnetic shielding anisotropy 3-43489
- acetylene nitrile, photodissociation and photoionisation in vacuum u.v., Rydberg states obs. 3-75093
- acetylene-air flames, atomic absorption of Hg, effect of standard Hg(II) solutions 3-48639
- acetylene- Cl_2 complexes, low temp. i.r. spectra 3-75014
- acetylene- N_2O gas shielded flame, Ba determination, atomic absorption spectrometry 3-48637
- acetylene- O_2 chemical laser characs. 3-59863
- acetylene- O_2 flame at extremely low pressures, ion recombination 3-76445
- N-acetylglycine, single crystals, X-ray damage, e.s.r. meas. 3-73146
- N-acetylglycine X-irradiated crystal, ENDOR under intense r.f. field 3-55504
- acridine, amino derivatives, quantum yields of interconversion 3-76480
- acridine dyes, dication $1 \rightarrow A$, band polarization meas. (*French*) 3-69050

organic compounds continued

- acridine mustard, monofunctional reversion of genetic alterations, X-irradiation, *Neurospora crassa* 3-48262
- acriflavin, stimulated cond. and photocurrent, relax. 3-75775
- acriflavine, dye film, activation of photocurrent 3-72382
- acriflavine, use in dye-mixture laser 3-78029
- acriflavine soln., excitation energy transfer 3-69047
- acrolein, cis and trans, near u.v. absorption spectra 3-52352
- acrolein, unsuccessful search for molecular lines in interstellar matter 3-61863
- acrolein- d_1 , near u.v. absorption spectra 3-52352
- acryl-lead layers, heterogeneous absorbers, form of electron cascade curves (*Russian*) 3-67626
- acrylic acid, Al surface adsorption, polymerisation, oxidation 3-72264
- acrylic acid radical anions in low temp. glasses, e.s.r. detection 3-65094
- acrylic monomers, hypersonic props., temp. depend., Brillouin spectra, thermal relax. effect 3-55990
- acyl peroxide oligomers, i.r. spectral analysis (*Russian*) 3-78777
- adamantane, self-diffusion in rotator cryst. phase, temp. depend. 3-64206
- adamantane angle crystals, Brillouin scatt. acoustic velocity, phonon modes, elastic constants, Debye freqs. (*German*) 3-68976
- adenine, energy level structure of ionised states, photoemission, photoconductivity 3-68669
- adenine sulphate, single crystals, growth and morphology 3-80149
- adenosine monophosphate, 3',5'-cyclic, p.m.r. study of conformations 3-63568
- adsorption on Pt electrode, electrochemistry studies using modulation spectroscopy 3-55965
- air-acetylene flame, oxygen-shielded, burner design atomic spectroscopy 3-70486
- β -alanine, X-irrad., recrystn. effect on e.s.r. spectra 3-55970
- alanine single cryst., nuclear spin-lattice relax. anisotropy 3-75907
- alcohol, monocrystals, deuteration effect on Davydov splitting and absorption band of OH stretching vibrations 3-47254
- alcohol, solns. of rhodamine dyes, conc. quenching of luminesc. 3-69075
- alcohol vapours, infra red studies, intramolecular interactions and self association 3-78770
- alcohol water liquid layers, finite amplitude oscill. motions in two component Benard problem 3-67950
- alcohols, ionization potential calc. 3-78672
- alcohols, i.r. spectra, intermolecular interaction, phase transition 3-72654
- alcohols, liquid, detection of intermolecular coupling in Raman spectra 3-57657
- aldehydes, static and dynamical pot. surface distortions in $^3\text{A}'(\pi\pi^*)$ states 3-63382
- alicyclic amines, Raman spectra, Bohlmann bands 3-75027
- aliphatic, additive character of displacements of inner atom levels 3-78684
- aliphatic, influence of substituents in $\pi\pi^*$ and $\pi\pi^*$ absorption bands (*Russian*) 3-43441
- alkali TCNQ salts, mag. props. 3-60954
- n-alkane, chain flexibility, Monte Carlo simulation 3-60400
- n-alkane liquid mixtures, infinite dilution diffusion coefficients 3-76489
- n-alkanes: aromatics, zero-phonon line width temp. depend. 3-68360
- 1-alkanes, dielec. consts. and losses, mean relax. times, chain length depend. 3-47204
- alkanes, halogenated, opt. mol. anisotropy in different media (*French*) 3-63424
- n-alkanes, light scatt. spectrum 3-80053
- n-alkanes, molecular optical anisotropy, depolarised Rayleigh scattering 3-49469
- alkanes, quantitative analysis, simple decomposition technique 3-61970
- alkanes, solvent effects in ^{13}C n.m.r. spectra ^1H 3-71580
- alkanes and intermediate solvents, for liquid scintillators 3-48526
- alkenes, C_2 to C_4 , Ar matrices, i.r. spectra, 20K, cryogenic studies 3-49470
- n-alkoxy-n-acyloxybenzol, liquid cryst., dynamic light scatt. 3-76027
- n-alkoxyazoxybenzenes, homologous series liquid crystals, struct. obs. 3-75470
- alkyl ammonium halides, spectra of polymorphic transitions 3-72755
- alkyl ammonium tetrachloromanganate and deuterated analogues, cryst. and mag. transitions 3-47045
- alkyl derivs., straight chain, electron density distrib. 3-71525
- n-alkyl fluorides, C-F stretching frequencies of rotational isomers 3-43426
- alkyl iodide aqueous solns., pulse radiolysis, transient ion pairs from OH radical reactions 3-76464
- alkyl mercaptans far i.r. spectra, torsional transitions 3-63457
- 1-alkyl-3-aryltriazenes, tautomerism, n.m.r. spectroscopy 3-74929
- 9 alkyl-substituted anthracene solutions, excimeric fluorescence, concentration quenching 3-65106
- alkylchlorosilanes, addition reactions with alpha-olefins, i.r. spectroscopic study (*Russian*) 3-80543
- alkylsilane, vibr. freq. obs. and force const. determ. 3-67776
- allene, excited states, CNDO calc. using ligand geometries in transition metal complexes 3-60419
- allyl cyanide, ^{13}C n.m.r., conformation anal., chem. shift, T_1 meas. 3-67855
- allyl halides photoelectron spectra 3-46336
- allyl radical, all-electron mol. orbital theory, symm. dilemma 3-43402
- aluminium guanidine sulphate hexahydrate, polarization switching process, hydrostatic press. effects 3-79986
- amide-water systems, deviations from ideal behaviour of mixtures 3-53356
- amides, simple primary and secondary, identification and origin of N-H overtone and combination bands in near i.r. spectra 3-46291
- amidoximes, valence vibr. bands of NH_2 , ND_2 and NHD groups, NH bonds inequivalence (*French*) 3-52365

organic compounds continued

- amine-SO₂ complexes, force consts. for charact. vibrs., i.r. and Raman spectra 3-60461
- amine-sulphur system, Raman spectra 3-78794
- amines, ionization potential calcs. 3-78672
- amines, non-planar aromatic, spin-forbidden electronic transitions 3-46237
- amino acetonitrile, microwave spectra, bond angles, dipole moment 3-63485
- amino acid tryptophan in frozen polar soln. at 77K, two-quantum ionisation 3-41866
- amino acids, transmission electron microscopy, 2.5 MeV, penetration meas. 3-56982
- amino acids containing S, γ -irrad., electronic structure parameters of free radicals, expanded Huckel meth. 3-78681
- amino group, two-component solns., spectroscopic study of intermolecular interactions (*Russian*) 3-80050
- 2-amino-7-nitrofluorene in polar solvents at low temp., dependence of fluorescence wavelength on excitation wavelength (*German*) 3-55689
- aminoacids, photoconductivity, role of mol. electronic structure (*Russian*) 3-46365
- aminodifluorophosphine, CNDO/2 approximation for conformational analysis (*French*) 3-63359
- aminoethyldithioacetic acid formation, X-radiation of cystamine and dithiodiglycolic acid, chain reaction 3-47566
- 1-aminoindan (IV), structure depend. of emission props., intramol. electron transfer 3-75061
- 2-aminoindan (V), structure depend. of emission props., intramol. electron transfer 3-75061
- aminoindenes, isostructural energy band structure, photogeneration mechanisms, effect of S substitution of O (*Russian*) 3-55304
- 6-aminopenicillic acid, i.r. vibrational spectrum, structural analysis (*Russian*) 3-78778
- p-aminophenol hydrolysis, reaction kinetics, thin-layer electrochemistry 3-69467
- aminophosphines, bonding, n.m.r., ¹⁵N-H coupling 3-71575
- 2-aminopyridine, fluoresc. lifetime, single photon counting apparatus 3-69085
- aminopyridines, phosphoresc. emission and polarization, triplet states 3-65101
- aminopyridines in chloroform soln., hydrogen bonding study 3-52349
- 1-aminopyridinium perchlorate, crystal, influence of pressure on i.r. spectrum of the perchlorate group 3-47265
- ammonium hydrogen bis(chloroacetate) ferroelectric phase transition, ³⁵Cl n.q.r. and i.r. spectra obs. 3-79992
- ammonium hydrogen oxalate hemihydrate, dislocation lines direction obs. 3-64037
- aniline, mol. configuration determination, models for internal rotation, n.m.r. lanthanide shift studies 3-46226
- aniline, single vibronic level fluorescence measurements, effects of anharmonicity and geometry change 3-80107
- aniline, u.v. spectra analysis, computational method (*German*) 3-46266
- aniline derivatives, u.v. absorpt. spectra, electronic transition 3-78730
- aniline in NbSe₂, intercalation complex, electron microscope examination 3-72039
- aniline-cyclohexane mixtures, critical exponents near critical conc. determ. by light scatt. (*German*) 3-65119
- anisal-p-aminoazobenzene nematic liq. cryst., proton mag. reson., degree of order 3-55485
- n-anisalaminoazobenzene, structure of nematic mesophase 3-79234
- n-anisalaminoacinnamic acid ethyl ether, application of optical modelling method to liquid crystal struct. determ. (*Russian*) 3-68152
- anthracene, ¹L_b transition location by dichroism meas. 3-76013
- anthracene, absorpt. spectra, polarisation props., line form of 2 photon transitions 3-66887
- anthracene, anharmonicity of lattice vibrs. 3-75583
- anthracene, carrier sign and mobility determ., photoconductivity (*Russian*) 3-55309
- anthracene, charge carrier generation by singlet-singlet exciton interaction under weakly absorbed illumination 3-64374
- anthracene, compressed powder disc, a.c. conductivity, freq. and temp. depend. 3-79685
- anthracene, cryst., exciton band structure, thermoabsorpt. obs. 3-55230
- anthracene, dielectric tensor as a function temp. and pressure 3-41471
- anthracene, dissociation of Frenkel excitons, influence of vibronic coupling, photoconductivity 3-79655
- anthracene, effect of doping on styrene fluoresc. 3-69081
- anthracene, elec. cond. in melting region (*Russian*) 3-44068
- anthracene, enhancement of photoconduction by detrapping 3-55303
- anthracene, exciton-phonon interaction, conservation laws, molecular crystal spectra 3-68972
- anthracene, expt., orbital calcs. for photocurrents 3-68675
- anthracene, fluoresc. at high exciton conc. 3-58549
- anthracene, fluorescence lifetime in polymethacrylate 3-80562
- anthracene, impurity effects on electrical conductivity 3-68615
- anthracene, in H₂SO₄, conc. depend. relax. times, spin echo expts. 3-41400
- anthracene, in n-hexane and n-heptane matrices, fluoresc., phonon struct. 3-72729
- anthracene, injection of electrons and electron trapping levels, s.c.l. current obs. 3-75755
- anthracene, low frequency Raman spectra, line intensities 3-64653
- anthracene, magnetic field dependence of delayed fluorescence, test of non-crossing pair state theorem 3-79661
- anthracene, molecular crystals, press. depend. of lattice freqs. 3-75585
- anthracene, n-hexane soln., photodimerization and fluorescence rates, press. depend. 3-69476
- anthracene, photocond., triplet exciton-impurity interaction rel. to carrier generation 3-46879
- anthracene, radiationless transitions, position-dependent deuterium effects, triplet lifetimes 3-65100
- anthracene, radiolysis at metal surfaces (*Russian*) 3-47567

organic compounds continued

- anthracene, reflection spectra, exciton band structs., optical consts. 3-64307
- anthracene, rhodamine B absorpt., triplet exciton luminesc. 3-69089
- anthracene, singlet-triplet absorpt. spectra, Franck-Condon factors 3-73159
- anthracene, small polaron model of electron motion 3-64334
- anthracene, superradiant light excited fluorescence 3-72703
- anthracene, tetracene doped, triplet exciton interactions, delayed fluoresc. (*German*) 3-50616
- anthracene, theory of singlet-triplet exciton fusion 3-64311
- anthracene, triplet exciton stimulated current pulses, delayed luminesc. 3-60895
- anthracene, triplet-triplet energy transfer to rhodamine dyes 3-69077
- anthracene, vibrational relaxation in triplet state 3-46312
- anthracene, with tetracene, rubrene surface states, mag. quenching of fluoresc. 3-72724
- anthracene and methyl derivatives in polymethylmethacrylate matrix, absorption and fluorescence spectra 3-63507
- anthracene as semiconductor, review 3-55253
- anthracene concentrated solutions, fluorescence quenching, role of processes of formation of excitons and photodimers (*Russian*) 3-44468
- anthracene crystal, absorption spectrum, resonance interband interaction and vibronic coupling 3-41161
- anthracene crystal, exciton dynamics, line shape analysis of reflectance spectra 3-64306
- anthracene crystal, surface states, Davydov splitting, low temp. refl. spectra 3-69017
- anthracene crystals, carrier mobilities and lifetimes, electron traps, dislocation effects due to deformation 3-41182
- anthracene crystals, difference between effective and mean light-wave fields in determ. of spectroscopic props. 3-62737
- anthracene crystals, effects on polarized reflection spectrum during cooling 3-69008
- anthracene crystals, exciton fluoresc., intensive pumping 3-66890
- anthracene crystals, nonlinear quenching of fluoresc., 1.8-4.2 K 3-58559
- anthracene crystals, nonradiative destruction of triplet excitons by excess electrons 3-44451
- anthracene crystals, two-photon absorption 3-48944
- anthracene crystals containing tetracene impurity, stimulated radiation emission study 3-80077
- anthracene crystals, fluoresc. quenching by singlet-singlet and singlet-triplet exciton interactions 3-58541
- anthracene derivatives, two-photon excited fluoresc., polarisation study 3-42986
- anthracene derivatives chemiluminescence during oxidation (*Russian*) 3-41862
- anthracene doped fluorene, time resolved fluorescence spectroscopy 3-55680
- anthracene electrodes, electrochem. reactions with exciton participation 3-55968
- anthracene mol. solids, polariton dynamics from band profile analysis 3-72642
- anthracene molecule, vacuum u.v. absorpt. spectrum 3-78745
- anthracene ring system containing cpds., photoemission in vacuum u.v. region 3-41613
- anthracene single crystals, intrinsic photoconduction, hole and electron quantum yields, electric field dependence 3-75769
- anthracene solution, delayed fluorescence, O₂ quenching, mag. field effects 3-46309
- anthracene stable dimer, fluorescence absorption energy gap 3-71570
- anthracene vapour, fluoresc. spectra, freq., temp. depend. 3-67846
- anthracene-Au system, extrinsic photocurrent production, role of singlet and triplet excitons 3-46815
- anthracene-N,N'-diethylaniline, excited CT complex form. rate meas., psec. laser pulses 3-76476
- anthracene-pyromellitic dianhydride, zone-refined crystals, charge-transfer spectra 3-61269
- anthraquinone single cryst., far-i.r. spectra, translational lattice vibrs., Fermi reson. 3-61034
- anthronitrile, absorption and fluorescence spectra, solvent and pressure dependence 3-41531
- antimony triphenyl-d₁₅, solid, deuterium quadrupole coupling at 77K 3-44348
- aqueous base solutions having i.r. absorption continua, very polarisable H-bonds 3-61285
- aromatic, Br-C bond distance 3-46600
- aromatic, fluoresc. state, heavy-atom collisional quenching, empirical law 3-52382
- aromatic, in n-paraffin matrices, local states of impurity aggregate formations 3-72738
- aromatic, influence of substituents on $\pi\pi^*$ and $\pi\pi^*$ absorption bands (*Russian*) 3-43441
- aromatic and heterocyclic molecules, reactions with F atoms, energy distrib. in reaction complex 3-73124
- aromatic compound soln., kinetics of energy degradation and relax. 3-76082
- aromatic compounds, absorption spectra, intensity of transition and intensity distribution correlation 3-60440
- aromatic cpds., radiative transition rate from π,π^* triplet state, external heavy-atom enhancement mechanism 3-40642
- aromatic hydrocarbon, efficiency of zone melting method 3-41641
- aromatic hydrocarbons, condensed, Stark effect 3-76012
- aromatic hydrocarbons, mag. circular dichroism, vibronic coupling 3-74993
- aromatic hydrocarbons, quenching of triplet states in solution by O₂ 3-61272
- aromatic hydrocarbons, quenching of triplet states in solution by O₂ 3-61273
- aromatic hydrocarbons, quenching of triplet states in solution by NO and free radicals 3-61274
- aromatic hydrocarbons, S₁→T₁, intersystem crossing process, PMDR obs. 3-44731
- aromatic hydrocarbons in vitreous media, identification of autoassociated species by absorption spectra (*French*) 3-50590

organic compounds continued

- aromatic molecules, effects of environment on excited states 3-60473
- aromatic molecules, electron excitation energy transfer to DPPH in solid solns., luminesc. yield 3-76484
- aromatic molecules, energy transfer from higher triplet levels (*Russian*) 3-41863
- aromatic molecules, ligand atom vacancy initial states 3-66464
- aromatic molecules in glassy matrices, spectra, internal energy transfer 3-69084
- aromatic molecules in soln., fluoresc. quantum yields from highly excited states 3-78830
- aromatic molecules in vapour phase, fluoresc. quantum yields from highly excited states 3-78831
- aromatic mol., force const. determ. using Coulson-Longuet-Higgins formula (*Russian*) 3-63420
- aromatic nitro derivatives, sensitisation of bisazide, mechanism 3-61280
- aromatic nitro-compounds, rate of combustion at high pressures, rel. to temp. of flame (*Russian*) 3-47539
- aromatic nitrogen heterocyclic ions, two-centre Coulomb repulsion integrals effect on spin densities 3-60426
- aromatic polynitro compounds, electrochemical circulation cell, electrolysis, electronic absorption spectra, optical density meas. 3-45534
- aromatic quinone derivatives, sensitisations of bisazides, mechanism 3-61280
- aromatic triple bond molecules, description of radiative triplet props. 3-67841
- aromatics in fluid dimethylmercury, room temp. phosphoresc. 3-47570
- arsabenzene, photoelectron spectra 3-46255
- arsonomethylanthranilic acid, oxidation-reduction indicator, titration Fe (II), Cr (VI) 3-48649
- aryldifluoromethyl ethers, dipole moments in benzene, calc. of moment μ_s from μ_n 3-71522
- aryldifluoromethyl sulphides, dipole moments in benzene, calc. of moment μ_s from μ_n 3-71522
- aryldifluoromethylsulphones, dipole moments in benzene, calc. of moment μ_s from μ_n 3-71522
- aryldifluoromethylsulphoxides, dipole moments in benzene, calc. of moment μ_s from μ_n 3-71522
- arylethylene, doping in naphthalene, vibronic spectrum phonon struct. 3-68357
- arylethylenes in solvents at low temp., dependence of fluorescence wavelength on excitation wavelengths (*German*) 3-55689
- arylketones in benzene soln., substituent effect on triplet lifetimes 3-76475
- ascorbic acid and 2-chloro-4-aninophenol single and combined photographic developers, kinetics of Ag formation, AgBr emulsion 3-47591
- ascorbic acid developer, AgBr photographic emulsion, kinetics of development, filamentary growth 3-53341
- asymmetric complexes, proton tunnelling effect on internal vibrs. 3-60427
- azaaromatic compounds and cations zero field splitting of triplet state 3-75875
- 3-azabicyclononane, plastic cryst. phase, self-diffusion, n.m.r. study 3-68438
- azanaphthalenes, triplet-triplet absorpt. spectra 3-53330
- aziridine-borane, electronic structure, BN bond, charge transfer 3-46242
- azo compounds, decomp., chem. induced nuclear polarisation, methyl radical 3-71579
- 7-azaindole, multiple excitation, biprotonic phototautomerism, hydrogen-bonded dimers, fluorescence 3-63548
- azole, additivity rules for ^{14}N chem. shifts 3-71599
- azomethane, azomethane- d_6 , Raman spectra and vibrational potential function 3-75017
- azomethanes, nonradiative transitions and properties of lower triplet state, SCF-MO and CI calc. 3-63504
- azomethine group, C=N bond calcs. in hypothetical formalimine 3-71523
- azomethine-, azo-compounds and their protonated species, barriers to rotation and inversion 3-67727
- p-azoxyanisole, liquid crystal, theory of anomalous mag. and elec. birefringence 3-80005
- n-azoxyanisole, nematic phase, electret effect 3-75940
- p-azoxyanisole nematic liquid crystal, proton spin relaxation of dipolar energy, frequency depend. 3-55491
- p-azoxyphenetole, liquid crystals, e.s.r., orientation of radicals containing N-O groups 3-79231
- azulene, B-X(3500 μ) transition, medium-depend. effects, vibronic coupling, Fermi reson. 3-75002
- azulene, in hydrocarbon matrices, electronic spectra struct. 3-72736
- azulene in soln., consecutive two-photon absorpt. using dye lasers 3-44730
- bacteriochlorophyll, one-electron oxidation, absorption and e.p.r. obs. (*Russian*) 3-51425
- barbituric acid, single cryst., electron irradiation at 77K radical pair formation 3-55973
- barbituric acid dihydrate, single crystals, 4.2K, oxidation and reduction by ionizing radiation 3-73147
- barium nitroprusside dehydrate, crystal and mol. structure 3-63991
- barium stearate built-up films, a.c. breakdown 3-47209
- barium stearate films, built-up, refr. index calc. 3-53076
- barium stearate films, static dielec. const., corrected calc. 3-53057
- benz(o)triazole, electrical conductivity meas. 3-58257
- benzaldehyde, in alcoholic soln., triplet state, absorpt. spectra obs. (*Russian*) 3-80067
- benzaldehyde electronic emission spectrum, molecular vibrations 3-67843
- benzaldehydes, dielectric props. in solutions, microwave meas. 3-55999
- benzaldehydes, substituted, benzene soln., microwave absorpt., dielec. props. 3-80585
- benzamide, in alcoholic soln., triplet state, absorpt. spectra obs. (*Russian*) 3-80067
- benzanthrane, quantitative determ. in mixed solutions by luminescence spectroscopy (*Russian*) 3-62364

organic compounds continued

- benzanthrone, i.r. absorpt., Davydov splitting due to arrangement changes 3-72636
- benzene, $^1\text{E}_g \leftarrow ^1\text{A}_1$ absorpt. transition 3-78728
- benzene, absorpt. spectra, polarization props., line form of 2 photon transitions 3-66887
- benzene, adsorption on Pt(111) and Pt(100) surfaces, Leed and work function investigation 3-55127
- benzene, adsorption on SiO_2 , anomalous sites characterisation 3-68489
- benzene, Born-Oppenheimer coupling contribs., vibronic intensity borrowing theory 3-40596
- benzene, $\text{C}_p\text{-C}_v$, calc. using temp. depend. of lattice freq. (*Russian*) 3-50007
- benzene, CH-stretching overtone spectrum analysis, phase coincidence problem 3-67777
- benzene, Cotton-Mouton const. calculated by free electron wave functions 3-57632
- benzene, cryst., $^1\text{B}_{1u} \leftarrow ^1\text{A}_1$ 0-0 transition obs. 3-76051
- benzene, deuteration effect on radiationless transition probability, multiphonon transitions approach (*Russian*) 3-80092
- benzene, dielectric constants and molar polarizations, 278-343 K 3-50861
- benzene, electronic model, stability conditions for maximum overlap Bruckner independent particle wave functions 3-67743
- benzene, ethyl acetate and cyclohexane mixture adsorption on activated C 3-76486
- benzene, exciton-phonon interaction, conservation laws, molecular crystal spectra 3-68972
- benzene, full II, ab initio valence bond calc. 3-71508
- benzene, in soln., effects of environment on excited states 3-60473
- benzene, in various solvents, orientational relax. rates, depolarised Rayleigh scatt. meas. 3-50574
- benzene, isotopic mixed crystals, 1.8 K, phosphorescence lifetimes 3-80102
- benzene, isotopic mixed crystals, heavily doped, resolved emission from compound states 3-61066
- benzene, liq., mol. motion from n.m.r. and neutron scatt. obs. 3-68875
- benzene, liquid, mol. motion, depolarised Rayleigh scatt. obs. 3-79223
- benzene, liquid, reorientational motions from press. depend. Rayleigh scatt. 3-80055
- benzene, mol. cryst., low-temp. luminesc., phonon structure 3-72715
- benzene, molecular crystals, press. depend. of lattice freqs. 3-75585
- benzene, n.m.r. consts., neutron spectra, molecular motion 3-68877
- benzene, photoelectron spectroscopy study 3-52394
- benzene, rotational mechanism near melting point and neutron scattering 3-60435
- benzene, self-diffusivity, neutron diff., n.m.r. spin echo, mol. dynamics methods 3-72217
- benzene, single cryst., 2000 μ absorpt. system in polarised light 3-58520
- benzene, solid, electron energy loss meas. of optical consts. 3-64622
- benzene, solidification in porous media, calorimetric method, latent heat determ. effect of pore radius, hysteresis (*French*) 3-75606
- benzene, T, L and S tensors, calc. from cryst. forces 3-79262
- benzene, third order susceptibility, absolute meas. from third harmonic generation 3-78064
- benzene, traces in Ar discharge, emission study of C_2 Swan bands 3-52368
- benzene, vibrational spectrum theory 3-74987
- benzene and derivatives, phosphoresc. microwave double reson. 3-75918
- benzene and methyl and deuterio derivatives, phosphorescence lifetime, solvent effects 3-72707
- benzene and methylene chloride mixture, dielectric polarisation, n.m.r., u.v. and i.r. studies 3-58817
- benzene cryst., determ. of exciton-phonon interact. in absorpt. spectrum 3-72630
- benzene derivatives, gas phase spectra 3-78786
- benzene derivatives, in solid matrices, quasiline phosphoresc. spectra 3-72741
- benzene homologues, in solid matrices, quasiline phosphoresc. spectra 3-72741
- benzene in rare gas hosts, triplet lifetimes and emission spectra, external heavy atom effects 3-55675
- benzene isotopic mixed crystals, band struct. calc. 3-55194
- benzene liquid, u.s. light diff. for laser beam generating third harmonic 3-41500
- benzene photoionisation, quasi-equilib. theory, unimolecular decomposition 3-57674
- benzene ring system containing cpds., photoemission in vacuum u.v. region 3-41613
- benzene single crystal, 2000 μ polarised light system, spectra 3-69019
- benzene single crystal, u.s. absorpt. meas. 3-43837
- benzene vapour, adsorption on sulphopolystyrene during heat treatment 3-61250
- benzene vapour, average energy per ion pair for α -particles 3-44728
- benzene vapour, thermal energy ion condensation reactions 3-41837
- benzene- Cl_2 solutions, i.r. and Raman spectra 3-78799
- benzene-cyclohexane-dioxane ternary mixtures, dielectric behaviour 3-73175
- benzene-oxygen contact complex, vapour phase absorpt. spectrum 3-54664
- benzene-tetracyanoethylene complex, calc. allowing for doubly-excited configurations (*Russian*) 3-67751
- benzenes, cyano-substituted, lowest excited triplet states, zero field splitting 3-78845
- benzenes, fluorinated, in liq. cryst. solvents, H-F and F-F nucl. mag. spin-spin coupling anisotropies 3-40655
- benzenes, monosubstituted, ν_8 and ν_{19} vibrs., i.r. band intensities 3-60456
- benzenes, monosubstituted, and mixtures, microwave absorpt. and relax. processes 3-68918
- benzenes, multi-homosubstituted, variable electronegativity SCF-MO calcs. 3-67736

organic compounds continued

- benzenes, substituted, molecules, magnetic circular dichroism 3-54669
- benzenes, substituted, perturbation MO calc. of ionisation potentials, effects of induction and resonance 3-46333
- benzenes with side-chain interacting groups, substituent effects on proton spin-spin coupling 3-60478
- benzenium cation, CNDO/SP calc. of spin-spin coupling consts. 3-74936
- benzenoid aromatic hydrocarbons, time-profiles of transient absorpt. obs. in kinetic spectrophotometry 3-63500
- benzil, new meas. method for electro-optical consts. at h.f. 3-48404
- benzil, position of phenyl rings 3-71486
- benzo-1,4-dioxane derivatives, electronic spectrum bands, hydrogen bonding 3-67764
- benzocoumarins as laser dyes 3-78031
- benzodioxane-1,4, i.r. absorpt. bands temp. depend. in deform. vibrations region (*Russian*) 3-54694
- benzoic acid, enthalpy of sublimation meas., thermal cond. manometer 3-45460
- benzoic acid, in alcoholic soln., triplet state, absorpt. spectra obs. (*Russian*) 3-80067
- benzoic acid, methyl derivatives, Pariser-Parr-Pople calc. of spectra and conformations (*French*) 3-63379
- benzoic acid, sublimation enthalpy and Gibbs energy function, microcalorimetric determ. 3-55079
- benzoic acid derivs., ionization pot., determ. 100-170°C, by photoionization method (*Russian*) 3-43503
- benzoic acids, highest occupied and lowest unoccupied mol. orbitals and total π -electronic energies, LCAO calc. 3-52318
- benzol emulsion, u.s. wave absorption and scattering, impulsion method (*Russian*) 3-50796
- benzonitrile, vibronic spectra, theoretical study 3-67783
- benzonitrile, vibrational analysis of the 2738 cm^{-1} system 3-40610
- 1,12-benzoperylene, in n-hexane, luminesc., zero-phonon lines and electron-phonon interaction 3-72727
- 1,12-benzoperylene, in n-hexane and n-heptane matrices, fluoresc., phonon struct. 3-72729
- 1,12-benzoperylene, in n-paraffin matrices, quasilinear spectra, solute-solvent interactions 3-72728
- benzophenone, enthalpy of sublimation meas., thermal cond. manometer 3-45460
- benzophenone, ethanol and water solution, electronic spectra, bonding 3-64710
- benzophenone, in binary solvent mixtures, electronic spectral intensities 3-46264
- benzophenone, in toluene, quasilinear luminesc. spectrum, theoretical interpretation 3-72740
- benzophenone, i.r., fluorescence spectra of photochemical reaction products 3-65110
- benzophenone, linear crystalliz. rate temp. depend. (*German*) 3-53184
- benzophenone, microwave-optical double resonance, study of lowest triplet states 3-80121
- benzophenone, quenching of phosphorescence in vitreous state by long-lived guest triplet states 3-64705
- benzophenone, solute dipole moment relax. in o-terphenyl 3-72571
- benzophenone, undistorted triplet state, static and dynamic paramagnetism 3-76478
- benzophenone and rhodamine 6G in soln., nonlinear absorpt., singlet-singlet energy transfer 3-78035
- benzophenone single crystal, Raman and polarised i.r. spectra, vibrational study (*French*) 3-47266
- benzophenone-aromatic hydrocarbon, mixed crystals, delayed fluoresc. 3-76089
- benzophenone-diphenylamine complex, form I, vibr. analysis of i.r. absorpt. spectrum (*French*) 3-57650
- benzophenone-naphthalene system in rigid solns., triplet-triplet excitation transfer obs. 3-53329
- benzophenones, orthosubstituted, conformational preferences, ^{13}C n.m.r., calc. torsional angles 3-49489
- benzopinacol, benzophenone photochemical reaction products, spectra 3-65110
- 1,2-benzopyrene, in n-paraffin matrices, luminesc., cooling rate effects 3-72730
- p-benzoquinone, ($-\text{H}_4$ and $-\text{d}_4$), fluoresc. obs., electronic struct. and dynamics 3-40648
- 1,4-benzoquinone, (and B0-d₄) single crystals, i.r. spectra 3-80045
- n-benzoquinone, adsorption on PbS film, role of surface complexes in photosensitivity 3-79734
- p-benzoquinone, gaseous, mol. geometry, electron diff. obs. 3-54606
- p-benzoquinone, photocycloaddition to cyclooctatetraene, laser excitation, effect of solvent acidity and oxygen 3-47580
- p-benzoquinone, single crystals, Stark effect on lowest $^1\text{B}_{1g}(\text{n}\pi^*)$ state 3-80065
- p-benzoquinone, single crystals, Stark effects on low energy electronic states 3-76468
- benzothiazolocarboaniline dyes, formation of epitaxial attachments on AgBr surface, ligand bonds, red shift 3-53342
- benzotrifluorides Fourier transform n.m.r. ^{19}F chemical shift intermolecular, intramolecular effects, high pressure 3-61003
- benzoyl peroxide, decomp., chem. induced nuclear polarisation, methyl radical 3-71579
- 1-benzoyl-8-benzyl-naphthalene, deuterium effects on phosphoresc. and photochem. activity 3-76470
- 1-benzoyl-8-benzyl-naphthalene and 1-benzoylnaphthalene, viscosity-depend. phosphoresc. 3-76469
- benzoylacetone, u.v. diffuse reflectance spectra 3-47291
- benzoylacetones, enol-enolic equilib., ^{13}C n.m.r. spectra 3-71592
- benzo[c]cinnolin, fluorescence, temperature dependence (*German*) 3-52379
- 1,12-benzoperylene, n-heptane soln., fluorescence emission, second excited π -singlet state to singlet ground state 3-50848
- 1,12-benzoperylene, short-wavelength fluoresc., subband obs. 3-63496
- 1,2-benzopyrene; naphthalene, thin layers, sensitised luminescence, concentration depend. of emission spectra 3-41572
- 3,4-benzopyrene, n-heptane soln., fluorescence emission, second excited π -singlet state to singlet ground state 3-50848

organic compounds continued

- benzpyrene, quantitative determ. in mixed solutions by luminescence spectroscopy (*Russian*) 3-62364
- benzvalene, six isotopic species, microwave structural study 3-78814
- benzyl ammonium iron chloride, mag. susceptibility 3-50352
- benzyl radical, electronic states assignment by three-step photoselection 3-44735
- benzyl radicals, fluorescence, photoexcitation of toluene thin films (*Russian*) 3-72701
- 2-benzyl-norborane (I), structure depend. of emission props., intramol. electron transfer 3-75061
- benzyl-type radicals, methyl substitution effect on electronic struct. and spectra 3-78731
- benzylcyanide, liq., internal rot., at high press., n.m.r. relax. obs. 3-68871
- 2-benzylidenecyclohexanones and 2,6-bis-benzylidenecyclohexanones, substituted, mass spectra 3-63529
- benzylpenicillin, i.r. vibrational spectrum, structural analysis (*Russian*) 3-78778
- biacetyl, electronic and vibrational relaxation 3-40649
- biacetyl, small molecule behaviour and $^3\text{B}_2$ state 3-75058
- biacetyl, vibr. relax. obs. by visible-i.r. double reson. technique 3-78885
- 9,9'-bianthranil, dianion triplet at low temp. 3-47573
- bicyclic alcohol, mol. configuration determination, models for internal rotation, n.m.r. lanthanide shift studies 3-46226
- bicyclo(3.1.0).hexane analogs, far i.r. spectra, ring puckering vibrs., mol. config. 3-63456
- bicyclo[3.2.1]octane derivatives, ^{13}C n.m.r. 3-71585
- binary liquid solutions, electron-beam excited, luminesc. intensity 3-40259
- biphenyl-naphthalene-d₈, polarisation of delayed fluorescence and phosphorescence emissions 3-69053
- biphenyl, emission spectra, exciton-phonon interactions 3-69071
- biphenyl, in liquid cyclohexane, photoionisation of negative ions 3-65107
- biphenyl crystal, high-resolution two-photon excitation spectra 3-80068
- biphenyl crystal, low energy magnetic and electric dipole transitions 3-47282
- biphenyl derivatives, quasi-linear absorption and luminescence 3-72747
- biphenyl fluorescence, quenching by inorganic ions in solution 3-73160
- biphenyl guest-carbazole host mixed crystal, phosphorescence spectrum, trap emission 3-76039
- biphenyl orthosubstituted derivatives, hydrogen bridges role in crystn. (*French*) 3-79475
- biphenyl radical anion in soln., ruby laser induced photoioniz., intensity depend. 3-47569
- biphenyl radical anions, ^1H and ^2D n.m.r. studies 3-43488
- biphenyl-tetracyanobenzene single crystals, mobile charge-transfer triplet excitons 3-64538
- biphenylene, Raman spectra, in-plane normal mode calc. and complete vib. assignment 3-61038
- bipyridyls and their protonated forms, ^{13}C n.m.r. spectra 3-71594
- bis(trimethylgermyl)ketene, mol. struct. by electron diff. 3-63361
- bis-(7-n-tolyl-6-methylquinolin-4)trimethylcyanineperchlorate liquid laser with diffraction grating resonator, generating characteristics (*Russian*) 3-57228
- bisazides, spectral sensitivity, quenching of phosphorescence, mechanism 3-61280
- 1,3-bisdiphenylene-2-p-chlorophenylallyl, paramag.-antiferromag. transition at 3.25 K 3-58375
- bis(trifluoromethyl) sulphide, sulphoxide and disulphide, Raman spectra, normal modes vibr. assignments and depolarisation meas. 3-47274
- bond lengths, dissociation energies and CH stretching frequencies 3-46229
- borazine, hexasubstituted crystals, mol. reorientation obs. by p.m.r. (*French*) 3-53026
- borine carbonyl, Green's function anal. of vibrs. 3-78696
- branched monocarboxylic and esters in carbonyl, ^{13}C n.m.r. spectra 3-71584
- brominebenzole emulsion, u.s. wave absorption and scattering, impulsion method (*Russian*) 3-50796
- 1-bromo-1-methylcyclohexane 3-78764
- 1-bromo-3,3,4-trifluorobutene-4, n.m.r. study, determ. of ^{19}F , ^{13}C , ^1H chemical shifts and coupling consts. 3-75072
- 2-bromo-5-chlorothiophene, n.m.r. AB spectrum, use of compensating device for parasitic beat signal 3-77595
- 1-bromo-5-nitronaphthalene in benzene soln., temp. variation of relax. time and activation energy 3-68921
- p-bromoanisole, ultraviolet absorption spectra 3-67795
- m-bromoanisole, u.v. absorpt. spectra assignments 3-67799
- bromocyclobutane, Raman spectra obs. 3-75035
- bromomethane, liquid, Raman spectroscopy, mol. reorientation 3-75984
- bromophenols, isomeric, fundamental frequency assignment, effect of Br substitution 3-78758
- 2-bromopyridine, n.m.r. of ^{13}C , long-range ^{13}C - ^1H spin coupling consts. 3-43483
- 5-bromotetrazole, single cryst., Raman active external phonon assignments, harmonic force const. calcs. 3-50573
- bromotrichloromethane, thermal decomp. phenomena, electron diff. obs. 3-65074
- bromotrifluoromethane as flame suppressant for cold fog seeding with propane spray 3-51189
- 1,3-butadiene, conformers and internal rotation barriers, MO-SCF study 3-54607
- trans-butadiene, low lying π -electron states, configuration interaction calc. 3-74958
- butadiene π -system, non-orthogonal pair theory of electronic structure 3-67756
- trans-butadiene radical, valence bond and mol. orbital calcs., convergence comparison 3-43401
- butadiene-1,3, p.m.r., spin-spin coupling consts. 3-43484
- butan-2-one solution, polystyrene translational diffusion, Rayleigh light scatt. obs. 3-67878

organic compounds continued

- butane, α -particle molecular stopping cross sections 3-56554
 butane absorption cross sections from 180 to 700 μ 3-67805
 n-butane photooxidation with OH, rate const. determ. 3-69478
 n-butanol vapour, chemisorption by silica surface 3-73165
 butanol-1, dielectric relaxation 3-64598
 Butanol-1-hexane mixture, dielectric relaxation 3-64598
 butanol-1-tetrachloromethane, dielectric relaxation 3-64598
 butanol-2-(+), circular dichroism, comparison of theoretical and expt. results of rot. strengths 3-78746
 butanol-(1) and -(2) and iso-butanol, refractive index meas., between 250 and 700 nm. 3-66190
 butene isomers, reactions with F, unimol. decomp. of long-lived complex 3-73121
 butene-1 on A- and Y-zeolites, mobility, proton spin relax. (German) 3-64245
 trans-butene-2 collisional deactivation of acetaldehyde, temp., pressure and excitation wavelength effect on photoluminescence 3-46313
 butenes, liquid, electron mobilities and activation energies 3-72354
 p-n-butoxybenzylidene-p-aminobenzonitrile nematic liquid crystal, with positive dielec. anisotropy, light diff. 3-68962
 p-n-butoxybenzal p-phenetidine nematic liquid crystal, p.m.r. 3-53025
 t-butyl alcohol aqueous solns., radical form. and solvation behaviour 3-58805
 butyl alcohol effect of surfactant solution on rate of moisture transfer in capillary porous bodies 3-65031
 t-butyl bromide- h_2 and d_2 , liquid and three solid phases, far i.r. spectra, lattice modes 3-55575
 t-butyl chloride, solvolysis, solvent isotope effects and the transition state 3-55957
 4-n-butyl-4'-methoxybenzene nematic solutions, use of INDOR technique 3-54720
 t-butylamine, p.m.r. absorption and relaxation study 3-55492
 t-butylamine clathrate deuterate, p.m.r. absorption and relaxation study 3-55492
 p,p'-di-n-butylazoxybenzene: 7,7,8,9-tetracyanoquinodimethane nematic liquid crystal having positive dielectric anisotropy, dynamic scattering 3-54917
 t-butylchloride, self-diffusion coeff. and rot. correlation time determ. 3-68872
 3-butyne-2-one, i.r. and Raman spectra 3-71560
 cadmium arachidate Langmuir film, freq. depend. cond., evidence for contact effects 3-68691
 cadmium formate, Mossbauer investigation of cation positions in iron formate mixture (German) 3-79967
 calcium stearate monolayers and multilayers, shear properties 3-64108
 camphor, mol. dynamics, ^{13}C n.m.r. relax. times 3-68881
 camphor- ^{14}C , reaction with H_2SO_4 , computer-assisted analysis 3-80531
 carbanic acid aryl and alkyl esters, i.r. spectra-structure correlations 3-57658
 carbamoylazides, and N-deuterated derivatives, i.r. and Raman spectra (German) 3-47271
 carbazole and hydrogen bonded complex with esters, fluorescence quenching mechanism 3-52383
 carbohydrate crystals, i.r. spectra, polysaccharide transition 3-72655
 carbon tetrabromide, plastic cryst., shear strength 275 to 375 K, 320 K polymorphic transform. 3-79407
 carbon tetrachloride, atmospheric concentration over Pacific and Ross Sea 3-69589
 carbon tetrachloride, collisions with NO , orientational anisotropy in total collision cross section 3-46355
 carbon tetrachloride, dielectric constants and molar polarizations, 278-343 K 3-50861
 carbon tetrachloride, liquid, absorpt. loss spectrum, thermo-optical meas. technique 3-62103
 carbon tetrachloride, liquid, Rayleigh scatt. meas. using optical fibres 3-62102
 carbon tetrachloride, neutron diff., ang. correl. effects 3-57979
 carbon tetrachloride, press. dependence of u.s. absorption 3-71995
 carbon tetrachloride, pressure dependence of excess ultrasonic absorption 3-49942
 carbon tetrachloride, Raman difference spectra with rotating cell of CHCl_3 mixture 3-68974
 carbon tetrachloride matrix, aromatic molecules, quasiline phosphoresc. spectra, external heavy atom effect 3-72743
 carbon tetrachloride vapour, average energy per ion pair for α -particles 3-44728
 carbon tetrachloride-cyclohexane system, thermogravitational thermal diffusion, end effects 3-41037
 carbon tetrachloride- H_2O -acetic acid, coexistence curve shape near plait point 3-75600
 carbon tetrafluoride, dissociative electron detachment processes 3-46343
 carbon tetrafluoride, energy loss and range straggling of α -particles from ^{238}Pu , comparison with Payne-Titeica model (Russian) 3-59638
 carbon tetrafluoride, force constants, kinematical evaluation 3-74969
 carbonyl fluoride, absorp. of CO_2 laser radiation, rel. to chemical laser efficiency 3-66810
 carbonyl fluoride convergence of reduced Hamiltonian, centrifugal distortion, z-axis choice 3-63425
 carbonyl group, 5-membered ring compounds, photoelectron spectroscopy, lone pair orbital ionisation potentials, INDO calcs. 3-54625
 carbonyl group, $\text{C}=\text{O}$ stretch region in vibr. spectrum 3-63410
 carbonyl group, two-component solns., spectroscopic study of intermolecular interactions (Russian) 3-80050
 carbonyl group intermol. electrostatic and mag. effects on proton shielding const. 3-63525
 carbonyl sulphide, COS^+ , interaction with $\text{He}(2^3\text{S})$, $\text{CO}^+(\text{A}^2\Pi)$ 3-54736
 carboranes, multi-centre bonding, ab initio and semi-empirical MO study 3-63391
 carboranes and organotin derivatives, $^{1\text{H}}$ - $^{11\text{B}}$ heteronuclear magnetic double resonance spectra 3-78848

organic compounds continued

- carboxylic acids, halogenated, far i.r. studies of the hydrogen bonding 3-78773
 carboxylic esters and derivatives, molecular structure and conformation 3-74927
 α -o-carboxyphenylcinnamic acids, u.v. spectra 3-60449
 α -carboxystilbenes, u.v. spectra 3-60448
 β -carotene, optical nonlinearities in conjugated systems 3-59888
 β -carotene and related compounds, Raman vibrational resonance, in-plane vibr. model 3-78755
 celluloid thin films, fading of alpha particle tracks by u.v. heating 3-59648
 ceresin-Al composite, thermal cond., effect of composition inhomogeneities 3-50033
 chalcones, substituted and vinyls, fluoresc. and absorp. spectra rel. to props. in excited state 3-64725
 charge-transfer complexes in liq. soln., deactivation mechanism, fluoresc. 3-41859
 chiral molecules, circular differential Raman spectra 3-78802
 chitosane fixer, effect on preservability of hydrotype colour images (Russian) 3-47597
 1-chloro-1-methylcyclohexane, i.r. spectra, conformational equilibrium 3-78764
 1-chloro-2,4-dinitrobenzene, n.q.r. study, Zeeman effect 3-43480
 2-chloro-4-aminophenol, single and combined photographic developers, kinetics of Ag formation, AgBr emulsion 3-47591
 2-chloro-4-aminophenol developer, AgBr photographic emulsion, kinetics of development, filamentary growth 3-53341
 2-chloroacrylonitrile, normal coordinate vibrational analysis 3-46252
 β -chloroalkyl radicals, struct. and conform., isotropic e.s.r. g-values and h.f.s. 3-60397
 4-chloroanthraquinonethiadiazole, Patterson function, electron density, struct. determ. 3-72072
 4-chloroanthraquinonoxadiazole, crystal and molecular structure 3-79331
 chlorobenzene, liquid, absorpt. loss spectrum, thermo-optical meas. technique 3-62103
 chlorobenzene, out-of-plane vibr. modes in ground and first excited singlet states 3-63408
 chlorobenzene, p.m.r. partially oriented in nematic phase, use of INDOR technique 3-54720
 chlorobenzene, u.s. scatt., nonlinear phenomena 3-68336
 chlorobiphenyls, space charge effects at solid/liquid interfaces 3-47210
 2-chlorobutane, torsion force consts. and low frequency bending assignments 3-71559
 chlorocyclohexane, equatorial, microwave rot. spectra anal. 3-78811
 chlorocyclohexane at low temp., FT ^{13}C n.m.r. spectra, conformational anal. 3-71582
 chlorocyclopentane, disordered cryst., vibr. spectr, i.r. absorpt. and Raman obs. 3-72638
 chloroform, and deuterated analogue, Raman spectra and cryst. struct. at 77 K 3-50576
 chloroform, liq., mol. reorient. at high press., n.m.r. relax. obs. 3-68871
 chloroform, liquid-vapour equil. in acetone mixture 3-64165
 chloroform, Raman difference spectra with rotating cell of CCl_4 mixture 3-68974
 d-chloroform, Raman vibrational line shapes, reorientational correlation functions, appl. to nuclear quadrupole coupling constants 3-46274
 chloroform crystalline, quadrupole relaxation of ^{35}Cl nucleus and effect on CCl_3 group mobility 3-75902
 chloroform intermol. complexes, spectroscopic and dielec. investig., comparison 3-74931
 chloroform soln., containing aminopyridines, hydrogen bonding study 3-52349
 chloroform solutions, saturated aqueous, rel. to X-ray irradiation, dose effect curve of dosimeter 3-63240
 chloromethane, Raman spectra in liquid and gaseous states (Russian) 3-63475
 chloromethanes, vacuum u.v. absorpt. spectra 3-52356
 chloronitromethane, gas phase, electron diffraction study of structure 3-78655
 4-chloronitricyclene, ^{35}Cl nuclear quadrupole coupling constant, microwave spectra 3-71567
 chlorophenol derivatives, complexes with acetone and dimethylformamide, hydrogen bond energies spectroscopic determ. (Russian) 3-49474
 chlorophyll, in soln., fluoresc., intermol. energy migration, appl. of fluorometer 3-76085
 chlorophyll, theory of singlet-triplet exciton fusion 3-64311
 chlorophyll A, fluoresc. in polymer matrices, laser excitation 3-69074
 chlorophyll A, in n-paraffin matrices, luminesc. and excitation spectra 3-72733
 chlorophyll-a, absorpt. spectra, optical activity, in micellar detergents 3-72680
 N-chloropiperidine, vibrational spectra and conformation (Russian) 3-63476
 2-chloropropane, torsion force consts. and low frequency bending assignments 3-71559
 3-chloropyridine hydrogen bonded complexes with quinoline, methyl- and ethyl-pyridines vibrational spectra 3-75029
 p-chlorostyrene, rot. band contour analysis of O_0^0 bands of $\text{A}^1\text{A}'-\text{X}^1\text{A}'$ systems 3-63446
 chlorosubstituted hydrocarbons, i.r. spectra, intensities of characteristic bonds of rotational isomers 3-78765
 2-chlorotetrahydropyran, ab initio mol. wavefunction calc. 3-49491
 2-chlorothiophene, microwave spectra, quadrupole coupling and rotational constants 3-43463
 chlorotrifluoromethane-He system, binary diffusion coefficients at 300 K, 1 atm., Chapman-Enskog theory test 3-52419
 β -chlorovinylketones, Pariser-Parr-Pople calculations, conformational assignment 3-67733
 chloryl fluorides, Urey-Bradley force fields 3-67782
 cholesteric liquid crystals, pitch changes, solute and temp. induced, pretransitional effects 3-75473

organic compounds continued

- cholesteric mixtures solute chromophores, electronic transitions of different polarization (*German*) 3-79235
 cholesteric planar structure, static distortions induced by mag. or a.c. elec. fields 3-71998
 cholesterol, solvent effects on ^{13}C n.m.r. spectra 3-63512
 cholesterol derivatives, optical study, blue phase in amorphous-cholesteric transition 3-72000
 cholesterol naphthylidene Schiff's base compounds, homologous series, liquid crystal props. 3-57983
 cholesteryl alkanoate liquid crystal, pure, and binary mixtures, structure effect on transition thermodynamics 3-52573
 cholesteryl decanoate liquid crystals, dynamic scatt., memory effect 3-75964
 cholesteryl ester, liquid crystalline phases 3-71999
 cholesteryl myristate, mesophase transitions, light scatt. and microscopic obs., cholesteric morphology 3-52571
 cholesteryl myristate, mesophase transitions, light scatt. and microscopic obs., spherulite growth kinetics 3-52572
 cholesteryl nonanoate, cholesteric-isotropic (solid) transitions, X-ray halo scatt. obs. 3-79230
 cholesteryl nonanoate, fluorec. of pyrene and phenanthrene impurities, phase transitions 3-55685
 cholesteryl oleyl carbonate, tricritical behaviour 3-60663
 cholesteryl valerate, liquid crystal, specific volume obs. up to 1000 atm and temp. range 80-129°C 3-57987
 cholesteryl esters, mesomorphic, spherulite growth kinetics 3-52570
 chlorinated copper phthalocyanine film, compensation effects in dark cond. and photocond. 3-44115
 chromatography, flame-ionization detector, Tsvet, model 2-65, additional heater 3-70474
 chromium carboxylate, Heisenberg exchange Hamiltonian 3-58359
 chromones, MO study of π -electronic struct. 3-71507
 chrysene, in n-paraffin matrix, absorpt. and fluorec. 3-72739
 cinnoline in durene and naphthalene host cryst., electronic absorpt. spectra analysis 3-69028
 cinnolines, (n,π^*) fluorec. quantum yields and lifetimes 3-76473
 circobiphenyl, phosphorescence, E-type delayed fluorescence (*German*) 3-69069
 citric acid, O determ. and distrib. from α tracks, $^{17}\text{O}(n,\alpha)^{14}\text{C}$ 3-66457
 n-Cl-aniline:pentafluorophenol compound, Raman spectra, phase transformation study 3-72198
 clathrates, far i.r. spectra, vibrs. 3-72661
 cobalt anhydrous acetates, struct. 3-40908
 cobalt corrinoids, selective enhancement of bond intensities in resonance Raman spectra 3-71668
 complex, [(pyridine-2,6-dicarboxylato)-(pyridine-2,6-dicarboxylic acid)]copper(II) hydrate, struct. (*French*) 3-46636
 complex hydrogen bonded cations, stretching and bending modes, vibrational spectra, proton potential 3-75031
 complex molecule, intramolecular relax. spectroscopic investig. 3-71536
 complicated molecules, in liq. cryst. matrices, absorpt. spectra 3-71543
 copper phthalocyanine, frequency dependence of conductivity and permittivity 3-72564
 copper phthalocyanine, phosphorescence spectra, temp. depend. and decay time 3-72710
 copper propionate monohydrate, Zn-doped single crystals., e.s.r. spectra 3-55465
 copper trisethylenediamine sulphate, Jahn-Teller anisotropy of paramagnetism 3-50341
 coronene, in n-heptane and CCl_4 matrices, quasiline phosphoresc. spectra, external heavy atom effect 3-72743
 coronene, in n-hexane, luminesc., zero-phonon lines and electron-phonon interaction 3-72727
 coronene, in n-nonane and n-decane, fluorec., doublet struct. at 77 K, isothermal exposure effects (*Russian*) 3-44475
 coronene, in n-paraffin matrices, luminesc., cooling rate effects 3-72730
 coronene, in n-paraffin matrices, quasilinear spectra, solute-solvent interactions 3-72728
 coronene, luminescence and vibrational spectra 3-60460
 coronene, quantitative determ. in mixed solutions by luminescence spectroscopy (*Russian*) 3-62364
 coronene in Shpol'skii matrix, laser excited luminescence 3-54712
 coumarin and methyl derivatives, σ and π electron contributions to long-range spin-spin coupling consts. 3-52387
 coumarin dye, formation mech. of excited reactions, laser saturation characs. obs. 3-51924
 coumarin laser dye, gain spectrum inhomogeneity, excited state reaction species 3-45800
 o-, m-cresols, i.r. absorption spectra, assignment of vibrational frequencies 3-78759
 cresyl violet-rhodamine 6G dye mixture, excitation transfer, gain spectra obs. 3-70818
 crude oil, atomic absorption spectroscopy, trace metal determ., evaluation of carbon rod atomiser 3-70485
 cryptocyanine, resonance spontaneous Raman scattering spectra 3-64655
 cryptocyanine, soln. in methanol, fluorescence spectra, fine periodic spectral structure, ruby laser excitation 3-55669
 cryptocyanine in methanol soln., hole burning by laser beam (*French*) 3-51943
 crystals, mag. effects on triplet exciton bands 3-68579
 cumene-tetraline mixture, chemiluminescence spectra, co-oxidation 3-41846
 cupric formate tetrahydrate, pressure effect on antiferroelectric phase transitions 3-79988
 cupric formate tetrahydrate single crystals., elastic consts., u.s. wave velocities meas. 3-79403
 cyanine dyes, electrical conductivity (*French*) 3-50207
 cyanine dyes, excited singlet-singlet absorption in solution 3-62739
 cyanine dyes, Huckel mol. orbital descriptions, contours approach 3-46232
 cyanine dyes, relation between degree of conjugation and elec. conductivity (*French*) 3-50208

organic compounds continued

- cyanine dyes in various solvents, use in liquid lasers (*Russian*) 3-57227
 cyanmelluric acid salts, cyanmelluric ring charact. freq. in i.r. spectra (*Russian*) 3-71565
 cyanoacrylate IS 12, bond strength expts. for photoelasticity sandwich technique 3-48351
 p-cyanobenzylidene-p'-octyloxyaniline, elastic constants near second order nematic-smectic phase change 3-58064
 cyanocyclobutane, μ -wave spectrum, dipole moment quadrupole coupling consts. and conformation study 3-40634
 cyanocyclobutane, microwave spectrum assignments 3-63484
 cyanomethane, Raman spectra in liquid and gaseous states (*Russian*) 3-63475
 α -cyanostilbene, nematic, with large negative dielec. anisotropy, instabilities in elec. fields 3-52575
 cyclic amides, opt. activity calcs. using INDO method 3-52322
 cyclic ammonium bromides in water, ^{13}C , ^{14}N nucl. relax. 3-68882
 cyclitols in solution, MO-LCAO calc. of conformations 3-60402
 cycloalkanes, dielectric constants and molar polarizations, 278-343 K 3-50861
 cycloalkanes, reactive state in photochem. 1,3-addition of benzene and alkylbenzenes 3-47574
 cyclobutadiene (and deuterated), ground state potential energy surfaces, relevance to i.r. data 3-78662
 π -cyclobutadienylium tricarboxyl, intramol. rot. obs. from nematic-phase n.m.r. 3-60481
 cyclobutane, C-H bond length and stretching force const. CNDO/2 calc. 3-74925
 cyclobutanol, fragmentation mechanism, mass spectra 3-75090
 cycloheptatriene, photoisomerisation, intermolecular energy transfer 3-65096
 1,3-cyclohexadiene, photochem. dimerisation, decay of light excited mols. 3-63549
 1,4-cyclohexadiene and 1,3-cyclohexadiene, ring-puckering vibrs. 3-78790
 cyclohexadienes, 1,4- and 1,3-, Raman spectra, barriers to planarity 3-60453
 cyclohexane: nitroxide free radical, molecular self-diffusion, nuclear spin-lattice relaxation and dynamic polarisation 3-49854
 cyclohexane, dielectric constant, solid state transition, density, 500 atm. 3-68910
 cyclohexane, i.r. absorpt. spectra near phase transition 3-55072
 cyclohexane, liq., mol. motion from n.m.r. and neutron scatt. obs. 3-68875
 cyclohexane, relationship between the phase transitions and fluorescence spectra of impurity molecules 3-47306
 cyclohexane, solvent for aromatic molecules, effect on excited states 3-60473
 cyclohexane, u.s. scatt., nonlinear phenomena 3-68336
 cyclohexane adsorption on Hg, interfacial tensions of pendant Hg drops 3-45420
 cyclohexane n.m.r. consts., neutron spectra, molecular motion 3-68877
 cyclohexane proton n.m.r. in nematic liquid crystal solvents, use of deuterium decoupling 3-46319
 cyclohexane vapour, average energy per ion pair for α -particles 3-44728
 cyclohexane-benzene, -toluene, binary mixtures, isobaric vapour-liquid equilibrium data, prediction method 3-72186
 cyclohexane-biphenyl solns., pulse radiolysis, ioniz. in track of high-energy electron 3-65092
 cyclohexanic derivatives, ^{13}C n.m.r., diamag. effect 3-71583
 cyclohexanone, solute dipole moment relax. in o-terphenyl 3-72571
 cyclohexene sulphide, microwave spectra, rotational consts. 3-43459
 cyclohexyl bromide, cis and trans 2-substituted, photoelectron spectra, ionisation potential 3-74992
 cyclohexyl percarbonate, decomp., chem. induced nuclear polarisation, methyl radical 3-71579
 cyclooctatetraene, in nematic solvents, n.m.r. studies of struct. and bond shift kinetics 3-71576
 cyclooctatetraene, photocycloaddition of p-benzoquinone, laser excitation, effect of solvent acidity and oxygen 3-47580
 trans-cyclooctene, electron diffraction study, chair conformation, bond lengths and angles 3-46225
 cyclopent-3-enone, microwave spectra, ring polarity, r_s -structure and dipole moment 3-60466
 cyclopent-3-enone, out-of-plane ring modes from far i.r., Raman and microwave spectra, pot. function 3-60467
 cyclopentadienide anions, cyano-substituted, mag. circular dichroism, electronic transitions 3-40607
 cyclopentadienone, microwave spectra analysis and assignments 3-78813
 π -cyclopentadienyl derivatives, ^{13}C n.m.r. spectra obs. by pulse Fourier transform spectroscopy 3-75897
 cyclopentane, cryst., vibr. spectra, phase transition, 168 K 3-50565
 cyclopentane, crystalline, impurity molecule fluorec. and phase transitions 3-64724
 cyclopentane, disordered cryst., vibr. spectra, i.r. absorpt. and Raman obs. 3-72638
 cyclopentane, extended Huckel theory, energy gradients, stable configurations 3-71489
 cyclopentane-benzene, binary systems, isobaric vapour-liquid equilibrium data, prediction method 3-72186
 cyclopentanone, vibrational analysis, i.r. and Raman spectra 3-67812
 cyclopentanone triplet state, microwave-microwave-optical triple reson., multiconfig. aspect 3-75919
 cyclopentene, i.r. and Raman spectra interpretation 3-54685
 cyclopentyl bromide, cis and trans 2-substituted, photoelectron spectra, ionisation potential 3-74992
 (2,2)p-cyclophane and related compounds, electronic structure and spectra 3-78734
 cyclopropane, and deuterated analogues, cryst. Raman spectra and assignments 3-41510
 cyclopropane, C-H bond length and stretching force const. CNDO/2 calc. 3-74925
 cyclopropane, perpendicular bands in 3000 cm^{-1} region, Q-branches 3-67819

organic compounds continued

- cyclopropane, photoionis. cross sections, He I and He II photoelectron spectra 3-78857
- cyclopropane, solid, and cyclopropane deuterate, molecular rotation determ. by p.m.r. and spin-lattice relax. 3-44346
- cyclopropane, vibr.-rot. Raman bands 3-63461
- cyclopropane isomerisation, CNDO study on alternative mechanisms 3-47548
- cyclopropane series ketones and thioketones, position and intensity of i.r. bands (French) 3-46273
- cyclopropenone, microwave spectrum, substitutional structure, Stark and Zeeman effects 3-63482
- cyclopropenone-d₀ (and -d₂), i.r. and Raman spectra 3-78785
- cystamine and dithiodiglycolic acid, X-radiation, formation of mixed disulphide aminoethyldithio acetic acid, chain reaction 3-47566
- cytidine, conformational analysis, hydrogen bonding 3-63363
- cytidine, X-irradiated, ENDOR and e.s.r. studies 3-44726
- decacyclene, in n-paraffin matrices, luminesc., cooling rate effects 3-72730
- decacyclene, quasi-linear fluorescence spectra 3-76080
- n-decane:coronene, fluoresc., doublet struct. at 77 K, isothermal exposure effects (Russian) 3-44475
- n-decane matrices, luminesc. and excitation spectra of chlorophyll A 3-72733
- n-decane matrix, multiplet struct. of quasiline spectra of Zn phthalocyanine, 4.2K 3-72734
- desmethylinurone-linurone mixture, quantitative absorption spectra and linear and convex programming 3-51763
- deuterated acetamide, n.q.r. of D, fine structure 3-63522
- N,N-deuterated propionamide, i.r. and Raman spectra 3-60452
- N,N-deuterated thiopropionamide, i.r. and Raman spectra 3-60452
- deuteriochloroform liquid, Raman spectroscopy, mol. reorientation 3-75984
- 6-deuterofulvene, μ -wave spectrum, methylene group struct. 3-49477
- dextran, thermal diffusion in distilled water and salt solutions 3-60500
- di(methyl-1-quinolyl)-2,2-trimethinecyanine iodide dye, electrical conductivity (French) 3-50207
- di-imide, gaseous, i.r. spectrum, ground state investigation 3-78779
- di-n-butyl phthalate, in o-terphenyl, supercooled liquid, dielectric relaxation 3-49850
- diacetoneglucose, mol. configuration determination, models for internal rotation, n.m.r. lanthanide shift studies 3-46226
- diacetyl, pure liq., active intramolecular motion in dielectric relax., spectral obs. 3-64602
- diacetyl in benzene or toluene, luminesc., photo, X-ray, triplet-triplet energy transfer 3-69083
- diacetylene, high resolution for i.r. spectrum obtained with a Michelson interferometer 3-60462
- dialkyl phosphites, γ -irradiated, e.p.r. identification of P-centred radicals 3-55974
- N,N-dialkyl-p-cyanoaniline, polar excimer fluorescence 3-54710
- N,N-dialkyl-p-cyanoanilines self-complex, electronic absorption and luminescence spectra 3-54674
- dialkylaminophosphines, determination of electronic character of P-N bond from optical props. (French) 3-49439
- 1-4-diaminopiperazine polymers and metal chelates, dynamic mechanical, thermal electrical and tensile props. 3-80462
- diaryl disulphides, conformational props. calc. from dipole moments 3-43395
- diastereomeric compounds, ¹³C n.m.r. spectra non-equivalence 3-71589
- 1,3-diazaazulene, polarized absorpt., fluoresc., phosphoresc., mixed cryst. obs. 3-41857
- 9,10-diazaphenanthrene solutions, fluorescence and absorption spectra at 77K 3-41574
- dibenzanthracene, quantitative determ. in mixed solutions by luminescence spectroscopy (Russian) 3-62364
- dibenzofuran, lowest singlet state obs. 3-67804
- dibutyl sulphide, K β X-ray emission spectra 3-52345
- 9,10-dibromanthracene in soln., triplet-singlet energy transfer from acetophenone 3-76088
- p-dibromobenzene:naphthalene, phosphorescence, 4.6K, T₁ absorption 3-80106
- p-dibromobenzene, host crystal, naphthalene, localisation of phonon sidebands, T₁ to S₀ 3-69051
- dibutyl phthalate, suspensions of PMMA, rheological props. 3-61231
- dibutylphthalate aerosol nucleation by NaCl and AgCl 3-58770
- dicalcium strontium propionate, ferroelec., e.s.r. of Mn²⁺, binding of Mn²⁺ ion 3-68832
- dicalcium strontium propionate, hydrostatic pressure effect on ferroelec. phase transition 3-68940
- 1,8-dichloro-10-methyl anthracene, phase transforms. 3-75622
- dichloro-fluoro-methane, vacuum u.v. photolysis, matrix isolation study, i.r. spectra 3-40629
- 9,10-dichloroanthracene, autoassociation in vitreous solutions, study by absorption spectra (French) 3-50591
- 9,10-dichloroanthracene, photocond. associated with triplet state 3-46870
- p-dichlorobenzene:naphthalene, phosphorescence 3-80106
- p-dichlorobenzene, α , γ phases, T₁ absorption and phosphorescence spectra, fine structure 3-69052
- p-dichlorobenzene, α - and γ -phases, T₁ absorption and phosphorescence 3-80104
- α -p-dichlorobenzene, host crystal, naphthalene, localisation of phonon sidebands, T₁ to S₀ 3-69051
- p-dichlorobenzene, irradiated, conditions and defects influence on recovery of free radicals (French) 3-53325
- α -para-dichlorobenzene, quadrupolar regime n.m.r., chem. shifts, asymm. parameter, ang. orientation 3-44338
- p-dichlorobenzene melt, viscosity meas., modified Ostwald viscometer 3-48693
- 4,4'-dichlorobiphenyl oriented in nematic M.B.B.A., structure and conformation determ. by n.m.r. 3-67853
- dichlorodifluoromethane, atmospheric level, Southern California 3-65372

organic compounds continued

- dichlorodifluoromethane, energy loss and range straggling of α -particles from ²³⁸Pu, comparison with Payne-Titeica model (Russian) 3-59638
- 4,4'-dichlorodiphenyl, in paraffin matrices, phosphoresc. spectra, low temp. 3-72731
- 1,2-dichloroethane, relax. time distrib. functions, temp. depend. (French) 3-79981
- dichloromethane, Raman spectra in liquid and gaseous states (Russian) 3-63475
- dichloromethane vapour, average energy per ion pair for α -particles 3-44728
- dichloronaphthalenes in benzene soln., temp. variation of relax. time and activation energy 3-68921
- dichloropentane, torsion force consts. and low frequency bending assignments 3-71559
- 3,6-dichloropyridazine-d₂, solid, deuteron quadrupole coupling at 77K 3-44348
- 6,7-dichloroquinoline, spin-spin coupling of peri-protons 3-50479
- 1,4-dicyanobenzene, anomalous total electric polarisation, i.r. absorption spectra 3-68915
- 1,1-dicyanocyclopropane, liquid and vapour phase, vibrational spectrum 3-46287
- N,N'-dideuteroarachloroaniline, mag. dipole interact. in ND₂ group, ¹⁴N n.q.r. Zeeman effects 3-75910
- dienes, liquid, electron mobilities and activation energies 3-72354
- dienes, reactions with F, unimol. decomp. of long-lived complexes 3-73122
- dietary fatty acids, tocopherol effect on mammalian erythrocytes, mouse, radiation induced haemolysis, K loss 3-48260
- diethyl 4,4'-azoxydibenzoate, smectic A, anisotropic u.s. vel. 3-79432
- diethyl 5-bromouracil-1-malonate, C π → π^* transition, assignment expr. verification and extended Huckel mol. orbital calc. 3-52324
- diethyl 5-nitrouacil-1-malonate, C π → π^* transition, assignment expr. verification and extended Huckel mol. orbital calc. 3-52324
- diethyl ether, liquid-vapour equil. in acetone mixture 3-64165
- diethyl uracil-1-malonate, C π → π^* transition, assignment expr. verification and extended Huckel mol. orbital calc. 3-52324
- 1,1'-diethyl-2,2'-cyanine hole-trapping mechanism, recomb. processes by J-aggregate, supersensitisation 3-61278
- diethyl-5-methyluracil-1-malonate, C π → π^* transition, assignment expr. verification and extended Huckel mol. orbital calc. 3-52324
- diethylamine, solid, p.m.r. second moment and spin-lattice relax., mol. motion study 3-55497
- diethylamine, vibrational spectrum, absorption bands integrated intensities calc. 3-63469
- diethylamine and Cu(II) complex, i.r. spectrum, structural investigation 3-78763
- diethylamine clathrate deuterate, solid, p.m.r. second moment and spin-lattice relax., mol., motion study 3-55497
- diethylamine copper chloride, mag. struct., from mag. torque meas. 3-64502
- 7-diethylamino-4-methylcoumarin, laser use 3-78029
- 7-diethylamino-4-methylcoumarin, tunable dye laser 3-74252
- 7-diethylamino-4-trifluoromethylcoumarin laser dye for blue-green spectral region 3-48904
- diethyloxadicarbocyanine iodide, flowing absorber for c.w. laser operation 3-66827
- 3,3'-diethylthiaticarbocyanine iodide, methanol soln., optical pumping, gain 3-70816
- diffusivities of amines in organic solvents 3-72216
- 3,3-difluoro-oxetane, ring puckering vibr., substituent effects 3-78716
- p-difluorobenzene, electronic struct. and geom., CNDO-CI calcs. for ground and excited states 3-60423
- m-difluorobenzene, mol. struct., electron diff. obs. 3-63356
- m-difluorobenzene, n.m.r. in nematic solvents, geom. and indirect F-F coupling anisotropy 3-60477
- 1,1-difluorocyclobutane, ring puckering vibr., substituent effects 3-78716
- 1,2-difluorodiimide, cis- and trans-, vibr. coupling effects and pot. functions 3-78702
- 1,2-difluoroethane, gauche structure determ. from n.m.r. in nematic solvents 3-43482
- 1,2-difluoroethane, molecular structure from gas phase electron diffraction 3-43392
- 1,1-difluoroethene, ¹⁹F chem. shift anisotropy 3-49490
- 1,1,1-difluoroethene, vibr. corrections of dipolar couplings 3-78700
- 1,2-difluoroethylene, cis- and trans-, vibr. coupling effects and pot. functions 3-78702
- difluoroethylene, dielec. second virial coeff. 3-52414
- 1,1-difluoroethylene, mass-spectrometric study in vacuum u.v., photoionisation curves and threshold energies 3-52395
- 1,1-difluoroethylene mass spectra, ion-molecule reactions 3-43506
- difluoromethane, hyperfine struct. meas. by beam maser spectroscopy 3-46303
- diglycine nitrate, γ -irrad., e.s.r. spectra 3-58426
- diglycine nitrate, ferroelectric phase transition, reciprocal dielectric constant, hydrostatic pressure effects 3-53067
- dihalocarbenes, isolated in rare gas matrices, i.r. spectra 3-75043
- 3,4-dihydro-2H-1,5-benzodioxepin-2,4-dicarboxylic acid, conformation 3-74921
- 2,3-dihydrofuran, Raman spectra, barrier to planarity 3-75021
- 2,3-dihydrofuran and 2,3-dihydrothiophene, ring-puckering vibr. 3-78790
- 2,3-dihydrothiophene, Raman spectra, barrier to planarity 3-75021
- 3,4-dihydroxy L-phenylalanine, cryst. and molecular structure, H-bonding 3-60720
- 1,8-diiodoanthraquinone, crystal and mol. structure 3-79332
- p-diiodobenzene, low frequency Raman spectra, line intensities 3-64653
- trans-1,4-diiodocyclohexane, vibrational spectra and conformation (Russian) 3-63476
- 4,4'-diiododiphenyl, in paraffin matrices, phosphoresc. spectra, low temp. 3-72731
- β -diketones, rare earth complexes, i.r. spectral band assignment 3-78751

organic compounds continued

dimers, strong coupling and spectral consequences 3-78699
 dimesitylbenzene anion-alkali cation radical, $^{85,87}\text{Rb}$ and proton ENDOR study 3-78849
 4,4'-dimethoxyazoxybenzene, mesophase, induced solute mol. deform. 3-58417
 dimethoxybenzene, ortho, meta and para, nuclear spin-lattice relaxation, cross correlation effects 3-55490
 2,4-dimethoxypentane, ^{13}C n.m.r. studies on stereochemical configurations 3-63577
 dimethyl ammonium phosphate, crystal structure determ., Patterson and Fourier syntheses 3-68237
 dimethyl cyanamide, microwave spectra, struct., dipole moment, i.f. vibrs. 3-60464
 dimethyl ether...HCl, H-bonded molecule in gas phase, i.r. spectrum 3-67813
 dimethyl of sulphoxide, n.m.r. spectra quadrupole coupling const. 3-64564
 1,3-dimethyl-2-chloro-diazaboracyclopentane, struct., electron diffraction determ. 3-74922
 dimethylacetylene cryst., phonon Raman spectra, mol. motions and phase transitions 3-55573
 dimethylacetylene substituted molecule, anal. of Hamiltonian, symmetry group and vibr. coords. 3-74975
 p-N,N-dimethylamino-benzonitrile derivatives, two fluoresc. bands, solvent influence 3-76083
 dimethylaminodifluorophosphine, CNDO/2 approximation for conformational analysis (French) 3-63359
 dimethylammonium copper(II) formate, crystal structure determ. by X-ray structural analysis 3-68236
 dimethylchloride, isotopic dilution effect on i.r. absorpt. bandshape 3-54679
 dimethylcyclobutanone, laser-excited fluorescence, ultra-short-lived excited molecules 3-50841
 3,3-dimethyldiazirine, i.r. and Raman spectra 3-78788
 dimethylformamide complexes with chlorophenol derivatives hydrogen bond energies spectroscopic determ. (Russian) 3-49474
 1,2-dimethylindole, dipole moment changes determ. from Stokes shift temp. depend. 3-67839
 N,N-dimethylnitrosamine, hindered rotation barriers 3-71529
 dimethylphthalate thermal conductivity 3-72236
 dimethylquinoline hydrochlorides with MnCl_2 , photoluminescence props. 3-41549
 dimethylsilane, in torsional excited states, rotational spectra analysis (German) 3-43428
 dimethylsilane, rotational spectrum, validity of Hamiltonian for torsional fine structure (German) 3-75053
 dimethylsulfide, in torsional excited states, rotational spectra analysis (German) 3-43428
 dimethylsulfoxide solution in water, self diffusion coeff., n.m.r. meas. 3-68868
 N,N-dimethylthiocarbamyl cyanide, hindered rotation barriers 3-71529
 m-dinitrobenzenes, various substituents, mesomeric moments 3-74928
 2,4-dinitrobenzenesulphonyl chloride, single cryst. struct. data 3-68240
 dinitroxydiethylnitramine (dina), in CO_2 and Ar, pulse calorimetry, reaction kinetics (Russian) 3-45432
 N,4-dinitroso-N-methylaniline reaction with polyamide resins, e.p.r. and i.r. study of products (Russian) 3-50851
 2,4-dinitrotoluene, π -, σ -electronic struct., conversion in ground state, CNDO/2 calcs. (Russian) 3-78678
 dinitroxide spin label oriented in crystal matrix, electron-electron dipolar splitting anisotropy 3-44316
 dinucleotides, backbone conformation, ^{13}P and ^1H fast Fourier transform n.m.r. spectroscopy 3-67850
 dioctyl phthalate aerosol, meas. of number conc. by light scattering method 3-50790
 α -, ω diols, intramolecular hydrogen bonding, i.r. study 3-46293
 3,6-dioxabicyclo[3.1.0]hexane, microwave spectrum, dipole moment, conformation 3-63486
 1,4-dioxacyclohexadiene-2,5, far i.r. spectra, struct., ring bending modes 3-40624
 dioxane in uranine solutions, fluorescence light intensity, influence of degree of dispersion 3-41575
 dioxane, α NPO excimer formation, thermodynamic properties, solvent effect 3-80584
 dioxane, PPO soln., radioluminesc. mechanism in scintillators 3-80085
 p-dioxane and H_2O_2 binary solutions, i.r. and Raman studies (French) 3-58512
 dioxolan, i.r. spectra, $\nu(\text{CH}_2)$ vibrs. of $\text{O}-\text{CH}_2-\text{O}$ group (French) 3-46270
 1-1'-dioxy-4-4'-dianthraquinonyl film, surface pyroelec. effect 3-55529
 diphenyl, in paraffin matrices, phosphoresc. spectra, low temp. 3-72731
 diphenyl, i.r. spectra, conformation 3-75016
 α -, α' -diphenyl β -picryl hydrazyl, solid free radical, elec. cond. and energy gap meas. 3-50200
 diphenyl sulphide, band position, oscill. forces and electron density distrib. (Russian) 3-50555
 diphenyl sulphide, sulphoxide, sulphone vibrational spectra 3-76011
 diphenyl sulphone, electron struct. and nature of absorpt. bands (Russian) 3-50555
 1,1-diphenyl-2-picryl hydrazyl recrystallised free radical powder, e.s.r. absorption 3-47601
 diphenyl-2-picryl hydrazyl recrystallised powders, static magnetic susceptibility 3-58374
 diphenylamine, in organic matrices at 77K role of solvent in delayed fluorescence by two photon excitation (French) 3-46314
 9,10-diphenylanthracene, fluoresc. quantum yield 3-76474
 1:2 diphenylbenzene, solidification behaviour 3-79252
 diphenylenesulphide, in n-heptane and CCl_4 matrices, quasiline phosphoresc. spectra, external heavy atom effect 3-72743
 diphenylmethyl radical, stereochem., e.s.r. data interpret., INDO-MO calcs. 3-46228

organic compounds continued

diphenylnitroxide radical, polarised absorption spectra, electronic structure 3-63442
 2,5-diphenyloxadiasole-1,3,4, in inert solvent, inhomogeneous broadening of fluoresc. spectra 3-69094
 2,5-diphenyloxadiazole, substitution effects on electronic structure and fluorescence (Russian) 3-63395
 2,5-diphenyloxasole-1,3, in inert solvent, inhomogeneous broadening of fluoresc. spectra 3-69094
 α -, ω -diphenylperfluoropolyenes, effect of fluorination on conjugation, UV and Raman spectra, steric struct. of mols. 3-71520
 diphenylpicrylhydrazyl radicals, electron excitation energy transfer from aromatic molecules in solid solns., luminesc. yield 3-76484
 diphenylpolyenes, conjugation and resonance Raman effect 3-76010
 diphenylpolyenes, conjugation and resonance Raman effect on Raman intensities 3-40623
 1,3-diphenylpropane, intramol. triplet excimer form. 3-44732
 diphenylsulphone-2-sulphonyl chloride, single cryst. struct. data 3-68240
 diphenyl sulphoxide, electron struct. and nature of absorpt. bands (Russian) 3-50555
 dipyrindyls, ($\alpha\alpha'$ - and $\gamma\gamma'$), i.r. spectra, conformation 3-75016
 disubstituted benzene derivatives containing two acceptor groups, pi-electron SCF-MO calc., numerical results 3-57638
 disubstituted benzene derivatives containing two acceptor groups, pi-electron SCF-MO calc. 3-63396
 1,2-disubstituted ethanes, ab initio MO calc. of internal rotation 3-49451
 disulphides, charge transfer complexes with various acceptors, u.v. spectra and bond angle study 3-46263
 cis-1,4-ditertiarybutylcyclohexane, combined electron diff., conform. energy and vibr. obs. 3-63357
 dithiophosphorinanes, [1,3,2] and [1,3,2]-dioxta-FT ^{13}C n.m.r. spectra 3-71591
 dithiodiglycollic acid and cystamine, X-radiation, formation of mixed disulphide aminoethyldithio acetic acid, chain reaction 3-47566
 DMSO: Eu^{3+} soln., radiative and radiationless processes 3-55683
 DMSO: Tb^{3+} , Eu^{3+} electronic excitation energy transfer 3-47300
 DMSO, radiative and nonradiative transitions rel. to energy transfer model of Tb^{3+} 3-64732
 DPPH and derivatives, high-resolution e.p.r. spectra of hydrazil radicals 3-78841
 DPPH in polystyrene, e.p.r. lineshape in wings of exchange narrowed systems 3-64539
 DPPH radical, mag. transition, infralow temp., e.p.r. obs. 3-79894
 duren, emission spectra, exciton-phonon interactions 3-69071
 duren, low frequency Raman spectra, line intensities 3-64653
 duren, methyl motions, vibr. exciton, temp. depend. 3-44042
 duren matrix, isolated p-fluoroaniline dipole moment determ., Stark spectroscopy 3-72600
 duren single crystals, ^{13}C chem. shielding tensors using proton-enhanced n.m.r. 3-64580
 dye, rigid film, anisotropic image form. 3-73798
 dye dimers, effect of local field on electronic spectra 3-53122
 dye laser, radiationless internal conversion rate meas. 3-78032
 dye laser, spectral narrowing with non-resonant feedback, fibre optics appl. 3-78027
 dye laser, superradiant slab, refractive index gradient effects 3-78033
 dye lasers, continuous freq. tuning, 2 mixed dyes 3-62714
 dye molecules aggregates, effect of local field in electronic spectra 3-67807
 dye sensitisation of AgBr(I) and AgBr photographic emulsions, effect on photovoltaic effect, electron and hole traps 3-53343
 dye solution lasers, generation spectra kinetics (Russian) 3-62715
 dye solutions, energy transfer to and from Eu^{3+} and Tb^{3+} , electrostatic interaction 3-76093
 dye solutions, two-photon excitation, fluoresc. quenching mechanisms 3-64715
 dyes, bleaching and fluoresc. in high viscosity solvent, polarisation 3-51926
 dyes, formation of epitaxial attachments on AgBr surface, ligand bonds, red shift 3-53342
 dyes, optimum spectral characteristics, computer simulation 3-47287
 dyes in laser with transverse flow cuvette 3-66833
 dyes sorbed on polymer globules, energy migration, quantum efficiency 3-69080
 dysprosium ethyl sulphate, exchange interactions effect on low temp. ordering 3-47015
 EDA complexes in polar solvents excited state dipole moment from solvent shift 3-71537
 EDA complexes with liquid donors, excited singlet-singlet absorpt. spectra 3-76471
 energy loss and range straggling of α -particles from ^{238}Pu , comparison with Payne-Titeica model (Russian) 3-59638
 enones, conjugated, spin-orbit coupling effects on the zero field splitting of (π, π^*) triplet states, ODMR obs. 3-65103
 eosin, in soln., fluoresc., intermol. energy migration, fluorometer appl. 3-76085
 eosin, soln., excitation energy transfer 3-69047
 epichlorhydrin, adsorption on SiO_2 , anomalous sites characterisation 3-68489
 epoxy resin, bending and elongation waves effects on stationary crack 3-75564
 erythrosin, in soln., fluoresc., intermol. energy migration, fluorometer appl. 3-76085
 erythrosin, soln., excitation energy transfer 3-69047
 esters, elec. dipole moment at 1 MHz for mol. config. determ. 3-52350
 esters, ionization potential calcs. 3-78672
 esters, mixed polyfluorinated, valency vibration absorption bands, carbonyl groups (Russian) 3-71530
 ethane, ^{13}C n.m.r., mag. shielding consts. calc. by Gaussian function 3-71593
 ethane, α -particle molecular stopping cross sections 3-56554
 ethane, at low reduced temps., second and third virial coeffs. meas. 3-54788

organic compounds continued

- ethane, effect on second-order inflammation of H₂ (*Russian*) 3-47540
- ethane, internal rot barrier calcs., comparison between SCF-LCAO-MO and SCF-X α -SW approxs. 3-40590
- ethane, liquid, specific heat and applicability of asymptotic laws near critical point 3-72203
- ethane, local bonding orbitals, FSGO model 3-71503
- ethane, mol. force fields and isotopic rules determ. 3-54653
- ethane, molecule, electron impact excitation, emission spectra 3-75122
- ethane, second-order props. calc. with virtual orbitals 3-54617
- ethane, two centre calc., Slater type orbitals, vertical electronic transitions, bond distances, force constants (*Russian*) 3-49444
- ethane absorption cross sections from 180 to 700 3-67805
- ethane-ethylene solutions, molecular thermodynamics in normal and critical regions 3-65121
- ethanol, boiling, heat transfer, effect of thermophys. props. of heating surface material 3-52693
- ethanol, glassy liquid and crystal state, supercooling rate 3-75484
- ethanol, limit of superheat 3-75612
- ethanol, liquid, hydrogen bonded, association and assignment of OH overtones 3-75023
- ethanol, PVA in solution, thermoelasticity, gels 3-63601
- ethanol, refractive index meas., between 250 and 700 nm. 3-66190
- ethanol, solvent for aromatic molecules, effect on excited states 3-60473
- ethanol, submillimetre refraction spectrum 3-69108
- ethanol glasses, deuterated, trapped electrons, 4K 3-76465
- ethanol in uranine solutions, fluorescence light intensity, influence of degree of dispersion 3-41575
- n-ethanol-propanol-water, diffusion coefficients, ternary, meas., apparatus, analysis (*Japanese*) 3-64198
- ethenes, fluorinated, in liq. cryst. solvents, H-F and F-F nucl. mag. spin-spin coupling anisotropies 3-40655
- ether in chloroform soln., association and anisotropic mol. reorientation, n.m.r. obs. 3-68873
- ethers, containing solvated electrons, optical absorpt. spectra by pulse radiolysis 3-44725
- p-ethoxybenzal p-aminoazobenzene, nematic liquid crystal, p.m.r. 3-53025
- ethyl acetate, solvent effects in hydrolysis reaction rate 3-69457
- ethyl bromide and deuterated derivatives, normal coord. analysis of force fields 3-63407
- N-ethyl butyramide solns., dimer-trimer formation, i.r. spectral evidence 3-46301
- n-ethyl carbazole, in n-paraffin matrix, fluoresc. and phosphoresc. emission and excitation spectra 3-72744
- ethyl cation, C₂H⁺, classical and non-classical struct. approach 3-74911
- ethyl chloroformate, vibrational spectra, rotational isomerism, normal coordinate analysis, mean amplitudes 3-54687
- ethyl compounds, uncoupled pulsed Fourier transform ¹³C n.m.r. spectra 3-75085
- ethyl cyanofornate, vibrational spectra, rotational isomerism, normal coordinate analysis, mean amplitudes 3-54687
- ethyl ether, α NPO excimer formation thermodynamic properties, solvent effect 3-80584
- ethyl fluoride, gaseous, submillimetre laser lines by optical pumping 3-51916
- ethyl fluoride, vibrational analysis 3-75037
- ethyl formate, vibrational spectra, rotational isomerism, normal coordinate analysis, mean amplitudes 3-54687
- ethyl radicals, ab initio calcs., mol. fragments 3-78668
- ethylcarbonium ion, nonempirical MO calcs. of energies rel. to geom. 3-63354
- ethylene, and similitudes, mols. symmetry effects in internal rotation 3-74974
- ethylene, expansion apparatus for measurement of Joule-Thomson effect 3-71708
- ethylene, harmonic force consts. determ. 3-60432
- ethylene, molecule, electron impact disoc., rotational and vibrational energy level distrib., luminesc. 3-75127
- ethylene, molecule, electron impact excitation, emission spectra 3-75122
- ethylene, Raman spectra of crystal molecular orientation intermolecular potential and crystal structure 3-72608
- ethylene, reaction with N atom, emission spectra obs. 3-44718
- ethylene, second-order props. calc. with virtual orbitals 3-54617
- ethylene, two centre calc., Slater type orbitals, vertical electronic transitions, bond distances, force constants (*Russian*) 3-49444
- ethylene absorption cross sections from 180 to 700 3-67805
- ethylene and C₂D₆ threshold electron-photoion coincidence mass spectrometric study 3-43499
- ethylene and fluoroethylene mixture, ion-molecule reactions, mass spectra 3-43508
- ethylene chlorine complex, struct determ. from spectra 3-54608
- ethylene glycol, dye laser, radiationless internal conversion rate meas. 3-78032
- ethylene glycol, with Cr(V) complexes, dynamic proton polarisation and spin-lattice relax. 3-72543
- ethylene glycol + water glassy mixture, trapped electron excitation mechanism, e.s.r., thermoluminescence 3-65099
- ethylene oxide, adsorption on SiO₂, anomalous sites characterisation 3-68489
- ethylene oxide, as clathrate deuterate, proton spin-lattice relax. time 3-54727
- ethylene oxide, C-H stretching and CH₂ wagging modes, i.r. spectra 3-54676
- ethylene oxide, Coriolis coupling coefficients, C-H stretching vibrations 3-49450
- ethylene oxide, vacuum-u.v. photolysis 3-73157
- ethylene oxide clathrate hydrate, stretching modes, ring breathing mode, i.r. spectra, 100K 3-54677
- ethylene oxide lines, collision broadening by quadrupolar mol. CO₂ 3-52397
- ethylene oxide-d₈, Coriolis coupling coefficients, C-H stretching vibrations 3-49450
- ethylene sulphide, Coriolis coupling coefficients, C-H stretching vibrations 3-49450

organic compounds continued

- ethylene sulphide, photoelectron spectrum obs. 3-54627
- ethylene sulphide, Rydberg transitions, vacuum u.v. spectra 3-54675
- ethylene sulphite and chlorophosphite, vibration and i.r. spectra, conformers. (*Russian*) 3-71492
- ethylene triplet state, ab initio calcs., mol. fragments 3-78668
- ethylene trithiocarbonate, solid, fundamental vibrations assignment from i.r. and Raman spectra 3-47261
- ethylene-acetone system, intermolecular triplet excitation transfer 3-69480
- ethylene-Cl₂ complexes, low temp. i.r. spectra 3-75014
- ethylene-glycol, relax. time distrib. functions, temp. depend. (*French*) 3-79981
- ethylene-O₂ flames, electron temp. meas. using double-probe current-voltage charact. 3-80523
- ethylenes, monosubstituted, absolute i.r. intensities, CNDO/2 calc. 3-46243
- ethylenes, substituted, electronegativity effect on bond lengths 3-67728
- ethylenic chromophores-trans-cyclooctene, absorption and circular dichroism spectra 3-71545
- o-, m-ethylphenols, molar polarization and dipole moment, mol. assoc. 3-68916
- 4-ethylpyridine hydrogen bonded complexes with quinoline, methyl- and chloro-pyridines, vibrational spectra 3-75029
- ethylsulphates of yttrium and some rare earths, Raman spectra 3-50564
- ethynyl ion, heat of formation 3-75092
- ethynyl-benzene and derivatives, absolute calc. radiationless decay of lowest triplet state 3-67842
- ethynylbenzene, vibronic spectra, theoretical study 3-67783
- eucarovne, protonated, electronic distrib. by ¹³C n.m.r. 3-75076
- eugenol, press. dependence of u.s. absorption 3-71995
- europium aromatic acid compounds, luminescence and i.r. spectra, structure 3-65108
- europium benzoylacetate complex in soln., spectral studies (*Russian*) 3-50559
- excited states of matter, symp., Lubbock, Texas, USA (Apr. 1971) 3-63547
- fatty acid salts, cond. meas. to illustrate tunnelling 3-42500
- fatty acids, i.r. spectra, intermolecular interaction, phase transition 3-72654
- fenchone, solute dipole moment relax. in o-terphenyl 3-72571
- ferrocene, enthalpy of sublimation meas., thermal cond. manometer 3-45460
- ferrocene, proton multiple pulse spectra, nuclear magnetic shielding anisotropies 3-79930
- ferrocene derivatives, ¹³C n.m.r. spectra obs. by pulse Fourier transform spectroscopy 3-75897
- film, principal index variation with wavelength (*French*) 3-80064
- filters, for spectrum width restriction in giant pulse ruby laser (*Russian*) 3-70823
- five-membered heterocycles, aromatic character, ring currents and proton chem. shifts, Hartree-Fock calcs. 3-60420
- flavonoids, with 5-OH group, luminesc. quenching mechanism 3-69082
- fluorene:anthracene, tetracene, time resolved fluorescence spectroscopy 3-55680
- fluorene, pyrene-d₁₀ doped, triplet annihilation behaviour 3-64708
- fluorenone, in o-terphenyl and mixed solvents, supercooled liquid, dielectric relaxation 3-49850
- fluorenone radical anions, ¹H and ²D n.m.r. studies 3-43488
- fluorescein, alcoholic soln., ozone induced chemiluminesc. 3-80569
- fluorescein, lifetime and time-resolved fluorescence meas. with ACO synchrotron radiation 3-40651
- fluorescein, soln., excitation energy transfer 3-69047
- fluorescein, X-ray chemiluminescence of aqueous solutions, effect of pH 3-47568
- fluorescence of mols. in solid. solns., band narrowing, vibronic struct. 3-46311
- fluorescein, alcoholic soln., ozone induced chemiluminesc. 3-80569
- fluoro(trifluoromethyl)benzenes, in gas phase, fluoresc. and singlet state emission quenching 3-55978
- fluoro(trifluoromethyl)benzenes, in gas phase, photophysical processes 3-55977
- 1-fluoro-2, 4-dinitrobenzene, i.r. spectrum, 4000 to 250 cm⁻¹, vibr. assignments 3-49465
- 1-fluoro-2 trifluoromethylbenzene, photolysis in gas phase 3-47581
- 4-fluoro-2-chlorotoluene vapour, near u.v. absorption spectrum, modes of vibration 3-46260
- 1-fluoro-3 trifluoromethylbenzene, photolysis in gas phase 3-47581
- 1-fluoro-4 trifluoromethylbenzene, photolysis in gas phase 3-47581
- fluoro-substituted quinolines π -electron densities, Pariser-Parr-Pople calc. 3-74957
- fluoroacetones, n.m.r. coupling consts. and rot. isomerism 3-46323
- fluoroacetones, n.m.r. study and rotational isomerism 3-78843
- fluoroacetophenones, elec. dipole moments and conformations, o-, m- and p- 3-67724
- p-fluoroaniline, dipole moments determ., orientational Stark splitting obs. 3-63433
- p-fluoroaniline, in durenne cryst., dipole moment determ., Stark spectroscopy 3-72600
- fluorobenzene, 4.2 K, exciton spectra, polarised u.v. light 3-69020
- fluorobenzene, electrophilic substitution calcs. 3-78677
- fluorobenzene-d₅, liq., mol. reorient. at high press., n.m.r. relax. obs. 3-68871
- fluorobenzenes, homo-substituted, ground state electronic struct., extended Huckel MO calcs. 3-67737
- fluorobenzenes, homosubstituted, all valence electron MO calcs. 3-67738
- p-fluorobenzotrifluoride, fluoresc. quantum yields and decay times, rate consts. 3-63495
- fluorocarbons, pulse irradiated, electron disappearance 3-73148

organic compounds continued

- fluorocyclopentenes, ^{19}F n.m.r. 3-57669
 fluoroethylene, ion-molecule reactions, mass spectra 3-75134
 fluoroethylene and ethylene mixture, ion-molecule reactions, mass spectra 3-43508
 fluoromethane, i.r. spectrum of solid at 20K 3-61037
 fluoromethane, time resolved i.r.-microwave double resonance, theory and expt. 3-71578
 fluoromethane collisions with CO_2 , vibrational relaxation 3-54752
 fluoromethane molecules, C and F X-ray emission and F K absorption spectra 3-43430
 fluoromethanes, vacuum u.v. absorpt. spectra 3-60451
 fluoromethanol, anomeric effect 3-60417
 fluoromethanol, localized MO, excited state geometry, gauche effect 3-74914
 p-fluorostyrene, rot. band contour analysis of O_2^0 bands of $\Delta^1\text{A}'-\text{X}^1\text{A}'$ systems 3-63446
 p-fluorotoluene, fluoresc. quantum yields and decay times, rate consts. 3-63495
 1-fluorovinyl cations, geometrical study, INDO calc. 3-52325
 formaldehyde, $2\nu_2$ band, i.r. spectra, constants 3-63494
 formaldehyde, anomalous hyperfine lines in L1436, interstellar dust cloud 3-56444
 formaldehyde, energy function calc. for geometry optimisation 3-71490
 formaldehyde, H_2CO^+ , interaction with $\text{He}(2^3\text{S})$, $\text{CO}^+(\text{A}^2\Pi)$ 3-54736
 formaldehyde, illustration of calculated orbitals 3-63375
 formaldehyde, interstellar, 6 cm excitation temp. in dark dust clouds 3-70046
 formaldehyde, microwave collision diameters in rot. spectrum 3-67858
 formaldehyde, photochemistry of single vibronic levels 3-41864
 formaldehyde, production and decay of excited states by photon impact 3-40665
 formaldehyde, sensitized decomposition to formyl radical, e.s.r. and electronic spectra 3-47577
 formaldehyde, unsuccessful search for molecular lines in interstellar matter 3-61863
 formaldehyde absorption of 2.7 K cosmic background radiation in interstellar dust clouds 3-70047
 formaldehyde radiation, absence in galactic plane cold region 3-51392
 formaldehyde- h_2 and - hd , fluoresc. lifetime meas. A_2-A_1 transition, N_2 laser 3-75057
 formalimine, hypothetical, $\text{C}=\text{N}$ bond theory 3-71523
 formamide, mol. fragment, polypeptide systems, procedure to examine large mol., appl. to polypeptide characterisation 3-46360
 formamide, protonation site, non-empirical LCAO-MO-SCF calcs. 3-63381
 formamide, unsuccessful search for molecular lines in interstellar matter 3-61863
 2-formamidoacetamide, mol. fragment, polypeptide systems, procedure to examine large mol., appl. to polypeptide characterisation 3-46360
 formates in soln., dielec. dispersion characts. and dipole moments 3-68919
 formic acid, gaseous, submillimetre laser lines by optical pumping 3-51916
 formic acid, HCOOH^+ , interaction with $\text{He}(2^3\text{S})$, $\text{CO}^+(\text{A}^2\Pi)$ 3-54736
 formic acid, ionic solvation, CNDO/2 calcs. on solvated univalent ions 3-53347
 formic acid, proton barrier, i.r. spectra, theory 3-63390
 formic acid, reaction coordinate eigenvalue effect on heavy atom kinetic isotope effects 3-76426
 formimide, microwave spectrum, gas phase conformational props. of amide bond 3-63483
 formyl, unsuccessful search for molecular lines in interstellar matter 3-61863
 formyl chloride, struct., decomp., i.r. spectra, vibr. assignments 3-78753
 formyl fluoride photochem. laser behaviour, HF i.r. emission 3-44733
 formyl radical, energy function calc. for geometry optimisation 3-71490
 formyl radical e.s.r. spectra, non-collinear Zeeman, hyperfine and fine structure tensors effect 3-47127
 free radicals, electronic structure, geometry change and substitution effects using INDO method 3-63387
 Fremy salt, orange-brown form, triplet state obs. by e.s.r. (French) 3-61275
 freon, electron attachment cross sections in energy range up to 10 eV 3-78880
 Freon, Freon-air mixture, sparking potentials and swarm coeffs. 3-52544
 freon, orthopositronium and free positron decay rate 3-74908
 freon gas ionisation sensitivity to pressure variation, applic. to transient velocity and pressure meas. 3-49528
 Freon R12, R113 and R114, nucleate boiling, heat transfer, maximum heat flux, and transition boiling 3-52694
 Freon-114 diabatic local void fraction meas. using hot-wire anemometer 3-46128
 Freon-11 atmospheric concentration over Pacific and Ross Sea 3-69589
 fuel oil hydrocarbons and mineral particles in seawater and marine sediments 3-53456
 fumaric acid, monoalkyl esters, hydrogen bonding, i.r. spectra conformations 3-63468
 fumaric acid proton multiplet pulse spectra, nuclear magnetic shielding anisotropies 3-79930
 2-furaldehyde and deuterio analog, vibr. spectra, band contours 3-67818
 furan, liquid, proton-spin relaxation and molecular motions 3-44344
 furan, rot. transitions, h.f.s. 3-54701
 furan, solid and liquid, i.r. spectra and struct. (French) 3-75033
 furan, vibr. rot., i.r. spectra of condensed phases 3-68996
 gelatin: Cu_2SO_4 , X-ray laser emission 3-66835
 glass, endurance under cyclic elastoplastic deform., liq. media influence (Russian) 3-80465

organic compounds continued

- glass, synthesised from C , O_2 and H_2 with radioactive admixtures rel. to (ν)-diffusion detector construction (Russian) 3-62240
 glass, yield of two-dimens. void assembly 3-58735
 glutamic acid, effect on neuromuscular transmission in stick insects 3-56495
 glycerine, Doppler optical velocimeter for small vel. flow meas. in fluid free convection 3-45619
 glycerine liquid film, deformation drop impact process (Russian) 3-40947
 glycerine-water solution, spin-lattice relax., Mn^{2+} ion effect 3-53035
 glycerol, 10 to 10⁷ poises, viscoelastic properties, relaxation range, u.s. frequencies 3-61993
 glycerol, absorpt. and dispersion of u.s. waves 3-49940
 glycerol, aqueous, PVA in solution, thermoelasticity, gels 3-63601
 glycerol, dynamic tensile failure, technique for liquids 3-39852
 glycerol, human serum albumin, liquid jet, monodispersed drops, production by forced vibration 3-71833
 glycerol, laminar pipe flow, non-isothermal, velocity profiles, pressure drops and heat transfer 3-63629
 glycerol, photon correlation study of scatt. depolarised ray at low temp. (French) 3-68966
 glycerol single crystals, l.f. vibr. assignment, Raman spectra (French) 3-58497
 glycine, ^{15}N enriched, aqueous soln., n.m.r. lineshape, relaxation time, chemical shift, pH depend. 3-64570
 glycine, mono-, di-, tri-, tetra-, and pentapeptides, SCF molecular fragment approach 3-78669
 glycine silver nitrate, ferroelec. transition, hydrostatic press. effects 3-64611
 glycine single cryst., nuclear spin-lattice relax. anisotropy 3-75907
 glycol monoformate, gaseous, electron diff., i.r. spectra, conformations, bond lengths 3-63362
 glycol PVA in solution, thermoelasticity, gels 3-63601
 glycolaldehydes, microwave spectra, substitution struct., intramolecular hydrogen bond and dipole moment 3-54703
 glyoxal, $(\text{HCO})_2^+$, interaction with $\text{He}(2^3\text{S})$, $\text{CO}^+(\text{A}^2\Pi)$ 3-54736
 glyoxal, and deuterated derivatives laser excited emission spectra, band assignments 3-54662
 cis-glyoxal, time and energy resolved fluoresc. 3-57663
 glyoxal vapour, singlet and triplet emission, spectra, 4358 3-80566
 glyoxal- d_1 and glyoxal- d_2 , 5207 μ band system, vibrational assignment 3-54660
 guanidine(III) aquo-carbonatolanthanidates, hydrogen bonds, i.r. absorpt. (French) 3-40620
 guanidinium ion, ^{14}N -NQR study 3-79943
 1-halo-3,3,3-trifluoropropynes, vibrational spectra 3-46296
 halobenzenes, π -orbitals, inductive and mesomeric effects 3-78690
 halocyclopentanes, n.m.r. spectra, conformations, calcs. 3-63366
 halogen substituted benzenes, temp. and phase dependence of positronium lifetimes 3-55221
 halobenzenes, mono- and disubstituted; tables of data for electronic struct. 3-74967
 halogenoalkanes, i.r. spectra in Ar matrices at 20K 3-61037
 halogenopyridines, vibrational spectra 3-46288
 α -haloketones, optically active, fluorine anomaly 3-63393
 2-halomethanes, intensity of valency vib. bands of C-Cl and C-Br bonds (Russian) 3-63478
 heptafulvalene mol., cause of nonplanarity, bond angle strain 3-46220
 heptafulvalene mol., cause of nonplanarity, ring strain, H repulsion 3-46221
 n-heptane, quasilinear spectra of trapped coronene, 1,12-benzoperylene and perylene, solute-solvent interactions 3-72728
 n-heptane, trapped perylene, anthracene and 1,12-benzoperylene, fluoresc., phonon struct. 3-72729
 heptane, u.s. scatt., nonlinear phenomena 3-68336
 n-heptane matrices, luminesc. and excitation spectra of chlorophyll A 3-72733
 n-heptane matrix, aromatic molecules, quasiline phosphoresc. spectra 3-72743
 heptyloxyazoxybenzene, smectic-phase order-parameter fluctuations in nematic phase 3-63952
 heterocycles with divalent sulphur, resonance energy calcs. from thermodynamical data 3-67753
 N-heterocyclic compounds, ortho, oxy, and methoxy substituted, electronic structure and fluorescence (Russian) 3-63395
 heterocyclics, n.m.r. obs. (French) 3-63518
 heteroorganic molecules, LCAO mol. orbital calcs., experimental criterion for correctness, energy of charge transfer 3-71499
 hexachlorocyclohexane, α , γ , δ and isomers, quantitative absorption spectra anal., linear and convex programming 3-51763
 hexachlorocyclopropane, molecular structure, electron diffraction determ. 3-54612
 hexafluoro-2-propanol and deuterated analogues, solid, liquid and gaseous states, i.r. and Raman spectra 3-46286
 hexafluoroazomethane, vibrational spectra and molecular configuration 3-43452
 hexafluorobenzene, Raman spectra, C-F bond length determ. 3-54691
 hexafluoroethane, α -cryst. phase, vibr. spectra 3-41508
 hexafluoropropanol-2, vibr. freq., force field, mean amplitudes 3-63412
 hexagens, rate of combustion at high pressures, rel. to temp. of flame (Russian) 3-47539
 hexamethyl benzene, emission spectra, exciton-phonon interactions 3-69071
 hexamethyl-tetracarbahexaborane(6), molecular struct. determ. (German) 3-43397
 hexamethylbenzene crystal, Raman, far i.r. studies, mol. motion, λ -phase transition 3-64134
 hexamethylbenzene single cryst., polarized Raman spectra, freqs. assignment 3-55572
 hexamethylenetetramine, proton and ^{14}N rotational correlation times in chloroform 3-75900
 hexamethylenetetramine crystals, interatomic forces, intermolecular mode frequencies 3-46686

organic compounds continued

- hexamethylphosphoramide, pulsed ^{14}N n.q.r., use of multichannel accumulators 3-73829
- hexamine, thermal diffuse scattering of X-rays, lattice dynamical models, theoretical maps, results comparison 3-40828
- hexamine, thermal diffuse scattering of X-rays, Laue method and interferim correlation 3-40827
- n-hexane, dielectric constants and molar polarizations, 278-343 K 3-50861
- n-hexane, electric field induced nucleation, bubble chamber study 3-77719
- n-hexane, for liquid scintillators 3-48526
- n-hexane, particulate charge carriers, electrohydrodynamic instability 3-46863
- n-hexane, quasilinear spectra of trapped coronene, 1,12-benzoperylene and perylene, solute-solvent interactions 3-72728
- n-hexane, solid, low frequency mol. vibrations by neutron inelastic scattering 3-75577
- n-hexane, superheated, nucleation, effect of elec. fields 3-49987
- n-hexane, trapped perylene, anthracene and 1,12-benzoperylene, fluoresc., phonon struct. 3-72729
- n-hexane matrices, luminesc. and excitation spectra of chlorophyll A 3-72733
- n-hexane matrix, 1,12-benzoperylene and coronene impurities, zero-phonon lines and electron-phonon interaction 3-72727
- n-hexane matrix, secondary radiation of trapped perylene molecule 3-72726
- n-hexane vapour, average energy per ion pair for α -particles 3-44728
- hexenes, liquid, electron mobilities and activation energies 3-72354
- high molecular materials, aq. soln., optical and dielec. props. (*Russian*) 3-50860
- hippuric acid, crystal twisting rel. to surface stress, approx. model 3-54931
- holmium ethyl sulphate, paramag. relax. rates of Ho^{3+} 3-50450
- holographic materials, storage of volume holograms 3-77528
- Hoppe-Paulus folded molecule procedure for determ. of molecule position in unit cell (*German*) 3-52617
- human serum albumin, liquid jet, monodispersed drops, production by forced vibration 3-71833
- hydrazinium halide, cryst., hydrogen bond vibr., i.r. and Raman spectra obs. 3-72640
- hydrocarbon, aromatic, in frozen polycryst. soln., quasiline spectra as zero-phonon lines 3-72635
- hydrocarbon, C/H ratio, laser pyrolysis, plasma stoichiometry analysis 3-70462
- hydrocarbon, force field calcs. using CNDO/2 method 3-74951
- hydrocarbon, liquid, quasi free electron energies and probability of localisation 3-50140
- hydrocarbon, solid, electron energy loss spectra and optical constants 3-79397
- hydrocarbon, unsaturated, collision with H atom, change in hyperfine state 3-63347
- hydrocarbon chains, correlation functions of internal motion 3-78847
- hydrocarbon conjugated free radicals, excitation spectra calc. using ensemble averaging schemes 3-67758
- hydrocarbon ions, polynuclear, mass assignments based on mobility meas. 3-66431
- hydrocarbon matrices, struct. of azulene electronic spectra 3-72736
- hydrocarbon mixtures, critical properties prediction methods 3-76488
- hydrocarbon partial pressure, ^{14}C -labelled, meas. using $\text{CaF}_2:\text{Eu}$ scintillation counter (*French*) 3-62039
- hydrocarbon radical cations, fluorinated, spin density distrib. 3-57631
- hydrocarbon systems from five-membered rings, Huckel $4n+2$ rule 3-78689
- hydrocarbon-carbon ratio, Lake Biwa deposits palaeomag. investigation, mag. control of climate 3-76675
- hydrocarbons, air pollutant automatic sampling and anal. 3-53783
- hydrocarbons, alternant, reson. energies calc. by semi-empirical method 3-67752
- hydrocarbons, ATDL dispersion model for chemically reactive pollutants 3-76704
- hydrocarbons, C_5 -unsaturated, ion-molecule reaction obs. by photoioniz. mass spectrometer 3-55932
- hydrocarbons, conformation and distortion, n.m.r. and i.r. spectra (*Russian*) 3-71491
- hydrocarbons, conjugated, energies and oscillator strengths of excited singlet states calc. 3-52344
- hydrocarbons, conjugated, graph theory applic. to topology depend. of π -electron parameters 3-46238
- hydrocarbons, conjugated, optical dipole polarisability calc. 3-43437
- hydrocarbons, conjugated, singlet-triplet and triplet-triplet spectra calc. 3-52343
- hydrocarbons, critical properties, prediction methods 3-76487
- hydrocarbons, interpretation of C-H coupling consts. for directly bonded nuclei 3-75073
- hydrocarbons, ionization potential calcs. 3-78672
- hydrocarbons, isotope effect on virial coefficients (*German*) 3-63605
- hydrocarbons, Leidenfrost temp. calc. 3-64169
- hydrocarbons, liq., proton spin-lattice relax., press. depend., mol. motions 3-41446
- hydrocarbons, liquid, electron mobility, phys. model 3-55262
- hydrocarbons, liquid, steady state and pulse radiolysis, charge scavengers effect on scavenging on opposite sign charges 3-41849
- hydrocarbons, long chain viscous, nuclear spin-lattice relaxation, rotational motion mechanism 3-54769
- hydrocarbons, low mol. weight, concs. rel. to air mass identification 3-73314
- hydrocarbons, mag. props. and ring current chem. shift calc. 3-57637
- hydrocarbons, MOA calculations of CH stretching frequencies and dissociation energies 3-43429
- hydrocarbons, mol. formulae, calc. from mol. weight, functional analysis (*Rumanian*) 3-71484

organic compounds continued

- hydrocarbons, molecule, electron impact excitation, Balmer β radiation, cross section meas. 3-75123
- hydrocarbons, monocyclic conjugated, mag. moments calc. 3-78724
- hydrocarbons, optimized extended Huckel calc. for ionisation potentials and dissociation energies 3-52313
- hydrocarbons, saturated, collisions with optically orientated Na atoms, disorientation (*German*) 3-43381
- hydrocarbons, supercooled liquids and derivatives, viscoelastic behaviour 3-46364
- hydrocarbons, vibr. deactivation of $\text{HF}(v=1,2)$, rate consts. 3-46350
- hydrocarbons adsorbed on zeolites, ^{13}C n.m.r. investigations (*German*) 3-47600
- hydrocarbons in Jovian thermosphere, i.r. cooling 3-76993
- hydrocarbons with delocalized electronic systems, molecular mechanics method for bond order determ. 3-67729
- hydroquinone β clathrates with H_2S , H_2Se , D_2S and D_2Se , far i.r. absorption spectra (*French*) 3-69031
- hydroxamic acid in nuclear fuel reprocessing solvents, spectrophotometric determ. 3-71225
- 6-hydroxy-2-formylfulvene, H-bonding, molecular symmetry, microwave spectra 3-54698
- trans-hydroxy-L-proline, proton NMR spectra, computer simulation, long range coupling constant, structural implications 3-75074
- hydroxyacetonitrile, microwave spectroscopy, rotational isomerism, barriers to internal rotation 3-49479
- 2-hydroxybenzophenone derivatives, intramolecular hydrogen bonding obs. (*Russian*) 3-71564
- hydroxylamine, interconversion of H_3NO , ab initio SCF calc. and rearrangements of substituted compounds 3-49430
- hydroxymethylcarbonium ion, nonempirical MO calcs. of energies rel. to geom. 3-63354
- hydroxyacetonitrile, barriers to internal rotation, group function and MO-LCAO-SCF computations 3-49432
- imidazole derivatives and complexes, high resolution ^{13}C n.m.r. spectra 3-75892
- imidazole-phenol complexes, hydrogen bonds, i.r. spectra (*French*) 3-40621
- 2,2'-iminobis(acetamidoxime), n.m.r. study of barrier to rotation 3-52331
- iminoxyl radical, in plastic cryst., inhomogeneous broadening of e.p.r. spectra, conditions of rapid rotational diffusion 3-79895
- 1-indanone, dual phosphoresc., triplet states 3-55975
- indole, dipole moment changes determ. from Stokes shift temp. depend. 3-67839
- indole, electrical conductivity meas. 3-58257
- interstellar methanol, $\text{E}_1\text{-E}_2$ labelling of energy levels and anomalous excitation 3-81190
- iodine-iodoform solns., laser flash photolysis, transient species obs. 3-65097
- 1-iodo-1-methylcyclohexane 3-78764
- iodobenzenes, o- and p-substituted, i.r. spectral band near 1000 cm^{-1} , substituent and solvent effects 3-46302
- iodoform, crystalline, vibrational spectrum 3-50575
- ion-molecule rate constants, absolute meas. by drift cell ion cyclotron reson. spectroscopy 3-57677
- iron (II) formate, Mossbauer investigation of cation positions in mixed crystals (*German*) 3-79967
- iron anhydrous acetates, struct. 3-40908
- isobutane collisional deactivation of acetaldehyde temp., pressure and excitation wavelength effect on photoluminescence 3-46313
- isomers of alkenes, alkylcycloalkanes, alkylcycloalkanol etc., C-chemical shift, conformational stability 3-71586
- isopropyl alcohol far i.r. spectra, torsional transitions 3-63457
- N-isopropyl carbazole, fluorescence quenching by aromatic and nonaromatic acids 3-76479
- 2',3'-isopropylideneadenosine, mol. interaction in soln., deuterium substitution effect on proton relax. times 3-75899
- isoquinoline, triplet-triplet absorpt. spectra 3-67803
- isoquinoline vapour, electronic absorpt. spectrum assignments 3-67798
- isoquinolines, π -electron densities, Pariser-Parr-Pople calc. 3-74957
- izoegenol in various solvents relative scintillation yield and radioluminescence (*German*) 3-64703
- kerosene u.s. beam edge effect 3-46679
- ketones, aromatic, quenching of triplet state by O_2 in liq. soln. 3-76482
- ketones, polyfluorinated, valency vibration absorption bands, carbonyl groups (*Russian*) 3-71530
- ketones, sensitised luminescence of Eu^{3+} , photochemical reactions 3-65109
- ketones in solution, triplet state, charge transfer rel. to quenching by aromatic molecules 3-69474
- lamellar potassium oleate- D_2O membrane bilayers, n.m.r. free induction decay, spin echoes 3-45258
- lanthanum ethyl sulphate, hyperfine interaction of ^{166}Er , γ - γ directional correl. obs. (*French*) 3-47179
- lanthanum ethyl sulphate, paramag. relax. rates of Pr^{3+} 3-50450
- laser dyes, continuous u.v.-photobleaching, quantum efficiencies 3-66834
- light hydrocarbons, sources, sinks and conc. in Gulf of Mexico 3-73273
- linurone-desmethylinurone mixture, quantitative absorption spectra anal., linear and convex programming 3-51763
- lipids, separated, chromatography, letter copying machines, secondary standards 3-70481
- liquid, thermal conductivity, nomogram method 3-72237
- liquid, u.v. region characts., dispersion curves (*Russian*) 3-64688
- liquid crystal, nematic, MPT, refr. indices, temp. depend. (*French*) 3-41526
- liquid crystalline cholesteryl esters, odd even effect 3-63949
- liquid fuel films, explosion in gas containers (*Russian*) 3-69446
- liquid mixtures steady state of gravitational thermal diffusion columns (*French*) 3-41035
- liquid scintillator in neutron detector, operational effectiveness calc. using Monte Carlo program (*German*) 3-59645

organic compounds continued

- liquid thin films, optical waveguides, molecular excitation techniques (*German*) 3-64752
 liquids, Brillouin scattering, thermal waves velocities determ. 3-61042
 liquids, CO₂ diffusivity at 25° and 50°C 3-79511
 liquids, transverse relaxation rates, measurement errors 3-79935
 liquids, u.s. absorption, amplitude coefficient, 10 MHz to 3 GHz, vibrational relaxation mechanism 3-58084
 lithium acetate Brillouin scattering measurement of photoelastic constants 3-68309
 lithium ammonium tartrate, sp. ht. anomaly near transition temp. 3-47221
 lithium formate crystals, refractive indices measurement, 0.35 to 1.5 micron, Sellmeier relation 3-40285
 lithium maleate dihydrate, crystal structure determ. with counter-measured X-ray intensities 3-68239
 lithium salicylate and citrate, aqueous and non-aqueous solns., Bachem's relation validity 3-69490
 lithium salicylate and citrate, aqueous and nonaqueous solns., u.s. vel., molar sound vel., adiabatic compressibility 3-69491
 lithium stearate spin-lattice relaxation n.m.r. measurements, saturation effects, polycrystalline, room temp. 3-58437
 lubricating oil, atomic absorption spectroscopy, trace metal determ., evaluation of carbon-rod atomiser 3-70485
 magnesium diethyl phosphate, structure, X-ray diffraction method 3-54951
 magnesium phthalocyanine, transition from aggregate to monomer state, spectral study 3-52753
 maleic acid, monoalkyl esters, hydrogen bonding, i.r. spectra conformations 3-63468
 maleic acid proton multiple pulse spectra, nuclear magnetic shielding anisotropies 3-79930
 malonic acid, irradiated single crystals, ELDOR study, nuclear spin exchange influence 3-53326
 malonic acid, proton multiple pulse spectra, nuclear magnetic shielding anisotropies 3-79930
 malononitrile, cryst. struct. at 25°C 3-54953
 malononitrile, mol. packing from Raman spectra 3-75521
 manganese formate, Mossbauer, investigation of cation positions in iron formate mixture (*German*) 3-79967
 MBBA, i.r. spectra, 2 crystallographic modifications 3-79226
 MBBA, nematic, i.r. absorpt. spectra, dynamic scatt. mode 3-64649
 MBBA, nematic, u.s. vel., density, order parameter 3-68338
 MBBA, nematic isotropic, soln. phase, intermol. modes from far i.r. spectra 3-53092
 MBBA, nematic liquid crystal, mean velocity measurements of electrodynamic flow 3-40845
 MBBA, nematic-isotropic (solid) transitions, X-ray halo scatt. obs. 3-79230
 MBBA, nematic-isotropic transition temp. depend. of mag. props. (*French*) 3-64474
 MBBA, Raman spectra of anisotropic liqs. (*French*) 3-50567
 MBBA, rotational correlation times by dielectric relaxation, i.r. line broadening, neutron scattering 3-68156
 MBBA α -hydroxy substituted liq. crystals., props. and synthesis 3-54922
 mercaptabenzthiazole, electrical conductivity meas. 3-58257
 mercaptan stabilisers, effect on blue luminescence of AgCl emulsions, colour photographic film (*Russian*) 3-47596
 mercaptan-type inhibitors, photographic development inhibition, latent-image bleaching 3-47589
 merocyanine solid dye, luminescence mechanism 3-53141
 mesospheric, photochemical model with vertical transport 3-73316
 metal-hexahalo species, (C₂H₅)₂NMX₆, M=Ti, Zr, Hf, Nb, Ta, X=Cl, Br force constants and mean amplitudes of vibration calc. 3-60436
 metallocenes, paramagnetic, ¹³C spin density distrib., pulse Fourier transform n.m.r. 3-75906
 methanol, dye laser, radiationless internal conversion rate meas. 3-78032
 methane, 3 ν_3 absorption band at 1.1 μ 3-71549
 methane, 3 ν_3 absorption band in Saturn's atmospheric spectra, rotational temp. and abundance 3-47913
 methane, ¹²CH₄, ν_3 band, spectral parameters (*French*) 3-57653
 methane, ¹²CH₄, hyperfine splittings in rot. F₁, F₂ levels of ground vibr. state 3-63401
 methane, ¹³C n.m.r., mag. shielding consts. calc. by Gaussian function 3-71593
 methane, ν_3 band of absorpt. spectrum from 2863-3132 cm⁻¹ (*French*) 3-49461
 methane, abundance in Titan's atm. 3-53618
 methane, analysis of the ν_3 band up to J'=12 3-40632
 methane, at low reduced temps., second and third virial coeffs. meas. 3-54788
 methane, atm. sources and sinks, conference (St. Petersburg, USA, 15-17 Aug. 1972) 3-73181
 methane, atomic X-ray photoemission cross-section modulation 3-44012
 methane, bideuterated, vibr.-rot. band ν_3 of 8 μ m line (*French*) 3-57652
 methane, binary mixtures with CD₄, CF₄, diffusion and thermal diffusion coeffs., mag. field effects, model calcs. 3-54789
 methane, CHD₃, Fermi resonance effects in CH₃ and CD₃ stretching regions 3-57643
 methane, collisions, excitation transfer rates in Cs, rotational effects 3-78516
 methane, collisions with H⁺, H₂⁺ and He⁺, K-shell X-ray emission and ionisation cross sections 3-46334
 methane, density localised mol. orbital calcs. 3-71501
 methane, deuterated, in inert liquids, rotational relaxation, i.r. spectra 3-78769
 methane, diffusion in moderator graphite rel. to manufacture conditions (*German*) 3-71272
 methane, equation of state, thermodynamic props., 0-225°C 3-67894
 methane, expt. obs. of second phase transition at 9.9 K 3-60793
 methane, fluoro-chloro derivatives, vacuum u.v. and photoelectron spectra, ionisation pots. 3-40617

organic compounds continued

- methane, force constants, kinematical evaluation 3-74969
 methane, force consts., from three term pot. energy function 3-72170
 methane, ground state energies and bond distances, stat. OCE calcs. (*German*) 3-67745
 methane, halide derivatives, bond rupture energies 3-78686
 methane, hot atom reactions with T, stochastic and analytical investigation 3-63114
 methane, hyperfine structure of vibration-rotation line, using laser saturated absorption 3-43456
 methane, in gaseous and liquid mixtures, i.r. band shapes and semi-classical rot. diffusion model 3-54681
 methane, induced Raman scatt. under cavity excitation, spectral width and line struct. 3-59895
 methane, intermolecular potential as effective cross section 3-71654
 methane, ion-molecule reactions with H₂O, H₂S and NH₃, resonant cyclotron ejection 3-73118
 methane, i.r.-r.f. double reson. study of pure rot. Q-branch transition 3-63405
 methane, J values determ. for $\nu_2 + \nu_3$ and $\nu_3 + \nu_4$ bands 3-40631
 methane, Lamb dip associated with measurements of freq. shifts 3.39 μ m Ne transition 3-78421
 methane, line strength meas. of ν_3 band 3-71554
 methane, mesospheric and stratospheric vertical distrib., model 3-73315
 methane, microwave spectrum, ground vibronic state, rot. transitions 3-75052
 methane, microwave-i.r. double resonance using 3.39 μ He-Ne laser line 3-43481
 methane, molecular beam scattering of Ar⁺, elastic differential cross-section 3-75142
 methane, molecule, electron impact, dissociative excitation, cross section meas. 3-75119
 methane, molecule, electron impact excitation, emission spectra 3-75122
 methane, molecule, NDDO calculations 3-52312
 methane, N₂, Ar ternary and binary systems, liquid-vapour equilibria at 112.00K, Gibbs free energy calc. 3-58120
 methane, nonlinear absorpt., He-Ne laser freq. stabilisation applic. 3-62706
 methane, one-centre HF calculations on ground and excited states 3-71509
 methane, pulsed microwave breakdown, with low degree of ionisation 3-57956
 methane, reforming using steam from high temperature reactor, pilot study (*German*) 3-69495
 methane, second-order props. calc. with virtual orbitals 3-54617
 methane, semi-empirical effective pair correl. parameters and correl. energies 3-54624
 methane, solid, cryst., band structure calc. in linear combination of mol. orbitals approx. 3-44013
 methane, solid, heavy and mixed crystals., i.r. absorpt. 3-72639
 methane, solid, plastic deform. mechanism and fracture behaviour (*Russian*) 3-79412
 methane, solid, spin conversion, proton magnetisation, spin-lattice relaxation 3-75903
 methane, solid, u.s. vel., mol. orientation and lambda anomaly 3-55031
 methane, solid deuterated, orientational order parameter 3-46694
 methane, temp. depend. of half widths of some self- and some foreign-gas-broadened lines 3-67836
 methane, theory of absolute intensities for vibration-rotation transitions 3-67820
 methane, tropospheric and stratospheric mixing ratio vertical profiles 3-73306
 methane, tropospheric photochemical model for methane removal 3-73311
 methane, valence electron binding energies and momentum space wave functions 3-74945
 methane, viscomagnetic effect, temp. depend. 3-52420
 methane, X-ray emission, K-shell ionisation by H⁺ and He⁺ impact 3-78606
 methane + methyl cation, ion-molecule crossed beam reaction, short-lived intermediate, scrambling, dissociation 3-73119
 methane + N₂ + inert gases crystals, heats of fusion calc. 3-73171
 methane + tritium hot atom reactions, energy-dependent cross sections 3-44737
 methane 3 ν_3 band obs. in 12000-4000 cm⁻¹ spectra of Jupiter 3-47899
 methane + H₂ elastic scatt., crossed beam expts., central-field pots. 3-54753
 methane absorption cross sections from 180 to 700 μ 3-67805
 methane and CD₄, threshold electron-photoion coincidence mass spectrometric study 3-43499
 methane and CH₃⁺, ten-electron hydride, ground state calc., field form of perturbation theory 3-71521
 methane and H₂ binary mixture, mutual diffusion const. meas. by spontaneous light scattering 3-54790
 methane atmospheric concentration over Pacific and Ross Sea 3-69589
 methane atom collisions with H atoms in energy range 80-2000 eV, H-production 3-46211
 methane charge transfer collisions with CO and CO₂ 3-75133
 methane collisional deactivation of HBr in (V=1) state 3-71624
 methane collisions with CO₂, vibrational relaxation 3-54752
 methane collisions with Cs atoms inducing fine structure transitions, rotational effects 3-67695
 methane conc. in ice samples indicating ancient atm. comp. 3-73313
 methane concs. in marine environments 3-73274
 methane derivative, CHFClBr, optical rot. calc. using polarisability theory 3-41493
 methane dissolved in southern ocean, surface seawater meas. 3-53451
 methane gas, desorption from quartz substrate by surface acoustic waves 3-50079
 methane gas, transport and equilibrium props., utility of m-6-8 potential function 3-60512
 methane pressure-broadened lines in Jupiter's atmosphere 3-47914

organic compounds continued

- methane selenol, μ -wave spectrum, internal rot. barrier, struct. and dipole moment meas. 3-54700
- methane spectral line Doppler broadening, band absorbance formula-tion in planetary atmospheres 3-52375
- methane sulfonyl chloride, mol. struct., electron diffraction study 3-74916
- methane thermal conductivity, Senftleben-Beenakker effect 3-71705
- methane-air mixture, ignition, critical duration of discharge (*Rus-sian*) 3-79186
- methane-Ar system, h.p. vapour-liquid equilibrium and activity coeffs. 3-64156
- methane-CO₂ gas mixture, vibrational relaxation, u.s. velocity measurements 3-57680
- methane-CO system, h.p. vapour-liquid equilibrium and activity coeffs. 3-64156
- methane-CO-CO₂ mixture, radiolytic oxidation of graphite moderator blocks, diffusion effects (*German*) 3-71273
- methane-formaldehyde-air mixture flames, propagation limits, Le-Chatelier rule deviations (*Russian*) 3-80529
- methane-N₂ (Ar), heats of mixing calc. by corresponding-states theory of mixtures 3-49524
- methane-N₂-Ar system, vapour-liquid equilibrium (*French*) 3-64145
- methane-Ne gas mixture, viscosity and nonpolar-polar molecular inte-ractions 3-60515
- methane-PCl₃-H₂ mixture, P,C codeposition 3-69376
- methane-propane gaseous mixtures, Van der Waals type eqn. for enthalpy departure 3-63608
- methane-stabilised laser, frequency shifts with laser power, temp. and press. of gas 3-78014
- methanes, deuterated, rare gas collision induced dissoc. (*French*) 3-71635
- methanes, halogen-substituted, second virial coeffs. and force consts. recalculation 3-40600
- methanes, halogenated, ¹⁸F substitution reactions, substituent effects and stereochem. mechanisms 3-76420
- methanes, solid isotopic, optical birefringence in lowest temp. phase 3-50556
- methanes, substituted, Raman spectra in liquid and gaseous states (*Russian*) 3-63475
- methanethiol + H* hot atom reactions 3-76485
- methanol, disordered hydrogen-bonded crystal, dynamics and struc-ture 3-68367
- methanol, hyperfine struct. in internal rotor molecules 3-78817
- methanol, limit of superheat 3-75612
- methanol, liq., mol. motion from n.m.r. and neutron scatt. obs. 3-68875
- methanol, liquid, ¹³C nuclear magnetic relaxation mechanism 3-44345
- methanol, liquid, hydrogen bonded, association and assignment of OH overtones 3-75023
- methanol, OH stretch, 3430 to 3940 cm⁻¹, torsional level transitions 3-78780
- methanol, solvent for aromatic molecules, effect on excited states 3-60473
- methanol, uncoupled pulsed Fourier transform ¹³C n.m.r. spectra 3-75085
- methanol, vacuum-u.v. photolysis, i.r. spectrum of CH₂OH radical 3-65105
- methanol + carbon disulphide liq. sytem, crit. region thermal expan-sion 3-68384
- methanol + heptane liq. system, crit. behaviour of sp. ht. and coexis-tence curve 3-68383
- methanol and methanol-d, ionisation and dissociation by electron impact 3-43496
- methanol n.m.r. consts., neutron spectra, molecular motion 3-68877
- methoxide ion tautomer, topomerization, tautomerization, gauche effect 3-78650
- n-p-methoxy-benzylidene-p-butylaniline liquid crystal, nematic, dis-tortion patterns in electric fields 3-60662
- p-methoxy-p'-n-butylaxoxybenzene, liquid cryst., i.r. circular and linear dichroism 3-43749
- p-methoxyacetophenone in soln., triplet-singlet energy transfer to 9,10-dibromoanthracene 3-76088
- n-methoxyacetophenone, in organic solvents emissive and non emissive transfer, heavy ions influence (*Russian*) 3-44469
- methoxylamine, reversion of genetic alterations, X-irradiation, Neu-rospora crassa 3-48262
- 2-methoxytetrahydropyran, anomeric effect 3-60417
- N-methyl acetamide crystal, molecular packing 3-43762
- methyl alcohol, adsorption on SiO₂, anomalous sites characterisation 3-68489
- methyl alcohol, internal rotation barriers rel. to localized charge dis-tributions 3-54633
- methyl alcohol, ion-polar mol. collision theory, reaction kinetic energy depend. 3-46338
- methyl alcohol waveguide laser in far i.r., CO₂ laser pumping 3-66850
- methyl allenyl sulphide gas electron diffraction study of molecular struct. 3-54610
- methyl ammonium iron chloride, crit. point exponents and mag. susceptibility, Ising antiferromagnet 3-50352
- methyl anion, inversion pot. surface, HF represent., augmented basis set 3-74910
- methyl bromide, i.r. spectra, 2 ν_2 band near 2600 cm⁻¹, rot. fine struct. 3-63454
- methyl bromide-n-hexane solutions, γ -irradiated, electron scavenging, external electric field effect 3-80560
- methyl chloride, Cl quadrupole coupling, variation of strength with isotopic substitution 3-49475
- methyl chloride adsorbed on NaCl and KCl, microwave absorption and potential barrier to orientation 3-72265
- methyl chloride gas mixtures with Ne, Ar, Kr and Xe, viscosity and nonpolar-polar molecular interactions 3-60515
- methyl chloride-d₂, i.r. spectra, geom. of methyl chloride 3-63455
- methyl chloroformate, microwave spectra, internal rot. barrier, mol. structure 3-75050

organic compounds continued

- methyl cyclohexane-benzene, -toluene, binary systems, isobaric vapour-liquid equilibrium data, prediction method 3-72186
- methyl cyclopentane-benzene, -toluene, binary systems, isobaric vapour-liquid equilibrium data, prediction method 3-72186
- methyl fluoride, 496 μ m intense superradiant emission, CO₂ laser pumped 3-53127
- methyl fluoride, gas laser, 30 kW peak, 496 micron characts., CO₂ TEA laser pumping 3-78020
- methyl fluoride, rot.-vibr. spectrum, 2000-2100 cm⁻¹ 3-63463
- methyl fluoride, Stark effect of transitions of ν_3 band (*French*) 3-46271
- methyl fluoride + T hot atom reactions, substitution processes 3-44738
- methyl formate, methyl fluoroformate, INDO calcs. of dipole moment and conformation 3-63369
- methyl group, group theory of nuclear magnetic relaxation 3-64575
- methyl group, weakly hindered, tunnelling rotation rate, e.p.r. and ENDOR meas. 3-47125
- methyl iodide, and deuterated cpd., liq., reorientational motion temp. depend., Raman spectra obs. 3-64667
- methyl iodide, Fermi and Coriolis resonances with $\nu_3 + \nu_6$ and ν_2 , ν_5 detailed analysis 3-71550
- methyl iodide, liq., rot. diffusion, Raman and n.m.r. spin relax. obs. 3-75976
- methyl iodide, liquid, collective excitation of mol. vibs., Raman spec-tra obs. 3-64668
- methyl iodide, liquid, mol. motion, depolarised Rayleigh scatt. obs. 3-79223
- methyl iodide, liquid, mol. motions and interactions, temp. dependent Raman study 3-47248
- methyl iodide, liquid, molecular vibration excitons, Raman band profiles (*German*) 3-53113
- methyl iodide, liquid, reorientational motions from press. depend. Rayleigh scatt. 3-80055
- methyl iodide, Raman scattering, orientational motions 3-43445
- methyl iodide, Raman scattering, vibrational correlation 3-43444
- methyl iodide, Raman vibrational line shapes, reorientational correla-tion functions, appl. to nuclear quadrupole coupling constants 3-46274
- methyl iodide and CD₃T, liquid, Raman line-shapes, rotation and vibration analysis 3-41509
- methyl iodide in solid and liquid Kr, Wannier states study by vacuum u.v. spectra 3-47294
- methyl malonic acid: free radicals, e.s.r. and ENDOR measurements, tunnelling rotation 3-55503
- methyl mercury associated deafness, ototoxic effect 3-48229
- methyl methacrylate, α NPO excimer formation, thermodynamic properties, solvent effect 3-80584
- 3-methyl pentene-2 isomers config. assignment, mol. struct., elec-tron diff. 3-63360
- methyl substituted aromatic radical ions, proton spin relax., CH₃ line-width 3-63517
- 1-methyl uracil single crystal, irradiation induced formation of radical pairs, e.s.r. obs. 3-69473
- methyl vinyl sulphide gas electron diffraction study of molecular struct. 3-54610
- 2-methyl-1,3-dioxolane solid liquid gas, infrared, Raman spectra 3-54692
- 2-methyl-butane and 2,3-dimethyl-butane, isomerism, Raman spectra 3-78793
- N-methyl-d₃-P,P,P-trimethylphosphine imide, vibr. spectra, struct. of P-N bond 3-75024
- N-methyl-ethylidenimine isotopes, matrix and gas, i.r. spectra, 4000-200 cm⁻¹ 3-78807
- N-methyl-N'-nitro-N-nitrosoguanidine, reversion of genetic altera-tions, X-irradiation, Neurospora crassa 3-48262
- methyl-substituted benzyl, triphenylmethyl and diphenylmethyl radi-cals, fluoresc. lifetimes 3-47571
- N-methylacetamide, mol. fragment, polypeptide systems, procedure to examine large mol., appl. to polypeptide characterisation 3-46360
- 9-methyladenine. 1-methylthymine complex, hydrogen bonding, struct. determ. by neutron diffraction 3-64022
- methylamine, internal rotation barriers rel. to localized charge distribu-tions 3-54633
- methylamine, laboratory microwave spectra 3-43458
- methylamine chloride, internal rot. and inversion doubling in micro-wave spectrum 3-67829
- methylamines, liquid, self-diffusion coeffs., n.m.r. obs. 3-68874
- methylaminoethane, rot.-inversion spectrum analysis 3-63491
- methylammonium alum, Ti³⁺ Orbach relax. rate anisotropy, dynamic Jahn-Teller effect 3-75877
- 9-methylanthracene, n-hexane soln., photodimerization and fluorescence rates, press. depend. 3-69476
- N-methylazoles, proton n.m.r., aryl substituent chemical shifts 3-75066
- methylbenzenes, phosphorescence lifetimes 3-80105
- methylbromide, mol. reorientation, Raman spectral obs. 3-64666
- N-methylcarbamoylhalogens, i.r. and Raman spectra, 150 to 4000 cm⁻¹, vibr. assignments (*German*) 3-47270
- methylchloride, and isoelectronic series, SCF-MO calcs. 3-60409
- methylchlorosilanes, L_{II-III} X-ray absorpt., electronic struct. calcs. 3-78671
- methylcyclohexane, solvent for aromatic molecules, effects on excited states 3-60473
- methylcyclohexane matrix, quasiline phosphoresc. spectra of benzene homologues and derivatives 3-72741
- methylcyclohexanol matrix, quasiline phosphoresc. spectra of benzene homologues and derivatives 3-72741
- methylcyclopentane solid liquid gas, infrared, Raman spectra 3-54692
- methylene, spin dipole-dipole parameters, ab initio calcs. 3-74939
- methylene blue, photoquenching, depend. of quantum yield on pulse intensity and duration 3-67840
- methylene blue-sodium lauryl sulphate solutions, luminescent life-times (*Russian*) 3-72719
- methylene chloride mixtures with toluene, benzene and xylenes, dielectric polarisation, n.m.r., u.v. and i.r. studies 3-58817
- methylene cyclobutadienyl radical, valence bond and mol. orbital calcs., convergence comparison 3-43401

organic compounds continued

- methylene fluoride, vibration-rotation spectra, mol. force field, deuteration effect 3-78761
- methylene iodide-decalin mixtures, wetting of polyethylene 3-43927
- 3-methylene oxetane, μ -wave spectrum, mol. Zeeman effect, mag. susceptibility anisotropy, quadrupole moment meas. 3-52372
- methylene thiocyanate, i.r. absorpt. spectra, 2 to 20 μ , point group C_{2v} conformation (*French*) 3-47273
- exo-methylenecycloalkanes, ^{13}C - ^{13}C coupling consts. and chem. shifts 3-75080
- methyleneiodide, wetting of polyethylene 3-43927
- methyleneimine, microwave spectra, molecular constants 3-75051
- methylfluoride, vibr. corrections of dipolar couplings 3-78700
- 3-methylhexane glass, energy level structure of trapped electrons from photoconductivity and bleaching meas. 3-64370
- 1-methylnaphthalene, in soln., effects of environment on excited states 3-60473
- 1-methylnaphthalene, non-radiative energy transfer to substituted oxazoles and oxadiazoles (*Russian*) 3-63510
- 1-,2-methylnaphthalene, vapour phase near u.v. absorpt. spectra assignments 3-67796
- N-methylpropionamide and N-deuterated N-methylpropionamide, normal coord. anal. 3-67774
- 3-methylpyridazine, asymmetric signal of terminal ring CH_3 group, origin 3-75088
- 4-methylpyridine hydrogen bonded complexes with quinoline, ethyl- and chloro-pyridines, vibrational spectra 3-75029
- methylquinoline, 2-, 4-, 6-, 7-, 8-, in crystalline n-paraffins, quasi-linear phosphorescence spectra, vibrational 3-50609
- methylsilylchlorides, i.r. and Raman spectra, vibr. assignments and torsional barrier heights 3-54680
- methylsulphonyl fluoride, chloride, and bromide, vibrational spectra and assignment (*German*) 3-43424
- 2-methyltetrahydrofuran glass, γ -irradiated, ELDOR study of trapped electrons mag. energy transfer between two different spin systems 3-44727
- 2-methyltetrahydrofuran solid liquid gas, infrared, Raman spectra 3-54692
- N-methylthiopropionamide, and N-deuterated analogue, i.r. and Raman spectra 3-49464
- 1-methylthymine, i.r. spectra, hydrogen bond behaviour, freq. and intensity distrib. 3-55574
- 4-methylumbelliferone, dye laser fluoresc., excited state structs. 3-78034
- 4-methylumbelliferone, spontaneous and stimulated emission 3-76064
- 4-methylumbelliferone and tautomer, extended Huckel molecule orbital calc. 3-52309
- 4-methylumbelliferone laser dye emission characts. 3-51927
- methylurea, ^{14}N n.q.r. at 77K and 296K 3-55500
- methyloxocarbenium ion trimer, geometry, CNDO/BW calc. 3-67726
- microdetermination, N, C and H, semiautomatic app., purification of O_2 3-48651
- molecular crystal, external, internal and semi-internal vibrs., spectroscopic identification criteria 3-79442
- molecular crystal, rigid hydrocarbons, lattice dynamics 3-46682
- molecular crystals, spin lattice relax. in localised triplet states, anisotropy and temp. depend. 3-75917
- monochloroamine, rotation-inversion transitions in microwave spectrum, inversion barrier of amine group 3-40639
- monoethanolamine PVA in solution, thermoelasticity, gels 3-63601
- monofluoroacetamide irradiated cryst., ELDOR 3-55972
- monofluorobenzene, electronic struct. and geom., CNDO-CI calcs. for ground and excited states 3-60423
- monosaccharides, amorphous, n.m.r. relaxation, electrical conductivity, viscosity, temp. depend. 3-79940
- N-methylacetamide, complex dielectric constant -185 to 20°C, 50 Hz to 3 MHz 3-60796
- n-pentane drop, effect of chemical kinetics on combustion (*French*) 3-76444
- naphthacene, in n-paraffin matrices, luminesc., cooling rate effects 3-72730
- naphthacene crystals, photoelectron spectroscopy by rare gas emission lines 3-47347
- naphthalamide, luminescence spectra (*Russian*) 3-44466
- naphthalene: dinaphthylethylene (:dibiphenylethylene) (:diphenylbutadiene), emission spectra 3-69090
- naphthalene, α -bromo- and β -chloro-, vibr. spectra and depolarisation ratio 3-52367
- naphthalene, adsorption on Pr(111) and Pt(100) surfaces, Leed and work function investigation 3-55127
- naphthalene, anharmonicity of lattice vibr. and lifetime of optical phonons 3-72644
- naphthalene, arylethylene doped, vibronic spectrum phonon struct. 3-68357
- naphthalene, Bridgman growth, reaction of foreign particles with crystn. front 3-75492
- naphthalene, C_p - C_v , calc. using temp. depend. of lattice freq. (*Russian*) 3-50007
- naphthalene, disordered mol. cryst., vibr. spectra, Davydov splittings 3-72637
- naphthalene, doped with naphthalene- β -substitutes, energy migration, temp. depend. 3-76092
- naphthalene, double space charge determ. method 3-75941
- naphthalene, elec. cond. in melting region (*Russian*) 3-44068
- naphthalene, emission spectra, exciton-phonon interactions 3-69071
- naphthalene, e.p.r. and optical absorpt. obs. of radiation-induced radicals 3-55473
- naphthalene, exciton-phonon interaction, conservation laws, molecular crystal spectra 3-68972
- naphthalene, for liquid scintillators 3-48526
- naphthalene, host crystal effects on phosphoresc. spectra 3-69073
- naphthalene, molecular crystals, press. depend. of lattice freqs. 3-75585
- naphthalene, phonon sidebands in $T_1 \rightarrow S_0$ transition, effect of host on localisation 3-69051
- naphthalene, phosphorescence in p-dichloro- and p-dibromobenzene, T_1 absorption, spin-orbit coupling 3-80106

organic compounds continued

- naphthalene, pyrene doped, direct and delayed emission phenomena 3-55672
- naphthalene, reson. interaction in vibronic spectra of local excitons 3-68970
- naphthalene, single crystal, limitation on injected space charge deep trapping 3-64328
- naphthalene, space-charge-limited currents and trap distrib. 3-52849
- naphthalene, triplet-triplet absorption spectrum, polarisation, meas., substitution effects 3-46257
- naphthalene, with tetracene, rubrene surface states, mag. quenching of fluoresc. 3-72724
- naphthalene crystal, anomalous exciton splitting in 3000 cm^{-1} region vibrational spectrum 3-64657
- naphthalene crystal, luminescence spectra, surface effects, exciton states 3-44483
- naphthalene crystals, γ -irrad., polarised absorpt. (*French*) 3-65093
- naphthalene Franck-Condon factors, correl. function anal. T_1 - S_0 transitions 3-64709
- naphthalene ion in low bulk dielec. const. media, e.s.r. linewidth studies 3-44314
- naphthalene mol. crystals, calc. of temp. dependence of thermal expansion coeff. using quasi-harmonic model (*Russian*) 3-68368
- naphthalene mol. struct. determ. by n.m.r. in a nematic solvent 3-74919
- naphthalene ring system containing cpds., photoemission in vacuum u.v. region 3-41613
- naphthalene single crystals, local electric field and dielectric tensor 3-72566
- naphthalene-anthracene sandwich pair, absorption and exciplex fluorescence spectra 3-47579
- α - and β -naphthalene- d_1 , excited state H-D exchange and fluorescence quenching 3-69475
- naphthalene-hs, triplet-triplet absorpt. absence in pure crystals. 3-61048
- naphthalene-perdeuterated naphthalene mixed crystals, fluoresc., energy transfer via guest excitons 3-53137
- naphthalenes, monosubstituted, electronic absorpt. spectra interpret. by config. analysis 3-67754
- naphthalenes, substituted, electronic systems, rot. band contour anal. 3-57641
- naphthalic anhydride and heterylsubstitutes, luminescence spectra (*Russian*) 3-44466
- 2-naphthol, lifetime and time-resolved fluorescence meas. with ACO synchrotron radiation 3-40651
- 2-naphthol and hydrogen bonded complex with esters, fluorescence quenching mechanism 3-52383
- β -naphthol excited systems, primary processes, pulsed laser photolysis study 3-73156
- 2-naphthol in water, mass transfer coeffs., fixed bed, cylindrical and oval-shaped pellets 3-79047
- naphthols and naphtholate anions, correspondence of fluorescing states, effect on calc. of pK_a from spectral shifts 3-54714
- 1,8-naphthylene-1,2'-benzimidazole solutions, role of triplet states (*Russian*) 3-61276
- naphthoylinbenzimidazole, luminescence spectra (*Russian*) 3-44466
- naphthyridine, symmetric, electronic density, ^{13}C n.m.r. spectra 3-71581
- 2-naphthyl acetate, intramolecular energy transfer, upper triplet states 3-69079
- 2-naphthyl-isobutyric ester intramolecular energy transfer, upper triplet states 3-69079
- 1-naphthylacetic acid, intramolecular energy transfer, upper triplet states 3-69079
- 1,6- and 1,8-naphthyridine, assignments of fundamental vibrs. 3-63458
- 1,5-naphthyridine in durene, polarized phosphoresc., assignment of lowest singlet n, π^* state 3-76472
- 1,5-naphthyridine in durene mixed cryst. spectra, isotope effect on localized phonons 3-58542
- neodymium acetate hydrates, cryst. growth and lattice parameters 3-60719
- neodymium benzoylacetate complex in soln., spectral studies (*Russian*) 3-50559
- neopentane, dielectric constant, solid state transition, density, 500 atm. 3-68910
- neopentane plastic crystal, i.r. and Raman band shape analysis, mol. reorientation 3-75983
- neutron diffusion, thermal using static method 3-63106
- nickel anhydrous acetates, struct. 3-40908
- nickel formate, Mossbauer investigation of cation positions in iron formate mixture (*German*) 3-79967
- nitrate esters, lower electronic states, CNDO config. interaction calcs. 3-49435
- nitride systems, calculation of one electron properties of CN^- ion 3-52327
- 4-nitrile-benzilidene-p-N-octyloxyaniline, smectic-A to nematic transition, second order, orientational order 3-54925
- p-nitrobenzylidene-p-octyloxyaniline, second order nematic to smectic phase transition 3-58507
- 5-nitro-6-methyluracil, electron irradiated, e.s.r. study of free radical formation 3-41852
- nitroalkanes, chemical shift, for N, O, n.m.r. calcs. 3-63521
- O-nitroaniline, electrical conductivity meas. 3-58257
- o-nitroanisole, liquid, optical Kerr effect, birefringence changes 3-58490
- nitrobenzene, π -, σ -electronic struct., conversion in ground state, CNDO/2 calcs. (*Russian*) 3-78678
- nitrobenzene, electric field behaviour rel. to Kerr cell 3-47229
- nitrobenzene, fluorescence quenching of p-2,5-phenyl-oxazolyl-benzene (*German*) 3-43474
- nitrobenzene, thermo-electret state, form. processes 3-72568
- nitrobenzene, u.v. spectra analysis, computational method (*German*) 3-46266
- nitrobenzene solns., high elec. field induced radicals identification 3-50858
- nitrobenzene-n-nonane system, u.s. absorption near critical region 3-49941

organic compounds continued

- nitrobenzene/2,2,4-trimethyl pentane binary solution, critical soln. temp., dielec. consts. and losses 3-44364
 nitrobenzole emulsion, u.s. wave absorption and scattering, impulsion method (*Russian*) 3-50796
 nitrocellulose, membrane intracavity tuning element for dye laser 3-54227
 nitroethane isooctane, critical liquid mixture, Mandelshtam-Brillouin spectra 3-80040
 nitroethane-3-methylpentane mixture, shear dependence of the viscosity in the critical region 3-41039
 nitroethylene, isotopic species, microwave spectra, ground and excited vibrational states 3-78812
 nitroethylene, torsion of nitro group, pot. parameters 3-63399
 nitrogenase active centre, energy transfer, e.s.r. for struct. determ. 3-67871
 nitroglycerine powder in CO₂ and Ar, pulse calorimetry, reaction kinetics (*Russian*) 3-45432
 nitromethane, lower electronic states, CNDO config. interaction calcs. 3-49435
 nitromethane, rotational Zeeman effect (*German*) 3-43432
 2-nitrophenol, microwave spectrum, struct. of hydrogen bond 3-40638
 nitrophenols, isomeric, i.r. absorption spectra, vibrational assignments 3-78760
 2-nitropropane, dispersion of dielec. const. and dipole moment 3-55997
 4-nitroquinoline 1-oxide, carcinogen HeLa S3 u.v. sensitive cells, repair of DNA damage 3-48168
 nitrosomethane, SCF-LCAO-MO calculations on the rotational barrier 3-43391
 o-nitrotoluene, π -, σ -electronic struct., conversion in ground state, CNDO/2 calcs. (*Russian*) 3-78678
 nitrotoluene, o-, m-type, liquid, optical Kerr effect, birefringence changes 3-58490
 p-nitrotoluene, reversible reduction, cyclic voltammetry, digital data acquisition system, data analysis 3-70445
 2,4,6-nonachloromesitylene, rotational isomerism, conformational energy, p.m.r. 3-67851
 n-nonadecane, rotator phase transition, inelastic neutron scattering study 3-49853
 n-nonane:coronene, fluoresc., doublet struct. at 77 K, isothermal exposure effects (*Russian*) 3-44475
 n-nonane, quasilinear spectra of trapped coronene, 1,12-benzoperylene and perylene, solute-solvent interactions 3-72728
 n-nonane matrices, luminesc. and excitation spectra of chlorophyll A 3-72733
 n-nonyloxybenzoic acid ethyl ether, application of optical modelling method to liquid crystal struct. determ. (*Russian*) 3-68152
 norbornadiene, plastic cryst. phase, self-diffusion, n.m.r. study 3-68438
 norbornadiene, vibrational spectra 3-72624
 norbornane, plastic cryst. phase, self-diffusion, n.m.r. study 3-68438
 norbornane, vibrational spectra 3-72624
 norbornylene, plastic cryst. phase, self-diffusion, n.m.r. study 3-68438
 n.q.r., ³⁵Cl Zeeman spectra of polycryst. cpds. 3-75911
 nuclear magnetic resonance of ¹³C, continuous wave proton spin decoupling, virtual coupling 3-71574
 nuclei acid bases, in-plane electronic spectra using all valence electron MO-Cl calcs. 3-63386
 nucleotides, 2',3'-cyclic, ¹³C and ¹H n.m.r. study of conformations 3-63570
 nucleotides, 3',5'-cyclic, ¹³C n.m.r. study of conformations 3-63569
 octadecane adsorption on Hg surface, interfacial tension meas. 3-50075
 octadecyl alcohol adsorption on Hg surface, interfacial tension meas. 3-50075
 octadecyl amine adsorption on Hg surface, interfacial tension meas. 3-50075
 n-octane, quasilinear spectra of trapped coronene, 1,12-benzoperylene and perylene, solute-solvent interactions 3-72728
 n-octane, solid, low frequency mol. vibrations by neutron inelastic scattering 3-75577
 octane, u.s. scatt., nonlinear phenomena 3-68336
 octane isomers, diffusion in He meas. by chromatographic broadening method 3-73177
 n-octane matrices, luminesc. and excitation spectra of chlorophyll A 3-72733
 n-octane matrix, absorpt. and fluoresc. of monosubstituted benzenes 3-72739
 p-n-octylhydroxybenzoic acid, smectic, domain rotation 3-75471
 octyloxybenzoic acid, paranormal, liquid crystals, domain structure orientation oscill. freq. 3-72002
 oil, effect on chemical properties of seawater 3-80710
 oil, flow measurement facilities at N.E.L., 1 May 1973 3-70506
 oil/water, drop rest times and films shapes for deformable drops 3-47484
 oil/water, mechanism of film drainage for deformable drops 3-50788
 oils, elastic behaviour during impact 3-60761
 α -olefins, i.r. spectra, intermolecular interaction, phase transition 3-72654
 α -olefins, addition reactions with alkylchlorosilanes, i.r. spectroscopic study (*Russian*) 3-80543
 olefins, liquid electron mobilities and activation energies 3-72354
 olefins, nonconjugated, vibrations, conformation, heats of hydrogenation, consistent force field calc. 3-71526
 olefins, reactions with F, unimol. decomp. of long-lived complexes 3-73122
 olefins + O reaction, direct rate meas. showing negative temp. depend. 3-65075
 olefins and radical cations, CNDO/2 calcs. of electronic props. 3-54649
 organic disulphides Raman spectra, S-S and C-S stretching regions 3-54682
 organic dye laser, harmful schlieren effects (*German*) 3-51923
 organic phosphates, dipole moments determ. 3-54637

organic compounds continued

- organic pseudohalides, and compounds containing halogen and P lone pairs, low energy photoelectron spectra interpretation 3-46256
 organic pseudohalides, high energy photoelectron spectra, interpretative methods 3-43431
 organo(seleno,telluro)phosphorus cpds., ³¹P n.m.r. obs. of ³¹P-⁷⁷Se, ³¹P-¹²⁵Te spin-spin coupling constants. 3-75087
 organo-element compounds, n.m.r. Fourier spectroscopy, chemical shift 3-72536
 organo-phosphorus compounds, EX₃ type, p- π conjugation, trivalent P, groups IV-VI, hybridisation of the at. orbital 3-71519
 organophosphorus asymmetric centres, n.m.r. Fourier transform spectroscopy 3-75894
 organophosphorus compounds, n.m.r. evidence of steric effects 3-46317
 organophosphorus cpds., spin coupling with ³¹P, exptl. determ. 3-75081
 organosilicon, ²⁹Si, ¹³C n.m.r. meas., substituent effect 3-72533
 organosilicon compounds, ¹J(¹³C-²⁹Si) spin-spin coupling const. calc. by max. overlap approx. 3-75070
 organosilicon compounds, ²⁹Si n.m.r. spectra and mol. struct. 3-71596
 organosilicon oil-talc mixture, acoustic contact material, u.s. investigations of polymers 3-73678
 organosulphur, additive character of displacements of inner atom levels 3-78684
 orthosubstituted diphenyl sulphones, n.m.r. data and conformational preferences 3-54718
 oxadiazole-1,3,4 derivatives, in aromatic solvent, non-radiative singlet-singlet energy transfer 3-76048
 1,2,5-oxadiazole and deuterated species, vibrational spectra and fundamental frequencies 3-46299
 oxalic acid, cryst., hydrogen bond vibr., i.r. and Raman spectra obs. 3-72640
 oxalic acid, proton multiple pulse spectra, nuclear magnetic shielding anisotropes 3-79930
 oxalic acid dihydrate, proton resonance spectrum, high resolution 3-47156
 oxalyl bromide gas, molecular structure, trans-gauche conformers, electron diffr. 3-74913
 oxalyl chloride, Raman spectra, study of structure of vapour phase 3-63459
 oxamides, mol. anal. phosphoresc. characts. 3-78833
 oxazole-1,3 derivatives, in aromatic solvent, non-radiative singlet-singlet energy transfer 3-76048
 3-oxetanone, μ -wave spectrum, mol. Zeeman effect, mag. susceptibility anisotropy, quadrupole moments meas. 3-52372
 oxidation by photoproduced holes in ZnO 3-41100
 oxirane, photoionis. cross sections, He I and He II photoelectron spectra 3-78857
 5-oxybenzodioxane-1,4, i.r. absorpt. bands temp. depend. in deform. vibrations region (*Russian*) 3-54694
 3-oxypiperidone-4, stereochemical structure (*Russian*) 3-71493
 3-oxytetrahydropyranone-4, stereochemical structure (*Russian*) 3-71493
 PAA, crystal, nematic, isotropic and soln. phases, intermol. modes from far i.r. spectra 3-53092
 PAA, rotational correlation times by dielectric relaxation, i.r. line broadening, neutron scattering 3-68156
 para-halostyrenes, thermodynamic functions calc. 3-52416
 para-substituted benzaldehyde, toluene soln., solute-solvent interactions, p.m.r. chemical shift obs. 3-44744
 paraffin, X-ray excitation of thermal spikes 3-43731
 n-paraffin crystals, lattice vibrs., Raman spectra 3-72641
 n-paraffin matrices, guest molecules, line spectra 3-76063
 n-paraffin matrices, local states of impurity aggregate formations 3-72738
 n-paraffin matrices, organic molecule luminesc., cooling rate effects 3-72730
 n-paraffin matrix, absorpt. and fluoresc. of naphthalene type molecules 3-72739
 n-paraffin matrix, fluoresc. and phosphoresc. emission and excitation spectra of n-ethyl-carbazole 3-72744
 paraffin matrix, phosphoresc. spectra of polyatomic molecules with non-rigid struct., low temp. 3-72731
 n-paraffin matrix, quasiline absorpt. and fluoresc. spectra of polyenes 3-72742
 n-paraffin solutions of aromatic compounds, frozen, absorption and fluorescence spectra at 77K 3-72745
 paraffinic hydrocarbons, benzene, binary systems, isobaric vapour-liquid equilibrium data, prediction method 3-72186
 paraffins, Hg(P) photosensitization, energy transfer mechanism 3-50844
 n-paraffins, i.r. spectra, intermolecular interaction, phase transition 3-72654
 pefluoro-n-hexane, solvent for aromatic molecules, effect on excited states 3-60473
 pentacene, photocarrier form. mechanism, incident light depend. 3-72381
 pentachlorobenzene compounds, dielectric absorption, molecular rotation 3-72572
 pentacyclic aromatic hydrocarbon transitions interpret., composite system approx. 3-54645
 pentaerythritol tetranitrate, U.V. absorption spectrum 3-54668
 pentaerythritol tetranitrate, glass microballoons, energy source simulation of mech. energy release, expanding vaporised Na coolant 3-74674
 pentafluorophenol-n-Cl-aniline compound, phase transformation study, Raman spectra 3-72198
 2,4,6,8,10-pentamethylundecane crystalline and glassy films, i.r. spectra and rotational isomerism 3-47268
 n-pentane:acenaphthene radical, multiplicity of the quasi-line fluoresc. spectrum 3-64716
 iso-pentane, electric field induced nucleation, bubble chamber study 3-77719
 n-pentane, solid, low frequency mol. vibrations by neutron inelastic scattering 3-75577
 n-pentane, tensile strength by acoustic cavitation 3-46476

organic compounds continued

- pentanes, 2,4-disubstituted, n.m.r. conformational analysis using local interaction model 3-71487
- pentaphene, in n-paraffin matrix, absorpt. and fluoresc. 3-72739
- peptide bond protonation, SCF ab initio study 3-43407
- peptides, INDO finite perturbation calcs. of spin-spin coupling consts. J_{H}^{PH} , $J_{15\text{NH}}$, $J_{15\text{I}^{13}\text{C}}$ 3-74952
- perbromyl fluoride, Urey-Bradley force field const. calcs., i.r. Raman data 3-78713
- perchlorodihydropentalene epsilon C_8Cl_8 , crystal structure, constitution (German) 3-75520
- perchloryl fluoride, Urey-Bradley force field const. calcs., i.r., Raman data 3-78713
- perdeuterobenzene, reaction with F, ang. depend. and recoil-energy spectrum of products 3-73123
- perdeuteronitrobenzene dissolved in benzene and CCl_4 , elec. field induced dipolar alignment 3-64565
- perfluoro-n-butane, negative ion formation by low energy electron impact 3-63546
- perfluorocarbons, ion-molecule reactions, ion cyclotron resonance mass spectrometric obs. 3-52401
- perfluorocyclopentene, i.r. and Raman spectra interpretation 3-54685
- perfluoromethylcyclohexane, dependence of radiolysis on dose, O_2 content, temp. and radiation type (German) 3-69481
- perfluoropolyether vacuum fluid, effect of ion and electron bombardment, comparison with other vacuum fluids 3-77421
- perinaphthyl free radical coherence effects on line shape in ENDOR spectrum (German) 3-57672
- perocetyl isopropyl carbonate, decomp., chem. induced nuclear polarisation, methyl radical 3-71579
- peroxylamine disulfonate dilute solns., line shape analysis for unresolved hyperfine splitting 3-75873
- perylene, electron and hole drift mobilities 3-52838
- perylene, in n-hexane and n-heptane matrices, fluoresc., phonon struct. 3-72729
- perylene, in n-paraffin matrices, quasilinear spectra, solute-solvent interactions 3-72728
- perylene, in n-paraffin matrix, absorpt. and fluoresc. 3-72739
- perylene, i.r. spectrum, out of plane vibrations 3-75040
- perylene, quantitative determ. in mixed solutions by luminescence spectroscopy (Russian) 3-62364
- perylene crystals, photoelectron spectroscopy by rare gas emission lines 3-47347
- perylene mol. solids, polariton dynamics from band profile analysis 3-72642
- perylene molecule, trapped in n-hexane matrix, secondary radiation 3-72726
- phenanthrene, effect of doping on styrene fluoresc. 3-69081
- phenanthrene, elec. cond. in melting region (Russian) 3-44068
- phenanthrene, in n-heptane and CCl_4 matrices, quasiline phosphoresc. spectra, external heavy atom effect 3-72743
- phenanthrene, i.r. absorpt. spectra near phase transition 3-55072
- phenanthrene, radical anions, ^1H and ^2D n.m.r. studies 3-43488
- phenanthrene, T, L and S tensors, calc. from cryst. forces 3-79262
- phenanthrene in triplet state e.p.r. hyperfine interactions and electron spin distribution 3-47583
- phenanthrene molecules in solid solutions, spectroscopic manifestation of ordering 3-64656
- 2-phenethyl-norborane (II), structure depend. of emission props., intramol. electron transfer 3-75061
- phenol, benzene soln., microwave absorpt., dielec. props 3-80585
- phenol, molecular rotation study by neutron scattering and n.m.r. 3-52567
- phenol, near u.v. spectrum, solvent effects and distribution in micellar solutions 3-52359
- phenol complexes with pyridines, dipole moments and struct. 3-63358
- phenol-formaldehyde resins, i.r. spectra and struct. (Russian) 3-49472
- phenol-OD, microwave and i.r. transitions analysis by rot.-internal rot. theory 3-63490
- phenols, ortho substituted, torsional frequencies and conformational equilibria 3-52310
- phenols, substituted, reactivity estimations by semiempirical MO-methods (German) 3-53314
- phenoxymethylpenicillin, i.r. vibrational spectrum, structural analysis (Russian) 3-78778
- phenyl, benzoyl- $(\text{CH}_2)_5$ -phenyl, phthalyl in n-paraffin matrices, absorption spectra, luminescence, alternation effect 3-72746
- phenyl radical, hyperfine coupling, INDO calc., σ framework 3-52316
- phenyl silane, ^{29}Si n.m.r. 3-68878
- 1-phenyl-4-(n-chlorodiphenyl)butadiene-1,3 liquid laser with prism resonator, generating characteristics (Russian) 3-57228
- n-phenyl-benzophenone, in organic solvents emissive and non emissive transfer, heavy ions influence (Russian) 3-44469
- p-2,5-phenyl-oxazolyl-benzene, fluorescence quenching by nitrobenzene (German) 3-43474
- 2-Phenylbenzothiazole in frozen solutions at 77°K high-resolved phosphorescence spectra 3-64706
- 2-Phenylbenzoxazole in frozen solutions at 77°K high-resolved phosphorescence spectra 3-64706
- phenyldichlorophosphine, electron diffraction study of molecular structure 3-78659
- p-phenylenediamine-based developer, photographic development inhibition, latent-image bleaching 3-47589
- phenylethylenes, steric inhibition of resonance studied by photoelectron spectroscopy 3-54613
- N-phenylglycine, Raman spectra between 200 and 1700 cm^{-1} , vibr. assignment 3-47241
- phenylhydroxycyclopropenone, prep. and cryst. data 3-58026
- 3-phenylsidon, solvent effect on spectrum, dipole moment determ. from first excited singlet state 3-47284
- phenylsilane, Si-phenyl ring bonding, photoelectron spectra 3-67749
- phenylsilanes, calc. of u.v. spectra, s.c.f. method 3-67808
- phosphabenzene, photoelectron spectra 3-46255
- phosphiran, i.r. spectra, normal modes, force field, barrier to inversion 3-75038

organic compounds continued

- phospholenes (I and II)-Ni(AcAc) $_2$, dispersion of ^1H - ^{31}P heteronuc. chem.-exchange spin decoupling 3-75086
- phosphonium salts, ^{31}P n.m.r. obs., electron delocalization through P rel. to d_{π} - p_{π} bonding 3-71597
- phosphoric acid chloranhydrides, unsaturated u.v. absorption spectra, intramol. interactions (Russian) 3-40609
- phosphorus compounds, cyclic, tetra-coord., calc. of ^{31}P chem. shifts 3-71600
- phosphorylated hydrocarbons, flame ionization-flame emission detector instrument, for vapours and aerosols 3-62342
- photoemission threshold law for solids 3-44521
- phthalocyanine, dissociation of Frenkel excitons, influence of vibronic coupling, photoconductivity 3-79655
- phthalic acid, proton multiple pulse spectra, nuclear magnetic shielding anisotropies 3-79930
- phthalic acids, highest occupied and lowest unoccupied mol. orbitals and total π -electronic energies, LCAO calc. 3-52318
- phthalimide derivative vapour, excited state lifetime, spectral depend. 3-63508
- phthalimide derivatives, two-photon excited fluoresc., polarisation study 3-42986
- phthalimide derivatives in alcoholic soln., fluorescence relaxation of intermolecular interaction and spectral depend. of extinction time (Russian) 3-49487
- phthalimide molecules, gas phase, lifetime of excited state under anti-Stokes excitation (Russian) 3-43469
- phthalocyanine, H_2Pc , elec. cond. mechanism and carrier trapping 3-68618
- phthalocyanine, in frozen polycryst. soln., quasiline spectra as zero-phonon lines 3-72635
- phthalocyanine solns., intersystem crossing probability calcs. 3-74281
- phthalocyanines, thin films and solutions, emission spectra 3-61074
- picolines, dielectric props. in solutions, microwave meas. 3-55999
- picryl N-amino carbazyl, solid free radical, elec. cond. and energy gap meas. 3-50200
- picryl N-amino carbazyl, static susceptibility of crystalline and recrystallised powder samples 3-58373
- picryl N-amino carbazyl, temp. depend. of spin-spin lattice relax. times 3-79898
- picryl N-amino carbazyl recrystallised free radical powder, e.s.r. absorption 3-47601
- pigment three-component agitated solutions, energy transfer (Russian) 3-41563
- pinacol and its two hydrates, i.r. spectra, principle vibrations, hydrogen bonding 3-47269
- β -pinene, electron diffraction meas. of molecular conformation 3-78660
- pinene (α and β), absorption and circular dichroism spectra 3-71545
- plivalic acid plastic crystal, Brillouin and Rayleigh scattering determ. of phonon lifetimes, elastic and optical consts. 3-44409
- plastic crystal, p.m.r., mol. self-diffusion and reorientation, press. depend. 3-61005
- plastic crystals, self-diffusion, n.m.r. study 3-68438
- γ -platinum phthalocyanine, band structure, mobility 3-79626
- polyacenes, absorpt. spectra, exciton band shape, structure 3-69021
- polyamide resins reaction with N,4-dininoso-N-methylaniline, e.p.r. and i.r. study of products (Russian) 3-50851
- polycyano-compounds, solvent effect on u.v. spectra, dipole moments in excited singlet states (French) 3-63440
- polycyclic hydrocarbons, ^{13}C chemical shift, π -electron current effect 3-71588
- polyenes, electronic structure 3-71544
- polyenes, in n-paraffin matrices, quasiline absorpt. and fluoresc. spectra 3-72742
- polyethylene differential thermogravimetric curves, thermal decomposition, derivative thermobalance 3-76442
- polyethyleneterephthalate, dielec. polarisation, in pulsed elec. fields 3-64594
- polyethyleneterephthalate, Lawsonite film, liquid hydrogen target production 3-48502
- polymethine dye, induced absorpt., laser excitation 3-65112
- polymethine dye lasers, flashlamp excited, i.r. emission, mode locking, tuning 3-45801
- polymethine dyes, intra-, intermolecular transform., energy transfer 3-69479
- polynuclear aromatic hydrocarbons, in atmospheric dust (French) 3-76705
- polypeptides in binary solvents, helix-coil transition, thermodynamics 3-54761
- polyphenyl ether, high-press. viscosity meas. 3-62386
- polyphenyls and benzene near melting point, neutron scattering difference rel. to rotational mechanism 3-60435
- polypropylene, oriented isotactic γ -form crystal, form. by α - γ transition 3-69149
- polystyrene latex, multiple scatt. in cylindrical cell 3-74206
- polystyrene-cyclohexane, mixture shear dependence of the viscosity in the critical region 3-41039
- polyvinyl carbazole, perylene doped, energy transfer 3-76062
- polyvinylcarbazole:trinitrofluorenone, amorphous films, absorption and electroabsorption spectra 3-61049
- polyvinylfluoride pyroelectric detectors, mathematical model for response analysis 3-77393
- porphin, free base, Shpolskii-matrix lowest triplet states obs. from microwave induced fluoresc. changes 3-76050
- porphin derivatives, Shpolski spectra 3-72735
- porphins, low temp., absorpt., luminesc. spectra of complexes 3-64711
- porphyrin and alkylsubstituted derivatives, ^{13}C Fourier transform n.m.r. spectroscopy 3-71601
- porphyrins, alkylsubstituted, f.t. ^{13}C n.m.r. spectra, chemical shift 3-72537
- porphyrins, excited states, effects of metallic substitution 3-63550
- porphyrins, fluoresc. polarisation time depend., imino H displacement 3-49485
- porphyrins, mag. circular dichroism, vibronic coupling 3-74993
- porphyrins meso-substituted, e.p.r. spectra, effect of alkyl substituents (Russian) 3-78852

organic compounds continued

- potassium acid phthalate crystals, coefficient of thermal expansion perpendicular to cleavage planes, X-ray diffraction application 3-64191
- potassium boromaleate, crystal structure 3-43779
- potassium caproate spin-lattice n.m.r. measurements, saturation effects, polycrystalline, room temp. 3-58437
- potassium hydrogen acetylenedicarboxylate, i.r. and Raman spectra, vibr. studies of hydrogen-bonding 3-76006
- potassium hydrogen di-trifluoroacetate i.r. and Raman spectra, symmetric hydrogen bonds 3-68990
- potassium hydrogen oxalate, elastic consts., by u.s. wave light diff. 3-49920
- potassium hydrogen oxydiacetate, crystal structure determ. from X-ray intensity data 3-68238
- potassium hydrogen succinate, i.r. and Raman spectra, symmetric hydrogen bonds 3-68990
- potassium methyl xanthate-d₀ and -d₃, vibrational spectra and force constants (*German*) 3-46297
- potassium salt of 1,1-dinitroethane anion, cryst. structure obs. 3-72074
- potassium terephthalate, X-ray exam., polymorphism, thermal stability 3-75519
- potassium tetrafluorophthalate, ¹⁹F chem. shielding tensors and cryst. struct. 3-61001
- powdered, optical second harmonic generation 3-57259
- propane, ¹³C n.m.r., mag. shielding consts. calc. by Gaussian function 3-71593
- propane, α -particle molecular stopping cross sections, 3-56554
- propane, Hg(PO) photosensitized decomposition 3-50843
- propane, in torsional excited states, rotational spectra analysis (*German*) 3-43428
- propane, relative Raman cross-section, from short pulse laser scatt. and photon counting obs. 3-57651
- propane, supercritical, electron scavenging by N₂O in γ radiolysis, density var. 3-73145
- n-propanol, adiabatic volume viscosity and structure by ultrasonics 3-68431
- propanol-(1) and -(2), refractive index meas., between 250 and 700 nm. 3-66190
- propargyl alcohol, barriers to internal rotation, group function anal., MO-LCAO-SCF computations 3-49432
- propene, internal rotation barriers rel. to localized charge distributions 3-54633
- propene, mol. struct. determ. by electron diffraction 3-74918
- propene, oxidation, activity enhancement and selectivity change by catalytic effect of hot electrons 3-41868
- propionic acid CNDO/2 calc., energy, electron distrib. dipole moment origin 3-63389
- propionaldehyde, mol. struct., ab initio and semi-empirical calc. 3-74920
- propionamide, i.r. and Raman spectra 3-60452
- propylene imine, i.r. and Raman spectra 3-78788
- n-propyl fluoride, i.r. spectra, vibrational analysis 3-75037
- propyl radicals, spin delocalisation mechanisms through sigma bonds delocalisation to gamma proton, SCF-MO-INDO method 3-43418
- n-propylamine polyhedral clathrate, struct. of low melting hydrate 3-46637
- propylene, dipole moment determ. 3-67750
- propylene, relative Raman cross-section, from short pulse laser scatt. and photon counting obs. 3-57651
- propylene, supercritical, electron scavenging by N₂O in γ radiolysis density var. 3-73145
- trans-propylene imine, microwave spectra, centrifugal distortion effects 3-60463
- propylene in CO₂ mixture, vapour-liquid crit. line, light scatt. obs. 3-79484
- propylene-Cl₂ complexes, low temp. i.r. spectra 3-75014
- propylene-CO₂ solutions, molecular thermodynamics in normal and critical regions 3-65121
- cis-propyleneimine, ¹⁴N quadrupole coupling consts., microwave spectra 3-63489
- propynal, CNDO/2 calcs. of electronic struct. 3-67755
- propynal, millimetre wave spectrum, ground vibr. state 3-78816
- propynal, rot. anal. of 0-0 band near 4145 Å 3-67793
- propynal CNDO/2 calc., energy, electron distrib. dipole moment origin 3-63389
- propyne-d₂, i.r. spectra, geom. of propyne 3-63455
- PTFE, deuteron irradi., yield of peroxy radicals, e.p.r. obs. 3-79893
- pyrazine, ab initio MO wave functions 3-63372
- pyrazine, Born-Oppenheimer coupling contrbs., vibronic intensity borrowing theory 3-40596
- pyrazine, crystalline, low temp.-high temp. phase transition study by i.r. and Raman spectra 3-75982
- pyrazine cryst., triplet excitation Davydov splitting calc. 3-60862
- pyrazoles, substituted, ¹⁴N chemical shift (*French*) 3-63518
- pyrazole-¹⁵N, p.m.r. spectra 3-54722
- pyrazoline compounds, molecular association in binary solvents (*Russian*) 3-80542
- pyrene, Born-Oppenheimer coupling contrbs., vibronic intensity borrowing theory 3-40596
- pyrene, emission-absorpt. asymmetry of S₁-S₀ transition, deuterium effect, vibronic coupling 3-54715
- pyrene, in liquid cyclohexane, photoionisation of negative ions 3-65107
- pyrene, magnetic field dependence of delayed fluorescence, test of non-crossing pair state theorem 3-79661
- pyrene, pure cryst., phosphoresc. emission struct. 3-64707
- pyrene, T, L and S tensors, calc. from cryst. forces 3-79262
- pyrene and derivatives, vapour-phase fluoresc. from second excited singlet state 3-67844
- pyrene doped naphthalene, direct and delayed emission phenomena 3-55672
- pyrene excimer, absorption spectrum by modulation excitation spectrophotometry 3-46258
- pyrene fluorescence in ethanol and cyclohexane under pressure 3-61061
- pyrene single cryst., light absorpt., 4 to 300 K, ground-to-excimer state absorpt. search 3-53150

organic compounds continued

- pyrene solution, delayed fluorescence O₂ quenching, mag. field effects 3-46309
- pyrene-d₁₀ doped fluorene, triplet exciton behaviour 3-64708
- pyrenes, monohalogenated, fluoresc. temp. depend., intramol. heavy-atom effect and intersystem-crossing 3-46310
- pyridazine-¹⁵N, p.m.r. spectra 3-54722
- pyridine, in solid matrices, quasiline phosphoresc. spectra 3-72741
- pyridinaldehydes, INDO calcs. of stereochem. and NMR parameters 3-60401
- pyridine, ab initio MO wave functions 3-63372
- pyridine, adsorption on Pt(111) and Pt(100) surfaces, LEED and work function investigation 3-55127
- pyridine, n.m.r. of ¹³C, long-range ¹³C-¹H spin coupling consts. 3-43483
- pyridine, protonated pyridine, INDO finite perturbation calcs. of spin-spin coupling consts. J_{hh}, J_{15hh}, J_{15n13c} 3-74952
- pyridine, quantum chem. determ. of intermediate ion structure in mass spectra 3-46241
- pyridine, solvent effects on ¹³C n.m.r. spectra 3-63512
- pyridine, uncoupled pulsed Fourier transform ¹³C n.m.r. spectra 3-75085
- pyridine, unsuccessful search for molecular lines in interstellar matter 3-61863
- pyridine, u.v. spectra, 3000 to 3400 Å, triplet-singlet absorpt., band assignments 3-49460
- pyridine asymmetric ion hydrogen bonded complexes, i.r. and Raman spectra 3-75030
- pyridine in NbSe₂, intercalation complex, electron microscope examination 3-72039
- pyridine N-oxides, far i.r. investigations and hydrogen bonding 3-46290
- pyridine nucleotides, conformation, ¹³P and ¹H fast Fourier transform n.m.r. spectroscopy 3-67850
- pyridine ring system containing cpds., photoemission in vacuum u.v. region 3-41613
- pyridine-4-d₁, near u.v. spectra, appl. of band contour anal. method 3-46307
- pyridine-bromine complex oriented in nematic phase, geometry, n.m.r. obs. 3-41432
- pyridines, BEEM- π calcs. and ¹⁴N n.q.r. 3-63526
- pyridines, dielectric props. in solutions, microwave meas. 3-55999
- pyridines, disubstituted, proton-proton coupling consts., additivity of substituent effects 3-60479
- pyridines, long chain, benzene soln., microwave absorpt., dielec. props. 3-80585
- pyridinium ion, in-plane vibrations calc. 3-74976
- pyridinium trihalides, Raman, i.r. and electronic absorption spectra, struct. 3-75032
- pyridinium-pyridine ion, complex hydrogen bonded cations, i.r. and Raman spectra obs. 3-75028
- pyrimidine, quantum chem. determ. of intermediate ion structure in mass spectra 3-46241
- pyrimidine derivatives, e.p.r. study of iminoxy radicals 3-78842
- pyrimidine dimers, yeast cell's DNA, u.v. induced budding delay 3-48265
- pyrimidine nucleosides, syn conformation stability, INDO method hydrogen bonding 3-63363
- L-pyrroglutamic acid, n.m.r. spectra and conformations, and related compounds (*French*) 3-63519
- pyrolyzed phenol formaldehyde resin, preparation and temp. depend. of d.c. conductivity 3-41179
- pyromellitic dianhydride-anthracene single crystals, charge transfer complex, piezoeffectance 3-55644
- pyrone, microwave spectrum, molecular Zeeman effect, magnetic susceptibility 3-63481
- pyrrol, cryst., hydrogen bond vibr., i.r. and Raman spectra obs. 3-72640
- pyrrole, ¹⁵N and ¹³C n.m.r. spectra 3-78846
- pyrrole, ¹⁵N enriched, natural abundance ¹³C n.m.r. obs. 3-75083
- pyrrole, beam maser spectroscopy, obs. of rotational transitions, nitrogen hyperfine parameters 3-78826
- quantitative analysis, simple decomposition technique 3-61970
- quaternary alkyl ammonium carbonate, solvent extraction, purification of Be 3-69184
- quinazoline in durene and naphthalene host cryst., electronic absorpt. spectra analysis 3-69028
- quinoline, hydrogen bonding effect on absorpt. spectra (*Russian*) 3-54658
- quinoline, liquid, rot.-vib. relax., Raman and i.r. spectral obs. 3-64670
- quinoline, phosphorescent, ENDOR in 3.601 GHz zero-field transition, ¹⁴N quadrupolar splitting 3-46316
- quinoline, stimulated scatt. Rayleigh line wing light, fine struct. 3-58502
- quinoline, triplet-triplet absorpt. spectra 3-67803
- quinoline hydrogen bonded complexes with methyl-, ethyl- and chloro-pyridines, vibrational spectra 3-75029
- quinoline in durene host, multiple spin echoes in photo-excited triplet state 3-80564
- quinoline N-oxides and isoquinoline N-oxides, i.r. spectra and behaviour of N-O group 3-54697
- quinolinium cation, dual fluorescence, pH and Hammett acidity depend. 3-63497
- quinolizidine alkaloids, ¹³C n.m.r. spectra 3-71587
- quinoxaline in durene host, phosphoresc. spectra from spin sublevels of low emissivity 3-80565
- radical ion and triplet form, in electron transfer fluoresc. quenching by nsec. laser spectroscopy 3-80563
- radicals, liq., Overhauser effect, weak and quasi-zero field phenomena (*French*) 3-55502
- RDT/TNT explosive, fracture, surface markings and brittle cleavage characts. 3-41815
- retinol, primary photoprocesses 3-47575
- Rhodamin 6G, two-photon absorption 3-40287
- rhodamine, effect of structure and degree of acidity on generating props. (*Russian*) 3-78037
- rhodamine 6 G, photochemical method for determ. of pumping light energy 3-62713
- rhodamine 6 G dye laser, time resolved spectroscopy 3-40255

organic compounds continued

- rhodamine 6G, dye film, activation of photocurrent 3-72382
 rhodamine 6G, dye laser, double cavity flash-pumped, amplification competition 3-51925
 rhodamine 6G, ESR triplet state meas. 3-78028
 rhodamine 6G, in soln., fluoresc. intermol. energy migration, fluorometer appl. 3-76085
 rhodamine 6G, O₂ quenching constant for triplet state from laser characs. 3-64728
 rhodamine 6G, passively mode locked dye laser, build up of picosecond pulse generation 3-54224
 rhodamine 6G, photobleaching rel. to triplet state population 3-45803
 rhodamine 6G, soln. generation by excitation, effect of detergent (*Russian*) 3-70819
 rhodamine 6G, theory of singlet-triplet exciton fusion 3-64311
 rhodamine 6G and benzophenone in soln., nonlinear absorpt., singlet-singlet energy transfer 3-78035
 rhodamine 6G laser, Ar⁺ pumped, c.w. operation 3-66827
 rhodamine 6G laser, flashlamp pumped, spectral line breadth, rate eqns. 3-40257
 rhodamine 6G laser, frequency locking analysis by Faraday filter 3-40258
 rhodamine 6G laser, high average power, low distortion, using face pumped zigzag configuration 3-54225
 rhodamine 6G laser, photodecomposition during intense lamp pumping (*Russian*) 3-78036
 rhodamine 6G laser, triplet quenching by O₂ 3-43014
 rhodamine 6G-sodium lauryl sulphate solutions, luminescent lifetimes (*Russian*) 3-72719
 Rhodamine B, dimer in aq. solns., visible spectra, conc. depend. 3-47584
 rhodamine B, use in dye-mixture laser 3-78029
 rhodamine B absorbed on anthracene, mag. field effect on luminesc., triplets 3-69089
 Rhodamine B dye laser light polarisation 3-78030
 rhodamine B solution, absorption processes associated with anti-Stokes fluorescence 3-61060
 rhodamine dyes, conc. quenching in luminesc. of alcohol solns. 3-69075
 rhodamine dyes, energy transfer from anthracene triplets 3-69077
 rhodamine-B, absorption and fluorescence spectra 3-69046
 rhodamine, dimeric structures, vibratory spectra calcs. (*Russian*) 3-75015
 rhodizone anion, in soln. and salts, Raman spectra, intensity and depolarisation ratio 3-78801
 rhodopsin and meta-rhodopsin, absorption spectra (*Japanese*) 3-50849
 riboflavin, absorption and fluorescence spectra 3-69046
 rubrene, surface states, on naphthalene, anthracene, mag. quenching of prompt fluoresc. 3-72724
 rubrene in benzene soln., surface generated photocurrent, ion-image state as intermediate 3-47578
 saccharides and polysaccharides, conformational analysis by n.m.r. (*Russian*) 3-63587
 salicylaldehyde, chemiluminescence 3-55945
 salicylaldehydic acid esters, spectrofluorometric investigation 3-54711
 salol single crystal, wetting by its own melt 3-75660
 saturated heterocycles, intermol. action of heteroatom, n.m.r. (*French*) 3-43475
 second harmonic generation, cryst. mol. struct. 3-62738
 selenium pentamethylene heterocycle, conformational analysis 3-78654
 selenophenes, 2-substituted, ⁷⁷Se n.m.r. spectra, substituent shifts 3-50481
 semiquinone radicals in aprotic media, spectral linewidth alternation (*French*) 3-44729
 silacyclopentanes, vibr. analysis of i.r. and Raman spectra 3-63464
 silacyclobutane, (1-d), (1-d₂), i.r. and Raman spectra, ring-puckering vibr. 3-78789
 silicon organic esters of phosphoric acids, crystalline roentgenofluorescent anal., Si and P determ. 3-48662
 siloxanes, modification of surface energy and surface tension of wetting, glass powders (*German*) 3-53279
 sodium biphenylide, e.s.r. spectra, ion-pairing dissociation consts. 3-76428
 sodium bromoacetate and sodium bromoacetate-d₂, vibrational spectra and struct. 3-75987
 sodium fluorescein in glycerol solution, Webers red edge effect, luminescent aggregates 3-69078
 sodium hydrogen diacetate, i.r. and Raman spectra, symmetric hydrogen bonds 3-68990
 sodium hydrogen oxalate monohydrate, deuteron magnetic resonance, hydrogen bond studies 3-72529
 sodium hydrogen oxydiacetate, crystal structure determ. from X-ray intensity data 3-68238
 sodium naphthalenide, e.s.r. spectra, ion-pairing dissociation consts. 3-76428
 sodium pyrenide in tetrahydrofuran, flash photolysis, photo-oxidation and Na⁰ existence 3-61270
 sodium-hydrogen oxalate monohydrate, γ -irrad. single crystals, radical obs. 3-47565
 solid solutions, laser excited luminesc., fine struct. and broad spectral bands 3-72725
 solvent with F traces, anodic oxidation of Si 3-41671
 solvents and thermoplastic polymers, influence on photoelectric properties of Se, interaction mechanism (*Russian*) 3-79740
 spirochromenes, of indoline series, holographic images, optimum exposure and storage times 3-42583
 spiropyran, coloured isomeric forms struct. stability, extended Huckel method study 3-74923
 squaric acid and anions, π electronic struct. determ., near u.v. aq. soln. spectra 3-52360
 stearic acid, adsorption on Fe, Ni, Cr and stainless steels, effect on contact angle 3-43933
 stearic acid, Langmuir-Blodgett layers, i.r. spectroscopic obs. of struct. 3-76002
 stearic acid adsorption on Ge, Al₂O₃, i.r. spectra 3-75986

organic compounds continued

- stearic acid adsorption on Hg surface, interfacial tension meas. 3-50075
 stearic acid film, prep. by Langmuir-Blodgett method, and elec. props. 3-41273
 stibabenzene, photoelectron spectra 3-46255
 stilbene, anharmonicity of lattice vibr. and lifetime of optical phonons 3-72644
 trans-stilbene, enthalpy of sublimation meas., thermal cond. manometer 3-45460
 stilbene, in n-octane matrix, absorpt. and fluoresc. 3-72739
 stilbene crystal, scintillator, neutron spectrometer, line shape, experimental, Monte Carlo calculation 3-70408
 stilbene powder, stimulated Raman scatt., energy and time characs., temp. effects 3-62751
 stilbenes and analogs, electronic overlap populations as reactivity meas. in electrocyclic reactions 3-52317
 stratospheric, photochemical model with vertical transport 3-73316
 strontium formate, phase matched second harmonic generation and optical mixing 3-40281
 strontium formate dihydrate, phase matched second harmonic generation and optical mixing 3-40281
 structured systems, highly elastic deform., kinetic curves 3-73070
 styrene, effect of polymerisation on energy level shift, energy transfer 3-69081
 styrene, nonplanar conformation 3-52387
 styrene thin film polymerisation in glow discharge, effect of O₂ on electrical props. 3-41280
 trans-2-styrylthiophene and some nitro derivatives, i.r. characteristics 3-54696
 sublimation enthalpy and Gibbs energy function, microcalorimetric determ. 3-55079
 substituted, picolines, flame-ionization chromatography, sensitivity coeff. 3-70473
 4-substituted α -methylstyrenes and α -t-butylstyrenes, substituent effects, n.m.r. obs. and CNDO/2 calculations 3-52386
 4-substituted styrenes, substituent effects, n.m.r. obs. and CNDO/2 calculations 3-52385
 succinic acid, irradiated, spectral confirmation of absence of CO₂ 3-61266
 succinic acid, proton multiple pulse spectra, nuclear magnetic shielding anisotropies 3-79930
 succinonitrile, energy difference between gauche and trans isomers (*French*) 3-68172
 succinonitrile, plastic crystals, Raman spectra, isomer equilib. position 3-72658
 succinonitrile plastic crystal, Rayleigh scatt. spectrum, interpretation (*French*) 3-47277
 sucrose powder, compaction mechanisms 3-47490
 sulphamic acid, carbonylation, formation of aromatic ring systems containing S 3-55942
 superconducting fluctuations in one-dimens. organic solid 3-58350
 supercooled liquids, Mossbauer line broadening 3-68907
 t-butyl alcohol-water system, u.s. absorption, frequency dependence, relaxation processes, model 3-59478
 tanane, ferroelastic-ferroelectric compound, paraferroelectric transition meas. 3-55536
 tanol linear chain free radical, proton relax time freq. and temp. depend. (*French*) 3-58441
 tartrate crystals, triboluminescence and simultaneous charge produced at fracture 3-69045
 TCNE negative ions, photodetachment of electrons 3-78856
 TCNE-benzene charge transfer complex, resonant Raman effect and charge distrib. 3-75977
 TCNQ-NH₄⁺, proton spin-lattice relaxation time, temp. dependence 3-55498
 TCNQ, electronic props. of one-dimensional solids, review 3-50134
 TCNQ, satellites in high energy photoelectron spectra 3-52326
 TCNQ and TCNQ-d₄ single crystals, polarised Raman spectra, vibrational modes 3-72625
 TCNQ anion radical salts, dimer approx. temp., mag. field and lattice distortion effects 3-55224
 TCNQ charge transfer salts, mag. props., review 3-55425
 TCNQ complex, supercond. fluctuations rel. to structural defects 3-55384
 TCNQ complexes, electron transport and mag. susceptibility, 2 K to room temp. 3-60869
 TCNQ complexes, high-conductivity, effect of vibronic interaction in i.r. spectra 3-72645
 TCNQ crystal, nucleation kinetics of allotropic transformation 3-79488
 TCNQ salt of methyltriphenylphosphonium, phase transitions, electrical cond. meas. 3-72194
 TCNQ salts, extended Frenkel excitons in one dimens. band, triplet states dipolar splitting 3-58233
 TCNQ salts, sp. ht. and mag. susceptibility, 1.4-4.4 K, rel. to band struct. 3-46795
 TCNQ salts, supercond. and Peierls instability 3-46941
 TCNQ/tetrathiofulvalene highly conducting complex, electron transfer 3-46824
 tellurium pentamethylene heterocycle, conformational analysis 3-78654
 1,4-telluroxan in vapour, liquid, amorphous and crystalline state, vibrational spectra 3-46292
 terephthalic aldehyde, cross linked PVA networks, thermoelasticity, gels 3-63601
 o-terphenylphenols, Fourier transform ¹³C n.m.r. spectra 3-71590
 p-terphenyl mixed crystals, with tetracene and pentacene, second-order Stark effect on ¹B_{2u} state 3-53128
 tertiary aliphatic amines in SO₂ solns., e.s.r., optical absorption 3-69477
 tertiary amides, mean square and mean amplitudes for in-plane vibrations of various linkages 3-46246
 tertiary amine extractants for Pu recovery from natural u irradi. fuel, anal. methods 3-57583
 tertiary butanol, liquid, hydrogen bonded, association and assignment of OH overtones 3-75023
 tetra-allyl silane, vibrational spectra 3-46294
 tetra-n-butyl-ammonium iodide in water (benzene)¹³C, ¹⁴N nucl. relax. 3-68882

organic compounds continued

- tetra-n-butylphosphonium bromide, CoBr_4^{2-} in soln. absorpt. spectra 3-64671
- tetraalkyl ammonium iodides, self-trapped exciton spectroscopy 3-69034
- tetrabenzoporphin, in n-octane, phototransform. of centres, rel. to multiplicity of Shpol'skii effect 3-58548
- tetrabromobenzene, symmetric, Br hyperfine and quadrupole fine struct. in MODR spectrum 3-53328
- tetrabromomethane, far i.r. spectra and octopole moments 3-49466
- tetrabutylammonium ions, effect on electroreflectance spectra of Pt and Au 3-47292
- tetracene, mol. cryst. film, Stark effect, electron absorpt. band 3-72678
- tetracene, surface states, on naphthalene, anthracene, mag. quenching of prompt fluoresc. 3-72724
- tetracene crystal, optically induced singlet fission 3-75723
- tetracene doped anthracene, triplet exciton interactions, delayed fluoresc. (German) 3-50616
- tetracene doped fluorene, time resolved fluorescence spectroscopy 3-55680
- tetracene mol. solids, polariton dynamics from band profile analysis 3-72642
- tetracene sandwich between Al and Au, electrical props. 3-46904
- 1,1,1,2-tetrachloro-2-methylpropane, solid, n.m.r. static and rotating frame relaxation 3-72538
- tetrachloroethylene, vibrational force fields, specific imposition of pots. parameters on nonbonded distances 3-71527
- 1,1,1,3-tetrachloropropane, Raman, i.r. spectra, rot. isomerism 3-72653
- 1,1,2,2-tetrachlorotetrafluorocyclobutane and 1-chloro-2,2,3,3-tetrafluorocyclobutane, i.r. and Raman spectra 3-78787
- tetracyanobenzene-biphenyl complex single crystals, spin alignment in charge transfer phosphorescent state 3-61059
- 1,1,2,2-tetracyanocyclopropane, cryst. and mol. struct. 3-46219
- tetracyanoethylene, radical anion salts, reson. Raman spectra and bond strengths 3-43446
- tetracyanoethylene with mesitylene and benzene, charge transfer complexes, solvent effect, thermodynamic props. and optical absorpt. spectra 3-44429
- tetracyanoethylene-benzene complex, calc. allowing for doubly-excited configurations (Russian) 3-67751
- tetracyanoethylene-toluene charge transfer complex in glassy soln., fluoresc. spectra 3-69076
- tetracyanomethane, i.r. spectra, vibrational assignment, normal coordinate analysis and thermodynamic functions 3-54684
- tetradeuteriomethane collisions with CO_2 , vibrational relaxation 3-54752
- 2,3,4,5-tetrafluoroaniline, i.r. absorption spectrum, vibrational assignments 3-78757
- tetrafluorobenzene, heat capacity, adiabatic calorimetry, 11-353K, phase transition enthalpy, liquid entropy 3-46714
- tetrafluoroethylene, mass spectra, thermal ion-molecule reactions by ion cyclotron resonance 3-43507
- tetrafluoroethylene/monotetracarbonyl, molecular structure, gas phase electron diffraction 3-60718
- tetrafluoromethane, far i.r. spectra and octopole moments 3-49466
- tetrafluoromethane, i.r. spectra in liquid Ar 3-71562
- tetrafluoromethane, mol. ESCA spectra, calc. by multiple-scatt.-X α method 3-40662
- tetrafluoromethane, number density remote sensing in hypersonic flow using Raman scattering 3-71699
- tetraglycine, energy minimisation 3-75163
- tetrahydrofuran, as clathrate deuterate, proton spin-lattice relax. time 3-54727
- tetrahydrofuran clathrate hydrate, far i.r. absorption, rotational oscillations 3-80062
- 1,2,3,4-tetrahydroisoquinoline (III), structure depend. of emission props., intramol. electron transfer 3-75061
- 2-O-tetrahydropranyluridine, dextrorotatory, crystal struct. 3-79329
- 1,2,4,5-tetramethyl benzene, moles., crystals, atom-atom pots., H atom coords. 3-72073
- 2,2,6,6-tetramethyl-4-hydroxypiperidine-1-oxyl-4-derivatives, mag. susceptibility, 1.8-300 K 3-64493
- 2,2,6,6-tetramethyl-4-piperidone 1-oxyl, ^{17}O and ^{14}N σ - π polarisation parameters and spin density distribution 3-52321
- N, N, N', tetramethyl-n-phenylenediamine in solid solution 3-methyl-pentane at 77K, electroluminescence (Russian) 3-44490
- N, N, N', tetramethyl-p-phenylenediamine, recombination luminescences resulting from photoionisation 3-41571
- tetramethyl-p-phenylenediamine, satellites in high energy photoelectron spectra 3-52326
- tetramethylammonium chloride, struct. transitions, config. entropy and polymorphism 3-79489
- tetramethylammonium manganese chloride, cation rotational motion, neutron scatt. obs. 3-49855
- tetramethylbiphosphine Raman spectra, isomers obs. 3-75036
- N,P,P,P-tetramethylphosphine imide, vibr. spectra, struct. of P-N bond 3-75024
- N,P,P,P-tetramethylphosphine imide and N-methyl- d_3 analogue, vibr. spectra analysis 3-78795
- 1,3,5,7-tetramethylsiladamantane, vibrational spectra (German) 3-43453
- 1,4,5,8-tetraoxanthraquinone, in octane matrix, fluoresc., electron-vibr. interactions 3-75060
- tetraphenylethylene, conformation of phenyl rings, using n.m.r. and Fraenkel relation 3-71485
- tetraphenylporphine halogen derivatives, fluorescence spectra, internal heavy atom effect 3-63503
- thalline laser, pulse generation lines (Russian) 3-78038
- thiirane, photoionis. cross sections, He I and He II photoelectron spectra 3-78857
- thiirane, vibration spectra, Davydov splitting, unit cell symmetry determ. 3-64652
- thiirane sulphone, Raman and i.r. spectra 3-57655
- thioacetamide, analysis of silver in photographic products, improved procedure 3-61281
- thioamides, hindered rotation barriers, p.m.r. determ. 3-71529

organic compounds continued

- thioamides, mean square and mean amplitudes for in-plane vibrations of various linkages 3-46246
- thiocarbonyl chloride, photoelectron spectra 3-43502
- thiocarbonyl fluoride, photoelectron spectra 3-43502
- thiochlorides, vibrational spectra (Russian) 3-63477
- thiodiglycolic acid molecule thermal vibrations 3-67773
- thioformaldehyde, ab initio calcs. for ground and low-lying triplet states 3-52323
- thiolic acids, self-association, low temp. i.r. spectra 3-64641
- thiomethyl group, characteristic Raman freq., stretching modes, substitution 3-67809
- thionine-sodium lauryl sulphate solutions, luminescent lifetimes (Russian) 3-72719
- thiophane, vibration spectra Davydov splitting, unit cell symmetry determ. 3-64652
- thiophene, compliance constants, iterative consistency method 3-74981
- thiophene, solid and liquid, i.r. spectra and struct. (French) 3-75033
- thiophene, valence electron density, calc. using IEHT approach 3-63380
- 2-thiopheneldehyde, gas, microwave study, O-S trans rotamer identification 3-63365
- thiophenes, ring proton-proton coupling consts., SCF INDO calcs. 3-60414
- thiophosgene, vapour phase absorpt. spectrum, vibrational structure 3-63441
- thiopropionamide i.r. and Raman spectra 3-60452
- thiourea, electrical conductivity meas. 3-58257
- thiourea, photosensitized oxidation method for determ. of triplet state conversion efficiency 3-76481
- thiourea and deuterated thiourea, phase transition phenomena, soft mode behaviour, Raman spectra (French) 3-61032
- thiourea and deuterium derivatives, vibr. spectrum calcs. 3-63415
- 4-thiouridine, decay kinetics, temp. depend., excited states deactivation 3-73154
- thioviolic acid, complex formation, photometric determination of Co in presence of Ni 3-48650
- thioxanthone, phosphorescence lifetime in rigid glass, 77K 3-80562
- thulium ethyl sulphate, ^{169}Tm n.m.r. study 3-64577
- thymidine monophosphate, 3',5'-cyclic, p.m.r. study of conformations 3-63568
- thymine dimers, repair of DNA damage HeLaS_3 u.v. sensitive cells, sensitivity to carcinogen 4-nitroquinoline 1-oxide, X-radiation 3-48168
- thymol, depend. of rate of crystn. on capillary dia. 3-63966
- TMPP-TCNQ, delocalised triplet state excitations, spin susceptibility, e.s.r. 3-60970
- TMPO, linear chain like free radical, sublattice magnetisation, proton n.m.r. 3-55486
- tocopherol, dietary fatty acids, effect on mammalian erythrocytes, mouse radiation induced haemolysis, K loss 3-48260
- tolane, in n-octane matrix, absorpt. and fluoresc. 3-72739
- toluene, α NPO excimer formation, thermodynamic properties, solvent effect 3-80584
- toluene, π , σ -electronic struct., conversion in ground state, CNDO/2 calcs. (Russian) 3-78678
- toluene, in soln., effects of environment on excited states 3-60473
- toluene, in various solvents, orientational relax. rates, depolarised Rayleigh scatt. meas. 3-50574
- toluene, liquid, Brillouin scattering obs. of acoustic relaxations 3-80038
- toluene, thermal conductivity 3-72236
- toluene, thermal diffusion of polystyrene 3-60500
- toluene, thin films, photoexcitation, fluorescence of benzyl radicals (Russian) 3-72701
- toluene, u.s. absorption rel. to pressure 3-43831
- toluene and methylene chloride mixture, dielectric polarisation, n.m.r. u.v. and i.r. studies 3-58817
- toluene in dilute solutions, fluorescence yields and decay processes 3-61065
- toluene matrix, benzophenone solute, quasilinear luminesc. spectrum, theoretical interpretation 3-72740
- toluene solid solution, mechanism of singlet, triplet state formation 3-76467
- trapped electron, acting potential calc. 3-41858
- trapped in single crystals, ^{13}C hyperfine coupling tensors from e.s.r. 3-55971
- tri-(3-bromo-2-thienyl) phosphine, ^{13}C - ^{31}P coupling, off resonance proton decoupling, n.m.r. 3-75069
- sym-triazine, electronic states, optical emission and e.p.r. 3-80103
- s-triazine, Stark, Zeeman effects on lower electronic states 3-64674
- s-triazine crystals, mag. sensitivity of 3330.8 Å state 3-61044
- triazol, cryst., hydrogen bond vibr., i.r. and Raman spectra obs. 3-72640
- triazoles, i.r. spectra and normal vibrations 3-71547
- 4-R-1,2,4-triazoline-3,5-diones, ($\text{R}=\text{H}$, CH_3 , CH_2CH_3 , $\text{CH}_2\text{CH}_2\text{CH}_3$), electronic spectra 3-49459
- tribenzyl-antimony dihalides, i.r. and Raman spectra 3-67821
- tribenzyl-arsenic dihalides, i.r. and Raman spectra 3-67821
- 1,2,3-tribromopropane, vibr. spectra, electron diff., conformation 3-63465
- trichloro-1,1,1 propanes, normal coord. calcs. and force consts. (French) 3-46250
- trichlorodeuteromethane, mol. reorientation, Raman spectral obs. 3-64666
- 1,1,1-trichloroethane, laser excited Raman bands and funds. 3-67814
- trichloroethylene in mixtures of HMPT and cyclohexane, ^{13}C and H chemical shifts as function of conc. and temp. 3-75898
- trichlorofluoromethane, atmospheric level, tracer for air and water mass movements 3-65372
- trichlorofluoromethane, electron bombarded 3-67860
- trichloromethyl derivatives of P, CCl_3PCl_2 and $(\text{CCl}_3)_2\text{PCl}_3$, n.q.r. spectroscopy and mol. dynamics 3-75912
- 1,2,3-trichloropropane, vibr. spectra, electron diff., conformation 3-63465

organic compounds continued

- tricyclic hydrocarbons, ^{13}C n.m.r. spectra for struct. determ. 3-75067
- n-tridecane, thermal cond., 30-400°C, press. up to 500 bar 3-52726
- trideuteromethanol ionisation and dissociation by electron impact 3-43496
- triethylene diamine, as clathrate deuterate, proton spin-lattice relax. time 3-54727
- triethylenediamine, mol. UV absorpt. spectrum anal. of struct. 3-78740
- triethylenediamine, plastic cryst. phase, self-diffusion, n.m.r. study 3-68438
- trifluoramine oxide, vibr. assignment and Urey-Bradley force field 3-40599
- 1,1,1-trifluoro-3-chloropropane, Raman, i.r. spectra, rot. isomerism 3-72653
- trifluoroacetic acid, solid, vibrational spectra and structure 3-50572
- trifluoroacetyl fluoride, i.r. spectrum and rotational isomerism 3-43455
- 1,3,5-trifluorobenzene, Raman spectra, C-F bond length determ. 3-54691
- trifluoroethanol-trimethylamine vapour phase complex, effect of temperature on H bond ν , band 3-46247
- trifluoroethylamine, vibrational spectra 3-71558
- trifluoroethylamine, vibrational spectrum and structure 3-76007
- trifluoroethylene, mass spectra, thermal ion-molecule reactions by ion cyclotron resonance 3-43507
- trifluoroethylene, microwave moments and rotational constants 3-43461
- trifluoromethane, dielec. second virial coeff. 3-52414
- trifluoromethane orientational anisotropy in total collision cross section 3-46355
- trifluoromethyl derivatives, phosphorescence lifetimes 3-80105
- trifluoromethyl group, three-spin system, nonexponential, spin lattice relaxation, orientation dependence 3-72539
- trifluoromethylacetophenones, elec. dipole moments and conformations, o-, m- and p- 3-67724
- trifluoromethyltrifluoroborate anion, Urey-Bradley force constant, vibration spectrum, i.r. and Raman spectra 3-57648
- 2,4,6-trifluoronitrobenzene, n.m.r. of ^1H , ^{19}F , ^{14}N , external electric field effects 3-68854
- 3,3,3-trifluoropropene, mol. struct. determ. by electron diffraction 3-74918
- triglycine fluoberyllate, spontaneous polarisation, temp. depend., dielectric hysteresis 3-53072
- triglycine selenate, spontaneous polarisation, temp. depend., dielectric hysteresis 3-53072
- triglycine sulphate:L-alanine, high internal bias fields, pyroelec. detector applications 3-44376
- triglycine sulphate: Pd^{2+} , single cryst. growth, domain struct. 3-55528
- triglycine sulphate, anomalies in elastic compliance as test for Janovec's theory 3-79406
- triglycine sulphate, equilibrium domain structure near Curie point 3-79997
- triglycine sulphate, ferroelectric switching, domain wall motion 3-64612
- triglycine sulphate, i.r. reflection spectra 3-80041
- triglycine sulphate, irradiation influence on ferroelec. props. (Polish) 3-50526
- triglycine sulphate, laser damage rel. to pyroelectric detectors 3-66859
- triglycine sulphate, molecular field theory, dielectric constant, spontaneous polarisation obs. 3-72565
- triglycine sulphate, phenomenological parameters, mol. field and thermodynamic theories 3-79991
- triglycine sulphate, temp. dependence of pyroelectric volt. response to step i.r. signals 3-44377
- triglycine sulphate, thermal gradient effects on intensity of diffracted X-rays (French) 3-63924
- triglycine sulphate, X-ray struct. damage 3-49903
- triglycine sulphate crystals, ferroelectric domain wall thickness, evaluation from thermal diffusivity data 3-50522
- triglycine sulphate crystals, influence of defects on optical behaviour near fundamental absorption edge 3-80081
- triglycine sulphate crystals, thermal conductivity, thermal diffusivity, ferroelectric and paraelectric, effect of growth conditions 3-50031
- 1, 2, 3-trihalogenobenzene, Raman spectra, detection of crystalline isomorphism 3-75991
- trihalomethyl radicals, isolated in rare gas matrices, i.r. spectra 3-75043
- triisopropyl phosphate and amine complex stability constant and dipole moment determ. from permittivity meas. 3-65118
- trimers, mag. circular dichroism, vibronic coupling 3-74993
- 1,2,4-trimethyl benzene, donor in binary solutions, energy transfer 3-80108
- trimethyl bismuth, mol. struct. determ. by electron diffraction 3-74926
- trimethyl derivatives, $(\text{CH}_3)_3\text{M}$ (M=N, P, CH, SiH), conform. analysis, CNDO/2 calcs. 3-46222
- trimethylamine, mol. A_2 torsional frequency by computer aided microwave anal. 3-78821
- trimethylamine-borane, microwave spectra, struct., dipole moment, rot. consts. 3-60465
- trimethylchlorosilane, nuclear quadrupole coupling and rotational const. determ. from microwave spectra (German) 3-60468
- trimethylcyanosilane, ^{29}Si n.m.r. 3-68878
- trimethylene chloroarsenite, heterocyclic, vibrational spectra and conformation 3-63472
- trimethylene chlorophosphite, heterocyclic, vibrational spectra and conformation 3-63472
- trimethylene oxide, far i.r. spectra, double minimum potential function 3-75022
- trimethylene oxide, p.m.r. spectra, ring puckering vibr., chem. shifts and spin-spin coupling meas. 3-54726
- trimethylene sulphide, deuterated analogues, ring puckering 3-78792
- trimethylene sulphide, p.m.r. spectra, ring puckering vibr., chem. shifts and spin-spin coupling meas. 3-54726

organic compounds continued

- trimethylenecyclophosphite, molecular structure, electron diffraction 3-78656
- trimethylphosphate, molecular structure determ. (German) 3-60403
- trimethylphosphine oxide with carboxylic acid complexes, $\nu\text{P}=\text{O}$, $\nu\text{C}=\text{O}$ bands, i.r. spectra 3-75989
- trimethylsilyl cyanide and isocyanide, microwave spectra, rotational consts. and structure 3-43462
- 1,3,5-trinitrobenzene, single crystal growth, precipitant infusion method, X-ray examination 3-80153
- 1,3,5-trinitrobenzene-aromatic hydrocarbon charge-transfer complexes in glassy solns., temperature effects on absorption and fluorescence spectra (French) 3-50847
- s-trinitrobenzene-s-triaminobenzene crystal complex, i.r. spectrum 3-76008
- 1,3,5-trinitrohexahydro-s-triazine, i.r. and Raman study, heat capacity determ. 3-80059
- 2,4,6-trinitrotoluene, single crystal growth, precipitant infusion method, X-ray examination 3-80153
- 2,8,9-trioxadamantane, microwave spectrum 3-40636
- 1,3,5-triphenylbenzene, elastic-vibration amplitudes, thermal diffuse scattering obs. 3-64118
- triphenylcarbonium derivatives absolute fluorescence yields and bond order change during electronic transition (German) 3-57665
- triphenylene:Zn porphyrin, low temp. optical absorption spectra 3-55653
- triphenylmethyl radical, ^{13}C -E.S.R. coupling constants, π -radicals, hyperconjugation 3-78850
- 1,3,5-triphenylpyrazoline, substitution effects on electronic structure and fluorescence (Russian) 3-63395
- triphenylsilane, ^{29}Si n.m.r. 3-68878
- 2,4,6-triphenyltriazine, Raman active lattice spectrum, 300 and 30K 3-55578
- triptycenes, substituted, optical activity theory and absolute config. meas. 3-47288
- 1,1,2-trisubstituted ethanes, p.m.r. spectrum, theoretical appl. of coupling consts. depend. on internal rot. pot. function 3-46318
- trisubstituted methanes, ab initio MO calc. of conformations and stabilities 3-49429
- 1,6,6a ^{34}Si -trithiapentalene oxygenated isologues, CNDO/2-SCF-MO calc., $\text{S} \dots \text{O}$ interactions (French) 3-43412
- 1,6,6a ^{34}Si -trithiapentalene substituted oxygenated derivatives, CNDO/2 calc. of preferred conformations (French) 3-43413
- tropolone, near u.v. absorpt. vibr. anal. 3-54671
- tropone, microwave spectrum, molecular Zeeman effect, magnetic susceptibility 3-63481
- trotyl nitroethers, rate of combustion at high pressures, rel. to temp. of flame (Russian) 3-47539
- tryptophan, far u.v. absorption and circular dichroism spectra 3-63574
- tryptophan in ethylene glycol/water glass, recombination luminescence and trapped electron decay 3-55695
- Tschiischibabin (quinoid) type hydrocarbons, triplet state, e.s.r. meas. and Huckel calc. (German) 3-63511
- TTF TCNQ, low temp. specific heat, 89.5 K Debye temp. meas. 3-79500
- TTF-TCNQ, giant cond. 3-68741
- TTF-TCNQ, metal-insulator transition, BCS pairing suppression, Peierls instability 3-64388
- TTF-TCNQ, thermopower, 10-300K, metal-insulator transition 3-64387
- two-proton system with hindered rot., methyl group tunnelling, n.m.r. lineshapes 3-64562
- unsaturated hydrocarbons, bond order-bond length relationship, VESCF method 3-54605
- unsaturated molecule threshold electron energy-loss spectra 3-67789
- uranin, low conc. in aqueous soln., emission spectra rel. to ionic balance 3-58791
- uranine, aqueous solutions, fluorescence light intensity, influence of degree of dispersion 3-41575
- uranyl acetate, vibronic interaction, luminescence spectra 3-72748
- uranyl butyrate, vibronic interaction, luminescence spectra, 3-72748
- uranyl compounds, spectra of optically active mol. crystals, vibr., symm. 3-72603
- uranyl diformate, anhydrous and monohydrate, luminescence spectra, 77K (French) 3-69065
- uranyl propionate, vibronic interaction, luminescence spectra 3-72748
- urea, electrical conductivity meas. 3-58257
- urea, proton second moments at 77 K 3-72071
- urea, Raman spectra, external modes, vibr. amplitudes 3-72658
- urea and deuterium derivatives, vibr. spectrum calcs. 3-63415
- uridine, solvent effects on ^{13}C n.m.r. spectra 3-63512
- vanadium salts, X-ray photoelectron spectra, binding energy 3-50642
- vanadyl tartrate, binuclear, soln. e.s.r., electron exchange interaction sign 3-58416
- vanillic aldehyde, chemiluminescence 3-55945
- vapours rel. to characteristics of Geiger counter gases in detection of exo electrons 3-59642
- vinyl, substituted compound, u.s. relax. of conformational equilibria 3-54615
- vinyl cation, C_2H_3^+ , classical and non-classical struct. approach 3-74911
- vinyl cpds., indirect H-H and ^{13}C -H spin-spin coupling consts., CNDO/2 calcs. (German) 3-63528
- vinyl groups on cyclopropane rings, torsional barriers INDO calc. 3-74924
- vinyl halides photoelectron spectra 3-46336
- vinyl monomers, chemical shift rel. to electron density, quantum theory calc. (German) 3-63527
- vinyl radicals, 1-substituted, geometrical study, INDO calc. 3-52325
- vinyl radicals, ab initio calcs., mol. fragments 3-78668
- vinyl-fluoride, dipole moment determ. 3-67750
- vinyl-Pt complexes, n.m.r., i.r., Raman data, coupling consts, hybridisation 3-75065
- vinylchloride, mass-spectrometric study in vacuum u.v., photoionisation curves and threshold energies 3-52395

organic compounds continued

- vinylfluoride, mass-spectrometric study in vacuum u.v., photoionisation curves and threshold energies 3-52395
 vinylous amides, hindered rotation, N-C bond, chemical shift, coupling constants 3-57668
 vinyltrimethylsilane, charge transfer reactions with Ar, in r.f. discharge, mass spectrometric ion sampling 3-73941
 vinyltrimethylsilane ion-molecule reactions with Ar in discharge apparatus, ion sampling 3-73940
 vitamin B₁₂, low symmetry e.s.r. spectra computer simulation 3-43528
 water-benzene-ethyl alcohol ternary system, shear viscosity and u.s. absorpt. near plat pt. 3-64204
 Wurster's blue perchlorate, aq. solns., temp. depend. scalar coupling, electron-nucl. Overhauser effect study 3-57671
 xanthine, polycrystalline, i.r. and vibrational spectra 3-76004
 o-xylene, in soln., effects of environment on excited states 3-60473
 p-xylene, in various solvents, orientational relax. rates, depolarised Rayleigh scatt. meas. 3-50574
 o-xylene, microwave spectra, methyl rot. barrier, methyl conform. and dipole moment 3-67832
 xylene, spray electrification 3-79759
 xylenes, effect of environment on decay times lifetime meas., phosphorescence 3-65098
 xylenes and methylene chloride mixture, dielectric polarisation, n.m.r., u.v. and i.r. studies 3-58817
 o-xylyl, rotational contour analysis of electronic origin band in emission spectrum at 4683 Å 3-67794
 yttrium ethyl sulphate: Dy, Yb, proton polarisation and relaxation, pulsed refrigerator optimal conditions 3-47161
 yttrium ethyl sulphate: Er, c.w. n.m.r. spectrometer for H₁ field meas. 3-45538
 yttrium ethyl sulphate, hyperfine interaction of ¹⁶⁶Er, γ - γ directional correl. obs. (French) 3-47179
 yttrium ethyl sulphate, hyperfine interactions of ¹⁶⁶Ho³⁺, influence on directional correl. of $\gamma\gamma$ cascade (French) 3-53039
 yttrium ethyl-sulphate 9H₂O:Yb³⁺, nuclear spin diffusion barrier obs. 3-75904
 zinc acetate, irradiated single crystals, ELDOR study, nuclear spin exchange influence 3-53326
 zinc formate, Mossbauer investigation of cation positions in iron formate mixture (German) 3-79967
 zinc phthalocyanine, in n-decane matrix, multiplet struct. of quasiline spectra 3-72734
 zinc phthalocyanine, photoconductivity induced by ruby and glass lasers, thermally stimulated current, drift mobility 3-50237
 zinc porphyrin, in Shpol'ski hosts, optical and Zeeman studies 3-72737
 α -particle, molecular stopping cross sections 3-56554
 N-aryl substituted hydroxamic acids, i.r. spectra (Russian) 3-63480
 As(C₂F₃)₃, i.r. and Raman spectra and ¹⁹F n.m.r. 3-71561
 2-benzylidenecyclohexanone oximes, substituted, mass spectra 3-63530
 n-butylacetylene, i.r. spectrum, Fermi resonance 3-44410
 CH₄, rotational transitions in v₃=1 excited state, i.r. microwave double resonance method 3-52373
 CO⁺ (A² Π) formation from He(2³S) interaction with COS⁺, H₂CO⁺, HCOOH⁺ and (HCO)₂⁺ 3-54736
 difluoro-chloro-methane, vacuum u.v. photolysis, matrix isolation study, i.r. spectra 3-40629
 N,N-dimethylamides, chalcogen replaced, hindered rot. about N-C amido band 3-52389
 FeOCl-pyridine complex, mag. props., Mossbauer obs. 3-58450
 p-fluorophenylalanine labelled ¹⁸F, for pancreas/liver scanning in rats 3-42370
 HB-40, thermal conductivity 3-72236
 H₂CO, collision-induced transitions, velocity depend., obs. by triple resonance method 3-52384
 H₂NO...HF hydrogen bonded radical, ab-initio study of stable configurations 3-43398
 H₂TBP, paramag., polarisation, simulation, frozen hydrocarbon matrices, para and nonparamag. porphyrins 3-48125
 hexamethylbenzene, phase transition at 116 K, phase III morphology, vib. spectra and absorpt. anisotropy 3-60794
 macromolecule, methyl group behaviour, internal rotation and nonexponential nuclear relaxation 3-79936
 methane, ionization and dissociation by electron impact, expt. obs. 3-54742
 methane-He mixture, phase equilibria at high press., astron. appl. 3-42162
 Na₃[Ce(C₂H₃NO₄)₂].15H₂O, thermal contact with liq. He, millikelvin temps. 3-45458
 P(C₂F₃)₃, i.r. and Raman spectra and ¹⁹F n.m.r. 3-71561
 n-paraffins, low frequency Raman-active lattice vibrations 3-55577
 Sb(C₂F₃)₃, i.r. and Raman spectra and ¹⁹F n.m.r. 3-71561

organic insulating materials

- see also insulating oils; paper; plastics; rubber; silicones; varnish; waxes
 chlorobiphenyls, space charge effects at solid/liquid interfaces 3-47210
 epoxy resin, tree growth characs. caused by discharges in artificial cavities 3-50519
 epoxy resins cured by acid anhydride, electrical conductivity rel. to struct. features 3-47467
 n-hexane, particulate charge carriers, electrohydrodynamic instability 3-46863
 impregnated paper, dielectric loss under simultaneous action of a.c. and d.c. fields 3-47207
 internal discharge, SEM obs. 3-47212
 perspex, dielectric breakdown 3-64604
 poly(ethylene terephthalate) film, electron irradi., cross-linking and chain scission 3-6596
 polyethylene, γ -ray irradi., elec. cond., after annealing 3-46864
 polyethylene, electrical treeing resistance, effect of liquid absorption 3-47216
 polyethylene, low density, tree growth characs. caused by discharges in artificial cavities 3-50519
 polyethylene, oxidised, electric breakdown at -196°C and -65°C 3-50515
 polyethylene, treeing, growth and forms rel. to generated gas volume 3-50518

organic insulating materials continued

- polyethylene sheet, effects of corona discharges, SEM obs. 3-63899
 polyimide, photocond. under electrical stress 3-46878
 polymer, discharge channel initiation and propagation 3-47213
 polymer, treeing breakdown, voltage induced mechanism, review 3-47214
 polymeric, examination of discharge and chemical treeing 3-50516
 polymers, electrical properties, review 3-44363
 polymethylmethacrylate, tree growth characs. caused by discharges in artificial cavities 3-50519
 polymethylmethacrylate, void free, ambient O₂ effect on a.c. tree generation 3-47215
 polypropylene film-trichlorobiphenyl system, a.c. conduction and dielectric losses 3-47211
 transparent polymer, tree propagation under oil using needle electrode 3-47217
 volume discharges and treeing, sharp pointed electrode obs. 3-50517
 xylene, spray electrification 3-79759

organic molecule configurations and dimensions

- 1,2-bis-(4-pyridyl) ethanes conformations of the rot. isomers, Raman and i.r. spectra 3-78772
 N-(diphenylmethylene)-aniline, dihedral angle of A ring determ. by n.m.r., e.s.r. and from Fraenkel relation 3-71486
 acenaphthene vinyl ethers, i.r. spectra, config., vib. (Russian) 3-63479
 acetonitrile, and liq. struct., X-ray scatt. (German) 3-63944
 acetonitrile-phenol complex, CNDO/2 calcs. (French) 3-43390
 acetophenones, substituent effects on acetyl group config. rel. to carbonyl frequency 3-63353
 acetylated glycopyranosyl chlorides, ³⁵Cl pure n.q.r., coupling const. and mol. conformation relation 3-49491
 acyl peroxide oligomers, i.r. spectral analysis (Russian) 3-78777
 alicyclic amines, Raman spectra, Bohlmann bands 3-75027
 n-alkane, chain flexibility, Monte Carlo simulation 3-60400
 1-alkyl-3-aryltriazenes, tautomerism, n.m.r. spectroscopy 3-74929
 alkylsilanes, force consts. determ. 3-67776
 allene, excited states, CNDO calc. using ligand geometries in transition metal complexes 3-60419
 aminodifluorophosphine, CNDO/2 approximation for conformational analysis (French) 3-63359
 6-aminopenicillanic acid, vibrational spectra, structural analysis (Russian) 3-78778
 aniline, mol. configuration determination, models for internal rotation, n.m.r. lanthanide shift studies 3-46226
 7-azaindole, multiple excitation, biprotonic phototautomerism, hydrogen-bonded dimers, fluorescence 3-63548
 benzil, phenyl ring positions determ. by n.m.r., e.s.r. and from Fraenkel relation 3-71486
 benzo-1, 4-dioxane derivatives, electronic spectrum bands, hydrogen bonding 3-67764
 benzoic acid, methyl derivatives, Pariser-Parr-Pople calc. of conformations (French) 3-63379
 benzophenones, orthosubstituted, conformational preferences, ¹³C n.m.r., calc. torsional angles 3-49489
 p-benzoquinone, gaseous, electron diff. obs. 3-54606
 benzvalene, six isotopic species, microwave structural study 3-78814
 benzylpenicillin, vibrational spectra, structural analysis (Russian) 3-78778
 beryllocene, and cryst. struct., X-ray diff. obs. 3-52308
 bicyclic alcohol, mol. configuration determination, models for internal rotation, n.m.r. lanthanide shift studies 3-46226
 bicyclo(3.1.0)hexane analogs, far i.r. spectra, ring puckering vibr., mol. config. 3-63456
 bis(trimethylgermyl)ketene, electron diff. of vapour, meas. parameters 3-63361
 bromotrichloromethane, thermal decomp. phenomena, electron diff. obs. 3-65074
 1,3-butadiene, conformers and internal rotation barriers, MO-SCF study 3-54607
 butanol-2-(+), circular dichroism, comparison of theoretical and expt. results of rot. strengths 3-78746
 carbohydrate crystals, i.r. spectra, polysaccharide transition 3-72655
 carboxylic esters and derivatives, vapour, liquid phases 3-74927
 chain molecules, n.m.r. conformational analysis using local interaction model 3-71487
 β -chloroalkyl radicals, struct. and conform., isotropic e.s.r. g-values and h.f.s. 3-60397
 4-chloroanthraquinonoxadiazole, crystal and molecular structure 3-79331
 chlorobenzene, geometric variations with orientation in nematic phase, INDOR determ. 3-54720
 chlorocyclohexane, equatorial, microwave rot. spectra anal. 3-78811
 chloroform intermol. complexes, spectroscopic and dielec. investig., comparison 3-74931
 chloronitromethane, gas phase, electron diffraction 3-78655
 N-chloropiperidine, vibrational analysis and conformation (Russian) 3-63476
 p-chlorostyrene, rot. band contour analysis of O₀⁰ bands of A'A'-X'A' systems 3-63446
 β -chlorovinylketones, Pariser-Parr-Pople calculations, conformational assignment 3-67733
 complex hydrogen bonded cations, stretching and bending modes, vibrational spectra, proton potential 3-75031
 conformational anal. by ¹³C n.m.r., lanthanide shift reagents, T₁ meas. 3-67855
 conjugated systems, barriers to internal rotation magnitude estimation from Raman spectra 3-63368
 cyanmelluric acid salts, cyanmelluric ring charact. freq. in i.r. spectra (Russian) 3-71565
 cyanocyclobutane, μ -wave spectrum, dipole moment quadrupole coupling consts. and conformation study 3-40634
 cyanocyclobutane, ring conformation, microwave spectra 3-63484
 cyclofols in solution, MO-LCAO calc. of conformations 3-60402
 cyclobutadiene (and deuterated), ground state potential energy surfaces, relevance to i.r. data 3-78662

organic molecule configurations and dimensions continued

- cyclobutane, C-H bond length and stretching force const. CNDO/2 calc. 3-74925
- 1,3-cyclohexadiene, photochem. dimerisation, decay of light excited mols. 3-63549
- cyclohexadienes, 1,4- and 1,3-, Raman spectra, barriers to planarity 3-60453
- cyclooctatetraene, in nematic solvents, n.m.r. studies of struct. and bond shift kinetics 3-71576
- trans-cyclooctene, electron diffraction study, chair conformation, bond lengths and angles 3-46225
- cyclopent-3-enone, microwave spectra, ring polarity, r_s -structure and dipole moment 3-60466
- cyclopent-3-enone, out-of-plane ring modes from far i.r., Raman and microwave spectra, pot. function 3-60467
- cyclopentadienone, microwave spectra analysis and assignments 3-78813
- cyclopentane, extended Huckel theory, energy gradients, stable configurations 3-71489
- cyclopropane, C-H bond length and stretching force const. CNDO/2 calc. 3-74925
- cyclopropenone, microwave spectrum, Stark and Zeeman effects 3-63482
- deformation induced by liq. cryst. solvents 3-58417
- diacetoneglucose, mol. configuration determination, models for internal rotation, n.m.r. lanthanide shift studies 3-46226
- dialkyl cadmium, magneto-optical conformational analysis (*French*) 3-54609
- dialkyl mercury, magneto-optical conformational analysis (*French*) 3-54609
- dialkyl zinc, magneto-optical conformational analysis (*French*) 3-54609
- diaryl disulphides, conformational props. calc. from dipole moments 3-43395
- 4,4'-dichlorobiphenyl oriented in nematic M.B.B.A., structure and conformation determ. by n.m.r. 3-67853
- diethylamine and Cu(II) complex, i.r. spectrum, structural investigation 3-78763
- p-difluorobenzene, CNDO-CI calcs. for ground and excited states 3-60423
- m-difluorobenzene, electron diff. obs. 3-63356
- m-difluorobenzene, n.m.r. in nematic solvents, geom. and indirect F-F coupling anisotropy 3-60477
- 1,2-difluoroethane, from gas phase electron diffraction 3-43392
- 1,2-difluoroethane, gauche structure determ. from n.m.r. in nematic solvents 3-43482
- 11,11-difluoroethene, vibr. corrections of dipolar couplings 3-78700
- 3,4-dihydro-2H-1,5-benzodioxepin-2,4-dicarboxylic acid, conformation 3-74921
- 2,3-dihydrofuran, Raman spectra, barrier to planarity 3-75021
- 2,3-dihydrothiophene, Raman spectra, barrier to planarity 3-75021
- 3,4-dihydroxy L-phenyl-alanine, cryst. and molecular structure, H-bonding 3-60720
- 1,8-diiodoanthraquinone, crystal and mol. structure 3-79332
- trans-1,4-diiodocyclohexane, vibrational analysis and conformation (*Russian*) 3-63476
- β -diketones, rare earth complexes, i.r. spectral assignments, symm. 3-78751
- 2,4-dimethoxypentane, ^{13}C n.m.r. studies on stereochemical configurations 3-63577
- dimethyl and diethyl-2,2-stanna-1,3-cyclopentanes, conformation (*French*) 3-43454
- dimethyl cyanamide, bond lengths and angles, microwave spectra 3-60464
- 1,3-dimethyl-2-chloro-diazaboracyclopentane, struct., electron diffraction determ. 3-74922
- dimethylacetylene substituted molecule, anal. of Hamiltonian, symmetry group and vibr. coords. 3-74975
- dimethylaminodifluorophosphine, CNDO/2 approximation for conformational analysis (*French*) 3-63359
- dimethylaminodifluorophosphine, microwave spectra data 3-49476
- m-dinitrobenzenes, various substituents 3-74928
- dinucleotides, backbone conformation, ^{13}P and ^1H fast Fourier transform n.m.r. spectroscopy 3-67850
- 3,6-dioxabicyclo[3.1.0]hexane, microwave spectrum, dipole moment, conformation 3-63486
- 1,4-dioxacyclohexadiene-2,5, far i.r. spectra, struct., ring bending modes 3-40624
- diphenyl, i.r. spectra, conformation 3-75016
- diphenylmethyl radical, stereochem., e.s.r. data interpret., INDO-MO calcs. 3-46228
- α,ω -diphenylperfluoropolyenes, effect of fluorination on conjugation, UV and Raman spectra, steric struct. of mols. 3-71520
- dipyridyls, ($\alpha\alpha'$ - and $\gamma\gamma'$), i.r. spectra, conformation 3-75016
- 1,2-disubstituted ethanes, ab initio MO calc. of conformational preferences 3-49451
- disulphides, charge transfer complexes with various acceptors, u.v. spectra and bond angle study 3-46263
- cis-1,4-ditertiarybutylcyclohexane, combined electron diff., conform. energy and vibr. obs. 3-63357
- dithiophosphorinanes, [1,3,2] and [1,3,2]-dioxo-, FT ^{13}C n.m.r. spectra 3-71591
- esters, elec. dipole moment at 1 MHz for mol. config. determ. 3-52350
- ethyl cation, C_2H^+ , classical and non-classical struct. approach 3-74911
- ethyl chloroformate, vibrational spectra, rotational isomerism, normal coordinate analysis, mean amplitudes 3-54687
- ethyl cyanoformate, vibrational spectra, rotational isomerism, normal coordinate analysis, mean amplitudes 3-54687
- ethyl fluoride, conform., i.r. spectra obs. 3-75037
- ethyl formate, vibrational spectra, rotational isomerism, normal coordinate analysis, mean amplitudes 3-54687
- ethylcarbonium ion, nonempirical MO calcs. of energies rel. to geom. 3-63354
- ethylene, and similitudes, mols. symmetry effects in internal rotation 3-74974
- ethylene chlorine complex, struct. determ. from spectra 3-54608

organic molecule configurations and dimensions continued

- ethylene sulphite and chlorophosphite, vibration and i.r. spectra, conform. (*Russian*) 3-71492
- ethylenes, substituted, electronegativity effect on bond lengths 3-67728
- fluoroacetones, n.m.r. coupling consts. and rot. isomerism 3-46323
- fluoroacetophenones, elec. dipole moments and conformations, o-, m- and p- 3-67724
- fluoromethanol, anomeric effect 3-60417
- fluoromethanol, conformation, localized molecular orbitals, excited state geometry, gauche effect 3-74914
- p-fluorostyrene, rot. band contour analysis of O_0^0 bands of $\text{A}^1\text{A}'-\text{X}^1\text{A}'$ systems 3-63446
- 1-fluorovinyl cations, geometrical study, INDO calc. 3-52325
- formaldehyde, energy function calc. for geometry optimisation 3-71490
- formimide, microwave spectrum, gas phase conformational props. of amide bond 3-63483
- formyl chloride, struct., decomp., i.r. spectra, vibr. assignments 3-78753
- formyl radical, energy function calc. for geometry optimisation 3-71490
- fumaric acid, monoalkyl esters, hydrogen bonding, i.r. spectra conformations 3-63468
- furan, reorientation, effect on i.r. bandwidth 3-68996
- furan, solid and liquid, i.r. spectra and struct. (*French*) 3-75033
- glycine, mono-, di-, tri-, tetra-, and pentapeptides, SCF molecular fragment approach 3-78669
- glycol monoformate, gaseous, electron diff., i.r. spectra, conformations, bond lengths 3-63362
- glycolaldehydes, microwave spectra, substitution struct., intramolecular hydrogen bond and dipole moment 3-54703
- 1-halo-1-methylcyclohexanes, conformational equilibrium, i.r. spectra 3-78764
- halocyclopentanes, n.m.r. spectra, conformations, calcs. 3-63366
- heptafulvalene mol., cause of nonplanarity, bond angle strain 3-46220
- heptafulvalene mol., cause of nonplanarity, ring strain, H repulsion 3-46221
- hexachlorocyclopropane, electron diffraction determ. 3-54612
- hexafluoroazomethane, trans. configuration 3-43452
- hexafluorobenzene, C-F bond length 3-54691
- hexamethyl-tetracarbaheptaborane(6), molecular struct. determ. (*German*) 3-43397
- hydrocarbon chains, correlation functions of internal motion 3-78847
- hydrocarbons, conformation and distortion, n.m.r. and i.r. spectra (*Russian*) 3-71491
- hydrocarbons, conjugated, graph theory applic. to topology depend. of π -electron parameters 3-46238
- hydrocarbons, mol. formulae, calc. from mol. weight, functional analysis (*Rumanian*) 3-71484
- hydrocarbons with delocalized electronic systems, molecular mechanics method for bond order determ. 3-67729
- 6-hydroxy-2-formylfulvene, H-bonding, molecular symmetry, microwave spectra 3-54698
- trans-hydroxy-L-proline, proton NMR spectra, computer simulation, long range coupling constant, structural implications 3-75074
- hydroxymethylcarbonium ion, nonempirical MO calcs. of energies rel. to geom. 3-63354
- liquid crystals, correlation with liq. cryst. state of matter 3-71999
- maleic acid monoalkyl esters, hydrogen bonding, i.r. spectra conformations 3-63468
- methane, bond distances, stat. OCE calcs. (*German*) 3-67745
- methane selenol, μ -wave spectrum, internal rot. barrier, struct. and dipole moment meas. 3-54700
- methane sulfonyl chloride, mol. struct., electron diffraction study 3-74916
- methoxide ion tautomer, topomerization, tautomerization, gauche effect 3-78650
- 2-methoxytetrahydropyran, anomeric effect 3-60417
- methyl allenyl sulphide gas electron diffraction study of molecular struct. 3-54610
- methyl anion, inversion pot. surface, HF represent., augmented basis set 3-74910
- methyl chloride, geom., i.r. spectra analysis of methyl chloride- d_2 3-63455
- methyl chloroformate, microwave spectra, internal rot. barrier, mol. structure 3-75050
- methyl formate, methyl fluoroformate, INDO calcs. of dipole moment and conformation 3-63369
- 3-methyl pentene-2 isomers config. assignment, mol. struct., electron diff. 3-63360
- methyl vinyl sulphide gas electron diffraction study of molecular struct. 3-54610
- methylene thiocyanate, i.r. absorpt. spectra, 2 to 20 μ , point group C_2 GG conformation (*French*) 3-47273
- methyl fluoride, vibr. corrections of dipolar couplings 3-78700
- 4-methylumbelliferone and tautomer, extended Huckel molecular orbital calc. 3-52309
- methyloxocarbonium ion trimer, geometry, CNDO/BW calc. 3-67726
- molecular crystals, symm., vibr. transitions, optical activity 3-72603
- monofluorobenzene, CNDO-CI calcs. for ground and excited states 3-60423
- naphthalene mol. struct. determ. by n.m.r. in a nematic solvent 3-74919
- nitroethylene, isotopic species, microwave spectra, ground and excited vibrational states 3-78812
- 2,4,6-nonachloromesitylene, rotational isomerism, conformational energy, p.m.r. 3-67851
- olefins, nonconjugated, conformation, consistent force field calc. 3-71526
- oligomers and polymers, effect of chain length and conformation on i.r. spectra (*Russian*) 3-63583
- orthosubstituted diphenyl sulphones, n.m.r. data and conformational preferences 3-54718

organic molecule configurations and dimensions continued

- oxaly bromide gas, trans gauche conformation, internal rotation, electron diffraction 3-74913
- oxaly chloride, Raman spectra, study of structure of vapour phase 3-63459
- 3-oxypiperidone-4, stereochemical structure (Russian) 3-71493
- 3-oxytetrahydrothiopyranone-4, stereochemical structure (Russian) 3-71493
- pentanes, 2,4-disubstituted, n.m.r. conformation analysis using local interaction model 3-71487
- peptides, INDO finite perturbation calcs. of spin-spin coupling constants. J_{HPI} , J_{15H} , J_{15H13C} 3-74952
- perchlorodihydropentalene epsilon C_8Cl_8 , crystal structure, constitution (German) 3-75520
- phenol complexes with pyridines, dipole moments and struct. 3-63358
- phenol-formaldehyde resins, i.r. spectra and struct. (Russian) 3-49472
- phenols, ortho substituted, torsional frequencies and conformational equilibria 3-52310
- phenoxymethylpenicillin, vibrational spectra, structural analysis (Russian) 3-78778
- phenyldichlorophosphine, electron diffraction study of molecular structure 3-78659
- phenylethylenes, steric inhibition of resonance studied by photoelectron spectroscopy 3-54613
- β -pinene, electron diffraction meas. of conformation 3-78660
- planar conjugated hydrocarbon molecules, graphical model 3-66108
- porphyrin and alkylsubstituted derivatives, ^{13}C Fourier transform n.m.r. spectroscopy 3-71601
- porphyrins, fluoresc. polarisation time depend., imino H displacement 3-49485
- propene, mol. struct. determ. by electron diffraction 3-74918
- propionaldehyde, mol. struct., ab initio and semi-empirical calc. 3-74920
- n-propyl fluoride, conform., i.r. spectra obs. 3-75037
- propynal, CNDO/2 calcs. 3-67755
- propyne, geom., i.r. spectra analysis of propyne- d_2 3-63455
- pyridinaldehydes, energy conform. obs., INDO calcs. 3-60401
- pyridine asymmetric ion hydrogen bonded complexes, i.r. and Raman spectra 3-75030
- pyridine hydrogen bonded complexes, vibrational spectra 3-75029
- pyridine nucleotides, conformation, ^{13}P and ^1H fast Fourier transform n.m.r. spectroscopy 3-67850
- pyridinium trihalides, Raman, i.r. and electronic absorption spectra, struct. 3-75032
- pyridinium-pyridine ion, complex hydrogen bonded cations, i.r. and Raman spectra obs. 3-75028
- pyrimidine nucleosides, syn conformation stability, INDO method hydrogen bonding 3-63363
- L-pyrogutamic acid, n.m.r. spectra and conformations, and related compounds (French) 3-63519
- quinolizidine alkaloids, structure and conformational states, ^{13}C n.m.r. spectra 3-71587
- radicals, e.s.r., β -proton splittings 3-67730
- selenium pentamethylene heterocycle, conformational properties 3-78654
- sodium bromoacetate, and - d_2 , vibr. spectra and structure 3-78798
- sodium bromoacetate and sodium bromoacetate- d_2 , vibrational spectra and struct. 3-75987
- spiropyran, coloured isomeric forms struct. stability, extended Huckel method study 3-74923
- styrene, nonplanar conformation 3-52387
- tellurium pentamethylene heterocycle, conformational properties 3-78654
- 1,1,2,2-tetracyanocyclopropane, cryst. and mol. struct. 3-46219
- tetrafluoroethylenetetracarboxyl, molecular structure, gas phase electron diffraction 3-60718
- 2'-O-tetrahydropyranlyluridine, dextrorotatory, crystal struct. 3-79329
- N,P,P-tetramethylphosphine imide and N-methyl- d_3 analogue, vibr. spectra analysis 3-78795
- tetramethyltin derivs., $(\text{CH}_3)_4\text{-xSnX}_x$, effect of donor atom and ligand size on struct. 3-79330
- tetraphenylethylene, conformation of phenyl rings, using n.m.r. and Fraenkel relation 3-71485
- thiophene, solid and liquid, i.r. spectra and struct. (French) 3-75033
- 2-thiopheneldehyde, gas, microwave study, O-S trans rotamer identification 3-63365
- 1,2,3-tribromopropane, vibr. spectra, anti-gauche conformer 3-63465
- 1,2,3-trichloropropane, vibr. spectra, anti-gauche conformer 3-63465
- triethylenediamine, UV absorpt. spectrum anal. of struct. 3-78740
- 1,3,5-trifluorobenzene, C-F bond length 3-54691
- trifluoroethylene, equilibrium configuration 3-43461
- trifluoromethylacetophenones, elec. dipole moments and conformations, o-, m- and p- 3-67724
- 3,3,3-trifluoropropene, mol. struct. determ. by electron diffraction 3-74918
- trimethyl bismuth, mol. struct. determ. by electron diffraction 3-74926
- trimethyl derivatives, $(\text{CH}_3)_3\text{M}$ (M=N, P, CH, SiH), conform. analysis, CNDO/2 calcs. 3-46222
- trimethylamine-borane, bond lengths and angles, microwave spectra 3-60465
- cis-1,2,3-trimethylcyclopropane, stereochemistry of free radical ring cleavage by Br 3-47547
- trimethylene chloroarsenite, heterocyclic, vibrational spectra and conformation 3-63472
- trimethylene chlorophosphite, heterocyclic, vibrational spectra and conformation 3-63472
- trimethylenechlorophosphite, electron diffraction 3-78656
- trimethylphosphate, molecular structure determ. (German) 3-60403
- trimethylsilyl cyanide and isocyanide, microwave spectra data 3-43462
- triphenylmethyl radical, ^{13}C -E.S.R. coupling constants, π -radicals, hyperconjugation 3-78850

organic molecule configurations and dimensions continued

- tritylenes, substituted, optical activity theory and absolute config. meas. 3-47288
- trisubstituted methanes, ab initio MO calc. of conformations and stabilities 3-49429
- 1,6,6aSi^{IV}-trithiapentalene substituted oxygenated derivatives, CNDO/2 calc. of preferred conformations (French) 3-43413
- Tschitschibabin (quinoid) type hydrocarbons, triplet state, twisting angles (German) 3-63511
- vinyl, substituted compound, u.s. relax. of conformational equilibria 3-54615
- vinyl cation, C_2H_3^+ , classical and non-classical struct. approach 3-74911
- vinyl groups on cyclopropane rings, torsional barriers INDO calc. 3-74924
- vinyl radicals, 1-substituted, geometrical study, INDO calc. 3-52325
- o-xylene, microwave spectra, methyl rot. barrier, methyl conform. and dipole moment 3-67832
- N-aryl substituted hydroxamic acids, i.r. spectra (Russian) 3-63480
- $\text{H}_2\text{NO}\dots\text{HF}$ hydrogen bonded radical, ab-initio study of stable configurations 3-43398
- organic molecule electronic structure**
- di- μ -(pyridine N-oxide)bis [bisnitrate (pyridine N-oxide) copper (II)], e.p.r. spectrum, triplet ground state, computer simulation 3-75075
- acetaldehyde, localized charge distribution and internal rotation barriers 3-54633
- acetonitrile-phenol complex, CNDO/2 calcs. (French) 3-43390
- acetylene, vertical electronic transitions, Slater-type orbitals, two-centre calc. (Russian) 3-49444
- aldehydes, static and dynamical pot. surface distortions in $^3\text{A}''(\pi\pi^*)$ states 3-63382
- aliphatic compounds, additive character of displacements of inner atom levels 3-78684
- aliphatic cpds., influence of substituents on $\pi\pi^*$ and $\pi\pi^*$ absorption bands (Russian) 3-43441
- alkyl derivs., straight chain, electron density distrib. 3-71525
- alkyl mercaptans far i.r. spectra, torsional transitions 3-63457
- amines, non-planar aromatic, spin-forbidden electronic transitions 3-46237
- amino acids containing S, γ -irrad., electronic structure parameters of free radicals, expanded Huckel meth. 3-78681
- aminoacids, rel. to photoconductivity obs. (Russian) 3-46365
- 2-aminopyridine, solvent effect on levels, fluoresc. 3-69085
- aminopyridines, phosphoresc. emission and polarization, triplet states 3-65101
- aromatic cpds., influence of substituents on $\pi\pi^*$ and $\pi\pi^*$ absorption bands (Russian) 3-43441
- aromatic cpds., radiative transition rate from π,π^* triplet state, external heavy-atom enhancement mechanism 3-40642
- aromatic nitrogen heterocyclic ions, two-centre Coulomb repulsion integrals effect on spin densities 3-60426
- arsabenzene, data from photoelectron spectra 3-46255
- aziridine-borane, electronic structure, BN bond, charge transfer 3-46242
- azulene, benzophenone (naphthalene), impurity change of polarisability and dipole moment, $^1\pi\pi^*$ state 3-72662
- benzene, electronic model, stability conditions for maximum overlap Brueckner independent particle wave functions 3-67743
- benzene, full Π , ab initio valence bond calc. 3-71508
- benzene anion, effects of orbital degeneracy on g-values 3-54723
- benzene derivatives, structure depend. of emission props., intramol. electron transfer 3-75061
- benzene-tetracyanoethylene, weak π -complex, calc. allowing for doubly-excited configurations (Russian) 3-67751
- benzenes, cyano-substituted, lowest excited triplet states, zero field splitting 3-78845
- benzenes, multi-homosubstituted, variable electronegativity SCF-MO calcs. 3-67736
- benzo-1,4-dioxane derivatives, electronic spectrum bands, hydrogen bonding 3-67764
- benzoic acid, methyl derivatives, Pariser-Parr-Pople calc. (French) 3-63379
- benzoic acids, highest occupied and lowest unoccupied mol. orbitals and total π -electronic energies, LCAO calc. 3-52318
- benzonitrile, vibronic spectra, theoretical study 3-67783
- benzophenone n, π^* triplet states, microwave-optical double resonance 3-80121
- p-benzoquinone, single crystals, Stark effects on low energy electronic states 3-76468
- benzotrifluorides Fourier transform n.m.r., high pressure, ^{19}F chemical shift 3-61003
- 1,12-benzperylene, n-heptane soln., fluorescence emission, second excited π -singlet state to singlet ground state 3-50848
- 3,4-benzpyrene, n-heptane soln., fluorescence emission, second excited π -singlet state to singlet ground state 3-50848
- benzyl radical, electronic states assignment by three-step photoselection 3-44735
- benzyl-type radicals, methyl substitution effect on electronic struct. and spectra 3-78731
- bicyclo [2,1,1] hexane, LCAO-MO-SCF calcs. using optimised minimal set of Gaussian functions 3-67761
- trans-butadiene, low lying π -electron states, configuration interaction calc. 3-74958
- trans-butadiene radical, valence bond and mol. orbital calcs., convergence comparison 3-43401
- carboranes, multi-centre bonding, ab initio and semi-empirical MO study 3-63391
- 4-chloronortricylene, ^{35}Cl nuclear quadrupole coupling constant, microwave spectra 3-71567
- 2-chlorotetrahydropyran, ab initio mol. wavefunction calc. 3-49491
- β -chlorovinylketones, Pariser-Parr-Pople calculations, conformational assignment 3-67733
- chromones, MO study of π -electronic struct. 3-71507
- conjugated moles. mag. props. and ring current chem. shift calc. 3-57637
- conjugated non-planar systems, two-centre Coulomb repulsion and overlap integrals 3-60425
- conjugated systems, application of RPA theory to excited states 3-52328

organic molecule electronic structure continued

- cryptocyanine, resonance spontaneous Raman scattering spectra 3-64655
- cyanine dyes, Huckel mol. orbital descriptions, contours approach 3-46232
- cyclopentadienide anions, cyano-substituted, mag. circular dichroism, electronic transitions 3-40607
- (2,2)p-cyclophane and related compounds 3-78734
- cyclopropanone, microwave spectrum, Stark and Zeeman effects 3-63482
- dibenzofuran, lowest singlet state obs. 3-67804
- p-difluorobenzene, CNDO-CI calcs. for ground and excited states 3-60423
- 2,4-dinitrotoluene, π -, σ -electronic struct., conversion in ground state, CNDO/2 calcs. (Russian) 3-78678
- diphenylnitroxide radical, polarised absorption spectra 3-63442
- α,ω -diphenylperfluoropolyenes, effect of fluorination on conjugation, UV and Raman spectra, steric struct. of mols. 3-71520
- disubstituted benzene derivatives containing two acceptor groups, p-electron SCF-MO calc., numerical results 3-57638
- disubstituted benzene derivatives containing two acceptor groups, p-electron SCF-MO calc. 3-63396
- 1,2-disubstituted ethanes, ab initio MO calc. of internal rotation 3-49451
- DNA, excited states, triplet quenching, photosensitisation 3-63588
- EDA complexes with liquid donors, excited singlet-singlet absorpt. spectra 3-76471
- π -electron energies estimation 3-78680
- ethane, vertical electronic transitions, Slater-type orbitals, two-centre calc. (Russian) 3-49444
- ethylene, band structure, self consistent field perturbation treatment 3-64289
- ethylene, vertical electronic transitions, Slater-type orbitals, two-centre calc. (Russian) 3-49444
- ethylene sulphide, photoelectron spectrum obs. 3-54627
- ethylenes, substituted, electronegativity effect on bond lengths 3-67728
- ethynylbenzene vibronic spectra, theoretical study 3-67783
- excited states of matter, symp., Lubbock, Texas, USA (Apr. 1971) 3-63547
- five-membered heterocycles, aromatic character, ring currents and proton chem. shifts, Hartree-Fock calcs. 3-60420
- fluoro-substituted quinolines π -electron densities, Pariser-Parr-Pople calc. 3-74957
- fluorobenzene, electrophilic substitution calcs. 3-78677
- fluorobenzenes, homo-substituted, ground state electronic struct., extended Huckel MO calcs. 3-67737
- fluorobenzenes, homosubstituted, all valence electron MO calcs. 3-67738
- fluoromethanol, anomeric effect 3-60417
- formaldehyde, illustration of calculated orbitals 3-63375
- formaldehyde energy function calc. for geometry optimisation 3-71490
- formic acid, ionic solvation, CNDO/2 calcs. on solvated univalent ions 3-53347
- formyl radical, energy function calc. for geometry optimisation 3-71490
- free radicals, organic, geometry change and substitution effects using INDO/CI formalism 3-63387
- ground state asymmetry, optical nonlinearities 3-62738
- guanidinium ion, ^{14}N -NQR study, quadrupole coupling obs. of bond electronic population 3-79943
- halobenzenes, π -orbitals, inductive and mesomeric effects 3-78690
- halogenbenzenes, mono- and disubstituted, tables of data 3-74967
- α -haloketones, optically active, fluorine anomaly 3-63393
- heptafluoro-n-propyl cyanide, ionisation, low electron energies, time-of-flight technique 3-57679
- heteroaromatic compounds, quantum chem. method for determ. intermediate ion structure 3-46241
- heterocycles with divalent sulphur, resonance energy calcs. from thermodynamical data 3-67753
- N-heterocyclic compounds, ortho, oxy, and methoxy substituted (Russian) 3-63395
- heteroorganic molecules, LCAO mol. orbital calcs., experimental criterion for correctness, energy of charge transfer 3-71499
- hydrocarbon, force field calcs. using CNDO/2 method 3-74951
- hydrocarbon conjugated free radicals, excitation spectra calc. using ensemble averaging schemes 3-67758
- hydrocarbon radical cations, fluorinated, spin density distrib. 3-57631
- hydrocarbon systems from five-membered rings, Huckel $4n+2$ rule 3-78689
- hydrocarbons, alternant, reson. energies calc. by semi-empirical method 3-67752
- hydrocarbons, conjugated, graph theory applic. to topology depend. of π -electron parameters 3-46238
- hydrocarbons, second moment of electronic charge distrib., additivity eqn. 3-74960
- hydrocarbons with delocalized electronic systems, molecular mechanics method for bond order determ. 3-67729
- ions, unrestricted CNDO/2, INDO methods 3-60424
- isopropyl alcohol far i.r. spectra, torsional transitions 3-63457
- isoquinoline vapour, electronic absorpt. spectrum assignments 3-67798
- isoquinolines, π -electron densities, Pariser-Parr-Pople calc. 3-74957
- ketones, aromatic, quenching of triplet state by O_2 in liq. soln. 3-76482
- metalloporphyrins, luminesc., triplet-triplet energy transfer 3-67847
- methane, $^{12}\text{CH}_4$, hyperfine splittings in rot. F_1 , F_2 levels of ground vibr. state 3-63401
- methane, ground state energies, stat. OCE calcs. (German) 3-67745
- methane, i.r.-r.f. double reson. study of pure rot. Q-branch transition 3-63405
- methane, molecule, NDDO calculations 3-52312
- methane, one-centre HF calculations on ground and excited states 3-71509
- 2-methoxytetrahydropyran, anomeric effect 3-60417

organic molecule electronic structure continued

- methyl alcohol, localized charge distribution and internal rotation barriers 3-54633
- methylamine, localized charge distribution and internal rotation barriers 3-54633
- N-methylazoles, chemical shift correl., substituent effect 3-75066
- methylene cyclobutadienyl radical, valence bond and mol. orbital calcs., convergence comparison 3-43401
- 3-methylene oxetane, μ -wave spectrum, mol. Zeeman effect, mag. susceptibility anisotropy, quadrupole moment meas. 3-52372
- molecular crystal, Davydov splitting, multipole approximation based on transition charge densities 3-80014
- monofluorobenzene, CNDO-CI calcs. for ground and excited states 3-60423
- naphthalenes, monosubstituted, electronic absorpt. spectra interpret. by config. analysis 3-67754
- naphthalenes, substituted, electronic systems, rot. band contour anal. 3-57641
- 1,5-naphthyridine in durene, polarized phosphoresc., assignment of lowest singlet n,π^* state 3-76472
- nitrile systems, calculation of one electron properties of CN^- ion 3-52327
- nitrobenzene, π -, σ -electronic struct., conversion in ground state, CNDO/2 calcs. (Russian) 3-78678
- o-nitrotoluene, π -, σ -electronic struct., conversion in ground state, CNDO/2 calcs. (Russian) 3-78678
- nucleic acid bases, in-plane electronic spectra using all valence electron MO-CI calcs 3-63386
- olefins and radical cations, CNDO/2 calcs. 3-54649
- organic three membered ring molecules, protonation, electrostatic versus SCF CNDO calc. 3-46234
- organo-phosphorus compounds, EX_3 type, $p-\pi$ conjugation, trivalent P, groups IV-VI, hybridisation of the at. orbital 3-71519
- organosilicon compounds, ^{13}C - ^{29}Si spin-spin coupling consts. calc. by max. overlap approx. 3-75070
- organosilicon compounds, ^{29}Si n.m.r. spectra 3-71596
- oxamides, mol. anal. phosphoresc. characts. 3-78833
- 3-oxetanone, μ -wave spectrum, mol. Zeeman effect, mag. susceptibility anisotropy, quadrupole moment meas. 3-52372
- pentacyclic aromatic hydrocarbon transitions interpret., composite system approx. 3-54645
- pentafluoroethyl cyanide, ionisation, low electron energies, time of flight technique 3-57679
- peptide bond protonation, SCF ab initio study 3-43407
- peptide systems, fragment studies, appl. to polypeptide characterisation 3-46360
- phenyl radical, hyperfine coupling, INDO calc., σ framework 3-52316
- phenylalanine, π -inductive effects rel. to π polarization effects 3-67747
- phenylalanine, π -inductive effects rel. to π polarization effects 3-67747
- phenylalkanes with polar or charged substituents, π -inductive effects rel. to π polarization effects 3-67747
- phenylglycine, π -inductive effects rel. to π polarization effects 3-67747
- phenylsilane, Si-phenyl ring bonding, photoelectron spectra 3-67749
- phosphabenzene, data from photoelectron spectra 3-46255
- phosphonium salts, ^{31}P n.m.r. obs., electron delocalization through P rel. to $d_{\pi}-p_{\pi}$ bonding 3-71597
- phthalic acids, highest occupied and lowest unoccupied mol. orbitals and total π -electronic energies, LCAO calc. 3-52318
- polycyenes, absorpt. spectra, exciton band shape, temp. depend. 3-69021
- polyatomic molecules and ions, genealogy in mol. spectroscopy, aromatic π -electron spectroscopy 3-63432
- polycyclic hydrocarbons, ^{13}C chemical shift, π -electron current effect 3-71588
- polymeric complexes, spectral study 3-63963
- polynucleotide chains, internal rot. barriers 3-46358
- polypeptides, rel. to photoconductivity obs. (Russian) 3-46365
- porphyrins, excited states, effects of metallic substitution 3-63550
- propene, localized charge distribution and internal rotation barriers 3-54633
- propionic acid CNDO/2 calc., energy, electron distrib. dipole moment origin 3-63389
- propylene, dipole moment determ. 3-67750
- propynal, CNDO/2 calcs. 3-67755
- propynal CNDO/2 calc., energy, electron distrib. dipole moment origin 3-63389
- proteins, rel. to photoconductivity obs. (Russian) 3-46365
- pyrazine, ab initio MO wave functions 3-63372
- pyridine, ab initio MO wave functions 3-63372
- pyridines, BEEM- π calcs. and ^{14}N n.q.r. 3-63526
- radicals, core level binding energies, multiplet splitting, unpaired orbital spin density distrib. 3-46236
- radicals, spin density calc. by modified INDO and MZDO methods 3-46231
- rhodamine 6G, ESR triplet state meas. 3-78028
- solutions under h.p., optical activity induced by chiral solvents 3-46254
- squaric acid and anions, π electronic struct. determ., near u.v. aq. soln. spectra 3-52360
- stibabenzene, data from photoelectron spectra 3-46255
- stibenes and analogs, electronic overlap populations as reactivity meas. in electrocyclic reactions 3-52317
- styrene, polymerisation effect on spectra, energy transfer 3-69081
- sulphur compounds, additive character of displacements of inner atom levels 3-78684
- TCNE-benzene charge transfer complex, resonant Raman effect and charge distrib. 3-75977
- TCNQ, satellites in high energy photoelectron spectra 3-52326
- tellurophene, microwave spectra, rot. consts., bonding 3-67826
- 1,1,2,2-tetracyanocyclopropane, cryst. and mol. struct. 3-46219
- tetramethyl-p-phenylenediamine, satellites in high energy photoelectron spectra 3-52326
- thioformaldehyde, ab initio calcs. for ground and low-lying triplet states 3-52323

organic molecule electronic structure continued

- thiophene, valence electron density, calc. using IEHT approach 3-63380
 thiophosgene, 2780 angstroms absorpt. system, vibrational structure 3-63441
 toluene, π -, σ -electronic struct., conversion in ground state, CNDO/2 calcs. (*Russian*) 3-78678
 toluene solid solution, mechanism of singlet, triplet state formation 3-76467
 s-triazine, lowest states, Stark, Zeeman effects 3-64674
 4-R-1,2,4-triazoline-3,5-diones, (R=H, CH₃, CH₂CH₃, CH₂CH₂CH₂CH₃) 3-49459
 triphenylmethyl radical, ¹³C-E.S.R. coupling constants, π -radicals, hyperconjugation 3-78850
 1,6,6aSiV-trithiapentalene oxygenated isologues, CNDO/2-SCF-MO calc., S...O interactions (*French*) 3-43412
 1,6,6aSiV-trithiapentalene substituted oxygenated derivatives, CNDO/2 calc. of preferred conformations (*French*) 3-43413
 Tschischibabin (quinoid) type hydrocarbons, triplet state (*German*) 3-63511
 urea, band structure, self consistent field perturbation treatment 3-64289
 vinyl monomers, chemical shift rel. to electron density, quantum theory calc. (*German*) 3-63527
 vinyl-fluoride, dipole moment determ. 3-67750
¹⁴C beta-decay chemical consequences 3-80570
 (N(C₂H₅)₄)₂ZnI₂:NiI₂²⁻, mag. circular dichroism spectrum, spin-orbit splitting, quenching 3-50601

organometallic compounds

- di- μ -(pyridine N-oxide)bis [bisnitrate (pyridine N-oxide) copper (II)], e.p.r. spectrum, triplet ground state, computer simulation 3-75075
 aniline intercalated transition metal dichalcogenide, absorpt. spectra 3-55607
 tert-benzylic metal compounds, structure and hindered rotation determ. by n.m.r. 3-63514
 beryllocene, mol. config. and cryst. struct., X-ray diffr. obs. 3-52308
 biferricenium, biferricenylum cations, ⁵⁷Fe Mossbauer spectra and intervalence transfer electronic absorpt. study 3-55507
 bis(cyclooctatetraene)iron, n.m.r. study, line-width and second moment rel. to temp. 3-50477
 chlorophyll assay, ocean and coastal zone, Earth Resources Technology Satellite 3-80717
 copper porphyrin, low temp. absorpt. and luminesc. spectra 3-64711
 π -cyclobutadienyliron tricarbonyl, intramol. rot. obs. from nematic-phase n.m.r. 3-60481
 cyclopropylamine intercalated transition metal dichalcogenide, absorpt. spectra 3-55607
 dialkyl cadmium, magneto-optical conformational analysis (*French*) 3-54609
 dialkyl mercury, magneto-optical conformational analysis (*French*) 3-54609
 dialkyl zinc, magneto-optical conformational analysis (*French*) 3-54609
 dibromotrimethylantimony, ¹²¹Sb Mossbauer quadrupole patterns 3-58455
 dimethyl and diethyl-2,2-stanna-2 dithia-1,3-cyclopentanes, vibrational spectra and conformation (*French*) 3-43454
 dimethylmercury solution, dipole moment, temp. depend., 8.5-50°C 3-79976
 ferricenium ion, distortion, parameters from low temp. absorpt., MCD and ESR spectra 3-75004
 ferrocene derivatives, n.m.r. spectra, meta couplings 3-63524
 ferrocene i.r. absorption spectra at low temp., phase transition, rotational barrier (*French*) 3-47260
 ferrocene vibrational study 3-67780
 Fourier transform n.m.r. spectroscopy 3-75893
 iron (phenanthroline)Cl₂, powder, ferromag. props. 3-58369
 isopropyl ammonium chloroplatinate, ferroelast. 3-60762
 isopropyl ammonium chlorotriacetate, ferroelast. 3-60762
 metal porphyrins, mag. circular dichroism, vibronic coupling 3-74993
 metal-dibenzotetraazaannulenes, electrocatalytic activities, meas. for O₂-reduction using standardised dispersion electrode method (*German*) 3-53324
 metal-metal bonded species, vibrational spectra and bonding 3-78797
 metal-phthalocyanines, electrocatalytic activities, meas. for O₂-reduction using standardised dispersion electrode method (*German*) 3-53324
 metalloenes, transition metal complexes, high energy photoelectron spectroscopy, binding energies, mol. orbital calc. 3-49441
 metalloporphyrins, luminesc., triplet-triplet energy transfer 3-67847
 metalloporphyrins, spin-orbit coupling and heavy atom effect on radiationless transitions 3-63498
 nickel porphyrin, low temp. absorpt. and luminesc. spectra 3-64711
 n-octadecylamine intercalated transition metal dichalcogenide, absorpt. spectra 3-55607
 organosilicon, ²⁹Si nuclear spin lattice relaxation, ²⁹Si-¹H overhauser enhancement 3-64574
 organotin covalent compounds, vibr. modes from Mossbauer effect and Raman data 3-44355
 phenylferrocenes, chemical shift explanation 3-63524
 porphyrin/cafeine complexes, n.m.r. and e.p.r. studies, chemical shift determ. 3-78851
 porphyrins, excited states, effects of metallic substitution 3-63550
 pyridine intercalated transition metal dichalcogenide, absorpt. spectra 3-55607
 ruthenocene vibrational study 3-67780
 selective determination by dual channel detector based on flame conductivity and emission 3-66418
 spherical top mols., Raman band contour analyses and Coriolis constants. 3-67816
 tetra-allyl tin, vibrational spectra 3-46294
 tetraethyl tin, ¹¹⁷Sn, ¹¹⁹Sn, spin-lattice relax. meas., temp. depend. 3-68884
 tetramethyl tin, ¹¹⁷Sn, ¹¹⁹Sn, spin-lattice relax. meas., temp. depend. 3-68884
 tetramethyltin derivs., (CH₃)_{4-x}SnX_x, effect of donor atom and ligand size on struct. 3-79330

organometallic compounds continued

- tetramethyltin/tetramethylaluminium, methyl group exchange, d.m.r. obs. 3-75089
 tetrapropyl tin, ¹¹⁷Sn, ¹¹⁹Sn, spin-lattice relax. meas. temp. depend. 3-68884
 transition metal dichalcogenide, organic mol. intercalated, absorpt. spectra 3-55607
 triphenyltin fluoride, chloride, bromide, and hydroxide, mol. motion study from spin-lattice relax. times and second moments meas. 3-46325
 trimethylenemethaneiron tricarbonyl in nematic solvent, p.m.r. anal. 3-54728
 vanadyl complex of porphyrins, quasiline phosphorescence spectra, vibrational analysis at 77 K 3-53138
 zinc porphyrin, low temp. absorpt. and luminesc. spectra 3-64711
 [Fe(C₅H₅)₂]BF₄, spectra of ²E_{1u} ← ²E_{2g} band system at 4.2 K 3-41532
 [Fe(C₅H₅)₂](CCH₃CO₂H)₂ - (CCH₃CO₂⁻) spectra of ²E_{1u} ← ²E_{2g} band system at 4.2 K 3-41532
 [Fe(C₅H₅)₂]PF₆, spectra of ²E_{1u} ← ²E_{2g} band system at 4.2 K 3-41532
 As(C₃F₃)₃, i.r. and Raman spectra and ¹⁹F n.m.r. 3-71561
 FeTBP, interstellar polarisation simulation 3-48125
 MgTBP interstellar polarisation simulation 3-48125
 (N(C₂H₅)₄)₂ ZnI₂:NiI₂²⁻ mag. circular dichroism spectrum, spin-orbit splitting, quenching 3-50601
 P(C₃F₃)₃, i.r. and Raman spectra and ¹⁹F n.m.r. 3-71561
 Pd complexes of etioporphyrin and mesoporphyrin, nonfluorescent, quantum yield for intermolecular conversion (*Russian*) 3-49488
 Rh π -complexes, ¹³C n.m.r., Rh-C coupling 3-63513
 Sb(C₃F₃)₃, i.r. and Raman spectra and ¹⁹F n.m.r. 3-71561

organs (artificial body) see artificial organs**origin of elements** see element origin**orthicons** see television camera tubes**oscillations**

- see also circuit oscillations; electromagnetic oscillations; harmonics; liquid oscillations; mechanical oscillations; piezoelectric oscillations; plasma oscillations; resonance; stability
 asteroid orbits with aphelia near Jupiter 3-56301
 atmospheric tidal oscill. effects on nighttime Na layer 3-53485
 body decelerating in atmosphere, oscill., damping effect of internal moving load 3-48710
 boundary layer, oscillatory, growth over the top and bottom plates of a rotating channel 3-63696
 chemical reactions illuminated systems, oscillations, multiple steady states and instabilities 3-55976
 chemical systems, nonlinear oscillations 3-41838
 circular cylinders, analysis of dynamically possible circulation preserving finite deformations 3-40113
 differential eqns., higher order, oscillatory properties of solns., theorems of Mikusinski and Kiguradze (*Russian*) 3-70528
 differential equations, Banach spaces, qual. behaviour involving oscillation and non-oscillation 3-73988
 dipolar fluid, wave propagation from oscillating infinite plate 3-79001
 earth, Q⁻¹ determ. of free oscils. 3-61388
 earth core-mantle, free oscillations for Colombian 31 July 1970 event 3-61386
 fluctuating flow and heat transfer from vertical surface 3-63682
 galactic models, uniformly rotating stellar discs 3-53697
 gas-fluidised bed, spontaneous oscillation 3-43620
 heat conduction, transient two-dimensional in solids, stability and oscillation characteristics of finite-element, finite-difference and weighted residual methods 3-62625
 hypersonic flow, excited degrees of freedom, frozen energy (*Russian*) 3-63716
 Kelvin wave oscils. at 50 mb level climatological analysis 3-44880
 linear differential eqn. nth order, necessary and sufficient conditions for non-oscillation and oscillation 3-70533
 lunar tidal oscill. in horizontal ionospheric drift at equator 3-53524
 Maclaurin stellar disc, oscil. spectrum 3-61640
 magnetically distorted polytropes, structure and radial oscill. 3-53639
 neutron stars, radial pulsations near onset of instability 3-61770
 non-linear resonance, method of averaging and simulation of language CSM 3-40094
 nonlinear acoustic streaming effects associated with oscillating cylinders 3-60559
 Nonlinear resonant oscillations in open tubes 3-75241
 ocean-atmosphere system, simulation 3-80712
 pitot tube fluid oscillations in unsteady flow 3-52477
 proton beam, Maxwellian 1 dimens., normal oscill. modes in linear space charge approx. 3-57269
 reaction schemes, homogeneous phase, damped oscillations (*French*) 3-76429
 reactivity, for zero power transfer function measurement of nuclear reactors (*Portuguese*) 3-46060
 shallow rectangular cavities, adjacent to compressible flow, possible excitation frequencies 3-46464
 shock profiles, calculated by difference methods (*French*) 3-46454
 solar 5-minute oscillation, vertical phase var. and mechanical flux 3-80934
 solar 5-minute oscillations of large horizontal scale, theory rel. to observations 3-47884
 solar mag. field, short-period oscill., correlation anal. 3-65657
 Stueckelberg oscillations of differential cross-section, tunnelling remnants 3-71462
 temperature oscill. in F-region over St-Santin 3-53529
 time function, spectrum recovery, Fourier transforms 3-42054
 viscoplastic media, oscillating MHD flows in a plane channel (*Russian*) 3-57820

oscillators

- see also microwave oscillators; relaxation oscillators; swept-frequency oscillators
 cell-membrane resistance meas. (*German*) 3-42271
 electron-cavity interactions, quantum theory 3-62726
 high-frequency, amplitude modulator circuit, in unipolar mass spectrometer 3-73888
 linearly coupled, transformation of Hamiltonian system, existence of linear integrals (*Russian*) 3-66581

oscillators continued

- non-linear analogue transfer function generator, for NAL bend magnet 3-56958
- physical quantities meas. from natural vibrations attenuation of oscillator circuit (*Czech*) 3-56695
- rigid body, torque-free rotational dynamics, nonlinear oscillator analogue 3-66514
- single coil service resonant circuit, for pulsed nuclear resonance 3-45540
- spectroscopy, pulsed ion cyclotron resonance, solid state marginal oscillator, design 3-62265
- spin generator, for n.m.r. spectroscopy 3-56707
- temperature controllers, for crystal growth by Czochralski method 3-53181
- ultrastable Rb, H₂ clocks and He-Ne laser, navigation applic. (*French*) 3-62679
- voltage source for metrology research, characts. 3-77566

oscillator effect *see* **oscillators****oscillators**

No entries

oscillograms *see* **oscillographs****oscillograph recorders** *see* **oscillographs****oscillographs**

- see also* **cathode-ray oscilloscopes**
- energy-current spectra, charged particle, photographic method 3-73807
- radioisotope imaging, blur rectification 3-61923

oscilloscopes, cathode-ray *see* **cathode-ray oscilloscopes****Oseen method** *see* **flow****osmium**

- magnetic susceptibility of single crystals, mag. field dependence 3-55417
- muonic atom, magnetic hyperfine splitting due to magnetization density 3-49209
- muonic atoms, magnetic hyperfine splitting of 2⁺ rotational states (*German*) 3-52302
- Cs₂ZrBr₆:Os⁴⁺, absorpt. and mag. circular dichroism spectra, 17000 to 31000 cm⁻¹ 3-44437
- Os-Mo system, interdiffusion coeff., electron microprobe study, polycrystalline couples 3-68442

osmium alloys

see also **osmium compounds**

- LaOs₂, supercond. transition temps. of 5.9K, 8.9K for hexagonal, cubic forms 3-52919

osmium compounds

see also **osmium alloys**

- OsO₄, centrosymmetric struct., neglect of dispersion effect 3-68212
- OsO₄, He(I) photoelectron spectra, low energy transitions 3-40608
- OsO₄, mag. circular dichroism assignment of longest wavelength band 3-54663
- OsO₄, Raman band contour analyses and Coriolis consts. 3-67816
- OsO₄, rotational-vibr. spectra, narrow saturation resons. induced by CO₂ laser radiation 3-46279

osmosis

see also **membranes**

- conducting solid particles, ideally polarised thin double layer, electrophoresis 3-73074
- electroosmosis, depend. on conc. of uni-univalent electrolyte 3-61259
- electroosmotic transport is saturated disperse systems, temp effect 3-62279
- endosmosis fluid mechanics, double layer characts. determ. 3-47562
- liquid DL/spherical solid particle 3-73076
- membrane, for H₂ partial press. meas. 3-48397
- muscle fibres, without membranes, Donnan and osmotic effects, explanation 3-65982
- polymer semi-dilute solns., screening length 3-49515
- turbulent flow along semipermeable barrier, hyperfiltration (*Russian*) 3-63636
- two-phase laminar flow along plane barrier, hyperfiltration (*Russian*) 3-63753
- water treatment, using reverse osmosis, for semiconductor processing 3-50668
- ⁴He-³He, very dilute mixture, osmotic pressure 3-55119

osmotic pressure *see* **osmosis****otology** *see* **ear****oven**

see also **electric heating**

- heat-pipe, for containment of atomic and molecular vapours 3-39877
- high temp. vitreous C thermal cavity, for mass spectrometric studies 3-45451
- hot air gun heating, 400°C for ultrahigh vacuum bake-out 3-70297

Overhauser effect

- azo compounds, decomp., chem. induced nuclear polarisation, methyl radical 3-71579
- benzoyl peroxide, decomp., chem. induced nuclear polarisation, methyl radical 3-71579
- camphor, ¹³C relax, dipolar, spin-rot separation 3-68881
- cyclohexyl percarbonate, decomp., chem. induced nuclear polarisation, methyl radical 3-71579
- enhancement suppression in ¹³C n.m.r. using chemical shift reagents 3-56709
- free radicals, chemically induced dynamic spin polarization, hydrodynamic effect 3-80537
- glycine, ¹⁵N enriched, aqueous solution, n.m.r., pH depend. 3-64570
- large molecules, ¹³C spin-lattice relax. 3-67874
- macromolecules, homonuclear effects 3-75166
- n.m.r., permanent magnet, chemically induced nuclear dynamic polarisation, nuclear and electron spin coupling 3-48324
- organic radicals, liq., weak and quasi-zero field phenomena (*French*) 3-55502
- organosilicon compounds, ²⁹Si-H enhancement, spin-lattice relaxation 3-64574
- solutions, coupled spin systems, intermolecular nuclear Overhauser effect 3-50489

Overhauser effect continued

- tanol linear chain free radical, proton relax time freq. and temp. depend. (*French*) 3-58441
- Wurster's blue perchlorate, aq. solns., temp. depend. scalar coupling 3-57671
- Cr³⁺ aquacomplex in viscous soln., intermediate effect between Overhauser and solid effects 3-75079
- Mn²⁺ ions in aq. solns., temp. depend. scalar coupling 3-57671
- Ni³⁺ aquacomplex in viscous soln., intermediate effect between Overhauser and solid effects 3-75079
- ³¹P-(¹H), ¹H-(³¹P) heteronuclear n.m.d.r., nonlinearities and nucl. Overhauser effect 3-75082
- Si compounds, ²⁹Si n.m.r. 3-68878

overhead lines

- h.v., current measurement, optical technique using laser beam 3-51961

oxidation

see also **combustion; corrosion**

- acetylene-O₂ chemical laser characts. 3-59863
- acrylic fibre oxidation stage in carbon fibre formation 3-41817
- alloy, two-phase, internal oxidation, model approach 3-64813
- anodic oxide film growth on GaP 3-50652
- anthracene derivatives chemiluminescence during oxidation (*Russian*) 3-41862
- p-arsonophenylanthranilic acid, oxidation-reduction indicator, titration Fe (II), Cr (VI) 3-48649
- bacteriochlorophyll, one-electron oxidation, absorption and e.p.r. obs. (*Russian*) 3-51425
- barbituric acid dihydrate, single crystals, 4.2K, oxidation and reduction by ionizing radiation 3-73147
- c TiO₂, rutile, vacuum reduction 3-41800
- cumene-tetraline mixture, chemiluminescence spectra 3-41846
- cyclic testing and data interpret. 3-73096
- glass/iron substrate systems, interfacial reactions and enhanced wetting 3-55880
- glass/metal substrate systems, interfacial reactions and adherence 3-55882
- graphite, gasification reaction with CO₂-based mixtures, irradiation effect (*German*) 3-71274
- graphite, reactor, reaction rate in damp atmosphere, mech. strength, stress effect (*German*) 3-71271
- graphite block, reactor moderator, CH₄-CO-VO₂ mixture exposure, irradiation, diffusion effects (*German*) 3-71273
- haematite, effect of magnetic field on reduction 3-61257
- Havero meteorite, interpretation of obs. 3-45070
- infrared internal reflectance spectrometry, metal and C film use 3-73164
- Lunar fines, surface reduction by H₂, relevance to solar wind effects 3-42179
- lunar orange soil, low oxidation states of Fe and Ti 3-65849
- magnetite, reduction at 750°C, growth of Fe (*German*) 3-47365
- metal, ion migration rel. to growth kinetics in thin films under electron equilib. 3-43950
- metal, ionic transport equation for cryst. solid film 3-43949
- metal, reactive sputtering in oxidizing atmosphere, model 3-64758
- metal or metal oxide, oxidation rate const. maximum value w.r.t. temp. 3-65085
- metal oxides in water-cooled reactor, thermodynamics 3-57582
- microanalysis of oxide surface layer by ¹⁸O(p,α)¹⁵N nuclear reaction 3-42695
- m.o.s., on (111), (100) n-Si, elec. props., influence of HCl in thermal oxidation 3-79771
- nitrogen oxides, reduction, rare earth manganites as catalysts with low ammonia yield 3-55943
- p-nitrotoluene, reversible reduction, cyclic voltammetry, digital data acquisition system, data analysis 3-70445
- oceanic basalts, low temperature oxidation causing carriers of natural remanence to become superparamagnetic 3-58971
- optical microscopy, application to electrochemical studies, review 3-66198
- organic compounds, parallel determ. of N, C and H, semiautomatic app., purification of O₂ 3-48651
- organic molecules, by photoproduced holes in ZnO 3-41100
- oxide film formation, space charge and conc. gradient effects 3-50651
- polyethylene, γ-ray irradi., rel. to elec. cond. after annealing 3-46864
- polyethylene film, heat-treated, adhesion strength on steel and Al, metal-catalysed oxidation 3-73057
- polymer sliding on metals, chem. change obs. (*Russian*) 3-80466
- polymers, induction period meas., DTA apparatus 3-77397
- powder metallurgic magnetic protection against oxidation during heat treatment 3-50751
- propene, activity enhancement and selectivity change by catalytic effect of hot electrons 3-41868
- radiation damage mechanisms, e.s.r. spectroscopy study, reviews 3-55459
- rare earth phosphides, cryst. chem. and phys. props., reviews 3-64018
- sodium pyrenide in tetrahydrofuran, flash photolysis, photo-oxidation and Na⁰ existence 3-61270
- steel, cooling rate during solidification effect on dislocation struct. internal oxidation (*Russian*) 3-53220
- steel, low-C electromelted, comp. and complex deoxidizing effects on mech. props. (*Russian*) 3-58647
- steel tube, degree of oxidation influence on glass coating quality (*Russian*) 3-58657
- thermogravimetric system for multiple specimen oxidation studies 3-77753
- thin film, logarithmic rate law 3-41101
- thiourea, photosensitized oxidation method for determ. of triplet state conversion efficiency 3-76481
- titanomagnetite, low-temp. oxidation and palaeomagnetic implications 3-69512
- titanomagnetite, natural and synthetic, rotational hysteresis characts. with oxidation 3-58867
- Zircaloy-2, accelerated oxidation in steam at high pressure following heat treatment 3-71300
- Zircaloy-2, morphology of thick oxide films 3-43951

oxidation continued

- Ag alloys, internal oxidation at h.p. and in atomic O (*German*) 3-41056
- Ag surface sensors, interaction with free O₂ gas stream (*Russian*) 3-66461
- Al, anodic, behaviour of ion-implanted atoms, Rutherford backscatt. obs. 3-68511
- Al, super purity, anodizing by molten KNO₃ 3-73142
- Al, temp. depend. of surface oxide thickness 3-53260
- Al anodic oxide layers, nuclear microanalysis and ¹⁸O tracer techniques 3-50088
- AlN, high temp. oxidation 3-72954
- α -Al₂O₃, whisker crystal growth, Al₂O₃ reduction, condensation of Al nucleation centres (*Russian*) 3-41624
- B₄C, hot-pressed, high-temp. characteriz. 3-69348
- C, interaction kinetics, surface diffusion 3-75662
- C black, electrochem. in H₃PO₄, mechanisms 3-69461
- CS₂-O₂ mixture, kinetics of pulsed chem. laser with photoinitiated oxidation 3-74234
- CS₂ + O₂ → CO, SO₂, oxidation, electron vibr. population inversion, chemilum. 3-47554
- Cd, climb of super-jogs and dislocation configs. (*French*) 3-64047
- Co, reactive sputtering in oxidizing atmosphere, expt. confirmation of model 3-64758
- Co-Ni-Cr alloys, precipitates formed by internal oxidation (*French*) 3-47384
- Cr, surface reactions investigation, static method of secondary ion mass spectrometry 3-75682
- Cr, thin film, thermochemical interaction of laser radiation 3-58797
- Cr binary alloys with 1st period metals, comp. depend. 3-58661
- Cr(100) and (110) surfaces, adsorption of O₂ and oxide formation 3-41098
- Cu, charact. secondary ion mass spectra for depth analysis of CuO 3-59706
- Cu oxidation kinetics and internal irregular structure of Cu₂O layer 3-75681
- Cu-Al dil. alloys, internal oxidation, dispersed phase morphology 3-64848
- Cu-Be (0.25 wt.%) alloy, oxide particle size and distrib. (*French*) 3-44586
- Er, confirmation of f.c.c. phase by weight increase on oxidation to Er₂O₃ 3-79276
- Fe, kinetics of thin film formation using proton impact excited X-ray analysis 3-50087
- Fe, reactive sputtering in oxidizing atmosphere, expt. confirmation of model 3-64758
- Fe-Al-Cr, alloys, effect of Ti and Mo additions 3-61179
- Fe-Co films, effect on mag. props. and constitution (*Russian*) 3-72481
- Fe-Cr(18 wt.%) sealing alloy, oxide film resist. rel. to Al and Ti additions (*Japanese*) 3-72905
- Fe-Mn-Cr sealing alloy, high temp. oxidation and sealability, effects of Al, Mn and Si additions (*Japanese*) 3-44615
- Fe-Ni films, effect on mag. props. and constitution (*Russian*) 3-72481
- Fe-Si alloys, polycryst., thin oxide film growth phenomena (*Czech*) 3-55165
- Fe-X-O alloy, scale struct., (X=Ni, Cr, Mo) (*German*) 3-76195
- (Fe₂Mg_{1-x})SiO₄, low temperature, gravimetric and magnetic study 3-76537
- GaAs anodic oxidation, in aq. H₂O₂ soln. 3-80552
- GaAs junction laser, rel. to degradation and passivation 3-40272
- GaAsP, m.i.s. struct. fabrication by thermal oxidation 3-64789
- GaP, growth and composition of anodic thin film 3-79590
- GaP, oxidation in aq. H₂O₂ soln. 3-41672
- Gd film, new f.c.c. phase, identification and oxidation characts. 3-79589
- Ge, obs. of (111) surface by LEED during O₂ adsorption 3-50078
- HfB₂, effect of SiC, 1200 to 1550°C 3-72953
- LaB₆ cathode, Auger electron spectroscopy obs. of oxidation 3-68510
- La₂(CrO₃)₃, oxidation-vaporiz. kinetics 3-72955
- LiH, LiOH reaction layer structure 3-43952
- NO prod. in the stratosphere by N₂O oxidation 3-61450
- NO⁺ + O₃ → NO₂⁺ + O₂, laboratory expt. and ionospheric implications 3-51108
- Nb, surface reactions investigation, static method of secondary ion mass spectrometry 3-75683
- Nb (100) surface, reaction kinetics, interaction of O and N, Auger spectroscopy 3-55166
- Nb surface, thin oxide film form, ellipsometric obs. (*French*) 3-46761
- Ni (100) surface, atomic positions in C (2 × 2) oxygen struct., dynamical LEED obs. 3-64233
- Ni-Be dil. alloys, internal oxidation, rel. to oxygen diffusivity determ. in Ni 3-58147
- Ni-Be dil. alloys, internal oxidation, rel. to oxygen diffusivity determ. in Ni 3-58148
- Ni-Cr-Hf alloy, fine HfO₂ dispersion prod. through internal oxidation 3-76187
- Ni-Cr(20 wt.%) alloys with oxide dispersions, high temp. oxidation 3-76188
- Ni-P films, partial oxidation to NiO at 350°C (*Russian*) 3-60843
- NiO powder, reduction, nucleation rate, kinetics rel. to Neel transition 3-55164
- Pb-In(Sn) alloys, corrosion-resistant, surface obs. by ESCA 3-76209
- Pt(110) surface, S + O₂ adsorption, catalytic CO oxidation 3-73166
- Pu, voloxidation for reprocessing 3-54539
- Sb₂O₃, formation of epitaxial layer of Sb₂O₄ (*Russian*) 3-40854
- Si, anodic oxidation in organic solvent with F traces 3-41671
- Si, B diffusion anisotropy under oxidizing atm. 3-50077
- Si, dislocation free crystals, float-zoned, dislocation generation along swirls, thermal oxidation 3-41648
- Si, point defect injection, rel. to IC fabrication 3-55745
- Si, transmission electron microscopy of oxide film, defect effects on surface 3-72276
- Si (111) surface, by steam, Auger electron emission obs. 3-41097
- Si (111) surface, O₂ adsorption kinetics 3-55160

oxidation continued

- Si p-n junction diode, elec. characts., oxidation-induced stacking fault effects 3-41259
- Si single crystals, adsorbed water and oxygen effects in electron exoemission 3-64759
- Si surfaces, Auger electron spectroscopy, rapid oxidation and carbonisation of upper layers 3-68472
- Si:Ge, oxide interface properties, surface state density function measurement 3-60921
- Si-oxide interface, boron redistribution in oxidising atmosphere 3-44151
- SiC, Si-bonded, fission fragment irradi. effect on passive oxidation, 950°C 3-67551
- SiO₂ film, grown in Cl₂ and HCl atmosphere, Cl profile 3-41643
- SiO₂ films, high-temperature, internal stresses obs. 3-58191
- Ta, anodic oxidation, O migration 3-80553
- Ta, surface reactions investigation, static method of secondary ion mass spectrometry 3-75683
- Ta₂N anodisation, thin film, basic properties (*German*) 3-46762
- Te, electrodisolution, graphite electrode, HCl and HBr 3-73137
- Th + O(O₂)(N₂O) vapour, chemi-ioniz. 3-80533
- Ti, from 25 to 100°C, ellipsometry, Auger and surface pot. difference obs. 3-55167
- Ti, stress corrosion cracking, neutral methanolic and ethanolic, NaCl soln., electrochem. behaviour 3-55959
- Ti and alloys, anodic oxidation, review 3-41096
- Ti and TA6V alloy, oxid. products, diffuse reflectance spectra obs. (*French*) 3-69287
- Ti-Al-V-Sn alloy, stress corrosion cracking, influential factors and effect on anodic oxidation 3-47406
- Ti-Zr alloys, wear resist. in H₂O, increase by oxide surface layer formation 3-58697
- (U,Pu)₂O₃ solid solns., oxidation props., model interpret. 3-54542
- U + O(O₂) vapour, chemi-ioniz. 3-80533
- UO₂, high temp. oxidation, effect of compaction, exposed area and initial composition 3-60275
- V, surface reactions investigation, static method of secondary ion mass spectrometry 3-75683
- V₂O₅, thermal and low energy electron bombardment induced O₂ loss, transition into V₆O₁₃ 3-41099
- W field emitter, field induced oxidation 3-64767
- WO₃:Be doped powder, reduction, W filament production, secondary β -W formation (*Hungarian*) 3-72986
- W(100), secondary ion mass spectrometry and electron-induced desorption investigation 3-75669
- Y, metallothermic reduction in molten fluoride bath 3-65091
- Zr alloys in molten salts, 300-500°C, current-voltage characteristics and oxidation rate 3-72918
- ZrO₂/W and ZrO₂/ZrO₂ fibre composites, thermal shock resist. 3-76353
- oxide coated cathodes**
see also coating techniques; thermionic electron emission
SnO₂ film cold cathodes, electron emission into vacuum, obs. 3-41621
- oxide semiconductors**
thin film oxidation, logarithmic rate law 3-41101
- Ag₂O:Cd, photocond. and luminesc., 4.2 and 77K, participation of excitons 3-47312
- B₂O₃, liq. and amorphous, switching effect 3-55315
- Bi_{1-x}GeO_{2x}, carrier transport and current oscill. in relaxation semiconductor regime 3-44084
- CdO-B₂O₃-SiO₂ glasses, phase separation effects on photocond. props. 3-75767
- (Co,Ni)O, cation diffusion, semiconductivity and nonstoichiometry 3-41050
- Cu₂O, modulated excitonic spectra in elec. field 3-55638
- EuO, Kramers-Kronig analysis of reflection at room temp., 0-14 eV, energy level determ. (*German*) 3-53117
- EuO, optical constants, magnetic field modulated magnetorefectance, Kramers-Kronig relation 3-55614
- EuO thin film, optical absorpt. and photocond., mag. order effect 3-55307
- EuO:Gd, amorphous, threshold and memory switch behaviour, Ovshinsky effect (*German*) 3-50246
- EuO:Gd, photoemission, excited energy states, absorpt. edge behaviour (*German*) 3-50646
- Fe₃O₄, magnetite, pure and substituted, hopping of localised electrons, 4.2-300 K 3-46833
- β -Ga₂O₃, conductivity and thermoelectric power, 650-900K 3-68631
- β -Ga₂O₃, electrical conductivity meas. 3-52845
- Ho₂O₃, quasi-stoichiometric, electronic cond. mechanism (*French*) 3-79746
- In₂O₃, n-type semiconductor, meas. of elec. props. 3-79686
- MnO-NiO, resistivity and energy constant, obs. 3-75744
- MoO₃ based binary oxides, amorphous semicond., localized d¹ electron e.s.r. meas. 3-68847
- Mo₂V_{1-x}O₂ whiskers, metal-semicond. transition phenomena, comp. depend. 3-60907
- NiO, conc. depend. diffusion of Cr 3-64212
- PbO, anodized, tetragonal, photoproperties 3-79727
- PbO, single crystals, illumination effect on Hall mobility of charge carriers (*Russian*) 3-41177
- Sb₂O₃, liq. and amorphous, switching effect 3-55315
- SiO films, cond. mechanism, metallic impurities influence (*French*) 3-50199
- SnO₂, anal. of exciton absorpt. spectrum at 1.5, 4.2 K 3-41164
- SnO₂ film, prep. by vapour deposition, elec. props., chemical composition depend. 3-44073
- SnO₂-CdSe n-n heterojunction, elec. and optical props. (*Korean*) 3-72399
- SnO₂-CdSe-CdS n-n double heterojunction, elec. and optical props. (*Korean*) 3-72399
- Ta₂O₅ anodic film, elec. cond., rectification, transport processes and electronic struct. 3-46839
- Ti Oxides, crystal growth and props., semiconductor-to-metal transitions (*German*) 3-53194
- TiO₂, rutile, thermodynamic analysis of lattice defects, and H and D impurities 3-55218
- TiO₂:H,D, rutile, i.r. absorpt., impurity conc. detn. 3-58530

oxide semiconductors continued

- Ti₂O₃, pressure effects on the semiconductor-semimetal transition 3-79750
 Ti₂O₃, pure and V-doped, thermoelectric effects, semiconductor to semimetal transition 3-58290
 V oxides, crystal growth and props., semiconductor-to-metal transitions (*German*) 3-53194
 (V_{0.3}Nb_{0.7})O₂, electrical transport props. 3-41239
 V_{1-x}Nb_xO₂, (0 ≤ x ≤ 0.33), vapour phase prep. and characteriz. of single crystals. (*French*) 3-72802
 VO₂, passage of current across semicond.-metallic phase boundary 3-44149
 VO₂, coplanar switching devices, pulse response theory 3-79747
 V₂O₅, metal-insulator transition, current carriers density discontinuous change 3-72326
 V₂O₅, single cryst. prep. by chem. transport reaction 3-72801
 V₂O₅-Sc₂O₃ system, elec. cond. transition 3-72388
 V₂O₅, electric field effect on electronic struct., electroreflectance spectra 3-76021
 V₂O₅, liquid semicond.-metal interface, nonlinearity of current-voltage characts. 3-41265
 V₂O₅, single cryst., electroreflectance, resonance due to conduction band fine struct. 3-50598
 V₂O₅ binary oxides, amorphous semicond., localized d¹ electron e.s.r. meas. 3-68847
 V₂O₅ thin film resistor, low energy laser pulse calorimeter applic. 3-53918
 ZnO, band structure, density of states and reflectivity computation 3-46292
 ZnO, elec. cond. in atomic N, recombination-adsorpt. model (*Russian*) 3-75740
 ZnO, extended defects rel. to nonstoichiometry, transmission electron microscope obs. 3-79333
 ZnO, i.r. absorption by acoustoelectric domains 3-72617
 ZnO, modulation spectroscopy, surface electron states photoconductivity 3-55323
 ZnO, photoproduced holes in oxidation of organic compounds 3-41100
 ZnO, surface state spectroscopy, modulated photoconductivity measurements 3-55325
 ZnO (0001) surfaces, electronic and structural characteristics 3-79756
 ZnO aqueous suspensions, reproducible e.s.r. spectra 3-75872
 ZnO film, prep. by cold plasma condensation, growth kinetics (*French*) 3-52772
 ZnO thin films, dye sensitised, photoresponse, self-quenching effect 3-46871
 ZnO thin layers as u.s. transducers, prep. (*German*) 3-53193
 ZnO whiskers, antiphase boundaries, transmission electron microscope obs. 3-79597
 ZnO:Ag,Cl phosphors, photolum. emission characts. 3-69056
 ZnO:Li, photo-induced persistent internal quadrupole moment 3-46876
 (ZnO-MgO):Fe(O) photoconductor, thermally stimulated current curves for different cooling schedules 3-46883
 ZnO₂, castable, elec. resist. from 900-1700K, calcia stabilisation rel. to furnace appl. 3-52832

oxygen

- absorption cross sections from 180 to 700 Å 3-67805
 acetylene-O₂ chemical laser characts. 3-59863
 acetylene-O₂ flame at extremely low pressures, ion recombination 3-76445
 adsorbed layer on Fe(001) epitaxial film, behaviour of impurity atoms 3-55132
 adsorbed on PbS film, effect on photocond. 3-75778
 adsorption, on Ag, single crystals, (111) face, electron and argon ion bombardment cleaned under ultra high vacuum, work function 3-43938
 adsorption, on Ag thin films, kinetics, sticking probabilities, slow and fast adsorption 3-46755
 adsorption, on Ni-SiO₂ catalysts, magnetic methods, strong and weak field, preferential fixation (*French*) 3-44741
 adsorption, photostimulated by CdTe film, mech. stress changes obs. 3-50095
 adsorption by tungsten 1800-2750 K, Auger spectroscopy meas. (*German*) 3-52749
 adsorption on Ag, field emission obs., heating effects, changes in average work function 3-55147
 adsorption on Cr(100) and (110) surfaces, oxide formation 3-41098
 adsorption on Cu faces, LEED and RHEED study (*French*) 3-79575
 adsorption on Ge(111) surface, LEED obs. 3-50078
 adsorption on Ir(110) surfaces, LEED and Auger studies 3-60831
 adsorption on Mo (100) face, LEED obs. (*French*) 3-79563
 adsorption on Ni(111), Auger electron spectroscopy, chemical shift and valence spectra 3-41090
 adsorption on Pt (111) and Ni (111), CFSSO-BEBO calcs. 3-68501
 adsorption on Si, model for adsorption complex 3-55149
 adsorption on Si(111) surfaces, influence of residual water vapour 3-75670
 adsorption on Si (111) surface 3-55160
 adsorption on stainless steel 304 at 20°C 3-60836
 adsorption on ThO₂, luminesc. phenomena 3-79561
 adsorption on transition metals at high temps., interaction model (*French*) 3-68495
 adsorption on W, coverage at 78 and 973K, field ion investigation 3-46752
 adsorption on W (110) single cryst. surface 3-79564
 adsorption on ZnO powder, logarithmic time law (*German*) 3-64239
 aerosol, acoustic coagulation, elimination from gases 3-76390
 air-water interface, transfer of O₂, CO₂ and water vapour 3-44855
 antiferromagnetic, double excitonic bands, doublet structure 3-61031
 in Ar, solid, luminesc. and absorpt. spectra 3-44472
 Atlantic Ocean, dissolved O₂, isotopic anal., mass spectrometry (*Russian*) 3-47695
 N. and W. Atlantic Ocean, in situ O. meas. 3-53446
 Atlantic Ocean, isotopic formation of surface waters, distrib. of salinity and ¹⁸O (*Russian*) 3-47694

oxygen continued

- atmospheric, absorption spectra by N₂ and O₂ complexes near 4.3 μ (*Russian*) 3-73294
 atmospheric, photodissociation, solar u.v. flux variations 3-80756
 atmospheric conc. determ. by shock-layer radiometry during PAET entry-probe expt. 3-56187
 atmospheric microwave spectrum rel. to attenuation and phase dispersion 3-49480
 atmospheric negative ions, collisional detachment of electrons 3-46212
 atom, (2¹D₂), quenching of atomic resonance radiation in vacuum ultraviolet by gases 3-71370
 atom, absorpt. by Nb, kinetics at low press. and high temp. (*German*) 3-43880
 atom, electron capture and loss in H₂, cross sections, charge-state distrib. 3-78632
 atom, electron scatt., total cross sections, multi-config. expansion 3-67699
 atom, electron scattering, cross section calc. 3-74862
 atom, electronic correls. role in X-ray and fast electron scatt. 3-52248
 atom, excitation cross section from CO₂ photodissoc. 3-44736
 atom, excitation state following dissociative recombination processes e + NO⁺ 3-78881
 atom, gas discharge plasma, electron impact excitation, effective cross section determ. 3-74871
 atom, ground state, single excitations in multiconfig. wavefunctions 3-71351
 atom, He and Li like, spectra, lifetime meas., decay time 3-49389
 atom, ionisation by fast neutral inert gas atoms, anal. of autoionising states 3-74846
 atom, multiconfiguration and polarized orbital close coupling calc., comparative study 3-71443
 atom, partial wave calc. of scattering amplitude, reln. to electron diffraction determ. of molecular structure 3-78661
 atom electron scattering, free-free absorption coefficients calc. 3-43371
 atom reactions with positive and negative ions, cross sections for charge-transfer and ion-molecule reactions 3-78635
 atomic, scattering from (001) LiF by fast adsorption-desorption process 3-41600
 atomic O red line photometer, ISIS-II, auroral and airglow obs. 3-65514
 atomic orbitals, SCF, Gaussian expansions, radial weighting effects 3-67649
 atoms, h.f.s., orbit depend., Hartree-Fock wave functions 3-67648
 atoms and ions, electron scatt., config. interaction effects, cross sections 3-63328
 atoms collisions with CO, vibrational relaxation 3-46348
 atoms in metastable ⁵S₀ state, quenching rates 3-43380
 Auger spectroscopy of reaction with Nb (100) surface, reaction kinetics 3-55166
 beam-folite lifetime meas. in vacuum u.v. 3-78747
 p-benzoquinone, photocycloaddition to cyclooctatetraene, laser excitation, effect of solvent acidity and oxygen 3-47580
 biological materials, α-tracks determ. using ¹⁷O tracer 3-66457
 blood pO₂, in vivo radial telemetry 3-73922
 in CaS phosphors, effect on optical characts. (*Russian*) 3-76055
 chemical reactions with metal vapours, chemilum. and photolum. of products 3-76421
 chemical shift calcs., n.m.r. 3-63521
 chemisorption, on Ta, polycrystalline tapes, helium molecular beam reflection study, chemical interactions (*French*) 3-44742
 chemisorption, rel. to development of oriented cryst. growth during condensation in vacuum 3-52763
 chemisorption at Ag and Cu surfaces, X-ray and u.v. induced photoelectron spectroscopy 3-55159
 chemisorption in CdS, influence on luminescence spectra 3-80100
 chemisorption on Ag film, effect on elec. resist. 3-41094
 chemisorption on Mo, incidence reflectance studies 3-55157
 chemisorption on Mo surface, composition of two-dimensional oxide film 3-50082
 chemisorption on transition metals, high temp. (*French*) 3-79574
 chemisorption on ZnO, e.p.r. obs. 3-43942
 collision induced broadening of CO lines (*French*) 3-67835
 crystalline absorption spectra, excited mol. interactions 3-69022
 current growth, detachment and attachment coeffs. 3-54889
 cyclooctatetraene, photocycloaddition of p-benzoquinone, laser excitation, effect of solvent acidity and oxygen 3-47580
 deoxyhemoglobin and deoxymyoglobin, binding mechanism, Fe ion fine struct. obs. 3-42269
 diffusion, in Ag, solid and liquid, solubility enthalpy of dissolution, diffusion coefficients 3-50019
 diffusion, in ZnO, by proton activation analysis of ¹⁸O 3-64208
 diffusion calculations, reaction of refractory materials with steel melts (*German*) 3-72969
 diffusion in Cu, coeff. determ. from dissolved oxygen conc. (*French*) 3-60802
 diffusion in Na₂O₂ melt or SiO₂ film, reaction with SiC 3-68508
 diffusion in Si wafers, X-ray double crystal method, lattice strain meas. 3-41662
 diffusion in vitreous SiO₂ 3-76331
 diffusion in Zr, using ¹⁸O(p,α)¹⁵N reaction (*Russian*) 3-58142
 diffusivity and solubility in liq. Sn, solid Ag and solid Ni 3-41051
 diffusivity in liq. Ag, electrochem. meas. (*Japanese*) 3-41038
 diffusivity in Ni, determ. by internal oxidation of dil. Ni-Be alloys 3-58147
 diffusivity in Ni, determ. by internal oxidation of dil. Ni-Be alloys 3-58148
 discharge, high speed anodization 3-54884
 dissociation in r.f. discharge 3-57952
 dissolved in aqueous solution, Na₂WO₃ as potentiometric indicating electrode 3-62326
 effect on expansion of failed (Pu,U)O₂ fuel rods 3-63224
 electrocatalysis of O₂-cathode by metal-phthalocyanines and -dibenzotetraazaannulenes (*German*) 3-53324
 electron energy distrib. and attachment coeff. for electron swarms 3-54792
 energy transfer collisions with Na (3²P) doublet in flames 3-52300

oxygen continued

- equation of state, selection of functional form, least squares fitting 3-75593
- ethylene-O₂ flames, electron temp. meas. using double-probe current-voltage charact. 3-80523
- excitation transfer collisions with Rb, quenching and doublet mixing cross sections 3-67694
- F₁-layer O/N₂ ratio, seasonal variation from vertical sounding data during solar activity minima 3-69660
- fugacity control in solid media high-pressure apparatus 3-73896
- gas, transport and equilibrium props., utility of m-6-8 potential function 3-60512
- glow discharge, metastable level deactivation processes 3-52546
- interaction with Ag surface sensors, degree of dissociation meas. (*Russian*) 3-66461
- interstellar clouds, u.v. absorption spectra, ionisation of C, N and O, effects of X-ray flux 3-48129
- interstitial, effect on mech. props. of Nb and Ta 3-80340
- interstitial in Zr, effect on elastic moduli 3-76204
- interstitials in Nb, pinning of dislocations (*Russian*) 3-72854
- ion, electron capture and loss in H₂, cross sections, charge-state distrib. 3-78632
- ion coordination, ZrO₂:Er³⁺, Y₂O₃-stabilised, absorpt. spectrum, crystal structure 3-41539
- ion extraction from layer of air flowing around electrometer electrode (*Polish*) 3-73278
- ion implantation in Al and Ti films, cermet struct. formation 3-72112
- ion projectiles, Cu k-shell ionisation, impact-parameter dependence of the probability 3-43374
- ionised atom and molecule, X-ray spectra with various targets 3-78446
- ions beam-foil spectra, 6-42 MeV 3-74816
- isotope analysis, ion receiver for mass spectrometer 3-73892
- isotope separation plant, thermal diffusion, automatic control system 3-77743
- K-ionisation cross sections by H⁺ impact, $e < 100$ keV (*German*) 3-54597
- layers on Ti, eddy current testing, megahertz frequencies 3-45531
- LEED investigation of reaction with Nb (100) surface 3-55124
- liquid, hypersonic velocity meas. by Brillouin scattering 3-75570
- liquid, optical absorpt. bands at 0.58 and 0.63 μ , mag. field effect on intensity 3-64654
- liquid density 3-58060
- lower thermosphere, effect of O on N₂ vibrational temp. 3-53512
- lunar soil, Apollo 17 sample ¹⁸O/¹⁶O 3-65823
- magnetosphere, (6300 Å) emission near plasmopause predawn enhancement 3-69684
- mammalian cells, Chinese hamster fibroblasts, generation time, rel. to partial pressure of O₂, effect of hypoxia 3-48167
- mammalian cells, hypoxia, X-radiation survival curves, rel. to partial pressure of O₂ 3-48259
- mass spectrometer ion source O loss, appl. to sounding rocket meas. 3-51184
- mass transfer, fermentations, effect of pressure 3-66696
- migration during anodic oxidation of Ta 3-80553
- molecular, resonant vibr. excitation by slow electron impact 3-71616
- molecular beam elementary interactions obs. 3-78907
- molecule, atomic resonance radiation quenching of O(2D₂) in vacuum ultraviolet 3-71370
- molecule, collision broadening of acetaldehyde lines 3-67834
- molecule, electron impact, dissociative excitation, extreme vacuum u.v. spectra 3-75117
- molecule, gas discharge plasma, electron impact excitation and dissociative cross section determ. 3-74871
- molecule, natural orbitals calc. by perturbation theory, diagonalization of one-electron density matrix 3-74942
- molecule, quenching of excited iodine atoms, opto-acoustic spectra obs. 3-78883
- molecule, quenching of triplet state of aromatic ketones in liq. soln. 3-76482
- molecule, vibrational excitation, electron impact, 4-15 eV 3-75106
- molecule in N₂ and CO condensed matrices, < 10 K, torsional oscills., ¹⁷O hyperfine splitting 3-43477
- in Nb, creep deformed, mass spectrographic exam., laser vapourisation (*Russian*) 3-41722
- neutral particle mass spectrometer data, gas surface interactions on walls of instrument 3-69603
- neutron activation analysis of rocks 3-70494
- neutron-activation analysis, ¹⁶N isotope rel. to O content 3-51764
- in nuclear fuel, metal oxide, macrodetermination by graphite reduction method 3-66411
- O I day airglow emissions of 5577 and 6300 Å lines in Martian atmosphere 3-65742
- overlay on Ni(001), chemisorption bonding, LEED study 3-60829
- overlay on Ni (100) surface, dynamical LEED obs. of atomic positions of C (2 × 2) struct. 3-64233
- paramagnetism, bonding theory, difference between valence bond and mol. orbital approaches, demonstration for students 3-48326
- photoabsorpt. cross-section at He 584 Å line 3-49407
- photoabsorption coefficients from 400 to 650 Å using synchrotron radiation 3-40566
- photochemical role, e.p.r. susceptibility meas. of C black (*French*) 3-68825
- photodissociation continuum determ., appl. to upper atm. emission 3-49497
- photoelectron spectra, autoionisation, Rydberg series 3-63532
- photosorption on ZnO powder, max. cover definition, apparatus (*Russian*) 3-48572
- planetary nebulae contrib. of charge exchange and optically thick condensations to [O I] radiation 3-73554
- plasma jet, high-energy propagation 3-43695
- plasmas, recombining, continuum emission 3-54835
- precipitation, in Si, heat treatment, X-ray anomalous transmission and topography 3-68413
- pressure dependent absorption cross sections, between 2000 and 2500 Å 3-78732
- purification attachment, microdeterm. C, N, H in org. compounds, decomposition 3-48651

oxygen continued

- quenching constant, for rhodamine 6G triplet state, from lasing characteristics 3-64728
- quenching delayed fluorescence, anthracene soln., mag. field effects 3-46309
- radiation recovery in Tenebrionid beetles, suppression by hypoxia 3-77266
- Raman cross section, relative, short-pulse laser scatt. and photon counting obs. 3-57651
- reaction with HCl in electrodeless r.f. discharge 3-80530
- red atmospheric band system, line intensities and half widths of A and B bands 3-65375
- resonances in electron impact, energies and width 3-52288
- rhodamine 6G laser, triplet quenching by O₂ 3-43014
- river, biochemical oxygen demand, three dimens. analytical soln. 3-59209
- saturated and compressed fluid, thermodynamic props. from acoustic wave velocity obs. 3-49964
- solar abundance corrections based on forbidden transition probabilities 3-45016
- solid, direct exchange interaction Hamiltonian 3-46951
- solubility in V, temp. dependence from 200 to 750°C 3-49998
- sorption, by Zr, kinetics, at very low press. 3-55140
- source and sensor, use of stabilized ZrO₂ solid electrolyte in ultrahigh vacuum 3-73713
- spin-orbit quenching of Te(5²P₁) and Te(5²P₀) 3-71371
- stars, C-O core growth phase 3-77047
- stellar evolution, abundance variation, effect on horizontal branch models 3-77045
- thermosphere, latitudinal and temporal variations in O, O₂ and O₃ abundance 3-61512
- thermosphere, lower, quenching of vibrationally excited N₂ by O, temp. depend. 3-69621
- thermosphere, O and He variations associated with geomagnetic activity 3-80768
- thermospheric atomic O comp. meas. using quadrupole mass spectrometer with strongly focusing ion source 3-51185
- Townsend's first ionisation coeff. measurement in time resolved avalanche studies 3-68121
- transport of O in lower thermosphere rel. to hemispheric imbalance 3-51100
- transport properties calc. 3-52417
- in upper atmosphere, comparison of concentration with that of impurity CO₂ 3-61506
- in upper atmosphere, concentration above 85 km measured by rocket-borne mass spectrometer 3-61505
- in upper atmosphere, number densities measured during geomagnetic activity at high latitudes 3-61504
- upper atmosphere, photochem. air pollution, O and O₃ concs., discharge flow method 3-69605
- upper atmosphere, production of vibrationally excited state 3-69601
- upper atmosphere, quenching profile between 75 and 115 km 3-76796
- vacuum u.v. absorption spectra in solid Ar, Kr and N₂ matrices 3-53130
- vibrational relaxation in an unsteady expansion wave 3-71629
- vibrational relaxation in presence of atomic O 3-54738
- vibrationally excited, produced in flash photolysis of NO₂ 3-80568
- water-air interface, rate of Rn exchange rel. to that of O₂ and CO₂, film model 3-80722
- C-O plasma, transition probabilities of CI lines, near i.r. 3-63866
- CO-He-O₂ laser, vibrational temp. meas. 3-54222
- CO₂, defect equilibria for extended point defects, effect of O₂ pressure 3-79340
- Cr-Ni films, evaporated, structural and electrical props. as function of gas pressure 3-58247
- in CuCl, absorpt. spectrum, e.p.r. of point defects, colour centres 3-68844
- n-GaAs, O₂-doped, radiative recombination at low temp., photocond. 3-52854
- GaAs:O, epitaxial layers, distribution coeff., temp. depend. 3-52758
- GaAs:O, impurity state electroabsorption measurements at 300 K 3-55664
- GaP, liquid phase epitaxy, Te and O₂ incorporation 3-50090
- GaP:O, photocapacitance measurements for study of nonradiative centres 3-58227
- Ge localised vibr. modes for implanted O ions 3-43854
- Ge:Li, O, precip. of Li, influence of O 3-43806
- Ge:O p-n junction, effect on VI characteristics (*Russian*) 3-52896
- Ge/Cs/O (100) surface, structural analysis and photoemissive props. 3-69134
- KCl(Br), photocond., influence of O ions 3-60902
- N₂:O₂, e.p.r. theory, effective zero-field splitting parameter calc. 3-50449
- NaCl:O²⁻, u.v. illuminated, photoplastic effect 3-58077
- O, beam-foil forbidden lines transition probabilities rel. to astronomical spectra 3-78430
- O, ionisation potential calc. 3-63305
- O⁵⁵⁷⁷ Å line, photometric investigation of auroral emission 3-44913
- O and O⁺ multiplets effective cross sections and excitation functions 3-43512
- O column density variations, u.v. photometry from OGO-6 satellite 3-61511
- O I 1304 and 1356 Å emissions from atmosphere of Venus rel. to rocket and Venera data 3-56346
- O I 4368 Å, airglow emission, conjugate photoelectron excitation 3-51097
- O I 5577 Å and 6300 Å forbidden lines in nightglow, seasonal and diurnal variations 3-51088
- O I 5577 Å radiation and differential photoelectron flux spectrum in twilight airglow 3-53508
- O I forbidden red lines in nightglow of Naini Tal 3-61492
- O I permitted line emissions, excitation in tropical nightglow 3-53509
- O II, O III, O IV, excited ions, quantum-beat g-factor meas. 3-60370
- O III 5007 Å line profiles in spectra of old planetary nebulae rel. to expansion velocities 3-45232

oxygen continued

- O V to VIII beam-foil spectra, tandem Van der Graaf energies 3-78447
 O VII line in solar corona, X-ray survey 3-65712
 O-H Van der Waals dipole-dipole interaction 3-63350
 O+C collision integrals for different electronic states 3-71395
 O+CS₂→SO+CS, reactive scattering in crossed beams 3-76452
 O+HBr→OH+Br, react. probabilities, quantum and transition state theories 3-80534
 O+HBr→OH+Br, react. probabilities, quantum and transition state theory 3-80535
 O+O₂+O₂→O₃+O₂ recomb. reaction, vibr. excitation of O₃ 3-76477
 O+olefins reaction, direct rate meas. showing negative temp. depend. 3-65075
 O- charge transfer reactions with O₃ 3-46349
 O- implantation effects on depth profiles by secondary ion emission mass spectrometry 3-66439
 O- molecule collision processes, electron exchange, mass spectrometric anal. (German) 3-78891
 O+He, collisions, autodetaching state obs., electron spectra 3-63339
 O+O₂, rate constants for charge transfer reactions, endothermic 3-63554
 O+O₂→O+O₂+e, electron affinities from collisional electron detachment rates in nonthermal fields 3-74808
 O⁺, beam-foil mean-life meas., cascade effect suppression 3-78429
 O⁺ bombardment of NaCl:Ti, luminescence, influence of channelling (Russian) 3-41550
 O⁺ charge exchange reaction with CO 3-40678
 O⁺ electron induced desorption from W, cross section, temp. depend. 3-75675
 O⁺ low energy collisions with Ne atoms radiation phase interference and optical polarisation effects 3-67715
 O⁺+H₂, reactive scatt. at relative energies below 15 eV, dynamics study 3-49414
 O⁺+N₂, product ion peaks near centroid scatt. mechanisms 3-40671
 O⁺+N₂ to NO⁺+N, reaction rate coeff. for ionospheric F-region, drift tube meas. 3-69742
 O⁺+N₂→NO⁺+N, low energy study 3-40668
 O⁺+Ne, low-energy collisions, phase-interference effects 3-71465
 O₂, adhesion coeffs. on W (100) and (110) planes, 78-950K (Russian) 3-79558
 O₂, adsorption on C, surface diffusion 3-75662
 O₂, adsorption on Pt, surface anal. in flow system (German) 3-79571
 O₂, adsorption on W(100), secondary ion mass spectrometry and electron-induced desorption investigation 3-75669
 O₂, adsorption on W(100) surface, work function obs. 3-75666
 α-O₂, at 1.3 K, bimol. series (Σ_g⁺→(ΔΔ) and (ΣΣ), absorpt. band fine struct. 3-44411
 O₂, chemisorption on Pt, sticking probability obs. as function of time 3-75678
 O₂, chemisorption on Pt, sticking probabilities 3-75679
 O₂, ionisation and fragmentation by 5-45 keV Ne⁺, Na⁺ ions, and Ne atoms 3-78898
 O₂, photoabsorpt. coeffs., 400-600 Å 3-52364
 O₂, vibrational excitation in low-energy electron impact, role of negative ionic states 3-78874
 O₂, X³Σ_g⁻ state, resolution of discrepancies 3-78736
 O₂ and water vapour binary mixture, thermal conductivity and viscosity calc. 3-63609
 O₂ content in C black during H₃PO₄ oxidation 3-69461
 O₂ minimum layer in SE Atlantic, structure and characteristics 3-41939
 O₂/CO₂ mixtures, vibr. relax. meas. 3-43516
 O₂-CS₂ flame laser emission rel. to CO, CO₂, N₂O and NO₂ additives (Russian) 3-62696
 O₂+CS₂, chemical laser, output parameters 3-70813
 O₂+D₂(H₂) elastic scatt., crossed beam expts., central-field pots. 3-54753
 O₂+H₂+N₂ flames, alkali metal atom collision process rates 3-80525
 O₂+H(H⁺) impact, electronic excitation cross-sections 3-78895
 O₂+N₂ mixtures, N₂(C³Π_u); v⁺=0, 1) de-excitation, luminesc. study 3-49483
 O₂+O₂, vibr. scatt., pot. well effect, SSH theory validity 3-49503
 O₂+O₂ interactions, absolute total scatt. cross sections meas. 3-71394
 O₂+Sn→SnO₂, matrix isolation i.r. study, characterisation of products 3-76427
 O₂⁻ alkali halide crystal impurity centre 3-68361
 O₂⁻ stimulated emission phenomena in high-frequency discharge (French) 3-52549
 O₂⁺, A₂Π_u-X²Π_g second negative band system 3-78735
 O₂⁺, electron impact excitation, collision strengths 3-71440
 O₂⁺ dissociative recombination rel. to O(¹S) excitation in pulsating aurora 3-80785
 O₂⁺ first negative system, effective cross sections and excitation functions 3-43512
 O₂⁺ second negative and N₂⁺ Meinel bands, laser theory 3-74223
 O₂⁺+Ar double charge transfer, translational energy spectrum of O₂⁻ ions 3-71634
 O₂⁺+NO, charge exchange in energy range 0.04 to 2 eV 3-71644
 (O₂)₂, van der Waals molecule, i.r. and visible spectra 3-43447
 O₃, general quartic force field calc. 3-46251
 O₃, relative Raman cross sections, for four Ar⁺ laser freqs. 3-63452
 O₃ molecular potential function, second order anharmonic, force constants obtained from zero order wave numbers (French) 3-43422
 O₃⁺, photoionisation cross section calcs. 3-71383
 O₄⁺, core description with small basis sets of SCF-MO-LCGO method (German) 3-52246
 O⁺+Ar high-energy collisions, electron loss 3-78584
 O(¹D) quenching with N₂, vibrational relaxation 3-75137
 OH+O₂→HO₂+O₂ reaction, rate const., 220-450 K, u.v. fluorescent scatt. obs. 3-41835
 OI 5777 Å laboratory emission, discharge expt. on oxygen and hydrogen gas mixture 3-57601
 OI 6300 Å airglow, morning twilight enhancement 3-59132

oxygen continued

- OI 6300 Å night airglow emission at low latitudes, Ogo 4 obs. in map-form 3-80782
 OI(6300 Å) emission data from Ogo 4, geomagnetic anomaly of equatorial airglow 3-69639
 O(¹S) auroral green line excitation by N₂(A³Σ_u⁺) molecules energy transfer 3-41997
 O(¹S) photodissociative production from CO₂, O₂, O₃ and N₂O at the 1216-Å Lyman-α line 3-40660
¹⁶O ions, mica irradiation, tracks, scatt. recoil nuclei process 3-66327
¹⁸O/¹⁶O ratios in cherts assoc. with East African lake deposits 3-53388
 O₂(2×1)-W(110) surface structure, RHEED intensities, kinematic analysis 3-55126
 O₂(a¹Δ_g), collisional quenching studied by time-resolved absorption spectroscopy in vac. u.v. 3-46269
 Rb/O dipole layer on Si, negative electron affinity surfaces 3-44128
 Si, conc., solubility, and equilibrium distrib. coeff. of N₂ and O₂ 3-58046
 in Si crystals, effect of growth medium, kinetics 3-68175
 Si:O, irradiated, influence on luminesc. spectra 3-61069
 Si:O e.s.r., oxygen content in floating zone single crystals, method (German) 3-53018
 SiO₂, films, annealing, influence on ion drift 3-60922
 Ta, thin film resistors, ion bombardment effect on resistance 3-58054
 in U oxides, macrodetermination by graphite reduction method 3-66411
 V:O neutron irradi., and radiation anneal hardening, recovery and temp. depend. 3-79383
 W-X-O-H systems, X-halogen, gas phase composition and chem. transport reactions (German) 3-44747
 W(112)-O₂ system, adsorbed layer models, LEED and optical diffraction pattern comparison 3-68500
 ZnS:Cu,Fe(Co,Ni)O, rise, decay and temp. depend. of photocurrents 3-46867
 Zr-O₂ system, quasi-equilibrium approach to combustion 3-58793
 ZrC, solubility of O₂, X-ray diffraction 3-41804
- oxygen compounds**
 hydride, influence of polarisation functions on molecular orbital hydrogenation energies 3-67744
 metal oxides, sintering, pore size rel. to grain size 3-64973
 oxides, melting, electron processes 3-75609
 oxides, nonstoichiometric, chem. of defects 3-68243
 oxides, oxygen partial molar parameters and stoichiometry deviations, model (French) 3-68419
 oxides, oxygen partial molar parameters rel. to nonstoichiometry (French) 3-52709
 oxides, sputtering coeffs., temp. depend. 3-69119
 X-ray emission spectra rel. to chem. bonding (Japanese) 3-69106
 CO+H→CO₂+H, rate consts. determ. 3-41840
 H₂+OH→H₂O+H, rate consts. determ. 3-41840
 HF, semi-empirical effective pair correl. parameters and correl. energies 3-54624
 Hf-O₂ superstructure and order-disorder transform. of interstitial O 3-58111
 KBr:OH⁻ oscillatory radiation of OH⁻ induced by electronic excitation (Russian) 3-44470
 KCl:OH⁻, microhardness and ionic cond., temp. depend. (Russian) 3-68644
 KCl(Br):OH⁻ single crystals, photocond. and optical bleaching of F-centres 3-60902
 MgO:Li, polycryst., O self-diffusion 3-79524
 O-Cu-Mn-Fe system, props. of spinel solid soln. 3-68411
 O₂, resonances in electron impact, energies and configurations 3-52400
 O₂-Ar Van der Waals complex, i.r. absorption spectra, internal rotation 3-78805
 O₂⁻ charge transfer reactions with O₃ 3-46349
 OCS, crystals i.r., Raman spectra, 2 phonon absorpt. 3-69001
 OCS, isotopically enriched, ground state and vibr. excited, microwave spectra 3-67830
 OCS, perturbation of electronic transitions under foreign gas pressure 3-75012
 OCS, vibrational relaxation in inert gases 3-60490
 OCS microwave transient nutation measurement, Bloch eqns. for relaxation times 3-63539
 OD, A₂²Σ⁺ state, dipole moment and hyperfine consts. by SCF and configuration interaction calc. 3-40606
 OD, A₂²Σ⁺ state, Stark studies and high field level crossing 3-40654
 OF₂, moments, orbital energy, charge distrib., SCF calcs. 3-52320
 OH, conc. on macropore surface and in ultrapores of glasses 3-61236
 OH, crossing of ⁴Σ⁻ and A²Σ⁺ states, comment 3-60474
 OH, interstellar, maser amplification, radioastronomical spectra (Dutch) 3-70036
 OH, OD, optical r.f. double reson. studies and zero-field level crossing 3-40653
 OH (A²Σ⁺-X²Π) rotational line strengths and energy level population in water vapour arc plasmas 3-43688
 OH emissions, upper atmosphere, rel. to stratospheric warmings 3-65320
 OH free radicals, sensitized fluoresc. by Hg(6³P₀) metastables 3-60484
 OH in water vapour arc plasmas, rotational lines meas. 3-43687
 OH interstellar emission polarization, density matrix techniques rel. to saturated OH-maser 3-42243
 OH molecular lines and oscillator strengths in photosphere 3-69829
 OH nightglow intensities in Europe-Africa sector, diurnal, annual and solar cycle var. 3-51101
 OH radicals reaction with n-butane, rate const. determ. 3-69478
 OH vibrational excitation, possible mechanisms rel. to upper atmospheric radiation 3-80779
 OH+NH₃→NH₂+H₂O reaction absolute rate const., pulsed photolysis obs. 3-65076
 OH+O₃→HO₂+O₂ reaction, rate const., 220-450 K, u.v. fluorescent scatt. obs. 3-41835
 OH+OH→H₂O+O, rate consts. determ. 3-41841

oxygen compounds continued
OH⁻, alkali halide crystal impurity centres 3-68361
OH⁻, in alkali halides, charge transfer excited states 3-68573
OH⁻, in alkali halides, librational and tunnelling levels 3-79453
OH⁻, in KCl, role in quasi-metallic centre formation (*Russian*) 3-68253
OH⁻, paraelec. behaviour in alkali halides 3-41476
OH⁻, photodetachment spectra, rot. line strengths 3-40659
OH⁻ ion effect on 18 Cr-8 Ni stainless steel, pitting and crevice corrosion (*Japanese*) 3-72907
OH radical, microwave and magnetic resonance spectra of vibrationally excited states, Λ -doubling 3-78853
ONF, vibr. deactivation of CO₂ upper laser level 3-45790
U-Nd-O system, oxygen pot. meas. 3-72933
W-halogen-O-H reaction systems, C influence on chem. reactions and transport processes (*German*) 3-53362

ozone
air pollutant, automatic sampling and anal. 3-53783
alkali metal ozonides, M⁺O₃⁻, Raman spectrum, Ar, Kr plasma excitations 3-78754
alkali metal ozonides, M⁺O₃⁻ type, Ar matrix, reson. Raman spectrum and vibr. analysis 3-78808
atmospheric, absorption spectra, 2.7 mm 3-76707
atmospheric, increase due to haze scattering 3-65386
atmospheric, low latitude, var. 3-73285
atmospheric conc. determ. from Earth daytime horizon meas. 3-51032
atmospheric concentration decrease with decreasing ionization during PCA event 3-69594
atmospheric concentration var., nighttime obs. in N. Carolina Piedmont boundary layer 3-65350
atmospheric heating due to O₃ absorpt., analytic formula 3-61470
atmospheric negative ions, collisional detachment of electrons 3-46212
atomic resonance radiation quenching of O(2¹D₂) in vacuum ultraviolet 3-71370
charge transfer reactions with O⁻, O₂⁻, OH⁻, NO₂⁻, F⁻, Cl⁻, CO₃⁻ 3-46349
chemiluminescent monitors 3-77295
concentrations in mesosphere and lower thermosphere at sunset, rocket obs. 3-51099
continuous u.v. absorption O₃ photometer 3-59716
i.r. fluorescence, laser induced, air pollution remote sensing 3-76043
i.r. spectrum, isolated in inert gas matrices, test for this technique 3-60455
martian polar region, seasonal variation, Mariner 9 u.v. spectra obs. 3-45038
matrix isolated, i.r. spectra, bonding, geometry and thermodynamic functions 3-75044
molecule, non-empirical SCF studies of ring and open forms 3-78667
molecule, vibr. deactivation of CO₂ upper laser level 3-45790
photolysis, time-resolved absorption spectroscopy in vac. u.v. of O₃(a¹ Δ_g) 3-46269
photolysis at 3130 Å, quantum efficiency for O(¹D) prod. 3-41860
stratosphere, NO production from past nuclear explosions, O₃ measurements 3-65348
stratospheric, effect of nitrogen oxides from nuclear explosion and jet engines 3-61476
stratospheric, effects of water vapour and nitrogen oxides 3-76741
stratospheric and mesospheric ozone, perturbations 3-59103
submillimetre laser lines by optical pumping 3-51916
upper atmosphere, photochem. air pollution, O and O₃ concs., discharge flow method 3-69605
u.v. spectrum, features of photochemical interest 3-73155
vibrational excitation using O + O₂ + O₂ → O₃ + O₂ recomb. reaction 3-76477
vibrational relaxation of CO₂(001), laser fluorescence technique 3-78888
NO + O₃ → NO₂ + O₂, O₂(¹ Δ_g) and O₂(¹ $\Sigma_g^+) possible production 3-47572
O₃-D₂-N₂O, mixture laser oscillation, optical gain and laser emission by flash photolysis 3-48873
O₃-D₂(H₂)-CO₂, mixture laser oscillation, optical gain and laser emission by flash photolysis 3-48873
O₃⁻, CNDO-MO calculations 3-67735
O₃⁺, rotational diffusion equation, Markov process 3-79245
¹⁶O₃, low temp. i.r. spectrum, zero order parameters 3-78782
¹⁸O substituted molecules, microwave spectra, rotational consts. 3-78782
¹⁸O₃, low temp. i.r. spectrum, zero order parameters 3-78782$

ozonosphere
No entries
P invariance
hyperon non-leptonic decays, parity conserving, medium strong mass symmetry-breaking effects 3-66969
neutral current parity violating, detection in e⁻e⁺ colliding beams 3-66959
nuclear e.m. transitions, spatial parity nonconservation effects including higher approxs. (*Russian*) 3-74529
nuclear parity-violating expts., exchange effects 3-40444
nucleon one-meson exchange potentials, parity-violating, in current-current quark model 3-48994
review of symmetries in physical laws (*German*) 3-66939
space-time symmetries for system of particles with electric and magnetic charges 3-51983
spatial violation, in nuclear fission through the two hump barrier, detection 3-67379
unified gauge theories of hadronic weak interactions, P violation in nuclei 3-66972
violation, hyperon decay, NN π vertex, scalar meson pole model 3-62809
violation in π N interactions, off mass shell effects, renormalisable σ -model 3-74349
 γ circular polarisation, correction from divergent P-violating NN ρ vertex in $\pi p \rightarrow d\gamma$ 3-78198
 μ decay, phenomenological model of weak lepton interactions 3-78118
 ρ - ω mixing parameter phase from unitarity relation 3-78230

p-n heterojunctions
amorphous chalcogenide semiconductors, photoelectric phenomena 3-41231
chalcogenide glass-Si heterojunctions, switching and photoelectric behaviour 3-60913
GaAs/Ga_{1-x}Al_xAs single-heterostructure diode laser, external cavity controlled, time delays 3-66845
III-V quaternary alloy epitaxial layer application 3-41684
interface states, Aerts model 3-55332
lasers, catastrophic and slow degradation 3-48926
mesa stripe double heterostructure laser, fabrication and performance 3-54236
photoconductographic system with p-n junction, dark current compensation 3-73801
semiconductor laser, time delays and Q-switching 3-54237
p-Si:B on n type Si, piezoresistive effect 3-79984
theory (*Czech*) 3-52891
(AlGa)As-GaAs, cold cathode electron emitter 3-58586
(AlGa)As-GaAs, refractive index step and carrier confinement rel. to lasing props. 3-70825
Al_{1-x}Ga_xAs photodiode, micro-cathodoluminesc. obs. 3-58320
Al_{1-x}Ga_xAs-GaAs, single heterojunction injection laser, self-switching 3-70829
Cu_{1-x}S-CdS, field induced absorption 3-64406
CdO-NaCl containing colour centres, electrically stimulated photocond. inversion 3-50241
(GaAl)As-GaAs, double heterostruc., high peak power injection laser 3-51935
GaAlAs-GaAs, localised gain within resonator type laser with narrow active region 3-54234
GaAs/Ga_{1-x}Al_xAs single heterostructure diode laser, threshold, spectral and output power characts. 3-66846
GaAs-Al_{1-x}Ga_xAs double heterostructure, luminesc. spatial pattern obs. 3-66848
GaAs-Ga_{1-x}Al_xAs double heterostructure laser, threshold and electron lifetime, acceptor conc. depend. 3-57236
GaAs-Ga_{1-x}Al_xAs double heterostructure lasers, composition profile effect on characts. 3-43021
GaAs-Ga_{1-x}Al_xAs light emitting diode, emission spectrum 3-41584
GaAs-GaAlAs junction-stripe-geometry lasers, room-temp. continuous operation 3-43023
Ge-CdS diode, current-voltage charact., resist. states 3-72398
Ge-GaAs alloy junctions, photoelectric characts. (*Russian*) 3-58318
Se-As₂Se, thin films, switching phenomena and memory effect 3-79749
Si₃Ge_{1-x}, current-voltage characts. 3-41627
n-ZnS-p-GaAs, negative resistance at 77 to 293 K (*Russian*) 3-79761
ZnSe-SnO₂, obs. of donor acceptor pair recombination in ZnSe 3-80110
ZnTe thin films on GaAs, InAs and GaP, epitaxially grown heterostructures 3-44138
ZnTe-CdSe, growth, elec. props., interface parameters 3-68698
ZnTe-CdSe heterojunctions, photoelectric and luminescent props. 3-79767
ZnTe-Ge, irreversible switching of conductivity states 3-68702
ZnTe-ZnSe, blue electrolum. 3-64740
ZnTe-ZnSe, electroluminesc., red and green emission (*French*) 3-53151

p-n homojunctions
capacitance of diode, function of forward bias and freq. 3-68699
charge injection, into SiO₂ coating with reverse bias below breakdown 3-55333
diamond, formation by B and Sb implantation 3-46846
diffused, with deep impurities, barrier capacitance calc. 3-46891
hole and electron traps, p-n junction capacitance studies 3-64300
many layer structs. with p-n junctions, nonequilib. cond. relax., memory effects 3-44140
p-n-p semiconductor negative resistance origination by minority carrier injection (*Czech*) 3-55277
semiconductor laser, time delays and Q-switching 3-54237
CdP₂, diffused, prep. and characts. 3-44142
CdS:Bi, ion implanted, characs. rel. implanted layer behaviour 3-69167
CdTe, prep. by Al vapour-diffusion 3-79764
CdTe p-n junction, photomagnetic effect, current-voltage characts. 3-44139
CuInSe₂, small signal analysis, doping levels and band diagrams 3-46844
Ga_{1-x}Al_xAs:Si p-n structure, delay of electrolum., rel. to barrier capacitance 3-47316
GaAs, liquid phase epitaxial, hole and electron traps detn., capacitance obs. 3-41263
GaAs, photovoltaic effect due to two photon process in presence of built-in field 3-68696
GaAs, photovoltaic effects, laterally illuminated 3-52869
GaAs, prep. by solid-to-solid S diffusion, injection luminescence 3-41189
GaAs IMPATT structures, multiple layer liquid phase epitaxy 3-41687
GaAs microwave diode applications, IMPATT varactor, abrupt junction, liquid phase epitaxy 3-50662
GaAs:Cr, p-i-n structure, impurity photocapacitance effects, photoionisation cross sections spectra 3-41260
GaAs:Ge, Te, epitaxial, compensation effects on electrolum. 3-41261
GaAsP negative electron affinity cold cathode, characts. 3-68693
GaP, electroluminesc. delay time on applic. of forward pulse 3-58566
GaP, epitaxial p-n junctions, cathodolum., scanning electron microscope obs. 3-44496
GaP, green-emitting diode, high-efficiency, LPE overcompensation growth 3-79762
GaP, modulation of He-Ne laser light at near grazing incidence 3-40279
GaP, modulation of laser light, birefringence, waveguide properties (*German*) 3-53079
GaP, phase modulation of He-Ne laser light by Pockels effect 3-53922

p-n homojunctions continued

- GaP:N, electrolum. at high excitation levels 3-76098
 GaP:N, yellow electrolum. 3-80115
 Ge, effect on O on VI characs. (*Russian*) 3-52896
 Ge, p-i-n structure, gradually graded, produced by electron irradiation, magnetoresistance 3-52894
 Ge, p-n junction depth of occurrence, electronic probe determ. (*Russian*) 3-77717
 InAs, electrolum. max., temp. depend. 3-64743
 $\text{In}_x\text{Ga}_{1-x}\text{As:Ge}$, amphoteric props. of Ge, liquid epitaxial growth and elec. props. 3-50266
 $\text{In}_{1-x}\text{Ga}_x\text{P}$, epitaxial p-n structure, electrolum. 3-64742
 $\text{In}_{1-x}\text{Ga}_x\text{P}$ vapour growth, p-n junction electroluminescence characs. 3-58599
 $\text{In}_{1-x}\text{Ga}_x\text{P}$ vapour growth technique, p-n junction electroluminescence 3-58598
 InP, single cryst. diffused and liquid phase epitaxial, elec. and optical props. 3-41587
 InSb, electron energy dissipation nr. impact ionisation threshold, photoelectric effect obs. 3-58305
 InSb, photosensitivity spectra, 0.5-3.4 eV, at 90 K 3-44143
 InSb, scanning electron microscopic study 3-68695
 PbSe, photovoltaic spectra, temp. and substrate impurity conc. depend. 3-58298
 Si, alloyed, avalanche breakdown characs. 3-52893
 Si, avalanche radiation, resistivity inhomogeneity meas. 3-41258
 Si, breakdown voltage lowering due to C impurity precipitation 3-52890
 Si, characterisation of defects, thermally stimulated meas. capacitance and current 3-41257
 Si, diffused, avalanche breakdown voltage 3-64399
 Si, epitaxial, electron and hole ionisation rates, photomultiplication obs. 3-68642
 Si, epitaxial growth, p-n junctions, thyristor manufacture 3-41256
 Si, generation-recombination characteristic behaviour 3-79765
 Si, insulating, epitaxial structure, leakage current meas., four-probe method 3-42601
 Si, p-n junction depth of occurrence, electronic probe determ. (*Russian*) 3-77717
 Si diode, elec. characs., oxidation-induced stacking fault effects 3-41259
 Si $p^+ - n - n^+$ vertical junction diodes, ionizing radiation, second breakdown 3-64402
 Si transference and change of mesoplasma characteristics in p-n junction (*Russian*) 3-68697
 Si:Au $p^+ - n$ reverse-biased junctions, thermal and optical generation current 3-46889
 Si:B, carrier generation levels in forbidden band, function of implanted ion energy 3-44144
 Si:P, prep. by ion implantation through oxide layer 3-46845
 Si:Zn, thermal capture of electrons and holes at Zn centres, obs. 3-68562

p-n junctions

- see also p-n heterojunctions; p-n homojunctions*
 abrupt, analytical approx. under high level conditions using simple model 3-46890
 avalanche multiplication calculation, simple approximation, abrupt junction (*Hungarian*) 3-68694
 capacitance, thermodynamic considerations 3-64400
 capacitance of junction with deep centres, influence of mobile charge carriers 3-79766
 carrier heating effect, very low currents 3-64401
 carrier injection, triggering of trapped plasma in $p^+ - n - n^+$ structure 3-68692
 contrast distortion, limit of electron microscope investigation, with and without oxide layers (*German*) 3-52895
 current flow rel. to electron gas heating 3-44141
 depletion region thicknesses 3-44136
 Ebers-Moll eqns., modified for junction voltage drops and leakage currents 3-75790
 electronic probe, for determ. of depth of occurrence (*Russian*) 3-77717
 gas flowmeter, p-n junction sensor 3-48690
 inhomogeneous structures, photo-effects 3-58299
 inhomogeneously doped, depletion width determination 3-64397
 mathematical framework, solved problems, book contrib. 3-58219
 microplasma phenomena theory, avalanche multiplication process 3-41262
 m.o.s. capacitor, collection inversion charge, p-n junction collector, minority carrier recombination 3-41202
 n-p-i structure, negative-resistance, temp. dependence of parameter spread (*Russian*) 3-44137
 negative differential resistance, p-n-p-n-p-structure, theoretical formulae (*Russian*) 3-50264
 neutral region carrier concentration, detn. using quasi Fermi levels 3-52892
 p-n-p-n structure, propag. of turned on state 3-60914
 p-n-p-n structures, charge carrier distrib. on disconnection of control pulse 3-68701
 p-n-p-n-p-structure, voltage-current characteristics calc. (*Russian*) 3-58319
 photovoltage response, surface effects in p-i-n structures 3-68665
 photovoltaic effects, laterally illuminated, theory 3-52869
 planar, effect of Al_2O_3 film on electrical characs. 3-79763
 pulsar magnetospheres, charge boundaries, p-n junction effect 3-81124
 space charge region, effect of recombination on photocurrent under parallel illumination 3-64369
 temperature coefficients of drift voltage (*German*) 3-50265
 thermal switching and breakdown rel. to law of electrical conductivity 3-60877

P-V-T relations *see equations of state***pacemakers**

- see also patient treatment*
 electrostimulation, field strength hypothesis, pacemaker electrodes, experimental results (*German*) 3-65985
 online control, using process computers (*Italian*) 3-54022

packaging

- see also modules*
 microelectronic, laser beam sealing 3-74287
 nuclear fuel, spent, Yankee Atomic Electric Co. shipping experience 3-67576
 nuclear spent fuel, NFS-4 cask 3-67575
 radioactive materials, licensing and analytical techniques of evaluation 3-67413
 reactor fuel in transit effect of reflection material on reactivity 3-63183
 superinsulation, Al coated plastic foils 3-62024

packing *see packaging***pair algebra** *see algebra***pair annihilation, electron** *see positron annihilation***pair production, electron** *see electron pair production***pairs, electron** *see electron pairs***palaeomagnetism**

- analytical representation of past epochs, using superposition of travelling magnetic waves 3-69543
 archaeomagnetism and secular geomagnetic var. rel. to dynamics of drifting eccentric dipole field 3-41914
 Archean volcanics, Blake river syncline, Ontario 3-58941
 Azores, Terceira island, geomagnetic secular variation 3-58960
 Baffin diabase dikes, data and revised Franklin pole 3-47663
 Brunhes epoch, excursions and secular variations in Indian Ocean region 3-76673
 Brunhes normal polarity epoch, occurrence of 3 field reversals 3-53435
 Cambrian Gondwanaland reconstruction rel. to palaeomagnetism of Central India 3-50984
 Canary Islands and Madeira, results from 359 igneous rocks 3-58915
 Carboniferous rapid polar motion of North America 3-58931
 Central Cascades, Washington, palaeomagnetism of granitic rocks rel. to Miocene pole 3-53433
 clay tilt deposition relation, study of Port Alma, Ontario 3-76651
 Crozet Basin, deep sea core, rel. to mag. reversals 3-58961
 deep sea cores, time averaged geomag. fields, distinction between axial symmetry and geocentricity 3-80676
 deep sea sediment cores, paleomag. record, effect of sedimentation on magnetisation 3-80677
 dolerite, pliocene, pre-Balkans, natural remanent magnetisation, thermomagnetisation curves, palaeomagnetic stability 3-56099
 earth, earth's crust, evolution 3-76586
 Elmina sandstone, Ghana, NRM studies 3-73253
 ensialic model for Precambrian Africa and South America 3-76573
 Eocene Green River sediments, annually banded, large discrepancy between virtual magnetic and rotation poles 3-73247
 equatorial palaeopoles and dipole field behaviour during polarity transitions 3-56102
 field reversal in Pliocene, changes in declination inclination and field intensity 3-65238
 Foyers plutonic complex, Invernesshire, palaeomagnetism, direction of magnetisation 3-41905
 Greater Antilles Outer Ridge, giant piston core reversed polarity event 3-58963
 Greenland, Cape Biot formation 3-58948
 Grenville Front, Labrador, Seal and Croteau rocks, polar wander and tectonic implications 3-76657
 Grenville Province, Ontario, giving Precambrian pole posns. 3-76655
 Grenville Province, palaeopoles rel. to plate convergence in Late Precambrian 3-56137
 Guam, curvature of southern Mariana island arc 3-58958
 Gulk of Mexico latest Pleistocene deep-sea sediment, paleomag. excursion 3-53427
 igneous rocks, unequal co-axial dipole pair model for data analysis 3-58955
 intensity of Earth's mag. field during late Upper Cretaceous and Oligocene 3-61405
 Jurassic Topley Intrusions, Endako, British Columbia 3-76654
 Kahochella Group, Canada 3-58942
 Kayenta formation, Upper Triassic, anomalous field behaviour 3-58949
 Kirkland Lake, Ontario, Archean mafic volcanics, palaeomagnetic and petrologic correlations 3-58969
 Late Mesozoic, Spitzbergen, evidence for continental drift in Arctic 3-73248
 lavas, palaeosecular variation, Norfolk and Philip Islands 3-76664
 Libya, palaeomagnetism of Tertiary basalts 3-58917
 magmatic formations, separation by gravitational and magnetic anomalies (*Russian*) 3-76677
 mantle roll, comparison of plume traces with palaeomagnetic data 3-76577
 Marianas island arc, secular variation studies 3-58959
 marine anomalies, linear filtering application 3-59163
 marine near-bottom magnetic anomalies rel. to field over last 5 m.y. 3-58932
 Martin Formation, Saskatchewan, stratigraphic correlation between sedimentary basins of Canadian Shield 3-58943
 Mesozoic palaeomagnetic scale from sedimentary formations in USSR 3-65245
 metamorphic rocks from Churchill Structural Province, Canadian Shield 3-76652
 Mid-Atlantic Ridge, magnetic results from Median Valley basalt drill cores 3-56025
 N. Atlantic and Caribbean oceanic rocks natural remanent magnetism intensities and susceptibility 3-73217
 Neogene sedimentary rocks, Oga Peninsula, Japan 3-80674
 Oregon Cascade lava flows study of NRM 3-76672
 palaeointensity studies on magnetite by Thellier technique 3-58972
 palaeozoic rocks, Australia, a.c. demagnetisation method, pole positions 3-41904
 Pliocene basalt, North Bulgaria, natural remanent magnetisation, thermomagnetisation curves, palaeomagnetic stability 3-56099
 polar wandering, Precambrian, India 3-61415
 polarity changes and duration of volcanism in lava flows 3-76671
 polarity sequence and radiolarian zones, Epoch 17-Matuyama 3-58962

palaeomagnetism continued

- pre-Cambrian dolerite dykes, Vestfold Hills of East Antarctica 3-76665
 Precambrian red beds N.W. Scotland 3-58944
 western Pyrenees plate boundary, magnetisation of Permian basaltic flows and dikes 3-73246
 pyrrhotite, significance of mag. transitions at 5-16 kbar 3-58865
 Reunion geomagnetic polarity event, age and duration 3-80655
 reversal history to earliest Miocene, sediment cores from eastern equatorial Pacific 3-58965
 reversal record from Osuzuyama intrusion eastern Kyushu, comparison with Tathoosh intrusion 3-58956
 reversal stratigraphy, Lake Rudolph, Kenya, dating of associated artefacts and fossils 3-58957
 Sardinian volcanic rocks, evidence of rotation during Early Miocene 3-44795
 secular geomagnetic field var. rel. to archeomagnetic and palaeomagnetic data 3-41908
 stratigraphic appl. (*Russian*) 3-65232
 stratigraphy of Equatorial Pacific core, oxygen isotopes, temperatures, ice volumes 3-76693
 titanomagnetite, low-temp. oxidation and palaeomagnetic implications 3-69512
 Tororo ring complex, SE Uganda, palaeomagnetism of carbonatite volcanics 3-80654
 Trenton limestone, New York State 3-58945
 Upper Cretaceous volcanic rocks in Sicily, palaeomagnetism rel. to motion 3-56101
 Vancouver Island, Oligocene East Sooke gabbro characteristic magnetisation retained after demagnetisation 3-73245
 volcanogene formations of Carpathian region (*Russian*) 3-65231
 West Pyrenees, delineation of plate boundary between Iberian Peninsula and Europe, evolution of Bay of Biscay 3-58946
 Western Alps, Permian and Triassic rocks (*French*) 3-44854
 western equatorial Pacific, sediment accumulation rates, remanence, correlation of magnetically disturbed intervals 3-58964

palladium

- band structure calc., of cubic 4d Pd 3-72313
 conduction electron characs. and optical constants, 1-9 μ spectral range obs. 3-75992
 Debye temperature, temp. depend., sp. ht. data 3-72155
 elastic moduli meas. under hydrostatic press. by u.s. vel. method (*French*) 3-54994
 e.s.r., spin-orbit coupling effect, numerical calc. 3-41395
 f.c.c., lattice dynamics, extended de Launay's model 3-55056
 Fermi edge isochromat spectroscopic localization in conduction band 3-79624
 film, on Au substrate, misfit dislocation generation 3-64259
 foil, Knight shift and spin-lattice relax. of ^6Li , nucl. mag. dipole moment determ. 3-40409
 liquid, resistivity and thermopower, d resonance calc. 3-44059
 localized modes of interstitial H, neutron scatt. study 3-55063
 magnetoelectric and thermomag. props., 77 to 750 K, temp. depend. (*Russian*) 3-75738
 neutron irradiation, fast vs thermal neutrons, defect production, elec. cond. monitoring 3-64073
 nucleation and growth on amorphous C by vapour deposition 3-41632
 phonon dispersion, freq. spectrum and sp. ht. calc. 3-79444
 surface, polycryst., oblique Ar^+ bombardment in 1 keV range, sputtering yield, ion incident angle depend. (*German*) 3-47342
 surface, with chemisorbed CO, equil. comp. 3-79577
 thin crystals, charact. X-ray prod., electron beam orientation depend. 3-40833
 triglycine sulphate: Pd^{2+} , single cryst. growth, domain struct. 3-55528
 Hg/Pd interfacial and adhesion energy meas. by SEM 3-75659
 Pd-Fe-He, improved thermal contact at ultralow temps. 3-52740
 Pd:H system on metallic hydrogen, superconducting transition temperature 3-58330
 Pd-H, supercond. transition temp., h.p. effect, isotope effect 3-60931
 Pd-M system, compositional dependence of superconducting critical temp. 3-64423
 ^{105}Pd , nucl. quadrupole moment from h.f.s. consts. 3-52261

palladium alloys

- see also palladium compounds*
 absorption of H in Pd-Pt, Pd-Ni and Pd-Rb 3-55789
 actinide-Pd phases, prep. and props. 3-46604
 lanthanide-Pd phases, prep. and props. 3-46604
 metallic glasses, bending deform., brittleness 3-41783
 rare earth-Pd, 7:3 phases, cryst. struct. and mag. props. 3-79274
 Ag-Pd alloys, electronic states 3-72311
 Ag-Pd films, prep. and optical props. (*French*) 3-41527
 Au-Pd alloys, H_2 diffusion 3-53230
 Ca-Pd system, new cubic phase 3-58008
 CePd_3 , Kondo system, anomalously large thermoelec. cooling figure of merit 3-50182
 Cr-Pd, composition dependence of shrinkage in sintering of systems charact. by eutectic constitution diagrams 3-80395
 Cu-Pd, disordered, electron diffraction study of short-range order diffuse scattering 3-63978
 Cu-Pd, investigation of disordering processes (*Russian*) 3-69190
 Cu-Pd system, origin of formation of one- and two-dimensional superlattices 3-68197
 FePd_3 , ordered and disordered, electronic specific heat rel. to hydrogen solubility 3-55090
 $\text{Fe}(\text{Pd}_{0.53}\text{Pt}_{0.47})_3$, magnetisation and hysteresis curves at 77 K and 4.2 K, magnetic structure determ. 3-52996
 Gd_2Pd_3 , ferromag., isotopic with R_2Pd_3 ($\text{R}=\text{La}, \text{Ce}, \text{Pr}, \text{Nd}, \text{Sm}$), non-centrosymmetric ThFe_3 structure 3-52601
 Ni-Pd, forced magnetostriiction, temp. and comp. depend. 3-47120
 Ni-Pd, magnetocryst. anisotropy const., comp. depend. 3-47084
 NiPd, concentration depend. of magnetic hyperfine fields, Mossbauer effect of ^{61}Ni 3-41457
 $\text{Pb}_3\text{MnSb}_2\text{S}_{10}$, Heusler type alloys, mag. hyperfine fields, spin transfer mechanism 3-46948
 Pd-Ag, chemisorbed CO, surface composition, in equilib. 3-79577
 Pd-Ag, localized modes of interstitial H, neutron scatt. study 3-55063

palladium alloys continued

- Pd-Co, mag. ordered, dilute, induced into supercond. state, anomalous tunnelling 3-68736
 Pd-Cr, localised spin fluctuations, low temp. mag. props. obs., Pd-Ni comparison 3-68768
 β^1 -Pd-Ni, electronic susceptibility, Fermi energy influence 3-72448
 Pd-Ni, Debye temperature, temp. depend., sp. ht. data 3-72155
 Pd-Ni-P, comp. depend. of glass transition temp. 3-68167
 Pd-Pb mixture phase characterization (*German*) 3-63983
 Pd-Rh:Ni, spin fluctuation resist., 1.3-20 K 3-64480
 Pd-V, dil., incremental resist., 1.4-300K, high spin-fluctuation and Kondo models 3-55245
 Pd-W solid soln., interdiffusion coeffs., conc. depend., correl. with solidus line shape (*Russian*) 3-41712
 $\text{Pd}_{1-x}\text{Ag}_x\text{Hn}$, electrical resistance anomaly, from 4 to 300K and phonon resistivity 3-79673
 $\text{Pd}_{1-x}\text{Al}_x$, ($x<0.03$), impurity atom electronic struct. calc., rel. to spin-lattice relax. time 3-44034
 $\text{Pd}_{1-x}\text{Cu}_x$, ($x<0.03$), impurity atom electronic struct. calc., rel. to spin-lattice relax. time 3-44034
 PdEu, mag. props. and cryst. struct., Mossbauer and X-ray obs. 3-79954
 PdFe type alloy, dilute, nonmagnetic impurity effects on Curie temp. 3-55430
 $(\text{Pd}_{0.997}\text{Fe}_{0.003})_{1-x}\text{Gd}_x$, dilute ternary alloy, ferromag. props. depend. on x 3-50351
 β^1 -PdIn phase, constitutional and thermal defects, heating and quenching effects, exptl. obs. 3-49887
 Pd_3Mn thin films, antiphase domain boundaries 3-41739
 PdMnGe, crystal atomic structure and magnetic properties 3-49878
 $\text{Pd}_{11}\text{MnSb}$, Heusler type alloys, mag. hyperfine fields, spin transfer mechanism 3-46948
 Pd_2MnSb , n.m.r. study, magnitude and sign of hyperfine fields at ^{55}Mn and ^{123}Sb 3-50485
 Pd_2MnSn , local mag. ordering of ^{57}Fe impurities 3-79832
 $\text{Pd}_1\text{-R}_x$, R=rare earth, magnetic properties, crystal field effects, e.p.r., magnetic moment 3-47129
 $\text{Pd}_{52}\text{Si}_{18}$, amorphous, splat cooled, physical props. 3-60758
 PdZn-PdGa mixture, crystalline structure (*German*) 3-58006
 Rh-Pd alloys, H_2 absorption, at high pressures 3-53229

palladium compounds

- see also palladium alloys*
 Cu-Ni ores, X-ray spectrometric anal., segregation 3-48659
 Pd complex, $\text{Pd}_2\text{Cl}_2(\text{C}_2\text{H}_4)_2$, torsional potential for ethylene ligands 3-54656
 Pd complex, phthalocyanine, dynamics of triplet state in zero field 3-50846
 Pd complexes, $\text{Pd}(\text{PPh}_3)_2\text{X}_2$, $\text{Pd}(\text{PPhO})_3\text{X}_2$, ($\text{X}=\text{Cl}, \text{Br}$), vibrational spectra and structure 3-54689
 Pd complexes of etiopyrphyrin and mesoporphyrin, nonfluorescent, quantum yield for intermolecular conversion (*Russian*) 3-49488
 Pd II complex, diiodobis(triphenylphosphine)palladium(II), cryst. and mol. struct. 3-46611
 Pd-Ag-H system, superconductivity, temp. depend. of relative electrical resistance 3-79793
 Pd-D system, superconductivity theory 3-46928
 Pd-H system, superconductivity theory 3-46928
 Pd-H $_2$ and Pd-D $_2$ system, thermodynamic props. at low D $_2$ and H $_2$ concentrations over wide temp. range 3-44580
 Pd-Pr-H system, superconductivity, temp. depend. of relative electrical resistance 3-79793
 Pd-Rh-H system, superconductivity, temp. depend. of relative electrical resistance 3-79793
 PdH $_x$, hydriding pressure effect on supercond. transition temp. 3-68721
 Pd(II) azide complex, resonance Raman effect (*German*) 3-78775
 Pd(II) complex, trans-planar, energy transfer to ligand-field states 3-41854
 Pd(II) complexes, $[\text{X}_2\text{Pd}(\text{C}_5\text{H}_5)_2]$, ($\text{X}=\text{Cl}, \text{Br}$), i.r. and Raman spectra, vibr. assignments 3-46300
 PdRh $_2\text{H}_3$, hydriding pressure effect on supercond. transition temp. 3-68721

paper

- see also paper industry*
 electrostatic copy paper, automatic testing system 3-66729
 impregnated, dielectric loss under simultaneous action of a.c. and d.c. fields 3-47207
 moisture measurement, infrared absorption method 3-62338
 photographic, disc sound recording 3-39960

paper industry

- noise abatement problems 3-51481

piezoelectric materials *see dielectric materials***piezoelectric resonance** *see dielectric resonance***parallel processing**

- computational algorithm, subsonic compressible flow 3-71777
 optical parallel image processor, on-board spacecraft, design concepts 3-45475

parallel resonator filters *see band-pass filters***paramagnetic properties of substances**

- see also paramagnetic resonance; paramagnetism*
 alkali TCNQ salts, mag. susceptibility 3-60954
 1,3-bis(diphenyl)-2-p-chlorophenylallyl, paramag.-antiferromag. transition at 3.25 K 3-58375
 copper formate dihydrate, ferromag. (100) and paramag. (200) interlayer interaction 3-64499
 copper trisethylenediamine sulphate, Jahn-Teller anisotropy of paramagnetism 3-50341
 DPPH radical, mag. transition, infralow temp., e.p.r. obs. 3-79894
 ferrites, cubic, valencies of Mn and Fe ions, paramag. Mossbauer obs. 3-55510
 ionic salts, γ -irradiated, impurity cent. form. 3-68254
 liquid metals, magnetic susceptibility calc. 3-72449
 magnetic glass, review 3-46977
 magneto-acoustic waves, distribution, phase diagram (*Russian*) 3-47123
 metalloenes, ^{13}C spin density distrib., pulse Fourier transform n.m.r. 3-75906
 polyacrylonitrile thermal transformation products 3-63600

paramagnetic properties of substances continued

- rare earth single cryst., translation balance adapted for paramag. susceptibility meas. 3-42609
- rare earth-Fe, thermal expansion rel. to Curie temp. pressure depend. 3-58385
- rare earth-group VIII metal systems, 7:3 phases, paramag. susceptibility 3-79274
- ruby, susceptibility, γ -irrad. effects 3-41325
- steel, phase anal. by Faraday method 3-75853
- TiCN salts, sp. ht. and mag. susceptibility, 1.4-4.4 K, rel. to band struct. 3-46795
- Van Vleck paramagnet, single-singlet model, high temp. dynamical props. 3-64464
- SmS:La, cond. electron enhancement of exchange interactions, Van Vleck susceptibility obs. 3-55413
- Ag-Gd, dilute, mag. susceptibility, n.m.r. and thermoelec. power obs. of impurity state 3-68765
- As₂Te₃-As₂Se₃ glasses, 40-80% composition range, of magnetic susceptibility 3-75826
- B₂O₃-MnFe₂O₄ partially devitrified glass, mag. props. and recrystallisation study 3-55410
- BaFe_{12-x}In_x³⁺O₁₉, BaFe_{12-x}Al_x³⁺O₁₉, susceptibility, temp. depend., molecular field coeffs. (Russian) 3-55414
- Bi₂Ti₂Fe₂O₂₇, ferroelec., susceptibility and mag. moment 3-60961
- C black, e.p.r., irrad. influence, susceptibility meas. (French) 3-68825
- CdCr₂S₄:Cu, influence of dopant on paramag. Curie point 3-75842
- α -Ce film, strongly disordered, rel. to resist., 1.5-300 K 3-68593
- Ce_{1-x}La_x, press.-temp. phase diagram, transition from Curie to Pauli paramagnetic phase 3-72444
- Ce_{1-x}R_xAl₃, (R=Gd,Tb,Er), n.m.r. and mag. susceptibility 3-41434
- CeSn₃, d.c. electrical resistivity determ., influence of 4f electrons 3-79674
- Co-transition metal intermetallics, orbital susceptibility and ⁵⁹Co Knight shift, d-electron motion (Russian) 3-52954
- β -CoAl(Ga), mag. moments rel. to defect antistructure Co conc. 3-58367
- CoO, paramagnon symmetries and magnon dispersion relations 3-68796
- CoTiSb, Heusler type alloy, cryst. structure, Pauli paramag. props. 3-58003
- CoTiSb and Co₂TiSb Heusler alloys, mag. and chem. order 3-68791
- Cr-Fe alloy, magnetic excitations, inelastic neutron scattering 3-41329
- Cr-Mn alloy, itinerant antiferromag. coexistence with localised mag. moments 3-64487
- Cr-Mn spinels, susceptibility obs. 3-68777
- Cr_{5-x}Si₃ solid solutions, Pauli paramagnetism, 78 to 300K (Russian) 3-68611
- Cs-NH₃ solution, paramag. susceptibility meas. by Gouy method 3-73172
- Cu-Al alloys, solid and liq., susceptibility, 20-1200°C (Russian) 3-52953
- Cu-Mn spinels, susceptibility, Curie-Weiss const. 3-68776
- Cu-Ni alloy, susceptibility, influence of clustering 3-52957
- Cu-Rh alloys, f.c.c., Pauli behaviour 3-79277
- β -Cu(IO₃)₂, Cu(IO₃)₂.2H₂O(γ -H₂O), cryst. struct., paramag. props. to 1.4 K 3-79306
- Cu(NH₃)₄PtCl₄, spin correl. functions from e.p.r. data 3-55458
- Dy, pure elec. quadrupole interaction, PAC obs., cond. electron contrib. to EFG 3-41468
- Dy₂Gd_{1-x}, paramag. susceptibility meas., single-ion and exchange interaction anisotropy 3-75828
- Er(OH)₃, magnetic susceptibility and Schottky sp. ht., crystal field studies 3-79840
- EuO, surface paramag. layer, photoelectron spin polarisation obs. (German) 3-50407
- EuYb₂O₄, orthorhombic, susceptibility, Curie-Weiss behaviour (French) 3-46979
- Fe phosphate glasses, temp. dependence of magnetic susceptibility, 2.0 to 300K 3-75830
- γ -Fe-Mn alloys, Mossbauer effect obs. of temp. and conc. depend. singularities (Russian) 3-44353
- Fe-Mn(18 wt.%) alloy, second order transform., ϵ -phase behaviour (Russian) 3-72462
- FeAl, electron transport and mag. susceptibility 3-44053
- Fe₂Al, paramagnetic susceptibility as probe into atomic ordering 3-60957
- Fe₂GeS₄, paramag.-antiferromag. transition (French) 3-47052
- FeNH₄(SO₄)₂.12H₂O, paramagnetic with pure dipole-dipole coupling, Mossbauer spectra, relaxation phenomena, spin wave model (German) 3-58463
- α -Fe₂O₃:Sn, hematite, Morin transition temp., Sn⁴⁺ impurity effects 3-72472
- Fe₂Si₂S₄, paramag.-antiferromag. transition (French) 3-47052
- Fe₂TiS₂, intercalation cpds., susceptibility, 78-340 K 3-46623
- FeTiSb, Heusler type alloy, cryst. structure and Curie-Weiss paramag. props. 3-58003
- Fe₂TiSn, Heusler type alloy, cryst. structure and Curie-Weiss paramag. props. 3-58003
- GaAs, paramagnetism, obs. of photolum. circular polarisation in weak mag. field 3-46980
- Gd:Mg, single impurity effect on electron-hole T-matrix 3-55220
- Gd(Al_{1-x}M_x)₂, (M=Cu,Ni), Curie temp. meas. rel. to cond. electron number 3-58376
- Gd₂MF₇, GdK₃F₆, and cryst. struct. and phase behaviour (French) 3-64017
- Gd₂O₃, reduction of effective paramag. and saturation moment 3-68762
- GdP, Heisenberg paramag., dynamics, pulsed n.m.r. obs. 3-41447
- Gd₂(SO₄).8H₂O, reduction of effective paramag. and saturation moment 3-68762
- Gd_{0.5}Y_{1.5}O₃, reduction of effective paramag. and saturation moment 3-68762
- HgCo(SCN)₄, susceptibility temp. depend. to 5K 3-52952
- KO₂ crystals, sp. ht., transforms. (German) 3-50361
- K₂Pt(CN)₄.Br_{0.3}.2.3H₂O, susceptibility temp. depend., model of linear metallic strands interrupted by insulating lattice defects 3-50340
- LaCo_{5-x}Ni_x-s_x, mag. props., lattice consts., and H absorpt. 3-58380

paramagnetic properties of substances continued

- LaCuO₃, mag. susceptibility, Pauli paramag., superexchange enhancement (French) 3-60955
- LaNiO₃, mag. susceptibility, Pauli paramag., superexchange enhancement (French) 3-60955
- LaP:Gd, Heisenberg paramag., dynamics, pulsed n.m.r. obs. 3-41447
- LaSn₃, d.c. electrical resistivity determ. 3-79674
- LaSn₃In_{3(1-x)}, local electronic props., paramag. susceptibility and n.m.r. meas. 3-46803
- Lu, high purity, meas. by Faraday method, 1.5-300 K, impurity effects 3-75827
- LuP:Gd, Heisenberg paramag., dynamics, pulsed n.m.r. obs. 3-41447
- Mg-Cd alloys, influence of melting on mag. props. (Russian) 3-68763
- α -Mn, paramag. susceptibility maximum, Fermi-liq. model 3-55416
- α -Mn-Fe alloy, paramag. susceptibility maximum, Fermi-liq. model 3-55416
- MnAlF₆, mag. interactions nature w.r.t. MnF₂ (French) 3-64486
- MnAs, elastic constants rel. to ferromagnetic and paramagnetic states 3-40953
- MnCO₃, symm. in paramag. and antiferromag. states, Mn²⁺ ion absorpt. spectrum obs. (French) 3-47064
- MnCrO₃, ilmenite type, susceptibility, Curie-Weiss law behaviour 3-60709
- Mn₂(Mg_{1-x}Y₂S₄), polycryst. solid soln., mag. susceptibility, Curie-Weiss behaviour 3-41328
- MnO-P₂O₅ glasses, magnetisation studies, high and low temp. susceptibility 3-75831
- Mo, susceptibility of single crystals, plastic strain influence (Russian) 3-79822
- MoS₂, semiconductor layer structure, magnetic susceptibility, Van Vleck theory of paramag. susceptibility 3-41327
- Na-NH₃ solution, paramag. susceptibility meas. by Gouy method 3-73172
- Nb₃Au, Pt_(1-x)A₁₅ type phases, superconductivity, structure and magnetic susceptibility 3-58334
- Nb₃X A-15 cpds., low temp. paramag. susceptibility and supercond. crit. temp. (French) 3-68724
- Ni, hyperfine struct. of Mossbauer spectra, influence of paraprocesses near Curie temp. (Russian) 3-44215
- NiAl, electron transport and mag. susceptibility 3-44053
- Ni₃Al(Ga):Fe, giant moments in paramag. alloys, depend. on ferro-mag. crit. comp., Mossbauer obs. 3-64585
- Ni₂Al_{25-x}Ga_x, x=0 and 10, mag. ordering, 2-50K 3-64504
- Ni₃Ga alloy, magnetisation, susceptibility, t<80K 3-64476
- Ni₃Ga alloy, paramag. props., Stoner-Edwards-Wohlfarth model 3-55415
- Ni(II) complex, bis-isopropylsilylaldiminato, single crystal, mag. anisotropy and susceptibility 3-72447
- NiO, antiferromag.-paramag. transition, crit. behaviour of spontaneous magnetisation 3-58382
- NiO, paramagnon symmetries and magnon dispersion relations 3-68796
- NiS₂, magnetic susceptibility, temp. depend., mag. transition at 31K 3-64496
- NiS₂, pyrite type, weak ferromag. T_c equiv. to antiferromag. M2-mode T_n, neutron diff. obs. 3-68783
- NiS_{2-x}Se_x, metal-semicond. phase diagram, resist., susceptibility and calorimetric meas. 3-72328
- NiTiSb, Heusler type alloy, cryst. structure, Pauli paramag. props. 3-58003
- O₂, bonding theory, difference between valence bond and mol. orbital approaches, demonstration for students 3-48326
- β -Pd-In alloy, electronic susceptibility, Fermi energy influence 3-72448
- Pr, d.h.c.p., paramag. excitons, temp. depend. excitation spectra 3-46821
- Pr₂In, Curie-Weiss props. above 80 K, mag. susceptibility meas. 3-79828
- Pr₂Tl Van Vleck paramagnet, spin-phonon coupling 3-46981
- Pu, electron-paramagnon electrical resistivity, high-temp. behaviour 3-44062
- rare earth-gold compound, RAu₂, Curie-Weiss law, temp. depend. of magnetic susceptibility 3-46999
- RbMnF₃, spin diffusion coeff., room temp. to critical region 3-55412
- Rh-Mn-Sb alloys, Cl₃ type, reciprocal susceptibility 3-64490
- Sc high purity, effect of impurities on magnetic susceptibility 3-46985
- SmZn₁₂, Curie-Weiss law, paramagnetic susceptibility 3-44198
- Sr₂FO₃F, Curie-Weiss, magnetic susceptibility above 50K 3-46978
- 1sTaS₂, semiconductor, layer structure, magnetic susceptibility, Van Vleck theory of paramag. susceptibility 3-41327
- Ta₂S metal intercalation compounds, preparation and properties 3-72050
- Th-Dy alloys, susceptibility, temp. depend., Curie-Weiss behaviour (Russian) 3-60956
- TiCo, mag. susceptibility meas. from 300 to 1500K, overlapping band electron model 3-52956
- Tm_{0.25}Y_{0.75}Al₃, neutron crystal field spectroscopy, paramagnetic phase, energy distribution, field parameters 3-52955
- UP-ThP solid soln., lower temp. antiferro-paramag. transition, susceptibility obs. 3-68782
- V₁₀Sb, with B8-type structure, Pauli type paramag. 3-60960
- V₂Si-V₂Ge, low temp. paramag. susceptibility and supercond. crit. temp., comp. depend. (French) 3-68723
- V₃X A-15 cpds., low temp. paramag. susceptibility and supercond. crit. temp. (French) 3-68724
- YCo₂, paramag. susceptibility, press. depend., correl. with Curie temp. of LnCo₂ alloys 3-55419
- YFe₂, temp. depend. mag. behaviour (French) 3-72547
- Y(OH)₃:Er³⁺, magnetic susceptibility and Schottky sp. ht., crystal field studies 3-79840
- Zn₁₃Fe, zeta phase, more paramag. susceptibility than pure diamag. Zn 3-64477
- ZrFe₂, thermal expansion rel. to Curie temp. pressure depend. 3-58385

paramagnetic resonance

- see also *acoustic paramagnetic resonance*; *ENDOR*; *paramagnetic resonance of ions*; *spin-lattice relaxation*; *spin-spin relaxation*
- N-(diphenylmethylene)-aniline, determ. of dihedral angle of A ring 3-71486
- di- μ -(pyridine N-oxide)bis [bisnitrate (pyridine N-oxide) copper (II)], e.p.r. spectrum, triplet ground state, computer simulation 3-75075
- N-acetylglycine, single crystals, X-ray damage, e.s.r. meas. 3-73146
- β -alanine, X-irrad., recrystn. effect 3-55970
- aliphatic ester radicals and complexed radical from photolysis of azo-compounds 3-55979
- alkali metal, radical anion soln., n.m.r. studies, comparison with n.m.r. 3-44734
- alkali tellurite glass, heat-treated, e.p.r. of radiation centres (*Russian*) 3-44324
- amino acids containing S, γ -irrad., e.s.r., electronic structure parameters of free radicals, expanded Huckel meth. 3-78681
- anthracene-pyromellitic dianhydride, zone-refined crysts., charge-transfer spectra 3-61269
- antiferromagnet, two-dimens., crit. exponents for n.m.r., e.p.r. linewidths 3-58418
- aromatic hydrocarbons, $S_1 \rightarrow T_x$ intersystem crossing process, PMDR obs. 3-44731
- atom, spin reson. and parametric interactions with counter-rotating terms, theory 3-67671
- p-azoxyphenetole, liquid crystals, e.s.r., orientation of radicals containing N-O groups 3-79231
- bacteriochlorophyll, one-electron oxidation, absorption and e.p.r. obs. (*Russian*) 3-51425
- barbituric acid dihydrate, 4.2K, oxidation and reduction by ionising radiation, e.s.r., ENDOR meas. 3-73147
- benzene anion radical, effects of orbital degeneracy on g-values 3-54723
- benzenes, cyano-substituted, lowest excited triplet states, zero field splitting 3-78845
- benzil, position of phenyl rings 3-71486
- benzophenone, undistorted triplet state, static and dynamic paramagnetism 3-76478
- 9,9'-bianthranyl, dianion triplet at low temp. 3-47573
- bimodal cavity spin inductors field theory analysis 3-62194
- biphenyl-tetracyanobenzene single crysts., mobile charge-transfer triplet excitons 3-64538
- cell for electron resonance spectra up to 100 kbar 3-51559
- β -chloroalkyl radicals, struct. and conform., isotropic e.s.r. g-values and h.f.s. 3-60397
- cholesteric mesophase struct., perturbed by mag. field, electron reson. spectroscopy 3-54921
- conference, Athens, Georgia, USA, Oct. 1972 3-54719
- copper phthalocyanine polymorph, dimeric struct., i.r., X-ray, electronic, e.p.r. spectra 3-52599
- copper propionate monohydrate, Zn-doped single crysts. 3-55465
- cross relaxation probability, dependence on angle between axes of spin quantisation 3-64540
- cytidine, X-irradiated, ENDOR and e.s.r. studies 3-44726
- defect centres in solids, e.p.r. and paraelec. reson. studies 3-64552
- dialkyl phosphites, γ -irradiated, e.p.r. identification of P-centred radicals 3-55974
- diamond, e.p.r. of single ionised N-C-N centre 3-47145
- diglycine nitrate, γ -irrad., e.s.r. spectra 3-58426
- dimers triplet EPR spectra simulation, g and D tensors not coaxial 3-64546
- N,4-dinitroso-N-methylaniline reaction with polyamide resins, e.p.r. and i.r. study of products (*Russian*) 3-50851
- dinitroxide spin label oriented in crystal matrix, electron-electron dipolar splitting anisotropy 3-44316
- 1,1-diphenyl-2-picryl hydrazyl recrystallised free radical powder, e.s.r. absorption 3-47601
- diphenylmethyl radical, stereochem., e.s.r. data interpret., INDO-MO calcs. 3-46228
- DPPH and derivatives, high-resolution e.p.r. spectra of hydrazil radicals 3-78841
- DPPH in polystyrene, e.p.r. lineshape in wings of exchange narrowed systems 3-64539
- DPPH radical, infrared temp., mag. transition 3-79894
- ELDOR of monofluoroacetamide irradiated cryst. 3-55972
- electron, microwave, applic. of IMPATT diodes as r.f. source 3-39979
- electron cyclotron resonance spectra in vacuo by photoejection and thermionic emission from metal films 3-72503
- electron spin echo envelope spectrometry, superhyperfine splitting 3-39978
- enones, conjugated, spin-orbit coupling effects on the zero field splitting of (π, π^*) triplet states, ODMR obs. 3-65103
- e.p.r. absorption spectra, improvement of r.f. spectrometer 3-73823
- e.p.r. information storage, handling, multichannel analyser 3-73822
- e.p.r. line, second moment of dipolar broadening finite temperatures, lattice sum of truncated dipolar interaction 3-41397
- e.s.r. spectra, non-collinear Zeeman, hyperfine and fine structure tensors effect 3-47127
- ethane + R(stable radical), local conc. near critical liquid-gas point, e.p.r. obs. 3-50862
- ethanol glasses, deuterated, trapped electrons, 4K 3-76465
- ethylene + R(stable radical), local conc. near critical liquid-gas point, e.p.r. obs. 3-50862
- ethylene glycol + water glassy mixture, trapped electron excitation mechanism, thermoluminescence obs. 3-65099
- exponential time constants, computer meas., noise present 3-62191
- external voltage sweep, for field-regulated magnets 3-42617
- field-swept fixed-frequency spectra, eigenfield expansion technique for efficient computation, from relaxation master equations 3-60476
- fine structure e.s.r. spectra, in strong crystal fields, spin Hamiltonian constrs. determ. numerical solution 3-44312
- formyl radical, from sensitized decomposition of formaldehyde 3-47577
- free radicals, chemically induced dynamic spin polarization, hydrodynamic effect 3-80537
- free radicals in aq. environments, line shape calc. 3-47603
- Fiemy salt, orange-brown form, triplet state obs. (*French*) 3-61275

paramagnetic resonance continued

- gas-phase e.p.r. linewidths and intermolecular potentials, exper. results F-He-F₂ system 3-71368
- gas-phase e.p.r. linewidths and intermolecular potentials, theory 3-71367
- Gaussian condensation methods for fast diagonalization of complex Hermitian matrices 3-44315
- germanate glasses, e.s.r. spectra of microdefects, energy levels and struct. models 3-50459
- glass matrix, optical and paramag. absorpt. of Ag particles, size effect 3-55563
- graphite, pyrolytic, g-factor anisotropy and e.p.r. linewidths, 300-4.2K, neutron irrad. effects (*French*) 3-47124
- halogen atoms, thermally produced, forbidden electron reson. transitions 3-46188
- Heisenberg ferromagnet spin relax., high-temp., exchange-narrowed e.p.r. 3-79897
- Heisenberg linear chain, damping constant 3-68753
- high polymer, stressed, free radical obs. (*German*) 3-61223
- hyperfine structure, cepstral anal. for mag. parameters 3-63520
- iminoxy radicals of pyrimide derivatives 3-78842
- iminoxy radical, in plastic cryst., inhomogeneous broadening of e.p.r. spectra, conditions of rapid rotational diffusion 3-79895
- iminoxy radicals, ¹⁵N e.p.r. spectral linewidths, mol. reorientation effects 3-43486
- iminoxy radicals, spin exchange frequency determ. from poorly resolved spectra 3-58795
- ion-implanted films, giant transmission e.p.r. theory 3-41402
- Jahn-Teller effect, e.p.r. spectra of ²E_g state, vibronic reduction factors 3-72507
- Jahn-Teller effects, intermediate coupling for ²E states in cubic symmetry 3-60987
- line broadening, caused by cavity Q-factor variation 3-42616
- line shape analysis for unresolved hyperfine splitting, effect of field modulation amplitude and frequency 3-75873
- lipid bilayers, e.p.r. spectra of spin labels 3-73571
- liquid, paramagnetic probe motion from electron spin relaxation 3-64542
- liquid crystal, viscous nematic, second-order phase change nonexistence 3-55456
- magnetic susceptibility change, absolute determination, automatic compensation method 3-62195
- magnetisation, periodic longit., of transverse r.f. wave irrad. spin system at e.s.r. 3-50441
- malonic acid, irradiated single crystals, ELDOR study, nuclear spin exchange influence 3-53326
- matching circuit and bucking current stabilizer for detector in e.s.r. spectrometer 3-42618
- metal, conduction e.s.r., microwave cavity size effects 3-47146
- metal, large samples, second derivative detection theory 3-60986
- metal, thin samples, conduction electron spin resonance saturation theory, surface relaxation 3-64553
- metals, conduction electrons and localized moments, derivation of Bloch equations including anisotropy field 3-60985
- metals, Doppler-shifted spin resonance in electron fluid 3-50387
- methane, microwave-i.r. double resonance using 3.39 μ He-Ne laser line 3-43481
- methyl group, weakly hindered, tunnelling rotation rate, e.p.r. and ENDOR meas. 3-47125
- 1-methyl uracil single crystal, irradiation induced formation of radical pairs, e.s.r. obs. 3-69473
- 3-methylhexane glass, energy level structure of trapped electrons, optical bleaching meas. 3-64370
- 2-methyltetrahydrofuran glass, γ -irradiated, ELDOR study of trapped electrons mag. energy transfer between two different spin systems 3-44727
- microwave cavity, for high temp. expts. 3-39980
- molecular excited states, optically detected electron spin locking and rotary echo trains 3-43492
- molecular excited triplet states, absolute sign of electron spin dipolar and nucl. quadrupole interactions 3-57667
- monitoring of anisotropic dielectric rods with paramagnetic impurities 3-77587
- monofluoroacetamide irradiated cryst., ELDOR role of F p-orbital anisotropy 3-55972
- naphthalene, e.p.r. and optical absorpt. obs. of radiation-induced radicals 3-55473
- 5-nitro-6-methyluracil, electron irradiated, e.s.r. study of free radical formation 3-41852
- nitrobenzene solns., high elec. field induced radicals identification 3-50858
- nuclear photoemulsions, due to presence of tanning agent 3-62248
- nuclear polarisation, dynamic, electronic spin-spin interactions contrib., theory 3-79890
- nuclear polarisation, dynamic, electronic spin-spin interactions contrib., expt. 3-79891
- nucleic acid, e.s.r. study of radiation damage in single crystals, free radical formation 3-41851
- optically transparent magnetic materials, nature of laser radiation, e.s.r. influence (*Russian*) 3-43016
- organic free radicals, computer program for interpreting e.s.r. spectra 3-73151
- organic free radicals, effects of orbital degeneracy on g-values 3-54723
- organic molecular crystals, spin-lattice relax. in localised triplet states 3-75917
- phenanthrene in triplet state e.p.r. hyperfine interactions and electron spin distribution 3-47583
- picryl-N-amino carbazyl, static magnetic susceptibility, reln. to ESR line width 3-58373
- picryl-N-amino carbazyl recrystallised free radical powder, e.s.r. absorption 3-47601
- polyacrylonitrile, e.s.r. data, stereoregularity 3-63600
- polymer with system of conjugated bonds in solution, e.s.r. spectra 3-60499
- polymeric complexes, e.s.r. spectra 3-63963
- polystyrene, dynamic polarisation of protons, electronic spin-spin interactions contrib. 3-79891
- polystyrene containing paramagnetic impurity, spin-lattice relaxation of protons 3-72540

paramagnetic resonance continued

- polyvinyl-iso-propenylacetylene ladder polyene with three fibre chains, thermal transformations, electrophysical props. 3-60503
 porphyrins meso-substituted, e.p.r. spectra, effect of alkyl substituents (*Russian*) 3-78852
 probe analysis, 10 GHz, rotatable h.f. field (*French*) 3-77588
 propyl radicals, spin delocalisation mechanisms through sigma bonds delocalisation to gamma proton, SCF-MO-INDO method 3-43418
 proteins, e.s.r. study of radiation damage in single crystals, free radical formation 3-41851
 PTFE, deuteron irradi., obs. of yield of peroxy radicals 3-79893
 quartz, X-irrad., e.p.r. and paraelec. reson. study 3-64552
 quartz glass, structural changes during heat treatment, optical and e.p.r. meas. 3-80428
 radiation damage mechanisms, e.s.r. spectroscopy study, review 3-55459
 radical, transient effects in time resolved ESR 3-80536
 radicals, core level binding energies, multiplet splitting, unpaired orbital spin density distrib. 3-46236
 radicals, di-substituted, β -proton splittings, conformational properties 3-67730
 radicals, estimation of CC bond lengths 3-63367
 radicals in solids, mechanism of discrete spectral diffusion 3-64541
 radicals trapped in single crysts., ^{13}C hyperfine coupling tensors 3-55971
 rhodamine 6G, ESR triplet state meas. 3-78028
 ruby, effects of internal stresses on spectrum 3-79886
 saturation method, microwave, for $\Delta M_s = 2$ transition probability determ. 3-48490
 semiconductor, electron spin relax. meas. by optical pumping 3-68845
 semiconductor, e.s.r. correction to hot electron elec. cond. 3-72367
 semiquinone radicals in aprotic media, linewidth alternation (*French*) 3-44729
 DL-serine, irradiated at 4.2 K, e.s.r. and ENDOR studies 3-76466
 solid, low temp., theory of saturation 3-50442
 spectral diffusion coefficient, electron-nucl. cross-relax. contrib., calc. 3-68830
 spin exchange frequency determ. from poorly resolved spectra 3-58795
 spin Hamiltonian for low symmetry, second-order perturbation treatment for energy levels 3-72506
 spin probe spectra in weakly anisotropic media 3-54716
 stopped flow control system, operational characteristics 3-66289
 student laboratory microwave experiment 3-56603
 succinic acid, irradiated, spectral confirmation of absence of CO_2 3-61266
 superconductor, gapless, dirty, type II, e.p.r. theory 3-46935
 tertiary aliphatic amines in SO_2 solns., e.s.r., optical absorption 3-69477
 theory at low temp., e.p.r., acoustic e.p.r. and spontaneous spin-lattice relax. (*Russian*) 3-79889
 TMPD-TCNQ, delocalised triplet state excitations, spin susceptibility, e.s.r. 3-60970
 sym-triazine, electron states 3-80103
 triphenylmethyl radical, ^{13}C -E.S.R. coupling constants, π -radicals, hyperconjugation 3-78850
 Tschitschibabin (quinoid) type hydrocarbons, triplet state determinations (*German*) 3-63511
 tumbling system, low symmetry e.p.r., motionally averaged hyperfine structure and assymetries 3-79896
 uniaxial crystals, mosaic and block structure, axis directions, method 3-53013
 vanadyl tartrate, binuclear, electron exchange interaction sign 3-58416
 vitamin B_{12} , low symmetry e.s.r. spectra computer simulation 3-43528
 zero-field spectrometer, new design 3-77594
 zinc acetate, irradiated single crystals, ELDOR study, nuclear spin exchange influence 3-53326
 $[\text{CuCl}_4 \cdot 2\text{NH}_3]^{2-}$ complex, spin hamiltonian parameters, Π bonding, e.p.r. study 3-41401
 AgCl, e.s.r. of self trapped holes, Ag^{2+} centres, at liquid nitrogen temps. 3-72521
 Al, spin relaxation of surface conduction electrons 3-72522
 $\text{Al}_{1-x}\text{Ga}_x\text{As}$ mixed crystals, e.p.r., carrier conc. and Si donor props. 3-55467
 $\alpha\text{-Al}_2\text{O}_3$, reactor-irrad., F^+ centres, e.s.r. obs. 3-41409
 $\text{Al}_2\text{O}_3\text{-Cr}_2\text{O}_3$ powders, condensed from plasma, e.p.r. struct. exam. 3-47448
 B, β -rhombohedral cryst., photocond. and photo-e.p.r. at 77 K, mechanism and quantitative description 3-52877
 $\beta\text{-B}$, rhombohedral, e.p.r. obs. of paramagnetic centres 3-79914
 $\text{B}_2\text{O}_3\text{-SiO}_2\text{-PbO-Fe}_2\text{O}_3$ glass, mag. ordered 3-58402
 C black, e.p.r. meas., illum., photochemical effects (*French*) 3-68825
 C fibre, e.s.r. g-value, resist., thermolec. power and magnetoresist., correlations 3-80477
 CN radical, gas phase ODMR 3-40656
 CaO:Mg F_a^+ centre e.p.r. and optical absorption spectra 3-43786
 CaS, plastically deformed, colour centres (*Russian*) 3-76032
 CaTiO_3 , Nb substituted, cryst. chem. 3-72044
 CaWO_4 , e.p.r. of divacancy centres 3-55475
 $\text{CdCr}_2\text{Se}_4(\text{S}_4)$, mag. semicond., temp. depend., Raman relax. process 3-79899
 ClO_2 , ^{17}O -labelled, isotropic hyperfine const., dipolar tensor, spin density 3-60480
 CrTe, 100-360K, press. up to 50 kbar, mag. transitions 3-64500
 CsBr, e.p.r. of triplet state of self-trapped exciton, obs. by microwave optical double resonance 3-58428
 CuCl, group VI impurities, e.p.r. of point defects 3-68844
 Cu(II) complexes, polycrystalline, glasses, e.s.r. spectra, computer analysis 3-79903
 $\text{Cu}(\text{NH}_3)_4\text{PtCl}_4$, spin correl. functions 3-55458
 EuB_6 , CsCl-structure, e.s.r. studies, compared to GdS and $\text{Y}_{1-x}\text{Gd}_x\text{S}$ 3-41407
 Fe complexes, acetate chloroplatinate, anomalous g factors, triads of Fe atoms 3-75874
 Fe(III) complexes, tris(2-thio-oxalato) salts, microcrystallite spectra interpretation using line-shape calcs. 3-55457

paramagnetic resonance continued

- GdB_6 , $\text{La}_{1-x}\text{Gd}_x\text{B}_6$, CsCl-structure, e.s.r. studies, compared to GdS and $\text{Y}_{1-x}\text{Gd}_x\text{S}$ 3-41407
 $\text{Gd}_2\text{B}_{1-x}\text{Ru}_x$ ($\text{B} = \text{Th, Ce, La}$), e.p.r. and supercond. correl. transition temp. Gd conc. depend. 3-72417
 $\text{Gd}_2\text{La}_{1-x}\text{B}_6$, e.s.r. spectra, exchange narrowing, linewidth measurements 3-47128
 $\text{Gd}_2\text{Th}_{1-x}\text{Ru}_x$, re-entrant crit. field behaviour, e.p.r. correl. 3-72418
 Ge, atom-free single-cryst. surface, states determ. (*Russian*) 3-64394
 Ge:As, high conc. region, e.s.r. line width 3-47130
 H atoms reaction with H_2S , e.s.r. study 3-47555
 $\text{H} + \text{NF}_3$ reactions in moderately fast flow system, kinetic study by high temp. e.s.r. 3-76430
 H_2 , para, $d(3p^2)\pi_u$ ($v=0-3$) fine structure via microwave ODMR induced by electrons 3-40657
 HfO_2 single crystals, $^{10}\text{e.s.r. obs.}$ 3-72518
 H_2O_2 and H_2O in aqueous solutions at 77K 3-55980
 H_2SO_4 glasses, γ -irrad., study of disappearance of trapped H atoms 3-73149
 H_2SO_4 :anthracene, conc. depend. relax. times, spin echo expts. 3-41400
 $\text{Hf}(\text{BH}_4)_4\text{-U}(\text{BH}_4)_4$, Zeeman spectra, cryst. field parameters 3-76033
 KAsF_6 , γ -irradiated, e.s.r. study of F_2^{2-} 3-41408
 KBr, e.p.r. of triplet state of self-trapped exciton; obs. by microwave optical double resonance 3-58428
 KBr, self-trapped exciton, optical detection 3-75882
 KCl F centres, optical detection of e.p.r. and luminescence bleaching effects (*French*) 3-53021
 KCl, e.p.r. spectra, decoloration of F-band (*Russian*) 3-54961
 KClO_3 , formation and annealing of free radicals created by irradiation 3-61268
 KH_2PO_4 , e.p.r. after γ -irradiation 3-69472
 K_2MnF_4 , two-dimens. antiferromagnet, crit. exponents for e.p.r. linewidths 3-58418
 K_2MnF_4 , two-dimensional Heisenberg paramagnet, min. linewidth obs. 3-41396
 $\text{K}_2\text{Pt}(\text{CN})_4\text{Br}_0.3(\text{H}_2\text{O})_{2.3}$, e.p.r., mag. susceptibility 3-52958
 $\text{LaAl}_2\text{-Gd, Ce, Th, U}$, conduction electron spin flip scattering obs. 3-41411
 $\text{La}_{1-x}\text{Gd}_x\text{B}_6$, CsCl-structure, e.s.r. studies, compared to GdS and $\text{Y}_{1-x}\text{Gd}_x\text{S}$ 3-41407
 Li-Bi, liquid alloy electronic transport, spin-flip scattering, e.s.r., thermoelectric power, conductivity 3-50180
 LiF, growth of V_k -centres by beta-rays from irradiation produced tritium, e.p.r. 3-72519
 LiF crystal, obs. of neutron irradi. prod. F-like centres 3-79912
 LiNbO_3 crystal, laser damage susceptibility rel. to growth and purity control 3-69358
 $\text{Li}_2\text{O-Al}_2\text{O}_3\text{-SiO}_2$ glass, nucleation and crystn. phenomena 3-54928
 Li(TCNQ), spin susceptibility, low temp. sp. ht., e.s.r. linewidths 3-58415
 MgAl_2O_4 , spinel, orthorhombic Cr^{3+} centre, spin Hamiltonian for e.s.r. spectra 3-43788
 MgO , ^{25}Mg hyperfine confirmation of localised ground state model of V^- centre 3-58429
 MgO , F^+ centre obs. 3-68886
 MgO , V^- centre, combined e.p.r. and mag. circular dichroism double reson. study 3-55474
 MgO crystal, u.v. excitation, deep hole trap, hole-release Auger mechanism 3-72776
 MgOH radical, e.p.r. spectra at 4K, CNDO struct. calc. 3-46321
 $\text{MnCl}_2 \cdot 4\text{H}_2\text{O}$, X-band and Q-band obs., 10/3 effect (*French*) 3-44313
 MnF_2 , low-field resonance and zero-field relaxation 3-60989
 Mn(II) complexes, multi-freq. e.p.r. study, 10/3 effect 3-47126
 $\text{MnSO}_4 \cdot 4\text{H}_2\text{O}$, X-band and Q-band obs., 10/3 effect (*French*) 3-44313
 MoO_3 cpds., amorphous semicond., localized d^1 electron e.s.r. meas. 3-68847
 $\text{N}_2\text{:O}_2$, effective zero-field splitting parameter calc. 3-50449
 N_2^- molecular ions, electronic magnetic resonances 3-52390
 NO_2 , electronically excited, microwave optical double resonance 3-43479
 NaCl:Ni, X-irradiated, stimulated processes, conductivity, thermoluminescence, absorption and e.s.r. spectra 3-41592
 NaClO_3 , formation and annealing of free radicals created by irradiation 3-61268
 NaF, $\text{H}_2(\text{Li}^+)$ paramag. centre caused by electron irradi., e.s.r., hyperfine interaction, line splitting 3-41410
 NaNO_2 , triplet state of NO_2^- , e.s.r., phosphoresc., level crossing 3-72509
 NaO_2 , e.p.r. spectra, g tensors and h.f.s. interaction 3-54717
 NaSO_2 e.p.r. spectra, g tensors and h.f.s. interaction 3-54717
 $\text{Na}_2\text{ZnGeO}_4$, Zn-Mn isomorphism, e.s.r. study 3-72068
 NiCl_2 , antiferromagnet, crit. e.p.r. spin dynamics, linewidth divergence behaviour 3-47136
 $\alpha\text{-NiSO}_4 \cdot 6\text{H}_2\text{O}$ e.p.r. measurements, single crystals, spin Hamiltonian parameters, direction cosines of crystalline field 3-50440
 O_2 in N_2 and CO condensed matrices, $<10\text{ K}$, torsional oscils., ^{17}O hyperfine splitting 3-43477
 POX_2 , PSX $_2$, PX $_4$, free radicals, e.p.r. spectra 3-43487
 PbF_2 , pure and rare-earth activated, colour centres 3-54960
 Pb, spin-orbit coupling effects, numerical calc. 3-41395
 Pt(II) complexes, Magnus's green salt, e.p.r. study, impurity effects 3-53017
 RbBr(I), unstressed crystal, three reorientation processes of O_2^- centres 3-44325
 $\text{SH}(\pi_{3/2})$ radical in two lowest rotational levels, gas phase e.p.r. spectra, proton hyperfine interactions 3-43490
 Si, atom-free single-cryst. surface, surface states determ. (*Russian*) 3-64394
 Si, defect centres and amorphous phase produced by ion implantation, e.s.r. obs. 3-7913
 Si, e.s.r. obs. of interaction between defects and impurities 3-40910
 Si, self-interstitial migration and implant damage annealing, ionisation effects 3-60806

paramagnetic resonance continued

- n-Si, surface inversion layers, g-factor determ. for cond. electrons 3-58430
 Si film, rel. to refractive index increase by dangling bonds 3-76109
 Si surface, passivation mechanism, e.s.r. obs. 3-43943
 Si:B, stress depend. of g-tensor 3-68842
 Si:P, ion implanted, conduction electrons 3-68846
 Si₃Te₂ crystals, photoluminescence and e.p.r. of defects 3-58556
 Ti₂PbCu(NO₂)₆, obs. rel. to phase transitions and Jahn-Teller effect 3-50136
 U(BH₄)₄/Hf(BH₄)₄, optical and e.p.r. spectra of mol. crystals, exciton theory 3-68973
 V₂O₅ cpds., amorphous semicond., localized d¹ electron e.s.r. meas. 3-68847
 Y₃Ga₂O₁₂, magnetoelastic coupling in YIG detn. 3-47119
 ZnO, e.p.r. of chemisorbed O₂ 3-43942
 ZnO aqueous suspensions, reproducible e.s.r. spectra 3-75872
 ZnS, thermal stability of S vacancies (*Russian*) 3-75881
 ZnS:Cu,Cr,Cl, Cr⁺ centres, glow peaks, efficiency of phosphorescence 3-76101
 ZrZn₂ intermetallic phase, very weak itinerant electron ferromagnet 3-68771

paramagnetic resonance of colour centres *see colour centres; paramagnetic resonance*

paramagnetic resonance of conduction electrons *see charge carriers; paramagnetic resonance*

paramagnetic resonance of crystal defects *see crystal defects; paramagnetic resonance*

paramagnetic resonance of ions

- acrylic acid radical anions in low temp. glasses, e.s.r. detection 3-65094
 alkali-metal silicate glass:Cu, Cu(II) e.s.r. spectra at liquid N temperature 3-58423
 azaaromatic compounds and cations zero field splitting of triplet state 3-75875
 azides, irradiated, N₃ or N₂⁻ radicals identification 3-61267
 crystal slightly doped with paramag. ions, X-band guided wave rot. and ellipticity, obs. (*French*) 3-50632
 crystals, Sn impurity, optical characts., interactions 3-68565
 dicalcium strontium propionate, ferroelec., of Mn²⁺, binding of Mn²⁺ ion 3-68832
 dilute mag. alloys, spin-orbit interaction rel. to e.s.r. 3-55466
 o-dimesitylbenzene-alkaline earth metal chelates, biradical species obs. 3-64545
 exchange-coupled ion pairs, spin Hamiltonian parameters derivation 3-46950
 ferricinium ion, distortion, parameters from low temp. absorpt., MCD and ESR spectra 3-75004
 fluoride series, effect of indirect exchange interactions on crystal field parameters of Er³⁺ centres 3-50139
 g-matrix of Zeeman spin Hamiltonian, diagonalization for low symmetry transition ions 3-64450
 glass:Ag⁺, ion-polyvalent ion (As, Sb, Bi) interaction, colloid form, opt. and e.s.r. spectra 3-58427
 glass:Gd³⁺, e.s.r., crystal field parameters 3-72510
 glasses, two component:Fe³⁺, e.p.r. obs. (*Russian*) 3-50458
 hexakisantipyrine metal perchlorate, Mn(II) e.s.r. spectra 3-55462
 inorganic luminescent materials, e.p.r. study of ²S_{1/2} ions (*Russian*) 3-44318
 inorganic materials, ²S_{1/2} state ions, varying ligand ions, 1.6 K to 450 K 3-76041
 metal porphyrin/caffeine complexes chemical shift determ. 3-78851
 methyl malonic acid: free radicals, deuterated, tunnelling rotation at 4.2 K 3-55503
 methylammonium alum, Ti³⁺ Orbach relax. rate anisotropy, dynamic Jahn-Teller effect 3-75877
 monocrystal: impurity γ -radioactive nucleus, e.s.r. spectra, defection mechanism 3-79961
 muscovite:Fe³⁺, e.s.r. spectra obs. 3-44322
 naphthalene ion in low bulk dielec. const. media, e.s.r. linewidth studies 3-44314
 phosphate glass:Fe³⁺, gamma-ray induced e.p.r. spectra (*Russian*) 3-79911
 polyacrylonitrile, glassy and rubber like states, relax of [Cr(H₂O)₆]³⁺ and [Mn(H₂O)₆]²⁺ 3-72511
 quartz glass, symmetry of Ti³⁺ activator centres 3-64296
 rare earth ions in diamag. host, zero-field e.p.r. spectrometer for obs. 3-77594
 ruby:Cr³⁺, Mg²⁺, electron irradiated, e.p.r. line splitting (*Russian*) 3-55472
 ruby, mag. susceptibility, with microwave saturation of Cr³⁺ e.p.r., γ -irrad. effects 3-41325
 silicate glass:Cr³⁺, e.p.r. spectra 3-68833
 silicate glass:Fe³⁺, gamma-ray induced e.p.r. spectra (*Russian*) 3-79911
 sodium biphenylide, e.s.r. spectra, ion-pairing dissoc. consts. 3-76428
 sodium naphthalenide, e.s.r. spectra, ion-pairing dissoc. consts. 3-76428
 spin-lattice relaxation of nuclei of paramagnetic ions 3-55471
 transition metal complexes, Fermi-contact term calc. from unrestricted Hartree-Fock MO method 3-74934
 zeolite: Cu²⁺, e.s.r. study 3-53019
 AgBr, of Rh²⁺ 3-79900
 AgCl:Cr³⁺, e.s.r. spectrum of 135K after illumination 3-47140
 Al₂O₃, sapphire, of Co²⁺, lattice disturbances due to H⁺ positioning (*German*) 3-50447
 α -Al₂O₃:Co²⁺, H⁺ and α -Al₂O₃:Co²⁺, X⁺, sapphire e.p.r. spectra and mag. consts. 3-55460
 Al₂O₃:Co²⁺, e.s.r. spectra, effects of distortion by H⁺ (*German*) 3-50446
 Al₂O₃:Cr²⁺, Fe²⁺, elec. field induced thermally detected e.p.r. of non-Kramers ions 3-44319
 Al₂O₃:Cr³⁺, e.p.r. obs. in E(2E) optically excited state for H perpendicular to c₃ 3-68837
 α -Al₂O₃:Mn²⁺, corundum, angle depend. of forbidden e.p.r. line intensities 3-44321
 Al₂O₃:Mn²⁺, e.p.r. hyperfine line intensity determ. 3-47137
 BaF₂, e.p.r. of V²⁺ at 77K 3-50456

paramagnetic resonance of ions continued

- BaF₂:Gd³⁺, cubic splitting parameter, press.-induced changes 3-60990
 BaO-P₂O₅ glass:V⁴⁺, Cu²⁺, Co²⁺, e.p.r. ultrafine structure, depend. on Co content 3-58424
 Be₂SiO₄ phenacite crystals, e.p.r. of Cr³⁺ at tetrahedral sites 3-68836
 CaCO₃:XO₃, X=C, P, As, hyperfine structure splitting measurement, temp. depend. 3-41403
 CaF₂:Dy³⁺, crystalline field study 3-52799
 CaF₂:Gd³⁺, cubic splitting parameter, press.-induced changes 3-60990
 CaF₂:Nb³⁺, 9-40 GHz 3-58425
 CaMg(SiO₃)₂:Fe³⁺, e.p.r. study 3-55461
 CaO:Ag²⁺, e.p.r. spectra, Jahn-Teller effects, static to dynamic transition 3-53016
 Ca(OH)₂:Gd³⁺, spin-Hamiltonian parameters 3-58422
 CaO.2Al₂O₃:Nd³⁺, e.p.r. and optical spectra rel. to ion site energy levels 3-44320
 CaRu₂:Fe, superconductor, g-value 3-79905
 CaS:Cr phosphors, complex centre obs. (*Russian*) 3-75876
 CaWO₄:Mn²⁺, tetragonal symm., angular variation of e.p.r. linewidth 3-44323
 CdF₂:Cr²⁺, e.p.r. spectra at X band at 4.2 K 3-60988
 CdF₂:Cr²⁺, interactions of Cr²⁺ with F⁻ ligands, s.h.f.s. 3-72514
 CdS:Ti²⁺, e.p.r. spectra at 27K and 77K 3-47138
 CdSe:Ti²⁺, e.p.r. spectra at 27K and 77K 3-47138
 CdWO₄:Co²⁺, monoclinic, spin-lattice relax., conc. and freq. depend. 3-50453
 CeRu₂:Gd, local moment e.s.r. in normal and supercond. states 3-44171
 Cr complex, [(Cr₂Fe₃O(CH₃COO)₆(H₂O))NO₃CH₃COOH, e.p.r., exchange integral 3-47132
 Cr complex, [(CrFe₂O(CH₃COO)₆(H₂O))NO₃CH₃COOH, e.p.r., exchange integral 3-47132
 Cr complexes, acetate chloroplatinate, anomalous g factors, triads of Cr atoms 3-75874
 CsEu(MoO₄)₂, e.p.r. of Gd³⁺ at 293K 3-50457
 Cs₂HfCl₆:Yb³⁺, e.s.r. and fluoresc. obs. rel. to octahedral symm. 3-68840
 CsI:Na⁺, Tl⁺, for obs. of V_k centres 3-64035
 CsY(MoO₄)₂, e.p.r. of Gd³⁺ at 293K 3-50457
 Cu complexes, EPR spectra and covalent bonding in CuCl₄²⁻ and CuBr₄²⁻ ions 3-79901
 Cu complexes in NH₄Cl, ND₄Cl and CsCl, e.s.r. spectra, temp. depend. 3-47135
 Cu diethyldithiophosphate crystals diluted with Ni, h.f.s. 3-57670
 Cu:Cr, Mn, doubly bottlenecked e.p.r. 3-47142
 CuO-MgO polycryst. solid solutions, characterization rel. to catalytic activity 3-73176
 F₂:V, charge conversion, e.p.r. 3-55659
 Fe complex, [(Cr₂Fe₃O(CH₃COO)₆(H₂O))NO₃CH₃COOH, e.p.r., exchange integral 3-47132
 Fe complex, [(CrFe₂O(CH₃COO)₆(H₂O))NO₃CH₃COOH, e.p.r., exchange integral 3-47132
 Fe³⁺ in lunar plagioclases, e.p.r. spectra 3-51303
 Fe³⁺ symmetrically coordinated ⁶S spin-state ions in soln., e.s.r. and crystal field anisotropy 3-41398
 GaAs:Fe, rel. to inhomogeneous distrib. of ferromag. props. 3-64489
 β -Ga₂O₃:Cr₂O₃, e.p.r. study of Cr ions, magnetic interactions 3-79902
 HgCr₂Se₄, g-factor determ. 3-79909
 KCl:Ag⁺, X-irradiated, e.p.r. spectrum at 300K 3-79907
 KH₂PO₄:Cr³⁺, e.p.r., ferroelectric and ferroelastic phase transitions 3-55463
 KMgF₃:Ni²⁺, K₂MgF₄:Ni²⁺, exchange interactions obs. (*Japanese*) 3-50357
 K₂SO₄:Mn²⁺, e.p.r. spectra, temp. depend. 3-55464
 KY(MoO₄)₂-KDy(MoO₄)₂ system, energy spectrum of Dy³⁺ ion obs. 3-64682
 KZnF₃:Ni²⁺, K₂ZnF₄:Ni²⁺, exchange interactions obs. (*Japanese*) 3-50357
 K₂ZnF₄:Mn²⁺, axial anisotropy of Mn²⁺, overlap contribs., e.p.r. obs. 3-50444
 La_{1-x}Gd_xAl₂, g-shift and linewidth of Gd³⁺ 3-47133
 LaMg double nitrate, of Mn²⁺ and Cu²⁺, mag. environment, spin-echo decay obs. 3-50448
 La₂Mg₃(NO₃)₁₂.24H₂O:⁵⁹Co²⁺, e.p.r. and ENDOR obs., g-factors determ. 3-72515
 La₂O₃S single crystals, e.p.r. of Tb³⁺ and Pr³⁺ 3-68835
 LaRu₂:Gd, local moment e.s.r. in normal and supercond. states 3-44171
 Li-Ga spinel, ordered, Co²⁺, ion e.s.r. 3-75880
 LiAl(SiO₃)₂:Fe³⁺, e.p.r. study 3-55461
 LiGaO₃:Cr³⁺, angular depend. rel. to internal cryst. field 3-53020
 LiIO₃:Mn²⁺, e.s.r. spectra at room temp. 3-79908
 MgO:Ag²⁺, e.p.r. spectra, Jahn-Teller effects, static to dynamic transition 3-53016
 Mg₂SiO₄:Fe³⁺, e.p.r. study at 35 and 9 GHz 3-41399
 MgWO₄:Mn²⁺, e.s.r. spectrum at room temp., external field effects 3-75879
 Mn²⁺ in lunar plagioclases, e.p.r. spectra 3-51303
 Mn²⁺ ions in solutions, comparison of linewidths (*German*) 3-64543
 Mn²⁺ symmetrically coordinated ⁶S spin-state ions in soln., e.s.r. and crystal field anisotropy 3-41398
 Mn(II) complex, (RNH₃)₂MnBr₄ salt, e.s.r. linewidths rel. to two-dimens. nature 3-68828
 MnMoO₄ and hydrate, temp. dependence of width of Mn²⁺ e.p.r. lines (*Russian*) 3-68831
 MnSO₃ in aqueous soln., linear conc. depend. of e.p.r. signal width (*French*) 3-58419
 MnWO₄ and hydrate, temp. dependence of width of Mn²⁺ e.p.r. lines (*Russian*) 3-68831
 MoS₂:As, natural and synthetic, e.p.r. of As acceptors, g-values 3-50452
 NH₄Cl:Cu²⁺, optical and e.p.r. spectra 3-55468
 (NH₄)₂SO₄:Mn²⁺, paraelec.-ferroelec. phase transition rel. to 215K e.s.r. discontinuity 3-50454

paramagnetic resonance of ions continued

- $\text{Na}_2\text{Cd}(\text{SO}_4)_2 \cdot 2\text{H}_2\text{O} \cdot \text{Co}^{2+}$, spin lattice relax., one phonon and Raman scatt. processes 3-50455
 NaCl , exchange-coupled pairs of Mn^{2+} ions, e.s.r. 3-55470
 $\text{NaCl}[\text{Ni}(\text{CN})_4]^{2-}$, X-irrad., paramag. species identification 3-64544
 $\text{NaCl}:\text{Mn}^{2+}$, aggregation products involving divalent cation-cation vacancy complexes 3-50458
 $\text{NaCl}:\text{Sb}^{2+}$, Sb^{3+} , for defect centre obs. 3-60739
 NaVO_3 , Cr^{3+} , Cr^{5+} , e.s.r. spectra at room temp. and 77K 3-72516
 $\text{Na}_2\text{Zn}(\text{SO}_4)_2 \cdot 4\text{H}_2\text{O} \cdot \text{Co}^{2+}$, spin-lattice relax., one phonon and Raman scatt. processes 3-50455
 $\text{NiSiF}_6 \cdot 6\text{H}_2\text{O}$, zero-field splittings, e.p.r. thermometer applic. 3-44317
 Pb silicate glass: Cu , $\text{Cu}(\text{II})$ e.s.r. spectra at liquid N temperature 3-58423
 Pb silicate glass: Fe^{3+} , reduced and unreduced, e.s.r. spectrum 3-79910
 $\text{PbCl}_2(\text{Br}_2)$, u.v. irrad., Pb^+ ions and exchange coupled Pb^+ ion pairs 3-64552
 Pd :rare earth ions, magnetic properties of dilute alloys 3-47129
 PrAlO_3 : Gd^{3+} , e.p.r. obs. of phase transitions 3-55083
 α -quartz: Ti^{3+} , 9300 MHz, 77K 3-79904
 $\text{RbCl}:\text{Mn}^{2+}$, e.s.r. spectrum at 77 K 3-72512
 SO_2Cl_2 radical anion struct. determ. 3-55969
 SCF_3 : Gd^{3+} (Mn^{2+}), 290 and 77 K 3-55469
 Si , determ. of crit. ion implantation for amorphous form. 3-68302
 Si , ion implanted, amorphisation obs. 3-68838
 $\text{Si}:\text{Ar}$, ion implanted, paramag. centre obs. 3-68834
 $\text{Si}:\text{O}$ e.s.r., oxygen content in floating zone single crystals, method (German) 3-53018
 α - SiO_2 , e.p.r., defect anion radical traps struct. 3-68843
 SmS , press. depend. exchange coupling, e.s.r. g-shifts of S-state ion trace impurities 3-64491
 $\text{SmS}:\text{La}$, cond. electron enhancement of exchange interactions, e.p.r. obs. 3-55413
 SmSe , press. depend. exchange coupling, e.s.r. g-shifts of S-state ion trace impurities 3-64491
 SrCl_2 : ^{243}Cm (^{247}Cm), obs. of nuclear spins and mag. moments 3-68841
 SrCl_2 : Cu^{2+} e.p.r. obs. for model of centre 3-50451
 SrF_2 : Gd^{3+} , cubic splitting parameter, press.-induced changes 3-60990
 SrMoO_4 : Gd^{3+} , elec. field effect on e.s.r. 3-72517
 $\text{SrO}:\text{Ag}^{2+}$, e.p.r. spectra, Jahn-Teller effects, static to dynamic transition 3-53016
 SrTiO_3 , light-induced oxygen centres 3-47144
 SrTiO_3 , of Fe^{3+} - V_0 centre, phase transform. dynamics implications (German) 3-53015
 SrTiO_3 , tetragonal, Fe^{3+} - V_0 centre obs. (German) 3-50445
 SrTiO_3 : Fe^{3+} , electric field effect on e.p.r. spectrum 3-72513
 $\text{Te-As-Ge-Si}:\text{Mn}^{2+}$, amorphous, e.s.r. obs. from 420 to 77K and at 4.2K 3-64550
 ThB_4 : Gd^{3+} , ThB_6 : Gd^{3+} , e.s.r., mag. susceptibility meas. influence of U admixture 3-41406
 ThO_2 : Er^{3+} , axial g values 3-41405
 ThO_2 : Gd^{3+} , temp. dependence of hyperfine interaction 3-64551
 Ti^{3+} in lunar plagioclases, e.p.r. spectra 3-51303
 TiO_2 : Fe^{3+} , hyperfine struct., e.p.r. obs. 3-58421
 TiO_2 : SiO_2 glasses, e.p.r. study of Ti^{3+} - Ti^{4+} reaction 3-76418
 VO^{2+} in dimethylformamide and dimethylacetamide solns., n.m.r., e.p.r. study of coordination 3-41433
 $\text{Y}:\text{Gd}$, single cryst., e.p.r. and antiferromagnetic reson. study 3-47143
 $\text{Y}_3(\text{Al}_{1-x}\text{Ga}_x)_2\text{O}_{12}:\text{Nd}^{3+}$, study of clustering 3-78040
 YAsO_4 , pair interaction and mag. relax. of Yb^{3+} (German) 3-53014
 $\text{YGaG}:\text{Re}^{3+}$ garnet, strain variation of Ru ion energy levels, magnetostriiction calcs., e.p.r. obs. (French) 3-58420
 Y_2GaO_7 : Pb^{3+} diamag. garnet cryst., e.s.r. anal. of Pb^{3+} ions in dodecahedral sites 3-47141
 YPO_4 , pair interaction and mag. relax. of Yb^{3+} (German) 3-53014
 $\text{ZnSO}_4 \cdot 7\text{H}_2\text{O}:\text{Cu}^{2+}$ e.p.r. spectra as function of orientation of mag. field 3-64549
 ZnWO_4 : Co^{2+} , monoclinic, spin-lattice relax., conc. and freq. depend. 3-50453
 ZnWO_4 : Fe^{3+} , e.s.r. spectrum at low concentrations, superhyperfine structure 3-41404
 ZrO_2 : Gd^{3+} e.s.r. experiments 3-47139
 ZrSiO_4 , e.p.r., defect anion radical traps struct. 3-68843
 ZrSiO_4 : Ti^{3+} , 9300 MHz, 77K 3-79904

paramagnetism

- see also *paramagnetic properties of substances*
 Curie-Weiss system, classical limit of n-vector spin models 3-66691
 electron gas, non-interacting, rel. to volume expansion and magnetostriiction 3-50339
 Green's function theory of Heisenberg ferromagnet, temperature dependence of thermodynamic properties 3-64462
 Heisenberg ferromagnet, surface paramag. layer, photoelectron spin polarisation obs. (German) 3-50407
 h.f. phonon scattering by spins 3-55050
 Hubbard chain, strong-coupling, Curie law for spin susceptibility 3-50338
 induced moment system, containing impurities, susceptibility calc. 3-44199
 induced moment system, impurity excitations, exchange coupling effects 3-41330
 induced moment system, transverse mag. field influence on mag. ordering (German) 3-50309
 itinerant electron model, effect of exchange interaction on dielec. response 3-44194
 Kinetic diamagnetism and paramagnetism in the presence of illumination 3-75777
 metal, thin films, spin-wave reson. 3-72524
 modified Zener model, for ferromagnetism, paramag. susceptibility calc. 3-44193
 noble muonic atoms, electron paramag., spin-orbit interaction effects 3-46217
 oceanic basalts, low temperature oxidation causing carriers of natural remanence to become superparamagnetic 3-58971

paramagnetism continued

- Pauli's master equation, continuum thermodynamic limit 3-57166
 polymer with conjugated bonds, Mott semiconductor, one-dimensional theory 3-75715
 relativistic correction term to spin orbit coupling 3-46801
 thermodynamics, upper bounds on magnetostriction and magnetoelec. susceptibility 3-47006
 Wurster's blue perchlorate, aq. solns., temp. depend. scalar coupling, electron-nucl. Overhauser effect study 3-57671
 $\text{Fe}(\text{II})$ complexes, bis[2,4-bis(2-pyridyl)thiazole] $\text{Fe}(\text{II})$, Mossbauer spectra, $^5\text{T}_2$ - $^1\text{A}_1$ spin transition and residual paramagnetism 3-53037
 GdP , Heisenberg paramag., dynamics, pulsed n.m.r. obs. 3-41447
 $\text{LaP}:\text{Gd}$, Heisenberg paramag., dynamics, pulsed n.m.r. obs. 3-41447
 $\text{LuP}:\text{Gd}$, Heisenberg paramag., dynamics, pulsed n.m.r. obs. 3-41447
 Mn^{++} ions in aq. solns., temp. depend. scalar coupling 3-57671

parametric amplifiers

- critical, oscillatory behaviour, time-dependent pump amplitude, phase 3-59894
 four photon exchange effect, amplification and oscillation near pump field (German) 3-78056
 quartz, acoustic surface waves, second harmonic generation and parametric amplification, nonlinear, theory and obs. 3-70196
 radiation-meter, 4 cm, RATAN 600 radiotelescope, liquid nitrogen cooled input parametric amplifier, description (Russian) 3-81220
 He-Ne laser focusing in $\text{Ba}_2\text{Na Nb}_2\text{O}_{15}$ (German) 3-39953
 LiNbO_3 acoustic surface waves, second harmonic generation and parametric amplification, nonlinear, theory and obs. 3-70196

parametric devices

- i.r. detector, operating on freq. conversion, noise 3-70850
 optical, review 3-54248
 proustite, parametric freq. upconverter, background light 3-51944
 InSb difference frequency mixer, for tunable far i.r. generation 3-54239
 PrCl_3 quantum counter, direct i.r. image upconversion 3-57247
 $\text{Si p}^+ \text{-n-n}^+$ photoparametric upconverter diode, base parameter effects on signal to noise ratio 3-66885

parametric oscillators

- far i.r. generator, phase matching by periodic variation of nonlinear coeffs. 3-59892
 four photon exchange effect, amplification and oscillation near pump field (German) 3-78056
 i.r. sources, tunable, state-of-the-art 3-78008
 Josephson junctions, mixing and parametric effects, analogue computer simulation 3-41303
 light sources, one and two resonators, transient processes 3-48948
 optical, applications of nonlinear crystals, review 3-40288
 optical, for tunable laser radiation, review 3-48935
 statistical theory of instabilities in stationary non-equilibrium systems 3-70801
 Ag_2AsS_3 , singly resonant, tuned from 1.22 to 8.5μ 3-40280
 CdSe , pumped by HF laser 3-78059
 α - HIO_3 , spontaneous parametric emission and light scatt. by polaritons 3-48945
 LiNbO_3 , i.r. optical parametric fluoresc. 3-43031

parametric up-convertors see *parametric devices***parametric varactor diodes** see *varactors***parametrons** see *parametric oscillators***parity**

- see also *hyperon spin and parity; meson spin and parity; nuclear spin and parity*
 baryon parity doubling, spin formalism, Regge pole model without parity doubling 3-60002
 doublet contributions to baryon exchange, πN elastic scattering 3-60025
 non-Abelian gauge theories with parity and strangeness conservation 3-57393

partial differential equations

- see also *boundary value problems*
 atmospheric dynamics and circulation numerical simulation 3-51071
 averaged lagrangians containing higher derivatives 3-57043
 axial radiation reception, multidimensional, nondispersive, uniform, unbounded propagative medium 3-66607
 boundary-value problem for elliptic type linear eqns. and second order elliptic systems, geometric criterion (Russian) 3-62416
 chemical kinetics, steady-state approx. in differential eqns. 3-44712
 circular cylindrical shell theory, fourth-order differential eqns. 3-70596
 conservation laws, soln. by generalized two-step Richtmyer method 3-45625
 coupled, nonlinear, elliptic, false transient method 3-75184
 cylindrical shells under axial compression, postbuckling behaviour 3-70595
 decaying spherical shocks in solid, linear Q effects, finite difference calcs. 3-70648
 elastic solid, stress singularity at corners or terminations of crack edges, eigenvalue problem 3-74042
 elastic wave propagation problems, use of modal solns. 3-51795
 elastodynamics, similarity solns. for plane problems 3-45645
 electric arc gas heater, calc. of enthalpy distrib. from energy eqn. 3-40822
 external boundary-value problem, numerical soln. in finite domain (Russian) 3-62420
 Falkner Skan equation, solution 3-49532
 Faraday type MHD generators with nonequilibrium plasmas, end effects calc. 3-46558
 finite element calculations, variational principle, math. aspects 3-63111
 flow, unsteady one dimensional, soln. by characteristics at fixed time interval 3-71782
 fluid flow in heated closed cavity, numerical soln. 3-57710
 fluid mixture and polarised fluid phase equilb. 3-66711
 fourth order with elliptic type coeff., Cauchy problem and general representation (Russian) 3-77781
 function minimization, Davidson-Fletcher Powell method modification 3-62391

partial differential equations continued

- heat conduction, physical constant determ. using intersecting graph technique 3-51838
- Helmholtz, generalized axisymmetric soln. of mixed boundary value problem using integral representation 3-74001
- Helmholtz eqn., soln. of boundary problem for axially-symmetric spatial layer (*Russian*) 3-70576
- hermitian, with elliptical type derivatives, soln. of boundary value problem by method of dynamic programming (*Russian*) 3-62410
- hydrothermal system modelling, finite element approach 3-59212
- hyperbolic, asymptotic properties of solns. to mixed problems (*Polish*) 3-70535
- hyperbolic second order, boundedness, stability and uniqueness of solns. (*Polish*) 3-66499
- iterative soln. of nonlinear system of eqns. in implicit form with partial differentials with delay 3-77779
- Jeffery-Hamel flow of dissipative plasma, similarity transformation 3-75302
- Kolmogorova, in theory of Markovian processes (*Russian*) 3-62431
- Korteweg-de Vries equation, scattering theory, Schrodinger equation, analogue of Fourier's method 3-74118
- Lagrangian eqns., governed by velocity-dependent potential energy, general soln. and invariants 3-43097
- mixtures, fluid dynamics, conservation laws, theory and numerical methods 3-49531
- modified Korteweg-de Vries eqn. and scattering theory 3-62565
- nonlinear, gauge invariance and conservation laws 3-45853
- nonlinear boundary problems quasi-linearisation of soln. using iterative method, convergence (*Russian*) 3-70526
- nonlinear hyperbolic, boundedness and stability of solns. (*Polish*) 3-66500
- nonlinear transformations, effect on computation of weak solns. 3-71731
- nonlinear wave modulation, perturbation method, integro-partial differential eqns. 3-77864
- nuclear reactor spare-time kinetics and heat flow problems, numerical soln. 3-46063
- ore sintering furnace simulation, solution by orthogonal eigenfunction expansions 3-41794
- orthotropic plate, clamped, estimation of natural numbers of differential problem (*Russian*) 3-40141
- oscillatory chemical reactions, phase waves, diffusion equation 3-50826
- parabolic system in three-dimensional space, intrinsic estimate (*Russian*) 3-62421
- plane parallel unstable flow, numerical study of mildly non-linear partial differential equation 3-49545
- plate, orthotropic annular, postbuckling behaviour 3-70592
- pluriparabolic, relationship between fundamental soln. (*Russian*) 3-77783
- porous catalyst, heat and mass transfer, nonlinear boundary value problem solution 3-42911
- quantum statistical thermodynamics, spatial distrib. function calc., linear partial differential equation, Schrodinger equation 3-70769
- quasi-linear hyperbolic systems, generalised solns., entropy conditions 3-78996
- quasilinear elliptic, unbounded domains, weaker monotonicity conditions 3-70529
- river, biochemical oxygen demand, three dimens. analytical soln. 3-59209
- scalar wave and diffusion eqns., variational formulation 3-40088
- scattering theory, existence of wave operators 3-40151
- Schrodinger eqn., variation-of-parameters method of soln. for scatt. problem, improved method 3-42843
- Schrodinger eqn. finite difference boundary value method of soln., comparison with Cooley-Cashion-Zare method 3-42844
- Self energy differential formalism 3-66954
- sound propagation in viscous gas, Poisson type estimate for correcting Petrovski eqn. (*Russian*) 3-62419
- stability, dynamic, of pipe conveying pulsatile flow 3-67944
- Stefan problem, melting of ice block (*French*) 3-79474
- Sturm-Liouville eqn. with periodic boundary conditions, iterative determ. of ground state eigenvalues and eigenfunction 3-70516
- thick axisymmetric boundary layers, turbulent skin friction analysis 3-71776
- torsion of prismatic bars, soln. by numerical and analytic techniques 3-48715
- transonic flow around airfoils, time dependent calc. 3-49592
- two-dimensional flows, unsteady with free boundary, numerical methods 3-75185
- unsteady and three-dimensional boundary layer flows, numerical soln. 3-71761
- $\Pi_{l=1}^n(\Delta^2 + k_l^2)\Psi = 0$, solution 3-48700

particle accelerator accessories

- see also storage rings
- abort system, main accelerator Batavia USA, safe proton beam dumping, description 3-56866
- active filters, for NAL quadrupole power supply 3-56954
- beam current monitor, charged particles, coaxial cable transmission line, pulsed transformer techniques 3-56905
- beam phase locking circuitry, amplitude limited pulse comparison, ZGS Argonne USA, description 3-56894
- beam profile monitor, high energy, low intensity, secondary emission in dielectric layer, measurements 3-56904
- beam scrapers for luminosity improvement, background reduction and chamber protection in ISR 3-56819
- beam-monitoring system, SPEAR Stanford USA, synchrotron light diagnosis, TV system 3-56900
- beam-viewer, radial position width and brightness, CCTV system, ZGS Argonne USA, description 3-56893
- bending magnets with Fe yokes and rectangular coils, multipole field distortions 3-56801
- Bevatron, rectangular vacuum windows 3-56864
- booster, proton synchrotron, CERN, 800 MeV, present performance 3-56741
- bremsstrahlung fluxmeter, linear relative monitor, for 680 MeV synchrotron 3-70335
- buncher ring, Astron accelerator Livermore USA, control system, application of crossbar relays 3-56897

particle accelerator accessories continued

- CAMAC crate controller, serial control system, neutrino meson and proton beams, Batavia USA, description 3-56898
- CAMAC experimental beam line control system 3-56778
- coils, for zero gradient synchrotron, failures analysis 3-56803
- computer system, for multiparameter measurements 3-40030
- control system, meson physics facility, Los Alamos USA, central control room man/machine interface, development, description 3-56899
- control systems, cross-wire touch panel man/machine interface, c.r.t. monitors, computer control, Stanford USA 3-56789
- cyclotron, isochronous, Oak Ridge USA, computer control system, progress and description 3-56787
- cyclotron, TRIUMF Canada, H⁻ ions, components, construction costs, performance 3-56744
- cyclotron axial injection system, minimizing disturbing magnetic fields 3-62203
- dipole magnet with circular Fe shield, design 3-56802
- fast-spinning stripper, for zero gradient synchrotron booster 3-56762
- high current test facility injector 3-56859
- High gradient stack investigations at AWRE 3-70353
- injector system, for zero gradient synchrotron polarized proton beam program 3-56764
- intercomputer links, in real time control systems 3-56955
- ion sources, polarised ions, H isotopes, atomic beam, Lamb shift NSF electrostatic accelerator UK, process design operation 3-70375
- LAMPF low energy pion channel, mechanical design 3-56854
- magnet coil diagnostic tests at zero gradient synchrotron 3-56805
- magnet coil protection, in zero gradient synchrotrons 3-56804
- measurement, dump line, CERN 800 MeV proton synchrotron booster, emittance, spectrometry, dumping 3-56903
- measurement system, beam position, CERN 800 MeV proton synchrotron booster, description 3-56902
- monitoring system, beam position and intensity, Stanford positron-electron asymmetric ring USA, description 3-56788
- MP-tandem, emittance measuring system 3-45541
- NAL booster synchrotron magnet, power supply servo 3-56953
- NAL computer control system 3-56776
- NAL main ring, radiation survey vehicle 3-56775
- non-linear analogue transfer function generator, for NAL bend magnet 3-56958
- Omega detector for use on CERN 25 GeV and 300 GeV proton synchrotrons, trajectory obs. (*Danish*) 3-77704
- phase detector system for cavity tuning, at national accelerator laboratory, USA 3-56959
- pole face winding equipment, for eddy current correction at zero gradient synchrotron 3-56765
- poleface winding system, for independent multipole fields in AGS magnets 3-56796
- pulsed beam preparation systems 3-62204
- pulsed beam shutter magnet, for r.f. separated beams at zero gradient synchrotron 3-56806
- pulsed magnets, for bubble chamber experiments 3-56908
- pulsed quadrupole system, for depolarization prevention of proton beam in ZGS 3-56830
- quadrupole magnet, field computation considering grain orientation effect 3-56799
- quadrupole magnets, parameter study for synchrotrons 3-56832
- ramped superconducting dipoles, for NAL doubler 3-56807
- r.f. modulated electron gun, for NINA injection equipment 3-56766
- r.f. phase control system, for electron synchrotrons 3-56785
- r.f. structure monitor, for zero gradient synchrotron 3-56786
- r.f. system, for NIMROD 3-56769
- r.f. system, for Oak Ridge Isochronous Cyclotron 3-56768
- r.f. system for SPEAR, operation 3-56951
- sector magnet shimming for NIMROD 70 MeV injector, computer program GFUN 3-70342
- septum magnets, for secondary beams at NAL 3-56800
- sextupole magnet, for 200 GeV line 3-56798
- shielding blocks, response to earthquake motions 3-56773
- SLAC main control center, operational aspects 3-56777
- spark gaps, for d.c. accelerators 3-70356
- SPEAR, automatic control program 3-56783
- Stockholm cyclotron, fast beam pulsing system 3-62202
- strippers, foil, Erlangen EN tandem Germany, development, operational experience, designs 3-73847
- superconducting accelerator magnet cooling systems 3-56726
- superconducting cavities, electron multiplication 3-56714
- superconducting helical resonators, electronic tuning and phase control 3-56725
- superconducting magnets, for intersecting storage accelerations 3-56795
- superconducting magnets, pulsed, recent progress, trends, review 3-56794
- superconducting r.f. cavities, resonant freq. control 3-56724
- superconducting separator, deflecting cavities, r.f. tests 3-56860
- superconducting stretcher ring, resonance injection 3-56763
- synchrotron, Argonne National Laboratory, booster injector for Zero Gradient Synchrotron, operating results 3-56737
- synchrotron, internal electron beam, collimation using beam scrapers 3-62200
- tandem, beam-chopper system for high-energy side, optimum dimensioning (*German*) 3-59634
- tandem, pulsing system for ion beams (*German*) 3-59633
- target, internal beam, condensed H₂ jet, installation, tests 3-70370
- timing system, PRIMET, Batavia USA, control system synchronisation, single line clock transmission, serial encoding 3-56901
- transducers, for zero gradient synchrotron performance for current measurement and control 3-56767
- tube, accelerating, electrostatic, high gradient design criteria 3-70362
- tube, accelerating, magnetically suppressed design and performance, Van de Graaff, tandem 3-73849
- tube, inclined field, 5 MV Van de Graaff KFKI Budapest, design, manufacture, operational experience 3-73850
- tubes, accelerating, suppressed, tandem, injector, Oxford UK, operational experience, failure analysis 3-70365
- tubes, acceleration, Brookhaven MP tandem, electrical breakdown, failure analysis 3-70364

particle accelerator accessories continued

- tubes, inclined field accelerating, conditioning, X-ray survey, technique, Orsay MP tube France 3-70363
 Van de Graaff injector, linear stabilizer 3-59624
 video tape recorder and computer for data acquisition 3-54023
 Al magnet coils, radiation resistant, for Nevis synchrocyclotron 3-56797
 C stripper foils, heavy ion bombardment, behaviour, improvements 3-73846
 Nb S-band superconducting cavity, with large beam tubes 3-56861
 Nb superconducting cavities, attaining high fields 3-56722
 Nb superconducting cavities, frozen-in flux, additional losses 3-56723
 Nb superconducting cavity, surface preparation techniques 3-56862
 SF₆, gaseous insulator for d.c. accelerators 3-70354

particle accelerators

- see also beam handling equipment; cyclotrons; electron accelerators; linear accelerators; proton accelerators; synchrotrons*
 beam containment devices, safety problems 3-56879
 Bevalac, Berkeley Laboratory USA, high energy heavy ions, SuperHilac linked to Bevatron, description 3-56729
 computer aided data and control systems, recursive digital filter algorithm for analogue signals 3-56793
 conference, San Francisco, Calif., USA (1973) 3-56711
 contoured cavity design using computer program 3-56848
 control system, computer aided, satellite minicomputers, decentralisation advantages 3-56792
 cyclic, accelerating superconducting resonator, interaction with high-current single bunch of particles (Russian) 3-48492
 cyclical, beams longitudinal stability 3-73839
 electrostatic, charging induction, fabric belts, problems, systems development, Argonne USA 3-70361
 e.s., conference, Daresbury, England (1973) 3-70343
 heavy ion, superconducting helix resonators, variation r.f. control 3-56715
 heavy ions, multiaccelerator system, Oak Ridge, design 3-56732
 heavy ions accelerated from 10-1000 MeV/nucleon, ionisation energy loss and penetration tables (French) 3-62219
 heavy-ion, applications in nuclear, atomic, astro- and solid-state physics and chemistry 3-51673
 helical resonators, short, field distributions, measurements, calculations 3-59625
 high energy, shielding calc., CASIM, Monte Carlo program 3-56772
 high energy physics horizons, review 3-56857
 high power polarized photon beam at SLAC 3-56770
 intense electron beam interruption, particle acceleration 3-48495
 intersecting storage accelerator, design study 3-56855
 intersecting storage accelerator, injection models 3-56825
 intersecting storage accelerators, experimental insertions 3-56817
 ion source, Penning, doubly-negative charged ions, tandem accelerator Heidelberg Germany, experimental evidence 3-70372
 ions, metallic, Harwell tandem generator UK, charge-state distribution, analysis 3-73848
 ISABELLE, electron ring for ep option 3-56814
 with LC tuned circuit, stabilization of particle energy 3-53967
 in Mossbauer spectroscopy 3-42683
 multiharmonic field in azimuthally varying gap 3-73838
 negative ions, technology, properties, sources, review 3-57281
 NG-150 neutron generator, for activation analysis 3-53973
 proton, r.f. noise effect on bunching 3-56828
 r.f. cavity beam loading 3-56849
 SAMES 150 kV accelerator, external beam pulsing method 3-51672
 separated-function periodic magnetic structure 3-70339
 SPEAR, closed orbit correction 3-56912
 stopped K-mesons, high intensity beams, Bevatron 3-56771
 superconducting storage accelerator, controlling nonlinear resonances 3-56826
 tandem accelerator upgrading, at Univ. of Rochester, USA 3-56761
 tandem generators, heavy ion beams, energy spectra, 3 to 5 MeV, measurements 3-78072
 twin-tank accelerator, for h.v. electron microscopy 3-56760
 Van de Graaf, 4MV, accelerating tube for 3-70337
 ZGS injector-booster accelerator for intense neutron generator 3-48508
³H(d,n)⁴He reaction in ion accelerators for neutron production (French) 3-56917

particle backscattering

- auroral electrons, twin payload obs. 3-51093
 channelling, theory of backscattering yield oscill. 3-68294
 compound semiconductors, analysis of backscattering spectra 3-61089
 electron backscattering angular distribution dependence on target atomic number 3-80123
 fission fragments, back-scatt. from thin metal films 3-61090
 heavy target ion bombard., coeff. calcs., keV energy 3-69116
 ion surface interactions, 30 keV instrument 3-48587
 neutron backscattering diffractometer, Bragg refl. meas. from Si (German) 3-63933
 random solid, energy distrib. of scatt. particles 3-61099
 SEM, electron backscatt. and secondary electron prod., Monte Carlo calc. 3-70432
 semiconductor impurity analysis, applic. of MeV ⁴He⁺ 3-41644
 semiconductor impurity analysis, applic. of MeV ⁴He⁺ 3-41670
 solid target surface investigation using low energy ion backscattering 3-48586
 solids, thin films, ion beam techniques for, structure and composition analysis 3-57973
 surface study by noble gas ion backscatt. technique 3-60837
 Al, behaviour of ion implanted atoms during anodic oxid., He backscatt. obs. 3-68511
 Al-Mn(0.09 at. %), irradi.-induced dumbbells, ion backscatt. obs. 3-75551
 doped Al₂O₃, of He⁺ ions backscattering, ion implantation range distribution measurement 3-49918
 Al₂O₃ films, compositional information from ion-induced X-rays and Rutherford backscattering 3-43960
 Au film, dechannelling from 2-MeV He⁺ damage 3-52656
 CaF₂ single crystals with disordered surface layers, channelling 3-49915

particle backscattering continued

- Cu, polycryst., electron backscatt. coeff., meas. using spherical retarding-field analyzer 3-53162
 Cu sputtering yield dependency on proton energy and backscattered ions 3-80128
 Ge, dechannelling of MeV protons, obs. 3-52655
 InSb, ion-implanted Al₂O₃ and SiO₂ protective layers, backscatt. study 3-41677
 KCl, 1 MeV He⁺ irradi., backscatt. ion yield 3-52652
 LiF, 1 MeV He⁺ irradi., backscatt. ion yield 3-52652
 MnBi film, formation process obs. using α -particles 3-44298
 NaCl, 1 MeV He⁺ irradi., backscatt. ion yield 3-52652
 Ni single cryst., energy distrib. for protons with 15 keV primary energy 3-61100
 Si, dechannelling of MeV protons, obs. 3-52655
 Si, gettering action of phosphosilicate glasses and ion implementation damage layers, MeV ⁴He⁺ backscatt. obs. 3-41644
 doped Si₃N₄, of He⁺ ions backscattering, ion implantation range distribution measurement 3-49918
 doped SiO₂, of He⁺ ions backscattering, ion implantation range distribution measurement 3-49918
²⁸Si, neutron elastic and inelastic backscattering at 14.2 MeV, time-of-flight spectroscopy, energy level obs. 3-74575
 W, dechannelling of H⁺, ³He- and ⁴He-ions 3-49916

particle beams

- see also atomic beams; electron beams; ion beams; molecular beams; particle optics*
 16 to 60 MeV neutron beams, dose rate measurements in phantoms 3-56559
 acceleration, produced by microcritical mass of fissioning matter 3-54513
 ACO, Orsay storage ring, beam dynamics 3-56812
 aerosol beam spectrometry, recent developments 3-55904
 atmospheric MHD and v.l.f. emissions produced by electron and proton beams 3-51183
 bunch-length measurement, using mode-locked laser 3-56888
 bunched, longitudinal stability criterion 3-57264
 bunched proton beams, neutralization 3-57267
 charged, motion, axisymmetric E × B fields equilibrium orbit, linear oscillations, theory, electron ring accelerators 3-59626
 charged particles, emittance, entropy, information carrying, thermodynamic analysis 3-74291
 circulating, momentum and betatron amplitude distributions by two-probe method 3-56910
 closed orbit correction in SPEAR 3-56912
 colloidal particle beams, visual display of spatial distribution 3-45616
 focussing, permanent multipole mag. fields stored in superconductors 3-42631
 intensity increase in injector of proton synchrotron 3-51676
 intersecting storage accelerator, injection models 3-56825
 longitudinal stability in cyclical accelerators and storage rings with resonant systems 3-73839
 matching to linac of beam in bunching injection scheme 3-56913
 Maxwellian 1 dimens., normal oscillating modes in linear space charge approx. 3-57269
 multibunch injection into synchrotrons 3-56871
 phase-space fluid, stochasticity limit and turbulent motion 3-57266
 pion production by high energy protons, from cancer treatment 3-59442
 plasma diagnostics using particle beams 3-71960
 plasma fusion expt., high intensity neutral beams development 3-71937
 polarized beam depolarization in transport system, transfer matrices (French) 3-53966
 prebunching single gap cavities, space charge effects 3-57270
 proton, in ISR at CERN, extension of energy by acceleration of stacked beams 3-56821
 proton beam, of NAL booster synchrotron, correction for particle loss 3-56911
 proton beam bunching parameters with six-dimensional matching to linac acceptance 3-57268
 proton beam monitoring, at NAL main accelerator 3-56933
 proton relativistic beams, coherent longitudinal instability 3-57265
 r.f. cavity loading 3-56849
 r.f. separated beam line, 50 μ s 3-56967
 subnanosecond high intensity pulse, bunching system 3-56841
 synchrocyclotron, vertical plane space charge effects during injection 3-56833
 synchronous transfer of beam from national accelerator laboratory booster synchrotron to main ring system 3-56870
 synchrotron closed orbit distortion correction 3-56836
 synchrotron phase motion, effect of random fluctuations 3-56835
 transport, superconducting quadrupole lenses, design and construction (German) 3-62199
 velocity filter, separated fields, improved stigmatic focusing (German) 3-70410
 NaI, crystal gamma-ray spectrum, non-constant Bevatron beam, photomultiplier resolution, feedback compensation circuit 3-77703

particle counters *see counters***particle detectors**

- see also bubble chambers; counters; ionisation chambers; particle track visualisation; radiation detectors; streamer chambers*
 air-filled ion chambers, for beam loss monitoring at zero gradient synchrotron 3-56934
 channel plate arrays, particle and photon counting, high gain, resolution improvement 3-77623
 channel secondary electron multiplier, for electrons, protons, ions 3-77569
 charged particles, relativistic, transition radiation techniques, review 3-77631
 charged particles, ultrarelativistic, X-ray transition radiation, detectors 3-77632
 collector system, on-line isotope separator, separate backings for collection and measurement 3-77621
 colloids, superheated, superconducting, metastability with large grain size, development 3-77638
 continuous energy dependence of triple angular charged particle- γ -ray, correlations (Russian) 3-73858
 cosmic ray detector, electron calibration 3-42258

particle detectors continued

- crystals, relativistic particle identification by quasiperiodic scattering radiation 3-77637
 dielectric track detectors, track-diameter kinetics 3-48540
 drift counter, for particle location (*French*) 3-62228
 effective centre of long counters, calculation by two-group diffusion equations (*German*) 3-48521
 Faraday cup and collimator assembly design 3-77603
 foamed plastic, transition radiation, 13-130 keV 3-56943
 glass track chamber, operation characteristics 3-40022
 hadron-shower calorimeter, for muon detection at high energies 3-40010
 heavy non-relativistic sea level particle detection, ionisation and track measurements (*Russian*) 3-62235
 high energy particle detector, 3-dimensional projection chamber (*French*) 3-70394
 high-vacuum gas counter for charged particles and gamma rays 3-66318
 hypervelocity particles, 25 μm diameter, optical in-flight detection technique 3-51738
 ion cyclotron resonance spectroscopy, frequencies > 1 MHz 3-77628
 jet detector, Coulter counter blood platelets, sizing and counting 3-73930
 liquid in underpressure condition, detection of nuclear fragments by local boiling (*German*) 3-51693
 low energy, charged, position sensitive, for mass spectrometer 3-56976
 molecular beams, based on charged particle oscillator 3-77617
 neutron, 145 scintillator elements, on-line electroproduction experiment, calibration, performance 3-77636
 neutron detector of fast time response 3-51704
 plastic scintillation counter, of effective attenuation length of 25m using gradient activation 3-40008
 plastic scintillation Gd-loaded detector for neutrons 3-40019
 position sensitive detectors and multi-counter arrays for neutron studies 3-56940
 Rutherford scatt. apparatus, design and expt. results 3-42504
 scattering chamber, remote control, universal application, design, construction 3-70371
 secondary electron multiplier, electrons, protons, ions, construction 3-77568
 solid-state nuclear track detectors, precautions in etching 3-51723
 spectrometric, amplitude analyzers, $E^{1/2}$ scale, nonlinear conversion, circuits 3-66313
 split field magnetic, geometrical fit program for proton-proton collision data 3-60047
 thin-film, response to passage of accelerated heavy ions, results 3-77625
 threshold detectors, ionisation losses, collision cross-sections generalisation of formulas (*Russian*) 3-62218
 (β - γ) chamber, for nuclide determination in off-gas samples 3-40012
 P, recoil counters and multiple scattering, theory 3-59641
 ^8Be , ground and excited states array detector, spectroscopic study of particle producing reactions, techniques 3-77620
 Rh neutron detector, flux and fluence, explicit solns. 3-42651
 Si, surface barrier detector, damage by 0.5 to 1.5 MeV electrons 3-77618
 Si detectors, analytically determined response to polyenergetic neutron beam 3-42650
 Si(Li) position and energy sensitive detector 3-70389
 SrTiO_3 :Fe colour changes for energetic heavy particle detection 3-49911

particle focusing *see focusing; particle optics***particle lenses, electrostatic** *see electrostatic lenses***particle lenses, magnetic** *see magnetic lenses***particle optics**

- see also aberrations; electrodynamics; electron optics; ion optics*
 axisymmetric E \times B fields equilibrium orbit, linear oscillations, theory, electron ring accelerators 3-59626
 beam line design, minimization of aberrations 3-56882
 cylindrical electrostatic analyser, perfect direction and velocity focus at $254^\circ 34'$ 3-45841
 einzel symmetric lenses, analysis 3-48961
 electron beam self-focusing, rel. to beam pinching in plasma production 3-63846
 electron beams focusing, in pulsed accelerators 3-57278
 focusing, momentum free, AG e.m. field 3-59655
 helical resonators, short, field distributions, measurements, calculations 3-59625
 magneto-periodic focusing, eliminating end effects (*Russian*) 3-45840
 mass spectrometers, second order image aberrations calcs. (*Japanese*) 3-59656
 proton accelerator, linear, 550 keV, with asymmetrical alternating-phase focusing 3-53962
 proton accelerator, linear, with quadrupole r.f. focusing, alignment of accelerating electrodes 3-53968
 superconducting separator, deflecting cavities, r.f. tests 3-56860
 SuperHILAC, beam transport systems 3-56881
 μ , beam dynamics in magnetised Fe 3-73840
 He atomic beam, focusing array, fused glass capillaries, axial density, beam width, throughput, measurements 3-66308

particle range *see energy loss of particles***particle scattering**

- see also collision processes; elementary particle scattering; energy loss of particles; ion scattering; nuclear reactions and scattering; particle tracks; potential scattering; S-matrix theory*
 analytic continuation of scattering amplitude in scattering angle using impact-parameter representation 3-57125
 central potentials, l-wave reduction to s-wave 3-60087
 chamber, remote control, universal application, design, construction 3-70371
 charged, fast, inelastic scatt., by first and second row atoms, systematics of total cross sections 3-71442
 charged, three, below ionization threshold, integral eqns. 3-70707
 Fredholm integral method, calc. of scatt. amplitude 3-74101

particle scattering continued

- by harmonic oscillator, applic. to electron-molecular collisions 3-71618
 integral equations, N-particle transition operators 3-62562
 Mitra three-body model derived from Faddeev theory 3-57126
 nonlocal pots., semiclassical approxs., appl. to atomic collisions 3-45698
 nonrelativistic, direct and inverse, amplitude eqns. (*Russian*) 3-62795
 nonspherically symmetric potential, zero energy limit 3-51807
 orbital clustering, elastic and inelastic scatt., solar system appl. 3-65627
 program for differential and integral cross sections from reactance and transition matrices 3-66617
 program for solution of coupled second-order differential equations 3-66616
 radial equation, cylindrically symmetric potential, s-waves, semiclassical approximation 3-70692
 radial Schrodinger equation, nearly exact calc. of soln., program description 3-48752
 Relativistic particles identification by quasi periodic scattering radiation in crystals 3-77637
 rotational excitation scattering parameters, radial asymptotic expansions 3-40150
 three nonrelativistic pairwise interacting, amplitudes, variational principles 3-70708
 three-particle, Alt-Grassberger-Sandhas perturbation theory 3-49237
 time independent, with Coulomb potential 3-70706
 two-body scattering with separable potentials, polarisation 3-52110
 upper and lower-bound estimates of particle with potential $V(r)$, amplitudes of multichannel processes (*Russian*) 3-62551
 Van de Graaf generator, nuclear spectroscopy study (*French*) 3-59619
 variational methods, relationship 3-57122
 LIF (001) cleavage plane, atomic O scattering process by fast adsorption-desorption 3-41600

particle separators

- Lovelace aerosol particle separator, design and performance, reply to comments 3-77711
 Lovelace aerosol particle separator 3-66146
 powder particle separator 3-44697
 r.f. separated beam line, 50 μs 3-56967

particle size

- aerosol, ambient, in air, size distribution, environmental effects 3-44693
 aerosol, high dispersed, bimodal size distrib., dynamical diffusion, electron microscopy 3-73085
 aerosol beam spectrometry, recent developments 3-55904
 aerosol size distribution, effect on integrating nephelometer accuracy 3-47836
 aerosols, errors in logarithmically normal distrib. 3-65030
 aerosols and liquid dispersions, low angle laser light scattering 3-76389
 air pollutants, laser detection and meas. (*German*) 3-70193
 Airborne-particle sizing using optical-extinction measurements 3-80860
 analyser, using laser beam 3-48359
 analysis rel. to precision of X-ray diff. analysis of thin quartz layers 3-59674
 atmospheric dust, radioactivity 3-53555
 atmospheric particle size distribution determ. from forward scattering data 3-51198
 centrifuge, for submicron particle size determ. (*German*) 3-53829
 ceramic, microstruct. characts., eval. using rapid quantitative SEM image analysis 3-80409
 ceramic powder, binary size system, compaction 3-80423
 chromatography, gas, columns having known size distrib. of sorbent particle, moment analysis of elution curves 3-66434
 clustering, dynamic theory (*Russian*) 3-64863
 disperse system, particle size and concentration distribution determ. from mutual dispersion coefficients attenuation (*Russian*) 3-80506
 in gas-solid transitions, distribution effect for spherical particles 3-65116
 graphite powder, high temp. reactor fuel pressings, struct., grain size distrib. (*German*) 3-71268
 iron hydroxide gel, effect of freezing 3-44685
 isodiametric spherical, microtome sections 3-57004
 latex particle size distrib. rel. to ion exchange, electron micrograph quality improvement 3-41822
 light scatt. photometer for kinetic studies of flowing aerosols, particle size distrib. 3-40082
 log-probability paper application 3-65024
 magnetic alloy, prep. from metal and phthalate ions in dimethyl sulfoxide, for recording media 3-47098
 measurement by low-angle laser light scattering from liquids 3-40293
 metal oxides, sintering, pore size rel. to grain size 3-64973
 metal powder, milling, specific surface, grain size distrib. rel. to additives 3-80390
 microparticle classification, dimension range, computer anal. 3-48599
 molecule-size nuclei, coagulation 3-73088
 multiphase materials, scanning electron microscopy 3-70420
 2-naphthol in water, mass transfer coeffs., fixed bed, cylindrical and oval-shaped pellets 3-79047
 non-spherical object, size distrib., photomicrography 3-69397
 ocean, light scattering indicatixes, meas. and calc., Junge type particle size distrib. (*Russian*) 3-50998
 oil-in-water emulsions, particle size analysis by polymer film impression technique 3-45564
 ρ Ophiuchi, dark clouds, extinction and polarisation wavelength dependence 3-48046
 particle eddy diffusivity, concn. profiles, turbulent Schmidt numbers 3-79032
 polydisperse systems, particle size analysis by microscopy and computer 3-42677
 polymer latexes, particle size distribution determ. with an ultracentrifuge (*German*) 3-41825

particle size continued

- polystyrene latex colloidal suspensions, size distribution by light scattering 3-47485
- powder particle separation according to shape, lab. device 3-44697
- powders, metallic, grain size, specific resistivity, temp. depend., Q-meter measurement method 3-62179
- Raleigh-Gans scatterers, size distrib. determ. by forward scattering lobe method 3-76388
- refractory concretes, calcium aluminate bonded, thermal shock testing 3-80405
- suspension, sampler for size analysis 3-65040
- Tauri, dark clouds, extinction and polarisation, wavelength dependence 3-48046
- tectonics, sliding friction and stick-slip rel. to foliation, grain size and comp. 3-76624
- transition metal compounds, ultrafine powder 3-41827
- transmission electron microscopy, distributions computer program for extinction spectra 3-56983
- Ag alloys, cold-worked, Voigt profile analysis from single reflection 3-61141
- Ag halide, particle size distrib., effect on optical sensitisation of ammonical negative emulsions (*Russian*) 3-50856
- Ag halides, photographic emulsion grain size distrib. determination, electrolytic reduction technique 3-51661
- Ag-Sb alloys, determ. by method of variance 3-44575
- AgI, adsorption, dielectric determ. 3-65028
- Al-Al₂O₃ alloys, ball-milled, room and elevated temp. props. 3-44613
- Al-CuAl₂ eutectic composites, lamellar and particulate, phase size influence on elevated temp. deform. 3-64958
- Al₂O₃ compacts, effect on shrinkage during sintering, kinetic study (*French*) 3-72996
- Al₂O₃ in flames, average particle diameter and spectral characteristics determ. (*Russian*) 3-62365
- Al₂O₃ particles, flame photometry, size obs. and stimulated part of refractive index (*Russian*) 3-59711
- C black, explosion decomposition of acetylene, particle size of carbon black rel. to temp. (*Russian*) 3-47543
- Cr(OH)₃ sols in size range of less than 0.5 μ m, particle size analysis, structure 3-76383
- Cu alloys, cold-worked, Voigt profile analysis from single reflection 3-61141
- Fe-Ni-Ta alloy, coherency strains influence on precipitate shape 3-69246
- NH₄ClO₃ and its polystyrene mixtures, catalytic decomposition, kinetics and mechanism, effect of grain radii (*Russian*) 3-47538
- NaCl aerosol, activation supersaturation meas., particle size rel. to nucleation 3-44896
- PbZr_{0.5}Ti_{0.5}O₃ synthesis, microstruct. development, effect of ZrO₂ particle size and struct. 3-61201
- Pt catalysts, supported and unsupported, electron microscopic determ., distrib. 3-73179
- Si₃N₄-SiC composite system, microstruct. effect on strength 3-76296
- SiO₂ support, NaOH addition effects on morphology and struct. 3-58773
- SmCo₅ powder, effect on microstruct. and mag. props. (*Russian*) 3-58403
- SmCo₅ powder, rel. to coercivity distrib. 3-44276
- ThO₂ powders, phys. props. and influence on sinterability 3-80402
- TiO₂ compacts, effect on shrinkage during sintering, kinetic study (*French*) 3-72996
- α -Zr(HPO₄)₂·H₂O, crystalline, prep. and characterisation 3-55730

particle sources

- see also ion sources; neutron sources; radioactive sources*
- electron, pulsed plasma, power supply circuit 3-73853
- electrons, cold-cathode tube, compact, fast electrons, nanosecond pulses, operation 3-66310
- low energy electron source, for drift velocity experiments 3-42738
- proton generator, ³He(D,P)⁴He reaction, sealed instrument, description 3-66309
- β , using tritium (*French*) 3-53972

particle spectrometers

- see also alpha-particle spectrometers; beta-ray spectrometers; gamma-ray spectrometers; neutron spectrometers; x-ray spectrometers*
- analyzers, hemispherical, large aperture, geometrical factor, fringing fields, calculations 3-62264
- Anger scintillation camera systems, deadtime calculation 3-62260
- Auger electron spectroscopy meas. of gas-solid interface interactions at high temp. (*German*) 3-52749
- capacitor, parallel plate, as relativistic particle analyzer 3-77708
- capacitor, parallel plate, as relativistic particle analyzer, improvement of props. 3-77709
- charged particles coincidences, from nuclear reactions, BOL-system including computer 3-66334
- Cherenkov shower spectrometer with glass radiator, energy resolution 3-53992
- cosmic ray ionization spectrometer, energy calibration 3-48552
- cosmic ray shower spectrometers, Cherenkov, energy resolution, effect of radiator shape, computer calculations 3-70057
- discrimination system, high resolution, analysis 3-77699
- electron, for angular and energy distrib. obs. of ejected electrons in heavy particle collisions, 10-150 keV (*French*) 3-42660
- electron, improvement for ESCA 3-66444
- electron, spectrometer function of parallel plate analyser 3-42659
- electron, spherical electrostatic, transmission properties, theoretical analysis 3-77707
- electrostatic analyser, toroidal, cosmic charged particle streams, description 3-70055
- fringing field effect minimization, parallel plate electrostatic spectrograph 3-77710
- magnetic spectrograph, helical cathode proportional chamber 3-62261
- magnetic spectrograph for energy measurements 3-42661
- meson spectrometer, frozen spin polarised targets, feasibility study 3-77612
- multichannel, for simultaneous storage of spectra and additional signals 3-48549
- multiparticle spectrometer magnets, design 3-56966

particle spectrometers continued

- Omega CERN, magnet, detectors, trigger, general description 3-77712
- Omega detector for use on CERN 25 GeV and 300 GeV proton synchrotrons, trajectory obs. (*Danish*) 3-77704
- Omega project at CERN, implementation of on-line data acquisition system 3-66333
- pair, spark chambers, magnetostriuctive read-out, computer on-line data storage, appl. to photon materialisation (*French*) 3-48554
- pulse amplifier 3-73882
- pulsed ion cyclotrons resonance spectroscopy, solid state marginal oscillator, design 3-62265
- retarding potential analyzers, errors due to grid plane potential nonuniformities 3-53993
- scintillation single crystal time spectrometer, excited state lifetimes of nuclei, description 3-70409
- sparkchamber spectrometer, filmless, invariant mass reduction 3-77713
- sparkstictive wire-chamber, K_K⁺+K_{K π ⁺ decay 3-70411}
- time-of-flight spectrometer, using electrostatic particle guide, for high-resolution charged-particle mass identification 3-48553
- velocity filter, separated fields, improved stigmatic focusing (*German*) 3-70410
- Ge(Li), correlation between cryst. and spectrometer props. 3-56970
- NaI(Tl) signal shaping, energy response, large crystal assembly at NAL USA 3-77706
- particle track visualisation**
- see also bubble chambers; cloud chambers; nuclear track emulsions; scintillation chambers; spark chambers; streamer chambers*
- ALICE flying spot digitizing system, application to spark chamber and oscilloscope data 3-40024
- appearance time, theoretical considerations (*French*) 3-51725
- automatic plate scanner, developments, on-line computer program 3-40025
- celluloid film, gamma-irradiation effects, influence on registration of alpha tracks 3-70399
- Chapark chambers, cylindrical set, MADKA system, design, performance 3-77681
- cosmic ray track visualisation using laser technique 3-59647
- device for tracking and data processing of events recorded on videotape 3-56946
- dielectric track detectors, track-diameter kinetics 3-48540
- dipolar medium, ion tracks, anal. allowing for electrostriction (*Russian*) 3-77641
- discharge-condensation chamber, high resolution time, long memory time, charged particle detection (*Russian*) 3-62250
- drift chambers, 50 cm drift length, SPES1 spectrometer Saclay, France, operation 3-77687
- drift chambers, in magnetic fields, very high accuracy, operational characteristics 3-77684
- drift chambers, large area, array, operation and further development, description 3-77676
- drift chambers, proportional, 16m², high spatial and time resolution, read-out electronics system 3-77698
- drift chambers, proportional, very large (16m²), high spatial and time resolutions, design, performance 3-77677
- driftchamber, multiwire, high space and time resolution, operation, performance, calibration 3-73873
- driftchambers, multiwire, large, multiple system, location accuracy, analysis, performance 3-77644
- fission fragments, back-scatt. from thin metal films 3-61090
- fission track registration technique, for estimation of ²³⁵U in U samples 3-51722
- flash tube hodoscopes, study of properties 3-77674
- flash tube recovery time 3-77675
- glass fission-fragment track detectors, angular characteristics 3-53985
- glass track chamber, operation characteristics 3-40022
- grain density of tracks determ. from cavity lengths distrib. (*French*) 3-56941
- gypsum, surface tracks (S tracks) from external source of fissile nuclei 3-56945
- heavy ion discrimination by track detectors 3-48511
- heavy nuclei, low-energy, track regression in plastic detectors and photoemulsion due to prolonged exposure (*Russian*) 3-66323
- hodoscope chambers, developments, plastic chambers 3-77665
- hodoscope chambers, fast flashtube, operation, advantages 3-73874
- holographic track chambers, appl. of holography to high energy physics 3-70401
- low-pressure streamer chamber in mag. field 3-48544
- Measuring projector with analogue servo system 3-77691
- mica, ¹⁶O ion irradiat., scatt. recoil nuclei tracks, process 3-66327
- mica detectors, coincidence spectroscopy of fission fragments 3-48542
- mixing of solid particles, radioactive tracer technique, collimating system and scintillation detector 3-48339
- MOLLY, automatic scanning and measuring system 3-77694
- multivariable chambers, inert liquid filled, proportional and ionisation modes, high resolution 3-77685
- multiwire proportional chamber, 5 wires per mm design, construction 3-77686
- multiwire proportional chamber, cylindrical, low mass, simultaneous axial and azimuthal measurements 3-77680
- multiwire proportional chamber readout, strip delay line, design, operation 3-77688
- multiwire proportional chamber system, decision wired logic (*French*) 3-53983
- multiwire proportional chambers, sense wire support, melinex strip compared to nylon cord 3-77682
- multiwire proportional chambers for photon beam experiments, construction, performance 3-77683
- muscovite, surface tracks (S tracks) from external source of fissile nuclei 3-56945
- particles, radioactive tracer techniques, collimator efficiency calc. 3-48340
- plastic chambers, electrically pulsed, design features 3-77673
- plastic nuclear track detector, range-energy relns. for heavy charged particles 3-77642
- plastics, identification of fission fragments 3-62247

particle track visualisation continued

- plexiglas track sensitive target in cryogenic bubble chamber, physics run 3-70402
- proportional chamber system, 50000 wires, design, construction, electronics, description 3-77679
- solid track detectors, surface track counting instrument 3-53986
- solid-state detectors, fission fragment energy spectrum 3-48541
- solid-state nuclear track detectors, precautions in etching 3-51723
- solid-state track detector, particle identification and energy measurement, light nuclear particles, new method 3-77646
- streamed chamber, working range investigation 3-53984
- streamer chamber, $100 \times 60 \times 40$ cm., 3 electrode design, operation in a magnetic field 3-70396
- streamer chamber, development for use with ISR, CERN 3-77667
- streamer chamber, IHEP proton synchrotron, μ polarisation measurement 3-77668
- streamer chamber, ionisation measurements in quark experiments 3-77672
- streamer chamber, JINR, for detection of K^0 , K^\pm , π^\pm , nuclei, optimum operational mode 3-77669
- streamer chamber, multiple firing, conical Blumlein line, fast rise time, low amplitude jitter 3-77670
- streamer chamber, three electrodes, neon filling < 1 atm., ns HV pulse generator rel. to cosmic ray detection (*Russian*) 3-62252
- streamer chamber, three-electrode Blumlein line, design description 3-51728
- streamer chambers, for use with CERN hyperon beam, brief description 3-77666
- streamer chambers, H_2 , technical problems, performance evaluation 3-77645
- streamer chambers, recent technical improvements, SLAC chamber accuracy and resolution 3-77664
- streamer chambers, use in high energy experiments 3-77663
- thermal neutron fluence meas. by fission track method using standard U glasses 3-51726
- track sensitive targets, geometrical construction of events 3-77656
- track sensitive targets, review 3-77649
- track-etch radiography, alpha particles, protons, fast and thermal neutrons 3-67627
- wire chamber, glow memory, readout of multiple track event, design, operation 3-77689
- wire chambers, proportional, large, Split Field Magnet detector at ISR CERN, operation 3-77678
- H_2 , track sensitive targets, in Ne/H_2 bubble chamber 3-77655
- H_2/D_2 track sensitive target, neutrino interaction studies in BEBC 3-77657
- 4He streamer chamber, for missing mass spectrometer 3-77671
- LiF, surface tracks (S tracks) from external source of fissile nuclei 3-56945

particle tracks

- see also *energy loss of particles*
- alpha-particle, fading by u.v. heating, hot air and hot liquid circumstances 3-59648
- cosmic ray tracks in lunar dust, to theories of cold accumulation 3-65794
- cosmic rays, fossil ion tracks in rock silicates 3-61294
- cosmic rays, in lunar materials and meteorites, calc. for surface exposure 3-44971
- lunar fossil cosmic ray track meas. of Luna 16 and 20 missions 3-47954
- lunar microstratigraphic chronology using mechanical erasure of particle tracks 3-69899
- lunar rocks (Apollo 17) 3-65832
- mica, fission-track aging 3-44779
- neutron temperature, rel. to temp. of medium, fission track detectors 3-48539
- U content, in minerals induced fission track technique geochronology appl. 3-44831

particle velocity analysis

- see also *energy loss of particles; ion mobility; mass spectrometers; particle spectrometers*
- device for tracking and data processing of events recorded on video tape 3-56946
- electrostatic deflection, ions, electrons, energy anal. 3-77705
- molecular beams, space modulation of radiofrequency field, shift of Zeeman pattern, devices (*French*) 3-49507
- retarding field, ions electrons, energy anal. 3-77705

particles, elementary see elementary particles**parton model**

- anomalous dimension of parton field 3-66926
- Bjorken scaling hypothesis, applicability at energies ~ 30 GeV (*Hungarian*) 3-62841
- Bjorken-Paschos model, inelastic electron-nucleon scattering 3-45883
- charge distrib. of partons in $pp \rightarrow 1^+1^- + \text{anything}$ 3-74459
- charge meas. in electroproduction expts. 3-67054
- composite models of conformal field theory with nonintegral number of partons 3-59987
- current interactions, field theoretic formulation 3-78146
- deep inelastic one-particle inclusive processes 3-52015
- deep inelastic phenomena, complementary descriptions using resonances and partons 3-67033
- deep inelastic processes, hadronic final states in simple quark-parton models 3-59980
- deep-inelastic scattering, single hadron inclusive distrib., parton model and duality 3-57366
- dual, deep inelastic νN scattering description 3-70903
- dual, for photoproduction of pseudoscalar and vector mesons in high energy region 3-74372
- dynamics, recent developments, total virtual photoabsorption cross sections 3-70941
- electroproduction, comparison with SLAC-MIT experimental data 3-62829
- electroproduction data, deep inelastic, model analysis 3-43112
- electroproduction of hadrons, $e^+e^- \rightarrow e^+e^- + \text{hadrons}$, logarithmic enhancements 3-78142
- e.m. mass shifts, renormalisation of Cottingham formula and $SU(3)$ consistency 3-62827
- field theory in infinite momentum limit 3-40312

parton model continued

- Fritzsch-Gell-Mann bilocal algebra representation by unified approach to resonances and partons 3-66946
- g-2, with intrinsic anomalous moment at photoabsorption vertex 3-67047
- general, of deep inelastic lepton scattering, weak cross-sections and electroproduction moments 3-45881
- gluon-exchange model for high transverse momentum hadron jet production in pp inclusive reaction 3-70945
- hadron collisions, inclusive cross section of pion production, energy depend. 3-78215
- hadron-hadron wide-angle scattering, model from inelastic lepton-nucleon scattering 3-74457
- hard collisions of parton pairs, theory for new effects obs. in ISR region 3-49065
- high transverse momentum secondaries in 10^3 GeV cosmic ray interactions 3-57444
- inclusive lepton-hadron scattering, constraints on current fragments, parton-quark identification 3-52012
- lepton-hadron scattering, quark-parton model, duality relation 3-78151
- light cone, Regge behaviour and single-particle electroproduction, scaling regions in large- ω limit 3-67046
- non-perturbative, for inelastic electroprod., fixed-mass sum rules 3-40323
- parton-antiparton annihilation mechanism, boson prod. in high energy pp collisions 3-78208
- photoabsorption sum rule derivation 3-70887
- proton reactions, exclusive and inclusive, description in regions of high transverse momenta 3-57371
- quark, rel. to detection of W boson in high energy N-N collisions (*Russian*) 3-67062
- quark parton, for deep inelastic processes, reln. between quark fragmentation and distribution functions 3-74380
- quark parton, for final state production in deep inelastic lepton-hadron scattering 3-70933
- quark parton for deep inelastic electroproduction in photon fragmentation region 3-70930
- quark-parton, for hadronic production of muon pairs, structure functions 3-78226
- quark-parton, mixed symmetry scheme for valence component of parton distrib. 3-62842
- quark-parton analogy 3-59984
- quark-parton form factors, validity of Drell-Yan formula 3-74340
- quark-parton model for deep inelastic and semi-inclusive annihilation processes, duality and constraints 3-54312
- quark-parton model for deep inelastic inclusive electroproduction 3-74385
- quark-parton model for deep inelastic lepton-nucleon scattering, charge symmetry 3-40355
- quark-parton model in current fragmentation region, inclusive pion electroproduction 3-54313
- quark-parton puzzle, vacuum polarisation 3-66995
- relativistic model of baryons, solution of spinor-scalar Bethe-Salpeter equation 3-57297
- relativistic models of composite hadrons, group theoretical approach, zero-width approx. 3-67056
- relativistic partonlike eqns., difficulty in formulation 3-54257
- review of parton picture of elementary particles 3-67061
- scaling laws, with Regge analysis, π^+/π^- asymmetry in inclusive electroproduction of hadrons 3-57361
- single muon spectra in $pN \rightarrow \mu^+ \mu^-$ hadrons and $W \rightarrow \mu\nu$ hadrons processes 3-40396
- structure functions, deep, inelastic, differences between νW_2^p and νW_2^n 3-62843
- sum rules, derivation in Dashen-Gell-Mann's program 3-40322
- sum rules and positivity 3-54294
- three-triplet currents, internal symmetries and analysis of bilocal operator and partons 3-67035
- unsymmetric core, massive lepton pair production 3-59985
- vector meson dominance effects, partonic content of virtual photon 3-67032
- Weinberg's renormalizable theory, calc. of semileptonic neutral currents 3-70905
- $e^+e^- \rightarrow e^+e^- + \text{hadrons}$, Regge and parton model for photon photon annihilation 3-43116
- eN scattering, deep inelastic, anal. and comparison with vector dominance anal. 3-74382
- eN scattering, deep inelastic, scaling of individual channels, unified approach to resonances and partons 3-78140
- $ep \rightarrow e + \text{anything}$, scaling behaviour in parton model 3-52019
- $\nu\gamma \rightarrow X$ cross section, prediction of equivalent-photon method for $ee \rightarrow ee + X$ 3-70934
- νN deep inelastic scattering, parton model for cross-section x-dependence 3-78117
- νN production process, comparison with CERN data 3-62810
- νp - νn behaviour and Adler sum rule 3-43077
- p.p., scattering total cross section rise, e.m. structure of proton and partons 3-67057
- pp collisions, causality, scaling bounds on high transverse momenta 3-67148
- pp inclusive charged multiplicity distribution, 13-300 GeV/c, truncated gaussian 3-71017
- pp scattering, moderate energy, scaling limit rel. to parton, field theory scaling 3-78192
- π^+p elastic high-energy scattering, parton model and multiple scattering effects 3-60024

Paschen-Back effect see Zeeman effect**passive attenuators see attenuators****patient diagnosis**

- Aberdeen section scanner for rectilinear, arc, transverse and longitudinal section scanning 3-42368
- auditory recruitment (*Italian*) 3-56505
- brain examination, X-ray technique (*Danish*) 3-51463
- brain tumour, automatic detection and location (*Danish*) 3-51462
- cancerous tissue, spin echo n.m.r. obs. 3-42366
- cerebral vascular lesions, proton radiography 3-70140
- cerebrovascular disease, radionuclide angiography 3-56534
- chest X-ray with monoenergetic beam, appl. of Monte Carlo method 3-73600

patient diagnosis continued

- digital gamma camera tomography, theory, nuclear medicine 3-70153
 disease, in maxillofacial region, X-ray obs. 3-53747
 e.e.g. photic alpha blocking, nonstationary spectrum analysis 3-48178
 e.e.g. rel. to medical data 3-59439
 evoked potential audiometry applic., special purpose computer for data processing (*Hungarian*) 3-73575
 excitation thyroid laminography, fluorescence scanning 3-70152
 eye, Cherenkov radiation from the use of ^{32}P for diagnosis of malignant conditions (*Czech*) 3-70136
 foetal development (*Italian*) 3-54033
 Gamma camera tomographic magnifying collimator systems 3-70155
 gamma camera tomography system, digital, clinical experience 3-70168
 gamma-gamma coincidence detection, three-dimensional imaging of radionuclides distributions 3-70162
 high energy therapy, using computer (*Italian*) 3-56546
 isotope applications 3-66042
 isotope applications 3-66043
 lung scanning employing ^{131}I MAA and $^{99\text{m}}\text{Tc}$ ferrous hydroxide 3-42369
 medical thermography, convective heat transfer effects 3-77258
 myelosclerosis, using ^{52}Fe and $^{99\text{m}}\text{Tc}$ 3-42371
 ocular fundus, digital stereophotogrammetry 3-53743
 online blood analysis (*Italian*) 3-54032
 ophthalmological, electric stimulation of retina, excitability, method (*German*) 3-65997
 Polytome, image intensifier fluoroscopy and tomography 3-66388
 positron camera, Massachusetts General Hospital 3-70161
 positron tomography, three dimensional reconstruction technique 3-70163
 positron-transverse section detector, 32-crystal 3-70160
 radiocardiology, basic concepts and applications 3-53754
 radiographic computer image enhancement 3-66040
 radiographic image processing by computer for heart disease detection 3-66041
 radioisotope diagnostics, release to environment through excreta, control 3-77296
 radioisotope scans, automated analysis 3-42374
 radiology, development, trends 3-70139
 renal transplant cases, gamma-camera renography using ^{123}I -Hippuran and ^{125}I -albumin 3-40063
 rotational cine-scintiphotography, three dimensional organ images 3-70165
 stereophotography, practical ophthalmology, applications, theoretical considerations (*German*) 3-70125
 stereoscintiphotography, brain scanning applic., depth perception experimental studies 3-70164
 subdural hematomas, radionuclide detection, rapid sequential scintiphotography 3-56535
 by thermography 3-48629
 tomocamera, tomographic imaging, clinical experience 3-70167
 Tomographic imaging with a Fresnel zone plate system 3-70157
 tomographic scanner, multiplane, clinical results 3-70171
 tomographic scanner, multiplane, nuclear medicine 3-70148
 tomographic scintillation camera, performance parameters 3-70154
 tomographic system in nuclear medicine, multiple view of isotope distribution 3-70158
 tomography, circular, clinical artifacts encountered 3-70169
 tomography, computer-controlled colour-coded digitised images, display system 3-70156
 tomography, radionuclide, clinical perspective 3-70173
 tomography, transverse axial, computerized 3-70166
 tomoscanner, clinical experience 3-70172
 tomoscanner, theory, prototype nuclear medicine 3-70151
 transverse section brain scanning, tomoscanner, multicrystal cylindrical imaging device 3-70150
 transverse section scanner, analogous to transverse roentgen tomography, nuclear medicine 3-70149
 transverse section scanning, brain 3-70170
 by u.s. imaging 3-48631
 X-ray examination, ferrite powder applications 3-42372
 X-ray TV system, dose reducing fluoroscopy 3-45329
 ^{123}I production 3-45316
 ^{127}Xe , appl. to biomedical imaging with Anger camera 3-42373

patient monitoring

- see also *electrocardiography; electroencephalography*
 automatic inflight respiratory gas analyser 3-48665
 biological phenomena, polygraphs improving efficiency 3-48604
 blood flow, cranial scintiphotography, cerebral vascular disease, $^{99\text{m}}\text{Tc}$ injection 3-73595
 foetal development (*Italian*) 3-54033
 neonate pulse and respiration obs. hemodensitometer 3-56996
 respiratory mass spectrometer 3-45601
 respiratory waveforms monitoring 3-59684
 section scanning and imaging, orthogonal tangent correction, appl. to clinical brain scanning 3-51458
 vocal-tract, X-ray films, computer assisted measurement system 3-77210
 π^- , dose in soft tissue, bone, calc. 3-77286
 ^{67}Ga -citrate photoscan, tumour location 3-48252
 ^{125}I , labelled thrombosis monitor, for deep vein obs. 3-56530
 ^{239}Pu in lungs, correction factors for different body builds between phantom and subject 3-73601
 $^{99\text{m}}\text{Tc}$, brain scans, tuberous sclerosis, vascularity 3-51461
 $^{99\text{m}}\text{Tc}$ -S colloid, lung uptake, heart and lung time-activity curves, reticuloendothelial mechanism 3-51459
 $^{99\text{m}}\text{Tc}$ -streptokinase, localisation of deep vein thrombosis, animal studies, appl. to man 3-48253
 $^{99\text{m}}\text{TcO}_4^-$, radionuclide cerebral angiograms, effect of injection volume 3-51460

patient treatment

- see also *surgery*
 blind rehabilitation programme, Veterans Administration USA, experience with CCTV for low vision patients 3-77229
 brain tumours, inoperable, Natulan + telecobalt radiation (*French*) 3-53751

patient treatment continued

- bronchial cancer, treatment by electrontherapy (*French*) 3-53752
 clinical mass spectrometry applic. 3-48664
 isotope applications 3-66042
 microwave therapy, 460 MHz, 100 W generator 3-53746
 X-ray therapy apparatus RT 255, RT 305, operation method, practical experience 3-66389
- pattern recognition**
 see also *character recognition; speech recognition*
 binary classification of patterns by humans, experiments (*German*) 3-45305
 biological pattern formulation, morphogenesis 3-48166
 electron probe image analysis system, automatic, Quantimet 720 3-42715
 forest tree species, computer-aided spectral recognition 3-53908
 Fourier hologram filter, pattern recognition and size determ. of signals (*French*) 3-66770
 iconics problems, image matrix representation 3-51887
 image intensifier, effect of noise on visual detection threshold 3-61900
 mass spectra of small organic molecules, simulation, computerised pattern recognition techniques, improved technique 3-57017
 medical radiosciintigraphy, classification, rejection/acceptance of small fluctuations, likelihood ratio test 3-51464
 microscope images, particle characterisation using Quantimet 720 3-73731
 optical information processing, incoherent, applications 3-77978
 PEPR II system, at Oxford and Padova 3-77702
 radiometric information, reflection classification, image recognition applic. (*Russian*) 3-77023
 scanning optical patterns with acoustic surface waves 3-39865
 three dimensional objects, laser beam orthogonal light section method (*Japanese*) 3-45835
 visual, masking, effects of two dimensional filtered noise, experiments 3-73584
 visual information redundancy reduction, probabilistic analysis of feature information (*Russian*) 3-70130
- Patterson diagrams** see *X-ray crystallography calculation methods*
p.c.m. see *pulse-code modulation*
p.c.m. links see *pulse-code modulation links*
peaking circuits see *differentiating circuits*
Peltier effect see *thermoelectricity*
PEM effect see *photoelectromagnetic effects*
Pendellosung fringes see *X-ray crystallography*
pendulums
 see also *mechanical oscillations; time measurement*
 acceleration and tilt meas. using pendulums and accelerometers 3-56233
 ballistic pendulum struck by arrow, student experiment 3-70244
 double, approx. formulae for oscillations (*Italian*) 3-77840
 Earth crust tiltmeter, servo-controlled horizontal pendulum apparatus 3-47807
 errors, systematic, influence of damping (*Russian*) 3-74077
 gyropendulum mounted on moving base, combinative parametric resonance, analysis (*Russian*) 3-59546
 gyroscopic, subjected to random vibrations, analysis of motion (*Russian*) 3-66578
 high pressure torsion pendulum, for viscoelastic studies on polymers 3-51529
 high vacuum torsion pendulum with low instrumental decrement 3-61988
 hydromechanical oscillatory system, for study of elastic oscillations 3-76852
 plane-corrector pendulum in rocking boat, motion under damping (*Russian*) 3-62438
 resonance in forced vibr., coupled pendulum meas. system (*Russian*) 3-66133
 rubber band pendulum, behaviour 3-66513
 tidal tide meas., instrumentation and techniques 3-47804
 trifilar, inherent errors in measurement of moment of inertia 3-39845
 vibration, normal modes, demonstration to students 3-48321
 Ni rod, torsional spring element, magnetomech. amplification and generation of mech. vibrs. (*German*) 3-58408
- pentary algebra** see *algebra*
pentodes
 No entries
perception (hearing) see *hearing*
perfusion see *diffusion*
periodic system of elements
 see also *elements (chemical)*
 rel. to critical temperature prediction 3-61967
peripheral equipment (computers) see *computer peripheral equipment*
peripheral models
 ϕ^2 multiperipheral model with strong coupling, Regge trajectories 3-60013
 absorptive A_2 exchange in $\pi^-p \rightarrow \pi^-p^*n$, 17.2 GeV/c, polarised target predictions 3-60039
 average multiplicity calcs. in FESR scheme including Harari Pomeron-intercept hypothesis 3-52032
 baryon exchange model, limiting fragmentation, and Bjorken scaling 3-60055
 charge channel analysis, $\text{NN} \rightarrow (\Sigma\text{K})\text{N}$, $(\text{AK})\text{N}$, without I-spin-exchange interference OPE and Deck models 3-78197
 Chew-Pignotti model of charged multiplicities in high energy interactions 3-54360
 Deck effect, diffraction-dissociation process of $\pi\text{N} \rightarrow \pi\text{pN}$ reaction 3-74404
 double peripheral Regge model for B^- production in $\pi^-p \rightarrow \rho\omega\pi^-$ at 9.1 GeV/c 3-78200
 gas model, one-dimens., transverse-momentum limitation 3-52031
 hadronic production, short-range correlation, role of secondary Regge singularities rapidity clusterings 3-67081
 hypercharge-exchange reactions, analysis of data, impact parameter representation 3-67134
 inclusive pionization spectrum internal structure 3-49062
 inclusive reactions, multiperipheral model implications on correls. between charged pions 3-62903

peripheral models continued

- inclusive reactions in fragmentation domain, absorptive corrections and pion-exchange contribs. 3-54361
- inclusive two-particle rapidity correlations at ISR energies, multiperipheral fireball model 3-52060
- light pion interactions and PCAC hypothesis, S-matrix theory 3-62789
- multiparticle production, magnitude of t_0 -cut 3-67075
- multiparticle production at ISR energies, analysis of unitarity eqn. 3-67152
- multiparticle production in heavy nuclei, multiperipheral collisions 3-60045
- multiperipheral, azimuthal corrections for 20-70 GeV proton-proton collisions 3-78214
- multiperipheral, elastic scattering exam. using multiparticle impact parameter 3-67093
- multiperipheral, for high-energy collisions, role of nucleons 3-43128
- multiperipheral, for inclusive two-particle correlation, 18 GeV/c-ISR energies, energy-momentum conservation effects 3-62907
- multiperipheral, for nucleon-nucleon inelastic interactions at 200 GeV, comparison with cosmic ray data (*Russian*) 3-67133
- multiperipheral, for which full multiparticle S-matrix is unitary, multi-chain forces 3-70961
- multiperipheral, forward peak slope, s-channel analysis 3-70962
- multiperipheral, investigation of mean pion multiplicity of high missing mass 3-62866
- multiperipheral, Kp inclusive reactions, $|x| < 0.6$, account taken of Regge poles 3-62912
- multiperipheral, massive muon pair production in pp collisions 3-74468
- multiperipheral, new dual quark diagrams for diffractive dissociation processes 3-67068
- multiperipheral, of high energy πN and NN interactions (*Russian*) 3-67099
- multiperipheral, properties of proton and pion spectra in pp and $\pi\pi$ interactions (*Russian*) 3-40400
- multiperipheral, rel. to asymptotics of $T=1$ $\pi\pi$ scattering (*Russian*) 3-62870
- multiperipheral, representation of inclusive cross-sections by kinematically corrected densities 3-43163
- multiperipheral, transverse momenta and overlap functions 3-70963
- multiperipheral, transverse momentum distribution 3-67083
- multiperipheral, unification by eikonal formulation 3-67086
- multiperipheral, value of triple-pomeron vertex 3-67085
- multiperipheral ABFT model, Morrison rule for $\pi\pi \rightarrow \pi A_2$ 3-67092
- multiperipheral and diffractive production mechanisms for two-particle correlation in pp interactions 3-60010
- multiperipheral arguments in diffraction dissociation multiplicity distrib., nova-type model 3-57446
- multiperipheral Chan Loskiewicz Allison, in study of 1, 12.7 GeV/c 3-67141
- multiperipheral cluster model of high-energy inelastic collisions 3-57389
- multiperipheral dynamics, self-contained treatment, application to inclusive distribs. 3-43131
- multiperipheral dynamics and KNO scaling 3-52030
- multiperipheral dynamics for grand partition function in high energy hadron collisions 3-67091
- multiperipheral eikonal estimates and cancellations of high energies, elastic scattering in modified ϕ^4 theory 3-67095
- multiperipheral inclusive distribs., harmonic analysis on one-sheet hyperboloid 3-57453
- multiperipheral integral eqn. and semigroup contained in SL_2 , 3-49031
- multiperipheral model for charge transfer processes, comparison with fragmentation picture 3-57390
- multiperipheral model for low-multiplicity interactions at ultrahigh energies 3-54331
- multiperipheral model with long range correlations, generalization, Van der Waals approx. 3-57387
- multiperipheral models, charge transfer 3-54333
- multiperipheral plus diffractive production, multiplicity distrib. 3-57388
- multiperipheral secondaries in N-particle cross-sections for pp scattering, 50-300 GeV/c 3-62910
- multiperipheral shower production at high energy, reln. to Regge cut theory of multiplicity distribs. 3-49033
- multiperipheral theory, description of pion spectra from pp collisions, assumed similarity of photon and pion properties (*Russian*) 3-74407
- multiperipheral-like, two-body correlation functions rel. to high-energy hadronic collisions 3-67098
- multiplicity distrib. in multiperipheral fireball model 3-45902
- non-diffractive production of meson resonances, peripheral cross sections 3-52014
- one-pion exchange, adsorption effects for reactions of type $Bp \rightarrow B\pi^+ n$, spin dependence 3-57386
- one-pion exchange in single pion production reaction, strength of absorptive corrections 3-49055
- pion exchange and missing-mass spectra near phase-space boundary for $pp \rightarrow p + \text{anything}$ 3-74456
- s-channel model for high-energy inelastic two body problems, amplitudes, peripheral resonances 3-78196
- self-consistent multiperipheral, inclusive cross section factorisation 3-78173
- semimultiperipheral dual N-point amplitudes, factorization using $SL(2, R)$ representation 3-70953
- short-range correlations, extension of Mueller-Regge formalism 3-70958
- single particle exchange amplitudes, localisability, renormalisation 3-78171
- stripping reactions, (d,p), nuclear coupling const. determ. including form factor effect (*Russian*) 3-74598
- two cluster production via Reggeon exchange, multiplicity distrib. in very-high-energy collisions 3-57385
- unitary multiperipheral, diffractive production, bootstrap solution, constant total cross section at high energies 3-60012
- unitary multiperipheral, nonleading Regge poles, high energy behaviour 3-62869

peripheral models continued

- urbaryon rearrangement diagrams, πN , KN reactions, baryon exchange 3-78174
- vector and tensor meson exchange amplitude systematics in complex pole model 3-67078
- A_2 exchange amplitudes in $\pi^- p \rightarrow \eta n$ and $K^- p \rightarrow \eta \Lambda(\Sigma)$ reactions 3-52046
- pp elastic scattering slope, multiparticle momentum correlation effect on angular distributions 3-60029
- $\pi^+ p \rightarrow \eta^0 \Delta^{++}$, 1.28-2.67 GeV/c, meas. and analysis using effective trajectory parameterization 3-54353
- $^3H(p, \gamma)^4He$, 156 MeV radiative capture, differential cross section calc. in peripheral model 3-52164
- peripheral processors** see *satellite computers*
- peripheral speed** see *velocity*
- Permalloy**
- electroplated thin film, isochronal annealing behaviour 3-79881
- film, coercive force and domain boundary creep (*Russian*) 3-58396
- film, cylindrical, surface roughness and thickness depend. of coercive force (*Russian*) 3-53003
- film, electrodeposited, effect of Mn and In on magnetic and storage properties 3-41385
- film, ferromag. reson., exchange cond. const. damping versus two-magnon relax. model 3-64558
- film, irradi. influence on anisotropy energy (*Russian*) 3-68798
- film, preparation and magnetoresistive props. 3-79882
- film, vacuum-deposited, macrostresses, mol. beam angle of incidence and condensation rate depend. (*Russian*) 3-79587
- film, with perpendicular anisotropy, domain struct. (*Russian*) 3-58395
- films, electrolytically deposited, inner effective field due to bidirectional rotation 3-41379
- films, perpendicular anisotropy, mag. treatment effect on domain structure 3-75862
- garnet composite films bubble vel. measurements. 3-72490
- garnet-permalloy composite structure, domain wall velocity, hard-bubble-free garnet epitaxial films 3-52995
- magnetic texture influence on resist. to irradi. and temp. variations (*Russian*) 3-50406
- magnetically saturated overlay interaction with mag. bubble 3-44272
- Mossbauer effect of ^{57}Fe in alloys with Mo additions, annealing effects (*Russian*) 3-53038
- Permalloy/Mn films with exchange anisotropy, l.f. region of spin wave reson. (*Russian*) 3-79918
- T-bar cct., on orthoferrite, bubble generation and propagation characs. 3-50410
- thin film, temp. step anneal effects on mag. props., sheet resistivity and stresses 3-41384
- thin films, determination of resonance s.h.p. permeability (*Russian*) 3-60991
- thin layer, suppression of hard bubbles in garnet films 3-47086
- Mo-Permalloy/Cu core mag. composite wire characteriz. for memory applics. (*Japanese*) 3-50394
- permanent magnets**
- 2-dimensional plane and axisymmetric systems, computer-aided analysis for magnetic potential (*Russian*) 3-45756
- Cavity type permanent magnet suspension 3-73818
- focusing system, end effects corrections (*Russian*) 3-57271
- magnetic field intensity measurement, using potential measuring coil 3-48476
- magnetisation, up to 500°C, meas. method (*Russian*) 3-59613
- rare earth: Fe(Co)(Ni), characterisation (*Rumanian*) 3-68816
- rare earth-cobalt, LnCos, prepared by liq. phase sintering 3-64521
- rare earth-transition metal alloy, hard mag. props. 3-44266
- Ticonal alloys, critical temp. of mag. change pt., apparatus development 3-53956
- CeCos:Fe, Cu modified, sintered, magnetic props. 3-47101
- Co-Sm, quenching, oxides identified by X-ray diffr. 3-47100
- Co-Sm alloy, temp. depend. of coercivity 3-44269
- Co₂R, R = Y, La, Pr, prep. by liquid phase sintering, mag. props. 3-44268
- GdCos, single crysts., hysteresis singularities rel. to domain struct. form. (*Russian*) 3-72485
- Sm₂Ce_{1-x}(Co_{1-x-y}Fe_xCu_y)₂, bulk hardening effect in case of nonstoichiometric composition 3-50416
- Sm(Co, Cu)₂ alloys, mag. props. temp. depend. 3-50424
- SmCos, powder-based magnets, texture perfection degree, particle orientation angles distrib. (*Russian*) 3-61135
- SmCos, single crysts., hysteresis singularities rel. to domain struct. form. (*Russian*) 3-72485
- SmCos, single-domain state with mag. energy 32 million G-Oe 3-55446
- SmCos, sintered, magnetic domains, powder pattern obs. 3-52992
- SmCo₅ and Sm₂Pr₂Co₅, sintered, annealing temp. depend. of mag. props. (*Russian*) 3-44259
- SmCo₅ magnets, liquid-phase sintering 3-44643
- SmCos powder, microstruct. and mag. props. (*Russian*) 3-58403
- SmCos powder, sintering mechanisms 3-47438
- Y(Co_{1-x}Fe_x)₂, composition and stability of CaCu₂-type compds., permanent mag. application 3-50679
- permeability**
- see also *diffusion; mechanical permeability*
- aquifer, math. modelling of ground-water flow, heterogeneous permeability distrib. 3-56277
- gelatin films, effect of H₂SiO₄, kaolin and silver halide conc., effect of developers (*Russian*) 3-46773
- living cell, semipermeable properties, role of polarised water and of lipids, theory 3-81263
- membranes, homogeneous swollen, hydraulic permeability rel. to diffusion 3-54773
- membranes permeability meas. 3-58813
- porous circular discs, squeeze film behaviour, design of clutch plates 3-40970
- soil, infiltration models, steady rain 3-56052
- surface, frictional drag, heat transfer, effect of free convection (*Russian*) 3-57746
- thermoplastic films, permeability of gases and vapours 3-69401

permeability continued

vacuum material, gas in solids, rel. to alloys, pure metals, refractory oxides, ceramics, organic 3-59570

Ni, H₂ permeation, diffusion and solubility 3-53238

permeability (electric) *see* **permittivity****permeability (magnetic)** *see* **magnetic permeability****permeability measurement (magnetic)** *see* **magnetic permeability measurement****permittivity**

see also **electric strength**

(K_{1/2}Pb_{1/2})(Zn_{1/6}Nb_{5/6})O₃, dielectric constant, temp. depend. 3-72562

acetates, determ. of dielectric relax. at microwave freq. 3-72569

alkali halide crystals, h.f. dielectric constant, calc. 3-61017

1-alkanes, dielec. consts. and losses, mean relax. times, chain length depend. 3-47204

amide-water systems, deviations from-ideal behaviour of mixtures 3-53356

anthracene, dielectric tensor as a function temp. and pressure 3-41471

aqueous electrolyte solns., and dielec. relax. (*German*) 3-69460

bacteria, dielectric const. at low frequencies 3-48169

barium stearate films, static dielec. const., corrected calc. 3-53057

basalts, dielectric constant and loss tangent 3-50911

benzene, dielectric constant and molar polarizations, 278-343 K 3-50861

benzene, solid, electron energy loss meas. of optical consts. 3-64622

benzene solutions of binary mixtures, phenol, pyridines, benzaldehyde, microwave absorpt. 3-80585

benzophenone, in binary solvent mixtures, dielec. const., effect on electronic spectral intensities 3-46264

binary mixtures in dilute solutions, long chain pyridines, picolines and benzaldehydes, microwave meas. 3-55999

boundary effects, random dielectric media, effective permittivity, theory 3-75933

carbon tetrachloride, dielectric constants and molar polarizations, 278-343 K 3-50861

cellulose hydroxyalkyl ethers, dielectric props. below glass-transition temp. (*Russian*) 3-72574

ceramic, high dielec. const., temp. coeff. 3-75935

cholesteryl decanoate liquid crystals, scatt. erasure correl. 3-75964

computer program for simultaneous analysis of multiproperty data 3-72166

condensed nonpolar media, suboptical dielectric losses 3-55519

conductor-dielectric heterogeneous mixtures, formulae 3-79973

continental ice caps, dielec. const. depth depend. 3-59205

corrugated dielectric rod, surface wave and radiation characts. 3-77939

cycloalkanes, dielectric constants and molar polarizations, 278-343 K 3-50861

cyclohexane, density, dielectric const., phase transition, 500 atm. 3-68910

1,2-dichloroethane, relax. time distrib. functions, temp. depend. (*French*) 3-79981

dielectric constant, relationship with surface tension, Lifshitz macroscopic forces theory 3-43926

diglycine nitrate, reciprocal dielectric constant, temp. depend. at different hydrostatic pressures 3-53067

effective dielectric constant bounds of inhomogeneous material 3-68913

electron tunnelling into single trapping in dielectric 3-44369

e.m. wave diffraction from conducting wedge loaded with dielectric slab 3-57200

e.m. wave scattering from sphere coated with inhomogeneous sheath 3-57199

emulsion, with dispersed conducting phases (*French*) 3-80502

ethylene-glycol, relax. time distrib. functions, temp. depend. (*French*) 3-79981

o-, m-ethylphenols, molar polarization and dipole moment, mol. assoc. 3-68916

ferroelectric, rel. to domain nucleation, under influence of very low elec. fields 3-53069

fluid heat transfer and dielec. props. determ. method using capacitance meas. 3-62019

glass, mixed alkali silicate, electric field relaxation, mechanical relaxation rel. to ionic diffusion 3-76327

glycine silver nitrate, ferroelec. transition, hydrostatic press. effects 3-64611

heterogeneous mixture, correl. with component permittivities 3-53054

n-hexane, dielectric constants and molar polarizations, 278-343 K 3-50861

high energy storage capacitor single crystals. evaluation 3-72580

high-molecular organic materials, aq. soln., dielec. const. and loss tangent, conc. depend. (*Russian*) 3-50860

hydrocarbon, solid, dielectric constant calc. from electron energy loss spectra 3-79397

ice, grown from KCl soln. 3-47195

ice, zone-melted, time-dependence of complex dielectric constant in 0.3 Hz-0.3 MHz range (*German*) 3-53052

ice single crystal, Cl⁻ doped (*Japanese*) 3-55518

ice with KCl in low concentration (*Japanese*) 3-55517

itinerant electron system, effect of exchange interactions 3-44194

light absorption by impurity centres, theory 3-72691

liquid crystal, nematic, with large negative dielec. anisotropy, instabilities in elec. fields 3-52575

liquids with polarisable dipoles, static electric permittivity 3-47197

Lorentz factors calc. for crystals with various unit cell shapes 3-75937

Lorenz-Lorentz eqn., generalised, applic. to mol. spectroscopy using absorbing solvent 3-74997

lossless layer, measured path difference graphical method 3-51649

metal, structural depend., free electron calcs. 3-68536

metal films, granular, i.r. permittivity, rel. to calc. of intergranular forces of coalescence (*French*) 3-64268

mica, 3-36.8 GHz (*Russian*) 3-50512

moist n-element capillary-porous material 3-79970

permittivity continued

molecular complex, stability constants and dipole moments, determ. from permittivity meas. 3-65118

molecular electric dipole moments from meas. in soln., ALGOL program 3-73180

multiphase mixture, dielectric theory 3-68911

N-methylacetamide, complex dielectric constant -185 to 20°C, 50 Hz to 3 MHz 3-60796

nearly-one-dimensional metallic conductor, model approach 3-50099

nearly-one-dimensional metallic conductor, model approach 3-50100

neopentane, density, dielectric const., phase transition, 500 atm. 3-68910

nitrobenzene/2,2,4-trimethyl pentane binary solution, critical soln. temp., dielec. consts. and losses 3-44364

2-nitropropane, dispersion and dipole moment 3-55997

organic resin/inorganic filler mixture, dielec. const. calc. 3-76367

pentachlorobenzene compounds, dielectric absorption, molecular rotation 3-72572

polyethylene filled with wood flow, dielectric and thermophysical props. meas. 3-65006

polymers, dielectric consts. above 100 by nomadic polarisation 3-47199

polyvinylidene fluoride film, metal ions injection in an electric field, effect on complex dielectric constant 3-58466

rare earth sesquioxides, dielectric constants meas. 3-79974

Rochelle salt powder, variation with particle size 3-72563

rock samples, dielectric constant and loss tangent spectra, meas. techniques 3-50910

rocks with high permittivity and high loss, meas. techniques 3-51160

rubber mixtures, polar, Cole-Cole plots, 500-10¹⁰ Hz 3-55516

rutile, single crystal, dielectric relaxation and effect of residual polarisation from 20 to 140°C (*Russian*) 3-61019

saline solutions, aqueous, metastable state rupture, transitions to liquid state phenomena (*French*) 3-79492

s.c.l. current, theoretical anal., including effect of charge exchange between traps on permittivity 3-75748

semiconductor, n-type, linear correction due to virtual interband transitions 3-55554

semiconductor, photoconducting, electron component of permittivity, external-pumping-induced change 3-58307

semiconductor, tetrahedral, average nuclear effective charge 3-79265

semiconductors, reln. to energy gas changes, temperature dependence 3-41472

solids, optical props. measurement, review (*French*) 3-41494

in solution, dilute, static, complex and optical dielec. const. meas. for relax. determ. 3-68908

sub-monolayer molecular films 3-47333

surface inelastic light scattering, semiclassical study, cross section rel. to dielectric constant 3-50536

thermophysical properties computation and production of self-consistent tables and Mollier charts 3-60510

triglycine sulphate, ferroelec., irradi. effects (*Polish*) 3-50526

triglycine sulphate, reciprocal dielectric constant, temp. depend., molecular field theory 3-72565

triisopropyl phosphate and amine complex, stability constant and dipole moment determ. from permittivity meas. 3-65118

water emulsions, metastable state rupture, transitions to liquid state phenomena (*French*) 3-79492

AgCl, d.c. and very low freq. fields (*French*) 3-41480

AgI, gigantic low freq. dispersion theory 3-65028

AgNa(NO₂)₂, dielectric constant as function of temp. hydrostatic-pressure effects 3-50510

As₄₀Se₅₀Ge₁₀, amorphous film, a.c. cond. obs., heat treatment and light irradi. effects 3-68620

Au, separation of free and bound electron contrib. 3-64592

Ba-mica/Al₂O₃ composites characteriz. 3-76342

Ba(ClO₄)₂·H₂O single crystal, dielectric props. from 32 to 325°C 3-41473

Ba₂Ti₂Nb₂O₁₀, temp. depend. 3-72584

BaTiO₃, doped, permittivity and conductivity dispersion (*Russian*) 3-58465

BaTiO₃, explosively compacted, characteristic behaviour 3-55533

BaTiO₃, rel. to temperature changes (*Polish*) 3-47203

BaTiO₃ ceramic, TiO₂ enriched (*German*) 3-75956

BaTiO₃:LiF-MgO, weak field, stress, temp. depend. 3-80415

BaTiO₄:ZnO-SnO₂, polycryst. solid soln., crit. field for permittivity changes, pressure depend. 3-50529

CdGeP₂, i.r. absorpt. and refl. spectra, 2 to 100μ, dielec. const. and refr. index calc. 3-44412

CdIn₂S₄, microwave dielec. const., and its press. depend., 9.25 GHz 3-68912

CdTiO₃ ceramics, dielectric constant, hydrostatic pressure and temp. depend. 3-68943

Co-Cl trigonal boracites, dielectric and thermal anomalies 3-79998

Cr₂O₃, rel. to off-diagonal magnetoelectric susceptibility 3-47002

Cs halides, strain derivatives of static and high frequency dielectric constants 3-47198

CsMnF₃, i.r. refl. spectra, dielec. const., lattice freqs. and interionic pot. calc. 3-47272

Cu-Zn ferrites, dielectric behaviour from -130° to +120°C 3-53055

Fe-Cl and Fe-Br trigonal boracites, dielectric and thermal anomalies 3-79998

Fe-Ni alloy films, freq. depend. of permittivity tensor components (*Russian*) 3-61045

GaAs, microwave conductivity and permittivity meas. 3-50225

Ge, microwave conductivity and permittivity meas. 3-50225

Ge, nonlinear interaction of Gaussian e.m. beam, kinetic treatment 3-58294

HCl, static dielectric const. calc. 3-54791

HF liquid, dielec. const. and assoc. anal. indicates extended chainwise assoc. 3-72561

³He, P-V-T relations and critical indices obs. 3-60823

⁴He, thermophysical properties, 4 to 3000 R, pressures up to 15000 PSIA 3-50043

permittivity continued

- ⁴He, thermophysical props. tables from 2 to 1500 K with pressures to 1000 atmospheres 3-60822
- n-InSb, e.m. wave propagation, permittivity, penetration depth, dispersion relations 3-68662
- InSb, nonlinear dielec. consts., e.m. beam self-focussing study 3-57249
- K halides, fundamental spectra obs. in Schumann u.v. region 3-58518
- KCl:OH⁻ paraelectric system with small zero-field splitting, low temp. applications (*German*) 3-50509
- KH₂PO₄, influence of gamma-radiation dose rate on dielectric props. 3-79975
- KH₂PO₄ powder, variation with particle size 3-72563
- KMgF₃, i.r. refl. spectra, dielec. const., lattice freqs. and interionic pot. calc. 3-47272
- KMnF₃, cubic-tetragonal transition at 186K, press. effects., dielec. const. obs. 3-58127
- KNbO₃ single crystals, low frequency dielectric studies 3-53053
- K_{1/2}La_{1/2}Nb_{1-x}O₃Sn_{0.001}, flux grown, dielec. const., elec. cond. anomaly (*Japanese*) 3-41490
- La_{0.1}Li_{0.1}NaBa_{0.8}Nb_{0.5}O₁₅, temp. depend. 3-64610
- LiD₂(SeO₃)₂, meas. of permittivity, spontaneous polarisation and coercive field 3-79999
- LiF, crystal, immersion method, effects of adsorbed H₂O, lattice defects 3-41470
- LiGaO₂ single crystal 3-50520
- LiF and natural LiF, i.r., calc. using shell model lattice dynamical data 3-41516
- MoSe₂, static and high freq. dielec. const., i.r. absorpt. obs. 3-47279
- (NH₄)₂BeF₄, anomaly at phase transitions 3-72207
- (NH₄)₂BeF₄, freq. depend., 1 kHz-1 MHz 3-68945
- NaCl, under simultaneous action of a.c. and d.c. voltages, 15-90°C 3-55521
- NaNbO₃ dielectric constant in ferroelectric phase, Curie-Weiss law 3-50523
- Na₂SO₄, dielectric props. temp. and freq. depend. 3-75936
- Na₃BO₃, natural antimonite cryst., permittivity anomalies at phase transition, Curie temp. (*Russian*) 3-58481
- NiFe₂O₄, CaO impurity influence on dielectric behaviour 3-53056
- Pb₂(Ge₂Si₂O₁₁), optically active ferroelec., Si conc. depend. 3-61025
- Pb_{1-x}La_xTi_{1-x/4}O₃, dirty displacive ferroelec., clamped dielec. const. meas. from lattice vibr. modes 3-58483
- PbO, freq. and temp. depend., disc specimens (*French*) 3-79971
- PbO-PbX₂-SiO₂ system glasses, X-halogen, rel. to anionic cond. 3-55099
- PbO-SiO₂ glasses, dielectric constant, depend. on PbO conc. 3-55266
- Pb(Zr,Ti)O₃ ceramics, fabrication process and props. characteriz. 3-72965
- Pb(Zr,Ti)O₃ ceramics, hydrostatic press. and high elec. field combined effects 3-72579
- PbZrO₃-SrCu_{1/3}Nb_{2/3}O₃ system, temp. depend. X-ray diff. phase anal. 3-72591
- PbZr_{0.5}Ti_{0.5}O₃, effect of ZrO₃ particle size and struct. 3-61201
- Rb halides, strain derivatives of static and high frequency dielectric constants 3-47198
- RbFeF₃, i.r. refl. spectra, dielec. const., lattice freqs. and interionic pot. calc. 3-47272
- RbMnF₃, i.r. refl. spectra, dielec. const., lattice freqs. and interionic pot. calc. 3-47272
- Se-As(0-24 at.%As), determ. from fast electron c.e. losses, atomic arrangement 3-72288
- Si, microwave conductivity and permittivity meas. 3-50225
- Si₃N₄, effect of fabrication conditions 3-76294
- Si₃N₄ vapour deposited thin films 3-55272
- SiO₂ films, dielectric constant, measurement in very low frequency by thermally stimulated current 3-50507
- Sn, gray, zero-gap semiconductor, stress-dependent dielectric constant 3-44365
- SrTiO₃, permeability in vicinity of phase transition at 110 K 3-79490
- Ta₂O₅ pyrolytic film characterisation 3-58591
- TiO₂, film, in m.i.s. struct. 3-50276
- TiO₂, in 15 kG field, liquid He temp., phonon aided polaron hopping 3-79647
- YIG, n-type, inhomogeneous polycryst., non-Ohmic current behaviour 3-72363
- Zn-Cl trigonal boracites, dielectric and thermal anomalies 3-79998
- ZnS film, temp. and freq. depend., 78-380 K and 10⁻²-10⁵ Hz 3-41474
- ZnTe, frequency dependence of relative permittivity 3-64364
- ZrO₂, Y₂O₃ stabilized, current-blackened single crystals. 3-79972

permittivity measurement

- capacitor, for use at high press. and low temp. 3-39971
- complex, remote sensing by multipole resonance meas. in radar cross section 3-47196
- complex dielectric constant using Fabry-Perot interferometer as resonator (*Japanese*) 3-59593
- dielectric materials, in TEM resonator, 100-1000 MHz band (*Polish*) 3-73804
- electrolyte solns., simultaneous cond. and permittivity meas. by Maxwell-Wagner effect (*French*) 3-50508
- immersion method, effects of adsorbed H₂O and lattice defects from LiF obs. 3-41470
- liquid, capacitance of capacitor containing material, rel. to dielectric constant 3-53947
- liquid, low loss, automatic acquisition of dispersion data, voltage standing wave amplitude obs. 3-42602
- liquid, pulse waveguide method, technique, apparatus 3-75934
- liquid with high microwave losses, X-band interferometric apparatus modifications (*French*) 3-59608
- liquids, broad band interferometric technique (*French*) 3-56698
- liquids, complex permittivity, 5 to 40 GHz, theoretical analysis of reflected power method 3-73810
- liquids, flow method, microwave region, errors 3-77570
- polymers, dielectric constant and loss tangent, heated meas. cell, temp. dependence 3-48469

permittivity measurement continued

- very low frequency, meas. by thermally stimulated current 3-50507
- personnel**
- see also education; management; teaching; training
- Advanced Test Reactor, available operating time improvement, instrument, component and maintenance modifications, personnel training 3-74695
- nuclear instrument and control technicians, basic elec. and electronics course 3-73645
- nuclear plant, operator training 3-52223
- nuclear plant instructors, selection and development guidelines 3-73647
- nuclear power plant, safety 3-63144
- nuclear power plant, training simulator 3-52225
- nuclear power plant operator, Brunswick Nuclear Plant training programme 3-73644
- nuclear power plant operator, on-site systems training, operator requalification 3-73643
- nuclear power plant operators, candidate selection, training 3-73629
- nuclear power plant operators, cold licence AEC exam., on-site systems training 3-73646
- nuclear power plant operators, selection and training 3-73628
- nuclear power plant operators, training, use of simulators 3-73648
- nuclear power plants, Brunswick Steam Electric Plant, startup and operating procedures, emergency and fuel handling procedures 3-73641
- nuclear power plants, operating procedures, manual for plant safety 3-73639
- nuclear power plants, operating procedures, min. risk to health and safety 3-73638
- nuclear power plants, Pilgrim Station, operating procedures, plant safety 3-73640
- nuclear power plants, standards and operating procedures, personnel, safe and reliable plant operation 3-73642
- nuclear reactor, operator training, present state and future trends 3-52221
- nuclear reactor, staff training 3-52222
- nuclear reactor, training simulator, computer controlled 3-52226
- nuclear reactor operation, procedures, experience and standards, personnel training, conf., Myrtle Beach, South Carolina, USA (Aug 1973) 3-74691
- nuclear reactor plant operators, training, in-plant production of black and white video tapes 3-73649
- nuclear ship, seamen training 3-52224
- operator selection and training 3-73628
- welders' health hazards of arc radiation and heat 3-59456

perturbation techniques

- alkali halide:Ti⁴⁺-like ion, method of moments evaluation of electron-lattice interaction in absorpt. spectra 3-72684
- axisymmetric plate with stabilised rotation, vibrations (*Russian*) 3-62525
- book, similarities, differences, advantages and limitation of various methods 3-62423
- boundary rel. to diffraction of plane compressional elastic wave with rigid spheroidal inclusion 3-74079
- circular plates, unsymmetric wrinkling, edge thrust and lateral pressure effects, post-wrinkling behaviour, perturbation expansion 3-74054
- conductivity, electron-impurity system, first corrections to Boltzmann result 3-72341
- direct-interaction approximation by modal-interaction perturbation technique 3-63654
- dynamic buckling, finite column resting on a nonlinear elastic foundation, step loaded two-time perturbation expansion 3-70633
- e.m. wave reflection from randomly uneven surface, asymptotic development method of determ. (*French*) 3-54197
- flexural vibrations in orthotropic plates, natural freq. calc. 3-42809
- fluid-structure interaction problems, i.f., perturbation method 3-74081
- inverse problems, appl. in geophysics, medicine and engineering 3-54064
- Kleinmen forbidden nonlinear optical coeffs., magnitude and dispersion 3-59891
- linear systems, effects of determinant perturbation and random perturbation (*Russian*) 3-62409
- linear time scales, for linear perturbation problems, expansion terms 3-74121
- liquid metals, magnetic susceptibility calc. 3-72449
- microwave low-loss nonresonant circuit, elec. field distrib. meas. (*Polish*) 3-42939
- nonlinear pulsations of vibrationally unstable upper main sequence stars 3-42188
- nonlinear vibration system analysis (*Polish*) 3-66587
- nonlinear wave propagation 3-45632
- nuclear reactivity change calcs., generalized perturbation method, second-order term evaluation 3-60265
- nuclear reactor calcs., higher order perturbation method 3-60262
- nuclear reactor shield weight optimization by perturbation method, computer program 3-74690
- Poincare-Lighthill, for linear perturbation problems, secular behaviour 3-74121
- radiation transport, deep penetration, class of second-order approx. formulations 3-63243
- semiconductor electrons, kinetic equations in strong electric field, Green's resolvent (*Russian*) 3-68632
- skew stiffened plates, parametric reson. problems 3-70662
- spherical pressure vessel, non-linear viscoelastic material, random loading 3-70564
- vibrating beams, uniform elastic, time dependent boundary conditions 3-74056
- perturbation theory**
- see also quantum theory
- absorption spectra, impurities in solids, fourth order 3-72689
- Adler anomaly, compensation by evanescent couplings 3-70885
- alkali halides, diatomics, perturbation theory, ionic modes, dipole moment and interaction energy calc. 3-40682
- alkaline earth dihydrides, nearly free electron model for equil. behaviour 3-75497
- alloys, binary, disordered, electronic structure using diagrammatic approach tight binding approximation 3-43982

perturbation theory continued

- anthracene crystals, nonradiative destruction of triplet excitons by excess electrons 3-44451
- atom, multiphoton effects, anal. by Keldysh method, and perturbation method 3-74825
- atom, multiphoton ioniz., Reiss approximation at moderate intensities 3-71387
- atom and ion, isoelectronic energy levels, interpolation formulae for Z, 1 to 137 3-74791
- atom dispersion energy coefficients, bounds 3-43383
- atomic dynamic polarisabilities, dipole-dipole and dipole-quadrupole contributions to dispersion energy calc. 3-43386
- atomic system, dynamic multipole polarizability, perturbation operator from unitary transform of HF Hamiltonian 3-67665
- atomic systems, Heisenberg Uncertainty magnitude (*French*) 3-46167
- atoms, multiphoton effects, appl. perturbation theory 3-74824
- atoms electron correlation, multiperturbation theory 3-43329
- bimolecular reactions, collinear, vibrational transitions 3-73126
- binding energy calculation, for metallic H₂, zero press., second and third order theory 3-58001
- biphenyl, triplet-triplet transition absorption spectrum 3-74946
- Bloch electrons in uniform elec. field, rigorous solns. 3-43973
- boundary value problem, single perturbation type, resonance, improved method of matching asymptotic expansions 3-70532
- chain fraction expansion of S-operator 3-74325
- collisionless damping of plasma waves, quantum perturbation theory of plasmons 3-49678
- controlled fusion blankets and shields, perturbation theory for neutron and photon transport calcs. 3-74743
- convergence of perturbation series in field theory models containing fermions 3-54283
- creeping flows, liquid droplet in shear flow, computer generated analytic solutions, perturbation solution 3-71834
- degenerate state, diagrams, perturbation expansions, eigenfunctions, secular matrix elements (*Russian*) 3-48768
- dense fluid transport properties, viscosity, thermal conductivity 3-72221
- diatomic mol., electron density quotient, delta-function model (*German*) 3-54646
- diatomic mol., electron-density quotient, internucl. distance depend. (*German*) 3-54647
- disordered anharmonic chain with symmetric potential, modulated waves 3-43856
- double, nondegenerate systems, secular equations 3-66632
- effective interaction properties for simple 2×2 matrix 3-67222
- electron diffraction, absorption coeffs. of degenerate Bloch waves 3-40839
- energy corrections for bound, virtual and resonance states, Hilbert-Schmidt method 3-70879
- equation integration procedure based on transformational behaviour 3-66618
- excited state CI studies, reduced partitioning procedure 3-74953
- excited states, effect of perturbations, mol. orbital LCAO method 3-71498
- extended average energy perturbation calculation of resonance state energies in 2 electron atoms 3-67666
- ferromagnet, Heisenberg model, spin 1/2, rel. to equivalence of two spin operator approaches 3-79811
- Feynman diagrams, computer generation, general algorithm 3-70875
- Feynman diagrams, computer generation, program description for atomic and molecular appl. 3-70876
- first order, molecular vibrations, isotopic properties 3-74989
- first order, operator expectation values 3-45700
- fluctuation-dissipation theorem for open system 3-66687
- Fokker-Planck equation, stationary soln. near detailed balance 3-77909
- geostationary satellites, first order perturbation theory (*German*) 3-51248
- gravitation, as self-interacting massless spin-2 field theory, perturbation calcs. 3-45720
- Hartree-Fock equation, perturbation theory 3-52245
- Hartree-Fock perturbation theory, upper and lower bounds for second order energy 3-57599
- hydrides, ten-electron, ground state calc., field form of perturbation theory 3-71521
- hydrocarbons, conjugated, optical dipole polarisability calc. 3-43437
- hydrogenic wavefunctions derivation 3-63266
- III-V semiconductor, drag photocurrent, due to photon momentum in direct interband transitions 3-58304
- inelastic and rearrangement scatt. processes, variation-perturbation treatment 3-62569
- infinite momentum, consistent soln. for annihilation and electroproduction cross sections 3-67019
- inhomogeneous medium, perturbation theory for field moments 3-62645
- invariant, for chiral Lagrangian, calc. of higher orders 3-66937
- Ising model with long-range interaction, calc. of correlation functions 3-54175
- Kato's expansion by generalizing relative bound condition 3-48759
- Kirkwood-Salsburg eqn., series soln. and radius of convergence 3-62406
- linked diagram, electric dipole sum rule enhancement factor calc. 3-78240
- liquid mixtures, perturbation theory and excess props. 3-43744
- liquid-gas mixtures, solubility investig. 3-53357
- liquid-solid phase transitions, phenomenological theory 3-75605
- Lowdin orthogonalization and square root of positive self-adjoint matrix 3-60407
- magnetic properties of molecules, influence of perturbations 3-57636
- many-body perturbation methods applic. in discrete orbital basis 3-46233
- Mathieu equation, two-timing solution to second order, perturbation technique 3-74120
- metal, bulk moduli and pseudopotential perturbation theory 3-46657
- modified Rayleigh-Schrodinger expts., singlet state polarizabilities, conjugated mols. 3-74099

perturbation theory continued

- molecular complexes, double perturbation theory for interacting theory 3-57676
- molecular natural orbitals calc., diagonalization of one-electron density matrix 3-74942
- molecular orbital, substituent induced ¹³C chemical shifts 3-63374
- molecular states 1s2p, 1s²2p, 1s²2s perturbation correction calcs. 3-71505
- molecule, heteronuclear diatomic, closed form perturbation theory of, multiphoton transitions 3-71517
- molecule, heteropolar, diatomic, multiphoton processes, time-dependent, Born-Oppenheimer, approx. 3-67760
- molecule, homopolar diatomic, multiphoton processes, time dependent, Born-Oppenheimer approx. 3-71516
- Moller operators, predictions 3-70866
- mononuclear systems, diamag. susceptibility calc. using Brandus method 3-67640
- multidimensional linear problems, Poincare-Lighthill and linear-time-scales methods 3-74121
- multipole polarisabilities and London dispersion forces between Ne and He atoms, using double perturbation theory 3-40588
- neutron cross-section sensitivity analysis for discrete ordinates calcs., perturbation approach 3-74637
- nondegenerate system, multiple perturbations, Rayleigh-Schrodinger formalism (*Spanish*) 3-74086
- nonideal Bose gas, hydrodynamic Hamiltonian 3-54167
- nonlinear wave modulation, perturbation method, integro-partial differential eqns. 3-77864
- nonpolynomial Lagrangians, higher perturbation orders in principle coupling constant 3-54277
- nonsemisimple matrices, perturbation series for eigenvalues and eigenvectors 3-40084
- nuclear matter, asymmetric, second order perturbation theory 3-62976
- nuclear reactor reactivity due to cross-section perturbations, Monte-Carlo calcs. 3-49331
- nuclear reactor shield design, application of second-order perturbation theory to sensitivity studies 3-74689
- nuclear reactor system, sample worth analysis, group collapsing effect 3-60257
- nuclear reactors, fast, calc. of reactivity, Doppler effect, void coeffs. (*Czech*) 3-74651
- phonons, optical, coupling in presence of external forces, first and second order theories 3-46684
- plane layer, dynamic coupled thermoelastic problem, dynamic perturbation, oscillating load (*Russian*) 3-70582
- polyatomic mols., potential energy function, unitary transformation operator for perturbation treatment of the Hamiltonian 3-40601
- for projected states 3-42851
- projection operators, product form and scheme for approximate projection 3-67229
- quantum freq. converter, quantum theory, time depend. perturbation theory 3-66883
- quantum systems, eqn. of state, finite range Kac pot. at high temp. 3-42892
- reacting Coulomb gases, quantum-statistical-mechanical formulation 3-71698
- reggeon-particle amplitude in a+b→c+d+e, perturbation theory model of analytic structure 3-78163
- renormalizable interactions, composite operators in perturbation theory 3-43057
- renormalizable interactions, normal products and short distance expansion in perturbation theory 3-43058
- satellite coupled vibration-rotation motion, Lie transform perturbation theory 3-69808
- Schrodinger equation approximate solution by minimizing deviation 3-59781
- seismology, low frequency motions 3-76592
- self consistent field, band structure of mol. crystals 3-64289
- semi-classical time dependent approach to polar diatom-atom scatt. 3-71636
- semiconductor laser, band to level transition, spectral hole burning and nonlinear gain decrease calc. 3-66847
- spectroscopy of impurity centres, parametrisation of equivalent Hamiltonian 3-69033
- spin Hamiltonian for low symmetry, second-order perturbation treatment for energy levels 3-72506
- sum rule examination, causality, DGS representation 3-59940
- super radiance, level shifts of N atom system 3-62678
- super-radiance interpretation in classical diffraction theory terms 3-62677
- superconducting transition temp., magnetic impurity effect, two-band model 3-79780
- superconductor, response to static spatially dependent perturbation of interaction const. 3-60939
- symmetry reduction of system by perturbation (*French*) 3-42837
- symmetry-adapted perturbation expansions using unitary transforms. 3-62559
- t₂^g config. in low symm. cryst. fields, mag. props. calc. 3-44181
- T-matrix perturbation theory in three nucleon bound state 3-60065
- tetrachloroethylene, vibrational force fields, specific imposition of pots. parameters on nonbounded distances 3-71527
- thermodynamic second order, study short range potential (*Russian*) 3-74172
- thin film overlay, perturbation theory for electric potential acoustic surface wave transducer 3-41075
- three-particle scattering, Alt-Grassberger-Sandhas perturbation theory 3-49237
- time-dependent variational principle derivation from Hamilton's expression 3-74098
- transport coefficients evaluation, analogy between Frisch-Berne and Watts perturbation theories 3-42910
- unitary transform of Hartree-Fock Hamiltonian giving rise to perturbation operator 3-67665
- unrestricted Hartree-Fock perturbation theory for molecules 3-54623
- vacuum polarization by external field, Stieltjes summability and convergence of Pade approximants 3-74362
- Van der Waals dipole-dipole interaction for C-H and O-H systems 3-63350

perturbation theory continued

- variational formula in quantum mechanics 3-66608
- vertex functions and polarisation operator in (4- ϵ)-dimensional field theory 3-59928
- vibrational energy transfer collisions between polyatomic mols. (*German*) 3-63552
- wave diffraction, finite bodies of revolution, stationary diffraction, method of perturbation of boundary forms (*Russian*) 3-70545
- Wilson's theory of critical phenomena 3-66710
- Yang Mills theory, deep Euclidean Green's functions, perturbative results for strong interactions 3-51980
- Yukawa potential, large coupling expansions for eigenenergies and Regge trajectories 3-74326
- ep interactions, influence of proton structure 3-59967
- ²⁴¹Am polycrystalline source, perturbation of α - γ angular correlation 3-43225
- Ge, drag photocurrent due to photon momentum in direct interband transitions 3-58304
- Ge, migration energy calc. of interstitial 3-50026
- H, high-order bound-bound transitions 3-71349
- H₂, polarisability depend. on internuclear distance 3-63435
- H₂ + H₂ near Van der Waals min., intermol. energy, perturbative procedure 3-49508
- H₂⁺, short range atomic interactions, Van Vleck perturbation treatment 3-71477
- He, dispersion energies by distinguishable electron perturbation method 3-78449
- He, perturbation-variational calc. for 1s² 1S 3-60351
- HeH²⁺, short range atomic interactions, Van Vleck perturbation treatment 3-71477
- (³He,t) reaction mechanism, 2nd order perturbation method with (He- α -t) process and DWBA 3-71123
- ³He in superfluid ⁴He, dilute soln., theory in nonorthogonal basis 3-55118
- NaCl many-electron theory of distorted lattices 3-55177
- P(ϕ) quantum field Hamiltonian perturbation 3-48977
- Si, migration energy calc. of interstitial 3-50026
- Ti II, lifetime, transition moments and energy calcs. HF and perturbation theory 3-71352

petrol engines see *internal combustion engines***petroleum industry**

- atomic absorption spectroscopy, trace metal determ., lubricating and crude oils, evaluation of carbon-rod atomiser 3-70485

pH

- ammoniacal negative emulsions, optical sensitisation, effects of silver halide particle size distrib., pH and Br⁻ conc. (*Russian*) 3-50856
- p-benzoquinone, photocycloaddition to cyclooctatetraene, laser excitation, effect of solvent acidity and oxygen 3-47580
- cyclooctatetraene, photocycloaddition of p-benzoquinone, laser excitation, effect of solvent acidity and oxygen 3-47580
- glass, electrolyte pH depend. of crack propag. 3-61211
- glass membrane potentials, heterogeneous-site, solid state theory 3-69484
- glycine, ¹⁵N enriched, aqueous solution, n.m.r., chemical shift, line shape, relaxation times 3-64570
- oscillations in one-dimensional membrane, computer simulation 3-73167
- quinolinium cation, acidity depend. of dual fluorescence 3-63497
- scales, based on synthetic sea water 3-65258
- water, pH, effect of various gases 3-53359
- Al₂O₃ colloidal dispersions, rheological props. 3-53287
- B(OH)₃ acidity constant in sea water 3-65257
- Fe(III) complexes with oxygen-containing ligands, effect on electronic spectra (*Russian*) 3-71524
- H₂CO₃, dissociation constant in sea water 3-65257
- U in acid media, electrochem. behaviour, influence of V, Cr and C additions (*French*) 3-47561

pH control

- No entries

pH factor see *pH***pH measurement**

- No entries

phase angle meters see *phase meters***phase changers** see *phase converters***phase comparators**

- electromagnetic, heat treated steel inspection appl. (*German*) 3-69417

phase-contrast microscopy see *microscopy***phase converters** see *phase converters***phase converters**

- see also *phase shifters*
- crystal oscillator, automatic phase tuning cct., with controlled phase inverter 3-54250

phase diagrams

- see also *phase equilibrium; phase transformations*
- acetone-chloroform, liquid-vapour equilibrium, const. temp. 3-64165
- acetone-diethyl ether, liquid-vapour equilibrium, const. temp. 3-64165
- antiferromagnet, order-disorder transition in mag. field, Monte Carlo method 3-68752
- cast structures, expanded TTD diagrams for homogenization description (*German*) 3-55764
- III-V compounds, mixed, solid/gaseous system, thermodynamic equilibrium 3-58186
- III-V semiconductor, thermodynamics of solns. of n-components 3-79468
- liquid crystal, nematic PAA, coherent neutron scattering determ. 3-40847
- methanol + carbon disulphide liq. sytem, crit. region thermal expansion curve 3-68384
- methanol + heptane liq. system, crit. behaviour of sp. ht. and coexistence curve 3-68383
- multicomponent systems, polynomial approximation for construction 3-75597
- polystyrene-cyclohexane system, cloud point curves near critical pt. 3-80489
- Potts model, three-state, anomalous tricritical points 3-62608

phase diagrams continued

- quantum lattice gas model rel. to supersolid existence 3-46735
- rare earth-Fe(Co)(Ni) alloys, Fe, Co, Ni magnetic and structural properties (*Rumanian*) 3-63982
- saline solutions, aqueous, metastable state rupture, transitions to liquid state phenomena (*French*) 3-79492
- saline solutions, aqueous, spontaneous rupture of supercooling and supersaturation states (*French*) 3-79493
- saline solutions, metastable aqueous, spontaneous rupture of supercooling and supersaturation states (*French*) 3-79491
- steam-water-ice, 2 dimensional bonded lattice model, first order approximation, long range and short range order 3-41006
- steel, microalloyed structural, metallographic investigations (*German*) 3-80202
- superconducting thin films, tricritical points 3-44163
- ternary, composite adsorption isotherm analysis 3-68491
- transitions in systems with long-range potential 3-74185
- variable composition mixtures, homogeneity region determ. 3-75625
- water emulsions, metastable state rupture, transitions to liquid state phenomena (*French*) 3-79492
- wustite, oxygen activities and phase boundaries 3-55843
- AgBr-CuBr mixed crystals, phase behaviour and lattice disorder, calorimetric obs. (*German*) 3-64184
- AgI-Ag₂WO₄, rel. to solid-state electrolyte formation for battery applic. 3-43892
- Al-Ga-P system 3-79467
- Al-W alloys, Al-rich, liquid-quenched, metastable phase behaviour 3-41696
- B-C system, electron microprobe studies, ZAF method (*French*) 3-48672
- BaF₂-(Y,Ln)F₃, Ln = Sm-Lu, at 880 C, using X-ray crystallography 3-79470
- BaFeO₄, thermal decomposition products of BaFeO₄, Mossbauer obs. 3-58451
- BaO-Nb₂O₅-Li₂O, tetragonal bronze phase homogeneity region 3-68230
- BaO-ZrO₂-Al₂O₃ subsolidus 3-72177
- BaO.5.5 Fe₂O₃, mag. phase analysis 3-58381
- Bi-Sb alloys, solidus construction, intercrystalline liquation 3-72836
- Bi₂O₃-Sm₂O₃ eutectoid, transform. deform., stress and temp. depend. 3-76231
- Bi₂O₃-WO₃ system, phase relations 3-76242
- Ca-Hg system, between -39 and 1000°C 3-60785
- CaF₂-NdF₃(YF₃) system phase relations and characteriz. (*German*) 3-47443
- Ca₂Ni_{1-x}Fe₂O₄ system, cryst. structure of NiFe₂O₄, CaFe₂O₄, Ca₂Fe₂O₅ phases 3-64144
- CaO-Al₂O₃-FeO-Fe₂O₃ system, phase relations, liquidus temp. 3-76340
- CaO-CaO.Al₂O₃-11 CaO.7 Al₂O₃.CaF₂, constructed from high temp. equilibrium, seven pertinent joins 3-76321
- CaO-Fe₂O₃ system, Mossbauer spectrometry (*German*) 3-47177
- CaO-MgO-SiO₂-V₂O₅ system, 1500°C 3-76337
- CaO-MgO-SiO₂-V₂O₅ system, 1450°C 3-76338
- CaSiO₃-Gd₂SiO₃ system, phase equilib., annealing and quenching method 3-68385
- CdS-CdTe, solidus and liquidus curves, DTA obs. 3-68388
- Co-Cr system, binary phase diagram calc. 3-41701
- Co-Ni system, binary phase diagram calc. 3-41701
- Co-Si eutectic alloy, struct. and mag. props. of phases 3-80201
- CoCr₂S_{4-x}Se_x system, new ferrimag. spinels 3-55074
- Cr-Fe-Si alloys, liquidus temperatures, ferrochromium silicide alloy composition range 3-50689
- Cr-Ir, intermediate beta, epsilon phases with Cr₃Si type, h.c.p. cryst. structures 3-53204
- Cr-N system, thermodynamic props. characteriz. 3-55845
- Cr-Ni system, binary phase diagram calc. 3-41701
- Cr-Rh alloy system, metallography, X-ray diffr., electron probe obs. 3-69193
- Cr-Si alloys, thermodynamic properties of liquid system at 1900 K 3-72835
- CrAs_{1-x}Sb_x mixed crystals 3-41347
- Cr₂O₃-Fe₂O₃-TiO₂-ZrO₂ system, compounds based on intergrowth of α -PbO₂, V₂O₅ structure types 3-68389
- CsCl melt-plasma, P- ρ -T phase diagram 3-49636
- Cu-Au, binary system, order-disorder transform. theory, phase diagram calc. 3-44562
- Cu-Au alloys, strain energy effect and melting 3-72832
- Cu-B eutectic alloy, unidirectionally solidified 3-76155
- Cu-S, rel. to Cu₂S cpd. formation, X=1.95-2.00, 80-105°C 3-75603
- Cu-Se-Sn system, DTA, X-ray phase analysis, microhardness, thermo-e.m.f. 3-72174
- Cu-Sn-Se system, DTA, microstructural and X-ray phase analysis, cross sections 3-72175
- Cu-Te system, Cu_{2-x}Te region, DTA anal. (*French*) 3-72181
- CuPt alloy, crystallographic ordering mechanism and modified microstruct. 3-80215
- DyInO₃, pressure-temperature stability fields 3-79469
- EuInO₃, pressure-temperature stability fields 3-79469
- Fe-Al-Ge alloy, solid solution, structure, hardness, elec. resist., conc. depend. 3-76159
- Fe-C system, metastable phase diagram 3-41693
- Fe-C system, pseudohexagonal Fe₂C₃ and Fe₃C-Fe₂C₃ eutectic studies 3-41692
- Fe-Co system, binary phase diagram calc. 3-41701
- Fe-Cr system, binary phase diagram calc. 3-41701
- Fe-Cr-Co(Mn)(Ni) systems, α + γ/ψ phase boundary determ. (*Czech*) 3-55757
- Fe-Cr-V, correl. between exper. and theoretical diagram based on binary comp. systems 3-72841
- Fe-Ni system, binary phase diagram calc. 3-41701
- Fe-Ni-Co system characteriz. 3-64815
- Fe-V system, thermodynamic props. and equil. diagram 3-69191
- Fe-V(W) alloys, thermodynamic variables, calcs., from phase diags. 3-64818
- Fe-Zn, diffusion of Zn into γ and α -iron 3-72840

phase diagrams continued

- Fe-Zn binary system, evaluation of p -loop, comparison with expt. results (*German*) 3-47356
 Fe-Zn-Al system, phase constitution at 450°C 3-53208
 FeCr₂S_{4-x}Se_x system, new ferrimag. spinels 3-55074
 Fe₂P, cryst. structure refinement, homogeneity range determ. 3-68232
 Ga-Mg (*German*) 3-80211
 GaAs_{1-x}Sb_{1-y} alloy single phase solid soln. range 3-75602
 GdInO₃, pressure-temperature stability fields 3-79469
 H, molecular solid, metallic solid and fluid phases, astron. appl. 3-42163
 H₂O-acetic acid-carbon tetrachloride, coexistence curve shape near plait point 3-75600
 He-methane mixture at high press., astron. appl. 3-42162
 HfO₂-CaO, HfO₂-Y₂O₃, phase relns. using X-ray analysis 3-75599
 HfO₂-Y₂O₃ solid solution, boundary detn., X-ray analysis 3-64153
 In-S system, downcooling obs. (*Russian*) 3-75596
 In₂Se₃, p-T-x, variable composition 3-64147
 K-Cs, calc. using heat of solution in solid and liquid phases 3-41007
 K-Rb, calc. using heat of solution in solid and liquid phases 3-41007
 KCl-LiCl-FeCl₃, KCl-LiCl-AlCl₃, immiscible systems, diagrams of melting, thermography (*Russian*) 3-52691
 Kf-ErF₃ system, phase diagram, cpd. structs. (*French*) 3-60703
 KNO₃-CsNO₃-NaNO₃, thermodynamic calc., thermography (*Russian*) 3-52692
 Kf-TbF₃, differential thermal, X-ray, crystalloptical anal., struct. 3-64148
 LiNbO₃-KNbO₃ system, X-ray diffr., Curie temp. 3-72590
 Li₂Se-Se (LiBr-RbBr eutectic) pseudoternary system, physicochemical and e.m.f. obs. 3-43863
 Li(Ta,Sb)_{1-x}O₃, X-ray diffr. study, ferroelec. props. 3-72589
 Mg-In system, thermodynamic props. of solid phases 3-58139
 MgO-Al₂O₃-TiO₂ system, phase relations, 1100-1550°C 3-76339
 MnCr₂S_{4-x}Se_x system, new ferrimag. spinels 3-55074
 MnSb-Sb-Bi system, determ. of MnSb liquidus close to eutectic line (*French*) 3-53205
 Mo-C-O, rel. to compound formation during sintering of Mo in organic binder 3-69353
 Mo-Cu-Ni alloys, boundaries of single-phase side fields 3-80221
 Mo-Ni system, determ. using diffusion couples and equilibrated alloys 3-53209
 Mo-Pt system, revision using resistivity, superconductivity, hardness and X-ray diffraction meas. (*French*) 3-58329
 Na₃AlF₆-CaF₂, differential thermal anal. in sealed crucible 3-75604
 NaCl-CdCl₂-SrCl₂ thermography, X-ray methods, Na₂CdCl₄ binary combination, eutectics, Van Rein point (*Russian*) 3-52692
 Na(D,H)_{1-x}(SeO₃)₂ crystals induction of β -phase by elec. field in y direction 3-72587
 Na₂O-Al₂O₃ system, polymorphism and Na₂O.2Al₂O₃ cpd. characterization. 3-72932
 Na₂O-B₂O₃-SiO₂ system, tie lines in metastable immiscibility region 3-55075
 Na₂O-Ca₃Al₂O₆, polymorphism, cubic, orthorhombic I, II and tetragonal cryst. forms (*French*) 3-72179
 Na₃PO₄-Pb₃(PO₄)₂ system, liquidus diagram 3-46697
 Na₂P₂O₇-Mg₂P₂O₇, D.T.A., hot stage microscopy and X-ray diffraction analysis 3-64149
 Nb-Au alloys (*German*) 3-44565
 Ni-C equil. diagram from carbon activity and solubility studies (*Czech*) 3-55769
 Ni-S(Se)(As)(Sb) systems, equiatomic comp. region studies (*French*) 3-46804
 Ni-W solid soln., interdiffusion coeffs., conc. depend., correl. with solidus line shape (*Russian*) 3-41712
 NpF₄-TlF, solid-liq. equilib. diag., phase identification (*French*) 3-60787
 PbBr₂-NaBr-CdBr₂, diagram of melting, thermodynamic calc. (*Russian*) 3-49967
 PbO-B₂O₃ system, miscibility gap 3-69360
 PbS_{1-x}Se_x, pseudobinary phase diagram and existence regions 3-79471
 PbZrO₃-SrCu_{1/3}Nb_{2/3}O₃ system, X-ray diffr. phase anal. dielec. props., Curie point determ. 3-72591
 Pd-W solid soln., interdiffusion coeffs., conc. depend., correl. with solidus line shape (*Russian*) 3-41712
 PrCo₃, Pr₂Co₁₇, Al substituted, struct. and phase relations, X-ray obs. 3-69194
 ϵ -Pu b.c.c. solid solution, retention at room temp. 3-76154
 Rb-Cs, calc. using heat of solution in solid and liquid phases 3-41007
 RbI, phase diag. at high press., comparison with KCl 3-68404
 Sb₂Se₃/Ti₂Se system, existence of Ti₉SbSe₆ and TiSbSe₂ by DTA (*German*) 3-55073
 Sb₂Se₃-GeSe₂, Sb₂Se₃-GeSe₂ systems, condition state diagrams, thermal, X-ray and microstructure anal. (*Russian*) 3-49968
 Se-I system, equilibrium, liquid state, viscosity, solid state 3-72173
 Si-C phase diagram, Czochralski growth of Si, influence of C 3-41645
 Sm-Co-Cu system, hypothetical ternary phase diagram 3-50424
 SmCo₅, Sm₂Co₁₇, Al substituted, struct. and phase relations, X-ray obs. 3-69194
 SrFe₁₅O₂₇, oxygen partial pressure and temp. variation 3-52690
 SrMnO_{3-x}Mn₃O₄, phase relations, elevated temps. 3-43864
 SrO-BaO-Al₂O₃ system, solid state equilib., X-ray struct. anal. 3-72998
 TaS_{2-x}Se_x, phase diagram, X-ray analysis, atomic scattering factors 3-41016
 TbF₃-Kf, differential thermal, X-ray, crystalloptical anal., struct. 3-64148
 TeO₂-Fe₂O₃, phase equilibrium and elec. conductivity 3-60784
 Ti-S system polytypes characterization (*French*) 3-46633
 TiO₂-K₂B₂O₇ system, thermal analysis 3-68387
 TiO₂-Na₂O-B₂O₃ system, thermal analysis 3-68387
 U-B system, temp.-comp. diagram 3-72940
 U-C system, phase boundary between UC₁₄ and β -UC₂ 3-43298
 U-Se and U-Se-C systems, solid-state relationships 3-43299
 UO₂-SiO₂ system melts, spinodal decomp. and primary crystn. 3-72984

phase diagrams continued

- U_{0.8}Pu_{0.2}C-W system, peritectic behaviour 3-47451
 V_{1-x}Cr_xO₂, (0 $\leq x \leq 0.15$), magnetic susceptibility, DTA, X-ray diffr. meas. (*French*) 3-79472
 V₂O₅-MoO₃, melting points, binary system 3-80582
 YEu garnet, empirical binary phase diag. rel. to liquid phase epitaxy 3-44287
 Y₂O₃-CaO system characteriz. 3-76241
 Yb-Pd system 3-64151
 ZnGeP₂ pseudo-binary, ZnP₂-Ge join in system, eutectics 3-72180
 Zr-H, γ - and δ -phase hydride form. on cooling from α -phase field 3-72864
- phase equilibrium**
see also phase diagrams; phase transformations; solutions
 alkali halide aerosols, relaxation behind shock wave 3-54824
 alloy, f.c.c. solid solution, homogeneous, ordered configs., Bragg-Williams-Gorsky model 3-41703
 alloy, thermodynamic props. of condensed phases, eval. and analysis, model approach (*German*) 3-41702
 alloys, phase analysis, methodology (*German, English*) 3-69202
 chain molecule liquids, calculation of vapour-liquid and liquid-liquid phase equilibria using Prigogine theory 3-65124
 dimers, rigid, linear, restricted lattice model, symmetry breakdown in equilibrium states 3-59815
 ethane-ethylene solutions, molecular thermodynamics in normal and critical regions 3-65121
 fluid mixture and polarised fluid phase equilib. 3-66711
 glasses, semi-liquid, activator segregation and energy transfer between Nd³⁺ and Yb³⁺ (*Russian*) 3-64735
 interfacial behaviour, stability analysis 3-78941
 Lennard-Jones fluid, surface density and tension, stat. mech. and quasithermodynamic calcs. 3-60790
 liquid metal alloys, simple mean field approach to phase separation 3-58132
 liquid mixtures theoretical treatment by means of equilibrium models (*German*) 3-44746
 liquid-liquid equilibrium data correlations, properties of NRTL equation 3-46713
 liquid-liquid partition coefficient, static and dynamic chromatography 3-73169
 liquid-vapour, heat conducting fluids in e.m. field 3-72165
 liquid-vapour system, molecular exchange 3-49983
 liquid-vapour system, propagation near the critical point 3-60773
 metal surfaces, adsorption, equilib. and reversibility (*French*) 3-79559
 methane-Ar system, h.p. vapour-liquid equilibrium and activity coeffs. 3-64156
 methane-CO system, h.p. vapour-liquid equilibrium and activity coeffs. 3-64156
 methanol + carbon disulphide liq. system, crit. region thermal expansion 3-68384
 methanol + heptane liq. system, crit. behaviour of sp. ht. and coexistence curve 3-68383
 minerals, liquidus boundary shifts, effect of dissolved metal oxides on SiO₂ content, significance in magma genesis 3-80653
 multicomponent liquid-liquid equilibrium, Renon's and Black's activity equations 3-58130
 multicomponent systems, equal-g surfaces for heterogeneous equilibria 3-56000
 muscovite plus quartz, high temp. stability, hydrothermal studies, nucleation mechanism 3-44770
 nitrobenzene/2,2,4-trimethyl pentane binary solution, critical soln. temp., dielec. consts. and losses 3-44364
 one-dimensional kinetic system, equilibrium props. simulation 3-59809
 potentiostat, phase anal., anal. of nonmetallic inclusions 3-48472
 propylene-CO₂ solutions, molecular thermodynamics in normal and critical regions 3-65121
 solid solution, double pseudobinary, boundary phase stability and crit. phenomena 3-80212
 solutions in normal and critical regions, molecular thermodynamics 3-65120
 stainless steel, martensitic cast, phase anal., microprobe anal., electron microscopy 3-76179
 stationary, silica-containing polymers, for gas chromatography 3-66428
 stationary phase, effect of mol. wt. on gas chromatographic data, activity coeff. 3-66429
 stationary phase, standard, rel. to gas chromatography 3-62333
 steel, low-alloy, phase anal., microprobe anal., electron microscopy 3-76179
 steel, phase analysis, methodology (*German, English*) 3-69202
 ternary aqueous solutions, water activity from binary data 3-65122
 transition metal alloys of extraordinary stability, generalized Lewis-acid-base interactions 3-64823
 vapour-liquid equilibrium, overall area tests for thermodynamic consistency, effect of random error 3-58119
 vapour-liquid equilibrium and gas PVT props., precision apparatus 3-62025
 water-benzene-ethyl alcohol ternary system, shear viscosity and u.s. absorpt. near plait pt. 3-64204
 Al-Fe alloys, rapidly solidified, iron precip. behaviour (*German*) 3-41744
 Al-Ga-As-Sn quaternary III-V system 3-46764
 Al-W alloys, Al-rich, liquid-quenched, metastable phase behaviour 3-41696
 Al₂O₃-Na₂O system, range of existence and stability of β and β' alumina (*French*) 3-69365
 Ar-CO system, h.p. vapour-liquid equilibrium and activity coeffs. 3-64156
 Ar-N₂ solutions, molecular thermodynamics in normal and critical regions 3-65121
 As-Bi(Pb) alloys, liq., thermodynamics props. (*German*) 3-72839
 Au-Cr cosputtered films, up to 49 at.% Cr 3-43963
 Au-Sn phase prepared by splat cooling, metastability 3-64821
 BaO-CeO₂-TiO₂ system, subsolidus phase relations 3-44650
 BaO-Ln₂O₃ system, intermediate cpds. 3-72172
 CaO-Al₂O₃-FeO-Fe₂O₃ system, phase relations, liquidus temp. 3-76340
 CaO-MgO-SiO₂ system, stability relations of bredigite 3-76239

phase equilibrium continued

- CaO-MgO-SiO₂-V₂O₅ system, 1500°C 3-76337
 CaO-MgO-SiO₂-V₂O₅ system, 1450°C 3-76338
 CaO-MgO-iron oxide system, TiO effects on equil. among refractory phases 3-44655
 CaO-P₂O₅-H₂O system, 300 to 600°C at 2 kb H₂O pressure 3-69488
 CaSiO₃-Gd₂SiO₅ system, annealing and quenching method 3-68385
 CeO₂-SmO_{1.5} and CeO₂-NdO_{1.5}, MO₂ (fluorite)-MO_{1.5} type mixed oxides, phase relations 3-64181
 Cr-Fe-Si-C alloys, high carbon ferrochromium alloy composition range 3-50688
 Cr-S system, nonstoichiometry and thermodynamics 3-41019
 Cr-TiC and Cr-ZrC pseudobinary systems 3-53270
 CrAs_{1-x}Sb_x mixed crystals 3-41347
 CrO₂-Cr₂O₃ phase boundary, high O₂ press. 3-69354
 Cu₂Mn₃O₄ system, stability range of cubic spinel struct. 3-60786
 (Fe, Ni)₂S₃, eolite nodules, kimberlite pipe, South Africa, phase equilib. 3-44764
 Fe-Cr system, α/γ equil. thermodynamics, chromium distrib. between ferrite and austenite 3-69197
 Fe-Cr-V, correl. between exper. and theoretical diagram based on binary comp. systems 3-72841
 Fe-Cr-V-C system, carbide equil. with α and γ solid solns., chem. comp. (Czech) 3-55759
 Fe-Mn system, α/γ equil. thermodynamics, chromium distrib. between ferrite and austenite 3-69197
 Fe-Mn-C alloy, liquidus and solidus temps., Nb additive effects (Russian) 3-44561
 Fe-Ni alloys, struct. modifications during recovery of equil. by tempering subsequent to cooling 3-64930
 FeO-Fe₂O₃-TiO₂ for study of magnetomineralogical alteration trends, interpretation of magnetic anomaly patterns and contrast profiling 3-58933
 Ga-As-Ge-Sn system, 800°C liquidus isotherm 3-46765
 GaAs_{1-x}He system, equilib. comp. of gas phase, 800-1300 K, transport of GaAs 3-72798
 He-methane mixture, high-press. meas. appl. to Jupiter and Saturn 3-42162
³He-nO₂ and ³He-nH₂ binary systems, liquid vapour equilibrium 3-50041
⁴He-nD₂ and ³He-nH₂ binary systems, liquid vapour equilibrium 3-50041
 KNO₃-LiNO₃-AgNO₃ ternary system, equilibrium study 3-60788
 Mn-B-O system, phase relations, influence of Mn:B ratio 3-79466
 Mn_{1-x}Fe_xAs phase, crystal structure, mag. props. 3-40901
 N₂, Ar, methane ternary and binary systems, liquid-vapour equilibria at 112.00K, Gibbs free energy calc. 3-58120
 N₂-Ar-CH₄ system, vapour-liquid equilibrium (French) 3-64145
 NaAlO₂-SiO₂-H₂O mineral, phase equilibria, Gibbs energy of formation 3-44773
 NaNO₃-LiNO₃-AgNO₃ ternary system, equilibrium study 3-60788
 Na₂O-SiO₂ glass, immiscibility temp., Al₂O₃ and Ga₂O₃ additions effect 3-69383
 Nb-Al-Si alloy, at. absorption spectroscopy (French) 3-50678
 Nb-Al-Si alloy, isothermal sections at 1500°C and 1300°C, Nb(Si,Al)₂ phase behaviour (French) 3-50677
 Nb-W-Mo-Zr, aged, acrbide phase distrib., electron microscope studies (Russian) 3-41721
 NbCl₅, molten, Raman spectra, 220-320°C (German) 3-52702
 A-Nd₂O₃-A-La₂O₃ and A-Nd₂O₃-C-Y₂O₃, investigation of the binary systems (French) 3-64152
 Ni alloy, cast, phase anal., microprobe anal., electron microscopy 3-76179
 Ni alloys, phase analysis, methodology (German, English) 3-69202
 Ni-Ta-Cr-Mn system dendritic duplex crystals, topography 3-41725
 NiAl-G(Mo) eutectic composites, directionally solidified, stability 3-69198
 Pb_{1-x}Cd_xSe, phase widths 3-75601
 PbF₂-Ln₂O₃ system, new phases 3-72176
 Pb_{1-x}Mg_xSe, phase widths 3-75601
 PbO-B₂O₃ system, miscibility gap 3-69360
 Pt_(s)+Cl_{2(g)}, Pt₆Cl₆ formation (German) 3-80539
 Re-ZrC system, microscopy, X-ray phase, chem. anal., high temp. 3-72978
 Se, DTA study 3-72005
 SiO₂-Al₂O₃ system, stable and metastable equil. 3-76238
 Sn₄As₃-Pb-SnAs ternary subsystem 3-49966
 Sr-Mo-O system, compound formation, X-ray obs. 3-68386
 Sr(NO₃)₂-Nd(NO₃)₃-Na₂WO₄-H₂O system, aqueous solutions, solid phase 3-76422
 SrNb₂O₆-NaNbO₃, DTA, Curie point, crystallographic meas. (French) 3-79994
 SrO-BaO-Al₂O₃ system, solid state, X-ray anal., 1400°C 3-72998
 Sr₂SiO₄-Sr₂GeO₄-Ba₂GeO₄-Ba₂SiO₄, solid solubility, polymorphism, lattice constants 3-41803
 TeO₂-Fe₂O₃, phase equilibrium and elec. conductivity 3-60784
 Ti alloys, solid soln. strengthening and phase stability, physical basis 3-64809
 TiC-Cr pseudobinary systems 3-53270
 TiO₂-K₂O-B₂O₃ system, thermal analysis 3-68387
 TiO₂-Na₂O-B₂O₃ system, thermal analysis 3-68387
 TiO₂-SnO₂ system, subsolidus equil. 3-76240
 U-Pu-N ternary system, equil. assessments 3-46136
 U-Se and U-Se-C systems, solid-state relationships 3-43299
 UC₂, bainitic transforms., carbide phase nomenclature 3-55836
 UO₂-MgO system, using X-ray diffraction methods 3-74725
 V₂O₅-Na₂O-Fe₂O₃(Cr₂O₃)(MgO), ternary, solid-liq. 3-46696
 WC-ZrC system, solid solubility limits 3-72939
 ZrC-Cr pseudobinary systems 3-53270
 ZrO₂, Sc₂O₃-stabilized, high temperature neutron diffraction study 3-64150
 ZrO₂-Er₂O₃(La₂O₃)(Y₂O₃) cubic solid soln. stability below 1500°C (French) 3-76309

phase equilibrium diagrams *see* **phase diagrams****phase-locked loops**

- ECL universal counter application 3-40026
 microwave frequency lock system, digital, design and performance 3-77578

phase measurement

- equipment for dynamic measurements 3-51651

phase measurement continued

- laser distance meas. system comparing phase of modulating signal 3-51960
 multiscale system, maximum likelihood estimation 3-70259
 radiation field, microscopic, using ideal laser amplifier 3-66892
 sky wave direction at l.f. and v.l.f. 3-80791

phase meters

- for dynamic measurements of phase of electrical signal 3-51651

phase modulation*see also* **phase shift keying**

- guided optical wave, bulk acoustic wave interaction 3-55545
 laser pulse shaping, self-phase modulation in ruby, high power amplification, theory and experiment 3-48939
 of light by u.s. (Russian) 3-66758
 Mossbauer γ -rays, sideband intensities treatment 3-67257
 t.w. laser phase modulator, using rectangular waveguide loaded with electro-optical material (Korean) 3-77544
 GaP, p-n junction, of He-Ne laser light, by Pockels effect 3-53922

phase shift circuits *see* **phase shifters****phase shift keying**

- s.w. ionospheric propagation, phase instability distribution parameters (Russian) 3-42020

phase shift microphones *see* **microphones****phase shifters***see also* **phase converters**

- latching, using GdYFe garnet: Co²⁺ material props. 3-47097

phase space methods

- circularly symmetric waves in nonlinear medium, phase-plane analysis 3-54196
 neutron transport eqn., one-dimensional, application of phase-space finite elements 3-60247
 quantum statistics, reconstruction, refutation of Bell Wigner locality argument 3-74154
 rigid body, torque-free rotational dynamics, nonlinear oscillator analogue 3-66514

phase transformations*see also* **liquid-vapour transformations**; **order-disorder transformations**; **phase diagrams**; **phase equilibrium**; **solid-liquid transformations**; **solid-state phase transformations**; **solid-vapour transformations**

- apparatus, press. up to 40 kbar, temp. 2 to 400 K 3-39885
 BEA liq. cryst. transition at 25°C 3-54924
 ceramic, thermoplastically produced, ion-exchange, BL material 3-76317
 cholesteric-smectic phase transitions, cholesteric pitch change 3-54920
 cholesterol derivatives, optical study, blue phase in amorphous-cholesteric transition 3-72000
 cholesteryl nonanoate, fluoresc. of pyrene and phenanthrene impurities, phase transitions 3-55685
 cholesteryl valerate, liquid crystal, specific volume obs. up to 1000 atm and temp. range 80-129°C 3-57987
 critical exponents, higher order contrbs. 3-49963
 critical points of third order, scaling hypothesis and data collapsing 3-45742
 critical region, quantum field theory, validity of bootstrapping and length scaling 3-74178
 cryogen, liquid, thermodynamic instability, contact with warmer host liquid 3-49997
 p-cyanobenzylidene-p'-octyloxyaniline, elastic constants near second order nematic-smectic phase change 3-58064
 Earth crust, motion due to subcrustal phase transition 3-65190
 eigenvalue degeneracy of eight-vertex transfer matrix 3-42906
 ferroelectric, interacting an harmonic oscillators model, phase transition 3-41489
 first-order, melting, entropy determ. 3-72183
 glass transition, confidence limits for the abscissa of intersection of two linear regressions 3-66504
 glassy polymers, thermodynamics 3-46718
 Goldstone mode freq., phase transitions, symmetry breaking and asymptotic props. 3-49956
 Goldstone-mode frequency, phase transitions, symmetry breaking, asymptotic properties 3-70731
 gravitational radiation from relativistic phase transitions, generation and detection 3-59801
 hard sphere system, thermodynamic properties (German) 3-62628
 Heisenberg hamiltonian with single-ion anisotropy and antisymmetric Dzialoshinsky-Moriya interactions, critical behaviour 3-58358
 hierarchical model, Dyson, spherical, simulation of long-range Ising problem, phase transition critical temperature 3-59816
 ideal Boson film, specific heat, scaling functions 3-66689
 Ising model, 3-body interactions, lower bound for magnetisation and critical temperature 3-66693
 Ising model, simple cubic structural transformations at interface 3-59821
 Ising model, two dimensional, transfer matrix for pure phase, pair correlations, relation between phase transition and spectrum degeneracy 3-60946
 isotropic Bose system, helicity modulus, superfluidity, scaling 3-70734
 liquid crystal, nematic to isotropic, static solutions for pipe 3-68159
 liquid crystal, nematic-cryst. transition, lattice theory 3-79232
 liquid crystal, smectic A-nematic, 2nd order, dynamics of fluctuations (French) 3-49845
 liquid crystal, smectic-A to nematic transition, second order, orientational order 3-54925
 liquid crystals., angular correls., integral eqn. approach, transition props. 3-43750
 many-particle systems, macroscopic collective excitations 3-74181
 MBBA, mag. susceptibility through liquid cryst.-isotropic liquid phase transition 3-49842
 metal-ammonia solns., metal-nonmetal transition, transport props. anal. 3-44126
 mixture exhibiting phase separation, mean spherical model 3-54183
 p-nitrobenzylidene-p'-octyloxyaniline, second order nematic to smectic phase transition 3-58507
 nuclear, superfluid to normal state, schematic two-level model of rotation at high angular momenta 3-57483

phase transformations continued

- nuclear matter, $N=Z$, multiparticle nuclear forces, from pi-meson spectrum 3-60105
 nuclear matter, pion condensation 3-67248
 order parameter fluctuations in external fields near phase transition points (*Russian*) 3-40196
 particle fluid mass transfer, multiparticle system 3-63759
 partition function in several complex variables, zeros limiting distribution 3-66713
 polymer combinations, plasticity elasticity phase boundary, effect of intermediate layer (*German*) 3-61215
 polystyrene, thermodynamic stability limits, rel. to glass transition (*German*) 3-60675
 probability, adiabatic and nonadiabatic, 2 unidimensional linear terms with inclinations of differing sign (*Russian*) 3-64154
 quantum fluid-solid transition, short range, square well repulsive potential 3-57155
 rubber, stress relaxation, effect of infrasonic vibration (*German*) 3-65011
 spectral density method applied to systems showing phase transitions 3-62599
 statistical mechanics of long-range order, method of symmetry-breaking potential 3-59817
 thermodynamic, critical points of complex systems, classification scheme by order, notation 3-42907
 thin films, role of size-effects, bulk sample instability (*German*) 3-46771
 topological classification, critical exponents 3-77930
 tricritical phase transitions theory, renormalisation group approach 3-47024
 Van der Waals fluid near critical point, Yang-Lee distrib. 3-57175
 Webster dunite, shock compression and phase transitions at high pressure 3-59512
 Cr-Ni steel, austenitic stainless, a.c. electroetching for metallographic differentiation of δ -ferrite (*German, English*) 3-64866
 Cu-Al system, martensitic and eutectoid transformations, thermodynamics 3-80200
 Fe, molten, structural, polymorphic, short-range order 3-58616
 He, liquid heat flow below the second order transition point 3-58161
 ^3He , liq., B transition, first order character 3-79543
 $\text{PrO}_x\text{-O}$ system, pseudophase behaviour in epsilon and iota regions 3-64180
 Se film, glass, crystalline, liquid, vapour reversible transformations, electron beam induced 3-72006

phase transitions see *phase transformations***phased locked oscillators** see *parametric oscillators***phi mesons**

- boson triad (ρ', ω', ϕ') approach to $\text{pp} \rightarrow \text{KK}$, 700 MeV/c 3-62873
 electroprod. at high virtual-photon four-momentum 3-52009
 0 cross-section, width and S-wave production in $\pi\text{-p}$ interaction 3-70975
 $e^+e^- \rightarrow \phi + \text{anything}$, low, high energy, $\phi \rightarrow \text{K}^+\text{K}^-$, study of reactions 3-59968
 $e^+e^- \rightarrow \text{hadrons}$, duality relation between vector meson formation and scaling behaviour 3-70932
 ep electroproduction of ϕ , 19.5 GeV, cross section 3-67039
 K^0K^0 decay via ϕ reson., charge asymmetry 3-52000
 $\text{IN} \rightarrow \text{IN}_0$, lepton polarisation, one-photon approximation anal., decay 3-78145
 $\omega\phi$ mixing hypothesis, description of e.m. decay of neutral meson 3-59966
 $\rho - \phi$ e.m. mixing parameter, appl. to $\phi \rightarrow \pi\pi$ decay and $e^+e^- \rightarrow \pi\pi$ 3-49005

philosophical aspects

- see also *humanities*
 conceptually complete physics and Weizsackers hypothesis (*German*) 3-42491
 Galileo and the progress of science, criticism of Feyerabend's work 3-56593
 generalised quantisation, reformulation of fundamentals of microscopic physics, comments 3-48748
 generalised quantisation, reformulation of fundamentals of microscopic physics (*French*) 3-48749
 logical analysis of physical theories 3-61952
 quantum mechanics, criticism of Houtof's work 'Quantification Generalisee' 3-66611
 quantum mechanics, natural philosophy based on induction 3-74092
 quantum mechanics, realistic explanation, new approach 3-66626
 quantum mechanics and interpretations of probability theory 3-53807
 quantum theory generalised quantification, reply to criticisms (*French*) 3-66612
 reality and understanding in science 3-70223
 reciprocity in uncertainty relations 3-74119

phonographs see *gramophones***phonon drag** see *electron-phonon interactions***phonon-electron interactions** see *electron-phonon interactions***phonon-phonon interactions**

- anisotropic insulator, three-phonon scatt. processes, variational treatment 3-68374
 clathrates, vibrs. far i.r. spectra, mol. crystals 3-72661
 dielectric crystals, estimation from heat pulse interaction 3-55051
 eigenvector for interaction matrix, phonon relax. 3-43846
 lattice thermal conductivity, theory 3-68377
 optical, long-wavelength, coupling in presence of external forces 3-46684
 quantum crystal, harmonic single-particle basis, transformation to self-consistent harmonic approximation 3-48760
 quasiparticles in solid state, theory, expt. (*Japanese*) 3-72334
 thermal, lattice cond., high-temp., three-phonon scatt. 3-50034
 thermal conductivity, high temp., relax. time approx. 3-68375
 thermal conductivity, low temp., relax. time approx. 3-68376
 Al_2O_3 , corundum, multiphonon absorpt., 1100-2500 cm^{-1} (*Russian*) 3-80048
 Bi, hypersonic attenuation, Bragg light scatt. by sound obs. (*Russian*) 3-79435
 $(\text{Bi}_{1-x}\text{Sb}_x)_2\text{Te}_3$, $\text{Bi}_2(\text{Te}_{1-x}\text{Se}_x)_3$, semicond., rel. to thermal cond. 3-68451

phonon-phonon interactions continued

- He, second sound in solid, effects of collinear and non-collinear three phonon processes 3-55120
 $\text{NH}_4\text{Br}(\text{Cl})$, lambda order-disorder transition, u.s. obs., mode-mode coupling theory 3-41000
 NaF, second sound in solid, effects of collinear and non-collinear three phonon processes 3-55120
- phonons**
 see also *elastic waves; electron-phonon interactions; lattice dynamics; lattice phonons; phonon-phonon interactions; spin-phonon interactions*
 n-alkanes, liq., hypersonic phonon velocity, 20-140°C 3-80053
 detection, using supercond. tunnel junction 3-44175
 Goldstone mode freq., phase transitions, symmetry breaking and asymptotic props. 3-49956
 He II liquid/solid interface, h.f. phonon transmission 3-64226
 Kapitza thermal boundary resistance, theory including phonon scattering within either material 3-60779
 liquid alloy, rel. to partial struct. factors and electronic correl. functions 3-57981
 liquid metal, rel. to partial struct. factors and electronic correl. functions 3-57981
 many interacting waves far from thermal equilibrium, statistics 3-43039
 metal solid-liquid interface, phonon thermal resistance 3-75588
 noncrystalline solids, theory of phonon-like excitations 3-79454
 nuclear, self-consistent random phase approximation amplitudes, many fermion model 3-78273
 organic liquids, Brillouin scattering, thermal waves velocities determ. 3-61042
 scattering by paramagnetic ions, drone-fermion representation, spin-phonon system lifetimes 3-40990
 Al tunnel diodes, 870 GHz phonon emission 3-55381
 Au:Gd- ^3He , improved thermal contact at ultralow temps. 3-52740
 CdS phonon maser structures, u.s. wave propagation 3-53788
 CdS phonon masers, light diffraction studies 3-53785
 He, solid, b.c.c. ground state energy and phonon dispersion, numerical calcs. 3-64231
 He II, liquid, multi-branch structure of excitation spectra 3-60818
 He II, phonon dispersion curve, eff. of weak intermed.-range attraction on low-momentum part 3-52733
 He II, sound propag. transport eqn., numerical soln. 3-64229
 He II, superthermal monochromatic phonon dispersion and attenuation 3-68462
 He II solid body boundary, Kapitza temp. discontinuity, sound attenuation 3-75650
 He II/solid interface, h.f. transmission probability, spectrum 3-72247
 HeII, few-phonon structure functions 3-68457
 ^3He , anisotropic phonon energy, effect on normal fluid density, second and fourth sound 3-68466
 ^3He - ^4He liquid mixtures elementary excitations energy spectrum 3-75651
 ^3He - ^4He soln., splitting of phonon spectrum 3-68468
 ^4He , liquid, excitation spectrum, three phonon vertex corrections, liquid struct. function 3-79537
 ^4He , superfluid, dissipative coefficients calc., Boltzmann equation solution for phonons and rotons 3-43915
 ^4He , superfluid, inelastic neutron scatt. from free surface, ripplon spectrum 3-68463
 ^4He II, liquid, phonon scattering effects on electron bubble mobility 3-72243
 ^4He II under pressure 3-43913
 ^4He liquid, structure and excitations, review 3-58158
 Ni, pulse heating, thermal energy transfer to liquid He, mechanism 3-72246
 Pd:Fe- ^3He , improved thermal contact at ultralow temps. 3-52740
- phosphorescence**
 see also *fluorescent screens; phosphors*
 acetaldehyde, photoluminescence, temperature, pressure, and excitation wavelength effect 3-46313
 acridine, amino derivatives, quantum yields of interconversion 3-76480
 acridine dyes, dication $1 \rightarrow A_n$ band polarization meas. (*French*) 3-69050
 aldehydes, static and dynamical pot. surface distortions in $^3A''(n\pi^*)$ states 3-63382
 alkaline earth sulphides, stimulation spectra structure and trap processes (*Russian*) 3-76059
 amines, non-planar aromatic, spin-forbidden electronic transitions 3-46237
 aminopyridines, phosphoresc. emission and polarization, triplet states 3-65101
 anthracene-pyromellitic dianhydride, zone-refined crystals, charge-transfer spectra 3-61269
 aromatic hydrocarbons, $S_1 \rightarrow T_1$ intersystem crossing process, PMDR obs. 3-44731
 aromatic molecules, electron excitation energy transfer to DPPH in solid solns., luminesc. yield 3-76484
 aromatic triple bond molecules, description of radiative triplet props. 3-67841
 aromatics in fluid dimethylmercury, room temp. phosphoresc. 3-47570
 arylketones in benzene soln., substituent effect on triplet lifetimes 3-76475
 benzaldehyde electronic emission spectrum, molecular vibrations 3-67843
 benzene, isotopic mixed crystals, 1.8 K, lifetimes, trap-trap triplet energy transfer 3-80102
 benzene and methyl and deuterio derivatives, phosphorescence lifetime, solvent effects 3-72707
 benzene in rare gas hosts, triplet lifetimes and emission spectra, external heavy atom effects 3-55675
 benzophenone, ethanol, water solution, hydrogen bonding, blue shift 3-64710
 benzophenone, quenching and bimolecular annihilation rate const. by long-lived guest triplet states determ. 3-64705
 benzophenone, undistorted triplet state, static and dynamic paramagnetism 3-76478

phosphorescence continued

- benzophenone-naphthalene system in rigid solns., triplet-triplet excitation transfer obs. 3-53329
 1-benzoyl-8-benzyl-naphthalene, deuterium effects on phosphoresc. and photochem. activity 3-76470
 1-benzoyl-8-benzyl-naphthalene and 1-benzoyl-naphthalene, viscosity-depend. phosphoresc. 3-76469
 biacetyl, small molecule behaviour and 3B_g state 3-75058
 biphenyl:naphthalene- d_8 , polarisation of delayed fluorescence and phosphorescence emissions 3-69053
 biphenyl guest-carbazole host mixed crystal, temp. depend. of spectra, trap emission 3-76039
 carbon tetrachloride matrix, aromatic molecules, quasiline phosphoresc. spectra, external heavy atom effect 3-72743
 circobiphenyl, phosphorescence, E-type delayed fluorescence (German) 3-69069
 complex organic molecules, decay kinetics, high aperture ratio installation 3-73725
 copper phthalocyanine, spectra, temp. depend. and decay time 3-72710
 coronene, luminescence and vibrational spectra 3-60460
 N,N-dialkyl-p-cyanoanilines self-complex in glassy solutions 3-54674
 1,3-diazaazulene, mixed cryst. polarization obs., nitrogen substitution effects 3-41857
 dibenzofuran, lowest singlet state obs. 3-67804
 p-dichlorobenzene, α - and γ -phases, defect sites 3-80104
 p-dichlorobenzene, T₁ spectra, modes, fine structure 3-69052
 1,3-diphenylpropane, intramol. triplet excimer form. 3-44732
 DNA, excited states, triplet quenching, photosensitisation 3-63588
 fluorene, pyrene- d_{10} doped, triplet annihilation behaviour 3-64708
 glass face plate of LI 604 dissector, pulse noise dependence (Russian) 3-77501
 glyoxal vapour, yields, lifetimes, quenching, 4358 Å 3-80566
 n-heptane matrix, aromatic molecules, quasiline phosphoresc. spectra 3-72743
 1-indanone, dual phosphoresc., triplet states 3-55975
 metalloporphyrins, energetics, triplet-triplet energy transfer 3-67847
 metalloporphyrins, spin-orbit coupling and heavy atom effect on radiationless transitions 3-63498
 methylbenzenes, impurity emission 3-80105
 methylcyclohexane matrix, quasiline phosphoresc. spectra of benzene homologues and derivatives 3-72741
 methylcyclohexanol matrix, quasiline phosphoresc. spectra of benzene homologues and derivatives 3-72741
 methylquinoline, 2-, 4-, 6-, 7-, 8-, in crystalline n-paraffins, quasiline phosphorescence spectra, vibrational 3-50609
 molecular excited states, optically detected electron spin locking and rotary echo trains 3-43492
 molecules oriented in stretched polymers, phosphoresc. polarization 3-40641
 naphthalene, localisation of phonon sidebands, T₁ to S₀, host crystals 3-69051
 naphthalene, spectra, in chemically mixed crystals 3-69073
 naphthalene Franck-Condon factors, correl. function anal. T₁-S₀ transitions 3-64709
 naphthalene in p-dihalogenated benzene host crystals 3-80106
 1,5-naphthylidene in durene, polarized phosphoresc., assignment of lowest singlet n,π^* state 3-76472
 1,5-naphthylidene in durene mixed cryst. spectra, isotope effect on localized phonons 3-58542
 organic molecules, luminescence spectrometry, at low temperatures 3-59700
 oxamides, emission and absorption spectra anal. of excited singlet states 3-78833
 oxygen dominated phosphors, excitation spectrum in 3-21 eV region (Russian) 3-50611
 n-paraffin matrix, fluoresc. and phosphoresc. emission and excitation spectra of n-ethyl-carbazole 3-72744
 paraffin matrix, phosphoresc. spectra of polyatomic molecules with non-rigid struct., low temp. 3-72731
 paramagnetic metal complexes, with porphyrin, quasiline luminesc. and absorpt. spectra 3-72732
 2-Phenylbenzothiazole in frozen solutions at 77°K high-resolved phosphorescence spectra 3-64706
 2-Phenylbenzoxazole in frozen solutions at 77°K high-resolved phosphorescence spectra 3-64706
 phthalocyanines, thin films and solutions, emission spectra 3-61074
 pyrene, pure cryst., phosphoresc. emission struct. 3-64707
 quinazoline in durene and naphthalene host cryst., $\pi^* \rightarrow \pi$ phosphoresc. 3-69028
 quinoline, phosphorescent, ENDOR in 3.601 GHz zero-field transition, ^{14}N quadrupolar splitting 3-46316
 quinoline in durene host, multiple spin echoes in photo-excited triplet state 3-80564
 quinoxaline in durene host, phosphoresc. spectra from spin sublevels of low emissivity 3-80565
 rhodamine 6G, O₂ quenching constant for triplet state from laser characs. 3-64728
 Shpol'ski systems, intensity of solute-solvent interactions 3-72728
 spectrometer, high resolution, for simultaneous recording of phosphorescence and luminesc. 3-42563
 tetracyanobenzene-biphenyl complex single crystals, spin alignment in charge transfer phosphorescent state 3-61059
 N, N', N'- tetramethyl-p-phenylenediamine, added electron trap effects 3-41571
 4-thiouridine, decay kinetics, temp. depend., excited states deactivation 3-73154
 thioxanthone, lifetime in rigid glass, 77K 3-80562
 toluene solid solution, mechanism of singlet, triplet state formation, via aromatic additives radioluminescence 3-76467
 transition metal complexes, $^2E_g \rightarrow ^4A_g$ transition, vibr. anal. 3-76061
 transition metal phosphine and arsine complexes, metal localized emission 3-41855
 trifluoromethyl derivatives 3-80105
 triplet state zero-field transitions determ. by PMDR, absolute polarization meas. 3-61009

phosphorescence continued

- vanadyl complex of porphyrins, quasiline phosphorescence spectra, vibrational analysis at 77 K 3-53138
 xylenes, effect of environment on decay times lifetime meas. 3-65098
 AgBr (J) photographic emulsions, phosphorescence in gamma radiation, latent image formation (Russian) 3-50607
 AgCl (I) photographic emulsions, phosphorescence in u.v. radiation latent image formation (Russian) 3-50607
 AgNO₃, polarised, in single cryst. 3-64729
 AlN:Eu²⁺ phosphors, luminescent props. 3-41547
 BX₃, x=halogen, electronic absorption spectra, singlet-triplet transitions 3-43439
 CaF₂:PrF₃(NdF₃, DyF₃, HoF₃, ErF₃, TmF₃), gamma-luminescence, phosphorescence, photoluminescence 3-53140
 β -Ca₃(PO₄)₂:Ga⁺, Ge²⁺, In⁺, Sn²⁺, Sb³⁺, Tl⁺, Pb²⁺, phosphorescence (Russian) 3-50613
 CaS:Bi phosphors, effect of didymium ions on emission characteristics 3-47301
 Cr(III) complexes, anomalous phosphoresc. spectra interpret., Stokes shifts 3-44453
 HgO, orthorhombic and rhombohedral, local cryst. field effects (French) 3-44452
 KCl, activated, monomolecular recombination (Russian) 3-44456
 KCl:Ag⁺(Cu⁺), ionization of different impurity electron states (Russian) 3-44455
 K₂CrF₆, temp. depend. of phosphorescence and fluorescence (German) 3-58561
 KI, divalent ion doped, elec. field effect (French) 3-55693
 LiAl₂O₈:Cr³⁺, and excitation spectra in ordered and disordered phases 3-53135
 LiAl₂O₈:Mn²⁺, effect of ordering on phosphorescence 3-55682
 NO₃⁻, electronic absorption spectra, singlet-triplet transitions 3-43439
 NaCl:Ag⁺(Cu⁺), ionization of different impurity electron states (Russian) 3-44455
 NaNO₂, triplet state of NO₂⁻, e.s.r. spectra 3-72509
 Na₂ZnGeO₄, Mn²⁺ activation Zn-Mn isomorphism 3-72068
 Ru complex, Ru(dipy)₂²⁺ phosphorescence quenching by Cr(CN)₆³⁻, diffusion controlled mechanism 3-53332
 SiC, n-type hexagonal, thermoluminescence phosphorescence and cryoluminescence 3-55681
 Sr₃(PO₄)₂:Eu³⁺, radiationless recombinations in surface layers (Russian) 3-50612
 Y₂O₃:Eu³⁺, Tb³⁺, radiationless recombinations in surface layers (Russian) 3-50612
 ZnS, stimulation spectra structure and trap processes (Russian) 3-76059
 ZnS:Ag, Cu phosphor, spectral response to fast ions 3-50628
 ZnS:Ag/ZnS:CdS:Ag/Bi₂S₃ luminescent screens, spectral characteristics (Russian) 3-50623
 ZnS:Cu,Co phosphor, phosphoresc. decay obs. of trap distrib. (French) 3-80089
 ZnS:Cu,Cr,Cl, Cr⁺ centres, efficiency 3-76101
- phosphorescence microwave double resonance** see magnetic double resonance
- phosphors**
 see also fluorescent screens; luminescence
 alkali metal halides, phosphors, ionisation of luminescence centres by unrelaxed vacancies (Russian) 3-41559
 alkaline earth sulphides, structure of stimulation spectra and trap processes (Russian) 3-76059
 alkaline earth tellurates:U⁶⁺, emission characs. 3-44478
 charged point defects, electronic states 3-41567
 detector for visual display of spatial distribution of colloidal particle beams 3-54616
 double-pumped, with energy transfer, materials and devices 3-44449
 fluorescence quenching by reson. transfer of excitation energy between luminesc. centres, random lattice statics 3-58551
 fluoroaluminates activated by lanthanide ions, effect of Ce impurities (Russian) 3-64733
 oxygen dominated phosphors, excitation spectrum in 3-21 eV region (Russian) 3-50611
 phosphor-transparent membrane-photosensitive material system, modulation transfer function of membrane 3-66768
 silicate oxyapatite:Eu³⁺, fluoresc., emission and excitation spectra obs. 3-41569
 X-ray, noise equivalent absorption, rel. to integrated scintillation obs. 3-77733
 AlN:Eu²⁺ phosphors, luminescent props. 3-41547
 CaO doped with Tl, In and Ga impurities in different valency states (Russian) 3-76052
 CaO phosphors, preparation conditions, emission and optical absorption spectra 3-76068
 CaO:GeO₂, emission of Eu³⁺ 3-55676
 CaO:Bi, kinetics of radical reform. luminesc. with N excitation (Russian) 3-80091
 β -Ca₃(PO₄)₂:Ga⁺, Ge²⁺, In⁺, Sn²⁺, Sb³⁺, Tl⁺, Pb²⁺, Bi³⁺, phosphorescence (Russian) 3-50613
 CaS, optical characteristics of Cr centres using e.s.r. (Russian) 3-75876
 CaS, role of O in formation and properties (Russian) 3-76055
 CaS, structure and optical characteristics of Bi centres (Russian) 3-76053
 CaS doped with Tl, In and Ga impurities in different valency states (Russian) 3-76052
 CaS phosphors, luminescence centre formation, effects of one-, two- and three-valence activators (Russian) 3-44460
 CaS:Ag, Zn, spectral characteristics, formation of [AgV⁺]+e⁻ traps (Russian) 3-76060
 CaS:Bi phosphors, effect of didymium ions on emission characteristics 3-47301
 Ca(Si:Se):Sb³⁺ phosphors activated with ions having s² configuration, luminescence centres 3-72711
 CaSb₂O₇:Mn(Bi) (Russian) 3-44459
 GaAs:Si, double heterostructure i.e.d., excitation source for up-converting phosphors 3-41584
 KCl:Tl, photoluminescence (Russian) 3-41556

phosphors continued

- KCl-Eu, radiation centres, plastic deformation effect on optical props. 3-76077
 KI:TL type, double luminesc., A band excitation, theory 3-69087
 MgO-B₂O₃:Tb, thermoluminescence relation to composition for radiation dosimetry (*Russian*) 3-44499
 MgO-SiO₂:Tb, thermoluminescence relation to composition for radiation dosimetry (*Russian*) 3-44499
 Sc₂O₃:Bi phosphor, luminescence centres (*Russian*) 3-44458
 Sr₃(PO₄)₂:Eu³⁺, radiationless recombinations in surface layers (*Russian*) 3-50612
 SrS, photolum. characts., effect of Bi and Cu activators 3-69054
 SrS:Cu, preparation and spectral props. (*Russian*) 3-76057
 Tl⁺ absorpt. and emission spectra in glasses 3-58547
 Y₂O₃:Bi phosphor, luminescence centres (*Russian*) 3-44458
 Y₂O₃:Eu³⁺, Tb³⁺, radiationless recombinations in surface layers (*Russian*) 3-50612
 Y₂O₃:S:Eu, emission colour detn. 3-44494
 ZnO, kinetic of radical recomb. luminesc. with N excitation (*Russian*) 3-80091
 ZnO:Ag,Cl, photolum. emission characts. 3-69056
 ZnS, structure of stimulation spectra and trap processes (*Russian*) 3-76059
 ZnS phosphors, surface energy losses, electron and hole diffusion (*Russian*) 3-44462
 ZnS:Ag, Cu phosphor, spectral response to fast ions 3-50628
 ZnS:Ag/ZnS:CdS:Ag/Bi₂S₃ luminescent screens, spectral characteristics (*Russian*) 3-50623
 ZnS:Cu, cubic and hexagonal, thermoluminescence glow curves (*German*) 3-69103
 ZnS:Cu,Co, phosphoresc. decay obs. of trap distrib. (*French*) 3-80089
 ZnS:Cu,H, double band electrolum., synthesis and emission characts. 3-69095
 ZnS:Cu double band electroluminescence, emission, freq. depend. 3-72756
 ZnS:Mn, Cu, powder, d.c. electroluminescence investigation, brightness, efficiency 3-58563
 ZnS:Mn, powdered, d.c. electroluminescence, pulse response 3-61075
 ZnS-Cu, space charge relax. during electrolum. (*Russian*) 3-80109

phosphorus

- Atlantic tropical zone, distrib. and dynamics of dissolved mineral P, seasonal effects (*Russian*) 3-80701
 atoms and ions, computed lifetimes of 3s3pⁿ lifetimes 3-78435
 atoms in ³²DJ and ³²PJ states, kinetic study by atomic absorption spectroscopy 3-49397
 chemical vapour codeposition with C, prep., props. 3-69376
 cooperative diffusion with B in Si, mathematical model 3-68433
 detection in streams and soil, radioactive thin-walled proportional counter low level background meas. 3-51719
 diffusion, in Si, point defect injection, rel. to IC fabrication 3-55745
 diffusion in Si, concentration dependent 3-41045
 diffusion in Si, mechanism (*Russian*) 3-43890
 excited atoms, PCl₃, collisional quenching, kinetics rel. to ionisation potential, atomic spectroscopy 3-49415
 films on Si substrate, secondary electron characteristic energies 3-41601
 ion, fast, electron capture cross section in He and N₂ 3-78630
 in iron, friction and wear 3-64957
 radial distribution in Si cryst., radioactivation analysis, electrical measurements 3-72098
 spectrochemical determination in high alloy steel (*Japanese*) 3-70478
 Vembanad lake, distribution in sediments 3-77305
 X-ray states, central atom vacancy, photoemission spectra 3-66464
 Ge:P, As, Li, i.r. absorpt. by donor impurities 3-44443
 P⁺ + Ar, collisions, prod. and decay of double L vacancies 3-63341
 P₂, equilibrium dissociation, mass spectroscopic investigation 3-46329
 P₂ radical, electronic system bands analysis, π-π transition (*French*) 3-52353
 P₄, Raman band contour analyses and Coriolis consts. 3-67816
 p-Si, use of Mg diffout to meas. residual P conc. by i.r. absorpt. 3-61054
 Si:P, As, Sb shallow donor ground states, pseudopot. theory, effective mass 3-50146
 Si:P, ion implanted, conc. profile, annealing effects 3-53191
 Si:P, ion implanted, conduction electrons, e.s.r. 3-68846
 Si:P, ion implanted, lateral spread, oblique incidence and CV plot obs. 3-80179
 Si:P, ion implanted, profiles of channelled and dechannelled impurities 3-54974
 Si:P, quadratic Zeeman effect, variational calc. 3-58515
 Si:P layer, ion implanted through oxide, elec. props. 3-46845
 in SiO₂ films, i.r. spectra, struct., stability 3-64646

phosphorus compounds

- glasses, Fe phosphate, coordination states and magnetic structure determ. by Mossbauer spectroscopy 3-75922
 glasses, Fe phosphate, temp. dependence of magnetic susceptibility, 2.0 to 300K 3-75830
 organo-phosphorus compounds, EX₃ type, p-π conjugation, trivalent P, groups IV-VI, hybridisation of the at. orbital 3-71519
 organophosphorus asymmetric centres, n.m.r. Fourier transform spectroscopy 3-75894
 organophosphorus compounds, n.m.r. evidence of steric effects 3-46317
 phosphate glass:Fe³⁺,²⁺, gamma-ray induced e.p.r. spectra (*Russian*) 3-79911
 phosphates, analysis of mean bond lengths 3-40875
 phosphates in sediments off S.W. Africa 3-56144
 phosphonium salts, ³¹P n.m.r. obs., electron delocalization through P rel. to d_π-p_π bonding 3-71597
 phosphonium salts dipole-dipole molecular interaction with acetone, i.r. spectra obs. (*Russian*) 3-50850
 PO valence shell states, spin-orbit coupling consts. variation with internuclear distance 3-71514
 radicals, e.p.r. identification in γ-irradiated dialkyl phosphites 3-55974
 radicals, X₂PO, X₂PS, X₄P, e.p.r. spectra 3-43487

phosphorus compounds continued

- silicon organic esters of phosphoric acids, crystalline roentgenofluorescent anal., Si and P determ. 3-48662
 trichloromethyl derivatives, CCl₃PCl₄ and (CCl₃)₂PCl₃, n.q.r. spectroscopy and mol. dynamics 3-75912
 trimethylphosphate, molecular structure determ. (*German*) 3-60403
 Al-Ga-P phase diagram 3-79467
 C-P system, equilibria, mass spectrometric studies and enthalpy determ. 3-44711
 CaCO₃:PO₃²⁻, molecule-ion, hyperfine structure splitting, temp. depend. 3-41403
 CaO-MgO-P₂O₅-SiO₂ glass containing fluorine, crystallisation, EPMA (*Japanese*) 3-68170
 CeO₂-P₂O₅ glasses, characteriz. w.r.t. struct. 3-76273
 CeO₂-P₂O₅ glasses, heat treatment temp. effect on microstruct. 3-76262
 Co-P, Co-Ni-P film, annealing behaviour rel. to mag. props. 3-47111
 Co-p laminated film, influence of intermediate layers on coercive force 3-47099
 Cu-P, interactions of impurity atoms with dislocations in dilute copper solutions (*Russian*) 3-72131
 FeO-K₂O-P₂O₅ glasses, preparation and properties, agricultural application in supply of soluble Fe to soil 3-76260
 GaP doped with nitrogen, obs. (*German*) 3-64064
 MnO-P₂O₅ glasses, magnetisation studies, high and low temp. susceptibility 3-75831
 Nd₂O₃-POCl₃-SnCl₄ solutions Nd³⁺ luminescence, self-quenching 3-64713
 Ni complex, bis(O,O'-diethyldithiophosphato)nickel(II) and related cpds., P atom-ligand bonding probe 3-52381
 P(CN)₃, harmonic force fields, vibrational analysis 3-74977
 PCl₃, chem. shifts and nuclear spin-spin coupling calcs. 3-71598
 PCl₃, composition of P, C from CH₄-PCl₃-H₂ mixture 3-69376
 PCl₃, collisional quenching of excited P atoms, kinetics rel. to ionisation potential, atomic spectroscopy 3-49415
 PF₃, chem. shifts and nuclear spin-spin coupling calcs. 3-71598
 PF₃ and PF₃⁺ geometry, SCF MO calculations 3-60399
 PF₃, Gillespie-Nyholm calculations of force fields 3-63398
 PF₃, photoelectron spectrum, band assignments 3-78719
 P₂F₄, i.r. and Raman spectra, vibr. and mol. struct. 3-43457
 PH₃, force constants and frequencies calc. 3-71528
 PH₃, ground state rot. consts., i.r. determ. 3-40626
 PH₃, ionization and dissociation by electron impact, expt. obs. 3-54741
 PH₃ adsorption on clean Si(111), LEED and Auger electron spectra study 3-44513
 PH₃ and PH₃⁺, geometry, SCF MO calculations 3-60399
 PH₃BF₃, barrier to internal rotation, electronic struct. 3-46223
 PHCl₂, chem. shifts and nuclear spin-spin coupling calcs. 3-71598
 PH₂Cl, chem. shifts and nuclear spin-spin coupling calcs. 3-71598
 PHF₂, chem. shifts and nuclear spin-spin coupling calcs. 3-71598
 PH₂F, chem. shifts and nuclear spin-spin coupling calcs. 3-71598
 PN, resonance fluorescence from A¹Π states, vibronic transition probabilities 3-78838
 (PNBr)₃, oriented single crystal Raman spectra and vibrational assignments 3-47259
 (PNCI)₃, oriented single crystal Raman spectra and vibrational assignments 3-47259
 PO₄³⁻, electronic structure, two atom differential overlap approx. 3-78685
 PO₄³⁻ adsorption on Sb₂O₄ determ. using ³²P tracer 3-46756
 PO₄³⁻ Raman intensities and force constants 3-67822
 P₂O₅ ceramic, in SiO₂-Na₂O glass, composite material for prosthetic applic. 3-55876
 P₂O₅ in lunar soil, analysis of 5 Apollo 17 samples 3-65831
 P₂O₅-(Na₂O)_{1-x}-(Ag₂O)_x, phosphate glass, elec. cond. meas. 3-72355
 P₂O₅-CaO-H₂O system, phase relations at 300 to 600°C./2 kb H₂O pressure 3-69488
 P₂O₅-Na₂O(Ag₂O), phosphate glass, elec. cond. meas. 3-72355
 P₂O₅-transition metal glasses, radiation effect on elec. cond. 3-79683
 POCl₃:SnCl₄ with Eu³⁺ ion, solvent effect on luminesc. characts. 3-69055
 POCl₃:SnCl₄:Nd³⁺ liquid laser, spectral luminescent characts. effect of SOCl₂ on generation conditions 3-70817
 PS₄³⁻, vibrational spectra 3-46298
 P₂Se₃, semiconductor, glass-crystal phase transition, NMR of P¹ (*Russian*) 3-72197
 P[Cl₃F]₃, i.r. and Raman spectra and ¹⁹F n.m.r. 3-71561
 SiO₂-PbO-P₂O₅ system glasses, microstruct., heat treatment effects 3-76261
 WO₃-P₂O₅-Li₂O, semiconducting glass, resistivity and thermoelectric polarisation obs. (*Polish*) 3-41176

photocatalysis see catalysis**photocathodes**

- see also photoemission
 aging, effect on photometric and colorimetric meas. 3-66212
 for i.r. and low-light-level imaging 3-48372
 phosphor-transparent membrane-photocathode system, modulation transfer function of membrane 3-66768
 semiconductor, physical model for negative electron affinity 3-47343
 Ag-O-Cs emission mechanism, refractive index, absorption constant, quantum yields, thermal emission (*German*) 3-64260
 Cs₃Sb, scanning electron diff. study during formation 3-53166
 GaAs liquid phase epitaxial layer, transmission mode 3-47345
 GaAs negative electron affinity, performance calc. 3-47344
 SbNa₂K, Cs film, optical and photoelectric props. detn. (*French*) 3-41612
 Si, Li, adsorbed layer characterisation by photoemission obs. (*French*) 3-44516

photocells see photoelectric cells**photochemistry**

- see also photochromism; photolysis
 acetaldehyde predissociation, photoluminescence, temp., pressure and excitation wavelength effect 3-46313

photochemistry continued

- acidine, amino derivatives, quantum yields of interconversion 3-76480
- amino acid tryptophan in frozen polar soln. at 77K, two-quantum ionisation 3-41866
- aminopyridines, phosphoresc. emission and polarization, triplet states 3-65101
- anthracene, n-hexane soln., photodimerization and fluorescence rates, press. depend. 3-69476
- anthracene, radiationless transitions, position-dependent deuterium effects, triplet lifetimes 3-65100
- anthracene, singlet-triplet absorpt. spectra, Franck-Condon factors 3-73159
- anthracene derivatives chemiluminescence during oxidation (*Russian*) 3-41862
- anthracene-N,N'-diethylaniline, excited CT complex form. rate meas., psec. laser pulses 3-76476
- anthracene-pyromellitic dianhydride, zone-refined crystals, charge-transfer spectra 3-61269
- aromatic cpds., radiative transition rate from π, π^* triplet state, external heavy-atom enhancement mechanism 3-40642
- aromatic hydrocarbons, quenching of triplet states in solution by O₂ 3-61272
- aromatic hydrocarbons, quenching of triplet states in solution by O₂ 3-61273
- aromatic hydrocarbons, quenching of triplet states in solution by NO and free radicals 3-61274
- aromatic hydrocarbons, S₁ → T₁ intersystem crossing process, PMDR obs. 3-44731
- aromatic molecules, energy transfer from higher triplet levels (*Russian*) 3-41863
- arylketones in benzene soln., substituent effect on triplet lifetimes 3-76475
- azaphthalenes, triplet-triplet absorpt. spectra 3-53330
- azomethanes, nonradiative transitions and properties of lower triplet state, SCF-MO and CI calc. 3-63504
- azulene, fluoresc. quantum yield 3-76474
- azulene in soln., consecutive two-photon absorpt. using dye lasers 3-44730
- bacteriochlorophyll, one-electron oxidation, absorption and e.p.r. obs. (*Russian*) 3-51425
- benzophenone, i.r., fluorescence spectra of reaction products 3-65110
- benzophenone, microwave-optical double resonance, n, π^* triplet states 3-80121
- benzophenone, undistorted triplet state, static and dynamic paramagnetism 3-76478
- p-benzoquinone, photocycloaddition to cyclooctatetraene, laser excitation, effect of solvent acidity and oxygen 3-47580
- p-benzoquinone, single crystals, Stark effects on low energy electronic states 3-76468
- 1-benzoyl-8-benzyl-naphthalene, deuterium effects on phosphoresc. and photochem. activity 3-76470
- 1-benzoyl-8-benzyl-naphthalene and 1-benzoylnaphthalene, viscosity-depend. phosphoresc. 3-76469
- benzyl radical, electronic states assignment by three-step photoselection 3-44735
- biacetyl, electronic and vibrational relaxation 3-40649
- 9,9'-bisanthryl, dianion triplet at low temp. 3-47573
- biphenyl, in liquid cyclohexane, photoionisation of negative ions, photoconductivity 3-65107
- biphenyl fluorescence, quenching by inorganic ions in solution 3-73160
- biphenyl radical anion in soln., ruby laser induced photoioniz., intensity depend. 3-47569
- biphenyl-tetracyanobenzene single crystals, mobile charge-transfer triplet excitons 3-64538
- n-butane photooxidation with OH, rate const. determ. 3-69478
- chlorophyll A luminescence, changes in polymer medium 3-69074
- cinnolines, (n, π^*) fluoresc. quantum yields and lifetimes 3-76473
- cryostat, for flash photolysis installation 3-53861
- cycloalkanes, reactive state in photochem. 1,3-addition of benzene and alkylbenzenes 3-47574
- cycloheptatriene, photoisomerisation, intermolecular energy transfer 3-65096
- 1,3-cyclohexadiene, photochem. dimerisation, decay of light excited mols. 3-63549
- cyclooctatetraene, photocycloaddition of p-benzoquinone, laser excitation, effect of solvent acidity and oxygen 3-47580
- diatomic free radicals, sensitized fluoresc. by Hg(6³P₀) metastables 3-60484
- 1,3-diazaazulene, polarized absorpt., fluoresc., phosphoresc., mixed cryst. obs. 3-41857
- dimethylcyclobutane, laser-excited fluorescence, ultra-short-lived excited molecules 3-50841
- N,4-dinitroso-N-methylaniline reaction with polyamide resins, e.p.r. and i.r. study of products (*Russian*) 3-50851
- dinucleotide, polarization of excimer fluoresc. 3-41856
- dyes, bleaching and fluoresc. in high viscosity solvent, polarisation 3-51926
- E-region, ion composition and photochemistry, density variations with time and solar activity 3-69661
- enones, conjugated, spin-orbit coupling effects on the zero field splitting of (π, π^*) triplet states, ODMR obs. 3-65103
- europium aromatic acid compounds, luminescence and i.r. spectra, structure 3-65108
- fluorene, pyrene-d₁₀ doped, triplet annihilation behaviour 3-64708
- fluoro(trifluoromethyl)benzenes, in gas phase, fluoresc. and singlet state emission quenching 3-55978
- fluoro(trifluoromethyl)benzenes, in gas phase, photophysical processes 3-55977
- formaldehyde, photochemistry of single vibronic levels 3-41864
- frozen aqueous solutions at 77 K, electron tunnelling 3-47576
- glyoxal vapour, excited at 4358 Å, collision induced intersystem crossing, photophysics 3-80566
- hydrocarbon, liquid, quasi free electron energies and probability of localisation 3-50140
- III-V semiconductors, thermal decomp. by laser beam, mechanism 3-73152

photochemistry continued

- illuminated systems, oscillations, multiple steady states and instabilities 3-55976
- 1-indanone, dual phosphoresc., triplet states 3-55975
- ketones, aromatic, energy transfer from triplet states to O₂ in liq. soln. 3-76482
- lamps for photochemical irradi., electrodelessly discharged 3-53881
- laser separation of isotopes, historical review 3-80567
- latent image formation and photographic sensitivity 3-58809
- 9-methylanthracene, n-hexane soln., photodimerization and fluorescence rates, press. depend. 3-69476
- methylene blue, photoquenching, depend. of quantum yield on pulse intensity and duration 3-67840
- molecular crystal, PMDR in exciton states and coherent states of triplet spin ensemble 3-72546
- molecular structure, photostability, SCF LCAO MO calc. 3-50845
- 1,8-naphthoylene-1,2'-benzimidazole solutions, role of triplet states (*Russian*) 3-61276
- 1,5-naphthyridine in durene, polarized phosphoresc., assignment of lowest singlet n, π^* state 3-76472
- oxidation of organic molecules by photoproduced holes in ZnO 3-41100
- phenanthrene in triplet state e.p.r. hyperfine interactions and electron spin distribution 3-47583
- phosphonium salts dipole-dipole molecular interaction with acetone-trile, i.r. spectra obs. (*Russian*) 3-50850
- photochemically unstable compounds, digital integration method for fluorimetric studies 3-48634
- photochromic sodalite, synthesis by struct. conversion method 3-41865
- photoinduced molecular aggregation and precipitation 3-53331
- photoquenching of large molecule depend. of quantum yield on pulse intensity and duration 3-67840
- phthalocyanine complexes of the platinum metals, dynamics of triplet state in zero field 3-50846
- phthalocyanine solns., intersystem crossing probability calcs. 3-74281
- polymer secondary chromophoric group identification, stability determ. from fluorescence (*Russian*) 3-61277
- polymethine cyanine dyes, bleaching kinetics, fluoresc. decay time 3-48877
- polycycliccarbazole, triplet excitons, number, heterogeneous photosensitisation 3-65111
- porphyrin, free base, Shpolskii-matrix lowest triplet states obs. from microwave induced fluoresc. changes 3-76050
- potassium halides, activated with NO₂⁻ and NO₃⁻, u.v. irradi., coloration (*Russian*) 3-44432
- pyrene, in liquid cyclohexane, photoionisation of negative ions, photoconductivity 3-65107
- pyrene, pure crystal, phosphoresc. emission struct. 3-64707
- quinoline in durene host, multiple spin echoes in photo-excited triplet state 3-80564
- quinoxaline in durene host, phosphoresc. spectra from spin sublevels of low emissivity 3-80565
- reaction, control by selective laser excitation 3-76483
- retinol, primary photoprocesses 3-47575
- rhodamine 6 G, photochemical method for determ. of pumping light energy 3-62713
- rhodamine 6G, photobleaching rel. to triplet state population 3-45803
- rubrene in benzene soln., surface generated photocurrent, ion-image state as intermediate 3-47578
- sunlight applications for direct energy conversion 3-58808
- tertiary aliphatic amines in SO₂ solns., e.s.r., optical absorption 3-69477
- tetrabromobenzene, symmetric, Br hyperfine and quadrupole fine struct. in MODR spectrum 3-53328
- tetracyanobenzene-biphenyl complex single crystals, spin alignment in charge transfer phosphorescent state 3-61059
- thiourea, photosensitized oxidation method for, determ. of triplet state conversion efficiency 3-76481
- 4-thiouridine, decay kinetics, temp. depend., excited states deactivation 3-73154
- transition metal phosphine and arsine complexes, metal localized emission 3-41855
- trapped electron, acting potential calc. 3-41858
- triplet state zero-field transitions determ. by PMDR, absolute polarization meas. 3-61009
- upper atmosphere, photochem. air pollution, O and O₃ concs., discharge flow method 3-69605
- C black, O₂ effect on e.p.r. susceptibility meas. (*French*) 3-68825
- CO, 147 nm Xe-sensitized fluoresc., phase shift obs. 3-46308
- CO₂ photodissoc., CO and O excitation cross sections 3-44736
- CO₂ and hydrate, photodetachment cross section, reply 3-71605
- CO₂ and hydrate, photodetachment cross sections, comment 3-75091
- CaF₂, reversible photochemical reactions in additively coloured crystals 3-55660
- CdS, pure and doped, mechanisms of photochem. reactions (*Russian*) 3-79737
- CdS:Cu, photolum. and photoelec. prop. changes with photochem. reactions, recomb. centre form 3-61071
- Eu³⁺ photochemical reactions in solution with ketones, sensitised luminescence 3-65109
- F gas phase reaction rates w.r.t. F + NO + Ar chemilum. process 3-69441
- Hg(3P) photosensitization of paraffins, energy transfer mechanism 3-50844
- Hg6(3P₀) photosensitized decomposition of propane 3-50843
- Hg6(3P₁) photosensitization band fluorescence spectra 3-50842
- I atom recombination by flash photolysis, kinetic isotope effect 3-73153
- I₂, excited atom quenching by O₂, opto-acoustic spectra obs. 3-78883
- I₂ photodissociation laser, kinetics of generation spectrum 3-62708
- Ne, photodissoc. continuum determ., appl. to upper atm. emission 3-49497
- O₂, photodissoc. continuum determ., appl. to upper atm. emission 3-49497

photochemistry continued

- O₂ atmospheric, photodissociation, solar u.v. flux variations 3-80756
 O₃, u.v. spectrum, features of photochemical interest 3-73155
 OH + O₃ → HO₂ + O₂ reaction, rate const., 220-450 K, u.v. fluorescent scatt. obs. 3-41835
 Rh(III) complex, halopentammine, radiative and radiationless decay processes 3-73158
 Ru complex, Ru(dipy)₃²⁺ phosphorescence quenching by Cr(CN)₆³⁻, diffusion controlled mechanism 3-53332
 T + methane hot atom reactions, energy-dependent cross sections 3-44737
 T + methyl fluoride hot atom reactions, substitution processes 3-44738

photochromism

- glass, alkali aluminoborosilicate, containing Ag, Cl and Br, comp. of Ag halide cryst. precip. 3-80437
 glass, Ce-activated, effect of melt conditions on photochromic props. 3-62075
 glass, volume hologram recording by optical bleaching process 3-62148
 holographic recording substrate, chromatic photosensitization (*French*) 3-73775
 organic photochromatic bulk materials, high information capacity, principal properties 3-48450
 photochemical imaging processes, non-conventional, photochemical formation of dyes, photochromism, photopolymerisation 3-50852
 polymeric matrix photochromic spiran, electrochromic effect 3-71694
 sodalite, for electro-optic device appl., prep. and props. 3-50656
 AgCl crystal, laser irr. interaction, bleaching (*Rumanian*) 3-65113
 SrTiO₃:Fe, valence states rel. to colour changes, Mossbauer obs. 3-58461

photoconducting devices

- see also photoconductive cells; photodiodes; phototransistors*
 chalcogenide glass-Si heterojunctions, switching and photoelectric behaviour 3-60913
 holographic storage media, thermoplastic-photoconductor ghost images 3-77982
 semiconductor, electron component of permittivity, external-pumping-induced change, appl. to device development 3-58307
 semiconductor photoconductor-graphic system with p-n junction, dark current compensation 3-73801
 thermoplastic, holographic storage 3-40229
 InSb hot-electron photoconductor, liquid helium cooled, for radiometry at 1 mm 3-77180

photoconducting materials

- see also photoconductivity*
 acriflavine, dye film, activation of photocurrent 3-72382
 anthracene, triplet exciton stimulated current pulses, delayed luminesc. 3-60895
 anthracene single crystals, intrinsic photoconduction, hole and electron quantum yields, electric field dependence 3-75769
 biphenyl, in liquid cyclohexane, photoionisation of negative ions, photoconductivity 3-65107
 for holographic recording, thermoplastic photoconductor mats. improvement 3-77525
 N-isopropyl carbazole, fluorescence quenching by acids 3-76479
 KRS 5 crystal, thermal, photon depolarisation currents, light polarisation 3-68671
 merocyanine solid dye, luminescence mechanism, electric field effect on photoconductivity 3-53141
 pentacene, photocarrier form. mechanism, incident light depend. 3-72381
 polyethylene, absorption currents and photocurrents 3-58300
 pyrene, in liquid cyclohexane, photoionisation of negative ions, photoconductivity 3-65107
 rhodamine 6G, dye film, activation of photocurrent 3-72382
 semiconductor, electron component of permittivity, external-pumping-induced change 3-58307
 n-Si, Zn-compensated, very high resistivity, photocurrent decay, temp. depend. 3-79725
 n-Cd_{1-x}Hg_xTe solid solutions, nonequilib. carrier lifetime meas. 3-72369
 CdO-B₂O₃-SiO₂ glasses, phase separation effects on photocond. props. 3-75767
 CdS, acoustoelect. amplification of Bleustein-Gulyaev waves (*French*) 3-44121
 CdS, multisaturations of I-V charact. 3-41227
 CdS, photoelectret state, anal. 3-58470
 CdS, powder, effect of heat treatment on photoconductive properties 3-60896
 CdS, reflectivity, spectral sensitivity, particle diameter measurements, relationship with chemical precipitate 3-46872
 CdS powders, electrical charging obs. 3-52871
 CdS single crystals, ohmic contacts using pure In, soldering and diffusion techniques 3-77575
 CdS single crystals in indifferent electrolyte solns., photo-effects due to localised electron levels in space charge region 3-53315
 CdSe films, field quenching, conduction electron mobility using Hall effect, illumination and field depend. 3-46873
 n-InSb nonlinear photoconductive response, room temp., high intensity 5.3 μm radiation 3-41228
 PbO, anodized, tetragonal, photocurrent depend. on incident radiation 3-79727
 Sb₂S₃ semiconductor metal contacts, work functions, contact types 3-46893
 Sb₂Se₃, high-resistivity, prep. by two-step refining process 3-61116
 ZnO (0001) surfaces, electronic and structural characteristics 3-79756
 ZnO:Li, photo-induced persistent internal quadrupole moment 3-46876
 (ZnO-MgO):Fe(O), thermally stimulated current curves for different cooling schedules 3-46883
 ZnS:Cu,Fe(Co,Ni)O, rise, decay and temp. depend. of photocurrents 3-46867

photoconductive cells

No entries

photoconductivity

- see also photoconducting devices; photoconducting materials*
 acriflavine, stimulated cond. and photocurrent, relax. 3-75775
 acriflavine, dye film, activation of photocurrent 3-72382
 adenine, relative quantum efficiency, energy level structure of ionised states 3-68669
 aminoacids, role of mol. electronic structure (*Russian*) 3-46365
 aminoidenes, isostructural energy band structure effect of S substitution of O (*Russian*) 3-55304
 amorphous chalcogenide semiconductors 3-41231
 anthracene, carrier sign and mobility determ. (*Russian*) 3-55309
 anthracene, charge carrier generation by singlet-singlet exciton interaction under weakly absorbed illumination 3-64374
 anthracene, enhancement of photoconduction by detrapping 3-55303
 anthracene, expt., orbital calcs. for photocurrents 3-68675
 anthracene, triplet exciton-impurity interaction rel. to carrier generation 3-46879
 anthracene activation energy, Frenkel excitons 3-79655
 anthracene-Au system, extrinsic photocurrent production, role of singlet and triplet excitons 3-46815
 carrier lifetime measurement, decay time obs. 3-50243
 n-CdSe, influence of mobility at high excitation energy 3-79733
 chlorinated copper phthalocyanine film, compensation effects in dark cond. and photocond. 3-44115
 9,10-dichloroanthracene, photocond. associated with triplet state 3-46870
 dielectric, double space charge determ. method 3-75941
 dielectric, radiation induced, theory 3-46877
 electrometric amplifier for current, voltage, resist. meas. 3-77565
 n-GaAs drag effect in interband two photon transitions 3-44114
 hydrocarbon, liquid, quasi free electron energies and probability of localisation 3-50140
 III-V semiconductors, drag photocurrent, due to photon momentum in direct interband transitions, theory 3-58304
 intensity dependence and recombination center parameters 3-68666
 ionosphere, early morning, electron temperature increase 3-73354
 KRS 5 crystal, thermal, photon depolarisation currents, light polarisation 3-68671
 light intensity modulated, temperature, trapping and mobility effects 3-75768
 magnetic semiconductors, photoconductivity, band structure, Hall effect 3-41214
 3-methylhexane glass, energy level structure of trapped electrons 3-64370
 molecular crystals, anal. of quantum yield for ionised level determ. 3-69140
 p-n junction, space charge region, effect of recombination on photocurrent under parallel illumination 3-64369
 pentacene, photocarrier form. mechanism, incident light depend. 3-72381
 phthalocyanine, activation energy, Frenkel excitons 3-79655
 polar semiconductor, electrical conduction, influence of strong e.m. wave (*Russian*) 3-44106
 poly(N-vinylcarbazole) films, cond. and photocond., carrier generation processes 3-52873
 polyethylene, temp. depend. of photocurrent 3-46874
 polyethylene, u.v. transient photocurrents with zero external field 3-79728
 polyimide insulation, electrically stressed 3-46878
 polypeptides, role of mol. electronic structure (*Russian*) 3-46365
 proteins, role of mol. electronic structure (*Russian*) 3-46365
 quartz, elementary electronic excitations, 4-22.8 eV 3-64314
 rhodamine 6G, dye film, activation of photocurrent 3-72382
 rubrene in benzene soln., surface generated, ion-image state as intermediate 3-47578
 semiconductor, compensated, effective cross section of deep centre optical ionisation 3-61072
 semiconductor, compensated, impurity photocond., influence of double optical transitions 3-75772
 semiconductor, deep levels, detection, method based on high-field domain generation 3-58232
 semiconductor, in strong mag. field, quasilinear relax. of electron plasma 3-58296
 semiconductor, negative differential resist. controlled by photoinjection from metal contact 3-60881
 semiconductor, nonequilib. carrier distrib. after illum., ambipolar equation 3-60882
 semiconductor, optical phonon effect 3-41188
 semiconductor, spectral sensitization (*German*) 3-50233
 semiconductor, totally depleted, transient current theory 3-64376
 semiconductor, transverse wave excitation with optical creation of carriers 3-60901
 semiconductor surface quantisation meas. technique, review 3-50261
 semiconductors, Demmer type voltage, temp. depend., traps influence 3-52874
 semiconductors, luminescence intensity dependence and photoconductivity for electron-electron, electron-exciton and exciton-exciton interactions 3-41548
 semiconductors, photo-carrier generation and recombination theory 3-58299
 semiconductors with deep traps, influence of interband recombination on photocond. and photoelectromagnetic effect 3-55306
 spectra measuring device, automatically controlled (*Russian*) 3-73752
 zinc phthalocyanine, ruby and glass laser induced, thermally stimulated currents and carrier drift mobility obs. 3-50237
 3CdS-CdSe cryst., residual cond. after ruby laser irr. 3-64379
 Ag chalcogenides, pure form, electronic properties (*German*) 3-50202
 Ag₃AsS₃, proustite, temp. depend., 573-90K (*Russian*) 3-79735
 AgBr, emulsion, spectral sensitization, orthorhombic PbO, photocond. meas., photographic diode 3-47588
 AgCl, emulsion, spectral sensitization, orthorhombic PbO, photocond. meas., photographic diode 3-47588
 Ag₂O:Cd, photocond. and luminesc., 4.2 and 77K, participation of excitons 3-47312

photoconductivity continued

- Ag₂S, semiconductor thin film, struct. and props. (*Rumanian*) 3-64417
- Ag₃SbS₂, pyrrargyrite, temp. depend., 573-90K (*Russian*) 3-79735
- Al/tetracene/Au sandwich cell 3-46904
- Al-SiO₂-Au structure, internal photocurrent (*French*) 3-41274
- AsSe glassy film, with Ag electrodes, negative photocurrents 3-58306
- As₂Se₃, amorphous, chopping freq. depend. 3-64372
- As₂Se₃, amorphous film, photocond. in visible and X-ray regions 3-44112
- As₂Se₃, glassy semicond., and recomb. 3-64378
- As₂Se₃, vitreous, influence of surface conditions 3-79731
- As₂Se₃, vitreous, relaxation processes between 286 and 314K 3-68670
- B, β -rhombohedral cryst., photocond. and photo-e.p.r. at 77 K, mechanism and quantitative description 3-52877
- Bi₂GeO₂₀, carrier transport and current oscill. in relaxation semiconductor regime 3-44084
- BiI₃, low temp. spectra, fine structure near absorption edge 3-75780
- Bi₂O₃ anodic films 3-50236
- BiOCl single crystals, photocond. and photolum. (*Russian*) 3-50234
- Bi₁₂SiO₂₀, Al doped and undoped, transport processes of photoinduced carriers 3-46868
- CdBr₂(PbI₂) stationary, delocalisation of activator excitations (*Russian*) 3-55308
- CdGeAs₂, valence band splitting obs. 3-64686
- Cd₂Hg_{1-x}Te epitaxial film, optical and elec. props. 3-58188
- CdIn₂S₄, multi-quantum photoconductivity 3-60897
- CdO-NaCl heterojunction, containing colour centres, electrically stimulated photocond. inversion 3-50241
- CdS, effect of parameter of fast recomb. centres (*Russian*) 3-41234
- CdS, frozen-in X-ray cond. 3-44117
- CdS, high ohmic layer, longitudinal conductivity (*Russian*) 3-72380
- CdS, hot carrier temp. depend. on lattice temp., photon excitation 3-58276
- CdS, influence of O₂ chemisorption on photocurrent 3-80100
- CdS, multisaturations of I-V charact. 3-41227
- CdS, photosensitive, current oscills. associated with impurity breakdown 3-44086
- CdS, pure and doped mechanisms of photochem. reactions (*Russian*) 3-79737
- CdS, reflectivity, spectral sensitivity, particle diameter measurements, relationship with chemical precipitate 3-46872
- CdS, spectral obs. near fundamental absorpt. band edge (*Russian*) 3-44105
- CdS, surface electron states, modulation spectroscopy 3-55323
- CdS cryst., residual cond. after ruby laser irradi. 3-64379
- CdS powders, electrical charging obs. 3-52871
- CdS single crystal, thermomodulated photoconductivity 3-60894
- CdS:Bi film, ion implanted, dose level and post annealing effects 3-50244
- CdS:Cu, Ni(Fe), stimulated cond. at 77 K, Ni(Fe) impurities rel. to electron deep traps 3-41203
- CdS:Na(K)(Li)(Cs), polycryst. film, photomemory effect 3-41232
- p-CdSb, recomb. processes, photocond. and photomag. effects, 350-100K (*Russian*) 3-72384
- CdSe, low voltage instability at potential probe 3-75771
- CdSe:Ti, (Co), CdTe:Ti, (V), impurity excited states, absorption and photocond. spectra (*Polish*) 3-41154
- CdSe_{1-x}Te_x:Cu solid solution, effect of Cu, 85 to 400 K, photoluminescence (*Russian*) 3-52876
- CdTe, n-type, oscillations and photo-Hall effect spectra 3-79732
- CdTe:Ge, elec. cond. and Hall effect meas. at equilib. and under illumination 3-41186
- CdTe:Se layers, recrystallized, electron capture processes (*Russian*) 3-50235
- EuO thin film, mag. order effect 3-55307
- GaAs, carrier ionisation rate from photomultiplication obs. in Schottky barrier 3-55271
- n-GaAs, epitaxial, recomb. processes near surface, photocond. and photomag. effect obs. 3-75756
- p-GaAs, epitaxial films, extrinsic, far i.r., acceptor states investigation 3-64299
- GaAs, laser excited, non radiative recombination of electrons and holes 3-79711
- n-GaAs, O₂-doped, radiative recombination at low temp., photocond. 3-52854
- GaAs, photoconductivity technique for meas. of electron mobility 3-41196
- GaAs, photoinjected free carrier conc., m.m. refl. determ. 3-50238
- GaAs epitaxial film, high resist. layer 3-41225
- n-GaAs photovoltaic effect, single crystals, spectral distributions, sensitivity 3-50232
- GaAs:Cr, excess carrier lifetime, injection depend. obs. 3-79726
- GaAs:Cr, photocurrent decrease above 0.9 eV, optical absorption curves 3-52870
- GaAs:Cr, recomb. singularities and elec. instability (*Russian*) 3-79736
- GaAs:Ti, Co compensated, and photo-Hall effect 3-58266
- GaAs(Cr), semi-insulating, donor-acceptor interaction effect on recombination and electrical instability 3-41156
- GaP, high-resist., i.f. oscills. of current 3-75754
- GaP-ZnS(Se) solid solutions, soln. grown, characterization 3-64797
- Ge, A⁺ and D⁻ centre effects 3-60900
- Ge, amorphous, electronic density of states, optical absorption, photoemission, photoconductivity 3-41119
- Ge, drag photocurrent, due to photon momentum in direct interband transitions, theory 3-58304
- n-Ge, impact ionization of excitons 3-68672
- Ge, impurity interaction effect upon ionisation energy of donor electrons 3-68558
- Ge, ionised impurity scatt., carrier excitation by H₂O laser, cyclotron reson. obs. 3-79729
- Ge, laser excitation, carrier recomb. in deep and shallow surface centres 3-41253

photoconductivity continued

- p-Ge, plastically deformed, photoelec. effects and minority carrier lifetime 3-58279
- Ge, recombination through shallow surface centres at power optical excitation 3-60899
- Ge, submillimetre exciton photoconductivity 3-50239
- Ge, surface electron states, modulation spectroscopy 3-55323
- Ge band-to-band Auger recombination of optically infected carriers, theoretical model 3-76072
- Ge exciton condensation, model for anomalous photoconductivity 3-55319
- Ge film, amorphous, spectral depend. 3-64380
- n-Ge heating photocond. in mm range 3-44116
- n-Ge:Ni, illuminated, negative diff. resist. in presence of elec. domains and high surface recomb. rate 3-79708
- Ge:Sb, far i.r. photoconductivity and photo-Hall effect 3-68667
- n-Ge-electrolyte (0.1 N H₂SO₄) interface, field effect, large variable signal, stationary photoconductivity, shunting and polarisation effects 3-44135
- Ge-GaAs alloy junctions, photoelectric characts. (*Russian*) 3-58318
- He, liquid, photomobility of electron bubbles with near i.r. irradi. 3-50036
- HgI₂ high resolution X-ray spectrometers 3-66382
- n-InAs, heating electrons with light, meas., mechanism 3-75779
- InP:Cu, thermal quenching, static N-type negative differential conductivity 3-52850
- In₂S₃, optical transitions involving different numbers of photons 3-74272
- InSb, electron energy dissipation, near impact ionisation threshold 3-58305
- n-InSb, rel. to microwave absorpt. at low temp. 3-60891
- InSb, two photon interband magnetoabsorpt., photocond. obs. 3-41504
- n-InSb, under optical and elec. carrier heating conditions 3-75776
- n-InSb nonlinear photoconductive response, room temp., high intensity 5.3 μ m radiation 3-41228
- InSb p-n junction, photosensitivity spectra, 0.5 to 3.4 eV, at 90 K 3-44143
- KBr, photocurrent measurements, F-centre concentration effects 3-41230
- KBr:Ag⁰, conduction band separation from Ag⁰ 3-72685
- KBr:OH⁻ single crystals, photocond. and optical bleaching of F-centres 3-60902
- KCl, photocurrent measurements, F-centre concentration effects 3-41230
- KCl:OH⁻ single crystals, photocond. and optical bleaching of F-centres 3-60902
- PbS film, physically treated, role of surface complexes in photosensitivity 3-79734
- PbS film, with adsorbed O₂, anomalous adsorpt. hysteresis of photocond. 3-75778
- SbSI, excitation of trapped electrons, photocond. and photodiffusion study 3-44109
- Se, amorphous, electronic states model for band gap 3-58200
- Se, amorphous film, influence of long-lived traps pot. function parameters 3-75781
- Se films, Hg activated, U-centre potential barrier shape 3-58303
- Si, A⁺ and D⁻ centre effects 3-60900
- Si, amorphous, electronic density of states, absorption, photoemission, photoconductivity 3-41119
- Si, effect of edge dislocations 3-55270
- Si, electron irradi., effective recomb. levels, carrier lifetime obs. 3-68646
- Si, laser excitation, carrier recomb. in deep and shallow surface centres 3-41253
- n-Si, overdepleted, s.c.l.c. transients, light pulse excited 3-64335
- Si, surface electron states, modulation spectroscopy 3-55323
- Si, surface-sensitive photoeffects, theory (*Russian*) 3-79738
- Si, surface-sensitive photoeffects, expt. (*Russian*) 3-79739
- Si, thermally treated, decay of excess carrier concentration 3-68561
- Si band-to-band Auger recombination of optically infected carriers, theoretical model 3-76072
- Si film, amorphous, effect of voids, model 3-68629
- Si film, amorphous, spectral depend. 3-64380
- Si:Ag, impurity photocond. edge shift under influence of combined illumination 3-46875
- Si:Au p+n reverse-biased junctions, thermal and optical generation current 3-46889
- Si:Ni(Zn), short wavelength quenching of photocond. 3-50240
- Si:Rh, impurity states obs. 3-64377
- Si:Zn, induced impurity photocond. 3-41233
- Si-SiO₂ spectra, diffusion length and coeff. determ. (*Russian*) 3-58322
- β -SiC, n-type, impurity photoconductivity (*Russian*) 3-68664
- Si_{1-x}Te_x amorphous thin films and bulk samples 3-58556
- SnI₄, narrow-band charge transport, temp. depend. of carrier mobility 3-55263
- StrTiO₃:Cr³⁺, thermally stimulated, luminesc. excitation mechanism obs. 3-64704
- Te, thin layer, temp. depend. of elec. resist. 3-64368
- Te₄₀As₃₅Ge₇Si₁₈, threshold switching in presence of photo-excited charge carriers 3-41244
- TlInSe₂, piezophotorestrictive effect in single cryst. 3-68674
- Zn_xCd_{1-x}S:Cu, Cl solid soln., peculiarities of recombination processes 3-52875
- ZnO, surface electron states, modulation spectroscopy 3-55323
- ZnO, surface state spectroscopy, modulated 3-55325
- ZnO-rhodamine B thin films, dye sensitised, illumination effect on conductance, self-quenching effect 3-46871
- ZnO(0001) surfaces, electronic properties, correlation with LEED expts. 3-68689
- ZnS, two-photon photocond., spectral and intensity-depend. meas. 3-41229
- ZnS:Te, autoionisation of ³Ti(³P) state, photoconductivity meas. and absorption spectra 3-64375
- ZnTe, deep traps obs. 3-68673
- ZnTe-CdSe heterojunctions, photoelectric and luminescent props. 3-79767

photoconductivity continued

ZnTe-CdTe solid solutions, negative photocond., field depend. (*Russian*) 3-72383

photoconductors see *photoconducting materials***photocopying**

see also *electrophotography*

chromatography, letter copying machines, secondary standards 3-70481

microcircuitry, diffraction problem 3-62162

photocurrent see *photoconductivity; photoemission***photodetectors**

autocollimator, internal stray light 3-39906

far u.v. NBS detector standard 3-51507

optical communication link, dynamic range limiting information capacity 3-48855

optical sensor for tracing edge of work 3-66204

photocount statistics rel. to atmospheric turbulence, laser binary communication system applic. 3-57207

pulsatile blood flow, velocity in transilluminated microvessels 3-42691

semiconductor, conference, Pugnoliuso, Italy (1972) 3-58539

spectroscopic apparatus, review 3-56669

Ge photon drag detector, performance at high CO₂ laser intensity 3-62154

InSb p-n junction, photosensitivity spectra, 0.5 to 3.4 eV, at 90 K 3-44143

Si photodiode linear arrays, self-scanning, spectrometry appl. 3-70309

Si photodiode system, multichannel emission spectrochemical analysis 3-73958

photodiodes

in laser Doppler instrument for vibration measurement 3-66144

laser Doppler systems, choice of photodetector for specific operating conditions 3-66265

light flux power measurement, 0.6328 μ 3-73746

meteorological satellite, photodiode for weather forecasting, visible spectrum operation 3-51197

position sensing, for refractive power meas. in small regions (*German*) 3-73742

AgBr-PbO, spectral sensitization of AgBr, photocond. meas. 3-47588

AgCl-PbO, spectral sensitization of AgCl, photocond. meas. 3-47588

Al_{0.5}Ga_{1-x}As heterojunction, micro-cathodoluminesc. obs. 3-58320

Si, linear detector arrays, self-scanning, spectrometry appl. 3-70309

Si, p⁺-n-n⁺, photoparametric upconverter, base parameter effects on signal to noise ratio 3-66885

Si, planar arrays, multichannel emission spectrochemical analysis 3-73958

Si carrier recombination after light pulse excitation for medium-high carrier conc. levels 3-46858

ZnTe-CdSe heterojunctions, photoelectric and luminescent props. 3-79767

photodisintegration

see also *deuteron photodisintegration; photofission*

emulsion nuclei, cross section determ. for 1-4.5 GeV bremsstrahlung (*Russian*) 3-40481

⁴⁰Ar photoneutron disintegration, 13-23 MeV 3-49238

¹²C, de-excitation gamma ray meas., interpretation 3-52166

⁴⁰Ca, de-excitation gamma ray meas., interpretation 3-52166

³He, two-body, cross section calc. using ³He and proton-deuteron wave functions 3-67301

³He(p,d)³H, differential cross-section meas., 11-65 MeV 3-74554

⁴He(p,p)³H, 180 to 320 MeV, photon energies, meas. differential cross section, proton angular distribution 3-67302

⁶Li, threshold-12 MeV, low-energy total cross section in sequential-decay model 3-63035

¹⁶O, de-excitation gamma ray meas., interpretation 3-52166

¹⁶O(p,p)¹⁵N, bremsstrahlung and 50-80 MeV energies, cross-section meas. 3-52170

photodissociation see *dissociation; photochemistry***photoelasticity**

see also *mechanical birefringence; piezo-optical effects*

Beltrami-Michell type stress equations of motion, uniqueness of solns. 3-51784

birefringence meas. (*French*) 3-59586

ceramic structures, photoelastic methods approach to stress investigation (*German*) 3-44645

composite cylinder, axially connected, thermal stresses 3-66534

crystals under static uniaxial compression, investigation apparatus 3-73673

cyanoacrylate IS 12, bond strength expts. for photoelasticity sandwich technique 3-48351

cylindrical shell, pressurized ribbed, with reinforced hole, stress analysis 3-58781

dual-beam polariscope and framing camera for dynamic photoelastic stress patterns 3-73112

dynamic, resolution of principal stresses 3-58081

epoxy resin, bending and elongation waves effects on stationary crack 3-75564

garnet, Czochralski-grown, perfection and charact. for gems, lasers and substrates 3-76131

glass fibre orthotropic ring, diametral compression, photoelastic analysis 3-73000

instability, absolute, of photoelastic interaction of optical and acoustic waves 3-70844

lithium acetate, birefringent crystal, Brillouin scattering measurement of photoelastic constants 3-68309

mechanical structure measurements, comparison with, numerical calc. (*French*) 3-56620

non-Gaussian polymeric networks, photoelastic props. (*Russian*) 3-49517

photoelasticimetric meas., stress separation by finite element method 3-66559

plate, axially loaded, with circular hole, three-dimens. photoelastic anal. 3-66137

polycarbonate, craze formation, kinetics, stress intensity factor 3-55887

polymer creep stress and strain, deformation 3-61219

photoelasticity continued

polymers, light-scattering method for obs. of fine scale structure 3-59578

polymethylmethacrylate, craze formation, kinetics, stress intensity factor 3-55887

rubbers, statistical thermodynamic theory 3-45666

shear stress measurement, Hertzian contact, below asperities 3-76225

stress analysis, dynamic, incident stress waves, stress concentration, apparatus, techniques (*Japanese*) 3-61991

stress concentration measurement, perforated tube, star-shaped profiles, internal and external pressures (*Russian*) 3-74053

stress meas. technique simultaneously recording birefringence in transmitted and in scattered light 3-39859

titania-silica glasses, thermal expansion meas. by photoelastic and u.s. techniques 3-51593

two-dimensional structures, photoelastic model investigations of optimum shapes (*Polish*) 3-59750

Ag₃AsS₃, proustite, determ. of six photoelastic consts. by Bragg scatt. of laser light 3-75558

Al₂O₃, sapphire, mol. scatt. of light obs. 3-75998

CdS, anisotropy, Brillouin scattering of thermal phonons 3-50577

GaAs single crystal photoelastic constants, stresses in crystal ingots (*German*) 3-53082

KCl:Sr plastically deformed slip band internal structure by precipitation 3-52632

Si, single crystal constants, stresses in crystal ingots (*German*) 3-53082

photoelectrets see *electrets; photoelectricity***photoelectric cells**

see also *photoconductive cells; photovoltaic cells*

arteriography, injected media detection, photo-electric method 3-66397

discriminator, frog's eye type, preprocessor for visual data, small body astronomy 3-53733

CdS, in bridge circuit for automatic focusing of projectors (*Japanese*) 3-53876

photoelectric devices

see also *photocathodes; photoconducting devices; phototubes*

lightning detector, all-sky 3-59185

microscopes for length meas., accuracy comparison (*Slovak*) 3-48409

neonate pulse and respiration obs. hemodensitometer 3-56996

photoelectrocolorimeter, liquid optical density, scanistors meas. 3-73728

smoke/dust density meters, error sources (*Dutch*) 3-73606

spectrophotometer, double-beam recording, photoelectric system 3-48431

thermo-optic deflector with photoelectric registration (*Russian*) 3-66262

GaAs:Cr, p-i-n structure, impurity photocapacitance effects, photoionisation cross sections spectra 3-41260

photoelectric effects see *photoelectricity***photoelectric electron emission** see *photoemission***photoelectric emission** see *photoemission***photoelectric tubes** see *phototubes***photoelectricity**

see also *photoconductivity; photoelectromagnetic effects; photoemission; photovoltaic effects*

amorphous chalcogenide semiconductors, photo-electromotive forces, photoelectret state, injection and thermally stimulated currents 3-41231

characean cells, photoelectric effects 3-56475

direct and exchange types of scattering in e.m. fields 3-75963

Fabry-Perot interferometers, photoelectric control of untreated plane surface thickness (*French*) 3-42576

ferroelectric material, hologram storage applic. 3-53917

p-Ge, anisotropic props. of photon drag effect 3-68668

gyroscope, gimballless electrostatic, accuracy of photoelectric angle-measuring system, effect of rotor pattern 3-66192

holographic interferometry exptl. results prediction method 3-73783

microscope, photoelectric, rotating plane-parallel plate, treatment of output (*Czech*) 3-51589

m.o.s. structure, spectral distrib., theoretical analysis (*Russian*) 3-72408

p-i-n semiconductor structure, surface effects on photovoltage 3-68665

photovoltage spectroscopy, role of surface trapping 3-55328

plasma, laser produced, energy absorpt. mechanism and evolution (*Rumanian*) 3-63856

radiation spectra emitted due to incident radiation fd. at specific density boundary (*Italian*) 3-77940

solids, measurement methods, review (*French*) 3-41494

AgBr-GaAs, interface heterojunction, photoelectric properties 3-44110

AgBr-Si, interface heterojunction, photoelectric properties 3-44110

Au-CdS diodes, field-induced absorption 3-64406

BaTiO₃ ferroelectric, photoactive light effects on domain formation kinetics, and structure, Curie point 3-50528

CU₂S-CdS diodes, field induced absorption 3-64406

CdS, photoconducting, anal. of photoelectret state 3-58470

CdS, sintered, prod. of high mobility photosensitive layers (*Russian*) 3-72818

CdS:Cu, and photolum. prop. changes with photochem. reactions, recomb. centre form 3-61071

Cu evaporated films, photoelectric and optical studies (*French*) 3-58301

GaAs, space charge region, elec. field modulation by laser light, photorefl. obs. 3-75773

GaAs-electrolyte interface, nonequilibrium depletion, surface-barrier photoeffect (*Russian*) 3-73144

n-GaP, inadvertent deep centres, Schottky barrier photocapacitance obs. 3-52868

GaP:O, photocapacitance measurements for study of nonradiative centres 3-58227

p-Ge-electrolyte boundary, photoeffect kinetics (*Russian*) 3-44107

Se properties, influence of organic solvents and thermoplastic polymers, interaction mechanism (*Russian*) 3-79740

photoelectricity continued

- Si, epitaxial, photomultiplication in p-n junction, electron and hole ionisation rates, detn. 3-68642
 Si:Ag, photocapacitance and its quenching, impurity levels, 77K 3-44113
 β -SiC, rel. to struct. defects, volt ampere charact. 3-72097

photoelectromagnetic effects

- contactless measurement apparatus 3-73812
 Kinetic diamagnetism and paramagnetism in the presence of illumination 3-75777
 light-electric field near plasma frequency 3-41224
 liquid metals, photomagnetic waves 3-50242
 quartz, elementary electronic excitations, Dember effect, 4-22.8 eV 3-64314
 semiconductor, collective relax. of nonequilib. photoelectrons in quantized mag. fields 3-75782
 semiconductors, Dember type voltage, temp. depend., traps influence 3-52874
 semiconductors, photo-carrier generation and recombination theory 3-58299
 semiconductors with deep traps, influence of interband recombination on photocond. and photoelectromagnetic effect 3-55306
 n-Cd, Hg_{1-x}Te solid solutions, nonequilib. carrier lifetime meas. 3-72369
 p-CdSb, recomb. processes, photocond. and photomag. effects, 350-100K (Russian) 3-72384
 CdTe film, exhibiting anomalously high photo-e.m.f., anomalous Dember effect 3-75770
 CdTe p-n junction, photomagnetic effect, current-voltage characts. 3-44139
 n-GaAs, epitaxial, recomb. processes near surface, photocond. and photomag. effect obs. 3-75756
 GaAs:Cr, excess carrier lifetime, injection depend. obs. 3-79726
 p-Ge, plastically deformed, photoelec. effects and minority carrier lifetime 3-58279
 n-InAs, photomagnetic effect meas., heating electrons with light 3-75779
 Si, surface-sensitive photoeffects, theory (Russian) 3-79738
 Si, surface-sensitive photoeffects, expt. (Russian) 3-79739

photoelectron spectra

- see also Auger effect; photoemission
 alkali halides, core level binding energies 3-44517
 alkali metal halides and other crystalline salts, binding energies determ. from inner-orbital photoelectron spectra 3-50648
 allyl halides, photoelectron spectra 3-46336
 arsabenzene, data from photoelectron spectra 3-46255
 atom, trivalent, circularly polarised two photon sources of polarised electrons 3-74809
 autoionisation resonances, photoelectron angular distributions 3-43360
 benzene, photoelectron spectroscopy study 3-52394
 carbonyl group 5-membered ring compounds, carbonyl lone pair orbital ionisation potentials 3-54625
 counting statistics, quasimonochromatic light clipped correlation function 3-57217
 cyclohexyl bromide, cis and trans 2-substituted, photoelectron spectra, ionisation potential 3-74992
 cyclopentyl bromide, cis and trans 2-substituted, photoelectron spectra, ionisation potential 3-74992
 cyclopropane, photoionis. cross sections, He I and He II photoelectron spectra 3-78857
 diamond, X-ray photoemission cross-section modulation in valence bands 3-44012
 diamond, X-ray spectroscopic investigation of electronic structure 3-64294
 discharge emission identification 3-63894
 ESCA, X-ray photoelectrons, surface sensitivity, angular dependence 3-44522
 ethylene sulphide, ioniz. pots., orbital types and symmetries 3-54627
 glass, surface comp. from photoelectron spectra (French) 3-54037
 graphite intercalation compounds, electronic props., ESCA (German) 3-72391
 halobenzenes, π -orbitals, inductive and mesomeric effects 3-78690
 inert gas photoelectron ang. distribution meas. using synchrotron radiation 3-40579
 Jupiter dayglow, photoelectron impact contribution for atmospheric model with and without He 3-56345
 metal, IIB, $^2D_{3/2}$ / $^2D_{5/2}$ branching ratios meas. at 584 Å 3-71393
 metal complexes containing trimethylsilylmethyl and neopentyl, HeI spectra 3-54642
 metal vapours and compounds 3-40577
 metallocenes, transition metal complexes, high energy photoelectron spectroscopy, binding energies, mol. orbital calc. 3-49441
 metals, two photon photocurrent calc., multiple beam illum. 3-72782
 methane, fluoro-chloro derivatives, vacuum u.v. and photoelectron spectra, ionisation pots. 3-40617
 molecular ionic states theoretical description observed by high energy photoelectron spectroscopy 3-46335
 molecular ionization potentials determ. method 3-63536
 multiplet hole theory, core electron binding energies, transition metal ions, X-ray photoelectron spectra 3-52794
 naphthalene crystals, photoelectron spectroscopy by rare gas emission lines 3-47347
 organic cpds. containing benzene, naphthalene, pyridine and anthracene ring systems, vacuum u.v. meas. 3-41613
 organic pseudohalides, and compounds containing halogen and P lone pairs, low energy photoelectron spectra interpretation 3-46256
 organic pseudohalides, high energy photoelectron spectra, interpretative methods 3-43431
 oxirane, photoionis. cross sections, He I and He II photoelectron spectra 3-78857
 perylene crystals, photoelectron spectroscopy by rare gas emission lines 3-47347
 phenylsilane, Si-phenyl ring bonding 3-67749
 phosphabenzene, data from photoelectron spectra 3-46255
 photoelectron spectra, binding energy shifts 3-54638
 photoionization cross sections for states split by spin-orbit coupling 3-67684
 quartz, SCF X α scattered wave method calcs. of valence orbitals 3-52793
 radicals, core level binding energies, multiplet splitting, unpaired orbital spin density distrib. 3-46236
 rare-earth ion, core electron binding energy multiplet hole splitting obs. 3-44021
 review of photoelectron spectroscopy for the study of atoms, mols. and solids 3-61104
 silyl pseudohalides, d functions role in Si-N bond by stereochemistry dipole moments and photoelectron spectra 3-43419
 soft X-ray appearance potential spectroscopy X-ray filtering for improved signal to noise ratio 3-73917
 soft X-ray source, for photoelectron spectroscopy 3-45570
 solid, energy distrib. of photoelectrons, band struct. (Russian) 3-72778
 spectrometer, photoelectron counting, 60 channel, description 3-66331
 stibabenzene, data from photoelectron spectra 3-46255
 tetramethyl-p-phenylenediamine and TCNQ, satellites in high energy spectra 3-52326
 thirane, photoionis. cross sections, He I and He II photoelectron spectra 3-78857
 thiocarbonyl chloride, photoelectron spectra 3-43502
 thiocarbonyl fluoride, photoelectron spectra 3-43502
 transition metal iodides, S-containing complexes, adsorbed iodide, chem. shift meas. 3-41617
 transition metal ion, core electron binding energy multiplet hole splitting obs. 3-44021
 transition metal monoxide, band struct., and electronic props. obs. 3-46791
 u.v. photoelectron spectroscopy, energy resolution, fringing emitter field 3-40047
 vinyl halides, photoelectron spectra 3-46336
 X-ray, binding energy meas., surface charge errors, external standards 3-72777
 X-ray, review 3-57646
 Ag, freq. depend. of photoelec. emission 3-55726
 Ag surface, chemisorption of O, X-ray induced spectroscopy 3-55159
 AgGaS₂, valence band density of states and core level shifts, X-ray photoemission obs. 3-55720
 Al foil surfaces, ESCA studies rel. to oxide film thickness 3-61105
 Al-noble metal alloy, valence bands, X-ray photoelectron obs. 3-64287
 Au, L-shell photoelec. cross section of 32.88 keV photons 3-50641
 Au, modulated s-p band photoemission data 3-55724
 Au foil, X-irrad., valence band spectrum determ. from emitted electron energy distrib. 3-50119
 Au/H₂O adsorbed layer system, HeI spectra at low temperature, surface sensitivity 3-55148
 Au-Ag alloys, X-ray, valence band structure 3-64284
 BF₃-nitrogen base complexes, bonding, mol. orbital calc., photoelectron spectra 3-49440
 B₂H₆, band assignments 3-71532
 CO₂, fluorescence excitation and photoelectron spectra induced by vacuum u.v. 185-176 Å radiation 3-63448
 CS₂, autoioniz. process mechanism 3-63537
 Ce, X-ray photoemission spectra near Fermi energy 3-53168
 CoSi, electron struct. determ. (Russian) 3-58568
 Cr complexes, ESCA, ioniz. energies and multi-peak struct. 3-52314
 CrO₄²⁻, X-ray, valence electron levels obs. 3-63388
 Cr₂O₇²⁻, X-ray, valence electron levels obs. 3-63388
 Cs halide vapours, He I photoelectron spectra, rel. to ionic bonds 3-71610
 Cu, chemisorption of O, u.v. induced spectroscopy 3-55159
 Cu, clean cryst., photoemission, surface effect characts. 3-41615
 Cu, freq. depend. of photoelec. emission 3-55726
 Cu-Au alloy, X-ray, density of states in valence band obs. 3-79601
 DF, spin-orbit coupling consts. and ioniz. pots. determ. 3-71609
 Dy, 4f and valence bands, X-ray photoemission obs. 3-80144
 FeO₄²⁻, X-ray, valence electron levels obs. 3-63388
 FeSi, electron struct. determ. (Russian) 3-58568
 GaAs, polar (111) and (111) faces, surface states obs. 3-72394
 Gd, 4f and valence bands, X-ray photoemission obs. 3-80144
 Ge, amorphous film, cond. band, secondary emission and photoemission modulation spectra 3-55188
 Ge, fine structure details in LMM Auger spectra 3-69139
 Ge, normal and anomalous absorpt. cross sections, X-ray energies from 5 to 25 keV 3-43724
 Ge, X-ray photoemission cross-section modulation in valence bands 3-44012
 Ge compounds, photoelectron spectra, binding energy shifts 3-54638
 GeTe, amorphous and crystalline, valence band density of states obs. 3-41121
 H₂, ioniz. pots. determ. 3-63536
 H₂O, ioniz. pots. determ. 3-63536
 Hg, freq. depend. of photoelec. emission 3-55726
 I₂, variable temp. photoelectron spectra, adiabatic ioniz. pot. 3-40658
 InSb, real surface, meas. of fast and slow surface state distrib. 3-55326
 La, X-ray photoemission spectra near Fermi energy 3-53168
 La³⁺ ion core levels, monopole excitation and electrostatic coupling, X-ray photoelectron obs. 3-46802
 LiF, valence band, X-ray photoelectron obs. rel. to Hartree-Fock calcs. 3-79628
 Mg, meas. in vacuum u.v., surface plasmon excitation 3-44520
 Mg₂Ge, using He resonant radiation, effect of surface contamination 3-64761
 Mg₂Si, Mg₂Sn and Mg₂Ge, X-ray excitation, band structure investigation 3-55722
 Mg₂Si, using He resonant radiation, effect of surface contamination 3-64761
 Mg₂Sn, using He resonant radiation, effect of surface contamination 3-64761
 MnO₄⁻, X-ray, valence electron levels obs. 3-63388

photoelectron spectra continued

- NH₃, liquid, containing K and Na, solvated electrons photoelectron emission, 1.55 to 5.4 eV 3-41614
 NO⁺, valence states, spectroscopic consts. 3-63427
 N₂O⁺, geometries of X and A states 3-63422
 NaBr, electron energy distrib., comparison with densities of state calcs. 3-44015
 NaCl, anomalous behaviour of X-ray induced photoelectron lines (*German*) 3-50645
 NaCl, X-ray study of angle distrib. of photoelectrons using double-focusing spectrometer (*German*) 3-53165
 Ne, subshell photoionization cross sections, absolute exptl. determ. 3-78481
 Ni-Au alloy, X-ray, density of states in valence band obs. 3-79601
 NiS, valence band structure, X-ray photoelectron obs. of density of states 3-50124
 NiSi, electron struct. determ. (*Russian*) 3-58568
 O₂ autoionisation, application to Rydberg series 3-63532
 OsO₄, low energy transitions assignment 3-40608
 PF₃, band assignments 3-78719
 PH₃, PF₃, interpretation of low-energy spectra 3-60399
 Pb, L- and higher-shell cross sections of 32.88 keV photons 3-50641
 Pb compounds, photoelectron spectra, binding energy shifts 3-54638
 Pb-In(Sn) alloys, corrosion-resistant, surface obs. by ESCA 3-76209
 PbS, energy distribution spectra of photoemitted electrons 3-58584
 PbS(Se)(Te), valence bands, high resolution X-ray photoemission results 3-44011
 PbSe, energy distribution spectra of photoemitted electrons 3-58584
 PbTe, 6.25-8.74 eV 3-55723
 PbTe, energy distribution spectra of photoemitted electrons 3-58584
 Pt, X-ray photoemission spectra near Fermi energy 3-53168
 Pt-Au alloy, X-ray, density of states in valence band obs. 3-79601
 Re(V, VII and III) complexes, X-ray photoelectron spectra, Re-O and Re-halogen binding energies, struct. 3-74994
 RuO₄, low energy transitions assignment 3-40608
 S₂, molecule config. from gas-phase spectroscopy at 140°C 3-52307
 SO₂, assignment, third band obs. 3-60439
 SO₂, SOX₂ (X=halide), photoelectron spectra rel. to bond lengths and angles 3-67784
 Se, amorphous and trigonal, valence band density of states, X-ray, u.v. photoemission obs. 3-50117
 Si, normal and anomalous absorpt. cross sections, X-ray energies from 5 to 25 keV 3-43724
 Si, real surface, meas. of fast and slow surface state distrib. 3-55326
 Si, X-ray photoemission cross-section modulation in valence bands 3-44012
 Si compounds, photoelectron spectra, binding energy shifts 3-54638
 Tb, 4f and valence bands, X-ray photoemission obs. 3-80144
 Tb thin film, photoelectron spectrum, struct. effects 3-61106
 TiC, single crystals and thin films, ESCA spectra 3-80142
 TiF₃, large satellite separations from core electron emission 3-69136
 (TiF)_x, x=1 or 2, photoelectron spectra 3-49495
 U, L-shell photoelec. cross section of 32.88 keV photons 3-50641
 U compounds, 4f binding energies 3-76119
 V compounds, X-ray photoelectron spectra, binding energy 3-50642
 VO₂³⁺, X-ray, valence electron levels obs. 3-63388
 W, directional photoemission normal to (100), (110) faces, surface states and band structure 3-55725
 W, L-shell photoelec. cross section of 32.88 keV photons 3-50641
 ZnO(0001) polar surfaces, contaminated, X-ray photoelectron spectroscopy, impurity investigation 3-75653

photoemission

see also *photoelectron spectra*

- adenine, quantum yield, energy level structure of ionised states 3-68669
 alkali halide crystals, X-irrad. or u.v.-irrad., photostimulated electron emission temp. depend. (*Russian*) 3-44518
 alkali halides, X-ray photoelectron spectra, core level binding energies 3-44517
 alkali metal halides and other crystalline salts, binding energies determ. from inner-orbital photoelectron spectra 3-50648
 allyl halides photoelectron spectra 3-46336
 angular distrib. of photoelectrons after photoionisation 3-72780
 arsa benzene, photoelectron spectra 3-46255
 atom, intense wave interactions anal. by hydrodynamical model, high field emission 3-74126
 atomic, experimental total cross-sections 3-52273
 autoionisation resonances, photoelectron angular distributions 3-43360
 benzene, photoelectron spectroscopy study 3-52394
 carbonyl group, 5-membered ring compounds, ionisation potentials, photoelectron spectroscopy 3-54625
 Coulomb correlation energy in solids, estimates from X-ray photoemission data 3-43975
 CuI, X-ray photoelectron study of valence bands 3-52789
 diamond, X-ray photoemission cross-section modulation in valence bands 3-44012
 diffusion coefficients, photoemission electron microscope determ. 3-70418
 Earth satellite photoelectron sheath, properties rel. to photoemission laboratory meas. 3-56226
 electron cyclotron resonance spectra in vacuo by photoejection and thermionic emission from metal films 3-72503
 elements, photoelectric cross-section meas. for 100, 280, 662 keV gamma rays, indirect method 3-80143
 far-u.v., photoelectric yield, attenuation length determ., thickness and optical consts. depend. (*French*) 3-47346
 graphite, π -band structure (*German*) 3-72315
 historical review (*French*) 3-41609
 inert gas photoionisation cross section and photoelectron ang. distribution using synchrotron radiation 3-40579
 metal, solid surface photoemission, laser multiphoton phenomena 3-76121
 metal complexes containing trimethylsilylmethyl and neopentyl, HeI photoelectron spectra 3-54642
 metal vapours and compounds, photoelectron spectroscopy 3-40577
 metallocenes, transition metal complexes, high energy photoelectron spectroscopy, binding energies, mol. orbital calc. 3-49441
 metals, two photon photocurrent calc., multiple beam illum. 3-72782
 methane, atomic X-ray photoemission cross-section modulation 3-44012
 methane, fluoro-chloro derivatives, vacuum u.v. and photoelectron spectra, ionisation pots. 3-40617
 molecular crystals, anal. of quantum yield for ionised level determ. 3-69140
 molecular ionic states theoretical description observed by high energy photoelectron spectroscopy 3-46335
 Moon, photoelectron layer above sunlit surface, simple models rel. to solar proton flux 3-61719
 naphthalene crystals, photoelectron spectroscopy by rare gas emission lines 3-47347
 organic cpds. containing benzene, naphthalene, anthracene and pyridine ring systems, condensation effect 3-41613
 organic pseudohalides, and compounds containing halogen and P lone pairs, low energy photoelectron spectra interpretation 3-46256
 organic pseudohalides, high energy photoelectron spectra, interpretative methods 3-44341
 organic solid, photoemission threshold law 3-44521
 perylene crystals, photoelectron spectroscopy by rare gas emission lines 3-47347
 phenylethylenes, steric inhibition of resonance studied by photoelectron spectroscopy 3-54613
 phosphabenzene, photoelectron spectra 3-46255
 photoelectric yield measurements, optical properties, electron attenuation lengths, optical constants, method 3-69135
 quadratic response formalism, microscopic theory 3-72779
 rare-earth ion, core electron binding energy multiplet hole splitting, X-ray photoelectron spectra obs. 3-44021
 semiconductor, noncryst. mag., spin polarized photoelectron emission, multiparticle effect (*German*) 3-50644
 semiconductor, physical model for negative electron affinity 3-47343
 semiconductor-metal junctions 3-50268
 shell-wire photoelectric cross-sections of 60-keV gamma rays 3-40575
 silyl pseudohalides, role of d functions in Si-N bond by stereochemistry, dipole moments and photoelectron spectra 3-43419
 soft X-ray source, for photoelectron spectroscopy 3-45570
 solids, measurement methods, review (*French*) 3-41494
 solids, photoelectron spectroscopy, band structure of nonmetals, review 3-50649
 spacecraft surfaces, low plasma densities 3-61562
 stibabenzene, photoelectron spectra 3-46255
 surveying of deformed metal surface, structural distortion 3-48406
 swarms produced by Q-switched ruby laser light 3-60652
 TCNQ, satellites in high energy photoelectron spectra 3-52326
 tetramethyl-p-phenylenediamine, satellites in high energy photoelectron spectra 3-52326
 theoretical problems, review (*French*) 3-41611
 thiocarbonyl chloride, photoelectron spectra 3-43502
 thiocarbonyl fluoride, photoelectron spectra 3-43502
 transition metal compounds, photoemission, valence-band structure 3-47348
 transition metal iodides, S-containing complexes, adsorbed iodide, photoelectron spectra 3-41617
 transition metal ion, core electron binding energy multiplet hole splitting, X-ray photoelectron spectra obs. 3-44021
 transition metal monoxide, band struct., and electronic props., X-ray photoelectron spectra obs. 3-46791
 transition metals, ferromagnetism and photoemission 3-46969
 u.v. photoelectron spectroscopy, energy resolution, fringing emitter field 3-40047
 vinyl halides, photoelectron spectra 3-46336
 X-ray photoelectron spectra, binding energy 3-50642
 Ag, photoelec. cross sections, Z-depend. 3-67681
 Ag, photoelectric cross section for 145 keV gamma rays 3-49406
 Ag-O-Cs photocathodes, emission mechanisms, refractive index, absorption constant, quantum yields, thermal emission (*German*) 3-64260
 Ag(111) and (100) single cryst. films, energy distrib. and quantum yields, band struct. 3-64763
 Al, meas. of energy distrib. (*German*) 3-53167
 Al, photoelectric cross section for 145 keV gamma rays 3-49406
 Al, photoemissive threshold, ratio of photoyields, p- to s-polarized light 3-72781
 As, cryst. and amorphous, covalent bonding, X-ray photoelectron spectra obs. 3-49868
 Au, L-shell photoelec. cross section of 32.88 keV photons 3-50641
 Au, meas. of energy distrib. (*German*) 3-53167
 Au, photoelec. cross sections, Z-depend. 3-67681
 Au foil, X-irrad., valence band spectrum determ. from emitted electron energy distrib. 3-50119
 BF₃-nitrogen base complexes, bonding, mol. orbital calc., photoelectron spectra 3-49440
 Be, meas. of energy distrib. (*German*) 3-53167
 Bi, cryst. and amorphous, covalent bonding, X-ray photoelectron spectra obs. 3-49868
 C, bulk and evaporated layers, meas. of energy distrib. (*German*) 3-53167
 Ca, film, elec. field effect on photoelec. efficiency, work function 3-64760
 Cd, d band location 3-58585
 CdSe, photoemission and density of valence states 3-69138
 CdTe, photoemission and density of valence states 3-69138
 Ce, X-ray photoemission spectra near Fermi energy 3-53168
 Co film, caesiated, photoelectron spin polarization, photon energy depend. 3-50643
 Cs, pure thick layer in u.h.v., spectral range 250-630 nm (*French*) 3-41610
 Cu, clean cryst., surface effect characts. 3-41615
 Cu, photoelec. cross sections, Z-depend. 3-67681
 Cu, photoelectric cross section for 145 keV gamma rays 3-49406
 Cu, photoelectric work function for clean surfaces, meas. by Fowler method 3-41616

photoemission continued

- Cu X-ray spectra, valence band structure, comparison with emission spectroscopy 3-46790
- CuBr, X-ray photoelectron study of valence bands 3-52789
- CuCl, X-ray photoelectron study of valence bands 3-52789
- EuO, ferromag., paramag. surface sheet, photoelectron spin polarisation obs. 3-47061
- EuO, surface paramag. layer, photoelectron spin polarisation obs. (German) 3-50407
- EuO:Gd, excited energy states, absorpt. edge behaviour (German) 3-50646
- Fe-Si alloy (100) single crystals, photoelectric work function and Auger electron spectroscopy 3-61082
- GaAs, escape probability elec. field enhancement of negative electron affinity surfaces 3-61103
- Ga, exoelectron emission rel. to melting, freezing characts. 3-58583
- GaAs, carrier ionisation rate from photomultiplication obs. in Schottky barrier 3-55271
- GaAs, liquid phase epitaxial layer, in reflection and transmission mode 3-47345
- GaAs, photon energies up to 12 eV, pair scatt. effects 3-69137
- GdP, noncryst., spin polarized photoelectron emission, multiparticle effect (German) 3-50644
- Ge, amorphous, electronic density of states, optical absorption, photoemission, photoconductivity 3-41119
- Ge, normal and anomalous absorpt. cross sections, X-ray energies from 5 to 25 keV 3-43724
- Ge, X-ray induced electron emission under (111) Bragg refl. conditions 3-55727
- Ge, X-ray photoemission and electronic structure 3-64762
- Ge, X-ray photoemission cross-section modulation in valence bands 3-44012
- Ge film, density of state changes at amorphous-cryst. transition, photoemission obs. 3-43987
- Ge/Cs/O (100) surface, structural analysis and photoemissive props. 3-69134
- GeH₄, germane, atomic X-ray photoemission cross-section modulation 3-44012
- GeTe, amorphous and crystalline, X-ray and u.v., valence band density of states measurement 3-41121
- Hg, liquid, density of states determination 3-79604
- Hg, solid and liquid, photoelectron energy distrib., density of states (German) 3-50647
- HgSe, photoemission and density of valence states 3-69138
- HgTe, photoemission and density of valence states 3-69138
- I₂, variable temp. photoelectron spectra, adiabatic ioniz. pot. 3-40658
- In, liquid, meas. rel. to electron structure 3-50107
- K, pure thick layer in u.h.v., spectral range 250-630 nm (French) 3-41610
- KI, photoemission, electronic structure and scattering props. 3-55721
- La, X-ray photoemission spectra near Fermi energy 3-53168
- La³⁺ ion core levels, monopole excitation and electrostatic coupling, X-ray photoelectron obs. 3-46802
- Mg, photoelec. meas. in vacuum u.v., surface plasmon excitation 3-44520
- Mo (100) crystal face, molecular orbital excitation (French) 3-79563
- MoS₂ layer crystals, directional dependence, simple model 3-44519
- NH₃, liquid, containing K and Na, solvated electrons photoelectron emission, 1.55 to 5.4 eV 3-41614
- Na, pure thick layer in u.h.v., spectral range 250-630 nm (French) 3-41610
- NaBr, photoemitted electron energy distrib., comparison with densities of state calcs. 3-44015
- NaCl, anomalous behaviour of X-ray induced photoelectron lines (German) 3-50645
- NaCl, X-ray study of angle distrib. of Auger and photoelectrons using double-focusing spectrometer (German) 3-53165
- Nd, X-ray photoemission spectra near Fermi energy 3-53168
- NiS, valence band structure, X-ray photoelectron obs. of density of states 3-50124
- OsO₄, He(I) photoelectron spectra, low energy transitions 3-40608
- Pb, L- and higher-shell photoelec. cross sections of 32.88 keV photons 3-50641
- Pb, photoelec. cross sections, Z-depend. 3-67681
- Pb, photoelectric cross section for 145 keV gamma rays 3-49406
- PbS, energy distribution spectra of photoemitted electrons 3-58584
- PbS(Se)(Te), valence bands, high resolution X-ray photoemission spectra obs. 3-44011
- PbSe, energy distribution spectra of photoemitted electrons 3-58584
- PbTe, energy distribution spectra of photoemitted electrons 3-58584
- Pr, X-ray photoemission spectra near Fermi energy 3-53168
- Pt, photoelec. cross-sections of γ -rays, L- and M-shell 3-67682
- Rb, pure thick layer in u.h.v., spectral range 250-630 nm (French) 3-41610
- RbCl, electronic core levels binding energy, valence band structure, X-ray photoemission meas. 3-50125
- RuO₄, He(I) photoelectron spectra, low energy transitions 3-40608
- Sb, cryst. and amorphous covalent bonding, X-ray photoelectron spectra obs. 3-49868
- SbNa₂K, Cs photocathode, optical and photoelectric props. detn. (French) 3-41612
- Se, amorphous and trigonal valence band density of states, X-ray, u.v. photoemission obs. 3-50117
- Si, amorphous, electronic density of states, absorption, photoemission, photoconductivity 3-41119
- Si, Cs-O activation and apparent negative electron affinity (French) 3-44515
- Si, escape probability elec. field enhancement of negative electron affinity surfaces 3-61103
- Si, Li, adsorbed layer characterisation (French) 3-44516
- Si, normal and anomalous absorpt. cross sections, X-ray energies from 5 to 25 keV 3-43724
- Si, X-ray photoemission and electronic structure 3-64762
- Si, X-ray photoemission cross-section modulation in valence bands 3-44012
- Si negative electron affinity surfaces using Rb/o dipole layer 3-44128

photoemission continued

- SiH₄, silane, atomic X-ray photoemission cross-section modulation 3-44012
- Sn, liquid, meas. rel. to electron structure 3-50107
- Sn, photoelec. cross sections, Z-depend. 3-67681
- Sn, photoelectric cross section for 145 keV gamma rays 3-49406
- Ta, photoelectric cross section for 145 keV gamma rays 3-49406
- (TiF)₃, x=1 or 2, photoelectron spectra 3-49495
- U, L-shell photoelec. cross section of 32.88 keV photons 3-50641
- W, L-shell photoelec. cross section of 32.88 keV photons 3-50641
- Zn, d band location 3-58585
- ZnTe, photoemission and density of valence states 3-69138
- Zr, photoelectric cross section for 145 keV gamma rays 3-49406
- photoemissive devices**
see also photocathodes; photoemission
- III-V quaternary alloy epitaxial layer application 3-41684
- photoemissivity** see emissivity
- photofission**
²⁴⁰Pu, influence of double barrier on quadrupole absorption component 3-60237
- ²³²Th, 25-40 MeV, mass yield distrib., γ -spectra 3-67377
- ²³²Th, influence of double barrier on quadrupole absorption component 3-60237
- ²³²Th, photofission cross-sect. meas., threshold to 8 MeV 3-46046
- ²³⁵U, 5 to 8 MeV, cross-section from yield curve 3-78359
- ²³⁵U, cross section and anisotropy for photofission 3-60230
- ²³⁶U, photofission cross-sect. meas., threshold to 8 MeV 3-46046
- ²³⁸U, 25-40 MeV, mass yield distrib., γ -spectra 3-67377
- ²³⁸U, 5 to 8 MeV, cross-section from yield curve 3-78359
- ²³⁸U, 800 MeV, meas. of peak-to-valley ratio 3-74617
- photoflash lamps** see flash lamps
- photoglow tubes** see phototubes
- photographic applications**
see also photolithography
- aerial mapping of coastal wetland natural resources 3-53933
- air pollution detection by digital correlation of multispectral stereo photographs 3-42383
- astronomical, imaging of outer planets and satellites 3-48160
- astronomical electronography 3-73566
- astronomical photography with naturally-cooled emulsion at -35°C 3-65949
- beam-foil experiments, study of light emission from ion beam and target (French) 3-77497
- biomedical photography at Rochester Institute of Technology, USA, two-year degree program 3-62313
- colour radiographs for examination of heart and blood vessels (Czech) 3-56992
- computer data plotting, true-perspective three dimensional plots photographic method 3-48460
- computer enhanced i.r. photography, for cutaneous thermal burn wound 3-48621
- corona photography, electrode effects and streamer phenomena 3-56998
- current measurements, Lake Superior, 1971, aerial photography and photogrammetry 3-47683
- dark-field, appl. of holography to high energy physics 3-70401
- electron microscopy, stereophotography, parallax, tilt angle, setup, description 3-66347
- faint astronomical objects detection, image orthicon system, effective quantum efficiency 3-48145
- fingerprint low contrast image, enhancement by spatial filtering 3-66199
- flow visualisation technique using front light laser photography 3-48688
- free molecular to continuum flow transition 3-40731
- geophysical exploration, passive remote sensing, natural surfaces, reflective techniques 3-76848
- geophysics, fault displacement meas. by optical parallax and photographs 3-51164
- HZ Herculis, 'on' and 'off' eclipse phenomena, photographs, 1890 to 1972 3-48075
- high speed X-ray flash, study of target penetration by metal jet (Russian) 3-69263
- holographic, fast processes, paired radiation pulses 3-74210
- instant photography, for mapping acoustic fields 3-51644
- integrated circuit manufacture, aligning and exposure devices 3-45513
- interferogram, with increased sensitivity, using neg-positive charac. of photographic material 3-62128
- i.r. airflow, photographic studies, detailed struct. determ. 3-80787
- i.r. airflow, photographic studies, detailed struct. determ. 3-80790
- jet engine inspection, using 'cold' light 3-53928
- Lichtenberg figures, obs. by high speed image convertor cameras 3-68123
- line printers, laser recording on dielectric coated paper 3-48960
- lunar surface, Apollo 15, panoramic photographs, stereophotogrammetric reduction 3-65970
- magnetic particle and penetrant indications, colour photography 3-47519
- mapping, stereophotograph space model 3-53936
- maps, hemispherical palaeogeographic, direct photographic method of production, terrascop 3-76835
- Mariner 9 photography, photogrammetric evaluation 3-70058
- Mars, Mariner 9 observations, volcanic structure, CO₂ and water ice crystal clouds 3-47903
- meteorological satellites and picture interpretation, review 3-80734
- moire topography, photographic representation of 3-D object 3-77546
- NGC 1566, Seyfert galaxy, luminosity distribution, long and short-exposure photographs 3-48105
- optical processing, contour generation from stereo photography 3-77981
- orthophoto mapping technique requirements 3-53934
- oscillograph energy-current spectra, charged particle 3-73807
- photolithographic operations in IC manufacture, statistical analysis (Russian) 3-42592
- photometry, use of photographic exposure meters, corrections and calibrations 3-77473

photographic applications continued

- plan position indicator photographs, probability of encountering weather-echo near Gan 3-73401
- planetary mapping, Mars chart from Mariner photographs 3-76996
- printed circuit and IC manufacture, artwork and film generation, review (*German*) 3-56688
- radioactivity distribution, 2D sample, photographic recording technique, apparatus 3-73859
- remote sensing from space platforms (*Italian*) 3-61595
- resource surveillance from space (*Italian*) 3-61593
- satellites, electronic imaging trends (*Japanese*) 3-73373
- Skylab experiments 3-53728
- small movement and vibrations meas., by laser photography 3-48361
- spectral reflectivity difference detection, isoluminous additive colour method, lunar orbital multispectral photography 3-45517
- spectrometry, Thorn image-retaining panel, photography of spectral lines from 0.7 to 1.5 microns 3-66221
- stereophotography, practical ophthalmology, applications, theoretical considerations (*German*) 3-70125
- striated high efficiency photographic plates for recording conversion and/or Auger electron spectra 3-48567
- student spectral analysis using 35 mm camera and projected slides 3-73653
- surf swash, velocity, western Kamchatka 3-80711
- surveillance, using super 8 equip., review 3-66278
- time-average-holography, for recording of vibration pattern on excited hollow cylinder (*German*) 3-48446
- Titan, toroidal ring, u.v. photography 3-80998
- turbulent flow, velocity distrib. in rough channel, cinematographic method obs. 3-54802
- viewing screen, rear projection, production using holographic and interferometric techniques 3-66178
- water quality, use of technique 3-65542
- N₂ plasma, exact meas. of continuous emission 3-46555

photographic developers see *photographic materials***photographic development** see *photographic process***photographic emulsions**

- ammoniacal negative emulsions, optical sensitisation, effects of silver halide particle size distrib., pH and Br⁻ conc. (*Russian*) 3-50856
- astronomical photography with naturally-cooled emulsion at -35°C 3-65949
- characterization techniques 3-77551
- coherent optical systems, higher orders in diffraction patterns of random scenes 3-42980
- dyes adsorbed on grains, flash photolysis 3-55982
- electric field effect, polarised grains, response to high intensity exposures, results, model 3-70321
- electron beam exposure, electron micrography 3-54014
- for electron microscopy at 100 and 1000 kV 3-45565
- e.p.r. centres due to presence of tanning agent 3-62248
- film grain noise meas. by laser scatt. 3-77557
- granularity, alternating renewal model 3-48459
- hologram, image quality, depend. on photographic emulsion layer, diffr. efficiency 3-51879
- holography, bleaching agent efficiency 3-51630
- J-aggregates supersensitization, to luminescent evidence for hole trapping mechanism 3-47585
- latent-image distrib., ionic cond., interstitial Ag⁻ 3-53336
- modulation transfer function, meas. by image anal. method 3-51874
- nonreciprocal substitution, surface, sub-surface and conventional developers, activation energy of first resorbed Ag atoms (*Russian*) 3-50854
- optical constants calc., developed Ag grains, filamentary thickness 3-47224
- propagation of α -particles, calc. (*Russian*) 3-49274
- quantum sensitivity data, Silberstein curves 3-47590
- radioactive Ag effects during storage 3-50853
- resolution and modulation transfer function of systems comprising fly's-eye lenslets and photographic emulsion 3-62164
- striated high efficiency photographic plates for recording conversion and/or Auger electron spectra 3-48567
- for super-8 optical-sound prints (*German*) 3-53923
- transparent type PE-1, ultra fine grain, synthesis, gelatin content rel. to stability, setting and sensitising processes (*Russian*) 3-47598
- Ag, filamentary, e.m. theory applied to optical behaviour 3-59606
- Ag complex formation, (NH₄)₂S₂O₃, fixing rates, rate of diffusion, Br inhibition 3-47592
- Ag complex formation, NH₄SCN, NaSCN, fixing rates, Br inhibition 3-47593
- Ag halide microcrystals, effect of u.s. waves on growth mode during emulsification, electron microscopy (*Russian*) 3-47595
- Ag halides, grain size distrib. determination, electrolytic reduction technique 3-51661
- Ag halides e.m. theory applied to optical behaviour of colloidal particles 3-59606
- AgBr, kinetics of Ag formation, ascorbic acid and 2-chloro-4-aminophenol single and combined developers 3-47591
- AgBr, kinetics of development, ascorbic acid and 2-chloro-4-aminophenol, filamentary growth 3-53341
- AgBr, phosphorescence in gamma radiation, latent image formation (*Russian*) 3-50607
- AgBr, photographic emulsion, behaviour of space charge in impulsed elec. field, effect of sensitisation and presence of crystal impurities, latent-image formation 3-53345
- AgBr, photostimulated thermoluminesc., electron and hole traps 3-53340
- AgBr, photovoltaic effect, effect of dye sensitisation, electron and hole traps 3-53343
- AgBr, spectral sensitization, orthorhombic PbO, photocond. meas., photographic diode 3-47588
- AgBr and AgBr(Cl) crystals, behaviour in pulsed electrostatic field, space charge concept (*Russian*) 3-47594
- AgBr filter deposits, technique, characteristics 3-70322
- AgBr photographic emulsions and crystals, luminesc. spectra, luminesc. flash, thermal quenching, electron trapping 3-55983
- AgBr sensitivity centres calc. 3-66325
- Ag(BrCl) photographic emulsion, behaviour of space charge in impulsed elec. field, effect of sensitisation and presence of crystal impurities, latent-image formation 3-53345

photographic emulsions continued

- AgBr(I), luminesc. spectra, luminesc. flash, thermal quenching electron trapping 3-55983
- AgBrI, photographic emulsions, gelatin soln. influence of [Br⁻] and [NH₃] on crystal shape, Ostwald ripening 3-53337
- AgBr(I), photographic emulsions, photovoltaic effect, effect of dye sensitisation, electron and hole traps 3-53343
- AgCl, phosphorescence in u.v. radiation, latent image formation (*Russian*) 3-50607
- AgCl, spectral sensitization, orthorhombic PbO, photocond. meas., photographic diode 3-47588
- AgCl crystal habit rel. to absorption spectra of adsorbed dyes 3-47587
- AgCl emulsion, colour photographic film, blue luminescence, effect of mercaptan stabilisers (*Russian*) 3-47596

photographic filters see *optical filters***photographic lenses**

- copying, for microfilm photography 3-77550
- fly's-eye lenslets and photographic emulsion system, resolution and modulation transfer function 3-62164
- Japanese single lens camera, design and testing of lenses 3-77548
- lunar camera, description, modified Hasselblad 500 EL Data camera 3-70079
- micropattern imaging 3-45511
- modulation transfer for analysis, wavelength weighting 3-77549
- night vision, with image intensifiers 3-66279
- objective, three-component, with telecentric ray path and symmetrical interior component 3-66276
- objectives, standardization of diaphragm settings (*German*) 3-42591
- pancratic, variable-focus, tolerances on component motion 3-66275
- Polaroid Land lenses, testing 3-77547
- telephoto lenses, design for reduced secondary spectrum 3-62165
- wide-angle, phase frequency functions 3-48461
- wide-angle camera lenses, modulation transfer functions, new direct measurement method 3-53940

photographic light sources see *light sources; photography***photographic material sensitivity**

- acoustic pressure distribution, shadow-optical method, analysis accounting for nonlinear relations 3-77320
- ammoniacal negative emulsions, optical sensitisation, effects of silver halide particle size distrib., pH and Br⁻ conc. (*Russian*) 3-50856
- bisazides, spectral sensitivity, phosphorescence quenching 3-61280
- chalcogenide glass films, reversible hologram recording 3-66257
- cyclized rubber, spectral sensitivity 3-61280
- 1,1'-diethyl-2,2'-cyanine hole-trapping mechanism, recomb. processes by J-aggregate, supersensitisation 3-61278
- electrophotographic films, spectral sensitivity, amorphous Se, indirect exposure InSe, Sb₂Se₃ semiconducting layer (*Russian*) 3-50855
- emulsion, electric field effect, polarised grains, response to high intensity exposures, results, model 3-70321
- emulsion type PE-1, transparent, ultrafine grain, synthesis, gelatin content rel. to stability, setting and sensitising processes (*Russian*) 3-47598
- film, Kodak 101-01, Pathe SC5, SC7, in vacuum u.v. 3-62161
- frequency-contrast, determination, holographic technique, results (*Russian*) 3-77560
- holographic recording substrate, chromatic photosensitization (*French*) 3-73775
- imaging processes, non-conventional photochemical formation of dyes, photochromism, photopolymerisation 3-50852
- J-aggregates supersensitization, to luminescent evidence for hole trapping mechanism 3-47585
- Kodak RM films, γ -ray latent image stability rel to temp., humidity 3-77561
- nuclear emulsions sensitivity temp. depend., theoretical expression 3-66326
- photochromic solid films, kinetic model of photobleaching, photocoloration, thermal bleaching 3-53333
- physical-chemical theory 3-58809
- quantum sensitivity data, Silberstein curves 3-47590
- reversible film, black and white, microgranularity of negative and positive images (*Russian*) 3-51646
- sensitisers, spectral sensitivity, phosphorescence quenching by bisazides, mechanism 3-61280
- AgBr, anodically formed, positive relief images photographic sensitivity 3-53334
- AgBr, emulsions, spectral sensitization, orthorhombic PbO, photocond. meas., photographic diode 3-47588
- AgBr, photographic emulsion, photovoltaic effect, effect of dye sensitisation, electron and hole traps 3-53343
- AgBr, photographic emulsion, behaviour of space charge in impulsed elec. field, effect of sensitisation and presence of crystal impurities, latent-image formation 3-53345
- AgBr grains, latent-image formation, photographic sensitising and desensitising phenomena, photoelectron capture by electron traps 3-53339
- AgBr moisture effects, latent-image fading, possible mechanisms 3-59604
- Ag(BrCl) photographic emulsion, behaviour of space charge in impulsed elec. field, effect of sensitisation and presence of crystal impurities, latent-image formation 3-53345
- AgBrI, anodically formed, negative images, photographic sensitivity 3-53334
- AgBr(I), photographic emulsion, photovoltaic effect, effect of dye sensitisation, electron and hole traps 3-53343
- AgBrI grains, latent-image formation, photographic sensitizing and desensitising phenomena, photoelectron capture by electron traps 3-53339
- AgCl, emulsion, spectral sensitization, orthorhombic PbO, photocond. meas., photographic diode 3-47588

photographic materials

- Agfacontour film, for aerial photograph interpretation 3-53931
- ascorbic acid and 2-chloro-4-aminophenol single and combined photographic developers, kinetics of Ag formation, AgBr emulsion 3-47591
- black and white film, corona reflection and image sharpness, contact and projection methods (*Russian*) 3-45522

photographic materials continued

- characteristics determinations, frequency contrast, holographic method, technique, results (*Russian*) 3-77560
- 2-chloro-4-aminophenol single and combined photographic developers, kinetics of Ag formation, AgBr emulsion 3-47591
- cine film, aging, effect of atmospheric temp., humidity and H₂S pollution (*Russian*) 3-50857
- colour film, AgCl emulsion, blue luminescence, effect of mercaptan stabilisers (*Russian*) 3-47596
- colour film, CPN-1, duplicates from reversed positive, comparison with Eastman Colour Internegative type 7271 (*Russian*) 3-48463
- developers, surface, sub-surface and conventional, nonreciprocal substitution, emulsions, activation energy of first resorbed Ag atoms (*Russian*) 3-50854
- dye, rigid film, anisotropic image form. 3-73798
- dye sensitized fine grain emulsions, sensitivity, light induced e.p.r. signal (*Russian*) 3-58811
- Earth resources, photographic techniques (*French*) 3-73379
- electrophotographic layers, optical constants and structure properties, diffuse reflection spectra, binding material (*Russian*) 3-77559
- electrophotography, image formation, correlation between perceived noise and spatial arrangement of toner particles 3-77556
- exposure calculations for scientific motion-pictures 3-62166
- film, for holograms, development 3-62152
- film, Kodak 101-01, Pathe SC5, SC7, sensitivity meas. in vacuum u.v. 3-62161
- films, black-and-white, new specifications 3-39963
- films, developed linear deformation in photographic photometer, meas. (*German*) 3-39964
- films, shrinkage stresses, formation mechanism effect of drying temp. and humidity use of counterbalancing gelatin layer (*Russian*) 3-46675
- fine grain photoemulsion, for nuclear research, dosimetry and autoradiography 3-53943
- fixers, effect on preservability of hydrotype colour images, chitosane and polyvinylbenzyltriethylammonium chloride (*Russian*) 3-47597
- fixing solutions, Ag⁺ recovery, phenylthiourea selective resins, ion exchange, polarographic Ag anal. 3-53335
- gelatin, dichromated, dye sensitised, for hologram recording 3-56681
- gelatin films, effect of H₄SiO₄, kaolin and silver halide conc., effect of developers (*Russian*) 3-46773
- glass, alkali aluminoborosilicate, containing Ag, Cl and Br, comp. of Ag halide cryst. precip. 3-80437
- granularity of layers, computer evaluation (*German*) 3-51643
- holographic materials, storage of volume holograms 3-77528
- holographic recording on photoconductor-thermoplastic device at 1.15 μ m 3-59596
- paper disc sound recording 3-39960
- PbI₂ decomposition of microcrystalline sample by giant pulse ruby laser light, one step imaging 3-59607
- phosphor-transparent membrane-emulsion system, modulation transfer function of membrane 3-66768
- photochromic glass, volume hologram recording, using optical bleaching process 3-73780
- photochromic glasses, photographic charact. curves 3-48448
- photochromic solid films, kinetic model of photobleaching, photocoloration, thermal bleaching 3-53333
- photopolymer, holographic material, study by thick grating 3-77529
- photoresist exposure parameters, grey scale 3-59605
- polymer semiconductors, electrophotographic properties (*Russian*) 3-55986
- resolution, 440 to 2960 mm⁻¹, LIR 1 interference resolution measuring instrument, specifications, operation, design 3-53937
- thermoplastic photoconducting film, recording media for real time holographic 3D display 3-39951
- wash-off film, high contrast, emulsion and processing characts. 3-53925
- Ag salts, analysis, novel titrator assembly, increased reaction rate of thioacetamide 3-61281
- AgBr sol conversion to AgI, reaction kinetics, turbidimetric studies, effect of gelatin-protection and unsubstituted polyethylene oxides 3-53338
- AgCl, thermoluminescence determ. of electron trap depth, reln. to latent-photographic-image formation 3-55696
- Pb halides, photolysis, image recording, e.p.r., mechanism of initial and printout processes 3-61279
- photographic process**
see also photochemistry
- black and white reversible film, microgranularity of negative and positive images (*Russian*) 3-51646
- composite photographs, description of device for obtaining (*Russian*) 3-77187
- development inhibition, latent-image bleaching, Br⁻ and mercaptan-type inhibitors 3-47589
- Earth resources, photographic techniques (*French*) 3-73379
- emulsion crystals, latent-image distrib., ionic cond., interstitial Ag⁺ 3-53336
- emulsion layers, electron beam exposure, electron microscopy 3-54014
- emulsion response, quantum sensitivity data, Silberstein curves 3-47590
- enlarging, optimum exposure time determ. 3-42593
- exposure calculations for scientific motion-pictures 3-62166
- fixing and washing in rapid processing 3-47586
- half tone image registration on cholesterol type liquid crystals, reflection coeff. (*Russian*) 3-45521
- hydrotype colour images, effect of fixers on preservability, chitosane and polyvinylbenzyltriethylammonium chloride (*Russian*) 3-47597
- image processing, review 3-62167
- imaging processes, non-conventional photochemical formation of dyes, photochromism, photopolymerisation 3-50852
- Kodak RM films, γ -ray latent image stability rel. to temp., humidity 3-77561
- latent image, phosphorescence, AgCl (J) emulsions in u.v. radiation, AgBr (J) emulsions in gamma radiation (*Russian*) 3-50607
- latent image and undevelopment 3-77554

photographic process continued

- latent image centres, activation energy of first resorbed Ag atoms, nonreciprocal substitution, emulsions (*Russian*) 3-50854
- latent image formation 3-58809
- latent-image, moisture effects 3-59604
- photolithographic operations in IC manufacture statistical analysis (*Russian*) 3-42592
- photomicrography of a rapidly moving meniscus using an i.r. sensor 3-62163
- raster reproduction, structure evaluation (*Russian*) 3-53941
- semiconductor photoconductographic system with p-n junction, dark current compensation 3-73801
- semiconductor-metal systems, reciprocity violation in electron irradiation (*Russian*) 3-55984
- wash-off film, high contrast, emulsion and processing characts. 3-53925
- Ag filamentary developed grains, optical constants calc. 3-47224
- Ag⁺ recovery, photographic fixing soln., phenylthiourea selective resins, ion exchange, polarographic Ag anal. 3-53335
- AgBr, anodically formed, positive relief images photographic sensitivity 3-53334
- AgBr, photographic emulsion, kinetics of development, ascorbic acid and 2-chloro-4-aminophenol, filamentary growth 3-53341
- AgBr, photographic emulsion, behaviour of space charge in impulsed elec. field, effect of sensitisation and presence of crystal impurities latent-image formation 3-53345
- AgBr, pure and doped crystals, existence of subsurface layer of space charges, effect on latent-image process 3-53344
- AgBr emulsion, kinetics of Ag formation, ascorbic acid and 2-chloro-4-aminophenol single and combined developers 3-47591
- AgBr grains, latent-image formation, photographic sensitising and desensitising phenomena, photoelectron capture by electron traps 3-53339
- AgBr sol conversion to AgI, reaction kinetics, turbidimetric studies, effect of gelatin-protection and unsubstituted polyethylene oxides 3-53338
- Ag(BrCl), photographic emulsion, behaviour of space charge in impulsed elec. field, effect of sensitisation and presence of crystal impurities latent-image formation 3-53345
- AgBrI, anodically formed, negative images, photographic sensitivity 3-53334
- AgBrI grains, latent-image formation, photographic sensitizing and desensitising phenomena, photoelectron capture by electron traps 3-53339
- AgCl, thermoluminescence determ. of electron trap depth, reln. to latent-photographic-image formation 3-55696
- As-S amorphous film, photographic effects, 77 and 293 K, interpretation 3-69015
- GaAs crystal, photographic image formation 3-58810
- NH₄SCN fixing rates, complexing with Ag, Br inhibition 3-47593
- (NH₄)₂S₂O₈ fixing rates, rate of diffusion, complexing with Ag, Br inhibition 3-47592
- NaSCN fixing rates, complexing with Ag, Br inhibition 3-47593
- PbS film, photographic image formation 3-58810
- photographic recording media** see photographic materials
- photographic techniques** see photography
- photography**
see also cinematography; colour photography; electrophotography; microphotography; photographic applications; photographic lenses; photographic materials; photographic process; radiography
- aperture ratios, standardisation of diaphragm settings (*German*) 3-42591
- Apollo 15, Itek optical-bar panoramic camera 3-65807
- astronomical, calibration using brightness profiles of field stars 3-45235
- camera exposure time, stability, precise measurement, method and unit (*Russian*) 3-48464
- cameras, exposure control, electronic applic. 3-53924
- corona reflection, contact and projection methods, image sharpness, black and white film (*Russian*) 3-45522
- detector characts., quantum efficiency 3-77558
- diffusimetry, review (*German*) 3-53944
- electron-optic shutter having μ sec duration 3-56690
- equidensitometer, lines of equal density, photographic image (*Russian*) 3-45520
- equivalent projection density meas. of silver and vesicular films 3-39966
- exposure setting device, amateur camera, programmed automatic mechanism, design 3-53939
- exposure time, using cine camera shutter 3-45509
- high-speed, multistage image converter tubes 3-48462
- high-speed photochronograph, with 2×10^{-11} time resolution, using image converter 3-53930
- image enhancement by holography 3-56694
- image rectification, using electro-optical rectifier 3-53926
- image structure analysis, 2 dims. Fourier transform meas. 3-42594
- image-sharpness criteria 3-77555
- instant photography, for mapping acoustic fields 3-51644
- kymography with intravital microscope (*German*) 3-51757
- laser image recording, flat vs. cylindrical surfaces 3-56692
- laser system, aeroballistic range, in-flight model contour measurements, hypervelocity models, techniques 3-56686
- light, colour and photography, teaching course for artists 3-51485
- lines of equal density, production by sharp mask method (*German*) 3-53945
- microelectronics characteristics keys to high resolution plate images 3-66273
- Newton's laws on photographs for teaching (*Hungarian*) 3-39847
- night photography systems, built around image intensifiers 3-66280
- photogrammetric, depth of field and image scale of object 3-73802
- photogrammetry, camera analytical self-calibration 3-53932
- projector slides using sound track system (*Spanish*) 3-42595
- pseudo-solarization, fringe boundaries sharpening 3-66274
- random-carrier, optical modulation techniques, theory and experimental results 3-66271
- satellite observations, Automatic Camera for Astrogeodesy, photographic obs., active and passive artificial satellites 3-48152
- scientific, quasi holographic scheme 3-73799

photography continued

- scintillation scanning, recording of images on 35mm film 3-66039
 security and policing instrumentation, conference, New York, USA, 20-21 Sept (1972) 3-66277
 semiconductor-dielectric system, electrostatic contrast, charge transfer method, effect of various exposures on discharge potential (*Russian*) 3-45523
 stellar, removal of atmospheric turbulence 3-81254
 stereometry with mirror stereoscope facilitated by interpreter's table 3-53935
 system camera, in high resolution photography 3-45518
 transmission density meas. of photographic layer in microfilming 3-39965
 Nd³⁺:YAG burst mode freq. doubled laser for high speed photography and holography application 3-43015

photoionisation

see also photoionisation of gases

- acetonitrile, photodissociation in vacuum u.v. meas. of yield curves and thermochemical parameters 3-75093
 acetylene, molecular and dissociative photoionisation, hot bands obs. ethynyl ion heat of formation 3-75092
 acetylene nitrile, photodissociation in vacuum u.v. meas. of yield curves and thermochemical parameters 3-75093
 angular distrib. of photoelectrons 3-72780
 atom, ionisation cross-section calcs. for circularly and linearly polarised light 3-43353
 atom, multiphoton effects, anal. by Keldysh method, and perturbation method 3-74825
 atom, multiphoton impact ionisation mechanism, contribution of electron collisions 3-74817
 atom, multiphoton ioniz., polarisation phenomena 3-63303
 atom, multiphoton ioniz., Reiss approximation at moderate intensities 3-71387
 atom, multiphoton processes, description of intense laser interactions 3-74823
 atom, multiphoton processes, expt. results for H and inert gases 3-74826
 atom, neutral, in 3p⁶ and 5p⁶ subshells 3-78482
 atom, photoioniz. cross sections for states split by spin-orbit coupling 3-67684
 atom, Stark effect, influence of high-frequency fields 3-74800
 atom, trivalent, circularly polarised two photon sources of polarised electrons 3-74809
 atom multiphoton ionisation, selection rules, nonperturbative theory 3-52277
 atom radiation absorption due to photoeffect in a magnetic field 3-63306
 atomic beam, detection of upper level optical resons. (*French*) 3-57603
 atomic total photoelectric cross-sections 3-52273
 atoms, multiphoton effects, appl. perturbation theory 3-74824
 atoms, photoionisation probability, variational method 3-43356
 atoms and ions, cross sections calc., approx. method 3-63307
 atoms and molecules, dependence of cross section on photon energy 3-40578
 auroral arcs, role 3-65427
 benzene, photoelectron spectroscopy study 3-52394
 benzene, unimolecular decomposition, fragmentation thresholds, energy dependence, theory 3-57674
 benzoic acid derivs., ionization pot., determ. 100-170°C, by photoionization method (*Russian*) 3-43503
 biphenyl, in liquid cyclohexane, photoionisation of negative ions 3-65107
 biphenyl radical anion in soln., ruby laser induced photoioniz., intensity depend. 3-47569
 cyclopropane, photoionis. cross sections, He I and He II photoelectron spectra 3-78857
 1,1-difluoroethylene, mass-spectrometric study in vacuum u.v., photoionisation curves and threshold energies 3-52395
 diphenylamine, in organic matrices at 77K role of solvent in delayed fluorescence by photoionisation (*French*) 3-46314
 elements Z=1 to Z=94, photon cross sections from 0.1 keV to 1 MeV, tables 3-49404
 ethylene and C₂D₆, threshold electron-photoion coincidence mass-spectrometric study 3-43499
 gas atoms at focus of ruby laser 3-78476
 Green's function theory 3-78489
 hydrocarbons, C₃-unsaturated, ion-molecule reaction obs. by photoioniz. mass spectrometer 3-55932
 inert gas atoms, polarization of electrons ejected by circ. polarized light 3-78488
 ion sources, for investigation of nonvolatile substances on mass spectrometer 3-51679
 isoelectronic sequences, cross sections 3-78483
 mass spectra prediction, energy deposition functions 3-63531
 metal, group IIB; branching ratios, ²D_{5/2}; ²D_{3/2} ratios meas. by photoelectron spectroscopy 3-71393
 molecular crystals, anal. to determine ionised levels 3-69140
 molecule, diatomic heteropolar, multiphoton processes, Born-Oppenheimer approx. 3-67760
 molecule, heteronuc. diatomic, perturbation theory in closed form for multiphoton processes 3-71517
 molecule, high energy charged particle ionisation collisions, Bethe theory, photoabsorption data 3-75100
 molecule, homopolar diatomic multiphoton processes, Born-Oppenheimer approx. 3-71516
 multiphoton, non-perturbative approaches to semiclassical theory 3-71388
 multiphoton, polarisation effects to measure ratios of bound-free matrix elements 3-78478
 multiphoton excitation and ionis. rates, momentum-translation method, fallacy 3-78491
 multiphoton ionisation of excited atoms, resonance phenomena 3-46197
 multiphoton radiative collisions, in e.m. fields 3-78490
 one-electron atom, multiphoton ionisation rel. to light polarisation 3-52278
 organic cpds. containing benzene, naphthalene, pyridine and anthracene ring systems, photoemission, vacuum u.v. 3-41613
 photoionisation strengths determ. using double and triple coincidence techniques (*Dutch*) 3-39922
 oxirane, photoionis. cross sections, He I and He II photoelectron spectra 3-78857
 photoelectron ang. distrib. in jj coupling, relativistic theory 3-52274
 planetary nebulae contrib. of charge exchange and optically thick condensations to [O I] radiation 3-73554
 polar liquids, energy distribution and cross section 3-76120
 protogalaxies, photoionization by u.v. radiation from massive stars 3-42228
 pyrene, in liquid cyclohexane, photoionisation of negative ions 3-65107
 shell-wire photoelectric cross-sections of 60-keV gamma rays 3-40575
 sodium pyridine in tetrahydrofuran, flash photolysis, photo-oxidation and Na⁰ existence 3-61270
 solids, energies, electrostatic suspension method 3-45558
 stellar atmospheres, radiation absorption through photoionisation in magnetic field 3-77049
 TCNE negative ions, photodetachment of electrons 3-78856
 N, N, N', N'-tetramethyl-p-phenylenediamine, thermal glow curves and delayed luminescence 3-41571
 thiirane, photoionis. cross sections, He I and He II photoelectron spectra 3-78857
 trapped electron, acting potential calc. 3-41858
 two-photon photoionization absorpt. of optical, X-ray quanta 3-66878
 vinylchloride, mass-spectrometric study in vacuum u.v., photoionisation curves and threshold energies 3-52395
 vinylfluoride, mass-spectrometric study in vacuum u.v., photoionisation curves and threshold energies 3-52395
 Ag photoelec. cross sections, Z-depend. 3-67681
 Al I photoionization cross section and 3p²P°-3s3p²S_{1/2} autoionization doublet 3-80926
 Ar, Ar⁺, Ar²⁺, 3p subshell, cross sections 3-78483
 Ar⁺, photodetachment threshold law, exptl. investig. 3-78494
 Au, photoelec. cross sections, Z-depend. 3-67681
 Ba, absolute absorpt. cross section at 237.9 nm 3-71382
 Be, cross sections, quantum defect theory applic. 3-63302
 C³⁺, cross section calcs. 3-71383
 CO⁺, photofluoresc. by electron impact, relative oscillator strength for B²Σ state form. 3-46327
 CO₂, form. of excited mol. ions by photon impact, cross section structs. 3-78865
 CO₂, photon impact to produce CO₂⁺(A²Π_u) and CO₂⁺(B²Σ_u⁺) 3-78866
 CO₂⁺ 2890 Å band, photoionization excitation rel. to column excitation rates for planetary atmospheres 3-54732
 CO₂⁺ fluorescent cross sections and yields from threshold to 185 Å 3-40646
 CaF₂, M centre reorientation under u.v. excitation 3-40915
 CdSe:Cr, optical photoionisation spectra of Cr impurity 3-55661
 CdSe:Cr, temp. depend., anomalous impurity absorption 3-55651
 Cs, (6²P_{3/2}) state, photoioniz. cross section 3-74822
 Cs, multiphoton ionisation and absorpt. of ruby laser light (*French*) 3-64195
 Cs atom, multiphoton, bound electron state perturbation 3-54584
 Cs atoms, in 6²P excited states, binary collisions, photosensitised ionisation 3-46196
 Cs vapour, effective cross section for step photoionisation near threshold 3-71392
 Cu, photoelec. cross sections, Z-depend. 3-67681
 F₂, dissociative ionization and dissociation energy, calc. of curves 3-49494
 F₂O, photoionisation mass spectrometry 3-63533
 GaAs:Cr, p-i-n structure, impurity photocapacitance effects, photoionisation cross sections spectra 3-41260
 Ge, impurity interaction effect upon ionisation energy of donor electrons 3-68558
 H, multiphoton ionisation induced by circularly polarised radiation 3-43361
 H-like atoms, non resonant, intense fields, Ramon processes 3-71384
 H⁺, photodetachment, spontaneous, from 2p² ³P° state 3-78492
 H⁺, polarisation effects in high-order multiphoton ionisation by CO₂ laser 3-49405
 H₂, cross section calc. from threshold to 30 eV 3-57673
 He, 1¹S state, continuous oscillator strengths calc. 3-52276
 He, resonance multiphoton ionisation 3-49411
 He, simultaneous multiphoton ioniz. and excitation in intense laser beam 3-52275
 He atom, double ionization by high energy photons 3-78485
 Hg, atomic electron struct. distortion due to high-intensity laser field 3-74772
 I₂, variable temp. photoelectron spectra, adiabatic ioniz. pot. 3-40658
 K⁻, photodetachment cross section 3-78493
 Kr, cross section of 4s² subshell 3-78487
 Kr, photoproduction of Kr⁺ in vicinity of outer d-subshell threshold 3-78486
 Li atom, Green's function theory 3-78489
 methane and CD₄, threshold electron-photoion coincidence mass spectrometric study 3-43499
 Mg selectively excited 3s3p ¹P^o state, photoionisation to the 3p² ¹S₀ autoionisation level 3-54585
 Mg³⁺, cross section calcs. 3-71383
 N atom, cross section calc. 3-78484
 N⁺ plasmas, recombining, continuum emission, ionisation cross sections 3-54835
 NO, photoabsorpt. cross sections, 380-660 Å region 3-71606
 N₂O, dissociative excitation and ionisation excitation with synchrotron radiation 3-43504
 N₂O, form. of excited mol. ions by photon impact, cross section structs. 3-78865
 Na, theory of multiphoton ionisation by ruby laser 3-71381
 Na atoms, resonant two-photon ionisation, photoelectron angular distribution 3-67690
 Ne, Ne⁺, Ne²⁺, 2p subshell, cross sections 3-78483

photoionisation continued

- Ne, subshell photoionization cross sections, absolute exptl. determ. 3-78481
 Ne³⁺, cross section calcs. 3-71383
 O⁺ plasmas, recombining, continuum emission, ionisation cross sections 3-54835
 O³⁺, cross section calcs. 3-71383
 OH⁻, photodetachment spectra, rot. line strengths 3-40659
 Pb, photoelec. cross sections, Z-depend. 3-67681
 Pt, photoelec. cross-sections of γ -rays, L- and M-shell 3-67682
 Se⁻, photodetachment spectra, rot. line strengths 3-40659
 Se⁻, photodetachment, high resolution pulsed dye laser study 3-67687
 SeH⁻, photodetachment spectra, rot. line strengths 3-40659
 Sn, photoelec. cross sections, Z-depend. 3-67681
 Xe, photoproduction of Xe⁺ in vicinity of outer d-subshell threshold 3-78486

photoionisation of gases

- combustion gas-K medium, rel. to MHD generators 3-49665
 diatomic, in extreme u.v. 3-78863
 formaldehyde, production and decay of excited states by photon impact 3-40665
 inert gas metastable atoms, cross sections near threshold 3-74821
 inert gases, photoionisation cross sections using synchrotron radiation 3-40579
 interstellar matter, photoionisation rate using OAO-2 data 3-81197
 laser induced, effective photon theory, expt. verification 3-49527
 laser plasma, effect of Cs 3-66805
 metal vapours and compounds 3-40577
 quasi-stellar objects, models for emission-line regions. 3-53683
 Ar, photoabsorpt. cross-section at He 584A line 3-49407
 CO₂, excited CO₂⁺ ion formation by vacuum u.v. radiation 3-40664
 CO₂, photoionisation excitation to obs. CO₂⁺ band strengths 3-75059
 CO₂ TEA laser, electron density meas., with microwave interferometer, u.v. excitation 3-70802
 CS₂, autoionisation processes, photoelectron spectra obs. 3-63537
 Cs halide vapours, He I photoelectron spectra, rel. to ionic bonds 3-71610
 D₂, photoabsorpt. cross-section at He 584A line 3-49407
 H⁻, two photon detachment cross section, linear and circularly polarised light 3-74810
 H₂, photoabsorpt. cross-section at He 584A line 3-49407
 H₂ autoionisation meas. lifetimes discrepancy due to config. interaction effect in electron capture method 3-71608
 He, simultaneous excitation-photoionisation by synchrotron radiation, high resolution optical meas. 3-40580
 Kr, photoabsorpt. cross-section at He 584A line 3-49407
 N₂, photoabsorpt. cross-section at He 584A line 3-49407
 NO₂ ionisation potential, 9.62 to 9.25 eV assoc. mass spectrometer 3-71604
 Ne, 2s2p³(P-) state, ang. distrib. and shape var. of resonance lines of photoelectrons 3-74819
 O₂, photoabsorpt. cross-section at He 584A line 3-49407
 Xe, photoabsorpt. cross-section at He 584A line 3-49407

photolithography

- see also masks; photoresists
 bisazide compounds, spectral sensitization 3-61280
 colour TV laser-recorded microtrack records (Polish) 3-43043
 high resolution plate images, for microelectronics 3-66273
 operations in IC manufacture, statistical analysis (Russian) 3-42592
 printed circuit and IC manufacture, artwork and film generation, review (German) 3-56688

photoluminescence

- A₂BWO₆ (A=alkaline earth), ordered perovskites, electronic emission spectra 3-41577
 acetaldehyde, photoluminescence, temperature, pressure, and excitation wavelength effect 3-46313
 alkali halides:Sm²⁺, luminescence and energy levels 3-55679
 alkali halides, Z₂ centres, triplet state, emission and absorpt. spectra 3-58546
 alkali metal halides, phosphors, ionisation of luminescence centres by unrelaxed vacancies (Russian) 3-41559
 alkyl ammonium halides, polymorphic transition study 3-72755
 anthracene, fluorescence lifetime in polymethylacrylate 3-80562
 anthracene-N,N'-diethylaniline, excited CT complex form. rate meas., psec. laser pulses 3-76476
 Ar, solid, with trapped oxygen, luminesc. and absorpt. spectra 3-44472
 benzene, mol. cryst., low-temp. luminesc., phonon structure 3-72715
 1,2-benzpyrene: naphthacene, thin layers, sensitised, concentration depend. of emission spectra 3-41572
 AlO clouds, temps., diffusion coeffs. and densities 3-59136
 crystal: rare earth ion ³⁺, two-photon excitation spectra of luminesc. 3-64730
 diacetyl in benzene or toluene, triplet-triplet energy transfer, photo-X-ray spectra 3-69083
 diamond, X-ray luminesc. centres, spectral and kinetic characts. 3-76079
 diamond, yellow-green, spectra, vibr. replicas 3-76078
 diffusion pump oils, rel. to contamination in vacuum deposition of optical films 3-69048
 dioxane, PPO soln. scintillators, radioluminesc. quenching mechanism 3-80085
 europium tetra-O-dibenzoyl-methanates, luminescence spectra (Russian) 3-41561
 excitation intensity, direct meas. of nonlinear dependence 3-51613
 F-centre i.r. quantum yield, probability calcs. 3-69039
 fluorescence intensity control, liquid crystals 3-76073
 fluorimeter, decay time meas., 77-500 K (French) 3-66455
 fluorite series, effect of indirect exchange interaction on crystal field parameters of Er³⁺ centres 3-50139
 n-GaAs:Te, laser excited, low energy emission bands at 77 K and 300 K 3-61068
 gadolinium tetra-O-dibenzoyl-methanates, luminescence spectra (Russian) 3-41561
 glass, Ce and Tb activated, differences during photo- and cathodic excitation 3-64719

photoluminescence continued

- III-V compounds and alloys, spectra of direct and indirect band gap 3-58210
 III-V semiconductors, direct gap, shallow donor and acceptor obs. 3-55690
 mercury-like ions dependence of ³P₁ level on difference between radii of activator and substituted cation (French) 3-64712
 metal vapour + halogen reactions, products identification 3-76421
 molecular crystal, line shape theory, exciton motion 3-80073
 molecular spectra, line shapes, radiationless transitions 3-67845
 naphthalamide, luminescence spectra (Russian) 3-44466
 naphthalene crystal, luminescence spectra, surface effects, exciton states 3-44483
 naphthalic anhydride and heterylsubstitutes, luminescence spectra (Russian) 3-44466
 naphthoylinbenzimidazole, luminescence spectra (Russian) 3-44466
 organic solid solutions, laser excited luminesc., fine struct. and broad spectral bands 3-72725
 n-pentane:acenaphthene radical, multiplicity of the quasi-line fluoresc. spectrum 3-64716
 perovskites, A₂BWO₆ (A=Ca, Sr, Ba; B=Mg, Ca, Cd, Sr, Ba), luminescence of WO₆ (Russian) 3-41558
 photochromic sodalites, sodium-alumino-silicate to sodalite structure conversion 3-41865
 phthalocyanines, thin films and solutions, emission spectra 3-61074
 polymers, luminescence during deformation, breaking and friction, gas-discharge processes (Russian) 3-47313
 quartz, elementary electronic excitations, 4-22.8 eV 3-64314
 rare earth chelates, under intense pulse excitation, kinetics and energy transfer 3-76087
 ruby, radiative and nonradiative transitions, temp. depend., emission quenching 3-41568
 ruby, u.v. anti-Stokes, mechanism 3-64723
 semiconductor, carrier radiative recomb., strong elec. field modification 3-61070
 semiconductor, compensated, effective cross section of deep centre optical ionisation 3-61072
 semiconductors, analysis 3-69180
 semiconductors, luminescence intensity dependence and photoconductivity for electron-electron, electron-exciton and exciton-exciton interactions 3-41548
 silicate glass: Cr³⁺, Yb³⁺, energy transfer and fluoresc. sensitisation 3-72705
 solids, X-irradiated, apparatus for luminescence properties meas. (Russian) 3-48560
 solution, fluoresc. quenching and nonradiative energy transfer 3-69060
 tetraalkyl ammonium iodides, self-trapped exciton spectroscopy 3-69034
 thioxanthone, phosphorescence in rigid glass, 77K 3-80562
 tryptophan in ethylene glycol/water glass, recombination luminescence and trapped electron decay 3-55695
 uranyl acetate, vibronic interaction, luminescence spectra 3-72748
 uranyl butyrate, vibronic interaction, luminescence spectra 3-72748
 uranyl compounds, luminescence props. (Russian) 3-44471
 uranyl diformate, anhydrous and monohydrate, luminescence spectra, 77K (French) 3-69065
 uranyl propionate, vibronic interaction, luminescence spectra 3-72748
 visualisation methods of long-wave radiation (Russian) 3-44465
 X-ray luminescence, use in chemical analysis (Russian) 3-42700
 AgCl, in different atmospheres, surface luminescence centre origin 3-80087
 AgCl emulsion, colour photographic film, blue luminescence, effect of mercaptan stabilisers (Russian) 3-47596
 AgNO₃, polarised phosphoresc. and absorp. in single cryst. 3-64729
 Ag₂O, exciton luminesc., temp. depend., 4 to 77 K 3-53139
 Ag₂O: Cd, photocond. and luminesc., 4.2 and 77K, participation of excitons 3-47312
 Al_{1-x}Ga_xAs, melt-grown, impurity obs. and recombination mechanisms (German) 3-53182
 Al_{1-x}Ga_x-P: Zn, green light emission 3-50608
 As₂S₃, amorphous, obs. down to 4 K, excitation spectra 3-44480
 As₂Se₃, glassy, photoluminesc., optical quenching, midgap localized states evidence 3-50618
 As₂Se₃:As₂Te₃, glassy, photoluminesc., optical quenching, midgap localized states evidence 3-50618
 As₂Se_{1.5}Te_{1.5}, glassy, excitation spectra and carrier diffusion lengths 3-50617
 Au, activation energy and frequency factor of traps, u.v. amplitude modulated excitation 3-41570
 BaF₂:Gd³⁺, X-irrad., V_k centre emission 3-47302
 BaO microwave optical double resonance spectra 3-75063
 BiI, spectroscopic investigation of the energy level of a bi-electron or a bi-hole (Russian) 3-44473
 BiOCl single crystals, photocond. and photolum. (Russian) 3-50234
 Bi₁₂SiO₂₀, Al doped and undoped, transport processes of photoinduced carriers 3-46868
 CaF₂:Er³⁺, Ho³⁺, two-photon excitation spectra of luminesc. 3-64730
 CaF₂:Er³⁺, i.r. to visible upconversion, sequential pair process 3-54241
 CaF₂:PrF₃(NdF₃, DyF₃, HoF₃, ErF₃, TmF₃), gamma-luminescence, phosphorescence, photoluminescence 3-53140
 CaI₂, cryst., pure and doped, X-ray luminesc. and thermoluminesc., 90 to 300 K, scintillation props. 3-44482
 CaO:GeO₂ phosphors, emission of Eu³⁺ 3-55676
 Ca(S:Se):Sb³⁺ phosphors activated with ions having s² configuration, luminescence centres 3-72711
 Ca₃SiO₄Cl₂:Pb²⁺, Eu²⁺, host lattice, luminesc. of phosphors 3-47307
 CaWO₄:Nd³⁺-LaNa(WO₄)₂:Nd³⁺ composite active medium, laser luminescence spectra 3-62720
 CdF₂:Gd³⁺, X-irrad., V_k centre emission 3-47302
 CdS, activation energy and frequency factor of traps, u.v. amplitude modulated excitation 3-41570

photoluminescence continued

- CdS, effect of surface on reflection and luminescence spectra 3-53149
- CdS, luminesc. kinetics of free and bound excitons 3-55687
- CdS, luminescence, influence of dislocations (*Russian*) 3-41555
- CdS, pure, doped and surface contaminated, excitation spectra of luminescence 3-55686
- CdS, resonant luminescence of free excitons (*Russian*) 3-41553
- CdS, single crystal platelets, electron bombardment, photoexcitation and gas adsorption effects 3-41573
- CdS, spontaneous and stimulated luminescence excited by multiphoton optical pumping 3-58557
- CdS single crystals doped with different donors and acceptors 3-53148
- CdS:Cu, and photoelec. prop. changes with photochem. reactions, recomb. centre form 3-61071
- CdS:Li, spectra, excitonic line and phonon replica 3-61067
- CdSe, edge luminesc. spectra at high excitation densities 3-58560
- CdSe, hot-exciton luminescence from 4.2 to 300 K, LO phonons 3-80099
- CdSe, luminescence, influence of dislocations (*Russian*) 3-41555
- CdSe, $\text{Te}_{1-x}\text{S}_x$ Cu solid solution, effect of Cu, 85 to 400 K, photoconductivity (*Russian*) 3-52876
- CdTe, edge and donor-acceptor pair emissions 3-80095
- CdTe lattice defects study 3-60724
- CsBr, e.p.r. of triplet state of self-trapped exciton obs. by microwave double resonance 3-58428
- CuI, magnetic circular polarisation of exciton resonance luminescence 3-80094
- Cu₂O, exciton luminesc., temp. depend., 4 to 77 K 3-53139
- Cu₂O, luminescence, resonant interaction between ortho and para-excitons with assistance of phonons (*Russian*) 3-41554
- GaAs, epitaxial, from Me_2Ga and AsH_3 3-79713
- GaAs, free and bound excitons, energy shift in mag. fields up to 12 T, photolum. study 3-46820
- GaAs, impurity recomb. radiation excited by strongly absorbed radiation 3-50622
- GaAs, paramagnetism, obs. of photolum. circular polarisation in weak mag. field 3-46980
- GaAs, self-excited luminescence 3-44477
- GaAs, shallow donor and acceptor obs. 3-55691
- GaAs, surface luminescence at laser excitation, surface treatment and cleavage effects 3-44484
- GaAs minority carrier diffusion length, obs. 3-64354
- GaAs single cryst., recovery kinetics after 600 keV electron irradiation 3-72716
- GaAs:C(Si)(Ge)(Zn)(Cd), acceptor binding energies, free to bound and bound exciton luminesc. meas. 3-47303
- GaAs:Cu, radiative recomb. at repulsive Cu centres 3-41578
- n-GaAs:Se, near bandgap photolum. meas. at transparent CrAu-GaAs Schottky contact 3-44450
- GaAs:Si, Ge, epitaxially grown, donor and acceptor energy levels 3-69177
- GaAs:Te, Ge, radiative recomb. depend. on degree of compensation 3-41579
- GaAs:Te, ion-implanted, photolum. degradation, dose depend. 3-64074
- GaAs-Al_{1-x}Ga_xAs double heterostructure, luminesc. spatial pattern obs. 3-66848
- GaAs-ZnSe solid solutions, epitaxial layers, spectral shift 3-75685
- GaAs_{1-x}P_x, i.r. emission band at 1.3 eV 3-69064
- GaAs_{1-x}P_x, photoluminesc. characterisation for electroluminesc. light emitting junctions 3-41580
- Ga_{1-x}In_xP alloys, solution-grown, composition depend. 3-80183
- Ga_{1-x}In_xP epitaxial films, $0.3 < x < 1$ 3-76075
- GaN:Be, Mg, yellow-green and blue-violet luminesc. 3-69058
- α -Ga₂O₃:Cr³⁺, excitation and emission spectra 3-41576
- α -Ga₂O₃:Fe³⁺, excitation and emission spectra 3-41576
- GaP, spectra, isoelectronic traps, complex centres 3-58225
- GaP, two-step excitation process 3-80098
- GaP:Cu, photoquenching and photostimulation spectra meas. rel. to photoionisation cross section determ. 3-80101
- GaP:N, epitaxial layers, minority carrier lifetime, luminesc. efficiency green l.e.d. 3-41585
- GaP:N, Zeeman splitting of B-line at low mag. fields 3-50615
- GaP-ZnS(Se) solid solutions, soln. grown, characterization 3-64797
- GaSe, recomb. radiation emitted under two photon excitation 3-44487
- GaSe, spectra, temp. depend., exciton recombination 3-58550
- GaSe, $\text{Se}_{1-x}\text{S}_x$, spectra, temp. depend., exciton recombination 3-58550
- GaSe p- and n-type, 4.2 K to room temperature, free exciton emission, structured emission, impurity states emission 3-53146
- Ge, doped, spectra at 4.2 and 1.7 K, effect of impurity centres 3-76076
- Ge, laser excitation, carrier recomb. in deep and shallow surface centres 3-41253
- Ge, optical pumping threshold new phenomena in exciton condensation 3-55319
- Ge, uniaxial deformed, low temp. obs. of excitons, electron-hole drops 3-75725
- HCl(Br):CN⁻ aqueous solution, nonradiative transitions in luminesc. centres (*Russian*) 3-72717
- HCl(Br):CN⁻ frozen solutions, absorpt. and luminesc. (*Russian*) 3-69067
- He, liquid, stimulated u.v. luminescence, injection of positive and negative ions 3-75642
- Hg_{1-x}Cd_xTe, spectra at various stages of annealing, electron irradiation effects 3-54982
- Hg₂I, high density excitons, biexciton annihilation, emission obs. 3-52806
- In_{0.5}Ga_{0.5}P, vapour phase epitaxial layer 3-55674
- In_{1-x}Ga_xP heteroepitaxial layer, on GaAs, vapour grown, gas phase stoichiometry effect 3-41683
- InP, donor and acceptor impurities 3-41581
- InP, shallow donor and acceptor obs. 3-55691

photoluminescence continued

- InP epitaxial layer, grown by closed-space method, characterisation 3-41680
- InSb, radiation recombination, light hole role at low temp. 3-50220
- K plasma, laser selective excitation spectroscopy for diagnostics 3-68086
- KBr, e.p.r. of triplet state of self-trapped exciton obs. by microwave double resonance 3-58428
- KBr, optical detection of paramag. reson. of self-trapped exciton 3-75882
- KBr:OH⁻ oscillatory radiation of OH⁻ induced by electronic excitation (*Russian*) 3-44470
- KBr:TI, Ag and pure crystals, tunnel luminescence (*Russian*) 3-41560
- KCl F centres, optical detection of e.p.r. and luminescence bleaching effects (*French*) 3-53021
- KCl, F-centres luminescence, electron tunnel transfer (*Russian*) 3-41551
- KCl:Te(In) two photon multistage radiation during interaction of a single electron-vacancy pair with activating centres (*Russian*) 3-41557
- KCl:TI, Ag and pure crystals, tunnel luminescence (*Russian*) 3-41560
- KCl:TI, photoluminescence (*Russian*) 3-41556
- KCl:TI⁺, Jahn-Teller effect in 3000 Å emission, time resolved spectroscopy 3-69061
- K₂(Cr³⁺O₆Mo₆O₁₈H₆).nH₂O, absorpt. and luminescence spectra, vibr. structure 3-72679
- KI, phonon structure in excitation spectra of luminescence under two-photon excitation 3-80093
- KI:Ag crystals, stimulated, nonisothermal relaxation 3-76036
- KI:Sn²⁺, negative mag. circular polarisation of A-band emission 3-44486
- KI:TI, Ag and pure crystals, tunnel luminescence (*Russian*) 3-41560
- KI:TI thermoluminescence, electric field effect 3-55694
- KMgF₃:Eu²⁺, f-f transition obs. 3-64726
- KN₃, spectral distrib. and intensity (*Russian*) 3-44476
- La₃AlO₅:Cr³⁺, temp. broadening and shift of R line 3-64718
- La₂Be₂O₅:Nd³⁺, spectra and decay time 3-44485
- LaCl₃:Pr³⁺, energy transfer processes 3-72706
- LaF₃:Pr³⁺, energy transfer processes 3-72706
- LiCl-Ni X-ray photolum. and thermolum. (*Russian*) 3-69068
- LiCl(Br):CN⁻ frozen solutions, absorpt. and luminesc. (*Russian*) 3-69067
- MnCl₂ with dimethylquinoline hydrochlorides, photoluminescence props. 3-41549
- MnF₂:Er³⁺, energy transfer between Mn²⁺ and Er³⁺ (*Russian*) 3-44464
- Mn(IV), efficient emission in FI coordination 3-58545
- N₂ solid, vibr. relax. phenomena of N₂ mol. 3-44463
- (NH₄)₂(Cr³⁺O₆Mo₆O₁₈H₆).nH₂O, absorpt. and luminescence spectra, vibr. structure 3-72679
- NaCl, perturbation of intrinsic luminesc. by lattice defects 3-80096
- NaCl:TI, Ag and pure crystals, tunnel luminescence (*Russian*) 3-41560
- NaCl:TI, luminescence, influence of channelling under the influence of positive ions (*Russian*) 3-41550
- Na₂(Cr³⁺O₆Mo₆O₁₈H₆).8H₂O, absorpt. and luminescence spectra, vibr. structure 3-72679
- NaLa(WO₄)₂, NaY(WO₄)₂, spectra 3-69009
- NaMgF₃:Eu²⁺ f-f transition obs. 3-64726
- NaN₃, spectral distrib. and intensity (*Russian*) 3-44476
- Nd³⁺ impurity in ionic crystals, excitation energy transfer, phonon stimulation (*Russian*) 3-41564
- PbBr₂ layers, exciton absorption range, temp. range 180 to 220 K (*Russian*) 3-55981
- PbBr₂, low temp. luminescence in excitation energy range 4 to 12 eV (*Russian*) 3-50614
- PbBr₂, low temperature, thermal quenching, cation exciton model (*Russian*) 3-44454
- PbCl₂, low temperature, thermal quenching, cation exciton model (*Russian*) 3-44454
- PbCl₂ low temp. luminescence in excitation energy range 4 to 12 eV (*Russian*) 3-50614
- PbF₂, low temperature, thermal quenching, cation exciton model (*Russian*) 3-44454
- Pb(OH)I, gel-grown single cryst. 3-44479
- Rh(III) complex, halopentammine, radiative and radiationless decay processes 3-73158
- Se, trigonal, electrophotoluminescence at 4 K with a.c. and d.c. voltages 3-69062
- Si, energy of formation of biexcitons 3-50156
- Si, laser excitation, carrier recomb. in deep and shallow surface centres 3-41253
- Si, laser-excited electron-hole recomb. at deep impurity centres 3-76074
- Si, thermally treated, decay of excess carrier concentration 3-68561
- Si:B, emission lines and model of multiple exciton complexes bound to impurities 3-58553
- Si:O, irradiated, annealed, low temp. spectra 3-61069
- Si:P, emission lines and model of multiple exciton complexes bound to impurities 3-58553
- SiC, 4H polytype, grown from Si melt, u.v. excited 3-61063
- SiC, exciton-impurity complexes spectra, impurity centres interaction, photolum. 3-44046
- 6H SiC, H- and D-implanted, efficient luminescence centres 3-58558
- α -SiC(6H), of excitons localised at donor-acceptor dipoles 3-72714
- Si₂Te₃ crystals, photoluminescence and e.p.r. of defects 3-58556
- SrCl₂:Yb²⁺, single crystals, photoluminescence (*Russian*) 3-41552
- SrS phosphors, effect Of Bi and Cu activators 3-69054
- SrTiO₃:Cr³⁺, thermally stimulated, luminesc. excitation mechanism obs. 3-64704
- TaBO₄, u.v. excited, low temp. luminesc. 3-68989
- YAG:Nd³⁺, energy level temp. shift obs. 3-64727
- YAlO₃:Ce³⁺, 5d-4f fluorescence, and sensitised fluoresc. with Nd and Cr codoping 3-58531
- YAlO₃:rare earth, absorpt. and emission intensities for trivalent rare earth ions 3-47296

photoluminescence continued

- YAlO₃: rare earth, nonradiative relax. by multiphonon emission 3-47309
- YLAG: Nd³⁺, spectral props. and induced emission 3-53131
- Y₂O₃: Eu³⁺, energy transfer interaction between Eu³⁺ ions situated in different lattice positions (*Russian*) 3-41565
- Zn₂Cd_{1-x}S: Cu, Cl solid soln., peculiarities of recombination processes 3-52875
- ZnGa₂O₄, exchange interactions of nearest neighbour Cr³⁺ pairs, spectra obs. 3-53142
- ZnO, and stimulated emission after two-quantum excitation, free, bound exciton form. (*German*) 3-58529
- ZnO: Ag, Cl phosphors, emission characts. 3-69056
- Zn(S, Se): I annealed in liquid Zn, resistivity and photoluminescence 3-58544
- ZnS, Ag and Zn ion implanted, characteriz. 3-72817
- ZnS, photolum., visible region, electron irradi. effects 3-47318
- ZnS, spontaneous and stimulated luminescence excited by multiphoton optical pumping 3-58557
- ZnS: Cu, blue centres, emission mechanism 3-44436
- ZnS: Cu, gamma ray and u.v. irradiation, dose dependency meas., electron hole pair production (*Russian*) 3-76056
- ZnS: Cu, photoelectronum., u.v. flux and appl. voltage amplitude and freq. depend. 3-58565
- ZnS: Cu, spectral effect of exciting frequency and temperature 3-80112
- ZnS: Cu monocrystals, shift in band maxima with temp. (*Russian*) 3-72722
- ZnS: Cu, ZnS- Mn, activation energy and frequency factor of traps, u.v. amplitude modulated excitation 3-41570
- ZnS- Cu luminophore, quenched in vacuum, effect of milling 3-80086
- ZnSe, pair spectra and shallow acceptors 3-58555
- ZnSe: Mn, excitation and emission spectra obs. at 85K 3-61064
- ZnSe: Mn, luminescence origin 3-53147
- ZnTe, at 77-295K, obs. of seven bands from green to i.r. 3-61073
- ZnTe: Cu, impurity and native defect levels determ. 3-41153
- ZrO₂ powder, analysis of complex spectra (*Russian*) 3-64737

photolysis

- ammonia, collisional deactivation of c¹π and A³π states of imino radicals 3-65102
- aqueous solutions at 77K, e.s.r. obs. and calculations of trapped H₂O²⁺ and H₂O 3-55980
- azo compounds, e.s.r. of aliphatic ester radicals and complexed radical 3-55979
- benzenoid aromatic hydrocarbons, time-profiles of transient absorpt. obs. in kinetic spectrophotometry 3-63500
- cryostat, for flash photolysis installation 3-53861
- dichloro-fluoro-methane, vacuum u.v. photolysis, matrix isolation study, i.r. spectra 3-40629
- diffuoro-chloro-methane, vacuum u.v. photolysis, matrix isolation study, i.r. spectra 3-40629
- dual beam flash photolysis system, for transients 3-42671
- dyes adsorbed on emulsion grains, flash photolysis 3-55982
- EDA complexes with liquid donors, excited singlet-singlet absorpt. spectra 3-76471
- ethylene oxide, vacuum-u.v. photolysis 3-73157
- flash-photolysis, pulsed source, continuous spectrum, visible and u.v., description 3-73755
- 1-fluoro-2 trifluoromethylbenzene, photolysis in gas phase 3-47581
- 1-fluoro-3 trifluoromethylbenzene, photolysis in gas phase 3-47581
- 1-fluoro-4 trifluoromethylbenzene, photolysis in gas phase 3-47581
- formaldehyde, sensitized decomposition to formyl radical, e.s.r. and electronic spectra 3-47577
- formyl fluoride photochem. laser behaviour, HF i.r. emission 3-44733
- gases in v.u.v., apparatus for flash photolysis 3-48673
- iodine-iodoform solns., laser flash photolysis, transient species obs. 3-65097
- Jovian atmospheric reactions, qualitative picture 3-69879
- Martian atmosphere, photolytic stability rel. to convection and low altitude aerosol 3-65768
- methanol, vacuum-u.v. photolysis, i.r. spectrum of CH₂OH radical 3-65105
- β-naphthol excited systems, primary processes, pulsed laser photolysis study 3-73156
- polymethine dye, induced absorpt., laser excitation 3-65112
- polymethine dyes, study of electron excitation energy transfer 3-69479
- radical ion and triplet form. in electron transfer fluoresc. quenching by nsec. laser spectroscopy 3-80563
- retinol, primary photoprocesses 3-47575
- rhodopsin and meta-rhodopsin, absorption spectra (*Japanese*) 3-50849
- sodium pyrenide in tetrahydrofuran, flash photolysis, photo-oxidation and Na⁰ existence 3-61270
- AgI hydrosols, ice-nucleating properties, UV radiation 3-44897
- AgX absorption spectra (X = halide), early photolytic stages, quasimetallic centres, fluctuation theory, effects (*Russian*) 3-80084
- Cl atom recombination obs. by flash photolysis 3-41861
- DAr₄⁺ in solid Ar, i.r. absorption 3-65104
- Fe(CO)₅ vapours in air, condensation nuclei formation 3-61271
- HA₄⁺, in solid Ar, i.r. absorption 3-65104
- H₂S₂, flash photolysis, HS₂ radical obs. 3-75003
- H⁺ + methanethiol hot atom reactions 3-76485
- I atom recombination by flash photolysis, kinetic isotope effect 3-73153
- I₂ photodissoc. laser, apparent late-time gain 3-62693
- NH₃ in Jupiter's atmosphere, photolysis rel. to composition and temperature 3-61681
- NO + O₃ → NO₂ + O₂, O₂(¹Δ_g) and O₂(¹Σ_g⁺) possible production 3-47572
- NO₂, energy disequilibrium meas. 3-80568
- O + O₂ + O₂ → O₃ + O₂ recomb. reaction, vibr. excitation of O₃ 3-76477
- O₃, 1330 Å, quantum efficiency for O(¹D) prod. 3-41860

photolysis continued

- O₃, time-resolved absorption spectroscopy in vac. u.v. of O₂(a¹Δ_g) 3-46269
- O₃-D₂-N₂O flash, optical gain and laser emission 3-48873
- O₃-D₂(H₂)-CO₂ flash, optical gain and laser emission 3-48873
- OH + NH₃ → NH₂ + H₂O reaction absolute rate const., pulsed photolysis obs. 3-65076
- Pb halides, initial and printout processes, e.p.r., image formation 3-61279
- PbBr₂, layers, exciton absorption range, temp. range 180 to 220K (*Russian*) 3-55981
- PbCl₂(Br₂)(I₂), role of anion vacancy migration 3-72229
- Pd(II) complex, trans-planar, energy transfer to ligand-field states 3-41854
- SO₂, flash excitation, SO(³Σ⁻) prod. 3-58807

photomagnetic effect *see photoelectromagnetic effects***photomagnetolectric effect** *see photoelectromagnetic effects***photometers**

- see also photometry; spectrophotometers*
- astronomical two-beam multi-mode nebular-stellar photometer 3-42251
- Atmosphere Explorer, airglow photometer for thermospheric emission measurements 3-42076
- Atmosphere Explorer, e.u.v. photometer for solar observ. 3-42262
- aurora latitude time behaviour obs. using meridian scanning photometer 3-69741
- auroral photometer, ISIS-II scanning instrument 3-65513
- automatic exposure system, for low light intensities (*German*) 3-48419
- brightness meter, meas. of area and time distrib. of luminous objects 3-66216
- calibration rel. to air, directed light, attenuation coeff. meas., effect of salinity and temp. (*Russian*) 3-45483
- computerized digital light scattering photometer for molecular weight determ. 3-42714
- continuous u.v. absorption O₃ photometer 3-59716
- cosmic ray nuclei charge determ. in photonuclear emulsions 3-56462
- digital for chemical analysis 3-45602
- electronic, use with electron microscope, charge measurement based on operational amplifier 3-56691
- exposure meter, use of CdS PPF7-1 photoresistors, prod. and testing procedures 3-39916
- exposure setting device, amateur camera, programmed automatic mechanism, design 3-53939
- f.d.m. multichannel photoelectric photometers, astron. appl. 3-53726
- flame, for Na-concentration deter. (*Polish*) 3-62094
- flame ionization-flame emission detector instrument, for response and aerosols of phosphorylated hydrocarbons 3-62342
- flow microfluorometer, dual parameter, mammalian cell analysis, operation 3-66400
- light scatt. photometer for kinetic studies of flowing aerosols, particle size distrib. 3-40082
- light scattering, slit arrangements (*German*) 3-48416
- microphotometry of spots produced by electron-photon cascades on X-ray film, semi-automatic device (*Russian*) 3-66270
- mirror-geiger tube photometers for obs. of galactic far u.v. backgrounds 3-48103
- modulated beam, for thin film transmission and reflectance monitoring 3-53901
- nephelometer, integrating, absolute calibration method 3-59465
- photodiode, flux power meas. at 0.6328 μ 3-73746
- photoelectric photometer with msec. integration time for lunar occultations of stars 3-45248
- photographic, meas. of deformation of developed films (*German*) 3-39964
- photographic exposuremeters, application to photometry, correlations and calibrations 3-77473
- polyvinyl fluoride optical detectors, mathematical model for response analysis 3-77393
- rocketborne, for rotational temp. meas. in aurora 3-65534
- scanning, photoelectric, for astronomical problems (*German*) 3-77190
- scanning microscope photometer, with programmed control (*German*) 3-73748
- shutter exposure time testing instruments 3-39962
- skylight intensity measurement, scanning field apparatus 3-80861
- small contrast photographic pictures digital readout (*Slovak*) 3-53929
- K trace analysis, modification to flame photometer 3-45587
- O red line photometer, ISIS-II, auroral and airglow obs. 3-65514

photometric light sources

No entries

photometry

- see also brightness; colorimetry; densitometry; spectrophotometry*
- aerosol size distribution, effect on integrating nephelometer accuracy 3-47836
- airborne, optical properties of coastal waters 3-77477
- astronomical photoelectric photometry in u.v.-i.r. band up to 1 μ, optimum operating modes 3-42255
- calibration procedures, NBS, report 3-42562
- Comet Bennett (1969 i), equidensity method (*Russian*) 3-77014
- Comet Tago-Sato-Kosaka (1969 g), equidensity method (*Russian*) 3-77013
- dynamic magnetostriction meas. by photometric method (*Russian*) 3-56703
- electro-optical studies, NBS 3-53854
- filter-fluorimeter based on compensation in electronic measuring cct. (*Hungarian*) 3-62097
- flame, for Na-concentration deter. (*Polish*) 3-62094
- galactic nebulae at |b| > 20°, Hβ photometry 3-56452
- galaxies, comparison of parameters of southern galaxies measured at Cordoba and Mt. Stromlo 3-48112
- galaxies, nuclear magnitudes 3-77174
- K-giant stars, N₂ enrichment due to meridional circulation, rel. CN-strength 3-69949
- grating target, brightness additivity 3-51454

photometry continued

- heterochromatic using synchrotron radiation calibrated detector 3-39995
- human cones, optical density 3-51456
- image structure analysis of photographic records, 2 dimens. Fourier transform meas. 3-42594
- Jovian atmosphere, data of photolytic reactions examined 3-69879
- L-929 cells, phase duration by impulescycophotometry (*German*) 3-77202
- I.e.d.s., lasers, sun, discussion of measuring methods 3-66213
- light scattering microscopic rough surface, scattering indicatrix shape, gloss measurement (*German*) 3-59842
- Mauna Kea, Hawaii, evaluation as an observatory site 3-77194
- measurement techniques and equipment, review (*German*) 3-53902
- metallography applies. of microrefl. 3-47379
- meteor trails, variation of colour index 3-77016
- minimally-distinct-border, chromaticity difference, method, review 3-66214
- modular aurora and airglow photometer system 3-44956
- Neptune, wavelength dependence of albedo from 0.3 to 1.1 μ photoelectric photometry 3-80982
- NGC 1068, Seyfert galaxy, i.r. photometry, quiescent period, i.r. outburst variability 3-48106
- photocathode aging effect on measurements 3-66212
- photoelectron spectroscopy in XUV 3-39918
- quartz rich metamorphic rocks, determ. preferred orientation of optic axis 3-57971
- reflectivity, measurement of diffuse and specular components 3-77476
- Saturn's rings, deconvolution of raw photometric curves (*French*) 3-56341
- Seyfert galaxies, two component photometric model, nuclear magnitude correction, appl. to luminosity distrib. 3-51384
- thiovioluric acid, complex formation, photometric determination of Co in presence of Ni 3-48650
- Uranus, wavelength dependence of albedo from 0.3 to 1.1 μ photoelectric photometry 3-80982
- zodiacal light obs. from space, OSO-6 meas. 3-53630
- zodiacal light perturbation in Earth-Moon system 3-53631
- He 1 584 A diffuse radiation, evidence and model of interplanetary source 3-47977
- OH airglow, structure and fluctuations in i.r. 3-76791
- OI 5577 A airglow satellite obs. 3-76794
- OI(6300 A) emission near plasmopause predawn enhancement 3-69684
- Pr₆O₁₁ thin films, optical properties meas. by photometry and ellipsometry 3-53159

photomultiplier tubes *see photomultipliers***photomultipliers**

- apparatus for luminescence properties meas. of X-irradiated solids (*Russian*) 3-48560
- Lallemand's, physics and non-linear effects 3-70376
- in laser Doppler instrument in vibration measurement 3-66144
- laser Doppler systems, choice of photodetector for specific operating conditions 3-66265
- luminescence decay time meas. errors caused by photomultiplier saturation 3-73898
- phase response measurement, high freq. heterodyning mode 3-73747
- photoelectric methods, for ultra low light intensity meas. 3-45575
- for scintillation counting, IEEE standard test procedure 3-59639
- secondary electron emission, intrinsic nonlinearity 3-41598
- secondary emission, search for intrinsic nonlinearities 3-77442
- sensitivity, effect of toroidal magnets 3-73563
- stabilization of receiving-amplifying path 3-56964
- GaP(Cs) dynodes, five stage photomultiplier 3-76115
- NaI, crystal gamma-ray spectrum, non-constant Bevatron beam, photomultiplier resolution, feedback compensation circuit 3-77703

photon counting

- atomic fluorescence spectrometry, photon counting or lock in amplification, comparison 3-70456
- channel plate arrays, particle and photon counting, high gain, resolution improvement 3-77623
- chaotic and modulated coherent fields M-mode superposition, photon counting distribution 3-57216
- correlation spectroscopy, factors affecting accuracy 3-62109
- dead time correction technique 3-78001
- fluorescence, lifetime meas., single photon apparatus 3-69085
- Gaussian light, photoelectric counting statistics, spatial coherence effect 3-42987
- interference spectroscopy apparatus, Fabry Perot linear scanning, method (*French*) 3-66238
- light propagation through random medium, photon counting statistics 3-77998
- light propagation through random medium dynamic field eqns., quasi-distributions, characteristic functions 3-77997
- many interacting waves far from thermal equilibrium, statistics 3-43039
- mixed coherent and chaotic radiation, statistics, approximate formula 3-77999
- photoelectron probability distribution of laser in several axial modes, analysis 3-62731
- radiation field, microscopic, phase meas., using ideal laser amplifier 3-66892
- spatial coherence function parameters, statistical errors 3-48865
- Statistics of photocount products 3-78002
- thermal light consisting of two spectral lines, counting statistics 3-59851
- thermal light containing two spectral lines, counting statistics 3-66782
- two-level system in interaction with linearly polarized e.m. field, energy spectrum 3-42983

photon interactions

- see also gamma-ray interactions; hadron photoproduction; nuclear reactions and scattering due to photons*
- annihilation, Regge and parton models 3-43116
- coherent photoprocesses on nuclei, optical concepts 3-48993
- Dirac electron in field of quantised e.m. wave and in homogeneous magnetic field, eigenfunction determ. 3-70911

photon interactions continued

- meson production, point spinless pair, by two photons 3-52010
- photoabsorption, real and virtual, model of diffractive parton scattering from hadrons 3-67057
- photoabsorption and e-N inelastic scatt., SU(6) \times O(3) model of higher baryon couplings 3-43115
- photoabsorption sum rule derivation in parton model 3-70887
- photon-neutrino weak coupling and self-consistent theory for weak interactions 3-45864
- threshold values for scattering of light by light in vacuum free of field influences 3-70843
- total cross sections, energy dependence, Regge theory 3-57458
- triplet production by polarized photons 3-74384
- two-photon and possible weak interferences in inclusive e^+e^- annihilation 3-52011
- two-photon exchange production of lepton pairs in hadron-hadron collisions 3-67130
- two-photon inclusive hadron production, role in high-energy e^+e^- collisions 3-57360
- virtual, partonic content, vector meson dominance effects on parton cluster models 3-67032
- virtual photoabsorption total cross sections, parton dynamics 3-70941
- $e^+\gamma \rightarrow e^+A$, deep inelastic diff. cross section, comparison with $e^+\gamma \rightarrow e^+e^-e^-$ 3-43108
- $\gamma d \rightarrow d\pi^0$, differential cross section, wave functions influence 3-70918
- γe , pair production, differential cross sections, $E_\gamma < 5$ MeV, energy spectra, angular distributions 3-59972
- $\gamma\gamma \rightarrow h(\text{hadrons})$, diffractive excitation and sum rule 3-45880
- $\gamma\gamma \rightarrow X$, parton model, prediction of equivalent-photon method for $ee \rightarrow ee + X$ 3-70934
- $\gamma\gamma \rightarrow \nu\bar{\nu}$ Salam-Weinberg model, 2 BeV 3-80919
- $\gamma\gamma \rightarrow \pi^+\pi^-$ anything, predicted differential cross section by factorisation of Regge trajectories 3-60052
- $\gamma\gamma \rightarrow \pi^+\pi^-\pi^+\pi^-$, 18 GeV, photon dissociation into four pions, evidence for ρ enhancement in 4π mass spectrum 3-57364
- $\gamma\gamma \rightarrow \pi^+\pi^-\pi^+\pi^-$, 9-18 GeV, spin-parity analysis of ρ' 3-57365
- $\gamma\gamma$ total and partial cross sections at 9.3 GeV, bubble-chamber expt. 3-70936
- $\gamma\tau$, rotational properties of production amplitude, reln. to e.m. form factor 3-49006
- $\pi\nu \rightarrow \pi\nu$, kinematics, gauge invariance and helicity conservation 3-54318

photon-phonon excitations *see polaritons***photon polarisation**

- circular, correction from divergent P-violating NN ρ vertex in $np \rightarrow d\gamma$ 3-78198
- Compton scattering by polarized electrons, photon polarization plane obs. (*German*) 3-62840
- Compton scattering of off-shell photons on polarised nucleons, invariant amplitudes 3-67018
- low-energy linear polarisation meas. by pair production, asymmetry ratios 3-59969
- photoproduction polarisation theorems for all spin-J boson exchanges 3-52013
- triplet production by polarized photons 3-74384
- $\gamma d \rightarrow \pi^- + \text{anything}$, 7.5 GeV, linearly polarised photon beam 3-67040
- γN , 16 GeV polarised photons, charged pion production asymmetries 3-45878
- $np \rightarrow d\gamma$, circular polarisation of γ and weak P-odd NN ρ vertex (*Russian*) 3-40376
- ^{12}C , resonance fluorescence of 1^+ state at 15.1 MeV, production 3-71102
- $^{54}\text{Cr}(\text{p},\text{n})^{54}\text{Mn}$, meas. of polarisation of deexciting gamma-rays (*Russian*) 3-52126
- $^{64}\text{Ni}(\text{p},\text{n})^{64}\text{Cu}$, meas. of polarisation of deexciting gamma-rays (*Russian*) 3-52126

photon scattering

- see also Compton effect; gamma-ray scattering; nuclear reactions and scattering due to photons*
- bubbles of photons in scattering atmosphere 3-53651
- coherent-incoherent, by atoms, discrete ordinates transport calcs., computer program 3-74756
- electroproduction of hadrons, parton model, logarithmic enhancements 3-78142
- inelasticity, excitation and dissociation modes at high energy 3-52041
- in planetary atm., path length distrib. for diffuse reflection 3-65739
- semitransparent plasma, photon scatt. by Langmuir oscill., effect on spectra, astron. appl. 3-60611
- wavelength selection, scattering process simulation, Monte Carlo programme, parallel computers 3-62433
- ep , compton kernel from invariant 4-vector representation 3-74374
- γN , high energy, extended hadronic structure 3-57363
- γN scalar scatt., Jost-Lehmann-Dyson representation and scaling 3-54315
- H, 1-s state, retardation in elastic scattering calc. (*Russian*) 3-63262

photons

- see also cosmic ray photons; gamma-rays; light; X-rays*
- 150 MeV-600 MeV, experimental study (*French*) 3-60063
- bubbles of photons in scattering atmosphere 3-53651
- emission in static e.m. field, quasi-classical soln. (*Russian*) 3-43118
- gauge particle, model of electromagnetic interactions, no neutral currents or heavy leptons 3-59950
- inclusive production in pp interactions at 69 GeV 3-74449
- massless particle decay, phase restrictions, conservation laws 3-59965
- materialisation, pair spectrometer, magnetostrictive read-out, computer on-line data storage (*French*) 3-48554
- nonzero mass existence, physical consequences (*French*) 3-40230
- position operator construction in photon's own reference system 3-45842
- production in 69 GeV pp interactions, conversion into electron pairs 3-67157

photons continued

- production in neutron transport through air and sodium, emission anisotropy effects 3-49305
- properties, similarity to pion properties, description of spectra from pp collisions (*Russian*) 3-74407
- quantum electrodynamics without ultraviolet infinities 3-49000
- radiation monitoring of personnel rel. to photons and neutrons standardisation of dosage 3-63241
- rest mass, in rel. to mean mass density of Universe and clusters of galaxies, existence of intergalactic magnetic field 3-65624
- rest mass, upper limit in reln. to intergalactic magnetic fields 3-51386
- retinue, electron induced, i.r. divergence problem in QED 3-66994
- stability with respect to decay to graviton plus photon 3-70940
- structure functions for $e^+e^- \rightarrow n\pi^+n\pi^- \gamma$ 3-67043
- structure functions from $e^- \gamma \rightarrow e^- A$, deep inelastic diff. cross section, comparison with $e^- \gamma \rightarrow e^- e^+ e^-$ 3-43108
- synchrotron radiation, soft photon emission, domination by radiation damping effects 3-70917
- transverse force on light refracted by matter 3-40231
- two-photon exchange in ed scattering, Glauber theory 3-67042
- virtual, partonic content, vector meson dominance effects on parton cluster models 3-67032
- $\gamma \rightarrow 3\pi$ vertex, low energy theorem 3-40344
- $\nu\nu$ description, in framework of local Lagrangian field 3-62816
- He atom, double ionization by high energy photons 3-78485
- Se, two photon photo-generation in amorphous state, Poole-Frenkel model 3-55305

photonuclear reactions see *nuclear reactions and scattering due to photons*

photophoresis

- radiation press. on absorbing spheres, and phosphoresis, heat source function 3-51849

photoplasticity

- celluloid, lateral contraction coeff., similarity condition (*Polish*) 3-61213
- elasto-visco-plastic material, isoclinic parameter expt. 3-43822
- polycarbonate as model material for three-dimens. photoplasticity 3-73064
- Al, alloys, lateral contraction coeff., similarity condition (*Polish*) 3-61213
- NaCl:O $^{2-}$, u.v. illuminated 3-58077

photoresistors

- inertial, for investigation of shape of short light pulses 3-51582
- CdS, FPF7-1 type, for use in exposure meters, prod. and testing procedures 3-39916

photoresists

- bisazide compounds, spectral sensitization 3-61280
- exposure parameters 3-59605
- glass, 0.1 μ m periodic surface struct. prod. by laser interference on surface photoresists 3-59901
- holographic diffraction gratings, profile formation 3-66780
- photocopying, diffraction problem 3-62162
- semiconductor wafer processing chemicals 3-76142

photosphere

- 5-minute oscill., high-vel. horizontal phase propag. 3-65674
- A5-V class stars, model construction using Mustel's method (*Russian*) 3-73490
- arch filament systems, mag. structure 3-65709
- coronal helmet development compared with photospheric and chromospheric activity 3-65713
- element abundance, survey of f-values needed for calculations 3-80976
- equatorial currents detection from spectra 3-61664
- filament feet positions determ. rel. to supergranular Ca network 3-65669
- geomagnetic Kp-index variations rel. to photospheric activity 3-65715
- granular vels., effect of finite spectral and spatial resolution on Doppler shifts 3-65672
- granulation, dynamics rel. to models 3-45005
- granulation plate record, statistical anal. 3-65972
- isotopic composition, photospheric and sunspot spectra, atomic line studies 3-61672
- large-scale distrib. of activity during Cycle 19 period 3-51269
- limb darkening at extreme solar limb during 1972, July 10 eclipse 3-47883
- limb darkening eqn., Phillips-Twomey method in presence of noise 3-80933
- magnetic field behaviour, interpretation of obs. (*Italian*) 3-61665
- magnetic field representation, force-free, practical method 3-69830
- magnetic field vertical distribution, study of Fraunhofer lines (*Russian*) 3-76976
- magnetically active regions, 5-minute oscill. 3-65675
- moustaches, rel. to chromospheric and photospheric phenomena 3-65706
- multichannel diode array for solar photoelectric measurements 3-81218
- one-component model, radiative transfer and statistical equilibrium eqns. 3-80925
- optical heterodyne radiometry of solar surface 3-61654
- photoelectric profiles, damping constants and turbulence velocities by Voigt method 3-76986
- quasiperiodic wavelike motions, direct spectroscopic meas. 3-53613
- radio sources connection with sunspot groups and local magnetic field, study during partial eclipse (*Russian*) 3-76981
- solar atmosphere, response to granular excitation forced by convection 3-45004
- solar granulation, cinematography using red continuum filtergrams 3-80951
- source function determ. for upper photosphere 3-59257
- spectra, C $_2$, CH, CN, MgH, NH and OH molecular lines and oscillator strengths 3-69829
- spontaneous bound-free transitions for 2p 2 $^3P^e$ state of H $^-$ 3-73440
- stellar, coefficient of absorption of radiation by H $^+$ ions (*Russian*) 3-73491
- sunspot umbra, physical parameters (*Russian*) 3-76977
- sunspots visible observations in Poland for 1971 3-73441
- u.v. continuous opacity sources, search 3-65649

photosphere continued

- velocity fields, from radial velocities (*Russian*) 3-76975
- C $_2$ Phillips bands, absence in photospheric spectrum 3-61661
- CO isotope bands in i.r. spectrum, solar $^{13}\text{C}/^{12}\text{C}$, $^{18}\text{O}/^{16}\text{O}$ and $^{17}\text{O}/^{16}\text{O}$ abundance ratios 3-61651
- Ca II flocculae, structural changes and regularities during Cycle 19 period 3-51268
- Fe I lines, effect of LTE departures and microturbulence 3-65673
- Mn I and II abundance, beam-foil spectra lifetimes 3-78442
- RbI resonance lines at 7800 and 7949 Å in photosphere, isotopic effects 3-42134
- Si abundance from analysis of 19 photospheric Si I lines 3-59255
- Tm II abundance, beam-foil spectra lifetimes 3-78442

phototransistors

- animal activity-analysing system, infrared l.e.d.'s, three arrays, computer analysis 3-73933

phototubes

- see also *photocathodes; photomultipliers*
- electronographs, astronomical 3-73566
- spectral sensitivity measurement, interlaboratory comparison 3-66218

photovoltaic cells

- GaAs p-n junction, photovoltaic effect due to two photon process in presence of built-in field 3-68696

photovoltaic effects

- m.o.s. structure, with nonstationary depletion layer, rel. to ionising radiation detection (*Russian*) 3-52905
 - p-n junction, laterally illuminated, theory 3-52869
 - semiconductor layered structure, potential distrib. at arbitrary illumination, calc. 3-55301
 - semiconductor photoconductographic system with p-n junction, dark current compensation 3-73801
 - semiconductor two-layer structure, potential distrib. for illumination at one point 3-55302
 - triglycine sulphate, temp. dependence of pyroelectric volt. response to step i.r. signals 3-44377
 - xerographic discharge characts. of photoreceptors with bulk generation, time varying exposure 3-44108
 - xerographic discharge characts. of photoreceptors with bulk generation, flash exposure 3-46869
 - AgBr, photographic emulsions, photovoltaic effect, effect of dye sensitisation, electron and hole traps 3-53343
 - AgBr(I), photographic emulsions, photovoltaic effect, effect of dye sensitisation, electron and hole traps 3-53343
 - Al/tetracene/Au sandwich cell 3-46904
 - As $_2$ S $_3$:Ag, amorphous film, obs. in Ag photodoping, energy band model 3-58302
 - Au-GaP, Schottky barrier, wavelength modulated photovoltage spectra 3-55618
 - CdTe film evaporated obliquely in high vacuum, anomalous photovolt. effect, thickness effects 3-75774
 - CuInSe $_2$, semicond., band gap obs. 3-46844
 - Cu $_2$ -xS-CdS system, distribution changes of photovoltaic effect 3-60893
 - GaAs minority carrier diffusion length, obs. 3-64354
 - GaAs p-n junction, laterally illuminated 3-52869
 - GaAs p-n junction, two photon process in presence of built-in field 3-68696
 - n-GaAs single-crystals, spectral distributions, sensitivity, photoconduction 3-50232
 - GaP-ZnS(Se) solid solutions, soln. grown, characterization 3-64797
 - GaSe single crystals, homogeneity obs. using 'optical probe' technique 3-60898
 - Ge, obliquely film, signal reversal of anomalous photovoltaic effect 3-79730
 - Hg $_{1-x}$ Cd $_x$ Te, spectra at various stages of annealing, electron irradiation effects 3-54982
 - In $_x$ Ga $_{1-x}$ As:Ge p-n junction, grown by liquid phase epitaxy 3-50266
 - InSb, electron energy dissipation, near impact ionisation threshold 3-58305
 - PbSe, p-n junction temp. and substrate impurity conc. depend. 3-58298
 - Si amorphous film-electrolyte interface, mobility gap obs. 3-52867
 - Si carrier recombination after light pulse excitation for medium-high carrier conc. levels 3-46858
 - Si film, amorphous, annealed 3-64380
 - Si solar cell junctions, surface photovoltage obs. 3-41226
 - p-Si:N $^+(N_2^+)$, lateral photovoltage, dose depend. 3-52872
 - SnO $_2$ -CdSe n-n heterojunction elec. and optical props. (*Korean*) 3-72399
 - ZnS, anomalous photovoltaic effect 3-44111
- photovoltaic generators, solar** see *solar cells*
- physical chemistry**
- see also *chemical analysis; chemical equilibrium; chemical reactions; chemical structure; crystal chemistry; electrochemistry; nuclear chemistry; pH; photochemistry; quantum chemistry; radiation chemistry; radiochemistry; solvated electrons; surface chemistry; thermochemistry*
 - analog computer soln. of particle infinite well, expt. for college curricula 3-53812
 - benzene-cyclohexane-dioxane ternary mixtures, dielectric behaviour 3-73175
 - bibliography, introductory physical chem. course 3-77357
 - collagen fibres, hydrated, proton exchange and molecular orientation of H $_2$ O and D $_2$ O, n.m.r. studies 3-55993
 - data acquisition expt. for instrumental analysis, for inclusion in college curricula 3-53820
 - gas solubility effective hard sphere diameter, temperature dependence 3-41870
 - gases at infinite dilution in liquids, liquid compressibility and partial molar volumes, states correlations 3-58815
 - group theory, chem. applications, overhead projection of character tables 3-77371
 - heats of vaporisation, calculation from hard sphere equations of state 3-41871
 - homogeneous swollen films, binary diffusivities 3-80574
 - hydrocarbons adsorbed on zeolites, ^{13}C n.m.r. investigations (*German*) 3-47600

physical chemistry continued

- molecular complex formation equilibria, solvent effects, nonpolar analog model 3-53358
- rate of solution of horizontal surface of solid body in liquid, free convective cellular motion 3-46390
- solute adsorption, restricted diffusion in liquids with fine pores 3-80579
- solvated electrons in polarised dielec., ab initio Hartree-Fock calcs. 3-50827

physical data, collections of *see collections of physical data***physical metallurgy** *see metallurgy***physical optics**

- scattering of radiation and information content 3-42975

physics

see also computational physics

- 56th Physics Exhibition, Alexandra Palace, March 1972, report 3-51482
- bibliography No.25 of unclassified documents published by AWRE 3-73627
- careers for physics students, seminar for graduating seniors 3-66097
- chemical, book 3-57595
- chemical, student exercises, book 3-60347
- conceptually complete physics and Weizsackers hypothesis (German) 3-42491
- conference, Norwegian Physical Society, Tromsø, Norway, (June 1972) 3-39842
- conference, Swiss Physical Society, Berne (Apr. 1972) 3-48319
- Copernican revolution influence on physics and cosmology development (Polish) 3-51264
- course with illustrative material from biology and medicine 3-53810
- degree courses, in Britain, a comparison 3-51488
- dictionary, concise 3-70226
- environmental physics teaching course 3-51486
- examinations, grading system 3-53817
- general physics, student textbook 3-51504
- high school project, based on Personalized System of Instruction (Keller Plan) 3-59519
- microcomputers for introductory physics laboratories 3-51502
- Personalized System of Instruction, college physics 3-59518
- Personalized System of Instruction rel. to high school project physics 3-59519
- student textbook, Physics, the foundation of modern science 3-51505
- Swiss Physical Society Meeting, Lucerne (Oct. 1972) 3-42490
- teaching, high school, students' view of current practices 3-59517
- tests, computer-generated 3-59520

physics fundamentals

see also classical field theory; complementarity; cosmology; elementary particles; fundamental law tests; mechanics; quantum field theory; quantum theory; relativity; thermodynamics; units (measurement)

- acausality and renormalizability 3-48982
- causality, absorpt., dispersion made signal rel. to Fourier spectroscopy 3-64535
- causality and g-factor for spin-one particle 3-51976
- causality and particle-like soln. of classical scalar field 3-48747
- causality from equal-time commutation relations 3-78077
- causality in pion-nucleon-delta hyperon interaction 3-51975
- Dirac relationship between fundamental constants, interpretation 3-76957
- equivalence of action and entropy, cohomology and interdepend. of universal const. (French) 3-54137
- extragalactic radioresources, review of new data, consequences for physics 3-81121
- generalised quantisation, reformulation of fundamentals of microscopic physics, comments 3-48748
- generalised quantisation, reformulation of fundamentals of microscopic physics (French) 3-48749
- individuality in nature rel. to barriers and cells 3-73622
- logical analysis of physical theories 3-61952
- Newton's laws on photographs for teaching (Hungarian) 3-39847
- nonequilibrium system, principle of causality, rel. to soln. of Schwinginger equation (Russian) 3-42840
- symmetry and invariance in laws (German) 3-70224
- tensor analysis on fundamental principles of mechanics 3-42759
- time, absolute, development of concept during 16th and 17th centuries 3-59511

physiological models

see also brain models; electrophysiology; neurophysiology; physiology

- achromatic human vision, edge-contrast phenomena, review (Russian) 3-48235
- auditory receptor, mechanical-to-neural transduction model 3-42300
- biological pattern formulation, morphogenesis 3-48166
- blood circulatory system, theoretical and operational problems in driving physical model 3-53737
- defective human colour vision, testing of Fick's shifting hypothesis (German) 3-48249
- eye head coordination, in monkeys 3-56515
- eye movements during fixation stationary target, stochastic model 3-45304
- frog's visual analyser, information processing principles (Russian) 3-48241
- heat transfer, biological tissue perfused by blood of arbitrary temperature, model, steady state analysis, cooling 3-77204
- human and animal visual analysers, neural network model (Russian) 3-48237
- human monocular field of view during motion of visual axis (Russian) 3-48236
- human thermoregulation 3-42273
- human visual perception mechanism, model of regulated image-edge intensification (Russian) 3-70120
- idealised torso, e.c.g. studies 3-51432
- inner ear, diagnosis (Italian) 3-56505
- innervated left ventricle, mathematical model of function 3-77247
- large systems, biochemical membranes with enzymes, modelling/simulation/identification and optimal control 3-53738
- living systems visual information (Italian) 3-56524
- modulated retinal discharge, spectrum and autocorrelation 3-45312

physiological models continued

- muscle tissue, continuous mechanical and chemical model (Russian) 3-70094
- neural system modelling, applicability of Fourier-Bessel expansions of evoked cortical potentials 3-59420
- peripheral auditory system, lateral inhibitory mechanism 3-77211
- response to flash of light, mechanism characteristics 3-70122
- stabilised retinal image (Japanese) 3-70126
- vestibulo-oculomotor reflex (Italian) 3-56523
- white-noise techniques for insect visual nervous system studies 3-45307

physiological optics *see vision***physiology**

- see also blood; electrophysiology; haemodynamics; hearing; neurophysiology; physiological models; speech; vision*
- fluid, electrical conductivity, dynamic measurement, studying anti-diuretic hormones, electronic conductometer (Rumanian) 3-59613
- living organisms' physiological parameters recording, radio-biotelemetry systems design (Russian) 3-73936
- peripheral glomerular basement membrane, thickness distrib., statistical anal. 3-56484
- thoracic electrical impedance and regional ventilation of the lung, associated change, expt. 3-73931
- voluntary movement, quantitative relationship between surface and intramuscular e.m.g. activity 3-48183

pi mesons *see pions***pick-up reactions**

- DWBA, finite-range, matrix elements calc. method 3-60139
- nucleon-nucleus optical potential, contrib. to self-energy 3-78301
- radial form factor determ. using Green's function method rel. to alpha-decay width calc. 3-60133
- two nucleon transfer, multipole expansion method for finite range calculations 3-67294
- (p,d) and complementary (d,p) reactions, comparative treatment of spectroscopic factors 3-40502
- $^{27}\text{Al}(\text{He},\alpha)^{26}\text{Al}$, 18 MeV neutron pickup, angular distrib., ^{26}Al level structure 3-67355
- $^{36}\text{Ar}(\text{He},\alpha)^{35}\text{Ar}$, 18 MeV neutron pick-up, determ. of ^{35}Ar level structure 3-67354
- $^{10}\text{B}(\text{d},\text{t})$, j-dependence of triton angular distrib. (Russian) 3-52191
- $^{11}\text{B}(\alpha,\text{He})$, $E_\alpha=65$ MeV, α -transfer feasibility studies 3-63073
- $^9\text{Be}(\text{d},\text{t})$, j-dependence of triton angular distrib. (Russian) 3-52191
- $^9\text{Be}(\text{p},\alpha)^6\text{Li}$, 6 MeV multi-interaction, finite-range, two-mode DWBA analysis 3-67297
- $^{12}\text{C}(\text{d},\text{He})^{10}\text{B}^*$, ^3He continuous spectrum calculated, direct reaction mechanism 3-60207
- $^{13}\text{C}(\text{d},\text{t})$, j-dependence of triton angular distrib. (Russian) 3-52191
- $^{23}\text{C}(\alpha,\text{He})$, $E_\alpha=65$ MeV, α -transfer feasibility studies 3-63073
- ^{40}Ca , proton elastic scattering, coupling to pickup channels, contrib. to optical potential 3-46031
- $^{42}\text{Ca}(\text{He},\alpha)^{41}\text{K}$, meas. differential cross sections, use DWBA to study ^{43}Ca protons in ^{42}Ca 3-74480
- Co isotopes, Hartree-Fock-Bogoliubov calc. of pick-up strengths 3-67246
- $^{19}\text{F}(\text{d},\text{He})^{18}\text{O}$, analogue state, distorted wave theory extended to include charge exchange channel 3-60203
- $^{19}\text{F}(\text{d},\text{t})^{18}\text{F}$, analogue state, distorted wave theory extended to include charge exchange channel 3-60203
- $^{56}\text{Fe}(\text{d},\text{t})^{55}\text{Fe}$, low-lying levels study 3-74485
- $^{56}\text{Fe}(\text{d},\alpha)$ reaction, 12 MeV, analysis in terms of DWBA theory 3-60201
- $^{24}\text{Mg}(\text{p},\text{p}')^{24}\text{Mg}$, strongly coupled, spinless nucleon model, deformation parameters 3-54473
- $^{25}\text{Mg}(\text{p},\text{d})^{24}\text{Mg}$, study of particle-hole nature of lowest 3- states in ^{24}Mg 3-49151
- $^{26}\text{Mg}(\text{d},\text{t})^{25}\text{Na}$, 29 MeV, angular distrib. meas., ^{25}Na structure determ. 3-52095
- Mn isotopes, Hartree-Fock-Bogoliubov calc. of pick-up strengths 3-67246
- $^{22}\text{Ne}(\text{p},\text{t})^{20}\text{Ne}$, 4.97 MeV 2^- transition, excitation of unnatural parity states from O^+ targets 3-78326
- $^{58}\text{Ni}(\text{p},\text{t})^{56}\text{Ni}$, $E_p=45$ MeV, finite range effects by multipole expansion method 3-67294
- ^{16}O , α -pickup to ground state rotational bands of ^{20}Ne , shell-model calcs. 3-45980
- $^{16}\text{O}(\alpha,\text{He})$, $E_\alpha=65$ MeV, α -transfer feasibility studies 3-63073
- $^{16}\text{O}(\text{p},\text{He})$, violation of isospin conservation, $E_p=27$ MeV 3-63056
- $^{16}\text{O}(\text{p},\text{t})$, violation of isospin conservation, $E_p=27$ MeV 3-63056
- ^{208}Pb , ^{11}B induced transfer reactions above Coulomb barrier, selective excitation of particle, hole states 3-60219
- ^{208}Pb , single neutron transfer, sub-Coulomb, form factor calcs. and single-particle potentials 3-67298
- $^{208}\text{Pb}(\text{d},\text{t})$, 12.5 MeV, vector analysing power, differential cross section, ^{207}Pb deduced levels, DWBA analysis 3-60199
- $^{208}\text{Pb}(\text{p},\text{t})$, two step (p,d)-(d,t) mechanism 3-74582
- $\text{Pb}(\text{p},\text{t})$, $A=208, 206, 204, 35$ MeV, two-neutron pick-up strengths, transition from single-particle to collective 3-60187
- $^{152}\text{Sm}(\text{He},\alpha)^{151}\text{Sm}$, transfer l values ^{151}Sm ground state, wave function 3-74594
- $^{152}\text{Sm}(\text{d},\text{t})^{151}\text{Sm}$, transfer l values ^{151}Sm ground state, wave function 3-74594
- $^{154}\text{Sm}(\text{p},\text{t})^{152}\text{Sm}$, finite range DWBA calcs. 3-78327
- $^{86}\text{Sr}(\text{He},\alpha)^{85}\text{Rb}$, 15 MeV, meas. α -particle spectra, determ. levels ^{85}Rb 3-71056
- $^{128}\text{Te}(\text{p},\text{d})^{127}\text{Te}$ and complementary (d,p) reactions, comparative treatment of spectroscopic factors 3-40502
- $\text{Te}(\text{t},\alpha)\text{Sb}$, study of captured proton wave function and Sb isotope structures (Spanish) 3-74484
- $^{169}\text{Tm}(\text{d},\text{t})^{168}\text{Tm}$, $E_d=17$ MeV, rot. bands of ^{168}Tm 3-63069
- V isotopes, Hartree-Fock-Bogoliubov calc. of pick-up strengths 3-67246
- $^{183}\text{W}(\text{He},\alpha)^{182}\text{W}$, 20.3 MeV, ^{182}W deduced levels, two quasiparticle configurations 3-57475
- $^{183}\text{W}(\text{d},\text{t})^{182}\text{W}$, 12.1 MeV, ^{182}W deduced levels, two quasiparticle configurations 3-57475

pick-up tubes, television *see television camera tubes***pick-ups**

- Gardon radiometer, for convective thermal fluxes 3-51544
- gramophone, vibration displacement measurement applic. 3-59544

pick-ups continued

- long-period torsional vibration pickup, design and performance 3-61580
- pressure and temp. measurement, in high-pressure chambers 3-51560

pickups *see pick-ups*

picture processing

- see also pattern recognition*
- image enhancement by holography 3-56694
- image rectification, using electro-optical rectifier 3-53926
- Mariner 9 TV from Mars orbit, digital image processing 3-59275

piezo-magneto-optical effects *see magneto-optical effects*

piezo-optical effects

- see also piezoreflectance*
- alkali halides, refr. index and refl. spectra, uniaxial deform. effects 3-58528
- alkali halides, strain-optical constant ratios, u.s. determ. 3-80007
- alkaline earth oxides, deformed, compression depend. of luminesc. 3-69049
- laser, solid electrooptic, piezooptic control, mode selection 3-48914
- modulation spectroscopy, review 3-55643
- modulation spectroscopy 3-55621
- semiconductor, modulation spectroscopy under uniaxial stress, review 3-55642
- Ba(NO₃)₂, stress-optical coeffs., temp. depend., 30 to 250°C 3-50539
- CsCl structure crystals, birefringence 3-80006
- GaAs single crystal photoelastic constants, stresses in crystal ingots (*German*) 3-53082
- Pb(NO₃)₂, stress-optical coeffs., temp. depend., 30 to 200°C 3-50539
- Si, single crystal photoelastic constants, stresses in crystal ingots (*German*) 3-53082
- Sr(NO₃)₂, stress-optical coeffs., temp. depend., 30 to 300°C 3-50539

piezoelectric devices

- see also crystal filters; crystal resonators; piezoelectric transducers*
- acoustic surface wave correlator, using space charge nonlinearity 3-52747
- beam chopper, high vacuum applications 3-77571
- bulk, r.f. piezoelectric waves, theory (*French*) 3-50521
- ferroelectric materials, properties and applic. 3-61024
- moisture in gas streams, nonexplosionproof piezoelectric analyser 3-59720
- quartz piezoelectric vibrations determ. of superficial mass of vacuum deposition of Au and Cu films (*French*) 3-59661
- rare gas condensation measurement, using quartz crystals (*French*) 3-66138
- thermal radiation detectors 3-66268
- u.s. interferometer, wide-band piezosemiconductor unit absorption coeff. and velocity meas. of liquid 3-42522
- vibration viscometer, bimorphous plates, gas viscosity 3-70498
- CdS phonon maser structures, u.s. wave propagation 3-53788
- CdS phonon masers, light diffraction studies 3-53785

piezoelectric filters *see crystal filters*

piezoelectric materials

- acoustic surface wave propagation, multilayers of arbitrary anisotropy, piezoelectricity and conductivity, matrix description 3-50066
- ceramics, effect on efficiency of plain tuning fork, measurement of constants 3-61950
- ceramics, physics of piezoelectric effect, device manufacture, properties 3-68928
- ceramics coupled to mirrors, investigation for interferometric application 3-48353
- crystals, phonon echoes, e.m. wave effect (*French*) 3-72146
- elastic constants, dynamical determination by means of electromechanically excited resonators 3-51533
- electric field echoes, mechanism 3-72576
- III-V semiconductors, nonlinear interaction of e.m. and acoustic waves, hypersound generation 3-50542
- one-dimensional superlattice, coherent phonon generation by optical mixing 3-41499
- piezoceramics, perovskite-type structure, anomalous polarisation (*Russian*) 3-64606
- PVC, piezoelec. currents due to temp. and pressure changes obs. 3-47220
- Rochelle salt, piezoelec. lines, meas. elastic stiffnesses 3-79983
- semiconducting crystal, inhomogeneous, u.s. propagation, acoustoelectric interaction, nonuniformities 3-58310
- semiconductor, interaction of plasma and lattice waves 3-79743
- semiconductor, recomb. amplification of sound, theory 3-75783
- semiconductors, heating of electrons by acoustic waves, theory 3-75785
- semiconductors, sound attenuation and amplification 3-68676
- spectroscopic determination of lanthanide elements (*Russian*) 3-62362
- surface waveguide problem, thin semiconducting guiding layer 3-64605
- tartrate crystals, triboluminescence and simultaneous charge produced at fracture 3-69045
- thin film overlay, perturbation theory for electric potential acoustic surface wave transducer 3-41075
- tourmaline, stereographic projection of indicative surface 3-72018
- transducer materials, for vibration detection and excitation, review 3-68932
- transverse surface waves on piezoelectric material with metallic layer 3-41073
- u.s. applications, discovery and development of new materials 3-42410
- AgGaS₂, piezoelectric nonlinear optic, crystal structure determ. 3-72049
- AlN epitaxial film, on sapphire, acoustic surface wave props. 3-55135
- BaTiO₃, explosively compacted, characteristic dielec. behaviour 3-55533
- BaTiO₃:LiF-MgO, room temp., poling conditions, internal stress 3-80415
- Bi₁₂GeO₂₀, Bi₁₂SiO₂₀, Bi₁₂(Ge_{0.5}Si_{0.5})₂₀, anomalous u.s. attenuation, selection rule existence for vibration mechanism 3-58085

piezoelectric materials continued

- Bi₁₂GeO₂₀, harmonic generation of u.s. surface wave (*French*) 3-41079
- Bi₁₂GeO₂₀, minimal diffraction cuts for acoustic surface wave propagation 3-58172
- Cd,Hg_{1-x},Te solid soln., piezoresist. under uniaxial compression 3-61021
- CdS, for enhanced u.s. Rayleigh surface wave convolver 3-42421
- CdS, impurity electroabsorption obs. 3-76037
- CdS crystals, analysis of u.s. fields by light diffraction 3-53787
- CdS phonon maser structures, u.s. wave propagation 3-53788
- CdS phonon masers, light diffraction studies 3-53785
- GaAs piezoelectric semiconductor, theory of phonon-assisted hopping conduction 3-58264
- GaN epitaxial film, on sapphire, acoustic surface wave props. 3-55135
- LiIO₃, Bleustein-Gulyaev waves, props. 3-52748
- LiNbO₃, acoustic radiation from a high-coupling cut 3-55136
- LiNbO₃, dispersion relation for acoustic wave propag. along z-axis 3-41485
- LiNbO₃, elastic wave propag., domain struct. effect 3-75568
- LiNbO₃, harmonic generation of u.s. surface waves (*French*) 3-41079
- LiNbO₃, optical probing of u.s. surface wave nonlinear effects 3-39902
- LiNbO₃, piezoelec. coeffs. determ. by interference dilatometer method 3-58477
- LiNbO₃, third order elastic constants, u.s. wave obs. 3-68929
- LiNbO₃ acoustic surface wave generation, Al interdigital transducers on piezoelectric substrate, optical spectroscopy 3-50065
- LiNbO₃-Si layered structure, acoustoelec. effects 3-58308
- LiNbO₃-Si(CdSe), layered structure, acoustoelec. effect due to elec. fields of u.s. surface waves 3-44120
- LiTaO₃, crystal growth 3-64783
- (NH₄)₂BeF₄, coeff. meas., freq. depend. below phase transition 3-68945
- Pb₂KNb₅O₁₅, single crystal growth and piezoelectric props. 3-68927
- (Pb_{0.92}La_{0.08})(Zr_{0.65}Ti_{0.35})_{0.98}O₃ ceramics, elec. and opt. props. characterization, porosity and grain size effects 3-55532
- Pb(Zr,Ti)O₃ transducer ring, strength anisotropy 3-75944
- Pb(Zr,Ti)O₃ transducer rings, mech. failure 3-72966
- Sb-Te-I-solvent-H₂O systems, high temp. and press., piezoelec. single cryst. form. 3-72790
- SbNbO₄, synthesis, piezoferroelec. props. 3-75955
- TiO₂, trace element spectrochemical analysis (*Polish*) 3-73955
- ZnS film, surface elastic wave motion, computer analysis (*Japanese*) 3-41482
- ZrO₂, trace element spectrochemical analysis (*Polish*) 3-73955

piezoelectric oscillations

- ceramic, elastic moduli and mech. Q of small specimens, resonant beam technique 3-70263
- crystal surfaces plated with electrodes, two-dimensional dynamic theory of h.f. vibrations 3-41082
- e.m. radiation from vibrating quartz plate 3-41483
- gravitational wave detection by obs. of stresses produced in piezoelectric crystals 3-70723
- gravitational wave detector configurations sensitivity analysis (*French*) 3-51827
- gravitational wave detector response to gravitational shocks, signal dispersion (*French*) 3-51829
- mechanical displacement for slab sandwiched between elastic and visco-elastic material 3-42805
- quartz oscillator, film thickness measurement, theoretical models, relationships with frequency and period (*French*) 3-45426
- r.f. waves in insulators, theory (*French*) 3-50521
- semi-infinite, coated with conducting thin film, effect of time-depend. heat flow on disturbances 3-74073
- vibrating bar mech. parameters meas. rel. to gravitational wave detection (*French*) 3-51828
- LiIO₃, Bleustein-Gulyaev waves, props. 3-52748

piezoelectric resonators *see crystal resonators*

piezoelectric transducers

- acoustic surface wave amplification 3-48279
- ceramics, physics of piezoelectric effect, device manufacture, properties 3-68928
- crystal ultrasonic absorption, transducer, bond energy losses 3-75573
- dynamic piezoelectric pressure transducer system, pulsed plasma flow diagnostics 3-40806
- flexure mode piezoelectric transducer, for ossicular chain activation 3-40064
- interdigital, on piezoelec. substrate, Rayleigh wave prod. and detect. (*French*) 3-45369
- thin film overlay, perturbation theory for electric potential acoustic surface wave transducer 3-41075
- u.s., for depletion and diffusion layer transducers 3-42410
- u.s. freq., piezoelec. material props. rel. to transducer limitations 3-41484
- u.s. wave generation and detect. beyond 100 GHz 3-42411
- vibration and pressure applications, comparison with charge amplifier systems 3-56623
- vibration detection and excitation, materials, review 3-68932
- wideband piezosemiconductor, loss and bandwidth characts. 3-42525
- LiNbO₃, interdigital, high coupling cut 3-55136
- LiNbO₃, piezoelec. transducer, nuclear reactors, u.s. inspection 3-65061
- Pb(Zr,Ti)O₃ rings, cold pressed, strength anisotropy 3-75944
- Pb(Zr,Ti)O₃ rings, mech. failure 3-72966
- ZnO thin layers as u.s. transducers, prep. (*German*) 3-53193
- ZnS thin film, surface elastic wave motion, computer analysis (*Japanese*) 3-41482

piezoelectricity

- see also electrostriction; piezoelectric devices; piezoelectric materials; piezoelectric oscillations; piezoresistance*
- acoustic amplification in piezoelectrics with double injection 3-41238
- anisotropy in crystal physical props. represented by surfaces of rotation 3-79247

piezoelectricity continued

- bound piezoelectric polaron, ground state energy 3-46818
- earthquake lightning, piezoelectric theory 3-50925
- II-VI semiconductors, rel. to zincblende and wurtzite structure stability (*German*) 3-75496
- linear, variational principles for complete set of governing equations 3-55526
- noble metals, longitudinal piezo-thermoelectric effect in polycrystalline wires 3-72347
- nonlinear optical crystals, applications, review 3-40288
- periodic structure, dispersion relation 3-41485
- polaron, theory 3-75728
- polymer film, induced by charge injection, rel. to three layer capacity microphone 3-68931
- PVC, piezoelec. currents due to temp. and pressure changes obs. 3-47220
- pyroelectric contributions 3-68933
- Rochelle salt, piezoelec. lines, meas. elastic stiffnesses 3-79983
- semi-infinite medium, disturbances due to time decaying elec. field and elastic compliance, use of transform calculus 3-48717
- semi-infinite rod, heat generation near finite end, distrib. of temp., displacement, stress, electric field, and entropy density 3-72575
- semiconductor, combination freq. in nonlinear wave interactions during supersonic carrier drift 3-75784
- semiconductor laser compound cavity, tuning 3-62723
- semiconductors, piezoelectric, renormalised viscosity for high acoustic flux 3-60904
- symmetry by second harmonic generation 3-48951
- u.s. applications, discovery and development of new materials 3-42410
- u.s. surface wave in piezoelec. crystal, harmonic generation (*French*) 3-41079
- u.s. waves with opposite propag. directions on piezoelec. surface, nonlinear interactions (*French*) 3-41078
- wurtzite structure crystals, bond-bending parameter calc. from elastic properties 3-47218
- wurtzite type crystals, longitudinal constant calc. phenomenological model 3-47219
- zincblende structure crystals, bond-bending parameter calc. from elastic properties 3-47218
- zincblende type crystals, longitudinal constant calc. phenomenological model 3-47219
- AlN, epitaxial film growth and piezoelec. props. 3-80189
- GaAs, epitaxial film growth and piezoelec. props. 3-80189
- GaAs, piezoelec. amplified phonon spectra, X-ray scatt. obs. 3-55057
- GaN, epitaxial film growth and piezoelec. props. 3-80189
- Gd₂(MoO₄)₃, morphic piezoelectric and elastic coefficients (*German*) 3-53071
- LiGaO₂ single crystal 3-50520
- LiNbO₃, elastic wave propag., domain struct. effect 3-75568
- LiNbO₃, piezoelec. coeffs. determ. by interference dilatometer method 3-58477
- LiNbO₃, third order elastic constants, u.s. wave obs. 3-68929
- SbNbO₄, hydrostatic piezoelec. modulus meas. 3-75955
- SrTeO₃, ferroelectric single crystal 3-68938

piezomagnetism *see magnetostriction***piezorefectance**

- degenerate semiconductors, calc. of piezomodulation parameters 3-55548
- phase of reflectivity determ., appl. to ZnTe exciton spectrum 3-53887
- pyromellitic dianhydride-anthracene single crystals, charge transfer transitions 3-55644
- semiconductors, modulation spectroscopy, Raman and Brillouin scattering 3-55593
- Au film, piezo, thermo and electroreflectance spectra, comparative props. 3-55631
- GaP, piezorefectivity spectra investigation of band structure 3-55546
- Ge, piezorefectivity spectra investigation of band structure 3-55546
- HgTe, band structure, electro-, thermo- and piezorefectance obs. 3-55635
- ZnTe, exciton spectrum, reflectivity phase determ. 3-53887

piezoresistance

- semiconductors, surface quantisation meas. technique, review 3-50261
- p-Si:B epitaxial layers on n-type Si 3-79984
- Ag thin film, strain coeff. of resist., calc. 3-52813
- Cd_{1-x}Hg_xTe solid soln., under uniaxial compression 3-61021
- Cu-Mn-Ni alloy, manganin, impact loaded, nonlinearity 3-68930
- n-Ge, carrier density depend. under mixed scatt. conditions 3-58286
- Si diffused layers, piezoresistive coeffs. 3-41217
- n-Si electron-phonon interactions, quadrupole and octupole, mobility and piezoresistance, and experiment calculation 3-46842
- Si(001)/Al(0112) films, anisotropy in electrical props. 3-41269
- TlInSe₂, piezophotorestrictive effect in single cryst. 3-68674

piezoresistive devices *see piezoelectric devices***piles (nuclear fission)** *see nuclear reactors***pinch effect**

- belt pinches, compression limitations 3-79163
- Bett Pinch, slab models, for classical diffusion 3-63862
- buried conductor system, feasibility study 3-60626
- collisional preionisation in large pinch vessels obs. 3-68053
- conical theta-pinch gun, effects of multipole field on plasma production 3-63848
- double inverse, magnetoplasma equilibria with planar symmetry 3-79160
- ion beam interaction with θ -pinch turbulent plasma, low press. region (*Russian*) 3-40785
- linear, MHD instability, finite element method 3-75303
- linear pinch, MHD stability using finite element method 3-79165
- magnetic stars, pinch instabilities 3-51332
- magnetospheric plasma, development of pinch effect rel. to drift current instability in plasma blob 3-42048
- neo-classical transport equations, steady-state solutions, trapped-particle pinch effect 3-49646

pinch effect continued

- plasma, theta pinch, relativistic effect in light scatt. spectrum 3-63884
- relativistic electron beam filamentation theory 3-40778
- rotating magnetic field pinch, slowly varying magnetic induction obs. 3-57936
- semiconductors, universality of current-voltage characteristics 3-68637
- sheet-pinch in plane geometry, MHD waves decay by phase mixing 3-52505
- spot formation on anode of high intensity arcs 3-63917
- theta, dense cold plasma, light scattering meas. 3-79171
- theta, heating by flux compression 3-71939
- theta, high-beta, plasma density and beta distributions 3-79164
- theta, reference reactor, discrete ordinates neutronic analysis 3-60326
- theta, staged, with implosion heating, feasibility study 3-60622
- theta, toroidal, magnetic field feedback stabilisation 3-79166
- theta pinch, e.m. radiation origin 3-79076
- theta pinch, negative, in caulked cusp torus field, heated by r.f. oscillating field 3-60626
- theta pinch, slow, anomalous loss instabilities in hot electron plasma 3-79153
- theta pinch and Z pinch expts. at Los Alamos Scientific Laboratory 3-60643
- theta pinch pulsed thermonuclear reactor, plasma cooling by means of a neutral gas layer 3-63850
- theta pinch thermonuclear reactor, plasma energy direct conversion by high magnetic compression and expansion 3-63234
- theta-pinch in plane geometry, MHD wave decay by phase mixing 3-52506
- Tokamak devices toroidal diffuse pinch, plasma processes discussion (*Dutch*) 3-49768
- toroidal, MHD and resistive instabilities, theory and expt. 3-75352
- Z pinch, MHD instabilities, surrounding gas effect 3-63828
- Z-pinch, continuous flow, high-density plasma beam formation, expt. obs. 3-49740
- Z-pinch, non-cylindrical, study by holographic interferometry (*French*) 3-57942
- Z-pinch, noncylindrical, matching discharge circuit with membrane movement, neutron density, two dimensional snow plough model (*Russian*) 3-57950
- Z-pinch, plasma turbulence, h.f. field meas. forbidden He I line satellites intensity (*Russian*) 3-71955
- z-pinch, thermonuclear possibilities 3-71963
- Z-pinch instabilities, expt. obs. 3-49775

pin cushion distortion *see aberrations***pion-baryon interactions**

see also pion-hyperon interactions; pion-nucleon interactions

pion-baryon scattering

see also pion-hyperon scattering; pion-nucleon scattering

pion decay

- pseudoscalar decay constant as energy scale for hadron dynamics, asymptotic cross-section 3-66967
- $\pi \rightarrow e\nu$, effect of e.m., strong interaction corrections on (ussian) 3-78111
- $\pi \rightarrow e\nu$, energy spectra in terms of single Kemmer currents 3-57322
- $\pi \rightarrow \mu\nu$, coupling const. calc. from strong gravity theory 3-40331
- $\pi \rightarrow \mu\nu$, effect of e.m., strong interaction corrections on (ussian) 3-78111
- π^0 anomalous vertices, chiral-symmetric limit, Ward identity predictions 3-59937
- $\pi^0 \rightarrow e^+e^-$, reasons for experimentally search continuation, unitarity limit (*Russian*) 3-66968
- $\pi^0 \rightarrow \gamma\gamma$, decay rate and PCAC calc. 3-43105
- $\pi^0 \rightarrow \gamma\gamma$, PCAC and gauge models with heavy pion 3-54297
- $\pi^0 \rightarrow \gamma\gamma$, PCAC sum rule for anomalous vertex functions 3-54293
- $\pi^0 \rightarrow \gamma\gamma$, SU(2)@U(1) gauge theories of generalised σ model 3-57346
- $\pi^0 \rightarrow \gamma\gamma$ vertex function, exact bound derivation 3-45876
- $\pi^0 \rightarrow \gamma\gamma\gamma$, search for process using $K^\pm \rightarrow \pi^\pm \pi^0$ on pion source 3-52006
- π^+ identity of strong-interaction coupling constants, avoidance of neutral currents 3-66963
- $\pi_\pi \rightarrow \eta\pi$, decay widths of scalar mesons from generalised nonlinear Lagrangian 3-66932

pion-hyperon interactions

No entries

pion-hyperon scattering

No entries

pion interactions

- see also pion-baryon interactions; pion-pion interactions*
- Adler anomalies in pion electrodynamics, reln. to $\eta \rightarrow \pi\pi\pi$ puzzle 3-52001
- chiral perturbation theory, effects of renormalisation on nonanalyticity of S-, and current matrix elements 3-62776
- total cross sections, energy dependence, Regge theory 3-57458
- $\gamma\pi$, rotational properties of production amplitude, reln. to e.m. form factor 3-49006
- $\pi d \rightarrow \pi p n$, cross-section, near threshold 3-62877
- $\pi^+ d$, 7 GeV/c, B meson production, mass, width 3-60042
- $\pi^+ d$, 7 GeV/c, production of KK and $KK\pi$ systems, diffraction dissociation mechanism 3-43149
- $\pi^+ d = pp$, impulse approx. and multiple-scattering series at high energy 3-54354
- $\pi^+ n \rightarrow K^0 \Sigma^+$, Σ^+ polarization, 1.2 to 2.4 GeV/c 3-57437
- π NA interaction, covariant derivation of characteristic surfaces, causality 3-51975
- $\pi\rho \rightarrow \pi\rho$, location of zeros in helicity amplitudes, rel. to duality (*French*) 3-67125
- $\pi\nu \rightarrow \pi\nu$, kinematics, gauge invariance and helicity conservation 3-54318

pion-nucleon interactions

see also pion-proton interactions

- 3-3 phase shifts, no-pole S-matrix fit to $\Delta(1236)$ resonance 3-59931
- 3-3 resonance, 3-parameter formula for phase shift, reln. to pole position 3-43137

pion-nucleon interactions continued

3-3 resonance pole, residue determ. 3-57408
bremsstrahlung, differential cross section, off energy shell effects 3-78180
cascade evaporation model for π -nucleus collisions at energies $> > 10$ GeV (Russian) 3-60194
charge exchange amplitudes, application of optimised finite energy sum rule 3-45914
charge and hypercharge exchange reactions in a Regge pole model 3-67072
charge exchange, comparison between phase-shift analysis amplitudes and high-energy amplitudes 3-57429
charge exchange, slope of amplitude at $t=0$, dispersion method calc. 3-57405
charge exchange at large momentum transfer, amplitude analysis 3-60036
coherent production of $K^+\pi^+\pi^-$ on nuclei at 10, 13 and 16 GeV/c (German) 3-52208
coherent production of three pions on nuclei 9 to 15 GeV, total cross section determ. using optical model 3-67368
cross section inside nucleus in $^{27}\text{Al}(\pi^+, \pi^0)^2\text{Si}$ reaction 3-54506
current algebra applications, S-wave pion-nucleon effective range (Rumanian) 3-45860
finite range effect on π d scattering length, calcs. 3-78178
inelastic, high energy, on heavy emulsion nuclei, secondary particle characteristics analysis 3-67369
inelastic interaction of heavy nuclei, ω -pole exchange, 3π coupling const. (Russian) 3-40517
low-energy, application of transition operator for matrix potentials 3-70852
multiperipheral theory at high energies elastic and charge exchange amplitudes near $t=0$ (Russian) 3-67099
parity violating, off mass shell effects, renormalisable σ model 3-74349
renormalisation const. of nucleon, rigorous upper bound 3-59989
resonance (3/2,3/2), obs. of $^{12}\text{C}(\pi^+, \pi^+n + \pi^+p)$ reaction, cross section 3-60225
scattering cross sections in reln. to $(\pi, \pi\pi)$ reactions on ^{14}N and ^{19}F at (3/2, 3/2) resonance 3-49284
sum rule for production of doubly charged exotic meson resonances 3-43145
 π coherent production from π^+ -nuclei interactions, $\sim 10\text{GeV}/c$, 3π branching ratios 3-74440
 $\pi\pi$ interactions on nuclei, 9 and 15.1 GeV/c, spin-parity analysis of coherently produced $\pi^+\pi^-\pi^+$ 3-49052
 $\pi\pi$ - ^{132}Xe producing photons, 9 GeV, correlation between longit. and transverse momenta 3-78351
 π^+ + nucleus $\rightarrow \pi^+\pi^+\pi^0$ + nucleus, 11.7 GeV/c, obs. of B(1235) and $\rho(1710)$ resonances 3-40397
 $\pi A \rightarrow \pi X$ where A =nucleus composed of A nucleons, approach to scaling in composite system scattering 3-67059
 $\pi^-C \rightarrow \pi^+\pi^-\pi^-C^*$ (4.44) at 6.0 GeV/c, mass distrib. and spin-parity analysis of 3π system 3-67138
 $\pi^-d \rightarrow n\pi$, meas. of final state nn scattering length using time-of-flight technique 3-78181
 $\pi^-d \rightarrow \pi^-\pi^+p$, 9.0 GeV/c, study of $I=2\pi\pi$ scattering using Chew-Low extrapolation method 3-67139
 π^+d , 7.87 GeV/c, search for four-pion decay mode of $f_0(1260)$ 3-54359
 $\pi^+d \rightarrow p, \pi^+\pi^-$, 4 GeV/c, density matrix study of p^0 and f^0 production, Estabrooks-Martin analysis 3-71014
 $\pi^+d \rightarrow \pi^+$ + anything at large transverse momenta, energy dependence of inclusive cross section 3-67156
 $\pi N \rightarrow K\Sigma(\Lambda)$, hypercharge exchange, 4-16 GeV/c, impact parameter representation 3-67134
 $\pi N \rightarrow NX$, finite mass sum rules and duality, relns. for two-body reactions, resonance production 3-45920
 $\pi N \rightarrow \pi\Delta$ phases of resonant amplitudes modified SU(6)_w 3-62894
 $\pi N \rightarrow \pi N^*(\frac{1}{2}, \frac{3}{2}-)$, multipole (kinematic) analysis, invariant, spiral and scalar amplitudes (Russian) 3-54342
 $\pi N \rightarrow \pi$ + anything, spin dependent, triple Reggeisation, single particle spectrum 3-62914
 $\pi N \rightarrow \pi N$, 3, 4 and 6 GeV/c high statistics expt., study of ρ - ω interference 3-71013
 $\pi N \rightarrow \pi N$, interaction Lagrangian by study of $\pi^+\pi^-\pi^+\pi^+$, 230 MeV, ratio of isospin invariant amplitudes (Russian) 3-60020
 $\pi N \rightarrow \pi p N$, single peripheral model properties, of Deck effects 3-74404
 πN -vector meson + Δ baryon, dipole coupling model 3-74442
 πN -vector-meson N, Reggeized higher symmetry model, vector-meson dominance test 3-78167
 π^-n , 40 GeV/c, charged-prong multiplicity distribns., scaling behaviour and local excitation model 3-43151
 π^-N , 40 GeV/c, γ quanta prod. 3-74428
 π^-N , in light nuclei, multiplicity distribns. of charged particles (Russian) 3-40516
 π^-n , multiple particle production at 40 GeV 3-52029
 $\pi^-N(A) \rightarrow \pi^- \Delta^- \pi^- N(A^+)$, 3.9 GeV/c obs. secondary pion momentum spectra, longitudinal and transverse components (Russian) 3-67142
 $\pi^-n \rightarrow \pi^-\pi^+\pi^-n$, 3.9 GeV/c interactions on quasifree neutrons of light nuclei, resonance production (Russian) 3-40515
 $\pi^-N \rightarrow \pi^- \pi^+ N$, 3-6 GeV/c, study of π scattering using Argonne Effective Mass Spectrometer 3-70988
 $\pi^-n \rightarrow p^-\pi^-\pi^+$, low-mass enhancement, doubled charged A_1^{--} and existence of true A_1 resonance 3-57401
 $\pi^-n \rightarrow \omega p$, 6.0 GeV/c differential cross section, spin density matrix elements, Regge exchange models 3-57435
 $\pi^-n \rightarrow \pi^+\pi^-\pi^-p$, 6 GeV/c, study of $\pi\pi$ scattering in 0.6-1.42 GeV region, phase shift analysis 3-70991

pion-nucleon scattering

see also pion-proton scattering
 $\pi N \rightarrow \pi N$ data, Coulomb interference effects in $\pi\pi$ off-shell scatt. 3-78176
 σ commutator, value of 86 ± 12 MeV 3-70976
 σ -model, nonanalytic corrections, low energy limit 3-45852
amplitude analysis and models for intermediate and high energy interactions 3-40385
amplitudes at intermediate energies, impact parameter expansion 3-54343

pion-nucleon scattering continued

amplitudes determ. at large momentum transfer 3-71000
backward, high-energy, dual relativistic quark model, scaling limits 3-74381
backward, possible existence of elementary nucleon 3-40392
baryon exchange, urbaryon rearrangement diagrams 3-78174
charge exchange, Regge pole and cut contributions 3-57428
charge exchange scatt., Regge-cut models 3-62884
charge-exchange forward scatt. at high energies 3-54369
Chew-Low integral eqn. analysis, cut-off functions and strong-coupling limit 3-57402
 σ commutator contribution to amplitude of scattering (Russian) 3-62875
coupling constant and s-wave scattering length determ. using fixed t dispersion relations 3-74422
coupling constant and scattering length determ. from fixed t dispersion relations 3-49040
diffractive production of nonstrange mesons in harmonic-oscillator quark model 3-57370
elastic, 300-600 MeV, anomalous isospin breaking in S-wave 3-49039
elastic, cross sections, nucleon polarisation, parity doublet contributions 3-60025
elastic, diffractive excitation of hadron resonances, phenomenological model 3-67096
elastic, $E < 300$ MeV, effect of Coulomb barrier, difference in resonance widths 3-57407
elastic, K-matrix absorption model including Pomeranchuk contribution 3-74402
elastic, phase-shift ambiguities for differential cross section 3-51995
elastic, phenomenological analysis, duality, existence of Z_1^* and phase shift soln. 3-74432
forward amplitudes up to 30 GeV/c, tabulation 3-71006
forward elastic, duality and vacuum Regge singularities with zero intercept 3-74391
forward isospin even amplitude with zero-mass pions, reln. to isovector photon forward Compton amplitude 3-62834
forward scattering amplitudes, total cross-section, tabulation, treatment of errors 3-49043
impact parameter analysis in intermediate energy region 3-57404
inclusive, on nuclear target, scaling 3-74467
low energy, nucleon sigma terms estimate 3-67109
moments of absorptive parts of elastic scatt. amplitude, bounds 3-54348
multiple scattering by nucleons in deuteron, rel. to $\pi d \rightarrow \pi p n$ cross section 3-62877
off-shell and on-shell amplitudes, static limit, three-body forces 3-78261
optical model anal., with dynamically modified optical potential, pion-nucleon (3,3) resonance 3-67370
optical model potential for pion-nucleon scattering 3-74608
optimal bounds on total cross section moments 3-57421
 P_{33} partial wave, energy dependence of $\Delta(1236)$ width, background effect 3-71011
parity, helicity flip non-flip amplitudes, transformation ambiguity 3-60002
partial wave amplitude, $\Delta(1236)$ pole position 3-78165
phase-shift analysis, tests of bounds obtained from polarisation and differential cross section data 3-43140
pomeron and P' exchange amplitudes 3-52042
Regge amplitude determ. using continuous moment sum rules and phase-shift data 3-40394
Reggeized symmetry model, forward and backward scattering, high energy 3-78195
relativistic eikonal model, nucleon spin introduction 3-52036
sigma term recalc. in broad-area subtraction sum rule for on-shell scattering amplitude 3-74420
spin rotation parameters discrepancies between CERN and Saclay phase shifts predictions above and below 1.5 GeV/c 3-74419
Veneziano-type amplitudes, charge-exchange polarisations, differential cross sections 3-62876
 $\Delta(1236)$, relativistic parametrization in Breit-Wigner formalism, coupling constants 3-67074
 $\Delta N\pi$ interaction and σ term at low-energies, model 3-57410
 π -nucleus optical potential, density expansion second order terms 3-63086
 π -nucleus optical potentials, low-energy, local potentials 3-43257
 π^- -He, elastic small angle scattering at 3.48 and 6.13 GeV/c, determ. total elastic cross section (Russian) 3-67124
 πd , corrections for multiple scattering, total and differential cross sections (Russian) 3-70922
 πd , high-energy, overlapping isospin-dependent interactions 3-62880
 πd , in $\Delta(1236)$ resonance region, three body problem using Faddeevs eqns. 3-78177
 πd scattering length, generalisation of Brueckner formula 3-49044
 πN backward scatt., dual absorptive model 3-45906
 πN backward scattering, 6 GeV/c, amplitudes, Regge pole model with absorption 3-62897
 $\pi N \rightarrow \omega N(pN)$, non-linear π -B exchange degenerate Regge trajectory 3-60004
 $\pi N \rightarrow \pi N$, amplitude structure in Pomeron exchange reaction and s-channel helicity nonconservation 3-74406
 $\pi N \rightarrow \pi N^*$, production cross section and SU(6) \times O(3) structure 3-62892
 $\pi N \rightarrow pN$ nondiffractive scattering, direct channel effects 3-71009

pion-pion interactions

coupled channels, inelastic, π -exchange production mechanism and absorption 3-70998
low energy phase shifts in $K^+ \rightarrow \pi^+\pi^-e^+e^-$ decay 3-70895
total cross section meas. using inclusive reaction $\pi^+\pi^+ \rightarrow \Delta^{++} + \text{anything}$ 3-70998
 $\pi\pi \rightarrow \pi A_2$, Morrison rule in ABFST multiperipheral model 3-67092
 $\pi\pi \rightarrow \pi^-\pi^+\pi^0\pi^+\pi^-$, g meson production 3-57448
 $\pi^+\pi^- \rightarrow K^+K^-$, coupled channel analysis 3-70998
 $\rho\pi\pi$ Regge residue function from sum rules and new representation for $\pi\pi$ amplitudes 3-74444

pion-pion scattering

σ -model, nonanalytic corrections, low energy limit 3-45852

pion-pion scattering continued

- Argonne Effective Mass Spectrometer study of $\pi^-N \rightarrow \pi^- \pi^+ N$ in 3-6 GeV/c region 3-70988
 asymptotic cross sections, pion decay constant as energy scale 3-66967
 Chew-Low extrapolation of $\pi^- p \rightarrow \pi^- \pi^+ n$ data at 4.5 GeV/c 3-71015
 conference, Tallahassee, U.S.A. (March 1973) 3-70977
 Coulomb interference effects, $\pi N \rightarrow \pi \pi N$ data 3-78176
 coupled channel phase-shift analysis in KK threshold region using $\pi^+ p \rightarrow \pi^+ \pi^+ n$ and $\pi^- p \rightarrow K^+ K^- n$ data 3-70981
 cross section, Chew Low extrapolation with complex transformations 3-70986
 crossing relations, ρ meson existence, S-wave lengths 3-78187
 crossing sum rules applied to inequalities on $\pi\pi$ S and P waves 3-52039
 crossing-symmetric model, low-energy behaviour 3-43138
 dual $\pi\pi$ partial wave amplitudes, asymptotic behaviour 3-59998
 dual $\pi\pi$ partial wave amplitudes, threshold behaviour, scattering lengths and effective ranges 3-62859
 dual crossing-symmetric representations with finite-width resonances and Regge asymptotic behaviour 3-57375
 elastic, 600-1900 MeV phase-shift analysis using $\pi^- p \rightarrow \pi^- \pi^+ n$ reaction 3-70983
 elastic, duality, generalized potentials and failure of ρ meson bootstrap 3-43122
 elastic, phase-shift ambiguities 3-51994
 elastic large-angle, differential cross section, quark model and auto-modellism 3-62850
 e.m. scattering amplitude from two-particle Klein-Gordon equation, retardation effects 3-62878
 hard pion amplitudes, threshold, S_2 and P wave scattering lengths 3-67113
 $I_1 = 1\pi\pi$ absorptive part, t-dependence, sum rule reln. to integrals over total cross section 3-52040
 $I = 2\pi\pi$ scattering from reaction $\pi^- d \rightarrow \pi^- \pi^- p, p$ at 9.0 GeV/c 3-67139
 inelastic, review, current algebra and pion form factor 3-70995
 inelastic final states and resonance parameter determ. from partial wave analysis of $2 \rightarrow 3$ body reactions 3-70982
 interaction Lagrangian by study of $\pi^+ p \rightarrow \pi^+ \pi^+ n$, 230 MeV, scattering length (Russian) 3-60020
 isospin 2 phase shifts from $\pi^+ p \rightarrow \pi^+ \pi^+ n$ at 12.5 GeV/c 3-70994
 lengths calc. using non-linear chiral $SU(2) \times SU(2)$ dynamics and asymptotic restrictions 3-40381
 low energy s- and p-wave phase shifts calc. using Padé approximant technique 3-70992
 low-energy, crossing symmetry calcs. of partial wave amplitudes current algebra type zeros 3-67114
 low-energy amplitudes, zero contours and ρ dominance 3-74425
 moments of absorptive parts of elastic scatt. amplitude, bounds 3-54348
 optimal bounds on total cross section moments 3-57421
 phase shift analysis, from $\pi^- p \rightarrow \pi^- \pi^+ n$ extrapolation to π exchange pole 3-71016
 phase shift analysis in 0.6 to 1.42 GeV region using $\pi^+ n \rightarrow \pi^+ \pi^- p$ reaction 3-70991
 phase shift analysis in range $440 < M_{\pi\pi} < 1400$ MeV using $\pi^- p \rightarrow \pi^- \pi^+ n$ data at 17.2 GeV/c 3-70979
 phase-shift analysis, relativistic resonance propagators 3-70993
 phenomenological analysis for low-energy amplitudes 3-52037
 phenomenology, appl. of Roy's eqns. 3-70997
 phenomenology below 1100 MeV, crossing, unitarity and analyticity requirements, Roy eqns. 3-70996
 Roy's equations to resolve up-down ambiguity and reproduce S^* resonance 3-57419
 smoothness of pion amplitudes and PCAC 3-52038
 $T=1$, asymptotics explained in a multiperipheral model with a constant total cross section (Russian) 3-62870
 total cross section, scale, massless pion limit 3-57418
 upper bounds on energy averaged cross sections, crossing dispersion sum rules 3-57432
 Weinberg's low-energy model, continuation of zero contours into ρ region 3-43139
 Weinberg scattering lengths, dispersion sum rule correction 3-74426
 zeros, reln. to dynamical properties of scattering amplitude 3-70980
 A_2 -exchange and polarization effects using $\pi^- p \rightarrow \pi^- \pi^- \pi^+ n$ data at 17.2 GeV/c 3-70987
 $\pi^- p \rightarrow$ high energy scattering using $\pi^- p \rightarrow \pi^- \pi^- \Delta^{++}$ elastic and total cross sections 3-71001
 $\pi^- \pi^-$, elastic and total cross neutron studies using final states of $\pi^- p$ interactions 3-57448
 $\pi^- \pi^0$ elastic, from two-prong events in $\pi^- p$ interactions at 4.45 GeV/c, cross-sections 3-49056
 $\pi^- \pi^+$, elastic and total cross neutron studies using final states of $\pi^- p$ interactions 3-57448
 $\pi^- \pi^+$ elastic, from two-prong events in $\pi^- p$ interactions at 4.45 GeV/c, cross-sections 3-49056
 $\pi^- \pi^+$ high energy scattering using $\pi^- p \rightarrow \pi^- \pi^+ n$, elastic and total cross sections 3-71001
 $\pi^0 \pi^0 \rightarrow \pi^0 \pi^0$, bounds on derivatives of S and D partial waves 3-45911
 $\pi^0 \pi^0 \rightarrow \pi^0 \pi^0$, rigorous constraints between low partial waves 3-45910
 $\pi^+ \pi^-$ cross section meas., extrapolation technique used by SLAC group on $\pi^- p \rightarrow \pi^+ \pi^- X^0$ reaction 3-70985
 $\pi^+ \pi^- \rightarrow \pi^0 \pi^0$, elastic and differential cross sections, threshold-1 GeV, phase shift analysis 3-70990
 $\pi^+ \pi^-$, in $I=2$ channel in $\pi^+ p$ reactions at 5.45 GeV/c, cross-sections and phase shifts, Chew-Low extrapolation method 3-67135

pion production

- coherent, three pions on nuclei, 9 to 15 GeV, optical model to determ. total cross section 3-67368
 coherent phase hypothesis of P wave amplitudes in ρ^0 production, validity 3-71012
 coherent production from π^+ -nuclei at ~ 10 GeV/c, 2 to 5 π^+ 3π branching ratios 3-74440
 condensation in $N=Z$ nuclear matter, spectrum determ. 3-60105
 correlations between neutral and charged pions produced in high energy collisions, critical fluid gas model 3-70960
 correlations of identical pions in multibody production, Pomeranchuk model 3-49064

pion production continued

- current algebra applications, low energy weak single pion prod. (Rumanian) 3-45860
 dual fireball decay, pion spectrum 3-67066
 dynamic characteristics, angular, momentum distribution, for pp interactions, 19.1 and 10 GeV/c (Russian) 3-60046
 electron-positron annihilation, hadron production at 4-GeV centre of mass energy 3-49017
 electroproduction, application of pion gauge condition as mass extrapolation constraint 3-40362
 electroproduction, light cone dominance technique, scaling law 3-70931
 electroproduction, PCAC constraints 3-78143
 electroproduction on nucleons, low energy, current algebra model with hard pions (Russian) 3-40361
 hadron collisions, inclusive cross section of pion production, energy depend. 3-78215
 hadron high-energy collisions, reasons for SU_3 violation, quark model 3-54355
 hadron resonance decay, current-constituent quarks, $SU(6)_w$ 3-78152
 inclusive π^\pm production, quark-parton model, duality relation 3-78151
 inclusive correlations for fixed prong number, two-component model 3-52057
 inclusive cross sections calc. in pionization region from PCAC 3-78220
 inclusive distribution, average multiplicity, impact picture 3-62916
 inclusive electroproduction in current fragmentation region, duality and quark-parton model 3-54313
 inclusive nucleon and pion production from proton-nucleus collisions, semiempirical model 3-57465
 inclusive pionization spectrum internal structure, peripheral models 3-49062
 inclusive reactions, ρ dominance and Regge coupling 3-49061
 inclusive single-particle spectra in pp interactions at 102 GeV/c 3-71020
 inclusive spectra in central region, approach to scaling limit in resonance dominance framework 3-49059
 inclusive charged particle production and inelastic proton spectra at CERN ISR 3-71027
 K-matrix formalism, minimal 3-to-3 scattering amplitudes 3-54281
 LAMPF low energy pion channel, mechanical design 3-56854
 large acceptance pion channel, cancer therapy 3-77252
 on light nuclei by 600 MeV protons, forward cross-section calc. 3-57520
 multipion production, charge distribution 3-57451
 multiplicity distribution analysis in inclusive reactions using correlation integrals and two-component picture 3-62904
 multiplicity production of high missing mass, multiperipheral model investigation 3-62866
 neutral and charged correlations in high-energy multiparticle production 3-52052
 neutron star cores, possibilities of pion condensation and nucleon crystallization 3-81033
 p-wave single production amplitudes phase coherence 3-67094
 pair production from time-like photons in e^+e^- annihilation 3-49011
 photoproduction, evaluation of resonance-saturated dispersion relations for all charge states 3-62832
 photoproduction, high-energy, dual relativistic quark model, scaling limits 3-74381
 photoproduction, PCAC constraints 3-78143
 photoproduction, test of amplitude signs predicted by transformation from current to constituent quarks 3-78138
 photoproduction and electroproduction, 1-5 GeV, model (Russian) 3-67027
 photoproduction in high energy region, dual parton model, 3-74372
 photoproduction process recording, equipment, results 3-66312
 quark fragmentation model, explanation of abundance in high energy collisions 3-62852
 radiotherapy using π^- from racetrack microtron 3-59445
 strength of absorptive corrections in single pion production reactions 3-49055
 weak, nuclear targets, test for neutral currents 3-43082
 0 photoproduction, application of PCAC anomalies in quark-vector gluon model 3-67020
 d induced, on nuclear target, energy, cross section (Russian) 3-60206
 e^+e^- annihilation processes, $SU(3)$ symmetry breaking and branching ratios 3-62837
 $e^+e^- \rightarrow$ hadrons, SU_3 inclusive sum rules for bounds on K/π production ratio 3-78141
 $e^+e^- \rightarrow \pi^+ \pi^-$, coupled channel model explanation of qualitative features 3-74376
 $e^+e^- \rightarrow \pi^+ \pi^- \pi^0$, coupled channel model explanation of qualitative features 3-74376
 $ep \rightarrow e^+ \pi^+ n$, electroproduction on hydrogen, four momentum transfers, 0.2, 0.4, 0.6 GeV² 3-62844
 $ep \rightarrow \pi n^+$, azimuthal angle dependence near threshold 3-62846
 $ep \rightarrow \pi n^+$, current algebra and π^+ meson and distrib. (Russian) 3-40360
 $ep \rightarrow \pi n^+$, electroproduction on hydrogen near threshold, total cross section, electron neutron coin. meas. 3-62845
 $ep \rightarrow e \pi^+ + \text{anything}$, $0.1 < |q^2| < 0.8$ GeV² and $3.15 < W < 2.8$ GeV 3-40357
 $e^- p \rightarrow e^- \pi^- n$, comparison with Berends dispersion-theory model, pion e.m. form factor 3-59979
 $\gamma d \rightarrow \pi^+ + \text{anything}$, 7.5 GeV, linearly polarised photon beam 3-67040
 $\gamma d \rightarrow \pi^0 p(\text{ps})$, 3.4 GeV, linearly polarised photons, meas. asymmetry of reaction 3-67036
 $\gamma d \rightarrow \pi^0 d$, corrections for multiple scattering, total and differential cross sections (Russian) 3-70922
 $\gamma N \rightarrow N \pi$, Reggeized higher symmetry model, vector-meson dominance test 3-78167
 $\gamma n \rightarrow \pi^+ X$, 7-5 GeV, str. functions, γp comparison 3-78144
 $\gamma N \rightarrow \pi \Delta$ threshold effect on πN coupling of $P_{11}(1470)$, quark model and exptl. data (Spanish) 3-67031
 $\gamma N \rightarrow \pi N$, $E_\gamma < 450$ MeV, multichannel dispersion theory 3-62838

pion production continued

- $\gamma n \rightarrow \pi^0 n$, photoproduction, differential cross section, 500-900 MeV 3-57349
- $\gamma p \rightarrow \pi^+ \pi^- \pi^0$, $\pi^0 \pi^0$, cross-sect. meas., $E_6 = 600$ to 900 MeV 3-49015
- $\gamma p \rightarrow \pi^- X^{++}$ inclusive reaction mediated by ρ meson production pion spectrum study 3-74375
- $\gamma p \rightarrow \pi^0 p$, 4 GeV, target asymmetry 3-70919
- $\gamma p \rightarrow \pi^0 p$, dip region, amplitude constraints, dual absorption model 3-57352
- $\gamma p \rightarrow \pi^+ n$, 0.4-1.8 GeV, backward anal., differential cross sections 3-78135
- $\gamma p \rightarrow \pi^+ n$, numerical study of phase of backward amplitude 3-57355
- $K^+ p \rightarrow K^+ \pi^- p$, 4.1-6.2 GeV, longitudinal phase space analysis, one pion exchange and dual models 3-57362
- $\gamma p \rightarrow \pi^+ \pi^- \pi^+ \pi^- p$, 18 GeV, photon dissociation into four pions, evidence for p' enhancement in 4π mass spectrum 3-57364
- $\gamma p \rightarrow \pi^+ \pi^- \pi^+ \pi^- p$, 9-18 GeV, spin-parity analysis of ρ' 3-57365
- $\gamma p \rightarrow \pi^\pm + X$, 7.5 GeV, struct. functions, γn comparison 3-78144
- $K^- \rightarrow \pi^- \pi^- \pi^+$, 400 MeV/c, τ^- mode, Dalitz plot distribution 3-66977
- $K^\pm \rightarrow \pi^\pm \pi^0 \pi^0$, charge asymmetry, total decay rates, CP violation 3-78113
- $K^- p$ interaction, 10, 16 GeV, π^+ , π^- momentum distrib. 3-78205
- $K^+ p \rightarrow K^+ \pi^+ \pi^- \pi^+ \pi^- p$, 12.7 GeV/c, comparison with Chan Loskiewicz Allison, and quark models 3-67141
- $\bar{K}\pi$ system in $K^- p \rightarrow \bar{K}\pi\pi N$ reactions at 14.3 GeV/c, Q-production 3-67136
- $K^+ \pi^+ \pi^-$, coherent production on nuclei at 10, 13 and 16 GeV/c (*German*) 3-52208
- NN annihilation into pions, statistical model with new charge weight factor 3-67137
- NN interaction, polarisation structure of reactions with four spin $1/2$ particles 3-74550
- nn interaction, secondary pion energies, approximation of experimental data (*Russian*) 3-62902
- NN $\rightarrow \pi^\pm +$ anything at rest, soft-pion limits of inclusive pion distrib., test of PCAC 3-52056
- νN interactions, application of soft-pion techniques 3-57332
- pd annihilations at rest into two pions, obs. 3-43136
- pN inelastic collisions, 200 GeV/c, ang. characts. of secondary relativistic charged particles 3-78213
- $pn \rightarrow \pi^+ \pi^- \pi^-$ annihilation at rest, two-variables expansions, analysis of Dalitz plot 3-57397
- pp annihilations, average transverse momentum of produced pions, uncorrelated jet model 3-45916
- pp collisions, 20-70 GeV, azimuthal corrections 3-78214
- pp collisions, 53.4 GeV c.m. energy, π^0 transverse-momentum distrib. 3-52059
- pp collisions, π , K and p production ratios in central region at CERN ISR 3-49068
- pp collisions at CERN ISR, charged pion spectra at 44.4 and 52.7 GeV 3-49069
- pp elastic scattering, spatial extension of pion cloud in p hadronic matter distrib., ISR energy 3-62879
- pp high energy collisions, multiperipheral description of π spectra, assumed similarity of γ and π properties (*Russian*) 3-74407
- pp interactions, multiplicity distrib. at very high energy, Reggeized production model 3-57385
- pp interactions, semi-inclusive, pion distrib. in fragmentation model 3-45917
- $\bar{p}p \rightarrow \bar{K}K$, $\pi^+ \pi^-$, possible polarisation meas. 3-40390
- $\pi\pi$ non-diffractive multiple production, high energy, evidence for strong correlation 3-78211
- pp \rightarrow pions, high energy, uncorrelated jet model predictions on multiplicity distribution 3-57440
- pp $\rightarrow p\pi\pi$, properties of π and p momentum spectra in multiperipheral scheme (*Russian*) 3-40400
- pp $\rightarrow p\pi^0$, production cross sections at 6.6 GeV/c, two-prong events 3-54350
- pp $\rightarrow p\pi^+ \pi^- \pi^0$, 19 GeV/c, diffraction dissociation, longitudinal phase space analysis 3-74446
- pp $\rightarrow \pi^+ \pi^-$, production cross sections at 6.6 GeV/c, two-prong events 3-54350
- pp $\rightarrow \pi^- +$ anything, 19 GeV/c, inclusive production spectrum, comparison with two centre thermal model 3-57455
- pp $\rightarrow \pi^0 +$ anything, 23.5-62.4 GeV, invariant-cross sections and obs. of large transverse momentum $\pi^0 n$ 3-78227
- pp $\rightarrow \pi^0 +$ anything, 52.7 and 44.8 GeV, large transverse momentum phenomena 3-74453
- pp $\rightarrow \pi^+ +$ anything, 20 to 1500 GeV, semiempirical formula for cross section, consistency with scaling, limiting fragmentation 3-57461
- pp $\rightarrow \pi^+ \pi^-$, 0.7 to 2.4 GeV/c, to study heavy boson coupling to π system, folded angular distributions, total cross sections 3-57396
- pp $\rightarrow \pi^+ \pi^- \pi^+ \pi^- \pi^0$, 2.1-2.24 GeV, over T-region, reson. anal. 3-78209
- pp $\rightarrow \pi^+ \pi^+ \pi^+ \pi^- \pi^- \pi^- (\pi^0)$, test of invariance under charge conjugation (*French*) 3-49053
- pp $\rightarrow \pi X$, spectral representation, scaling limit, light cone dominance 3-78222
- π photoproduction backward, 0.4 to 2.2 GeV, differential cross section 3-78133
- π -p mass spectrum in πN interaction, single peripheral model of Deck effect 3-74404
- π^- , in πp inclusive reactions in fragmentation region at CERN ISR 3-77454
- π^- , multiplicity distributions, 100, 200, 300 GeV, hydrodynamic model 3-60044
- π^- beam transport channel for radiation therapy and radiobiology 3-59447
- π^- inclusive distributions from 205 GeV/c pp interactions 3-62915
- π^- inclusive spectra from electroproduction in streamer chamber $0.3 < Q^2 < 1.5(\text{GeV})^2$, $1.3 < W < 2.8$ GeV 3-40354
- π^- photoproduction from ${}^1\text{H}$ 3-43234
- π^-/π^+ asymm., photoprod. on nucleons by 16 GeV polarised photons 3-45878
- π^0 , from $\pi^- p$ and pp collisions, charged multiplicity distribution using phenomenological model 3-62905
- π^0 , in $ee \rightarrow e\pi^0$, effect of anomalies terms in Ward identities 3-70935

pion production continued

- π^0 , thermodynamical spectra of neutral particles, 3-49060
- π^0 inclusive production at 14 GeV/c in $\pi^+ p$ interactions 3-71030
- π^0 multiplicity in $\pi^+ p$ interactions at 10.5 GeV/c 3-60040
- π^0 photoprod. on deuterons, differential cross section, wave function influence 3-70918
- π^0 photoproduction cross section calc. using two-body composite baryon model 3-74368
- π^+ , in ${}^{12}\text{C}(p, \pi^+){}^{13}\text{C}$ at 185 MeV, DWBA calcs. 3-40492
- π^+ , π^- , from 740 MeV protons on nuclei, nuclear effects, and two-body input cross sections corrections 3-67331
- π^+ in ep inelastic scattering, cross section meas. 3-49016
- π^+ photoprod. from ${}^{27}\text{Al}$ and ${}^{51}\text{V}$ 3-60159
- π^+ photoproduction from ${}^{16}\text{O}$, study using different dynamical amplitudes, particle-hole correlations 3-54461
- π^+ photoproduction from ${}^3\text{He}$ in first π -N resonance region, impulse approx., cross section 3-67300
- π^+/π^- asymmetry in inclusive electroproduction of hadrons, Regge analysis, scaling laws of parton model 3-57361
- π^\pm , in K π inclusive reactions at 13 GeV/c 3-54364
- π^\pm , photo- and electroproduction on nuclei at high energies (*Russian*) 3-54462
- π^\pm electroproduction, subtraction constant in fixed-t dispersion relations 3-62833
- π^\pm inclusive production at CERN ISR 3-74454
- π^\pm inclusive production at medium angles at CERN ISR 3-71029
- π^\pm inclusive production in pp interactions at 303 GeV/c, cross section determ. 3-74447
- π^0 in $\gamma n \rightarrow \pi^0 n$, 500-900 MeV, differential cross sections, resonance production 3-40347
- π^0 photoproduction, 1000 to 1800 MeV, recoil proton polarisation, summary fits 3-59978
- π^0 photoproduction from hydrogens, differential cross section in range 350-1175 MeV 3-62831
- π^0 production at 90°, large transverse momentum, constituent interchange model 3-62851
- $\pi^\pm +$ missing mass, electroproduction off protons, from factor, scaling behaviour 3-70929
- $\pi^- + p \rightarrow \pi^- + X$ inclusive interactions 3-54367
- $\pi^- C \rightarrow \pi^+ \pi^- \pi^- C^*$ (4.44) at 6.0 GeV/c, mass distrib. and spin-parity analysis of 3π system 3-67138
- $\pi^+ d \rightarrow \pi^- +$ anything at large transverse momenta, energy dependence of inclusive cross section 3-67156
- $\pi^+ \Delta^+(1236)$ and $\pi^+ \Delta^0(1236)$, electroproduction on hydrogen 3-40356
- $\pi^- N(A) \rightarrow \pi^- \Delta^- \pi^+ N(A^*)$, 3.9 GeV/c obs. secondary pion momentum spectra, longitudinal and transverse components (*Russian*) 3-67142
- $\pi^- n \rightarrow \pi^\pm +$ anything, 40 GeV/c, cross section (*Russian*) 3-71034
- $\pi^- p \rightarrow (n\pi)p$, parametrisation, diffractive props., energy dependence of exclusive reactions 3-74445
- $\pi p \rightarrow p\pi\pi$, properties of π and p momentum spectra in multiperipheral scheme (*Russian*) 3-40400
- $\pi p \rightarrow \pi +$ anything, 10.0 and 15.5 GeV/c, meas. of single particle distrib. 3-71031
- $\pi^- p \rightarrow \pi^\pm +$ anything, 40 GeV/c, cross section (*Russian*) 3-71034
- $\pi^- p \rightarrow \pi^- + (n-1)$ charged + neutrals, 7.5 and 21 GeV/c, scaling, reduced charged multiplicity 3-78225
- $\pi^- p \rightarrow \pi^- +$ anything, new parametrization, π^- spectra fit, Bose-Einstein distrib. 3-62908
- π^+ photoproduction and T_\perp versus T_\parallel analogue states in $N > Z$ nuclei 3-57508
- $\pi^+ \pi^- \pi^-$, coherent production by π^- on nuclei, 9 and 15.1 GeV/c, spin-parity analysis 3-49052
- $\Sigma^\pm \rightarrow \pi^\pm \gamma$, π spectrum up to 150 MeV/c, branching ratios, decay rates, parity 3-78115
- ${}^{12}\text{C}(p, \pi^+)$, cross-section for π^+ production calc. in Jastrow model, comparison with IPM 3-49259
- ${}^{12}\text{C}(p, \pi^+){}^{13}\text{C}$, $E = 185$ MeV, energy spectra, angular distribution, comparison with one-nucleon model 3-67323
- ${}^2\text{H}(p, \pi^+)H$ 340 to 670 MeV, study using Yao-Barry model 3-78307
- ${}^{16}\text{O}(p, \pi^+){}^{16}\text{N}$, effect of Woods-Saxon wave functions on cross sections for charged-pion photoproduction 3-63034

pion-proton interactions

- asymmetry, contribs. to total cross sections, 16-40 GeV/c (*Russian*) 3-67143
- diffractive three pion production on hydrogen, forward diffractive cross section, mass spectrum 3-67368
- final state obs. at 4 GeV/c, determ. of K^0 and Λ^0 masses 3-74476
- inelastic overlap function structure in diffractive dissociation model 3-57430
- total cross sections, Regge-pole model 3-67151
- universal multiplicity formula based on thermodynamics 3-49034
- $\pi^- \rightarrow \pi^0 n$, continuous moment sum rules (*Russian*) 3-40325
- π^0 production from $\pi^- p$ and pp collisions, charged multiplicity distribution using phenomenological model 3-62905
- $\pi^- + p \rightarrow \pi^- (K^0, \Lambda) + X$ inclusive interactions 3-54367
- $\pi^- n \rightarrow \pi^\pm +$ anything, 40 GeV/c, cross section (*Russian*) 3-71034
- $\pi p \rightarrow (n\pi)p$, parametrisation, diffractive props., energy dependence of exclusive reactions 3-74445
- $\pi p \rightarrow$ missing mass $+\eta$, mass width and cross-sections of η , ω , X^0 and 0 3-70975
- $\pi p \rightarrow p\pi\pi$, properties of π and p momentum spectra in multiperipheral scheme (*Russian*) 3-40400
- $\pi p \rightarrow \pi^0 n$ charge exchange, meas. using NaI scintillation counter, 120-270 MeV (*French*) 3-51698
- $\pi p \rightarrow \pi +$ anything, 10.0 and 15.5 GeV/c, meas. of single particle distrib. 3-71031
- $\pi^- p$, 40 and 50 GeV/c, charged-prong multiplicity distrib., scaling behaviour and local excitation model 3-43151
- $\pi^- p$, 40 GeV/c, γ quanta prod. 3-74428
- $\pi^- p$, 50 GeV/c, topological cross sections and charged particle multiplicities 3-57441
- $\pi^- p$, 7 GeV/c, production of KK and $KK\pi$ systems, diffraction dissociation mechanism 3-43149
- $\pi^- p$, average multiplicity and total cross section at 200 GeV/c 3-74448
- $\pi^- p$, inclusive reaction study at 11.2 GeV/c and average multiplicity detn. 3-43152
- $\pi^- p$, multiple particle production at 40 GeV 3-52029

pion-proton interactions continued

- π^-p , strange particle production at 1.69 GeV/c, obs. of $\Sigma\pi K$ and $\Lambda\pi K$ final states 3-45915
- π^-p , two-prong events at 4.45 GeV/c, cross-section meas., ρ^0 , f^0 , ρ^- production 3-49056
- $\pi^-p \rightarrow \pi^+n$, 17.2 GeV/c, phase-shift analysis of elastic $\pi\pi$ scattering, 600-1900 MeV 3-70983
- $\pi^-p \rightarrow A_1p$, 4.45 GeV/c, helicity conservation, ρ matrix elements and A_1 maximum decay 3-62890
- $\pi^-p \rightarrow A_2^-p$, discussion of form of A_2 resonances (*Slovak*) 3-62888
- $\pi^-p \rightarrow c + \text{anything}$ at 16 GeV/c, description in the triple Regge limit 3-67145
- $\pi^-p \rightarrow \lambda^0(\rightarrow \gamma\gamma)n$, production cross sections at 3.8, 6, 8 and 12 GeV/c 3-78210
- $\pi^-p \rightarrow \Delta^{++}X^-$, at 15 GeV/c, study of Δ^{++} production 3-60056
- $\pi^-p \rightarrow e^+e^-n$, dispersion model analysis, pion, nucleon form factors (*Russian*) 3-59963
- $\pi^-p \rightarrow \eta n$ charge exchange reactions in Regge-cut Van Hove model 3-57436
- $\pi^-p \rightarrow \eta(\rightarrow \gamma\gamma)n$, production cross sections at 3.8, 6, 8 and 12 GeV/c 3-78210
- $\pi^-p \rightarrow \eta n$, forward, Regge pole model of charge and hypercharge exchange reactions 3-67072
- $\pi^-p \rightarrow \eta n$, illustration of tensor exchange amplitudes, absorption model, effective rescattering 3-67082
- $\pi^-p \rightarrow \eta n$, Regge amplitudes in forward and backward directions, peripheral nature of A_2 exchange amplitude 3-52046
- $\pi^-p \rightarrow \eta n$, s-channel analysis in model of higher baryon couplings 3-43107
- $\pi^-p \rightarrow K^-K^+n$, Argonne Effective Mass Spectrometer study 3-70988
- $\pi^-p \rightarrow K^0_s + \text{anything}$, 11.2 GeV/c, various presentations of data 3-60048
- $\pi^-p \rightarrow K^0\Lambda$, 8, 10.7 and 15.7 GeV/c, differential and total cross sections 3-60034
- $\pi^-p \rightarrow K^0\Lambda$, brief survey of experimental data, parity doublet contributions 3-60025
- $\pi^-p \rightarrow K^0\Lambda$, pseudoscalar production line reversed reaction, amplitude analysis 3-71008
- $\pi^-p \rightarrow K^0\Sigma$, 8, 10.7 and 15.7 GeV/c, differential and total cross sections 3-60034
- $\pi^-p \rightarrow K^-K^+n$, coupled-channel phase-shift analysis for $\pi\pi$ scattering in KK threshold region 3-70981
- $\pi^-p \rightarrow K^*0\Lambda$, vector-meson production reaction, amplitude analysis 3-71008
- $\pi^-p \rightarrow \Lambda^0 + \text{anything}$, 11.2 GeV/c, various presentations of data 3-60048
- $\pi^-p \rightarrow \Lambda K$, search for struct. at ΣK threshold 3-67126
- π^-p neutrals, production cross sections at 3.8, 6, 8 and 12 GeV/c 3-78210
- $\pi^-p \rightarrow \pi^0\pi^0$, 1.6-2.4 GeV/c, di-pion system obs. 3-62900
- $\pi^-p \rightarrow pX$, dual properties and scaling behaviour 3-40402
- $\pi^-p \rightarrow pX$, dual properties study from scaling behaviour 3-49070
- $\pi^-p \rightarrow pd$, 4.6 GeV/c, differential cross sections analysis 3-62893
- $\pi^-p \rightarrow \rho^0\pi^-$, 9.1 GeV/c, production cross section for B- resonance 3-78200
- $\pi^-p \rightarrow \pi^-\pi^0$, $\pi^+\pi^-\pi^-$, 11.2 GeV/c, helicity conservation tests 3-43147
- $\pi^-p \rightarrow \rho\rho$ (1710) $\rightarrow \pi^+\pi^-\pi^-\pi^0$, 8 and 18.5 GeV/c. decay mode study 3-43148
- $\pi^-p \rightarrow \pi^-(^+) \text{anything}$, predicted differential cross section by factorisation of Regge trajectories 3-60052
- $\pi^-p \rightarrow \pi^-\Delta^+(1236)$, s-channel profile factor model for Regge- ρ exchange and duality 3-62887
- $\pi^-p \rightarrow \pi^-X$, $X = \text{fireball}$, decay, phase space effects, diffraction model 16 GeV 3-78172
- $\pi^-p \rightarrow \pi^- + (n-1) \text{ charged} + \text{neutrals}$, 7.5 and 21 GeV/c, scaling, reduced charged multiplicity 3-78225
- $\pi^-p \rightarrow \pi^-\pi^-\Delta^+$, study of $\pi^-\pi^-$ high energy scattering 3-71001
- $\pi^-p \rightarrow \pi^-\pi^0\pi^-\pi^+$, 25 GeV/c, study of high energy $\pi\pi$ scattering processes 3-57448
- $\pi^-p \rightarrow \pi^-\pi^+\Delta^+$, 25 GeV/c, study of high energy $\pi\pi$ scattering processes 3-57448
- $\pi^-p \rightarrow \pi^-\pi^+n$, 17.2 GeV/c, absorptive A_2 exchange, polarised target predictions 3-60039
- $\pi^-p \rightarrow \pi^-\pi^+n$, 17.2 GeV/c amplitude analysis and extrapolation to pion exchange pole 3-71016
- $\pi^-p \rightarrow \pi^-\pi^+n$, 25 GeV/c, study of high energy $\pi\pi$ scattering processes 3-57448
- $\pi^-p \rightarrow \pi^-\pi^+n$, 4.5 GeV/c, Chew-Low extrapolations to pion pole 3-71015
- $\pi^-p \rightarrow \pi^-\pi^+n$, absorption model for π -exchange calculation of spin dependence 3-57386
- $\pi^-p \rightarrow \pi^-\pi^+n$, proton polarisation, high energy predictions of a $\pi + A_2$ model 3-74443
- $\pi^-p \rightarrow \pi^-\pi^+n$, strength of absorptive corrections to pion exchange Born term 3-49055
- $\pi^-p \rightarrow \pi^-\pi^+n$, study of $\pi^+\pi^+$ high energy scattering 3-71001
- $\pi^-p \rightarrow \pi^-\pi^+n$ 3-70979
- $\pi^-p \rightarrow \pi^-\pi^+n$ A_2 -exchange and polarization effects in analysis of $\pi\pi$ scattering 3-70987
- $\pi^-p \rightarrow \pi^0n$, 6 GeV/c, amplitude by s-channel model 3-78196
- $\pi^-p \rightarrow \pi^0n$, charge exchange reaction, dispersion relations 3-43143
- $\pi^-p \rightarrow \pi^0n$, high energy, analysis of explt. data, violation of Pomeranchuk theorem (*Russian*) 3-62898
- $\pi^-p \rightarrow \pi^0n$, Regge pole and cut model of charge exchange 3-54341
- $\pi^-p \rightarrow \pi^0n$ charge exchange reactions in Regge-cut Van Hove model 3-57436
- $\pi^-p \rightarrow \pi^0\pi^0n$, 2 GeV/c, $\pi\pi$ phase shift analysis 3-70990
- $\pi^-p \rightarrow \pi^+\pi^-X^0$, extrapolation technique used by SLAC group for $\pi^+\pi^-$ cross section meas. 3-70985
- $\pi^-p \rightarrow \pi^+\pi^-n$, 200 to 260 MeV, matrix element near threshold (*Russian*) 3-78179
- $\pi^-p \rightarrow \pi^+ + \text{anything}$, 40 GeV/c, cross section (*Russian*) 3-71034
- $\pi^-p \rightarrow \rho^-p$, 6 GeV/c, differential cross sections, density matrix elements, simple model proposed 3-67129
- $\pi^-p \rightarrow \rho^0n$, 6 GeV/c, differential cross sections, density matrix elements, simple model proposed 3-67129
- $\pi^-p \rightarrow pN$, 2.3 GeV/c, obs. of structure in momentum transfer distrib. 3-71010

pion-proton interactions continued

- $\pi^-p \rightarrow X^-p$, 6.0 GeV/c, meas. of missing mass spectrum in A_2^- region 3-57434
- $\pi^-p \rightarrow X^-p$, cross sections of S, T and U mesons, 25 GeV/c 3-57452
- $\pi^-p \rightarrow Xp$, missing mass experiments, implications for Regge cuts 3-43126
- π^+p , 10.5 GeV/c, π^0 multiplicity meas., inclusive cross section, correlation parameters 3-60040
- π^+p , 8 GeV/c, strange particle production in five and six body final states (*Rumanian*) 3-49058
- π^+p , 8 GeV. ten prong events, phase space deviation 3-78206
- π^+p , strange particle production at 3.7 GeV/c 3-54352
- $\pi^+p \rightarrow \Delta^{++} + \text{anything}$, determ. of $\pi\pi$ total cross section 3-70998
- $\pi^+p \rightarrow \eta\Delta^{++}$, 1.28-2.67 GeV/c, meas. and analysis using effective trajectory parametrization 3-54353
- $\pi^+p \rightarrow \pi^+\pi^+p$, two-prong fitted channels at 11.7 GeV/c, cross-sections 3-57439
- $\pi^+p \rightarrow \pi^+\pi^+$, polarization parameter meas., description of on-line computer system 3-66322
- $\pi^+p \rightarrow \pi^+\pi^+\pi^+$, $\pi^+\pi^0$, $\pi^+\pi^+\pi^-$, 11.7 GeV/c, helicity conservation tests 3-43147
- $\pi^+p \rightarrow \pi^- + \dots$ and $\pi^- + \dots$, proton fragmentation analysis 3-57416
- $\pi^+p \rightarrow \pi^0\Delta^{++}(1236)$, s-channel profile factor model for Regge- ρ exchange and duality 3-62887
- $\pi^+p \rightarrow \pi^+\eta p$, 230 MeV, cross section estimation (*Russian*) 3-60020
- $\pi^+p \rightarrow \pi^+\eta p$, bremsstrahlung process in 1236 resonance region, Schrodinger current operator calc. 3-57403
- $\pi^+p \rightarrow \pi^+\pi^0p$, at 2.67 GeV/c, ρ^+ production, obs. of interference effects 3-40399
- $\pi^+p \rightarrow \pi^+\pi^0p$, two-prong fitted channels at 11.7 GeV/c, cross-sections, $\pi^0\Delta^{++}$ and ρ^+ channels 3-57439
- $\pi^+p \rightarrow \pi^+\pi^0p$, 230 MeV, cross section estimation (*Russian*) 3-60020
- $\pi^+p \rightarrow \pi^+\pi^+n$, 12.5 GeV/c, study of isospin 2 $\pi\pi$ phase shifts 3-70994
- $\pi^+p \rightarrow \pi^+\pi^+n$, 5.45 GeV/c, cross sections and phase shifts for $I=2$ $\pi^+\pi^+$ scattering, Chew-Low extrapolation method 3-67135
- $\pi^+p \rightarrow \rho^+\pi^+$, low mass enhancement, doubled charged A_1^- and existence of the true A_1 resonance 3-57401
- $\pi^+p \rightarrow \rho^+p$, 6 GeV/c, differential cross sections, density matrix elements, simple model proposed 3-67129
- $\pi^+p \rightarrow \Sigma^+K^+$, polarization parameter meas., description of on-line computer system 3-66322
- π^+p , charged multiplicity data analysis, Nova and Chew-Pignotti models 3-54360
- π^+p , energy dependence of difference of total cross sections and curvature of the ρ trajectory 3-43158
- $\pi^+p \rightarrow B^+p$, 11 GeV/c, production and decay props. of B-meson 3-43144
- π^+p helicity amplitudes, unitarity and analyticity 3-54340
- $\pi^+p \rightarrow p + \text{pions}$ ($p + \text{anything}$), average transverse momentum of produced particles, uncorrelated jet model 3-45916
- $\pi^+p \rightarrow \pi^- + \text{anything}$, new parametrization, π^- spectra fit, Bose-Einstein distrib. 3-62908
- $\pi^+p \rightarrow \pi^0X$, 14 GeV/c, differential cross section meas. 3-71030
- $\pi^+p \rightarrow \pi^+\pi^+n$, coupled-channel phase-shift analysis for $\pi\pi$ scattering in KK threshold region 3-70981
- π^+p systems, Ericson fluctuations in energy range 2 to 3.5 GeV 3-57460
- $\pi^+p \rightarrow \pi^+\pi^+n$, 230 MeV, cross section, interaction Lagrangian for $\pi\pi$ and πN reactions (*Russian*) 3-60020
- $\pi^+p \rightarrow p + \text{anything}$, 10.0 and 15.5 GeV/c, meas. of single particle distrib. 3-71031

pion-proton scattering

- σ commutator, value of 86 ± 12 MeV 3-70976
- elastic, crossing even, strong central absorption prescription 3-74431
- elastic, scaling and kinematic variable n^2 3-57450
- elastic large-angle, differential cross section, quark model and auto-modellism 3-62850
- elastic large-angle at 5 GeV/c, cross-section fluctuations 3-57426
- nondiffractive, direct channel effects, 6 GeV/c 3-71009
- topological cross-section, phenomenological model 3-45918
- p form factors, inelastic, determ. in multiparticle production processes 3-74436
- pp, high-energy, Bethe phase shift and meas. of Ref/Imf ratio (*Russian*) 3-67165
- $\pi p \rightarrow \pi p$, high energy, backward, rel. to dominance of light cone singularities 3-71003
- $\pi p \rightarrow \pi p$ baryon exchange reaction, line reversal and energy dependence of dip locations 3-54351
- πp , 88 to 292 MeV, elastic differential cross sections 3-57406
- πp , 88 to 310 MeV, phase shift analysis 3-60019
- πp , elastic, at 25 and 40 GeV/c meas. differential cross sections and diffraction cone slopes (*Russian*) 3-67123
- πp , elastic at 25 and 40 GeV/c, differential cross sections and diffraction slopes 3-57424
- πp , elastic scattering, 5 GeV/c, backward and forward peaks 3-78189
- πp elastic scattering at 40 GeV/c, polarisation parameter meas. 3-49048
- $\pi^-p \rightarrow X^-$, missing mass spectra, Boson spectrometer obs. (*French*) 3-52050
- $\pi^-p \rightarrow \pi^0n$, limits on charge-exchange polarization 3-57409
- $\pi^-p \rightarrow \pi^+n$, real parts, differential cross sections, polarisations 3-62896
- π^+p , 88 to 292 MeV, elastic, differential cross sections 3-57406
- π^+p , elastic, meas. of polarisation parameter between 2.50 and 5.15 GeV/c 3-71004
- π^+p , elastic scattering, 5 GeV/c, backward and forward peaks 3-78189
- π^+p backward elastic scattering at 2.0, 3.5 and 4.0 GeV/c, polarisation meas. 3-57422
- π^+p large angle elastic scatt. at 13.8 GeV/c 3-40389
- $\pi^+p \rightarrow \pi^+\pi^+$, dual absorptive model and polarization 3-45906
- $\pi^+p \rightarrow \pi^+\pi^+$, two-prong fitted channels at 11.7 GeV/c, cross-sections 3-57439

pion-proton scattering continued

- π^+p , elastic, forward and backward, polarisation meas. at high energy 3-74429
- π^+p elastic, differential cross section meas., 88-292 MeV 3-74423
- π^+p elastic high-energy scattering, parton model and multiple scattering effects 3-60024
- π^+p elastic scatt., analytic phase shift analysis 3-54339
- π^+p forward elastic scattering amplitude, 50-5000 GeV, ratio of real to imaginary parts 3-49046
- π^+p partial waves, lower bound for number necessary for exptl. analysis 3-43134
- $\pi^+p \rightarrow \pi^+p$ forward amplitudes, zeros 3-74418
- π^+p scattering, 88-310 MeV, phase shift solutions 3-74421
- π^+p total cross sections, upper bound for sum above 60 GeV 3-54362
- π^+p , 88 to 310 MeV, phase shift analysis 3-60019

pion scattering

- see also pion-baryon scattering; pion-pion scattering
- $e\pi$ elastic large-angle, differential cross section, quark model auto-modellism 3-62850
- $K\pi$, low energy, general features from physical region method, dispersion relation 3-78188
- $K\pi$, study using Argonne Effective Mass Spectrometer 3-70988
- $K\pi$ inelastic final states and resonance parameter determ. from partial wave analysis of $2 \rightarrow 3$ body reactions 3-70982
- $K\pi$ scattering study using k^+p reaction at 13 GeV, SLAC expt. 3-70989
- $K\pi$ system with mass below 1 GeV produced in $K^+p \rightarrow \Delta^+ + K^+ \pi^-$ reaction, partial wave analysis 3-70978
- $K^-\pi^+$, elastic scattering cross section measured in $K^-p \rightarrow K^-\pi^-\Delta^{++}$ at 14.3 GeV/c 3-57423
- $K^+\pi^-$, elastic cross section, obs. in $K^+p \rightarrow K^+\pi^-\Delta^{++}$, 3-13 GeV/c 3-40398
- pd, 15-60 GeV, energy dependence of shadow term, regenerative effects 3-52058
- πd , effect of πN interaction range on scatt. length 3-78178
- πd , elastic, calc. of scattering length using Faddeev integral eqns. 3-49042
- π^+d , pion absorption and elastic scattering, Faddeev eqns., contribs. to scattering length 3-67108
- π^+d elastic scattering near 3-3 resonance, angular distribns., cross sections, 141-256 MeV 3-40379
- π^+d , determ. Bethe phase shift and Ref./Imf ratio, meas. total scattering cross section (Russian) 3-67165
- $\pi\eta$, chiral $SU(2) \times SU(2)$ symmetry 3-45870
- $\pi^3\text{He}$, at 100 MeV rel. to determ. of $\pi^+{}^3\text{He}$ coupling constant using $d\sigma/d\Omega$ extrapolations to ${}^3\text{H}$ pole (Russian) 3-67304
- πK , low energy, chiral $SU(2) \times SU(2)$ symmetry, amplitudes consistent with unitarity and crossing 3-57420
- $\pi\omega$, static model, description of ρ meson properties. 3-62921

pions

- charge radius, from current algebra sum rule and short range correlation model 3-49006
- charge radius determ. from meas. $2S_{1/2}-2P_{1/2}$ energy level shift of $\pi\text{-u}$ atom 3-66996
- e.m. form factor and derivative, new bounds 3-57344
- e.m. mass splitting, tensor gravity, sum rules 3-62822
- e.m. radius determ. from $\pi^+{}^4\text{He}$ scattering 3-78305
- exchange effects on nuclear magnetic moments 3-45928
- excitation, vector and axial-vector, to arbitrary single particle state 3-74386
- form factor, electric, restrictions imposed by timelike e.m. current 3-45874
- form factor and inelastic $\pi\pi$ scattering, review 3-70995
- form factors, elastic e.m., asymptotic behaviour, reln. to scale dimensions of interpolation field 3-78126
- form factors, from dispersion model analysis of $\pi^+p \rightarrow e^+e^-n$ (Russian) 3-59963
- gauge condition, application as mass extrapolation constraint 3-40362
- low energy, experimental study (French) 3-60063
- mass, gauge model, current algebraic treatment 3-70864
- mass, gauge model realising pseudo-Goldstone idea 3-70862
- nuclear and neutron star matter, pion condensation, equilb. thermodynamic conditions 3-49183
- nuclear matter, pion condensation as in neutron 3-54417
- parton model, general features 3-45883
- properties, similarity to photon properties, description of spectra from pp collisions (Russian) 3-74407
- proton production, for cancer treatment 3-59442
- Regge trajectory functions, bounds below threshold 3-45895
- scintillation counter, organic liquid, energy deposition and fluctuations 3-73869
- soft pion extrapolation problem in highly virtual photon-induced reactions 3-57309
- spectra, fragmentation in central region, possibility of discontinuity at $x=0$ 3-43162
- stopped, cellular response 3-66052
- π , weak and e.m. mass diff. 3-54307
- π^- , dose in soft tissue, bone, calc. 3-77286

pitch detection see acoustic variables measurement**planes** see sun**plane polarisation** see polarisation**planet Mercury** see Mercury (planet)**planetary atmospheres**

- anisotropic non-conservative scatt. in semi-infinite media 3-56332
- boundary layer, non-stationarity effects 3-65317
- boundary layer, Richardson number profiles through instability wave regions 3-61599
- boundary layer gravity wave generation by shear instability 3-61458
- diffuse reflection by semi-infinite atmosphere, approx. formulae (Russian) 3-61677
- dynamic process parameterization 3-73322
- giant planets, spacecraft radio occultation experiments planned for Pioneer and Mariner missions 3-65969
- inhomogeneous, plane parallel, emergent radiation calculated by adding method 3-73455
- inner planets, weather systems, Mars and Venus probe obs., comparison with Earth 3-65767

planetary atmospheres continued

- ionization levels, implications of H_3^+ and H_5^+ electron-ion recomb. coeffs. 3-63882
- Jovian atmosphere structure determ. from i.r. meas., iterative method 3-56335
- Jovian electron radiation belts, decimetric radiation obs. and electron energy and density 3-69848
- Jovian ionosphere, structure and time variations 3-42173
- Jovian ionospheric models 3-69888
- Jovian magnetosphere, radio wave propag. 3-47897
- Jovian magnetospheric diffusion rates, expected X-ray flux at Earth 3-47898
- Jovian radiation belt, simultaneous soln. of electron energy and number densities 3-69847
- Jupiter, 12000-4000 cm^{-1} spectra by Fourier Transform spectroscopy, obs. of $3\nu_3$ methane band 3-47899
- Jupiter, Alfvén wave propagation along Io's flux tube 3-65771
- Jupiter, atmospheric belt intensity rel. to solar activity 3-51290
- Jupiter, atmospheric structure and clouds from obs. of methane and H_2 quadrupole lines 3-47914
- Jupiter, auroral activity, electron excitation 3-69889
- Jupiter, convective instability, internal heat source, Boussinesq equations solution 3-76992
- Jupiter, D fractionation 3-59264
- Jupiter, Great Red Spot rel. to Taylor column theory 3-42166
- Jupiter, greenhouse models 3-56343
- Jupiter, HD 7467 A absorption line obs. rel. to D/H ratio 3-80988
- Jupiter, He-methane system, phase equilibria meas. at high-pressure 3-42162
- Jupiter, infrared high resolution maps at 5μ 3-69850
- Jupiter, ionosphere and magnetosphere rel. to ionization and temperature 3-65769
- Jupiter, ionospheric physical and chemical processes 3-47937
- Jupiter, Lyman- α albedo rel. to atmospheric models 3-61675
- Jupiter, magnetospheric interaction of Io and I.f. MHD wave emission 3-65770
- Jupiter, methane 1.1μ $3\nu_3$ band absorption, Lorentz half-width, photoelectric obs. 3-61682
- Jupiter, methane absorption line formation from high dispersion spectra 3-59269
- Jupiter, microwave brightness temp. determ. using model atm. 3-42158
- Jupiter, NH_3 absorption coefficients in 2100-2250 Å region rel. to Jovian albedo 3-56330
- Jupiter, NH_3 photolysis rel. to atmospheric composition and temperature 3-61681
- Jupiter, occultation of β_1 Scorpii, photometric obs. 3-45035
- Jupiter, outer atmosphere, review 3-65778
- Jupiter, photochemical analysis 3-69879
- Jupiter, photochemistry of hydrocarbons 3-65745
- Jupiter, photoelectron excitation of dayglow 3-69890
- Jupiter, polarimetric obs. of atmosphere rel. to two models 3-47910
- Jupiter, radiative transfer, ammonia spectral data for ν_2 bands 3-76995
- Jupiter, rotation profiles, short-term (1970-72) 3-69858
- Jupiter, south equatorial belt disturbance, June 1971 initial development 3-65744
- Jupiter, spectroscopic obs. at 8000-3000 cm^{-1} , search for minor atm. constituents 3-69891
- Jupiter, temp. variation with depth from 2 cm obs. 3-61825
- Jupiter, thermosphere temperature, importance of solar e.u.v. flux 3-76993
- Jupiter's cloud bands, radiative instability of cloud deck, flow model 3-61680
- Jupiter dayglow, photoelectron impact contribution for atmospheric model with and without He 3-56345
- Jupiter radiation belt, source and structure 3-65779
- Jupiter shock-layer temps. appropriate for entry, meas. of H_2 -He radiation 3-69881
- Jupiter temperature and ammonia profiles from inversion of i.r. spectrum 3-80983
- Langmuir probes, current collection characteristics rel. to motion in atmospheres 3-60632
- localised turbulence, remote sensing by radio spectrum analysis 3-42176
- major planets, atm. dynamics rel. to planetary dynamics 3-47936
- major planets, atm. meas. rel. to interior models 3-47934
- major planets' thermal structure determ. from radio obs. 3-47938
- Mars, α -particle experiment for chemical analysis of surface and atmosphere 3-51410
- Mars, analysis of Mariner 9 occultation data 3-61708
- Mars, approx. using Mariner 9 occultations 3-69869
- Mars, atm. and radiative props. 3-65741
- Mars, atm. scatt. props., Mariner 9 u.v. spectrometer data 3-65763
- Mars, atmosphere, latitudinal dependence of surface pressure 3-61709
- Mars, atmospheric temperature, Mariner 9 ultraviolet spectroscopy, OI 1304-Å emission 3-69875
- Mars, Boundary layer over sloping terrain, temp. and wind oscillations 3-45036
- Mars, circulation, Mariner 9 global results 3-65759
- Mars, CO_2 2μ band obs. by Mars 3 spacecraft for altitude detn. 3-65782
- Mars, CO emission in dayglow 3-65743
- Mars, CO fourth positive system in airglow rel. to dissociative recombination of CO_2^+ ions 3-78860
- Mars, dayglow, emission of excited CO third positive bands 3-80990
- Mars, dust-filled, radiation regime 3-61696
- Mars, extent and structure of ionosphere 3-56347
- Mars, H_2O content, Mars 3 spacecraft obs. 3-65781
- Mars, He abundance determ. method and estimate of x.u.v. dayglow 3-69883
- Mars, ionospheric refr. of H.F. waves, electron-neutral particle collision effects 3-42174
- Mars, Mariner 9 Extended Mission TV results 3-69865
- Mars, Mariner 9 i.r. spectroscopic meas. 3-65762
- Mars, Mariner 9 S band occultation meas. of atm. and topography 3-69868
- Mars, Mars-2 preliminary results 3-42175

planetary atmospheres continued

- Mars, O I day airglow emissions of 5577 and 6300 Å lines 3-65742
 Mars, obliquity var., climatic effects 3-76997
 Mars, photolytic stability rel. to convection and low altitude aerosol 3-65768
 Mars, polar cap matter rel. to CO₂ frosts 3-53620
 Mars, polar region, ozone, seasonal variation, Mariner 9 u.v. spectra obs. 3-45038
 Mars, theoretical calc. of airmass 3-47926
 Mars, upper atmosphere column density of CO 3-61706
 Mars, wave-induced eddy diffusion coefficients in upper atmosphere 3-80991
 Mars, winds and dust clouds 3-65775
 Mars, yellow cloud prod. mechanism and nature (*French*) 3-80989
 Mercury, atmospheric density determ. from solar wind interaction 3-69885
 Mercury, interaction with solar wind, determ. of atm. density 3-61686
 Mie phase matrix for multiple scattering calcs. in four-component Stokes vector representation 3-51870
 modified two-stream approx. of Sagan and Pollock (1967) 3-56342
 multiple scatt. of polarised light in semiinfinite atmospheres 3-61691
 Neptune, ionospheric physical and chemical processes 3-47937
 Neptune and Uranus 3-65780
 occultation curve spikes, critique of Brinkmann's method 3-47912
 outer planet magnetospheres, scaling laws 3-47939
 outer planets, chemical comp. and structure rel. to solar system origin 3-47932
 PAET, entry probe experiment in Earth's atmosphere 3-47730
 photon path lengths, probability distrib. for diffuse reflection 3-65739
 physics and chemistry of terrestrial and planetary upper atmospheres 3-41982
 pressure profile, entry probe base pressure expt. 3-59401
 radiation field in deep layers for anisotropic scatt. 3-61692
 radiative instability of cloudy planetary atmosphere 3-61679
 radiative transfer, multiple scattering theory in inhomogeneous atmospheres 3-48815
 radiative transfer 3-69880
 radius occultation of spacecraft, utilization in studying atmospheres 3-65968
 Reflection and transmission of radiation by planetary atmospheres with reflecting surfaces 3-80993
 refraction, eqn. of radiative transfer 3-73453
 remote sounding from artificial satellites and space probes of Earth and planets 3-47767
 Rossby number similarity theory, A B (μ) functions, variability of empirical determ. 3-65319
 Saturn, 0.62 μ methane band absorpt. and near-u.v. characts. 3-61695
 Saturn, He-methane system, phase equilibria meas. at high press. 3-42162
 Saturn, ionospheric physical and chemical processes 3-47937
 Saturn, methane $3\nu_3$ absorption band in atmosphere spectra, rotational temp. and abundance 3-47913
 Saturn, methane $3\nu_3$ band obs. along planet's central meridian 3-56331
 Saturn, microwave brightness temp. determ. using model atm. 3-42158
 scattering and transmission functions of atm. with reflecting surfaces 3-69852
 solar Lyman- α radiation transfer through plane-parallel atm. 3-53615
 solar wind, weakly shocked flow through cometary comas and planetary atmospheres 3-73446
 solar wind interaction rel. to ionization and mass loss 3-65783
 solar wind interaction with magnetized planet 3-65774
 spectral line Doppler broadening, band absorbance formulation in planetary atmospheres 3-52375
 spectroscopic techniques, education 3-59521
 temperature structure determ., numerical method 3-47920
 terrestrial planets origin and evolution 3-65773
 Titan, escape of H₂ from various hypothetical atmospheres 3-76994
 Uranus, ionospheric physical and chemical processes 3-47937
 Uranus and Neptune, review 3-65780
 Venus, atmosphere, stability of CO₂, removal of photodecomposition products 3-61705
 Venus, circulation model driven by polar and diurnal surface temp. variations 3-47924
 Venus, CO₂ absorpt. strength variations 3-45034
 Venus, CO₂ production kinetics rel. to inferred surface temp. 3-61683
 Venus, dayside upper ionosphere, model for ion and electron gases 3-65785
 Venus, determ. of characts. light-scatt. particles 3-59267
 Venus, H₂SO₄ in clouds, chemical processes and spectrum 3-69857
 Venus, helium content estimation from radioactive progenitors and ionization profiles 3-61704
 Venus, high altitude retrograde horizontal winds rel. to cloud layers 3-69886
 Venus, ionosphere, estimation of He content 3-69876
 Venus, ionospheric heating on simple one-dimensional model 3-65784
 Venus, i.r. radiative heating and cooling of mesosphere, day-to-night var. 3-51292
 Venus, limb radiance profiles, derivations, 600 to 700 cm⁻¹, application to spacecraft navigation 3-73452
 Venus, lower ionosphere, ionization rates and ion chemistry model 3-69887
 Venus, microwave meas., absence of water vapour 3-51296
 Venus, O I 1304 and 1356 Å emissions from atmosphere rel. to rocket and Venera data 3-56346
 Venus, stratosphere, gravity wave-mean flow interactions, 4-day circulation 3-65406
 Venus, upper atmospheric 4 day circulation, dynamical aspects 3-65777
 Venus upper atmosphere, 4-day rotation from u.v. photographs 3-65776

planetary atmospheres continued

- water vapour, production from lunar breccia by exposure to hydrogen and outgassing, implications 3-73462
 waves, vertical structures (*German*) 3-65321
 CO₂* 2890 Å band, photoionization excitation rel. to column excitation rates for planetary atmospheres 3-54732
 D₂, liquid, shock wave compression to 0.9 Mbar 3-75594
 H-He planet, convective portion of atmosphere rel. to internal structure 3-51289
 H₂, statistical mechanics at high pressure 3-60508
 H₂ quadrupole absorption in Jovian atmosphere Curtis-Godson approx. 3-47911
 H₂SO₄ solution in water rel. to composition, structure, characteristics and spectra of clouds of Venus 3-47909
 NH₃ solid, optical properties, scattering parameters for cloud particles 3-76991
- planetary nebulae**
 BD + 30°3639, 8-13 μ spectrum 3-65941
 BD + 30°3639, H β meas. rel. to scattered continuum, optical depth 3-51402
 central stars rel. to hot liquefying white dwarfs, cores, masses and luminosity 3-61877
 condensations, H radio recombination lines strengths 3-61875
 Crab Nebula, origin of h.f. radiation 3-61876
 expansion velocities in six old nebulae, O III 5007 Å line profiles 3-45232
 formation rel. to red giants with H and He shell sources (*Polish*) 3-45090
 galactic absorption map based on planetary nebulae extinctions 3-45213
 identification of 20 objects within elliptical galaxies 3-45230
 ionisation structure, contrib. of charge exchange and optically thick condensations to [O I] radiation 3-73554
 i.r. emission mechanism and energy sources 3-42219
 i.r. photometry of 28 objects between 1.6 and 3.5 microns 3-56455
 in Local Group galaxies NGC 185, NGC 205 and NGC 221, identifications 3-70045
 M2-9, [FeII] emission-lines and i.r. continuum 3-56456
 M 1-11, i.r. object, radio emission detection at 10.63 GHz 3-65901
 magnetic DC white dwarfs, evolutionary connection with planetary nebulae nuclei 3-81027
 new object formerly designated as Wray 1876, Be star 3-53716
 NGC 185-1, planetary nebula in elliptical galaxy, chemical abundances 3-45231
 NGC 6302, 0.35-20 μ obs. 3-73553
 NGC 6445 (p-k 008 + 03°1), irregular ring nebula, spectrophotometric study 3-56451
 NGC 6572, 8-13 μ spectrum 3-65941
 NGC 6572, 9.0 μ obs. 3-59392
 NGC 6720, comparison of Pulkovo and Harvard meas. of ang. expansions 3-53717
 NGC 6778, line identifications 3-61874
 NGC 6853, comparison of Pulkovo and Harvard meas. of angular expansions 3-53717
 NGC 7027, 8085 MHz obs., fine structure 3-59393
 NGC 7027, 8-13 μ spectrum 3-65941
 NGC 7027, 9.0 μ obs. 3-59392
 NGC 7027, obs. of high-n Balmer transitions 3-53714
 NGC 7027, relative line intensities in spectral range 3000-5000 Angstroms 3-45228
 NGC 7293, meas. of ang. expansion rate 3-45233
 NGC 7293, trigonometric parallax determ. for central star 3-45234
 NGC 7662, comparison of Pulkovo and Harvard meas. of ang. expansions 3-53717
 nuclei, relation with DA and DB white dwarfs 3-81028
 nuclei, spectra rel. to massive Population I stars 3-81212
 nuclei evolution compared with evolution of C-rich stars with He envelopes 3-45075
 optical positions for 153 objects 3-45227
 radial velocities 3-77167
 recognition, colour photography, anomalous images, visual examination 3-81056
 FG Sagittae, observational evidence of thermal pulse in old planetary nebula 3-69960
 FG Sagittae, symmetrical emission nebulosity expansion 3-70044
 search in globular clusters for new objects, H α observations 3-45229
 He envelopes, upper bounds of mass 3-81211
- planetary satellites**
see also moon
 Callisto, improved data during Jupiter's close approach to 21 Capricorn 1973 May 3-76990
 Deimos, Mariner 9 TV obs. 3-69866
 Europa, occultation obs. indicating polar cap 3-61690
 Galilean satellites, eclipses and occultation obs. during 1973-74 period 3-47908
 Galilean satellites, surface colour variations 3-47919
 Galilean system, dynamical motion (*French*) 3-42107
 intermediate satellite orbital elements, differential eqns. for perturbed motion 3-53592
 Io, 100 KeV electron prod., model 3-65788
 Io, Alfvén wave propagation along flux tube to Jovian ionosphere 3-65771
 Io, effect of ionosphere on Jovian decametric radiation 3-56334
 Io, interaction with Jovian magnetosphere and i.f. MHD wave emission 3-65770
 Io, post eclipse brightening, review 3-69859
 Io, post eclipse brightening (June 25 1971) 3-69860
 Io-controlled decametric radiation rel. to Alfvén wave emission 3-65772
 Jovian, potential atmospheres of Galilean satellites 3-51294
 Jovian decametric emission periodicities rel. to innermost satellites and solar activity 3-42138
 Jovian satellite-satellite eclipses and occultations 3-47918
 of Jupiter, radiation belt fluxes meas. by Pioneer 10, satellites effects 3-65786
 Jupiter, sweeping effect of inner satellites in radiation belts 3-56344
 Jupiter's Galilean satellites, narrow-band photometry in 0.3-1.1 microns range 3-69855

planetary satellites continued

- Jupiter's Galilean satellites, outer two, 3-7 commensurability 3-69853
- Jupiter's Galilean satellites, spectral albedos from 0.36-3.4 micron photometry 3-69856
- Jupiter radio emissions, decametric, modulation by Io, triggering mechanism 3-65789
- libration cloud, theoretical possibility in restricted three body problem 3-69803
- major planets, survey of dynamical data 3-42155
- mean distances distrib. in Sun, Jupiter, Saturn and Uranus systems 3-59265
- Mercury, satellite loss, effect of solar tidal friction 3-69837
- outer planets, chemical comp. and structure rel. to solar system origin 3-47932
- outer planets, survey of present knowledge 3-45039
- outer planets and satellites, imaging techniques 3-48160
- Phobos, Mariner 9 obs. (*Czech*) 3-59266
- Phobos, Mariner 9 TV obs. 3-69866
- properties, review of known facts 3-42153
- radius determ. using radiometry and photometry 3-48148
- size determ. independent of angular diameter 3-53730
- terrestrial natural moonlets, analysis of Bagby's work 3-61714
- tidal evolution of satellite resonances by tidal energy dissipation 3-42106
- Titan, atmospheric dynamics and temp. variations 3-56339
- Titan, bulk comp. of atm. 3-53618
- Titan, escape of H₂ from various hypothetical atmospheres 3-76994
- Titan, greenhouse models of atm. 3-47921
- Titan, H₂ detection 3-53617
- Titan, model from observational data 3-42141
- Titan, polarimetric obs. rel. to optically thick atmosphere 3-47916
- Titan, polarization obs. rel. to opaque cloud layer with strong u.v. absorption 3-47917
- Titan, possible H₂ greenhouse effect rel. to atmospheric temp. 3-47915
- Titan, potential atmospheric composition 3-51294
- Titan, role of noble gases on greenhouse effect 3-61688
- Titan, toroidal ring, u.v. photography 3-80998
- Titan, upper limit on 4.9 μ flux 3-65740
- Titan atmosphere, strong temp. inversion from i.r. spectra 3-80987
- topography on satellite surfaces and shape of asteroids 3-47967
- Triton, potential atmospheric composition 3-51294
- Venus, satellite loss, effect of solar tidal friction 3-69837

planetoids see asteroids**planets**

- see also asteroids; comets; earth; Jupiter; Mars; Mercury (planet); Neptune; planetary satellites; Pluto; Saturn; Uranus; Venus*
- accretion process in formation of planets and comets 3-42122
- Barnard's Star, planetary system rel. to proper motion obs. 3-59349
- core models, unstable outer Fe₂O core 3-65765
- crustal evolution, oceanisation and continental growth, comparative planetology evidence 3-61366
- deep planetary interiors, structure and dynamics 3-42167
- extra-solar, detection by wavelength optimisation of signal noise 3-81253
- extrasolar planetary systems, origin and characteristics 3-42242
- figure theory, integration of eqns. 3-61693
- fluid rotating planet, density distrib. rel. to particular solutions of Clairaut eqn. 3-42140
- formation, core production by Ramsey phase change, mountain building 3-65766
- formation from solar nebula, role of cometary nuclei 3-53599
- fundamental catalogue zero points accuracy determ. from major and minor planets obs. (*Russian*) 3-61880
- giant, precession constants 3-76998
- gravitational fields of major planets 3-47933
- hypothetical tenth planet, mass and position limits from residuals of Neptune 3-47929
- interior physical properties rel. to Earth's inner core and Venus 3-42169
- interiors, high-pressure, physics, conference (Houston, 1-3 March 1972) 3-42151
- internal convection evidence from first-order topography 3-47930
- i.r. ground-based obs. at 34 microns 3-69994
- magnetism in outer planets 3-47941
- magnetized, solar wind interaction 3-65774
- major planets, survey of dynamical data 3-42155
- mantles, penetrative thermal convection, hydrodynamic equations 3-73451
- mass and dynamical flattening determ. methods 3-42157
- mean distances distrib. in Sun, Jupiter, Saturn and Uranus systems 3-59265
- in meteorite stream, force analysis, gravitational interaction 3-42186
- micrometeorite capture mechanism 3-65628
- modelling, isentropic compression of fused quartz and liquid H to several Mbar 3-39886
- orbital secular variation, element plots for 10⁷ years 3-69854
- outer, formation mechanism 3-61689
- outer, remote sensing of i.f. nonthermal radio emission 3-47940
- outer, solar wind interaction, shock shapes and locations 3-69827
- outer layers, quantum statistical mechanics of dense partially ionised H 3-42160
- outer planet magnetospheres, scaling laws 3-47939
- outer planets, chemical comp. and structure rel. to solar system origin 3-47932
- outer planets, development of US space program 3-48158
- outer planets and satellites, imaging techniques 3-48160
- outer planets elemental and isotopic abundances of volatile elements 3-47931
- outer planets exploration, mission building blocks 3-48159
- outer planets formation from gaseous solar nebula 3-47876
- outer solar system, planetary magnetism 3-47941
- patrol programme, international 3-65967
- planetary system, physical limitations rel. to technology development (*Hungarian*) 3-76946
- planetary system formation, jetstreams 3-42124
- planetesimals, accretion from gaseous solar nebula on cooling 3-69849

planets continued

- properties, review of known facts 3-42153
- shockwave determ. of shear velocity at very high pressures rel. to planetary interiors 3-42170
- solar system, smaller bodies, evolution and potential atmospheric composition 3-51294
- solid planet with or without liquid interior, elastic energy and quakes 3-42168
- surface mapping using ground-based radar 3-65956
- surface temperatures, methods and problems in their measurement 3-65741
- terrestrial, core comp., Fe₂O occurrence 3-42149
- terrestrial planets, present thermal state, viscosity-temp. relationship 3-42171
- thermal radio emission from major planets 3-47938
- very long baseline interferometric obs. of radio sources 3-65908
- very long baseline interferometry, appl. 3-65957
- H, liquid metal, transport props. under high press. 3-42172
- H-He planet, convective portion of atmosphere rel. to internal structure 3-51289

planimeters see area measurement**plants (industrial) see industrial plants****plants (power) see power plants****plasma**

- see also discharges (electric); plasmons; thermonuclear reactions*
- atmospheric supercooled plasma in equatorial exosphere, Ogo 6 meas. 3-53504
- column changes at small solar elongations, Mariner 9 meas. 3-65640
- fundamentals of plasma physics, book 3-71847
- Galactic cosmic ray propagation and isotropization, role of plasma effects 3-51218
- gravitational wave dispersion by collisionless gas 3-54148
- interplanetary microscale fluctuations, statistical props. 3-65864
- interplanetary space plasmas (*German*) 3-53629
- ionospheric clouds, two level model for deformation and striation, numerical simulation 3-61550
- ionospheric spread-F instability model for temperate high latitude, numerical simulation technique 3-61552
- ionsphere, velocity of weak inhomogeneities 3-69635
- magnetospheric plasma sheet structure at geocentric distance of 17-18 R_e 3-69702
- magnetospheric polar sub-storm, two fluid homogeneous model 3-61563
- multicomponent ionospheric plasma, particle streams along force lines of magnetic field (*Russian*) 3-69637
- plasma and gas discharge physics (symposium Amsterdam, Netherlands, May 1973) 3-49631
- plasma engineering, monograph 3-49632
- plasmoids motion in non uniform mag. field (*Russian*) 3-71878
- primordial gas, role of electron-neutrino interaction 3-56310
- research in space and laboratory, review 3-43651
- solar flare non-thermal ionisation and recombination processes 3-45022
- solar wind, magnetic field annihilation at tangential or rotational discontinuity, effect 3-63809
- solar wind, rotational discontinuities, classification, orientation characteristics and examples 3-69834

plasma applications*see also plasma devices*

- antenna system, electronically scannable, using isotropic plasma column with central conductor along axis excited by magnetic ring source 3-49657
- arc welding, swirling effects 3-49765
- coating deposition, powder heating in plasma stream (*Russian*) 3-53176
- coating deposition, powder particle acceleration in plasma stream (*Russian*) 3-53175
- coatings, mixed composition plasma-sprayed, thermal conductivity 3-53267
- cutting metals, plasma arc, magnetic control 3-68103
- etching polymers, h.f. oxygen discharge, surface temps. 3-64253
- ferrite thin film prod. by plasma spraying 3-58590
- low-pressure microwave induced plasmas as excitation sources for spectroanalytical chemistry 3-43697
- metal removal by a plasma torch, effects of vibration and pulsation 3-64946
- metallic particle spraying by jets 3-43968
- metallic plasma coating form. kinetics (*Russian*) 3-80318
- narrow beam antenna, using cylindrical columns of isotropic plasma 3-63820
- polymer etching, distortion due to working gas and electron conc. in discharge (*Russian*) 3-73068
- pulsed electron source, power supply circuit 3-73853
- thick films production of Ni-Zn ferrites 3-55731
- transition metal compounds, ultrafine powder 3-41827
- v.u.v. source for determining neutral H atom density distribution in thermonuclear machine 3-79172
- X-ray emission, from laser produced plasma numerical calc. of char. acs. 3-63893
- He plasma spectrometric detector for quantitative determ. of CO, CO₂, SO₂, N₂O in air 3-45611
- Si surface layer treatment, r.f. glow effects on recombination rates (*Russian*) 3-68685
- SiC, surface film etching, chemical and discharge treatment (*Russian*) 3-68509
- SiO₂ film bombardment by Ar ions in r.f. plasma, low temp. prop. change (*Russian*) 3-68706
- WC-Co compound powder, plasma spraying on hard metals (*German*) 3-50752

plasma collision processes*see also plasma transport processes*

- beam-plasma interaction in Astron 3-46518
- charged particle energy loss and stopping power 3-63815
- charged particle trapping in quadrupole r.f. field, Markov process 3-68080
- classical, generalised collision integral theory (*Russian*) 3-79061
- classical dynamics, book 3-71847
- collisional resistivity in low aspect ratio tori 3-63812

plasma collision processes continued

- column, anomalous impedance at r.f.'s, Maxwell's and Boltzmann's eqns., soln. 3-49651
- Coulomb-collision corrected electron-plasma line profiles 3-43655
- in Crab Nebula, second-order plasma interaction 3-61872
- dense plasma, overlapping neutral-atom lines, electron broadening, quadrupole contribs. 3-46520
- drift cyclotron instability, collision effects 3-52515
- electrical conductivity in mag. field, electron and ion momentum transfer 3-71860
- electron beam interaction with plasma, intermittent microwave generation 3-43664
- electron effective collision frequency in gases 3-49648
- electron gas temp. in shock precursors calc. 3-54840
- electron transport coefficients determ. using motion of heavy collision partners, Lorentz approach (*German*) 3-57882
- electron-electron, effect on test charge potential 3-79059
- electrons, spontaneous scatt. of light, mean square freq. shift 3-63613
- electrostatic instabilities driven by velocity gradients, collision effects 3-63838
- e.m. wave nonlinear, propagation in plasma containing random irregularities 3-46523
- e.m. wave propag. classical study incorporating collision processes 3-49656
- e.m. wave propag. in magnetoactive plasma, damping due to electron-ion and electron-electron collisions 3-68002
- fast MHD wave collisional damping, ion heating mechanisms 3-68066
- field-free plasma, mag. pulse anomalous penetration, two-fluid eqns. numerical integration calc. 3-46536
- h.f. discharge electron distrib. function when elec. field alternation freq. \gg elastic electron atom collision freq. 3-40821
- hydromagnetic composite plasma, dynamic stability, finite resistivity effect 3-43666
- instability in cold collisional and warm magnetoplasma 3-67992
- ion density determ. of electron beam in a gas 3-52500
- ion neutral collisions and ion acoustic waves 3-79138
- ion wave damping and collision frequency determination 3-79088
- ion-acoustic and drift wave stability in weakly collisional plasma, temp. perturbations effect 3-40780
- ion-acoustic wave stability in infinite plasma with electric field, collision effects 3-57901
- ion-ion collisions in two fluids model 3-57885
- ionisation of a neutral medium by an electron beam (*Russian*) 3-68054
- ionospheric electron thermal conductivity for weakly ionised gas 3-47785
- kinetic equation for vel. distrib. fns., collision cross sections 3-71856
- kinetic theory of a collision dominated plasma 3-60594
- Langmuir probe, spherical, in partially ionised plasma with uniform mag. field, theory 3-49753
- large pinch vessels, collisional preionisation 3-68053
- longitudinal waves instability in collisional plasma 3-79120
- low density plasma with cosmic abundances, ionisation and heating by energetic particles 3-56304
- low energy electron, obs. using swarm and transport meas. methods, book 3-60598
- low-density plasma, collision integral, quantum interpretation 3-71863
- magneto-active, solid, SHF e.m. wave propagation in waveguide (*Russian*) 3-79066
- magnetoplasma, high-freq. cond. calc., close collisions quantum mech. treatment 3-49650
- magnetoplasma partially ionized Lorentzian, transport coeff. calc. including interparticle collisions 3-75289
- MHD turbulence, interaction of fast particles and accel. by Alfvén waves 3-46516
- microturbulent magnetoactive plasma, weak nonlinear interactions, scattering of magnetoionic waves 3-75310
- mirror confined, calc. of α -particle heating using binary collision theory 3-60618
- neutral gas between plasma and wall, kinetic model 3-67991
- nonideal plasma, quantum kinetic equations 3-71853
- normal Doppler-shifted cyclotron radiation from cold plasma 3-52497
- parametric instabilities, nonlinear saturation, turbulence spectrum, enhanced collision frequency 3-75355
- partially ionised plasma, radiative recombination coefficient approximation 3-79060
- positive column, second harmonics of finite amplitude oscillations 3-40781
- positive column, steady-state nonisothermal, in magnetic field, theory 3-68113
- random electron density fluctuations, effect of collisions 3-57877
- recombination in three body collisions, potential curve crossing 3-79064
- relativistic electron beam interaction with plasma in waveguide (*Russian*) 3-43661
- relativistic electrons slowing down in plasma 3-49647
- resistivity, collisional, in low aspect ratio tori 3-67994
- r.f. cond. in mag. field presence, freq. shift meas. 3-54837
- scattering function, effect of collisions 3-49658
- shock wave structure in Ar or H, translational inequilibrium effects (*Italian*) 3-79083
- spectral line broadening by electrons in nonequilibrium plasma 3-63808
- spherical surface function tensors of collision integrals for weakly ionised plasma (*German*) 3-67988
- steady-state confinement regime in stellarators, idealised collisional diffusion model 3-49738
- stimulated Compton interaction between matter and radiation, plasma effects 3-71964
- surface oscillations of a magnetoactive plasma, influence of collisions 3-49686
- toroidal plasma, transport props. at low to intermediate collision frequencies 3-49649
- toroidal plasma modes, transport and particle scattering 3-60605

plasma collision processes continued

- transverse electron thermal conductivity meas. in mag. field 3-54841
- turbulent effective, physical meaning, review 3-75324
- two stream instability, Krook model collisions effect 3-63840
- wall interaction effects on steady-state operation for controlled fusion expts. 3-60625
- wave propagation in drifting warm plasma under Grad's thirteen-moment approximation 3-49705
- wave propagation in partially, ionised chemically reacting plasma 3-46532
- weakly ionised Lorentz plasmas in an external electric and magnetic field arbitrarily orientated, electron kinetics (*German*) 3-71857
- whistler ray paths, lower ionosphere 3-80801
- Ar afterglow, electron thermal conductivity along the magnetic field collision theory calc. 3-49786
- Ar-H₂ microwave afterglow, plasma decay obs. 3-52532
- Ar⁺, collision induced transitions in levels of 4p configuration 3-70807
- CO₂ laser discharge, ionisation instability 3-43670
- CO₂-N₂-He laser discharges, plasma chemistry 3-43654
- Cs, dense high temp. plasma, electron-ion recombination rate meas. 3-57939
- Cs, diffusion cross section for atomic electron scatt. 3-49644
- Cs plasma diode, ionisation and recombination 3-49655
- D-T plasma heating, escape of α particles 3-49737
- D₂ plasma, energy deposition of a fast deuteron 3-60614
- H, ion motion effects on spectral lines 3-46514
- H, n- α lines, high principal quantum number, Stark broadening 3-40802
- H₃⁺ and H₅⁺ electron-ion recomb. coeffs., afterglow meas. 3-63882
- HCO⁺ electron-recomb. coeffs., afterglow meas. 3-63883
- He, ion motion effects on spectral lines 3-46513
- He, ionisation equilib., atomic collision cross sections in shock wave 3-78501
- He, laser produced, afterglow, recomb. of doubly ionized atoms 3-40808
- He decay, ion recomb. coeffs. meas., electron temp. depend. 3-40801
- He I, excited state population lowering in He plasma due to laser beam 3-49639
- He ion-electron recombination at several atmospheres pressure, spectra and lifetime 3-79065
- He plasma jet, electronic recombination coefficient meas. 3-54838
- He positive column, ion acoustic instability, collision processes 3-49695
- He-Cs plasma, He⁺, He₂⁺, Cs⁺ ion densities, time depend. determ., rate const. ion decay rates 3-68094
- He-H₂ mixtures, decaying plasma obs. 3-63881
- Na discharge, optically thick, 250 Torr, electron and gas temp. profiles, non-LTE plasma, collision processes 3-40768
- U-D thermonuclear plasma, controlled fusion, obtained by composite macro-particle collisions 3-49733
- plasma confinement**
- see also magnetic traps; pinch effect
- Ambipolar diffusion as a singular perturbation problem 3-79062
- astron, electron distributions for small field cancellation in quiescent E layer 3-60624
- belt pinches, compression limitations 3-79163
- charged particle confinement in quadrupole r.f. field Markov process 3-68080
- diffusion, anomalous in magnetized plasma due to hydrodynamic effect 3-71862
- directional transport eqns. applic. 3-63818
- energy recovery from energetic plasma stream by travelling waves 3-49742
- extragalactic radio sources, ram pressure confinement models, relativistic motion, plasma cloud 3-48059
- fusion plasma control of the energy balance 3-57930
- high temperature walls, continuous operating ion laser (*French*) 3-78024
- highly ionised cylindrical column, radial particle loss 3-71944
- internal-ring devices, plasma confinement, review 3-49739
- laser produced, solid targets (*Rumanian*) 3-63856
- levitron, supercond., hot-electron plasma confinement 3-52529
- magnetic field interaction of laser irradiation produced plasma, capture containment (*French*) 3-43678
- magnetic pumping in spatially inhomogeneous magnetic fields 3-49744
- MHD equilibrium in a slightly asymmetric Tokamak 3-40797
- MHD nonlinear stability 3-75304
- neo-classical transport equations, steady-state solutions 3-49646
- noncircular plasma cylinder, singularities of the vacuum magnetic field 3-40798
- particle trapping by nonlinear waves, influence on dispersion props. 3-52519
- plasma drift motion and adiabatic invariance of magnetic moment in a nonstatic magnetic field 3-40762
- Q-machine, effect of high frequency mag. field on plasma diffusion 3-49653
- rotating magnetic field pinch, slowly varying magnetic induction obs. 3-57936
- steady-state confinement regime in stellarators, idealised collisional diffusion model 3-49738
- theta pinch equilibrium model, density and beta distributions 3-79164
- Tokamak devices toroidal diffuse pinch, plasma processes discussion (*Dutch*) 3-49768
- Tokamak TO-1, with automatic control, plasma filament confinement, discharge characts. 3-46547
- toroidal plasma simulations, low-pressure axisymmetric, stability analysis 3-46546
- two-dimensional collision-free plasmas, stability 3-75412
- wall interaction effects on steady-state operation for controlled fusion expts. 3-60625
- Z-pinch, continuous flow, high-density plasma beam formation, expt. obs. 3-49740
- D-T pulsed reactor, calc. of Lawson criteria for exponentially decaying ion density and temp. 3-60623

plasma containment *see plasma confinement*

plasma devices

see also plasma diodes; plasma guns; plasma probes; stellarators; Tokamak devices
 acceleration by means of applied azimuthal mag. field (*Russian*) 3-79079
 accelerator with closed electron drift, effect of feedback system on plasma flux 3-75341
 accelerators, steady-state interactions 3-71962
 air-heating plasma torch, high-pressure, development (*German*) 3-46559
 all-metal liner for RF heating 3-49732
 apparatus for producing high intensity relativistic electron beam 3-57948
 Astron, beam-plasma interaction 3-46518
 astron, electron distributions for small field cancellation in quiescent E layer 3-60624
 astron, relativistic electrons confined in axisymmetric mirror field, numerical simulation 3-43682
 astron, resistive rings effect on rotating electron beams 3-68083
 astron E-layers, electron spatial distributions, loss rates 3-71946
 Astron linear accelerator beam transport, delay line 3-57945
 Astron-like experiments, injection current limitation 3-75424
 CLEO Tokamak neutral injection system 3-49769
 closed electron drift accelerator, driven electrostatic oscillations 3-75340
 coaxial accelerator, plasmoid production, initial gas conditions effect 3-71929
 coaxial plasma injector 3-49770
 collisionless thermionic converter, oscillations obs. 3-49771
 controlled fusion research in 17 countries 3-71329
 coupler, e.m. surface waves, cylindrical plasma, interdigital metallic rings, results 3-49764
 cutting metals, plasma arc, magnetic control 3-68103
 d.c. Octopole, effect of field errors on the confinement 3-43679
 discharge between modules of cold insulated wall, expt. study 3-49766
 double plasma device, for plasma wave studies 3-40045
 electron bombardment ion thrusters, evidence of fireball phenomena in hollow cathode 3-52535
 Faraday type MHD generators with nonequilibrium plasmas, end effects calc. 3-46558
 focus, two-stream instability and plasma heating interferometric meas. 3-75394
 focus device, ion kinematics 3-60596
 heliotron, electron beam injection through divertor 3-75401
 Heliotron D, material limiter effect, ohmic discharges 3-75411
 high current diode, ion acceleration 3-54874
 homopolar type rotating plasma device, vel. limitation 3-54875
 inductive energy-storage devices for plasma injectors, transients 3-68102
 inert gas ion continuous operation lasers (*German*) 3-57223
 internal-ring devices, plasma confinement, review 3-49739
 ion acceleration in electron beams 3-57283
 large nonequilibrium MHD generator, electrode and gasdynamic effects 3-43693
 laser apparatus for obs. of impact waves (*Czech*) 3-57938
 laser-plasma ions, acceleration in cyclotron 3-57946
 levitated spherator, hot-electron plasma confinement 3-75410
 levitron, magnetic island formation and destruction 3-63860
 magnetically driven shock tube, poor separation 3-75321
 manometer, ionisation, noise immune, 10^{-9} to 10^{-3} torr, design, construction, operation 3-73714
 MHD compression of coaxial plasma accelerator flow for micrometeoroid simulation 3-40810
 MHD convertor channel, non-equilibrium laminar flow study (*Russian*) 3-79080
 MHD generator, discharge struct. obs. 3-79180
 MHD generator, discharge struct. obs. 3-79181
 MHD generator, ionisational waves, parametric two-dimensional study 3-75380
 MHD generator, plasma annular duct flow (*German*) 3-57898
 MHD generators, MHD instabilities discussion (*Dutch*) 3-49667
 MHD generators, shock formation by a moving force field 3-79182
 MHD generators ionisation instability, channel size effect 3-79179
 MHD Hall generator, steady-state, magneto-acoustical response, flow stability calc. 3-79183
 MHD-arc thruster exhausts electron number density and temp., temporal characts. 3-46557
 Neptune accelerator, plasma effect on current density of relativistic electron beam 3-52501
 Ogra-2T mirror device, instabilities obs. 3-79154
 partially ionised plasma centrifuge for element and isotope separation 3-43696
 plasma engineering, monograph 3-49632
 plasma torch, 100 KW DC for varied steel cutting 3-72928
 Polytion, toroidal Hall accelerator, employing cusp containment 3-75413
 pulse plasma accelerator, broadening of spectral lines obs. (*Russian*) 3-63889
 pulsed MPD-arc thruster, exhaust flow and propulsion characteristics 3-63891
 pulsed plasma accelerator, investigation of heat fluxes 3-60635
 Q-device, single-ended, ion acoustic waves obs. 3-75365
 Q-machine, collisionless, step-like density perturbations meas. 3-75421
 Q-machine, effect of high frequency mag. field on plasma diffusion 3-49653
 radiometer, transpiration, annular, edge cooled, measurement of total thermal radiation from flowing plasma, results 3-56643
 review of present-day position (*Dutch*) 3-40761
 superconducting 12-coil bumpy torus magnet facility, performance 3-60639
 switching devices 3-57962
 thermonuclear devices, mag. fringe fields from the solenoids 3-46164
 torch, arc cutting for dismantling of power reactors 3-71339
 torch using Ar, for emission spectroscopy 3-45607
 Tornado trap device, drift approximation for particle motion 3-52530

plasma devices continued

Tuman-1, ohmic heating, longitudinal thermal conductivity effect 3-71930
 z-pinch, thermonuclear possibilities 3-71963
 CO₂ laser discharge, ionization instability 3-43670
 CO₂-N₂-He laser discharge, plasma chemistry 3-43654
 D-T small mirror fusion device, 14 MeV neutron flux capabilities 3-63857
 MHD generator, conducting grids to stabilise ionisation instabilities 3-57947
plasma diagnostics
see also plasma probes
 afterglow plasmas, mass spectrometer diagnostic technique 3-54871
 air plasma, electrical conductivity and total emission coefficient meas. 3-71947
 air plasma components, ionisation energy level shifts, effect of Debye screening (*Russian*) 3-46508
 arc, d.c. in air at atmospheric pressure, volatilization rate of free particles 3-63914
 atmospheric, ion mobility, plasma chromatograph measurements, clear dry air, 760 Torr, 200 C 3-61484
 bremsstrahlung meas. of coaxial gun plasma, density and temp. determ. (*Russian*) 3-71951
 capillary discharge emission screening study in a plasma jet (*Russian*) 3-49761
 characteristics determ. of plasma produced by TEA-CO₂ laser 3-57927
 charge collection meas. for CO₂ laser induced preionisation plasma 3-71924
 charged particle energy, continuous measurement technique, multigrid electrostatic analyser 3-71957
 collisional preionisation in large pinch vessels obs. 3-68053
 conductivity coeffs. in Tokamaks expt., possible direct meas. 3-49758
 cyclotron radiation from a rarefied inhomogeneous magnetoplasma, use as diagnostic tool 3-68048
 D⁺ plasma, kilovolt ions, energy distribution meas. in modified Penning discharge 3-57929
 dense cold plasma, light scattering meas. 3-79171
 dense plasma, high press., opaque, mag. probes, X-rays meas. (*Russian*) 3-71953
 density and temperature, direct display meter, using Langmuir probe 3-68092
 density distribution meas. using an open barrel-shaped cavity 3-49760
 double Langmuir probe device for diagnostics in pulsed discharges (*Czech*) 3-54870
 Druyvesteyn electron plasma, electron temp., Langmuir probe meas. 3-46553
 electric arc gas heater in plasma jets of temp. up to 12000 K, calc. of work 3-40824
 electric field fluctuations, probability distrib., meas. for turbulent plasma 3-52512
 electrical polarisation in magnetic field flow (*Russian*) 3-71873
 electron beam, enhanced microwave emission due to transverse energy 3-68093
 electron beam distribution function, time-resolved meas. 3-40799
 electron beams, hollow intense relativistic, destructive instabilities 3-49704
 electron density, antenna admittance determ. 3-79167
 electron density, bounded plasma, from ion-acoustic wave obs. 3-63831
 electron density and electron collision frequency, r.f. nonimmersive probe obs. 3-68089
 electron density and temperature measurement, in H plasma, using Ar laser 3-46550
 electron density determ. from H₂ lines broadened by combined Stark and Zeeman effect 3-43691
 electron density determ. from laser beam refraction meas. 3-40804
 electron density distributions at high altitudes around entry vehicles, theory and expt. comparison 3-44911
 electron density meas., laser excited Fabry Perot interferometer 3-49755
 electron energy distributions, soft X-ray bremsstrahlung meas. 3-71961
 electron temp. meas. in quasi-stable pulsed discharge in spark gaps with high overvoltages 3-63876
 electron temperature, by Langmuir probe, cooling effects in high pressure plasma 3-63869
 electron temperature, meas. in recomb. plasma, possible use of double probe 3-49752
 electrostatic-wave topside sounder for electron plasma resonances 3-44958
 e.m. wave in plasma, direct meas. of skin depth 3-79067
 energy spectra of ions in plasma heated by collisionless shock wave 3-40793
 far-field potential of moving test charge in turbulent plasma, inverse square dependence 3-60604
 flow, local velocity vector, meas. by electrostatic probes 3-49666
 flow, microwave interferometry visualisation meas. 3-79081
 flow in non uniform magnetic field, probe obs. (*Russian*) 3-71878
 fluctuation characts. of dense plasma of high current discharge produced by exploding wire, mag. meas. 3-71975
 focus, two-stream instability and plasma heating interferometric meas. 3-75394
 focused CO₂ laser beam perturbation, piezoelec. probe obs. 3-54862
 fusing plasma neutron diagnostics 3-63888
 gas, laser induced breakdown, optical emission time depend. 3-46554
 gas composition analysis, plasma jets, cooled tube probe (*German*) 3-60627
 gas discharge, effect of weak r.f. signal on electron energy distribution 3-63897
 He plasma, cavity perturbation technique for determ. presence of molecular ions 3-63870
 h.f. field measurement, turbulence, forbidden He I line satellites intensity (*Russian*) 3-71955
 h.f. properties using wideband power amplifier (*Russian*) 3-43694

plasma diagnostics continued

- high power impulse discharge channel, structural and spectroscopic studies (*Russian*) 3-49787
- high z plasma, laser heating, temp., density and drift velocity meas. 3-43677
- highly ionised atoms spectra in laser produced plasmas and from sun 3-79173
- homogeneous arc plasmas, quasi-monochromatic meas. of OH rotational lines 3-43687
- inert gas afterglows, magnetized, meas. in 200-1500 MHz range 3-46563
- inert gas plasma behind shock waves, thermodynamic variables, interferometric meas. (*German*) 3-68099
- inert gas plasmas luminescent, spectral line decay obs. (*German*) 3-68084
- interferometric method, accuracy when optical components become heated 3-63877
- ion acoustic instability growth from slow electron drift, BGK-like modes evaluation 3-49703
- ion acoustic wave excitation, intensity distrib. in k -space, meas. 3-52507
- ion acoustic waves in boundary layer at a conducting sphere, phase velocity meas. 3-57915
- ion beam source and free-stream diagnostic techniques 3-40000
- ion density fluctuations meas. by optical absorption method 3-75422
- ion wave detection in electron-beam-plasma interaction by optical correlation 3-49680
- ionisation waves dispersion curves measurement method 3-79170
- ionospheric, polar, investigation using mother-daughter sounding rocket ELECTRA 1 3-42064
- Langmuir cylindrical probe charact. 3-46552
- Langmuir double probe, Thomson laser scattering 3-63885
- Langmuir probe, cylindrical or spherical, sheath thickness calc. 3-63873
- Langmuir probe system, multiple sweep, floating potential 3-79176
- Langmuir probes, contaminated surface and reliability of electron temp. meas. 3-57940
- laser apparatus for obs. of impact waves (*Czech*) 3-57938
- laser produced plasmas, neutron emission 3-40803
- laser produced systems, electron temp. and ioniz. state 3-68047
- laser-produced plasma, dynamic mass spectrometer for study of ions blown off 3-79177
- laser-supported detonation wave in air, emission spectra 3-40788
- leakage magnetic field measurement from iron core in shell-less tokamak device 3-52527
- light reflection at 1.06, 0.53 micron wavelength in laser heating 3-71931
- local parameters of ionized gas flow, meas. device 3-49751
- low plasma density measurement by microwave heterodyne technique 3-49756
- low-pressure microwave induced plasmas as excitation sources for spectroanalytical chemistry, fundamental props. 3-43697
- magnetic field, determ. from contour of H spectral lines 3-40807
- magnetic field interaction, spatially periodic (*Russian*) 3-71874
- magnetized, density determ., Langmuir probe meas. (*French*) 3-75419
- magnetoplasma, quiescent, cross spectral meas. of electron density fluctuations 3-68088
- MHD generator, discharge struct. obs. 3-79180
- MHD generator, discharge struct. obs. 3-79181
- MHD-arc thruster exhausts electron number density and temp., temporal characts. 3-46557
- microwave electron density meas., calibration procedure for correction of dielectric container effect 3-40800
- microwave reflection from plasma column in rectangular waveguide 3-46551
- microwave reflection method for plasma column in waveguide, analysis 3-43684
- using microwave resonators, open (*Rumanian*) 3-46556
- microwave scatt. in plasma-beam discharge 3-68096
- microwave signal modulation, in fluctuating plasma, parameters determ. 3-75420
- minimum-B field extremely quiescent plasma stabilised with permanent magnets, properties 3-57937
- negative glow of cylindrical hollow cathode discharges, mechanisms and plasma diagnostics (*German*) 3-49747
- non resonant Rayleigh scattering by a weakly ionised inhomogeneous plasma (*Dutch*) 3-49757
- nonlinear wave-plasma interactions, technique to display particle distribution function in phase-space 3-57944
- particle beam meas. 3-71960
- particle flux, measurement, double elec. probe, fluctuations (*Russian*) 3-71954
- phase-space diagrams meas. technique 3-68087
- plasma engineering, monograph 3-49632
- plasmoid energy meas. in time-varying mag. field 3-52533
- plasmoid frequency measurement, microwave interferometer (*Russian*) 3-71952
- poloidal current in mag. field (*Russian*) 3-71875
- polyethylene plasma, laser prod., shock hydrodynamic phenomena, core-corona decoupling 3-54872
- positive column, strongly magnetised, noise radial distribution and mean density 3-68085
- potential distribution meas. near an electron beam using thermionic probe 3-54873
- probe ion current characteristics in plasma flow 3-71948
- probe measurement errors, due to inadequate reference electrode 3-63874
- pulse plasma accelerator, broadening of spectral lines obs. (*Russian*) 3-63889
- pulsed arc plasma, laser light scattering 3-40805
- pulsed MPD arcjet, quasi-steady operation establishment, diagnostic meas. 3-43692
- pulsed plasma flow diagnostics, dynamic piezoelectric pressure transducer system 3-40806
- Q-machine, collisionless, step-like density perturbations meas. 3-75421

plasma diagnostics continued

- radiation analysis of high-temperature, high density plasmas, review 3-43685
- radiometer, transpiration, annular, edge cooled, measurement of total thermal radiation from flowing plasma, results 3-56643
- reaction channel, ion intensity meas. 3-79168
- refractive index measurement, Michelson interferometer, stabilised, calibrated, gas laser light source 3-62131
- relativistic beam-plasma system, conductivity determ. technique by magnetic diffusion times meas. 3-43690
- Satellite spectra for helium-like ions in laser-produced plasmas 3-74771
- self-igniting pulsed optical discharge in erosion laser plasma 3-40792
- shock-heated plasma, electron temp. determ. from microwave meas. 3-63880
- spatial Fourier analyser, bandwidth DC to 10 MHz 3-68095
- spectrum temporal variation of cathode plasma, obs. 3-68130
- stabilized arc plasma, density distrib., determ. by double holography method 3-63867
- stellator, plasma density determ. using open microwave resonator 3-52531
- streaming plasma diagnostics application of cylindrical Langmuir probes 3-63879
- student laboratory microwave experiment 3-56603
- temperature meas. using self-absorbed spectral lines, solutions of radiative transfer equation 3-43689
- test wave for studying sideband instability of electron plasma wave 3-57913
- theta pinch, relativistic effect in light scatt. spectrum 3-63884
- Thompson scattering, increased laser efficiency (*Russian*) 3-71956
- Tokamak TO-1, with automatic control, plasma filament confinement, discharge characts. 3-46547
- topside ionosphere plasma density irregularities power spectra 3-61540
- transient gas discharges, time resolved Langmuir probe meas. 3-53951
- transverse electron thermal conductivity meas. in mag. field 3-54841
- turbulent heating in linear discharge, diagnostic meas. 3-68043
- vacuum interrupters, post arc current mechanism, plasma decay, dynamic sheath, density 3-46564
- v.u.v. continuum radiation from laser vaporized high Z -material 3-79172
- wakes, projectile Mach 16, electron density fluctuations, turbulent scattering spectra 3-79169
- X-ray emission, coaxial plasma gun in deuterium 3-68101
- Z-pinch, non-cylindrical, study by holographic interferometry (*French*) 3-57942
- Ar, Cs seeded plasma, MHD power generation, characteristics determ. 3-63892
- Ar, high density plasma in explosively driven shock wave, radiation intensity and spectrum 3-54869
- Ar, shocked-plasma flows, double search-coil cond. probe study 3-63872
- Ar cascade arc, spectral meas., non-LTE effects 3-79178
- Ar low temperature submersed plasma jet, conductivity, velocity and temperature profiles (*Russian*) 3-68006
- Ar plasma above the cutoff frequency, recombination emission meas. 3-60628
- Ar plasma decay, and collisional radiative recombination 3-63878
- Ar plasma decay, early stages investigation 3-60629
- Ar plasma in r.f. discharge, intensity calibration for level populations determ. 3-68091
- Ar positive column, in medium pressure discharge, bremsstrahlung continuum obs. 3-63907
- Ar-H₂ microwave afterglow, plasma decay obs. 3-52532
- Ar⁺ laser plasma, temperatures study (*German*) 3-70814
- C V and VI $\Delta n=1$ transitions Stark broadening in laser-produced plasma 3-63871
- C-O plasma, transition probabilities of CI lines, near i.r. 3-63866
- C₂ Swan bands from discharge through Ar + trace benzene, emission study 3-52368
- CO₂ plasma, radiative capacity, 7000-9000K, 2100-10000 Å 3-49750
- CO₂ TEA lasers, u.v. photoionisation density meas., with microwave interferometer 3-70802
- Cs, dense high temp. plasma, electron-ion recombination rate meas. 3-57939
- Cs discharge, cooling and heating of electrons in decay and development 3-52534
- Cs ionized vapour, electron distrib. function (*French*) 3-49748
- Cs plasma, decaying, excited states relaxation obs. 3-60630
- Cs plasma, nonideal, equation of state, shock wave investigation 3-49759
- Cs plasma diode, ionisation and recombination 3-49655
- Cs plasma diode, microwave oscillations and visible emission 3-68097
- D discharge, Stark broadening of Paschen lines 3-43334
- D-plasma, in toroidal geometry, pre-ionisation and pre-heat conditions, density and temp. meas. 3-49730
- D₂ stationary glow plasma, isotopic effects in establishment of thermal equilibrium 3-71959
- Fe XVIII and Fe XIX transitions near 100 Å obs. in laser-prod. plasma 3-65630
- H, n - α lines, high principal quantum number, Stark broadening 3-40802
- H₂ stationary glow plasma, isotopic effects in establishment of thermal equilibrium 3-71959
- H₃⁺ and H₃⁺ electron-ion recomb. coeffs., afterglow meas. 3-63882
- HCO⁺ electron-recomb. coeffs., afterglow meas. 3-63883
- He, laser produced, afterglow, recomb. of doubly ionized atoms 3-40808
- He afterglow, electron energy balance and distrib. function, metastable population effects 3-63910
- He afterglow, electron radiation temp. meas., 300K 3-71972
- He arc, laser light scattering spectrum 3-71958

plasma diagnostics continued

- He decay, electron temp. meas., spectroscopic methods comparison 3-40801
 He I plasma spectral lines, Stark shifts 3-63868
 He plasma, ion temp. meas. in range 0.1-1 eV by Doppler broadening of He II 4686 Å line 3-57941
 He r.f. plasma in steady mag. field, electric and spectroscopic props. 3-71949
 He-CdI: positive column used for I⁺ laser, electron temp. and density 3-48879
 He-Cs, He⁺, He₂⁺, Cs⁺ ion densities, time depend. determ., rate const. 3-68094
 He-H₂ mixtures, decaying plasmas, collision processes 3-63881
 I₂⁺-I₃⁺ plasma, Langmuir probe characteristics 3-79175
 K plasma, decaying, excited states relaxation obs. 3-60630
 K plasma, laser selective excitation spectroscopy 3-68086
 Li exploded wire plasma, light scattering 3-43686
 Li plasma, electron concentrations determ. by spectroscopic method (*Russian*) 3-49762
 Li-In discharge, high-current, space-time distrib. of plasma optical density 3-49749
 N₂ gas flow interaction with plasma, turbulence, light emission fluctuations 3-68008
 N₂ isothermal, spectral determ. of temp. and electron conc. (*Russian*) 3-63890
 N₂ plasma, exact meas. of continuous emission 3-46555
 N₂ plasma, glow discharge, Langmuir probe study, electron density, electron energy distrib. (*Russian*) 3-57943
 N₂ plasma, recombination rates meas. 3-43500
 N₂O, discharge excited, vibr. luminesc., level populations (*French*) 3-52380
 Na spectral line profile, inhomogeneity and reversal temp. effect 3-63875
 Ne plasma, electron velocity distribution function computation from probe data 3-49754
 OH (A₂X-X₂I) rotational line strengths and energy level population in water vapour arc plasmas 3-43688
 U_i emission coeff. meas., theory comparison for design calcs. 3-78385
 Xe, shock ionized, radiative energy loss, struct. determ. 3-68090
- plasma diodes**
 plasmatron, laser-supported, in metals 3-72999
 plasmatron, N₂ plasma arc, convective arc model, limiting operating conditions (*Russian*) 3-40809
 sectored duoplasmatron (*Russian*) 3-71922
 s.h.f. plasmatron, spectrum excitation source, apparatus 3-73947
 switching device in HVDC circuit interrupter for inductive energy storage systems 3-60638
 Cs, microwave oscillations and visible emission 3-68097
- plasma equilibria** *see plasma confinement*
- plasma flow**
see also magnetohydrodynamics
 annular duct flow in crossed field device (*German*) 3-57898
 boundary layer with external magnetic field perpendicular to flow 3-60601
 coaxial flow stabilisation 3-75309
 coaxial plasma accelerator flow, MHD compression, for micrometeoroid simulation 3-40810
 coupling, magnetically induced, between counterstreaming plasmas 3-57910
 critical flow due to powerful laser beam effects, passivity criteria (*Russian*) 3-49671
 dissipative compressible Jeffery-Hamel flow, similarity transformation 3-75302
 dynamics in pulsed magnetic gate field (*Russian*) 3-71876
 electron velocities in crossed magnetic and electric fields, statistics 3-52504
 electrostatic potential created by test particle in one, two and three dimensions in flowing plasma 3-57876
 e.m. wave in counterstreaming electron plasma, thermal effects on instability 3-54842
 flow in magnetic field, induced current, solenoid (*Russian*) 3-71881
 gas cross flow interaction with e.m. fields 3-49669
 geomagnetic pulsations of diminishing period rel. to motion of magnetospheric plasma inhomogeneities 3-80660
 geomagnetic tail, plasma flow and field reversals, Pioneer 7 obs. 3-69711
 high Mach number plasma flows, laminar interactions 3-63826
 high velocity collisionless flow use of cylindrical Langmuir probes for diagnostics 3-63879
 induced current in steady flow in axially-symmetric mag. field (*Russian*) 3-71881
 ion boundary layer on a flat plate 3-79077
 ion heating in thermal plasma flows in upper ionosphere and inner magnetosphere 3-56202
 ionised gas layer, pulse electromag. signal, boundaries move at speed of light (*Russian*) 3-71871
 ionospheric flowing plasma, multiring probe 3-80853
 ionospheric interhemispheric transport, effect on plasma temp. at low latitudes 3-80795
 jet, turbulent, heterogeneous electron behaviour 3-46527
 jets, pressure and free stream velocity relation heat transfer and viscosity effects 3-57894
 local parameters of ionized gas flow, meas. device 3-49751
 local velocity vector, meas. by electrostatic probes 3-49666
 magnetic field interaction, spatially periodic (*Russian*) 3-71874
 magnetic lines of force reconnection 3-46529
 magnetised plasma, flow round discs and cylinders, effect of body potential (*Russian*) 3-57899
 magnetised plasmas, non-turbulent electric fields in soliton and shock-like structures 3-57896
 magnetised positive column, diffusion under turbulent flow 3-68085
 magnetospheric within ring current and near-earth plasma sheet, IMP 6 obs. 3-65484
 magnetotail plasma flow, Vela 4A meas. 3-80815
 MHD channel flow, boundary layers, thermal instabilities 3-75308
 MHD converter channel, non-equilibrium laminar flow study (*Russian*) 3-79080

plasma flow continued

- MHD Hall generator, steady-state, magneto-acoustical response, flow stability calc. 3-79183
 microwave interferometry visualisation meas. 3-79081
 moving plasma in quickly changing mag. field, current vortices development (*Russian*) 3-79078
 multi-ion isothermal astrophysical plasmas, motion in gravit. field 3-47863
 multi-ion plasmas, critical points existence criteria in astrophysical appl. 3-47862
 non-isothermal plasma flow through a magnetic nozzle 3-49670
 nonequilibrium plasma, in mag. field, influence of viscosity on motion of nonuniformities 3-49673
 partially ionized gas flow around permeable surface, heat exchange near stagnation point 3-63825
 particles velocity dispersion across non uniform magnetic field (*Russian*) 3-71880
 plasmasphere, penetration of magnetospheric electric fields and plasma convection 3-80833
 plasmoids formation, magnetic deflection of slow component (*Russian*) 3-71877
 probe ion current characteristics in plasma flow 3-71948
 pulsed MPD-arc thruster, exhaust flow and propulsion characteristics 3-63891
 relaxation, diffusion and recombination processes in discharge, boundary value problem 3-71967
 slabs, laser irradiated, plasma motion, ellipsoidal coordinate system 3-71883
 solar wind, ionising high-beta flows, h.f. electrostatic instabilities 3-80978
 steady state ion acceleration in magnetic nozzle for 2-20 keV 3-54847
 stream in axially symmetric mag. field, electrical polarisation (*Russian*) 3-71873
 thermal expansion expt. obs. 3-71884
 Tokamak plasma, poloidal rotation decay 3-68072
 toroidal diffusion and stationary shocks 3-49694
 toroidal equilibrium shift, plasma flow effect 3-79162
 toroidal MHD equilibrium with toroidal flow 3-71885
 transverse ionizing MHD detonation waves, numerical simulation 3-57904
 viscous, hypersonic blunt body problem in shock heated plasma, numerical analysis 3-46525
 viscous flow of inhomogeneous plasma in coaxial structure with a thermionic cathode 3-54846
 wake past an obstacle in a magnetised plasma flow 3-40774
 wakes, projectile Mach 16, electron density fluctuations, turbulent scattering spectra 3-79169
 Z-pinch, continuous flow, high-density plasma beam formation, expt. obs. 3-49740
 A, rotation freq., mag. field effect (*Russian*) 3-71872
 Ar, Cs seeded plasma, MHD power generation, characteristics determ. 3-63892
 Ar, shocked-plasma flows, double search-coil cond. probe study 3-63872
 Ar plasma jet, local heat transfer to a sphere, effect of local gas velocity and temp. 3-68100
 H plasma, toroidal flow (*Russian*) 3-71879
 Kr, rotation freq., mag. field effect (*Russian*) 3-71872
 N₂ supersonic nozzle flow in high current arc, turbulence development 3-68008
 Ne, rotation freq., mag. field effect (*Russian*) 3-71872
 Xe, rotation freq., mag. field effect (*Russian*) 3-71872
- plasma generation** *see plasma production*
- plasma guns**
 coaxial, construction and operation 3-68042
 coaxial, in mode I operation, focusing action in deuterium 3-68101
 coaxial, operation, freq., energy spectra (*Russian*) 3-71921
 coaxial, outer electrode of cage structure near fast acting valve 3-49767
 cold cathode discharge, large area electron beam, characteristics 3-49763
 deflagration, formation of high-density plasma beam by continuous-flow Z-pinch 3-49740
 electron beam, high intensity production 3-57948
 for electron beam pumping, of semiconductor lasers 3-54232
 pulsed plasma accelerator, struct. of current front and turbulent acceleration of ions 3-49718
 pulsed plasma accelerator, struct. of current front and turbulent accelerations of ions in fast regime 3-49719
- plasma heating**
 absorbed r.f. power calc. at perpendicular ion cyclotron resonance of 'H-D plasma' 3-49725
 adiabatic compression in toroidal devices 3-68073
 adiabatic gamma for two-dimensional compression of unstable plasma 3-49637
 all-metal liner for RF heating 3-49732
 anomalous absorption and heating, parametric instabilities 3-68033
 anomalous absorption of radiation 3-68076
 anomalous heating of dense plasma by laser radiation 3-49735
 Astron linear accelerator beam transport, delay line 3-57945
 beam-plasma system, counterstreaming, turbulent heating 3-79158
 belt pinches, compression limitations 3-79163
 bootstrap equilibria including energy balance 3-75406
 bounded dense plasma systems, r.f. props. rel. to heating, resonances 3-68036
 charged particle scattering, energy transfer in strong e.m. field 3-66999
 CLEO Tokamak neutral injection system 3-49769
 collisionless drift instabilities stabilisation by electron-cyclotron resonance heating 3-52513
 collisionless electron-cyclotron damping along weak mag. beach, meas. 3-52523
 collisionless heating of plasma ions by ion beam 3-49736
 combined heating by electron beam and intense ion-cyclotron wave 3-75399
 concentric compression by laser implosion of thin 'heavy' coating, numerical method 3-57922
 controlled fusion at Wisconsin University, education and research 3-63238

plasma heating continued

- controlled thermonuclear fusion expts. and engineering aspects, conference, Austin, Texas, USA (Nov. 1972) 3-60295
- controlled thermonuclear reactions research, atomic parameters 3-79155
- current-carrying plasma, anomalous heating and momentum transfer, ion-reson. broadening influence 3-52524
- cybernetics methods application to controlled fusion (*Russian*) 3-71923
- cyclotron radiation loss from a rarefied inhomogeneous magnetoplasma 3-68048
- D⁺ plasma, kilovolt ions, energy distribution meas. in modified Penning discharge 3-57929
- dense plasma anomalous heating by laser radiation 3-68077
- deuterium, hot, infinite, Coulombian transparency, finite deuterons 3-52525
- electrical conductivity meas., resist., oscill. effects (*Russian*) 3-71858
- by electron beam, intense pulsed 3-40789
- electron beam intense relativistic, motion in toroidal field 3-57934
- Electron cyclotron heating as inverse cyclotron radiation 3-71926
- electron cyclotron heating in mag. mirror field, energetic electrons generation 3-46543
- electron cyclotron heating in magnetic mirror field 3-43676
- electron cyclotron heating magnetic mirror field 3-68062
- electron cyclotron resonance heating of mirror trapped plasmas, stochastic theory 3-75407
- electron gas temp. in shock precursors calc. 3-54840
- electron heating, parametric instability, mode coupling saturation 3-71903
- electron heating resonances in Penning source, max. temperature rel. to mag. field 3-51685
- electron tail, hot nonthermal, produced by anomalous microwave absorption 3-57926
- e.m. wave, nonlinear propagation in plasma containing random irregularities electron heating effects 3-46523
- e.m. wave transmission coefficient, coupling to lower-hybrid resonance 3-75298
- e.m. waves in plasma density gradient, irreversible energy transfer, possible heating mechanism 3-49660
- excitation of open resonator, starter radiation from strong current discharge, oscillations, geometrical resonance (*Russian*) 3-54867
- extraordinary wave propag. near low hybrid resonance freq. 3-68003
- fast magnetic compression in tokamak like geometries 3-68074
- by flux compression 3-71939
- focus, two-stream instability and plasma heating interferometric meas. 3-75394
- focused CO₂ laser beam perturbation, piezoelec. probe obs. 3-54862
- fusion laser systems 3-68044
- fusion plasma control of the energy balance 3-57930
- fusion technology at Michigan university, educational and research activities 3-61955
- fusion technology first year graduate course at Illinois University 3-61954
- heating and injection (Conf. Varenna, Italy, Sept. 1972) 3-68056
- high intensity neutral beams development 3-71937
- high z plasma, laser heating 3-43677
- high-frequency heating, particles nonlinear dragging 3-57931
- hybrid fission-fusion reactor, energy balance eqn. and particle conservation eqns. 3-67392
- inhomogeneous laser plasma, second harmonic generation 3-71928
- intense electron beam, dense plasma heating 3-75403
- intense light source generation, by optimising imploding detonations with laser energy 3-63849
- by intense relativistic electron beam, density-temp. ranges 3-71940
- intense relativistic electron beam applic. 3-52520
- intergalactic medium heating by electron heat conduction 3-61858
- interstellar clouds, heating rel. to H₂ dissociation by u.v. photons 3-42240
- ion acoustic resonances obs. in RF power absorption expt. of a bounded plasma in the electron and magneto-ion domain 3-40790
- ion and electron transit time magnetic pumping and ion cyclotron heating, neoclassical aspects 3-68059
- ion component, by collisionless shock wave 3-40793
- ion cyclotron wave generation, heating efficiency 3-71895
- ion cyclotron heating expts. in ST Tokamak 3-68064
- ion cyclotron resonance and turbulent heating studies at Nagoya university 3-68061
- ion cyclotron wave, coil-to-plasma coupling, effect of inhomogeneous density profile 3-46544
- ion cyclotron wave excitation, associated ion heating, by two counter-streaming electron beams 3-40791
- ion heating in thermal plasma flows in upper ionosphere and inner magnetosphere 3-56202
- ion heating mechanisms based on absorption of fast MHD wave around ion cyclotron frequency 3-68066
- ion intense heating by parametrically driven ion cyclotron waves 3-54865
- ionospheric interhemispheric transport, effect on plasma temp. at low latitudes 3-80795
- Jeffery-Hamel flow of dissipative plasma, similarity transformation 3-75302
- KMS laser fusion experiments 3-63099
- laser, applic. of supersonic thermal sources in perfect gas 3-75173
- laser, electron temp., theory and expt. obs. 3-75405
- laser, Nd:glass, with second harmonic converter 3-74245
- laser concentric cumulation of D-T plasma, heat of nuclear fusion consideration 3-63855
- laser cumulative heating of plasma focus, averaged eqns., thermonuclear fusion contrib. 3-63854
- laser fusion, thermal conduction limitations 3-46517
- laser heated target plasmas, high-energy electrons occurrence and surface expansion 3-49734
- laser heating of magnetically confined underdense plasmas 3-71941
- laser heating refl., saturation effects in stimulating scatt. 3-46542
- laser induced, c.w., in atmospheric pressure air, ignition and maintenance, CO₂ laser 3-49723
- laser irradiation, review of processes involved 3-62749

plasma heating continued

- by laser irradiation of solid targets (*Rumanian*) 3-62732
- laser produced systems, electron temp. and ioniz. state 3-68047
- laser-plasma ions, acceleration in cyclotron 3-57946
- light reflection at 1.06, 0.53 micron wavelength in laser heating 3-71931
- low density plasma with cosmic abundances, ionisation and heating by energetic particles 3-56304
- magnetically confined, effect of laser pulse rise time 3-40787
- magnetoplasma, laser beam heating, fundamental equations (*Japanese*) 3-75389
- magnetoplasma, parametric instabilities, anomalous absorption and heating 3-79159
- magnetoplasma with strong longitudinal, microwave absorption 3-68004
- metal liner for T.T.M.P. heating calc. 3-68063
- MHD shock wave heating 3-68075
- MHD wave heating in Tokamak plasmas 3-68060
- microwave high power injection into overdense magnetoactive plasma in waveguide 3-57923
- mirror confined, calc. of α -particle heating using binary collision theory 3-60618
- neutral injection heating in open and closed systems 3-68070
- neutral injection techniques 3-68071
- nonlinear effects near lower hybrid resonance frequency 3-68065
- nonlinear heating in Tokamak plasma 3-46545
- nuclear applications of lasers 3-62709
- obliquely incident radiation, parametric decay 3-60599
- ohmic, collective interactions in high current gas discharge, instability (*Russian*) 3-71919
- ohmic heating, direct, of ions in ionising shock 3-68050
- ohmic high current gas discharge, efficiency (*Russian*) 3-71920
- ohmic in Tuman-I, longitudinal thermal conductivity effect 3-71930
- ohmic and neutral injection heating 3-71938
- parametric excitation by laser, role of Landau damping, inverse-bremsstrahlung, ion wave (*Japanese*) 3-75390
- parametric instabilities and anomalous absorption 3-68034
- parametric instabilities and turbulent heating of plasma in the field of fast MHD wave 3-68049
- parametric instabilities expts., review 3-75384
- particle acceleration by moving laser focus, focusing front, or ultra-short pulse front 3-40794
- plasma heating, elec. cond. meas. (*Russian*) 3-71858
- plasma heating, high current, instabilities (*Russian*) 3-71919
- plasma torch, high-pressure air-heating, development (*German*) 3-46559
- power absorption in nonuniform collisionless magnetoplasma 3-63852
- pulsed plasma accelerator, struct. of current front and turbulent acceleration of ions 3-49718
- pulsed plasma accelerator, struct. of current front and turbulent accelerations of ions in fast regime 3-49719
- pulsed thermonuclear reactor, plasma cooling by means of a neutral gas layer 3-63850
- relativistic electron beam heating of fully ionized system 3-63853
- relativistic electrons slowing down in plasma 3-49647
- relativistic plasma, long range ordering 3-79184
- resonant inhomogeneous layer, rel. to h.f. field increase 3-57909
- r.f. absorption by magnetised hot electron-ion column 3-68069
- r.f. heating processes 3-68058
- rocket driven liners for fusion triggers and for very high density reactors 3-49372
- shock-heated plasma, electron temp. determ. from microwave meas. 3-63880
- by short laser pulses 3-54866
- solar wind, non-thermal heating by supra-thermal secondary ions 3-65689
- solar wind, two-fluid models 3-44999
- staged θ pinches with implosion heating, feasibility study 3-60622
- stellar spherical systems, gravitational shock heating 3-69920
- step heat waves dynamics 3-54861
- stochastic acceleration, survey 3-71936
- stochastic heating of particles in turbulent plasma, theory 3-40795
- stochastic ion heating due to parametric ion-acoustic decay instability 3-54864
- suprathermal particle generation, laser produced plasmas, role of strong magnetic fields 3-49722
- symposium on heating and injection, concluding report 3-71943
- thermonuclear plasma, radiation losses calc. 3-75408
- thermonuclear plasma energy direct conversion by high magnetic compression and expansion 3-63234
- theta pinch, high-beta, plasma density and beta distributions 3-79164
- tokamak, large, inductive energy storage requirements for pulsed expts. 3-60306
- Tokamak, ST, ion cyclotron and fast hydromag. wave generation 3-54863
- Tokamak, turbulent heating, high electric field effect on design 3-60644
- Tokamak low density reactor ignition by fast neutral atom injection, density build up with moving limiter 3-78388
- Tokamak plasma, poloidal rotation decay 3-68072
- Tokamak plasma heating 3-68057
- Tokamaks, Bootstrap equilibria, neutral injection, energy balance 3-79156
- toroidal, injection of neutralised relativistic electron ring 3-49724
- toroidal plasma stability subject to neutral injection 3-68037
- toroidal turbulent heating expt. 3-71935
- transit time, in toroidal plasmas 3-71942
- turbulent, with intense relativistic electron beam 3-71934
- turbulent heating (*Dutch*) 3-49729
- turbulent heating 3-71932
- turbulent heating expts., lineal geometry 3-71933
- turbulent heating in linear discharge, diagnostic meas. 3-68043
- two temperature, general equations for heating by short laser impulses 3-60617
- two-temperature, conduction-type laser, numerical analysis, incl. recovered nuclear fusion energy 3-75396
- two-temperature, laser, in focus system, numerical analysis of averaged eqns., incl. fusion energy 3-75397

plasma heating continued

- two-temperature plasma, laser heating, plane wave general solution 3-60616
- Venus, ionospheric heating on simple one-dimensional model 3-65784
- viscous, hypersonic blunt body problem in shock heated plasma, numerical analysis 3-46525
- z-pinch, thermonuclear possibilities 3-71963
- Ar low pressure arc of high power laser, intensification of 4880 Å line and temperature (*German*) 3-52522
- Ar plasma, fully ionised, nonresonant laser light absorption meas. 3-60615
- D, laser created plasma, role of spontaneous mag. fields, numerical simulation 3-63851
- D solid target, laser light absorption, wavelength depend. 3-49731
- D-D, fusion power balance calcs., equilibrium parameters 3-60620
- D-plasma, in toroidal geometry in millitorr pressure range, pre-ionisation and pre-heat conditions 3-49730
- D-T, pulsed high-beta fusion reactor based on θ pinch 3-60303
- D-T fusion reactor, stationary and start up heating with fast neutral beam injection 3-79157
- D-T inhomogeneous fusion plasma, control, thermal instability 3-75393
- D-T plasma, laser compression, averaged equations allowing for fusion heat 3-68040
- D-T plasma, laser compression, averaged description 3-68041
- D-T pulsed reactor, calc. of Lawson criteria for exponentially decaying ion density and temp. 3-60623
- D₂, solid, evaporation in a fusion plasma 3-78389
- D₂ plasma, energy deposition of a fast deuteron 3-60614
- DT plasma, fast α particle reactions 3-57925
- H, high temp. fusion, impurity radiation loss estimation 3-60621
- He, excited state populations lowering of HeI due to laser beam 3-49639
- MHD nonlinear waves propagation in a magnetic neutral sheet, shock heating 3-43668
- U-D thermonuclear plasma, controlled fusion, obtained by composite macro-particle collisions 3-49733

plasma instability

see also *plasma oscillations*

- absolute and convective instabilities, review 3-75347
- absolute whistler instabilities, nonlinear theory 3-79146
- adiabatic gamma for two-dimensional compression of unstable plasma 3-49637
- anisotropic cyclotron instability in an inhomogeneous mag. field 3-49687
- anomalous heating of dense plasma by laser radiation, instability threshold conditions 3-49735
- anomalous loss instabilities in hot electron plasma in slow theta pinch 3-79153
- atmospheric v.l.f. hiss, incoherent Cherenkov radiation amplification by Landau instability 3-51158
- beam plasma discharge, h.f. wave transform. rel. to l.f. instabilities 3-49684
- beam-magnetoplasma system, e.s. instability, absolute to convective transition 3-49702
- beam-plasma and two-stream instability, numerical simulation, expt. obs. 3-79195
- beam-plasma instabilities, surface waves propagation 3-75322
- beam-plasma instabilities suppression by HF pressure in bounded systems 3-79118
- beam-plasma instability, nonlinear development 3-71914
- beam-plasma instability, quenching, by mode mixing at a density discontinuity 3-60609
- beam-plasma interaction, beam velocity distribution function deformation 3-79115
- beam-plasma interaction, high pressure nonlinear effects, volumetric waves 3-68017
- beam-plasma system, captured electrons role in plasma waves (*Dutch*) 3-49685
- beam-plasma system, nonlinearities, instabilities in cold energetic system 3-75387
- BGK waves decay instability, unstable oscills. 3-49690
- bounded electron beam, parametric instability 3-52516
- bunching instability mechanism 3-63844
- cold plasma, with group of hot ions with anisotropic velocity distrib. function, low freq. instabilities (*Russian*) 3-71910
- collisional drift instability obs. 3-79086
- collisionless drift instabilities, stabilising effect of electron temp. gradient 3-52513
- collisionless drift waves in toroidal hexapole, obs. 3-52514
- counterstreaming instability in collisionless anisotropic plasmas 3-80913
- coupling, magnetically induced, between counterstreaming plasmas 3-57910
- current carrying toroidal plasma filament, dynamic stabilisation in stellarator 3-52528
- current-carrying plasma, instability at cyclotron harmonics and anomalous resist., theory 3-71909
- cyclotron and Cherenkov instability, caused by e.m. wave excitation by relativistic electron beam 3-63824
- cyclotron harmonic waves, nonlinear instability 3-68010
- cyclotron wave of finite amplitude, instability (*Russian*) 3-68029
- decay instability, modified, nonlinear theory 3-75311
- decay instability by large amplitude Bernstein waves, effect on ion temperature 3-79103
- decay instability threshold in inhomogeneous plasma 3-52509
- destructive instabilities in hollow intense relativistic electron beams 3-49704
- diffusion, effect of high frequency mag. field Q-machine 3-49653
- dissipative trapped ion instability, anomalous transport 3-63835
- drift cyclotron instability, collision effects 3-52515
- drift MHD wave instabilities due to magnetic drift resonance 3-46528
- drift temperature and Kelvin-Helmholtz, excitation due to neutral injection 3-68037
- drift waves dynamic stabilisation by h.f. e.m. fields 3-79125
- drift waves growth rate, instabilities, critical shear 3-75379
- drift waves in nonuniform current-carrying plasma, critical shear and growth rates 3-49696
- drift waves stabilisation expts. 3-75372
- electric field fluctuations, probability distrib., meas. for turbulent plasma 3-52512
- electrojet, equatorial, small scale instabilities rel. to local drift velocity with large irregularities 3-51106
- electron beam, relativistic, in plasma, stability in strong longitudinal mag. field 3-54859
- electron beam, relativistic, low frequency hydromagnetic kink mode 3-60600
- electron beam, relativistic, unneutralised, instability 3-54858
- electron beam, relativistic propagating in plasma, hollow equilibrium and stability 3-49741
- electron beam, unneutralised, rigidly rotating, stability 3-48964
- electron beam parametric instability when modulated by external electrostatic electric field 3-48966
- electron beam stability in an inhomogeneous dielectric medium 3-75338
- electron beams interacting in plasma, obs. of nonlinear stabilisation 3-49682
- electron cyclotron drift instability obs. 3-75376
- electron drift instability in high β plasmas, nonlinear theory 3-75378
- electron plasma wave, nonlinear saturation and harmonic generation 3-54849
- electron plasma wave, side-band instability studied by launching small test-wave 3-57913
- electron-electron two-stream instability, relativistic electron beam heating 3-71940
- electrostatic in collisional and thermal magnetoplasma 3-67992
- electrostatic instabilities, ion bunching 3-75358
- electrostatic instabilities driven by velocity gradients, collision effects 3-63838
- electrostatic instabilities in hot-electron plasma 3-75332
- electrostatic low threshold instability in a weakly ionised plasma 3-49720
- electrostatic modulational instabilities due to resonant particles 3-75362
- electrostatic plasma waves, frequency exceeding gyrofrequency in the magnetosphere, propagation, instability 3-69671
- electrostatic stability of modulated plasma profiles 3-79144
- electrostatic surface waves parametric excitation and instabilities in plasma layer (*German*) 3-71887
- electrostatic turbulence, collisionless dissipation of a cross-field electric current 3-49698
- electrostatic waves, instability with nonlinear Landau effect 3-60603
- e.m. instabilities in non-uniform anisotropic plasmas 3-79073
- e.m. instabilities in plasma with transverse current 3-75296
- e.m. instabilities in plasma with transverse current 3-75297
- e.m. instabilities of finite anisotropic plasma with hot electrons 3-40779
- e.m. instability in counterstreaming plasma 3-40769
- e.m. microinstabilities in nonuniform anisotropic streaming magnetoplasmas 3-79147
- e.m. streaming instability 3-79090
- e.m. surface wave instability, in bounded plasma stream 3-63821
- e.m. wave in counterstreaming electron plasma, thermal effects on instability 3-54842
- e.m. wave propag. in magnetoactive plasma, stability of ordinary and extraordinary waves 3-68002
- e.m. waves in plasma density gradient, nonlinear interaction 3-49660
- energy dissipation in magnetic neutral point 3-79152
- equilibrium in Tokamak, numerical calc. 3-49745
- expanding multicomponent plasma instabilities and laser scattering 3-52510
- explosive in stabilities stabilisation by nonlinear frequency shifts 3-49709
- explosive instabilities, coupling strength, dissipation, random-phase description 3-79129
- explosive instabilities of waves, dissipation and phase effects 3-49707
- explosive instability and soliton generation 3-52517
- explosive instability due to anomalous resistance 3-63817
- F-region, diffuse radio reflections (*Russian*) 3-69665
- feedback controlled instabilities hard excitation 3-79124
- field-free plasma, mag. pulse anomalous penetration, turbulent resistivity calc. 3-46536
- finite pressure plasma, cyclotron instabilities 3-43671
- firehose, loss-cone and mirror instabilities in finite- β plasma with hot electrons 3-75333
- five wave interaction, enhancement of optical or microwave radiation by nonlinear coupling to explosively unstable plasma waves 3-49708
- flute instability, l.f., in bounded plasma column 3-63830
- flute instability suppression in open system by magnetic feedback 3-75329
- flute low-frequency instability in hollow cathode arc discharge, theory and expt. 3-60607
- flute stability in toroidal plasma 3-75330
- flute-like modes in inhomogeneous plasmas 3-75377
- flutes magnetic feedback stabilisation in mirror machines 3-79123
- geophysical, drift mirror and ion cyclotron instabilities 3-76814
- gradient instabilities in system of gravitating point masses 3-77152
- gravitational instability, finite Larmor radius effects 3-75353
- heating, due to h.f. instability (*Russian*) 3-71919
- heavy current discharge, in open-ended tube with evaporating walls 3-49775
- helix instability in convection stabilised high-current, high-pressure, arc (*German*) 3-68132
- h.f. instabilities in arbitrary configurations, numerical method 3-79150
- high current diode, ion acceleration due to two-stream plasma instability 3-54874
- high power laser simulation, plasma stability of electric discharges in mol. gases 3-66821
- high-power-density mirror fusion reactor 3-54549
- hydrodynamic instability, appearance of turbulence during interaction of monoenergetic beam with plasma 3-71906

plasma instability continued

- hydromagnetic composite plasma, dynamic stability, finite resistivity effect 3-43666
- hydromagnetic composite plasma, including neutral gas friction, Hall currents, viscosity 3-68007
- inhomogeneous phase space fluids, stability problems 3-75348
- instabilities, basic features, review 3-75346
- instabilities, nonlinear, simulation 3-79121
- instabilities prediction in laser production target model 3-75395
- ion acoustic instability, electron trapping inability for stabilisation 3-49701
- ion acoustic instability, temperature gradient driven 3-75375
- ion acoustic instability growth from slow electron drift, BGK-like modes evaluation 3-49703
- ion beams, counterstreaming, e.m. instability 3-49659
- ion cyclotron instability of rotating plasma cylinder (*Russian*) 3-40786
- ion cyclotron wave excitation, associated ion heating, by two counter-streaming electron beams 3-40791
- ion wave turbulence, current-driven, electron drift velocity and frequency meas. at onset of instability 3-79084
- ion-acoustic and drift wave stability in weakly collisional plasma, temp. perturbations effect 3-40780
- ion-acoustic dissipative instability, quasi-linear theory 3-79095
- ion-acoustic instability, and associated multimode phenomena 3-63832
- ion-acoustic instability, nonlinear theory, angular spectrum 3-75356
- ion-acoustic instability causing anisotropic turbulence in a collisionless shock 3-57906
- ion-acoustic wave turbulence, current-driven 3-54850
- ion-resonance broadening influence on anomalous heating and momentum transfer in current-carrying plasma 3-52524
- ionisation instabilities obs. in MHD generator 3-79180
- ionisation instability in MHD generators, channel size effect 3-79179
- ionisation wave instability, evolution, nonlinear effect 3-71889
- ionisation waves, non-linear stability (*Russian*) 3-54860
- ionospheric F region unstable drift 3-53526
- ionospheric spread E caused by cross-field plasma instability 3-73359
- isothermal MHD shock waves stability 3-79093
- kinetic instability in relativistic electron beam, limiting currents 3-71907
- laser-driven instabilities, partial coherence effect 3-63841
- levitron, supercond., hot-electron plasma confinement 3-52529
- longitudinal waves instability in collisional plasma 3-79120
- loss-cone, electric drift effect 3-68027
- lossfree plasma, feedback stabilisation for reactive instabilities 3-49677
- low frequency electrostatic motions stability, energy principle 3-75349
- magnetic field annihilation, expt. obs. 3-79082
- magnetic stars, pinch instabilities 3-51332
- magnetoactive plasma stability with relativistic electron beam in r.f. electric field 3-68026
- magnetoplasma, highly ionized, inhomogeneous, low freq. self-oscillating instability meas. 3-68012
- magnetoplasma, unstable flute-like cyclotron modes caused by presence of suprathermal particles 3-49672
- magnetosheath, nonlinear theory of plasma instability 3-53537
- magnetosphere, drift instabilities, finite β effects, Vlasov-Maxwell equations 3-80834
- magnetosphere, instability in ring current protons 3-69695
- magnetosphere current instability in neutral sheet, anisotropic plasma instability theory 3-42050
- magnetospheric plasma, rayed auroral structures 3-42048
- MHD channel flow, boundary layers, thermal instabilities 3-75308
- MHD generators, MHD instabilities discussion (*Dutch*) 3-49667
- MHD instabilities in toroidal theta pinch 3-79166
- MHD instabilities obs. 3-75381
- MHD stability of cospherical plasma, finite Larmor radius effects 3-80911
- microinstabilities in short mirror plasmas 3-79148
- mirror machines with multicomponent plasmas, finite-length criteria 3-79149
- mode coupling saturation in unstable plasmas, model equations 3-49693
- modulated electron beam interaction, instability development 3-68024
- molecular beam-plasma instabilities obs. 3-78907
- non-linear waves, effect of temp. and particle trapping on dispersion props. 3-52519
- nonlinear cold stationary waves stability 3-79127
- nonlinear cold waves stability 3-79092
- nonlinear instability due to parametric interaction of waves 3-54851
- Ogra-2T mirror device, instabilities obs. 3-79154
- ordinary mode instability, electrons' negative press. effect, using linearized Vlasov-Maxwell eqns. 3-49700
- oscillating two-stream instability, nonlinear stabilisation 3-71901
- outer radiation zone-plasma sheet boundary, obs. of current driven plasma instability 3-51152
- parametric, in inhomogeneous plasma with hot ions 3-68025
- parametric decay instabilities in laboratory plasmas 3-79102
- parametric excitation, instabilities, anomalous dissipation in strong e.m. fields 3-75383
- parametric excitation model by an imperfect pump 3-43674
- parametric instabilities, anomalous absorption and heating 3-68033
- parametric instabilities, anomalous absorption and heating 3-79159
- parametric instabilities, linear and nonlinear theory, review 3-75382
- parametric instabilities, low freq., in variable elec. field (*Russian*) 3-79100
- parametric instabilities, nonlinear saturation, turbulence spectrum, enhanced collision frequency 3-75355
- parametric instabilities, nonlinear saturation spectrum in the structure 3-75385
- parametric instabilities, purely growing in bounded homogeneous magnetoactive plasmas, threshold fields 3-79111
- parametric instabilities and anomalous absorption 3-68034
- parametric instabilities and harmonic generation in Tonks-Dattner resonances theory 3-57900

plasma instability continued

- parametric instabilities and turbulent heating of plasma in the field of fast MHD wave 3-68049
- parametric instabilities expts., review 3-75384
- parametric instabilities in bounded plasmas 3-54857
- parametric instabilities in plasma, review 3-68015
- parametric instabilities theory 3-71888
- parametric instability, excitation in magnetoactive plasma by microwave pumping wave 3-71908
- parametric instability, mode coupling saturation, electron heating 3-71903
- parametric instability, nonlinear theory, with comparable electron and ion temperatures 3-68035
- parametric instability, self-action of e.m. wave 3-71869
- parametric instability, stimulated back scattering from diffusion modes 3-79108
- parametric instability excitation by u.h.f. pump wave 3-79105
- parametric instability of nonlinear relativistic oscillations 3-79109
- Parametric instability of whistler solitary waves 3-79107
- parametric interaction with h.f. field in magnetoactive plasma, theory 3-75327
- parametric reson. in inhomogeneous plasma, theory 3-75326
- positive column, second harmonics of finite amplitude oscillations 3-40781
- pulsed plasma accelerator, struct. of current front and turbulent acceleration of ions 3-49718
- pulsed plasma accelerator, struct. of current front and turbulent accelerations of ions in fast regime 3-49719
- Rayleigh-Taylor instability in presence of horizontal mag. field, resistivity and ion viscosity effects 3-57916
- relativistic electron beam, microwave omission from anisotropic instability 3-71902
- relativistic electron beam filamentation theory 3-40778
- relativistic intense beam-plasma system, instabilities 3-75386
- repetitive explosive instabilities 3-49710
- resistive force-free fields, marginal modes growth rates 3-75305
- runaway electron discharge instability in Tokamak-6 device 3-63834
- saturation spectrum of ion-acoustic instability in current-carrying plasma 3-49688
- sausage type oscillations parametric build up 3-49692
- sideband instability of large amplitude collisionless electron plasma wave 3-57911
- solar corona plasma and MHD instabilities investigation (*Dutch*) 3-51285
- solar plasma irregularities and instabilities, obs. of interplanetary scintillations 3-65714
- solar wind, ionising high-beta flows, h.f. electrostatic instabilities 3-80978
- solar wind stability rel. to e.m. streaming instability 3-61649
- soliton decay instability and shock profile formation 3-46541
- spectral line broadening by electrons in nonequilibrium plasma 3-63808
- stabilized arc plasma, density distrib., determ. by double holography method 3-63867
- superheat instability in dense plasma formed by exploding wire 3-71975
- supersonic jet, stability investigations in magnetic field (*Russian*) 3-68009
- surface waves in semi-infinite plasma, kinetic theory of parametric excitation 3-49714
- surface waves parametric excitation in an inhomogeneous magnetized plasma 3-49721
- synchrotron instability, increments of longitudinal waves 3-40784
- tearing mode in cylindrical Tokamak 3-60608
- tearing mode instability in partially ionised gas 3-57914
- thermal flute perturbations in open device with feedback 3-75339
- thermal instability, in D-T fusion reactor, inhomogeneous plasma 3-75393
- thermodynamic stability of a current-carrying collisionless plasma column 3-57880
- tokamak reactor, thermal stability analysis including anomalous diffusion and synchrotron radiation 3-60636
- tokamak-like CTR, self-consistent energy balance studies 3-60637
- toroidal discharge, in longitudinal mag. field, dynamic stabilisation 3-49717
- toroidal effects on MHD modes in tokamaks 3-63827
- toroidal pinch system MHD and resistive instabilities, theory and expt. 3-75352
- toroidal plasma confinement effect of trapped particle instability 3-54868
- turbulence, low amplitude, dispersive waves, weak instabilities, review 3-60610
- turbulent, electron plasma, nonlinear instability 3-68010
- two stream instability, Krook model collisions effect 3-63840
- two-dimensional collision-free plasmas, tearing modes 3-75412
- two-stream instability, asymptotic behaviour 3-49697
- two-stream instability in plasma focus 3-75394
- two-stream ion cyclotron instability in presence of magnetic shear 3-75318
- unmagnetised plasma, purely growing instability, parametric excitation 3-54856
- unstable three wave coupling for time-dependent dissipation and coupling strength, soln. to random phase eqns. 3-49711
- vortex sheet MHD instability 3-75260
- wave dispersion and stability in presence of Coriolis force 3-75351
- wave propagation along static mag. field, parametric interaction, absolute instabilities 3-49699
- waves and instabilities (conf. Innsbruck, Austria, Apr. 1973) 3-75345
- weakly ionized collisional magnetoplasma, stability of oblique ion-acoustic waves 3-63836
- Weibel instability, nonrelativistic theory solns., numerical simulation 3-79145
- whistler decay instability in three dimensions 3-79106
- whistler mode instability, nonlinear development and Fourier analysis 3-46522
- Z pinch, MHD instabilities, surrounding gas effect 3-63828
- Ar, gross structure and instabilities 3-75370
- CO₂ laser discharge, ionization instability 3-43670

plasma instability continued

- D-T inhomogeneous fusion, numerical analysis of thermal stability rel. to fuel injection 3-60619
- H lines, Stark broadened, structure effect of plasma instability 3-49661
- He positive column, ion acoustic instability 3-49695
- He plasma wave propagation in an ion sheath, effect on immersed antenna (French) 3-49712
- MHD generator, conducting grids to stabilise ionisation instabilities 3-54827

plasma interactions *see* plasma collision processes

plasma jets

- capillary discharge emission screening study (Russian) 3-49761
- osmium flow stabilisation 3-75309
- current structure, in mag. field, Hall effect (Russian) 3-71882
- electric arc gas heater in plasma jets of temp. up to 12000 K, calc. of work 3-40824
- gas composition, analysis by means of cooled tube probe (German) 3-49827
- metal removal by a plasma torch, effects of vibration and pulsation 3-49826
- powder, spectral analysis in plasma jet, grain size depend. (Russian) 3-49752
- pressure and free stream velocity relation heat transfer and viscosity effects 3-57894
- pulsed MPD arc, quasi-steady operation, environmental, diagnostic means 3-49690
- pulsed plasma accelerator, investigation of heat fluxes 3-60635
- supersonic, stability investigations in magnetic field (Russian) 3-68100
- synthesised, oscillations obs. 3-52518
- turbulent, heterogeneous electron behaviour 3-49507
- As flow heat transfer to a sphere, effect of total gas velocity and temp. 3-68100
- As low temperature submersed plasma jet, conductivity, velocity and temperature profiles (Russian) 3-68006
- He local heat transfer to a sphere, effect of local gas velocity and temp. 3-68100
- He plasma jet, electronic recombination coefficient meas. 3-54826
- He high-energy propagation 3-49696

plasma measurement techniques *see* plasma diagnostics

plasma oscillations

- see also* plasma waves
- anisotropic cyclotron instability in an inhomogeneous mag. field 3-49687
- auroral E region density oscill. 3-51128
- auroral E-region electric field and plasma density oscill. 3-51128
- beam-plasma interaction, high pressure nonlinear effects, volumetric waves 3-68017
- beam-plasma nonlinear interaction obs. 3-79113
- beam-plasma system, bounded, magnetised, longitudinal oscillations, spectral distribution rel. to electron scattering 3-79113
- BOK waves decay instability, unstable waves 3-49690
- charged particle energy loss and stopping power 3-60615
- cold plasma, with group of hot ions with anisotropic velocity distribution, low freq. instabilities (Russian) 3-49690
- collective oscillations and separation of wave modes 3-79102
- collisionless parametric converter, oscillations obs. 3-49771
- current-coupled ion Langmuir oscillations, nonlinear phase of development 3-75328
- discharge with oscillating electrons, freq., current, pot. drop meas. 3-75327
- dispersion of LF oscillations in magnetic and gravitational fields (Russian) 3-49689
- drift and drift-diffusive, suppressing, diffusion, effect of high frequency mag. field Q-machine 3-49633
- drift oscillations, inhomogeneous plasma, h.f. electric field shielding effect 3-71891
- driven electrostatic oscillations in closed electron drift accelerator 3-75326
- electron, nonlinear effects in parametric excitations 3-79096
- electron beam modulated by low frequency oscillations, interaction with plasma 3-49743
- electron oscillating two-stream instability, nonlinear stabilisation 3-71414
- electron-wave amplitude oscillation due to an initial spatial distribution 3-57919
- electrostatic, in hot-electron plasma 3-75360
- electrostatic, low-free plasma, dispersion rel., energy eq. 3-49677
- electrostatic in accelerator with closed electron drift, effect of feedback system on plasma flux 3-75341
- electrostatic surface, interaction with inhomogeneous longitudinal electron beam 3-75331
- electrostatic-wave topology sounder for electron plasma resonances 3-44954
- em. instabilities in plasma with transverse current 3-75396
- em. instabilities in plasma with transverse current 3-75397
- em. oscillations in relativistic electron beam in plasma 3-54856
- excitation of open resonator, start-up radiation from ionizing current discharge, oscillations, geometrical resonances (Russian) 3-54856
- geomagnetic tail neutral sheet, production of low plasma oscill. 3-55555
- geomagnetic tail oscill. study using Chew-Goldberger-Low eqns 3-57110
- g. properties using wideband power amplifier (Russian) 3-49692
- mer. gas afterglows, magnetized, meas. in 300-1500 MHz range 3-49583
- inhomogeneous plasmas in field of two line currents 3-75377
- interaction of plasma with modulated relativistic beam 3-75345
- ion cyclotron instability of rotating plasma cylinder (Russian) 3-49746
- ionospheric, heating, disc ord meas. (Russian) 3-71458
- ionospheric second harmonic, amplitude oscillations obs. 3-71902
- ionospheric wave, in bounded plasma 3-68105
- ionospheric, Langmuir oscillations, parametric excitation (Russian) 3-49771
- ionospheric, polar, investigation using mother-daughter sounding technique ELBCTRA 3-45164

plasma oscillations continued

- jet, synthesised, oscillations obs. 3-52518
- Langmuir, in relativistic electron beam 3-79119
- l.f. oscill. effect on transport processes across mag. field 3-52499
- long-wave, damping 3-49715
- longitudinal and transverse, nonlinear interaction in the h.f. hybrid resonant region 3-68006
- magnetospheric highly ionized, inhomogeneous, low freq. self-excited, oscillations obs. 3-49692
- magnetospheric drift instabilities, finite Ω effects, Vlasov-Maxwell equations 3-50134
- magnetospheric, hydromagnetic propagation, mechanical analogue for magnetospheric oscillations 3-68115
- magnetospheric, plasma-wave excitation at low freqs. 3-61560
- magnetospheric tail, model for hydromagnetic eigenoscillations 3-49554
- MHD mode, dynamic stabilisation, nonlinear coupling theory 3-75011
- n-n-nr., physical mechanism 3-41254
- non-linear, effect of temp. and particle trapping on dispersion props. 3-52519
- nondegenerate plasma in quantised mag. field 3-75325
- nonlinear, effect of capture of particles by plasma waves on stability 3-75326
- nonlinear ion-acoustic resonance frequencies, expt. 3-75323
- nonlinear relativistic, parametric instability 3-79109
- nonlinear standing striations reaction on pulse disturb. 3-49681
- parametric instabilities, low freq., in variable elec. field (Russian) 3-79100
- parametric reson. in inhomogeneous plasma, theory 3-75326
- photospheric 5-minute oscill., high-vel. horizontal phase propag. 3-65674
- photospheric magnetically active regions, 5-minute oscill. 3-65675
- plasma engineering, monograph 3-49632
- point charge oscillating, interference structure near resonant zone 3-75117
- positive column, relaxation oscillations obs. 3-68126
- positive column, second harmonics of finite amplitude oscillations 3-40781
- quasineutral ion beam, amplitude of oscills. of potential 3-54852
- relativistic oscillation of charged particles in laser fields and pair production 3-40811
- Resonant oscillations in radiative magnetogasdynamics 3-79050
- responses of oscillator and dispersive medium to fields of moving point charge, analysis 3-49633
- sawtooth type oscillations, parametric point up 3-49690
- scattering function, effect of oscillations 3-49654
- semitransparent plasma, proton beam effects on spectra, astroph. appl. 3-606
- solid wind 3-65736
- sunspot umbral flashes and running penumbral waves 3-65679
- surface oscillations of a magnetoactive plasma 3-49686
- surface waves in semitransparent plasma, kinetic theory of parametric scattering 3-49714
- three pinch, 8 m radiation origin, unstable longitudinal oscillations 3-79016
- Tonks-Darmer resonances, theory of subharmonic excitation in bounded plasmas 3-68015
- toroidal discharge, in longitudinal mag. field, dynamic stabilisation 3-49717
- turbulent h.f. field, meas. forbidden He I line satellites intensity (Russian) 3-71955
- Van der Pol oscillators collisional drift instability obs. 3-79086
- wake, turbulent plasmas, oscillation centre quasilinear theory 3-63839

plasma probes

- see also* Langmuir probes
- Atmospheric Explorer 4E, D, E, electrostatic probes for electron temp. and ion concentration 3-42075
- cooled tube, gas composition analysis of plasma jets (German) 3-60627
- cylindrical conductor, ionosphere transition region, charged particle measurements 3-61602
- double probe, possible use for electron temp. determ. in recomb. plasma 3-49752
- double-sphere probe, antenna self-impedance in warm anisotropic plasma 3-75714
- electron temperature measurement in ethylene-O₂ flames, from current-voltage charact. 3-80523
- electrostatic double, finite Larmor radius effects upon ion current collection 3-75423
- emitting, disturbance of plasma potential 3-60601
- fast paced cylindrical, positive ion collector produced by Monte Carlo method 3-61601
- flow field velocity vector meas. by electrostatic probe 3-49696
- flush-mounted, characteristics in forward stagnation region, ion current in plasma flow 3-71948
- hollow cathode discharge, probe meas. of plasma charact. (French) 3-49773
- hydrodynamic eqns. for probe in highly ionized plasma 3-60604
- ionospheric probe meas. theory for lower ionosphere 3-53554
- Langmuir type and RFA, interaction between spacecraft and ionospheric plasma 3-61524
- local parameters of ionized gas flow, meas. device 3-49751
- Mixing probe in a flowing ionospheric plasma 3-80853
- orifice, characteristics 3-63887
- pulsed plasma flow diagnostics, dynamic pressure/velocity pressure transducer system 3-49746
- reference electrode, inadequate, meas. errors 3-63874
- RF impedance probe for ionospheric meas., orientational depend. 3-53560
- r.f. noninterfering, for electron density and electron stream freq. obs. 3-68069
- solar wind distribution function meas. 3-65978
- spacecraft interaction, collisionless plasmas rel. to Laframboise and Parker theory 3-60602
- spherical electrostatic, symmetrical model for current collectors 3-60631
- split Langmuir probe, near wakes of planar disc and cylindrical geometries on sounding rockets 3-61603

plasma probes continued

- thermionic potential distribution meas. near an electron beam 3-54873
- transverse energy meas., in mag. field (*Russian*) 3-71950
- turbulence measurement, double elec. probe in mag. field (*Russian*) 3-71954
- Ar, shocked-plasma flows, double search-coil cond. probe study 3-63872

plasma production

- air, low threshold breakdown by CO₂ laser beam, recoil momentum 3-49727
- alpha radiation induced, Monte Carlo simulation model 3-75426
- British fusion research, history and future prospects 3-49728
- coaxial plasma gun, properties, obs. 3-68042
- coaxial plasma gun with outer electrode of cage structure near fast acting valve 3-49767
- coaxial plasma-waveguide system, microwave breakdown 3-68051
- collisional preionisation in large pinch vessels obs. 3-68053
- concentric compression by laser implosion of thin 'heavy' coating, numerical method 3-57922
- conical theta-pinch gun, effects of multipole field on plasma production 3-63848
- cylindrical plasma sources with densities high above critical density, excited by r.f. helix with and without mag. field 3-68068
- electron beam, simultaneous beam pinching obs. 3-63846
- electron beam injection through heliotron divertor 3-75401
- expanding multicomponent plasma instabilities and laser scattering 3-52510
- fast electrons production by microwave power at electron cyclotron frequency harmonics 3-75404
- focus experiment, neutron yield improvement (*French*) 3-71925
- focused CO₂ laser beam perturbation, piezoelec. probe obs. 3-54862
- gas, laser induced breakdown, optical emission time depend. 3-46554
- gas, laser induced breakdown, similarity principles 3-60612
- helical dense microwave source in large mag. field, operational props. (*French*) 3-68067
- Heliotron D, material limiter effect, ohmic discharges 3-75411
- intense light source generation, by optimising imploding detonations with laser energy 3-63849
- ionisation of a neutral medium by an electron beam (*Russian*) 3-68054
- large valence microwave plasmas 3-49726
- laser, TEA-CO₂ produced, characteristics determ. and wavelength scaling law 3-57927
- laser induced, c.w., in atmospheric pressure air, ignition and maintenance, CO₂ laser 3-49723
- laser induced, preionisation, charge collection meas. 3-71924
- laser induced gas breakdown rel. to transverse elec. field 3-60613
- laser irradiated target, momentum transfer indicating nonlinear interaction force 3-52521
- laser irradiation, parametric scatt. instabilities 3-68052
- laser irradiation of solid surface, satellite lines 3-74771
- by laser irradiation of solid targets (*Rumanian*) 3-62732
- by laser on solid targets, energy absorpt. mechanism and evolution (*Rumanian*) 3-63856
- laser plasma, anomalous generation of neutrons, model 3-68039
- laser plasma, Cs effect on photoionisation 3-66805
- laser produced, electron temp., theory and expt. obs. 3-75405
- laser produced, high intensity, rapid growth, spectral broadening 3-71927
- laser produced, neutron emission, collisionless electrostatic shock waves 3-75398
- laser produced, neutron emission 3-40803
- laser produced, X-ray emission, characs., numerical calc. 3-63893
- laser produced from C, Be and polyethylene targets, heating studies 3-43677
- laser produced systems, electron temp. and ioniz. state 3-68047
- laser production, bibliography, (1969-1972) 3-57932
- laser target model 3-75395
- laser vaporized from high Z-material, v.u.v. continuum emission 3-79172
- laser-induced evaporation of metallic targets, theory 3-61102
- laser-thin target interaction, temp. laws 3-63847
- metal, evaporation by laser radiation, gas-dynamic struct. of plasma flare 3-75400
- off resonance microwave created plasmas 3-57928
- plasma-beam discharges → beam-plasma system (*Russian*) 3-68110
- plasmoid obtained from coaxial source, parameters depend. on polarity of central electrode 3-52526
- plasmoid production in coaxial accelerator, initial gas conditions effect 3-71929
- plasmoids formation, magnetic deflection of slow component (*Russian*) 3-71877
- plasmoids production from coaxial gun, initial gas conditions, energy (*Russian*) 3-71921
- plasmoids production with pulsed magnetic gate field (*Russian*) 3-71876
- polyethylene plasma, laser prod., shock hydrodynamic phenomena, core-corona decoupling 3-54872
- preionisation in Tokamak by TM mode 3-75402
- rocket driven liners for fusion triggers and for very high density reactors 3-49372
- self-igniting pulsed optical discharge in erosion laser plasma 3-40792
- shock waves, hemispherical, laser produced with Al or C targets 3-71886
- solid sublimation with varying energy liberation by laser radiation, motion of sublimation products (*Russian*) 3-68055
- solid surface in air, emission spectra of laser-supported detonation wave 3-40788
- suprathermal particle generation, laser produced plasmas, role of strong magnetic fields 3-49722
- target manufacture, solid hydrogen and deuterium 3-77414
- Al foil, by CO₂ TEA laser 3-57924
- Al surface, rel. to impulse reaction to in air irradiation by pulsed CO₂ laser beam 3-68045
- Ar, wide aperture fast neutral atom injectors (*Russian*) 3-71922
- At low pressure arc of high power laser, intensification of 4880 Å line and temperature (*German*) 3-52522

plasma production continued

- CO₂, wide aperture fast neutral atom injectors (*Russian*) 3-71922
 - Cs, by reson. absorpt., physical props. 3-68046
 - D, laser created plasma, role of spontaneous mag. fields, numerical simulation 3-63851
 - D solid target, laser light absorption, wavelength depend. 3-49731
 - D-plasma, in toroidal geometry in millitorr pressure range, pre-ionisation and pre-heat conditions 3-49730
 - D₂ solid, laser irradiation 3-75388
 - He, laser produced, afterglow, recomb. of doubly ionized atoms 3-40808
 - He, preionised, CO₂ laser induced breakdown, electron cascade theory 3-75391
 - Li exploding wire production of dense plasma of high current discharges, fluctuation characts. 3-71975
 - Mg vapour, wide aperture fast neutral atom injector (*Russian*) 3-71922
 - W surface, laser induced, energetic ion origin 3-75392
- plasma sheaths**
see also plasma confinement
 breakdown between cathode sheath and anode in spark gap, ionisation and flow velocity effect 3-46565
 diameter meas. near probe, comparison with theory 3-63886
 E-polarised wave scatt. by plasma-coated cylinder 3-75291
 electrode sheath electric field and Bohm criterion 3-52550
 formation around transmitter, effect of free streaming electrons 3-57921
 ion boundary layer on a flat plate, flow fields in ion sheath region 3-79077
 ionosphere, transition region probe analysis, effects of payload potential and sheath size 3-61602
 Langmuir probe, spherical, in partially ionised plasma with uniform mag. field, theory 3-49753
 plasmagmap, effects on charged particle measurement 3-61561
 pulsed plasma accelerator, struct. of current front and turbulent acceleration of ions 3-49718
 pulsed plasma accelerator, struct. of current front and turbulent accelerations of ions in fast regime 3-49719
 shock-driving current sheaths, non-planar shocks and energy concentration 3-79151
 spacecraft, theoretical studies, computer simulation, satellite measurements 3-61562
 spherical antenna radiation in inhomogeneous over-dense plasma layer 3-79075
 surface waves parametric excitation in inhomogeneous sheath 3-75336
 theta pinch, density and beta distributions, drift velocity and sound speeds in sheath region 3-79164
 transmitter sheath effect on free-streaming electron 3-71898
 vacuum interrupters, post arc current mechanism, plasma decay, dynamic sheath, density 3-46564
 Hg plasma wave propagation in an ion sheath, effect on immersed antenna (*French*) 3-49712
- plasma shock waves**
 accelerators, steady-state interactions 3-71962
 collisionless, electrostatic, in laser produced plasma 3-75398
 collisionless, heating of plasma ion component 3-40793
 collisionless, review 3-79096
 collisionless, turbulence anisotropy 3-57906
 electron, bounded collisionless plasma, Mach number and period depend. on amplitude 3-49675
 electron density distribution at high altitudes around entry vehicles, viscous shock-wave analysis 3-44911
 electron gas temp. in shock precursors calc. 3-54840
 electron-acoustic, current front structure 3-75337
 Electrostatic shock waves in collisionless plasmas 3-75371
 generation by acoustic turbulence 3-63655
 hemispherical, laser produced 3-71886
 inert gas plasma behind shock waves, thermodynamic variables, interferometric meas. (*German*) 3-68099
 interplanetary, from chromospheric flares, space probe meas. 3-61755
 ion density discontinuity disruption, heavy particle method (*Russian*) 3-46540
 ionising shock waves, structural determ. of electric field conditions, MHD parameters 3-57902
 isothermal MHD shock waves stability 3-79093
 magnetic field line reconnection in compressible conducting fluids 3-51252
 magnetically driven shock tube, poor separation 3-75321
 magnetised plasmas, non-turbulent electric fields in soliton and shock-like structures 3-57896
 magnetohydrodynamic blast wave, planar and spherical, numerical soln. 3-57895
 MHD, in upstream solar wind, radiation emission 3-51218
 MHD, nonlinear waves propagation in a magnetic neutral sheet, shock formation 3-43668
 MHD, plasma heating effects 3-68075
 MHD generators, shock formation by a moving force field 3-79182
 MHD shock polar, exact solution in aligned fields 3-46526
 microwave meas. determ. of electron temp. of shock-heated plasma 3-63880
 non-planar and energy concentration in shock-driving current sheaths 3-79151
 nonstationary, propagating at arbitrary angle to magnetic field (*Russian*) 3-68030
 ohmic heating, direct, of ions in ionising shock 3-68050
 parallel high β shocks, collisionless, relaxation phenomena, shock structure, turbulence 3-69670
 perpendicular, electrostatic potential rise 3-75320
 Pioneer 8 observations of shock front shape, perturbation, magnetic and electric fields 3-69914
 polyethylene plasma, laser prod., shock hydrodynamic phenomena, core-corona decoupling 3-54872
 quasi-neutral solitary wave, stationary electrostatic solutions for a non-neutral two fluid model 3-57918
 solid surface in air, emission spectra of laser-supported detonation wave 3-40788
 soliton decay instability and shock profile formation 3-46541
 steady state high Mach shock waves theory 3-79126

plasma shock waves continued

- structure in Ar or H, translational inequilibrium effects (*Italian*) 3-79083
- structure in fully ionized gas 3-57908
- toroidal diffusion and stationary shocks 3-49694
- transverse ionizing MHD detonation waves, numerical simulation 3-57904
- transverse ionizing MHD detonation waves, structure, Hugoniot curves and Chapman-Jouguet limit 3-57903
- turbulence in normal wave, laser light scatt. investigation 3-57912
- two-temperature plasma, laser heated, thermal and shock wave fronts separation 3-60616
- type II solar radio bursts, plasma radiation from MHD shock waves 3-56316
- viscous, hypersonic blunt body problem in shock heated plasma, numerical analysis 3-46525
- Ar, high density plasma in explosively driven shock wave, radiation intensity and spectrum 3-54869
- Ar, shock adiabats calc. (*Russian*) 3-68032
- Ar, shock produced ionized, supersonic current interaction with elec. and mag. fields (*French*) 3-40776
- Ar, shock-plasma flows, double search-coil cond. probe study 3-63872
- Ar, wall boundary layer effects on ionising shock structure 3-71892
- Cs, state functions behind ionizing shock waves 3-63807
- Cs plasma, nonideal, equation of state, shock wave investigation 3-49759
- D₂, solid, laser irradiation, plasma production, shock wave effects 3-75388
- He, ionisation equilib., atomic collision cross section. 3-78501
- He-H plasma behind shock front, stepwise excitation and local thermodynamic equilibrium of H levels 3-71369
- K, state functions behind ionizing shock waves 3-63807
- Xe, ionised radiative energy loss, struct. determ. 3-68090
- Xe, shock adiabats calc. (*Russian*) 3-68032

plasma simulation

- beam-plasma and two-stream instability, numerical simulation, expt. obs. 3-71915
- bumpy tori, effect of magnetic field errors on confinement 3-63865
- drift wave turbulence, expt. study using digital spectral analysis techniques 3-75354
- electron velocities in crossed magnetic and electric fields, statistics 3-52504
- equilibrium in toroidal configurations, numerical solution methods 3-63863
- free expansion of collisionless plasma plane, cylindrical and spherical one dimensional models comparison 3-67983
- fusion plasma control of the energy balance 3-57930
- h.f. instabilities in arbitrary configurations, numerical method 3-79150
- instabilities, nonlinear, simulation 3-79121
- ionospheric plasma surrounding satellite, laboratory simulation 3-44915
- laser production, target model 3-75395
- many-particle models, energy-conservation requirements 3-71966
- microwave stochastic reflection, Walsh spectral analysis 3-75301
- Monte Carlo model, rel. to α -induced noble gas plasma, electron energy distrib. 3-75426
- non linear differential equations, computer use (*Russian*) 3-71965
- nonequilibrium plasma in segmented electrode duct, current and density distributions, numerical investigation 3-67990
- nonlinear interaction of small resonant electron beam with cold electron-cyclotron wave 3-54853
- nonlinear wave interactions, computer simulation 3-79137
- nonphysical self forces in some electromag. plasma-simulation algorithms 3-57874
- on-line correlation measurements 3-57951
- radiation-induced plasmas, Monte Carlo simulation 3-46560
- relativistic electrons confined in axisymmetric mirror field, numerical simulation 3-43682
- satellite-ionosphere interaction using 'plasma wind tunnels' 3-61530
- thermal (nonthermal), electric field probability distrib., density and temp. 3-67985
- Tokamak plasma generator, magnetic field analysis by finite element analysis 3-68078
- transport processes, error characterisation of analytic methods 3-71328
- transverse ionizing MHD detonation waves, numerical simulation 3-57904
- turbulent plasma, spectral index determ. from digitally computed power spectra 3-71899
- two-dimensional guiding centre plasma, negative temperature states, numerical simulation 3-57875
- Weibel instability, nonrelativistic theory solns., numerical simulation 3-79145
- whistler mode instability, nonlinear development and Fourier analysis 3-46522
- Z-pinch, noncylindrical, matching discharge circuit with membrane movement, neutron density, two dimensional snow plough model (*Russian*) 3-57950
- D, laser created plasma, role of spontaneous mag. fields, numerical simulation 3-63851
- D-T inhomogeneous plasma, numerical analysis of thermal stability rel. to fuel injection 3-60619

plasma theory

- charged particle acceleration and radiation reaction in strong plane and spherical waves 3-46521
- charged particle moving in bounded cold magnetoplasma 3-71848
- collisionless damping of waves, quantum theory 3-49678
- constitutive equations of a plasma with bound charges 3-57878
- Coulomb pot. generalized screened, critical screening parameters 3-70694
- Coulomb-collision corrected electron-plasma line profiles 3-43655
- Debye plasma bremsstrahlung 3-67981
- definite Fourier integrals, computation 3-71850
- deuterium, hot, infinite, Coulombian transparency, finite deuterons 3-52525
- electrodynamics of nonequilibrium plasma, state of the art 3-49640

plasma theory continued

- electrostatic potential created by test particle in one, two and three dimensions in flowing plasma 3-57876
- fluctuations and correlations, transition probability approach 3-49642
- fluctuations and nonlinear susceptibilities 3-49641
- free expansion of collisionless plasma plane, cylindrical and spherical one dimensional models comparison 3-67983
- fully ionised plasma, homogeneous, high frequency, equilibrium electrons distribution function 3-52498
- high-density, new integral eqns. for radial distribution function 3-40174
- homogeneous nonstationary plasma, charge radiation (*Russian*) 3-71854
- inhomogeneous plasma, contribution of various processes in the density distribution 3-67986
- ionic fluids, equil. field theory 3-48794
- ionic fluids, onset of short-range order 3-48795
- ionisation, recombination, low temperature, modified diffusion theory 3-63816
- ionised systems, three component, classical kinetic eqns. derivation 3-43653
- ionization effects 3-79056
- Jeffery-Hamel flow of dissipative plasma, similarity transformation 3-75302
- kinetic theory of a collision dominated plasma 3-60594
- laser plasma, kinetic processes 3-49643
- locally ionised, afterglow, electron density calc. 3-75285
- matter-antimatter plasma, fluid-type eqns. for macroscopic behaviour 3-46509
- microturbulent magnetoactive plasma, weak nonlinear interactions, scattering of magnetoionic waves, polarised radiation, nonlinear conversion of microturbulence 3-75310
- moving test particles shielding in warm isotropic plasma 3-46512
- non-L.T.E., particle densities, He atoms 3-79058
- non-Markovian effects, microscopic theory of linearized hydrodynamical eqns. 3-79057
- nonideal plasma, quantum kinetic equations 3-71853
- nonlinear wave interaction and fluctuations 3-49706
- nonphysical self forces in some electromag. plasma-simulation algorithms 3-57874
- partially ionised gases, density fluctuations theory 3-40764
- particle conc. and electric potential in vicinity of rapidly moving charge 3-75287
- planetary outer layers, quantum statistical mechanics of dense partially ionised H 3-42160
- plasma engineering, monograph 3-49632
- plasma particle moving in bounded cold magnetoplasma 3-71848
- quantum plasma, time-depend. microfield, distrib. 3-46515
- radial distribution function for long-range and short-range interaction potential, integral eqns. 3-74151
- random electron density fluctuations, effect of collisions 3-57877
- rarefied plasma, inconsistency of classical theory with cut-off for X-ray power density 3-67984
- relaxation to equilibrium, two dimensional 3-71852
- responses of oscillator and dispersive medium to fields of moving point charge, analysis 3-49633
- review of present-day position (*Dutch*) 3-40761
- screening factors for nuclear reactions, intermediate screening and astrophysical appl. 3-47861
- screening factors for nuclear reactions in dense plasma, general theory 3-47860
- short-range order, HNC approx. 3-46511
- slightly ionised plasma, continuum theory, diamagnetic effects 3-57879
- stochastic kinetic theory of plasma in strong e.m. fields 3-75288
- test charge potentials in collisional plasmas 3-79059
- thermal (nonthermal), electric field probability distrib., density and temp. 3-67985
- thermodynamic stability of a current-carrying collisionless plasma column 3-57880
- thermodynamic states, numerical soln. of Abel integral equations, piecewise polynomials 3-71849
- two component nondegenerate systems with Coulomb interaction, theory 3-49635
- two fluids model 3-57885
- two-dimensional guiding centre plasma, negative temperature states 3-57875
- two-dimensional plasma, equilibrium pair correlation function 3-75286
- Vlasov-Maxwell operators in self-adjoint form 3-52496
- Zeeman sublevel transitions, in homogeneous magnetoactive plasma (*Russian*) 3-43652
- Ar-H plasmas, equilib. compositions and thermodynamic props., 10^{-2} - 10^3 atmos., 2000-35000K calc. and tables 3-71855
- Cs, state functions behind ionizing shock waves 3-63807
- Cs plasma, local thermodynamic equilibrium in short space 3-57881
- CsCl, strongly nonideal ion plasma, thermodynamics 3-49636
- H diffusion dominated non LTE plasma, electron temp. determ. 3-67987
- H plasma, partially ionised, dense, Lymann- α asymmetry calc. 3-71851
- He I, excited state population lowering in He plasma due to laser beam 3-49639
- K, state functions behind ionizing shock waves 3-63807
- N⁺ plasmas, recombining, continuum emission, photoionisation cross sections 3-54835
- N₂, Debye type corrections influence on compressibility factor (*French*) 3-46510
- Na plasma optically dense, temp. and particle density calc. (*Dutch*) 3-49638
- O⁺ plasmas, recombining, continuum emission, photoionisation cross sections 3-54835

plasma thermocouples see *plasma devices; thermocouples*

plasma torches see *plasma devices*

plasma transport processes

see also *Vlasov equation*

air plasma, electrical conductivity and total emission coefficient meas. 3-71947

Alfven wave accel. of fast particles 3-46516

plasma transport processes continued

- Ambipolar diffusion as a singular perturbation problem 3-79062
- anomalous conductivity 3-71864
- anomalous electrical conductivity, reln. to turbulence processes 3-75324
- anomalous resistance, role of non-linear effects 3-63817
- anomalous resistivity, particle diffusion, mag. field penetration 3-75307
- anomalous resistivity and ion-acoustic turbulence 3-75357
- anomalous resistivity in magnetic neutral point 3-79152
- arbitrary fluctuation spectrum of particle velocity 3-49654
- astron, electron distributions for small field cancellation in quiescent E layer 3-60624
- astrophysical, strongly magnetised, enhanced diffusion 3-80914
- Bett Pinch, slab models, for classical diffusion 3-63862
- Brownian motion of charged particles in rotating fluid embedded in mag. field 3-71859
- charged particle diffusion and mobility in a neutral gas, Boltzmann eqn. treatment 3-40765
- charged particle transport in turbulent mag. fields, exact soln. and quasilinear approx. comparison 3-43657
- and collision at low electron energies, obs. using swarm and transport meas. methods, book 3-60598
- collision processes in plasma, kinetic eqn. for vel. distrib. fns. 3-71856
- collisional resistivity in low aspect ratio tori 3-63812
- collisional resistivity in low aspect ratio tori 3-67994
- column, anomalous impedance at r.f.'s, Maxwell's and Boltzmann's eqns., soln. 3-49651
- conductivity, nonlinear, hydrodynamic model, warm plasmas 3-60595
- conductivity, tensor components, Grad's method, collisional plasma 3-67989
- conductivity coeffs. in Tokamaks expt., possible direct meas. 3-49758
- conference, Providence, USA (1973) 3-70748
- coupled radiation with turbulent convection in electric arcs 3-79185
- current vortices development in moving plasma in quickly changing mag. field (*Russian*) 3-79078
- current-carrying plasma, instability at cyclotron harmonics and anomalous resist., theory 3-71909
- current-driven modes in two-dimensional plasma configurations 3-68038
- diffusion, anomalous in magnetized plasma due to hydrodynamic effect 3-71862
- diffusion due to parametric instability turbulence driver field, coeff. 3-71894
- diffusion of weak inhomogeneities in two-ion magnetically active plasma 3-54836
- diffusion spreading of weak plasma inhomogeneities with two kinds of positive ions 3-40767
- directional transport eqns. deriv., applic. to confinement 3-63818
- dissipative trapped ion instability, anomalous transport 3-63835
- drain diffusion in two fluids model 3-57885
- drift and drift-dissipative, suppression, diffusion, effect of high frequency mag. field, Q-machine 3-49653
- drift motion and adiabatic invariance of magnetic moment in a non-static magnetic field 3-40762
- drift tubes, transport equation for ions 3-43535
- electrical conductance and temperature decay, in arc plasma 3-63811
- electrical conductivity calc. 3-79063
- electrical conductivity in mag. field, electron and ion momentum transfer 3-71860
- electrical conductivity meas., resist., oscill. effects (*Russian*) 3-71858
- electrical conductivity of partially ionised gas mixtures, approximate calc. (*Czech*) 3-43534
- electrodynamical plasma acceleration, relaxation processes 3-60634
- electron, in radiation-induced plasma, Monte Carlo simulation 3-46560
- Electron fluctuations and transport in toroidal plasmas 3-67995
- electron runaway rate under uniform elec. field 3-63814
- electron transport coefficients determ. using motion of heavy collision partners, Lorentz approach (*German*) 3-57882
- e.m. wave propagation in plasma using transport theory 3-57888
- F-region, incoherent scatter meas. of plasma influx 3-65464
- focus device, ion kinematics 3-60596
- Green-Kubo formalism and conditions for linear relationships among transport coefficients 3-63813
- heat transfer, 1972 literature 3-75188
- h.f. discharge, diffusion under strong skin effect conditions 3-60653
- ion acceleration on expansion of rarefied plasma 3-60597
- ionospheric electron thermal conductivity for weakly ionised gas 3-47785
- jets, pressure and free stream velocity relation heat transfer and viscosity effects 3-57894
- laser fusion, thermal conduction limitations 3-46517
- laser heated target plasmas, limitations on electron thermal conduction 3-49734
- laser production, target model, heat flow 3-75395
- l.f. oscill. effect on transport processes across mag. field 3-52499
- locally ionised, afterglow, electron density calc. 3-75285
- magnetic fields, force-free, resistive media, models, elec. current density rel. to mag. field, elec. field an plasma velocity 3-69813
- magnetic mirror device with positive plasma potential, electron Coulomb diffusion 3-75417
- magnetoplasma, high-freq. cond. calc., close collisions quantum mech. treatment 3-49650
- magnetoplasma partially ionized Lorentzian, transport coeff. calc. including interparticle collisions 3-75289
- multi-ion isothermal astrophysical plasmas, motion in gravit. field 3-47863
- multi-ion plasmas, critical points existence criteria in astrophysical appl. 3-47862
- multiple ion species plasma, neo-classical transport theory 3-46519
- neo-classical transport equations, steady-state solutions 3-49646
- non-Markovian effects, microscopic theory of linearized hydrodynamical eqns. 3-79057

plasma transport processes continued

- nonequilibrium plasma, in mag. field, influence of viscosity on motion of nonuniformities 3-49673
 - nonequilibrium plasma in segmented electrode duct, current and density distributions, numerical investigation 3-67990
 - nonideal plasma, quantum kinetic equations 3-71853
 - optically thick, radiative transfer mechanism 3-49645
 - partially ionised in electric field, transport props. 3-71865
 - particles non adiabatic motion in inhomogeneous mag. fields, change in mag. moment 3-49634
 - plasma steady state ion acceleration in magnetic nozzle for 2-20 keV 3-54847
 - plasma sphere, penetration of magnetospheric electric fields and plasma convection 3-80833
 - poloidal current in mag. field (*Russian*) 3-71875
 - Rayleigh-Taylor instability in presence of horizontal mag. field, resistivity and ion viscosity effects 3-57916
 - recombination ionisation, low temperature plasma, modified diffusion theory 3-63816
 - relativistic beam-plasma system, conductivity determ. technique by magnetic diffusion times meas. 3-43690
 - resistance, anomalous, nonlinear processes, one-dimens. numerical expt. 3-43658
 - resistivity, anomalous ion-sound turbulence effects 3-57883
 - r.f. cond. in mag. field presence, freq. shift meas. 3-54837
 - steady-state confinement regime in stellarators, idealised collisional diffusion model 3-49738
 - striations as eigensolns. of electron motion in elec. field (*German*) 3-63918
 - thermal conductivity, longitudinal, effect on ohmic heating in Tuman-1 3-71930
 - thermal conductivity calc. 3-75290
 - tokamak plasma, poloidal rotation decay 3-71861
 - Tokamak plasma heating, thermal conduction 3-68057
 - toroidal diffusion and stationary shocks 3-49694
 - toroidal plasma, particle diffusion and drift-surface-island formation 3-63859
 - toroidal plasma, stationary convection 3-57884
 - toroidal plasma, transport props. at low to intermediate collision frequencies 3-49649
 - toroidal plasma modes, transport and particle scattering 3-60605
 - toroidal plasma modes transport and particle scattering 3-67993
 - transverse electron thermal conductivity meas. in mag. field 3-54841
 - two-temperature plasma, laser heated, thermal conduction mechanism 3-60616
 - viscosity and neutral-gas friction, determination of hydromagnetic stability of composite plasma 3-68007
 - wave propagation in drifting warm plasma under Grad's thirteen-moment approximation 3-49705
 - Ar, decaying plasma, doubly charged ions obs. 3-63810
 - Ar, shocked-plasma flows, double search-coil cond. probe study 3-63872
 - Ar low temperature submersed plasma jet, conductivity, velocity and temperature profiles (*Russian*) 3-68006
 - Ar plasma jet, local heat transfer to a sphere, effect of local gas velocity and temp. 3-68100
 - CO₂, electron-beam ionised, electrical conductivity 3-54839
 - Cs weakly-ionized, elec. cond., electron-Cs atom scatt. cross section determ. 3-49644
 - D₂ plasma, isotopic effects in establishment of thermal equilibrium, ambipolar diffusion 3-71959
 - H₂ plasma, isotopic effects in establishment of thermal equilibrium, ambipolar diffusion 3-71959
 - He plasma jet, local heat transfer to a sphere, effect of local gas velocity and temp. 3-68100
 - K⁺ diffusion in He and Ne gases, experimental variables and interaction potential depend. 3-40766
 - K⁺ in N₂, longitudinal-diffusion coefficient meas. at 293 K 3-43536
 - N₂ electron-beam ionised, electrical conductivity 3-54839
 - N₂ gas, electron swarm parameters, diffusion coeff., mobility, amplification coeff., Townsend ionisation coeff. 3-49526
 - Ne, decaying plasma, doubly charged ions obs. 3-63810
 - O₂, electron energy distrib. and attachment coeff. for electron swarms 3-54792
- plasma turbulence**
- acoustic, shock wave generation 3-63655
 - anisotropy of turbulence in a collisionless shock 3-57906
 - anomalous mag. field penetration, turbulent fields effect 3-75307
 - beam-plasma nonlinear interaction obs. 3-79113
 - beam-plasma system, counterstreaming, turbulent heating 3-79158
 - conductivity, anomalous and turbulent, expt. and theory 3-71864
 - coupled radiation with turbulent convection in electric arcs 3-79185
 - Crab Nebula, origin of h.f. radiation 3-61876
 - current-driven ion wave turbulence 3-54850
 - D⁺ plasma, kilovolt ions, energy distribution meas. in modified Penning discharge 3-57929
 - diffusion coefficient, driver field, parametric instability 3-71894
 - drift wave turbulence, expt. study using digital spectral analysis techniques 3-75354
 - drift waves, h.f. microturbulence influence 3-75373
 - electric field fluctuations, probability distrib., meas. for turbulent plasma 3-52512
 - electron beam deceleration, new turbulent state 3-49713
 - electron velocities in crossed magnetic and electric fields, statistics 3-52504
 - electrostatic macro-turbulence in magnetised plasma 3-75359
 - electrostatic turbulence, collisionless dissipation of a cross-field electric current 3-49698
 - e.m. wave propagation in turbulent plasma using transport theory 3-57888
 - far-field potential of moving test charge, inverse square dependence 3-60604
 - field-free plasma, mag. pulse anomalous penetration, two-fluid eqns. numerical integration calc. 3-46536
 - heating, collisionless, of plasma ions by ion beam, nonlinear interaction of waves 3-49736
 - heating, turbulent 3-71932
 - heating expts., lineal geometry 3-71933

plasma turbulence continued

- heating in linear discharge, diagnostic meas. 3-68043
- h.f. field measurement, intensity of forbidden He I line satellites (*Russian*) 3-71955
- highly ionised cylindrical column, radial particle loss 3-71944
- hydrodynamic tensor wave equation 3-75350
- inhomogeneous system, repeated-cascade theory 3-63843
- intense relativistic electron beam turbulent heating 3-71934
- interstellar radioscintillations due to plasma irregularities with power law spectra 3-51397
- ion and electron transit time magnetic pumping and ion cyclotron heating, neoclassical aspects 3-68059
- ion beam interaction with θ -pinch turbulent plasma, low press. region (*Russian*) 3-40785
- ion cyclotron resonance and turbulent heating studies at Nagoya university 3-68061
- ion heating in relativistic intense beam-plasma system 3-75386
- ion sound turbulence and the theory of anomalous resistivity 3-57883
- ion wave turbulence, current-driven, electron drift velocity and frequency meas. at onset of instability 3-79084
- ion-acoustic, and anomalous resistivity 3-75357
- ion-acoustic, nonlinear theory, angular spectrum 3-75356
- ion-acoustic turbulence due to relativistic electron beam relaxation 3-79119
- ionosphere, artificial plasma inhomogeneity, turbulent motions 3-76800
- low amplitude, review 3-60610
- magnetised positive column, diffusion under turbulent flow 3-68085
- magnetosphere, threshold of appearance of anomalous resistance 3-42051
- MHD generators, electrical conductivity of turbulent non-equilibrium plasma 3-54848
- MHD turbulence, interaction of fast particles and accel. by Alfvén waves 3-46516
- microturbulent magnetoactive plasma, weak nonlinear interactions, scattering of magnetoionic waves, polarised radiation, nonlinear conversion of microturbulence 3-75310
- monoenergetic beam interaction with plasma 3-71906
- nonequilibrium plasma, in mag. field, influence of viscosity on motion of nonuniformities 3-49673
- nonlinear Landau damping of electron plasma waves, weak turbulence theory modification 3-49676
- nonlinear wave kinetics, wave packet formulation, weak turbulence 3-75314
- parametric instabilities, nonlinear saturation, turbulence spectrum, enhanced collision frequency 3-75355
- parametric instabilities and turbulent heating of plasma in the field of fast MHD wave 3-68049
- plasma engineering, monograph 3-49632
- pulsed plasma accelerator, struct. of current front and turbulent acceleration of ions 3-49718
- pulsed plasma accelerator, struct. of current front and turbulent accelerations of ions in fast regime 3-49719
- reflex discharge, double elec. probe, fluctuation meas. (*Russian*) 3-71954
- relativistic particle generation as in new and supernova stars (*Russian*) 3-65617
- resonant inhomogeneous layer, rel. to h.f. field increase 3-57909
- review, including elementary excitations, method of statistical averaging and effective turbulent collisions 3-75324
- saturation spectrum of ion-acoustic instability, turbulent field effects 3-49688
- semitransparent plasma, photon scatt. by Langmuir oscill., effect on spectra, astron. appl. 3-60611
- shock wave, laser light scatt. study 3-57912
- solar convection zone, appl. of dynamo eqns. and α -effect to mag. fields 3-53606
- spectral index determ. from digitally computed power spectra 3-71899
- stellar atmospheres, F, G and K type, microturbulence rel. to temp., luminosity and metal abundance 3-69932
- stochastic heating of particles in turbulent plasma, theory 3-40795
- strong trapped particle turbulence theory 3-71916
- Tokamak, turbulent heating, high electric field effect on design 3-60644
- toroidal, low- β plasmas, trapped particle scattering by electrostatic turbulence 3-63833
- toroidal turbulent heating expt. 3-71935
- turbulent heating (*Dutch*) 3-49729
- wakes, projectile Mach 16, electron density fluctuations, turbulent scattering spectra 3-79169
- weak, renormalization of wave-particle interaction 3-43656
- weak turbulence theory, modification due to perturbed orbit effects 3-43672
- weakly turbulent plasmas, oscillation centre quasilinear theory 3-63839
- N₂ gas flow interaction with plasma, turbulence, light emission fluctuations 3-68008

plasma waves

- see also magnetohydrodynamic waves; plasma oscillations
- absorption and emission in beam-plasma system 3-75335
- acoustic waves modulation of e.m. second harmonic amplitude, in a dispersive plasma 3-57892
- Alfvén, large amplitude, nonlinear interaction 3-65863
- Alfvén wave accel. of fast particles 3-46516
- Alfvén wave damping at high beta 3-49668
- asymmetric wave stress tensors and wave spin, Hamiltons variational principle 3-43586
- beam plasma discharge, h.f. wave transform. rel. to l.f. instabilities 3-49684
- beam-plasma interaction, density gradients and static magnetic field effects 3-79116
- beam-plasma interaction below threshold, wave spectrum obs. 3-71897
- beam-plasma scattering and wave amplitude meas. 3-79114
- beam-plasma system, captured electrons role in plasma waves (*Dutch*) 3-49685

plasma waves continued

- beam-plasma system, nonresonant, unstable, wave-wave coupling 3-71900
- beam-plasma wave interaction, electron velocity distribution function variation 3-68028
- Bernstein, electron cyclotron damping 3-49689
- Bernstein, large amplitude, decay instability, effect on ion temperature 3-79103
- Bernstein, linear temporal echoes 3-71893
- Bernstein modes, transformation from high frequency e.m. waves 3-57889
- Bernstein wave dispersion relation meas. 3-75376
- Bernstein-Greene-Kruskal waves, two-stream instability 3-49697
- BGK waves decay instability, unstable oscils. 3-49690
- bounded dense plasma systems, r.f. props. rel. to heating, resonances 3-68036
- bunching instability mechanism 3-63844
- charge density regular waves amplification and transformation in anisotropic waveguide 3-79136
- cold electron-cyclotron wave, nonlinear interaction of small resonant electron beam, simulation 3-54853
- collective effects in magnetoactive plasma 3-79133
- collisionless damping, Weisskopf-Wigner theory of line broadening 3-49678
- collisionless drift waves in toroidal hexapole, obs. 3-52514
- combined heating by electron beam and intense ion-cyclotron wave ion-cyclotron and electron beam combined heating 3-75399
- correlation functions in magnetoplasma 3-79131
- coupled waves in stratified plasmas, with tensor press. perturbations 3-54843
- current-driven modes in two-dimensional plasma configurations 3-68038
- cyclotron, nonlinear propagation in collisionless plasmas 3-75312
- cyclotron harmonic Bernstein-mode waves, nonlinear instability due to parametric interaction 3-54851
- cyclotron wave of finite amplitude, instability (*Russian*) 3-68029
- cyclotron waves, multiveLOCITY electron beam, interaction with electrodynamic systems (*Russian*) 3-67982
- decay instability threshold in inhomogeneous plasma 3-52509
- dispersion and stability in presence of Coriolis force 3-75351
- dispersion function approximations 3-57905
- dispersion relations, decay and parametric instabilities, anomalous absorption and heating 3-68033
- dispersion theory, inhomogeneous medium, h.f. elec. field. (*Russian*) 3-46539
- double plasma device investigation 3-40045
- drift MHD wave instabilities due to magnetic drift resonance 3-46528
- drift wave turbulence, expt. study using digital spectral analysis techniques 3-75354
- drift wave-electron interaction, electron trapping instability effect on toroidal confinement 3-54868
- drift waves, h.f. microturbulence influence 3-75373
- drift waves, parametric excitation and suppression by lower hybrid fields 3-75374
- drift waves dynamic stabilisation by h.f. e.m. fields 3-79125
- drift waves growth rate, critical shear in nonuniform current carrying plasmas 3-75379
- drift waves in nonuniform current-carrying plasma, critical shear and growth rates 3-49696
- drift waves stabilisation expts. 3-75372
- Earth's magnetosphere, Ogo 5 obs. of ion cyclotron waves in polar cusp 3-56227
- electroacoustic waves interaction with e.m. waves in laboratory quiescent plasma 3-75368
- electron, excitation, propagation, free-streaming electrons obs. 3-71898
- electron, free streaming obs. 3-57921
- electron beam interaction with plasma, meas. of evolution in phase space, cyclotron wave damping 3-49652
- electron cyclotron harmonics emission from non-Maxwellian plasma 3-46537
- electron cyclotron waves excitation by high-current-counter streaming electron beam 3-75342
- electron energy distribution evolution due to trapping in the wave potential 3-75369
- Electron fluctuations and transport in toroidal plasmas 3-67995
- electron plasma wave, nonlinear saturation and harmonic generation 3-54849
- electron plasma wave, side-band instability studied by launching small test-wave 3-57913
- electron waves, influence of low frequency fluctuations 3-57917
- electron waves, nonlinear Landau damping, weak turbulence theory modification 3-49676
- electron waves, oscillating two-stream instability, nonlinear stabilisation 3-71901
- electron-wave amplitude oscillation due to an initial spatial disturbance 3-57919
- electronic in inhomogeneous plasma, obs. of effect of induced transparency of barrier 3-49683
- electronic longitudinal modes propagation in non Maxwellian plasma obs. 3-79139
- electrostatic, coherent, interaction with particles trapped in mag. field 3-75361
- electrostatic, frequency exceeding gyrofrequency in the magnetosphere, propagation, instability 3-69671
- electrostatic, in nonuniform warm plasma 3-60606
- electrostatic, instability with nonlinear Landau effect 3-60603
- electrostatic, low frequency, stability, energy principle 3-75349
- electrostatic, reflection from a plasma density gradient 3-75317
- electrostatic diffusion modes, stimulated back scattering of radiation 3-79108
- electrostatic direct nonlinear coupling with e.m. waves 3-63837
- electrostatic ion cyclotron harmonic wave coupling in a spiraling electron beam-plasma interaction 3-40782
- electrostatic microturbulence in magnetised plasma 3-75359
- electrostatic modes excitation, power absorption in nonuniform collisionless magnetoplasma 3-63852
- electrostatic modes excitation, transport and particle scattering 3-67993

plasma waves continued

- electrostatic modulational instabilities due to resonant particles 3-75362
- electrostatic surface modes of a toroidal plasma 3-63842
- electrostatic surface wave parametric excitation in plasma-layer 3-79110
- electrostatic surface waves parametric excitation in plasma layer (*German*) 3-71887
- electrostatic turbulent waves effects on trapped particles in low- β toroidal plasmas 3-63833
- e.m. surface wave instability, in bounded plasma stream 3-63821
- energy recovery from energetic plasma stream by travelling waves 3-49742
- excitation, nonlinear damping, parametric instability theory 3-68035
- excitation of transverse extraordinary mode in inhomogeneous magnetoplasma 3-49674
- explosive in stabilities stabilisation by nonlinear frequency shifts 3-49709
- explosive instabilities of waves, dissipation and phase effects 3-49707
- explosive instability and soliton generation 3-52517
- finite amplitude, in scattering expts. 3-75334
- finite amplitude and solitary, in anisotropic waveguide, nonlinear theory 3-79135
- five wave interaction, enhancement of optical or microwave radiation by nonlinear coupling to explosively unstable plasma waves 3-49708
- flute instability, l.f., in bounded plasma column 3-63830
- heating, collisionless, of plasma ions by ion beam, nonlinear interaction of waves 3-49736
- h.f., in upstream solar wind, radiation emission 3-51282
- h.f. electrostatic waves in magnetospheric plasmas 3-53541
- impact waves obs. with laser apparatus (*Czech*) 3-57938
- inhomogeneous beams eigenmodes 3-79122
- inhomogeneous system, parametric scatt. instabilities rel. to laser penetration 3-68052
- ion acoustic, excitation in positive column intensity distrib. in k-space, meas. 3-52507
- ion acoustic, Green's functions study 3-79142
- ion acoustic, modified Korteweg-de Vries eqn. 3-79141
- ion acoustic, nonlinear excitation in bounded plasma (*Russian*) 3-46538
- ion acoustic, nonlinear Landau damping and wave modulation 3-79140
- ion acoustic and h.f. electron, generation and suppression in beam-plasma system 3-75363
- ion acoustic and Langmuir, parametric excitation 3-75360
- ion acoustic damping, ion neutral collisions 3-79138
- ion acoustic in boundary layer at a conducting sphere, phase velocity meas. 3-57915
- ion acoustic instability, electron trapping inability for stabilisation 3-49701
- ion acoustic instability, temperature gradient driven 3-75375
- ion acoustic instability in He positive column 3-49695
- ion acoustic nonlinear interaction with radiation in optically active media 3-49662
- ion acoustic resonances obs. in RF power absorption expt. of a bounded plasma in the electron and magneto-ion domain 3-40790
- ion acoustic solitary wave propagation in collisionless plasma, ion temperature effect 3-75319
- ion acoustic wave response to an impulse disturbance 3-57920
- ion acoustic waves, collisionless damping 3-79099
- ion acoustic waves due to resonant electrons, modified Korteweg-de Vries equation 3-46533
- ion acoustic waves enhanced damping due to harmonic generation 3-79143
- ion acoustic waves in single-ended Q device 3-75365
- ion Bernstein modes excitation and propagation 3-75367
- ion Bernstein modes nonlinear amplification in Tokamak plasma 3-46545
- ion Bernstein waves, dispersion, cyclotron damping 3-75315
- ion cyclotron, finite amplitude waves, excited by external plates, decay characteristics 3-54865
- ion cyclotron, resonant inhomogeneous layer, h.f. field increase 3-57909
- ion cyclotron harmonics excitation by ion injection 3-75366
- ion cyclotron wave, coil-to-plasma coupling, effect of inhomogeneous density profile 3-46544
- ion cyclotron wave excitation, associated ion heating, by two counter-streaming electron beams 3-40791
- ion cyclotron wave generation, plasma density profile effect 3-71895
- ion cyclotron wave instabilities in Ar plasma 3-75370
- ion cyclotron waves dispersion and energy relations 3-79193
- ion sound turbulence and the theory of anomalous resistivity 3-57883
- ion wave damping and collision frequency determination 3-79088
- ion wave detection in electron-beam-plasma interaction by optical correlation 3-49680
- ion wave dispersion in presence of finite-amplitude electron-plasma wave 3-40777
- ion wave turbulence, current-driven, electron drift velocity and frequency meas. at onset of instability 3-79084
- ion-acoustic, MHD and e.m. instabilities of a finite anisotropic plasma with hot electrons 3-40779
- ion-acoustic, nonlinear, resonance frequencies, expt. 3-75323
- ion-acoustic, parametric decay instability, stochastic ion heating 3-54864
- ion-acoustic, second harmonic, amplitude oscillations obs. 3-71904
- ion-acoustic and drift, in weakly collisional plasma, temp. perturbations effect 3-40780
- ion-acoustic and electron, formation from parametric decay of obliquely incident radiation 3-60599
- ion-acoustic instability, and associated multimode phenomena 3-63832
- ion-acoustic instability causing anisotropic turbulence in a collisionless shock 3-57906
- ion-acoustic instability in current carrying plasma, saturation spectrum 3-49688

plasma waves continued

- ion-acoustic solitary wave expts. 3-71912
- ion-acoustic turbulence, and anomalous resistivity 3-75357
- ion-acoustic turbulence due to relativistic electron beam relaxation 3-79119
- ion-acoustic unstable waves, electric field fluctuations, probability distrib. meas. 3-52512
- ion-acoustic wave, in bounded plasma 3-63831
- ion-acoustic wave response to an impulse disturbance 3-68023
- ion-acoustic wave stability in infinite plasma with electric field 3-57901
- ion-acoustic wave train, or soliton decay instability, shock profile formation 3-46541
- ion-acoustic wave turbulence, current-driven 3-54850
- ion-cyclotron and electron beam combined heating 3-75399
- ion-ion hybrid resonance, dispersion relation 3-68011
- ion-ion hybrid resonances obs. in H₂ and D₂ plasmas 3-68020
- ion-sound pulsations, interaction with mag. pulsations in nonisothermal plasma 3-60602
- ionic Bernstein mode coupling with wake in magnetised plasma flow past an obstacle 3-40774
- ionisation, in inert gases, residual gas effect 3-79085
- ionisation, in longitudinally inhomogeneous plasma 3-75343
- ionisation, spatially growing, feedback controlled instabilities 3-79124
- ionisation wave instability, evolution, nonlinear effect 3-71889
- ionisation waves, non-linear stability (*Russian*) 3-54860
- ionisation waves, Pekarek-Krejci eqn., electron temp., density var. 3-68021
- ionisation waves dispersion curves measurement method 3-79170
- ionisational waves, in MHD generator, parametric two-dimensional study 3-75380
- ionospheric artificially induced plasma waves 3-51114
- ionospheric wave decay interaction obs. during topside sounding meas. 3-56266
- Landau damping, influence of transverse mag. field 3-52511
- Langmuir soliton, damping and amplification 3-52508
- Langmuir wave, nonlinear theory of modified decay instability 3-75311
- Langmuir waves, nonlinear Schrodinger eqn. 3-43675
- laser plasmas stability, wave modes excitation 3-66821
- laser radiation decay into ion-acoustic and reflected wave 3-49661
- launched waves on a beam-plasma system 3-43673
- linear mode conversion 3-71918
- long-wave oscill., damping 3-49715
- longitudinal, propagation in plasma with small temp. gradient 3-79087
- longitudinal and transverse modes in cold transcendent plasma, dispersion relations 3-79098
- longitudinal waves instability in collisional plasma 3-79120
- loop antenna, corner driven, in warm plasma, plasma wave radiation 3-67999
- lower hybrid resonance in an inhomogeneous cold and collisionless plasma slab 3-54854
- magnetosphere, plasma waves near plasmapause, S³-A obs. during 1971, December 16-17 storm 3-69686
- magnetospheric, at 2-3 mHz at 6.6 Earth radii 3-69698
- in magnetospheric disturbed polar cusp region, Ogo 5 meas. 3-51150
- magnetospheric substorms of 15 August 1968, Ogo 5 plasma wave observations 3-56123
- MHD, magnetoacoustic wave-traps, trap geometry and density variation effects (*French*) 3-63858
- MHD, nonlinear propagation in a magnetic neutral sheet 3-43668
- MHD, torsional, effect of resistivity gradient 3-57897
- MHD fast and slow wave characteristics in layered plasmas 3-46530
- MHD signals generation by pulsed acoustic wave in anisotropic conducting medium (*Russian*) 3-43665
- MHD waves decay by phase mixing in sheet-pinch in plane geometry 3-52505
- MHD waves decay by phase mixing in theta-pinch in cylindrical geometry 3-52506
- microturbulent magnetoactive plasma, weak nonlinear interactions, scattering of magnetoionic waves, polarised radiation, nonlinear conversion of microturbulence 3-75310
- mode coupling saturation in unstable plasmas, model equations 3-49693
- non-homogeneous plasma, three modes interaction 3-57907
- non-linear, effect of temp. and particle trapping on dispersion props. 3-52519
- nonlinear, evolution in a dissipative medium with dispersion, numerical simulation (*Russian*) 3-68031
- nonlinear, trapped electron sideband instability 3-57911
- nonlinear cold stationary waves stability 3-79127
- nonlinear cold waves stability 3-79092
- nonlinear ion acoustic waves with Landau damping 3-68014
- nonlinear quasi-monochromatic, amplitude modulation theory 3-79091
- nonlinear wave interaction and fluctuations 3-49706
- nonlinear wave interactions, computer simulation 3-79137
- nonlinear wave kinetics, wave packet formulation 3-75314
- nonlinear wave processes 3-71917
- nonlinear wave theory aspects of currents 3-68019
- nonlinear wave-particle interaction of whistler modes in nonuniform mag. field 3-75364
- nonlinear wave-plasma interactions, technique to display particle distribution function in phase-space 3-57944
- nonlinear waves in a waveguide partially filled with plasma 3-40775
- nonlinearly coupled modes with different linear damping rates, relax. 3-79097
- parametric downconversion from lower-hybrid frequency waves 3-79104
- parametric excitation, instabilities, anomalous dissipation in strong e.m. fields 3-75383
- parametric excitation at electron cyclotron harmonics 3-49716
- parametric excitation by laser, role of Landau damping, inverse-bremsstrahlung, ion wave (*Japanese*) 3-75390
- parametric excitation model by an imperfect pump 3-43674
- plane nonlinear waves in warm weakly dissipative plasma 3-79134

plasma waves continued

- plasma engineering, monograph 3-49632
- plasma-beam resonator, eigenmode spectra theory 3-63845
- propagation along static mag. field, parametric interaction 3-49699
- propagation in drifting warm plasma under Grad's thirteen-moment approximation 3-49705
- propagation in partially ionized chemically reacting plasma 3-46532
- propagation of frequency-modulated pulses in randomly stratified plasma 3-46535
- pseudowaves phase-space diagrams meas. technique 3-68087
- quasi-neutral solitary wave, stationary electrostatic solutions for a non-neutral two fluid model 3-57918
- quasicylindrical electrostatic waves, excitation connected with electron Bernstein modes 3-68022
- radar aurora, electrostatic ion cyclotron waves prod. type III spectra 3-61497
- refraction in ionosphere, topside sounding (*Russian*) 3-69664
- in relativistic electron gas 3-79130
- relativistic plasmas, longitudinal and transverse wave mode-mode coupling, energy conversion 3-75425
- repetitive explosive instabilities 3-49710
- small amplitude, book 3-71847
- solar wind, MHD waves (*Russian*) 3-69835
- space charge waves transformation on density discontinuities 3-79117
- spatial electron cyclotron damping 3-71891
- stationary nonlinear longitudinal waves in cold magnetoplasma 3-79128
- step heat waves dynamics 3-54861
- step-like density perturbations in collisionless Q-machine 3-75421
- strongly magnetised degenerate electron plasma with anisotropic pressure, dispersion relation 3-71896
- supercyclotron electrostatic waves in plasma with loss cone 3-49691
- surface wave propagation, density gradient and mag. field effects 3-75322
- surface waves in semi-infinite plasma, kinetic theory of parametric excitation 3-49714
- surface waves interaction with electron beams 3-79118
- surface waves parametric excitation in an inhomogeneous magnetized plasma 3-49721
- surface waves parametric excitation in inhomogeneous sheath 3-75336
- synchrotron instability, increments of longitudinal waves 3-40784
- Tonks-Dartner resonances, theory of subharmonic excitation in bounded plasmas 3-68013
- toroidal plasma modes, transport and particle scattering 3-60605
- trapping of particles, effect on nonlinear oscillations 3-75344
- turbulence, low amplitude, dispersive waves, weak instabilities, review 3-60610
- unidirectional energy transfer in nonlin. wave-wave interactions 3-48816
- unstable in beam-plasma system, Van der Pol model 3-75316
- unstable three wave coupling for time-dependent dissipation and coupling strength, soln. to random phase eqns. 3-49711
- Vlasov eqn., nonlinear, comparison of Fourier-Hermite and power transform solutions 3-46534
- wave-particle interactions in weakly turbulent plasmas, oscillation centre quasilinear theory 3-63839
- wave-trains in ideal isotropic one-fluid plasma, appl. to solar wind 3-47879
- waves and instabilities (conf. Innsbruck, Austria, Apr. 1973) 3-75345
- weakly turbulent, renormalization of wave-particle interaction 3-43656
- Ar grid excited, discontinuous phase velocity variation rel. to oscillatory damping 3-54855
- Hg plasma wave propagation in an ion sheath, effect on immersed antenna (*French*) 3-49712

plasmatrons *see plasma diodes***plasmons**

- Auger effect, dynamic theory, plasmon-electron interaction (*French*) 3-80138
- charged Fermi systems, rel. to long-wave fluctuations (*Russian*) 3-72413
- collisionless damping of plasma waves, quantum perturbation theory of plasmons 3-49678
- crystalline solid, Raman scatt. by collective excitations 3-80025
- diffraction gratings, sinusoidal, light absorpt. and re-emission due to surface plmons 3-74201
- electron gas, De Gennes correlation function method, appl. 3-46776
- electron mean free path, spatial variation near surface 3-41251
- excitation by X-rays, review 3-44047
- liquid alloy, rel. to partial struct. factors and electronic correl. functions 3-57981
- liquid metal, rel. to partial struct. factors and electronic correl. functions 3-57981
- magnetic semiconductor, plasmon-magnon interaction 3-79858
- metal, contrib. to surface energy 3-58315
- metal, surface-plasmon dispersion relation calc. using variational principle 3-55324
- metal, with overlapping d-, s-bands, acoustic plasmon excitation 3-58234
- metal-vacuum interface, image charge, surface plasmon contrib. 3-41246
- observation using X-rays within context of random phase approx. 3-41595
- plasmoid energy meas. in time-varying mag. field 3-52533
- plasmoid obtained from coaxial source, parameters depend. on polarity of central electrode 3-52526
- plasmoids formation, magnetic deflection of slow component (*Russian*) 3-71877
- plasmoids motion in non uniform mag. field (*Russian*) 3-71878
- plasmoids production from coaxial gun neutral gas effect on frequency and energy spectra (*Russian*) 3-71921
- plasmoids production with pulsed magnetic gate field (*Russian*) 3-71876
- semiconductor, damping of local vibrs. caused by reson. interaction with plasmons, theory 3-55297

plasmons continued

- semiconductor, plasmon-l.o. phonon system, mode-crossing behaviour 3-41188
 - surface, dynamical image interactions of charged particles, classical theory 3-75554
 - surface, principal mode, nonlocal shift in quantizing mag. field 3-50252
 - surface dispersion relation for plasma slab in magnetic field 3-60910
 - surface excitations in absorbing media 3-52885
 - surface magnetoplasmon obs. 3-52884
 - surface-plasmon dispersion and damping to pot. barrier shape, sensitivity calc. 3-41247
 - transition metal dichalcogenides, position of plasmon peaks from energy loss function 3-64618
 - transition metals, collective excitation phenomena (*Russian*) 3-68571
 - X-ray spectra following O bombardment 3-72768
 - Ag film, nonradiative surface plasmons roughness induced decay, emitted radiation polarisation 3-46811
 - Al, epitaxial, surface plasmons, LEED obs. 3-50257
 - Al, surface plasmon dispersion, electron energy loss expts. 3-50253
 - Al film, surface plasmon dispersion from LEED 3-50258
 - Be, Auger spectrum, plasmon energy gain and double ionization satellites 3-47340
 - Be, X-ray emission, appearance pot. spectroscopy, plasmon satellites 3-55699
 - Be single crystal, X-ray plasmon scattering 3-55227
 - C surface, soft X-ray incidence potential spectroscopy (*German*) 3-72763
 - Cu thin films, surface plasma oscillations 3-44133
 - In, liquid, energy gain of fast electrons reflected at surface 3-69114
 - InSb, surface magnetoplasmon-optic phonon modes, meas. 3-68687
 - K₂Pt(CN)₄Br_{0.3}·3H₂O, rel. to dielec. function 3-68958
 - Mg, refl., absorpt. and photoelec. meas. in vacuum u.v., surface plasmon excitation 3-44520
 - Mg, surface plasmon dispersion, electron energy loss expts. 3-50253
 - Mg, X-ray emission, appearance pot. spectroscopy, plasmon satellites 3-55699
 - Se, amorphous and crystalline thin films, volume plasmon energies, dependence on density 3-41221
 - Si, absence of plasmon gain satellites in Auger spectrum 3-58581
 - α -Sn and β -Sn thin films, volume plasmon energies, dependence on density 3-41221
 - Ti, single and polycrystal thin films, volume plasmon energies, dependence on density 3-41221
- plastic crystals**
- acetylene, deuterated, molecular reorientation, n.m.r. 3-79246
 - adamantane, self-diffusion in rotator cryst. phase, temp. depend. 3-64206
 - t-butyl bromide-h₂ and d₂, liquid and three solid phases, far i.r. spectra, lattice modes 3-55575
 - t-butylchloride, self-diffusion coeff. and rot. correlation time determ. 3-68872
 - carbon tetrabromide, shear strength 275 to 375 K, 320 K polymorphic transform. 3-79407
 - cyclohexane: nitroxide free radical, molecular self-diffusion, nuclear spin-lattice relaxation and dynamic polarisation 3-49854
 - cyclopropane, solid, and cyclopropane deuterate, molecular rotation determ. by p.m.r. and spin-lattice relax. 3-44346
 - dinitrocarbanion reorientation in alkali salts, i.r. and u.v. spectra 3-69003
 - halopropanes, high temp. isomers 3-72653
 - N-methyl acetamide crystal, molecular packing 3-43762
 - molecular rotation, nonperiodic, quasi-elastic neutron scatt. (*German*) 3-60679
 - neopentane, i.r. and Raman band shape analysis, mol. reorientation 3-75983
 - n-nonadecane, rotator phase transition, inelastic neutron scattering study 3-49853
 - pivalic acid plastic crystal, Brillouin and Rayleigh scattering determ. of phonon lifetimes, elastic and optical consts. 3-44409
 - p.m.r., mol. self-diffusion and reorientation, press. depend. 3-61005
 - polyethylene, molecular motion, n.m.r. line shape analysis (*German*) 3-61007
 - review of props. for substances with orientational freedom of mols. (*Polish*) 3-49856
 - succinonitrile, energy difference between gauche and trans isomers (*French*) 3-68172
 - succinonitrile, Rayleigh scatt. spectrum, interpretation (*French*) 3-47277
 - 1, 1, 1, 2-tetrachloro-2-methylpropane, solid, n.m.r. static and rotating frame relaxation 3-72538
 - tetrahydrofuran clathrate hydrate, far i.r. absorption, rotational oscillations 3-80062
 - two isotropically rotating molecules, magnetic dipolar interaction 3-46599
 - CsSH, rot. dynamics and phase transitions, neutron scatt. investigation 3-40852
 - CsSh in cubic phase, SH⁻ reorientation, neutron quasielastic scattering study 3-46597
 - NH₄Cl, phase II, reorientational motion of NH₄⁺ ions, neutron scatt. obs. 3-68173
 - NaSH, rot. dynamics and phase transitions, neutron scatt. investigation 3-40852
 - RbSH in cubic phase, SH⁻ reorientation, neutron quasielastic scattering study 3-46597
- plastic deformation**
- see also Bauschinger effect; buckling; creep; ductility; elastoplasticity; ferroelasticity; plastic flow; slip*
 - alkali halide, dislocation density, rel. to plastic deform. at initial stage of compression curve (*Russian*) 3-79360
 - alkali halides, refr. index and refl. spectra, uniaxial deform. effects 3-58528
 - alkali halides plastic deformation polarity, indenter penetration, X-ray irradi. (*Russian*) 3-40959
 - alkali metal halides, pure and Ca-doped, d.c. conductivity during plastic deformation (*German*) 3-53060

plastic deformation continued

alloy, machine parts, surface work hardening for increase of low cycle fatigue resist. 3-44632
 alternating bend testing, amplitude of deformation, meas. and control, resonant type e.m. machines 3-55913
 anisotropic metal, bulge test and simple tension test data 3-68311
 anisotropic metals, bulge caused by rolling 3-69271
 anisotropic shells, theory 3-70628
 anthracene crystals, carrier mobilities and lifetimes, electron traps, dislocation effects due to deformation 3-41182
 austenitic stainless steel, low temp. deformation, mag. susceptibility, martensitic transformation 3-50720
 axisymmetric shells deformed by fluid pressure, influence of back pressure on point of instability 3-54111
 bars, naturally uniformly twisted, plastic torsion and tension 3-40132
 beam, axially creeping with random material parameters, damped lateral vibration 3-42806
 beam with distributed load, deflexion effect on plastic collapse 3-57092
 bodies with variable geometry, plastic flow, extension of the methods of limit analysis 3-66563
 bonded half spaces, continuous distrib. of dislocations 3-68259
 bone, analysis as three component system with mineral phase, organic phase and pores 3-50771
 brass, deep-drawing into h.p. medium, plastic instability conditions 3-58700
 α -brass, prestrained, stress corrosion cracking and dislocation arrays (Japanese) 3-44577
 buckling, cylindrical panels, non-uniform axial compression, load distrib. rel. to crit. stress 3-45675
 buckling loads, nondestructive determination, elastic plates and bars 3-47494
 buckling of cylindrical shell subject to external fluid pressure 3-62506
 buckling under shear, diagonal stiffeners reinforcing clamped infinitely long plate, optimum distribution 3-57088
 ceramic specimens, miniature, high temp. tensile test 3-72961
 circular elastic-plastic columns, numerical study of uniaxial compression 3-51794
 circular plate, variable-thickness, limit loads accounting for transverse shear 3-57093
 composite, fibrous, strength, ductility, fibre-matrix interface effect 3-80454
 composite, plastic, C-fibre reinforced, hysteresis behaviour 3-80442
 composite, plastic deform. anisotropy and work hardening rate 3-76356
 composite beam elastoplastic deformation, models 3-80456
 composite beam elastoplastic deformation, quasihomogeneity problem 3-80457
 conical shell inversion, approx. energy analysis 3-48735
 conical shells, elastically constrained and stiffened, buckling anal., hydrostatic pressure, collocation method 3-45641
 constitutive eqns. rate type, for elastic-plastic solids under large deformation 3-48732
 constrained bodies, yield condition 3-70616
 creep deformation of solids, stress relaxation and time-dependent boundary conditions, numerical soln. 3-70626
 cyclic deformation processes, elastoplastic constitutive law 3-70609
 cyclic elastic-plastic deformation, methods of anal. kinetic characteristics, fatigue damage, crack development 3-55910
 cylinder, axially symmetric temp. field, shifts, influence of cylinder extremities (Rumanian) 3-70618
 cylindrical bar, longit. elastic-plastic final duration pulse propag. 3-70635
 cylindrical shell, three-layer, rigid-plastic direct design, Mises and Tresca yield conditions, variational problem (Russian) 3-70631
 cylindrical shells loaded by axial compression, circular hole effect on buckling 3-45672
 cylindrical specimen, friction coeff. estimation at interfaces (Polish) 3-59744
 diamond, natural framesite, relief polished striations 3-61323
 disclinations, continuous and discrete in anisotropic elasticity 3-64044
 dislocation cell size in deformed crystals 3-43760
 dynamic plasticity, macroscopic and microscopic aspects, review 3-49923
 dynamic plasticity under combined stresses, medium rate tension-torsion machine 3-48354
 edge buckling of cylindrical shells with low in-plane shear moduli 3-57087
 elastic-plastic continua, finite deformation, minimum principle, impulsive loading of rigid-plastic beams 3-70559
 elastic-plastic finite strain, geometrical concept of intermed. config. 3-54087
 elastic-plastic solids, stress/strain rates reln. 3-54109
 elastic/viscoplastic media, cylindrical plane strain wave propag. 3-57091
 elasto plastic media, shock wave structure (Russian) 3-42815
 elastoplastic rod, centrally compressed, with cross-like cross-section stability (Russian) 3-42795
 elastoplastic solid body weakened by two round openings, plane deformation (Russian) 3-42796
 extrusion, axial symmetric, determ. of geometry and force, variation calc. (German) 3-69325
 fading memory materials with internal variables, equilibrium state 3-66562
 fading memory materials with internal variables, general theory 3-66561
 failure under simple and composite stresses, deform. criteria 3-58686
 fatigue crack propagation, two theoretical models 3-46671
 FFTF fuel assembly, duct pressure response anal., stainless steel, ANSYS computer code 3-71293
 fibre-glass shells manufactured in vacuum, tensile and deforming characteristics (Russian) 3-64990
 fibreglass-reinforced composite, fracture possibility under transverse tension and shear (Russian) 3-64991
 finite plasticity, minimum principles 3-51793

plastic deformation continued

glass, static fatigue, crack formation, fracture (German) 3-69380
 glass fibre, mech. props., comp. (Polish) 3-44681
 glass reinforced plastic cylinders, thin walled load bearing capacity and deformation under torsional loading 3-58714
 glassy polymers, post-yield behaviour 3-46666
 glassy polymers, yield behaviour 3-46665
 graphite, reactor, neutron irradiation, tensile stress expansion (German) 3-71263
 groove formation in sheet metal under tension, forming limit diag. 3-76197
 hardening of G31, Cu and Ni by shock waves (Russian) 3-64898
 heat-resistant materials, failure at low number of cycles of simultaneous temp. and load fluctuations 3-44625
 heterogeneous system, review (Russian) 3-55752
 history, internal parameter descriptions, state of stress 3-74046
 hot torsion test, plotting of flow curves, effect of specimen dimensions on slope (German) 3-73098
 HTR helium environment, high temperature mechanical properties 3-67583
 indentation of plastic rigid halfspace by a smooth spherical stamp (Russian) 3-70623
 industrial metals and alloys, micro-yield region behaviour (Russian) 3-58648
 inert gas solids, mechanism 3-58076
 inhomogeneous, Johnston-Gilman's theory of yielding 3-49922
 ionic crystals, dislocation struct. development during plastic deform., deform. luminesc. obs. 3-40929
 ionic crystals, maximum and work analysis for slip on $\{110\langle 110 \rangle$ and $\{100\langle 110 \rangle$ systems 3-64090
 ionic crystals, uniaxial deform. and axisymmetric flow for slip on $\{110\langle 110 \rangle$ and $\{100\langle 110 \rangle$ systems 3-64091
 isotropic incompressible elastic-inelastic solids with temp. indepdt. response, dynamically possible finite deformations 3-42800
 isotropic materials, local strains theory, variants for soln. of complex loading problems 3-55005
 Kapron monofilaments, breakdown surface, microdeformation, cracks, scanning electron microscope studies (Russian) 3-47480
 lamina, inherently aging, on flexible base, bending stresses under transverse forces (Russian) 3-45677
 laminated plastics, effect of interlaminar stiffness and strength, plane stress 3-73023
 liquid crystal, smectic-A, buckling instability of layers 3-49847
 lower yield stress rel. to dislocation mobility 3-68313
 lunar anorthosite rocks, natural exoemission, recrystallisation, deform. history 3-77007
 materials with memory, thermomech. coupling, history of temp. gradient, deformation gradient and temp. 3-70766
 metal, cyclic deform. at high temps., math. interpret. 3-69311
 metal, cylindrical specimen, cross rolled, internal stresses produced by disloc. 3-69302
 metal, delay of yield and hardening in high-speed deform., model 3-76222
 metal, frictional forces deform. chars. generation under influence of surface-active lubricants (Russian) 3-58079
 metal, hysteretic internal friction due to attractive dislocation junction breakdown 3-79430
 metal, investigation using exoelectron emission 3-48585
 metal, laser beam irradiat., mech. deform. and disruption (Russian) 3-40958
 metal, plastic anisotropy, Lankford calc. (French) 3-72912
 metal, plastic deform. degree assessment in crater with ball imprint, etch pit method 3-64938
 metal, short-time stress/strain characteristic, temp. depend., thermally activated models 3-69309
 metal, softening during supercond. transitions (Russian) 3-72415
 metal, stress wave propagation, obeying the constitutive eqn. of the Johnston-Gilman type 3-64088
 metal and alloy shear props., high strain rates 3-58787
 metal rings in plastic states destruction (Russian) 3-80305
 metal SEM obs., chip formation during machining, dynamic viewing 3-58610
 metal surfaces, impact boundary instability (Russian) 3-64086
 metal thin films, fatigue phenomena under boundary friction 3-41109
 metallic bodies, transition from static contact to displacement (Russian) 3-55017
 metals, force-distance diagrams, dislocation-obstacle interactions rel. to deformation 3-49893
 metals, load-elongation curves of pure b.c.c. structure at low temp. 3-72118
 metals and alloys, magnetic anisotropy meas., indirect method of grain struct. determ. 3-53226
 methane, solid, deform. mechanism and fracture behaviour (Russian) 3-79412
 Mg-Cd (10 at.%) twinning contrib. to tensile deformation at 293K, 77K (German) 3-52665
 micro-indentation method and apparatus for studies in temp. zone near brittle failure (Russian) 3-80514
 mineral powders, cold compaction, time-depend. deform. 3-47489
 multilayer cylindrical shell with non-isothermal loading, numerical analysis by incremental technique (Russian) 3-40133
 neck formation, effect on true strain at max. load, effect on longitudinal stress (German) 3-69254
 non-isothermal elastic-plastic, thermodynamic considerations of phenomenological theory 3-40129
 non-linear material beam, structural behaviour at finite deformation 3-54112
 nonhomogeneous circular plate, dynamical bending 3-70607
 nonlinear panels, equilibrium states, original imperfections influence 3-54114
 orthotropic shells, low shear stiffness, solvents in theory, force moments and stress functions 3-70630
 perforated tube, star-shaped profiles, stress conc. meas., photoelastic methods, internal and external pressures (Russian) 3-74053
 photostimulated emission, surveying of deformed metal surface, structural distortions 3-48406
 plane stress, yield criterion, second order effects, tension-torsion loading 3-62489

plastic deformation continued

- plastic shell, three-layer, free oscillation, boundary conditions, Bubnov-Galerkin method, effect of angle of layer anisotropy (*Russian*) 3-70632
- plastics, amorphous, post-yield behaviour 3-46666
- plate with external slits, elastoplastic deform. and failure under concentrated loads (*Russian*) 3-77827
- PMMA, biaxial orientation, birefringence, rel. to degree of deformation 3-71682
- PMMA, creep and low-cycle fatigue, hereditary theory 3-65015
- PMMA, glassy state, cyclically changing temps. effect during subsequent loading 3-55900
- polyethylene, high density, electron microscope, X-ray analysis of crystal distortion (*Russian*) 3-71692
- polyethylene, oriented, deform. mechanisms, tensile tests 3-58730
- polyethylene, tensile deformation, calorimetry 3-61216
- polyethylene, tensile deformation, effect on melting point, specific vol., vol. coeff. of expan. 3-80483
- polyethylene melt, stresses, periodic deformations, effect of vibration frequency and amplitude variations, Weissenberg rheogoniometer 3-76380
- polyethylene single crysts., by dislocation motion 3-40961
- polymers, deformability, wide temp. range, device for plotting thermomechanical curves, constant load, continuous heating 3-55915
- polymers, local stress distrib. and deformation props., effect of microcracks, network model 3-49928
- polymers, luminescence during deformation, breaking and friction, gas-discharge processes (*Russian*) 3-47313
- polymers, plastic relaxation via twist disclination motion 3-40972
- polymers amorphous, biaxial orientation, macromol. orientation distrib. function, rel. to birefringence 3-71682
- polystyrene, oriented, deform. mechanisms, tensile tests 3-58730
- polystyrene, craze morphology rel. to shear-band morphology 3-58732
- polystyrene, deform., fracture, crazing, shear bands interaction 3-55892
- porous bodies, elastic-plastic compressibility, pore vol. depend. 3-77830
- Prandtl Reuss materials, stress analysis on elastoplastic deformation (*German*) 3-65008
- pressing of thin rigid body into elasto-plastic medium, linearised approx. (*Russian*) 3-77831
- propagating deformation bands, disloc. velocity and density detn. 3-54965
- propagating deformation bands, velocity and density detn. 3-54966
- quantitative strain and stress state criterion, failure in the vicinity of sharp cracks 3-66568
- quartz, deform. dislocations, X-ray obs. 3-75539
- quartz, transmission electron microscopy obs. of dislocation structure 3-58038
- rectangular beam, elasto-plastic deform. under combined compression and bending stresses (*Italian*) 3-48733
- refractories, electron microscopy, slip bands, grain growth 3-72976
- residual stress distrib. calc. methods 3-48738
- rheonomic media, deform. instability effects, instantaneous hardening and deform. aging 3-42797
- rigid, plastic struct. at yield-point load, stability 3-51792
- rigid viscoplastic structures, dynamically loaded, lower bound theorem 3-70608
- rock dilatancy recovery upon unloading 3-58903
- rod, resistance analogies 3-80365
- sandwich circular plate, buckling beyond elastic limit (*Polish*) 3-59765
- sandwich shells of revolution nonlinear bending and buckling, finite element analysis 3-62490
- shallow shells, compression-bent, rigid-plastic collapse, limit analysis solns. 3-70620
- shell, shallow spherical, inelastic buckling under external pressure 3-48736
- shells, cylindrical with two adjacent circular cut outs, limiting pressure determ. 3-74050
- shells, nonlinear dynamic response under blast waves 3-42458
- spherical shells, rigid plastic, rate problem for finite deform. under hydrostatic press. 3-62498
- spring alloy, cold deformation, ageing, relaxation resist., elec. resist. 3-76210
- steel, acoustic emission, spectrum anal., deformation and crack propagation 3-47509
- steel, austenite, recrystallisation kinetics, Nb effect (*French*) 3-72872
- steel, austenite, transformation rel. to thermomechanical treatment (*German*) 3-76151
- steel, austenitic, high-Mn, 110G13L, fine structure after high-speed straining (*Russian*) 3-64836
- steel, austenitic, intergranular corrosion, Huey test (*German*) 3-76194
- steel, austenitic, stainless, deformed Type 316, microstructural characterization as function of deformation 3-47393
- steel, austenitic stainless, cyclic stress/strain curves in M_s - M_d range 3-64829
- steel, austenitic stainless, warm extruded, struct. and mech. props. 3-50749
- steel, automatic testing device, heat resistance, distortion due to temp. fluctuation 3-42531
- steel, balls, rupture testing, ultracentrifuge, rotating mag. field, stress at centre of ball, residual deformation 3-53304
- steel, carbon, ultrasonic vibro-indentation hardness, resistance to plastic deformation 3-41753
- steel, Cr-Mo-Ni, softening of austenite, effect of deformation to fracture by tensile stress (*German*) 3-72888
- steel, cracking rel. to δ -ferrite content 3-80280
- steel, embrittlement, 500°F, fracture toughness (*Japanese*) 3-76202
- steel, ferrite-class, substructure and its effects on mech. behaviour (*Russian*) 3-53225
- steel, G.TsK polycrystals, microstructure, effects of deformation, hydrostatic pressure, X-ray examination, dislocations (*Russian*) 3-55787
- steel, hardened high C, hardening in NaCl soln., annealing, uniaxial compression diag. (*Russian*) 3-41767

plastic deformation continued

- steel, heat-resistant, deform. and destruction in thermal fatigue and creep 3-64937
- steel, high tensile, effects of geometrical shape of sample (*Russian*) 3-76221
- steel, high-Mn, dislocation structure and strain hardening (*Russian*) 3-69218
- steel, high-Ni, martensitic transform. kinetics of deformed austenite (*Russian*) 3-80206
- steel, high-strength, hydrogenated, relax. effect on mech. props. (*Russian*) 3-80315
- steel, influence on struct. and mech. props. (*Russian*) 3-69265
- steel, internal friction rel. to thermomechanical treatment 3-80352
- steel, low C austenitic, high temp. creep, surface struct. (*Japanese*) 3-76168
- steel, low-C, effect of chem. heterogeneity on distortion during thermal cycling 3-80383
- steel, low-C, effect of interruptions in loading on mech. props. 3-55916
- steel, low-C, microyield region, dislocations, electron microscopy 3-80287
- steel, low-C, plastic instability phenomena (*French*) 3-69301
- steel, low-C, prestrained, temp. effect on mech. props. anisotropy 3-47427
- steel, low-C austenite, transform. to ferrite after small plastic strains 3-58615
- steel, mag. field induced rot. sphere method of mech. props. obs. (*Russian*) 3-80313
- steel, martensite, loading effect in macroelastic range on X-ray diff. linewidth (*Russian*) 3-61133
- steel, medium-C, cyclic loading, dynamic aging, struct. 3-80364
- steel, mild, cavitation erosion for low cavitation intensity 3-41751
- steel, mild, tubular specimens, precise meas. of plastic behaviour under combined torsion/axial force 3-76199
- steel, monotonic concentration factor, localised and gross plasticity effects 3-64903
- steel, of microstruct. below honed surfaces (*German*) 3-41743
- steel, phase anal. by Faraday method 3-75853
- steel, plastic bending of edge-cracked specimen 3-64897
- steel, quenched, tempered, fine struct. rel. to wear 3-80279
- steel, residual austenite behaviour during deform. (*Russian*) 3-41756
- steel, serrated grain boundaries form. during hot deform. (*Russian*) 3-80252
- steel, stainless, 18Cr-8Ni, rapidly deformed, temperature rises meas. (*Japanese*) 3-41781
- steel, stainless, mech. props. determined in high-speed extension (*Russian*) 3-53250
- steel, stainless, strengthening by deform., martensitic transform. and ageing 3-50731
- steel, strengthening mechanism, high-temp. thermomech. treatment (*Russian*) 3-80309
- steel, structural, tests for localized heating effects determ. 3-69436
- steel, surface layer under hydrostatic pressing, MoS₂ lubrication (*Russian*) 3-72896
- steel, wear resistance rel. to additions 3-80347
- steel, X-ray obs. of stacking faults, effect on resistance to plastic deformation (*Russian*) 3-69269
- steel bar reinforcement, fatigue strength, spot welding effect (*German*) 3-44638
- steel castings, Cr-Mo-V, creep-rupture investigations (*German*) 3-47400
- steel constructions, brittle failure and means of prevention 3-47428
- steel plate, notched, elastic stress distribution rel. to curvature 3-80370
- steel reinforcing, cyclic loading, Ramberg-Osgood type function 3-64935
- straight bar, deformation determ., discontinuous transverse loading (*Rumanian*) 3-74047
- strain curve relations in static and cyclical loading 3-80380
- strain gauge, direct measurement, uniaxial stress condition 3-73100
- strain gauge meas. of plastic deform. under tension (*German*) 3-65052
- superconductor, plasticity change in N-S transition, mechanism 3-79802
- surface phenomena during fracture and deformation in adsorption active media 3-50084
- surface phenomena in solids during course of deformation and failure 3-79557
- tension specimens under lateral press., fluid-press. eigenstates and bifurcation 3-62499
- thermally activated dislocation motion past point obstacle including dislocation shape effects 3-54969
- thin metallic shells under transverse loading, literature review (*Russian*) 3-76220
- transient thermal stresses in disc of linearly strain-hardening material 3-54107
- transversely-isotropic materials with memory, constitutive equations, reduced forms 3-70610
- two-dimensional finite, noncoaxiality implications 3-64965
- two-layered shell, dynamically loaded, elastoplastic deformation theory (*Russian*) 3-62496
- vertical cut stability in plastic media, wall collapse problems 3-74051
- viscoelastic material, circular twist disclinations 3-64041
- viscoelasticity, stress relax. at mech. deformations (*German*) 3-60767
- viscoplasticity, thin circular plate, dynamic yield surface, uniformly distributed transverse pressure 3-62488
- Ag, deformed by rolling, recrystn. kinetics from internal friction (*French*) 3-55029
- Ag, dislocation recovery before onset of recrystn. (*French*) 3-54999
- Ag, elec. resist. and thermo-e.m.f. meas. of recovery stages, defects contrib. (*Russian*) 3-79663
- Ag, local internal friction determ. during recrystn. (*French*) 3-55028
- Ag, recrystn., point defects influence, internal friction obs. (*French*) 3-64111
- Al, 6061-T6 rings, elastic-plastic expansion 3-80299

plastic deformation continued

- Al, cylindrical shell, dynamic deformation behaviour, compression wave 3-80374
- Al, effect on diffusivity, vacancy prod. by thermal jogs (*German*) 3-64218
- Al, energy scatt. of vibrs. after plastic deform. and annealing 3-55807
- Al, hot deformed, yield stress, dependence on subgrain size, texture and orientation (*Russian*) 3-41720
- Al, load relaxation studies of high purity polycrysts. 3-41748
- Al, microscopic discontinuities in surface layers 3-76224
- Al, plastic wave propag., tensile and compressive wave profiles 3-58660
- Al, polycryst., deform. nonhomogeneity, dislocation mechanism of slip 3-64846
- Al, polycryst., single [111] fibre texture development (*Japanese*) 3-61143
- Al, rapidly deformed, temperature rises meas. (*Japanese*) 3-41781
- Al, thermo-activation parameters (*Russian*) 3-44603
- Al alloy, 2024-T3, fatigue crack delay and arrest due to single-peak tensile overloads 3-58789
- Al alloy, cyclic concentration factor, localised and gross plasticity effects 3-64903
- Al alloy D16, microstructures during stabilized hot deform. stage (*Russian*) 3-53219
- Al alloy shells, cylindrical, stability to axial compression and external side pressure (*Russian*) 3-72915
- Al bicrystal, grain boundary dislocations after shear deform. 3-55826
- Al crystal, diamond scratched surface, cell structure, dislocations (*Japanese*) 3-72867
- Al single cryst., flow stress down to 1.4 K, temp. depend. singularities 3-52663
- Al single crystal, deform. rate depend. of yield limit (*Russian*) 3-72916
- Al single crystals, temp. depend. of strength, high plasticity phenomena, 1.4-300K (*Russian*) 3-55003
- Al-Mg alloy single crystals, crit. shear stress temp. depend., 1.6-300 K 3-64942
- Al-Mg-Si 6061 alloys, mechanical props. after very rapid heating, microstruct. changes 3-47405
- Al-Zn alloys, axisymm. extrusion, activation enthalpy and material consts. depend., relation to recrystn., substruct., mech. props. 3-47403
- Al-Zn-Mg alloys, axisymm. extrusion, activation enthalpy and material consts. depend., relation to recrystn., substruct., mech. props. 3-47403
- Al-Zn(50 wt.%), supersaturated, precip. process, plastic deformation effects (*Polish*) 3-50690
- Al₂O₃, abrasion, debris, microstrain, X-ray exam. 3-69357
- Al₂O₃, fracture process and crack struct. 3-72957
- Al₂O₃, scratching, near surface microplasticity, damage penetration 3-80420
- Ar, solid deform. mechanism and fracture behaviour (*Russian*) 3-79412
- As-se glass, thermal expansion coeff., glass transition temp. and deform. point (*Japanese*) 3-79510
- Au, deformed, P₄ peak, model interpret. (*French*) 3-55027
- Au, dislocation recovery before onset of recrystn. (*French*) 3-45999
- Au, elec. resist. and thermo-e.m.f. meas. of recovery stages, defects contrib. (*Russian*) 3-79663
- BaSO₄, barite, rel. to longit. u.s. propag. vel. and twin orientation 3-46663
- Be, elec. resist. variation during recovery kinetics (*Russian*) 3-69266
- Be single cryst., deformation under laser action, defect obs. (*Russian*) 3-52661
- Bi₂Te₃-Bi₂Se₃, linear expansion coefficient, mechanical props. 3-75628
- C fibre, band like plane smoothing rel. to extension velocity (*German*) 3-76373
- C fibre, microstructural changes induced by plastic deformation at elevated temperatures 3-53286
- CaS, colour centre formation, optical absorption spectra characteristics (*Russian*) 3-76032
- Ca₂SiO₄, crystal defects, $\beta \rightarrow \gamma$ polymorphic transition 3-72192
- Cd-Zn alloy single crystals, crit. resolved shear stress, temp. and conc. depend. 3-58069
- Co-Ni-Mo-Cr alloy, structural mechanisms (*French*) 3-53211
- Cr-Fe(45 at.%) alloy, deform. mechanism and low temp. embrittlement (*Russian*) 3-41757
- Cr-Ni alloy, stress relaxation resist. rel. to training loading, 850°C 3-80368
- Cu, cubic centred, axes of anisotropy and work hardening rates 3-68311
- Cu, deformed in polyslip, structure sensitive recovery 3-76172
- Cu, deformed in wide range of loading rates, substructure (*Russian*) 3-44568
- Cu, discrepancy between sp. ht. and stored energy data 3-64186
- Cu, effect on diffusivity, vacancy prod. by thermal jogs (*German*) 3-64218
- Cu, elec. resist. and thermo-e.m.f. meas. of recovery stages, defects contrib. (*Russian*) 3-79663
- Cu, force-distance diagrams, dislocation-obstacle interactions rel. to deformation 3-49893
- Cu, high temp. creep, surface struct. (*Japanese*) 3-76168
- Cu, high temp. deform. mechanisms 3-76223
- Cu, hydrostatically extruded, heavy deform. influence on UTS and elongation (*Russian*) 3-72892
- Cu, plastic tensile deformation resistance, effect of grain size and deformation rate 3-69303
- Cu, polycryst., amplitude independ. internal friction and modulus defect 3-64114
- Cu, polycryst., deform. nonhomogeneity, dislocation mechanism of slip 3-64846
- Cu, pure, pressurizing effect 3-50717
- Cu, softening of single crystals deformed by rolling (*Russian*) 3-44573

plastic deformation continued

- Cu, surface indentations made by cone indenters on cube face, apex-angles influences (*Japanese*) 3-58169
- Cu recrystn. and recovery after heavy rolling, h.v. electron microscope obs. 3-50702
- Cu single crystal, deform. rate depend. of yield limit (*Russian*) 3-72916
- Cu strengthening curves for thread-like crystals, orientation dependence during deformation by elongation and torsion 3-80360
- Cu/Mo composite, stress deformation state, microhardness obs. 3-80369
- α -Cu-Al(As)(Ga)(Ge)(In) alloys, Portevin-Le Chatelier effect (*German*) 3-41746
- Cu-Be(1.87 wt.%) alloy, stress relax., deform. dynamics 3-64908
- Cu-P alloy, recrystn. and recovery after heavy rolling, h.v. electron microscope obs. 3-50702
- α -Fe, carbon interstitial diffusion retardation by lattice defects (*Russian*) 3-58143
- Fe, cast, torsional deform., hydrostatic press. 3-64886
- α -Fe, discontinuous Luders band propag. in blue brittleness temp. range (*Japanese*) 3-50699
- Fe, high-purity, substructure, effect of rolling, wire drawing and stretching deformation processes (*German*) 3-69204
- Fe, pure single crystals, electron irradiation effects, softening 3-68280
- Fe, technical, deform. and fracture mechanisms in complex stress state, low temp. 3-44624
- Fe crystal, crack apex, plastic slip 3-80376
- Fe crystal, surface layer scratch deformation, electron microscopy (*Japanese*) 3-72871
- Fe low temperature irradiation effects on deform. characts. 3-79376
- Fe single crystals, ZrH₂ refined, with C and N in soln., low temp. mech. props. 3-58696
- Fe-(23 wt.%)Ni-(0.38 wt.%)C alloy, martensite induced by plastic deformation, morphology and crystallography 3-44566
- Fe-Cr-Ni alloys, deform. recovery and recrystn. of austenite 3-69285
- Fe-Cu-Ti(C) alloys, micro- and macro-deform. resist., temp. depend. (*Russian*) 3-64835
- Fe-Ge alloy, texture, recrystallisation struct. 3-76177
- Fe-Mn alloy, form restoration process after bending, memory process 3-41784
- γ -Fe-Mn alloys, dislocation motion in antiferromagnetic structure 3-53009
- Fe-Mo alloys, yield stress and alloy softening, conc. depend. (*Japanese*) 3-41775
- Fe-Mo(3.5 at.%) alloy, steady state creep, Ar atmosphere, microstructure, internal stress (*Japanese*) 3-72906
- Fe-Ni alloy, form restoration process after bending, memory process 3-41784
- Fe-Ni alloys, effect on Invar phenomena (*Russian*) 3-58409
- Fe-Ni-C alloy, martensite burst in deformed and thermally stabilized austenite 3-64826
- Fe-Ni-C alloy, martensite form. during plastic deform. of metastable austenite 3-80209
- Fe-Ni(31.15 wt.%) alloy, effect on martensite burst kinetics 3-41782
- Fe-Si, shock loaded, struct. changes during heating (*Russian*) 3-80248
- Fe-Ti(0.16 wt.%) single crystals, orientation, temp. and strain rate effects on deform. 3-64909
- GaAs single crystals, bend, tension 3-75559
- GaP, deformation pot. const. for pure shear, double refraction obs. 3-40963
- Ge, dislocation form., structure, two beam tilt lattice image obs. 3-68263
- Ge, heating of electron-hole drops in inhomogeneous deform. field 3-79697
- p-Ge, plastically deformed, photoelec. effects and minority carrier lifetime 3-58279
- Ge:Zn⁺, excitation spectrum under uniaxial compress., symmetries and deform. pot. consts. 3-44439
- H₂, solid, brittle failure susceptibility, mol. orientation effect (*Russian*) 3-79419
- In single crystals, rel. to spasmodic creep, 78 and 180K (*Russian*) 3-64954
- Insb, effect of deformation on conduction band 3-58214
- KCl, abrupt, spasmodic nature, nonuniformity of internal stress field 3-75561
- KCl, F and F-aggregate centres 3-60725
- KCl, hot worked, strength and deformation behaviour 3-76252
- KCl, press forged, strengthening effects 3-45502
- KCl:Sr slip band internal structure by precipitation 3-52632
- KCl-Eu phosphors, radiation centres, effect on optical props. 3-76077
- Kr, solid, deform. mechanism and fracture behaviour (*Russian*) 3-79412
- LiF, abrupt, spasmodic nature, nonuniformity of internal stress field 3-75561
- LiF, preliminary deform. effects on cryst. stability (*Russian*) 3-55002
- LiF, single cryst., creep deform., dislocation climb, 650-750°C 3-55011
- LiF dislocation dynamics, single crystals, strain rate cycling and stress relaxation methods, 77 to 673K, velocity measurements 3-43799
- LiF:Mg, deform. hardening under simple slip conditions 3-58075
- LiNbO₃, crystal hypersonic waves at 9.4 GHz, associated power, displacement amplitude, deformation and stress (*Russian*) 3-68341
- Mg, compressed along c-axis, twinning deform. 3-80263
- Mg, rolling, recrystallisation, rel. to deformation temp. and purity (*French*) 3-69234
- Mg, single cryst., crit. shear stress temp. and rate depend. for basal slip, obs. and mechanism 3-80381
- Mg twinning contrib. to tensile deformation at 293K, 77K (*German*) 3-52665
- Mg-In solid soln. single crystals, conc. depend. (*Japanese*) 3-41776
- Mg-Li(8%) alloy, steel reinforced 3-73011
- MgO, bombardment damage due to Al₂O₃ microspheres 3-72128
- MgO, deformation effect on optical absorption 3-64697

plastic deformation continued

- MgO, pure crystals., dislocation dynamics and thermally-activated deform. 3-72081
- MgO, pure single crystals., edge and screw dislocation behaviour 3-72080
- MgO dislocation dynamics, single crystals, strain rate cycling and stress relaxation methods, 77 to 673K, velocity measurements 3-43799
- MgO single crystals., Fe²⁺ and Fe³⁺ doped, edge and screw dislocation behaviour 3-72082
- Mg₂O₃ compacts, densification during hot-pressing, plastic deformation model (*Japanese*) 3-47454
- Mo, He⁺ ion implantation and re-emission temp. depend. and surface deformation 3-79394
- Mo, impure, temp. and strain rate influence on plasticity and stress/strain diagram appearance (*Russian*) 3-80344
- Mo, low-alloy, plastic deform. degree influence on struct. and mech. props. (*Russian*) 3-58625
- Mo, neutron irradiation and plastic deformation, recovery model critical testing 3-79382
- Mo, plastic strain influence on paramag. susceptibility of single crystals. (*Russian*) 3-79822
- Mo alloy, recrystallized, carbide segregation behaviour and effects (*Russian*) 3-55782
- Mo thin foils, in situ deform., 800 keV electron microscopy 3-50703
- Mo/Al fibre composites, deformation and fracture effect on brittle interfacial compounds 3-47457
- NaCl, compression along cubic face, etching, dislocation distrib. 3-75532
- NaCl, estimation of elec. charge carried by dislocations 3-72119
- NaCl, shear apparatus, simple slip on (110) and (100) planes (*German*) 3-46661
- NaCl single crystals, deformed, annealing, n.m.r. studies (*Russian*) 3-64093
- Nb, enhanced strain aging by cyclic deform., interstitial solute-moving dislocation interaction 3-50722
- Nb, high purity single crystal., tensile tests at 2.17-300 K (*French*) 3-55004
- Nb, interstitial effects on tensile behaviour, 20 to 1000°C (*French*) 3-80291
- Nb, low temp. deform. mechanisms, 20-300K (*French*) 3-79409
- Nb alloys with small alloying additions, resist. to light plastic deform. (*Russian*) 3-72890
- Nb He⁺ ion implantation and re-emission temp. depend. and surface deformation 3-79394
- β -Nb-Zr, deform. temp. depend., slip, twinning and dislocations rel. to yield and fracture 3-52662
- Ni, deformed in polyslip, structure sensitive recovery 3-76172
- Ni, grain boundary fracture mechanism (*Russian*) 3-61132
- Ni, high temp. creep, surface struct. (*Japanese*) 3-76168
- Ni, polycrystalline, cyclic push-pull, coercive force change within single load cycle 3-60979
- Ni-Al alloys with large vol. contents of γ' -phase, ageing, mechanism (*Russian*) 3-61162
- Ni₃(Al,W) single crystals, yield stress, dislocation rearrangements 3-80298
- NiAl single crystals., stoichiometric, steady-state creep, orientation depend. of deform. mode 3-64913
- Ni₄Mo alloy, twinning for ordered phase, slip in disordered phase 3-79408
- Pb, exoemission obs. under recrystalliz. conditions 3-69146
- Pb, in supercond. transition, temp. depend. due to electronic drag of dislocations 3-41285
- Pb bar, exptl. study of plastic wave propagation, meas. of stress and strain histories 3-41752
- RbCl, first-order recovery, migration of Sr²⁺ impurity-vacancy dipoles 3-43902
- Sb₂Te₃-Bi₂Te₃ linear expansion coefficient, mechanical props. 3-75628
- Si, deformed crystals, dislocation structure, surface and bulk layers, electron microscopy (*Russian*) 3-40922
- Si, deformed layers with different orientations and dopants (*Russian*) 3-52628
- Si, dislocation struct. during stage II 3-58074
- Si, exoelectron emission, temp. effects, extended and abraded mat., activation energy (determ.) (*Russian*) 3-53170
- Si, microdeform. of surface layers in brittle transition temp. region, surface-volume dislocation interactions (*Russian*) 3-79411
- Si, prod. of donor and acceptor centres, Fe atoms influence on elec. props. 3-41157
- Si single crystals, dynamical yielding 3-79416
- Ti, under static and cyclic loading (*Russian*) 3-41762
- Ti alloy, effects of geometrical shape of sample (*Russian*) 3-76221
- Ti alloy, fatigue failure, creep resistance, temp. depend. 3-76212
- Ti alloy, high-strength, strengthening and rupture characteriz. 3-47429
- Ti alloy, two-phase, fatigue failure in vacuum (*Russian*) 3-41759
- Ti alloys, mech. props. determined in high-speed extension (*Russian*) 3-53250
- Ti alloys, strain curves, 20-400°C 3-58680
- Ti alloys, two-phase, microstruct. singularities of deform., rel. to ductility (*Russian*) 3-69216
- Ti and alloys, stress relaxation data interpret. 3-64926
- Ti-Fe alloys, conc. depend. (*Russian*) 3-58640
- TiCr₂, Laves phase, X-ray diffr. study 3-69238
- TiNi intermetallic, phase memory effect obs. (*Russian*) 3-80310
- γ -U-Mo, fast burst reactor fuel, deformation and fracture behaviour 3-63207
- UO₂, hyperstoichiometric single crystals., deform. model 3-55849
- V, He⁺ ion implantation and re-emission temp. depend. and surface deformation 3-79394
- V, highly deformed, point defects 3-44587
- W, hydroextrusion effect (*Russian*) 3-72922
- W, W-Cu-Ti and W-Re alloys, micro- and macrodeform. characts., foreign atom binding effects (*Russian*) 3-80271
- W microcrystals, interstitial plasticity, FIM study 3-60766
- W single crystals., struct. changes during plastic deform. and annealing (*Russian*) 3-58624
- W-Ta-Zr alloy, recrystallization, microstructure 3-76334

plastic deformation continued

- Y, h.c.p., deform. modes, 77-497K 3-64912
- Zn, cyclic deformation, dissipated energy 3-40962
- Zn, during friction in food-industry media (*Russian*) 3-40967
- Zn, effects on acoustic and elec. emission (*Russian*) 3-79413
- Zn, motion of basal dislocations, influence of thermal jogs 3-60736
- Zn, thermally activated glide of single crystals., 4.2 to 373 K 3-40957
- ZnSe, electric field effects, temp. depend. 3-58071
- Zr and alloys, stress relaxation data interpret. 3-64926
- Zr single crystals., compression parallel to c-axis, 78-1100 K 3-46659
- plastic flow**
see also ductility; rheology
 activation entropy w.r.t. Gibbs free energy and effective stress 3-64092
- anisotropic rigid/plastic materials, plane strain slip line theory 3-47469
- axisymmetric shells under impulsive loadings, viscoelastoplastic response 3-57086
- Bingham liquid, convective stability of vertical layer 3-60544
- bodies with variable geometry, plastic flow, extension of the methods of limit analysis 3-66563
- creep meas. using helically coiled springs, Bingham flow 3-45422
- electrohydrodynamic flow of a visco-plastic fluid (*Russian*) 3-43608
- extrusion, material behaviour influence on force requirements and velocity (*German*) 3-41795
- filamentary materials under plane stress 3-51790
- halide laser windows, press forged, mech. props., grain size and alloying depend. 3-73786
- hot rolling, math. predictions, temp. distrib. effects 3-80339
- ideally plastic orthotropic material, general plane problem for stress and velocity fields (*Russian*) 3-64087
- ionic crystals, uniaxial deform. and axisymmetric flow for slip on {110}<110> and {100}<110> systems 3-64091
- landslides and avalanches, static and kinematic solns. 3-40128
- materials with different tension, compression and yield strengths, stress-strain relations 3-45674
- metal, b.c.c., struct. factor changes near ductile/brittle transition (*Russian*) 3-55753
- metal, direct study by X-ray motion picture filming 3-76402
- metal, hot torsion testing for flow stress determ. 3-76416
- metal particles, dislocation generation during early stage sintering 3-69243
- metallic plates, yielding in front of through cracks in pure bending 3-76382
- metals, load-elongation curves of pure b.c.c. structure at low temp. 3-72118
- metals and alloys, superconducting phase transition rel. to plastic properties 3-55355
- microyielding in cyclic loading using time monitoring technique 3-41747
- nonlinear thermoelastoplastic and creep analysis by finite element method 3-66570
- orthotropic materials, stress and velocity field eqns. for plane flow (*Russian*) 3-66567
- plate, impulsively loaded, nonoccurrence of von Mises yielding 3-70636
- polymer flow between calender roll, force and energy parameters 3-61218
- polymeric plates, yielding in front of through cracks in pure bending 3-76382
- sandwich circular plate, buckling beyond elastic limit (*Polish*) 3-59765
- solid solution hardening in crystals with randomly distributed solute atoms 3-41710
- spinel based ceramic/ceramic composites, plastically deformed, microstruct. features 3-76343
- steel, eutectoid-composition, finely spheroidized, thermal mech. treatments influence 3-53258
- steel, low-C, pressurized, Portevin-Le Chatelier effect 3-80289
- steel, microhardness indentations method for irregularity study, fracture zone 3-76399
- steel, torsional prestrain effect on Bauschinger effect 3-64928
- strip, weakened by array of holes, uniaxial tension, initiation and propagation of plastic zones 3-70611
- superplastic, activation energy determ. 3-60765
- superplastic alloys, diffusion-accommodated flow 3-40964
- thermally activated dislocation motion, selection methods 3-64052
- ultimate strength and plasticity of materials in complex stress state, stat. criteria 3-58685
- Al, strain rate cycling, thermally activated flow, 77-403 K mobile dislocation density (*Japanese*) 3-41741
- Al alloy 2024, axisymmetric extrusion, temp. and ram speed effects on flow pattern 3-53266
- Al-Ge (0.75 wt.%) single crystals., strengthening due to precipitates 3-46660
- Al-Mg alloy, cold work effect on strain rate sensitivity 3-69300
- Al-Mg alloys, discontinuous flow at high temps., Portevin-Le Chatelier effects 3-69299
- Al-Mg-Zn alloys, soln. softening effect of zinc at high temps. 3-64948
- Al-Mg(1 at.%) alloy, strain rate cycling, thermally activated flow, 77-403 K mobile dislocation density (*Japanese*) 3-41741
- Al₂O₃, hot-pressing, analysis with rate equations (*Japanese*) 3-50762
- Au-Cu(14 at.%) alloy, Portevin-Le Chatelier band characts. 3-80293
- Cd, critical shear stress, metal purity and temp. depend., single crystals. (*Russian*) 3-52660
- Cu, pure, pressurizing effect 3-50717
- Fe, cast, damping mechanisms rel. to graphite inclusions 3-64900
- Fe, plastic asymmetry phenomena 3-80295
- Fe-Mn alloy, fatigue cracked fracture toughness, sulphur content and grain size effects 3-69292
- FeAl single crystal., cooperative slip systems, orientation depend. 3-58073
- He, solid, force-displacement curve, motion of dislocations 3-79546
- KCl, pure and doped, flow stress, microhardness and rosette size intercomparisons 3-79415

plastic flow continued

- KCl:KBr mixed crystals flow stress, microhardness and rosette size intercomparisons 3-79415
 MgO, polycryst., microyield and fracture, model approach 3-58067
 MgO, polycryst., microyield and fracture, model interpret. 3-58068
 MgO single crystals, dynamic strain ageing characters. 3-58072
 Mo alloy, as cast, group VIII metals influence on struct. and props. (Russian) 3-55778
 NaCl, strength of attractive junctions formed by primary and secondary dislocations 3-60735
 Nb, dehydrogenated, dislocation struct. and high flow stress 3-80283
 Nb, interstitial effects on tensile behaviour, 20 to 1000°C (French) 3-80291
 Ni-Co alloys, dispersion-hardened, stacking fault energy effect on stress/strain curves 3-58670
 Ni₃Fe and Ni₃FeCr alloys, dislocation struct. at various strain hardening stages (Russian) 3-58626
 Ni₃Mn alloy, ordering effect on crit. shear stress magnitude (Russian) 3-44570
 Pb-In (4 at.%) alloy, flow stress in normal and supercond. states, thermal cond. model approach 3-68727
 Ta, strain rate cycling, thermally activated flow, 77-403 K mobile dislocation density (Japanese) 3-41741
 Ti alloys, commercial, low temp. deform. phenomena (Japanese) 3-44616
 U, high purity, high temp. plastic flow in α , β and γ phases 3-41772
 W, vacancy generation by rapid rate deform. at elevated temps. 3-80234
 Zn, coated with liq. metal, failure under brittle fracture to plastic flow transition conditions 3-50741
 Zn, critical shear stress, metal purity and temp. depend., single crystals. (Russian) 3-52660
 Zr, pre-exponential factor in rate eqn. 3-46662
 Zr single crystals, compression parallel to c-axis, 78-1100 K 3-46659

plastic strain see plastic deformation

plastic theory see plasticity

plasticity

- see also elastoplasticity; photoplasticity
 acceleration wave vel. in finitely deforming medium, Mandel inequalities extension (French) 3-54110
 beams and plates, rigid-plastic, in-plane displacement effects at boundaries 3-62493
 beetle shell design, rel. to composites 3-41807
 blocks with transverse sections in form of multiconnected regions, plastic torque 3-42798
 book on elastic and plastic solids and the formation of cracks 3-62485
 circular orthotropic plate, lower bound plastic analysis 3-48731
 circular plate, limiting equilibrium allowing for shear stress (Russian) 3-66566
 Coulomb material, rigid plastic, Prandtl stress fields, static extension (French) 3-70613
 cylindrical shell, flexural equilibrium beyond elastic limit (Russian) 3-62497
 cylindrical shell, rigid-plastic collapse 3-48737
 cylindrical shell, three-layer, rigid-plastic direct design, Mises and Tresca yield conditions, variational problem (Russian) 3-70631
 dislocation theory, constitutive equations for dislocation speeds 3-70621
 dynamic, 'plateau' existence using rate-type constitutive equations 3-40131
 elastoplastic crystal plates, symmetric and asymmetric flexure and eff. of stress distrib. (Russian) 3-42799
 failure diagram, calculation from energy criterion (Russian) 3-57056
 ideal, axisymmetric problem, exact soln. (Russian) 3-57097
 ideal, stress tensor calculation, viscous fluid flow applic. 3-45671
 inertia movement of plastic ring under impulse load (Russian) 3-45678
 longitudinal shear crack, steady motion in narrow plastic zone (Russian) 3-57055
 material and/or geometrically nonlinear structural analysis, evaluation of solution procedures 3-45673
 metals, yield surface shape, offset influence, different loading paths, slip theory model anal. 3-72889
 plastic material with sequence of ray-like loading paths vectors E and S relation 3-55006
 plastic shell, three-layer, free oscillation, boundary conditions, Bubnov-Galerkin method, effect of angle of layer anisotropy (Russian) 3-70632
 plate with complex periphery, load capacity (Russian) 3-54113
 polymer combinations, plasticity elasticity phase boundary, effect of intermediate layer (German) 3-61215
 reinforced beam and plate, contact problem 3-59766
 rigid standard materials, duality of unit theorems (French) 3-40130
 rigid viscoplastic bodies, finite element analysis of dynamics 3-66564
 rigid viscoplastic structures, dynamically loaded, lower bound theorem 3-70608
 shell, axisymmetric, load capacity determ. under conditions of piece-wise linear plasticity (Russian) 3-57094
 shell, stiffened cylindrical, minimum weight optimisation using random search analysis (Russian) 3-62504
 shell intersections, dynamically loaded, approx. rigid plastic analysis 3-48739
 shock wave, spherical, in plastic compressible medium, temp. distrib. (Russian) 3-42826
 shock wave effect of viscous and plastic properties of medium (Russian) 3-57796
 stochastic analysis 3-54108
 strip, weakened by array of holes, uniaxial tension, initiation and propagation of plastic zones 3-70611
 structures, min.-volume design through variational principles 3-74045
 thermoplasticity, uncoupled, principles for stress rate, strain rate 3-77828
 thermoviscoplasticity, crystalline solids, unified theory 3-70619

plasticity continued

- thin shells, Ilyushin-Shapiro yield surfaces accounting for transverse shear 3-70614
 two-dimensional continuum with nonlinear characts., transient response and failure simulation 3-48729
 vertical cut stability in plastic media, wall collapse problems 3-74051
 viscoplastic media, oscillating MHD flows in a plane channel (Russian) 3-57820
 viscoplasticity, finite element soln. based on elastoviscoplastic constitutive relations 3-40098
 viscoplasticity, mechanisms affecting strain rate and temperature sensitivity 3-57090
 viscoplasticity, thermodynamic theory of rheological material with internal structure changes 3-57089
 viscoplasticity, thin circular plate, dynamic yield surface, uniformly distributed transverse pressure 3-62488
 yield surface for thin shells, effect of transverse shear stresses 3-45676
 yield surfaces curvature, dissipation rate as single-valued function of strain rates (German) 3-66569
 Cu, high temp. deform. mechanisms 3-76223
 p-Ge, whiskers, microplasticity due to dislocations 3-72299
 NaCl type crystals, calc. of thermoplastic and residual stresses 3-79417
 Ni alloy, u.s. treatment during vacuum arc melting, ingot struct. refinement, plasticity, corrosion-resistance (Russian) 3-53263
 Pb-Sb alloy, increase at supercond. transition, quenching and aging effects 3-55001
 Rh, thin plastic foil, electrodeposition, addition of H₂O₂ soln. to electrolyte 3-76461

plastics

- ABS, plated, atm. exposure effect 3-73065
 acrylonitrile-butadiene-styrene composite, review of processes and applics. 3-64981
 adhesive fibrous nonfabric material with polyurethane binders, thermomechanical props. 3-58715
 amorphous, post-yield behaviour 3-46666
 anisotropic rigid/plastic materials, plane strain slip line theory 3-47469
 Asbetextolit sheet exposed to high temps. on load-bearing zone surface, mech. failure 3-47472
 board, nonlinear viscoelastic, cubical approximation method of calc. (German) 3-65009
 Brillouin scatt. obs. of shear waves in Lexan plastic 3-80028
 caprolon, self-heating and thermal fatigue during cyclic compression 3-61220
 celluloid, photoplasticity, lateral contraction coeff., similarity condition (Polish) 3-61213
 composite, C fibre reinforced, shear damage effect on torsional behaviour 3-55856
 composite, C fibre reinforced plastics, bulk compressibility rel. to shear strength 3-53277
 composite, carbon fibre reinforced, hysteresis behaviour 3-80442
 composite, carbon fibre-reinforced, microhardness, depend. on indenter/fibre relative orientation 3-47459
 composite, glass reinforced epoxy resin, crit. stress intensity factors 3-55862
 composite, glass ribbon reinforced, fabrication and characteriz. 3-76348
 composite, glass ribbon reinforced, isotropy of strength 3-76349
 drawability, effects of temp. and punch speed 3-65000
 epoxy composite, glass fibre reinforced, adverse environmental conditions influence on resin/glass interface 3-64982
 epoxy laminates, glass fibre reinforced orthotropic characts. under plane stress 3-53274
 epoxy resin, cast, linear elastic characts. 3-58741
 epoxy resin, glass reinforced, with Vulkador A crosslinking agent, mech. props. enhancement 3-58709
 epoxy resin composite, CFRP, impact and shear strength 3-76363
 epoxy resin used for photoelastic models, mech. and optical creep (Polish) 3-61214
 fibre, light guides, application to optical instruments 3-51588
 fibre reinforced, fatigue failure mechanisms 3-73008
 fibre reinforced, microstructure rel. to processing dwell time 3-50768
 fibre reinforced epoxy resins, specimen and testing variables effect on fracture 3-55857
 fibre reinforced thermoplastics, high-strength, improved prod. method 3-69368
 foam, effect of cellular struct. on mech. props. 3-65014
 foamed plastic, transition radiation, 13-130 keV 3-56943
 foils, Al coated, for superinsulation packaging 3-62024
 glass fibre reinforced, flexural strength, optimum volume fraction 3-50765
 glass fibre reinforced, low-cycle fatigue strength and notch factor obs. 3-69373
 glass plastics, longevity of structures 3-55901
 glass reinforced, cylindrical shell, elastic core, torsional stability 3-80449
 glass reinforced, effect of dynamic loading on mech. props. 3-50776
 glass reinforced, interlaminar shear modulus, thermal conductivity 3-80445
 glass reinforced, shells of revolution, geodesic windings characteristics 3-80446
 glass reinforced, thermal expansion coeffs. at low and high temps. 3-47465
 glass reinforced, wound cylinders, residual stress distrib. 3-80447
 glass reinforced cylindrical shells, axial compression, optimal parameters for min. weight structure 3-80452
 glass reinforced plastic, creep and recovery, in uniaxial tension 3-58711
 glass reinforced plastic, effect of composition and porosity on tensile strength and elasticity 3-58713
 glass reinforced plastics, solution of boundary value problems using experimental and theoretical values of relaxation properties and pliability 3-58717
 glass Textolites, damping props. under bending vibrs., 213-363K 3-58763

plastics continued

- glass-plastic, ageing and media effects on struct., X-ray shadow microscopy obs. (*Russian*) 3-41814
- glass-reinforced, compressed, elastic constants, strength characteristics 3-73021
- glass-reinforced, dynamic loading, review 3-55899
- glass-reinforced, orthotropic shells, low shear stiffness, resolvents in theory, force moments and stress functions 3-70630
- glass-reinforced, resist. to long-term shear failure 3-55873
- glass-reinforced, stability, mech. loading, temp. effect of shear strength 3-70580
- glass-reinforced, surfaces of equicritical planar stress distrib., fourth degree polynomial description 3-55872
- glass-reinforced, winding, change in degree of anisotropy, elastic and strength props. 3-73024
- glass-reinforced plastics under high pressure for oceanography 3-69374
- glassfibre reinforced, mean thermal cond., elastic modulus, 4-77 K, 4-300 K 3-73702
- for holographic recording, thermoplastic photoconductor mats. improvement 3-77525
- laminated, effect of interlaminar stiffness and strength, plane stress, deformation characteristics 3-73023
- magnetic carrier type composites, short-time strength and deformability at high temps. 3-47463
- mechanical testing, monograph 3-53309
- melt, non-Newtonian flow, viscosity, molecular position change, temp. depend. (*German*) 3-65010
- metal-plastic adhesion band, shear strength determ., response to lubrication 3-73055
- multilayers, shock adiabats meas. (*Russian*) 3-80464
- Nylon 6, glass fibre reinforced, compressive creep and recovery 3-47456
- Nylon 6, glass fibre reinforced, tensile creep 3-47455
- nylon 6, plane bending fatigue, crack nucleation (*Japanese*) 3-80463
- penton film, molten, morphology, heat treatment effect (*Polish*) 3-53282
- Perspex, water-jet erosion of prestressed materials 3-72902
- phenol formaldehyde industrial resins, structural changes during heat treatment (*Russian*) 3-63603
- plastic nuclear track detectors 3-62247
- Plexiglas, laser-induced shock effects 3-43028
- Plexiglas, pressure in discharge channel produced by breakdown 3-55525
- plexiglas, symmetric branching of cracks 3-65007
- polycaprolactam, glass fibre addition rel. to mech. props. (*Polish*) 3-58710
- polycarbonate, track-etch radiography, alpha particles, protons, fast and thermal neutrons 3-67627
- polyester, fibre reinforced, breakdown mechanism in interface region by artificial weathering 3-41808
- polyester, glass fibre reinforced, impact strength 3-64980
- polyester and epoxide resin systems, ASTM standards 3-64983
- polyester dough moulding materials, fibre reinforced, stiffness and strength 3-73007
- polyethylene filled with wood flow, dielectric and thermophysical props. meas. 3-65006
- pyrocatechin-formaldehyde resins, structural changes during heat treatment, i.r. spectra (*Russian*) 3-63604
- reinforced with three dimensional woven multilayer glass fabric, deformation and strength characteristics 3-58712
- rubber reinforced, transition magnitudes and impact improvement 3-50783
- rubber reinforced thermoplastics, toughening behaviour 3-47481
- scintillation counters, review 3-77640
- Teflon FEP electrets, liquid charged, stability 3-68914
- thermally stable thermoplastics and molybdenum disulphide compounds, temperature dependence of friction, relaxation and autohesion 3-58753
- thermoplastic films, permeability of gases and vapours 3-69401
- thermoplastics, glass-reinforced, properties 3-61204
- thermoplastics, resist. strain gauge meas., current heating effect 3-50785
- unidirectional reinforced, creep and long-time strength compression 3-73019
- Vickers microhardness meas. diagonal length and indentation depth relaxation (*German*) 3-47525
- vitreous, fibres, determ. of strength limit for shearing, anal. method 3-53281

plated wire stores

- Magnetization creep in composite plated wires 3-75850

plates (anodes) see anodes**plating (electroplating) see electroplating****platinum**

- additive, in ZrC, thermionic emission 3-69131
- adsorbate interactions on (110) surface, H₂S, S and CO adsorption 3-41869
- adsorption and interaction of H₂, CO, i.r. spectroscopic study 3-79573
- adsorption of benzene, naphthalene, pyridine, LEED and work function investigations 3-55127
- adsorption of Co, O, CO₂, CFSO-BEBO calcs. 3-68501
- adsorption of H₂, O₂, surface anal. in flow system (*German*) 3-79571
- adsorption of H, electrical double layer study, modulated specular reflectance spectroscopy 3-55966
- adsorption of organic compounds, electrochemistry studies using modulation spectroscopy 3-55965
- atom, photoelec. cross-sections of γ -rays, L- and M-shell 3-67682
- bamboo structure, rheological props. under flexural loads 3-47426
- capsules containing low-boiling liquids, containment technique 3-39887
- catalysts, particle size distrib., dark field electron microscopy 3-73179
- chemisorption of O₂, sticking probabilities 3-75679
- chemisorption of O₂, sticking probability obs. as function of time 3-75678

platinum continued

- conical hot Pt film probes, limitations as oceanographic flow sensors 3-51201
- desorption, dissociation, adsorption of CO, electron induced, Auger spectra 3-55152
- desorption of H₂ from Pt surface, spatial distrib. 3-55154
- electrode, electroreflectance spectra, effect of I⁻ and (n-C₄H₉)₄N⁺ adsorption 3-47292
- electron induced desorption of H 3-55141
- energy loss of 2.0-MeV ⁴He ions, meas. 3-40944
- film, chemical vapour deposition for semiconductor devices 3-44547
- foil, Knight shift and spin-lattice relax. of ⁸Li, nucl. mag. dipole moment determ. 3-40409
- Frenkel pair prod. by electron irradi., threshold energy anisotropy 3-49907
- Frenkel pairs, cross section of radiation induced recomb. 3-72079
- hemispherical total emittance from hot wires as function of temperature 3-62021
- melt, free surface energy, contact angle, density, meas. installation, lying-drop method 3-73687
- nugget, composition, chromian aluminian magnetite, Rh alloys, Alaska 3-44763
- reduced resist. temp. scale based on (*German*) 3-59540
- resistance element, linear temp. bridge design, math. approach 3-51543
- resistance thermometer, as reciprocal Kelvin temp. sensor 3-77403
- specific heat meas., pulsed electron beam method 3-45447
- subthreshold radiation effects, Frenkel defects, recombination 3-68282
- superconducting, Knight shift and nuclear spin relax. calc. 3-55356
- surface, ion beam neutralisation by scatt., emission angle depend. 3-58576
- surface adsorbate interactions, S effect on catalytic CO oxidation 3-73166
- surfaces, single cryst., low- and high-Miller-index planes, H₂ + D₂ exchange, mol.-beam study 3-47599
- thermal expansion, cooperative meas. techniques from 1000-2600°C 3-48376
- thin film sputtered in Ar discharge, optical and mass spectrometric analysis 3-43961
- thin film sputtered in Ar/N₂ discharge, optical and mass spectrometric analysis 3-43962
- wetting of glass sessile drops, contact phenomena 3-58175
- wires, quenched, field ion microscopy and elec. resist. obs. of vacancy defects 3-43780
- wires, quenched, field ion microscopy and elec. resist. obs. of vacancy defects 3-43781
- Eu₃Ga₅O₁₂:Pt, dispersion like line shape rel. to Eu³⁺-Pt⁴⁺ two centre absorpt. 3-58536
- NaCl/Pt interface, charging and discharging currents 3-79769
- Pt thermal resistance, DTA cell block 3-73690
- Pt:⁵⁷Fe, foil, Mossbauer fraction, impurity-host to host-host coupling const. variation 3-68896
- Pt/Fe²⁺, Fe³⁺ electrochemical electrode reaction study by relaxation method 3-44723
- Pt/Fe(CN)₆⁴⁻, Fe(CN)₆³⁻ electrochemical electrode reaction study by relaxation method 3-44723
- Pt-GaAs interface, energy structure, Schottky barrier height, Fermi level 3-60916
- Pt-Si contact, heat treatment, alloyed layers, solid state reaction kinetics 3-69485

platinum alloys*see also platinum compounds*

- actinide-Pt phases, prep. and props. 3-46604
- lanthanide-Pt phases, prep. and props. 3-46604
- metallic glasses, bending deform., brittleness 3-41783
- rare earth-Pt, 7:3 phases, cryst. struct. and mag. props. 3-79274
- Au-Pt alloy structure using field electron and field ion microscopes (*German*) 3-57972
- CePt₃, low temp. specific heat and magnetic susceptibility measurements, crystal field model 3-46946
- CoPt, thermal neutron radiation damage, Mossbauer effect obs. on ¹⁹⁷Au 3-79958
- CrPt-Cr₃Pt transition with increasing Cr at%, ferrimagnetic-antiferromagnetic transition 3-64498
- Cu-Pt, disordered, electron diffraction study of short-range order diffuse scattering 3-63978
- Cu-Pt, origin of formation of one- and two-dimensional superlattices 3-68197
- Cu-Pt alloys, short-range order in hardened alloys (*Russian*) 3-69270
- CuPt, crystallographic ordering mechanism and modified microstruct. 3-80215
- CuPt, ordered, geometrical anal. of field-ion images 3-68196
- Fe-Pt, crack propagation during cathodic charging, role of Fe dissolution 3-43948
- Fe-Pt, martensite transform. near Fe₃Pt comp., austenite ordering effect 3-64822
- Fe-Pt, martensite transform. near Fe₃Pt comp., austenite ordering effect 3-69201
- Fe-Pt, ordered equiatomic, mag. and atomic struct., neutron and X-ray diff. (*Russian*) 3-68787
- Fe(Pd_{0.53}Pt_{0.47})₃, magnetisation and hysteresis curves at 77 K and 4.2 K, magnetic structure determ. 3-52996
- GdPt₃, ferromagnetic, hyperfine fields determ. by n.m.r. 3-79927
- LaPt₃, low temp. specific heat and magnetic susceptibility measurements, crystal field model 3-46946
- Mo-Pt system, homogeneous domains of superconducting phases (*French*) 3-58329
- Nb₃Au, Pt_{(1-x)A-15} type phases, superconductivity, structure and magnetic susceptibility 3-58334
- NdPt₃, low temp. specific heat and magnetic susceptibility measurements, crystal field model 3-46946
- Ni-Pt, mass-defect disordered alloy, phonon modes 3-64127
- NiPt, concentration depend. of magnetic hyperfine fields, Mossbauer effect of ⁶¹Ni 3-41457
- Pd-Ni, localised spin fluctuations, comparison with Pd-Cr, Pt-Cr low temp. mag. props. 3-68768
- Pd-Pt, absorption of H 3-55789

platinum alloys continued

- PtPt₃, low temp. specific heat and magnetic susceptibility measurements, crystal field model 3-46946
 Pt-Au, density of states in valence band from X-ray photoelectron spectra 3-79601
 Pt-Cr, localised spin fluctuations, low temp. mag. props. obs., Pd-Ni comparison 3-68768
 Pt-Ni-P, comp. depend. of glass transition temp. 3-68167
 Pt-W, anomalous mag. susceptibility and conc. depend. of supercond. transition temp. (*German*) 3-41286
 PtCo, dilute, nature of impurity ordering, near-neighbour, antiferro- and ferromag. 3-68767
 PtCo, interpretation of FIM image with atom probe 3-52595
 PtFe, dilute, nature of impurity ordering, near-neighbour, antiferro- and ferromag. 3-68767
 Pt₃Fe, Mossbauer spectra isomer shift, pressure depend. 3-72554
 Pt(II)/Pt electrodes, impedance study on LiCl-KCl eutectic 3-65090
 PtMnSn, Mossbauer obs. of hyperfine field at ¹¹⁹Sn site 3-68899
 PtSb₂, conductivity, Hall effect, thermoelectric power, Nernst-Ettinghausen effect obs. 3-68650
 PtSi-Al reaction, electrical and mechanical features rel. to Schottky diodes 3-64403
 PtSn n.m.r. measurements, energy band structure, Knight shift, spin-lattice relaxation time 3-41440
 U₂Pt_{1-x}, pressure induced loss of ferromagnetism; magnetisation curves, differential paramagnetic susceptibility 3-47095

platinum compounds

- see also *platinum alloys*
 phthalocyanine, γ -polymorph, band struct. and carrier mobility 3-79626
 CaPt(OH)₆, crystal structure (*German*) 3-79319
 Cu-Ni ores, X-ray spectrometric anal., segregation 3-48659
 K₂Pt(CN)₄Br_{0.3}·3H₂O, one-dimensional conductor, giant Kohn anomaly observation 3-43849
 K₂Pt(CN)₄Br_{0.3}·3H₂O, optical cond. and electron interaction 3-68958
 K₂Pt(CN)₄Br_{0.3}·nH₂O quasi one-dimens. conductor, ¹⁹⁵Pt n.m.r. and p.m.r., temp. depend. behaviour (*German*) 3-50482
 K₂Pt(CN)₄Br_{0.3}·xH₂O, low temp. phase transition, condensation of soft modes by Kohn anomaly 3-64177
 Li₂Pt(OH)₆, Na₂Pt(OH)₆, crystal structure (*German*) 3-79318
 Pd complex, cyclic olefin, bonding vibr. spectra obs. 3-78726
 Pd-Pt-H system, superconductivity, temp. depend. of relative electrical resistance 3-79793
 Pt complex, Cu(NH₃)₄PtCl₄, spin correl. functions from e.p.r. data 3-55458
 Pt complex, cyclic olefin, bonding, vibr. spectra obs. 3-78726
 Pt complex, K₂Pt(CN)₄Br_{0.3}·3H₂O, one dimens. conductor, ¹⁹⁵Pt Mossbauer effect 3-53044
 Pt complex, K₂[Pt(CN)₄]Cl_{0.3}·xH₂O, stability in wet and dry atmospheres 3-46627
 Pt complex, K[PtCl₃(C₂H₅)₂]H₂O, torsional potential for ethylene ligands 3-54656
 Pt complex, phthalocyanine, dynamics of triplet state in zero field 3-50846
 Pt complexes, K₂Pt(CN)₄Br_{0.3}·2.3H₂O and K₂Pt(CN)₄Cl_{0.3}·3.6H₂O, thermoelectric power 3-50185
 Pt complexes, vinyl-Pt, n.m.r., i.r. Raman data, coupling consts, hybridisation 3-75065
 Pt metal silicides and germanides, ordered pyrite structure, diamagnetism, semiconducting, valence electron conc. 3-40906
 PtC, Franck-Condon factors, r-centroids, α -averaging of Morse potential functions 3-78720
 Pt₄Cl_{m(g)}, formation from Pt_(s) and Cl_{2(g)} (*German*) 3-80539
 PtFe₂²⁺, force consts. and mean vibr. amplitudes 3-67771
 PtGe, cryst. struct. and linear thermal expansivities 3-68214
 PtGeSe with cobaltite structure, ternary variant of pyrite structure 3-60691
 Pt(II) azide complex, resonance Raman effect (*German*) 3-78775
 Pt(II) complexes, [X₂Pt(C₃H₅)₂], (X=Cl, Br), i.r. and Raman spectra, vibr. assignments 3-46300
 Pt(II) complexes, Magnus's green salt, e.p.r. study, impurity effects 3-53017
 Pt(N₂), rare gas and N₂ matrices, 14 K, i.r. study 3-78810
 Pt(N₂) complex in low temp. matrices, i.r. identification 3-46277
 Pt(N₂)₂, rare gas and N₂ matrices, 14 K, i.r. study 3-78810
 Pt(N₂)₂ complex in low temp. matrices, i.r. identification 3-46277
 PtO, Franck-Condon factors, r-centroids, α -averaging of Morse potential functions 3-78720
 PtSi, cryst. struct. and linear thermal expansivities 3-68214
 PuO₂-UO₂ nuclear reactor fuel elements, irradiated, data evaluation (*German*) 3-71310

pleochroism

- see also *dichroism*
 No entries

plexiglas see *plastics***plotters**

- digital, computer controlled, synthetic holograms, compensation of plot distortions 3-45776
 electric field, apparatus design 3-42503
 phase-plane technique 3-66121
 photographic method, computer true-perspective, three-dimensional plots 3-48460

plugs (electric) see *electric connectors***Pluto**

- interferometer obs. of 11.1 and 3.7 cm 3-56333
 observations at Padova and Asiago Observatories, astrometric programs (*Italian*) 3-61886
 polarimetry obs. 3-80981
 rotational axis orientation, model 3-47904
 survey of present knowledge 3-45039

plutonium

- atomic, Pu I and II ground multiplets, hyperfine structure 3-78414
 bend strength, room temp., of α -Pu 3-54540
 content of Japanese river water 3-69750
 criticality studies, Dow Rocky Flats Nuclear Safety Laboratory 3-63229
 decontamination of plutonia contaminated thermal reactor systems 3-57589

plutonium continued

- deposited in lungs, correction factors for different body builds between phantom and subject 3-73601
 diffusion in UC_x, high temp. 3-43298
 electron-paramagnon electrical resistivity, high-temp. behaviour 3-44062
 fuel, isotopic composition, calorimetric determ. prior to irradiation 3-71287
 fuel, recovery by fluorination process using BrF₃ 3-43289
 fuel, recycling, neutronics 3-57578
 fuel elements, buckling meas. from cooling-channel temp. coeffs. (*German*) 3-67588
 fuel recycling in PWR, reliability assessment of CNEN neutronic codes 3-49362
 fuel reprocessing, polarographic determination of small quantities in solution (*German*) 3-71325
 high-burnup solns., computer calcs. of critical parameter using two isotopic approx. 3-46153
 Interim Decay Storage Facility, upper Pu limit, transport and diffusion theory calc. 3-71298
 ionisation energy calc. 3-60376
 mass spectrometric determ. by isotope dilution method (*Czech*) 3-42708
 monitoring, nondestructive instrument techniques, criticality safety 3-63252
 nondestructive assay, criticality prevention, scrap recovery 3-63249
 nuclear fuel reprocessing, value from throwaway cycle 3-57575
 nuclear fuel technology, processing and fabrication technology 3-57576
 nuclear fuel technology, radiation exposure consideration in LWR fuel manufact. 3-57588
 phase transformations, α = β , cinematic obs. 3-47359
 phase transformations, β - α and γ - α quenching obs. 3-47360
 recovery from natural U irradi. fuel using tertiary amine extractants, anal. methods 3-57583
 recycle fuelled reactors, behaviour of transient Xe concentration as functions of core Pu fraction 3-49340
 recycled, fuel use in heavy water reactor, technical and economic feasibility (*German*) 3-71316
 recycled, optimal use as fuel, PWR example (*German*) 3-67598
 recycling in boiling water reactor, economic investigation (*German*) 3-67597
 self-irradiation damage obs. by positron annihilation 3-63194
 spherical metal assemblies, neutron importance, comparison of theory and expt. 3-71204
 subcritical fast reactor, reactivity meas., Pu fuel, rod drop method 3-71208
 subcritical fast reactor, reactivity meas., Pu fuel rod drop method 3-71208
 voloxidation for reprocessing 3-54539
 Pu-Be neutron sources, fabrication 3-62213
 Pu-U mixtures, criticality safety, effect of Gd, B-containing Raschig rings 3-63228
 Pu³⁺, electronic spectra, f-level intermediate spin-orbit coupling 3-69011
²³⁹Pu, ²⁴¹Pu, use in nuclear power stations (*German*) 3-46163

plutonium compounds

- factors affecting swelling at high temperatures 3-63198
 (Pu, U)₂ mixtures, exptl. examination after irradiation in HWR (*German*) 3-67614
 (Pu, U)₂O₂, early-in-life failures, release of fuel and fission products 3-63223
 (Pu, U)₂O₂ fuel rods, failed, effect of O₂ availability on expansion 3-63224
 Pu-U nitrate solns., computer calcs. of criticality factors based on exptl. data 3-46152
 PuAl₂, nuclear spin-lattice relax. of ²⁷Al, spin fluctuation effects 3-41441
 PuAs, ferromagnet, static magnetization 3-68774
 Pu(NO₃)₃ nuclear reactor criticality safety at pipe intersections (*German*) 3-67543
 Pu(NO₃)₄ solutions, slag geometry, criticality experiments 3-63197
 PuO₂, criticality safety in LWR fuel fabrication 3-57577
 PuO₂ aerosol, release during LMFBR large core disruptive accident, transfer to second containment, calc. models 3-71178
 PuO₂ sols, solvent extraction process, description 3-65039
 PuO₂/UO₂ fuel elements, electron microprobe analysis of radiation induced changes (*German*) 3-71311
 PuO₂-ThO₂ HTGR lattice, temp. dependence of infinite-medium neutron multiplication factor 3-49345
 PuO₂-ThO₂ lattice, temp. dependence of conversion ratio 3-71171
 PuO₂-UO₂, creepage under neutron irradiation up to 1000°C (*German*) 3-71324
 PuO₂-UO₂, nuclear reactor fuel, performance and design, GE BWR, Oyster Creek 3-67567
 PuO₂-UO₂-polystyrene mixtures, LWR, 7.6 wt% Pu, criticality expts., computer calcs. 3-46154
 PuWC_{1.75} ternary phase, cryst. struct. and comp. 3-44649
²³⁸PuO₂, annealing of self-radiation damage 3-79389
²³⁸PuO₂, annealed sample, self radiation damage due to alpha particles and recoil atoms 3-79388
²³⁹Pu, ²³⁸U oxide-fuelled LMFBR, calcs. of fission product poisoning 3-49356
 (U, Pu)-Co-O system, thermal diffusion mechanisms 3-63232
 (U, Pu)C pellets manufacture by reactive sintering (*German*) 3-43302
 (U, Pu)O_{2-x}, oxygen redistrib. behaviour 3-43308
 (U, Pu)O₂ pellets, sintering variable effects on chem. and phys. characteriz. 3-78379
 (U, Pu)O₂, fuel, cladding attack causes and control 3-78383
 (U, Pu)O₂, fuel fabrication, chem. process characteriz. 3-78380
 (U, Pu)O₂, LMFBR fuel rods, thermal and mech. eval. of oxide microstruct. 3-78381
 (U, Pu)O₂, thermoelec., resist., and u.s. centreline thermometry 3-45455
 (U, Pu)O₂ fuel, brittle fracture behaviour 3-43309
 (U, Pu)O₂ fuel, conservation eqns. governing porosity and actinide redistrib. 3-46145
 (U, Pu)O₂ fuel, irradi., O/M ratio effect on Pu redistrib. 3-46147

plutonium compounds continued

- (U,Pu) O_2 fuel pins, in-pile radial temp. profiles, simulation 3-46142
 (U,Pu) O_2 fuel pins, plutonium redistrib. considerations 3-46141
 (U,Pu) O_2 fuel rods, irradi., Pu and U diffusion 3-46143
 (U,Pu) O_2 mixed fuels, thermodynamic behaviour 3-57569
 (U,Pu) O_2 pellets, parametrically designed, atmospheric stability obs. 3-78382
 (U,Pu) O_2 pellets, quantification of processing parameter effects on chem. and phys. characts. 3-78378
 (U,Pu) O_2 solid solns., oxidation props., model interpret. 3-54542
 (U,Pu) O_{2-x} fuel pellets, creep at high stress 3-72950
 (U,Pu) O_{2-x} fuel pellets, compressive creep, comp. depend. 3-74728
 U-Pu, nuclear fuel, fission gas release, effect of vol. swelling, probabilistic model 3-63208
 U-Pu carbide nuclear reactor fuels, summary of development, properties and uses 3-63211
 U-Pu-N ternary system, equil. assessments 3-46136
 UO_2 -Pu O_2 , fuel use in thermal reactors 3-57579
 UO_2 -Pu O_2 fuel pins, irradi., oxygen pot. gradient 3-63189
 $U_{0.79}Pu_{0.21}C_{1.02}$, compressive creep and hot hardness 3-61188
 $U_{0.8}Pu_{0.2}C$ -W system, phase diagram obs. 3-47451
 $U_{0.75}Pu_{0.25}O_{2-x}$ fuels, equil. oxygen pot., conc. depend. 3-54541

PMDR see magnetic double resonance

Pockels effect see birefringence

point contacts

- apparatus, for supercond. device tunnelling expts. 3-64437
 Josephson junction arrays, electromag. props., radiation detector applications 3-46939
 W-Ge-Ni, submillimetre wave detector (Russian) 3-73805

point defects

- see also colour centres; interstitials; vacancies (crystal)
 anelastic and dielec. relax. due to point defects, partial relax. magnitudes 3-58083
 β -CoAl(Ga), paramag. props. rel. to antistructure Co conc. 3-58367
 crystal, GaP, defects rel. to growth from non-stoichiometric melts 3-44555
 diffusing, spatial distrib., computer code DEPORT 3-64032
 dynamics, extension to conc. dislocation 3-72084
 elastic field of point defect, vibr. freq. of dislocation, calc. 3-58041
 α -Fe, irradi. defect annealing, computer anal. 3-79346
 II-VI compounds, associated point defects, state-of-the-art review 3-58030
 interactions, physical cluster theory 3-75523
 ionic crystal of polarizable ions of high symmetry containing point defects, electrostatic energy calc. 3-64025
 isotropic crystal containing random defect distrib., elastic X-ray and neutron scatt., static correl. functions (German) 3-52561
 luminescent materials, charged point defects, electronic states, luminescent semiconductors, phosphors 3-41567
 mathematical framework, solved problems, book contrib. 3-58032
 metal, b.c.c., defect kinetics during annealing, computer anal. 3-79345
 metal, f.c.c., correlated point defects, annealing simulation using Monte Carlo methods 3-79531
 metal, field-ion image interpretation 3-75527
 molecular and ionic crystals, spectral effects, vibr., electronic, U-centres, theory 3-72652
 Mossbauer effect, resonance vibration modes, effect on recoilless fraction 3-75923
 niobium oxides, stoichiometric variability in block structure and tunnel structures 3-40909
 nuclear reactor mats., neutron irradi., prod., detection and annealing 3-58052
 oxides, nonstoichiometric, chem. of defects 3-68243
 semiconductors, nondegenerate, influence of linear and point defects on hypersonic attenuation by free carriers 3-55310
 superconductor pinning, statistical theory 3-79798
 Ag films, ultrahigh vacuum deposited on cold substrate, reverse recovery process interpret. 3-64263
 AgX quasicrystalline centres, (X=halide), fluctuation theory, effect on absorption spectra in early photolytic stages (Russian) 3-80084
 Al, harmonically deformed, u.s. attenuation, contrib. of point defect diffusion along dislocations (Russian) 3-43833
 Ba $_2$ NaNb $_5$ O $_{15}$, form., dissoc., vac. heat treatment, γ -ionisation 3-72078
 (Bi $_{1-x}$ Sb $_x$) $_2$ Te $_3$, Bi $_2$ (Te $_{1-x}$ Se $_x$) $_3$, semicond., rel. to three phonon processes in thermal cond. 3-68451
 CaF $_2$:NaF(YF $_3$), following γ and p irradiation and annealing 3-72694
 CaZrO $_2$ nonstoichiometric, effect on Raman spectra of massive point defects conc. 3-80037
 Cu, form. energy, use of pair pot. of atom interaction (Russian) 3-75522
 Fe low temperature irradiation effects on deform. characts. 3-79376
 Fe $_2$ O $_3$, tempered, ordering of nonstoichiometric defects (French) 3-72076
 GaAs, nature and conc., effect of melt comp. during growth 3-75526
 KBr, u.v. and electron irradi., defect formation, exciton decay, electron microscope obs. (Russian) 3-43807
 KBr single crystal in electric field, dislocations and inclusions due to point defect diffusion 3-79520
 KBr:Na, thermal recovery of radiation hardening, thermoluminescence and thermal decay of V_1 band 3-68247
 KBr(Cl), filamentary crystals, internal friction peak due to dislocation-point defect interaction 3-75569
 KCl single crystal in electric field, dislocations and inclusions due to point defect diffusion 3-79520
 LiF, effect on dislocation mobilities (Spanish) 3-75528
 LiF, preliminary deform. effects on cryst. stability (Russian) 3-55002
 Mo, neutron irradiation and plastic deformation, recovery model critical testing 3-79382
 NaCl, filamentary crystals, internal friction peak due to dislocation-point defect interaction 3-75569

point defects continued

- NaCl, rel. to influence of ageing on dislocation movement (Russian) 3-79353
 NaCl, X-irradiated, defect distrib. of crystals aged after quenching 3-58028
 NaClO $_3$, d.c. elec. conductivity determ. 3-79342
 Nb, density of fluctuation, pinning theory, statistics 3-68735
 Ni single crystal, Ar $^+$ bombard., ion scatt., LEED obs. 3-68292
 Pb, dislocation pinning by point defects, u.s. detection, migration energies 3-54979
 Pb, dislocation pinning by point defects, u.s. detection, model 3-54980
 β -PdIn phase, constitutional and thermal defects, heating and quenching effects, exptl. obs. 3-49887
 Si, anomalous residual damage, after annealing of 'through-oxide' As implantations 3-68299
 Si, dislocation-free crystals, distribution of point defects Cu decoration, X-ray topography, etching 3-41650
 Si, injection during nonequilibrium diffusion processes, rel. to IC fabrication 3-55745
 TiO $_2$, rutile, rel. to vacuum reduction 3-41800
 V, highly deformed, sensitivity technique 3-44587
 W, quenched, defects behaviour, superfluid He quench 3-79344
 W, W $^+$ irradi. field ion microscope study of point defect struct. 3-79392
 Zr, neutron irradi. at 24K, point defect creation and elimination (French) 3-52643

point groups see crystal atomic structure

point to point radio links see radio links

Poiseuille flow see laminar flow

Poisson ratio see elastic constants

polar cap absorption see ionospheric electromagnetic wave propagation

polar cap flow see airglow

polar crystal lattice vibrations

- alkali halides; small mol. ions, centres 3-68361
 alkali halides, mixed, coherent potential approximation reflectivity rel. to lattice mode 3-53110
 alkali halides, multiphonon i.r. absorpt. temp. depend. 3-64659
 alkali halides, multiphonon i.r. absorpt. temp. depend. 3-64660
 alkali halides, multiphonon i.r. absorpt. temp. depend. 3-68985
 alkali halides, NaCl lattice struct., thermodynamic props. 3-52685
 ethylsulphates of yttrium and some rare earths, Raman spectra 3-50564
 F-centre theory, electron-phonon interactions, Jahn-Teller effect 3-69039
 α -HgS, cinnabar, birefringence indices (French) 3-53080
 ionic crystals, diatomic and polyatomic, mechanical and electrical anharmonicity 3-68359
 magnetic field depend. of electron-phonon correlation effects 3-41159
 BaClF, i.r.-active lattice vibrs., phonon freqs. 3-75575
 CaCO $_3$, calcite, lattice dynamics, theory and i.r. spectra obs. 3-72628
 CdF $_2$:Co $^{2+}$, mag. circular dichroism of vibr.-induced $^4A_{2g}(F) \rightarrow ^4T_{1g}(P)$ transition 3-64631
 Cs halides, dielec. consts., strain derivatives, two ion polarizable shell model 3-47198
 KCl:CN $^-$, absorpt., orientational tunnelling of mol. defects 3-69040
 KI, far i.r. anharmonic optical props., absorpt., 12-300K 3-53104
 KNCS crystal, polarised i.r. and Raman spectra lattice vibrations 3-72609
 Rb halides, dielec. consts., strain derivatives, two ion polarizable shell model 3-47198
 TeO $_2$, i.r. refl., polar phonon spectrum 3-53106

polarimeters

see also polarimetry

- Biot's polariscope, working model 3-59533
 birefringent compensator, rotating 3-59579
 double image chopping polarimeter using plane parallel calcite slab 3-77177
 dual-beam polariscope and framing camera for dynamic photoelastic stress patterns 3-73112
 ellipsometer, for interface optical const. meas. 3-73727
 ellipsometer, modulated, for study of film optical props., surface dynamics 3-53885
 ellipsometer, rotating analyser, Fourier transform computer detection system 3-56661
 ellipsometer, using stable polarization modulator 3-45484
 ellipsometer calibration, component imperfections effects 3-59575
 ellipsometers, computer controlled for study of anodic Ta $_2$ O $_5$ films 3-80122
 ellipsometry of anisotropic surfaces 3-59576
 integrated polariscope response 3-39859
 lidar, remote water quality meas. 3-42384
 low cost recording spectropolarimeter, design and evaluation 3-45584
 movable detector ellipsometer design 3-66185
 for neutrons of 3 MeV (German) 3-45549
 optoelectronic system, for interferometric ellipsometry 3-62139
 photon counting polarimeter, linear polarisation meas., non-stellar stars, extragalactic objects (Russian) 3-42560
 Pioneer 10, imaging photopolarimeter optical system 3-48138
 Polanet variable densiphase microscope, for optical imaging 3-56659
 polarovisor for lunar and planetary work 3-77196
 three-crystal X-ray polarimeter, collimator and spectrometer 3-66385
 weak light source polarisation meas. method (Russian) 3-62077
 γ -ray, figure of merit 3-40051
 $^{12}C(p,p)^{12}C$, absolute polarizations measured at 50° in range 2.0-4.5 MeV 3-63029
 Ge(Li) Compton polarimeter for γ -rays 3-40013

polarimetry

see also ellipsometry; polarimeters

- comet Bennett (1969 i), spectropolarimetric obs. of head (Russian) 3-77012

polarimetry continued

Galactic X-ray polarimetry and high-resolution X-ray spectroscopy 3-81259
stationary dynamic birefringence meas. method (*French*) 3-77426

polarisability

see also *atomic polarisability; molecular polarisability*
gas, nonlinear polarisability in laser transition with reson. radiation trapping 3-51918
ionic crystal of polarisable ions of high symmetry, generalised polarisability function 3-64026
metal-semiconductor interface, covalent-ionic transition, microscopic theory 3-55334
metallic particles, electronic polarisability 3-50511
metallic thin film, electronic polarisability 3-50511
p-terphenyl mixed crysts. with tetracene and pentacene, second-order Stark effect on 1B_u state 3-53128
uniaxial cryst., electronic polarisabilities of ions in trigonal system (*French*) 3-75961
uniaxial cryst., tetragonal system 3-72567
n electric, effect on two-neutron scattering length 3-45978
Li⁺ gas, harmonic power generation using nonlinear optical polarisabilities 3-57260
²¹⁰Po, M1 core polarizabilities of 8⁺ and 6⁺ states, shell model calcs. 3-49117
Xe harmonic power generation using nonlinear optical polarisabilities 3-57260

polarisation

see also *beta-ray polarisation; deuteron polarisation; dielectric polarisation; light polarisation; neutron polarisation; nuclear polarisation; photon polarisation; polarisation in nuclear reactions and scattering; proton polarisation*
acoustic waves in solids (*French*) 3-43830
astronomical radiosources, depolarisation and luminescence 3-81122
charge cloud, effect on elastic small angle electron scattering from inert gases 3-71431
chemically induced electron spin polarisation, level convergence processes 3-44716
chiral molecules, circular differential Raman spectra 3-78802
conducting solid particles, thin diffuse double layer, electrophoresis 3-73074
crystal slightly doped with paramag. ions, X-band guided wave rot. and ellipticity, obs. (*French*) 3-50632
current and charge densities on surface of conducting cylinder scattering e.m. waves 3-77952
Cygnus X-3, 8 GHz obs. during September 1972 outburst 3-70001
depolarization of polarized beam in transport system, transfer matrices (*French*) 3-53966
Earth's bow shock 0.5-3 Hz waves, circular polarisation meas. 3-69713
electron beam, in e⁺e⁻ storage rings, use in determining e.m. structure function 3-57350
e.m. waves, propag. in ferrimag. materials, field eqns. (*French*) 3-75966
f.c.c. crystal, (001) surface, adsorbed monolayer, wave polarisation and frequencies (*French*) 3-79566
frequency and time domain induced, multilayered Earth survey for mineral exploration 3-65149
gamma quanta, cosmic, linear polarisation, measurement by Compton effect, feasibility 3-70056
geomagnetic pulsations, wave polarisations at high latitudes on Earth's surface 3-56114
gravitational wave, rotation by weak gravitational field 3-66669
hadron, possibility of determination from hadronic atoms 3-67722
hadron inclusive spectra, effect of initial polarisation (*Russian*) 3-78228
inclusive reactions, applications of properties of six body helicity amplitude 3-62913
interstellar, polarisation, simulation, frozen hydrocarbon matrices, para and nonparamag. porphyrins 3-48125
ionospheric r.f. propagation, polarisation parameters 3-59138
maximum selectivity, with minimum interference (*Russian*) 3-42963
microturbulent magnetoactive plasma, nonlinear conversion of micro-turbulences, theory of polarised radiation 3-75310
near field polarisation ellipse 3-48836
nucleon, for reactions meson + nucleon → meson + meson + nucleon, general description 3-74443
ρ Ophiuchi, dark clouds, extinction and polarisation wavelength dependence 3-48046
partially polarised e.m. fields, polarisation state representation by Poincare sphere 3-45760
particles in inclusive reactions using invariant Reggeon vertices formalism (*Russian*) 3-67167
Pc1 micropulsation polarisation, obs. at low-latitude sites 3-61403
photoelectron emission from trivalent atoms in two-photon ioniz., polarised electron source 3-74809
Pi2 micropulsations, latitude depend. of sense 3-41928
Pluto, polarimetry 3-80981
polymers, nomadic, for dielectric constns. above one hundred 3-47199
pulsar pulses, observations between 110 and 1400 MHz 3-77123
radiative transfer in inhomogeneous magnetic field, numerical integration of equations (*Russian*) 3-77043
radio sky polarization distribution, appl. of entropy measure 3-70061
radio source depolarisation rel. to existence of intergalactic gas 3-53706
radio sources, polarisation variation in self-absorbed synchrotron sources 3-51361
radioastronomical, circular repolarization in compact sources 3-69977
radioastronomical meas. using Westerbork synthesis radio telescope 3-61879
radioastronomical observations of supernova remnants, high resolution interferometry 3-77093
radiosources, linear polarisation, time variation at 2.8 and 4.5 cm 3-77109
radiosources, linear polarisation at 2.8 and 4.5 cm. 3-77108
radiowave emission from pulsars, limiting polarization 3-42216

polarisation continued

radiowaves, ordinary wave reflected from ionosphere, vertical incidence, vertical magnetic field 3-76797
reflection and transmission by unidirectionally conducting screen 3-57193
ruby cylinders, transversely pumped 3-78000
self-gravity-induced electric polarisation of rotating massive body, magnetic field generation 3-59791
sky, Earth surface albedo in i.r. (*Russian*) 3-80752
solar microwave circular polarised radiation from solar hemispheres 3-65658
solar type III bursts at 80 MHz, non-existence of linear polarisation 3-45026
solar type III radio bursts, time dependence of polarization 3-53614
space-charge polarisation theory and electrode-discharge effects 3-44072
spherical solid particles, electrophoresis 3-73076
spin-1/2, -1 polarisation analyzing tensors, measurement techniques 3-42622
spin-projection invariance in null-plane formalism 3-62796
Tauri, dark clouds, extinction and polarisation, wavelength dependence 3-48046
Tauri, optical and infrared obs., model for wavelength dependence of polarisation 3-73511
two-body scattering with separable potentials, polarisation 3-52110
two-photon excited fluoresc., polarisation study 3-42986
uncollimated beam wave in turbulent medium, mean square depolarisation, analysis 3-40207
Van der Waals forces, nonlocal conductivity systems, external polarisation, calc. 3-70772
Δ (1236), from ep → eΔ, hadronic current tensor, polarisation density matrix 3-67024
μ, streamer chamber for measurement 3-77668
πN scattering, Veneziano-type amplitudes, charge-exchange polarisations, differential cross sections 3-62876
π⁺p → ηn, illustration of tensor exchange amplitudes, absorption model, effective rescattering 3-67082
BaTiO₃, rel. to temperature changes (*Polish*) 3-47203
Cs atom, 62P, depolarization by collisions with inert gases in variable mag. field 3-78515
Cu electrode, alternatively polarised, moisture effects (*Polish*) 3-58802
GaAs-electrolyte interface, non-equilibrium depletion, surface-barrier photoeffect, effect of doping and surface treatment (*Russian*) 3-73144
H atom, metastable, quenching in elec. field, polariz. of Ly-α radiation 3-78471
Hg atom, spin polarisation, elastically scattered electrons (*Russian*) 3-49417
(N(C₂H₅)₂ZnL₂:NiL₂²⁻ mag. circular dichroism spectrum, ligand field transition, linear polarisation meas. 3-50601

polarisation in nuclear reactions and scattering
elastic scattering of deuterons, medium energy, polarisation effects on cross sections and spin tensors (*Russian*) 3-74595
inelastic proton scattering, analysing capability reln. to reaction amplitude (*Russian*) 3-67318
inelastic scattering of polarised protons, identification of collective modes 3-60101
light nuclei, obs. of S-wave levels near threshold for tensor-polarised deuteron reaction 3-49261
light nuclei interactions with electrons, polarisation of emitted protons (*Russian*) 3-63038
rank-1 polarizations, linear relations 3-43231
reactions with four spin-1/2 particles, structure determ. 3-74550
scattering of polarised neutrons on zero-spin nuclei, methods of polarisation measurement (*German*) 3-60156
spin-1/2, -1 polarisation analyzing tensors, measurement techniques 3-42622
transfer coeff. determination techniques 3-42623
vector analysing power, semi-classical model, for sub-Coulomb neutron transfer reactions 3-60146
(d,p) reactions, compound nucleus contribs. to T₂₀ analysing power 3-67343
²H, neutron scatt., polarisation asymmetry, 35 MeV 3-74553
(n,d) scattering at 2.45 MeV, depolarisation, angular distrib. of Wolfenstein parameter (*German*) 3-46022
⁹Be, polarised proton scattering, 8-15 MeV, angular distrib. of polarisation analysing powers 3-52184
⁹Be(p,p)⁹Be 0.8 to 2.7 MeV, analysing power, deduced phase shifts, ¹⁰B deduced levels 3-63047
¹²C, polarized proton scattering, 9.5-11.5 MeV, obs. of T=1/2 ¹³N levels (*German*) 3-49139
¹²C(d,p) to ¹³C unbound states, comparison with DWBA theory 3-54488
¹²C(n,n), 2.5 MeV, absolute polarisation, cross sections using R-function theory anal. 3-78325
¹²C(p,p)¹²C, absolute polarization measured at 50° in range 2.0-4.5 MeV, use as polarimeter 3-63029
¹³C(α,n)¹⁶O, 2.075-2.43 MeV, neutron polarisation angular distrib., parity assignments of ¹⁶O 7.97-8.197 MeV states 3-67189
¹⁴C(d,n)¹⁵N, deuteron energies, 1.3 to 1.9 MeV, neutron polarisation ang. distrib. (*German*) 3-52197
⁵⁹Co(n,p)⁵⁹Co, polarised target and thermal neutrons, meas. of γ-ray asymmetry 3-60175
⁵²Cr(d,p)⁵³Cr, 10 MeV, tensor polarised deuteron beam, meas. of analysing powers and cross sections 3-49266
D(p,n)pp, breakup neutrons polarisation meas. at 21.5 MeV 3-52163
¹⁹F(p,p')¹⁹F, core-polarisation effects, DWBA analysis 3-52134
Fe, A=54, 56, 58, scattering of polarised 12.3 MeV deuterons, vector analysing power and cross sections 3-52194
⁵⁴Fe(d,p)⁵⁵Fe, 10 MeV, tensor polarised deuteron beam, meas. of analysing powers and cross sections 3-49266
¹H(d,d)¹H scattering, 30 MeV, meas. of vector and tensor analysing power 3-49235
²H(d,d)²H, 3-11.5 MeV polarised deuterons, meas. of vector and tensor analysing powers (*German*) 3-49233
²H(d,n)³He, 3-11.5 MeV polarised deuterons, meas. of vector and tensor analysing powers (*German*) 3-49233

polarisation in nuclear reactions and scattering continued

- ³H(d,n)³He, polarised deuteron beam, 3.3-14.9 MeV, meas. of longitudinal polarization transfer at 0 degrees 3-57506
- ²H(d,p)³H, 3-11.5 MeV polarised deuterons, meas. of vector and tensor analysing powers (*German*) 3-49233
- ³He in elastic scattering from ²⁷Al and ²⁸Si nuclei, determ. optical model parameters 3-67349
- ⁴He(d,d)⁴He, 11.5 to 17 MeV, incident vector polarised ²H, meas. vector analysing power *i*T₁₁ 3-74552
- ⁶Li(d,α)⁴He, 3-11.5 MeV, tensor analysing power and differential cross section meas. (*German*) 3-52188
- ⁷Li(d,n)⁸Be, polarised 800 keV deuterons, meas. of analysing powers and relative cross section 3-60197
- ⁷Li(p,p)⁷Li, 0.4-2.5 MeV, polarisation and phase shift analysis, resonances and ⁸Be level structure 3-46025
- ²⁴Mg(³He,n)²⁶Si, 5.0 and 5.8 MeV, meas. of angular distrib. of neutron polarisation, DWBA analysis 3-67352
- ¹⁴N(d,d)¹⁴N vector analyzing powers comparison with ¹⁴N(d,t)¹³N 3-74597
- ¹⁴N(d,t)¹³N, vector analyzing powers comparison with ¹⁴N(d,d)¹⁴N 3-74597
- ²⁰Ne(d,d)²⁰Ne, 11.6 MeV polarised deuterons vector analysing power, optical model, differential cross section 3-52193
- ²²Ne(d,d)²²Ne, 11.6 MeV polarised deuterons vector analysing power, optical model, differential cross section 3-52193
- ⁵⁸Ni(d,p)⁵⁹Ni, 10 MeV, meas. of angular distrib. of vector analysing power and absolute cross section 3-52077
- ⁵⁸Ni(p,p')⁵⁸Ni, E_p = 60 MeV polarized protons, giant reson. excitation 3-74584
- ⁶⁰Ni scattering of polarised 12.3 MeV deuterons, vector analysing power and cross sections 3-52194
- ⁶⁰Ni(d,p)⁶¹Ni, 10 MeV, vector analysing power, ang. distrib. meas., DWBA calcs. 3-78239
- ⁶²Ni(p,p)⁶²Ni, isobaric analogue resonances, double-scattering techniques, 2.43-2.75 MeV 3-63045
- ¹⁶O(d,d)¹⁶O, 11.6 MeV polarised deuterons vector analysing power, optical model 3-52193
- ¹⁶O(d,d)¹⁶O, 11.6 MeV polarised deuterons vector analysing power, optical model 3-52193
- ¹⁶O(d,p) to ¹⁷O unbound states, comparison with DWBA theory 3-54488
- ²⁰⁸Pb(d⁺,d) 12.3 MeV, vector analysing power, differential cross section, deduced optical model parameters 3-60199
- ²⁰⁸Pb(d⁺,p), 12.3 MeV, vector analysing power, differential cross section, ²⁰⁹Pb deduced levels, DWBA analysis 3-60199
- ²⁰⁸Pb(d⁺,t), 12.3 MeV, vector analysing power, differential cross section, ²⁰⁷Pb deduced levels, DWBA analysis 3-60199
- ³²S(d,³He)³¹P vector analyzing powers comparison with ³²S(d,d)³²S 3-74597
- ³²S(d,d)³²S, vector analyzing powers comparison with ³²S(d,³He)³¹P 3-74597
- ³²S(p,p'), polarised, hexadecapole phonon state 3-74583
- ²⁸Si(p,p')²⁸Si, 25.25 MeV polarised protons, ground state rotational band excitation 3-52174
- ³⁰Si(d,d)³⁰Si vector analyzing powers comparison with ³⁰Si(d,t)²⁹Si 3-74597
- ³⁰Si(d,t)²⁹Si vector analyzing powers comparison with ³⁰Si(d,d)³⁰Si 3-74597
- Si(p,p)Si, 17-29 MeV, analysing powers and cross sections in ²⁹P giant resonance region, optical model analysis 3-67327
- ²³⁵U, neutron-induced fission, spin determ. of reson. 3-74614
- ¹⁷⁶Yb(p,t)¹⁷⁴Yb, 16 MeV polarised protons, meas. of vector analysing power and differential cross section 3-49257
- ⁹⁶Zr(d,p)⁹¹Zr, 10 MeV, tensor polarised deuteron beam, meas. of analysing powers and cross sections 3-49266

polariscopes see polarimeters**polaritons**

- anthracene mol. solids, polariton dynamics from band profile analysis 3-72642
- crystalline solid, Raman scatt. by collective excitations 3-80025
- ionic crystals, biaxial finite, dispersion, macroscopic theory (*German*) 3-58103
- ionic crystals, uni- and bi-axial, polariton Raman lines, eigenvectors and intensities (*German*) 3-53114
- molecular crystal, spectra, Fermi reson exchange 3-69000
- molecular crystals, theory of hyper-Raman effect 3-66891
- perylene mol. solids, polariton dynamics from band profile analysis 3-72642
- β-quartz phonon and polariton spectra, longitudinal E₁ modes 3-55582
- Raman scattering spectra, determ. of effective charge of ions 3-54942
- Raman spectrum in presence of mass defects 3-41514
- resonant Raman effect with damping, Coulomb exciton-phonon interaction, polariton effect 3-69006
- semiconductors, interaction of exciton-polaritons with charged impurities 3-55228
- surface polaritons, study by transition radiation 3-46888
- tetracene mol. solids, polariton dynamics from band profile analysis 3-72642
- two-photon absorpt. rel. to exciton-polariton generation, theory 3-44043
- virtual excitation type, on anisotropic media 3-41163
- CO, solid, u.v. spectrum, exciton-phonon coupling role (*German*) 3-50586
- CdS, exciton-polariton relax., bottleneck expt. evidence 3-46812
- CuCl, two-photon absorption line shape 3-79653
- GaAs film on substrate, props. of surface polaritons 3-58505
- GaAs thin film, Raman scatt. from surface polaritons 3-58504
- α-HfO₂, spontaneous parametric emission and light scatt. by polaritons 3-48945
- InSb, surface magnetoplasmon-optic phonon modes, meas. 3-68687
- LiF, parametric and polariton light scatt. 3-51957
- LiNbO₃, parametric and polariton light scatt. 3-51957
- NaCl, film, surface optical vibrations, frustrated total internal reflection obs. 3-50063
- NiO, small particles, i.r. surface modes 3-41524

polarization see polarisation**polarography**

- a.c., stationary Hg electrode, effect of potential sweep rate on peak height, reversible and irreversible electrochem. reactions 3-53318
- concentration polarization transfer between serially polarized drops, laser interferometric obs. 3-45597
- concentration polarization transfer between serially polarized drops, laser interferometric obs. 3-48663
- d.c., multiparametric curve filtering, minicomputer programming 3-70447
- d.c., rapid, anodic Hg waves rel. to drop times 3-70448
- differential pulse, stationary Hg electrode, effect of potential sweep rate on peak height, reversible and irreversible electrochem. reactions 3-53318
- digital smoothing of data based on Fourier transformation 3-40065
- electrode process, first order chem. reactions, charge transfer step, mechanisms 3-65089
- electrophoresis of charged Hg drops in aqueous electrolyte soln. 3-59610
- Ilkovi standard d.c. and a.c. equations at short drop time; validity study 3-55962
- impedance bridge for differential capacity measurement at dropping mercury electrode (*French*) 3-62343
- maxima, depend. on capillary characteristics and depolariser conc. 3-70477
- polarograph, averaging, with digital output 3-66437
- vibrating indicator electrode, polarography, amperometric titration, polarometry 3-48652
- Ag⁻ recovery, photographic fixing soln., phenylthiourea selective resins, ion exchange, polarographic Ag anal. 3-53335
- Cd-ethylenediaminetetraacetate chelate 3-69451
- Pu, determination of small quantities in solution, reprocessing of nuclear fuel (*German*) 3-71325
- TlBr-KBr single crystal, lattice consts., luminescence centres 3-64722

polarons

- anthracene, small polaron model of electron motion 3-64334
- Boltzmann equation, collision term. rel. to high freq. cond. 3-55225
- bound piezoelectric polaron, ground state energy 3-46818
- free, Pekar 1:2:3:4 and ground state theorems 3-41162
- ground state discontinuity, Feynman's path integral method 3-50151
- hydrated electron structure modified CNDO/2 method for water and ice 3-73174
- ionic crystal, phonon effects in lattice statics anal. of defects and polarons 3-43853
- large polaron, dynamical theory 3-50150
- magnetic condensation, polaron state form., cond. electron interactions in strong mag. fields 3-72150
- many-valley crystals, strong interactions between electron and polarization oscills., of lattice, theory 3-75727
- m.i.m. system, charge relay transport via impurities or polaron states 3-60923
- mobility of small polarons, strong elec. fields, theory 3-55278
- piezoelectric polaron, theory 3-75728
- polar cryst., polaron bound in Coulomb pot. 3-52809
- polar crystal, Frohlich, energy spectrum in mag. field 3-79656
- polar crystals, magnetic field depend. of electron-phonon correlation effects 3-41159
- polar fluids, solvated electron, radiative processes, long range interactions via polaron modes 3-55995
- semiconductor, electron transport, optical phonon effect, mag. field effects 3-41188
- semiconductor, polar, i.r. free polaron absorpt., temp. depend. 3-55591
- transport mechanism, small polaron tunnelling 3-64312
- AgBr, rel. to hole cyclotron reson., 34 GHz and 1.7 K 3-46796
- α-AlB₂, current carrying mechanism, elec. props., refl. spectrum 3-72357
- CeO₂, defect equilibria for extended point defects, effect of O₂ pressure 3-79340
- CeO₂, nonstoichiometric, defect struct. above 700°C 3-68244
- EuO, bound mag. polarons, susceptibility to 700K 3-50348
- Ge, excitonic polaron obs. at cyclotron reson. 3-55200
- TiO₂, phonon aided hopping of polarons, dielectric props. meas. 3-79647

poles and towers

- antenna tower alignment system for radome boresight error meas. 3-45831

polishing

- see also electrolytic polishing*
- corundum plates, single-crystal, process for grinding and polishing 3-62088
- glass, microindentation hardness rel. to comp. 3-55883
- lenses, temp. fluctuations meas., conditions 3-62091
- optical component mounting, uniform colour of block 3-62092
- optical glass, ion polishing 3-62087
- semiconductor, compound, for device manufacture 3-76141
- semiconductor wafer, chemical-mechanical polishing, thickness variations 3-76143
- Al₂O₃, environment effect on surface damage penetration 3-80420
- Al₂O₃, sapphire, hardness and damage resist. depend. on surface finishing 3-69342
- Cu, effect on fatigue process, cracking 3-64883
- Cu mirror surfaces, for high power i.r. lasers, polishing and coating techniques 3-62153
- GaAs, etch polishing with sodium hypochlorite 3-58182
- GaAs, with perhydrol-alkaline mixture (*Polish*) 3-76138
- GdGa garnet substrate, for bubble domain device 3-44528
- LiF single crystals, for use in far u.v. optics 3-62090
- Si, prep. for planar technology 3-69179
- TiO₂, rutile, chemical polishing with KOH-NaOH melt mixture 3-55162
- Zr and Zircaloy-2, oxidized, wear in water, characteriz. 3-57573

pollution

- see also air pollution; pollution detection and control; water pollution; water treatment*
- analysis, cassette data loggers for 3-70190
- analysis instrumentation, conference, San Francisco, Calif., USA (1972) 3-61929
- conference, Washington, D.C., USA, Oct. (1972) 3-42378
- design optimisation of anti-pollution device 3-48275

pollution continued

- Earth Resources Technology Satellite, earth imaging systems, appl. to pollution monitoring 3-80851
 environmental contamination by ^{14}C from HTRs and fuel reprocessing plants 3-71335
 environmental surveillance from space, Italian participation (*Italian*) 3-61592
 ERTS multispectral scanning system for earth monitoring 3-44951
 food processing industry, control, instrumentation, process control, computer control, symposium, Pittsburgh (1972) 3-59721
 fusion reactor power plants, environmental contamination 3-60319
 gas. conc. meas. by stimulated anti-Stokes scatt. 3-66438
 hydrodynamic dispersion of injected contaminant in fractured rock aquifer, model 3-51212
 light, concern to astronomers, high pressure Na lamps 3-76778
 lungs and other organs, ferromagnetic contamination 3-59438
 methylmercury compounds, concentration and distribution in estuarine sediments 3-73410
 nuclear power facilities, effluent and environmental sample meas. by gamma ray spectrometry 3-62233
 pollutant detection by absorpt., Mie scatt. and topographic targets as retroreflectors 3-53778
 radioactive waste disposal, alternative storage areas 3-71338
 radiological, U.S. atomic energy programme, radiation standards 3-43319
 remote sensing from space rel. to man's effect on environment 3-51074
 synthetic fuel energy system based on fusion reactors, environmental effects 3-67619
 trace element analysis by high flux neutron activation 3-62356

pollution detection and control

- heading is late addition, see also pollution; chemical variables control measurement
 air particulates, multielement analysis, X-ray emission spectrometry 3-59718
 air pollution, instrumentation study 3-66083
 air pollution, Raman and fluorescent spectrum 3-78832
 airborne radioactive effluents, estimation procedure 3-77303
 analysis instrumentation, conference, San Francisco, Calif., USA (1972) 3-61929
 atmosphere, urban diffusion model for predicting concentrations of inert vehicle-generated pollutants 3-61454
 atmospheric aerosol fluorescence, implications for lidar detection 3-77294
 atmospheric i.r. thermal emission 2.5-4.2 μ , detection technique 3-76714
 atmospheric particulate material, instrumental photon activation analysis 3-70458
 atmospheric particulates, nuclear activation techniques 3-66081
 cassette data loggers for 3-70190
 dust concentration, development of low cost sampler 3-66071
 Earth Resources Technology Satellite, earth imaging systems, appl. to pollution monitoring 3-80851
 Electronic automatic advance for automobile internal combustion engines 3-77293
 environmental surveillance, by neutron capture γ -rays 3-66079
 food processing industry, conference, Pittsburgh, USA (1972) 3-59721
 fuel sensor for faster analysis 3-66073
 gas conc. meas. by stimulated anti-Stokes scattering 3-66438
 historical survey, neutron activation analysis of human hair 3-66080
 marine and fresh water, remote sensing of chlorophyll content and temp. 3-73607
 nuclear installations, airborne effluents, WEERIE program 3-77297
 ocean and coastal zone, Earth Resources Technology Satellite, imaging 3-80717
 ocean surface slicks, i.r. characs., comparison between natural and oil slicks 3-69744
 oil, on water surface, remote sensing techniques 3-70194
 radioiodine, airborne, monitoring, improvement of collecting efficiency under high relative humidity 3-73608
 radioisotopes, medical diagnostics, release to environment through excreta, control 3-77296
 smoke/dust density meters, photoelectric, error sources (*Dutch*) 3-73606
 source concentration monitoring, low resolution i.r. derivative spectrometry 3-73609
 stack gases, continuous monitoring, optical instrumentation 3-61931
 urban planning and air pollution control, systems approach 3-81331
 water pollution, oil spills, cleanup using waste paper, technique 3-81330
 water pollution monitoring (*Japanese*) 3-66076
 water quality turbidity meas. 3-61930
 CO atmospheric concentration meas. by gas filter correlation instrument 3-81328
 $\text{H}_2\text{S}/\text{SO}_2$ ratio, S recovery plants, photometric analyser system 3-61932
 ^3H , conc. in air, continuous high sensitivity monitor 3-77301
 NO , NO_2 , atmospheric pollution fluorescence detn. 3-70189
 NO and NO_2 , emissions from stationary sources, monitoring, instrumental techniques 3-61933
 O_3 , i.r. fluorescence, laser induced, air pollution remote sensing 3-76043
 SO_2 , detection by laser excited fluorescence 3-81329
 T_2O , ruggedized field air sampler 3-77302

polonium

- radiohaloes, isomer precursors 3-60348
 ^{210}Po α -particle irradiator, high vacuum 3-62211

polonium compounds

No entries

polyelectrolytes see polymers**polymerisation**

- acetone, pressure effect on melting point 3-79476
 acrylic acid adsorbed on Al 3-72264
 diacetylenes, Raman spectral changes during the solid-state polymerisation 3-57685

polymerisation continued

- germanate glasses, mixed-cation, pseudo-alkali cation effects on network depolymerization 3-44679
 glass, heat treatment 3-68165
 holographic recording substrate, chromatic photosensitization (*French*) 3-73775
 human serum albumin, ^{60}Co gamma irradiation, polymerisation, cross-linkages, sedimentation velocity technique 3-48264
 mass, in heterogeneous systems, mathematical modelling (*German*) 3-65012
 photochemical imaging processes, non-conventional, photochemical formation of dyes, photochromism, photopolymerisation 3-50852
 polystyrene, intramolecular cross linking, synthesis and chemical characterisation 3-78913
 radiation nonuniformly initiated, mixing effect 3-57689
 sealants, gas evolution kinetics in vacuum optomechanical appls. 3-62040
 silicates, liq., thermodynamic props. of Masson polymerization models 3-65081
 styrene, effect on energy level shift, electronic excitation energy transfer 3-69081
 styrene thin film in glow discharge, effect of O_2 on electrical props. 3-41280
 H_2O , anal. of explanations and experimental data, review (*German*) 3-40841
 $\text{Ti}_2\text{O}-\text{GeO}_2-\text{SiO}_2$ glasses, i.r. detection of depolymerization 3-58500

polymerization see polymerisation**polymers**

see also elastomers; plastics

- ABA block copolymers, statistical thermodynamics microstructure model, free energy change calc. 3-54775
 acoustic phonons, propagation and influence on props. (*German*) 3-60777
 acrylic fibre oxidation stage in carbon fibre formation 3-41817
 adhesive bonds, strength anal. using mol. theory 3-55898
 adhesive fibrous nonfabric material with polyurethane binders, thermomechanical props. 3-58715
 aliphatic resin:polyethyleneepolyamine-epoxy resin models, metal surface finish, dimensional deviations 3-50812
 alkane derivatives, surface tension of homologous series of liquids 3-50070
 n-alkane systems, molar excess enthalpies, polymer solution theories 3-55998
 alkyl phenol polyethylene glycol ether, friction props., effect of surface-active agents 3-73056
 alternating copolymer of ethylene and tetrafluoroethylene, crystal structure 3-63959
 Amberlite XE-270 resin, use in ^{237}Np purification 3-67577
 amorphous, biaxial orientation, macromol. orientation distrib. function, rel. to birefringence 3-71682
 amorphous, in rubberlike elastic state, viscoelastic props. as function of nature and length of chain 3-73047
 amorphous, relaxation processes 3-44676
 amorphous, supermolecular structure model 3-60668
 amorphous, X-ray diffr. obs. of structure 3-46593
 amorphous and crystalline, durability study 3-61222
 antioxidants, influence on effective viscosity and tensile strength, polypropylene melt during processing and aging 3-73058
 aqueous solutions, hydrodynamic influence of polymer additives in external flow around a sphere 3-57830
 araldite-hardener mixtures, hardener effect on transition temps., rot. plate method 3-69381
 axisymmetrically heated orthotropic cylinder fastened to a pliable elastic cylinder, stability under shear 3-57084
 biaxial extensional flow, material functions 3-67888
 biopolymers oriented by hydrodynamic flow, dichroic spectra 3-43529
 bisphenol-A, diglycidyl ether, cured with methylenedianiline, pulsed n.m.r. studies, molecular motion 3-54771
 bisphenol-A uncured diglycidyl ether, pulsed n.m.r. study of molecular motion 3-58443
 boundary layer flow, similarity solution based on constitutive equation 3-63683
 branched, solutions, viscoelastic props. calc. based on Zimm-Kilb theory 3-54776
 breakdown under load, infrared spectroscopic obs. 3-58747
 Brillouin scatt. obs. of shear waves in amorphous polymers 3-80028
 bundle model, dielectric and mechanical relax. obs. (*German*) 3-60672
 butadiene, polymers and copolymers, Raman spectroscopy, sample preparation, quantitative analysis 3-58496
 butadiene-styrene copolymer, SKS-85, filled mixtures, microstructure of fracture surfaces, +60°C to -60°C 3-58748
 butyl rubbers, chain rigidity from i.r. spectra (*Russian*) 3-71670
 capron, electron irradi. rate and deform. rate effect on strength (*Russian*) 3-80467
 capron, submicrocrack formation and concentration, in loading and unloading 3-58742
 caprone, etching, distortion caused by working gas, electron conc. (*Russian*) 3-73068
 carboxymethylcellulose soln., flow curve determ., rolling-ball viscometer 3-71688
 carbon, film subject to static and fatigue loading, arterial crack growth 3-55895
 carrier transport, time of flight investigation 3-60876
 cast resins, dielectric property, effects of discharges in SF_6 gas (*German*) 3-54880
 cation-exchanger resins, modification under α - and γ -radiation (*German*) 3-73162
 cellophane and polyethylene films, adhesion, microrheological process effects 3-55893
 cellulose, di- and tri-acetyl, film, subject to static and fatigue loading, arterial crack growth 3-55895
 cellulose, gamma-irradiated, changes in strength, heat of wetting, during storage 3-73059
 cellulose, paracrystalline lattice disorders, powder X-ray diffraction, anal., two phase hypothesis 3-54932
 cellulose acetate, ultrathin and thick membranes, p.m.r. studies 'free' and restricted water 3-54770

polymers continued

- cellulose acetate fibres, heat-treated, peak resolution and crystallinity determ. 3-72016
 cellulose fibres, crystallinity and crystallite size meas. in Ramie and Fortisan 3-72017
 cellulose fibres, internal microstructure, electron microscopy, prep. technique (*Russian*) 3-47479
 cellulose hydroxyalkyl ethers, dielectric props. below glass-transition temp. (*Russian*) 3-72574
 cellulose nitrate, track-etch radiography, alpha particles, protons, fast and thermal neutrons 3-67627
 cellulose triacetate fibres, heat-treated, correl. crystallinity and phys. props. 3-72015
 cellulose tributylate molecules, sedimentation constant, diffusion coeff., intrinsic viscosity, optical anisotropy effect of different solvents (*Russian*) 3-46368
 chain, comblike branched, unperturbed dimensions calc., unequal branches 3-71663
 chain branching rel. to rheology and thermal props. (*German*) 3-63598
 chain molecules, n.m.r. conformational analysis using local interaction model 3-71487
 chain polymer solutions, transport of compact particles 3-47487
 chain type, absorption band intensity change under loading 3-63580
 chains, conformational energy, stereoregularity and role of nonstaggered conformations 3-57683
 characterisation, mechanical, electrical and thermal properties 3-41829
 chemical analysis, review 3-59696
 chromophoric group identification, stability determ. from fluorescence (*Russian*) 3-61277
 circularly polarised small-angle light scattering from an anisotropic sphere 3-57693
 cis-polybutadiene, chain rigidity from i.r. spectra (*Russian*) 3-71670
 coating on steel plate, effect of internal stresses in the coating on vibrations and static bending 3-58671
 coatings on sheet elements, damping of bending vibrs. 3-44683
 collagen, dielectric dispersions 3-58472
 combination, structure rel. to mech. props. (*German*) 3-61215
 concentrated solns., heterogeneous drag, reduction system, turbulent pipe flow, heat transfer 3-52434
 configuration, weighting methods for Monte Carlo calcs. 3-67867
 conjugated bonds, electronic structure, one-dimensional Mott semiconductors 3-75715
 π -conjugated heterocyclic, bond alternation 3-75164
 copolymer composition heterogeneity determ. by light scattering 3-63594
 cotton fibre, internal microstructure, electron microscopy, prep. technique (*Russian*) 3-47479
 Couette flow, viscoelastic, polymeric, stability prediction based on network rupture hypothesis, analysis 3-75277
 cracking and crazing, under tension, laser diffraction obs. 3-52667
 creep, long term, phenomenological prediction in time dependent systems 3-58745
 creep activation energy measurement, rapid temp. jump apparatus 3-42516
 creep stress and strain deformation 3-61219
 creeping deformation, irreversible, under stepwise stressing rel. to theory of hardening 3-58743
 cross-linked, for stably binding blood heparin 3-56473
 crosslinked, supermol. structure, determ. by structure of starting components, method of synthesis 3-71664
 crystalline, light scattering rel. to structure (*German*) 3-65013
 crystalline, stress-strain dependence, adiabatic and veritable processes (*Rumanian*) 3-73033
 crystalline, uniaxially oriented, elastic deformation, heat release, thermoelasticity rel. to supermol. structure 3-71683
 crystallinity, structural kinetic mechanism (*French*) 3-52583
 crystallisation, chain molecule crystal formation theory (*German*) 3-60676
 crystallisation, isotropic small angle scatt. models for lamellar struct. (*German*) 3-60670
 crystallisation mechanism, surface energy rel. to chain flexibility (*Russian*) 3-79243
 crystallization morphology, effect of mechanical field 3-79240
 deformability, wide temp. range, device for plotting thermomechanical curves, constant load, continuous heating 3-55915
 deformation properties, theoretical prediction (*Russian*) 3-58766
 dextran-mediated cellular interactions, electrostatic effects 3-61893
 dextran/erythrocyte systems, electrokinetic potential of cells and other charged particles 3-61892
 diacetylenes, Raman spectral changes during the solid-state polymerisation 3-57685
 1-4-diaminopiperazine polymers and metal chelates, dynamic mechanical, thermal electrical and tensile props. 3-80462
 dielectric constant and loss tangent, heated meas. cell, temp. dependence 3-48469
 diffusion of a solvent with small molcs., stress-dependent diffusion equation 3-57688
 digital computer applies. 3-69385
 dilute polymer solution jet, destruction of high C steel 3-72913
 dilute polymer solutions, thermomechanics, multiple-bead-spring model 3-43530
 dilute soln., non-Newtonian flow, mass transfer with rotating disc 3-71816
 dilute solns., round turbulent jet, laser-Doppler meas. 3-75283
 dilute solution, torsional quartz crystal method for viscoelastic measurements 3-77381
 dilute solution flow behaviour, frictional resist. of rotating disc 3-43628
 dilute solutions, mass transfer 3-57827
 dilute solutions, modified Huggins' eqn. of thermodynamic interaction parameter 3-47602
 dilute solutions, Taylor vortices and evaluation of material constants 3-60573
 dilute solutions flow over a rough surface, wall pressure fluctuations 3-54823
 diphenylene oxide, relaxation times (*Russian*) 3-71669
 discharge channel initiation and propagation 3-47213

polymers continued

- dissolved long chain alkanes, length effect on interaction 3-40686
 drag reducing solutions, in presence of high-phase velocity disturbances, laminar pipe flows stability 3-60570
 drain dimensions in bulk and soln. 3-65038
 dye molecules aggregates, effect of local field in electronic spectra 3-67807
 dynamic loading, review 3-55899
 elasticity, statistical thermodynamic theory 3-45666
 elastomer, chain rigidity from i.r. spectra (*Russian*) 3-71670
 electrical properties, review 3-44363
 electrification, during extrusion 3-47482
 electrochromic effect on polymeric matrix photochromic spiran 3-71694
 electron energy loss study during radiation damage 3-54987
 endpoint distribution of self-avoiding walks 3-51835
 epoxide, thick walled tubes, nonlinear creep under internal pressure rel. to nonlinear generalized Maxwell equations 3-58754
 epoxy resin, cured, filled with mica flake, dynamic mechanical props. 3-69379
 epoxy resin, laser absorption waves, coupling loss mechanism, explt. obs. with 5 ms 10.6 μ radiation 3-66858
 epoxy resin, short-term action of static loading and aggressive liq. media influence on mech. props. (*Russian*) 3-80469
 epoxy resin, thermoplastic mixture, n.m.r. study mol. mobility 3-64578
 epoxy resin, tree growth characs. caused by discharges in artificial cavities 3-50519
 epoxy resin curing reaction, analogue computer simulation 3-50831
 epoxy resin systems of reduced viscosity, gamma-irradiated, mechanical properties 3-50786
 epoxy resin-aliphatic resin:polyethylenepolyamine models, metal surface finish, dimensional deviations 3-50812
 epoxy resins, diamine-cured, dynamic mechanical props. 3-69378
 epoxy resins, impregnation of superconducting magnet windings 3-58786
 epoxy resins (ED5, ED6), relaxation times (*Russian*) 3-71669
 epoxy resins cured by acid anhydride, electrical conductivity rel. to struct. features 3-47467
 epoxythiokol bond, elastoplastic props. 3-58764
 e.s.r. spectra of polymers with a system of conjugated bonds in solution 3-60499
 etching, by h.f. oxygen discharge plasma, surface temps. 3-64253
 etching, distortion caused by working gas, electron conc. (*Russian*) 3-73068
 ethylene and vinyl acetate copolymers, partly crystalline, molecular mobility, dynamic meas. (*German*) 3-63589
 ethylene-1-olefin copolymer series, ^{13}C n.m.r. studies, chemical shift, short-chain branch distribution in low-density polyethylene 3-54763
 ethylene-phosphonic acid copolymers, X-ray study of structure 3-54934
 ethylene-propylene copolymer, effect of composition on electric props. 3-64352
 ethylene-vinyl acetate copolymer, dielectric loss, permeability and relaxation, elec. cond., dependence on composition (*Russian*) 3-47206
 ethylene-vinyl acetate copolymer, effect of composition on electric props. 3-64352
 ethylene-vinyl acetate copolymer, equilib. stress, temp. depend., 38-42°C 3-69386
 extensional flow through small orifices 3-63790
 fibre filter, hydrodynamics, ultrafine fibres of 3-71787
 fibre optics, use in, appls. 3-62071
 filled polymers, polymer-filler interaction energy effect on T_g of filled polymers 3-61202
 filler effects on structure and properties 3-80482
 film, induced piezoelectricity by charge injection, rel. to three layer capacitive microphone 3-68931
 film, low loss, with adjustable refr. index 3-53157
 film, viscoelastic deform. following extended Voigt model 3-40955
 films, critical angle refractometry 3-42553
 films, impact testing technique 3-50807
 films, laboratory methods of prep., review 3-48346
 flow between calender roll, force and energy parameters 3-61218
 flow between two rotating cylinders 3-40725
 flow of liquids with polymer admixture, applicability of viscoelastic hypothesis (*Russian*) 3-63771
 fluid behaviour in elongational flow (*Polish*) 3-60501
 fluorocarbon, thin films, struct. and props. depend. on sputtering conditions (*French*) 3-80157
 Fortisan, variance anal. of X-ray profile line broadening 3-79241
 fractographic method for brittle fracture transition determ. 3-58765
 fracture mechanics, review 3-76364
 fracture of solid polymer, cooperative kinetics, focus mechanism 3-72124
 fracture surface energy, dependence on mol. wt., entanglement model 3-63595
 free radicals, in stressed high polymers, e.s.r. obs. (*German*) 3-61223
 friction characts., prior loading effect (*Russian*) 3-58722
 friction initial stages of slip 3-65018
 frictional properties, surface temp. effect (*Russian*) 3-80470
 gelatin, dielectric dispersions 3-58472
 glass reinforced plastic cylinders, thin walled load bearing capacity and deformation under torsional loading 3-58714
 glass reinforced polyester, surface microcracking, artificial weathering 3-76359
 glass transition temp. rel. to expansion coeffs. 3-54935
 glass-fibre-reinforced polyester resin, Young's modulus, shear modulus, damping, fibre diam. effects 3-47460
 glassfibre reinforced Araldite epoxy resin, thermal contraction meas., use in thermal cond. app., 77-300 K 3-73005
 glassy, cracking and crazing 3-46672
 glassy, creep. 3-46669
 glassy, diffusion and sorption of gases, mechanism 3-46734
 glassy, environmental crazing, solvent absorpt. role 3-58729
 glassy, impact test, model exam. 3-58778
 glassy, physics, book 3-46591

polymers continued

- glassy, post-yield behaviour 3-46666
 glassy, relaxation processes 3-46676
 glassy, structure, packing density, free volume concepts, mech. behaviour 3-46592
 glassy, thermodynamics 3-46718
 glassy, toughening by rubber reinforcement, review 3-47481
 glassy, yield behaviour 3-46665
 glassy polymers, use of Rheoribron for meas. of dynamic moduli 3-42515
 globule, dye sorption, energy migration 3-69080
 glycidyl amine resin systems of reduced viscosity, gamma-irradiated, mechanical properties 3-50786
 heteropolymer melting, random two-component one-dimens. Ising model 3-63572
 hydrodynamics, sedimentation of chain in dilute solution 3-67877
 impregnated porous brittle materials, stress conc. factors 3-55839
 insulation, examination of discharge and chemical treeing 3-50516
 ion charge carrier transport in low field, minimum hole size (*Japanese*) 3-44067
 i.r. intensities calc. in disordered polymers 3-71673
 i.r. spectroscopy, multiple reflection, methods and instruments (*Polish*) 3-70311
 isotactic helical, conformational and packing stability 3-67869
 isotropic materials, strength criteria representation in two-dimens. invariant space 3-55897
 Kapron monofilaments, breakdown surface, microdeformation, cracks, scanning electron microscope studies (*Russian*) 3-47480
 lamellar structure, X-ray small angle scatt. analysis (*German*) 3-60671
 lamellar thickening, chain extended growth, annealing 3-69389
 latex film formation 3-80460
 latexes, particle size distribution determ. with an ultracentrifuge (*German*) 3-41825
 latexes, synthetic, mech. stability 3-50791
 lausan, etching, distortion caused by working gas, electron conc. (*Russian*) 3-73068
 lifetime rel. to bond rupture kinetics 3-65017
 light-scattering method for obs. of fine scale structure 3-59578
 linear, free volume rel. to temp., chain thickness, spectral factor (*Russian*) 3-71689
 linear chains, elastic interaction with periodic potentials 3-71681
 liquid crystal cholesteric polymer solutions, shear induced structural changes mechanism, reflectance spectra, rheological props. 3-49843
 liquids, equilibrium model based on cell theory extended to polymeric molecules 3-63940
 local diffusion, segmental solubility 3-73044
 local stress distrib. and deformation props., effect of microcracks, network model 3-49928
 lubricant films, friction coefficient as function of pressure, reply to comments 3-44676
 luminescence during deformation, breaking and friction, gas-discharge processes (*Russian*) 3-47313
 Makrolon, mechanical properties, prolonged storage effect 3-80488
 maleic acid-styrene, copolymer, conformational transition in NaCl soln., standard free energy, volume change 3-54765
 mathematical introduction, solved problems, book contrib. 3-58767
 mechanical properties, hydrostatic press. effect, review 3-80475
 melt, diffusion of long chain molecule, effect of entanglements 3-57686
 melt, effect of entanglements on viscosity 3-57687
 melt, effect of pressure on viscosity 3-65019
 melt rheology, recent publications, review 3-50784
 melts, flow between coaxial cylinders under complex shear conditions 3-73048
 melts, shearing flow, anisotropy, second normal stress difference meas. 3-71842
 melts, temperature-invariant rheological dependences obtained using Leonov-Vinogradov model 3-57699
 membranes, homogeneous swollen, hydraulic permeability rel. to diffusion 3-54773
 methacrylic acid-cotton fibre copolymer, internal microstructure, electron microscopy, prep. technique (*Russian*) 3-47479
 methylmethacrylate, polymers and copolymers, Raman spectroscopy, sample preparation, quantitative analysis 3-58496
 MHD elastico-viscous flow past plane porous plate, velocity field soln. 3-40736
 molecular weight determination, gel permeation chromatography, viscometry (*German*) 3-71662
 molecular weights calculation 3-54760
 molecular wt. and size by one conc. method in light scatt. 3-40687
 molecular wt. distribution determ. by temperature drop turbidimetry 3-57682
 molten, heat capacities 3-67883
 molten, helical flow, non-Newtonian fluid, cylindrical annulus, shear dependence of viscosity 3-73061
 molten flow, instability in extrusion 3-67889
 molten flow, pressure effect on shear viscosity 3-63599
 moulding, diametral test, finite element analysis 3-80493
 moulding, injection, Newtonian fluid filling a rectangular mould, theoretical analysis 3-76377
 multichain, mol. size distrib. theory, condensation products of R-A with R'-B 3-63567
 multiphase mixture properties, pair additivity principle 3-73042
 Mylar capacitor, reactor irradi. effect on dielec. loss peaks, crystallinity 3-68923
 n-bis ω -oxybutoxy methylphenylsilyl diphenylene oxide, relaxation times (*Russian*) 3-71669
 neutral polymer adsorption on cells and other charged particles, effect on diffuse double layer 3-61235
 neutral polymer effect on electrokinetic potential of cells and charged particles, zeta potential increases 3-61234
 Newtonian liquid, die swell 3-58760
 nitrocellulose, film, subject to static and fatigue loading, arterial crack growth 3-55895
 nomadic polarisation, for dielectric consts. above one hundred 3-47199
 non-Gaussian polymeric networks, photoelastic props. (*Russian*) 3-49517

polymers continued

- non-Newtonian fluid flow, frictionally heated, crit. parameters 3-63646
 non-Newtonian fluids, axial dispersion in porous media 3-57841
 non-Newtonian fluids, entrance flows 3-52485
 nonlinear panels, equilibrium states, original imperfections influence 3-54114
 nylon 6 fibre, highly oriented, creep failure, nucleation process 3-73049
 nylon capacitor, reactor irradi. effect on dielec. loss peaks, crystallinity 3-68923
 nylons, viscoelastic studies, high-press. torsion pendulum 3-51529
 oligomer, temp. depend. of relaxation times, bulk and thin layers (*Russian*) 3-71669
 opaque materials, subcrit. cracking, compliance method 3-44654
 organic resin/inorganic filler mixture, dielec. const. calc. 3-76333
 oriented, theoretical strength from intermolecular interaction and finite chain length 3-57698
 oriented amorphous, i.r. dichroism theory 3-80043
 oxidation studies, thermistor based DTA apparatus 3-77397
 partially crystalline, elec. breakdown (*German*) 3-55524
 particle engulfment by solidifying melts, thermodynamics 3-61210
 particle-polymer disperse systems, dynamic viscoelasticity (*Japanese*) 3-40693
 Pentaplant, effect of crystallinity degree on electric props. 3-64352
 percolation expts. 3-71677
 perspex, dielectric breakdown 3-64604
 phenol formaldehyde industrial resins, structural changes during heat treatment (*Russian*) 3-63603
 phenolformaldehyde resin binder for graphitic fuel elements, rheology under press. (*German*) 3-71267
 phenoxy resin, solvent effect on form. of crystalline entities 3-79239
 phenylthiourea selective resins, ion exchange, Ag⁺ recovery, photographic fixing soln. 3-53335
 photopolymer, holographic material, study by thick grating 3-77529
 physical tests, at cryogenic temp. 3-58726
 plastic relaxation via twist disclination motion 3-40972
 PMMA, accelerated removal of microcracks by dry friction 3-58752
 PMMA, amplitude behaviour of shock waves, theory 3-79426
 PMMA, biaxial orientation birefringence, rel. to degree of deformation 3-71682
 PMMA, brittle crack motion 3-75563
 PMMA, compression yield behaviour, temp. and strain rate depend. 3-58728
 PMMA, crack velocity at fracture, plastic zone model and heat output (*German*) 3-60770
 PMMA, creep and low-cycle fatigue, hereditary theory 3-65015
 PMMA, dynamic compliance, creep 3-80492
 PMMA, environmental crazing, solvent absorpt. role 3-58729
 PMMA, fatigue crack retardation and closure 3-76381
 PMMA, fraction mechanism in methanol at low temp. (*Russian*) 3-58723
 PMMA, fracture surface relief, rel. to kinetics of main crack growth 3-73054
 PMMA, friction props., effect of surface-active agents 3-73056
 PMMA, glassy state, cyclically changing temps. effect during subsequent loading 3-55900
 PMMA, heat outputs from plastic zones of fast running cracks 3-65002
 PMMA, impact tests, fracture toughness and absorbed energy release 3-58779
 PMMA, laser-irradiated, nontransparent inclusions, scattering centres, elastic-stress fields 3-73060
 PMMA, max. Newtonian viscosity and dipole relaxation polarisation (*Russian*) 3-80495
 PMMA, slowing down of cracks 3-58762
 PMMA, stereocomplex between isotactic and syndiotactic oligomers in soln., struct., n.m.r. obs. 3-75168
 PMMA, symmetric branching of cracks 3-65007
 PMMA suspension in dibutyl phthalate rheological props. 3-61231
 polyethylene, non-Newtonian flow under conditions of an inhomogeneous temp. distribution 3-63593
 poly(amide carboxylic acid) solution, flow birefringence, 30°C, molecular dimensions, triethylamine addition effect 3-54781
 poly(capromide), salted, rel. to melting behaviour 3-52410
 poly(dimethyl siloxane), glass transition temperature meas. 3-79242
 poly(dimethylsiloxane), Raman depolarization, temp. and strain depend., config. energy difference 3-40689
 poly(ethylene terephthalate), cyclic, statistical conformation, equilibrium concs. 3-54766
 poly(ethylene terephthalate) film, electron irradi., cross-linking and chain scission 3-46596
 poly(glycine), short chains conformational statistics, chains with constrained ends, partition function 3-75162
 poly(L-alanine), short chains conformational statistics, chains with constrained ends, partition function 3-75162
 poly(n-butyl methacrylate) networks, viscoelasticity, stress-strain behaviour, effect of reference chain dimension, thermoelastic meas. 3-55890
 poly(N-vinylcarbazole) films, cond. and photocond., carrier generation processes 3-52873
 poly(vinyl chloride) electrical conductivity theory 3-79706
 poly-1-butene, effect of allotropic form on static mech. props. (*French*) 3-63592
 poly-1-butene, heat capacity in molten and solid states 3-67883
 poly-4-methyl-1-pentene and poly-3-methyl-1-butene, crystall., conformational and packing stability 3-67869
 poly- γ -ethyl-L-glutamate soln. in ethyl acetate, diamag. susceptibility anisotropy 3-58365
 poly-L-alanine, i.r. spectra, n.m.r. study, config. transform., struct. 3-63581
 poly-L-glutamic acid, length depend. resolved pseudo-Raman spectra 3-78920
 poly-L-glutamic acid, partially resolved pseudo-Raman band 3-78919
 poly-L-glutamic acid sodium salt, Raman like non-fluorescent broad band 3-55586
 poly-L-leucine i.r. spectra, n.m.r. study, config. transform., struct. 3-63581

polymers continued

- poly-o-bromostyrene in benzene soln., high-resolution small-angle X-ray and light scatt. for mol. wt. determ. 3-67868
- polyacetaldehyde, cryst., conformational and packing stability 3-67869
- polyacrylamide admixture effect on turbulent flow of water in flat rough tubes (*Russian*) 3-67770
- polyacrylamide soln. flow curve determ., rolling-ball viscometer 3-71688
- polyacrylamide solutions, viscoelastic liquid, flow patterns upstream of orifices 3-71754
- polyacrylates and model compounds, ^{13}C n.m.r. 3-63576
- polyacrylic acid and model compounds, ^{13}C n.m.r. 3-63576
- polyacrylonitrile, effect of heat treatment on supermolecular structure (*Russian*) 3-71693
- polyacrylonitrile, glassy and rubber like states, relax of $[\text{Cr}(\text{H}_2\text{O})_6]^{3+}$ and $[\text{Mn}(\text{H}_2\text{O})_6]^{2+}$, e.s.r. 3-72511
- polyacrylonitrile, influence of macromolecular stereoregularity, thermal transform. prod. 3-63600
- polyacrylonitrile, Kr adsorption isotherms 3-68487
- polyacrylonitrile, struct. form. in aq. dispersion, elastic props. 3-65025
- polyacrylonitrile fibres, stress relaxation peculiarities 3-63602
- polyacrylonitrile fibres, u.v. dichroism of $\text{C}\equiv\text{N}$ valency vib. bands (*Russian*) 3-64689
- polyalkenamers, n.m.r. and i.r. spectroscopy, structural unit determ. 3-54046
- polyalkyl acrylates, spin-lattice and dielectric relaxation, effect of chain length and kinetic flexibility (*Russian*) 3-50487
- polyalkyl methacrylates, spin-lattice and dielectric relaxation, effect of chain length and kinetic flexibility (*Russian*) 3-50487
- polyalkyl vinyl ethers, ^{13}C n.m.r. studies on stereochemical configurations 3-63577
- polyamide 6,6, annealing, effect on crystallinity, density and heat of fusion (*German*) 3-60673
- polyamide-6 fibres, effect of drawing, X-ray diffraction patterns, intensity distrib. along layer lines (*Russian*) 3-47476
- polyamides aliphatic, struct., lower freq. i.r. spectra (*German*) 3-71666
- polyaminoborane $[\text{BH}_2-\text{NH}_2]_n$ (B-chloro- and N-chloro-derivatives), LCAO MO band structure 3-71667
- polyaurolactam, effect of N-substitution on crystallinity 3-63961
- polybutadiene, copolymer, three-block, structure, rheological properties and pouring index (*Russian*) 3-71690
- cis-1,4-polybutadiene chains, bound protons transverse magnetisation, fluctuation effects, Rouse model explanation 3-40690
- trans-1,4-polybutadiene i.r. evidence for folded chain model 3-72014
- polycapromamide, diffusion-stabilized, wear resist. (*Russian*) 3-58725
- polycapromamide and cellulose hydrate films supermolecular structs., dimens. 3-63582
- polycaprolactam, fracture surface relief, rel. to kinetics of main crack growth 3-73054
- polycaprolactam-resin crumbs, hydrodynamics of a spouting bed 3-63756
- polycarbonate, bisphenol-A, short range intermol. ordering obs. by radial distrib. functions 3-80473
- polycarbonate, Charpy notched impact strength, A and B forms comparison 3-80474
- polycarbonate, craze formation, kinetics, stress intensity factor 3-55887
- polycarbonate, creep and recovery behaviour under high tension and compression stresses 3-47470
- polycarbonate, dynamic fracture, shock damage 3-68331
- polycarbonate, mechanical properties, prolonged storage effect 3-80488
- polycarbonate, Raman spectra, using He-Ne laser 3-64658
- polycarbonate, solvent effect on form. of crystalline entities 3-79239
- polycarbonate, steel disc reinforced, strength improvement 3-80440
- polycarbonate and ABS resin, drawability, effects of temp. and punch speed 3-65000
- polycarbonate as model material for three-dimens. photoplasticity 3-73064
- polycarbonate plates, yielding in front of through cracks in pure bending 3-76382
- polychloroprene-microgel characterisation by light scattering (*German*) 3-41824
- polychlorotrifluoroethylene, viscoelastic studies, high-press. torsion pendulum 3-51529
- polydimethylsiloxane, used for toughening of polystyrene 3-55903
- polydimethylvinylsiloxane, toluene solution, light scatt., mol. wt., gyration radii, Zimm method (*Polish*) 3-57697
- polyelectrolyte immersed in 1:1 electrolyte, mean square radius 3-58801
- polyelectrolyte membranes, elec. cond. and persistent elec. polarization, coexistence 3-41475
- polyene, in frozen polycryst. soln., quasiline spectra as zero-phonon lines 3-72635
- polyene, SAMO method calcs. 3-54767
- polyester resin, unsaturated glycol derived, dielectric absorpt. rel. to struct., 65-190°C (*Japanese*) 3-53062
- polyethylene terephthalate, molecular mobility and structure 3-60502
- polyethylene, γ -ray irradi., elec. cond., after annealing 3-46864
- polyethylene, absorption currents and photocurrents 3-58300
- polyethylene, biaxially oriented linear, mech. α -relax. anisotropy 3-58727
- polyethylene, branching, X-ray diff. obs. 3-54930
- polyethylene, charge build up from electron irradiation 3-44372
- polyethylene, combined tension-torsion creep with abrupt stress changes 3-58740
- polyethylene, conductivity changes at first order phase transition 3-46865
- polyethylene, crystal defects, structure, transformation data, Maander model (*German*) 3-60677
- polyethylene, crystal twisting rel. to surface stress, approx. model 3-54931

polymers continued

- polyethylene, crystalline, specific heat C_p rel. to C_v vibrational spectra calc. 3-55089
- polyethylene, crystallite size distrib. and lattice distortion, Debye-Scherrer line profiles 3-40850
- polyethylene, drawn, annealed, relaxation processes, effect on conformation and orientation factors (*Russian*) 3-47477
- polyethylene, dynamic light scattering, expt. procedure 3-57694
- polyethylene, elasticity tensor, in 10-60°C range 3-58744
- polyethylene, electrical treeing resistance, effect of liquid absorption 3-47216
- polyethylene, electron irradiated, drawn fibres, structural defects rel. to molecular structure 3-55889
- polyethylene, environmental stress cracking 3-67885
- polyethylene, etching, distortion caused by working gas, electron conc. (*Russian*) 3-73068
- polyethylene, fibre and row struct., X-ray pole diag. obs. (*German*) 3-61224
- polyethylene, glassy, high elastic deform., kinetics, decrease 3-67881
- polyethylene, high density, crystallisation from dil. soln., heterogeneous nucleation 3-80461
- polyethylene, high density, electron microscope, X-ray analysis of crystal distortion (*Russian*) 3-71692
- polyethylene, high temp. thermoluminescence obs. 3-64746
- polyethylene, high-density, with single cryst. texture, structure 3-57993
- polyethylene, Kirkwood's model, exact phonon Green function 3-58089
- polyethylene, linear, effect of mol. wt. and crystallization conditions on dynamic mech. meas. (*Spanish*) 3-76368
- polyethylene, linear, low-temp. toughness below glass transition 3-49852
- polyethylene, linear, single-cryst. texture, thermal expansion, 0 to -190°C 3-58734
- polyethylene, linear, u.h. modulus, mod. weight effects on cold drawing, extended chain crystn. 3-50781
- polyethylene, liquid permeated membrane useful life determ. using electron microscopy 3-80576
- polyethylene, low density, effect of filling melt on the first difference of the normal stresses and on tangential stresses 3-58758
- polyethylene, low density, fatigue crack propagation, mean stress depend. (*Japanese*) 3-53278
- polyethylene, low density, tree growth characs. caused by discharges in artificial cavities 3-50519
- polyethylene, low freq. spectrum, conformational defect induced features, interpretation 3-43527
- polyethylene, low pressure, effect on rubber props. 3-73043
- polyethylene, low-density, short-chain branch distrib., ^{13}C n.m.r. studies of ethylene-1-olefin copolymers 3-54763
- polyethylene, mobility measurement at low temp., transient space charge limited current theory 3-52834
- polyethylene, molecular motion, n.m.r. line shape analysis (*German*) 3-61007
- polyethylene, molten, heat capacity 3-67883
- polyethylene, molten, steady flow, dynamic viscoelasticity 3-67886
- polyethylene, multiple transitions, glass temp., low-temp. toughness 3-63962
- polyethylene, negative coeff. of thermal expansion obs., following elongation 3-58140
- polyethylene, n.m.r. of molecule with fixed ends rel. to partly crystallised struct. (*German*) 3-60999
- polyethylene, optical absorption rel. to electrical conduction 3-41529
- polyethylene, oriented, plastic deform. mechanisms, tensile tests 3-58730
- polyethylene, oxidised, electric breakdown at -196°C and -65°C 3-50515
- polyethylene, paracrystalline lattice, small angle X-ray scatt. 3-72012
- polyethylene, periodically loaded, isotropic specimen lifetimes, superposition principle 3-80481
- polyethylene, pressure dependence of thermal conductivity, thermal diffusivity and specific heat 3-43881
- polyethylene, Raman spectra, devices for obs. up to 50 kbar pressure 3-80027
- polyethylene, SAMO method calcs. 3-54767
- polyethylene, small angle X-ray scatt. curve evaluation, two phase model validity 3-72013
- polyethylene, spherulites, twist model interpret., SEM obs. 3-57992
- polyethylene, spherulitic, crystal morphology and elastic moduli 3-68171
- polyethylene, struct. changes during annealing and fusion (*Russian*) 3-80498
- polyethylene, submicrocrack formation and concentration, in loading and unloading 3-58742
- polyethylene, temp. depend. of photocurrent 3-46874
- polyethylene, tensile deformation, calorimetry 3-61216
- polyethylene, tensile deformation, effect on melting point, specific vol., vol. coeff. of expsn. 3-80483
- polyethylene, thermoluminescence, due to molecular oxygen and aromatic molecules (*German*) 3-61080
- polyethylene, transcrystalline, morphology rel. to mechanical props. 3-40851
- polyethylene, treeing, growth and forms rel. to generated gas volume 3-50518
- polyethylene, use in nuclear reactors (*German*) 3-67595
- polyethylene, u.v. transient photocurrents with zero external field 3-79728
- polyethylene, valence and cond. band calcs. 3-79629
- polyethylene, wetting by water, methylene iodide and methyl iodide-decalin mixtures 3-43927
- polyethylene and cellophane films, adhesion, microrheological process effects 3-55893
- polyethylene carbon monoxide copolymer crystal, morphology, unit cell dimensions 3-69387
- polyethylene chains, conformational defects, group theoretical aspects 3-43525

polymers continued

- polyethylene composites, adhesion bond, temp. stresses at polymer-filler interface 3-80448
- polyethylene crystals, Moire fringes due to triple lamellae, electron microscope obs. 3-79355
- polyethylene dynamic light scattering, expt. results 3-57695
- polyethylene echelette gratings, double-ruled, large-constant, for long wavelength i.r. region 3-62060
- polyethylene fibres, effect of drawing, X-ray diffraction patterns, intensity distrib. along layer lines (*Russian*) 3-47476
- polyethylene film, chain extended crystallisation, lamellar thickening 3-69390
- polyethylene film, diffusion of antistatic agents, surface cond. study 3-65004
- polyethylene film, heat treated, adhesion strength on steel and Al, metal-catalysed oxidation 3-73057
- polyethylene glycol, adsorption on graphitised C black, gas chromatography 3-72263
- polyethylene glycol, i.r. absorpt. curve calcs. for different length and config. (*Russian*) 3-63584
- polyethylene glycol dilute soln. elastico-viscous liquid, oscillatory laminar flow, velocity profiles in tubes of circular section 3-54822
- polyethylene melt, effect of pressure on viscosity 3-65019
- polyethylene melt, shear and elongational flow, stress-time data, network theory predictions 3-73062
- polyethylene melt, stresses, periodic deformations, effect of vibration frequency and amplitude variations, Weissenberg rheogoniometer 3-76380
- polyethylene melt, viscoelastic flow through converging ducts, wall normal stresses, die swell behaviour 3-80459
- polyethylene oxide, viscoelastic flow, hole error meas. 3-67966
- polyethylene oxides unsubstituted, effect on AgBr photographic sol conversion to AgI, reaction kinetics, turbidimetric studies 3-53338
- polyethylene paper, liquid N₂ impregnated, elec. insulation, cryogenic power cable, simulated load tests 3-48389
- polyethylene plasma, laser prod., shock hydrodynamic phenomena, core-corona decoupling 3-54872
- polyethylene powder filter, spectral transmission 3-62072
- polyethylene Raman spectra, low frequency modes, lattice vibrations and pressure dependence 3-47249
- polyethylene sheet, effects of corona discharges, SEM obs. 3-63899
- polyethylene single cryst., amorphous surface layers thickness 3-58168
- polyethylene single crystals, melting and morphology 3-67884
- polyethylene single crystals, plastic deform. by dislocation motion 3-40961
- polyethylene solutions, Mark-Houwink relations 3-71680
- polyethylene terephthalate, amorphous, nuclear relaxation, spin dynamics 3-75909
- polyethylene terephthalate, amorphous state, annealing, change in supermolecular state 3-60667
- polyethylene terephthalate, carrier mobility, temp. depend. 3-64329
- polyethylene terephthalate, carrier mobility measurement by electron beam bombardment 3-50209
- polyethylene terephthalate, crystallinity determ. by X-ray diffraction 3-43758
- polyethylene terephthalate, crystallisation, kinetics of growth of spherulites 3-57690
- polyethylene terephthalate, molecular reorientation, polarized Raman scatt. 3-67873
- polyethylene terephthalate, molten, departure from Newtonian behaviour 3-53285
- polyethylene terephthalate electret, surface charge and i.r. absorp. characs. 3-68917
- polyethylene terephthalate fibre, effect of thermal treatment on thermomechanical props. (*Russian*) 3-80496
- polyethylene terephthalate film, solid-state transitions investigation by temperature tear strength method 3-61221
- polyethylene transmission of beta-particles in presence of elec. field (*Russian*) 3-79396
- polyethylene/fibrous fillers composites, coeffs. calcs. 3-80450
- polyethyleneglycol, effect of chain length and conformation on i.r. spectra (*Russian*) 3-63583
- polyethyleneglycol adipate, i.r. spectra and polymorphism (*Russian*) 3-63964
- polyethylenimine-polyacrylate, rotation viscometer study of Newtonian flow 3-43630
- polyethylenepolyamine cured aliphatic resin-epoxy resin models, metal surface finish, dimensional deviations 3-50812
- polyethylenepolyamines, effect of changes in conformation and units in chain on i.r. frequencies 3-54762
- polyethyleneterephthalate, crystallisation, meander model of microstruct. (*German*) 3-60669
- polyethyleneterephthalate, mech. relax. props., 100-525K, crystallinity effects (*Russian*) 3-80494
- polyethyleneterephthalate, n.m.r. study of crystallisation, orientation effect, molecular movement (*Russian*) 3-71691
- polyfluorocyclobutyl silanes, mass spectra fragmentation rel. to struct. (*Japanese*) 3-78921
- polyhexene-1, amorphous, cooling rate influence on heat capacity and thermal transitions 3-50008
- polyimide film, thermally assisted tunnelling in elec. cond. 3-46851
- polyimide insulation, photocond. under electrical stress 3-46878
- polyimides, strength and relaxation props. (*Russian*) 3-80499
- polymineborane [BH=NH]_n (B-chloro- and N-chloro-derivatives), LCAO MO band structure 3-71667
- polyisobutylene, viscoelastic props., bubble inflation technique 3-67890
- polyisobutylene fluids, normal stress data correlation 3-67892
- polyisobutylene in transformer oil, inf. of press. and temp. on u.s. absorption 3-75572
- polyisobutylene solution, conc., inflow into a flat slot, polarisation-optical study, stress anal. (*Russian*) 3-46366
- polyisobutylene solutions, dynamic viscosity and elasticity, effect of steady-state flow 3-71686
- polyisoprene, copolymer, three-block, structure, rheological properties and pouring index (*Russian*) 3-71690
- polyisopropyl acrylate, ¹³C n.m.r. 3-63576

polymers continued

- polyisoxazole and polyisoxazolines, resist. temp. depend., semicond. behaviour 3-58265
- poly-L-alanine, far-i.r. absorpt. spectra, 4-200 cm⁻¹, α -helix behaviour 3-78917
- polymer, treeing breakdown, voltage induced mechanism, review 3-47214
- polymer semiconductors, with conjugate C-N bonds electrophotographic properties (*Russian*) 3-55986
- polymer solution turbulent submerged jets, long-range nature 3-57860
- polymeric glasses, residual entropies calc. 3-58137
- polymethane, rigid, porous, vibrocreep, recovery 3-73052
- polymethine chains, alternating binding angles, max. overlap principle (*German*) 3-63571
- polymethine cyanine dyes, bleaching kinetics, fluoresc. decay time 3-48877
- polymethine dye laser, flashlamp-excited, quenching effects 3-66832
- polymethyl acrylates and model compounds, ¹³C n.m.r. 3-63576
- polymethyl methacrylate, glassy, Brillouin scatt. from transverse phonons 3-80030
- polymethyl methacrylate, in CO₂ and Ar, pulse calorimetry, reaction kinetics (*Russian*) 3-45432
- polymethyl methacrylate, photoinduced for holographic diffr. grating form. 3-62143
- polymethyl methacrylate, transmission of beta-particles in presence of elec. field (*Russian*) 3-79396
- polymethyl vinyl ether, ¹³C n.m.r. studies on stereochemical configurations 3-63577
- polymethylenes, Raman spectra, low frequency modes, lattice vibrations and pressure dependence 3-47249
- polymethylmethacrylate, craze formation, kinetics, stress intensity factor 3-55887
- polymethylmethacrylate, cryst., conformational and packing stability 3-67869
- polymethylmethacrylate, dynamics, spin lattice relax. study 3-67880
- polymethylmethacrylate, film, subject to static and fatigue loading, arterial crack growth 3-55895
- polymethylmethacrylate, fracture characteristics, under cubic compression, subject to laser radiation 3-58750
- polymethylmethacrylate, fracture under steady-state crack propag. conditions 3-58761
- polymethylmethacrylate, heat capacity in molten and solid states 3-67883
- polymethylmethacrylate, recharging effect by beam of fast electrons 3-75939
- polymethylmethacrylate, tree growth, caused by discharges in artificial cavities 3-50519
- polymethylmethacrylate, void free, ambient O₂ effect on a.c. tree generation 3-47215
- polymethylmethacrylate matrix absorption and fluorescence of anthracene 3-63507
- polynucleotide chains, internal rot. barriers 3-46358
- polyolefins, crystallisation, heterogeneous nucleation mechanism 3-57691
- polyoxyethylene oligomers, molecular optical anisotropy, depolarised Rayleigh scattering 3-49469
- polyoxymethylene, acicular single crystals, strength props. 3-54779
- polyoxymethylene, heat capacity, calc. from frequency distrib. 3-55088
- polyoxymethylene, paracrystalline lattice, small angle X-ray scatt. 3-72012
- polyoxymethylene, X-ray diffraction, structure determination 3-75485
- polypeptide in non-protonating solvents, helix-coil transition, n.m.r. obs. 3-67870
- polyphenylene oxide, solvent effect on form. of crystalline entities 3-79239
- polyphenylsiloxanes, ladder, electro-optical props. 3-64627
- polypropene-2-d₁ sulphide, effect of deuterium-decoupling on n.m.r. spectrum 3-63578
- polypropylene, cryst., conformational and packing stability 3-67869
- polypropylene, film, subject to static and fatigue loading, arterial crack growth 3-55895
- polypropylene, isothermal crystallis. and crystallis. by constant rate cooling obs. (*German*) 3-60674
- polypropylene, laser Raman spectrum, cryogenic temp. to melting point 3-46362
- polypropylene, molten, heat capacity 3-67883
- polypropylene, oriented, plastic deform. mechanisms, tensile tests 3-58730
- polypropylene, oriented isotactic γ -form crystal, form. by α - γ transition 3-69149
- polypropylene, u.s. anisotropy meas. and mech. props. 3-53308
- polypropylene, use in nuclear reactors (*German*) 3-67595
- polypropylene composites, thermoplastic fibre reinforced, transcrystalline morphology 3-64985
- Polypropylene film, effects of corona discharge treatment on surface properties 3-60651
- polypropylene film-trichlorobiphenyl system, a.c. conduction and dielectric losses 3-47211
- polypropylene melt, effect of micro-additions on viscoelasticity (*Russian*) 3-80497
- polypropylene melt, processing, aging, effective viscosity, tensile strength, effect of polymeric antioxidants 3-73058
- polypropylene melt, temp. meas., i.r. fibre optics 3-45436
- polypropylene melt, viscoelastic flow through converging ducts, wall normal stresses, die swell behaviour 3-80459
- polypropylene oxide and deuterated derivative, dynamics, spin lattice relax. and neutron scatt. 3-67880
- polysaccharides, aq. soln., spin-spin proton relaxation 3-68876
- polysaccharides, i.r. spectra of carbohydrate crystals, phase transition 3-72655
- polysaccharides and saccharides, conformational analysis by n.m.r. (*Russian*) 3-63587
- polysilicic acid gels, mol. structure 3-44686
- polysiloxanes, liquid, viscous flow at high pressures, free energy, enthalpy, entropy, vol. of activation calc. (*Russian*) 3-46367

polymers continued

- polydisodium acrylate and model compounds, ^{13}C n.m.r. 3-63576
 polystyrene, atactic, effect of plasticizer content on electric props. 3-64352
 polystyrene, copolymer, three-block, structure, rheological properties and pouring index (*Russian*) 3-71690
 polystyrene, crack growth kinetics and fracture morphology, temp./time factors influence (*Russian*) 3-80471
 polystyrene, craze layer density on fracture surface 3-58738
 polystyrene, craze morphology rel. to shear-band morphology 3-58732
 polystyrene, deform., fracture, crazing, shear bands interaction 3-55892
 polystyrene, dynamic polarisation of protons, electronic spin-spin interactions contrib. 3-79891
 polystyrene, electrostriction due to phenyl group induced dipole moments (*German*) 3-61022
 polystyrene, film, subject to static and fatigue loading, arterial crack growth 3-55895
 polystyrene, intramolecular cross linking, meas. of dimensions 3-78915
 polystyrene, intramolecular cross linking, synthesis and chemical characterisation 3-78913
 polystyrene, intramolecular crosslinked molecules, dimensions in soln. 3-78914
 polystyrene, mixture with elastomers, mol. wt. effect on rheology 3-71676
 polystyrene, molten, heat capacity 3-67883
 polystyrene, pressure effect on viscosity, rheological data 3-63599
 polystyrene, replica technique, Brinell hardness testing of steel 3-50806
 polystyrene, rubber-modified, fracture mechanics 3-80490
 polystyrene, silas balloon filled, flow props. 3-69377
 polystyrene, spectral shift on formation, localisation of excitation 3-69081
 polystyrene, thermal diffusion in toluene 3-60500
 polystyrene, thermodynamic stability limits rel. to glass transition (*German*) 3-60675
 polystyrene, time resolved laser induced degradation, mass spectroscopy 3-70460
 polystyrene, toughening with polydimethylsiloxane 3-55903
 polystyrene, translational diffusion in butan-2-one solution, Rayleigh light scatt. obs. 3-67878
 polystyrene, triboelec. props., xerographic powder manuf. (*Polish*) 3-76379
 polystyrene containing paramagnetic impurity, spin-lattice relaxation of protons 3-72540
 polystyrene dilute theta solns. in cyclohexane, translational diffusion 3-49514
 polystyrene films, growth rate determ., formation by electrodeless r.f. excitation 3-50092
 polystyrene foam, heat conductivity meas. (*German*) 3-65044
 polystyrene latex, multiple scatt. in cylindrical cell 3-74206
 polystyrene latex colloidal suspensions, size distribution by light scattering 3-47485
 polystyrene lattices, coagulation rate meas., low angle light scattering technique 3-73089
 polystyrene layer, semiconductor-dielectric photographic system, electrostatic contrast, charge transfer method (*Russian*) 3-45523
 polystyrene mixed lattices, flocculation by addition of KCl soln. 3-44690
 polystyrene particles in aqueous suspension, dielectric properties at microwave frequencies 3-44692
 polystyrene solns. in toluene, monodisperse, refr. index increment, mol. wt. depend. 3-49516
 polystyrene solutions, viscoelastic props. 3-53291
 polystyrene solutions, viscosity, effect of mol. weight, range of shear stresses, structure formation and orientation 3-71687
 polystyrene-CdS, three-layer system, propag. of elastic transversal waves, dispersion eqns. (*Russian*) 3-55026
 polystyrene-cyclohexane system, cloud point curves near critical pt. 3-80489
 polystyrene-cyclohexane system, diffusion, temp. dependence 3-54774
 polystyrene-microgel characterisation by light scattering (*German*) 3-41824
 polystyrene- NH_4ClO_4 mixtures, catalytic decomposition, kinetics and mechanism, dynamic mass spectrometry, thermogravimetry (*Russian*) 3-47538
 polystyrene-polybutadiene-polystyrene copolymer, macrolattice based on lamellar morphology 3-63960
 polystyrol transmission of beta-particles in presence of elec. field (*Russian*) 3-79396
 polysulphone, solvent effect on form. of crystalline entities 3-79239
 polytetrafluoroethylene, ^{19}F phase transition, far i.r. meas. lattice modes determ. 3-41511
 polytetrafluoroethylene, and Na-treated polytetrafluoroethylene, wettability, roughness and anisotropy effects 3-58739
 polytetrafluoroethylene, Raman spectra, devices for obs. up to 50 kbar pressure 3-80027
 polythene and borated polythene shielding, calc. of leakage neutron spectra 3-49378
 polypeptide films, Fermi resonance in i.r. spectra 3-75169
 polyurethane, creep under varying temperature for nonlinear uniaxial stress 3-53283
 polyurethane, cross-linked, near i.r. spectra, chain orientation and interaction energies (*Russian*) 3-63586
 polyurethane, elevated temp. creep under nonlinear torsional stress with step changes in torque 3-53284
 polyurethane, fracture toughness and impact strength, Dugdale model 3-80472
 polyurethane, rigid porous material, simple stressed state, vibr. creep study 3-55894
 polyurethane, vibrocreep, biaxial loading, small vibrations 3-80480
 polyurethane, vibrocreep, under composite loading 3-58746
 polyurethane, vibrocreep coefficient 3-65016
 polyurethane block copolymers, segment size and polydispersivity effect on props. 3-58759
 polyurethane film, light modes, refr. index, thickness, dispersion 3-47335

polymers continued

- polyurethane foam, thermal insulation, cryogenic power cable, simulated load tests 3-48389
 polyurethane type foams, cellular structure, mechanical props., model anal. 3-73090
 polyvinylcarbazole, triplet excitons, number, heterogeneous photosensitisation 3-65111
 polyvinyl acetate, crack self-healing, temp. and crosslinking effects 3-55896
 polyvinyl acetate, self healing of cracks, molecular weight, and environment effects 3-58749
 polyvinyl acetate, self-healing of cracks, medium and layer thickness effects 3-80486
 polyvinyl alcohol, ^{13}C , n.m.r. studies, stereochemical placements 3-54764
 polyvinyl alcohol, thermoelastic props., gel formation in solutions 3-63601
 polyvinyl butyl, adhesion to glass, temp., strain rate effects 3-80484
 polyvinyl esters, spin-lattice and dielectric relaxation, effect of chain length and kinetic flexibility (*Russian*) 3-50487
 polyvinyl-iso-propenylacetylene ladder polyene with three fibre chains, thermal transformations, electrophysical props. 3-60503
 polyvinylacetate, i.r. bands, temp. depend., 173 to 493 K, CH_3 rot. activation energy 3-46363
 polyvinylalcohol fibres, effect of drawing, X-ray diffraction patterns, intensity distrib. along layer lines (*Russian*) 3-47476
 polyvinylbenzyltriethylammonium chloride fixer, effect on preservability of hydrotype colour images (*Russian*) 3-47597
 polyvinylcarbazole:trinitrofluorenone, amorphous films, absorption and electroabsorption spectra 3-61049
 polyvinylchloride, structurally disordered, vibr. spectrum 3-71672
 polyvinylchloride, use in nuclear reactors (*German*) 3-67595
 polyvinylidene chloride carbon, absorpt. characts. 3-68485
 polyvinylidene fluoride, film flow of Hell over polarised media 3-68461
 polyvinylidene fluoride, pyroelectricity as function of poling treatment 3-41486
 polyvinylidene fluoride film, metal ions injection in an electric field, effect on complex dielectric constant 3-58466
 10- polyvinylphenothiazine, complex based on elec. cond., spectral props. 3-63963
 polywater, anal. of anomalous condensates 3-61286
 powder, substrate, influence of temp. on struct. and transport props., of Bi films 3-50091
 precipitation from supersaturated solutions, theory 3-63590
 propene-ethene block-copolymers, structure by i.r. spectroscopy (*Russian*) 3-63585
 propylene oxide-tetrahydrofuran copolymer, i.r. spectra, length distrib. of tetrahydrofuran units (*Russian*) 3-49511
 PTFE, crystalline, i.r. spectra, between ambient and 150 K 3-80060
 PTFE, estimation of depth of charge penetration in film corona electrodes (*Russian*) 3-58469
 PTFE, phase II and III, Raman spectra analysis, mol. and cryst. parameters 3-64643
 PTFE sheets with orthorhombic symmetry, extensional and shear compliances 3-55879
 PVC, long term strength, flat stressed state 3-58751
 PVC, piezo- and pyro-electricity 3-47220
 PVC board, nonlinear viscoelastic, cubical approximation method of calc. (*German*) 3-65009
 PVC coatings on tubes, crack form. processes in soil medium (*Russian*) 3-80468
 PVC degradation, kinetic parameters, DTA's 3-76439
 pyrocatechin-formaldehyde resins, structural changes during heat treatment, i.r. spectra (*Russian*) 3-63604
 random copolyamides, thermal behaviour and H-bonding effects in glassy state 3-67882
 real chain, self-avoiding walk model 3-49513
 regular, with stable points linking four chains, viscoelastic behaviour, theory 3-54777
 regular block copolymers, morphology 3-46594
 reinforced, unreinforced epoxy resin, effect of strain rate and temperature, deformation behaviour 3-50775
 reinforced polymers, tension normal to the fibres, strength and deformability 3-64989
 resin, liquid, 10 to 10⁷ poises, viscoelastic properties, relaxation range, u.s. frequencies 3-61993
 resin reinforced C fibres, large diameter, effects of varying process variables 3-50777
 resins, chelating ion exchange, for trace element analysis of geological samples using X-ray fluorescence 3-62329
 rheogoniometer, for viscoelastic properties of polymeric systems 3-53831
 secondary electron emission, yield curve, $E_p=50-2500\text{ eV}$ 3-69123
 SEM specimen, macroscopic math. model 3-70433
 semi-crystalline, amorphous transitions, review 3-49851
 semi-crystalline, multiple transitions esp. double glass, rel. to chem. structure, thermal expansion and glass temp. 3-63962
 semi-crystalline, small angle X-ray scattering 3-69388
 semi-dilute solns., screening length 3-49515
 semicrystalline, small angle X-ray scattering, theoretical models 3-57994
 silica-containing, as stationary phases for gas chromatography 3-66428
 simulated ab-initio mol. orbital method for band struct. 3-54767
 SIS three block copolymer, cubic struct. characteriz. 3-50782
 sliding on metals, chem. change obs. (*Russian*) 3-80466
 sodium polyaluminate solid electrolyte, resistivity meas., effect of Mg doping 3-46857
 solid, high polymeric, fatigue crack growth 3-61212
 solution, dil., behaviour in inlet region of pipe 3-75267
 solution, dilute, turbulent flow, spectral characts. of press. fluctuations 3-49559
 solution, high viscosity, wedge and channel flow stability 3-54825
 solution, rigid ellipsoid, intrinsic viscosity, shear rate depend. 3-80478
 solution, thermodynamic studies on diffusion (*Japanese*) 3-40692
 solution, zero shear viscosity, conc. depend. 3-71679
 solutions, capillary viscosimeter flow meas. 3-57831
 solutions, internal viscosity models evaluation 3-53288

polymers continued

- solutions, nonlinear viscoelastic functions, analysis and temp. dependence 3-53289
 solutions, normal stress difference meas., cone and plate rheo-
 niometer, flush-mounted pressure transducers 3-70503
 solutions, reduced drag in turbulent and transient laminar flows near a
 flat plate 3-63778
 solutions, rotational Couette flow stability 3-57749
 solutions, structure formation, light scattering studies (*Russian*)
 3-49518
 solutions, surface thermodynamics, applic. of Prigogine-Marechal
 theory 3-53346
 solutions, turbulent drag reduction in external rotational flows
 3-60571
 solutions, turbulent flow, influence of high-molecular weight addi-
 tives 3-57832
 solutions, viscoelasticity, hole size and soln. concentration effects
 3-53290
 solutions and melts, periodic deformation, viscous flow, under step-
 wise vibrations 3-58755
 solutions and melts, periodic deformation and viscous flow
 3-54780
 spectral distrib. of absorption coeff. in vibr. spectra 3-74998
 spherulite, light scatt. calc. internal struct. effect 3-71678
 spherulites, two-dimensional, tilted, light scattering 3-57692
 static fatigue, activator evaluation 3-61217
 stationary phase, rel. to gas chromatography 3-62333
 stiff chain dynamics, eqn. of motion, discrete bead transform. to conti-
 nuous model 3-67876
 streaming fluid, flow props. flow birefringence obs. (*German*)
 3-60592
 strength, change in process of orientation 3-71685
 structure, lamellar, of partially cryst. polymers, determ. from X-ray
 scatt. curves 3-72011
 styrene, polymers and copolymers, Raman spectroscopy, sample pre-
 paration, quantitative analysis 3-58496
 styrene-butadiene-styrene block copolymer, domain struct., hexagonal
 convection cell, anisotropy, X-ray diffraction studies 3-54933
 styrene-divinyl benzene copolymers, disperse structures, porosity
 3-44698
 styrene-methyl, ethyl and butyl methacrylate copolymers, triboelec.
 props., xerographic powder manuf. (*Polish*) 3-76379
 styrene-methyl methacrylate copolymer, epoxy resin mixture, n.m.r.
 study 3-64578
 styrene-related polymers, dielectric relaxation at low temperatures
 3-58471
 sulphopolystyrene, adsorption of Ar, benzene, water vapours, heat
 treatment 3-61250
 superstructure in dissolved long chains 3-40685
 surface energy of substrates determ. method 3-46750
 suspensions, rheological equations 3-73083
 teflon, aq. suspension, modelling of hydrophobic interactions
 3-65026
 teflon cell, for pressure measurements up to 40 kilobars 3-45463
 Teflon films, investigation of homocharge (*Russian*) 3-58468
 Teflon high pressure cell 3-73710
 Teflon valves, mass spectrometer, quick introduction of gases
 3-48557
 terpolymer solution, ductile fracture anal. using light scattering
 method 3-80491
 tetrahydrofuran-propylene oxide copolymer, i.r. spectra, length dis-
 trib. of tetrahydrofuran units (*Russian*) 3-49511
 thermal conductivity measurement device, -40° to $+250^{\circ}\text{C}$
 3-48367
 thermal diffusivity, by light heat wave irradi. and two layer slab
 method 3-68448
 thermal diffusivity, by two layer slab method, edge effect losses
 3-68450
 thermal diffusivity, by two layer slab method, temp. sensor transient
 response 3-68449
 thermal expansion, entropy and vel. coeff., rel. to specific vol., effect
 of hydrostatic pressure 3-73053
 threads, drag reduction 3-40739
 time-dependent strength and failure, eqn. development 3-65020
 transparent, tree propagation under oil using needle electrode
 3-47217
 unperturbed chain dimensions from intrinsic viscosities determ. in
 good solvents 3-52407
 unstable, viscoelastic integral equation solution, Il'yushin approx-
 imation, time varying properties 3-57083
 u.s. anisotropy measurements and mechanical properties 3-53308
 u.s. investigations, 2.1 to 240 K, acoustic contact, organosilicon oil-
 talc mixture 3-73678
 u.s. velocity, at liq. He temp. 3-43532
 vinly, dynamic rot. isomer model using irreversible statistical mech.
 3-40691
 vinyl acetate and ethylene copolymers, partly crystalline, molecular
 mobility, dynamic meas. (*German*) 3-63589
 vinylidene chloride (vinyl chloride) copolymer, film, strain proper-
 ties (*Russian*) 3-73067
 10-vinylphenothiazine, complex based on elec. cond., spectral
 props. 3-63963
 viscoelastic behaviour, teaching demonstrations 3-42499
 viscoelastic flow in square cavity, comparison with Newtonian
 fluid (*French*) 3-79055
 viscoelastic hereditary media, temp.-time analogy, conditions for exis-
 tence 3-54778
 viscoelastic props. of melts and solns., effect of mol. wt. and mol. wt.
 distrib. 3-69384
 viscoelastic studies, high-pressure. torsion pendulum 3-51529
 viscoelastic systems, equations of motion, derived from conservation
 laws, phenomenological theory of nonequilib. processes 3-71684
 viscometer, frictional heat meas., capillary rheometry, calorimetric
 method, appl. to extrusion 3-70502
 viscose, film, subject to static and fatigue loading, arterial crack
 growth 3-55895
 viscose fibres and formaldehyde, supermolecular structs., dimens.
 3-63582
 viscosity, zero-shear, of monodisperse polymers, depend. on mol. wt.
 distrib. 3-57696

polymers continued

- water flows with polymer additives, hydraulic losses investigation
 3-57829
 water streams containing some macromolecular substances, boundary
 layer turbulence 3-71819
 water/polymer emulsions, medium and high internal phase ratio
 3-50792
 weak polymer solns., turbulent flow in a pipe, expt. obs. 3-71818
 Young's modulus determination, metal coatings 3-73672
 H₂O polymers molecular interactions studies comparison using differ-
 ent MO basis sets 3-40679
- polymorphism**
see also crystal structure; isomorphism
 alkyl ammonium halides, transitions, spectroscopic display 3-72755
 bronzite rocks, eqns. of state for high-pressure. polymorphic transform.
 3-47629
 carbon tetrabromide, plastic cryst., shear strength 275 to 375 K, 320 K
 polymorphic transform. 3-79407
 ceramic materials, cordierite Mg₂Al₄Si₅O₁₈, infrared and X-ray diffrac-
 tion studies 3-53271
 copper phthalocyanine polymorph, dimeric struct., i.r., X-ray, elec-
 tronic, e.p.r. spectra 3-52599
 1,8-dichloro-10-methyl anthracene orientational relationship between
 crystal lattices 3-75622
 dinitrocarbanion reorientation in alkali salts, i.r. and u.v. spectra
 3-69003
 dunite rock, eqns. of state for high-pressure. polymorphic transform.
 3-47629
 ideal fluid, polytypic hypersonic transform. (*French*) 3-62590
 metal, thermodynamic prop. changes during A1 to A2, A3 to A2
 polymorphic transitions 3-58136
 metals, polymorphic transitions A3→A2 or A1→A2, temp./melting
 pt. relationship 3-43877
 mica-type minerals, relative stabilities 3-80643
 pentafluorophenol-n-Cl-aniline compound, Raman spectra, changes
 on polymorphic transition 3-72198
 poly-1-butene, effect of allotropic form on static mech.
 props. (*French*) 3-63592
 polyethyleneglycoladipate, i.r. spectra (*Russian*) 3-63964
 potassium terephthalate, X-ray exam., thermal stability 3-75519
 rare earths of TRNbTiO₆ and TRTaTiO₆ types, aeschynite-euxenite
 polymorphic transition 3-41015
 rocks, wave vel. and attenuation 3-53395
 solid elements, density periodicity rel. to pressure-induced polymor-
 phic transformations 3-43872
 tartaric derivs., coordination cpds., external vib. freqs. of active and
 racemic forms, i.r. and Raman spectra 3-55581
 TCNQ crystal, nucleation kinetics of allotropic transformation
 3-79488
 tetrahydrite, comp. variation and polymorphism in Cu-Sb-S system
 below 400°C 3-50877
 tetramethylammonium chloride, struct. transitions, config. entropy
 and polymorphism 3-79489
 Ag₂Se, phase transformation obs., electron microscope investigation
 3-58129
 Ag₂Te, elec. props. and X-ray studies 3-68406
 Al, electromigration of polygonization substructures 3-79523
 Al₂O₃, alumina, polygonized boundaries, form. kinetics and interfacial
 energies 3-72947
 CaSiO₃ (wollastonite), X-ray diffraction examination 3-68277
 CaSiO₃, $\beta \rightarrow \gamma$ transition, u.s. dispersion effects 3-72192
 CdI₂, crystal structures of six new polytypes 3-68200
 CdI₂, feeble occurrence of polytypes based on 2H basic phase
 3-60695
 Co coordination cpds., external vib. freqs. of active and racemic
 forms, i.r. and Raman spectra 3-55581
 CsSCN, orthorhombic and high temp. cubic forms, cryst. struct.
 3-46624
 CuCrO₄ transition ranges 3-72048
 Fe, molten, structural transformations, short-range order 3-58616
 Fe-Ni, alloys, polymorphic $\gamma \rightarrow \alpha$ transform. kinetics (*Russian*)
 3-69188
 Gd film, new f.c.c. phase, identification and oxidation characts.
 3-79589
 GdF₃-MF (M=K, Rb, Cs) and GdF₃-Gd₂O₃, crystal structure, phase
 behaviour (*French*) 3-64017
 Ir coordination cpds., external vib. freqs. of active and racemic forms,
 i.r. and Raman spectra 3-55581
 K₂CO₃, polymorphic transform. behaviour 3-60792
 K₄(Ni₂(CN)₆), symmetry, polytypism, twinning (*German*) 3-40893
 LiIO₃, phase transforms. behaviour (*German*) 3-49992
 MoO₂Cl₂·H₂O, polycrysts. and stereochemistry 3-49874
 MoO₂Cl₂·H₂O, polytype struct. from non-space group extinctions
 3-49873
 Na₂O-Al₂O₃ system, X-ray obs. 3-72932
 Na₂O-CaAl₂O₆, cubic, orthorhombic I, II and tetragonal cryst.
 forms (*French*) 3-72179
 A-Nd₂O₃-A-La₂O₃ and A-Nd₂O₃-C-Y₂O₃, investigation of the
 binary system (*French*) 3-64152
 PbI₂, polytypic crystals, transform. 290-310°C, stacking fault
 mechanism 3-43874
 RbI, phase diag. at high press., comparison with KCl 3-68404
 Rh coordination cpds., external vib. freqs. of active and racemic
 forms, i.r. and Raman spectra 3-55581
 SiC, reaction-sintered, growth characts., polytype distrib., 6H₂ struct.
 absence 3-76299
 SiC, reaction-sintered, self-bonding characts., TEM obs. 3-76301
 SiC, relation between elastic constants of hexagonal and cubic poly-
 types 3-54997
 SiC, solution growth from liquid Si, X-ray obs. of polytypes
 3-64771
 SiC polytypes, structural stability and growth 3-64007
 Sr₂SiO₄-Sr₂GeO₄-Ba₂GeO₄-Ba₂SiO₄, solid solubility, polymorphism,
 lattice constants 3-41803
 TM, high press. phase transformation, X-ray obs. 3-75500
 Ti-S system polytypes characterization (*French*) 3-46633
 TiC-ZrC system, rel. to comp. depend. of monochromatic emittance.
 1800K 3-52703
 YSeF polytypes, cryst. struct. (*French*) 3-46632

polymorphism continued

- ZnS, polytype form., layer transposition mechanism inapplicability 3-54947
 ZnS, polytypes, TEM obs. 3-58044
 Zr, allotropic α - β transform. kinetics (*Russian*) 3-53201

polynomials

- approximation, and distrib. of electrons 3-54070
 boson, reln. to canonical tensor operators in unitary groups 3-74106
 conical shells, elastically constrained and stiffened, buckling anal., hydrostatic pressure, collocation method 3-45641
 convergent series expansions solutions, computer programming for algebraic (literal) operations 3-78709
 fatigue crack growth rates eval. by polynomial curve fitting 3-72123
 ferromagnetic and antiferromagnetic for various lattices, Ising model 3-72435
 finite element analysis, two-dimensional diffusion, effects of discontinuous props., smooth polynomials 3-63113
 fourth degree, surfaces of equicritical planar stress distrib., description for glass-reinforced plastics 3-55872
 high field, for various lattices, Ising model 3-72434
 Jacobi, Series equations, reduced to Fredholm integral equations, solution by Legendre-Gauss quadrature formula, appl. to boundary-value-problems 3-74000
 Jacobian polynomials for description of gamma-ray ang. distrib. in multiparticle eqns. 3-40553
 Jacoby, rel. to soln. of kinetic eqn. in cylindrical geometry (*Russian*) 3-74641
 Legendre, spherical harmonics, useful relations 3-57042
 orthogonal, series expansion, application of Pade approximants 3-62428
 Pade approximants, mathematical theory 3-62425
 piecewise, for one-dimensional multiparticle kinetics eqns. 3-46062
 piecewise, mathematical soln. of Abel integral equations, thermodynamic states, radiating plasma columns 3-71849
 problem-specific, Gram-Schmidt orthogonalization process generated 3-62390
 rotation group, new basis for representation, Lamé and Heun polynomials 3-62396
 SU₂ vector coupling coefficients, for n-particles, applic. to analytical formulation 3-48989
 transforms with orthogonal polynomial kernels 3-48698
 triatomic molecule, linear, computer appl. to calc. of pot. energy function 3-78710
 Tschebyscheff orthogonal, representation of atmospheric circulation patterns, rel. to weather 3-80856
 zero-order classical orthogonal, estimated soln. (*Russian*) 3-62398
 Ge probe, low temperature, approximation of R(θ) (*Czech*) 3-53848

polytypism *see polymorphism***Pomeranchuk poles and trajectories**

- see also hadron scattering*
 average multiplicity calcs. using Harari Pomeron-intercept hypothesis in FESR scheme 3-52032
 correlations of identical pions in multiparticle production, Pomeranchuk model 3-49064
 couplings of Pomeranchuk cut in reln. to inclusive cross sections 3-57382
 decoupling of two Pomeranchuk-cut from two Pomeranchuk-Regge poles at zero momentum transfer 3-60006
 diffraction dissociation into high masses at NAL-ISR energies, triple pomeron picture 3-57445
 double-Pomeron coupling strength in dual resonance model, reln. of exclusive to inclusive expts. 3-67067
 dual B₆-model with Pomeron background modified for ISR single-particle distrib. at $x=0$ 3-67146
 dual Pomeron, absence of ghost state 3-40367
 exchange reactions, amplitude structure of $\gamma p \rightarrow \rho^0 p$, and $\pi N \rightarrow \pi N$ reactions 3-74406
 fixed poles, t-channel unitarity and rising cross-sections 3-52028
 form factors, elastic, convergence 3-66951
 forward peak slope, s-channel analysis 3-70962
 hadronic high-energy collisions, asymptotic properties of charge distrib. 3-78216
 high-energy relations for scattering of particles and antiparticles having given properties under crossing 3-40391
 inclusive one-particle cross sections, cut contribs. in triple-Pomeron limit 3-52026
 inelastic two-to-three particle production processes, Pomeranchuk theorems 3-74399
 intercept of the Pomeranchuk singularity 3-43125
 K-matrix absorption model for pion nucleon system including Pomeranchuk contribution 3-74402
 multiple hadron production, Pomeranchuk model, reln. to statistical bootstrap model 3-67065
 multiple hadron production, statistical bootstrap and Pomeranchuk model 3-59990
 multiple-Pomeron exchange amplitudes, iterative conditions and intermediate states 3-40372
 multipomeron exchange in sum rules for inclusive cross sections and correlation functions (*Russian*) 3-74472
 Pomeron coupling constraints from multiple diffractive dissociation 3-67079
 Pomeron dynamics, self-consistent without decoupling 3-60008
 Pomeron eqn. linearisation, from one-loop amplitudes in dual resonance models 3-52021
 pomeron factorization in general dual models 3-57376
 Pomeron in hadron physics, theory of strong interactions, Regge pole model 3-74400
 Pomeron sector of dual model, no-ghost theorem 3-49027
 self-reproducing-cut Pomeron, phenomenological compatibility with ABSC mechanism in pp diffraction scattering 3-43155
 singularity in models without short-range order, azimuthal correlations 3-54365
 triple Pomeron vertex and complex Pomeron trajectories 3-60007
 triple-pomeron vertex within multiperipheral model 3-67085
 unbounded total cross sections, Pomeranchuk theorem, proof 3-52027
 pp collisions, ISR inclusive hadron spectra, triple-Regge model, triple-pomeron coupling determ. 3-67154

Pomeranchuk poles and trajectories continued

- pp elastic cross sections, magnitude of triple-Pomeranchuk coupling 3-57398
 pp scatt models, review 3-71005
 pp scattering, elastic large angle, dual model with logarithmic trajectories 3-60026
 pp scattering, ISR rising cross section and finite energy effects, Pomeranchuk mechanism 3-67077
 πN scatt., pomeron and P' exchange amplitudes 3-52042
 $\pi p \rightarrow pX$ inclusive spectra, triple-Pomeron coupling 3-49070
 $\pi p \rightarrow \pi n$ high energy reaction violation of theorem (*Russian*) 3-62898

Pontryagin maximum principle *see maximum principle***Poole-Frenkel effect**

- Al-SiO-Au structures conduction phenomenon, current-voltage characteristics. (*French*) 3-72411
 As₂Se₃, amorphous film, in d.c. cond. meas. before switching 3-41242
 GeSe amorphous film, Poole-Frenkel conduction mechanism 3-55276
 Se, two photon photo-generation in amorphous state, Poole-Frenkel model 3-55305
 TiO₂, amorphous thin film, d.c. and a.c. construction 3-75798

population inversion

- see also laser theory*
 product state in chemical reactions, vibr. temp. concept 3-65070
 two-level system, semiclassical theory of saturated absorpt. 3-62746
 Ar gas laser, continuous, population inversion, output (*French*) 3-48943
 CO, low temp., vibr. energy transfer rates in CO laser beam 3-74230
 CO₂, with electric discharge excitation (*Russian*) 3-43010
 CO₂ laser, pulsed, effect of temp. and gas mixture composition 3-59858
 CO₂ upper laser level vibr. deactivation by ONF, COF₂ and O₂ 3-45790

population inversion in lasers *see laser theory***porosity**

- see also porous materials*
 anisotropic media, reciprocity theorem, quasi-stationary state 3-73187
 Bunter Sandstone, Northwest England 3-76544
 ceramic, effects on strength and fracture 3-76244
 ceramics, porosity, dep. of creep rate 3-41805
 clay content, radioactive logging data (*Russian*) 3-76895
 diffusion of gases, influence of finite pore length, porous materials (*German*) 3-50799
 drainable porosity of silt/clay soils as function of physical properties 3-76931
 elastic-plastic compressibility, pore vol. press. depend., theory 3-77830
 electrode, bipolar porous, theory 3-58799
 fabrication pores, migration during irradiation 3-67454
 fibre, electron microscopic methods, transmission and stereoscaning (*Polish*) 3-73902
 fibre, mercuric porometry and physical adsorption methods 3-69400
 glass frit, diffusion of ortho/para H₂, influence of finite pore length (*German*) 3-50799
 glass laminate, effect of porosity on strength 3-64987
 glass reinforced plastic, effect of composition and porosity on tensile strength and elasticity 3-58713
 glass-plastic, X-ray shadow microscopy obs. of ageing and media effects (*Russian*) 3-41814
 granular materials, effect of moistening and demisting, influence of porosity (*German*) 3-47488
 insulating thin films, determ. by electrolysis (*German*) 3-45415
 lunar soil, upper layer, compaction parameter using opposition effect (*Russian*) 3-77003
 microporosity of graphite matrix material and pyrocarbon in HTR fuel elements (*German*) 3-71319
 nuclear fuel, thermal cond. depend. 3-40537
 propene-pyrocarbon layers, structural changes under thermal treatment and neutron irradiation (*German*) 3-67600
 reactor matrix material, microporosity, annealing and neutron irradiation effects (*German*) 3-71252
 refractory spinels, elastic moduli, porosity depend. 3-72942
 reservoir sandstones, computer classification of pore structure 3-80630
 sandstone, porosity dependence and mechanism of brittle fracture 3-53407
 sintering process, dispersed porous body, thermodynamic anal. 3-69364
 solid conducting inclusions, resistivity logging data (*Russian*) 3-76896
 solidification in porous media, dependence of energy of transformation on curvature of interfaces, effect of capillary radius (*French*) 3-75607
 solidification in porous media, thermogram, calorimetric method, effect of pore size distrib., transformation hysteresis (*French*) 3-75608
 solidification of H₂O and benzene in porous media, calorimetric method, latent heat determ., effect of pore radius, hysteresis (*French*) 3-75606
 squeeze film, load capacity and time height relations 3-64106
 steel, sintered, rel. to fracture-resistance 3-69307
 styrene-divinyl benzene copolymers, disperse structures 3-44698
 tuffaceous rocks, shock wave response, porosity and saturation effects 3-58876
 Zircaloy-2, morphology of thick oxide films 3-43951
 Al₂O₃, alumina, microstruct. effects on fracture energy meas. 3-44651
 Al₂O₃, hot-pressed, annealing effect on fracture energy, strength and microstruct. 3-72935
 Al₂O₃, sintered, grain boundary segregation, impurities role in densification 3-69343
 BaTiO₃-CaZrO₃ solid solution Curie point, sintering temp., ferroelectric material manufacture (*Polish*) 3-68946
 C, electron microprobe method (*German*) 3-76375

porosity continued

- C, glassy, submicroscopic void obs. 3-58737
 C/C composites, fibre volume percent depend. 3-55854
 Cu-Ni multilayer system, u.s. vibrs. effect on pore form. and Kirken-dall effect (*Russian*) 3-79518
 Gd₂O₃, polycrystalline monoclinic, elastic moduli 3-76326
 Ni, pure, pore form. on 40 keV Ni⁺ ion irradiat. 3-72106
 (Pb_{0.92}La_{0.08})(Zr_{0.65}Ti_{0.35})₂O₇ ceramics, rel. to elec. and opt. props. characteriz. 3-55532
 Pb(Zr,Ti)O₃ transducer rings, rel. to mech. failure 3-72966
 (U,Pu)O₂, LMFBR fuel rods, thermal and mech. eval. of oxide microstruct. 3-78381
 (U,Pu)O₂ fuel, conservation eqns. governing porosity and actinide redistrib. 3-46145
 (U,Pu)O₂ pellets, parametrically designed, atmospheric stability obs. 3-78382
 UO₂, irradi., morphology and growth rate of interlinked porosity 3-43306
 UO₂ microsphere fabrication by hydrolysis from uranyl nitrate soln., controlled porosity 3-46146
 α -Zr(HPO₄)₂·H₂O, crystalline, prep. and characterisation 3-55730
 ZrSiO₄, plasma sprayed, reheating, pore contraction 3-76332

porous materials

- see also flow through porous media; mechanical permeability*
 anisotropic, reciprocity theorem, quasi-stationary state 3-73187
 bone, analysis as three component system with mineral phase, organic phase and pores 3-50771
 bulk compressibility rel. to pore strains, theoretical calculations 3-50801
 capillary pressure, moist granular materials, influence of porosity (*German*) 3-47488
 capillary-porous materials, moisture content determ. by microwave absorption 3-73093
 catalyst, heat and mass transfer, nonlinear boundary value problem solution 3-42911
 cellulose fibre, swollen state (*Polish*) 3-53292
 ceramic nuclear materials, applic. of surface anal. to porosity study (*Czech*) 3-61237
 containing NaCl solution, n.m.r. relaxation of ²³Na 3-60993
 density meas. device 3-70266
 diffusion analogy with electrical conductivity 3-73092
 diffusion of gases, influence of finite pore length (*German*) 3-50799
 effective pressure in porous solids 3-53409
 elastic wave diffraction by smooth wedge in infinite porous-elastic medium (*Russian*) 3-42825
 electrical conductivity analogy with diffusion 3-73092
 energy deposition, effects of porosity on pressure generation 3-74761
 fibre, electron microscopic methods, transmission and stereoscan-ning (*Polish*) 3-73902
 fluid penetration rate, Washburn eqn. 3-41828
 fluid saturated rocks, effective stress laws 3-76558
 foamed plastic, transition radiation, 13-130 keV 3-56943
 fractionated quartz river sand, effect of porous struct. and absorbed moisture on u.s. propagation 3-61238
 gas-porous solid system, non-catalytic with chemical reactions and diffusion 3-69442
 glass, OH group content in ultrapores, on macropores 3-61236
 glass fibre, surface microcrack volume on etching (*Russian*) 3-53280
 graphite, isotherms of metal chloride vapours 3-68486
 half-space, transpiration cooled, temp. distrib. determ. by variational method 3-54178
 interface refraction, boundary between porous layers 3-54827
 isotropic, homogeneous, variational theorem, quasi-static case 3-65043
 marine sediment, acoustic wave reflection (*French*) 3-76862
 mass transport, absorbents expt. (*German*) 3-50800
 metal oxides, sintering, pore size rel. to grain size 3-64973
 metallic, thermal and electrical conductivity prediction 3-76392
 MHD flow of conducting fluid due to rotatory vibrations of porous disc over fixed disc 3-54818
 moist n-element capillary-porous material dielectric const. 3-79970
 moisture transfer rates, capillary impregnation with butyl alcohol solutions 3-65031
 nuclear fuel, thermal cond. depend. on porosity 3-40537
 oscillations induced by acoustic waves, elastic matrix, motion and continuity equations 3-59507
 particles, in liquid chromatographic columns, packing technique 3-66421
 polymer-impregnated brittle materials, stress conc. factors 3-55839
 polystyrene foam, heat conductivity meas. (*German*) 3-65044
 polyurethane, simple stressed state, vibr. creep study 3-55894
 pore fluids rel. to P and S velocity ratio, earthquake aftershocks, fault creep and magnetic precursors 3-76512
 rheology, nonlinear and semilinear 3-69509
 rock, porosity and grain struct. by SEM 3-69729
 rocks, freezing and supercooling of water in pores (*Japanese*) 3-56034
 silica gels, correlation of orthopositronium annihilation and surface props. as a function of temp. 3-40936
 silt/clay soils, drainable porosity as function of physical properties 3-76931
 solidification in porous media, dependence of energy of trans-formation on curvature of interfaces, effect of capillary radius (*French*) 3-75607
 solidification in porous media, thermogram, calorimetric method, effect of pore size distrib., transformation hysteresis (*French*) 3-75608
 solidification of H₂O and benzene in porous media, calorimetric method, latent heat determ., effect of pore radius, hysteresis (*French*) 3-75606
 squeeze film, load capacity and time height relations 3-64106
 strength measurement 3-44699
 structured systems, highly elastic deform., kinetic curves 3-73070
 sulfolipolystyrene, microporosity on heat treating 3-61250
 surface structure, replica technique for electron microscopy 3-68142
 tensile strength, moist granular materials, influence of porosity (*German*) 3-47488

porous materials continued

- thermal conductivity measurement, high temp., electron bombardment heating (*German*) 3-42542
 Al₂O₃, alumina, microstruct. effects on fracture energy meas. 3-44651
 Al₂O₃, high-density, white spots analysis 3-69349
 C, polyvinylidene chloride based, absorpt. characts. 3-68485
 Fe sintered, elastic modulus and ductility, stress concentration factors due to pores 3-50753
 He superfluid, flow conductivity, Ginzburg-Pitaevskii eqn. 3-75646
 MgO-P₂O₅ system glass, isothermal crystn. behaviour (*Japanese*) 3-65022
 SiO₂, porous powder compact, specific surface area, pore struct. rel. to compaction, adsorpt. obs. 3-41801
 Ta powder compacts, porous, shrinkage in sintering (*Korean*) 3-53265
 UO₂, stoichiometric and hyperstoichiometric, thermal cond., 670-1270 K 3-43304
 UO₂ microsphere fabrication by hydrolysis from uranyl nitrate soln., controlled porosity 3-46146
 UO₂ microspheres, compressibility determ., microscopy, struct. depend. 3-80424
 ZrO₂, porous powder compact, specific surface area, pore struct. rel. to compaction, adsorpt. obs. 3-41801

porous media *see porous materials***Portevin-Le Chatelier effect** *see stress/strain relations***positors**

No entries

position control*see also attitude control*

- h.v. electrodes assembly, alignment device in high vacuum apparatus 3-53870
 oceanographic instrument depth control techniques 3-65541
 optimal longitudinal travel control of liquid-filled elastic tank (*Rus-sian*) 3-59773
 plasma, in Scyllac MHD feedback system 3-60317
 power reaction, control of spatial Xe-induced oscillations 3-57556
 precision hydromechanical displacement micropositioner 3-39860
 projector automatic focusing device with CdS photocells (*Japanese*) 3-53876
 radiotelescopes, on-line computer control, operation, hardware and architecture 3-70091
 underground workings, laser guidance and control system 3-48959

position finding *see navigation***position measurement**

- asteroids, position determ. of 19 objects (*French*) 3-73465
 carriage feeding accuracy of screw cutting lathe using laser interfe-rometer 3-59903
 Centering Projector-10, VEB Carl Zeiss JENA, positioning device, workpiece alignment 3-51600
 extragalactic radiosources, VLBI meas. 3-45143
 eye, by digital techniques 3-51755
 Fine-Positioning Device FAE-4, VEB Carl Zeiss JENA, optical sym-metry adjustment 3-51601
 FKSZ stars, catalogue of R.A. and comparison with other catalogues 3-59239
 geodetic position meas. using Doppler satellite obs. 3-56248
 laser tracking stations, relative position determ. 3-56074
 marks on object surface using optical sensors incorporating photodetect-or 3-66204
 Mars landing position estimation, in presence of ephemeris biases 3-59403
 NGC 7293, planetary nebulae, trigonometric parallax determ. for cen-tral star 3-45234
 optico-electronic system for brief displacements, calibration 3-51617
 planetary nebulae, optical positions for 153 objects 3-45227
 radiosources, VLBI, geodetic appl. 3-56246
 satellite position corrections for sudden increases in electron content 3-51104
 tracking station coordinates of Goddard Earth Model 3-56072
 vector baseline meas. using VLBI 3-56062

positioning *see position control***positive column***see also glow discharges*

- electric arc in a gas flushed channel, development of equations (*Rus-sian*) 3-71968
 gas discharge, low pressure, electron energy distrib., deviation from Maxwellian 3-68112
 hollow cathode discharge, probe meas. of plasma characts. (*French*) 3-49773
 hollow cylinder, with annular cross section, props. calc. 3-75441
 ion acoustic wave excitation, intensity distrib. in k-space, meas. 3-52507
 microwave reflection from plasma column in rectangular waveguide 3-46551
 oscillations, finite amplitude, second harmonics 3-40781
 plasma, strongly magnetised, noise radial distribution and mean den-sity 3-68085
 positive column, steady-state nonisothermal, in magnetic field, theory 3-68113
 radial pressure inhomogeneity calc. 3-54891
 relaxation oscillations obs. 3-68126
 steady-state nonisothermal, in magnetic field, theory 3-68113
 thermal contraction by dissociative recombination 3-75443
 Ar, medium pressure discharge, diagnostics using bremsstrahlung con-tinuum 3-63907
 Ar, population density and l.t.e. of excited atoms 3-52545
 Ar discharge, continuous emission spectrum of electron deceleration 3-63320
 Ar low pressure columns, influence of local transverse magnetic field on self-excited running layers (*German*) 3-63904
 Ar positive column at medium pressures, concentration of atoms in excited 3p⁴s levels 3-52269
 Ar positive column at moderate pressures, theory and experiment 3-49783
 Cs ionized vapour, electron distrib. function (*French*) 3-49748
 D₂, ion-ion hybrid resonances obs. 3-68020

positive column continued

- H₁, nonlinear standing striations reaction on pulse disturb. 3-49681
 H₂, ion-ion hybrid resonances obs. 3-68020
 He positive column, ion acoustic instability 3-49695
 He-Ar mixture, gas separation, effects of steady state elec. discharge 3-60649
 I⁺ laser, plasma characts. of He-CdI₂ positive column 3-48879
 Ne-Hg mixture, cathaphoretic segregation effects 3-57959
 Ne-Xe-Hg mixture, cathaphoretic segregation effects 3-57959

positive feedback *see feedback***positive ray sources** *see ion sources***positive rays** *see ion beams***positive temperature coefficient thermistors** *see thermistors***positons** *see positrons***positron annihilation**

- alkali silicate multicomponent glass, struct., SO₂ treatment 3-68165
 brass, subjected to different thermal treatments (*Russian*) 3-79375
 bremsstrahlung, prod. by high-energy electron-positron collision in mag. field 3-43110
 bremsstrahlung angular distribution (*Russian*) 3-70923
 circular polarization correl. of annihilation quanta 3-67030
 cross-section, consistent soln. from perturbation theory at infinite momentum 3-67019
 decay rate and Z_e in freon, Ar, N₂ and Kr 3-74908
 doppler broadened radiation, various metals, electron effective mass ratio 3-68541
 duality constraints, processes producing meson or baryon octets 3-59991
 galactic positronium-formation red shift of 511 keV annihilation line 3-70018
 gamma ray buildup factor determ. in Pb shielding using Monte Carlo methods 3-71336
 Gribov-Lipatov reciprocity relation, group theoretical derivation 3-48985
 hadron production at 4-GeV centre of mass energy 3-49017
 into hadrons, use of beam polarisation for e.m. structure function meas. in one-photon approx. 3-57350
 inclusive current induced interactions, scaling behaviour due to light-cone singularities 3-40320
 inclusive reaction, light-cone dominance 3-52016
 inclusive sum rules for hadron production, asymptotic behaviour of multiplicity 3-49012
 inelastic, deep, continuation of scaling function from deep inelastic electron scattering, dynamic models 3-57359
 ionic crystals, exciton energy spectrum 3-68578
 for lattice defect obs., vacancy trapping 3-68245
 liquid metal, theory using Green function method 3-50110
 metal, formation entropy of single vacancy, evaluation from positron annihilation data 3-46640
 metals, strongly deformed, lifetime and lineshape factor, influence of dislocations 3-52805
 multihadronic production cross section at Adone e⁺e⁻ storage ring up to 3 GeV c.m. energy 3-49019
 neutron star radiation producing 473 keV feature 3-61759
 one-particle inclusive, two-photon and possible weak interferences 3-52011
 quark-parton model, duality constraints 3-54312
 quasi two-body annihilation, helicity formalism, vector meson dominance expectations 3-70924
 silica gels, correlation of orthopositronium annihilation and surface props. as a function of temp. 3-40936
 SU(3) symmetry breaking and branching ratios 3-62837
 universal multiplicity formula based on thermodynamics 3-49034
 vector meson decays into lepton pairs, deviation from e-μ universality 3-45885
 e⁺e⁻ → γ-hadrons, broken-scale invariance canonical trace identities, anomalies 3-45859
 e⁺e⁻ → μ⁺μ⁻, sign of muon charge asymmetry and models of unified e.m.-weak interactions (*Russian*) 3-67029
 e⁺e⁻ → p + anything, deep-inelastic limit, structure function threshold behaviour, reln. to electroproduction 3-45884
 e⁺e⁻ → resonance + anything, low, high energy, study of reactions, resonances decaying into two charged mesons 3-59968
 e⁺e⁻, from the light cone, annihilation structure functions 3-60061
 e⁺e⁻ colliding beam expts., production and decays of short lived particles 3-59977
 e⁺e⁻ → e⁺e⁻γ, cross section meas. at Adone storage ring, new limit for heavy electron existence 3-49018
 e⁺e⁻ → γγ, 4 GeV centre-of-mass energy, cross section meas., exptl. test of QED 3-57348
 e⁺e⁻ → γγ, hard photon corrections, cross section calcs. 3-78136
 e⁺e⁻ → h + anything, deep inelastic one-particle inclusive process in parton model 3-52015
 e⁺e⁻ → hadron + X, SU(3) prediction for single particle distribns. 3-57367
 e⁺e⁻ → hadrons, application of correspondence arguments 3-70937
 e⁺e⁻ → hadrons, role of radially excited vector mesons, relativistic quark model 3-70925
 e⁺e⁻ → hadrons, SU₃ inclusive sum rules for bounds on K/π production ratio 3-78141
 e⁺e⁻ high-energy collisions, role of two-photon inclusive hadron production 3-57360
 e⁺e⁻ → L[±]L[±] meas. of s-dependence of time-like e.m. form factors of pseudoscalar mesons 3-70913
 e⁺e⁻ → μ⁺μ⁻, complex angular momentum theory, high energy 3-78107
 e⁺e⁻ → μ⁺μ⁻, cross-section for annihilation, W⁰ exchange 3-59948
 e⁺e⁻ → μ⁺μ⁻ radiative corrections and neutral currents in unified gauge theories 3-67015
 e⁺e⁻ → μ⁺μ[±], differential cross section calcs., hard photon corrections 3-57353
 e⁺e⁻ → nπ⁺nπ⁻γ, photon structure functions 3-67043
 e⁺e⁻ → p + anything, threshold relation with e⁻p deep inelastic scatt. 3-45886
 e⁺e⁻ → ϕ → K⁰K⁰, decay charge asymmetry 3-52000
 e⁺e⁻ → π⁰γ, low energy theorem 3-40344
 e⁺e⁻ → π⁺π⁻, coupled channel model explanation of qualitative features 3-74376

positron annihilation continued

- e⁺e⁻ → π⁺π⁻ (K⁺K⁻), 1.5, 1.6, 1.7 GeV, pair production from time-like photons 3-49011
 e⁺e⁻ → π⁺π⁺π⁻π⁻, coupled channel model explanation of qualitative features 3-74376
 e⁺e⁻ → π + anything, conformal invariance, singular bilocal operators and scaling 3-67034
 e⁺e⁻ → ππ, appl. of ρ-φ e.m. mixing parameter 3-49005
 Ag vacancy formation energy, positron annihilation gamma rays, trapping model 3-49888
 Al₂O₃, positron annihilation investigation of valence electrons 3-72317
 As₂S₃, cryst. and amorphous 3-60746
 As₂Se₃(Te₃), crystalline 3-60746
 Au, positron trapping by vacancies, temp. independ. 3-60741
 Bi-Pb(Sn) binary alloy, effect of ternary addition, m.p. effects 3-68279
 Cu, OFHC, deformation effects, lineshape factor obs. 3-58039
 Cu, subjected to different thermal treatments (*Russian*) 3-79375
 Cu vacancy formation energy, positron annihilation gamma rays, trapping model 3-49888
 Cu:Ni(Co)(Fe)(Cr), with impurity core electrons 3-64301
 GaAs, angular distrib. of γ quanta, influence of temp. 3-75548
 KBr, angular distrib. of γ quanta, influence of temp. 3-75548
 KBr, coloured single crystal, bleaching by positron irradiation 3-64696
 KBr, effective mass measurements, γ-ray angular correlation curves at 300 K and 90 K 3-44008
 KCl, angular distrib. of γ quanta, influence of temp. 3-75548
 KCl, effective mass measurements, γ-ray angular correlation curves at 300 K and 90 K 3-44008
 KCl, trapping in F-colour centres, positronium-like state 3-40916
 KH₂PO₄, ang. correl. curves, valence states 3-64066
 Na, liquid, theory using Green function method 3-50110
 Na, liquid, volume dependence, up to 4 kbar 3-50115
 NaCl, angular distrib. of γ quanta, influence of temp. 3-75548
 NaCl, effective mass measurements, γ-ray angular correlation curves at 300 K and 90 K 3-44008
 NaCl:Ca²⁺, rel. to Ca²⁺ conc. 3-79373
 NbH_{0.95}, angular γ-correlation study, proton model 3-50131
 Ni, ferromag., band structure obs. 3-58361
 Pu, self-irradiation damage obs. 3-63194
 Si, angular distrib. of γ quanta, influence of temp. 3-75548
 Si, positron annihilation, angular correlation of radiation 3-72318
 SiO₂ powder, mag. quenching of orthopositronium, effects of chemisorbed water 3-52642
 WO₃, powdered and sintered 3-79372
 YH_{1.95}, angular γ-correlation study, proton model 3-50131
⁶⁴Zn(p,n)⁶⁴Zn cross section meas. from 20.4 to 21.9 MeV, annihilation photopeaks meas. 3-52167
 ZrH_{1.97}, angular γ-correlation study, proton model 3-50131

positron annihilation in solids

No entries

positron states

see also positron annihilation

metal, with voids, vacancies and surfaces, positron behaviour 3-46808

KCl, existence of positronium-type bound states, angle correlation expt. (*German*) 3-50144

positronium

see also electron pairs

formation in positron + H scattering, integral approach 3-78555

galactic cosmic ramma-ray feature at 476 keV, positronium origin rel. to explosive nucleosynthesis 3-61617

ground level, hyperfine shift contrib. calc. using polarization operator from quasi-potential eqn. 3-70910

halogen substituted benzenes, temp. and phase dependence of positronium lifetimes 3-55221

h.f.s., fourth order vacuum polarisation correction 3-40340

hydride, SCF calculations 3-78648

positron systems with H⁻ and other negative ions, SCF calculations 3-78648

positron systems with negative ions and atoms, quasi-stationary states calc. 3-78649

o-positronium, natural decay rate in freon, Ar, N₂, Kr 3-74908

silica gels, correlation of orthopositronium annihilation and surface props. as a function of temp. 3-40936

Zeeman and motional Stark effects, relativistic contrib. 3-71483

in SiO₂ powder, mag. quenching of orthopositronium, effects of chemisorbed water 3-52642

positrons

see also electron pairs; electrons

autoionisation spectra in heavy ion collisions produced in over critical fields 3-67356

channelling in single crystals, computer simulation 3-54989

Coulomb field production during interaction of heavy nuclei 3-74604

electron-positron pair production in extremely high intensity laser fields 3-40811

positron camera, Massachusetts General Hospital 3-70161

radiation belts, trapped positron investigation by satellite 3-65489

stopping power law, empirical formula 3-51689

tomography, three dimensional reconstruction technique 3-70163

transverse section detector, 32-crystal 3-70160

e⁺-He bound state, variational calc. 3-43388

potassium

anharmonic lattice dynamics 3-58093

atom, collisional excitation by mols., population of 6S and K5P states 3-63309

atom, electron collision, momentum transfer cross sections, from elec. conductivity of arc discharge 3-71430

atom, electron impact ionisation, binary encounter calcs. 3-71412

atom, electron scatt., frozen core Glauber approx. 3-46202

atom, ion induced K X-ray de-excitation spectra 3-54596

autoionisation in electron impact 3-74881

binding energy, compressibility, pseudopot. calcs. 3-54941

combustion gas-K medium, photoionisation rel. to MHD generators 3-49665

potassium continued

- Compton profile, influence of electron correlation and crystal structure 3-75544
 Compton profile calcs., momentum wave functions of APW 3-79616
 covering on W-emitters, noise spectral densities, field emission flicker noise theories 3-76122
 desorption of N_2 , activation energy, low temp. obs. (German) 3-43941
 earth core, radioactive decay heat source 3-76545
 electron elastic scattering, variational calc. 3-43365
 electron-phonon interaction, far IR cyclotron reson. study 3-43851
 electronic band struct. and Fermi surface, pseudopot. calc. 3-52779
 energy levels of $1s^2 2s^2 2p^4$ configurations 3-43332
 Fermi surface, augmented-plane-wave Hartree-Fock first-principles calc. 3-58203
 fluorescence obs. in laser excited NaK vapour mixture 3-40650
 ion implanted, in Al, behaviour during anodic oxid., He backscatt. obs. 3-68511
 K partitioning between silicates and sulphide melts rel. to composition of primitive Earth core 3-41899
 liquid, effective pair potentials, calc. from X-ray data 3-49825
 liquid, pair interaction pot. calcs. 3-49838
 liquid, struct. factor, press. effects, X-ray study 3-49823
 liquid, thermodynamic properties calc. using perturbation theory (Russian) 3-55092
 magnetoresistance, longit. and transverse high field 3-55248
 mammalian erythrocytes, mouse, radiation induced haemolysis, K loss, effect of dietary fatty acids and tocopherol 3-48260
 photo emission and optical constants, of pure thick layers in u.h.v., 250-630 nm (French) 3-41610
 plasma, decaying, excited states relaxation obs. 3-60630
 plasma, laser selective excitation spectroscopy for diagnostics 3-68086
 plasma, state functions behind ionizing shock waves 3-63807
 residence time on clean tungsten, mol. beam meas. 3-60839
 self-diffusion in KN_3 , 85-254°C 3-43898
 stellar, η Canis Major spectrum 3-69957
 surface tension, up to 850°C, maximum bubble pressure meas. apparatus 3-70272
 trace analysis, modification to flame photometer 3-45587
 vapour, elec. conductivity, pressure depend. including atomic clustering effects 3-63612
 vapour pressure, 2100 F up to critical temp., pressure tube meas. method 3-75616
 Cds:K, polycryst. film, photomemory effect 3-41232
 K + Ar, (Kr), (Xe) collisional excitation, new system of oscillations 3-74843
 K + I scattering, differential cross-sections 3-71398
 K + I_2 collisions at superthermal energies, Monte Carlo simulation 3-71615
 K + Na(K) collisions, threshold energies for excitation to $K(4^2P)$ 3-78514
 K-, electron detachment by electron collisions 3-67702
 K-, photodetachment cross section 3-78493
 K+, chemical gradient, sedimentary marine pore waters, sampler 3-73381
 K+, desorption from Mo, energy determ. 3-55153
 K+, in Ar gas, mobilities and longitudinal diffusion coeffs. 3-40700
 K+, in $RbMnF_3$, ^{19}F nuclear acoustic resonance obs. 3-41431
 K+, optical pumping charge-exchange method for nuclear spin orientation, 1S_0 3-67677
 K+ diffusion in He and Ne gases, experimental variables and interaction potential depend. 3-40766
 K+ in N_2 , longitudinal-diffusion coefficient meas. at 293 K 3-43536
 K+ ion reduced mobility in gas mixtures 3-46373
 K+ spectra, lifetimes and Lande g-factors calc. (French) 3-67658
 K+ + Ar, absolute scattering cross-sections and interaction potential 3-71454
 Li:Na,K, singly and doubly ionized states, Auger transitions 3-69122
 in NH_3 , liquid, solvated electrons photoelectron emission, 1.55 to 5.4 eV 3-41614
 Si slice processing, flame emission analysis of K 3-54045

potassium compounds

- (see also *Rochelle salt*)
 $(K_{1/2}Pb_{1/2})(Zn_{1/6}Nb_{5/6})O_3$, dielectric and electro-optic properties 3-72562
 acid phthalate, coeff. of thermal expansion perpendicular to cleavage planes, X-ray diffraction application 3-64191
 boromaleate, cryst. struct. 3-43779
 caproate spin lattice relaxation n.m.r. measurements, saturation effects, polycrystalline, room temp. 3-58437
 1,1-dinitroethane salt, cryst. struct. determ. 3-72074
 dipotassium tartrate crystals, triboluminescence and simultaneous charge produced at fracture 3-69045
 Fremy salt, orange-brown form, triplet state obs. by e.s.r. (French) 3-61275
 halides, mol. orbital calcs. for dimer activator centres 3-68566
 hydrogen acetylenedicarboxylate, i.r. and Raman spectra, vibr. studies of hydrogen-bonding 3-76006
 hydrogen oxalate, elastic const., by u.s. wave light diff. 3-49920
 hydrogen oxydiacetate, crystal structure determ. from X-ray intensity data 3-68238
 ice:KCl low concentration, dielectric properties (Japanese) 3-55517
 KBr, dielectric loss due to OH^- defects, electrical susceptibility calcs. 3-41477
 $KI:Ti^+$, phonon props. and electron-phonon interaction 3-58098
 KI, chromate- and nitrite-activated, absorpt. at 300 k, 80 k and 4 K (Russian) 3-44432
 lamellar potassium oleate- D_2O membrane bilayers, n.m.r. free induction decay, spin echoes 3-45258
 potassium hydrogen di-trifluoroacetate, i.r. and Raman spectra, symmetric hydrogen bonds 3-68990
 potassium hydrogen succinate, i.r. and Raman spectra, symmetric hydrogen bonds 3-68990
 potassium methyl xanthate- d_0 and - d_3 , vibrational spectra and force constants (German) 3-46297

potassium compounds continued

- terephthalate, X-ray exam., thermal stability 3-75519
 tetrafluorophthalate, ^{19}F chem. shielding tensors and cryst. struct. 3-61001
 (Ag + K) NO_3 , molten binary mixtures, external transport numbers, ionic mobility, cooperative mechanism, ionic conductivity (French) 3-75747
 $BaF_2:KF$, ionic conductivity and disorder parameters determ. 3-60879
 $CKI(Br)(I)$, off-centre Cu^+ ions, ionic thermocurrent study 3-41478
 $(FeF_3)_{1-x}(KMnF_3)_x$ mixed system, mag. and crystallographic characterization. 3-60965
 $FeO-K_2O-P_2O_5$ glasses, preparation and properties, agricultural application in supply of soluble Fe to soil 3-76260
 $(K,NH_4)_2CuCl_4 \cdot 2H_2O$, 3-dimensional Heisenberg ferromagnet, magnetic interactions, n.m.r. obs. 3-60998
 $K,Pt(CN)_4Br_{0.3}(H_2O)_{2.3}$, diamagnetic one-dimensional metal 3-52958
 K halide cryst., model pot. with short range three-body interaction 3-63976
 K-Cs, phase diagram calcs. using heat of soln. in solid and liquid phases 3-41007
 K-Rb, phase diagram calcs. using heat of soln. in solid and liquid phases 3-41007
 K-Rb liquid alloys, electrical resistivity calc. 3-60866
 KAl_2Br_7 crystal structure, X-ray diffraction study 3-54943
 $KAl(Cr)(SO_4)_2 \cdot 12 H_2O$, crystallisation, rate of growth of (100) and (111) faces under various conditions 3-52588
 $KAl(NH_2)_4$, H-N lengths and H-N-H angles (French) 3-46605
 $KAl_3(OH)_6(SO_4)_2$, Mossbauer study of magnetic hyperfine fields in Fe^{3+} ions 3-50498
 $KAsFe_6$, p -irradiated, e.s.r. study of F_2^{2-} 3-41408
 $KAuCl_4$, crystal structure of anhydrous compound 3-63992
 KBr, anharmonic vibrational effects on the Debye-Waller factors 3-40988
 KBr, chromate- and nitrite-activated absorpt. at 300, 80 and 4 K (Russian) 3-44432
 KBr, coloured single crystal, bleaching by positron irradiation 3-64696
 KBr, containing BO_2^- , anharmonic force field calc. 3-43421
 KBr, damage region form., changes in giant laser pulses and luminous plasma 3-74262
 KBr, e.p.r. of triplet state of self-trapped exciton; obs. by microwave optical double resonance 3-58428
 KBr, energy spectrum of electrons emitted after ion and atom bombardment 3-80132
 KBr, F-centres, photoconduction kinetics 3-41230
 KBr, filamentary crystals, internal friction peak due to dislocation-point defect interaction 3-75569
 KBr, flux, distrib. of impurities from InAs melt, radioactive isotope method 3-75626
 KBr, fundamental spectra in Schumann u.v., temp. depend. 3-58518
 KBr, Gruneisen parameters and thermal expansion, calc. using anharmonic models 3-40997
 KBr, optical absorption and luminescence of I-centres 3-46642
 KBr, paramagnetic resonance, self-trapped exciton, optical detection 3-75882
 KBr, photo-stimulated electron emission temp. depend. (Russian) 3-44518
 KBr, positron annihilation, γ -ray angular correlation curves, effective mass measurements 3-44008
 KBr, positron annihilation, influence of temp. 3-75548
 KBr, Raman scattering from CrO_2^{2-} ions at low temp. 3-53109
 KBr, single crystals, laser induced transient bleaching, F-centres 3-76031
 KBr, stored energy meas. after 4.6K reactor irradiation 3-54984
 KBr, thermal expansion from lattice const. temp. depend. 3-52712
 KBr, U centre i.r. absorpt. side bands Gruneisen const., hydrostatic press. depend. 3-55657
 KBr, u.v. and electron irradiation, defect formation, exciton decay, electron microscope obs. (Russian) 3-43807
 KBr, u.v. irradiation, electron microscope and opt. obs. (Russian) 3-43921
 KBr, vibr. excited, inelastic scatt. by Ar and CO_2 3-54746
 KBr, whisker crystals, ionic conductivity at 40 to 300C and effects of X-ray irradiation (Russian) 3-79598
 KBr crystal, crystal lattice structure, optical information recording (Czech) 3-53129
 KBr crystals with PO_2^- impurity, effect of pressure on luminescence 3-69023
 KBr pellet method for hygroscopic compounds i.r. spectral meas. 3-45491
 KBr pure and Ca doped, d.c. conductivity during plastic deformation (German) 3-53060
 KBr single crystal in electric field, dislocations and inclusions appearance 3-79520
 KBr single crystals, grown from aq. solns., (100) and (111) faces, microstruct. 3-52585
 KBr soln., crystn. and nucleation, thermal effects, analysis method 3-43759
 KBr whiskers, point defects, absorpt. spectra, U-centres, surface water effect 3-72652
 $KBr:Ag^0$, optical absorption bands, excited states 3-72685
 $KBr:CrO_4^{2-}$, impurity oscillatory absorpt. (Russian) 3-47299
 $KBr:Cu^+$, absorpt. from optically pumped relaxed excited $3d^9 4s$ state of Cu^+ 3-50603
 $KBr:HS^-$, lattice sideband structure in i.r. absorpt. spectra 3-68366
 KBr:In, thermoluminescence energy meas., alpha and gamma irradiation at 100 to 700 K (Russian) 3-76100
 KBr:KCl crystal mixtures, flow stress, Vickers hardness, and wing size intercomparisons 3-79415
 $KBr:NO_2^-$, SH^- , impurity local modes, Raman and i.r. absorpt. obs. 3-72696
 KBr:Na, composite structure of V_L -band, thermal annealing obs. 3-64699
 KBr:Na, thermal annealing of interstitial halogen ions 3-64033
 KBr:Na, thermal recovery of radiation hardening, thermoluminescence and thermal decay of V_L band 3-68247

potassium compounds continued

- KBr:Na⁺, H, H_a centre form. with dynamic interstitial interactions, temp. depend. 3-58034
 KBr:Na⁺, Li⁺, H-centre interactions during thermal annealing, V-centre form. 3-43787
 KBr:OH⁻ oscillatory radiation of OH⁻ induced by electronic excitation (*Russian*) 3-44470
 KBr:OH⁻ single crystals, photocond. and optical bleaching of F-centres 3-60902
 KBr:Pb, optical absorption spectra, A, B, and C bands 3-69030
 KBr:Pb⁺, absorpt. bands of Pb⁺ centres 3-58532
 KBr:SH⁻, effect of press. on Raman spectra 3-69004
 KBr:SH⁻, h.p. effects on Raman scatt. 3-80019
 KBr:Ti, Ag and pure crystals, tunnel luminescence (*Russian*) 3-41560
 KBr:Ti, phonon dispersion relations 3-55596
 KBr:Ti⁺, phonon props. and electron-phonon interaction 3-58098
 KBr:TiBr single crystal, luminescence centres, characts. 3-64722
 KBr + KCl:Ca⁺⁺ mixed crystals, dielectric relaxation by vacancy dipole mechanism 3-64599
 KBr + LiF, miscibility gaps study 3-72202
 KCl:F centres, optical detection of e.p.r. and luminescence bleaching effects (*French*) 3-53021
 KCN, cubic, anomalous thermoelastic behaviour 3-54998
 KCN, i.r. spectra from 4000 to 140 cm⁻¹ 3-47240
 KCN, liquid, spectroscopic props., method of mol. dynamics simulation 3-80051
 KCN, order-disorder phase transition study, Raman scattering 3-72648
 KCN, Raman and i.r. spectra, phase transition phenomena (*French*) 3-58509
 K₂CO₃, in alkali carbonate molten binary mixture, conductance, fuel cell material 3-69462
 K₂CO₃, polymorphic transform. behaviour 3-60792
 K₂CdF₃:Mn²⁺, hyperfine interactions, ENDOR study 3-47172
 KCl, (KBr), (K):Ti⁺, luminesc., slow electron impact excitation 3-41590
 KCl, activated, monomolecular recombination (*Russian*) 3-44456
 KCl, activation energy anal. after reactor irradiation 3-79378
 KCl, aq. soln., hypersonic vel., molar conc. depend., Brillouin scatt. meas. 3-49934
 KCl, containing BO₂⁻, anharmonic force field calc. 3-43421
 KCl, containing impurity complexes, bleached, temp. depend. of cond. 3-55279
 KCl, damage region form., changes in giant laser pulses and luminous plasma 3-74262
 KCl, deuteron induced damage 3-79391
 KCl, dislocation loops induced by electron irradiation, Burgers vectors 3-72090
 KCl, dislocation mobility, determ. from expts. on dislocation multiplication (*Russian*) 3-43793
 KCl, dislocation struct. determ., appl. of methods of X-ray scatt. dynamic theory (*Russian*) 3-68274
 KCl, existence of positronium-type bound states, angle correlation expt. (*German*) 3-50144
 KCl, F-centres, photoconduction kinetics 3-41230
 KCl, F-centres luminescence, electron tunnel transfer (*Russian*) 3-41551
 KCl, filamentary crystals, internal friction peak due to dislocation-point defect interaction 3-75569
 KCl, flow stress, Vickers hardness, and wing size intercomparisons 3-79415
 KCl, flux, distrib. of impurities from InAs melt, radioactive isotope method 3-75626
 KCl, hot worked, strength and deformation behaviour 3-76252
 KCl, ion irradi., channelling meas. of damage 3-52652
 KCl, isotope-induced far i.r. absorpt. 3-44402
 KCl, lattice dynamics model using band struct. props. 3-40982
 KCl, liquid, spectroscopic props., method of mol. dynamics simulation 3-80051
 KCl, low temp. sp. ht., influence of heavy Pb²⁺ impurities 3-58135
 KCl, M₂ centres, high density optical memory using dichroic absorpt. 3-44431
 KCl, magnetic circular dichroism of M- and R-centres 3-69026
 KCl, magnetic circular dichroism, R-centres, moments technique analysis 3-69027
 KCl, mechanical bleaching of F and F-aggregate centres 3-60725
 KCl, molten, Pauling potential Monte Carlo computations 3-68150
 KCl, multiphonon i.r. absorpt. temp. depend. 3-68985
 KCl, mutual transformation of V₃=V centres, thermoluminescence and e.p.r. spectra (*Russian*) 3-54961
 KCl, neutron diffraction study at room temp. 3-64128
 KCl, photo-stimulated electron emission temp. depend. (*Russian*) 3-44518
 KCl, photothermal conversion of F-centres to X-centres, light intensity dependence (*Russian*) 3-68250
 KCl, polarised luminescence and Mossbauer effect of Sn impurity centres 3-41456
 KCl, positron annihilation, γ -ray angular correlation curves, effective mass measurements 3-44008
 KCl, positron annihilation, influence of temp. 3-75548
 KCl, positronium-like state in F-colour centres 3-40916
 KCl, press forged, strengthening effects 3-45502
 KCl, pure and OH⁻ doped, microhardness and ionic cond., temp. depend. (*Russian*) 3-68644
 KCl, quasi-metallic centre formation, role of impurities (*Russian*) 3-68253
 KCl, Raman scattering from CrO₂⁻⁴ ions at low temp. 3-53109
 KCl, shear elastic constant C₄₄ rel. to phase transformation 3-43876
 KCl, single cryst., thermal depolarisation currents, electret effect (*Russian*) 3-75938
 KCl, sputtered, preferential ejection pattern 3-41603
 KCl, stability of droplets migrating in thermal gradient 3-43887
 KCl, substrate for Au condensation, spatial distrib., mechanism 3-72023
 KCl, theoretical analysis of type I F_a(Na) and type II F_a(Li) centres, point ion model 3-58229
 KCl, thermal coagulation of F-centres in additively coloured crystals (*Russian*) 3-68249

potassium compounds continued

- KCl, thermal coagulation of F-centres, alkali metal dopants 3-76035
 KCl, three-phonon umklapp resistivity, variational calc. 3-68378
 KCl, V_k centres in surface region self-trapping energy calcs. 3-40918
 KCl, vacancy and interstitial hardening, conc. effect on flow stress 3-60723
 KCl, whisker crystals, ionic conductivity at 40 to 300C and effects of X-ray irradiation (*Russian*) 3-79598
 KCl abrupt deformation and nonuniformity of internal stress field 3-75561
 KCl aqueous solutions, restricted diffusion 3-61283
 KCl aqueous solutions, temperature anomaly of energy-volume coefficient 3-68382
 KCl billet, optical quality, crack free, constrained hot pressing technique 3-69362
 KCl cryst., F-centre transform. to F₃(R), F₄(N) aggregates by optical bleaching 3-64034
 KCl crystal, crystal lattice structure, optical information recording (*Czech*) 3-53129
 KCl dilute solution, dielectric properties of ice single crystal (*Japanese*) 3-55518
 KCl low density dielectric films, controllable secondary electron emission at high energies (*Russian*) 3-58574
 KCl pure and Ca doped, d.c. conductivity during plastic deformation (*German*) 3-53060
 KCl single crystal in electric field, dislocations and inclusions appearance 3-79520
 KCl soln., ice cryst. formation, dielec. props. 3-47195
 KCl solution, artificial membrane potential at NaCl solution interface, Ca²⁺ effect 3-69486
 KCl solutions, aqueous, metastable state rupture, transitions to liquid state phenomena (*French*) 3-79492
 KCl whiskers, point defects, absorpt. spectra, U-centres, surface water effect 3-72652
 KCl:Ag⁺, X-irradiated, e.p.r. spectrum at 300K 3-79907
 KCl:Ag⁰, optical absorption bands, excited states 3-72685
 KCl:Ag⁺, Cu⁺, Pb²⁺, f-centres study (*French*) 3-52625
 KCl:Ag⁺(Cu⁺), ionization of different impurity electron states (*Russian*) 3-44455
 KCl:Al porous film, Al effect on transmitted secondary electron emission 3-50633
 KCl:CN, acoustic relax. and internal strains 3-55032
 KCl:CN⁻, vibr. absorpt., orientational tunnelling of defects 3-69040
 KCl:Co₃²⁻, Pb²⁺(Sr²⁺), mol. impurity centre form. during electrolysis, i.r. absorpt. bands 3-50604
 KCl:Ca²⁺, Mg²⁺, Sr²⁺, ionic conductivity measurements as function of temp. 3-68639
 KCl:Ca(Sr) flow stress, Vickers hardness, and wing size intercomparisons 3-79415
 KCl:F₂, semiclassical interpretation for large quadrupole interaction 3-55215
 KCl:HS⁻, lattice sideband structure in i.r. absorpt. spectra 3-68366
 KCl:In, Ag, thermoluminescence energy meas., alpha and gamma irradiation at 100 to 700 K (*Russian*) 3-76100
 KCl:In, tunnel ionization of excited In⁺ centres, 7-300 K 3-55688
 KCl:K₂SO₄, X-irrad., i.r. absorpt. 3-69044
 KCl:K₂SO₄ single crystals, interaction of mol. impurities and vacancies 3-72102
 KCl:KBr crystal mixtures, flow stress, Vickers hardness, and wing size intercomparisons 3-79415
 KCl:Li, paraelectric reson., random internal strain effects 3-53051
 KCl:Li, single crystals, vacancy mechanism of Li diffusion 3-72231
 KCl:Li⁺, spin-lattice relax. of F, F₂ centres 3-72520
 KCl:Li⁺, Zeeman nuclear relax. of tunnelling centres 3-72542
 KCl:LiF, NaF, LiCl, new bands in absorption spectrum 3-44438
 KCl:NO₂⁻, SH⁻, impurity local modes, Raman and i.r. absorpt. obs. 3-72696
 KCl:OH⁻, tunnel levels for librator in Devonshire O_k potential 3-52803
 KCl:OH⁻ acoustic paraelectric resonance, acoustic transition probability, adsorption coefficient, theoretical study (*Russian*) 3-55522
 KCl:OH⁻ paraelectric system with small zero-field splitting, low temp. applications (*German*) 3-50509
 KCl:OH⁻ single crystals, photocond. and optical bleaching of F-centres 3-69002
 KCl:Pb⁺, absorpt. bands of Pb⁺ centres 3-58532
 KCl:Pb(Tl) fine struct. of impurity A-absorpt. bands 3-69038
 KCl:SH⁻, effect of press. on Raman spectra 3-69004
 KCl:SH⁻, h.p. effects on Raman scatt. 3-80019
 KCl:SO₄²⁻ - M₂⁺ (CO₂⁻ - M₂⁺), band width var. with temp. 3-68364
 KCl:Sl plastically deformed, slip band internal structure by precipitation 3-52632
 KCl:Te(In) two photon multistage radiation during interaction of a single electron-vacancy pair with activating centres (*Russian*) 3-41557
 KCl:Ti, Ag and pure crystals, tunnel luminescence (*Russian*) 3-41560
 KCl:Ti, hole diffusion absorption method, 170 K-177 K (*Russian*) 3-55267
 KCl:Ti, lattice sp. ht., force const. change effects 3-41026
 KCl:Ti, photoluminescence (*Russian*) 3-41556
 KCl:Ti luminescence at excitation in region of fundamental absorption 3-80116
 KCl:Ti⁰, tunnelling transitions (*Russian*) 3-44447
 KCl:Ti⁺, Jahn-Teller effect in 3000 Å emission, time resolved spectroscopy 3-69061
 KCl:Ti⁺, phonon props. and electron-phonon interaction 3-58098
 KCl/adsorbed methyl chloride, microwave absorpt. 3-72265
 KCl:Eu phosphors, plastic deformation effect on optical props. 3-76077
 KCl:H₂O-HCl system isothermal diffusion studies at 25°C 3-55994
 KCl-In, KCl-In, Ti, ionic crystals containing electron traps, thermally stimulated luminescence peaks 3-76105
 KCl-LiCl molten eutectic, impedance study of metal-metal ion electrodes 3-65090
 KCl-LiCl-FeCl₃, KCl-LiCl-AlCl₃, immiscible systems, diagrams of melting, thermography (*Russian*) 3-52691

potassium compounds continued

- KCl-RbCl, solid soln., chem. diffusion 3-43896
 KCl-RbCl solid solution single crystals, linear expansion coeff., 25-500°C (*Russian*) 3-79507
 KCl + KBr:Ca⁺⁺ mixed crystals, dielectric relaxation by vacancy dipole mechanism 3-64599
 KCl + LiCl, additive coloured, roentgenised, transformation processes of F=F_a centres, electron-hole recomb. (*Russian*) 3-54962
 KCl(Br), dislocation density, rel. to plastic deform. at initial stage of compression curve (*Russian*) 3-79360
 KCl(Br), hygromech. effect 3-58174
 KCl₁Br_(1-x), additively coloured, aggregate bands, spectral positions, half width 3-69037
 KCl(Br)(I), paraelec. behaviour of OH⁻ ions, electrooptical and electrocaloric studies 3-41476
 KCl(Br)(I), refr. index and refl. spectra, uniaxial deform. effects 3-58528
 KClO₃, formation and annealing of free radicals created by irradiation 3-61268
 KCl:Ca, short-term electric relaxation (*Russian*) 3-64597
 KCoF₃, antiferromagnetic, supertransferred hyperfine interaction, perturbed angular correlation of ^{111m}Cd 3-44360
 K₂Co₂Mg_{1-p}F₄, diluted antiferromagnets, susceptibility meas. 3-75833
 KCo[Fe(CN)₆], treated with CuSO₄, CuCo[Fe(CN)₆] adsorbent, ¹³⁷Cs/^{137m}Ba radioisotope generator system, ^{137m}Ba recovery 3-48505
 K₃Cr(CN)₆ crystal and solution, Raman spectra, struct. and vibrational assignments 3-75988
 K₃CrF₆, temp. depend. of phosphorescence and fluorescence (*German*) 3-58561
 K₂Cr₂O₇, crystalline molten and aqueous, vibrational spectra 3-55587
 K₂Cr₂O₇, Fe (II) titrimetric determination, p-aronophenylanthranilic acid, oxidation-reduction indicator 3-48649
 K₃(Cr³⁺·O₆Mo₆O₁₈H₆)·nH₂O, absorpt. and luminescence spectra, vibr. structure 3-72679
 KCuF₃, one-dimens. antiferromagnet, anisotropic, anomalous susceptibility, temp. depend. 3-68773
 KCuF₃, one-dimens. antiferromagnet, neutron diff. obs. 3-68789
 K₂CuF₄, two-dimens. ferromag., magnetisation, n.m.r. obs., 1.66-4.21K 3-58399
 K₂CuF₄, two-dimens. ferromag., Heisenberg symm., neutron diff. obs. 3-79845
 K₂Cu(ZrFe₂)₂·6H₂O, crystal structure, binuclear complex in [ZrFe₂]⁴⁺ (*French*) 3-68209
 K(D,H_{1-x})₂PO₄, different deuteration degrees, Curie temp. depend. of electro-optical coeffs. 3-75965
 KD₂PO₄, X-ray structural study at 20°C 3-49879
 KD₂PO₄ growth from aqueous soln., temperature decrease method (*French*) 3-72789
 K₂MoO₄, phase transition at 10K due to cooperative Jahn-Teller effect 3-43875
 KF, aq. soln. hydrothermal crystn. of Sb₂O₃ 3-68174
 KF, fundamental spectra in Schumann u.v., temp. depend. 3-58518
 KF-ErF₃ system, phase diagram, cpd. structs. (*French*) 3-60703
 K₂Fe(CN)₆·3H₂O ferroelectric crystals, discontinuity in conductivity at transition point 3-79694
 K_{0.9}FeF₃, crystalline structure of pseudo-tetragonal bronze (*French*) 3-63988
 K₂FeO₄, cryst. structure, same type as Rb₂FeO₄, Cs₂FeO₄ 3-68231
 K₂AsO₄, ferroelectric, H bonded, Raman spectra, mol. struct. 3-72649
 K₂AsO₄, low frequency dielectric relaxation obs. 3-58473
 KHF₂, ionic conduction meas. as function of temp., determ. of transition temps. 3-43897
 KHF₂, long wavelength i.r. active phonons, assignment 3-41512
 K₂H₂PO₄, 90° phase matched, second harmonic generation in u.v. 3-51946
 K₂H₂PO₄, crystal growth from aq. soln. layer motion 3-75488
 K₂H₂PO₄, direct current conduction, proton vacancies migration 3-41198
 K₂H₂PO₄, dislocation influence on crystal growth 3-68177
 K₂H₂PO₄, dispersion of nonlinear refractive index 3-75959
 K₂H₂PO₄, e.p.r. after γ -irradiation 3-69472
 K₂H₂PO₄, effect of frozen-in radiation-induced radicals on ferroelectric loss and relaxation 3-79371
 K₂H₂PO₄, film flow of HeII over ferroelec. material 3-68461
 K₂H₂PO₄, influence of gamma-radiation dose rate on dielectric props. 3-79975
 K₂H₂PO₄, new meas. method for electro-optical consts. at h.f. 3-48404
 K₂H₂PO₄, noncollinear second harmonic generation 3-66875
 K₂H₂PO₄, obs. of domain structure by low-temp. X-ray photography 3-50527
 K₂H₂PO₄, obs. of underdamped soft lattice mode, pressure effect 3-58506
 K₂H₂PO₄, polarisation in phase transition region, nonlinearity 3-72588
 K₂H₂PO₄, positron annihilation ang. correl. curves, valence states 3-64066
 K₂H₂PO₄, Raman susceptibility, stimulated Raman effect 3-51953
 K₂H₂PO₄, second harmonic converter, for Nd:glass laser 3-74245
 K₂H₂PO₄, vector synchronous interaction of light waves 3-62741
 K₂H₂PO₄, X-ray diff. intensity var. with changing temp. gradient 3-79295
 K₂H₂PO₄, X-ray diffraction intensity contrast and Pendellosung fringes obs. due to lattice distortions 3-68267
 K₂H₂PO₄ 45° Y-cut crystal, effects of domains on optical properties and Raman scattering 3-61036
 K₂H₂PO₄ and KD₂PO₄, ferroelectric transitions, i.r. polarised reflection obs. 3-58482
 K₂H₂PO₄ finite-ice-rule ferroelectric models, statistical mechanics 3-75947
 K₂H₂PO₄ growth from aqueous soln., temperature decrease method (*French*) 3-72789
 K₂H₂PO₄ powder, dielectric constant 3-72563
 K₂H₂PO₄ relaxation, slow response of polarisation to external field, above transition point, relaxation time 3-47200

potassium compounds continued

- KH₂PO₄:Cr³⁺, e.p.r., ferroelectric and ferroelastic phase transitions 3-55463
 KH₂PO₄:K₂SeO₄ mixed crystals, ferroelec. props., e.s.r. study 3-68826
 K₃HP₂O₇·3H₂O, crystal structure, refinement by least squares method (*French*) 3-63987
 KHSO₄, HSO₄⁻ SK _{β} emission spectra 3-47328
 KH₃(SeO₃)₂, antiferroelectric, vibr. spectra and hydrogen bond pot. study 3-47256
 KH₃(SeO₃)₂, Raman and i.r. spectra, hydrogen bond potential well 3-53090
 KHgBr₃·H₂O, and KHgI₃·H₂O, polarised Raman and i.r. spectra, 10 to 4000 cm⁻¹, Urey-Bradley-Shimanouchi force field (*French*) 3-47258
 KI, anionic impurities, transformations unduced by electrolytical colouration with F and V centres 3-53134
 KI, divalent ion doped, elec. field effect on luminesc. (*French*) 3-55693
 KI, electroluminescence, expt. obs. (*Russian*) 3-41582
 KI, exciton level prediction, modulation spectroscopy 3-55229
 KI, far i.r. anharmonic optical props., absorpt., 12-300K 3-53104
 KI, fundamental spectra in Schumann u.v., temp. depend. 3-58518
 KI, molecular beam, electron scattering, total cross section 3-75109
 KI, phonon structure in excitation spectra of luminescence under two-photon excitation 3-80093
 KI, photo-stimulated electron emission temp. depend. (*Russian*) 3-44518
 KI, photoemission, electronic structure and scattering props. 3-55721
 KI, single crystals, laser induced transient bleaching, F-centres 3-76031
 KI, thermorefectance spectrum, Rydberg series of gamma₁ exciton 3-55623
 KI, whisker crystals, ionic conductivity at 40 to 300C and effects of X-ray irradiation (*Russian*) 3-79598
 KI crystals with PO₂⁻ impurity, effect of pressure on luminescence 3-69023
 KI mol. quadrupole hyperfine structure meas., obs. in vibrational states (*German*) 3-57660
 KI solution, depolarized Rayleigh wing scatt. 3-72607
 KI:Ag crystals, colour centres, recombination luminescence 3-76036
 KI:Ag⁻ and KI:Ag⁻(Li), anomalous C* emission 3-69059
 KI:Ca²⁺, Mg²⁺, Sr²⁺, ionic conductivity measurements as function of temp. 3-68639
 KI:ClO₄-(ReO₄)⁻, i.r. absorpt. and local symmetry of impurity ions (*Russian*) 3-41542
 KI:HS⁻, lattice sideband structure in i.r. absorpt. spectra 3-68366
 KI:NO₂⁻, SH⁻, impurity local modes, Raman and i.r. absorpt. obs. 3-72696
 KI:nitrates, spectral frequency shifts, uniaxial pressure 3-68568
 KI:Pb, optical absorption spectra, A, B, and C bands 3-69030
 KI:SH⁻, effect of press. on Raman spectra 3-69004
 KI:SH⁻, h.p. effects on Raman scatt. 3-80019
 KI:Sn²⁺, negative mag. circular polarisation of A-band emission 3-44486
 KI:TL type phosphor, double luminesc. excited in A band, theory 3-69087
 KI:Ti, Ag and pure crystals, tunnel luminescence (*Russian*) 3-41560
 KI:Ti, enhancement of vacuum u.v. excited luminescence by electric field (*Russian*) 3-50624
 KI:Ti, γ -scintillations 90 K-300 K (*Russian*) 3-55684
 KI:Ti, low temp. irradiation, static electric field effect on thermoluminescence (*French*) 3-53153
 KI:Ti, luminesc., hot photoelectron impact excitation processes (*Russian*) 3-44493
 KI:Ti thermoluminescence, electric field effect 3-55694
 KI + LiF, miscibility gaps study 3-72202
 KI + MI (M = Ag, Cu) molten systems, thermoelectric power 3-72375
 KICl₂, KICl₂·H₂O, cryst. struct. and bonding 3-79284
 K₂MF₄:Mn²⁺ (M = Mg, Zn, Cd), ENDOR, nuclear quadrupole interaction, zero-point spin deviation 3-75915
 KMM'X₆, pyrochlore-tetragonal transition (*French*) 3-63988
 KMgF₃, covalency parameters for Fe³⁺, comparison with LaFeO₃ and YFeO₃ 3-40860
 KMgF₃, i.r. refl. spectra, dielec. const., lattice freqs. and interionic pot. calc. 3-47272
 KMgF₃:Co²⁺, fluoresc. lifetime, multiphonon nonradiative decay at isolated impurity centre 3-47308
 KMgF₃:Eu²⁺, f-f transitions, absorp. and luminesc. spectra obs. 3-64726
 KMgF₃:Fe²⁺, far i.r. absorpt. 3-47298
 KMgF₃:Mn²⁺, hyperfine interactions, ENDOR study 3-47172
 KMgF₃:Ni²⁺, K₂MgF₄:Ni²⁺, exchange interactions, e.s.r. and mag. suscept. obs. (*Japanese*) 3-50357
 K(Mn, Ni)F₃, Heisenberg antiferromagnetic alloys, insulating, coherent potential approximation 3-55395
 K₂(Mn, Ni)F₄, Heisenberg antiferromagnetic alloys, insulating, coherent potential approximation 3-55395
 KMnF₃, cubic-tetragonal transition at 186K, press. effects., dielec. const. obs. 3-58127
 KMnF₃, equilibrium spin configuration and antiferromagnetic resonance for low temp. phase 3-72523
 KMnF₃, mag. susceptibility, temp. depend. below 80K, and field depend. 3-47008
 KMnF₃, spontaneous birefringence and order parameter below 186K transition 3-44391
 KMnF₃, weakly ferromagnetic, Bethe and Davydov mag. splittings 3-75968
 K₂MnF₄, critical magnetic scattering, neutron diffraction measurements 3-72474
 K₂MnF₄, Heisenberg antiferromagnet, two magnon light scattering 3-72619
 K₂MnF₄, quadratic layer, antiferromag. reson. 3-50463
 K₂MnF₄, quadratic-layer antiferromag., spin-wave anal. 3-50384
 K₂MnF₄, two-dimens. antiferromagnet, crit. exponents for e.p.r. linewidths 3-58418

potassium compounds continued

- K_2MnF_4 , two-dimensional Heisenberg paramagnet, e.p.r. min. line-width obs. 3-41396
 K_2MnF_4 , planar antiferromag., spin waves and mag. ordering 3-50385
 $KMn_2Mg_{1-p}F_3$, diluted antiferromagnets, susceptibility meas. 3-75833
 $K_2Mn_2Mg_{1-p}F_4$, diluted antiferromagnets, susceptibility meas. 3-75833
 $KMnF$ and $KMnAs$ powders, synthesis, crystal structure, X-ray studies 3-40900
 K_2MoCl_6 , force consts. and mean vibr. amplitudes 3-67771
 K_0MoS_2 , room temp. resistivity obs. 3-79691
 K_2MoS_4 , Raman, i.r. spectra, force constants 3-63450
 KN_3 , photolum. spectral distrib. and intensity (Russian) 3-44476
 KN_3 , self-diffusion of K, 85-254°C 3-43898
 $KNCS$ crystal, polarised i.r. and Raman spectra lattice vibrations 3-72609
 KNO_3 crystal, model for coupled rotation-displacement modes 3-79440
 KNO_3 , molten, at 400 C and 6-10 V, super purity Al anodizing 3-73142
 KNO_3 - $Ca(NO_3)_2$ mixtures, low temp. spectra of external modes 3-75974
 KNO_3 - $CsNO_3$ - $NaNO_3$ phase diagram, thermodynamic calc., thermography (Russian) 3-52692
 KNO_3 - $LiNO_3$ - $AgNO_3$ ternary system, equilibrium study 3-60788
 KNO_3 - $M(II)(NO_3)_2$ glass, thermodynamic props. 3-72009
 $KNaNbO_3$, ferroelectric, sputter machining, rel. to use as acoustic transducer 3-64966
 $KNbO_3$, cubic-tetragonal-orthorhombic-rhombohedral ferroelectric transitions, neutron powder profile refinement technique 3-64609
 $KNbO_3$, intracavity second harmonic generation of YAlG/Nd laser 3-51948
 $KNbO_3$, nonlinear optical coeffs., at 1.06 μ , Marker fringe method 3-68954
 $KNbO_3$ single crystals, low frequency dielectric studies 3-53053
 $KNbO_3$ thick crystals, ferroelec. domain struct. obs. 3-79993
 $KNbO_3$ - $LiNbO_3$ system, X-ray diffr., phase diagram, Curie temp. 3-72590
 $K(Ni, Zn)F_3$, Heisenberg antiferromagnetic alloys, insulating, coherent potential approximation 3-55395
 $K_2(Ni_2(CN)_6)$, struct. from X-ray diffr. (German) 3-40894
 $K_2(Ni_2(CN)_6)$, symmetry, polytypism, twinning (German) 3-40893
 $KNiF_3$, antiferromagnetic, supertransferred hyperfine interaction, perturbed angular correlation of ^{111}mCd 3-44360
 $KNiF_3$, crystal field and exchange parameters, decoupling transformation method 3-55208
 $KNiF_3$, lattice constants measurement, double-crystal diffractometry using white X-rays 3-52559
 K_2NiF_4 , quadratic-layer antiferromag., spin-wave anal. 3-50384
 K_2NiF_4 , structure of transition metal oxide systems, rel. to electron transport props. 3-41241
 K_2NiF_4 : ^{19}F , two-dimensions. antiferromagnet, crit. exponents for n.m.r. linewidths 3-58418
 $KNiPO_4$, antiferromagnetic, crystal structure, basis atoms coordinates and interatomic distances calc. 3-60715
 KO_2 crystals, sp.ht., mag. transforms. (German) 3-50361
 K_2O - B_2O_3 melts isothermal viscosity behaviour by ultrasonic relaxation studies 3-41040
 K_2O - B_2O_3 + MnO_2 glasses, optical and magnetic properties, alkali oxide content depend. 3-55411
 K_2O - BaO - B_2O_3 , glasses rheological properties, viscosity 3-58070
 K_2O - SiO_2 : Dy^{3+} glass, luminesc. centres (Russian) 3-72721
 K_2O - SrO - SiO_2 glasses, i.r. spectra, struct., depolymerizing effect 3-68164
 K_2O - TiO_2 - SiO_2 - Li_2O glass, n.m.r. spectra of 7Li , ion struct. 3-72528
 $(K_2O-P_2O_5)_x$ -(WO_3) $_{1-x}$ glass, microphase separation, electron microscope obs. of surface replicas 3-72007
 $(16-x)K_2O \cdot 2xKCl \cdot 84B_2O_5$ glasses, Tl^+ phosphor characteriz. 3-58547
 KPF_6 , chemical shift in n.m.r. of ^{19}F 3-61002
 KPF_6 , pulsed n.m.r., F spin-lattice relaxation 3-47159
 $K_2P_2O_4F_2$, n.m.r. investigation of P-P bond 3-54721
 K_2Pd , diamagnetic lattice for EPR of Cu complexes 3-79901
 $K_2Pt(CN)_4Br_{0.3}(H_2O)$, reflection meas. for polarised light in f.r. region (German) 3-50568
 $K_2Pt(CN)_4Br_{0.3}(H_2O)$ unidimensional metallic conductor optical const. determ. by laser light reflection meas. (German) 3-50532
 $K_2Pt(CN)_4Br_{0.3} \cdot 2.3H_2O$, susceptibility temp. depend., model of linear metallic strands interrupted by insulating lattice defects 3-50340
 $K_2Pt(CN)_4Br_{0.3} \cdot 3H_2O$, one dimens. conductor, ^{195}Pt Mossbauer effect 3-53044
 $K_2Pt(CN)_4Br_{0.3} \cdot 3(H_2O)$, anisotropic Seebeck effects, temp. dependence, reln. to metal-insulator transition (German) 3-50184
 $K_2Pt(CN)_4Br_{0.3} \cdot 3H_2O$, n.m.r. obs. of low temp. insulating phase in one-dimensional conductor 3-55489
 $K_2Pt(CN)_4Br_{0.3} \cdot 3H_2O$, one-dimensional conductor, giant Kohn anomaly observation 3-43849
 $K_2Pt(CN)_4Br_{0.3} \cdot 3H_2O$, optical cond. and electron interaction 3-68958
 $K_2Pt(CN)_4Br_{0.3} \cdot 3(H_2O)$, Pt Mossbauer meas. as test for metal-insulator transition with localisation of conduction electrons (German) 3-50492
 $K_2Pt(CN)_4Br_{0.3} \cdot 3H_2O$, Peierls instability, tight-binding theory of electron-phonon interaction 3-72148
 $K_2Pt(CN)_4Br_{0.3} \cdot 3(H_2O)$ quasi-unidimensional conductor, optical transmission spectrum for perpendicularly polarised light (German) 3-50588
 $K_2Pt(CN)_4Br_{0.3} \cdot 3H_2O$, optical excitation of electronic plasma oscillation in one-dimensional conductor 3-52810
 $K_2Pt(CN)_4Br_{0.3} \cdot nH_2O$ quasi one-dimens. conductor, ^{195}Pt n.m.r. and p.m.r., temp. depend. behaviour (German) 3-50482
 $K_2Pt(CN)_4Br_{0.3} \cdot xH_2O$, one dimens. cond., Peierls distortion, Kohn anomaly 3-49900
 $K_2Pt(CN)_4Br_{0.3} \cdot xH_2O$, low temp. phase transition, condensation of soft modes by Kohn anomaly 3-64177

potassium compounds continued

- K_2PtCl_6 structure, X-ray diffraction refinement, single crystal and powder 3-58013
 $K_xRb_{1-x}SO_4$ (0.3 < x < 0.55), alkali metal ordering and hydrogen bonding 3-46607
 K_2ReCl_6 , 110.9 K displacive phase transform., order parameter meas. 3-46712
 $K_2S_2F_6$, K_2GeF_6 and K_2TiF_6 , efficient Mn(IV) emission in FL coordination 3-58545
 K_2SO_4 , e.p.r. spectra of Mn^{2+} , temp. depend. 3-55464
 K_2SO_4 , neutron irradiation effects on single crystals 3-79379
 K_2SO_4 , Raman scattering from CrO_4^{2-} ions at low temp. 3-53109
 K_2SO_4 multiparticle crystal growth rates in vertical cones 3-47352
 K_2SO_4 - AgI , seeding of warm clouds, steady flow cloud chamber 3-80865
 $K_2S_2O_8$, $S_2O_8^{2-}$ - SK_6 emission spectra 3-47328
 $KSc(EO_4)_2$ (where E=Mo, W), crystal parameters 3-79328
 $K_2Sc_2(Ge_2O_7)(OH)_2$, synthetic basic, crystalline structure, cation-anion interatomic distances 3-60714
 K_2SiO_3 , glass melt, super-crit. conc. fluctuations at high viscosity, light scatt. obs. 3-79238
 $K_{1-x}Ta_xNb_{1-x}O_3$ Sn $_{0.001}$, flux grown, dielec. const., elec. cond. anomaly (Japanese) 3-41490
 $KTaO_3$, electronic band structure, LCAO calcs. 3-41139
 $KTaO_3$, ferroelec. mode freq., thermal expansion and compressibility 3-55071
 $KTaO_3$, wavelength-modulated spectrum, temp. variation of band gap 3-55569
 K_2TeO_3 glass, heat-treated, e.p.r. of radiation centres (Russian) 3-44324
 $K_2TiSi_2O_8$, crystal structure and hydrothermal synthesis 3-60716
 $K_3(UO_2)_2F_7 \cdot 2H_2O$, X-ray diffraction, crystal structure 3-79311
 $K_xV_{1-x}Mo_{1-x}O_3$ crystal structure of hexagonal phase determ. (French) 3-79302
 $K_{0.37}WO_3$, tetragonal structure, alkali metal distrib., X-ray diffractometer data 3-63995
 K_2WO_3 , optical props. determ. from 0.1 to 38 eV 3-80072
 $KY(MoO_4)_2$ - $KDy(MoO_4)_2$ system, energy spectrum of Dy^{3+} ion, absorp. and e.p.r. spectrum obs. 3-64682
 $KY(WO_4)_2:Nd^{3+}$ crystal spectroscopic and generation study for laser 3-64691
 $KY(WO_4)_2:Nd^{3+}$ stimulated emission in $^4F_{3/2} \rightarrow ^4I_{13/2}$ transition 3-43018
 $KZnF_3:Mn^{2+}$, hyperfine interactions, ENDOR study 3-47172
 $KZnF_3:Ni^{2+}$, $K_2ZnF_4:Ni^{2+}$, exchange interactions, e.s.r. and mag. suscept. obs. (Japanese) 3-50357
 $KZnF_3:V^{2+}$, Cr^{3+} , fluorine hyperfine interactions, ENDOR obs. 3-79947
 $K_2ZnF_4:Mn^{2+}$, axial anisotropy of Mn^{2+} , overlap contribs., e.p.r. obs. 3-50444
 $K_2[Pt(CN)_4]Cl_{0.3} \cdot xH_2O$, stability in wet and dry atmospheres 3-46627
 $K_4[Zr_2(SO_4)_6 \cdot 4H_2O]$, complete X-ray structure, heavy-atom method determ. 3-79309
 $Kf-TbF_3$ system, differential thermal, X-ray, crystalloptical anal., phase diagrams 3-64148
 $KmnF_3$, antiferromag., magnon-phonon sidebands temp. depend., optical absorpt. obs. 3-47238
 $Na-K$ liquid alloys, electrical resistivity calc. 3-60866
 $Na_2K(CO_3)_2(SO_4)Cl$ hanksite crystal structure 3-73201
 Na_2O - K_2O - SiO_2 system glasses, He migration behaviour 3-75632
 $SbNa_2K$, Cs film photocathode, optical and photoelectric props. detn. (French) 3-41612
 TiO_2 - K_2O - B_2O_3 system, phase equilb. diagram 3-68387
- potential dividers** see voltage dividers
potential energy between molecules see intermolecular mechanics
potential scattering
 see also particle scattering
 analytic continuation of scattering amplitude in scattering angle using impact-parameter expansion 3-57125
 Born series, variational bounds on radius of convergence. 3-66619
 central potential, l-wave reduction to s-wave 3-60087
 Coulomb corrections to $\pi\pi$ scattering, retardation effects in the vector potential 3-62878
 cutoff potentials, expansion of scattering matrix in momentum power series, analytic continuation 3-62546
 cylindrically symmetric potential, radial equation, semiclassical approximation 3-70692
 eikonal approx. and additivity for partial-wave phase shifts 3-71110
 eikonal expansions of eqns., general formalism for rearrangement processes 3-62570
 equivalent variational functionals 3-62557
 exchange reactions, derivations of absorptive corrections using eikonal approx. 3-62864
 high energy, Green functions and projection operators in semiclassical approx. 3-59789
 inverse problems; approx. soln. using generalised WKB method 3-62572
 inverse scattering calcs. of energy independent potentials 3-62545
 method for hyperon-nucleon scattering, low energy 3-62874
 N/D method, exponential potentials 3-62792
 nonrelativistic from spherically symmetric potential, additivity of phase shifts 3-77865
 nuclear reaction theory transition matrix application 3-60138
 quasipotential formalism for system of two particles with spin 0 and 1/2 3-70874
 relativistic spinless particle scattering by complex potential, high-energy limit 3-66924
 S matrix, linked cluster decomposition, generalisation of eikonal approx. 3-62779
 spin-dependent spheroidal potential, iterative soln. 3-74107
 two-body, with long-range interaction, modified Lippmann-Schwinger eqn. 3-74108
 two-bump barrier penetration, influence of fission potential (Russian) 3-67223
 upper and lower-bound estimates of particle with potential V(r), amplitudes of multichannel processes (Russian) 3-62551
 variational procedures 3-66623
 velocity dependent, phase shift low energy behaviour 3-62871

potential scattering continued

nd elastic scattering with local potentials, Fadeev formalism
3-62872

potentials (bioelectric) *see bioelectric potentials***potentials (crystals)** *see crystal internal fields***potentials (electric)** *see electric potential***potentiometers**

see also voltage measurement

chronopotentiometry, improved, use of potentiostat and capacity-current addition device 3-73950

heating rate control in device with automatic recording potentiometer 3-73688

Kelvin-Varley, high precision, calibration 3-51662

powder diffraction cameras *see cameras; X-ray crystallography apparatus***powder metallurgy**

cathode materials for electric vacuum devices 3-80398

combustion quenching model with variable surface temperature (*Russian*) 3-69334

drop spheroidisation during solidification, effect of melt thermophys. props. 3-80394

e.m. compaction, density determ. (*Russian*) 3-72923

explosive compaction processes (*German*) 3-47444

gas evaporation with electron beam heating, fine metal particle prep. 3-80389

magnet protection against oxidation during heat treatment 3-50751

metal matrix composite, analysis of energy expended in dynamic hot pressing 3-80453

milling, specific surface, grain size distrib. rel. to surface active additive 3-80390

sintering, early stage, dislocation generation 3-69243

sintering, stress induced diffusional transport, material continuity requirements 3-69332

sintering, stress induced diffusional transport, material continuity requirements 3-69333

sintering of powder compacts, anisotropy in linear shrinkage (*Polish*) 3-72921

sintering of two-component systems with eutectic constitution diagrams, comp. depend. of shrinkage 3-80395

sponge-iron powder, lubrication effects on compaction at low and high speeds 3-69335

steel, Ni-Mo, post-sintering heat treatment and microstruct. phenomena 3-69306

steel, R18, sintered, structure and props. 3-80396

steel, sintered, fracture-resistance, Cu and carbon addition effects 3-69307

strain hardening effects in powder compaction 3-69336

AlNi, gas-free burning of metal mixtures and self-propagating high-temp. synthesis (*Russian*) 3-58699

Cu-Fe powder mixtures, degree of mixing (*German*) 3-47439

Fe, sintered, elastic modulus and ductility 3-50753

Fe-Si sintered alloys, mag. props. 3-80397

Fe₃O₄-CaO-SiO₂, self-fluxing agglomerate, sintering, reaction conditions (*French*) 3-69330

Nb₃Sn, supercond., shock wave synthesis from powder mixtures 3-69328

Ni, pack-aluminizing, boundary conditions for diffusion 3-64964

SmCo₅, microstruct. and mag. props. characteriz. (*Russian*) 3-58403

SmCo₅, powder-based magnets, texture perfection degree, particle orientation angles distrib. (*Russian*) 3-61135

Ta powder compacts, porous, shrinkage in sintering (*Korean*) 3-53265

TaC_{1-x}TaN_x-HfN system, hot pressed, annealed, lattice parameters, microhardness rel. to comp. (*Germany*) 3-80392

W after hydroextrusion, physico-mech. props. (*Russian*) 3-72922

W powder compacts, low temp. sintering (*Korean*) 3-53264

W-Ni-Fe system, liq. phase sintering, microcrack behaviour (*German*) 3-80391

WC/Co, sintering, shrinkage rel. to milling 3-80393

WC-Co compound powder, plasma spraying on hard metals, mechanical props. meas. (*German*) 3-50752

W_{0.3}Be doped, reduction, W filament production, strength rel. to comp. (*Hungarian*) 3-72986

Zn powder electrolytic deposition on steel, effect of foreign atoms 3-80556

ZrC and ZrC-B alloys, arc melting and homogenization 3-80430

powders

see also densification; granular structure; particle size; sintering agglomerated, properties rel. to structure (German) 3-50797

alunite ore, attachment to URS-50IM system, X-ray diffractometer, alunite content determ. 3-48593

ballistic fuels, combustion, effect of catalysts CuS, CuH and PbS, combustion products and rate (*Russian*) 3-47546

burning, surface refl. of plane acoustic wave (*Russian*) 3-69445

ceramic, binary size system, compaction 3-80423

ceramic powders and mixtures, explosive compaction (*German*) 3-47444

coal, compaction mechanisms 3-47490

compressed, Poisson's ratio, X-ray diffr. determ. (*Czech*) 3-54993

1,1-diphenyl-2-picryl hydrazyl recrystallised free radical powder, e.s.r. absorption 3-47601

fluidization types and criteria 3-55909

glass, kinetics of wetting, surface energy and surface tension, modification by siloxanes (*German*) 3-53279

granular solids, flow profile and void fraction in moving bed 3-44696

graphite, electrical resistivity variation during heating in air (*Japanese*) 3-79688

graphite, high temp. reactor fuel pressings, struct., grain size distrib., radiation effects (*German*) 3-71268

heating in plasma stream for deposition of coatings, effectiveness inverse (*Russian*) 3-53176

mechanical properties, temp. effect, coating with liq. films 3-80507

metallic, grain size, specific resistivity, temp. depend., Q-meter measurement method 3-62179

metallic, r.f. echoes in n.m.r. 3-79923

metallic particles electronic polarisability 3-50511

powders continued

microscopic specimen prep. by powder separation technique 3-42556

mineral, cold compaction, time-depend. deform. 3-47489

motion in plasma stream for deposition of coatings (*Russian*) 3-53175

particle redispersion system, disaggregation without fracture 3-69399

particle separation according to shape, lab. device 3-44697

photosorption of gases, powdered adsorbents, max. cover definition, apparatus (*Russian*) 3-48572

picryl-N-amino carbazyl recrystallised free radical powder, e.s.r. absorption 3-47601

polymer, substrate, influence of temp. on struct. and transport props. of Bi films 3-50091

porous metallic materials, thermal and electrical conductivity prediction 3-76392

pressing, triaxial compaction technique 3-80422

Raman spectra of powder composed of small crystals, vibr. modes 3-58095

random and non-random mixtures, stat. props., variance of sample comp. 3-55907

Rochelle salt, dielectric constant of powder 3-72563

sintering, dispersed porous body 3-69364

solid fuel, reaction kinetics on surface, linear nonstationary effects, instability (*Russian*) 3-47545

spectral analysis, two-stage spectrum excitation technique 3-54042

spectral analysis in plasma jet, grain size depend. (*Russian*) 3-77752

standard specimens, by vacuum evaporation 3-55906

stilbene powder, optical characteristics by nonstationary diffusion method (*Russian*) 3-70851

sucrose, compaction mechanisms 3-47490

transition metal compounds 3-41827

URS-50IM attachment, X-ray diffraction, material content, continuous monitoring 3-48593

vehicle hot pressing technique 3-76306

X-ray powder diffractometry, low temp., 65 to 320 K (*French*) 3-49800

Al₂O₃, flame- and plasma-prepared, metastable phase formation 3-47447

Al₂O₃-Cr₂O₃, condensed from plasma, struct. exam. 3-47448

B₁₂C₂, void morphologies 3-71282

B₂C₃-KBF₄-NaCl-Al₂O₃ mixture, boriding of steel parts 3-80350

BN, sintering under pressure (*Polish*) 3-47452

Be, tensile behaviour under hydrostatic pressure, effect of surface conditions, ductility 3-61182

CO₂R R=Pr, Sm and mischmetal, prep. by rapid quenching technique for magnet applic. 3-44278

¹⁴C, sepn. from neutron-irrad. AlN by dry procedure 3-44739

Cd₂Co_{1-x}Cr₂S₄, mag. semiconductor, hot pressing for magneto-optical props. 3-47230

CdS, powder, effects of heat treatment on photoconductive properties 3-60896

CdS, with Cu acceptors and halide donors, elec. cond. 3-64331

CdSe compressed powder, d.c. cond., temp. depend. 3-68621

(Co_{0.7}Fe_{0.3})₂MM₂, MM=Ce rich mischmetal, mag. props. obs. rel. to permanent magnets and recording media 3-44277

KH₂PO₄ powder, dielectric constant 3-72563

Mg₂Mn_{1-x}Fe₂O₄, phase composition, Mossbauer spectral studies 3-53041

NaCl, compaction mechanisms 3-47490

Ni, multiaxial, Wohlfarth-Kondorskii relation applicability (*Russian*) 3-60980

NiO, reduction, nucleation rate, kinetics rel. to Neel transition 3-55164

(Pb, La)(Zr, Ti)O₃ powders, chem. prep. from aqueous nitrate sols. 3-76247

SiC, very high pressure hot pressing 3-50755

SiO₂ powder, mag. quenching of orthopositronium, effects of chemisorbed water 3-52642

SmCo₅, sintering mechanisms, rel. to magnet prod. 3-47438

SmCo₅ domain wall pinning centres, particle size and coercivity 3-44276

Sm₂Co₁₇, liquid phase sintering, mag. props. obs. 3-44694

ThO₂, phys. props. and influence on sinterability 3-80402

UO₂, microstruct. evolution during press. sintering 3-78377

UO₂, thermal precip. from sols 3-67555

W, swaged, diffusion, autoradiography, 1300-1900°C (*Hungarian*) 3-72987

Y₂O₃-ThO₂ (10 mole%)-Nd₂O₃ (1 mole%), transparent powder prep. and processing 3-64968

ZnO, adsorption of O₂, logarithmic time law (*German*) 3-64239

ZnO, photosorption of O₂, max. cover definition, apparatus (*Russian*) 3-48572

ZrO₂, partially stabilized with calcia, SiO₂ role in sintering 3-69346

power amplifiers

fibre laser amplifiers, for detectors 3-48458

wideband, for h.f. plasma properties (*Russian*) 3-43694

power cables

cryogenic, liquid N₂ cooled, simulated load tests, Al stranded hollow conductor, insulation 3-48389

power control

see also load regulation

reactor core power distrib. smoothing by fuzzy automaton using search technique of control rod pattern 3-71160

power factor measurement

No entries

power factor meters *see power factor measurement***power factor Q** *see Q-factor***power generation, electric** *see electric power generation***power lines** *see power cables***power measurement**

see also wattmeters

laser pulse, low energy, V₂O₅ thin film resistor calorimeter 3-53918

laser pulse energy, calorimeter, digital meter 3-70283

light flux at 0.6328 μ, photodiode 3-73746

power measurement continued

- nuclear reactor, using gamma compensated pulsed ionisation chamber 3-45547
- Siemens training reactor, absolute power calibration, real time correlator-spectrum display system 3-62196
- CO₂ laser, absolute calorimeter design 3-42588

power packs *see power supplies to apparatus***power plants**

- noise abatement, employee protection 3-42473
- noise abatement, OSHA compliance plans 3-42472
- noise abatement 3-42471
- oil-fired, nearby fallout by precip. 3-73280
- pump, design considerations for noise reduction 3-42476

power stations

- see also energy resources; geothermal power stations; nuclear power stations; power plants; steam power stations*
- balloons appl. 3-56257
- gases, Na-concentration deter. (Polish) 3-62094
- steam fog, formation from warm water lagoon for power station cooling 3-65292
- thermal, of Electricite de France, development (German) 3-67618

power supplies to apparatus

- see also cells (electric); power plants; power supply circuits*
- capacitor discharge unit, mobile, radiographic examination of chest, practical experience 3-66390
- current stabiliser, controlled, for supercond. solenoid 3-77567
- energy discharge power supply at National Accelerator Laboratory, USA 3-56952
- for NAL booster synchrotron magnet 3-56953
- for national accelerator laboratory main ring system 3-56948
- pulse generator, for laser electro-optical Q-switch 3-73791
- for solid laser with repetition frequency of several Hz 3-51636

power supply circuits

- see also power supplies to apparatus*
- constant current, high resolution, high stability 3-39973
- electron beam welding guns, during breakdown 3-49772
- lamp current supply, programmable, for atomic absorpt. spectrophotometry 3-62115
- magnetron, for microwave excited electrodeless discharge lamp for spectroscopy 3-62112
- matching circuit and bucking current stabilizer for detector in e.s.r. spectrometer 3-42618
- microlamp radiation stabilisation ccts. 3-39917
- for pulsed plasma electron source 3-73853
- for solid laser with repetition frequency of several Hz 3-51636

power supply systems *see power systems***power system control**

- see also load regulation*
- International Convention and Exposition, New York, (1973) 3-78372

power systems

- see also transmission networks*
- electromechanical plant, e.m. field control problems (Russian) 3-48835

power transformers

- distribution, overhauling standards 3-59539
- oils, detection of DBPC antioxidant by gas chromatography 3-66443

power transmission

- see also transmission networks*
- at planar interface, Hilbert-space formulation of ang. spectrum representation 3-42952

power transmission line carrier systems *see carrier transmission on power lines***power transmission lines**

- cables and insulated conductors, protection against contact voltage with neutral conductor, standard (Slovenian) 3-66127

power transmission networks *see transmission networks***power utilisation**

- see also drives; environmental engineering; heating; metering; refrigeration; transportation*
- and control, International Convention and Exposition, New York, (1973) 3-78372
- current leads, cooling, thermodynamic optimisation, refrigerator min. power input calc. 3-48382

praseodymium

- absorption spectra, 1.13-4.42 eV, dispersion depend., quantum transitions (Russian) 3-80066
- atom, spectrum analysis 3-78415
- elastic constants, temp. range 4.2-300 K 3-68307
- electrical resistance minimum in crystals with Fe impurities, mag. field effects (Russian) 3-52816
- Lorenz number, high purity polycrystalline specimen, 2-40 K 3-55235
- paramagnetic excitons in d.h.c.p., Pr, temp. depend. excitation spectra 3-46821
- reflectivity of synchrotron radiation and surface plasma resonances 3-41538
- singlet ground-state system, elastic consts., cryst.-field level effects 3-52658
- X-ray photoemission spectra near Fermi energy 3-53168
- Pr³⁺, shielding of quadrupole crystalline electric field 3-41146
- CaS:Bi phosphors, effect of didymium ions on emission characteristics 3-47301
- LaCl₃:Pr³⁺, energy transfer processes 3-72706
- LaCl₃:Pr³⁺, Nd³⁺, energy transfer between low-lying energy levels of Pr³⁺ and Nd³⁺ 3-53145
- LaF₃:Pr³⁺, energy transfer processes 3-72706
- La₂O₃S single crystals, e.p.r. of Tb³⁺ and Pr³⁺ 3-68835
- Pr³⁺, in Y cpds., multiphonon relax. of excited states 3-53143
- Pr³⁺, paramag. relax. in yttrium and lanthanum ethyl sulphates 3-50450
- Pr³⁺ ion in soln., magnetooptical activity calc. for forbidden transitions 3-61030
- SeOCl₂:SnCl₄ solution, Pr³⁺ doped, fluorescence spectra 3-76049
- YIG:Pr, ferromag. resonance, high pressure effects on anisotropy and relax. 3-41421

praseodymium compounds

- acetate sesquihydrate, cryst. growth and lattice parameters 3-64023
- binary chalcogenides, mag. props., metal-insulator transition, superconductivity 3-41326
- praseodymium benzoyletacetate, u.v. diffuse reflectance spectra 3-47291
- 2Pr₂O₃.xSb₂O₃, tetragonal cryst. structure for 3.0<x<3.8, X-ray obs. 3-52603
- {Pr₃}[Lu₂](Ga₃)O₁₂ garnet dodecahedral and octahedral site filling, structure factor calc. 3-40877
- CaF₂:PrF₃(NdF₃, DyF₃, HoF₃, ErF₃, TmF₃), gamma-luminescence, phosphorescence, photoluminescences 3-53140
- Pr III complex, acetylacetonate, absorption spectra, energy levels 3-52354
- Pr III complex, benzoyletacetate, absorption spectra, energy levels 3-52354
- Pr III complex, thenoyltrifluoroacetate, absorption spectra, energy levels 3-52354
- Pr-Sm-Co, mag. props. as function of composition 3-47088
- PrAlO₃, phase transitions obs. using Raman scattering, optical fluorescence spectroscopy and e.p.r. 3-55083
- PrB₆ X-ray diffr. anal., thermal props. 3-68423
- PrBO₃, flux growth of single crystals 3-58595
- PrCl₃ quantum counter, direct i.r. image upconversion 3-57247
- PrCo₂ thermal-decomposition, PrCo₂→PrCo₃+Pr, high temp. and vacuum 3-47558
- PrCo₃, liquid phase sintered, mag. props. 3-44268
- PrCo₃, sputter deposited permanent mag. material, heat treatment and hysteresis 3-44251
- PrCo₃ powder, prep. by rapid quenching technique for magnet applic. 3-44278
- PrCrSe₃, mag. and elec. charact. 3-64497
- PrF₃, far u.v. refl. spectra, 6-40 eV 3-58521
- PrF₃, reflectivity and surface plasma resonances 3-41538
- PrN, cryst. field splitting of ³H₄ ground multiplet, neutron scatt. obs. 3-58352
- PrO, visible and IR spectra 3-75026
- PrO_x-O system, pseudophase behaviour in epsilon and iota regions 3-64180
- PrO₁₁ thin films, optical properties meas. by photometry and ellipsometry 3-53159
- Pr₂O₃(hexagonal), Pr₂O₃(cubic), PrO_{1.833}, enthalpies of formation 3-65084
- PrSb, singlet ground-state system, elastic consts., cryst.-field level effects 3-52658
- PrScFe₄O₁₂, anisotropy and microwave linewidth due to Pr³⁺ anomalous behaviour 3-50396
- PrTiNbO₆, polycrystalline specimens, electrical conductivity, temperature dependence 3-75787
- Pr(Zn,Mg) nitrates, improved analysis and double perturbations in spectra 3-55663

preamplifiers

- bioelectric voltage signals, measuring apparatus (German) 3-66399
- multichannel emission spectrochemical analysis, solid state photodiode system matched to d.c. and lock-in amplifiers 3-73958
- noise in proportional counter measurements 3-56935
- solid state, for biological purposes 3-70443

precipitation

- see also flocculation*
- alloy, binary, form. of carbide, nitride dispersions from coprecipitated hydroxides (French) 3-53231
- alloy, creep, bypassing past coherent mismatch-free precipitates by climbing 3-64869
- alloy, discontinuous precipitate cells, growth rates (German) 3-64879
- alloy, elastic stabilization of arrays of precipitates 3-69244
- alloy, f.c.c. ternary, segregation of atoms at antiphase boundaries (Russian) 3-50692
- alloy, hydrogen induced grain boundary cracking, quantitative model 3-69206
- Auger spectroscopy applic. for impurity segregation to grain boundaries obs. 3-55768
- binary melts, obs. of unidirectional solidification with natural convection 3-72877
- β-brass, Widmanstätten precipitates morphology 3-47378
- clustering, dynamic theory (Russian) 3-64863
- dielectric, perfect, spinodal decomposition, elec. field effects 3-72201
- dispersed particle stabilization by coherent strain energy 3-64867
- dispersed particle stabilization by elastic strain energy 3-61160
- electron metallography, microstruct. anal., bright field images, struct. factor, strain contrast 3-76181
- electron microscopy, 1 MeV, in situ obs. 3-50704
- Fe-C-V, crystal segregations, eutectic carbide precipitations, effect of alloying elements, Cr, Mo, W and V (German) 3-72845
- field-ion atom-probe analysis applics. in iron and steel 3-76170
- glass, alkali aluminoborosilicate, containing Ag, Cl and Br, comp. of Ag halide cryst. precip. 3-80437
- grain boundary precipitation density rel. to atomic struct., intergranular germination sites defn. (French) 3-47370
- heterogeneous systems, and mass polymerisation, mathematical modelling (German) 3-65012
- Inconel 718 sheet, time-depend. edge-notch sensitivity rel. to mech. and microstruct. characts. 3-64952
- Inconel 718 type alloys, morphology of precipitates and thermal stability 3-69232
- ionic crystal, vacancy subsystem behaviour in temp. gradient field (Russian) 3-40911
- metal, irradi., void nucleation kinetics, impurity effects 3-64072
- metallographic applics. of electron microscope microanalysis (German) 3-69230
- Nimonic PE16, effect of isothermal aging on precipitate yield strength 3-58698
- photoinduced molecular aggregation and precipitation 3-53331
- polymer theory of precipitation from supersaturated solutions 3-63590
- polymers, molecular wt. distribution determ. by temperature drop turbidimetry 3-57682
- polystyrene-cyclohexane system, cloud point curves near critical pt. 3-80489

precipitation continued

- salts, from aqueous solutions, high press. and temp., γ -ray study 3-50859
- solid solution, decomp. curve asymmetry, elastic distortions influence (*Russian*) 3-72855
- spinodal decomposition, early-stage theory 3-53198
- spinodal decomposition kinetics, higher derivative terms 3-41689
- steel, 17 wt.% Cr stainless, microsegregation of alloying elements, high temperatures 3-76205
- steel, A19 alloy, Be, Ti and Zr additions effect on struct. and mech. props. (*Russian*) 3-72850
- steel, austenite, dissolution kinetics of $M_{23}C_6$ carbides 3-64839
- steel, austenite EI-257, prolonged ageing influence (*Russian*) 3-80273
- steel, austenite transform., Mn dendritic segregation effect 3-50684
- steel, austenitic, analysis of precipitation of σ phase (*Polish*) 3-72843
- steel, austenitic, containing Nb, neutron irradiation induced swelling, influence of quenching conditions (*French*) 3-40538
- steel, austenitic, containing Si on Ti, phase characteriz. 3-69222
- steel, austenitic, solid soln. decomp., dislocation effects 3-50710
- steel, austenitic, time-temp. diagram, X-ray and electron microscope obs. (*German*) 3-47364
- steel, austenitic stainless, irradiation, with Ti and B additions, high-temp. deform. and fracture 3-63188
- steel, austenite-ferrite stainless, struct. development by holding between 600 and 1100°C (*French*) 3-44582
- steel, bainite Fe-C-Si, austenite decomp. kinetics (*French*) 3-47358
- steel, cementite dissolution, in situ obs., h.v. electron microscopy 3-50706
- steel, converter, Nb-microalloyed, precip. processes (*Slovak*) 3-55773
- steel, Cr and Cr-Ni, electron microscopic detection, potentiostatic structure development (*German*) 3-47369
- steel, Cr-Ni, of Cr_2N solubility of N, temp. depend. (*German*) 3-47367
- steel, Cr-Ni type, austenite struct. and strength changes during ageing (*Russian*) 3-80277
- steel, Cu-bearing, isothermal internal friction technique applic. to precip. 3-80268
- steel, dispersion hardening, time-to-rupture and substruct. under u.s. treatment (*Russian*) 3-53247
- steel, duplex, heat treatment, aging, ferrite and austenite grain comp., electron probe analysis 3-64850
- steel, Fe-Mn-C type, isothermal transform. induced struct. and props. 3-69224
- steel, ferrite, vanadium carbide precip. phenomena 3-69225
- steel, ferritic, anisothermal stress relax. processes 3-69279
- steel, ferritic stainless, 475°C embrittlement phenomena 3-64914
- steel, hardened, segregation phenomena and fractography (*Russian*) 3-55781
- steel, high-C, chromium effect on hardenability (*Korean*) 3-53256
- steel, high-speed maraging Fe-Co-W type, strengthening phases nature (*Russian*) 3-80308
- steel, local mag. struct. of carbides formed during ϵ - χ - θ transforms (*Russian*) 3-79951
- steel, low-C, form. of δ -nitride and niobium carbonitride (*Russian*) 3-72856
- steel, low-C unalloyed, strengthening by small Nb additions 3-64922
- steel, low-C vanadium, controlled-rolled and continuously cooled, microstruct. obs. by TEM 3-80259
- steel, maraging, Co influence on ageing mechanism (*Russian*) 3-53243
- steel, maraging, synergistic Co-Mo age-hardening interaction in Fe-10%Mn martensite 3-69284
- steel, martensitic; internal friction and isothermal aging, -50 to 25°C (*French*) 3-64931
- steel, martensitic Ni-Cr-Mo-Co, toughness and strength characteriz. 3-64915
- steel, microalloyed structural, metallographic investigations by phase diagrams (*German*) 3-80202
- steel, phase anal. by Faraday method 3-75853
- steel, precip. strengthening, heat treatment effect on niobium precipitates 3-72862
- steel, quenchability influence on carbide precip. during continuous cooling (*French*) 3-47416
- steel, quenched, substruct. changes during heating (*Russian*) 3-53213
- steel, resulphurized, solidifying rate and form. of sulphide inclusions 3-61181
- steel, secondary martensite struct., atomic ordering effect (*Russian*) 3-61134
- steel, silicon-type, morphology and substruct. of upper bainite (*Czech*) 3-55772
- steel, stainless, high-silicon, intercryst. corrosion susceptibility 3-50713
- steel, stainless, intercryst. corrosion causes 3-50711
- steel, stainless, nitrided, phase identification 3-64838
- steel, strength, corrosion resist. rel. to tempering temp. and H_2 absorption 3-80355
- steel, tempering, carbide form. (*Russian*) 3-53242
- steel, tempering and reheating effects 3-55821
- steel, W-Mo high-speed, carbide phase behaviour 3-55813
- steel, maraging, heat treatment influence 3-44598
- steel pressure vessels, struct. stability characteriz. 3-69322
- teflon, aq. suspension, struct., mech. props. of precipitate 3-65026
- Ticonal alloy, $\alpha \rightarrow \alpha + \gamma$ transformation, rare earth additions effect 3-80220
- Zircaloy, hydrogen supercharging during corrosion 3-44610
- Zircaloy-2, quenched and aged, vacancy precip. phenomena 3-80231
- Zircaloy-H system, hydride precip., resistometric obs. 3-64875
- Al-Ag alloy, liquid-quenching, decomp. products 3-80261
- Al-Ag alloys, γ phase dissolution 3-80223
- Al-Ag-Zn, (5 at.% Ag, Zn), liquisol quenched, GP zone form. 3-72865
- Al-Ag(Cu) solid solns., dissolution kinetics of grain boundary allotriomorphs 3-80233

precipitation continued

- Al-Cu oriented bicrystals, quenching and tempering, intercrystalline density (*French*) 3-69233
- Al-Cu thin films, precipitation and solid soln. effects on electromigration 3-43958
- Al-Cu-Li alloy, microstruct. after isothermal heat treatment, precipitation behaviour (*German*) 3-44590
- Al-Cu-Li alloy, precipitation kinetics by hardness and electrical resistance meas. (*German*) 3-53237
- Al-Cu(Zn) alloys, single crystals, alloying effects on acoustic props. (*Russian*) 3-72138
- Al-Cu(3 wt.% alloy, strain fields at Guinier-Preston zones, lattice resolution meas. 3-41705
- Al-Fe alloys, rapidly solidified, iron precip. behaviour (*German*) 3-41744
- Al-Ge, alloys formation of Ge nuclei, supersaturated alloy, below 140C, X-ray and resistivity analysis, vacancies 3-53234
- Al-Ge (0.75 wt.% single crystals, strengthening due to precipitates 3-46660
- Al-Ge alloys, high temp. precipitation, Ge nuclei effect (*German*) 3-44592
- Al-Ge(4 wt.% solid soln. decomp. phenomena (*Russian*) 3-58619
- Al-Li-Mg alloys, precip. characts., solid soln. strengthening 3-69219
- Al-Mg alloys, Al-rich, preprecip. phenomena, Guinier-Preston zones, neutron diffraction obs. (*French*) 3-80242
- Al-Mg alloys, u.s. vibr. effects on mech. props. and fine struct. (*Russian*) 3-72849
- Al-Mg-Zn, Al-Mg-Zn-Cu, alloys, nucleation, Guinier-Preston zone, ageing, 130-225°C, elec. resist. obs. (*Japanese*) 3-72868
- Al-Mg(11 wt.% alloys, microstruct. and corrosion resist. after long-time natural ageing (*Russian*) 3-80249
- Al-Mn (1.8 wt.% high temp. decomp. 3-76184
- Al-Ti alloys, grain refinement by metastable phases 3-55793
- Al-Zn (22 at.% alloy, liq.-quenched, spinodal decomp. 3-64868
- Al-Zn (28 at.% alloy, liquid-quenched, phase decomp. 3-41740
- Al-Zn (28at%) alloy, discontinuous precip., h.v. electron microscope in situ obs. 3-50708
- Al-Zn-Mg alloy, grain boundary precipitate effects on stress corrosion cracking (*Japanese*) 3-50725
- Al-Zn-Mg alloys, high-strength, tensile deform. and fracture props. 3-76207
- Al-Zn-Mg-Cu alloy 7075, improved fatigue resist. through thermomech. processing 3-64917
- Al-Zn-Mg-Cu-Cr alloy, as-cast, ingot processing effects on subgrain struct. 3-80264
- Al-Zn(50 wt.%), supersaturated, precip. process, plastic deformation effects (*Polish*) 3-50690
- Al-Zn(9 at.%)-Ag(1 at.%), Al(90 at.%)-Zn(10 at.%), supersaturated, structural features of decomposition process (*Russian*) 3-41723
- Al-Zr alloys, grain refinement by metastable phases 3-55793
- AlCuMg, electrical resistivity during precipitation, temp. depend. (*German*) 3-50161
- AlMgSi ductile alloy, electrical resistivity, tuning precipitation, temp. depend. (*German*) 3-50161
- Al₂O₃, sintered, grain boundary segregation, impurities role in densification 3-69343
- Al₂O₃:Ti, creep and sintering, anomalously high activation energies origin 3-55842
- Au-Fe alloy, heterogeneous precip., rel. to mag. props. 3-79875
- B, coprecipitation from the sea, using Fe(OH)₃, effect of pH, conc., quantity of coprecipitant (*Russian*) 3-80700
- Bi₂C₂, void morphologies 3-71282
- Ba(NO₃)₂ supersaturated solution 3-53361
- Be fine wire, mech. props. characteriz. rel. to prep. conditions 3-55811
- C impurity, in Si diode, lowering of breakdown voltage obs. 3-52890
- Co alloy, liq., Ostwald ripening of transition metal carbides (*German*) 3-41745
- Co-Co₂Si system, γ - ϵ transform. phenomena (*German*) 3-53207
- Co-Ni-Cr alloys, precipitates formed by internal oxidation (*French*) 3-47384
- Cr, interstitials influence on cellular struct. form. and brittle behaviour (*Russian*) 3-41711
- Cr-Fe-Si-C alloys, high carbon ferrochromium alloy composition range 3-50688
- Cr-Rh alloy system, metallography, X-ray diffraction, electron probe obs. 3-69193
- Cu-Ag alloy, high temp. internal friction, grain boundary peak (*Japanese*) 3-44579
- Cu-Al alloys, X and α_2 phase form. by annealing of martensitic β_1 phase (*French*) 3-47382
- Cu-Al alloy, internally oxidized, particle size effect on yield stress 3-80294
- Cu-Bi alloys, Bi segregation to grain boundaries, intergranular fracture 3-80228
- Cu-Co alloy, n.m.r. of ^{59}Co obs. 3-50473
- Cu-Co solid solution, hydrostatic stress in coherent β Co particles, Mossbauer obs. 3-47376
- Cu-Fe alloy single crystals, containing γ -Fe precipitates work hardening phenomena 3-80226
- α -Cu-Mn solid soln., coherent precipitates in ordered phase, Cu₂O contrib. to diffraction pattern 3-53236
- Cu-Ni alloy, thermopower meas., Nordheim-Gorter plot, Ni clusters 3-68598
- Cu-Ni alloys, mag. permeability correl. with microstruct. 3-75856
- Cu-Ni-Co alloy, n.m.r. of ^{59}Co obs. 3-50473
- Cu-Ni-Zn alloys, high strength microduplex, characteriz. 3-64911
- Cu-Si-Mn alloys, annealing-induced structural changes (*Russian*) 3-58641
- Cu-Zn system, lattice relationships in α - β transform. caused by diffusion 3-50687
- EuAlO₃ coprecipitation, aqueous soln. 3-73117
- (Fe, Cr)-(Cr, Fe)-C₃ in-situ grown unidirectionally solidified composite primary precipitates influence on tensile strength 3-58664
- Fe, molten, nitrogen impurity role in hydrogen embrittlement mechanism (*French*) 3-80244
- α -Fe, tempered, C and N behaviour, internal friction obs. (*French*) 3-72879

precipitation continued

- Fe alloys containing V, twin morphology 3-41708
 Fe alloys with Sb and C impurities, grain boundary segregation and intercryst. brittleness (*Russian*) 3-55775
 Fe phosphate glasses, heat treatment, precipitation of crystalline phases 3-75922
 Fe:N, nitrided, heat treatment, resist. obs., electron microscopy (*French*) 3-72873
 Fe-Al-C alloys, martensite decomp. mechanism and kinetics, atomic ordering influence (*Russian*) 3-53214
 Fe-Al-C alloys, quenched, atomic ordering and carbide form. during heating (*Russian*) 3-69209
 Fe-Al-N alloy, deformed, precip. sites 3-58633
 Fe-C alloy, Widmanstätten ferrite morphology 3-80224
 Fe-C alloys, struct. development in specimens placed in temp. gradient after quenching (*French*) 3-44583
 Fe-C-X alloys, precipitate growth kinetics 3-64861
 Fe-Cu alloy, precip. and grain boundary hardening combination 3-64870
 Fe-Cu-Ti(-C) alloys, micro- and macro-deform. resist., temp. depend. (*Russian*) 3-64835
 Fe-Fe₃C-X alloys, secondary precip. behaviour (*German*) 3-64878
 Fe-Mn-Ti-Si alloys, martensitic, precip. hardening mechanism (*French*) 3-80303
 Fe-N(0.1 wt.%) alloy, precipitation, resistivity and thermoelectric power behaviour 3-80297
 Fe-N(1.5 wt.%) alloy, tempering of martensite, precip. processes 3-64859
 Fe-Ni-Al alloy, nitriding, hardness, struct., mech. props. (*German*) 3-76193
 Fe-Ni-Al alloys, Mossbauer effect of ⁵⁷Fe, spinodal decomp. obs. (*Japanese*) 3-61145
 Fe-Ni-Ta alloy, coherency strains influence on precipitate shape 3-69246
 Fe-Ni-Ti alloys, continuous decomp. of γ -solid soln. (*Russian*) 3-58621
 Fe-Ni-W alloys, struct. changes during ageing of martensite (*Russian*) 3-80247
 Fe-Si, Fe-P, Fe-Si-P alloys, effect on thermal diffusion (*German*) 3-80240
 Fe-Si(3 wt.%) sheet, kinetics of MnS precipitate coarsening 3-64856
 Fe-Sn system α -solid solns., continuous and discontinuous precip. behaviour 3-64860
 Fe-Ti (0.16 wt.%) single crystals, orientation, temp. and strain rate effects on deform. 3-64909
 Fe-W alloys, redistrib. of atoms, Mossbauer obs. (*Russian*) 3-53223
 α -Fe-Zn, precipitation behaviour, effect of Si, Ge, Sn and Cu, morphology and kinetics of precipitation (*German*) 3-72847
 Fe-Zn ferritic alloys, cellular precipitation, kinetics (*German*) 3-44591
 Fe₃C crystn., rel. to reaction between graphite and liquid, melting pt. data 3-69192
 Fe₃Ga, L1₂ type, antiphase wall obs. (*French*) 3-58618
 Fe₃N in Fe, effect on coercive force anisotropy 3-72494
 FeS₂ on nuclei of iron thiospinel from aqueous alkali suspension 3-75491
 Fe-Cr-Nb alloys, precip. hardening phenomena 3-69281
 GaAs, precipitation during Zn diffusion 3-80188
 GdAlO₃ coprecipitation, aqueous soln. 3-73117
 GdF₃-MF(M=K, Rb, Cs) and GdF₃-Gd₂O₃, crystal structure, phase behaviour (*French*) 3-64017
 Gd₃Ga₅O₁₂ with large inclusions, dislocation loop interpret. w.r.t. second phase precip. 3-64054
 Ge:Li, kinetics, density of Li precip. centres 3-60797
 Ge:Li, O, of Li, influence of O 3-43806
 KCl:Sr plastically deformed slip band internal structure by precipitation 3-52632
 Mg-Ce(1.3 wt.%) alloy, isochronal annealing, elec. resist. and electron microscopy obs. (*Japanese*) 3-76165
 MgO, single cryst., prismatic disloc. loops on impurity precipitates 3-64040
 MgO:3.5 Al₂O₃ spinel single crystals, precip. strengthening 3-72959
 Mo, cast, boundary strength increase by V microadditions 3-61177
 Mo alloy, recrystallized, carbide segregation behaviour and effects (*Russian*) 3-55782
 Mo alloy, ZnO₂ form. on grain-, sub-boundaries and within grains during annealing (*Russian*) 3-76161
 Mo alloys, grain boundary precipitate constitution and conc., annealing influence (*Russian*) 3-44572
 Mo alloys, recrystallized, intercryst. fracture and carbide dissolution (*Russian*) 3-55777
 Mo alloys, recrystallized, ductile-brittle transition, group VIII element effects (*Russian*) 3-55776
 Mo-Re-C alloy, ageing, heat treatment, 1400-1800°C, microscopy, X-ray analysis 3-76174
 Mo-Re(34 at.%), σ -phase precip. and flux pinning, electron microscope obs. and mag. hysteresis 3-50697
 NaCl: Cd, dissolution kinetics of precip., ionic thermocond. study 3-41020
 NaCl:Mn²⁺ e.p.r. study of aggregation products involving divalent cation-cation vacancy complexes 3-64548
 NaCl:Ti,Cd,Cs, impurity precipitates meas. by u.s. velocity changes 3-64060
 Nb-Ta(20 at.%) alloy, nitride precipitate morphology and struct. 3-64872
 Nb-W-Mo-Ti-Zr-C alloy, quenching, ageing, high strength 3-76176
 Ni alloy, liq., Ostwald ripening of transition metal carbides (*German*) 3-41745
 Ni alloy, ternary, segregation of elements (*German*) 3-72881
 Ni based superalloy, precip.-hardened, high temp. creep behaviour of single crystals 3-64916
 Ni composite, W(Mo) wire reinforced, diffusion, carbide layer formation, recrystallisation rel. to weakening (*Russian*) 3-53272
 Ni-Al alloys, ageing, spatial distrib. of second phase precipitates, correl. parameters (*Russian*) 3-44571
 Ni-base alloys, quenched, critical voltage analysis in high voltage electron microscope 3-61154

precipitation continued

- Ni-C ingot, unidirectionally solidified, periodic macrostructure 3-61159
 Ni-Co-W alloys, struct. changes during ageing of martensite (*Russian*) 3-80247
 Ni-P films, Ni and Ni₃P phase precip. phenomena (*Russian*) 3-60843
 NiCr, ThO₂ dispersed, high temp. stability and coarsening 3-64855
 Ni(NH₄)₂SO₄·6H₂O, from aq. solns., 20-35°C 3-72795
 Ni(NH₄)₂(SO₄)₂·6H₂O, rate obs. for agitated and non-agitated systems between 0 and 35°C 3-52589
 NiO-CaO solid soln., exsoln. kinetics and microstruct. development 3-72941
 (Pb, La)(Zr, Ti)O₃ powders, chem. prep. from aqueous nitrate solns. 3-76247
 Pb-Ca alloys, during room-temp. ageing (*German*) 3-55790
 Pb-Cd(1.5 wt.%), isothermal ageing, -25-150°C, micro-hardness, elec. resist. obs. (*Japanese*) 3-72866
¹⁰⁶Ru complexes effect on coprecipitation yields from seawater, obs. 3-69556
 Si, Cu precipitate colony growth, electron microscope obs. 3-68412
 Si, float-zoned crystals, growth striation and swirl precipitates, electron microscopy 3-41649
 Si, of Cu, habit and morphology, dislocation mechanism 3-40932
 Si, of Cu, habit and morphology, critical evolution of mechanism 3-40933
 Si:B, ion implanted, α -particle channelling analysis 3-55738
 Si:Fe, of Fe, electron irradi. effects 3-43810
 Si-Sb, solid solution, dislocation loops, transmission electron microscopy obs. 3-75535
 Sn, segregation coeff. of Zn 3-69227
 Sn minerals, precipitation and separation of single phases, metallurgical products, Sn production 3-50671
 Ta, surface-carburized, carbide precip. phenomena (*French*) 3-61153
 Ti alloys, metastable β -phase, hydrogen effect (*Japanese*) 3-41726
 Ti-Al alloys, stress corrosion cracking mechanisms in methanol-ACI solns., Ti₃Al precipitation 3-47401
 Ti-Cr alloys, aged, decomp. processes prior to omega phase detection 3-61148
 Ti-Nb(35 at.%) alloy, heat treatment effect on microstruct. and supercond. 3-79800
 U-Nb alloys, niobium segregation phenomena 3-61149
 UC, irradi., microprobe obs., precipitate distrib. (*German*) 3-57567
 UC+N₂ reaction, graphitization of precipitating free carbon 3-47553
 UO₂ powders, thermal precip. from sols 3-67555
 UO₂-SiO₂ system melts, spinodal decomp. and primary crystn. 3-72984
²³⁵U nuclear reactor fuel refabrication and production by chemical precipitation process (*German*) 3-67607
 V₃N, precipitate in α -V, structure, morphology and orientation relationships 3-50698
 WC-Co composite materials, sintered, coercivity and saturation magnetisation obs. 3-60973
 WC-Co sintered compacts, precip. effect on mag. props. from expts. on Co-W alloys 3-64527
 WC-ZrC system, phase equil. and microstruct. 3-72939
 Zn-Al (30 wt.%) alloy, solid soln. decomp. and superplasticity behaviour (*French*) 3-47418
 ZnO, extended defects rel. to nonstoichiometry, transmission electron microscope obs. 3-79333
 Zr-Al alloys, quenched and aged, vacancy precip. phenomena 3-80231
 Zr-H, γ - and δ -phase hydride form. on cooling from α -phase field 3-72864
 Zr-H system, γ -phase formation by peritectoid reaction 3-58617
 Zr-H system, hydride precip., resistometric obs. 3-64875
 ZrO₂-Er₂O₃(La₂O₃)(Y₂O₃) cubic solid soln. stability below 1500°C (*French*) 3-76309
- precipitation (atmospheric)** see *atmospheric precipitation*
precipitation (meteorology) see *atmospheric precipitation*
precipitation hardening see *dispersion hardening*
precipitators see *precipitation*
prediction theory see *filtering and prediction theory*
predictor-corrector methods
 see also *Runge-Kutta methods*
 forced convection with variable thermal conductivity on a flat plate, numerical soln. 3-40707
 high-speed viscous flow over cone at incidence, predictor corrector method 3-49586
 Navier-Stokes equation, difference schemes for the solution, comparative study 3-49536
 nuclear reactor space-time kinetics, fully implicit matrix decomposition 3-46064
 plasma simulation, radiation-induced, using piecewise linearised predictor-correct iterative scheme 3-46560
 Runge-Kutta method for dynamic behaviour of intrinsic thermocouple 3-45444
 supersonic and hypersonic flow, nonlinear hyperbolic eqns. soln. based on Runge-Kutta technique 3-43568
- prerotation** see *rotation*
presentation methods, radar see *radar displays*
presintering see *sintering*
pressure
 see also *atmospheric pressure and density; vapour pressure*
 air and water, effects on water flow through unsaturated stratified vertical sand column 3-46485
 contact potential for hot circular die on transversely-isotropic semispacer with heat transfer at interface (*Russian*) 3-40191
 FFTF fuel assembly, duct pressure response anal., stainless steel, ANSYS computer code 3-71293
 hexagonal fuel assembly response to internally generated pressures, effect of coolant STRAW dynamic finite element code 3-71294
 HTGR design basis accidents, primary cooling system, depressurisation 3-74678
 lunar surface gas sources, role of press. transient in detection and identification 3-51302

pressure continued

molten fuel-coolant interaction, damage to reactor structures, model, REXCO-H code, radial compliance effects peak pressures 3-71295
 perforated tube, star-shaped profiles, stress conc. meas., photoelastic methods, internal and external pressures (*Russian*) 3-74053
 profiles, across fast nuclear reactor fuel element assemblies, thermal hydraulic anal. (*German*) 3-67589
 pump, up to 1 kbar 3-53866
 sea-ice, internal press. changes due to artificial deform. (*Japanese*) 3-56271
 teflon cell, for pressure measurements up to 40 kilobars 3-45463
 thermal conductivity cell as pressure gauge 3-42546

pressure, atmospheric *see atmospheric pressure and density***pressure control**

see also vacuum control
 intracranial 3-42685
 Mannheim power reactor, circulating system modifications due to outlet pressure fluctuations in BWR at Wurgassen 3-67459
 outlet valve malfunction and failure in Wurgassen BWR circulating system (*German*) 3-67460
 reduction system in nuclear reactor, condensation meas. by relief valve blow-off (*German*) 3-74710
 steam condenser chamber failure in a nuclear reactor, cause and countermeasures (*German*) 3-74707

pressure measurement

see also vacuum measurement; vapour pressure measurement
 absolute high press. determ. method 3-45462
 acoustic pressure distribution, shadow-optical method, quantitative analysis method 3-77320
 blood employing microminiature solid state capacitive transducer with improved sensitivity 3-42692
 blood pO₂, in vivo radio telemetry 3-73922
 catheter manometer and catheter-tip micromanometer, in vivo comparison, measuring max. left ventricular rate of pressure 3-62310
 coolant in nuclear reactor, calc. pressure drop for parallel flow through roughened rod cluster 3-74666
 detecting circuit, absolute, for ion gauge controllers 3-62277
 diurnal and semidiurnal barometric oscillations global distrib., annual variations 3-44906
 fission gas pressure measurement by null-balance pressure sensor 3-70294
 gravity dams during earthquakes (*Japanese*) 3-61361
 in high-pressure chambers 3-51560
 intracranial using implantable pressure transducers 3-42685
 nuclear reactor, local pulsed pressure field at blowdown, tests in condenser chamber (*German*) 3-74709
 piezoelectric transducer electronics, vibration and pressure applications, comparison with charge amplifiers 3-56623
 planetary atmosphere, entry probe base pressure expt. 3-59401
 propagation velocities of pressure and void by cross correlation of fluctuations in N₂O flow 3-70499
 rapidly varying pressure, Si and GaAs p-n junc. transducer applic. 3-70293
 respiration monitoring, airway pressure waveform, analogue signals 3-59684
 RMO-4S omegatron, for partial pressures of hydrocarbons 3-54051
 seismometers, seismic noise, prediction convolving the microbarogram with a transfer function 3-80838
 soil, pneumatic device (*Russian*) 3-53864
 supersonic flow, stagnation pressure probe, new, high pressure recovery, cylindrical compression surface 3-57033
 supersonic jet engine inlet distortion measurement, steady and time variant, high response pressure measurement 3-57032
 teflon cell, for pressure measurements up to 40 kilobars 3-45463
 using thermal conductivity cell 3-42546
 transient velocity and pressure meas. by gaseous ionisation 3-49528
 two-phase pressure losses calc. by evaluation of two phase friction in fluid flow 3-74668
 viscoelastic flow, hole error, analysis 3-67887
 H₂, partial press. meas. osmotic membrane 3-48397
 He gas, large pressurized vessels, leak-rate measurement 3-73712

pressure sintering *see sintering***pressure transducers**

flush-mounted, cone and plate rheogoniometer, normal stress difference meas., polymer solutions 3-70503
 intracranial pressure monitoring 3-42685
 viscoelastic fluid flow, stress meas., hole error 3-67966
 GaAs p-n junction, for rapidly varying pressure meas. 3-70293
 Si integrated circuit for blood pressure 3-42692
 Si p-n junction, for rapidly varying pressure meas. 3-70293

primary cells

e.m.f. comparison 3-56610
 AgCl solid electrochemical cell, polarization, complex admittance study 3-69470
 T battery, theory and performance, for microwatt range 3-53950

primary cosmic radiation *see primary cosmic rays***primary cosmic rays**

γ rays, investigation using acoustic spark camera in telescope (*Russian*) 3-65550
 altitude dependence and intensities near Moon's surface (*Russian*) 3-65576
 atmospheric temperature dependence of muon flux, reln. to primary radiation (*German*) 3-53586
 average daily values of streams of particles at 'Prognoz' sputniks (*Russian*) 3-65556
 bombardment of meteorites, rel. to solar system history 3-77027
 detection from artificial Earth satellite 'Intercosmos 6', apparatus description (*Russian*) 3-69752
 dust grain model, discussion of difficulties 3-69755
 electron, 1 to 20 GeV, spectrum and interpretation 3-51224
 electron detection using gas threshold Cherenkov counter (*Russian*) 3-62239
 excess radiation at low altitudes rel. to primary cosmic ray intensity 3-56285
 galactic cosmic rays in interplanetary medium near Earth, mean energy losses 3-42094
 galactic with energies ≥ 200 GeV, distribution anisotropy 3-42096
 gamma-rays, from galactic north pole region, satellite study (*Russian*) 3-65918

primary cosmic rays continued

hadron interactions at energies of 10^{13} eV at mountain altitude, study of elementary events (*Russian*) 3-69782
 heavy nuclei, detection by plastic detectors and photoemulsion, track regression due to prolonged exposure (*Russian*) 3-66323
 interplanetary shock wave interaction 3-76937
 lunar particle track record of Luna 16 and 20 missions 3-47954
 Magellanic Clouds and Galactic central region, gamma-ray astronomy and cosmic-ray studies 3-45205
 nuclear component, Forbush effect (August 1972) (*Russian*) 3-65578
 origin and propagation, measurement parameters (*Hungarian*) 3-59226
 photoemulsion events in stratosphere, $E > 5 \times 10^{12}$ eV, formation of superheavy fireballs (*Russian*) 3-69784
 search for rays streaming out of Galaxy 3-51223
 spectrum, $5.10^{14} \leq E_p \leq 2.10^{16}$ eV, from size spectrum of EAS 3-69779
 spectrum, and multiplicity distribution of shower particles underground at $E > 10^3$ BeV 3-69793
 spectrum changes above atmosphere, zenith-angle dependence of total particle count (*German*) 3-53582
 total energy spectrum, $3 \times 10^{17} \cdot 10^{20}$ eV 3-73415
 $Z \geq 60$, nucl. energy spectrum near 1 GeV/amu, new cosmic ray source evidence 3-53581
 γ -rays, production of electron-photon showers in copper, fluctuations in overall path of charged particles (*Russian*) 3-69790
 γ -rays, reln. of energy of magnitude of fluctuations of Cherenkov radiation of electron photon shower (*Russian*) 3-69773
 μ charge ratio meas. and hadronic scaling prediction 3-76945
 N interactions with air nuclei at energies > 30 GeV, possible inelastic cross section behaviour (*Russian*) 3-42102
 P, vertical showers, calc. of spatial distrib. of electrons at sea level in energy region $10^{15} \cdot 10^{21}$ eV (*Russian*) 3-76941
 p prod. in interstellar pp collisions, fraction expected at top of earth's atm. 3-47855
 π charged multiplicity in interactions with air nuclei, scaling validity 3-73421

printed circuits

artwork and film generation, review (*German*) 3-56688
 photoresist exposure parameters, grey scale 3-59605

printers

contact and optical, picture image modulation transfer functions, Russian (*Russian*) 3-45519
 line printers, laser recording on dielectric coated paper 3-48960

printing

contact and optical, picture image modulation transfer functions, Russian (*Russian*) 3-45519

prisms (optical) *see optical prisms***probabilistic logic**

logistic distribution as approx. to normal probability function 3-42747
 U alloys, nuclear fuel, fission gas release, effect of vol. swelling, probabilistic model 3-63208
 U-Pu, nuclear fuel, fission gas release, effect of vol. swelling, probabilistic model 3-63208

probability

see also game theory; Monte Carlo methods; queuing theory; random processes; statistics
 astrophysical hypotheses evaluation using probability theory and Bayes' rule 3-56297
 bounded extremal value like freq. distrib. fitting, occurrence of natural events 3-54068
 cloud-free line-of-sight probabilities determ. methods 3-47744
 coexistence of two props., anal. of theory rel. to quantum mechanics 3-74097
 earthquake prediction studies in Japan 3-73207
 hydrology, two distrib. method for seque data generation 3-56278
 information theory, conditional entropy concept (*Hungarian*) 3-77926
 isotropic random flights, probability density and distribution function 3-42900
 logistic distribution as approx. to normal probability function 3-42747
 meteorological variable, probability score, vector partition 3-76907
 non-coherent scattering spherical shell media, probabilistic model for resolvent kernel 3-51840
 nuclear reactor shield analysis, radiation transport 3-60341
 nuclear reactors, engineered safety features, design, probability, statistical risk 3-71179
 occupation, satellite i.r. terrestrial targets, successive estimation scheme 3-76850
 one-degree-of-freedom mechanical system with jump-like variable mass, probabilistic problems (*Polish*) 3-66590
 Pearson type 3 distribution, random variable, moment and max. likelihood estimates 3-56241
 philosophy, quantum mechanics and interpretations of probability theory 3-53807
 in quantum mechanics, 2-slit expt. 3-40159
 radiative transfer, probabilistic, mean number of scatterings, numerical soln. 3-42914
 random point process, restricted rewards 3-74006
 steel wire fatigue, cycles to failure and stress to failure Weibull distributions 3-41833
 stochastic streamflow synthesis technique, transition probability matrices 3-54797
 transitions, adiabatic and nonadiabatic, average transition probability, calc. (*Russian*) 3-68969
 transitions between states, anal. of theory rel. to quantum mechanics 3-74097
 transport processes, first flight escape probability for spherical shell with empty central region 3-60245
 turbulent boundary layer, probability distributions and correlations 3-49574
 two simply coupled spectral lines, probabilistic radiative transfer 3-51892
 vibrations, high amplitude systems with random excitations synthesis of parameters (*Polish*) 3-66591

probability continued

vibrations of n -degree-of-freedom systems, determ. of probability characteristics using Fokker-Planck eqn. (*Polish*) 3-66593
weather forecasting, skill and probability scores 3-47757

probes

see also electron probes; plasma probes
atmospheric turbulence, refractive index calc. 3-76749
atom probe, 10 cm, field ion microscope, channel plate photomultiplier detector, no tip movement, operation 3-62288
bioelectric potentials (*Italian*) 3-56501
bubble size distributions, gas/solid fluidized layers, capacitive probe (*German*) 3-45617
conductance probe, for thickness measurement 3-61989
conical hot Pt film probes, limitations as oceanographic flow sensors 3-51201
cryogenic liquid level detection, universal probe, simple and cheap design 3-56647
electric field meas. in air discharge by surface electrode fields (*French*) 3-63912
electric field meter, rotating probe type for precision measurement 3-45536
electric field strength meas. (*German*) 3-59609
electro-mechanical for in-pile monitoring of dimensional changes in SNR-300 fuel cans (*German*) 3-71305
electrostatic field measurement, ionosphere, magnetosphere (*German*) 3-73405
e.p.r. 10 GHz probe analysis, rotatable h.f. field (*French*) 3-77588
gamma-gamma log collimated probes for geophysical borehole spectrometry (*Russian*) 3-47820
high current spark channels radial recovery 3-43705
hot film, MHD heat transfer in Hg 3-46393
ion, ceramic surface anal. 3-80418
ion scattering spectrometry, surface composition analysis 3-40041
multiparticle atom probe time-of-flight meas., 10 nsec resolution counter 3-40043
Pioneer, gravitational whiplash from Jupiter 3-59522
ring potential probe for determ. of strata resistivity (*Russian*) 3-47654
sampling for molten Fe and steel, evaluation and testing (*German*) 3-76190
semiconductor, cylindrical, degree of uniformity calc., elec. cond., four-probe method 3-42599
sounding rocket, effect of wake boundaries on boom mounted probes 3-75284
supersonic flow, stagnation pressure probe, new, high pressure recovery, cylindrical compression surface 3-57033
thermocouple, recovery characteristics measurement, low pressure, subsonic speeds 3-77398
u.s., sound field, automatic measurement installations (*German*) 3-69416
 ^{13}C Fourier transform apparatus at 14.2 kG, probe for 20 mm spinning sample tubes 3-73827
Ge, low temperature, approximation of $R(\Theta)$ (*Czech*) 3-53848
Ge, rectangular plates, electrical conductivity measurement, four-probe method, effect of inhomogeneity and dimensions 3-45525

process control

see also control engineering applications of computers; online operation

ceramics, microwave applications 3-47491

chromatography, gas, automated preparative scale, use of cut and backflush devices, performance and economy 3-66433

colour matching system employing computer 3-51605

food processing industry, instrumentation, pollution control, computer control, symposium, Pittsburgh (1972) 3-59721

industrial, neutron source applic. (*German*) 3-56916

laser Raman spectrometer application 3-66237

measurement engineering education (*German*) 3-59537

standardisation, trends and views (*German*) 3-48332

Procopiu effect *see* magnetoelectric effects; magnetomechanical effects

product control *see* quality control

production

this heading is restricted to industrial production

see also integrated circuit production; manufacture; quality control; reliability

HTGR fuel elements, environmental and safety

considerations (*German*) 3-67591

organic coatings on metals, electrostatic fluidised bed technique,

limitations 3-66720

thermonuclear and thermal power plants, facilities, French development (*German*) 3-67618

^3H , French facilities (*French*) 3-57550

production control

see also process control; quality control

Fabry-Perot interferometers, photoelectric control of untreated plane surface thickness (*French*) 3-42576

production schedules *see* production control

production testing

microelectronics, measuring projector MP 320 appl. 3-45514

petrochemical plants, gas extraction from petrol, quality

control (*German*) 3-66456

professional aspects

atomic absorption spectrometry, writing a paper, topics to be included

3-70225

program interpreters

magnetic anomalies, two-dimensional algorithms, thick plate model

3-76660

programmed control

see also process control; production control

fatigue testing, choice of number of steps in programme, stress below

fatigue limit 3-55911

scanning microscope photometer (*German*) 3-73748

programmer training *see* training

programming

see also computer software; hybrid computer programming; systems analysis

in ALGOL of digital computers, applic. to polymers 3-69385

Fourier program for X-ray crystal structure analysis using Coley-Tukey

algorithm 3-43719

programs (computer) *see* computer software

project engineering

see also design engineering; electromagnetic compatibility; quality

control; reliability; systems engineering

nuclear fusion research using TOKAMAK type medium beta torus

JFT-2 (*Japanese*) 3-60293

projectiles

see also ballistics; missiles; rockets; weapons

spinning, equations of motion, analytical solution, computer method

3-74013

projectors (optical) *see* optical projectors

promethium

Ap type stars problems in search for Tc II lines rel. to promethium

controversy 3-81049

identification tests and consequences for Pm in Hr 465, Ap-star

3-48021

$\text{LaCl}_3\text{:Pm}^{3+}$, absorption spectrum 3-76034

$\text{Pm}^{3+}\text{:LiYF}_4$, lasing action 3-59865

^{147}Pm , mag. struct., neutron scatt. obs. 3-50373

promethium compounds

No entries

prominences (solar) *see* solar prominences

propagation, wave *see* wave propagation

propagators *see* quantum field theory

proportional counters

β -ray detection system, low level background meas., environmental

studies 3-51719

drift multiwire proportional chamber with adjustable electric field,

operation in strong magnetic fields 3-40007

encapsulated radiation service life, limiting causes, anode deposits,

effects 3-70381

energy deposition spectra calc., computational technique, 45 MeV and

600 MeV protons, tissue equivalent gas mixtures 3-48254

field distribution, in gas counters of box-type geometry 3-48534

gas counters, proportional region investigation 3-53982

gas-discharge, spectrometric, cylindrical, lock chamber for source

changing, operating characteristics 3-70379

gasflow, soft X-ray detection, compact design, construction

3-73867

helical cathode, magnetic spectrograph 3-62261

hyperbolic Charpak chambers, design, operation, advantages

3-77630

low-energy proton detection 3-51700

miniature (ϕ , 1, 3, 4 mm) low background, meas. supersmall quantities

of ^{37}Ar and ^3H , sensitivity limit (*Russian*) 3-65403

Mossbauer spectroscopy of steel by scattered electrons 3-66384

coupled to multichannel analyser, thermally stimulated exoelectrons

3-62225

multifilament, for photonuclear reactions 3-51702

multilayer, high-energy particle identification 3-73866

multiwire, for $4\pi\beta$ - γ coincidence measurements 3-40003

multiwire chamber, technique of particle position localization

3-51709

multiwire chambers, with monofilar helical cathodes and high spatial

resolution 3-51705

multiwire proportional chamber system, decision wired

logic (*French*) 3-53983

multiwire proportional-surface, performance in particle

beam (*German*) 3-51695

particle coordinate determ. by potentiometric method 3-51701

preamplifier noise in measurements 3-56935

scaled multiwire proportional chamber, design description 3-48523

scintillation, gas, peak shifts under high X-ray fluxes 3-77619

secondary charged particle multiplicity, incident particle charge, deter-

mination rel. to ionization calorimeter (*Russian*) 3-62237

tissue equivalent, neutron dose determ. 3-77275

with tissue equivalent gas, time distribution of spurious pulses

3-51699

wire chambers, 1 mm pitch, high gain, gas mixture, chamber proper-

ties 3-77622

X-ray counter, unlimited operating service life, construction, param-

eters 3-70380

for X-rays, gas density control system 3-65950

μ identification external to bubble chamber, high energy νp interaction

test of principle 3-77629

n spectrometer, 25 keV to 1 MeV, through nuclear reactor shield, H_2O

and Fe 3-74752

^3H identification and exact meas. in gas sample (*French*) 3-57019

^3He high-pressure, meas. of energy distribution of delayed fission

neutrons 3-54515

Kr gas-filled proportional counters, for ^{161}Dy (26 keV) Mossbauer

studies 3-40036

$^{14}\text{N}(\text{n,p})^{14}\text{C}$, use in neutron beam strength measurement 3-73864

Xe liquid multiwire proportional chambers, study of parameters

3-48525

propulsion

see also aerospace propulsion; electric propulsion

axisymmetric body in water with artificial cavity collapse and

reformation (*Russian*) 3-63795

disc with artificial nonstationary gaseous cavity development (*Rus-*

sian) 3-63796

gas/liquid reactive propeller with ballast-boosted traction (*Russian*)

3-63794

prospecting (geophysical) *see* geophysical prospecting

prosthetics

see also artificial limbs; artificial organs

bioceramic vascular prosthesis, surface props. rel. to blood compatibil-

ity etc. 3-64969

glass-ceramic materials, for physiological bond between living bone

and implant 3-55876

liver transplant, blood circulation study using radioactive tracer (*Ital-*

ian) 3-56545

renal transplant cases, gamma-camera renography using ^{123}I -Hippuran

and ^{123}I -albumin 3-40063

protactinium

diffusion in UC_x , high temp. 3-43298

ionisation energy calc. 3-60376

isotope discovery and naming 3-51484

protactinium compounds

No entries

protection

see also alarm systems; corrosion protection; protective coatings; radiation protection; safety
 contact voltage with neutral conductor, standard JUS N.CO.010 (Slovenian) 3-66127
 h.v. standardisation problems (German) 3-48333
 LMFBF, heat transfer system design, safety 3-67508
 nuclear reactor shielding, advances, book 3-60337
 PWR core, three-dimensional kinetic analysis of reactivity insertion, necessity of protection-grade circuits 3-46089
 PWR protection system, effects of electrical underfrequency transients 3-46085

protective coatings

see also corrosion protection
 enamel, composite section method eval. for elastic props. determ. 3-47528
 fission product containment by coating a kernel of nuclear fuel 3-67581
 glass, on steel, degree of oxidation influence on quality (Russian) 3-58657
 metal, wear resistance from electrical resistance 3-73103
 mixed composition plasma-sprayed coatings thermal conductivity 3-53267
 nonconductive samples in SEM, partial charging prevention 3-70435
 polyethylene, heat treated, adhesion strength on steel and Al, metal-catalysed oxidation 3-73057
 polymer-coated square plates, bending vibrs., damping 3-44683
 polymeric, on soda-lime glass, effects on bend strength 3-76265
 polymeric coating on metal, Young's modulus, Poisson's ratio 3-73672
 powder metallurgic magnetic protection against oxidation during heat treatment 3-50751
 PVC coatings on tubes, crack form. processes in soil medium (Russian) 3-80468
 steel, diffusion Cr plated, corrosion stability in nitric acid medium (Russian) 3-80336
 X-ray diffraction method for thickness meas. 3-73676
 Al coated steel, fatigue strength 3-55797
 Al coatings on steel, technique description for strength meas. 3-55802
 Cr plating of Armco iron by diffusion from liq. metal melts (Russian) 3-41758
 SiC, pyrolytic coatings of fuel particles, strength characteriz. 3-43311
 Sn diffusion coatings on steel, corrosion resist. 3-80338
 TiN in Ni-based composite material diffusion protection (Russian) 3-73012

protective relays see relay protection**proteins**

see also DNA; gelatin
 carboxypeptidase, crystal and in solution, struct., laser Raman scatt. 3-75165
 chlorophyll in n-paraffin solid solutions, quasilinear spectra (Russian) 3-44488
 cooperative mechanism, modelling using grand partition function, occupational and conformational interaction 3-57684
 dinucleotide, polarization of excimer fluoresc. 3-41856
 egg-white, pulse radiolysis, e_{aq}^- , cystine disulphide anion-radicals, yield and decay 3-77251
 Faraday spectra obs., structure and dynamics of heme containing proteins 3-71671
 ferricytochrome b_5 , determ. of principal axis of G-tensor by p.m.r. (German) 3-49510
 globular protein solutions, diffusion consts., Rayleigh light scatt. obs. 3-67879
 glycine, X-ray radical yield 3-66047
 haemoglobin, Heitler-London calc. on bonding of O_2 , diamagnetism of oxyhaemoglobin 3-67872
 heme proteins, resonant Raman bands of differing polarization, intensity origin 3-54768
 hemeproteins, resonant Raman scattering 200 cm^{-1} to 3000 cm^{-1} , cytochrome-c 3-78918
 hemoproteins, stereochem. of porphyrin and electronic struct. 3-46359
 human serum albumin, ^{60}Co gamma irradiation, polymerisation, cross-linkages, sedimentation velocity technique 3-48264
 interacting systems, calculation of sedimentation equilibrium in density gradients 3-71675
 locust, adult female, rheological props. of extensible intersegmental membrane 3-42272
 lysozyme, refinement of X-ray data to relieve atomic overlaps 3-58025
 lysozymes, p.m.r. spectra, resolution enhancement using difference between broadened and normal spectrum 3-71665
 macromolecular vibrations, low freq., possibility of revealing properties by conformation 3-60497
 molecular conformations, H and ^{13}C n.m.r. spectroscopy 3-67875
 ovalbumin, structure characteristics detn. by dielectric relaxation method (Rumanian) 3-43526
 photoconductivity, role of mol. electronic structure (Russian) 3-46365
 phytoene isomers, n.m.r. of ^1H and ^{13}C 3-46361
 p.m.r. spectra, resolution enhancement using difference between broadened and normal spectrum 3-71665
 polypeptide energy minimisation by method of partial energies and cubic subdivision 3-75163
 polypeptides, photoconductivity, role of mol. electronic structure (Russian) 3-46365
 radiation damage, e.s.r. study of single crystals, free radical formation 3-41851
 ribonuclease A, crystal and in solution, struct., laser Raman scatt. 3-75165
 DL-serine, irradiated at 4.2 K, e.s.r. and ENDOR studies 3-76466
 tobacco mosaic virus, X-ray phases, direct determ. using non-crystallographic symmetry 3-63925
 transferrin, ^{57}Fe Mossbauer effect, h.f.s., spectra analysis 3-63575

proteins continued

two-dimensional formamide network, CNDO/2 and MINDO/2 energy band structs. 3-54772

proton absorption

see also nuclear reactions and scattering due to protons
 beam stop, steel, 28 GeV protons, particle distribution measurement 3-59632
 tissue absorbed dose and dose equivalent for 3.5 GeV-1.0 TeV protons 3-52234

proton accelerators

see also cosmotrons
 beam transformer system, Serpukhov synchrotron, fast ejection efficiencies 3-59651
 CERN proton storage rings (German) 3-53961
 colliding beam expts. at CERN ISR 3-53965
 cyclograaff, Livermore USA, combined cyclotron and tandem Van de Graaff, pulsed beam capabilities 3-59622
 cyclotron, SIN Switzerland, 590 MeV, $100\text{ }\mu\text{A}$ c.w. proton beam at 50 MHz, construction progress, test results 3-56738
 electromagnet coils, precision production 3-73832
 EPIC electron proton intersecting ring complex, possible construction 3-66305
 high current test facility injector 3-56859
 intersecting storage rings, CERN 3-42628
 ion source, duoplasmatron system, high intensity, description 3-56922
 Lawrence Berkeley laboratory 184-in synchrocyclotron proton beam intensity improvements 3-56746
 linear, 550 keV, with asymmetrical alternating phase focusing 3-53962
 linear, 800 MeV, operating results 3-56838
 linear, increase of beam intensity, design data, theory and experiment 3-66301
 linear, with quadrupole r.f. focusing, alignment of accelerating electrodes 3-53968
 superconducting linacs, helical structures, review 3-56713
 synchrotron, 200 GeV, computer controlled (Czech) 3-56710
 synchrotron, alternating-gradient, Brookhaven USA, 30 GeV, operation, performance results 3-56742
 synchrotron, NAL Batavia, 200 to 400 GeV, operating results, first year of operation 3-56736
 synchrotron, zero-gradient, Argonne USA, acceleration of polarised protons, depolarisation problems, corrections, operation 3-56740
 synchrotron booster, CERN, 800 MeV, present performance 3-56741
 synchrotron dense critical beam interaction 3-53964
 synchrotron vacuum system (Japanese) 3-48493
 USSR, medical uses for treatment of malignant tumours 3-59440

proton angular distribution

see also proton spectra
 compound nucleus decay, A=56-66 test of independence hypothesis and isospin conservation 3-71093
 inelastic scattering of polarised protons on nuclei, asymmetry meas. (Russian) 3-67318
 interactions with tungsten emulsion nuclei, 200 GeV 3-71024
 magnetosphere, low energy IMP 6 obs. 3-65484
 photoprotons, decay of isobaric analogue states, spectra (Russian) 3-57477
 ring current protons, energy spectra and pitch angle distrib. during 1971, December 17 storm 3-73363
 spark chamber expt. $^4\text{He}(p,p)^3\text{H}$, meas. differential cross section, 180 to 320 MeV proton energies 3-67302
 K⁺p, elastic scatt., complete ang. distrib. meas., incident momenta 1368 to $2259\text{ MeV}/c$ 3-60032
 pp elastic scattering, 290 to 450 MeV liquid target 3-74414
 pp elastic scattering, high energy, distribution of absorption, correction term 3-67120
 from pp interactions, 19.1 and 10 GeV/c, comparison with theory (Russian) 3-60046
 pp scattering at 4.21 MeV, relative cross section determ., gas target 3-74558
 pp scattering at high energies, break in angular distrib., hard core radius model 3-62881
 $^{138}\text{Ba}(d,p)^{139}\text{Ba}$, 19 MeV, angular distrib. meas., determ. of orbital angular momentum transfer and spectroscopic factors 3-46033
 ^9Be proton scattering, 6-30 MeV, differential cross section excitation functions and angular distributions 3-52184
 Bi, deuteron disintegration in Coulomb field, angular and energy distrib. of products (Russian) 3-67340
 ^{12}C , elastic and inelastic scattering of 1.04 GeV protons, angular distrib. meas. 3-57522
 ^{12}C , polarized proton scattering, 9.5-11.5 MeV, obs. of $T=1/2$ ^{13}N levels (German) 3-49139
 $^{12}\text{C}(^{12}\text{C},p)^{23}\text{Na}$, low energy, rel. to carbon burning era of nucleosynthesis in stellar evolution 3-40511
 $^{12}\text{C}(\text{He},n)^{14}\text{O}(p)^{15}\text{N}$, E=12 MeV, ang. correl. meas., excited states of ^{14}O 3-40509
 $^{12}\text{C}(\text{He},p)^{14}\text{N}$, 3-11 MeV, reaction mechanism study by use of p-p angular-correlation method 3-63074
 $^{12}\text{C}(\text{He},p)^{14}\text{N}$, 7 to 17 MeV, total cross section, compound nuclear effects 3-63078
 $^{12}\text{C}(d,p)^{13}\text{C}$, determ. of angular distrib. of protons near resonances by shape-studies of p-ray lines 3-40501
 ^{40}Ca , inelastic proton scatt., ^{41}Sc doorway state struct. 3-78319
 $^{40}\text{Ca}(e,p)$, 710 MeV, momentum distrib. interpret. 3-43235
 $^{42}\text{Ca}(\alpha,n)^{45}\text{Ti}$, 10.2-14.2 MeV, study of $K=3/2^+$ rotational band 3-74494
 $^{42}\text{Ca}(\alpha,p)^{45}\text{Si}$, 10.2-14.2 MeV, study of $K=3/2^+$ rotational band 3-74494
 $^{106}\text{Cd}(d,p)$ 12MeV, meas. energy, ang. distributions, l-transfer, spin-parity assignments 3-67345
 ^{54}Fe , ^{56}Fe , inelastic scattering, proton spin-flip at 12 MeV 3-63048
 $^{56}\text{Fe}(\text{He},p)^{58}\text{Co}$, product energy levels, spin assignments 3-54428
 $^{56}\text{Fe}(\text{He},p)^{58}\text{Co}$, product energy levels, spin assignment 3-54428
 Ge, nucl. lifetimes by blocking technique, computer simulation 3-40443
 $^3\text{He}(e,e'p)^2\text{H}$, cross section, depend. on p-d relative motion energy 3-78310
 $^6\text{Li}(\pi^-, \pi^+p)^5\text{He}$, $q < 170\text{ MeV}/c$, meas. of cross sections, angular and momentum distrib., reaction mechanisms (Russian) 3-40514

proton angular distribution continued

- ⁵⁸Ni, elastic and inelastic scattering of 1.04 GeV protons, angular distrib. meas. 3-57522
- ³¹P(d,p)³²P, E = 10 MeV, angular distributions, ³²P deduced ln, spectroscopic factors 3-60198
- ³³P excited state ang. correl. studies 3-40449
- Pb, deuteron disintegration in Coulomb field, angular and energy distrib. of products (*Russian*) 3-67340
- ²⁰⁸Pb, elastic and inelastic scattering of 1.04 GeV protons, angular distrib. meas. 3-57522
- ²⁰⁸Pb(p,p'), 54 MeV, study of collective excitations in ²⁰⁸Pb 3-63056
- ³²S(α , p)³⁵Cl, 12-16 MeV, study of high spin states in ³⁵Cl by $\gamma\gamma$ -coincidence, angular distrib., yield function meas. 3-74493
- ³²S(p,p'), differential cross sections and inelastic scattering asymmetry for first 3- levels excitation (*Russian*) 3-74569
- ³²S(p,p)³²S, 5-6 MeV, meas. of excitation functions and angular distrib., optical model description of cross-section (*Russian*) 3-52180
- ³⁴S(p,p'), differential cross sections and inelastic scattering asymmetry for first 3- levels excitation (*Russian*) 3-74569
- ²⁸Si(p,p)²⁸Si, 5-6 MeV, meas. of excitation functions and angular distrib., optical model description of cross-section (*Russian*) 3-52180
- ²⁸Si(t,p)³⁰Si, 6-12.1 MeV, excitation energies of levels in ³⁰Si, angular distrib. of proton groups 3-62940
- ²⁹Si(d,p)³⁰Si, angular distrib. of proton groups, 10 MeV 3-62940
- ³⁰Si(d,p)³¹Si, low deuteron energies, proton angular distrib. comparison of direct and compound nucleus mechanisms (*Russian*) 3-71119
- ⁴⁸Ti, ³⁰Ti, inelastic scattering, proton spin-flip at 12 MeV 3-63048

proton beam effects *see* **proton effects****proton belt** *see* **radiation belts****proton detection and measurement**

- beam transformer system, Serpukhov synchrotron, fast ejection efficiencies 3-59651
- channel secondary electron multiplier, construction 3-77569
- dosimeter, design for distributed body organs 3-77627
- high-energy, multilayer proportional counter identification 3-73866
- marine proton magnetometer, APM-1, automated, selection of optimum sensor, meteorological tests (*Russian*) 3-47841
- scintillation counter, organic liquid, energy deposition and fluctuations 3-73869
- secondary electron multiplier, high vac. 3-77568
- synchrotron at NAL, monitoring proton losses 3-56933
- using telescope consisting of proportional counters and semiconductor detector in β background 3-51700
- track-etch radiography, alpha particles, protons, fast and thermal neutrons, polycarbonate plastics, cellulose nitrate 3-67627

proton-deuteron scattering

- backward elastic scattering below 1 GeV, energy dependence 3-52109
- elastic, 10 to 26 GeV, deuteron form factor from Glauber theory (*Russian*) 3-57343
- pd \rightarrow ppn at 600 MeV, proton polarisation and energy spectra with account for rescattering (*Russian*) 3-67106

proton effects

- see also nuclear reactions and scattering due to protons*
- cerebral vascular lesions, proton radiography 3-70140
- dosimeter development for distributed body organs, space mission application 3-53777
- eyes, Beagle dog, thermoluminescent dosimetry, 20, 35 and 45 MeV protons 3-48258
- glass reinforced plastic and components, effect of proton-electron rad. on strength 3-61207
- lunar rock luminescence, effect of u.v.-proton excitation 3-61718
- metal, u.s. excitation by proton beams 3-55034
- optical materials, calc. of distrib. of monoenergetic, moderate-energy protons 3-64075
- photon dose rates from interactions of 200 GeV protons in Fe and Fe-Pb beam stops 3-54556
- proportional counter energy deposition spectra calc., computation technique, 45 MeV and 600 MeV protons, tissue equivalent gas mixtures 3-48254
- proton beam radiotherapy, effects of multiple scattering 3-77253
- Proton energy degradation in water vapor 3-71637
- protons, 8 BeV spectra, flux meas. with satellite of Cosmos series hazard estimation (*Russian*) 3-65607
- sputtering of Cu film, yield dependence on incident energy of proton 3-80128
- steel, stainless, Type 316, irradi., void form. and hydrogen effects 3-46138
- superheavy elements in natural and proton-irradiated materials 3-60231
- water, trace element analysis by proton activation 3-66415
- AgBr, thermal disorder study by proton channelling (*French*) 3-52650
- alkali halides, U centre formation, u.v. and i.r. spectra 3-52623
- Au thin film single crystal, proton scattering 3-49912
- CaF₂:NaF(YF₃), optical absorption following γ and p irradiation and annealing, colour centres obs. 3-72694
- Cu, proton, neutron and fission neutron damage comparison 3-72105
- Fe oxidation, kinetics of thin film formation using proton impact excited X-ray analysis 3-50087
- H₂, solid, desorption obs. 3-60838
- Mo, proton bombardment, electron emission, energy spectra 3-55716
- NaF, induced F aggregate centres at low temp. thermal aggregation and annihilation 3-68251
- NaF, microhardness, depth profile of damage 3-49910
- Si defect form. under electron, proton irradi., dynamic obs. 3-54954
- Ta, irradi., void form. and hydrogen effects 3-46138
- ZnS-CdS:Cu, effect on protons on radical recombination luminescence, radiation defects 3-53152

proton interactions

see also nuclear reactions and scattering due to protons; pion-proton interactions; proton-proton interactions

- 30 GeV, angular distribution of forward cone secondaries, effect of target nature 3-57449
- absorptive corrections to Primakoff effect (*Russian*) 3-60014
- cross section compilation for proton and antiproton induced reactions on proton, neutron and deuteron targets 3-70973
- deep inelastic, proton-neutron structure function difference in resonance region 3-67037
- electroproduction from parton chains, comparison with SLAC-MIT data 3-62829
- electroproduction off protons, obs. of hadronic final states 3-70929
- hadron electroproduction from deuterium and hydrogen 3-67038
- inclusive, target asymmetries 3-60054
- inclusive spectra, effect of initial polarisation $\Delta(1236)$ -resonance alignment (*Russian*) 3-78228
- large angle production of stable particles heavier than proton, search for quarks, CERN ISR 3-71035
- neutrino and antineutrino high energy events 3-43093
- nuclear emulsion collisions of 200 GeV protons, white star formation, pair production 3-74451
- nuclear emulsion of tungsten 200 GeV collisions 3-71024
- nuclear emulsion target, 200 GeV collisions, mean-free-path and charged multiplicity determ. 3-74452
- nuclear emulsion target, 200 GeV interaction, multiplicity distrib., Castagnoli method 3-71025
- parton model description, exclusive and inclusive reactions in regions of high transverse momenta 3-57371
- Pomeron dynamics, self-consistent without decoupling, reln. to ISR expts. 3-60008
- proton-proton collisions, 1-300 GeV/c, semi-inclusive scaling curve for charged multiplicity distrib. 3-67155
- total cross sections, energy dependence, Regge theory 3-57458
- total cross-sections, correlation between structures for p-p, p-p, p-n and K⁺-p interactions 3-45905
- vector meson prod. by polarized photons at 2.8, 4.7 and 9.3 GeV 3-54310
- dp \rightarrow d + missing mass, high-energy interaction, obs. of inelastic coherent production 3-67127
- dp \rightarrow NX quasinuclear meson production via pole mechanism, spin effects (*Russian*) 3-40377
- dp $\rightarrow\eta\gamma$, 2.8 to 3.8 GeV/c 3-62895
- dp $\rightarrow\pi\gamma$, 2.8 to 3.8 GeV/c, angular distrib. and differential cross sections 3-62895
- e-p gravitational interaction, possible existence of massless scalar particle 3-66923
- e⁺e⁻ pair prod., 200 GeV protons 3-71018
- ep, electroproduction in streamer chamber $0.3 < Q^2 < 1.5(\text{GeV})^2$, $1.3 < W < 2.8$ GeV, charged multiplicities, π^- inclusive spectra 3-40354
- ep, heavy intermediate bosons and leptons, production cross sections (*Russian*) 3-59952
- ep, possible expts. for an intersecting ring complex 3-66305
- ep $\rightarrow e^+ \pi^+ + n$, electroproduction, four momentum transfers, 0.2 to 0.6 GeV/2 3-62844
- ep $\rightarrow e^+$ anything, Bjorken scale invariance in φ^3 ladder model 3-78147
- ep $\rightarrow e^+$ anything, scaling behaviour in parton model 3-52019
- ep $\rightarrow e^+$ hadron + X, SU(3) prediction for single particle distrib. 3-57367
- ep $\rightarrow e\pi^+ \pi^+$, azimuthal angle dependence near threshold 3-62846
- ep $\rightarrow e\pi^+$, current algebra and π^+ meson and. distrib. (*Russian*) 3-40360
- ep $\rightarrow e\pi^+$, electroproduction near threshold, total cross section 3-62845
- ep $\rightarrow e\pi^+ +$ anything, $0.1 < |q^2| < 0.8 \text{ GeV}^2$ and $3.15 < W < 2.8 \text{ GeV}$ 3-40357
- ep $\rightarrow e\Delta(1236)$, diff. cross section detn. 3-40356
- ep $\rightarrow e\Delta^+$ (1236), analysis in terms of $\Delta\gamma$ form factors 3-43102
- e⁺p $\rightarrow e^+ +$ anything, deep-inelastic limit, structure function threshold behaviour, reln. to annihilation 3-45884
- e⁺p $\rightarrow e^+ \pi^+ \eta$, value of experimental study 3-70902
- e⁺p $\rightarrow e^+ \pi^+ n$, comparison with Berends dispersion-theory model, pion e.m. form factor 3-59979
- e⁺p $\rightarrow e^+ \pi^+ n$, electric Born model and pion form factor 3-59976
- e⁺p $\rightarrow e^+ \pi^+ n$, value of experimental study 3-70902
- e⁺p $\rightarrow e^+ e^+ p$ in hydrogen bubble chamber, direct pair production, cross section determ. 3-54314
- η p, hadronic state prod., scaling, asymptotic form factors 3-78127
- η p $\rightarrow \Delta^+$, analysis in terms of $\Delta\gamma$ form factors 3-43102
- η p $\rightarrow \eta$ p, < 2.24 GeV, direct channel isobar model, electromagnetic widths of resonance states 3-57357
- η p $\rightarrow \eta$ p s-channel analysis in model of higher baryon couplings 3-43107
- η p $\rightarrow K^+ \Lambda$, amplitude analysis 3-71008
- η p $\rightarrow \omega$ p, unnatural parity contribs., pion exchange 3-67017
- η p $\rightarrow \rho$ v Salam-Weinberg model, 2 BeV 3-80919
- η p $\rightarrow \rho$ n, 0.4 to 2.2 GeV backward photoproduction, differential cross section 3-78133
- η p $\rightarrow \pi^+ \pi^-$, ρ n ρ , cross-sect. meas., $E_\gamma = 600$ to 900 MeV 3-49015
- η p $\rightarrow \pi^-$ anything, predicted differential cross section by factorisation of Regge trajectories 3-60052
- η p $\rightarrow \pi^0$ p, dip region, amplitude constraints, dual absorption model 3-57352
- η p $\rightarrow \pi^+ n$, 0.4-1.8 GeV, backward anal., differential cross sections 3-78135
- η p $\rightarrow \pi^+ n$, numerical study of phase of backward amplitude 3-57355
- η p $\rightarrow \pi^+ \pi^- p$, 4.1-6.2 GeV, longitudinal phase space analysis, one pion exchange and dual models. 3-57362
- η p $\rightarrow \pi^+ \pi^- \pi^+ \pi^- p$, 18 GeV, photon dissociation into four pions, evidence for ρ^0 enhancement in 4π mass spectrum 3-57364
- η p $\rightarrow \pi^+ \pi^- \pi^+ \pi^- p$, 9-18 GeV, spin-parity analysis of ρ^0 3-57365
- η p $\rightarrow \pi^0$ p, photoproduction, differential cross section in range 350-1175 MeV 3-62831
- η p $\rightarrow \rho^0$ p amplitude structure in Pomeron exchange reaction and s-channel helicity nonconservation 3-74406
- η p total and partial cross sections at 9.3 GeV, bubble-chamber expt. 3-70936

proton interactions continued

- K⁺p, 10, 16 GeV, momentum distrib. of π^+ , π^- , K⁻, K⁰, p, Λ 3-78205
- K⁺p, 10 GeV/c, Ω^- prod., decay, mass, lifetime values 3-78231
- K⁺p, 13 GeV/c, statistical measure of clustering in multiparticle final states 3-70964
- K⁺p, 2.885 GeV/c, η' production, decay study 3-60041
- K⁺p, 33.8 GeV/c, topological cross sections and charged particle multiplicities 3-57441
- K⁺p, 8.25 GeV/c, cross sections for common final states and prominent resonances 3-60038
- K⁺p, five-body final states at 6, 10 and 16 GeV/c, separation into sub-reactions, quantum number transfer 3-62899
- K⁺p, one- and two-particle inclusive-reaction cross sections at 13 GeV/c 3-54364
- K⁺p (ω , ϕ) Λ , vector-meson production reaction, amplitude analysis 3-71008
- K⁺p (ω , ϕ) Λ , 3.9 and 4.6 GeV/c, transversity-amplitude analysis 3-40395
- K⁺p charge transfer, 10 and 16 GeV/c, use of squared four-current transfer variable 3-57433
- K⁺p $\rightarrow \eta(\Lambda)$, Regge amplitudes in forward and backward directions, peripheral nature of A_2 exchange amplitude 3-52046
- K⁺p $\rightarrow K^-\pi^+\Delta^{++}$, 14.3 GeV/c, measurement of $K\pi$ elastic scattering cross section 3-57423
- K⁺p $\rightarrow K^-\pi^+n$ absorption model for π -exchange calculation of spin dependence 3-57386
- K⁺p $\rightarrow K^0X$, $|x| < 0.6$, multiperipheral model taking account of Regge poles 3-62912
- K⁺p $\rightarrow K^0X^0$, 8.25 GeV/c inclusive reaction, triple-Regge and absorptive behaviour 3-57457
- K⁺p $\rightarrow K^0\Xi^0$, 1.8 GeV/c, angular distribution, differential cross section 3-57414
- K⁺p $\rightarrow K^0n$, 39 GeV/c, comparison with Regge-pole model (*Russian*) 3-74438
- K⁺p $\rightarrow K^0n$, 3.13, 3.30, 3.59 GeV/c, differential cross section meas. 3-57413
- K⁺p $\rightarrow K^0n$, comparison with $K^+n \rightarrow K^0p$, 3.8 GeV/c, total and differential cross sections 3-60035
- K⁺p $\rightarrow K^0n$ charge exchange, 8 GeV/c, polarization meas. 3-74437
- K⁺p $\rightarrow K^*(890)X^+$, 8.25 GeV/c inclusive reaction, triple-Regge and absorptive behaviour 3-57457
- K⁺p $\rightarrow K^*(890)p$, $K^*(1420)p$, $K^*(890)\Delta^+$, results for 12 event/ μ b bubble-chamber expt., 3.13 and 3.3 GeV/c 3-40393
- K⁺p $\rightarrow K\pi\pi$ n reactions at 14.3 GeV/c, study of $K\pi\pi$ system, Q-production 3-67136
- K⁺p $\rightarrow \Lambda\Sigma\pi^+\pi^-$, measurement of Λ lifetime 3-67140
- K⁺p $\rightarrow \Lambda\eta$, 0.8 to 1.84 GeV/c, new data, hyperon resonance formation 3-57411
- K⁺p $\rightarrow \Lambda\eta$, 3.13, 3.30, 3.59 GeV/c, differential cross section meas. 3-57413
- K⁺p $\rightarrow \Lambda\pi^0$, 3.13, 3.30, 3.59 GeV/c, differential cross section meas. and Λ polarisation distrib. 3-57413
- K⁺p $\rightarrow \Lambda\pi^+\pi^-\pi^0$, Λ lifetime measurement 3-67140
- K⁺p $\rightarrow pK^*(nK^0)$ 777 to 1226 MeV, $K^*(892)$ prod. study 3-78182
- K⁺p $\rightarrow \pi^-(+)$ anything, 8.25 GeV/c, differential cross sections prediction by factorisation of Regge trajectories 3-60052
- K⁺p $\rightarrow \pi^-Y^{*+}$ (1385), amplitude analysis 3-71008
- K⁺p $\rightarrow \pi^+ + \dots$ and $\pi^- + \pi^- + \dots$, proton fragmentation analysis 3-57416
- K⁺p $\rightarrow \Sigma^-\pi^+$, 1.5-4.0 GeV/c, dispersive part of box diagram amplitude 3-62889
- K⁺p $\rightarrow \Sigma^-\pi^+$, Σ^- decay rate, branching ratio, test of $\Delta S = -\Delta Q$ selection rule 3-59954
- K⁺p $\rightarrow \Sigma^+\pi^-$, 250-550 MeV/c, meas. of Σ^+ magnetic moment 3-54309
- K⁺p $\rightarrow \Sigma^+\pi^-\Sigma^+$ decay, $\Delta S = -\Delta Q$ selection rule 3-59954
- K⁺p $\rightarrow \Sigma\pi\pi$, in region of $\Lambda(1520)$ resonance, cross sections and branching ratios 3-54345
- K⁺p $\rightarrow D^+K^+\pi^-$, 12 GeV/c, obs. of $K\pi$ scattering below 1 GeV mass, partial wave analysis 3-70978
- K⁺p elastic scattering, differential cross section meas., 1368-2259 MeV/c 3-78190
- K⁺p four or five bodies, 2.11 to 2.72 GeV/c, reaction channel, resonance cross sections 3-78204
- K⁺p $\rightarrow K^0X$, $|x| < 0.6$, multiperipheral model taking account of Regge poles 3-62912
- K⁺p $\rightarrow K^+\pi^+\pi^+\pi^-$, 12.7 GeV/c, comparison with Chan Loskiewicz Allison, and quark models 3-67141
- K⁺p $\rightarrow K^+\pi^-\Delta^{++}$, 3-13 GeV/c, determ. of $K^+\pi^-$ elastic scattering cross section 3-40398
- K⁺p $\rightarrow K^+\pi^+\pi^-p$, 4.6 GeV/c, cross-sections and ($K\pi\pi$) system production and decay properties 3-57442
- K⁺p $\rightarrow K^0(1420)\Delta^{++}$ in quark model, test of t-channel parity exchange 3-62886
- K⁺p $\rightarrow \pi^+ + \dots$ and $\pi^- + \pi^- + \dots$, proton fragmentation analysis 3-57416
- K⁺p $\rightarrow \pi^-\pi^+ +$ anything, two-component model of inclusive correlations for fixed prong number 3-52057
- K⁺p, 13 GeV SLAC expt., $K\pi$ scattering study 3-70989
- K⁺p charged multiplicity data analysis, Nova and Chew-Pignotti models 3-54360
- μ pair production, quark parton model, proton and neutron structure function effects 3-78226
- μp , 16 GeV inelastic scattering in hybrid bubble chamber, obs. of hadronic final states 3-70927
- np $\rightarrow dp$, circular polarisation of γ and weak P-odd $NN\rho$ vertex (*Russian*) 3-40376
- np $\rightarrow dp$, γ circular polarisation, correction from divergent P-violating $NN\rho$ vertex 3-78198
- np total cross section, 0.7 to 3.6 GeV/c, n-n total cross section evaluation 3-60057
- νp , μ identification external to bubble chamber 3-77629
- $\nu p \rightarrow \mu^+\pi^+p$, ~ 1 GeV/c, dominance by $\nu p \rightarrow \mu^+\Delta^{++}$ (1236), N- Δ axial current transition matrix elements, model predictions 3-57333
- $\nu p \rightarrow \mu^+\pi^+p$, value of experimental study 3-70902
- $\nu p \rightarrow \mu^+$ hadrons, application of correspondence arguments 3-70937
- $\nu p \rightarrow \nu l^+l^- +$ hadrons, cross sections for $E_\nu = 50$ -1000 GeV (*Russian*) 3-40337

proton interactions continued

- $\nu_\mu p \rightarrow \mu^-\Delta^{++}$, test of Weinberg model at CERN 3-66964
- $\nu_\mu p \rightarrow \nu_\mu\Delta^+$, test of Weinberg model at CERN 3-66964
- $\nu_\mu p \rightarrow \nu_\mu\pi^+\pi^-$, used in search for neutral weak currents, isovector or isoscalar 3-62818
- p-hadron collisions, limiting behaviour of inclusive baryon spectra 3-74460
- p-nucleus, cross sections calc., dependence on nucleon structure in b-space 3-67160
- p + N $\rightarrow W(\rightarrow l\nu l) +$ (hadrons), lepton spectra analysis rel. to detection of W boson, quark model application (*Russian*) 3-67062
- pd $\rightarrow {}^3\text{He} +$ meson, η , ω , ρ^0 cross section meas., 5 GeV 3-78199
- pd annihilations at rest into two pions, obs. 3-43136
- pd $\rightarrow NX$ quasinuclear meson production via pole mechanism, spin effects (*Russian*) 3-40377
- pn, 25-60 GeV total cross section calc., shadow corrections including inelastic screening (*Russian*) 3-67166
- pn, 70 GeV, unsuccessful search for heavy quasistable leptons 3-60022
- pn annihilation and bound states 3-57399
- pn inelastic collisions, 200 GeV/c, ang. characts. of secondary relativistic charged particles 3-78213
- pn $\rightarrow \mu^+\mu^-$ hadrons, single muon spectra in parton model 3-40396
- pn $\rightarrow NN\pi$, 1.0 to 1.6 GeV/c, cross-section study 3-52053
- pn $\rightarrow pp\pi^+\pi^-$, 28 GeV/c, statistical analysis of event-to-event fluctuations, evidence for strong clustering effects 3-74441
- pn $\rightarrow \pi^+\pi^-\pi^-$ annihilation at rest, two-variables expansions, analysis of Dalitz plot 3-57397
- pn $\rightarrow \pi\pi\pi$, Dalitz-plot distrib. explanation 3-57375
- pn $\rightarrow YN$ low energies, one-pion exchange contribution to cross section (*Russian*) 3-60017
- π^0 production at 90°, large transverse momentum, constituent interchange model 3-62851
- $\pi^-p \rightarrow A_2^-p$, discussion of form of A_2 resonances (*Slovak*) 3-62888
- $\pi^-p \rightarrow \pi^-\pi^0\pi^+\pi^-p$, 25 GeV/c, study of high energy $\pi\pi$ scattering processes 3-57448
- $\pi^-p \rightarrow \pi^-\pi^+\Delta^+$, 25 GeV/c, study of high energy $\pi\pi$ scattering processes 3-57448
- $\pi^-p \rightarrow \pi^-\pi^+n$, 25 GeV/c, study of high energy $\pi\pi$ scattering processes 3-57448
- $\Sigma^-p \rightarrow \Lambda n$, determ. of $\Lambda\Sigma\pi$ coupling const., test of charge-independence hypothesis and T invariance 3-70974

proton magnetic moment

- fundamental constant, new determination in terms of nuclear magneton to within $4.3 \times 10^{-9}\%$ 3-48486
- SL₃, unitary irreducible representations, relations among baryon magnetic moments 3-59958
- SU₃ predictions, exact reduced-vertex symmetry 3-51986

proton magnetic resonance

- acetone, (CH₃)₂CO-(DC₃)₂CO mixture, determ. of ratio of proton and deuteron nuclear mag. moments 3-62936
- acetone, oriented, D spectra quadrupole coupling const. 3-64564
- acetone, partially deuterated, determ. of ratio of proton and deuteron nuclear mag. moments 3-62936
- acetoxybenzal p-phenetidine, nematic liquid crystal, p.m.r. 3-53025
- acetoxybenzal p-aminoazobenzene nematic liq. cryst., proton mag. reson., degree of order 3-55485
- acetoxybenzal p-anisidine nematic liq. cryst., proton mag. reson., degree of order 3-55485
- acetylene in different liquid crystals, proton magnetic shielding anisotropy 3-43489
- adenosine monophosphate, 3',5'-cyclic, ¹H n.m.r. spectra, conformation investigation 3-63568
- anisol-p-aminoazobenzene nematic liq. cryst., proton mag. reson., degree of order 3-55485
- aryl N-methylazoles, chemical shift effects 3-75066
- azo compounds, decomp., chem. induced nuclear polarisation, methyl radical 3-71579
- benzenes with side-chain interacting groups, substituent effects on proton spin-spin coupling 3-60478
- benzoyl peroxide, decomp., chem. induced nuclear polarisation, methyl radical 3-71579
- biphenyl radical anions ¹H and ²D n.m.r. studies 3-43488
- borazine, hexasubstituted crysts., mol. reorientation obs. (*French*) 3-53026
- 1-bromo-3,3,4-trifluorobutene-4, determ. of chemical shift and coupling consts. 3-75072
- butadiene-1,3, spin-spin coupling consts. 3-43484
- butene-1 on A- and Y-zeolites, mobility, proton spin relax. (*German*) 3-64245
- p-n-butoxybenzal p-phenetidine, nematic liquid crystal, p.m.r. 3-53025
- t-butylamine, p.m.r. absorption and relaxation study 3-55492
- t-butylamine clathrate deuterate, p.m.r. absorption and relaxation study 3-55492
- t-butylchloride, self-diffusion coeff. and rot. correlation time determ. 3-68872
- carbonyl group intermol. electrostatic and mag. effects on proton shielding const. 3-63525
- cellulose acetate, ultrathin and thick membranes, p.m.r. studies 'free' and restricted water 3-54770
- chemically induced nuclear dynamic polarisation, nuclear and electron spin coupling, student experiment 3-48324
- chlorobenzene partially oriented in nematic phase, use of INDOR technique 3-54720
- chlorocyclohexane at low temp., FT ¹³C n.m.r. spectra, conformational anal. 3-71582
- collagen fibres, hydrated, proton exchange and molecular orientation of H₂O and D₂O, n.m.r. studies 3-55993
- coumarin and methyl derivatives, σ and π electron contributions to long-range spin-spin coupling consts. 3-52387
- cyclohexane in nematic liquid crystal solvents, use of deuterium decoupling 3-46319
- cyclohexyl percarbonate, decomp., chem. induced nuclear polarisation, methyl radical 3-71579
- cyclooctatetraene, in nematic solvents, n.m.r. studies of struct. and bond shift kinetics 3-71576
- cyclopropane, solid, and cyclopropane deuterate, molecular rotation determ. 3-44346

proton magnetic resonance continued

- deuteron decoupling in nematic liquid crystal solvents, theory 3-46320
- 6,7-dichloroquinoline, spin-spin coupling of peri-protons 3-50479
- diethylamine, solid, p.m.r. second moment and spin-lattice relax., mol. motion study 3-55497
- diethylamine clathrate deuterate, solid, p.m.r. second moment and spin-lattice relax., mol., motion study 3-55497
- dimethyl sulphoxide; D spectra, quadrupole coupling consts. 3-64564
- dinucleotides, backbone conformation, ^{13}P and ^1H fast Fourier transform n.m.r. spectroscopy 3-67850
- elastomer, rapidly rotated, line narrowing effect, monomer ratio and conform. struct. obs. 3-78916
- p-ethoxybenzal p-aminoazobenzene, nematic liquid crystal, p.m.r. 3-53025
- ethylene glycol, with Cr(V) complexes, dynamic proton polarisation and spin-lattice relax. 3-72543
- ethylene oxide, as clathrate deuterate, proton spin-lattice relax. time 3-54727
- ferricytochrome b_5 , determ. of principal axis of G-tensor (German) 3-49510
- ferrocene; monosubstituted, meta couplings 3-63524
- fluorenone, radical anions, ^1H and ^2D n.m.r. studies 3-43488
- fluoroacetones, coupling consts. and rot. isomerism 3-46323
- free radicals, chemically induced dynamic, hydrodynamic effect 3-80537
- furan, liquid, proton-spin relaxation and molecular motions 3-44344
- Helmholtz coil pair application, uniform magnetic field study 3-45574
- hexamethylenetetramine, proton rotational correl. time in chloroform 3-75900
- hydrates, solid echo expt. for direct meas. of spin-1/2 pair dipolar interactions 3-79934
- hydrocarbons, liq., spin-lattice relax., press. depend., mol. motions 3-41446
- trans-hydroxy-L-proline, computer simulation, long range coupling constant, structural implications 3-75074
- 2',3'-isopropylideneadenosine, mol. interaction in soln., deuterium substitution effect on proton relax. times 3-75899
- lineshape analysis of mutually coupling equinegetic two-site exchange system using PDP-8 computer 3-46322
- liquid crystals, smectic, n.m.r. studies 3-55483
- metal porphyrin/caffeine complexes chemical shift determ. 3-78851
- methyl substituted aromatic radical ions, proton spin relax., CH_3 linewidth 3-63517
- molecular interaction in soln., deuterium substitution effect on proton relax. times 3-75899
- montmorillonite, adsorption of water, spin-lattice relaxation in single and double layer system 3-68867
- 2,4,5-nonachloromesitylene, rotational isomerism, conformational energy 3-67851
- oligomer, temp. depend. of relaxation times, bulk and thin layers (Russian) 3-71669
- organic acids, proton multiple pulse spectra, nuclear magnetic shielding anisotropies 3-79930
- organophosphorus cpds., spin coupling with ^{31}P , exptl. determ. 3-75081
- oxalic acid dihydrate, high resolution spectrum measurements 3-47156
- para-substituted benzaldehyde, toluene soln., solute-solvent interactions, chemical shifts 3-44744
- perocetyl isopropyl carbonate, decomp., chem. induced nuclear polarisation, methyl radical 3-71579
- phenanthrene, radical anions, ^1H and ^2D n.m.r. studies 3-43488
- phytoene isomers, struct. obs. 3-46361
- plastic crystal, mol. self-diffusion and reorientation, press. depend. 3-61005
- plastic crystals, self-diffusion, relax. time and linewidth obs. 3-68438
- polyethyleneterephthalate, n.m.r. study of crystallisation, orientation effect, molecular movement (Russian) 3-71691
- polypropylene-2-d, sulphide, effect of deuterium-decoupling on n.m.r. spectrum 3-63578
- polysaccharides, aq. soln., spin-echo for spin-spin relax. time 3-68876
- polystyrene, dynamic polarisation of protons, electronic spin-spin interactions contrib. 3-79891
- polystyrene containing paramagnetic impurity, spin-lattice relaxation of protons 3-72540
- protein conformations, n.m.r. spectroscopy 3-67875
- protein spectra, resolution enhancement using difference between broadened and normal spectrum 3-71665
- pyrazole[^{15}N], spin-spin coupling coeffs. 3-54722
- pyridazine[^{15}N], spin-spin coupling coeffs. 3-54722
- pyridine nucleotides, conformation, ^{13}P and ^1H fast Fourier transform n.m.r. spectroscopy 3-67850
- pyridines, disubstituted, proton-proton coupling consts., additivity of substituent effects 3-60479
- ribonucleic acid, transfer, high resolution spectra, chemical shift 3-75167
- saturated heterocycles, intermol. action of heteroatom (French) 3-43475
- tanol linear chain free radical, proton relax time freq. and temp. depend. (French) 3-58441
- TCNQ-NH_4^+ , proton spin-lattice relaxation time, temp. dependence 3-55498
- tetrahydrofuran, as clathrate deuterate, proton spin-lattice relax. time 3-54727
- thioamides, hindered rotation barriers determ. 3-71529
- thymidine monophosphate, 3',5'-cyclic, ^1H n.m.r. spectra, conformation investigation 3-63568
- TMPO, linear chain like free radical, sublattice magnetisation 3-55486
- trichloroethylene in mixtures of HMPT and cyclohexane, chemical shift as function of conc. and temp. 3-75898
- triethylene diamine, as clathrate deuterate, proton spin-lattice relax. time 3-54727
- 2,4,6-trifluorobenzene, external electric field effects 3-68854

proton magnetic resonance continued

- trimethylene oxide, p.m.r. spectra, ring puckering vibr., chem. shifts and spin-spin coupling meas. 3-54726
- trimethylene sulphide, p.m.r. spectra, ring puckering vibr., chem. shifts and spin-spin coupling meas. 3-54726
- triphenyltin fluoride, chloride, bromide, and hydroxide, mol. motion study from spin-lattice relax. times and second moments meas. 3-46325
- trismethylenemethaneiron tricarbonyl in nematic solvent, p.m.r. anal. 3-54728
- 1,1,2-trisubstituted ethanes, p.m.r. spectrum, theoretical appl. of coupling consts. depend. on internal rot. pot. function 3-46318
- vector, obs. of change in nuclear susceptibility and angular momentum transfer 3-41435
- water, proton spin-lattice relaxation time meas. 3-71577
- AlCl_3 , aqueous soln., proton n.m.r. shifts and local elec. field 3-79921
- Cr^{3+} in aqueous solns., p.m.r. field shift meas. 3-68860
- Cu^{2+} in aqueous solns., p.m.r. field shift meas. 3-68860
- N,N-dimethylamides, chalcogen replaced, hindered rot. about N-C amido band 3-52389
- Fe^{3+} in aqueous solns., p.m.r. field shift meas. 3-68860
- Fe_2 , solid, 0.2-4.2K 3-68866
- HBr, pure gaseous, proton chemical shift and magnetic shielding 3-54724
- HCl, chem. shift, temp. and density depend. 3-75068
- $\text{H}_2\text{O-D}_2\text{O}$ mixture, determ. of ratio of proton and deuteron nuclear mag. moments 3-62936
- $\text{Hg}_2(\text{NO}_3)_2 \cdot 2\text{H}_2\text{O}$, H_2O molecule orientation 3-60992
- $\text{K}_2\text{Pt}(\text{CN})_4\text{Br}_{0.3} \cdot \text{nH}_2\text{O}$ quasi one-dimens. conductor, temp. depend. behaviour (German) 3-50482
- $\text{MgCl}_2 \cdot 6\text{H}_2\text{O}$, solid, proton n.m.r. shifts and local elec. field 3-79921
- Mn^{2+} in aqueous solns., p.m.r. field shift meas. 3-68860
- NH_4Br , proton magnetic resonance study of tunnelling of NH_4^+ ions 3-44332
- NH_4Br , time-depend. n.m.r. spectra, 4.2K 3-79920
- $(\text{NH}_4)_2\text{C}_2(\text{SO}_4)_3$, distortion of langbeinite structure, p.m.r. meas. of NH_4^+ location 3-68234
- NH_4ClO_4 , proton spin-lattice relax. and exchange splitting of torsional ground state 3-44343
- $(\text{NH}_4)_2\text{CrO}_4$, proton magnetic resonance study of tunnelling of NH_4^+ ions 3-44332
- $\text{NH}_4\text{H}_2\text{AsO}_4$, mol. reorientation, spin-lattice relax. obs., Curie pt. behaviour, high temp. phase transition 3-61004
- NH_4I , proton magnetic resonance study of tunnelling of NH_4^+ ions 3-44332
- NH_4IO_3 , time-depend. n.m.r. spectra, 4.2K 3-79920
- NH_4NO_3 , proton magnetic resonance study of tunnelling of NH_4^+ ions 3-44332
- NH_4SCN , proton magnetic resonance study of tunnelling of NH_4^+ ions 3-44332
- $\text{Sc}(\text{HPO}_3)_3$, structural investigation 3-78657
- $\text{Sc}(\text{H}_2\text{PO}_2)_3$, structural investigation 3-78657
- $\text{Sc}(\text{H}_3\text{PO}_3)_3$, structural investigation 3-78657
- $\text{Sc}(\text{HPO}_3)_3 \cdot 4\text{H}_2\text{O}$, structural investigation 3-78657
- $\text{UF}_6 \cdot 2.5\text{H}_2\text{O}$, position and mobility of H_2O 3-79925

proton polarisation

- bounds, calc. from H hyperfine interval recoil corrections 3-66998
- elastic scattering by nuclei, diff. theory of polarization (Russian) 3-78328
- inelastic scattering on nuclei, analysing capability reln. to reaction amplitude (Russian) 3-67318
- light nuclei interactions with electrons, polarisation of emitted protons (Russian) 3-63038
- strong-absorption model for elastic, polarisation and inelastic proton scattering 3-52183
- target, frozen spin polarised, 50 mK meson spectrometer 3-77612
- targets, predictions based on absorptive A_2 exchange in $\pi^-p \rightarrow \pi^-n$, 17.2 GeV/c, polarised target predictions 3-60039
- $\pi p \rightarrow \pi^0 p$, 4 GeV, target asymmetry 3-70919
- $\text{K}^-p \rightarrow \text{K}^0 n$ charge exchange, 8 GeV/c, polarization meas. 3-74437
- NN interactions, polarisation structure at high energies, simple models 3-70969
- np scattering, elastic, 612 MeV, depolarization 3-40375
- p-n polarisation role in models for atomic mass dependence of photo-nuclear giant resonance energy 3-74546
- pd \rightarrow ppn at 600 MeV, separation of single and double scatterings (Russian) 3-67106
- pp elastic scattering, 220 MeV, polarization meas. 3-74412
- pp elastic scattering, 2.5 to 5.15 GeV/c, 0.2 to 2.0 (GeV/c) 2 3-60027
- pp \rightarrow KK, $\pi^+\pi^-$, possible polarisation meas. 3-40390
- pp \rightarrow nn charge exchange at 8 GeV/c; polarisation meas. 3-49050
- p scattering, spin correlation parameters, 50 MeV reln. to nuclear forces 3-63030
- pp scattering, total cross section meas., in pure spin states, 3.5 GeV/c 3-67121
- π^0 photoproduction, 1000 to 1800 MeV, recoil proton, summary fits 3-59978
- π^-p elastic scattering at 40 GeV/c, polarisation parameter meas. 3-49048
- $\pi^-p \rightarrow \pi^-n$, general description, high energy predictions of a $\pi^+ + \text{A}_2$ model 3-74443
- $\pi^-p \rightarrow \pi^0 n$, real parts of amplitudes, differential cross sections 3-62896
- π^+p backward elastic scattering at 2.0, 3.5 and 4.0 GeV/c, polarisation meas. 3-57422
- $\pi^\pm p$ elastic scattering, meas. of polarisation parameter between 2.50 and 5.15 GeV/c 3-71004
- scattering, relation to differential cross section in baryon exchange, parity-doublet contributions 3-60025
- $^{40}\text{Ar}(p,p)$, 40 MeV polarised protons, asymmetry meas. at small angles 3-40487
- $^2\text{H}(d,p)^3\text{H}$, 6-15 MeV, meas. of polarisation transfer coeffs. at angle of 0° 3-74555
- $^2\text{H}(p,n)p$, enhancement of total and differential cross section 3-71096
- $^{32}\text{S}(p,p')$, polarized scattering, hexadecapole phonon state 3-74583

proton polarisation continued

^{28}Si inelastic scattering of 25.25 MeV polarised protons, ground state rotational band excitation 3-52174

proton production

p^2 theory, effect of nucleons in high energy collisions (*Russian*) 3-67132
 deuteron electrodisintegration matrix element, reln. to neutron-proton phase shifts 3-70939
 dynamic characteristics, angular, momentum distribution, for pp interactions, 19.1 and 10 GeV/c (*Russian*) 3-60046
 generator, $^3\text{He}(\text{D},p)^4\text{He}$ reaction, sealed instrument, description 3-66309
 inclusive, in pp interactions at 303 GeV/c, cross section determ. 3-74447
 inclusive nucleon and pion production from proton-nucleus collisions, semiempirical model 3-57465
 low-energy, under 600 MeV proton bombardment of C, Al, Ni, Cu, Au, cascade-plus-evaporation model 3-57528
 $K^+d \rightarrow K^0p$, spectator momentum distrib., effect of final-state interaction 3-67111
 K^-p interaction, 10, 16 GeV, momentum distrib. 3-78205
 p , in pp inclusive reactions in fragmentation region at CERN ISR 3-57454
 p , inclusive charged particle production and inelastic proton spectra at CERN ISR 3-71027
 p , p inclusive production at CERN ISR 3-74454
 p, p inclusive production at medium angles at CERN ISR 3-71029
 p + missing mass, electroproduction off protons, scaling behaviour 3-70929
 pp collisions, π , K and p production ratios in central region at CERN ISR 3-49068
 $\Sigma^+ \rightarrow pp$, proposed explanation of experimental results 3-66971

proton-proton interactions

azimuthal corrections for 20-70 GeV collisions and multiperipheral model 3-78214
 bremsstrahlung, 156 MeV, off-shell effects 3-78335
 charged multiplicity data analysis, Nova and Chew-Pignotti models 3-54360
 charged particle multiplicity distrib. at high energy, scaling parameter to give Poisson distrib. 3-45921
 charged particle multiplicity distrib. at high energy correlation parameters 3-43156
 charged particle production at large transverse momentum at CERN ISR, 23.2-52.7 GeV, pion and γ -ray spectra 3-49069
 charged-prong multiplicity distrib., 50-303 GeV/c, evidence for systematic behaviour 3-43159
 coherent generation of particles on emulsion nuclei at 200 GeV/c 3-74439
 cosmic jets, $1-10^{10}$ GeV pp interactions, total cross section (*French*) 3-53585
 cosmic rays, extraction of high-energy particle information from emulsion data 3-56295
 cross section compilation for proton and antiproton induced reactions 3-70973
 diffractive production, threshold effects 3-74461
 fireball production, energy-independent distribution, explicit KNO function 3-67153
 fragmentation models and unitarity, diffractively excited inelastic processes, apparent breakdown of factorisations 3-67090
 high energy, correlation between neutral and charged pions, critical fluid gas model 3-70960
 high-energy, correlation between pionization region and fragmentation region 3-49066
 high-energy, fit of charged particle multiplicity data to double Poisson distrib. 3-49057
 inclusive, at 205 GeV/c is 30-inch bubble chamber, single particle distrib. 3-71021
 inclusive, high transverse momentum hadron jet production, gluon-exchange model 3-70945
 inclusive, limiting fragmentation, exptl. tests at CERN ISR, 31-53 GeV 3-52062
 inclusive, proton leading-particle spectrum at 14, 19, 24 GeV/c, Regge Regge Pomeron model 3-67150
 inclusive, short range correlations in central region at ISR energies, cluster formation 3-67149
 inclusive π , K and p production ratios in central region at CERN ISR 3-49068
 inclusive at ISR scaling properties of charged particle multiplicity distrib. 3-71028
 inclusive charged particle production and inelastic proton spectra at CERN ISR 3-71027
 inclusive charged particle production at CERN ISR 3-74454
 inclusive charged particle production at medium angles at CERN ISR 3-71029
 inclusive hadron spectra, ISR data, determ. of triple-pomeron coupling 3-67154
 inclusive in ISR region, hard collision of parton pairs theory for new effects 3-49065
 inclusive nucleon and pion production from proton-nucleus collisions, semiempirical model 3-57465
 inclusive production of π^- , K^- and p in fragmentation region at CERN ISR 3-57454
 inclusive production of high transverse momentum particles in central region at CERN ISR 3-49067
 inclusive reaction, 53-4 GeV c.m. energy, π^0 transverse-momentum distrib. 3-52059
 inclusive studies of p , K^0 and Λ^0 production at 303 GeV/c 3-43157
 inclusive two-particle rapidity correlations at ISR energies, multiperipheral fireball model 3-52060
 inelastic, $>10^{11}$ eV, heavy cluster theory, topological cross section props. (*Russian*) 3-78229
 inelastic collisions, 200 GeV/c, ang. characts. of secondary relativistic charged particles 3-78213
 inelastic cross sections at ISR energies, maximal e.m. contribution 3-74465
 ISR at CERN, report on first twenty months of operation 3-56858
 KNO scaling behaviour at finite energies, unitarity generation of long range correlations 3-74471
 lepton production at ISR, review 3-66991
 multigamma events search at high energy at ISR 3-71026

proton-proton interactions continued

multiparticle production at ISR energies, analysis of unitarity eqn. 3-67152
 multiperipheral and diffractive production mechanisms rel. to two-particle correlation 3-60010
 multiple production, fireball model, comparison of cosmic ray data and ISR results, rapidity distrib. 3-78168
 multiple production, non-diffractive, high energy, evidence for strong correlation 3-78211
 multiplicity dependence on recoil momentum at 28.5 GeV/c 3-78211
 multiplicity distrib. at high-energy, asymptotic expansions 3-7103
 multiplicity distribution at 205 GeV/c. fluctuation analysis 3-574
 multiplicity distributions, charged, empirical formula possessing scaling property 3-60043
 pair production, approximately normal model, 5-300 GeV/c 3-60023
 parton model and causality, scaling bounds on high transverse momenta 3-67148
 Pomeranchuk mechanism for ISR rising cross sections and finite energy effects 3-67077
 $pp \rightarrow p\pi^+n$, appl. of invariant description of peripheral three-particle final state reaction 3-43150
 quark model for inclusive spectra in central region $|p_T^m| \leq 0.3 p_{\text{max}}$ 3-74464
 rising total cross-sections at ISR energies, new parametrization 3-78218
 semi-inclusive, pion distrib. in fragmentation model 3-45917
 semi-inclusive interactions at 303 GeV/c, production angle distrib. meas. 3-52063
 semi-inclusive scaling, early onset 3-57467
 single-particle distrib. at $x=0$, ISR data, dual B_6 -model with Pomeron background modifications 3-67146
 single-particle production at ISR, c.m. angles 45° - 90° , cross sections 3-40404
 storage ring expts. at energies up to 2000 GeV, review of progress 3-40384
 total cross section, Regge-pole model 3-67151
 total cross-sections, correlation between structures for p-p, p-p, p-n and K-p interactions 3-45905
 two-particle rapidity correlations at ISR, independent emission of clusters mechanism 3-74463
 universal multiplicity formula based on thermodynamics 3-49034
 p annihilation in hydrogen, 0-600 MeV, radiative transitions (*Russian*) 3-40378
 \bar{p} , effective cross sections, 720 MeV/c 3-74411
 $pp \rightarrow (n\pi^+)p$ data, split field magnet geometry fit program: NICOLE 3-60047
 $pp \rightarrow (p^-, K^- \text{ and } \pi^-) + \text{anything}$ up to ISR energies, new form of scaling 3-43154
 p annihilations, average transverse momentum of produced pions, uncorrelated jet model 3-45916
 $pp \rightarrow d\pi^+$ backward process, 1.0-2.8 GeV, model of N and N* exchanges 3-67128
 $pp \rightarrow \gamma X$, 303 GeV/c inclusive production process, cross section meas. 3-74447
 $pp \rightarrow \gamma X$, 69 GeV, photon conversion into electron pairs, scaling behaviour 3-67157
 $pp \rightarrow \gamma X$ processes at 69 GeV, cross sections and scaling 3-74449
 $pp \rightarrow \gamma + \text{anything}$, cross section meas. at large transverse momentum 3-71023
 $pp \rightarrow \gamma + \text{charged particles} + \text{anything}$, inclusive two-particle production at storage ring energies, rapidity correlations 3-49063
 pp increasing total cross sections rel. to growth of p-nucleus cross sections 3-67160
 $pp \rightarrow K^0 X$, 303 GeV/c inclusive production process, cross section meas. 3-74447
 $pp \rightarrow K^0 + \text{anything}$, 19 GeV/c, inclusive production spectrum comparison with two centre thermal model 3-57455
 $pp \rightarrow K^- K^+$ resonance parametrization and reln. to dual models 3-52034
 $pp \rightarrow K^0, K^0$ in hydrogen, relative suppression of $pp \rightarrow K^0, K^0$ process, reln. to quasi-nuclear meson interference 3-70970
 $pp \rightarrow K^0, K^0$, cross section difference for hydrogen and deuterium, reln. to quasi-nuclear meson interference 3-70970
 $pp \rightarrow K^0 K^0$, 700-1100 MeV/c, new cross section and angular data 3-70971
 $pp \rightarrow K^0 X$, 69 GeV, cross sections, scaling behaviour 3-67158
 $pp \rightarrow K^0 X$ processes at 69 GeV, cross sections and scaling 3-74449
 $pp + K^+ K^-$, 0.7 to 2.4 GeV/c, to study heavy boson coupling to system, folded angular distributions, total cross sections 3-57396
 $pp \rightarrow K^+ K^-$, annihilation interaction, 5 GeV/c backward and forward peaks 3-78189
 $pp \rightarrow KK$, 700 MeV/c, analysis on basis of boson triad (ρ^+ , ω^+ , ϕ^+) 3-62873
 $\bar{p}p + \bar{K}K$, $\pi^+ \pi^-$, possible polarisation meas. 3-40390
 $pp \rightarrow KKn\pi$, 1.5-2.0 GeV/c (*French*) 3-52048
 $pp \rightarrow l^+ l^-$, high energy, effects of W^0 , cross-sections for annihilation 3-59948
 $pp \rightarrow l^+ l^- + \text{anything}$, charge distribution of partons and scaling 3-74447
 $pp \rightarrow \Lambda^0 X$, 303 GeV/c inclusive production process, cross section meas. 3-74447
 $\bar{p}p \rightarrow \Lambda\Lambda$, 1.5 to 2.0 GeV/c 3-52044
 $pp \rightarrow \Lambda X$, 69 GeV, cross sections, scaling behaviour 3-67158
 $pp \rightarrow \Lambda X$ processes at 69 GeV, cross sections and scaling 3-74449
 $pp \rightarrow \Lambda + \text{anything}$, 19 GeV/c, inclusive production spectrum, comparison with two centre thermal model 3-57455
 $pp \rightarrow \mu^+ \mu^-$ anything, multiperipheral theory 3-74468
 $pp \rightarrow \mu^+ \mu^- X$, spectral representation, scaling limit, light cone dominance 3-78222
 $pp \rightarrow Nn\pi$, π , 200 GeV/c, independent-emission model 3-40405
 $pp \rightarrow N^* N^*$, prediction of differential cross-section slope using factorization of diffractive exchange 3-52047
 $pp \rightarrow nn$, charge exchange at 8 GeV/c, differential cross section, π -exchange effects (*German*) 3-52045
 $\bar{p}p \rightarrow \bar{n}n$ charge exchange at 8 GeV/c, polarisation meas. 3-4905
 $pp \rightarrow p$ inclusive process at high energy, double Regge exchange model 3-52055

proton-proton interactions continued

- pp \rightarrow p π^+ , high-energy wide-angle differential cross section in DRM, absence of universal behaviour 3-52043
- pp \rightarrow pX, 205 GeV/c reaction characts. 3-74462
- pp \rightarrow pX, 303 GeV/c, separation of diffractive and nondiffractive compr. of multiplicity distribution 3-62919
- pp \rightarrow pX, 303 GeV/c inclusive production process, cross section meas. 3-74447
- pp \rightarrow pX, diffractive multiplicity distrib., two-component model, prong cross-sections 3-70959
- pp \rightarrow pX, energy dependence between 40 and 260 GeV/c using internal H_2 jet target at NAL 3-71022
- pp \rightarrow pX, in diffractive region at 200 GeV, meas. of doubly differential cross section 3-74450
- pp \rightarrow p + anything, 102 GeV/c, inclusive spectra meas. 3-71020
- pp \rightarrow p + anything, diffractive-excitation model, comparison with ISR data 3-74466
- pp \rightarrow p + anything, pion exchange and missing-mass spectra near phase-space boundary 3-74456
- pp \rightarrow pions, high energy, uncorrelated jet model predictions on multiplicity distribution 3-57440
- pp \rightarrow p $\pi^+\pi^+\pi^-$, 19.1 GeV/c, production cross sections, angular and momentum distributions, comparison with theory (Russian) 3-60046
- pp \rightarrow pp, production cross sections at 6.6 GeV/c, two prong events 3-54350
- pp \rightarrow p $\pi^+\pi^-$, properties of π and p momentum spectra in multiperipheral scheme (Russian) 3-40400
- pp \rightarrow pp π^0 , production cross sections at 6.6 GeV/c, two-prong events 3-54350
- pp \rightarrow pp $\pi^+\pi^-$, 19.1 GeV/c, production cross sections, angular and momentum distributions, comparison with theory (Russian) 3-60046
- pp \rightarrow pp $\pi^+\pi^-$, 28 GeV/c, statistical analysis of event-to-event fluctuations, evidence for strong clustering effects 3-74441
- pp \rightarrow pp $\pi^+\pi^-\pi^0$, 19 GeV/c, diffraction dissociation, longitudinal phase space analysis 3-74446
- pp \rightarrow pp $\pi^+\pi^-\pi^0$, 19.1 GeV/c, production cross sections, angular and momentum distributions, comparison with theory (Russian) 3-60046
- pp \rightarrow pp $\pi^+\pi^-\pi^-\pi^+$, 28 GeV/c, statistical analysis of event-to-event fluctuations, evidence for strong clustering effects 3-74441
- pp \rightarrow pp $\pi^+\pi^-\pi^-\pi^-\pi^+$, 28 GeV/c, statistical analysis of event-to-event fluctuations, evidence for strong clustering effects 3-74441
- pp \rightarrow p π^+ n, energy dependence of cross-section in Deck type models 3-49051
- pp \rightarrow p π^+ n, production cross sections at 6.6 GeV/c, two-prong events 3-54350
- pp \rightarrow p π^+ n absorption model for π -calculation of spin dependence 3-57386
- pp \rightarrow px, 303 GeV/c, diffraction excitation analysis, mean charged multiplicity 3-62918
- pp \rightarrow px, three-reggeon description of inclusive proton spectra 3-62906
- pp \rightarrow π^- + anything, 19 GeV/c, inclusive production spectrum, comparison with two centre thermal model 3-57455
- pp \rightarrow $\pi^-\pi^+$, resonance parametrization and reln. to dual models 3-52034
- pp \rightarrow π^0 + anything, 23.5-62.4 GeV, invariant-cross sections and obs. of large transverse momentum π^0 n 3-78227
- pp \rightarrow π^0 + anything, 52.7 and 44.8 GeV, large transverse momentum phenomena 3-74453
- pp \rightarrow $\pi^0\eta$, large cross section due to existence of quasi-nucleon meson interference 3-70970
- pp \rightarrow $\pi^0\eta$, large cross section due to existence of quasi-nucleon meson interference 3-70970
- pp \rightarrow π^+ + anything, 20 to 1500 GeV, semiempirical formula for cross section, consistency with scaling, limiting fragmentation 3-57461
- pp \rightarrow π^+ + anything, diffractive-excitation model, comparison with ISR data 3-74466
- pp \rightarrow π^- , 0.7 to 2.4 GeV/c, to study heavy boson coupling to pp system, folded angular distributions, total cross sections 3-57396
- pp \rightarrow $\pi^+\pi^-$, 2-10 GeV, upper bounds on cross sections for $\pi\pi$ scattering, crossing dispersion sum rules 3-57432
- pp \rightarrow $\pi^+\pi^-$, annihilation interaction, 5 GeV/c, backward and forward peaks 3-78189
- pp \rightarrow $\pi^+\pi^-\pi^+\pi^-$, 2.1-2.24 GeV, over T-region, reson. anal. 3-78209
- pp \rightarrow $\pi^+\pi^-\pi^+\pi^-\pi^-\pi^+$ (π^0), test of invariance under charge conjugation (French) 3-49053
- pp \rightarrow $\pi^+\pi^-\pi^+\pi^-\pi^-\pi^+$ (π^0), annihilation at 1.1 and 1.4 GeV/c (French) 3-52049
- pp \rightarrow $\pi^+\pi^-\pi^+\pi^-\pi^-\pi^+$ 5.7 GeV/c, two-particle correlation study 3-54358
- pp \rightarrow π^+X , 303 GeV/c inclusive production process, cross section meas. 3-74447
- pp \rightarrow π^+ + anything, 102 GeV/c, inclusive spectra meas. 3-71020
- pp \rightarrow π^+X , ISR pionization spectrum internal structure, peripheral models 3-49062
- pp \rightarrow π^+X , spectral representation, scaling limit, light cone dominance 3-78222
- pp \rightarrow $\pi\pi$ baryon exchange reaction, line reversal and energy dependence of dip locations 3-54351
- pp \rightarrow $\pi\pi\pi$, contribution of ρ' (1650) to nucleon form factor 3-57339
- pp \rightarrow Xp missing mass experiments, implications for Regge cuts 3-43126
- π multiplicity distrib. at very high energy, Reggeized production model 3-57385
- π production, multiperipheral description of spectra, assumed similarity of ν and π properties (Russian) 3-74407
- π spectra, inclusive transverse momentum, relationship of diffractive excitation model and thermodynamic model 3-67163
- π^- distribution from 205 GeV/c obs. 3-62915
- π^0 production from π^- p and pp collisions, charged multiplicity distribution using phenomenological model 3-62905

proton-proton scattering

- 1S_0 p-p potential, shape, phase shifts 3-78257
- angular distribution at high energies, hard core radius model 3-62881

proton-proton scattering continued

- diffraction, phenomenological compatibility of self-reproducing-cut Pomeron with ABCS mechanism 3-43155
- diffraction and production of uncorrelated pairs of resonances in high-multiplicity reactions 3-52051
- diffraction mechanisms and s-dependence of $d\sigma/dt$ at fixed t 3-40388
- diffractive dissociation at 24 GeV/c, factorizable diffraction excitation model estimate 3-43146
- elastic, 10 to 26 GeV, deuteron form factor from Glauber theory (Russian) 3-57343
- elastic, 2.5 to 5.15 GeV/c, 0.2 to 2.0 (GeV/c) 2 , polarisation 3-60027
- elastic, 290 to 450 MeV, meas. ang. distrib. from liquid target 3-74414
- elastic, 8-400 GeV, diffr. peak slope meas. 3-74434
- elastic, absolute cross-section meas., 500-2000 keV (German) 3-49231
- elastic, at large momentum transfer, agreement with $d\sigma/dt = s^{-n}f(t)$ under restrictions 3-49047
- elastic, changing slope of $d\sigma/dt$ at small $|t|$ in CERN data, multiple quark scattering 3-49022
- elastic, high-energy small angle, spatial extension of pion cloud in p hadronic matter distrib. 3-62879
- elastic, in region of Coulomb interference, slope parameter (Russian) 3-62883
- elastic, infinite energy, model description including spin 3-60031
- elastic, ISR data, Gribov's Reggeon calculus 3-74430
- elastic, moderate energy, scaling limit rel. to parton, field theory scaling 3-78192
- elastic, near 50 MeV, phase-shift analysis 3-70972
- elastic, scaling and kinematic variable n^2 3-57450
- elastic, slope, various models, multiparticle momentum correlation effect on angular distributions 3-60029
- elastic cross sections, magnitude of triple-Pomeron coupling 3-57398
- elastic differential cross section 30 GeV/c in extended bremsstrahlung model 3-67087
- elastic diffractive, shadow approach 3-57391
- elastic forward, 6-17.5 GeV/c, polarisation meas. 3-74429
- elastic high energy, distribution of absorption, correction term 3-67120
- elastic large angle, dual model with logarithmic trajectories 3-60026
- elastic large-angle, differential cross section, quark model and auto-modellism 3-62850
- elastic model-independent analysis of structure at $t \approx -1.1$, Regge shrinkage 3-78193
- elastic scatt. in Coulomb interference region, 1.1-1.7 GeV 3-40386
- final-state interaction in $^2H(p,n)pp$ reaction, scattering length determ. 3-71098
- forward elastic scattering amplitude, 50-5000 GeV, ratio of real to imaginary parts 3-49046
- forward scattering, high energy, analytic parametrization 3-78224
- forward spin-non flip amplitude by Ciulli-Cutkosky-Deo method 3-57427
- forward-angle, bremsstrahlung cross section at 156 MeV, relativistic and noncoplanar effects 3-67104
- geometrical scaling, forward differential, elastic and total cross sections 3-74427
- high energy, analysis using impact parameter representation, quark model 3-74433
- high energy, elastic, p layered substructure model explanation of dip 3-60028
- high-energy elastic, spin effects due to $X^0(960)$ meson exchange, Regge trajectory (Russian) 3-78194
- inelastic, charged multiplicity distribution 13-300 GeV/c, truncated gaussian, parton-like model 3-71017
- inelastic, high energy, massive boson production, gauge models 3-78208
- inelastic, multiplicity distrib., two-component model and Regge trajectory intercept. 3-54356
- ISR data, shadow scattering explanation, s-channel unitarity 3-67118
- lengths, determ. from $^2H(p,n)2p$ spectra 3-78337
- models reviewed, including Regge-pole, dual, Pomeron parametrizations and scaling models 3-71005
- multiparticle production cross-section, 50-300 GeV/c, model with SU(3) singlet uncorrelated fireballs 3-62910
- muon pair production, exact expression for mass spectrum 3-57358
- partial waves, lower bound for number necessary for exptl. analysis 3-43134
- rising cross-sections and real part of forward amplitude, ISR energies, dispersion relation calcs. 3-60050
- slope of cone, quasipole model 3-40387
- small-angle scatt., 290-570 MeV, differential cross section (French) 3-52033
- spin correlation parameters, 50 MeV 3-63030
- topological cross-section, phenomenological model 3-45918
- total cross section growth mechanism 3-57459
- total cross section increase in high-energy region, effect on slope parameter of diffraction peak 3-67147
- total cross section meas., in pure spin states, 3.5 GeV/c 3-67121
- total cross section rise, e.m. structure of proton and partons 3-67057
- p form factors, inelastic, determ. in multiparticle production processes 3-74436
- pp, <350 MeV/c, phenomenological models, cross section threshold behaviour 3-57395
- pp, elastic, 220 MeV, polarisation meas. 3-74412
- pp, elastic, at 25 and 40 GeV/c meas. differential cross sections and diffraction cone slopes (Russian) 3-67123
- pp, elastic at 25 and 40 GeV/c, differential cross sections and diffraction slopes 3-57424
- pp, elastic scattering, 5 GeV/c, backward and forward peaks 3-78189
- pp, elastic scattering, spectral function shape, Mandelstam analyticity 3-62882
- pp, missing mass spectra, Boson spectrometer obs. (French) 3-52050
- pp, s-channel resonance duality model explanation of exotic peaks and cross sections 3-74395

proton-proton scattering continued

- pp elastic scattering, spectral function shape, Mandelstam analyticity 3-62882
 pp forward elastic scattering amplitude, 50-5000 GeV, ratio of real to imaginary parts 3-49046
 pp forward scattering, high energy, analytic parametrization 3-78224
 pp \rightarrow nn, differential cross section, exchange degenerate Regge pole model 3-60033
 pp \rightarrow pN*, scaling and new kinematic variable n^2 3-57450
 pp partial waves, lower bound for number necessary for exptl. analysis 3-43134
 pp \rightarrow pp, 2.32 GeV/c, forward scattering amplitude, total cross section and s-channel resonance excitation 3-45912
 pp \rightarrow pp, high-energy wide-angle differential cross section in DRM, absence of universal behaviour 3-52043

proton scattering

- see also electron-proton scattering; neutron-proton scattering; nuclear reactions and scattering due to protons; pion-proton scattering; proton-deuteron scattering; proton-proton scattering
 Bethe phase shift, contribution from inelastic intermediate states (Russian) 3-67165
 Compton, non-forward using O(3,1) symmetry model 3-62836
 current proton scattering amplitude, reln. to light-cone commutators by spin-dependent FESR 3-51989
 elastic backward in reactions $\pi^+p \rightarrow p\pi$ and $K^+p \rightarrow pK$, test of theoretical models 3-57396
 meson-proton, target, frozen spin, 50 mK, meson spectrometer frozen spin polarised target 3-77612
 recoil counters and multiple scattering, theory 3-59641
 ep deep inelastic, review 3-54321
 K⁻ elastic, at 25 and 40 GeV/c meas. differential cross sections and diffraction cone slopes (Russian) 3-67123
 K_p, K_f-K_f, regeneration 3-40332
 K⁻p, elastic at 25 and 40 GeV/c, differential cross sections and diffraction slopes 3-57424
 K⁻p, missing mass spectra, Boson spectrometer obs. (French) 3-52050
 K⁻p, s-channel resonance duality model explanation of exotic peaks and cross sections 3-74395
 K⁻p elastic, 3.59 GeV/c, differential cross section, forward peak 3-78191
 K⁻p elastic, crossing even, strong central absorption prescription 3-74431
 K⁰p \rightarrow $\pi^+ \Lambda^0$, differential cross sections for near 90° scattering, 1.0 to 7.5 GeV/c 3-49041
 K⁰p \rightarrow $\pi^+ \Sigma^0$, differential cross sections for near 90° scattering, 1.0 to 7.5 GeV/c 3-49041
 K⁺p, elastic complete ang. distrib. meas., incident momenta 1368 to 2259 MeV/c 3-60032
 K⁺p backward elastic scattering 1.5 GeV/c parity doublets and Mandelstam-Sommerfeld-Watson transformation 3-71007
 K⁺p large angle elastic scatt. at 13.8 GeV/c 3-40389
 K⁺p, elastic scattering, 5 GeV/c, backward and forward peaks 3-78189
 K⁺p, elastic scattering, spectral function shape, Mandelstam analyticity 3-62882
 K⁺p backward elastic, 1.5-7.0 GeV/c, existence of Z₁* 3-43141
 K⁺p elastic forward scattering 6-17.5 GeV/c, polarisation meas. 3-74429
 K⁺p forward B amplitude determ., hyperon coupling const. 3-57425
 K⁺p forward elastic scattering amplitude, 50-5000 GeV, ratio of real to imaginary parts 3-49046
 K⁺p forward scattering amplitudes, pole extrapolation 3-74424
 K⁺p partial waves, lower bound for number necessary for exptl. analysis 3-43134
 K⁰p \rightarrow K⁰p, differential cross sections for near 90° scattering, 1.0 to 7.5 GeV/c 3-49041
 ν p deep inelastic spin-dependent, determ. of sum rules in SU₂, bilocal algebra 3-62812
 ν _pp \rightarrow ν _pp, test of Weinberg model at CERN 3-66964
 pd, backward inelastic at 1.0 GeV, nucleon and isobar exchange effects 3-49038
 pd backward scattering, 1.0-1.5 GeV, rescattering effects 3-40374
 K⁺p elastic large-angle collisions at high energies, rescattering model 3-67117

proton spectra

- A=12 to 209, 30 to 60 MeV, proton bombardment comparison with intranuclear cascade model 3-74588
 auroral proton glow, energy spectra and pitch angle of electrons and protons 3-42005
 compound nucleus decay, A=56-66 test of independence hypothesis and isospin conservation 3-71093
 delayed fine structure statistical fluctuations rel. β^+ transition matrix elements (Russian) 3-40467
 delayed proton and alpha precursors, decay properties 3-54439
 diffractive-excitation model calculation, for reaction pp \rightarrow p + anything 3-74466
 inclusive, three-reggeon description 3-62906
 inclusive charged particle production and inelastic proton spectra at CERN ISR 3-71027
 inclusive single-particle in pp interactions at 102 GeV/c 3-71020
 isobaric analogue resonances, proton decay, multiple-particle mechanism (Russian) 3-52155
 nuclear track emulsion meas., artificial satellite of Cosmos series, radiation hazards, 200-400 km, 8 BeV (Russian) 3-65607
 photoprotons, decay of isobaric analogue states, angular distribution (Russian) 3-57477
 plasmopause, proton spectra and fluxes in 1.0-300 keV range, satellite obs. 3-73365
 radiation belt protons, omnidirectional energy spectra below 750 km altitude 3-69719
 ring current protons, energy spectra and pitch angle distrib. during 1971, December 17 storm 3-73363
 solar cosmic rays, calc. near Earth and at source for flares in 1956-1967 period (Russian) 3-65562
 threshold effects from (d,p) reactions at the neutron threshold 3-71121

proton spectra continued

- p-hadron collisions, limiting behaviour of inclusive baryon spectra 3-74460
 pd \rightarrow ppn at 600 MeV, polarisation and energy spectra with account of rescattering (Russian) 3-67106
 pp inclusive reaction, proton leading-particle spectrum at 14, 19, 27 GeV/c, Regge Regge Pomeron model 3-67150
 pp \rightarrow p π m π , properties of π and p momentum spectra in multiperipheral scheme (Russian) 3-40400
 π p \rightarrow p π m π , properties of π and p momentum spectra in multiperipheral scheme (Russian) 3-40400
¹⁹⁷Au(n,p), E_n=14 MeV, proton spectra anal. 3-67319
¹⁴C(d,p)¹³C, analysis with magnetic spectrograph rel. to ¹³C states determ. 3-67208
⁶³Cu(α ,p)⁶⁶Zn 3-78346
⁵⁴Fe(α ,p)⁵⁷Co, 23 MeV, selective population of highly excited states 3-78346
⁵⁴Fe(α ,p)⁵⁹Co 3-78346
⁵⁷Fe(α ,p)⁶⁰Co 3-78346
¹H(d, 2p)n, 12.6 MeV, two-dimensional coincidence spectra, p-n final state interaction 3-40477
²H(n,p)n, 14 MeV, spectra meas., validity of impulse approx. for scattering length 3-78339
⁶Li(γ ,p)⁵He at E_p=60 MeV, excitation of (1p)⁻¹, (1s)⁻¹ hole states 3-71100
⁷Li(γ ,p)⁶He, 60 MeV, excitation of residual hole states 3-71100
²¹Mg, β^+ -delayed proton decay, half-life meas. 3-60128
⁵⁸Ni(α ,p)⁶¹Cu 3-78346
⁶¹Ni(α ,p)⁶⁴Cu 3-78346
³¹P, photoprotons in giant reson. regions (γ , p₀), (γ , p₁) reactions 3-54458
³¹P(γ , p₀)³⁰Si, photoprotons in giant reson. region, for ³¹P 3-54458
 π p \rightarrow p + anything, 10.0 and 15.5 GeV/c, meas. of single particle distrib. 3-71031
³⁵S(α ,p)³⁵Cl, obs. states of ³⁵Cl from proton spectra meas., 20 MeV 3-62947
³²S(γ , p)³¹P, photoprotons in giant reson. region, for ³¹P 3-54458
¹⁰⁹Tc, delayed proton emission, statistical model analysis (Russian) 3-57497
¹¹³Xe, β -delayed proton emission energy spectrum, nuclear emulsion method 3-54438

protonium see protons**protonosphere see upper atmosphere****protons****see also cosmic ray protons**

- 76 GeV synchrotron, operation at high intensities 3-56751
 bunched proton beams, neutralization 3-57267
 crystal lattice scattering, shadow effect 3-75553
 crystallography, protonograms from arbitrarily ordered crystals (Russian) 3-63922
 e.m. form factor determ. at squared four-momentum transfers up to (GeV/c)² 3-62823
 form factor, dipole fit, elastic ep scattering 0.05-0.30 (GeV/c)² 3-67022
 form factor, magnetic, derived from ep elastic scattering data 3-59970
 gyromagnetic ratio, progress report 3-61982
 inclusive production in pp interactions at 303 GeV/c, cross section determ. 3-74447
 inner radiation belt, equilibrium equatorial proton flux using albedo neutron measurements 3-69683
 Lawrence Berkeley laboratory 184-in synchrocyclotron proton beam intensity improvements 3-56746
 mass difference, proton-neutron, contributions based on vector meson dominance 3-59957
 multigramma events search at high energy at ISR in pp collisions 3-71026
 nuclear, spin-orbit coupling, quasi-free scattering determ. 3-60030
 radiography, as diagnostic tool 3-66030
 semiconductor proton recoil counters with radiator of finite thickness response function calculation 3-48532
 stability, reln. to limits on tachyon masses 3-43168
 structure, quasi-potential description of proton-electron interaction 3-59967
 substructure, layered, explanation of dip in high energy pp scattering 3-60028
 therapy, prospects 3-59444
 n-p diff. in gauge theories of weak and e.m. interactions, cancellation of log. divergences 3-59964
 n-p mass difference, calc. from isospin gauge group models 3-59961
 n-p mass difference, cancellation of logarithmic divergences in unified theory of weak and e.m. interactions 3-70914
 np bremsstrahlung, one-pion-exchange-current contrib. 3-54396
 p-n mass difference, convergence of deep inelastic contribution to Cottingham formula 3-52005
 p-n mass difference, reln. to neutral weak currents, Weinberg's model 3-51997
 p-n mass difference in gauge theories of weak and e.m. interaction 3-74367
 Ge, multiple scatt. and planar dechannelling of MeV protons 3-52655
 Si, multiple scatt. and planar dechannelling of MeV protons 3-52655

proving, theorem see theorem proving**pseudopotential methods**

- alkali alloys, dilute, residual resistivity, effect of lattice strain 3-44055
 alkali metal alloys, zero model in pseudopot. theory, solid solubility limit (Russian) 3-80245
 alkali metal and alkaline earth metal alloys, liq., enthalpy of mixing (German) 3-79504
 alkali metals, Krasko-Gurskii model, cohesive energy and mech. props. calc. 3-75499
 alloy, ordered, of noble metals, total electronic energy (Russian) 3-79614
 amorphous semiconductors, KKR approach to electronic spectra 3-64277

pseudopotential methods continued

- band structure, calc. for elemental semicond. and their alloys 3-58212
- band structure, calc. for II-VI semiconduct. and their alloys 3-58212
- band structure and Fermi surface, calc. for Al, Pb, Li, Na and K 3-52779
- band structure calculation, rel. to photoemission and pair scatt. in GaAs 3-69137
- binding energy and stable crystal structure calcs. 3-41115
- conductor, pseudopot. in mag field (*Russian*) 3-72310
- dialkali halide systems, chem. reactions, semiempirical pseudopot. surfaces 3-44715
- electronic charge density calc. for GaSe (*German*) 3-50123
- electronic energy bands calc. for PbI_2 3-43999
- electronic energy bands calc. for SnS_2 and SnSe_2 3-43998
- f.c.c. and h.c.p. stacking sequence energies from asymptotic potential approx. 3-54973
- form factors for Al, rel. to electron-impurity scatt. pot. 3-44050
- form factors for Al and In, rel. to Fermi surface stress depend. 3-43990
- group IV semiconductors, model pseudopotential calc. of electronic and bonding props. 3-58215
- Hartree-Fock equation with correlation pseudopotentials (*Russian*) 3-54561
- interionic potentials, simple metals, interatomic force constants, elastic constants 3-68193
- interstitial defect, (1/2, 1/2, 1/2) in Al, relax. and formation energy, calc. 3-54956
- liquid metals, electronic density of states, effective mass, Knight shift 3-50114
- local model pseudopotential optimization (*Russian*) 3-63977
- many-band calcs. of impurity states in Si 3-44032
- metal, bulk moduli and pseudopotential perturbation theory 3-46657
- metal, driving forces for electromigration, pseudopotential based theory 3-41047
- metal, effective interionic pair potentials (*German*) 3-63972
- metal, monovalent, elec. cond. behaviour at melting pt. (*Russian*) 3-79664
- metal, non-transition, estimate of energies by pseudopotential method 3-60682
- metal, rel. to theory of vacancy-impurity interactions 3-64030
- metal, simple, binding energy, compressibility, pseudopot. calcs. 3-54941
- metals, electronic exchange and correlation effects, equilib. lattice constants and bulk properties 3-46780
- metals, Fermi energy depend. on atomic number 3-68542
- metals, multi-ion interaction, asymptotically exact form 3-72301
- noble metal, generalized magnetic pseudopotential 3-44195
- ordering behaviour, calc. for Cd-Mg(Zn) alloys 3-69195
- positive ions, general model pseudopotential in closed analytic form 3-67635
- quantum structure of solids 3-55565
- semiconductor, impurity states calcs. using screened local pseudopotential 3-44035
- semiconductors, III-V and group IV solution of secular determinants in pseudopotential method 3-60855
- shallow donor ground states, pseudopot. theory, effective mass 3-50146
- surface electron states calc. 3-55329
- surface electronic states and complex band structure calc. (*French*) 3-72395
- Ag, calc. of twin boundary elec. resist. 3-44056
- Ag, second-order elastic shear consts., pseudopot. calcs. 3-68308
- Al, electrical resistivity of voids 3-44054
- Al, electronic properties, study by considering electron gas screening, dielectric function effects 3-44058
- Al:Sn, Cu, impurity-impurity interaction, pseudopot. calcs. 3-54976
- Au, second-order elastic shear consts., pseudopot. calcs. 3-68308
- Ba, phonon frequencies and binding energy calcs. 3-46602
- Be, dispersion curves, simple pseudopot. theory breakdown, expt. evidence 3-40993
- Ca, f.c.c.-b.c.c. phase transition rel. to s-d hybridisation 3-58128
- Ca, phonon frequencies and binding energy calcs. 3-46602
- CdSnAs_2 , pseudopot. calc. of band struct. at points in Brillouin zone, electrorefl. spectra 3-43996
- Cu, second-order elastic shear consts., pseudopot. calcs. 3-68308
- Cu-Co alloys, electron lifetime and Dingle-Robinson temps. 3-44063
- Cu-Ni alloys, electron lifetime and Dingle Robinson temps. 3-44063
- Hg alloys liquid, form factor, resistivity, anomalous thermopower, experimental determination 3-50104
- In, liquid, n.m.r. and n.q.r. properties, temp. depend. of Knight shift and nuclear spin relaxation rate 3-47169
- $\text{InSb}_{1-x}\text{Bi}_x$ alloys, theoretical estimate of band gap (*French*) 3-79632
- Li, calc. of charge densities, comparison with self-consistent results 3-75699
- Li, phonon freq. along symmetry directions, model pseudopotential calc. 3-68351
- Li phonon dispersion, influence of conduction band-core exchange and correlation on pseudopotential calc. 3-58090
- Mg, electrical resistivity of voids 3-44054
- Na, calc. of charge densities, comparison with self-consistent results 3-75699
- Na, electrical resistivity calc. from lattice dynamical structure factors 3-55243
- Na, electrical resistivity of voids 3-44054
- Nb, electronic struct. and density of states, empirical pseudopot. method calcs. 3-55192
- Pb, model for electronic prop. calc. in solid and liquid states 3-64279
- PbS , electronic band structure and optical props. 3-58523
- PbSe , electronic band structure and optical props. 3-58523
- PbTe , electronic band structure and optical props. 3-58523
- Si band structure, self-consistent pseudopotential 3-58216
- SnS_2 , SnSe_2 , energy band calcs. 3-41138
- Sr, f.c.c.-b.c.c. phase transition rel. to s-d hybridisation 3-58128
- Sr, phonon frequencies and binding energy calcs. 3-46602

pseudopotential methods continued

- Zn Fermi surface, calc. of stress depend. 3-41127
- ZnGeP_2 , band struct. and reflectivity spectra, empirical calc. 3-41135
- ZnO , band structure, density of states and reflectivity computation 3-64292
- ZnS wurtzite and zincblende structures, electronic charge density 3-41117
- PSK** see phase shift keying
- psychological optics** see vision
- psychology**
 - colour perception 3-45314
 - mechanics of individuality in nature rel. to barriers and cells 3-73622
 - visual recognition/detection, symposium, USA 1973 3-70121
- PTC thermistors** see thermistors
- pulp industry** see paper industry
- pulsars**
 - see also neutron stars
 - 8.4 GHz detection of 9 objects 3-59359
 - 15.1 GHz detection of 5 objects 3-59359
 - 408 MHz pulsar search with Bologna Cross radiotelescope, sensitivity and results 3-70052
 - accreting magnetic neutron star, radiation beaming rel. to X-ray pulsars 3-45083
 - Alven waves effect of relativistic mass of magnetic fields 3-69811
 - CP 0950, periodic analysis of arrival times in delayed cosmic-ray coincidences 3-53580
 - CP 1133, periodic analysis of arrival times in delayed cosmic-ray coincidences 3-53580
 - Crab Nebula, origin of h.f. radiation 3-61876
 - Crab Nebula, relativistic particle and magnetic field distributions, synchrotron radiation mechanism 3-77166
 - Crab pulsar and energy spectrum of relativistic electrons in nebula 3-70042
 - distance estimates from 21 cm. absorption spectra of 8 examples 3-69988
 - electron gas ferromag. state to maintain strong mag. fields, density of states calc. 3-51256
 - emission mechanism for radio, optical and X-ray emission 3-45156
 - energy generation from gravitational collapse via rapid rotation and magnetic fields 3-44991
 - evolution, phases and reln. to distance comment 3-51367
 - fluctuation spectra and generalized drifting-subpulse phenomenon 3-51365
 - fluxes and spectra of 12 pulsars, simultaneous six-frequency obs. 3-48069
 - frequency distribution function, according to age and lifetime, astronomical phenomena 3-76951
 - Galactic centre, radio pulse search 3-69978
 - intensity fluctuations, obs. of 5 objects 3-59358
 - interstellar medium props. determ. from pulsar obs. 3-70037
 - interstellar scintillation patterns of pulsars rel. to density irregularities of interstellar medium 3-48118
 - limiting polarization of radiowave emission 3-42216
 - magnetic field time variations rel. to detailed observations 3-51366
 - magnetosphere model, partial differential eqn. for rotating star in aligned magnetic field 3-69984
 - magnetosphere model of Goldreich-Julian 3-77121
 - massive star explosions, cosmic ray origin and nucleosynthesis 3-80890
 - MP0736-40, upper limit to X-ray flux 3-61830
 - MP0835-40, upper limit to X-ray flux 3-61830
 - new, 406 and 410 MHz obs. of 13 objects 3-56407
 - NO 0532, expected radiative var. rel. to angular velocity changes 3-77124
 - nonlinear effects due to bending of a weak ionised D-type front (*Russian*) 3-53687
 - NP0532, arrival times of 100-400 keV pulses 3-53689
 - NP 0525, X-ray obs. 3-61829
 - NP 0532, optical polarisation, relativistic vector model 3-69986
 - NP 0532, optical pulsations rel. to detection of pulsed high energy gamma rays from Crab Nebula 3-48074
 - NP 0532, optical pulses coincident with pulsed high energy γ -rays in Crab Nebula 3-81128
 - NP 0532, optical timing obs. 3-53686
 - NP 0532, periodic gamma ray emission in 10^{11} - 10^{12} range 3-73527
 - NP 0532, relativistic vector model, observational results and fits 3-69987
 - NP 0532, synchrotron source model rel. to optical emission 3-69971
 - NP 0532, variability of dispersion and scatt. 3-61827
 - NP 0532, X-ray obs. 3-61829
 - optical, search in extragalactic supernovae 3-65909
 - origins rel. to C ignition in degenerate C cores (*Polish*) 3-45090
 - p-n junctions in magnetospheres 3-81124
 - parameters, improved meas. for 15 objects 3-61828
 - physics course 3-77348
 - polarisation of pulses, observations between 110 and 1400 MHz 3-77123
 - properties, optical and radio, interpretations 3-65910
 - PSR0329+54, pulse profile changes at 10.7 GHz 3-69989
 - PSR0833-45, upper limit to X-ray flux 3-61830
 - PSR 0301+19, periodic power fluctuations at 430 MHz, spectrum analysis 3-42215
 - PSR 0329+54, pulse profile variations at 2695 MHz 3-77120
 - PSR 0531+21, optical obs. of steady and discontinuous changes and period of rotation (*German*) 3-81125
 - PSR 0531+21 giant pulses at 146 MHz, analysis of polarization 3-69985
 - PSR 0809+74, sub-pulse obs. at 81.5 and 151 MHz 3-56406
 - PSR 0833-45, X-ray structure observed from Uhuru 3-73530
 - PSR 0950+08, radio spectrum of short subpulses 3-48067
 - PSR 1919+21, notches in average pulse profile 3-45151
 - PSR 2020+28, periodic fluctuations at 430 MHz, spectrum analysis 3-42215
 - PSR 2021+51, assoc. with supernova remnant HB 21 indicated by 21 cm obs. 3-65894
 - pulses with wide integrated profiles rel. to pulsar radiation and models 3-45157

pulsars continued

- quakes rel. to model of solid planet and neutron stars 3-42168
- radio emission mechanism based on Chiu-Canuto model 3-59357
- rotating neutron star model and observational evidence, review 3-53688
- rotation measurement, galactic mag. field, dependence on galactic coordinates 3-48071
- signal processing techniques 3-65911
- slow intensity variations 3-77122
- slowdown, MHD theory of rotating neutron stars under external torque 3-69943
- spatial distrib. in Galaxy rel. to supernovae 3-42214
- stimulated linear accelerated radiation, possible pulsar emission mechanism 3-48070
- stimulated linear acceleration radiation, Einstein coeff. method, for electrons 3-73528
- subpulse time scales and intensity fluctuations in 74-318 MHz range 3-48068
- supernovae remnant-pulsar genetic relationship 3-61831
- supernovae remnants search for compact radio sources at 53-318 MHz 3-45155
- synchrotron radiation, soft photon emission, domination by radiation damping effects 3-70917
- synchrotron radiation from cosmic sources, stimulated amplification 3-53680
- Vela, giant glitches rel. to neutronic quantum cryst. formation 3-56408
- very long baseline interferometric obs. 3-65908
- weak continuum radio emission from vicinity of 18 pulsars rel. to haloes 3-42217
- X-ray emission rel. to X-ray sources 3-81126
- X-ray UHURU satellite obs. 3-51368

pulse amplifiers

- gaseous molecular amplifiers, short-pulse, output energy relaxation losses 3-70809
- nuclear spectroscopy 3-73882

pulse amplitude analysers *see pulse height analysers***pulse circuits**

- see also digital circuits; modulators; pulse generators; pulse shaping circuits*
- amplitude recorder, of coincidence multiplicity and number of inputs, nsec range 3-53989
- BD-9 integral discriminator, fast n scintillation counter, γ -radiation pulse elimination 3-70387
- gas laser excitation 3-77543
- interference-suppressing device, for radiometers 3-56634
- linear gate circuit, for photomultiplier pulses 3-40031
- linear scanistor, for processing graphical information 3-51727
- Penning discharge formative time 3-43706
- p.r.f. discriminator with complete harmonic suppression 3-48545
- sampling, 0.2 to 10.0 V range 3-40032
- shaper, integrating discriminator, AND-NOT, AND-OR-NOT for time and amplitude analysis 3-53987

pulse-code modulation

- stochastic-ergodic measuring techniques, comparison, cross-correlation function measurement (German) 3-70258

pulse-code modulation links

- optical repeater, using GaAs, laser, error-rate obs. 3-66897

pulse control systems *see sampled data systems***pulse generators**

- see also multivibrators*
- birefringence, electrical, experimental apparatus, high ionic strength solutions, Kerr effect 3-62180
- burst shaper, examination of hearing capability and echo location of dolphins 3-73935
- for control of camera with image converter 3-56689
- electro-optical shutter control, Q-switching of laser 3-73791
- high voltage, for streamer chamber (French) 3-42654
- impulse generator, discharge, damping resistors, calculation 3-66718
- klystron system for pulsing of ion beams in tandem accelerator (German) 3-59633
- n.m.r. spectroscopy, high speed digital control 3-66296
- radiosonde recorder, calibration, multi-pulse generator 3-80857
- three-electrode Blumlein line for streamer chamber 3-51728
- GaAs diode laser fast current drive circuit 3-45807

pulse height analysers

- information storage and handling, operation, appl. to e.p.r. meas. 3-73822
- Mossbauer digital spectrometer, multichannel analyser controlled 3-70438
- multichannel, for unfolding neutron spectra from proton recoil data 3-51734
- radiation intervals distribution meas. 3-62257
- real time, 448000 closed, multiparameter, small programmed computer 3-62227
- ^{234}Th β -decay, precision meas. of γ -ray energies 3-74539

pulse modulation

- see also modulators; pulse-code modulation*
- reactivity of nuclear reactor, rel. to kinetic tests on reactors using cross-correlations method (German) 3-67483

pulse motors *see stepping motors***pulse oscillators** *see pulse generators***pulse shaping circuits**

- discharge lamps, electrodeless, chopping in very short times, circuit and method, optical pumping 3-45507
- for preliminary analysis of spectrometric signal 3-53988
- unitized output shaper, in nuclear electronic circuits 3-56965

pulse width modulation

- ohmmeters, digital, designed for resistances of transducers for nonelectrical quantities 3-70326

pulverised coal *see pulverised fuels***pulverised fuels**

- see also coal*
- reaction kinetics on surface, linear nonstationary effects, instability (Russian) 3-47545

pulverized fuels *see pulverised fuels***pumping** *see pumps***pumping (optical)** *see optical pumping***pumps**

- see also vacuum pumps*
- bellows pump for pumpover of gases, construction, capability 3-77415
- condensation nuclei, production by peristaltic pump friction on rub and silicone 3-46674
- electromagnetic, for liquid metals in fast reactors 3-43275
- e.m. pump, method of measuring the pressure drop (Russian) 3-59566
- gas circulating pump, positive displacement 3-66479
- peristaltic pumping, inertia and streamline curvature effects 3-52
- power-plant pump, design considerations for noise reduction 3-42476
- pressure, up to 1 kbar 3-53866
- single stage radial for SNR 300 reactor, cavitation and oscillation tests (German) 3-74714
- He, gas filtering pump fluid vapours, ceramic filter, method 3-77720

punched paper tape equipment *see punched tape equipment***punched tape equipment**

- X-ray diffractometer automatic information output 3-73915

Purkinje effect *see vision***push pull amplifiers** *see differential amplifiers***push pull microphones** *see microphones***p.w.m.** *see pulse width modulation***pylons** *see poles and towers***pyroelectricity**

- alkali halides, paraelec. behaviour of OH^- ions, electrooptical and electrocaloric studies 3-41476
- detector as basis for chopper-stabilized null radiometer 3-7739
- insulating thin film, surface pyroelec. effect 3-55529
- m.i.m. ferroelectric structure, pyroelectric effect (Russian) 3-72577
- nonlinear optical crystals, applications, review 3-40288
- piezoelectricity, pyroelectric contributions 3-68933
- polyvinylfluoride optical detectors, mathematical model for response analysis 3-77393
- polyvinylidene fluoride, pyroelectricity as function of poling treatment 3-41486
- PVC, pyroelec. currents due to temp. and pressure changes obs. 3-47220
- transient thermal analysis, rel. to radiation detectors 3-68935
- triglycine sulphate:L-alanine, high internal bias fields, pyroelec. detector applications 3-44376
- triglycine sulphate: Pd^{2+} , single cryst. growth, domain struct. 3-55528
- triglycine sulphate, laser damage rel. to radiation detector applications 3-66859
- triglycine sulphate, temp. dependence of pyroelectric volt. response step i.r. signals 3-44377
- $\text{BaTiO}_3\text{:Fe}$, Curie pt. region behaviour (French) 3-68934
- $\text{Gd}_2(\text{MoO}_4)_3$, detection props. 3-44375
- KH_2PO_4 , polarisation nonlinearity, temp. depend. meas. 3-72
- LiInS_2 , electrooptic and pyroelec. coeffs., linear relationship 3-61029
- LiInSe_2 , electrooptic and pyroelec. coeffs., linear relationship 3-61029
- $\text{Sr}_{1-x}\text{Ba}_x\text{Nb}_2\text{O}_6$, preparation and props. of ferroelec. single crystals 3-80170

pyrolysis *see chemical reactions***pyromagnetic effects** *see magnetothermal effects***pyrometers***see also temperature measurement*

- high temp. meas., optimal utilization of redundant inform. in therm radiation 3-70290
- infra-red, selective absorption, high temperature monitoring of wall gases from industrial furnaces 3-70284
- infrared photoelectric pyrometer, f.p. meas. of Cu 3-46698
- i.r., testing devices, displays, image converters, new instruments E.Europe, review (German) 3-73685
- i.r. pyrometer, temp. monitoring, train wheels, jet engine rotors 3-45435
- micro, with i.r. microscope and scanning device, for small surface areas (German) 3-59561
- optical pyrometry, analytical procedures, errors (German) 3-483
- polyvinylfluoride pyroelectric detectors, mathematical model for response analysis 3-77393
- three-colour, for high temp. meas. (Russian) 3-51552
- visual, brightness values calc. in mesopic range (German) 3-566

Q *see Q-factor***Q-factor**

- electro-optical modulation, solid state laser modulator components (Russian) 3-57230
- e.s.r. cavity, variation causing line broadening 3-42616

Q-factor measurement

- physical quantities meas. from natural vibrations attenuation of oscillator circuit (Czech) 3-56695

Q-meters

- metallic powders, grain size, specific resistivity, temp. depend., measurement method 3-62179

Q power factor *see Q-factor***Q-switching***see also lasers*

- electro-optical shutter, power supply block 3-73791
- giant laser pulse generation, reproducible, using optically regenerative Q-switch 3-66263
- laser resonator Q-factor, switching by stimulated Mandelstam Bragg scattering 3-70836
- pulsed laser switching using exploding film Q-switch 3-45785
- Q-switching resonator laser, dynamics (Russian) 3-62724
- ruby laser, decomposition of photographic materials, one-step imaging 3-59607
- ruby pulsed laser, with Q-switched multiple cavities, characts. 3-40264
- semiconductor homostructure and heterostructure lasers 3-5423
- solid laser, spikes due to self Q-switching 3-40266

Q-switching continued

- superhigh-pressure gas breakdown by Q-switched lasers, threshold minima 3-60518
- variable path cell, Q-switch attachment, Laser Mirospectral Analyzer, VEB Carl Zeiss, JENA, optimisation of anal. results 3-51766
- CO laser, operating at 5.307 μ , using magnetically tuned NO 3-66812
- CO₂ laser, Q-switched pulse duration, rot. relax. effect 3-66804
- N₂O laser, self-mode locking, rotating mirror Q-switching 3-78015
- Nd: glass laser, single freq. operation 3-45805

QC *see quality control***quadratic programming**

- rigid viscoplastic bodies, finite element analysis of dynamics 3-66564

quadrupole crystal field interactions *see crystal hyperfine field interactions***quadrupole lenses** *see electron lenses; electrostatic lenses; magnetic lenses***quadrupole moments**

- see also atomic electric moment; molecular moments; nuclear electric moment; nuclear quadrupole resonance*
- atomic dynamic polarisabilities, dipole-dipole and dipole-quadrupole contributions to dispersion energy calc. 3-43386
- 4-chloronortricyclene, ³⁵Cl nuclear quadrupole coupling constant, microwave spectra 3-71567
- 2-chlorothiophene, microwave spectra, quadrupole coupling and rotational constants 3-43463
- cyanocyclobutane, μ -wave spectrum, dipole moment quadrupole coupling consts. and conformation study 3-40634
- cyclic molecules, quadrupole moments and diamag. susceptibilities calc. 3-63377
- electric, evaluation from exptl. hyperfine interaction constants 3-74803
- inert gases, at. quadrupole moments of excited states 3-71364
- molecule, maximum overlap criterion approach 3-78651
- strontium formate dihydrate, deuterated, quadrupolar consts. from deuteron mag. reson. 3-64569
- Au, muonic, fund. level (French) 3-54603
- Bi₂Fe₂O₉, antiferromagnetic, transition temp., magnetisation, quadrupole moments, Mossbauer obs. 3-79952
- CH, valence excited states, props. 3-71513
- D₂, electric field gradient and magnetic spin-spin interactions 3-43438
- Fe(III) complex, basic carboxylate, effect of asymmetric Hamiltonian on Mossbauer spectra 3-79955
- GeO magnetic susceptibility anisotropy, mol. g_J-factor, quadrupole moments (German) 3-71539
- H₂ electric field gradient and magnetic spin-spin interactions 3-43438
- HD, electric field gradient and magnetic spin-spin interactions 3-43438
- N₂ r.f. spectrum of metastable (A³ Σ_u^+) state, fine struct., mag. hyperfine struct., electric quadrupole consts. for 13 vibrational levels 3-40635
- NCN₃, microwave spectra, anal. four nuclear quadrupole problem 3-78819
- N₂O, far-i.r. absorpt. and quadrupole moment determ. 3-74999
- O₂, determ. from collision broadened rot. linewidths of acetaldehyde 3-67834
- PbO magnetic susceptibility anisotropy, mol. g_J-factor, quadrupole moments (German) 3-71538
- PbO magnetic susceptibility anisotropy, mol. g_J-factor, quadrupole moments (German) 3-71539
- SnO magnetic susceptibility anisotropy, mol. g_J-factor, quadrupole moments (German) 3-71538
- ZnO:Li, photo-induced persistent internal quadrupole moment 3-46876

quality control

- see also reliability*
- electronic components, in Europe 3-39849
- instrument manufacture, mathematical analogue with LC oscillator (German) 3-53827
- Lamb wave u.s. bond inspection, airframe struct. 3-47512
- measurement process performance and assurance programmers 3-48331
- meteorological data 3-59092
- national standards and quality assurance, dependence 3-66129
- nuclear fuel rod, gamma scan system, enrichment, fuel column density, uniformity, ²³⁵U content meas. 3-66320
- nuclear reactor fuel, structural materials, reactivity testing, quality control 3-63210
- nuclear reactors, quality assurance and in-service inspection 3-67401
- petrochemical plants by production analysis equipment (German) 3-66456
- radioactive material packaging licensing and analytical techniques of evaluation 3-67413
- radioactive sterilisation of doses of protective and steroid hormones (Italian) 3-54050
- X-ray analysis, clinical chemistry, pharmacology (Italian) 3-66409
- Al-Mg (AMG6), quality rating, macroscopic failure diagrams effect of stress on crack length 3-44608

quality factor *see Q-factor***quantic theory of chemical binding** *see bonds (chemical)***quantisation**

- bosons and fermions, product vector basis and occupation-number basis in Fock space 3-48767
- canonical field quantization in Riemannian space-time, nonuniqueness 3-54261
- charged π_2 field interactions, quantisation, consistency problem 3-66934
- conjugate pair of preferred fields interactions with spinor field, operator relns. in Heisenberg picture 3-74311
- digital correlation spectrometer for multi-level quantisation, radioastron. appl. 3-70076
- elastic continuum, one-dimensional, detailed wave eqn. for classical and quantum mechanics 3-59994
- few-body problem in nonrelativistic field theory 3-67224
- Feynman's path integration method 3-48766

quantisation continued

- field models of particles, a generator, centrosymmetric metrics 3-66660
- generalised, reformulation of fundamentals of microscopic physics, comments 3-48748
- generalised, reformulation of fundamentals of microscopic physics (French) 3-48749
- gravitation, as self-interacting massless spin-2 field theory, perturbation calcs. 3-45720
- gravitational field, covariant gauges and point sources 3-57133
- gravitational field model of non charged particle, OK₁ model 3-66659
- infinite component wave equation, causal ghost-free covariant harmonic oscillator model 3-48984
- Kepler's third law and possibility of quantized planetary and satellite orbits (Russian) 3-44982
- Lagrangian, non-linear, quantisation, point mechanics and scalar field cases 3-62774
- Lagrangians, equivalent, in generalized mechanics 3-48763
- light-cone, unitary transformations relating current to constituent quarks 3-70942
- light-cone quantisation of dual models and structure functions 3-51978
- local field theory of dual string 3-54329
- massive spin one vector field in external potential, causality Lorentz invariance 3-57289
- massive vector field, spontaneously broken gauge theory, gauge transformations of propagation 3-74310
- massless relativistic string, light string, quantum dynamics 3-45891
- massless spin 1/2 eqn. neutrinos, unusual group of external symmetries 3-40310
- Maxwell field with three polarisation directions, quantisation 3-66992
- Minkowski metric for multidimensional geometry in quantal units, light-cone relations 3-51817
- m.o.s. structure, inversion layer quantisation, exptl. verification, temp. range 25-75 K 3-55339
- non-linear fields, energy-density commutation relation, integrability condition 3-45847
- null-plane field algebra, Dirac's canonical quantisation method, scaling relations 3-62787
- quantum crystals, harmonic single-particle basis, transformation to self-consistent harmonic approximation 3-48760
- relativistic wave equations for zero-mass particles with invariant helicities 3-45843
- relativity theory and quantization of action (French) 3-57135
- Schrodinger, generalised, extension to include classical counterparts 3-74090
- skew-symmetric field quantisation, A₁ and ρ mesons from violation of local Lorentz invariance 3-48986
- spin-optimized SCF methods in second quantization formalism (French) 3-57617
- spinor field, constant curvature space-time, limit to quantised field in the flat world (Russian) 3-48988
- string of spinning material, quantisation, Hamiltonian and Lagrangian formulation 3-66930
- super-quantisation in construction of unitary S-matrix 3-59930
- unified field model of charged particle 3-66661
- Weyl quantisation rule from functional integral representation of operators 3-48756
- He, rotating, macroscopic spatial quantization of angular momentum, expt. evidence 3-79539

quantitative analysis *see chemical analysis***quantum chemistry**

- alkali metal atom, excited, fine structure transitions in collisions with rare gas atoms 3-78513
- benzyl-type radicals, methyl substitution effect on electronic struct. and spectra 3-78731
- charge-conserving integral approxs. in ab initio calcs. 3-57616
- chemical SN2 reactions, reaction path calc. by ab initio LCAO-MO-SCF method 3-55954
- chemionisation of H₂ by He(2-3S) metastable atoms, potential energy surface calc. 3-78902
- collinear electronically non-adiabatic reactions, quantum mechanical formulation 3-69453
- diatomic molecule, virial theorems, adiabatic representation 3-78670
- diatomic molecules, Born-Oppenheimer approx. corrections and electronic effects on isotopic exchange equil. 3-74959
- dimers, strong coupling and spectral consequences 3-78699
- electron transfer probability calc. by outer-sphere bridge mechanism 3-58803
- ensemble-representable reduced density matrices suggested by X α transition state 3-78401
- excited state CI studies, reduced partitioning procedure 3-74953
- frontier molecular orbitals, link between kinetics and bonding theory, elementary university chem. teaching 3-77355
- group-function expansions of correlated wave functions 3-57627
- Hamiltonian eigenvalue derivatives to fifth order, rel. to mol. characts. 3-59786
- integrals in bases of Laguerre functions, 2l+2 order functions 3-57597
- interacting systems, double perturbation theory 3-57676
- local energy calcs., many-points local procedures accuracy 3-74774
- Lowdin orthogonalization and square root of positive self-adjoint matrix 3-60407
- mass spectra of heteroaromatic compounds, intermediate ion structure determ. 3-46241
- off-diagonal operator equivalents, matrix elements 3-62560
- one-electron diatomic molecule, non-crossing rule for potential curves 3-71497
- organic three membered ring molecules, protonation, electrostatic versus SCF CNDO calc. 3-46234
- oscillatory chemical reactions, phase waves, diffusion equation 3-50826
- phenylsilanes, calc. of u.v. spectra, s.c.f. method 3-67808
- photographic emulsions, quantum sensitivity data, Silberstein curves 3-47590
- proton transfer reactions in soln., tunnelling 3-55956

quantum chemistry continued

- radial factor in bipolar expansion of $r^{-1}{}_{12}$, convergence of series form 3-59780
- reaction transition states (Conf. Paris, France, Sep. 1970) 3-55950
- review of development of subject, suggested introduction into chemistry courses (*German*) 3-67742
- screened potential eqn. in RPA 3-57630
- sequence-adapted mol. tensors, algebraic methods and cryst. field theory applies. 3-57620
- spin-optimized SCF methods in second quantization formalism (*French*) 3-57617
- ternary homonuclear systems, dipole moment 3-78664
- time-dependent variational principle derivation from Hamilton's expression 3-74098
- trajectory analysis of transition states 3-55958
- 3d transition metal complexes with N_2 , electronic struct. calc., N_2 bonding 3-71518
- two-electron systems, fund. electron energy calc. method (*French*) 3-46170
- two-level systems, variational principle for weak stimulated absorpt. with energy minimizing fields 3-52341
- valence-bond wavefunctions and population analyses 3-78665
- $F + H_2 \rightarrow FH + H$ collinear reaction, large quantum effects 3-44710
- $F + H_2 \rightarrow FH + H$ collinear reaction, quantum, quasi-classical and semi-classical reaction probabilities 3-76457
- H, through barrier of double-well pot. 3-57594
- $H + H_2 \rightarrow H_2 + H$, distorted wave approximation 3-47533
- $H + H_2 \rightarrow H_2 + H$ collinear reaction, streamlines of probability current density and tunnelling fractions 3-76458
- $H_2 + CL \rightarrow H + HCl$, force field and tunnelling effects, kinetic-isotope effects 3-50833
- H_2^+ , existence of discrete spectrum, Lippmann-Schwinger eqn. analysis 3-74947

quantum counters *see photon counting***quantum electrodynamics**

- see also electromagnetism; experimental tests of quantum electrodynamics*
- asymptotic operators for Coulomb scattering 3-54323
- Bloch-Siegert shift of r.f. resons., power series expansion 3-67667
- bound state properties using Lippmann-Schwinger eqn., fine structure and perihelion advance 3-59923
- charged $\frac{3}{2}$ field interactions, quantisation, consistency problem 3-66934
- dimension-selecting duality principle for hadrodynamics and electrodynamics 3-54328
- divergent e.m. masses, analyticity, scaling and light cone 3-40342
- electron beam modulation by laser, Kapitza-Dirac effect 3-74298
- electron counting statistics from QED treatment of electron multiplier 3-62760
- electron in a quantised plane wave and in a constant magnetic field 3-52004
- electron motion in field of two monochromatic e.m. waves, classical and quantised fields 3-74114
- electron moving in weakly focussing magnetic field, radiation (*Russian*) 3-43095
- electron scatt., bremsstrahlung and Compton scatt. effects in high intensity laser 3-74263
- e.m. interaction of massive spin-one field with magnetic dipole moment, causality and Lorentz invariance 3-57292
- e.m. mass differences of elementary particles, calc. 3-59956
- gauge-theory tree graphs, high-energy behaviour and massive vector meson prod. 3-54273
- high energy, review, speculations, experimental implications 3-67005
- hydrogenic radial r^k matrix elements, closed form, factorisation method 3-67647
- infinite-range interactions and Lorentz covariance 3-54322
- Lagrangian eqns., governed by velocity-dependent potential energy, general soln. and invariants 3-43097
- light scattering by charged particle in external e.m. field (*Russian*) 3-59983
- muon- and electron-nuclear interactions, limits on difference, possibility of anomalous interactions 3-57513
- muonic atom, $2p \rightarrow 1s$ transition energy discrepancies, possibility of scalar, mass dependent, lepton-hadron interaction 3-57514
- null-plane field algebra, Dirac's canonical quantisation method, scaling relations 3-62787
- photon rest mass, upper limit in reln. to intergalactic magnetic fields 3-51386
- pseudodual transformations (*Russian*) 3-43096
- quark-parton puzzle, vacuum polarisation 3-66995
- radiation from charge, Lorentz transformation for spectral angular distrib. (*Russian*) 3-67049
- radiative frequency shifts, QED approach, comment and correction 3-54208
- relativistic Fermi system in external field, renormalization 3-70870
- renormalised coupling constants, spontaneously broken gauge symmetries, i.r. and u.v. divergences 3-57337
- Schwinger term, positivity in forward direction 3-66921
- second-order radiative corrections in unified gauge theories, cancellation of infinities 3-67014
- superconductivity and macroscopic quantum phenomena 3-44160
- synchrotron radiation, induced, for helical trajectory (*Russian*) 3-43117
- tests, applications of heavy-ion accelerator 3-51673
- triangle diagram in spin Q.E.D., comment (*Russian*) 3-45887
- validity and experimental work (*German*) 3-43099
- vertex functions with arbitrary spin rel. to asymptotic conservation of helicity 3-62775
- e, μ states subspaces, connection by conserved axial current, conserved currents in each subspace 3-59915
- p,p, scattering total cross section rise, e.m. structure of proton and partons 3-67057
- D, muonic atom, vacuum polarisation contribs. to Lamb shift 3-52303

quantum electronics *see quantum optics***quantum field theory**

- see also Bethe-Salpeter equation; Clebsch-Gordan coefficients; dispersion relations; Lee model; meson field theory; quantisation; quantum electrodynamics; quantum field theory of interactions; quantum field theory of scattering; relativistic quantum field theory; scaling phenomena*
- σ model and $(3,3) \oplus (3,3)$, chiral symmetry breaking and isospin breaking 3-43075
- σ -model, nonanalytic corrections, low energy limit 3-45852
- ϕ_3^4 Hamiltonian, positivity 3-70857
- $(\phi^4)_2$, Euclidean, as classical Ising model, proof of Lee-Yang theorem 3-75820
- Abelian gauge model with spontaneously broken symmetry, verification of multiplicative renormalization 3-70865
- acausality and renormalizability 3-48982
- algebraic classifications of fields and particles 3-78084
- anomaly-free irreducible representation of compact Lie groups 3-48980
- asymptotic freedom of renormalizable theories and non-Abelian gauge fields 3-70859
- axiomatic approach, review 3-78097
- axiomatic structure, Neumann Hilbert model 3-70696
- Bogoliubov-Parasiuk-Hepp-Zimmermann renormalized Lagrangian field theorem, equivalence thm. 3-54266
- boson models, mathematical foundations 3-78098
- bosons, Goldstone, non-existence in two-dimensions 3-48972
- broken symmetry systems, self-consistency conditions 3-59933
- broken-scale invariance canonical trace identities, anomalies 3-45859
- C* algebra for canonical commutations relations 3-59913
- canonical, current-current energy momentum tensor for chiral dynamics 3-57290
- canonical model, determ. of field operator representation 3-43067
- canonical quantization in Riemannian space-time, nonuniqueness 3-54261
- causality from equal-time commutation relations 3-78077
- charged spin $\frac{3}{2}$ field, equivalence of Lagrange and Heisenberg equations of motion 3-66935
- chiral perturbation theory, effects of renormalisation on nonanalyticity of S-, and current matrix elements 3-62776
- coherent states for Hermitian symmetric spaces, bounded homogeneous domains 3-48987
- conformal invariance, kinematical aspects 3-40314
- conformal invariance and short distance behaviour, bootstrap approach 3-43071
- contemporary physics mathematics, conference, London, England (Aug-Sept. 1971) 3-77771
- convergence of perturbation series in field theory models containing fermions 3-54283
- correlation inequalities and mass gap in $P(\phi)_2$, domination by two point Schwinger function 3-43063
- covariance, physical analysis 3-48969
- dilation charge, behaviour of Ward identity in asymptotic Gell-Mann-Low limit 3-78083
- double Wilson expansions, products of three-spinor operators 3-57296
- doubly constrained self consistent field calculation and RPA 3-54292
- dressing operators 3-74316
- energy-density commutation relation, integrability condition 3-45847
- equal-time canonical commutation rules, break-down 3-45858
- equivalence theorem on Lagrangian field theories, localizability 3-66933
- exponential superpropagator, limit processes 3-57291
- fermion field models, ultralocal, formulation and solution, positive, definite Hilbert space 3-57285
- gas of two boson systems in thermal contact, C* algebraic model 3-57156
- gauge fields, spontaneous symmetry breaking in path integral method, Goldstone theorem 3-66928
- gauge fields, zero mass limits and broken symmetries, normal-product algorithm 3-43072
- gauge invariance and conservation laws for a class of nonlinear partial differential equations 3-45853
- gauge potentials, Wilson expansion and Durr-Winter identification 3-45850
- gauge theories, invariant regularisation 3-74320
- gauge theories, non-Abelian, Ward-Takahashi identities for proper vertices, renormalization 3-70860
- gravitational collapse, influence of f gravity 3-57151
- Green's function properties under finite transformation of soft-broken-symmetry group 3-66942
- Haag theorem, generalisation in terms of n-point functions 3-45851
- hadron states containing condensed phase of quark-antiquark excitations, properties 3-54260
- induced dispersion and symmetry breaking phenomena, statistical approach 3-48974
- infinite momentum limit, reln. to parton model calcs. and light-cone formulation 3-40312
- infinite-component wave eqn. with linear mass spectrum, completeness of solns. 3-51977
- interacting fields, axiomatic formalism 3-70867
- isospin gauge group model calc. of n-p mass difference 3-59961
- Lagrangian, local, description of photon as $\nu\bar{\nu}$ pair 3-62816
- Lagrangian, non-linear, quantisation, point mechanics and scalar field cases 3-62774
- Lagrangians, ghost free, massless and massive tensor fields 3-77886
- light-cone analysis of virtual processes, errata on Lagrangian 3-54272
- light-cone singularities and asymptotic domains of momentum space 3-54270
- light-cone structure of vertex functions for composite fields 3-40308
- linear fields according to I.E. Segal 3-78099
- local products as operators 3-74301
- massive gauge theory, equivalence of U-gauge and R-gauge formulations 3-59922

quantum field theory continued

- massless vector currents, role in joining matter-antimatter worlds, removal of pinch-off singularity 3-76960
- massless yang-mills field theory, renormalizability 3-74320
- maximal additive field, Neumann algebras 3-74315
- Mercer's theorem application, states of finite systems of bosons or fermions 3-66927
- neutrino-f-g gravity combined field 3-48788
- nonlinear, renormalized operator eqns. 3-78081
- nonlinear c-number field, $\lambda\phi^4$ model, plane wave modes, energy density 3-57286
- nonlinear chiral symmetry and PCAC Bogoliubov-Parasiuk-Hepp-Zimmermann renormalization 3-54267
- nonlocal, S-matrix unitarity proof 3-40316
- nonpolynomial, evaluation of Fourier transform of zero-mass exponential superpropagator 3-57293
- nonpolynomial Lagrangians, higher perturbation orders in principle coupling constant 3-54277
- operator product expansions, Wilson's short distance and light cone expansions 3-40315
- parafermi field, cluster property, relation to fermi field with hidden variable 3-62598
- parafermi field theory, statistical quantum number and gauge groups 3-45724
- parafermi operators, non-relativistic, cluster restrictions 3-42893
- parton field, anomalous dimension meas. 3-66926
- perturbation of $P(\phi)_2$ quantum field Hamiltonian 3-48977
- perturbative calculations of symmetry breaking for renormalizable gauge theories 3-54263
- Poincare group, asymptotic properties of unitary representations 3-59912
- Poincare group, unitary representation, Hilbert space 3-74336
- quantum crystals, phenomenological theory, microscopic justification 3-40998
- renormalisation group, continuous dimensional regularisation 3-78087
- renormalization group for small coupling constants and asymptotic behaviour 3-59924
- renormalized ϕ^4 theory, Callan-Symanzik equations and ϵ expansions 3-54265
- representations of group $SL(2, C)$ 3-74318
- scalar theories, vacuum energy density as function of bare mass 3-74321
- sesquilinear forms continuous positive, using positive linear functionals 3-74305
- single spinor field; spin differential forms (Russian) 3-43065
- softened field theory, vector gluons, light cone algebra, scaling 3-78086
- spin-two field eqns. from Dirac-like eqn. 3-51972
- spontaneous T violation theory, complex spin-0 fields 3-70881
- structure functions in Bjorken limit, light-cone and non-light-cone contrs. 3-54274
- $SU(2) \times L$ spin up-invariant non linear spinor equation construction (Russian) 3-62785
- $SU(3)$ symmetry and asymptotic props. of quantum number Ω 3-54275
- Subgroups of the complex Lorentz group 3-74317
- superpropagator for nonpolynomial field 3-54262
- Thirring's equations for unbounded field operators 3-45845
- Thirring model, anomalous spin, quantized coupling constant for confirmed covariance 3-74308
- Thirring model, representation theory of conformal group in two dimensions 3-45849
- tree graphs and Schwarzschild soln. 3-42856
- U_3 symmetry between baryons and mesons 3-57305
- unified field theory for synthesis of gravitation and electromagnetism 3-57152
- unified gauge theories, upper bounds on masses of unobserved particles 3-54271
- unstable-particle theory and spectral function interpret. 3-45844
- vertex functions and polarisation operator in $(4-\epsilon)$ -dimensional field theory 3-59928
- Ward identities, chiral and scaling, axial vector current anomaly 3-62790
- Weyl systems for the $(\phi^4)_3$ model 3-48978
- Wightman type, charges as generators of unitary symmetry groups 3-74303
- Wigner 9j coeffs., structure of Alisauskas-Jucys form 3-74304
- Wilson's fixed point condition for the renormalised coupling constant 3-66929
- Wilson's theory of critical phenomena and Callan-Symanzik eqns. in $4-\epsilon$ dimensions 3-66716
- Yang-Mills field, curvature tensor variations (French) 3-48971
- π , weak and e.m. mass diff. 3-54307

quantum field theory of interactions

- see also elementary particle coupling constants; elementary particle interactions; Feynman diagrams; quantum field theory of strong interactions; quantum field theory of weak interactions
- ϕ^3 ladder model, Bjorken scale invariance 3-78147
- ϕ^4 theory, comparison with multilinear theory of scalar fields, colouring problem of Feynman graphs 3-57288
- $(\phi^4)_2$, Griffiths-Hurst-Sherman inequalities and Lee-Yang theorem 3-40311
- $(\phi^4)_3$ Hamiltonian, semiboundedness 3-57287
- bound state properties using Lippmann-Schwinger eqn., fine structure and perihelion advance 3-59923
- conjugate pair of preferred fields interacting with spinor field, internal symmetry and particle interpretation 3-78092
- conjugate pair of preferred fields interactions with spinor field, operator relns. in Heisenberg picture 3-74311
- current-induced, scaling behaviour due to light-cone singularities 3-40320
- current-mixing gauge theories of weak anal. e.m. interactions of hadrons 3-45866
- electroproduction, deep inelastic, parton model, field theory formulation in current interactions 3-78146
- exchange interaction, spin and field of vacuum, classical approach 3-70688
- fermion-neutral-vector-gluon model, eikonal approx. for bilocal vertex function and structure function 3-78063

quantum field theory of interactions continued

- functional methods and models, book 3-51981
- gauge fields, neutral, spontaneous symmetry breaking, physical nature of Goldstone fields (Russian) 3-59927
- gauge theories, renormalizable, weak and e.m. interactions, current algebra rel. to symmetries of strong interactions 3-62791
- gauge theories of weak and e.m. interactions, proton-neutron mass differences 3-74367
- gauge theory, unified weak e.m., based on three dimensional unitary group 3-62800
- gauge-theory tree graphs, high-energy behaviour and massive vector meson prod. 3-54273
- Gribov-Lipatov reciprocity relation, group theoretical derivation 3-48985
- heavy vector mesons, spontaneously broken gauge theories, uniqueness 3-45848
- high energy behaviour and gauge symmetry, Yang-Mills structure in vector meson theories 3-70861
- higher-spin particles, ξ -limiting process and additive $\delta L(\sim i\delta^4(0))$ term 3-59921
- Legendre transforms of generating functionals 3-70873
- light cone expansion rel. to e^-e^+ annihilation 3-60061
- light-cone commutators and chiral symmetry effects in deep-inelastic processes 3-54269
- light-cone quantisation of dual models and structure functions 3-51978
- local Higgs-Kibble type theories in unitary gauge 3-51979
- massive Yang-Mills field, impossibility of covariant equation derivation for many-point functions 3-62768
- massless bosons, chiral self-interaction, Feynman rules 3-78080
- meson field interaction with heavy source, SCF approx. 3-54268
- models with derivative couplings and isotropic spin 3-62763
- nonlinearly realized theories, self-interacting, Wilson operator products 3-66920
- nonlocal, Mossbauer effect on ν , limits on elementary length 3-66979
- nonpolynomial interactions of harmonic oscillation, Efimov-Fradkin formalism 3-57294
- $O(4)$ gauge theory with three-triplet quarks, e.m. and weak interactions 3-62801
- PCAC and gauge models with heavy pion, rel. to $\pi^0 \rightarrow \gamma\gamma$ 3-54297
- quadratic interaction Hamiltonian, exact soln. 3-70866
- quarks, massive, field theory of hadrons and deep-inelastic phenomena 3-54325
- relativistic wave eqn. for two particles of arbitrary spin with instantaneous interaction 3-78076
- relativistic convergent quantum mechanics of interacting particles, realistic model, S-matrix elements 3-59920
- renormalizable interactions, composite operators in perturbation theory 3-43057
- renormalizable interactions, normal products and short distance expansion in perturbation theory 3-43058
- renormalization of Cottingham formula, $SU(3)$ consistency and e.m. mass shifts in parton models 3-62827
- repulsive core, limitations on short distance behaviour 3-67217
- scalar $\lambda\phi^4$ interaction and Fermi interac. in less than 4-dimens. 3-54264
- Schwinger term, positivity in forward direction 3-66921
- self-interacting systems, Lagrangian approach 3-62769
- selfinteracting quark field gauge invariant model, light cone algebra 3-62786
- spin $1/2$ wave eqn., explicit representations for hierarchy of algebras 3-78090
- spin $3/2$, consistency problems, quantisation of charged spin field 3-66934
- spin-two fields, minimal e.m. coupling 3-78082
- Thirring model with $U(n)$ symmetry, scale invariance only for fixed values of coupling constant 3-74341
- unified gauge theories, light-cone approach to hadron mass differences 3-67011
- unified gauge theories, radiative corrections to $e^+e^- \rightarrow \mu^+\mu^-$ and neutral currents 3-67015
- unified gauge theories, reln. to electron-muon mass ratio 3-78106
- unified lepton-hadron symmetry and gauge theory of basic interactions 3-70884
- unified model of weak and e.m. interactions of nucleons 3-78105
- unified theory of weak and e.m. interactions, cancellation of logarithmic divergences in neutron-proton mass difference 3-70914
- unrenormalizable theory for interaction between current of spinning particles and fixed point charge source, solvable model 3-70872
- Weinberg model, additional gauge fields, local lepton symm. representation 3-78095
- e-p gravitational interaction, possible existence of massless scalar particle 3-66923
- $\pi\Delta\Delta$ interaction, covariant derivation of characteristic surfaces, causality 3-51975

quantum field theory of scattering

- see also elementary particle scattering; relativistic scattering theory
- ϕ^2 theory, construction of Bogolyubov scattering operator 3-54280
- amplitude phase, asymptotic behaviour, rel. to energy depend. (Russian) 3-78096
- asymptotic behaviour of elastic form factors and light-cone 3-43066
- asymptotic operators for Coulomb scattering 3-54323
- asymptotic properties of scattering amplitudes bounded by Martin-Froissart bound 3-48979
- axiomatic, concentratable functions and asymptotic relations 3-45846
- deep inelastic structure functions in field theory with computable large-momenta behaviour 3-49014
- duality diagrams formulation and ur-citon scheme 3-78159
- formal scattering theory with shadow states, indefinite metric theory 3-59932
- hadron forward elastic scattering amplitude, 50-5000 GeV, ratio of real to imaginary parts 3-49046
- hadron-hadron wide-angle scattering, model from inelastic lepton-nucleon scattering 3-74457
- indefinite metric, interpretation and unitarity of S-matrix 3-74313
- infinite momentum limit approach, scatt. amplitude, spinless particles (Rumanian) 3-62793

quantum field theory of scattering continued

- Klein-Gordon eqn., two-particle, for e.m. scattering amplitude of equal mass spinless particles 3-62878
 man shift model, measure theoretic considerations 3-78093
 multichannel nonrelativistic, interpolating fields and long-range forces 3-74302
 multiparticle systems 3-77872
 null-plane formalism and polarisation, helicity and canonical formalism relations 3-62796
 operator product expansions and high mass phenomenology at light-like distances 3-74299
 Padé approximations for fixed sources (*Russian*) 3-43070
 potential scattering of relativistic spinless particle, high-energy limit 3-66924
 quasipotential formalism for system of two particles with spin 0 and $1/2$ 3-70874
 quasipotential phase shift calcs. in first and second order 3-54295
 renormalized scattering theory for Lee model 3-70871
 S-matrix construction using super-quantisation method, bi-local field, non-flat space time metric 3-59930
 scale invariance, elementary particles and high-energy scattering 3-51973
 scaling asymptotics for deep inelastic electron-nucleon scattering in local field theory 3-70869
 scaling asymptotics for deep inelastic electron-proton scattering 3-74319
 Schwinger-term sum rule 3-66951
 tree diagram scattering amplitudes, gauge theory, vector mesons 3-78085
 two-body amplitude, relativistic field-theoretic description on Born term 3-40307
 unstable particles, $V-\theta$ sector of Lee model 3-74309
 AN potential, two-pion exchange contrib. from field-theoretical amplitude 3-52035
 pp moderate energy, scaling limit rel. to parton, field theory scaling 3-78192

quantum field theory of strong interactions

- see also elementary particle strong interactions*
 asymptotic behaviour of trajectory functions and size of classical orbits 3-66931
 Bogolyubov transformation in strong coupling theory 3-54279
 composite models of conformal field theory with nonintegral number of partons 3-59987
 conformal invariance, 2- and 3-point functions 3-40313
 eikonal approx. techniques in elastic scattering and production processes 3-43130
 gauge theories, non-Abelian, u.v. behaviour 3-48983
 hadron Hamiltonian function of Cabibbo angle by station projection 3-74314
 internal space, reinterpretation for conformal-spin zero case in dual-resonance model 3-45894
 K-degeneracy in nonadditive dual resonance models, renormalisation 3-59999
 lecture notes, book 3-40364
 multiple particle production in the straight-line path approximation 3-52029
 non-polynomial, chirality, regularisation 3-62770
 optimisation of collision amplitudes under constraints 3-43166
 Padé approximation applications 3-62849
 phenomenological field theory for high-multiplicity reaction, fireball model 3-67088
 quark-gluon model, Goldstone bosons as bound states 3-59988
 relativistic models of composite hadrons, group theoretical approach, zero-width approx. 3-67056
 relativistic string, classical and quantum mechanics 3-59994
 renormalisation const. of nucleon rigorous upper bound, pion-nucleon coupling const. 3-59989
 second-order radiative corrections in unified gauge theories, cancellation of infinities 3-67014
 sigma model, corrections to the axial anomaly 3-74403
 single particle exchange amplitudes, localisability, renormalisation 3-78171
 vacuum polarisation, influence of strong interactions 3-49007
 Yang-Mills theory, deep Euclidean Green's functions, perturbative results 3-51980

quantum field theory of weak interactions

- see also elementary particle weak interactions*
 Abelian gauge theory, second order corrections to triangle anomalies 3-70893
 anomalous origin of masses, vacuum energy density as function of bare parameters 3-57338
 chiral current-mixing gauge theories, nonleptonic $\Delta I = 1/2$ rule 3-62807
 fermion field models, ultralocal, formulation and solution, positive, definite Hilbert space 3-57285
 gauge theories, sum rules for verification from neutrino scattering 3-74358
 gauge theories with superweak CP violation, $O(4)$ and $O(4) \times G$ groups 3-66960
 gauge theory of Bars, Halpern and Yoshimura for semi-leptonic decays 3-62806
 gauge theory tests in deep inelastic region 3-59947
 Goldstone neutrino interaction with e.m. field 3-52002
 hadronic, unified gauge theories, enhancement of parity violation in nuclei 3-66972
 Lagrangian, nonpolynomial, interactions of muons, hadrons, charged W boson (*Russian*) 3-74351
 non-local current-current, anomalous magnetic moments of leptons and Lamb shift 3-66958
 nonleptonic, hadron Hamiltonian, function of Cabibbo angle by station projection 3-74314
 nonleptonic decays with exact field algebra 3-57326
 nonlocal, $\nu\nu$ interactions, ν e.m. form factor, four-fermion and W boson models (*Russian*) 3-59926
 nonrenormalizable interactions on low-energy limits of renormalizable ones, virtual field concept 3-74306
 $O(3)$ gauge, with three-triplet models of hadrons, symmetry breaking 3-62802
 renormalisation of spontaneous symmetry breaking model in the unitary gauge 3-66925

quantum field theory of weak interactions continued

- renormalizable gauge theory, $\Delta I = 1, 2$ rule, schizon scheme formulation 3-66961
 renormalizable model of neutrino interactions, heavy lepton production 3-45872
 renormalizable models, sideways dispersion calcs. for lepton magnetic moment 3-67009
 Salam-Weinberg model, ν processes, stellar energy loss rates 3-80919
 second-order radiative corrections in unified gauge theories, cancellation of infinities 3-67014
 stability of originally massless lepton fields against spontaneous mass formation 3-70907
 $SU_2 \times U_1$ gauge models, determ. of mixing angle by general method 3-51984
 unified gauge theory, tests of scaling from high energy neutrino scattering 3-74359
 unified gauge theory for weak and e.m. interactions, $SU(3) \times SU(3)$ symmetry and quark structure 3-70894
 universal length, a new constant 3-54299
 Weinberg's renormalizable theory, calc. of semileptonic neutral currents assuming partons 3-70905
 Yang-Mills, $\nu\nu$ scattering, gauge invariance, cancellation of divergences (*Russian*) 3-74322
 Yang-Mills-Maxwell system in Weinberg model 3-48981
 $K \rightarrow \pi\mu(e)\nu$, $(1,8) + (8,1)$ symmetry breaking, soft-pion approach in σ model 3-45867

quantum fluids

- see also boson systems; fermion systems; liquid helium*
 Ashcroft-Lekner hard sphere model, generation for struct. factor calc. 3-45727
 cryogenic heat transfer, nucleate pool boiling 3-77408
 gas, eqns. of state, S-matrix representation of second virial coeff. 3-70727
 Liouville perturbation expansion, renormalization, reduced density matrices 3-59814
 phase diagrams of lattice gas model rel. to supersolid existence 3-46735

quantum generators (optical) *see lasers***quantum mechanics *see quantum theory*****quantum numbers *see quantum theory*****quantum optics**

- see also photon counting*
 anthracene crystals, difference between effective and mean light-wave fields in determ. of spectroscopic props. 3-62737
 atom multiphoton ionisation, selection rules, nonperturbative theory 3-52277
 atom radiation absorption due to photoeffect in a magnetic field 3-63306
 bound electron in strong light field, Green's function including many-photon transitions 3-54581
 clipped photocount autocorrelation formulae for nongaussian light 3-42985
 coherent Glauber state characts. from interaction of two-level system with polarized field (*French*) 3-51890
 coherent interaction of particle beam with matter 3-48868
 Coulombic Green function in parabolic coordinates 3-62680
 e.m. field interactions with matter, book 3-74186
 gases, theory of e.m. wave scatt. (*Russian*) 3-43540
 inverted media, superluminal velocity of multiple-level and multipole systems 3-51894
 light waves four-photon forced dispersion during nonmonochromatic pumping (*Russian*) 3-48952
 light-echo type signals, theory of multi-pulsed excitation 3-48867
 master equation, strongly interacting systems 3-70794
 medium with negative permittivity, excited molecules 3-74216
 mode locking phenomena 3-40233
 multi-level atoms, quantum statistical theory of coherent emission 3-66784
 multilevel systems, coherent spontaneous emission 3-40232
 non-Markoffian effect on superradiance from harmonic oscillators 3-48864
 nonlinear model for population interaction (*French*) 3-51891
 nonlinear susceptibility tensor, permutation symmetry relation to photon number conservation laws in the dissipative media 3-57250
 nonzero photon mass existence, physical consequences (*French*) 3-40230
 Optical Soc. America meeting, Rochester, N.Y., USA (1973) 3-77430
 Optical Society of America, conference, Rochester, USA (1973) 3-77431
 photoelectron counting statistics, quasimonochromatic light, clipped correlation function 3-57217
 photographic process, detector characts., quantum efficiency 3-77558
 photon echoes, doubly resonant, in three-level system 3-66783
 photon statistics and coherence of stimulated superradiant pulses 3-59853
 point sources of light, resolution analysed by quantum detection theory 3-59850
 quantum freq. converter, quantum theory, time depend. perturbation theory 3-66883
 quantum statistical props. of radiation, book 3-74217
 quasienergy and quasienergetic states, strong monochromatic e.m. wave perturbation of atoms and mols. 3-74219
 radiative frequency shifts, QED approach, comment and correction 3-54208
 Rhodamin 6G, two-photon absorption 3-40287
 second harmonic frequency light generation in a Gaussian light 3-66868
 single mode radiation in cavity, approach to equilibrium 3-42984
 spatial coherence function parameters, statistical errors in photon counting technique 3-48865
 super radiance, perturbation theory, level shifts of N atom systems 3-62678
 super-radiance, perturbation theory, interpretation in classical diffraction theory terms 3-62677
 superradiance, atomic coherent state representation from exact soln. of Fokker-Planck eqn. 3-66872

quantum optics continued

- superradiance, statistical treatment by generalized master equation 3-70754
- superradiance, two-photon, and optical free-induction decay, theory 3-45824
- thermal radiation, black-body, transparent medium, spectral energy distrib., two-level system 3-45783
- three photon process, absorpt. cross section and spin analysis 3-51952
- three-level system, linear susceptibility using general relax. theory 3-62681
- transverse force on light refracted by matter 3-40231
- two simply coupled spectral lines, probabilistic radiative transfer 3-51892
- two state system, non-resonant levels effect, Schrodinger eqn. representation, Stark shift 3-45782
- two-atom system, higher order retardation effects 3-51893
- two-level atom system, polarisation effects, self-focusing (*Russian*) 3-57251
- two-level atom system, superradiant fluctuations, Brownian motion model, Fokker Planck eqn. soln. 3-54212
- two-level quantum oscillations rel. to analysis of regenerative nuclear spin system (*Russian*) 3-64568
- two-level system, carrier-frequency distance depend. of pulse propagation 3-70795
- two-level system, coherent radiation interaction, evolution of observables (*French*) 3-54207
- two-level system, photon statistics influence on Bloch-Siegert shift 3-52266
- two-level system in interaction with linearly polarized e.m. field, energy spectrum 3-42983
- two-level system interacting with one-mode quantized field, r.f. reson. phenomena 3-63289
- two-level system of weakly interacting particles, radiation theory 3-74215
- two-photon excited fluoresc., polarisation study 3-42986
- wave packet motion in constant homogeneous electrical and mag. fields (*Russian*) 3-59852
- wave quanta in inhomogeneous material media, bending effect, finite rest masses 3-51889

quantum statistical mechanics

- see also many-body problems; quantum fluids*
- applications in optics and solid-state physics 3-70736
- asymptotic operators for stationary-homogeneous states, correlation weakening and ergodic relationships 3-70735
- Bernoulli schemes in one dimension, Ising model 3-57162
- binary mixtures, space-time correlation function determ. 3-74152
- Bose gas, interacting, ground state energy calc. 3-54164
- Bose gases, dilute, finite volume Green's functions, existence 3-42889
- Bose-Einstein condensation of the gapless Hartree-Fock model Hamiltonian (*Korean*) 3-70730
- Brownian motion, Boltzmann and Fermi-Dirac statistics 3-70739
- C_p theorems, continuity of multiplication, convergence of operators 3-73981
- charge transfer in polar solvents, quantum theories (*French*) 3-65088
- classical random variable, statistical dynamics 3-62600
- contemporary physics mathematics, conference, London, England (Aug-Sept. 1971) 3-77771
- correlation functions, method of calculating quasiperiodicities 3-62602
- correlation inequalities and mass gap in $P(\phi)_2$, domination by two point Schwinger function 3-43063
- equation of state of quantum systems, finite range Kac pot. at high temp. 3-42892
- equilibrium thermodynamics between charged particles and e.m. radiation (*French*) 3-77900
- exchange energies and potentials at finite temp., Hartree-Fock-Slater calc. 3-54165
- Fermi-Dirac function, computation of stellar configurations using Chebyshev approximations 3-61769
- fermion operators, normal ordering of disordered product, problem of rooks 3-66682
- finite quantum systems, operators ergodicity 3-74158
- fluctuation-dissipation theorem for open system 3-66687
- Fokker-Planck eqn. for systems far from equil., Boltzmann distrib. function 3-62605
- free Fermi gas, asymptotic orbits 3-66680
- Friedrichs model, collision operator in physical representation 3-66683
- Gartenhaus-Schwartz transform. rel. to centre-of-mass motion in many-particle systems 3-40179
- Goldstone-mode frequency, phase transitions, symmetry breaking, asymptotic properties 3-70731
- hard non-spherical molecule system, eqn. of state simulation 3-54161
- hard-sphere collision operator, eigenfunctions and spectrum, numerical soln. 3-40176
- heat bath, time evolution of harmonic oscillator 3-77912
- instabilities in stationary non-equilibrium systems, appl. to lasers and nonlinear optics 3-70801
- kinetic eqns., nonlinear, for expectation values of physical quantities of non-equilibrium states, general derivation 3-74159
- Langevin equations, generalised linear and nonlinear 3-62595
- Liouville's theorem, distribution function, n-time, BBGKY hierarchy (*German*) 3-70732
- location of zeroes of partition function for lattice systems 3-48800
- logics, anal. of probability concepts of coexistence, and transitions between states 3-74097
- long-range order, method of symmetry-breaking potential 3-59817
- many universes interpretation, statistical postulate deviation 3-74095
- many-body system, weak self-consistent approx. scheme 3-40181
- many-particle systems, Bloch equation soln. in terms of path integral 3-70728
- maser, infinite atom Dicke model, dynamics 3-78003
- maximum information entropy of quantum states 3-42924
- n-body problems, nonrelativistic scattering into cones 3-42891
- non-equilibrium thermodynamics theory 3-70771
- nonequilibrium, models construction 3-62596

quantum statistical mechanics continued

- nonequilibrium system, kinetic eqns., Markoffian soln. of Liouville eqn. 3-77902
 - nonideal Bose gas, hydrodynamic Hamiltonian 3-54167
 - nonlinear coupled oscillators, modal equation approach 3-57157
 - nonlinear dynamics of fluctuations, renormalization of kinetic coeffs. by projector-operator method 3-42901
 - open system, linear Langevin equation derivation 3-66688
 - open systems, treatment of generalized master equation 3-70754
 - parafermi field, cluster property, relation to fermi field with hidden variable 3-62598
 - parafermi field theory, statistical quantum number and gauge groups 3-45724
 - parafermi harmonic oscillators considered as canonical ensemble 3-74155
 - parastatistics and cluster property, symmetrization postulate 3-51833
 - partition function, integral representation and classical limit of spin systems 3-48799
 - phase-space reconstruction, refutation of Bell Wigner locality argument 3-74154
 - planetary outer layers, theory of dense partially ionised H 3-42160
 - pure thermodynamic phases, facial aspects of superposition principle 3-74110
 - quantum statistical props. of radiation, book 3-74217
 - reacting Coulomb gases, quantum-statistical-mechanical formulation 3-71698
 - regional stationary principles and regional virial theorems 3-62594
 - semiclassical fermion μ -space density, quantum oscillations 3-42886
 - spectral density method applied to systems showing phase transitions 3-62599
 - spin systems, 1-d, finite range potential, uniqueness of states satisfying Kubo-Martin-Schwinger boundary condition 3-62601
 - states and dynamics of infinitely extended physical systems, C^* algebraic formalism 3-66681
 - states and representations, C^* algebraic approach 3-77904
 - Stefan Boltzmann formula, abelian and tauberian theorems 3-66684
 - stochastic collision models and radiative equilibrium, line shape constraints 3-42888
 - stochastic symmetry breaking of time reversal invariance 3-70729
 - stochastic theory approach to reformulating quantum mech. motion 3-62597
 - superfluid density, conserving approx. within pair theory of Fermi or Bose statistics 3-52729
 - systems far from thermal equil., Fokker-Planck eqn. soln., distrib. function 3-54163
 - thermal relax. rate eqns., n-level system, decay eigenfunctions and eigenstates 3-40177
 - thermodynamic derivation of $\epsilon = \hbar\nu$, teaching approach 3-51499
 - thermodynamics, spatial distrib. function calc., linear partial differential equation, Schrodinger equation 3-70769
 - Toeplitz hamiltonian systems, collision operator 3-74157
 - Toeplitz Hamiltonian systems, quantum dynamics 3-74156
 - transitions under influence of local interaction in stochastic motion 3-40180
 - von Neumann's theorem, introduction of hidden parameters 3-66640
 - Wigner distribution and reduced distribution functions 3-45725
 - Wilson's theory of critical phenomena and Callan-Symanzik eqns. in 4- ϵ dimensions 3-66716
- quantum statistics** *see quantum statistical mechanics*
- quantum statistics of many-particle systems** *see quantum statistical mechanics*
- quantum theories of fluid structure**
- inert gas liquid, struct. factor, effect of softness of interparticle repulsive potential 3-49816
 - liquid metal, struct. factor, effect of softness of interparticle repulsive potential 3-49816
 - soft-core model, molecular dynamics method, velocity autocorrelation, self-diffusion constant, density 3-49818
- quantum theory**
- see also complementarity; correspondence principle; harmonic oscillators; indeterminacy; perturbation theory; quantisation; quantum chemistry; quantum field theory; quantum theories of fluid structure; spin hamiltonians; wave mechanics*
 - algebraic, facial aspects of superposition principle 3-74110
 - analytic nonlocal potentials, forward dispersion relation 3-62558
 - anharmonic oscillator, λx^{2m} , eigenvalues determ. using Hill determinants 3-74102
 - anharmonic oscillator, velocity-dependent perturbations, hypervirial and Hellmann-Feynman theorems 3-42846
 - atom, multiphoton effects, anal. by Keldysh method, and perturbation method 3-74825
 - atomic spectral-line broadening and Kirchhoff's law, quantum mech. theory, classical limit 3-49481
 - atomic system, oscillatory mag. and elec. field effects, quantum interpret. (*French*) 3-52264
 - atoms, multiphoton effects, appl. perturbation theory 3-74824
 - axiomatic, field of real numbers 3-74112
 - axiomatic mechanics, quantum logic approach 3-70696
 - Born expansions, equivalence of wave and impact parameter approx. 3-59782
 - boson polynomials, reln. to canonical tensor operators is unitary groups 3-74106
 - bound state wave functions, exponential decay 3-59779
 - bra and ket formalism is extended Hilbert space 3-74109
 - Brownian motion, Boltzmann and Fermi-Dirac statistics 3-70739
 - canonical commutation relations, coordinate free, algebraic treatment 3-48757
 - charged particle emission from crystals, quantum calcs. 3-41620
 - charged particle in low magnetic field with finite boundary conditions 3-66609
 - charged solid Hamiltonian and scalar wave eqn. of spin corpuscle in nonrelativistic mechanics (*French*) 3-42838
 - coherent states and magnetic operators 3-42857
 - complex gamma function, approx. use in wave propagation problems 3-48755
 - complex Hilbert space, necessity for quantum mechanics 3-42853

quantum theory continued

- conformal groups, correspondence with pseudoscalar geometry in a plane (*Italian*) 3-77855
- correlation functions, orthogonal operator expansion, zero-freq. anomaly 3-77856
- Coulombic pot. energy integrals and approxs. 3-40148
- density matrix elements and exotic conservation laws 3-42847
- density of states and Jacobians (*French*) 3-51806
- dipole oscillator strength distrib., partial, systematics, and moments for atoms of first two rows 3-78400
- Dirac particle, quantum mechanical Hamiltonian formalism, observables 3-54136
- dynamical system with N degrees of freedom, regular and irregular spectra 3-66622
- dynamics of classical relativistic particles, circular orbit solns. and nonrelativistic limit 3-48758
- eigenvalue bounds, relative accuracies 3-70693
- eikonal approximation, remarkable properties 3-45703
- Einstein, Podolski and Rosen paradox fallacy 3-66630
- Einstein-Lorentz formula for fluctuation of energy in enclosure of blackbody radiation 3-42855
- Einstein-Podolsky-Rosen paradox, quantum mechanical prediction understanding 3-66631
- elastic scattering amplitudes, uniformation calc. arbitrarily many open channels 3-66636
- elementary particle physics, quantum mech. rel. to classical reson. scattering (*Czech*) 3-70889
- energy levels repulsion phenomenon, statistical measure 3-57474
- exchange of quantum-numbers in hadronic collisions 3-67116
- expectation values error limits 3-51804
- exponential decay law, quantum foundations 3-51810
- few body bound states location using linear fractions 3-74100
- finite algebra, Fermi operators and systems 3-74122
- free Landau electron, canonical transformations 3-74103
- functional integral representation of operators, Weyl quantisation rule 3-48756
- Galilei-invariant single particle action 3-54135
- gas laser under high-energy conditions 3-43006
- generalised quantification, reply to criticism (*French*) 3-66612
- generalised WKB method for approximate soln. of inverse scattering problems 3-62572
- Green's function rearrangement, circular symmetrization, generalized isoperimetric inequalities 3-73995
- Hamiltonian eigenvalue derivatives to fifth order, rel. to mol. characts. 3-59786
- Hamiltonian system, constants of motion and degeneration 3-62393
- harmonic oscillator, anisotropic, with rationally related frequencies, decomposition, reln. to SU(n) 3-48754
- harmonic oscillator, creation and annihilation operators 3-59783
- harmonic single-particle basis, transformation to self-consistent harmonic approximation 3-48760
- Heisenberg operators, representation of simplex algebra in space of all polynomials 3-62552
- high school mechanics (*Hungarian*) 3-73633
- Hilbert space, sequence of finite dimension subspaces convergence to subspace of dimension (*Spanish*) 3-40156
- Hilbert spaces, generalised operator domains 3-77765
- Hooke's symmetries and nonrelativistic cosmological kinematics, irreducible projective representations 3-42850
- hydrodynamical model, intense wave interactions with atoms 3-74126
- interpretative rules of quantum mechanics, possible strengthening 3-59790
- Kato's perturbation theory, expansion by generalizing relative bound condition 3-48759
- Klein-Gordon equation, spectral and scattering theory 3-45696
- Lagrangian, consistent theory for one degree of freedom based on Frechet derivative 3-40154
- Lagrangian, for several degrees of freedom, use of Frechet calculus, stationary action 3-66629
- Lagrangian quantum mechanics with velocity-dependent potential, invariance of action and conservation law 3-57123
- Lippmann-Schwinger eqn., modified, for two-body scattering theory with long-range interactions 3-74108
- logics, anal. of probability concepts of coexistence, and transitions between states 3-74097
- logics, manuals of operation 3-74113
- LSZ reduction formalism and generalized Green's functions 3-74146
- magnetic white dwarfs, polarised radiation, exact soln. of Kemp's (1970) model 3-53658
- Majorana equation, infinite component, internal coordinates introduction 3-42852
- many electron systems, matrix elements evaluation of spin-dependent two-body operators 3-63258
- many universes interpretation, statistical postulate deviation 3-74095
- many-body problem, pseudometric, generalized, soln. in Hilbert space and use of Pauli principle 3-40153
- many-electron atoms, non-stationary states, theory 3-78399
- Mathieu equations, matrix solutions 3-45626
- matrix elements, bound-state, stationary and quasistationary bounds 3-62568
- matrix elements, upper and lower bounds 3-62567
- measurement process, information, entropy concepts 3-77860
- mechanics, criticism of Hautot's work 'Quantification Generalisee' 3-66611
- mechanics, realistic interpretation using concept of information 3-74089
- mechanics of individuality in nature rel. to barriers and cells 3-73622
- moment expansion and eigenvalues 3-51809
- multichannel scattering, transition from time-dependent to time-independent theory 3-74105
- multichannel stationary scattering theory in two-Hilbert space formulation 3-48764
- multiple scattering by two centres of force 3-51805
- natural philosophy based on induction 3-74092
- nonconservative systems, stationary state concept (*French*) 3-48751

quantum theory continued

- nonequilibrium system, soln. of Schwinger equation, Green's function method (*Russian*) 3-42840
- nonequilibrium systems, dynamic description, inclusion of causality principle (*Russian*) 3-57116
- nonlinear evolution eqns. of phys. significance, soln. using inverse scatt. method 3-51811
- nonlinear parameters, least squares estimation, matrix evaluation 3-40155
- nonlinear periodic waves in inhomogeneous medium, scatt. and transform. 3-40158
- nonrelativistic mechanics, integrated classical and quantum approach, book 3-70698
- nonrelativistic quantum mechanics, invariance algebras and interactions 3-66625
- nonspherically symmetric potentials, iterative inversion procedure 3-42845
- observation, physical concept of information 3-74091
- octahedral spinor group, irreducible tensors 3-62561
- off-diagonal operator equivalents, matrix elements 3-62560
- one-particle problem, known eigenstates, connection with OPW and COPW pseudopotential theories 3-74116
- optical potentials in time-dependent quantum theory 3-54133
- order, implicate and explicate in physical law 3-74093
- oscillator, anisotropic, canonical transformations and accidental degeneracy 3-45701
- oscillator in sector, isotropic, canonical transformations and accidental degeneracy 3-45702
- oscillator phase states, thermal equilibrium and group representations 3-42848
- oscillators coupled as student illustration of many body system 3-70234
- particle creation in expanding Universe, quantum mechanical analogue 3-76958
- particle in uniformly rotating reference system, relativistic quantum mechanics 3-62578
- particle motion in relativistic invariant quantum pot. (*French*) 3-54156
- particle scattering, nonspherically symmetric potential, zero energy limit 3-51807
- periodic potential, one-dimensional, soln. using Laplace transform method 3-77853
- permutation group in hyperspherical formalism, matrix elements and recurrence relation 3-57482
- perturbation energy variational formula 3-66608
- philosophy, quantum mechanics and interpretations of probability theory 3-53807
- potential scattering, appl. of Pade approximants 3-62573
- potential scattering cross sections in semiclassical limit 3-62554
- probability in quantum mechanics, 2-slit expt. 3-40159
- projection operators, product form and scheme for approximate projection 3-67229
- propositional calculus, algebraic formulation 3-74123
- quantum mechanical measurement problem 3-51501
- quantum mechanical problem of measurement 3-51500
- quantum-mechanical system in oscill. field, steady states and quasienergies 3-45709
- quasistationary states, semi-classical eigenvalue eqns. 3-54134
- quaternion charge, reln. to baryon conservation 3-51982
- radial momentum operator 3-51493
- rare earth metals and compounds w.k.b. approximation, tunnelling probability calcs. by quasi-particle approach 3-41375
- realistic explanation, new approach 3-66626
- rearrangement Green's function, generalised isoperimetric inequalities 3-73994
- relativistic, position operators, algebraic operator relationships 3-48762
- relativistic equivalent oscillator, group structure 3-48765
- relativistic invariance and discrete symmetries 3-59777
- representation using functions in phase space (*French*) 3-57127
- r.f. resonances, validity of semiclassical description 3-45704
- rotational coordinates for description of spin, relation of quantum mechanical and classical theories 3-62553
- scattering, inelastic and reactive, sudden and semiclassical approxs. 3-42842
- scattering, inverse calcs. of energy independent potentials 3-62545
- scattering, principle value integral evaluation by differential equation method 3-70690
- scattering, time independent, with Coulomb potential 3-70706
- scattering amplitudes for central Yukawa potential, soln. using continuous space-filling curves 3-66628
- scattering by nonlocal pots., semiclassical approxs., appl. to atomic collisions 3-45698
- scattering by spin-dependent spheroidal potential, iterative soln. of infinitely coupled integral eqns. 3-74107
- scattering quantum theory of multiparticle system 3-77872
- scattering theory, computer calc. for student 3-77362
- scatterings by nonlocal pots., effective-mass method, semiclassical approx. 3-42841
- Schwinger's variation principle by means of Q-number variation for non-lin. Lagrangians 3-45707
- Schwinger's variational principle in quantum mechanics with velocity dependent potential 3-74117
- Schwinger's variational principle with velocity dependent potentials reducible multi-dimensional case 3-62564
- simultaneous meas. of several observables, concept of fuzzy probability meas. 3-74087
- simultaneous measurements theory, state preparation and state determination concepts 3-74088
- solid molecular H, eqn. of state at high press., astron. appl. 3-4216
- spectrum generating algebra sl_4 , for Coulomb system 3-77866
- spin corpuscles, nonrelativistic approach, fluid interpret. (*French*) 3-42839
- stochastic and deterministic aspects of classical approach 3-62564
- stochastic theory approach to reformulating quantum mech. motion 3-62597
- SU_n unitary unimodular groups, structural props. 3-59778
- symmetry reduction of system by perturbation (*French*) 3-4283
- symmetry-adapted perturbation expansions using unitary transforms. 3-62559

quantum theory continued

- t matrix, utility of separable expansions, appl. to trinucleon system 3-74506
- Tamm-Dancoff method, new, level dependent 3-66639
- teaching plan for quantum mechanics in secondary schools (*Hungarian*) 3-61960
- Thomas-Fermi approximation, quantum corrections, Kirzhnits method 3-54132
- Thomas-Fermi theory, simple derivation of expression for electron density 3-56597
- three charged particles system below threshold, integral eqns. 3-70707
- three nonrelativistic pairwise interacting, amplitudes, variational principles 3-70708
- three-body problem, complete set of basis functions 3-74397
- three-dimensional quartic oscillator, energy levels and matrix elements 3-74973
- unitarity bound on evolution of nonstationary states 3-57124
- unstable states, correspondence with resonances, potential scattering 3-42834
- unstable system, finite energy states decay rate 3-40146
- vinyl monomers, chemical shift rel. to electron density, quantum theory calc. (*German*) 3-63527
- von Neumann's theorem, introduction of hidden parameters 3-66640
- wave propagation through potential barrier system, exact and approx. methods 3-59787
- wavepacket propagation through square wells and potential barriers, simple calc. method for students 3-66104
- Weyl group, survey 3-51812
- Wick's theorem, general statistical, general subsystem Hamiltonian in 3D Hilbert space 3-45705
- Wigner's quantum distribution functions, calc. of mean values of physical consts. (*Russian*) 3-66621
- Wigner quasiclassical theory for particles (*French*) 3-57118
- WKB energy levels for a class of one-dimensional potentials, teaching approach 3-53814
- zero-point energy in a bounded continuum 3-51803
- $\text{Br}_2 + \text{Br}_2$, vibr. scatt., pot. well effect, SSH theory validity 3-49503
- $\text{Cl} + \text{Cl}_2$, vibr. scatt., pot. well effect, SSH theory validity 3-49503
- H. operator domain paradox and relativistic correction to energy levels 3-66107
- H atom, symmetry in weak mag. field, degeneracy problem 3-67638
- H energy level relativistic mass correction 3-66105
- H operator domain paradox and relativistic correction to energy levels 3-66106
- H_2 , para, at room temperature, heat conductivity, Senftleben-Beenakker effect, quantum mechanical calc. 3-52418
- $\text{O}_2 + \text{O}_2$, vibr. scatt., pot. well effect, SSH theory validity 3-49503

quantum theory applications

- amplitude-phase method, attractive r^{-2} potential 3-70703
- boundary effects on dispersion force between oscillators 3-57120
- coupled channel code for Coulomb excitation of higher lying nuclear states 3-46014
- crossing of two systems of potential curves 3-74125
- distorted wave approx. calc. of resons. in electron-ion scatt. 3-52283
- eikonal Born approximation with angle trajectories 3-70704
- harmonic oscillator, maximal kinematical invariance group 3-62549
- harmonic oscillator, particle scattering, applic. to electron-molecular collisions 3-71618
- harmonic oscillator, three dimensional, dynamical group construction 3-77868
- inverse problem with constraints, reln. to method of completely orthogonalized plane waves 3-66638
- particle scattering, computer program for solution of coupled second-order differential equations 3-66616
- Planck's equation, numerical solution 3-77913
- scattering, computer program for differential and integral cross sections from reactance and transition matrices 3-66617
- $\text{SU}(n)$, $\text{SU}(n,1)$ representations connected with n dimensional isotropic harmonic oscillator 3-57303
- three-body problems, non-relativistic spinor regularization 3-70695
- transport processes, variation principles 3-57167
- van der Waals attraction in symmetric array of macroscopic bodies 3-57121
- Wigner R-matrix approach to inelastic collinear collisions 3-71397
- x^6 anharmonic oscillator, approximate formula for energy level determ. 3-59785
- $\text{He}^+ + \text{Ar}$ charge transfer collisions, application of WKB theory 3-74900

quantum theory of gravitation

- ambiguity-free, class of gauges with suppressed u.v. divergences 3-74145
- gravitating particles model in quantum theory 3-54155
- space-time properties (*German*) 3-42878

quantum theory of light *see quantum optics***quantum theory of many-body problems** *see many-body problems***quark model** *see quarks***quarks**

- asymptotic nonet-symmetry model, similarity with quark model 3-43104
- baryon resonances partial decay widths, quark model analysis, internal orbital angular momentum 3-43120
- baryon spectroscopy and regularities between SU_6 and SU_3 mass-breaking parameters, quark model study 3-78150
- baryon-number conservation, quark approach 3-59945
- bootstrap model, complete, of quarks, mesons, baryons, Yukawa coupling and $\text{SU}(3)$ symmetry 3-70946
- Cabibbo's weak Hamiltonian, nonrelativistic quark model and octet dominance 3-74355
- charge, direct meas. in deep inelastic lepton scattering 3-57372
- Compton cross sections, virtual, longitudinal, quark model light cone algebra determining rate of tendency to zero 3-59973
- constituent, breakdown of scaling 3-78154
- constituent and current, Melosh transformation, pionic decays of resonances 3-49021

quarks continued

- cosmic ray studies, artificial satellites of the Proton series, meas. high energy electrons, particle search (*Russian*) 3-65577
- cosmic rays, source of penetrating paris 3-69801
- cosmic-ray delayed shower particles underground, new interpretation as alternative to quarks 3-59233
- current and constituent, pionic transitions as tests of connection 3-67058
- current content of hadrons, Melosh transformation 3-67051
- current to constituent picture mapping, broken collinear $\text{SU}(6)$ symmetries and suppression of $|\Delta S|=1$ amplitude 3-48995
- current to constituent transformation, test of amplitude signs in pion photoproduction 3-78138
- deep inelastic inclusive processes, reln. between quark fragmentation functions and quark distribution functions 3-74380
- deep inelastic processes, hadronic final states in simple quark-parton models 3-59980
- deep inelastic processes and quarks 3-66965
- diffractive dissociation and hadron structure, dual quark model 3-67068
- diffractive production of nonstrange mesons in harmonic-oscillator quark model 3-57370
- dual amplitude construction from quark diagram considered as lowest order Feynman diagram 3-62857
- in dual model, method in which non-zero triality particles cannot be made free (*Russian*) 3-40368
- dual resonance model, simple nonadditive quark like operators, Neveu-Schwarz operators 3-60000
- e.m. decays, $\text{SU}_w(6)$ of constituents and $\text{SU}(3) \times \text{SU}(3)$ of currents 3-67016
- exotic baryon resonances, possible assignments in SU_3 , utility of quark model 3-40318
- fractionally charged, identification with partons, inclusive lepton scattering problem 3-52012
- fragmentation models, high energy production processes, experimental elusiveness explanation 3-62852
- fragmentation processes, quark model, possible consequences 3-54324
- hadron inclusive spectra, effect of initial polarisation in quark theory (*Russian*) 3-78228
- hadron photoproduction, quark model with vector-meson dominance hypothesis (*Russian*) 3-59975
- hadron scattering, elastic large-angle, automodellism and structure of hadrons 3-62850
- hadron states containing condensed phase of quark-antiquark excitations, properties 3-54260
- Han-Nambu, in Weinberg's gauge model 3-51998
- Han-Nambu, rel. to symmetry breaking in $\text{O}(3)$ gauge theories with three-triplet models of hadrons 3-62802
- harmonic oscillator model, $\pi N \rightarrow \pi N^*$ production cross section and $\text{SU}(6) \times \text{O}(3)$ structure 3-62892
- inclusive electroproduction, deep inelastic, quark parton model 3-74385
- inclusive one-particle distrib. and reaction asymmetries within completely symmetric duality scheme 3-60054
- inclusive reaction model, expl. check of predictions 3-40403
- inclusive spectra in central region $|p_T| \leq 0.3 p_{\text{max}}$, quark model 3-74464
- interacting, Melosh-like operator construction 3-74388
- lepton-hadron scattering, quark-parton model, duality relation 3-78151
- light cone commutator, quark model, analyticity and scaling of divergent e.m. masses 3-40342
- light-cone algebra of quark currents, positivity inequalities for spin-dependent lepton-hadron scattering 3-40350
- light-cone quantisation, unitary transformations relating current to constituent quarks 3-70942
- magnetic charge, relativistic strings as lines of quantised magnetic flux 3-74393
- masses, for a given value of $\pi\text{-N}$ term, parton models 3-62827
- massive, field theory of hadrons and deep-inelastic phenomena 3-54325
- meson-baryon scattering, total cross-section relns., quark-line picture 3-52054
- model, problems rel. to masses, quark-parton analogy, relativistic couplings and hierarchical status 3-59984
- model, production of higher resonances, configuration mixing 3-67053
- model for hypercharge exchange reactions, amplitude analysis 3-71008
- model in study of $K^+p \rightarrow K^+\pi^+\pi^+\pi^-$, 12.7 GeV/c 3-67141
- model symmetry $\text{SU}(6)$ or $\text{U}(6)$ (*Russian*) 3-74389
- multiparticle and inclusive reaction model 3-40365
- multiple quark scattering model for changing slope of $d\sigma/dt$ at small $|t|$ in pp scattering 3-49022
- non-Abelian gauge theories with parity and strangeness conservation 3-57393
- nonlinear theory of fields of spin $s=2$ (*Russian*) 3-43119
- parity-violating nucleon one-meson exchange potentials in current-current quark model 3-48994
- parton chains, pN production process, comparison with CERN data 3-62810
- parton chains, electroproduction, comparison with SLAC-MIT experimental data 3-62829
- parton model, for final state production in deep inelastic lepton-hadron scattering 3-70933
- photoproduction, high-energy, dual relativistic quark model, scaling limits 3-74381
- pionic resonance decays, current-constituent transform., $\text{SU}(6)_w$ 3-78152
- proton scattering, high energy, analysis using impact parameter representation, quark model 3-74433
- quark-gluon model, deep-inelastic scattering and state properties of baryons 3-62847
- quark-gluon model, Goldstone bosons as bound states 3-59988
- quark-neutral vector gluon system, Melosh-like operator construction 3-74388
- quark-parton form factors, validity of Drell-Yan formula 3-74340
- quark-parton model, duality constraints for deep inelastic semi-inclusive and annihilation processes 3-54312

quarks continued

- quark-parton model, for hadronic production of muon pairs, structure functions 3-78226
- quark-parton model, possibility of detecting W boson in high-energy NN interactions (*Russian*) 3-67062
- quark-parton model for deep inelastic lepton-nucleon scattering, charge symmetry 3-40355
- quark-vector-gluon model, light-cone commutators and chiral symmetry effects 3-54269
- quasi-independent model, asymptotic behaviour of hadron e.m. form factors 3-57340
- relativistic, diffractive excitation of hadron resonances 3-67096
- relativistic model, nucleon form factors and Markov-Yukawa conditions 3-67052
- relativistic model, vector meson e.m. props. 3-70925
- relativistic quark model, appl. to current algebra, high energy hadron-hadron scattering 3-70943
- review, shortcomings of different theories and hypothesis of weak interactions (*Hungarian*) 3-62811
- scattering, deep inelastic, valence quark model of mixed symmetry and s-channel picture 3-62842
- search, at CERN intersecting storage rings, charge greater than or equal to $2/3$ 3-71035
- search for, in cosmic rays and accelerator studies, review 3-61620
- search for in terrestrial matter, review 3-61615
- second-order radiative corrections in unified gauge theories, cancellations of infinities 3-67014
- selfinteracting field, light cone algebra, gauge invariant model 3-62786
- SL(3, C), principal degenerate series of unitary representations 3-62784
- strange particle interactions, prediction of branching rules between partial cross-sections 3-70944
- streamer chamber search of high energy air showers 3-77672
- strong interactions at large transverse momentum, metals of Blankenbecler, Brodsky and Guinon 3-67060
- SU₆-breaking pattern implied by transformations from constituent to current quarks 3-74332
- SU(2) × U(1) gauge theories of weak and e.m. interactions using Han-Nambu quarks 3-45865
- symmetric model, summation of direct-channel resonances, inelastic structure function relations 3-43109
- t-channel parity exchange for $K^+ + p \rightarrow K^*(1420) + \Delta^{++}$ reaction in quark model 3-62886
- three-triplet, O(4) gauge theory, e.m. and weak interactions 3-62801
- three-triplet model of third integral charges and integrally charged three-triplet model of Han-Nambu type 3-67054
- three-triplet quark currents for weak and e.m. interaction, internal symmetry groups 3-67035
- three-triplet realisations of gauge models for weak and e.m. interactions 3-59962
- total cross sections for particle-neutron interactions, shadow corrections including inelastic screening (*Russian*) 3-67166
- triality, exotics and dynamical basis of quark model 3-59986
- two-body scattering, quark counting picture, hadronic matter pool 3-78153
- unified gauge theory for weak and e.m. interactions, SU(3) × SU(3) symmetry and quark structure 3-70894
- unified lepton-hadron symmetry and gauge theory of basic interactions 3-70884
- vacuum polarisation, quark-parton puzzle 3-66995
- vector mesons, interaction with quarks, tensor current divergence principle 3-70886
- 0 photoproduction, application of PCAC anomalies in quark-vector gluon model 3-67020
- $ep \rightarrow eN^*$, modified Woods-Saxon potential for quark-diquark potential 3-78132
- $\nu N \rightarrow \pi \Delta$ threshold effect on νN coupling of $P_{11}(1470)$, quark model and exptl. data (*Spanish*) 3-67031
- $K_S^0 \rightarrow \pi^+ \pi^- \gamma$, consistency test of current-current quark model 3-57330
- $K_S^0 \rightarrow \nu \bar{\nu}$, decay width calc. in relativistic quark model 3-78130
- $K^* \rightarrow K \rho / K^* \rightarrow K^* \pi$, calc. of quark mass ratios 3-43086
- ν high energy scattering, unified gauge theory, tests of scaling 3-74359
- ν scattering, deep inelastic, three triplet realisation of gauge models 3-43094
- νN inclusive scattering as probe of nucleon core structure 3-62813
- ν inclusive electroproduction in current fragmentation region, duality and quark-parton model 3-54313
- π production in high-energy hadron collisions, reasons for SU₃ violation, quark model 3-54355
- ^3H magnetic moment, quark model study, nucleon and nuclear resonance effects 3-52073
- ^4He magnetic moment, quark model study, nucleon and nuclear resonance effects 3-52073

quartz

- acoustic surface wave focussing, Y-cut surface with Au deposit, laser probing study 3-58171
- acoustic surface waves, second harmonic generation and parametric amplification, nonlinear, theory and obs. 3-70196
- amorphous, optical characteristics in 1400-200 cm⁻¹ region, calc. using Kramers-Kronig relations 3-53096
- boundary layer formation, liquid solns. at quartz surface 3-43932
- colouration due to neutron irradiation, colour centre model (*Russian*) 3-64702
- critical opalescence, during α - β inversion 3-58571
- crystal growth structure, etching obs. (*German*) 3-52586
- cultured, growth on rhombohedral surfaces, microcrystals acting as nucleus centres 3-52584
- Dauphine twins, direct obs. using second harmonic light 3-52637
- deformation dislocations, X-ray obs. 3-75539
- deformation lamellae in ion thinned foils of naturally deformed quartz 3-69522
- deformed, basal lamellae substruct. 3-65187
- desorption of gases from quartz substrate by surface acoustic waves 3-50079
- diorite, jointed, friction and deformation meas. 3-76625

quartz continued

- dislocation structs. near cracks, transmission electron microscope obs. 3-69527
- elastic constant, u.s. velocity meas. as a function of pressure 3-80650
- enthalpy of solution of low quartz in aq. HF acid. 3-65078
- exciton creation, absorpt., photolum. excitation, photocond. and Dember effect studies 3-64314
- fused, CO₂ laser drilling, kinetic effects 3-66895
- fused, reaction with halides 3-73116
- glass, emissivity meas. 3-70289
- glass, experimental apparatus for determining emissivity, high temp. 3-70307
- glass, fused, hydrolytic surface defects and high-strength state 3-72274
- glass, integral normal radiating power, 600-1400 K 3-50005
- glass, structural changes during heat treatment, optical and e.p.r. meas. 3-80428
- glass, surface, periodic wave struct. formation by TEA CO₂ laser pulses 3-57246
- glass, symmetry of Ti³⁺ activator centres, e.s.r. and optical spectra studies 3-64296
- Hadrian's wall, quartz dolerite, age of viscous remanent magnetisation, a.c. demagnetisation techniques 3-44927
- heat transfer study 3-64223
- Hertzian fracture strength 3-58736
- high temp. stability, hydrothermal studies, muscovite plus quartz 3-44770
- high temperature phase, phonon and polariton spectra, longitudinal E₁ modes 3-55582
- hydrolytic weakening, Haasen-type dislocation multiplication model 3-65188
- impurity leaching process, high yield method of anomalous water 3-80151
- ion damage in synthetic crystals. 3-60748
- margarite, upper stability in presence of quartz 3-41885
- matrix isolation of radioactive waste 3-71334
- microchemical determination in granite dust by size selective methods on membrane filters 3-54047
- microdrilling technique for ceramics and crystalline materials 3-64970
- microimpurities determ. by neutron activation analysis 3-40075
- monocrystalline, thermal disintegration under vacuum 3-73115
- nanometre stability, suspended in catenary, for strain meter test base 3-44935
- natural, thermoluminescence study of geological differences from glow peaks 3-69499
- optical waveguides, using fused silica and quartz, light absorpt. at 1.06 μ 3-73732
- oscillator, film thickness measurement, theoretical models, relationships with frequency and period (*French*) 3-45426
- α -phase, Raman spectrum rel. to uniaxial stress, liq. He temps. 3-53102
- piezoelectric vibrations determ. of superficial mass of vacuum deposition of Au and Cu films (*French*) 3-59661
- planetary modelling, isentropic compression to several Mbar 3-39886
- plastically deformed, transmission electron microscopy obs., of dislocation structure 3-58038
- polycrystalline, magnification in X-ray diffraction patterns 3-76855
- α -quartz:Ti³⁺, electron spin resonances 3-79904
- quartz-phenolic composite, quasistatic uniaxial strain and Hugoniot tests compared 3-73111
- for rare gas condensation measurement, at low temperature (*French*) 3-66138
- resonator, thickness meas. of thin films, stress effects (*Czech*) 3-56612
- self-focusing ultrashort laser pulses 3-74273
- shock induced transition to stishovite, X-ray and optical obs. 3-76560
- stellar spectrophotometer with oscillating plateholder, review of appl. (*French*) 3-70064
- stress waves, at free boundary 3-48280
- subcritical crack growth in irrad. single cryst. slabs 3-58078
- surface, isotherm of separating pressure for water film 3-46751
- surface wave attenuation along rod in dissipative medium 3-66747
- susceptibility, third order, absolute meas. from third harmonic generation 3-78064
- syntectonic recrystallisation and texture development 3-61326
- synthetic, hydrothermally grown, charact. growth patterns 3-58014
- tectonic fault-gouge, effect on sliding mode and stick-slip stress drops 3-76627
- thermal contact conductance correlations in vacuo 3-47430
- thermal phonon radiation into quartz substrates 3-55043
- thermoluminescence, effect of radiation from radioactive material 3-76104
- thermometer probe, as fluid stirring agitator 3-42438
- transmission and reflection spectra in vac. u.v. 3-69016
- veins in rocks of late metamorphic event rel. to pressure-temp. estimates 3-61333
- vibrating plate, e.m. radiation 3-41483
- X-irradiated, e.p.r. and paraelec. reson. study 3-64552
- X-ray photoelectron, X-ray emission and u.v. spectra, valence orbitals SCF X α calcs. 3-52793
- μ^+ , polarised, anomalous precession, study via asymm. decay 3-52305
- CdS-fused quartz film-substrate system, transverse normal waves (*Russian*) 3-41080

quartz resonators see crystal resonators**quasars**

- see also cosmology; galaxies; stars
- absolute optical luminosity relation with optical variability 3-8112
- absorpt. red shifts rel. to black holes and jet mechanism 3-48066
- absorption line spectra formation, model 3-59354
- absorption spectra of large redshift quasars rel. to microwave background temp. 3-59352
- angular diameters of quasars with unusual colour 3-53684
- bright galaxies-QSO associations 3-51363

quasars continued

- 5C3 radiosources, M 31 region, optical identifications of quasars and galaxies 3-42212
 4C 05.34, absorption spectra, search for high ionisation redshift systems 3-77116
 3C 13, attempt to detect 21 cm absorption in spectra 3-77118
 3C 232, attempt to detect 21 cm absorption in spectra 3-77118
 3C 273, model for He abundance 3-59355
 3C 273, obs. of variable fluxes (*Russian*) 3-45145
 3C 273, optical variability 3-56404
 3C 273, structure and apparent motion 3-77119
 3C 275.1, attempt to detect 21 cm absorption in spectra 3-77118
 3C 279, structure and apparent motion 3-77119
 3C 286, 21 cm absorpt. at $z=0.692$, implications for intergalactic medium 3-73525
 4C 29.03, attempt to detect 21 absorption in spectra 3-77118
 4C 31.63, spectroscopic and photometric obs. 3-51364
 3C and 4C sources and candidates between -4° and $+40^\circ$ declination 3-45153
 classification into 2 types according to red shift and nearby galaxy-
 assoc. 3-45150
 clustering effects, statistical test 3-61836
 depolarisation and luminescence obs. of double radio sources 3-81122
 energy derived from gravitational collapse via rapid rotation in magnetic field 3-44991
 faint variable objects in M31 region 3-48064
 Faraday depolarization of radio galaxies and quasars with simple spectra 3-48065
 galaxy-quasar pairing, z-angular separation relations 3-53685
 gravitation-lens quasar density estimate 3-56402
 Hubble diagram for quasar groups 3-48096
 integrated contribution to X-ray diffuse background 3-81154
 intergalactic matter enrichment by matter ejection by quasi-stellar sources 3-53695
 interplanetary scintillation obs. of 203 radiosources identified as radio galaxies or quasars 3-48055
 BL Lacertae, radio structure variations 3-56405
 linear polarisation, time variation at 2.8 and 4.5 cm 3-77109
 linear polarisation at 2.8 and 4.5 cm 3-77108
 luminosity evolution rel. to pure density evolution, Parkes radio data 3-42213
 Markarian 132, absorpt.-line spectrum 3-59356
 Markarian 132, absorption lines in coude spectra using integrating television scanner 3-77117
 optical identification by coincidence of radio and optical positions 3-77107
 optical identification problems 3-81108
 optically selected, and from radio catalogues, luminosity function comparison 3-69980
 OQ172, redshift meas. 3-45207
 origin, discussion 3-45154
 observations at Padova and Asiago Observatories, astrometric programs (*Italian*) 3-61886
 PHL957, system A absorption spectra in H I cloud 3-81203
 PHL 938, absorption spectra, search for high ionisation redshift systems 3-77116
 PHL 957, absorption spectra, search for high ionisation redshift systems 3-77116
 photoionisation models for quasi-stellar object emission-line region 3-53683
 PKS 0237-23, absorption spectra, search for high ionisation redshift systems 3-77116
 QSO 1331 + 170, absorption line spectrum in visible and near i.r. 3-69982
 QSO historical light curves rel. to optical variability of 20 objects 3-48063
 QSOs in direction of Abell clusters of galaxies 3-69983
 red shift assoc. with clusters of galaxies 3-56403
 redshift distributions, their interpretation 3-73526
 redshift-angular size diagram interpretation, cosmological aspects 3-51362
 redshift-magnitude banding among QSS 3-48107
 redshift-magnitude bands visibility and charact. rel. to cosmological model 3-48086
 redshift-magnitude relation for QSOs 3-69981
 review of new data, consequences for physics 3-81121
 RHL5 model universe, predicted redshifts and number counts of extragalactic objects 3-80920
 TON 1530, absorption spectra, search for high ionisation redshift systems 3-77116
 Ton 256, spectrum of extranuclear regions 3-45183
 U1 model universe, predicted redshifts and number counts of extragalactic objects 3-80920
 V/V_m test and source-count anal. 3-73524
 wavelength dependence of degree of polarization, Faraday rotation 3-61826
 H α broad emission line, origin model 3-45152

quasi-particles

- see also *excitons; helicons; magnons; plasmons; polaritons; polarons; quantum fluids*
 alloy, disordered dispersion, anomalous, leading to non-propagating states and a mobility gap 3-72309
 electron gas, two-dimens., oscillatory quasiparticle g factor, surface electron density and mag. field depend. 3-52886
 ferroelectrics, non-conservation, bound states 3-41160
 nuclear matter, model space calc. of quasiparticle interaction 3-57487
 nuclear matter, quasiparticle interaction 3-45990
 nuclear pairing forces, methods of treatment, quasiparticle approximation (*Rumanian*) 3-62973
 solid state physics concepts, mutual interaction, hybridisation (*Japanese*) 3-72334
 superconductors, strong-coupling, quasiparticle phenomenology for thermodynamics 3-72416
 two quasiparticle systems, effects of strong rotation-particle coupling on nuclear energy levels 3-62942
 two-phonon states in even-even nuclei, microscopic theory 3-74518
 He II, liquid, line width of rotons for wave numbers $2A^{-1}$ to $3A^{-1}$, collective description 3-75647

quasi-particles continued

- He II, liquid, multi-branch structure of excitation spectra 3-60818
³He, liquid, quasiparticle interaction 3-43916
⁴He liquid, structure and excitations, review 3-58158
 MnCO₃, parametric excitation of mixed pair of quasiparticles 3-41354
 NaCl type crystals, relaxed and non-relaxed excitations (*Russian*) 3-44041
quasi-stellar objects see *quasars*
quasi-stellar sources see *quasars*
quenching (optical) see *radiation quenching*
queueing theory see *queueing theory*
queueing theory
 No entries
R and D management see *research and development management*
R waves see *Rayleigh waves*
Racah coefficients see *angular momentum theory*
radar
 see also *Doppler effect; optical radar*
 atmospheric stably stratified zones, thin radar echo layers 3-65296
 aurora, type III spectra, interpretation 3-61497
 f.m.-c.w. and optical, simultaneous obs. in meteorology 3-42085
 incoherently scattered radar signals in ionosphere, Faraday effect 3-42015
 ionospheric radar scatter, anal. and interpretation of data 3-65445
 optical processing of linear phased array radar signals 3-48856
 reflectivity, loss of information on weather patterns due to finite sample volume 3-76761
 student demonstration using chirp system to meas. distance 3-56602
 synthetic aperture data, optical processing, review 3-77977
radar altimeters see *radiocaltimeters*
radar antennas
 auroral radar scattering parameter measurement, ideal antenna configuration determ. 3-80788
 ionospheric scatter meas., aperture rel. to coherence length 3-65445
radar applications
 Apollo 17 sounding radar, surface obs. of moon 3-61730
 atmospheric Doppler spectra of diffuse radar aurorae at 50 MHz 3-73341
 atmospheric inversion above convective boundary layer, pulsed Doppler radar study of structure 3-65297
 Black Hills, radar climatology of summertime convective clouds 3-51056
 clear air convective field, intensive probing by radar and drone aircraft 3-47755
 clear air turbulence, radar detection 3-44962
 comet nucleus identification within coma, for automated space missions 3-51311
 Dee weather radar project, area precip. meas. 3-73404
 Doppler radar laser, for length and speed meas. (*German*) 3-45833
 earth's surface, aerial survey 3-73372
 f.m.-c.w. radar as remote probe of Pacific Trade-Wind Inversion 3-65520
 f.m.-c.w. radar atmospheric sounding, new developments and applications 3-65519
 ionospheric reflections in dynamics study, data processing systems 3-44961
 lunar dark mantling area of Apollo 17 nature and extent from earth-based meas. 3-61727
 lunar dual-freq. bistatic radar meas., Apollos 14 and 15 results 3-69900
 mapping North Atlantic winds 3-59174
 mountain glaciers, radar sensing 3-76868
 moving objects, Einstein-Minkowski equations (*German*) 3-40160
 ocean wave height meas. by two frequency radar interferometry 3-59197
 oceanography, remote sensing of sea states using skywave radar 3-44967
 oil spill detection using 13.3 GHz radar scatterometer 3-51213
 plan position indicator photographs, probability of encountering weather-echo near Gan 3-73401
 planetary surface mapping using ground-based radar 3-65956
 polar auroral radar, location of auroral oval 3-65411
 probing of waves and turbulence in statically stable clear-air layers 3-65516
 pulsed Doppler weather radar, storm wind velocity isotach displays 3-76911
 rain shower records, vertical motion of patterns 3-51055
 rain showers, wind gradients and Doppler spectra variance from radar obs. 3-76762
 sea ice growler detection, anomalous performance 3-76922
 sea ice imagery using airborne multifrequency side-looking radar 3-51200
 sea ice probing with video pulse sequence 3-73406
 sea slope spectrum meas. by two-frequency microwave radar 3-42089
 sea surface mapping, centimetre radiowave scattering, analysis under different hydrometeorological conditions 3-65287
 sea surface pollution meas. by satellite (*Italian*) 3-61609
 sensing, remote, correlation of insect distribution with atmospheric structure, results 3-73320
 stratospheric obs. for lee waves during glider flight 3-47761
 temperature, electron and ion, radar and OGO 6 meas., comparison 3-51181
 VHF Doppler spectra of radar echoes assoc. with visual auroral form 3-51089
radar cross-sections
 backscatter from V-shaped thin wire, theory and 9.8 GHz expt. 3-40212
 e.m. wave reflection from randomly uneven surface, asymptotic development method of determ. (*French*) 3-54197
 multipole resonance meas. for remote sensing of complex permittivity 3-47196
 rough oscillating surfaces using spectral Fourier method 3-57201
radar displays
 see also *cathode ray tube displays; fluorescent screens*
 mountain glaciers, radar sensing 3-76868
radar echo areas see *radar cross-sections*

radar equipment

- altimeter optimisation for geodesy over sea 3-44932
- pencil beam radar for ionospheric research 3-47844
- scanning f.m.-c.w. radar sounder for tropospheric sensing 3-42083

radar interference

- radiometer, protection from radar pulse interference, use of amplitude limiter (*Russian*) 3-81242

radar measurement

- atmospheric boundary layer, Doppler radar pulse for turbulent dissipation rate meas. 3-59189
- atmospheric ionization and radar wave attenuation due to nuclear explosion 3-54550
- Doppler radar characteristics of precipitation at vertical incidence 3-47768
- E-region, measurement of electron-temperature, Langmuir probe, incoherent scatter radar, results, review 3-73356
- F-region electron density 3-59175
- Geminids 1959-1969, overdense echoes, mass-distribution analysis 3-77015
- moon, Mare Imbrium lava flows, earth based radar response meas. 3-59308
- ocean wave height meas. by two frequency radar interferometry 3-59197
- tropopause detect. using forward scatter c.w. radar 3-59188
- troposphere stratified layers, trans-horizon propagation techniques for examining disturbances 3-65522
- Venezuelan rainstorm, mesoscale 1969 obs. 3-47752
- weather Doppler radar, possibility of increased velocity capability and reduced range ambiguities 3-76904

radar systems

- back-scatter, design, Thumba, India, 54.95 MHz, electrojet irregularities 3-73400
- landing aid, all-weather, meteorological measurements (*French*) 3-51194
- laser, for air pollution monitoring 3-66896
- laser radar system, Langley Research Center, description 3-40301
- weather, remote-controlled, data processing using computer 3-42059

radar telescopes *see radiotelescopes***radar theory**

- hologram matrix application 3-48447
- scattering matrix definition 3-42953
- sea ice growler detection, anomalous performance 3-76922

radarscopes *see radar displays***radiance** *see brightness***radiation**

- see also* airglow; atmospheric radiation; beta-rays; cathode rays; electromagnetic waves; heat radiation; radiation effects; radiative transfer; stellar radiation
- acoustic array, by laser-beam excitation 3-42399
- acoustic cylindrical transducer, perturbation effects of rigid cylinders 3-45367
- acoustic waves, source near reflecting boundary, sound characteristics 3-42392
- background, $\text{CaF}_2\text{:Mn}$, dosimeter, background radiation measurement 3-77284
- electric dipole in gyrotropic medium (*Russian*) 3-42946
- e.m. waves, from directional rotating source of particles (*Russian*) 3-42950
- graphite, dose absorbed, absolute calorimetric determ. (*French*) 3-74754
- laser, measurement device (*Russian*) 3-73797
- laser, measurement using calorimeter with two reflecting mirror sections (*Russian*) 3-73796
- nuclear, interaction with matter for reactor shield analysis 3-60339
- nuclear physics, book 3-62922
- radiotherapy, dosimetry, nominal standard dose, introduction of time, dose and fractionation, TDF 3-70135
- resonance radiation redistribution, magnetic fields effect 3-48838
- short surface waves, radiation and scattering, partially immersed bodies effect 3-49604
- short surface waves, radiation and scattering 3-49603
- Smith-Purcell radiation, from line charge moving parallel to reflection grating 3-42943
- sound, infinite plate with reinforcing beams 3-45352
- sound field potential on rigid cylindrical baffle by coaxial radiation 3-45354
- transition, prod. of cosmic X-rays 3-51217
- travelling sources, induction of two-dimensional field 3-75259
- vibratory prolate spheroids, local radiation impedance 3-59470

radiation belts

- see also* atmospheric electron precipitation; atmospheric proton precipitation
- alpha particles, trapped, response to geomagnetic disturbed conditions 3-69720
- auroral electrojets and evening sector electron dropouts at synchronous orbit 3-61564
- dipole theory, motion of particles in rotational symmetric e.m. field (*Hungarian*) 3-59146
- drift shell splitting by internal geomagnetic multipoles 3-50971
- electron acceleration in outer radiation belt during magnetic disturbances 3-56219
- electron diffusion driven by magnetospheric electrostatic waves 3-69697
- electron precipitation and trapped positron investigation by satellite 3-65489
- electrons, quiet time equilibrium structure 3-51151
- electrons trapped by geomagnetic field at altitudes below inner radiation belt 3-51155
- electrostatic turbulent loss of ring current protons 3-53542
- fast electron injection dynamics between belts, comparison with 1967 polar substorm 3-69677
- geocoronal hydrogen, excitation of low luminosity Balmer emissions 3-76813
- geomagnetically trapped α -particles at equator, $\text{S}^3\text{-A}$ obs. 3-69685
- high energy protons, review of present theories and expts. 3-80832
- inner, dynamic variations in intensity and energy spectra of electrons 3-69681
- inner belt electrons, OGO-5 obs. 3-69718

radiation belts continued

- inner belt equilibrium equatorial proton flux using albedo neutron measurements 3-69683
- inner zone energetic electron replenishment 3-69717
- ions, possibility of C/O ratio as a method of determining source 3-80831
- Jupiter, rel. to solar wind 3-65778
- Jupiter, source and structure 3-65779
- L, B coordinate calc., error analysis of approximation methods (*Russian*) 3-65493
- NASA/MPE barium ion cloud project, geomagnetic and geoelectric expt. 3-80822
- outer, rel. to solar wind parameters and magnetic activity and magnetotail 3-42049
- outer, simulation of gyroresonant electron-whistler interactions 3-61559
- outer, temporal variation of radial diffusion coefficient for relativistic electrons 3-69682
- outer belt dynamics during IQSY 3-56217
- outer zone electron fluxes, effect of sudden magnetospheric compression 3-65476
- outer zone-plasma sheet boundary, obs. of current driven plasma instability 3-51152
- proton ring current and magnetic field during 1971 December storm period, $\text{S}^3\text{-A}$ obs. 3-73367
- protons of low energy, resonance acceleration during storm time 3-56218
- pseudotrapping region, solar proton behaviour during magnetospheric substorm 3-61565
- pulsed magnetic field (terrella) model for expts. with radiation belts and solar wind 3-69545
- radial diffusion coefficient for relativistic electrons, temporal var. 3-61573
- relativistic electron precipitation event, rocket-borne electron spectrometer meas. 3-61574
- review of near space environment 3-56222
- ring current buildup at magnetic storm onset 3-61568
- ring current decay by charge-exchange mechanism during magnetic storm 3-51157
- ring current decay rate and polar disturbances 3-80812
- ring current particle distrib. during 1971, December 16-18 magnetic storms 3-73362
- ring current protons, energy spectra and pitch angle distrib. during 1971, December 17 storm 3-73363
- ring current protons at low altitudes, variable intensities 3-53539
- solar proton flux rel. to HF absorption during PCA events 3-80830
- solar wind interaction with magnetized planet 3-65774
- third adiabatic invariant of charge particle motion in axially symmetric fields 3-57272
- trapped protons, omnidirectional energy spectra below 750 km altitude 3-69719
- trapped protons in 0.24-0.96 MeV range, enhancement during 1967 May 25 storm 3-80817
- wave-particle interactions in ring current and plasma sheet, IMP-6 obs. 3-65483
- α particles trapped in inner radiation belt 3-80818

radiation biology *see biological effects of radiation***radiation chemistry**

- see also* chemical effects of nuclear reactions and scattering; photolysis; radiochemistry; radiolysis
- N-acetylglycine, single crystals, X-ray damage, e.s.r. meas. 3-73146
- acrylic acid radical anions in low temp. glasses, e.s.r. detection 3-65094
- azides, irradi., N_3 or N_3^{2-} radicals identification by e.s.r. and INDO calcs. 3-61267
- barbituric acid, single cryst., electron irradiation at 77K radical pair formation 3-55973
- barbituric acid dihydrate, single crystals, 4.2K, oxidation and reduction by ionizing radiation 3-73147
- cathodochromic sodalite, synthesis by struct. conversion method 3-41865
- chloroform saturated aqueous solns., X-irradiation, dose-effect curve 3-63240
- cytidine, X-irradiated, ENDOR and e.s.r. studies 3-44726
- dialkyl phosphites, γ -irradiated, e.p.r. identification of P-centred radicals 3-55974
- p-dichlorobenzene, irradi. conditions and defects influence on recovery of free radicals (*French*) 3-53325
- ethanol glasses, deuterated, trapped electrons, 4K 3-76465
- fluorescein, X-ray chemiluminescence of aqueous solutions, effect of pH 3-47568
- human serum albumin, ^{60}Co gamma irradiation, polymerisation, cross-linkages, sedimentation velocity techniques 3-48264
- Japan Radiation Research Soc. 15th meeting, Kanazawa (1972) 3-70134
- kryptonates, radioactive, in plastic substances, dosimetric application (*Russian*) 3-73150
- methyl bromide-n-hexane solutions, γ -irradiated, electron scavenging external electric field effect 3-80560
- 1-methyl uracil single crystal, irradiation induced formation of radical pairs, e.s.r. obs. 3-69473
- 2-methyltetrahydrofuran glass, γ -irradiated, ELDOR study of trapped electrons mag. energy transfer between two different spin systems 3-44727
- naphthalene crystals, γ -irrad., polarised absorpt. (*French*) 3-6509
- 5-nitro-6-methyluracil, electron irradiated, e.s.r. study of free radical formation 3-41852
- nucleic acid, e.s.r. study of radiation damage in single crystals, free radical formation 3-41851
- polymerisation, radiation nonuniformly initiated, mixing effect 3-57689
- proteins, e.s.r. study of radiation damage in single crystals, free radical formation 3-41851
- DL-serine, irradiated at 4.2 K, e.s.r. and ENDOR studies 3-76466
- succinic acid, irradiated, spectral confirmation of absence of CO_2 3-61266
- trapped in single crystals, ^{13}C hyperfine coupling tensors from e.s.r. 3-55971

radiation chemistry continued

- vapours of dielectric liquids, average energy per ion pair for α -particles 3-44728
- water and H₂O₂ aqueous solutions, depolarization of negative muons 3-41853
- water vapour, energy distrib. of secondary electrons released by fast electrons 3-80561
- H₂SO₄ glasses, γ -irrad., e.s.r. study of disappearance of trapped H atoms 3-73149
- KH₂PO₄, e.p.r. after γ -irradiation 3-69472
- Na₂Al₆Si₆O₂₄ · 1.2 NaCl · 0.4 Na₂SO₄, solid solution, optically erasable cathodochromic coloration 3-41850

radiation counters *see* **counters****radiation damage** *see* **radiation effects****radiation detectors**

- see also* dosimeters; infrared detectors; ionisation chambers; photodetectors; ultraviolet detectors
- activation, using photonuclear and neutron reaction for use in high γ -ray flux field 3-40006
- airborne particulate radioactivity, selection of monitors 3-63246
- annular, geometrical problems, beam focusing technique 3-62226
- beam diagnostic device, using optical transition radiation 3-56932
- bremssstrahlung, linear relative monitor, for 680 MeV synchrotron 3-70335
- collimator, coaxial circular aperture, for space radiation meas., optimum design 3-62231
- cosmic-rays, high-energy physical instrumentation, techniques, review 3-77633
- directional charged particle meas., digital optimization device 3-59650
- electron capture, tritiated Sc evaluation 3-66419
- fissile detectors, for neutron spectrum measurement in L54 reactor 3-48528
- flash tube hodoscopes, study of properties 3-77674
- gamma-ray spectrometry, radiological surveillance, Ge(Li) detector 3-62233
- high-vacuum gas counter for charged particles and gamma rays 3-66318
- hodoscope chambers, developments, plastic chambers 3-77665
- hydrophysical instruments, cylindrical sensors, spectral characteristics, design (Russian) 3-47848
- integral pulse, ionising radiation detection, ionisation chamber and spark gap, operating characteristics 3-70378
- jOsephson junction, point-contact arrays 3-46939
- monitoring methods and instruments, review 3-48516
- Mont Blanc cosmic ray muon hodoscope telescope expt. 3-65610
- noble gases, liquefied, ioniz. by α -particles, characterization 3-65095
- nonlinear, selective, automatic correction of differential absorption spectra (Russian) 3-73770
- nuclear power reactor instrumentation, book 3-59617
- polyvinyl fluoride optical detectors, mathematical model for response analysis 3-77393
- position sensitive detectors and multi-counter arrays for neutron studies 3-56940
- protection equipment, principles, design, construction and operation (Spanish) 3-61924
- pyroelectric, transient thermal analysis 3-68935
- radioisotopes, for medical use, integrated magnetic recorder (French) 3-53757
- radiometer sensitivity to distance of source from window and effective anode length (Czech) 3-42646
- resonance counter, for Mossbauer effect in ¹²⁵Te nuclei 3-54019
- response function of charge collection process, rigorous proof 3-40021
- scintillation counter, with high amplitude resolution for cosmic ray studies 3-56463
- submillimetre waves, W-Ge-Ni point contacts, technique, performance (Russian) 3-73805
- triglycine sulphate:L-alanine, pyroelec. detector 3-44376
- triglycine sulphate pyroelectric detector, laser radiation damage 3-66859
- universal meter, for industrial measurement techniques (German) 3-48517
- ⁴¹Ar, mobile detector, description 3-42645
- Cd₃As₂, Nernst radiation detector 3-51546
- Ge(Li), Ortec, coaxial, time resolution 3-53981
- Ge(Li) efficiency curve near Ge K-edge, method of determination 3-77624
- NaI detectors, for Cs-137 half-life meas. 3-73863
- Nal(Tl) γ -ray detector, high counting rates, discriminator 3-73881
- Nal(Tl) total-absorption counters, high energy physics, recent applications 3-77634
- Pu monitoring, nondestructive instrument techniques, criticality safety 3-63252
- Si, partially depleted surface-barrier detectors, use in low energy β -nuclide estimation 3-62350
- p-Si, position sensitive (Russian) 3-70392
- Si, surface barrier detector, damage by 0.5 to 1.5 MeV electrons 3-77618
- Si(Li), escape peaks, energy dispersive X-ray spectra, electron probe analysis 3-42730
- Si(Li) diodes used as detectors in 4π beta spectrometer, fabrication 3-59643
- T₂O, ruggedized ultrasensitive field air sampler 3-77302
- U accumulations, diffusion plant equipment, radiation monitoring, nuclear criticality 3-63250

radiation dosimetry *see* **dosimetry****radiation effects**

- see also* acoustic wave effects; alpha-particle effects; beta-ray effects; biological effects of radiation; electron beam effects; gamma-ray effects; hyperon effects; ion beam effects; laser beam effects; meson effects; neutron effects; proton effects; radiation chemistry; radiation hardening; voids (solid); x-ray effects
- alkali halide substrate surface microrelief change induced by radiation damage causing mechanical unreliefs in thin films 3-52770
- alkali halides, elementary mechanisms in radiation-induced coloration (Russian) 3-43784

radiation effects continued

- alkali tellurite glass, heat-treated, e.p.r. of radiation centres (Russian) 3-44324
- alloy, b.c.c., defects, conf. Gaithersburg, USA, (Aug., 1973) 3-79367
- atmospheric environment following nuclear weapon burst, importance of delayed radiation 3-76788
- AVR elements, post irradiation studies (German) 3-67593
- barbituric acid dihydrate, 4.2K, oxidation and reduction by ionising radiation, e.s.r., ENDOR meas. 3-73147
- cloud condensation nuclei production by u.v. radiation 3-51020
- corrosion of austenitic steel cans encasing FBR oxide fuel elements after prolonged in pile irradiation (German) 3-71313
- corundum doped with Be, Mg, Fe, u.v. irradiated, colour centre formation 3-52624
- creep, modified Orowan eqn. for case of internal stress due to energetic particle bombardment 3-64095
- damage in crystals caused by ultrasound 3-43832
- damage mechanisms, e.s.r. spectroscopy study, review 3-55459
- damage obs., i.r. spectra of cryst. defects, book 3-72693
- defect centres in solids, e.p.r. and paraelec. reson. studies 3-64552
- diamond, damage centre, optical absorption obs., neutral vacancy 3-68246
- dielectric material, induced conductivity 3-46877
- Dragon reactor, irradiation facility, HTR fuel concepts and fuel element designs 3-67458
- fading of alpha particle tracks by u.v. heating 3-59648
- ferroelectric, transparent, dispersing, irradiation discharge, intensity, spectral distribution (Russian) 3-54978
- fusion reactor technology studies at ORNL 3-60320
- GCFR pressure equalization system, irradiation results 3-63171
- genetic, exposure from man made sources, review (German) 3-74744
- graphite, gasification reactions with CO₂-base mixtures, irradiation effect (German) 3-71274
- graphite block, reactor moderator, radiolytic oxidation in CH₄-CO-CO₂ mixture, diffusion effects (German) 3-71273
- graphite irradiation for high temperature reactors (Dutch) 3-57564
- heating, blowoff impulse technology 3-74760
- HTR fuel elements, dimensional and density changes (German) 3-67592
- ionic solid, radiation induced thermally activated depolarization phenomena, nonlinear mechanisms 3-53061
- leakage, nuclear fission products, rates and amounts, water-cooled reactors 3-74749
- metal, b.c.c., defects, conf. Gaithersburg, USA, (Aug., 1973) 3-79367
- metal, elastic modulus decrease, interstitial behaviour 3-72144
- metals, lower and upper irradiation temp. limits for void formation 3-68242
- monochromatic radiation, interaction with matter, spectral theory (Russian) 3-57221
- m.o.s. capacitor, plasma irrad., oscillatory C-V curves 3-60920
- myeloclerosis, using ⁵²Fe and ⁹⁹Tc^m 3-42371
- nuclear explosions, underground, seismic moment, long-period radiation, value of explosive point source model 3-80609
- nuclear fuel, irradiated, combustion rate meas. using adiabatic calorimeter (French) 3-73694
- permissible limits of radiation, regulation of hazard, safety, National Bureau of Standards 3-53761
- photographic emulsions, effect of radioactive Ag 3-50853
- point defects, spatial distrib., diffusion, computer code DEPORT 3-64032
- polymer materials, physical tests at cryogenic temp. 3-58726
- radiative magnetogasdynamics, growth of pressure shocks 3-44925
- rock salt, behaviour under particle irradiation from high level nuclear waste (German) 3-53420
- semiconductor devices, rel. reliability and device technology (German) 3-55740
- sphere gaps and crossed cylinder gaps stressed with impulse voltages, influence of radiation 3-52548
- strain measurement, microwave frequencies, radiation environments 3-66147
- succinic acid, irradiated, spectral confirmation of absence of CO₂ 3-61266
- temperature measurement, radiation sources, coloured flames, reversal of spectral lines method 3-48366
- thin metallic targets, mech. vibrs. excited by relativistic charged particles 3-52641
- TMV-RNA, inactivation by u.v. radiation in sunlight 3-59454
- transition radiation, ultrarelativistic charged particle, laminar media, general macroscopic theory 3-79368
- triglycine sulphate, on ferroelec. props. and thermal expansion (Polish) 3-50526
- Victoreen R-meters, inherent nonlinearity 3-62312
- void growth termination in irrad. mats. 3-79336
- voids, gas-filled, equil. shape 3-68241
- γ e scattering, Compton kernel from invariant 4-vector representation 3-74374
- AgCl, illuminated, e.s.r. detection of Cr³⁺ centres 3-47140
- As₂S₂, cryst. film, photo-induced shift of transmission edge, structure changes 3-58525
- As₄₀Se₅₀Ge₁₀, amorphous film, light irrad. effect on a.c. cond. 3-68620
- CdSe films, photoconductive, illumination, conduction electron mobility, field quenching 3-46873
- α -Fe, displacement cascades due to 1-7 keV primary knock-on atoms (Russian) 3-52646
- α -Fe, displacement cascades due to 0.5 20 keV primary knock-on atoms (Russian) 3-52647
- Fe₃Al, computer simulation of radiation damage 3-79366
- He II, stimulated surface scattering of light caused by ponderomotive effect of radiation 3-55105
- KBr, u.v. and electron irrad., defect formation, exciton decay, electron microscope obs. (Russian) 3-43807
- KBr, u.v. irrad., electron microscope and opt. obs. (Russian) 3-43921
- NaCl whiskers, radiative coloration and recombination luminescence (Russian) 3-44497
- Nb, blistering due to D⁺ ions at 300 keV and above 3-40943

radiation effects continued

- PbCl₂(Br₂), u.v. irradi., e.p.r. study 3-64552
 Si collective processes in the formation of primary radiation defects 3-58050
 Si p⁺-n-n⁺ vertical junction diode, second breakdown 3-64402
 Si:O, effect on luminesc. spectra 3-61069
 SiO layer on Si, cathodoluminesc. from centres responsible for radiation induced space-charge build up 3-50275
 SiO₂ film, stress relief induced by u.v. radiation 3-64266
 SrTiO₃:Fe colour changes for energetic heavy particle detection 3-49911
 UO₂/PuO₂ fuel elements, electron micro-probe analysis of radiation induced changes (*German*) 3-71311

radiation hardening

- alloy, b.c.c., neutron irradi. effect on tensile props. 3-79386
 alloy, b.c.c., neutron irradi. temp. effect on hardness 3-79387
 alloy, radiation-induced disordering, model approach (*Russian*) 3-72831
 metal, b.c.c., neutron irradi. damage effect on mech. props. 3-79380
 metal, b.c.c., neutron irradi. effect on tensile props., embrittlement 3-79386
 metal, b.c.c., neutron irradi. temp. effect on hardness 3-79387
 neutron irradiation softening and effect of interstitials 3-79343
 CaF₂, hardening and colour centre growth after gamma irradiation 3-79349
 Cu, electron at 78K and 300K 3-60743
 Cu-Ge, electron at 78K and 300K 3-60743
 Cu-Ni, electron at 78K and 300K 3-60743
 Cu-Si, electron at 78K and 300K 3-60743
 Fe low temperature irradiation effects on deform. characts. 3-79376
 KBr:Na, thermal recovery of radiation hardening, thermoluminescence and thermal decay of V_i band 3-68247
 NaCl, X-irrad., dislocation density and radiation hardening 3-52631
 Nb, neutron irradi. hardening, oxygen impurity effects, defect agglomeration 3-40937
 V:O neutron irradi., and radiation anneal hardening, recovery and temp. depend. 3-79383
 V-Ti, and V interstitial alloys, neutron irradi., anneal hardening 3-79384
 V-Ti, neutron irradi. effect on high temp. mech. props. 3-79385

radiation injuries *see biological effects of radiation***radiation monitoring***see also dosimetry*

- ³H, conc. in air, continuous high sensitivity monitor 3-77301
 α -detector for monitoring waste water 3-53765
 β -active aerosols, Xe monitor (*German*) 3-67632
 acrylic-lead layers, heterogeneous absorbers, form of electron cascade curves (*Russian*) 3-67626
 airborne particulate radioactivity, selection of monitors 3-63246
 airborne radioactive effluents, estimation procedure from data 3-77303
 albedo, earth's surface, compared with excess or deficiency of radiated energy, Nimbus 3 satellite (*German*) 3-73329
 BWR at Nine Mile Point, survey of radiation levels and shielding 3-71340
 Concorde instrumentation, for warning of solar flares and increased radiation levels at high altitude 3-48515
 digital display system, gamma dosimeter, beta-gamma ratemeter 3-77282
 dismantling of Elk River Reactor, radioactive operations 3-71339
 dose calc. internal, using absorbed fractions concept, exact and approximate soln. (*German*) 3-77270
 dose distribution calc. using matrix, decremental line and Monte Carlo methods (*German*) 3-77269
 environmental contamination by ¹⁴C from HTRs and fuel reprocessing plants 3-71335
 environmental radioactivity, International Reference Centre, activities 3-54554
 fission products in reactor gas coolant using monitoring loop (*German*) 3-67465
 light-water reactor automatic coolant activity monitor based on Ge(Li) detector 3-67629
 methods and instruments, review 3-48516
 NIMROD, prediction of induced activity levels 3-73841
 nuclear power stations, γ -ray fields, N-16 content 3-74747
 nuclear power stations, by CEGB 3-53759
 nuclear power stations, water-cooled, routine monitoring system 3-74750
 nuclear reactor, Braunschweig research, organisation of radiation protection service 3-63255
 nuclear reactor coolant activity supervision, γ -ray spectrometry (*German*) 3-71327
 nuclear reactor fuel elements, cask loading, inverse multiplication meas. in situ, criticality safety 3-63251
 passive gamma neutron monitor, fissile content of waste and scrap, criticality safety 3-63254
 personnel rel. to photons and neutrons standardisation of dosage 3-63241
 plume exposure, BWR, calculated and measured 3-63244
 protection equipment, principles, design, construction and operation (*Spanish*) 3-61924
 pulsed neutron source techniques, criticality safety determination, reactivity of a reactor core 3-63231
 radioactivity measurement in dust around 400 MeV LINAC 3-40549
 radioiodine, airborne, monitoring improvement of collecting efficiency under high relative humidity 3-73608
 radionuclide concs. in marine animals, monitoring sensitivity San Onofre Nuclear Generating Station 3-74767
 reactor fuel, exposed, criticality control parameters 3-46151
 real time monitor, for field shape and intensity 3-66063
 sapphire radiation monitoring loop rel. to determ. fission product conc. in reactor coolant (*German*) 3-67464
 secondary standard dosimetry, WHO Regional Reference Centres 3-54555
 single channel analyzer, temp. compensated, for monitoring of fission products 3-40029
 tasks and problems 3-45325
 thermoluminescence dosimetry system, for radiotherapy monitoring 3-53775

radiation monitoring continued

- transport of radiation, directional-biasing soln. for cases of deep penetration 3-52236
 units, SI rationalisation, problems, recommendations of ICRU 3-77245
 u.v., radiation hazard meas., optical spectrophotometer 3-73753
 u.v. biologically weighted hazard monitor. 3-77281
 waste, radioactive, monitoring information system 3-74751
 welding, elec., radiation meas., eye protection (*German*) 3-51466
 X-ray monitor calibration, ¹²⁹I, colour television 3-73911
 X-rays and γ -rays, methods (*French*) 3-66315
 Al-Pb layers, heterogeneous absorbers, form of electron cascade curves (*Russian*) 3-67626
 B, soluble poison meter, neutron detection 3-63253
²⁵²Cf neutron radiography device, comparison of a multiplied and unmultiplied facility 3-63247
 Cu-Pb layers, heterogeneous absorbers, form of electron cascade curves (*Russian*) 3-67626
⁶⁷Ga-citrate photocan, tumour location 3-48252
 Gd, soluble poison meter, neutron detection 3-63253
 I, A = 129-135, emission from nuclear reactors, accumulation in Federal German Republic (*German*) 3-67631
 Pb-Al, Pb-Cu and Pb layers, heterogeneous absorbers, form of electron cascade curves (*Russian*) 3-67626
 Pu, nondestructive assay, criticality prevention, scrap recovery 3-63249
 Pu, nondestructive instrument techniques, criticality safety 3-63252
²³⁹Pu in lungs, correction factors for different body builds between phantom and subject 3-73601
^{99m}Tc, brain scans, tuberous sclerosis, vascularity 3-51461
^{99m}Tc-S colloid, lung uptake, heart and lung time-activity curves, reticuloendothelial mechanism 3-51459
 U accumulations, diffusion plant equipment, nuclear criticality 3-63250

radiation monitors *see radiation monitoring***radiation patterns, antenna** *see antenna radiation patterns***radiation pressure**

- see also acoustic streaming; solar corpuscular radiation*
 absorbing spheres, and phosphoresis, heat source function 3-51849
 acoustic wave diffraction by plates joined at right angles, pressure determ. (*Russian*) 3-45344
 cosmic dust under influence of radiation pressure and gravity 3-70050
 early-type stars, heavy ion acceleration 3-81042
 galaxies, expulsion of interstellar dust by radiation pressure 3-42229
 Mariner 9 Mars orbiter, solar radiation pressure calc. 3-56318
 multilayer media, radiation force due to plane e.m. waves 3-45761
 phonon concepts rel. to acoustical mirage and radiation pressure (*French*) 3-40989

radiation protection*see also radiation monitoring*

- beam containment devices, safety problems 3-56879
 charcoal filters, absolute and activated, testing 3-71344
 concrete, thermoluminescence, γ -ray transmission curve and build-up factors 3-43318
 containment building leak rate, regression approach calc. 3-49377
 decontamination of Al, steel, and Al/steel couples 3-60283
 decontamination of plutonia contaminated thermal reactor systems 3-57589
 dosage received by nuclear reactor staff over seven year period, and positional activity data (*German*) 3-74769
 dump for high-energy high-intensity beam, design calcs. 3-57590
 environmental, atomic energy industry's approach to the problem 3-74745
 fissile metal, criticality study for handling and storage 3-43315
 fusion reactor, radiological implications 3-42380
 gamma-ray ceiling attenuation factors, basement, determ. from finite field data 3-60336
 health phys. conf. Miami Beach, USA (1973) 3-77246
 helium dewar, portable, gas-cooled radiation shields, use with superconducting magnetometers 3-48384
 hot cell modification for alpha work (*German, English*) 3-63242
 instrumentation for UK nuc. prog. 3-54531
 Japan Radiation Research Soc. 15th meeting, Kanazawa (1972) 3-70134
 laser protective materials, selection and testing, filter measurements 3-73789
 leakage neutron spectra calc. for monoenergetic, fission and reactor sources and for various shields 3-49378
 medical sources, ²⁵²Cf, storage and handling facility, design 3-70179
 mice, pulse radiation exposure, AET protection 3-70180
 microwaves in spectroscopic sources 3-66061
 monitoring equipment, principles, design, construction and operation (*Spanish*) 3-61924
 NAL main ring, radiation survey vehicle 3-56775
 neutron shielding, transport calcs., duct streaming, Japanese activities (*Japanese*) 3-71333
 nuclear installation, airborne effluents, WEERIE program 3-77297
 nuclear power plant, general public and operating personnel 3-63144
 nuclear power stations, underground containment system 3-77268
 nuclear reactor, Braunschweig research, organisation of radiation protection service 3-63255
 nuclear reactor, shield attenuation calc. 3-60342
 nuclear reactor experimental shielding, design 3-60345
 nuclear reactor fuel elements, cask loading, inverse multiplication meas. in situ, criticality safety 3-63251
 nuclear reactor shield analysis, Monte Carlo methods 3-60341
 nuclear reactor shield design 3-60343
 nuclear reactor shield design 3-60346
 nuclear techniques, protection technology 3-63256
 nuclear waste, nondestructive assay, criticality problems and solutions 3-63248
 organisation and standardisation, French central service (*French*) 3-66060
 passive gamma neutron monitor, fissile content of waste and scrap, criticality safety 3-63254
 permissible doses of ionizing radiation, standards (*Dutch*) 3-78392

radiation protection continued

- permissible limits of radiation, regulation of hazard, safety, National Bureau of Standards³ 3-53761
 portable exposure meter, requirements and test procedures 3-48538
 power station build-up of radioactive materials, detection and control 3-74768
 pulsed neutron source techniques, criticality safety determination, reactivity of a reactor core 3-63231
 radioactive waste, selection of ground disposal site using computer (*Japanese*) 3-43517
 radioactivity measurement in dust around 400 MeV LINAC 3-40549
 Rauscher leukemia virus, SJL/J mouse, development of radioresistance, distrib. of mortality, X-radiation 3-48269
 reactor shielding, neutron cross-sections of Egyptian marble, evaluation 3-67625
 reactor shielding, radiation sources 3-60338
 reactor shielding analysis, Boltzmann transport eqn., soln. 3-60340
 shield analysis, radiation interaction with matter 3-60339
 standards, U.S. atomic energy programme, pollution control 3-43319
 standards hierarchy and interrelationships 3-67380
 teletherapy room and maze-protected doors, shielding calculation using γ -ray albedo 3-53760
 Universal Cells at Chalk River nuclear laboratories 3-57592
 welding, electric, radiation meas., eye protection (*German*) 3-51466
 X-ray diffraction equipment in New Zealand, safety features 3-48268
 X-ray diffractometer, divergence slit assembly shield, elimination 3-63928
 X-ray generation and application apparatus, standardisation (*French*) 3-70178
 X-rays at high-energy, attenuation obs. rel. to shielding, betatron expts. (*Japanese*) 3-42630
¹³⁷Cs γ -ray backscatt. by finite barriers 3-60333
³H handling, protective measures (*French*) 3-59458
 Pu fuel technology, radiation exposure consideration in LWR fuel manufact. 3-57588
 Pu monitoring, nondestructive assay, criticality prevention, scrap recovery 3-63249
 Pu monitoring, nondestructive instrument techniques, criticality safety 3-63252
 U accumulations, diffusion plant equipment, radiation monitoring, nuclear criticality 3-63250
 Zr, total neutron cross section meas. for Zircaloy-2, ⁹⁰Zr 3-60285

radiation quenching

- acetone in solution, triplet state, charge transfer rel. to quenching by aromatic molecules 3-69474
 9 alkyl-substituted anthracene solutions, excimeric fluorescence, concentration quenching 3-65106
 anthracene crystals, nonlinear quenching of fluoresc., 1.8-4.2 K 3-58559
 anthracene crysts., fluoresc. quenching by singlet-singlet and singlet-triplet exciton interactions 3-58541
 anthracene solution, delayed fluorescence, O₂ quenching, mag. field effects 3-46309
 aromatic compounds fluoresc. state, heavy-atom collisional quenching, empirical law 3-52382
 biacetyl, small molecule behaviour and ³B_g state 3-75058
 biphenyl fluorescence, quenching by inorganic ions in solution 3-73160
 dioxane, PPO soln., radioluminesc. mechanism in scintillators 3-80085
 DNA, excited states, triplet quenching, photosensitisation 3-63588
 dye laser, polymethine, flashlamp-excited, quenching effects 3-66832
 flavonoids, with 5-OH group, luminesc. mechanism 3-69082
 fluorescence, internal quenching, compensation law 3-60471
 fluorescence quenching rel. to use as laser material 3-48907
 fluoro(trifluoromethyl)benzenes, in gas phase, fluoresc. and singlet state emission quenching 3-55978
 cis-glyoxal, time and energy resolved fluoresc. 3-57663
 glyoxal vapour, excited at 4358 Å, collision induced intersystem crossing, photophysics 3-80566
 N-isopropyl carbazole, fluorescence quenching by aromatic and nonaromatic acids 3-76479
 ketones, aromatic, quenching of triplet state by O₂ in liq. soln. 3-76482
 ketones in solution, triplet state, charge transfer rel. to quenching by aromatic molecules 3-69474
 liquid scintillation counters, methods for quenching correction 3-62245
 methylene blue, photoquenching, depend. of quantum yield on pulse intensity and duration 3-67840
 α - and β -naphthalene-d₁₀, excited state H-D exchange and fluorescence quenching 3-69475
 nitrogenase active centre, tracers, energy transfer, dimens. meas. 3-67871
 organic dye solutions, two-photon excitation, fluoresc. quenching mechanisms 3-64715
 photoquenching of large molecule depend. of quantum yield on pulse intensity and duration 3-67840
 pyrene solution, delayed fluorescence O₂ quenching, mag. field effects 3-46309
 radical ion and triplet form. in electron transfer fluoresc. quenching by nsec. laser spectroscopy 3-80563
 rhodamine dyes, conc. quenching of luminesc. in alcohol solns. 3-69075
 ruby, nonlinear optical, mechanism 3-64723
 ruby, radiative and nonradiative transitions, temp. depend., emission quenching 3-41568
 solution, fluoresc. quenching and nonradiative energy transfer 3-69060
 terbiu aromatic dyes, nonradiative energy transfer 3-64714
 As₂Se₃, glassy, photoluminesc., optical quenching, midgap localized states evidence 3-50618
 As₂Se₃:As₂Te₃, glassy, photoluminesc., optical quenching, midgap localized states evidence 3-50618
 B + Cl₂ chemilum. quenching, BaCl₂* radiative lifetime 3-55927
 CO(A π), deactivation rel. to individual vib. levels 3-75150

radiation quenching continued

- H₂ quenching and trapping of Lyman- α fluorescence at large optical depths 3-60362
 H atom, metastable, quenching in elec. field, polariz. of Ly- α radiation 3-78471
 H metastables, photon scatt. theory of quenching 3-63270
 I₂, excited atom quenching by O₂, opto-acoustic spectra obs. 3-78883
 I₂(B³ Π_{ou}^+), fluoresc. lifetimes, self- and foreign gas quenching cross sections 3-40647
 N₂, solid kinetics, relaxation mechanisms, electronic quenching in luminesc. 3-69072
 (N(C₂H₅)₄)₂ZnI₄:NiI₄²⁻, mag. circular dichroism spectrum, spin-orbit splitting, quenching 3-50601
 NO₂, fluoresc., mag. quenching study, 0 to 15 kG 3-43471
 NO₂, fluorescence, magnetic field effect 3-78836
 Na fluorescence in Hg-Na-N₂ mixture, collisional quenching by N₂ 3-54571
 Nd³⁺ ion excited state crystals, investigation of elementary cross-relaxation 3-64305
 Nd₂O₃-POCl₃-SnCl₄ solutions Nd³⁺ luminescence, self-quenching 3-64713
 O(2¹D₂), quenching of atomic resonance radiation in vacuum ultraviolet by gases 3-71370
 P atoms, electronically excited by PCl₃, collisional quenching, kinetics rel. to ionisation potential, atomic spectroscopy 3-49415
 Rb(5²P_{3/2,1/2}) doublet, quenching and doublet mixing cross sections by N₂, O₂, H₂, H₂O 3-67694
 Rh(III) complex, halopentammine, radiative and radiationless decay processes 3-73158
 SO₂, collision-free time-resolved fluoresc. 3-75056
 SO₂, decay fluoresc. from single vibronic levels 3-54708
 Te(5³P₁), Te(5³P₀), spin-orbit quenching by gases 3-71371
 V₂Ga composite wires, processing and superconducting props. 3-68726
- radiative shifts** see *relativistic corrections*
- radiative transfer**
- Ablation and radiation coupled viscous hypersonic shock layers 3-78985
 absorption capacity of hollow vessels calcs. (*Russian*) 3-77920
 air suspension with Al₂O₃, heat transfer from a reflected shock wave (*Russian*) 3-52470
 Algal-type binary secondary component, departures from LTE 3-51326
 angular quadrature perturbations, numerical solution 3-42913
 anisotropic non-conservative scatt. in semi-infinite media 3-56332
 annular rings and hemispherical sectors radiation configuration factors calc. 3-66705
 astronomical X-ray spectra effect of Compton scattering 3-81047
 atmosphere, radiative slip between two absorbing-emitting gases rel. to air pollution 3-53474
 atmospheric window, airborne radiative transfer from tropical sea, band surfaces 3-59100
 axial radiation reception, multidimensional, nondispersive, uniform, unbounded propagative medium 3-66607
 bibliography of Soviet works 3-62620
 binary stars, atmospheric temperature distrib. (*Russian*) 3-73488
 blackbody cavity, radiative equilib., integral eqns. 3-45734
 blackbody simulators, polythermal, theory 3-77914
 blast wave propagation in inhomogeneous medium, analytic soln. 3-78993
 boundary layer of radiating gas, nonlinear effect of Rosseland approx. 3-78953
 Chandrasekhar's S and T functions relationship 3-74169
 cloudy atmosphere containing water drops, clearing by intense monochromatic radiation (*Russian*) 3-79485
 combined conduction, convection and radiation, plate temp. determ. 3-75190
 composite material, heat transfer, photon mean free path depend. 3-55103
 Compton-scattering atmosphere with continuous energy dependence 3-70761
 coupled radiation with turbulent convection in electric arcs 3-79185
 dayglow, excitation of OII at 834 Å 3-41999
 diffuse galactic light rel. to interstellar dust albedo in 1500-4250 Å region 3-53701
 dusty atmosphere, i.r. radiative fluxes, model, appl. to Rajasthan Desert atmosphere, India 3-44885
 Earth's interior, opacities of transparent minerals rel. to temp. and wavelength 3-65217
 Earth-atmosphere system, effect of atmospheric aerosols, soln. of radiative transfer eqn. 3-80775
 electrical simulation models 3-70765
 electrically conducting and thermally radiating gas, temperature decay 3-60509
 extended stellar atmospheres with pure absorption, curvature effects 3-51325
 flat ocean, irradiance refl., radiative transfer eqn. 3-53438
 fluids, radiative, thermal stability, asymm. slot problem 3-40712
 gas, confined, radiatively driven harmonic acoustic waves, expt. 3-71712
 gas, confined, radiatively driven harmonic acoustic waves, theory 3-71711
 gas, heat absorption, approximate method at high temperatures 3-57172
 gas, radiating, nonlinear resonant wave motion 3-57702
 gas flow, plane, heated by radiation in presence of strong overirradiation (*Russian*) 3-43644
 gas-cooled nuclear reactor, by solid suspension laminar flow with radiating fluid 3-40529
 gaseous suspension flow of solid and liq. particles with internal heating, analysis 3-60576
 gases and plasmas, step heat waves dynamics 3-54861
 graphite, massively ablating, chemical nonequilibrium 3-80401
 gray medium in rectangular enclosure, radiative equilibrium temp. distributions 3-54180
 H-matrix, existence and uniqueness theorems 3-56373
 heat and mass transfer, bibliography, Soviet works 3-52435
 heat and mass transfer bibliography of Soviet works 3-40190
 heat transfer bibliography, Japanese works 3-57735

radiative transfer continued

- hemisphere with radiating surface, thermal stresses due to internal heat source 3-54096
- high-speed turbulent radiating boundary layers, numerical solns. of integro-differential equations 3-52453
- inhomogeneous magnetic field, numerical integration of equations (*Russian*) 3-77043
- integral eqns. asymptotic solns. with convolution kernel 3-48699
- interface functions calc. 3-51841
- interstellar gas, radiative cooling of hot low density gas 3-56436
- interstellar masers, radiative transport calcs. 3-61861
- isothermal spherical layer, radiative flux, effect of line or band shape 3-66700
- Jovian atmosphere structure determ. from i.r. meas., iterative method 3-56335
- Jupiter, greenhouse models of atm. 3-56343
- Jupiter's cloud bands, radiative instability of cloud deck, flow model 3-61680
- Jupiter atmosphere, ammonia spectral data for ν_2 bands 3-76995
- Jupiter shock-layer temps. appropriate for entry, meas. of H_2 -He radiation 3-69881
- laminar liquid flow, radiative transfer 3-60540
- laser cavity, density inhomogeneity due to energy release 3-45789
- line radiative transport in nonhomogeneous media, improved separability approximation 3-42912
- linear-operator equations on spherical shell 3-48814
- local characteristics, study and calc. using iterative-zonal method 3-48820
- lunar surface radiative transfer, effects of scattering and thermal conduction 3-61684
- RR Lyrae variable star models, non-linear pulsations and grey radiative transfer 3-47993
- magnetogasdynamics, radiative, resonant oscillations 3-79050
- Mercury, surface radiative transfer, effects of scattering and thermal conduction 3-61684
- multidimensional line transfer equation, exact solution 3-66701
- multiple scattering theory in inhomogeneous atmospheres 3-48815
- non-coherent scattering in infinite medium, resonance radiation transfer problem (*Russian*) 3-42971
- non-coherent scattering spherical shell media, probabilistic model for resolvent kernel 3-51840
- non-stationary gas-dynamics, soln. including radiational heat exchange by angular averaging (*Russian*) 3-43645
- nongray medium, radiative decay times for thermal perturbations 3-51839
- nongray medium with arbitrary configurations, radiative decay time 3-70763
- nongray radiative transport in a cylindrical medium 3-45741
- optically deep absorbing media, interior radiances, one-dimensional model exact solutions 3-74168
- optically deep absorbing media, interior radiances, Rayleigh scattering 3-70760
- packed beds, radiating gas effect on effective thermal conductivity 3-40706
- participating, non-participating media, fundamental concepts, mathematical treatment, book 3-77921
- photon bubbles, analogy with fluidized bed 3-53651
- Planck's equation, numerical solution 3-77913
- planetary atm., modified two-stream approx. of Sagan and Pollock (1967) 3-56342
- planetary atm., photon path length distrib. for diffuse reflection 3-65739
- planetary atm., refraction problems 3-73453
- planetary atm., scattering and transmission functions of atm. with reflecting surfaces 3-69852
- planetary atmospheres, far i.r. H_2 spectrum 3-69880
- planetary atmospheres, inhomogeneous, plane parallel, emergent radiation calculated by adding method 3-73455
- planetary atmospheres, multiple scatt. of polarised light 3-61691
- planetary atmospheres, radiation field in deep layers 3-61692
- planets, radiative instability of cloudy atmosphere 3-61679
- plasma, optically thick, radiative transfer mechanism 3-49645
- plasma temperature meas. using self-absorbed spectral lines, solutions of radiative transfer equation 3-43689
- plastic foils, Al coated, for superinsulation packaging 3-62024
- probabilistic model for transfer problems in cylindrical shell media 3-53643
- probabilistic radiative transfer, mean number of scatterings, numerical soln. 3-42914
- radial radiative heat flux in a cylinder 3-66706
- radiation-conduction heat transfer, integral equation 3-59823
- rarefied gas, thermal conduction analog 3-67943
- resonance radiation redistribution, magnetic fields effect 3-48838
- resonance radiation transfer, role of branching ratio 3-70762
- scattering from maritime haze, matrix operator theory of radiative transfer 3-41952
- semi transparent solids, heat transfer study 3-64223
- semitransparent cylindrical medium solidification, heat conduction and radiation 3-46701
- smooth air-water interface, thermal radiative props. 3-45736
- solar one-component model, radiative transfer and statistical equilibrium eqns. 3-80925
- solar radiation transfer through cirrus clouds 3-53475
- solids temperature fields under natural heat exchange conditions with the atmosphere 3-77916
- spectral line broadening, non-coherent scattering study 3-52376
- spectral line profile inversion, numerical method 3-51333
- specular reflection from a curved surface, view function in generalised curvilinear coordinates 3-45737
- specular reflectors for prescribed disturbed radiant heating from a point energy source 3-45442
- specularly reflected radiation properties of absorbing films, at normal incidence 3-51858
- spherical circumstellar dust shell, radiative transfer eqn. for polarised light scatt. 3-69954
- spherical shell media with complete freq. redistrib., probabilistic models 3-56374
- steam, turbulent flow in pipe, radiative transport 3-52436
- stellar atm., multiple scatt. of resonance radiation in plane layer and sphere 3-69918

radiative transfer continued

- stellar atm., non-LTE line transfer, interpolation method for soln. 3-73484
 - stellar atm., plane-parallel, matrix method for determ. of internal radiation field 3-69929
 - stellar atm., transfer of polarised radiation 3-53637
 - stellar atm. curvature effects, absorpt. and scatt. 3-69928
 - stellar atmosphere numerical evaluation of formal soln. in spherical geometry 3-69935
 - stellar atmospheres, integrated kernels and exact solns. to problems in spherical geometries 3-61758
 - stellar atmospheres, multiplet formation in spectra 3-71359
 - stellar atmospheres, superposition of layers 3-47994
 - stellar envelopes, meridian circulation with rapid differential rotation 3-53636
 - stellar hydrodynamics, eqns. describing rotating gaseous medium 3-47865
 - stellar moving atm., coupling between thermal conduction and radiative transfer 3-73483
 - stellar spectral line formation in spherical atm. 3-45087
 - stellar stationary outflowing envelope models 3-69931
 - Sun, source function determ. for upper photosphere 3-59257
 - sunspot radiative model in magnetohydrostatic equil., possibility of construction 3-65678
 - supergiant stars, line effects on radiative accel. 3-47981
 - terrestrial atmospheric model, two-level general circulation, response to solar radiation reduction 3-59098
 - terrestrial infrared, effects of particulate matter on radiance 3-76721
 - time dependent radiative cooling of hot low-density interstellar gas 3-48119
 - time dependent radiative transfer, development of formalism 3-59333
 - Titan, greenhouse models of atm. 3-47921
 - transport equations, nonlocal variational formulation 3-70751
 - two simply coupled spectral lines, probabilistic radiative transfer 3-51892
 - two-level source function, dependence on own radiation field 3-48000
 - two-phase flow, radiation interrogation dynamic-bias 3-46394
 - V-groove and rectangular cavities, directional thermal emission optimisation 3-45443
 - H_2O molecule masering in protostellar gas clouds 3-45215
 - H_2O pure rotation spectrum, approximate mean absorption coefficient 3-67833
- radicals, free** see free radicals
- radio applications**
 see also radioastronomy; radionavigation
 glaciers, radiointerferometry depth sounding 3-80659
 Mars lander position estimation, in presence of ephemeris biases 3-59403
 meteorological broadcasts, outline of information 3-73335
 radiointerferometry depth sounding, theoretical wave nature of electromagnetic fields, appl. to meas. of elec. props. 3-80843
 time scale clamping and frequency collation, using v.l.f. radiowave propagation 3-51510
- radio broadcasting**
 ionospheric wave propagation curves at night in broadcasting range 3-69633
- radio links**
 see also microwave links
 balloons appl. 3-56257
 s.w. ionospheric propagation, phase instability distribution parameters (*Russian*) 3-42020
- radio receivers**
 see also superheterodyne receivers
 meteorological equipment 3-73335
- radio relay systems** see radio links
- radioactive age determination** see radioactive dating
- radioactive chemical analysis**
 see also radiochemistry
 β -nuclide estimation at low energy using partially depleted surface-barrier Si detectors 3-62350
 biological systems using radioactive tracers (*Italian*) 3-54035
 charged particle activation analysis, isotopic concentrations for light elements 3-62371
 environmental radiocativities, active charcoal method 3-69582
 light water reactor rods, ^{235}U content meas., Sb-Be neutron source 3-67558
 lunar surface, expected emission spectra as function of chemical composition 3-77004
 meteorites, Haverö ureilite, anal. of cosmogenic radionuclides 3-45062
 nakhlite meteorites, Lafayette and Nakhla, thermal history by ^{40}Ar - ^{39}Ar method 3-56360
 neutron activation analysis, advantages, limitations and applications 3-62373
 neutron activation analysis in geochemistry 3-65512
 nucleic acid, T-labelled, scintillation counting obs. in salt solutions (*German, English*) 3-66452
 radioisotope applications, new techniques (*Afrikaans*) 3-62198
 steel, thermodynamic activity meas., ^{14}C radiometric method, equilibrium and kinetic study 3-54039
 trace analysis techniques, advantages and disadvantages 3-48669
 tritiated water, internal contamination, dose equivalent determ. 3-73604
 whey, radioactive sterilisation and dosage (*Italian*) 3-54050
 Cd metal loaded chromatographic columns, radiochemical separation by adsorption 3-40069
 ^{238}Pu , ^{241}Am sequential determ. in environmental samples 3-66451
 Pu isotopic composition in nuclear reactor fuels, calorimetric determ. prior to irradiation 3-71287
 ^{124}Sb -Be (p,n) assay system, fissile content meas., 4He gas tube detectors 3-67557
 U-Pb systematics in lunar basalts, response to comment 3-53621
 UF_6 , partial pressure determ. from meas. on U radioactivity (*German*) 3-66462

radioactive dating

- see also earth age
- apatite fission-track dating of porphyry type deposits 3-65133
- Apollo 17 material, isotopic ages 3-65845
- applications in art and archaeology, review 3-53809
- Archaean granulite facies metamorphic event in W. Greenland, $^{207}\text{Pb}/^{206}\text{Pb}$ ages 3-56044
- blueschists of Seldovia, Alaska, tectonic significance 3-50936
- Columbia plateau basal production rate, K/Ar age data 3-76596
- Dembe-Divula complex, whole rock Th-Pb age determ. 3-47622
- fission-track, volcanic glass from Mt. Edziza, British Columbia 3-76515
- flow distrib. of environmental tracers, finite state mixing cell models 3-56275
- Galaxy, r-process path termination in nuclear yield ratio dating 3-73437
- geological samples and tektites, thermal annealing of latent damage trails 3-61359
- granitic rocks of Nova Scotia, Rb-Sr ages 3-76517
- igneous rocks near Hedley B.C., K-Ar ages constraints on petrological model for Similkameen batholith 3-76521
- Juvinas achondrite, use of ^{146}Sm for dating of planetary materials 3-47966
- Lac St. Jean anorthosite and associated rocks, Rb-Sr ages and petrologic studies 3-65136
- lunar soils and rocks (Apollo 17) 3-65832
- Masuke complex, whole rock Th-Pb age determ. 3-47622
- Matatchewan dike swarm, Rb-Sr dating, evaluation of method 3-65137
- meteorites, ages of eight recently fallen objects 3-61744
- mica, fission-track aging 3-44779
- minerals containing U, suitability for fission track geochronology 3-44831
- Orgueil meteorite, magnetite, $^{129}\text{I}/^{129}\text{Xe}$ method 3-77025
- radiocarbon, reln. to atmospheric content, geomagnetic variations and cosmic radiation (Russian) 3-65233
- tree rings, effect of lightning production of neutrons on ^{14}C dates 3-76745
- zircons from early Precambrian Godthaab District Amitsoq Gneisses 3-47619
- K-Ar, slates from Meguma Group, Nova Scotia 3-73204
- $^{207}\text{Pb}/^{206}\text{Pb}$ ratio, radiometric ages of meteorites 3-77026
- Th-Pb whole rock dating on eight granites 3-65219

radioactive decay periods

- delayed proton and alpha precursors, decay properties 3-54439
- half-life measurements with unequal time bins, analysis of method 3-48491
- measurement method using multichannel analyzer (French) 3-51697
- perturbation of decay rates, review 3-54442
- ^{31}Al , $T_{1/2}=5/2$ nuclide, mass and β decay half-life 3-54373
- ^{37}Ar , half-life by gas proportional counters (French) 3-57493
- ^aAs , $A=84-86$, produced in ^{235}U neutron induced fission, delayed-neutron meas., half-life determ. 3-43202
- ^{177}Au , deduced half-life and α -particle energy 3-54499
- ^{197m}Au , from $^{197}\text{Au}(\gamma, p')$, 100-800 MeV 3-67308
- ^{143}Ba , half-life and γ -ray energy by direct meas. 3-78281
- ^{10}Be half-life, modification of cross sections for $^{10}\text{Be}(\text{d}, p)^{11}\text{Be}$, $^{10}\text{Be}(\text{d}, \alpha)^8\text{Li}$ and $^{10}\text{Be}(p, p\gamma)^{11}\text{B}$ 3-40505
- ^{189}Bi , deduced half-life and α -particle energy 3-54499
- ^{39}Ca β -decay, meas. of half-life, ft values, and Gamow-Teller matrix elements 3-67275
- ^{248}Cf , α -decay, total half-life obs., spontaneous fission half-life determ. 3-46013
- ^{54}Co , half-life meas. 3-40461
- ^{132}Cs , gamma activity, half-life 3-67268
- ^{134}Cs , half-life meas. by mass spectrometry over 9.8 yrs. 3-57494
- ^{137}Cs , half-life meas. by mass spectrometry over 11 yrs. 3-57494
- ^{252}Es , half life by decay of α count rate, decay scheme 3-54443
- ^{22}F β decay, half-life 3-43221
- ^{251}Fm , α -decay, determ. half life, multiplicities of prominent transitions from α -e $^{-}$ ion expt. 3-67281
- $^{65}\text{Ge} \rightarrow ^{65}\text{Ga}$, positron decay, half-life meas. 3-60131
- ^{172}Hf , half-life meas. 3-52143
- ^{178}Hf high-spin isomeric state, half life and neutron capture production cross section 3-62987
- ^{194}Hf , half-life meas. 3-52143
- ^{177m}Hf , half-life meas. 3-63007
- $^{179m2}\text{Hf}$, half-life meas. 3-63007
- ^{130}I , half-life meas. 3-67214
- ^{115m}In , from $^{115}\text{In}(\gamma, p')$, 100-800 MeV 3-67308
- ^{198}Ir , existence and half-life, evidence from γ -transition obs. on $^{198}\text{Pt}(\text{n}, p)$ 3-63008
- ^{72}Kr , produced in $^{58}\text{Ni}^{(16}\text{O}, 2\text{n})^{72}\text{Kr}$, gamma decay, $T_{1/2}$ determ. 3-74532
- ^{73}Kr , produced in $^{58}\text{Ni}^{(16}\text{O}, \text{n})^{73}\text{Kr}$, gamma decay, $T_{1/2}$ determ. 3-74532
- ^{178}Lu , from ^{178}Yb decay and $^{176}\text{Yb}(\text{t}, \text{n})$ reaction, half-life, β and γ energies and coincidences, log ft. values 3-67276
- ^{21}Mg , β^{+} -delayed proton decay, half-life meas. 3-60128
- ^{50}Mn , half-life meas. 3-40461
- ^{24}Na , effect of chemical combination on half life (German) 3-49221
- ^{26}Na , beta decay $T_{1/2}$ meas., mass excess, and ^{26}Mg excited states determ. 3-74541
- ^{27}Na , beta decay $T_{1/2}$ meas., mass excess determ. 3-74541
- ^{173}Pr , deduced half-life and α -particle energy 3-54499
- ^{103m}Rh , half-life determination 3-40438
- $^{132}\text{Sb} \rightarrow ^{132}\text{Te}$, β -decay of two states with half-lives 3.4 and 4.9 mins. (Russian) 3-74538
- ^{41}Sc β -decay, meas. of half-life, and ft values, and Gamow-Teller matrix elements 3-67275
- ^{133}Sn , β -decay, half-life determ. 3-71050
- ^{154}Te , isomeric state half lives and branching ratios determ. 3-67263
- ^{135}Te β -decay, half-life determ. 3-71050
- ^{218}Th , α -decay energies and half lives meas. 3-54445
- ^{219}Th , α -decay energies and half-lives meas. 3-54445
- ^{220}Th , α -decay energies and half-lives meas. 3-54445
- Tm to Hg short-lived neutron deficient nuclei, spectroscopic investigation of half-life (Russian) 3-52142
- ^{46}V , half-life meas. 3-40461

radioactive decay periods continued

- $^{47}\text{V} \rightarrow ^{47}\text{Ti}$ β -decay, meas. of γ -ray spectra, half-life and log ft values 3-52146
- ^{163}W , from $^{144}\text{Sm}^{(24}\text{Mg}, \text{n})$ and $^{147}\text{Sm}^{(24}\text{Mg}, \text{n})$, α -decay 3-57498
- ^{164}W , from $^{144}\text{Sm}^{(24}\text{Mg}, 4\text{n})$ abd $^{147}\text{Sm}^{(24}\text{Mg}, \text{n})$, α -decay 3-57498
- ^{13}Xe , β -delayed proton emission, energy spectrum 3-54438
- ^{129m}Xe , half-life determ. 3-52127
- ^{95}Y , half-life (French) 3-71087
- ^{89m}Y , from $^{89}\text{Y}(\gamma, p')$, 100-800 MeV 3-67308
- ^{178}Yb , meas. of half-life, β and γ energies and coincidences, log ft. values, deduced ^{178}Lu levels 3-67276

radioactive decay schemes

- $^{210}\text{Rn} \rightarrow ^{210}\text{At}$, electron capture decay and spin assignments 3-43223
- delayed proton spectrum, fine structure statistical fluctuations rel. β^{+} transition matrix elements (Russian) 3-40467
- electron emission, secondary, from radioactive precipitates 3-49228
- $^{9,3}\text{Ru}$, high spin state de-excitation study, ^{92}Mo radioactivity meas. 3-78249
- $^{105}\text{Ag} \rightarrow ^{105}\text{Pd}$, γ -ray and β -decay intensities (Russian) 3-74522
- ^{106m}Ag decay, gamma ray spectra and transition multipolarity 3-71076
- ^aAs , $A=84-86$, produced in ^{235}U neutron induced fission, delayed-neutron meas., half-life determ. 3-43202
- $^{190}\text{Au} \rightarrow ^{190}\text{Pt}$ decay scheme assignments 3-67278
- $^{195}\text{Au}^{(183\text{d})} \rightarrow ^{195}\text{Pt}$, decay schemes, ^{195}Pt excited states, spin and parity assignments 3-52137
- ^{198m}Au , obs. of isomeric transition in ^{198}Au 3-43209
- ^{206}Bi in Ni, γ -ray distrib. meas., transition determ. of ^{206}Pb 3-78286
- ^{105}Cd , multiparticle levels, decay scheme (Russian) 3-74487
- $^{131}\text{Ce} \rightarrow ^{131}\text{La}$, determ. of partial level scheme for ^{131}La (French) 3-52148
- ^{57}Co , radioactive precipitate, secondary electron emission 3-49228
- $^{165}\text{Dy} \rightarrow ^{165}\text{Ho}$, γ -ray spectra study 3-43207
- $^{165m}\text{Dy} \rightarrow ^{165}\text{Ho}$, γ -ray spectra study 3-43207
- ^{252}Es , α decay and electron capture decay 3-54443
- $^{147}\text{Eu} \rightarrow ^{147}\text{Sm}$, γ -ray spectrum meas., obs. of new levels in ^{147}Sm (Russian) 3-74525
- $^{155}\text{Eu} \rightarrow ^{155}\text{Gd}$, effects of microscopical theory of Coriolis forces 3-63011
- $^{155}\text{Eu} \rightarrow ^{155}\text{Gd}$, first-forbidden β decays, correction matrix element effects 3-63012
- ^{22}F β decay 3-43221
- ^{146}Gd , γ -ray spectra meas. with Ge(Li) spectrometer (Russian) 3-74524
- ^{149}Gd , γ -ray spectra meas. with Ge(Li) spectrometer (Russian) 3-74524
- $^{167}\text{Hf} \rightarrow ^{167}\text{Lu}$, 2.05 min, meas. of K/ β^{+} ratio, determs. of total decay energy, Nilsson model assignments 3-52147
- $^{169}\text{Hf} \rightarrow ^{169}\text{Lu}$, 3.25 min, meas. of K/ β^{+} ratio, determs. of total decay energy, Nilsson model assignments 3-52147
- $^{184}\text{Hf} \rightarrow ^{184}\text{Ta}$, identification 3-60129
- $^{131}\text{I} \rightarrow ^{131}\text{Xe}$, product 341.2 and 404.8 keV level lifetime meas. (German) 3-52139
- $^{119}\text{In} \rightarrow ^{119}\text{Sn}$, β -decay, obs. of gamma transitions between low-lying levels in ^{119}Sn 3-49212
- $^{130}\text{In} \rightarrow ^{130}\text{Sn}$, obs. of excited two-neutron-hole states in ^{130}Sn (Russian) 3-71086
- ^{108m}In , β^{+} /electron capture decay, spin and parity, j-j coupling model 3-63004
- ^{192}Ir , electron capture and β^{+} decay to ^{192}Os , β^{-} decay to ^{192}Pt levels 3-40414
- $^{195}\text{Ir}^{(2,3\text{h})} \rightarrow ^{195}\text{Pt}$, decay scheme, ^{195}Pt excited states, spin and parity assignments 3-52137
- $^{195}\text{Ir}^{(3,7\text{h})} \rightarrow ^{195}\text{Pt}$, decay scheme, ^{195}Pt excited states, spin and parity assignments 3-52137
- ^{72}Kr , gamma decay, $T_{1/2}$ determ., produced in $^{58}\text{Ni}^{(16}\text{O}, 2\text{n})^{72}\text{Kr}$ reaction 3-74532
- ^{72}Kr , new $N=Z$ isotope, obs. of β -delayed γ -rays, determ. of decay scheme 3-46011
- ^{73}Kr , produced in $^{58}\text{Ni}^{(16}\text{O}, \text{n})^{73}\text{Kr}$, gamma decay, $T_{1/2}$ determ. 3-74532
- $^{134}\text{La} \rightarrow ^{134}\text{Ba}$, obs. of β -spectra, conversion electron spectra, γ -rays and $\gamma\gamma$ coefficients (Russian) 3-52141
- ^{178}Lu , from ^{178}Yb decay and $^{176}\text{Yb}(\text{t}, \text{n})$ reaction, half-life, β and γ energies and coincidences, log ft. values 3-67276
- $^{20}\text{Na} \rightarrow ^{20}\text{Ne}$ β^{+} decay, mirror symmetry props. and Fermi decay strength to isobaric analog state 3-60127
- $^{136}\text{Nd} \rightarrow ^{136}\text{Pr}$, obs. of new γ -ray transitions, multipolarity determ. (Russian) 3-71084
- $^{137}\text{Nd} \rightarrow ^{137}\text{Pr}$, from γ -ray, X-ray, conversion electron, β^{+} and $\gamma\gamma$ coincidence spectra (Russian) 3-52140
- $^{141}\text{Nd} \rightarrow ^{141}\text{Pr}$, obs. of γ -ray, X-ray, $\gamma\gamma$ -coincidence, conversion electron and positron spectra (Russian) 3-52092
- ^{235}Np , energy level spacings, transition probabilities, interpretation by strong Coriolis interaction 3-57499
- $^{93,231}\text{Np}$ electron capture decay, energies and rel. intensities for γ -ray transitions 3-54434
- $^{93,231}\text{Np}$ electron capture decay, energies and rel. intensities for γ -ray transitions 3-54434
- $^{232}\text{Pa} \rightarrow ^{232}\text{U}$, obs. using semiconductor detectors and coincidence techniques 3-74535
- $^{234m}\text{Pa}/\text{UX}_2$ (French) 3-40465
- $^{136}\text{Pr} \rightarrow ^{136}\text{Ce}$, obs. of new γ -ray transitions, multipolarity determ. (Russian) 3-71084
- $^{137}\text{Pr} \rightarrow ^{137}\text{Ce}$, from γ -ray spectra, internal conversion electrons, positron emission, γ - γ coincidences and ^{137}Ce lifetimes (Russian) 3-49222
- ^{187}Pt , spin, parity and probability of depopulating transitions for excited levels in ^{187}Ir 3-71049
- ^{235}Pu , electron capture type 3-40462
- RaE, determ. of configuration mixing ratios consistent with beta-decay and magnetic moment 3-52144
- ^{209}Rn , electron capture decay to levels in ^{209}At , obs. of gamma rays and conversion electrons 3-74542
- ^{117}Sb , multiparticle levels, decay scheme (Russian) 3-74487
- ^{130}Sn , β -decay of 7- isomer and ground state to excited states in ^{130}Sb , obs. of γ -transitions (Russian) 3-71085
- $^{132}\text{Sn} \rightarrow ^{132}\text{Sb}$, obs. of proton-neutron-hole type states populated in ^{132}Sb (Russian) 3-74486
- ^{147}Tb , short-lived isomer behaviour 3-40464

radioactive decay schemes continued

- ¹⁴⁸Tb, short-lived isomer behaviour 3-40464
¹²⁹Te beta decay to ¹²⁹I, gamma ray meas., decay schemes 3-74537
¹²⁹Te^{m.s.} → ¹²⁹I, meas. of γ -ray angular distrib., orientation study of ¹²⁹I excited states 3-52131
²³¹Th, energy level spacings, transition probabilities, interpretation by strong Coriolis interaction 3-57499
⁴⁴Ti → ⁴⁴Sc → ⁴⁴Ca, meas. of γ -ray spectra (*Russian*) 3-52124
 Tm to Hg short-lived neutron deficient nuclei, spectroscopic investigation (*Russian*) 3-52142
¹⁷⁷W → ¹⁷⁷Ta, $\gamma\gamma$ coincidence meas., determ. of ¹⁷⁷Ta level scheme (*Russian*) 3-74521
¹²²Xe, half-lives of ¹²²I excited levels 3-54424
¹³³Xe → ¹³³Cs, charge distrib., vacancy-cascade model 3-60107
⁸³Y^{m.s.} → ⁸³Sr, decay schemes and spin-parity assignments 3-46007
⁸⁸Y → ⁸⁸Sr, a directional correlations meas. for 898-1836 keV cascade (*German*) 3-60118
⁹⁵Y → ⁹⁵Zr, γ -ray assignments (*French*) 3-71087
¹⁷⁸Yb, meas. of half-life, β and γ energies and coincidences, log ft. values, deduced ¹⁷⁸Lu levels 3-67276

radioactive lifetimes see *radioactive decay periods***radioactive sources**see also *radioisotopes*

- 4 π sources on electrosprayed ion exchange resin, for standardization 3-56927
 α -particle irradiator, high vacuum using ²¹⁰Po 3-62211
 β -ray emission for X-ray excitation (*Rumanian*) 3-62301
 applications and contamination hazards (*French*) 3-62222
 ion-molecule collisions obs. by nucl. reson. fluoresc. 3-63009
 kryptonates in plastic substances, dosimetric application (*Russian*) 3-73150
 mass spectrometer for, design (*Japanese*) 3-59704
 β -emitter circular disc source, standardization by β^+ annihilation and $\gamma\gamma$ coincidence methods 3-42634
⁹⁰(Sr + Y) extended source, influence of chemical and physical factors on electrolytic deposition rate 3-62212
²⁴²Cm, α -particle source for Surveyor, preparation 3-62208
⁵⁸Co high activity source preparation by separation from Ni and electrodeposition 3-62205
⁶⁰Co radioactive source, nuclear excitation by gamma rays 3-67305
¹³⁷Cs/^{137m}Ba radioisotope generator system, separation of ^{137m}Ba, CuCo[Fe(CN)₆] adsorbent 3-48505
¹⁸F, in-cyclotron production by ¹⁶O(d, α)¹⁸F on water 3-39998
⁸⁵Kr incorporation into Ni, Fe, Cu by film evaporation 3-39997
²⁴Na radioactive source, nuclear excitation by gamma rays 3-67305
³²P beta source, absorption of particles in Cu, Ag, Sn and Pb foil targets 3-49376
⁴²Pr radioactive source, nuclear excitation by gamma rays 3-67305
⁴⁶Sc radioactive source, nuclear excitation by gamma rays 3-67305
⁸⁹Sr, beta source, absorption of particles in Cu, Ag, Sn and Pb foil targets 3-49376
⁹⁰Sr + ⁹⁰Y source in radiometer, sensitivity to distance of source from window (*Czech*) 3-42646
²³⁵U^m source preparation and detecting system for decay rates 3-42635
⁹¹Y beta source, absorption of particles in Cu, Ag, Sn and Pb foil targets 3-49376

radioactive tracers

- Aberdeen section scanner for rectilinear, arc, transverse and longitudinal section scanning 3-42368
 applications and contamination hazards (*French*) 3-62222
 atmospheric vertical diffusion coefficients between 0 and 100 m. using ²²²Rn and ²¹²Pb tracers (*French*) 3-51011
 autoradiography, high resolution electron microscopy, radioactive tracers, metal structural defects (*French*) 3-48561
 cerebral circulation, flow of radioactive tracers, multichannel system 3-51457
 cerebrospinal fluid shunt function assessment 3-81325
 fluid flow in cylindrical channel, response to tracer pulse injection 3-42736
 insulators, surface impurity effect on tracer diffusion 3-58149
 liver transplant, blood circulation study (*Italian*) 3-56545
 lung scanning employing ¹³¹I MAA and ^{99m}Tc^m ferrous hydroxide 3-42369
 lung uptake during liver imaging 3-81326
 mixing of solid particles, radioactive tracer techniques, collimator efficiency calc. 3-48340
 mixing of solid particles, tube mixer, radioactive tracer technique 3-48339
 nucleic acid, T-labelled, scintillation counting obs. in salt solutions (*German, English*) 3-66452
 placenta studies 3-81324
 proportional counter, thin walled, β -ray detection system, low level background meas., environmental studies 3-51719
 sand particles sieved to different sizes, ⁶⁰Co activated, study of binary system in tube mixer 3-44695
 two-phase annular flow, interchange and entrainment from tracer meas. 3-63750
 water, self-diffusion meas. 3-68430
 Ar, liq., self-diffusion meas. 3-68430
¹⁴C, radiometric method, thermodynamic activity meas., C in steel and alloys 3-54039
¹⁸F-p-fluorophenylalanine for pancreas/liver scanning in rats 3-42370
⁵²Fe and ^{99m}Tc^m for myeloscrosis studies 3-42371
⁶⁷Ga-citrate photostan, tumour location 3-48252
³H participation in water cycle (*French*) 3-59047
¹²³I-Hippuran and ¹²³I-albumin in gamma-camera renography 3-40063
⁴⁰K, total body in 1-12 month old infants, whole body counting, age and weight correlation 3-73594
⁸⁵Kr, label Ni films, adsorption of H₂, radiorelease, 273 K 3-43939
¹⁷O(n, α)¹⁴C, O determ. and distrib. in biological materials from α tracks 3-66457
³²P for determ. of adsorption of PO₄³⁻ ions on Sb₂O₄ 3-46756
²³¹Pa for ²³²Th analysis (*Japanese*) 3-59698
⁸⁶Rb extraction, blood flow changes, mouse tissue, X-irradiation appl. to clinical radiation therapy 3-48263
^{99m}Tc, intravenous bolus injection, cranial scintiphotographic blood flow defects, cerebral vascular disease 3-73595

radioactive tracers continued

- ^{99m}Tc labelled diphosphonate, uptake by bone lesions rel. to radiation therapy 3-73597
^{99m}Tc, brain scans, tuberosus sclerosis, vascularity 3-51461
^{99m}Tc-S colloid, lung uptake, heart and lung time-activity curves, reticuloendothelial mechanism 3-51459
^{99m}Tc-streptokinase, localisation of deep vein thrombosis, animal studies, appl. to man 3-48253
^{99m}TcO₄⁻, radionuclide cerebral angiograms, effect of injection volume 3-51460
 Ti/⁴⁷Sc, corrosion, radiometric studies 3-42703
- radioactivity**
 see also *alpha decay; atmospheric radioactivity; beta-decay; beta-rays; muon capture; nuclear decay theory; radioactive decay periods; radioactive decay schemes; radioactivity measurement*
 cyclotron isotope production, target-holder and vacuum cleaner design 3-39999
 dismantling of Elk River Reactor, radioactive operations. 3-71339
 earth core, potassium decay as heat source 3-76545
 environmental, International Reference Centre, activities 3-54554
 ground disposal site for radioactive wastes, internal dose estimation by sensitivity analysis 3-40550
 inert gas isotopes, external X-ray emission following hypothetical reactor hazards 3-67623
 lunar surface, Apollo 15 and 16 γ -ray spectra 3-45049
 macromolecular kryptonates, physico-chemical problems (*Czech*) 3-69482
 nuclear reactor fuel Interim Decay Storage Facility, upper Pu limit, transport and diffusion theory calc. 3-71298
 productive strata, porosity and clay content, logging procedure (*Russian*) 3-76895
 reactor waste ground disposal, site selection migration of multiple nuclides 3-78393
 Bi isotopes, low temperature orientation in ferromagnetic BiMn, use in nuclear structure studies 3-46008
 Rn, daughter aerosols, closed vessel storage, mobility spectrum, time variation 3-62981
^{117m}Sn, as bone-scanning agent, evaluation 3-53748
- radioactivity measurement**
 see also *radioactivity measuring apparatus*
 area scans, computer focusing, use of digital phantoms and scanning process simulation 3-56531
 biological systems (*Italian*) 3-54035
 clip circuit application (*Japanese*) 3-45544
 digital gamma camera tomography, theory, nuclear medicine 3-70153
 distribution, 2D sample, photographic recording technique, apparatus 3-73859
 in dust around 400 MeV LINAC 3-40549
 electron-capture radioactivity, total cross-sections by X-ray detection 3-48531
 environmental radioactivities, active charcoal method 3-69582
 Gamma camera tomographic magnifying collimator systems 3-70155
 gamma-gamma coincidence detection, three-dimensional imaging of radionuclides distributions 3-70162
 gamma-ray spectrometry, radioactivity assay 3-63202
 gamma-ray spectrometry, radiological surveillance, nuclear power facilities 3-62233
 Haverro meteorite, ³⁷Ar, ³⁹Ar and ³H radioactivity meas. 3-45066
 lifetime meas. method using multichannel analyzer (*French*) 3-51697
 liver phantom, computer smoothing of numerical scintillograms (*French*) 3-56532
 marine samples near nuclear power stations 3-69557
 motion tomography, general theory 3-70159
 positron tomography, three dimensional reconstruction technique 3-70163
 power station build-up of radioactive materials, detection and control 3-74768
 pressurized water reactor, radioactive waste, activity conc. calc., primary to secondary leakage 3-52239
 primary coolant of HTR experimental plant, discharge of radioactive material (*German*) 3-67632
 proportional counter, thin walled, β -ray detection system, low level background meas., environmental studies 3-51719
 radiation intervals distribution meas. 3-62257
 regional air transport model, effect of source characteristics and meteorological variables 3-53494
 river sediment and soil, method of determ. of ⁹⁰Sr and ¹³⁷Cs, report 3-73398
 rotational cinescintiphography, three dimensional organ images 3-70165
 sample changer, for automatic irradiation apparatus 3-39982
 section scanning and imaging, orthogonal tangent correction, appl. to clinical brain scanning 3-51458
 stereoscintiphography, brain scanning applic., depth perception experimental studies 3-70164
 tomographic imaging in nuclear medicine, Conference, USA, 15-16 Sept. (1972) 3-70146
 Tomographic imaging with a Fresnel zone plate system 3-70157
 tomography, circular, clinical artifacts encountered 3-70169
 tomography, radionuclide, clinical perspective 3-70173
 tomoscanner, multicrystal cylindrical imaging device, transverse section brain scanning 3-70150
 transverse section scanning, brain 3-70170
 whey, dosage standards (*Italian*) 3-54050
^{238,239}Pu, ²⁴¹Am sequential determ. in environmental samples 3-66451
- radioactivity measuring apparatus**
 airborne radioiodine monitoring, improvement of collecting efficiency under high relative humidity 3-73608
 distribution, 2D sample, photographic recording technique, apparatus 3-73859
 gamma camera tomography system, digital, clinical experience 3-70168
 nuclear debris, school experiment 3-61974
 positron camera, Massachusetts General Hospital 3-70161
 positron-transverse section detector, 32-crystal 3-70160
 tomocamera, tomographic imaging, clinical experience 3-70167

radioactivity measuring apparatus continued

- tomographic scanner, multiplane, clinical results 3-70171
- tomographic scanner, multiplane, nuclear medicine 3-70148
- tomographic system in nuclear medicine, multiple view of isotope distribution 3-70158
- tomoscanner, clinical experience 3-70172
- tomoscanner, theory, prototype nuclear medicine 3-70151
- transverse section scanner, analogous to transverse roentgen tomography, nuclear medicine 3-70149
- ¹²⁵I, labelled thrombosis monitor, for deep vein obs. 3-56530

radioactivity protection *see radiation protection***radioaltimeters**

- see also aircraft instrumentation; radionavigation*
- geodesy over sea, radar altimeter optimisation 3-44932
- geodetic satellite-borne altimeter 3-59155

radioastronomical observations*see also radiosources (astronomical)*

- 2.7°K cosmic background radiation, search for anisotropy at 3.56 cm 3-56401
- 327 MHz observation of galactic centre, possible deuterium absorption line 3-77154
- 408 MHz pulsar search with Bologna Cross radiotelescope, sensitivity and results 3-70052
- 1633;38, identification with visible object 3-77111
- 2695 MHz survey of weak sources, source count 3-45144
- aperture synthesis of interstellar H I 21 cm. absorption 3-81106
- Apollo 17 sounding radar, surface obs. of moon 3-61730
- Apollo Lunar Rover tracking using VLBI 3-65958
- apparent angular size of source, influence of scattering phenomena 3-77179
- atmospheric ozone and absorption spectra, 2.7 mm 3-76707
- B2 catalogue of radiosources at 408 MHz, differential log S-log N relationship 3-81110
- B2 sky survey sources, spectral index distrib. between 408 and 5000 MHz 3-73522
- bright galaxies, 80 MHz obs. 3-51391
- 3C120, Seyfert galaxy, 7.85 GHz outbursts, 1972 April to Oct., Goldstone-Haystack interferometer obs. 3-65902
- 3C120, Seyfert galaxy, 7.85 GHz outbursts, 1972 June to Nov., Goldstone-Haystack interferometer obs. 3-69975
- 3 C 10, high resolution 21 cm. obs. 3-53676
- 3C 13, attempt to detect 21 cm absorption in spectra 3-77118
- 3C 144, angular dimensions meas. at 25 MHz (*Russian*) 3-81113
- 3C 147, angular dimension meas. at 408 MHz (*Russian*) 3-81112
- 3C 196, angular dimensions meas. at 25 MHz (*Russian*) 3-81113
- 3C 196, radiointerferometric obs. at 85.5 MHz (*Russian*) 3-81114
- 3C 232, attempt to detect 21 cm absorption in spectra 3-77118
- 3C 254, angular dimensions meas. at 25 MHz (*Russian*) 3-81113
- 3C 273, angular dimensions meas. at 25 MHz (*Russian*) 3-81113
- 3C 273, obs. of variable fluxes (*Russian*) 3-45145
- 3C 273B, angular dimension meas. at 408 MHz (*Russian*) 3-81112
- 3C 275.1, attempt to detect 21 cm absorption in spectra 3-77118
- 3C 286, 21 cm absorpt. at $z=0.692$, implications for intergalactic medium 3-73525
- 3C 286, angular dimension meas. at 408 MHz (*Russian*) 3-81112
- 4C 29.03, attempt to detect 21 absorption in spectra 3-77118
- 3C 298, radiointerferometric obs. at 85.5 MHz (*Russian*) 3-81114
- 3C 327, radiogalaxy, u.h.f. polarisation meas. of intergalactic gas density 3-45142
- 3C 345, obs. of variable fluxes (*Russian*) 3-45145
- 3C 382, 452 and 465, obs. at 2.7 and 5 GHz 3-81117
- 4C 38.41, identification with visible object 3-77111
- 3C 391, supernova remnant, 18 and 21 cm recombination-line emission 3-70034
- 3C 391 remnant, high freq. obs. and theoretical interpretation of recombination line emission 3-77153
- 3C 398 (W49B), supernova remnant, 21 cm recombination-line emission 3-70034
- 3C 454.3, angular dimension meas. at 408 MHz (*Russian*) 3-81112
- 3C 461, high resolution 21 cm. obs. 3-53676
- 3C 52 at 2.7 and 5 GHz 3-69976
- 3C 52 obs. at 2.7 and 5 GHz 3-69976
- 3C 84, obs. of variable fluxes (*Russian*) 3-45145
- 3C 84, Seyfert galaxy, long baseline interferometry 3-53705
- Carina nebula NGC 3372 obs. at 30 MHz 3-61871
- Cassiopeia A, angular dimensions meas., by independent reception interferometer at 9 MHz (*Russian*) 3-81111
- Cassiopeia A, flux density meas. at 1440 MHz 3-56397
- Cassiopeia A, Perseus arm feature, aperture synthesis of interstellar H I absorption 3-81105
- Cassiopeia A, scintillation at 26 MHz during artificial ionospheric modification 3-80796
- cassiopeiae-A, 26.3 MHz obs., interferometry 3-48047
- Ceres, 3.7 cm radio emission, interferometry 3-81001
- clusters of galaxies, 1400 MHz obs. 3-70002
- Coma cluster of galaxies, detection of hot gas from scattering of background 3 K radiation 3-53709
- compact source 2048+31 in Cygnus Loop, interferometric meas. 3-65906
- compact sources, structure at 2.8 cms 3-77113
- corona, scattering causing type I radio bursts 3-73443
- cosmic microwave background, fine-scale anisotropy upper limit at 3.5 mm 3-45141
- Crab nebulae, scanning the diagram of the variable profile antenna (*Russian*) 3-81248
- P Cygni, detection of radio emission at 5 and 10.68 GHz 3-81119
- V1016 Cygni, radio emission at 10.63 GHz 3-65899
- Cygni-A, scanning the diagram of the variable profile antenna (*Russian*) 3-81248
- Cygnus A, scintillation at 26 MHz during artificial ionospheric modification 3-80796
- Cygnus X-2, peculiar blue star counterpart, obs. of radio emission 3-45148
- Cygnus X-3, 8 GHz obs. during September 1972 outburst 3-70001
- dark cloud ionization, failure to detect radio recombination lines 3-81207
- dark interstellar clouds, H₂CO 6 cm. excitation temperatures 3-70046
- dark nebulae search for 165 α and 166 α radio recombination lines 3-77163

radioastronomical observations continued

- depolarisation and luminescence obs. of double radio sources 3-81122
- differential interferometry, lunar and planetary applications 3-45249
- discrete sources, obs. at 2 cm at Pulkovo Obs. 3-61825
- DR21, H II region, 5 GHz obs. of small-scale structure 3-48061
- elliptical galaxies, upper limit to H I content 3-53704
- extragalactic radiosources, component separation velocity from 178 MHz luminosity 3-42210
- extragalactic sources, 1 mm radiometry, cryogenic optical system 3-77180
- extragalactic sources, position determ. from VLBI obs. 3-45143
- extragalactic Uhuru X-ray sources, radio structure 3-81129
- Faraday depolarization of radio galaxies and quasars with simple spectra 3-48065
- formaldehyde absorpt. in front of galactic sources 3-59379
- G0.5-0.0, galactic centre H II region, anomalous He abundance 3-42248
- G 355.3+0.1, identification as H II region 3-77110
- Galactic, background radio emission, 3.75 cm-3.5 m 3-77151
- Galactic background spectrum 130-2600 kHz, IMP-6 satellite measurements 3-77139
- Galactic centre, fine structure obs. at 2695 and 8085 MHz 3-45203
- Galactic centre, neutral H obs. of nuclear disc 3-61841
- Galactic centre, obs. of HI, contour diagrams of antenna temp. 3-81176
- Galactic centre, radio pulse search 3-69978
- galactic centre, sensitive search for microwave pulses 3-70024
- Galactic centre and 3-kpc arm, 21 cm line obs. 3-77134
- galactic nebulae, 1 mm radiometry, cryogenic optical system 3-77180
- galactic nebulae, correlation study of C and OH lines 3-48122
- galactic spiral structure, theories rel. to radio observations 3-42234
- galactic spiral structure map from 21 cm obs. 3-45188
- Galactic spiral structure outside solar circle, new 21 cm. map 3-70014
- Galactic X-ray sources, radio obs., review 3-81146
- galaxies, 1415 MHz obs. of 45 bright spiral galaxies 3-45202
- galaxies, head-tail, brightness and polarisation distrib. at 1415 MHz 3-61821
- galaxies, radio maps around five spiral and peculiar objects 3-70009
- galaxies in chains and groups, u.h.f. observations 3-51383
- Galaxy, linear polarisation at 210 MHz (*Russian*) 3-81178
- gas-dust ratio, H I column density in direction of known colour excess globular clusters 3-81170
- Geminids 1959-1969, overdense echoes, mass-distribution analysis 3-77015
- Giacobinid meteor shower 1972, 16.6 MHz obs. 3-61746
- giant dust complex detection in Perseus arm 3-51403
- globular clusters, neutral H obs. in 8 objects 3-45198
- Green Bank 1400 MHz sky survey, anisotropy and counts of sources 3-61819
- Gum Nebula, obs. below 20 MHz 3-51401
- H I filament, radio mapping, association with supernova shell 3-77158
- HB 21 supernova remnant assoc. with PSR 2021+51 indicated by 21 cm obs. 3-65894
- HD37806, i.r. object, radio emission detection at 10.63 GHz 3-65901
- HDE 226868 (Cygnus X-1), radio variability of spectroscopic binary 3-51359
- HI regions, galactic spiral structure density wave map 3-45190
- HI regions (galactic), rel. residuals determ. 3-45189
- IC 2574, H I 21 cm-line aperture-synthesis map 3-81163
- IC 443, supernova remnant, radio spectrum 3-77098
- interplanetary scintillation obs. of 203 radiosources identified as radio galaxies or quasars 3-48055
- interplanetary scintillations, three spaced receiver analysis rel. to solar wind velocity 3-61754
- interstellar background, OH line obs. (*Russian*) 3-81116
- interstellar dust cloud, absence of 6 cm. hyperfine anomalies 3-59388
- interstellar dust clouds, H₂CO absorption of 2.7K cosmic background radiation 3-70047
- interstellar dust clouds, OH obs. 3-61864
- interstellar hydrogen absorption of soft X-rays 21 cm obs. of H column density in the Galaxy 3-81156
- interstellar matter, search, unsuccessful, for organic molecular lines 3-61863
- interstellar methanol lines obs. at 2 mm 3-65937
- interstellar methylacetylene and isocyanic acid, 85.4 GHz obs. 3-42244
- interstellar neutral hydrogen, effect of Loop III, velocity distribution analysis 3-77155
- interstellar rotating dust cloud, OH 1667 MHz obs. 3-61878
- interstellar scintillation patterns of pulsars rel. to density irregularities of interstellar medium 3-48118
- interstellar SO emission 9.9 and 138.2 GHz column density meas. 3-81198
- isolated, dispersed r.f. pulses, search at 110 cm 3-48058
- Jovian decametric emission periodicities rel. to innermost satellites and solar activity 3-42138
- Jovian electron radiation belts, decimetric radiation obs. and electron energy and density 3-69848
- Jupiter, decametric radiation, bursts, high resolution spectral recordings, 20 to 26 MHz, anal. 3-47907
- Jupiter, decametric radiosource B, fine structure 3-56348
- Jupiter, dynamic spectra at 2.5-18 MHz 3-51295
- Jupiter, obs. at 11 cm to locate mag. dipole 3-47923
- Jupiter, radio disk temp. at 1.35 cm rel. to Mars 3-42148
- Jupiter decametric rotation period rel. to Source-A emission beam 3-42156
- L1436, interstellar dust cloud, ¹²C¹⁸O emission rel. to formaldehyde lines 3-81188
- AR Lacertae, Algol-type eclipsing and spectroscopic binary, obs. of radio emission 3-45148
- BL Lacertae, radio structure variations 3-56405
- BL Lacerte, structure and apparent motion 3-77119

radioastronomical observations continued

- Loop III, effect of galactic spur on H I regions velocity distrib. 3-45182
 M17 (Omega nebula), flux density meas. at 0.955, 1.65 and 2.73 cm 3-45225
 M31, radio obs. of clusters of H II regions 3-45201
 M33, radio obs. of clusters of H II regions 3-45201
 M51, radio obs. of clusters of H II regions 3-45201
 M8, HCN radio emission from Hourglass region 3-51395
 M 1-11, i.r. object, radio emission detection at 10.63 GHz 3-65901
 Magellanic Clouds, supernova remnant discovery 3-61839
 major planets, nonthermal radio observations 3-42154
 major planets, thermal structure of atm. 3-47938
 Markarian galaxies, attempt to detect emission at 408 MHz 3-51360
 Markarian galaxies, obs. at 75 cm wavelength (*Russian*) 3-81179
 Mars, gravity field analysis, Mariner 9, radiotracking data 3-80996
 Mars, Mariner 9 occultation, topographic and atm. approx. 3-69869
 Mars, Mariner 9 S band occultation meas. of atm. and topography 3-69868
 Mars, radio disk temp. at 1.35 cm rel. to Jupiter 3-42148
 Mars atmosphere, Mars-2 preliminary results 3-42175
 MD167362, i.r. object, radio emission detection at 10.62 MHz 3-65900
 Mercury, 21-cm. radio interferometer obs. of brightness temp., effects of background confusion sources 3-56329
 microwave H₂O vapour emission from Galactic sources 3-59381
 Molonglo Radio Source Catalogue 1, 1545 objects at 408 MHz 3-59351
 moon, 1 mm radiometry, cryogenic optical system 3-77180
 moon, black spots, reflectivity and radio backscatter, comparison with surface structure and composition 3-77005
 moon, dual-freq. bistatic radar meas., Apollos 14 and 15 results 3-69900
 moon, Mare Imbrium lava flows, earth based radar response meas. 3-59308
 MWC957, 2.8 cm 3-69979
 MWC 349, optical, radio and i.r. obs. 3-73520
 nearby stars, search for narrow band 21-cm signals from other civilizations 3-59353
 Neptune, interferometer obs. of 11.1 and 3.7 cm 3-56333
 neutral hydrogen radio line, computer reductions of obs., stationary antenna (*Russian*) 3-81247
 neutral stellar objects, identification with radio sources 3-53679
 NGC1265, radio galaxy, peculiar morphology and tail, high resolution 5 GHz map 3-65905
 NGC7538, H II region, 2.7 and 5 GHz obs. 3-61870
 NGC 253, spiral galaxy, 2695 MHz obs. 3-48094
 NGC 2798/9, double galaxy system, search for associated radio-sources at 1415 MHz 3-48056
 NGC 3372 (Carina Nebula), OH 1667 MHz absorpt. and formaldehyde band obs. 3-48134
 NGC 4651, attempt to detect 21 cm absorption in spectra 3-77118
 NGC 5128 (Centaurus A), high resolution obs. of radio galaxy 3-73545
 NGC 5128 (Centaurus A), size and nature of X-ray source 3-53692
 NGC 6618, (Omega nebula), flux density meas. at 0.955, 1.65 and 2.73 cm 3-45225
 NGC 7027, planetary nebula, 8085 MHz obs. 3-59393
 NGC 7319 in Stephan's quintet, non-velocity redshift rel. to NGC 7320, radio obs. 3-48092
 NGC 7538, H 94 α recombination line obs. 3-70038
 NGC 7640, H I 21 cm-line aperture-synthesis map of Sbc galaxy 3-81163
 NP 0532, variability of dispersion and scatt. 3-61827
 OH 471, flux density records rel. to variability 3-48062
 Ohio-survey radiosources, flux densities and positions at 430 MHz 3-42205
 ON-1 (OH 69.5-1.0), associated compact radiosource rel. to H II region 3-45147
 Ooty radiosources, lunar occultation obs. at 327 MHz of 6 objects with flat spectra 3-42206
 Orion A, search for D92 α recombination line emission and D/H ratio 3-81107
 Orion B, 7.8 GHz recombination lines of H, He, and C spectroscopic mapping 3-61868
 Orion Nebula, OII brightness and HCHO radio emission rel. to globules 3-61865
 Orionis-A, scanning the diagram of the variable profile antenna (*Russian*) 3-81248
 outer solar system, remote sensing of l.f. nonthermal radio emission 3-47940
 partial solar eclipse, Sept. 1968, study of local sources (*Russian*) 3-76981
 β Persei, 5GHz obs. 3-61816
 β Persei (Algol), optical and radio determ. of position 3-81102
 planetary brightness temp. meas. at 8.6 mm and 3.1 mm 3-47922
 planets, surface temperature measurement, methods and problems 3-65741
 Pluto, interferometer obs. of 11.1 and 3.7 cm 3-56333
 linear polarisation survey of region around $l=140^\circ$, $b=+8^\circ$ at 240.5 MHz 3-61822
 PSR0329+54, pulse profile changes at 10.7 GHz 3-69989
 PSR 0301+19, periodic power fluctuations at 430 MHz, spectrum analysis 3-42215
 PSR 0329+54, pulse profile variations at 2695 MHz 3-77120
 PSR 0531+21 giant pulses at 146 MHz, analysis of polarization 3-69985
 PSR 0809+74, sub-pulse obs. at 81.5 and 151 MHz 3-56406
 PSR 0950+08, radio spectrum of short subpulses 3-48067
 PSR 1919+21, notches in average pulse profile 3-45151
 PSR 2020+28, periodic fluctuations at 430 MHz, spectrum analysis 3-42215
 PSR 2021+51, assoc. with supernova remnant HB 21 indicated by 21 cm obs. 3-65894
 pulsar distance estimates from 21 cm. absorption spectra of 8 examples 3-69988
 pulsar intensity fluctuations, obs. of 5 objects 3-59358
 pulsar subpulse time scales and intensity fluctuations in 74-318 MHz range 3-48068
 pulsars, 406 and 410 MHz obs. of 13 new objects 3-56407

radioastronomical observations continued

- pulsars, 8.4 and 15.1 GHz obs. of 11 objects 3-59359
 pulsars, fluxes and spectra of 12 objects, simultaneous six-frequency obs. 3-48069
 pulsars, improved parameters for 15 objects 3-61828
 pulsars, polarisation of pulses, observations between 110 and 1400 MHz 3-77123
 pulsars, slow intensity variations 3-77122
 pulsars, weak continuum radio emission from vicinity of 18 objects rel. to haloes 3-42217
 pulsars, wide integrated pulse profiles rel. to radiation and models 3-45157
 quasar luminosity evolution rel. to pure density evolution, Parkes radio data 3-42213
 quasars, angular diameters of objects with unusual colour 3-53684
 quasars 3C 273 and 279, structure and apparent motion 3-77119
 quasistellar object redshift distributions, their interpretation 3-73526
 radio sources, bright, precision of measuring the coordinates Pulkova and RATAN-600 radiotelescopes (*Russian*) 3-81251
 radiogalaxy 3C 120, structure and apparent motion 3-77119
 radiosource flux density measurements relative to Cas A at 21.8 GHz 3-77112
 radiosource positions for 59 objects from 2695 and 8085 MHz obs. 3-69972
 radiosources, linear polarisation, time variation at 2.8 and 4.5 cm 3-77109
 radiosources, linear polarisation at 2.8 and 4.5 cm. 3-77108
 radiosources, optical identification by coincidence of radio and optical positions 3-77107
 radiosources, optical identification problems 3-81108
 radiosources, spectral flux density, radio emission at 3.5 cm (*Russian*) 3-45146
 recombination lines toward galactic centre, 1.621 GHz obs. 3-51379
 Sagittarius A, meas. at mm and meter wavelengths (*Russian*) 3-81115
 Sagittarius B1, meas. at mm and meter wavelengths (*Russian*) 3-81115
 Sagittarius B2, meas. at mm and meter wavelengths (*Russian*) 3-81115
 Sagittarius B2, negative search for acrylonitrile, pyrimidine and pyridine 3-81193
 Sagittarius B4, meas. at mm and meter wavelengths (*Russian*) 3-81115
 Saturn, 21-cm. line obs. by new method of radio interferometry of faint moving sources 3-61674
 Saturn, upper limit to the 11.2 m- λ flux, VLBI system, fringe rate and amplitude 3-47906
 Saturn's radio flux at 26.3 MHz, upper limit from VLBI 3-42150
 Sharpless H II regions, H₂O sources, obs. of microwave emission 3-61869
 solar, 3.71, 11.1 cms, McMath Region 12094 3-76967
 solar, distribution of 2, 4, 6, 8 mm wavelengths over disc (*Russian*) 3-76982
 solar 810 MHz emission, daily values (1957-1967) 3-69828
 solar active regions, high-resolution radio meas. and sunspot diameters 3-47889
 solar active regions, obs. at 9 and 3.5 mm under disturbed conditions 3-65660
 solar chromospheric flares, relation between chemical composition of cosmic rays and radiospall duration spectrum (*Russian*) 3-65575
 solar determined component investigations, at 9.0 cm (*Russian*) 3-80967
 solar differential rotation determ. from optical, radio and interplanetary data 3-65697
 solar flare emissions, review 3-65717
 solar fluctuations, obs. over diurnal interval (*Russian*) 3-80964
 solar neighbourhood, H I distribution about local standard of rest 3-48127
 solar polar region, dark ring in brightness at 3 cm., 1971 eclipse obs. (*Russian*) 3-80965
 solar radio emission, local sources, 9 cm wavelength, slowly varying component characteristics, statistical investigation (*Russian*) 3-80968
 solar type II burst, derivation of interplanetary electron density scale 3-65856
 solar type III bursts, second harmonic radiation at km wavelengths 3-45028
 solar type III radio bursts, decay time at km wavelengths 3-65688
 solar wind, power spectrum of small-scale irregularities, 81.5 scintillation obs. 3-65647
 source counts at 408 MHz using MC1 catalogue data 3-56399
 source strengths at 29.9 MHz between -4° and -64° declinations 3-53672
 spiral galaxies, conditions of nuclear radio component 3-77137
 Stark broadening effects in radio recombination line temperatures for radiosources 3-42209
 Stephan's quintet, non-velocity redshift of NGC 7319 rel. to NGC 7320, radio obs. 3-48092
 Stephan's Quintet of interacting galaxies, H II region and supernova obs. 3-70004
 sun, 1 mm radiometry, cryogenic optical system 3-77180
 sun, 350 MHz obs. during 1972 November 3-45014
 sun, 3.71 and 11.1 cm obs. using NRAO 3-element interferometer 3-42131
 sun, correlation and spectral analysis of daily radio flux 3-65686
 sun, fluctuation at 3 cm. emission, correlations with chromospheric height variations (*Russian*) 3-80961
 sun, height of radio regions from 9.1 cm wavelength emission 3-47890
 sun, interferometric. obs. of pulsating source assoc. with type IV burst 3-65665
 sun, l.f. modulation, sunspot magnetic field oscillations (*Russian*) 3-80962
 sun, McMath zone 11482, polarization inversions in 237 MHz radio emission 3-65693
 sun, noise storm source structure during 1968 total eclipse (*Russian*) 3-45011
 sun, quasiperiodic fluctuations at 3 cm., using two telescope 1500 km apart (*Russian*) 3-80960

radioastronomical observations continued

- Sun, reduced radiobrightness regions, in 8 mm range (*Russian*) 3-80966
- Sun, spectral index and fluctuations at 3 cm. (*Russian*) 3-80963
- Sun, type I storm, evidence of twisted bi-polar mag. fields 3-65711
- Sun limb brightening, distribution of radio brightness (*Russian*) 3-45012
- supernova remnants, high resolution interferometry 3-77093
- supernova remnants, high resolution obs. at 80 MHz 3-56398
- supernova remnants, obs. of galactic sources at 1.7 and 2.7 GHz 3-59348
- supernova remnants near galactic plane, 8.8 GHz radio obs., brightness distrib. and flux densities 3-53671
- supernovae 1970g in M101, obs. at 2.8, 6 and 21 cm 3-42204
- Supernovae remnants, search for 1415 MHz emission from young extragalactic objects 3-56400
- supernovae remnants search for compact radio sources at 53-318 MHz 3-45155
- thermal radioresources in H II regions, 8.2 mm high resolution survey 3-77115
- (1685) Toro, asteroid, radar obs. 3-61735
- type III radio bursts, energetic solar electron interactions 3-80957
- type III radiobursts, simultaneous obs. of fast solar electrons 3-80892
- type IV solar emission of 28.6 MHz, decay times and flux densities 3-80930
- Universal Time, UT1, determ. using Cambridge 5 km telescope 3-65952
- Uranus, 21-cm. line obs. by new method of radio interferometry of faint moving sources 3-61674
- Uranus, interferometer obs. of 11.1 and 3.7 cm 3-56333
- Venus, atmosphere, microwave meas. absence of water vapour 3-51296
- Venus, brightness temperature and absolute flux density scale at 608 MHz 3-69851
- Venus microwave brightness temps. at 430 MHz 3-73449
- very long baseline interferometric obs. of radio sources 3-65908
- Virginis-A, scanning the diagram of the variable profile antenna (*Russian*) 3-81248
- Vy2-2, i.r. object, radio emission detection at 10.62 MHz 3-65900
- W51, kinematic distance estimate of non-thermal source using OH absorpt. line meas. 3-48057
- W 43 region at 4.5 cm, automatic reduction of radio maps 3-65904
- W 49 A, B, 18 cm OH absorpt. meas. 3-61820
- Wolf-Rayet stars 3-77078
- CO and HCN mm.-wave emission from stars 3-69974
- D₂ in the Galaxy 3-42236
- H I regions, 21 cm emission outside plane of spiral galaxies 3-81204
- H I regions, obs. of C recombination lines 3-48128
- H I regions, two-component equilibrium model of interstellar regions rel. to radio obs. 3-77160
- H II region, search for r.f. transition from metastable states of H₂ and CO 3-45222
- H II regions, aperture synthesis obs. of group around $l=111^\circ$ 3-70041
- HCN radio emission from Hourglass region of M8 nebula 3-51395
- HI local structure, small scale individual features, 21 cm. obs. 3-59389
- HI region, Galactic anticentre, detection against background spatial fluctuations 3-77159
- HI survey in low galactic latitudes at 21-cm. 3-65939
- HNCO detection in Galactic centre at 21.98 GHz 3-53711
- H₂O, interstellar masers, resonance Stark effect 3-81194
- H₂O sources assoc. with OH emission in H II regions 3-51394
- H₂O sources in Sharpless H II regions, obs. of microwave emission 3-61869
- H66 α recombination line obs. in 6 H II regions 3-56448
- OH, interstellar masers, resonance Stark effect 3-81194
- OH clouds, obs. of H α emission-line stars 3-45219
- OH emission sources, accurate positions at 1665 and 1667 MHz 3-69973
- OH extended emission at 1720 MHz 3-81109
- OH stars, type I, optical props. 3-61781
- OH/IR stars, search in globular clusters at 1665 MHz 3-61840

radioastronomical techniques

- 408 MHz pulsar search with Bologna Cross radiotelescope, sensitivity and results 3-70052
- Apollo 17 site, electrical structure from r.f. interferometry 3-61890
- Apollo Lunar Rover tracking using VLBI 3-65958
- Astrometry with the 5-km radiotelescope 3-77189
- automatic reduction of radio maps 3-65904
- Bordeaux 8 mm interferometer, electronic systems techniques 3-70068
- celestial bodies, radio images obtained with resolution $>10^{-2}$ sec. of arc, global radiotelescope (*Russian*) 3-81245
- Culgoora radioheliograph operation at 43.25, 80 and 160 MHz 3-70071
- data processing systems for 160 MHz compound interferometer (*Japanese*) 3-70086
- Deep Space Network of large antennas, low-noise microwave receiving system 3-65965
- double-cavity maser, wavelength 1.35 cm (*Russian*) 3-51407
- Earth-rotation aperture synthesis 3-65955
- faint moving sources, new method of radio interferometry, obs. of Uranus and Saturn 3-61674
- gravitational red shift meas. using earth satellites 3-53729
- heterodyne detection of black body radiation, 10.6 μ m 3-42254
- high-resolution methods 3-61885
- interferometry of moving sources at 21-cm., effects of background confusion sources 3-56329
- interstellar communication, frequency selection 3-77191
- Mars, radar-ranging and effect of planet's figure 3-61676
- meteor trails drift optimum processing (*Russian*) 3-77022
- meteors detection, optimum processing (*Russian*) 3-77021
- meteors information processing (*Russian*) 3-77020
- microwave, low temp. bolometer heterodyne receiver, Kitt Peak Arizona, description 3-65971
- National Radio Astronomy Obs. spectrum control procedures 3-65966
- NRAO tape-recorder interferometer system 3-65960

radioastronomical techniques continued

- occultations of spacecraft by outer planets, Pioneer and Mariner missions 3-65969
- planetary atmosphere, remote sensing by radio spectrum analysis 3-42176
- planetary atmosphere study by radio occultation of spacecraft 3-65968
- planetary surface mapping using ground-based radar 3-65956
- polarisation meas. using Westerbork synthesis radio telescope 3-61879
- polarization of radio sky, appl. of entropy measure for partially polarized radiation 3-70061
- Pulkovo large radiotelescope, illumination of the variable profile reflector, technical methods (*Russian*) 3-81249
- pulsar signal processing techniques 3-65911
- radio sources, bright, precision of measuring the coordinates Pulkova and RATAN-600 radiotelescopes (*Russian*) 3-81251
- radioheliograph, mm-wave, for two-dimens. mapping 3-70072
- RATAN-600, astrophysical problems to be solved with this radiotelescope (*Russian*) 3-81244
- RATAN-600, methods of radioastronomical obs., azimuthal aperture synthesis, variable profile antenna (*Russian*) 3-81222
- RATAN-600, radiotelescope, antenna parameters, calibration of sensitivity, 8 mm in the radar regime, radioastronomical method (*Russian*) 3-81246
- RATAN-600, radiotelescope, characteristics of periscopic part, surveying the sky (*Russian*) 3-81243
- RATAN-600, radiotelescope, control of antenna parameters, radioastronomical obs. (*Russian*) 3-81238
- restoration of radio maps, new method 3-81215
- ruby maser for 8 mm band, appl. 3-42989
- selenodesy using differential VLBI 3-56470
- solar cosmic-rays, weak flux detection by ground-based radio methods 3-56255
- solar radio patrol network of AFCRL 3-69838
- solar wind velocity fine structure, new method of search and analysis 3-42128
- spectrography, electro-optical device with wide freq. range 3-70073
- standards, 21 cm, four regions 3-56460
- supernova search in galaxies at 70 Mpc 3-77178
- supersynthesis radiotelescope, interactive computer data processing 3-70053
- telescope control and mm-wave spectral line obs., computer program in FORTH 3-70078
- telescope pointing and receiver calibration, accuracy 3-56447
- Universal Time, UT1, meas. method 3-65952
- variable profile antenna, adjustment, radioastronomical method (*Russian*) 3-81237
- variable profile antenna, adjustment by geodetic and radiotechnical methods (*Russian*) 3-81236
- variable profile antenna, scanning the diagram, obs. of Orion-A, Virgo-A, Cygnus-A, Crab nebulae (*Russian*) 3-81248
- very long baseline interferometry, appl. 3-65954
- very long baseline interferometry, appl. 3-65957
- very-long-baseline-interferometry, spectral line anal. of data 3-65959
- VLBI, appl. to lunar librations study 3-59154
- VLBI for position determ. of extragalactic radio sources 3-56062
- VLBI for radio source position meas., geodetic appl. 3-56246
- HI spectroscopy, Dominion supersynthesis radio telescope 3-70066
- radioastronomy**
see also pulsars; quasars; radiotelescopes; solar radiofrequency radiation
- array simulation facility 3-48301
- civilizations, galactic, their detectivity 3-59399
- data processing systems for 160 MHz compound interferometer (*Japanese*) 3-70086
- Deep Space Network of large antennas, low-noise microwave receiving system 3-65965
- digital correlation spectrometer for multi-level quantisation 3-70076
- E-W rotation-synthesis array, main beam and ringlobes 3-51405
- evolution of radio astronomy, book 3-56468
- Galactic disc continuum radio structure, model based on density wave theory 3-77140
- Harvard minicorrelator incorporating minicomputer 3-48146
- history of obs. and telescopes 3-45253
- interstellar radiosintillations due to plasma irregularities with power law spectra 3-51397
- Josephson junction receiver for mm obs. 3-45240
- Jovian magnetosphere, radio wave propag. 3-47897
- maser, travelling-wave system, appl. 3-70074
- meteor information automatic processing machine (*Russian*) 3-77023
- microwave astronomy with 25 m or greater reflectors, state of the art vs. practice 3-48143
- microwave background isotropy rel. to rotation and distortion of Universe 3-51262
- molecules, interstellar, obs., discussion 3-45220
- number-flux-density distrib. of sources, maximum likelihood estimation 3-65943
- outer solar system, remote sensing of l.f. nonthermal radio emission 3-47940
- Project Cyclops, detection of radio signals of extraterrestrial intelligent origin, conclusions 3-59400
- QSO's near bright galaxies, Parkes 2700 MHz survey objects 3-51363
- RATAN-600, astrophysical problems to be solved with this radiotelescope (*Russian*) 3-81244
- spectrograph, electro-optical, wide freq. range device 3-70073
- total power filter spectrometer appl. 3-59176
- wideband antenna array application 3-59398
- radiocarbon dating** see radioactive dating
- radiochemistry**
see also radioactive chemical analysis; radioactive tracers
- tracer applications and contamination hazards (*French*) 3-62222
- ¹⁴C, sepn. from neutron-irrad. AlN by dry procedure 3-44739
- ¹⁴C beta-decay effects on org. mol. electronic struct. 3-80570
- Cu spallation, induced by 65 MeV π^+ and π^- and by 205 MeV protons, radiochemical yield determ. 3-67373
- ²⁴Na, effect of chemical combination on half life (*German*) 3-49221

radiochemistry continued²³⁸U, spontaneous fission and radio-chemical yield 3-57543**radiocrystallography** *see crystallography; radiography***radiofrequency amplifiers***see also preamplifiers*
for n.m.r. spectrometer 3-56706**radiofrequency cosmic radiation***see also pulsars; quasars; radioastronomy*

2.7°K cosmic background radiation, search for anisotropy at 3.56 cm 3-56401

aural substorm, cosmic radio noise absorption and H β emission 3-42009

Carina nebula NGC 3372 obs. at 30 MHz 3-61871

EAS, obs. of radioemission at 32 and 58 MHz at Moscow State Univ., geomagnetic mechanism (*Russian*) 3-69770

EAS, radio emission resulting from geomagnetic charge separation 3-44975

galactic centre, sensitive search for microwave pulses 3-70024

large antenna meas. using cosmic radio sources 3-48060

l.f. radio spectra, deviations from power law, possible mechanism for point sources 3-42208

limiting polarization of radiowave emission from pulsars 3-42216

microwave background, cosmic ray nucleon interactions, production of ultrahigh energy photons, universal hypothesis 3-42093

microwave background, fine-scale anisotropy upper limit at 35 mm 3-45141

microwave background, X-ray flux due to Compton scatt. of fast electrons 3-45161

microwave background radiation, temp. at large redshifts 3-59352

non-linear Compton scattering, phase vel. effects 3-53675

PSR0329+54, pulse profile changes at 10.7 GHz 3-69989

pulsars, nonlinear effects due to bending of a weak ionised D-type front (*Russian*) 3-53687

synchrotron radiation from cosmic sources, stimulated amplification 3-53680

radiofrequency heaters *see radiofrequency heating***radiofrequency heating**

lower E-region, r.f. heating effects on electron density 3-80805

radio wave heating of air rl. to isothermal ionization of lower ionosphere 3-42013

Ar plasma, for emission spectroscopy 3-45607

radiofrequency interferenceradiotelescope interferometry, RT22 CrAO telescope, 3 cm, sensitivity increase, high angular resolution (*Russian*) 3-81219radiowave propagation through rain at 17.7 to 19.7 GHz (*Norwegian*) 3-61481**radiofrequency spectra of diatomic inorganic molecules***see also nuclear magnetic resonance; paramagnetic resonance*AlI, quadrupole hyperfine structure, coupling constants (*German*) 3-57661AlBr, quadrupole h.f.s. of rot. transition (*German*) 3-57662AlCl, hyperfine structure of rotational transition J=1 \rightarrow 2 (*German*) 3-57662

BaO, microwave optical double resonance obs. using c.w. dye laser 3-78039

BaO microwave optical double resonance spectra 3-75063

¹²C¹⁸O emission from interstellar dust cloud L1436 rel. to formaldehyde anomalous hyperfine lines 3-81188

GeO, rotational magnetic moment and magnetic susceptibility, from mol. beam electric resonance spectroscopy 3-78727

HCl, blended isotopic doublets, equivalent spectral widths 3-78823

IF, rotational spectrum, hyperfine structure analysis (*German*) 3-78822KI, quadrupole hyperfine structure meas. obs. in vibrational state (*German*) 3-57660⁶Li ⁹F, J=1 \rightarrow 0 rotational transition, partial resolution 3-54704N₂ r.f. spectrum of metastable (A³ $\Sigma_u^+) state, fine struct., mag. hyperfine struct., electric quadrupole const. for 13 vibrational levels 3-40635$

NO, r.f. excited, emission spectra from 200 to 600 nm 3-78815

O₂, X³ Σ_g^- state, resolution of discrepancies 3-78736O₂ atmospheric microwave spectrum rel. to attenuation and phase dispersion 3-49480OH radical, microwave and magnetic resonance spectra of vibrationally excited states, Λ -doubling 3-78853

SF radical, microwave spectra 3-40637

SiO, rotational magnetic moment and magnetic susceptibility, from mol. beam electric resonance spectroscopy 3-78727

radiofrequency spectra of inorganic solids*see also nuclear magnetic resonance; paramagnetic resonance*
elbaite, n.m.r. studies, ⁷Li, ¹¹B, ²³Na and ²⁷Al, crystal structure 3-44768

piezoelectric crystals. X-band echo 3-72576

tourmaline minerals, n.m.r. studies, ¹H, ⁷Li, ¹¹B, ²³Na, ²⁷Al, crystal structure 3-44768

Al superconducting tunnel diodes, 870 GHz phonon emission 3-55381

CdGeP₂, semiconductor, glass-crystal phase transition, NMR of ³¹P (*Russian*) 3-72197EuB₆, CsCl-structure, e.s.r. studies, compared to GdS and Y_{1-x}Gd_xS 3-41407GaI, (n²P⁰-n²D_J) resonance lines, collision broadening, cross-sections (*Russian*) 3-72770GdB₆, La_{1-x}Gd_xB₆, CsCl-structure, e.s.r. studies, compared to GdS and Y_{1-x}Gd_xS 3-41407

Ge, ultrapure, photoexcitation spectra of free excitons by submm. radiation 3-58570

HSiF₃, excited vibr. states, structure, force field models 3-63487InI, (n²P⁰-n²D_J) resonance lines, collision broadening, cross-sections (*Russian*) 3-72770

n-InSb, compensated, reson. absorpt. by electrons localised on donor pairs 3-47330

InSb plasma, possibility of acoustic amplification and microwave radiation 3-68677

La_{1-x}Gd_xB₆, CsCl-structure, e.s.r. studies, compared to GdS and Y_{1-x}Gd_xS 3-41407NbSe₂, microwave absorption, critical fluctuations 3-41302P₂Se₃, semiconductor, glass-crystal phase transition, NMR of ³¹P (*Russian*) 3-72197**radiofrequency spectra of inorganic solids** continuedThB₄:Gd³⁺, ThB₆:Gd³⁺, e.s.r., mag. susceptibility meas. influence of U admixture 3-41406TlI, (n²P⁰-n²D_J) resonance lines, collision broadening, cross-sections (*Russian*) 3-72770**radiofrequency spectra of organic molecules and substances***see also nuclear magnetic resonance; paramagnetic resonance*di- μ -(pyridine N-oxide)bis [bisnitrate (pyridine N-oxide) copper (II)], e.p.r. spectrum, triplet ground state, computer simulation 3-75075acetaldehyde, collision broadening of rot. lines by O₂ 3-67834alcohols, ¹³C multiplets, cross relaxation effects 3-68879

1-alkyl-3-arylthiazenes, tautomerism, n.m.r. spectroscopy 3-74929

amino acetonitrile, microwave spectra, bond angles, dipole moment 3-63485

aniline, mol. configuration determination, models for internal rotation, n.m.r. lanthanide shift studies 3-46226

benzophenone, microwave-optical double resonance, n π^* triplet states 3-80121

benzvalene, six isotopic species, microwave structural study 3-78814

bicyclic alcohol, mol. configuration determination, models for internal rotation, n.m.r. lanthanide shift studies 3-46226

2-bromo-5-chlorothiophene, n.m.r. AB spectrum, use of compensating device for parasitic beat signal 3-77595

chlorocyclohexane, equatorial, microwave rot. spectra anal. 3-78811

chloroform crystalline, quadrupole relaxation of ³⁵Cl nucleus and effect on CCl₃ group mobility 3-759024-chloronortricylene, ³⁵Cl nuclear quadrupole coupling constant 3-71567

2-chlorothiophene, microwave spectra, quadrupole coupling and rotational constants 3-43463

cyanocyclobutane, μ -wave spectrum, dipole moment quadrupole coupling const. and conformation study 3-40634

cyanocyclobutane, microwave spectrum assignments 3-63484

cyclohexene sulphide, microwave spectra, rotational const. 3-43459

cyclopent-3-enone, microwave spectra, ring planarity, r_s-structure and dipole moment 3-60466

cyclopent-3-enone, out-of-plane ring modes, microwave spectra obs. 3-60467

cyclopentadienone, microwave spectra analysis and assignments 3-78813

cyclopropanone, isotopic species, substitutional structure 3-63482

6-deuterofulvene, μ -wave spectrum, methylene group struct. 3-49477

diacetoneglucose, mol. configuration determination, models for internal rotation, n.m.r. lanthanide shift studies 3-46226

diacetyl, pure liq., active intramolecular motion in dielectric relax., spectral obs. 3-64602

difluoromethane, hyperfine struct. meas. by beam maser spectroscopy 3-46303

dimethyl cyanamide, microwave spectra, struct., dipole moment, i.f. vibrs. 3-60464

dimethylaminodifluorophosphine 3-49476

dimethylsilane, rotational spectrum, validity of Hamiltonian for torsional fine structure (*German*) 3-75053

3,6-dioxabicyclo[3.1.0]hexane, microwave spectrum, dipole moment, conformation 3-63486

DNA, excited states, triplet quenching, photosensitisation 3-63588

ethylene oxide lines, collision broadening by quadrupolar mol. CO₂ 3-52397

formaldehyde, absence of 6 cm. hyperfine anomalies in interstellar dust cloud 3-59388

formaldehyde, absorpt. in front of strong galactic sources 3-59379

formaldehyde, comment on anomalous hyperfine lines from interstellar dust cloud 3-81188

formaldehyde, microwave collision diameters in rot. spectrum 3-67858

formaldehyde radiation, absence in galactic plane cold region 3-51392

formamide, interstellar detection at 19 cm 3-61860

formimide, gas phase conformation props. of amide bond 3-63483

fulvene, interstellar, upper limit determ. 3-56438

furan, rot. transitions, h.f.s. 3-54701

glycolaldehydes, microwave spectra, substitution struct., intramolecular hydrogen bond and dipole moment 3-54703

6-hydroxy-2-formylfulvene, H-bonding, molecular symmetry, microwave spectra 3-54698

hydroxyacetoneitrile, microwave spectroscopy, rotational isomerism, barriers to internal rotation 3-49479

interstellar molecular clouds in The Galaxy 3-65938

methane, i.r.-r.f. double reson. study of pure rot. Q-branch transition 3-63405

methane, microwave spectrum, ground vibronic state, rot. transitions 3-75052

methane selenol, μ -wave spectrum, internal rot. barrier, struct. and dipole moment meas. 3-54700

methanol, hyperfine struct. in internal rotor molecules 3-78817

methanol lines obs. at 2 mm in interstellar matter 3-65937

methyl chloride, ³⁵Cl and ³⁷Cl quadrupole coupling determ. with mol. beam maser spectrometer 3-49475methyl chloroformate, microwave spectra, internal rot. barrier, ³⁵Cl quadrupole coupling, conform. 3-75050

methylamine, laboratory microwave spectra 3-43458

methylamine chloride, internal rot. and inversion doubling in microwave spectrum 3-67829

methylaminoethane, rot.-inversion spectrum analysis 3-63491

3-methylene oxetane, μ -wave spectrum, mol. Zeeman effect, mag. susceptibility anisotropy, quadrupole moment meas. 3-52372

methylenimine, microwave spectra, molecular constants 3-75051

monochloroamine, rotation-inversion transitions in microwave spectrum, inversion barrier of amine group 3-40639

nitroethylene, isotopic species, microwave spectra, ground and excited vibrational states 3-78812

2-nitrophenol, microwave spectrum, struct. of hydrogen bond 3-40638

non-polar liquids, dielec. absorpt. in microwave and far infrared region 3-80120

radiofrequency spectra of organic molecules and substances continued

- 3-oxetanone, μ -wave spectrum, mol. Zeeman effect, mag. susceptibility anisotropy, quadrupole moments meas. 3-52372
 phenol-OD, microwave and i.r. transitions analysis by rot.-internal rot. theory 3-63490
 porphyrin, free base, Shpolskii-matrix lowest triplet states obs. from microwave induced fluorescence changes 3-76050
 trans-propylene imine, microwave spectra, centrifugal distortion effects 3-60463
 cis-propyleneimine, ^{14}N quadrupole coupling consts., microwave spectra 3-63489
 propynal, millimetre wave spectrum, ground vibr. state 3-78816
 pyrone, zero-field microwave spectra, rotational constants determ. 3-63481
 pyrrole, beam maser spectroscopy, obs. of rotational transitions, nitrogen hyperfine parameters 3-78826
 tellurolene, microwave, rot. consts., struct. 3-67826
 tetrabromobenzene, symmetric, Br hyperfine and quadrupole fine struct. in MODR spectrum 3-53328
 2-thiophenalddehyde, gas, identification of O-S trans rotamer 3-63365
 trifluoroethylene, microwave spectra and struct. 3-43461
 trimethylamine, mol. A_2 torsional frequency by computer aided microwave anal. 3-78821
 trimethylamine-borane, microwave spectra, struct., dipole moment, rot. consts. 3-60465
 trimethylchlorosilane, nuclear quadrupole coupling and rotational const. determ. from microwave spectra (German) 3-60468
 trimethylsilyl cyanide and isocyanide, microwave spectra 3-43462
 2,8,9-trioxadamantane, microwave spectrum 3-40636
 tropene, zero-field microwave spectra, rotational constants determ. 3-63481
 o-xylene, microwave spectra, methyl rot. barrier, methyl conform. and dipole moment 3-67832
 CF_2 , microwave spectra, centrifugal distortion anal. force field and dipole moment 3-78820
 CH_4 , rotational transitions in $v_3=1$ excited state, i.r. microwave double resonance method 3-52373
 H_2CO , collision-induced transitions, velocity depend., obs. by triple resonance method 3-52384

radiofrequency spectra of polyatomic inorganic molecules

- see also nuclear magnetic resonance; paramagnetic resonance
 transient nutation effect obs. in microwave transitions 3-49478
 Ar-HCl, struct. determ. from microwave and r.f. spectra 3-75049
 ArHCl complex, structure determ. by mol. beam electric resonance spectroscopy 3-78824
 BrCN, pressure broadened line widths in microwave region 3-67837
 BrF₃, microwave meas. of J8-9 transition 3-63492
 BrF₃, rot. spectra, 70 and 140 GHz (French) 3-43460
 CHO radical, microwave spectrum, obs. of K doubling transition in rotational states, hyperfine interaction 3-78827
 CO₂, microwave, i.r. laser transitions, high resolution frequency measuring techniques 3-48420
 COF₂, beam maser spectra, pin-rotation interaction, ^{19}F hyperfine struct. 3-71573
 COS, dipole moment function determ. 3-78768
 D₂ ^{17}O and D₂ ^{18}O , microwave spectra 3-78818
 (D₂O)₂, microwave and r.f. transitions obs. by mole. beam electric resonance method 3-78825
 F₂CS, microwave spectrum, structure and dipole moment 3-67827
 HCO nonlinear free radical, Zeeman effect, microwave spectra theory and analysis 3-46306
 H₂D⁺, radio spectrum and dipole moment rel. to interstellar clouds 3-70031
 HNO and DNO, microwave spectra analysis 3-63488
 H₂O pure rotation spectrum, approximate mean absorption coefficient 3-67833
 (H₂O)₂, microwave and r.f. transitions obs. by mol. beam electric resonance method 3-78825
 H₂PBH₃, dipole moment, internal rotation barrier, staggered conformation, microwave obs. 3-54699
 NCl₃, microwave spectra, anal. four nuclear quadrupole problem 3-78819
 NCO, Renner-Teller effect and vibronically induced bands in electronic spectrum 3-75048
 NH₃, inversion spectrum, collision broadening and shifting 3-67838
 NH₃, rot. energy transfer, direct obs. by time-resolved i.r.-microwave double reson. 3-78886
 NH₃ microwave absorption lineshift by non resonant i.r. laser radiation (French) 3-54702
 NO₂, microwave optical double resonance lines 3-78835
 N₂O₂, N quadrupole hyperfine splitting 3-46305
 O₃, ^{18}O substituted, microwave, rotational consts. 3-78782
 OCS, isotopically enriched, ground state and vibr. excited, microwave spectra 3-67830
 SF₂Cl, rot. spectrum, K-type splitting (French) 3-57659
 S₂O, centrifugal distortion consts., microwave spectra analysis 3-67828
 SO³²Cl₂, nuclear quadrupole coupling constants 3-78839
 SiF₄, microwave spectrum in excited vibr. states, equil. struct., pot. function, Coriolis reson. 3-67831
 TeF₃Cl isotopic species, rot. consts. 3-46304

radiofrequency spectrometers

- digital correlation spectrometer for multi-level quantisation, radioastron. appl. 3-70076
 e.s.r., absorption spectra investigation, improvement 3-73823
 e.s.r., Bloch arrangement for X-band (German) 3-66288
 many-channel, operating at 21 cm, Pulkova large radiotelescope (Russian) 3-81241
 n.q.r. pulse radiospectrometer, resolving power, effect of spectral width, passband of receivers 3-48487
 RATAN-600, radiotelescope, receiving equipment (Russian) 3-81240
 spectrograph, electro-optical, astron. appl. 3-70073
 spectrograph, for recording solar radio emission 3-56461

radiofrequency spectroscopy

- see also nuclear magnetic resonance; paramagnetic resonance; radiofrequency spectrometers
 atomic g-factor beam-foil meas. techniques 3-78458
 beam-foil spectroscopy, improved resolution methods 3-77492

radiofrequency spectroscopy continued

- Bloch equations and adiabatic rapid passage with radiation damping 3-68822
 cryostat, gas-flow, r.f. measurements, design, operation 3-77411
 electron spin echo envelope spectrometry, superhyperfine splitting 3-39978
 Fourier transform n.m.r., computerised 3-66293
 Fourier transform n.m.r. spectroscopy 3-53957
 l.f. parallel pumping, below 500 MHz, for ferrite and garnet mag. relax. obs. 3-64555
 magnetic field homogeneity anal., using atomic beam r.f. spectroscopy 3-73899
 microwave e.p.r., applic. of IMPATT diodes as r.f. source 3-39979
 molecular beams, velocity distrib., space modulation of radiofrequency field, shift of Zeeman pattern, devices (French) 3-49507
 multifrequency methods and their application 3-75871
 n.m.r., computer for processing and display 3-66294
 n.m.r., continuous Fourier anal. method 3-66295
 n.m.r., digital program controlled generator 3-66296
 n.m.r., spectrometer, two pulse experiments, interfaced minicomputer, techniques 3-73828
 nuclear mag. spin-lattice relax. time meas. using repetitive sweep techniques 3-59616
 pulsed NMR spectrometer, interface to Varian 620/i computer 3-39981
 spin lattice relax. time meas., progressive saturation methods (Rumanian) 3-64537
 tunable lasers, use in spectroscopy 3-66898

radiogalaxies see galaxies; radiosources (astronomical)**radiogoniometers see goniometers****radiographs (x-ray photography) see radiography****radiography**

- see also neutron radiography; nondestructive testing
¹³³I Hippurium renogram, computer-aided statistical analysis 3-56533
 acquired cardiovascular disease, radionuclide angiocardiology 3-53756
 automated analysis of brain, thyroid, liver and lung radioisotope scans 3-42374
 blood vessel imaging with screen film systems, effect of radiographic magnification 3-66032
 blood vessel phantom, X-ray pattern, X-ray spectrum and screen-film unshortness effect 3-66033
 brain examination (Danish) 3-51463
 capacitor discharge unit, mobile, radiographic examination of chest, practical experience 3-66390
 cerebral angiography, phantom study using different film-screen combinations 3-66034
 chest X-ray diagnosis with monoenergetic beam, Monte Carlo appl. 3-73600
 classification, rejection/acceptance of small fluctuations, likelihood ratio test 3-51464
 collimation, rectilinear scanners, camera imaging equipment, designs, review 3-70143
 colour radiographs for examination of heart and blood vessels (Czech) 3-56992
 computer evaluation, high energy X-radiography, detectability of cracks prediction 3-45572
 computer image enhancement in medicine 3-66040
 computer image processing for heart disease diagnosis 3-66041
 concrete, prestressed, reinforcement strength and position, non-destructive X-ray test, strain meas. (German) 3-69418
 diagnostic X-radiography, radiation quality and anode effect, in Hiroshima and Nagasaki 3-56552
 digital gamma camera tomography, theory, nuclear medicine 3-70153
 disease diagnosis, in maxillofacial region, X-ray obs. 3-53747
 dual-isotope angiocardiology, for diagnosis of intracardiac shunts 3-66024
 egg-white, pulse radiolysis, e_{aq}^- , cystine disulphide anion-radicals, yield and decay 3-77251
 electron linear accelerator, for radiation therapy, review 3-53753
 electron microscope, high resolution, autoradiography radioactive tracers, metal structural defects (French) 3-48561
 electronic image processing in X-ray diagnosis 3-48628
 electradiography, technique and future 3-77256
 equivalent penetrometer sensitivity, for X-rays and γ -rays in steel 3-65050
 excitation thyroid laminography, fluorescence scanning 3-70152
 Fresnel zone plate imaging, high resolution by spatially coded source 3-73598
 gamma, industrial applications in South Africa (Afrikaans) 3-65064
 Gamma camera tomographic magnifying collimator systems 3-70155
 gamma camera tomography system, digital, clinical experience 3-70168
 gamma-gamma coincidence detection, three-dimensional imaging of radionuclides distributions 3-70162
 health phys. conf. Miami Beach, USA (1973) 3-77246
 hemopoietic marrow scanning, comparison of ^{52}Fe and ^{111}In 3-70137
 high energy X-radiography, precision meas., dimensional change monitoring 3-45569
 hypotonic duodenography 3-56540
 image enhancement by spatial frequency filtering, application to non-destructive testing 3-80509
 image processing, review 3-62167
 image quality evaluation 3-66036
 imaging systems, instrumentation, performance analysis, review 3-70142
 imaging systems, radiotracers, collection and analysis factors, instrumentation, review 3-70145
 isotope imaging 3-66043
 L-929 cells, phase duration by autoradiography (German) 3-77202
 larynx, soft tissue intensification in frontal roentgenography 3-56544
 left ventricular volume and ejection fraction, radionuclide angiography determ. 3-53755

radiography continued

- lymphography and supplementary procedures 3-56541
- medical X-ray diagnosis, ferrite powder applications 3-42372
- motion tomography, general theory 3-70159
- multiple γ -camera images recorded on one X-ray film 3-77257
- myocardial blood flow, Anger radionuclide determ. 3-56538
- neutron imaging, with thin Gd converters 3-48566
- patient positioner, for radiation therapy 3-59446
- pericardial effusion, radionuclide angiocardiology 3-56539
- physics in nuclear medicine, proceedings of American Association of Physicists, Chicago, USA, 30 Nov to 1 Dec, 1972 3-61914
- planigraphy, influence of intensifying screens 3-45318
- Polytome, image intensifier fluoroscopy and tomography 3-66388
- positron camera, Massachusetts General Hospital 3-70161
- positron tomography, three dimensional reconstruction technique 3-70163
- positron-transverse section detector, 32-crystal 3-70160
- proton, as diagnostic tool 3-66030
- proton, visualisation of cerebral vascular lesions 3-70140
- proton accelerators of USSR, medical uses for treatment of malignant tumours 3-59440
- proton beam radiotherapy, effects of multiple scattering 3-77253
- proton radiation therapy, prospects 3-59444
- proton scattering, edge pattern intensity 3-69423
- pulsed reactor fuel, NDT, dye penetrant, u.s. reflection, X-radiography, immersion density methods 3-67559
- radiation therapy at TRIUMF, using π^- beam 3-59447
- radiocardiology, basic concepts and applications 3-53754
- radiology, densitometry, development, trends 3-70139
- radiotherapy using π^- from racetrack microtron 3-59445
- Roentgen photographs, influence of object motion using modulation transfer functions 3-66021
- roentgenmicrography of human neonatal lung 3-56543
- rotational cinescintiphotography, three dimensional organ images 3-70165
- scintillation camera, portable, clinical appls. 3-73596
- SI units in radiology and radiation measurement 3-53773
- simulated radiographic signal, factors affecting detectability 3-66035
- spatial frequency filtering of radiographs, optical Fourier transform enhancement 3-48594
- steel, rare-earth inoculated, contact microradiography obs. 3-61146
- stereoscintiphotography, brain scanning applic., depth perception experimental studies 3-70164
- stressed rocks, h.v. radiography, dual microdensitometry 3-45516
- subdural hematomas, radionuclide detection, rapid sequential scintiphotography 3-56535
- Theratron 80 radiotherapy machine, collision detection computer programs 3-66037
- tomocamera, tomographic imaging, clinical experience 3-70167
- tomographic imaging in nuclear medicine, Conference, USA, 15-16 Sept. (1972) 3-70146
- Tomographic imaging with a Fresnel zone plate system 3-70157
- tomographic scanner, multiplane, clinical results 3-70171
- tomographic scanner, multiplane, nuclear medicine 3-70148
- tomographic scintillation camera, performance parameters 3-70154
- tomographic system in nuclear medicine, multiple view of isotope distribution 3-70158
- tomography, basic principles, nuclear medicine applic. 3-70147
- tomography, circular, clinical artifacts encountered 3-70169
- tomography, computer-controlled colour-coded digitised images, display system 3-70156
- tomography, modulation transfer function and thickness of cut 3-66031
- tomography, radionuclide, clinical perspective 3-70173
- tomography, radionuclide, systems, current state of the art review 3-70144
- tomography, transverse axial, computerized, X-rays 3-70166
- tomoscanner, clinical experience 3-70172
- tomoscanner, multicrystal cylindrical imaging device, transverse section brain scanning 3-70150
- tomoscanner, theory, prototype nuclear medicine 3-70151
- total body counting 3-77250
- total body neutron activation analysis, neutron source selection 3-77254
- total-body skeletal imaging 3-66027
- tracer applications and contamination hazards (French) 3-62222
- track-etch radiography, alpha particles, protons, fast and thermal neutrons, polycarbonate plastics, cellulose nitrate 3-67627
- transverse section scanner, analogous to transverse roentgen tomography, nuclear medicine 3-70149
- transverse section scanning, brain 3-70170
- venography, using $^{99m}\text{TcO}_4^-$ 3-66026
- welded joints with artificial flaws, fatigue strength determ. (German) 3-69412
- X-ray renal arteriography 3-56542
- X-ray TV system, dose reducing fluoroscopy 3-45329
- γ -cameras, intrinsic efficiencies and modulation transfer fns. 3-77255
- Al, creep, X-radiographical study, mosaic block fragmentation (Russian) 3-58629
- Al alloy, fatigue crack detection, u.s., X-radiographic and eddy current techniques 3-47511
- B autoradiography appls. 3-66446
- Si:Sb(P), (Au), zone refined, distribution of impurity elements, quantitative autoradiography 3-41651
- Si_3N_4 , hot-pressed, impurities and inclusions identification 3-76284
- ^{87}Sr , combined lung-liver scan, preliminary expt. in animals 3-56536
- UO_2 , particles, TRISCO coated, thermochem. stability 3-78384
- ^{127}Xe , appl. to biomedical imaging with Anger camera 3-42373

radioisotope separation see isotope separation**radioisotopes**

- bed material transport in rivers, radioisotope meas. technique 3-73397
- concentration in marine animals, monitoring sensitivity San Onofre Nuclear Generating Station 3-74767
- gamma radiography industrial applications in South Africa (Afrikaans) 3-65064

radioisotopes continued

- gamma ray spectrometric determination of levels in materials 3-63202
 - gamma-ray spectrometry, radioactivity assay 3-63202
 - gamma-ray spectrometry, radiological surveillance, nuclear power facilities 3-62233
 - gamma-ray standards, National Bureau of Standards, gamma-ray meas. techniques 3-62303
 - lunar rocks and soils, Apollo 17 samples 3-61728
 - medical applications, radiation detector with integrated magnetic recorder (French) 3-53757
 - medical diagnostics, release to environment through excreta, control 3-77296
 - nucleation of ice, supercooled H_2O drops 3-76769
 - packaging, licensing and analytical techniques of evaluation 3-67413
 - production in cyclotron, characteristics (Afrikaans) 3-62214
 - radioiodine, airborne, monitoring improvement of collecting efficiency under high relative humidity 3-73608
 - Rhone sediments, diffusion coeffs. of radioelements 3-56142
 - technological applications, conference, Pelindaba, South Africa (October 1972) 3-62197
 - technology advances, applications (Afrikaans) 3-62198
 - thermoelectric generator, fuel capsule vent system, He, Viking mission to Mars 3-67402
 - in X-ray fluorescence analysis, review 3-62372
 - ^{14}C , sepn. from n-irrad. AlN by dry procedure 3-44739
 - ^{141}Ce : ^{144}Ce radioisotopic activity ratio obs. by γ spectrometry of rain-water 3-69581
 - ^{60}Co / ^{137}Cs content of coastal sediments near nuclear power station coolant discharge into seawater 3-69558
 - ^{137}Cs concentration in Japanese coastal sediments, obs. 3-69559
 - ^{137}Cs concentration in Japanese coastal waters, obs. 3-69560
 - ^{137}Cs concentration in Nishiyama soils, vegetables and human diets 3-69514
 - ^{137}Cs concentration in volcanic ash paddy soil, obs. 3-69515
 - ^{137}Cs content of soils in Niigata Prefecture, Japan 3-69513
 - ^{137}Cs / ^{137m}Ba radioisotope generator system, separation of ^{137m}Ba , $\text{CuCo}[\text{Fe}(\text{CN})_6]$ adsorbent 3-48505
 - ^{67}Ga , production by deuteron bombardment of Zn for medical applications 3-59448
 - ^{67}Ga scanning, for localization of psos abscess 3-66022
 - ^3H concentration in North Pacific, liquid scintillation counting 3-69561
 - I, A = 129-135, emission from nuclear reactors, accumulation in Federal German Republic (German) 3-67631
 - ^{125}I , labelled thrombosis monitor, for deep vein obs. 3-56530
 - ^{81}Kr , rate of formation in atmosphere, influence of cosmic ray intensity (Russian) 3-65322
 - ^{237}Np purification using Amberlite XE-270 exchange resin 3-67577
 - ^{150}O , production with Van de Graaff acceleration 3-73833
 - ^{238}Pu , ^{241}Am sequential determ. in environmental samples 3-66451
 - ^{220}Rn and ^{222}Rn atmospheric surface layer diurnal variations and vertical distributions 3-73326
 - ^{103}Ru : ^{106}Ru radioisotopic activity ratio obs. by γ spectrometry 3-69581
 - ^{106}Ru complexes effect on coprecipitation yields from seawater, obs. 3-69556
 - ^{117m}Sn , as bone-scanning agent, evaluation 3-53748
 - ^{90}Sr concentration in Japanese coastal waters, obs. 3-69560
 - ^{90}Sr concentration in volcanic ash paddy soil, obs. 3-69515
 - ^{90}Sr content of soils in Niigata Prefecture, Japan 3-69513
 - ^{235}U and ^{233}U , criticality research, Oak Ridge Critical Experiments Facility 3-63227
 - ^{135}Xe , measurement of neutron capture cross section by the activity depletion method 3-60171
 - ^{129m}Xe , half-life determ. 3-52127
- radiolysis**
- alkyl iodide aqueous solns., pulse radiolysis, transient ion pairs from OH radical reactions 3-76464
 - aminoethylthioacetic acid formation, X-radiation of cystamine and dithiodiglycolic acid, chain reaction 3-47566
 - anthracene at metal surfaces (Russian) 3-47567
 - t-butyl alcohol aqueous solns., radical form. and solvation behaviour 3-58805
 - cyclohexane-biphenyl solns., pulse radiolysis, ioniz. in track of high-energy electron 3-65092
 - cystamine and dithiodiglycolic acid, X-radiation, formation of mixed disulphide aminoethylthioacetic acid, chain reaction 3-47566
 - dithiodiglycolic acid and cystamine, X-radiation, formation of mixed disulphide aminoethylthioacetic acid, chain reaction 3-47566
 - egg-white, pulse radiolysis, e_{aq}^- , cystine disulphide anion-radicals, yield and decay 3-77251
 - ethers, containing solvated electrons, optical absorpt. spectra by pulse radiolysis 3-44725
 - fissiochemical loop, low temp. design and operational features 3-74649
 - fluorocarbons, pulse irradiated, electron disappearance 3-73148
 - hydrocarbons, liquid, steady state and pulse radiolysis, charge scavengers effect on scavenging on opposite sign charges 3-41849
 - ice, radiation produced trap phenomena in low temp. crystals 3-58806
 - perfluoromethylcyclohexane, dependence of radiolysis on dose, O_2 content, temp. and radiation type (German) 3-69481
 - propane, supercritical, electron scavenging by N_2O in γ radiolysis, density var. 3-73145
 - pulse radiolysis in aqueous solns., ionisation state determ. of e_{aq}^- adducts, a.c. conductivity method 3-53327
 - toluene solid solution, mechanism of singlet, triplet state formation, via aromatic additives radioluminescence 3-76467
 - water and aqueous solns., γ -radiolysis under N_2 gas bubbling, reln. to reactor cooling 3-71277
 - $\text{Sn}(\text{ClO}_4)_2 \cdot 3\text{H}_2\text{O}$, SnBu_4 , SnBu_2Cl_2 and SnBu_2SO_4 , Mossbauer absorption spectroscopy meas. of after-effects of ^{119m}Sn isomeric transition 3-55985
- radiometers**
- absolute radiometry, instrumental theory (French) 3-45438
 - airborne scanning i.r., meas. correction for atm. effects 3-59190
 - amplifier, selective, synchronous integrator 3-73560

radiometers continued

- APT scanning radiometer data, technique for real-time quantitative display 3-51168
 continuous spectrum, main parameters limits of sensitivity, RATAN-600 radiotelescope (*Russian*) 3-81239
 differential, remote sensing of chlorophyll and temp. in marine and fresh water 3-73607
 electrically calibrated pyroelectric detector basis 3-77394
 electro-optical studies, NBS 3-53854
 flow measurement application (*Polish*) 3-42739
 Gardon radiometer, for convective thermal fluxes 3-51544
 interference-suppressing device, for radiometers 3-56634
 i.r. heterodyne radiometer, appl. to remote detection of SO₂ and CO₂ 3-45330
 mesospheric and stratospheric temps. remote sensing by microwave radiometry 3-56260
 microwave, for remote sensing of soil moisture in Phoenix Arizona region 3-59166
 microwave S-band, use in sea surface temperature meas. 3-76920
 millimetric band, input mechanical switch, crossed waveguide system, description, operation (*Russian*) 3-80859
 modulation balance, principles of operation, RATAN-600 radiotelescope (*Russian*) 3-81240
 multichannel, for Earth's atmosphere composition determ. 3-56187
 multiple wavelength radiometer for atm. extinction meas. 3-51186
 NOAA satellite scanning radiometer for ocean surface temp. sensing, atm. effects 3-50994
 passive microwave radiometry, appl. to Earth resources surveys 3-51178
 polarised i.r., for ocean surface temp. meas. (*French*) 3-65536
 polarizing radiometer for improved meas. of sea surface temperature (*French*) 3-51207
 radar pulse interference, protection by using amplitude limiter (*Russian*) 3-81242
 radioactive aerosols concentrations, artificial, meas., for α and β rays, methods 3-42534
 satellite borne 16-channel selective chopper radiometer, IR and 15 μ m CO₂ band 3-69736
 sea surface water temp. meas. using airborne dual-channel i.r. radiometer 3-51204
 spectroradiometer, for field use, design description 3-39880
 transpiration, annular, edge cooled, measurement of total thermal radiation from flowing plasma, results 3-56643
 two-wavelength radiometer for meas. of heat flux from sea, divergence effects 3-51202
 Cf²⁵², use as detector in geophysical radiometry (*Rumanian*) 3-51171
 H arcs for vacuum u.v. radiometry 3-51549

radionavigation

- aerospace, specific effective scatt. area of Moon, Mars and Venus 3-56312

radios see radio receivers**radiosondes**

- see also *meteorological instruments*
 atmosphere temp., rocketsonde, radiosonde, NOAA-2 and NIMBUS-5 satellites, comparisons of meas. 3-59068
 baroswitch, automatic calibration, environmental testing chamber, for audiofrequency modulated radiosonde 3-80858
 calibration, multi-pulse generator 3-80857
 ionospheric station pulsed transmitter 3-42061
 objective analysis scheme, atmospheric wind field, spectral analyses 3-76860
 refractivity var., use of radiosonde data in range correction 3-76786
 stratosphere temp., radiosonde meas. rel. to NOAA-2 satellite meas. 3-56259

radiosources (astronomical)

- see also *pulsars; quasars*
 2.7°K cosmic background radiation, search for anisotropy at 3.56 cm 3-56401
 1633+38, identification with visible object 3-77111
 2695 MHz survey of weak sources, source count 3-45144
 active radio galaxies, assoc. galaxy formation and binding of rich clusters 3-59376
 apparent angular size, influence of scattering phenomena 3-77179
 B2 catalogue of radiosources at 408 MHz, differential log S-log N relationship 3-81110
 B2 sky survey sources, spectral index distrib. between 408 and 5000 MHz 3-73522
 background confusion sources, effects on radio interferometry of moving sources at 21-cm. 3-56329
 binary star radiosources rel. to X-ray binaries, possibly two types 3-61823
 bright, precision of meas. coordinates, Pulkovo and RATAN-600 radiotelescopes, variable profile antenna (*Russian*) 3-81251
 3C120, Seyfert galaxy, 7.85 GHz outbursts, 1972 April to Oct., Goldstone-Haystack interferometer obs. 3-65902
 3C120, Seyfert galaxy, 7.85 GHz outbursts, 1972 June to Nov., Goldstone-Haystack interferometer obs. 3-69975
 3C147, single-spacing obs. of interstellar H I absorption 3-81106
 3C353, aperture synthesis of interstellar H I absorption 3-81106
 5C3 sources, M 31 region, optical identifications of quasars and galaxies 3-42212
 3C 10 (Tycho's supernova remnant), interpretation of radio emission 3-42203
 3C 144, angular dimensions meas. at 25 MHz (*Russian*) 3-81113
 3C 147, angular dimension meas. at 408 MHz (*Russian*) 3-81112
 3C 192 obs. at 2.7 and 5 GHz 3-69976
 3C 196, angular dimensions meas. at 25 MHz (*Russian*) 3-81113
 3C 196, radiointerferometric obs. at 85.5 MHz (*Russian*) 3-81114
 3C 254, angular dimensions meas. at 25 MHz (*Russian*) 3-81113
 3C 273, angular dimensions meas. at 25 MHz (*Russian*) 3-81113
 3C 273, obs. of variable fluxes (*Russian*) 3-45145
 3C 273B, angular dimension meas. at 408 MHz (*Russian*) 3-81112
 3C 286, angular dimension meas. at 408 MHz (*Russian*) 3-81112
 3C 298, radiointerferometric obs. at 85.5 MHz (*Russian*) 3-81114
 3C 327, radiogalaxy, u.h.f. polarisation meas. of intergalactic gas density 3-45142
 3C 345; obs. of variable fluxes (*Russian*) 3-45145
 3C 353, extended OH emission at 1720 MHz 3-81109

radiosources (astronomical) continued

- 3C 382, 452 and 465, obs. at 2.7 and 5 GHz 3-81117
 4C 38.41, identification with visible object 3-77111
 3C 391, supernova remnant, 18 and 21 cm recombination line emission 3-70034
 3C 398 (W49B), supernova remnant, 21 cm recombination-line emission 3-70034
 3C 454.3, angular dimension meas. at 408 MHz (*Russian*) 3-81112
 3C 461 (Cassiopeia A), young supernova remnant, interpretation of radio emission 3-42203
 3C 465 rel. to morphology of outer regions of NGC 7720, associated galaxy 3-42226
 3C 52 obs. at 2.7 and 5 GHz 3-69976
 3C 83.1 B rel. to morphology of outer regions of NGC 1265, associated galaxy 3-42226
 3C 84, obs. of variable fluxes (*Russian*) 3-45145
 3C 84, Seyfert galaxy, long baseline interferometry 3-53705
 5C survey regions, flux density errors 3-73521
 Cassiopeia A, angular dimensions meas., by independent reception interferometer at 9 MHz (*Russian*) 3-81111
 Cassiopeia A, flux density meas. at 1440 MHz 3-56397
 Cassiopeia A, Perseus arm feature, aperture synthesis of interstellar H I absorption 3-81105
 Cassiopeia A, scintillation at 26 MHz during artificial ionospheric modification 3-80796
 Cassiopeia A (3C 461), young supernova remnant, interpretation of radio emission 3-42203
 celestial bodies, radio images obtained with resolution $>10^{-2}$ sec. of arc, global radiotelescope (*Russian*) 3-81245
 Centaurus A, 100 μ survey of Southern Milky Way 3-45158
 circular repolarization in compact sources 3-69977
 clusters of galaxies, dynamical models of tailed radiosources 3-61843
 compact, structure at 2.8 cms 3-77113
 compact source 2048+31 in Cygnus Loop, interferometric meas. 3-65906
 cosmic, use for meas. of large antennas 3-48060
 counts at 408 MHz using MC1 catalogue data 3-56399
 Crab Nebula, origin of h.f. radiation 3-61876
 Crab nebulae, radioastronomical obs., scanning the diagram of the variable profile antenna (*Russian*) 3-81248
 P Cygni, detection of radio emission at 5 and 10.68 GHz 3-81119
 V1016 Cygni, peculiar emission object, radio emission interpretation 3-77099
 V1016 Cygni, radio emission at 10.63 GHz 3-65899
 Cygni-A, radioastronomical obs., scanning the diagram of the variable profile antenna (*Russian*) 3-81248
 Cygnus A, aperture synthesis of interstellar H I absorption 3-81106
 Cygnus A, obs. of CO bands at 2.6 mm 3-45214
 Cygnus A, scintillation at 26 MHz during artificial ionospheric modification 3-80796
 Cygnus X-2, peculiar blue star counterpart, obs. of radio emission 3-45148
 Cygnus X-3, 8 GHz obs. during September 1972 outburst 3-70001
 Cygnus X-3, model for second radio outburst rel. to source structure 3-61834
 depolarisation, size and red shift rel. to existence of intergalactic gas 3-53706
 depolarisation and luminescence obs. of double radio sources 3-81122
 discrete sources, obs. at 2 cm at Pulkovo Obs. 3-61825
 double sources, assoc. with radio halos 3-61824
 DR21, H II region, 5 GHz obs. of small-scale structure 3-48061
 energy generation due to gravitational contraction and rapid rotation in mag. field 3-44991
 extensive phenomena at high galactic latitudes, H I regions, nebulosity and giant radio loops 3-42230
 extragalactic, 1 mm radiometry, cryogenic optical system 3-77180
 extragalactic, extended, models 3-53677
 extragalactic, position determ. using VLBI 3-56062
 extragalactic, ram pressure confinement models, relativistic motion, plasma cloud 3-48059
 extragalactic, review of new data, consequences of physics 3-81121
 extragalactic, stronger than 10 f.u. at 408 MHz, all-sky catalogue 3-53673
 extragalactic radio sources rel. to bubbles of relativistic plasma from galactic nuclei 3-53678
 extragalactic sources, position determ. from VLBI obs. 3-45143
 extragalactic sources, radio surveys review 3-65907
 Faraday depolarization of radio galaxies and quasars with simple spectra 3-48065
 flux density measurements relative to Cas A at 21.8 GHz 3-77112
 formaldehyde absorpt. in front of galactic sources 3-59379
 fundamental reference system, extension to radio sources and faint objects 3-59241
 G 355.3+0.1, identification as H II region 3-77110
 Galactic, background radio emission, 3.75 cm-3.5 m 3-77151
 galactic anticentre, soft X-ray flux rel. to radio continuum features 3-51376
 Galactic centre, fine structure obs. at 2695 and 8085 MHz 3-45203
 Galactic centre, radio pulse search 3-69978
 galactic centre, sensitive search for microwave pulses 3-70024
 Galactic radio spurs and spiral structure, optical and radio brightness distributions 3-61854
 galaxies, head-tail, brightness and polarisation distrib. at 1415 MHz 3-61821
 galaxies, radio maps around five spiral and peculiar objects 3-70009
 galaxies identified with 4C radiosources, redshifts for 51 objects 3-51382
 Galaxy, linear polarisation at 210 MHz (*Russian*) 3-81178
 Green Bank 1400 MHz sky survey, anisotropy and counts of sources 3-61819
 HDE 226868 (Cygnus X-1), radio variability of spectroscopic binary 3-51359
 HI regions in Sagittarius and Scutum arms, 21 cm radiation source 3-61867
 interplanetary scintillation, latitude dependence outside plane of ecliptic 3-77030

radiosources (astronomical) continued

- interplanetary scintillation obs. of 203 sources identified as radio galaxies or quasars 3-48055
 interstellar, OH line obs. (*Russian*) 3-81116
 interstellar matter, search, unsuccessful, for organic molecular lines 3-61863
 interstellar rotating dust cloud, OH 1667 MHz obs. 3-61878
 interstellar SO, 9.9 and 138.2 GHz emission column density meas. 3-81198
 isolated, dispersed r.f. pulses, search at 110 cm 3-48058
 Jovian decametric radiation, plasma physics 3-53616
 Jupiter, 10.4 cm and 21.3 cm, rel. to radiation belts 3-65779
 Jupiter, decametric radiosource B, fine structure 3-56348
 Jupiter, effect of Io's ionosphere on radio bursts 3-56334
 Jupiter, Io-controlled decametric radiation rel. to alfvén wave emission 3-65772
 Jupiter, microwave brightness temp. determ. using model atm. 3-42158
 Jupiter, radio disk temp. at 1.35 cm rel. to Mars 3-42148
 Jupiter decametric rotation period rel. to Source-A emission beam 3-42156
 AR Lacertae, Algol-type eclipsing and spectroscopic binary, obs. of radio emission 3-45148
 BL Lacertae, BV obs. and bibliographic informations (*French*) 3-73514
 BL Lacertae, peculiar properties, review 3-45149
 BL Lacertae, photographic and photoelectric obs. of optical variability 3-81095
 BL Lacerte, structure and apparent motion 3-77119
 l.f. radio spectra, deviations from power law, possible mechanism for point sources 3-42208
 linear polarisation, time variation at 2.8 and 4.5 cm 3-77109
 linear polarisation at 2.8 and 4.5 cm 3-77108
 loops as fossil, Stromgren spheres, radio and X-ray emission 3-56450
 M8, HCN radio emission from Hourglass region 3-51395
 M 17, effects of Stark broadening in radio recombination line temperatures 3-42209
 major planets, nonthermal radio observations 3-42154
 Markarian galaxies, attempt to detect emission at 408 MHz 3-51360
 Markarian galaxies, obs. at 75 cm wavelength (*Russian*) 3-81179
 Mars, radio disk temp. at 1.35 cm rel. to Jupiter 3-42148
 MC's 76 and 77, proximity to LMC X-1 rel. to optical candidate 3-53694
 microwave H₂O vapour emission from Galactic sources 3-59381
 Models of extended radio sources 3-77114
 Molonglo Radio Source Catalogue 1, 1545 objects at 408 MHz 3-59351
 Multiple explosions and the evolution of radio galaxies 3-77143
 MWC957, 2.8 cm 3-69979
 MWC 349, optical, radio and i.r. obs. 3-73520
 MWC 349, radio star, photoelectric obs. 3-61802
 nearby stars, search for narrow band 21-cm signals from other civilizations 3-59353
 neutral stellar objects, identification with radio sources 3-53679
 NGC1265, radio galaxy, peculiar morphology and tail, high resolution 5 GHz map 3-65905
 NGC 2798/9, double galaxy system, search for associated radio-sources at 1415 MHz 3-48056
 NGC 5128 (Centaurus A), high resolution obs. of radio galaxy 3-73545
 NGC 7552, i.r. obs. and identification with PKS radio sources 3-51388
 NGC 7582, i.r. obs. and identification with PKS radio sources 3-51388
 number-flux-density distrib. of sources, maximum likelihood estimation 3-65943
 OH 471, flux density records rel. to variability 3-48062
 Ohio-survey radiosources, flux densities and positions at 430 MHz 3-42205
 OJ 287, blue compact object, photoelectric sequence 3-73523
 OJ 287, peculiar properties, review 3-45149
 ON-1 (OH 69.5-1.0), associated compact radiosource rel. to H II region 3-45147
 Ooty sources, lunar occultation obs. at 327 MHz of 6 objects with flat spectra 3-42206
 optical identification by coincidence of radio and optical positions 3-77107
 optical identification problems 3-81108
 OQ 208, synchrotron source model rel. to radio emission 3-69971
 Orion A, effects of Stark broadening in radio recombination line temperature 3-42209
 Orion A, search for D92 α recombination line emission and D/H ratio 3-81107
 Orion B, 7.8 GHz recombination lines of H, He, and C spectroscopic mapping 3-61868
 Orionis-A, radioastronomical obs., scanning the diagram of the variable profile antenna (*Russian*) 3-81248
 β Persei, 5GHz obs. 3-61816
 β Persei, X-ray emission during radio flares, upper limits 3-65903
 PKS 2134 + 004, synchrotron source model rel. to spectrum turnover 3-69971
 planetary nebulae H radio recombination lines strengths 3-61875
 planets, thermal and nonthermal emission, conference (Houston, 1-3 March 1972) 3-42151
 linear polarisation survey of region around l=140°, b=+8° at 240.5 MHz 3-61822
 position meas. using VLBI, geodetic appl. 3-56246
 positions for 59 sources from 2695 and 8085 MHz obs. 3-69972
 PSR 0531 + 21 giant pulses at 146 MHz, analysis of polarization 3-69985
 quasi-stellar and unidentified radiosources, angular distrib. over sky 3-81118
 quasi-stellar sources, V/V_m test and source-count anal. 3-73524
 radiostars of group 4, observations (*German*) 3-81120
 RATAN-600, astrophysical problems to be solved with this radiotelescope (*Russian*) 3-81244
 recombination lines toward galactic centre, 1.621 GHz obs. 3-51379

radiosources (astronomical) continued

- Sagittarius A, meas. at mm and meter wavelengths (*Russian*) 3-81115
 Sagittarius A West, nonthermal properties rel. to galactic centre 3-42207
 Sagittarius B1, meas. at mm and meter wavelengths (*Russian*) 3-81115
 Sagittarius B2, meas. at mm and meter wavelengths (*Russian*) 3-81115
 Sagittarius B4, meas. at mm and meter wavelengths (*Russian*) 3-81115
 Saturn, microwave brightness temp. determ. using model atm. 3-42158
 scintillation effect of plasma velocity fine structure 3-77031
 scintillation time spectra rel. to velocity dispersion of interplanetary medium 3-53681
 separation velocity of components of extragalactic sources 3-42210
 Sharpless H II regions, H₂O sources, obs. of microwave emission 3-61869
 solar chromospheric flares, relation between chemical composition of cosmic rays and radiospash duration spectrum (*Russian*) 3-65575
 source strengths at 29.9 MHz between -4° and -64° declinations 3-53672
 spatial distrib. of radiosources rel. to number counts and redshift meas. 3-42211
 spectral flux density, radio emission at 3.5 cm (*Russian*) 3-45146
 spiral galaxy nuclei, optical properties and ionisation mechanism 3-77137
 stellar coronae, X-ray and radio emission rel. to soft X-ray background 3-45078
 supernova remnants, high resolution obs. at 80 MHz 3-56398
 supernova remnants, obs. of galactic sources at 1.7 and 2.7 GHz 3-59348
 supernova remnants near galactic plane, 8.8 GHz radio obs., brightness distrib. and flux densities 3-53671
 supernovae 1970g in M101, obs. at 2.8, 6 and 21 cm 3-42204
 Supernovae remnants, search for 1415 MHz emission from young extragalactic objects 3-56400
 synchrotron self-absorpt., variation in polarisation 3-51361
 synchrotron sources, extension of theory for small pitch angles 3-69970
 synchrotron sources, pulsars and compact extragalactic objects 3-69971
 thermal, in H II regions, 8.2 mm high resolution survey 3-77115
 very long baseline interferometric obs. 3-65908
 Virginis-A, radioastronomical obs., scanning the diagram of the variable profile antenna (*Russian*) 3-81248
 W12, single-spacing obs. of interstellar H I absorption 3-81106
 W51, kinematic distance estimate of non-thermal source using OH absorpt. line meas. 3-48057
 W 3, effects of Stark broadening in radio recombination line temperatures 3-42209
 W 41, 43 and 51, extended OH emission at 1720 MHz 3-81109
 W 43 region at 4.5 cm, automatic reduction of radio maps 3-65904
 W 49 A, B, 18 cm OH absorpt. meas. 3-61820
 wavelength dependence of degree of polarization, Faraday rotation 3-61826
 X-ray counterparts of radio stars 3-81147
 X-ray emission by Compton-synchrotron or Compton black-body effect, comparison 3-53674
 CO and HCN mm-wave emission from stars 3-69974
 H I regions, 21 cm emission outside plane of spiral galaxies 3-81204
 HI survey in low galactic latitudes at 21-cm 3-65939
 H₂O interstellar masers, resonance Stark effect 3-81194
 H₂O masers in protostellar gas cloud rel. to multi-level line transfer cocoon stars 3-59382
 H₂O sources, possible detection by rapid sky survey and constraints on maser intensity 3-53682
 H₂O sources assoc. with OH emission in H II regions 3-51394
 H₂O sources in Sharpless H II regions, obs. of microwave emission 3-61869
 OH emission sources, accurate positions at 1665 and 1667 MHz 3-69973
 OH interstellar masers, resonance Stark effect 3-81194
 OH sources, possible detection by rapid sky survey and constraints on maser intensity 3-53682
 OH stars, type I, optical props. 3-61781
- radiostars** see *radiosources (astronomical)*
- radiotelescopes**
 see also *radioastronomy*
 5 km radio telescope, astrometry 3-77189
 antenna, variable profile, plane periscopic reflector (*Russian*) 3-81224
 Arecibo, diffraction integral expansion in caustic region of spherical mirror 3-77953
 Arecibo spherical mirror, e.m. field structure in focal region, numerical study 3-77944
 Bordeaux 8 mm interferometer for solar radio astronomy 3-70068
 Cambridge 5-km, coordinate system determ. rel. to β Persei position 3-61816
 Clark Lake Array for solar and sidereal studies 3-70067
 control, on-line computer, operation, hardware and architecture 3-70091
 control and mm-wave spectral line obs., computer program in FORTH 3-70078
 cross array design, 34.3 MHz 3-77181
 Culgoora radioheliograph operation at 43.25, 80 and 160 MHz 3-70071
 Dominion super synthesis telescope for H I spectroscopy 3-70066
 E-W rotation-synthesis array, main beam and ringlobes 3-51405
 Effelsberg 100-meter telescope 3-70070
 Fleurs earth-rotation synthesis radio telescope 3-65963
 Fleurs telescope, data and comparison with other telescopes 3-51414
 global, radio images of celestial bodies, resolution > 10⁻² sec. of arc (*Russian*) 3-81245
 Hot Creek mm-wave interferometer 3-65964
 Llaheerne l.f. telescope, data 3-51416
 microwave astronomy with 25 m or greater reflectors, state of the art vs. practice 3-48143

radiotelescopes continued

- millimetric-wave, dielectric waveguide line feeder 3-42267
 Molonglo telescope, future plans 3-51415
 NRAO 300 ft., antenna-beam characteristics at 21 cm. 3-77172
 NRAO 300 ft., compensation for error beam at 21 cm. 3-77173
 NRAO interferometer, electronics 3-70075
 NRAO tape-recorder interferometer system 3-65960
 Ooty aperture synthesis interferometer, 327 MHz operation 3-70069
 parabolic aerial, phase errors at the aperture, feed shifted from the focus (*Russian*) 3-81227
 pointing accuracy 3-56447
 pointing accuracy of 6m. mm-wave telescope (*Japanese*) 3-70084
 Pulkova, many-channel radio spectrograph operating at 21 cm (*Russian*) 3-81241
 Pulkovo, illumination of the variable profile reflector, technical methods (*Russian*) 3-81249
 Pulkovo, variable profile antenna, precision of measuring the coordinates of bright radio sources (*Russian*) 3-81251
 radiation-meter, 4 cm, RATAN 600 radiotelescope, liquid nitrogen cooled input parametric amplifier, description (*Russian*) 3-81220
 radioheliograph, mm-wave, for two-dimens. mapping 3-70072
 radiointerferometer, calc. of sensitivity (*Russian*) 3-81250
 radiometer, protection from radar pulse interference, use of amplitude limiter (*Russian*) 3-81242
 RATAN-600, 0.4 to 21 cm., variable profile antenna, periscope, main parameters (*Russian*) 3-81221
 RATAN-600, antenna parameters, calibration of sensitivity, 8 mm in the radar regime, radioastronomical method (*Russian*) 3-81246
 RATAN-600, astrophysical problems to be solved with this radiotelescope (*Russian*) 3-81244
 RATAN-600, characteristics of periscopic part, surveying the sky (*Russian*) 3-81243
 RATAN-600, circular reflector, reading and setting device (*Russian*) 3-81231
 RATAN-600, circular reflector, reference reading and setting device (*Russian*) 3-81232
 RATAN-600, circular reflector sections, geodetic layout of the foundations (*Russian*) 3-81235
 RATAN-600, construction of reflecting elements and the secondary mirror (*Russian*) 3-81229
 RATAN-600, distortion of reflecting surface, thermal effect, radial errors (*Russian*) 3-81233
 RATAN-600, geodesy in the process of mounting and adjustment (*Russian*) 3-81234
 RATAN-600, main parameters of radiometers, limits of sensitivity (*Russian*) 3-81239
 RATAN-600, methods of radioastronomical obs., azimuthal aperture synthesis, variable profile antenna (*Russian*) 3-81222
 RATAN-600, receiving equipment, radiometers, spectro-analysers, operation of a modulation balance radiometer (*Russian*) 3-81240
 RATAN-600, reflecting elements size determ., calc. of elec. parameters (*Russian*) 3-81223
 RATAN-600, reflecting sections, monomotor drive, double-reduction condenser breaking (*Russian*) 3-81230
 RATAN-600, variable profile antenna, calc. of noise temp., effect of field of scattering (*Russian*) 3-81228
 RATAN-600, variable profile antenna, precision of measuring the coordinates of bright radio sources (*Russian*) 3-81251
 RATAN-600 control of antenna parameters, radioastronomical obs. (*Russian*) 3-81238
 reflector surface of 6m. mm-wave telescope (*Japanese*) 3-70083
 reflector tolerance determ. by separation of aberrant and phase errors 3-70077
 Sensitivity increase of RT22 CrAO radio telescope at 3 CM wavelength for radio interferometer with high angular resolution (*Russian*) 3-81219
 Stanford five-element array, appl. of earth rotation synthesis 3-65961
 supernova search, 1.4×10^9 Hz, description of system 3-77178
 supersynthesis type, interactive computer data processing 3-70053
 variable profile antenna, aberrations of main mirror, scanning the antenna pattern by shifts of the primary feed (*Russian*) 3-81226
 variable profile antenna, adjustment, radioastronomical method (*Russian*) 3-81237
 variable profile antenna, adjustment by geodetic and radiotechnical methods (*Russian*) 3-81236
 variable profile antenna, operation near the zenith, parallel aperture synthesis (*Russian*) 3-81225
 variable profile antenna, scanning the diagram, obs. of Orion-A, Virgo-A, Cygnus-A, Crab nebulae (*Russian*) 3-81248
 weak source detection, digital integration of signals (*Japanese*) 3-56466
 Westerbork synthesis radio telescope 3-65962

radiowave propagation

- see also *electromagnetic wave propagation*
 absorption, ionospheric, 2.4 MHz, Waltair India, Al technique, variations, results 3-73347
 atmosphere, 5 mm band, effect of H₂O vapour, admixture gases and cloudness on brightness temp. (*Russian*) 3-69570
 atmosphere, rain effect at 17.7 to 19.7 GHz (*Norwegian*) 3-61481
 atmosphere, VLF phase changes and absorption during August 4-5 1972 SC 3-80669
 atmospheric Doppler spectra of diffuse radar aurorae at 50 MHz 3-73341
 atmospheric l.f. radio emission from EAS 3-69778
 atmospheric stably stratified zones, thin radar echo layers 3-65296
 attenuation measurement, ionosphere, 9.303 MHz, ISIS-II to ground 3-61525
 audio frequency size effect seen in modulation of r.f. size effect 3-46788
 auroral absorpt., latitudinal variation at different longitudes 3-65414
 auroral radar scattering parameter measurement, ideal antenna configuration determ. 3-80788
 circumterrestrial signal azimuthal characts. in winter 3-42018
 dayside-cusp ionosphere Whistler mode hiss and soft electron fluxes 3-69638
 Earth-flattening approx. in theory of radiowave propagation near Earth's surface 3-44899
 in earth-ionosphere waveguide, field representation 3-59139

radiowave propagation continued

- effect of waves and turbulence in stable layers, symposium (La Jolla, June 1972) 3-65295
 Ellis window problem, numerical solution for ionospheric model 3-42026
 F₂-region, global evolution of foF₂ 3-76808
 fading, ionospheric, frequency dependence, characteristics of ionospheric irregularities 3-73348
 f.m., theory, definite Fourier integrals, computation 3-71850
 foliage and diffraction losses at u.h.f. and X-band 3-80753
 frequency analysis of calculated ionospheric reflection coefficients 3-44918
 geomagnetic absorption effect, latitudinal variation in W. Hemisphere 3-56109
 group refractive index curves for r.f. propagation through ionosphere over Calcutta 3-51103
 impulsive radio noise environment at quiet site, v.h.f. background 3-48155
 ionosphere, D₁ method used to measure sequential wind profiles 3-76793
 ionosphere, instrument constant determ., in nighttime absorption by Al method 3-69730
 ionosphere, particle precipitation in Brazilian geomagnetic anomaly during magnetic storms 3-73352
 ionosphere, polarisation of reflected ordinary wave, vertical incidence, vertical magnetic field 3-76797
 ionosphere, VHF, second order corrections for refraction, phase path and curvature 3-69634
 ionospheric, group path difference determ. by interference method 3-42019
 ionospheric, phase characts. 3-56204
 ionospheric absorpt., phase integral corrections for model layers 3-65447
 ionospheric D-region radio waves, winter absorption anomaly, analysis 3-76805
 ionospheric fading, computer simulation of spaced-receiver drift expt. 3-65449
 ionospheric lateral incidence, electron density inhomogeneity effects 3-42017
 ionospheric LF radio absorpt. events during major meteor shower 3-61524
 ionospheric LF wave upward propag., Poynting vector turning towards geomag. field 3-65448
 ionospheric radar dispersion meas. 3-61527
 ionospheric reflected radio waves, ground diffraction pattern during spread-F conditions 3-80799
 ionospheric r.f. propagation, polarisation parameters 3-59138
 ionospheric seasonal anomaly of radiowave absorption 3-47786
 ionospheric v.l.f. penetration and reflection coefficients, full wave calcs. with ground effect 3-47784
 ionospheric wave propagation curves at night in broadcasting range 3-69633
 Jovian magnetosphere, radio wave propag. 3-47897
 l.f., SID effects, solar flares, apparatus, measurements 3-61526
 l.f., sudden ionospheric disturbance effects (*Japanese*) 3-56207
 l.f. and v.l.f. lower ionosphere study 3-80791
 lower E-region, r.f. heating effects on electron density 3-80805
 magnetosphere, whistler nose frequency and min. group delay 3-76816
 Mars, ionospheric refr. of H.F. waves, electron-neutral particle collision effects 3-42174
 multiple scattering, from random plasma inhomogeneities 3-75292
 NWC signal (22.3 kHz) phase changes over transequatorial path 3-80792
 ocean wave height spectra, LORAN-A transmission scattering by 7 second period waves 3-58982
 polarization during partial scattering in ionosphere 3-56194
 precipitation media, anisotropy meas. 3-41965
 rain attenuation at 7 to 8 GHz 3-51017
 rain attenuation meas. at millimetre waves over short paths 3-41964
 rainfall rates statistics 3-69577
 refraction spectrum of liquid water at submillimetre wavelengths, direct meas. 3-47331
 satellite communications, effect of rain on Earth-space paths 3-44905
 Schumann earth-ionosphere e.l.f. cavity reson. line splitting rel. to solar activity 3-65456
 short-wave ionospheric absorption models (*German*) 3-51121
 solenoid coil, Schumann cavity resonances, variation with solar ionizing radiation, zenith angle and storms 3-76747
 spread-F (equatorial) irregularities obs. at Nairobi and on transequatorial path Lindau-Tsumeb 3-42043
 s.w., in ionosphere, phase instability distribution parameters (*Russian*) 3-42020
 troposphere, effect of small scale variations of temperature, humidity and refractive index 3-65313
 tropospheric, above 1000 MHz (*German*) 3-76785
 UHF signal propagation above sea at zero angles, fluctuations 3-44876
 v.l.f., for time scale clamping and frequency collation 3-51510
 v.l.f., non-linear propagation in magnetoplasma, inc. ion effects 3-67998
 v.l.f., reflection from lower ionosphere 3-80793
 v.l.f. and e.l.f. in whistler mode, sunrise and sunset effects 3-76750
 v.l.f. and e.l.f. whistler waves absorption during night 3-76751
 v.l.f. radio wave field, distortion by vertical metal poles 3-76900
 whistler induced amplitude perturbation in subionosphere VLF transmissions 3-69667

radium

- Antarctic Ocean Ba conc. rel. to geochemistry of ²²⁶Ra 3-65260
²²⁶Ra, mass unit measurement standard 3-51509
²²⁶Ra and ²²⁸Ra abundance in interstitial water from Pacific Ocean sediment 3-65267

radium compounds

- NaCl soln. film, evaporation from rotating disc, heat transfer 3-63641

radium emanation see *radon***radius of curvature measurement** see *curvature measurement*

radon

- atmospheric, sources and sinks, ocean air masses 3-59077
- atmospheric concentration over Pacific and Ross Sea 3-69589
- atmospheric convection, distribution below 4 km 3-76780
- atmospheric surface layer diurnal variations and vertical distributions 3-73326
- atomic quadrupole moments of excited states 3-71364
- daughter aerosols, closed vessel storage, mobility spectrum, time variation 3-62981
- dosimetry in mines 3-53549
- oceanography, excess-Rn profile temporal var. at first GEOSECS intercalibration station 3-58993
- oceanography, excess-Rn profiles in near bottom and surface Atlantic water, GEOSECS meas. 3-58994
- radiation exposure of rats and mice 3-66050
- water-air interface, rate of Rn exchange rel. to that of O₂ and CO₂, film model 3-80722
- Rn 220 study of atmospheric turbulent diffusion near ground (French) 3-65395
- ²²²Rn daughter ions in atm. 3-59073
- ²²²Rn emanation from lunar crater Aristarchus, Apollo 15 α -spectra obs. 3-45048

radon compounds

No entries

rain

- Africa, recent rainfall trends 3-51064
- Arabian Sea monsoon activity rel. to beat low over W. Pakistan 3-65323
- attenuation meas. at millimetre waves over short paths 3-41964
- charge, size, raindrops, urban area, magnetic tape recording device 3-59081
- convectively active regions, rainfall estimation 3-47751
- drop size distrib. effects on visibility (German) 3-47764
- drops, oblate, scattering of radiowaves, crosstalk in microwave link systems, 19.3 and 34.8 GHz, calculations 3-61473
- e.m. wave attenuation at 37 to 110 GHz 3-77949
- engineering and sanitary problems 3-65392
- equatorial rainfall, effect of disturbances in subtropical westerlies upon jet stream 3-80761
- fire-induced rain clouds over Illinois, radar obs. 3-65369
- graupel, conical, mechanism of origin, rain and hail formation 3-44889
- India, 700-mb. 5-day mean contours and 5-day rainfall anomaly during July 3-65325
- India, estimation of extreme rainfall 3-47725
- India, heaviest rainfall rel. to return period 3-47726
- India, mean precipitable water vapour and rainfall liability index 3-51014
- India, N.W., dust effects 3-65379
- India, recent rainfall trends 3-51064
- Indian west coast rainfall during 1969 SW monsoon 3-80728
- infiltration models, homogeneous soil, steady rain 3-56052
- i.r. attenuation in mist, fog and heavy rain (Russian) 3-73292
- large waterdrops. wake effect interactions rel. to cloud physics 3-51028
- linear conceptual catchment models, time variance, rainfall rel. to runoff 3-56242
- Mediterranean rainfall patterns and atm. circulation 3-76774
- methane concs. in marine environments 3-73274
- microwave attenuation at 7 to 8 GHz 3-51017
- Middle East, recent rainfall trends 3-51064
- Middle East rainfall patterns and atm. circulation 3-76774
- monsoon, Indian summer, break rel. to Eurasia circulation patterns 3-65381
- Nagpur, India, forecasting heavy rainfall during SW monsoon 3-80726
- New Zealand Earth strain meas., wind and rain effects 3-47638
- numerical simulation of cloud seeding experiments in selected Australian areas 3-65362
- orographic effect on wind and rain distribution around mountain gap 3-65327
- Pacific northwest coast, oceanic rainfall meas. 3-51034
- Patna City area, 1967 September 19-20, exceptional rainfall rel. to mid-tropospheric easterly and westerly waves interaction 3-51016
- patterns in cyclonic systems, frontal zones and convective storms, NIMBUS-5 obs. 3-56175
- patterns of rainfall over US from Nimbus 5 radiation data 3-59112
- Poona, district, India, rainfall over 1955-64 period 3-80725
- probabilistic study for Charente and Seudre river basins (France) (French) 3-61464
- Puerto Rican marine atm., chemistry of aerosols, cloud droplets and rain 3-51035
- radar shower records, vertical motion of patterns 3-51055
- radiowave propagation at 17.7 to 19.7 GHz (Norwegian) 3-61481
- radiowave propagation effect 3-69577
- rain-gauge on mast-top, performance during field test 3-44960
- raindrop falling at terminal velocity in vertical electric field, stresses, numerical method 3-47766
- rainfall intensity freq. patterns, snow melt and seasonal effects 3-59064
- rainfall var. in urban industrial region near Bombay rel. to pollution 3-51043
- runoff estimation, dynamic contrib. area model 3-56173
- Sahel Zone, India, rainfall patterns and atm. circulation 3-76774
- salt composition of rain and river water in USSR, role of sea salts 3-51066
- satellite communications, effect of rain on Earth-space paths 3-44905
- showers, wind gradients and Doppler spectra variance from radar obs. 3-76762
- soil moisture of sagebrush rangelands, Idaho, max., min. storage for snow and rain 3-58869
- southwest monsoon period, India, 1971, rainfall and floods, Ganga Basin 3-80736
- spectra for 5 different climates, comparison (German) 3-47763
- statistical freq. distrib. to predict floods, droughts and rainfall 3-56172
- statistical properties and rainfall rate of precipitation patterns of convective storm 3-65361

rain continued

- storm hydrograph partial area model for storm flow synthesis 3-59065
- terminal vel. under vertical elec. stress 3-59052
- time scale independence of rainfall in India during monsoon season 3-65328
- trace elements in atmospheric environment at rural site in NW England 3-65404
- tropical cloud cluster, growth rate of rain area, boundary layer flow, movable CISK analysis 3-44882
- tropical cyclone systems crossing Appalachians, max. rainfall 3-47746
- troposphere over India, seasonal changes in pressure gradient, wind circulation and rainfall 3-80747
- Venezuelan rainstorms, radar obs. 3-47752
- warm rain development in cumulus cloud model 3-47737
- ¹⁴¹Ce/¹⁴⁴Ce radioisotopic activity ratio obs. by γ spectrometry 3-69581
- ¹⁰³Ru/¹⁰⁶Ru radioisotopic activity ratio obs. by γ spectrometry 3-69581
- Sr in rain and air after 9th Chinese atmospheric nuclear test 3-53476

rainfall see rain

Raman spectra

- see also molecular rotation; molecular vibration; Raman spectra of inorganic substances; Raman spectra of organic substances
- A₂BWO₆ (A=alkaline earth), ordered perovskites, vibr. spectra 3-41577
- air pollution, remote sensing spectrometer 3-56563
- anion radicals and dianions in solution, resonance spectra of spontaneous Raman scattering 3-49468
- antiferromagnet, rutile type, photon pumped spin wave instability, Raman scatt. 3-79851
- antiferromagnetic insulator, Raman scatt. by two-magnon excitation due to s-d exchange interaction 3-53097
- atmospheric pollutants, Raman scattering 3-66070
- atom and mol. scatt. nonlinear Rayleigh and Raman 3-74282
- coherent beat phenomenon analysis using coupled Maxwell-Schrodinger eqns. 3-62748
- coherent system, light scatt. by excited impurity particles 3-62743
- crystalline solid, Raman scatt. by collective excitations 3-80025
- cyclopentanone, vibrational analysis, i.r. and Raman spectra 3-67812
- depolarisation and inelastic scattering of light in gases and liquids 3-78063
- digital laser Raman spectrometer system, online control of data acquisition 3-62105
- electrode reaction obs., total refl. Raman scatt. due to evanescent wave 3-73938
- fluorescence elimination, three techniques 3-77482
- gas, separation of scatt. traces, band assignment problems (French) 3-78749
- gases, stimulated Raman scatt., spatially bounded phase capture, anti-Stokes radiation 3-51951
- Grating Double Monochromator GDM 1000, VEB Carl Zeiss JENA, appl. to Raman and fluorescence spectroscopy 3-51610
- highly coloured crystals, surface scanning technique 3-48423
- ionic crystals, uni- and bi-axial, polariton Raman lines, eigenvectors and intensities (German) 3-53114
- large k-vector phonon generation by stimulated Raman scattering from picosecond pulses 3-55041
- laser beam improved trapping using glassy water films 3-53904
- laser Raman spectrometer, for process control 3-66237
- lattice vibrations, relax. and dynamic characts. resonance optical pumping effects 3-58101
- liquid, i.r. and Raman band profile analysis mol. vib. 3-64665
- liquid, line width and intensity temp. depend., mol. reorientation and intermol. interaction 3-68994
- liquid, molecular motion, conf., Orsay, France, Jul.(1973) 3-64192
- liquid, simple, anisotropy in mol. reorientational motions 3-68995
- liquids, gases, high speed recording unit 3-73756
- low temperature Raman cell for the Cary model 81 laser instrument 3-42572
- luminescence, vibrational relax. theory of electronic excitation transfer 3-76084
- magnetic crystals, theory of spin-dependent phonon Raman scattering 3-72616
- molecular crystals, lattice vibrs., intermolecular interactions 3-76001
- molecular crystals, rel. to n.q.r. spectral parameters 3-75914
- molecular crystals, scatt. efficiency, mol. reorientation, theory 3-72656
- molecular crystals, theory of hyper-Raman effect 3-66891
- molecular orbital admixture coeffs. rel. to Raman scatt. 3-57624
- molecular vibration, stimulated Raman scatt. of phase modulated light pulses 3-62742
- molecular vibrational frequencies tables 3-75039
- molecule, excited, anal. of resonant scatt. 3-75041
- molecule, theory of Rayleigh light scattering with Brownian motion 3-62664
- plasma, inhomogeneous, parametric scatt. instabilities rel. to laser penetration 3-68052
- polarised scattering, small single crystals, 90 degree viewing, simple experimental technique 3-56668
- polaritons, determ. of effective charge of ions 3-54942
- powder composed of small crystals, vibr. modes 3-58095
- quantitative analysis by laser Raman spectroscopy (French) 3-66460
- resonant Raman effect with damping 3-69006
- rotation, vibration-rotation hyper-Raman spectra, selection rules 3-54693
- scattering tensor, analytical expression development (French) 3-78748
- self-focused light beams, backward stimulated light scatt. and limiting diameters 3-62745
- soft modes, Raman activity, proof of Worlock's conjecture 3-79462
- solid and fluid media, Rayleigh, Brillouin and Raman lines rel. to microscopic processes 3-80024
- solid state anti-Stokes Raman oscillator, stationary behaviour 3-80044

Raman spectra continued

- stimulated Raman scattering, effect of spontaneous Raman line parameters 3-78065
- symmetric top molecules, pure rotational Raman scattering 3-60454
- temperature dependent, technique, appls. 3-72658
- thin films, meas. method (*German*) 3-45488
- three mirror Raman cell for gases 3-62111
- two-magnon, helical spin system, Green's function method 3-41519
- vibro-electronic Raman effect, obs. of impurities in solid 3-69005
- vibroelectronic Raman effect 3-72612
- GaP with plasma of charge carriers, dielectric parametrization of Raman lineshapes 3-50563
- α -HgS, cinnabar, Raman scattering by phonons 3-58508
- KBr Raman scattering from CrO_2^{2-} ions at low temp. 3-53109
- KCl, Raman scattering from CrO_2^{2-} ions at low temp. 3-53109
- K_2SO_4 , Raman scattering from CrO_2^{2-} ions at low temp. 3-53109
- NaBrO_3 , Raman spectra of irradiated crystals, internal oscill. 3-55654
- Si amorphous solids, coupling constants, l.f. 3-41520

Raman spectra of inorganic substances

- alkali metal ozonides, M^+O_3^- , Ar, Kr plasma excitations 3-78754
- alkali metal ozonides, M^+O_3^- type, Ar matrix, vibrational analysis 3-78808
- alkali metal ozonides, matrix isolated, resonance Raman spectrum, vibrational analysis 3-71553
- antiferromagnets, one-magnon light scattering in spin-flop phase at low temps. 3-72477
- arsenates, paraelectric, ferroelec. phases, H bonding, transition mechanism 3-72649
- azide and metacarbonyl complexes, resonance Raman effect (*German*) 3-78775
- complex salts, l.f. vibrs., metal-ligand and complex ion-outer ion interactions 3-47246
- electrolytes, 1-1 valent, comparison with water, quasi-Fermi resonance effects 3-75046
- garnet, Al, Ga, Fe, Raman active phonons, laser, reflection and transmission spectra 3-72613
- gas, inelastic photon re-emission, air pollutants detect. 3-78832
- glasses, vibrational study 3-76005
- gypsum, vibrational spectrum, high press. effects 3-76003
- halide salts, C_{2v} , C_3 , symmetry group impurities, spectral props. 3-69043
- hydric acids, solid, theory, expt. 3-72660
- inert gases, solid, theory expt. 3-72660
- insulators, Raman effect under resonance conditions, study by Green's function technique 3-50553
- ionic glasses, low temp. spectra of external modes 3-75974
- metal pyridine tetracyanonickelate complexes, analysis 3-63467
- molecular crystals, two phonon absorpt. 3-69001
- niobates, crystalline, vibrational spectra 3-55602
- oxides, with fluorite struct. 3-72610
- polaritons, mass defect effects 3-41514
- poly(dimethylsiloxane), Raman depolarization, temp. and strain depend., config. energy difference 3-40689
- pyrogermanates with linear bridge, vibr. spectra and isotopic shifts 3-46285
- pyrosilicates with linear bridge, vibr. spectra and isotopic shifts 3-46285
- β -quartz, phonon and polariton spectra, longitudinal E_1 modes 3-55582
- α -quartz, uniaxial stress effects at liq. He temps. 3-53102
- rare earth molybdate (tungstate), vibr. spectra obs. and crystal struct. 3-80039
- rutile-structure fluorides, elastic and optical props. in rigid ion approximation 3-68987
- scattering from conduction electrons, momentum distrib. function 3-50578
- semiconductor, defect zinc-blende struct. type 3-72621
- semiconductor, reson. Raman scatt. at critical points 3-53101
- semiconductors, group IV, III-V, resonant scattering by optical phonons at E_1 energy gap 3-55595
- semiconductors, resonant scattering, modulation spectroscopy, piezoreflectance, birefringence 3-55593
- SF_6 , OOSO_2SF_6 in liquid phase, vibrational spectra 3-46295
- spherical top mol's., Raman band contour analyses and Coriolis const. 3-67816
- tetrahalegenic ions, space group, atom sites 3-72658
- transition metal tungstates, assignment, MnWO_4 valence force field calc. (*French*) 3-80020
- vitreous state, Rayleigh, Brillouin and Raman lines 3-80026
- water, comparison with 1-1 valent electrolytes, quasi-Fermi resonance effects 3-75046
- water, depolarization ratio spectra, band shapes 3-75020
- water, heavy water, effect of hydrogen bonding on intramolecular vibrations 3-80022
- water, stimulated short-wave radiation due to single freq. reson. of third-order nonlinear susceptibility 3-66882
- AgNO_3 , and alkali nitrate molten mixtures 3-80023
- $\text{Al}(\text{BD}_4)_3$, i.r. and Raman spectra 3-72623
- $\text{Al}(\text{BH}_4)_3$, i.r. and Raman spectra 3-72623
- AlF_3 , solid, i.r. and Raman spectra 3-72627
- Ar_2O_3 thin films between alkali halide discs, obs. of surface interaction effects in Raman spectra 3-64638
- AsBr_3 and tributylphosphate complexes, Raman and i.r. spectra (*French*) 3-46281
- AsI_3 , molecular cryst., lattice dynamical props., phonon spectrum 3-76009
- As_2O_3 glass, vibrational spectra obs., reln. to arsenolite and claudetite structures (*Italian*) 3-72604
- As_2S_3 , amorphous, Raman and depolarisation spectra, struct. models 3-53105
- BCl_2Br , BClBr_2 , vibrational spectra 3-46298
- B_2F_4 , gaseous and cryst. spectra, 25 to 1500 cm, normal vibr. assignments and intermol. force const. calc. 3-47250
- B_2S_3 ring compounds, vibr. study 3-78784
- $^{10}\text{B}_2\text{H}_6$, $^{11}\text{B}_2\text{H}_6$, B_2D_6 , ring-puckering vibr. 3-78791
- $\text{Ba}(\text{ClO}_3)_2$, $\text{H}_2\text{O}(\text{D}_2\text{O})$, Davydov components, intramolecular and collective modes 3-75973
- BaF_2 , Raman spectra rel. to uniaxial stress at 15 K 3-53103

Raman spectra of inorganic substances continued

- $\text{Ba}(\text{NO}_3)_2$ crystals, stimulated Raman scattering, combitones 3-66888
- $\text{Ba}(\text{NO}_3)_2$ crystals, temperature dependence of low frequency spectrum (*Russian*) 3-64663
- BaSO_4 , vibr. spectra and isomorphism 3-72634
- BaTiO_3 , cubic, temp. depend. of Raman cross section and light absorpt. 3-41522
- Be_2F_3^- , and more complex species, obs. in cryst. and molten state 3-53091
- $\text{Bi}_{12}\text{GeO}_{20}$, Raman spectra rel. to uniaxial stress at 15K 3-53103
- BiOBr , 40-600 cm^{-1} , vibrational band assignments 3-44404
- BiOCl , 40-600 cm^{-1} , vibrational band assignments 3-44404
- BiOI , 40-600 cm^{-1} , vibrational band assignments 3-44404
- Br_2 crystal, spontaneous and forced Raman spectra at 77 K (*Russian*) 3-50585
- BrO_4^- Raman intensities and force constants 3-67822
- CF_3 compounds, $-\text{PH}_2$, $-\text{PD}_2$, $-\text{AsH}_2$, $-\text{AsD}_2$, vibr. spectra and normal coord. anal. (*German*) 3-46282
- CO , CO_2 , relative cross-section, short laser pulse scatt. and photon counting obs. 3-57651
- CO_2 , Raman spectra, rotational const. determ. 3-49471
- C_2O_2 , far i.r. and Raman spectra, potential function, low frequency bending mode 3-71548
- C_3O_2 , skeletal bending mode 3-78791
- C_3O_2 crystals, overtones of ν_2 and ν_3 3-55583
- CS_2 , fine structure, effect of Fermi, resonance, Bethe and Davidov splitting 3-75990
- CS_2 crystals, mol. and lattice modes assignments 3-61033
- CS_2e^{2-} , $\text{CS}_2\text{Se}^{2-}$, CS_2S^{2-} , $\text{CS}_2\text{Se}^{2-}$, vibrational spectra 3-46298
- CaCO_3 , calcite picosecond pumping, group retardation effects 3-78058
- CaF_2 , elastic deform. splitting of Raman lines 3-72629
- CaF_2 , Raman spectra rel. to uniaxial stress at 15K 3-53103
- $\text{CaF}_2:\text{Eu}^{3+}$ tetragonal single crystal, features, phonon band, Raman tensor 3-64644
- $\text{Ca}(\text{OH})_2$, and polarised i.r. spectra 3-44406
- CaSO_4 , vibr. spectra and isomorphism 3-72634
- CaSO_4 crystal, vibrs. of complex ions 3-72633
- CaZrO_2 nonstoichiometric, effect of massive point defects conc. 3-80037
- $\text{Cd}(\text{II})$ complex, CdX_2 ($\text{X}=\text{Cl}, \text{Br}, \text{I}$) in tri-n-butylphosphate soln., vibrational spectra 3-75034
- CdS , spin-flip Raman scatt. near 5145 Å, resolution improvements 3-5582
- CdS , two-photon reson. Raman scatt., widths of peaks 3-58501
- CdS electric field modulated scattering by l.o. phonons 3-55594
- CdTe , Raman scatt. dispersion below absorpt. edge 3-41523
- $\text{Ce}(\text{NO}_3)_3$ aqueous solutions 3-44407
- $(\text{ClHCl})^-$ system, H bond activity, Cl-Cl vibr., theory (*German*) 3-71563
- ClO_4^- Raman intensities and force constants 3-67822
- Co coordination compounds, external vibration frequencies of active and racemic forms 3-55581
- CoCO_3 , optical phonons and electron excitation at Neel temp. obs. 3-47243
- $\text{Co}(\text{CO})_3\text{NO}$, potential const. from vibrational spectra of six isotopic species 3-43442
- Co_2GeO_4 and CoF_2 calc. of mag. susceptibility of Co^{2+} 3-68997
- Co_2Br^- vibrational spectra, normal coordinate analysis rel. to MO_2X_n ($\text{M}=\text{Cr}, \text{Mn}, \text{Tc}, \text{Re}; \text{X}=\text{F}, \text{Cl}, \text{Br}, \text{S}; n=0,1$) (*German*) 3-71557
- $\text{Cs}_2\text{LiM}(\text{CN})_6$ ($\text{M}=\text{Cr}, \text{Mn}, \text{Fe}, \text{Co}$), vibr. spectra and neutron diffr. cryst. struct. 3-79294
- CSO_2 in Ar matrix, Raman spectra 3-52371
- CSH , lattice dynamics and order-disorder transitions 3-55590
- $\text{CuBr}(\text{I})$, peaks due to zone centre optic phonon mode scatt. 3-58516
- CuCl , linewidths, frequency shifts, temp. depend. in range 300 K to 45 K 3-72615
- CuCl monocrystal, first and second order Raman scattering 3-68986
- $\text{CuCl}:\text{CuBr}$, mixed cryst., optic phonon modes, Raman scatt. and i.r. absorpt. obs. 3-58099
- Cu_2O , 1S yellow exciton, reson. quadrupole-dipole Raman scatt. 3-53100
- Cu_2O , reson. Raman scatt., with absorpt. followed by luminesc. 3-53107
- Cu_2O , reson. Raman scatt. at blue and indigo excitons 3-41521
- Cu_2O , symmetry forbidden resonant Raman scattering 3-58511
- O-D_2 , density-dependent phase transition and anisotropic interactions 3-75995
- D_2 , solid, ordered phase, Q branch 3-80016
- D_2O , broadband picosecond continuum and light gate, time resolution and characteristics 3-45820
- EuGa garnet, crystal field splittings in electronic Raman spectra field parameters 3-41312
- n-EuTe , reson. Raman scatt. from screened LO phonons 3-55592
- F_2^- , molecular anion, alkali metal atom- F_2 matrix reaction products 3-63451
- $\text{F}_2\text{SO}-$, bonding, CNDO MO calcs. (*German*) 3-74966
- FeBO_3 , two-magnon Raman scatt., 2-300K 3-68981
- FeCO_3 , natural siderite, optical phonons and electron excitation at Neel temp. obs. 3-47243
- FeF_2 , paramag. crystal, distortion parameters, energy level diagram 3-64645
- FeGeO_4 and FeF_2 calc. of mag. susceptibility of Fe^{2+} 3-68997
- GaAs , optical phonon lifetimes, photoexcited hot phonons, Raman lineshape 3-52679
- GaAs amorphous film, far i.r. absorption 3-68988
- GaAs film on substrate, props. of surface polaritons 3-58505
- GaAs thin film, Raman scatt. from surface polaritons 3-58504
- GaF_3 , solid, i.r. and Raman spectra 3-72627
- Ga_2L , Ga_2I_3 , Ga_2S_3 , constitution studies 3-44405
- $\text{GaP}:\text{Mn}(\text{As})$, impurity mode 3-55585
- β - GaS , energies and symmetries of first order Raman active phonon modes 3-47278
- GaSe , phonon modes, temp. depend. 3-80042
- Ge , amorphous, i.r. and Raman spectra theory 3-41513
- Ge amorphous film, far i.r. absorption 3-68988
- GeD_4 , rovibrational const. 3-63460

Raman spectra of inorganic substances continued

- (GeF₂)₃GeF₄, spectral characteriz. 3-55599
 O-H₂, density dependent phase transition and anisotropic interactions 3-75995
 H₂, HD, D₂, solids, theory, expt. 3-72660
 H₂, resonance collisions in rotational energy transfer 3-67864
 H₂, scattering cross section, $\lambda > 1200\text{Å}$ 3-67810
 H₂, solid, ordered phase, Q branch 3-80016
 HBr, HCl, glass-like solutions with molecular anion admixture 3-64720
 HDO, liquid Raman intensities of uncoupled OD oscillators 3-75979
 HDO in rare earth chloride soln., Raman spectra 3-75980
 H₂O, broadband picosecond continuum and light gate, time resolution and characteristics 3-45820
 H₂O and H₂O-trimethylamine complex, gas phase 3-78800
³He-⁴He solutions, roton energies and linewidths meas. from Raman scattering 3-41062
³He-⁴He solutions, two-roton Raman scattering 3-43919
 HgBr, molecular cryst., lattice dynamical props., phonon spectrum 3-76009
 Hg(II) complex, HgX₂ (X=Cl, Br, I) in tri-n-butylphosphate soln., vibrational spectra 3-75034
 I₂, reson. Raman scatt., spectral var., excitation freq. depend. 3-40633
 ICl₃.SbCl₅, and ICl₃.AlCl₃, laser Raman spectra and freqs., ICl₃⁺ ionic struct. study 3-47255
 InFe³⁺, solid, i.r. and Raman spectra 3-72627
 InP, Raman scatt. dispersion below absorpt. edge 3-41523
 InSb, conditions, for existence of double resonance effects 3-80046
 p-InSb, interband electronic Raman scatt., threshold characts. 3-50580
 InSb, near reson. spontaneous spin-flip Raman scatt. 3-44415
 InSb, Raman spin flip tunable laser, high power pulsed operation 3-57257
 InSb, spontaneous spin-flip Raman line width, non reson. non linearly, 2K 3-57258
 InSb, theory of spin-flip Raman amplification 3-78049
 Ir coordination compounds, external vibration frequencies of active and racemic forms 3-55581
 KBr:SH⁻, effect of pressure on Raman spectra 3-69004
 KBr:TI, differential impurity induced spectra, phonon dispersion reln. 3-55596
 KBr:TI⁺, phonon props. and electron-phonon interaction 3-58098
 KBr(Cl), whiskers, point defects, U-centre theory 3-72652
 KBr(Cl)(I) with SH⁻ impurities, h.p. effects 3-80019
 KBr(Cl)(I):NO₂⁻, SH⁻, impurity local modes, Raman and i.r. absorpt. obs. 3-72696
 KCN, order-disorder phase transition study 3-72648
 KCN, phase transitions influence, phonon modes and librations obs. (French) 3-58509
 KCl:TI⁺, phonon props. and electron-phonon interaction 3-58098
 KCl- effect of pressure on Raman spectra 3-69004
 K₃Cr(CN)₆ crystal and solution, Raman spectra, struct. and vibrational assignments 3-75988
 K₂Cr₂O₇, crystalline molten and aqueous, vibrational spectra 3-55587
 KH₂PO₄, 45° Y-cut crystal, effects of domains on optical properties 3-61036
 KH₂PO₄, obs. of underdamped soft lattice mode, pressure effect 3-58506
 KH₂PO₄, Raman susceptibility, stimulated Raman effect 3-51953
 KH₃(SeO₃)₂, antiferroelectric, vibr. spectra and hydrogen bond pot. study 3-47256
 KH₃(SeO₃)₂, Raman and i.r. spectra, hydrogen bond potential well 3-53090
 KHgBr₃.H₂O, and KHgI₃.H₂O, polarised Raman and i.r. spectra, 10 to 4000 cm⁻¹, Urey-Bradley-Shimanouchi force field (French) 3-47258
 KI:SH⁻, effect of pressure on Raman spectra 3-69004
 KI:TI⁺, phonon props. and electron-phonon interaction 3-58098
 K₂MnF₄, Heisenberg antiferromagnet, two magnon light scattering 3-72619
 KNCS crystal, polarised spectra, lattice vibrations 3-72609
 La₂(SO₄)₃.9H₂O, polarised, obs. at room temp. 3-53173
 La₂(SO₄)₃.9H₂O single cryst., water mol. orientation obs. by Raman effect (French) 3-68978
 LiBr, LiCl, glass-like solutions with molecular anion admixture 3-64720
 LiH₃(SeO₃)₂, ferroelectric, vibr. spectra and hydrogen bond pot. study 3-47256
 LiIO₃, hexagonal and tetragonal, vibr. and ¹²⁷I n.q.r. spectra (Russian) 3-79945
 LiN₃, Raman active phonons, temp. depend., phase transition 3-72611
 LiNO₃ solns. in liq. ammonia, vibr. spectra, solvent effects 3-55991
 LiNbO₃, Li₃NbO₄, LiZnNbO₄, crystal spectra 3-55602
 LiXVO₄, (X=Mg, Co, Ni, Cu, Zn), vibr. spectra obs. of order-disorder phenomena 3-52689
 MgAl₂O₄ synthetic and natural crystals, Raman characteristic studies, phonon modes 3-41507
 MgAl₂O₄:Cr³⁺, Raman selection rule violation, fluorescence, impurity resonant Raman effects 3-50581
 Mg₂Cd_{1-x}Te mixed crystals, lattice vibrations, i.r. and Raman obs. 3-80036
 Mg(ClO₄)₂.H₂O system, Raman studies 3-53094
 MgNO₂.water systems, Raman and i.r. study 3-53353
 Mg₄Nb₂O₉, crystal spectra 3-55602
 MgO microcrystals, Raman scattering, crystal vibrations study 3-75994
 Mg(OH)₂, and polarised i.r. spectra 3-44406
 Mg₂SiO₄, isotopic species, i.r. and Raman spectra, vibr. studies and shift meas. 3-46284
 MnO₄⁻.H₂O solution, rotating cell, solvent line cancellation 3-68974
 MoF₅, vibrational spectra 3-46278
 MoO₄²⁻, force field, isotope shift, in Na₂MoO₄ 3-63450
 MoS₂, force field, isotope shift, in K₂MoS₄, Cs₂MoS₄ 3-63450
 N₂, $\alpha \rightarrow \gamma$ phase transition, librational modes 3-72650

Raman spectra of inorganic substances continued

- N₂, induced Raman scatt. under cavity excitation, spectral width and line struct. 3-59895
 N₂, relative cross-section, short laser pulse scatt. and photon counting obs. 3-57651
 N₂, solid, theory, expt. 3-72660
 N₂, vibr. excitation from N+NO reaction, Raman scatt. study 3-43517
 N₂ dissolved in liquids, vibr. Raman bands, collisional narrowing effect 3-75019
 N₂ Raman scattering, density effect, scattering polarisation, intensity, frequency shift, and line shape study 3-71551
 N₂ vibrational Raman spectra 3-49471
 N₂-Ar solute-solvent systems, computer simulation of correl. functions, bandshapes and relax. times 3-64651
 NH₃, liquid and in solution 3-55584
 NH₄⁺ halides, disordered phases, phonon modes, polarisation characts. 3-72651
 NH₄NO₃ solns. in liq. ammonia, vibr. spectra, solvent effects 3-55991
 NH₄PF₆ and ND₄PF₆, polycrystals, i.r. and Raman spectra, phase transitions study 3-47263
 NO, relative cross-section, short laser pulse scatt. and photon counting obs. 3-57651
 NO₂, separation of overlapping fluorescence and Raman lines 3-78756
 Na₂Cd(SO₄)₂.2H₂O:Co²⁺, spin lattice relax., one phonon and Raman scatt. processes 3-50455
 NaCl:OH⁻, motion of OH⁻ ion studied by Raman scattering at low freq. shifts and in O-H stretching region 3-75981
 NaH₂(SeO₃)₂, ferroelectric, vibr. spectra and hydrogen bond pot. study 3-47256
 NaN₃, Raman active phonons, temp. depend., phase transition 3-72611
 NaNCS-water system, intermolecular interactions, Raman spectroscopic study (Russian) 3-72632
 NaNO₂, ferroelec., vibr. spectrum near Curie point, elec. field effects 3-72631
 NaNiF₃, one and two magnon Raman scatt., mag. coeffs. 3-50561
 Na₂O, mol. and lattice vibrs., struct. changes at 230 and 201 K (German) 3-50569
 NaSH, lattice dynamics and order-disorder transitions 3-55590
 Na₂WO₃ semiconducting crystals, Raman scattering cross section dependence on laser intensity 3-41517
 Na₂Zn(SO₄)₂.4H₂O:Co²⁺, spin-lattice relax., one phonon and Raman scatt. processes 3-50455
 Na₂[Ln(CO₃)₂](H₂O)₂.wH₂O, band assignments, struct. obs. (French) 3-60457
 NbCl₅, molten, equilibrium, 220-320°C (German) 3-52702
 NiSO₄.6H₂O and NiSO₄.6D₂O, vibrational spectra, frequency and temp. effects 3-44420
 NiSnCl₆.6H₂O and NiSnCl₆.6D₂O, vibrational spectra, frequency and temp. effects 3-44420
 O₂, relative cross-section, short laser pulse scatt. and photon counting obs. 3-57651
 O₃, relative cross sections, for four Ar⁺ laser freqs. 3-63452
 P₂F₄, i.r. and Raman spectra, vibr. and mol. struct. 3-43457
 (PNBr₂)₃, oriented single crystal Raman spectra and vibrational assignments 3-47259
 (PNCI₂)₃, oriented single crystal Raman spectra and vibrational assignments 3-47259
 PO₄³⁻, Raman intensities and force constants 3-67822
 POCl₃.SnCl₄.Nd³⁺ liquid laser, spectral luminescent characts. 3-70817
 PS₃³⁻, vibrational spectra 3-46298
 Pb(NO₃)₂ crystals, stimulated Raman scattering, combitones 3-66888
 Pb(Ti_{1-x}Zr_x)O₃, ferroelec., soft optical phonons rel. to morphotropic phase transition, Raman scatt. obs. 3-41491
 Pd complexes, Pd(PPh₃)₂.X₂, Pd(PPhO)₃.X₂, (X=Cl, Br) 3-54689
 Pd(II) complexes, [X₂Pd(C₂H₅)₂], (X=Cl, Br), i.r. and Raman spectra, vibr. assignments 3-46300
 PtAlO₃, phase transitions obs. 3-55083
 Pt(II) complexes, [X₂Pt(C₂H₅)₂], (X=Cl, Br), i.r. and Raman spectra, vibr. assignments 3-46300
 RbCl, second order Raman spectra, 80 and 300 K 3-68991
 RbH₂AsO₄, low frequency χ spectra, soft mode behaviour of ferroelectric model 3-61041
 RbO₂ in Ar matrix, Raman spectra 3-52371
 RbSH, lattice dynamics and order-disorder transitions 3-55590
 Rh coordination compounds, external vibration frequencies of active and racemic forms 3-55581
 SF₆, liq., mol. reorient. 3-68993
 SF₆, liquid, stimulated Raman scatt. 3-70847
 SF₂OOSF₂ in liquid phase, vibrational spectra 3-46295
 SO₂, relative cross-section, short laser pulse scatt. and photon counting obs. 3-57651
 SO₄²⁻, Raman intensities and force constants 3-67822
 S₂O₇, unstable, matrix isolated vibrational spectra, identification of new species 3-78803
 SO₂Cl₂, solid, Raman and infrared spectra rel. to crystallographic structure 3-61035
 SbBr₃ and tributylphosphate complexes, Raman and i.r. spectra (French) 3-46281
 α -S₈ crystals, intermolecular vibratory terms splitting 3-72659
 SeO₄²⁻, Raman intensities and force constants 3-67822
 Si, amorphous, i.r. and Raman spectra theory 3-41513
 p-Si, heavily doped, interaction of electronic and vibronic Raman scatt. 3-58514
 Si, second-order spectrum and phonon density of states 3-68984
 Si, selective reson. enhancement of two-phonon Raman spectrum 3-80033
 Si, spectral growth of stimulated emission 3-50579
 SiC, relation between elastic constants of hexagonal and cubic polytypes 3-54997
 n-Sn, grey, interband electronic Raman scatt., threshold characts. 3-50580
 SnCl₄(SnBr₄) and tributylphosphate complexes, i.r. and Raman spectra (French) 3-46280

Raman spectra of inorganic substances continued

- SnI₄ in soln., reson. Raman effects, stretching vibrs. enhancement 3-75013
- Sn(IV) complex, bis(2,4-pentanedionato)dimethyltin(IV), oriented single-cryst. and solns., laser Raman spectra 3-47257
- SrCl₂, phonon dispersion curves, i.r. and Raman spectra obs. 3-49951
- TaBO₄, i.r. and Raman spectra 3-68989
- TbAl garnet, crystal field splittings in electronic Raman spectra field parameters 3-41312
- Tel, zero-centre phonon behaviour 3-72059
- TiCl₆B₂O₄, one and two phonon bands obs. 3-64639
- TiF₆³⁻, solid, i.r. and Raman spectra 3-72627
- TiNO₃III, Davydov and interset splitting rel. to cryst. struct. 3-75997
- UO₂Cl₂·3H₂O, crystal struct., space group (*French*) 3-68221
- UCl₄ in soln., reson. Raman effects, stretching vibrs. enhancement 3-75013
- YIG, Raman-Nath scatt. of light by magnetostatic waves 3-55439
- YNbO₄, internal vibration modes of NbO₄³⁻ tetrahedra, i.r. and Raman spectra obs. 3-53095
- YTaO₄, internal vibration modes of NbO₄³⁻ tetrahedra, i.r. and Raman spectra obs. 3-53095
- Zn(II) complex, ZnX₂ (X=Cl, Br, I) in tri-n-butylphosphate soln., vibrational spectra 3-75034
- ZrF₄-alkali fluoride systems, melts and polycryst. solids, Zr(IV) fluoride complex ions 3-72614
- ZrO₂·Ca²⁺, massive point defect behaviour 3-68975

Raman spectra of organic substances

- 1,2-bis-(4-pyridyl) ethanes conformations of the rot. isomers 3-78772
- acetic acid, cryst., rel. to hydrogen bond vibr. 3-72640
- acetonitrile, CH₃CN and CD₃CN, Raman spectra and phase transition, lattice modes 3-55588
- acetonitrile, liq., mol. reorientational motion, Raman bandshapes, diffusion consts. and activation energy 3-60661
- alcohols, liquid, detection of intermolecular coupling 3-57657
- alicyclic amines, Raman spectra, Bohlmann bands 3-75027
- n-alkanes:aromatics, zero-phonon line width temp. depend. 3-68360
- amine-SO₂ complexes, force consts. for charact. vibrs. 3-60461
- amine-sulphur system, bands due to polysulphide ions 3-78794
- anisotropic liquid, energy levels determ. (*French*) 3-50567
- anthracene, low frequency Raman spectra, line intensities 3-64653
- azomethane, azomethane-d₆, Raman spectra and vibrational potential function 3-75017
- benzene-Cl₂ solutions, charge transfer interaction 3-78799
- benzonitrile theoretical study of vibronic spectra 3-67783
- benzophenone single crystal, Raman and polarised i.r. spectra, vibrational study (*French*) 3-47266
- biphenylene, in-plane normal mode calc. and complete vib. assignment 3-61038
- bis(trifluoromethyl) sulphide, sulphoxide and disulphide, Raman spectra, normal modes vibr. assignments and depolarisation meas. 3-47274
- bromocyclobutane, Raman spectra obs. 3-75035
- bromomethane, liquid, Raman spectroscopy, mol. reorientation 3-75984
- 5-bromotetrazole, single cryst., Raman active external phonon assignments, harmonic force const. calcs. 3-50573
- butadiene, polymers and copolymers, sample preparation, quantitative analysis 3-58496
- 3-butyne-2-one, i.r. and Raman spectra 3-71560
- carbamoylazides, and N-deuterated derivatives, i.r. and Raman spectra (*German*) 3-47271
- carbon tetrachloride-chloroform mixture, rotating cell 3-68974
- carboxypeptidase, crystal and in solution, structure 3-75165
- β-carotene and related compounds, vibrational resonance 3-78755
- chiral molecules, anomalies, polarisation depend. 3-71566
- chiral molecules, circular differential spectra 3-78802
- 2-chlorobutane, torsion force consts. and low frequency bending assignments from i.r. and Raman spectra 3-71559
- chlorocyclopentane, disordered cryst., vibr. spectra, i.r. absorpt. and Raman obs. 3-72638
- chloroform, and deuterated analogue, Raman spectra and cryst. struct. at 77 K 3-50576
- d-chloroform, Raman vibrational line shapes, reorientational correlation functions, appl. to nuclear quadrupole coupling constants 3-46274
- N-chloropiperidine, liquid (*Russian*) 3-63476
- 2-chloropropane, torsion force consts. and low-frequency bending assignments from i.r. and Raman spectra 3-71559
- cobalt corrinoids, selective enhancement of bond intensities in resonance Raman spectra 3-71668
- conjugated systems, barriers to internal rotation magnitude estimation from Raman spectra 3-63368
- coronene, luminescence and vibrational spectra 3-60460
- cryptocyanine, reson. spontaneous scattering, structural interpretation 3-64655
- 1,4-cyclohexadiene and 1,3-cyclohexadiene, ring-puckering vibrs. 3-78790
- cyclohexadienes, 1,4- and 1,3-, Raman spectra, barriers to planarity 3-60453
- cyclopent-3-enone, out-of-plane ring modes from far i.r., Raman and microwave spectra, pot. function 3-60467
- cyclopentane, cryst., vibr. spectra, phase transition, 168 K 3-50565
- cyclopentane, disordered cryst., vibr. spectra, i.r. absorpt. and Raman obs. 3-72638
- cyclopentene, i.r. and Raman spectra interpretation 3-54685
- cyclopropane, and deuterated analogues, cryst. Raman spectra and assignments 3-4510
- cyclopropane, vibr.-rot. Raman bands 3-63461
- cyclopropenone-d₆ (and -d₂) solid, liquid and gas phases 3-78785
- N,N-deuterated propionamide, i.r. and Raman spectra 3-60452
- N,N deuterated thiopropionamide, i.r. and Raman spectra 3-60452
- deuteriochloroform liquid, Raman spectroscopy, mol. reorientation 3-75984
- diacetylenes, Raman spectral changes during the solid-state polymerisation 3-57685
- Raman spectra of organic substances continued**
- dichloropentane, torsion force consts., low frequency bending assignments from i.r. and Raman spectra 3-71559
- 1,1-dicyanocyclopropane, liquid and vapour phase, vibrational spectrum 3-46287
- 2,3-dihydrofuran, Raman spectra, barrier to planarity 3-75021
- 2,3-dihydrofuran and 2,3-dihydrothiophene, ring-puckering vibrs. 3-78790
- 2,3-dihydrothiophene, Raman spectra, barrier to planarity 3-75021
- p-diiodobenzene, low frequency Raman spectra, line intensities 3-64653
- dimethyl and diethyl-2,2-stanna-2 dithia-1,3-cyclopentanes (*French*) 3-43454
- dimethylacetylene cryst., phonon spectra, mol. motions and phase transitions 3-55573
- 3,3-dimethyldiaziridine, vibr. of strained ring systems 3-78788
- p-dioxane and H₂O₂ binary solutions, i.r. and Raman studies (*French*) 3-58512
- α,ω-diphenylperfluoropolyenes, effect of fluorination on conjugation, UV and Raman spectra, steric struct. of mols. 3-71520
- diphenylpolyenes, conjugation and resonance Raman effect 3-76010
- diphenylpolyenes, conjugation and resonance Raman effect on Raman intensities 3-40623
- disulphides Raman spectra, S-S and C-S stretching regions 3-54682
- durene, low frequency Raman spectra, line intensities 3-64653
- ethylene, Raman spectra of crystal molecular orientation intermolecular potential and crystal structure 3-72608
- ethylene trithiocarbonate, solid, fundamental vibrations assignment from i.r. and Raman spectra 3-47261
- ethylsulphates of yttrium and some rare earths, low temp. obs. 3-50564
- ethynylbenzene theoretical study of vibronic spectra 3-67783
- glycerol single crystals, l.f. vibrs. assignment (*French*) 3-58497
- haemoproteins, 200 cm⁻¹ to 3000 cm⁻¹, cytochrome-c 3-78918
- 1-halo-3,3,3-trifluoropropenes, vibrational spectra 3-46296
- halogenopyridines, vibrational spectra 3-46288
- heme proteins, resonant Raman bands of differing polarization, intensity origin 3-54768
- hexafluoro-2-propanol and deuterated analogues, solid, liquid and gaseous states, i.r. and Raman spectra 3-46286
- hexafluoroazomethane, vibr. spectra and mol. config. 3-43452
- hexafluorobenzene, C-F bond length 3-54691
- hexafluoroethane, α-cryst. phase, vibr. spectra 3-41508
- hexafluoropropanol-2, vibr. freq., force field, mean amplitudes 3-63412
- hexamethylbenzene crystal, Raman, far i.r. studies, mol. motion, λ-phase transition 3-64134
- hexamethylbenzene single cryst., polarized spectra, freqs. assignment 3-55572
- holopropanes, rot. isomerism, temp. depend., fast freezing 3-72653
- hydrazinium halide, cryst., rel. to hydrogen bond vibr. 3-72640
- iodoform, crystalline, vibrational spectrum 3-50575
- malononitrile, mol. packing from Raman spectra 3-75521
- 2-mercaptoethanol, liq., vibr. spectra and rot. isomerism 3-47245
- methane, induced Raman scatt. under cavity excitation, spectral width and line struct. 3-59895
- methanes, substituted, liquid and gaseous states, comparison (*Russian*) 3-63475
- methyl iodide, and deuterated cpd., liq., reorientational motion temp. depend., Raman spectra obs. 3-64667
- methyl iodide, liq., rot. diffusion obs. 3-75976
- methyl iodide, liquid, collective excitation of mol. vibrs., Raman spectra obs. 3-64668
- methyl iodide, liquid, mol. motions and interactions, temp. dependent Raman study 3-47248
- methyl iodide, liquid, molecular vibration excitons, Raman band profiles (*German*) 3-53113
- methyl iodide, Raman scattering, orientational motions 3-43445
- methyl iodide, Raman scattering, vibrational correlation 3-43444
- methyl iodide, Raman vibrational line shapes, reorientational correlation functions, appl. to nuclear quadrupole coupling constants 3-46274
- methyl iodide and CD₃I, liquid, Raman line-shapes, rotation and vibration analysis 3-41509
- 2-methyl-1,3-dioxolane, solid, liquid, gas, infrared spectra, molecular vibration, rotation 3-54692
- 2-methyl-butane and 2,3-dimethyl-butane, rot. isomerism 3-78793
- N-methyl-d₃-P,P,P-trimethylphosphine imide, vibr. spectra, P-N bond struct. 3-75024
- methylbromide, mol. reorientation, Raman spectral obs. 3-64666
- N-methylcarbamoylhalogens, i.r. and Raman spectra, 150 to 4000 cm⁻¹, vibr. assignments (*German*) 3-47270
- methylcyclopentane, solid, liquid, gas, infrared spectra, molecular vibration, rotation 3-54692
- methylmethacrylate, polymers and copolymers, sample preparation, quantitative analysis 3-58496
- methylsilylchlorides, i.r. and Raman spectra, vibr. assignments and torsional barrier heights 3-54680
- methylsulphonyl fluoride, chloride, and bromide (*German*) 3-43424
- 2-methyltetrahydrofuran, solid, liquid, gas, infrared spectra, molecular vibration, rotation 3-54692
- N-methylthiopropionamide, and N-deuterated analogue, i.r. and Raman spectra 3-49464
- molecular crystal, external, internal and semi-internal vibrs., spectroscopic identification criteria 3-79442
- molecular crystal, Fermi reson. exchange 3-69000
- naphthalene, α-bromo- and β-chloro-, vibr. spectra and depolarisation ratio 3-52367
- naphthalene, anharmonicity of lattice vibr. and lifetime of optical phonons 3-72644
- 1,6- and 1,8-naphthyridine, assignments of fundamental vibrs. 3-63458
- neopentane plastic crystal, i.r. and Raman band shape analysis, mol. reorientation 3-75983
- norbornadiene, vibrational spectra 3-72624
- norbornane, vibrational spectra 3-72624
- organometallic compounds, metal-metal bonding, vibr. analysis 3-78797

Raman spectra of organic substances continued

- organotin covalent compounds, vibr. modes from Mossbauer effect and Raman data 3-44355
 1,2,5-oxadiazole and deuterated species, vibrational spectra and fundamental frequencies 3-46299
 oxalic acid, cryst., rel. to hydrogen bond vibr. 3-72640
 oxalyl chloride, structure of vapour phase 3-63459
 n-paraffin crystals, lattice vibrs. 3-72641
 pentafluorophenol:n-Cl-aniline compound, phase transformation study 3-72198
 perfluorocyclopentene, i.r. and Raman spectra interpretation 3-54685
 N-phenylglycine and Na salt, between 200 and 1700 cm^{-1} , vibr. assignment 3-47241
 poly-L-glutamic acid, length depend. resolved pseudo-Raman spectra 3-78920
 poly-L-glutamic acid, partially resolved pseudo-Raman band 3-78919
 poly-L-glutamic acid sodium salt, Raman like non-fluorescent broad band 3-55586
 polycarbonate, using He-Ne laser 3-64658
 polyethylene, devices for obs. up to 50 kbar pressure 3-80027
 polyethylene, Raman spectra, low frequency modes, lattice vibrations and pressure dependence 3-47249
 polyethylene terephthalate, molecular reorientation, polarized Raman scatt. 3-67873
 polymethylenes, Raman spectra, low frequency modes, lattice vibrations and pressure dependence 3-47249
 polypropylene, laser Raman spectrum, cryogenic temp. to melting point 3-46362
 polytetrafluoroethylene, devices for obs. up to 50 kbar pressure 3-80027
 potassium hydrogen acetylenedicarboxylate, crystal struct., vibr. studies of hydrogen-bonding 3-76006
 potassium hydrogen di-trifluoroacetate, i.r. and Raman spectra, symmetric hydrogen bonds 3-68990
 potassium hydrogen succinate, i.r. and Raman spectra, symmetric hydrogen bonds 3-68990
 potassium methyl xanthate- d_3 and - d_5 , vibrational spectra and force constants (*German*) 3-46297
 propane, relative cross-section, from short pulse laser scatt. and photon counting obs. 3-57651
 1,2-propanedithiol, vibr. spectra and rot. isomerism 3-53093
 propionamide, i.r. and Raman spectra 3-60452
 propylene, relative cross-section, from short pulse laser scatt. and photon counting obs. 3-57651
 propylene imine, vibration of strained ring systems 3-78788
 PTFE, phase II and III, mol. conform., cryst. struct., phase transition, vibr. assignment 3-64643
 pyrazine, crystalline, low temp.-high temp. phase transition study by i.r. and Raman spectra 3-75982
 pyridine asymmetric ion hydrogen bonded complexes, i.r. and Raman spectra 3-75030
 pyridine hydrogen bonded complexes, vibrational spectra 3-75029
 pyridinium trihalides, Raman, i.r. and electronic absorption spectra, struct. 3-75032
 pyridinium-pyridine ion, complex hydrogen bonded cations, i.r. and Raman spectra obs. 3-75028
 pyrrol, cryst., rel. to hydrogen bond vibr. 3-72640
 quinoline, liquid, rot.-vib. relax., Raman and i.r. spectral obs. 3-64670
 rhodanine dimers, comparison with vibratory spectra calcs. (*Russian*) 3-75015
 rhodizone anion, in soln. and salts, intensity and depolarisation ratio 3-78801
 ribonuclease A, crystal and in solution, structure 3-75165
 silacyclopentanes, vibr. analysis 3-63464
 silacyclobutane, (1-d), (1- d_2), silacyclopent-3-ene, ring-puckering vibrs. 3-78789
 sodium hydrogen diacetate, i.r. and Raman spectra, symmetric hydrogen bonds 3-68990
 spherical top molcs., Raman band contour analyses and Coriolis constants. 3-67816
 stilbene, anharmonicity of lattice vibr. and lifetime of optical phonons 3-72644
 stilbene powder, stimulated Raman scatt., energy and time characts., temp. effects 3-62751
 styrene, polymers and copolymers, sample preparation, quantitative analysis 3-58496
 tartaric derivatives, external vibration frequencies of active and racemic forms 3-55581
 TCNE-benzene charge transfer complex, resonant Raman effect and charge distrib. 3-75977
 TCNQ and TCNQ- d_4 single crystals, polarised Raman spectra, vibrational modes 3-72625
 1,4-telluroxan in vapour, liquid, amorphous and crystalline state, vibrational spectra 3-46292
 tetra-allyl silane, vibrational spectra 3-46294
 tetra-allyl tin, vibrational spectra 3-46294
 1,1,2,2-tetrachlorotetrafluorocyclobutane and 1-chloro-2,2,3,3-tetrafluorocyclobutane 3-78787
 tetracyanoethylene, radical anion salts, reson. Raman spectra and bond strengths 3-43446
 tetrafluoromethane, number density remote sensing in hypersonic flow using Raman scattering 3-71699
 tetramethylbiphosphine Raman spectra, isomers obs. 3-75036
 N,P,P,P-tetramethylphosphine imide, vibr. spectra, struct. of P-N bond 3-75024
 N,P,P,P-tetramethylphosphine imide and N-methyl- d_3 analogue, vibr. spectra analysis 3-78795
 1,3,5,7-tetramethylsilaadamantane (*German*) 3-43453
 thiirane sulphone, vibr. spectra 3-75655
 thiochlorides (*Russian*) 3-63477
 thiomethyl group, characteristic freq., stretching modes 3-67809
 thiopropionamide, i.r. and Raman spectra 3-60452
 thiourea and deuterated thiourea, phase transition phenomena, soft mode behaviour (*French*) 3-61032
 triazol, cryst., rel. to hydrogen bond vibr. 3-72640
 tribenzyl-antimony dihalides, i.r. and Raman spectra 3-67821
 tribenzyl-arsenic dihalides, i.r. and Raman spectra 3-67821

Raman spectra of organic substances continued

- 1,2,3-tribromopropane, anti-gauche conformer in crystals, stretching vibrs. 3-63465
 trichlorodeuteromethane, mol. reorientation, Raman spectral obs. 3-64666
 1,1,1-trichloroethane, laser excited Raman bands and funds. 3-67814
 1,2,3-trichloropropane, anti-gauche conformer in crystals, stretching vibrs. 3-63465
 trifluoroacetic acid, solid 3-50572
 1,3,5-trifluorobenzene, C-F bond length 3-54691
 trifluoroethylamine, vibrational spectra 3-71558
 trifluoromethyltrifluoroborate anion, 4000 to 50 cm^{-1} , vibrational spectrum, Urey-Bradley force constants 3-57648
 1, 2, 3-trihalogenobenzene, lattice vibrations, detection of crystalline isomorphism 3-75991
 1,3,5-trinitrohexahydro-s-triazine, vibrational spectrum analysis, heat capacity determ. 3-80059
 2,4,6-triphenyltriazine, Raman active lattice spectrum, 300 and 30K 3-55578
 vinyl-Pt complexes, coupling consts. Pt hybridisation 3-75065
 $\text{As}(\text{C}_2\text{F}_3)_3$, i.r. and Raman spectra and ^{19}F n.m.r. 3-71561
 hexamethylbenzene, phase transition at 116 K, phase III morphology, vib. spectra and absorpt. anisotropy 3-60794
 $\text{Pl}(\text{C}_2\text{F}_3)_3$, i.r. and Raman spectra and ^{19}F n.m.r. 3-71561
 n-paraffins, low frequency Raman-active lattice vibrations 3-55577
 $\text{Sb}(\text{C}_2\text{F}_3)_3$, i.r. and Raman spectra and ^{19}F n.m.r. 3-71561

Ramsauer effect see *electron absorption; electron scattering*

random functions

see also *random processes*

entropy production in functional random-walk model 3-74177

random noise

see also *thermal noise*

filters, Nth root stack nonlinear multichannel, for seismic refraction and teleseismic array data 3-65147

random number generation

growth time generation for mammalian cells 3-59413

random-phase approximation, nuclear see *nuclear models; nuclear theory*

random processes

see also *Brownian motion; fluctuations; Markov processes; probability; queuing theory; stochastic processes*

1/f noise theory 3-62603

autocorrelation function, statistical evaluation (*Polish*) 3-70538
 classical gas, macroscopic observables time-correl. function 3-62591

critical temperature of Ising system, properties of random and self avoiding walks 3-62606

density of states in tetrahedrally bonded solids in terms of number of returns to origin 3-72304

Dirichlet problem soln. using Monte Carlo technique (*Italian*) 3-74003

elasticity, random external load problems soln. (*Russian*) 3-57079

endpoint distribution of self-avoiding walks 3-51835

errors in maximum values of stationary random process using discrete methods (*Russian*) 3-53824

functional random-walk model for irreversible processes steady-state 3-40195

harmonic analysis of relative number of sunspots 3-42136

isotropic random flights, probability density and distribution function 3-42900

lattice statics, random rel. to fluorescence quenching by resonance transfer of excitation energy 3-58551

mixtures, turbulent flows, concentration probabilities distribution and alternation (*Russian*) 3-54800

multicorrelated random processes, simulation using fast Fourier transform algorithm 3-42479

nonlinear conversion equations, non Gaussian, anal. (*Russian*) 3-74005

nonlinear perturbed stochastic integral equation, Volterra type, random solution 3-74004

Pearson type 3 distribution, random variable, moment and max. likelihood estimates 3-56241

plate, random wideband vibr. due to point forces (*Russian*) 3-54123

point process, restricted rewards, probability 3-74006

self-avoiding random walk on triangular or honeycomb lattice, numerical study 3-40183

self-avoiding walks, simple cubic lattice 3-70744

simultaneous meas. of several observables, concept of fuzzy probability meas. 3-74087

stationary ergodic processes, comparison of Fourier transform method with a correlation method, spectral density estimation (*Russian*) 3-70312

string, random wideband vibr. due to point forces (*Russian*) 3-54123

temperature variations rel. to non linear creep buckling in reactor materials 3-74671

vapour-liquid equilibrium, overall area tests for thermodynamic consistency, effect of random error 3-58119

vibration response, probabilistic and deterministic approaches 3-74066

walk, calcs. of number of distinct sites visited 3-40182

Ca apatites, diffusion coeff. determ. using random walk statistics 3-41053

range finding see *distance measurement*

range of particles see *energy loss of particles*

ranging (sonar) see *sonar*

rare earth alloys

see also *lanthanum alloys; rare earth compounds*

crystal chemistry of CeCu_2 -type structure 3-79266

crystal field splittings and electronegativity, correl. 3-55216

elastic constant in applied magnetic field, finite strain calc. 3-64532

excitation spectrum, hyperfine and Heisenberg exchange interaction 3-72432

with Fe, Co, Ni magnetic and structural properties (*Rumanian*) 3-63982

rare earth alloys continued

- group VIII metal alloys, 7:3 phases, metallographic and X-ray obs. and mag. props 3-79274
- heavy, binary, mag. props. 3-68780
- intermetallic compounds, magnetic properties 3-52962
- lanthanide-noble metal phases, prep. and props. 3-46604
- liquid, Hall coeff., elec. resist. and susceptibility, rel. to electronic struct. 3-50112
- magnetic props. of hard mag. rare earth-3d metal alloys, permanent RCo magnets (*Rumanian*) 3-44220
- magnetic transitions, compressibility and thermal expansion meas. 3-79834
- melt growth by crystn. 3-44537
- rare earth transition metal silicides, structure types, X-ray obs. 3-58010
- rare earth-Al-Fe(Co), ordering, X-ray and neutron diffr. obs. 3-79273
- rare earth-Co, coercivity, theory and exptl. 3-47089
- rare earth-cobalt, LnCo_2 , Curie temp., press. depend., correl. with YCo_2 susceptibility 3-55419
- rare earth-cobalt, permanent magnets, LnCo_5 , prepared by liq. phase sintering, mag. props. 3-64521
- rare earth-transition metal compounds, 3d states influence on stability, Fermi level, mag. props. 3-58002
- transition metal, hard mag. props. rel. to permanent magnets 3-44266
- zinc intermetallic, $\text{RE}(\text{Zn})_5$ type, $\text{RE}=\text{Ce, Pr, Nd, Sm, Gd, Gy}$ and Er , lattice parameter for CaCu_5 (D_{2d}) struct. 3-68198
- Ag-Gd, dilute, mag. susceptibility, n.m.r. and thermoelec. power obs. of impurity state 3-68765
- Al-rare earth, n.m.r. (*Rumanian*) 3-68863
- Ce-Co, CeMM-Co, mag. and mech. props. of R_5Co_{19} , RCo₅ phases (*German*) 3-79844
- Ce-La-Co, mag. and mech. props. of R_5Co_{19} , RCo₅ phases (*German*) 3-79844
- CeAl₃, elec. resist. meas. up to 17 kbar pressure, Kondo effect 3-50168
- CeCo₅:Fe, Cu modified, sintered magnet 3-47101
- $\text{Ce}_2(\text{Co}_{1-x}\text{Fe}_x)_{17}$, phase instability rel. to permanent mag. props. 3-44558
- CeIn₃ thermoelectric cooling figure of merit, large anomaly, Kondo system, Peltier effect, thermopower, low temps. 3-50182
- $\text{Ce}_{1-x}\text{La}_x$, press.-temp. phase diagram, transition from Curie to Pauli paramagnetic phase 3-72444
- CePd₃ thermoelectric cooling figure of merit, large anomaly, Kondo system, Peltier effect, thermopower, low temps. 3-50182
- CePt₅, low temp. specific heat and magnetic susceptibility measurements, crystal field model 3-46946
- $\text{Ce}_{1-x}\text{R}_x\text{Al}_3$, ($\text{R}=\text{Gd, Tb, Er}$), n.m.r. and mag. susceptibility 3-41434
- CeRu₂:Fe, superconductor, e.p.r. obs. 3-79905
- CeRu₂:Gd, local moment e.s.r. in normal and supercond. states 3-44171
- CeSn₃, d.c. elec. resist. meas. influence of 4f electrons 3-79674
- $\text{CeSn}_2\text{In}_{3-x}$, ^{119}Sn n.m.r. Knight shifts and spin lattice relax. time 3-50480
- (Co,Fe)₁₇R₂, R=rare earth metal easy magnetis. directions and Curie temp. 3-47082
- with Co, magnetic structure and characteristics (*Rumanian*) 3-68816
- Co-Fe-Cu-R permanent magnet alloy, R=rare earth metal, intrinsic mag. props and magnetic process 3-44252
- Co-rare earth metal, domain wall energies detn. 3-44248
- Co-rare earth metal, wall pinning model for coercive force 3-44249
- Co-Sm, for permanent magnets, temp. depend. of coercivity 3-44269
- Co-Sm magnet, quenching, oxides identified by X-ray diffr. 3-47100
- Co-Sm permanent magnet alloy, lattice parameter variation with composition and temp. 3-43763
- Co₅R, R=Y, La, Pr, prep. by liquid phase sintering for permanent magnets 3-44268
- Co₅R, R=heavy rare earth, magnetic moments and easy directions 3-47001
- Co₅R powder, R=Pr, Sm and mischmetal, prep. by rapid quenching technique, for magnet applic. 3-44278
- Co₅Sm, sintered magnets, magnetic domains obs. using polarised light 3-68811
- Co₅Sm, temp. depend. of nucleating fields and coercive force 3-44267
- DyFe₂-DyAl₂ and DyFeAl, ordering, X-ray and neutron diffr. obs. 3-79273
- DyFe₂-xCo_x, mag. moments, Curie and compensation temps. 3-41342
- Dy₂Gd_{1-x}, paramag. susceptibility meas., single-ion and exchange interaction anisotropy 3-75828
- Dy₂Sb, mag. structure, type II antiferromag. ordering 3-50379
- ErAu, metamag. props., susceptibility and magnetization studies 3-47039
- ErCo₂-ErAl₂, effect of replacement of Co by Al on mag. props. 3-41373
- ErCo₂-ErAl₂ and ErCoAl, ordering, X-ray and neutron diffr. obs. 3-79273
- ErFe₂, magnetostrictive compound, u.s., magnetostrictive compounds, u.s. determination of elastic moduli 3-43820
- ErFe₂, thermal expansion rel. to Curie temp. pressure depend. 3-58385
- ErFe₂ and ErFe₃, susceptibility, anomalous behaviour near mag. compensation point 3-58370
- ErFe₃, thermal expansion rel. to Curie temp. pressure depend. 3-58385
- Er₂Fe₁₇, thermal expansion rel. to Curie temp. pressure depend. 3-58385
- Er₄Fe₂₃, thermal expansion rel. to Curie temp. pressure depend. 3-58385
- Er_{0.75}Lu_{0.25}, mag. struct., transitions to c-axis longit. spin wave, antiferromag. conical structs. 3-79847
- Er_{1-x}Th_xCo₅, ferromag. props., antiferromag. Gd-Co coupling after Th addition, Co moment reduct. 3-68772

rare earth alloys continued

- Er_{1-x}Al_x, crystalline electric field levels, determ. by neutron spectroscopy 3-50312
- Er_{1-x}Y_xFe₂, Mossbauer effect, dipolar contributions to mag. hyperfine fields 3-79959
- ErZn₁₂, antiferromagnetic, low temp. props. 3-79835
- EuAl₄, Mossbauer obs. of hyperfine field contribs. 3-47187
- Eu_{1-x}Al_x alloys, Mossbauer meas. of coexistence of superconductivity and magnetism 3-44164
- Eu_{1-x}La_{1-x}Al₂, Mossbauer obs. of hyperfine field contribs. 3-47187
- Eu₂Yb_{1-x}Al₂, Mossbauer obs. of hyperfine field contribs. 3-47187
- Eu₂Yb_{1-x}Cu₂, Mossbauer obs. of hyperfine field contribs. 3-47187
- with Fe, magnetic structure and characteristics (*Rumanian*) 3-68816
- Gd-Co and Gd-Fe film for bubble domain applications 3-47109
- Gd-Co thin films, amorphous, structural and mag. changes, electron microscopy 3-68523
- Gd-Dy alloys, mag. resistivity 3-79671
- Gd-Y alloys, magnetocrystalline anisotropy, susceptibility, saturation magnetisation, temp. depend. 3-50390
- GdAl₂, ferromagnetic, hyperfine fields determ. by n.m.r. 3-79927
- Gd(Al_{1-x}Cu_x)₂, Curie temp. meas. rel. to cond. electron number 3-58376
- Gd(Al_{1-x}Ni_x)₂, Curie temp. meas. rel. to cond. electron number 3-58376
- Gd₂B_{1-x}Ru_x (B=Th,Ce,La), e.p.r. and supercond. correl. transition temp. Gd conc. depend. 3-72417
- GdBe₁₃, susceptibility, mag. moment and ⁹Be nuclear mag. relax. (*French*) 3-55427
- GdCo₅, single cryst., hysteresis singularities rel. to domain struct. form. (*Russian*) 3-72485
- Gd₂Co₁₇, spin echo obs., 77 K (*French*) 3-79933
- GdIr₂, ferromagnetic, hyperfine fields determ. by n.m.r. 3-79927
- Gd₂Pd₃, ferromag., isotopic with R₂Pd₃ (R=La,Ce,Pr,Nd,Sm), non-centrosymmetric Th₂Fe₃ structure 3-52601
- GdPt₂, ferromagnetic, hyperfine fields determ. by n.m.r. 3-79927
- GdRh₂, ferromagnetic, hyperfine fields determ. by n.m.r. 3-79927
- Gd_{1-x}Th_xCo₅, ferromag. props., antiferromag. Gd-Co coupling after Th addition, Co moment reduct. 3-68772
- HoAg, Neel temp. and mag. struct., neutron diffr. obs. 3-47057
- HoAu, metamag. props., susceptibility and magnetization studies 3-47039
- HoCo₂-HoAl₂, magnetisation props. at cryogenic temp., neutron diffr. obs. 3-44222
- Ho₂Co₁₇, permanent mag. material, modified Czochralski growth 3-44529
- HoFe₃, susceptibility, anomalous behaviour near mag. compensation point 3-58370
- HoFe₂-xCo_x, mag. moments, Curie and compensation temps. 3-41342
- Ho_{1-x}Th_xCo₅, ferromag. props., antiferromag., Gd-Co coupling after Th addition, Co moment reduct. 3-68772
- HoZn, mag. anisotropy 3-68801
- HoZn₂, magnetocrystalline anisotropy, applied field effect on sinusoidal mag. structure 3-60972
- In-Gd, supercond. film, electron thermal cond., strong coupling effects 3-41300
- (La,Ce)Al₂, Kondo system, magnetoresist. 3-68770
- La_{1-x}Gd_xAl₂, g-shift and linewidth of Gd³⁺ 3-47133
- La_{0.8}Lu_{0.2}-xTb_x, supercond. crit. fields with short-range mag. order, transition temp. 3-68716
- Lu, high purity, physical and metallurgical properties 3-63981
- LuPb₃, high pressure synthesis of f.c.c. compound 3-58007
- Lu_{1-x}Th_xFe₃, magnetisation vs. temp. behaviour hybrid local moment-band model 3-47094
- Mg-Ce(1.3 wt.%), isochronal annealing, precipitation, elec. resist. and electron microscopy obs. (*Japanese*) 3-76165
- Nb-Ru system, martensitic transitions, temp. and conc. depend. (*French*) 3-58126
- NdPt₅, low temp. specific heat and magnetic susceptibility measurements, crystal field model 3-46946
- NdSn₃, d.c. elec. resist. meas. influence of 4f electrons 3-79674
- with Ni, magnetic structure and characteristics (*Rumanian*) 3-68816
- Pb-Gd, supercond. film, electron thermal cond., strong coupling effects 3-41300
- PdEu, mag. props. and cryst. struct., Mossbauer and X-ray obs. 3-79954
- (Pd_{0.997}Fe_{0.003})_{1-x}Gd_x, dilute ternary alloy, ferromag. props. depend. on x 3-50351
- Pd_{1-x}R_x, R=rare earth, magnetic properties, crystal field effects, e.p.r., magnetic moment 3-47129
- Pr-Sm-Co, mag. props. as function of composition 3-47088
- PrCo₅, Pr₂Co₁₇, Al substituted, structure and phase relations, X-ray obs. 3-69194
- PrCo₅ and Sm₂Pr_{1-x}Co₅ permanent magnets, prepared by liq. phase sintering, mag. props. 3-64521
- Pr₃In, determ. of magnetic properties in range 4.2 to 300 K at 80 KOe 3-79828
- PrPt₅, low temp. specific heat and magnetic susceptibility measurements, crystal field model 3-46946
- PrSn₃, d.c. elec. resist. meas. influence of 4f electrons 3-79674
- Pr₂Th Van Vleck paramagnet, spin-phonon coupling 3-46981
- Pr₂Y_{1-x}Al_x, crystalline electric field levels, determ. by neutron spectroscopy 3-50312
- RBe₁₃ intermetallic compounds, (R=La,Ce,Nd,Gd) magnetic properties, hyperfine interactions, spin dynamics 3-52969
- rare earth-gold compound, RAu₂, magnetic susceptibility study, temp. depend., first order magnetic transition 3-46999
- Sm-Co intermetallic compounds, hyperfine interactions, ⁵⁷Fe Mossbauer study 3-61014
- Sm-Co-MM, MM=mischmetal, mag. props. as function of composition 3-47088
- Sm₂Ce_{1-x}(Co_{1-x-y}Fe_yCu_y)₂, bulk hardening effect in case of nonstoichiometric composition 3-50416
- Sm(Co,Cu)₅, mag. props. temp. depend. 3-50424
- Sm₂(Co,Fe)₁₇, mag. props. of permanent mag. material 3-44253

rare earth alloys continued

- SmCo₅, coercive field and structure between 780 and 1150°C 3-60981
 SmCo₅, mag. after effect, mag. viscosity 3-50420
 SmCo₅, permanent magnet material, heat treatment and mag. phase analysis 3-44250
 SmCo₅, powder-based magnets, texture perfection degree, particle orientation angles distrib. (*Russian*) 3-61135
 SmCo₅, single crystals, hysteresis singularities rel. to domain struct. form. (*Russian*) 3-72485
 SmCo₅, single-domain state with mag. energy 32 million G-Oe 3-55446
 SmCo₅, Sm₂Co₁₇, Al substituted, structure and phase relations, X-ray obs. 3-69194
 SmCo₅ and Sm_{0.5}Pr_{0.5}Co₅ of mag. props. (*Russian*) 3-44259
 SmCo₅ and Sm₂Pr_{1-x}Co₅ permanent magnets, prepared by liq. phase sintering, mag. props. 3-64521
 SmCo₅ magnets, liquid-phase sintering 3-44643
 SmCo₅ powder, domain wall pinning centres, particle size and coercivity 3-44276
 SmCo₅ powder, microstruct. and mag. props. (*Russian*) 3-58403
 SmCo₅ powder, sintering mechanisms, rel. to magnet prod. 3-47438
 SmCo₅ sintered magnet, magnetic domains, powder pattern obs. 3-52992
 Sm₂Co₁₇, cryst. structure, high temperature phase of CaZn₃ type 3-52600
 Sm₂Co₁₇, liquid phase sintering, mag. props. obs. 3-44694
 SmCo₅Cu_{1.5}, magnetic after effect domain structure and critical remagnetising field (*Russian*) 3-79867
 SmCo_{5-x}Cu_x, magnetocrystalline anisotropy constant determ. 3-50393
 Sm(Fe,Co,Cu)₅, magnetocrystalline anisotropy constant determ. 3-50393
 SmZn₁₂, paramagnetic susceptibility, Curie-Weiss law 3-44198
 Tb-light rare earth alloys mag. and cryst. struct., neutron diffr. obs. 3-68790
 Tb-Te films, simple cubic structure 3-52768
 TbAl₂:Dy ferromagnetic internal fields and relaxation effects for Dy, perturbed angular correlation meas. 3-53046
 TbBe₁₃, susceptibility, mag. moment and ⁹Be nuclear mag. relax. (*French*) 3-55427
 TbCo₂-TbAl₂, magnetisation props. at cryogenic temp., neutron diffr. obs. 3-44222
 TbFe₂ and TbFe₃, magnetostrictive compounds, u.s. determination of elastic moduli 3-43820
 TbFe₂-TbAl₂, magnetisation props. at cryogenic temp., neutron diffr. obs. 3-44222
 Tb₂Fe₁₇-Tb₂Al₁₇, ordering, X-ray and neutron diffr. obs. 3-79273
 TbSb, elec. resistivity, effect of mag. field 3-41171
 Tb₂Y_{1-x}Fe₂, Mossbauer effect, dipolar contributions to mag. hyperfine fields 3-79959
 TbZn, mag. anisotropy 3-68801
 TbZn₂, magnetocrystalline anisotropy, applied field effect on sinusoidal mag. structure 3-60972
 Th-Dy, mag. susceptibility, temp. depend. (*Russian*) 3-60956
 Tm₂Fe₁₇, mag. phase transition, Mossbauer and magnetis. obs. 3-64495
 TmSb, form factor rel. to cryst. field 3-64501
 Tm, Y_{1-x}Al₂, crystalline electric field levels, determ. by neutron spectroscopy 3-50312
 Tm_{0.25}Y_{0.75}Al₂ neutron crystal field spectroscopy, paramagnetic phase, energy distribution, field parameters 3-52955
 YCo₅ permanent magnets, prepared by liq. phase sintering, mag. props. 3-64521
 Y₂Co₁₇, permanent mag. material, modified Czochralski growth 3-44529
 Y₂Co₁₇, spin echo obs., 77 K (*French*) 3-79933
 Y(Co_{1-x}Fe_x)₅, composition and stability of CaCu₂-type compds., permanent mag. application 3-50679
 Y_{21x}(Co_{1-x}Fe_x)_{17-2x} intermetallic compound, magnetocryst. anisotropy, X-ray diffr. obs. 3-44230
 YFe₂, Mossbauer parameters, mag. props., temp. depend. (*French*) 3-72547
 YbAl₂ and YbAl₃, ambivalence of Yb, lattice const., sp.ht., and elec. props. study 3-68552

rare earth compounds

- see also under the individual compounds e.g. cerium compounds
 see also rare earth alloys
 aluminium garnets, elec. field gradients at Al³⁺ nucleus 3-79635
 amorphous materials, new magnetism model 3-52949
 arsenates, mag.-field induced crystallographic domains 3-72495
 borates, RBO₃ type, flux growth of single crystals 3-58595
 borides, lattice const. corrls. 3-68222
 borides, perovskite structure, preparation, X-ray and metallographic studies 3-40907
 bromide hexahydrates, ⁷⁹Br and ⁸¹Br n.q.r. 3-75913
 carbides, perovskite structure, preparation, X-ray and metallographic studies 3-40907
 chalcogenide-silver chalcogenide system cpds., cryst. struct. (*French*) 3-46631
 chalcogenides, cryst. chem. and semiconduction (*French*) 3-46847
 chalcogenides, thermophysical props., electronic struct. 3-72322
 chlorides solns., HDO Raman spectra 3-75980
 complexes, electron transfer, f-d absorpt. bands, theory 3-76491
 complexes with β -diketonates, i.r. spectral band assignments 3-78751
 cubic, mag. ordering and phase changes 3-52976
 dicarbides, mixed, lattice constants rel. to composition 3-58017
 double nitrates, double and multiple perturbations of non-Kramers ions in trigonal lattice 3-55662
 electrical resist. and thermoelec. power for R₂NiO₄(R₂CuO₄), band structure interpretation 3-41180
 exchange interactions effect on low temp. ordering of rare earth hydroxides 3-47015
 ferrimagnets, R₂Fe₁₇, effective field at ⁵⁷Fe 3-75926
 fluorozirconate, crystal struct. similarities to ReO₃ type (*French*) 3-79299
 garnet, mixed rare earth iron type, epitaxial film development 3-79583
 garnet, R_{0.3}Y_{2.7}Fe₅O₁₂, ⁵⁷Fe n.m.r. by spin echo method 3-50475
 garnet, sixfold coordination of ions 3-72065

rare earth compounds continued

- garnets:Er³⁺, Eu³⁺, Nd³⁺, crystal field theory Stark effect 3-72331
 garnets, Al, Ga, Fe, Raman active phonons, laser reflection and transmission spectra 3-72613
 garnets, bubble, liquid phase epitaxy, isothermal diffusion theory 3-68514
 garnets, optical props. for coherent mag. vibrs. 3-47235
 garnets, paramagnetoelectric effect 3-41204
 garnets containing Sc, RE₃Sc₂Al₃O₁₂ and RE₃Sc₂Ga₃O₁₂, crystal stoichiometry 3-72806
 germanates, flux growth, mag. transition temps. 3-41638
 germanates, synthesis, elec. cond., mechanism 3-76315
 germanates, synthesis, physicochem. classifications, solid solns. 3-76314
 hexagonal compounds, A_nB_nC₂X₁₄ with n=1/2, 2/3, 1, 4/3 and 2 (*French*) 3-64016
 inorganic microcrystals, regularity of energy transfer between lanthanide ions 3-76090
 intermetallic, Re-Al₂ type, neutron diffraction examination 3-50375
 ionic, exchange interaction effective field approx., neutron scatt. obs. 3-60963
 iron garnets, Curie pts., 60 kbar press. effect (*French*) 3-72463
 luminescence of rare earth chelates, under intense pulse excitation, kinetics and energy transfer 3-76087
 manganites, catalysts with low ammonia yield in reduction of nitrogen oxides 3-55943
 mesoperoxide tetrahydrates, X-ray diffr., isostructurality, unit cell dimensions 3-72067
 mixed metal oxides, rare earth luminescence, crystal chemistry 3-64008
 molybdate, vibr. spectra and cryst. struct. 3-80039
 molybdates, Ln₂(MoO₄)₃ and Ln₂MoO₆, structural and physical properties 3-64009
 monochalcogenides, pressure induced semiconductor-metal transition 3-44031
 niobates, perovskite structure, vibr. spectra 3-53111
 organic microcrystals, regularity of energy transfer between lanthanide ions 3-76090
 orthoferrite, anisotropy and exchange interactions 3-44211
 orthoferrite, domain structure and elastic properties, mag. state changes with temp. 3-79874
 orthoferrites, optical props. for coherent mag. vibrs. 3-47235
 oxide-PbF₂ system, new phases 3-72176
 oxide/metal composites, unidirectional solidification 3-76347
 oxides, form., decomp. of solid soln. with ZrO₂ 3-76314
 oxides, impurity determ., atomic absorpt., fluoresc., pulsed volatilisation 3-73946
 perovskite type compounds, non-stoichiometry investigation (*French*) 3-64014
 perovskites, Ln_{0.22}(M_{2/3}W_{1/3})O₃ and Ln_{0.05}(M_{0.15}W_{0.85})O₃ type, crystallographic characterization (*French*) 3-54949
 phosphides, cryst. chemistry and phys. props., review 3-64018
 polymorphism of TRnTiO₆ and TRTaTiO₆ types, aeschonite-euxenite transition 3-41015
 with pyrochlore structure, i.r. absorption characteristics 3-44401
 pyrochlores, Ln₂O₈O₇, prep. and characterization 3-60708
 rare earth chromium sulphides, LnCrS₃, (Ln=Y, Gd, Dy, Ho, Er), cryst. growth, struct., and absorpt. 3-40869
 rare earth complexes, benzoyltrifluoroacetylacetonate lanthanide solid chelates, fluorescence and intermolec. energy transfer 3-47304
 rare earth complexes, degradation processes of excitation energy, struct. factor effects 3-76094
 rare earth iron garnet films, epitaxial, wavelength modulation spectroscopy, derivative absorption and reflectance spectra 3-55570
 rare earth metal Fe₂, magnetocrystalline anisotropy 3-47077
 rare earth-alkali fluorides, M=alkali metal, character study of binary systems 3-64182
 rare earth-Fe compounds, REFe₂, susceptibility and magnetisation analysis by mol. field theory (*German*) 3-64488
 sesquioxides, surface steps (*French*) 3-60832
 sesquioxides, cubic, dielectric props., effective ionic charges, IR absorption 3-79974
 sesquioxides, thin crystals, electron microscope obs. of mechanical twins, role of microtwins (*French*) 3-68278
 silicates, synthesis, physicochem. classification, solid solns. 3-76314
 solubility enhancement of Nd³⁺ in rare earth-Al garnet by lattice expansion with Sc³⁺ 3-68415
 sulphides, containing two III_a elements, comparison of cryst. struct. (*French*) 3-58021
 superexchange interaction in insulator cryst., rel. to Neel and Curie temps. 3-72458
 symmetry tendencies, f-degeneracy 3-72030
 tetaborates, ¹¹B Knight shifts at the three different crystallographic sites 3-41439
 titanoniobates, Ln TiNbO₆, Ln=Ce, Nd, Sm, Eu, Pr, polycrystalline specimens, electrical conductivity, temperature dependence 3-75787
 tungstate, vibr. spectra and cryst. struct. 3-80039
 tungstates, Ln₂WO₆ types, Ln=Ce to Lu, refined cell parameters 3-64001
 vanadates, mag.-field induced crystallographic domains 3-72495
 [LnW₁₀O₃₃]⁷⁻, isostructural series, Judd-Ofelt parameters var. 3-44025
 BaLn₂O₃, Ba₃Ln₂O₉ types, physicochemical props. 3-72172
 CaLn³⁺BO₄, isomorphism with warwickite 3-46625
 CaLnCrO₄, (Ln=Pr, Nd, Sm, Eu, Gd), new series of phases, preparation and structure (*French*) 3-79317
 Ca₁₁Ln₁₋₃CrO₄, (Ln=Pr, Nd, Sm, Eu, Gd), solid solns., preparation and structure (*French*) 3-79317
 Fe garnet, liquid phase epitaxial growth kinetics, influence on mag. props. 3-43953
 RCoGe₂ type, R=La, Ce, Pr, Nd, Sm, Gd, Tb, Dy, Ho, Er, Tm, Yb, Lu, lattice parameters 3-58016

rare earth elements see rare earth metals

rare earth metals

- see also the individual metals e.g. cerium
 abundances in acid and basic rocks in Iceland 3-80626
 Allende meteorite, rare-earth elements in matrix, inclusions, and chondrules 3-61741

rare earth metals continued

- atom, doubly and triply ionized, ioniz. energies 3-71378
 atom, self-consistent relativistic Dirac-Hartree-Fock calc. 3-67651
 atoms and ions, energy levels and spectra theory 3-78431
 chondritic meteorites with peculiar rare-earth patterns 3-81008
 chromatographic analysis using ion exchange displacement technique (*French*) 3-62351
 conduction electron m.f.p. and concentration 3-79679
 electric field gradient, cond. electron contrib. 3-44027
 energy levels, comparison of calc. and exptl. values 3-52795
 energy transfer and degradation of rare earth ions in non-aqueous solvent 3-76081
 e.p.r. of rare earth ions in diamag. host, zero-field spectrometer for obs. 3-77594
 excitation of 4d electrons by inelastic scattering of high energy electron beam 3-64280
 ferromagnetic, PAC obs. of mag. hyperfine field 3-64591
 heavy, magnetoelectric interaction effect on elastic consts. 3-47113
 inclusions in steel, contact microradiography obs. 3-61146
 ion, core electron binding energy multiplet hole splitting 3-44021
 ion, in YAlO_3 , fluoresec. sensitisation using Cr ions 3-69057
 ions, in alcohol, acetone and acetonitrile, nonradiative energy transfer processes 3-64717
 ions, in microcrysts., regularity of energy transfer 3-76090
 laser emission spectrography 3-45582
 liquid, Hall coeff., elec. resist. and susceptibility, rel. to electronic struct. 3-50112
 localization of 5d electrons, calc. 3-79639
 luminescence in phosphors, effect of Ce impurities (*Russian*) 3-64733
 lunar fines 74220 Apollo 17 sample, rare earth elements and Ba distribution 3-65846
 magnetic anisotropy due to combination of cryst. field and indirect exchange interactions 3-47079
 magnetic phase transition, sound propagation effects nr. transition 3-46709
 magnetic properties, review (*French*) 3-64478
 melt growth by crystn. 3-44537
 multiplet structure 3-40563
 noble metals, rare earth doped, exchange corrections to fourth order cryst. field parameter 3-52800
 optical spectra, classification (*French*) 3-63276
 oxidation potential (II-III), correlation technique 3-76491
 spectroscopic determination in ferroelectric and piezoceramic materials (*Russian*) 3-62362
 trace metals detection by X-ray excited optical fluorescence in YPO_4 and YVO_4 3-48635
 trivalent ions in soln., magnetooptical activity calc. for forbidden transitions 3-61030
 viscosity, liquid metals, rare earth and actinide, viscous flow models, f-orbital electronic contribution 3-50021
 CaF_2 :R, i.r. spectra of defects 3-72693
 in Fe garnet, effect on spin wave linewidths 3-41422
 in GaAs, distribution ratios, solubility curves 3-72099
 Gd: rare earth impurities, magnetic anisotropy study to analyze torque measurement results 3-50391
 PbF_2 , rare-earth activated, coloration by γ -irrad. and elec. props. 3-54960
 YAlO_3 :Dy (Ho)(Er)(Tm)(Yb), absorpt., luminesc. spectra, Stark levels, stimulated emission 3-72674
 YAlO_3 :rare earth, absorpt. and emission intensities for trivalent rare earth ions 3-47296
 YAlO_3 :rare earth, nonradiative relax. by multiphonon emission 3-47309
 YAlO_3 : TR^{3+} (TR=rare earth), colour centres, absorption and thermoluminescence spectra 3-44441

rare gases see inert gases**rarefied fluid dynamics**

- see also atomic beams; molecular beams*
 air, heat transfer between coaxial cylinders, meas. ranges 3-63640
 binary gas mixtures, heat conduction between concentric cylinders 3-49525
 binary gas mixtures, mass transfer 3-67942
 Clausing's contribution, review 3-43579
 cylindrical Poiseuille flow and thermal creep 3-49600
 drag coefficients for cones and cylinders using Schamberg's model 3-52474
 flow rate measurement, drift of marker ion electron beam produced supersonic and nonisotropic currents (*Russian*) 3-45622
 free molecular flow, impulsive tridimensional interaction model with solid surface 3-57802
 free molecular flow on concave surfaces, heat transfer and forces 3-46461
 free molecular to continuum flow transition photographic obs. 3-40731
 free-molecule, body drag, Knudsen accommodation coeff. 3-78998
 gas slip, effect on fibrous filters resist. 3-71786
 gas slip flow through porous solids, determ. of mass-flow rate depend. 3-40732
 heat flow birefringence calc. 3-52475
 heat transfer in Knudsen layer, ellipsoidal model 3-54816
 high-speed leading edge problem 3-49599
 hypersonic blunt body merged layer problem, numerical soln. of Navier-Stokes eqns. 3-52466
 hypersonic inlet collection devices for free molecular flow 3-77755
 Knudsen molecular gas, effect of periodic variation of coeff. of heat transfer in mag. field 3-75174
 molecular beams interaction with surfaces 3-57801
 multilayer insulation system, gas flow analysis 3-78997
 nonlinear radial wave propagation in low density expanding flows, application to free jet 3-49628
 plane Poiseuille flow with arbitrary accommodation of tangential momentum (*Russian*) 3-63722
 polyatomic gas, thermomag. gas torque, horizontal field effect 3-60522
 polyatomic gases, behaviour in static mag. field 3-52476
 polymer fibre filter materials, hydrodynamics 3-71787
 rarefied gas, thermal conduction analog 3-67943
 self-diffusion, Green-Kubo formulas and long tail of velocity autocorrelation function 3-54158

rarefied fluid dynamics continued

- shock wave reflection from thermally accommodating wall, molecular simulation 3-71788
 slip flow, hydrodynamic force resisting approach of sphere to wall 3-75230
 sonic nozzle, low-density streams, high pressure drops, transition between continuous and rarefied flow, flow behind a Mach disc (*Russian*) 3-57873
 surface flow, irreversible thermodynamics, straight and cross-coefficients, diffusion and self diffusion 3-46460
 tangential momentum accommodation, Poiseuille flow 3-75231
 temperature measurement, rarefied gas flow, binary gas mixtures, He (*Russian*) 3-46370
 temperature slip problem with arbitrary accommodation at the surface 3-63723
 transient exhaust plume interaction with a rarefied atmosphere 3-43643
 variational principle study of gas flow 3-71785
 weak shock waves in dilute gases, nonlinear Boltzmann kinetic equation 3-71780
 Ar, heat transfer between coaxial cylinders, meas. ranges 3-63640
 Ar, press. ratio effects on flow through square tubes 3-49602
 N_2 , thermomagnetic torque between 75 and 300 K due to boundary layer 3-54787
 N_2 expanding into $\text{CO} + \text{N}_2$ atmosphere, low density supersonic stream, diffusion processes, electron beam techniques (*Russian*) 3-46462

rarefied gas dynamics see rarefied fluid dynamics**rarefied gas flow see rarefied fluid dynamics****Rayleigh law see Rayleigh scattering****Rayleigh limit see Rayleigh scattering****Rayleigh scattering**

- alkanes, halogenated, opt. mol. anisotropy in different media (*French*) 3-63424
 n-alkanes, molecular optical anisotropy, depolarised Rayleigh scattering 3-49469
 atmospheres of late-type stars, importance of molecular Rayleigh scattering 3-65874
 atom and mol. scatt. nonlinear Rayleigh and Raman 3-74282
 benzene, in various solvents, orientational relax. rates, depolarized Rayleigh scatt. meas. 3-50574
 carbon tetrachloride, liquid, meas. using optical fibres 3-62102
 circular polarisation by single scatt. of unpolarised light from lossless nonspherical particles 3-51318
 collision induced in liquids, binary collision model 3-80017
 double well molecule, role of exchange 3-63471
 electrolyte aqueous solns., Rayleigh-Brillouin intensity ratios 3-55992
 gas, rotating linear mol.s., depolarized Rayleigh line, non-Lorentzian shape 3-78828
 globular protein solutions, diffusion consts. 3-67879
 inert gases, low-power He-Ne laser meas. 3-49388
 late-type stellar atm., effects of scatt. by atoms and negative ion absorpt. 3-51330
 liquid, meas. using optical fibres 3-62102
 liquid, mol. motion, high pressure depolarised Rayleigh scatt. obs. 3-79223
 liquid, press. depend. of reorientational motions 3-80055
 macromolecules, very large, in dilute soln., Rayleigh line spectrometry 3-43531
 macromolecules in soln., diffusion consts. determ. 3-78922
 molecular aggregates, microscopic theory, random-phase-modulation theory and stochastic theory 3-70784
 molecule, Brownian motion, spectral density, theory 3-62664
 molecules in liq. state, nonlinear third order polarisability, Kerr effect and Rayleigh scatt. Obs. 3-40605
 p-nitrobenzylidene-p-octyloxyaniline, second order nematic to smectic phase transition 3-58507
 non resonant Rayleigh scattering by a weakly ionised inhomogeneous plasma (*Dutch*) 3-49757
 optically deep absorbing media, interior radiances 3-70760
 partially ionised gases, density fluctuations, e.m. wave scattering theory 3-40764
 pivalic acid plastic crystal, Brillouin and Rayleigh scattering determ. of phonon lifetimes, elastic and optical consts. 3-44409
 planetary atmospheres, multiple scatt. of polarised light 3-61691
 polyoxyethylene oligomers, molecular optical anisotropy, depolarised Rayleigh scattering 3-49469
 polystyrene/butan-2-one dilute solution, translational diffusion 3-67878
 quartz, rel. to critical opalescence, during α - β inversion 3-58571
 quinoline, stimulated scatt. Rayleigh line wing light, fine struct. 3-58502
 ruby laser rod, obser. of scattering pattern of parallel line fringes 3-48953
 simulation with glass tank and light source, student experiment 3-70250
 solid and fluid media, Rayleigh, Brillouin and Raman lines rel. to microscopic processes 3-80024
 succinonitrile plastic crystal, interpretation (*French*) 3-47277
 toluene, in various solvents, orientational relax. rates, depolarised Rayleigh scatt. meas. 3-50574
 vitreous state, Rayleigh, Brillouin and Raman lines 3-80026
 water, depolarised Rayleigh wing scatt. 3-72607
 in waters, radiant energy transfer, effect of multiple scatt. 3-59206
 p-xylene, in various solvents, orientational relax. rates, depolarised Rayleigh scatt. meas. 3-50574
 Al_2O_3 , sapphire, mol. scatt. of light 3-75998
 CO_2 , modification in calc. half-width of depolarised Rayleigh line 3-63436
 CS_2 -carbon tetrachloride soln., optical Kerr effect, depolarised Rayleigh scatt. 3-44403
 n-D_2 , modification in calc. half-width of depolarised Rayleigh line 3-63436
 H_2 , compressed, normal and para, Rayleigh-Brillouin scatt. 3-80032
 n-H_2 , modification in calc. half-width of depolarised Rayleigh line 3-63436
 H_2 , scattering cross section, $\lambda > 1200 \text{ \AA}$ 3-67810

Rayleigh scattering continued

- H₂ mutual diffusion const. in methane, meas. by spontaneous light scattering 3-54790
 4He, spectra obs. near gas-liquid crit. point, dynamic props. determ. 3-50039
 KI, depolarized Rayleigh wing scatt. 3-72607
 K₂SiO₃, glass melt, obs. of super-crit. conc. fluctuations at high viscosity 3-79238
 MgSO₄ solution, depolarized Rayleigh wing scatt. 3-72607
 MnBi films, Rayleigh curve and coercive force 3-68804
 N₂, gas, low-power He-Ne laser meas. 3-49388
 N₂, modification in calc. half-width of depolarised Rayleigh line 3-63436
 NaF, forced Rayleigh scatt. meas. 20 to 300K 3-53099

Rayleigh waves

- Aleutian Island Arc, upper mantle structure determ. from Rayleigh wave dispersion data 3-50895
 amplitude yield scaling, underground nuclear explosions, slope parameter 3-76505
 anisotropic crystal, method for Rayleigh velocity calc., using dislocation theory 3-46749
 anisotropic elastic half-space propag. of seismic waves 3-47611
 atmospheric explosions, theoretical seismograms for Rayleigh waves, yield and burst height effects 3-58879
 attenuation and magnitude relations for eastern North America 3-50921
 azimuthal dependence of Love and Rayleigh surface wave propag. in slightly anisotropic medium 3-61307
 buried explosive sources, topography and Rayleigh wave generating efficiency 3-61308
 Canadian Shield, crustal surface-wave group-vel. anal. 3-61369
 CANNIKIN nuclear explosion, seismic wave meas. 3-50891
 convolver, enhanced Rayleigh surface wave, using piezoelec. CdS 3-42421
 crystal, surface layer, interaction with dislocations, theory 3-64236
 cubic crystals, propag. on (111) face, elastic const. bounds, damping consts. 3-68477
 dispersion, multilayered medium, effect of anisotropic layer 3-44828
 earth mantle group vel., dispersion data 3-56017
 earthquake, southeastern Missouri, surface wave attenuation, crustal anelasticity 3-80618
 earthquake focal depth determ. precision using spectral ratio of Love/Rayleigh surface waves 3-58821
 earthquake M_s, Rayleigh wave magnitude scale 3-61358
 homogeneous three-quarter space, acoustic surface-wave scattering 3-41074
 long-period surface wave enhancement by time-varying adaptive filters 3-61321
 metal, electron absorpt. of Rayleigh sound waves in parallel mag. field 3-49939
 metal, Rayleigh wave absorpt. in mag. fields 3-55453
 mid-ocean ridges, compressive stress effects on wave amplitudes 3-41880
 mode dispersion in spherical earth, equivalent flat-Earth transform. 3-61389
 nuclear explosions and cavity collapses in S. Nevada, radiation of Rayleigh wave energy 3-44785
 oceanic Rayleigh waves, group velocities rel. to oceanic mantle 3-44820
 piezoelectric overlay acoustic surface wave transducer, perturbation theory for electric potential 3-41075
 point mass defect in solid, elastic surface wave scattering 3-58173
 radiation and attenuation of Rayleigh waves from the SE Missouri 1965 October 21 earthquake 3-50922
 reflection and transmission of Rayleigh waves in elastic wedge 3-65151
 reflection in elastic wedge by rigid obstacle, seismological appl. 3-53378
 San Fernando Valley, propag. along N-S section 3-53373
 scattering at vertical discontinuities, finite difference analysis 3-53412
 seismic distance corrections for Rayleigh-wave magnitudes 3-53368
 seismic source parameters determ. using radiation patterns 3-61370
 signal persistence, half-amplitude decay times, random model 3-58899
 Somigliana waves, Rayleigh equation, degeneration to evanescent waves 3-73182
 steel, case hardening depth, detn. using ultrasonics (French) 3-58790
 surface wave propag., spatial coherence 3-58880
 surface waves recorded by large-base quartz extensometers, comparison with long period seismic equipment 3-65164
 surface-to-bulk mode conversion 3-60833
 symmetric undulations of the surface, effect on dispersion curve 3-76503
 teleseismic displacements due to underground nuclear explosions 3-56011
 transducer, interdigital, on piezoelec. substrate, Rayleigh wave prod. and detect. (French) 3-45369
 tsunami and Rayleigh ground waves, warning system using ionospheric technique 3-69748
 Cds, harmonic generation of elastic surface waves, under u.s. amplification conditions 3-64381
 LiNbO₃, acoustic radiation from a high-coupling cut 3-55136
 LiNbO₃, surface acoustic wave attenuation, effect of 80 keV ion implantation 3-52746
 LiNbO₃, guidance, theoretical approach using optical analogy 3-41071

reactance

see also capacitance; inductance

No entries

reactance measurement

see also capacitance measurement; inductance measurement
 h.f., analysis and construction (Japanese) 3-70325

reaction kinetics

see also catalysis; chemical exchanges; chemical reactions; explosions

- acetone heterogeneous decomposition on 20% Cr/25%Ni niobium stabilised stainless steel, kinetics, deposit characterisation 3-71299
 activation parameter determination, modified Varytemp procedure 3-65068
 alkali atom + Br₂ reaction cross-sections 3-73132
 alkali atom + Br₂ reaction cross-sections 3-76454
 alkali atom-dimer exchange reactions, semi-empirical pot. energy surfaces 3-63541
 alkylchlorosilanes with alpha-olefins, addition reactions, i.r. spectroscopic study (Russian) 3-80543
 aromatic hydrocarbons, quenching of triplet states in solution by O₂ 3-61272
 aromatic hydrocarbons, quenching of triplet states in solution by O₂ 3-61273
 aromatic hydrocarbons, quenching of triplet states in solution by NO and free radicals 3-61274
 aromatic nitro-compounds, rate of combustion at high pressures, rel. to temp. of flame (Russian) 3-47539
 Arrhenius' parameters, calc. from Polanyi-Evans equation 3-55944
 asymptotic stability, Onsager fluxes, admissible entropy functions 3-65073
 atom-molecule rearrangement collisions, eikonal approximation in theory 3-76455
 atomic reactions, photochem. air pollution, O and O₃ concs., discharge flow method 3-69605
 attractive nonbonded interactions in organic molecules 3-63373
 ballistic fuel powders, effect of catalysts CuS, CuH and PbS, combustion products and rates (Russian) 3-47546
 bimolecular reactions, collinear, perturbation theory for vibrational transitions 3-73126
 biochemical system, nonequilibrium steady states, finite fluctuation effects, stochastic model 3-65082
 n-butane photooxidation with OH, rate const. determ. 3-69478
 carbothermic, ThN with graphite, effects of temp. and particle size, ThC₂N_{1-x} formation 3-74724
 chemical kinetics, steady-state approx. in differential eqns. 3-44712
 cold flame propagation, speed, limit, chain branching (Russian) 3-69444
 collinear A + BC reaction with model pot. energy surfaces, quantum mech. computational studies 3-44717
 combinatorial theory, stereochem. invariance law and statistical mechanics of flexible molecules 3-53313
 combustion reactions numerical soln. (Russian) 3-80528
 complex reaction systems, parameterisation, model fitting, fundamental kinetics 3-80521
 computer analysis of results 3-73657
 computer simulation, student expt. 3-53822
 cyclopropane isomerisation, CNDO study on alternative mechanisms 3-47548
 differential scanning calorimetry, thermal decomp. solids, activation energy 3-76441
 1,1-difluoroethylene mass spectra, ion-molecule reactions 3-43506
 dimethylcyclobutane, laser-excited fluorescence, ultra-short-lived excited molecules 3-50841
 dinitroxydiethylnitramine (dina), in CO₂ and Ar, pulse calorimetry (Russian) 3-45432
 electrochemistry, thin-layer techniques, applic. to p-aminophenol hydrolysis obs. 3-69467
 electrode-electrolyte interface, multisteady states, reaction path, impedance, local stability (French) 3-73139
 electron transfer reactions, theory 3-53311
 electron transfer reactions theory 3-41842
 exactly soluble kinetic equation, approximation schemes 3-80527
 excimer formation, pulse fluorometry data analysis, decay function Laplace transform 3-62337
 fast highly exothermic reactions, nonequil. vel. distrib. and reaction rates 3-61252
 fluctuations around steady states, phase-space and stochastic descriptions 3-65083
 fluoroethylene and ethylene mixture, ion-molecule reactions, mass spectra 3-43508
 formic acid, reaction coordinate eigenvalue effect on heavy atom kinetic isotope effects 3-76426
 free radical ring cleavage of cis-1,2,3-trimethylcyclopropane by Br, stereochemistry 3-47547
 gas-solid reaction kinetics, rate determ. by filament resistance monitoring 3-45559
 gas-solid transitions, effect of particle size distribution for spherical particles 3-65116
 glass, powder, kinetics of wetting, surface energy and surface tension, modification by siloxanes (German) 3-53279
 graphite, nuclear, reaction with H₂, 600-1150°C, 1-40 atms. (German) 3-71246
 hexagens, rate of combustion at high pressures, rel. to temp. of flame (Russian) 3-47539
 hydrolysis of acetamide and ethyl acetate, solvent effect on reaction rates 3-69457
 impedance plane display of reaction with solution soluble intermediate 3-69450
 internal reflection spectroscopy, electrochem. studies 3-66226
 ion decomposition kinetics, use of double focusing field ionisation mass spectrometer 3-73885
 ion-molecule rate constants, absolute meas. by drift cell ion cyclotron reson. spectroscopy 3-57677
 ion-molecule reactions, surroundings influence on reaction rate and centre 3-55955
 irreversible chemical reactions, stochastic formulation of the kinetics 3-47560
 isotope effect on ion-mole. reaction, energy <10 eV (Rumanian) 3-67859
 kinetic parameters, thermogravimetric data, comparison real and ideal TG curves 3-76437
 laminar boundary layer with combustion on a flat plate 3-40723
 linear macromolecules, kinetics of one dimensional lattice and triplet closure 3-52409

reaction kinetics continued

metal, b.c.c., defect kinetics during annealing, computer anal. 3-79345
 methane, ion-molecule reactions with H_2O , H_2S and NH_3 , resonant cyclotron ejection 3-73118
 methane + methyl cation, ion-molecule crossed beam reaction, short-lived intermediate, scrambling, dissociation 3-73119
 methyl alcohol, ion-polar mol. collision theory, reaction kinetic energy depend. 3-46338
 n-pentane drop, effect of chemical kinetics on combustion (French) 3-76444
 α - and β -naphthalene- d_1 , excited state H-D exchange and fluorescence quenching 3-69475
 nitroglycerine powder, in CO_2 and Ar, pulse calorimetry (Russian) 3-45432
 p-nitrotoluene, reversible reduction, cyclic voltammetry, digital data acquisition system, data analysis 3-70445
 non-isothermal, solid-state thermogravimetric curve 3-76438
 non-isothermal methods, condensed phase, slow and fast reactions, stage reactions (Russian) 3-47535
 perfluoromethylcyclohexane, dependence of radiolysis on dose, O_2 content, temp. and radiation type (German) 3-69481
 polyethylene, struct. changes during annealing and fusion (Russian) 3-80498
 polymeric materials, lifetime rel. to bond rupture kinetics 3-65017
 polymethyl methacrylate in vacuum, CO_2 and Ar, pulse calorimetry (Russian) 3-45432
 Pourbaix diagram, application to molten FI systems and MSR (Spanish) 3-74645
 PVC degradation DTA, Flynn-Wall, Freeman Carroll method 3-76439
 quadratic kinetic potentials, continuously perturbed equivalent classes of asymptotically stable kinetic equations 3-47557
 quasi-thermodynamic mass-action systems, complex graphs 3-73129
 quasi-thermodynamic mass-action systems, reaction diagrams 3-73128
 quasi-thermodynamic mass-action systems, three short complexes 3-73130
 rate constant, first-order, rapid calc. in the student laboratory 3-77360
 rate constants for first order reactions, data acquisition expt. for instrumental analysis 3-53820
 rate of reaction, rational definition for systems of changing volume 3-44714
 rational approach, constitutive equations isothermal, non-isothermal kinetics 3-76433
 reaction schemes, homogeneous phase, damped oscillations (French) 3-76429
 reaction transition states (Conf. Paris, France, Sep. 1970) 3-55950
 salicylic and vanillic aldehydes, chemiluminescence 3-55945
 single component system, reaction in heavy-gas thermostat, disturbance of Maxwellian distrib., effect on reaction rate 3-73131
 singular perturbation method application, Lindemann scheme 3-58796
 solid fuel powder, surface phenomena, linear nonstationary effects, instability (Russian) 3-47545
 solid-fluid reactions, steady state kinetic control 3-58794
 solid-state reactions of particulate ensembles with size distrib. 3-55940
 solvated electrons, attachment to pyrene in several ethers, absolute rate consts. determ. 3-44725
 solvent effect on reaction rates 3-69457
 solvolysis reactions, solvent isotope effects and the transition state 3-55957
 specular reflection spectroscopy, electrode-solution interphase, review 3-66227
 spin exchange frequency determ. from e.s.r. spectra 3-58795
 steel, X18H10T, meas. of corrosion kinetics under n,p-radiation in N_2O_4 3-40546
 steel (4% Mn), kinetics and morphology of surface layer formation in liquid zinc (Polish) 3-72842
 stopped-flow apparatus, with temp. control 3-62383
 symmetry and the activated state 3-55951
 tetrafluoroethylene, mass spectra, thermal ion-molecule reactions by ion cyclotron resonance 3-43507
 thermal curve analysis, conf., Budapest, Hungary, (Jul. 1972) 3-76431
 thermal decomposition, condensed substances, computer-aided kinetic anal. (Russian) 3-47537
 thermal decomposition, under vacuum kinetics 3-76434
 thermal explosion, branched chain reactions, critical conditions (Russian) 3-69443
 thermal explosion during linear heating, mathematical treatment, monomol., bimol. and autocatalytic reactions (Russian) 3-47536
 thermoanalytical measurements evaluation, approximation of temperature integral 3-55947
 thermogravimetric curve, second deriv. kinetic constants, decomposition reactions 3-76436
 thermogravimetric data analysis, graphical methods comparison 3-55948
 thermogravimetry, reaction order estimation from differential curve 3-55949
 thermokinetic study of slow reactions by conduction microcalorimetry (French) 3-55946
 thin film nucleation kinetics, additional processes 3-79596
 trajectory analysis of transition states 3-55958
 transfer of heat and mass for 2 reacting species with temp. dependent reaction constant 3-65065
 trifluoroethylene, mass spectra, thermal ion-molecule reactions by ion cyclotron resonance 3-43507
 trolyl nitroethers, rate of combustion at high pressures, rel. to temp. of flame (Russian) 3-47539
 turbulent, flame anal., combustion of gas mixture, thermochemistry, kinematic characteristics (Russian) 3-47542
 in turbulent flow system, consecutive chem. reactions 3-49619
 AgBr, photographic emulsion, kinetics of development, ascorbic acid and 2-chloro-4-aminophenol, filamentary growth 3-53341

reaction kinetics continued

AgBr photographic sol conversion to AgI, reaction kinetics, turbidimetric studies effect on gelatin protection and unsubstituted polyethylene oxides 3-53338
 Ar, dimer formation, mol. dynamics study 3-40680
 $Ba(OH)_2 \cdot 8H_2O$ decomposition, solid state, kinetic parameters 3-76432
 Br, ground state, recomb. kinetics at 298K 3-47556
 C black, thermal self-ignition, nonuniform surface, critical temp. computer calc., reaction kinetics (Russian) 3-50830
 CO pulsed chemical laser with photoinitiated oxidation of CS_2 3-74234
 $CO + OH \rightarrow CO_2 + H$, rate consts. determ. 3-41840
 CO^+ collision-induced dissociation near threshold, energy dependence of cross-section 3-76451
 CO_2 production kinetics in Venus' atmosphere rel. to inferred surface temp. 3-61683
 $CO_2H^+ + CH_4 = CH_3^+ + CO_2$, equilib. const. meas. at variable temps. 3-55930
 $CaCO_3$ thermal analysis of kinetic data, heterogeneous processes 3-76435
 α $CaSO_4 \cdot 1/2 H_2O$ thermal analysis of kinetic data, heterogeneous processes 3-76435
 $Cd_{1-x}Mn_xFe_2O_4$ ferrite, formation kinetics, densification 3-76304
 $Cl + DH \rightarrow DCl + H$, temp. dependence of intramolecular kinetic isotope effect 3-76424
 $Cl + HD \rightarrow HCl + D$, temp. dependence of intramolecular kinetic isotope effect 3-76424
 Cs + RbCl collisions, branching ratios, statistical approximation 3-75146
 $CsI + Xe \rightarrow Cs^+ + I^- + Xe$, collisional dissociation 3-76449
 CuO in phosphoric acid, using pH meter 3-76423
 $D^+ + H_2 \rightarrow HD + H^+$, reaction rate meas., interstellar appl. 3-65936
 DNO, chemilum. spectra in reaction of $O(P)/O_2$ with NO and hydrocarbons or aldehydes 3-76419
 F gas phase reaction rates w.r.t. F + NO + Ar chemilum. process 3-69441
 F + $C_6D_6 \rightarrow D + C_6D_5F$, ang. depend. and recoil-energy spectrum of products 3-73123
 F + $DF(v) \rightarrow DF(v') + F$ vibr. relax. process, rate consts., Monte Carlo calcs. 3-60486
 F + $H_2 \rightarrow FH + H$ collinear reaction, quantum, quasi-classical and semi-classical reaction probabilities 3-76457
 F + $H_2 = HF + H$, variational calc. of reaction rates 3-73120
 F + $HF(v) \rightarrow HF(v') + F$ vibr. relax. process, rate consts., Monte Carlo calcs. 3-60486
 F + olefins (dienes), unimol. decomp. of long-lived complexes 3-73122
 Fe oxidation, kinetics of thin film formation using proton impact excited X-ray analysis 3-50087
 H transfer, reaction kinetic isotope effect rel. to substituents in systems with benzene derivatives (German) 3-44709
 H + Br_2 , rate consts. determ., classical trajectory calcs. 3-41844
 H + $Cl_2 \rightarrow HCl + Cl$, H isotope effects and rate consts., reaction coord. eigenvalue and eigenvector variations 3-47552
 H + $ClF_3 \rightarrow HF + Cl + 2F$, kinetic study 3-73125
 H + H_2 , isotopic collinear reactions, exact quantum mech. reaction probabilities and rate consts. 3-55937
 H + H_2 collinear reaction, time delays, phase behaviour and resonances 3-76456
 H + $H_2 \rightarrow H_2 + H$ collinear reaction, streamlines of probability current density and tunnelling fractions 3-76458
 H + HBr, rate consts. determ., classical trajectory calcs. 3-41844
 H + NF_3 reactions in moderately fast flow system, e.s.r. and mass spectrometric studies 3-76430
 H + negative ions, associative-detachment reactions at thermal energy 3-49418
 H_2 , inflammation and combustion, numerical anal. of kinetic models, delay time meas., effect of H_2O vapour (Russian) 3-47541
 H_2 , second-order inflammation effect of ethane additions (Russian) 3-47540
 $H_2 + OH \rightarrow H_2O + H$, rate consts. determ. 3-41840
 $H_2^+ + He \rightarrow H + HeH^+$, crossed-beam meas. 3-75144
 $H_3^+ + D_2 \rightarrow D_2H^+ + H_2$, energetics of proton transfer 3-75145
 HCl, reaction with O_2 in electrodeless r.f. discharge 3-80530
 $HCl + e^- \rightarrow H + Cl^-$ reversible, kinetics of Cl^- formation in atmospheric pressure flames 3-73127
 $H(D) + NO_2$, isotope effect on reactive differential cross-section 3-73133
 HNO, chemilum. spectra in reaction of $O(P)/O_2$ with NO and hydrocarbons or aldehydes 3-76419
 H_2O_2 , Fe(III) catalysed decomp., calc. rate consts., activation energy, computer program 3-77373
 $He^+ + O_2 \rightarrow He + O + O^+$, dissociative charge transfer, chemical dynamics 3-76450
 $Hg(P)$ photosensitization of paraffins, energy transfer mechanism 3-50844
 $Hg_6(P_6)$ photosensitized decomposition of propane 3-50843
 I, atomic recomb. reactions and rate const. determ., classical trajectory calcs. 3-41843
 $MgCO_3$ thermal analysis of kinetic data, heterogeneous processes 3-76435
 N + N + N $\rightarrow N_2 + N$ recombination velocity const., low temp. non catalytic coatings (Russian) 3-63610
 N_2-N_2O mixture, expanding supersonic jet, rapid cooling, dissociation reactions (Russian) 3-57872
 $NH_2^- + H_2 = H^- + NH_3$, rate consts. and $D^0(NH_2-H)$ derivation 3-55931
 NH_3 ion-molecule reactions, relative rate constant 3-63556
 NH_4ClO_3 , and its polystyrene mixtures, catalytic decomposition, kinetics and mechanism, dynamic mass spectrometry, thermogravimetry (Russian) 3-47538
 $N_2O_4 \rightarrow 2NO_2 \rightarrow 2NO + O_2$ reversible reaction in turbulent flow heat and mass transfer determ. (Russian) 3-76447
 N_2O_4 chemically reacting system, thermodynamic parameters (Czech) 3-44713
 $N_2OH^+ + CO = COH^+ + N_2O$, equilib. const. meas. at various temps. 3-55930
 Na + $N_2O \rightarrow N_2 + NaO$, room temp., photometric obs. 3-80524

reaction kinetics continued

- NiO powder, reduction, nucleation rate, kinetics rel. to Neel transition 3-55164
 $O + CS_2 \rightarrow SO + CS$ in crossed beams 3-76452
 $O + HBr \rightarrow OH + Br$, react. probabilities, quantum and transition state theories 3-80534
 $O + HBr \rightarrow OH + Br$, react. probabilities, quantum and transition state theory 3-80535
 $O +$ olefins reaction, direct rate meas. showing negative temp. depend. 3-65075
 $O + N_2$ to $NO + N$, reaction rate coeff. for ionospheric F-region, drift tube meas. 3-69742
 $OH + NH_3 \rightarrow NH_2 + H_2O$ reaction absolute rate const., pulsed photolysis obs. 3-65076
 $OH + O_3 \rightarrow HO_2 + O_2$ reaction, rate const., 220-450 K, u.v. fluorescent scatt. obs. 3-41835
 $OH + OH \rightarrow H_2O + O$, rate consts. determ. 3-41841
P atoms, electronically excited by PCl_3 , collisional quenching, kinetics rel. to ionisation potential, atomic spectroscopy 3-49415
Pt-Si contact, heat-treated, interface struct., solid state reaction kinetics 3-69485
SiC, etching by Na_2O_2 , effect of dislocations 3-68508
 SiH_4 , endothermic ion-mol. reactions 3-40666
 $Sr(OH)_2 \cdot 8H_2O$ decomposition, solid state, kinetic parameters 3-76432
 $T + H_2$, $T + D_2$, and $R + HD$ exchange collisions in 10 eV range, prediction of spectator stripping dynamics 3-76453
 $Th + O(O_2)$ (N_2O) vapour oxidation, chemi-ioniz. 3-80533
 TiO_2 - SiO_2 glasses, e.p.r. study of Ti^{3+} - Ti^{4+} reaction 3-76418
 $U + 3/2H_2 \rightarrow UH_3$, kinetics study 3-61255
 $U + O(O_2)$ vapour oxidation, chemi-ioniz. 3-80533
UC, compatibility with stainless steel bonded with sodium, carbon transfer kinetics 3-43307
W, chem. vapour deposition kinetics, 6-60 Torr, 500-870°C 3-41628
Zn thin film deposition on surfaces of Ge single crystals 3-61110

reaction rates see *reaction kinetics***reactions (chemical)** see *chemical reactions***reactions (nuclear)** see *nuclear reactions and scattering***reactors (nuclear)** see *nuclear reactors***read-only storage**

magnetoelectric effect application 3-44202

readout, digital see *digital readout***real time computer systems** see *real-time systems***real-time systems**

see also *online operation*

- APT scanning radiometer data, technique for real-time quantitative display 3-51168
computer control of marine exploration, handling seismic, gravitational and magnetic data 3-65494
holography, large mirror structures, elastic behaviour (*German*) 3-45480
liquid crystal Fourier plane filter 3-77428
three-dimensional display system 3-77523

receivers

see also *acoustic receivers*; *radio receivers*

- n.q.r. pulse radiospectrometer, resolving power, effect of spectral width, passband of receivers 3-48487

receiving antennas

- v.l.f. radio wave field, distortion by vertical metal poles 3-76900
wideband, appl. to radioastronomy 3-59398

recombination, electron-hole see *electron-hole recombination***recombination, ion** see *ion recombination***reconnaissance satellites** see *artificial satellites***record players** see *gramophones***recorders**

see also *recording*; *tape recorders*

- analogue recorder for geophysical appl. 3-56236
dielectric dispersion, data acquisition, for low loss liquids, voltage standing wave amplitude obs. 3-42602
ectopic beat recording display system 3-48605
maxometer for sensing and recording peak wind speed 3-56254
Mossbauer spectrometer, multichannel pulse analyzer, const. vel. mode 3-73914
optical absorption spectra, automatic recording on tape (*Russian*) 3-62100
seismic digital recording system 3-53544
startle response of small animals, digital isometric recording system 3-62304
tensometer, with air gap capacitance transducer, for linear meas. 3-53842
two-coordinate, stress/strain measurement applic. 3-76406
video-to-film colour image recorder, laser applic. 3-73800
X-Y tape recorder, polar coordinate design, for recording small light sources (*German*) 3-45469

recording

see also *audio recording*; *magnetic recording*; *video recording*

- acoustic hologram, using 2MHz transmitter/receiver 3-53846
automatic water uptake by plants 3-59685
bioassay, urine automatic, urine flow, conductivity, antidiuretic-hormone bioassay 3-73932
biological phenomena, polygraphs improving efficiency 3-48604
boreholes, e.m. logging by attenuation (*Russian*) 3-76898
central nervous system employing photoengraved microelectrodes 3-45262
computer-generated holograms, low-noise recording methods 3-54201
electrostatic, pressure electrode arrangements (*German*) 3-59835
holographic, spatial frequency multiplexing, storage density improvement 3-59598
hydraulic cylindrical probe, boreholes, resistivity data (*Russian*) 3-76897
i.r. laser addressing of media 3-48957
ocean devices, legal problems (*French*) 3-52623
porosity, solid conducting inclusions, from specific resistivities (*Russian*) 3-76896
radioactive data, productive strata, porosity and clay content (*Russian*) 3-76895

recording continued

- Raman spectra, high speed system, image conversion, oscilloscope output 3-73756
spark gaps, predischarges (*German*) 3-60646
spectra, automation of meas. by points 3-73758

recording instruments see *recorders***recovering** see *recovery***recovery**

- alloy, precip. hardened, heat treated under relative stable conditions, recovery creep props. 3-69313
alloys, long-lived vacancies, relaxation technique, elec. resistivity, kinetics of adjustment to temp. jump 3-48466
glass reinforced plastic, and creep, in uniaxial tension 3-58711
graphite, Young's modulus, annealing and pre-stressing effect 3-41816
metal, b.c.c., low temp. neutron irradi. effects, annealing recovery depend. 3-79381
Nimonic 90 and 108, tensile and compressive creep behaviour interpret. 3-58667
Nylon 6, glass fibre reinforced, compressive creep and recovery 3-47456
PMMA, creep and low-cycle fatigue, hereditary theory 3-65015
polycarbonate, creep and recovery behaviour under high tension and compression stresses 3-47470
polyethylene, periodically loaded lifetime and recovery of isotropic specimens, superposition principle 3-80481
polymethane, rigid, porous, vibrocreep, recovery 3-73052
quench hardening, isothermal recovery 3-64920
rubber, creep and stress relax., stress history and temp. changes 3-58731
steel, austenitic, stainless, Type 316, microstruct. stability of thermal-mechanically pretreated type 3-47392
steel, austenitic stainless, irradi., with Ti and B additions, high-temp. deform. and fracture 3-63188
steel, extra mild, recrystallisation, texture, Al passivation (*French*) 3-76173
steel, ferrite-class, substructure and its effects on mech. behaviour (*Russian*) 3-53225
steel, neutron irradiation, embrittlement and annealing, model based on Davidenkov criterion 3-72914
steel, UHB stainless 724LN, austenitic, improved creep strength mechanism 3-69324
uniaxial creep recovery and stress relax., model based on residual stress distrib. 3-58666
wire, work hardening induced residual stress recovery, temp. and holding time depend. (*French*) 3-61170
Ag, plastically deformed, elec. resist. and thermo-e.m.f. meas., defects contrib. (*Russian*) 3-79663
Ag, recrystallisation, moving grain boundaries, internal friction (*French*) 3-72875
Ag films, ultrahigh vacuum deposited on cold substrate, reverse recovery process interpret. 3-64263
Ag⁺, photographic fixing soln., phenylthiourea selective resins, ion exchange, polarographic Ag anal. 3-53335
Al-Zn-Ag alloy, structural change determ. $AgZn_3$ metastable phase characteristics (*Russian*) 3-80256
Au, plastically deformed, elec. resist. and thermo-e.m.f. meas., defects contrib. (*Russian*) 3-79663
Au sputtering yield variation with ion dose, dislocation loop explanation of recovery time 3-61087
Be, deformed, elec. resist. variation during recovery, kinetics (*Russian*) 3-69266
BeO, neutron irradi. sintered, He gas release and diffusion processes (*German*) 3-57568
Cu, deformed in polyslip, structure sensitive recovery 3-76172
Cu, high temp. creep, stress-change expts. 3-76206
Cu, plastically deformed, elec. resist. and thermo-e.m.f. meas., defects contrib. (*Russian*) 3-79663
Cu alloys, dil., electron-irradi., stage II recovery 3-79374
Cu recrystn. and recovery after heavy rolling, h.v. electron microscope obs. 3-50702
Cu-Al alloy, deformed, recovery during heating, mechanism (*Russian*) 3-58643
Cu-P alloy recrystn. and recovery after heavy rolling, h.v. electron microscope obs. 3-50702
Cu-Sn alloy, martensitic transform., deform. and recovery of form (*Russian*) 3-69189
Fe, high temp. creep, stress-change expts. 3-76206
Fe, $YbNDK35T5$, damage-recovery heat treatment effects (*Russian*) 3-72486
Fe alloys, substitutional, static strain aging 3-69280
Fe-Co-V atomic order recovery, influence of vacancies, X-ray diffraction study (*French*) 3-58638
Fe-Cr-Ni alloys, recovery and recrystn. of austenite 3-69285
Fe-Ni alloys, struct. modifications during recovery of equil. by tempering subsequent to cooling 3-64930
Fe-Ni-Mo and Fe-Ni-Co-Mo maraging alloys, redistrib. of alloying elements during recovery (*Russian*) 3-80312
Fe-Ni-W alloys, struct. changes during ageing of martensite (*Russian*) 3-80247
Fe-V alloys, low temp. ductility, recovery heat treatments influence 3-53257
GaAs, photolum. and laser props., recovery kinetics after 600 keV electron irradi. 3-72716
Ge, deformed threadlike crystals on annealing 3-68312
n-Ge, electron bombardment induced annealing stages, model 3-64067
KBr, stored energy meas. after 4.6K reactor irradi. 3-54984
KBr:Na, thermal recovery of radiation hardening, thermoluminescence and thermal decay of V_i band 3-68247
KCl, ion irradi., channelling study 3-52652
LiF, ion irradi., channelling study 3-52652
 Li_2O - ZnO - SiO_2 , glass-ceramic, compression creep and recovery, 590-750°C 3-76320
Mo, electrical resistivity recovery stages III and IV, vacancy vs. interstitial migration 3-60722
Mo, neutron irradiation and plastic deformation, recovery model critical testing 3-79382
NaCl, ion irradi., channelling study 3-52652

recovery continued

NaCl single crystals, deformed, annealing, n.m.r. studies (*Russian*) 3-64093

Nb, cold deformed, short-term heat resist., gaseous medium influence (*Russian*) 3-80427

Nb, recovery after fast neutron irradiation at low temp. 3-68287

Ni, deformed in polyslip, structure sensitive recovery 3-76172

Ni-Co-W alloys, struct. changes during ageing of martensite (*Russian*) 3-80247

²³⁸PuO₂, annealing of self-radiation damage 3-79389

RbCl, migration energy of Sr²⁺ impurity-vacancy dipoles 3-43902

Si, plastic deform. during stage II 3-58074

TiNi intermetallic, shape memory effect obs. (*Russian*) 3-80310

UO₂, in-reactor radiation induced creep behaviour 3-54543

UO₂ bars, thermally shocked, crack healing, isothermal annealing effect 3-74727

V, recovery after fast neutron irradiation at low temp. 3-68287

V:O neutron irradi., and radiation anneal hardening, recovery and temp. depend. 3-79383

Zn, high temp. creep, stress-change expts. 3-76206

Zn, low-temperature electron irradiation effects 3-60744

Zr, neutron irradi., resist. changes, recovery changes 3-69288

Zr, neutron irradi. at 24K, point defect creation and elimination (*French*) 3-52643

Zr and alloys, cold work and stress-relieving effect on irradiation growth behaviour 3-41773

recrystallisation

β -alanine, X-irradi., recrystn. effect on e.s.r. spectra 3-55970

alkali borate + TiO₂ mixtures, fused, acid-based reactions 3-58818

alloy, recrystn. texture prediction (*Russian*) 3-72848

Berycolloy, effect of additives on annealing texture 3-61136

CZC, effect of additives on annealing texture 3-61136

electron microscopy, 1 MeV, in situ obs. 3-50704

Fe film, cylindrical, annealing effect on long. and transverse Procopiu effect (*Rumanian*) 3-68817

Havero meteorite, interpretation of obs. 3-45070

lunar anorthosite rocks, natural exoemission, recrystallisation, deformation history 3-77007

metal, recrystn. texture prediction (*Russian*) 3-72848

Nimcolloy, effect of additives on annealing texture 3-61136

Nimonic 108, grain boundary sliding and recrystn. during creep 3-58634

quartz, plastically deformed, transmission electron microscopy obs. of dislocation structure 3-58038

quartz, syntectonic recrystallisation and texture development 3-61326

quartz, synthetic, ion damage, fluence depend. 3-60748

refractories, kinetics of grain growth, deformation 3-72976

steel, austenitic, stainless, Type 316, microstruct. stability of thermal-mechanically pretreated type 3-47392

steel, austenitic stainless, α -irradi., recrystn. influence on high-temp. embrittlement 3-44614

steel, austenitic stainless, crit. work hardening of nucleation and migration for recrystn. (*French*) 3-61152

steel, Cr-Mo-Ni, softening of austenite, effect of deformation, appl. to recrystn. (*German*) 3-72888

steel, deformation, Nb effect, thermodynamic calc. (*French*) 3-72872

steel, extra mild, texture, Al passivation effect (*French*) 3-76173

steel, ferrite-class, substructure and its effects on mech. behaviour (*Russian*) 3-53225

steel, high-C, dynamic elasticity and vib. decrement, 20-1200°C, obs. and mechanism (*Russian*) 3-53249

steel, high-strength 4340M, grain refinement effect on microstruct. and mech. props. 3-64854

steel, low-C austenite, transform. to ferrite after small plastic strains 3-58615

steel, low-C chromium, M₂C to M₇C₃ transform. 3-80210

steel, metastable austenite form. during heating (*Russian*) 3-44601

steel, structural inheritance, overheating and tempering temp. depend. 3-80282

steel melt, precipitation hardening 3-76214

texture of sheet, three-dimens. represent. (*French*) 3-61151

welding, grain growth inside material and at joints (*Russian*) 3-72925

Ag, deformed, local internal friction determ. during recrystn. (*French*) 3-55028

Ag, deformed by rolling, recrystn. kinetics from internal friction (*French*) 3-55029

Ag, high internal friction, dislocation network (*French*) 3-72875

Ag, point defects influence, internal friction obs. (*French*) 3-64111

Al, energy scatt. of vibrs. after plastic deform. and annealing 3-55807

Al, imperfect structure after low-temp. rolling and annealing (*Russian*) 3-69208

Al alloy D16, microstructures during stabilized hot deform. stage (*Russian*) 3-53219

Al compressed commercial pure, annealing behaviour, polygonisation, recrystallisation and grain growth kinetics 3-41769

Al etch pit shapes rel. to recrystn., orientation relationships (*French*) 3-44584

Al-Zn alloys, axisymm. extrusion, activation enthalpy and material consts. depend., relation to recrystn., substruct., mech. props. 3-47403

Al-Zn-Mg alloys, axisymm. extrusion, activation enthalpy and material consts. depend., relation to recrystn., substruct., mech. props. 3-47403

Au films on NaCl (001) substrate, electron microscopy and diffraction obs. 3-72293

Au films on NaCl (001) substrate, X-ray measurement of strains 3-72294

B₂O₃-MnFe₂O₄ partially devitrified glass, mag. props. and recrystallisation study 3-55410

BaFe₁₂O₁₉, recrystallisation under 20 bar of O₂ 3-72808

Cd, recrystallized during hot deform., orientation of grain boundaries 3-80262

Cr thin films, recrystallisation during aging (*Russian*) 3-60845

Cu, crit. work hardening of nucleation and migration (*French*) 3-61152

recrystallisation continued

Cu, deformation in high speed cutting, cut surface obs. (*Russian*) 3-80257

Cu, driving force depend. of recrystn. rate, single crystals. (*German*) 3-55791

Cu, polycryst., moving grain boundary interaction with surface foreign particles (*Russian*) 3-80246

Cu, recrystn. and recovery after heavy rolling, h.v. electron microscope obs. 3-50702

Cu, recrystn. kinetics, omnidirectional press. influence (*Russian*) 3-50691

Cu, softening of single crystals. deformed by rolling (*Russian*) 3-44573

Cu, under hydrostatic press. up to 15 kbar during annealing 3-47373

Cu-Ni-Zn alloys, high strength microduplex, characteriz. 3-64911

Cu-P alloy recrystn. and recovery after heavy rolling, h.v. electron microscope obs. 3-50702

Fe, high-purity, dislocation pattern, recrystn., influence of tempering, rolling (*German*) 3-72846

Fe alloy, high-C, dynamic elasticity and vib. decrement, 20-1200°C, obs. and mechanisms (*Russian*) 3-53249

Fe-Cr-Ni alloys, deform. recovery and recrystn. of austenite 3-69285

Fe-Ge alloy, deformation texture 3-76177

Fe(CIO₄)₂.6H₂O aqueous soln., frozen, Mossbauer effect, thermal analysis, phase separation 3-41453

Fe(CIO₄)₂.6H₂O aqueous soln., frozen, Mossbauer effect, thermal analysis, phase separation 3-41452

KCl, hot worked, strength and deformation rel. to microstruct. 3-76252

KCl, press forged, strengthening effects 3-45502

Mg, rel. to deformation temp. and purity (*French*) 3-69234

Mo, deformed, struct. stability and mech. characteriz. under prolonged influences of temp. and stress 3-44630

Mo alloy sheet, surface layer struct., X-ray analysis 3-76175

Nb, cold deformed, short-term heat resist., gaseous medium influence (*Russian*) 3-80427

Nb single crystals, deformed in rolling at 77K, defect struct. (*Russian*) 3-58627

Ni, annealed, centre growth rate, X-ray diffraction study 3-72861

Ni, deformation in high speed cutting, cut surface obs. (*Russian*) 3-80257

Ni, electrodeposited dispersion-hardened thin films, electron micrographic exam. 3-61142

Ni, etch pit shapes rel. to recrystn., orientation relationships (*French*) 3-44584

Ni, thoriated, impurity induced recrystn. 3-64849

Ni 270 work hardened in tension, annealing twins role in primary recrystn. (*French*) 3-44585

Ni composite, W(Mo) wire reinforced, diffusion, carbide layer formation, recrystallisation rel. to weakening (*Russian*) 3-53272

Pb, during plastic deformation, rel. to exoemission 3-69146

α -SiC, recrystallisation during reactive sintering 3-80433

Ti-C system, grain growth kinetics 3-64877

β -Ti-Mo-Cr-Fe-Al alloy, microstructure, texture 3-76178

Ti-O system, grain growth kinetics 3-64876

Ti-V-Cr-Al metastable alloy, recrystallisation and X-ray diff. invest. of age-hardening (*German*) 3-72880

W, wire, creep, impurities, research review (*Hungarian*) 3-72989

W sheets, recrystn. texture (*German*) 3-55792

W-Ta-ZrC alloy, deformation depend., microstructure 3-76334

W-ThO₂ (1 wt.%) wire, heating rate effects 3-64857

Zr single crystals, compression parallel to c-axis, 78-1100 K 3-46659

rectangular waveguides

e.m. wave, SHF, propagation in magneto active plasma (*Russian*) 3-79066

junctions partially dielectric-filled, e.m. wave propagation 3-42832

microwave reflection from plasma column 3-46551

open dielectric resonator, forced oscillations 3-70686

partially loaded with electro-optical material, travelling wave laser phase modulator applic. (*Korean*) 3-77544

transition radiation in a rectangular waveguide (*Russian*) 3-57192

rectification

image rectification, using electro-optical rectifier 3-53926

Al/tetracene/Au sandwich cell 3-46904

Ta₂O₅ anodic film, elec. cond., rectification, transport processes and electronic struct. 3-46839

rectifier tubes

No entries

rectifier valves see rectifier tubes

recursive functions

seismograph transfer function numerical inversion by recursive filtering (*French*) 3-76511

red giants see stars

red shift

see also cosmology; Doppler effect; gravitational red shift

4C 05.34, absorption spectra, search for high ionisation redshift systems 3-77116

3C 286, 21 cm absorpt. at z=0.692, implications for intergalactic medium 3-73525

clusters of galaxies, possible systematic red shifts 3-56420

clusters of galaxies, redshift-magnitude bands 3-48086

Coma cluster, redshift magnitude banding, model 3-48107

Coma cluster of galaxies, red shift-morphological type relationship 3-61842

companion galaxies, study of differential vels. 3-56431

galactic clusters and pairs relation with surface brightness 3-77138

galactic positronium-formation red shift of 511 keV annihilation line 3-70018

galaxies, distant clusters 3-77146

galaxies, redshift-distance relation, absolute magnitudes of brightness galaxies in clusters 3-70007

galaxies, redshift-distance relation rel. to Galactic latitude and models 3-70005

galaxies, redshift-distance relation rel. to Hubble diagram for rich clusters and sparse groups 3-70006

galaxies, velocity-distance relation clusters, brightest galaxy forms 3-81166

red shift continued

- galaxies identified with 4C radiosources, redshifts for 51 objects 3-51382
- galaxies redshifts for nine objects below declination 60°S 3-48087
- galaxy-quasar pairing, z-angular separation relations 3-53685
- Hoyle and Narlikar's (1971, 72) cosmology, critique 3-56309
- intergalactic absorption effect on magnitude-redshift and count-magnitude relations 3-70023
- intergalactic matter enrichment rel. to red shift 3-53695
- liquid crystal, cholesteric mesophases, helical struct. press. depend. 3-46586
- Markarian 132, QSO, identification of lines of absorpt. spectrum 3-59356
- metagalaxy kinematics, apparent magnitude-redshift relations, special relativity 3-76961
- microwave background radiation, temp. at large redshifts 3-59352
- NGC 1068, Seyfert galaxy, red shift of H α and H β lines 3-56422
- NGC 7319 in Stephan's quintet, non-velocity redshift rel. to NGC 7320, radio obs. 3-48092
- OQ172, second QSO with $z > 3$, Lick obs. 3-45207
- PHL 938, absorption spectra, search for high ionisation redshift systems 3-77116
- PHL 957, absorption spectra, search for high ionisation redshift systems 3-77116
- PKS 0237-23, absorption spectra, search for high ionisation redshift systems 3-77116
- QSOs, redshift-magnitude relation 3-69981
- quasar absorpt. red shifts rel. to black holes and jet mechanism 3-48066
- quasar redshift-angular size diagram interpretation, cosmological aspects 3-51362
- quasar-clusters of galaxies red shift associations 3-56403
- quasars, division into two types 3-45150
- quasars, Hubble diagram 3-48096
- quasars, redshift rel. to scintillation visibility 3-48055
- quasars with $Z \geq 0.3$ rel. to Abell clusters 3-61836
- quasistellar object redshift distributions, their interpretation 3-73526
- radio sources, existence of intergalactic gas 3-53706
- radiosources, spatial distrib. rel. to number counts and redshift meas. 3-42211
- review of new data, consequences for physics 3-81121
- RHL 5 model universe, predicted redshifts and number counts of extragalactic objects 3-80920
- Stephan's quintet, non-velocity redshift of NGC 7319 rel. to NGC 7320, radio obs. 3-48092
- Stephan's Quintet of interacting galaxies, H II region and supernova obs. 3-70004
- Tom 256, galaxy/quasar-like object, spectrum of extra-nuclear regions 3-45183
- TON 1530, absorption spectra, search for high ionisation redshift systems 3-80920
- U1 model universe, predicted redshifts and number counts of extragalactic objects 3-80920
- Virgo cluster, apparent distribution and radial velocity 3-81173
- AgBr, epitaxial attachment of dye aggregates to surface, ligand bonds red shift, benzothiazolocarboquinone 3-53342
- AgBr, optical absorption from room temp.-1000K, obs. of red-shift of absorption edge (German) 3-53119
- AgCl, optical absorption from room temp.-1000K, obs. of red-shift of absorption edge (German) 3-53119
- AgI, optical absorption from room temp.-1000K, obs. of red-shift of absorption edge (German) 3-53119

reduction (chemical) see oxidation**redundancy**

- visual information, redundancy reduction by contour separation (Russian) 3-70130

redundancy theory see redundancy**reed relays**

- chopper application, magnetically driven, for potentiometry on thermoelectric samples 3-39970
- contact plating, d.c. sputtering, modified configuration for improved deposition rates 3-53873

reeling see winding (process)**reference circuits**

- reference voltage source 3-45411

references (standards) see standards**reflectance** see reflectivity**reflection**

- see also acoustic wave reflection; electromagnetic wave reflection; neutron reflection; reflectivity
- close binary stars, eclipsing, model, reflection effects, temp. distrib. 3-51327

- corona, black and white photographic film, contact and projection methods (Russian) 3-45522
- elastic waves, from free boundary in hexagonal metals 3-46677
- ellipsometry, principles of technique, application to electrochem. studies, review 3-66196
- geological cross section, methods of processing seismic recordings (Russian) 3-76887
- Helmholtz eqn. and wave propagation in inhomogeneous media 3-48708
- internal, multiple, in fluorescence spectrometry 3-66414
- internal reflection spectroscopy, electrochem. studies 3-66226
- internal reflection spectroscopy, water, aqueous solutions, i.r. spectra 3-75042
- planetary atm., photon path length distrib. for diffuse reflection 3-65739
- Rayleigh wave reflection in elastic wedge by rigid obstacle, seismological appl. 3-53378
- seismic data, three dimensional interpretation, velocity distributions 3-76840
- seismic data interpretation, structure and modification of optimum algorithms (Russian) 3-47650
- seismic wave shear reflection method for Tatariya region (Russian) 3-47651
- seismic waves, common-depth point time-depth curve for nonlinear boundary and reference overlying layer (Russian) 3-47649
- shock wave, glancing, in parallel flow of ideally dissociative gas in magnetic field (Russian) 3-67936

reflection continued

- single and multiple waves, dynamic properties (Russian) 3-76647

reflection nebulae see nebulae**reflectivity**

- see also electroreflectance; magnetorelectance; piezorelectance; thermorelectance
- adsorbed species, effect of surface roughness of interface 3-47334
- alkali halides, refl. meas., surface effects 3-58494
- alkali metal nitrates and carbonates, longit. mode freqs., PSR i.r. spectra 3-75975
- alkaline earth nitrates and carbonates, longit. mode freqs., PSR i.r. spectra 3-75975
- antireflection coating incident light illuminator, measuring microscope, VEB Carl Zeiss JENA 3-51586
- asteroids, polarisation curve slope albedo relationship 3-56363
- asteroids, spectral reflectivities of 36 objects rel. to 22 ordinary chondritic meteorites 3-61740
- dielectric mirror coating, meas. using laser beam 3-66186
- diffuse and specular components, apparatus for measurement 3-77476
- fluorescent samples, comparison of methods for reflectivity determination 3-77475
- III-V compounds and alloys, modulated reflectance measurements for direct band gap 3-58210
- ionospheric meas. from 6 to 35 kHz 3-65446
- i.r. measurement using lamination screen interferometer (German) 3-48434
- irradiance reflectivity in and above ocean 3-59024
- laser mirrors, periodic multilayer dielectric system of ZnS and MgF₂, normal incidence, design formulae and graphs 3-45505
- layers, multiple, reflectance and transmittance rel. to Kubelka-Munk theory (German) 3-77967
- liquid crystals, cholesterol type, reflection coeff., registration of half tone photographic images (Russian) 3-45521
- lunar dust, far u.v. meas. of Apollo 11, 12 and 14 samples 3-45041
- lunar soil, remote optical analysis 3-65802
- lunar spectral reflectivity, meas. of Mare Humorum 3-56352
- meteorites, spectral reflectivities of 22 ordinary chondrites rel. to 36 asteroids 3-61740
- pyrrhotite, comparison with troilite 3-50879
- radar, loss of information on weather patterns due to finite sample volume 3-76761
- rare earth metals, free-ion energy levels, comparison of calc. and expl. values 3-52795
- reflectometers analysis, power equation concepts 3-57115
- sea ice radiation, Antarctica, spectral composition, reflectivity rel. to sea ice 3-80774
- solids, optical props. measurement, review (French) 3-41494
- spectral reflectivity difference detection, isoluminous additive colour method, lunar orbital multispectral photography 3-45517
- sub-monolayer molecular films, equation for specular reflectance 3-47333
- troilite, comparison with pyrrhotite 3-50879
- Sb_{1-x}Se_x, amorphous films, reflectivity spectra, electronic structure 3-64754
- Ag film, effects of residual gas during deposition on optical props. 3-80001
- AgI-Ag photosensitive film, refl. spectra, 370 to 500 nm 3-53121
- AgNO₃, longit. mode freqs., PSR i.r. spectra 3-75975
- Ag₂S(Se) semiconductor-metal transition, i.r. reflectivity obs. (German) 3-50571
- Al reflectance coatings, LiF-protected, use in u.v. space optics 3-81252
- Au thin films, goniospectrophotometer, reflectance and transmittance measurements, 0.25 to 1 micron polarised light (French) 3-39926
- CdS, photoconductor and chemical precipitate relationship 3-46872
- CdTe, band structure, fundamental reflectivity spectra (Polish) 3-41132
- Cu₂HgI₂, thermochromic, cryst. growth and refl. 3-61047
- EuO:Gd i.r., 250 μ to 12 eV photon energy, Kramers-Kronig analysis, coupled modes 3-41518
- (Fe, Ni)₂S₁₁, elongite nodules, kimberlite pipe, South Africa, phase equilib. 3-44764
- GaTe, layer compound, exciton photorelectance, Kramers-Kronig relations 3-55610
- Ge film, amorphous, spectrum 3-55550
- GeTe, optical props. and energy gap from reflectance spectra 3-64685
- Hg₂Br₂, for i.r. reflectivity meas., polar optic phonons study 3-55571
- Hg₂Cl₂, for i.r. reflectivity meas., polar optic phonons study 3-55571
- HgTe, band structure, fundamental reflectivity spectra (Polish) 3-41132
- K₂Pt(CN)₄Br_{0.3}·3H₂O, optical cond. and electron interaction 3-68958
- ⁷LiF and natural LiF, i.r., calc. using shell model lattice dynamical data 3-41516
- Mo, incidence reflectance studies, effect of chemisorption of O₂, CO, H₂ 3-55157
- MoS₂, optical functions calculated from reflectivity data by Kramers-Kronig analysis 3-64618
- NH₄I, u.v. spectra for NaCl and CsCl structures 3-64677
- NbSe₂, optical functions calculated from reflectivity data by Kramers-Kronig analysis 3-64618
- Ni reflectance measurements, precision, 2 to 3 eV, fine structure, spin-orbit effects in exchange-split energy bands 3-52780
- Pb(NO₃)₂, longit. mode freqs., PSR i.r. spectra 3-75975
- PbS, electronic band structure and optical props. 3-58523
- PbSe, electronic band structure and optical props. 3-58523
- PbTe, electronic band structure and optical props. 3-58523
- Ru evaporated thin films, in v.u.v. from 300 to 2000 Å 3-80069
- Si films, optical interference phenomena, wave number calc. 3-58488
- α -SiC, polarity, reflection spectra of polished faces 3-43772
- Th, itinerant 5f states observation by reflectivity meas. 3-43992
- TiO₂ thin films, goniospectrophotometer, reflectance and transmittance measurements, 0.25 to 1 micron polarised light (French) 3-39926

reflectivity continued

- TiNO₃, longit. mode freqs., PSR i.r. spectra 3-75975
 ZnO, pseudopotential method of computing band structure, density of states and reflectivity 3-64292
 ZnTe, band structure, fundamental reflectivity spectra (Polish) 3-41132

reflector antennas

see also antenna reflectors

- acoustic, parabolic, retroreflection calibration 3-39871
 Deep Space Network of large antennas, low-noise microwave receiving system 3-65965
 parabolic, phase errors at the aperture, feed shifted from the focus (Russian) 3-81227
 radiotelescope reflector tolerance determ. by separation of aberrant and phase errors 3-70077
 RATAN-600, radiotelescope, antenna parameters, calibration of sensitivity, 8 mm in the radar regime, radioastronomical method (Russian) 3-81246
 RATAN-600, radiotelescope, control of antenna parameters, radioastronomical obs. (Russian) 3-81238
 RATAN-600, radiotelescope, reflecting elements size determ., calc. of elec. parameters (Russian) 3-81223
 variable profile, aberrations of main mirror, scanning the antenna pattern by shifts of the primary feed (Russian) 3-81226
 variable profile, adjustment, radioastronomical method (Russian) 3-81237
 variable profile, adjustment by geodetic and radiotechnical methods (Russian) 3-81236
 variable profile, operation near the zenith, parallel aperture synthesis (Russian) 3-81225
 variable profile, plane periscopic reflector (Russian) 3-81224
 variable profile, precision of measuring the coordinates of bright radioresources, Pulkova and RATAN-600 radiotelescopes (Russian) 3-81251
 variable profile, RATAN-600, methods of radioastronomical obs., azimuthal aperture synthesis (Russian) 3-81222
 variable profile, RATAN-600 radiotelescope, 0.4 to 21 cm (Russian) 3-81221
 variable profile, RATAN-600 radiotelescope, calc. of noise temp., effect of field of scattering (Russian) 3-81228
 variable profile, scanning the diagram, obs. of Orion-A, Virgo-A, Cygnus-A, Crab nebulae (Russian) 3-81248

reflex klystrons

No entries

refraction

see also acoustic wave refraction; electromagnetic wave refraction; refractive index

- Alfven wave refr. by interplanetary inhomogeneities 3-51315
 crustal, time-term analysis, iterative method 3-44926
 elastic-plastic shock wave, refraction at material interface 3-49594
 geodesic, S. Slovakia (German) 3-58852
 mean universal curve for optical angle of refraction 3-51077
 ocean waves, linear profile of descending bottom (German) 3-76917
 plasma waves, ionosphere, topside sounding (Russian) 3-69664
 porous media, interface refraction, boundary between porous layers 3-54827
 seismic, on continental shelves, detection with seismometers on sea floor 3-76837
 seismic refraction methods, use of obs. space for dipping structures 3-47794
 seismic waves, refraction field measurement, interpretation by computer model of earth 3-65143
 Vibroseis data, enhanced by linearly swept frequency vibratory field procedures 3-65144

refractive index

see also refractometers

- air, effect of time fluctuations on accuracy of long range measurements (Russian) 3-73338
 air, room temp. meas. using Michelson interferometer (Korean) 3-49529
 alkali halides, refr. index and refl. spectra, uniaxial deform. effects 3-58528
 amorphous semicond., lone-pair, pressure depend. rel. to chem. bonds and comp. 3-44390
 atmospheric, structural constant rel. to blurring of extended object viewed through 20 km of turbulence (Russian) 3-65524
 atmospheric turbulence 3-76749
 barium stearate films, built-up, calc. 3-53076
 benzene-cyclohexane-dioxane ternary mixtures, far i.r. and Na D-line 3-73175
 BO₆-type O-octahedra ferroelectrics, two oscillator description 3-41498
 Brundheim meteorite, complex refractive index between 1.1 and 5.2 μ m 3-59325
 clear air turbulence effect on line-of-sight e.m. wave propagation 3-65310
 corneal refractive index rel. to thickness and pachometric meas. errors 3-70123
 cytochrome c, dispersion in α - and β -absorp. band regions 3-63596
 dielectric film on Si, refr. index and thickness, ellipsometric method, accuracy 3-51591
 dye laser, superradiant slab, refractive index gradient effects 3-78033
 electro-optical crystal, optically induced changes, measurement with sharp edged illumination pattern 3-64624
 fibres synthetic, interferometric meas. of microstruct. (German) 3-41818
 fluid, nonpolar, corrections in critical region 3-71722
 garnet, Czochralski-grown, perfection and charact. for gems, lasers and substrates 3-76131
 gas, compressed, virial coeffs., coeffs. of expansion of optical complex and refractometric virial coeffs., connection 3-49962
 gases, rel. to propag. of coherent light of large amplitude (Russian) 3-43539
 germanate glasses, mixed-cation, pseudo-alkali cation effects on network depolymerization 3-44679
 glass, mixed nitrate, M(I)NO₃ + M(II)(NO₃)₂ 3-72009
 refractive index continued
 glass, multicomponent, concentration fluctuation scattering, reln. to fibre optical waveguides 3-73737
 graphite (0001) face, Xe layers, phase difference (French) 3-79560
 group, Whistler mode propagation in drifting plasma 3-68001
 group refractive index curves for r.f. propagation through ionosphere over Calcutta 3-51103
 heterogeneous, plane, uniform e.m. waves, heterogeneity index notion (French) 3-66748
 high-molecular organic materials, aq. soln., optical density and refr. index, conc. depend. (Russian) 3-50860
 holographic thin-beam reconstruction, to study 3D refractive index field 3-66245
 ice, spectral reflectance in i.r. 3-44387
 inhomogeneity in optical windows, surface correction 3-77468
 liquid, u.v. region charact., dispersion curves (Russian) 3-64688
 liquid crystal, nematic, MPT, temp. depend. (French) 3-41526
 liquid crystals, nematic, refractive index, density and diamagnetic susceptibility meas. 3-54918
 lithium formate crystals, refractive indices measurement, 0.35 to 1.5 micron, Sellmeier relation 3-40285
 Lorenz-Lorentz eqn., generalised, applic. to mol. spectroscopy using absorbing solvent 3-74997
 MBBA, isotropic phase, field-induced refractive index meas., mol. ordering study 3-40846
 meteorological variables, microstructure, dry cold fronts 3-76758
 microwaves, generation and dissipation of fluctuations in boundary layer 3-65307
 momentum of a light wave in a refracting medium 3-42957
 nematocysts, interference microscopic determ. (German) 3-54028
 noble metal thin film, transmission in vis. and near u.v. spectra regions (French) 3-76112
 noncentrosymmetric crystals, nonlinear, dispersion in fundamental absorption region 3-75959
 one dimensional fields, light deflection effects 3-40217
 optical coating of variable refr. index 3-62093
 optical windows, surface correction for refr. index in homogeneity 3-51578
 optically pumped ruby, verification of Kramers-Kronig relations 3-48909
 organic film, principal index variation with wavelength (French) 3-80064
 oxyhaemoglobin, dispersion in α - and β -absorp. band regions 3-63596
 plagioclase, shock effects, refractive index and birefringence obs. 3-61367
 polymer film, low loss, with adjustable refr. index 3-53157
 polystyrene, craze layer density on fracture surface 3-58738
 polystyrene solns. in toluene, monodisperse, refr. index increment, mol. wt. depend. 3-49516
 polyurethane film, light modes, refr. index, thickness, dispersion 3-47335
 pyroxene, shock effects, refractive index and birefringence obs. 3-61367
 rare earth sesquioxides, dispersion 3-79974
 ruby, change on R-line transition saturation, Jones optical lever method 3-80003
 silica glass, optical prop. modification by ion bombardment 3-59584
 thin films, multiple-beam interferometry study 3-73766
 thin films on glass substrates optical constants calc. by ellipsometry 3-53158
 transition metal iodate, 3d, for characterisation 3-53120
 triglycine sulphate crystals, influence of defects near fundamental absorption edge 3-80081
 troposphere stratified turbulent layers, forward scatter radio techniques 3-65521
 uniaxial cryst., electronic polarisabilities of ions in trigonal system (French) 3-75961
 uniaxial crystal, electronic polarisability of ions, tetragonal systems 3-72567
 water, imaginary part determ., 4400 to 50 cm⁻¹ 3-61039
 water, optical dispersion eval. using two-state theory 3-68951
 (AlGa)As-GaAs heterojunction, index step at lasing freq. obs. 3-70825
 Al₂O₃ particles, flame photometry, size obs. and stimulated part of refractive index (Russian) 3-59711
 As-Se-Tl glasses, refractive index, density, polarisation, absorption spectra (Russian) 3-50584
 B₂O₃ glass, pressure compaction, volume relaxation 3-76325
 B₂O₃-SiO₂-GeO₂ glasses, characteriz. w.r.t. struct 3-76271
 Ba₂Sr_{1-x}Nb₂O₆, Ba₂NaNb₂O₁₅, single cryst. growth, refr. index homogeneity 3-50653
 CO₂, room temp. meas. using Michelson interferometer (Korean) 3-49529
 CaF₂-NdF₃(YF₃) system phase relations and characteriz. (German) 3-47443
 Ca(IO₃)₂·6H₂O, indices at 0.53 microns 3-46606
 CdGeP₂, i.r. absorpt. and refl. spectra, 2 to 100 μ m, dielec. const. and refr. index calc. 3-44412
 CdSb, i.r. radiation filter 3-64619
 CdTe, 300-1100 nm (Russian) 3-47225
 F₂, refractive index determ. 3-75182
 n-GaAs, calc. rel. to heterostruct. lasers 3-68952
 Ge, Brillouin spectra lineshape analysis 3-50566
 HF, refractive index determ. 3-75182
 α -HfO₃, principal value n₂ of refractive index calc. (Russian) 3-50537
 H₂O, refractive index meas. up to dynamic press. of 10 kbar 3-41495
 He, room temp. meas. using Michelson interferometer (Korean) 3-49529
⁴He, freezing liquid, thermophysical properties, 4 to 3000 R, pressures up to 15000 PSIA 3-50043
 HgTe, 300-1100 nm (Russian) 3-47225
 InPAs, positive uniaxial, transparent crystals 3-80004
 LiF film, light modes, refr. index, thickness, dispersion 3-47335
 LiInS₃, linear and nonlinear optical props. 3-45819
 NaLa(WO₄)₂, NaY(WO₄)₂ 3-69009
 NH₄Cl, temp. depend., near order-disorder transition 3-68956

refractive index continued

- Pb_{1-x}La_x(Zr_{0.65}Ti_{0.35})_{1-x/4}O₃, dirty displacive ferroelec., rel. to local disorder 3-58484
 Pb₃(MnNb₂)O₉, (M=Zn,Mg), dirty displacive ferroelec., rel. to local disorder 3-58484
 PbO-GeO₂ glasses characteriz. w.r.t. comp. 3-76270
 PbO-TiO₂-BaO-Al₂O₃-B₂O₃-ZnO glass microspheres coated on an Al surface, reflex-reflective characteristics 3-47441
 Rb vapour, anisotropy due to laser radiation 3-63292
 SbNa₂K, Cs photocathode, optical and photoelectric props. detn. (French) 3-41612
 Sb₂O₃ thin film, 300-4000 nm, rel. to microstruct. 3-76113
 Si, Brillouin spectra lineshape analysis 3-50566
 Si films, and dangling bonds 3-76109
 SrTeO₃, ferroelec., optical props. 3-68938
 Ta₂O₅ pyrolytic film characterisation 3-58591
 Te₆₀As₂₅Ge₁₅S(Se)₂ glass, physico-chem. props. (French) 3-60666
 TiO₂-GeO₂-SiO₂ glasses, i.r. detection of depolymerization 3-58500
 YAlO₃, biaxial cryst. 3-41492
 Y₂O₃-ThO₂(10 mole%)-Nd₂O₃(1 mole%), transparent, powder prep. and processing rel. to refractive index variation 3-64968
 ZnS film, visible region 3-41474
 ZnS-MgF₂ optical coating of variable refr. index 3-62093

refractive index measurement

see also refractometers

- ACD-solution, between 250 and 700 nm. 3-66190
 Abinet compensator, deflection mapping, refractive index changes, sensitivity, applications 3-62133
 Bruderheim meteorite, complex index of refraction, 1.1 to 5.2 μ m 3-81013
 butanol -(1) and -(2) and iso-butanol, between 250 and 700 nm. 3-66190
 double beam interferometry, electrochem. studies, review 3-66236
 ethanol, between 250 and 700 nm. 3-66190
 films, refr. index and thickness from single angle refl. meas. 3-51594
 gas phase, interferometry, undergraduate teaching 3-45401
 gases and liquids, at high pressure, interferometer applic. (German) 3-73768
 interpolation of data 3-51596
 i.r. refractive index temp. coeff. meas. using CO₂ laser 3-51592
 laser application, school expt. 3-59526
 laser application, school expt. 3-59527
 microscopic refractometer, VEB Carl Zeiss JENA, refractive index meas., biology, medicine, technical products 3-51587
 phase microscopy, variable contrast 3-56659
 plasma, Michelson interferometer, stabilised, calibrated, gas laser light source 3-62131
 polymer films, critical angle refractometry 3-42553
 profiles produced by ion implantation, ellipsometric meas. method 3-45478
 propanol-(1) and -(2), between 250 and 700 nm. 3-66190
 refractometer, recording, measurement of i.r. transmitting solids, 8 to 14 microns, accuracy of 0.0001, description 3-70299
 Ringer's soln., between 250 and 700 nm. 3-66190
 by shearing method, using interference microscope (German) 3-56670
 solids, exptl. methods, review (French) 3-41494
 systematic errors, analysis, solid and liquid homogeneous isotropic materials (Czech) 3-53880
 temperature depend., meas. using thermal self-phase modulation 3-51595
 thin film, methods, review 3-77462
 translucent isotropic solids, Pulrich refractometer application (Slovak) 3-39903
 transparent film, on metal substrate, dispersion, ellipsometric method 3-62049
 tropospheric fluctuations meas. using laser beam, interferometric and diffraction methods (Russian) 3-69732
 water, between 250 and 700 nm. 3-66190
 NaCl, 9%, soln., between 250 and 700 nm. 3-66190

refractivity see refractive index**refractometers**

- holographic type 3-73777
 microscopic, VEB Carl Zeiss JENA, refractive index meas., biology, medicine, technical products 3-51587
 Pulrich, PR-2 Zeiss Jena, application to translucent isotropic solids (Slovak) 3-39903
 recording, measurement of i.r. transmitting solids, 8 to 14 microns, accuracy of 0.0001, description 3-70299
 scanning, for in-line dissolved solids monitor 3-59581

refractometry see refractive index measurement**refractories**

see also ceramics; clay

- atomic absorption spectroscopy, flameless, trace metal impurity determination 3-48640
 borides, recrystallisation kinetics, deform. 3-72976
 brittle materials, thermal stability for prismatic samples 3-58703
 carbides, recrystallisation kinetics, deform. 3-72976
 compatibility with ²⁴⁴Cm₂O₃ as fuel for radioisotopic applications 3-69363
 concrete, calcium aluminate bonded, thermal shock testing 3-80405
 dispersion form. of carbides, nitrides in alloys (French) 3-53231
 fireclay, strength, fracture and thermal shock behaviour 3-80414
 fireclay, thermal-expansion-under-load behaviour 3-80407
 graphite, and graphite-containing materials, reaction with liquid Fe calc. O₂ diffusion (German) 3-72969
 hardness meas., high-temp., with B-C-Ti 3-80515
 liquid opaque systems, surface tension determ. 3-72260
 metal, heat resistance estimation method for variable temp. conditions (Russian) 3-80425
 metals, film defects screening by current noise meas. 3-68709
 metals, preparation of bicrystals, controllable orientations, zonal melting technique 3-80174
 mullite fibre, fine diameter, characteriz. for high temp. use 3-76275
 nuclear reactor fuels, factors affecting swelling at high temperatures 3-63198

refractories continued

- oxide fibre eval. for high temp. rigidized insulation applic. 3-76276
 oxides, oxide compounds, h.f. heating, melting 3-72979
 polycrystalline compounds, thermal expansion coefficients, temp. depend. 3-76310
 rare earth germanates, meas. and nature of elec. cond. 3-76315
 rare earth silicates, germanates, oxides, synthesis, physicochem. classification 3-76314
 refractories, atomic absorption spectroscopy, flameless, trace metal impurity determination 3-48640
 sintered, thermal conductivity meas., modified Krishnan and Jain method, 1000-2200°C (Czech) 3-70288
 sintered bodies, grain shapes in two-dimens. sections 3-44647
 sintered metallic materials, elec. resist. (Polish) 3-44665
 spinel, elastic moduli, density depend. 3-80412
 spinel, elastic moduli, porosity depend. 3-72942
 steel G₁₃, 45, R₁₈ F5K, eutectic Sn-Zn alloy effect on drilling (Russian) 3-76311
 thermal expansion under load, test program 3-80406
 thermal shock damage resistance 3-80404
 thermal stability, dispersion of fracture temp. drops. 3-47453
 thermal stress resistance of brittle refractories caused by anisotropic behaviour of grains in polycryst. matrix (German) 3-61187
 thermally loaded, deformed state studies 3-44636
 variable composition compounds, sintering 3-80434
 work of fracture measurement, frictional forces effect 3-76307
 X-ray fluorescent and atomic absorpt. anal. methods characteriz. 3-80410
 Zircaloy cladding, high temp. testing for use as thermocouple sheath in PWR 3-47431
 Al₂O₃, phase changes during service in high temp. kiln 3-80411
 Al₂O₃ systems, defects ordering phenomena, X-ray anal. (French) 3-76335
 Al₂O₃:Ti, creep and sintering, anomalously high activation energies origin 3-55842
 B₄C, hot-pressed, high temp. props., oxidation resist., thermal expansion, fracture 3-69348
 C, low density, thermal conductivity 3-72974
 C, pyrolytic, negative magnetic resist., crystallization, semiconductor-metal transition, 1.5-300K (German) 3-72387
 CaO-Al₂O₃-FeO-Fe₂O₃ system, phase relations, liquidus temp. 3-76340
 CaO-MgO-SiO₂-V₂O₅ system, phase equilib. diagram, 1500°C 3-76337
 CaO-MgO-SiO₂-V₂O₅ system, phase equilib. diagrams, 1450°C 3-76338
 CaO-MgO-iron oxide system, TiO effects on equil. among refractory phases 3-44655
 CeO₂, nonstoichiometric, defect struct. above 700°C 3-68244
 Cr-Ni alloy Zh S6K, eutectic Sn-Zn alloy effect on drilling (Russian) 3-76311
 Fe-B-C hard facing alloy characteriz. 3-50740
 MgO-Al₂O₃-TiO₂ system, phase relations, 1100-1550°C 3-76339
 MgO-BOF brick, compressive creep, 1200-1500°C 3-80408
 Mo, anisotropic surface struct. change during directional transport processes 3-55130
 Mo, diffusion of Fe impurities, 1000-1350°C (Japanese) 3-72985
 Mo, international practical temperature scale, reference points 3-73661
 Mo, thermal expansion, 1800-2546°C 3-69351
 Mo alloy sheet, surface layer struct. rel. to recrystallization, X-ray analysis 3-76175
 Mo and alloys, creep rel. to long-term fracture 3-58677
 Mo and alloys, neutron irradiat. temp. effect on hardness 3-79387
 Mo organic binder, sintering props., chemical stability in reducing atmosphere 3-69353
 Mo-Re-C alloy, ageing, heat treatment, 1400-1800°C 3-76174
 MoS₂(Se₂), lubricating action mechanism (Russian) 3-41798
 MoSi₂ recrystallisation kinetics, deform. 3-72976
 Nb, carburizing in glow discharge plasma 3-76217
 Nb, cold deformed, short-term heat resist., gaseous medium influence (Russian) 3-80427
 Nb, enthalpy in solid and liq. state 3-72209
 Nb and alloys, neutron irradiat. temp. effect on hardness 3-79387
 Nb-Mo system, anomalous behaviour during interdiffusion 3-72860
 Nb-W-Mo-Ti-Zr-C alloy, quenching, ageing, carbide precipitation 3-76176
 Nb-Zr (1 wt.%) alloy, sp. heat, electrical resistivity and hemispherical total emittance determination 3-64971
 NbSe₂, lubricating action mechanism (Russian) 3-41798
 PuWC_{1.75} ternary phase, cryst. struct. and comp. 3-44649
 SiC, bonded, strength, fracture and thermal shock 3-76288
 SiC, high density, thermal cond., 25-1300°C 3-76293
 SiC, microstruct. analysis 3-80413
 SiC, slow crack growth at elevated temps. 3-76290
 Si₃N₄, hot pressing, high temp. flexure strength rel. to impurities, 1375°C 3-76305
 Si₃N₄, hot-pressed, low cycle fatigue 3-76287
 Si₃N₄, hot-pressed, UTS, room temp. to 2800°F 3-76291
 Si₃N₄, reaction sintered, creep obs. and mechanism, 1200-1400°C (German) 3-61186
 Si₃N₄, shape and thermal shock behaviour 3-76289
 Si₃N₄, slow crack growth at elevated temps. 3-76290
 SiO₂, and silica-containing materials, reaction with steel melts, calc. O₂ diffusion (German) 3-72969
 SnO₂, sintering, MnO₂ content effect (Polish) 3-44663
 TaC_{1-x}Ta_{N_x}-HfN system, hot pressed, annealed, lattice parameters, microhardness rel. to comp. (Germany) 3-80392
 (Ti, W)C solid solution form., diffusion mechanism 3-64975
 TiB₂, thermal expansion, 25-1200°C, X-ray diff. obs. 3-44657
 UC+N₂ reaction, graphitization of precipitating free carbon 3-47553
 V-N dil. alloys, metastable phase behaviour 3-64976
 V₆Cs, V₆Cr₃, vacancy ordering effects on thermodynamic props. 3-72973
 W, anisotropic surface struct. change during directional transport processes 3-55130
 W, carburizing in glow discharge plasma 3-76217
 W, electron spectroscopy, surface struct. (Hungarian) 3-72256

refractories continued

- W, monochromatic emissivity, 1200-2600K 3-69352
 W, powder metal, hydroextrusion effect (*Russian*) 3-72922
 W, thermal expansion, 1950-3335C 3-69351
 W, thermophysical props. 3-72975
 W powder, swaged, diffusion of ^{59}Fe and ^{185}W , autoradiography, 1300-1900°C (*Hungarian*) 3-72987
 W wire, high temp. creep, grain boundary cavity formation rel. to filament lifetime (*Hungarian*) 3-72988
 W wire, research review (*Hungarian*) 3-72989
 W:B doped filament development (*Hungarian*) 3-72986
 W-Mo alloys, electrical resistivity and thermal conductivity 3-72972
 W-Ta-ZrC alloy, recrystallization, deform. depend. 3-76334
 W/Co powder, sintering, shrinkage rel. to milling 3-80393
 WS₂(Se₂), lubricating action mechanism (*Russian*) 3-41798
 ZrBr₂, pyrolytic, thermal diffusivity at high temps. 3-61200
 ZrC, nonstoichiometric, C distrib. var. during creep testing, laser microanalyser 3-72977
 ZrC and ZrC-B alloys, arc melting and homogenization 3-80430
 ZrO₂, calcia-stabilized, fluorite type solid soln., ordering (*French*) 3-72991
 ZrO₂, castable, elec. resist. from 900-1700K, calcia stabilisation rel. to furnace appl. 3-52832
 ZrO₂, comparison with HfO₂-MO systems (*French*) 3-72993
 ZrO₂, Y₂O₃ stabilized, current-blackened single crystals, dielec. consts. and loss tangent 3-79972
 ZrO₂ and ZrO₂-CaO, elec. cond. and thermoelec. force, 1000 to 1700°C, 1 to 10⁻¹⁶ O₂ partial press. (*German*) 3-68604
 ZrO₂ oxygen-pump die for hot pressing 3-76256
 ZrO₂ systems, defects ordering phenomena, X-ray anal. (*French*) 3-76335
 ZrO₂/W and ZrO₂/ZrO₂ fibre composites, thermal shock resist. 3-76353
 ZrO₂-Er₂O₃(La₂O₃)(Y₂O₃) cubic solid soln. stability below 1500°C (*French*) 3-76309
 ZrSiO₄, plasma sprayed, reheating, pore contraction 3-76332

refractory materials see **refractories****refrigeration**

- see also *cryogenics; freezing*
 heat pipe performance, meas. of liquid on solid contact angles 3-70273
 nucleate pool boiling heat transfer coeff. pressure dependence, obs. and calc. (*German*) 3-68393
 superconducting accelerator magnet cooling systems 3-56726

refrigerators

- continuous, flow impedance construction, liquid ⁴He and ³He 3-51553
 miniature, Stirling-cycle machine, appl. to cooling of i.r. detectors 3-48381
 minimum power input, thermodynamic optimisation, cooling of current leads 3-48382
 He refrigerator cycle with cascade coupling of expansion engines, optimisation 3-62632
³He dilution type, for Mossbauer spectroscopy down to 0.1 K 3-68895

regenerative receivers see **radio receivers****Regge poles and trajectories**

- see also *hadron scattering*
 3-to-3 amplitude asymptotic upper bound in helicity-pole-Regge-pole limit 3-45897
 ϕ^3 multiperipheral model with strong coupling 3-60013
 absorption models, duality 3-57378
 analyticity and finite energy sum rule for reggeon-particle amplitude in $a+b \rightarrow c+d+e$ 3-70957
 asymptotic behaviour of real part of trajectory as $s \rightarrow \infty$ 3-66949
 asymptotic behaviour of trajectory functions and size of classical orbits 3-66931
 average multiplicity, secondary trajectory and Mueller analysis 3-57384
 baryon, total decay widths of resonances and trajectories 3-60005
 baryon octet spectra, lin. depend. of mass spectrum on isospin (*Russian*) 3-43124
 baryon spectrum and reflection partners, SU(3) Regge scheme 3-45900
 baryon-antibaryon amplitudes from Reggeon-particle scatt., duality test 3-57466
 baryon-antibaryon elastic scattering, test of duality from Reggeon-particle reactions 3-49026
 bounds from unitarity and analyticity on forward slopes of overlap functions 3-49036
 broken conformal symmetry of strong interactions 3-67070
 charge, and hypercharge exchange reactions, including KN, πN and $\pi p \rightarrow \eta n$ 3-67072
 charge and hypercharge exchange reactions, properties of corrections to Regge pole amplitudes 3-62863
 charged hadron multiplicity, energy depend., high energy inclusive collisions 3-78166
 complex pole model, systematics of vector and tensor-meson exchange amplitudes 3-67078
 coupling constraints from inequalities based on duality and unitarity 3-67080
 couplings from SU(2) \times SU(2) saturation schemes 3-78162
 current-hadron amplitudes in deep Regge region algebra of strengths 3-57308
 decay of heavy Regge recurrences, Brower and Harte theorem 3-57381
 decoupling of two Pomeranchon-cut from two Pomeranchon-Regge poles at zero momentum transfer 3-60006
 diffractive mechanism for multiparticle production processes 3-67076
 dipole coupling model of reggeon exchange for double resonance reaction $\pi N \rightarrow$ vector meson + Δ baryon 3-74442
 discontinuity of second-order correction to Regge trajectory, calc. in dual resonance model 3-74390
 double-Regge-pole model, phenomenological fits to high-energy data 3-40371
 dual $\pi\pi$ partial wave amplitudes, threshold behaviour 3-62859
 dual absorption model, colliding-Regge-cut representation, high energies 3-62856
 dual crossing-symmetric representations with finite-width resonances and Regge asymptotic behaviour 3-57375
 dual model investigation of meson photoproduction, $\gamma B \rightarrow MB'$ 3-57351
 dual model of current, off-shell amplitudes, Regge limit and scaling 3-59993
 dual model pomeron-reggeon vertex operator, gauge props. 3-78158
 dual model with Regge cuts deep inelastic limit 3-57374
 eikonal representation for scattering amplitude containing virtual Veneziano blocks 3-62860
 electroproduction, deep inelastic, dual reson. models, phenomenological approach 3-54320
 exchange degenerate Regge pole model for np and pp charge exchange scattering 3-60033
 factorizing dual amplitude with Mandelstam analyticity 3-59995
 fermionic trajectories, asymptotic behaviour 3-52024
 Gribov's Reggeon calculus for ISR elastic proton-proton scattering data 3-74430
 hadron high energy collision phenomena, Regge poles, reviews 3-54330
 hadron physics, Reggeization and kinematical props. of helicity amplitudes, inclusive reactions 3-74400
 hadron-carbon scattering, Regge-pole model analysis, factorization 3-67073
 hadronic level degeneracy, statistical bootstrap condition, linear Regge trajectories 3-49024
 hadronic production, short-range correlation, role of secondary Regge singularities rapidity clusterings 3-67081
 hadronic scaling in high energy, large momentum transfer reactions and broken conformal symmetry 3-67159
 hard Regge cuts consistent with elastic unitarity 3-45896
 impact parameter analysis of KN and πN scattering in intermediate energy region 3-57404
 inclusive cross sections, anomalous singularities and nature of Regge singularities 3-54363
 inclusive electroproduction, matrix elements of bilocal operators, rel. to scaling regions in large- ω limit 3-67046
 inclusive one-particle distrib. and reaction asymmetries within completely symmetric duality scheme 3-60054
 inclusive reactions, ρ dominance and Regge coupling 3-49061
 inclusive reactions, exotic SU(3) representation in b fragmentation region 3-57462
 inclusive reactions, Regge analysis of correlations in central plateau 3-78219
 inclusive reactions, Regge singularities of twisted loop graphs, phenomenological treatment 3-49025
 inclusive reactions, single-particle cross sections, duality and Regge approach 3-57468
 inclusive two-particle processes, Regge phenomenology, scaling 3-43160
 linear, nucleon form factors in the relativistic quark model 3-67052
 meson charge exchange reactions in Regge-cut Van Hove model 3-57436
 meson trajectories and multiple production 3-52025
 meson trajectory functions, bounds below threshold 3-45895
 mesonic trajectory, maximum behaviour at infinity 3-70955
 model construction, without parity doubling, linear trajectories 3-60002
 model for momentum transfer dependence of differential cross section in $K^-p \rightarrow K^0n$ (*Russian*) 3-74438
 Mueller's analysis, with scaling laws of parton model, π^+/π^- asymmetry in inclusive electroproduction of hadrons 3-57361
 multi-Regge model, transverse momenta and overlap functions 3-70963
 multi-Regge theory for $a+b \rightarrow 1+2+\dots+N$ 3-57383
 multiple-Reggeon exchange cuts, dynamics 3-40372
 multiplicity distrib., two-component model of particle production, Regge trajectory intercept 3-54356
 multiplicity distrib. at high energy, multiperipheral showers and Regge cut contribution 3-49033
 non-diffractive mechanism for multiparticle production, magnitude of t_{\perp} -cut 3-67075
 non-linear π -B exchange degenerate, rel. to $\pi N \rightarrow \omega N(\rho N)$ processes 3-60004
 nonleading, in unitary multiperipheral models with two input trajectories, high-energy behaviour 3-62869
 nonparallel trajectory family, group-theoretical approach 3-70956
 particle polarisation in inclusive reactions for particles with arbitrary spins (*Russian*) 3-67167
 Pomeron dynamics, self-consistent without decoupling 3-60008
 Regge-Mueller bootstrap model of inclusive reactions, total and partial cross sections 3-62853
 Regge-Regge-Pomeron model for proton leading-particle spectrum at accelerator energies 3-67150
 reggeon calculus, application to dual models 3-57377
 reggeon exchange, inclusive spectra characteristics, fluctuations in inelastic processes (*Russian*) 3-74473
 reggeon F/D ratio, baryon exchange degeneracy, crossing invariant solution 3-78156
 Reggeon-Reggeon-particle vertex, singularity structure from analytic properties of Feynman graphs 3-60009
 scattering amplitude, props. of two-variable expansions 3-51990
 six body helicity amplitude, massive particles, various properties 3-62913
 softened field theory, vector gluons, fixed pole struct. 3-78086
 spinor-spinor Bethe-Salpeter eqn., expansion methods, calc. of Regge trajectories 3-43055
 structure function ratio $\nu W_2^{\pi}(x)/\nu W_2^{\eta}(x)$ and Regge model 3-54311
 SU₃ Regge pole model for total cross sections at high energy 3-67151
 SU(3) \otimes SU(3) symmetry breaking and Regge behaviour reln. to dispersion relns. 3-54287
 SU(3) symmetry and exchange degeneracy of baryon Regge residues 3-54288
 sum rule, finite-energy, for $a+b \rightarrow c+d+e$ reggeon amplitude 3-78163

Regge poles and trajectories continued

- sum rules for amplitudes involving space-like reggeons, pairs of helicity singularities 3-59941
- symmetry model, Reggeized, high energy pion-nucleon scattering 3-78195
- symmetry model, Reggeized, test of vector-meson dominance model 3-78167
- total cross sections for protons, kaons, pions and photons, energy dependence, Regge theory 3-57458
- trajectory, from Feynman diagrams, dual amplitude construction 3-62857
- triple Regge limit in the description of $\pi^- p \rightarrow c + \text{anything}$ at 16 GeV/c, exchange trajectory parameters 3-67145
- triple Reggeization of spin dependent reaction $\pi N \rightarrow \pi + \text{anything}$, single particle spectrum 3-62914
- two-body scattering, high-mass exotic resonances and plane consistency 3-78175
- two-body scattering amplitude, relativistic field-theoretic description on Born term 3-40307
- two-current planar amplitudes, dual resonance model, large-s behaviour of Compton-like amplitude 3-59992
- two-Reggeon cut, from inclusive type sum rules, dual resonance model use 3-74401
- vector meson production, pomeron exchange component 3-57431
- weak leptonic interactions, high energy, massless particle exchange 3-78107
- Yukawa potential, large coupling expansions for eigenenergies and Regge trajectories 3-74326
- zeros of triple Regge vertex in HPRP limit of one-particle inclusive cross sections 3-45898
- $\Delta(1236)$, second sheet pole position, partial wave anal. 3-78165
- $e^- e^+ \rightarrow e^- e^+ + \text{hadrons}$, Regge and parton models for photon-photon annihilation 3-43116
- $\gamma p \rightarrow \pi^-$ anything, predicted differential cross section by factorisation of Regge trajectories 3-60052
- K^+ electroproduction, extension of Regge absorption model for photoproduction 3-40349
- K^+ photoproduction, Regge model from kaon and exchange degenerate $K^*(892)$ - $K^{*0}(1420)$ trajectories 3-40348
- K^\pm -charge exchange differential cross sections, expt. comparison 3-78207
- KK and $K\bar{K}$ scattering, Veneziano model 3-62854
- Kn elastic scattering, Regge analysis of data above 4 GeV/c 3-67119
- $K^+ n \rightarrow K^0 p$, 3.8 GeV/c, total, differential cross sections, comparison with Regge model 3-60035
- Kp inclusive reactions, $|x| < 0.6$, multiperipheral model taking account of Regge poles 3-62912
- $K^- p \rightarrow \eta/\Lambda(\Sigma)$, Regge amplitudes in forward and backward directions, peripheral nature of A_2 exchange amplitude 3-52046
- $K^- p \rightarrow K^0 X^0$, 8.25 GeV/c inclusive reaction, triple-Regge and absorptive behaviour 3-57457
- $K^- p \rightarrow K^{*0}(890)X^+$, 8.25 GeV/c inclusive reaction, triple-Regge and absorptive behaviour 3-57457
- $K^+ p$ backward elastic scattering 1.5 GeV/c parity doublets and Mandelstam-Sommerfeld-Watson transformation 3-71007
- $K^+ p$ elastic scattering, differential cross section anal. 3-78190
- p inclusive spectra, three-reggeon description 3-62906
- pp collisions, ISR inclusive hadron spectra, triple-Regge model, triple-pomeron coupling determ. 3-67154
- pp diffraction scattering, effective-normal-Regge trajectory of strong-exchange degeneracy type 3-43155
- pp interactions, multiplicity distrib. at very high energy, Reggeized production model 3-57385
- $pp \rightarrow p$ inclusive process at high energy, double Regge exchange model 3-52055
- pp scatt models, review 3-71005
- pp scatt., growth of total cross sections, mechanism 3-57459
- p scattering, elastic, model-independent analysis of structure at $t \approx -1.1$, Regge shrinkage 3-78193
- $pp \rightarrow Xp$ missing mass experiments, implications for Regge cuts 3-43126
- π , bounds on trajectory functions below threshold 3-45895
- πN amplitudes determ. at large momentum transfer 3-71000
- πN backward scattering, 6 GeV/c, amplitudes, Regge pole model with absorption 3-62897
- πN charge exchange, Regge pole and cut contributions 3-57428
- πN charge exchange at large momentum transfer, amplitude analysis 3-60036
- πN charge exchange scatt., Regge-cut models 3-62884
- πN forward scattering, duality and vacuum Regge singularities with zero intercept 3-74391
- πN scattering, Regge amplitude determ. using continuous moment sum rules 3-40394
- πN scattering, tests of bounds obtained from polarisation and differential cross section data 3-43140
- $\pi^+ n \rightarrow \omega p$, 6.0 GeV/c differential cross section, spin density matrix elements, Regge exchange models 3-57435
- $\pi^- p \rightarrow \eta n$, Regge amplitudes in forward and backward directions, peripheral nature of A_2 exchange amplitude 3-52046
- $\pi^- p \rightarrow pX$ inclusive spectra, energy-dependent triple Regge analysis 3-49070
- $\pi^- p \rightarrow \pi^{(*)}$ anything, predicted differential cross section by factorisation of Regge trajectories. 3-60052
- $\pi^- p \rightarrow \pi^- \Delta^+(1236)$, s-channel profile factor model for Regge- ρ exchange and duality 3-62887
- $\pi^- p \rightarrow Xp$, missing mass experiments, implications for Regge cuts 3-43126
- $\pi^+ p \rightarrow \rho^0 \Delta^{++}$, 1.28-2.67 GeV/c, meas. and analysis using effective trajectory parametrization 3-54353
- $\pi^+ p \rightarrow \rho^0 \Delta^{++}(1236)$, s-channel profile factor model for Regge- ρ exchange and duality 3-62887
- $\pi\pi$, S^* resonance, consistency with Roy's equations, resolution of up-down ambiguity 3-57419
- $\pi^- \rho \rightarrow \pi^0 n$, pole and cut model of charge exchange 3-54341
- ρ Regge trajectory, linearly rising, bootstrapping calculation using Balazs method 3-74345
- ρ trajectory curvature, reln. to difference of $\pi^\pm p$ total cross section 3-43158

Regge poles and trajectories continued

- $\rho\pi\pi$ residue function from sum rules and representation for $\pi\pi$ amplitudes 3-74444
- $X^0(960)$, Regge trajectory, exchange spin effect on elastic pp high-energy scattering (Russian) 3-78194
- $^4\text{He}(\alpha,\alpha')^4\text{He}$, Regge representation including background term 3-52162
- region of escape** see *exosphere*
- regulators** see *controllers*
- Rehbinder effect** see *mechanical properties of substances; surface phenomena*
- relative density** see *density*
- relative humidity** see *humidity*
- relativistic corrections**
 - heading is late addition, see also *atomic spectra; atomic structure*
 - atoms, Hartree-Fock ionisation potentials 3-78473
 - isoelectronic atom and ion energy levels, interpolation formula 3-74791
 - Lamb dip of CH_4 associated with freq. shift measurements of 3.39 μm Ne transition 3-78421
 - Lamb shift, absolute wavelength of $2s^2S-2p^2P$ transition in LiII 3-78407
 - Lamb shift in heavy one-electron ions 3-78409
 - magnetic hyperfine structure of $3d^4s^2$ atoms 3-74796
 - many-electron atoms, non-stationary states, theory 3-78399
 - two-electron ions, multiply-charged, transition energy calcs. 3-74795
 - Ar I isoelectronic series, dipole polarizabilities from nf term values 3-78450
 - Ga, relativistic Hartree-Fock-Slater oscillator strengths 3-78406
 - H, quantum beat meas. of fine struct., $n=2$ state 3-78437
 - H atom excitation, fine structure of $n=4$ state, Lamb shift transition 3-78452
 - H $n=3$ Lamb shift, separated oscillatory field measurements, line shape 3-78410
 - In, relativistic Hartree-Fock-Slater oscillator strengths 3-78406
 - Mn^{2+} , relativistic effects in the ground-state splitting parameters 3-79637
 - Na I isoelectronic series, dipole polarizabilities from nf term values 3-78450
 - Ne I isoelectronic series, dipole polarizabilities from nf term values 3-78450
 - Tm I, h.f.s. of even levels $4f^{12}5d6s^2 + 4f^{13}6s6p$ (French) 3-74794
- relativistic fluid dynamics**
 - continuous media, rigid motion, Riemann, Killing and Rosen (Italian) 3-75272
 - Einstein-Maxwell-Boltzmann system, existence, uniqueness and local stability 3-74163
 - irrotational steady-state flow of ideal gas 3-43632
 - MHD, exceptional waves 3-60583
 - shear free normal flows of perfect fluid Petrov Type I space-time of static or degenerate fields 3-71828
 - shock waves, special-relativistic eqns., astrophysical appl. 3-60582
 - steady relativistic gas dynamics reduction to equivalent Newtonian flow 3-49618
 - viscous fluids and continuous media concept (French) 3-54140
 - vortex motion, general relativity eqn., astron. appl. 3-60584
 - wave front propagation velocity, appl. to adiabatic flow (Italian) 3-43588
- relativistic plasmas**
 - Crab Nebula, second-order plasma interaction 3-61872
 - Crab Nebula, weak Landau damping, heating of high energy electrons 3-73551
 - electron beam heating of fully ionized system 3-63853
 - e.m. wave theory, large amplitude, thermal effects 3-68104
 - extragalactic radio sources, ram pressure confinement models, relativistic motion, plasma cloud 3-48059
 - long range ordering in hot plasma 3-79184
 - longitudinal and transverse wave mode-mode coupling, energy conversion 3-75425
 - MHD generalised flux-vorticity theorem 3-40812
 - moving isotropic plasma slab, reflection and transmission of obliquely incident e.m. waves 3-40770
 - oscillation of charged particles in laser fields and pair production 3-40811
 - parametric instability of nonlinear relativistic oscillations 3-79109
 - particle acceleration by moving laser focus, focusing front, or ultra-short pulse front 3-40794
 - pulsars Alven waves effect of relativistic mass of magnetic field 3-69811
 - relativistic electrons confined in axisymmetric mirror field, numerical simulation 3-43682
 - stimulated Compton interaction between matter and radiation, plasma effects 3-71964
 - strong e.m. wave propagation, steady-state solns. 3-71870
 - synchrotron instability, increments of longitudinal waves 3-40784
 - theta pinch, relativistic effect in light scatt. spectrum 3-63884
 - Vlasov-Maxwell equation, solution of initial value problem using contraction mapping theorem 3-57949
 - waves in relativistic electron gas 3-79130
- relativistic quantum field theory**
 - 4-point-function and the Wilson-Zimmermann expansion 3-43064
 - ϕ^2 theory, construction of Bogolyubov scattering operator 3-54280
 - bound state properties using Lippmann-Schwinger eqn., fine structure and perihelion advance 3-59923
 - causal ghost-free covariant harmonic oscillator model for boson respecting CPT 3-48984
 - charged spinless particles in external vector fields 3-48973
 - complex Lorentz group, vector parametrization 3-62401
 - conformal group, analytic spinor representations in four and five dimensions connected with differential eqns. 3-62767
 - conformal invariance of mass condition for light-like particles, helicity 3-59918
 - conformal spinor fields, two-dimensional internal space associated with dual resonance models 3-59919
 - conformal symmetry, equal-time commutators with improved energy momentum tensor 3-62777
 - conformally covariant spinor fields, scale dimension 3-51971
 - conformally invariant spinor field equations 3-40305

relativistic quantum field theory continued

- convergent quantum mechanics of interacting particles, realistic model, S-matrix elements 3-59920
- covariant Hamiltonian formalism for Dirac particle, physical interpretation 3-48970
- Curzon field, generalised, soln. of Einstein eqns. in coupled e.m. and zero-mass scalar meson field 3-48976
- Dirac eqn. solns. in infinite de Sitter space, representation of $SO_{3,2}$ 3-66922
- Dirac particles in constant external vector potential, asymptotic group invariance, determ. of $\alpha=e^2 2\pi/\hbar c$ 3-57336
- elastic continuum, one-dimensional, detailed wave eqn. for classical and quantum mechanics 3-59994
- electrons, wave packet construction, light cone 3-78078
- essentially nonlinear scalar fields and geometry of space-time 3-54278
- Euclidean Green's functions, axioms to define unique Wightman field theory 3-43062
- Euclidean-Markov field interpret. in Minkowski space-time framework 3-74312
- extended S-matrix method 3-62781
- factorized wave eqns. on homogeneous spaces of Poincaré group 3-74307
- functional methods and models, book 3-51981
- gravity, existence of class of gauges free from u.v. divergences 3-74145
- gravity, nonperturbative solution to one-loop correction to tree diagrams 3-66676
- gravity-modified QED, higher order infinity regularization 3-49001
- handedness of neutrinos, indefinite metric 3-62772
- handedness of neutrinos, lagrangians, mass and interaction 3-62773
- harmonic oscillator, charged, relativistic algebraic analogs 3-43069
- harmonic-oscillator model extension with SU_6 multiplet structure 3-51985
- Hartree-Fock method applications, nuclear force problem 3-54259
- helicity spinor phase 3-74300
- hydrodynamics, relativistic, quantum field 3-54276
- interacting scalar field in $\lambda(\Phi^4)_4$ theory 3-51974
- ions, hydrogen-like, ground state polarisability, Green's function, external elec. field (Russian) 3-71366
- Klein-Gordon eqn. in Riemannian space 3-62778
- Klein-Gordon operator, iterated, causal elementary solns. 3-62766
- Lagrangians for particles of spins 3/2, 2 and 5/2 in Gel'fand-Naimark formalism 3-62771
- light cone expansion, four point function 3-78079
- light cone singularities, asymptotic behaviour of matrix elements of operator products in momentum space 3-59914
- lightlike charges, vacuum annihilation property, lightlike asymptotic behaviour of local operators 3-59925
- Lorentz-covariant fields, conformal transformation matrix 3-43054
- massive spin one vector field in external potential, causality Lorentz invariance 3-57289
- massive Yang-Mills field, causality, Lorentz invariance 3-57292
- massless spin 1/2 eqn. neutrinos, unusual group of external symmetries 3-40310
- models of composite hadrons, group theoretical approach, zero-width approx. 3-67056
- multi mass wave equations, theory 3-78091
- neutrino fields with zero energy and momentum determ. of admitting space-times 3-48975
- nonrenormalizable interactions on low-energy limits of renormalizable ones, virtual field concept 3-74306
- nonzero rest mass particles and spin algebras for irreducible unitary representations 3-43060
- photon position operator construction in its own reference system 3-45842
- point source of quantised gravitational field, Schwarzschild solution, comparison with de Donder gauge 3-57133
- polaron, relativistic, without cutoffs, interaction with scalar boson field 3-40306
- position operators, algebraic operator relationships 3-48762
- quark model, vector meson e.m. props. 3-70925
- relativistic invariance, unitary and nonunitary representations, Poincaré group 3-70868
- renormalization for relativistic Fermi system in external field 3-70870
- spin 1/2 wave eqn., explicit representations for hierarchy of algebras 3-78090
- spin-one particle, causality and g-factor in Shay-Good formalism 3-51976
- spinor field quantisation, constant curvature space-time, limit to quantised field in the flat world (Russian) 3-48988
- spinor fields interaction with gravitation, massless Dirac eqn. rel. to Heisenberg's Unified Field Theory 3-59806
- spinor-spinor Bethe-Salpeter eqn., mass-symmetries 3-78089
- spinor-spinor Bethe-Salpeter amplitudes, short distance behaviour 3-43056
- spinor-spinor Bethe-Salpeter amplitudes, symmetry of energy dependence 3-78088
- spinor-spinor Bethe-Salpeter eqn., expansion methods, calc. of Regge trajectories 3-43055
- string of spinning material, quantisation, Hamiltonian and Lagrangian formulation 3-66930
- system with variable spin, relativistic motion equations (Russian) 3-78094
- tachyon field model, interacting (Korean) 3-70858
- three-dimensional formulation, configuration representation of three-body problem 3-70888
- two-body scattering amplitude, relativistic field-theoretic description on Born term 3-40307
- Ward identities for arbitrary Lie groups, anomalies 3-57295
- wave eqn. for two particles of arbitrary spin with instantaneous interaction 3-78076
- wave eqns., classical non linear relativistic, integration using Lie series 3-62765
- wave eqns. for particles with $m>0$ and fixed spin, difficulty in formulating partonlike eqns. 3-54257
- wave equations for zero-mass particles with invariant helicities, quantisation 3-45843

relativistic quantum field theory continued

- wavefunctions and form factors of bound system 3-43059
 - weak interactions, universal length role 3-54299
 - zero rest-mass fields in the vicinity of zeros, behaviour 3-43061
 - $^{12}C(p,\pi^+)$, relativistic field theoretic description 3-46044
 - $^{12}C(\pi^+,p)$, relativistic field theoretic description 3-46044
- relativistic scattering theory**
see also elementary particle scattering; quantum field theory of scattering
- additivity of phase shifts, Glauber approach 3-77865
 - asymptotic behaviour of real part of Regge trajectory as $s \rightarrow \infty$ 3-66949
 - convergent iterative solution 3-57313
 - differential cross section and overlap function at high energies, stationary values (Russian) 3-78103
 - dilatation-invariant two-body relativistic S-matrix, partial wave analysis 3-66953
 - eikonal approximation for three-body generalized ladder graphs in QED 3-51991
 - Faddeev equations, three-body symmetrical basis 3-48992
 - impact-parameter representation, analytic properties and dispersion relations 3-51992
 - kinematical analysis, amplitudes, M-function symmetries 3-59943
 - multi-particle helicity amplitudes, regularization 3-57314
 - multichannel bond method and Faddeev's equations, solutions for systems above disintegration threshold (Russian) 3-62797
 - N/D eqns., optimisation and tautologies 3-66950
 - nuclear two-body relativistic kinematics, computer calc. of transformation relations 3-71090
 - nucleon spin modification, rel. to relativistic eikonal model using ladder graph model, Feynman parameters 3-67089
 - null-plane formalism and polarisation, helicity and canonical formalism relations 3-62796
 - parametrization of $\Delta(1236)$ resonance in Breit-Wigner formalism 3-67074
 - partial-wave scattering amplitude in quasipotential model, analytic properties 3-43073
 - parton picture of elementary particles, review 3-67061
 - potential scattering of relativistic spinless particle, high-energy limit 3-66924
 - quantum theory for charged spinless particles in external vector fields 3-48973
 - quasixchange group, integration of infinitesimal transformations 3-57312
 - quasipotential amplitudes, spurious singularities in soln. of eqns. 3-74347
 - quasipotential phase shift calcs. in first and second order 3-54295
 - resonance propagators for π - π resonances and N-N interaction 3-70993
 - scattering amplitude, props. of two-variable expansions 3-51990
 - three-body problem, configuration representation 3-70888
 - trace-class operators, asymptotic behaviour of cross section at high energy 3-62555
 - two particle, direct and inverse, amplitude eqns. (Russian) 3-62795
 - two-body, high energy, partial wave analysis for absorption model, computer program descrip. 3-49029
 - two-particle reactions of any spin, definite-parity amplitudes free of kinematical singularities 3-51993
 - ye scattering, Compton kernel from invariant 4-vector representation 3-74374
 - H atom, as relativistic elem. particle, scatt. and photo-effect problems 3-67634
 - H atom as relativistic elem. particle, wave eqn. and mass formulae 3-67652
- relativity**
see also general relativity; relativistic quantum field theory; relativistic scattering theory; special relativity
- 4-surface of stationary volume embedded in 5-dimens. pseudo-Euclidean space 3-48770
 - 4-surface of stationary volume embedded in 5-dimensional pseudo-Euclidean space 3-48769
 - covariant disturbances and exceptional waves 3-48771
 - covariant field theories on two-dimens. indefinite metric, soluble models 3-42859
 - dynamics of classical relativistic particles, circular orbit solns. and nonrelativistic limit 3-48758
 - electric charge and energy equivalence 3-51814
 - lunar orbit perturbation, post-Newtonian gravitational effects in lunar laser ranging 3-45047
 - Michelson, role in relativity development 3-73621
 - pulsar NP 0532, optical polarisation, relativistic vector model 3-69986
 - pulsar NP 0532, relativistic vector model, observational results and fits 3-69987
 - relativistic astrophysics, book 3-61626
 - variable point mass dynamics, first integrals (Italian) 3-74127
- relaxation**
see also anelasticity; dielectric relaxation; elastic relaxation; magnetic relaxation; molecular relaxation; viscoelasticity
- glass fibres, long-loaded, relaxation of curvature 3-64094
 - linear system, vector-valued, theory 3-66709
 - plasma electrodynamic acceleration, relaxation processes 3-60634
 - semiconductor non equilibrium surface potential, thermally stimulated, anal. (Russian) 3-75717
 - solid, high heat flux, relaxation model 3-66707
 - thermal relax. rate eqns., n-level system, decay eigenfunctions and eigenstates 3-40177
 - transient chemical reactions, acoustic effects, nonequilibrium relaxation methods 3-41836
- relaxation oscillators**
 cardiac pacemaker cell's similarity to relaxation oscillator illustrated 3-61897
- relaxation time, carrier** *see carrier relaxation time*
- relay protection**
 differential-phase relay, from corona on carrier channel 3-52541
- relay systems (radio)** *see radio links*
- relay systems (satellite)** *see satellite relay systems*

relays

see also reed relays; switches

- carrier channel, corona interference reduction 3-52541
operate time measurement, digital millisecond meter 3-77564
Ag electrodeposition, effect of temp. and metaphosphate, relay timing in electronic circuit 3-50836

relays (repeaters) see repeaters**reliability**

- see also circuit reliability; quality control; standards; testing
bathythermographs, mechanical, reliability study 3-76921
camera NEOPHOT 2, VEB Carl Zeiss JENA 3-47495
fast reactor, Na cooled, heat removal systems, design 3-67504
fast reactor core design 3-67517
nuclear, fast breeder reactor, design engineering 3-67502
nuclear, fast breeder reactor operation, safety and reliability, conference, Karlsruhe, Germany (1972) 3-67501
nuclear, fast reactor core design 3-67503
nuclear reactor components, operating experience (French) 3-67515
nuclear reactor operation, scram system trip, obs. (Russian) 3-67514
pressure tank system, totally automated probabilistic approach 3-46069
steam generators for Na cooled fast reactor, design 3-67505
structural creep reliability eval. using entropy principles 3-58668
structural reliability and minimum creep life at elevated temp., stat. eval. method 3-62494
Au-Ni metallisation, for IC and semiconductor devices, diffusion study 3-79528
IC, electromigration and metallisation lifetimes 3-43891
Nd:glass laser, mode locked, improvement 3-62718

remance

see also coercive force

- (35-x)NiO.8ZnO.xCoO.57Fe₂O₃, freq. depend. of permeabilities, induced anisotropy in magnetic spectra 3-47104
basalt from Pacific Ocean, magnetic properties 3-58967
basalt powder, multidomain, pseudo-single-domain moments, low field t.r.m. meas. 3-58866
CANNIKIN nuclear explosion, quasi-static mag. field changes 3-50962
chemical remanent magnetisation, Fe₃O₄ at 345°C 3-76537
Crozet Basin, deep sea core, rel. to mag. reversals 3-58961
Deccan Trap basalts, n.r.m. stability 3-58838
detrital remanent magnetisation of clay till deposits from glaciers 3-76651
dolerite, pliocene, pre-Balkans, natural remanent magnetisation, thermomagnetisation curves, palaeomagnetic stability 3-56099
garnet film, magnetic imperfections, remanent domain pattern obs. 3-44294
geomagnetic field drift in 1885-1965 period 3-56107
geomagnetic remanent field rel. to other geophysical and geological phenomena 3-56108
Hadrian's wall, age of viscous remanent magnetisation, a.c. demagnetisation techniques 3-44927
Jurassic Topley Intrusions, Endako, British Columbia 3-76654
limestone, Trenton, New York State 3-58945
lunar breccias thermal demagnetisation 3-47960
magnetite powder, multidomain, pseudo-single-domain moments, low field t.r.m. meas. 3-58866
microwave ferrite, temp. and stress sensitivities, review 3-41366
mineral constituents of intrusive rocks, relationship to natural remanent magnetisation 3-58970
oceanic basalts, low temperature oxidation causing carriers of natural remanence to become superparamagnetic 3-58971
Pacific western equatorial, palaeomagnetic study, sediment accumulation rates, correlation of magnetically disturbed intervals 3-58964
palaeo-poles determ. 3-59163
palaeointensity studies on magnetite by Thellier technique 3-58972
palaeomagnetic results from Martin Formation, Saskatchewan, stratigraphic correlation between sedimentary basins of Canadian Shield 3-58943
palaeomagnetic results from West Pyrenees, delineation of plate boundary between Iberian Peninsula and Europe, evolution of Bay of Biscay 3-58946
palaeomagnetic study of Guam, curvature of southern Mariana island arc 3-58958
palaeomagnetic study of Kahochella Group, Canada 3-58942
particulate assemblies, interaction effects on saturation remanence 3-50426
Pliocene basalt, North Bulgaria, natural remanent magnetisation, thermomagnetisation curves, palaeomagnetic stability 3-56099
pre-Cambrian dolerite dykes, palaeomagnetism 3-76665
Precambrian red beds N.W. Scotland 3-58944
rare earth-cobalt, permanent magnets, LnCo₅, prepared by liq. phase sintering 3-64521
rocks, ang. depend. of secondary magnetisation and demagnetisation 3-44792
rocks, anhysteretic remanent magnetisation, appl. to bore core reorientation (French) 3-61287
rocks, props. of Fe-containing minerals during chemical transforms. 3-61297
rocks, rel. to magnetic anomalies 3-58934
rocks, thermoremanent magnetisation in uniaxial compression at 20-200°C 3-44789
sedimentary rocks-dike contact point, natural remanence anomaly 3-44793
thermal demagnetisation studies to determine 3-58947
titanomagnetite, ultrafine intergrowths effect 3-56095
viscous magnetization in oceanic igneous rocks 3-58968
Co alloy, Cobaloy, magnetic particle for tape applic. 3-44262
Cr₂O₃ tapes, temp. dependence of relative saturation remanence and coercive force, obs. 3-55448
Fe-Co(49 wt.%)-V(2 wt.%) alloy, work hardened tempered, character. for high flux density apparatus (French) 3-68810
γ-Fe₂O₃ tapes, Co-doped and undoped, temp. dependence of relative saturation remanence and coercive force, obs. 3-55448
γ-Fe₂O₃:Co particles, temp. and conc. depend. 3-41362
GdYFe garnet: Co²⁺, props. rel. to latching phase shifter applic. 3-47097

remance continued

- Li₂O-Fe₂O₃-SiO₂ compositions, magnetic, elec. and physical props. 3-64967
MgMn ferrite, arc-plasma sprayed, for microwave applic. 3-41796
Sm₂Co₁₇, prep. by liquid phase sintering 3-44694

remant magnetism see remanence**remote control see telecontrol****remote control equipment see telecontrol equipment****remote metering see telemetering****repackaging see packaging****repeaters**

- optical, p.c.m., using GaAs laser, error-rate obs. 3-66897

replica techniques

- direct-replica prep. from steel fatigue specimen 3-46581
electron microscopy of porous surfaces 3-68142
epoxy resin-aliphatic resin:polyethylenepolyamine models, metal surface finish, dimensional deviations 3-50812
human articular surfaces, contour examination, profile recorder, stereomicroscopy, replication 3-59409
metallographic exam. method using replica made after thermal etching (German) 3-58632
relief-phase holograms for precoded video 3-77524
steel, Brinell hardness testing, difficult to reach areas, polystyrene replica 3-50806
GaAs specimen preparation, electron microscope examination (German) 3-52618
(K₂O-P₂O₅)_x-(WO₃)_{1-x}, glass, microphase separation, electron microscope obs. of surface replicas 3-72007

replicas see replica techniques**reproduction (copying)**

- see also photocopying; printing
electrostatic copy paper automatic testing system 3-66729
image-replicator, multiple-objective projection system 3-53938
Microfilm Duplicator, DOKUMATOR, VEB Carl Zeiss JENA, expose and development of diazo film 3-51642
organic photoconductor electrophotography, development 3-42596
CrO₂:S modified magnetic tape, for thermomagnetic duplication 3-41363

research and development management

- atomic energy, Japanese policy 3-63141
CIRENE pressure tube H.W.R., comparison with other systems 3-63135
fast-breeder reactor, in Holland (Dutch) 3-46057
SAGO company developing automatic systems for health organisation (Italian) 3-54034

residual stresses see internal stresses**resins see polymers****resistance (electric)**

- see also contact resistance; electrical conductivity; magnetoresistance; negative resistance; piezoresistance; skin effect
electrochemical cell, two probe, resistance component of potential, automatic compensation 3-48468
plasma heating, elec. cond. meas. (Russian) 3-71858
plasma ohmic heating, anomalous (Russian) 3-71919
soil during freezing (Japanese) 3-56036
Au-Al₂O₃-Au diode, series resist. and series capacitance, time depend. (French) 3-64415

resistance coupled amplifiers see d.c. amplifiers**resistance measurement**

- see also ohmmeters
cell-membrane, using oscillator (German) 3-42271
cryostat for high-ohmic samples (Czech) 3-51555
furnace system, two-, four-terminal resist. meas. 3-77406
gas-solid reaction kinetics, rate determ. by filament resistance monitoring 3-45559
high resistivity semiconductors, by van der Pauw method 3-42606
ion exchange membrane, elec. cond. determ., effect of temp., resistance meas. 3-51658
low-ohm low-temp. resistance box, design description 3-51654
low-resistance specimens, small resistance changes, a.c. synchronous detection 3-48471
meg-meg ohm meas., direct coupled current amplifier, constructional details 3-51648
metal films, rel. to diffusion coeff. determ. 3-51657
metal specimens, apparatus for measuring and recording elec. resist. during mech. testing 3-45535
ohmmeter, internal calibration (Spanish) 3-66283
photoconductivity, electrometric amplifier construction 3-77565
physical quantities meas. from natural vibrations attenuation of oscillator circuit (Czech) 3-56695
ratio determ. technique rel. to high purity Cu evaluation 3-64804
rectangular anisotropic material, principal resistivities, extension of van der Pauw's method 3-45533
semiconductor, four point probe meas., correction devisors, cylindrical coordinates 3-68619
solid bulk and surface resistivity, d.c., improved guarded electrode method 3-42605
superconducting thin films, internal friction and electrical resistance measurement, cryostat apparatus 3-48385
Ga:Ge, spreading resistance, rel. to quantitative detn. of dopant segregation during growth 3-69171
Nb-Al-Ge superconducting ribbon, study from 4.2 to 16 K 3-56696

resistance noise see thermal noise**resistance thermometers**

- bridge circuit, for low temp. resistance thermometry 3-42537
carbon resistor, temp. meas., 0.3 to 4.2K, empirical function between resistance and temp. 3-48387
cryogenic linear temperature sensor, Micro-Measurements Ltd., magnetoresistance, 4.2 to 300 K 3-59565
digital, resistance to time-interval convertor, -60 to 100°C (Russian) 3-66161
low temp., self-balancing resistance bridge 3-48393
quick-response thermometer for small temp. variations meas. 3-56633
Pt, as reciprocal Kelvin temp. sensor 3-77403
Pt, temp. measurement, on IPTS-68 scale (German) 3-42530
(U,Pu)₂O₃, centreline thermometry 3-45455

resistance welding

composite electrical contact, electron probe analysis 3-42722

resistivity *see electrical conductivity***resistors**

see also photoresistors; posistors; thermistors; thick film resistors; thin film resistors; varistors
carbon, temp. meas., 0.3 to 4.2K, empirical function between resistance and temp. 3-48387

resolving power (optical) *see optical resolving power***resonance**

see also circuit resonance; dielectric resonance; magnetic resonance; oscillations

audio frequency size effect seen in modulation of r.f. size effect 3-46788

boundary value problem, single perturbation type, resonance, improved method of matching asymptotic expansions 3-70532

building response to vibrations 3-59482

Coral Sea, tidal resonance obs. 3-53455

cylinder, thin flexible, towed in viscous fluid 3-42811

cylindrical shells, forced oscillations with gas-pressure fluctuations, variable stress analysis (*Russian*) 3-62535

damping, vector response loci, numerical analysis 3-70651

elastic constant, internal friction resonance-impulse method of determ., resonant frequency meas. room temp. to 2200 C 3-51527

elastic structure, dynamic parameters, orthogonality method using ground resonance test (*German*) 3-66527elementary particle physics, quantum mech. rel. to classical reson. scattering (*Czech*) 3-70889

e.m. field interactions with matter, book 3-74186

flexural vibrations in orthotropic plates, natural freq. calc. 3-42809

flute, mouth cavity resonance effects on frequency, experimental results 3-77336

forced vibr., coupled pendulum meas. system (*Russian*) 3-66133

frequency, vector response loci, numerical analysis 3-70651

geostationary satellites, first order perturbation theory (*German*) 3-51248gyropendulum mounted on moving base, combinative parametric resonance, analysis (*Russian*) 3-59546

Hamiltonian system, autonomous, third and fourth order resonances 3-66515

heated cylinders, vibrating vertical array, heat transfer rate 3-71736

helicopter, motion stability in nonlinear resonance conditions (*Russian*) 3-62441

isotropic materials, disc-shaped specimens, resonant frequency measurement, elasticity modulus and Poisson ratio determ. 3-51525

non-linear, method of averaging and simulation language CSMP 3-40094

nonstationary nonlinear multidegree-of-freedom systems, resonances 3-77833

oceanic internal wave resonant generation 3-73270

oscillations in harbour of arbitrary shape (*Polish*) 3-43589

particle, non-linear effects in spiral galaxies 3-59371

planetary motion, global soln. in resonance problem of Poincaré 3-51245

radiation redistrib., collisional effects 3-52262

r.f., validity of semiclassical description 3-45704

ring, discontinuously constrained and damped, forced resonance 3-40145

shells, fluid filled spherical, characteristic freq. 3-54127

skew stiffened plates, parametric reson. problems 3-70662

stellar atm., multiple scatt. of resonance radiation in plane layer and sphere 3-69918

system with two degrees of freedom, in mixed resonance, parametric vibrations 3-74070

trigonal system, dynamical, Jahn-Teller problem 3-68555

upper hybrid resonance, Imp 6 obs. of assoc. noise bands 3-51112

vibrating-systems, multiple-degree-of-freedom, stability limit of non-linear resonances 3-70641

He atom steady-state eqns. in matrix form 3-60374

resonance reactions and scattering, nuclear *see nuclear resonance reactions and scattering***resonances, baryon** *see baryon resonances***resonances, meson** *see meson resonances***resonant absorption of gamma-rays** *see Mossbauer effect***resonant cavities** *see cavity resonators***resonant gamma-ray interactions in crystals** *see Mossbauer effect resonators*

see also acoustic resonators; cavity resonators; crystal resonators; resonance

compound-mirror open resonator 3-53877

Fabry-Perot interferometer for complex dielectric constant meas. (*Japanese*) 3-59593

helical heavy particle accelerators, short, field distributions, measurements, calculations 3-59625

Josephson junction, resonator connected, electrodynamic props. in Aslamazov-Larkin model 3-75817

optical parametric oscillators, for tunable laser radiation, review 3-48935

orthotron, signal detecting element interaction with radiation, 2 to 2.8 mm (*Russian*) 3-66916reflection-type, in maser, direct i.f. generation (*Russian*) 3-57219superconducting, accelerating, interaction with high-current single bunch of particles (*Russian*) 3-48492**retrieval, information** *see information retrieval***revaporisation** *see vaporisation***reverberation**

see also anechoic chambers; architectural acoustics; echo

acoustic transducers, calibration, in reverberant water tank 3-42528

acoustic wave reverberation, diurnal variation in California current, 3 to 30 kHz, frequency dependence 3-77329

bounded space, steady state and transient responses 3-42430

characteristics meas. 3-53791

dome, of drive-in bank 3-42427

microwave, meas. by sampling technique (*German*) 3-54195

monaural and binaural free-field speech reception through ear-level hearing aids under noise and reverberation 3-48232

perception of spectrum, effect of late arriving reverberation 3-42293

reverberation continued

Philadelphia Academy of Music, reverberation time meas. 3-42432

reverberant room expts., design and analysis 3-39867

reverberation chamber, qualification procedure, effect of absorption and rotating vanes 3-39868

room, average sound power determ. for discrete freq. sources 3-48293

semireverberant fields, minimum measuring distance, bias and variance 3-42393

speech, anomalous loudness function, role of reverberation, experimental results 3-81276

toll centre switching meas., acoustic noise meas. 3-66089

volume reverberation signals, backscatter, level and zero crossings 3-45340

reviews

4f-band superconductors, high pressure effects 3-50291

A=4 nuclei, compilation of energy levels 3-43181

ab initio calcs. on small molecules 3-57626

Abbe's theory and holographic imaging (*German*) 3-54198Abbe's theory of optical microscope and subsequent developments (*German*) 3-53879achromatic human vision, mathematical models of edge-contrast phenomena (*Russian*) 3-48235

acoustic holography and imaging 3-70788

acoustic noise in industry, measurement and control 3-42469

acoustic test facilities, techniques and instruments at I.S.V.R. 3-56625

acoustical signal processing 3-45385

acquisition of scientific knowledge, practicability of controls (*German*) 3-73624

acrylonitrile-butadiene-styrene composite, review of processes and appls. 3-64981

aerodynamic noise generation 3-57739

air sampling, filter paper tape samplers 3-56564

alloys, splat cooling and metastable phases 3-80358

amorphous chalcogenide semiconductors, photoelectric phenomena 3-41231

amorphous Si and Ge, structural aspects, critical review of data and models 3-46589

analytical chemistry, new reactions and reagents 3-48648

anodic oxidation of Ti and alloys 3-41096

Antarctica, natural resource potential 3-47614

anthracene as semiconductor 3-55253

Apollo lunar exploration programme 3-45046

articulation index, evolution and modification 3-81267

astronomical optics, review of recent advances 3-53721

Atmosphere Explorer, scientific objectives 3-42066

atmospheric particulate matter, occurrence and chemistry 3-61447

atmospheric surface boundary layer, review 3-65301

atom-probe FIM 3-51745

atomic and molecular scattering of electrons in reln. to space travel, upper atmosphere, sun (*Dutch*) 3-63317

atomic fluorescence spectrometry 3-59697

atomic structure, role of spectroscopy, historical (*Hungarian*) 3-48318Auger electron spectroscopy (*Hungarian*) 3-80124

auroral He precipitation 3-47778

auroral oval, reevaluation rel. to particle precipitation, all-sky photographs 3-47777

axiomatic quantum field theory 3-78097

bats, echolocation behaviour, zoological survey 3-70108

beam-foil spectra, structure theory, review of results since 1970 3-78434

beam-foil spectroscopy, recent developments 3-77488

beta decay, superallowed, of O⁺ (T=1) states, summary of current data 3-74545

binary star systems as X-ray sources 3-81143

biological effects of e.m. radiation 3-45319

biomagnetism, direct interaction of magnetic fields 3-42365

Bloch's electrons and phonons interaction with a crystal surface (*French*) 3-50249

brain wave research, US Naval Academy 3-77207

bubble chamber techniques in high energy physics 3-56944

building vibrations and acoustics 3-59482

capacitance micrometers, design and applications 3-45419

capacitive discharge, formation processes 3-46561

carboxylic esters and derivatives, molecular structure and conformation 3-74927

cholesteric liq. crystals, mag. props. 3-55385

clay mineral crystal phase, water adsorption in intersheet space (*Polish*) 3-44832

clear air turbulence, radar detection 3-44962

coatings, methods of chemical analysis 3-59693

colour measurement, instrumentation, applications to food processing industry, methods, review 3-59588

colour perception, recent research 3-81303

composite material, directionally solidified eutectic, appls. 3-50766

compound semiconductor alloys, band structure 3-50135

concert halls, evaluation methods 3-42431

condensation, film, binary vapour mixtures, completely miscible mutually insoluble condensed phases (*German*) 3-64157

continental drift and paleoclimate 3-65128

coronary blood flow assessment, using ¹³³Xe and ⁸⁴Rb 3-56537cosmic rays, origin (*French*) 3-65559

cosmic-rays, high-energy physical instrumentation, techniques, review 3-77633

cryoelectronics, developments 3-59612

crystal growth from solution, theory difficulties 3-63968

crystallisation, gas bubble nucleation 3-63967

CW metal vapour lasers 3-48900

data processing systems for Earth resources surveys 3-51174

deep sea sediment cores, paleomag. record, effect of sedimentation on magnetisation 3-80677

detection techniques, charged relativistic particles, transition radiation techniques, review 3-77631

diffraction gratings, design and production methods 3-62081

digital correlation techniques 3-42463

dispersion sum rules for strong and e.m. interactions 3-43078

displacive phase transitions, theory 3-46692

reviews continued

- distance meas. in Universe rel. to age estimates (*Danish*) 3-44996
 Doppler broadening effect on collision cross section functions 3-60485
 double beam interferometry, electrochem. studies 3-66236
 double pumped phosphors, materials and devices 3-44449
 dynamic plasticity, macroscopic and microscopic aspects 3-49923
 E-region, measurement of electron-temperature, Langmuir probe, incoherent scatter radar, results, review 3-73356
 earth's near space environment 3-56222
 Earth's polar oscillation and migration, historical (*Hungarian*) 3-50963
 earth's shape determination (*German*) 3-58820
 earthquake focal mechanism studies 3-65224
 echolocation, marine dolphins, fresh water dolphin 3-70112
 elastoplastic deformation and load carrying capacities of thin metallic shells (*Russian*) 3-76220
 electrochemical detection and analysis instruments, ion selective electrodes, pH meters 3-40072
 electromagnetic pumps and flowmeters, for fast reactors 3-43275
 electron deep inelastic scattering 3-54321
 electron laser, review of stimulated bremsstrahlung 3-56684
 electron micrograph analysis, practical methods 3-66350
 electron microscope, scanning 3-59673
 electron microscope superconducting lenses (*Czech*) 3-73904
 electron microscopy, h.v., studies of metals and other materials 3-49807
 electron ring accelerator, of Univ. of Maryland, status report 3-56758
 electron ring accelerator experiments in Karlsruhe, Germany 3-56755
 electron ring accelerators research in Japan 3-56754
 electron spectroscopy for study of atomic and molecular energy levels 3-60380
 electron-phonon interaction and characteristics of metal electron 3-75703
 electronic props. of one-dimensional solids 3-50134
 electrophotography 3-77552
 elemental semiconductor thin film prep. and props. 3-76146
 ellipsometry, electrochem. studies, surfaces and surface films 3-66197
 ellipsometry, principles of technique, application to electrochem. studies 3-66196
 ellipsometry of fluid interfaces and membrane-like systems, review 3-77427
 embrittlement by liquid metals 3-47421
 equatorial ionosphere electric fields, techniques and measurements 3-42062
 exchange interactions and spin wave theory 3-64451
 exciton theory 3-58240
 extractive concentration, anal. of microquantities of elements 3-48647
 fast reactor physics in France 3-49353
 fast reactor physics program in Japan, review of current status 3-49337
 fast reactor physics progression Federal Republic of Germany 3-49336
 fast reactor program in USA 3-49338
 fatigue-damage theory 3-76185
 ferrite, polycryst., microwave relaxation 3-41393
 ferrites, after-effects due to ion and electron motion, review (*German*) 3-68803
 ferroelectricity and applications 3-55539
 ferroelectrics, bibliography, of literature from April to June 1972 3-44383
 ferromagnetic domain theory, thermodynamics, recent results 3-75863
 ferromagnetic fluids thermodynamics (*Russian*) 3-79878
 Filler-Elastomer interactions 3-80439
 fine grain photoemulsion, for nuclear research, dosimetry and autoradiography 3-53943
 flame spectroscopic temp. meas. review 3-42713
 fusion reactor technology studies at ORNL 3-60320
 fusion reactors, computer models (*Dutch*) 3-74740
 Galactic X-ray sources, radio obs. 3-81146
 gas lasers, frequency stabilization 3-62155
 gas phase n.m.r. 3-60521
 gaseous ion recombination 3-57678
 generator coord. method for nucl. bound states and reactions 3-52116
 geomagnetic field of external origin 3-56138
 geomagnetic micropulsations, review of research in January 1969 to July 1972 period 3-41924
 hadron resonances, classification schemes, coupling 3-52023
 heavy and superheavy nuclei, calcs. of fission barriers 3-54520
 heterojunction injection lasers 3-74247
 high energy physics horizons 3-56857
 high polymers, stressed, e.s.r. obs. of free radicals (*German*) 3-61223
 high powered solid-state/molecular, properties and applic. 3-62685
 holograms as optical elements 3-45501
 human engine, cell mitochondria, energy requirements 3-56474
 hydroacoustic transduction 3-42456
 hyperfine interactions of trans-lead elements, nuclear radiation studies 3-68904
 II-VI compounds, associated point defects 3-58030
 II-VI semiconductors, injection electroluminesc., review (*Polish*) 3-41586
 II-VI semiconductors, large energy gap, interaction between electrons and acoustic waves, review (*Polish*) 3-41236
 III-V semiconductor, liquid phase epitaxial growth 3-69162
 image processing 3-62167
 injection laser applications 3-48930
 interstellar molecules, formation mechanisms, spectroscopy 3-42245
 Io, post eclipse brightening 3-69859
 ionic solids, superexchange coupling, review of theory 3-47012
 ionospheric behaviour in the region of the magnetic equator 3-59137
 ionospheric E-region and irregularities in equatorial electrojet 3-42038

reviews continued

- ionospheric h.f. strong r.f. waves absorption 3-76812
 i.r. and low-light-level imaging, Si technology impact 3-48373
 i.r. astrophysics, theories of emission mechanism and energy sources 3-42219
 i.r. sources, celestial, maximum known brightness 3-45160
 i.r. sources, tunable, state-of-the-art 3-78008
 i.r. spectroscopy 3-51547
 i.r. spectroscopy at subambient temps. 3-59589
 i.r. testing devices, pyrometers, displays, image converters, new instruments in E. Europe, review (*German*) 3-73685
 i.r. transmitting materials 3-77545
 isospin impurities in nuclei 3-54382
 isotope separation, laser appl., historical review 3-80567
 ISR, at CERN, layout, physics equipment and use for experiments 3-56823
 jet noise 3-57740
 Jupiter, outer atmosphere 3-65778
 laboratory filtration 3-45557
 large bubble chambers 3-77648
 large cryogenic bubble chambers 3-77647
 laser injection locking 3-66791
 laser irradi. of solid targets, expts. (*Rumanian*) 3-62732
 lasers and glass technology 3-74243
 lasers in chemistry 3-57222
 layered lunar/earth surfaces, measurement of electrical parameters, bibliography 3-45241
 LEED for surface structural analysis 3-50060
 lenses, manufacture and testing 3-77450
 lepton production in pp collisions, expts. at ISR 3-66991
 light velocity measurement techniques over last 300 years (*Norwegian*) 3-70261
 liquid, transport processes, state-of-the-art 3-72214
 liquid crystal, nematic, behaviour in electric field, review (*German*) 3-75465
 liquid crystals, spectroscopy 3-43747
 liquid crystals, texture 3-79227
 liquid metal, struct. and dynamics 3-49822
 liquid metal and alloy, struct., expt. and theory 3-49821
 liquid metals, atomic transport properties, viscosity, self-diffusion, results, techniques, theories, models, correlations, review 3-50015
 liquid metals, electronic structure, transition and rare earth metals and alloys, electrical and magnetic props., theories 3-50112
 liquid metals and alloys, spin relaxation of conduction electrons, theory 3-50460
 liquid metals and alloys, thermodynamic props. interpretation, review 3-50010
 liquid statistical theory, method of integral eqns., esp. Percus-Yevick eqn., review 3-79221
 liquid-crystal applications (*Italian*) 3-43753
 LMFBR design considerations, performance and safety 3-71192
 low-latitude ionosphere, solar and lunar tidal effects 3-42022
 low-light-level imaging, using television camera tubes and direct-view intensifiers 3-48413
 Lunar and Planetary Laboratory and its telescopes 3-70054
 magnetic field, megagauss, production, meas., appl. 3-74193
 magnetic glass, mag. order in amorphous materials 3-46977
 magnetic nucleation fields for superconductor in contact with normal metal (*French*) 3-55382
 magnetospheric substorms 3-47664
 Maine-Yankee Power Station, design, initial operation 3-74694
 Mariner 9 geological data 3-65747
 Mars, active and ancient volcanism 3-73448
 Martian surface markings and crust 3-61685
 mass spectrometry of ion cyclotron resonance 3-54000
 material and/or geometrically nonlinear structural analysis, evaluation of solution procedures 3-45673
 material damping, mathematical models and experimental techniques 3-66093
 mean turbulent field closure models, survey 3-63624
 mechanics, solid, heterogeneous materials, statistical theory, recent developments, review 3-74017
 meson-baryon scatt. and baryon resonances, partial wave analysis 3-45907
 metals analysis in particulate pollutants by emission spectroscopy 3-45332
 metals and alloys, creep behaviour, basic mechanisms, review 3-46667
 metals and alloys, superconducting phase transition rel. to plastic properties 3-53555
 metastable atomic states, hyperfine and Zeeman studies by atomic-beam magnetic resonance, review 3-49393
 meteorological data, objective analysis 3-80731
 MHD generators, electrical conductivity of turbulent non-equilibrium plasma 3-54848
 microcontinuum fluid mechanics 3-62448
 microwave ferrite, temp. and stress sensitivities 3-41366
 molecular crystal, ionic states 3-72306
 molecules, luminescence, solvation shell composition (*Polish*) 3-60472
 m.o.s. structures, Si based, transient behaviour and recombination processes (*Hungarian*) 3-68707
 m.o.s. technology, review 3-50278
 multidimensional kinetic problems, diffusion theory, state-of-art 3-71151
 multiparticle production processes, combination of inclusive and exclusive data 3-43127
 Navier-Stokes equations, numerical soln. methods 3-49534
 negative ions, technology, properties, sources, accelerators 3-57281
 nematic liq. crystals, mag. props. 3-55385
 neutron scattering obs. of mol. motion in solids and liqs. 3-68140
 noise abatement zones 3-56586
 nonferrous metal chemical analysis 3-59695
 nonferrous metals, methods of chemical analysis 3-59694
 nonlinear acoustics 3-48312
 nonlinear mechanics problems solved by method of variable scale (*Polish*) 3-66584
 nonlinear optical and electro-optical props. of dielects. and ferroelects. 3-43032
 nonlinear optical crystals and their applications 3-40288

reviews continued

- nonlinear optical susceptibilities and parametric interactions 3-54248
- nonsinusoidal e.m. waves (*German*) 3-54193
- nuclear applications in art and archaeology 3-53809
- nuclear decay rates, perturbation 3-54442
- nuclear e.m. transitions and moments 3-54433
- nuclear fission and production of superheavy nuclei (*Japanese*) 3-71133
- nuclear fuel assays, instrumentation, gamma-ray spectroscopy, neutron system, calorimetry 3-47502
- nuclear fuel elements, Clementine reactor, development 3-67562
- nuclear fuel financing 3-67408
- nuclear fusion, laser induced, present state and future prospects (*German*) 3-43316
- nuclear level densities 3-54394
- nuclear medicine in India 3-45317
- nuclear moments of short-lived high-spin states, exptl. techniques 3-45930
- nuclear reactor, H.B. Robinson Unit No.2, operating experience 3-74692
- nuclear reactor fuel elements, development for Clinton, Hanford and Brookhaven reactors 3-63212
- nuclear reactor fuel elements, EBR-I, history of development 3-67563
- nuclear reactor power plants, safety-related occurrences, 1972 review 3-74700
- nuclear science annual review (1972), book 3-53808
- nuclear shell model, present status and reasons for success 3-67231
- nuclear structure, new facets 3-78268
- nuclear thermal breeder reactors 3-54537
- ocean current meter technology 3-69747
- one-electron theories of solids description in terms of projection operators 3-52775
- optical activity, spontaneous generation 3-73635
- optical and photoelectric measurements in solids (*French*) 3-41494
- optical data processing, lasers, holography, data storage, systems, techniques 3-59849
- optical microscopy, application to electrochemical studies 3-66198
- optical parametric oscillators 3-48935
- optical spectroscopy, radiation sources, monochromatization, detectors and spectrometer systems 3-56669
- organic dye lasers 3-54226
- osteoporosis, methods of in-vivo measurement 3-66406
- parametric artificial talker 3-81266
- parametric instabilities in plasma 3-68015
- parton dynamics, recent developments 3-70941
- parton picture of elementary particles 3-67061
- PEP design study 3-56856
- photoelectron spectroscopy, band structure of nonmetals 3-50649
- photoelectron spectroscopy in atomic molecules and solid state studies 3-61104
- photoemission, history (*French*) 3-41609
- photoemission, theoretical problems (*French*) 3-41611
- photographic diffusimetry (*German*) 3-53944
- photographic surveillance 3-66278
- photometric measurement techniques and equipment (*German*) 3-53902
- photometry, minimally-distinct-border, chromaticity difference, method 3-66214
- physico-chemical aspects of neutron studies of molecular motion 3-57645
- picosecond spectroscopy and molecular relaxation 3-57647
- piezoelectric materials, for vibration detection and excitation, review 3-68932
- planetary atmospheres, Uranus and Neptune 3-65780
- plasma absolute and convective instabilities 3-75347
- plasma collisionless shock waves 3-79096
- plasma confinement in internal-ring devices 3-49739
- plasma diagnostics of high-temperature, high density plasmas by radiation analysis 3-43685
- plasma instabilities, basic features 3-75346
- plasma parametric instabilities, linear and nonlinear theory 3-75382
- plasma parametric instabilities expts. 3-75384
- plasma physics, present-day position (*Dutch*) 3-40761
- plasma turbulence, including elementary excitations method of statistical averaging and effective turbulent collisions 3-75324
- plasma-sphere-plasma-pause, characteristics and research 3-47793
- plasmon excitation by X-rays 3-44047
- plastic, scintillation counters, review 3-77640
- plastic crystals, with orientational freedom of mols. (*Polish*) 3-49856
- plastic deformation and brittle fracture in heterogeneous system (*Russian*) 3-55752
- Polar Experiment 3-56155
- polymer, hydrostatic press. effect on mech. props. 3-80475
- polymer, treeing breakdown, voltage induced mechanism, review 3-47214
- polymer chemical analysis 3-59696
- polymer films, laboratory methods of prep., review 3-48346
- polymer fracture mechanics 3-76364
- polymer melt rheology, recent publications 3-50784
- polymer with conjugated bonds, Mott semiconductor, one-dimensional theory 3-75715
- polymeric materials, dynamic loading 3-55899
- polymeric streaming fluid, flow props., flow birefringence obs. (*German*) 3-60592
- polymers, electrical properties 3-44363
- polymers, semi-crystalline, amorphous transitions 3-49851
- polywater, anal. of explanations and experimental data, review (*German*) 3-40841
- position sensitive detectors and multi-counter arrays for neutron studies 3-56940
- printed circuit and IC manufacture, artwork and film generation (*German*) 3-56688
- pulsar properties, theoretical interpretation 3-65910
- pulsars; rotating neutron star model and observational evidence, review 3-53688
- Quad-Cities Station, operating experience 3-74693
- quark search in terrestrial matter 3-61615

reviews continued

- quartz spectrograph with oscillating plateholder, appl. (*French*) 3-70064
- radiation damage mechanisms, e.s.r. spectroscopy 3-55459
- radiocardiology, basic concepts and applications 3-53754
- radiography, collimation, rectilinear scanners, camera imaging equipment, designs 3-70143
- radiography, imaging systems, instrumentation, performance analysis 3-70142
- radiography, imaging systems, radiotracers, collection and analysis factors, instrumentation 3-70145
- radiography, tomography, radionuclide, systems, current state of the art review 3-70144
- radioisotopes in X-ray fluorescence analysis, review 3-62372
- rare earth phosphides, cryst. chem. and phys. props., review 3-64018
- residual stress 3-55025
- rotating blades noise generation 3-57741
- satellite meteorology 3-80734
- scales and reticles, optical instrument manufacture, classification in terms of material and manufacture 3-53899
- O. Yu Schmidt's ideas in atm. science 3-47606
- scintillation counters, design factors, fundamentals, performance 3-66319
- scintillation counting equipment 3-62224
- sea floor spreading, fluid dynamic models 3-80639
- seismology, instrument developments 3-44934
- semiconductor, bound exciton complexes (*Polish*) 3-58236
- semiconductor, size effect theory 3-58253
- semiconductor lattice dynamics 3-72142
- semiconductor relaxation regime behaviour 3-55259
- semiconductor surface quantisation 3-50261
- semiconductors, excitons bound to defects, binding energy, theoretical 3-50160
- semiconductors, highly excited, experimental aspects 3-50158
- semiconductors, highly excited, theoretical aspects 3-50159
- shear flow, stably stratified, linear viscous stability theory 3-60551
- shells weakened by holes, stability, stress distrib. around holes (*Russian*) 3-45654
- shutter exposure time testing instruments 3-39962
- Si clean surface physics 3-50059
- solar flare radio emissions 3-65717
- solid, transport processes 3-72339
- solid lasers, optically pumped, sensitized energy transfer and near i.r. operation 3-48917
- solid multiparticle systems, fluidisation, sedimentation 3-79030
- soliton, current status of research, inverse method 3-66508
- spectral density method applied to systems showing phase transitions 3-62599
- spectral wings in a low pressure atomic gas due to formation of quasi-molecules 3-60349
- spectrochemical analysis instrumentation 3-40073
- specular reflection spectroscopy, electrode-solution interphase 3-66227
- storage rings, in Novosibirsk 3-56810
- storage rings, usefulness and practicability in high energy physics 3-56858
- stratified fluid turbulent mixing away from boundary layer influence 3-60532
- strong interactions at high and very high energies, exptl. progress 3-40384
- superconducting magnets, pulsed, particle accelerator applications, recent progress, trends 3-56794
- superconducting proton linacs 3-56713
- synchrotron radiation, uses in research 3-56986
- synchrotron radiation as u.v. source, 10-1000 Å, spectroscopy applications 3-39930
- TCNQ charge transfer salts, mag. props. 3-55425
- technological activities at "Laboratori Gas Ionizzati", Frascati, Italy 3-60640
- thermal radiation atmos. transmission from 4π source to 2π receiver, survey report 3-53463
- thermodynamic props. of metals and alloys, exptl. meas. techniques (*German*) 3-42539
- thermodynamic props. of metals and alloys, exptl. method (*German*) 3-53200
- thermometer screen design 3-48371
- thermonuclear fusion, laser-induced 3-71330
- thin film refractive index meas. 3-77462
- time-interval meters, digital, methods, design principles, comparison, review 3-66281
- time-of-flight signals, distortions 3-42608
- track chambers, bubble chambers, filament chambers, scintillation chambers, discharge and condensation chambers 3-70400
- track sensitive targets and rapid cycling bubble chambers 3-77649
- transition metal alloy, chemist's view 3-41309
- transition metal alloys, physicist's view 3-41320
- transition metal liquid alloys, mag. susceptibility (*German*) 3-55418
- transition metals and alloys, magnetic susceptibility 3-46982
- turbulence, low amplitude 3-60610
- turbulence theory, Navier-Stokes eqns. closure problems 3-78956
- u.s. holography, surface relief technique, theory and practice (*French*) 3-51882
- vacuum breakdown, rel. to device design limitations 3-57704
- vacuum pumps, performance characteristics 3-56653
- van der Waals attraction in and between solids 3-49869
- Venus' transits, obs. from Japan, Dec. 9, 1874 event 3-61700
- vibration \rightarrow vibration energy transfer 3-57681
- viscoelastic nonlinear wave propagation 3-70646
- water quality turbidity meas. 3-61930
- wave mechanics, the first fifty years, book 3-77871
- weather forecasting, by computers 3-44908
- Weinberg model tests at CERN with Gargamelle, review 3-66964
- Wigner quasichlassical theory for particles (*French*) 3-57118
- X-ray absorption spectra of solids, atomic one-electron vs. band calcs. 3-47323
- X-ray crystallography, biographical review (*German*) 3-77346
- X-ray photoelectron spectroscopy 3-57646

reviews continued

- N-N effective range expansion parameters 3-54397
 pp scatt. models reviewed, including Regge-pole, dual, Pomeron parametrizations and scaling models 3-71005
 π N amplitudes at intermediate and high energies 3-40385
 Ag ion conductors high conductivity solids 3-61260
 CO₂ high power CW laser 3-43007
 CO₂ laser technology 3-48901
¹³C, n.m.r., methods and chem. appl. 3-54729
 GaP single crystal growth technology 3-50660
 He/H solar abundance 3-47894
⁴He liquid, structure and excitations, review 3-58158
 Lu, high purity, physical and metallurgical properties 3-63981
 NO and NO₂ emissions from stationary sources, monitoring, instrumental techniques 3-61933
 Pb chalcogenides, small energy gap semiconductor, band structure, review (Polish) 3-41131
 Pb-salt tunable diode lasers 3-48929
 Sb₂Bi_{1-x}, small energy gap semiconductor, band structure, review (Polish) 3-41131
 Sn chalcogenides, small energy gap semiconductor, band structure, review (Polish) 3-41131
 Th, isolation from ores, atomic energy programme 3-67560
 U, isolation from ores, atomic energy programme 3-67560
 U, nuclear fuel rods for CP-3 methods of fabrication 3-67561
 U resources and production in United States 3-74722
 W wire, recrystallisation, creep (Hungarian) 3-72989
 Y₃Al₅O₁₂:Nd lasers, current status 3-48916

revolution see rotation

revolving see rotation

rewinding see winding (process)

Reynolds number see flow

r.f. amplifiers see radiofrequency amplifiers

r.f. heating see radiofrequency heating

r.f.i. see radiofrequency interference

rhenium

- atom, partial wave calc. of scattering amplitude, reln. to electron diffraction determ. of molecular structure 3-78661
 chemical reaction with ZrC, high temp., phase equil. 3-72978
 desorption of H₂, isotope replacement reactions 3-41092
 electron-phonon interaction, from neighbour electron gas model 3-79447
 FEM tip, microcrater form, on microparticle bombard. at limited field emission currents 3-44523
 LEED from (0001), multiple-scatt. resonances within atomic monolayer 3-41067
 pump filament in new catalytic pump for H pumping 3-39888
 u.s. attenuation measurements, transverse and longitudinal waves along c axis in normal and superconducting states 3-58337
 X-ray L_{III} absorption discontinuity, fine struct. 3-47327

rhenium alloys

see also rhenium compounds

- Mo-Re alloy, analysis of lattice specific heat 3-58134
 Mo-Re (35 at.%) interaction of twins with grain boundaries, substructures 3-41707
 Mo-Re-C, ageing, heat treatment, 1400-1800°C, hardness, microstructure 3-76174
 Mo-Re(34 at.%), α -phase precip. and flux pinning, electron microscope obs. and mag. hysteresis 3-50697
 Mo-Re(50%), fast reactor neutron irradi., tensile props. 3-79386
 Ni-Re, thermo-e.m.f., temp. depend., 77-1300K (Russian) 3-72346
 Pd-Rh-Ni, spin fluctuation resist., 1.3-20 K 3-64480
 W-Re, micro- and macrodefect. characts., foreign atom binding effects (Russian) 3-80271
 W-Re, thermal expansion coeff., anomalous conc. depend. 3-72213
 W-Re b.c.c. solid solns., electronic struct. anomalies (Russian) 3-79621

rhenium compounds

see also rhenium alloys

- ReS₄²⁻, mag. circular dichroism assignment of longest wavelength band 3-54663
 Cu-Ni ores, X-ray spectrometric anal., segregation 3-48659
 ReO₃, electronic structure and press. dependence by Korringa-Kohn-Rostoker method 3-58204
 ReO₄⁻, in KI and CsI, i.r. absorpt. and local symmetry (Russian) 3-41542
 Re₂O₃, struct., electron microscope obs. (French) 3-60705
 Re₂O₇, molecular structure, electron diffraction determ. 3-54611
 ReOF₄, vibrational spectra 3-72626
 Re(V, VII and III) complexes, X-ray photoelectron spectra, Re-O and Re-halogen binding energies, struct. 3-74994

rheology

see also plasticity; viscoelasticity

- colloidal dispersions, meas. of microrheology by microtube technique 3-59722
 coniferous wood tissues molecular rheology 3-52412
 deformation instability effects in rheonomic media, instantaneous hardening and deform. aging 3-42797
 epoxy resin used for photoelastic models, mech. and optical creep (Polish) 3-61214
 PMMA suspension in dibutyl phthalate, properties 3-61231
 polymer, rel. to chain branching (German) 3-63598
 polymer flow between calender roll, force and energy parameters 3-61218
 polymer melt rheology, recent publications, review 3-50784
 porous solids, nonlinear and semilinear rheology 3-69509
 resin binder for graphitic fuel particles (German) 3-71267
 rock rheology from wavelength selection in tectonic folding 3-76603
 rocks, rheological models and spatially continuous mass creep 3-47657
 structured systems, dispersions and high mol. wt. compounds 3-73073
 structured systems, kinetic curves of shear stresses 3-73070
 viscometer, rotation, bell-type coaxial cylinders, reduction of edge effects, rheological characteristics, highly viscous liquids 3-54054

rheology continued

- viscoplastic Shvedov-Bingham material over infinite plate, transient flow 3-71765
 viscosity measurement, eccentric cylinder and displaced hemisphere rheometers, Weissenberg rheogoniometer, anomalous results, highly viscous fluids, cavitation 3-39854
 Weissenberg rheogoniometer for dynamic properties (French) 3-47493
 Al₂O₃ colloidal dispersions, rheological props. 3-53287
 K₂O-BaO-B₂O₃ glasses, viscosity obs., activation energy 3-58070
 Mg-Li(8%) alloy, steel reinforced, model for behaviour prediction (Russian) 3-73011
- rho mesons**
 ρ - ω interference, isolation in $\pi^-N \rightarrow \pi^-\pi^+N$ interactions, 3-6 GeV/c 3-70988
 boson triad (ρ', ω', ϕ') approach to $pp \rightarrow KK$, 700 MeV/c 3-62873
 coupled channel model, qualitative features of reactions $e^+e^- \rightarrow \pi^+\pi^-$ and $e^+e^- \rightarrow \pi^+\pi^-\pi^+\pi^-$ 3-74376
 dominance and zero contours in low-energy $\pi\pi$ scattering 3-74425
 duality, generalized potential and failure of ρ meson bootstrap 3-43122
 inclusive reactions, ρ dominance and Regge coupling 3-49061
 matrix elements in $\pi^-p \rightarrow A_1p$ reaction at 4.45 GeV/c, helicity conservation 3-62890
 photoproduction in high energy region, dual parton model 3-74372
 production, obs. by phase-shift analysis of elastic $\pi\pi$ scattering, 600-1900 MeV 3-70983
 production by $K^+p \rightarrow$ four or five bodies at 2.11 to 2.72 GeV/c, cross section 3-78204
 production in $\gamma p \rightarrow \pi^+X^+$ reaction, vector meson dominance 3-74375
 production in $\pi^-p \rightarrow \rho N$ interaction at 2.3 GeV/c, structure in momentum transfer distrib. 3-71010
 production on nucleons, isoscalar exchange contribs. 3-57431
 properties, nonpolynomial Lagrangian theory, static $\pi\omega$ scattering 3-62921
 Regge trajectory curvature, reln. to difference of π^+p total cross section 3-43158
 skew-symmetric field quantisation, A_1 and ρ mesons from violation of local Lorentz invariance 3-48986
 Weinberg's low-energy $\pi\pi$ model, continuation of zero contours into ρ region 3-43139
 $e^+e^- \rightarrow \rho^0 +$ anything, low, high energy, $\rho^0 \rightarrow \pi^+\pi^-$, study of reactions 3-59968
 $e^+e^- \rightarrow$ hadrons, duality relation between vector meson formation and scaling behaviour 3-70932
 ep electroproduction of ρ^0 , 19.5 GeV, mass spectrum shape, momentum transfer distribution, polarisation 3-67039
 $\gamma N \rightarrow \rho^0 + X$, 7.5 GeV, vector dominance model 3-78144
 $lN \rightarrow lN\rho$, lepton polarisation, one-photon approximation anal., decay 3-78145
 NN ρ vertex, weak P-odd, in $np \rightarrow d\gamma$ reaction (Russian) 3-40376
 $pd \rightarrow {}^3\text{He}\rho^0$, 5 GeV, cross section meas. 3-78199
 π - ρ mass spectrum in πN interaction, single peripheral model of Deck effect 3-74404
 $\pi^+p \rightarrow \rho N$, 6 GeV/c, differential cross sections, density matrix elements, simple model proposed 3-67129
 $\pi\pi$ phase shift analysis in ρ resonance region in $\pi^-p \rightarrow \pi^-\pi^+n$ reaction 3-70979
 $\pi\pi$ scattering lengths, current algebra, unitary constraints 3-78187
 $\pi\rho \rightarrow \pi\rho$, location of zeros in helicity amplitudes, rel. to duality (French) 3-67125
 $\rho(1710)$, decay modes study at 8 and 18.5 GeV/c in π^-p interaction 3-43148
 $\rho(1710)$, production on nuclei by 11.7 GeV/c, π^+ induced reactions 3-40397
 $\rho \rightarrow e^+e^-$ identity of strong-interaction coupling constants, avoidance of neutral currents 3-66963
 $\rho \rightarrow \pi\gamma$, anomalous magnetic moments of nucleon, strong interaction coupling consts., one-pion approximation 3-59959
 ρ Regge trajectory, linearly rising, bootstrapping calculation using Balazs method 3-74345
 ρ - ω interference in $\pi N \rightarrow \pi\pi N$ interaction at 3, 4 and 6 GeV/c 3-71013
 ρ - ω mixing parameter phase from unitarity relation 3-78230
 ρ^0 , ρ^- production in π^-p two-prong events at 4.45 GeV/c 3-49056
 $\rho^0(765)$, vector meson-current coupling consts. 3-70925
 ρ^0 amplitude separation for Pomeranchuk and f exchange reactions, dual absorption model 3-74406
 ρ^0 electroprod. at high virtual-photon four-momentum 3-52009
 ρ^0 production, coherent phase hypothesis of p-wave amplitudes 3-67094
 ρ^0 production, coherent phase hypothesis of P wave amplitudes, validity 3-71012
 ρ^0 production in $\pi^-N \rightarrow \pi^-\pi^+N$ reaction at 3-6 GeV/c, obs. with Argonne Effective Mass Spectrometer 3-70988
 ρ^0 production in π^+d interactions at 4 GeV/c, Estabrooks-Martin analysis 3-71014
 ρ^+ production in π^+p reaction at 11.7 GeV/c, two-prong fitted channels 3-57439
 ρ^+ production in $\pi^+p \rightarrow \pi^+\pi^0$ at 2.67 GeV/c, interference effects 3-40399
 ρ^+ , universal coupling in Veneziano-type representation 3-67007
 $\rho^{(0)}(1600)$, vector meson-current coupling consts. 3-70925
 ρ^0 production in π^- interactions with quasifree neutrons of light nuclei, decay asymmetry (Russian) 3-40515
 ρ^+ , produced in $\gamma p \rightarrow \pi^+\pi^-\pi^+p$ at 18 GeV, mass, width and spin-parity assignment 3-57364
 $\rho^+(1650)$, contribution to nucleon form factor, analysis using $\bar{p}p \rightarrow \pi^+\pi^+\pi^0$ data 3-57339
 ρ^+ production, obs. by phase-shift analysis of elastic $\pi\pi$ scattering, 600-1900 MeV 3-70983
 ρ^+ production in $\gamma p \rightarrow \pi^+\pi^-\pi^+p$ at 9-18 GeV, spin-parity analysis 3-57365
 ρ^+ vector boson, gauge model, current algebraic treatment 3-70864
 ρ^+ vector boson in gauge model realising pseudo-Goldstone idea for pion 3-70862
 ρ^0 - ϕ e.m. mixing parameter, appl. to $\phi \rightarrow \pi\pi$ decay and $e^+e^- \rightarrow \pi\pi$ 3-49005

rho mesons continued

- $\rho^0 N_1 \rightarrow \pi N_2$, vector meson dominance and mass dependence of Ball's invariant amplitudes 3-67084
 $\pi\pi$ Regge residue function from sum rules and new representation for $\pi\pi$ amplitudes 3-74444

rhodium

- adsorption of N_2 at room temp., sticking probability 3-68498
 band structure calc., of cubic 4d Rh 3-72313
 cation, impurities in AgBr and AgBr(Cl) crystals, photographic emulsions, behaviour in pulsed electrostatic field, space charge concept (*Russian*) 3-47594
 e.p.r. in AgBr 3-79900
 films, mirrors, evaporated, reflectance, transmittance, optical constants, effect of surface dielectric films 3-66203
 Hall and Nernst-Ettingshausen coeffs., thermo-e.m.f., resist., temp. depend. (*Russian*) 3-52825
 neutron detector, flux and fluence, explicit solns. 3-42651
 solid thermal props. at high temps. 3-79666
 solubility of hydrogen, temp. depend. 3-41017
 thin plastic foil, electrodeposition, addition of H_2O_2 soln. to electrolyte 3-76461
 Rh:Er, Dy, Yb, γ -ray angular correlation by implanted ions, crystal effects 3-41460
 Si:Rh, photoelectric. obs. of impurity states 3-64377

rhodium alloys

- see also rhodium compounds*
 actinide-Rh phases, prep. and props. 3-46604
 rare earth-Rh, 7:3 phases, crystal. structure and mag. props. 3-79274
 Cr-Rh system, constitution diagram, metallography, X-ray diffraction, electron probe obs. 3-69193
 Cu-Rh, f.c.c., lattice parameters, magnetic properties 3-79277
 FeRh, antiferro-ferromagnetism transition in pulsed mag. field up to 300 kOe 3-50368
 FeRh, near equiatomic alloys, magnetisation curves, elec. resist. in fields to 370 kOe 3-47096
 GdRh₂, ferromagnetic, hyperfine fields determ. by n.m.r. 3-79927
 Ni-Rh, electronic density of states determ. 3-79603
 Ni-Rh, giant mag. moments critical behaviour near Curie point, magnetisation obs. 3-47031
 NiRh₃, hyperfine interactions, ²³⁷Mossbauer obs. 3-68905
 NiRh₃, magnetic susceptibility and electrical resistivity measurements, stabilisation of 5f energy band 3-46983
 Pd-Rh, absorption of H 3-55789
 Pt nugget composition, chromian aluminian magnetite, Rh alloys, Alaska 3-44763
 PuRh₃, magnetic susceptibility and electrical resistivity measurements, stabilisation of 5f energy band 3-46983
 Rh-Mn-Sb, Cl₃ type, lattice parameters, mag. props. 3-64490
 Rh-Pd alloys, H_2 absorption, at high pressures 3-53229
 RhMnGe, crystal atomic structure and magnetic properties 3-49878
 Rh₄Pb₅, crystal. structure. determ. (*German*) 3-79275
 ThRh₃, magnetic susceptibility and electrical resistivity measurements, stabilisation of 5f energy band 3-46983
 URh₃, magnetic susceptibility and electrical resistivity measurements, stabilisation of 5f energy band 3-46983

rhodium compounds

- see also rhodium alloys*
 coordination compounds, Raman and i.r. spectra external vibration frequencies of active and racemic forms 3-55581
 Pd-Rh-H system, superconductivity, temp. depend. of relative electrical resistance 3-79793
 Rh complex, phthalocyanine, dynamics of triplet state in zero field 3-50846
 RhBO₃, calcite-type borate, structure and props. 3-40871
 Rh(III) complex, halopentammine, radiative and radiationless decay processes 3-73158
 Rh(III) complexes, phosphine and arsine complexes, metal localized emission 3-41855
 Rh(N₂)_n, n=1-4, low temperature matrices, i.r. examination 3-78809
 Rh₂O₃, corundum structure, thermal expansion 3-69340
 Rh₂O₃, corundum structure, directional thermal expansion coeffs. meas. 3-41032
 Rh π -complexes, ¹³C n.m.r., Rh-C coupling 3-63513

Richardson effect *see Einstein-de Haas effect***ridge waveguides** *see rectangular waveguides***Riemann-Cristofel tensors** *see general relativity; tensors***Righi-Leduc effect** *see magnetothermal effects***ring lasers**

- beat frequency, external mag. field effect, with nonreciprocal phase shifter 3-74236
 caustic surface eqn. (*Russian*) 3-57244
 difference freq. fluctuations study 3-43027
 gas, three mode oscillation, stability, pumping depend. 3-62704
 gas lasers with anisotropic resonator, competition between longitudinal modes 3-45813
 linear and ring, general method for determining natural frequencies (*Russian*) 3-57243
 locking, frequency depend. 3-74239
 mode locking using saturable absorbers 3-40275
 resonator, mirror effects on modes and losses 3-78052
 single mode, method for freq. of beats calc. 3-70832
 solid, generation regimes 3-51931
 time characts. of laser with bleachable filter 3-45814
 tunable CW dye laser, ring cavity configuration, travelling wave operation 3-45802
 unidirectional unstable travelling wave type, props. 3-43026
 He-Ne, oppositely travelling waves polarised in different planes, generation 3-48932
 He-Ne, use in angular velocity measurement (*Japanese*) 3-66900
 LiNbO₃, mode synchronisation, resonant modulation, ultra short light pulse excitation, 10⁻¹⁰ sec (*Russian*) 3-57235

riometers *see ionospheric measuring apparatus***rivers and lakes**

- see also water pollution*
 Antarctic ice sheet, radio echo sounding discovery of water pockets 3-76932

rivers and lakes continued

- bed material transport in rivers, radioisotope meas. technique 3-73397
 biochemical oxygen demand of river, three dimensions analytical soln. 3-59209
 canals, seismic surveying using marine techniques 3-56043
 CANNIKIN nuclear explosion, ground shock effects on shallow onshore waters 3-51209
 CANNIKIN nuclear explosion, hydrological effects 3-51208
 CANNIKIN nuclear explosion, lake formation 3-50901
 cavern development by thermal springs 3-61402
 Central N. American rift system, source of midcontinent gravity high 3-73219
 Charente and Seudre river basins, probabilistic study of rainfall (*French*) 3-61464
 chlorophyll content and temperature, remote sensing using airborne differential radiometer 3-73607
 Colorado River Basin Pilot Project, runoff increase due to precipitation management 3-51215
 Combarjua canal, flow characteristics 3-76687
 current measurements, Lake Superior, 1971, aerial photography and photogrammetry 3-47683
 dam, effect of severe frost, air and water temp., bending of the dam 3-73407
 deep temperate lakes, seasonal thermal structure 3-65547
 drainage subsurface routes, development along bedding phases rel. to Karst hydrology 3-58870
 drained lakes exposed to permafrost aggradation, growth of pingos 3-65545
 Earth Resources Technology Satellite, hydrological applications 3-80716
 East African saline lake deposits, ¹⁸O/¹⁶O ratios in assoc. cherts 3-53388
 ecological modelling for Lake George NY 3-47714
 engineering and sanitary problems 3-65392
 estuarine sediments, concentration and distribution of methylmercury compounds 3-73410
 flow, vertical component of velocity in along-shore currents (*Russian*) 3-63621
 flow distrib. of environmental tracers, finite state mixing cell models 3-56275
 fresh waters, evidence for buffering of dissolved Si 3-44970
 gravity surveying for ground-water study in Great Basin 3-59167
 Great Lakes, planetary boundary layer modification 3-76733
 Great Masurian Lakes, water level periodicity rel. to precipitation (*German*) 3-76845
 ground-water flow, heat transfer 3-59211
 ground-water temp. distrib. in shallow aquifer 3-59213
 groundwater, flowing, mass transport, appl. to prediction and control of contaminants 3-47853
 groundwater basin, coupled salt and water flow 3-80689
 groundwater flow, functional coeffs., finite element analysis 3-46488
 groundwater hydrographs, barometrically conditioned fluctuations, elimination (*German*) 3-73276
 heat and mass transport in a hydrologic system, math. modelling 3-59214
 hydrogeochemical analysis, flameless atomic absorption methods 3-48642
 hydrothermal system modelling, appl. to Wairakei, New Zealand 3-59212
 Italian, surface temperature i.r. obs. (*Italian*) 3-61613
 Kakhovka reservoir, suspended sediment flow rate 3-76928
 Kelvin wave generation, near shore thermocline, Lake Michigan 3-47674
 lacustrine sediment cores, rapid meas. of magnetic susceptibility 3-65495
 Lagoon of Venice, tide level telemetry system (*Italian*) 3-51206
 lake, evaporation and cooling under unstable atmos. conditions 3-56149
 Lake Baykal area, depth of heat source from geometric anomalies 3-65165
 lake effect snowstorms, role in hydrology, Lake Erie 3-47773
 Lake Ontario, kinetic energy spectra in nearshore region 3-58977
 Lake Superior, origin of valleys on floor, sonar and sampling studies 3-69562
 lepidolite, hydrothermal, anal. deposition from Ojo Caliente hot spring, Yellowstone National Park 3-80597
 Liverpool Bay, effect of rivers Dee, Mersey and Ribble 3-65262
 Lonar lake, India, impact crater in basalt, shocked fragments discovery 3-59320
 long waves in shallow triangular river channels 3-56153
 longitudinal dispersion in rivers, fractional Brownian motion model 3-59208
 Mandovi estuary, premonsoon tidal flow characteristics 3-76688
 modelling of ground-water flow in unconfined aquifer, heterogeneous permeability distrib. 3-56277
 natural reservoirs, age distrib. and transit time 3-47852
 oscillating stratified lake of varying cross section, diffusion eqns. for vertical transport 3-73411
 oscillations of levels due to unsteady wind stress 3-42091
 Paktia, E. Afghanistan, aquifer location 3-50966
 pollution dispersal and seepage, beneath open channels through porous media 3-56562
 pollution monitoring (*Japanese*) 3-66076
 pollution of ground water, longit. dispersion with nonlinear adsorption in porous media 3-56276
 pumped well, unconfined aquifer, unsteady radial flow, model 3-46489
 pumped well, water table drawdown, unconfined aquifer, unsteady radial flow 3-46490
 Quaternary alluvial stratigraphy rel. to drainage system development and evolution 3-47632
 radiant energy transfer, effect of multiple scatt. 3-59206
 radioactive pollution, dosimetric implications for man 3-77300
 reservoir, turbulence structure of thermally stratified air-flow layer near water surface under wind gust conditions 3-59048
 reservoir surfaces, wind induced tidal oscillations 3-76682
 Rhone sediments, diffusion coeffs. of radioelements 3-56142

ivers and lakes continued

- river sediment and soil, method of determ. of ^{90}Sr and ^{137}Cs , report 3-73398
- salt composition of rain and river water in USSR, role of sea salts 3-51066
- seiche, lake Biwa ko, numerical experiments using nonlinear two dimensional model 3-76925
- Seneca Lake, internal undular surges as naturally occurring solitons 3-50988
- sequential data generation, two distrib. method, appl. to Sangamon river, Illinois 3-56278
- South Saskatchewan River, example of isostatic rebound 3-47618
- streamflow, stochastic methods in hydraulics and hydrology 3-56280
- streamflow, stochastic methods in hydraulics and hydrology 3-76930
- streamflow regression simulation to evaluate hydrologic parameter accuracy 3-59215
- Swiss lakes, heat flow meas. 3-76699
- T-S structures rel. to long period internal waves 3-59218
- temperature changes in rivers, math. model 3-44969
- temperature structure of freshwater lake, temporal changes 3-61610
- tidal estuary, turbulent flow obs. 3-51214
- time variable waste input, dynamic water quality response, effect of longitudinal dispersion 3-56272
- transport of cohesionless, fine graded, flaked sediment by water 3-80705
- Trent Catchment, atmospheric attenuation of sunlight and potential evapotranspiration 3-61486
- turbulent streams, lifetime of inhomogeneities, definition (*Russian*) 3-67909
- Upper Colorado River, economic-hydrologic-air pollution model 3-59216
- valley rebound, prediction by mathematical model based on elastic behaviour 3-65544
- Vellar estuary, distribution of dissolved silicon 3-77304
- Vembanad lake, distribution of phosphorus in sediments 3-77305
- Venice, isotopes and circulations in aquifers (*French*) 3-53571
- wind gust factor over lake 3-51010
- wind-driven currents in shallow lake or sea 3-76692
- Mn freshwater deposits in lacustrine environments, accretion rates for ferromanganese nodules 3-47634
- P, radiation detection, thin-walled proportional counter, low level background meas. 3-51719
- Pu content of Japanese river water 3-69750

road traffic

- noise, urban main roads, L_{10} prediction 3-81341
- visibility of highway objects, nighttime driving situations 3-53469

road vehicles

- vibration diagnostic, source, synchronous integration technique, problems, feasibility 3-56622

Rochelle salt

- Curie points, model approach to existence of two points 3-64615
- ferroelectric props., domain structure stabilisation, crystn. temp. influence 3-44378
- growth data, (001)(002) type faces, BCF theory 3-72022
- piezoelectric and ferroelec. props. for use as u.s. transducer 3-41484
- piezoelectric lines meas., elastic stiffnesses 3-79983
- powder, dielectric constant 3-72563
- Seignette salt, pure, irradiated, Mo, Cu impurities, i.r. reflection spectra 3-80041
- triboluminescence and simultaneous charge produced at fracture 3-69045

rock magnetism

see also *palaeomagnetism*

- aeromagnetic maps, attenuation of near surface noise 3-59157
- analytic signal concept, use for interpretation of magnetic anomalies 3-59158
- basalt, magnetic properties, sample from western North Atlantic magnetic quiet zone 3-58966
- basalt, Pacific Ocean, petrology observations, Curie temperature, remanence 3-58967
- Deccan Trap basalts, n.r.m. stability 3-58838
- deep tow measurements, implications for emplacement of oceanic crust 3-58950
- diffusion aftereffects due to impurity atoms 3-69507
- dike-sedimentary rocks contact point, natural remanence anomaly 3-44793
- dipoles, randomly oriented, net moment 3-72499
- Jharia coal field, mag. survey, correl. with tectonics 3-44852
- Jurassic Topley Intrusions, Endako, British Columbia 3-76654
- Libya, palaeomagnetism of Tertiary basalts 3-58917
- magnetic anomalies related to rock type 3-58934
- magnetisation (secondary) and demagnetisation, ang. depend. 3-44792
- magnetomineralogical alteration trends, interpretation of magnetic anomaly patterns and contrast profiling 3-58933
- metamorphic Churchill Structural Province, Canadian Shield, palaeomagnetic data 3-76652
- Mid-Atlantic Ridge, magnetic results from Median Valley basalt drill cores 3-56025
- model construction, analysis of magnetic anomalies keweenawan volcanic rocks, Lake Superior 3-59159
- multidomain type alternating-field in igneous rocks 3-53397
- natural remanent magnetism, relationship to mineral constituents of intrusive rocks 3-58970
- oceanic basalts, low temperature oxidation causing carriers of natural remanence to become superparamagnetic 3-58971
- palaeomagnetism of Canary Islands and Madeira, results from 359 igneous rocks 3-58915
- sediment cores, rapid meas. of magnetic susceptibility 3-65495
- sediments, reprecipitated, oriented magnetisation 3-76670
- stress effects, press, uniaxial, nonmagnetic, tiltable piston 3-70330
- viscosity, by distrib. function method 3-58919
- viscous magnetization in oceanic igneous rocks 3-58968
- Western Alps, Permian and Triassic, palaeomagnetic study (*French*) 3-44854
- rock magnetism continued**
- ($\text{Fe,Mg}_{1-x}\text{SiO}_4$), low temperature oxidation, gravimetric and magnetic study 3-76537
- rocket vehicles** see *rockets*
- rockets**
- see also *missiles; space vehicles; weapons*
- 1965-11D (Cosmos 54 rocket), orbit anal. 3-53591
- Earth environment monitoring using rockets 3-50874
- ELECTRA I, mother-daughter sounding rocket for investigation of upper polar atmospheric plasma 3-42064
- environmental satellites carrier vehicles, Italian participation (*Italian*) 3-61592
- exhaust plumes, effect of nozzle boundary layers 3-49620
- motor case liner, thickness meas., laser gauge technique 3-45423
- relativistic rockets, variational theory 3-66654
- rocket astronomy, history of developments 3-45254
- solid propellant burning, effect of neutron irradi., safety analysis 3-49322
- sounding, geophysical research appl. (*Italian*) 3-61596
- sounding rocket mass spectrometer ion sources, O loss 3-51184
- three-dimensional liquid rocket nozzle admittances, expt. determ., combustion stability 3-46496
- wake boundaries effect on boom mounted probes 3-75284
- wake measurement of planar disc and cylindrical geometries on sounding rockets 3-61603
- rocks**
- see also *geology; minerals; rock magnetism*
- aerial gamma-ray surveying with continuous allowance for atm. radioactivity 3-69725
- alkaline granite from Golden Horn Batholith, North Cascades, Washington, anal. of calcic and alkali amphiboles 3-80594
- alkaline rocks from Vermont, petrology, Mesozoic alkaline magmatism 3-76522
- anhysteretic remanent magnetisation, appl. to bore core reorientation (*French*) 3-61287
- anorthite, liquid, viscosity meas. 3-69511
- Apollo 17, major and trace element chemistry of 30 samples 3-65842
- Apollo 17 material, isotopic ages 3-65845
- Archaean granulite facies metamorphic event in W. Greenland, $^{207}\text{Pb}/^{206}\text{Pb}$ ages 3-56044
- basalt, i.f. electrical impedance parameters 3-53389
- basalt fragments pyroxene relations, Apollo 17 sample from Station 5 3-65825
- basalt from Snake River Plain, comp. anal. 3-80588
- basaltic magmas, analysis of possible source rocks 3-50914
- basalts, dielectric properties 3-50911
- basalts, experiments simulating weathering in humid climates 3-61400
- basalts from Heimae and Surtsey eruptions, comparison of Sr isotopes and rare earth element comp. 3-41884
- basalts from Pacific Ocean layer 2, velocities, elastic moduli and weathering 3-76531
- Bearpaw shale, computer modelling of underground explosive cratering 3-58877
- Birch's law, exponential representation for minerals and rocks 3-65203
- Birch's Law, power law representation 3-73209
- brillite, prefailure initiation behaviour 3-76553
- bronzeite, high pressure u.s. velocity data, application of Q ellipsoid method 3-65211
- bronzeite polymorphic transform. under press., eqns. of state 3-47629
- Bunter Sandstone, Northwest England, hydrogeophysical properties 3-76544
- calcite strain-gauge calculation, expt. test 3-76608
- Cane Valley diatreme, Utah, carbonatite-kimberlite relations 3-53404
- Central Cascades, Washington, palaeomagnetism of granitic rocks rel. to Miocene pole 3-53433
- cherts assoc. with East African lake deposits, $^{18}\text{O}/^{16}\text{O}$ ratios meas. 3-53388
- chondrites, Yilmia enstatite, mineralogy and petrology 3-45054
- clay, i.f. survey, membrane polarisation, apparent specific resistivity variations (*German*) 3-73256
- comagmatic, petrology of Mt. Tuororame (*Italian*) 3-76495
- composition effect on formation of garnet 3-76516
- cross-anisotropic deposits, settlement using isotropic theory 3-80600
- Deccan Trap basalts, n.r.m. stability 3-58838
- deep-sea basalts, effect of seawater interaction on Sr isotope composition 3-56029
- Dembe-Divula complex, whole rock Th-Pb age determ. 3-47622
- density rel. to vertical crustal velocity (*Russian*) 3-65155
- diffusion aftereffects due to impurity atoms 3-69507
- dilatancy, premonitory variations of P, S travel times, shear and compressional waves, earthquakes 3-80623
- dilatancy model, earthquake prediction, anomalous seismic velocity ratio 3-80649
- dilatancy recovery upon unloading 3-58903
- drainage subsurface routes, development along bedding planes rel. to Karst hydrology 3-58870
- drape folds and upthrusts, petrofabric anal. 3-76607
- dry sample, dielectric constant and loss tangent spectra, meas. techniques 3-50910
- dunite, high pressure u.s. velocity data, application of Q ellipsoid method 3-65211
- dunite, torsional shear strength under near-homogeneous confining stress 3-50959
- dunite, Twin Sisters, frictional props. 3-76629
- dunite polymorphic transform. under press., eqns. of state 3-47629
- dunitites, electrical conductivity meas. rel. to pressure and temperature 3-50904
- East African saline lake deposits, $^{18}\text{O}/^{16}\text{O}$ ratios in assoc. cherts 3-53388
- effective pressure in porous solids 3-53409
- elasticity of water-saturated rocks rel. to temp. and pressure 3-61306
- elasticity theory, finiteness of stress conditions rel. to rock mechanics and crack theory 3-47659

rocks continued

- electrical characteristics of rocks with high permittivity and high loss, meas. techniques 3-51160
 electrical nonlinear phenomena 3-50909
 electrical parameters of rocks, symposium Salt Lake City, Utah, USA, March 1972 3-50903
 electrical parameters rel. to development of geophysical techniques 3-50908
 electrical relaxation, decay-time distributions 3-50906
 electrolytic reaction measurement of electric potential between dissimilar specimens 3-65247
 Elliot Lake area, mechanical properties and stress state before mining 3-76514
 exposure meas. using e.m. wave diffraction (*Polish*) 3-42928
 failure for isotropic medium, invariant description 3-53410
 failure time, prediction from fluctuation mechanism of crack growth 3-47658
 fault creep events, dislocation theory anal. 3-58905
 flexible thin section preparation 3-59152
 Foyers plutonic complex, Invernessshire, palaeomagnetism, direction of magnetisation 3-41905
 fracture, finite element models 3-61368
 fracture, initiation from compressive stress concentrations round elastic flaws 3-76552
 fracture growth around openings in thick-walled cylinders, hydrostatic press. effects 3-65169
 fractured, stress-flow method of fluid injection anal. 3-61375
 fractured rock aquifer, model of hydrodynamic dispersion of injected contaminant 3-51212
 gabbro, frictional sliding at high temp. and press., time-depend. 3-76631
 gabbro, frictional strength of faults at high temp. and press. 3-76630
 garnet clinopyroxene xenolith from Dish Hill, California 3-56027
 geochemistry, neutron activation analysis 3-65512
 geological samples, thermal annealing of latent damage trails 3-61359
 granite, electrical conductivity, high pressures, 300 to 1500°C 3-76659
 granite, frictional strength of faults at high temp. and press. 3-76630
 granite, inelasticity and rupture under triaxial constraints (*French*) 3-47613
 granite, I.f. electrical impedance parameters 3-53389
 granite, static mech. props. rel. to shock loading response 3-69528
 granite, Westerly, dynamic fatigue phenomenon 3-69529
 granite, Winnsboro, tensile anisotropy at 0.5 kbar 3-76611
 granite and granite/serpentine, frictional characters. at high press. 3-76626
 granite dust, microchem. determ. of quartz by size selective methods on membrane filters 3-54047
 granitic, proportions of normative minerals, calc. method 3-76510
 granitic rocks of Nova Scotia, Rb-Sr ages 3-76517
 granodiorite, holocrystalline igneous rock, eqn. of state under compression to 20 kb 3-76559
 granodiorite, torsional shear strength under near-homogeneous confining stress 3-50959
 granular aggregates, acoustic velocities and energy losses 3-50798
 graywacke, elastic fingering sedimentary rock, eqn. of state under compression to 20 kb 3-76559
 Great Bear batholith, volcanism and plutonism 3-76525
 Haast Schists containing myrmekites, New Zealand 3-44778
 haematitic sandstone, effects of atmospheric moisture on electrical resistivity 3-53399
 heat transfer from high temp. underground explosion gas filled cavity, isotropic, homogeneous 3-65160
 high pressure phases, from Hugoniot data 3-76539
 high pressure phases from Hugoniot data 3-65216
 igneous, multidomain type alternating-field demagnetisation 3-53397
 igneous rocks near Hedley B.C., K-Ar ages constraints on petrological model for Similkameen batholith 3-76521
 igneous with water saturation under high pressure u.s. velocity (*Russian*) 3-65158
 inelastic deformation, effect on seismic vels. 3-76636
 internal friction, test of Lomnitz theory by creep expts. 3-76570
 Isua Fe formation, W. Greenland, Pb-Pb isochron age 3-73223
 Ivera zone, longitudinal P-wave velocity anisotropy in mantle rock 3-65206
 jointed masses, continuum characterisation, low shear modulus significance 3-76555
 jointed masses, general constitutive equations 3-76554
 Kakagi Lake (Ontario), nature and origin of salic pyroclastic rocks 3-47617
 kimberlite pipes containing flowing magma, diamond synthesis by cavitation 3-50944
 Kolar Gold Fields, India, properties of lab. specimens 3-80631
 Lonar lake, India, impact crater in basalt, shocked fragments discovery 3-59320
 low pressures, change of seismic wave velocity (*Italian*) 3-73184
 lunar, ages, ion tracks and rare gases (Apollo 17) 3-65832
 lunar, geochemical aspects of soil, basalts and breccia 3-65838
 lunar, geochemistry of various types 3-47959
 lunar, holocrystalline from North Massif, petrology and genesis (Apollo 17 samples 76055 and 77135) 3-65850
 lunar anorthosite rocks, natural exoemission, recrystallisation, deform. history 3-77007
 lunar basalt, large coarse grained and predominantly basalt particles (Apollo 17) 3-65829
 lunar basalt 70035, Apollo 17, multistage cooling history 3-65843
 lunar glass, Apollo 15 and 17, orange and green 3-65840
 lunar glasses, orange and green, props. rel. to mare basalts, model 3-65839
 lunar ilmenite basalt, Apollo 17 sample 70035, petrology 3-65851
 lunar ilmenite basalt (Apollo 17 sample 75055) 3-65833
 lunar Taurus-Littrow mare basalt and dark mantle soil 3-65824
 lunar volcanic glass, orange and black, Apollo 17 sample 74220 from Shorty crater 3-65835
 magmas, contemporaneous basaltic and rhyolitic, composition, evolution 3-44761
 magnetisation (secondary) and demagnetisation, ang. depend. 3-44792

rocks continued

- marine sediments, worldwide unconformities rel. to eustatic changes of sea level 3-56042
 Masuke complex, whole rock Th-Pb age determ. 3-47622
 metamorphic, quartz rich, optic axis preferred orientation determ. 3-57971
 metamorphics, mineral weight percentages using principle of constituent analysis 3-53381
 metasedimentary from Wind River mountains, Wyoming, ferroan garnite 3-80589
 metavolcanic rocks, petrology of Grenville Province 3-56022
 mica syenite porphyry dikes, distribution of elements, chilled border effects 3-80642
 microcrack, grain boundary cracks due to P, T changes 3-65182
 microfracture growth during dilation 3-58902
 Mid-Atlantic ridge basalts and meas. of primordial rare gases in deep Earth 3-58843
 mineral-groundmass partition coefficients for Ti rel. to Rb. in volcanic rocks 3-56030
 Neogene sedimentary rocks, Oga Peninsula, Japan, palaeomagnetism 3-80674
 neutron activation analysis for oxygen determ. 3-70494
 neutron distrib. from spontaneous fission of U nuclei 3-61301
 oceanic crust-seawater geophysical and geochemical reactions 3-41879
 Oka carbonatite complex, X-ray fluorescence anal. of Sc abundance 3-80587
 olivinites, electrical conductivity meas. rel. to pressure and temperature 3-50904
 ophiolites, representation of oceanic crust, sea floor spreading 3-76640
 optical properties in 0.2-50 μ range 3-58830
 palaeozoic rocks, Australia, palaeomagnetism, a.c. demagnetisation method, pole positions 3-41904
 partially molten rock analogues, extensional wave velocity meas. technique 3-65204
 Pennsylvanian fissile shale, multi-method investigation of internal structure 3-65218
 peridotite, hydrated, anelastic creep at high temps, holographic interferometry obs. 3-65183
 peridotites, electrical conductivity meas. rel. to pressure and temperature 3-50904
 petrofabric analysis holographic interferometry, thermal expansion tensors, preferred orientation determ. 3-80652
 petrogenetic rel. of acid and basic rocks in Iceland 3-80626
 pillow lavas, magnetic properties and submarine weathering 3-58862
 plane waves propagated by transient shock load, characteristic method (*Russian*) 3-69508
 Pliocene basalt, North Bulgaria, natural remanent magnetisation, thermomagnetisation curves, palaeomagnetic stability 3-56099
 pliocene dolerite, pre-Balkans, natural remanent magnetisation, thermomagnetisation curves, palaeomagnetic stability 3-56099
 poikilo-macrospherulitic feldspar, crystallization in Rhum peridotite 3-41894
 polymorphic transforms, wave vel. and attenuation 3-53395
 pore pressure effects in creep and earthquakes 3-61379
 porosity and grain struct. by SEM 3-69729
 porous, fluid-saturated, effective stress laws 3-76558
 porous solids, nonlinear and semilinear rheology 3-69509
 porphyry Cu mineralization, complex electrical resistivity spectra 3-50907
 Precambrian gneisses, Nagar Untari, India, microcline minerals, texture and struct. 3-80632
 Precambrian rocks drilled on Rockall Bank, geological interpretation 3-56040
 pressure coefficient of sound velocity for holocrystalline igneous rocks 3-65205
 property determ. by induced polarisation 3-59150
 pseudotachylyte problem 3-76513
 pyroxene-garnet rocks, shock-wave high-pressure phases 3-65214
 Quaternary continental sediments, correlation between geomagnetic var. and precession 3-58925
 quartz veins in rocks of late metamorphic event rel. to pressure-temp. estimates 3-61333
 quartzite, I.f. electrical impedance parameters 3-53389
 quartzite, nonlinear model for folds 3-76604
 radioactive waste self burial utilising decay heat to melt rock 3-67415
 radiometry, use of Cf²⁵² as detector (*Rumanian*) 3-51171
 remanence, props. of Fe-containing minerals during chemical transforms. 3-61297
 reservoir sandstones, computer classification of pore structure 3-80630
 rheological models and spatially continuous mass creep 3-47657
 rheology from wavelength selection in folding 3-76603
 Rize and Gumusane crystalline massifs, geochronology (*French*) 3-47661
 salic pyroclastic rocks at Kakagi Lake, nature and origin 3-47617
 Salt Range Formation, partial extension of evaporite facies to Hazara, Pakistan 3-61337
 San Andreas fault, pore pressure changes during creep events 3-50919
 San Jose, geophysical investigations of landslides 3-47623
 sandstone, deformation behaviour, strength and interaction of joints 3-76634
 sandstone, drape folds and upthrusts, petrofabric anal. 3-76607
 sandstone, Navajo, elasticity, dilatancy and failure in effective tension 3-76612
 sandstone, porosity dependence and mechanism of brittle fracture 3-53407
 sandstone, timing, amount and nature of dilatancy 3-61374
 sandstone beams, folded, microfracture anal. 3-76610
 sandstone partial melting during frictional sliding in triaxial expt. 3-76628
 sedimentary, electrical resistivity and strength dependence on changes of pore pressure 3-65163
 sedimentary, Mexico zeolite identification, X-ray diffraction and electron microscope studies 3-44774
 seismic props. in lunar conditions 3-69898

rocks continued

- silicates, characts. of on tracks 3-61294
 silicates, liquid immiscibility, study of synthetic compositions, possible factor in rock formation 3-73226
 sill periphery, 'finger' formation by fluid instability 3-76615
 slates, Meguma Group, Nova Scotia, K-Ar radioactive dating 3-73204
 Soroy, Norway, noncylindrical, incongruous and aberrant folding in Eo-Cambrian rocks 3-50957
 Soroy, Norway, synfold stretching lineation in evolution of noncylindrical rock folding 3-50958
 South Harris complex rel. to Precambrian oceanic crustal slice over continental crust 3-44797
 South Sandwich Islands volcanic rocks, $^{87}\text{Sr}/^{86}\text{Sr}$ ratios 3-61293
 spinel gabbro xenoliths, Kerguelen Archipelago plagioclase stability at high pressures 3-44772
 St. Lucia volcanic rocks, Sr isotopic ratios 3-53396
 St. Vincent volcanic rocks, Sr isotopic ratios 3-53396
 steady state igneous and sedimentary fluxes, evolution of continental crust 3-61401
 strain patterns and magnitudes in 5 different tectonic regions 3-47644
 strain-durability, samples with loading history (Russian) 3-65157
 strata resistivity determ. from logging data during drilling (Russian) 3-47654
 stress in Earth crust, global meas. of bedrock 3-47647
 stressed specimens, h.v. radiography, dual microdensitometry 3-45516
 syenitic intrusion, K, U and Th distrib. between dry and wet facies 3-53382
 tectonics, sliding friction and stick-slip rel. to foliation, grain size and comp. 3-76624
 tektites, Georgia, fission track ages and stratigraphic occurrence 3-69510
 terrigenous, in Kamsk-Kinel'sk basin, shear reflection method (Russian) 3-47651
 thermal and elastic moduli of rocks and crystals, holographic interferometric technique 3-61398
 thermalized neutron detection, time of establishment of equilibrium spectrum (Russian) 3-73391
 thermophysical parameters determ. by plane temp. wave method 3-69505
 thermoremanent magnetisation in uniaxial compression at 20-200°C 3-44789
 tholeiites from Galapagos Islands and adjacent ridges, chemistry and petrology 3-80636
 tholeiites from Reykjanes Ridge and Charlie Gibbs Fracture zone, chemistry 3-61334
 time-depend. behaviour meas. by servocontrolled hydraulic testing machine 3-65170
 titanomagnetite, low-temp. oxidation and palaeomagnetic implications 3-69512
 tuff (Nevada Test Site), effect of strain rate in loading 3-58904
 tuffaceous rocks, shock wave response, porosity and saturation effects 3-58876
 underground nuclear explosions, rock melt, shock wave energy deposition 3-58875
 Upper Bhandar sandstones of Central India palaeomagnetism rel. to Cambrian Gondwanaland reconstruction 3-50984
 Upper Cretaceous volcanic rocks in Sicily, palaeomagnetism rel. to motion 3-56101
 u.s. travel-times in rocks under uniaxial compression 3-76635
 viscous heat prod. in a slab 3-50937
 volcanic, popping rocks and lava tubes from Mid-Atlantic rift valley 3-76578
 water supercooling and freezing processes in pores internal friction measurement (Japanese) 3-56034
 water-saturated, variation of elasticity, at melting point of ice 3-76530
 Webster dunite, shock compression and phase transitions at high pressure 3-65212
 Wedowee Group, Piedmont, USA, stratigraphy, metamorphism 3-80602
 Woo Dale borehole near Buxton, Derbyshire, sedimentology 3-41887
 X-ray fluorescence, conc. determ., rock-forming elements, error anal. 3-48654
 xenoliths in Maar-type volcanoes and diatremes rel. to Moon, Mars and Venus 3-53403
 Cu-bearing pillow basalts from La Desirade, Lesser Antilles island arc 3-53383
 Pb isotopic composition rel. to episodic U-Pb models 3-47655
 Th-Pb whole rock dating on eight granites 3-65219
 W abundance in oceanic and continental basalts 3-65221

Roentgen ray see X-rays

rolling

- anisotropic metals, bulge caused by rolling 3-69271
 plastic flow in hot rolling, math. predictions, temp. distrib. effects 3-80339
 sheet metal in tension, influence of plastic properties on forming limit drag 3-76197
 spherical debris, in rolling contact fatigue 3-55830
 spherical particle formation, in rolling contact fatigue 3-55829
 steel, austenite grain refining, deform. effect 3-55825
 steel, eutectoid-composition, finely spheroidized, thermal mech. treatments influence on mech. props. 3-53258
 steel, low-C, texture form. during deform. (Russian) 3-53218
 steel, low-C vanadium, controlled-rolled and continuously cooled, microstruct. obs. by TEM 3-80259
 steel, serrated grain boundaries form. during hot deform. (Russian) 3-80252
 steel, with type II MnS inclusions, effects on fracture 3-69223
 steel plates, low cycle fatigue anisotropy 3-69256
 steel/Ti explosion welding Ti to steel, effect of hot and cold rolling 3-72927
 texture determination, X-ray diffraction technique, combination of inverse polar and direct figures 3-53227
 texture of sheet, three-dimens. represent. (French) 3-61151
 Al, failure during transverse rolling, effect of single reductions 3-50743

rolling continued

- Al, imperfect structure after low-temp. rolling and annealing (Russian) 3-69208
 Al-Cu(4 wt.%) alloy, substruct. and dispersion hardening 3-69231
 Cr bronze, rolling texture determ., X-ray diffraction technique, combination of inverse polar and direct figures 3-53227
 Cu, softening of single crystals. deformed by rolling (Russian) 3-44573
 Fe, high-purity, dislocation pattern, recrystn., influence of tempering, rolling (German) 3-72846
 Fe, high-purity, substructure, effect of rolling, wire drawing and stretching deformation processes (German) 3-69204
 Fe-Cr-Ni alloys, deform. recovery and recrystn. of austenite 3-69285
 Fe-Si(3 wt.%) single crystals., deform. texture form. (Russian) 3-58622
 Mo, low-alloy, plastic deform. degree influence on struct. and mech. props. (Russian) 3-58625
 Mo/Cu, Mo/Cu-Cr fibre reinforced composites, cold rolling, ultimate tensile strength (Japanese) 3-73017
 Nb single crystals., deformed in rolling at 77K, defect struct. (Russian) 3-58627
 U, warm working effects on mech. and fabrication props. 3-72904
 W single crystals., struct. changes during plastic deform. and annealing (Russian) 3-58624
 W/Cu fibre reinforced composite, cold rolling, ultimate tensile strength (Japanese) 3-73017
- roots of polynomials see polynomials
- rotating bodies
 see also angular velocity measurement; centrifuges; gyroscopes
 astronomical radiosources energy generation with rotation in mag. fields, gravitational contraction 3-44991
 axisymmetric plate with stabilised rotation, vibrations (Russian) 3-62525
 basin, semi-infinite, with abruptly changing depth, existence of Kelvin waves 3-71796
 black hole, time evolution in static scalar field 3-53594
 black holes, angular momentum change caused by distribution of outside matter 3-69817
 Cosserat surfaces of revolution, rotationally symmetric deformations 3-57065
 Crab pulsar, PSR 0531+21, optical obs. of steady and discontinuous changes and period of rotation (German) 3-81125
 curvilinear flow incompressible simple fluid, between rotating concentric spheres 3-43541
 cylinder with inhomogeneous surface impedance, e.m. wave scatt. 3-66755
 cylindrical, amplification of reflected e.m. waves 3-40204
 cylindrical mass shell, relativistic mechanics of particle near axis 3-57132
 discs loaded by concentrated force, dynamic stability (Russian) 3-62443
 Earth rotational dynamics estimation using stellar obs. 3-56005
 elastic media, two-dimensional wave problems 3-70637
 elastic shells, natural and forced oscillations, calculated from boundary problem for integro-differential eqns. (Russian) 3-62521
 elasticity effect in rotational decay experiments 3-42752
 ellipsoid under concentrated load, stress distrib. (Russian) 3-45655
 equilibrium of charged spinning masses in general relativity 3-51821
 finite-amplitude convection in stars, combined effect of rotation and mag. field 3-51258
 fluid mass, asymptotic solns. of Clairaut eqn. 3-80916
 fluid rotating planet, density distrib. rel. to particular solutions of Clairaut eqn. 3-42140
 galaxies, Gaussian density distrib. 3-77141
 galaxies, nonlinear theory of gravit. instability 3-53707
 galaxies, origin of rotation rel. to shock wave generated vorticity 3-42227
 galaxies, rotation curves for different spirals rel. to mass distribution 3-61844
 generalised three-body problem, uniform circular movement of centres of inertia (French) 3-56298
 K-giant stars, N_2 enrichment due to meridional circulation, rel. CN-strength 3-69949
 gyrocompass, analytically dynamic, numerical soln. (Russian) 3-62439
 gyroscopic, heavy, regular precessions determ. by integration of Zhukovskii eqns. (Russian) 3-77794
 gyroscopic motion in external gravitational field 3-57149
 gyroscopic pendulum subjected to random vibrations, analysis of motion (Russian) 3-66578
 gyrotachometer, determ. of probability distrib. for nonlinear case using Fokker-Planck eqn. (Polish) 3-66517
 high speed objects, exam. technique, non-stroboscopic system 3-48410
 Hubble's law applied to relativistic torque on rotor 3-73438
 main sequence stars, N_2 enrichment, due to meridional circulation 3-69949
 metal poor stars, mass loss in stellar wind for fast rotation 3-77060
 moving object orientation determ. from ang. vel., error estimation (Russian) 3-54072
 multi-disc rotor, joint deflectional-torsional oscillations (Russian) 3-42817
 neutron stars, radial pulsations near onset of instability 3-61770
 non-symmetrical hard, in process of orientation, angular movements dynamics (Russian) 3-45634
 orthotropic discs of variable thicknesses, elastic stresses and displacements 3-66535
 oscillation of solid body filled by arbitrary viscous liquid (Russian) 3-70658
 paraboloid of resolution loaded at top by axial concentrated force, equilibrium, numerical analysis (Russian) 3-62468
 Pluto, rotational axis orientation, model 3-47904
 pulsar NP 0532, expected radiative var. rel. to angular velocity changes 3-77124
 pulsar slowdown, MHD theory of rotating neutron stars under external torque 3-69943
 radiating Kerr metric, nonstatic soln. of Einstein's eqns. 3-59799

rotating bodies continued

- rapidly rotating neutron stars 3-45091
- relativistic rotating stars, review of known properties (Polish) 3-65619
- rigid, torque-free rotational dynamics, nonlinear oscillator analogue 3-66514
- rigid body, orientation determ., Pikkati's equation, rotary motion expressed in canonical form (Russian) 3-70546
- rods and plates, buckling behaviour 3-57070
- satellite coupled vibration-rotation motion, Lie transform perturbation theory 3-69808
- self-gravity-induced electric polarisation of rotating massive body, magnetic field generation 3-59791
- shaft, whirling, with internal and external damping, stability of motion 3-57047
- solar differential rotation determ. 3-65697
- solar spin-down, internal time-scales for Boussinesq fluid 3-80945
- spinning aeolotropic disc, transverse vibration 3-42804
- spiral galaxies, angular momentum, models and correlations for 17 objects 3-81168
- spiral galaxies, angular momentum and rotation-wave analysis 3-81167
- stability analysis using Lyapunov function (Russian) 3-42755
- stability of oscillations of body partly filled with viscous fluid, boundary layer method (Russian) 3-62536
- stability of steady state rot. of solid body with cavity containing liquid (Russian) 3-57049
- stars, A-type dwarfs, rotation and shell spectra 3-61774
- stars, axisymmetric oscillations allowing for gravitational radiation 3-45715
- stars, differential rotation including spatial dependence of meridional circulation 3-81053
- stars, Fm-type, incidence and abundance anomalies 3-47987
- stars, magnetic, oblique rotator model 3-69936
- stars, magnetic, toroidal and poloidal oscill. in decay field 3-77074
- stars, magnetoelastic rotating, variational principle 3-61632
- stars, oscillations and stability of rotating masses with magnetic fields 3-47986
- stars, photospheric magnetic fields rel. to rapid rotation 3-48019
- stars, radiative equilib., model, multipole mag. fields 3-69946
- stars, secular stability of uniformly rotating fluid masses, effect of gravitational radiation 3-45076
- stars, struct., J^2 method, for uniform rotation, Roche approx. 3-69937
- stars, supermassive, stability conditions 3-69933
- stars, T Tauri-type, mass loss through stellar wind 3-77061
- stars, viscous effects with appl. to white dwarf models 3-65871
- stars, viscous Maclaurin spheroids, evolution of secular instability 3-47985
- stratified rotating conducting fluids, universal stability under influence of mag. field and Coriolis force 3-40735
- sun, differential rotation, pole-equator temp. difference 3-65695
- sun, interpretation of rotational vel. obs. (Italian) 3-61665
- sun, meas. in chromospheric and coronal e.u.v. lines 3-65696
- Sun, rotation changes rel. to 11 years solar energy generation cycle 3-53604
- synchronously rotating close binary stars, equi-density surfaces 3-53646
- thick walled, slowly rotating cylinder, deformation undergravitational load 3-59754
- Thomas precession of macroscopic objects 3-57143
- twisting of nonuniform body of rotation with variable shear moduli (Russian) 3-40111
- wave diffraction, finite bodies of revolution, stationary diffraction, method of perturbation of boundary forms (Russian) 3-70545
- white dwarf stars, line profiles and rotation meas. 3-45120
- white dwarf viscous evolutionary sequences 3-65872
- white dwarfs quasiradial pulsation freq. determ. using general relativity theory 3-53653
- work-energy equation, teaching 3-61962

rotation

- see also angular velocity measurement; earth rotation; molecular rotation; optical rotation; rotating bodies; rotational flow
- beam, random vibrations, in-core finite difference method, separable boundary value problems 3-70548
- centrifugal force and rot. motion, teaching approach 3-42497
- differential, rel. to solar neutron flux 3-53605
- earth's magnetic field, main field models 3-65246
- galactic rotation, anal. of gravitational instability in quiet universe as source of galactic rot. 3-81182
- galactic rotation, invalidity of conservation of circulation allowing gravitational stability as cause of rot. 3-81183
- parallel coaxial discs rot. at different speeds, heat transfer, temp. profile and Nusselt's number, rot. effect 3-49553
- plane harmonic waves, rotating elastic media, centripetal and Coriolis accel. 3-74078
- pulsar, galactic mag. field, dependence on galactic coordinates 3-48071
- pyrrhotite (mineral), comparison of Ar meas. with troilite 3-50879
- rigid body, orientation determ., Pikkati's equation, rotary motion expressed in canonical form (Russian) 3-70546
- stars, radiative equilib., model, multipole mag. fields 3-69946
- stellar envelopes, meridional circulation with rapid differential rotation 3-53636
- stick-propeller device, why does it rotate 3-59523
- student experiments, friction free force table 3-70254
- troilite (mineral), comparison of Ar meas. with pyrrhotite 3-50879
- uniform, rotating stars, struct., J^2 method, for uniform rotation, Roche approx. 3-69937

rotation by magnetisation see Einstein-de Haas effect**rotational flow**

see also vortices

- amplification and decay of long nonlinear waves in rotating fluids 3-46468
- angular momentum mixing, turbulence and secondary circulations 3-78957
- atmospheric asymmetric mean westerly current in rotating fluid, instability studies 3-69579
- axisymmetric flow through shaped gauze screens, velocity profiles simulation 3-43554

rotational flow continued

- baroclinic vortex, two-layer fluid, instability, separate circulations 3-46426
- barotropic vorticity equation, lateral boundary conditions 3-44891
- Bingham fluid, conducting, non-steady flow in annulus in presence of time-varying toroidal pressure gradient 3-46423
- boundary layer due to rotating sphere in stationary medium, laminar flow soln. (French) 3-49573
- circular cylinder, flow field survey and aerodynamic force meas. 3-43551
- coaxial cylinders with outer rot. cylinder, frictional moment and press. drop of flow 3-54805
- combined free and forced convective heat transfer and fluid flow in rotating curved rectangular tubes, numerical soln. 3-46404
- compressible swirling, stability and Richardson number 3-54808
- conducting fluid rotational motion between two discs in crossed electric and magnetic fields (Russian) 3-79020
- conducting liquid near stationary disc, high suction in transverse mag. field 3-71797
- convection, nonlinear, rot. effect 3-52425
- Couette flow, circular, with const. finite acceleration, linear stability anal. 3-71758
- Couette flow, time-dependent, rotational, numerical experiments 3-49564
- cylinder rotation in a conducting fluid in an axial magnetic field (Russian) 3-57815
- density-stratified spiral flows, hydrodynamic stability 3-57752
- differentially heated annulus of fluid, rotating, heat transfer, thermal boundary layers, high amplitude waves 3-43544
- Earth core, nonlinear resistive boundary layer in rotating hydromagnetic flow 3-44822
- Ekman and Stewartson nonlinear layers in rotating fluid 3-57755
- electrically conducting fluid entrain by rot. walls of cylinder in mag. field, eqns. of motion (French) 3-67959
- electrically conducting liquid rotation with a free surface in a rotating field (Russian) 3-57817
- fluid ellipsoid, influence of Coriolis force on convection (Russian) 3-78948
- fluid layer, rotating, effect of shear and stratification on the stability 3-52448
- fluids with couple stresses, secondary flow caused by rotation of sphere 3-54806
- friction factors, tube rotating around its own axis 3-67912
- gas motion on a rotating sphere with gravity, Euler's eqns. soln. 3-75206
- gas-liquid mixtures, swirl flow heat transfer in a vertical tube fitted with twisted-tapes 3-52437
- heat transfer for laminar flow, rotating straight annular pipe, series expansion soln. 3-71742
- inert turbulent boundary layer swirl flows prediction 3-78958
- Kelvin waves in rotating semi-infinite basin with abruptly changing depth 3-71796
- laminar mixed convection from a horizontal rotating disc 3-46396
- laminar tube flows, behaviour of falling and suspended sphere, rotation, tubular pinch effect 3-71821
- linear spin up, stratified fluid, small Prandtl number 3-75204
- liquid, Newtonian and non-Newtonian, rotational flow, interaction with stationary surface 3-40715
- liquid, rotational, symm. flow near static disc, high suction in transverse mag. field 3-71797
- liquid metal MHD rotating flow, expt. obs. 3-75254
- liquid rapid rotation in a strong inhomogeneous electric field 3-49610
- liquid sphere, rotating, oscillation in presence of toroidal mag. field (Russian) 3-57812
- mass transfer from base of an agitated cylindrical tank 3-57748
- mass transfer from stationary disc to a fluid in Bodewadt flow 3-57747
- mass transfer peculiarities of a disc rotating in a non-Newtonian fluid 3-46386
- MHD flow of conducting fluid due to rotatory vibrations of porous disc over fixed disc 3-54818
- MHD rotating Couette flow in a coplanar field, expt. obs. (Russian) 3-60562
- MHD system, uniformly rot., variational principle and virial theorem 3-57821
- multiply-circulating flows in channels of simple shape (Russian) 3-52445
- oceanic straits and sills, model of two-layer rotating fluid flow 3-59004
- oscillatory boundary layer growth over the top and bottom plates of a rotating channel 3-63696
- oscillatory instability, in revolving fluid of variable density 3-71789
- perfect fluid with free surface, continuous corner-type flow existence (French) 3-52444
- plasma, mag. field effect (Russian) 3-71872
- polyacrylamide solutions, viscoelastic liquid, flow patterns upstream of orifices 3-71754
- polymer solutions, rotational Couette flow stability 3-57749
- polymer solutions, turbulent drag reduction in external rotational flows 3-60571
- polymers, molten, helical flow, non-Newtonian fluid, cylindrical annulus, shear dependence of viscosity 3-73061
- radial flow passage, wakes and eddies, flow model 3-75208
- radial-flow passage, wakes and eddies, experimental observations 3-75207
- relaxing gas flows geometry 3-78960
- rotating fluid layer, convection, buoyancy-surface tension instability 3-71790
- rotating pipe, wavy flow under Coriolis force 3-67911
- secondary flow between rotating coaxial cylinders (Russian) 3-67916
- sharp spinning body at incidence, laminar symmetry-plane boundary layer 3-57764
- shear layers in a rotating stratified fluid with bottom topography 3-44862
- solar wind, rotational discontinuities, classification, orientation characteristics and examples 3-69834
- sound refraction 3-81335

rotational flow continued

- sphere spinning in air stream, rot. influence on heat transfer 3-63650
- spin-up of fluid in cylinder using rotating laser Doppler velocimeter 3-57029
- spinning bodies of revolution, Magnus effect 3-57751
- spiral motion of a cylinder in a non-Newtonian fluid 3-63672
- steady and unsteady rotating flows velocity profiles for finite cylindrical geometry 3-49566
- stratified fluid, β plane, length scales, model 3-46427
- stratified fluid in circular cylinder, heat-up process 3-43545
- stratified fluid in rotating annulus, steady state, upwelling, numerical soln. 3-52447
- stratified rotating conducting fluids, universal stability under influence of mag. field and Coriolis force 3-40735
- stratified Taylor column 3-47669
- streaming around oscillating circular cylinder at low Reynolds number 3-67914
- swirl decay in round tube (*Russian*) 3-43553
- swirl resistance 3-54833
- Swirling flows in streamtubes of variable cross section 3-78959
- swirling fluid flow, reduction of independ. variables and optimization 3-57753
- swirling supersonic jet obs. 3-78982
- swirling turbulent pipe flows expt. 3-75205
- thermal convection, rotation and magnetic field combined effect 3-78934
- tidal oscillations, predictability surface waves rotating fluid 3-47675
- toroidal fully developed viscous flow in coiled circular pipes 3-57750
- torque coefficient functional dependence of coaxial cylinders on gap width and Reynolds numbers 3-63673
- torsional oscillating sphere induced flow of a rotating viscous incompressible fluid 3-63671
- travelling forcing effects, two-dimens. wave pattern 3-79005
- turbulent skin friction on a rotating disc, integral calc. 3-57721
- two-dimensional relaxed flow of gas in convergent-divergent pipe (*French*) 3-52462
- viscid spiral flows, hydromag. stability 3-57813
- viscous fluid, with free surface, branching of symmetric solns. (*Russian*) 3-57757
- viscous incompressible fluid, unsteady flow between porous coaxial rotating cylinders 3-54807
- viscous incompressible fluid flow between porous fixed disc and nonporous rotating disc (*French*) 3-63693
- wakes, two-dimensional, smoke visualization of three-dimensional flow patterns, axial helical flow 3-63802
- water, swirling cavity flow, through straight circular pipe 3-57754
- water subcooled boiling, in top-generated swirl flow 3-68401
- water vapour condensation in swirling wake following longitudinal flow along a plate 3-57859
- wave solutions for nonlinear equations of rot. incompressible viscous fluid 3-75237
- Fe_2O_3 dielectric ferromagnetic suspension, flow in a rotating magnetic field (*Russian*) 3-63776
- He, rotating superfluid, damping of transverse waves 3-60816

rotator phase in solids see *nuclear magnetic resonance*

rotatory dispersion power see *optical rotation*

rotors

- gyro suspension, 4-pole, magnetic/geometric asymmetries, drift moments (*Russian*) 3-66134
- gyroscopic, gimballess electrostatic, accuracy of photoelectric angle-measuring system, effect of rotor pattern 3-66192
- in-core finite difference method, separable boundary value problems, random vibration, rotating beam 3-70548
- slotted, travelling e.m. field, investigation (*Russian*) 3-66734
- spherical, magnetic suspension gyroscopic, effect asphericity moments (*Russian*) 3-59544
- spherical ferrite, rotating in magnetic field, eddy current effects (*Russian*) 3-45755

RS coupling see *Russell-Saunders coupling*

rubber

- additive to epoxy resin matrix of C unidirectional composites, impact and shear strength 3-76363
- adhesive joint, rubber-glass, shrinkage and peel strength 3-80476
- anomalous behaviour, elasticity, thermodynamics general review (*Hungarian*) 3-76376
- carbon black-rubber interactions 3-80439
- condensation nuclei, production by peristaltic pump friction 3-46674
- creep and stress relax., stress history and temp. changes 3-58731
- dynamic properties under working conditions 3-76408
- elasticity, non-Gaussian theory 3-73046
- elasticity, statistical thermodynamic theory 3-45666
- elastomer mixtures, polyethylene effect on props. 3-73043
- frictional properties, surface temp. effect (*Russian*) 3-80470
- inflated circular cylindrical rubber membranes, bending rigidity 3-47466
- latex particle size distrib. rel. to ion exchange, electron micrograph quality improvement 3-41822
- natural, cross-linked by dicumyl peroxide, shear modulus, exptl. obs. 3-65003
- natural, oriented crystallisation, strain-induced, axial stress changes 3-54929
- Neoprene latex films, diffusion of Ca^{2+} , model 3-43895
- neoprene-filled rubber system, electron emission adhesive strength 3-61208
- Perbunan rubber-carbon black mixture, dielec. function, 500-10¹⁰ Hz 3-64593
- polar mixtures, dielec. props., 500-10¹⁰ Hz 3-55516
- reinforced plastics, transition magnitudes and impact improvement 3-50783
- reinforcement of glassy polymers, toughening behaviour 3-47481
- stoppers, removal of glass tubing 3-48345
- stress relaxation, effect of infrasonic vibration (*German*) 3-65011
- vulcanizate, Rivlin-Thomas criterion for cut growth, finite element calc. of J integral 3-73045
- wettability and stability in aqueous solns. (*Russian*) 3-41813

rubber continued

C-filled, relaxation times (*Russian*) 3-73066

rubbing (abrasion) see *abrasion*

rubidium

- atom, $2p_{1/2}$ excited states, h.f.s., g_j factors and lifetimes, optical double reson. meas. 3-46189
 - atom, electron collision, momentum transfer cross sections, from elec. conductivity of arc discharge 3-71430
 - atom, electron impact ionisation, binary encounter calcs. 3-71412
 - atom, electron spin exchange collisions, cross section, temp. depend. 3-67705
 - atomic beam, excited by short coherent optical pulse, incoherent reson. fluoresc. 3-63295
 - atomic beam, incoherent reson. fluoresc. from coherently excited state, neoclassical radiation theory test 3-63296
 - atoms, nutation echoes obtained by nonresonant oscill. field 3-78455
 - autoionisation in electron impact 3-74881
 - binding energy, compressibility, pseudopot. calcs. 3-54941
 - birefringence induced circular, when laser radiation passes through vapour 3-63292
 - critical properties, high temperature saturated phase densities 3-75619
 - dielectric function, optical props. meas., 2.07 to 6.2 eV, sum rule tests 3-80070
 - excitation collisions in flames, quenching and doublet mixing cross sections of $5^2P_{3/2,1/2}$ doublet by N_2 , O_2 , H_2 , H_2O 3-67694
 - granular thin films, surface plasma oscill., light absorption (*French*) 3-55702
 - ion implanted, in Al, behaviour during anodic oxid., He backscatt. obs. 3-68511
 - liquid, collective excitations, neutron scatt. study 3-49833
 - liquid, effective pair potentials, calc. from neutron scatt. data 3-49825
 - liquid, electron-ion triplet correlations 3-52778
 - liquid, neutron scatt., coherent and incoherent, relation 3-49832
 - mineral-groundmass partition coefficients for Tl rel. to Rb. in volcanic rocks 3-56030
 - n.m.r., rot. frame coherent resons. on fund. level of ^{85}Rb (*French*) 3-54574
 - optical pulse self steepening with possible shock formation in Rb vapour 3-57261
 - photo emission and optical constants, of pure thick layers in u.h.v., 250-630 nm (*French*) 3-41610
 - resonance lines, radiation frequency shift and linewidth 3-52270
 - rotar isotopic composition, photospheric and sunspot spectra, atomic line studies 3-61672
 - vapour, adiabatic following and slow optical pulse propag. 3-45823
 - vapour press. meas., at 330 K, by optical absorption 3-48396
 - vapour pressure, saturated, 683-1649°C, 0.97-101.5 atm. 3-49981
 - vapour pressure measurement, 1400 F up to critical temp., pressure tube method 3-75617
 - Rb I vacuum-u.v. absorption spectrum between 350 and 810 Angstroms 3-67655
 - Rb II Zeeman effect analysis in discharges, atomic spectrum, hyperfine structure, experimental 3-71379
 - Rb/o dipole layer on Si, negative electron affinity surfaces 3-44128
 - Rb-Cs spin-exchange collisions, relaxation of Rb electronic polarisation 3-54587
 - Rb-Sr dating of granitic rocks in Nova Scotia 3-76517
 - Rb⁺, electron detachment by electron collisions 3-67702
 - Rb⁺ optical pumping charge-exchange method for nuclear spin orientation ^{150}S 3-67677
 - RbI resonance lines at 7800 and 7949 Å in photosphere, isotopic effects 3-42134
 - ^{87}Rb maser, light shift and light broadening 3-54209
 - ^{87}Rb maser, short-term frequency stability 3-57218
 - ^{87}Rb vapour, optically pumped, parametric frequency conversion of resonance radiation 3-43350
 - $\text{SrCl}_2\text{:Rb}^+$, F* centre bleaching, annihilation probability 3-40917
- rubidium compounds**
- halides, strain derivatives of static and high frequency dielectric constants 3-47198
 - halides, thermal expansion at low temps. 3-43885
 - Cs + RbCl collisions, branching ratios, statistical approximation 3-75146
 - K-Rb, phase diagram calcs. using heat of soln. in solid and liquid phases 3-41007
 - K-Rb liquid alloys, electrical resistivity calc. 3-60866
 - KCl-RbCl solid solution single crystals, linear expansion coeff., 25-500°C (*Russian*) 3-79507
 - $\text{Li}_2\text{Se-Se-(LiBr-RbBr eutectic)}$ pseudoternary system, phase diagram, physicochemical and e.m.f. obs. 3-43863
 - Nb-Rb liquid alloys, electrical resistivity calc. 3-60866
 - PbPF₆, pulsed n.m.r., F spin-lattice relaxation 3-47159
 - Rb halide cryst., model pot. with short range three-body interaction 3-63976
 - Rb-Cs, phase diagram calcs. using heat of soln. in solid and liquid phases 3-41007
 - RbAg₄S, Cu-substituted, Cu ion conducting solid electrolyte 3-41046
 - RbAg₄S, Hall effect measurement using double a.c. method 3-77574
 - RbAg₄S, solid electrolyte, far i.r. meas., low freq. lattice absorpt. 3-83115
 - RbAlSiO₄, crystal structure (*German*) 3-64005
 - RbBr, Debye-Waller factors, mean-square displacement of atoms calc. 3-64129
 - RbBr, thermal expansion from lattice const. temp. depend. 3-52712
 - RbBr, unstressed crystal, e.s.r. meas., three reorientation processes of O_2^- centres 3-44325
 - RbBr + LiF, miscibility gaps study 3-72202
 - RbCdF₃:Mn²⁺, hyperfine interactions, ENDOR study 3-47172
 - RbCl, aq. soln., hypersonic vel., molar conc. depend., Brillouin scatt. meas. 3-49934
 - RbCl, conduction band structure computation by model potential approach 3-44006
 - RbCl, Debye-Waller factors, mean-square displacement of atoms calc. 3-64129

rubidium compounds continued

- RbCl, electronic core levels binding energy, valence band structure, X-ray photoemission meas. 3-50125
 RbCl, i.r. emissions of the F centre and of compound colour centres 3-41566
 RbCl, migration energy of Sr^{2+} impurity-vacancy dipoles 3-43902
 RbCl, second order Raman spectra, 80 and 300 K 3-68991
 RbCl, thermal expansion using shell model 3-52714
 RbCl: Mn^{2+} , e.s.r. spectrum at 77 K 3-72512
 RbCl:Pb fine structure of impurity A-absorpt. bands 3-69038
 RbCl-KCl, solid soln., chem. diffusion 3-43896
 RbCl(Br), F-centre growth kinetics and thermolum. 3-69101
 RbCl(Br)(I), paraelec. behaviour of OH^- ions, electrooptical and electrocaloric studies 3-41476
 RbClO₃, absolute config., X-ray study 3-60710
 RbCoCrF₆ pyrochlores, new cryst. positions for Rb^+ in Fd3m space group (French) 3-40885
 RbCoF₃, magnons, excitons energies, linewidths, light scatt. obs. 3-41356
 Rb₂CoF₄, two-dimensional Ising antiferromagnet, neutron diffraction obs. of critical behaviour 3-75837
 Rb₂CrO₃, crystal struct. 3-79285
 RbF, Debye-Waller factors, mean-square displacement of atoms calc. 3-64129
 RbFeF₃, i.r. refl. spectra, dielec. const., lattice freqs. and interionic pot. calc. 3-47272
 RbFeF₄, multilayer crystals, Mossbauer recoilless factor behaviour, Debye-Waller factor (German) 3-50493
 Rb₂FeO₄, cryst. structure, same type as K_2FeO_4 , Cs_2FeO_4 3-68231
 RbH₂AsO₄, ferroelectric, H bonded, Raman spectra, mol. struct. 3-72649
 RbH₂AsO₄, low frequency xy Raman spectra, soft mode behaviour of ferroelectric model 3-61041
 RbHF₂, ionic conduction meas. as function of temp., determ. of transition temps. 3-43897
 RbHSO₄, alkali metal ordering and hydrogen bonding 3-46607
 Rb₂HfF₆,¹⁸¹Ta, relax. phenomena, PAC obs. 3-79957
 RbI, Debye-Waller factors, mean-square displacement of atoms calc. 3-64129
 RbI, exciton level prediction, modulation spectroscopy 3-55229
 RbI, hygromech. effect 3-58174
 RbI, thermorefectance spectrum, Rydberg series of gamma; exciton 3-55623
 RbI, unstressed crystal, e.s.r. meas., three reorientation processes of O_2^- centres 3-44325
 RbI, X-irradiated, F-centres, optical density, 80-160 K (German) 3-52626
 RbI:Ti, γ -scintillations 90 K-300 K (Russian) 3-55684
 RbI + LiF, miscibility gaps study 3-72202
 RbI + MI (M=Ag, Cu) molten systems, thermoelectric power 3-72375
 Rb₂MF₄: Mn^{2+} (M=Mg, Zn, Cd), ENDOR, nuclear quadrupole interaction, zero-point spin deviation 3-75915
 RbMnBr₃, antiferromag. props., neutron diff. and susceptibility obs. 3-47056
 Rb₂MnBr₄.2H₂O, magnetic phase diagram 3-50366
 RbMnF₃, antiferromag. reson. near Neel temp., u.s. wave coupling to antiferromag. spin waves (French) 3-41427
 RbMnF₃, antiferromagnetic, supertransferred hyperfine interaction, perturbed angular correlation of ^{111m}Cd 3-44360
 RbMnF₃, heat capacity near mag. phase transition 3-44217
 RbMnF₃, i.r. refl. spectra, dielec. const., lattice freqs. and interionic pot. calc. 3-47272
 RbMnF₃, impurity doped, ¹⁹F nuclear acoustic resonance 3-41431
 RbMnF₃, magnetic transition, sound propagation effects nr. transition 3-46709
 RbMnF₃, nonlinear effects in nuclear echo 3-64567
 RbMnF₃, spin diffusion coeff., room temp. to critical region 3-55412
 Rb₂MnF₄, quadratic layer, antiferromag. reson. 3-50463
 Rb₂MnF₄, quadratic-layer antiferromag., spin-wave anal. 3-50384
 Rb₂MoCl₆, force consts. and mean vibr. amplitudes 3-67771
 Rb_{0.8}MoS₂, room temp. resistivity obs. 3-79691
 RbNO₃ structure transformation, NaCl type to CsCl type, orientation relation 3-52696
 RbNO₃-Cd(NO₃)₂ glass, thermodynamic props. 3-72009
 RbNb₂O₃F pyrochlores, new cryst. positions for Rb^+ in Fd3m space group (French) 3-40885
 RbNiF₃, spin wave sp. ht., a.c. temp. calorimetry, 1.5-4K 3-50381
 Rb₂NiF₄, magnetic susceptibility, antiferromagnet, optical absorption and magnetic circular dichroism spectra 3-44204
 RbO₂ in Ar matrix, Raman spectra 3-52371
 Rb₂PtS₄, synthesis and structure (German) 3-49880
 RbReO₄, mass spectrometric investigation of sublimation 3-49990
 RbSH, lattice dynamics and order-disorder transitions, Raman scatt. study 3-55590
 RbSH in cubic phase, SH⁻ reorientation, neutron quasielastic scattering study 3-46597
 RbSc(EO₄)₂ (where E=Mo, W), crystal parameters 3-79328
 Rb-U complex fluorides, far i.r. absorption spectra 3-58499
 Rb[In₆O₁₀], preparation and crystallography (German) 3-79322
 Rb[Tl₆O₁₀], preparation and crystallography (German) 3-79322
 RbCoCrF₆ pyrochlores, new cryst. positions for Rb^+ in Fd3m space group (French) 3-40885

ruby

- ENDOR, spin-echo, for Cr-Al hyperfine and elec. quadrupole interactions determ. 3-47173
 e.p.r. spectrum, effects of internal stresses 3-79886
 growth, for lasers, comparison of Verneuil and Czochralski methods 3-66839
 hydrothermal growth from HCl soln. 3-58589
 laser, complex resonator, interference effects, coherence in terms of scattering (Russian) 3-57231
 laser, cooled illuminator for investigation of lasing 3-73794
 laser, free-running external signal effect 3-62719
 laser, generation with moving mirror and selector in resonator 3-48911
 laser, giant pulse, spectrum width resolution by clarifying filters (Russian) 3-70823
 laser, pulsed, with Q-switched multiple cavities, characts. 3-40264

ruby continued

- laser, quasistationary lasing technique 3-51638
 laser, reorganised, generation of internal cyclic modes (Russian) 3-59868
 laser, self-mode-locked, shape of radiation pulses 3-40267
 laser, self-termination of free-oscills. at low temp. 3-74246
 laser induced thermal damage, absorbing impurities role 3-74261
 laser Q factor electro-optical modulation, modulator components (Russian) 3-57230
 laser rod, obser. of Rayleigh scattering pattern 3-48953
 lasers, for machining of nonmetals 3-59902
 maser, multicomponent frequency mixing under magnetic resonance conditions (Russian) 3-57220
 maser for 8 mm band using miniaturized cooling system producing 35°K 3-42989
 negative electron temperatures, role of Al nucleus (Russian) 3-64547
 optical absorption spectra at high shock pressure 3-76858
 optical spectrum due to exchange-coupled Cr^{3+} ions 3-44435
 optically pumped, verification of Kramer-Kronig relations 3-48909
 orange colour, origin (Russian) 3-64036
 phonon bottleneck at 29 cm⁻¹ 3-55049
 polarisation properties of transversely pumped cylinder 3-78000
 push pull ruby maser, inversion ratio 3-51895
 radiation locked photon echoes, optical free induction 3-54243
 radiative and nonradiative transitions, temp. depend., emission quenching 3-41568
 refractive index change on R-line transition saturation, Jones optical lever method 3-80003
 ruby:Cr³⁺, Mg²⁺, electron irradiated, e.p.r. line splitting (Russian) 3-55472
 ruby:Cr, population determ. of metastable level (Russian) 3-50149
 self-induced transparency, temp.-depend. phase memory 3-62747
 spin lattice relax. time meas., progressive saturation methods (Rumanian) 3-64537
 u.v. luminescence, non linear quenching, mechanism 3-64723
 Cr ion pairs, energy spectrum calc. effective Hamiltonian method 3-68564

Runge-Kutta methods

- Faraday type MHD generators with nonequilibrium plasmas, end effects calc. 3-46558
 forced convection with variable thermal conductivity on a flat plate, numerical soln. 3-40707
 laminar film condensation on the inside of slender, rotating truncated cones 3-68400
 Maxwell equations for harmonic generation by intense microwave in weakly ionised nitrogen plasma 3-63822
 multilayer insulation system, gas flow analysis 3-78997
 optically deep absorbing media, interior radiances, one-dimensional model exact solutions 3-74168
 supersonic and hypersonic flow, nonlinear hyperbolic eqns. solns. based on Runge-Kutta technique 3-43568

rupture

- alloy, precip. hardened, heat treated under relative stable conditions, recovery creep props. 3-69313
 brass, elevated temp. and volume stressed state obs. 3-58676
 brittle materials, rel. to heat resist. problems 3-58702
 caprolon, self-heating and thermal fatigue during cyclic compression 3-61220
 capron, electron irradi. rate and deform. rate effect on strength (Russian) 3-80467
 composite, directionally solidified, yield pt. phenomenon interpret. 3-64992
 Couette flow, viscoelastic, polymeric, stability prediction based on network rupture hypothesis, analysis 3-75277
 creep-rupture testing machine, biaxial-tension 3-58780
 glass, torsional strength under hydrostatic pressure 3-65021
 glass-crystalline materials, cast, rupture character 3-47475
 granite, triaxial constraint effects (French) 3-47613
 graphite fibre/Li₂O.Al₂O₃.8SiO₂, high strength composites, development and strength props. 3-47458
 Inconel 718 sheet, time-depend. edge-notch sensitivity rel. to mech. and microstruct. characts. 3-64952
 laminates, free edge model for catastrophic delamination 3-69369
 liquid films, meas. of breakdown times 3-60835
 Makrolon, prolonged storage effect 3-80488
 metal, failure process in complex stress state, mechanism 3-58689
 metal, pair interaction influence (Russian) 3-72891
 microobjects, small sized precision testing machine 3-76404
 nuclear fuel pin-to-pin failure propagation, pressure pulse loading, fission gas release, buckling failure criterion 3-74732
 nuclear reactor containments, safety margin in pressure-temperature transients calc. 3-46091
 nuclear reactor piping, analysis of effects 3-67434
 polycarbonate, prolonged storage effect 3-80488
 polyethylene terephthalate film, temperature transitions investigation by tear-strength method 3-61221
 polymeric materials, time marker for long-term strength and instant of rupture 3-53834
 steel, 27%Cr, defect behaviour under creep conditions 3-69319
 steel, austenitic stainless, He-injected, cold working effect on creep rupture props. 3-44612
 steel, balls, rupture testing, ultracentrifuge, rotating mag. field, stress at centre of ball, residual deformation 3-53304
 steel, computerized time-temp. parametric analysis of stress-rupture data 3-50746
 steel, Cr-Mn type, effect of carbon addition 3-47432
 steel, Cr-Mo-V, low-alloy, creep rupture strength, effect of carbide repartition (German) 3-69255
 steel, Cr-Mo-V type, creep rupture of tubular specimens under axial loads and internal press. 3-69308
 steel, Cr-Ni austenitic, creep rupture as cause of operational damage (German, English) 3-61174
 steel, crack development resist. and yield stress, temp.-rate relationships (Russian) 3-58651
 steel, creep behaviour, 500-700°C, Rajakovics method (German) 3-47397
 steel, creep rupture as cause of operational damage (German, English) 3-61174

rupture continued

- steel, dispersion hardening, time-to-rupture and substruct. under u.s. treatment (*Russian*) 3-53247
- steel, high-strength, creep rupture behaviour, effect of interruption in mechanical stress (*German*) 3-69253
- steel, high-strength, hydrogenated, relax. effect on mech. props. (*Russian*) 3-80315
- steel, high-strength, quenched, short-term testing props. correl. with fatigue limit (*Russian*) 3-80321
- steel, low-C, prestrained, temp. effect on mech. props. anisotropy 3-47427
- steel, mag. field induced rot. sphere method of mech. props. obs. (*Russian*) 3-80313
- steel, martensitically-aged, cracking in H_2S and NH_4CNS solns. (*Russian*) 3-58659
- steel, Mn-Mo and Mn-Mo-Ni type, normalizing and austenizing effects 3-50747
- steel, plastic low-alloy, alkaline cracking under steady pot. (*Russian*) 3-41719
- steel, soft, rupture probability and quasi-brittle fracture (*German*) 3-47396
- steel, spring, fatigue phenomena in large plate specimens after shot-peening treatment (*Japanese*) 3-41779
- steel, stainless, creep-rupture, instantaneous strain and proof stress meas. 3-47437
- steel, stainless, Type 304, shielded metal-arc weldments 3-47435
- steel, stainless, Type 316, characteriz. for LMFBR cladding 3-47394
- steel, temp. and strain rate influence 3-69312
- steel, weld metal, Type 316, tensile and creep-rupture props. 3-47434
- steel welded joint, high temp. Cr-Mo-V type, creep behaviour rel. to structure (*German*) 3-47398
- steel wires, tensile strength in aqueous-alcoholic and lacholic HCl soln. with added Sb_2O_3 (*Russian*) 3-80331
- stress corrosion cracking susceptibility test procedure 3-69402
- structural creep reliability eval. using entropy principles 3-58668
- structural reliability and minimum creep life at elevated temp., stat. eval. method 3-62494
- testing of biaxial stressed specimens at low temps., machine attachment 3-47529
- Ag, creep rupture as cause of operational damage (*German, English*) 3-61174
- Al, deformed, microscopic discontinuities in surface layers 3-76224
- Al alloy, creep rupture of plain and notched specimens 3-69320
- Al alloy, creep under variable uniaxial tensile loading, strain accumulation and rupture 3-69405
- Al alloy, elevated temp. and volume stressed state obs. 3-58676
- Al/graphite fibre reinforced composite, creep rupture tests (*Japanese*) 3-44669
- Al_2O_3 , high integrity body design using chem.-mineralogical phase anal. 3-76274
- B_4C , hot-pressed, high-temp. characteriz. 3-69348
- Bi_2Te_3 - Bi_2Se_3 , linear expansion coefficient, mechanical props. 3-75628
- CaB_6 , hot pressing, strength and fracture 3-69347
- Fe-Al-Cr, alloys, effect of Ti and Mo additions 3-61179
- Li_2O - Al_2O_3 - $4SiO_2$ graphite fibre reinforced composite, elevated temp. props. 3-76351
- Li_2O - Al_2O_3 - $nSiO_2$ graphite fibre reinforced composite, fabrication and low temp. props. 3-76350
- Mg sintered composites, cladding material of U fuel elements, mechanical properties, creep and rupture (*Czech*) 3-67556
- Mg-Li(8%) alloy, steel reinforced (*Russian*) 3-73011
- Mo, deformed, struct. stability and mech. characteriz. under prolonged influences of temp. and stress 3-44630
- Ni, creep rupture as cause of operational damage (*German, English*) 3-61174
- Ni, grain boundary fracture mechanism (*Russian*) 3-61132
- NiCrCo alloy, defect behaviour under creep conditions 3-69319
- α -Pu, room temp. bend strength 3-54540
- Sb_2Te_3 - Bi_2Te_3 linear expansion coefficient, mechanical props. 3-75628
- SiC refractories, microstruct. analysis 3-80413
- Si_3N_4 , effect of fabrication conditions 3-76294
- Si_3N_4 , hot-pressed, creep and tensile strength 3-76286
- Ti alloy, brittle rupture resistance (*Russian*) 3-80323
- Ti alloy, creep and fracture, stress-rupture strength energy criterion, 400-550°C 3-58692
- Ti alloy, high-strength, strengthening and rupture characteriz. 3-47429
- Ti alloys, strain curves, 20-400°C 3-58680
- Ti-Al-Mn alloy, hydrogen embrittlement, tensile and stress-to-rupture tests 3-69277
- (U,Pu) O_2 fuel, brittle fracture behaviour 3-43309
- W wire, high temp. creep, grain boundary cavity formation rel. to filament lifetime (*Hungarian*) 3-72988
- ZrO_2 -MgO system, directional solidification and oriented eutectic composite behaviour 3-76236

Russell-Saunders coupling

- beam-foil spectra, zero field, quantum beats in L-S coupling without cascades 3-78644
- correlation effects on isotope shifts 3-67642
- rules, ground state Russell-Saunders symbols, student teaching 3-48322
- two-electron ions, multiply charged, relativistic calcs. of transition energies 3-74795
- Ar I isoelectronic sequence, Hartree-Fock calcs. for $np^n p$ config. terms, Slater integrals 3-63263
- $CaF_2:Dy^{3+}$, f^n -electrons in cubic crystal fields 3-79638
- Co II spectra, energy level structure (*Spanish*) 3-40564
- F, isoelectronic sequence, LS-term depend. of Slater integrals in pp' config. 3-74784
- Ne I, LS-term depend. of Slater integrals, single-config. approx. deviations 3-67641
- Ne I, parametric study of isotope shifts 3-67643
- Ne I isoelectronic sequence, Hartree-Fock calcs. for $np^n p$ config. terms, Slater integrals 3-63263
- Sc II, semiempirical calculation of gf values, LS transition arrays, transition integrals, eigenvectors 3-74786

Russell-Saunders coupling continued

- Ti, X-ray emission $K\beta$, β' spectrum, fine struct. 3-67661

rust prevention see *corrosion protection***ruthenium**

- film, evaporated, reflectivity and optical constants, in v.u.v. from 300 to 2000 Å 3-80069
- Hall and Nernst-Ettingshausen coeffs., thermo-e.m.f., resist., temp. depend. (*Russian*) 3-52825
- solubility of hydrogen, temp. depend. 3-41017
- YGaG:Re $^{3+}$ garnet, strain variation of Ru ion energy levels, magnetstriction calcs., e.p.r. obs. (*French*) 3-58420

ruthenium alloyssee also *ruthenium compounds*

- $Ce_{1-x}Gd_xRu_2$, sp. ht., mag. transition, supercond. transition, 1.8-20K 3-55350
- $CeRu_2$:Fe, superconductor, e.p.r. obs. 3-79905
- $CeRu_2$:Gd, local moment e.s.r. in normal and supercond. states 3-44171
- $Ce_{1-x}Tb_xRu_2$, sp. ht., mag. transition, supercond. transition, 1.8-20K 3-55350
- $Ce_{1-x}Y_xRu_2$, sp. ht., mag. transition, supercond. transition, 1.8-20K 3-55350
- Cr-Ru, elec. resist. at Neel temp. 3-52819
- $Gd_2B_{1-x}Ru_x$ (B=Th,Ce,La), e.p.r. and supercond. correl. transition temp. Gd conc. depend. 3-72417
- $Gd_2Th_{1-x}Ru_x$, re-entrant crit. field behaviour, e.p.r. correl. 3-72418
- $LaRu_2$:Gd, local moment e.s.r. in normal and supercond. states 3-44171
- V-Ru, near-equiatomic, electronic transition, ^{51}V n.m.r. study 3-53032

ruthenium compoundssee also *ruthenium alloys*

- ruthenocene vibrational study 3-67780
- Ru complex, $Ru(dipy)_2^{2+}$ phosphorescence quenching by $Cr(CN)_6^{3-}$, diffusion controlled mechanism 3-53332
- $Ru(II)$ complex, tris(2,2'-bipyridine)ruthenium(II) cation, multiple-state emission 3-80090
- RuO_2 , sinterability, 800-1000°C (*Japanese*) 3-44666
- RuO_2 , thick film resistor material, laser beam reactions rel. to trimming 3-45838
- RuO_4 , He(I) photoelectron spectra, low energy transitions 3-40608
- ^{106}Ru complexes effect on coprecipitation yields from seawater, obs. 3-69556

rutile see *titanium compounds***S-matrix theory**see also *dispersion relations*

- $\Delta(1236)$ resonance, no-pole S-matrix fit 3-59931
- adiabatic definition when i.r. divergences are present 3-54282
- Adler condition and pole dominance, light pions and PCAC hypothesis 3-62789
- analytic continuation of S-matrix for cut-off potentials 3-43074
- analytic properties of box diagram amplitudes, spectral representation 3-74324
- bounds from unitarity and analyticity on forward slopes of overlap functions 3-49036
- bremstrahlung model for high-energy collisions, extension to include secondary particle correlations 3-67087
- chain fraction expansion of S-operator 3-74325
- Clebsch-Gordan coeffs., dynamical invariant amplitudes and universal coupling constants, selection 3-66938
- convergence of perturbation series in field theory models containing fermions 3-54283
- coupled channel analysis in $K\bar{K}$ threshold region 3-70981
- cross section expression, using quantum mechanics representation with functions in phase space (*French*) 3-57127
- cutoff potentials, expansion of scattering matrix in momentum power series and analytical extension 3-62546
- definition and properties 3-42953
- deuteron electrodisintegration matrix element, reln. to neutron-proton phase shifts 3-70939
- dilatation-invariant two-body relativistic S-matrix, partial wave analysis 3-66953
- dressing operators for translationally invariant Hamiltonian 3-74316
- Ericson fluctuations in presence of direct reactions, Hauser-Feshbach theory 3-74549
- Euclidean QED, S-matrix element eqns., generating operator and perturbation series 3-54303
- extended S-matrix method in quantum field theory 3-62781
- field theory at infinite momentum, calc. of matrix elements 3-40312
- Fredholm solution of integral equation for analytic continuation 3-59929
- gauge theories, non-Abelian, Ward-Takahashi identities for proper vertices, renormalization 3-70860
- handedness of neutrinos, indefinite metric 3-62772
- handedness of neutrinos, lagrangians, mass and interaction 3-62773
- invariant perturbation theory for chiral Lagrangian, calc. of higher order 3-66937
- K-matrix formalism, minimal 3-to-3 scattering amplitudes 3-54281
- Korteweg-de Vries equation, scattering theory, Schrodinger equation, analogue of Fourier's method 3-74118
- Lee model, S-matrix diagonal structure, eigenvalue equation for $V2\theta$ -type eigenvalue 3-57298
- linked cluster decomposition, generalisation of eikonal approx., numerical test for Yukawa potentials 3-62779
- long-range correlations, nonplanar contrs. to scatt. amplitudes 3-62780
- low-energy behaviour of few body scattering amplitudes 3-70878
- many-channel S-matrix in quasi-classical approximation 3-74124
- meson production, from high-energy nucleon-nucleon interactions, unitary eikonal formalism 3-78203
- multichannel stationary scattering theory in two-Hilbert space formulation 3-48764
- multiple complex energy poles in continuum shell-model calcs., analytic properties 3-60095
- nonanalyticity, renormalisation effects, chiral perturbation theory 3-62776

S-matrix theory continued

- nonpolynomial Lagrangians, higher perturbation orders in principle coupling constant 3-54277
- operator product expansions and high mass phenomenology at light-like distances 3-74299
- partial-wave scattering amplitude in quasipotential model, analytic properties 3-43073
- perturbation theory for energy corrections for bound, virtual and resonance states, Hilbert-Schmidt method 3-70879
- quantum gas, equation of state, S-matrix representation of second virial coeff. 3-70727
- reduction formula in QED for expressing S matrix in terms of Green's functions 3-40341
- Reggeon-Reggeon-particle vertex, singularity structure from analytic properties of Feynman graphs 3-60009
- relativistic convergent quantum mechanics of interacting particles, realistic model, S-matrix elements 3-59920
- Saxon-Woods potential, computer program for s-state binding energy and wave functions 3-67289
- scattering amplitude representation by analytic functions, Hilbert-space approx. technique 3-40317
- single-photon exchange diagrams in quasi-potential approach, calc. using polarization operator 3-70910
- spin dynamics, anisotropy effects study from second moment behaviour 3-44226
- strong interactions Pade approximation applications 3-62849
- threshold phenomena and their observation, S-matrix unitarity basis 3-67285
- transition operator for matrix potentials, application to pion-nucleon interaction 3-70877
- U-gauge residual divergences, cancellations, R-gauge formulations of massive gauge theory 3-59922
- unitarity, proof in nonlocal quantum field theory 3-40316
- unitarity and interpretation in the indefinite metric quantum field theory 3-74313
- unitarity at ISR energies, analysis in impact-parameter space 3-67152
- unitarity constraints on model for multiparticle production 3-45901
- unitary construction, super-quantisation method, bi-local field, non-flat space-time metric 3-59930
- unitary multiperipheral models, multichain forces 3-70961
- unrenormalizable theory for interaction between current of spinning particles and fixed point charge source, solvable model 3-70872
- zeros in $\pi\pi$ scattering, reln. to dynamical properties of scattering amplitude 3-70980
- $\Delta(1236)$, $N(1470)$ pole position determination 3-74475
- $K \rightarrow \mu(e)\pi$, kinematics of decay amplitudes and relativistic eqns. for spin-0 particles 3-57323
- pp scattering diffractive production, threshold effects 3-74461
- πN 3-3 resonance pole, residue determ. 3-57408

safety

- see also accidents; alarm systems; health hazards; protection
- CIRENE prototype, H.W.R. design features 3-63134
- coolant-slug-impact accident, fast reactor head cover, impulsive loading, nonlinear dynamic anal. 3-74673
- deep-sea disposal of radioactive waste, safety evaluation models 3-70192
- Dynamic Slug Impact Model, coolant-reactor vessel head impact, safety anal., MIMIC simulation 3-71176
- electrostatic spray guns, ignition test procedure, safety assessment 3-70778
- electrotechnical products regulations (Slovenian) 3-61978
- environmental contamination by ^{14}C from HTRs and fuel reprocessing plants 3-71335
- fast breeder reactor, critical excursion 3-67622
- fast nuclear reactors, design basis accidents, loss of coolant, safety and containment provisions 3-71181
- fast reactor, assessment, Bethe-Tait approximation 3-67538
- fast reactor, local fuel failure, simulation experiments 3-67521
- fast reactor core, research studies and experiments 3-67526
- fast reactor core design 3-67517
- fast reactor disassembly analysis, space-energy-dependent, safety 3-46083
- fast reactor fuel pins, sodium bonded 3-43293
- fast reactor overpower excursion, molten fuel/coolant dynamics, accident mitigation 3-71290
- fast reactor subassemblies, local blockages, calc. 3-67522
- FFTF fuel assembly, duct pressure response anal., stainless steel, ANSYS computer code 3-71293
- FFTF subassembly, potential for fuel failure propagation, fission gas release 3-71292
- fissile material storage, calcs. on double latching cell loadings 3-46156
- fissile materials, computerized nondestructive neutron interrogation technique for safeguards application 3-46072
- fissile materials in water-sprinkled noncubic storage arrays, computer calcs. of criticality 3-46155
- fissile solution storage, vessel design and analysis 3-63149
- fission products from breeder reaction, atmospheric distrib. and safety measures 3-40551
- fusion reactor, radiological implications 3-42380
- gas-cooled fast reactor design studies in Federal Republic of Germany 3-46103
- ground disposal site for radioactive wastes, internal dose estimation by sensitivity analysis 3-40550
- heavy water reactors, light water infiltration reactivity effects, Ames Laboratory Research Reactor, safety considerations 3-74736
- HTGR design basis accidents, primary cooling system, depressurisation 3-74678
- HTR, with coated fuel particles rel. to fission product Cs transport mechanism (German) 3-71320
- human vision from laser irradiation 3-42360
- hypothetical core disruptive accidents, LMFBR, simulation of mech. energy release, reactor energy source characterisation 3-74674
- hypothetical core disruptive accident, mech. energy yield, energy dissipation mechanism 3-74675
- laser, regulations, scientific foundations and biophysical effects (German) 3-77259
- laser beam effects on human tissue, TEA CO_2 laser, 30 mJ pulses with 100 kW 3-45816

safety continued

- laser safety performance standards in United States 3-66788
- liquid scintillation counting 3-70388
- LMFBR, backup safety device, evaluation, poison rod insertion, coolant poisoning 3-74672
- LMFBR, criterion for free-contact fragmentation in molten-fuel-coolant interaction 3-46092
- LMFBR, effect of noncondensibles on rate of Na vapour condensation from single rising HCDA bubble 3-46158
- LMFBR, fuel pin transient behaviour, obs. 3-67519
- LMFBR, heat transfer system design 3-67508
- LMFBR, interrelationships between core design, reactor physics and safety 3-71198
- LMFBR, local molten fuel-coolant interaction, pressure pulse on subassembly wall 3-46073
- LMFBR, prevention of local fault propagation arising from local cooling disturbances 3-46096
- LMFBR, system for protection against local core malfunction 3-46097
- LMFBR, uncontrolled energy releases 3-67534
- LMFBR, voided-core disassembly, fuel-coolant interactions 3-46075
- LMFBR accident analysis, model for Na droplet combustion 3-46076
- LMFBR design, experiments with fast oxide reactor 3-67516
- LMFBR design considerations, review 3-71192
- LMFBR disassembly calcs. fuel-coolant interaction and differential motion effects 3-46074
- LMFBR fuel assemblies, dynamic expts. for heat transfer and mixing studies 3-46113
- LMFBR fuel rods, failed, fission gas release rate, porous flow model 3-71291
- LMFBR fuel subassemblies, determ. of wrapper-can meltthrough using THTB code 3-46079
- LMFBR fuel subassembly with wire-wrap spacers, exptl. determ. of subchannel coolant crossflow 3-46111
- LMFBR large core-disruptive accident, PuO_2 aerosol release, transfer to second containment, calc. models 3-71178
- LMFBR power temp. accident, fuel melting, shutdown mechanism, axial molten-fuel motion model 3-74731
- LMFBR safety analysis, hexagonal fuel assembly response, effect of coolant STRAW dynamic finite element code 3-71294
- low energy excursions, reactor containment, implicit continuous Eulerian containment code 3-71175
- microwave shielding and surveys near spectroscopic sources 3-66061
- molten fuel-coolant interaction, damage to reactor structures, model, REXCO-H code, containment anal. 3-71295
- multidimensional kinetic problems, diffusion theory, state-of-art 3-71151
- nuclear, fast breeder reactor, design engineering 3-67502
- nuclear, fast breeder reactor operation, safety and reliability, conference, Karlsruhe, Germany (1972) 3-67501
- nuclear, fast reactor core design 3-67503
- nuclear criticality safety, measurement requirements 3-67406
- nuclear fuel facilities in Japan, criticality safety control (Japanese) 3-43277
- nuclear fuel handling criteria, supporting critical lattice data 3-67405
- nuclear fuel pin-to-pin failure propagation, pressure pulse loading, fission gas release, buckling failure criterion 3-74732
- nuclear fuel storage, accident prevention (German) 3-57563
- nuclear LMFBR, loss-of-flow accidents, in-pile simulations 3-67420
- nuclear power plant, acoustic surveillance system 3-66156
- nuclear power plant, design for pipe break outside of containment 3-67433
- nuclear power plant, general public and operating personnel 3-63144
- nuclear power plant, THTR 300 MWe, removal of decay heat and release of activity (German) 3-71237
- nuclear power plants, Brunswick Steam Electric Plant, startup and operating procedures, emergency and fuel handling procedures 3-73641
- nuclear power plants, operating procedures, manual for plant safety 3-73639
- nuclear power plants, operating procedures, min. risk to health and safety 3-73638
- nuclear power plants, Pilgrim Station, operating procedures, plant safety 3-73640
- nuclear power plants, standards and operating procedures, personnel, safe and reliable plant operation 3-73642
- nuclear pressure vessel fracture and safety analysis 3-63133
- nuclear reactor, after-cooling systems design and operation (German) 3-71235
- nuclear reactor, considerations for after heat removal (German) 3-71234
- nuclear reactor, fast test, minimization of double-release problem in gas-tagged core 3-67427
- nuclear reactor, fault tree analysis, new approach 3-46068
- nuclear reactor, light water, catalyst performance for post loss-of-coolant accident recombiner applications 3-67423
- nuclear reactor, loss-of-target analysis, safety criteria 3-67421
- nuclear reactor, pressurized water, conceptual in-vessel design for containment of molten core 3-67422
- nuclear reactor, primary pump shutdown, temp.-time behaviour in MTR type fuel elements (German) 3-74644
- nuclear reactor, SLOWPOKE, inherent safety 3-70368
- nuclear reactor, stochastic decision making procedure 3-46084
- nuclear reactor containments, safety margins in pressure-temperature transients calc. 3-46091
- nuclear reactor criticality accidents, CRAC expt. 3-67407
- nuclear reactor criticality safety at pipe intersections for Pu nitrate solns. (German) 3-67543
- nuclear reactor fast neutron irradiated, fatigue crack propagation 3-69296
- nuclear reactor fuel elements, cask loading, inverse multiplication meas. in situ, criticality safety 3-63251
- nuclear reactor fuel Interim Decay Storage Facility, upper Pu limit, transport and diffusion theory calc. 3-71298

safety continued

- nuclear reactor fuel storage, $\text{Pu}(\text{NO}_3)_4$ solutions, slab geometry, criticality experiments 3-63197
- nuclear reactor operating experience, procedures and standards, conf., Myrtle Beach, South Carolina, USA (Aug 1973) 3-74691
- nuclear reactor operation, scram system trip, obs. (Russian) 3-67514
- nuclear reactor power plants, safety-related occurrences, 1972 review 3-74700
- nuclear reactor primary containment, dynamic response calc. using hydrodynamic elastic-plastic computer code 3-46080
- nuclear reactor safety vessel construction and materials (German) 3-74716
- nuclear reactors, design basis accidents, evaluation 3-71180
- nuclear reactors, design basis accidents, evolution of technology 3-74677
- nuclear reactors, engineered safety features, design, probability, statistical risk 3-71179
- nuclear reactors, quality assurance and in-service inspection 3-67401
- nuclear waste, nondestructive assay, criticality problems and solutions 3-63248
- passive gamma neutron monitor, fissile content of waste and scrap, criticality safety 3-63254
- power plant employee protection from noise 3-42473
- power reactor steam generators, safety against sodium-water reaction 3-67615
- propane spray for cold fog seeding, bromotrifluoromethane as flame suppressant 3-51189
- pulsed neutron source techniques, criticality safety determination, reactivity of a reactor core 3-63231
- radiation, permissible limits, regulation of hazard, safety, National Bureau of Standards 3-53761
- radioactive iodine emission from nuclear reactors, accumulation in Federal German Republic (German) 3-67631
- radioactive waste, selection of ground disposal site using computer (Japanese) 3-43317
- radioactive waste, site for ground disposal, migration of multiple nuclides 3-78393
- radioactive wastes in ground, point-rating chart for safety evaluation 3-70191
- reactor fuel, exposed, criticality control parameters 3-46151
- reactor thermal analysis, treatment of uncertainties by expanded method of correlated temperatures 3-46070
- rocket solid propellant burning, effect of neutron irradi., safety analysis 3-49322
- SPR II, fast burst reactor, control and burst generation, nonfissile external reflector element 3-71212
- ultrasound, diagnostic and therapeutic applications, tolerance range of dosage (German) 3-77249
- X-ray diffraction equipment in New Zealand, radiation protection 3-48268
- Na, liquid, two-phase and subcooled, thermodynamic props., calc. molten fuel-coolant interactions, potential accidents 3-71288
- Pu, criticality studies, Dow Rocky Flats Nuclear Safety Laboratory 3-63229
- Pu high-burnup solns., computer calcs. of critical parameter using two-isotope approx. 3-46153
- Pu monitoring, nondestructive assay, criticality prevention, scrap recovery 3-63249
- Pu monitoring, nondestructive instrument techniques, criticality safety 3-63252
- Pu-U mixtures, criticality safety, effect of Gd, B-containing Raschig rings 3-63228
- Pu-U nitrate solns., computer calcs. of criticality factors based on exptl. data 3-46152
- $\text{PuO}_2\text{-UO}_2$ -polystyrene mixtures, LWR, 7.6 wt% Pu, criticality expts., computer calcs. 3-46154
- ^{239}Pu , nitrate solutions, criticality studies, effect of acid molarity and ^{240}Pu content 3-63230
- U, criticality studies, Dow Rocky Flats Nuclear Safety Laboratory 3-63229
- U accumulations, diffusion plant equipment, radiation monitoring, nuclear criticality 3-63250
- ^{235}U and ^{233}U , nitrate solutions, criticality studies, effect of acid molarity and ^{240}Pu content 3-63230
- ^{235}U and ^{233}U isotopes, criticality research, Oak Ridge Critical Experiments Facility 3-63227

safety systems

- see also alarm systems
- accelerator abort system, main accelerator Batavia USA, safe proton beam dumping, description 3-56866
- criticality switching in SNR-300 due to Na-void effect (German) 3-67473
- LMFBR, backup safety device, evaluation, poison rod insertion, coolant poisoning 3-74672

Sakata model see quarks**samarium**

- alkali halides: Sm^{2+} , luminescence and energy levels 3-55679
- crystal structure rel. to phase transitions from 77 to 300K 3-49996
- magnetic scatt. amplitudes, approx. ground states 3-50372
- quadrupole interaction with recoiling ^{150}Sm nuclei, calc. of electric field gradient 3-45943
- solubility in Pb-Li liquid alloys 3-58131
- X-ray isotope shifts and variations of nuclear charge radii 3-67662
- $\text{CaF}_2\text{:Sm}^{2+}$, high press. optical absorpt. studies 3-41540
- $\text{CaF}_2\text{:Sm}^{2+}$, nonradiative and fluorescent lifetimes 3-72708
- LaO:Sm film, r.f. sputtered, luminesc. during sputtering 3-69097
- LaO:Sm film, r.f. sputtered, luminesc. during sputtering 3-69097
- MgO:Sm film, r.f. sputtered, luminesc. during sputtering 3-69097
- ^{146}Sm , existence in Juvinas achondrite 3-47966
- $^{146}\text{Sm}/^{149}\text{Sm}$ ratio determ. in Apollo 16 soils 3-56351

samarium compounds

- ethylsulphate, Raman spectra 3-50564
- samarium benzoylacetate, u.v. diffuse reflectance spectra 3-47291
- $\text{Bi}_2\text{O}_3\text{-Sm}_2\text{O}_3$ eutectoid, transform. deform., stress and temp. depend. 3-76231

samarium compounds continued

- Co-Sm alloy, for permanent magnets, temp. depend. of coercivity 3-44269
- Co-Sm magnet, quenching, oxides identified by X-ray diffr. 3-47100
- Co-Sm permanent magnet alloy, lattice parameter variation with composition and temp. 3-43763
- Pr-Sm-Co, mag. props. as function of composition 3-47088
- Sm-Co-MM, MM=mischmetal, mag. props. as function of composition 3-47088
- SmBr₂, determination of lattice constant (German) 3-64011
- $\text{Sm}_2(\text{Co}, \text{Fe})_{17}$, mag. props. of permanent mag. material 3-44253
- SmCo_5 , cryst. struct. 3-49871
- SmCo_5 , domain wall energies detn. 3-44248
- SmCo_5 , permanent magnet material, heat treatment and mag. phase analysis 3-44250
- SmCo_5 , sputter deposited permanent mag. material, heat treatment and hysteresis 3-44251
- SmCo_5 , temp. depend. of nucleating fields and coercive force 3-44267
- SmCo_5 powder, domain wall pinning centres, particle size, and coercivity 3-44276
- SmCo_5 powder, prep. by rapid quenching technique for magnet applic. 3-44278
- SmCo_5 powder, sintering mechanisms, rel. to magnet prod. 3-47438
- $\text{Sm}_2\text{Co}_{17}$, liquid phase sintering, mag. props. obs. 3-44694
- Sm_2CuO_4 , semicond. props. from 120 to 1000 K rel. to K_2NiF_4 structure 3-41241
- SmFeO_3 , antiferromag. reson. and phase transition 3-41429
- SmFeO_3 , hysteresis of magnetization reversal 3-58401
- $\text{Sm}_3\text{Fe}_2\text{O}_{12}$, effect of 60 kbar pressure on Curie point (French) 3-72463
- $\text{Sm}_{1-x}\text{La}_x\text{S}$, Van Vleck exchange coupled ions mag. susceptibility 3-50355
- $\text{SmM}_2\text{X}_{2-x}$, (M=Fe, Co, Ni, Ag), (X=Si, Ge), ferromag. Sm, Ce and diamag. M sublattices 3-64475
- SmO, unusual 6R struct. 3-40895
- $\text{SmO}_{1.5}\text{-CeO}_2$, $\text{MO}_{1.5}\text{-MO}_2$ (fluorite) type mixed oxide, phase relns. 3-64181
- SmS, optical properties of discontinuous semiconductor-metal phase transformation (German) 3-53118
- SmS, press. depend. exchange coupling, e.s.r. g-shifts of S-state ion trace impurities 3-64491
- SmS, region of homogeneity, comp. effect on physical props. 3-64178
- SmS, thermal and electrical conductivity, thermopower, Hall effect, temp. and composition depend. 3-60871
- SmS:Gd, temp.-induced explosive first-order electronic phase transition 3-64297
- SmS:La, cond. electron enhancement of exchange interactions 3-55413
- SmSe, press. depend. exchange coupling, e.s.r. g-shifts of S-state ion trace impurities 3-64491
- SmSe and $\text{Sm}_{1-x}\text{Se}_x$ n.m.r., exchange-induced hyperfine fields at ^{77}Se 3-58439
- $\text{Sm}_x(\text{Ta}_{3-x}\text{W}_{1-3-x})\text{O}_3$, $0.04 \leq x \leq 0.33$, struct. evolution as function of composition (French) 3-54948
- SmTiNbO_6 , polycrystalline specimens, electrical conductivity, temperature dependence 3-75787
- $\text{Sm}_{0.75}\text{Yb}_{0.25}\text{Fe}_2\text{O}_{12}$ and $\text{Sm}_{1.5}\text{Yb}_{1.5}\text{Fe}_2\text{O}_{12}$, epitaxial film development 3-79583
- SmZrF_7 , crystal struct. similarities to ReO_3 type (French) 3-79299

sampled data systems

see also discrete time systems

- Bevatron, ion gun power supply regulation 3-56780

sand

- andesitic sand rel. to elastic properties of granular media in uniaxial compression 3-65207
- basaltic sand rel. to elastic properties of granular media in uniaxial compression 3-65207
- binary system in tube mixer study of ^{60}Co activated component 3-44695
- depositional histories, surface texture examination 3-69517
- fractionated quartz river sand, effect of porous struct. and absorbed moisture on u.s. propagation 3-61238
- granular aggregates, acoustic velocities and energy losses 3-50798
- heaving force when freezing under constraint (Japanese) 3-56035
- Martian craters and aeolian features 3-59274
- offshore bars, mechanism for origin and corrosion 3-59041
- ridges and waves on tidal sea shelves 3-47706
- submarine longshore sand bar formation rel. to slowly var. Stokes waves 3-65265
- transverse sand bar formation, model 3-53449
- triaxial compression test, effects of specimen height and strain rate 3-69422
- u.s. velocities, frozen ottawa sand, dilatational and shear velocities, variation with water content 3-47660
- vortex formation over rippled beds by progressive waves 3-58992
- water flow, numerical solns., allowance for hysteresis effects 3-46486
- waterflow, unsaturated stratified vertical sand column, effects of air and water pressure 3-46485

satellite computers

- control systems, particle-accelerators, decentralisation, advantages 3-56792

satellite links

see also artificial satellites

- Antarctic unmanned geophysical observatory with satellite link to California 3-56001
- earth photography, electronic imaging, trends (Japanese) 3-73373
- ionospheric scintillation at 4 and 6 GHz near geomagnetic equator, obs. 3-56193
- ISIS-II to ground, radiowave attenuation by ionosphere 9.303 MHz, measurement 3-61525
- loop antenna, corner driven in warm plasma, theory 3-67999
- rain effect on Earth-space paths 3-44905

satellite relay systems

- meteorological data centralization, Eole expt. (Italian) 3-61605

satellite vehicles see artificial satellites

satellites, artificial *see* artificial satellitessatellites, planetary *see* planetary satellites

saturable core reactors

transducers, for zero gradient synchrotron performance for current measurement and control 3-56767

saturable reactors *see* saturable core reactorssaturation measurement *see* chemical variables measurement

Saturn

21-cm. line obs. by new method of radio interferometry of faint moving sources 3-61674

astrolabe obs. during 1971-72 winter (*French*) 3-56336

atmosphere dynamics rel. to planetary dynamics 3-47936

atmospheric structure, 0.62 μ methane band absorpt. and near-u.v. characts. 3-61695

brightness temp. meas. at 3.1 and 8.6 mm 3-47922

cloud layer and overcloud atmosphere by photographic obs. between 3620 and 6250 Å (*Russian*) 3-76988

comet origins and orbits rel. to Jupiter-Saturn system 3-42184

condensed molecular H, electrical cond. rel. to mag. field generation 3-42159

figure theory, integration of eqns., determ. of gravit. moments 3-61693

fringe rate and amplitude, upper limit to the 11.2 m- λ flux VLBI system 3-47906

gravitational field constraints on model of interior 3-47933

horseshoe and Trojan orbits associated with Jupiter-Saturn system 3-42137

interior processes model testing using atm. meas. 3-47934

ionospheric physical and chemical processes 3-47937

mass determ. from motion of Trojans 3-47900

metallic H prod., correlation of theory and expt. 3-40684

methane 3 ν_2 absorption band in atmospheric spectra, rotational temp. and abundance 3-47913methane 3 ν_2 band obs. along planet's central meridian 3-56331

microwave brightness temp. determ. using model atm. 3-42158

new ring prediction 3-61699

nonthermal radio emission 3-42154

radiative transfer by fundamental methane bands in atmosphere 3-69880

radio flux at 26.3 MHz, upper limit from VLBI 3-42150

rings, brightness temp. meas. at 20 μ 3-47902rings, deconvolution of raw photometric curves (*French*) 3-56341

rings, effective optical thickness and dark-side illumination 3-42139

rings, photographic obs. (*French*) 3-56340

rings, spectral reflectivities of ices 3-61703

solid molecular H, eqn. of state at high press. 3-42164

structural models 3-69884

survey of present knowledge 3-45039

Titan, model from observational data 3-42141

Titan, polarimetric obs. rel. to optically thick atmosphere 3-47916

Titan, polarization obs. rel. to opaque cloud layer with strong u.v. absorption 3-47917

Titan, possible H₂ greenhouse effect rel. to atmospheric temp. 3-47915

Titan atmosphere, strong temp. inversion from i.r. spectra 3-80987

toroidal ring, u.v. photography 3-80998

H model, eqn. of state and phase diagram for dense H 3-42163

H planet, high-pressure phenomena 3-42152

H quadrupole lines in (3-0) and (4-0) bands 3-80984

H-He atm., thermodynamics props. at high press. 3-42161

He-methane system, phase equilibria meas. at high-pressure. 3-42162

SC (sudden commencement) *see* magnetic stormsscale invariance *see* scaling phenomenascalars (circuits) *see* scaling circuitsscales *see* balances

scaling circuits

decade scaler with commutator, 100 MHz 3-56962

direct-reading arithmetic unit, for nondestructive assay of nuclear materials 3-51729

molecular beam velocity analysis using time-of-flight method with PDP-11 multiscale interface 3-78908

multichannel, operation of an AI-100-1 amplitude analyser 3-73879

scaling phenomena

see also elementary particle theory ω_p scaling 3-67047axial current scale dimensionality (*Russian*) 3-59938

axial vector current, short-distance behaviour, canonical scaling 3-67003

Bjorken, in ϕ^3 ladder model 3-78147

Bjorken scaling, limiting fragmentation in baryon exchange model 3-60055

Bjorken scaling hypothesis, applicability ~ 30 GeV (*Hungarian*) 3-62841

charged-prong multiplicity distrib. in hadronic collision, scaling behaviour 3-43151

Compton cross sections, virtual, longitudinal, scaling limit 3-59973

conformal symmetry, scale dimensionality of currents and field derivatives, equal-time commutators 3-62777

dilatation invariance used to derive scaling laws for ep scatt., μ -pair production, and inclusive reactions 3-74337

divergent e.m. masses, analyticity, scaling and light cone 3-40342

dual amplitudes, dilatation and scale invariance 3-54327

dual model of currents, off-shell amplitudes, Regge limit and scaling 3-59993

electroproduction, bremsstrahlung model and scaling 3-59981

form factors, hadronic store prod., asymptotic behaviour 3-78127

function continuation from deep inelastic electron scattering into annihilation 3-57359

geometric scaling in high energy collisions of hadrons, KNO scaling function 3-67055

hadron interactions at short distances, quantum field theory 3-51973

hadronic collision, scaling and new kinematic variable n^2 3-57450

hadronic processes, two-body and quasi-two-body, geometrical scaling 3-74427

hadronic scaling, scattering of composite systems 3-74467

hadronic scaling and broken conformal symmetry 3-67159

inclusive pp interactions at 303 GeV/c 3-74447

inclusive single-particle spectra, new form of scaling 3-43154

scaling phenomena continued

inclusive two-particle processes, Regge phenomenology 3-43160

Koba, Nielsen, Olesen scaling law, exptl. study at low energy and validity for definite rapidity interval 3-78201

Koba Nielsen Olesen scaling and scaling in partial wave inelasticities 3-78202

Koba-Nielsen-Olesen scaling at finite energies 3-74471

Koba-Nielsen-Olesen scaling function for energy-independent distrib. of fireballs 3-67153

Koba-Nielsen-Olesen scaling restrictions on fireball production in statistical bootstrap model 3-67063

Koba-Nielsen-Olesen scaling for charged prong multiplicity distrib. 3-62909

longitudinal structure function of inelastic neutrino and electron scattering quark gluon model 3-62847

multiperipheral model, transverse momentum distribution 3-67083

neutron-lepton amplitude at threshold, polarisability contrib. 3-78134

null-plane field algebra, Dirac's canonical quantisation method, scaling relations 3-62787

phase transition, critical region, validity of bootstrapping and length scaling 3-74178

pion decay constant on energy scale for hadron dynamics 3-66967

proportionality of hadronic and e.m. amplitudes 3-62834

quarks with structure, breakdown of scaling 3-78154

scaling asymptotics in quantum field theory of deep inelastic electron-proton scattering 3-74319

scaling in some deep inelastic scattering and annihilation processes 3-67034

scaling law for general inclusive reactions induced by current 3-49013

scaling laws of parton model, pion asymmetry in hadron electroproduction 3-57361

scaling models of high-energy multiparticle production in hadron-hadron collisions 3-62868

scattering of composite systems, approach to scaling 3-67059

semi-hadronic inclusive reactions, operator approach 3-57368

semi-inclusive scaling curve for charged multiplicity distrib. in high energy collisions 3-67155

softened field theory, vector gluons, light cone singularities 3-78086

t/s scaling in exclusive and inclusive proton reactions 3-57371

Thirring model with U(n) symmetry at fixed values of coupling constant 3-74341

Ward identities and axial-vector current anomaly, Adler-Bardeen theorem proof 3-62790

Wilson's theory of critical phenomena and Callan-Symanzik eqns. in 4-E dimensions 3-66716

e-hadron collisions, quasi-inclusive processes, dual resonance model and scaling 3-43113

e⁺e⁻→e⁺e⁻X, very high energy, possible tests of scale invariance 3-52017

eN deep inelastic scattering, scaling of individual channels 3-78140

ep→e⁺+anything, scaling behaviour in parton model 3-52019

interactions charged multiplicity distributions, empirical formula having scaling property 3-60043

Kp inclusive reactions scaling $|x| > 0.6$ 3-62912 ν high energy scattering, tests of scaling from total cross-sections 3-74359 ν interactions, consequence of scaling 3-62819 ν N scattering, inelastic, spin sum rules, light cone scaling 3-78116

pion inclusive spectra, approach to scaling limit in resonance dominance framework 3-49059

pp collision, parton model and causality, scaling bounds on high transverse momenta 3-67148

pp collisions, early onset of semi-inclusive scaling 3-57467

pp→l⁺l⁻+anything, charge distrib. of partons and scaling 3-74459pp→ $\mu^+\mu^-X(\pi X)$, scaling limit, light cone dominance, spectral representations 3-78222pp→ $\mu^+\mu^-$ anything, scaling function multiperipheral theory 3-74468pp→ π^+ +anything, 20 to 1500 GeV, semiempirical formula for cross section 3-57461

pp scattering, moderate energy, scaling limit rel. to parton, field theory scaling 3-78192

 $\pi^-p \rightarrow \pi^- + (n-1)$ charged + neutrals, 7.5 and 21 GeV/c scaling, reduced charged multiplicity 3-78225 $\pi\pi$ total cross section, scale and massless pion limit 3-57418scaling tubes *see* counting tubes

scandium

alkaline earth fluorides: Sc, Y, La, thermoluminescence, donor-acceptor pairs (*Russian*) 3-44500

conduction electron m.f.p. and concentration 3-79679

electronic struct., Knight shift, nuclear spin relax., mag. susceptibility anisotropy 3-50333

high purity, effect of impurities on magnetic susceptibility 3-46985

Oka carbonatite complex, X-ray fluorescence anal. of Sc abundance 3-80587

semiempirical calculation of gf values, LS transition arrays, transition integrals, eigenvectors 3-74786

tritiated, for electron capture detector 3-66419

Al, cond. electron charge density around Sc impurity, n.q.r. obs. 3-47168

CaF₂:Sc³⁺, Bridgman grown, impurity distrib. 3-58048Sc³⁺, eightfold coordination in garnet 3-72065YAG:Sc³⁺, Nd³⁺, solubility enhancement of Nd³⁺ by lattice expansion with Sc³⁺ 3-68415

scandium compounds

sulphides, containing two III_a elements, comparison of cryst. struct. (*French*) 3-58021K₂Sc₂(Ge₂O₇)(OH)₂, synthetic basic, crystalline structure, cation-anion interatomic distances 3-60714

Sc alkali borosilicates, crystallochemical features, stereometrically mixed framework 3-72063

ScBO₃, thermal expansion, temp. depend., 30-702°C 3-68422ScCl₃, NaCl structure, band structure calc. 3-41142Sc(ClO₄)₃, aqueous solutions, density, compressibility, expansibility, sound velocity (*Russian*) 3-72114ScF₃:Gd³⁺(Mn²⁺), e.p.r. spectra, 290 and 77 K 3-55469Sc(H₂PO₄)₃, i.r., p.m.r. spectra 3-78657

scandium compounds continued

- Sc(H₂PO₃)₃, i.r., p.m.r. spectra 3-78657
 Sc₂(HPO₃)₃, i.r., p.m.r. spectra 3-78657
 Sc₂(HPO₃)₃·4H₂O, i.r., p.m.r. spectra 3-78657
 Sc₂(MoO₄)₃, ferroelastic transition from monoclinic to orthorhombic phase at 9°C 3-52664
 ScN, NaCl structure, band structure calc. 3-41142
 ScO, NaCl structure, band structure calc. 3-41142
 Sc₂O₃-V₂O₅ system, elec. cond. transition 3-72388
 ScRu₂C_{1-x}, ScRh₂C_{1-x}, ScIr₂C_{1-x}, perovskite structure, preparation, X-ray and metallographic studies 3-40907
 Wc₂O₃:Bi phosphor, luminescence centres (Russian) 3-44458

scattering

- see also acoustic wave scattering; backscatter; beta-ray scattering; electromagnetic wave scattering; nuclear reactions and scattering; particle scattering; potential scattering
 abstract differential eqns. of second order, existence of wave operators 3-40151
 additivity of phase shifts, nonrelativistic scattering from spherically symmetric potential, Glauber approach 3-77865
 aerosols, polydisperse, method for calculating scattering indicatrices (Russian) 3-43631
 amplitude-phase method, attractive r^{-2} potential 3-70703
 analytic continuation of data, necessity of nearly-best possible methods 3-62556
 bounds for scattering matrix and transition probabilities 3-70702
 bra and ket formalism is extended Hilbert space 3-74109
 C* algebra and automorphisms for problem of return to equilibrium 3-45630
 classical approach to semi-classical scattering theory 3-71613
 cutoff potentials, expansion of scattering matrix in momentum power series and analytical extension 3-62546
 discrete ambiguities and equivalent potentials 3-66634
 eikonal Born approximation with angle trajectories 3-70704
 eikonal expansion of eqns., general formalism for rearrangement processes 3-62570
 eikonal expansion of potential scattering T-matrix 3-42835
 elastic, involving central Yukawa potential, soln. using continuous space-filling curves 3-66628
 elastic scattering amplitudes, uniformation calc. arbitrarily many open channels 3-66636
 Fredholm calculations using L² functions with complex coordinates 3-70701
 Fredholm determinants calc. on L² basis, equivalent quadrature extraction method 3-70700
 generator-coordinate amplitude, boundary conditions, solution to Hill-Wheeler equation 3-63020
 H-function for isotropic scattering, approximate form 3-45697
 hard spheres, multiple scatt. problem 3-66614
 high-frequency, asymptotic analysis, circular and parabolic cylinders 3-66507
 inelastic and reactive, sudden and semiclassical approxs. 3-42842
 inelastic scatt. elements from approx. wavefunctions in L² basis 3-45695
 inverse problems, approx. soln. using generalised WKB method 3-62572
 JWKB phase shifts, optimum numerical calcs. 3-70689
 Kato's lemma on Schwinger's variational principle for scattering phase, new proof 3-45706
 Klein-Gordon equation, spectral and scattering theory 3-45696
 L² expansion scattering calculations, new approach 3-70699
 Lippmann-Schwinger equation, moment methods for numerical solutions 3-62563
 many-channel S-matrix in quasi-classical approximation 3-74124
 method convergent long wavelength expansion for 2 dimensional problems 3-54069
 modified Korteweg-de Vries eqn. and scattering theory 3-62565
 multichannel, stationary, in two-Hilbert space formulation 3-48764
 multichannel quantum, transition from time-dependent to time-independent theory 3-74105
 multiple scattering by two centres of force 3-51805
 nonlinear evolution eqns. of phys. significance, soln. using inverse scatt. method 3-51811
 nonlinear periodic waves in inhomogeneous medium 3-40158
 nonspherically symmetric potentials, iterative inversion procedure 3-42845
 optical potentials in time-dependent quantum theory 3-54133
 particle by nonlocal pots., effective-mass method, semiclassical approx. 3-42841
 phase shifts, spherically symmetric potentials 3-74115
 potential, appl. of Pade approximants in Lippmann-Schwinger eqn. and zero-energy amplitude 3-62573
 potential, equivalent variational functions from differential and integral eqns. 3-62557
 potential scatt., variational bounds on radius of convergence of Born series 3-66619
 potential scattering, variational methods 3-66623
 potential scattering cross sections in semiclassical limit 3-62554
 potentials, analytic nonlocal, forward dispersion relation 3-62558
 potentials, energy independent, inverse scattering calc. 3-62545
 principle value integral evaluation by differential equation method 3-70690
 quantum mechanical system, Green functions and projection operators in semiclassical approx. 3-59789
 quantum theory, computer calc. for students 3-77362
 quantum theory of multiparticle system 3-77872
 radial asymptotic expansions for singular potentials, numerical integration 3-40149
 rearrangement Green's function, generalised isoperimetric inequalities 3-73994
 resonant scatt. from inhomogeneous nonspherical targets 3-45631
 scalar wave, elastic medium with random rough boundary 3-42751
 Schrodinger eqn., variation-of-parameters method of soln. for scatt. problem, improved method 3-42843
 Schrodinger equation approximate solution by minimizing deviation 3-59781
 seismic wave pulses, scattering effect of embedded obstacle on seismic wave pulses 3-69500
 separable expansions of t-matrix 3-49164

scattering continued

- short surface waves, radiation and scattering, partially immersed bodies effect 3-49604
 short surface waves, radiation and scattering 3-49603
 by spherically symmetric potentials, existence and completeness of wave operators 3-42849
 spin-dependent spheroidal potential, iterative soln. of infinitely coupled integral eqns. 3-74107
 time dependent theory, algebraic, wave operators (French) 3-77854
 trace-class operators, asymptotic behaviour of cross section at high energy 3-62555
 two-body, with long-range interactions, modified Lippmann-Schwinger eqn. 3-74108
 unitary amplitude construction from differential cross section 3-78104
 unitary representation of SL(2,C) group in horospheric basis 3-62798
 unstable states, correspondence with resonances, potential scattering 3-42834
 wave, e.m. and quantum mechanical, random media 3-66510
 wave propagation, abstract theory on Hilbert space 3-51778
 weak reflection by slowly varying plane layered media, solns. near zeros of parameters, WKB method 3-74111
scattering matrix see S-matrix theory
scf methods see self-consistent field methods
schizons see elementary particle weak interactions
schlieren systems
 organic dye laser, harmful schlieren effects (German) 3-51923
 turbulent gas mixing meas. using a laser Schlieren technique 3-48689
Schottky-barrier diodes
 see also semiconductor-metal boundaries
 capacitance, freq. depend, deep impurity effects 3-64405
 conduction mechanism, quasi Fermi level position detn. 3-55336
 diamond, boron doped, current voltage characteristics 3-64404
 h.f. noise, unified theory 3-44146
 inhomogeneous semiconductor, deep level energy and density profiles, determ. method 3-60859
 m.i.s. type, VI characs. allowing for tunnelling through space charge region (Russian) 3-52908
 shot noise, during tunnelling through a space charge region (Russian) 3-72402
 GaAs, liquid phase epitaxial, hole and electron traps detn., capacitance obs. 3-41263
 GaAs, rectifying barrier props. (Russian) 3-75791
 PtSi-Al reaction, electrical and mechanical features 3-64403
 ZnSe, reverse-biased, electroluminescence obs. 3-58564
Schottky barriers see Schottky effect
Schottky defects
 alkali halides, Mott-Littleton model, successive approximations 3-79338
 ionic crystal of polarisable ions, polarisational energy of Schottky defect 3-64027
 ionic crystal of polarisable ions of high symmetry, generalised polarisability function 3-64026
 polarisation energy, cubic cryst., calcs., Mott-Littleton approximation 3-79263
 NH₄ClO₄, rel. to ionic conduction, computer simulation using polarisable point ion model 3-58146
 PbFCl, rel. to anisotropic ionic conduction 3-58145
 PbFCl, rel. to mixed anionic cond. 3-72230
Schottky effect
 see also work function
 conduction mechanism, quasi Fermi level position detn. 3-55336
 diamond, semiconducting, current-voltage characteristics 3-64404
 evidence for Schottky-emission-dominated dielectric breakdown 3-44373
 junctions, temperature coefficients of drift voltage (German) 3-50265
 metal-dielectric contact, rel. to I-V characs. (Russian) 3-44145
 metal-semiconductor interface, covalent-ionic transition, microscopic theory 3-55334
 m.i.s. structure, potential barrier transparency coefficient, calc. (Russian) 3-52907
 m.i.s. structure, VI characs. allowing for tunnelling through space charge region (Russian) 3-52908
 semiconductor, hole and electron traps, Schottky barrier capacitance studies 3-64300
 semiconductor epitaxial layer doping profile, Schottky barrier CV characs. obs. (Polish) 3-69161
 AgBr-GaAs, interface, rel. to photoelec. props. 3-44110
 AgBr-Si, interface, rel. to photoelec. props. 3-44110
 Al-SiO₂-Au structure, rel. to internal photocurrent (French) 3-41274
 Au-GaAs Schottky barrier, prebreakdown capacitance-voltage and current-voltage characs., obs. 3-55322
 Au-GaP, Schottky barrier, wavelength modulated photovoltage spectra 3-55618
 GaAs, carrier ionisation rate from photomultiplication obs. 3-55271
 GaAs, Schottky barrier electroreflectance meas. 3-41502
 GaAs, Schottky surface barriers, high-resolution electroreflectance meas. 3-55630
 GaAs-Au, Schottky barrier, electroreflectance spectra at GaAs discrete and continuum exciton states 3-55640
 GaAs-metal interface, energy structure, Schottky barrier height, Fermi level 3-60916
 n-GaP, inadvertent deep centres, Schottky barrier photocapacitance obs. 3-52868
 n-InP-Au Schottky barrier, elec. props. and appl. to majority carrier conc. determ. for n-InP 3-52898
 Mg placed in Ar, exoelectronic emission in Ar ambient (Rumanian) 3-69144
 Si:Ge, ion implanted, deep trap levels obs. 3-52802
Schottky noise see shot noise
Schrodinger equation
 amplitude-phase solution and attractive r^{-2} potential 3-70703
 approximate solution by minimizing deviation 3-59781
 boson system, many-body, extended Jastrow functions 3-68453
 Cauchy problem, soln. using quantum stochastic processes for particles with spin 3-62548

Schrodinger equation continued

- chemical reaction description, adiabatic reference functions determ. 3-47551
 coherent Raman beat phenomenon analysis using coupled Maxwell-Schrodinger eqns. 3-62748
 coherent states and magnetic operators 3-42857
 computer program giving numerical soln., for students 3-77361
 Coulombian transparency in hot infinite deuterium plasma, finite deuterons 3-52525
 deduction from classical mechanics (*Spanish*) 3-66613
 diffusion model, description of microphysical processes 3-59788
 double minimum Morse pot., analytical soln., intramol. inversion applic. 3-52332
 double perturbation theory for interacting systems 3-57676
 eikonal approx. for partial-wave phase shifts, high-energy collision processes on nuclei 3-71110
 electron in a quantised plane wave and in a constant magnetic field 3-52004
 envelope-soliton solutions, exact of nonlin. wave eqn. 3-48806
 exact motion of charged particle is noncentral electric field, Newton's and Schrodinger's mechanics 3-74104
 few-body problem in nonrelativistic field theory 3-67224
 finite difference analogues, relativistic three-body problem, configuration representation 3-70888
 finite difference boundary value method of soln., comparison with Cooley-Cashion-Zare method 3-42844
 free Landau electron, canonical transformations 3-74103
 generalised, quantisation procedure extension to include classical counterparts 3-74090
 Green's functions, calc. for homogeneous and const. elec. and mag. fields (*Russian*) 3-48753
 Green function calc. rel. to motion of wave packet of particle with $e < 0$ in crossed fields (*Russian*) 3-78122
 harmonic oscillator, maximal kinematical invariance group 3-62549
 linear abstract, existence and uniqueness of soln. in Beurling spaces (*Italian*) 3-40087
 magnetic Bloch functions 3-58362
 many-body Hamiltonian, decomposition technique, Thomas-Reiche-Kuhn sum rule 3-59784
 model crystal modified by external field, Houston-type solns to time dependent eqn from Bloch functions 3-64272
 modified Rayleigh-Schrodinger expan., singlet state polarizabilities, conjugated mols. 3-74099
 molecular vibrational-rotational spectra electronic-nuclear interaction effect 3-63428
 multichannel, solution to potential model for hyperon-nucleon scattering 3-62874
 nondegenerate system, multiple perturbations, Rayleigh-Schrodinger formalism (*Spanish*) 3-74086
 nonlinear, three dimensional rel. to cyclotron wave propagation in collisionless plasma 3-75312
 nonlinear dispersive waves, derivative-expansion method 3-77791
 nonlocal potentials, soln. (*German*) 3-66610
 ocean inertial frequency oscillations evolution eqn. 3-69555
 one-dimensional, approximate solutions by comparison equations 3-66637
 operators in infinite domains, non-existence of positive eigenvalues 3-40152
 in orthogonal curvilinear coordinates 3-73632
 paramagnetic atom in external mag. field, equivalence of classical motion and quantum mech. solns. 3-63285
 paramagnetic atom in mag. field with const. and oscillatory components, unitary perturbation method 3-63286
 particle scattering, Fredholm integral method, calc. of scatt. amplitude 3-74101
 phase shifts, spherically symmetric potentials 3-74115
 plasma electrostatic modulational instabilities due to resonant particles 3-75362
 plasma Langmuir waves, nonlinear Schrodinger eqn. 3-43675
 plasma nonlinear wave kinetics, wave packet formulation 3-75314
 quantum statistical thermodynamics, spatial distrib. function calc., linear partial differential equation, Schrodinger equation 3-70769
 quasiclassical approx. based on geometric and wave-optical relation 3-42854
 radial, approx. analytical expression for soln., mol. vibr. problems applic. (*French*) 3-77858
 radial, continued fraction generation, application to bound state problems 3-70691
 radial, nearly exact calc. of soln., program description 3-48752
 radial, solutions by using cubic-spline basis functions 3-40147
 radial, with atomic-like potentials, numerical approach to soln. 3-57119
 radial asymptotic expansions for singular potentials 3-40149
 random potential, functional integral approach to average density of states 3-77863
 relativistic for a particle with arbitrary spin 3-51813
 rotational excitation scattering parameters, radial asymptotic expansions 3-40150
 S-wave, solvable potentials derivation 3-57117
 scattering theory, analogue of Fourier's method for Korteweg-de Vries equation 3-74118
 symmetric Hooke systems, eqns. of state (*French*) 3-65623
 three-body system with Coulomb interaction, slow collisions 3-70697
 time-dependent application of Pade approximants in variational approach 3-62426
 two state system, non-resonant levels effect, Schrodinger eqn. representation, Stark shift 3-45782
 unbound solns., expansion in terms of harmonic oscillator wave functions multiplied by Gauss one 3-57128
 variation-of-parameters method of soln. for scatt. problem, improved method 3-42843
 variational estimation of a wide class of functionals $F(\psi, \phi)$ 3-66635
 wave packet motion in constant homogeneous electrical and mag. fields (*Russian*) 3-59852
 CH, valence excited states, potential curves from radial Schrodinger equation 3-71513
 H, single-particle bound-state radial wavefunction, Rayleigh-Ritz-Galerkin with cubic splines 3-74780

Schrodinger equation continued

- H atom, factorisation of radial equation, radial integral props. (*Russian*) 3-54560
 $H^+ + H$ collisions, semiclassical turning pt. approx. $2p\sigma_u - 2p\pi_u$ excitation 3-67716
Schrodinger equation *see* **Schrodinger equation**
Schwarz-Hora effect
 Kapitza-Dirac effect 3-74298
 modulated beam properties, quantum effects 3-43052
Schwarzschild metric
see also cosmology
 extended space, maximal foliations 3-42864
 Kerr-Schild metric, new interpretation 3-40166
 Lorentz invariant formalism 3-62587
 nongeodesic radial accretion in Schwarzschild geometry 3-59250
 nonstatic model of expanding or contracting star 3-45092
 observable quantities and tensor projection (*Russian*) 3-77895
 point source of quantised gravitational field, comparison with quantum theory, de Donder gauge 3-57133
 radial wave eqn., behavior of solns. near singular points 3-62582
 Schwarzschild-Kerr metric, complex coordinate transformations 3-45717
 singularity, discussion, scalar indeterminacies 3-66658
 synchrotron radiation, rotating searchlight effect, black hole mass 3-80917
 transformation from Schwarzschild space to plane space (*Russian*) 3-48780
Schwarzschild space *see* **Schwarzschild metric**
science education *see* **education**
scientific societies *see* **societies**
scintillation
see also phosphorescence; phosphors
 alkali iodides, TI-activated, γ -scintillation (*Russian*) 3-55684
 interplanetary, derivation of solar wind velocity 3-61754
 interplanetary, latitude dependence for radiosources outside plane of ecliptic 3-77030
 interplanetary, solar wind plasma density irregularities 3-51275
 interstellar, due to plasma irregularities with power law spectra 3-51397
 ionospheric scintillation at 4 and 6 GHz near geomagnetic equator, obs. 3-56193
 irradiance scintillation of optical beams in random medium 3-62663
 isoeugenol in various solvents relative scintillation yield and radioluminescence (*German*) 3-64703
 Radio scintillation on stellar signals during artificial ionospheric modification 3-80796
 radiosource scintillation time spectra rel. to velocity dispersion of interplanetary medium 3-53681
 space/Earth signal scintillation parameters as auxiliary reference for ionospheric irregularities meas. 3-51199
 supernovae high energy γ -ray flashes, liquid and plastic scintillators 3-77192
 tomographic scintillation camera, performance parameters 3-70154
 CaI_2 , cryst., pure and doped, X-ray luminesc. and thermoluminesc., 90 to 300 K, scintillation props. 3-44482
scintillation chambers
see also scintillation counters
 fast track devices, review 3-70400
scintillation counters
see also photomultipliers
 Anger scintillation camera systems, deadtime calculation 3-62260
 atomic absorption spectral analysis, scintillation recording (*Russian*) 3-59707
 automatic quench corrections using a desk top computer (*German*) 3-62220
 combined scintillation detector in omnidirectional radiation field, sensitivity improvement (*Czech*) 3-73861
 cosmic ray electron component, 1 to 10 BeV, EM asymmetry method (*Russian*) 3-62241
 for cosmic-ray studies 3-56463
 design factors, fundamentals, performance, review 3-66319
 design problems, increasing effectiveness through improved light collection, amplitude distributions due to cosmic ray muon (*Russian*) 3-62238
 detection system, for neutron studies with neutron-gamma discrimination 3-40014
 dioxane, PPO soln., radioluminesc. quenching mechanism 3-80085
 extensive atmospheric showers, amplitude analysis, feasibility, circuits 3-69734
 heavy non-relativistic sea level particle detection, ionisation and track measurements (*Russian*) 3-62235
 inorganic scintillation screen, for detection of fission fragments 3-48527
 Insta-Gel, T-labelled nucleic acids measurement (*German, English*) 3-66452
 large pulse loadings, time and amplitude characteristics, 56 AVP and 56 DVP photomultipliers 3-70405
 with light guide, energy resolution 3-56937
 liquid, calculating techniques 3-48520
 liquid, choosing equipment 3-51703
 liquid, counting equipment, review 3-62224
 liquid, for 3H measurements 3-42649
 liquid, meas. beta rays from chromatogram and pherogram apertures (*German*) 3-42642
 liquid, methods for quenching correction 3-62245
 liquid, performance and quenching choice and cleaning of vials 3-42647
 liquid, using commercial tissue solubilizers 3-59450
 liquid scintillation solutions, for pulse-shape discrimination 3-40017
 liquid scintillators, based on normal alkanes and intermediate solvents 3-48526
 luminescence yield, plastic scintillator, dependence on electron and proton energies, results 3-70384
 mixing of solid particles, radioactive tracer technique, collimating system and scintillation detector 3-48339
 Mossbauer effect, resonance detector description 3-54020
 neutron detector, 145 scintillator elements, on-line electroproduction experiment, calibration, performance 3-77636
 neutron detector of fast time response 3-51704

scintillation counters continued

- neutron detector with organic scintillator, operational effectiveness calc. using Monte Carlo program EFFI (*German*) 3-59645
 neutron flux density, by scintillator coincidence system 3-40033
 numerical scintillograms, computer smoothing, liver phantom obs. (*French*) 3-56532
 organic, liquid, efficiency compared with DETEPP, OSS predictions 3-73865
 organic liquid, energy deposition and fluctuations for incident protons and charged pions 3-73869
 particles, radioactive tracer techniques, collimator efficiency calc. 3-48340
 photomultipliers, IEEE standard test procedure 3-59639
 plastic, area 2m² rel. to cosmic ray meas., radial dependence of light collection, pulse amplitudes (*Russian*) 3-62244
 plastic, for measurement of radioactive aerosols 3-40011
 plastic, Gd-loaded, for neutron detection 3-40019
 plastic, of effective attenuation length of 25m using gradient activation 3-40008
 plastic, review 3-77640
 plastic, study of decay time 3-48522
 plastic, with meson supertelescope, coupling coeff. determ. (*Russian*) 3-65549
 polarisation parameter meas. in high-energy πp and $K p$ interactions, on-line computer system 3-66322
 portable camera, clinical appls. 3-73596
 proportional, gas, peak shifts under high X-ray fluxes 3-77619
 safety, liquid scintillation counting 3-70388
 satellite-borne, for obs. of primary γ -radiation from galactic north pole region (*Russian*) 3-65918
 scintiblocks, parameter dependence on relationship between crystal dimensions and photomultiplier dimensions 3-70385
 spectrometer, time single crystal, excited state lifetimes of nuclei, description 3-70409
 thin film scintillation detectors, response to light and heavy ions 3-48512
 time resolution study 3-53976
 time-of-flight spectrometer for fast neutrons, neutron-gamma discrimination (*German*) 3-59652
 time-parameters, deexcitation, luminescence, yield, electro-optic measuring apparatus, technique 3-70383
 tomography, transverse axial, computerized, X-rays 3-70166
 triggering telescope equipment, extra-terrestrial gamma-rays experiment, COS-B satellite, ESRO 3-62223
 universal nuclear radiation meter, for industrial measurement techniques (*German*) 3-48517
 windowless 4 π -scintillation counter with NaI(Tl) crystals 3-56936
 (β - γ) chamber, for nuclide determination in off-gas samples 3-40012
 n, fast, BD-9 integral discriminator for γ -radiation pulse elimination 3-70387
 CaF₂:Eu, u.h.v. use, ¹⁴C-labelled hydrocarbon partial press. meas. (*French*) 3-62039
³H counting by emulsion scintillators, external standard channel ratio method 3-66317
³H identification and exact meas. in gas sample (*French*) 3-57019
 NaI, large, performance and use in $\pi p \rightarrow \pi^n n$ charge exchange meas. (*French*) 3-51698
 NaI, well type, Monte Carlo calc. of gamma-ray efficiency values 3-62221
 NaI γ -ray spectra, reduction of neutron-induced background 3-51712
 NaI well-type detector, relative counting rate in isotopic neutron source activation analysis 3-48530
 NaI well-type detectors, photopeak efficiency by Monte Carlo calculations considering self-absorption in source 3-40004
 NaI(Tl), gain variation compensation with rate 3-40018
 NaI(Tl), total absorption counters, TASC and TANC 3-70391
 NaI(Tl) detectors, Compton scatter and K-edge escape, correction matrix 3-59644
 T, T₂O, ruggedized ultrasensitive field air sampler 3-77302
 U-Th ores, spectral assay, influence of resolution on accuracy (*Russian*) 3-73390

scintillation detectors see scintillation counters**scintillation spectrometers see particle spectrometers; scintillation counters****scintillators see scintillation counters****scintillometers see scintillation counters****scorching see combustion****s.c.r. see thyristors****screening see shielding****screens, fluorescent see fluorescent screens****screens, phosphorescent see fluorescent screens****screens (display)**

see also fluorescent screens

rear projection, produced by holographic and interferometric techniques 3-66178

rear projection screens 3-62079

ruled half-tone, radiant flux density distrib.-analysis 3-77444

scrubbing (abrasion) see abrasion**scuffing see abrasion****SDI see information dissemination****sealing see seals (stoppers)****seals (stoppers)**

see also glass-metal seals

for pressure vessels 3-51561

shaft seals in pressurized water, endurance tests 3-57562

ultrahigh vacuum slide type seal, metal gasketing 3-48399

Fe-Mn-Cr sealing alloy, high temp. oxidation and sealability, effects of Al, Mn and Si additions (*Japanese*) 3-44615

seawater

- acidity constants for boric and carbonic acid, by potentiometric titrations in synthetic seawater 3-65257
 Arctic Ocean water, wintertime surface layer convection rel. to sea ice formation 3-44856
 Black Sea, Ca₃(PO₄)₂, saturation 3-80709
 chemical properties, effect of oil 3-80710
 chemical reactions with oceanic crust in ocean layer II 3-65131

seawater continued

- chlorophyll content and temperature, remote sensing using airborne differential radiometer 3-73607
 clear ocean water, imaging in backscatt. light, inhomogeneities effects 3-41932
 corrosion of materials, effects of depth of submergence, temp., salinity, pH, velocity of currents and conc. of dissolved gases (*Russian*) 3-80697
 dense water formation, topographic effects, theoretical model 3-65256
 East Mediterranean, changes in isotopic comp. during Holocene 3-51000
 equation of state from sound velocity data 3-58987
 fuel oil hydrocarbons and mineral particles in seawater and marine sediments 3-53456
 global water exchange, mathematical theory 3-80765
 groundwater basin, coupled salt and water flow 3-80689
 heat capacity from 5 to 35°C and 0.5 to 22‰ chlorinity 3-65266
 high pressure density meas., preliminary results 3-58986
 hydrofoil ship, surface-piercing struts, ventilation, influence of waves 3-79003
 ice, brine content 3-80708
 ice obs. using satellite imagery 3-53546
 light scattering and particulate matter results from GEOSECS Atlantic cruise 3-58995
 N.W. Mediterranean, deep convective mixing preceding hydrographic conditions 3-65255
 methane concs. in marine environments 3-73274
 mineral content, search for and exploitation of marine raw materials in USSR (*German*) 3-61445
 ocean, effects of electric currents E-polarisation case, numerical models 3-80672
 oceanic crust-seawater geophysical and geochemical reactions 3-41879
 Pacific subarctic zone, warm intermediate layer, winter convection 3-80707
 pH-scales, based on synthetic sea water 3-65258
 phosphate-water isotopic temp. scale 3-61438
 radionuclide meas. in marine samples near nuclear power stations 3-69557
 resonant internal wave interactions rel. to driving frequency in salt solution 3-59003
 Rockall channel, temp., density, chemical comp. annual cycles 3-80678
 salt finger structure in heat-solute system 3-53442
 salt-fingering at interface of salty and fresher water, limiting conditions 3-53441
 salty hydrothermal soln., comp. rel. to oceanic chemical evolution 3-56143
 sampling bottle-cuvette for investigating optical properties 3-42087
 Sargasso Sea, Mg/Cl ratios 3-58978
 seasonal surface water temp. var. in World's Oceans 3-51002
 seepage flow, parallel line sinks, diffusing interface between fresh and saline water 3-54809
 shallow coastal water, temp. var., surface wave height and water motion 3-58989
 sorption of B and Si using granulated Zr(OH)₄, Black Sea (*Russian*) 3-80698
 sound velocity calculation for seawater from hydrologic data 3-51473
 southern ocean meas. of dissolved CO₂, methane and H₂ in surface seawater 3-53451
 surf swash, western Kamchatka, velocity measurement 3-80711
 surface conditions, microwave radiometric obs. 3-50991
 surface slicks, i.r. characs., comparison between natural and oil slicks 3-69744
 suspension, determ. of trace elements, by atomic absorption with arc atomiser 3-80875
 thermal expansion, adiabatic temp. gradient and potential temp., new polynomials 3-53444
 transfer of salts to atmosphere 3-80714
 turbidity currents, parameters, methods of computing 3-80713
 Vellar estuary, salinity rel. to Si distribution 3-77304
 vertical boundaries, South Atlantic Ocean, T-S analysis 3-80706
 volcanic clouds, Iceland, produced by lava in contact with seawater, lightning 3-80773
 western North Pacific, vertical profiles of temp., salinity, dissolved O₂, alkalinity and nutrients 3-73258
 Au concentration by reduction and spectrographic analysis 3-76918
 B, coprecipitation from the sea, using Fe(OH)₂, effect of pH, conc., quantity of coprecipitant (*Russian*) 3-80700
⁶⁰Co/¹³⁷Cs content of coastal sediments near nuclear power station coolant discharge 3-69558
¹³⁷Cs concentration in Japanese coastal sediments, obs. 3-69559
¹³⁷Cs concentration in Japanese coastal waters, obs. 3-69560
³H concentration in North Pacific, liquid scintillation counting 3-69561
 Mg/Cl ratios, Sargasso Sea samples 3-58978
 P, dissolved mineral, distrib. and dynamics, Atlantic tropical zone, seasonal effects (*Russian*) 3-80701
 Rn excess profile temporal var. at first GEOSECS intercalibration station 3-58993
 Rn excess profiles in near bottom and surface Atlantic water, GEOSECS meas. 3-58994
¹⁰⁶Ru complexes effect on coprecipitation yields, obs. 3-69556
⁸⁷Sr/⁸⁶Sr ratio of deep-sea basalts, effect of seawater interaction 3-56029
⁹⁰Sr concentration in Japanese coastal waters, obs. 3-69560

second sound

see also liquid helium sound propagation

- dielectric crystal, coeff. of sound absorption in region of existence of second sound 3-72135
 dielectric crystals, hydrodynamic eqns. 3-75574
 dielectric crystals, heat pulse propagation in solids 3-58108
 He II liquid/solid interface, h.f. phonon transmission 3-64226
 He, rotating, macroscopic spatial quantization of angular momentum, expt. evidence 3-79539
 He, solid, effects of collinear and non-collinear three phonon processes 3-55120

second sound continued

- He II, superfluid, inhomogeneous density distrib. near λ point, second sound investigation, theory 3-79538
¹He, anisotropic phonon energy, effect on normal fluid density, second and fourth sound 3-68466
³He, anisotropic superfluid, rel. to long range distortions 3-52739
⁴He-⁴He mixture, second sound damping coeff., near tricritical point, mode-mode coupling calc. 3-60825
⁴He under press. near T_{λ} , sound vel. and superfluid density meas. 3-46741
NaF, phonon-phonon interaction, estimation from heat pulse interaction 3-55051
NaF, solid, effects of collinear and non-collinear three phonon processes 3-55120
Ne, isotopic mixtures, thermal conductivity measurements, phonon scattering relaxation rates 3-55067

secondary cells

- battery grid alloys, Pb-Ca-Sn, grain struct., mech. props., corrosion 3-41724
Ag₂LiWO₄, solid electrolyte with high ionic cond., for solid state battery applic. 3-43892
Na/ β -alumina interphase impedance rel. to Na-S battery separator applic. 3-69465

secondary electron emission

- dielectric thin film, surface potential and continuous current struct. determ. by charged particle bombardment 3-69120
dielectrics, coeff. by new method 3-51652
energy distrib., effect of mean free path constancy and source function (*French*) 3-64757
energy spectrum, angular distrib. (*French*) 3-80139
glass, theoretical and experimental techniques, depend. on surface conditions, temp. and energy distrib. 3-41602
glow discharges, secondary electron emission involving charge exchange 3-46566
graphite, π -band structure (*German*) 3-72315
graphite, free film, electron inelastic scatt., fast secondary electrons 3-76117
ion-electron converter, high vacuum, pre-breakdown cond., gas press. depend., comments 3-48400
ion-electron converter, high vacuum, pre-breakdown cond., gas-press. depend., reply to comments 3-48401
multiple diffusive reflection system, density function, linear Fredholm integral equation soln. 3-51965
one-sided secondary electron resonance discharge in lattice-type fields in 3 cm band, experimental investigation 3-63913
photomultiplier, intrinsic nonlinearity 3-41598
photomultipliers, search for intrinsic nonlinearities 3-77442
polymers, yield curve, $E_p = 50-2500$ eV 3-69123
SEM, electron backscatt. and secondary electron prod., Monte Carlo calc. 3-70432
from solid targets under ionic bombard., angular, energetic distrib., Auger peaks 3-61098
spacecraft surfaces, low plasma densities 3-61562
thermal gas, electron, proton and X-ray ionization, secondary electrons and energy per ion-pair 3-43354
water vapour, energy distrib. of secondary electrons released by fast electrons 3-80561
Au polycrystal surface, under 4keV ion bombard., energy spectrum 3-58573
Be, charact. energy gain, double ionisation and ionisation loss 3-55714
BeO, charact. energy gain, double ionisation and ionisation loss 3-55714
BeO, electron stimulated desorption of C effects 3-75674
Cu, polycryst., total yield and spectrum, meas. using spherical retarding-field analyzer 3-53162
Cu, single crystal, ion bombardment of (100) surface, He⁺ and Ne⁺ ions, 3 keV, energy distribution, long magnetic lens 3-44512
Cu-Be, Auger and slow secondary electron spectra 3-50636
GaP(Cs) dynodes, five stage photomultiplier 3-76115
Ge, amorphous film, cond. band, secondary emission and photoemission modulation spectra 3-55188
KCl low density dielectric films, controllable secondary electron emission at high energies (*Russian*) 3-58574
KCl:Al porous film, Al effect on transmitted emission 3-50633
Mg, polycryst., slow emission peak, fine struct. 3-47338
MgO-Au cermet, sputtered, for electron multiplier applic. 3-53160
Mo, proton bombarded, electron emission, energy spectra 3-55716
N₂, metastable particle impact in ioniz. growth expts. 3-68116
N₂, metastable particle impact in ioniz. growth expts. 3-68117
P film on Si substrate, characteristic energies 3-41601
Si, influence of impurity clusters 3-64063
Si, ion implanted, secondary electron emission, temp. depend. (111) surface 3-69121
Si, Li, adsorbed layer characterisation by photoemission obs. (*French*) 3-44516
W, anisotropy, 300 K 3-55715
Zn, single crystal ion bombardment of (0001) surface, He⁺ and Ne⁺ ions, 3 keV, energy distribution, long magnetic lens 3-44512

secondary emission

- see also secondary electron emission; secondary ion emission
No entries

secondary ion emission

- alloy, rel. to electronic structure 3-61096
ceramic surfaces, spectrometry technique, chemical comp. 3-80418
channelling influence on yield 3-61095
dilute alloy, screening of moving impurity, implications (*French*) 3-72330
energy distrib., analysed using e.s. mirror (*French*) 3-58580
energy distribution of emission from 15 polycrystalline targets 3-80135
impurity conc. profiles obs. in solid, use of secondary ion mass spectrometry 3-61122
light element targets, secondary emission of mol. ions 3-61086
mass spectrographic analysis of ion implantations (*French*) 3-40946
mass spectrometer, ion bombardment, spectra, intensity (*Japanese*) 3-59658
mass spectrometry, primary O⁻ implantation affects on depth profiles 3-66439

secondary ion emission continued

- mass spectroscopy, spectral interferences, mol. ions 3-64756
metal surface ion bombardment, apparatus for secondary ions study 3-40044
solid target, 30 to 70 keV electron bombardment, conditions for appearance and applicability 3-41604
Al target, solid and liquid, temp. dependence of emission 3-80136
Cr, oxidation investigation at room temp. 3-75682
LiF, ion-ionic scattering from (100) cleavage face, LEED studies (*Russian*) 3-50640
Mo surface, composition of two-dimensional oxide film, secondary ion-ion emission determ. 3-50082
Nb, oxidation investigation at room temp. 3-75683
PbS, ion-ionic scattering from (100) cleavage face, LEED studies (*Russian*) 3-50640
Si, influence of impurity clusters 3-64063
Si-SiO₂ structure, mass spectra analysis, Na impurity distrib. obs. (*Russian*) 3-52904
Ta, oxidation investigation at room temp. 3-75683
Ta film, surface and bulk analysis 3-62321
V, oxidation investigation at room temp. 3-75683
W(100), adsorption of O₂, secondary ion mass spectrometry 3-75669

sedimentation

- see also disperse systems; water treatment
aerosol particles, jet method for capture coeff., flow round sphere 3-63766
aerosol particles, Poiseuille flow in pipes, deposition by diffusion and sedimentation 3-73087
Atlantic deep-sea long-core samples, analysis 3-73227
cellulose tributylate molecules, sedimentation constant, diffusion coeff., intrinsic viscosity, optical anisotropy effect of different solvents (*Russian*) 3-46368
chain polymer solutions, transport of compact particles 3-47487
Combarjua canal, relation to tidal stages 3-76687
deep sea sediment cores, paleomag. record, effect of sedimentation on magnetisation 3-80677
deep-sea, late pleistocene-holocene, spectral analysis, non-random fluctuations 3-76782
deep-sea, Pacific N.E., late pleistocene-holocene oceanographic changes from radiolarian assemblages 3-76695
deep-sea, S.E. Pacific, stratigraphic and palaeoclimatic analysis 3-76694
deep-sea sediments, variations in intensity of magnetisation and inclination 3-59039
dust sedimentation on drops formed by liquid atomisation in rapid gas flow 3-80504
East Pacific ferromanganese sediments 3-65142
emulsion, statistical mean speed of sedimentation in dilute dispersion of droplets 3-69392
Equatorial Pacific core, oxygen isotope and palaeomagnetic stratigraphy 3-76693
in fibrous aerosol filters, theory 3-65034
Gulf of Maine, props. of sediments recovered with giant piston corer 3-58836
Gulf of Mexico latest Pleistocene deep-sea sediment, palaeomag. excursion 3-53427
human serum albumin, ⁶⁰Co gamma irradiation, polymerisation, cross-linkages, sedimentation velocity technique 3-48264
Indian Ocean sediment trapping of ¹⁴⁴Ce and ⁹¹Y 3-65281
isolated reefs, Midland Basin, Texas, telluric anomalies, resistivity distrib., reef-reef sediments 3-80658
longshore energy flux, longshore flux and longshore sediment transport 3-59043
marine sedimentary pore waters in situ sampler 3-73381
Moravian Palaeozoic, Southern part, synsedimentary tectonics 3-44836
oceanic sedimental logic and stratigraphic patterns 3-59040
in oceanic thermocline zones, particle displacement 3-59031
oriented magnetisation of reprecipitated sediments 3-76670
Peru-Chile trench, major and marginal provinces 3-80638
polyacrylonitrile particles, in aq. dispersion, electrolyte effect 3-65025
polymer chain in dilute solution 3-67877
proteins, interacting systems, calculation of sedimentation equilibrium in density gradients 3-71675
river sediment, method of determ. of ⁹⁰Sr and ¹³⁷Cs, report 3-73398
spherical solid particles, Reynolds number and drag coeff. definitions, review 3-79030
suspensions, fixed and free, settling speed, viscous fluid 3-73091
Vembanad lake, distribution of phosphorus 3-77305
Yamato Rise sedimentary layer structure from seismic reflection profiles 3-65280
Hg conc. in marine sediments from Santa Barbara Basin 3-61325
ThO₂ powders, phys. props. and influence on sinterability 3-80402

Seebek effect see thermoelectricity**Seidel theory** see aberrations**Seignette salt** see Rochelle salt**Seignetteelectric materials** see ferroelectric materials**seismic waves**

- Amchitka Island Test Site events, seismic surface waves rel. to source mechanism 3-53413
amplitude yield scaling, underground nuclear explosions, slope parameter 3-76505
amplitude-distance relation of short period P-waves recorded at Iberian stations rel. to mantle structure 3-58825
anisotropic elastic half-space propag. of Rayleigh waves 3-47611
anisotropic P-wave vel. effects on hypocentre location 3-58901
anisotropic stratified-fractured media, seismic propag. vels. (*Russian*) 3-47648
apparent velocity, shear wave Sn, upper mantle 3-76504
atmospheric explosions, theoretical seismograms for Rayleigh waves, yield and burst height effects 3-58879
attenuation and magnitude relations for eastern North America 3-50921
Australian region, upper mantle P-wave velocities 3-58886
azimuthal dependence of Love and Rayleigh surface wave propag. in slightly anisotropic medium 3-61307

seismic waves continued

- azimuthally varying P-wave travel-time residuals, lateral inhomogeneity, Fennoscandia 3-76590
- Blue Mountain Lake earthquakes, premonitory P and S wave vel. changes 3-61378
- body wave amplitudes, ray theory amplitudes, simple approx. formula 3-58895
- body wave displacement spectra, derivation of rupture area and stress drop 3-47642
- body waves, normal and leaking modes, dispersion and excitation on the (+-) sheet, phase-velocity curves 3-80615
- body waves from dislocation source, theoretical amplitudes of core phases 3-50951
- body waves in 'real Earth' 3-56013
- body-wave amplitude anomalies, deep mantle lateral heterogeneity 3-53425
- buried explosive sources, topography and Rayleigh wave generating efficiency 3-61308
- CANNIKIN nuclear explosion, tectonic strain-release meas. from surface waves 3-50894
- common-depth point time-depth curve for nonlinear boundary and reference overlying layer (*Russian*) 3-47649
- computation, time-distance curves, dipping refractor, velocity increasing with depth in the overburden 3-76535
- core-mantle boundary, low velocity transition zone 3-73230
- core-mantle boundary beneath Hawaii, obs. of P-waves at San Andreas seismic network 3-58885
- core-mantle transition region thin layer model, P_cP wave characts. 3-44787
- Coyote Mountain earthquake California, aftershocks and source characteristics 3-76509
- crust, investigation by converted waves from remote earthquake 3-58833
- crust-mantle model, NORSAR area 3-76589
- deep earthquakes focusing due to inclined slab containing subducted material 3-58894
- deep mantle lateral heterogeneity from P-waves travel times 3-58883
- diffraction by anomalous regions in mantle 3-58824
- discrimination from noise of unknown properties using discrete quasi-optimal filters and minimax filters 3-65502
- distance corrections for Rayleigh-wave magnitudes 3-53368
- earth, from underground explosion, stress measurement determination of inelastic region 3-76549
- earth core, velocity model, revised, travel times and amplitudes, earthquakes and underground nuclear explosions 3-80619
- earth mantle, transmission of elastic waves through a soft layer, variational method 3-44930
- earthquake, structure model, micromorphic continuum, wave processes in focal region 3-44824
- earthquake M_s Rayleigh wave magnitude scale 3-61358
- earthquakes, grouped according to S-P interval, statistical method of detection and prediction 3-80839
- earthquakes, recording on mag. tape, observatory tape recorder, multiflex f.m. system 3-80837
- elastic layer, transient disturbance by a buried spherical source 3-76864
- elasticity variation, water saturated rocks at melting point of ice 3-76530
- energy and plane waves in linear viscoelastic media 3-53411
- explosion, under soft ground, size of effective elastic-wave emitter 3-76548
- explosions, North America, compressional velocity distrib., upper mantle, lower crust 3-80612
- explosions, prestressed media, stress wave radiation 3-44783
- explosions, second pulses on recordings in near zone, relation to spalling 3-76550
- explosive source, freq. domain response, comparison with BOXCAR nuclear explosion 3-58878
- fault expansion mechanism at earthquake foci, radiation of body waves 3-44812
- filtering, multiple filter and time variable filter techniques 3-73205
- G-waves in mantle 3-65152
- geometrical body wave obs. rel. to Earth structure nonuniqueness 3-47656
- ground motion, prediction, source time function rel. to fracturing process 3-80613
- h.f., guided by continuous lithosphere, western South America 3-76538
- horizontal inhomogeneities investigation from recordings 3-76551
- India (S.), regional gravity low determ. by seismic surface waves 3-56069
- Ivrea zone, longitudinal P-wave velocity anisotropy in mantle rock 3-65206
- Kamchatka focal zone, velocities 3-76547
- layered half space, ellipsoidal volume source surface wave response 3-57111
- layered medium, seismic wave field rel. to heterogeneous block 3-58834
- l.f. spectra of waves from explosions 3-58827
- long period surface waves, reflection, refraction and mode conversion 3-61388
- long period wave propagation, synthetic seismograms from 17° to 40° 3-76830
- long-period P and S waveforms rel. to focal process of deep and intermediate earthquakes around Japan 3-44810
- long-period surface wave enhancement by time-varying adaptive filters 3-61321
- Love, in non-uniform channels over homogeneous half space, dispersion 3-61349
- Love wave dispersion analysis, laterally inhomogeneous Himalayas, crustal struct., Severnaya Zemlya earthquake 3-80624
- Love wave generation by point source in nonuniform medium 3-44788
- Love wave phase velocities, contamination free, by surface wave analysis method 3-58898
- Love waves, earth-flattening transformation from a point source to a sphere, Biswas-Knopoff transformation 3-80614

seismic waves continued

- Love waves, earthquake, southeastern Missouri, surface wave attenuation, crustal anelasticity 3-80618
- Love waves, inhomogeneous anisotropic elastic solids, velocity, frequency equation 3-44825
- Love waves, modulation, travel times, variational method, nonhorizontally layered struct. 3-80616
- Love waves, torsional free modes, simple algorithm for computation of attenuation factors 3-80620
- Love waves group velocity reduction due to leaking modes 3-58897
- low velocity zone, spectral characteristics (*Russian*) 3-76649
- lower mantle lateral heterogeneity from ScS-S differential travel times 3-58882
- lower mantle shear wave travel times from nuclear explosions 3-58887
- mantle heterogeneity rel. to body wave multipathing 3-58884
- mantle Rayleigh wave group vel. dispersion data 3-56017
- marine sediment, acoustic wave reflection (*French*) 3-76862
- Mendocino escarpment, aftershock sequence, seismicity, ocean bottom seismic measurements 3-76502
- microearthquakes, Nevada region, use in determining mechanism of faulting, stresses, source characteristics 3-76546
- microseism propag. in oceanic waveguides 3-61342
- microseism variations around Gulf of Gascogne (*French*) 3-61343
- microseismic oscill. emission from region with standing ocean waves 3-44791
- microseismic P wave sources 3-65177
- microseisms, sea wave origin during storms 3-65264
- model of crust and upper mantle, central Chile, P- and S-wave arrival times, structural parameter determ. 3-80607
- Montana Lasa, P wave scatt. rel. to Chernov theory 3-50932
- multiple core reflections of $PnKP$ and $SnKP$ type 3-80627
- New Hebrides-Fiji Islands travel times, low vel. zone beneath Fiji plateau 3-61315
- Newtonian self-gravitating body under elastic perturbations, response derivation 3-74138
- nuclear explosions, underground, seismic moment, long-period radiation, value of explosive point source model 3-80609
- ocean seismic sounding, resolution assessment using reflected-wave method 3-47851
- ocean-ridge mantle structure from seismic wave ray tracings 3-58888
- oceanic Rayleigh and Love waves, group velocities rel. to oceanic mantle 3-44820
- oceans, pendulum system for study and recording 3-76852
- P_n , Western Sicily, January 1968, travel times (*Italian*) 3-73183
- P, amplitude spectrum rel. to focal depth 3-61348
- P and P_cP wave reflection from Earth's core 3-44786
- P and P_cP waves, amplitude ratio 3-44790
- P and PL wave arrivals on 55 seismograms rel. to low-velocity zone var. in SW United States 3-53406
- P and pP waves attenuation behind island arcs and above inclined seismic zones 3-58890
- P and S wave displacements rel. to earthquake focal mechanisms (*Spanish*) 3-56047
- P and S waves, use in earthquake focal mechanism studies, review 3-65224
- P and SV waves, polar radiation patterns, multi-layered medium mathematical model 3-76508
- P phases, array studies for determ. of mantle D' D'' region structure 3-73210
- P signals, complexity 3-76540
- P waves, influence of station conditions on spectra 3-76600
- P- and S-waves, damping 3-76541
- P-phase spectrum rel. to earthquake magnitude calculation 3-61357
- P-wave magnitudes, NORSAR and ISC data, bias analysis 3-59168
- P-wave observations, inversion, long-range profile, France, 1971, lower lithosphere fine structure 3-73236
- P-wave rise time, small earthquakes, determination of source parameters 3-76828
- P-wave upper mantle structure of western United States 3-53405
- P-wave velocity variation before San Francisco earthquake, earthquake prediction 3-58849
- P-waves spectra, effect of crust structure in region of seismic station (*Russian*) 3-65159
- PcP from Pacific earthquakes 3-73206
- $PKIKP$ phases, amplitude meas., identification from nuclear explosions and earthquakes 3-80648
- PKP precursors rel. to scattering regions in lower mantle 3-41892
- $PmKP$, large amplitude in multiple core phases 3-61393
- in polymorphic rocks, wave vel. and attenuation 3-53395
- pre-strained media, Fourier-Laplace transformation 3-44784
- pre-straining in the earth, ray theory 3-76843
- propagating crack, infinite medium, exact solution 3-76500
- propagation in medium with inhomogeneities of random distribution 3-58828
- radiation and attenuation of Rayleigh waves from the SE Missouri 1965 October 21 earthquake 3-50922
- radiation from explosion in non-uniformly pre-stressed medium 3-58826
- Rat Island earthquakes (1965), radiation patterns and amplitudes of Rayleigh and Love waves 3-76568
- ray velocity determination from reflected wave travel-time curves 3-65167
- Rayleigh wave amplitudes at mid-oceanic ridges 3-41880
- Rayleigh wave reflection in elastic wedge by rigid obstacle 3-53378
- Rayleigh waves, earthquake, southeastern Missouri, surface wave attenuation, crustal anelasticity 3-80618
- Rayleigh waves, signal persistence, half-amplitude decay times, random model 3-58899
- Rayleigh waves in elastic wedge, reflection and transmission 3-65151
- recordings, processing by different methods, effectiveness (*Russian*) 3-76887
- reflection and refraction at boundary of absorbing media using frequency dependence of absorption coefficient 3-65166
- reflection data, three dimensional interpretation, velocity distributions 3-76840

seismic waves continued

- reflection data interpretation, structure and modification of optimum algorithms (*Russian*) 3-47650
 refracted wave absorpt. coeffs. determ. from amplitude curves of head waves (*Russian*) 3-58822
 refraction, continental shelves, detectors on sea floor 3-76837
 refraction field measurement, interpretation by computer model of earth 3-65143
 rocks, low pressures, change of seismic wave velocity (*Italian*) 3-73184
 S_n regionalized velocities and composition of Atlantic lithosphere 3-53390
 S and P phases meas., radius of inner and outer core meas. 3-58848
 S and ScS from Pacific earthquakes 3-73206
 S and ScS waves, shear vels. at base of mantle 3-61392
 S. Nevada, nuclear explosions and cavity collapses, radiation of Rayleigh wave energy 3-44785
 S waves, influence of station conditions on spectra 3-76600
 San Fernando Valley, propag. of Love and Rayleigh waves 3-53373
 scattering effect of embedded obstacle on seismic wave pulses 3-69500
 ScP and ScS phases, spectral ratio rel. to mantle attenuation in Tasman Sea and Antarctic Region 3-53392
 ScS wave phase conversion to ScSp wave phase in Japanese region 3-58891
 Semipalatinsk underground nuclear explosions, source parameters, P-wave spectra 3-44826
 SH, P and SV waves, effect of topography on surface motion 3-76829
 shear and compressional, premonitory variations of P, S travel times, rel. to dilatancy, earthquakes 3-80623
 shear velocities at base of mantle 3-76563
 shear wave attenuation and melting beneath Mid-Atlantic ridges 3-76566
 shear-coupled PL waves, generation and props. 3-53375
 short period P and PcP phases, studied at Lasca, Montana 3-76564
 sinking slab, seismically dead, west USA, detect. by P-wave delays 3-58892
 Somigliana waves, Rayleigh equation, degeneration to evanescent waves 3-73182
 spallation and generation of surface waves by underground explosion 3-53414
 surface wave propag., spatial coherence 3-58880
 surface waves, band-pass filtering information on group velocities, spectral amplitudes 3-76831
 surface waves recorded by large-base quartz extensometers, comparison with long period seismic equipment 3-65164
 symmetric undulations of the surface, incident elastic waves 3-76503
 T-phase radiation from CANNIKIN underground nuclear explosion, solar hydrophone recordings 3-53401
 Tatariya region, shear reflection method (*Russian*) 3-47651
 travel times, corrections due to ellipticities and Radau's parameter for const. density surfaces 3-73231
 tsunamis, relation with sea bottom deformation caused by earthquakes 3-73228
 tsunami and Rayleigh ground waves, warning system using ionospheric technique 3-69748
 tuffaceous rocks, shock wave response, porosity and saturation effects 3-58876
 underground explosion waves, propag. in nearly-elastic range 3-53374
 underground explosions, simulation, generation of longitudinal and transverse waves, expression for transfer function 3-80603
 underground explosions, theoretical model, separation of large explosions from earthquakes 3-80604
 underground nuclear explosions, rock melt, shock wave energy deposition 3-58875
 upper mantle, gross velocity depth distribution, P- and S-waves, Europe, earthquake obs. 3-73238
 upper mantle, P-wave structure, long-range explosion observations 3-73237
 upper mantle discontinuities, PP' and precursors, reflection 3-76827
 velocity, Bunter Sandstone, Northwest England, hydrogeophysical properties 3-76544
 velocity determ. from reflected wave seismograms (*Russian*) 3-73240
 velocity in inner core, determ. of incompressibility and density at centre of Earth 3-73202
 viscoelastic media, plane waves propagated by transient shock load (*Russian*) 3-69508
 volcanic tremors analysis, S. Italy 3-61363

seismographs see seismometers

seismology

- see also earthquakes; lunar seismology; seismic waves; seismometers
 acceleration and tilt meas. using pendulums and accelerometers 3-56233
 Afghanistan seismotectonic model 3-47645
 aftershock, time of occurrence, magnitude, India 3-76591
 air-gun array system, use of far-field press. pulses 3-47796
 Alaska earthquake (1964), comments on model by Ben-Menahem 3-73233
 Aleutian Island Arc, upper mantle structure determ. from Rayleigh wave dispersion data 3-50895
 Aleutian Islands, geomorphic evidence of late Holocene vertical stability 3-50890
 ambient Earth motion in period range 0.1-2560 sec. 3-53377
 S. American continental margin, plate motion and seismology 3-65200
 Andes, centra, crystal struct. determ. 3-76598
 annual seismic energy release rel. to Chandler wobble 3-69518
 array installations, research prospects, nuclear explosion detection 3-65180
 asymmetric P'P' rays amplitude estimates for upper mantle 3-56012
 Atlantic fracture zones, geophysical study 3-58872
 Atlantic lithosphere, S_n regionalized velocities rel. to composition 3-53390
 Australian region, upper mantle P-wave velocities 3-58886

seismology continued

- Baffin Island earthquake, surface wave spectrum analysis, tectonic implications 3-76567
 bedrock depth determ. in glaciated mountain valleys 3-76519
 Birch-Murnaghan equation of state verification 3-56032
 body waves, normal and leaking modes, dispersion and excitation on the (+ -) sheet, phase-velocity curves 3-80615
 body-force calculations from permanent deformations around seismic events 3-58823
 Canadian Shield, crustal surface-wave group-vel. anal. 3-61369
 CANNIKIN nuclear, explosion, close-in ground motion 3-50899
 CANNIKIN nuclear explosion, ground deform. meas. 3-50900
 CANNIKIN nuclear explosion, predicted and postshot geological and geophysical factors 3-50891
 CANNIKIN nuclear explosion, seismic and tectonic related events 3-50893
 CANNIKIN nuclear explosion, strain and tilt data 3-50898
 CANNIKIN nuclear explosion strain and tilt meas. 3-50897
 CANNIKIN underground nuclear explosion at Amchitka, seismic results 3-44837
 Celebes Sea, seismic refraction profiles 3-61316
 Central Aleutians intermediate depth earthquake relocation by seismic ray tracing 3-69521
 central Chile, model of crust and upper mantle, P- and S-wave arrival times, structural parameter determ. 3-80607
 Central N. American rift system, source of midcontinent gravity high 3-73219
 Chile, subduction of Nazca oceanic plate, focal mechanism solns. and general seismicity 3-73213
 common-depth point data processing, appl. of signal quasi-multiplication algorithm (*Russian*) 3-47812
 compressional velocity distribution, upper mantle, lower crust, Early Rise explosions, North America 3-80612
 conductivity anomalies in Japan, review of recent studies 3-73252
 continental margin, seismic refr. and refraction meas. 3-58874
 core-mantle boundary, low velocity transition zone 3-73230
 core-mantle boundary beneath Hawaii, obs. of P-waves at San Andreas seismic network 3-58885
 Crimea-Caucasus region, seismic-risk zone determ. 3-69502
 crust, investigation by converted waves from remote earthquake 3-58833
 crust and upper mantle fine structure determ. 3-56235
 crustal profile; trans-California, Death Valley to Monterey Bay 3-73203
 crustal structure, Manitoba, seismic sounding, velocity model, sub-Mohorovicic event 3-80611
 data collection for modern seismograph systems 3-61587
 data processing and curve plotting rel. to zero travel time analysis (*Japanese*) 3-42056
 data reduction, computer programs and algorithms for digital filtering (*Russian*) 3-47811
 Deccan earthquakes, macroseismic study 3-47624
 deconvolution of seismograms and high fidelity seismometry techniques, conf. 3-76599
 deep earthquakes focusing due to inclined slab containing subducted material 3-58894
 deep mantle lateral heterogeneity from P-waves travel times 3-58883
 diffracted wave time-travel curves (*Russian*) 3-76886
 digitized strong-motion accelerograms, error anal. 3-56234
 distance corrections for Rayleigh-wave magnitudes 3-53368
 divergence effects, layered earth 3-80628
 earth core, velocity model, revised, travel times and amplitudes, earthquakes and underground nuclear explosions 3-80619
 earth flattening approximation, body wave seismograms for media with spherical symmetry 3-61362
 earthquake, San Fernando, prediction, change in seismic body wave velocities, dilatant-diffusion model 3-80647
 earthquake, southeastern Missouri, Love and Rayleigh waves, surface wave attenuation, crustal anelasticity 3-80618
 earthquake, structure model, micromorphic continuum, focal region props., deformation of microstructure 3-44824
 earthquake distribution, Calaveras Fault zone, California 3-76834
 earthquake magnitude, rel. to stress-drop and fault size, seismic energy, characteristic stress 3-80622
 earthquake magnitude correlation for M_{th} (USSR) and m_{pv} (ISC) using recurrence curves 3-61355
 earthquake magnitude determ., inconsistency of broad-band and short-period instruments 3-61353
 earthquake magnitude values, comparison of obs. of Soviet and American stations 3-61356
 earthquake magnitude values, distortion and use of broad band instrumentation 3-65179
 earthquake prediction, anomalous seismic velocity ratio, rock dilatancy model 3-80649
 earthquake prediction methods 3-44952
 earthquake prediction velocity variation before San Francisco earthquake 3-58849
 earthquake swarms, Volcano Aso, Japan 3-76529
 earthquake teleseismic depth determ. for depth range 35 to 100 km 3-58900
 earthquake-explosion discrimination, statistical capabilities, false alarm probabilities at given deterrence 3-80621
 earthquakes, frequency distribution, cumulative frequency moment equation 3-44782
 earthquakes, Hindu Kush region, focal depth, frequency magnitude relationship dependence of strain energy release 3-73186
 earthquakes, Italy, long-period seismic network, seismometers (*Italian*) 3-73370
 earthquakes, premonitory variations of P, S travel times, rel. to dilatancy, shear and compressional waves 3-80623
 earthquakes, recording on mag. tape, observatory tape recorder, multiflex f.m. system 3-80837
 earthquakes, response of soil struct. and struct. foundation of multi-storey buildings, computer program 3-80617
 earthquakes, statistical method of detection and prediction 3-80839
 east Pacific Ocean, earthquake epicentre evaluation 3-73221
 East Pacific Rise, seismic refr. results near 14°N, 104°W 3-61396
 Eastern Alps macroseismic data, model experiments for interpretation (*German*) 3-56054

seismology continued

- elastic energy storage and release in Earth rel. to seismic activity 3-50946
- elastic waves from explosions, crust-mantle model, NORSAR area 3-76589
- energy and plane waves in linear viscoelastic media 3-53411
- estimation of magnitudes of future earthquakes, Japan 3-76836
- explosion magnitude estimates, variance, joint magnitude determ. and anal., least squares procedure 3-80608
- explosions, prestressed media, stress wave radiation 3-44783
- explosions, second pulses on recordings in near zone, relation to spalling 3-76550
- explosions, stress measurement determination of inelastic region 3-76549
- fan filters, mixers, comparison of use (*Russian*) 3-76889
- fast reactor, aseismic design, research and development in Japan 3-67511
- fault creep obs. using water level changes in wells 3-61376
- filters, Nth root stack nonlinear multichannel, for seismic refraction and teleseismic array data 3-65147
- geological discontinuities mapping rel. to seismic meas. (*German*) 3-61590
- geophysical prospecting in Gulf of Mexico, three dimensional model giving geological composition 3-65145
- ground motion, prediction, source time function rel. to fracturing process 3-80613
- ground motion, topographic effects 3-56018
- group earthquake locations, global calibration 3-76844
- Gulf of Gascogne, microseism variations (*French*) 3-61343
- Hawaiian volcanic chain, seismic array evidence of core boundary source 3-50934
- high-attenuation low-velocity zone, possible mechanisms 3-50949
- Himalayan mountain belt, aftershock activity rel. to crystal structure 3-65161
- hypocentre location, effect of anisotropic P wave vel. 3-58901
- Iberia, amplitude-distance relation of short period P-waves rel. to mantle structure 3-58825
- implementation errors, statistical modelling methods, geophone array design 3-76533
- information processing equipment resistant capacity 3-69526
- informational seismicity, use of earthquake informational energy and entropy (*Rumanian*) 3-50961
- inland waterways, seismic surveying using marine techniques 3-56043
- inverse problem informative solution 3-58848
- isostasy rel. to seismic activity, gravity anomalies 3-44807
- Japan, earthquake prediction studies 3-56096
- SW Japan margin, seismic reflection meas. rel. to major tectonics 3-53417
- local magnitude (M_L) scale and microearthquake magnitude scale discrepancies 3-56020
- location comparison, accuracy of hypocentres, Kilauea Volcano 3-76833
- long period surface waves, reflection, refraction and mode conversion 3-61388
- long-period torsional vibration pickup, design and performance 3-61580
- longitudinal shear cracks, stress conc. and unsteady propag. 3-61314
- Love wave dispersion analysis, laterally inhomogeneous Himalayas, crustal struct., Severnaya Zemlya earthquake 3-80624
- Love waves, earth-flattening transformation from a point source to a sphere, Biswas-Knopoff transformation 3-80614
- Love waves, effects of transverse isotropy and inhomogeneity 3-56009
- Love waves, inhomogeneous anisotropic elastic solids, velocity, frequency equation 3-44825
- Love waves, modulation, travel times, variational method 3-80616
- Love waves, torsional free modes, simple algorithm for computation of attenuation factors 3-80620
- low rate, first order perturbation theory 3-76592
- lower lithosphere, fine structure, long range profile, France, 1971, P-wave obs., inversion 3-73236
- lower mantle lateral heterogeneity from ScS-S differential travel times 3-58882
- lower mantle shear wave travel times from nuclear explosions 3-58887
- LVL depth determ. from closely spaced seismic stations 3-58829
- mantle, compressional and shear velocity profiles from Fe^{2+} and Mg^{2+} distributions 3-73229
- mantle heterogeneity rel. to body wave multipathing 3-58884
- mantle sounding by method of seismically conjugate points 3-69724
- marine, appl. of homomorphic deconvolution 3-61372
- marine seismic data, resolution improvement 3-61373
- microearthquakes, Los Angeles, correl. with water flooding, Newport-Inglewood Fault 3-80610
- microseism propag. in oceanic waveguides 3-61342
- microseism storms, spectral development at Oulu Finland 3-61341
- microseismic P wave sources 3-65177
- microseismic vibration, complex of phenomena 3-61346
- microseisms, conference (Moscow, USSR, Aug. 1971) 3-61340
- microseisms, USSR data 3-61344
- microseisms generation, hydrometeorological conditions 3-61345
- microseisms near coast lines, analytical methods 3-65178
- microseisms theory, illustration by examples (*French*) 3-61347
- microzonning with emphasis on Thessaloniki, Greece 3-61350
- mid-Atlantic plate boundary in Iceland, hypocentre and fault plane solns. for microearthquakes 3-73215
- MILROW nuclear explosion, close-in ground motion 3-50899
- MILROW nuclear explosion, seismic and tectonic related events 3-50893
- mining application, detection of hazardous conditions 3-50902
- N. Atlantic oceanic rocks, compressional wave velocities as a function of pressure 3-73218
- Ninety East ridge, origin from seismic, gravity and geomagnetic obs. 3-76565
- nomogram for earthquake magnitude data 3-61588
- normal modes identification using spectral stacking and stripping 3-61387
- E. North America, seismic hazard index rel. to elevation 3-58908

seismology continued

- northwestern African margin, sea floor spreading from six geophysical profiles 3-73259
- nuclear explosions, underground, seismic moment, long-period radiation, value of explosive point source model 3-80609
- nuclear reactor seismic qualifications, Category I equipment, structures, systems and components 3-69537
- ocean seismic sounding, resolution assessment using reflected-wave method 3-47851
- ocean-ridge mantle structure from seismic wave ray tracings 3-58888
- P and pP waves attenuation behind island arcs and above inclined seismic zones 3-58890
- P-wave magnitudes, NORSAR and ISC data, bias analysis 3-59168
- Papua-New Guinea-Solomon Islands region, 1959 to 1970, magnitude domain study 3-80605
- polymorphic rocks, wave vel. and attenuation 3-53395
- pore fluids rel. to P and S velocity ratio, earthquake aftershocks, fault creep and magnetic precursors 3-76512
- pre-straining in the earth, ray theory 3-76843
- quartz fibre accelerometer for seismic and tidal meas. 3-47805
- ray tracing, 3 dimensional model of plane or curved surfaces, general algorithm 3-80844
- Rayleigh-type waves, propagation, dispersion, multilayered medium, effect of anisotropic layer 3-44828
- recordings, processing by different methods, effectiveness (*Russian*) 3-76887
- records modification for effect of local soil conditions 3-53371
- reflection data, three dimensional interpretation, velocity distributions 3-76840
- reflection survey of mag. lineations in quiet zone 3-61417
- refraction methods, use of obs. space for dipping structures 3-47794
- Rhinegraben rift system, local interference and temporal interaction with Alpine orogenesis 3-73208
- rock inelastic deformation, effect on seismic vels. 3-76636
- rocks, low pressures, change of seismic wave velocity (*Italian*) 3-73184
- N. Rocky Mtns., seismic evidence of intermediate layer 3-58912
- Ross Sea, seismic profiler and sonobuoy meas. 3-61317
- S. Nevada, nuclear explosions and cavity collapses, radiation of Rayleigh wave energy 3-44785
- San Andreas fault, tilting meas. 3-58881
- San Andreas Fault Experiment, simulation 3-56061
- San Andreas fault system, recurrence of seismic migrations 3-56039
- San Fernando earthquake, source parameters, finite element analysis of residual displacements for rupture 3-73214
- San Fernando earthquake 1971 focal mechanisms and tectonics 3-80640
- San Francisco Bay region, tidal tilt data evaluation and prediction 3-47806
- ScS wave phase conversion to ScSp wave phase in Japanese region 3-58891
- sedimentary basins in Baffin Bay giving main structural features 3-76524
- seismic arrays, location capabilities, computer simulation 3-76826
- seismic intensity data, three California earthquakes, significant conclusions to seismology, earthquake engineering 3-73371
- seismic noise, prediction convolving the microbarogram with transfer function 3-80838
- seismic noise background in Alma-Ata and Tashkent 3-69504
- seismic recordings, kinematic corrections (*Russian*) 3-76885
- seismic reflection obs. during marine geophysical study off western India 3-53391
- seismic source parameters determ. using freq. depend. radiation patterns 3-61370
- seismic station instruments, distortions comparative study 3-59151
- seismogram anal., generalised operators connected with interference transforms. 3-61295
- seismograph phase response determ. from amplitude response 3-53372
- seismograph transfer function numerical inversion by recursive filtering (*French*) 3-76511
- seismological practice, meeting (Moscow, August 1971) 3-61352
- Semipalatinsk underground nuclear explosions, source parameters, P-wave spectra 3-44826
- SH-wave source, elastic half-space, non-homogeneous surface layer 3-44827
- simulation, earthquakes, sine-beat method, environment and damage potential 3-53552
- sinking slab, seismically dead, west USA, detect. by P-wave delays 3-58892
- SKS and SKKS obs., determ. of core constraints 3-58911
- slowness, azimuth, Uppsala array, calibration and event location 3-76863
- Sn to Lg conversion at continental margins 3-58913
- solid Earth tides rel. to changes in situ seismic vel. 3-50930
- Somigliana waves, Rayleigh equation, degeneration to evanescent waves 3-73182
- source parameters of large earthquakes using macroseismic data 3-44814
- South America, and Japan, comparison of Q-struct. 3-58889
- spectral peaks and earthquake source dimension 3-50942
- station errors and correlation of P mean residuals 3-65150
- stick-slip propag. vel. and seismic source mechanism 3-53369
- strength of crust and upper mantle in seismically active regions 3-61351
- Sulu Sea, seismic refraction profiles 3-61316
- Tadzhik, U.S.S.R., study of the Dushanbe-Vakhsh system (*Russian*) 3-56031
- Tasman Sea, evidence of seafloor spreading 3-50945
- Tasman Sea and Antarctic Region, ScP and ScS phases rel. to mantle attenuation 3-53392
- teleseismic residuals for earthquake prediction 3-73224
- teleseismic signals, short-period, earth crust and mantle structure determ. 3-73382
- thin absorbing layer, amplitude-depend. freq. characts. 3-61299
- time-term analysis, iterative method, crustal refraction data 3-44926
- tsunami, relation with sea bottom deformation caused by earthquakes 3-73228
- tsunami model, generation and open-sea characts. 3-53440

seismology continued

- underground explosion waves, propag. in nearly-elastic range 3-53374
- underground explosions, simulation, generation of longitudinal and transverse waves, expression for transfer function 3-80603
- underground explosions, theoretical model, separation of large explosions from earthquakes 3-80604
- underground nuclear explosions, local seismic phenomena immediately after event 3-50933
- underground nuclear explosions, seismic magnitudes 3-56011
- underground nuclear explosions, Yucca Flat, Seismic spectra 3-44780
- SW United States, low-velocity zone var. in upper mantle from 55 seismograms 3-53406
- W United States, P-wave upper mantle structure 3-53405
- unsteady boundary layer flow, induced by rigid wavy plate, Laplace transform method 3-75214
- upper crust, state of stress from mines and tectonophysical and seismological studies 3-44803
- upper mantle, gross velocity depth distribution, P- and S-waves, Europe, earthquake obs. 3-73238
- upper mantle, P-wave structure, long-range explosion observations 3-73237
- upper mantle discontinuities, PP' and precursors, reflection 3-76827
- upper mantle velocity determ., travel-time tables 3-80606
- W. Venezuela, seismicity and tectonics 3-53376
- Vibroseis refraction data enhanced by linearly swept frequency vibratory field procedures 3-65144
- viscoelastic half space deformation by shear dislocations 3-58896
- volcanic tremors analysis, S. Italy 3-61363
- Wadati diagram interpretation with relaxed assumptions 3-61371
- Western USA, intermountain seismic belt, intraplate tectonics, seismicity 3-69536
- western U.S.A., rock accelerations and attenuation curves recorded during earthquakes 3-76506
- Wharton basin, NE Indian Ocean, crustal deformation, bathymetric and seismic data 3-50918
- Wiener filter equations, solution by gradient or steepest descent methods 3-65146
- Yamato Rise sedimentary layer structure from seismic reflection profiles 3-65280

seismometers

- accuracy of hypocentres, Kilauea Volcano 3-76833
 - air-gun array system, use of far-field press. pulses 3-47796
 - bilateral recursive deconvolution in time domain 3-76878
 - deconvolution, influence of round off errors in digital filters 3-76877
 - deconvolution by reiterative convolution for a seismogram 3-76871
 - deconvolution of seismograms, time domain soln. 3-76873
 - digital filter technique for ground motion recovery in seismographs 3-76876
 - digital recording system 3-53544
 - digitized strong-motion accelerograms, error anal. 3-56234
 - earthquake magnitude determ., inconsistency of broad-band and short-period instruments 3-61353
 - earthquake magnitude values, distortion and use of broad band instrumentation 3-65179
 - electrodynamic seismograph, true ground motion by numerical integration of seismograms 3-76872
 - electronic seismographs, noise in galvanometer substitute, inverse filter and negative feedback systems 3-76882
 - event selecting system with digital recording 3-65496
 - galvanometer-seismometer, zero-coupled, calibration 3-80840
 - implementation errors, seismic source and geophone array design 3-76533
 - improvements and developments, review 3-44934
 - inverse time operator approx. 3-76870
 - long period seismographs, noise suppression and stability 3-76883
 - long period wave propagation, synthetic seismograms from 17° to 40° 3-76830
 - long-period, near earthquakes, Italy, long-period seismic network (Italian) 3-73370
 - lowly astatized short period, design of high precision long period seismic channels 3-76880
 - micro-earthquake activity obs. using local radio-linked seismometer networks 3-47809
 - microseismic obs. device for deep wells 3-61584
 - mining application, detection of hazardous conditions 3-50902
 - P signals, complexity 3-76540
 - phase response determ. from amplitude response 3-53372
 - portable seismograph, data processing system, long and short period information 3-76825
 - processing by different methods, effectiveness (Russian) 3-76887
 - recordings, kinematic corrections (Russian) 3-76885
 - refraction, continental shelves 3-76837
 - seismic noise, prediction convolving the microbarogram with transfer function 3-80838
 - seismic station instruments, distortions comparative study 3-59151
 - seismogram approx. deconvolution of finite functions with Fourier transforms 3-76874
 - seismogram input signal restoration for a linear dynamic system 3-76869
 - seismogram restoration in the frequency domain 3-76875
 - seismograph system, feedback controlled broadband modifications 3-76881
 - seismograph systems, transmission of dynamic disturbances 3-76846
 - Sempalatinsk underground nuclear explosions, P-wave spectra, shot depth, yield estimate 3-44826
 - shake table expts., true ground motion determ. 3-76879
 - spectral vibration seismic prospecting apparatus (Russian) 3-76888
- selective dissemination of information** see *information dissemination*
- selenium**
- amorphous, electronic states model for band gap using conductivity and photoconductivity obs. 3-58200
 - amorphous, mech. strength and fracture characts., crystn. role 3-76366
 - amorphous, monoclinic, electrical resistance and optical properties, pressure depend. 3-44074

selenium continued

- amorphous, semiconductor-dielectric photographic system, electrostatic contrast, charge transfer method (Russian) 3-45523
 - amorphous, spectral sensitivity of electrophotographic films, direct or indirect exposure, interposed InSe or Sb₂Se₃ semiconducting layer (Russian) 3-50855
 - amorphous materials, Se-based, photocrystallisation, thermodynamics (French) 3-75624
 - anisotropic chemical shift of n.m.r., theoretical analysis 3-41437
 - capacitance of potential barriers in trigonal single crystals 3-79705
 - critical substrate temperatures, critical straight lines (German) 3-72803
 - critical substrate temperatures, energy analysis of vapour deposition (German) 3-72804
 - crystallisation, elec. field effects, resist. temp. depend. meas., freq. var. 3-72004
 - DTA, various grades, wide temperature range, thermal effects 3-72005
 - electroabsorption spectra of excitons in trigonal, α -monoclinic Se, high field regime 3-55639
 - electron probe microanalysis, mass absorption coeffs. for CuL α line (Japanese) 3-57022
 - electrophotoluminescence at 4K with a.c. and d.c. voltages 3-69062
 - epitaxial growth on Te crystal planes, non-symm. 3-68516
 - film, glass, crystalline, liquid, vapour reversible transformations, electron beam induced 3-72006
 - film, trigonal, vapour-phase epitaxial growth on (1010) cleavage surface of Te 3-80182
 - films, Hg activated, U-centre potential barrier shape 3-58303
 - glassy film, transient s.c.l.c., mobility detn. 3-58268
 - growth of single crystals from vapour, effect of impurity addition 3-69152
 - hexagonal and liquid in 298 to 1000 K range, enthalpy and temperature of fusion measurement 3-68416
 - hydrosols, monodisperse, effect of particle size 3-61233
 - liquid, elec. cond., temp. depend., 10¹⁰Hz 3-55298
 - liquid, non-ohmic conduction and current oscill. 3-68634
 - modulation spectroscopy obs., band structure 3-55567
 - Monte Carlo model of atomic arrangement in sputtered vitreous Se film 3-64264
 - negative ion formation by electron impact in dissociative reattachment region (German) 3-71403
 - optical waveguide, Se diffused into CdS, TE, TM modes 3-66756
 - overlay on Ni(001), chemisorption bonding, LEED study 3-60829
 - photoconductivity of amorphous Se film, influence of long-lived traps 3-75781
 - photoelectric properties, influence of organic solvents and thermoplastic polymers, interaction mechanism (Russian) 3-79740
 - polariser, thin layer transmission and degree of polarisation 3-73724
 - potential barrier limited current, analysis of barrier model, I-V characteristics, hole trapping 3-64339
 - specific heat measurements, trigonal and vitreous, 3 to 300 K, heat pulse method 3-52707
 - thin film, amorphous and cryst., volume plasmon energy, density depend. 3-41221
 - two photon photo-generation in amorphous state 3-55305
 - valence band density of states of amorphous, trigonal Se, X-ray, u.v. photoemission obs. 3-50117
 - vapour, In₂Se₃ evaporation, Se_n polymers 3-64147
 - viscous flow behaviour, stress and temperature depend. 3-55000
 - Au-Se-SnO₂ system, amorphous optical memory obs., depend. on Se film thickness 3-50541
 - Be-Se, barrier heights, surface density of states, Fermi level location (Rumanian) 3-64395
 - CdTe:Se layers, recrystallized, electron capture processes, dark cond. and photocond. (Russian) 3-50235
 - in CuCl, absorpt. spectrum, e.p.r. of point defects, colour centres 3-68844
 - GaAs_{1-x}P_x:Te, Se, deep levels due to shallow donors, i.r. absorpt. and Hall effect obs. 3-44039
 - GaAs_{1-x}P_x:Te,Se, impurity levels, activation energies, Hall effect, carrier mobility, 100-800K 3-44037
 - GaDb:Se, impurity level scheme 3-75722
 - GaSb:Se, segregation coeff. of Se rel. to growing rate 3-58049
 - He-Cd-Se gas laser, characts. 3-51913
 - InAs:SE, band struct., impurity conc. effect obs. 3-75708
 - Se:¹²⁵Te, nucl. quadrupole interactions, Mossbauer spectra 3-50501
 - Se-Ag₂Se, thin film heterojunction, switching phenomena and memory effect 3-79749
 - Se-, photodetachment, high resolution pulsed dye laser study 3-67687
 - Si I, spectra, observed in PbS region 3-40560
 - Zn-Se, interfaces, barrier heights and surface state density (Rumanian) 3-64395
- selenium compounds**
- Ag-Se-Te glasses, thermal stability, energies and rates of crystallization 3-75478
 - As-Se glasses, atomic radial distribution functions 3-57990
 - As-Se system glasses, elastic props., u.s. vel. obs. (Japanese) 3-64084
 - As-Se-I vitreous semiconductor, anisotropisation of conductivity in oriented samples 3-58260
 - As-Se-Pb, glass formation (Russian) 3-73069
 - As-Se-Tl glasses, refractive index, density, polarisation, absorption spectra (Russian) 3-50584
 - As₄₀Se₅₀Ge₁₀, amorphous film, a.c. conductivity, heat treatment and light irradi. effects 3-68620
 - As₂Se₃Tl_x, electrical conductivity and thermoelectric power, temp. depend. 3-55265
 - Cu-Se-Sn system, DTA, X-ray phase analysis, microhardness, thermo-e.m.f. 3-72174
 - Cu-Sn-Se system, DTA, microstructural and X-ray phase analysis, cross sections 3-72175
 - Ge-As-Se glasses, multiphonon absorption obs. in i.r. spectra 3-75972
 - Ge-Se glasses, electron microscopy examination of chemically etched surfaces 3-41064
 - Ge-Se semiconductor glasses, mag. susceptibility, temp. dependence, glass-fusion transition (Russian) 3-72456

selenium compounds continued

- Ge₂₈Sb₁₂Se₆₀, laser window material, stress and temp. analysis for surface heating and cooling 3-70319
 Li-Se system, thermodynamic props., e.m.f. obs. 3-43884
 Li₂Se-Sc-(LiBr-RbBr eutectic) pseudoternary system, phase diagram, physicochemical and e.m.f. obs. 3-43863
 Se-As(0-24 at.%As), atomic arrangement, fast electron energy losses rel. to optical constants. 3-72288
 Se-Ge, glassy semicond., temp. depend. of u.s. absorpt. (French) 3-40976
 Se-I system, equilibrium, liquid state, viscosity, solid state 3-72173
 Se-Te alloys, transition in conducting from extrinsic to intrinsic semiconducting mechanism 3-52881
 Se-Te melt, high temp. semicond. to metallic cond. transition 3-72390
 SeCn⁻ spectroscopic props. of admixture in HCl, HBr, LiCl, LiBr 3-64720
 SeF₆, Raman band contour analyses and Coriolis consts. 3-67816
 SeF₆⁻ square pyramidal ions, mean amplitudes of vibration calc. (German) 3-67781
 SeH⁻, photodetachment spectra, rot. line strengths 3-40659
 SeO₂, matrix isolated, i.r. spectra, bonding, geometry and thermodynamic functions 3-75044
 SeO₂²⁻ Raman intensities and force constants 3-67822
 SeOCl₂:SnCl₄ solution, Pr³⁺ doped, fluorescence spectra 3-76049
 SeO₂(OH)₂ molecule, thermodynamic props., 100-1000 K 3-60395
 Se_xTe_{1-x}, liq., elec. cond., temp. depend., 10¹⁰Hz 3-55298

self-absorption see absorption**self-consistent field methods**

- ab initio LCAO MO SCF calc. of electronic struct. and geometry of HOF 3-46235
 approximate molecular orbital theory, balance and predictive capability 3-43399
 atomic scattering factors, isoelectronic sequence of first row atoms, calc. from analytical SCF functions 3-79201
 atomic scattering factors, neutral first row atoms, aspherical charge distrib., anal. s.c.f. functions 3-79202
 azomethanes, nonradiative transitions and properties of lower triplet state, SCF-MO and CI calc. 3-63504
 bicyclo[2.1.1]hexane, LCAO-MO calcs. using optimised minimal set of Gaussian functions 3-67761
 bond lengths optimisation in all-valence electron SCF-MO calcs. 3-46227
 bond order, SCF MO theory, zero differential overlap approx. 3-54616
 1,3-butadiene, conformers and internal rotation barriers, MO-SCF study 3-54607
 trans-butadiene, low lying π -electron states, configuration interaction calc. 3-74958
 chemical SN₂ reactions, reaction path calc. by ab initio LCAO-MO-SCF method 3-55954
 disubstituted benzene derivatives containing two acceptor groups, pi-electron SCF-MO calc., numerical results 3-57638
 disubstituted benzene derivatives containing two acceptor groups, pi-electron SCF-MO calc. 3-63396
 1,2-disubstituted ethanes, ab initio MO calc. of conformational preferences 3-49451
 electric quadrupole moments evaluation from exptl. hyperfine interaction consts. 3-74803
 elements Z=1 to Z=94, photon cross sections from 0.1 keV to 1 MeV, calc. by relativistic SCF method, tables 3-49404
 ensemble-representable reduced density matrices suggested by X α transition state 3-78401
 fluorobenzene, electrophilic substitution calcs. 3-78677
 formamide, protonation site, non-empirical LCAO-MO-SCF calcs. 3-63381
 General SCF operator satisfying correct variational condition 3-71495
 glycine, mono-, di-, tri-, tetra-, and pentapeptides, molecular fragment approach 3-78669
 hydrated electron structure modified CNDO/2 method for water and ice 3-73174
 hydrogenation energies, polarization functions influence 3-67744
 hydrogenlike systems, electron elastic scattering, SCF calculations 3-43363
 LCAO SCF wave functions, one-electron props. 3-57618
 LCAO-MO, energy functional direct minimization 3-60406
 LCAO-MO and X α -Sw approxs., comparison for ethane internal rot. barrier calcs. 3-40590
 local orbitals, self-consistent equations to second order in overlap 3-43404
 many-electron calcs., pre-processing two-electron integrals 3-52244
 MCSCF study of ground and excited states of systems CN and AlO 3-78693
 molecular crystals, Raman scatt. efficiency, mol. reorientation 3-72656
 molecular ESCA spectra, calc. by multiple-scatt.-X α method 3-40662
 molecular structure, photostability, SCF LCAO MO calc. 3-50845
 molecular wavefunctions, new basis set 3-71506
 multi-configuration, convergence guarantees 3-67740
 multiconfiguration, closed shell systems, model and Brillouin theorem 3-78675
 multiple scattering method calc. of electronic spectra of octahedral transition metal fluorides 3-52340
 nitrosomethane, SCF-LCAO-MO calculations on the rotational barrier 3-43391
 optimization technique for Slater orbital exponents and SCF energy (French) 3-57621
 organic three membered ring molecules, protonation, electrostatic versus SCF CNDO calc. 3-46234
 peptide bond protonation, SCF ab initio study 3-43407
 perturbation improvement of SCF orbitals 3-40555
 perturbation treatment, band structure of mol. crystals 3-64289
 phenylsilanes, quantum-chemical calc. of u.v. spectra 3-67808
 potential energy curves calc. for HCl⁺ and DCl⁺ 3-52393
 propyl radicals, spin delocalisation mechanisms through sigma bonds delocalisation to gamma proton, SCF-MO-INDO method 3-43418
 radial weighting effects in Gaussian expansions of SCF atomic orbitals B-F 3-67649

self-consistent field methods continued

- relativistic effects in magnetic hyperfine structure of 3dⁿ4s² series 3-74796
 rotating superconducting cylinders, London moment current generation calc. by SCF method 3-41283
 SCF X α SW calcs. of pot. barriers for NH₃ and H₂O₂ 3-46224
 sectorial horn radiation calc., superior to successive-diffraction and Kirchhoff methods 3-70782
 semiconductors, doped, model for self-consistent cluster calc. using SCF X α scattered wave method 3-75700
 spectra of organic compounds, correl. functions 3-64681
 spin-optimized methods in second quantization formalism (French) 3-57617
 spin-restricted open-shell SCF theory, off-diagonal Lagrangian multipliers, elimination method 3-78666
 trisubstituted methanes, ab initio MO calc. of conformations and stabilities 3-49429
 two-electron atoms, exponential or scaled SCF orbitals in correlated wavefunctions 3-40557
 VESCF approach to bond order-bond length relationship in unsaturated hydrocarbons 3-54605
 water cyclic polymers stability LCAO-SCF-MO calc. 3-46584
 X α method comparison with ensemble average method 3-67646
 X α scattered wave method calcs. for quartz 3-52793
 B⁺, core description with small basis sets of SCF-MO-LCGO-method (German) 3-52246
 BeAr, atomic contraction coefficients, valence shell correlation, LCAO-MO-SCF calc. using Gaussian basis functions 3-43410
 BeNe, atomic contraction coefficients, valence shell correlation, LCAO-MO-SCF calc. using Gaussian basis functions 3-43410
 C⁺, wavefunctions and energies for valence and excited states 3-74773
 C²⁺, core description with small basis sets of SCF-MO-LCGO-method (German) 3-52246
 CN radical, multiconfiguration self-consistent field theory for excited states 3-46230
 CO⁺, dipole moment, SCF calcs. 3-49437
 (ClHCl)⁻ system, i.r., Raman activity of H bonds, theory (German) 3-71563
 F₂ molecule, SF-CI calculations for ground and some excited states (German) 3-43406
 F³⁺, core description with small basis sets of SCF-MO-LCGO-method (German) 3-52246
 H₂NO interconversion with H₂NOH, ab initio SCF calculations and rearrangements of substituted compounds 3-49430
 H₂O, Rydberg states, ionisation and excitation energies calc. 3-46268
 H₂O polymers molecular interactions studies comparison using different MO basis sets 3-40679
 H₂O₂⁺, STO double zeta wavefunctions, solvation process 3-71504
 H₂O₂⁺, tunnelling in proton transfer between water mols. 3-78867
 He atom pair, polarizability calc. 3-60392
 He-Be²⁺ interaction energy at small internuclear distances, MO-SCF calc. 3-54601
 Li₂, valence-only model pot. and all-electron ab initio LCAO SCF MO calcs. comparison 3-74935
 LiH, valence-only model pot. and all-electron ab initio LCAO SCF MO calcs. comparison 3-74935
 N⁺, wavefunctions and energies for valence and excited states 3-74773
 N³⁺, core description with small basis sets of SCF-MO-LCGO-method (German) 3-52246
 NH₃-H₂O, LCAO calcs. for H bond energy (French) 3-71502
 NH₃-H₂O, SCF MO LCGO studies on hydrogen bonding 3-54648
 (NO)₂, dimer, bond lengths and angles, ab initio calcs. 3-74912
 Ni(CO)₄ and Ni(CN)₄²⁻ LCAO-MO-SCF contracted Gaussian, pi back-bonding analysis 3-67762
 O₃, non-empirical SCF studies of ring and open forms 3-78667
 O⁴⁺, core description with small basis sets of SCF-MO-LCGO-method (German) 3-52246
 OD, A² Σ ⁺ state, dipole moment and hyperfine consts. by SCF and configuration interaction calc. 3-40606
 PO valence shell states, spin-orbit coupling consts. variation with internuclear distance 3-71514

self-diffusion see diffusion**self-focusing**

- heading is late addition, see also nonlinear optics
 glass, ultrashort laser pulses, formation of filamentary defects 3-74273
 leucosapphire, ultrashort laser pulses, formation of filamentary defects 3-74273
 light beam, existence and stability of eigenmodes 3-70840
 limiting diameters and backward stimulated light scattering of self-focused light beams 3-62745
 quartz, ultrashort laser pulses, formation of filamentary defects 3-74273
 transparent materials, parameter meas. using intrinsic optical damage 3-59583
 CuSO₄:gelatin, of Nd laser beam, X-ray laser emission 3-66835
 GaAs, two-photon absorption of Nd laser radiation 3-66864

self inductance see inductance**semi-insulating materials see semiconductor materials****semiconductor counters**

- charge collection, universal description independent of detector geometry 3-42652
 dynamic display, avoidance of separation of counting and display processes (Russian) 3-73877
 flip-flops JK and D appl. (French) 3-56947
 heavy charged particle detectors, phys. processes 3-73868
 low energy proton detection 3-51700
 proton recoil counters with radiator of finite thickness, response function calculation 3-48532
 spectral data handling, in semiautomatic system containing storage devices and electronic computer 3-56938
 subnanosecond coincidence resolution by means of three parameter analysis, on-line processing (German) 3-51696
 telescope, obs. of ⁵⁸Co beta decay, positron asymmetry meas., telescope, obs. of 474 keV, 0.013K 3-63005

semiconductor counters continued

- Au-silicon n-type surface barrier detector, depletion depth 300-500 microns 3-66321
 Ge(Li), correlation between cryst. and spectrometer props. 3-56970
 Ge(Li) coaxial detectors, absolute efficiency calibration in range 160 to 1330 keV 3-48524
 Ge(Li) Compton polarimeter for γ -rays 3-40013
 Ge(Li) detector, for particle identification 3-42648
 Ge(Li) detector, method of fitting of detection peaks (*French*) 3-51715
 Ge(Li) detector with automatic sample changer for neutron fluence probe activation meas. 3-73862
 Ge(Li) detector with separated sensing regions, for γ -ray spectrometry with Compton background suppression 3-53978
 Ge(Li) detectors, use of ^{16}O as efficiency calibration standard 3-48335
 Ge(Li) five-sided coaxial detectors, solid-angle correction factors 3-48533
 Si, surface barrier detector, damage by 0.5 to 1.5 MeV electrons 3-77618
 Si detector, for stereoscan scanning electron microscope 3-62284
 Si detectors, thickness measurement of sensing region 3-53979
 Si radial position sensitive detectors, fabrication by ion implantation technique 3-51714
 Si surface barrier detectors, mechanism of Al contacts aging 3-40009
 Si surface barrier detectors, variable detector mounting assembly 3-48535
 Si(Li) detector, Au-layer and dead-layer thickness determ. 3-51713
 Si(Li) detectors, for proton-induced C(K α) X-rays 3-51707

semiconductor defects

- crystal, i.r. microscopy study of defects 3-54955
 degenerate, diffusive-mobility ratio temp. and doping dependence 3-68612
 Dember type voltage, temp. depend., traps influence 3-52874
 diffusivity-mobility ratio determ. in degenerate semiconductors from linewidth meas. in laser diodes 3-43020
 galvanomagnetic effects, anisotropy, influence of layer distrib. of charged defects (*Russian*) 3-55292
 p-Ge, annealing of thermal defects 3-52620
 IC fabrication, nonequilibrium diffusion processes, point defect injection 3-55745
 II-VI compounds, associated point defects, state-of-the-art review 3-58030
 luminescent materials, charged point defects, electronic states, luminescent semiconductors, phosphors 3-41567
 m.o.s. structure, surface charge density (*Slovak*) 3-46894
 periodic nonuniformity, stochastic temperature fluctuations in melt 3-72815
 SEM observation of defect kinetics 3-63936
 trapping levels, one dimens. model describing thermally stimulated relax. of non-equilib. surface potential (*Russian*) 3-75717
 zinc-blende struct. type, lattice vibrs., i.r. and Raman spectra 3-72621
 n-AlAs, reflection spectrum, influence of defect centres (*German*) 3-50560
 Al $_{1-x}$ Ga $_x$ As, effect of impurities of on growth and electrophysical properties (*German*) 3-53182
 (Bi $_{1-x}$ Sb $_x$) $_2$ Te $_3$, Bi $_2$ (Te $_{1-x}$ Se $_x$) $_3$, rel. to three phonon processes in thermal cond. 3-68451
 n-Bi $_2$ Se $_3$ crystals, free carrier scattering by ionised impurities 3-79681
 Bi $_2$ Te $_3$, dislocations, etch pits (*Russian*) 3-49890
 CdS, dislocation-induced anisotropic absorpt. of polarized light 3-55666
 CdSb, X-ray obs. (*Russian*) 3-75541
 GaAs, dislocation etch-memory effect 3-43801
 GaAs, growth by liquid encapsulation, effect of Sn and Te on perfection (*German*) 3-53183
 GaAs, point defect nature and conc., effect of melt comp. during growth 3-75526
 GaAs epitaxial layers, effect of growth rate and crystallisation conditions on defect formation 3-80192
 GaP epitaxial layers, effect of growth rate and crystallisation conditions on defect formation 3-80192
 Ga $_2$ Te $_3$, unstable equilibrium and radiation defects 3-52645
 Ge, charge carrier recomb. at dislocations 3-68645
 Ge, effect of B doping and neutron irradiation on X-ray diffraction 3-68286
 n-Ge, electron bombardment induced annealing stages, model 3-64067
 p-Ge, plastically deformed, dislocation states, rel. to minority carrier lifetime 3-58279
 Ge, radiation defect form. after 600K electron bombard. 3-60745
 Ge crystal growth from melt, dislocation-free, prevention of vacancy cluster formation 3-72810
 p-Ge:Ga, In, annealing of γ -induced defects, impurity depend., minority carrier lifetime 3-79709
 Hg $_{1-x}$ Cd $_x$ Te, phonon scatt., thermoelec. power and thermal cond. obs. 3-60809
 In $_2$ Te $_3$, unstable equilibrium and radiation defects 3-52645
 Sb $_2$ Te $_3$, dislocations, etch pits (*Russian*) 3-49890
 Si, 1.0 MeV electron irradi. defect centres, energy levels, impurity depend. and annealing behaviour 3-41155
 Si, annealed, defect kinetics, SEM obs. 3-63936
 Si, anomalous residual damage, after annealing of 'through-oxide' As implantations 3-68299
 Si, carrier lifetime doping by edge dislocations 3-55270
 Si, effect of B doping and neutron irradiation on X-ray diffraction 3-68286
 Si, electron irradiated, effective recomb. levels, carrier lifetime obs. 3-68646
 Si, high-purity crystal, investigation by Li decoration 3-43782
 Si, interaction of defects and impurities generated by ion bombard. and implantation 3-40910
 Si, Li $^+$ ion bombarded, radiation defects, i.r. absorpt. study 3-46652
 Si, microdeform. of surface layers in brittle transition temp. region, surface-volume dislocation interactions (*Russian*) 3-79411

semiconductor defects continued

- Si, p-n junctions, characterisation of defects, thermally stimulated meas. capacitance and current 3-41257
 Si, plastic deform. during stage II 3-58074
 Si, wafers, surface defect detection, scattered light meas., He-Ne laser 3-41663
 Si crystal growth from melt, dislocation-free, prevention of vacancy cluster formation 3-72810
 Si p-n junction diode, elec. characs., oxidation-induced stacking fault effects 3-41259
 Si:O e.s.r., oxygen content in floating zone single crystals, method (*German*) 3-53018
 Si:P, ion implanted, effect on e.s.r. 3-68846
 α -SiC, 6H and 15R polytypes, intensities of X-ray refl. from basal plane 3-55131
 SiC, 6H polytype, diffusion-doped, struct. imperfections 3-55741
 SiC, etching, rate of reaction with fused Na $_2$ O $_2$, dislocation effects 3-68508
 β -SiC, struct. defects and photoelec. props., relation 3-72097
 Si $_2$ Te $_3$ crystals, photoluminescence and e.p.r. of defects 3-58556
 α -Sn, electron beam induced n \rightarrow p transition, resistance and thermoelec. e.m.f. obs. 3-68614
 Te, acceptor action of dislocations, theory and expt. 3-79692
 ZnO, extended defects rel. to nonstoichiometry, transmission electron microscope obs. 3-79333
 ZnO:Li, photo-induced persistent internal quadrupole moment 3-46876

semiconductor device manufacture

- see also integrated circuit production*
 compound semiconductor polishing 3-76141
 doping concentration profile, rediffusion problem 3-64792
 IC, photolithographic process, statistical analysis (*Russian*) 3-42592
 impurity and contact materials, electron beam microanalysis (*German*) 3-48646
 ion implantation, radiation damage and technology (*German*) 3-55740
 material selection and preparation 3-80185
 mesa stripe double heterostructure laser, fabrication and performance 3-54236
 m.o.s. device, local drive-in diffusion sources, Silox process, parasitic channel prevention applic. 3-58607
 m.o.s. device, n and p-channel Si gate technologies, comparison 3-58608
 m.o.s. devices, Si slice evaluation, use of Sirtl etch 3-41673
 packaging, laser beam sealing 3-74287
 Pt film, for contacts, chemical vapour deposition 3-44547
 silicate glass, doped, etch rates in buffered HF, rel. to passivation and diffusion 3-64790
 wafer polishing, chemical-mechanical polishing, thickness variations 3-76143
 wafer processing chemicals 3-76142
 water treatment facility, using reverse osmosis 3-50668
 GaAs f.e.t., epitaxial film prep. 3-41625
 GaAs n $^+$ -n-n $^+$ transferred electron diode, continuous multilayer epitaxial growth 3-41688
 GaP i.e.d., LPE overcompensation growth 3-79762
 GaP i.e.d., monolithic matrix, liquid phase epitaxy 3-80195
 GaP i.e.d., vapour doped liquid phase epitaxial growth 3-64791
 HfSi $_3$, HfSi $_2$, formation on silicon from Hf films sputters deposited 3-69166
 InP p-n junction light emitting diode, single cryst. diffusion and liquid phase epitaxy 3-41587
 Si, concealed n $^+$ layer prod., from As silicate glass layer (*Bulgarian*) 3-69163
 Si, devices and processing materials, Na contamination monitoring, using flame emission spectrometry 3-69169
 Si material process modelling, integrated circuit and device parameter control 3-41668
 Si microwave diode, epitaxial growth from dichlorosilane 3-55747
 Si planar technology, mechanical props. of surfaces rel. to prep. and meas. 3-69179
 Si:Au wafers, EIDP deposited, Si $_2$ W crystallite growth on surface 3-72813
 Si(Li) position and energy sensitive detector 3-70389
 ZnS:Mn thin film electroluminescent cell, using ion implantation 3-41588
 ZnTe thin films on GaAs, InAs and GaP, epitaxially grown heterodiodes 3-44138

semiconductor device models

- Ebers-Moll eqns., modified for junction voltage drops and leakage currents 3-75790
 m.o.s. device modelling by computer, surface state density peaks, Gray-Brown studies 3-50270
 negative electron affinity photoemitter, physical model 3-47343
 p-n junction, abrupt, analytical approx. under high level conditions 3-64890
 Schottky barriers, semiconducting diamond, boron doped data analysis 3-64404

semiconductor device testing

- failure analysis using electron probe 3-48674
 p-i-n Si rectifier, pulse response meas. with portable X-ray generator 3-73918

semiconductor devices

- see also field effect devices; Gunn devices; integrated circuits; oscillators; semiconductor counters; semiconductor diodes; semiconductor lasers; space-charge limited devices; thermistors; thyristors; transferred electron devices; transistors; transit time devices; varistors*
 Auger electron spectroscopy in SEM 3-55707
 metallisation, Al-Cu stripes, electromigration 3-64214
 noise calc. by impedance field method, application to single injection 3-68638
 scanistor photoelectrocalorimeter, liquid optical density meas. 3-73728
 solid-state devices, conference, Lancaster, England, 12-15 Sept. (1972) 3-55743
 unipolar conduction, space charge effects 3-64327

semiconductor devices continued

- wideband piezosemiconductor transducers, loss and bandwidth char-
acts. 3-42525
- X-ray spectrometers, trace element determ. 3-66412
- Au-Ni metallisation, diffusion studies rel. to reliability 3-79528
- GaAs p-n junction pressure transducer, for rapidly varying pressure
meas. 3-70293
- GdS-EuS-GdS, film junction, elec. and mag. props. 3-41381
- Ge photon drag detector, for CO₂ lasers 3-42589
- Ge photon drag detector, performance at high CO₂ laser intensity
3-62154
- Se polariser, thin layer transmission and degree of polarisation
3-73724
- p-Si, radiation detectors, position sensitive (*Russian*) 3-70392
- Si, vapour deposition, single crystal and polycryst. films 3-41656
- Si device technology, i.r. spectroscopy, dielectric films on Si
3-41665
- Si p-n junction pressure transducer, for rapidly varying pressure meas.
3-70293

semiconductor diode light emitters *see light emitting diodes***semiconductor diodes**

- see also avalanche diodes; charge storage diodes; Gunn diodes; light
emitting diodes; photodiodes; Schottky-barrier diodes; solid-state
rectifiers; tunnel diodes; varactors; Zener diodes*
- capacitance meter, capacitive-resistive divider method 3-73806
- capacitance of abrupt p-n junction, forward bias, freq. depend.
3-68699
- laser, heterojunction, high power, progress and applic. 3-45808
- p-n, depletion region thicknesses 3-44136
- transition processes, analysis allowing for free surface of base
3-64398
- GaAs, as temp. transducer in hydrostatic pressure region (*Polish*)
3-39876
- GaAs, high resistivity, nonlinear IV characts. 3-58278
- GaAs laser diodes, influence of heat treatment on characts.
3-48923
- GaAs n⁺-n-n⁺ transferred electron, continuous multilayer epitaxial
growth 3-41688
- GaAs:Ti,Co compensated, IV characts. 3-58266
- Ge, point contact, electronic states of impurity centres (*Japanese*)
3-68703
- Ge-CdS p-n heterojunction, current-voltage charact, resist. states
3-72398
- Pb_{1-x}Sn_xTe diode lasers with improved mirror quality, high-power
output 3-43024
- Si, breakdown voltage lowering due to C impurity precipitation
3-52890
- Si, generation-recombination characteristic behaviour 3-79765
- Si, high voltage epitaxial diode, blocking voltages, carrier lifetime
3-41653
- n-Si, surface barrier diodes, light pulse excitation, transient currents
3-64335
- Si p-n junction diode, elec. characts., oxidation-induced stacking fault
effects 3-41259
- Si:P n⁺-p junction, prep. by ion implantation through oxide layer
3-46845
- ZnTe thin films on GaAs, InAs and GaP, epitaxially grown hetero-
diodes 3-44138

semiconductor doping

- see also ion implantation*
- concentration profile, rediffusion problem 3-64792
- diffused layer profile, i.r. reflectivity obs. (*German*) 3-50661
- diffusion in Si, concentration dependent 3-41045
- epitaxial and diffused layers, meas. methods for resistivity and doping
profiles (*Czech*) 3-72814
- epitaxial layer doping profile, Schottky barrier CV characs.
obs. (*Polish*) 3-69161
- IC fabrication, nonequilibrium diffusion processes, point defect injec-
tion 3-55745
- impurity material, electron beam microanalysis (*German*) 3-48646
- ion backscattering analysis, applic. of MeV ⁴He⁺ 3-41670
- ion implantation, beam heating effects, expt. simulation 3-64798
- ion implantation, method, equipment and advantages of this tech-
nique 3-41675
- mass spectrometry, secondary ion, for impurity conc. profiles obs.
3-61122
- mass transport in capsule diffusion process, physical and mathematical
analysis 3-58045
- microwave transistor, base impurity atom profile, m.o.s. capacitance
obs. 3-69181
- model, M₃ crit. point, screening-enhanced optical absorpt. spectrum
3-41505
- m.o.s. capacitor, collection inversion charge minority carrier recom-
binations, heavily doped layers 3-41202
- m.o.s. capacitor, effects of nonuniform doping on generation lifetime
meas. 3-79770
- m.o.s. device, local drive-in diffusion sources, Silox process
3-58607
- m.o.s. structure, CV doping profile obs., correction for interface state
errors 3-55338
- m.o.s. structure, near surface impurity density distrib., CV charac.
obs. 3-64408
- p-n junction, inhomogeneously doped, depletion width determination
3-64397
- semi-infinite medium, diffusion from thin layer, conc. depend. diffu-
sion coeff. case 3-69172
- As₂S₃:Ag, amorphous film, photodoping, photovoltage obs.
3-58302
- B, single crystal, characterization 3-44552
- CdS:I, Hall effect and self diffusion studies of I donor 3-55286
- GaAs, epitaxial on high resistivity substrate, impurity profile, elec-
trolyte interface method 3-69178
- GaAs, epitaxy, control of n-n⁺ interfaces, diffusion analysis
3-55749
- GaAs, homoepitaxial, influence of substrate treatment on electron and
impurity distrib. (*Russian*) 3-50663
- GaAs, liquid phase epitaxial, incorporation of Sn 3-43955
- n-GaAs, O₂-doped, radiative recombination at low temp., photocond.
3-52854

semiconductor doping continued

- GaAs, rare earth dopants, distribution ratios, solubility curves
3-72099
- GaAs, solid-to-solid S diffusion, n-type layer and p-n junc. prep.
3-41189
- GaAs autoepitaxial layers, influence of crystallisation temp. on
growth and doping (*Russian*) 3-58183
- GaAs autoepitaxial layers, effect of crystallisation temp. on growth and
doping (*Russian*) 3-58184
- GaAs deformation characteristics, Cr, Zn, tE dopants 3-75559
- GaAs epitaxial films, submicron, for f.e.t. 3-41625
- GaAs epitaxial layer, i-region analysis by direct image and spark mass
spectrometry 3-41686
- GaAs films, epitaxial growth, effect of substrate orientation on growth
rate in (111)-(100) range (*Russian*) 3-64255
- GaAs:Ge,Sn, epitaxial growth from liquid, electrical props.
3-46765
- GaAs:Si, Ge, vapour phase epitaxy, energy levels detn. 3-69177
- GaAs:Te(Zn), donor and acceptor conc., charge carrier mobility and
Hall conc. meas. 3-44544
- GaAs-electrolyte interface, non-equilibrium depletion, surface-barrier
photoeffect, effect of doping and surface treatment (*Russian*)
3-73144
- GaP, green-emitting p-n junction, high-efficiency, LPE overcom-
pensation growth 3-79762
- GaP, liquid phase epitaxy, Te and O₂ incorporation 3-50090
- GaP, liquid phase epitaxy using doped vapour, for green l.e.d. produc-
tion 3-64791
- GaP, vapour growth method using single flat temp. zone, uniformity
of doping 3-64775
- GaP doped with nitrogen, obs. (*German*) 3-64064
- GaP:N, epitaxial layers, minority carrier lifetime, lumines-
cence green l.e.d. 3-41585
- GaP:O, Mg diffusion and luminesc. props. 3-80186
- n-GaP:Zn, dopant diffusion and solid solubility 3-72228
- GaSb, doping effect on thermal cond., Angstrom method, thermal
diffusivity meas. (*French*) 3-75639
- GaSb:Se, segregation coeff. of Se rel. to growing rate 3-58049
- Ge, effect of B doping and neutron irradiation on X-ray diffraction
3-68286
- n-Ge, increase of phonon viscosity and thermoelastic absorpt. of u.s.
waves with doping 3-40979
- Ge:Ga, quantitative detn. of dopant segregation during growth
3-69171
- In₂Ga_{1-x}As films, epitaxial growth, effect of substrate orientation on
growth rate in (111)-(100) range (*Russian*) 3-64255
- InP, vapour phase epitaxy of doped material 3-55748
- InP:Te, Zn, carrier density rel. to solubility of donor, acceptor
dopants 3-60886
- InSb, current-controlled liq. phase epitaxy and dopant modulation
3-41636
- InSb:Te, e.m.f. meas., low conc. soln. thermodynamic properties
3-44071
- Ir as ion source for Al and In ion beams 3-41599
- Pb_{1-x}Sn_xTe, carrier conc. reduction, by Cd diffusion and Zn doping
3-69173
- Si, amorphous, B-implanted, non-Gaussian range profiles 3-40934
- Si, B diffusion and interface reactions of B₂O₃-Si system 3-58047
- Si, by B, P, Ni, Cu, Au, radial distrib., radioactivation analysis, elec-
trical measurements 3-72098
- Si, by B diffusion source glass, selective etching 3-79578
- Si, concealed n⁺ layer prod., from As silicate glass layer (*Bulgarian*)
3-69163
- Si, deformed layers with different orientations and dopants (*Russian*)
3-52628
- Si, determ. of location of interstitial Na atoms by charged particle
channelling 3-64062
- Si, doped epitaxial layer, controlled preferential etching, HF, HNO₃
and acetic acid 3-41659
- Si, doping inhomogeneities meas. by electroreflectance 3-54977
- Si, effect of B doping and neutron irradiation on X-ray diffraction
3-68286
- Si, epitaxial layers, donor conc. levels, effect of etching and autodop-
ing, low temp. i.r. studies 3-41653
- Si, epitaxially grown from SiH₄-H₂ and SiH₄-He mixtures, compari-
son 3-41626
- Si, float zone crystals, gas doping 3-58601
- Si, non-equilib. behaviour of dopants during epitaxial deposition using
silane 3-44554
- Si, penetration of B channelled ions; implantation angle influence
3-79365
- Si, single crystal films, vapour deposition, effect of minority carrier
lifetime, epitaxy, autodoping 3-41656
- Si, solid-solid vac. diffusion doping process 3-58600
- Si, vapour deposition, thin polycryst. layers, epitaxy, kinetics of
growth, doping 3-41652
- Si epitaxial layer, impurity conc. profile meas. for material selection
3-64800
- Si epitaxial layer, materials for diffusion 3-64801
- Si epitaxial layer, profile tailoring by enhanced diffusion in ion bom-
barded region 3-55746
- Si epitaxial layers, transport of B from source during sublimation in
vacuum 3-76145
- Si:Al, limit solubility determ., temp.-gradient fusion zone method
3-44543
- Si:As, epitaxial growth process, vapour etching, autodoping, impuri-
ty profiles 3-41654
- Si:Au, effect of growth medium on O content 3-68175
- Si:B, diffusion orientation depend., profiles obs. 3-55744
- Si:B, fast electron irradiated, diffusion profile changes obs.
3-60740
- Si:B, in oxidizing atmosphere 3-80178
- Si:B, P, ion implanted, conc. profiles, annealing effects 3-5319
- Si:B, polycryst. films, effect of doping on growth, microstructure and
elec. props. 3-41657
- Si:B, polycryst. films, elec. cond., effect of growth from SiH₄, carrier
conc. 3-41658
- Si:B, vacancy diffraction length at 1000°C, rel. to impurity profile
3-64788
- Si:B film, chemical vapour deposition, 300 to 550°C 3-80180

semiconductor doping continued

- Si:B films, low temp. CVD, struct., elec. and opt. props. 3-80193
 Si:P, epitaxial growth, surface band bending, surface Fermi level 3-41655
 Si:P, slow neutron irradiation, uniform standard specimens, resistivity meas. accuracy check 3-47353
 Si:Sb(P), (Au), zone refined, distribution of impurity elements, quantitative autoradiography 3-41651
 Si-oxide interface, boron redistribution in oxidising atmosphere 3-44151
 SiC, 6H polytype, diffusion-doped, struct. imperfections 3-55741
 SiO₂ film, grown in Cl₂ and HCl atmosphere, Cl profile 3-41643
 SiO₂:P, B, Zn, i.r. spectra of films, stability, struct. 3-64646
 SrF₂:Na, conversion of colour centres by doping 3-53133
 Te, influence of acceptor concentration on Hall effect 3-41205
 ZnS, ion implantation, annealing, luminesc., cond. change 3-72817
 ZnS:(In, Cu), laminar morphology, energy storage, thermoluminescence 3-76103

semiconductor electron states *see crystal electron states***semiconductor growth**

- chemical vapour deposition on hot substrate, laser beam local heating 3-44549
 deposition of polycrystalline Si and Al layers, heat-treating cycle, shallow diffused transistors 3-41661
 electron-beam alloying, local temp. fields, calc. method and exptl. obs. (Russian) 3-53192
 elemental thin film prep. and props., review 3-76146
 films, amorphous, surface irregularity formation during deposition, voids 3-55173
 float-zoned crystals, dislocation-free, [115] crystallographic orientation 3-50664
 III-V compound, liquid phase epitaxy, review 3-69162
 III-V compounds, mixed, solid/gaseous system, thermodynamic equilibrium 3-58186
 III-V quaternary alloy, liquid phase epitaxy for heterostructures 3-41684
 III-V semiconductor thin films, molecular beam epitaxy 3-72812
 IV-VI compounds, epitaxial films, preparation methods review 3-58603
 microwave devices, material selection and prep. 3-80185
 monocrystals for optoelectronics (German) 3-50669
 periodic nonuniformity, stochastic temperature fluctuations in melt 3-72815
 solid-state devices, conference, Lancaster, England, 12-15 Sept. (1972) 3-55743
 vacuum deposition of semicond. layers, using porous carbide evaporation sources 3-50657
 Ag₂S, semiconductor thin films, structure and properties (Romanian) 3-64417
 Ag₃SbS₃, preparation and physical-chemical props. 3-53195
 Al_{1-x}Ga_xAs, effect of impurities (German) 3-53182
 Al_{1-x}Ga_{1-x}As:Sn, liquid phase epitaxial growth, electrical props. 3-46764
 AlN, epitaxial film growth and piezoelec. props. 3-80189
 As₂S₃, thin film growth by laser sputtering, mol. comp. of condensate vapours 3-55176
 AsSe, thin film growth by laser sputtering, mol. comp. of condensate vapours 3-55176
 As₂Se₃, thin film growth by laser sputtering, mol. comp. of condensate vapours 3-55176
 As₂Se₃, thin films, preparation method for high induced conductivity 3-69182
 B, single crystal, characterization 3-44552
 BP, high-pressure synthesis from elemental vapours 3-69175
 BP crystal growth from metal phosphide solns. 3-50665
 Cd₃As₂-Zn₃P₂ semiconducting, preparation, physical and electrical properties 3-53188
 Cd_{1-x}Hg_x-Te, epitaxial, evap.-conc.-diffusion method, growth rate 3-58188
 Cd_{1-x}Hg_x-Te, epitaxial growth on CdTe in H₂ atmosphere 3-69176
 Cd_{1-x}Hg_x-Te thin films, deposition of HgTe onto CdTe, isothermal conditions, new method 3-53189
 CdS film on Ge, growth conditions effect on resist. states 3-72398
 CdS single crystals doped with different donors and acceptors photoluminescence 3-53148
 CdSe, thin films, chemical deposition using selenurea as depositing agent 3-58605
 CdSe single crystals with n- and p-type cond. approaching intrinsic 3-61120
 CdSnAs₂:Cu, preparation by diffusive saturation (Russian) 3-64298
 CdTe, electrolytic synthesis 3-69168
 CdTe, epitaxial growth in quasi-closed cell 3-79594
 CdTe, on Ge epitaxial, thin films, electron beam evaporation, structure and orientation 3-43957
 CdTe, semi-insulating undoped crystal growth for gamma ray detectors 3-64803
 Cd_{1-x}Zn_xS, production by isovalent cation diffusion 3-80191
 EuS thin film, by evaporation 3-75689
 Ga:Si, liquid, Si contamination rate determ. 3-61118
 Ga_{1-x}Al_xAs, discrete and planar monolithic structures 3-58602
 Ga_{1-x}Al_xAs, epitaxial, temp. grad. liquid phase method 3-41681
 Ga_{1-x}Al_xAs, heteroepitaxy on GaP, soln. growth and characterisation 3-41682
 GaAs, analysis of epitaxial layers using MeV α -particles 3-53196
 GaAs, chem. transport, optimum conditions in GaAs-I₂-He system 3-72798
 GaAs, Czochralski growth using molten B₂O₃ liquid seal 3-64795
 GaAs, epitaxial, from Me₃Ga and AsH₃, Hall effect and photolum. 3-79713
 GaAs, epitaxial film growth and piezoelec. props. 3-80189
 GaAs, epitaxial layers, distribution coeff., of O impurity, temp. depend., carrier concentration, impurity profile 3-52758
 GaAs, epitaxial layers grown from vapour, surface struct. rel. to condition 3-58592
 GaAs, epitaxy, control of n-n⁺ interfaces, diffusion analysis 3-55749
 GaAs, growth by liquid encapsulation, effect of Sn and Te on perfection (German) 3-53183

semiconductor growth continued

- GaAs, heteroepitaxy on GaP, soln. growth and characterisation 3-41682
 GaAs, homoepitaxial, influence of substrate treatment on electron and impurity distribns. (Russian) 3-50663
 GaAs, liq. phase epitaxy, isothermal diffusion theory 3-68514
 GaAs, liquid phase epitaxial, incorporation of Sn 3-43955
 GaAs, liquid phase epitaxy for Gunn devices 3-55750
 GaAs, point defect nature and conc., effect of melt comp. during growth 3-75526
 GaAs, related compounds, conference, Boulder, Colo., USA, Sept. (1972) 3-41678
 GaAs, selective epitaxy, anisotropy effect 3-72816
 GaAs, thin film, vapour deposition on sapphire 3-80184
 GaAs, vapour phase epitaxial, deep-level impurity conc., depth profile for various As vapour pressures (Japanese) 3-55736
 n⁺ GaAs {100} substrates, HCl-vapour etched 3-41629
 GaAs autoepitaxial layers, influence of crystallisation temp. on growth and doping (Russian) 3-58183
 GaAs autoepitaxial layers, effect of crystallisation temp. on growth and doping (Russian) 3-58184
 GaAs epitaxial films, submicron, for f.e.t. 3-41625
 GaAs epitaxial layer, high purity growth by liquid phase epitaxy in vacuum 3-41679
 GaAs epitaxial layers, effect of growth rate and crystallisation conditions on defect formation 3-80192
 GaAs films, epitaxial growth, effect of substrate orientation on growth rate in (111)-(100) range (Russian) 3-64255
 GaAs whiskers, vapour-liquid-crystal growth mechanism 3-72300
 GaAs:Ge, epitaxial, for microwave devices 3-50662
 GaAs:Ge,Sn, epitaxial growth from liquid, electrical props. 3-46765
 GaAs:Si, double heterostructure l.e.d. 3-41584
 GaAs:Si, Ge, vapour phase epitaxy, energy levels detn. 3-69177
 GaAs-ZnSe, liq. phase epitaxy, and characterization 3-75685
 GaAs_{1-x}P_x, discrete and planar monolithic structures 3-58602
 GaAs_{1-x}P_x, epitaxial, pyrolytic method, for electroluminesc. diodes 3-44545
 GaAs_{1-x}P_x vapour growth, thermochemical calc. of AsH₃-PH₃-HCl-Ga₂H₆ system 3-41676
 Ga_{1-x}In_xP alloys, solution growth method 3-80183
 GaIn, epitaxial film growth and piezoelec. props. 3-80189
 GaN, synthesis by reacting active N₂ with GaCl at 600°C 3-61114
 GaP, defects rel. to growth from non-stoichiometric melts 3-44555
 GaP, discrete and planar monolithic structures 3-58602
 GaP, epitaxial growth on Si substrate, chloride transport process 3-58604
 GaP, from Ga-rich soln. (French) 3-61121
 GaP, green-emitting p-n junction, high-efficiency, LPE overcompensation growth 3-79762
 GaP, liq. phase epitaxy, isothermal diffusion theory 3-68514
 GaP, liquid phase epitaxy, growth characs. and surface morphology 3-41685
 GaP, liquid phase epitaxy, Te and O₂ incorporation 3-50090
 GaP, low-strain, liq. encapsulation vertical gradient freeze method 3-41637
 GaP, n-p double epitaxial growth using vertical furnace system 3-46766
 GaP, selective liquid phase epitaxy for l.e.d. monolithic matrix 3-80195
 GaP, single crystals, 35 mm diameter, liq. encapsulated Czochralski growth 3-44531
 GaP, vapour doped liquid phase epitaxy, for green l.e.d. production 3-64791
 GaP, vapour growth method using single flat temp. zone 3-64775
 GaP by synthesis, solute diffusion for light emitting diodes 3-50670
 GaP epitaxial layers, effect of growth rate and crystallisation conditions on defect formation 3-80192
 GaP single crystals, liquid encapsulated Czochralski pulling 3-72811
 GaP normal melting, crucible free, installation, description 3-80173
 GaP-ZnS(Se) solid solutions, soln. growth and characterization 3-64797
 GaP single crystals, high pressure liquid-encapsulated Czochralski method, technology review 3-50660
 GaS, thermodynamical calc. on chemical transport in closed tube system 3-80159
 Ge, epitaxial, on Si substrate, zone melting method (Russian) 3-55735
 Ge, smooth epitaxial films, iodide method, diffusive mass transfer 3-76144
 Ge crystal growth from melt, dislocation-free, prevention of vacancy cluster formation 3-72810
 Ge epitaxial layers, anisotropy of growth and alloying, in Ge-I₂ system 3-76130
 Ge melt, apparatus for meas. temp. fluctuations (Russian) 3-66160
 Ge thin film, vapour deposited and ion implanted, scanning electron diffraction obs. 3-58189
 Ge whiskers, vapour-liquid-crystal growth mechanism 3-72300
 Ge:Ga, quantitative detn. of dopant segregation during growth 3-69171
 HfS₃, layer trichalcogenide single crystals, optical absorption, intrinsic edge, simple model 3-44428
 HgTe, electrolytic synthesis 3-69168
 HgTe crystal platelets, from Hg solution, growth mechanism, physical properties, growth methods 3-53190
 In_{1-x}Ga_xAs films, epitaxial growth, effect of substrate orientation on growth rate in (111)-(100) range (Russian) 3-64255
 In_{1-x}Ga_{1-x}As:Ge p-n junction, single stage liquid phase epitaxy 3-50266
 In_{1-x}Ga_xP, from vapour, mass spectrometric and thermodynamic studies 3-40855
 In_{1-x}Ga_xP, heteroepitaxy on GaAs, gas phase stoichiometry effects on props. 3-41683
 In_{1-x}Ga_xP vapour growth, p-n junction electroluminescence characs. 3-58599
 In_{1-x}Ga_xP vapour growth technique, p-n junction electroluminescence 3-58598

semiconductor growth continued

- InP, criteria for tipping during liquid phase epitaxial growth 3-80181
- InP, epitaxial, closed-space method 3-41680
- InP, epitaxial growth of pure and doped material, vapour phase method 3-55748
- InP films, chem. transport, and characterization 3-72286
- InSb, current-controlled liq. phase epitaxy and dopant modulation 3-41636
- InSb, liquid phase epitaxy on CdTe, metallurgical aspects (*French*) 3-64794
- InSb, thin film, prep. and appl. to bubble domain devices 3-80187
- NiSe_{2-x} pyrites, prep. by chem. transport with Cl₂ 3-60906
- PbS vapour phase growth, low dislocation density and impurity conc. 3-69151
- PbTe, electrolytic synthesis 3-69168
- Sb-Se, amorphous film, vacuum evaporation, comp. range 3-68522
- SbSI crystallization thin layers, heat-dissipation, temp. fluctuation effects 3-72289
- Sb₂Se₃, high-resistivity, prep. by two-step refining process 3-61116
- Se, effect of impurity addition on growth of single crystals from vapour 3-69152
- Se, on (1010) cleavage surface of Te, heteroepitaxial, electron microscope examination 3-80182
- Se on Te crystal planes, non-symm. epitaxy 3-68516
- Si, by internal work coil float zoner 3-64796
- Si, Czochralski growth, influence of C, Si-C phase diagram 3-41645
- Si, dislocation-free crystals, distribution of point defects Cu decoration, X-ray topography, etching 3-41650
- Si, epitaxial, choice of materials 3-64801
- Si, epitaxial, on spinel and sapphire, using SiH₄-H₂ and SiH₄-He mixtures, comparison 3-41626
- Si, epitaxial, thickness measurement down to 0.5 μ m 3-44548
- Si, epitaxial, using dichlorosilane, growth on single crystal hemispheres 3-76140
- Si, epitaxial growth, p-n junctions, thyristor manufacture 3-41256
- Si, epitaxial growth from dichlorosilane 3-55747
- Si, epitaxial layers, donor conc. levels, effect of etching and autodoping, low temp. i.r. studies 3-41653
- Si, filamentary growth from soln., mechanism 3-69164
- Si, float-zone growth, resistivity topography rel. facet growth 3-41646
- Si, float-zoned crystals, growth striations and swirls, electron microscopy 3-41649
- Si, growth on thermal oxide layer, decomposition of SiH₄, effect of growth on elec. props. 3-41658
- Si, non-equilib. behaviour of dopants during epitaxial deposition using silane 3-44554
- Si, selective epitaxy, orientation depend. 3-44546
- Si, soln. and etching in Sn, 600-1000°C, rel. to liq. phase epitaxy 3-69165
- Si, vapour deposition, semiconductor devices, single crystal and polycryst. films 3-41656
- Si, vapour deposition, thin polycryst. layers, epitaxy, kinetics of growth, doping 3-41652
- Si (111) epitaxy, geometry displacement and distortion model 3-50667
- Si crystal growth from melt, dislocation-free, prevention of vacancy cluster formation 3-72810
- Si epitaxial film, on sapphire, with microsec. carrier lifetime 3-41623
- Si epitaxial layers, transport of B from source during sublimation in vacuum 3-76145
- Si film, chem. deposited, effect of deposition conditions on struct. 3-41112
- Si homoepitaxy with ion sputtering, growth mechanism 3-44550
- Si slice processing, flame emission analysis of K 3-54045
- Si swirls, interaction with dislocations, comparison to striations 3-41647
- Si thick film ribbon, for large-area solar cells and arrays 3-61119
- Si whiskers, vapour-liquid-crystal growth mechanism 3-72300
- Si:As, epitaxial growth process, vapour etching, autodoping, impurity profiles 3-41654
- Si:As, effect of medium on O content, kinetics 3-68175
- Si:B, polycryst. films, effect of doping on growth, microstructure and elec. props. 3-41657
- Si:B, polycryst. films, elec. cond., effect of growth from SiH₄, carrier conc. 3-41658
- Si:B film, chemical vapour deposition, 300 to 550°C 3-80180
- Si:B films, low temp. CVD, struct., elec. and opt. props. 3-80193
- Si:P, epitaxial growth, surface band bending, surface Fermi level 3-41655
- Si-H-Br and Si-H-I equilibrium behaviour 3-50666
- SiC, whisker growth by vapour-liquid-solid phase mechanism (*Russian*) 3-72297
- SiC crystal growth by vapour-liquid-solid mechanism in sublimation method 3-80160
- SiC single crystal, improved sublimation growth method (*Japanese*) 3-47354
- Si₂Ge_{1-x}, epitaxial, on Ge, by simultaneous thermal decomp. of SiH₄ and GeH₄ 3-41627
- SiO₂ film, grown in Cl₂ and HCl atmosphere, Cl profile 3-41643
- SnTe, electrolytic synthesis 3-69168
- Ti oxides, crystal growth and props., semiconductor-to-metal transitions (*German*) 3-53194
- V oxides, crystal growth and props., semiconductor-to-metal transitions (*German*) 3-53194
- V_{1-x}Nb_xO₂, (0 \leq x \leq 0.33), vapour phase prep. and characteriz. of single crystals. (*French*) 3-72802
- V₂O₃, single cryst. prep. by chem. transport reaction 3-72801
- ZnGeP₂, large single cryst. metal growth 3-72180
- ZnO film, prep. by cold plasma condensation, growth kinetics (*French*) 3-52772
- Zn₃P₂-Cd₃As₂ semiconducting, preparation, physical and electrical properties 3-53188
- ZnSiAs₂, growth by vapour transport 3-61112

semiconductor growth continued

- ZnTe thin films on GaAs, InAs and GaP, epitaxially grown hetero-diodes 3-44138
- ZrS₃, layer trichalcogenide single crystals, optical absorption, intrinsic edge, simple model 3-44428
- semiconductor imperfections** see *semiconductor defects*
- semiconductor-insulator boundaries**
- m.o.s. capacitor, oxide and interface charge stability 3-41202
- GaAs-AgBr photoelectric properties 3-44110
- n-GaAs-Si₃N₄, energy spectrum of states at boundary (*Russian*) 3-50271
- LiNbO₃-Si(CdSe), layered structure, acoustoelec. effect due to elec. fields of u.s. surface waves 3-44120
- Si:Ge, oxidised, oxide interface properties, surface state density function 3-60921
- Si-AgBr photoelectric properties 3-44110
- Si-insulator interface, interface state densities rel. to H annealing 3-46897
- Si-oxide, boron redistribution in oxidising atmosphere 3-44151
- Si-SiO₂, cathodoluminesc. from centres responsible for radiation induced space-charge build up 3-50275
- Si-SiO₂, change of interface charge by BT treatment 3-79773
- Si-SiO₂, charge injection, p-n junction reversed biased below break-down obs. 3-55333
- Si-SiO₂, effect of ambients on immobilisation of ionic contaminants 3-46902
- Si-SiO₂, inversion layer, localised states 3-79772
- Si-SiO₂, photoconductivity, photoelectromotive force, i.r. light absorption (*Russian*) 3-58322
- Si-SiO₂, secondary ion emission analysis, Na impurity distrib. obs. (*Russian*) 3-52904
- Si-SiO₂ interface, energy spectrum of surface states, determ. from m.o.s. C-V characts. 3-58321
- Si-SiO₂ interface, nonavalanche injection of hot carriers 3-46895
- Si-SiO₂ interface, use in m.o.s. technology, review 3-50278
- Si-SiO₂-Au, interface state occupancy, incremental conductance freq. depend. obs. 3-58323
- Si-SiO₂-Si₃N₄, effect of ambients on immobilisation of ionic contaminants 3-46902
- Si-TiO₂, in m.i.s. struct., elec. obs. 3-50276
- SiO₂ films on Si, ion bombardment effect on electrical props. 3-41268
- Si(001)/Al(0112), anisotropy in electrical props. 3-41269
- semiconductor integrated circuits** see *monolithic integrated circuits*
- semiconductor junctions**
- heterojunctions, electrostatic energy 3-58317
- n \pm n, with near-intrinsic conductivity, charge-carrier and heat balance distribution 3-68700
- p- π -n, carrier lifetime measurement method 3-64336
- Schottky junctions, temperature coefficients of drift voltage (*German*) 3-50265
- surface barrier junction, current instability 3-44157
- GaAs laser, degradation and passivation, native oxide influence 3-40272
- GaAs-Al_xGa_{1-x}As heterostructure laser, threshold current density reduction by separate optical and carrier confinement 3-43019
- Ge-Si p-p heterojunctions, electrostatic energy 3-58317
- p⁺-i-n⁺ type structure, magnetoresistive effect in double-injection regime 3-52897
- Si:Au, compensated, p-i-n structure, current-voltage characts. 3-60915
- SnO₂-CdSe, n-n heterojunction, elec. and optical props. (*Korean*) 3-72399
- SnO₂-CdSe-CdS n-n double heterojunction, elec. and optical props. (*Korean*) 3-72399
- semiconductor lasers**
- band to level transition, spectral hole burning and nonlinear gain decrease 3-66847
- compound cavity, electrooptical and piezoelectric tuning 3-62723
- conference, Pugnuchiso, Italy (1972) 3-58539
- diffusivity-mobility ratio determ. in degenerate semiconductors from linewidth meas. in laser diodes 3-43020
- electron beam excited, radiating mirror types, dynamics of radiation emission 3-59874
- electron beam pumped, c.r.t. screen applic. 3-54233
- electron beam pumping, using gas plasma gun 3-54232
- electron beam semicond. pulse amplifier for injection laser modulation 3-39956
- e.m. wave interaction derivation of wave function and electron spectra, dependence on quantisation size (*Russian*) 3-45809
- GaAs injection lasers, mesa type, fabrication (*German*) 3-59907
- GaAs/Ga_xAl_{1-x}As single-heterostructure diode laser, external cavity controlled, time delays 3-66845
- generation threshold, phototransitions between zone exponential tails, kinetic approach (*Russian*) 3-57242
- heterojunction, high power, progress and applic. diodes 3-45808
- heterojunction injection lasers, review 3-74247
- heterojunction lasers, catastrophic and slow degradation 3-48926
- holograms of transparencies, image reconstruction 3-45777
- homostucture and heterostucture, time delays and Q-switching 3-54237
- injection, degradation, aging, self-damage 3-57240
- injection laser applications 3-48930
- injection lasers, empirical estimation of service life from short term tests 3-48924
- injection lasers, statistical distribution of failure 3-48925
- i.r. sources, tunable, state-of-the-art 3-78008
- linewidth, highly degenerate semicond. low temp. diffusivity-mobility ratio detn. 3-44069
- mesa stripe double heterostructure, fabrication and performance 3-54236
- multidiode injection laser, far field diff. pattern rel. to diodes in array and cavity mirror reflectances 3-40271
- multimode laser emission, asymptotic nature of threshold conditions 3-70830
- spontaneous emission behaviour, effect of saturable absorption 3-54231
- stimulated emission and laser transitions 3-57237
- thermal deformation of emitting face 3-48928

semiconductor lasers continued

- threshold theory of laser generation in p-n junctions with exponential band tails 3-40270
time delay calcs. 3-51937
wide injection laser, modes of large cavity with sawed sides 3-62722
(AlGa)As-GaAs heterojunction, refractive index step and carrier confinement rel. to lasing props. 3-70825
(AlGa)As-GaAs heterostructure, radiation confinement, effect of GaAs refractive index 3-68952
Al_{1-x}Ga_xAs heterojunction, cooled, pulsed and cw red emission 3-78043
Al_{1-x}Ga_xAs heterostructure laser, c.w. optically pumped, degradation characts. 3-59871
Al_{1-x}Ga_xAs-GaAs, single heterojunction injection laser, self-switching 3-70829
Al_{1-x}Ga_xAs-GaAs, stripe geometry double heterostruct. amplified spontaneous emission superlum. diode 3-51938
Al_{1-x}Ga_xAs-GaAs double heterostructure, interface stresses due to different thermal expansion coeffs. rel. to laser operation 3-59872
Al_{1-x}Ga_yAs-Al_{1-x}Ga_{1-y}As-Al_{1-x}Ga_{1-y}As, double heterostructure, uniaxial stress effects 3-78045
CdS, electron-beam pumped, influence of mech. treatment of resonator 3-74249
CdS, spontaneous and stimulated luminescence excited by multiphoton optical pumping 3-58557
CdS, thermal shift of laser wavelength during excitation pulse of electron beam 3-78044
CdS laser, KGP-2, electron beam pumped 3-48922
CdSe, laser emission due to exciton-exciton, exciton-electron interactions 3-64692
(GaAl)As-GaAs, double heterostructure, high peak power injection laser 3-51935
GaAlAs-GaAs heterostructure, localised gain within resonator type laser with narrow active region, 3-54234
n-Ga_{1-x}Al_xAs-p-GaAs, injection, double heterostruct., physical basis for negative resist. 3-78042
GaAs, electron beam pumped scanning laser 3-48927
GaAs, electron beam pumped, radiating mirror, divergence of output radiation 3-74248
GaAs, high power narrow linewidth operation, using dispersive element in external cavity 3-51936
GaAs, injection, multimode laser emission, asymptotic nature of threshold conditions 3-70830
GaAs, junction, stripe geometry, filaments, fabrication, thermal design, modes, spontaneous pulsing 3-57239
GaAs, lidar applications in meteorology 3-76912
GaAs, press. tuning and high resolution 3-49386
GaAs, transversely adjusted gap, for optical communication systems 3-48919
GaAs, waveguide laser, optically pumped, fundamental 0.11 micron corrugation feedback 3-78048
GaAs diode, modulation (*German*) 3-59875
GaAs diode, with fast current drive circuit 3-45807
GaAs double heterojunction c.w. laser at 300°K 3-48921
GaAs double heterostructure, degradation due to nonradiative recomb. component 3-54235
GaAs double-heterostructure, c.w. degradation at 300K, spontaneous emission obs. 3-70826
GaAs double-heterostructure, c.w. degradation at 300K, electronic gain obs. 3-70827
GaAs epitaxial waveguide with corrugation feedback, laser oscill. 3-66844
GaAs homostructure and double heterostructure, degradation and passivation, native oxide influence 3-40272
GaAs injection laser, mode selection by Fresnel refl. 3-48920
GaAs laser diodes, influence of heat treatment on characts. 3-48923
GaAs laser diodes, SEM studies 3-80113
GaAs optically pumped, surface laser, corrugation feedback, fabrication, spectrum, pumping power 3-48918
GaAs/Ga_{1-x}Al_xAs single heterostructure diode laser, threshold, spectral and output power characts. 3-66846
GaAs-Al_{1-x}Ga_xAs, double heterostruct., planar stripe laser 3-78046
GaAs-Al_{1-x}Ga_xAs, double heterostruct., threshold current density and lasing transverse mode 3-78047
GaAs-Al_{1-x}Ga_xAs double heterostructure, luminesc. pattern obs. by photoluminesc. method 3-66848
GaAs-Al_{1-x}Ga_xAs heterostructure laser, threshold current density reduction by separate optical and carrier confinement 3-43019
GaAs-Ga_{1-x}Al_xAs injection, single heterostructure, threshold current, quantum efficiency and losses determ. 3-59873
GaAs-Ga_{1-x}Al_xAs double heterostructure lasers, composition profile effect on characts. 3-43021
GaAs-Ga_{1-x}Al_xAs double heterostructure, threshold and electron lifetime, acceptor conc. depend. 3-57236
GaAs-Ga_{1-x}Al_xAs double-heterostructure laser with 30°C half-life exceeding 1000 h, continuous operation 3-59870
GaAs-GaAlAs junction-stripe-geometry lasers, room-temp. continuous operation 3-43023
GeAs, optical gain, stimulated recombination, temp. depend. 3-57238
In_{1-x}Ga_xP vapour growth, p-n junction electroluminescence characts. 3-58599
In_{1-x}Ga_xP vapour growth technique, p-n junction electroluminescence 3-58598
InSb, Raman spin flip tunable laser, high power pulsed operation 3-57257
InSb, theory of spin-flip Raman amplification 3-78049
InSb, two-photon excited stimulated recomb. emission 3-40269
InSb Raman laser, spin-flip, low field, characteristics, closed cycle refrigerator, Raman gain measurement 3-48938
Pb salt diode, small band gap, use in high resolution spectroscopy 3-57241
Pb-salt tunable diode lasers, review 3-48929
Pb_{0.98}Cd_{0.02}S diode, tunable cw operation at 3.5 μ m, ultrahigh resolution spectroscopy applic. 3-51607
PbSe injection laser, tuning by hydrostatic press. 3-43025
Pb_{1-x}Sn_xTe diode, tuning characts. in 8-12 μ m region 3-70828

semiconductor lasers continued

- Pb_{1-x}Sn_xTe diode lasers with improved mirror quality, high-power output 3-43024
ZnS, spontaneous and stimulated luminescence excited by multiphoton optical pumping 3-58557
- semiconductor materials**
Specific materials only. See also amorphous semiconductor materials; elemental semiconductors; II-VI semiconductors; III-V semiconductors; ionic semiconductors; liquid semiconductors; oxide semiconductors. For generalities and properties of unspecified materials see semiconductors
acoustic wave amplification in strong electric fields, plasma oscillation effects 3-41237
acriflavin, stimulated cond. and photocurrent, relax. 3-75775
anisotropic, non-degenerate, energy band structure and scattering mechanisms from optical expts. 3-47223
anthracene, elec. cond. in melting region (*Russian*) 3-44068
anthracene, impurity effects on electrical conductivity 3-68615
anthracene, photocond., triplet exciton-impurity interaction rel. to carrier generation 3-46879
anthracene, review 3-55253
anthracene crystals, carrier lifetime and mobility deformation effects 3-41182
anthracene crystals containing tetracene impurity, stimulated radiation emission study 3-80077
Auger and radiative processes, recombination coeffs. 3-58577
band structure of I-III-VI₂ semiconds., electroreflectance obs. 3-55206
binary compounds, energy band gaps tables 3-75707
binding energy of exciton-neutral donor complex, non adiabatic calc. 3-46814
chalcogenides, magnetic semiconductors, spinel and europium, electrical conductivity, influence of magnetic props., applications 3-52831
chlorinated copper phthalocyanine film, compensation effects in dark cond. and photocond. 3-44115
compound, polishing methods, for device manufacture 3-76141
conductivity, electrical, Hall effect, measurement, high resistivity, 239 to 1000 K, apparatus, technique (*German*) 3-62170
copper phthalocyanine, frequency dependence of conductivity 3-72564
crystals, switching effect model, donor screening 3-72389
current-voltage characteristics, universality under pinch effect 3-68637
Dember type voltage, temp. depend., traps influence 3-52874
dielectric constant, reln. to energy gas changes, temperature dependence 3-41472
diffused layer profile, i.r. reflectivity obs. (*German*) 3-50661
diffusion of impurities, distrib. region near surface 3-75635
electric props., mathematical framework, solved problems, book contrib. 3-58219
electrical conductivity, noncontact measurement technique, ampoule filling (*Russian*) 3-48473
electroabsorption, electron-hole interaction effects 3-68967
electron transport, optical phonon effect 3-41188
exciton radiation recombination under high levels of excitation (*Russian*) 3-44474
ferromagnetic, mag. mechanism for switching near Curie point 3-68682
galvanomagnetic effects, anisotropy, influence of layer distrib. of charged defects (*Russian*) 3-55292
heavily doped, transport coeff. calcs. 3-44065
high frequency conductivity, magneto-optical and optical effects (*German*) 3-52866
hopping conductivity, a.c., sum rule derivation in limit of low site densities 3-52833
hopping Hall conductivity, low-freq. three-site impurity, temp. diagrammatic analysis 3-52859
I-III-VI₂, band gap determ. by refl. meas. with polarization modulation 3-68549
II-IV-V₂ semiconductors, effective charges of Fe impurity atoms from Mossbauer obs. 3-58456
intra-band electron pairing in presence of radiation field 3-41307
ion implanted, impurity profile, rate of ionisation enhanced diffusion 3-55737
IV-VI compounds, epitaxial films, preparation methods and properties 3-58603
large-group, light scattering and absorption, interactions with lattice vibrations and excitons 3-50553
layer structure, magnetic susceptibility, Van Vleck theory of paramag. susceptibility 3-41327
light absorption by carriers, coeff. calc. 3-75960
light scattering in external electric field, interband, intraband 3-55551
luminescence intensity dependence and photoconductivity for electron-electron, electron-exciton and exciton-exciton interactions 3-41548
luminescence role of the surface (*Russian*) 3-41544
luminescent materials, theory of associated defects 3-41567
magnetic, plasmon-magnon interaction 3-79858
magnetic semiconductors, photoconductivity, band structure, Hall effect 3-41214
microwave conductivity, influence of strong electric fields 3-79701
microwave devices, material selection and prep. 3-80185
modulation spectroscopy, Raman and Brillouin scattering 3-55593
naphthalene, elec. cond. in melting region (*Russian*) 3-44068
naphthalene, single crystal, limitation on injected space charge deep trapping 3-64328
nonparabolic, band gap determ. by measuring Faraday rot. in quantum limit 3-44399
optical spectroscopy in high magnetic fields using polarisation modulation 3-55615
organic, impurities optical absorption 3-80079
p-type, with chalcopyrite lattice, mag. susceptibility oscills. (*Russian*) 3-44000
passive layer, on Ni electrode, modulation spectroscopy 3-55964
perylene, electron and hole drift mobilities 3-52838
phenanthrene, elec. cond. in melting region (*Russian*) 3-44068

semiconductor materials continued

- photoconductivity, photoelectromagnetic effect, photo-carrier generation and recombination theory 3-58299
 phthalocyanine, β -H₂Pe, elec. cond. mechanism and carrier trapping 3-68618
 piezoelectric, heating of electrons by acoustic waves, theory 3-75785
 piezoelectric, interaction of plasma and lattice waves 3-79743
 γ -platinum phthalocyanine, band struct. and carrier mobility 3-79626
 polar, longit. magnetoresist. resonance minima in ohmic regime, mechanism 3-50223
 polyethylene, absorption currents and photocurrents 3-58300
 polyethylene terephthalate, carrier mobility measurement by electron beam bombardment 3-50209
 polyisoxazole and polyisoxazolines, resist. temp. depend. 3-58265
 polymeric complexes based on 10-vinylphenothiazine, elec. cond. and spectral props. 3-63963
 radiative recombination at donor-acceptor pairs and higher associates 3-58224
 rare earth chalcogenides, cryst. chem. and electronic cond. (French) 3-46847
 rare earth monochalcogenides, pressure induced semiconductor-metal transition 3-44031
 resonance scattering of current carriers, conductivity, thermopower and magnetoresistance calcs. 3-46831
 surface conductivity, effect of intervalley scattering (Russian) 3-55258
 TCNQ, electronic props. of one-dimensional solids, review 3-50134
 TCNQ salts, sp. ht. and mag. susceptibility, 1.4-4.4 K, rel. to band struct. 3-46795
 TCNQ/tetrathiafulvalene highly conducting complex, electron transfer 3-46824
 transition metal chalcogenides, cryst. chem. and electronic cond. (French) 3-46847
 transition metal cpds., conf., Geneva, Switzerland, (Apr. 1973) 3-40897
 transition metal rare earth chalcogenides, LnCrSe₃ group, extrinsic characts. 3-64497
 transition metal mixed valency pair compounds, electronic props. of one-dimensional solids, review 3-50134
 zinc-blende semiconductors, microscopic dielectric function 3-68546
 zinc-blende struct. type, lattice vibrs., i.r. and Raman spectra 3-72621
 Ag chalcogenides stoichiometric and temp. dependence of electronic ionic conductivity ratio (German) 3-50202
 Ag₂AsS₄, proustite, band structure, light absorpt. and refl. obs. 3-44017
 Ag₂AsS₄, proustite, i.r. absorpt. spectrum effect of partial electrolysis (Russian) 3-68992
 Ag₂AsS₄, proustite, n.q.r. spectrum and spin-lattice relax. time of ⁷⁵As, 300-4.2K (Russian) 3-79944
 Ag₂AsS₄, proustite, photocond. and thermally stimulated cond. (Russian) 3-79735
 Ag₂-Au₂Se₃ solid solution, semiconductor electronic cond., electron mobility 3-41190
 AgGaS₂, piezoelectric nonlinear optic, crystal structure determ. 3-72049
 AgGaS₂, valence band density of states and core level shifts, X-ray photoemission obs. 3-55720
 α -Ag₂S and β -Ag₂S, optical props. in i.r. and far i.r. 3-53108
 Ag₂S(Se) semiconductor-metal transition, i.r. reflectivity obs. (German) 3-50571
 Ag₂SbS₃, pyrrhite, photocond. and thermally stimulated cond. (Russian) 3-79735
 α -AlB₂, elec. props., refl. spectrum, polaron cond. mechanism 3-72357
 As₂S₃(Se₂)(Te₂), positron annihilation 3-60746
 As₂Se₃ thin films, preparation method for high induced conductivity 3-69182
 (BaSb)(TiZr)O₃, three-step positive temp. coeff. of resistivity 3-52836
 BaTiO₃, rare earth doped crystal, optical absorption, elec. cond., luminescence 3-75741
 BaTiO₃, sintered ceramic, elec. cond., luminescence, grain size, doping depend. 3-75742
 BaTiO₃-Bi₂O₃-La composite ceramic, a.c. characts. at various temps. and freqs. 3-79696
 Bi-Sb alloy, far i.r. refl. spectra, band struct. obs. 3-44019
 Bi-Sb crystals, magnetoresistance anisotropy at 4.2 and 89 K 3-55788
 Bi₂, low temp. photoconductivity and absorption spectra 3-75780
 Bi₂S₃, conduction band parameters from Shubnikov-de Haas investigations 3-55202
 BiSb, cyclotron resonance, quantum oscillations, helicon waves 3-64293
 Bi_{1-x}Sb_x, cooling due Ettingshausen and Peltier effects 3-64362
 n-Bi_{1-x}Sb_x, cyclotron resonance meas. 3-55203
 Bi_{1-x}Sb_x, narrow-band semiconductor, absorption spectra 3-50592
 Bi₂Sb₃, valence band struct. from magnetoplasma wave dispersion 3-44020
 Bi₂Sb₃ film, thermoelec. power, quantum size effects (French) 3-55293
 (BiSb)₂Te₃ film, elec. cond. and thermoelec. power, effect of mech. stresses 3-61123
 (Bi_{1-x}Sb_x)₂Te₃, Bi₂(Te_{1-x}Se_x)₃, thermal cond., charge carrier and phonon contrib. 3-68451
 Bi₂Se₃, electroreflectance and thermoreflectance spectra obs. 3-55611
 Bi₂Se₃, Shubnikov-de Haas effect with high carrier conc., band structure obs. 3-58285
 n-Bi₂Se₃, thermoelectric power in strong transverse magnetic fields 3-41216
 n-Bi₂Se₃ crystals, free carrier scattering mechanism 3-79681
 Bi₂Se₃:Te(In(Pb)), anisotropy of elec. cond., Hall coeff. and thermoelec. power, doping effects 3-41185
 Bi₂Te₃, arbitrary field theory developed from valence band properties by galvanomagnetic measurements 3-64291
 Bi₂Te₃, dislocations, etch pits (Russian) 3-49890

semiconductor materials continued

- Bi₂Te₃, electroreflectance and thermoreflectance spectra obs. 3-55611
 p-Bi₂Te₃, galvanomag. effects, two valence subband model 3-72373
 n-Bi₂Te₃, magneto-Seebeck effect and Shubnikov-de Haas effect 3-79717
 Bi₂Te₃, n- and p-type, precision lattice parameters 3-49882
 Bi₂Te₃-Bi₂Se₃, linear expansion coefficient, mechanical props. 3-75628
 Cd₃As₂, i.r. absorpt., band gap obs. 3-68983
 Cd₃As₂ film, electron mobility, meas. for thermal detector use 3-68651
 Cd₃As₂-Zn₃P₂ solid-solution, semiconducting, preparation, physical and electrical properties 3-53188
 Cd₃Co_{1-x}Cr₂S₄, magnetic hot pressing and magneto-optical props. 3-47230
 CdCr₂S₄ ferromagnetic semiconductor, theory of spin-dependent phonon Raman scattering 3-72616
 CdCr₂Se₄, ferromagnetic spin wave amplification factor 3-41355
 CdCr₂Se₄, magnetic, reflectivity near Curie temp. 3-68955
 CdCr₂Se₄(S₄), e.p.r., temp. depend., Raman relax. process 3-79899
 CdGeAs₂, optical and photoelec. props., band struct. obs. 3-64686
 p-CdGeAs₂, valence band structure from electroreflectance spectra 3-44427
 CdGeP₂(As₂), band structure and modulation spectra, review 3-55205
 CdIn₂S₄, edge absorption in region of indirect transitions 3-47286
 CdIn₂S₄, microwave dielec. const., and its press. depend., 9.25 GHz 3-68912
 CdIn₂S₄, multi-quantum photoconductivity 3-60897
 Cd₃P₂, density-of-states effective electron mass determ. 3-68548
 Cd₃Pb_{1-x}Te film, struct. and elec. props., effect of deposition conditions 3-64265
 CdSb, defect struct., X-ray obs. (Russian) 3-75541
 CdSb, i.r. radiation filter 3-64619
 p-CdSb, recomb. processes, photocond. and photomag. effects, 350-100K (Russian) 3-72384
 CdSiP₂, long-wavelength fundamental absorption edge 3-55648
 CdSiP₂(As₂), band structure and modulation spectra, review 3-55205
 CdSnAs₂, pseudopot. calc. of band struct. at points in Brillouin zone, electrorefl. spectra 3-43996
 CdSnAs₂, selective etchant 3-79582
 CdSnAs₂:Cu, behaviour of impurity centre (Russian) 3-64298
 CdSnAs₂-CdSe solid solution, thermal cond. in mag. field, 80-400K 3-58155
 (CdSnAs₂)_{1-x}(2CdSe)_x, elec. cond., Hall and Nernst-Ettingshausen mobilities, temp. depend. 3-60885
 CdSnP₂(As₂), band structure and modulation spectra, review 3-55205
 Cd_{3-x}Zn_xAs₂ solid solns. influence of pressure on electrical props. 3-79718
 Co_{1-x}Fe_xO₃, electrical conduction, a.c. resistivity and thermoelectric power measurements 3-50206
 CoFe_{2-x}Ti_xO₃, electrical conduction, a.c. resistivity and thermoelectric power measurements 3-50206
 Cr chalcogenides, ACr₂B₄, mag. semiconductor, band model, optical and transport props. (Polish) 3-41133
 Cr₃S_{4-x}Te_x, Cr₃S_{3-x}Se_x and Cr₃S_{4-x}Se_x; mag. props. and elec. cond. (French) 3-47051
 CuBr, biexciton binding energy, electron-phonon interaction effects 3-46817
 CuCl, biexciton binding energy, electron-phonon interaction effects 3-46817
 CuCl, modulated excitonic spectra in elec. field 3-55638
 CuCr₂Se₄, Hall effect, conductivity, thermoelectrical force, temp. depend. 3-72371
 Cu_{0.5}Fe_{0.5}Cr₂S_{4-x}Se_x, x=0-2, negative magnetoresist. and elec. cond., room temp. T_c 3-50221
 CuGaS₂, wavelength modulated absorpt., refl. spectra, excitonic structure and band gap shift 3-55636
 CuInSe₂, bulk electrical props. and device characteristics 3-46844
 Cu_{2-x}S, electrical cond. and phase transitions 3-68407
 Cu₂(Se)(Te), thermo-e.m.f., and elec. cond., temp. depend., 500-1200°C 3-50203
 Cu₂Se, refl. spectrum, 0.8-8 μ m, optical effective mass, carrier relax. time 3-44418
 EuB₆, elec. cond. and Seebeck coeff., comparison with YbB₆ (French) 3-64332
 EuS, optical constants, magnetic field modulated magnetoreflectance, Kramers-Kronig relation 3-55614
 n-EuTe, reson. Raman scatt. from screened LO phonons 3-55592
 FeCr₂S₄, magnetoresist. anisotropy 3-58282
 FeS₂, transverse magnetoresistance at 77 K and 4.2 K as function of magnetic field 3-52860
 Ga_{0.5}Mo_{0.5}S₄(Se₄) spinels, ferromag. semicond., charactetiz. 3-72467
 β -GaS, energies and symmetries of first order Raman active phonon modes 3-47278
 GaS, optical absorption, photoluminescence and electroluminescence spectra 3-58550
 GaS, recomb. radiation emitted under two photon excitation 3-44487
 GaS, thermodynamical calc. on chemical transport in closed tube system 3-80159
 GaS, wavelength modulation spectra at 5K, 77K, 300K 3-55568
 GaS layer compound, switching and memory properties 3-64389
 Ga₂Se_{1-x}, optical absorption, photoluminescence and electroluminescence spectra 3-58550
 GaS₂Se_{1-x} (0 < x < 1) layer compound, switching and memory properties 3-64389
 GaSe, electrolum., bound exciton phenomena (French) 3-55692
 GaSe, electronic charge density, pseudopot. calc. (German) 3-50123
 GaSe, hole mobility anisotropy 3-50201
 GaSe, long-lifetime photoluminescence temp. and excitation intensity depend. 3-69063
 GaSe, optical absorption, photoluminescence and electroluminescence spectra 3-58550

semiconductor materials continued

- GaSe, optical second harmonic generation, nonlinear susceptibility coeff. (*French*) 3-54240
- GaSe, phonon Raman scattering spectra, temp. depend. 3-80042
- GaSe, photolum., 4.2 K, charact. emission line identification (*French*) 3-55673
- GaSe, photoluminescence, p- and n-type, 4.2K to room temperature, free exciton emission, structural emission, impurity states emission 3-53146
- GaSe, wavelength modulation spectra at 5K, 77K, 300K 3-55568
- GaSe layer compound, switching and memory properties 3-64389
- GaSe single crystals, photovoltaic investigation of homogeneity 3-60898
- GaSe(Te), effective ionic charge and bonding, from chem. shift of K-absorpt. discontinuities 3-54940
- GaTe, exciton photoreflectance, reflectance modulation Kramers-Kronig relations 3-55610
- Gd₃S₄, transport props. rel. to Coulombic and mag. disorder 3-50198
- Gd_{3-x}V_xS₄, semiconductor conductivity activation energy, thermoelectric power, effect of applied mag. field 3-41215
- Ge-Si alloy, band structure effect on recomb. radiation, comparison with pure Ge, Si 3-50621
- Ge_{1-x}Si_x film, electrorefl. spectra 3-76020
- GeTe, optical props. and energy gap from reflectance spectra 3-64685
- HfS₃, layer trichalcogenide single crystals, growth, optical absorption, simple model 3-44428
- HgCr₂Se₄, paramagnetic resonance study 3-79909
- Hg₂P₂X (X=Cl, Br), electrical props. 3-40883
- InAs-CdTe, solid soln., tetrahedral structure rel. to heterovalent substitution 3-40888
- InAs-CdTe solid soln., electron effective mass, thermoelectric power and i.r. refl. meas. 3-41141
- In₂S₃, optical transitions involving different numbers of photons 3-74272
- InS(Se)(Te), thermal expansion and isothermal compressibility 3-55094
- In₂Se₃, resist. and Hall coeff., 110-600K 3-68616
- LaRu₂Ga_{1-x}O₃, charge of conductivity over conc. range 3-41168
- LiInS₂, linear and nonlinear optical props. 3-45819
- Mg₂Si, Mg₂Sn and Mg₂Ge, X-ray excitation, photoelectron spectra and band structure 3-55722
- Mn_{1-x}Mg_xTe₂, crystallographic parameters and semiconduction 3-68229
- MnTe, thermoelec. power near Neel temp. 3-68655
- MoS₂, alkali metal intercalated, room temp. resistivity obs. 3-79691
- MoS₂, layer type structure, electronic props. of two dimensional solids 3-50133
- MoS₂, reflectivity in extreme u.v. range, band structure investigation 3-55609
- Na₂WO₃ semiconducting crystals, Raman scattering cross section dependence on laser intensity 3-41517
- NbSe₂, layer type structure, electronic props. of two dimensional solids 3-50133
- NbSe₂, reflectivity in extreme u.v. range, band structure investigation 3-55609
- Ni complex, bisquinoxaline-2,3-dithiol nickel frequency dependence of conductivity 3-72564
- NiS₂, high-pressure effect on semiconductor-metal transition temp. 3-79751
- NiS_{2-x}Se_x, metal-semicond. phase diagram, resist., susceptibility and calorimetric meas. 3-72328
- NiSe_{2-x} pyrites, prep. and elec. props. 3-60906
- Pb chalcogenides, small energy gap semiconductor, bond structure, review (*Polish*) 3-41131
- Pb_{1-x}Cd_xS, small band gap diode lasers, use in high resolution spectroscopy 3-57241
- PbF₂, pure and rare-earth activated, coloration by γ -irrad. and elec. props. 3-54960
- Pb_{1-x}Ge_xTe, small band gap diode lasers, use in high resolution spectroscopy 3-57241
- PbI₂, energy bands, empirical pseudopot. approach 3-43999
- PbS, absorpt. edge shift rel. to electron density, forbidden band optical widths 3-44018
- PbS, electronic band structure and optical props. 3-58523
- PbS, high field resist. meas., phonon mechanisms 3-68641
- PbS, valence bands, high resolution X-ray photoemission results 3-44011
- PbS film, physically treated, role of surface complexes in photosensitivity 3-79734
- PbS film, with adsorbed O₂, anomalous adsorpt. hysteresis of photocond. 3-75778
- PbS vapour phase growth, low dislocation density and impurity conc. 3-69151
- PbS_{1-x}Se_x, pseudobinary phase diagram and existence regions 3-79471
- PbS_{1-x}Se_x, small band gap diode lasers, use in high resolution spectroscopy 3-57241
- PbS(Se)(Te), two-photon absorpt. and optical orientation of free carriers, theory 3-54245
- PbSe, electronic band structure and optical props. 3-58523
- PbSe, energy distribution spectra of photoemitted electrons 3-58584
- PbSe, multivalley semicond., Knight shift, hyperfine coupling const. determ. 3-44342
- PbSe, p-n junction, photovoltaic spectra, temp. and substrate impurity conc. depend. 3-58298
- PbSe, small bandgap, band structure and optical properties 3-58211
- PbSe, thermodynamic props. 3-64187
- PbSe, valence bands, high resolution X-ray photoemission results 3-44011
- Pb_{1-x}Sn_xSe and Pb_{1-x}Sn_xTe, stimulated emission of light at 10 μ 3-50600
- Pb_{1-x}Sn_xTe, carrier conc. reduction, by diffusion and Zn doping 3-69173
- Pb_{1-x}Sn_xTe, small band gap diode lasers, use in high resolution spectroscopy 3-57241
- PbTe, electrolytic synthesis 3-69168
- PbTe, electronic band structure and optical props. 3-58523
- PbTe, energy distribution spectra of photoemitted electrons 3-58584

semiconductor materials continued

- PbTe, film, prep. by closed vol. method, thermoelec. and elec. props. 3-60873
- PbTe, magnetoabsorption theory, multiphonon, two-photon absorpt. only for transverse polarisation 3-44400
- PbTe, multivalley semicond., Knight shift, hyperfine coupling const. determ. 3-44342
- PbTe, photoelec. spectra, 6.25-8.75 eV 3-55723
- PbTe, small bandgap, band structure and optical properties 3-58211
- PbTe, valence bands, high resolution X-ray photoemission results 3-44011
- n-PbTe solid solution, thermal cond., separation of lattice and electronic components in strong mag. field 3-58154
- PbTe:Bi, energy spectrum and electron scatt., Bi impurities effects 3-44038
- Pbs, energy distribution spectra of photoemitted electrons 3-58584
- Pt metal silicides and germanides, ordered pyrite structure, diamagnetism, semiconducting, valence electron conc. 3-40906
- PtSb₂, conductivity, Hall effect, thermoelectric power, Nernst-Ettingshausen effect obs. 3-68650
- Sb-Te-I-solvent-H₂O system, high temp. and press., photosemicond. cryst. form. 3-72790
- Sb₂Bi_{1-x}, small energy gap semiconductor, band structure, review (*Polish*) 3-41131
- SbSI, excitation of trapped electrons, photocond. and photodiffusion study 3-44109
- SbSI, ferroelec., absorpt. edge not affected by ferroelec.-paraelec. transition 3-61051
- SbSI, ferroelec. semicond. optical absorpt. rel. to elec. field in Curie point region 3-44395
- Sb₂Se₃, high-resistivity, prep. by two-step refining process 3-61116
- Sb₂Te₃, dislocations, etch pits (*Russian*) 3-49890
- p-Sb₂Te₃, Shubnikov-de Haas obs., two valence band model 3-64357
- Sb₂Te₃-Bi₂Te₃ linear expansion coefficient, mechanical props. 3-75628
- SiAs, cryst. struct., elec., optical props., layers (*Japanese*) 3-72070
- SiC, 4H polytype, grown from Si melt, photolum. 3-61063
- α -SiC, 6H and 15R polytypes, intensities of X-ray refl. from basal plane 3-55131
- α -SiC, 6H polytype, activated by u.v. illumination, i.r. absorpt. 3-55600
- SiC, 6H polytype, diffusion-doped, struct. imperfections 3-55741
- α -SiC, 6H-polytype, impurity i.r. absorpt. (*Russian*) 3-80083
- SiC, far i.r. absorpt. bands, narrow doublet lines 3-44445
- β -SiC, n-type, impurity photoconductivity (*Russian*) 3-68664
- n-SiC, optical absorption associated with superlattice 3-41533
- SiC, p- and n-type, i.r. absorpt., role of free carriers 3-75996
- SiC, solution growth from liquid Si, using modified travelling heater method 3-64771
- β -SiC, struct. defects and photoelec. props., relation 3-72097
- SiC crystal growth by vapour-liquid-solid mechanism in sublimation method 3-80160
- SiC polytypes, elec. cond., temp. depend. of anisotropy, comparison 3-58272
- SiC:B,N, cathodolum., intensity depend. on excitation 3-61078
- SiTe₂, absorption spectra, optical properties between 300 K and 100 K 3-47285
- SmS, optical properties of discontinuous semiconductor-metal phase transformation (*German*) 3-53118
- SmS, thermal and electrical conductivity, thermopower, Hall effect, temp. and composition depend. 3-60871
- SmS:Gd, temp.-induced explosive first-order electronic phase transition 3-64297
- Sn chalcogenides, small energy gap semiconductor, bond structure, review (*Polish*) 3-41131
- Sn_{1-x}In_xTe, Hall coeff., thermoelec. power, elec. cond., rel. to In content 3-44098
- Sn_{1-x}Mn_xTe, resistivity and Hall effect spin depend., exchange coupling const. 3-46859
- SnS, absorption spectra and valence band spectra 3-41534
- SnS₂, energy band calcs. by pseudopotential methods 3-41138
- SnS₂(Se₂), electronic energy bands, local empirical pseudopot. approach 3-43998
- SnSe, absorption spectra and valence band spectra 3-41534
- SnSe₂, energy band calcs. by pseudopotential methods 3-41138
- SnTe, electrolytic synthesis 3-69168
- Ta₂S₃, 4Hb-type, prep. and props. 3-55084
- Tl(I)(Tl(III)Cl₂Br₂), electrical conductivity meas. 3-58258
- TlInSe₂, piezophotorestrictive effect in single cryst. 3-68674
- TlTe, low temp. electronic transport props. 3-52844
- TlTe, single cryst. growth and elec. props. 3-80176
- Tl₂Te, thermal cond., 300-625 K 3-79535
- Tl₂VSA, switching effect 3-46881
- V₃Co, valence and conduction band structures, X-ray spectra (*Russian*) 3-55207
- V₃Ga, valence and conduction band structures, X-ray spectra (*Russian*) 3-55207
- V₃Ge, valence and conduction band structures, X-ray spectra (*Russian*) 3-55207
- V₃Si, valence and conduction band structures, X-ray spectra (*Russian*) 3-55207
- V₃Sn, valence and conduction band structures, X-ray spectra (*Russian*) 3-55207
- WO₃-P₂O₅-Li₂O glass, resistivity and thermoelectric polarisation obs. (*Polish*) 3-41176
- YIG, n-type, inhomogeneous polycryst., non-Ohmic current behaviour 3-72363
- YbB₆, elec. cond. and Seebeck coeff., comparison with EuB₆ (*French*) 3-64332
- ZnAs₂-Zn₃P₂ solid solutions, prep., X-ray anal., Hall coeff., resist. meas. 3-79712
- ZnGeP₂, band struct., electrorefl. study 3-41136
- ZnGeP₂, calc. band struct. and reflectivity spectra 3-41135
- ZnGeP₂, chalcopyrite crystals, thermorefectance spectra and energy band structure 3-44007
- ZnGeP₂, electrical props. of high resistance single crystals 3-44077

semiconductor materials continued

- ZnGeP₂, Hall effect, conductivity, hole mobility, temp. depend. 3-68625
 ZnGeP₂(As₂), band structure and modulation spectra, review 3-55205
 ZnIn₂S₄ layer compound, switching and memory properties 3-64389
 ZnP₂-Cd₃As₂ solid-solution, semiconducting, preparation, physical and electrical properties 3-53188
 p-ZnSiAs₂ crystals, conductivity in high temp. region 3-52842
 ZnSiP₂, band struct., electrorefl. study 3-41136
 p-ZnSiP₂, conductivity, Hall effect, mobility, temp. depend. 3-68624
 ZnSiP₂-ZnSiAs₂ range, optical absorption edges at 300 K and 80 K 3-55604
 ZnSiP₂(As₂), band structure and modulation spectra, review 3-55205
 p-ZnSnP₂, electrorefl. spectra, 1.5-4.5 eV, 77 and 295 K 3-44430
 ZnSnP₂(As₂), band structure and modulation spectra, review 3-55205
 ZrS₂, layer type structure, electronic props. of two dimensional solids 3-50133
 ZrS₃, layer trichalcogenide single crystals, growth, optical absorption, simple model 3-44428

semiconductor materials testing

- channelling effect technique 3-41674
 cyclotron resonance measurements, submillimetre waves, pulsed magnetic fields, apparatus 3-66341
 impurity analysis by MeV ⁴He backscattering 3-41670
 infrared television microscope studies, resolution 3-41664
 photoluminescence analysis 3-69180
 Si, gettering action of phosphosilicate glasses and ion implementation damage layers, MeV ⁴He⁺ backscatt. obs. 3-41644
 Si, wafers, surface defect detection, scattered light meas., He-Ne laser 3-41663
 Si epitaxial layer, impurity conc. profile and resistivity 3-64800

semiconductor-metal boundaries

- see also Schottky-barrier diodes
 anthracene-Au system, extrinsic photocurrent production, role of singlet and triplet excitons 3-46815
 channelling effect technique for examination 3-41674
 chemical/thermodynamic approach for electron exchange analysis of materials in contact (French) 3-79760
 covalent-ionic transition, microscopic theory 3-55334
 h.f. noise, unified theory 3-44146
 hole and electron traps, Schottky barrier capacitance studies 3-64300
 liquid V₂O₅-metal interface, nonlinearity of current-voltage characs. 3-41265
 magnetic semiconductors, phase transition, narrow forbidden band, paramagnetic-antiferromagnetic, magnetisation 3-50367
 photoemission, quantum efficiency 3-50268
 quantum and electronic theory, junction capacitance expression with free electron tunnelling 3-44148
 Schottky barrier, capacitance freq. depend., deep impurity effects 3-64405
 Schottky barrier, I-V characs., image force and tunnelling effects (Russian) 3-41266
 surface barrier structure, semicond. impurity centre parameter determ. from relax. of reverse current 3-50267
 tunnel effect, phonon contrib., pot. fluctuations (French) 3-44150
 V-I characteristics, non-diffusion theory, with space charge limited current (Russian) 3-72403
 Al-Si contacts, resistivity inhomogeneity meas. spreading resistance method 3-41258
 Au-CdS, field induced absorption 3-64406
 Au-Si, mass spectrometric studies of interface contamination 3-41264
 Be-Se, barrier heights, surface density of states, Fermi level location (Rumanian) 3-64395
 CdS epitaxial layer, ohmic contacts using evap. Al film 3-52900
 CdS-Al barriers, junction tunnelling 3-44147
 CuInSe₂, rectifying contact, doping levels and band diagrams detn. 3-46844
 GaAs, alloying and annealing behaviour of evaporation Au-In layers, channelling effect technique 3-41674
 GaAs, low resistance contact using sequential deposition of Ag and Sn (Russian) 3-52899
 GaAs, potential barrier formation, mirror image force effects (Russian) 3-72401
 GaAs, rectifying barrier props., energy diagrams (Russian) 3-75791
 GaAs-Al alternating film growth, mol. beam epitaxy 3-61108
 GaAs-Au, Schottky barrier, electroreflectance spectra at GaAs discrete and continuum exciton states 3-55640
 n-GaAs-Au surface barrier structure, impurity centre parameter determ. from relax. of reverse current 3-50267
 GaAs-CrAu, transparent Schottky contact, near bandgap photolum. of n-GaAs:Se 3-44450
 GaAs-metal, energy structure, Schottky barrier height, Fermi level 3-60916
 n-GaAs-Sn nonrectifying contact, resist. obs. 3-75793
 GaAs_{1-x}P_x-metal contact carrier density determination, reverse biased junction comparison with R_h values 3-46843
 n-GaP, Au-Ni ohmic contact, current and temp. depend., activation energy 3-46892
 GaP-Au, Schottky barrier, wavelength modulated photovoltage spectra 3-55618
 n-InP-Au Schottky barrier, elec. props. and appl. to majority carrier conc. determ. for n-InP 3-52898
 Pt-Si contact, heat-treated, interface struct., solid state reaction kinetics 3-69485
 Pt-Si-Al reaction, electrical and mechanical features 3-64403
 SbS₃-metal photoconducting film, work functions, contact types 3-46893
 Si, photostimulated adhesion of Al, I-V charact. studies 3-75792
 p-Si-Au, high resistivity, compensated, bound space charge 3-58270
 n-Si-metal, electron energy distrib. rel. to current 3-79768
 VO₂, passage of current across semicond.-metallic phase boundary 3-44149

semiconductor-metal boundaries continued

- Zn-Se, barrier heights and surface state density (Rumanian) 3-64395

semiconductor properties see semiconductors

semiconductor storage devices

- chalcogenide glass diode, threshold and memory switching mechanisms, electron microscope obs. 3-55318
 m.n.o.s., discharge mechanisms at applied voltages and elevated temps. 3-55342
 m.n.o.s. memory, trap centres, thermally stimulated current meas. 3-79774
 m.n.o.s. memory device, discharge at low and zero gate voltages 3-46899
 m.o.s., with SiO₂ films prep. by SiH₄-H₂O system, memory performance 3-46896
 ZnTe film, memory switching device 3-68683

semiconductor switches

- amorphous, threshold on-state maintenance, cw bias, temp., freq., and bias interruption effects 3-55313
 chalcogenide glass, temp. depend. of switching 3-79745
 chalcogenide glass diode, threshold and memory switching mechanisms, electron microscope obs. 3-55318
 n-p-i structure, negative-resistance, temp. dependence of parameter spread (Russian) 3-44137
 thin film coplanar device, static characts., theory 3-79748
 time interval deviation measurement, nanosecond 3-73670
 TL150 ultrathermostat, contactless heater switch 3-70279
 Ge₃₀Te₃₀As₄₀, T-L type package, design and performance 3-55316
 SiTeAsGe film, injection processes and switching characs. 3-55317
 VO₂ coplanar switching devices, pulse response theory 3-79747
 ZnTe film, memory switching device 3-68683

semiconductor theory see semiconductors

semiconductor thin films

- acoustoelectric amplification, of surface waves in semicond.-piezoelectric layered medium, numerical soln. 3-68680
 amorphous, growth instabilities in deposition, voids 3-55173
 amorphous, holographic recording of information 3-74212
 chalcogenide glass thin amorphous films, reversible switching 3-60908
 coplanar thermal switching, static characts., theory 3-79748
 double injection and field ionisation, in current jump region (Russian) 3-52852
 electrical conductivity, effect of intervalley scattering on dimensional effect 3-55257
 electron probe microanalyser, cathodoluminesc. attachment 3-42704
 elemental, prep. and props., review 3-76146
 epitaxial and diffused layers, meas. methods for resistivity and doping profiles (Czech) 3-72814
 epitaxial layer, thickness meas., computer approx., interference pattern 3-41667
 epitaxial layer doping profile, Schottky barrier CV characs. obs. (Polish) 3-69161
 excitons, non-localised, scattering on phonons (Russian) 3-58088
 graphite, free film, electron inelastic scatt., fast secondary electrons 3-76117
 growth and application (Croatian) 3-58596
 III-V semiconductor thin films, molecular beam epitaxy 3-72812
 IV-VI compounds, epitaxial, preparation methods and properties 3-58603
 laser radiation, heating regime, steady and transient temp. field calcs. (Russian) 3-40277
 laser radiation damage, 10 μm hole formation (Russian) 3-69110
 optical absorption edges, quantum mech. broadening 3-41537
 optical density, detn. on transparent substrate 3-75958
 oxidation, logarithmic rate law 3-41101
 poly(N-vinylcarbazole) films, cond. and photocond., carrier generation processes 3-52873
 polyethylene terephthalate, carrier mobility measurement by electron beam bombardment 3-50209
 polyvinylcarbazole:trinitrofluorenone, amorphous, absorption and electroabsorption spectra 3-61049
 resistance of thin films on different dielectric backing, four-probe method 3-55269
 Schottky-emission-dominated dielectric breakdown evidence 3-44373
 semimetals, three dimensionally quantised, carrier density and mag. props. 3-58263
 stress determ. using automatic Bragg angle control 3-41669
 thermal switching and breakdown rel. to law of electrical conductivity 3-60877
 thickness meas. from lattice absorption bands 3-56616
 waveguiding layer, piezoelectric crystals, amplification of surface waves 3-64605
 Sb_{1-x}Se_x amorphous films, reflectivity spectra, electronic structure 3-64754
 Ag₂S, structure and properties (Rumanian) 3-64417
 Ag₃SbS₃ single crystals and amorphous films, light absorption, band structure 3-64679
 Ag₂Se-Se, heterojunction, switching phenomena and memory effect 3-79749
 Al_{1-x}Ga_xAs, cathodoluminescence, electron probe microanalyser 3-42704
 AlN, epitaxial film growth and piezoelec. props. 3-80189
 Al₂O₃ electrochem. obtained, thermolum., emission centres activation energy 3-47320
 Ar₂O₃, between alkali halide discs, i.r. and Raman spectra, surface interaction effects 3-64638
 As-S, amorphous, photographic effects, 77 and 293 K, interpretation 3-69015
 As-Te-Si-Ge, chalcogenide glass film, recovery of switching voltage 3-64390
 As₂S₃, thin film growth by laser sputtering, mol. comp. of condensate vapours 3-55176
 As₂S₃:Ag, amorphous, photodoping, photovoltage obs. 3-58302
 As₂S₃-Ge glasses, amorphous film, absorpt. edge depend. on comp. 3-64701

semiconductor thin films continued

- As₂S₃-Ge_x amorphous film, annealing and temp. influence on absorpt. edge 3-72673
- AsSe, glassy, transient s.c.l.c., mobility detn. 3-58268
- AsSe, thin film growth by laser sputtering, mol. comp. of condensate vapours 3-55176
- AsSe, with Ag electrodes, negative photocurrents 3-58306
- As₂Se₃, amorphous film, photocond. in visible and X-ray regions 3-44112
- As₂Se₃, thin film growth by laser sputtering, mol. comp. of condensate vapours 3-55176
- As₂Se₃ thin films, preparation method for high induced conductivity 3-69182
- As₂Se₃, amorphous, Poole-Frenkel effect in d.c. cond. meas., memory switching 3-41242
- As₄₀Se₆₀Ge₁₀, amorphous, a.c. conductivity, heat treatment and light irradiat. effects 3-68620
- As₂Te₃ film, amorphous, electron diffr. exam. (Russian) 3-46772
- Bi, elec. props. and struct. 3-64267
- Bi, epitaxial, struct. anal. 3-52761
- Bi, galvanomagnetic properties, influence of structure defects 3-75761
- Bi, optical const., determ. by ellipsometry 3-64621
- Bi, thermoelec. power, quantum size effects (French) 3-55293
- Bi, transport props. and struct., influence of polymer powder substrate temp. 3-50091
- Bi film, quantum temp. size effect, temp. depend. of thermal expansion 3-72212
- Bi films from 180 to 40000 Å, meas. of electrical props. 3-41243
- Bi on BeO substrates, resistivity variation with temperature 3-52913
- Bi semimetal, electrical conductivity thermoelectric power, grain boundary theory, grain size de Broglie wave (French) 3-46910
- Bi thin films partial superposition of Te thin films, microrelief appearance (French) 3-52769
- Bi₂O₃ anodic films, photoconductivity 3-50236
- Bi₁Sb_{1-x}, thermoelec. power, quantum size effects (French) 3-55293
- (BiSb)₂Te₃, elec. cond. and thermoelec. power, effect of mech. stresses 3-61123
- Bi₂Te₃, resistivity, composition and Hall coefficient measurement 3-41279
- C, temp. depend. elec. resist. 3-68606
- CaS, electronic states and optical props. from u.v. reflectance spectra (Russian) 3-76014
- Cd₃As₂, electron mobility meas. for fast thermal detector use 3-68651
- Cd₃As₂, evap. onto dielec. substrate, elec. props. (Russian) 3-52843
- Cd₃Hg_{1-x}Te, elec. props. and cryst. struct., temp. depend. (Russian) 3-72359
- Cd₃Hg_{1-x}Te, epitaxial, optical and elec. props. 3-58188
- Cd₃Hg_{1-x}Te preparation, deposition of HgTe onto CdTe, isothermal conditions, new method 3-53189
- Cd₃Pb_{1-x}Te, struct. and elec. props., effect of deposition conditions 3-64265
- CdS, electron irradiation effect on crystalline struct. 3-52771
- CdS, epitaxial, optical and elec. props., rel. to suitability for use as transparent electrode 3-64330
- CdS, evaporated, elec. resist. rel. to thickness 3-46908
- CdS, frozen-in X-ray cond. 3-44117
- CdS, optical absorpt. edges, quantum mech. broadening 3-41537
- CdS, sintered, prod. of high mobility photosensitive layers (Russian) 3-72818
- CdS, surface morphology, substrate effects, transverse field effect on elec. cond. (Korean) 3-72356
- CdS platelets, growth mechanism 3-43965
- CdS resistivity, rel. to exorption of boat material and superimposed oxide dielectric film 3-46911
- CdS:Bi, ion implanted, photocond., dose level and post annealing effects 3-50244
- CdS:Na(K)(Li)(Cs), polycryst. film, photomemory effect 3-41232
- CdS-Ge (fused quartz) film-substrate systems, transverse normal waves (Russian) 3-41080
- CdS-Te alloy thin films, energy gap variations and struct. phase changes 3-76028
- CdSe, chemical deposition using selenurea as depositing agent 3-58605
- CdSe, photoconductive, field quenching, conduction electron mobility using Hall effect, illumination and field depend. 3-46873
- CdSe, polycryst., Hall mobility meas., influence of applied elec. field (Polish) 3-68609
- CdTe, evaporated obliquely in high vacuum, anomalous photovolt. effect, thickness effects 3-75774
- CdTe, mech. stress changes caused by photostimulated adsorption of O₂ 3-50095
- CdTe epitaxial growth on Ge substrate, electron beam evaporation, structure and orientation 3-43957
- CdTe exhibiting anomalously high photo-e.m.f., anomalous Dember effect 3-75770
- CdTe:Se layers, recrystallized, electron capture processes (Russian) 3-50235
- Cu₂Se, struct. and elec. cond., tetragonal to cubic phase transition (Russian) 3-75688
- Eu_{1-x}Gd_xS, elec. and ferromag. props. 3-41381
- EuO, optical absorpt. and photocond., mag. order effect 3-55307
- EuS, growth, electrons diffr., absorpt. spectra, stability 3-75689
- n-Ga_{1-x}Al_xAs, epitaxial, variable gap, elec. cond. 3-79693
- GaAs, analysis of epitaxial layers using MeV α-particles 3-53196
- p-GaAs, epitaxial, acceptor states, far i.r. extrinsic photoconductivity obs. 3-64299
- GaAs, epitaxial, cathodolum. correlation with electron mobility 3-60874
- GaAs, epitaxial, from Me₃Ga and AsH₃, Hall effect and photolum. 3-79713
- GaAs, epitaxial, high-resist. layer, elec. props. 3-41225
- GaAs, epitaxial, nomogram for conversion of Hall mobility to ion scatt. limited mobility 3-44158
- n-GaAs, epitaxial, recomb. processes near surface, photocond. and photomag. effect obs. 3-75756

semiconductor thin films continued

- n-GaAs, epitaxial film, surface sensitive effect at 20K, carrier depletion 3-60912
- GaAs, epitaxial film growth and piezoelec. props. 3-80189
- GaAs, epitaxial submicron, for f.e.t. 3-41625
- GaAs, epitaxial overcritically biased, potential profile 3-46848
- GaAs, homoepitaxial, influence of substrate treatment on electron and impurity distrib. (Russian) 3-50663
- GaAs, surface morphology of layers grown by liquid phase epitaxy, photomicrograph studies 3-68513
- GaAs, vapour deposition on sapphire 3-80184
- GaAs amorphous film, far i.r. absorption 3-68988
- GaAs epitaxial waveguide with corrugation feedback, laser oscill. 3-66844
- GaAs film on substrate, props. of surface polaritons 3-58505
- GaAs films, epitaxial growth, effect of substrate orientation on growth rate in (111)-(100) range (Russian) 3-64255
- GaAs thin film, Raman scatt. from surface polaritons 3-58504
- GaAs thin films, glow discharge optical spectroscopy for chemical analysis 3-42705
- Ga_{1-x}In_xP, epitaxial, 0.3 < x < 1, photolum. 3-76075
- GaN, epitaxial film growth and piezoelec. props. 3-80189
- GaP, vapour growth method using single flat temp. zone 3-64775
- GdP, noncryst., spin polarized photoelectron emission, multiparticle effect (German) 3-50644
- Ge, amorphous, cond. band, secondary emission and photoemission modulation spectra 3-55188
- Ge, amorphous, photoelec. props. 3-64380
- Ge, amorphous, reduced intensity function and structure factor for diamond cubic, amorphon, and random network models 3-64262
- Ge, amorphous, refl. and electrol. spectra 3-55550
- Ge, amorphous, structure study by electron diffr. 3-63937
- Ge, density of state changes at amorphous-cryst. transition, photoemission obs. 3-43987
- Ge, epitaxial, RHEED investigation 3-41105
- Ge, epitaxial film, preparation of samples for galvanomag. meas. by Van der Pauw method 3-76139
- Ge, obliquely film, signal reversal of anomalous photovoltaic effect 3-79730
- Ge, replicated on flexible organic substrate, for stress and thermal energy transducers 3-56615
- Ge, smooth epitaxial growth, iodide method, diffusive mass transfer 3-76144
- Ge, sputtered amorphous, velocity of propag. in shock crystn. 3-58190
- Ge amorphous, defect elimination, resistivity measurements, crystallisation, structure models 3-52767
- Ge amorphous, semiconducting to metallic phase transition, pressure induced, low temp. superconductivity 3-50247
- Ge amorphous, structure change in annealing process 3-68410
- Ge amorphous film, elec. cond. and struct. 3-50281
- Ge amorphous film far i.r. absorption 3-68988
- Ge epitaxial films on GaAs and Si, film morphology, growth process, high energy electron diffraction 3-46767
- p-Ge layers, on unoriented substrates, elec. cond. and Hall effect (Russian) 3-50204
- Ge thin film, vapour deposited and ion implanted, scanning electron diffraction obs. 3-58189
- Ge thin films, energy spectra of transmitted electrons 3-49812
- Ge:Sb, amorphous electrical conductivity, freq. depend. in range 20 Hz to 26 GHz 3-58273
- Ge/Al films, evaporated, kinetics of crystallisation processes 3-43967
- GeSe amorphous film, Poole-Frenkel conduction mechanism 3-55276
- Ge_{1-x}Si_x, electrol. spectra 3-76020
- GeTe(Se), amorphous thin film, change in sp. conductivity and structure under pulse-heating (Russian) 3-52865
- In₂Ga_{1-x}As films, epitaxial growth, effect of substrate orientation on growth rate in (111)-(100) range (Russian) 3-64255
- In_{1-x}Ga_xP vapour growth, p-n junction electroluminescence characts. 3-58599
- In_{1-x}Ga_xP vapour growth technique, p-n junction electroluminescence 3-58598
- InP, growth on substrates, struct. anal. 3-72286
- InSb, Corbino magnetoresist., fields up to 20 kG 3-41213
- InSb, prep. and appl. to bubble domain devices 3-80187
- InSb Hall effect bubble domain detector 3-47110
- p-InSb:Cu, negative magnetoresist., localised mag. states model 3-41209
- InTlS₂, struct., electron diffr. obs. 3-75693
- MgF₂, elec. cond. mechanisms (French) 3-46909
- PbS, epitaxial, thermorefectance spectra from 0.7 to 5.6 eV 3-55622
- PbS, epitaxial film, micromorphology, dome-shaped growth figures 3-75687
- PbS, formation of photographic images 3-58810
- PbS, physically treated, role of surface complexes in photosensitivity 3-79734
- PbSe, epitaxial, thermorefectance spectra from 0.7 to 5.6 eV 3-55622
- PbTe, electron irradiation effect on crystalline struct. 3-52771
- PbTe, epitaxial, thermorefectance spectra from 0.7 to 5.6 eV 3-55622
- PbTe, prep. by closed vol. method, thermoelec. and elec. props. 3-60873
- Pbs, with adsorbed O₂, anomalous adsorpt. hysteresis of photocond. 3-75778
- Sb-Se, amorphous, evaporation, comp. depend. of optical and transport props. 3-68522
- Sb₂S₃ metal contacts, photoconducting film, work functions, contact types 3-46893
- SbSI crystallization thin layers, heat-dissipation, temp. fluctuation effects 3-72289
- Se, amorphous, electronic states model for band gap using cond. and photocond. obs. 3-58200
- Se, amorphous, photocond., influence of long-lived traps pot. function parameters 3-75781
- Se, glass, crystalline, liquid, vapour reversible transformations, electron beam induced 3-72006

semiconductor thin films continued

- Se, glassy, transient s.c.l.c., mobility detn. 3-58268
 Se, Hg activated, U-centre potential barrier shape 3-58303
 Se, photocrystallisation of amorphous solid, differential thermal anal. (French) 3-75624
 Se, sputtered vitreous, Monte Carlo model of atomic arrangement 3-64264
 Se, vapour-phase epitaxial growth on (1010) cleavage surface of Te 3-80182
 Se growth on Te crystal planes, non-symm., epitaxy 3-68516
 Se polariser, transmission and degree of polarisation 3-73724
 Se-As(0.24 at.%As), atomic arrangement, fast electron energy losses rel. to optical consts. 3-72288
 Si, amorphous, optical and elec. props., model for effect of voids 3-68629
 Si, amorphous, photoelec. props. 3-64380
 Si, amorphous and crystalline, impurities and ion clusters, mass spectra analysis 3-69170
 n-Si, carrier redistrib. between valleys due to size effect 3-75760
 Si, chem. deposited, effect of deposition conditions on struct. 3-41112
 Si, deposition on Be(0001) surface, LEED obs. 3-68521
 Si, epitaxial, on sapphire, with microsec. carrier lifetime 3-41623
 Si, epitaxial film, oblique slice fabrication, etching technique 3-43945
 Si, epitaxial film, thermal e.m.f. meas. 3-45526
 Si, epitaxial thin film, resistivity and Hall e.m.f. meas., distribution of resistivity, conc. and mobility 3-45527
 Si, epitaxially grown from SiH₄-H₂ and SiH₄-He mixtures, comparison 3-41626
 Si, optical interference phenomena, reflectivity vs. wave number curves 3-58488
 Si, refractive index and dangling bonds 3-76109
 Si, vapour deposition, semiconductor devices, single crystal and polycryst. films 3-41656
 Si, vapour deposition, thin polycryst. layers, epitaxy, kinetics of growth, doping 3-41652
 Si amorphous film-electrolyte interface, photovoltaic effect, mobility gap obs. 3-52867
 Si epitaxial film, preparation of samples for galvanomag. meas. by Van der Pauw method 3-76139
 Si epitaxial films, error analysis of thickness measurement by interference of i.r. rays 3-61985
 Si homoepitaxial, defects, electron microscopy, formation processes 3-52765
 Si homoepitaxy with ion sputtering, growth mechanism 3-44550
 Si:B, polycryst. films, effect of doping on growth, microstructure and elec. props. 3-41657
 Si:B, polycryst. films, elec. cond., effect of growth from SiH₄, carrier conc. 3-41658
 Si:B film, chemical vapour deposition, 300 to 550°C 3-80180
 Si:B films, low temp. CVD, struct., elec. and opt. props. 3-80193
 Si/Ag films, evaporated, kinetics of crystn. 3-43967
 SiC, surface film etching, chemical and discharge treatment (Russian) 3-68509
 SiC, thin film structure, morphology and growth on silicon substrate (Russian) 3-68515
 Si₂Ge_{1-x}, epitaxy on Ge, by simultaneous thermal decomp. of SiH₄ and GeH₄ 3-41627
 SiO, elec. cond. mechanism, metallic impurities influence (French) 3-50199
 SiO₂, grown in Cl₂ and HCl atmosphere, Cl profile 3-41643
 Si₃Te₂, amorphous sample, optical and electrical props. 3-58556
 SiTeAsGe, injection processes and threshold switching characs. 3-55317
 Si(001)/Al(011̄2) films, anisotropy in electrical props. 3-41269
 SnO₂, prep. by vapour deposition, elec. props., chemical composition depend. 3-44073
 SnO₂-CdSe n-n heterojunction, elec. and optical props. (Korean) 3-72399
 SnO₂-CdSe-CdS n-n double heterojunction, elec. and optical props. (Korean) 3-72399
 SnTe, epitaxial, thermoreflectance spectra from 0.7 to 5.6 eV 3-55622
 Ta₂O₅ anodic film, elec. cond., rectification, transport processes and electronic struct. 3-46839
 p-type Te, evaporated films, resistivity meas., strain sensitivity 3-41278
 Te, optical absorption between 39 and 250 eV 3-58522
 Te, photoelec. effects, temp. depend. of elec. resist. 3-64368
 Te, resist., Hall coeff. and thermoelec. power, 78-450 K 3-41187
 Te thin films, partial superposition of Bi thin films, microrelief appearance (French) 3-52769
 Te₈₁Ge₁₅As₄ amorphous, laser induced crystallisation, writing-in 3-70839
 TiSbS₂, structure and some electrophysical props. (Russian) 3-79588
 VO₂ coplanar switching devices, pulse response theory 3-79747
 V₂O₅ resistor, low energy laser pulse calorimeter applic. 3-53918
 ZnO, prep. by cold plasma condensation, growth kinetics (French) 3-52772
 ZnO thin layers as u.s. transducers, prep. (German) 3-53193
 ZnO-rhodamine B, dye sensitised, photoresponse, self-quenching effect 3-46871
 ZnS, dielec. props., temp. and freq. depend., 78-380 K and 10²-10⁵ Hz 3-41474
 ZnS, in h.f. sputtered metal/ZnS/metal struct., dielec. characts. (French) 3-58474
 ZnS, on Sb substrate, thickness and dispersion meas., ellipsometric method 3-62049
 ZnS, piezoelec., surface elastic wave motion computer analysis (Japanese) 3-41482
 ZnS heteroepitaxial film on GaAs, leaky wave propagation 3-41597
 ZnS:Cu,Cl, Franz-Keldysh effect in electroluminescence 3-80114
 ZnS:Er³⁺, electrolum., impact excitation by hot electrons 3-80111
 ZnS:Mn, Cu, Cl, electroluminescent, electron diffraction study of Cu-rich layer 3-47315
 ZnS:Mn, ion implanted, for electroluminesc. cell fabrication 3-41588

semiconductor thin films continued

- ZnSe heteroepitaxial film on GaAs, leaky wave propagation 3-41597
 ZnTe, electron irradiation effect on crystalline struct. 3-52771
 ZnTe, frequency dependence of electrical conductivity 3-64364
 ZnTe, non-polarised memory switching characts. 3-68683
 ZnTe thin films on GaAs, InAs and GaP, epitaxially grown heterodiodes 3-44138
 ZnTe vacuum evaporated film conductivity rel. to substrate temp. (20 to 440°C) and ambient atmosphere 3-58324
- semiconductors**
Generalities and properties of unspecified materials only. For specific materials see semiconductor materials.
see also crystal electron states; photoconductivity; photovoltaic effects; semiconductor devices; tunnelling
 absorption coeff. of 1s-2p line of deep impurity centres 3-64700
 antiferromagnetic, thermoelec. power near Neel temp., calc. 3-68655
 bounded, theory of size effects, review 3-58253
 carrier diffusion in strong elec. fields 3-72366
 carrier distrib., nonequilib., ambipolar equation 3-60882
 carrier lifetime, steady-state recombination conditions 3-44090
 carrier lifetime measurement, in p-n structure 3-64336
 carrier lifetime measurement, photoconductive decay time obs. 3-50243
 carrier mobility and density distrib., inhomogeneous layer, van der Pauw method 3-58269
 carrier mobility of Esaki superlattice 3-46830
 carrier multiplication processes with equal ionisation rates under high field, statistics (Russian) 3-64341
 carrier recombination, in space-charge region 3-60883
 cathodoluminescence in direct gap semiconds., temp. variation 3-72761
 channelling effect technique for examination 3-41674
 compensated, impurity photocond., influence of double optical transitions 3-75772
 compensated, spatial charge exchange waves and thermoelec. current instability 3-64349
 compensated, with high impurity conc., atomic cyclotron reson. line width 3-44309
 compound semiconductors, analysis of backscattering spectra 3-61089
 crystal orientation, determination using He-Ne laser 3-68183
 crystalline and amorphous, reson. aspect of chem. bonding 3-50128
 cubic, Debye temperatures and Lindemann-Gilvay melting law 3-75587
 cubic, two-photon absorpt. and optical orientation of free carriers, theory 3-54245
 current operator definition, application to Hubbard model 3-55255
 cyclotron reson. linewidth in quantum limit with high field anisotropic shielding 3-44014
 cyclotron-phonon conductivity oscillations 3-58255
 cylindrical, degree of uniformity calc., elec. cond., four-probe method 3-42599
 deep centres, photoionization section, formula (Russian) 3-79641
 deep levels, detection, method based on high-field domain generation 3-58232
 defect parameter validity based on computer analysis of temp. dependence of Hall meas. (Russian) 3-68648
 degenerate, diffusivity-mobility ratio temp. and doping dependence 3-68612
 degenerate, diffusivity-mobility ratio rel. to spontaneous emission linewidth 3-72699
 degenerate polar, superconductivity, theory 3-41293
 degenerate semiconductors, calc. of piezomodulation parameters 3-55548
 dichroism and optical anisotropy of media with oriented spins of free electrons 3-64632
 disordered, electroabsorption coeff., calc., random fields produced by charged impurity centres (Russian) 3-68603
 disordered, hopping conduction, effect of electric field and temperature gradient 3-64333
 donor magneto-optical spectra, inhomogeneous line broadening 3-50558
 doped, l.f. impurity pair cond. 3-52840
 double injection and field ionisation, in thin layer in current jump region (Russian) 3-52852
 dynamic screening of oscillating charge centres by free charge carriers (Russian) 3-64325
 Einstein relation, generalised, approximation for solution 3-68627
 electrical cond. in strong elec. fields, e.s.r. effects 3-72367
 electrical conduction, influence of strong e.m. wave (Russian) 3-44106
 electrical conductivity, static, of doped semiconductors (Russian) 3-68610
 electrical conductivity of disordered materials, 'inhomogeneous regime' theory 3-58262
 electroabsorption for elec. field profile determ. 3-55645
 electron charge density calc. 3-50105
 electron conc. rel. to quantising mag. field 3-41206
 electron distribution function and current, semiconductors with superlattices, theory 3-75750
 electron gas, heating and cooling by e.m. radiation in quantising mag. field 3-72303
 electron kinetic equation in strong electric field, Green's resolvent (Russian) 3-68632
 electron plasma, Einstein relation in quantising mag. field 3-68660
 electron plasma, quasilinear relax. in strong mag. field 3-58296
 electron scatt. by optical phonons under recomb. instability conditions 3-64350
 electron spin relaxation, meas. by optical pumping 3-68845
 electron-hole 'liquid' drops 3-72339
 electron-hole degenerate plasma, magnetoresist. 3-44097
 electron-hole plasma, Kadomtsev-Nedospasov helical instability in strong pinch effect 3-75764
 electronic spectrum, influence of extended defects 3-55223
 electoreflectance, excitonic effect, t-matrix theory 3-72598
 electoreflectance of bound excitonic states 3-55641
 e.m. wave interactions, nonparabolic cond. bands 3-72377

semiconductors continued

- energy diffusion equation in hot electron problems, polar optical phonon distrib. 3-58275
- equilibrium disperse phase containing metallic particles, electronic structure 3-60861
- equivalent diffusion effect, due to dielec. relax. effect 3-64323
- exciton, Wannier-Mott, in non-polar semicond., binding probability of free electrons, holes 3-58235
- exciton excitations, layer crystals, Van der Waals interaction, energy spectra 3-50155
- exciton-polariton interaction with charged impurities 3-55228
- excitons, Bose condensation, in strong mag. field 3-75726
- excitons, bound complexes, review (*Polish*) 3-58236
- excitons bound to defects, binding energy, theoretical review 3-50160
- excitons bound to neutral acceptors in direct-gap semiconds., transition line strengths 3-44044
- Faraday rotation, hot electron, in semicond. with non-parabolic energy bands 3-64630
- Fermi energy depend on temp. in doped semiconductors, computer calc. for students 3-66117
- ferrimagnetic semiconductors, current carriers and electron impurity centres, weak interaction 3-52987
- four point probe measurement, correction devisors, cylindrical coordinates 3-68619
- frozen (metastable) conductivity, theory using generalised barrier model 3-68602
- galvanomagnetic surface recomb. depend. on field electrode pot. (*Russian*) 3-55287
- galvanothermoelectric effects, low temp., theory 3-75759
- gapless with acceptor levels, S-shaped current-voltage charact. 3-44079
- generation-recombination meas. by m.o.s. capacitor nonequilibrium current 3-44089
- Hall and drift mobility in polar p-semicond., appl. to ZnTe(Se), CdTe 3-79716
- Hall and drift mobility in polar p-semicond., theory 3-79715
- Hall coeff. determ. with non-symm. arrangement of 4-probe gauge (*Russian*) 3-75757
- Hall effect, apparatus for high temp. meas. 3-42604
- Hall sample, field pattern calc. using conformal mapping 3-55290
- heavily doped, hopping conduction, temp. depend. 3-58267
- high field conduction, quantum transport theory 3-68635
- high field domain mode, carrier concentration effects 3-68633
- highly degenerate, diffusivity-mobility ratio determ. at low temp. by meas. of wavelength shift with cavity Q junction lasers 3-68605
- highly degenerate, low temp. diffusivity-mobility ratio, junction laser linewidth obs. 3-44069
- highly excited, experimental aspects, review 3-50158
- highly excited, theoretical aspects, review 3-50159
- highly resistive, drift mobility meas. (*Polish*) 3-58261
- hole and electron traps, energy levels and density, determ. from capacitance meas. 3-64300
- hopping conduction, in strong elec. field, theory 3-50217
- hot electron noise, calc. 3-41199
- III-V and II-VI nonlinear optical props., simple molecular orbital theory 3-48940
- impurities, limit solubility determ., temp.-gradient fusion zone method 3-44543
- impurity absorption, theory for materials with complicated band struct. 3-58537
- impurity centre parameters, determ. from relax. of reverse current in surface barrier structs. 3-50267
- impurity states calcs. using screened local pseudopotential 3-44035
- injection-field effect in semicond. with deep impurity levels, negative resist. region 3-64351
- inorganic, Wannier excitation, classical ion-electron interaction energy calc. 3-79264
- intra-band light absorption, by free carrier interactions 3-50597
- intrinsic size-quantized semiconductor, energy spectrum in presence of strong e.m. wave 3-75762
- ionisation coefficients, nonlocalised property 3-58256
- isotropic model, biexciton dissociation energy and binding energy, theorem 3-46816
- isotropic model, elastic, inelastic and symm. carrier scatt. steady-state kinetic coeffs. (*Russian*) 3-55254
- Kinetic diamagnetism and paramagnetism in the presence of illumination 3-75777
- Knight shift in multivalley semicond., hyperfine coupling const. determ. for PbSe(Te) 3-44342
- Knight shift theory in multivalley semicond., spin-orbit interaction and relativistic effects 3-44341
- laser beam propagation in semiconductor under two photon resonance conditions 3-48950
- laser radiation, high power, superconducting transition 3-50290
- lattice dynamics, model analyses, review 3-72142
- layer inhomogeneous, impurity effects on carrier mobility 3-52847
- layered structure, photovoltaic effect, potential distrib. at arbitrary illumination, calc. 3-55301
- light absorpt. in periodic semicond. structures 3-61058
- light scatt. on sound near plasma freq., refl. light diffr. 3-55547
- local vibrations, damping caused by reson. interaction with plasmons, theory 3-55297
- magnetic, carrier autolocalised fluctuation states 3-46810
- magnetic, equations of motion for electron spin and trajectory 3-44093
- magnetic, NaCl type lattices, structural disorder, photoelectric measurements 3-52951
- magnetic noncrystalline, spin polarized photoelectron emission, multi-particle effect (*German*) 3-50644
- magnetically active semicond. plasma, nonpot. surface waves along semicond.-vacuum boundary 3-44132
- magnetoabsorption, multiphonon, equiv. to perturbation theory 3-44400
- magnetophonon oscillations, discontinuities 3-44096
- magnetoresistance of many-valley semiconds., size depend. 3-64355
- many-valley crystals, polarons, theory 3-75727
- measurement of electrical properties (*Czech*) 3-52864
- melting, electron processes 3-75609

semiconductors continued

- mixed semiconductors, band theory, graded band-gap, effective mass (*Polish*) 3-41134
- mobility measurement, Hall effect obs., sample geometry effects 3-55261
- modulation spectra, final-state interactions, excitons effect, electroabsorpt. 3-55637
- modulation spectroscopy under uniaxial stress, review 3-55642
- multiphoton ionisation, in the presence of impurity levels 3-64373
- n-type, electrooptical effect due to virtual interband transitions 3-55554
- negative affinity, photoemission, theoretical problems, review (*French*) 3-41611
- negative differential mobility, current instabilities in long samples 3-41201
- negative differential resist. controlled by photoinjection from metal contact 3-60881
- negative electron affinity photoemitter, physical model 3-47343
- negative magnetoresistance theory for semicond. with impurity bands (*French*) 3-58281
- non-ohmic transport (*Korean*) 3-72365
- nondegenerate, influence of linear and point defects on hypersonic attenuation by free carriers 3-55310
- nonequilibrium photoelectrons, collective relax. in quantized mag. field 3-75782
- nonparabolic, method for estimation of effective mass band gap 3-52791
- nuclear average effective charge in tetrahedral semiconds. 3-79265
- optical absorpt. by impurities, linewidth, elec. field effect 3-44444
- optical and elec. props., doped semicond. in strong e.m. field 3-75765
- optical ionisation of deep centres in compensated semiconds., effective error section 3-61072
- optical properties of electrons in electric and magnetic fields 3-55560
- periodic structures nonlinear effects 3-64344
- photoconducting, electron component of permittivity, external-pump-induced change 3-58307
- photoconductivity, spectral sensitization (*German*) 3-50233
- photoconductivity and photoelectromagnetic effect, influence of inter-band recombination in presence of deep traps 3-55306
- photoluminescence analysis 3-69180
- photoluminescence band, strong elec. field modification 3-61070
- piezoelectric, combination freq. in nonlinear wave interactions during supersonic carrier drift 3-75784
- piezoelectric, recomb. amplification of sound, theory 3-75783
- piezoelectric, renormalised viscosity for high acoustic flux 3-60904
- piezoelectric, sound attenuation and amplification 3-68676
- piezoelectric crystal, inhomogeneous, u.s. propagation, acoustoelectric interaction, nonuniformities 3-58310
- plasma, carrier heated electron-hole instability 3-41195
- plasma, electron-hole, surface e.m. wave propag. in uniform mag. field 3-64367
- plasma, microwave emission, hydromag. turbulence theory (*French*) 3-68656
- plasma wave amplification by acoustic wave viscous absorpt. 3-44104
- plasma-semiconductor boundary, kinetic reflection coefficient for inelastic electron energy relaxation 3-68663
- plates, thick, classical reson. effect due to Landau damping and Fermi degeneracy 3-41129
- polar, i.r. free polaron absorpt., temp. depend. 3-55591
- polar, uniaxial, influence of spatial dispersion on high-freq. wave props. 3-55294
- polar optical scatt. mechanism for holes 3-68601
- quasi-monopolar, field theory of static VI characs., main approx. (*Russian*) 3-52853
- with quasiperiodic dopant distribution, IV characs., theory 3-58254
- Raman reson. scatt. at critical points 3-53101
- recombination waves, spectrum and attenuation in h.f. elec. field 3-44103
- relaxation regime behaviour, review 3-55259
- relaxation-case, cond. calc. including diffusion term 3-46853
- relaxation-type, transport processes 3-55273
- resistance measurement, by van der Pauw method 3-42606
- resistivity characterization of crystal ingots 3-41178
- screened exchange contribution to band gap, simple model, dynamic electron-electron interactions 3-41147
- screw instability in three-component electron-hole plasma 3-58293
- self-induced transparency by single-photon excitation by ultrashort light pulse 3-74270
- single carrier model, for wave propagation effects 3-64366
- small band gap semiconductors, collision integrals for high field transport 3-55274
- space charge limited conduction, thermal noise 3-68628
- space charge waves effects on adjacent plasma layers 3-79724
- space-charge-limited current pulse in presence of traps 3-50213
- spin-magneto-phonon resonance and nuclear d.c. polarisation 3-55455
- static cond., effect of acoustic waves 3-44125
- static domain, influence of injection 3-75752
- surface carrier waves, transverse mag. field effect 3-55321
- surface quantisation, review 3-50261
- surface reconstruction, electronic free energy, possible appl. 3-79758
- surface structure of electron-hole droplets 3-60911
- surface topography after Ar ion sputtering 3-61085
- thermo-e.m.f. in applied mag. field, size depend. 3-60887
- thermodynamic compensation law, obs. in elec. cond. of organic and amorphous semiconductors 3-45744
- thermodynamics of hot electron system, phonon temp. gradient 3-55275
- thermoelectric properties, meas. technique 3-60889
- totally depleted, transient photo currents, theory 3-64376
- transferred electron dynamics, Monte-Carlo simulation 3-55280
- transferred electron effect, instabilities, Boltzmann equation soln. 3-44085
- transport in one dimens. superlattice 3-60868
- transverse wave excitation with optical creation of carriers 3-60901

semiconductors continued

- travelling wave amplification and Gunn effect, power flow 3-64345
- two-layer structure, photovoltaic effect, potential distrib. for illumination at one point 3-55302
- uniaxial crystals with zero forbidden band 3-50132
- unipolar conduction, space charge effects 3-64327
- univalley, superadiation responses in combined reson. transitions (*Russian*) 3-69096
- u.s. wave amplification by transverse elec. current prod. hot electrons 3-58309
- wave propagation, through highly restrained solid-state plasma 3-68658
- zero-gap, possibility of negative resist. effects, solid-state oscillator appl. 3-79698
- GaAs, related compounds, conference, Boulder, Colo., USA, Sept. (1972) 3-41678
- GaAs diode laser, stripe geometry, light coupling into optical fibre with spherical end 3-43022
- $\text{In}_{1-x}\text{Ga}_x\text{P}$ heteroepitaxial layer, on GaAs, vapour grown, gas phase stoichiometry effect on elec. props. 3-41683
- InP, donor and acceptor impurities, elec. props. 3-41581

semileptonic decays

- gauge theories with superweak CP violation, $O(4)$ and $O(4) \times G$ groups, distinct intermediate bosons 3-66960
- gauge theory of Bars, Halpern and Yoshimura, use of spin-zero hadron field 3-62806
- higher-order correction, reln. to high-energy behaviour of lepton-lepton weak scattering amplitude 3-45868
- hyperon, contribs. of second-class currents 3-40333
- $K_1 \rightarrow \pi\mu\nu$, meas. energy level shift $2S_{1/2}-2P_{1/2}$ in $\pi\mu$ atom, determ. pion charge radius 3-66996
- widths, from new form of universality based on ur-citon schemes 3-66962
- $K \rightarrow e\pi\nu$, local action of leptonic action (*French*) 3-51999
- $K \rightarrow \pi\mu(e)\nu$, $(1,8) + (8,1)$ symmetry breaking, soft-pion approach in σ model 3-45867
- $K \rightarrow \pi\mu(e)\nu$, current algebra formalism (*Rumanian*) 3-45860
- $K \rightarrow \pi\mu(e)\nu$, hard-meson $(3, 3^*) + (3^*, 3)$ model, potentialities and applicability conditions 3-48998
- $K \rightarrow \Pi\mu(e)\nu$, hyperbolic metric for bounds on form factors 3-78112
- $K \rightarrow \pi\mu(e)\nu$ form factor, optimal lower bound on quadratic functional integrals using Watson theorem 3-43103
- $K \rightarrow \pi\mu(e)\nu$ form factors, improved optimal bounds for hadronic contrib. using Watson theorem 3-57345
- $K \rightarrow \pi\mu(e)\nu$ scalar form factor, semimonotonic bounds 3-70898
- $K \rightarrow \pi\mu(e)\nu$, study using $\text{SU}_3 \times \text{SU}_2$ light-cone algebra, sum rules and form factors 3-57320
- $K^- \rightarrow e^- \nu \pi^0$, Dalitz pairs for detection of π^0 3-66978
- $K^- \rightarrow \mu^- \nu \pi^0$, Dalitz pairs for detection of π^0 3-66978
- K^0 , evidence for T invariance violation, Bell-Steinberger sum rules in non Hermitian interactions 3-74327
- $K^0 \rightarrow \pi^- e^+ \nu$, time distrib. of three-body decays 3-43085
- $K^0 \rightarrow \pi^+ e^- \nu$, time distrib. of three-body decays 3-43085
- $K^0 \rightarrow \pi e \nu$, test of $\Delta S = \Delta Q$ rule 3-70896
- $K^+ \rightarrow e^+ \pi^0 \nu$, search for rare decay modes in bubble chamber expt., branching ratios 3-70897
- $K^+ \rightarrow \mu^+ \pi^0 \nu$, search for rare decay modes in bubble chamber expt., branching ratios 3-70897
- $K^+ \rightarrow \pi^0 \pi^0 e^+ \nu$, search for rare decay modes in bubble chamber expt., branching ratios 3-70897
- $K^+ \rightarrow \pi^+ e^+ e^-$, decay probability, neutral scalar meson mass (*Russian*) 3-74354
- $K^+ \rightarrow \pi^+ \nu$, search for rare decay modes in bubble chamber expt., branching ratios 3-70897
- $K^{\pm} \rightarrow \pi^{\mp} \pi^{\mp} e^{\pm} \nu$, determ. of low-energy $\pi\pi$ -phase shifts 3-70895
- K_{π} , reln. between $f_1(0)$ and S, D amplitudes in 1^+ decays, Fubini-Furlan method 3-43084
- $K_1^0 \rightarrow \pi^+ \pi^- \nu_{\mu}$, muon polarisation meas. as time-reversal invariance expt. test 3-40334
- $K_1^0 \rightarrow \pi^{\pm} e^{\mp} \nu$, Dalitz plot and contribs. to weak current 3-57321
- $K_1^0 \rightarrow \pi\mu\nu$, form factors meas. 3-54298
- $K^0 \bar{K}^0$ decay via ϕ reson., charge asymmetry 3-52000
- $\Sigma \rightarrow e\nu$, decay rate and branching ratio, $\Delta S = -\Delta Q$ selection rule 3-59954
- $E^- \rightarrow \Sigma^0 \nu (\Sigma^0 \rightarrow \Lambda \gamma)$ β decay, Λ distrib. and polarization 3-70899
- $K^+ \rightarrow \pi^+ \mu^+ \mu^-$, decay probability, neutral scalar meson mass (*Russian*) 3-74354
- $W \rightarrow \mu\nu$ hadrons, single muon spectra in parton model 3-40396

semimetals

- see also *antimony; arsenic; bismuth*
- e.m. generation of sound 3-50540
- excitonic transition in doped anisotropic semimetal 3-75724
- in garnet, laser generated coherent mag. vibrations 3-44396
- magnetic nonlinearity of current dependence on electric field, caused by intrinsic field 3-50190
- magnetosonic waves coupling with longitudinal lattice waves 3-72316
- optoelectric effect in quantizing mag. fields, theory 3-58297
- plasma oscillations, spectrum 3-55296
- plates, thick, classical reson. effect due to Landau damping and Fermi degeneracy 3-41129
- superconductor-excitonic dielec. phase transition 3-75811
- thin films, three dimensionally quantised, carrier density and mag. props. 3-58263
- two-band model, magnetic props. 3-55407

sensing devices see *detectors***sensing devices, electric** see *electric sensing devices***sensing devices, nonelectric** see *nonelectric sensing devices***sensitivity**

- 408 MHz pulsar search with Bologna Cross radiotelescope, sensitivity and results 3-70052
- carbon fibre reinforced plastics skinned honeycomb, by holography 3-39947
- chromatography, flame-ionization, sensitivity coeff., substituted picotines 3-70473
- gas ionisation sensitivity to pressure variation, applic. to transient velocity and pressure meas. 3-49528

sensitivity continued

- global circulation model, predictive capability and sensitivity 3-47745
- interferometer, double sensitivity, by polarisation multiplexing 3-77512
- ionospheric h.f. partial reflection experiment, sensitivity study 3-53557
- microminiature solid state capacitive blood pressure transducer with improved sensitivity 3-42692
- photoelectric methods, for ultra low light intensity meas. 3-45575
- photomultiplier sensitivity, effect of toroidal magnets 3-73563
- Q-switched gas-laser superregenerator, limiting characteristics 3-43008
- radiography, equivalent penetrameter sensitivity, for X-rays and γ -rays in steel 3-65050
- radiointerferometer, calc. of sensitivity (*Russian*) 3-81250
- remote sounding methods, comparison 3-42084
- spectrophotometric analysis, theoretical estimate of accuracy, multi-component systems 3-42702
- strain sensitivity factor, var., strain-gauge resistors 3-73099
- vision spectral sensitivity meas. by flicker threshold procedure 3-70132

sensitivity analysis

- see also *dynamic response; transient response*
- vision, human central fovea, sensitivity variations, eigenvectors, measurements 3-77234

sensors, nonelectric see *nonelectric sensing devices***separation**

- see also *distillation; drying; isotope separation*
- chromatography, using compressed fluids in critical temp. range as mobile phases (*German*) 3-45593
- grains, density separation in liquid 3-73961
- liquid metal alloys, simple mean field approach to phase separation 3-58132
- Hg manometer outlet trap combination of cyclone separator and fibrous filter 3-62036
- Sn minerals, precipitation and separation of single phases, metallurgical products, Sn production 3-50671

series (mathematics)

- atmospheric spherical harmonics series summation, alternative algorithm 3-47758
- Chebyshev, soln. of Painleve differential eqns. 3-70515
- convergence of approximation to function by general finite sums 3-70511
- convergent series expansions solutions, computer programming for algebraic (literal) operations 3-78709
- correlation function, disordered binary alloys 3-72162
- Coulomb field wave functions, power series solution 3-70687
- crack problems, internal, analysis using Laurent series expansion 3-40120
- cylindrical shell, segmental line load, convergence of solution 3-77814
- e.m. boundary-value problems, numerical soln. using zonal harmonic series 3-48833
- equations, Jacobi polynomials, reduced to Fredholm integral equations solution by Legendre-Gauss quadrature formula, appl. to boundary-value problems 3-74000
- expansion of ray theory for sound velocity depth profile in ocean 3-70217
- Fourier, application of Pade approximants 3-62428
- Fourier, divergence, generalisation of Kolmogoroff's theorem 3-40086
- Fourier, for Green's function of water wave, finite depth ocean, circular cylinder internal boundary 3-73263
- Fourier, truncated, computation of Fourier integrals of exponentials 3-71850
- Fourier-Bessel, applic. to thin circular elastic plate in Winkler type foundation 3-66521
- infinite, numerical calc. including asymptotic props. 3-66489
- linearized functions, estimation of the error, and region of applicability (*Russian*) 3-70756
- Neumann series of partial wave Lippmann-Schwinger eqn., summation by Pade approximants 3-62573
- Pade approximants, mathematical theory 3-62425
- Pade approximants, Summer School, Canterbury, England (July 1972) 3-62424
- Pade approximants for vacuum polarization by external field, Stieltjes summability and convergence 3-74362
- power, effects of random errors on convergence of Pade approximants 3-62429
- quasi-linear system, asymptotic reduction (*Russian*) 3-66490
- radial factor in bipolar expansion of $r^{-1/2}$, convergence of series form 3-59780
- saturated liquids spherical solidification, perturbation solutions 3-46702
- stress-deformed finite cylinder, under action of dynamic loads, soln. by series expansion (*Russian*) 3-77825
- sums of integral powers of consecutive integers using combinatorial theory 3-70510
- thin elastic shells, arbitrary edge loads, effect on stress and deformation, asymptotic expansion of tensor eqn. 3-70785
- triatomic molecule, linear, computer appl. to calc. of pot. energy function 3-78710

services, information see *information services***servomotors**

- thyristor servo drive, single-phase reversible, long-duration slow-cycle testing 3-73106

servos see *servomotors***set theory**

- Menger systems, densely embedded left ideals 3-54071
- supermetric props. of mol. structs. 3-71494

sets (mathematics) see *set theory***sferics** see *atmospherics***shadow universe** see *cosmology***shear flow**

- aerodynamic noise emission from turbulent shear layers 3-60534
- axisymmetric free shear layers, stability, jets, wakes 3-75280

shear flow continued

- bentonite-water suspensions structure in shear flow, mechanical props. 3-50794
- bentonite-water suspensions structure in shear flow, optical properties 3-50795
- boundary layer separation at a free streamline, detached downstream shear layers 3-57866
- carboxymethylcellulose soln., flow curve determ., rolling-ball viscometer 3-71688
- computer generated analytic solutions, perturbation solution, liquid droplet suspended in shear flow 3-71834
- convective Couette-Poiseuille shear flow with massive blowing 3-57842
- Couette turbulent flow, wall shear flow 3-60543
- Cross flows in bounded three-dimensional turbulent boundary layers 3-71769
- disperse systems, electroviscous nonaqueous, shear flow in transverse electric field 3-73080
- earth mantle convection in shear flow 3-76646
- elastic sphere transverse motion in a shear field 3-49614
- flow through non-uniform gauze screens 3-57772
- fluctuating flow and heat transfer from vertical surface 3-63682
- incompressible conducting liquid with power law, shear flow in time varying magnetic field (*Russian*) 3-60563
- instability and turbulence transition in layer between 2 streams of different salinities and speeds 3-60531
- jet, plane wall, self-preserving pressure gradient 3-79048
- jets, reattaching shear layer heat transfer 3-52488
- Kelvin-Helmholtz billows, finite amplitude 3-61459
- laminar boundary layer flow with assigned wall shear, numerical solns. 3-49578
- linear spin up, stratified fluid, small Prandtl number 3-75204
- liquid droplet, suspended in linear shear field, bursting and deformation 3-79002
- liquid films, wavy, in horizontal shear flow, convective diffusion 3-57714
- oscillating MHD flows of viscoplastic media in plane channel (*Russian*) 3-57820
- pipe and channel flows, moderately large Reynolds number 3-78954
- planetary boundary layer gravity wave generation by shear instability 3-61458
- planetary boundary layer Richardson number profiles, through instability wave regions 3-61599
- polar fluids, shearing flow, between two rotating coaxial cones 3-71843
- polyacrylamide soln. flow curve determ., rolling-ball viscometer 3-71688
- polyethylene melt, shear and elongational flow, stress-time data, network theory predictions 3-73062
- polyisobutylene solutions, dynamic viscosity and elasticity, effect of steady-state flow 3-71686
- polymer melts, flow between coaxial cylinders under complex shear conditions 3-73048
- polymer melts, shearing flow, anisotropy, second normal stress difference meas. 3-71842
- polymer solutions, normal stress difference meas., cone and plate rheogoniometer, flush-mounted pressure transducers 3-70503
- polymer solutions, reduced drag in turbulent and transient laminar flows near a flat plate 3-63778
- polymers, molten, helical flow, non-Newtonian fluid, cylindrical annulus, shear dependence of viscosity 3-73061
- pulsatile flow in tubes of varying cross section 3-63806
- rotating fluid layer, effect of shear and stratification on the stability 3-52448
- rotating stratified fluid with bottom topography, shear layers 3-44862
- rotation rheometer, voltage meas., during shear flow (*German*) 3-70504
- separated shear layer, inviscid reattachment 3-49591
- slightly stratified shear flow, wave induced distortions, nonlinear critical layer effect 3-43585
- sound waves in ducts, energy, group velocity small damping 3-61938
- spiral motion of a cylinder in a non-Newtonian fluid 3-63672
- stability, non-parallel flow corrections, application to jets and wakes 3-60586
- stably stratified, linear viscous stability theory, review 3-60551
- stratified, internal wave generation in tank expt. 3-63726
- stratified, stability, linear inviscid theory, linear initial value problem 3-63678
- surface flow for predicting crosshatch patterns 3-75216
- suspension, slow viscous shear flow, particle motion, laser obs. 3-40746
- synthetic lattices, rheology, influence of shear rate and temp. 3-69393
- turbulence in stratified shearing flow 3-60533
- turbulent, generation and maintenance mechanisms 3-75194
- turbulent boundary layer, two and three dimensional, velocity profiles, wall shear stress inference 3-63695
- turbulent channel flow for mean turbulent energy closures, asymptotic analysis 3-71747
- turbulent shear flow, mag. field influence (*Russian*) 3-43603
- turbulent supersonic boundary layer flow downstream from 90° corner 3-54811
- two arbitrary sized touching spheres in a linear shear field, creeping motion 3-52486
- two-dimensional free mixing flows, numerical solution 3-63662
- viscoelastic fluid, combined steady and oscillatory flows 3-71832
- viscous flow over solid surface, no-slip boundary condition 3-57771
- vortex shedding from bluff bodies in a shear flow 3-67915
- water surface waves growth rates due to turbulent channel airflow 3-46467

shear strength

- calcium stearate monolayers and multilayers 3-64108
- carbon tetrabromide, plastic props. 275 to 375 K, 320 K polymorphic transform. 3-79407
- composite, C fibre reinforced, interlaminar shear strength under impact conditions 3-55860

shear strength continued

- composite, C fibre reinforced plastics, bulk compressibility rel. to shear strength 3-53277
- composite, C fibre reinforced plastics, shear damage effects on torsional behaviour 3-55856
- composite, CFRP, impact and shear strength, epoxy resin prop. effects 3-76363
- composite, fibre reinforced, nonlinear elastic behaviour 3-55858
- composite, laminated, nonlinear behaviour 3-55869
- composite, shear toughening by stiff fibre reinforcement 3-76355
- composite, unidirectional, in-plane shear stress/strain response 3-55924
- composite, unidirectional, yielding under external loads and temp. changes 3-55865
- composite laminates, post-yielding behaviour, inelastic micromechanics 3-55864
- composite plate, impact resistance 3-73006
- concrete, prestressed, nuclear reactor vessels, loading to failure, stress conditions 3-60271
- dunite, torsional shear strength under near-homogeneous confining stress 3-50959
- dynamic shear modulus determination, thin ribbons, torsional vibration frequency meas. 3-51526
- fibre reinforced thermoplastics, high-strength, improved prod. method 3-69368
- fibreglass, fatigue strength, cyclic strength under shear loading, stress weakening by notches or steps 3-53297
- fibreglass-reinforced composite, fracture possibility under transverse tension and shear (*Russian*) 3-64991
- glass reinforced plastics, interlaminar shear modulus, relation with thermal conductivity 3-80445
- glass-fibre-reinforced polyester resin, Young's modulus, shear modulus, damping, fibre diam. effects 3-47460
- glass-reinforced plastics, resist. to long-term shear failure 3-55873
- granodiorite, torsional shear strength under near-homogeneous confining stress 3-50959
- granular material, friction characteristics on horizontally vibrating plane 3-65042
- graphite fibre/ $\text{Li}_2\text{O} \cdot \text{Al}_2\text{O}_3 \cdot 8\text{SiO}_2$ high strength composites, development and strength props. 3-47458
- Griffiths criterion, allowing for the critical shearing stress (*Russian*) 3-72120
- isogrid, integral stiffened waffle with pattern of 60° triangles 3-59763
- metal and alloy shear props., high strain rates 3-58787
- metal-plastic adhesion band, shear strength determ., response to lubrication 3-73055
- ocean sediments, vertical var. of shear strength, rel. to geotechnical properties 3-44864
- orthotropic shells, low shear stiffness, solvents in theory, force moments and stress functions 3-70630
- plasma coatings, device for shear testing 3-53835
- polyacrylonitrile in aq. dispersion, struct. depend. 3-65025
- polyester dough moulding materials, fibre reinforced, stiffness and strength 3-73007
- polymer latexes, synthetic, mech. stability 3-50791
- quench hardening, isothermal recovery 3-64920
- rocks, low shear modulus effect on stability of jointed masses 3-76555
- shearing crack, half-plane, plane strain conditions 3-70606
- shell, simply supported circular cylindrical, transverse shear acting on edge of circ. cutout 3-66530
- silicate glass bonded with polyvinyl butyral, polymer plasticization effect 3-80484
- structured systems, highly elastic deform., kinetic curves 3-73070
- thin shells, Ilyushin-Shapiro yield surfaces accounting for transverse shear 3-70614
- transversely isotropic shells, elastic filler, stability, mech. loading, temp. effect of shear strength 3-70580
- twisting of nonuniform body of rotation with variable shear moduli (*Russian*) 3-40111
- vitreous plastic fibres, determ. of strength limit for shearing, anal. method 3-53281
- Ag, second-order elastic shear const., pseudopot. calc. 3-68308
- Al single crystals, temp. depend. of strength, high plasticity phenomena, 1.4-300K (*Russian*) 3-55003
- Au, second-order elastic shear const., pseudopot. calc. 3-68308
- C fibre/glassy C composites, graphitization effects 3-55859
- C/C composite, reinforced (*German*) 3-73003
- C/C composites, fibre volume percent depend. 3-55854
- Cu, second-order elastic shear const., pseudopot. calc. 3-68308
- Cu monocrystals, annealed under load, shear modulus defect, dislocations (*Russian*) 3-55828
- Fe, cast, damping capacity correl. with mech. props. and microstruct. 3-50721
- $\text{Li}_2\text{O} \cdot \text{Al}_2\text{O}_3 \cdot \text{nSiO}_2$ graphite fibre reinforced composite, fabrication and low temp. props. 3-76350
- NaCl-type ionic crystals, effective valences and repulsive parameters using Born model on ultrasonic data for Ca_{44} 3-64082
- Ti/ferrite ceramic vacuum brazed joints 3-76229
- WC-Co compound powder, plasma spraying on hard metals, mechanical props. meas. (*German*) 3-50752

sheaths, plasma see plasma sheaths**shell model (nuclear) see nuclear shell model****shielding**

- see also magnetic shielding; radiation protection
- backscattering of fast neutrons from Al, Fe, Pb, 0.5-1.8 MeV 3-60250
- basement ceiling attenuation factors, exptl. study 3-52237
- BWR at Nine Mile Point, survey of radiation levels and shielding 3-71340
- BWR system, study of radiation shielding in operational and shutdown conditions 3-71341
- concrete, neutron penetration data, calc. of dose distrib. by moments method 3-74766
- controlled fusion blankets and shields, perturbation theory for neutron and photon transport calcs. 3-74743
- cryostat heat leak, multiple vapour cooled shields, positional tolerances 3-53858

shielding continued

- electron accelerator, 400 MeV, neutron source spectra in soil, concrete, FeTiO₃ and iron shields 3-71342
- e.m. field in screening semi-infinite solid, distribution due to currents in parallel conductors (*Polish*) 3-57181
- FTR/EMC shield test program, analysis of thermoluminescent dosimeter irradiations 3-71223
- gamma dosage calc. from Compton scattering in or outside shield (*Spanish*) 3-74746
- gamma ray moments computer code 3-54557
- manned space vehicles, against galactic cosmic ray alpha-particles 3-71343
- neutron cross-section library, medium- and low-energy, compilation 3-57526
- nuclear reactor, advances, book 3-60337
- nuclear reactor, attenuation calc. 3-60342
- nuclear reactor, shield analysis, radiation interaction with matter 3-60339
- nuclear reactor experimental shielding, design 3-60345
- nuclear reactor shield analysis, radiation transport 3-60341
- nuclear reactor shield design, application of second-order perturbation theory to sensitivity studies 3-74689
- nuclear reactor shield design 3-60343
- nuclear reactor shield design 3-60344
- nuclear reactor shield design 3-60346
- nuclear reactor shield weight optimisation, perturbation method, computer program 3-74690
- nuclear reactors, employing magnetite and serpentine 3-60332
- nuclear reactors, radiation sources 3-60338
- plasma, warm isotropic, moving test particles shielding 3-46512
- plasma screening theory with effects on thermonuclear detonation in evolved stellar cores 3-47996
- PWR, exptl. verification of temp. distrib. in primary shield during power operation 3-54536
- PWR, shielding design and analysis methods 3-74685
- radiation heating effects, blowoff impulse technology 3-74760
- radiation transport, deep penetration, class of second-order approx. formulations 3-63243
- reactor shielding analysis, Boltzmann transport eqn., soln. 3-60340
- space vehicle, manned, against galactic cosmic ray protons and alpha-particles, dose rate calc. 3-71337
- steel, benchmark expt. for neutron transport 3-74633
- transport of gamma-rays and electron, calcs. using Monte Carlo computer code 3-52235
- Fe, 2 in thick, with H₂O, neutron shielding, 25 keV to 1 MeV, spectrometer meas. 3-74752
- Fe, benchmark expt. for neutron transport 3-74633
- Fe, elemental, meas. and evaluation of neutron total cross-section minima, 24-750 keV 3-54523
- H₂O, neutron shielding, 25 keV to 1 MeV, spectrometer meas. 3-74752
- Pb, gamma ray buildup factor calc. using Monte Carlo methods 3-71336
- ²³⁸U, γ ray spectra, calcs. for slow and fast neutron capture, rel. to reactor shielding 3-67322

shielding, magnetic *see magnetic shielding***ships**

- see also navigation*
- nuclear, seamen training 3-52224

shock control

- thermal in liquid Na, fuel element spacing optimisation (*German*) 3-67586

shock measurement

- hydroshock determ., of vapour-gas content of liquid 3-63720
- laser interferometer for high shock velocity meas. 3-48349
- shear velocity determ. using shockwaves at very high pressures rel. to planetary interiors 3-42170

shock tubes

- see also shock waves*
- calorimetric, for entropy determ. (*French*) 3-62013
- condensation study of supersaturated vapours 3-79478
- ejected gas, quasistationary (*Russian*) 3-63792
- gas dynamic laser processes obs. in large diameter shock tube (*Russian*) 3-78012
- high Reynolds number shock-tunnel technology refinements 3-77754
- magnetically driven, poor separation 3-75321
- supersonic wind tunnel application 3-51773

shock wave effects

- air suspension with Al₂O₃, heat transfer from a reflected shock wave (*Russian*) 3-52470
- almandine-garnet, shock wave Hugoniot data 3-50913
- asbestos-textolite multilayers, shock adiabats meas. (*Russian*) 3-80464
- binary alloys, surface struct. due to plane shock wave (*Russian*) 3-80306
- BN shock induced graphite to wurtzite phase transformation, stacking 3-72193
- building response to sonic booms 3-59482
- CANNIKIN nuclear explosion, ground shock effects on shallow onshore waters 3-51209
- ceramic, quantitative thermal shock test 3-73094
- ceramic powders and mixtures, explosive compaction (*German*) 3-47444
- composites, fibre reinforced, shock unloading phenomena 3-44668
- condensed media, initial temp. effect on negative erosion (*Russian*) 3-79425
- condensed media compression, temp. estimation by thermodynamic method (*Russian*) 3-79423
- cryogenic liq. drop breakdown by shock wave, fuel atomisation process 3-40729
- cylindrical shell, forced axially symmetric vibrs. induced by periodic shock waves (*Russian*) 3-57106
- dynamic analysis of structures, shock spectra eval. 3-70661
- explosion, fuel films, mass exchange, boundary burning (*Russian*) 3-69446
- flow separation, shock induced, dynamic effects 3-57799
- galaxies, origin of rotation rel. to shock wave generated vorticity 3-42227

shock wave effects continued

- half-space under action of thermal shock on bounding surface 3-54095
- human response to transportation noise and vibration 3-59435
- interference heating in hypersonic flows, press. and heat transfer meas. 3-46452
- isentropic compression effects (*Russian*) 3-79424
- laser action termination, coaxial flash lamp dye lasers 3-48903
- metal powders and mixtures, explosive compaction (*German*) 3-47444
- metal rings in plastic states destruction (*Russian*) 3-80305
- metallic wedge shaped cavity interaction (*Russian*) 3-80304
- metals, compressibility, high vel. impact, gas-dynamic model (*Russian*) 3-66573
- meteorites, transformation in explosive shock experiments at 500 and 1000 kbar (*Russian*) 3-81009
- orthoclase, shock-induced phase change 3-50927
- plastic deformation hardening of G31, Cu and Ni by shock waves (*Russian*) 3-64898
- Plexiglas, pressure in discharge channel produced by breakdown 3-55525
- polycarbonate, dynamic fracture, shock damage 3-68331
- pyroxene-garnet rocks, shock-wave high-pressure phases 3-65214
- pyrrhotite, shock compression expts. and possible S content of Earth's core 3-44798
- shells, nonlinear dynamic response 3-42458
- shock tube interaction-region boundary layer, nonlinear problem 3-57794
- solar low-energy cosmic ray proton confinement ahead of interplanetary shock waves 3-65572
- solar proton events, Monte Carlo model including shock effects 3-42135
- solar wind proton temp. following interplanetary shocks, mag. bottles 3-51277
- steel, cylindrical shell, dynamic deformation behaviour 3-80374
- steel, fatigue strength change during explosive strengthening 3-64944
- steel, laser shock-hardening 3-69291
- stellar spherical systems, gravitational shock heating 3-69920
- textolite multilayers, shock adiabats meas. (*Russian*) 3-80464
- thermoelasticity, dilatational wave propagation, shock structures, low temp. 3-62509
- underground nuclear explosions, rock melt, shock wave energy deposition 3-58875
- water and ice, freezing and melting 3-43865
- weak shock wave interactions with rigid wall or free surface, flow similarity (*Russian*) 3-78991
- Webster dunite, shock compression and phase transitions at high pressure 3-65212
- Al, cylindrical shell, dynamic deformation behaviour 3-80374
- Al, laser shock-hardening 3-69291
- Al effect on textured, rolled, coarse-grained plates X-ray study (*Russian*) 3-69264
- laminar Al-Cu composites, behaviour under shock (*French*) 3-58718
- BaTiO₃, depolarization by shock waves 3-58486
- Bi, thermal waves preceding shock front, oscillographic obs. using thermoelectric effect (*Russian*) 3-64188
- C₂, oscillator strength of B² Σ -X² Σ transition, shock-tube determ. 3-54670
- CO₂-Ne-He laser, population inversion in blast waves, numerical calc. 3-40236
- Cu effect on textured, rolled, coarse-grained plates X-ray study (*Russian*) 3-69264
- Cu-Al-Ni alloys, plane shock waves influence on martensitic transformations. (*Russian*) 3-72829
- Cu-Mn-Ni alloy, manganin, piezoresistance coeff. nonlinearity 3-68930
- D₂ liquid, compression to 0.9 Mbar 3-75594
- glass-textolite multilayers, shock adiabats meas. (*Russian*) 3-80464
- o-H₂, matrix treatment of dissociation rotation-vibration relaxation times 3-67857
- LiNbO₃, depolarization by shock waves 3-58486
- Nb₃Sn, supercond., shock wave synthesis from powder mixtures 3-69328
- PbTiO₃, depolarization by shock waves 3-58486
- Ti alloy, brittle rupture resistance (*Russian*) 3-80323
- Ti alloy, laser shock-hardening 3-69291

shock waves

- see also detonation; explosions; plasma shock waves; shock tubes; shock wave effects; supersonic flow*
- Ablation and radiation coupled viscous hypersonic shock layers 3-78985
- acoustic nonlinear oscillations in pipes, shock wave formation 3-51478
- acoustic spark camera in telescope for obs. of primary cosmic γ -rays, shock wave effects (*Russian*) 3-65550
- airborne noise generation, shock structure 3-40730
- alkali halide aerosols, relaxation processes 3-54824
- attenuation in a 'gradual' area expansion 3-67934
- attenuation in air, explosive disturbance in spherical cavity (*Russian*) 3-66572
- blast wave propagation in inhomogeneous medium, radiative transfer, analytic soln. 3-78993
- blast wave propagation problems, numerical solns. 3-52473
- bow shock crossings, Greenstadt's binary index criterion 3-51153
- bow shock crossings, struct. of turbulence, effect of cold and heated solar wind, satellite obs. 3-80836
- building responses 3-59482
- channel flow, shock-losses induced by discontinuities 3-63126
- composite, steady shock waves, Hugoniot eqns. 3-55871
- concentric, uniform elastic spherical wave, excited by thermal explosions of envelope, soln. 3-52468
- condensing steam, flow through Laval nozzle 3-71831
- corner expansion wave interaction with a laminar hypersonic boundary layer 3-78978
- cosmic ray flux variations near geomagnetic pole, reln. to shock wave interactions in magnetosphere (*Russian*) 3-65568
- Coyote Mountain earthquake California, aftershocks and source characteristics 3-76509

shock waves continued

cryogen, liquid, thermodynamic instability, contact with warmer host liquid, shock wave initiation 3-49997
 cylindrical bar, longit. elastic-plastic final duration pulse propag. 3-70635
 damping, effect of viscous and plastic properties of medium (*Russian*) 3-57796
 detonation waves stimulated by intense light, gas dispersion (*Russian*) 3-67938
 diffraction theory, antisymmetric problems 3-67941
 Earth's atmosphere composition by shock-layer radiometry during the PAET entry probe experiment 3-56187
 Earth's bow shock structures, solar wind interaction with Earth's magnetic field 3-65242
 Earth's MHD bow shock, solar wind interaction with Earth's magnetic field 3-61411
 Earth entry, nonequilibrium effects on shock-layer radiometry 3-56188
 elastic bar, bilinear, propag. of plane loading shock wave 3-62530
 elastic-plastic, refraction at material interface 3-49594
 in elasto-plastic media, soln. of eqns., thermodynamic functions (*Russian*) 3-42815
 entropy, measurement using shock tube calorimetry (*French*) 3-62013
 entropy conditions, quasi-linear hyperbolic system of conservation laws 3-78996
 entry vehicle dynamics, instability caused by forebody blowing 3-43571
 exothermic systems, detonative Mach stem structure 3-46455
 expanding gas cloud, dynamical evolution 3-81206
 explosion at half-space boundary containing perfect gas, uniform wave propagation 3-46459
 flow discontinuities, improved constant time technique for the method of characteristics 3-49597
 flow of metals, explosive ejection from hemispherical depression Reynolds number (*Russian*) 3-69263
 fluidised beds, homogeneous to heterogeneous fluidisation transition, dynamic shock wave and velocity criteria (*German*) 3-46480
 fluids with internal state variables, behaviour of shock wave amplitude 3-71781
 Galactic local spiral arm, evidence of assoc. shock 3-45178
 Galactic shocks and nonlinear gaseous density waves 3-70010
 Galaxy, effect on star formation 3-61853
 gas, metallic oxide dust suspension, thermionic emission 3-67935
 gas bubble-liquid medium, shock wave structure (*Russian*) 3-67940
 gas dynamic, three dimensional curved, Beltrami and complex lamellar flows 3-71784
 gas-liquid mixed medium, structure of weak shock wave front 3-43577
 gasdynamic theory (*Russian*) 3-67939
 generation, in randomly inhomogeneous gas 3-43576
 generation, statistical effects 3-43575
 generation by acoustic turbulence 3-63655
 generation by supersonic thermal sources in perfect gas 3-75173
 generation in air from spherical TNT charges, expt. obs. 3-43578
 gravitational, creation by e.m. shock waves (*French*) 3-77888
 heat transfer from hypersonic layer to blunt body (*Russian*) 3-67933
 heat-conducting fluid behind shock wave with mass transfer and chemical reactions in boundary layer (*Russian*) 3-43648
 hypersonic blunt body merged layer problem, numerical soln. of Navier-Stokes eqns. 3-52466
 hypersonic concentric thermal wave in elastic medium soln. 3-52469
 hypersonic-shock/boundary layer interaction problem, initial conditions 3-57793
 intense light source generation, by optimising imploding detonations with laser energy 3-63849
 interplanetary, caused by solar flares, (August 1972) (*Russian*) 3-65631
 interplanetary, interaction with galactic cosmic rays 3-76937
 interplanetary and flare-generated coronal shock waves, close relationship 3-47892
 interplanetary in solar wind, perpendicular magnetofluid dynamic 3-65727
 interplanetary m.h.d. shocks, graphical representation 3-65862
 interplanetary shock scattering by tangential discontinuities in the solar wind 3-65726
 interplanetary shocks due to solar flares, Pioneer 10 obs. (August 1972) 3-65860
 interplanetary shocks rel. to flares and radio bursts 3-65861
 interstellar shock waves and molecule formation 3-42239
 isentropic, drag in irrotational transonic flow, numerical calc. 3-78984
 isothermal expansion of a proton into an inhomogeneous medium 3-78992
 Jupiter shock-layer temps. appropriate for entry, meas. of H₂-He radiation 3-69881
 liquid, weak shock wave attenuation 3-40973
 liquid-vapour system, propagation near the critical path shock wave development 3-60773
 magnetogasdynamics, weak, occurrence in tube 3-79050
 magnetosphere, interaction with cosmic radiation, kinetic description (*Russian*) 3-65586
 magnetospheric interaction with cosmic radiation, reln. to Forbush effect (*Russian*) 3-65470
 metal solid-liquid interface, phonon thermal resistance, shock mechanism 3-75588
 multishocked three dimensional supersonic flowfields with real gas effects around space shuttle 3-63705
 negative shock waves 3-57795
 nonlinear resonant oscillations in open tubes, shocks formation 3-75241
 nonsteady, propag. in hypersonic flow second order diff. method (*German*) 3-54815
 oblique MHD shock wave decay calc. 3-63721
 oblique partly dispersed, steady two-dimensional reflection from a plane wall 3-78994

shock waves continued

one-dimensional shock front caused by a disturbance moving on a circle, locus 3-52467
 oscillations in shock profiles, calculated by difference methods (*French*) 3-46454
 outer planets, solar wind interaction, shock shapes and locations 3-69827
 perfect gas unsteady transonic flows with shock waves in two-dimensional channels 3-67929
 plane, attenuation in high speed impact (*Russian*) 3-78990
 plastic compressible medium, explosion of spherical charge, temp. distrib. (*Russian*) 3-42826
 plate, transition of symmetrical deformation wave process to asymmetric process (*Russian*) 3-54126
 plenum, rapidly filling unsteady flow processes 3-46453
 pressure fields over hypersonic wing bodies at moderate incidence 3-57784
 propagation in an inhomogeneous medium 3-49595
 propagation in gravitational field, self-generated flows, energy dependence on Mach number (*Russian*) 3-67937
 propagation in solid, explosion in spherical air cavity (*Russian*) 3-66572
 propagation in three-component medium with elastic unloading 3-74071
 propagation of strong radiative shock into density gradient, soln. by characteristics at fixed time interval 3-71782
 propagation vel. of shocks assoc. with solar flares 3-56322
 protostars, radiative energy loss from shock front generated during collapse 3-65877
 radiation-driven, study of self-similar flows behind shock 3-63719
 radiative magnetogasdynamics, growth of pressure shocks 3-44925
 rarefaction, centred, nonstationary and stationary, propagation in nonviscous equilibrium media 3-57798
 reflecting, attenuation in a duct lined with lightweight polyurethane foam, results 3-71783
 reflecting oblique shock wave structure, numerical analysis 3-52472
 reflection at glancing incidence in parallel flow of ideally dissociative gas in magnetic field (*Russian*) 3-67936
 reflection from thermally accommodating wall, molecular simulation 3-71788
 relativistic gas dynamics, shock wave and nozzle flow 3-49618
 relativistic hydrodynamics, astrophysical appl. 3-60582
 rooms, pulse echograms, spectrum of mild blast effects in acoustical equality testing 3-77324
 seismic aftershock, time of occurrence, magnitude, India 3-76591
 shear velocity determ. using shockwaves at very high pressures rel. to planetary interiors 3-42170
 sinusoidal low amplitude acoustic sources, intrinsic nonlinear effect on flow field 3-77309
 solar chromosphere, interpretation of Ca II K-line 3-51287
 solar flare propagation mechanism in chromosphere (*Russian*) 3-76979
 solar wind shock fronts, flare produced 3-65725
 solid, elastic, prod. by supersonic thermal sources 3-62532
 solid, steady wave profiles, nonequil. eqn. of state, conservation laws 3-75567
 solid surface, shock and compression by TEA CO₂ laser pulses, liq. surface layer effects 3-57245
 sonic boom investigations with holographic recording 3-43573
 sonic booms, wind-tunnel investigation method 3-46451
 sonic-boom overpressures investigation, ballistic range investigation for various Mach numbers 3-57792
 spherical, in solid, effect of linear Q on decay determ. by finite difference technique 3-70648
 spherical, in water 3-40728
 spherically symmetric gas expansion into very low pressure, Navier-Stokes equations soln. 3-52471
 stability of plane shock waves 3-43574
 starting process in the nozzle of a nonreflected shock tunnel 3-46495
 steel, shock and rarefaction waves, structure rel. to heat treatment (*Russian*) 3-64110
 stellar evolution, blast wave hydrodynamics, cluster of galaxies, supernovae, intergalactic medium 3-47868
 strong shock over a sharp leading edge, Navier-Stokes eqns., finite difference treatment 3-49598
 supernovae, D prod. in envelopes 3-47991
 supersonic burning and pseudoshock in a tube, one dimensional model (*Russian*) 3-78987
 supersonic flow, around concave and convex bodies, shock shapes 3-63717
 supersonic flow, heterogeneous, stoichiometric hydrogen-air mixture with suspended Al and Mg powders in detonating wave (*Russian*) 3-63768
 supersonic jet, rel. to swirl effects 3-78982
 supersonic jet, shock associated noise 3-75229
 suspension of solid particles in gas flow, propagation of pressure waves 3-79029
 Tee-junctions, propagation across, one dimensional analysis, experimental and theoretical 3-75227
 tetrafluoromethane, number density remote sensing in hypersonic flow using Raman scattering 3-71699
 thermal, propagation in linear viscoelastic half-space (*Russian*) 3-42827
 thermoviscoelastic solid, crit. strain gradient, amplitude eqn. 3-79426
 transition into sound wave 3-45350
 transonic flows over blunt nosed geometries with detached bow shocks, relaxation method 3-52465
 turbulent boundary layer-shock wave interactions in rectangular channels 3-43572
 underwater explosions, loading of a submerged structure, shockwave propagation, numerical solution 3-75228
 underwater spark discharges, electromechanical efficiency (*German*) 3-54882
 unsteady flow with shocks, computational methods 3-49596
 upstream solar wind, plasma radiation from collisionless MHD shock waves 3-51282

shock waves continued

- viscoelastic media, plane waves propagated by transient shock load (*Russian*) 3-69508
 viscoelastic nonlinear wave propagation, review 3-70646
 viscosity, artificial, improved form from second Rankine-Hugoniot equation 3-46457
 vortex discontinuity in thermodynamic variables (*French*) 3-78986
 weak, turbulent thickening possibility 3-46458
 weak shock waves in dilute gases, nonlinear Boltzmann kinetic equation 3-71780
 Al, steady shock profile, hydrodynamic eqns. 3-68340
 CO vibrational relaxation by O atoms behind shock waves 3-46348
 CO₂ dissociation behind reflected shock waves 3-46332
 He, oblique shock-sound interaction at $M_\infty \approx 20$ 3-40727
 NF₃ dissociation in Ar, shock tube-spectrophotometric meas. 3-75094
 Rb vapour, optical pulse self steepening with possible shock formation 3-57261

shocks, electric *see electric shocks***short-range order**

- see also order-disorder transformations*
 acetonitrile, and liq. struct., X-ray scatt. (*German*) 3-63944
 alloy, disordered binary, spatial correlation function, high temp. series expansion 3-72162
 alloy, L1₂ superstruct., temp. depend. of order parameters, uniform and nonuniform ordering (*Russian*) 3-79270
 disordered alloys, moment approach for density of states 3-55185
 disordered system, effects rel. to metal-insulator transition and electronic props. 3-46807
 Heisenberg model, one-dimensional, dynamic properties, spin-wave-like excitations and lattice dimensionality 3-64461
 Heisenberg spin system, with uniaxial and exchange anisotropy, freq. moments, short range order effects 3-55400
 ionic fluids, onset of short-range order 3-48795
 liquid crystal, nematic, in isotropic phase, mag. birefr. theory 3-57988
 liquid structure, dynamic, correlation between molecules, position and time distrib. functions 3-49814
 liquid structure, mol. acoustic absorpt., review 3-54915
 micromagnetic alloys, complex mag. ordering, origin 3-47054
 noble metal binary alloys, order dependence of electrical resistivity 3-64317
 optical second harmonic generation for SRO obs. in disordered crystals. 3-64613
 plasma, one-component, HNC approx. 3-46511
 polycarbonate, bisphenol-A, short range intermol. ordering obs. by radial distrib. functions 3-80473
 solid solution, concentrated, model for partially ordered state (*German*) 3-55755
 superparamagnetism in alloy 3-47053
 ternary zincblende substitutional solid solutions, parameters 3-52596
 transition metal binary alloys order dependence of electrical resistivity 3-64317
 Ag-Ge liquid alloys of eutectic composition (*Russian*) 3-63946
 Au-Ag (15 at. %) alloy, resist. change during short-range order form. 3-64932
 Cd-Mg alloy, theory 3-69195
 CdGeAs₂, cryst. and glassy, i.r. electrorefl. obs., energy gap rel. to short-range order 3-64662
 α -Cu-Al (18.6 at. %), anneal-hardened, structure investigation with electron microscope and diffraction 3-72863
 Cu-Al alloy, slip plane dilation and disorder, electron microscope obs. 3-69235
 Cu-Al alloys, liq., mag. susceptibility depend. (*Russian*) 3-52953
 α -Cu-Al alloys, local atomic arrangements and anomalous behaviour 3-50715
 Cu-Au, order-disorder transform. theory, temp. and conc. depend. of SRO parameter 3-44563
 Cu-Mn alloy, antiferromag., temp. and heat treatment effects 3-47059
 Cu-Pt, Cu-Pd, disordered alloys, diffuse scattering obs. by electron diffraction 3-63978
 Cu-Pt alloys, short-range order in hardened alloys (*Russian*) 3-69270
 Cu-Au, atomic structure above critical ordering temp. 3-63980
 CuPt, ordered, geometrical anal. of field-ion images 3-68196
 Fe, molten, polymorphic transformations of clusters 3-58616
 Fe phosphate glasses, semiconducting, coordination states and magnetic structure determ. by Mossbauer spectroscopy 3-75922
 Fe-Al, atomic ordering energy parameters, Si content depend. (*Russian*) 3-76147
 Fe-Al (16.3 at. %) alloy, X-ray diff. obs. (*Russian*) 3-72893
 Fe-Al-C alloy, struct. changes at low temp., interstitial site ordering, resist. obs. (*Russian*) 3-80208
 Fe-Al-C alloys, martensite decomp. depend. (*Russian*) 3-53214
 Fe-Ni alloys, Invar phenomena, plastic deform. and heat treatment effect (*Russian*) 3-58409
 Fe-Ni alloys, Invar type, Ti addition effect on phys. props. (*Russian*) 3-79883
 Fe-Ni-Mo and Fe-Ni-Co-Mo maraging alloys, redistrib. of alloying elements during recovery (*Russian*) 3-80312
 Fe-P liquid alloy 3-49839
 Fe-Si alloy, annealing, ordering, elec. resist. (*Japanese*) 3-72837
 Ga_{0.16}Al_{0.84}As solid solutions, parameters 3-52596
 Ge, amorphous, structure, radial distrib. curves of density of atoms 3-60665
 LiFeO₂, high-resolution dark-field electron microscopy 3-63935
 NaNO₂, disordered paraelec. state, second harmonic generation for SRO obs. 3-64613
 Ni-Al alloys, ageing, spatial distrib. of second phase precipitates, correl. parameters (*Russian*) 3-44571
 Ni-Mn-Fe alloy with exchange anisotropy, ordering influence on anisotropy and galvanomag. effect (*Russian*) 3-60971
 Ni-Mo alloys, comp. and heat treatment conditions depend. (*Russian*) 3-80207
 Ni-Si alloys, liq., X-ray scatt. obs. (*Russian*) 3-41690
 Ni₃Al alloy, ordering transition, TEM obs. 3-80198
 Ni₃Fe, atomic structure above critical ordering temp. 3-63980

short-range order continued

- Ni₃Mn alloy, effect on crit. shear stress magnitude (*Russian*) 3-44570
 Pb_{1-x}La_x(Zr_{0.65}Ti_{0.35})_{1-x/4}O₃, refractive index rel. to local disorder 3-58484
 Pb₃(MnNb₂)O₉, (M=Zn,Mg), dirty displacive ferroelec., refractive index rel. to local disorder 3-58484
 Se-Te melt, electron energy band struct. smearing, cond. transition 3-72390
 Te disordered phases, effect of short-range order on energy spectrum 3-68534
 Ti b.c.c. solid solns., with ω -phase, short-range struct., diff. pattern interpretation 3-79198
 Ti-Al alloys, strengthening by Al, local order mechanism 3-64919
 Zr b.c.c. solid solns., with ω -phase, short-range struct., diff. pattern interpretation 3-79198
- shot noise**
 laser field, effect 3-70796
 Schottky-barrier diode, during tunnelling through a space charge region (*Russian*) 3-72402
- showers, cosmic ray** *see cosmic ray showers and bursts*
- Shubnikov-de Haas effect** *see magnetoresistance*
- SIC** *see monolithic integrated circuits*
- signal acquisition** *see signal detection*
- signal coding** *see encoding*
- signal delay lines** *see delay lines*
- signal detection**
 coherent optical detection, mutual coherence function for finite beam in random medium 3-66766
 hearing, click detection in noise 3-45302
 laser tracking system, detection relationships rel. to return signal fluctuations 3-53919
 meteors, optimum processing (*Russian*) 3-77021
 optical communication lines, information capacity 3-48855
 optical radar system, S/N ratio 3-66772
 orthotron, open resonator, interaction with radiation, 2 to 2.8 mm (*Russian*) 3-66916
 seismic waves, discrimination from noise using discrete quasi-optimal filters and minimax filters 3-65502
 simulated radiographic signal, factors affecting detectability 3-66035
 sky wave direction at l.f. and v.l.f. 3-80791
 visual recognition, masking, effects of two dimensional filtered noise, experiments 3-73584
- signal generators**
see also function generators; swept-frequency oscillators
 ocean bottom-sensing signal generator for use with STD systems 3-53563
 time-sampling observation of behaviour, tone signal generator 3-62308
 voltage source for metrology research, characts. 3-77566
- signal processing**
see also correlation theory; filtering and prediction theory; signal detection; Walsh functions
 acoustic array, vertical, hydrophones, maximum likelihood signal processing, technique 3-77389
 acoustic data, conference, Loughborough, England (1972) 3-53797
 acoustical, review 3-45385
 acoustics of external ear, transformations in impulsive stimuli 3-48224
 analogue data, digital analysis techniques 3-53798
 automatic machine, identification criteria for classification of signal reflections (*Russian*) 3-77023
 cochlear nerve potentials, digital signal processing analysis of evoked responses 3-42279
 correlation and spectral analysis of voluntary eye-movements (*German*) 3-48247
 diver speech distortion, rel. to HeO₂ environment 3-61945
 electron probe image analysis system, automatic, Quantimet 720 3-42715
 fan noise in ducts 3-53800
 Fourier hologram filter, pattern recognition and size determ. of signals (*French*) 3-66770
 meteor trails drift (*Russian*) 3-77022
 meteors detection (*Russian*) 3-77021
 microwave spectral analysis, discrete Fourier transform applic. 3-77577
 nonstationary data, digital analysis 3-53799
 optical data processing system, theory 3-77449
 optical processing of linear phased array radar signals 3-48856
 perceptive deafness, signal processing to improve speech intelligibility 3-59431
 p.r.f. discriminator with complete harmonic suppression 3-48545
 pulsar signal processing techniques 3-65911
 radiometric information (*Russian*) 3-77020
 seismogram input signal restoration for a linear dynamic system 3-76869
 SEM, improved processing systems 3-70422
 SEM, specimen current, time differentiated imaging 3-70425
 separate medium space-charge convolver 3-51479
 speech intelligibility for deaf subjects 3-48311
 Stochastic-ergodic measuring methods (*German*) 3-70258
 surface elastic wave devices, past, present and future 3-45370
- signal sources**
see also signal generators
 e.m. waves, from directional rotating source of particles (*Russian*) 3-42950
 sound signals, navigational, nearfield calibration 3-45386
- silica minerals** *see minerals*
- silicate minerals** *see minerals*
- silicon**
 adsorption, of PH₃, clean (111) surface, LEED and Auger electron spectra study 3-44513
 adsorption of O₂ on Si(111) surface 3-55160
 adsorption of O, influence of residual water vapour 3-75670
 adsorption of O, model for adsorption complex 3-55149
 amorphisation during different mass ion implantation 3-60754
 amorphous, B-implanted, non-Gaussian range profiles 3-40934

silicon continued

amorphous, electronic band structure and transport props. 3-72351
 amorphous, form. by ion implantation, model, e.p.r. 3-68302
 amorphous, hopping conduction, Mott's parameter evaluation 3-75743
 amorphous, i.r. and Raman spectra theory 3-41513
 amorphous, structural aspects, critical review of data and models 3-46589
 amorphous, tetrahedrally bonded, one-band density of states for Polk model 3-79610
 amorphous, tetrahedrally coord. random-network struct., model 3-52581
 amorphous film, photoelec. props. 3-64380
 amorphous film-electrolyte interface, photovoltaic effect, mobility gap obs. 3-52867
 amorphous semiconductor, electronic density of states, absorption, photoemission, photoconductivity 3-41119
 amorphous Si-Electrolyte interface, density of localised states 3-72397
 amorphous solids, Raman scattering, l.f. coupling constants 3-41520
 anodic oxidation in organic solvent with F traces 3-41671
 Ap stars, theoretical intensity of Si lines 3-53659
 appearance potential spectroscopy 3-64749
 atomic scatt. factors, electron densities and valence electron pot. calcs. (*Russian*) 3-58023
 atomic scatt. factors imaginary parts in nearly perfect crystal, Borrmann effect 3-43775
 Auger emission processes, spectroscopic technique (*Hungarian*) 3-80124
 Auger recombination coeffs. (*German*) 3-53164
 Auger spectroscopy of submonolayer Au deposits on (III) surfaces 3-44510
 Auger spectrum, absence of plasmon gain satellites 3-58581
 band struct. features, determ. from u.v. edge-absorpt. data 3-52787
 band structure, self-consistent pseudopotential 3-58216
 band-to-band Auger recombination of optically infected carriers, theoretical model 3-76072
 beam-foil lifetimes meas. in vacuum u.v. 3-78425
 biexcitons, energy of formation 3-50156
 bombarded with C^{+} , subsurface amorphous layers, annealing props. 3-54985
 Brillouin spectra, absorpt. line broadening, refr. indices determ. 3-50566
 bulk lifetime measurement, from m.o.s. capacitance and current obs. 3-55341
 carrier concentration and resistivity by low-temp. method 3-62030
 carrier lifetime doping, by edge dislocations 3-55270
 carrier lifetime radiation const. rel. to neutron spectrum 3-44078
 carrier recombination after light pulse excitation for medium-high carrier conc. levels 3-46858
 channelling of He ions, stopping power formula 3-60752
 channelling of protons along $\langle 111 \rangle$ direction, indirect meas. of energy loss coeff. 3-64077
 clean surface physics, review 3-50059
 commercial, microconstituent phases, rapid identification procedure 3-42732
 concealed n^{+} layer production, from As silicate glass layer (*Bulgarian*) 3-69163
 conduction band effective mass of electrons, plasma edge reflection study 3-44009
 cooperative diffusions of B and P, mathematical model 3-68433
 crystal, i.r. microscopy study of defects 3-54955
 crystal, uniformly bent, X-ray wavefield beam propag. 3-43723
 crystal binding, bond bending and stretching force const., high press. transform. into metallic dense form 3-49991
 crystal growth, by internal work coil float zoner 3-64796
 crystal growth from melt, dislocation-free, prevention of vacancy cluster formation 3-72810
 crystal lattice, model of diamond-type lattice dynamics including angular forces 3-79439
 crystals, Au doping, effect on O content of growth medium, kinetics 3-68175
 crystals, Borrmann effect, Compton scattering 3-69107
 Czochralski growth, anomalous resistivity profiles 3-68617
 Czochralski growth, influence of C, Si-C phase diagram 3-41645
 dechannelling of 5 MeV protons from planar channels, temp. depend. 3-60753
 defect centres, 1.0 MeV electron irradi., energy levels, impurity depend. and annealing behaviour 3-41155
 defect form. under electron, proton irradi., dynamic obs. 3-54954
 defect structure, after annealing of 'through-oxide' As implantations 3-68299
 defects and impurities generated by ion bombard. and implantation, interactions 3-40910
 deformed crystals, dislocation structure, surface and bulk layers, electron microscopy (*Russian*) 3-40922
 deformed layers with different orientations and dopants (*Russian*) 3-52628
 deposition of polycrystalline Si and Al layers, heat-treating cycle, shallow diffused transistors 3-41661
 detector, for stereoscan scanning electron microscope 3-62284
 detectors, analytically determined response to polyenergetic neutron beam 3-42650
 detectors, radial position sensitive, fabrication by ion implantation techniques 3-51714
 diffused layers, piezoresistive coeffs. 3-41217
 diffusion, of B, orientation depend., profiles obs. 3-55744
 diffusion curve, determ. by etching, impurity adsorption effects 3-55742
 diffusion in Cu, temp. depend., 700-1100°C (*Russian*) 3-68435
 diffusion of Au, low temp. interstitial mechanism 3-60805
 diffusion of Au atoms, LEED patterns (*Russian*) 3-50030
 diffusion of B and P, concentration dependent 3-41045
 diffusion of B into Si under oxidizing atm., anisotropy 3-50077
 diffusion of group III and group V elements, mechanism (*Russian*) 3-43890
 diffusion of interstitial, migration energy calc. using extended perturbation theory 3-50026

silicon continued

diffusion of P from oxylic source, impurity concentration (*German*) 3-43888
 diode, breakdown voltage lowering due to C impurity precipitation 3-52890
 diode, generation-recombination characteristic behaviour 3-79765
 discontinuous Compton scatt. by K- and L-electrons, intensity, chem. shift, fine struct. angular depend. 3-55701
 dislocation free crystals, float-zoned, dislocation generation along swirls, thermal oxidation 3-41648
 dislocation image evaluation, X-ray intensity distrib. in Bragg case 3-58037
 dislocation loops, electron microscopy weak-beam observ. 3-60726
 dislocation nodes study, by weak-beam technique of transmission electron microscopy 3-59666
 dislocation substructure induced by fatigue 3-54963
 dislocation-free crystals, distribution of point defects Cu decoration, X-ray topography, etching 3-41650
 dislocations, diffusion induced, simple planar structures, X-ray diffr. contrast study, Burgers vectors 3-43798
 divacancy-oxygen complex and A-centre form. on electron irradi. 3-41166
 dopants, non-equilib. behaviour during epitaxial deposition using silane 3-44554
 doped, metal to nonmetal transition in shallow donor states 3-55217
 doped, model for self-consistent cluster calcs. using SCF $X\alpha$ scattered wave method 3-75700
 doped epitaxial layer, controlled preferential etching, HF, HNO_3 and acetic acid 3-41659
 doping by B diffusion and interface reactions of B_2O_3 -Si system 3-58047
 doping process, solid-solid vac. diffusion 3-58600
 drift velocity, saturated, electron-optical phonon coupling, field dependence impact ionisation 3-50197
 electrical properties, single crystal in ultrahigh vacuum, instructional experiments for undergraduates 3-68684
 electron drift velocity near velocity saturation knee, temp. dependence 3-41197
 electron exoemission, thermally stimulated, adsorbed water and oxygen effects 3-64759
 electron irradi., defect formation threshold energy anisotropy 3-43811
 electron irradiated, effective recomb. levels, carrier lifetime obs. 3-68646
 electron negative differential mobility below 77K 3-44088
 electron-exciton interaction, time-resolved cyclotron resonance analysis 3-68572
 electron-phonon interactions and inter-valley scattering 3-72362
 electronic structure of (111) surface, Slater-Koster parameters 3-72392
 electroreflectance for doping inhomogeneities meas. 3-54977
 energy level spectra at (111), (110) and (100) surfaces, ion neutralisation spectroscopy 3-58578
 energy loss and stopping power meas. between 2 and 10 MeV/amu for 3He , 4He in Si 3-46654
 energy loss and stopping power meas. for ^{12}C , ^{4}N , ^{16}O in Si 3-46655
 enhanced diffusion of In and Ga, lattice location 3-46727
 epitaxial, electron and hole ionisation rates at high fields, p-n junction obs. 3-68642
 epitaxial and diffused layers, meas. methods for resistivity and doping profiles (*Czech*) 3-72814
 epitaxial film, oblique slice fabrication, etching technique 3-43945
 epitaxial film, on sapphire, with microsec. carrier lifetime 3-41623
 epitaxial film, preparation of samples for galvanomagn. meas. by Van der Pauw method 3-76139
 epitaxial film, thermal e.m.f. meas. 3-45526
 epitaxial growth, choice of materials 3-64801
 epitaxial growth, from dichlorosilane 3-55747
 epitaxial growth, p-n junctions, thyristor manufacture 3-41256
 epitaxial growth, thickness measurement down to 0.5 μm 3-44548
 epitaxial growth, using dichlorosilane, growth on single crystal hemispheres 3-76140
 epitaxial growth of Ge on Si substrate, zone melting method (*Russian*) 3-55735
 epitaxial layer, impurity conc. profile and resistivity for material selection 3-64800
 epitaxial layer, profile tailoring by enhanced diffusion in ion bombarded region 3-55746
 epitaxial layer, thickness measurement 3-64799
 epitaxial layer thickness meas., Fourier transform method, scanning Michelson interferometer 3-41666
 epitaxial layers, transport of B from source during sublimation in vacuum 3-76145
 epitaxial layers donor conc. levels, effect of etching and autodoping, low temp. i.r. studies 3-41653
 epitaxial thin film, resistivity and Hall e.m.f. meas., distribution of resistivity, conc. and mobility 3-45527
 epitaxy, (111) surface, geometry displacement and distortion model 3-50667
 e.s.r. obs. of defect centres and amorphous phase produced by ion implantation 3-79913
 etching, doping by B diffusion source glass 3-79578
 excess carrier concentration decay, photoconductivity, photoluminescence 3-68561
 exciton and plasma phase transitions 3-41167
 exoelectron emission, temp. effect, extended and abraded mat., activation energy determ. (*Russian*) 3-53170
 filamentary growth from soln., mechanism 3-69164
 film, amorphous, optical and elec. props., model for effect of voids 3-68629
 film, amorphous and crystalline, impurities and ion clusters, mass spectra analysis 3-69170
 film, chem. deposited, effect of deposition conditions on struct. 3-41112
 film, deposition on Be(0001) surface, LEED obs. 3-68521
 films, epitaxially grown from SiH_4 - H_2 and SiH_4 -He mixtures, comparison 3-41626
 films, optical interference phenomena, reflectivity vs. wave number curves 3-58488

silicon continued

- films, oxidation, struct., transmission electron microscopy, defects 3-72276
- float zone crystals, gas doping 3-58601
- float-zone growth, resistivity topography rel. facet growth 3-41646
- float-zoned crystals, dislocation-free, [115] crystallographic orientation 3-50664
- float-zoned crystals, growth striations and swirls, electron microscopy 3-41649
- fracture, X-ray Pendellosung fringe and double-cryst. diffractometry obs. 3-64102
- fresh waters, evidence for buffering of dissolved Si 3-44970
- g-factor of interacting electrons, in Si inversion layers 3-79754
- generation-recombination meas., using m.o.s. struct. nonequilibrium current 3-44089
- gettering action of phosphosilicate glasses and ion implantation damage layers, MeV $^4\text{He}^+$ backscatt. obs. 3-41644
- growth on thermal oxide layer, decomposition of SiH_4 , effect of growth on elec. props. 3-41658
- heat treatment, oxygen precipitation, X-ray anomalous transmission and topography 3-68413
- heavily doped, general transport eqns. 3-55260
- highly doped, metal insulator transition, metal-insulator transition, current carriers density discontinuous change 3-72326
- hole and electron traps, energy levels and density, determ. from capacitance meas. 3-64300
- homoeptaxial layer, misfit dislocs. on (110), (112), and (113) 3-64256
- homoeptaxy with ion sputtering, growth mechanism 3-44550
- impact ionisation thresholds derivation from band structure 3-64342
- implantation damage, by 80 keV Li^+ , i.r. absorpt. study 3-46652
- implantation of As, enhanced diffusion 3-44541
- implantation of B, angle influence on penetration of channelled ions 3-79365
- implantation of C^+ , X-ray interferometry of volume changes 3-43817
- implanted B ion conc. profile meas. with ion microprobe 3-52640
- impurity clusters, localization, comp. and influence on emission props. 3-64063
- impurity diffusion, carrier gas system and other methods compared 3-55739
- impurity distribution coefficients, ionic radius-lattice defect model, solubility, vacancies 3-52639
- impurity ions, shallow-donor, and spin-polarised electron transport 3-41181
- impurity level of N_2 and O_2 , conc., solubility, and equilibrium distrib. coeff. 3-58046
- impurity states, many-band pseudopotential calcs. of ground state energies 3-44032
- impurity states calcs., using screened local pseudopotential 3-44035
- indirect exciton absorption, derivative spectrum, anal. 3-47290
- infrared television microscope studies, resolution 3-41664
- interstitial Na atom, location determ. by charged particle channelling 3-64062
- intervalley repopulation and negative differential mobility, 8K 3-46852
- ion implantation, beam heating effects, expt. simulation 3-64798
- ion implantation, lateral spread for ^{31}P and ^{11}B , oblique incidence and CV plot obs. 3-80179
- ion implantation by trivalent or pentavalent elements (Italian) 3-58597
- ion implanted, amorphisation, e.s.r. obs. 3-68838
- ion irradiated, medium-energy ions, change in interplanar spacing 3-75552
- ion-implanted, precision lattice parameter meas. 3-43778
- i.r. absorption in p-type, use of Mg diffusion to meas. residual P conc. 3-61054
- i.r. spectroscopy, defect obs., book 3-72693
- i.r. spectroscopy, dielectric films on Si, device technology 3-41665
- isolated vacancy, ordering of energy levels using defect molecule method 3-72077
- laser excitation, carrier recomb. in deep and shallow surface centres 3-41253
- laser-excited, electron-hole recomb. at deep impurity centres 3-76074
- lateral photovoltaic effect, reln. between N ion dose and photovoltage 3-52872
- lattice phonon dispersion, Clark-Gazis-Wallis type angular force model 3-79446
- lattice repeat distance, visible wavelength meas. by He-Ne laser 3-73660
- layers elimination, by anode oxidation method 3-54005
- line stacking faults generation at coherent twist boundary 3-64058
- lunar soil, Apollo 17 sample $^{30}\text{Si}/^{28}\text{Si}$ 3-65823
- metal- Al_2O_3 - (SiO_2) -Si structure, C-V characteristics, effects of bias application 3-52901
- in mica, ^{16}O ion irradi., inelastic nuclear scatt. process 3-66327
- microdefects in high-purity crystal, investigation by Li decoration 3-43782
- microdeformation of surface layers in brittle transition temp. region, surface-volume dislocation interactions (Russian) 3-79411
- microwave conductivity and permittivity meas. 3-50225
- microwave meas. of K anisotropy factor (French) 3-60884
- migration in Au, low temp. obs. by means of e.s.c.a. 3-50028
- minority carrier lifetime meas. at low injection rates (German) 3-50219
- modulation spectroscopy, surface electron states photoconductivity 3-55323
- m.o.s. structures, effect of charge inhomogeneities on surface mobility 3-41270
- m.o.s. structures, transient behaviour and recombination processes (Hungarian) 3-68707
- Mossbauer spectra of implanted ^{57}Fe 3-47184
- multiple scatt. under [100] strain, metallised electron-hole droplets 3-46813
- multiple scattering and planar dechannelling of MeV protons 3-52655
- n-type, (111), (100) surfaces, thermal oxidation to produce m.o.s. structs., elec. props. 3-79771

silicon continued

- n-type, high resist., kinetic effects in electron field emission 3-72783
- n-type, large area contacts, layer of Si-Au eutectic alloy, low temp. techniques 3-48391
- n-type, longitudinal magnetoresist. in strong mag. fields, 77-150K 3-55291
- n-type, surface inversion layers, g-factor determ. for cond. electrons 3-58430
- n-type, surface lifetime degradation under low energy electron bombardment 3-44091
- n-type, thermoelec. and thermomag. props., crystal boundary effects (Russian) 3-75758
- n-type, Zn-compensated, very high resistivity, photocurrent decay, temp. depend. 3-79725
- n-type surface inversion layers, g-factor for electrons 3-46887
- n-type carrier redistrib. between valleys due to size effect 3-75760
- negative electron affinity surfaces on Si using Rb/o dipole layer 3-44128
- neutron backscattering from perfect single crystals. (German) 3-63933
- nonlinear absorpt. at 1.06 μm , indirect two-photon transition study 3-40286
- optical spectroscopy in high magnetic fields using polarisation modulation 3-55615
- oxidation and reduction of (111) surface by steam, Auger electron emission obs. 3-41097
- p^+ -n- n^+ vertical junction diodes, ionizing radiation, second breakdown 3-64402
- p^+ -n reverse-biased junctions, Au doped, thermal and optical generation current 3-46889
- p-n junction, alloyed, avalanche breakdown characs. 3-52893
- p-n junction, avalanche radiation, resistivity inhomogeneity meas. 3-41258
- p-n junction, depth of occurrence, electronic probe determ. (Russian) 3-77717
- p-n junction, diffused, avalanche breakdown voltage 3-64399
- p-n junction, insulating, epitaxial structure, leakage current meas., four-probe method 3-42601
- p-n junction, transference and change of mesoplasma characteristics (Russian) 3-68697
- p-n junction diode, elec. characs., oxidation-induced stacking fault effects 3-41259
- p-n junctions, characterisation of defects, thermally stimulated meas. capacitance and current 3-41257
- p-type, heavily doped, interaction of electronic and vibronic Raman scatt. 3-58514
- p-type, high resistivity, compensated, with Au contact, bound space charge 3-58270
- phonon dispersion relations with CGW type ang. force model 3-52677
- phonon interaction with stress-split acceptor states 3-55048
- photoconductivity kinetics, A^+ and D^- centre effects 3-60900
- photodiode system, multichannel emission spectrochemical analysis 3-73958
- photoelastic constants in single crystals, stresses in crystal ingots (German) 3-53082
- photoemission, Cs-O activation and apparent negative electron affinity (French) 3-44515
- photoemission, escape probability elec. field enhancement of negative electron affinity surfaces 3-61103
- photostimulated diffusion, reply to comments 3-43900
- planar technology, mechanical props. of surfaces rel. to prep. and meas. 3-69179
- point defect injection, during nonequilib. diffusion process, rel. to IC fabrication 3-55745
- polycrystalline gate, in m.o.s. struct., rel. to enhanced B diffusion through oxide from B_2O_3 source 3-58606
- positron annihilation, angular correlation of radiation 3-72318
- positron annihilation, influence of temp. 3-75548
- precipitate colonies, of Cu, growth, electron microscope obs. 3-68412
- precipitation of copper, habit and morphology, dislocation mechanism 3-40932
- precipitation of Cu, habit and morphology, critical evolution of mechanism 3-40933
- primary radiation defects, role of collective processes in formation 3-58050
- process modelling, integrated circuit and device parameter control 3-41668
- radial distribution of Ni, Cu, Au, P, B radioactivation analysis, electrical measurements 3-72098
- Raman spectrum, second-order, phonon density of states 3-68984
- Raman spectrum, two-phonon, selective reson. enhancement 3-80033
- range-energy relations for protons, electronic stopping constant, enhanced diffusion 3-52651
- recombination radiation, band structure effects, comparison with Ge-Si alloys 3-50621
- ribbon growth, for solar cell applic. 3-61119
- river pollution, distribution of concentration 3-77304
- rocking curve of vibrating single crystal, neutron diffraction 3-40836
- secondary electron emission, temp. depend., (111) surface at ion implanted crystal 3-69121
- selective epitaxial growth, orientation depend. 3-44546
- self-interstitial migration and implant damage annealing, ionisation effects 3-60806
- p-Si:B epitaxial layers, piezoresistive effect 3-79984
- silicide formation, from Hf films sputter deposited 3-69166
- single crystals, nearly perfect, lattice curvature, dislocation loops 3-60738
- slice evaluation, use of Sirtl etch 3-41673
- slice processing, flame emission analysis of K 3-54045
- in Sn solutions, 600-1000°C etching, solubility, effect of addition of metals rel. to liq. phase epitaxy 3-69165
- solar cell junctions, surface photovoltage obs. 3-41226
- solubility in cementite steels (German) 3-76160
- sorption from Black Sea using granulated $\text{Zr}(\text{OH})_4$ (Russian) 3-80698

silicon continued

- space charge limited conduction, thermal noise 3-68628
 space-charge-limited current of holes, expt. test of $S_V=4kT(U/I)$ 3-44076
 spectral growth of stimulated Raman emission 3-50579
 sputtering ion source, cluster obs. 3-61092
 sputtering yield with 15 and 45 keV ions 3-80130
 stacking faults, circular and hexagonal in bulk Si crystals. 3-49899
 Stark shift of Si I, Si II spectral lines from shock tube plasma 3-67659
 stopping cross section, for α -particles 3-64078
 strain determination, elastic, plastic, selected area channelling patterns 3-66379
 substrate, Ni film, thermal energy emission to liquid He 3-72246
 surface, condensation of metal vapours 3-79562
 surface, nitridation, LEED and Auger electron spectroscopy 3-43944
 surface, passivation mechanism, e.s.r. obs. 3-43943
 surface, with dielec. film, refr. index and thickness, ellipsometric method, accuracy 3-51591
 surface barrier detectors, mechanism of Al contacts aging 3-40009
 surface barrier detectors, variable detector mounting assembly 3-48535
 surface barrier diode, gold-on-n-type, light pulse excitation transient currents 3-64335
 surface electron states, calc. method within one-electron approx. 3-55329
 surface Fermi level position at 1350-1500 K 3-58314
 surface layer, in m.o.s. struct., carrier mobility, importance of phonon scattering 3-64409
 surface layer obs. after r.f. glow discharge, surface recombination rate meas. (Russian) 3-68685
 surface states, fast and slow distrib., of real Si surface, photoelec. meas. 3-55326
 surface states on atom free surfaces, obs. using e.p.r. and adsorption methods (Russian) 3-64394
 surface structure and chem., pre- and back-sputtering and cleaning processes 3-55161
 surface-sensitive photoeffects, expt. (Russian) 3-79739
 surface-sensitive photoeffects, theory (Russian) 3-79738
 surface-state transitions using electron energy-loss spectra 3-52887
 surfaces, Auger electron spectroscopy 3-68472
 surfaces properties using combined Auger electron spectroscopy and electron impact desorption 3-68505
 swirls, interaction with dislocations, comparison to striations 3-41647
 technology, appl. of ion-beam diagnostic techniques 3-57973
 thermal cond., boundary scatt. effects at room and dry-ice temps. 3-43904
 thermal conductivity, lattice, high temp., relax. time approx. 3-68375
 thermal conductivity, single cryst., dynamic obs., using cylindrical geometry 3-59559
 thin film, refractive index increase by dangling bonds 3-76109
 thin films, homoepitaxial defects, electron microscopy, formation processes 3-52765
 three-phonon umklapp resistivity, variational calc. 3-68378
 transmission electron microscopy, 2.5 MeV, penetration meas. 3-56982
 u.s. attenuation due to acceptor holes, internal stresses effects 3-50145
 valence band, spin-orbit effect 3-60857
 valence bands, X-ray photoemission cross-section modulation 3-44012
 valence electron momentum distrib. by Compton effect measurements 3-79633
 vapour deposition, semiconductor devices, single crystal and polycryst. films 3-41656
 vapour deposition, thin polycryst. layers, epitaxy, kinetics of growth, doping 3-41652
 wafers, diffusion of O, X-ray double crystal method, lattice strain meas. 3-41662
 wafers, surface defect detection, scattered light meas., He-Ne laser 3-41663
 whisker growth rate, vapour-liquid-crystal mechanism 3-72300
 X-ray diffraction, effect of neutron irradiation and B doping 3-68286
 X-ray dosimetry, adiabatic calorimeter, doses $>10^2$ rad., pulses of 1 sec. or less, description 3-66386
 X-ray emission, anomalous low energy $K\alpha$ lines after 30 MeV O⁺ irradi. 3-44503
 X-ray emission spectra, electron structure 3-55700
 X-ray normal and anomalous absorpt. 3-43724
 X-ray photoemission and electronic structure 3-64762
 yielding, dynamical of single crystals 3-79416
 μ^+ , polarised, anomalous precession, study via asymm. decay 3-52305
 Ag single crystal growth with selective electrochem. displacement in soln. 3-72787
 AgBr-Si, interface heterojunction, photoelectric properties 3-44110
 Al-Si contacts, resistivity inhomogeneity meas., spreading resistance method 3-41258
 n-AlAs, reflection spectrum, influence of Si donor centre (German) 3-50560
 Al_{1-x}Ga_xAs mixed crystals, e.p.r., carrier conc. and Si donor props. 3-55467
 Au-Si interface, mass spectrometric studies of contamination 3-41264
 B ion implantation, 3 to 8 MeV, electrical prop. meas. 3-79689
 Cu single crystal growth with selective electrochem. displacement in soln. 3-72787
 Ga-Si, liquid, Si contamination rate determ. 3-61118
 Ga_{1-x}Al_xAs:Si p-n structure, delay of electrolum., rel. to barrier capacitance 3-47316
 GaAs:Si, double heterostructure i.e.d., excitation source for up-converting phosphors 3-41584
 GaAs:Si, Ge, epitaxial growth, doping and energy levels 3-69177
 GaSb:Si, impurity level scheme 3-75722
 Ge/Si layer, dislocation nodes study, by weak-beam technique of transmission electron microscopy 3-59666

silicon continued

- lnP:Si, donor impurity, elec. and photoluminesc. props. 3-41581
 Mo/Au-SiO₂-Si, low-temp. treatment at 300 to 400 C, H₂ ambient, change of threshold voltage meas. 3-55337
 Na contamination, monitoring using flame emission spectrometry 3-69169
 Pt-Si contact, heat treatment, alloyed layers, solid state reaction kinetics 3-69485
 Si, Li, adsorbed layer characterisation by photoemission obs. (French) 3-44516
 Si detectors, thickness measurement of sensing region 3-53979
 n-Si electron-phonon interactions, quadrupole and octupole, mobility and piezoresistance, and experiment calculation 3-46842
 Si I, lifetime meas. of optical levels 3-54565
 Si I lines, absolute oscillator strengths in 2500-8000 Å region 3-60375
 Si I solar photospheric lines, Si abundance from analysis of 19 lines 3-59255
 Si II-IV, radiative lifetime meas. in the vacuum u.v. 3-40570
 Si VIII, transition probability for forbidden line in solar spectra 3-42132
 Si:Ag, impurity photocond. edge shift under influence of combined illumination 3-46875
 Si:Ag, photocapacitance and its quenching, impurity levels, 77K 3-44113
 Si:Al, limit solubility determ., temp.-gradient fusion zone method 3-44543
 Si:Ar, ion implanted, e.s.r. obs. 3-68834
 Si:As, epitaxial growth process, vapour etching, autodoping, impurity profiles 3-41654
 Si:Au, compensated, p-i-n structure, current-voltage characts. 3-60915
 n-Si:Au, deep impurity levels, injection field effect, negative resist. region 3-64351
 Si:Au, i.r. absorp. spectra, localised pair centre vibration and neutral centre obs. 3-72690
 Si:Au wafers, EIDP deposited, Si₂W crystallite growth on surface 3-72813
 Si:B, doping in oxidizing atmosphere 3-80178
 Si:B, emission lines and model of multiple exciton complexes bound to impurities 3-58553
 Si:B, fast electron irradiated, diffusion profile changes obs. 3-60740
 Si:B, ion implanted, acceptor profile from diffusive redistrib. during annealing 3-53187
 Si:B, ion implanted, precip. obs. by α -particle channelling analysis 3-55738
 Si:B, negative creep during bending 3-55012
 Si:B, polycryst. films, effect of doping on growth, microstructure and elec. props. 3-41657
 Si:B, polycryst. films, elec. cond., effect of growth from SiH₄, carrier conc. 3-41658
 Si:B, stress depend. of g-tensor 3-68842
 Si:B, vacancy diffraction length at 1000°C, rel. to impurity profile 3-64788
 Si:B,P, ion implanted, conc. profiles, annealing effects 3-53191
 Si:B film, chemical vapour deposition, 300 to 550°C 3-80180
 Si:B impurity, electron capture cross section study using microwave absorption technique 3-79710
 Si:C, state of impurity, electron diff. obs. (Russian) 3-72101
 Si:Cu, resistivity obs. of local disturbances due to Cu precipitates 3-60872
 Si:Fe, precip. of Fe, electron irradi. effects 3-43810
 Si:Fe plastically deformed, Fe atoms influence on energy spectrum and Hall mobility 3-41157
 Si:Ge, ion implanted, deep trap levels, Schottky barrier obs. 3-52802
 Si:Ge, oxide interface properties, surface state density function measurement 3-60921
 Si:Li, electron irradi. effects, comment 3-64069
 Si:Li, irradiated, spectra of Li-defect complexes 3-44434
 Si:Ni(Zn), short wavelength quenching of photocond. 3-50240
 Si:O, irradiated and annealed, influence on luminesc. spectra 3-61069
 Si:O e.s.r., oxygen content in floating zone single crystals, method (German) 3-53018
 Si:P, As, Sb shallow donor ground states, pseudopot. theory, effective mass 3-50146
 Si:P, emission lines and model of multiple exciton complexes bound to impurities 3-58553
 Si:P, epitaxial growth, surface band bending, surface Fermi level 3-41655
 Si:P, ion implanted, conduction electrons, e.s.r. 3-68846
 Si:P, ion implanted, profiles of channelled and dechannelled impurities 3-54974
 Si:P, quadratic Zeeman effect, variational calc. 3-58515
 Si:P, slow neutron irradiation, uniform standard specimens, resistivity meas. accuracy check 3-47353
 Si:P layer, ion implanted through oxide layer, elec. props. 3-46845
 Si:Rh, photoelectric. obs. of impurity states 3-64377
 Si:Sb(P), (Au), zone refined, distribution of impurity elements, quantitative autoradiography 3-41651
 Si:W, negative differential cond. in carrier capture by repulsive centres, double injection conditions 3-50216
 Si:Zn, induced impurity photocond. 3-41233
 Si:Zn, thermal capture of electronic and holes at Zn centres, p-n junction obs. 3-68562
 Si/Ag films, evaporated, kinetics of crystallisation processes 3-43967
 Si/SiO₂ interface, ion bombardment effect on electrical props. 3-41268
 Si-Al-Au alloy, zone refining, conc. depend. of motion, crystn. rate 3-68176
 Si-Au n-type surface barrier detector, depletion depth 300 to 500 μ 3-66321
 Si-CdS, three-layer system, propag. of elastic transversal waves, dispersion eqns. (Russian) 3-55026
 Si-Ge heterojunction, electrostatic energy 3-58317
 Si-H-Br and Si-H-I equilibrium behaviour, semiconductor growth 3-50666

silicon continued

- Si-LiNbO₃ layered structure, acoustoelec. effect due to elec. fields of u.s. surface waves 3-44120
 Si-LiNbO₃ layered structure, acoustoelec. effects 3-58308
 n-Si-metal system, electron energy distrib. rel. to current 3-79768
 Si-SiO₂, change of interface charge by BT treatment 3-79773
 Si-SiO₂, photoconductivity, photoelectromotive force, i.r. light absorption (*Russian*) 3-58322
 Si-SiO₂ interface, energy spectrum of surface states, determ. from m.o.s. C-V characts. 3-58321
 Si-SiO₂ interface, inversion layer, localised states 3-79772
 Si-SiO₂ interface, use in m.o.s. technology, review 3-50278
 Si-SiO₂ structure, secondary ion emission analysis, Na impurity distrib. obs. (*Russian*) 3-52904
 Si-SiO₂-Hg, struct. inhomogeneity, scanning Hg probe, capacitance, cond. meas. 3-72406
 Si-SiO₂-electrolyte system, rel. to electrorefl. spectra in strong surface elec. fields 3-50543
 SiII, spectral line and oscillator strength calcs., P, S series 3-78411
 Si(Li) detector, Au-layer and dead-layer thickness determ. 3-51713
 Si(Li) detectors, for proton-induced C(K_α) X-rays 3-51707
 Si(001)/Al(0112) films, anisotropy in electrical props. 3-41269
 Si(111), surface states and bonds, pot. construction 3-52888
 Si(111)7 surface, folding and nonfolding electron distrib. in ion neutralisation spectroscopy and electronic superlattice 3-58579
 W-Si(C), work function depend. on adsorbed layer thickness, electron field emission obs. 3-43930
 W/Au-SiO₂-Si, low temp. treatment at 300 to 400 C, H₂ ambient, change of threshold voltage meas. 3-55337
 YIG:Si, low temp. magnetostriction 3-58407
 YIG:Si, photoinduced linear dichroism, temp. depend. calc. 3-47226

silicon compounds

see also quartz; silicones

- alkylsilane, vibr. freq. obs. and force const. determ. 3-67776
 binary silicate relation of vitron theory to 2 layer-liquid immiscibility 3-63957
 carbide, whisker growth by vapour-liquid-solid phase mechanism (*Russian*) 3-72297
 condensation nuclei, production by peristaltic pump friction on rubber and silicone 3-46674
 glassy semiconductors based on Te, As, Si, Ge, temp. dependence of conductivity (*Russian*) 3-60870
 interstellar silicate grains, ice-coated, opacity calc., interstellar extinction curve 3-48124
 metal-Al₂O₃-(SiO₂-Si) structure, C-V characteristics, effects of bias application 3-52901
 mullite fibre, fine diameter, characteriz. for high temp. use 3-76275
 ores, X-ray fluorescent determ. of Si and Al, rel. error calc. 3-48655
 organosilicon, ²⁹Si, ¹³C n.m.r. meas., substituent effect 3-72533
 organosilicon compounds, ²⁹Si n.m.r. spectra 3-71596
 oxide coating for Ag surface optical film 3-56660
 photoelectron spectra, binding energy shifts 3-54638
 polysilicic acid gels, mol. structure 3-44686
 polysiloxanes, liquid, viscous flow at high pressures, free energy, enthalpy, entropy, vol. of activation calc. (*Russian*) 3-46367
 pyrosilicates with linear bridge, vibr. spectra and isotopic shifts 3-46285
 silica fibre compacts, sintering, model, densification of fibrous structure 3-50757
 silica gels, correlation of orthopositronium annihilation and surface props. as a function of temp. 3-40936
 silica glasses:TiO₂, small angle neutron scattering for inhomogeneous structure obs. 3-68169
 silica-reinforced composites, surface ablation 3-80438
 silicate ceramic, theoret. and exptl. mech. props. comparison 3-72956
 silicate glass:Fe³⁺, gamma-ray induced e.p.r. spectra (*Russian*) 3-79911
 silicate glass, complex, unslating struct. 3-76323
 silicate glass, isotropic, elastic constants, Brillouin scatt. obs. 3-64081
 silicate glass, volume composition relation 3-80479
 silicate grains, i.r. extinction cross sections 3-77170
 silicates, liq., thermodynamic props. of Masson polymerization models 3-65081
 silicoborate garrelsites, crystal structure determination 3-73225
 silicon organic esters of phosphoric acids, crystalless roentgenofluorescent anal., Si and P determ. 3-48662
 soda-lime-silica glasses, org. liq. environment effects on crack propagation 3-72968
 β-spodumene and β-spodumene-SiO₂ solid soln., electric conductivity versus temperature 3-44101
 system, phase equilib. diagram, 1500°C 3-76337
 tetra-allyl silane, vibrational spectra 3-46294
 titanite-silica glasses, thermal expansion meas. by photoelastic and u.s. techniques 3-51593
 vitreous silica uncalcd fibre, spectral loss meas. 3-53073
 Al-Cu-Si-Mn alloy, extruded bars and sections, coarse grain behaviour, prior thermal treatment influence (*German*) 3-44639
 Al-SiO₂ films, crystallisation (*German*) 3-68524
 Al-SiO₂-Al sandwich films, dielectric breakdown voltage obs. 3-58476
 Al-SiO₂-Au structure, internal photocurrent (*French*) 3-41274
 Al-SiO₂-Au structures conduction phenomena, Poole-Frenkel effect (*French*) 3-72411
 As-Te-Ge-Si, amorphous, local potential distrib. and I-V characts. 3-64343
 Au-SiO₂-Au thin film devices hot electron attenuation in oxide layer 3-41272
 B₂O₃-SiO₂ glass melts, cryst. growth kinetics 3-75481
 B₂O₃-SiO₂-GeO₂ glasses, characteriz. w.r.t. struct. 3-76271
 CaO-Al₂O₃-SiO₂-MgO, cordierite-based glass ceramic, metastable zoning, scanning electron microscopy 3-80429
 CaO-MgO-P₂O₅-SiO₂ glass containing fluorine, crystallisation, EPMA (*Japanese*) 3-68170
 CaO-MgO-SiO₂ glass, electron microscope investigation, crystallisation (*Russian*) 3-63958

silicon compounds continued

- CaO-MgO-SiO₂ glass system, crystallisation, electron microscope obs. (*Russian*) 3-52582
 CaO-MgO-SiO₂ system, stability relations of bredigite 3-76239
 CaO-MgO-SiO₂-V₂O₅ system, phase equilib. diagrams, 1450°C 3-76338
 CdO-B₂O₃-SiO₂ glasses, phase separation effects on photocond. props. 3-75767
 Cu/silica system, work hardening, diffusional stress relax., surface diffusion coeffs. 3-55827
 Cu-Si alloys, stress-strain characts. and slip band formation 3-47407
 Fe-Si(100) single crystals, photoelectric work function and Auger electron spectroscopy 3-61082
 Fe₃O₄-CaO-SiO₂, self-fluxing agglomerate, sintering, reaction conditions (*French*) 3-69330
 Ge_{1-x}Si_x film, electrorefl. spectra 3-76020
 Hg-SiO₂-Si structure, scanning Hg probe investigation 3-72406
 Li-Si-O-N system, comp., sialon struct. characts. 3-75474
 LiO₂-Al₂O₃-SiO₂ glass microstructure, dependence on composition, X-ray analysis 3-55902
 Li₂O-Al₂O₃-SiO₂ glasses, internal friction, crystn. effect, relax. peaks 3-76269
 Li₂O-Al₂O₃-SiO₂ glass ceramic, thermal expansion rel. to crystallinity 3-76302
 Li₂O-SiO₂ glasses crystallized after ion exchange below T_g, characteriz. 3-76266
 Li₂O-Al₂O₃-4SiO₂ graphite fibre reinforced composite, elevated temp. props. 3-76351
 Li₂O-Al₂O₃-nSiO₂ graphite fibre reinforced composite, fabrication and low temp. props. 3-76350
 Mo/Au-SiO₂-Si, low-temp. treatment at 300 to 400 C, H₂ ambient, change of threshold voltage meas. 3-55337
 Na₂O-CaO-SiO₂ glass rods, bend strength, thermal stress resist., abrasion effect 3-76328
 Na₂O-SiO₂ glass, He diffusion and solubility, phase separation effect 3-69382
 Na₂O-SiO₂ glass, immiscibility temp., Al₂O₃ and Ga₂O₃ additions effect 3-69383
 Na₂O-SiO₂ glasses, Nernst-Einstein relation 3-76459
 Na₂O-SiO₂ glasses, strength characteriz. 3-76267
 Na₂O-SiO₂(75%) glass, heat capacity, 1.5-25 K 3-72206
 2Na₂O.2Al₂O₃.3SiO₂ based glasses, crystn. 3-73032
 Nb-Al-Si alloy, at. absorption spectroscopy (*French*) 3-50678
 Nb-Al-Si alloy, isothermal sections at 1500°C and 1300°C, Nb(Si,Al)₂ phase behaviour (*French*) 3-50677
 Ni-SiO₂ film, granular metal, hopping cond., temp. depend. 3-52839
 PbO magnetic susceptibility anisotropy, mol. g_f-factor, quadrupole moments (*German*) 3-71539
 PbO-SiO₂ glasses, radiation induced absorpt. and decay after irradiation 3-76030
 PbO-TiO₂-SiO₂ system glass, Al₂O₃ addition effect on glassy phase separation and crystn. (*Japanese*) 3-65023
 Si-Al system, stability of zone melting with temp. gradient 3-80177
 Si-Al-O-N system, composition, sialon structure characts. 3-75474
 Si-As-Te, amorphous, relation of elec. and optical gaps, d.c. cond. and light absorpt. obs. 3-72308
 Si-Au, eutectic alloy, large area contacts on n-type Si, low temp. techniques 3-48391
 Si-Ge-Te-As system, amorphous, e.s.r. obs. of Mn²⁺ from 420 to 77K and at 4.2K 3-64550
 Si-Sb, solid solution, dislocation loops, high temp. precipitation 3-75535
 Si-SiO₂, change of interface charge by BT treatment 3-79773
 Si-SiO₂ interface, energy spectrum of surface states, determ. from m.o.s. C-V characts. 3-58321
 Si-SiO₂ interface, use in m.o.s. technology, review 3-50278
 Si-SiO₂ structure, secondary ion emission analysis, Na impurity distrib. obs. (*Russian*) 3-52904
 Si-SiO₂-electrolyte system, rel. to electrorefl. spectra in strong surface elec. fields 3-50543
 SiAs, cryst. struct., elec., optical props., layer structs. (*Japanese*) 3-72070
 SiB₆, hot pressing, densification, compressive strength, microhardness, fracture surfaces 3-80421
 SiBr molecules, centrifugal distortion constants determ. 3-74988
 SiC, 4H polytype, grown from Si melt, photolum. 3-61063
 α-SiC, 6H and 15R polytypes, intensities of X-ray refl. from basal plane 3-55131
 α-SiC, 6H polytype, activated by u.v. illumination, i.r. absorpt. 3-55600
 SiC, 6H polytype, diffusion-doped, struct. imperfections 3-55741
 α-SiC, 6H-polytype, impurity i.r. absorpt. (*Russian*) 3-80083
 SiC, ceramics, acoustic fatigue 3-76292
 SiC, chem. vapour deposited, nucleation and residual stress 3-72938
 SiC, dissolution kinetics in Fe melt (*German*) 3-76192
 SiC, etching by fused Na₂O₂, reaction rate, dislocations 3-68508
 SiC, exciton-impurity complexes spectra, impurity centres interaction, photolum. 3-44046
 SiC, far i.r. absorpt. bands, narrow doublet lines 3-44445
 SiC, fracture energy during slow crack growth 3-72936
 SiC, fracture energy eval. using notched beam test 3-72934
 6H SiC, H- and D-implanted, efficient luminescence centres 3-58558
 β-SiC, hexagonal pillar shape, surface polarities 3-43922
 SiC, high density, thermal cond., 25-1300°C 3-72944
 SiC, high temp. reaction with SrO, in air, Ar and in vacuum 3-74723
 SiC, hot-pressed, fabrication and strength characteriz. 3-76295
 SiC, hot-pressed, shear modulus meas., 350-1000°C 3-72944
 SiC, i.r. absorpt. on surface, multiple internal reflection method obs. 3-55580
 SiC, luminesc. rel. to high temp. annealing 3-44492
 β-SiC, n-type, impurity photoconductivity (*Russian*) 3-68664
 SiC, n-type hexagonal, thermoluminescence phosphorescence and cryoluminescence 3-55681
 SiC, neutron irradi. induced defects, TEM specimen prep. by ion-bombardment thinning 3-57977
 n-SiC, optical absorption associated with superlattice 3-41533

silicon compounds continued

- SiC, p- and n-type, i.r. absorpt., role of free carriers 3-75996
 SiC, plastic deformation in temp. zone near brittle failure, investig. method and apparatus (*Russian*) 3-80514
 α -SiC, polarity, reflection spectra of polished faces 3-43772
 SiC, pyrolytic, Cs migration 3-43296
 β -SiC, pyrolytic, irradi. induced void behaviour 3-63191
 β -SiC, pyrolytic, neutron-irrad., thermal cond. 3-40539
 SiC, pyrolytic, nuclear fuel particle coating, h.v. transmission electron microscope obs. 3-49368
 SiC, pyrolytic coatings of fuel particles, strength characteriz. 3-43311
 SiC, reaction-sintered, β -SiC growth during sintering, microstruct. characteriz. 3-76300
 SiC, reaction-sintered, growth characts., polytype distrib., 6H₂ struct. absence 3-76299
 SiC, reaction-sintered, self-bonding characts., TEM obs. 3-76301
 α -SiC, recrystallisation during reactive sintering 3-80433
 SiC, relation between elastic constants of hexagonal and cubic polytypes 3-54997
 SiC, Si-bonded, fission fragment irradi. effect on passive oxidation, 950°C 3-67551
 SiC, slow crack growth at elevated temps. 3-76290
 SiC, solution growth from liquid Si using modified travelling heater method 3-64771
 SiC, strength, vol., area and temp. depend. 3-76285
 SiC, strengthening by quenching 3-76283
 SiC, surface film etching, chemical and discharge treatment (*Russian*) 3-68509
 SiC, thermal shock testing 3-76394
 SiC, thermal-shock damage 3-61193
 SiC, thin film structure, morphology and growth on silicon substrate (*Russian*) 3-68515
 β -SiC, twin boundary, X-ray topography, optical probe exam. 3-72097
 SiC, very high pressure hot pressing 3-50755
 SiC, wetting by silicon and alloys, contact angle meas., rel. to reaction sintering 3-76298
 SiC addition in HfB₂, effect on high temp. oxidation 3-72953
 SiC coatings for fuel particles, fabrication and performance 3-43300
 SiC crystal growth by vapour-liquid-solid mechanism in sublimation method 3-80160
 SiC growth of SiC films by liquid-phase epitaxy 3-72278
 SiC polytype 189R, structure and growth, X-ray diffraction analysis 3-60689
 SiC polytypes, elec. cond., temp. depend. of anisotropy, comparison 3-58272
 SiC polytypes, structural stability and growth 3-64007
 SiC refractories, bonded, strength, fracture and thermal shock 3-76288
 SiC refractories, microstruct. analysis 3-80413
 SiC single crystal, improved sublimation growth method (*Japanese*) 3-47354
 SiC thin film on S, thickness meas. from lattice absorption bands 3-56616
 SiC:B, hot-pressed, strength correl. with grain struct. 3-76297
 SiC:B,N, cathodolum., intensity depend. on excitation 3-61078
 SiC+GdP+C system, atomisation energies of gaseous mols. produced, mass spectrometry 3-75096
 SiC(6H), exciton electroabsorpt. spectrum, cond. band localization 3-72677
 α -SiC(6H), photolum. of excitons localised at donor-acceptor dipoles 3-72714
 SiC and composites, characteriz. for turbine applics. 3-76281
 SiCl, rel. intensities of band spectra, vibrational overlap integral, calc. of Franck-Condon factors 3-78733
 SiF₂, microwave spectrum in excited vibr. states, equil. struct., pot. function, Coriolis reson. 3-67831
 SiF₄, bond length and vibr. amplitude by electron diff. 3-74915
 SiF₄, CO₂-laser induced dissociation 3-52391
 SiF₄, crystals i.r., Raman spectra, 2 phonon absorpt. 3-69001
 SiF₄ dissociative electron detachment processes 3-46343
 Si₂Ge_{1-x}, epitaxy on Ge, by simultaneous thermal decomp. of SiH₄ and GeH₄ 3-41627
 SiH₄, deposition of Si and Si:B, effect of growth on elec. props. 3-41658
 SiH₄, endothermic ion-mol. reactions 3-40666
 SiH₄, ground state energies and bond distances, stat. OCE calcs. (*German*) 3-67745
 SiH₄, ionization and dissociation by electron impact, expt. obs. 3-54742
 SiH₄, multiple-scatt. $\chi\alpha$ calcs. 3-54629
 SiH₄, ν_3 band, high resolution obs. (*French*) 3-54678
 SiH₄, one-centre HF calculations on ground and excited states 3-71509
 SiH₄, silane, atomic X-ray photoemission cross-section modulation 3-44012
 SiH₄-H₂O system, memory performance of m.o.s. transistors with SiO₂ films 3-46896
 SiH₄-He and SiH₄-H₂ mixtures, for Si epitaxial growth, comparison 3-41626
 Si₂H₆, Si₂D₆, mol. force fields and isotopic rules determ. 3-54653
 SiH₃N₃, (p \rightarrow d) π -bonding in Si-N bond 3-43419
 (SiH₃)₃N, (p \rightarrow d) π -bonding in Si-N bond 3-43419
 SiH₃NCO, (p \rightarrow d) π -bonding in Si-N bond 3-43419
 SiH(halogen)s, calc. of molecular Coriolis coupling constants 3-63418
 Si(Li) position and energy sensitive detector 3-70389
 SiN thin film, vapour deposited, physical, chemical and electrical properties variations with excess Si content 3-46850
 Si₃N₄, α and β phases, electron diff. data 3-60658
 Si₃N₄, α - and β -type, hot pressing 3-76282
 Si₃N₄, ceramics, acoustic fatigue 3-76292
 Si₃N₄, fracture energy during slow crack growth 3-72936
 Si₃N₄, hot pressing, high temp. flexure strength rel. to impurities, 1375°C 3-76305
 Si₃N₄, hot-pressed, creep and tensile strength 3-76286
 Si₃N₄, hot-pressed, impurities and inclusions identification 3-76284
 Si₃N₄, hot-pressed, low cycle fatigue 3-76287

silicon compounds continued

- Si₃N₄, hot-pressed, shear modulus meas., 350-1000°C 3-72944
 Si₃N₄, hot-pressed, UTS, room temp. to 2800°F 3-76291
 Si₃N₄, isothermal etch rates, HF dilution, temp. and conc. dependence 3-41660
 Si₃N₄, mech. and dielec. props., effect of fabrication conditions 3-76294
 Si₃N₄, pressureless densification 3-69350
 Si₃N₄, reaction sintered, creep obs. and mechanism, 1200-1400°C (*German*) 3-61186
 Si₃N₄, shape and thermal shock behaviour 3-76289
 Si₃N₄, slow crack growth at elevated temps. 3-76290
 Si₃N₄, strength, vol., area and temp. depend. 3-76285
 Si₃N₄, thermal shock testing 3-76394
 Si₃N₄, vapour phase reaction prep. 3-76129
 Si₃N₄, wetting by silicon and alloys, contact angle meas., rel. to reaction sintering 3-76298
 Si₃N₄ ceramic, sonic fatigue rel. to thermal shock treatment and microstructure 3-69359
 Si₃N₄ film, on Si-SiO₂ struct., effect of ambients on immobilisation of ionic contaminants 3-46902
 Si₃N₄ film, vapour deposited, thickness uniformity 3-53197
 Si₃N₄ ion implantation range distribution measurements, backscattering of 2 MeV He⁺ ions 3-49918
 Si₃N₄ vapour deposited thin films, conductivity in high fields 3-55272
 Si₃N₄/W, fibre reinforced, strength characteriz. for high temp. applics. 3-76352
 Si₃N₄-n-GaAs interface, energy spectrum of states at boundary (*Russian*) 3-50271
 Si₃N₄-SiC composite system, microstruct. effect on strength 3-76296
 Si₂NO, mass spectrometric evidence, heat of formation and atomisation 3-54731
 Si₃N₄ and composites, characteriz. for turbine applics. 3-76281
 SiO, absorpt. coefficients for CO₂ laser radiation, rel. to interaction at metal surface 3-70837
 SiO, in interstellar matter, E Σ^+ -X Σ^+ transition, radiative lifetimes and band oscillator strengths 3-73547
 SiO, in m.i.m. struct., breakdown strength using different cathode metals, avalanche theory 3-46907
 SiO, rotational magnetic moment and magnetic susceptibility, form mol. beam electric resonance spectroscopy 3-78727
 SiO, vacuum u.v. absorpt., electronic states analysis 3-63449
 SiO films, cond. mechanism, metallic impurities influence (*French*) 3-50199
 SiO in giant and supergiant atmospheres i.r. absorption 3-81054
 SiO layer on Si, cathodoluminesc. from centres responsible for radiation induced space-charge build up 3-50275
 SiO-Ag superlattices, switching effect 3-72400
 SiO-PbO-Fe₂O₃ glass, electronic cond. meas., mechanisms, comp., temp. depend. 3-79682
 SiO₂, adsorption of benzene, methanol, ethylene oxide, epichlorohydrin, anomalous sites characterisation 3-68489
 SiO₂, and silica-containing materials, reaction with steel, melts, calc. O₂ diffusion (*German*) 3-72969
 SiO₂, antireflection coatings, moisture resistant, vac. evaporation 3-62074
 SiO₂, charge build up from electron irradiation 3-44372
 SiO₂, charge injection from Si p-n junction reversed biased below breakdown 3-55333
 SiO₂, drift mobility and lifetime meas., applied field depend. 3-50211
 α -SiO₂, e.p.r., defect anion radical traps struct. 3-68843
 SiO₂, effect of dissolved metal oxides on content in minerals, shift of liquidus boundaries, significance in magma genesis 3-80653
 SiO₂, film on surface, Na₂O₂ etched SiC, oxygen diffusion 3-68508
 SiO₂, fused, Hertzian fracture strength 3-58736
 SiO₂, fused, W fibre reinforced composite, hot pressing, mech. strength 3-76360
 SiO₂, in m.o.s. struct., ion beam degradation of electric strengths, inert ambient annealing 3-60919
 SiO₂, in m.o.s. structure, KV electron energy dissipation in depth 3-72110
 SiO₂, inheritance of Si defects during oxidation of films, transmission electron microscopy 3-72276
 SiO₂, isothermal etch rates, HF dilution, temp. and conc. dependence 3-41660
 SiO₂, N.M.R. of adsorbed water layer 3-61000
 SiO₂, nonavalanche injection of hot carriers in MOS transistor 3-46895
 SiO₂, porous powder compact, specific surface area, pore struct. rel. to compaction, adsorpt. obs. 3-41801
 SiO₂, sputtering, surface binding energy, temp. depend. 3-69119
 SiO₂, time depend. of injection currents, homogeneous charge trapping 3-46841
 SiO₂, vitreous, diffusion of O₂ 3-76331
 SiO₂ antireflection coatings on fluorite lenses 3-62068
 SiO₂ coatings, thickness meas. by X-ray diff. 3-73676
 SiO₂ filler effects on dielec. props. of rubber 3-55516
 SiO₂ film, chemically-etched edge profile depend. on etchant conc. and temp. 3-80194
 SiO₂ film, differential spectral study (*Russian*) 3-72296
 SiO₂ film, etching of layers, structure by treatment with HF vapour 3-72287
 SiO₂ film, grown in Cl₂ and HCl atmosphere, Cl profile 3-41643
 SiO₂ film, image forces and behaviour of mobile positive ions 3-41267
 SiO₂ film, in m.i.m. struct., time dependent breakdown due to Na ions 3-52911
 SiO₂ film, on Si, effect of ambients on immobilisation of ionic contaminants 3-46902
 SiO₂ film, on Si, field enhancement dielec. breakdown, effect of mobile Na⁺ ions 3-79982
 SiO₂ film, on Si, ion drift rate 3-68447
 SiO₂ film, r.f. sputtered, dielec. props., 5 \times 10⁻⁴-10⁵ Hz freq. range 3-68924
 SiO₂ film, recoil Ag implantation, discrete cluster formation 3-72112

silicon compounds continued

- SiO₂ film, thickness meas. and chemical charac., by ATR i.r. spectroscopy 3-48442
- SiO₂ film defect exam. by scanning electron microscopy 3-68146
- SiO₂ film properties, effects of bombardment by Ar ions in r.f. plasma (*Russian*) 3-68706
- SiO₂ films, containing P, B, Zn, i.r. spectra 3-64646
- SiO₂ films, dipole relaxation time and dielectric loss factor in low frequency, thermally stimulated current 3-50507
- SiO₂ films, high-temperature oxidation of Si, internal stresses obs. 3-58191
- SiO₂ films, ion drift obs., influence of O annealing 3-60922
- SiO₂ films, memory performance of m.o.s. transistors prepared by SiH₄-H₂O system 3-46896
- SiO₂ films, plasma oxidized dielectric strength and interface-state density 3-44154
- SiO₂ films, thermally grown, role of protons 3-80190
- SiO₂ films on Si, ion bombardment effect on electrical props. 3-41268
- SiO₂ formation in SiC, SrO high temp. reaction in air, Ar and vacuum 3-74723
- SiO₂ impurity in partially stabilized zirconia, role in sintering 3-69346
- SiO₂ ion implantation range distribution measurements, backscattering of 2 MeV He⁺ ions 3-49918
- SiO₂ mass spectrometry evaporated by electron beam 3-75097
- SiO₂ noncatalytic surface for nitrogen recombination (*Russian*) 3-63610
- SiO₂ powder, mag. quenching of orthopositronium, effects of chemisorbed water 3-52642
- SiO₂ protective layers on ion-implanted InSb, backscatt. study 3-41677
- SiO₂ support, NaOH addition effects on morphology and struct. 3-58773
- SiO₂ surface, n-butanol vapour chemisorption 3-73165
- SiO₂ suspension, electroviscous nonaqueous, shear flow in transverse electric field 3-73080
- SiO₂ tapered windows by ion implantation 3-61117
- SiO₂ thin film, transmission, reflection and absorption of electrons, 4 to 30 keV, obs. 3-68285
- SiO₂/TiO₂ antireflection coating on glass, evaluation (*Czech*) 3-66189
- SiO₂-Al₂O₃, on Si, interface charge, traps due to oxygen vacancies 3-68705
- SiO₂-Al₂O₃ surface, CO₂ adsorption, quadrupole interaction 3-52750
- SiO₂-Al₂O₃ system, stable and metastable equil. 3-76238
- SiO₂-Al(V)(Cr)(Mo), heterogeneous reactions, deposition conditions, heat treatment 3-72405
- SiO₂-B₂O₃-Na₂O system, tie lines in metastable immiscibility region 3-55075
- SiO₂-C adsorbents, water vapour adsorption 3-43931
- SiO₂-Fe₂O₃-Li₂O compositions, magnetic, elec. and physical props. 3-64967
- SiO₂-Li₂O-Al₂O₃ glass, uniform introduction of OH group by addition of LiOH.H₂O 3-49849
- SiO₂-Li₂O-ZnO, glass-ceramic, high temp. creep, tension, compression 3-76319
- SiO₂-Li₂O-ZnO, glass-ceramic, compression creep and recovery, 590-750°C 3-76320
- SiO₂-metal systems, chemical reactions, voltage-capacitance characts., thermal instability 3-72404
- SiO₂-MgO-Al₂O₃ glass, e.p.r. spectra, theory 3-68833
- SiO₂-Na₂O glass, with CaO and P₂O₅ ceramics, composite material for prosthetic applic. 3-55876
- SiO₂-PbO glasses, electrical conductivity, dielectric constant, depend. on PbO conc. 3-55266
- SiO₂-PbO-P₂O₅ system glasses, microstruct., heat treatment effects 3-76261
- SiO₂-Si, photoconductivity, photoelectromotive force, i.r. light absorption (*Russian*) 3-58322
- SiO₂-Si interface, inversion layer, localised states 3-79772
- SiO₂-TiO₂ glasses, e.p.r. study of Ti³⁺-Ti⁴⁺ reaction 3-76418
- SiO₂-TiO₂-Li₂O-K₂O glass, n.m.r. spectra of ⁷Li, ion struct. 3-72528
- SiO₃ thin films, elec. microinhomogeneities, electron emission microscopy (*Russian*) 3-50282
- SiO₄ anions, e.p.r., defect radical traps struct. in ZrSiO₄, α-SiO₂ 3-68843
- SiO₄⁴⁻, electronic structure, mol. orbitals, two atom differential overlap approx. 3-78687
- SiO_x film, stress relief induced by u.v. radiation 3-64266
- SiO₂-K₂O-SrO glasses, i.r. spectra, struct. 3-68164
- SiP₂O₇, cubic, superstruct., soln. using computer simulation 3-46626
- SiP₂, absorption spectra, optical properties between 300 K and 100 K 3-47285
- Si₃Te_{1-x}, crystalline and amorphous props. 3-58556
- SiTeAsGe amorphous flss thin film switch, injection processes and threshold switching characs. 3-55317
- Si₃W₃O₁₂, tungsten bronze preparation by chemical transport process, X-ray study 3-53178
- Ta-Ta₂O₅-ZnS:Ti³⁺-SiO₂-Au, films electroluminescent, electron injection via tunnelling mechanism 3-50626
- TiO₂-SiO₂ glass, migration of Ne, activation energy, strain energy depend. 3-76330
- Ti₂O-GeO₂-SiO₂ glasses, i.r. detection of depolymerization 3-58500
- UO₂-SiO₂ system melts, spinodal decomp. and primary crystn. 3-72984
- UO₂-SiO₂ vitroceraic rods, Cu admission and distribution 3-57581
- W/Au-SiO₂-Si, low temp. treatment at 300 to 400 C, H₂ ambient, change of theshold voltage meas. 3-55337
- p-ZnSiP₂, conductivity, Hall effect, mobility, temp. depend. 3-68624
- ZnSiP₂ with pseudodirect energy gaps, band struct. 3-41136
- ZnSiP₂-ZnSiAs₂ range of semiconductor, optical absorption edges at 300 K and 80 K 3-55604

silicon controlled rectifiers *see* thyristorssilicon integrated circuits *see* monolithic integrated circuitssilicon reference diodes *see* avalanche diodes**silicones**

- liquid, electric breakdown under pulsed h.f. fields 3-68925

silver

- adsorption, of O, single crystals, (111) face, electron and argon ion bombardment cleaned under ultra high vacuum, work function 3-43938
- adsorption of O, field emission obs., heating effects, changes in average work function 3-55147
- alkali halide:Ti, Ag, tunnel luminescence (*Russian*) 3-41560
- atom, photoelec. cross sections, Z-depend. 3-67681
- atom, photoelectric cross section for 145 keV gamma rays 3-49406
- atom, resorption into latent image centres, activation energy calc., nonreciprocal substitution, emulsions (*Russian*) 3-50854
- atomic absorption spectroscopy, trace metal determ., lubricating and crude oils, evaluation of carbon-rod atomiser 3-70485
- band edge effects on strain modulation electron tunnelling in m.i.m. diode 3-55344
- Bordoni internal friction peak obs. 3-60772
- cathode sputtering coeff., Ar, He and Xe discharges, role of ion capture (*Russian*) 3-69128
- channelling, positive ions liberation under heavy ion bombardment 3-42641
- chemisorption of O, X-ray and u.v. induced photoelectron spectroscopy 3-55159
- chemisorption on metal and oxide substrates, obs. of sticking coefficients 3-60840
- colloidal, spectral extinction 3-44688
- concentration in biological samples, trace amount determ. by neutron activation 3-62359
- creep rupture as cause of operational damage (*German, English*) 3-61174
- crystal, (111) plane, Ar and Ne atoms scattering, velocity distribution meas. 3-47336
- Debye-Waller factors, temp. variation, calc. using modified non-central force model 3-43858
- deformation potentials under tetragonal, trigonal shears in Brillouin zone 3-55193
- deformed, dislocation recovery before onset of recrystn. (*French*) 3-54999
- deformed, local internal friction determ. during recrystn. (*French*) 3-55028
- deformed by rolling, recrystn. kinetics from internal friction (*French*) 3-55029
- deposition on Ni, model for Auger electron spectroscopy of layer growth systems 3-41605
- developed grains, optical constants calc., filamentary thickness 3-47224
- diffusion, in Li, impurities, force transport, electro- and thermo-transport, steady-state technique 3-52724
- diffusion of O₂, solid and liquid, solubility enthalpy of dissolution, diffusion coefficients 3-50019
- diffusivity and solubility of oxygen 3-41051
- dislocation mobility and temp. depend. of yield stress 3-49891
- effusion from Ta cell, surface diffusion, Knudsen determ. (*German*) 3-52754
- elastic shear const., second-order, pseudopot. calcs. 3-68308
- electrode, electroreflectance spectra, effect of I⁻ adsorption 3-47292
- electrodeposition, effect of temp. and metaphosphate, relay timing in electronic circuit 3-50836
- electromigration in Al (*French*) 3-46731
- electron diffraction obs., transmitted electron intensity measurement 3-49804
- electron impact ionisation cross sections between 40 and 250 eV, velocity of evaporated atoms 3-46200
- epitaxial growth, on NaCl: SO₄, doped and undoped crystals, electron microscope examination, nucleation and growth processes 3-46768
- etch pit rotation on (100) surface 3-79579
- exoemission current, electron work function depend., expt. confirmation of theory 3-58587
- f.c.c., lattice dynamics, extended de Launay's model 3-55056
- filamentary, optical behaviour in photographic emulsions/ e.m. theory 3-59606
- film, (111) and (100) single crysts., photoemission anisotropy obs. 3-64763
- film, condensation in vacuum, development of oriented cryst. growth 3-52763
- film, damping of mech. vibrs. (*Russian*) 3-72859
- film, effects of residual gas during deposition on optical props. 3-80001
- film, He⁺ ion passage, coherent Coulomb excitation 3-40587
- film, iodination in α-AgI phase region 3-55172
- film, nonradiative surface plasmons roughness induced decay, emitted radiation polarisation 3-46811
- film, O chemisorption, effect on elec. resist. 3-41094
- film, reaction with I vapour to form β-AgI crystals 3-55171
- film, thermal cond., emissivity and elec. resist., 300-900 K 3-62018
- film, ultrahigh vacuum deposited on cold substrate, reverse recovery process interpret. 3-64263
- film, vacuum deposited, optical const. by reflectance, inhomogeneities obs. 3-64617
- film, vacuum-deposited, internal friction peak due to stacking faults (*Russian*) 3-72284
- foil, absorption of beta particles from ⁹⁰Sr, ⁹¹Y and ³²P sources 3-49376
- glass:Ag⁺, ion-polyvalent ion (As, Sb, Bi) interaction, colloid form, opt. and e.s.r. spectra 3-58427
- heating surface, effect of thermophys. props. on heat transfer during boiling of water and ethanol 3-52693
- ideal resistivity and deviation from Matthiessen's rule meas. 3-64316
- impurity in Al, quasi-local vibrs. influence on heat capacity temp. depend. (*Russian*) 3-68417
- impurity in Al, quasi-local vibrs. influence on thermal expansion (*Russian*) 3-79506
- in InAs, distrib. in melt, under flux, radioactive isotope method 3-75626
- ion implantation of helium and deuterium by neutron collisions in reactors 3-60272

silver continued

- ion implantation of ZnS 3-72817
 K-shell ionization, differential cross section, ionization by electron bombardment 3-71411
 Kondo type resistivity anomaly caused by 3d metal impurities 3-55423
 liquid, diffusivity and solubility of oxygen, potentiostatic electrochem. meas. 3-64196
 liquid, diffusivity of oxygen, electrochem. meas. (Japanese) 3-41038
 liquid, impurity diffusion, solute diffusivity, radius and mass dependence 3-50016
 low resistance contact, for GaAs, formed by sequential deposition of Ag and Sn (Russian) 3-52899
 magnetic susceptibility around melting point 3-58368
 matrix isolation spectra using triode sputtering source 3-61046
 multiply charged ions, low-lying transitions, oscillator strengths systematics 3-78428
 nuclear orientation of ^{175}Yb , determ. from γ -ray anisotropy 3-47180
 nucleation and growth on amorphous C by vapour deposition 3-41632
 particles, in glass matrix, optical and paramag. absorpt., size effect 3-55563
 photoelectric emission, freq. depend. 3-55726
 photographic emulsions, effect of radioactive Ag 3-50853
 plastically deformed, elec. resist. and thermo-e.m.f. meas. of recovery, defects contrib. (Russian) 3-79663
 recoil implantation in SiO_2 film, discrete cluster formation 3-72112
 recrystallization, high internal friction, dislocation network (French) 3-72875
 recrystallization, point defects influence, internal friction obs. (French) 3-64111
 resistivity, structure factor from phonon frequencies, Moriarty's pseudopotentials 3-50166
 seawater suspension, determ. by atomic absorpt. with arc atomiser 3-80875
 seeded Alberta hailstorms, distribution in precipitation 3-76760
 self diffusion at low temps. 3-41054
 single crystal growth on Si, with selective electrochem. displacement in soln. 3-72787
 single crystals, dislocation free, growth by Czochralski method 3-44539
 spectrophotometric determ. in pure U samples 3-70472
 spherical crystals, LEED Bragg reflexes as function of electron energy, diffraction geometry 3-55128
 sputtering yield with 15 and 45 keV ions 3-80130
 supercooled melt, spontaneous crystn. (Russian) 3-58609
 surface, elastic and inelastic scattering of He atoms quantum theory 3-72774
 surface, polycryst., oblique Ar^+ bombardment in 1 keV range, sputtering yield, ion incident angle depend. (German) 3-47342
 surface film, coated with Al_2O_3 and Si, solar absorpt., thermal emissivity prep. 3-56660
 surface sensors, interaction with free O_2 gas stream (Russian) 3-66461
 thermal conductivity, heat flux depend., precise obs., 2-5 K 3-55236
 thin crystals, charact. X-ray prod., electron beam orientation depend. 3-40833
 thin film, aggregated, anomalous opt. absorpt. 3-76110
 thin film, strain coeff. of resist., calc. 3-52813
 thin film, transmission in vis. and u.v. spectral regions (French) 3-76112
 thin film (111) epitaxially grown on annealed Cu film 3-41108
 thin films, adsorption, of O_2 , kinetics, sticking probabilities, slow and fast adsorption, surface stoichiometry 3-46755
 thin films, crystallographic orientation, effect of Ar ion bombardment 3-55170
 trace sensitivity, superimposed pulses on stationary discharge (Russian) 3-70487
 twin boundary elec. resist., pseudopotential calcs. 3-44056
 vacancy formation energy, positron annihilation gamma rays, trapping model 3-49888
 vacuum arc cathode, erosion and ionisation 3-57957
 valence band Auger electron spectra 3-50638
 wetting on W, Mo and Ta, hot-filament vapour source 3-39892
 whiskers, mass production by reduction, effect of halide impurities 3-64269
 X-point, temp. dependence of optical props. 3-72672
 Ag:Er, Dy, Yb, γ -ray angular correlation by implanted ions, cryst. field effects 3-41460
 Ag/AgPyrex thin films, thickness measurement, comparative study of methods including Tolanski interference (Spanish) 3-73666
 Ag-AgCl electrodes for geophysical measurements 3-44948
 Ag-Au bicrystal, 111, escape of misfit disloc. from interface, electron microscope obs. 3-58167
 Ag-Cr thin film mixtures, optical constants 3-80002
 Ag-GaAs interface, energy structure, Schottky barrier height, Fermi level 3-60916
 Ag-He mixture, AgII line pulse excitation, coherent emission (Russian) 3-71375
 Ag-SiO superlattices, switching effect 3-72400
 Ag^+ , impurity electron state ionization in NaCl and KCl (Russian) 3-44455
 Ag^+ interdiffusion in molten TlNO_3 3-72215
 Ag^+ ion implanted in steel, friction changes 3-47410
 AgI-Ag photosensitive film, refl. spectra, 370 to 500 nm 3-53121
 ^{110m}Ag , diffusion in Li, thermotransport obs. 3-60803
 As_2S_3 :Ag, photodoping in amorphous film, photovoltage obs. 3-58302
 As_2S_3 :Ag(Cu), bulk glass, photo and thermal diffusions of Ag(Cu) 3-43903
 CaO : Ag^{2+} , e.p.r. spectra, Jahn-Teller effects, static to dynamic transition 3-53016
 CaO(S) :Ag, luminesc. centres (Russian) 3-76054
 CaS :Ag, Zn, spectral characteristics, formation of $[\text{AgVs}]^+e^-$ traps (Russian) 3-76060
 Cd film seeding on muscovite 3-72279
 CdS :Ag, origin of red and orange emission bands (Russian) 3-76058

silver continued

- KBr:Ag 0 , optical absorption bands, excited states 3-72685
 KCl:Ag $^{2+}$, X-irradiated, e.p.r. spectrum at 300K 3-79907
 KCl:Ag 0 , optical absorption bands, excited states 3-72685
 KCl:Ag $^+$, Cu $^+$, Pb $^{2+}$, f-centres study (French) 3-52625
 KCl:In, Ag, α - or γ -irrad., absolute thermolum. output (Russian) 3-76100
 KI:Ag $^-$ and KI:Ag $^-(\text{Li})$, anomalous C* emission 3-69059
 MgO:Ag $^{2+}$, e.p.r. spectra, Jahn-Teller effects, static to dynamic transition 3-53016
 NaCl:Ag enhancement of vacuum u.v. excited luminescence by electric field (Russian) 3-50624
 NaCl:Ag 0 , optical absorption bands, excited states 3-72685
 NaCl:Ag $^+$, Cu $^+$, Pb $^{2+}$, f-centres study (French) 3-52625
 Ni: ^{110}Ag , valence effect in electromigration 3-75637
 Si:Ag, impurity photocond. edge shift under influence of combined illumination 3-46875
 Si:Ag, photocapacitance and its quenching, impurity levels, 77K 3-44113
 Si/Ag films, evaporated, kinetics of crystallisation processes 3-43967
 SrO:Ag $^{2+}$, e.p.r. spectra, Jahn-Teller effects, static to dynamic transition 3-53016
 ZnS:Ag, Cu phosphor, spectral response to fast ions 3-50628
- silver alloys**
 see also silver compounds
 dilute, conduction electron scattering by impurity atoms 3-75720
 internal oxidation at h.p. and inatonic O (German) 3-41056
 Voigt profile analysis for particle size and strain determ. 3-61141
 Ag-Au-Cu, elastic moduli, effect of Cu 3-64806
 Ag-Bi, liq., thermodynamic props. (German) 3-55756
 Ag-Cd, dilute, localisation on temp. depend. impurity resistance 3-41170
 α -Ag-Cd, Fermi surface from polar-reflection Faraday effect 3-50121
 Ag-Cd, ferroelastic and superelastic behaviour 3-64830
 Ag-Cd, liq., density, temp. and comp. depend. (Japanese) 3-50672
 Ag-Cd solid solns., interdiffusion coeffs., conc. depend. (Russian) 3-72225
 Ag-Cu, eutectic, freezing and melting at very slow rates 3-53203
 Ag-Cu, liq., surface tension meas. by sessile drop method (French) 3-79554
 Ag-Cu (50 at.%) amorphous thin film, structure (German) 3-58192
 Ag-Gd, dilute, mag. susceptibility, n.m.r. and thermoelec. power obs. of impurity state 3-68765
 Ag-Ge liquid alloys of eutectic composition, short-range order (Russian) 3-63946
 Ag-In, liq., density, temp. and comp. depend. (Japanese) 3-50672
 Ag-In-Cd control rods in PWR, test of CNEN neutronic codes 3-74683
 α -Ag-Mg, Fermi surface from polar-reflection Faraday effect 3-50121
 Ag-Pb, liq., thermodynamics of solubility of S (German) 3-72882
 Ag-Pb-Cu, elastic moduli, effect of Cu 3-64806
 Ag-Pd alloys, electronic states 3-72311
 Ag-Pd films, prep. and optical props. (French) 3-41527
 Ag-Sb, liq., thermodynamic props. (German) 3-55756
 Ag-Sb, particle size and strain determ. by method of variance 3-44575
 Ag-Sn, dilute, dislocation mobility and temp. depend. of yield stress 3-49891
 Ag-Sn thermodynamics of solubility of S (German) 3-72882
 Ag-Zn, α -phase, rigidity modulus, temp. depend. 3-69183
 Ag-Zn solid solns., interdiffusion coeffs., conc. depend. (Russian) 3-72225
 AgCd, martensitic transition, anomalous stress-strain props. 3-58611
 AgI/Ag electrodes, impedance study on LiCl-KCl eutectic 3-65090
 Ag $_{10}\text{In}$, order-disorder transition phenomena 3-64831
 Ag $_{10}\text{Pd}_{10}\text{H}_{10}$, electrical resistance anomaly and phonon resistivity, 4 to 300K 3-79673
 β -AgZn, band structure and Fermi surface, APW calcs. 3-64281
 β -Ag-Al, splat-quenched, massive phase transform. phenomena 3-58613
 Al-Ag, γ phase dissolution 3-80223
 Al-Ag, liquid quenching effects and precip. 3-80261
 Al-Ag solid solns., dissolution kinetics of grain boundary allotriomorphs 3-80233
 Al-Ag-Zn, (5 at. % Ag, Zn), liquisol quenched, precipitation, GP zone form. 3-72865
 Al-Zn-Ag, changes in structure during recovery, metastable phase AgZn $_3$ characteristics (Russian) 3-80256
 Al-Zn(9 at. %)-Ag(1 at. %), structural features of formation in Al-Zn-Ag alloy (Russian) 3-41723
 Au-Ag, thermoelectric power obs., composition depend. at high temps. 3-68599
 Au-Ag, valence band structure, X-ray photoelectron spectra 3-64284
 Au-Ag (15 at. %), resist. change during short-range order form. 3-64932
 Cu-Ag, composition dependence of shrinkage in sintering of systems charact. by eutectic constitution diagrams 3-80395
 Cu-Ag, high temp. internal friction, grain boundary peak (Japanese) 3-44579
 Cu-Ag-Au liquid, heats of mixing, anomalous behaviour 3-50001
 Cu-Ag-Sn, elastic moduli, effect of Sn 3-64806
 Li-Ag, liq., struct., X-ray determ. 3-49827
 Pb-Au-Ag system, central atom model applic. to thermodynamic props. calc. (German) 3-64811
 Pd-Ag, chemisorbed CO, surface composition, in equilib. 3-79577
 Pd-Ag, localized modes of interstitial H, neutron scatt. study 3-55063
 ZnAg phonon resistivity 3-79669
- silver compounds**
 see also silver alloys
 AgBr photographic emulsions, effects of moisture on sensitivity, latent-image fading, possible mechanisms 3-59604
 α -AgI, iodination of Ag thin films 3-55172

silver compounds continued

- chalcogenides stoichiometric and temp. dependence of electronic ionic conductivity ratio (*German*) 3-50202
- halide, particle size distrib., effect on optical sensitisation of ammoniacal negative emulsions (*Russian*) 3-50856
- halide containing glasses, thin film phases, phototropism 3-76108
- halide crystal, precip. in alkali aluminoborosilicate glasses cont. Ag, Cl and Br, comp. 3-80437
- halide microcrystals, effect of u.s. waves on growth mode during emulsification, electron microscopy (*Russian*) 3-47595
- halides, conc. effect on permeability of gelatin films (*Russian*) 3-46773
- halides, photographic emulsion grain size distrib. determination, electrolytic reduction technique 3-51661
- halides depolarization and beta-decay of ^{110}Ag , n.m.r. obs. 3-61006
- proustite, difference freq. generation by mixing of dye lasers, 5.82-7.25 μm 3-57256
- rare earth chalcogenide-silver chalcogenide system cpds. (*French*) 3-46631
- salts, analysis in photographic products, novel titrator, data processing 3-61281
- Ag halides, e.m. theory, optical behaviour of photographic emulsions 3-59606
- Ag ion conductors, review 3-61260
- $\text{Ag}-(\text{NH}_4)_2\text{S}_2\text{O}_8$ complex, photographic fixing, rate of diffusion, Br-inhibition 3-47592
- Ag-AgCl electrodes for geophysical measurements 3-44948
- Ag-H solid solution, H solubility 3-41021
- $\text{Ag}-\text{NH}_4\text{SCN}$ complex, photographic fixing rates, Br inhibition 3-47593
- $\text{Ag}-\text{NaSCN}$ complex, photographic fixing rates, Br inhibition 3-47593
- Ag-Se-Te glasses, thermal stability, energies and rates of crystallization 3-75478
- (Ag+K)NO₃, molten binary mixtures, external transport numbers, ionic mobility cooperative mechanism ionic conductivity (*French*) 3-75747
- (Ag+Li)NO₃, molten binary mixtures, external transport numbers, ionic mobility, cooperative mechanism, ionic conductivity (*French*) 3-75747
- (Ag+Na)NO₃, molten binary mixtures, external transport numbers, ionic mobility, cooperative mechanism, ionic conductivity (*French*) 3-75747
- Ag⁻ recovery, photographic fixing soln., phenylthiourea selective resins, ion exchange, polarographic Ag anal. 3-53335
- AgAlTe_2 - AgGaTe_2 - AgInTe_2 , Mossbauer effect, elec. field gradients at ^{125}Te , ^{127}I impurity nuclei 3-72555
- AgAlX_2 - CuAlX_2 system, X=S, Se, limits of solid solubility 3-43879
- Ag_3AsS_3 , proustite, band structure, light absorpt. and refl. obs. 3-44017
- Ag_3AsS_3 , proustite, determ. of six photoelastic consts. by Bragg scatt. of laser light 3-75558
- Ag_3AsS_3 , proustite, i.r. refl. and transmission spectra 3-58503
- Ag_3AsS_3 , proustite, i.r. absorpt. spectrum effect of partial electrolysis (*Russian*) 3-68992
- Ag_3AsS_3 , proustite, light absorpt. and refl. obs. 3-44017
- Ag_3AsS_3 , proustite, n.q.r. spectrum and spin-lattice relax. time of ^{75}As , 300-4.2K (*Russian*) 3-79944
- Ag_3AsS_3 , proustite, photocond. and thermally stimulated cond. (*Russian*) 3-79735
- Ag_3AsS_3 , proustite nonlinear optics, conversion of i.r. into visible, mutually perpendicular pumped and signal beams, parameters, efficiency 3-40284
- Ag_3AsS_3 parametric oscillator, singly resonant, tuned from 1.22 to 8.5 μ 3-40280
- $\text{Ag}_{2-x}\text{Au}_x\text{Se}$, solid solution, semiconductor electronic cond., electron mobility 3-41190
- AgBr, absorpt. below band edge, Urbach rule, microscopic theory (*German*) 3-50554
- AgBr, anodically formed, positive relief images photographic sensitivity 3-53334
- AgBr, e.p.r. of Rh^{2+} 3-79900
- AgBr, emulsions, spectral sensitization, orthorhombic PbO, photocond. meas., photographic diode 3-47588
- AgBr, epitaxial attachment of dye aggregates to surface, ligand bonds red shift, benzothiazolocarboquinone 3-53342
- AgBr, hole cyclotron reson., 34 GHz and 1.7 K 3-46796
- AgBr, isotope effects for ^{105}Ag , ^{111}Ag diffusion, interstitiality and vacancy jumps 3-50027
- AgBr, mechanism of ion movement 3-79525
- AgBr, optical absorption from room temp.-1000K, obs. of red-shift of absorption edge (*German*) 3-53119
- AgBr, photographic emulsion, kinetics of Ag formation, ascorbic acid and 2-chloro-4-aminophenol single and combined developers 3-47591
- AgBr, photographic emulsion, kinetics of development, ascorbic acid and 2-chloro-4-aminophenol, filamentary growth 3-53341
- AgBr, photographic emulsion, photovoltaic effect, effect of dye sensitisation, electron and hole traps 3-53343
- AgBr, photographic emulsion, behaviour of space charge in impulsed elec. field, effect of sensitisation and presence of crystal impurities latent-image formation 3-53345
- AgBr, pure and doped crystals, existence of subsurface layer of space charges, effect on latent-image process 3-53344
- AgBr, thermal disorder study by proton channelling (*French*) 3-52650
- AgBr (J) photographic emulsions, phosphorescence in gamma radiation, latent image formation (*Russian*) 3-50607
- AgBr and AgBr(Cl) crystals, photographic emulsions, behaviour in pulsed electrostatic field, space charge concept (*Russian*) 3-47594
- AgBr grains, latent-image formation, photographic sensitizing and desensitising phenomena, photoelectron capture by electron traps 3-53339
- AgBr nucleation, formation kinetics, colloidal particles, temperature dependence 3-72021
- AgBr photographic emulsions and crystals, photostimulated thermoluminesc., electron and hole traps 3-53340

silver compounds continued

- AgBr photographic emulsions and crystals, luminesc. spectra, luminesc. flash, thermal quenching, electron trapping 3-55983
- AgBr photographic emulsions, sensitivity centres calc. 3-66325
- AgBr photographic layers, filter deposits, technique, characteristics 3-70322
- AgBr photographic sol conversion to AgI, reaction kinetics, turbidimetric studies effect on gelatin protection and unsubstituted polyethylene oxides 3-53338
- AgBr: Cd, diffusion of ^{22}Na , Frenkel defect conc. calc. 3-55098
- AgBr: CdBr₂, ionic cond., rel. contrib. of vacancies and interstitials 3-73636
- AgBr: CdS, three-layer system, propag. of elastic transversal waves, dispersion eqns. (*Russian*) 3-55026
- AgBr-CuBr mixed crystals, phase behaviour and lattice disorder, calorimetric obs. (*German*) 3-64184
- AgBr-GaAs, interface heterojunction, photoelectric properties 3-44110
- AgBr-Si, interface heterojunction, photoelectric properties 3-44110
- Ag(BrCl), photographic emulsion, behaviour of space charge in impulsed elec. field, effect of sensitisation and presence of crystal impurities latent-image formation 3-53345
- AgBrI, anodically formed, negative images, photographic sensitivity 3-53334
- AgBrI, photographic emulsions, gelatin soln. influence of [Br⁻] and [NH₃] on crystal shape, Ostwald ripening 3-53337
- AgBr(I), photographic emulsion, photovoltaic effect, effect of dye sensitisation, electron and hole traps 3-53343
- AgBrI grains, latent-image formation, photographic sensitizing and desensitising phenomena, photoelectron capture by electron traps 3-53339
- AgBr(I) photographic emulsions and crystals, luminesc. spectra, luminesc. flash, thermal quenching, electron trapping 3-55983
- AgCl, absorpt. below band edge, Urbach rule, microscopic theory (*German*) 3-50554
- AgCl, dielec. props. and space charge (*French*) 3-41480
- AgCl, diffusion of ^{22}Na , Frenkel defect conc. calc. 3-55098
- AgCl, e.s.r. of self trapped holes, Ag^{2+} centres, at liquid nitrogen temps. 3-72521
- AgCl, emulsions, spectral sensitization, orthorhombic PbO, photocond. meas., photographic diode 3-47588
- AgCl, illuminated, e.s.r. detection of Cr^{3+} centres 3-47140
- AgCl, in different atmospheres, surface luminescence centre origin 3-80087
- AgCl, ionic cond., hydrostatic press. effects 3-58151
- AgCl, isotope effects for ^{105}Ag , ^{111}Ag diffusion, interstitiality and vacancy jumps 3-50027
- AgCl, Knoop microhardness anisotropy, applic. to slip system identification 3-79410
- AgCl, mass spectrum, temp. depend. 3-78855
- AgCl, mechanism of ion movement 3-79525
- AgCl, molten, fragmentation when dropped in water, automatic picture scanner 3-74730
- AgCl, optical absorption from room temp.-1000K, obs. of red-shift of absorption edge (*German*) 3-53119
- AgCl, phonon dispersion props. 3-68350
- AgCl, thermoluminescence determ. of electron trap depth, reln. to latent-photographic-image formation 3-55696
- AgCl, Zn²⁺ tracer diffusion, 209-441°C, substitutional mechanism 3-68441
- AgCl (J) photographic emulsions, phosphorescence in u.v. radiation, latent image formation (*Russian*) 3-50607
- AgCl crystal, laser irradi. interaction, bleaching (*Rumanian*) 3-65113
- AgCl crystal habit in emulsion, rel. to absorption spectra of adsorbed dyes 3-47587
- AgCl emulsion, colour photographic film, blue luminescence, effect of mercaptan stabilisers (*Russian*) 3-47596
- AgCl high purity synthetic crystals, determ. of Fe, Cu, Pb, by spark source mass spectrometry 3-62327
- AgCl solid electrochemical cell, polarization, complex admittance study 3-69470
- AgCl: CdCl₂, physical cluster theory, cation vacancies interaction with impurity cations 3-75524
- AgCl: In single crystal, diffusion of In, temp. depend., varying In conc. (*German*) 3-79517
- AgCl: OH⁻, librational and tunnelling levels 3-79453
- AgCl-MnCl₂, ionic cond., hydrostatic press. effects 3-58151
- AgCl(Br), dynamical props. of dislocations, internal friction obs. 3-64112
- AgCrX_2 (X=S, Se), crystal structure and mag. structure 3-40881
- AgF, cohesive energy and elastic props., LCAO calc. 3-68188
- AgGaS_2 , piezoelectric nonlinear optic, crystal structure determ. 3-72049
- AgGaS_2 , valence band density of states and core level shifts, X-ray photoemission obs. 3-55720
- AgGaX_2 - CuGaX_2 system, X=S, Se, limits of solid solubility 3-43879
- $\text{Ag}_2\text{H}_2\text{IO}_6$, nucl. quadrupole interaction of ^{127}I , phase transform. behaviour (*German*) 3-53034
- $\text{Ag}_2\text{H}_2\text{IO}_6$, antiferroelec., proton-iodine cross relax. determ., of short quadrupolar spin-lattice relax. 3-47164
- $\text{Ag}_2\text{H}_2\text{IO}_6$, incoherent neutron scatt. and antiferroelec. modes 3-47222
- $\text{Ag}_2\text{H}_2\text{IO}_6$, incoherent neutron scatt. and i.r. spectra, assignment of vibrational modes 3-47222
- AgI, conversion from AgBr photographic sol, reaction kinetics, turbidimetric studies, effect of gelatin protection and unsubstituted polyethylene oxides 3-53338
- β -AgI, crystal growth from reaction of I vapour with Ag film 3-55171
- AgI, optical absorption from room temp.-1000K, obs. of red shift of absorption edge (*German*) 3-53119
- AgI, polycrystalline, thermal expansion, 170-500°C 3-75629
- AgI, seeded Lake Effect storms, diffusional deposition of ice, snow crystal struct., Ag content 3-76768
- AgI as contact or sublimation nuclei, electron-microscopic study 3-64173
- Ag(I) complex, bis(2-methyl benzothiozole) Ag(I) perchlorate, cryst. struct., X-ray obs. 3-72046

silver compounds continued

- AgI hydrosols, ice-nucleating properties, UV radiation 3-44897
 AgI nucleation of ice, electric field effects 3-47739
 AgI particles, size, surface charge 3-65028
 AgI-Ag photosensitive film, refl. spectra, 370 to 500 nm 3-53121
 AgI-K₂SO₄, seeding of warm clouds, steady flow cloud chamber 3-80865
 AgI + MI (M = Na, K, Rb, Cs) molten systems, thermoelectric power 3-72375
 AgI₂, thermoelectric effect, mechanistic analysis 3-79720
 Ag₂WO₄, solid electrolyte with high ionic cond., for solid state battery applic. 3-43892
 AgInX₂-CuInX₂ system, X = S, Se, limits of solid solubility 3-43879
 Ag₂MI₃ (M = Cs, Rb and K), thermal power of solid electrolytes and molten mixtures 3-50835
 AgNO₃, longit. mode freqs., PSR i.r. spectra 3-75975
 AgNO₃, polarised phosphoresc. and absorp. in single cryst. 3-64729
 AgNO₃ and alkali nitrate molten mixtures, Raman studies 3-80023
 AgNa(NO₂)₂, dielectric constant, relaxation time, Curie point, hydrostatic pressure effects 3-50510
 AgNa(NO₂)₂ ferroelec., dielec. relax., dispersion of dipolar polarisation 3-44381
 Ag₂O, exciton luminesc., temp. depend., 4 to 77 K 3-53139
 Ag₂O: Cd, photocond. and luminesc., 4.2 and 77K, participation of excitons 3-47312
 Ag₂O-Na₂O-SiO₂ glass, X-ray diffr. study 3-72008
 Ag₂O-P₂O₅, phosphate glass, elec. cond. meas. 3-72355
 (Ag₂O)_x-(Na₂O)_{1-x}-P₂O₅, phosphate glass, elec. cond. meas. 3-72355
 AgPF₆, chemical shift in n.m.r. of ¹⁹F 3-61002
 Ag₂S, crystal growth, thermal treatment in H₂S, scanning electron microscopy 3-80166
 Ag₂S, semiconductor thin films, structure and properties (*Rumanian*) 3-64417
 α-Ag₂S and β-Ag₂S, optical props. in i.r. and far i.r. 3-53108
 Ag₂S(Se) semiconductor-metal transition, i.r. reflectivity obs. (*German*) 3-50571
 Ag₃SbS₃, preparation and physical-chemical props. 3-53195
 Ag₃SbS₃, pyrrargyrite, photocond. and thermally stimulated cond. (*Russian*) 3-79735
 Ag₃SbS₃ single crystals and amorphous films, light absorption, band structure 3-64679
 Ag₃SbS₄, famatinitite, selection rules for inelastic neutron scatt. (*Russian*) 3-49948
 AgSbTe₂, liquid, electrical conductivity and thermoelectric power, temp. depend., activation energy 3-55264
 Ag₂Se, polymorphic transformation, electron microscopic investigation 3-58129
 Ag₂Se-Ge, heterojunction, switching phenomena and memory effect 3-79749
 Ag₂Te, polymorphism, elec. props. and X-ray studies 3-68406
 AgX absorption spectra (X = halide), early photolytic stages, quasimetallic centres, fluctuation theory, effects (*Russian*) 3-80084
 Ge-S-Ag, As-S-Ag system, glass forming regions 3-65005
 (Li, Ag, Na)NO₃ and (Li, Ag, K)NO₃ ternary systems, equilibria study 3-60788
 Pd-Ag-H system, superconductivity, temp. depend. of relative electrical resistance 3-79793
 RbAg₄I₃, Cu-substituted, Cu ion conducting solid electrolyte 3-41046
 Te-Ag, amorphous films, condensation, struct. obs. using electron microscope 3-75692

simulation

- see also *aerospace simulation; modelling; plasma simulation*
 di-μ-(pyridine N-oxide)bis [bisnitrate (pyridine N-oxide) copper (II)], e.p.r. spectrum, triplet ground state, computer simulation 3-75075
 analogue, epoxy resin curing reaction, analogue computer simulation 3-50831
 annealing of correlated point defects in f.c.c. metals following radiation damage 3-79531
 area scan process, use of digital phantoms to evaluate computer focusing 3-56531
 array simulation facility 3-48301
 atmospheric dynamics and circulation numerical simulation 3-51071
 atmospheric optical communication through clouds, computer simulation of light pulse propagation 3-76700
 atmospheric seeing, use of speckle interferometry 3-81255
 atmospheric surface layer, volumetric flow control, wind tunnel studies 3-53561
 atmospheric turbulence, quasi-geostrophic, numerical simulation 3-73324
 axisymmetric flow through shaped gauze screens, velocity profiles simulation 3-43554
 ball motion in ball bearing, digital simulation method 3-48711
 basilar membrane, computer simulation of motion, Schroeder's integrable model 3-42295
 binary photosensitive material, holographic characs., computer-aided 3-45773
 biological membrane pores, kinetics of diffusion and convection, computer simulation 3-56490
 blackbody cavities, polythermal theory 3-77914
 burn-up in AVR fuel elements, computer program (*German*) 3-71239
 cardiovascular circulation, by computer (*Italian*) 3-60593
 cardiovascular system simulator 3-51756
 chemical, energy release, pressure effects, comparison with nuclear excursions 3-67620
 chemical profiles during electrotransport segregation of liquid binary alloy 3-68429
 chemical reaction kinetics, student expt. 3-53822
 compartmental model neuron 3-51430
 cosmic ray air showers, computer simulation of optical Cherenkov emission 3-59232
 crystallography, computer simulation of cryst. struct., appl. to superstruct. of cubic SiP₂O₇ 3-46626
 dispersive dielectric fibres, transmission of stationary nonlinear optical pulses, numerical simulation 3-59886
 Dynamic Slug Impact Model, coolant-reactor vessel head impact, safety anal., MIMIC simulation 3-71176

simulation continued

- earthquake, sine-beat method, environment and damage potential 3-53552
 electric analogue simulation method for solving heat and mass transfer problems 3-70764
 electric field intensity in cylindrical waveguide employing analogue computer 3-74190
 electrochemical planar disc electrodes, digital simulation of edge effects 3-55963
 electrochemical rotating disc electrode convection diffusion process simulation by means of a model MN-7 analog computer 3-61263
 electrodeposition, three dimensional nucleation during potentiostatic pulse, simulation 3-69466
 electron diffraction effects, computer, contrast maps, profiles (*German*) 3-70442
 electronic conduction of insulators, one-carrier injection analogue (*Russian*) 3-75746
 external boundary layer flow using CSMP 3-52458
 fast reactor safety, local fuel failure, obs. 3-67521
 fluised bed coaters, motion of solids 3-67580
 fusion reactors, use of GERT IIIx simulation techniques for funding strategy analysis 3-60316
 galactic spiral structure dynamics, computer simulation 3-45193
 games, war between spaceships 3-66116
 gaseous discharges, computer simulation of streamers 3-57961
 GCFR plant using direct cycle, response to rapid loss of pressure due to duct rupture 3-46107
 grain boundary and vol. diffusion computer simulation of X-ray diffraction 3-41043
 hadronic cascades with new particle yield formation, Monte Carlo simulation 3-54349
 hair cell model, computer simulation 3-42301
 heat transfer simulator, one-dimensional, hydraulic network analogue, procedure 3-62016
 heterogeneous nucleation and growth, numerical method 3-63969
 hydrodynamic, approx. method for stress field distrib. around elliptical aperture and streamlined orifice (*Russian*) 3-45658
 hydrodynamic loading in PWR pressure vessels, computer model (*German*) 3-67492
 trans-hydroxy-L-proline, proton NMR spectra, computer simulation, long range coupling constant, structural implications 3-75074
 hypothetical core disruptive accidents, LMFBR, simulation of mech. energy release, reactor energy source characterisation 3-74674
 image intensifier noise, effect on visual detection threshold 3-61900
 image synthesis, by array systems, computer simulation 3-70786
 internal energy dissipation simulation in elastoplastic connections using analogue computers 3-57096
 ion scattering process, surface damage on Ni due to Ar⁺ bombard. 3-68292
 Josephson junctions, mixing and parametric effects, analogue computer simulation 3-41303
 Kronig-Penny model analogue computer simulation 3-51494
 large systems, biochemical membranes with enzymes, modelling/simulation/identification and optimal control 3-53738
 lightning strike, aircraft initiation 3-41980
 linear accelerator, for micrometers 3-42629
 linear accelerator, r.f. mass spectrometer, using computer 3-53996
 liquid, mol. motion 3-68432
 liquid drop oscillations, numerical method soln. 3-46465
 liquid spectroscopic props., method of mol. dynamics simulation 3-80051
 LMFBR demonstration plant, subcritical worth meas. of simulated control rod banks 3-49348
 Lung-equivalent material for fast neutron dose distribution studies 3-70138
 LWR core simulator PRESTO, characteristics and performance 3-49364
 mass spectra of small organic molecules, computerised pattern recognition techniques, improved technique 3-57017
 mass spectrometer field ionisation source, ion trajectories, electric field effects 3-56972
 molecular dynamics model, 10000 particle, with long range forces 3-78911
 molecular dynamics simulation of liquid-solid transition in two dimensions 3-79254
 moon capture origin, flyby encounter with earth, computer simulation model 3-59299
 multicorrelated random processes, simulation using fast Fourier transform algorithm 3-42479
 myelinated neuron, hybrid computer simulation of action potential generation and transmission 3-53740
 neutron elastic scattering simulation program 3-43142
 n.m.r., multipulse, Fourier transform, Bloch equations, effect on magnetisation vector 3-56708
 n.m.r. multipulse and Fourier transform expts., computer simulations using density matrix eqns. of motion 3-75868
 non-linear resonance, method of averaging and simulation language CSMP 3-40094
 nonlinear filtering algorithm for nuclear reactor reactivity monitoring 3-67437
 nonlinear heat and mass transfer problems, electric simulation 3-77917
 nuclear accidents, study by chemical simulation experiments 3-67535
 nuclear LMFBR, loss-of-flow accidents, in-pile simulations 3-67420
 nuclear magnetic resonance expts. 3-78854
 nuclear power plant operators, training, use of simulators 3-73648
 nuclear power plant training simulator 3-52225
 nuclear reactor, boiling water pressure tube, digital simulation for hydrodynamic processes and core heat-up 3-67396
 nuclear reactor, loss-of-coolant, emergency provisions, computer simulations and exptl. programs 3-71172
 nuclear reactor fuel assembly, LMFBR, air flow tests in bare rod bundle 3-67442
 nuclear reactor rod bundle geometries, two-phase mixing for annular flow 3-43281
 ore sintering furnace, numerical method 3-41794

simulation continued

- oxide fuel columns, in-reactor transient heating conditions, simulation 3-63203
 photon wavelength selection, scattering process simulation, Monte Carlo programme, parallel computers 3-62433
 plasma confinement, toroidal, low-pressure axisymmetric stability analysis 3-46546
 positron channelling in single crystals, computer simulation 3-54989
 pulsed neutron experiments, computer simulation, core reactivity determ., inhour method of interpretation 3-71206
 PWR, control procedures for spatial Xe oscillation, computer simulations and tests 3-46132
 PWR pressure vessel breach during blow-down phase (*German*) 3-71238
 radiative corrections and target wall contributions in electron scattering experiments 3-51669
 radiative transfer, electrical simulation models 3-70765
 random substitutional alloy, onset of ferromagnetic order, Monte Carlo computer method 3-47016
 reactivity, excess, determ. by meas. of prompt neutron decay constants (*German*) 3-63124
 reactor core elements handling, testing facility and manipulation sequences 3-43279
 Rossi- α -experiment, storage of time intervals of counter pulses for computer simulation 3-66328
 San Andreas Fault Experiment 3-56061
 semiconductor, ion implantation, beam heating effects, expt. simulation 3-64798
 simulated melting instability waves near stagnation region in hypersonic flow 3-46463
 simultaneous differential eqns., transient soln. using FORTRAN oriented simulation package 3-57044
 solid, phonon transport, Monte Carlo simulation 3-68379
 solids, polycryst., computer simulation of internal stresses 3-68305
 spectro-electrochemical working curves, implicit finite difference method 3-53323
 torsion testing machine, for programmed simulation of hot working 3-53836
 transferred electron dynamics, using Monte-Carlo methods 3-55280
 underground explosions, simulation, generation of longitudinal and transverse waves, expression for transfer function 3-80603
 underground water, simulation of flow (*Russian*) 3-63620
 u.s. interaction with defects, by computer 3-56571
 visual tracking, eye model 3-48616
 vitamin B₁₂, low symmetry e.s.r. spectra computer simulation 3-43528
 wind tunnel simulation of lower third of urban adiabatic boundary layer 3-63676
 wind tunnel simulation of urban boundary layer flow 3-63675
 X-ray high dose rate heating effect, reln. to nuclear weapon and missile design 3-74762
 Cu, computer simulation of weak-beam electron microscope images of extended dislocations 3-59669
 Cu, Frenkel pair creation, computer simulation of atomic dynamics at energies near displacement threshold 3-79341
 Fe₃Al, computer simulation of radiation damage 3-79366
 Ge, nucl. lifetimes by blocking technique 3-40443
 He, hcp single crystal growth technique, c-axis orientation of 0 and 90°, computer simulation of nucleation 3-51554
 NH₄ClO₄, ionic conduction, computer simulation using polarisable point ion model 3-58146
 Na boiling simulation using a water model, voiding and re-entry processes 3-46703

simulators see simulation**Sinanoglu's theory see atomic structure****single substrate integrated circuits see monolithic integrated circuits****sinks, heat see heat sinks****sintering**

- see also densification; powder metallurgy*
 alloy, binary, composition dependence of shrinkage in sintering of systems charact. by eutectic constitution diagrams 3-80395
 alloy, thermodynamic approach to analysis of diffusion controlled processes in interstitial phases 3-80361
 cathode materials for electric vacuum devices 3-80398
 ceramic, initial combined sintering, vol. and surface diffusion terms from shrinkage data 3-58705
 dispersed porous body, minimisation of free energy 3-69364
 hot pressing, densification rate, Newtonian and Bingham solids 3-64974
 i.r. transmitting mat., hot pressing 3-76253
 lunar glass, sintering and hot pressing of Apollo 14 samples 3-47942
 metal oxides, pore size rel. to grain size 3-64973
 metal particles, dislocation generation during early stage sintering 3-69243
 metal powder compacts, anisotropy in linear shrinkage during sintering (*Polish*) 3-72921
 niobate glass-ceramic, energy storage improvement by pressure crystallisation 3-75946
 nonporous particles, submicronic dimens., kinetic eqn., shrinkage (*French*) 3-72995
 ore sintering furnace simulation 3-41794
 pressure, kinetics of viscous flow, vol. diffusion, dislocation climb (*French*) 3-72994
 reactive, with liq. phase, math. model, appls. (*French*) 3-76336
 refractory compounds, variable composition 3-80434
 refractory materials, sintered, thermal conductivity meas., modified Krishnan and Jain method, 1000-2200°C (*Czech*) 3-70288
 refractory oxide fibre eval. for high temp. rigidized insulation applic. 3-76276
 SEM obs. using hot-stage technique 3-76257
 silica fibre compacts, sintering, model, densification of fibrous structure 3-50757
 sintered bodies, grain shapes in two-dimens. sections 3-44647
 sponge-iron powder, lubrication effects on compaction at low and high speeds 3-69335
 steel, R18, structure and props. 3-80396
 stress induced diffusional transport, material continuity requirements 3-69332

sintering continued

- stress induced diffusional transport, material continuity requirements 3-69333
 Al₂O₃, grain growth, inclusion and pore dragging, heat treatment 3-76324
 Al₂O₃, hot-pressing, analysis with rate equations (*Japanese*) 3-50762
 Al₂O₃ compacts, flash heating technique, kinetic study of shrinkage (*French*) 3-72996
 β -Al₂O₃ conductive ceramics for Na-S battery, microstructure control 3-80417
 Al₂O₃:Ti, anomalously high activation energies origin 3-55842
 Al₂O₃/WC composites prep. and characteriz. for cutting tools 3-69344
 BN, sintering under pressure (*Polish*) 3-47452
 (Ba,Nb)(Ti,Nb)O₃ polycryst. material prep. and prop. optimization 3-75945
 BaFe₂O₉, ferrite, liquid phase sintering of magnetically isotropic and anisotropic compacts 3-58701
 BaO.5Fe₂O₃ and BaO.6Fe₂O₃, sintering and characteriz. 3-61191
 BeO, effect of minor additions during sintering upon densification and microstructure 3-69366
 Cd₃Co_{1-x}Cr₂S₄, mag. semiconductor, hot pressing for magneto-optical props. 3-47230
 Cd,Mn_{1-x}Fe₂O₄ ferrite, formation kinetics, densification 3-76304
 CdS, prod. of high mobility photosensitive layers (*Russian*) 3-72818
 Co,R,R=Y, La, Pr, liquid phase, for permanent magnets 3-44268
 Fe, cleaning to high purity of chemically preliminary cleaned powder (*German*) 3-47399
 Fe, sintered, elastic modulus and ductility 3-50753
 Fe-Si sintered alloys, mag. props. 3-80397
 Fe₃O₄-CaO-SiO₂, haematite-lime-silica mixture, self-fluxing agglomerate, reaction conditions (*French*) 3-69330
 KCl billet, crack free, constrained hot pressing technique 3-69362
 LiFe₂O₈, LiMn_{0.3}Fe_{4.7}O₈, densification, effect of prep. technique and calcination temp. 3-76249
 MgAl₂O₄, transparent shaped mat., fabrication and props. 3-72967
 MgO, hot-pressing, anion effects 3-61189
 Mg₂O₃ compacts, densification during hot-pressing, plastic deformation model (*Japanese*) 3-47454
 MnO_{1+x}, nonstoichiometric, sintering kinetics 3-69345
 MnZn ferrite, prep. conditions, effect on mag. props. 3-50760
 Mo, in organic binder, chemical stability in reducing atmosphere 3-69353
 Mo-Cu-Ni alloys, boundaries of single-phase side fields 3-80221
 N-Fe alloys, microstructure examination and production by sintering 3-55766
 (Pb,La)(Zr,Ti)O₃ powders, chem. prep. from aqueous nitrate solns. 3-76247
 Pb_{1-x}La_x(Zr_{0.65}Ti_{0.35})_{1-(x/4)}O₃ transparent electrooptic ceramics, fabrication by atmosphere sintering 3-55838
 Pb(Zr,Ti)O₃ ceramics, fabrication process and props. characteriz. 3-72965
 PbZr_{0.5}Ti_{0.5}O₃ synthesis, microstruct. development, effect of ZrO₂ particle size and struct. 3-61201
 PbZr_{1-x}Ti_xO₃, continuous hot pressing 3-76255
 RuO₂, sinterability, 800-1000°C (*Japanese*) 3-44666
 SiC, reaction-sintered, β -SiC growth during sintering, microstruct. characteriz. 3-76300
 SiC, reaction-sintered, growth characts., polytype distrib., 6H₂ struct. absence 3-76299
 α -SiC, recrystallisation during reactive sintering 3-80433
 SiC, very high pressure hot pressing 3-50755
 SiC, wetting by silicon and alloys, rel. to reaction sintering 3-76298
 Si₃N₄, effect of fabrication conditions on mech. and dielec. props. 3-76294
 Si₃N₄, pressureless densification 3-69350
 Si₃N₄, wetting by silicon and alloys, rel. to reaction sintering 3-76298
 SiO₂ support, NaOH addition effects on morphology and struct. 3-58773
 SmCo₅ magnets, liquid-phase sintering 3-44643
 SmCo₅ powders, mechanisms, rel. to magnet prod. 3-47438
 Sm₂Co₇, liquid phase, mag. props. obs. 3-44694
 SnO₂, MnO₂ content effect (*Polish*) 3-44663
 SrFe₂O₉, ferrite, liquid phase sintering of magnetically isotropic and anisotropic compacts 3-58701
 SrO.5Fe₂O₃, sintering and characteriz. 3-61191
 Ta powder compacts, porous, shrinkage in sintering (*Korean*) 3-53265
 ThO₂ powders, phys. props. and influence on sinterability 3-80402
 TiO₂ compacts, flash heating technique, kinetic study of shrinkage (*French*) 3-72996
 (U, Pu)C pellets manufacture by reactive sintering (*German*) 3-43302
 (U,Pu)O₂ pellets, sintering variable effects on chem. and phys. characteriz. 3-78379
 (U,Pu)O₂ pellets, quantification of processing parameter effects on chem. and phys. characts. 3-78378
 UO₂, high temp. oxidation, effect of compaction, exposed area and initial composition 3-60275
 UO₂, mathematical model of process (*German*) 3-71323
 UO₂ pellets, crack sintering rates meas. 3-46144
 UO₂ powders, microstruct. evolution during press. sintering 3-78377
 W powder compacts, low temp. sintering (*Korean*) 3-53264
 W-Ni-Fe composite, with W wire fibres for reinforcement 3-69370
 W-Ni-Fe system, ductility, fracture resistance rel. to microstructure (*German*) 3-80391
 WC/Co powder, shrinkage rel. to milling 3-80393
 WC-Co composite materials, precipitation and magnetic hardening, coercivity and saturation magnetisation obs. 3-60973
 Y₂O₃-CaO system, phase diagram characteriz. 3-76241
 Y₂O₃-ThO₂ (10 mole%)-Nd₂O₃ (1 mole%), transparent powder prep. and processing 3-64968
 ZrO₂, partially stabilized with calcia, SiO₂ role in sintering 3-69346
 ZrO₂ oxygen-pump die for hot pressing 3-76256
 ZrSiO₄, TiO₂ addition effects (*Japanese*) 3-80436

size effect

- heading is late addition
audio frequency size effect seen in modulation of r.f. size effect 3-46788
glass matrix, optical and paramag. absorpt. of Ag particles 3-55563
metallic thin films, charge transport parameters determ. 3-55242
metallic thin films, electrical field dependence of resistance 3-68590
r.f., model for electron mean free path temp. depend. 3-55251
semiconductor, intrinsic size-quantized, energy spectrum in presence of strong e.m. wave 3-75762
semiconductor, many-valley, size depend. of magnetoresist. 3-64355
semiconductor, thermo-e.m.f. in applied mag. field, size depend. 3-60887
semimetal thin films, three dimensionally quantised, carrier density and mag. props. 3-58263
Shockley model, one-dimens. lattice terminated by arbitrary surface potentials, quantum size effect 3-58197
Bi film, quantum size effect 3-64267
Bi film, thermoelec. power, quantum size effects (French) 3-55293
Bi₂Sb_{1-x} film, thermoelec. power, quantum size effects (French) 3-55293
Cd, e.f. surface impedance and size effects on electronic m.f.p. 3-55252
Cd, electron mean free path determ. by r.f. size effect (French) 3-58252
InSb, size effect meas. at room temp. 3-58292
Sb, galvanomag. props. at low temp., size and static skin effects 3-72374
n-Si, carrier redistrib. between valleys due to size effect 3-75760
Sn, intermediate state, rel. to thermal cond. (French) 3-58336

skin effect

- h.f. discharge, diffusion under strong skin effect conditions 3-60653
Permalloy films, determination of resonance s.h.f. permeability (Russian) 3-60991
Permendur films, determination of resonance s.h.f. permeability (Russian) 3-60991
Ga, Azbel' Kaner cyclotron resonance at far i.r. frequencies 3-58313
Mn ferrite, with excess Fe, microwave reson. and relax., skin depth effect 3-68849
Sb, galvanomag. props. at low temp., size, surface, shape and static skin effects 3-72374
Sn, surface impedance in strong mag. field, cond. electron scatt. 3-72379

sky

- see also night sky; sky brightness
cloud amount, determinations using automatic instrument systems 3-65529
light scattering in the atmosphere, simulation with glass tank 3-70250

sky brightness

- see also airglow; twilight
artificial night-sky illumination and seeing at astronomical observatories 3-65374
Blue Mesa Observatory, contrib. by artificial illum. 3-47718
daytime Li vapour trails in thermosphere rel. to sky brightness 3-65418
diffuse Galactic light and interstellar dust albedo in 1500-4250 Å region 3-53701
Direct fluxes of illumination over India 3-80746
Fraunhofer line depth in daytime sky spectrum, brightness and polarisation 3-45033
intensity measurement, scanning field apparatus 3-80861
light pollution, high pressure Na lamps, concern to astronomers 3-76778
night sky radiation in u.v. and visible, Kosmos 51 and 213 obs. in space (Russian) 3-44878
night sky radiation in u.v. and visible kosmos 51 and 213 observations in space (Russian) 3-44877
phase function, altitude transform. and polarisation between 0.8 and 2.2 µ 3-73302
point light source, detection probability rel. to stellar magnitude and sky brightness 3-51418
pollution from outdoor lighting, astronomical implications 3-51240
solar atmosphere, velocity fields, mag. fields, brightness meas. (Russian) 3-45008
threshold brightness as function of location of source in instrument field of view 3-62062
visibility threshold of stars with unaided eye at different background brightnesses 3-70080

sky surveys see astronomical catalogues

sliderules see calculating apparatus

sliding contacts, electrical see electrical contacts

slip

- see also plastic flow
alloy, B2-type, work-hardening, thermal and nonthermal cross-slip effect 3-47374
anisotropic rigid/plastic materials, plane strain slip line theory 3-47469
blood flow and viscometry 3-56492
β-brass binary and ternary alloys, embrittlement by liq. metals and aqueous ammonia 3-80343
cross slip of superlattice dislocations 3-40928
dislocation acceleration through sonic barrier, computer simulation obs. 3-75531
dislocation arrays, hexagonal screw, short range stresses 3-68272
dislocation pile-ups retarded by slip boundaries, equil. dislocation distrib. (Russian) 3-43791
earthquakes, Archambeau's source theory rel. to slip on fault 3-56010
fibrous filters, effect of gas slip on pressure drop 3-71825
gas, effect on fibrous filters resist. 3-71786
grain boundary dislocation role in grain boundary sliding 3-79350
ionic crystals, maximum work analysis for slip on {110} and {100} systems 3-64090

slip continued

- ionic crystals, uniaxial deform. and axisymmetric flow for slip on {110} and {100} systems 3-64091
Johnston-Gilman's theory of yielding due to inhomogeneous deformation 3-49922
metal, f.c.c. and b.c.c. lattices, rate relationships of dynamic yield pt. 3-43824
metal, laser beam irradi., mech. deform. and disruption (Russian) 3-40958
metal, slip plane interaction with subgrain boundary, double refr. pattern obs. (Russian) 3-55779
metal foil, thickness meas. using intersecting slip traces 3-47372
metal particles, dislocation generation during early stage sintering 3-69243
metals, yield surface shape, offset influence, different loading paths, slip theory model anal. 3-72889
metals and alloys, dislocation arrays, planar and cellular, slip behaviour (German, English) 3-69241
metals and alloys, rel. to basic mechanisms of creep behaviour, review 3-46667
polycrystalline nonmetals, high temp. creep, third-power stress depend. 3-55010
polymer friction, initial stages of slip 3-65018
refractories, deform., grain growth, electron microscopy 3-72976
in rolling contacts, microslip due to tangential surface tractions 3-49931
shear crack pair behaviour near planar interface 3-64103
steel, alloy El 435, intergrain slip, in molten zone, arc welding, interferometry, statistical anal. (Russian) 3-41790
steel, low-C, fatigue crack propag. under doubly repeated stress, residual stress and plastic strain (Japanese) 3-41734
steel, low-C, pressurized, Portevin-Le Chatelier effect 3-80289
steel, mild, cavitation erosion for low cavitation intensity 3-41751
steel, UHB stainless 724LN, austenitic, improved creep strength mechanism 3-69324
superplasticity, grain boundary glide, elastic resist. to shear (Russian) 3-72853
tectonic stick-slip stress drops, effect of quartz fault-gouge 3-76627
thermally activated dislocation motion, selection methods 3-64052
unvulcanized rubbers, unstable flow, in open and closed channels 3-58756
viscometry correction 3-77761
AgCl, Knoop microhardness anisotropy, applic. to slip system identification 3-79410
Al, coarse crystals, fatigue damage mechanism (Japanese) 3-41732
Al, polycryst., deform. nonhomogeneity, dislocation mechanism of slip 3-64846
Al, polycryst., single [111] fibre texture development (Japanese) 3-61143
Al alloy 7075 sheets, crack initiation mechanisms 3-64834
Al single crystals, temp. depend. of strength, high plasticity phenomena, 1.4-300K (Russian) 3-55003
Al-Cu(1 wt.%) alloy, stress corrosion cracking, slip characts., grain boundary misorientation (Japanese) 3-44578
Al₂O₃, polycryst., pyramidal and basal slip systems 3-55848
Al₂O₃, sapphire, hardness and damage resist. depend. on surface finishing 3-69342
Al₂O₃, sapphire, pure and Cr-doped, basal slip 3-76243
Al₂O₃, sapphire, yield pt. behaviour, dislocation-multiplication mechanism 3-55846
Al₂O₃, sapphire filament, creep mechanism 3-76318
BaF₂, Knoop microhardness anisotropy, applic. to slip system identification 3-79410
Be, mechanical hysteresis, temp. depend. of friction stress for (1010) <1120> type dislocations 3-43823
Be single cryst., deformation under laser action, defect obs. (Russian) 3-52661
Bi-Sb single crystals, double modified etch technique, dislocation motion and glide system determ. 3-68266
C fibre, plastic deformation, band like plane smoothing rel. to extension velocity (German) 3-76373
Cd, critical shear stress, metal purity and temp. depend., single crystals. (Russian) 3-52660
Co-Fe (8 wt.%) alloy single crystals, twin-slip, twin-twin and slip-twin interactions 3-40930
Cu, deformed in polyslip, structure sensitive recovery 3-76172
Cu, neutron irradi. single crystals, dislocation struct. 3-79377
Cu, polycryst., deform. nonhomogeneity, dislocation mechanism of slip 3-64846
Cu, surface indentations made by cone indenters on cube face, apex-angles influences (Japanese) 3-58169
Cu-Al alloy, slip plane dilation and disorder, electron microscope obs. 3-69235
Cu-Al alloys, stress-strain characts. and slip band formation 3-47407
Cu-Fe alloy single crystals, containing γ-Fe precipitates work hardening phenomena 3-80226
Cu-Ge alloys, stress-strain characts. and slip band formation 3-47407
Cu-Si alloys, stress-strain characts. and slip band formation 3-47407
Cu-Sn alloy, martensitic transform., phenomenological analysis (Japanese) 3-50680
Cu₃Au type alloy, ordered, incomplete cross-slip of superdislocation 3-69236
Fe, plastic asymmetry phenomena 3-80295
Fe crystal, crack apex 3-80376
Fe single crystals, ZrH₂ refined, with C and N in soln., low temp. mech. props. 3-58696
Fe-Al(40 at.%) alloy, ordered, slip systems, shear stress induced (French) 3-53212
Fe-Ni-Ti alloys, continuous decomp. of γ-solid soln. (Russian) 3-58621
Fe-Ti (0.16 wt.%) single crystals, orientation, temp. and strain rate effects on deform. 3-64909
FeAl single cryst., cooperative slip systems, orientation depend. 3-58073
Ga, creep, slip participation near melting pt., single crystals. (Russian) 3-52666
GaAs, rel. to hardness anisotropy (Russian) 3-72121
Ge, rel. to hardness anisotropy (Russian) 3-72121

slip continued

- In single crystals, rel. to spasmodic creep, 78 and 180K (*Russian*) 3-64954
- InSb, rel. to hardness anisotropy (*Russian*) 3-72121
- KCl:Sr slip band internal structure by precipitation 3-52632
- LiF:Mg, deform. hardening under simple slip conditions 3-58075
- Mg, magnesia strengthened, high temp. creep 3-64959
- Mg, single cryst., crit. shear stress temp. and rate depend. for basal slip, obs. and mechanism 3-80381
- Mg-In solid soln. single crystals., conc. depend. (*Japanese*) 3-41776
- MgO, polycryst., microyield and fracture, model approach 3-58067
- MgO, polycryst., microyield and fracture, model interpret. 3-58068
- MgO, rel. to deformation effect on optical absorption 3-64697
- Mo, line patterns at room temperature, surface transmission electron microscope obs. 3-58036
- Mo thin foils, in situ deform., 800 keV electron microscopy 3-50703
- NaCl, dislocation struct. study by etching, slip band form. 3-75532
- NaCl, Knoop microhardness anisotropy, applic. to slip system identification 3-79410
- NaCl, stress-strain curves for (110) and (100) planes (*German*) 3-46661
- NaCl cryst., slip band motion kinetics, leading dislocations 3-49925
- Nb monocrystals, blister form in He⁺ implantation, slip plane interaction 3-72111
- β -Nb-Zr, deform. temp. depend., slip, twinning and dislocations rel. to yield and fracture 3-52662
- Ni, deformed in polycryst., structure sensitive recovery 3-76172
- Ni, grain boundary fracture mechanism (*Russian*) 3-61132
- Ni-Al(36 at.%) alloy, martensite struct. and behaviour (*Russian*) 3-80250
- NiAl single crystals., stoichiometric, steady-state creep, orientation depend. of deform. mode 3-64913
- Ni₃Fe and Ni₃FeCr alloys, dislocation struct. at various strain hardening stages (*Russian*) 3-58626
- Ni₃Mn alloy, ordering effect on crit. shear stress magnitude (*Russian*) 3-44570
- Ni₃Mo alloy, plastic deform., twinning for ordered phase, slip in disordered phase 3-79408
- Si, plastic deform. during stage II 3-58074
- SrF₂, Knoop microhardness anisotropy, applic. to slip system identification 3-79410
- Ti, fatigue tests with const. strain amplitude 3-64891
- Ti, polycrystalline sheet, orientation dependent 3-76164
- Ti, under static and cyclic loading (*Russian*) 3-41762
- Ti alloy, two-phase, fatigue fracture topography 3-55816
- Ti alloy, two-phase, fatigue failure in vacuum (*Russian*) 3-41759
- Ti-Al alloys in methanol-HCl solns., stress corrosion cracking by slip induced grain boundary splitting 3-47401
- Ti-Fe alloys, conc. depend. of constitution and plastic deform. (*Russian*) 3-58640
- UO₂, hyperstoichiometric single crystals., deform. model 3-55849
- Y, h.c.p., deform. modes, 77-497K 3-64912
- Zn, critical shear stress, metal purity and temp. depend., single crystals. (*Russian*) 3-52660
- Zn, dislocation motion initiation stress and internal stress meas. (*Russian*) 3-58620
- Zn, thermally activated glide of single crystals., 4.2 to 373 K 3-40957
- Zn single crystals, critical resolved shear stress, biaxial loading effect 3-46658
- Zn-Al(40 wt.%) alloy, superplastic, basal plane pole figures 3-69220
- Zr single crystals., compression parallel to c-axis, 78-1100 K 3-46659

smectic phase see *liquid crystals***smoke**

- see also *air pollution; dust*
- air pollution detection using biological method 3-61928
- atmospheric turbidity rel. to sunlight and aerosols, water catchment problems 3-61486
- laser attenuation and backscatter at 2.36 and 0.63 μ (*Russian*) 3-59846
- light backscatter coeffs. and total scattering coeffs. (*Russian*) 3-62662

snap off varactors see *varactors***Snoek effect** see *elastic relaxation; interstitials***snow**

- area of snow and pack-ice in fall rel. to insolation income 3-59099
- atomic absorption, flame and flameless, Ca determination, glacial snow samples 3-48638
- avalanche study (*Japanese*) 3-56268
- avalanches, plasticity theory, static and kinematic solns. 3-40128
- buckling characteristics of sloping snow slab rel. to avalanches 3-51211
- crystal growth, vapour deposition, computation of meas. growth rate 3-76766
- crystals, ice nucleation, cloud seeding 3-73319
- Mt. Daisetsu hard snow, times, conditions and processes of formation (*Japanese*) 3-56270
- drifting, wind fluctuations near surface (*Japanese*) 3-56159
- drifting round obstacle, measurement of wind turbulence (*Japanese*) 3-56160
- dust particles, influence on light transmission (*Japanese*) 3-56267
- failure criterion for characterising fracture strength 3-69578
- fracture under triaxial compression (*Japanese*) 3-56158
- graupel, conical, mechanism of origin, attachment to snow crystals 3-44889
- Greenland, T and D content in firn samples 3-53572
- hardness, measurements down to -55°C for varying densities (*Japanese*) 3-56157
- lake effect snowstorms, role in hydrology, Lake Erie 3-47773
- Lake Effect storms, diffusional deposition of ice on AgI, snow crystal struct., Ag content 3-76768
- melt runoff in subarctic, energy balance, Labrador 3-56148
- melting rate altitude depend. rel. to atm. temp. vertical profiles (*Japanese*) 3-56162
- mosaic structure of snowflakes 3-51036
- perennial patches, distribution, mass balance (*Japanese*) 3-56269
- rainfall intensity freq. patterns, snow melt and seasonal effects 3-59064

snow continued

- rates of snowfall, reliability of optical measuring technique 3-65530
- satellite pictures, snow hydrology, Western Himalayas 3-80740
- Scottish Highlands, changing seasonal patterns 3-80771
- snow lines, snow melt quality, Earth Resources Technology Satellite, imaging 3-80716
- snowline mapping with NOAA-2 environmental satellite 3-56174
- soil moisture of sagebrush rangelands, Idaho, max., min. storage for snow and rain 3-58869
- stochastic snow model for water supply prediction and flood forecasting 3-59063
- storm, 4-5 March 1971, Montreal 3-73330
- tensile strength meas., volume strengths rel. to density and type 3-76789
- wave propagation in snow 3-53363
- He-Ne laser light propagation loss (*Japanese*) 3-47719
- social and behavioural sciences**
- see also *psychology; teaching*
- arms race, a questionnaire for physicists 3-77345
- population explosion, mathematical conditions 3-48704
- societies**
- No entries
- sociology** see *social and behavioural sciences*
- sockets (electrical)** see *electric connectors*
- sodium**
- in amine solns., Faraday effect interpret. 3-53348
- atmospheric nighttime meas. at 23°S 3-53485
- atom, ²³Na states, disorientation induced in collisions with inert gas atoms 3-78511
- atom, broadening and shift of D-lines at low press. 3-67693
- atom, electron collision, momentum transfer cross sections, from elec. conductivity of arc discharge 3-71430
- atom, electron impact excitation, polarization of reson. lines 3-63314
- atom, electron impact ionisation, binary encounter calcs. 3-71412
- atom, electron scatt., frozen core Glauber approx. 3-46202
- atom, electron scatt., threshold behaviour of inelastic scatt. cross sections 3-63324
- atom, electron spin exchange collisions, cross section, temp. depend. 3-67705
- atom, Hanle effect, inert gas influence 3-74807
- atom, ionisation, resonant two-photon, photoelectron angular distribution 3-67690
- atom, laser excited, electron scattering, differential cross section meas. 3-74863
- atom, resonance polarization by electron impact, Glauber theory applic. 3-71441
- atom emission from N₂ afterglows, excitation process and Doppler temp. 3-46174
- atom ground state wave functions, variational method 3-49380
- atomic, theory of multiphoton ionisation of gas by ruby laser 3-71381
- atomic fluorescence lifetime meas. using stepwise excitation by dye lasers 3-49392
- atoms, optically orientated, disorientation in collisions with saturated hydrocarbons (*German*) 3-43381
- binding energy, compressibility, pseudopot. calcs. 3-54941
- boiling simulation using a water model, voiding and re-entry processes 3-46703
- Compton profile, influence of electron correlation and crystal structure 3-75544
- Compton profile calcs., momentum wave functions of APW 3-79616
- contamination, in Si devices and processing materials, flame emission spectrometry monitoring 3-69169
- coolant, LMFBF fuel-coolant interaction, noncoherence and heat transfer cutoff 3-71289
- coolant, molten fuel-coolant interactions, fragmentation of UO₂ and stainless steel 3-74730
- coolant in fast nuclear reactors, structural design guidelines 3-40530
- discharge, optically thick, 250 Torr, electron and gas temp. profiles, non-LTE plasma, collision processes 3-40768
- discontinuous Compton scatt. by K- and L-electrons, intensity, chem. shift, fine shift angular depend. 3-55701
- distribution, in Si-SiO₂ struct., secondary ion emission analysis (*Russian*) 3-52904
- electrical resistivity calc. of solid from lattice dynamical structure factors 3-55243
- electrical resistivity of voids, calc. using phase shift and pseudopotential methods 3-44054
- electron elastic scattering, variational calc. 3-43365
- electron scattering, elastic, spin-exchange cross sections, differential meas. 3-71421
- electronic band struct. and Fermi surface, pseudopot. calc. 3-52779
- fast reactor, Na pool fire, sodium oxide and fission products, release functions 3-67540
- Fermi surface, augmented-plane-wave Hartree-Fock first-principles calc. 3-58203
- fires, charact. (*Dutch*) 3-57565
- flow in constant field, circular tubes resistivity effect (*Russian*) 3-79017
- flow in pipe with diaphragms in mag. field, resistance effects (*Russian*) 3-79018
- fluorescence in Hg-Na-N₂ mixture, collisional quenching by N₂ 3-54571
- fluorescence obs. in laser excited NaK vapour mixture 3-40650
- fusion reactor blanket, Na cooling, neutron and gamma heating rates 3-60328
- heat pipes, sonic limit, dissociation, condensation 3-63659
- in InAs, distrib. in melt, under flux, radioactive isotope method 3-75626
- interaction with molten fuel, modelling 3-67532
- interaction with nuclear fuel, kinetic energy and pressure calc. 3-67531
- ions, 0.3 to 2.0 MeV, excitation of N, N₂ and air, fluoresc. efficiencies 3-40644
- ions, in SiO₂ film, time dependent breakdown in m.i.m. structures 3-52911
- lattice dynamics, modified Bhatia's model 3-46685

sodium continued

- liquid, collective motions charact., molecular dynamics simulation 3-52569
- liquid, corrosion tests on stabilized steel fast nuclear reactor fuel cans (*German*) 3-71304
- liquid, dynamic structure factor calcs., neutron inelastic scatt. obs. 3-49835
- liquid, effective pair potentials, calc. from X-ray data 3-49825
- liquid, equilibration method for measurement of carbon activity 3-63199
- liquid, explosive vapour interaction following infection into molten UO_2 3-60284
- liquid, flow rate determ. using analysis of temp. noise signals in nuclear reactor (*German*) 3-67490
- liquid, flow velocity through FFTF fuel assembly, meas. using eddy-current flowmeter 3-45621
- liquid, heat removal from LMFBR fuel assembly by natural circulation 3-46114
- liquid, initial expulsion in direct heated channel, ejection vel. and residual film 3-60258
- liquid, jet, penetration of solid UO_2 layer, theory 3-80342
- liquid, nonmetallic impurities mutual interaction 3-49840
- liquid, nuclear magnetic relaxation rate of ^{23}Na spin, temp. depend. 3-47160
- liquid, nuclear reactor coolant, meas. temp. following local primary circuit blockage (*German*) 3-67491
- liquid, pair interaction pot. calcs. 3-49838
- liquid, pair potentials, from struct. factor 3-49826
- liquid, positron annihilation theory using Green function method 3-50110
- liquid, saturated properties, use in LMFBR fuel-coolant interaction analysis 3-46157
- liquid, struct. factor, press. effects, X-ray study 3-49823
- liquid, thermodynamic properties calc. using perturbation theory (*Russian*) 3-55092
- liquid, thermotransport of Be and Hg 3-64197
- liquid, turbulent transport properties for thermal design of LMFBR cores 3-46112
- liquid, two phase and subcooled, thermodynamic props., calc. molten fuel-coolant interactions, potential accidents 3-71288
- liquid, void coeffs. in LMFBR, analysis from direct k-calcs. 3-71201
- liquid, voiding effect in LMFBR, test of calcs. by approximate DB^2 method 3-71200
- liquid, voiding effects in a Pu fuelled fast reactor, calc. using computer program (*German*) 3-67472
- liquid as coolant in fast reactor, determ. optimum fuel element spacing to limit thermal shock (*German*) 3-67586
- liquid as coolant in fast reactor, ebullition onset in laminar and boundary layer flow (*German*) 3-67469
- liquid burning, effect of aerosol suppressants rel. to fast reactor containment (*German*) 3-67471
- liquid droplet, combustion model for LMFBR accident analysis 3-46076
- liquid metal, positron annihilation, volume dependence up to 4 kbar 3-50115
- liquid metal/ β -alumina interphase impedance rel. to Na-S battery separator applic. 3-69465
- liquid use as solvent for crystal growth 3-80150
- in LMFBR, boiling caused by local blockages, exptl. study 3-46095
- LMFBR, sodium cooled, water leaks into sodium, monitoring 3-63148
- melting entropy, rel. to relative volume change 3-68391
- melts, diffusion of Armco iron, diffusion acceleration mechanism (*Russian*) 3-41717
- neutron transport, effects of photon emission anisotropy 3-49305
- nightglow, NaI, 5890/6Å, emission rate depend. on atm. structure and dynamics 3-65423
- nightglow emission, diurnal variations 3-47779
- nightglow intensities in Europe-Africa sector, diurnal, annual and solar cycle var. 3-51101
- nuclear reactor coolant, flow meas., eddy current flowmeter, wet vs. dry performance 3-66477
- nuclear reactor coolant, temperature measurement by microwave techniques 3-70282
- nuclear reactor sodium loop, temperature noise measurement 3-67453
- nucleation of boiling from surface cavities containing inert gases 3-46704
- optical pumping by dye laser, for c.w. velocity selection of Na thermal atomic beam 3-78463
- oscillator strengths for 3d to 4p and 4p to 4d transitions 3-43331
- photo emission and optical constants, of pure thick layers in u.h.v., 250-630 nm (*French*) 3-41610
- photometer for Na day airglow detect. 3-65515
- plasma optically dense, temp. and particle density calc. (*Dutch*) 3-49638
- power reactor steam generators, safety against sodium-water reaction 3-67615
- primary coolant, meas. and anal. of fast neutron spectra, fast breeder reactor 3-71153
- pseudopotential calc. of charge densities, comparison with self-consistent results 3-75699
- reactor component design, material technology, problems (*French*) 3-67545
- reactor coolant, C activity meas. 3-63214
- reactor coolant, removal of Cs, by activated charcoal, in thermal convection capsule 3-63216
- reactor pulsed assembly neutron emission-time effects 3-49297
- resonance lines, D_2 , power broadening by optical nutation, laser saturation spectra 3-67669
- resonance spectroscopy, using Na atomic beam and c.w. single-freq. dye laser 3-77484
- resonances in electron impact, energies and width 3-52288
- solar Na D_2 line profile inversion 3-73442
- solid, isothermal compressibility and isobaric expansivity data 3-79414
- solid and liquid, optical consts. depend. on aggregation and temp. for $\lambda = 0.3$ to $2.5 \mu\text{m}$ (*German*) 3-72595

sodium continued

- spectra, D lines hyperfine struct. by atomic beam absorpt. from dye laser 3-46178
- spectral line profile, plasma inhomogeneity reversal temp. effect in thermal boundary layer 3-63875
- stellar, η Canis Major spectrum 3-69957
- technology, influence on reactor design and operation (*French*) 3-67546
- trace analysis by absorption using dye laser 3-54048
- turbulent channel flow, incipient-boiling superheats, temperature rise rate effect 3-64168
- upper atmosphere, Na enhancement rel. to sporadic extraterrestrial dust influxes 3-44912
- vacancies, atomic relax. and elec. resist., calc. 3-46639
- vaporised coolant, expanding, simulation of mech. energy release, reactor energy source characterisation 3-74674
- vapour, effect of noncondensibles on condensation rate from single rising HCDA bubble 3-46158
- vapour, elec. cond., 1100-1500 K 3-46374
- vapour, elec. conductivity, pressure depend. including atomic clustering effects 3-63612
- vapour, reaction with N_2O , reaction rate, chemiluminesc. obs., mechanism 3-80524
- vapour condensation, HCDA bubble, effect of noncondensibles 3-68397
- void effect in the SNR-300 (*German*) 3-67473
- $\text{CdF}_2\text{:Na}^+$ -anion vacancy complex dielectric polarisation, ionic thermocurrents, reorientation, space charge formation 3-44367
- CdS:Na , polycryst. film, photomemory effect 3-41232
- CsI:Na^+ , Ti^+ , V_k centres, e.p.r. and light absorpt. obs., thermolum. study of thermal migration 3-64035
- He-Na discharge, freq. locking of CW dye laser near atomic absorpt. line 3-59880
- K + Na(K) collisions, threshold energies for excitation to $\text{K}(4^2\text{P})$ 3-78514
- KBr:Na, composite structure of V_1 -band, thermal annealing obs. 3-64699
- KBr:Na, thermal recovery of radiation hardening, thermoluminescence and thermal decay of V_1 band 3-68247
- KBr:Na $^+$, H, H_2 centre form. with dynamic interstitial interactions, temp. depend. 3-58034
- KCl, theoretical analysis of type I $\text{F}_a(\text{Na})$ and type II $\text{F}_a(\text{Li})$ centres, point ion model 3-58229
- Li:Na,K, singly and doubly ionized states, Auger transitions 3-69122
- in NH_3 , liquid, solvated electrons photoelectron emission, 1.55 to 5.4 eV 3-41614
- Na I 5890-5896 Å lines in nightglow, seasonal and diurnal variations 3-51088
- Na I isoelectronic series, dipole polarizabilities from nf term values 3-78450
- Na II ion, radiation lifetimes 3-74785
- Na- NH_3 solns., chemical potentials, related thermodynamics 3-73135
- Na- NH_3 solution, magnetic susceptibility meas. by Gouy method 3-73172
- Na + He collisions, transitions among $3p^2\text{P}$ states of Na 3-74829
- Na + Hg vapour mixture, translational energy transfer collisions between metastable and admixed atoms, excitation function study 3-78537
- Na + Hg + N_2 , collisional excitation transfer and quenching 3-78519
- Na + I $\rightarrow \text{Na}^+ + \text{I}^-$, differential cross section, oscillations 3-60388
- Na $^+$, electron detachment by electron collisions 3-67702
- Na $^+$, sixfold coordination in garnet 3-72065
- Na $^+$ low energy collisions with Ne atoms radiation phase interference and optical polarisation effects 3-67715
- Na $^+$ mobile ions, effect on field-enhancement dielec. breakdown of SiO_2 films 3-79982
- Na $^+$ spectra, oscillator strengths calc. for resonance series $2p^6\text{-}2p^5\text{n}s$ 3-63290
- Na $^+$ + Li, Na + Li $^+$, excitation and electron capture cross-section, small impact parameter 3-71447
- Na $^+$ + Na, excitation and electron capture cross-section, small impact parameter 3-71447
- Na $^+$ + Ne, absolute scattering cross-sections and interaction potential 3-71454
- Na $^+$ + Ne collisions, low energy, strong polarization effects in optical radiation 3-63337
- Na $^+$ + Ne collisions at 1.0-5.0 keV, differential cross-sections for electron transitions 3-74897
- Na $^{3+}$, spark spectra 3-49385
- Na $^{4+}$, spark spectra 3-46180
- Na $^{5+}$ spark spectra 3-46180
- Na $^{5+}$ spark spectra 3-49385
- Na $^{6+}$ spark spectra 3-46180
- NaI, self broadening of principal series 3-71399
- ^{22}Na , diffusion in AgBr: Cd and AgCl, Frenkel defect conc. calc. 3-55098
- Na* + He collisional depolarization of ^2P states, weak spin-orbital coupling 3-54586
- Na*(^2P) + He collisions, inelastic transitions between J,M-states in Na*(^2P) 3-78518
- Na(3^2P) doublet in flames, quenching by H_2 and O_2 collisions 3-52300
- PbBr $_2\text{:Na}^+$, ionic cond., 60-320°C 3-46728
- $\text{SrCl}_2\text{:Na}^+$, F* centre bleaching, annihilation probability 3-40917
- SrF $_2\text{:Na}$, conversion of colour centres by doping 3-53133
- UO_2 -Na interactions, pressure pulses, estimates 3-67617
- ZnSe photoluminescence spectra, shallow acceptor 3-58555

sodium compounds

- see also *Rochelle salt*
- aqueous solution, i.r. spectra of water, internal reflection spectroscopy 3-75042
- brine, content in sea ice 3-80708
- bromacetate and bromoacetate- d_2 , vibrational spectra and struct. 3-75987
- fluorescein in glycerol, luminesc. aggregates, Webers red edge effect 3-69078
- halides, thermal expansion at low temps. 3-43885

sodium compounds continued

- hydrogen oxalate mesohydrate, deuteron magnetic resonance, hydrogen bond studies 3-72529
- hydrogen oxydiacetate, crystal structure determ. from X-ray intensity data 3-68238
- NaCl, growth rate, kinetics 3-72298
- rivadavite, crystal structure, symbolic addition method 3-75508
- saline emulsion, with dispersed conducting phases, dielec. paramet-ers (*French*) 3-80502
- saline solutions, aqueous, spontaneous rupture of supercooling and supersaturation states (*French*) 3-79493
- saline solutions, metastable aqueous, spontaneous rupture of super-cooling and supersaturation states (*French*) 3-79491
- silicate glasses, mechanical properties, effect of iron oxides 3-76378
- soda-lime glass, elec. effects in slow fracture 3-76264
- soda-lime glass, polymeric coating effects on bend strength 3-76265
- soda-lime glass, slow fracture characts 3-76268
- soda-lime silicate glasses, Na⁺-H⁺ ion exchange influence on crack propag. 3-55886
- soda-lime-silica glasses, org. liq. environment effects on crack prop-ag. 3-72968
- sodalites, synthesis of photochromic and cathodochromic sodalites
- sodium-alumino-silicate to sodalite structure conversion 3-41865
- sodium anthranilate, i.r. spectra, metal-ligand stretching frequencies 3-54688
- sodium bromoacetate, and -d₂, vibr. spectra and structure 3-78798
- sodium hydrogen diacetate, i.r. and Raman spectra, symmetric hydrogen bonds 3-68990
- sodium N-phenylglycine, Raman spectra between 200 and 1700 cm⁻¹, vibr. assignment 3-47241
- sodium-alumino-silicate to sodalite structure conversion synthesis of photochromic and cathodochromic sodalites 3-41865
- sodium-hydrogen oxalate monohydrate, γ -irrad. single crystals, radical obs. 3-47565
- tartrate crystals, triboluminescence and simultaneous charge produced at fracture 3-69045
- transient phenomena of polarisation reversal, neutron time-of-flight method 3-72582
- zeolites, hydrated and dehydrated struct. parameters statistical com-parison 3-52597
- (Ag + Na)NO₃, molten binary mixtures, external transport numbers, ionic mobility, cooperative mechanism, ionic conductivity (*French*) 3-75747
- AgNa(NO₂)₂, dielectric constant, relaxation time, Curie point, hydrosta-tic pressure effects 3-50510
- Al₂O₃-Na₂O system, range of existence and stability of β and β' alu-mina (*French*) 3-69365
- (Ba,Na)(Ti,Nb)O₃ polycryst. material prep. and prop. optimization 3-75945
- Ba₂NaNb₅O₁₅, ferroelec., struct. behaviour in Curie pt. region 3-41488
- Ba₂NaNb₅O₁₅ in excited state, absorption spectra (*Russian*) 3-50599
- Ba₃NaNb₅O₁₅, ferroelectric, polarised microwave echo obs. 3-75951
- CdO-NaCl heterojunction, containing colour centres, electrically stim-ulated photocond. inversion 3-50241
- CsPF₆, reorientation motions and spin-rotation interaction 3-53033
- Ge(Li)-NaI(Tl) Compton-suppression spectrometer with high resolu-tion and large volume 3-42662
- He discharge effect of NaCl on volt.-current characts. (*Russian*) 3-60648
- KCl:LiF, NaF, LiCl, new bands in absorption spectrum 3-44438
- KNO₃-CsNO₃-NaNO₃ phase diagram, thermodynamic calc., thermo-graphy (*Russian*) 3-52692
- La_{0.1}Li_{0.1}NaBa_{1.8}Nb₅O₁₅, ferroelec. props. 3-64610
- LiCl-NaCl solid solution, thermographic and X-ray study, crystn. temp., peritectical transformation (*Russian*) 3-72196
- Li_xNa_{1-x} solid solutions, thin films, persistence of first absorption peaks 3-72665
- Na bisilicate, packing density calc., relaxation properties (*Russian*) 3-47478
- Na polyaluminate solid electrolyte, resistivity meas., effect of Mg doping 3-46857
- Na-K liquid alloys, electrical resistivity calc. 3-60866
- Na-Rb liquid alloys, electrical resistivity calc. 3-60866
- Na₃AlF₆, molten, elec. cond. meas. (*Polish*) 3-70323
- Na₃AlF₆ film, cryolite, on Cr, thickness and dispersion meas., ellip-sometric method 3-62049
- Na₃AlF₆ type phosphors activated with lanthanide ions, effect of Ce impurities (*Russian*) 3-64733
- Na₃AlF₆-CaF₂, phase diagram, differential thermal anal. in sealed cru-cible 3-75604
- NaAlH₄, lib. motion, inelastic neutron scatt. obs. 3-60678
- NaAl(NH₂)₄, H-N lengths and H-N-H angles (*French*) 3-46605
- NaAlO₂-SiO₂-H₂O mineral, phase equilibria, Gibbs energy of forma-tion 3-44773
- Na₆Al₆Si₆O₂₄ . 1.2 NaCl . 0.4 Na₂SO₄, solid solution, optically eras-able cathodochromic coloration 3-41850
- Na₄As₂O₇, bond lengths and angles, phase transformations 3-68223
- Na₂B₂O₇ in B₂O₃, distrib. of impurities from InAs melt, radioactive isotope method 3-75626
- γ -Na₂BeF₄, X-ray diffr., precession photography 3-40892
- NaBr, aqueous soln., X-ray obs. of structure 3-71996
- NaBr, interatomic interaction, electron diffr. study (*Russian*) 3-68195
- NaBr, photoemission obs., comparison with densities of state calcs. for valence and cond. bands 3-44015
- NaBr: Cd, equil. distrib. coeffs. of impurities 3-75543
- NaBr: Cu⁺, absorpt. from optically pumped relaxed excited 3d⁹s state of Cu⁺ 3-50603
- NaBrO₃, Raman spectra of irradiated crystals, internal oscill. 3-55654
- NaCN, i.r. spectra from 4000 to 140 cm⁻¹ 3-47240
- Na₂CO₃, aq. soln. hydrothermal crystn. of Sb₂O₃ 3-68174
- Na₂CO₃, in alkali carbonate molten binary mixture, conductance, fuel cell material 3-69462
- Na₂CO₃, solubility in NaCl:CaCl₂ crystals, 75 to 530°C, from elec. cond. meas. 3-55086

sodium compounds continued

- Na₂CdCl₄, binary combination, NaCl-CdCl₂-SrCl system, phase diag-ram, thermography, X-ray methods (*Russian*) 3-52692
- Na₂Cd(SO₄)₂·2H₂O:co²⁺, spin lattice relax., one phonon and Raman scatt. processes 3-50455
- NaCl, 9% soln., refractive index meas., between 250 and 700 nm. 3-66190
- NaCl, (001) face, factors responsible for complex form. of Au decorat-ing particles 3-75671
- NaCl, anomalous behaviour of X-ray induced photoelectron lines (*German*) 3-50645
- NaCl, anomalous transmission of swift electrons along <100> axis 3-68293
- NaCl, aq. soln., hypersonic vel., molar conc. depend., Brillouin scatt. meas. 3-49934
- NaCl, aqueous soln., X-ray obs. of structure 3-71996
- NaCl, bending, annealing and sign-varying deformation effects 3-75560
- NaCl, bidimens. cryst. of dislocation lines (*French*) 3-52633
- NaCl, channelling of 1 MeV He⁺ ions, damage and temp. effects, 77-870 K 3-52654
- NaCl, complex thermoluminescence glow curves, analysis 3-76102
- NaCl, crystal growth from aq. soln. layer motion 3-75488
- NaCl, crystal growth from drop of melt and anisotropy of surface energy 3-76136
- NaCl, damage region form., changes in giant laser pulses and luminous plasma 3-74262
- NaCl, deuteron induced damage 3-79391
- NaCl, dielec. loss under simultaneous action of a.c. and d.c. voltages 3-55521
- NaCl, dislocation mobility, determ. from expts. on dislocation multip-lication (*Russian*) 3-43793
- NaCl, dislocation movement, influence of ageing (*Russian*) 3-79353
- NaCl, dislocation structure, compression along cubic face, etching 3-75532
- NaCl, effect on spectral analysis of microimpurities in concentrates (*Russian*) 3-77750
- NaCl, effects of electric field on starting stress and range of disloca-tions 3-79359
- NaCl, elec. charge carried by dislocations, meas. 3-72119
- NaCl, energy spectrum of electrons emitted after ion and atom bom-bardment 3-80132
- NaCl, exchange-coupled pairs of Mn²⁺ ions, e.s.r. 3-55470
- NaCl, filamentary crystals, internal friction peak due to dislocation-point defect interaction 3-75569
- NaCl, film, electron diff. intensities, elec. recording, electron filter 3-72292
- NaCl, γ -irrad., dislocation mobility, temp. depend. 3-54970
- NaCl, ion irradi., channelling meas. of damage 3-52652
- NaCl, isothermal diffusion of Ba²⁺, temp. depend. of diffusion coeff. 3-60804
- NaCl, isotope-induced far i.r. absorpt. 3-44402
- NaCl, Knoop microhardness anisotropy, applic. to slip system identification 3-79410
- NaCl, large k-vector phonon generation by stimulated Raman scatter-ing from picosecond pulses 3-55041
- NaCl, laser induced breakdown field strength, pulse duration depend. 3-51941
- NaCl, lattice parameter, at high pressure and low temp., X-ray obs. 3-63998
- NaCl, many-electron theory of distorted lattices, perturbation theory 3-55177
- NaCl, Mn⁰ centre theory, models for A, B, C, D, E-centres 3-43789
- NaCl, monocrystal growth from aqueous soln. (*French*) 3-58588
- NaCl, monodisperse aerosols, diffusion coefficient 3-73086
- NaCl, motion and deform. of cavities in temp. gradient field 3-58152
- NaCl, multiphonon i.r. absorpt. temp. depend. 3-68985
- NaCl, nuclear quadrupole spin-phonon coupling, u.s. wave, propag. 3-75891
- NaCl, paraelec. behaviour of OH⁻ ions, electrooptical and electrocal-oric studies 3-41476
- NaCl, perturbation of intrinsic luminesc. by lattice defects 3-80096
- NaCl, photo-stimulated electron emission temp. depend. (*Russian*) 3-44518
- NaCl, plastically deformed, strength of attractive junctions formed by primary and secondary dislocations 3-60735
- NaCl, polarised luminescence and Mossbauer effect of Sn impurity centres 3-41456
- NaCl, positron annihilation, γ -ray angular correlation curves, effective mass measurements 3-44008
- NaCl, positron annihilation, influence of temp. 3-75548
- NaCl, press. dependence of self-diffusion of ²²Na 3-58150
- NaCl, refr. index and refl. spectra, uniaxial deform. effects 3-58528
- NaCl, scratchig method for evaluation of X-ray effects 3-76398
- NaCl, simple slip on (110) and (100) planes, stress-strain curves (*German*) 3-46661
- NaCl, single cryst., thermal depolarisation currents, electret effect (*Russian*) 3-75938
- NaCl, solution, electrochem. behaviour and stress corrosion cracking of Ti, alcoholic soln. 3-55959
- NaCl, solution, maleic acid-styrene, copolymer, conformational transi-tion in NaCl soln., standard free energy, volume change 3-54765
- NaCl, three-phonon umklapp resistivity, variational calc. 3-68378
- NaCl, V_k centres in surface region self-trapping energy calcs. 3-40918
- NaCl, vaporisation kinetics of solid, rate meas. from 530C to m.p. 3-72189
- NaCl, whisker crystals, ionic conductivity at 40 to 300C and effects of X-ray irradiation (*Russian*) 3-79598
- NaCl, X-irradiated, point defect distrib. of crystals. aged after quench-ing 3-58028
- NaCl, X-irradiation hardening, interstitials, dislocation density 3-52631
- NaCl, X-ray coloured, thermoluminescence, isothermal decay 3-53154
- NaCl, X-ray study of angle distrib. of Auger and photoelectrons using double-focusing spectrometer (*German*) 3-53165

sodium compounds continued

- NaCl (001) substrate, recrystallisation of Au films, electron microscopy and diffraction obs. 3-72293
- NaCl (001) substrate, recrystallisation of Au films, X-ray measurements of strains 3-72294
- NaCl aerosol, activation supersaturation meas. particle size rel. to nucleation 3-44896
- NaCl cryst., γ -irrad., temp. depend. of screw dislocation mobility 3-75536
- NaCl cryst., slip band motion kinetics, leading dislocations 3-49925
- NaCl crystallisation in continuous-flow mixed suspension crystalliser, Pb^{2+} effect 3-72786
- NaCl crystals, H_2 , D_2 diffusion and solubility, desorption obs., isotopic effects 3-72233
- NaCl electrical structure of matching cleavage surfaces 3-52889
- NaCl epitaxial film, i.f. polarisation obs. 3-47202
- NaCl film, surface optical vibrations, frustrated total internal reflection obs. 3-50063
- NaCl internal standard technique rel. to press. induced f.c.c.-h.c.p. transform. in Pb 3-72834
- NaCl Mossbauer emission spectra, deformation induced 3-53048
- NaCl powder, compaction mechanisms 3-47490
- NaCl pure and Ca doped, d.c. conductivity during plastic deformation (German) 3-53060
- NaCl single crystals, deformed, annealing, n.m.r. studies (Russian) 3-64093
- NaCl single crystals, ion bombardment, luminescence, channelling effect 3-72718
- NaCl soln., steel hardening, plastic deformation, uniaxial compression diag. (Russian) 3-41767
- NaCl soln. pH, anodic activation of Al and Mg (Russian) 3-73134
- NaCl solution, artificial membrane potential at KCl solution interface, Ca^{2+} effect 3-69486
- NaCl solution, in porous media, n.m.r. relaxation of ^{23}Na obs. 3-60993
- NaCl substrate, vapour epitaxy of CaF_2 microstructure investigation 3-43954
- NaCl type, thick single cryst., orientation effects of electron scatt. 3-49811
- NaCl type point charge lattice, electrostatic potential calc. 3-75498
- NaCl whiskers, internal friction and reversible creep (Russian) 3-43828
- NaCl whiskers, radiative coloration and recombination luminescence (Russian) 3-44497
- NaCl:Ag SO_4 epitaxial growth, of Ag, doped and undoped, electron microscope examination, nucleation and growth processes 3-46768
- NaCl:[Ni(CN) $_4$] $^{2-}$, X-irrad., e.p.r., paramag. species identification 3-64544
- NaCl:Ag, e.s.r. and optical study of relaxed and hot holes and excitons, 80-360 K (Russian) 3-44041
- NaCl:Ag enhancement of vacuum u.v. excited luminescence by electric field (Russian) 3-50624
- NaCl:Ag 0 , optical absorption bands, excited states 3-72685
- NaCl:Ag $^+$, Cu $^+$, Pb $^{2+}$, F-centres study (French) 3-52625
- NaCl:Ag $^+$ (Cu $^+$), ionization of different impurity electron states (Russian) 3-44455
- NaCl:Ca, short-term electric relaxation (Russian) 3-64597
- NaCl:Ca $^{2+}$, Mg $^{2+}$, Sr $^{2+}$, ionic conductivity measurements as function of temp. 3-68639
- NaCl:Ca $^{2+}$, positron annihilation, Ca $^{2+}$ conc. depend. 3-79373
- NaCl:CaCl $_2$ crystals, solubility of Na $_2CO_3$, 75 to 530°C, from elec. cond. meas. 3-55086
- NaCl:Cd, dissolution kinetics of precip., ionic thermocond. study 3-41020
- NaCl:Cd, equil. distrib. coeffs. of impurities 3-75543
- NaCl:Cd $^{2+}$, activation energy of thermolum., F-centre form 3-72688
- NaCl:F $^-$, reson. modes due to impurity pairs, Green function calc. 3-46690
- NaCl:Mn $^{2+}$ e.p.r. study of aggregation products involving divalent cation-cation vacancy complexes 3-64548
- NaCl:Ni, X-irradiated, stimulated processes 3-41592
- NaCl:Ni $^{+}$, position and energy of Ni $^{+}$ ions (German) 3-58029
- NaCl:O $^{2-}$, u.v. illuminated, photoplastic effect 3-58077
- NaCl:OH $^-$, motion of OH $^-$ ion studied by Raman scattering at low freq. shifts and in O-H stretching region 3-75981
- NaCl:OH $^-$, tunnel levels for librator in Devonshire O $_h$ potential 3-52803
- NaCl:Pb $^{2+}$, absorpt. bands of Pb $^{2+}$ centres 3-58532
- NaCl: Sb $^{3+}$, Sb $^{3+}$, defect centres, optical absorpt., elec. cond., dielec. loss and e.p.r. obs. 3-60739
- NaCl:Ti, Ag and pure crystals, tunnel luminescence (Russian) 3-41560
- NaCl:Ti, luminescence, influence of channelling under the influence of positive ions (Russian) 3-41550
- NaCl:Ti, thermoluminescence glow peaks, intensity as function of Ti concentration 3-47321
- NaCl:Ti,Cd,Cs, impurity precipitates meas. by u.s. velocity changes 3-44600
- NaCl:V $^{2+}$ crystals, Z-like centres study 3-52812
- NaCl/adsorbed methyl chloride, microwave absorpt. 3-72265
- NaCl/Pt interface, charging and discharging currents 3-79769
- NaCl-CdCl $_2$ -SrCl phase diagram, thermography, X-ray methods, Na $_2$ CdCl $_4$ binary combination, eutectics, Van Rein point (Russian) 3-52692
- NaCl-H $_2$ O-HCl system, isothermal diffusion studies at 25°C 3-55994
- NaCl-heavy water solns., struct. determ. by neutron diff. 3-60660
- NaCl-NaBr solid solution, single crystals., elastic const., lattice dimensions and Debye temp. (Russian) 3-43818
- NaClO $_3$, cross relax., n.m.r. acoustic saturation obs. 3-68869
- NaClO $_3$, d.c. elec. conductivity of single crystals with point defects 3-79342
- NaClO $_3$, formation and annealing of free radicals created by irradiation 3-61268
- NaClO $_3$, n.m.r. u.s. saturation study on strain distrib. 3-68858
- NaClO $_3$, mol. crystal spectra, influence of polarising effect of medium in region of internal vibr. 3-72647
- Na $_2$ CoGeO $_4$, magnetic structures, propagation vector (French) 3-60968

sodium compounds continued

- Na $_3$ Co $_2$ O $_7$ ($x \leq 1$), structure of bronze type phases (French) 3-40874
- Na $_2$ CoSiO $_4$, magnetic structures, propagation vector (French) 3-60968
- Na $_3$ (Cr $^{3+}$ O $_6$ Mo $_6$ O $_{18}$ H $_6$).8H $_2$ O, absorpt. and luminescence spectra, vibr. structure 3-72679
- NaCrX $_2$ (X=S, Se), crystal structure and mag. structure 3-40881
- Na(D $_2$ H $_{1-x}$) $_3$ (SeO $_3$) $_2$ crystals induction of β -phase by elec. field in y direction 3-72587
- Na(D $_2$ H $_{1-x}$) $_3$ (SeO $_3$) $_2$ n.m.r. investigation, ferroelectric transitions 3-79938
- NaF, crystal growth from drop of melt and anisotropy of surface energy 3-76136
- NaF, F aggregate centres, radiation induced, thermal aggregation and annihilation 3-68251
- NaF, forced Rayleigh scatt. meas. 20 to 300K 3-53099
- NaF, H $_2$ (Li $^+$) paramag. centre caused by electron irradi., e.s.r., hyperfine interaction, line splitting 3-41410
- NaF, hygromech. effect 3-58174
- NaF, molten, elec. cond. meas. (Polish) 3-70323
- NaF, multiphonon i.r. absorpt. temp. depend. 3-68985
- NaF, N $^{2+}$ bombarded, F-centres, absorpt. study 3-43785
- NaF, NaCl, NaI and LiF, common reduced equation of state 3-41005
- NaF, nuclear quadrupole spin-phonon coupling, u.s. wave propag. 3-75891
- NaF, proton bombardment effects, depth profile of damage in microhardness 3-49910
- NaF, second sound in solid, effects of collinear and non-collinear three phonon processes 3-55120
- NaF, second sound propagation, phonon-phonon interaction, estimation from heat pulse interaction 3-55051
- NaF, thermal expansion from lattice const. temp. depend. 3-52712
- NaF in CaF $_2$, colour centre obs., following γ and p irradiation and annealing 3-72694
- NaF:Cd, equil. distrib. coeffs. of impurities 3-75543
- NaF:AlF $_3$ molten binary mixture, electrical conductivity 3-58800
- NaF:AlF $_3$ system, AlF $_3$ -rich, high press. study, solid-liq. transform., vaporiz., sublimation (French) 3-68392
- NaFeO $_2$, tetrahedral, mag. struct. (French) 3-47069
- Na $_2$ Fe $_2$ Si $_2$ O $_{11}$, Na $_2$ Co $_2$ Si $_2$ O $_{11}$ and Na $_2$ Ni $_2$ Si $_2$ O $_{11}$, glasses on metal substrates, interfacial reactions and adherence 3-55882
- Na $_2$ Fe $_2$ Si $_2$ O $_{11}$ and Na $_2$ - $_2$ Fe $_2$ Si $_2$ O $_5$ glasses on Fe substrates, interfacial reactions and enhanced wetting 3-55880
- NaGa(NH $_2$) $_4$, H-N lengths and H-N-H angles (French) 3-46605
- NaGdO $_2$ and NaErO $_2$, ALnO $_2$ type ternary oxides of rare earths with A=Li-Cs (German) 3-64015
- Na $_2$ Ge $_2$ Si $_2$ O $_{10}$, cryst. struct. (French) 3-79307
- NaHCO $_3$, thermal decomp., Arrhenius plot, sample mass eff. 3-76441
- NaHF $_2$, long wavelength i.r. active phonons, assignment 3-41512
- NaH $_2$ (SeO $_3$) $_2$, ferroelectric, vibr. spectra and hydrogen bond pot. study 3-47256
- NaH $_2$ (SeO $_3$) $_2$, proton configurational entropy 3-68370
- Na $_3$ HSiO $_4$.5H $_2$ O, cryst. struct. obs. 3-75515
- NaI, adsorption on W, field emission obs., work function determ. 3-80145
- NaI, crystal gamma-ray spectrum, non-constant Bevatron beam, photomultiplier resolution, feedback compensation circuit 3-77703
- NaI, nuclear quadrupole relaxation times calc., Breathing Shell Model 3-79451
- NaI detectors, for Cs-137 half-life meas. 3-73863
- NaI γ -ray spectra, reduction of neutron-induced background 3-51712
- NaI well-type detector, relative counting rate in isotopic neutron source activation analysis 3-48530
- NaI well-type detectors, Monte Carlo calcs. of gamma-ray efficiency values 3-62221
- NaI well-type detectors, photopeak efficiency by Monte Carlo calculations considering self-absorption in source 3-40004
- NaI:Cd, equil. distrib. coeffs. of impurities 3-75543
- NaI:Ti, γ -scintillations 90 K-300 K (Russian) 3-55684
- NaI+MI (M=Ag, Cu) molten systems, thermoelectric power 3-72375
- NaI(Tl), total absorption counters, TASC and TANC 3-70391
- NaI(Tl) crystals, for windowless 4π -scintillation counter 3-56936
- NaI(Tl) detectors, Compton scatter and K-edge escape, correction matrix 3-59644
- NaI(Tl) γ -ray detector, high counting rates, discriminator 3-73881
- NaI(Tl) scintillation counter, gain variation compensation with rate 3-40018
- NaI(Tl) spectrometer, particle, signal shaping, energy response, large crystal assembly at NAL USA 3-77706
- NaI(Tl) total-absorption counters, high energy physics, recent applications 3-77634
- NaK, laser excitation, obs. of molecular and atomic fluorescence spectra 3-40650
- NaK-N $_2$ two-phase flow in rectangular cross section channel with large aspect ratio, frictional pressure drop 3-71811
- Na $_2$ K(CO $_3$) $_2$ (SO $_4$) $_2$ Cl hankite crystal structure 3-73201
- Na $_2$ K $_2$ Ca $_2$ TiSi $_2$ O $_{10}$ (OH), triclinic tinaxite, structure soln. by method of vector subsystems 3-46628
- NaLa(WO $_4$) $_2$ cryst. growth from Na $_2$ WO $_4$ melt, optical characts. 3-69009
- NaLi collision-induced rotational transitions, laser excited fluorescence 3-63553
- Na $_2$ Mg(CO $_3$) $_2$, etelite, crystal structure, X-ray crystallography 3-44766
- NaMgF $_3$:Eu $^{2+}$, f-f transitions, absorpt. and luminesc. spectra obs. 3-64726
- Na $_5$ (Mn, Na) $_3$ Mn[Si $_6$ O $_{18}$], synthetic metasilicate, cryst. struct. 3-64019
- NaMnCl $_3$, struct. 3-46609
- Na $_2$ MoO $_4$, Raman, i.r. spectra, force constants 3-63450
- Na $_2$ MoO $_4$ whisker growth in aq. soln., continuous conc. meas. apparatus 3-72792
- Na $_3$, photolum. spectral distrib. and intensity (Russian) 3-44476
- Na $_3$, Raman active phonons, temp. depend., phase transition 3-72611

sodium compounds continued

- NaNCS-water system, intermolecular interactions, Raman spectroscopic study (*Russian*) 3-72632
- NaNH₂SeO₄·2H₂O, heat capacity, temp. depend. and anomaly at ferroelec. transition 3-50009
- NaNH₂SeO₄·2H₂O, ferroelectric, large spontaneous rotary electrooptic effect 3-75962
- NaNH₄SeO₄·2H₂O, paraelec. phase, cryst. struct. obs. 3-75516
- NaNO₂, disordered paraelec. state, second harmonic generation for SRO obs. 3-64613
- NaNO₂, ferroelec., Raman spectrum near Curie point, elec. field effects 3-72631
- NaNO₂, second harmonic generation, spontaneous polarization, temp. depend. 3-78060
- NaNO₂, spontaneous polarisation measurement, Curie point, dielectric constant 3-50523
- NaNO₂, structure at 150, 185, 225 degrees C rel. to ferroelec. transition 3-44380
- NaNO₂, triplet state of NO₂⁻, e.s.r., phosphoresc., level crossing 3-72509
- NaNO₃, crystal growth from aq. soln. layer motion 3-75488
- NaNO₃, hygromech. effect 3-58174
- NaNO₃, neutron irradiation effects on single crystals 3-79379
- NaNO₃, phonon dispersion and phonon densities 3-55059
- NaNO₃-Ca(NO₃)₂ glass, thermodynamic props. 3-72009
- NaNO₃-LiNO₃-AgNO₃ ternary system, equilibrium study 3-60788
- NaNbO₃, antiferroelec., crystal growth, Czochralski method (*Japanese*) 3-41634
- NaNbO₃, lattice parameters and domains obs. in phase transitions 3-63984
- NaNbO₃, low-temp. transition and struct. of low-temp. phase 3-79985
- NaNbO₃-SrNb₂O₆, phase equilibrium, dielectric characterisation, DTA, Curie point meas. (*French*) 3-79994
- NaNiF₃, one and two magnon Raman scatt., mag. coeffs. 3-50561
- NaO₂, e.p.r. spectra, g tensors and h.f.s. interaction 3-54717
- NaO₂, Raman spectra, mol. and lattice vibrs., struct. changes at 230 and 201 K (*German*) 3-50569
- Na₂O, borosilicate glass, internal friction change during ligation 3-68334
- Na₂O, borosilicate glass, internal friction charge during ligation 3-68335
- Na₂O content in abyssal tholeiites, Mid Atlantic Ridge, CaO/Na₂O ratio 3-69525
- Na₂O-Al₂O₃ system, polymorphism and Na₂O·2Al₂O₃ cpd. characteriz. 3-72932
- Na₂O-Al₂O₃-SiO₂ glass membrane potentials, heterogeneous-site, solid state theory 3-69484
- Na₂O-B₂O₃-SiO₂ glass, u.s. absorpt. in immiscibility region, structural relax. 3-72140
- Na₂O-B₂O₃-SiO₂ system, tie lines in metastable immiscibility region 3-55075
- Na₂O-B₂O₃+MnO₂ glasses, optical and magnetic properties, alkali oxide content depend. 3-55411
- Na₂O-Ca₃Al₂O₆, polymorphism, cubic, orthorhombic I, II and tetragonal cryst. forms (*French*) 3-72179
- Na₂O-CaO-SiO₂ glass rods, bend strength, thermal stress resist., abrasion effect 3-76328
- Na₂O-CaO-SiO₂ glass-forming system, nucleation and crystn. 3-72010
- Na₂O-GeO₂ glass, heat capacity, 1.5-25 K 3-72206
- Na₂O-P₂O₅, phosphate glass, elec. cond. meas. 3-72355
- Na₂O-SiO₂ glass, X-ray diffr. study 3-72008
- Na₂O-SiO₂ glass, He diffusion and solubility, phase separation effect 3-69382
- Na₂O-SiO₂ glass, heat capacity, 1.5-25 K 3-72206
- Na₂O-SiO₂ glass, immiscibility temp., Al₂O₃ and Ga₂O₃ additions effect 3-69383
- Na₂O-SiO₂ glasses, Nernst-Einstein relation 3-76459
- Na₂O-SiO₂ glasses, strength characteriz. 3-76267
- Na₂O-SiO₂:Dy³⁺ glass, luminesc. centres (*Russian*) 3-72721
- Na₂O-V₂O₅-Fe₂O₃(Cr₂O₃)(MgO) ternary, solid-liq. phase diagrams 3-46696
- (Na₂O)_{1-x}-(Ag₂O)_x-P₂O₅, phosphate glass, elec. cond. meas. 3-72355
- Na₂O, fused, etching SiC, reaction rate at defects 3-68508
- NaOH addition effects on morphology and struct. of silica support 3-58773
- Na₂O-B₂O₃-SiO₂ glass (*German*) 3-68162
- Na₂O-K₂O-SiO₂ system glasses, He migration behaviour 3-75632
- Na₂O·1.5R₂O₃·Fe³⁺, R=B³⁺, P⁵⁺, e.p.r. of Fe³⁺ (*Russian*) 3-50458
- 2Na₂O·2Al₂O₃·3SiO₂ based glasses, crystn. 3-73032
- (16-x)Na₂O·2xNaCl·84B₂O₃ glasses, Ti⁴⁺ phosphor characteriz. 3-58547
- Na₂O·3RO₂·Fe³⁺, R=Si⁴⁺, Ge⁴⁺, e.p.r. of Fe³⁺ (*Russian*) 3-50458
- NaPF₆, chemical shift in n.m.r. of ¹⁹F 3-61002
- NaPF₆, pulsed n.m.r., F spin-lattice relaxation 3-47159
- Na₃PO₄-Pb₃(PO₄)₂ system, liquidus diagram 3-46697
- Na₂P₂O₇-Mg₂P₂O₇, phase diagrs. 3-64149
- Na₂P₂O₇·F₂·12H₂O, n.m.r. investigation of P-P bond 3-54721
- Na₃(P₂O₆N₃H₃), reactions with aq. solns. of MCl₃, M=Al, Ga, In, form. props. 3-73114
- Na₂PrGeO₄(OH), struct., X-ray analysis 3-40887
- Na₂Pt(OH)₆, crystal structure (*German*) 3-79318
- Na₂S₄ crystal structure, X-ray measurements, linear diffractometer 3-60683
- NaSCN photographic fixing rates, complexing with Ag, Br inhibition 3-47593
- NaSH, lattice dynamics and order-disorder transitions, Raman scatt. study 3-55590
- NaSH, rot. dynamics and phase transitions, neutron scatt. investigation 3-40852
- NaSO₂ e.p.r. spectra, g tensors and h.f.s. interaction 3-54717
- Na₂SO₄, dielectric props. temp. and freq. depend. 3-75936
- Na₂SbO₃, natural antimonite cryst., permittivity anomalies at phase transition, Curie temp. (*Russian*) 3-58481
- Na₂Sb₂S₉·9H₂O, dispersion of nonlinear refractive index 3-75959
- Na₄Si₄S₁₀, cryst. struct. (*French*) 3-79307

sodium compounds continued

- Na₂TeO₃ glass, heat-treated, e.p.r. of radiation centres (*Russian*) 3-44324
- Na₂UO₄, prep., crystallographic struct. determ. (*French*) 3-72060
- NaVO₃, e.s.r. spectra of Cr³⁺ and Cr⁵⁺ at room temp. and 77K 3-72516
- Na₂WO₃, electrochem. deposition 3-80551
- Na₂WO₃ as potentiometric indicating electrode for dissolved O₂ in aqueous solution 3-62326
- Na₂WO₃ optical props. determ. from 0.1 to 38 eV 3-80072
- Na₂WO₃ phase form. by Na⁺ diffusion in soda glass-WO₃ thin film system (*French*) 3-55169
- Na₂WO₃ semiconducting crystals, Raman scattering cross section dependence on laser intensity 3-41517
- NaY(WO₄)₂ cryst. growth from Na₂WO₄ melt, optical characts. 3-69009
- Na₂ZnGeO₄, formation, Mn²⁺ activation, luminesc., e.s.r., Zn-Mn isomorphism 3-72068
- Na₂ZnGeO₄, Franz-Keldysh effect in impurity absorpt. region 3-55553
- Na₂Zn(SO₄)₂·4H₂O:Co²⁺, spin-lattice relax., one phonon and Raman scatt. processes 3-50455
- Na₃[Ce(C₇H₅O)₃]₃·15H₂O, thermal contact with liq. He, millikelvin temps. 3-45458
- Na₂[Ln(CO₃)₂(H₂O)₂]₂·wH₂O, i.r. and Raman spectra, struct. obs. (*French*) 3-60457
- PbBr₂-NaBr-CdBr₂, diagram of melting, thermodynamic calc. (*Russian*) 3-49967
- SbNa₂K, Cs film photocathode, optical and photoelectric props. detn. (*French*) 3-41612
- SiO₂-Na₂O glass, with CaO and P₂O₅ ceramics, composite material for prosthetic applic. 3-55876
- Sr(NO₃)₂-Nd(NO₃)₃-Na₂WO₄-H₂O system, aqueous solutions, solid phase 3-76422
- TiO₂-Na₂O·B₂O₃ system, phase equilib. diagram 3-68387
- sodium potassium tartrate tetrahydrate** see *Rochelle salt*
- software (computers)** see *computer software*
- sogicons** see *semiconductor devices*
- soil**
- aerial gamma-ray surveying with continuous allowance for atm. radioactivity 3-69725
- Apollo 17, major and trace element chemistry of 30 samples 3-65842
- Apollo 17 results, conference, USA (1973) 3-65817
- Central Europe loess record rel. to Last Interglacial and continental climate 3-41973
- cross-anisotropic deposits, settlement using isotropic theory 3-80600
- density meas. by gamma backscatter 3-44931
- ejection cone shape, explosion in soil with reinforced upper layer (*Russian*) 3-58850
- elastic relative displacements of soils, failure of extended structures 3-76501
- electrical resistance during freezing (*Japanese*) 3-56036
- e.m. pulse reflection from multilayered medium, geophysical applications 3-61582
- freezing time determ. by method of concentric isotherms 3-61583
- freezing water-soil system, heat and mass transfer, multiphase water distrib., irreversible thermodynamics 3-56053
- gas anomalies in soil or air rel. to ore deposit locations 3-59170
- granular aggregates, acoustic velocities and energy losses 3-50798
- ground surface motions, effects of local soil conditions 3-53371
- groundwater-soil balance, Boussinesq eqn. modified to accept recharge 3-73235
- heaving force when freezing under constraint (*Japanese*) 3-56035
- infiltration models, homogeneous soil, steady rain 3-56052
- landslides, plasticity theory, static and kinematic solns. 3-40128
- leaching with iron using FeO·K₂O-P₂O₅ glass system 3-76260
- low surface area systems, theory of heterogeneous dielectrics 3-80629
- lunar, 2-4 mm soil fragments from 5 Apollo 17 sites 3-65837
- lunar, ages, ion tracks and rare gases (Apollo 17) 3-65832
- lunar, Apollo 17, morphology and chemistry of particles 3-65820
- lunar, Apollo 17 sample, C, S and inorganic gas abundances 3-65826
- lunar, geochemical aspects of soil, basalts and breccia 3-65838
- lunar, orange, low oxidation states of Fe and Ti 3-65849
- lunar, orange, sample 74220, Apollo 17 from Shorty crater 3-65834
- lunar, orange and grey Apollo 17 samples from Shorty crater 3-65841
- lunar, orange and grey samples, magnetic characteristics 3-65818
- lunar, Taurus-Littrow, Apollo 17 samples in 1-2 mm size range 3-65822
- lunar and terrestrial, elec. props. 3-59306
- lunar Apollo 17 orange sample, glass particle composition 3-65827
- lunar Apollo 17 samples, ¹⁸O/¹⁶O, ³⁰Si/²⁸Si, ¹³C/¹²C, D/H, H and C concentrations 3-65823
- lunar Apollo 17 samples, electrical and magnetic properties 3-65836
- lunar fines 74220 Apollo 17 sample, rare earth elements and Ba distribution 3-65846
- lunar glass spherules in Apollo 17 sample 74220, origin 3-65844
- lunar soil, Apollo 17 samples, analysis for halogens, P₂O₅, U, Li, Te 3-65831
- lunar soil material, orange, viscous flow and crystallization (sample 74220) 3-65848
- lunar Taurus-Littrow mare basalt and dark mantle soil 3-65824
- moisture, remote sensing with microwave radiometers in Phoenix Arizona region 3-59166
- moisture of sagebrush rangelands, Idaho, max., min., storage for snow and rain 3-58869
- optical diffraction anal. in earth science, Fourier optics appl. 3-80847
- oscillatory flow dispersion, effect of intra-aggregate diffusion, effect of atmospheric turbulence 3-46487
- particle size analysis by microscopy and computer 3-42677
- particles as freezing nuclei in atmospheric precipitation development 3-76739
- plane waves propagated by transient shock load, characteristic method (*Russian*) 3-69508

soil continued

- pressure meas., pneumatic device (*Russian*) 3-53864
 river soil, method of determ. of ^{90}Sr and ^{137}Cs , report 3-73398
 San Jose, geophysical investigations of landslides 3-47623
 semi-remote acoustic, electric and thermal sensing in top 50 cm of soil 3-61581
 shield for 400 MeV electron accelerator, neutron transport calcs. 3-71342
 silt/clay, drainable porosity as function of physical properties 3-76931
 structure response to earthquakes, three-dimensional anal. model, computer program 3-80617
 temperature waves, soln. to a problem in nonlinear periodic diffusion 3-59741
 water flow, numerical solns., allowance for hysteresis effects 3-46486
 water-containing, propag. of plane shock wave 3-74071
 ^{137}Cs concentration in Nishiyama soils, vegetables and human diets 3-69514
 ^{137}Cs concentration in volcanic ash paddy soil, obs. 3-69515
 ^{137}Cs content of soils in Niigata Prefecture, Japan 3-69513
 P, radiation detection, thin-walled proportional counter, low level background meas. 3-51719
 ^{220}Rn and ^{222}Rn exhalation from surface soil layer 3-53478
 S, radiation detection, thin-walled proportional counter, low level background meas. 3-51719
 ^{90}Sr concentration in volcanic ash paddy soil, obs. 3-69515
 ^{90}Sr content of soils in Niigata Prefecture, Japan 3-69513
 U adsorption and desorption, effect of CO_2 -conc. 3-69516

solar activity

- see also solar flares; solar prominences; sunspots
 5-minute oscillations of large horizontal scale, theory rel. to observations 3-47884
 active region spectrum used to identify solar line emission and assess temperature 3-65645
 active regions, high-resolution radio meas. and sunspot diameters 3-47889
 active regions, statistical characteristics using yellow coronal line 3-76968
 alpha-particles and medium nuclei in Oct. 27 1972 solar event, angular and time variations 3-69841
 anisotropy variation with time in solar low energy cosmic ray events 3-65574
 annual variation of faculae and sunspot number 3-56319
 arch filament systems, mag. structure 3-65709
 atmosphere circulation at 700 mb, response to solar-geomag. disturbances 3-69597
 atmospheric light pulses of ms time scale assoc. with solar and magnetospheric activity 3-65156
 chromospheric events, anal. of 25 events 3-65707
 coronal 5303 Å intensity rel. to recurrent geomagnetic storms and solar magnetic sector structure 3-73445
 coronal injection profile of energetic particles during solar rotation 1517 3-65719
 correlation with eleven-year cycle in cosmic ray intensity (*Russian*) 3-65587
 cosmic ray 27-day variation 3-53584
 cosmic ray He abundances in January 24 and September 2, 1971 solar events 3-80894
 cosmic ray intensity relation for 1963-5 period (*Russian*) 3-65591
 cosmic ray magnitude, boundaries of modulation effect (*Hungarian*) 3-59230
 cycle variations detection in geomagnetic line spectra 3-53603
 double solar cycle evidence from sunspot power spectra 3-44998
 dynamo theory, estimates of mag. diffusivity and α -effect 3-53606
 eleven year cycle, relation to large scale solar wind characteristics (*Russian*) 3-65590
 emerging flux regions, spatial distrib. 3-47893
 energetic heavy ion obs. near solar max. 3-69658
 energy cycle rel. to geomagnetic activity 3-53602
 equatorial mesosphere temp. rel. to solar activity 3-59130
 evolution of active regions, multi-wavelength studies 3-47885
 F₂-layer thickness and height of maximum, global distribution rel. to solar activity 3-42034
 F-region, variation in positive ion density with solar activity 3-65460
 F-region Thomson scatter variations in 1966-67 period 3-42045
 Forbush decreases and preceding cosmic-ray intensity increases, statistical analysis rel. to solar and geomagnetic activity 3-42098
 force-free mag. field structures determ., numerical method 3-56317
 forecasting, techniques and problems 3-65644
 galactic cosmic radiation, anisotropy, diurnal, 27 day recurrent effects, correlation with solar activity 3-73418
 geoeffective chromospheric theory, sudden ionospheric disturbances (*Russian*) 3-69636
 geomagnetic, ionospheric and solar activity relations (*Spanish*) 3-56326
 geomagnetic, ionospheric and terrestrial currents rel. to solar activity and cosmic rays (*Russian*) 3-65593
 geomagnetic Kp-index variations rel. to photospheric activity 3-65715
 geomagnetic storm families rel. to interplanetary field and solar activity 3-41910
 harmonic analysis of relative number of sunspots 3-42136
 ionosphere, Thumba drift records during high solar activity, full-correlation analysis 3-65458
 ionospheric D-region electron concentration changes 1957 to 1971 period, cyclic and seasonal, E. Europe 3-69659
 ionospheric electron content response to activity fluctuations 3-53520
 ionospheric F-region electron temp. var. with sunspot cycle 3-51129
 ionospheric irregularities, anisotropy of parameter during high solar activity 3-65440
 ionospheric spread F (equatorial), variations rel. to solar cycle 3-61543
 IQSY, outer radiation belt dynamics 3-56217
 Jovian atmospheric belt intensity rel. to solar activity 3-51290
 Jovian decametric emission periodicities rel. to innermost satellites and solar activity 3-42138

solar activity continued

- large-scale distrib. of activity during Cycle 19 period 3-51269
 local sources, observation of partial eclipse by radio telescope (*Russian*) 3-76981
 loop structures, coronal graded height spectra and filtergrams 3-80959
 M regions rel. to coronal holes 3-80940
 magnetospheric cusp region position, seasonal and solar cycle dependence 3-59147
 McMath zone 11482, polarization inversions in 237 MHz radio emission 3-65693
 moustaches, H α filtergrams and H α spectra 3-65706
 moustaches, H emission lines, quantitative analysis (*Russian*) 3-76978
 oscillations in longitude of active zones (*French*) 3-76971
 periodicities assoc. with excitation of new solar cycles 3-65681
 periodicity of large sunspot groups 3-61656
 Pi2 micropulsations occurrence and source 3-41930
 plage regions, videomagnetograph meas. of mag. field diffusion 3-65656
 plasma column changes at small solar elongations, Mariner 9 meas. 3-65640
 polar coronal rays rel. to sunspot cycle 3-59260
 polar particle identifier, for meas. of 30 Oct.-2 Nov. 1972 solar event 3-70088
 proton events, Monte Carlo model including shock wave effects 3-42135
 proton flare region development using method of summation curves 3-51270
 proton injection into magnetic field, dispersal, reln. to solar particle flux variation (*Russian*) 3-65633
 radiation changes rel. to terrestrial meteorological var. 3-80972
 radio emission at 3 cm, spectral index and fluctuations (*Russian*) 3-80963
 radio obs. at 9 and 3.5 mm of active regions under disturbed conditions 3-65660
 rotation changes rel. to 11 years solar energy generation cycle 3-53604
 Schumann earth-ionosphere e.l.f. cavity reson. line splitting rel. to solar activity 3-65456
 search for periodic variations in geomagnetic activity and their solar cycle dependence 3-44849
 seasonal variations of relative sunspot number, comment 3-61659
 sector struct. rel. to terrestrial mag. activity and solar activity 3-69843
 short periodicities, statistical test 3-45019
 short-wave ionospheric absorption models (*German*) 3-51121
 solar cycle rel. polarity of mag. regions 3-51286
 solar cycle variations of different quantities, phase differences 3-47880
 solar-climatic effects in 1961, rel. between events 3-69599
 sudden ionospheric disturbances, microwave bursts and optical flares associated with solar X-ray flares 3-65442
 terrestrial aurorae, occurrence during 11-year solar cycle 3-51078
 terrestrial effects, delays and variations 3-69496
 thermospheric temperature variations with solar activity and time of day 3-69600
 thermospheric wind velocity, effect on F2 ionisation and crest positions 3-73355
 time-lag between cosmic and solar activities, reln. to interaction in magnetosphere/ionosphere (*Russian*) 3-65588
 transition region and corona, temp. conductive flux, electron density variations with line intensity 3-80952
 turbulent gases, topological dissipation and small-scale fields 3-56303
 type I radioburst at 169 MHz, scattering by inhomogeneities of coronal electron density 3-73443
 type IV solar emission of 28.6 MHz, decay times and flux densities 3-80930
 umbral flashes and running penumbral waves, source mechanism 3-45003
 upper atm. temp. rel. to solar and geomag. activity 3-69602
 upper atmospheric temp. var. during solar activity min. from topside ionosphere sounding data 3-80780
 variation of cosmic-ray gradient during solar activity cycle 3-42100
 variations and their geophysical effects (*French*) 3-53570
 variations rel. to geomagnetic obs., Istanbul 3-61416
 velocity field meas., double magnetograph obs. of active regions (*Russian*) 3-45009
 velocity fields, mag. fields, brightness meas. (*Russian*) 3-45008
 v.l.f. and e.l.f. in whistler mode, sunrise and sunset effects 3-76750
 effect on weather and climate 3-69595
 X-ray bursts in 20-200 keV range, obs. by OSO-6 satellite 3-45000
 XX cycle maxima, use of 7-month consecutive averages (*Polish*) 3-65646
 Ca II flocculae, structural changes and regularities during Cycle 19 period 3-51268
 Ca plage and 2800 MHz intensities rel. to thermospheric neutral temp., obs. analysis 3-51079
 He, C, N, O and Fe nuclei, abundances in 1971 solar events 3-65723
 He, Fe-group and M nuclei, relative abundances during Oct. 27 1972 solar event 3-65722

solar atmosphere

see also chromosphere; photosphere

- BCA photospheric model, dissociation equilibrium 3-76970
 differential rotation determ. from optical, radio and interplanetary data 3-65697
 granulation at 1.65 μ , centre to limb contrast variation 3-65671
 Harvard Smithsonian Reference Atmosphere, near u.v. flux 3-65668
 high latitudes, discussion of possibilities of out-of-ecliptic spacecraft research 3-76972
 inhomogeneities, reference models of mean values 3-65699
 ionization losses, effect on cosmic-ray generation conditions on Sun 3-56321
 magnetoatmosphere, trapped magnetoacoustic and magnetogravitational waves 3-80929
 meridional flow, validity of 2-dim. approx. in stellar wind modelling 3-77037

solar atmosphere continued

- plasma oscillations in magnetic and gravitational fields, dispersion relations (*Russian*) 3-43669
- pole-equator temp. differences, energetics and momentum balance 3-69823
- response to granular excitation forced by convection 3-45004
- spicules, morphological study 3-65676
- surge formation mechanism in solar atmosphere 3-65685
- tidal friction, satellite loss, Mercury, Venus 3-69837
- velocity field meas., double magnetograph obs. of active regions (*Russian*) 3-45009
- velocity fields, different levels in quiet regions, study of various spectral lines (*Russian*) 3-76974
- velocity fields, mag. fields, brightness meas. (*Russian*) 3-45008
- Al I autoionisation lines, non-LTE profiles 3-80958
- Fe abundance from Fe II absolute transition probabilities 3-63299
- Mg I 4571 Å line formation, effect of one-dimens. macroscopic vel. fields 3-65648
- Mg I 4571 Å formation, Holweger solar model 3-65692
- Mg I 4571 Å line, one-dimensional approx. to macroturbulent velocity field 3-80937
- Mg I 4571 Å formation, one-dimens. model atm. 3-65698
- Tl abundance determ. from umbral spectra 3-65716

solar batteries *see solar cells***solar cell arrays**

- Si thick film ribbon growth technique, application 3-61119

solar cells

- thick film ribbon growth technique, application 3-61119
- Si solar cell junctions, surface photovoltage obs. 3-41226

solar chromosphere *see chromosphere***solar constant** *see solar radiation***solar corona**

- 1972, July 10, airborne white light photometry of outer corona during eclipse 3-47882
- 5303 Å intensity rel. to recurrent geomagnetic storms and solar magnetic sector structure 3-73445
- active region development using e.u.v. spectroheliograms 3-80952
- active regions, statistical characteristics using yellow coronal line 3-76968
- Apollos 11-16 results, review 3-45046
- atomic and molecular beam-foil forbidden lines transition probabilities rel. to astronomical spectra 3-78430
- chromosphere-corona transition region structure obs. from limb/disc e.u.v. intensity ratios 3-69831
- chromosphere-corona transition zone, x.u.v. flash spectrum crescents formation 3-65650
- chromospheric-coronal transition layer model from e.u.v. obs. 3-65629
- density and temp. gradients, models 3-65655
- emission line at 5303 Å, height gradient 3-61658
- energetic particle, plasma, and magnetic field obs. over three solar rotations 3-81016
- e.u.v. line meas. for determ. of solar rotation 3-65696
- F corona, brightness and linear polarisation meas. during 1972 July 10 solar eclipse 3-47881
- F-corona, dust particle evolution rel. to comets and Poynting-Robertson effect 3-53632
- fast transient events in green coronal emission line 3-80949
- flare protons, large scale drift transport 3-65721
- flare-generated coronal and interplanetary shock waves, close relationship 3-47892
- green line, use as an index for cosmic ray modulation 3-76938
- helmets, evolution during solar cycle 20 ascending phase 3-65713
- hole, source of high vel. solar wind stream 3-65667
- injection profile of energetic particles during solar rotation 1517 3-65719
- inner F and K coronal continuum obs. below 2220 Å 3-45018
- interplanetary obs. rel. to corona structure during Carrington rotations, 1967 3-65720
- K-coronometric and photographic meas. during 1972 July 10 eclipse, comparison study (*French*) 3-61653
- line spectrum below 400 Å identifications 3-80974
- loop structures, coronal graded height spectra and filtergrams 3-80959
- M regions rel. to coronal holes 3-80940
- magnetic disturbance, evolution using generalized Ohm's Law 3-80938
- magnetoplasma, synchrotron radiation, low freq. suppression 3-73444
- McMath Region 12094, radio observations at 3.71, 11.1 cms, small-scale features 3-76967
- MHD stability, finite Larmor radius effects 3-80911
- model, transition zone from chromosphere to solar corona (*Russian*) 3-45010
- photography, early daylight attempts 3-65634
- physical conditions deduced from eclipse obs. (7 March 1970) (*Russian*) 3-61655
- polar coronal rays 3-59260
- proton propag. at low energies, particle transport theory (*Zmeczka Greeman*) 3-65638
- radio bursts, associated noise storm phenomena, polarised radiation 3-75310
- radio wave scatt. rel. to plasma instabilities 3-65714
- radio-burst positions interpretation in scatt. corona 3-51288
- solar corona plasma and MHD instabilities investigation (*Dutch*) 3-51285
- solar cycle variation, phase differences 3-47880
- spectra, forbidden lines, below 2200 Å 3-80975
- temperature and gradient from solar wind heavy ion data 3-65730
- type I radiobursts at 169 MHz, scattering by inhomogeneities of coronal electron density 3-73443
- Fe XII, transition probability for forbidden lines in solar corona 3-42132
- Fe XIII, determ. of radial parts, energy levels and transition probabilities 3-52250
- Fe XIII line transition probabilities 3-71356
- Fe XIV 5303 Å line, linear polarisation meas. 3-45001
- Ne IX, X-ray survey of forbidden lines 3-65712

solar corona continued

- Ni XIV, transition probability for forbidden lines in solar corona 3-42132
 - O VII, X-ray survey of forbidden lines 3-65712
 - SX, transition probability for forbidden lines in solar corona 3-42132
 - Si VIII, transition probability for forbidden lines in solar corona 3-42132
- solar corpuscular radiation**
see also solar cosmic ray particles
- Alfvén waves in solar wind, wave pressure, Poynting flux and angular momentum 3-65636
 - Alfvén waves in two-fluid model of solar wind 3-47878
 - Apollo 16 sample analysis, solar process charact. 3-59290
 - camera/spectrograph, for u.v., obs. of terrestrial interactions with solar wind from Moon 3-81216
 - corona temperature and gradient from heavy ion data 3-65730
 - detection of 1970, March 7-8 interplanetary shock by Heos 1 in geosynchronous orbit 3-53610
 - detection of unshocked solar wind by ATS 5 in synchronous orbit 3-53609
 - distribution function meas. probe 3-65978
 - EUV flux rel. to ionospheric behaviour 3-56201
 - Faraday rotation, l.f. waves 3-65732
 - fine structure of solar wind velocity, new method of search and analysis 3-42128
 - flare piston gas, heavy ions 3-65724
 - flare-associated disturbances in solar wind, simulation and dynamics 3-65635
 - heliosphere, interaction of solar wind with interstellar H₂ 3-56327
 - h.f. wave cyclotron damping by suprathermal electron and proton fluxes 3-65735
 - interplanetary scintillations, pattern rel. to wind velocities 3-51312
 - interplanetary shocks due to solar flares, Pioneer 10 obs. (August 1972) 3-65860
 - interplanetary shocks rel. to flares and radio bursts 3-65861
 - interstellar He ion interaction 3-51396
 - ion flux power, 0.1 to 1.0 Hz 3-65734
 - Jovian radiation belts production 3-65778
 - lower atmosphere, effect of variations on weather 3-80767
 - lower atmosphere response, correlation with geomagnetic fluctuations 3-76744
 - Lunar fines, surface reduction by H₂, relevance to solar wind effects 3-42179
 - lunar green spherule inert gas content origin 3-47957
 - magnetic field annihilation at tangential or rotational discontinuity 3-63809
 - magnetopause, plasma interaction with magnetic field boundary 3-65477
 - magnetopause boundary layer, finite ion Larmor radius, effect on Kelvin-Helmholtz instability 3-76815
 - Mariner 9 Mars orbiter, solar radiation pressure calc. 3-56318
 - model, two-fluid with hydromagnetic heating, spiral field and conduction 3-65729
 - neutrino flux model and flux-cross-section product calc. 3-69832
 - neutron flux obs. 3-69606
 - planetary magnetic field interaction 3-65774
 - planetary magnetism in outer planets due to solar wind interaction 3-47941
 - plasma oscillation 3-65736
 - plasma velocity and interplanetary magnetic field, obs. and statistical analysis of abrupt changes 3-61752
 - plasmas in interplanetary space (*German*) 3-53629
 - proton parameters, fluctuations 10⁻² to 10⁻³ Hz 3-65733
 - radial var. of magnetic fluctuations and cosmic-ray diffusion tensor in solar wind 3-56315
 - sectorial structure rel. to geomagnetic SC and SI events 3-77029
 - shock fronts, flare produced 3-65725
 - shock scattering by tangential discontinuities 3-65726
 - shock waves produced by interaction with magnetosphere, reln. to Forbush effect (*Russian*) 3-65470
 - shocks, magnetofluid dynamic, perpendicular 3-65727
 - solar-climatic effects in 1961, rel. between events 3-69599
 - stellar wind modelling, meridional flow, validity of 2-dim. approx. 3-77037
 - structure, 20 solar radii to Mars orbit 3-65728
 - structure rel. to rotational and tangential discontinuities, Mariner 5 obs. 3-51273
 - travelling regions of high solar wind density, temporal and spatial flow patterns 3-56325
 - wind, analysis of ionic comet tail orientations allowing for meridional flow divergence 3-77009
 - wind, anomalously low proton temp. following interplanetary shock waves, mag. bottles 3-51277
 - wind, configuration of interplanetary shock waves from chromospheric flares 3-61755
 - wind, convective and decelerative effects on cosmic ray emission 3-45030
 - wind, darkening of lunar silicate rocks by sputtering 3-65797
 - wind, directional anisotropy of Alfvén waves 3-44997
 - wind, double ion streaming 3-51278
 - wind, effect on Moon's grey appearance 3-47952
 - wind, effect on turbulence of bow shock, satellite obs. 3-80836
 - wind, electron density distrib. model based on km-wave type III bursts 3-45029
 - wind, enhanced diffusion in strongly magnetised astrophysical plasmas 3-80914
 - wind, He abundance compared with solar cosmic ray ⁴He/¹H ratio 3-65637
 - wind, high vel. stream, coronal hole as source 3-65667
 - wind, interaction with atm. of Mercury 3-61686
 - wind, interaction with Earth's magnetic field, magnetosphere modelling (*Hungarian*) 3-59145
 - wind, interaction with Earth's magnetosphere 3-53611
 - wind, interaction with lunar thermal ionosphere, electric potential 3-73456
 - wind, ionising high-beta flows, h.f. electrostatic instabilities 3-80978
 - wind, isotopic composition (*Russian*) 3-65565

solar corpuscular radiation continued

- wind, Jovian bow shock, oblique structure, Pioneer 10 planned trajectory 3-80992
- wind, Jovian magnetosphere, centrifugal instability, interaction with solar wind, plasma transfer 3-69893
- wind, large scale characteristics, reln. to solar activity (*Russian*) 3-65590
- wind, large-scale structures beyond 1 AU 3-51280
- wind, MHD waves in plasma (*Russian*) 3-69835
- wind, non-thermal heating by supra-thermal secondary ions 3-65689
- wind, nonlinear and nonstationary effects (*Russian*) 3-65632
- wind, nonlinear model of high-speed plasma streams 3-51274
- wind, note on large velocity discontinuities 3-56320
- wind, Ogo 5 mag. field obs. during 1968 Aug. 15 magnetospheric substorms 3-56119
- wind, parameters determ. from Apollo 12 and 15 data 3-69709
- wind, planetary and interstellar ions, effect of electrostatic instabilities 3-80970
- wind, plasma column changes at small solar elongation, Mariner 9 meas. 3-65640
- wind, power spectrum of small-scale irregularities, 81.5 MHz scintillation obs. 3-65647
- wind, properties at Earth rel. to two-fluid model 3-65690
- wind, props. in outer solar system 3-47895
- wind, proton models and mean free path in interplanetary gas 3-73474
- wind, pulsed magnetic field (terrella) model for expts. with radiation belts and solar wind 3-69545
- wind, rel. to magnetospheric substorm expansion phases 3-56117
- wind, restrictions on radial mag. field and flow solns. 3-45031
- wind, rotational discontinuities, classification, orientation characteristics and examples 3-69834
- wind, single-fluid model 3-56324
- wind, solar cycle variations, phase differences 3-47880
- wind, speed, photospheric activity rel. to geomag. variations 3-65715
- wind, steepening of nonlinear magnetoacoustic waves 3-80969
- wind, temperature-speed relations 3-51279
- wind, thermal conductivity of quiet plasma and consequences 3-61650
- wind, transverse oscillations in interplanetary magnetic field, spatial structure from satellite obs. 3-81015
- wind, upstream proton component, bow shock perturbation 3-69846
- wind, validity of CGL (double adiabatic eqns. of state) eqns. 3-65639
- wind, var. of α -particle abundance, satellite meas. 3-65694
- wind, velocity fine structure detection test 3-45007
- wind, wave-trains in ideal isotropic one-fluid plasma 3-47879
- wind, weakly shocked flow through cometary comas and planetary atmospheres 3-73446
- wind and Xe isotope composition of carbonaceous chondrite meteorites 3-61743
- wind field sector direction in 1965 rel. to polar cap geomag. field changes 3-51281
- wind heat conduction, effect of fluctuations in interplanetary magnetic field 3-56371
- wind heat transport near Earth's bow shock 3-61663
- wind heating, two-fluid models 3-44999
- wind interaction with Comet Bennett (1970 II) 3-65855
- wind interaction with Earth's magnetic field, bow shock structures 3-65242
- wind interaction with Earth's magnetic field, magnetosheath 3-61410
- wind interaction with Earth's magnetic field, MHD bow shock 3-61411
- wind interaction with interstellar medium, obs. by future outer planet mission 3-47896
- wind interaction with Mercury's atmosphere, atmospheric density determ. 3-69885
- wind interaction with outer planets, shock shapes and locations 3-69827
- wind interaction with planetary atmospheres rel. to atmospheric ionization and mass loss 3-65783
- wind parameters and geomagnetic activity rel. to interplanetary magnetic and electric fields 3-42049
- wind plasma, interaction with interstellar gas 3-42127
- wind plasma, power spectrum of density irregularities 3-51275
- wind stability rel. to e.m. streaming instability 3-61649
- wind upstream from bow shock, h.f. waves 3-51282
- wind velocity changes, reln. to amplitude and phase of changes of solar daily anisotropy (*Russian*) 3-65583
- wind velocity changes rel. to excitation of geomagnetic tail oscillations 3-56220
- wind velocity derivation from observations of interplanetary scintillations 3-61754
- wind velocity heliographic latitude depend. 3-69844
- wind-comet interaction, Comet Bennett tail peculiarities 3-56359
- wind-lunar limb interaction, cool photoelectron effects 3-47891
- wind-magnetosphere boundary, MHD wave refraction and stability 3-76817
- wind-moon interaction, continuum fluid model 3-51276
- He component variations 3-65731

solar corpuscular streams *see solar corpuscular radiation***solar cosmic ray particles**

- 1972, August 4, meas. of protons, He and heavy nuclei during flare event 3-80893
- access of solar protons to Earth's polar caps 3-53538
- alpha, and medium nuclei in Oct. 27 1972 solar event, angular and time variations 3-69841
- alpha particle abundance, comparison with other obs. 3-65637
- alpha particle flux, present day and past, lunar sample meas. 3-51226
- anisotropy of low energy particles, pitch angle distrib. 3-69761
- anisotropy variation with time in low energy solar events 3-65574
- Apollo 16, 17 obs., low energy rel. to solar flares 3-70090
- April 1969 event, rocket meas. of particle fluxes in magnetosphere 3-59229
- atmospheric neutrons and products from solar protons during particle events 3-56290

solar cosmic ray particles continued

- atomic and molecular scattering of electrons in reln. to space travel, upper atmosphere, sun (*Dutch*) 3-63317
- chemical composition, relation with radiospash duration spectrum (*Russian*) 3-65575
- diffusion eqn. for continuous emission of low energy particles 3-45030
- eleven-year cycle in intensity, correlation with solar activity (*Russian*) 3-65587
- emission, obs. from Explorer 47, Oct. 27-Nov. 10, 1972 3-69840
- energetic electrons interaction with type III radiobursts 3-80957
- energetic solar cosmic ray increase Nov. 18, 1968, statistical adjustment to data 3-51232
- energy losses in interplanetary space 3-65571
- energy response and diffusion coefficient of Jan. 28, 1967 burst (*Russian*) 3-65592
- fast electrons near 1 AU simultaneous type III radio burst obs. 3-80892
- flare particle propagation, analytic solution rel. to spacecraft meas. 3-53607
- flare particles, interplanetary, pitch angle distribution during initial anisotropic phase 3-51225
- flare particles at and beyond modulation boundary 3-56292
- flare protons, of Aug. 1972, characterisation from lunar samples analyses 3-69842
- flare protons and electrons, interplanetary, propagation anisotropies, Pioneer 7 obs. 3-51313
- flare-generated cosmic-ray emission during 1971 January 24 activity 3-51271
- flares, Aug. 1972, underground and surface obs., energy-dependence of Forbush-decrease (*Russian*) 3-65579
- flares, August 1972, intensity of streams in stratosphere, diffusion (*Russian*) 3-65563
- flares in Aug. 1972, cosmic rays, plasma clouds and interplanetary shock waves (*Russian*) 3-65631
- flux meas. over extended solar longitudes 3-65573
- intensity interrelation with different indices of solar activity during 1963-5 period (*Russian*) 3-65591
- interplanetary and polar cap fluxes during 1972 August 4-11 solar particle events 3-61670
- ionization losses, effect on cosmic-ray generation conditions on Sun 3-56321
- low energy solar protons, corrections to Compton-Getting theory 3-76936
- magnetospheric model depend. of cosmic ray access calcs. 3-69759
- magnetospheric nonadiabatic particle motion, effect on polar cap structure of solar protons 3-51140
- modulation in flux at 1 AU rel. to interplanetary shock waves 3-69762
- neutrino flux rel. to centrally concentrated magnetic field 3-42125
- neutrino flux rel. to differential rotation and mag. fields 3-53605
- neutrino flux rel. to early inhomogeneities of composition 3-65641
- neutrinos, anomalous gravitational red-shift 3-56283
- neutrinos, episodic mixing in solar-type stars, Praesepe cluster 3-61666
- neutrinos, luminosity variations rel. to evolution in the Galaxy 3-51238
- neutrinos, rotating solar model to explain low flux as measured by Davis 3-73439
- neutrinos, secular stability of solar-type stars, reaction kinetics of proton-proton chain 3-81021
- neutrinos, stability of Sun against spherical thermal perturbations 3-76964
- neutrinos, terrestrial glaciation evidence (*French*) 3-80896
- neutron flux, upper limit for 1-20 MeV range, OGO-6 meas. 3-65570
- nuclei, heavy, obs. at different periods of time at energies, 400-600 and 40-100 MeV/nucleon (*Russian*) 3-65561
- pitch angle distrib., anisotropic, of relativistic rays 3-69760
- polar particle identifier, for meas. of 30 Oct.-2 Nov. 1972 solar event 3-70088
- production, propag., detect. 3-80887
- propagation in solar system, periodicity on earth's surface convection-diffusion theory (*Hungarian*) 3-59220
- proton confinement ahead of interplanetary shock waves 3-65572
- proton diffusion coeff., comparison of explt. and theoretical estimates for 3 flare events 3-65666
- proton events, Monte Carlo model including shock wave effects 3-42135
- proton illumination of Earth's polar caps, magnetotail particle entry models 3-80814
- proton injection into magnetic field, dispersal, reln. to solar particle flux variation (*Russian*) 3-65633
- protons, 10-40 keV particles flux limit determ. from Apollo to meas. 3-61711
- protons, behaviour in pseudotrapping region during magnetospheric substorm 3-61565
- protons, from chromospheric flares, Aug. 1972, surface and stratospheric meas. (*Russian*) 3-65564
- protons, low-energy, propag. in corona (*Zmeczg Greann*) 3-65638
- protons, magnetospheric, strong pitch angle diffusion, 1.2 to 8.2 MeV 3-51133
- protons, penetration into magnetosphere tail as a regular process 3-69756
- protons and electrons, intensity in Moon's vicinity (*Russian*) 3-65576
- protons from flares, directional diffusion coeffs. inside and outside Earth's bow shock 3-47792
- protons in sub-MeV range, interplanetary intensity anisotropies 3-53608
- protons of low energy in pseudo-trapping region of Earth's magnetosphere 3-51141
- radial var. of magnetic fluctuations and cosmic-ray diffusion tensor in solar wind 3-56315
- radiation belt flux, HF absorption during PCA events 3-80830
- rare gases in meteorites, anal. of Khor Temiki aubrite 3-61668
- simultaneous recording near Venus and Earth's magnetosphere 3-80895
- solar activity compared with cosmic ray activity and geomagnetic, ionospheric and terrestrial currents (*Russian*) 3-65593

solar cosmic ray particles continued

- solar flares, anisotropic stage, time dependence obtained from nonstationary kinematic equation 3-69757
- time-lag between cosmic and solar activities, reln. to interaction in magnetosphere/ionosphere (*Russian*) 3-65588
- variations, Aug. 1972, ground obs. of increased intensity (*Russian*) 3-65580
- variations in flux near geomagnetic pole, reln. to shock wave interactions in magnetosphere (*Russian*) 3-65568
- weak flux detection by ground-based radio methods 3-56255
- α -particles, abundance var. in solar wind, satellite meas. 3-65694
- n spectrometer for 10 to 50 MeV range (*German*) 3-62258
- v, Davis expt., possible explanations of anomaly (*German*) 3-76935
- v, in solar cosmic streams (*Russian*) 3-65565
- v, low counting rate expt., reln. to neutrino spectrum of different masses 3-42097
- v flux, discrepancy between theory and observation 3-80902
- v, spectra near Earth and at source, calc. for flares in 1956-1967 period (*Russian*) 3-65562
- P low energy, boundary of region of intrusion into polar ionosphere (*Russian*) 3-65567
- v, gravitational potential, non-Newtonian theory (*Hungarian*) 3-77891
- ^{37}Cl solar neutrino expt., effect of radiative opacities on predicted capture rate 3-76934
- H isotopes in cosmic streams (*Russian*) 3-65565
- ^2H , solar flare produced, satellite obs. of $^2\text{H}/^1\text{H}$ ratio 3-65569
- ^3H , solar flare produced, satellite obs. of $^3\text{H}/^1\text{H}$ ratio 3-65569
- He, C, N, O and Fe nuclei, abundances in 1971 solar events 3-65723
- He, Fe-group and M nuclei, relative abundances during Oct. 27 1972 solar event 3-65722
- He abundances in January 24 and September 2, 1971 solar events 3-80894
- He isotopes in cosmic streams (*Russian*) 3-65565

solar cosmic ray photons

- high energy particle generation rel. to type IV microwave bursts 3-42133

solar disturbances see solar activity**solar eclipses**

- 1955 partial, sporadic E ionization effects 3-51124
- 1968, Sept. 22, anomalous F-region behaviour 3-65459
- 1968, September 22, noise storm source structure (*Russian*) 3-45011
- 1970, 7 March, stratospheric cooling and perturbation of meridional flow 3-65341
- 1970, March 7, corona conditions from spectral obs. (*Russian*) 3-61655
- 1970, March 7, NO concentrations in Earth's upper atmosphere var. of ion concentrations 3-69610
- 1971, February 25, radio brightness at 3 cm. wavelength (*Russian*) 3-80965
- 1971, February 25, X-rays and ionizing u.v. radiation in E-region during partial eclipse 3-56209
- 1972, July 10, airborne white light photometry of outer corona during eclipse 3-47882
- 1972, July 10, F corona and inner zodiacal light obs. 3-47881
- 1972, July 10, K-coronometric and photographic meas. of corona, comparison study (*French*) 3-61653
- 1972, July 10, limb darkening at extreme solar limb 3-47883
- 1972, July 10, partial, variations in ionospheric total electron content and plasma temp. 3-76803
- 1972, July 10, report of observation from arctic circle 3-76983
- 1973, 4 Jan., lower ionosphere, radioastronomy obs. 3-65457
- 1973, June 30, atmospheric gravity waves as travelling ionospheric disturbances 3-69586
- 1973, June 30, obs. 3-73447
- 1973, June 30, obs. expeditions 3-80977
- 1973, June 30, prediction of acoustic gravity wave enhancement 3-61523
- F-region anomalous behaviour, during solar eclipse of Sept 22, 1968 3-65459
- partial, Sept. 1968, a radio telescope observation of local sources (*Russian*) 3-76981
- polar coronal rays rel. to sunspot cycle 3-59260
- total, obs. from fixed station on Earth 3-65718
- Venus' transits, obs. from Japan, Dec. 9, 1874 event, reviews 3-61700

solar flares

- 1961, July 12, metal lines and emission region properties 3-76985
- 1967, March 27, impulsive e.u.v. spectra 3-80950
- 1969, May 19-20, type III radio burst during impulsive phase 3-65664
- 1972, Aug. 11 event, description of 4 stages 3-65684
- 1972, Aug. 4 event, multidirectional scanning obs. 3-65683
- 1972, August 2 flare, OSO-7 X-ray obs. 3-80948
- 1972, August 4, meas. of protons, He and heavy nuclei during flare event 3-80893
- 1972, August 7, 3643-8542 Å spectrograph obs. 3-80956
- 1972, August activity, comments 3-65670
- anisotropy of low energy particles produced by small west limb flare, 1971 3-69761
- chromospheric, anal. of 25 events 3-65707
- chromospheric, configuration of interplanetary shock waves 3-61755
- chromospheric, relation between chemical composition of cosmic rays and radiospall duration spectrum (*Russian*) 3-65575
- chromospheric events, Ha line obs. 3-65708
- chromospheric flares, populations of quantum levels of H atoms 3-61660
- corona, large scale drift transport of flare protons 3-65721
- cosmic ray continuous emission diffusion eqn. 3-45030
- cosmic ray particle flux meas. over extended solar longitudes 3-65573
- cosmic ray protons, from chromospheric flares, Aug. 1972, surface and stratospheric meas. (*Russian*) 3-65564
- cosmic ray time dependence from nonstationary kinematic equation 3-69757

solar flares continued

- cosmic rays, Aug. 1972, energy-dependence of Forbush decrease (*Russian*) 3-65579
- cosmic rays, August 1972, intensity of streams in stratosphere, diffusion (*Russian*) 3-65563
- cosmic rays, low energy rel. to flares, Apollo 16, 17 obs. 3-70090
- cosmic rays, plasma clouds and interplanetary shock waves, (August 1972) (*Russian*) 3-65631
- cosmic rays from solar flare at and beyond modulation boundary 3-56292
- cosmic-ray emission generated by 1971 January 24 flare 3-51271
- Earth's bow shock, directional diffusion coeffs. of low-energy solar protons during flare 3-47792
- earth rotation rate changes, effects on length of day 3-61329
- energetic solar cosmic ray increase Nov. 18, 1968, statistical adjustment to data 3-51232
- e.u.v. emission, comparison of OSO-6 obs. and SFD data 3-45023
- expanding mag. bottles rel. to moving type IV radiobursts development 3-42130
- flare-generated coronal and interplanetary shock waves, close relationship 3-47892
- force-free mag. field structures determ., numerical method 3-56317
- geoactive chromospheric theory, sudden ionospheric disturbances (*Russian*) 3-69636
- highly ionised atoms spectra in laser produced plasmas and from sun 3-79173
- interplanetary, low energy flare protons and electrons, propagation anisotropies, Pioneer 7 obs. 3-51313
- interplanetary particles, pitch angle distribution during initial anisotropic phase 3-51225
- interplanetary shocks due to solar flares, Pioneer 10 obs. (August 1972) 3-65860
- interplanetary shocks rel. to flares and radio bursts 3-65861
- ionising radiation, energy increase, theoretical approach from ionospheric data 3-73346
- ionosphere SID effects, various observation methods 3-76899
- K α line emission during solar flares rel. to X-ray bursts 3-47887
- lunar samples analyses of cosmogenic radionuclides, for Aug. 1972 flare characterisation 3-69842
- magnetic storm and Forbush decreases, propag. vel. of assoc. shock waves 3-56322
- McMath Region 12094, radio observations at 3.71, 11.1 cms 3-76967
- model, kinematic, shock effects in chromosphere 3-65682
- non-thermal ionisation and recombination processes 3-45022
- nonlinear magnetosonic wave propagation in magnetic neutral sheet 3-80912
- particle emission, Explorer 47 obs., Oct. 27-Nov. 10, 1972 3-69840
- particle leaking from magnetic confinement configurations (*Dutch*) 3-51284
- particle propagation from flares, analytic solution rel. to spacecraft meas. 3-53607
- piston gas, heavy ions 3-65724
- plage, prominence and sunspot flares, mechanisms and phenomena 3-42129
- propagation of excitation through chromosphere (*Russian*) 3-76979
- proton diffusion coeff., comparison of exptl. and theoretical estimates 3-65666
- proton event, small, detect. from spacecraft inside and outside magnetosphere 3-69743
- proton flare region development using method of summation curves 3-51270
- protons, low-energy, propag. in corona (*Zmeczka Greasam*) 3-65638
- radiation monitoring, in Concorde aircraft for warning of increased radiation levels at high altitude 3-48515
- radio bursts after flares, coherent emission mechanisms (*Dutch*) 3-51283
- radio emissions, review 3-65717
- rare gases in meteorites, anal. of Khor Temiki aubrite 3-61668
- relativistic solar electron events from western hemisphere flares, rise-time to max. flux 3-69839
- resistive diffusion of force free magnetic fields in passive media 3-80928
- Saha's equation, emission measurement 3-76952
- shock fronts in solar wind, flare produced 3-65725
- shock wave interaction with galactic cosmic rays, model 3-76937
- stratospheric air masses, influx into lower troposphere 3-41969
- sunspot flares, anal. of Ca II H and K lines 3-45021
- type IV microwave bursts rel. to high-energy cosmic ray photon generation 3-42133
- wind, flare-associated disturbances, simulation and dynamics 3-65635
- X-ray bursts rel. to SID effects, l.f. radiowave propagation, apparatus, measurements 3-61526
- X-ray flares, albedo determ. up to 300 keV 3-45025
- X-ray flares, continuous energy injection at bright points 3-65662
- X-ray spectra, Intercomos-4 and Vertical-2 obs. 3-65663
- X-ray spectra from 8.5 to 16 angstroms 3-45024
- X-ray thin-target emission from 26 February 1972 flare 3-80947
- Fe XVII and XVIII lines during flares, soft X-ray spectrum 3-61667
- Fe XVIII and Fe XIX transitions near 100Å 3-65630
- H ionisation in optical flares 3-65661
- ^2H , solar flare produced, satellite obs. of $^2\text{H}/^1\text{H}$ ratio 3-65569
- ^3H , solar flare produced, satellite obs. of $^3\text{H}/^1\text{H}$ ratio 3-65569

solar furnaces see furnaces**solar magnetic fields see solar magnetism****solar magnetism**

- abnormal granulation, cinematography using red continuum filtergrams 3-80951
- arch filament systems, mag. structure 3-65709
- atmospheric ^{14}C content, heliomag. modulation, sunspot and geomag. effects 3-65402
- behaviour based on Maxwell's, and hydrodynamic equations of ideal plasma (*Hungarian*) 3-59262
- bipolar magnetic region development rel. to magnetic outflow 3-80936
- centrally concentrated magnetic field rel. to low solar neutrino flux 3-42125

solar magnetism continued

- chromospheric acoustic energy heating variations due to magnetic fields 3-80953
 chromospheric magnetic field polarity correl. with interplanetary mag. field polarity near solar minimum 3-69845
 corona, evolution of magnetic disturbance using generalized Ohm's Law 3-80938
 coronal 5303 Å intensity rel. to recurrent geomagnetic storms and solar magnetic sector structure 3-73445
 dynamo theory, estimates of mag. diffusivity and α -effect 3-53606
 field sector direction in 1965 rel. to polar cap geomag. field changes 3-51281
 flare region mag. bottles rel. to moving type IV radiobursts development 3-42130
 force-free mag. field structures determ., numerical method 3-56317
 heliomagnetic equator rel. to interplanetary sector struct. 3-69917
 Hoyle's theory of solar system formation, role of solar mag. field (*Italian*) 3-61645
 local field connection with radio sources and sunspot groups, study during partial eclipse (*Russian*) 3-76981
 loop prominences of August 1972, magnetic field obs. 3-80939
 M-regions, effect on geomag. activity, periodic var. 3-44850
 magnetic sector structure, rel. to circulation of Earth's atmosphere 3-56328
 magnetosphere, trapped magnetoacoustic and magnetogravitational waves 3-80929
 neutrino flux rel. to differential rotation and mag. fields 3-53605
 oscillations, short-period, correlation anal. 3-65657
 photospheric field behaviour, interpretation of obs. (*Italian*) 3-61665
 photospheric force-free magnetic field representation, practical method 3-69830
 photospheric magnetically active regions, 5-minute oscill. 3-65675
 plage regions, videomagnetograph meas. of mag. field diffusion 3-65656
 prominences, helical magnetic structures, formation model and dynamical equilibrium 3-51272
 proton injection into magnetic field, dispersal, reln. to solar particle flux variation (*Russian*) 3-65633
 real-time digital videomagnetograph 3-59406
 recurrent mag. storms reo. to solar and interplanetary mag. fields 3-56126
 resistive diffusion of force free magnetic fields in passive media 3-80928
 sector struct., long term stability, sunspot cycle feature 3-65737
 sector struct. rel. to stratospheric circulation 3-65401
 sector struct. rel. to terrestrial mag. activity and solar activity 3-69843
 solar cycle rel. polarity of mag. regions 3-51286
 solar-climatic effects in 1961, rel. between events 3-69599
 spectral line contrast formation due to turbulent vel. suppression 3-45015
 sunspot groups, magnetic classification 3-65643
 sunspot umbrae, magnetic field intensity rel. to brightness 3-61657
 sunspots, l.f. magnetic field oscillations, l.f. radio emission modulation (*Russian*) 3-80962
 surge formation mechanism in solar atmosphere 3-65685
 turbulent diffusion, generation and dissipation of mag. fields 3-69826
 twisted fields, evidence from radio obs. of type I storm 3-65711
 type I storm, radio evidence of twisted bi-polar mag. fields 3-65711
 velocity fields, mag. fields, brightness meas. (*Russian*) 3-45008
 vertical distribution of field, from study of Fraunhofer lines (*Russian*) 3-76976
 wind radial mag. field restrictions 3-45031

solar noise *see noise; solar radiofrequency radiation*

solar prominences

- 1972 August loop prominences, magnetic field obs. 3-80939
 helical magnetic structures, formation model and dynamical equilibrium 3-51272
 limb prominence obs. in H β line 3-65659
 model, interpretation of quiescent conditions (*Italian*) 3-59261
 prominence flares, mechanisms and phenomena 3-42129
 Ca⁺ line luminescence, role of electronic impact in excitation 3-59258
 He abundance compared with solar cosmic ray ⁴He/¹H ratio 3-65637
 He I r. emission lines at 10830 Å and 20581 Å 3-80932

solar radiation

- see also solar corpuscular radiation; solar cosmic ray photons; solar radiofrequency radiation; solar spectra; sunlight*
 absolute flux meas. for calibration of V-magnitudes of stars 3-81081
 absolute solar intensities and constant, accuracy of aircraft and ground based obs. 3-80980
 aerosols, effect on energy transfer, model atmospheres 3-76908
 aerosols, effect on energy transfer, model atmospheres 3-76909
 Alfvén waves, propag. in interplanetary space and directional anisotropy in solar wind 3-44997
 Atmosphere Explorer, e.u.v. photometer for solar observ. 3-42262
 Atmosphere Explorer, e.u.v. spectrophotometer for observ. 3-42261
 atmospheric scattering theory, Monte Carlo method for spherical atm. 3-73299
 Barcelona meas., anal. of 54-month series of records (*Spanish*) 3-56166
 brightness temp. meas. at 345, 450 and 1000 μ 3-61652
 broad band e.u.v. absorption in Earth's upper atmosphere 3-53511
 calibration facility, integration sphere, pyranometer calibration description 3-56639
 changes rel. to terrestrial meteorological var. 3-80972
 cirrus cloud transfer of radiation, function of solar zenith angle 3-53475
 coronal 5303 Å intensity rel. to recurrent geomagnetic storms and solar magnetic sector structure 3-73445
 direct and diffuse radiation rel. to atmospheric turbidity 3-61486
 e.u.v. flux, effect on Jovian thermosphere temperature 3-76993
 e.u.v. fluxes rel. to ionospheric incoherent scatter meas. 3-80798

solar radiation continued

- far u.v. flux rel. to reflectivity of lunar dust 3-45041
 grazing height meas. by obs. of Earth's shadow on Li trail 3-53513
 ground level u.v. solar flux meas. in Pasadena, California 3-47716
 heating of Earth-atmosphere system, effect of atmospheric aerosols, soln. of radiative transfer equation 3-80775
 intensity measurements, stray light correction, computer programs 3-65738
 Lake Vanda, Antarctica, heat balance 3-76681
 limb darkening eqn., Phillips-Twomey method in presence of noise 3-80933
 Lyman α changes at Earth's exobase rel. to H density distribution 3-53507
 Lyman- α radiation transfer through plane-parallel atm. 3-53615
 measurement, discussion of method 3-66213
 neutrino flux, possible explanation of discrepancy between theory and expt. 3-45013
 night sky radiation in u.v. and visible, Kosmos 51 and 213 obs. in space (*Russian*) 3-44878
 night sky radiation in u.v. and visible kosmos 51 and 213 observations in space (*Russian*) 3-44877
 optical brightness, fluctuation predictions, temperature variation of Earth's surface (*Hungarian*) 3-76973
 optically deep absorbing media, interior radiances, Rayleigh scattering 3-70760
 photosphere, search for continuous u.v. opacity sources 3-65649
 simulator, direct meas. of absorption and transmitting factor for material element (*French*) 3-42970
 snow and pack-ice areas in fall rel. to insolation income 3-59099
 solar chromosphere, brightness temp. in far i.r. 3-80954
 solenoid coil, Schumann cavity resonances, variation with solar ionizing radiation, zenith angle and storms 3-76747
 stratospheric spectral features at 8 cm⁻¹ of probable solar origin 3-61477
 sunspot umbrae, magnetic field intensity rel. to brightness 3-61657
 terrestrial atmospheric model, two-level general circulation response to solar radiation reduction 3-59098
 terrestrial interaction, stratospheric air mass influx into troposphere following flare 3-41969
 thermal radiation remote sensing instrumentation, meas. from light aircraft 3-77176
 upper atmosphere absorption producing vibrationally excited O₂ 3-69601
 u.v. flux variations, atmospheric O₂ photodissociation and heating rates 3-80756
 u.v. irradiance variability, Nimbus 3 and 4 obs. 3-56323
 variations and their geophysical effects (*French*) 3-53570
 water vapour absorption of solar radiation meas., shortwave absorptivity rel. to water path 3-44895
 waters, radiant energy transfer, effect of multiple scatter. 3-59206
 X-ray bursts in 20-200 keV range, obs. by OSO-6 satellite 3-45000
 X-ray obs. from 2 August 1972 flares 3-80948
 X-ray thin-target emission from 26 February 1972 flare 3-80947
 CO₂, fluoresc. at 4.3 μ m in upper atm. rel. to 2.7 μ m, solar radiation absorpt. 3-69622
 H₂SO₄ aqueous solutions, droplets, solar radiation absorption and scattering, near i.r. 3-44886
 He I, 584 Å resonance scattering, intensity and distribution of glow 3-77028
 (NH₄)₂SO₄ particles, solar radiation absorption and scattering, near i.r., appl. to industrial pollution 3-44886
- solar radio emission** *see solar radiofrequency radiation*
solar radiobursts *see solar radiofrequency radiation*
solar radiofrequency radiation
 1 mm radiometry, cryogenic optical system 3-77180
 2.8 GHz flux rel. to ionospheric electron content 3-53520
 3.1 and 8.6 mm obs. 3-47922
 3.71 and 11.1 cm obs. using NRAO 3-element interferometer 3-42131
 10.7 cm flux rel. to equatorial mesosphere temp. 3-59130
 350 MHz obs. during 1972 November 3-45014
 810 MHz emission, daily values (1957-1967) 3-69828
 1968, September 22, structure of noise storm source during eclipse (*Russian*) 3-45011
 active regions, high-resolution radio meas. and sunspot diameters 3-47889
 active regions, obs. at 9 and 3.5 mm under disturbed conditions 3-65660
 AFCRL patrol network, appl. 3-69838
 coronal scatt. rel. to plasma instabilities 3-65714
 daily radio flux, correlation and spectral analysis 3-65686
 determined component investigations, at 9.0 cm. (*Russian*) 3-80967
 differential rotation determ. from radio flux 3-65697
 distribution of 2, 4, 6, 8 mm wavelengths over disc (*Russian*) 3-76982
 flare emissions, review 3-65717
 fluctuation at 3 cm. emission, correlations with chromospheric height variation (*Russian*) 3-80961
 fluctuations, obs. over diurnal interval (*Russian*) 3-80964
 height of radio regions from 9.1 cm wavelength emission 3-47890
 l.f. modulation, sunspot magnetic field oscillations (*Russian*) 3-80962
 limb brightening, distribution of radio brightness (*Russian*) 3-45012
 local source geometry, observed during partial eclipse (*Russian*) 3-76981
 local sources, 9 cm wavelength, slowly varying component characteristics, statistical investigation (*Russian*) 3-80968
 McMath Region 12094, 3.71, 11.1 cms, small scale features in upper chromosphere, lower corona 3-76967
 McMath zone 11482, polarization inversions in 237 MHz radio emission 3-65693
 microwave circular polarised radiation from solar hemispheres 3-65658
 microwave flux density absolute calibration, history and correction factors 3-45250
 microwave impulse bursts, self-absorpt. of gyro-synchrotron emission 3-65710
 mm-wave mapping in two dims. using radioheliograph 3-70072

solar radiofrequency radiation continued

- noise storm phenomena, polarised radiation from solar corona 3-75310
 polar region, dark ring in brightness at 3 cm., 1971 eclipse obs. (*Russian*) 3-80965
 quasiperiodic fluctuations at 3 cm., using two telescope 1500 km apart (*Russian*) 3-80960
 radio-burst positions interpretation in scatt. corona 3-51288
 radio-bursts, coherent emission mechanisms (*Dutch*) 3-51283
 recombination line search in 110-115 GHz range, negative result 3-69825
 reduced radiobrightness regions, in 8 mm range (*Russian*) 3-80966
 S- and B-components, spectrum, dm-wavelengths, correlation analysis 3-76969
 slowly varying component, source at cm and mm wavelengths 3-65687
 spectral index and fluctuations at 3 cm. (*Russian*) 3-80963
 type I radiobursts at 169 MHz, scattering by inhomogeneities of coronal electron density 3-73443
 type II and III bursts, scattering effects on fundamental and harmonic emission 3-42126
 type II burst, derivation of interplanetary electron density scale 3-65856
 type II bursts, plasma radiation from MHD shock waves 3-56316
 type III bursts, obs. of assoc. H α features 3-45027
 type III bursts, second harmonic radiation at km wavelengths 3-45028
 type III bursts, time dependence of polarization 3-53614
 type III bursts at 80 MHz, non-existence of linear polarisation 3-45026
 type III km-wave bursts, model for solar wind electron density distrib. 3-45029
 type III radio burst during impulsive phase of 19-20 May, 1969 flare 3-65664
 type III radio bursts, energetic solar electron interactions 3-80957
 type III radiobursts, simultaneous obs. of fast solar electrons 3-80892
 type III solar radio bursts, decay time at km wavelengths 3-65688
 type IV (moving) bursts development rel. to expand mag. bottles from flares 3-42130
 type IV burst, interferometric obs. of assoc. pulsating source 3-65665
 type IV emission of 26.6 MHz, decay times and flux densities 3-80930
 type IV microwave bursts rel. to high-energy cosmic ray photon generation 3-42133

solar radiowaves see solar radiofrequency radiation**solar spectra**

- see also solar activity; solar corona; solar radiation
 5-minute oscillations, near u.v. obs. of phase lags 3-80943
 5600 to 6300 Å, determination of sunspot umbra physical parameters (*Russian*) 3-76977
 absorption line shifts, interpretation in rel. to progressive sound waves 3-65700
 active region spectrum used to identify solar line emission and assess temperature 3-65645
 airglow in 150 to 1500 Å range, He reson. scatt. of solar 584 Å line 3-69740
 airglow in 150-1500 Å range, He⁺ reson. scatt. of solar 304 Å line 3-69739
 arch filament systems, H α structure, mag. structure 3-65709
 Arizona-NASA i.r. solar spectrum atlas for 13350-34100 Å range 3-69833
 atomic and molecular beam-foil forbidden lines transition probabilities rel. to astronomical spectra 3-78430
 Balmer lines and Harvard-Smithsonian Reference Atmosphere 3-47888
 chromosphere, spectrum and details in 1190 to 1320 Å range 3-51267
 chromosphere-corona transition region structure obs. from limb/disc e.u.v. intensity ratios 3-69831
 chromospheric and coronal e.u.v. lines, rotation meas. 3-65696
 chromospheric flare events, H α line obs. 3-65708
 chromospheric H α mottles, high-resolution photography 3-65651
 chromospheric high resolution spectra from rocket-borne spectrograph 3-80942
 chromospheric mottles near limb, H α contrast profiles 3-65652
 chromospheric obs. at 1.2, 0.8 and 0.4 mm, brightness temp. and limb brightening data 3-45017
 contrasts, formation mechanism in radiatively controlled lines 3-45015
 coronal emission line at 5303 Å, height gradient 3-61658
 coronal identifications below 400 Å 3-80974
 element abundance, survey of f-values needed for calculations 3-80976
 emission lines observed in March 7 1970 eclipse, corona deductions (*Russian*) 3-61655
 e.u.v. obs. by spectrometer aboard OSO-6 3-65944
 e.u.v. rocket spectrometer obs. of solar spectrum in 50-300 Å range 3-61648
 e.u.v. spectroheliograph on rocket or satellite, evaluation of pinholes in metal film filters 3-65946
 e.u.v. spectrum of active region 3-51266
 faint Fraunhofer line profiles, asymmetry and line width 3-59259
 fast transient events in green coronal emission line 3-80949
 flare, 1967, March 27, impulsive e.u.v. spectra 3-80950
 flare, 1972, August 7, 3643-8542 Å spectrograph obs. 3-80956
 flare of 1961, July 12, metal lines and emission region properties 3-76985
 flare X-ray spectra, Intercosmos-4 and Vertical-2 obs. 3-65663
 flare X-ray spectra from 8.5 to 16 angstroms 3-45024
 forbidden lines below 2200 Å, chromosphere and corona 3-80975
 Fraunhofer line depth in daytime sky spectrum, brightness and polarisation 3-45033
 Fraunhofer lines, central intensity oscillations, effect of progressive sound wave (*Russian*) 3-76966
 Fraunhofer lines, determination of vertical distribution of magnetic field (*Russian*) 3-76976
 ghost lines, solar-limb emission lines by Burton and Ridgeley (1972), grating defects 3-69836

solar spectra continued

- green line, use as an index for cosmic ray modulation 3-76938
 highly ionised atoms spectra in laser produced plasmas and from sun 3-79173
 inner F and K coronal continuum obs. below 2220 Å 3-45018
 isotope composition, photospheric and sunspot spectra, atomic line studies 3-61672
 K-line width-absolute magnitude relation 3-80979
 line profile determ. under pure absorpt. and LTE conditions 3-65703
 line profile inversion, numerical method 3-51333
 loop structures, coronal graded height spectra and filtergrams 3-80959
 moustaches, H α filtergrams and H α spectra 3-65706
 one-component model, radiative transfer and statistical equilibrium eqns. 3-80925
 photoelectric profiles, damping constants and turbulence velocities by Voigt method 3-76986
 photosphere, C₂, CH, CN, MgH, NH and OH molecular lines and oscillator strengths 3-69829
 photospheric equatorial currents detection 3-61664
 photospheric quasiperiodic wavelike motions, direct spectroscopic meas. 3-53613
 prominences, He I i.r. emission lines at 10830 Å and 20581 Å 3-80932
 radial velocities from various spectral lines, velocity fields, different levels in quiet regions (*Russian*) 3-76974
 recombination line search in 110-115 GHz range, negative result 3-69825
 resonance line intensities, chromospheric-coronal transition layer model 3-65629
 S- and B-components spectrum, radio emission at dm-wavelengths, correlation analysis 3-76969
 Skylab A, synoptic survey of the Earth and solar disc 3-80849
 solar radiation, Antarctic, spectral composition, reflectivity rel. to sea ice 3-80774
 sunspot 5250.216 Å profile determ. 3-65703
 sunspot 6610-6770 Å spectra, line identification 3-45002
 sunspot flares, spectral anal. 3-45021
 sunspot H₂O vapour line intensity determ. at 263°K and 3500°K 3-65705
 sunspot oscillations, multichannel spectrometry 3-80955
 sunspot power spectrum, double solar cycle evidence 3-44998
 sunspot umbral Na D₂-5890 Å line, min. intensity meas. 3-65704
 sunspot umbral spectra, determ. of Ti abundance 3-65716
 sunspots molecular line formation levels and rotational temps. 3-80931
 transition region and corona, temp, conductive flux, electron density variations with line intensity 3-80952
 transition zone from chromosphere to solar corona, model (*Russian*) 3-45010
 two-level source function, dependence on own radiation field 3-48000
 u.v. obs. with 3840 Å interference filter 3-80944
 x.u.v. flash spectrum anal. and comparison with model 3-65650
 Al I autoionisation lines, non-LTE profiles 3-80958
 Al I photoionization cross section and 3p²P⁰-3s3p²S_{1/2} autoionization doublet 3-80926
 C₂ Phillips bands, absence in photospheric spectrum 3-61661
 CN mol. band system, solar temp. determ. 3-61669
 CO isotope bands in i.r. spectrum, solar ¹³C/¹²C, ¹⁸O/¹⁶O and ¹⁷O/¹⁶O abundance ratios 3-61651
 CO lines in i.r. solar spectrum, balloon-borne observations 3-56314
 Ca II 8542 Å i.r. triplet, early obs. 3-45032
 Ca II k₃ line obs. of 5-minute oscillation, vertical phase var. and mechanical flux 3-80934
 Ca II K-line rel. to shock waves in chromosphere 3-51287
 Ca II resonance and subordinate lines, correlation analysis from high resolution spectra 3-80941
 Ca plage rel. to thermospheric neutral temperature obs. analysis 3-51079
 Ca XV 5694 Å line obs. of active regions 3-76968
 Ca⁺ line luminescence, role of electronic impact 3-59258
 Cr I absolute oscillator strengths and solar Cr abundance 3-80927
 Fe two-electron ion, mean life of 2P₁ metastable state 3-63294
 Fe XII, transition probability for forbidden lines in solar corona 3-42132
 Fe XIII coronal line, transition probabilities 3-71356
 Fe XIV 5303 Å coronal line, linear polarisation meas. 3-45001
 Fe XVII and XVIII lines during flares, soft X-ray spectrum 3-61667
 Fe XVIII and Fe XIX transitions near 100 Å 3-65630
 H emission line intensities for various electron temperatures, number densities and solar atmospheric thicknesses 3-63274
 H emission lines in moustaches, quantitative analysis (*Russian*) 3-76978
 H β line obs. of active limb prominence 3-65659
 He D₃ and 10830 Å lines, from active regions (*Russian*) 3-76980
 Mg I 4571 Å line formation, effect of one-dimens. macroscopic vel. fields 3-65648
 Mg I 4571 Å formation, Holweger solar model 3-65692
 Mg I 4571 Å line, one-dimensional approx. to macroturbulent velocity field in solar atmosphere 3-80937
 Mg XI and Mg XII, X-ray spectroheliograms 3-65654
 Mgl 4571 Å formation, one-dimens. model atm. 3-65698
 Mn photospheric abundance from lifetime measurements by beam-foil method 3-78442
 Na D₂ line profile inversion 3-73442
 Ni abundance, from level lifetime measurements 3-78441
 Ni XIV, transition probability for forbidden lines in solar corona 3-42132
 Rbl resonance lines at 7800 and 7949 Å in photosphere, isotopic effects 3-42134
 S X, transition probability for forbidden lines in solar corona 3-42132
 Si I photospheric lines, Si abundance from analysis of 19 lines 3-59255
 Si VIII, transition probability for forbidden lines in solar corona 3-42132

solar spectra continued

Tm photospheric abundance from lifetime measurements by beam-foil method 3-78442

solar system

see also celestial mechanics; planets; sun

accretion process in formation of planets and comets 3-42122
angular momentum loss, Hubble's law application 3-73438
Bode's law and resonant structure of solar system 3-56313
cosmic rays in outer planet region, rel. to interstellar gas and galactic evolution 3-47854
element abundance, effects of delayed neutron emission on r-process abundances 3-80924
extra-terrestrial life, possibilities, origin and evolution 3-65612
gravitational waves and gravitationally closed solar system 3-42119
heavy element abundances 3-73425
high latitudes, discussion of possibilities of out-of-ecliptic spacecraft research 3-76972
history, from cosmic ray bombardment of meteorites 3-77027
Hoyle's theory of solar system formation, role of solar mag. field (*Italian*) 3-61645
nebular hypothesis of Kant and Laplace 3-42123
numerical models of primitive solar nebula, interstellar gas cloud 3-42120
orbital clustering, elastic and inelastic scatt. 3-65627
origin, chemistry of outer planets and satellites 3-47932
origin, evidence from lunar surface examination 3-59254
origin, review of known facts 3-42153
outer planets, development of US space program 3-48158
outer planets exploration, mission building blocks 3-48159
outer planets formation from gaseous solar nebula 3-47876
particle accumulation processes in primitive solar nebula 3-42121
Pioneer 9 electric field expt., radial gradients and storm obs. 3-47877
planet formation from solar nebula, role of cometary nuclei 3-53599
planetary patrol programme, international 3-65967
planetary system, inertial frame location, differential radio interferometry 3-45249
radio obs. of outer solar system, l.f. nonthermal emission 3-47940
solar nebula, formation of Moon inside orbit of Mercury 3-65799
solar wind props. in outer solar system 3-47895
statistical dynamics of gravitational systems 3-66675
structure and evolutionary history, plasma processes and MHD aspects 3-51265
²⁴⁸Cm in early Solar System from primitive meteorites 3-76963
D abundance in solar nebula 3-47874

solar visible radiation *see* sunlight**solar wind** *see* solar corpuscular radiation**soldering**

ohmic contacts to CdS crystals using pure In 3-77575
vacuum process, Zircaloy-4 spacers for nuclear power station (*German*) 3-72930
Al alloys, wetting by low melting solders, u.s. tinning, joint formation (*Russian*) 3-41791
Cu alloys, wettability of liq. Sn, rel. to soldering 3-50754
n-Si, large area contacts, layer of Si-Au eutectic alloy, In soldering of leads, low temp. technique 3-48391

solenoids

see also coils; electromagnets

a.c. excited, e.m. field in hollow ferromagnetic cylinder, analysis, numerical method (*Russian*) 3-45754
axisymmetric, rectangular cross-section, radial magnetic field calc., rel. to supercond. magnets 3-77938
bivectorial solenoidal field, integral formulae for scalar and vector potentials (*Italian*) 3-42938
equipment for producing pulsed magnetic fields (*Czech*) 3-53953
Helmholtz pair, uniform magnetic field study 3-45574
latching valve, protection of vacuum systems 3-77422
magnetic field distribution on conducting screen, surface currents along solenoid as field source (*Russian*) 3-54190
n.m.r. spectrometer, superconducting 3-66293
push-type, used in controllable tendon taper 3-59682
superconducting, compensator for nonuniformity in mag. field, elimination of side bands in n.m.r. spectrometer 3-73820
superconducting, installation for mag. field prod. 3-77580
superconducting, installation for mag. field prod. with cryostat 3-77581
thermonuclear devices, mag. fringe fields from the solenoids 3-46164
Nb-Sn superconducting solenoid, 50 kG gas cooled, operated at 13 K 3-73700

solid electron states *see* crystal electron states**solid helium**

b.c.c. ground state energy and phonon dispersion. numerical calcs. 3-64231
growth with safe superfluid-tight pressure cell 3-76135
hardness of crystal, meas. with glass indenter 3-50050
plastic flow investigation, motion of dislocations 3-79546
positive ion mobility, vacancy ion mechanism 3-41063
quantum crystals, zero sound, phonon modes 3-72253
second sound, effects of collinear and non-collinear three phonon processes 3-55120
solid-liquid interface effect of defect scattering on phonon transmission 3-55134
thermal conductivity measurement, anisotropic heat conduction 3-52744
³He, b.c.c., low temperature specific heat anomaly 3-43920
³He, b.c.c., spin and interspin energy diffusion coeffs. evaluation 3-72541
³He, effect of magnetic field on melting curve 3-55121
³He, ground state energy, t-matrix calc. 3-72252
³He, Monte Carlo calcs. 3-46744
³He, Neel temp., three-body exchange effects 3-52745
³He, shell depend. correlation functions, Monte Carlo calc. of ground-state energy 3-68470
³He, t-matrix calcs. for ground-state energies 3-72251
³He submonolayers adsorbed on solid air, sp. ht. anomalies, 0.5-6K 3-46745
⁴He, h.c.p. cryst., thermal cond. meas., phonon scatt. by isotopic impurities 3-55122

solid helium continued

⁴He, hcp single crystal growth technique, c-axis orientation of 0 and 90°, computer simulation of nucleation 3-51554

⁴He, solid and liquid, pressure-vol.-temp. relations 3-52732

solid lasers

see also semiconductor lasers

electrooptic, piezoelectric control, mode selection 3-48914
fibre lasers and dispersion in fibres 3-48458
fluorescence quenching rel. to use as laser material 3-48907
frequency lasers based on glass, emission polarisation (*Russian*) 3-48915
garnet, Czochralski-grown, perfection and charact. for gems, lasers and substrates 3-76131
glass:Nd, high power, self-focusing damage 3-40262
glass, phase separation effects on lasing parameters, absorpt., fluoresc. and damage threshold 3-54229
glass, properties and applications, review 3-74243
glass, Q-switched, damage threshold improvement 3-66837
glass ceramics, Nd₂O₃ doped, fluorescence and induced emission 3-57232
glass containing Nd, quasistationary lasing technique 3-51638
glass laser, Nd³⁺ activated, apparatus for meas. of small nonactive absorption coefficients of the active elements (*Russian*) 3-48456
merocyanine solid dye, luminescence mechanism 3-53141
mixed garnets as intermediate gain laser materials 3-59864
multimode, stability of monochromatic generation mode 3-57234
Nd:YAlG, intracavity second harmonic generation using KNbO₃ 3-51948
Nd high efficiency, small, design, for pyrotechnic ignition, application 3-59867
Nd-glass, high-power multi-laser system emitting picosecond pulses 3-66843
optically pumped, sensitized energy transfer and near i.r. operation, review 3-48917
optically pumped, transient temp. distrib. for single shot and repetitively pulsed operation 3-59866
optically transparent magnetic materials, nature of laser radiation, e.s.r. influence (*Russian*) 3-43016
oscillations, influence of inversion inhomogeneity on transverse structure 3-48912
output oscillation amplitude stability, linear amplification mode (*Russian*) 3-40268
plasma impact waves obs. with laser apparatus (*Czech*) 3-57938
power supply and synchronisation network 3-51636
Q factor electro-optical modulation, modulator components (*Russian*) 3-57230
rhodamine 6G impregnated film, two-dimens. distributed-feedback laser 3-40261
ring laser, generation regimes 3-51931
ruby, complex resonator, interference effects, coherence in terms of scattering (*Russian*) 3-57231
ruby, cooled illuminator for investigation of lasing 3-73794
ruby, giant pulse, spectrum width restriction by clarifying filters (*Russian*) 3-70823
ruby, growth, comparison of Verneuil and Czochralski methods 3-66839
ruby, high power, ionisation of gas atoms at focus 3-78476
ruby, Q-switched, widening of emission spectrum 3-70822
ruby, reorganised, generation of internal cyclic modes (*Russian*) 3-59868
ruby, self-mode-locked, shape of radiation pulses 3-40267
ruby, self-termination of free oscills. at low temp. 3-74246
ruby, simple exponential photon echo decay, mag. field and conc. depend. 3-66841
ruby, spatial coherence function, holographic meas. method 3-74259
ruby, verification of Kramer-Kronig relations 3-48909
ruby laser, free-running external signal effect 3-62719
ruby laser, generation with moving mirror and selector in resonator 3-48911
ruby lasers, quasistationary lasing technique 3-51638
ruby pulsed laser, with Q-switched multiple cavities, characts. 3-40264
spikes due to self Q-switching 3-40266
two-channel generation in spectral inhomogeneous media, non-correlated freq. 3-51898
ultrashort pulses, equil. eqns. applic. (*Russian*) 3-70824
CdS, room temp. lasing in glow discharge 3-66838
Cr³⁺:YAG, laser generation at 6874 Å 3-74244
CuSO₄.gelatin, X-ray laser emission 3-66835
Dy²⁺:CaF₂, laser generation parameters, concentration depend. 3-66842
Dy³⁺:BaY₂F₈, laser emission at 3 μ 3-54228
GaAs injection laser, strain induced degradation, bonding procedure 3-59869
Ho³⁺:YAG epitaxial film, laser oscill. obs. 3-51929
KY(WO₄)₂:Nd³⁺ spectroscopic and generation study of cryst. 3-64691
LiNbO₃ ring laser, mode synchronisation, resonant modulation, ultra short light pulse excitation, 10⁻¹⁰ sec (*Russian*) 3-57235
Nd, mode-locked, fifth picosecond harmonic generation in multistage system 3-70849
Nd: glass, single freq., nonspiking free oscill. and Q-switched operation 3-45805
Nd: glass mode-lock laser, two-photon absorption by Rhodamin 6G 3-40287
Nd: glass pumping lamp, Xe, hollow, laser rods up to 45 mm diameter, design, laser tests 3-53921
Nd: glass, freq. tuning, mode locking 3-51930
Nd: glass, GOS-301, design and components 3-70820
Nd: glass, investigation of lasing transitions 3-62721
Nd: glass, mode locked, improving reliability 3-62718
Nd: glass, mode-locked, picosecond pulses, streak camera obs. 3-78041
Nd: glass, overshoot inversion 3-66840
Nd: glass, with second harmonic converter, 1.06, 0.53 μ light pulse generation, plasma heating appl. 3-74245
Nd: glass laser, mode-locked by saturable absorbers, spectral narrowing effect suppression 3-51932

solid lasers continued

- Nd:glass laser, recovery time of saturable absorbers for 1.06 μ mode-locking 3-59601
 Nd:glass laser action on $^4F_{3/2} \rightarrow ^4I_{13/2}$ transition manifold, lasing at 1.35 μ m 3-45804
 Nd:glass laser slabs, face pumped, inversion spatial distrib. 3-40260
 Nd:glass mode locked laser, picosecond pulse development, output signal 3-48908
 Nd:YAG, Q-switched, as ideal amplifier, for phase meas. of microscopic radiation field 3-66892
 Nd:YAG, stimulated emission cross section at 1061 microns 3-43017
 Nd:YAG, third harmonic generation for dye laser pump 3-66829
 Nd:YAG c.w. laser with vortex stabilised lamp 3-45806
 Nd:YAG laser, pumping by miniature diode 3-66836
 Nd:YAG laser action on $^4F_{3/2} \rightarrow ^4I_{13/2}$ transition manifold, lasing at 1.35 μ m 3-45804
 Nd:YAlO₃ laser action on $^4F_{3/2} \rightarrow ^4I_{13/2}$ transition manifold, lasing at 1.35 μ m 3-45804
 Nd-glass, angular divergence of beam using telescopic cavity 3-57233
 Nd-glass, controllable single pulse laser 3-48910
 Nd-glass disk laser amplifier, design and operation 3-62717
 Nd³⁺ in YAlO₃, Lu₃Al₅O₁₂, CaWO₄ and KY(WO₄)₂ crystals, stimulated emission investigation 3-43018
 Nd³⁺:CaWO₄, thin film waveguide laser, epitaxial growth 3-54230
 Nd³⁺:CaWO₄-Nd³⁺:LaNa(WO₄)₂ laser luminescence spectra 3-62720
 Nd³⁺:glass, parasitic oscils. calcs. with gain variation 3-74242
 Nd³⁺:LiLa(MoO₄)₂, investigation of stimulated emission 3-51934
 Nd³⁺:SrF₂-GdF₃, mixed fluoride 3-72682
 Nd³⁺:YAG, cavity dumped, instability due to time varying reflections 3-40263
 Nd³⁺:YAG, reproducible giant pulse generation, using optically regenerative Q-switch 3-66263
 Nd³⁺:YAG, test of semiempirical theory of beam divergence 3-78055
 Nd³⁺:YAG, thin film waveguide laser, epitaxial growth 3-54230
 Nd³⁺:YAG burst mode freq. doubled laser for high speed photography and holography application 3-43015
 Nd³⁺:YAG cryst., meas. of relax. time of laser transition 3-70821
 Nd³⁺:YAG epitaxial film, laser oscil. obs. 3-51929
 Nd₂O₃:glass ceramic, new laser host material 3-40265
 NdP₅O₁₄ fluorescence, energy transfer and level system rel. to laser use 3-50610
 NdP₅O₁₄ laser at 1.05 microns 3-48906
 Nd³⁺:glass, relaxation rates meas. 3-51933
 Pm³⁺:LiYF₄, lasing action 3-59865
 YAG:Nd, Lu, repetitively pulsed flashlamp-pumped material, thermal transient effects 3-62716
 Y₃(Al_{1-x}Ga_x)₅O₁₂:Nd³⁺ spectroscopic study of crystals 3-78040
 Y₃Al₅O₁₂:Nd lasers, current status 3-48916

solid-liquid transformations

- see also crystallisation; freezing; melting; solidification
 augite-pigeonite miscibility gap pyroxene from lunar basalt (12021) 3-77001
 excitation condensation and soft mode energy at transform. 3-55082
 halogen substituted benzenes, temp. and phase dependence of positronium lifetimes 3-55221
 hard sphere fluid and perturbation theory approach, Lennard-Jones 12-6 fluid 3-75605
 heat source effect on depression and deform. of liquid phase surface 3-46700
 ice-water, 2 dimensional bonded lattice model, first order approximation, long range and short range order 3-41006
 insulating oil, polymeric nature, glass transition temp. obs. 3-46595
 metal, superplasticity and surface tension at phase transition, fluctuation model 3-49924
 molecular dynamics simulation of liquid-solid transition in two dimensions 3-79254
 Percus-Yevick equation, modification, direct correlation function, hard sphere equation of state 3-49979
 Ramsey phase change, planetary core production 3-65766
 semi-infinite solid with temp. depend. thermal props., phase change problem soln. 3-64155
 stainless steel, fragmentation, molten fuel-coolant interactions, Na coolant 3-74730
 tetrafluorobenzene, heat capacity, adiabatic calorimetry, 11-353K, phase transition enthalpy, liquid entropy 3-46714
 viscous liquids, glass transition, thermodynamic equations 3-52580
 AgCl, liquid, fragmentation when dropped in water, automatic picture scanner 3-74730
 Al₂O₃, flame- and plasma-prepared, metastable phase formation 3-47447
 Ar, shear viscosity behaviour near triple point 3-55096
 Bi, liquid, fragmentation when dropped in water, automatic picture scanner 3-74730
 CaO-P₂O₅-H₂O system, 300 to 600°C at 2 kb H₂O pressure 3-69488
 NaF-AlF₃ system, AlF₃-rich, high press. study (French) 3-68392
 Pb, liquid, fragmentation when dropped in water, automatic picture scanner 3-74730
 Sn, liquid, fragmentation when dropped in water, automatic picture scanner 3-74730
 UO₂, fragmentation, molten fuel-coolant interactions, Na coolant 3-74730
 Zn, liquid, fragmentation when dropped in water, automatic picture scanner 3-74730

solid mechanics see mechanics**solid solution hardening** see dispersion hardening**solid solutions**

- solid solutions such as Au-Cu are indexed under alloys of the named elements i.e. 'gold alloys' and 'copper alloys' in this example
 see also alloys
 binary, grain boundary equil. segregation, BET analogue eqn. 3-64873
 concentrated, disperse order, model for partially ordered state (German) 3-55755
 decomposition curve asymmetry, elastic distortions influence (Russian) 3-72855

solid solutions continued

- double pseudobinary, boundary phase stability and crit. phenomena 3-80212
 elastic gradient energy coeff. concept 3-64810
 eutectic structures, characterisation from thermodynamic data 3-79495
 exciton spectra, Fermi-Davydov reson. 3-68998
 f.c.c. homogeneous, ordered configs., Bragg-Williams-Gorsky model 3-41703
 free energy calculation, convergence of cumulant expansion technique 3-41029
 hardening in crystals with randomly distributed solute atoms 3-41710
 interstitial, thermodynamic props., effect of third nearest neighbour interactions 3-43883
 metallic, dilute, number of electrons bound to implanted impurity atom 3-64304
 multicomponent, clustering and ordering, fluctuations and kinetics 3-55751
 nonuniform, first order diffusionless transforms. (Russian) 3-72830
 ordered, antiphase boundaries influence on band struct. (Russian) 3-43989
 phenanthrene molecules in solid solutions, spectroscopic manifestation of ordering 3-64656
 semiconductor, regular soln. interaction parameters, calc. 3-68414
 spinels, composition-property graphs of Cu-Mn-Fe-O system 3-68411
 spinodal decomposition, early-stage theory 3-53198
 spinodal decomposition kinetics, higher derivative terms 3-41689
 β -spodumene-SiO₂, electrical conductivity meas. 3-44101
 sulphides, containing two III_a elements, comparison of cryst. struct. (French) 3-58021
 ternary, containing two interstitial solutes, Onsager off diagonal coefficients determ. 3-80235
 ternary zincblende substitutional solid solutions, SRO parameters 3-52596
 Ag halide crystal, precip. in alkali aluminoborosilicate glasses cont. Ag, Cl and Br, comp. 3-80437
 Al-Zn(9 at.%)-Ag(1 at.%), Al(90 at.%)-Zn(10 at.%), supersaturated, structural features of decomposition process (Russian) 3-41723
 BaFe₂O₁₉, substituted, solid solns., intrinsic coercivity meas. 3-41357
 Bi_{1-x}Nd_xFeO₃, intrinsic weak ferromagnetism 3-46998
 BiSe-group IV tellurides, solubility, cond., heat transfer 3-64179
 CaF₂-Na₃AlF₆ phase diagram, differential thermal anal. in sealed crucible 3-75604
 Cao-MgO-SiO₂ glass system, electron microscope obs. of crystallisation (Russian) 3-52582
 CeO₂-SmO_{1.5} and CeO₂-NdO_{1.5}, MO₂ (fluorite)-MO_{1.5} type mixed oxides, phase relations 3-64181
 CeO₂-Y₂O₃ system, equilib. structure absence, X-ray obs. 3-69361
 (Co₂Mg_{1-x})O₂, (Co₂Mg_{1-x})₂SiO₄, point defect thermodynamics (German) 3-64028
 CuBr-CuI system, thermographic anal. 3-72164
 CuO-MgO polycryst., characterization by e.s.r. rel. to catalytic activity 3-73176
 Ga_{0.16}Al_{0.84}As, SRO parameters 3-52596
 GaAs_{1-x}Sb_x, alloy solid miscibility gap, peritectic reaction 3-75602
 GdF₃-MF(M=K, Rb, Cs) and GdF₃-Gd₂O₃, crystal structure, phase behaviour (French) 3-64017
 Ge-Cu₂Te, boundary determ., microstruct. anal., microhardness 3-72199
 GeTe-PbTe, X-ray anal., annealing, quenching, phases 3-64146
 HfO₂-MgO(CaO), transition temp., zirconia like (French) 3-72993
 HfO₂-Y₂O₃ solid soln., phase diagram boundaries detn., X-ray analysis 3-64153
 LiCl-NaCl solid solution, thermographic and X-ray study, crystn. temp., peritectic transformation (Russian) 3-72196
 A-Nd₂O₃-A-La₂O₃ and A-Nd₂O₃-C-Y₂O₃, investigation of the binary systems (French) 3-64152
 NiO-CaO, exsoln. kinetics and microstruct. development 3-72941
 Ni₂TiO₄-NiFe₂O₄(Fe₃O₄), mag. props., cationic distrib., neutron diff. 3-72454
 O₂-Zr(Ar), absorpt. spectra, excited mol. interactions 3-69022
 PbSi_{1-x}Se_x, pseudobinary phase diagram and existence regions 3-79471
 n-PbTe solid solution, thermal cond., separation of lattice and electronic components in strong mag. field 3-58154
 PbTe-GeTe, X-ray anal., annealing, quenching, phases 3-64146
 Si-Sb, dislocation loops, high temp. precipitation 3-75535
 Sr_{1-x}Ba_xTeO₃, Sr_{1-x}Ca_xTeO₃, phase transition temps. 3-68938
 SrF₂-GdF₃, phase composition 3-72682
 SrO-BaO-Al₂O₃ system, solid state phase equilib., X-ray anal. 3-72998
 Ta-O, thermodynamic props., e.m.f. meas. 3-41030
 Ta+H₂ solid solution, high temperature calorimetry 3-69196
 (Ti, W)C, diffusion mechanism during form. 3-64975
 ZrO₂, Ca stabilized, X-ray anal., anionic vacancy ordering (French) 3-76335
 ZrO₂-rare earth oxides, form., decomp. 3-76314

solid-state microwave devices

- bipolar transistor, base impurity atom profile, m.o.s. capacitance obs. 3-69181
 Gunn oscillator, coherence, under impact ionisation conditions 3-75749
 IMPATT diode, source for microwave e.p.r. 3-39979
 Josephson junctions, anomalous microwave impedance 3-50307
 material selection and preparation 3-80185
 α -Fe₂O₃, hematite, easy plane antiferromag. applic. 3-50382
 GaAs, related compounds, conference, Boulder, Colo., USA, Sept. (1972) 3-41678
 GaAs n⁺-n-n⁺ transferred electron oscillator, continuous multilayer epitaxial growth 3-41688
 GaAs:Ge, epitaxial, applic. 3-50662
 Si diode, epitaxial growth from dichlorosilane 3-55747

solid-state phase transformations

- see also ageing; ferroelasticity; ferroelectric transitions; martensitic transformations; order-disorder transformations
- acetonitrile, CH_3CN and CD_3CN , Raman spectra and phase transition, lattice modes 3-55588
- aliphatic hydrocarbons, i.r. spectra, Davydov splitting, reson. 3-72654
- alkali halide cryst. transition pressure and vol. calc. from model pot. with overlap 3-63976
- n-alkyl ammonium chlorides wide line n.m.r. study of molecular motion 3-68852
- alkyl ammonium halides, spectroscopic display, polymorphism 3-72755
- alkyl ammonium tetrachloromanganate and deuterated analogues, neutron diff. obs. 3-47045
- amorphous to crystalline, optically induced, characts. (French) 3-75624
- antiferromagnet, f.c.c., Ising model 3-44185
- austenite, effect of heat shocks on transform. kinetics and morphology in lower bainite region 3-64820
- austenite decomposition, mag. permeability and saturation magnetisation meas., design of bath for instruments 3-51663
- austenitic stainless steel, low temp. deformation, mag. susceptibility, martensitic transformation 3-50720
- berlinite, high-low inversion up to 6 kbar, differential thermal analysis 3-73200
- BN shock induced graphite to wurtzite phase transformation, stacking 3-72193
- bronzeite rock undergoing polymorphic transform. under press, eqns. of state 3-47629
- carbohydrate, amorphous to crystal, i.r. spectra, polysaccharide 3-72655
- carbon tetrabromide, plastic cryst., shear strength 275 to 375 K, 320 K polymorphic transform. 3-79407
- crystal-glass transition, anharmonicity effect on properties of amorphous solids 3-79236
- cyclohexane, dielectric constant, density, transition enthalpy, 500 atm. 3-68910
- cyclohexane, i.r. absorpt. spectra near phase transition 3-55072
- cyclohexane, relationship between the phase transitions and fluorescence spectra of impurity molecules 3-47306
- cyclopentane, cryst., vibr. spectra, phase transition, 168 K 3-50565
- cyclopentane, crystalline, impurity molecule fluoresc. and phase transitions 3-64724
- diamond, bond bending and stretching force consts., high press. transform into metallic dense form 3-49991
- dicalcium strontium propionate, hydrostatic pressure effect on ferroelec. phase transition 3-68940
- 1,8-dichloro-10-methyl anthracene 3-75622
- dimethylacetylene cryst., phonon Raman spectra and mol. rot. behaviour 3-55573
- dislocation motion across obstacles, analogy with diffusionless transition 3-72096
- displacive, theory 3-46692
- dunite rock undergoing polymorphic transform. under press. eqns. of state 3-47629
- earthquake, structure model, micromorphic continuum, deformation of microstructure, focal point props. 3-44824
- electron and ion effect on phonon spectra and structural phase transformations 3-49954
- electronically induced crystallographic transition, dynamic theory 3-49994
- elements, density periodicity rel. to pressure-induced polymorphic transformations 3-43872
- eutectic structures, characterisation from thermodynamic data 3-79495
- excitation condensation and soft mode energy at structure transform. 3-55082
- ferrocene i.r. absorption spectra at low temp., phase transition, rotational barrier (French) 3-47260
- ferroelastic, soft modes having wavelength equal to general rational number times lattice const. 3-44386
- ferroelectric, soft modes having wavelength equal to general rational number times lattice const. 3-44386
- ferroelectric ferromagnet, ferroelec. transition in mag. field 3-50530
- halopropanes, transition temp. determ., isomerisms 3-72653
- hexamethylbenzene, at 116 K, and phase III morphology, vib. spectra and absorpt. anisotropy 3-60794
- hexamethylbenzene crystal, λ transition, Raman, far i.r. studies 3-64134
- ice hydrogen bond spectral shifts temp. depend., vitreous to cubic I phase transformation 3-47262
- Ising-like model, Wilson theory, and Ginzburg critical region 3-68390
- Landau model for second order transitions, role of entropy fluctuations 3-49959
- lepidocrocite-hematite, magnetisation behaviour on transform. 3-65240
- limestone, acoustic wave propag. 3-50929
- lithium ammonium tartrate, sp. ht. anomaly near transition temp. 3-7221
- martensitic transformations, localised soft mode theory 3-46695
- massive transformation temperature, cooling rate depend. 3-61130
- matrix distortions influence on diffuse X-ray scatt. (Russian) 3-52557
- metal, superplasticity and surface tension at phase transition, fluctuation model 3-49924
- metal, thermodynamic prop. changes during A1 to A2, A3 to A2 polymorphic transitions 3-58136
- metals, polymorphic transitions A3 \rightarrow A2 or A1 \rightarrow A2, temp./melting pt. relationship 3-43877
- metastable phase stability compared with crystallisation front stability 3-79256
- methane, expt. obs. of second phase transition at 9.9 K 3-60793
- methane, u.s. vel., mol. orientation and lambda anomaly 3-55031
- microscopic approach to hydrodynamic description 3-46693
- molecular crystal, nematic, i.r. integral intensity temp. depend. 3-72657
- Mossbauer scatt. study of solid state phase transformations 3-55068

solid-state phase transformations continued

- muscovite plus quartz, high temp. stability, hydrothermal studies, nucleation mechanism 3-44770
- N-methylacetamide, complex dielectric constant -185 to 20°C, 50 Hz to 3 MHz 3-60796
- neopentane, dielectric constant, density, transition enthalpy, 500 atm. 3-68910
- n-nonadecane, rotator phase transition, inelastic neutron scattering study 3-49853
- nuclear acoustic resonance obs. 3-75896
- optical phonon and electronic instability induced, sound propagation effects nr. transition 3-46709
- orthoclase, shock-induced phase change 3-50927
- pentafluorophenol:n-Cl-aniline compound, Raman spectra, H bond changes 3-72198
- perovskites, crit. dynamics for $T \geq T_c$ 3-49958
- phenanthrene, i.r. absorpt. spectra near phase transition 3-55072
- polyethylene, conductivity changes at first order phase transition 3-46865
- polyethylene, multiple transitions, glass temp., low-temp. toughness 3-63962
- polymers, semi-crystalline, multiple transitions esp. double glass 3-63962
- polypropylene, oriented isotactic γ -form crystal, form. by α - γ transition 3-69149
- polytetrafluoroethylene, 19°C phase transition, far i.r. meas. lattice modes determ. 3-41511
- PTFE, phase II and III, Raman spectra analysis 3-64643
- pyrazine, crystalline, low temp.-high temp. phase transition study by i.r. and Raman spectra 3-75982
- quartz, critical opalescence, during α - β inversion 3-58571
- quartz-stishovite shock induced transition, X-ray and optical obs. 3-76560
- Raman activity of soft modes, proof of Worlock's conjecture 3-79462
- rare earths of TRNbTiO_6 and TRTaTiO_6 types, aeschynite-euxenite polymorphic transition 3-41015
- second order, isomorphism 3-41001
- silicate glass, semiconducting glaze, for porcelain insulator, phase changes, growth rate 3-47442
- solid solution, nonuniform, first order diffusionless transforms. (Russian) 3-72830
- spinel, Jahn-Teller induced phase transitions 3-41014
- SrTiO_3 , anharmonic interactions and struct. phase transitions 3-58112
- statistical mechanics, melting curve maxima and solid-solid transitions, high pressure, two species model 3-49976
- steel, 18-8 stainless, H embrittlement (Japanese) 3-76201
- steel, austenite, dissolution kinetics of M_{23}C_6 carbides 3-64839
- steel, austenite, nucleation of pearlite at grain boundaries 3-58635
- steel, austenite, thermomechanical treatment effect (German) 3-76151
- steel, austenite form. during accelerated heating (Russian) 3-41695
- steel, austenite transform., Mn dendritic segregation effect 3-50684
- steel, austenitic, quenched, reaction kinetics in bainitic region (French) 3-41700
- steel, austenitic stainless, γ - α transform. effects on phys. props. between 80 and 280K (Russian) 3-44604
- steel, austenitic stainless, a.c. electroetching for metallographic differentiation of δ -ferrite (German, English) 3-64866
- steel, austenitic stainless, warm extruded, struct. and mech. props. 3-50749
- steel, bainite Fe-C-Si, austenite decomp. kinetics (French) 3-47358
- steel, bainite ferrite nucleation and growth depend. on austenite pretransform. state (Czech) 3-55760
- steel, bainitic ferrite nucleation and growth depend. on pretransform. state of austenite (Czech) 3-55758
- steel, diffusion mobility of hydrogen, temp. and time depend. (Russian) 3-41718
- steel, Fe-Mn-C type, isothermal transform. induced struct. and props. 3-69224
- steel, graphitic cast, graphitization behaviour 3-50685
- steel, local mag. struct. of carbides formed during ϵ - χ - θ transforms (Russian) 3-79951
- steel, low-C, effect of chem. heterogeneity on distortion during thermal cycling 3-80383
- steel, low-C austenite, transform. to ferrite after small plastic strains 3-58615
- steel, low-C chromium, M_2C to M_7C_3 transform. 3-80210
- steel, low-temp. DTA obs. (German) 3-64832
- steel, metastable austenite form. during heating (Russian) 3-44601
- steel, Ni-P, martensite temp. decrease due to incoherent particles (German) 3-47357
- steel, pearlite transform., isothermal, manganese role (Japanese) 3-41697
- steel, residual austenite behaviour during deform. (Russian) 3-41756
- steel, stainless, and mech. props. determined in high-speed extension (Russian) 3-53250
- steel, stainless, strengthening by deform., martensitic transform. and ageing 3-50731
- steel, stainless, strengthening by direct and reverse martensitic transforms. 3-50732
- structural and dislocation transformations, lattice model 3-79460
- structural transition, nonlinear coupling and relaxation of fluctuations, central peak 3-79465
- of surface, superstruct. disappearance 3-79550
- tanane, ferroelastic-ferroelectric compound, paraferroelectric transition meas. 3-55536
- TCNQ crystal, nucleation kinetics of allotropic transformation 3-79488
- TCNQ salt of methyltriphenylphosphonium, phase transitions, electrical cond. meas. 3-72194
- tetramethylammonium chloride, struct. transitions, config. entropy and polymorphism 3-79489
- tetramethylammonium manganese chloride, cation rotational motion, neutron scatt. obs. 3-49855
- thiourea and deuterated thiourea, Raman spectra, soft mode behaviour (French) 3-61032

solid-state phase transformations continued

- Ticonal alloy, $\alpha \rightarrow \alpha + \gamma$ transformation, rare earth additions effect 3-80220
- trifluoroacetic acid, 220.5K 3-50572
- unified theory of transitions, esp. ferroelectric 3-75620
- Zircaloy-4, β - α phase transform. 3-47361
- β -Ag-Al alloys, splat-quenched, massive phase transform. phenomena 3-58613
- Ag₂AsS₃, proustite, n.q.r. spectrum and spin-lattice relax. time of ⁷⁵As, 300-4.2K (Russian) 3-79944
- AgCd alloy, martensitic transition, anomalous stress-strain props. 3-58611
- AgCrS₂, reversible phase transition at 397°C 3-40881
- AgCrSe₂, reversible phase transition at 202°C 3-40881
- AgH₃IO₆, nucl. quadrupole interaction of ¹²⁷I, phase transform. behaviour (German) 3-53034
- Ag₂Se, polymorphic, electron microscope investigation 3-58129
- Ag₂Te, $\alpha \rightarrow \alpha'$, X-ray obs. 3-68406
- Al polycrystalline film, B⁺, C⁺, N⁺, P⁺, As⁺ bombard., electron diff. 3-72195
- Al-Cu-Li-Mn-Cd alloy, complex phase behaviour 3-55761
- Al-Zn, eutectoid transformation, phase boundary diffusion as rate-determining step (German) 3-80218
- Al₂(MoO₄)₃, M=Mo, W, ferroelastic transition from monoclinic to orthorhombic phase at 200, 6°C 3-52664
- Al₂O₃ refractories, phase changes during service in high temp. kiln 3-80411
- Au-Cd, martensitic phase transformation, acoustic emission, e.m. detection 3-47498
- B-C system, electron microprobe studies, ZAF method (French) 3-48672
- BaTiO₃, CeO₂ addition effects on transition temps., subsolidus relations in BaO-CeO₂-TiO₂ system 3-44650
- BaTiO₃ cubic-tetragonal, zone structure calcs. (Russian) 3-41487
- Bi, determ. of press. distrib. in multianvil high press. device 3-77416
- BiFeO₃, Bi₂FeO₉, DTA and elec. resist. obs. 3-75621
- BiSeI, nonferroelec. phase transition, model 3-58116
- Ca, f.c.c.-b.c.c. phase transition rel. to s-d hybridisation 3-58128
- Ca₂SiO₄, crystal defects, $\beta \rightarrow \gamma$ polymorphic transition 3-72192
- Cd₃As₂, lattice parameter measurement between 23 and 700°C using X-ray diffractometer 3-68426
- Cd₂Hg_{1-x}Te alloys, hydrostatic pressure effects on conductivity and phase transitions 3-72386
- CdNb_{2-2x}Sn_{2x}O_{7-2x}F_{2x}, Mossbauer study of props. and phase transitions 3-79962
- CdS-Te alloy thin films, energy gap variations and struct. phase changes 3-76028
- CdS(Se)(Te), structural mechanism of high pressure transformation (German) 3-52699
- Ce, X-ray absorption spectrum, M_{4,5} obs. of γ - α phase transition, obs. using CeF₃, CeO₂ and metal 3-76106
- Ce_{1-x}La_x, press.-temp. phase diagram, transition from Curie to Pauli paramagnetic phase 3-72444
- Co, allotropic transforms., addition elements influence (French) 3-41698
- Co-Co₂Si system, γ - ϵ transform. phenomena (German) 3-53207
- Cr₂(MoO₄)₃, ferroelastic transition from monoclinic to orthorhombic phase at 385°C 3-52664
- CsCl thin films, X-ray irradiation influence 3-68409
- Cs₂CuBr₄, at high-pressure, transformation from tetrahedral to planar symmetry, absorption studies 3-55603
- Cs₂CuCl₄, at high-pressure, transformation from tetrahedral to planar symmetry, absorption studies 3-55603
- CsSCN, orthorhombic and high temp. cubic forms, cryst. struct. 3-46624
- CsSH, order-disorder transitions, Raman scatt. study 3-55590
- CsSH, rot. dynamics and phase transitions, neutron scatt. investigation 3-40852
- Cu/Zr-Nb and Cu/Zr-Cu diffusion couple behaviour, intermediate phase props. (Japanese) 3-58612
- Cu-Al, β phase, phase transforms. on extremely rapid cooling from melt (German) 3-72838
- Cu-Al alloy, β_1 to β_1' martensitic transform. crystallography (Japanese) 3-61128
- Cu-Al alloys, mag. susceptibility depend. (Russian) 3-52953
- Cu-Ni-Mn high temp. spring material characteriz. 3-69203
- Cu-Sn alloy, martensitic transform., phenomenological analysis (Japanese) 3-50680
- Cu-Zn alloy, bainitic $\beta \rightarrow \alpha$ transform., cryst. geom. obs. (Russian) 3-80205
- Cu-Zn system, lattice relationships in α - β transform. caused by diffusion 3-50687
- CuCrS₂, reversible phase transition at 402°C 3-40881
- Cu_{2-x}S, and electrical conductivity 3-68407
- Cu₂Se, film, struct. and elec. cond., tetragonal to cubic phase transition (Russian) 3-75688
- Cu₂Se, prep. of single crystals of α form 3-68405
- Cu₂Se, structural transform. studied by high temp. roentgenography 3-52700
- O-D₂, density dependent, Raman scattering studies 3-75995
- EuP(As)(Sb)(Bi), low temp. sp. ht. anomaly 3-55433
- Fe, b.c.c. \rightarrow f.c.c., effect on phonon distrib. function, neutron scatt. study (Russian) 3-72151
- Fe, cast, ductile, transform. superplasticity (Japanese) 3-44564
- Fe, diffusion mobility of hydrogen, temp. and time depend. (Russian) 3-41718
- α -Fe film, C⁺ bombard., ϵ -carbide, cementite form., electron diff. 3-72195
- Fe-C alloys, liq., b.c.c.-f.c.c. like transform. effects on mag. susceptibility (Russian) 3-52963
- Fe-Cr alloys, bulk and intergranular diffusion of Fe, rel. to $\alpha \rightleftharpoons (\alpha + \gamma)$ transforms. (French) 3-44581
- Fe-Cr-Ni alloy, isothermal martensitic transform. (Japanese) 3-50681
- Fe-Mn alloy, form restoration process after bending, memory process 3-41784
- Fe-Mn-C alloy, thermally cycled, morphological changes 3-50686
- Fe-Mn(18 wt.%) alloy, antiferromag. of ϵ -phase, second order transform. (Russian) 3-72462

solid-state phase transformations continued

- Fe-Ni, alloys, polymorphic $\gamma \rightarrow \alpha$ transform. kinetics (Russian) 3-69188
- Fe-Ni alloy, form restoration process after bending, memory process 3-41784
- Fe-Ni alloys, austenite phase stabilization by cumulative thermal cycling (French) 3-41699
- Fe-Ni alloys, austenite start temp., press. depend. 3-41694
- Fe-Ni alloys, diffusion role, potentiokinetic obs. (French) 3-47362
- Fe-Ni alloys, martensitic transform. in pulsed mag. field (Russian) 3-44559
- Fe-Ni alloys, struct. modifications during recovery of equil. by tempering subsequent to cooling 3-64930
- Fe-Ni and Fe-Ni-Cr alloys, stacking fault energy, conc. depend., effect on martensitic transform. (Russian) 3-41715
- Fe-Ni(31.15 st.%) alloy, plastic deform. and thermal stabilization of austenite effect on martensite burst kinetics 3-41782
- FeCl₂, cryst. phase changes at 1-2 kbar, Mossbauer obs. (French) 3-58460
- Fe₂(MoO₄)₃, ferroelastic transition from monoclinic to orthorhombic phase at 499°C 3-52664
- Ga thin films, amorphous and crystalline phases, temps., thickness dependence, low-temp condensed 3-50094
- GaAs, bond bending and stretching force consts., high press. transform into metallic dense form 3-49991
- GaSb, bond bending and stretching force consts., high press. transform into metallic dense form 3-49991
- Gd-Co alloy thin films, amorphous, transmission electron microscopy and diffraction investigation 3-68523
- Gd₂(MoO₄)₃, elec. field effect on elastic const. near ferroelastic phase transition 3-55007
- Gd₂(MoO₄)₃, paraelectric to ferroelectric transition, electric field effect 3-44366
- Ge, bond bending and stretching force consts., high press. transform into metallic dense form 3-49991
- Ge amorphous films, semiconducting to metallic phase transition, pressure induced, low temp. superconductivity 3-50247
- Ge amorphous films, structure change in annealing process 3-68410
- Ge-Ni, alloys amorphous films, semiconductor-metal transition, high pressure up to 100 kbar, electrical resistance, X-ray data 3-50248
- Ge-Te, amorphous alloys, non crystalline to crystalline state, thermally induced changes 3-58259
- H₂, evidence for additional phase transition 3-64175
- H₂, n.m.r., 0.2-4.2K 3-68866
- p-H₂, possible phase transition at 14K 3-75623
- H₂, transition to metallic phase at high densities 3-79487
- p-H₂ density dependent, Raman scattering studies 3-75995
- o-H₂ effect of correlations on transition temp. calc. 3-72163
- In-Tl alloys containing Cd and/or Sn, axial ratio and phase changes 3-79269
- In₂(MO₄)₃, M=Mo, W, ferroelastic transition from monoclinic to orthorhombic phase at 335, 252°C 3-52664
- KBr(Cl)(I) with SH⁻ impurities, h.p. effects on Raman scatt. 3-80019
- KCN, cubic, anomalous thermoelastic behaviour 3-54998
- K₂CO₃, polymorphic transform. behaviour 3-60792
- KCl, shear elastic constant C₄₄ rel. to phase transformation 3-43876
- KDy(MoO₄)₃, phase transition at 10K due to cooperative Jahn-Teller effect 3-43875
- KH₂PO₄:Cr³⁺, e.p.r., ferroelectric and ferroelastic phase transitions 3-55463
- KMM'X₆, pyrochlore-tetragonal transition (French) 3-63988
- KMnF₃, cubic-tetragonal transition at 186K, press. effects., dielec. const. obs. 3-58127
- KMnF₃, spontaneous birefringence and order parameter below 186K transition 3-44391
- K₂Pt(CN)₄Br_{10.30}·xH₂O, low temp. phase transition, condensation of soft modes by Kohn anomaly 3-64177
- K₂ReCl₆, 110.9 K displacive phase transform., order parameter meas. 3-46712
- La, thermal cond. in 80 to 750K range, over first phase transition, lattice contrib. 3-75734
- LaAlO₃, inelastic neutron scatt., soft phonon response function 3-55070
- LaCrO₃, hexagonal-cubic transform, high temp., lattice parameter changes (French) 3-52697
- LiCl-NaCl solid solution, thermographic and X-ray study, crystn. temp., peritectical transformation (Russian) 3-72196
- LiIO₃, polymorphic behaviour (German) 3-49992
- LiN₃, Raman active phonons, temp. depend., phase transition 3-72611
- N₂, $\alpha \rightarrow \gamma$ phase, Raman spectra, librational modes 3-72650
- NH₄Br, specific heat anomaly near orientational phase transition 3-49995
- NH₄Cl, specific heat near transition point, pressure effects up to 3.6 kbar 3-52701
- NH₄H₂AsO₄, high temp. transition, mol. reorientation, n.m.r. obs. 3-61004
- NH₄NO₃, twinning accompanying transform., Medangesetz 3-40931
- NH₄PF₆ and ND₄PF₆, polycrystals, i.r. and Raman spectra, phase transitions study 3-47263
- (NH₄)₂PtBr₆, displacive phase transition ⁷⁹Br n.q.r. and spin-lattice relaxation time meas. 3-41449
- (NH₄)₂SO₄:Mn²⁺, paraelec.-ferroelec. phase transition rel. to 215K e.s.r. discontinuity 3-50454
- NH₄XCl₃, (X=Mn, Fe, Co), ⁵⁷Fe Mossbauer obs. 3-79950
- NaAlO₂-SiO₂-H₂O mineral, phase equilibria, Gibbs energy of formation 3-44773
- Na₂As₂O₇, cryst. struct., bond lengths and angles 3-68223
- NaN₃, Raman active phonons, temp. depend., phase transition 3-72611
- NaNO₂, structure at 150, 185, 225 degrees C rel. to ferroelec. transition 3-44380
- NaNbO₃, antiferroelec., rel. to domain boundary formation during Czochralski growth (Japanese) 3-41634
- NaNbO₃, lattice parameters and domains obs. up to 800°C 3-63984
- NaO₂, Raman spectra, mol. and lattice vibr., struct. changes at 230 and 201 K (German) 3-50569

solid-state phase transformations continued

- NaSH, order-disorder transitions, Raman scatt. study 3-55590
 NaSH, rot. dynamics and phase transitions, neutron scatt. investigation 3-40852
 Nb-H systems 3-49993
 Nb-Ru system, martensitic transitions, temp. and conc. depend. (*French*) 3-58126
 Nb₄Br:Cu²⁺, phase III-IV, effect on optical absorption spectrum 3-72667
 Ni complex, hexapyridinenickel (II) nitrate, order-disorder transitions, 13-300 K (*French*) 3-49961
 Ni-Al(36.8 at.%) martensite, internal twins 3-50718
 NiFe_{0.6}Cr_{1.4}O₄, cubic to tetragonal, mag. and magnetostrictive props. 3-75861
 (Pb,La)(Zr,Ti)O₃ ceramics, phase characteriz. 3-76248
 Pb, f.c.c.-h.c.p. transformation, pressure induced, based on the NaCl internal standard 3-72834
 PbHfO₃, electric quadrupole interaction, temp. depend. 3-55531
 PbI₂, polytypic crystals, transform. 290-310°C, stacking fault mechanism 3-43874
 Pb₃P₂O₈, and solid soln. with Pb₃V₂O₈, dielectric props., thermal expansion, characterisation 3-72191
 Pb(Ti_{1-x}Zr_x)O₃, ferroelec., soft optical phonons rel. to morphotropic phase transition, Raman scatt. obs. 3-41491
 Pd-Ni-P, comp. depend. of glass transition temp. 3-68167
 PrAlO₃, Raman scattering, optical fluorescence spectroscopy and e.p.r. of Gd³⁺ impurity obs. 3-55083
 Pt-Ni-P, comp. depend. of glass transition temp. 3-68167
 Pu, $\alpha \rightarrow \beta$ transforms, cinematic obs. 3-47359
 Pu, β - α and γ - α transforms., quenching obs. 3-47360
 RbNO₃ structure transformation, NaCl type to CsCl type, orientation relation 3-52696
 RbSH, order-disorder transitions, Raman scatt. study 3-55590
 Sb₂Se₃-GeSe₂, Sb₂Se₃-GeSe₂ systems, condition state diagrams, thermal, X-ray and microstructure anal. (*Russian*) 3-49968
 Se₂(MoO₄)₃, ferroelastic transition from monoclinic to orthorhombic phase at 9°C 3-52664
 Si, bond bending and stretching force consts., high press. transform into metallic dense form 3-49991
 Si₃N₄, α and β phases, struct. differentiation from electron diffr. data 3-60658
 Sm, crystal structure rel. to phase transitions from 77 to 300K 3-49996
 Sr, f.c.c.-b.c.c. phase transition rel. to s-d hybridisation 3-58128
 Sr_{1-x}Ba_xTeO₃, Sr_{1-x}Ca_xTeO₃ solid solutions, transition temps. 3-68938
 Sr₂SiO₄-Sr₂GeO₄-Ba₂GeO₄-Ba₂SiO₄, solid solubility, polymorphism 3-41803
 SrTiO₃, crit. opalescence, light scatt. near structural phase transition 3-41535
 SrTiO₃, cubic-to-tetragonal, thermomodulation expts. 3-55085
 SrTiO₃, displacive phase transitions, theory 3-72160
 SrTiO₃, e.p.r. of Fe³⁺-V₀ centre, phase transform. dynamics implications (*German*) 3-53015
 SrTiO₃, heat capacity in vicinity of phase transition at 110 K 3-79490
 SrTiO₃, implications of e.p.r. of Fe³⁺-V₀ centre (*German*) 3-50445
 SrTiO₃, lattice const., 17-300 K, anomaly at cubic-tetragonal transform. 3-60701
 SrTiO₃ structural transition, Wilson theory of critical phenomena, classical isotropic Heisenberg antiferromagnet 3-41013
 Ta-H systems 3-49993
 Ta₂, 4Hb-type, susceptibility, resist. and heat capacity studies 3-55084
 Tb-light rare earth alloys, neutron diffr. obs. 3-68790
 Ti, $\alpha \rightarrow \omega$ transform. hysteresis, T-P diagram (*Russian*) 3-44560
 Ti, $\alpha \rightarrow \omega$, mechanism 3-72876
 Ti alloys, and mech. props. determined in high-speed extension (*Russian*) 3-53250
 Ti-Mo-Zr-Sn alloy, β_{III} , isothermal transforms. (*French*) 3-80203
 Ti-V alloys, athermal $\beta \rightarrow \omega$ transform., interstitial oxygen effect 3-64827
 TiC-ZrC system, rel. to comp. depend. of monochromatic emittance, 1800K 3-52703
 Ti₂PbCu(NO₂)₆, domain structure below 291 K rel. to Jahn-Teller effect, e.s.r. obs. 3-50136
 TIRF, III transformation to TIBF₄ IV high-pressure phase, D.T.A. and volumetric techniques 3-64176
 Tm, high press., X-ray obs. 3-75500
 TmVO₄, phonon instabilities, near Jahn-Teller phase transition 3-55069
 α -U, heat capacity and transforms, 2-70K 3-47041
 UC₂, bainitic transforms., carbide phase nomenclature 3-55836
 V-H systems, nonclassical phase transformations 3-49993
 V-Ru alloy, near equiatomic, electronic transition, ⁵¹V n.m.r. study 3-53032
 V₂D, V₄D₃, structural transitions at low temps., X-ray and neutron diffraction studies 3-46710
 V₂O₅, thermal and low energy electron bombardment induced O₂ loss, transition into V₆O₁₃ 3-41099
 V₆O₁₃, cryst. structure obs. at room and liquid nitrogen temps. 3-52698
 V₅Si, Bitterman-Barrett, pressure derivatives of elastic constants 3-79792
 V₅Si, mag. field induced structural phase transform. prediction 3-46711
 Xe, rel. to vacuum u.v. emission spectrum, temp. depend. 3-69066
 Yb, Hall effect and magnetoresist. through f.c.c.-h.c.p. transform., 1.8-420K 3-50183
 Zn die casting alloy, ageing, kinetic analysis (*Japanese*) 3-72910
 Zn₃As₂, lattice parameter measurement between 23 and 700°C using X-ray diffractometer 3-68426
 ZnS, effect of firing atm. on rate of cubic-hexagonal transformations 3-43873
 ZnS(Se)(Te), structural mechanism of high pressure transformation (*German*) 3-52699
 -Zn₂V₂O₇, to thortvettite struct. at 615°C 3-49875
 Zr, allotropic α - β transform. kinetics (*Russian*) 3-53201
 Zr, $\alpha \rightarrow \omega$ transform. hysteresis, T-P diagram (*Russian*) 3-44560
 Zr, $\alpha \rightarrow \omega$, mechanism 3-72876

solid-state phase transformations continued

- Zr, $\omega \rightarrow \alpha$ transform., rel. to phys. props. (*Russian*) 3-79665
 Zr, phases and compressibility up to 120 kbars 3-72833
 Zr-Nb (19 wt.%) alloy, transform. and age hardening behaviour 3-47412
 Zr-Nb (20 at wt.%), Mossbauer scatt. study of solid state phase transformations 3-55068
 ZrO₂, monoclinic-tetragonal transition, high temp. obs., twin form. 3-72931
 ZrO₂-Er₂O₃(La₂O₃)(Y₂O₃) cubic solid soln. stability below 1500°C (*French*) 3-76309
- solid-state plasma**
see also helicons; plasmons
 aggregated metal systems, optical resonances 3-68948
 chemical pot. behaviour of dense electron plasma in strong mag. field 3-50153
 dielectric, transparent, changes in giant laser pulses and luminous plasma, in damage region form. 3-74262
 electron-hole, surface e.m. wave propag. in uniform mag. field 3-64367
 e.m. wave excitation, interaction of electron beam 3-79721
 ferromagnet with periodic domain struct., low-freq. magnetoplasma oscills. 3-55299
 frequency superbroadening in light filaments, plasma form. influence 3-66874
 h.f. conductivity of slightly nonideal plasma, influence of quantum effects (*Russian*) 3-79722
 light-electric field near plasma frequency 3-41224
 magnetically active semicond. plasma, nonpot. surface waves along semicond.-vacuum boundary 3-44132
 magnetoplasma, two-component, coupling of longit. and transverse waves 3-41223
 metal, electron wind anisotropy, Fermi surface geom. and electron scatt. mechanism depend. (*Russian*) 3-79648
 metal, magnetoplasma waves in quantizing mag. field 3-58297
 metal, refl. spectroscopy, plasma reson. enhancement 3-44040
 metals, magnetic, plasma minimum determ. using Boltzmann's transport and Maxwell's eqns. 3-47237
 p⁺-n-n⁺ structure, carrier injection, triggering of trapped plasma 3-68692
 p-n junction, microplasma phenomena theory, avalanche multiplication process 3-41262
 piezoelectric semiconductor, interaction of plasma and lattice waves 3-79743
 plasma engineering, monograph 3-49632
 resonant props. of resistive instability 3-75763
 semiconductor, acoustoelec. plasma transport and recombination delay 3-55312
 semiconductor, compensated, spatial charge exchange waves and thermoelec. current instability 3-64349
 semiconductor, Einstein relation in quantizing mag. field 3-68660
 semiconductor, electron-hole degenerate plasma, magnetoresist. 3-44097
 semiconductor, equilibrium disperse phase containing metallic particles electronic structure 3-60861
 semiconductor, highly restrained plasma, wave propagation 3-68658
 semiconductor, in strong mag. field, quasilinear relax. of electron plasma 3-58296
 semiconductor, Kadomtsev-Nedospasov helical instability in strong pinch effect 3-75764
 semiconductor, microwave emission, hydromag. turbulence theory (*French*) 3-68656
 semiconductor, plasma wave amplification by acoustic wave viscous absorpt. 3-44104
 semiconductor plasmas, carrier heated electron-hole instability 3-41195
 semiconductor-plasma boundary, kinetic reflection coefficient for inelastic electron energy relaxation 3-68663
 semiconductors, acoustic wave amplification in strong electric fields 3-41237
 semiconductors, space charge waves effects on adjacent plasma layers 3-79724
 semimetal, magnetoplasma waves in quantizing mag. field 3-58297
 semimetal, spectrum of plasma oscills. 3-55296
 surface plasmon dispersion relation for plasma slab in magnetic field 3-60910
 transition metals, collective excitation phenomena (*Russian*) 3-68571
 uniaxial polar semiconductors, influence of spatial dispersion on high-freq. wave props. 3-55294
 Bi, Alfvén wave phase velocity diagrams, expt. 3-58291
 Bi₂Sb₃, valence band struct. from magnetoplasma wave dispersion 3-44020
 Cu thin films, surface plasma oscillations 3-44133
 Dy, current carrier plasma and relax. freqs. from optical props. in 1-20 μ m range (*Russian*) 3-44421
 p-GaAs, resonance, carrier concentration meas. 3-68661
 GaP with plasma of charge carriers, dielectric parametrization of Raman lineshapes 3-50563
 GaSb, screw instability in three-component electron-hole plasma 3-58293
 Ge, exciton and plasma phase transitions 3-41167
 Ge, exciton drop system, magnetoplasma reson. 3-46819
 n-Ge frequency shift due to uniaxial stress, free carrier dispersion, polarised radiation, electron transfer model 3-72376
 Ge:Mn,Sb, recomb. wave in mag. field, mag. field effect on crit. elec. instability field 3-58280
 n-InSb, degenerate, possible parametric reson. of plasma in strong h.f. field 3-50229
 n-InSb, e.m. wave propagation in magnetoplasma cutoff region 3-58295
 n-InSb, e.m. wave propagation 3-68662
 InSb, electron-hole plasma, enhanced diffusion Bohm-like behaviour 3-50226
 InSb, inductance of impact-ionized plasma 3-55295
 n-InSb, plasma, convective instability due to impact ionisation, influence of crossed electric and mag. field 3-75766

solid-state plasma continued

InSb, possibility of acoustic amplification and microwave radiation 3-68677

InSb, surface carrier wave amplification at X-band 3-68657
 $K_2Pt(CN)_4Br_{0.33} \cdot 3H_2O$, optical excitation of electronic plasma oscillation in one-dimensional conductor 3-52810

Rb, granular thin films, surface plasma oscill., light absorption (*French*) 3-55702

Si, exciton and plasma phase transitions 3-41167

solid-state radiation detectors *see crystal counters***solid-state rectifiers**

see also copper-oxide rectifiers; thyristors

p-i-n-Si, pulse response meas. with portable X-ray generator 3-73918

solid structure

see also crystal structure; long-range order; noncrystalline state structure; short-range order

No entries

solid theory

Born theory, appl. to thermal expansion calc. for LiH 3-68425

cubic crystals, exponentially attractive and repulsive interatomic potential function appl. 3-68303

f.c.c. crystal, theoretical strength calc. using exponentially attractive and repulsive interatomic interactions 3-68304

quantum structure of solids 3-55565

solids, polycryst., computer simulation of internal stresses 3-68305

text book, solved problems in mats. sci. 3-56601

transport processes, review 3-72339

solid-vapour transformations

see also sublimation

Ar, shear viscosity behaviour near triple point 3-55096

CO₂, frost formation in flow system 3-79486

solidification

alloy, binary, heat, mass transfer calcs. 3-62615

alloy, binary, morphological stability nr. grain boundary groove during solidification 3-64816

alloy, binary, solute redistrib. during solidification, constitutional supercooling (*French*) 3-76152

alloy, rapid quenching from melt, annotated bibliography 3-41771

alloy, ternary, directional solidification, melt vs. cryst. comp., ternary distrib. coeffs. (*German*) 3-55762

alloys solidification in cylinder with axial and radial-axial heat transfer 3-80217

benzene, porous media, calorimetric method, latent heat determ., effect of pore radius, hysteresis (*French*) 3-75606

controlled Green's function determ. of diffusion eqn. (*German*) 3-50676

1:2 diphenylbenzene, crystallisation behaviour 3-79252

glassy polymers, thermodynamics 3-46718

impurity diffusion in the melt during directional

solidification (*Russian*) 3-72182

kinetics, mathematical framework, solved problems, book contrib. 3-58122

lamellar eutectic cryst. imperfections characteriz. 3-47377

mathematical modelling methods, for solving problems (*Russian*) 3-53202

melt, effect of thermophysical props. on spheroidisation of drops using solidification 3-80394

metallic melt, effect of thermophysical props. on spheroidisation of drops 3-80394

neutron stars, solidification density, t-matrix calc. 3-42115

particle engulfment by solidifying melts, thermodynamics 3-61210

planar, of saturated liquid with convection at the wall, exact solution of perturbation method 3-58121

porous media, dependence of energy of transformation on curvature of interfaces, effect of capillary radius (*French*) 3-75607

porous media, thermogram, calorimetric method, effect of pore size distrib., transformation hysteresis (*French*) 3-75608

pure substance, solidification, grain boundary groove in interrace, morphological stability 3-57995

rare earth oxide/metal composites, unidirectional solidification 3-76347

saturated liquids spherical solidification, perturbation solutions 3-46702

semitransparent cylindrical medium solidification, heat conduction and radiation 3-46701

steel, calc. interdendritic C, O enrichment (*German*) 3-69251

steel, cooling rate during solidification effect on dislocation struct. internal oxidation and dislocation struct. (*Russian*) 3-53220

steel, dendritic structure dispersion rel. to solidification rate 3-80278

steel, graphitic cast, graphitization behaviour 3-50685

steel, quenchability influence on carbide precip. during continuous cooling (*French*) 3-47416

steel, rate calc., heat balance integral (*German*) 3-76148

steel, resulphurized, solidifying rate and form. of sulphide inclusions 3-61181

steel, sampling, H₂ evolution anal., effect of alloy composition and structure (*German*) 3-66441

steel castings, low-alloy, solidification behaviour 3-64901

steel melt, precipitation hardening, recrystallisation 3-76214

steel slab, simulation, thermohydraulic analog model (*German*) 3-76149

superheated melt, crystallisation in an e.m. field (*Russian*) 3-61129

thin films, stress due to vol. change on solidification 3-41008

two-dimensional mesophases, fluid-solid transition phenomena 3-57984

water, ice column formation during freezing in open

container (*Japanese*) 3-55076

water, porous media, latent heat determ., calorimetric method, effect of pore radius, transformation hysteresis (*French*) 3-75606

Ag, supercooled melt, spontaneous crystn. (*Russian*) 3-58609

Ag-Cu, eutectic alloy, freezing and melting at very slow rates 3-53203

Al-Al₃Ni eutectic composite, morphological factors affecting microstruct. coarsening 3-64858

Al-Cu alloy, casting, numerical analysis (*Japanese*) 3-76156

Al-Cu alloy, eutectic, nonstationary solidification 3-50683

solidification continued

Al-Cu-Li-Mn-Cd alloy, complex phase behaviour 3-55761

Al-CuAl₂ eutectic, unidirectional, fault structure obs. 3-64843

Al-CuAl₂ eutectic composites, lamellar and particulate, phase size influence on elevated temp. deform. 3-64958

Al-Mg₂Si monovariant eutectic, unidirectional growth, duplex struct. (*Japanese*) 3-76157

Al-Si alloys, splat cooling phenomena (*Japanese*) 3-50682

Al-Ti alloys, grain refinement by metastable phases 3-55793

Al-Zr alloys, grain refinement by metastable phases 3-55793

Al₂O₃, flame- and plasma-prepared, metastable phase formation 3-74447

Al₂O₃-ZrO₂(Y₂O₃) eutectic, directionally solidified, fracture surface energies 3-72937

Ba₂Sr_{1-x}Nb₂O₆-BaNb₂O₆ system, eutectic solidification and characterization. 3-76237

Cu, supercooled melt, spontaneous crystn. (*Russian*) 3-58609

Cu alloy rods, binary, crystn. characts. determ. by temp. meas. during zone melting (*German*) 3-55763

Cu-Al, β phase, phase transforms. on extremely rapid cooling from melt (*German*) 3-72838

Cu-B eutectic alloy, unidirectional structure 3-76155

Cu-Ni alloys, dendritic solidification, initial growth of dendrite structs. 3-69199

Cu-Ni alloys, dendritic solidification, microsegregation 3-69200

CuNi-Sn alloys, directional solidification, melt vs. cryst. comp., ternary distrib. coeffs. (*German*) 3-55762

Fe, cast, spheroidal graphite, shrinkage cavity (*Korean*) 3-53255

Fe-C, solidification process, temp. progression, thermal diffusivity of liquid Fe (*German*) 3-72884

Fe-C and Fe-C-Si alloys, cast, shape of graphite inclusions 3-50712

Ge, supercooled melt, spontaneous crystn. (*Russian*) 3-58609

HfO₂/W composites, Y₂O₃ stabilized, unidirectional solidification behaviour 3-61203

Mg alloy MA2-1, u.s. treatment during solidification effects 3-55812

Mg-Li alloy, orientated eutectic, directionally solidified, morphology (*French*) 3-44574

Ni-C ingot, unidirectionally solidified, periodic macrostructure 3-61159

Ni-Ta-Cr-Mn system dendritic duplex crysts., topography 3-41725

NiAl-G(Mo) eutectic composites, directionally solidified, stability 3-69198

Ni₃Al-Ni₃Nb eutectic, directionally solidified, microstruct. and mech. props. (*Russian*) 3-44605

SiO₂-Al₂O₃ system, stable and metastable equil. 3-76238

Sn-Cd unidirectionally solidifying binary melt, with natural convection, neutron radiography study 3-72877

Sn-Cd(Pb) alloys, mag. field effect on directional solidification 3-80213

Sn-In unidirectionally solidifying binary melt, with natural convection, neutron radiography study 3-72877

Sn-Pb alloy, eutectic solidification front, thermal

microanalysis (*French*) 3-59705

UO₂-cladding composite body, heat conduction with simultaneous solidification and melting 3-54548

Zn droplets quenched from liq. state, cryst. struct. (*Russian*) 3-69268

Zn-Ti alloys, hypereutectic, struct. controlling by unidirectional

solidification (*Japanese*) 3-53206

ZrO₂-MgO system, directional solidification and oriented eutectic composite behaviour 3-76236

solids

see also crystals; solid structure; solid theory

thermophysical props., conf., Atlanta, USA, (Aug 1973) 3-71702

solitions *see transducers***solitons**

active media, explosive instability and soliton generation 3-52517

disordered anharmonic chain with symmetric potential, modulated waves 3-43856

Korteweg de Vries equation with slowly varying coefficients, asymptotic solution 3-75245

Korteweg-de Vries eqn. decay of continuous spectrum for solutions 3-73993

Langmuir, in plasma, damping and amplification 3-52508

lattice solitons, nonlinear lumped networks, theoretical and experimental studies 3-66509

nonlinear envelope-soliton solns., exact 3-48806

nonlinear lumped network eqn., exact soln. 3-48705

nonlinear lumped self-dual network eqns., exact soln. 3-48706

nonlinear optics, bound state solutions of sine-Gordon and related equations 3-57045

plasma, with ion-acoustic wave train, decay instability and shock profile formation 3-46541

plasma explosive instabilities stabilisation by nonlinear frequency shifts, soliton-like solutions 3-49709

plasma ion acoustic solitary wave propagation 3-75319

plasma ion-acoustic solitary wave expts. 3-71912

plasma quasi-neutral solitary wave, stationary electrostatic solutions for a nonneutral two fluid model 3-57918

plasma shock waves, soliton-like pulses obs. 3-75371

plasma solitary waves in anisotropic waveguide, nonlinear theory 3-79135

plasmas, magnetised, non-turbulent electric fields in soliton and shock-like structures 3-57896

plasmas, unstable, mode coupling saturation, model eqns., soliton soln. 3-49693

review, current status of research, inverse method 3-66508

self-induced transparency, Maxwell-Bloch equation, N soliton solutions 3-62734

Seneca Lake, internal undular surges as naturally occurring solitons 3-50988

wave propagation, shallow water waves, solitons and synacetics 3-45633

whistler solitary waves parametric instability 3-79107

soils

see also colloids; sedimentation

coagulation rate meas., low angle light scattering technique 3-73089

coagulation threshold, lyophobic, theory 3-61226

sols continued

- heated sol process for thermal precip. of UO_2 powders 3-67555
 Kerr effect during aging 3-73075
 molecular capacitor, lyophobic, stability, fast coagulation barrier mechanism 3-61230
 molecular capacitor, stability, lyophobic, fast coagulation barrierless mechanism 3-61229
 AgBr photographic sol conversion to AgI, reaction kinetics, turbidimetric studies effect on gelatin protection and unsubstituted polyethylene oxides 3-53338
 $\text{Cr}(\text{OH})_3$ sols in size range of less than $0.5 \mu\text{m}$, particle size analysis, structure 3-76383
 PuO₂, solvent extraction process, description 3-65039
 Se hydrosols, monodisperse, effect of particle size 3-61233
 SiO₂ in water, ultramicroscopy, coagulation mechanism 3-65029
 ThO₂, particle size distrib., small angle X-ray scatt. anal. 3-73079
 ZrO₂ microspheres production, CaO stabilization, sol-gel process 3-72992

solubility

- see also phase equilibrium; solutions
 alkali borate glass, of He 3-68437
 alkali metal alloys, zero model in pseudopot. theory, solid solubility limit (Russian) 3-80245
 alkali silicate glasses, helium migration behaviour 3-75631
 alloy, liquid, activity coeffs. of nonmetallic elements, comp. depend. 3-79505
 alloys, splat cooling and metastable phases 3-80358
 augite-pigeonite miscibility gap pyroxene from lunar basalt (12021) 3-77001
 binary glasses, effect of minor third component on metastable immiscibility boundaries 3-75475
 borate glasses, gas solubility phenomena rel. to struct. 3-44678
 borosilicate glass, of He, alkali oxide effects 3-44677
 γ -Fe, of CeN and LaN 3-64862
 gas solubility effective hard sphere diameter, temperature dependence 3-41870
 gases at infinite dilution in liquids, liquid compressibility and partial molar volumes, states correlations 3-58815
 liquid, of gas, applic. of perturbation theory 3-53357
 liquid-liquid equilibrium data correlations, properties of NRTL equation 3-46713
 lyotropic liquid crystals, solubility 3-43748
 molten salts, of BF₃, rel. to reactor safety 3-46140
 molten salts, of gases, method and apparatus 3-70415
 polymer, local diffusion, segmental solubility 3-73044
 powder agglomerates (German) 3-50797
 rare earth-Al garnet:Sc³⁺, Nd³⁺, solubility enhancement of Nd³⁺ by lattice expansion with Sc³⁺ 3-68415
 silicates, liquid immiscibility, study of synthetic compositions, possible factor in rock formation 3-73226
 steel, boride layer growth, carbon influence (Czech) 3-55803
 steel, cementite, of alloying elements, Si, Mo and Cr (German) 3-76160
 steel, Cr-Ni, of N temp. and Cr content depend., dissolution of gaseous N and precipitation of Cr₂N (German) 3-47367
 steel, low-C, of hydrogen, room temp. obs. (Japanese) 3-41727
 two layer liquid immiscibility, relation with vitron theory 3-63957
 vacuum material, gas in solids, rel. to alloys, pure metals, refractory oxides, ceramics, organic 3-59570
 Water solubility in basic and ultrabasic magmas 3-80637
 Ag, diffusivity and solubility of oxygen 3-41051
 Ag, of H, temp. variation 3-41021
 Ag, of oxygen, potentiostatic electrochem. meas. 3-64196
 Ag-Pb, liq. alloys, solubility of S, thermodynamics of (German) 3-72882
 Ag-Sn liq. alloys, solubility of S, thermodynamics of (German) 3-72882
 Al-Ni alloys, Al-rich, rapidly quenched from vapour, metastable solid solubility 3-69247
 Au, of H, temp. variation 3-41021
 Ba(IO₃)₂, determination of equilibrium solubility 3-79494
 CO₂ in water, absorption in gas-liquid annular flow 3-63752
 CaO-MgO-iron oxide system, TiO effects on equil. among refractory phases 3-44655
 CdS, of I donor, temp. depend. 3-55286
 Co and alloys, of nitrogen and hydrogen data survey 3-44567
 Co-H₂O system, thermodynamics at elevated temps. 3-47605
 Cr-H₂, solubility, partial molar enthalpy, excess entropy 3-80236
 Cu, of H, temp. variation 3-41021
 Cu, of oxygen, potentiostatic electrochem. meas. 3-64196
 Cu-H₂O systems, thermodynamics, at elevated temps. 3-44748
 CuAlX₂AgAlX₂ system, X=S, Se, limits of solid solubility 3-43879
 CuGaX₂-AgGaX₂ system, X=S, Se, limits of solid solubility 3-43879
 CuInX₂-AgInX₂ systems, X=S, Se, limits of solid solubility 3-43879
 Cu₂Te, of Ge, solid soln. boundary determ., microstruct. anal., microhardness 3-72199
 α -Fe, of Fe₁₆N₂, Co, Ni, Mo and W additions effect, ageing, internal friction obs. (Japanese) 3-76166
 α -Fe, of Fe₄N, effect of Co, Mn and W (Japanese) 3-41728
 Fe, of N, temp. depend., α , δ and γ domains (German) 3-47367
 Fe alloys, central atoms model, graphite and N₂ solubility 3-80238
 Fe-Co(Ni) alloy systems, stagnant, absorpt. rates of nitrogen, 1600°C 3-64808
 Fe-H₂O system, thermodynamics at elevated temps. 3-44749
 Fe-V(W) binary systems, vanadium and tungsten solubility in α and γ phases (Czech) 3-55771
 Fe-Zn binary system, thermodynamic calc. of Γ -phase in α -Fe, metastable miscibility gap in ferrite (German) 3-47356
 Fe-Zn-Al system, phase constitution at 450°C 3-53208
 FePd₃, ordered and disordered, electronic specific heat rel. to hydrogen solubility 3-55090
 GaAs_{1-x}Sb_x alloy solid miscibility gap, peritectic reaction 3-75602
 n-GaP, of Zn, solid soln., function of source composition 3-72228
 GaSb:Cu, Zn, Te, Zn and Te influence on Cu diffusion and solubility 3-72232
 InP:Te, Zn, carrier density rel. to solubility of donor, acceptor dopants 3-60886

solubility continued

- In₂Se₃, of Se, limits, homogeneity region boundary 3-64147
 Ir, of hydrogen, temp. depend. 3-41017
 LiF+alkali halides, miscibility gaps study 3-72202
 NaCl crystals, H₂, D₂ diffusion and solubility, desorption obs., isotopic effects 3-72233
 NaCl:CaCl₂ crystals, solubility of Na₂CO₃, 75 to 530°C, from elec. cond. meas. 3-55086
 NaCl: Cd, dissolution kinetics of precip., ionic thermocond. study 3-41020
 Na₂O-B₂O₃-SiO₂ glass, u.s. absorpt. in immiscibility region, structural relax. 3-72140
 Na₂O-SiO₂ glass, of He, phase separation effect 3-69382
 Na₂O-K₂O-SiO₂ system glasses, He migration behaviour 3-75632
 Nb, solubility and diffusivity of H isotopes at high temps., reln. to CTR components 3-61161
 Nb-Zr alloys, solubility and diffusivity of H isotopes at high temps., reln. to CTR components 3-61161
 Ni, diffusivity and solubility of oxygen 3-41051
 Ni, H₂ permeation, diffusion and solubility 3-53238
 Ni, of hydrogen, temp. depend. 3-41017
 Ni, pure, carbon solubility and activity (Czech) 3-55769
 Pb-Li, liquid alloy, of Th and Sm 3-58131
 PbS:MnS solid solution 3-72200
 PbSe, of MgSe and CdSe, 400 to 800°C 3-75601
 PbTa₂O₆, ferroelec., rel. to single crystal growth 3-64772
 Pd-Pt, Pd-Ni, and Pd-Rh alloys, of hydrogen 3-55789
 Rh, of hydrogen, temp. depend. 3-41017
 Rh-Pd alloys, H₂ absorption, at high pressures 3-53229
 Ru, of hydrogen, temp. depend. 3-41017
 Si:Al, limit solubility determ., temp.-gradient fusion zone method 3-44543
 Sn, liq., diffusivity and solubility of oxygen 3-41051
 Sn, of Si, metal impurity effects, Semenchenko moment, rel. to liq. phase epitaxy 3-69165
 Ta-O solid solns., terminal solubility, e.m.f. meas. 3-41030
 U_{0.8}Pu_{0.2}C-W system, phase diagram obs. 3-47451
 V, solubility and diffusivity of H isotopes at high temps., reln. to CTR components 3-61161
 V-O system, temp. dependent from 200 to 750°C 3-49998
 W-H₂, solubility, partial molar enthalpy, excess entropy 3-80236
 WC-ZrC system, solid solubility limits 3-72939
 YAG:Sc³⁺, Nd³⁺, solubility enhancement of Nd³⁺ by lattice expansion with Sc³⁺ 3-68415
 Y₂O₃-CaO system, phase diagram characteriz. 3-76241
 ZrC, solubility of O₂, X-ray diffraction 3-41804

solution energy see heat of solution

solutions

- see also Debye-Huckel theory; heat of solution; liquids; solid solutions
 alkali metal-amine solns., Faraday effect interpret. 3-53348
 aniline-cyclohexane mixtures, critical exponents near critical conc. determ. by light scatt. (German) 3-65119
 aqueous, i.r. spectra of water, internal reflection spectroscopy 3-75042
 aqueous base solutions having i.r. absorption continua, very polarizable H-bonds 3-61285
 aqueous solutions, pressure dependence of equilibrium constants 3-55939
 binary mixtures of organic liquids, dielectric props., microwave meas. 3-55999
 binary solutions, restricted diffusion 3-61283
 cell theory with holes, development 3-63939
 complex ion struct. in aqueous media using n.m.r. in nematic phases 3-55484
 convection, finite amplitude sideways diffusive 3-49554
 coupled spin systems, intermolecular nuclear Overhauser effect 3-50489
 cryptocyanine in methanol soln., hole burning by laser beam (French) 3-51943
 1,3-dioxolane-water mixtures, u.s. velocity rel. to water shell stabilization hypothesis 3-65125
 ethane-ethylene solutions, molecular thermodynamics in normal and critical regions 3-65121
 ether in chloroform soln., association and anisotropic mol. reorientation, n.m.r. obs. 3-68873
 fluorescence, concentration depolarisation (Russian) 3-41562
 fluorescence quenching and nonradiative energy transfer 3-69060
 fluorescence solution viscosity and temp. effects on the concentration depolarisation 3-49486
 formic acid, ionic solvation, CNDO/2 calcs. on solvated univalent ions 3-53347
 gas solubility effective hard sphere diameter, temperature dependence 3-41870
 gases at infinite dilution in liquids, liquid compressibility and partial molar volumes, states correlations 3-58815
 linear polyelectrolyte solutions, ion density relaxation (Russian) 3-73143
 macromolecular, Rayleigh scatt., diffusion consts. determ. 3-78922
 molecular motions and mutual viscosities of polar molecules in solutions 3-47604
 molecular thermodynamics, in normal and critical regions 3-65120
 multi-component fluids, primary medium effect in electric field 3-73178
 nitrobenzene-n-nonane system, u.s. absorption near critical region 3-49941
 organic pigment three-component agitated solutions, energy transfer (Russian) 3-41563
 poly(amide carboxylic acid) solution, flow birefringence, 30°C, molecular dimensions, triethylamine addition effect 3-54781
 with polyatomic solute mols., tensorial correlation function (French) 3-64201
 polyethylene glycol dilute soln. elastico-viscous liquid, oscillatory laminar flow, velocity profiles in tubes of circular section 3-54822
 polymer, high viscosity, wedge and channel flow stability 3-54825
 polymer, rigid ellipsoid, intrinsic viscosity, shear rate depend. 3-80478
 polymer, surface thermodynamics, applic. of Prigogine-Marechal theory 3-53346

solutions continued

- polymer aqueous solutions, hydrodynamic influence of polymer additives in external flow around a sphere 3-57830
 polymer concentrated solns., heterogeneous drag, reduction system, turbulent pipe flow, heat transfer 3-52434
 polymer dilute solutions, modified Huggins' eqn. of thermodynamic interaction parameter 3-47602
 polymer dilute solutions flow over a rough surface, wall pressure fluctuations 3-54823
 polymer fluid behaviour in elongational flow (*Polish*) 3-60501
 polymer semi-dilute solns., screening length 3-49515
 polymer soln., dilute, turbulent flow, spectral characts. of press. fluctuations 3-49559
 polymer solution turbulent submerged jets, long-range nature 3-57860
 polymer solutions, capillary viscosimeter flow meas. 3-57831
 polymer solutions, internal viscosity models evaluation 3-53288
 polymer solutions, structure formation, light scattering studies (*Russian*) 3-49518
 polymer solutions, turbulent flow, influence of high-molecular weight additives 3-57832
 polymer solutions, viscoelasticity, hole size and soln. concentration effects 3-53290
 polymer solutions and melts, periodic deformation, viscous flow, under stepwise vibrations 3-58755
 polymer solutions and melts, periodic deformation and viscous flow 3-54780
 polystyrene solutions, viscoelastic props. 3-53291
 polystyrene-cyclohexane system, cloud point curves near critical pt. 3-80489
 propylene-CO₂ solutions, molecular thermodynamics in normal and critical regions 3-65121
 rubrene in benzene soln., surface generated photocurrent, ion-image state as intermediate 3-47578
 salt, thermal diffusion of dextran 3-60500
 saturation parameters, high temp., γ -ray study 3-50859
 solute-solute forces obs. by n.m.r. relax. 3-53350
 solute-solvent interactions determ. from dielectric relaxation data 3-53360
 solutions, nonlinear viscoelastic functions, analysis and temp. dependence 3-53289
 solvated electrons in H₂O, NH₃, HF, semiempirical unrestricted Hartree-Fock calc. 3-69492
 solvent effect on reaction rates 3-69457
 solvents, rational series for incremental gradient elution in liq.-solid chromatography 3-66420
 solvolysis reactions, solvent isotope effects and the transition state 3-55957
 ternary aqueous solutions, water activity from binary data 3-65122
 ternary systems, ideally associated vapour composition rel. to soln., thermodynamics (*Russian*) 3-50864
 thermodynamic stability diagrams of clay minerals in aqueous solution 3-41889
 transition metal carbonyls in gas and liq. soln., vib.-rot. coupling effects on correlation functions 3-67825
 trapped electron, acting potential calc. 3-41858
 1,3,5-trinitrobenzene-aromatic hydrocarbon charge-transfer complexes in glassy solns., temperature effects on absorption and fluorescence spectra (*French*) 3-50847
 turbulent flow along semipermeable barrier, hyperfiltration (*Russian*) 3-63636
 two-phase laminar flow along plane barrier, hyperfiltration (*Russian*) 3-63753
 Ar-N₂ solutions, molecular thermodynamics in normal and critical regions 3-65121
 BaCl₂-heavy water solns., struct. determ. by neutron diffr. 3-60660
 CS₂-carbon tetrachloride optical Kerr effect, depolarised Raleigh scatt. 3-44403
 Cs-NH₃ magnetic susceptibility meas. by Gouy method 3-73172
 H₂O-acetone mixtures, atomic absorption spectra 3-59701
 (NH₄)₂SO₄ aq. soln., optical consts. from attenuated total refl. spectroscopy 3-53074
 Na-NH₃ magnetic susceptibility meas. by Gouy method 3-73172
 NaCl-heavy water solns., struct. determ. by neutron diffr. 3-60660
 NiCl₂-heavy water solns., struct. determ. by neutron diffr. 3-60660

sonar

- see also navigation; underwater sound*
 array simulation facility 3-48301
 correction of ocean depth measurement using computer 3-65543
 dolphin, echolocation, measurement, acquisition, storage, analysis, problems 3-66153
 development and uses of new device (*German*) 3-61606
 echoes from fish and rocks, discrimination 3-51472
 echolocating, bats, sonar ranging, acuity of resolution, species comparison 3-70110
 echolocation, marine dolphins, fresh water dolphin, review 3-70112
 I.f. transmission loss, nomograms 3-42442
 optical information processing, incoherent, applications 3-77978
 sodar, probing of waves and turbulence in statically stable clear-air layers 3-65516
 underwater sound projectors directivity index meas. 3-61941

sonar continued

- video disc television display, improvements 3-51205
sonic boom see shock waves
sonic propagation see acoustic wave propagation
sonoluminescence
 No entries
Soret effect see thermal diffusion in liquids
sorption
see also adsorption; chemisorption; desorption; surface diffusion
 atmospheric heating due to O₃ absorpt., analytic formula 3-61470
 electrolytic mixture transportation across porous membranes, sorption-diffusion model (*Russian*) 3-55988
 gas and vapour, kinetics, high-sensitivity compensation method 3-70475
 glassy polymers, of gases, mechanism 3-46734
 halides with quartz 3-73116
 organic dyes on polymer globules, energy migration 3-69080
 pyrocarbon, Br sorption-desorption kinetics (*French*) 3-46757
 LaCo₅Ni₅-s_x, of H₂, effect on mag. props. and lattice constants 3-58380
 O₂, by Zr, kinetics, at very low press. 3-55140
 SnPb, of NO₂, alloy composition effect on interaction 3-68484
 Zr(OH)₄, granulated, of B and Si from Black Sea (*Russian*) 3-80698
sound see acoustic waves; acoustics
sound amplification see acoustic wave amplification
sound broadcasting see radio broadcasting
sound field see acoustic field
sound generators see acoustic generators
sound intensity see acoustic intensity
sound measurement see acoustic variables measurement
sound propagation see acoustic wave propagation
sound ranging see sonar
sound reproduction
see also audio recording; pick-ups
 photographic paper disc player, feasibility 3-39960
 quadruphonic reproduction, psychoacoustic phenomena 3-45296
 rooms, pulse echograms, spectrum of mild blast effects in acoustical equality testing 3-77324
 sound track system for projector slides (*Spanish*) 3-42595
sound waves see acoustic waves
space charge
see also limited space charge accumulation; space-charge-limited conduction; space-charge limited devices
 amorphous insulator, residual discharge current behaviour (*French*) 3-40481
 anodic oxide film formation, space charge and conc. gradient effects 3-50651
 borosilicate glass, charge build up from electron irradiation 3-44372
 dielectric, double space charge determ. method 3-75941
 dielectric solid, dissipation of uniformly charged layers 3-50514
 electron and ion beams, automated modelling (*Russian*) 3-45839
 electron beams and ion beams, modelling current by automatic equipment (*Russian*) 3-57280
 inhomogeneous mag. field, prism image shift (*Rumanian*) 3-66918
 insulating thin film, rel. to surface pyroelec. effect 3-55529
 insulator, effect of diffusion on space charge currents 3-79704
 mass spectrometer, quadrupole, three-dimensional storage, space charge effect 3-73895
 m.i.s. Schottky barrier diode, VI characs. allowing for tunnelling through space charge region (*Russian*) 3-52908
 m.i.s. structures, h.f. space charge capacitance, theory 3-44156
 m.o.s. structure, lifetime, small photoinjection levels, theoretical analysis (*Russian*) 3-72408
 n⁺-n-n⁺, oscillation mechanism 3-41254
 p-n junction, abrupt, description of space charge region under high level conditions using simple model 3-46890
 p-n junction, capacitance, thermodynamic considerations/ 3-64400
 particles, negatively charged, space charge flow in air, charge depletion mechanism 3-54819
 Penning's discharge cell, negative space charge and potential distribution 3-68125
 perspex, accumulation rel. to dielectric breakdown 3-64604
 piezoelectric substrate, acoustic surface wave correlation by space charge nonlinearity 3-52747
 plasma regular space charge waves amplification and transformation in anisotropic waveguide 3-79136
 plasma space charge waves transformation on density discontinuities 3-79117
 polarisation theory and electrode-discharge effects 3-44072
 polyethylene, charge build up from electron irradiation 3-44372
 prebunching by single gap cavities 3-57270
 proportional gas counters, space charge limited proportionality 3-53982
 Schottky-barrier diode, tunnelling, shot noise (*Russian*) 3-72402
 semiconductor, carrier recomb. in space-charge region 3-60883
 semiconductor, space charge domain mode, carrier concentration effects 3-68633
 semiconductor, unipolar conduction, space charge effects 3-64327
 semiconductor surface carrier waves, transverse mag. field effect 3-55321
 semiconductors, space charge waves effects on adjacent plasma layers 3-79724
 separate medium space-charge convolver 3-51479
 streamers, space charges measurement, probe electron avalanche method 3-40819
 synchrocyclotron, vertical plane space charge effects during injection 3-56833
 uniform dielec. layer, carriers of opposite polarity and equal mobility, admittance calc. 3-41481
 unipolar, electric field meas., soln. (*Czech*) 3-42598
 AgBr, photographic emulsion, behaviour of space charge in impulsed elec. field, effect of sensitisation and presence of crystal impurities latent-image formation 3-53345
 AgBr, pure and doped crystals, existence of subsurface layer of space charges, effect on latent-image process 3-53344

space charge continued

- AgBr and AgBr(Cl) crystals, photographic emulsions, behaviour in pulsed electrostatic field, space charge concept (*Russian*) 3-47594
- AgBr(Cl), photographic emulsion, behaviour of space charge in impulse elec. field, effect of sensitisation and presence of crystal impurities latent-image formation 3-53345
- AgCl, rel. to potential distrib. and permittivity (*French*) 3-41480
- Au-Al₂O₃-Au diode, rel. to time depend. of series resist. and series capacitance (*French*) 3-64415
- CdF₂ dielectric polarization, ionic thermocurrents, reorientation of Na⁺ vacancy and Y³⁺ interstitial complexes, space charge formation 3-44367
- CdS single crystals in indifferent electrolyte solns., photo-effects due to localised electron levels in space charge region 3-53315
- GaAs, space charge region, elec. field modulation by laser light, photorefr. obs. 3-75773
- n-GaAs-Si₃N₄ interface, rel. to energy spectrum of states at boundary (*Russian*) 3-50271
- Ge, nonlinear interaction of Gaussian e.m. beam, kinetic treatment 3-58294
- ⁴He II, liquid, electron bubble electrical props. 3-72243
- (Pb_{0.92}La_{0.08})(Zr_{0.65}Ti_{0.35})_{0.98}O₂ ceramics characterization, porosity and grain size effects 3-55532
- Se, liquid, current oscill. due to space charge domain build up 3-68634
- Se, semiconductor, barrier capacitance determ. 3-79705
- Se-Si, high resistivity, compensated, with Au contact, bound space charge 3-58270
- SiO₂, charge build up from electron irradiation 3-44372
- ZnS-Cu phosphors, relaxation of charge in electroluminescence (*Russian*) 3-80109

space-charge-limited conduction

- see also limited space charge accumulation*
- anthracene, injection of electrons and electron trapping levels, s.c.l. current obs. 3-75755
- current-voltage characteristic, influence of field ionization of traps and charge exchange between them 3-75748
- electron beam, relativistic, uncompensated 3-48965
- metal-insulator-luminor structure, electroluminescence, space-charge-limited injection from insulator 3-50272
- m.i.m. system, charge relay transport under carrier injection conditions 3-60923
- naphthalene, space-charge-limited currents and trap distrib. 3-52849
- naphthalene single crystal, limitation on injected space charge deep trapping 3-64328
- quasi-monopolar semiconductor, field theory of static VI characs., main approx. (*Russian*) 3-52853
- semiconductor, totally depleted, transient photocurrent theory 3-64376
- semiconductor, unipolar conduction, space charge effects 3-64327
- semiconductor with traps, passage of current pulse 3-50213
- semiconductor-metal junction, non-diffusion theory (*Russian*) 3-72403
- solids, general scaling rule derivation 3-72368
- solids thermal noise 3-68628
- Al/tetracene/Au sandwich cell 3-46904
- AsSe glassy film, transient, carrier mobility detn. 3-58268
- CdS single crystal, limitation on injected space charge deep trapping 3-64328
- Se glassy film, transient, carrier mobility detn. 3-58268
- Si, overdepleted, current transients, light pulse excitation 3-64335
- Si, p-n junction, insulating, epitaxial structure, leakage current meas., four-probe method 3-42601
- Si, thermal noise 3-68628
- Si space-charge-limited current of holes, expt. test of $S_V = 4kT(U/I)$ 3-44076
- YIG, n-type, inhomogeneous polycryst., non-Ohmic current behaviour 3-72363

space-charge limited devices

see also limited space charge accumulation

No entries

space-charge limited solid state diodes

see space-charge limited devices

space-charge limited solid state triodes

see space-charge limited devices

space communication links

- see also satellite links; space vehicles; telemetering*
- Jupiter, using Pioneer spin-stabilized vehicle, separation and communications geometry 3-42266
- Mariner 9 TV from Mars orbit, digital image processing 3-59275
- CO₂ laser appl. (*German*) 3-54251

space groups

- see also crystal atomic structure*
- dynamical resonance phenomena 3-68555
- higher-moment test 3-79258
- irreducible representations, matrices 3-52591
- magnetic groups, associated space groups with non-primitive lattices (*French*) 3-79842
- nonpyroelectric, conditions for antiferroelec. dipole config. 3-64614
- P1 and related space groups, symbolic addition procedure 3-49794
- P1 and other noncentrosymmetric symmorphic space groups, phase set 3-49864
- Patterson function as a vector segment system, Fedorov group P1 3-49865
- reality classification, reproduction of Herring test 3-57998
- rhomb degeneration patterns 3-49866
- symmetry projection of wave functions using computer 3-75495
- Ce(MoO₄)₂ structure 3-40876
- RbNb₂O₇F pyrochlores, new cryst. positions for Rb⁺ in Fd3m space group (*French*) 3-40885
- RbCoCrF₆ pyrochlores, new cryst. positions for Rb⁺ in Fd3m space group (*French*) 3-40885
- SnS₂, SnSe₂, energy band calcs. using local empirical pseudopotential method 3-41138
- TiNb₂O₇F pyrochlores, new cryst. position for Ti⁺ in Fd3m space group (*French*) 3-40885

space research

see also artificial satellites; astronomy and astrophysics; space vehicles

- Apollo 15 panoramic lunar photographs, stereophotogrammetric reduction, AS-11 Analytical Plotter system 3-65970
- Apollo 17 for u.v. spectrometer expt. 3-48157
- Apollo window meteoroid detection expt. 3-59328
- Apollo 11-16 results, review 3-45046
- bacterial spores, survival of simulated lunar impact 3-77200
- Earth-viewing missions simulation, global cloud model 3-47832
- energy spectrum of cosmic ray electrons meas. in OGO 5 satellite (*Dutch*) 3-51221
- lunar photography, Itek optical-bar panoramic camera 3-65807
- Mars atmosphere, Mars-2 preliminary results 3-42175
- Mars-2 and 3 automatic interplanetary space probes, optomechanical scanner, image readout system 3-42263
- Mercury, detection of atm. by Mariner-Venus-Mercury 1974 flyby mission 3-61686
- mycology, evaluation of environmental conditions 3-77199
- orbits selection for various missions 3-42111
- out-of-ecliptic craft for solar high latitude research 3-76972
- outer planets, development of US program 3-48158
- outer planets exploration, mission building blocks 3-48159
- Pioneer 10, imaging photopolarimeter optical system 3-48138
- Pioneer 10 probe, instrums. and expts. 3-45245
- Pioneer 9 electric field expt., radial gradients and storm obs. 3-47877
- proton dosimeter development for distributed body organs, use on long space missions 3-53777
- Skylab, expts. operating through scientific airlocks 3-48161
- solar wind interaction with interstellar medium, obs. by future outer planet mission 3-47896
- terrestrial environment monitoring from space, conference (Rome, March-April 1973) 3-50871
- Venera 8 mission and results 3-45040

space science

see space research

space-time configurations

see also general relativity

- 4-surface of stationary volume embedded in 5-dimens. pseudo-Euclidean space 3-48770
- 4-surface of stationary volume embedded in 5-dimensional pseudo-Euclidean space 3-48769
- atmospheric e.m. wave propagation, turbulence, transport velocity dispersion, influence of chaotic component of transport (*Russian*) 3-69592
- calculus based on pairs of null directions 3-48783
- canonical field quantization in Riemannian space-time, nonuniqueness 3-54261
- conformal transformations in space-time (*Russian*) 3-48781
- constraints, based on path independence of dynamical evolution 3-62576
- correlation functions in quantal and classical binary mixtures 3-74152
- covariant field theories on two-dimens. indefinite metric, soluble models 3-42859
- critical dimension in dual models, simple physical interpretation 3-59996
- curved space physical conception 3-51815
- curved space-time, requirement by physical phenomena 3-62587
- Curzon field, generalised, soln. of Einstein eqns. in coupled e.m. and zero-mass scalar meson field 3-48976
- Cylindrically symmetric charged perfect-fluid distribution in general relativity 3-70721
- de Sitter space, infinite, solns. of Dirac eqn., representations of SO_{3,2} 3-66922
- Einstein-Maxwell fields, spacetimes with Killing tensors 3-57140
- Einstein-Maxwell space-times and non-null field, struct. of groups of motions 3-40162
- Einstein-Rosen metric, class of exact solns. for coupled electromagnetic and scalar fields 3-51819
- energy conservation and localization in static Riemannian space-times 3-51822
- essentially nonlinear scalar fields and geometry of space-time 3-54278
- Euclidean-Markov field interpret. in Minkowski space-time framework 3-74312
- first derivative discontinuities of space-time metric tensor 3-40168
- Friedmann space, Coulomb-type soln. of Maxwell eqns. (*Russian*) 3-57142
- Galilei-invariant single particle action 3-54135
- global properties of spacetime manifolds and singularity theorems 3-57136
- gravitation, general covariant two-tensor theory (*German*) 3-48793
- gravitation, geometric interpretation in general relativity 3-74134
- gravitation theories, foundations for analysis of any theory in four-dimensional spacetime manifold 3-59804
- ground state mass and critical dimension of space-time in dual resonance model 3-78155
- imaginary Lobachevski space, relativistically invariant expansion of scalar function 3-73976
- invariant electrodynamics (*Rumanian*) 3-62646
- isotropic space-time, Einstein-Maxwell, place in Petrov classification (*French*) 3-74139
- Kasner space-time V, geodesic motion 3-48786
- kinematics, relativistic, unified space-time trigonometry application 3-51816
- long range forces and broken symmetries 3-57147
- Lorentz manifold V₄, dyadic approach to general relativity 3-74143
- Mach principle, matter representation in general relativity 3-66662
- manifold with projective structure, geometrical constructions 3-57139
- Maxwell's equations covariance 3-74131
- metric inside collapsing or expanding sphere, calc. using null co-ords 3-40164
- metric of two spinning charged sources in equilibrium 3-54147
- Minkowski metric for multidimensional geometry in quantal units, light-cone relations 3-51817
- neutrino field admitting, zero energy and momentum 3-48975
- neutrino fields, space-times admitting two, Petrov type D classes 3-62584

space-time configurations continued

- neutrino sea rel. to missing mass, space-time structure 3-80921
 normal-dominated singularities in static space-times 3-57138
 parallel planes in space-time and possible origin of particles 3-45862
 Petrov classification of class two space-times 3-77877
 Petrov Type I of shear free normal flows of perfect fluid 3-71828
 radiating Kerr metric, nonstatic soln. of Einstein's eqns. 3-59799
 Reissner Nordstrom geometries, existence of generalised ergosphere, energy extraction 3-61638
 Riemann-Cartan, conservation law for current of energy, momentum and/or spin 3-62579
 Schmidt's b-boundary analysis, tangent bundle submanifold 3-77764
 Schwarzschild extended space, maximal foliations 3-42864
 Schwarzschild space-time, radial wave eqn., behaviour of solns. near singular points 3-62582
 Schwarzschild-Kerr metric, complex coordinate transformations 3-45717
 singular space-times, local extensions 3-59794
 spaces of recurrent curvature in general relativity 3-48789
 spherically symmetric metrics, Petrov-Plebanski classification of trace-free Ricci tensors 3-40161
 spinor field quantisation, constant curvature space-time, limit to quantised field in the flat world (*Russian*) 3-48988
 static space-times, null hypersurfaces 3-59800
 symmetries for system of particles with electric and magnetic changes 3-51983
 time coordinate uniqueness for certain singular space-times in general relativity 3-48785
 time-like closed smooth curves, true time evaluation (*Russian*) 3-77880
 virial theorem in general relativity for spherical and stationary axisymmetric spacetimes 3-48774
 Weyl space-times, minimally charged 3-54144

space vehicle power plants

- radioisotope thermoelectric generator, fuel capsule vent system, He, Viking mission to Mars 3-67402

space vehicles

- see also artificial satellites; rockets*
 Apollo 16, 17 obs. of cosmic rays, low energy rel. to solar flares 3-70090
 Apollo 17, obs. of Earth's airglow at 1180-1680 Å 3-69738
 Apollo Lunar Rover tracking using VLBI 3-65958
 charts, space exploration 3-77198
 entry probe, base pressure expt. for planetary atmospheric pressure profile detn. 3-59401
 Explorer 17, obs. of solar event Oct. 27 1972 3-65722
 Explorer 33, obs. of coronal injection profile of energetic particles during solar rotation 1517 3-65719
 Explorer 47, for charged particle meas. expt. 3-70089
 Explorer 47, obs. of alpha-particles in Oct. 27 1972 solar event 3-69841
 Explorer 47, solar particle emission obs., Oct. 27-Nov. 10, 1972 3-69840
 hull puncturing by meteoric impact 3-59315
 interplanetary flight, energy requirements 3-42501
 joined cylindrical-conical-cylindrical shell, elastic wave propag. meas. and calc. 3-70684
 manned, shielding against galactic cosmic ray protons and alpha particles 3-71337
 Mariner 9 Mars orbiter, solar radiation pressure calc. 3-56318
 Mars lander position estimation, in presence of ephemeris biases 3-59403
 microthrusters vapour jets, emission due to light scatt 3-59128
 navigation application of Venus limb radiance, 600-700 cm⁻¹, calculations 3-73452
 navigation technique, optical 3-76999
 Pioneer, for Jupiter research, separation and communications geometry 3-42266
 Pioneer 10, obs. of galactic cosmic ray intensity to and beyond 3.0 A.U. 3-69765
 Pioneer 10 flyby, Jovian ground based obs. backup suggestion 3-69862
 Pioneer Jupiter, magnetic control programme, rel. to interplanetary mag. field meas. 3-48147
 planetary landing site selection system, exptl. and simulation study 3-59402
 plasma probe interaction, collisionless plasmas rel. to Laframboise and Parker theory 3-61612
 proton event, small, detect. from spacecraft inside and outside magnetosphere 3-69743
 re-entry and production of large amounts of NO in Earth's mesosphere 3-69609
 remote sounding from artificial satellites and space probes of Earth and planetary atmospheres 3-47767
 shielding against galactic cosmic ray alpha-particles 3-71343
 shuttle, fluctuating pressure environment prediction 3-46450
 spacecraft surfaces, low plasma densities 3-61562
 trajectory determ., selection of measurable parameters 3-56299
 Vela, solar cosmic ray flux modulation meas. 3-69762
 Venera 8 mission and results 3-45040

spacecraft *see space vehicles***spallation (nuclear) *see nuclear spallation*****spark chambers**

- acoustic, in telescope for obs. of primary cosmic γ -rays, shock wave effects (*Russian*) 3-65550
 ALICE flying spot digitizing system, application to spark chamber and oscilloscope data 3-40024
 calorimeters, rel. to cosmic ray particle energy determ. (*Russian*) 3-62242
 cameras, large wire, with outlet systems and information storage, construction (*Russian*) 3-66324
 controllable, rel. to background estimation in (pe)-diffusion detector (*Russian*) 3-62240
 cosmic ray electron component, 1 to 10 BeV, EM asymmetry method (*Russian*) 3-62241
 current limited, depleted electron columns 3-77643
 data analysis at CNAF 3-77701

spark chambers continued

- discharge isotropic properties, Ne filling at 1 atm., 300 KV pulse, cosmic ray detection (*Russian*) 3-62253
 electrodes, film, damage due to spark discharge, parameters, diagnostic possibilities 3-70398
 emulsion, effect of electron divergence in air gaps on cascade energy meas. (*Russian*) 3-62249
 extra-terrestrial gamma-rays experiment, COS-B satellite, ESRO 3-62223
 ferrite rings, with memory, characts., appls. 3-73872
 four-layer, alcohol vapours + Ne, and pure Ne, performance rel. to cosmic ray detection (*Russian*) 3-62251
 heavy non-relativistic sea level particle detection, ionisation and track measurements (*Russian*) 3-62235
 high-energy physics, supply systems (*Polish*) 3-48543
 pair spectrometer, magnetostrictive read-out, appl. to photon materialisation computer on-line data storage (*French*) 3-48554
 particle track coordinates recording by vidicon automatic system using computer 3-51720
 polarisation parameter meas. in high-energy $\pi\pi$ and Kp interactions, on-line computer system 3-66322
 sparkostrictive wire-chamber, spectrometer, $K_e^+ + K_{\pi^{ee}+}$ decay 3-70411
 superconducting magnets for, prospects (*German*) 3-73870
 threshold electric fields, by r.f. excitation (*French*) 3-40023
 wire, ferrite memory matrices, fabrication method 3-56942
 Pb-plate system, photon-initiated showers between 150 and 450 MeV 3-42637

spark counters

No entries

spark-gap voltmeters *see voltmeters***spark gaps**

- air, operate time, pulsed N₂ ultraviolet laser synchronisation 3-75431
 for d.c. accelerators, breakdown protection 3-70356
 electric field meas. using probe (*French*) 3-63912
 electron temp. meas in quasi-stable pulsed glow discharge in spark gaps with high overvoltages 3-63876
 high-pressure, pulsed, stable, construction and characts. 3-75430
 laser flash initiated, time characteristics of He discharge, experimental results 3-75432
 measurement, nitrogen laser applic. (*German*) 3-59904
 multistage, electrical properties, 4-stage switch description 3-77572
 predischARGE recording (*German*) 3-60646
 sphere gaps and crossed cylinder gaps stressed with impulse voltages, influence of radiation 3-52548
 switching, laser triggered, high pressure gas filled spark gap, 575 kV, nanosecond delay, subnanosecond jitter 3-63911
 trigger mechanism, laser beam applic. 3-66893
 ultra-fast triggered spark gap, for electro-optical devices (*French*) 3-49790

sparks

- see also electric breakdown; lightning*
 air, dry and humid, sparking potentials between concentric sphere-hemisphere electrodes 3-63908
 air, spark-over, fireball, laser irradiation, cooling of heated region, temp. and density distrib., rel. to degree of ionisation (*Russian*) 3-57968
 air laser spark, laser radiation absorption 3-75442
 artificial lightning, sound of thunder 3-41978
 discharge, spectral effects at nonuniform sample on electrodes (*Russian*) 3-70489
 electrostatic, low energy, radio detection 3-75434
 Freon, Freon-air mixture, sparking potentials and swarm coeffs. 3-52544
 gap recovery rel. to ionisation and flow velocity 3-46565
 high current channels radial recovery 3-43705
 high voltage d.c. breakdown, electrostatic criterion 3-68111
 ignition theory using $\mathcal{E}(r)$ -form heat source 3-57965
 laser flash initiated, time characteristics of He discharge, experimental results 3-75432
 laser induced breakdown, optical emission time depend. 3-46554
 sphere gaps and crossed cylinder gaps stressed with impulse voltages, influence of radiation 3-52548
 time consts., of spark discharges initiated by 0.3371 μ s laser beam 3-75448
 underwater, approx. calc. of spark energy (*German*) 3-54881
 underwater spark, resistance, energy balance equation 3-49782
 underwater spark discharges, electromechanical efficiency (*German*) 3-54882
 water vapour, sparking potentials between concentric sphere-hemisphere electrodes 3-63908
⁴He II liquid, charge carrier production by spark discharges 3-72242
 N₂O, electric breakdown, sparking potential measurements 3-63909
 Na⁺, spark spectra 3-49385
 Na⁺ spark spectra 3-49385
 Ne breakdown in large gaps under conditions of preliminary ionization 3-63915

spatial orientation control *see attitude control***special purpose computers**

- Aberdeen section scanner for rectilinear, arc, transverse and longitudinal section scanning 3-42368
 evoked potential audiometry, clinical applic., data processing (*Hungarian*) 3-73575
 hybrid sleep recording scoring system 3-56991
 radioastronomy, data processing systems for 160 MHz compound interferometer (*Japanese*) 3-70086
 single crystal diffractometer, Philips PW 1100, built-in computer for control 3-52560

special relativity

- see also Lorentz transformation*
 action and entropy equivalence, three principles of thermodynamics (*French*) 3-57129
 atomic nuclear charge shielding in electron shell in relation to Einstein's relations of mass velocity (*German*) 3-60353
 charged photon soln. to Maxwell's eqns., formulation 3-51801
 clock paradox, symmetrical definition of simultaneity, Langevin effect 3-62574
 clock paradox in Kerr metric formula 3-70711

special relativity continued

- Doppler effect, absolute space-time theory, Kantor's 2nd order experiment, relativistic and nonrelativistic treatment 3-45713
 e.m. field quantities and Minkowski relations 3-51802
 equilibrium conditions, pivot events, skew symmetric torque tensor, extended bodies 3-45712
 equivalence of action and entropy, cohomology and interdepend. of universal consts. (*French*) 3-54137
 ether theory with postulates taken over from special relativity 3-66643
 fibrous tangent on phase space and commutation rules (*French*) 3-54139
 first-order test, impossibility 3-59792
 Huggins-renormalized electrodynamics, 4-force on system of charged particles 3-48746
 interaction interpretation using Lorentz transformation, muon decay theory 3-74130
 kinematics, visual aids 3-70713
 Lorentz transformations, noncommutativity 3-42860
 Maxwell's equations covariance 3-74131
 medium at rest, modified Lorentz equation 3-66648
 metagalaxy kinematics, apparent magnitude-spectra shift 3-76961
 Minkowski metric for multidimensional geometry in quantal units, light-cone relations 3-51817
 moving objects localisation, Einstein-Minkowski equations (*German*) 3-40160
 multipole radiation from an extended charge-current distribution, relativistic treatment 3-45758
 principle of virtual power 3-57114
 right angled lever in equilibrium frames of reference paradox 3-66645
 rigid body dynamical problem 3-66646
 superluminal inertial frames 3-66649
 tachyons, charged e.m. field, eqns. of motion 3-70710
 tachyons in generalized special-relativity theory, non-emission of Cherenkov radiation in vacuum 3-51818
 twins aging paradox 3-66644
 unidirectional interferometer experiment 3-70712
 velocity of light, gravitational pull (*Spanish*) 3-66647

specific gravity *see density***specific gravity measurement** *see density measurement***specific heat**

- see also Debye temperature; Gruneisen coefficient; specific heat of gases; specific heat of liquids; specific heat of solids*
 antiferromagnet, Heisenberg model, calc. 3-52946
 binary fluid mixtures, λ line, thermodynamic limit and divergence 3-62636
 α -Co solid, lattice temp. dependence determ. using X-ray diffraction methods 3-79508
 critical amplitude discontinuities 3-66715
 critical binary mixture, rel. to coherence length, possible violation of two-parameter universality 3-51843
 electrically conducting materials, thermophysical prop. meas. apparatus, measurement errors 3-53855
 ferromagnet, Heisenberg model, calc. 3-52946
 Heisenberg model, crossover exponent calc. 3-47019
 Ising dilute systems, one-dimens., mag props. 3-46955
 liquid crystals, pretransition phenomena just above clearing point 3-63950
 measurement apparatus, 1.5 to 310 K, adiabatic method, temperature drift corrected, actinide compounds (*French*) 3-56628
 metallic elements, Gruneisen parameter rel. to atomic coordination number 3-41033
 n-vector model, anisotropic classical dominant singularity 3-57164
 n-vector model, specific heat exponent, breakdown of scaling law relations in $1/n$ expansion 3-59818
 planar and Heisenberg model, high temp. series 3-50317
 thermodynamics of anisotropic body of two-dimens. Ising model 3-50324
 thermophysical props. conf., Atlanta, USA, (Aug 1973) 3-71702
 H₂O and isotopes, isobaric specific heat, specific enthalpy at zero pressure, 250 K to 2000 K 3-71709
 Te heat capacity, 99.999% pure polycrystalline specimen, 1.5 to 20 K, Debye temperature 3-41024

specific heat at constant pressure *see specific heat***specific heat at constant volume** *see specific heat***specific heat of gases**

- bubbles, boiling water, heat exchange mechanism, laser diffraction interferometry (*Russian*) 3-46708
 diatomic, undergraduate computer calc. 3-61975
 methane, isobaric heat capacity, equation of state, 0-225°C 3-67894
 thermophysical properties computation and production of self-consistent tables and Mollier charts 3-60510
 H₂ thermodynamic and transport props. calc. using Tabcode-II computer programs 3-60511
 He, thermophysical properties, 4 to 3000 R, pressures up to 15000 PSIA 3-50043
 He, thermophysical props. tables from 2 to 1500 K with pressures to 1000 atmospheres 3-60822
 NH₃, -30-325°C, up to 125 bar 3-71710
 Ne, isobaric heat capacity, adiabatic throttling effect, from 30 to 70 K 3-71707
 O₂, compressed fluid, ht. capacity ratio, from acoustic wave velocity obs. 3-49964
 Xe, low freq. sound vel. meas. in crit. region, compressibility and sp. ht. calc. 3-43533

specific heat of liquids

- alumina, condensed phase, near m.p. 3-72208
 atomic motion in simple liquids, model approach 3-79215
 cast basalt stone, solid, liq., two-phase states, thermal cond., heat capacity, elec. modelling (*Russian*) 3-41057
 ethane, specific heat and applicability of asymptotic laws near critical point 3-72203
 ideal Boson film, specific heat, scaling function 3-66689
 methanol + heptane system, crit. behaviour 3-68383
 polymers, molten, heat capacities 3-67883
 seawater, heat capacity from 5 to 35°C and 0.5 to 22% chlorinity 3-65266

specific heat of liquids continued

- tetrafluorobenzene, adiabatic calorimetry, 11-353K, phase transition enthalpy, liquid entropy 3-46714
 thermophysical properties computation and production of self-consistent tables and Mollier charts 3-60510
 Ar, specific heat and applicability of asymptotic laws near critical point 3-72203
 Ga, rel. to thermal diffusivity and Lorenz ratio 3-68594
 He II, size effects below 1K, normal fluid density, specific heat calcs. 3-79536
 He, in porous media, size effects 3-55104
 He, thermophys. props., 4-3000 R, press. to 15000 PSIA 3-50043
 He, thermophysical props. tables from 2 to 1500 K with pressures to 1000 atmospheres 3-60822
 He submonolayer films, two dimensional evaporation and substrate heterogeneity effects 3-55107
 He superfluid transition under press., static scaling and universality 3-64228
 Ne + H₂ liq. mixtures, heat capacity ratio from molar volume obs., 25-31K, up to 34 atm. 3-49965
 O₂, saturated, ht. capacity ratio, from acoustic wave velocity obs. 3-49964
 Se, hexagonal and liquid in 298 to 1000 K range, enthalpy and temperature of fusion measurement 3-68416
- specific heat of solids**
 alloy, dirty BCS superconductor, vortex struct., specific heat and density of states calc. 3-52927
 amorphous solid, low temp. sp. ht., cellular model 3-55066
 anisotropic Ising system, gap exponents, scaling theory predictions 3-62610
 antiferromagnet, itinerant, model calcs. 3-64471
 1,3-bisdiphenylene-2-p-chlorophenyl-allyl, rel. to paramag.-antiferromag. transition 3-58375
 cast basalt stone, solid, liq., two-phase states, thermal cond., heat capacity, elec. modelling (*Russian*) 3-41057
 copper formate dihydrate, rel. to ferromag. (100) and paramag. (200) interlayer interaction 3-64499
 dilute magnetic alloy, calc. from cond. electron self energy 3-46993
 dilute magnetic alloy, calc. from cond. electron self energy 3-46994
 elastic ferroelectric model, 16-vertex, thermodynamics 3-53066
 ferroelectric finite-ice-rule models, statistical mechanics 3-75947
 ferroelectric KDP model of Wu, including elasticity, thermodynamics 3-68942
 ferromagnet, isotropic Heisenberg, spin pair correlation function determ. 3-75823
 ferromagnetic alloy, dilute, T^{1/2} specific heat term, impurity scatt. of spin waves 3-72464
 glass, mixed nitrate, M(I)NO₃ + M(II)(NO₃)₂ 3-72009
 glass, tunnelling model rel. to temp. laws below 1K, acoustic props. (*French*) 3-40975
 graphite, lattice dynamics, interatomic forces, thermal props., half-continuum model appl. (*German*) 3-72158
 graphite, range 1500 to 3000 K, pulse heating meas. method 3-75627
 graphite, thermal properties, theoretical exposition with associated experimental data 3-72153
 Heisenberg ferromagnet, second-order Green function approach 3-44191
 Heisenberg ferromagnetic spin system, direct temp. depend. 3-79819
 high temp. expression, one dimens. anharmonic lattice model 3-50006
 Hubbard model, half filled band, thermodynamic and dynamic high temp. props. 3-41324
 ice, relaxational proton ordering and glassy crystalline state, heat capacity meas. 3-64135
 inert gas, Gruneisen parameter at T=0 K, first-order self-consistent phonon calcs. 3-46691
 Ising amorphous ferromagnet, fluctuations, perturbation theory 3-79810
 Ising and Heisenberg models scaling functions, comparison with Ni 3-50329
 Ising model, three-dimens., two points correl. functions analysis 3-52941
 Ising model, transverse, calc. 3-58115
 liquid metals, 1100-2100 K, thermal capacity, diffusivity and conductivity, simultaneous meas. 3-42543
 lithium ammonium tartrate, sp. ht. anomaly near transition temp. 3-47221
 magnetic, high freq. relax. meas. method 3-48484
 magnetic, specific heat data in critical region 3-75836
 mathematical framework, solved problems, book contrib. 3-58133
 mean energy value of system with limited or band energy spectrum (*Russian*) 3-72302
 metal, changes during A1 to A2, A3 to A2 polymorphic transitions 3-58136
 metallic thin films at liquid He-3 temps., microcalorimetry meas. 3-55091
 molecular crystals, C_p-C_v, calc. using temp. depend. of lattice freq. (*Russian*) 3-50007
 nearly one-dimensional metallic conductor, model approach 3-50100
 polyethylene, crystalline, specific heat C_p rel. to C_v, vibrational spectra calc. 3-55089
 polyethylene, pressure dependence from 0 to 25 kbar 3-43881
 polyethylene filled with wood flow, dielectric and thermophysical props. meas. 3-65006
 polyhexene-1, amorphous, cooling rate influence on heat capacity and thermal transitions 3-50008
 polymer crystal, acoustic phonon effects (*German*) 3-60777
 polymers, heat capacities 3-67883
 polyoxymethylene, heat capacity, calc. from frequency distrib. 3-55088
 pulse method meas. at high pressure 3-77404
 pulsed electron beam method, simultaneous specific heat and thermal diffusivity meas. 3-45447
 rare earth platinides, RPt₃, R=La, Ce, Pr, Nd, low temp. sp. ht. and mag. props., model 3-46946
 Schottky sp. ht., effect of spin-phonon coupling 3-72205

specific heat of solids continued

- semimetal thin films, three-dimensionally quantised, electronic heat capacity 3-58263
- shock wave condensed media compression, temp. estimation by thermodynamic method (*Russian*) 3-79423
- superconducting thin film, specific heat, peaking, screening-approximation prediction 3-55354
- superconductor, small grains, theory 3-52921
- superconductor with cryst. field split impurities, specific heat and upper crit. field 3-68714
- superconductors, strong-coupling, quasiparticle phenomenology for thermodynamics 3-72416
- superconductors in mixed phase, measurement 3-62033
- TCNQ salts, sp. ht. and mag. susceptibility, 1.4-4.4 K, rel. to band struct. 3-46795
- tetrafluorobenzene, adiabatic calorimetry, 11-353K, phase transition enthalpy, liquid entropy 3-46714
- transition metal solid solns., electronic heat capacity, alternative to rigid band model 3-79497
- 1,3,5-trinitrohexahydro-s-triazine, heat capacity measurement in range 5 to 278K 3-80059
- TTF TCNQ, in low temp. phase, 89.5 K Debye temp. meas. 3-79500
- two-dimensional ferromagnetic Heisenberg spin systems 3-52942
- Ag, lattice heat capacities calc. using an extended de Launay's model 3-55056
- AgBr-CuBr mixed crystals., phase behaviour and lattice disorder, calorimetric obs. (*German*) 3-64184
- Ag₃In, order-disorder transition behaviour 3-64831
- Al, lattice heat capacities calc. using an extended de Launay's model 3-55056
- Al, temp. depend., influence of quasi-local vibrs. due to Ag addition (*Russian*) 3-68417
- Al and Al-Si(8 wt.%) alloy, 10-270K (*Russian*) 3-79499
- Al and dilute alloys, supercond., energy gap anisotropy obs. 3-60929
- Al₁₀V, Einstein solid, crystal struct., localised phonon mode domination 3-40865
- Al₁₀V, Einstein solid, low temp. specific heat and electrical resistivity meas. 3-43855
- Ar, calc. of lattice heat capacity 3-72147
- Au:V, lattice specific heat reduction due to V impurities 3-55065
- B₂O₃, suboxide, 40 to 600°C 3-68421
- Be, phonon dispersion relations, lattice specific heats 3-64121
- Bi:Te, nuclear quadrupole heat capacity 3-68559
- C, soft, sp. ht. at room temp. 3-46716
- Cd and dilute alloys, supercond., energy gap anisotropy obs. 3-60929
- CdHg₃, calorimetric and vibrational studies 3-52706
- CdO(c), heat capacity meas., 298-1800 K, drop calorimetry and differential scanning calorimetry 3-46717
- α -Ce, valency, electronic specific heat, mag. susceptibility, localised 4f with band states model 3-46973
- CeCl₃, mag. contrib. to sp. ht, Debye temp., mag. susceptibility, 0.05-4.2 K 3-41335
- Ce_{1-x}Gd_xRu₂ mag. transition, supercond. transition, 1.8-20K 3-55350
- Ce_{1-x}Tb_xRu₂ mag. transition, supercond. transition, 1.8-20K 3-55350
- Ce_{1-x}Y_xRu₂ mag. transition, supercond. transition, 1.8-20K 3-55350
- CoF₂, magnetic, temp. derivative of linear magnetic birefringence 3-47227
- CoO, range including Neel temp. 3-58379
- Cr, state-depend. potentials calcs. 3-79615
- Cr-N system, thermodynamic props. characteriz. 3-55845
- Cr₃Te₄ from 298 to 950 K, order-disorder transition 3-68408
- Cs halides, thermal expansion and Gruneisen parameters at low temp. 3-43885
- CsMnBr₃, antiferromag. ordering obs. 3-47060
- CsNiF₃, meas. rel. to ferromag. chain structure 3-58392
- Cu, by automatic calorimetry 3-42536
- Cu, lattice heat capacities calc. using an extended de Launay's model 3-55056
- Cu, plastically deformed, discrepancy between sp. ht. and stored energy data 3-64186
- Cu:Sn, low temp. lattice sp. ht. enhancement by Sn impurities 3-55087
- Cu-Al alloy, temp.-wave method, derivation from thermal diffusivity and conductivity 3-51545
- α -Cu-Al alloys, local atomic arrangements and anomalous behaviour 3-50715
- Cu-Au(Fe) alloy, Kondo effect obs. 3-50344
- Cu-Co alloy, dil., 1.6-4.2K, in mag. field 3-47042
- Cu_{0.4}Cd_{0.6}Fe₂O₄, crit. props. near Curie point 3-75840
- Dy, dispersion relations and lattice thermal expansion 3-79456
- Dy(OH)₃, Schottky anomaly calc. between 10 and 300 K 3-79840
- Er(OH)₃, Schottky anomaly calc. between 10 and 300 K 3-79840
- Er₂Ni₂, antiferromagnetic, low temp. props. 3-79835
- EuO, heat capacity near mag. phase transition 3-44217
- EuP(As)(Sb)(Bi), low temp. anomaly 3-55433
- Fe-Cr(Al)(V) alloys, Fe-rich, 600-1200K 3-72468
- Fe-Ti alloys, Fe-rich, 600-1150K, Curie temp. determ. 3-50363
- FeCo, ordered and disordered system at low temp., electronic and harmonic phonon contributions 3-64185
- FeF₂, magnetic, temperature derivative of linear magnetic birefringence 3-47227
- FePd₃, ordered and disordered, electronic specific heat rel. to hydrogen solubility 3-55090
- Ga₂O₃(c), heat capacity meas., 298-1800 K, drop calorimetry and differential scanning calorimetry 3-46717
- GaS(Te), adiabatic calorimeter, below room temp. 3-68418
- GaSb, Gruneisen coeff., temp. depend. of i.r. dispersion obs. 3-50583
- Gd, effect of impurities on heat capacities at paramagnetic to ferromagnetic transition 3-52975
- Gd, exchange coupling and macroscopic props. 3-47013
- GdNi₂, magnetic sp. ht. anomaly at critical point 3-47032
- ³He, b.c.c., low temperature specific heat anomaly 3-43920

specific heat of solids continued

- ³He submonolayers adsorbed on solid air, sp. ht. anomalies, 0.5-6K 3-46745
- Hg, calorimetric and vibrational studies 3-52706
- HoPo₄, magnetic phase transition to antiferromagnetic state, Neel temp. 3-55428
- In(SrTe), adiabatic calorimeter, below room temp. 3-68418
- Ir thermal props. at high temps. 3-79666
- KCl, low temp. sp. ht., influence of heavy Pb²⁺ impurities 3-58135
- KCl:Ti, lattice sp. ht., force const. change effects 3-41026
- KO₂ crystals., mag. transform. behaviour (*German*) 3-50361
- Kr phonon dispersion relations, lattice heat capacity 3-68346
- LaSn₃In_{3(1-x)}, electronic coeff. rel. to local electronic props. 3-46803
- LiHg₃, calorimetric and vibrational studies 3-52706
- Mg, phonon dispersion relations, lattice specific heats 3-64121
- MnF₂, magnetic, temperature derivative of linear magnetic birefringence 3-47227
- Mo:Re alloy, analysis of lattice specific heat 3-58134
- MoS₂, MoSe₂, MoTe₂, lamellar lattice, heat capacity, thermodynamic props. 3-41028
- (NH₄)₂BeF₄, temp. depend., nonlinearity, phase transitions 3-72207
- NH₄Br, specific heat anomaly near orientational phase transition 3-49995
- (NH₄)₂Cd₂(SO₄)₃, paraelectric to ferroelectric transition, specific heat meas. 3-55537
- NH₄Cl, near phase transition point, pressure effects up to 3.6 kbar 3-52701
- Na halides, thermal expansion and Gruneisen parameters at low temp. 3-43885
- NaNH₃SeO₄.2H₂O, temp. depend. and anomaly at ferroelec. transition 3-50009
- NaNO₃, phonon dispersion and phonon densities 3-55059
- Na₂O-GeO₂ glass, 1.5-25 K 3-72206
- Na₂O-SiO₂ glass, 1.5-25 K 3-72206
- Nb superconducting, anomalous sp. ht., supercond. energy gap 3-46920
- Nb-Zr (1 wt.%) alloy, sp. heat, electrical resistivity and hemispherical total emittance determination 3-64971
- Nb₃Sn, supercond., cubic A-15 phase stabilization, a.c. heat capacity meas. 3-64422
- Ni, complex, hexapyridinenickel (II) nitrate, heat capacity 13-300 K, order-disorder transitions (*French*) 3-49961
- Ni, lattice dynamical model approach 3-68343
- Ni, lattice heat capacities calc. using an extended de Launay's model 3-55056
- Ni, scaling functions, comparison with Ising and Heisenberg models 3-50329
- Ni-transition metal dil. alloys, electronic sp.ht., virtual bound levels model (*French*) 3-46715
- Ni₃Al, low temperature, heat treatment effect 3-44216
- NiF₂, antiferromagnetic, magnon contrib., magnetic field effects 3-47075
- NiF₂, magnetic, temp. derivative of linear magnetic birefringence 3-47227
- Ni₃Fe, heat capacity, exptl. data from 300 to 1670 K 3-79841
- Ni₂Ga, low temperature, heat treatment effect 3-44216
- Ni(II) complex, Ni(N₂H₃)₂(SO₄)₂, applicability of Heisenberg linear chain model 3-47007
- NiO, range including Neel temp. 3-58379
- (Ni_{1-x}T_x)₂B, electronic specific heat, transition metal impurities, density of states at Fermi level 3-41118
- Ni₃Te₄, 298-950K, order-disorder transition 3-68408
- Pb-Se, Debye temperature determ. 3-68372
- Pd, calculation using lattice dynamical model 3-79444
- Pd, lattice heat capacities calc. using an extended de Launay's model 3-55056
- Pd, Pd-Ni alloy, temp. depend. of Debye temp. 3-72155
- Pd-Cr, localised spin fluctuations, low temp. specific heat obs., Pd-Ni comparison 3-68768
- Pt, pulsed electron beam method, simultaneous specific heat and thermal diffusivity meas. 3-45447
- Pt-Cr, localised spin fluctuations, low temp. specific heat obs., Pd-Ni comparison 3-68768
- Pu-Fe, (10at.%Fe), eutectic, rel. to order-disorder and antiphase structure 3-60799
- Rb halides, thermal expansion and Gruneisen parameters at low temp. 3-43885
- RbMnF₃, heat capacity near mag. phase transition 3-44217
- RbNiF₃, spin wave sp. ht., a.c. temp. calorimetry, 1.5-4K 3-50381
- Rh thermal props. at high temps. 3-79666
- Se trigonal and vitreous, 3 to 300 K, heat pulse measurement method 3-52707
- SrTiO₃, heat capacity in vicinity of phase transition at 110 K 3-79490
- Ta-W (10wt.%W), elec. resist., specific heat and emittance at 1500-3200K, high-speed simultaneous meas. 3-52705
- Ta₂S₃, 4Hb-type, temp. depend. 3-55084
- Tb, exchange coupling and macroscopic props. 3-47013
- (Ti,V)₂O₃ systems, sp.ht. anomalies, electronic d levels 3-64303
- TiO₂, rutile, Gruneisen coeff. for soft mode 3-41027
- Ti₂O₃, anomalies in meas. near elec. transition 3-43882
- Ti₂O₃(c), heat capacity meas., 298-800 K, drop calorimetry and differential scanning calorimetry 3-46717
- α -U, heat capacity and transforms, 2-70K 3-47041
- UO₂, high temp. model, Debye approx. and anharmonicity terms 3-52704
- V, state-depend. potentials calcs. 3-79615
- V-Ta, phonon spectrum change with Ta addition, specific heat meas. 3-75580
- VO₂ single crystal, heat capacity meas. above and below metal-semicond. transition 3-41025
- W, comparison of meas. values at high and low temp. 3-72975
- W, normal state heat capacity 0.35-25 K, crit. field for supercond. 3-79785
- Y(OH)₃:Er³⁺, Ho³⁺, Schottky anomaly calc. between 10 and 300 K 3-79840
- YbAl₂ and YbAl₃, ambivalence of Yb 3-68552

specific heat of solids continued

Zn and dilute alloys, supercond., energy gap anisotropy obs. 3-60929

ZnO(c), heat capacity meas., 298-1800 K, drop calorimetry and differential scanning calorimetry 3-46717
 ω -Zr, temp. depend., 80-280K (*Russian*) 3-79665

specific volume see density**specimen preparation**

see also replica techniques

blood sampling device, rapid drawing of 10 samples 3-59679
 cellulose fibres, internal microstructure, electron microscopy, prep. technique (*Russian*) 3-47479
 cermet, oxides, colour contrast layer formation, gas etching technique, microscope obs. (*German, English*) 3-69240
 colour contrast layer formation in gas-ion-reaction chamber under electron irradi., microscope obs. (*German, English*) 3-69239
 composite materials, colour contrast layer formation, gas etching technique, microscope obs. (*German, English*) 3-69240
 composite metal powders, for X-ray fluorescence analysis 3-62336
 critical point drying, water miscible solvents, scanning electron microscopy, nematodes, barley leaves, clover roots 3-54027
 electron microscope disc specimens, by u.s. impact grinding 3-40049
 freeze dryer, centrifugal, for small-volume multiple fractions of solvents 3-66453
 glow-discharge cleaning 3-48562
 ion-bombardment thinning for TEM of ceramics 3-57977
 lung, lamellated osmiophilic bodies, electron microscopic methods, specimen preparation 3-54026
 mammalian tissue, ultrathin frozen dried sections, elemental composition, transmission electron microscopy, X-ray microanal. 3-56476
 metal, colour contrast layer formation, gas etching technique, microscope obs. (*German, English*) 3-69240
 metal, transmission electron microscopy specimen, thinning and dissolving out (*German, English*) 3-64865
 oriented clay mineral specimen preparation for X-ray diff. anal. by filter-membrane peel technique 3-51159
 oxides, colour contrast layer formation, gas etching technique, microscope obs. (*German, English*) 3-69240
 petrographic flexible thin section preparation 3-59152
 powder separation technique for microscopy 3-42556
 SEM, nonconductive samples, partial charging prevention 3-70435
 t.e.m., proportion of thin metallic sheets (*Slovak*) 3-54010
 thick biological sections, for h.v. electron microscopy 3-48578
 tissue cellulose, microfibrillar structures, effect of staining and freeze etching, electron microscopy 3-57000
 ultramicroscopic particles, SEM X-ray spectrometer 3-70421
 whole body sections, staining, spray-on mountant, Trycolac 3-56477
 Al, flat crystals., electrolytic edge planing, for plasticity meas. 3-80388
 GaAs, jet etching for transmission electron microscopy (*German*) 3-52618
 Ir thin films for transmission electron microscopy by electropolishing 3-48575
 Nb, twin-jet thinning technique for transmission electron microscopy 3-50085
 Ta, twin-jet thinning technique for transmission electron microscopy 3-50085
 Zr alloy corrosion film thinning for transmission electron microscopy (*German, English*) 3-61157

spectra

see also alpha-particle spectra; astronomical spectra; atmospheric spectra; atomic spectra; beam-foil spectra; beta-ray spectra; Brillouin spectra; chemical shift; electron spectra; energy level crossing; gamma-ray spectra; isomer shift; light scattering; luminescence; mass spectra; microwave spectra; molecular spectra; neutron spectra; nonradiative transitions; proton spectra; spectra of inorganic liquids and solutions; spectra of inorganic solids; spectra of organic molecules and substances; spectra of solids; spectral line breadth; spectrochemical analysis; Stark effect; x-ray spectra
 absorption line frequency, least square convolution, curve fitting 3-73750
 alkali metal in amine solns., absorpt. spectra decay rates, temp. and solvent depend. 3-53355
 attenuated reflection spectra, optical consts. determ. by Kramers-Kronig method 3-68957
 biexcitonic molecules in crystal, Jahn-Teller effect 3-68583
 birefringent materials, band gap determ. by refl. meas. with polarization modulation 3-68549
 blood, erythrocytes, size and concentration distribution functions determ., spectral transmission method (*Russian*) 3-81260
 condensed matter, absorpt. with simultaneous energy transfer from excited impurity 3-44440
 crystal impurity molecules, nonlinear oscillation i.r. spectra 3-68362
 crystal with impurity molecule, effect of electron-phonon interaction on mirror symmetry of spectra 3-69092
 crystals, differential, modulated by energy parameters complex dielectric function 3-50557
 crystals, stimulated antiresonance in optical spectra 3-58495
 discharge tube spectra, student experiment 3-70249
 disperse system, particle size and concentration distribution determ. from mutual dispersion coefficients attenuation (*Russian*) 3-80506
 Earth tide anal. using spectral summation 3-56245
 electrophotographic layers, optical constants and structure properties, diffuse reflection spectra, binding material (*Russian*) 3-77559
 energy cooperation, coherent and u.s.-stimulated via elementary excitations 3-75969
 energy-current, charged particle, photographic oscillograph method 3-73807
 exciton spectra, effect of exciton interactions 3-79650
 geomagnetic line spectra in 2 to 70 years range, detection of solar cycle variations 3-53603
 gravity curve anomalous force spectra, appl. of Feelon method (*Russian*) 3-47653
 gravity wave directional spectrum determ. using programmed aircraft laser altimeter 3-51165

spectra continued

impure crystals, hydrostatic pressure effects, model (*Russian*) 3-44433
 i.r., multiband systems, classical dispersion analysis, self-bracketing search technique 3-56667
 i.r. absorption by crystals in h.f. wing of fundamental lattice absorption 3-58094
 Lake Ontario nearshore region, kinetic energy region 3-58977
 liquid, far infrared, interpret. in terms of collision distrib. 3-80058
 liquid, i.r. absorpt. band profiles, mol. dynamics obs. (*French*) 3-80018
 mixed crystals, exciton absorpt. band profiles, theory 3-64634
 molecular crystals, absorpt., luminesc., exciton band struct. 3-69070
 molecular crystals, collective effects 3-68971
 molecular crystals, low temp. i.r. Fourier transform spectroscopy 3-76000
 multipole-multipole point interactions, planewise summation 3-55562
 ocean bubble spectra, effect of bubble soln. on air-sea gas exchange 3-50990
 ocean wave height spectra meas., shipboard obs. 3-53448
 oceanic seven second ocean waves, directional spectra 3-59018
 optical, degenerate exciton, Jahn-Teller effect 3-50152
 ordered magnetic crystals, effect of dipolar forces on response functions, and light scatt. spectra 3-68795
 photon spin echo phenomena, transient and stationary regimes (*French*) 3-55482
 Pi2 micropulsation spectra along meridional profile 3-56106
 polyexcitonic molecules in crystal, Jahn-Teller effect 3-68583
 power density spectra, by fast Fourier transform 3-42460
 quantal energy spectrum of dynamical system with N degrees of freedom 3-66622
 scanning system output, spatially periodic signal spectral struct. 3-42554
 sea surface, wind-roughened, and curvature spectra 3-59017
 seismic P-wave amplitude spectrum rel. to focal depth 3-61348
 seismic P-waves, effect of crust structure in region of seismic station (*Russian*) 3-65159
 semiconductor, polar, i.r. free polaron absorpt., temp. depend. 3-55591
 solid, two-photon transitions near thresholds, electric field effect 3-80008
 solvation dynamics of excess electron, picosec. spectroscopy obs. 3-61284
 stabilization without reference peaks, expt. 3-73760
 surface electric field effects in refl. and first-derivative modulation spectra 3-69013
 three-component solutions, statistical approach to electronic spectra 3-64633
 transition radiation in a.c. electric field 3-68298
 transitions, adiabatic and nonadiabatic, average transition probability, calc. (*Russian*) 3-68969
 turbulence, using solid state hot wire anemometer feedback controller 3-47830
 velocity response envelope spectra of Pacoima Dam accelerometer Feb. 9 1971 as function of time 3-56019
 Ag, colloidal, spectral extinction 3-44688
 Tb³⁺ in DMSO, radiative and nonradiative transitions rel. to energy transfer model 3-64732

spectra of diatomic inorganic molecules
see also radiofrequency spectra of diatomic inorganic molecules
 alkali halide optical spectra interpretation with aid of molecular beam scattering data 3-54667
 fine structure due to vibrational and rotational motion, astrophysics and atmospheric applications 3-40604
 HCl⁺, emission intensity of vibrational bands in A² Σ →X² Π transition, rel. to DCl⁺ and HBr⁺ 3-78744
 homopolar isotopically unsymmetric molecules, forbidden transitions 3-78708
 Hund's coupling case, rot. energy and fine struct. of electronic states 3-63423
 Hund's coupling case, rot. energy and fine struct. of electronic states 3-67785
 metal oxides, absorpt. coeffs. for CO₂ laser radiation, rel. to interaction at metal surface 3-70837
 molecular constants determination, term value approach 3-78707
 non-polar mol., in noble gas matrices, non-random trapping, frozen-oscillator model 3-76038
 photosphere, C₂, CH, CN, MgH, NH and OH molecular lines and oscillator strengths 3-69829
 reduction to molecular constants, construction of RKR potentials 3-78706
 RKR potentials, centrifugal distortion constants 3-78705
 RKR potentials and semiclassical centrifugal consts. 3-67779
 rotational line intensities, theory 3-78717
 rotational line intensity factors for transitions, computer checking 3-63426
 AlO, D² Σ^+ - X² Σ^+ system, u.v. region, rotational and vibrational constants 3-60450
 AlO, electric dipole transitions, band oscillator strengths 3-43433
 AlO, fundamental vibration-rotation bands, relative spectral absorption coefficients 3-54683
 AlO, Morse oscill., Franck-Condon factor calc. by generalised WKB approx. 3-74986
 AlS radical, A² Σ^+ - X² Σ^+ transition, emission spectrum (*French*) 3-46259
 Ar₂ vacuum u.v. spectra in solid Ne 3-71546
 AsF₃, Hund's coupling case 3-67785
 AsO, emission spectra, rot. analysis 3-63439
 AsO, pair perturbations in electronic spectra, exptl. data processing method (*French*) 3-52347
 AsS, analysis of A² π -X² π band system 3-40613
 AuGa, rot. struct., incompletely resolved 0-0 band, isotope effect determ., visible spectrum (*French*) 3-43423
 BBr, singlet-triplet transition, discharge spectroscopy (*French*) 3-67800
 BF, resonance fluorescence from A¹ Π states 3-78838
 BO- α system, τ -centroids calc. 3-71531

spectra of diatomic inorganic molecules continued

- BaO, microwave optical double resonance obs. using c.w. dye laser 3-78039
- C₂ molecular lines and oscillator strengths in photosphere 3-69829
- C₂ Phillips bands, absence in solar photospheric spectrum 3-6661
- C₂ Swan bands from discharge through Ar+ trace benzene, emission study 3-52368
- C₂⁻, oscillator strength of B²Σ⁻→X²Σ⁻ transition, shock-tube determ. 3-54670
- CH, term values and molecular parameters for rotational and vibrational levels in visible and near u.v. region 3-75010
- CH molecular lines and oscillator strengths in photosphere 3-69829
- CH⁺, oscillator strengths for X²Σ⁺→A¹Π system 3-70028
- CH⁺, term values and molecular parameters for rotational and vibrational levels in visible and near u.v. region 3-75010
- CN, electric dipole moment of A²Π state meas. by level anticrossing spectroscopy, Stark effect 3-75001
- CN, excitation cross sections of red system bands 3-75009
- CN, red system, model stellar atmosphere opacity code 3-69923
- CN molecular lines and oscillator strengths in photosphere 3-69829
- CO, absorpt. spectrum atlas, 1060-1900 Å 3-75007
- CO, Cameron system, oscillator strengths 3-52363
- CO, diatomic mols. trapped in Ne matrix, absorpt. spectra, vibr. and rot. struct. 3-75011
- CO, i.r. spectra of air pollutants 3-53471
- CO, Ne gas mixture, vibration relax. rates, Landau-Teller model, i.r. spectra 3-75140
- CO, pure and in Ar matrix, absolute i.r. absorption intensities, band shapes 3-80061
- CO, RKR pots. and semiclassical centrifugal consts. 3-67779
- CO, vibrational-rotational, classical calc. of intensity distribution 3-74984
- CO absorption cross sections from 180 to 700 Å 3-67805
- CO bands in spectra of χ Cygni, variable 3-45132
- CO beam-foil forbidden lines transition probabilities rel. to astronomical spectra 3-78430
- α -CO chemisorbed on polycrystalline tungsten, reflection-absorption i.r. spectra, ultra-high vacuum 3-44417
- CO emission in Martian dayglow 3-65743
- CO fourth positive system, excitation by dissociative recombination of CO₂⁺ ions 3-78860
- CO lines in i.r. solar spectrum, balloon-borne observations 3-56314
- CO obs. in 32 H II regions, 6 supernovae remnants and Cygnus A 3-45214
- CO(A¹π), deactivation rel. to individual vib. levels 3-75150
- CS, gas-phase, lifetime meas. 3-40603
- CS₂, emission spectrum meas., 3060-2680 Å, obs. of new band system, rotational analysis 3-78743
- C⁸⁰Se, emission spectrum analysis 3-60446
- ¹²C¹⁶O, absolute wavenumbers of 2←0 vibr. rot. band, near i.r. standards 3-56611
- ^{12,13}C¹⁶O vib.-rot. lines near 4.7 μ in i.r. sources IRC+10216, VY Canis Majoris and NML Cygni 3-69951
- CaF, u.v. thermal emission using vacuum furnace 3-54672
- CrS, thermal emission using vacuum furnace 3-54673
- CuBi, rotational analysis of A and B systems (French) 3-57642
- D₂, Lyman and Werner bands, vacuum u.v. spectra, vibr. and rot. level anal. 3-40615
- n-D₂, modification in calc. half-width of depolarised Rayleigh line 3-63436
- DCl, i.r. spectra, dipole moment function, vibration-rotation matrix elements determ. 3-52351
- DCl, vacuum u.v. absorption spectrum, analysis of autoionising Rydberg states 3-40618
- DCl⁺, emission intensity of vibrational bands in A²Σ⁺→X²Π transition, rel. to HCl⁺ and HBr⁺ 3-78744
- Eul 4f⁷(⁸S)6s² level, hyperfine struct. of y₈P-multiplet by determ. by level crossing method 3-46315
- F₂, beam-foil lifetime meas. in vacuum u.v. 3-78747
- F₂, F₂⁺, F₂²⁺, pot. energy curves and spectroscopic consts. calcs. 3-71496
- GeF, rotational structure in emission transitions of higher electronic states 3-78742
- GeO, emission band spectrum 3-52355
- GeO, Franck-Condon factors and r-centroids for (A-X) system 3-67797
- H⁺+H, quasi-molecule formed during collision 3-71455
- H₂, collision-induced fund. band in H₂-He and H₂-Ne mixtures 3-63540
- n-H₂, modification in calc. half-width of depolarised Rayleigh line 3-63436
- H₂ quadrupole lines in Jupiter's atmosphere 3-47914
- H₂-rare gas mixtures, i.r. absorpt. quadrupole-induced transitions, diffusional narrowing 3-78882
- HBr⁺, emission intensity of vibrational bands in A²Σ⁺→X²Π transition, rel. to DCl⁺ and HCl⁺ 3-78744
- HCl, 87 to 200 torr, 163 to 208 K, i.r. absorpt. spectra (French) 3-46283
- HCl, absorpt. line broadening by gases, fund. band, temp. depend. 3-63544
- HCl, i.r. spectra dipole moment function, vibration-rotation matrix elements determ. 3-52351
- HCl, in N₂ matrix, i.r. absorpt., isotopic effects 3-75045
- HCl, vacuum u.v. absorption spectrum, analysis of autoionising Rydberg states 3-40618
- HCl gaseous mixtures with HBr and HI, low temp. absorpt. spectra (French) 3-78750
- HCl i.r. bonds, amplification and displacement, depend. on hydrogen bond energy (Russian) 3-49473
- HCl lineshifts and widths due to inert gas broadening of vibration-rotation lines 3-43467
- HCl⁺, emission spectra of four isotopic combinations 3-78739
- H³⁵Cl, rot. consts. calc., optimum number and accuracy considerations 3-63416
- HI, i.r. spectra in solid matrices at 20 K 3-54690
- He₂, ab initio calc. of A¹Σ_g⁺←X¹Σ_g⁺ absorpt. spectrum 3-63445
- He₂, optical states caused by α irradiation of high pressure mixture 3-63343
- He₂, singlet and triplet states characteriz., emission spectra 3-67802
- HfBr, new emission spectrum in the visible 3-67806

spectra of diatomic inorganic molecules continued

- Hg₂, 550 nm emission band due to ²Δ_u→³Δ_u collision-induced transition 3-60444
- HgH, Hund's coupling case 3-67785
- H₂ quadrupole absorption in Jovian atmosphere, Curtis-Godson approx. 3-47911
- I₂, continuous absorption below the band convergence limit in the B←X transition 3-60445
- I₂, continuous spectra assignment by photofragment spectroscopy, C state obs. 3-63535
- I₂, excited atom quenching by O₂, opto-acoustic spectra obs. 3-78883
- I₂, high-resolution spectroscopy using laser-mol.-beam technique 3-40643
- I₂, improved spectroscopic data synthesis and J depend. predictions for transition intensities 3-63421
- I₂, RKR pots. and semiclassical centrifugal consts. 3-67779
- I₂, reson. Raman scatt., spectral var., excitation freq. depend. 3-40633
- I₂, variable temp. photoelectron spectra, adiabatic ioniz. pot. 3-40658
- I₂, visible emission spectra 3-78738
- Kr₂ vacuum u.v. spectra in solid Ne 3-71546
- LiO, A²Σ⁺←X²Π system predictions 3-43451
- LiO, electric dipole transitions, band oscillator strengths 3-43433
- LuH, electronic spectra, rotational analysis (French) 3-54659
- LuO, pair perturbations in electronic spectra, exptl. data processing method (French) 3-52347
- MgH molecular lines and oscillator strengths in photosphere 3-69829
- MgO, F¹Π-X¹Σ electronic transition 3-52361
- MgO, G¹Π-X¹Σ and G¹Π-A¹Π transitions assignment 3-71542
- MnS, thermal emission using vacuum furnace 3-54673
- N₂, ¹Δ_g⁺ state, correlation with unidentified 6895.5 Å and 8937.0 Å bands 3-74964
- N₂, deperturbation of Worley-Jenkins Rydberg series 3-49458
- N₂, diatomic mols. trapped in Ne matrix, absorpt. spectra, vibr. and rot. struct. 3-75011
- N₂, Einstein transition probability, for W³Δ_u←B³Π_g system 3-40627
- N₂, electron impact, dissociative excitation, extreme vacuum u.v. spectra 3-75117
- N₂, emission B³Π_g state vibrational levels, absolute populations determ. 3-75008
- N₂, isotopic analysis (Rumanian) 3-62113
- N₂, lifetime of D³Σ_g⁺ state 3-75005
- N₂, modification in calc. half-width of depolarised Rayleigh line 3-63436
- N₂, perturbation of electronic transitions under foreign gas pressure 3-75012
- N₂, photoabsorption coeffs. from 400 to 650 Å using synchrotron radiation 3-40566
- N₂, photoabsorption coeffs. in 300-700 Å region 3-46262
- N₂ absorption cross sections from 180 to 700 Å 3-67805
- N₂ beam-foil forbidden lines transition probabilities rel. to astronomical spectra 3-78430
- N₂ excited by Ne⁺ impact, emission cross-sections 3-78894
- N₂ first negative bands, electron fluorescence efficiencies, calculations 3-63509
- N₂ gas, Rayleigh scatt., low-power He-Ne laser meas. 3-49388
- N₂ Rydberg complexes band structures 3-40616
- N₂ second positive 3160 Å emission in aurora, spatial separation from N₂⁺ first negative 3914 Å emission 3-51098
- N₂ second positive bands, electron fluorescence efficiencies, calculations 3-63509
- N₂ second positive system bands in dayglow, Kosmos-224 data 3-41983
- N₂⁺, emission cross-sections for 3914 Å from H⁺ impact on N₂ 3-78893
- N₂⁺ 3914 Å daytime emission profiles during moderate solar activity, Kosmos-224 data 3-41984
- N₂⁺ 4278 Å band, photometric investigation of auroral emission 3-44913
- N₂⁺ first negative 3914 Å band charge-transfer excitation by protons, photon-particle coincidence meas. 3-63560
- N₂⁺ first negative 3914 Å emission in aurora, spatial separation from N₂ second positive 3160 Å emission 3-51098
- NF and NF⁺, pot. energy curves and spectroscopic consts. calcs. 3-71496
- NH molecular lines and oscillator strengths in photosphere 3-69829
- NO, a¹Π state, spin-forbidden lifetime, cooperative optical phenomena 3-54665
- NO, deviation from Lorentzian shape in the wings of collision broadened i.r. absorption lines 3-43466
- NO, diatomic mols. trapped in Ne matrix, absorpt. spectra, vibr. and rot. struct. 3-75011
- NO, Doppler-limited i.r. mag. rot. spectrum, line shape 3-43448
- NO, electron impact, dissociative excitation processes, spectroscopic investigations 3-75114
- NO, fund. and first overtone bands obs. in NO-rare gas mixtures, 10000 psi 3-63444
- NO, i.r. spectra of air pollutants 3-53471
- NO, molecule, electron impact excitation and dissoci., radiation spectrum 2000 to 9000 Å 3-75128
- NO, perturbation of electronic transitions under foreign gas pressure 3-75012
- NO, photoabsorpt. cross sections, 380-660 Å region 3-71606
- NO absorption cross sections from 180 to 700 Å 3-67805
- NO detection and comp. determ. in stratosphere (French) 3-51012
- NO laser, ²Δ-²Π near i.r. transition, rotational analysis of spectrum 3-66806
- NO⁺, valence states, spectroscopic consts. 3-63427
- NS, fluorescence and zero-field level crossing spectroscopy of C²Σ⁺ state 3-78837
- NaK, laser excitation, obs. of molecular and atomic fluorescence spectra 3-40650
- Ne₂, vacuum u.v. absorption, determ. of ground state potential energy curve 3-67865
- O₂, beam-foil lifetime meas. in vacuum u.v. 3-78747
- O₂, electron impact, dissociative excitation, extreme vacuum u.v. spectra 3-75117

spectra of diatomic inorganic molecules continued

- O₂, electronically excited by H(H⁺) impact 3-78895
 O₂, photoabsorpt. coeffs., 400-600 Å 3-52364
 O₂, photoabsorption coeffs. from 400 to 650 Å using synchrotron radiation 3-40566
 O₂, pressure dependent absorption cross sections, between 2000 and 2500 Å 3-78732
 O₂, X³Σ_g⁻ state, resolution of discrepancies 3-78736
 O₂ absorption cross sections from 180 to 700 Å 3-67805
 O₂ glow discharge, metastable level deactivation processes 3-52546
 O₂⁺, A₂I_u - X₂I_g second negative band system 3-78735
 OD, A²Σ⁺ state, Stark studies and high field level crossing 3-40654
 OD free radical, A²Σ⁺ - X²I₁, electronic band system, rotational term values 3-78737
 OH, crossing of ⁴Σ⁻ and A²Σ⁺ states, comment 3-60474
 OH, excited, vibration-rotation bands, i.r. airglow, correl. of fluctuations 3-80789
 OH (A²Σ⁺ - X²I₁) rotational line strengths and energy level population in water vapour arc plasmas 3-43688
 OH emission, upper atmosphere, rel. to stratospheric warming 3-65320
 OH in water vapour arc plasmas, rotational lines meas. 3-43687
 OH molecular lines and oscillator strengths in photosphere 3-69829
 O₂(a¹Δ_g), time-resolved absorption in vac. u.v. 3-46269
 P₂ radical, electronic system bands analysis, π-π transition (French) 3-52353
 PN, resonance fluorescence from A¹I₁ states, vibronic transition probabilities 3-78838
 PrO, visible and IR spectra 3-75026
 PtC, Franck-Condon factors, r-centroids, α-averaging of Morse potential functions 3-78720
 PtO, Franck-Condon factors, r-centroids, α-averaging of Morse potential functions 3-78720
 SO, Hund's coupling case 3-67785
 SO(³Σ⁻) prod. by flash excitation of SO₂, rate const. meas. 3-58807
 SiCl, rel. intensities of band spectra, vibrational overlap integral, calc. of Franck-Condon factors 3-78733
 SiO, in interstellar matter, E¹Σ⁺ - X¹Σ⁺ transition, radiative lifetimes and band oscillator strengths 3-73547
 SiO, vacuum u.v. absorpt., electronic states analysis 3-63449
 SnCl radical, analysis of the a-X system (3400-3900 Å) (French) 3-49462
 SnCl radical, rotational anal., excited by Ar high tension discharge, ¹²⁰Sn, B²Σ⁺ - X²I₁ transition (French) 3-75006
 SnI spectral bands between 215 and 250 nm 3-40612
 SrI, band spectrum in 6500-7200 Å region 3-63438
 SrI, band system in 3350-3560 Å region 3-52362
 TiO p-system band spectra rel. to vibrational temperature of stars δ₂ Lyr and α Her A (Russian) 3-61805
 UO, i.r. spectra, 700 to 900 cm⁻¹, stretching modes study 3-40625
 Xe vacuum u.v. spectra in solid Ne 3-71546
 YbH(D), Hund's coupling case 3-67785

spectra of inorganic liquids and solutions

- actinide complexes, electron transfer, f-d absorption bands 3-76491
 actinide ion electronic spectra, f-level intermediate spin-orbit coupling 3-69011
 alkali halide, colour centre absorption 3-80075
 alkali metal salts in propylene carbonate, far-i.r. spectra, ionic solvation obs. 3-79931
 aqueous solutions, i.r. spectra using Fourier transform spectroscopy 3-72622
 Baltic Sea, determination of suspended inorganic substance, attenuance spectral method (German) 3-76916
 i.r. and Raman band profile analysis, mol. vib. 3-64665
 liquid, molecular motion, conf., Orsay, France, Jul.(1973) 3-64192
 molten alkali metal salts, nitrates and chlorates, i.r. emission, 50 to 3000 cm⁻¹, Fourier transform spectrometry 3-55668
 ocean, Sr content, spectroscopic determination, Sr-Cl ratio (Russian) 3-47696
 polar fluids, solvated electron, radiative processes 3-55995
 rare earth ions in soln., magneto-optical activity calc. for forbidden transitions 3-61030
 rare earth metal complexes, electron transfer, f-d absorption bands 3-76491
 Seignetto salt solns., position of nat. absorpt. limits (Russian) 3-65126
 transition metal carbonyls in gas and liq. soln., vib.-rot. coupling effects on correlation functions 3-67825
 water, aqueous solutions, i.r. spectra, internal reflection spectroscopy 3-75042
 water, i.r. spectra, Lambert absorpt. coeff., refr. index determ. 3-61039
 water and aqueous solutions, i.r. spectra, 1.15 micron band, structure, effect of ions 3-72605
 Ar:H₂ liq. mixture, roto-translational spectrum of H₂ and intercollisional interference 3-80057
 Bi(III) complexes, 4, 5, and 6 coord. chloro- and bromo bismuthate anions in benzene soln., far i.r. and u.v. spectra 3-47276
 C₂N₂ liquid, comparison with far i.r. collision induced absorption in compressed gas 3-60458
 CS₂ liquid, depolarized Brillouin spectrum, broad doublet 3-80034
 CaSiO₃-Gd₂SiO₅ system, variable phase composition 3-68385
 Cd(II) complex, CdX₂ (X=Cl, Br, I) in tri-n-butylphosphate soln., vibrational spectra 3-75034
 Ce(NO₃)₃ aqueous solutions, i.r. spectra 3-44407
 CoBr₂·2 in fused organic salt, absorpt., charge-transfer, ligand-field transitions 3-64671
 D₂O, broadband picosecond continuum and light gate, time resolution and characteristics 3-45820
 Es³⁺ in solution spectra, intensity correlations and energy levels 3-72664
 Gd(III) complex with ligands in solution absorption spectra 3-64680
 H₂ liquid and solid, short wavelength collective excitations 3-75993
 H₂O, broadband picosecond continuum and light gate, time resolution and characteristics 3-45820
 H₂O, near i.r. spectra, further anal. concerning vibr. assignments 3-43450

spectra of inorganic liquids and solutions continued

- H₂O + organic base, near i.r. struct. study and vibr. assignments 3-46275
 H₂O₂ and p-dioxane, binary solutions, i.r. and Raman studies (French) 3-58512
 H₂SO₄ aqueous solutions, droplets, solar radiation absorption and scattering, near i.r., appl. to industrial pollution 3-44886
³He atoms in superfluid ⁴He, roton like dip 3-79544
⁴He, superfluid, spectral intensity of scatt. light 3-52734
 HgCl₂ solution, dipole moment, temp. depend., 8.5-50°C 3-79976
 Hg(II) complex, HgX₂ (X=Cl, Br, I) in tri-n-butylphosphate soln., vibrational spectra 3-75034
 In(III) chloro- and bromo-complexes, in benzene soln., far i.r. spectra, 413 to 33 cm⁻¹ 3-47275
 K₃Cr(CN)₆ crystal and solution, Raman spectra, struct. and vibrational assignments 3-75988
 K₂Cr₂O₇, crystalline molten and aqueous, vibrational spectra 3-55587
 LiNO₃ solns. in liq. ammonia, vibr. spectra, solvent effects 3-55991
 MgNO₃-water systems, Raman and i.r. study 3-53353
 N₂-Ar solute-solvent systems, computer simulation of correl. functions, bandshapes and relax. times 3-64651
 NH₃, Lambert absorption coeff. in visible region 3-44422
 NH₄NO₃ solns. in liq. ammonia, vibr. spectra, solvent effects 3-55991
 (NH₄)₂SO₄ aq. soln., optical consts. from attenuated total refl. spectroscopy 3-53074
 Na₂[Ln(CO₃)₂(H₂O)₂].wH₂O, i.r. and Raman spectra, struct. obs. (French) 3-60457
 O₂, absorpt. bands at 0.58 and 0.63 μ, mag. field effect on intensity 3-64654
 ReOF₄, vibrational spectra 3-72626
 SF₆OOSF₆ in liquid phase, vibrational spectra 3-46295
 SF₆OOSF₆ in liquid phase, vibrational spectra 3-46295
 Ti(III) chloro- and bromo-complexes, in benzene soln., far i.r. spectra, 413 to 33 cm⁻¹ 3-47275
 Xe solid and liq., band struct. from refl. spectra 3-50130
 Zn(II) complex, ZnX₂ (X=Cl, Br, I) in tri-n-butylphosphate soln., vibrational spectra 3-75034
- spectra of inorganic molecules**
see also Raman spectra of inorganic substances; spectra of diatomic inorganic molecules; spectra of polyatomic inorganic molecules
 objective analysis scheme, atmospheric wind field, spectral analyses 3-76860
 HCl and electron donating bases, matrix isolation i.r. spectra 3-71540
 LiCl and electron donating bases, matrix isolation i.r. spectra of Li-bonds analogous to H-bonds 3-71540
- spectra of inorganic solids**
see also luminescence of inorganic solids; radiofrequency spectra of inorganic solids; Raman spectra of inorganic substances
 A₂BWO₆ (A=alkaline earth), ordered perovskites, absorption and vibr. spectra 3-41577
 actinide ion electronic spectra, f-level intermediate spin-orbit coupling 3-69011
 alkali halide: TI⁺, moments of dichroic spectra of (s)² impurity ions 3-41541
 alkali halide: NH₄⁺, pressure var. of i.r. spectra 3-68363
 alkali halide: PO₂⁻, effect of pressure on luminescence 3-69023
 alkali halide: TI⁰, ²p_{1/2} to ²p_{3/2} optical transition rel. to Jahn-Teller electron-phonon interaction 3-64698
 alkali halide: TI⁺-like ion, method of moments evaluation of electron-lattice interaction in absorpt. spectra 3-72684
 alkali halide, u.v. absorpt. anisotropy factor and transition energies of OH⁻ molecule 3-68573
 alkali halide cryst., impurity mol. anion vibr. bands, temp. depend. of integral absorpt. 3-72695
 alkali halide crystals, vibration-induced absorption (B band) of S²⁻ configuration ions 3-58534
 alkali halides: molecular ion impurities, temp. var. of vibr. spectra 3-68365
 alkali halides; HS⁻, lattice sideband structure in i.r. absorpt. spectra 3-68366
 alkali halides, far-i.r. region reststrahlen props., model approach 3-68977
 alkali halides, mixed, coherent potential approximation reflectivity rel. to lattice mode 3-53110
 alkali halides, multiphonon i.r. absorpt. temp. depend. 3-64659
 alkali halides, multiphonon i.r. absorpt. temp. depend. 3-64660
 alkali halides, multiphonon i.r. absorpt. temp. depend. 3-68985
 alkali halides, refl. meas., surface effects 3-58494
 alkali halides, refr. index and refl. spectra, uniaxial deform. effects 3-58528
 alkali halides, U centres, u.v. and i.r. spectra, proton irradiation 3-52623
 alkali metal nitrates and carbonates, longit. mode freqs., PSR i.r. spectra 3-75975
 alkaline earth nitrates and carbonates, longit. mode freqs., PSR i.r. spectra 3-75975
 amorphous semicond., lone-pair, optical props. pressure depend. rel. to chem. bonds and comp. 3-44390
 amorphous semiconducting materials, optical and electronic props. 3-41123
 amorphous semiconductor films, rel. to holographic recording of information 3-74212
 Ar₂O₃ thin films between alkali halide discs, i.r. and Raman spectra, surface interaction effects 3-64638
 Ar, solid, with trapped oxygen, luminesc. and absorpt. spectra 3-44472
 β-B elec. resist. and i.r. absorpt. correl. 3-44419
 beryllium glasses, NiO, MnO admixtures 3-72606
 boehmite, crystal vibration modes, i.r. study (French) 3-58513
 borate glass: Pb, absorption, emission and excitation spectra 3-55656
 n-Cd_{0.2}Hg_{0.8}TE, transmission, 0.09-0.25 eV, 77 and 300K (Russian) 3-80021
 chalcogenide glasses, multiphonon absorption processes, obs. in i.r. spectra 3-75972
 complex salts, i.f. vibr., metal-ligand and complex ion-outer ion interactions 3-47246

spectra of inorganic solids continued

- copper phthalocyanine polymorph, dimeric struct., i.r., X-ray, electronic, e.p.r. spectra 3-52599
- crystals, impurity centres, temp. depend. 3-68563
- diaspore, crystal vibration modes, i.r. study (*French*) 3-58513
- enstatite, 2200-27000 cm⁻¹ polarised spectra at room and liquid He temps. 3-50880
- ferroelectrics, vibronic impurity spectra, features near T_c 3-72692
- fluorite series, effect of indirect exchange interactions on crystal field parameters of Er³⁺ centres 3-50139
- fundamental optical spectra, quantum structure of solids 3-55565
- fused silica glasses with transition element impurities, optical absorption characteristics 3-73739
- n-GaAs, electron distrib. at high elec. fields, electroabsorpt. study 3-72321
- germanate glass: Pb, absorption, emission and excitation spectra 3-55656
- germanate glass: Tm³⁺, Er³⁺, oscillator strengths, emission and excitation spectra 3-72712
- glass: Ag⁺, ion-polyvalent ion (As, Sb, Bi) interaction, colloid form, opt. and e.s.r. spectra 3-58427
- glass: Eu³⁺, germanate, fluoresc. and absorpt. spectra 3-61062
- glass: Tm³⁺, Er³⁺, intensity parameters from oscillator strengths of electronic transitions 3-58535
- glass, bulk, low-loss for optical fibers, impurity content and spectral losses 3-73738
- glass matrix, optical and paramag. absorpt. of Ag particles, size effect 3-55563
- glasses, i.r. spectra, vibrational study 3-76005
- halide salts, C_{2v}, C_{3v}, symmetry group impurities, spectral props. 3-69043
- hydric acids, i.r. theory, expt. 3-72660
- ice, i.r. spectral reflectance and refractive index 3-44387
- ice hydrogen bond spectral shifts temp. depend., vitreous to cubic I phase transformation 3-47262
- III-V semiconductor, intrinsic, absorpt. coeff., heavy-hole to cond. band transition 3-72676
- inert gas: Ag(Ta)(W)(Mo), matrix isolation spectra using triode sputtering source 3-61046
- inert gas mixtures, absorpt., luminesc., impurity centres 3-69086
- inert gases, i.r. theory, expt. 3-72660
- inert-gas crystals, H⁻ and D⁻ impurities, existence from i.r. absorpt. spectral exam. 3-49955
- insulators, absorption and scattering of light, interactions with lattice vibrations and excitons 3-50553
- intermolecular interactions in condensed systems, induced i.r. spectra 3-72697
- ionic cryst., excited electronic states and electron-lattice interac. from optic. abs. meas. of Cd²⁺, Cu²⁺, Ti⁴⁺ 3-55650
- i.r. spectra of cryst. defects, book 3-72693
- IV-VI compounds, matrix isolation studies of i.r. spectra, laser-excited emission bands 3-78804
- lanthanides, optical spectra, classification (*French*) 3-63276
- metal, multivalent, interband optical absorpt. phenomena (*Russian*) 3-68963
- metal, refl. spectroscopy, plasma reson. enhancement 3-44040
- metal complexes of 2,4 pentadiene ligands, 3-substituted, i.r. spectra, metal substitution effects 3-64650
- metals with incomplete shell optical spectra of core electrons, overall line shapes 3-72669
- metals with incomplete shells, optical spectra of core electrons 3-72668
- molecular crystals, i.r., Raman spectra, two phonon absorpt. 3-69001
- niobates, i.r. spectra in crystals 3-55602
- noble metal thin film, transmission in vis. and near u.v. spectra regions (*French*) 3-76112
- noncubic crysts., impurity-induced i.r. absorpt. theory 3-64694
- olivine, 200-45000 cm⁻¹ polarisation spectra at room and liquid He temps. 3-50881
- paramagnetic impurity centres, line shift and line broadening 3-58538
- paramagnetic metal complexes, with porphyrin, quasiline luminesc. and absorpt. spectra 3-72732
- perovskites, A₂BWO₆ (A=Ca, Sr, Ba; B=Mg, Ca, Cd, Sr, Ba), luminescence of WO₆, absorption spectra (*Russian*) 3-41558
- peroxo tungstates and molybdates, i.r. spectra 3-57656
- phosphate glass: Pb, absorption, emission and excitation spectra 3-55656
- potassium halides, chromate- and nitrite-activated, absorpt. at 300 k, 80 k and 4 K (*Russian*) 3-44432
- pyrochlore structure, i.r. absorption characteristics 3-44401
- quartz, amorphous, optical characteristics in 1400-200 cm⁻¹ region, calc. using Kramers-Kronig relations 3-53096
- quartz, elementary electronic excitations, 4-22.8 eV 3-64314
- quartz, neutron irradi., colour centres, absorpt. study, 0.35-0.7 μ (*Russian*) 3-64702
- quartz, SCF Xα scattered wave method calcs. of valence orbitals 3-52793
- quartz, transmission and reflection spectra in vac. u.v. 3-69016
- quartz glass, structural changes during heat treatment, optical and e.p.r. meas. 3-80428
- quartz glass, symmetry of Ti³⁺ activator centres 3-64296
- rare earth chromium sulphides, LnCrS₃, (Ln=Y, Gd, Dy, Ho, Er), absorpt., 0.15-1.7 eV 3-40869
- rare earth double nitrates, double and multiple perturbations of non-Kramers ions 3-55662
- rare earth metals, free-ion energy levels, comparison of calc. and exptl. values 3-52795
- rare earth niobates, perovskite structure, vibr. spectra 3-53111
- rare earth sesquioxides, Ir absorption 3-79974
- rare gas matrix containing Pt(N₂)_n complexes, 14 K, i.r. study 3-78810
- refractory metal compounds, X-ray spectra interpretation, band structure calc. 3-41594
- ruby, optical spectrum due to exchange-coupled Cr³⁺ ions 3-44435
- ruby with Cr ion pairs, energy calc., effective Hamiltonian method 3-68564
- rutile-structure fluorides, elastic and optical props. in rigid ion approximation 3-68987

spectra of inorganic solids continued

- semiconductor, cubic, two-photon absorpt. and optical orientation of free carriers, theory 3-54245
- semiconductor, defect zinc-blende struct. type 3-72621
- semiconductor, I-III-VI₂, band gap determ. by refl. meas. with polarization modulation 3-68549
- semiconductor, I-III-VI₂, band structure, electroreflectance obs. 3-55206
- semiconductor, II-IV-V₂, band structure, modulation spectra obs., review 3-55205
- semiconductor, intraband light absorption, by free carrier interactions 3-50597
- semiconductor, with complicated band struct., theory of impurity absorption 3-58537
- semiconductor diffused layer profile, i.r. reflectivity obs. (*German*) 3-50661
- semiconductor thin films, optical absorpt. edges, quantum mech. broadening 3-41537
- semiconductors, magneto-reflection spectra using polarisation modulation 3-5615
- silicate crystals, temp. depend. of A_u vibr. modes 3-79449
- sulphide minerals, pressure effects on optical transmission 3-64690
- Suprasil W, silica glass, vacuum UV irradiated, rapid transmission loss 3-64672
- synchrotron radiation absorption 3-40614
- transition metal iodate, 3d, prep. and characterisation, absorpt. from 35 to 33000 cm⁻¹ 3-53120
- transition metal iodides, S-containing complexes, adsorbed iodide, photo-electron spectra 3-41617
- UO₂²⁺ complexes, circular dichroism and interpretation of electronic spectra 3-76029
- Sb_{1-x}Se_x, amorphous films, reflectivity spectra, electronic structure 3-64754
- [Co(H₂O)₆](BrO₃)₂, electronic absorpt. and mag. circular dichroism spectra 3-44408
- Ag, X-point, temp. dependence of optical props. 3-72672
- Ag electrode, electroreflectance spectra, effect of I⁻ adsorption 3-47292
- Ag film, nonradiative surface plasmons roughness induced decay, emitted radiation polarisation 3-46811
- Ag-Pd alloy films, sputtered, reflector power (*French*) 3-41527
- Ag₃AsS₃, proustite, band structure, light absorpt. and refl. obs. 3-44017
- Ag₃AsS₃, proustite, i.r. refl. and transmission spectra 3-58503
- Ag₃AsS₃, proustite, i.r. absorpt. spectrum effect of partial electrolysis (*Russian*) 3-68992
- AgBr and AgBr-PbO coatings, spectral sensitization, photocond. meas., photographic diode 3-47588
- AgBr(Cl), absorpt. below band edge, Urbach rule, microscopic theory (*German*) 3-50554
- AgCl and AgCl-PbO coatings, spectral sensitization, photocond. meas., photographic diode 3-47588
- Ag₂H₂O₁₀, i.r., assignment of vibrational modes 3-47222
- AgI-Ag photosensitive film, refl. spectra, 370 to 500 nm 3-53121
- AgNO₃, longit. mode freqs., PSR i.r. spectra 3-75975
- AgNO₃, polarised phosphoresc. and absorpt. in single cryst. 3-64729
- Ag₂S, semiconductor thin film, struct. and props. (*Rumanian*) 3-64417
- α-Ag₂S and β-Ag₂S, optical props. in i.r. and far i.r. 3-53108
- Ag₂(Se) semiconductor-metal transition, i.r. reflectivity obs. (*German*) 3-50571
- Ag₃SbS₃ single crystals and amorphous films, light absorption, band structure 3-64679
- AgX absorption, (X=halide), early photolytic stages, quasimetallic centres, fluctuation theory, effects (*Russian*) 3-80084
- Al, absorption spectra of vapour quenched film deposited on another film 3-58572
- n-AlAs, reflection spectrum, influence of defect centres (*German*) 3-50560
- α-AlB₁₂, refl. temp. depend., polaron cond. mechanism 3-72357
- Al(BD₄)₃, i.r. and Raman spectra 3-72623
- Al(BH₄)₃, i.r. and Raman spectra 3-72623
- AlF₃⁻, solid, i.r. and Raman spectra 3-72627
- Al₂O₃, corundum, multiphonon absorpt., 1100-2500 cm⁻¹ (*Russian*) 3-80048
- Al₂O₃ containing Ti, synthesis conditions and optical spectra 3-80171
- Al₂(SO₄)₃, i.r. absorption, dehydration temp. 3-53098
- AlSb, edge absorpt., band gap and phonon energies detn. 3-58526
- n-AlSb:Te, intraband direct forbidden transition, i.r. absorpt. and Hall coeff. obs. 3-41140
- Ar:(H₂), (D₂), i.r. absorpt. due to phonon sidebands on vibr./rot. transitions, theory 3-47244
- Ar/N₂:Rh(N₂)_n, n=1-4, i.r. examination, 10K 3-78809
- As-S amorphous film, photographic effects, 77 and 293 K, interpretation 3-69015
- As-Se-Tl glasses, refractive index, density, polarisation, absorption spectra (*Russian*) 3-50584
- AsI₃, absorpt. spectra and optical transitions 3-55647
- AsI₃, molecular cryst., low freq. far i.r. spectra, phonon spectrum 3-76009
- As₂O₃ glass, i.r. vibrational spectra obs., reln. to arsenolite and claudetite structures (*Italian*) 3-72604
- As₂Se₃ glass, multiphonon absorption processes obs. in i.r. spectra 3-75972
- AsSeI glass, i.r. transmission, 5-413K (*Russian*) 3-80049
- Au electrode, electroreflectance spectra, effect of I⁻ and n-(C₄H₉)₄N⁺ adsorption 3-47292
- Au film, d-band position and width, low temp. thermomodulation meas. 3-55632
- Au-GaP, Schottky barrier, wavelength modulated photovoltage spectra 3-55618
- B, tetragonal filaments, i.r. transmission 3-47252
- BaClF, i.r.-active lattice vibrs., phonon freqs. 3-75575
- BaClF, U centres i.r. absorpt. spectrum 3-50602
- Ba(ClO₃)₂.H₂O(D₂O), i.r. and Raman spectra 3-75973
- Ba(NO₃)₂ mol. crystal spectra, influence of polarising effect of medium in region of internal vibr. 3-72647
- Ba(NO₃)₂.H₂O crysts., optical activity, absorpt. spectra and dispersion 3-76025

spectra of inorganic solids continued

- Ba₂NbNb₂O₁₅ in excited state, absorption spectra (*Russian*) 3-50599
- α -BaO·Al₂O₃·4H₂O, synthesis, struct., i.r. absorption, X-ray obs. 3-72057
- BaSO₄, i.r., far i.r. vibr. spectra, isomorphism 3-72634
- BaTiO₃, and band structure, imaginary dielec. function determ. 3-44003
- BaTiO₃, i.r. absorption measurements, ferroelectric phase transition 3-79995
- BaTiO₃, rare earth doped crystal, elec. cond., optical absorption, luminescence, Hall coeff. 3-75741
- Bi, far i.r. refl. spectra, band struct. obs. 3-44019
- Bi, far i.r. spectra, harmonic series of cyclotronlike resonances 3-44414
- Bi-Sb alloy, far i.r. refl. spectra, band struct. obs. 3-44019
- BiI₃, absorption, productivity at low temp. 3-75780
- BiI₃, absorption spectrum, effect of uniaxial deformation, 4.2K, line shifts 3-50595
- BiI₃, electroabsorpt. of excitons, high field regime 3-55639
- BiI₃ single crystal, absorpt., direct transitions in mag. field 3-64683
- BiOBr, i.r. and Raman spectra, 40-600 cm⁻¹, vibrational band assignments 3-44404
- BiOCl, i.r. and Raman spectra, 40-600 cm⁻¹, vibrational band assignments 3-44404
- BiOI, i.r. and Raman spectra, 40-600 cm⁻¹, vibrational band assignments 3-44404
- BiOI single crystals, absorpt. edge, effect of layered struct. 3-58527
- Bi_{1-x}Sb_x, narrow-band semiconductor, absorption spectra 3-50592
- Bi₂Si₂O₇, Al doped and undoped, transport processes of photoinduced carriers 3-46868
- BKCl₃, thin films, absorption spectrum, crystal field components, energy level scheme 3-41530
- CO, absorpt., refl., exciton-vibron (phonon) interactions 3-68358
- CO, pure and in Ar matrix, absolute i.r. absorption intensities, band shapes 3-80061
- CO, u.v. spectrum, exciton-phonon coupling role (*German*) 3-50586
- CO₂, cryst., two-phonon i.r. absorpt. spectra 3-47247
- CO₂, isotopically mixed crystal, i.r. absorption freqs., depend. on ¹²CO₂/¹³CO₂ concn. ratio 3-80063
- CO₂ crystal, biexciton spectra, i.r. absorpt. bands 3-68999
- CO₃²⁻ in crystal complexes, ν_2 i.r. out of plane active mode 3-47264
- Ca fluorapatite mol. crystal spectra, influence of polarising effect of medium in region of internal vibr. 3-72647
- CaCO₃, calcite, i.r., lattice dynamics 3-72628
- CaCl₂, hygroscopic compound i.r. spectra, improved KBr pellet method 3-45491
- CaF₂, hardening and colour centre growth after gamma irradiation 3-79349
- CaF₂, reversible photochemical reactions in additively coloured crystals 3-55660
- CaF₂:Er³⁺, optical Zeeman effect of type I crystal 3-55605
- CaF₂:Eu²⁺, Stark effect in zero-phonon spectra of local centres, modulation obs. 3-55665
- CaF₂:NaF(YF₃), optical absorption following γ and p irradiation and annealing, colour centres obs. 3-72694
- CaF₂:Sm²⁺, (Dy²⁺), (Tm²⁺), (Gd³⁺), high press. optical absorpt. studies 3-41540
- CaO, dense polycrystalline, transmission spectrum 3-76329
- CaO phosphors, preparation conditions, emission and optical absorption spectra 3-76068
- CaO thin film, sputtering rate determination by fluorescence of sputtered atoms 3-44508
- Ca(OH)₂ i.r. vibr. spectra around 3600 cm⁻¹ 3-58510
- CaO·2Al₂O₃:Nd³⁺, e.p.r. and optical spectra rel. to ion site energy levels 3-44320
- Ca₅(PO₄)₃:F:Eu³⁺, Stark effect in zero-phonon spectra of local centres, modulation obs. 3-55665
- CaS, plastic deformation, optical absorption spectra characteristics (*Russian*) 3-76032
- CaS thin films optical props. and electronic states determ. (*Russian*) 3-76014
- CaSO₄, i.r. absorption, dehydration temp. 3-53098
- CaSO₄, vibr. spectra and isomorphism 3-72634
- CaSO₄ crystal, vibrs. of complex ions, i.r. and far i.r. refl. spectra 3-72633
- Cd, reflectivity and surface plasma resonances 3-41538
- Cd₃As₂, i.r. absorpt., band gap obs. 3-68983
- Cd₃Co_{1-x}Cr_xS₄, mag. semicond., absorpt. bands, crystal field transitions obs. 3-47230
- CdCr₂S₄, ferromag., polarisation modulated magnetoref. rel. to mag. ordering 3-55616
- CdF₂, charge conversion of Cr and V ions 3-55659
- CdGeAs₂, absorpt. and electroabsorpt., band edge obs. 3-64686
- CdGeAs₂, cryst. and glassy, i.r. electrorefl. obs., energy gap rel. to short-range order 3-64662
- p-CdGeAs₂, electroreflectance, valence band structure determ. 3-44427
- CdGeP₂, i.r. absorpt. and refl. spectra, 2 to 100 μ , dielec. const. and refr. index calc. 3-44412
- p-Cd_{0.8}Hg_{0.2}Te, transmission, 0.09-0.13 eV, 231-295K (*Russian*) 3-80021
- Cd_{0.9}Hg_{0.1-x}Te epitaxial film, optical and elec. props. 3-58188
- CdIn₂S₄, edge absorption in region of indirect transitions 3-47286
- CdIn₂S₄, optical absorpt., indirect energy gap determ. at 2.5 eV, 0 K 3-80071
- CdS, dislocation-induced anisotropic absorpt. of polarized light 3-55666
- CdS, effect of surface on reflection and luminescence spectra 3-53149
- CdS, exciton refl. spectra for oblique incidence of light, spatial dispersion effects 3-55646
- CdS, light and electron beam modulated reflectance, A, B exciton lines 3-55634
- CdS, piezo-optic obs. of exciton spectrum 3-50596
- CdS, piezoelectric, impurity electroabsorption obs. 3-76037
- CdS monocrystals, photoref. spectra (*Russian*) 3-68968

spectra of inorganic solids continued

- CdS single crystal, uniaxial compression effect on two photon absorpt. 3-41536
- CdS thin film, optical absorpt. edges, quantum mech. broadening 3-41537
- CdS_xTe_{1-x}, mixed cryst., optical energy gap, absorpt. determ. 3-79630
- CdSe, Faraday effect in region of intrinsic absorpt. edge 3-55561
- CdSe:Cr, anomalous features of impurity absorpt., photoionisation temp. depend. 3-55651
- CdSe:Cr, optical photoionisation spectra of Cr impurity 3-55661
- CdSe:Cr, V, Ti, absorpt., oscill. strength, crystal field splitting and Racah parameters detn. 3-55652
- CdSe:Ti, (Co), CdTe:Ti, (V), impurity electron states, absorption and photocond. spectra (*Polish*) 3-41154
- CdSe_{1-x}Te_x solid solution, optical phonon freqs. from reflection spectrum, concn. depend. 3-75579
- CdSe_xTe_{1-x}, reflection, long-wavelength optical phonons 3-43850
- CdSiP₂, long-wavelength fundamental absorption edge 3-55648
- CdSnAs₂, pseudopot. calc. of band struct. at points in Brillouin zone, electrorefl. spectra 3-43996
- CdTe, band structure, fundamental reflectivity spectra (*Polish*) 3-41132
- CdTe, reflectivity peaks in vacuum u.v. thermorefectance spectra 3-55623
- CdTe, temp. dependence of fundamental absorption edge 3-53126
- CdTe reflection, uniaxial compression effect on intrinsic absorption edge 3-76024
- CdWO₄:Cr³⁺, single crystal, optical absorption, luminescence spectra 3-76070
- CeF₃, far u.v. refl. spectra, 6-40 eV 3-58521
- Ce(III)/Ce(IV) hydroxide, spectroscopic props. and interaction absorption 3-55606
- Ce(III)/Ce(IV) oxide, spectroscopic props. and interaction absorption 3-55606
- Cf⁴⁺, electronic spectra, spin-orbit coupling diagram prediction 3-69012
- Cm⁴⁺, electronic spectra, spin-orbit coupling diagram prediction 3-69012
- (Co,Mn)F₂, far i.r. powder spectra, antiferromag. resonance obs. 3-41424
- Co, ferromag., interband optical absorpt., rel. to density of states (*Russian*) 3-53089
- Co coordination cpds., external vib. freqs. of active and racemic forms, i.r. spectra 3-55581
- Co cpds., chemical shifts and fine struct. of K-absorption edge 3-72765
- CoBr₂·2H₂O, far i.r. absorpt. spectra, magnons, magnon bound states, phonons, magnon-phonon excitations 3-64636
- CoBr₂·2H₂O, magnon-phonon simultaneous excitation, new type of bound state 3-52983
- CoCl₂, fundamental absorpt., broad and charge transfer bands 3-58524
- CoCl₂ single crystals, polarised i.r. spectra 3-55576
- CoCl₂·2H₂O, far i.r. spin cluster excited states temp. broadening, liq. helium temps. 3-64637
- CoCr₂S₄, giant magnetorefl., visible and near i.r. 3-47239
- CoF₂, antiferromag., Davydov coupled transition, mag. circular dichroism 3-64673
- Co(NH₄SO₄)₆·6H₂O, solid dilution effect on vibr. perturbation and cryst. field parameters 3-47293
- Co(NH₃)₆X₂ (X=Cl, Br, I, BF₄), i.r. line profile 3-72646
- Cr, reflectivity and surface plasma resonances 3-41538
- Cr cpds., X-ray emission spectra rel. to chem. bonding (*Japanese*) 3-69106
- Cr(III) complex, $\mu\mu'$ -dihydroxotetrakisethylenediamine dichromium (III) salts, rel. to superexchange 3-79825
- Cr(III) complexes, Cr(NH₃)₅X²⁺ ions, ²E(ν_2) state splitting, Coulombic parameter significance 3-47305
- Cr(NH₃)₆³⁺ ion in non-cubic environments, ²E→⁴A transition 3-47283
- Δ -Cr₂O₃, new high temp. form, X-ray powder diffraction and i.r. spectrum meas. 3-75509
- Cr₂(SO₄)₃, i.r. absorption, dehydration temp. 3-53098
- Cs, conductivity sum rule for optical absorption 3-53125
- Cs₂CoBr₂ tetragonal crystals, anisotropy of Zeeman effect in optical absorption spectra 3-72670
- Cs₂CoBr₂ tetragonal crystals, anisotropy of Zeeman effect in optical absorpt. spectra, selection rules 3-72671
- Cs₂CoCl₂ tetragonal crystals, anisotropy of Zeeman effect in optical absorption spectra 3-72670
- Cs₂CoCl₂ tetragonal crystals, anisotropy of Zeeman effect in optical absorpt. spectra, selection rules 3-72671
- CsCrBr₃, complex visible, crystal structure, X-ray study, effect of exchange coupling 3-61043
- Cs₂CuBr₄, at high pressure, transformation from tetrahedral to planar symmetry, absorption studies 3-55603
- Cs₂CuCl₄, at high pressure, transformation from tetrahedral to planar symmetry, absorption studies 3-55603
- CsI:ClO₄-(ReO₄)₃, i.r. absorpt. and local symmetry of impurity ions (*Russian*) 3-41542
- CsI(Br), vacuum u.v. wavelength modulation spectrum 3-55625
- Cs₂LiM(CN)₆, (M=Cr, Mn, Fe, Co), vibr. spectra and neutron diff. cryst. struct. 3-79294
- Cs₃Ln(MoO₄)₃, Ln=La, Pr, Nd, i.r. 3-72064
- CsMnF₃, i.r. refl. spectra, dielec. const., lattice freqs. and interionic pot. calc. 3-47272
- Cs₂ZrBr₆:Os⁴⁺, absorpt. and mag. circular dichroism spectra, 17000 to 31000 cm⁻¹ 3-44437
- Cu thin film, struct. effects on far u.v. spectra (*French*) 3-76111
- Cu-Fe dil. alloy, reson.-like humps in far i.r. surface resist. (*German*) 3-50570
- Cu-Ga dilute alloys, optical reflection investigation of electronic structure 3-72686
- Cu-Ge dilute alloys, optical reflection investigation of electronic structure 3-72686
- Cu-Zn(Al)(Ni), compositional modulation, absorpt. peaks rel. to band structure 3-55633
- CuCl, absorpt. spectrum, e.p.r. of point defects, colour centres 3-68844

spectra of inorganic solids continued

- CuCl, absorption line corresponding to Bose condensation of excitons 3-79649
- CuCl, far i.r. absorpt., assignment of peaks 3-68982
- CuCl, modulated excitonic spectra in elec. field 3-55638
- CuCl, two-photon absorption line shape of polariton 3-79653
- CuGaS₂, wavelength modulated absorpt., refl. spectra, excitonic structure and band gap shift 3-55636
- Cu₂HgI₄, thermochromic, cryst. growth and refl. 3-61047
- Cu(II) complexes, chloro- and bromoacetates 3-76016
- Cu(II) halide complexes with N-ethanolsalicylideneimines determ. of structural factors affecting magnetic behaviour 3-44205
- Cu(II) oxalate-amine complexes, visible absorption spectra, correlation with structure 3-44206
- CuO, matrix isolated, visible absorption spectra, evidence for a ²I_g ground state 3-52357
- CuO₄ tetrahedra, Jahn-Teller distorted in oxidic solids, ligand field spectra (*German*) 3-61052
- Cu₂O, modulated excitonic absorpt. in mag. or parallel elec. and mag. fields 3-55617
- Cu₂O, modulated excitonic spectra in elec. field 3-55638
- Cu₂O cryst., electroabsorpt. spectrum of yellow exciton series 3-61050
- CuSO₄, hygroscopic compound i.r. spectra, improved KBr pellet method 3-45491
- Cu₂Se, refl. spectrum, 0.8-8 μm, optical effective mass, carrier relax. time 3-44418
- D₂, far vacuum u.v. absorpt., energy levels 3-76015
- Dy, 1-20 μm absorpt. spectra obs. of optical consts. (*Russian*) 3-44421
- EuF₂:Tm²⁺, high press. optical absorpt. studies 3-41540
- Eu₂Ga₂O₁₂:Pt, dispersion like line shape rel. to Eu³⁺-Pt⁴⁺ two centre absorpt. 3-58536
- Eu(II)/Eu(III) oxide, spectroscopic props. and interaction absorption 3-55606
- Eu(II)/Eu(III) sulphide, spectroscopic props. and interaction absorption 3-55606
- Eu(NO₃)₃, hydrated and anhydrous, i.r. and luminesc. spectra (*Russian*) 3-72720
- EuO, Kramers-Kronig analysis of reflection at room temp., 0-14 eV, energy level determ. (*German*) 3-53117
- EuO thin film, absorpt., mag. order effect 3-55307
- EuO:Gd i.r. reflectivity, 250 μ to 12 eV photon energy, Kramers-Kronig analysis, coupled modes 3-41518
- EuO(Gd), magnetorefectance, Kramers-Kronig analysis, optical consts. 3-50562
- EuS, magnetorefectance, Kramers-Kronig analysis, optical consts. 3-50562
- EuS thin films, absorpt., multiplet struct. 3-75689
- EuSe, ferromag., polarisation modulated magnetorefl. rel. to mag. ordering 3-55616
- (Fe,Mn)F₂, far i.r. powder spectra, antiferromag. resonance obs. 3-41424
- Fe-Ni alloy films, equatorial Kerr effect in visible spectrum range (*Russian*) 3-61045
- Fe³⁺ high-spin system, magnetic circular dichroism of spin forbidden transitions 3-72663
- FeBO₃, calc. of multi-magnon side band 3-68979
- FeBO₃, weak ferromagnet, absorpt. spectra, fine struct. obs. 3-69010
- FeCO₃, antiferromag., light absorp. under phase transition induced by strong ext. mag. field 3-52964
- FeCl₂, fundamental absorpt., broad and charge transfer bands 3-58524
- FeCl₂, ligand-field zero-phonon line intensity, antiferromag.-ferromag. transition 3-41528
- FeF₃, canted antiferromag., light scatt. by single magnons 3-79855
- Fe(II) high-spin complex (N,N'-dicyclohexylthiourea)₆(ClO₄)₂, orbital ground state reversal, i.r. spectra 3-75925
- Fe(III) complex tris (O,O'-diethyldithiophosphato), polarised crystal spectra 3-47289
- α-Fe₂O₃, far i.r. absorpt., antiferromag. resonance and dimensional interference obs. 3-41414
- γ-FeOOH, lepidocrocite, low freq. vibr. obs. by i.r. absorption 3-44416
- Fe₂P, Mossbauer spectroscopy, vacancy distribution, mag. transition 3-41469
- Ga, Azbel' Kaner cyclotron resonance at far i.r. frequencies 3-58313
- GaAs, Faraday rotation and ellipticity, exciton absorption region 3-47236
- GaAs, reflectivity peaks in vacuum u.v. thermorefectance spectra 3-55623
- GaAs, Schottky barrier electroreflectance meas. 3-41502
- GaAs, Schottky surface barriers, high-resolution electroreflectance meas. 3-55630
- GaAs, space charge region, elec. field modulation by laser light, photorefl. obs. 3-75773
- GaAs, spontaneous electroabsorpt., odd harmonics 3-72675
- GaAs, wavelength modulated and electroreflectance spectra, fast neutron irr. effects 3-55629
- GaAs, Zeeman spectroscopy of shallow donor states 3-41543
- GaAs flatband electroreflectance 3-55628
- GaAs:O, impurity state electroabsorption measurements at 300 K 3-55664
- GaAs:Ti,Co compensated, absorp., material props. 3-58266
- GaAs-Au, Schottky barrier, electroreflectance spectra at GaAs discrete and continuum exciton states 3-55640
- GaAs-CdSe solid solution, i.r. refl. spectra and electron effective mass (*Russian*) 3-80047
- GaAs_{1-x}P_x, fundamental absorpt. edge, effect of band struct. parameter changes 3-76019
- GaCl₃:Nd³⁺ complexes, spectral broadening, struct. relax. 3-69036
- GdF₃, solid, i.r. and Raman spectra 3-72627
- Ga_{1-x}In_xP alloy, electroreflectance for band structure obs. 3-55204
- α-Ga₂O₃:Cr³⁺, excitation and emission, photoluminescence 3-41576
- GaP, piezorefectivity spectra investigation of band structure 3-55546

spectra of inorganic solids continued

- GaSb, i.r. dispersion of lattice reflection, temp. depend. obs. 3-50583
- GaSb, i.r. modulated electroreflectance, band structure obs. 3-55598
- GaSb, magnetoemission, free and bound excitons, g-factor 3-79654
- GaSb, multiphonon absorpt., I.R. transmission 3-55601
- GaTe, layer compound, exciton photorefectance, Kramers-Kronig relations 3-55610
- Gd, Kerr magneto-optical effects, 1-5 eV, interpretation 3-55559
- GdCl₃, u.v. absorpt. spectra, single ion induced magnon sideband 3-64693
- Ge, amorphous, electronic density of states, optical absorption, photoemission, photoconductivity 3-41119
- Ge, amorphous, pressure effects on electronic and optical props. 3-43985
- Ge, band struct. features, determ. from u.v. edge-absorpt. data 3-52787
- Ge, flatband electroreflectance 3-55628
- Ge, i.r. absorpt. meas. rel. to divacancy centres 3-43783
- Ge, i.r. and Raman spectra theory 3-41513
- Ge, localised vibr. modes for implanted O ions, i.r. spectra 3-43854
- Ge, piezorefectivity spectra investigation of band structure 3-55546
- Ge, reflectivity peaks in vacuum u.v. thermorefectance spectra 3-55623
- Ge, uniaxially stressed, low temp. Franz-Keldysh oscills. 3-69014
- Ge, wavelength modulation spectra, surface elec. field, carrier conc. effects on reflectivity 3-55627
- Ge film, amorphous, refl. and electrorefl. 3-55550
- Ge:As, excitation spectrum of donors, concentration depend. 3-50589
- Ge:B, Tl, excitation spectra, Zeeman effect 3-50594
- Ge:Zn⁺, energy state obs., symmetries and deform. pot. consts. 3-44439
- Ge-As-Se glasses, multiphonon absorption processes obs. in i.r. spectra 3-75972
- GeO₂, amorphous, hexagonal and tetragonal, reflection spectra, optical consts. detn., 4000-200 cm⁻¹ region 3-64616
- GeSe₂(Se₂), far i.r. spectra, cryst. struct. singularities 3-55579
- Ge_{1-x}Si_x film, electrorefl. spectra 3-76020
- GeTe, optical props. and energy gap from reflectance spectra 3-64685
- H₂, far vacuum u.v. absorpt., energy levels 3-76015
- H₂, HD, D₂, i.r. theory, expt. 3-72660
- o-H₂, solid, light absorpt., libron-libron interaction (*Russian*) 3-64137
- H₂ liquid and solid, short wavelength collective excitations 3-75993
- H₂ quantum diffusion 3-80015
- HA_n⁺, DA_n⁺, in Ar lattice, i.r. absorption, stabilization 3-65104
- HCl(Br):CN⁻ frozen solutions, absorpt. and luminesc. (*Russian*) 3-69067
- HCO₂, energy loss neutron inelastic scattering spectra in optical and far IR range, hydrogen bonding 3-60775
- HCrO₂, energy loss neutron inelastic scattering spectra in optical and far IR range, hydrogen bonding 3-60775
- HI, i.r. spectra in solid phase at 20 K 3-54690
- Hf(BH₄)₄:U(BH₄)₄, electronic absorpt. and optical spectra, vibr., cryst. field parameters 3-76033
- HgBr, molecular cryst., low freq. far i.r. spectra, phonon spectrum 3-76009
- Hg₂Br₂, far i.r. reflectivity meas., polar optic phonons study 3-55571
- Hg₂Cl₂, for i.r. reflectivity meas., polar optic phonons study 3-55571
- HgSe, conduction band structure from i.r. spectra 3-53112
- HgSe-HgS solid soln., conduction band structure from i.r. spectra 3-53112
- HgTe, band structure, electro-, thermo- and piezorefectance obs. 3-55635
- HgTe, band structure, fundamental reflectivity spectra (*Polish*) 3-41132
- Hg₂Zn_{1-x}Cr₂Se₄, i.r. absorpt. due to lattice vibrations 3-80035
- InAs, band struct., impurity conc. effect obs. 3-75708
- n-InAs, heavily-doped, effective mass 3-68623
- n-InAs, scanning laser i.r. microscopy, optical absorption and transmission 3-80082
- InAs-CdTe solid soln., band structure and light absorption (*Russian*) 3-64676
- InAs-CdTe solid soln., electron effective mass, thermoelectric power and i.r. refl. meas. 3-41141
- InAs-CdTe solid solns., band structure and optical props. (*Russian*) 3-64675
- InFe³⁺, solid, i.r. and Raman spectra 3-72627
- InP, Zeeman spectroscopy of shallow donor states 3-41543
- In₂S₃, optical transitions involving different numbers of photons 3-74272
- n-InSb, i.r. modulated electroreflectance, band structure obs. 3-55598
- InSb, reflectivity peaks in vacuum u.v. thermorefectance spectra 3-55623
- InSb, two photon interband magnetoabsorpt. 3-41504
- InSb, wavelength modulation spectra, surface elec. field, carrier conc. effects on reflectivity 3-55627
- inert, gas:O₂, vacuum u.v. absorption spectra, vibrational analysis 3-53130
- Ir coordination cpds., external vib. freqs. of active and racemic forms, i.r. spectra 3-55581
- K, conductivity sum rule for optical absorption 3-53125
- K halides, temp. depend. in Schumann u.v. region 3-58518
- KBr, optical absorption of I-centres 3-46642
- KBr, U centre i.r. absorpt. side bands Gruneisen const., hydrostatic press. depend. 3-55657
- KBr:Ag⁺, optical absorption bands, excited states 3-72685
- KBr:CrO₄²⁻, impurity oscillatory absorpt. (*Russian*) 3-47299
- KBr:Cu⁺, absorpt. from optically pumped relaxed excited 3d⁹4s state of Cu⁺ 3-50603
- KBr:Na, composite structure of V₁-band, thermal annealing obs. 3-64699

spectra of inorganic solids continued

- KBr:Na, thermal recovery of radiation hardening, thermoluminescence and thermal decay of V_1 band 3-68247
 KBr:Pb, optical absorption spectra, A, B, and C bands 3-69030
 KBr:Ti⁴⁺, phonon props. and electron-phonon interaction 3-58098
 KBr-TlBr single crystal, characts. of luminescence centres 3-64722
 KBr(Cl) whiskers, absorpt., U-centre theory, point defects 3-72652
 KBr(Cl)(I):NO₂⁻, SH⁻, impurity local modes, Raman and i.r. absorpt. obs. 3-72696
 KCN, i.r. spectra from 4000 to 140 cm⁻¹ 3-47240
 KCN, phase transitions influence, phonon modes and librations obs. (French) 3-58509
 KCl, isotope-induced far i.r. absorpt. 3-44402
 KCl, multiphonon i.r. absorpt. temp. depend. 3-68985
 KCl:Ag⁰, optical absorption bands, excited states 3-72685
 KCl:CN⁻, vibr. absorpt., broadening, tunnelling 3-69040
 KCl:CO₃²⁻, Pb²⁺(Sr²⁺), mol. impurity centre form. during electrolysis, i.r. absorpt. bands 3-50604
 KCl:K₂SO₄, X-irrad., i.r. absorpt. 3-69044
 KCl:LiF, NaF, LiCl, new bands in absorption spectrum 3-44438
 KCl:Na, Li, Cs, Rb, absorption, F-centres 3-76035
 KCl:SO₄²⁻-M₂⁺(CO₃²⁻-M₂⁺), band width var. with temp. 3-68364
 KCl:Ti⁴⁺, phonon props. and electron-phonon interaction 3-58098
 KCl(Br):Pb²⁺, absorpt. bands of Pb²⁺ centres 3-58532
 KCl, Br_(1-x), additively coloured, aggregate bands, spectral positions, half width 3-69037
 K₂Cr₂O₇, crystalline molten and aqueous, vibrational spectra 3-55587
 K₃(Cr³⁺O₆Mo₆O₁₈H₆).nH₂O, absorpt. and luminescence spectra, vibr. structure 3-72679
 KHF₂, long wavelength i.r. active phonons, assignment 3-41512
 KH₂PO₄ and KD₂PO₄, ferroelectric transitions, i.r. polarised reflection obs. 3-58482
 KH₃(SeO₃)₂, antiferroelectric, vibr. spectra and hydrogen bond pot. study 3-47256
 KH₃(SeO₃)₂; Raman and i.r. spectra, hydrogen bond potential well 3-53090
 KHgBr₃.H₂O, and KHgI₃.H₂O, polarised Raman and i.r. spectra, 10 to 4000 cm⁻¹, Urey-Bradley-Shimanouchi force field (French) 3-47258
 KI, far i.r. anharmonic optical props., absorpt., 12-300K 3-53104
 KI, thermorefectance, Rydberg series of gamma₁ exciton 3-55623
 KI:Ag, optical absorption, thermo- and photo-stimulated luminescence 3-76036
 KI.ClO₄-(ReO₄⁻), i.r. absorpt. and local symmetry of impurity ions (Russian) 3-41542
 KI:Pb, optical absorption spectra, A, B, and C bands 3-69030
 KI:Ti⁴⁺, phonon props. and electron-phonon interaction 3-58098
 KMgF₃, i.r. refl. spectra, dielec. const., lattice freqs. and interionic pot. calc. 3-47272
 KMgF₃:Eu²⁺, absorpt., f-f transition obs. 3-64726
 KMgF₃:Fe²⁺, far i.r. absorpt. 3-47298
 KNCS crystal, polarised far infrared spectra, lattice vibrations 3-72609
 K₂O-B₂O₃+MnO₂ glass, valence state of Mn 3-55411
 K₂O-SrO-SiO₂ system glasses i.r. spectra, struct. 3-68164
 K₂Pt(CN)₄Br_{0.3}(H₂O), reflection meas. for polarised light in far i.r. region (German) 3-50568
 K₂Pt(CN)₄Br_{0.3}.3(H₂O) quasi-unidimensional conductor, optical transmission spectrum for perpendicularly polarised light (German) 3-50588
 K₂WO₃, optical props. determ. from 0.1 to 38 eV 3-80072
 KY(MoO₄)₂-KDy(MoO₄)₂ system, energy spectrum of Dy³⁺ ion, absorpt. obs. 3-64682
 KmnF₃, antiferromag., magnon-phonon sidebands temp. depend., optical absorpt. obs. 3-47238
 Kr:H₂, i.r. absorpt. due to phonon sidebands on vibr./rot. transitions, theory 3-47244
 Kr:Hg trapped atoms, triplet splitting of ¹P state 3-64695
 La, absorpt. spectra, 1.13-4.42 eV, dispersion depend., quantum transitions (Russian) 3-80066
 LaAlO₃:Cr³⁺ crystals, electronic-vibrational spectrum, temp. var. 3-64721
 La₂Be₂O₃:Nd³⁺, absorption spectra 3-44485
 LaCl₃:Pm³⁺, absorption spectrum 3-76034
 LaF₃, reflectivity and surface plasma resonances 3-41538
 La₂O₃, infrared spectra 3-64661
 Li atoms in inert gas matrices, absorption and luminescence spectra 3-61055
 LiCl(Br):CN⁻ frozen solutions, absorpt. and luminesc. (Russian) 3-69067
 LiF, alkali ion implantation, correlation with absorption bands 3-80080
 LiF, proton irrad., 3400 Å absorpt. band due to metallic state hydrogen (French) 3-80078
 LiF, Stark effect in zero-phonon spectra of local N_i colour centres, modulation obs. 3-55665
 LiH₃(SeO₃)₂, ferroelectric, vibr. spectra and hydrogen bond pot. study 3-47256
 LiIO₃, hexagonal and tetragonal, vibr. and ¹²⁷I n.q.r. spectra (Russian) 3-79945
 LiNC, i.r. spectra from 4000 to 140 cm⁻¹ 3-47240
 Li₂Na_{1-x}I solid solutions, thin films, persistence of first absorption peaks 3-72665
 LiNbO₃, Li₃NbO₄, LiZnNbO₄, i.r. spectra 3-55602
 LiNbO₃ acoustic surface wave generation, Al interdigital transducers on piezoelectric substrate, optical spectroscopy 3-50065
 Li₂O-B₂O₃+MnO₂ glass, valence state of Mn 3-55411
 Li₂SO₄.D₂O, i.r. spectra, thermodynamic props. 3-72618
 Li₂SO₄.H₂O, i.r. spectra, thermodynamic props. 3-72618
 LiXVO₄, (X=Mg, Co, Ni, Cu, Zn), vibr. spectra obs. of order-disorder phenomena 3-52689
 LiX₂O₈ spinels (X=Ga, Fe, In, and Y=Cr, Rh) i.r. studies, ⁶Li-⁷Li shifts 3-47267
⁷LiF and natural LiF, i.r. props., calc. using shell model lattice dynamical data 3-41516
 Lu₃Al₅O₁₂:Ho³⁺, Er³⁺, Tm³⁺, absorption, luminescence, stimulated emission investigation 3-61053

spectra of inorganic solids continued

- LuFeO₃, wavelength modulated reflectivity, crystal field transitions obs. 3-47281
 Mg, refl., absorpt., and photoelec. meas. in vacuum u.v., surface plasmon excitation 3-44520
 MgBr₂ in solid Ar, matrix isolation i.r. study 3-64635
 Mg₂Cd_{1-x}Te mixed crystals, lattice vibrations, i.r. and Raman obs. 3-80036
 MgCl₂ in solid Ar, matrix isolation i.r. study 3-64635
 MgF₂, impurity ion absorpt. enhancement by radiation defects 3-53132
 Mg(H₂O)₆²⁺ salts i.r. spectra stretching vibr. water absorpt. bands, hydrogen bonds. (French) 3-63466
 Mg(H₂PO₄)₂.4H₂O and anhydrites, X-ray diffr., i.r. spectra, DTA 3-52616
 Mg(NH₃)₆Cl₂, Mg(ND₃)₆Cl₂, i.r. spectroscopy, strength of coordination band (French) 3-75985
 Mg₂Nb₂O₉, i.r. spectra 3-55602
 MgO, optical absorption, deformation effect 3-64697
 MgO:Ni²⁺, i.r. absorption, circular magnetical dichroism expts. (French) 3-41515
 MgO:Ni²⁺, MCD spectra of ³A_{2g}→³T_{2g} band, zero-phonon lines and phonon sidebands 3-64642
 MgSO₄, i.r. absorption, dehydration temp. 3-53098
 Mn cpds., X-ray emission spectra rel. to chem. bonding (Japanese) 3-69106
 MnCO₃, symm. in paramag. and antiferromag. states, Mn²⁺ ion absorpt. spectrum obs. (French) 3-47064
 MnCl₂, fundamental absorpt., broad and charge transfer bands 3-58524
 MnF₂, antiferromag., light absorpt. under phase transition induced by strong ext. mag. field 3-52964
 MnF₂, antiferromagnetic, spectroscopic investigation of intermediate state 3-75835
 MnF₂, impurity-induced i.r. absorpt. theory 3-64694
 Mn(II) complexes, CsMnX₃.2H₂O, (X=Cl, Br), N(CH₃)₄MnCl₃, antiferromagnets, polarised spectra, electronic transitions, temp. depend. and absorpt. mechanism 3-47253
 MnK₄(SO₄)₄.2H₂O, absorption spectra and Zeeman effect of Mn²⁺ at low temp. 3-44423
 MnO, matrix isolated, visible absorption spectra 3-52357
 α-MnS, visible absorpt., fine structure rel. to ligand field 3-58519
 MnSO₄, i.r. absorption, dehydration temp. 3-53098
 MnSiO₃, optical absorption spectrum of Mn²⁺, crystal field parameters 3-61056
 MoS₂, reflectivity in extreme u.v. range, band structure investigation 3-55609
 MoSe₂, i.r. absorpt. spectrum 3-47279
 N₂, i.r. theory, expt. 3-72660
 N₂ matrix containing Pt(N₂)_n complexes, 14 K, i.r. study 3-78810
 N₂O₂, vacuum u.v. absorption spectra, vibrational analysis 3-53130
 N₂:Rh(N₂)_n, n=1-4, i.r. examination, 10K 3-78809
 NH₄Br:Cu²⁺ absorption, effect of phase transition, phase III-IV 3-72667
 NH₄Cl:Cu²⁺, absorption spectrum, crystal parameters ¹³C-72687
 NH₄Cl:Cu²⁺, optical and e.p.r. spectra 3-55468
 NH₄Cl(I), u.v. reflectivity obs., ordered and disordered phases 3-80074
 (NH₄)₃(Cr³⁺O₆Mo₆O₁₈H₆).nH₂O, absorpt. and luminescence spectra, vibr. structure 3-72679
 NH₄H₂PO₄, NH₄H₂AsO₄, (NH₄)₂H₃IO₆, i.r. absorption spectra at room temp., NH₄ motion obs. 3-79996
 NH₄I, u.v. reflectivity for NaCl and CsCl structures 3-64677
 NH₄PF₆ and ND₄PF₆, polycrystals, i.r. and Raman spectra, phase transitions study 3-47263
 (NH₄)₂SO₄ particles, solar radiation absorption and scattering, near i.r., appl. to industrial pollution 3-44886
 Na peroxo tungstates and molybdates, i.r. spectra 3-57656
 NaBr:Cu⁺, absorpt. from optically pumped relaxed excited 3d⁹s state of Cu 3-50603
 NaCN, i.r. spectra from 4000 to 140 cm⁻¹ 3-47240
 NaCl, film, surface optical vibrations, frustrated total internal reflection obs. 3-50063
 NaCl, isotope-induced far i.r. absorpt. 3-44402
 NaCl, multiphonon i.r. absorpt. temp. depend. 3-68985
 NaCl:Ag⁰, optical absorption bands, excited states 3-72685
 NaCl:Ni, X-irradiated, stimulated processes, conductivity, thermoluminescence, absorption and e.s.r. spectra 3-41592
 NaCl:Pb²⁺, absorpt. bands of Pb²⁺ centres 3-58532
 NaClO₃ mol. crystal spectra, influence of polarising effect of medium in region of internal vibr. 3-72647
 Na₃(Cr³⁺O₆Mo₆O₁₈H₆).8H₂O, absorpt. and luminescence spectra, vibr. structure 3-72679
 NaF, multiphonon i.r. absorpt. temp. depend. 3-68985
 NaHF₂, long wavelength i.r. active phonons, assignment 3-41512
 NaH₃(SeO₃)₂, ferroelectric, vibr. spectra and hydrogen bond pot. study 3-47256
 NaLa(wO₄)₂, NaY(WO₄)₂, absorpt. and luminesc. spectra 3-69009
 NaMgF₃:Eu²⁺, absorpt., f-f transition obs. 3-64726
 Na₂O-B₂O₃+MnO₂ glass, valence state of Mn 3-55411
 Na₂WO₃, optical props. from 0.1 to 38 eV, absorpt. and refl. obs. 3-80072
 Na₂[Ln(CO₃)₂(H₂O)₂].wH₂O, i.r. and Raman spectra, struct. obs. (French) 3-60457
 Nb, reflectivity and surface plasma resonances 3-41538
 NbSe₂, reflectivity in extreme u.v. range, band structure investigation 3-55609
 Nd, absorpt. spectra, 1.13-4.42 eV, dispersion depend., quantum transitions (Russian) 3-80066
 NdF₃, far u.v. refl. spectra, 6-40 eV 3-58521
 Ni, precision reflectance 2-3 eV, spin-orbit effects 3-41525
 Ni, refl., 2-3 eV 3-52780
 Ni complex, 1-10 phenanthroline, crystal electronic absorpt. spectrum anal. 3-80076
 Ni films, adsorption of CO, multireflection i.r. spectra at room temp. and low pressure 3-68497
 Ni-Fe(25 wt.%) alloy, i.r. region obs. (Russian) 3-64664
 NiAl-based ternary β Hume-Rothery phases, optical consts., rel. to valence electron conc. and defect struct. 3-68965

spectra of inorganic solids continued

- NiCl₂, fundamental absorpt., broad and charge transfer bands 3-58524
- NiF₂, antiferromag., freq. moments of mag. light scatt. 3-47242
- NiF₆⁴⁻, NiCl₆⁴⁻ clusters, mol. orbital calcs., interatomic effects 3-68553
- Ni(II) complex, o-hydroxy-4-benzamidothio semicarbazide, distorted octahedral, visible absorption spectra 3-58517
- Ni(II) complex iminodiacetonickel(II), hygroscopic compound i.r. spectra, improved KBr pellet method 3-45491
- Ni(NH₃)₆X₂ (X=Cl, Br, I, BF₄), i.r. line profile 3-72646
- NiO, small particles, i.r. surface modes 3-41524
- NiSO₄·6H₂O and NiSO₄·6D₂O, vibrational spectra, frequency and temp. effects 3-44420
- NiSnCl₆·6H₂O and NiSnCl₆·6D₂O, vibrational spectra, frequency and temp. effects 3-44420
- NiWO₄, absorption spectrum, effect of antiferromagnetic ordering 3-44413
- NiWO₄, antiferromag. reson. lines in far i.r. absorpt. spectrum 3-50469
- O cpds., X-ray emission spectra rel. to chem. bonding (*Japanese*) 3-69106
- α-O₂, antiferromagnetic, double excitonic bands, doublet structure 3-61031
- α-O₂, at 1.3 K, bimol. series (Σ_g⁺→(ΔΔ) and (ΣΣ), absorpt. band fine struct. 3-44411
- O₂, cryst., excited mol. interactions, absorpt. 3-69022
- Pb halides, absorption, optical constants 3-44389
- PbBr₂, reflectance and luminescence at low temp., cation exciton model (*Russian*) 3-44454
- PbBr₂ film, absorpt. spectra, 3.5-11.0 eV, optical constants obs. 3-76017
- PbCl₂, reflectance and luminescence at low temp., cation exciton model (*Russian*) 3-44454
- PbCl₂ film, absorpt. spectra, 3.5-11.0 eV, optical constants obs. 3-76017
- PbF₂, pure and rare-earth activated, colour centres 3-54960
- PbF₂, reflectance and luminescence at low temp., cation exciton model (*Russian*) 3-44454
- PbI₂, band edge exciton parameters from refl. meas. (*German*) 3-50587
- PbI₂, electroabsorpt. of excitons, high field regime 3-55639
- PbI₂, single crystals, absorption and emission spectra at 1.8 K and 8 K respectively 3-72666
- PbMoO₄:Nd³⁺, cryst. Stark splitting, optical absorpt. and Zeeman spectra obs. 3-47297
- PbN₆:Bi, Ti, and pure thin films, i.r. absorption spectra 3-64647
- Pb(NO₃)₂, longit. mode freqs., PSR i.r. spectra 3-75975
- Pb(NO₃)₂ mol. crystal spectra, influence of polarising effect of medium in region of internal vibr. 3-72647
- PbO-SiO₂ glass, comp. effects 3-55266
- PbS, electronic band structure and optical props. 3-58523
- PbS(Se)(Te), epitaxial film, thermorefectance spectra from 0.7 to 5.6 eV 3-55622
- PbSe, electronic band structure and optical props. 3-58523
- Pd, electronic band structure and optical props. 3-58523
- Pd, 1-9 μ range, optical consts. and conduction electron characs. obs. 3-75992
- Pr, absorpt. spectra, 1.13-4.42 eV, dispersion depend., quantum transitions (*Russian*) 3-80066
- PrF₃, far u.v. refl. spectra, 6-40 eV 3-58521
- PrF₃, reflectivity and surface plasma resonances 3-41538
- Pr(Zn,Mg) nitrates, improved analysis and double perturbations 3-55663
- Pt electrode, electroreflection spectra, effect of I⁻ and n-(C₄H₉)₄N⁺ adsorption 3-47292
- Pt sputtered films in Ar discharge, H conc. 3-43961
- Pt sputtered films in Ar/N₂ discharge, water vapour press. 3-43962
- Pt/adsorbed H₂ and CO, i.r. spectroscopic study 3-79573
- Rb, conductivity sum rule for optical absorption 3-53125
- Rb, dielec. function meas. 2.07 to 6.2 eV, sum rule tests 3-80070
- RbAgI₃, solid electrolyte, far i.r. meas., low freq. lattice absorpt. 3-53115
- RbCl, i.r. emissions of the F centre and of compound colour centres 3-41566
- RbFeF₃, i.r. refl. spectra, dielec. const., lattice freqs. and interionic pot. calc. 3-47272
- RbI, F-centres, optical density, 80-160 K (*German*) 3-52626
- RbI thermorefectance, Rydberg series of gamma₁ exciton 3-55623
- RbMnF₃, i.r. refl. spectra, dielec. const., lattice freqs. and interionic pot. calc. 3-47272
- Rb-U complex fluorides, far i.r. absorption spectra 3-58499
- ReOF₄, vibrational spectra 3-72626
- Rh, coordination cpds., external vib. freqs. of active and racemic forms, i.r. spectra 3-55581
- Ru evaporated thin films, in v.u.v. from 300 to 2000 Å 3-80069
- SO₄²⁻, vibr. freq., environmental influence 3-75999
- SO₂Cl₂, solid, Raman and infrared spectra rel. to crystallographic structure 3-61035
- Sb₂O₃, crystalline, i.r. spectra, ion-exchange properties 3-75978
- Sb₂S₃ monocryst., optical dielec. const. and valent electron plasmonic oscill. freq. calcs. (*Russian*) 3-55540
- SbSI, ferroelec. semicond., absorpt. edge not affected by ferroelec.-paraelec. transition 3-61051
- SbSI, wavelength modulation spectrum rel. to band structure 3-55625
- Se, trigonal, α-monoclinic, electroabsorpt. of excitons, high field regime 3-55639
- Si, amorphous, electronic density of states, absorption, photoemission, photoconductivity 3-41119
- Si, amorphous, i.r. and Raman spectra theory 3-41513
- Si, band struct. features, determ. from u.v. edge-absorpt. data 3-52787
- Si, derivative spectrum of indirect exciton absorpt., anal. 3-47290
- Si, doping inhomogeneities meas. by electroreflectance 3-54977
- Si, epitaxial layers, donor conc. levels, effect of etching and autodoping, low temp. i.r. studies 3-41653
- Si, Li⁺ ion bombarded, radiation defects, i.r. absorpt. study 3-46652

spectra of inorganic solids continued

- p-Si, use of Mg diffusion to meas. residual P conc. by i.r. absorpt. 3-61054
- Si amorphisation during different mass ion implantation 3-60754
- Si:Au, i.r. absorption, localised pair centre vibration and neutral centre obs. 3-72690
- Si:Li, irradiated, spectra of Li-defect complexes 3-44434
- Si-As-Te, amorphous, relation of elec. and optical gaps, d.c. cond. and light absorpt. obs. 3-72308
- Si-SiO₂, i.r. light absorption, photoelectric props. (*Russian*) 3-58322
- Si-SiO₂-electrolyte system, electrorefl. spectra in strong surface elec. fields 3-50543
- α-SiC, 6H polytype, activated by u.v. illumination, i.r. absorpt. 3-55600
- α-SiC, 6H-polytype, impurity i.r. absorpt. (*Russian*) 3-80083
- SiC, far i.r. absorpt. bands, narrow doublet lines 3-44445
- SiC, i.r. absorpt. on surface, multiple internal reflection method obs. 3-55580
- n-SiC, optical absorption associated with superlattice 3-41533
- SiC, p- and n-type, i.r. absorpt., role of free carriers 3-75996
- α-SiC, polarity, reflection spectra of polished faces 3-43772
- SiO₂ film, differential spectral study (*Russian*) 3-72296
- SiO₂ film properties, effects of bombardment by Ar ions in r.f. plasma (*Russian*) 3-68706
- SiO₂ films, i.r. study, P, B, Zn impurities, stability, struct. 3-64646
- SiTe₂, absorption, optical properties between 300 K and 100 K 3-47285
- Si₃Te_{1-x} amorphous thin films and bulk samples 3-58556
- SmS, optical properties of discontinuous semiconductor-metal phase transformation (*German*) 3-53118
- SnO₂, anal. of exciton absorpt. spectrum at 1.5, 4.2 K 3-41164
- SnS, absorption spectra and valence band spectra 3-41534
- SnSe, absorption spectra and valence band spectra 3-41534
- SnTe, epitaxial film, thermorefectance spectra from 0.7 to 5.6 eV 3-55622
- SrCl₂, phonon dispersion curves, i.r. and Raman spectra obs. 3-49951
- SrCl₂:H⁺, U-centres, i.r. absorpt. study 3-69032
- SrF₂:Na, conversion of colour centres by doping 3-53133
- SrF₂:Tm²⁺, high press. optical absorpt. studies 3-41540
- StO, vibronic props. of F⁺ centre, absorpt. study 3-55062
- Ta sputtered films in Ar discharge, H conc. 3-43961
- Ta sputtered films in Ar/N₂ discharge, water vapour press. 3-43962
- TaBO₄, i.r. and Raman spectra 3-68989
- TbAlG:Tb³⁺, analysis, 4K, 77K 3-76067
- Tb(OH)₃:Er³⁺ ferromagnetic, anisotropic exchange effects 3-47010
- Te, absorption spectra for polarisation E ⊥ c, intervalence band transitions 3-79631
- Te thin films, optical absorption between 39 and 250 eV 3-58522
- Te, i.r. spectra, zero-centre phonon behaviour 3-72059
- TeO₂, i.r. refl., polar phonon spectrum 3-53106
- TeO₂:Ca²⁺ (Y³⁺), absorpt. edge behaviour, doping effect, rel. to fluoresc. 3-55678
- Ti optical constants and electronic characs. 3-72594
- Ti(III)/Ti(IV) hydroxide, spectroscopic props. and interaction absorpt. 3-55606
- TiO₂:Cr³⁺, Zeeman effect of no-phonon ⁴A_{2g}-⁴T_{2g} transition 3-53124
- TiO₂:H,D, rutile, i.r. absorpt., impurity conc. detn. 3-58530
- Ti₂O₃, oxid. products of Ti and TA6V alloy, diffuse reflectance obs. (*French*) 3-69287
- Tl, optical absorption over energy range 0.6-3.8 eV 3-44425
- TlBr, electroabsorpt. of excitons, high field regime 3-55639
- TlF₃⁺, solid, i.r. and Raman spectra 3-72627
- TiNO₃, longit. mode freqs., PSR i.r. spectra 3-75975
- TiNO₃III, i.r. absorpt., Davydov and intersite splitting rel. to cryst. struct. 3-75997
- Ti₂O-GeO₂-SiO₂ glasses, i.r. detection of depolymerization 3-58500
- U(BH₄)₄/Hf(BH₄)₄, optical and e.p.r. spectra of mol. crystals, exciton theory 3-68973
- UO₂Cl₂, exciton-phonon interactions, line shape anal. 3-72751
- UO₂(NO₃)₂, exciton-phonon interactions, line shape anal. 3-72751
- UO₂SO₄, uranyl ion orientation, electron-vibr. fine struct. 3-72752
- V₂O₃, rhombohedral, empirical band scheme, optical and soft X-ray data 3-41130
- V₂O₃:Cr, strongly correlated electrons in narrow band, impurity effects on absorpt. spectra 3-55195
- V₂O₅, single cryst., electroreflectance, resonance due to conduction band fine struct. 3-50598
- V₂O₅ electroreflection, reverse piezoelec. effect, electrostriction 3-76021
- W/α-CO chemisorbed layer, i.r. refl. and absorpt. 3-44417
- Xe, u.v. absorption, deposition temp. depend. 3-69018
- Xe, vacuum u.v. emission band obs. 3-55649
- Xe solid and liq., band struct. from refl. spectra 3-50130
- YAG:Nd³⁺, absorpt., energy level temp. shift obs. 3-64727
- YAG:Nd³⁺ single crystals, absorption bands (*Russian*) 3-69025
- Y₃(Al_{1-x}Ga_x)₅O₁₂:Nd³⁺, study of clustering 3-78040
- YAlO₃:Ce³⁺, i.r. and u.v. absorpt. spectra, 4f and 4d energy levels derived 3-58531
- YAlO₃:rare earth, absorpt. and emission intensities for trivalent rare earth ions 3-47296
- YAlO₃:TR³⁺ (TR=rare earth), colour centres, absorption and thermoluminescence spectra 3-44441
- YIG, optical absorption and Faraday rotation in range 1 to 0.35 μ at 300, 20 and 6 K 3-64684
- YIG, reflection spectra in range 9000 to 200000 cm⁻¹ 3-76023
- YIG, Sn-substituted, stretching vibrations from i.r. spectra 3-41464
- YIG, wavelength modulated reflectivity, crystal field transitions obs. 3-47281
- YIG epitaxial films, optical transmission and magneto-optical props. 3-44505
- YIG:Ga substituted, wavelength modulated reflectivity, crystal field transitions obs. 3-47281
- YLAG:Nd³⁺, spectral props. and induced emission 3-53131
- YNbO₄, internal vibration modes of NbO₄³⁻ tetrahedra, i.r. and Raman spectra obs. 3-53095

spectra of inorganic solids continued

- YTaO₄, internal vibration modes of NbO₄³⁻ tetrahedra, i.r. and Raman spectra obs. 3-53095
 Zn₃Cd_{1-x}Te, grown from melt, reflectivity in lowest band gap region 3-69154
 Zn₃Cd_{1-x}Te, multiphonon resonance combination scattering at 77K 3-76022
 ZnGa₂O₄, exchange interactions of nearest neighbour Cr³⁺ pairs, spectra obs. 3-53142
 ZnGeP₂, chalcopyrite crystals, thermorefectance, energy band structure 3-44007
 ZnGeP₂, wavelength modulation spectrum rel. to band structure 3-55625
 Zn(II) complexes, organophoric anions, halogen and pseudohalogen perturbations (*French*) 3-75505
 ZnO, i.r. absorption by acoustoelectric domains 3-72617
 ZnO sputtered films, diagnostic rate monitoring by interference spectroscopy 3-45418
 ZnP₂, edge absorpt. spectrum at 4.2K 3-44424
 ZnS, i.r. absorption and stimulated, optical and thermal depth of shallow traps 3-60860
 ZnS-Mn²⁺, excitation and emission spectra, lines due to stacking faults 3-50619
 ZnSe, donor-acceptor pair recomb. obs. of electro-luminescence edge emission 3-80110
 ZnSe:Mn²⁺ splitting, fine structure of ⁴E level, uniaxial stress method 3-47295
 ZnSe:Ti, autoionisation of ³Ti(³P) state, photoconductivity meas. and absorption spectra 3-64375
 ZnSiP₂-ZnSiAs₂, range of semiconductors, optical absorption edges at 300 K and 80 K 3-55604
 p-ZnSnP₂, electrorefl. spectra, 1.5-4.5 eV, 77 and 295 K 3-44430
 ZnTe, band structure, fundamental reflectivity spectra (*Polish*) 3-41132
 ZnTe, exciton effect in electrorefl. spectra 3-64678
 ZnWO₄:Cr³⁺, single crystal, optical absorption, luminescence spectra 3-76070
 α-Zr(HPO₄)₂·H₂O, crystalline, prep. and characterisation 3-55730
 ZrO₂, yttria stabilised, current blackening, optical absorpt. study 3-47449
 ZrO₂:Ce⁴⁺, Pr⁴⁺ and Tb⁴⁺, electron transfer spectra 3-55655
 ZrO₂:Er³⁺, Y₂O₃-stabilised, absorpt. spectrum, O²⁻ coordination, crystal structure 3-41539

spectra of organic molecules and substances

- see also infrared spectra of organic molecules and substances; luminescence of organic solids; radiofrequency spectra of organic molecules and substances; Raman spectra of organic substances
 absorption and emission in mol. cryst., line shape theory, exciton motion 3-80073
 absorption spectrum of local centres, correl. functions, multiplet structure 3-64681
 acenaphthene, quasi-linear absorption and luminescence 3-72747
 acetone in solution, triplet state, charge transfer rel. to quenching by aromatic molecules 3-69474
 acetonitrile, photodissociation and photoionisation in vacuum u.v., Rydberg states obs. 3-75093
 acetophenone, in alcoholic soln., triplet state, absorpt. spectra obs. (*Russian*) 3-80067
 acetylene, molecule, electron impact dissoc., rotational and vibrational energy level distrib., luminesc. 3-75127
 acetylene + oxygen flames, reduced-pressure, spectroscopic obs. of methene and methyl radicals 3-47532
 acetylene nitrile, photodissociation and photoionisation in vacuum u.v., Rydberg states obs. 3-75093
 acriflavine soln., fluorescence and absorption spectra 3-69047
 acrolein, cis and trans, near u.v. absorption spectra 3-52352
 acrolein-d₁, near u.v. absorption spectra 3-52352
 amino group, two-component solns., spectroscopic study of intermolecular interactions (*Russian*) 3-80050
 aniline derivatives, u.v. absorpt. spectra, electronic transition 3-78730
 anthracene, ¹L_b transition location by dichroism meas. 3-76013
 anthracene, absorpt. spectra, polarisation props., line form of 2 photon transitions 3-66887
 anthracene, cryst., exciton band structure, thermoabsorpt. obs. 3-55230
 anthracene, crystals, exciton-phonon interaction, conservation laws 3-68972
 anthracene, singlet-triplet absorpt. spectra, Franck-Condon factors 3-73159
 anthracene and methyl derivatives in polymethylmethacrylate matrix, absorption and fluorescence spectra 3-63507
 anthracene crystal, absorption, resonance interband interaction and vibronic coupling 3-41161
 anthracene crystal, low temp. refl. surface excitons 3-69017
 anthracene crystal reflectance, exciton dynamics, line shape analysis 3-64306
 anthracene crystals, effects on polarized reflection spectrum during cooling 3-69008
 anthracene mol. solids, polariton dynamics from band profile analysis 3-72642
 anthracene molecule, vacuum u.v. absorpt. spectrum 3-78745
 anthracene ring system containing cpds., photoemission in vacuum u.v. region 3-41613
 anthracene solution, delayed fluorescence, O₂ quenching, mag. field effects 3-46309
 anthronitrile, absorption and fluorescence spectra, solvent and pressure dependence 3-41531
 aromatic compounds, absorption spectra, intensity of transition and intensity distribution correlation 3-60440
 aromatic hydrocarbons, condensed, Stark effect 3-76012
 aromatic hydrocarbons in vitreous media, identification of autoassociated species (*French*) 3-50590
 aromatic polynitro compounds, electrochemical circulation cell, electrolysis, electronic absorption spectra, optical density meas. 3-45534
 aromatic systems, effect of B, N atoms on internal energy transfer 3-69084
 aromatic triple bond molecules, description of radiative triplet props. 3-67841

spectra of organic molecules and substances continued

- azaphthalenes, triplet-triplet absorpt. spectra 3-53330
 azulene, B-X(3500 Å) transition, medium-depend. effects, vibronic coupling, Fermi reson. 3-75002
 azulene, benzophenone (naphthalene), impurity change of polarisability and dipole moment, ¹ππ* state 3-72662
 azulene in soln., consecutive two-photon absorpt. using dye lasers 3-44730
 bacteriochlorophyll, one-electron oxidation, absorption and e.p.r. obs. (*Russian*) 3-51425
 benzaldehyde, in alcoholic soln., triplet state, absorpt. spectra obs. (*Russian*) 3-80067
 benzaldehyde electronic emission spectrum, molecular vibrations 3-67843
 benzamide, in alcoholic soln., triplet state, absorpt. spectra obs. (*Russian*) 3-80067
 benzene, ¹E_{2g} ← ¹A_{1g} absorpt. transition 3-78728
 benzene, CH-stretching overtone spectrum analysis, phase coincidence problem 3-67777
 benzene, cryst., ¹B_{1u} ← ¹A_{1g} 0-0 transition obs. 3-76051
 benzene, crystals, exciton-phonon interaction, conservation laws 3-68972
 benzene, single cryst., 2000 Å absorpt. system in polarised light 3-58520
 benzene absorpt. spectra, polarisation props., line form of 2 photon transitions 3-66887
 benzene cryst., determ. of exciton-phonon interact. in absorpt. spectrum 3-72630
 benzene derivatives, structure depend. of u.v. absorpt., intramol. electron transfer 3-75061
 benzene ring system containing cpds., photoemission in vacuum u.v. region 3-41613
 benzene single crystals 2000 Å polarised light absorpt. 3-69019
 benzene-oxygen contact complex, vapour phase absorpt. spectrum 3-54664
 benzenes, multi-homosubstituted, variable electronegativity SCF-MO calcs. 3-67736
 benzenes, substituted, molecules, magnetic circular dichroism 3-54669
 benzoic acid, in alcoholic soln., triplet state, absorpt. spectra obs. (*Russian*) 3-80067
 benzoic acid, methyl derivatives, Pariser-Parr-Pople calc. (*French*) 3-63379
 benzonitrile, vibrational analysis of the 2738 Å system 3-40610
 benzophenone, in binary solvent mixtures, electronic spectral intensities 3-46264
 benzophenone, microwave-optical double resonance, study of lowest triplet states 3-80121
 benzophenone, phosphorescence, absorption, hydrogen bonding in solution, blue shift 3-64710
 p-benzoquinone, single crystals, Stark effect on lowest ¹B_g(ππ*) state 3-80065
 p-benzoquinone, single crystals, Stark effects on low energy electronic states 3-76468
 benzoylacetone, u.v. diffuse reflectance spectra 3-47291
 benzyl-type radicals, methyl substitution effect on electronic struct. and spectra 3-78731
 biacetyl, vibr. relax. obs. by visible-i.r. double reson. technique 3-78885
 biphenyl, triplet-triplet transition absorption spectrum 3-74946
 biphenyl crystal, high-resolution two-photon excitation spectra 3-80068
 biphenyl crystal, low energy magnetic and electric dipole transitions 3-47282
 bitumens, industrial, spectra as means of identification (*Russian*) 3-64687
 p-bromoanisole, ultraviolet absorption spectra 3-67795
 m-bromoanisole, u.v. absorpt. spectra assignments 3-67799
 butane absorption cross sections from 180 to 700 Å 3-67805
 butanol-2-(+), circular dichroism, vacuum UV, rot. strengths 3-78746
 carbon tetrachloride, liquid, absorpt. loss spectrum, thermo-optical meas. technique 3-62103
 carbon tetrachloride, liquid, Rayleigh scatt. meas. using optical fibres 3-62102
 carbonyl fluoride convergence of reduced Hamiltonian, centrifugal distortion, z-axis choice 3-63425
 carbonyl group, two-component solns., spectroscopic study of intermolecular interactions (*Russian*) 3-80050
 carboxylic esters and derivatives, molecular structure and conformation 3-74927
 α-o-carboxyphenylcinnamic acids, u.v. spectra 3-60449
 α-carboxystilbenes, u.v. spectra 3-60448
 cerium benzoylacetate, u.v. diffuse reflectance spectra 3-47291
 chalcones, substituted and vinyls, absorpt. spectrum rel. to props. in excited state 3-64725
 chlorobenzene, liquid, absorpt. loss spectrum, thermo-optical meas. technique 3-62103
 chlorobenzene, out-of-plane vibr. modes in ground and first excited singlet states 3-63408
 chloromethanes, vacuum u.v. absorpt. spectra 3-52356
 chlorophyll-a in detergent, absorpt., optical activity, micelle form. 3-72680
 p-chlorostyrene, rot. band contour analysis of O_p⁰ bands of A¹A' - X¹A' systems 3-63446
 cholesteric mixtures solute chromophores, electronic transitions of different polarization (*German*) 3-79235
 cinnoline in durene and naphthalene host cryst., electronic absorpt. spectra analysis 3-69028
 cyanine dyes, excited singlet-singlet absorption in solution 3-62739
 cyclopentadienide anions, cyano-substituted, mag. circular dichroism, electronic transitions 3-40607
 (2,2)p-cyclophane and related compounds, electronic structure 3-78734
 decacyclene saturated solutions, quasi-linear fluorescence spectra 3-76080
 n-decane matrix, multiplet struct. of quasiline spectra of Zn phthalocyanine, 4.2K 3-72734
 diacetyl in benzene or toluene, luminesc., photo, X-ray, triplet-triplet energy transfer 3-69083

spectra of organic molecules and substances continued

- N,N-dialkyl-p-cyanoanilines self-complex electronic absorption spectra 3-54674
- 9,10-diazaphenanthrene solutions, fluorescence and absorption at 77K 3-41574
- dibenzofuran, lowest singlet state obs. 3-67804
- 9,10-dibromo- and dichloro-anthracene in vitreous solutions, autoassociation (*French*) 3-50591
- p-dichlorobenzene, α , γ phases, T_1 absorption and phosphorescence spectra, fine structure 3-69052
- p-dichlorobenzene, α - and γ -phases, T_1 absorption and phosphorescence 3-80104
- 1,1-difluoroethylene, mass-spectrometric study in vacuum u.v., photoionisation curves and threshold energies 3-52395
- dimers, strong coupling and spectral consequences 3-78699
- dinitrocarbanion reorientation in alkali salts, i.r. and u.v. spectra 3-69003
- diphenyl sulphide, band position, oscill. forces and electron density distrib. (*Russian*) 3-50555
- diphenyl sulphone, electron struct. and nature of absorpt. bands (*Russian*) 3-50555
- diphenylnitroxide radical, polarised absorption spectra, electronic structure 3-63442
- α,ω -diphenylperfluoropolyenes, effect of fluorination on conjugation, UV and Raman spectra, steric struct. of mols. 3-71520
- diphenyl sulphoxide, electron struct. and nature of absorpt. bands (*Russian*) 3-50555
- disulphides, charge transfer complexes with various acceptors, u.v. spectra and bond angle study 3-46263
- durane matrix, isolated p-fluoroaniline dipole moment determ., Stark spectroscopy 3-72600
- dye dimers, effect of local field on electronic spectra 3-53122
- dye molecules aggregates, effect of local field in electronic spectra 3-67807
- dyes, optimum spectral characteristics, computer simulation 3-47287
- EDA complexes in polar solvents excited state dipole moment from solvent shift 3-71537
- EDA complexes with liquid donors, excited singlet-singlet absorpt. spectra 3-76471
- eosin, soln., fluorescence and absorption spectra 3-69047
- erythrosin, soln., fluorescence and absorption spectra 3-69047
- esters, mixed polyfluorinated, valency vibration absorption bands, carbonyl groups (*Russian*) 3-71530
- ethane, electron impact excitation, emission spectra 3-75122
- ethane absorption cross sections from 180 to 700 Å 3-67805
- ethers, containing solvated electrons, optical absorpt. spectra by pulse radiolysis 3-44725
- ethylene, electron impact excitation, emission spectra 3-75122
- ethylene, molecule, electron impact dissociation, rotational and vibrational energy level distrib., luminesc. 3-75127
- ethylene, reaction with N atom, emission spectra obs. 3-44718
- ethylene absorption cross sections from 180 to 700 Å 3-67805
- ethylene chlorine complex, struct. determ. from spectra 3-54608
- ethylene sulphide, Rydberg transitions, vacuum u.v. spectra 3-54675
- ethylenic chromophores-trans-cyclooctene, absorption and circular dichroism spectra 3-71545
- ethynyl-benzene and derivatives, absolute calc. radiationless decay of lowest triplet state 3-67842
- europium tetra-O-dibenzoyl-methanates, luminescence and absorption spectra (*Russian*) 3-41561
- excited states of matter, symp., Lubbock, Texas, USA (Apr. 1971) 3-63547
- ferrocenium ion, distortion, parameters from low temp. absorpt., MCD and ESR spectra 3-75004
- fluorescein, soln., fluorescence and absorption spectra 3-69047
- 4-fluoro-2-chlorotoluene vapour, near u.v. absorption spectrum, modes of vibration 3-46260
- p-fluoroaniline, dipole moments determ., orientational Stark splitting obs. 3-63433
- fluorobenzene, 4.2 K, exciton spectra, polarised u.v. light 3-69020
- fluoromethanes, vacuum u.v. absorpt. spectra 3-60451
- p-fluorostyrene, rot. band contour analysis of O_0^0 bands of $A^1A' - X^1A'$ systems 3-63446
- formyl radical, from sensitized decomposition of formaldehyde, electronic spectra 3-47577
- gadolinium tetra-O-dibenzoyl-methanates, luminescence and absorption spectra (*Russian*) 3-41561
- glycerol, photon correlation study of scatt. depolarised ray at low temp. (*French*) 3-68966
- glyoxal- d_1 and glyoxal- d_2 5207 Å band system, vibrational assignment 3-54660
- N-heterocyclic compounds, ortho, oxy, and methoxy substituted, electronic spectra (*Russian*) 3-63395
- hydrocarbon matrices, struct. of azulene electronic spectra 3-72736
- hydrocarbons, conjugated, energies and oscillator strengths of excited singlet states calc. 3-52344
- hydrocarbons, conjugated, singlet-triplet and triplet-triplet spectra calc. 3-52343
- hydrocarbons, electron beam excitation, Balmer β radiation, cross section meas. 3-75123
- isoquinoline, triplet-triplet absorpt. spectra 3-67803
- isoquinoline vapour, electronic absorpt. spectrum assignments 3-67798
- ketones, polyfluorinated, valency vibration absorption bands, carbonyl groups (*Russian*) 3-71530
- ketones in solution, triplet state, charge transfer rel. to quenching by aromatic molecules 3-69474
- lanthanum benzoylacetate, u.v. diffuse reflectance spectra 3-47291
- liquid, u.v. region charact., dispersion curves (*Russian*) 3-64688
- liquid crystal, nematic, MPT, refr. indices, temp. depend. (*French*) 3-41526
- liquid crystal matrix, absorpt. by complicated molecules 3-71543
- liquid crystals, spectroscopy, review 3-43747
- magnesium phthalocyanine, transition from aggregate to monomer state, spectral study 3-52753
- methane, $3\nu_3$ absorption band in Saturn's atmospheric spectra, rotational temp. and abundance 3-47913

spectra of organic molecules and substances continued

- methane, ν_3 band of absorpt. spectrum from 2863-3132 cm^{-1} (*French*) 3-49461
- methane, electron impact excitation, emission spectra 3-75122
- methane $3\nu_3$ band of Saturn's atmosphere, obs. along planet's central meridian 3-56331
- methane absorption cross sections from 180 to 700 Å 3-67805
- methane absorption line formation in Jovian atmosphere, high dispersion spectra 3-59269
- methane pressure-broadened lines in Jupiter's atmosphere 3-47914
- methanes, solid isotopic, optical birefringence in lowest temp. phase 3-50556
- n-methoxyacetophenone, in organic solvents, fluorescence and absorption spectra (*Russian*) 3-44469
- methyl iodide in solid and liquid Kr, Wannier states study by vacuum u.v. spectra 3-47294
- methylene blue, photoquenching, depend. of quantum yield on pulse intensity and duration 3-67840
- methylene chloride mixtures with toluene, benzene and xylenes, dielectric polarisation, n.m.r., u.v. and i.r. studies 3-58817
- methylene thiocyanate, i.r. absorpt. spectra, 2 to 20 μ , point group C_{2v} GG conformation (*French*) 3-47273
- 1,2-methylnaphthalene, vapour phase near u.v. absorpt. spectra assignments 3-67796
- 3-methylpyridazine, n.m.r. and u.v. spectral changes due to intramolecular transform. 3-75088
- methylquinoline, 2-, 4-, 6-, 7-, 8-, in crystalline n-paraffins, quasi-linear phosphorescence spectra, vibrational 3-50609
- molecular crystal, absorpt. band structure and origin of high nonlinear dielec. susceptibility 3-62740
- molecular crystal, Davydov splitting, multipole approximation based on transition charge densities 3-80014
- molecular crystals, excitons, Fermi-Davydov reson. 3-68998
- monomethyl cadmium radical, u.v. absorption spectra 3-46261
- monomethyl tellurium radical, u.v. absorption spectra 3-46261
- monomethyl zinc radical, u.v. absorption spectra 3-46261
- naphthalene, arylethylene doped, vibronic phonon struct. 3-68357
- naphthalene, crystals, exciton-phonon interaction, conservation laws 3-68972
- naphthalene, c.p.r. and optical absorpt. obs. of radiation-induced radicals 3-55473
- naphthalene, ring system containing cpds., photoemission in vacuum u.v. region 3-41613
- naphthalene, triplet-triplet absorption spectrum, polarisation, meas., substitution effects 3-46257
- naphthalene crystal, anomalous exciton splitting in 3000 cm^{-1} region vibrational spectrum 3-64657
- naphthalene crystal, reson. interaction in vibronic spectra of local excitons 3-68970
- naphthalene-anthracene sandwich pair, absorption and exciplex fluorescence spectra 3-47579
- naphthalene-hs, triplet-triplet absorpt. absence in pure crystals. 3-61048
- naphthalenes, monosubstituted, electronic absorpt. spectra interpret. by config. analysis 3-67754
- 1,8-naphthoylene-1,2'-benzimidazole solutions, role of triplet states (*Russian*) 3-61276
- 2-naphthyl acetate, intramolecular energy transfer from upper triplet states 3-69079
- 1-naphthyl acetic acid, intramolecular energy transfer from upper triplet states 3-69079
- 2-naphthyl-isobutyric acid, intramolecular energy transfer from upper triplet states 3-69079
- neodymium benzoylacetate, u.v. diffuse reflectance spectra 3-47291
- n-octane matrix, absorpt. and fluoresc. of monosubstituted benzenes 3-72739
- organic complex molecule, intramolecular relax. 3-71536
- organometallic, organic mol. intercalated transition metal dichalcogenide, band structure obs. 3-55607
- oxamides, mol. anal. phosphoresc. charact. 3-78833
- n-paraffin matrices, luminesc. and excitation spectra of chlorophyll A 3-72733
- n-paraffin matrix, absorpt. and fluoresc. of naphthalene type molecules 3-72739
- n-paraffin matrix, quasiline absorpt. and fluoresc. spectra of polyenes 3-72742
- n-paraffin solutions of aromatic compounds, frozen, absorption, fluorescence at 77K 3-72745
- pentaerythritol tetranitrate, U.V. absorption spectrum 3-54668
- perylene mol. solids, polariton dynamics from band profile analysis 3-72642
- phenanthrene molecules in solid solutions, spectroscopic manifestation of ordering 3-64656
- phenol, near u.v. spectrum, solvent effects and distribution in micellar solutions 3-52359
- phenyl, benzoyl-(CH_2) $_n$ -phenyl, phthalyl in n-paraffin matrices, absorption, alternation effect 3-72746
- n-phenyl-benzophenone, in organic solvents, fluorescence and absorption spectra (*Russian*) 3-44469
- 3-phenylsidon, solvent effect on spectrum, dipole moment determ. from first excited singlet state 3-47284
- phenylsilanes, calc. of u.v. spectra, s.c.f. method 3-67808
- phosphoric acid chloranhydrides, unsaturated u.v. absorption spectra, intramol. interactions (*Russian*) 3-40609
- photoquenching of large molecule depend. of quantum yield on pulse intensity and duration 3-67840
- phthalimide derivative vapour, excited state lifetime, spectral depend. 3-63508
- phthalocyanines, thin films and solutions, emission spectra 3-61074
- pinene (α and β), absorption and circular dichroism spectra 3-71545
- polycyano, absorpt., exciton band shape, mol. crystals 3-69021
- polyatomic, quasiline absorpt. spectra (*Polish*) 3-57664
- polyatomic molecules and ions, genealogy in mol. spectroscopy, aromatic π -electron spectroscopy 3-63432
- polycyano-compounds, solvent effect on u.v. spectra, dipole moments in excited singlet states (*French*) 3-63440
- polyenes, electronic structure 3-71544

spectra of organic molecules and substances continued

- polyethylene, optical absorption rel. to electrical conduction 3-41529
- polyethyleneterephthalate, rel. to meander model of crystallis. (*German*) 3-60669
- polymeric complexes, u.v. study of structure 3-63963
- polymethine dye, induced absorption spectra 3-65112
- polymethine dyes, triplet-triplet energy transfer, fluoresc. 3-69479
- polyvinylcarbazole:trinitrofluorenone, amorphous films, absorption and electroabsorption 3-61049
- porphyrins, excited states, effects of metallic substitution 3-63550
- praseodymium benzoylacetate, u.v. diffuse reflectance spectra 3-47291
- propynal, rot. anal. of 0-0 band near 4145 Å 3-67793
- pyrazoline compounds, molecular association in binary solvents, absorption, dissociation energies calcs. (*Russian*) 3-80542
- pyrene, emission-absorpt. asymmetry of S_1 - S_0 transition, deuterium effect, vibronic coupling 3-54715
- pyrene excimer, absorption spectrum by modulation excitation spectro-photometry 3-46258
- pyrene single cryst., light absorpt., 4 to 300 K, ground-to-excimer state absorpt. search 3-53150
- pyrene solution, delayed fluorescence, O_2 quenching, mag. field effects 3-46309
- pyridine, u.v. spectra, 3000 to 3400 Å, triplet-singlet absorpt., band assignments 3-49460
- pyridine ring system containing cpds., photoemission in vacuum u.v. region 3-41613
- pyridine-4-d₁, near u.v. spectra, appl. of band contour anal. method 3-46307
- pyromellitic dianhydride-anthracene single crystals, charge transfer complex, piezoreflectance 3-55644
- quinazoline in durene and naphthalene host cryst., electronic absorpt. spectra analysis 3-69028
- quinoline, hydrogen bonding effect on absorpt. spectra (*Russian*) 3-54658
- quinoline, stimulated scatt. Rayleigh line wing light, fine struct. 3-58502
- quinoline, triplet-triplet absorpt. spectra 3-67803
- quinolinium cation, absorption and dual fluorescence 3-63497
- rhodamine 6G, soln. generation by excitation, effect of detergent (*Russian*) 3-70819
- Rhodamine B, dimer in aq. solns., visible spectra, conc. depend. 3-47584
- rhodamine dyes, conc. quenching in luminesc. of alcohol solns. 3-69075
- rhodamine-B, absorption and fluorescence spectra 3-69046
- riboflavin, absorption and fluorescence spectra 3-69046
- samarium benzoylacetate, u.v. diffuse reflectance spectra 3-47291
- Seignetto salt solns., position of nat. absorpt. limits (*Russian*) 3-65126
- semiconductors, impurities optical absorption 3-80079
- Shpol'ski systems, intensity of solute-solvent interactions 3-72728
- singlet-triplet and triplet-triplet spectra, closed and restricted open shell semiempirical methods, configuration interaction 3-52342
- sodium fluorescein in glycerol, luminesc. aggregates, Webers red edge effect 3-69078
- solutions under h.p., optical activity induced by chiral solvents 3-46254
- squaric acid and anions, π electronic struct. determ., near u.v. aq. soln. spectra 3-52360
- stretched film technique for fluoresc. and phosphoresc. polarization meas. 3-40641
- styrene, polymerisation effect, absorpt., fluoresc., doping 3-69081
- succinic acid, u.v. spectral confirmation of absence of CO_2 radical 3-61266
- TCNQ complexes, high-conductivity, effect of vibronic interaction in i.r. spectra 3-72645
- p-terphenyl mixed crystals, with tetracene and pentacene, second-order Stark effect on B_{2u} state 3-53128
- tetracene, mol. cryst. film, Stark effect, electron absorpt. band 3-72678
- tetracene mol. solids, polariton dynamics from band profile analysis 3-72642
- tetracyanoethylene with mesitylene and benzene, charge transfer complexes, solvent effect, thermodynamic props. and optical absorpt. spectra 3-44429
- thiurane, vibration spectra Davydov splitting, unit cell symmetry determ. 3-64652
- thiophane, vibration spectra Davydov splitting, unit cell symmetry determ. 3-64652
- thiophosgene, 2780 angstroms absorpt. system, vibrational structure 3-63441
- trapped electron, acting potential calc. 3-41858
- s-triazine, lower electronic states, 1.8°K optical study 3-64674
- sym-triazine, optical emission and e.p.r. 3-80103
- s-triazine crystals, mag. sensitivity of 3330.8 Å state 3-61044
- 4-R-1,2,4-triazoline 3,5-diones, ($R=H, CH_3, CH_2CH_3, CH_2CH_2CH_3$), electronic spectra 3-49459
- triethylenediamine, UV absorpt. spectrum anal. of struct. 3-78740
- triglycine sulphate crystals, influence of defects on optical behaviour near fundamental absorption edge 3-80081
- trimethylene chloroarsenite, heterocyclic, vibrational spectra and conformation 3-63472
- trimethylene chlorophosphite, heterocyclic, vibrational spectra and conformation 3-63472
- 1,3,5-trinitrobenzene-aromatic hydrocarbon charge-transfer complexes in glassy solns., temperature effects (*French*) 3-50847
- triphenylene:Zn porphyrin, low temp. optical absorption spectra 3-55653
- tritycenes, substituted, u.v. spectra and circular dichroism meas., absolute config. determ. 3-47288
- tropolone, near u.v. absorpt. vibr. anal. 3-54671
- uranyl molecular crystals, vibr. transitions, optical activity, symm. 3-72603
- u.v. spectra analysis, computational method (*German*) 3-46266
- vinylchloride, mass-spectrometric study in vacuum u.v., photoionisation curves and threshold energies 3-52395

spectra of organic molecules and substances continued

- vinylfluoride, mass-spectrometric study in vacuum u.v., photoionisation curves and threshold energies 3-52395
- wax, microcrystalline, i.r. rel. to structure detn. 3-54952
- o-xylol, rotational contour analysis of electronic origin band in emission spectrum at 4683 Å 3-67794
- $[Fe(C_5H_5)_2]BF_4$, spectra of ${}^2E_{1u} \leftarrow {}^2E_{2g}$ band system at 4.2 K 3-41532
- $[Fe(C_5H_5)_2](CCl_3CO_2H)_2 \cdot (CCl_3CO_2^-)$ spectra of ${}^2E_{1u} \leftarrow {}^2E_{2g}$ band system at 4.2 K 3-41532
- $[Fe(C_5H_5)_2]PF_6$, spectra of ${}^2E_{1u} \leftarrow {}^2E_{2g}$ band system at 4.2 K 3-41532
- CH radiative props., meas. by time sampling technique 3-78741
- CH⁺ radiative props., meas. by time sampling technique 3-78741
- Eu(benzoylacetate)₃ complex in soln., spectral studies (*Russian*) 3-50559
- $(N(C_2H_5)_4)_2 ZnL_2 \cdot NiL_2$ -mag. circular dichroism spectrum, spin-orbit splitting, quenching 3-50601
- Nd(benzoylacetate)₂ complex in soln., spectral studies (*Russian*) 3-50559
- Pr III complex, acetylacetate, absorption spectra, energy levels 3-52354
- Pr III complex, benzoylacetate, absorption spectra, energy levels 3-52354
- Pr III complex, thenoyltrifluoroacetate, absorption spectra, energy levels 3-52354
- spectra of polyatomic inorganic molecules**
see also radiofrequency spectra of polyatomic inorganic molecules
- alkali metal chlorate monomers, matrix isolation study of modes, metal-chlorate vibration 3-78806
- alkali metal ozonide molecules, i.r. spectra, isotopic shifts, stretching modes 3-71552
- BD₃-ND₃, matrix isolated, i.r. spectra 3-40628
- bridged metal-metal bonded species, spectra 3-78796
- IV-VI compounds, matrix isolation studies of i.r. spectra, laser-excited emission bands 3-78804
- metal pyridine tetracyanonickelate complexes, i.r. spectra analysis 3-63467
- peroxo tungstates and molybdates, i.r. spectra 3-57656
- pyrogermanates with linear bridge, vibr. spectra and isotopic shifts 3-46285
- pyrosilicates with linear bridge, vibr. spectra and isotopic shifts 3-46285
- pyroxene, Allende meteorite, crystal structure and optical props. 3-45052
- rare earth molybdate (tungstate), vibr. spectra obs. and crystal struct. 3-80039
- sodium bromoacetate, and -d₃, vibr. analysis and structure 3-78798
- transition metal carbonyls in gas and liq. soln., vibr.-rot. coupling effects on correlation functions 3-67825
- transition metal complex, $[M(1,8\text{-naphthyridine})_4](ClO_4)_2$; and $K_4[M(oxalate)_4]$, l.f. i.r. obs. 3-78776
- transition metal complexes, group IIIB and IVB, cis-1,2-dicyanoethylenedithiolate ion, electronic and vibrational spectra 3-57654
- transition metal complexes, linear relationships in ligand field theory rel. to optical spectra interpret. 3-63437
- transition metal diarsine complexes, containing high oxidation state metals, i.r. study 3-78774
- transition metal fluorides, octahedral, electronic spectra calc. by multiple scatt. method 3-52340
- transition metal tungstates, assignment, $MnWO_4$ valence force field calc., i.r. (*French*) 3-80020
- transition metal-DL- β -phenylalanine chelates, i.r. absorpt. spectra, normal coord. analysis 3-78771
- water, i.r. spectra, Lambert absorpt. coeff., refr. index determ. 3-61039
- water vapour, weak absorpt. line detection, using glass:Nd laser 3-39933
- water vibrational spectra isolated in D₂ matrices 3-43443
- Al(BD₄)₃, i.r. and Raman spectra 3-72623
- Al(BH₄)₃, i.r. and Raman spectra 3-72623
- AsBr₃ and tributylphosphate complexes, Raman and i.r. spectra (*French*) 3-46281
- Au(III) complex, formed by reaction Au halide and S containing ligand structure obs. 3-69448
- BBr₃, vacuum u.v. absorption spectra 3-46267
- BCl₃, vacuum u.v. absorption spectra 3-46267
- BCl₂Br, BClBr₂, vibrational spectra 3-46298
- BF₃, vacuum u.v. absorption spectra 3-46267
- B₂F₄, gaseous and cryst., Raman spectra, 25 to 1500 cm⁻¹, normal vibr. assignments and intermol. force consts. calc. 3-47250
- BH₃-NH₃, matrix isolated, i.r. spectra 3-40628
- BH₃-Nd₃, matrix isolated, i.r. spectra 3-40628
- B₂S₃ ring compounds, vibr. study 3-78784
- BX₃, x=halogens, electronic absorption, phosphorescence, singlet-triplet transitions 3-43439
- ¹⁰BH₃CO, mol. consts. of vibr.-rot. bands from i.r. study 3-78752
- Ba(ClO₄)₂·H₂O(D₂O), i.r., Raman spectra, intramolecular and colattice modes 3-75973
- CF₃ compounds, -PH₂, -PD₂, -AsH₂, -AsD₂, vibr. spectra and normal coord. anal. (*German*) 3-46282
- C₂N₂, far i.r. collision induced absorption in compressed gas, comparison with liquid phase absorption 3-60458
- CO₂, calc. of population relaxation for rotational levels 3-63559
- CO₂, fluorescence excitation and photoelectron spectra induced by vacuum u.v. 185-176 Å radiation 3-63448
- CO₂, mixed mode contribs. to absorpt. at 10.6 μ m 3-40619
- CO₂, modification in calc. half-width of depolarised Rayleigh line 3-63436
- CO₂ absorption cross sections from 180 to 700 Å 3-67805
- CO₂ gas, exponential decay of continuous absorption beyond 4.3 μ band head 3-63470
- CO₂ i.r., microwave spectroscopy, high resolution frequency measuring techniques, laser transitions 3-48420
- CO₂⁺, band strengths of, produced by photoionisation excitation of CO₂ 3-75059
- CO₂⁺ 2890 Å band, photoionization excitation rel. to column excitation rates for planetary atmospheres 3-54732
- C₃O₂, far i.r. and Raman spectra, potential function, low frequency bending mode 3-71548
- CS₂, analysis of ${}^1A_g \leftarrow {}^1\Sigma_g^+$ transition in the near ultraviolet 3-54661
- CS₂, i.r. spectra, hot bands associated with vibr. transitions 3-67817

spectra of polyatomic inorganic molecules continued

- CS₂, intermolecular spectra, 77-293 K (*Russian*) 3-43505
 CS₂, the $4\nu_2 + \nu_3$ band and general quartic force field 3-46289
 CSe₂²⁻, CS₂Se₂²⁻, CS₂²⁻, CSSE₂²⁻, vibrational spectra 3-46298
¹²C¹⁸O, absolute wavenumbers of 2⁺←0 vibr. rot. band, near i.r. standards 3-56611
¹²C¹⁸O₂, rot. const. from beats between Lamb dip stabilized lasers 3-63474
 Co cpds., chemical shifts and fine struct. of K-absorption edge 3-72765
 Co(CO₃)NO, potential const. from vibrational spectra of six isotopic species 3-43442
 Co(II) complex, chelate of anthranilic acid i.r. spectra, metal-ligand stretching frequencies 3-54688
 CrN₂, matrix isolated, sideways bonded N₂, i.r. obs. 3-43440
 Cr(CO₃)L, L=ligand, direct evaluation of π -bonding 3-71556
 CrO₂²⁻, X-ray photoelectron spectra, valence electron levels obs. 3-63388
 Cr₂O₇²⁻, X-ray photoelectron spectra, valence electron levels obs. 3-63388
 CrO₃Br⁻ vibrational spectra, normal coordinate analysis rel. to MO₃Xⁿ⁻ (M=Cr, Mn, Te, Re; X=F, Cl, Br, S; n=0,1) (*German*) 3-71557
 Cu(II) complex, chelate of anthranilic acid, i.r. spectra, metal-ligand stretching frequencies 3-54688
 Eu complexes, effect of line intensities in vibronic spectra 3-63506
 F₂CS, B¹A₁←X¹A₁, π^* ← π transition at 2000 Å 3-46265
 Fe complexes, tris(2,2'-bipyridyl)iron(II) and tris(glyoxal-bis-N-methylimine)iron(II), electronic spectra 3-63378
 Fe(II) complexes with oxygen-containing ligands, charge-transfer bands in electronic spectra (*Russian*) 3-71524
 FeO₄²⁻, X-ray photoelectron spectra, valence electron levels obs. 3-63388
 GeD₄, i.r. spectra, rovibrational const. 3-63460
 GeH₄, forbidden rot. spectrum in ground vibronic state 3-67811
 GeH₄, pure rot. transitions, spectral meas. 3-43449
 H₂ + alkali metal ions, low energy collisions, L_{ca} excitation cross sections 3-78892
 HCO, absorpt. spectra, detection by intracavity dye laser technique 3-54666
 HCl + Ar mixtures, low press. and temp. induced i.r. absorpt. spectra (*French*) 3-46283
 HI complexes in solid matrices at 20 K, i.r. spectra 3-54690
 HNO₃ vapour, u.v. absorption spectrum 3-52358
 H₂O, electron impact, dissociative excitation processes, spectroscopic investigations 3-75114
 H₂O, Fourier transform spectrum, between 2930 and 4255 cm⁻¹ 3-78767
 H₂O, mol. structure, quadratic force field, spectral analysis calcs. 3-78715
 H₂O, Rydberg states, ionisation and excitation energies calc. 3-46268
 H₂O, strengths and broadened widths in 2950-3400 cm⁻¹ region 3-71568
 H₂O, vibrational spectra, effect of intermolecular interactions, i.r. absorpt. intensity 3-63473
 H₂O molecule, IR vacuum spectra of vapour 3-78762
 H₂O vapour transitions, tunable laser meas., 5 μ m region 3-40622
 H₂¹⁶O, $3\nu_2$ band study, rotational levels 3-67823
 H₂¹⁶O, (000) and (020) states, rotational study, 2930 to 4255 cm⁻¹ region 3-78766
 H₂¹⁶O, high resolution i.r. spectra of $\nu_n + \nu_2$ and $\nu_2 + \nu_3$ bands (*French*) 3-75025
 H₂O.Cl₂ complex, i.r. and CNDO/2 study 3-54686
 H₂O.HCl complex in solid N₂, i.r. spectrum 3-52369
 HS₂ radical, u.v. absorpt. spectrum and geometry 3-75003
 H₂S, mol. structure, quadratic force field, spectral analysis calcs. 3-78715
 Mg (II) complex, MgX₂nMe₂O, i.r. spectra, stretching const. (*French*) 3-67824
 Mg(H₂O)₆²⁺ salts i.r. spectra stretching vibr. water absorpt. bands, hydrogen bonds. (*French*) 3-63466
 Mg₂SiO₄, isotopic species, i.r. and Raman spectra, vibr. studies and shift meas. 3-46284
 Mn(II) complex, chelate of anthranilic acid i.r. spectra, metal-ligand stretching frequencies 3-54688
 MnO₄⁻, X-ray photoelectron spectra, valence electron levels obs. 3-63388
 MoF₅, vibrational spectra 3-46278
 MoO₄²⁻, vibrational, force constants, i.r., Raman 3-63450
 MoS₄²⁻ and MoO₄²⁻, mag. circular dichroism assignment of longest wavelength band 3-54663
 MoS₄²⁻ vibrational, Raman, i.r., force constants 3-63450
 N₂-Ar Van der Waals complex, i.r. absorption spectra, internal rotation 3-78805
 NH₂, absorpt. spectra, detection by intracavity dye laser technique 3-54666
 NH₃, perturbation of electronic transitions under foreign gas pressure 3-75012
 NH₃, rot. energy transfer, direct obs. by time-resolved i.r.-microwave double reson. 3-78886
 NH₃, rotational lines, $\nu_1 + \nu_3$, $\nu_2 + \nu_3$ combination bands, intensity formula 3-78781
 NH₃, weak absorpt. line detection, using glass:Nd laser 3-39933
 NH₃ absorption coefficients in 2100-2250 Å region rel. to Jovian albedo 3-56330
 NH₃ i.r. absorption, expt. 3-71555
 NH₃ in N₂ and Ar matrices, i.r. spectra 3-55589
 NO₂, $2B_2$ - $2A_1$ transition, resonance fluorescence, rotational const. 3-78783
 NO₂, N₂O, i.r. spectra of pollutants 3-53471
 NO₂, vibr. struct. of $2B_1$ - $2A_1$ system 3-78729
 NO₂ ionisation potential, 9.62 to 9.25 eV assoc. mass spectrometer 3-71604
 NO₃⁺, vibr. freqs., correl. with cation polarising power and polarisability 3-49456
 N₂O, far-i.r. absorpt. and quadrupole moment determ. 3-74999
 N₂O absorption cross sections from 180 to 700 Å 3-67805
 NSF, rot. analysis of $1A''$ - $1A'$ band system 3-60447
 Na peroxo tungstates and molybdates, i.r. spectra 3-57656

spectra of polyatomic inorganic molecules continued

- Na₂[Ln(CO₃)₂(H₂O)₂].wH₂O, i.r. and Raman spectra, struct. obs. (*French*) 3-60457
 Nd³⁺+2-hydroxy-3-naphthoic acid complex, i.r. spectra, vibr. modes 3-67815
 Ni(II), complex, chelate of anthranilic acid, i.r. spectra, metal-ligand stretching frequencies 3-54688
 Ni(II) complex, ethyl xanthato, i.r. spectra assignments, normal coordinate analysis 3-54695
 Ni(II) complex, methyl xanthato, i.r. spectra assignments, normal coordinate analysis 3-54695
 NiX₂, complexes far-infrared, (X = Cl, Br, I), pyridine and gamma-picoline, metal-ligand vibrations, isotope shifts 3-57649
 NO₃⁻, electronic absorption, phosphorescence, singlet-triplet transitions 3-43439
 O₂-Ar Van der Waals complex, i.r. absorption spectra, internal rotation 3-78805
 (O₂)₂, van der Waals molecule, i.r. and visible spectra 3-43447
 O₃, i.r. spectrum in inert gas matrices at 20.4 K, test of matrix isolation technique 3-60455
 O₃, matrix isolated, i.r. spectra, bonding, geometry and thermodynamic functions 3-75044
 O₃, u.v. spectrum, features of photochemical interest 3-73155
 O₄, pressure dependent absorption cross sections, between 2000 and 2500 Å 3-78732
 OCS, perturbation of electronic transitions under foreign gas pressure 3-75012
¹⁶O₃, low temp. i.r. spectrum, zero order parameters 3-78782
¹⁸O₃, low temp. i.r. spectrum, zero order parameters 3-78782
 OsO₄, He(I) photoelectron spectra, low energy transitions 3-40608
 OsO₄, mag. circular dichroism assignment of longest wavelength band 3-54663
 OsO₄, rotational-vibr. spectra, narrow saturation resons. induced by CO₂ laser radiation 3-46279
 P₂F₄, i.r. and Raman spectra, vibr. and mol. struct. 3-43457
 PH₃, ground state rot. const., i.r. determ. 3-40626
 PS₂²⁻, vibrational spectra 3-46298
 PbF₂, matrix isolated, i.r. spectra 3-40630
 Pd complex, cyclic olefin, bonding, vibr. spectra obs. 3-78726
 Pd complexes, Pd(PPh₃)₂X₂, Pd[P(PhO)₃]₂X₂, (X=Cl,Br), i.r. spectra 3-54689
 Pd(II) complex, trans-planar, energy transfer to ligand-field states 3-41854
 Pd(II) complexes, [X₂Pd(C₅H₅)₂], (X=Cl, Br), i.r. and Raman spectra, vibr. assignments 3-46300
 Pt complex, cyclic olefin, bonding, vibr. spectra obs. 3-78726
 Pt(II) complexes, [X₂Pt(C₅H₅)₂], (X=Cl, Br), i.r. and Raman spectra, vibr. assignments 3-46300
 Pt(N₂) complex in low temp. matrices, i.r. identification 3-46277
 Pt(N₂)₂ complex in low temp. matrices, i.r. identification 3-46277
 Pt(N₂)₃ complexes in rare gas and N₂ matrices, 14 K i.r. study 3-78810
 ReOF₄, vibrational spectra 3-72626
 ReS₄²⁻, mag. circular dichroism assignment of longest wavelength band 3-54663
 Rh(N₂)_n, n=1-4, low temperature matrices, i.r. examination 3-78809
 RuO₄, He(I) photoelectron spectra, low energy transitions 3-40608
 SF₆, spectra, absorpt. lines, using CO₂ laser 3-45795
 SF₃Cl, K type |R₆| splitting coeff. (*French*) 3-46253
 SO₂, ³B₁-¹A₁ band system, rotational analysis of (010), (100), and (110) bands 3-40611
 SO₂, 3400-3000 Å absorpt., vibr. analysis 3-67801
 SO₂, i.r. spectra of air pollutants 3-53471
 SO₂, matrix isolated, i.r. spectra, bonding, geometry and thermodynamic functions 3-75044
 SO₂, u.v. spectrum in matrix isolation, vibr. struct. of 2348 Å system 3-63443
 SO₂, vibrational spectra, effect of intermolecular interactions, i.r. absorpt. intensity 3-63473
 SO₂ convergence of reduced Hamiltonian, centrifugal distortion, z-axis choice 3-63425
 S₂O₃, unstable, matrix isolated vibrational spectra, identification of new species 3-78803
³²S¹⁶O₂, $\nu_1 + \nu_3$ combination band obs. 3-63453
 SbBr₃ and tributylphosphate complexes, Raman and i.r. spectra (*French*) 3-46281
 Sc(H₂PO₃)₃, i.r., p.m.r. spectra 3-78657
 Sc(H₃PO₃)₃, i.r., p.m.r. spectra 3-78657
 Sc₂(HPO₃)₃, i.r., p.m.r. spectra 3-78657
 Sc₂(HPO₃)₃4H₂O, i.r., p.m.r. spectra 3-78657
 SeO₂, matrix isolated, i.r. spectra, bonding, geometry and thermodynamic functions 3-75044
 SiH₄, ν_3 band, high resolution obs. (*French*) 3-54678
 SnCl₄(SnBr₄) and tributylphosphate complexes, i.r. and Raman spectra (*French*) 3-46280
 SnF₂, matrix isolated, i.r. spectra 3-40630
 SnO₂, from Sn + O₂ reaction matrix isolation i.r. study, characterisation 3-76427
 TeO₂, matrix isolated, i.r. spectra, bonding, geometry and thermodynamic functions 3-75044
 Ti³⁺ fassaite, Allende meteorite, crystal structure. optical props. 3-45052
 UCl₄, vapour spectrum interpretation using cryst. field model 3-71541
 UO₂, UO₃, i.r. spectra, 700 to 900 cm⁻¹, stretching modes study 3-40625
 VO₄³⁻, X-ray photoelectron spectra, valence electron levels obs. 3-63388
 V₂O₅MoO₃, i.r. spectra 3-80582
 VS₄²⁻ and VO₄³⁻, mag. circular dichroism assignment of longest wavelength band 3-54663
 WS₄, mag. circular dichroism assignment of longest wavelength band 3-54663
 YF₂, YF₃, matrix isolated compounds, i.r. spectra, 40 to 800 cm⁻¹, freq. assignments 3-52370
 Zn(II) complex, chelate of anthranilic acid, i.r. spectra, metal-ligand stretching frequencies 3-54688

spectra of solids

- impurities, in solids, absorption spectra, fourth order perturbation theory 3-72689
- molecular crystals, exciton-phonon interaction and spectra of Davydov multiplet of excitons (*Russian*) 3-72336
- molecular crystals, optimum conditions of application of Kramers-Kronig method 3-72643
- Shpol'ski hosts, absorpt. and emission spectra of Zn porphyrin 3-72737

spectral analysers

- see also wave analysers
- u.s. attenuation meas. 3-42523
- u.v.-visible absorbance, computer controlled spectrophotometer 3-66217

spectral line breadth

- see also chemical shift; Doppler effect; Stark effect; Zeeman effect
- A-type stars, microturbulence from line profiles of six objects 3-51339
- acetaldehyde, collision broadening of rot. lines by O_2 3-67834
- alkali metal atoms, optically pumped, spin-exchange shift and narrowing of magnetic resonance lines 3-54580
- atomic line profiles emitted by hollow-cathode lamps and $C_2H_2-N_2$ flames, interferometric meas. 3-62352
- atomic self-absorption data, relative oscillator strengths calc. of lines 3-52251
- atomic spectral-line broadening and Kirchhoff's law, quantum mech. theory, classical limit 3-49481
- band contour anal. method, appl. to pyridine-4-d, near u.v. spectra 3-46307
- beam-foil spectroscopy, factors determining emission line shape, time-window spectra theory 3-77490
- bibliography on atomic line shapes and shifts, 1889-March 1972 3-52259
- bis(cyclooctatetraene)iron, n.m.r. study, line-width and second moment rel. to temp. 3-50477
- complex contours, resolution into two symmetrical bands, model curves method (*Russian*) 3-77500
- contour of single spectral line or band, optimal recording conditions, monochromator, second order system 3-53912
- correction to abstr. A27685 of 1971 3-78567
- cryptocyanine, soln. in methanol, fluorescence spectra, fine periodic spectral structure, ruby laser excitation 3-55669
- diatomic mols., pressure broadened spectral lines, intermolecular potential, nonrigidity influence 3-75157
- Doppler broadening, band absorbance formulation 3-52375
- $E\otimes e$ system, singlet to doublet transition, lineshape calculation 3-43465
- electron-plasma line profiles, Coulomb-collision corrected 3-43655
- e.p.r. line, second moment of dipolar broadening finite temperatures, lattice sum of truncated dipolar interaction 3-41397
- e.s.r., line broadening, cavity Q-factor variation effects 3-42616
- e.s.r. line shape analysis for unresolved hyperfine splitting, effect of field modulation amplitude and frequency 3-75873
- ethylene oxide lines, collision broadening by quadrupolar mol. CO_2 3-52397
- faint Fraunhofer line profiles, asymmetry and line width 3-59259
- fast-beam sources, spectrometer optimum settings for side-on viewing mode 3-77489
- formaldehyde, $2\nu_2$ band, i.r. spectra, constants 3-63494
- formaldehyde, microwave collision diameters in rot. spectrum 3-67858
- Fourier transform relationship between n.m.r. free induction decay and c.w. lineshape, reply to comment 3-60995
- Fourier transform spectroscopy, for linewidth determ. 3-51623
- free radicals in aq. environments, e.p.r. line shape calc. 3-47603
- gas, heat absorption, overlapping hot bands, approximate method at high temperatures 3-57172
- gas-phase e.p.r. linewidths and intermolecular potentials, exper. results F-He- F_2 system 3-71368
- gas-phase e.p.r. linewidths and intermolecular potentials, theory 3-71367
- Heisenberg linear chain, paramagnetic spin resonance line width 3-68753
- n-hexane, 1,12-benzoperylene and coronene impurities, luminesc., zero-phonon lines and electron-phonon interaction 3-72727
- iminoyl radicals, ^{15}N e.p.r. spectral linewidths, mol. reorientation effects 3-43486
- information theoretical lineshape, general case 3-48707
- ion beams, origin and reduction of line broadening 3-42669
- ion source, pulsed Penning (*Japanese*) 3-73854
- ionic crystals, uni- and bi-axial, polariton Raman lines, eigenvectors and intensities (*German*) 3-53114
- isothermal spherical layer, radiative flux, effect of line or band shape 3-66700
- laser transitions, determination of line shape parameters based on line-narrowing meas. 3-42566
- liquids, resonance line shapes for semi-integer spins 3-41394
- long-lived isomer spectroscopy, pulsed-beam expts., influence of time-windows on NMR-PAC line shapes 3-45995
- magnetic circular dichroism for C_{51} defect centre, line shape function 3-58533
- methane, in gaseous and liquid mixtures, i.r. band shapes and semi-classical rot. diffusion model 3-54681
- methane, temp. depend. of half widths of some self- and some foreign-gas-broadened lines 3-67836
- methyl iodide, liquid, mol. motions and interactions, temp. dependent Raman study 3-47248
- molecular electronic radiationless transitions, perturbation effect 3-67845
- molecular fluids, long range many mol. interactions, effect on absorpt. spectra 3-52405
- molecular rotation spectra, halfwidth, intensity, determination, iterative solution of nonlinear least squares problem, method (*French*) 3-70310
- n.m.r. c.w. line shape, Fourier transform relationship with free induction decay, comment 3-60994
- n.m.r. line shape, motional narrowing, analysis 3-41436
- n.m.r. lineshapes, asymmetry due to nonrandom mag. field inhomogeneities 3-64563

spectral line breadth continued

- n.m.r. spectra, many-site exchange problems, line shape calculation, Kubo-Sack probability matrices 3-80540
- non-coherent scattering study 3-52376
- n.q.r. pulse radiospectrometer, resolving power, effect of spectral width, passband of receivers 3-48487
- n.q.r. spectrum spectrometer system for lineshape determ. 3-48489
- paramagnetic impurity centres, light absorpt. 3-58538
- passive system susceptibility, frequency dependence, analyticity 3-42749
- perinaphthyl free radical coherence effects on line shape in ENDOR spectrum (*German*) 3-57672
- photon correlation spectroscopy, factors affecting accuracy 3-62109
- plasma, nonequilibrium, electron broadening 3-63808
- polyatomic mols., radiationless transitions effect on absorpt. lineshapes and fluoresc. decay curves 3-63501
- polyethylene, n.m.r. spectra, molecular motion obs. (*German*) 3-61007
- predissociation linewidths Franck-Condon factors and isotope effects, numerical calcs. (*French*) 3-43472
- pressure line shape, semiclassical and quantum mechanical calculations 3-54705
- profiles of H emission lines in solar moustaches, quantitative analysis (*Russian*) 3-76978
- quasi-stationary states in large mols., linewidth depend. 3-60469
- Raman vibrational line shapes, reorientational correlation functions, appl. to nuclear quadrupole coupling constants 3-46274
- rare equation description, generating operator 3-63493
- refractory metal compounds, X-ray spectra interpretation, spectral lineshape calc. 3-41594
- ruby laser, giant pulse, spectrum width resolution by clarifying filters (*Russian*) 3-70823
- satellite bands, semiclassical shape 3-43338
- satellite bands due to interatomic interaction with foreign gas atoms 3-74830
- Sco X-1, Bragg spectroscopy in search of Fe XXV emission lines 3-69996
- semiconductor, degenerate, diffusivity-mobility ratio rel. to spontaneous emission linewidth 3-72699
- semiconductor, donor magneto-optical spectra, inhomogeneous line broadening 3-50558
- semiconductor, optical absorpt. by impurities, linewidth, elec. field effect 3-44444
- singly ionised atoms, comparison of measured and calculated Stark parameters 3-43336
- spontaneous emission, radiative corrections 3-74363
- Stark broadening effects in radio recombination line temperatures for radiosources 3-42209
- stellar absorption line equivalent widths, from 105 Her, K4 II star (*Russian*) 3-77096
- stellar Ca II H and k-line absorption features, luminosity effect 3-81045
- stellar linewidth-luminosity relations and chromospheric velocity fields 3-69944
- stochastic collision models and radiative equilibrium, line shape constraints 3-42888
- succinonitrile plastic crystal, rel. to Rayleigh scatt. spectrum, interpretation (*French*) 3-47277
- three-component solutions, statistical approach to electronic spectra 3-64633
- uranus spectrum, molecular H_2 , 3-0 band obs. 3-47905
- Voigt function, spectral-line profile analysis 3-59594
- white dwarf stars, line profiles and rotation meas. 3-45120
- wing contours, self-broadened lines 3-75054
- wings in low pressure atomic gas due to formation of quasimolecules 3-60349
- Ar II, Lorenz and Doppler widths, Ballik method (*Russian*) 3-78444
- Ar positive column at medium pressures, resonance broadening 3-52269
- β -B, rhombohedral, e.p.r. obs. of paramagnetic centres 3-79914
- BrCN, pressure broadened line widths in microwave region 3-67837
- CO, pure solid and in Ar matrix, i.r. intensities and band shapes 3-80061
- CO lineshifts and widths calc. due to inert gas broadening of vibration-rotation lines 3-54707
- CO spectral line widths self-broadened and broadened by N_2 , O_2 , H_2 , HCl, NO and CO_2 (*French*) 3-67835
- CO-SF₆, dipole-hexadecapole interaction, theory of linewidth broadening 3-67863
- CO₂, modification in calc. half-width of depolarised Rayleigh line 3-63436
- Ca spectrum, absorption line half widths, 422.67 nm line in hydrogen diffusion flame spectroscopy 3-57600
- CaV garnet, polycryst., ferrimagnetic resonance, linewidth field depend. 3-47149
- CaV garnet: Zr, Ti substituted, ferrimag. resonance 3-47148
- CdCr₂S₄, ferromag. resonance obs. 3-47150
- CdCr₂Se₄, ferromag. resonance obs. 3-47150
- CdS, two-photon reson. Raman scatt., widths of peaks 3-58501
- Co crystal whisker, h.c.p., ferromag. resonance linewidths obs. 3-41418
- CuCl, temp. depend. in range 300 K to 45 K 3-72615
- CuMn alloy, n.m.r., near neighbour wipeout and satellites obs. 3-47152
- D discharge, Stark broadening of Paschen lines 3-43334
- n-D₂, modification in calc. half-width of depolarised Rayleigh line 3-63436
- EuS, mag. resonance linewidth, temp. and orientation depend. 3-41413
- EuSe, mag. resonance linewidth, temp. and orientation depend. 3-41413
- ^{151}Eu , hyperfine broadening of X-ray lines 3-49391
- Fe garnet, rare earth ion effects on spin wave linewidths 3-41422
- Fe transition metals, shape of X-ray $K\alpha$ lines, fine structure obs. 3-71362
- Fe(III) complexes, tris(dithio-oxalato) salts, microcrystallite spectra interpretation using line-shape calcs. 3-55457

spectral line breadth continued

- FeNH₄(SO₄)₂·12H₂O, paramagnetic with pure dipole-dipole coupling, Mossbauer spectra, relaxation phenomena, spin wave model (*German*) 3-58463
- GaI, (n²P⁰-n²D₁) resonance lines, collision broadening, cross-sections (*Russian*) 3-72770
- GdFe garnet:Tb, ferromag. resonance, high pressure effects 3-41421
- Gd₂La_{1-x}B_x, exchange narrowing in e.s.r. spectra, linewidth measurements 3-47128
- Ge, Brillouin spectra, absorpt. line broadening, refr. indices determ. 3-50566
- Ge:As, high conc. region, e.s.r. line width 3-47130
- H, resonant multiphoton processes, higher-order effects, induced shifts and breadths 3-43349
- H, separated oscillatory field measurements, line shape 3-78410
- H lines, Stark broadened, structure effect of plasma instability 3-40640
- H plasma, ion motion effects on spectral lines 3-46514
- H plasma, partially ionised, dense, Lyman- α asymmetry calc. 3-71851
- H₂, collision-induced fund. band in H₂-He and H₂-Ne mixtures 3-63540
- n-H₂, modification in calc. half-width of depolarised Rayleigh line 3-63436
- H₂, resonance collisions in rotational energy transfer, Raman linewidth measurement 3-67864
- o-H₂, solid, light absorpt., libron-libron interaction (*Russian*) 3-64137
- H₂-He mixtures, quantum scattering theory of rotational relaxation and spectral line shape 3-46351
- H₂-rare gas mixtures, i.r. absorpt. quadrupole-induced transitions, diffusional narrowing 3-78882
- HCl, absorpt. line broadening by gases, fund. band, temp. depend. 3-63544
- HCl, blended isotopic doublets, equivalent spectral widths 3-78823
- HCl gaseous mixtures with HBr and HI, low temp. absorpt. spectra (*French*) 3-78750
- HCl lineshifts and widths due to inert gas broadening of vibration-rotation lines 3-43467
- HCl lineshifts and widths calc., due to inert gas broadening of vibration-rotation lines 3-54706
- HF chemical laser, pressure broadened, Lorentzian parameters from Lamb dip 3-66796
- H₂O, strengths and broadened widths in 2950-3400 cm⁻¹ region 3-71568
- H₂O vapour transitions, tunable laser meas., 5 μ m region 3-40622
- He D₃ and 10830 Å lines from solar spectra, active regions (*Russian*) 3-76980
- He I 6678 Å line strength in OB supergiant stars 3-65883
- He plasma, ion motion effects on spectral lines 3-46513
- He plasma, ion temp. meas. in range 0.1-1 eV by Doppler broadening of He II 4686 Å line 3-57941
- Hy equivalent width rel. to stellar absolute magnitude determ., calibration 3-81078
- InI, (n²P⁰-n²D₁) resonance lines, collision broadening, cross-sections (*Russian*) 3-72770
- K₂MnF₄, two-dimensional Heisenberg paramagnet, e.p.r. min. line-width obs. 3-41396
- La₃AlO₃:Cr³⁺, luminescence spectrum, temp. broadening and shift of R line 3-64718
- La_{1-x}Gd_xAl₂, e.p.r. of Gd³⁺ 3-47133
- Mg II lines near 2800 Å, equivalent widths in spectra of 31 stars 3-45098
- MnF₂, antiferromag. resonance linewidth and relax. obs. 1.5-40 K 3-41412
- Mn(II) complexes, multi-freq. e.p.r. study, 10/3 effect 3-47126
- Mn(II) salts in solutions, comparison of e.s.r. linewidths (*German*) 3-64543
- MnMoO₄ and hydrate, temp. dependence of width of Mn²⁺ e.p.r. lines (*Russian*) 3-68831
- MnWO₄ and hydrate, temp. dependence of width of Mn²⁺ e.p.r. lines (*Russian*) 3-68831
- N excitation of K shell, ESCA, XUV spectra, theory 3-63278
- N₂, modification in calc. half-width of depolarised Rayleigh line 3-63436
- N₂ dissolved in liquids, vibr. Raman bands, collisional narrowing effect 3-75019
- N₂ Raman scattering, density effect, scattering polarisation, intensity, frequency shift, and line shape study 3-71551
- NH₃, inversion spectrum, collision broadening and shifting 3-67838
- NH₃ line profiles, deviations from the Lorentz shape 3-52377
- NH₃ spectral data for ν_2 bands, rel. to radiative transfer in Jupiter atmosphere 3-76995
- NH₃-SF₆, quadrupole-hexadecapole interaction, theory of linewidth broadening 3-67863
- NO, deviation from Lorentzian shape in the wings of collision broadened i.r. absorption lines 3-43466
- NO, Doppler-limited i.r. mag. rot. spectrum, line shape 3-43448
- Na, broadening and shift of D-lines at low press. 3-67693
- Na spectral line profile, plasma inhomogeneity and reversal temp. effect in thermal boundary layer 3-63875
- NaI, self broadening of principal series 3-71399
- Ne autoionising states line profiles in electroionisation curve 3-78474
- Ne* + Ne collisions, saturated absorpt., collisional broadening study 3-46199
- Ni single cryst. platelet, ferromag. resonance linewidth temp. depend. 3-41419
- Ni-Fe, film, ferromag. resonance linewidth angle and thickness depend. 3-41420
- NiCl₂, antiferromagnet, crit. e.p.r. spin dynamics, linewidth divergence behaviour 3-47136
- O III 5007 Å line profiles in spectra of old planetary nebulae rel. to expansion velocities 3-45232
- O₂ red atmospheric band system, line intensities and half widths of A and B bands 3-65375
- Pd, e.s.r., spin-orbit coupling effect, numerical calc. 3-41395
- Rb resonance lines, radiation frequency shift and linewidth 3-52270
- ⁸⁷Rb maser, light shift and light broadening 3-54209

spectral line breadth continued

- SO₂, linewidth parameters for $\Delta J=1$, $0 \leq J \leq 43$ rotational transitions 3-43464
- ¹²¹Sb, hyperfine broadening of X-ray lines 3-49391
- Si, Brillouin spectra, absorpt. line broadening, refr. indices determ. 3-50566
- SiCl₄, rel. intensities of band spectra, vibrational overlap integral, calc. of Franck-Condon factors 3-78733
- Ta, nuclear acoustic resonance, anomalous line broadening rel. to elastic constants 3-64080
- Tl vapour laser, superradiant pulse power, Fabry-Perot interferometry, isotopic and hyperfine splitting (*Russian*) 3-66823
- TlI, (n²P⁰-n²D₁) resonance lines, collision broadening, cross-sections (*Russian*) 3-72770
- VO₂⁺ in dimethylformamide and dimethyl acetamide solns., n.m.r. linewidths temp. depend. 3-41433
- YIG type materials, evaluation, ferromag. resonance obs. 3-50462
- YIG:Tb, Pr, ferromag. resonance, high pressure effects 3-41421
- spectral line profiles** see *spectral line breadth*
- spectral line shift**
see also *chemical shift; isomer shift; isotope shifts; red shift; Stark effect; Zeeman effect*
alkali earth metal atoms, singly ionised, Stark broadening and shift 3-54566
bibliography on atomic line shapes and shifts, 1889-March 1972 3-52259
excited atoms, multiphoton ionisation, resonance phenomena, Stark shift 3-46197
ice hydrogen bond spectral shifts temp. depend., vitreous to cubic I phase transformation 3-47262
liquids, resonance line shapes and shifts for semi-integer spins 3-41394
paramagnetic impurity centres, light absorpt. 3-58538
ruby, radiative and nonradiative transitions, temp. depend., emission quenching 3-41568
singly ionised atoms, comparison of measured and calculated Stark parameters 3-43336
spontaneous emission, radiative corrections 3-74363
CO lineshifts and widths calc. due to inert gas broadening of vibration-rotation lines 3-54707
FeNH₄(SO₄)₂·12H₂O, paramagnetic, Mossbauer spectra, relaxation phenomena, spin wave model (*German*) 3-58463
H resonant multiphoton processes, higher-order effects, induced shifts and breadths 3-43349
HCl lineshifts and widths due to inert gas broadening of vibration-rotation lines 3-43467
HCl lineshifts and widths calc., due to inert gas broadening of vibration-rotation lines 3-54706
La₃AlO₃:Cr³⁺, luminesc. spectra, temp. broadening and shift of R line 3-64718
NH₃ microwave absorption lineshift by nonresonant i.r. laser radiation (*French*) 3-54702
N₂ Raman scattering, density effects, polarisation, intensity, frequency shift, line shape study 3-71551
Rb resonance lines, radiation frequency shift and linewidth 3-52270
⁸⁷Rb maser, light shift and light broadening 3-54209
- spectral linewidths** see *spectral line breadth*
- spectral methods of temperature measurement**
see also *pyrometers*
atmospheric, covariance matrices, means of atmospheric Planck function profiles, satellite meas. 3-44959
dark interstellar clouds, H₂CO 6 cm. excitation temperatures 3-70046
flame spectroscopic temp. meas. review 3-42713
flames, using atomic-absorption method (*Russian*) 3-62022
glass, hot, errors, thermocouple and spectral methods 3-66169
i.r. pyrometer, temp. monitoring, train wheels, jet engine rotors 3-5435
liquid-crystal contact lens for corneal temp. distrib. meas. 3-56995
n.m.r. millidegree thermometer, continuous wave, design, low temp. applications 3-48388
nuclear reactor fuel, apparatus for temp. fluctuation meas. (*French*) 3-49310
ocean, internal wave strain, temp. perturbations, vertical spectra 3-47677
radiation sources, temp. meas., coloured flames, reversal of spectral lines method 3-48366
sea-air-interface, momentum and sensible heat fluxes meas. 3-47678
three-colour pyrometry, for high temps. (*Russian*) 3-51552
upper atmosphere, homodyne detection, luminous optically dense gas layer 3-69731
Cu, f.p. meas., infrared photoelec. pyrometer 3-46698
N₂ plasma, isothermal, and electron conc. determ. (*Russian*) 3-63890
- spectrochemical analysis**
absorption, fluoresc., comparison, low conc. region 3-73945
absorption instruments, flameless, calibration 3-62344
absorption line frequency, least square convolution, curve fitting 3-73750
air particulates, multielement analysis, X-ray emission spectrometry 3-59718
air pollution, i.r. spectroscopy, parts per billion levels, scanning Michelson interferometer, cooled solid state detectors, minicomputer 3-59461
air pollution, particulates, metals, Chicago metropolitan area USA, atomic absorption spectroscopy, Fe, Cu, Mg, Ca 3-59460
air pollution, using remote Raman spectroscopy 3-56563
air-acetylene flame, oxygen-shielded, burner design 3-70486
alkali metals determ. by flame photometry using Cs as internal standard (*Russian*) 3-62367
alloys, in-depth compositional profile analysis using optical emission glow discharge spectrography 3-45586
alloys, systematic errors in spectral analysis by vacuum quantometer 3-54041
analyzer, colorimetric, absorption-type, with luminescent screen 3-62354
arc discharge, atom distrib. in interelectrode gap (*Russian*) 3-59709

spectrochemical analysis continued

- arc discharge, terminal-spark migration products spectral line intensity, effect of Ar (*Russian*) 3-59710
- aromatic hydrocarbons determination in petrol by electronic absorption spectra (*Rumanian*) 3-45608
- atomic, air-acetylene flame, oxygen-shielded, burner design 3-70486
- atomic absorption, scintillation method of recording (*Russian*) 3-59707
- atomic absorption, ultramicro spectroscopy, W filament atom reservoir 3-45613
- atomic absorption and emission determ. of Hg using 184.9 nm line 3-54049
- atomic absorption bibliography (January-June 1973) 3-77740
- atomic absorption determ. of trace elements by pulse evaporation in flame and adapter (*Russian*) 3-62363
- atomic absorption measurements, alloys, pulsed hollow cathode lamps, Q-switched laser induced transient plasmas 3-57014
- atomic absorption spectrometry, indirect methods 3-45612
- atomic absorption spectrometry, pulse u.s. nebulizer system 3-45581
- atomic absorption spectrometry, writing a paper, topics to be included 3-70225
- atomic absorption spectroscopy, non-dispersive systems 3-48670
- atomic absorption spectroscopy, trace metal determ., lubricating and crude oils, evaluation of carbon-rod atomiser 3-70485
- atomic fluorescence and absorpt. flame photometry, comparative sensitivities (*Russian*) 3-59708
- atomic fluorescence spectrometry, photon counting or lock in amplification, comparison 3-70456
- atomic fluorescence spectrometry, review 3-59697
- atomic fluorescence spectrometry metals, graphite rod atomiser and thermostated electrodeless discharge lamp 3-57015
- atomic line profiles emitted by hollow-cathode lamps and $C_2H_2-N_2$ flames, interferometric meas. 3-62352
- biological materials, foreign metals identification 3-70444
- calculation of element content, intensity of anal. line, mass coeff. of absorption, surface density 3-48661
- cell holder, Beckman DK-2A Spectrophotometer, temp.-regulated 3-77368
- combustion intermediates and products, detection limits with line-centre absorption and derivative laser spectroscopy 3-65066
- complex gaseous mixtures, with He, calculation method for analysis using spectral line intensities (*Russian*) 3-48680
- dielectric films on Si, i.r. spectroscopy, device technology 3-41665
- discharge electrode prep., standardisation, grinding equipment (*Russian*) 3-62369
- dual wavelength spectrophotometer, new design, construction specifications 3-57016
- electrocast materials, physical methods of chem. analysis (*French*) 3-70468
- electron impact spectrometer, retarding field, gas molecule qualitative analysis, operation 3-62348
- electron probe microanalysis, computer control 3-73960
- electron spectrometer improvement 3-66444
- elemental, characteristic X-rays, proton and X-ray induced 3-59719
- ellipsometry, modulation, appl. to electrode-electrolyte interface study 3-53886
- e.s.r. studies, stopped flow control system, operational characteristics 3-66289
- flame photometer, FLAPHO 4, VEB Carl Zeiss JENA, Na, K, Ca, Li, Rb anal. 3-51765
- flame photometry, using stylometer with internal standard (*Russian*) 3-62367
- flame spectroscopic temp. meas. review 3-42713
- fluorimetry, correction for scatter peak interference 3-59703
- fluorimetry, signal vs. conc. relationship 3-45614
- foreign metals identification atomic absorpt. technique 3-70444
- free radical detection by intracavity dye laser technique 3-54666
- gas chromatograph peak, online grating i.r. spectrophotometry 3-62322
- gas chromatography and optical emission technique combination for chemical analysis 3-40071
- gas chromatography-i.r. spectrometry on-the-fly technique using cholesteric liq. cryst.-effluent interface 3-66416
- gas conc. meas. by stimulated anti-Stokes scatt. 3-66438
- gas concentration detector, opto-thermal, laser beam absorption 3-70471
- gases in v.u.v., apparatus for flash photolysis 3-48673
- generator, wide range, for industrial spectral control, specifications (*Russian*) 3-70491
- geochemical objects, study of possible use of a laser for atomic absorption analysis (*Russian*) 3-48681
- glass, surface comp. from photoelectron spectra (*French*) 3-54037
- graphite, neutron activation analysis, impurity determ., gamma-spectra 3-52638
- Hadamard-transform spectrometer, spectral Imaging HTS-255-15 3-59713
- hydrogeochemical analysis, natural waters, flameless atomic absorption methods 3-48642
- hydroxamic acid in nuclear fuel reprocessing solvents, spectrophotometric determ. 3-71225
- impulse fluorimeter using excitation from picosecond laser (*Russian*) 3-62370
- instrumental precision theory, reading error, electrical noise 3-62320
- instrumentation, modern, a review 3-40073
- i.r. gas analysers, using solid-state devices 3-48683
- i.r. internal reflection spectrometry, thin film appl. 3-73164
- lanthanide elements, determ. in ferroelectric and piezoceramic materials (*Russian*) 3-62362
- laser for absorption trace analysis of Na in flame 3-54048
- light source, hollow cathode with separate evaporation and excitation (*Russian*) 3-62366
- low cost recording spectropolarimeter, design and evaluation 3-45584
- low resolution i.r. derivative spectrometry for source concentration monitoring 3-73609
- low-pressure microwave induced plasmas as excitation sources for spectroanalytical chemistry 3-43697

spectrochemical analysis continued

- luminescence, decay time meas., 77-500 K (*French*) 3-66455
- luminescence quantitative determ. of polycyclic aromatics in mixed solutions (*Russian*) 3-62364
- luminescence quantum yield determination, finite excitation bandpass errors 3-62324
- metals analysis in particulate pollutants by emission spectroscopy, review 3-45332
- microimpurities in concentrates, effect of NaCl (*Russian*) 3-77750
- modulation spectroscopy, electrochem. appl. 3-55967
- multichannel emission, planar Si photodiode arrays, preamplifier, high-gain low-noise d.c. and lock-in amplifiers 3-73958
- multicomponent mixtures, absorpt. spectra, analytical position selection 3-73944
- multicomponent systems, spectrophotometric anal., theoretical estimate of accuracy 3-42702
- multiple internal reflection fluorescence spectrometry 3-66414
- nonlinear i.r. gas analyser calibration by exponential washout and polynomial curve fitting 3-73949
- organic molecules, luminescence spectrometry, at low temperatures 3-59700
- organometallics, selective determination by dual channel detector based on flame conductivity and emission 3-66418
- photochemically unstable compounds, digital integration method for fluorimetric studies 3-48634
- photodiode detector arrays, self-scanning, characts. 3-70309
- polyalkenamers, n.m.r. and i.r. spectroscopy, structural unit determ. 3-54046
- polymer X-ray filters for dispersionless analysis for light elements (*Russian*) 3-70492
- powders in plasmatron discharge, spectral line depend. on grain size (*Russian*) 3-77752
- programming, linear and convex, hexachlorocyclohexane isomer mixture, linurone and desmethyllinurone mixture 3-51763
- programming, linear and convex, reduction of random errors, accuracy improvement 3-51762
- pulse fluorimetry, data analysis excimer formation kinetics, Laplace transform. of decay function 3-62337
- quantitative analysis by laser Raman spectroscopy (*French*) 3-66460
- Raman scatt., evanescent wave in total refl., electrode reaction obs. 3-73938
- rare earth elements, laser emission spectrography 3-45582
- rare earth oxides, impurity determ., atomic absorpt., fluoresc., pulsed volatilisation 3-73946
- rare earth trace metals detection by X-ray excited optical fluorescence in YPO_4 and YVO_4 3-48635
- refractories, atomic absorption spectroscopy, flameless, trace metal impurity determination 3-48640
- refractory, X-ray fluorescent and atomic absorpt. anal. methods and characteriz. 3-80410
- seawater, determ. of trace elements, by atomic absorpt. with arc atomiser 3-80875
- silicon organic esters of phosphoric acids, crystallless roentgenofluorescent anal., Si and P determ. 3-48662
- slag, liquid, evaporation rate as function of melting point, discharge current (*Russian*) 3-70488
- using solid-state devices, air pollution study 3-48684
- spark discharge, spectral effects of nonuniform sample on electrodes (*Russian*) 3-70489
- spectrophotometry, far u.v. solution, techniques, apparatus, problems, applications, spectrochemistry 3-57013
- steel, high alloy, P determ. (*Japanese*) 3-70478
- steel, laser spectral analysis in plasma with controlled excitation delay (*Russian*) 3-70490
- steel, photometric determ. of Al after separation on a cation-exchanger (*German*) 3-45603
- styluscope SL-12, for analysis of iron and steel (*Russian*) 3-62368
- surface erosion during pulse discharge in magnetic field (*Russian*) 3-77748
- thin film, by ATR i.r. spectroscopy 3-48442
- trace element sensitivity, superimposed pulses on stationary discharge (*Russian*) 3-70487
- trace elements in TiO_2 and ZrO_2 (*Polish*) 3-73955
- trace metals, atomic absorption spectroscopic methods, techniques and results, conf., London, England (Nov 1972) 3-48636
- trace metals, human body fluids and tissues, sampling techniques 3-48643
- trace-impurity gas detection, with tunable semiconductor laser 3-77744
- variable path cell, Q-switch attachment, Laser Mirospectral Analyzer, VEB Carl Zeiss, JENA, optimisation of anal. results 3-51766
- volatilization rate of free particles in d.c. arc plasma in air at atmospheric pressure 3-63914
- wolframite, laser spectral analysis in plasma with controlled excitation delay (*Russian*) 3-70490
- X-ray analysis, As impurities, H_2SO_4 catalyst, AsK α line intensity rel. to composition 3-48656
- X-ray fluorescence, Fe ores and mixtures, determ. Si and Al, rel. error calc. 3-48655
- X-ray fluorescence, rocks, rock-forming elements, conc. determ., error anal. 3-48654
- X-ray fluorescence analysis, of heavy elements using electrodeposit technique (*Japanese*) 3-62355
- X-ray fluorescence analysis, Z=47(Ag) to 92(U), L spectra, primary radiation 3-48653
- X-ray fluorescence analysis of trace elements using semiconductor detector spectrometer 3-66412
- X-ray luminescence, use in chemical analysis (*Russian*) 3-42700
- ALNICO magnet alloys, spectrographic analysis 3-62339
- Ag spectrophotometric determ. in pure U samples 3-70472
- Ag trace sensitivity, superimposed pulses on stationary discharge (*Russian*) 3-70487
- Al_2O_3 in flames, average particle diameter and spectral characteristics determ. (*Russian*) 3-62365
- Al_2O_3 particles, flame photometry, size obs. and stimulated part of refractive index (*Russian*) 3-59711
- Al_2O_3/B_2C ceramics, extraction-flame photometric determ. of boron 3-78376
- Au concentration in seawater 3-76918

spectrochemical analysis continued

- Ba determination, N_2O -acetylene gas shielded flame, atomic absorption spectrometry 3-48637
 Ca absorption line half widths, 422.67 nm line in hydrogen diffusion flames spectroscopy 3-57600
 Ca determination, flame and flameless atomic absorption, glacial snow samples 3-48638
 CaTiO_3 , Nb substituted, cryst. chem. 3-72044
 Cd-Se thin film, spectrophotometric analysis, precision and accuracy, statistical analysis 3-51758
 Cr traces in nuclear pure Th samples, spectrochemical determ. 3-70493
 Cu, saturated vapour pressure determ. by atomic absorption method (*Russian*) 3-48679
 Cu based solders, impurity determ., s.h.f. plasmatron excitation 3-73947
 Cu-Ni ores Pt, Rh and Pd determ., X-ray spectrometry, segregation 3-48659
 F, measurement of intensity decays using ultraviolet beam foil spectra 3-59702
 GaAs, rare earth dopants, distribution ratios, solubility curves 3-72099
 GaAs thin films, glow discharge optical spectroscopy for chemical analysis 3-42705
 GaP-GaAs, GaAs-InAs, X-ray spectra, inhomogeneities, statistical models in local anal. 3-48658
 H_2O -acetone mixtures, dependence of atomic absorption spectra on solvent composition 3-59701
 $\text{H}_2\text{S}/\text{SO}_2$ ratio, S recovery plants, photometric analyser system 3-61932
 He plasma spectrometric detector for quantitative determ. of CO , CO_2 , SO_2 , N_2O in air 3-45611
 Hg, air-acetylene flames, effect of standard $\text{Hg}(\text{II})$ soln. 3-48639
 Hg, determ. by atomic absorption and emission using 184.9 nm line 3-54049
 Hg-Cd-Te thin film, spectrophotometric analysis, precision and accuracy, statistical analysis 3-51758
 K trace analysis, modification to flame photometer 3-45587
 LiF, spectrographic determ. of impurities (*Russian*) 3-48678
 NO , NO_2 , atmospheric pollution, fluorescence detn. 3-70189
 Na absorption trace analysis using dye laser 3-54048
 Na-concentration deter. in power station cycle fluid (*Polish*) 3-62094
 Nb-Al-Si alloy, at. absorption spectroscopy (*French*) 3-50678
 O_2 interaction with Ag surface sensors, degree of dissociation meas. (*Russian*) 3-66461
 Pb, gunshot residues, flameless atomic absorption spectrophotometric method 3-48644
 Pb determination in blood, filter paper punched disc method, atomic absorption spectroscopy 3-48641
 S_2O_2 , unstable, formation in electrodeless discharge in SO_2 , O_2 , Ar, matrix isolated vibrational spectra 3-78803
 SO_2Cl_2 , solid, Raman and infrared spectra rel. to crystallographic structure 3-61035
 Si devices and processing materials, Na contamination monitoring, flame emission obs. 3-69169
 Si slice processing, flame emission analysis of K 3-54045
 Si_3N_4 , hot-pressed, impurities and inclusions identification 3-76284
 Sr resonance fluorescence quenching meas. in CO and H_2 flames 3-42707
 Ta, industrial effluent, chemico-optogenospectral fluorescence 3-48657
 Ti, fractional distillation for increased sensitivity (*Russian*) 3-77751
 Ti, saturated vapour pressure determ. by atomic absorption method (*Russian*) 3-48679
 Ti-Al(Fe) alloys, elec. erosion behaviour, interatomic bond strength depend. (*Russian*) 3-77749
 TiO_2 - SiO_2 glasses, e.p.r. study of Ti^{3+} - Ti^{4+} reaction 3-76418
 U, d.c. arc in air at atmos. press., transport of particles 3-73959
 V, saturated vapour pressure determ. by atomic absorption method (*Russian*) 3-48679
 Xe Zeeman tuned laser differential absorpt. apparatus 3-42694
 Zn-Mn ferrites, estimation of Ca by X-ray fluorescence method 3-62340

spectrography see spectroscopy**spectrometer accessories**

- see also mass spectrometer accessories
 absorption spectrophotometry, wide band reversing transformer as automatic backing-off device 3-39928
 air-acetylene flame, oxygen-shielded, burner design, atomic spectroscopy 3-70486
 atomiser, carbon rod, evaluation, atomic absorption spectroscopy, trace metal determ., lubricating and crude oils 3-70485
 CAMAC system for computer control of spectrometry at Daresbury Synchrotron Radiation Facility 3-39990
 cell holder, Beckman DK-2A Spectrophotometer, temp.-regulated 3-77368
 cryostat, Joule-Thomson, gas delivery system, use with Mariner 6 and 7 i.r. spectrometer 3-77184
 double vacuum monochromator, 800-2800 Å, toroidal concave diffraction gratings, fixed entrance and exit slits (*Russian*) 3-66225
 gated ion source for time of flight spectroscopy 3-62263
 glass face plate of LI 604 dissector, phosphoresc. and pulse noise (*Russian*) 3-77501
 Grating Double Monochromator GDM 1000, VEB Carl Zeiss JENA, appl. to Raman and fluorescence spectroscopy 3-51610
 image-retaining panel, Thorn, photography of spectral lines from 0.7 to 1.5 microns 3-66221
 i.r. spectra of solids, automation of meas. by points 3-73758
 low energy electron source, for drift velocity experiments 3-42738
 low temperature Raman cell for the Cary model 81 laser instrument 3-42572
 microwave cavity, for high temp. expts. for e.p.r. 3-39980
 Mossbauer spectra recorder, multichannel pulse analyzer, const. vel. mode 3-73914
 multichannel diode array for solar photoelectric measurements 3-81218
 multiparticle spectrometer magnets, design 3-56966

spectrometer accessories continued

- photon correlator, multi-channel 3-77487
 pulse amplifier, for particle spectrometers 3-73882
 pulsed n.m.r. apparatus, thyatron switch 3-66290
 pulsed NMR spectrometer, interface to Varian 620/i computer 3-39981
 Raman, rotating cell, gated electronic systems 3-68974
 Raman scattering, high speed recording unit 3-73756
 refrigerator, ^3He dilution type, for Mossbauer spectroscopy down to 0.1 K 3-68895
 sample changer, pneumatic ejection, gravity-feed, for γ -ray spectrometer 3-77736
 sources, microwave excitation, radiation danger 3-66061
 three mirror Raman cell for gases 3-62111
 tunable InSb detector, for far i.r. grating spectrometer 3-66239
 vacuum u.v. spectra, apparatus for absolute intensity meas. (*Japanese*) 3-66224
 windowless sample cell rel. to luminescence spectrometry, front surface excitation 3-59700

spectrometers

- see also interference spectrometers; magnetic resonance spectrometers; mass spectrometers; microwave spectrometers; particle spectrometers; radiofrequency spectrometers; x-ray spectrometers
 acoustic, phonon, using optical modulation methods, mag. circular dichroism detect. 3-53847
 Apollo 17 for u.v. spectrometer expt. 3-48157
 Atmosphere Explorer, fixed-grating Ebert u.v. spectrometer for NO density measurements 3-42077
 atomic fluorescence, photon counting or lock in amplification, comparison 3-70456
 automatic recording spectrometer UV2 (*Russian*) 3-66215
 cell spectrometer, volume distribution of blood cells, semi-automatic determination 3-73921
 Cherenkov, for γ -astronomy, Monte Carlo calc. of linearity and resolving capability (*Russian*) 3-65948
 constant deviation grazing incidence, synchrotron radiation facility 3-39935
 Czerny-Turner spectrograph, improved stigmatic focus, computer verification 3-77483
 digital laser Raman system, online control of data acquisition 3-62105
 Hadamard transform spectrometer for airborne i.r. astronomy 3-45236
 Hadamard-transform spectrometer, spectral Imaging HTS-255-15 3-59713
 high shock pressure spectrographic system, optical absorption spectra of ruby and periclase 3-76858
 high-resolution c.w. dye-laser spectrometer 3-77485
 i.r., based on IKS-6 monochromator 3-51609
 i.r., for NIMBUS satellite measurement of atmospheric temperature profiles (*Hungarian*) 3-76725
 light transmission derivative meas. 3-77496
 luminescence spectrometer, high resolution, for simultaneous recording of phosphorescence and luminesc. 3-42563
 luminescence spectrometer, with programmed wavelength control 3-62107
 missing mass, diffractive dissociation study, helium streamer chamber 3-77671
 Mossbauer, interferometric calibration problems and solutions 3-70437
 multispectral scanner for Skylab, use of model for calibration 3-77461
 optical, review 3-56669
 optical heterodyne, movement of living microorganisms (*French*) 3-48626
 optimum settings for side-on viewing mode, refocusing technique 3-77489
 plane grating, Ebert-Fastie or Czerny-Turner, dispersion 3-62106
 radiometer, for field use, design description 3-39880
 Raman, for remote analysis of air pollution 3-56563
 Raman rotational-vibrational spectra, instrument description 3-53905
 rapid scanning, cathodoluminescence (*French*) 3-69098
 real-time digital videomagnetograph for sunspot magnetic fields 3-59406
 reflectometer, far u.v., for optical props. of solids 3-42568
 refocusing method to reduce optical blends 3-60370
 remote sensing application, in u.v., i.r., and visible regions 3-51172
 specular reflection spectroscopy, electrode-solution interphase, review 3-66227
 spin-phonon application to detection of v.h.f. pulsed phonons 3-54006
 vacuum u.v., absorpt., excitation of solids, installation 3-73757
 vacuum u.v., automation 3-62110
 wavelength modulation spectrometer, 2000-8000 Å 3-45485
 wavelength modulation type, appl. to solids 3-55624
- spectrophotometers**
 see also spectrophotometry
 for airglow detect., Na day 3-65515
 airglow obs. in 150-1500 Å range from satellite photometer 3-69739
 Atmosphere Explorer, e.u.v. spectrophotometer for solar radiation 3-42261
 cell holder, Beckman DK-2A Spectrophotometer, temp.-regulated 3-77368
 derivative light scattering photometer 3-66219
 DNA, helix coil transition, u.v. photometer, student experiment 3-51422
 double beam photon-counting spectrometer high resolving power (*Russian*) 3-45242
 double-beam recording spectrophotometer, photoelectric system 3-48431
 dual wavelength, new, design, construction, specifications, operation 3-57016
 exponential nonlinearity meas. method 3-39919
 far i.r., ultrahigh sensitivity detection system 3-45481
 flame, FLAPHO 4, VEB Carl Zeiss JENA, Na, K, Ca, Li, Rb anal. 3-51765
 goniospectrophotometer, reflectance and transmittance measurements, 0.25 to 1 micron polarised light (*French*) 3-39926

spectrophotometers continued

- grating infrared online, gas chromatograph peak identification 3-62322
- impulse fluorimeter using excitation from picosecond laser (*Russian*) 3-62370
- i.r., light passing, sector discs for checking photometric scales 3-51612
- microspectrophotometer, capable of recording absorpt. spectrum first derivative 3-48428
- microspectrophotometers, description (*Danish*) 3-66220
- modulation excitation spectrophotometry lens 3-66222
- multichannel, performance under observing conditions 3-77195
- null error elimination, by method of double modulation of source flux 3-53903
- for optical absorption of aqueous samples at high temp. and pressure during irradiation 3-48417
- recording systems, comparative evaluations 3-48429
- reference spectrophotometer, precision, accuracy 3-51606
- scanning spectrophotometer, using stable polarization modulator 3-45484
- SPEKTR-1, SFPA-4, atomic absorption analysis accuracy 3-53900
- stellar, operating in Hartley band, optics/electronics/measurement systems (*French*) 3-73561
- twin beam, for meas. of glass bulk, attenuation 3-53907
- u.v.-visible recording of absorbance spectra, computer controlled 3-66217
- vacuum u.v., totally integrated system 3-42567
- for v.v. radiation hazard meas. 3-73753

spectrophotometry

- see also colorimetry; spectrophotometers; stellar spectrophotometry*
- absorption, wide band reversing transformer as automatic backing-off device 3-39928
- absorption band anisotropy in lunar, meteoritic and terrestrial pyroxenes 3-65795
- airglow hydroxyl emission intensities in 0.3-2.3 μ range 3-76795
- atomic absorption, programmable lamp current supply 3-62115
- automatic recording on tape of solid state absorption spectra (*Russian*) 3-62100
- 4C 31.63, quasar, spectroscopic and photometric obs. 3-51364
- clusters of galaxies, Mariner 9 u.v. obs. 3-45199
- colour matching system employing computer 3-51605
- colour measurement, instrumentation, applications to food processing industry, methods, review 3-59588
- X Comae Berenice, optical variability, UVB colours 3-81171
- data enhancement procedure 3-66228
- far u.v. solution, techniques, apparatus, problems, applications, spectrochemistry 3-57013
- film thickness measurement, epitaxial, dielects., i.r. 3-73759
- flame, electrocast materials, physical methods of chem. analysis (*French*) 3-70468
- galaxies, emission-line, obs. of 3 objects 3-59369
- Galilean satellites, surface colour variations 3-47919
- haze scattering effect on atmospheric ozone 3-65386
- hydroxamic acid in nuclear fuel reprocessing solvents, spectrophotometric determ. 3-71225
- instrumental precision theory, reading error, electrical noise 3-62320
- interstellar molecular H, Copernicus satellite obs. 3-48116
- i.r. cell for catalyst studies 3-42570
- i.r. spectrum of zodiacal light 3-81017
- lamp current supply, programmable, for atomic absorpt. spectrophotometry 3-62115
- luminance fields, scaling of spatial spectra 3-62118
- Martian maria in equatorial zone of southern hemisphere, spectral values of contrast (*Russian*) 3-73450
- meteor radiation problems, bright fireballs 3-77017
- molecular dissociation energies, determ. for Ca and Ba cpds. 3-49493
- moon, monochromatic phase curves and albedos for lunar disk 3-45042
- multicomponent systems, spectrophotometric anal., theoretical estimate of accuracy 3-42702
- NGC 1300 barred spiral, UVB photoelectric drift scan 3-77133
- NGC 2276, late-type spiral galaxy, detailed UVB photometry (*Russian*) 3-45167
- night sky radiation in u.v. and visible, Kosmos 51 and 213 obs. in space (*Russian*) 3-44878
- nuclei of bright galaxies, UVVHKL obs. 3-51387
- offset device for high level interference in low level detectors 3-62114
- OJ 287, blue compact object, photoelectric sequence 3-73523
- phototubes, spectral sensitivity measurement, interlaboratory comparison 3-66218
- Scorpius X-1 flares, UVB obs. 3-48085
- Seyfert galaxies, photoelectric UVB obs. beyond nucleus 3-77149
- southern galaxies, JHKL colours of barred spirals 3-73543
- spectral irradiance measurement, fluorescent and incandescent lamps, interlaboratory comparison 3-66126
- (1685) Toro, asteroid, visible and near i.r. spectral reflectivity curve derivation 3-61733
- turbid media, optimum reference wavelength selection, dual wavelength 3-62101
- Vela X supernova remnant, emission line spectrum 3-81098
- Al diffusers, spectrophotometric props. 3-48418
- CoBr₂ in fused organic salt, absorpt., charge-transfer, ligand-field transitions 3-64671
- N₂, isotopic analysis (*Rumanian*) 3-62113

spectroscopes *see spectrometers***spectroscopic light sources**

- 130-280 Å region 3-51750
- atomic line profiles emitted by hollow-cathode lamps and C₂H₂-N₂ flames, interferometric meas. 3-62352
- beam-foil, as absolute intensity standard, near i.r. to vacuum u.v. and X-ray region 3-77503
- beam-foil, modulation spectroscopy 3-53910
- beam-foil spectroscopy, highly ionised emitters 3-78423
- BRV continuum pulsed light source 3-48424
- coaxial lamp, emission characteristics with reference to external magn. field (*Russian*) 3-77502

spectroscopic light sources continued

- electrodeless discharge lamp, microwave excited, stabilisation and modulation 3-62112
 - electrodeless discharge lamps, stabilizing device 3-66223
 - excitation arc source, sonic methods for potential and potential gradient meas. (*Russian*) 3-77498
 - excitation source, use of s.h.f. plasmatron 3-73947
 - flash-photolysis, pulsed source, continuous spectrum, visible and u.v., description 3-73755
 - furnace system, for high temp. vacuum u.v. obs. of atomic, mol. species 3-62104
 - hollow cathode with separate evaporation and excitation for spectral analysis (*Russian*) 3-62366
 - inert gas continuous source for vac. u.v. 3-62116
 - i.r., miniature highly stable ceramic 3-70315
 - laser irradiation appl. (*Rumanian*) 3-62732
 - microscopic, plane-wave complex spectrum, far-field interf. anal. 3-77480
 - offset device for high level interference in low level detectors 3-62114
 - quartz halide lamps, visible spectra (*German*) 3-48425
 - sectional lamp with planar solid luminescence of high intensity based on surface discharge (*Russian*) 3-62119
 - spark-arc discharge generator, device for stabilising emission spectrum, reduction of meas. error 3-73754
 - standard and excitation types, review 3-56669
 - synchrotron radiation as u.v. source, 10-1000 Å, spectroscopy applications, review 3-39930
 - tungsten halogen incandescent lamps, spectral irradi. standards, 300-1200 nm 3-39920
 - u.v., metallic discharge lamp, discharge plasma compression 3-73757
 - Cs electrodeless high intensity source 3-77478
 - H arcs for vacuum u.v. radiometry 3-51549
 - H₂ lamp, LiF and CaF₂ windows, effect of vac. u.v. on transmittance 3-62117
 - Hg/SnI₂ arcs, absorpt., emission and temp. meas. 3-54887
 - Na, thermal atomic beam, c.w. velocity selection by dye laser optical pumping 3-78463
 - Pb_{0.9}Co_{0.05} diode laser, tunable cw operation at 3.5 μ m, ultrahigh resolution spectroscopy applic. 3-51607
 - W ribbon lamps, self calibration by relative meas. of spectral, integral radiant energy 3-73751
 - Xe arc lamp, spectroscopic study of plasma (*Russian*) 3-77499
- spectroscopy**
- see also beam-foil spectroscopy; electron spectroscopy; mass spectroscopy; modulation spectroscopy; radiofrequency spectroscopy; X-ray spectroscopy*
 - aberration elimination in plane grating spectrographs and monochromators by using circular grooves 3-48861
 - adhesive bond strength, metal-to-metal joint, prediction 3-69410
 - aerosol beam spectroscopy, recent developments 3-55904
 - astronomical, using 16-inch telescope 3-51417
 - astronomical spectrograph camera, effect of component separation on image quality 3-73562
 - atomic absorption, continuous primary light source, monochromator, effect of spectral transmission function (*German*) 3-62108
 - ATR i.r., thin film, thickness meas. and chemical charac. 3-48442
 - automatic peak analysis, using minicomputer 3-48421
 - beam-foil, modified Lamb-dip technique using tunable laser sources 3-77494
 - beam-foil experiments, study of light emission from ion beam and target (*French*) 3-77497
 - beam-foil spectroscopy, conference, Tucson, Ariz., USA (1972) 3-78422
 - beam-foil spectroscopy, highly ionised emitters 3-78423
 - beam-foil spectroscopy, review of recent developments 3-77488
 - beam-laser, Doppler tuned, cascade free precision lifetimes 3-77493
 - Cloud-droplet size distribution measurement by laser optical-heterodyne spectroscopy 3-77758
 - complex contours, resolution into two symmetrical bands, model curves method (*Russian*) 3-77500
 - cryostat, variable temperature, 5.5-100 K, for i.r. and u.v. spectroscopy 3-70292
 - data processing system, PUMSM 3-74996
 - double wave, applications review 3-39924
 - electrochemistry, optical techniques, book 3-66195
 - fast beam high resolution, use of Fabry-Perot off-axis interferometer 3-77522
 - fast-scan spectroscopy, for luminescent decay studies 3-51614
 - ferrocene derivatives, Fourier transform n.m.r., chemical shift 3-75897
 - fluorescence lifetime meas., distortion of electric pulse 3-39929
 - fluorescence spectroscopy, multiple internal reflection 3-66414
 - fluorescence spectroscopy, applications review 3-39925
 - forest tree species, computer-aided recognition 3-53908
 - Fourier, fast-scanning spectrometer, characts., apodization 3-62140
 - Fourier, photon noise limited 3-42578
 - Fourier transform, equivalence with slow passage expt. 3-67791
 - Fourier transform, for air pollution study 3-48433
 - Fourier transform, for linewidth determ. 3-51623
 - Fourier transform, mm transmission of glasses, on line technique for thickness control 3-77486
 - Fourier transform spectroscopy, apodisation and phase information 3-45495
 - gravimetric data, calculation errors (*Russian*) 3-76894
 - high resolution spectroscopic application of atomic beam deflection by resonant light 3-53906
 - high-resolution spectroscopy, use of energy level crossing (*Russian*) 3-71376
 - holographic Fourier transform spectroscopy, heterodyning technique 3-77535
 - impurity complexes, parametrisation of equivalent Hamiltonian, perturbation theory 3-69033
 - internal reflection, electrochem. studies 3-66226
 - ion beams, origin and reduction of spectral line broadening 3-42669
 - i.r., applications review 3-39923
 - i.r., at subambient temps. 3-59589
 - i.r., for vacuum and surface studies, developments of technique 3-51547

spectroscopy continued

- i.r., multiband systems, classical dispersion analysis, self-bracketing search technique 3-56667
- i.r., multiple reflection, methods and instruments, appl. to polymers and fibres (*Polish*) 3-70311
- i.r., rapid recording method for chemical laser applic. 3-53920
- i.r. atomic wavenumber library 3-54558
- i.r. internal reflection, use of thin films 3-73164
- i.r. reflection ATR methods for optical constns. determ. (*Polish*) 3-48426
- i.r. spectra of solids, melting point, 20 to 120C, improved procedure 3-77359
- laser, quantum-beat detection method, discussion 3-40571
- laser spectroscopy, absorpt. line parameter meas., comments 3-45486
- light beating technique, for high-resolution Brillouin scatt. 3-77481
- line intensity rel. to weight of sample vaporised with laser microprobe 3-45556
- luminescence over broad spectral range, absolute quantum yield meas. 3-48430
- matrix-isolated species, far i.r. Fourier transform spectroscopy 3-45496
- molecular motion study in liquids 3-72214
- molecular rotation spectral line, halfwidth, intensity, determination, iterative solution of nonlinear least squares problem, method (*French*) 3-70310
- molecules and molecular crystals, synchrotron radiation from 5 to 260 eV 3-40061
- multiple beam holographic spectroscopy, interpretation of holographic interferograms 3-62151
- multiplet interpretation and spectral analysis, role of spectroscopic instrumentation (*French*) 3-39927
- n.m.r., molecular biological research, basic concepts, methods (*German*) 3-54029
- n.m.r. spectroscopy, using spin generator 3-56707
- nonlinear controlled dispersion spectrography 3-59590
- nuclear, in 1 GeV energy range (*French*) 3-59620
- nuclear fuel, irradiated, combustion rate meas. comparison with adiabatic calorimeter (*French*) 3-73694
- nuclear radiation, filters for improving energy resolution, fast pulse rates (*German*) 3-62269
- optical, radiation sources, monochromatization, detectors and spectrometer systems 3-56669
- optical cavities for spectral line absorption meas. 3-42565
- optical oscillator theory for photoionisation process, double and triple coincidence techniques (*Dutch*) 3-39922
- organo-element compounds, n.m.r. Fourier transform, chemical shift 3-72536
- photodiode detector arrays, self-scanning, characts. 3-70309
- photoluminescent excitation intensity, direct meas. of nonlinear dependence 3-51613
- photon correlation spectroscopy, factors affecting accuracy 3-62109
- picosecond, and molecular relaxation, review 3-57647
- planetary atmospheres, techniques, education 3-59521
- Raman, for study of thin films (*German*) 3-45488
- Raman, highly coloured crystals, surface scanning technique 3-48423
- Raman polarised scattering, small single crystals, 90 degree viewing, simple experimental technique 3-56668
- Raman spectra, laser beam improved trapping using glassy water films 3-53904
- Raman spectra obs. up to 50 kbar pressure, devices 3-80027
- Rayleigh scatt. meas. in liquids using optical fibres 3-62102
- Reflection spectroscopy of optically active materials 3-68950
- resonance spectroscopy, using Nd atomic beam and c.w. single-freq. dye laser 3-77484
- r.f. argon plasma torch appl. 3-45607
- sea surface pollution meas. by satellite (*Italian*) 3-61609
- sectoral modulator, for suppression of scattered light in recording of luminescence spectra 3-51608
- solids, photoacoustic spectroscopy 3-45490
- spectral components of lines, displacement determ. method 3-48427
- spectral density estimation, stationary random ergodic processes comparison of Fourier transform method with a correlation method, engineering design (*Russian*) 3-70312
- spectral line contours determ., meas. by an instrument with known apparatus function (*Russian*) 3-48432
- Stark spectroscopy, molecular dipole moment determ., environmental effects 3-72600
- student expt. in geometrical isomerism studies 3-53821
- student spectral analysis using 35 mm camera and projected slides 3-73653
- subsonic and sonic flow in heat pipe, spectroscopic obs. 3-40726
- synchrotron radiation, Daresbury Facility, CAMAC system for computer control 3-39990
- synchrotron radiation as u.v. source, 10-1000 Å, spectroscopy applications, review 3-39930
- Synchrotron Radiation Facility at Daresbury, recent development 3-39991
- thermo-optical technique for absorpt. loss spectrum meas. in liquids 3-62103
- time function, spectrum, recovery, Fourier transforms, harmonic and damped oscillations 3-42054
- tunable-wavelength high resolution spectroscopy 3-39921
- two-photon excitation spectroscopy, high-resolution technique 3-80068
- visual detection of stimulated emission or absorption from excited states, sunspot technique 3-45489
- water soluble solids, technique for studying i.r. spectra at ambient and elevated temp. 3-42571
- weak absorption line detection, using glass:Nd laser 3-39933
- KBr pellet method for hygroscopic compounds i.r. spectral meas. 3-45491
- Pb salt diode lasers, small band gap, absorption spectra, Zeeman splitting obs. 3-57241

spectrum *see spectra***spectrum analysers** *see spectral analysers***speech***see also hearing*

- articulation, vowel stress, jaw and tongue positions, differentiation 3-77208
 - automatic formant extraction, using linear prediction 3-45391
 - consonant durations in cluster environment 3-48306
 - deaf adolescents training, comparison of visual display devices 3-48189
 - diver distortion rel. to HeO₂ environment 3-61945
 - excised dog larynx, vibration patterns 3-48193
 - fake vowel length and three degrees of vowel length in Yupik Eskimo 3-48309
 - hearing, anomalous loudness function, role of reverberation, experimental results 3-81276
 - hearing stapedius reflex., articulation scores, stapedius paralysis effects 3-81277
 - jaw movements, influence of gamma motor system, theory and observations 3-77209
 - linguistic boundaries in English, acoustic and articulatory properties 3-48308
 - linguistic structure and speech shadowing at very short latencies 3-65988
 - monaural and binaural free-field speech reception through ear-level hearing aids under noise and reverberation 3-48232
 - movements of lip and jaw, strain gauge transduction system, two dimensions, design, calibration 3-73927
 - privacy in offices, background noise, graphic method 3-56575
 - production, rhythmic units and syntactic unit 3-48313
 - production and perception, unified theory 3-48201
 - production theory and linguistic units 3-48199
 - repaired cleft palate patients, velopharyngeal mechanism 3-45270
 - segmental timing, neural control 3-48188
 - tongue displacements, on-line pulsed through-transmission ultrasonic monitoring system 3-73925
 - velar movement, forward coarticulation 3-45269
 - vocal-tract, X-ray films, computer assisted measurement system 3-77210
 - vocal-tract area function for given lip impedance, noniterative computation 3-45394
 - volume velocity waveform at glottis during voiced speech, inverse filtering technique 3-59501
 - vowel duration as function of syllabic structure of English words 3-48307
 - young children, effect of oral anesthetization 3-48197
 - in He rich atmosphere, identification of vocal register shift 3-48196
- speech analysis**
- articulation index, evolution and modification 3-81267
 - articulatory model, midsagittal X-ray trace analysis 3-48185
 - consonant clusters, aspiration and voice onset time 3-45267
 - by delayed long-time averaged compression amplification method 3-48310
 - digital encoding of waveforms 3-81268
 - digital inverse filtering 3-77215
 - Dutch vowels, male speakers 3-48187
 - English, rhythmical and physiological constraints 3-81269
 - Fo, physiological factors, correlation analysis 3-48195
 - frequency analysis, Dutch vowels, female speakers, classification spectra 3-70218
 - Japanese sentences, semantic information processing, time concept (*Japanese*) 3-66096
 - laryngeal muscles, response time, correlation analysis 3-48194
 - Noise resistant larynx synchronous speech processing 3-77213
 - without oral sensation, acoustic characteristics 3-73578
 - palatoglossus activity, speech organization 3-45268
 - personality perception, hearing, manipulation of acoustical parameters 3-70107
 - spontaneous and read speech, acoustic analysis of phonological processes 3-48315
 - syntactic decoding and prosodic units 3-48200
 - vocal tract behaviour, waveform matching in glottal cycles 3-77214
 - Vocal tract damping and cavity wall vibrations 3-77211
 - vocal tract shape estimation 3-61943
 - vowels personal quality, multidimensional representation 3-61944
- speech intelligibility**
- communication quality, interference test 3-48186
 - consonant attributes, effect of noise 3-42337
 - deaf, computer aid 3-61898
 - deaf children, similarity scale to evaluate sub-intelligible speech patterns 3-48192
 - deaf children, speech production errors 3-48191
 - deep-diving communication, after H mixture breathing 3-42338
 - by delayed long-time averaged compression amplification method 3-48310
 - dichotic listening for simultaneous and time-staggered CVs, phonetic errors 3-42314
 - fidelity evaluation, interference test 3-77212
 - hearing impairment criteria 3-45272
 - helium speeds, He-N₂-O₂ gas mixture under pressure, syllable articulation tests, perceptual analysis 3-61946
 - initial consonant, hearing impaired children 3-73577
 - interference by speech and nonspeech signals 3-42315
 - masked speech, effect of practice 3-42330
 - modified rhyme test scores, closed-response format effect 3-48297
 - monosyllable words, for half-octave bandpass filtering conditions 3-45284
 - perception, attentional control 3-42331
 - perception of dichotically presented speech and non-speech, effect of asynchrony 3-42312
 - perceptive deafness, signal processing to improve speech intelligibility 3-59431
 - phonological contrast, stop consonants in French-English bilinguals, voice onset time study 3-77337
 - sensorineural hearing impairment, speech cue discrimination 3-48190
 - signal processing for deaf subjects 3-48311
 - stop consonants, artificial, time taken to perceive 3-45280
 - system for continuous speech understanding 3-45388
 - system for speech understanding, syntactic and semantic components 3-45389

speech recognition

- adaptation model 3-81270
- automatic, graph theoretic approach 3-81272
- automatic, phonological processes in English 3-48314
- basic English, automatic system 3-81271
- brief vowels, identification and discrimination 3-42333
- dichotic listening, effect of varying syllable microstructure on voiceless preponderance 3-42313
- dichotic speech perception, temporal offset effects 3-45271
- discrimination, decision processes, confidence rating 3-42329
- English consonants embedded in sentence 3-42336
- glottal source characteristics, identification in absence of inter-subject differences 3-59504
- hearing, effect of varying labels 3-42309
- perception of the F₃ cue for [r-l] distinction, Japanese, English cross study 3-61951
- phonetic levels of processing, reaction time 3-42332
- short vowels, forward and backward masking 3-42334
- speaker identification, using nasal coarticulation 3-45392
- two-pole spectral model 3-45390

speech synthesis

- deaf children, speech production errors 3-48191
- digital encoding of waveforms 3-81268
- modulation method, spectral generator with magnetic devices (*Japanese*) 3-66095
- parametric artificial talker, review 3-81266
- two-pass procedure, for synthesis by rule 3-45393

speed *see velocity***speed control** *see velocity control***speed indicating instruments** *see velocity measurement***speed measurement** *see velocity measurement***spherical aberration** *see aberrations***spicules** *see solar prominences***spin**

- see also electron spin; hyperon spin and parity; meson spin and parity; nuclear spin and parity; spin hamiltonians*
- classical particle with magnetic moment interacting with e.m. field, eqn. of motion determ. (*French*) 3-66603
- correlation parameters for 50 MeV proton-proton scattering 3-63030
- gravitational singularities, effect of intrinsic spin 3-54150
- Lagrangians for particles of spins 3/2, 2 and 5/2 in Gel'fand-Naimark formalism 3-62771
- Maxwell and Einstein's field equations, formulation in medium with 'particles' having internal spin 3-66655
- nucleon, modification of relativistic eikonal model using ladder graph model, Feynman parameters 3-67089
- null-plane formalism, helicity and canonical formalism relations 3-62796
- precession of charged particle in magnetic field including effects of general relativity 3-57148
- rotational coordinates for description of spin, relation of quantum mechanical and classical theories 3-62553
- Schrodinger eqns. for particle with spin, soln. of Cauchy problem using quantum stochastic processes 3-62548
- sounding rocket spin rate sensor 3-47831
- tagging, polarised neutron beams from deuteron beam break up 3-67168
- Wigner quasiclassical theory for particles (*French*) 3-57118

spin arrangements *see magnetic structure; spin systems***spin dynamics**

- alloys, nearly magnetic, Lorenz number and thermal resistivity 3-72343
- Anderson model for nonmag. limit of mag. impurity, localised spin fluctuations 3-52960
- anisotropy effect, from study of second moment behaviour 3-44226
- antiferromagnet, spin-flip transition dynamics 3-75839
- Bloch equations and adiabatic rapid passage with radiation damping 3-68822
- Brownian motion, Langevin equation method 3-62604
- cross relaxation probability, dependence on angle between axes of spin quantisation 3-64540
- dilute mag. alloys, Kondo problem, impurity spin dynamics 3-46997
- dilute magnetic alloys, spin diffusion and relax., electron-electron interactions 3-46996
- dynamic polarisation by solid effect, equivalence of rate equation and diffusion theory for isotropic distributions 3-68887
- ferromagnetic relaxation of magnetisation fluctuations above Curie point, dipole-dipole interactions 3-50465
- ferromagnetism, itinerant electron, Stoner theory modification for spin fluctuations 3-68756
- ferromagnetism, spin current correlation, free fermion system 3-64440
- flip-flop sequence for restoring Zeeman order in laboratory reference frame 3-53029
- gravitation-spin interaction, Zeeman effect analogue (*Russian*) 3-77879
- Heisenberg and X-Y magnets, spectral weight function of spin-pair correlation 3-46965
- Heisenberg ferromagnet, decoupling of single-ion functions by Green's function method 3-64463
- Heisenberg spin system, with uniaxial and exchange anisotropy, freq. moments, short range order effects 3-55400
- metal, retardation effects in longit. spin relax., dynamical impurity susceptibility 3-68827
- molecules and excitons in strong mag. fields, spin rearrangement 3-72337
- neutron inelastic scatt. theory for local spin fluctuation systems 3-55420
- Peierls transition, fluctuation effects 3-58107
- phonon Raman scattering, spin-dependent, of mag. crystals 3-72616
- polyethylene terephthalate, amorphous, nuclear relaxation 3-75909
- singlet ground state dynamics 3-64467
- stochastic Ising chain kinetics in a class of spin flip models 3-60948
- CdS, spin-flip Raman scatt. near 5145 Å, resolution improvements 3-50582
- Cr₂O₃, stress included spin flop 3-44227
- spin dynamics continued**
- Dy, resistivity meas., electron scatt. from spin fluctuations above Neel point 3-58245
- Fe(II) complex, diethiocyanatobis (1,10-phenanthroline)Fe(II), ligand substituent effects on ⁵⁷Ta = ¹A₁ transition 3-68779
- ³He, liquid, diffusion near crit. pt. 3-50045
- InSb, near reson. spontaneous spin-flip Raman scatt. 3-44415
- InSb, theory of spin-flip Raman amplification 3-78049
- NiCl₂, antiferromagnet, crit. e.p.r. spin dynamics, linewidth divergence behaviour 3-47136
- Pd-Cr, localised spin fluctuations, low temp. susceptibility, specific heat obs., Pd-Ni comparison 3-68768
- Pt-Cr, localised spin fluctuations, low temp. susceptibility, specific heat obs., Pd-Ni comparison 3-68768
- RBe₁₃ intermetallic compounds, (R = La, Ce, Nd, Gd), magnetic properties hyperfine interactions, spin dynamics 3-52969
- RbMnF₃, spin diffusion coeff., room temp. to critical region 3-55412
- UP₂, UBi₂, spin disorder resistivity 3-41219
- YFe_{0.8}Mn_{0.2}O₃, spin reorientation, Mossbauer and neutron diffr. obs. 3-55434
- spin echo method (electron)** *see paramagnetic resonance*
- spin echo method (nuclear)** *see nuclear magnetic resonance*
- spin Hamiltonians**
- Appelbaum-Kondo's trial ground state of Kondo's Hamiltonian, bound particle spatial density distrib. 3-55393
- atom pair direct exchange interaction Hamiltonian 3-46951
- charged solid Hamiltonian and scalar wave eqn. of spin corpuscle in nonrelativistic mechanics (*French*) 3-42838
- classical spin, Brownian motion, Langevin equation method 3-62604
- correlation functions, time depend., rigorous upper and lower bounds 3-41313
- critical point investigation in classical spin models of type of Dyson's hierarchical models 3-72431
- dimers triplet EPR spectra simulation, g and D tensors not coaxial 3-64546
- e.s.r. spectra, non-collinear Zeeman, hyperfine and fine structure tensors effect 3-47127
- exchange interactions and spin wave theory, review 3-64451
- exchange-coupled ion pairs, parameters derivation 3-46950
- ferromagnet, Hamiltonian, Schrodinger spin-exchange operator, Curie temp. anomalies 3-50316
- ferromagnet, parametric magnon excitation, theory, self consistent field method 3-58390
- ferromagnet, spin-one model, suscept. high temp. series expansion 3-47022
- fine structure e.s.r. spectra, in strong crystal fields, spin Hamiltonian consts. determ. numerical solution 3-44312
- glass:Gd³⁺, e.s.r., crystal field parameters 3-72510
- Heisenberg spin models, computational approach 3-75821
- hexakisantipyrine metal perchlorate, Mn(II) e.s.r. spectra 3-55462
- low symmetry, second-order perturbation treatment for energy levels 3-72506
- magnetic impurity problem, functional integral approach, two variable method 3-60944
- magnetism, biquadratic exchange and spin exchange operator effects 3-44180
- magnon Hamiltonian, itinerant electron ferromagnetism, magnon interaction problems 3-50380
- magnon Hamiltonian, itinerant-electron ferromagnetics, magnon interactions, method 3-50331
- molecular excited triplet states, absolute sign of electron spin dipolar and nucl. quadrupole interactions 3-57667
- n.m.r. spectra dipolar operators, broadening effects interpret. 3-68823
- nuclear spin diffusion phenomenon, new approach 3-75901
- perovskite fluorides: Mn²⁺, hyperfine interactions, ENDOR study 3-47172
- single ion anisotropy, generating function of anisotropy Green functions 3-79809
- symmetrical spin system with arbitrary spin I, theory of n.m.r. spectra (*German*) 3-53031
- symmetrical spin systems with I=Y₂, theory of n.m.r. spectra (*German*) 3-53030
- transferrin, ⁵⁷Fe Mossbauer spectra analysis 3-63575
- transition metal magnetism, effect of electron correlation on orbital interactions 3-72442
- two-phase system, nucl. spin relax. theory (*German*) 3-68865
- Wick's theorem, general statistical, general subsystem Hamiltonian in 3D Hilbert space 3-45705
- XY model, algebraic methods 3-79812
- [CuCl₄.2NH₃]²⁻ complex, spin hamiltonian parameters, Π bonding, e.p.r. study 3-41401
- Al₂O₃:V³⁺, spin-phonon coupling by quantitative spectroscopy with phonons 3-58104
- CaMg(SiO₃)₂:Fe³⁺, e.p.r. study 3-55461
- Ca(OH)₂:Gd³⁺, parameters from electron spin resonance spectra 3-58422
- CdF₂:Cr²⁺, e.s.r., interactions of Cr²⁺ with F⁻ ligands, s.h.f.s. 3-72514
- CdS:Ti²⁺, CdSe:Ti²⁺, e.p.r. spectra at 27K and 77K 3-47138
- Eu₂(MoO₄)₂, e.p.r. of Gd³⁺ at 293K 3-50457
- CsY(MoO₄)₂, e.p.r. of Gd³⁺ at 293K 3-50457
- D₂, electric field gradient and magnetic spin-spin interactions 3-43438
- H₂, electric field gradient and magnetic spin-spin interactions 3-43438
- HD, electric field gradient and magnetic spin-spin interactions 3-43438
- K₂MF₄:Mn²⁺ (M = Mg, Zn, Cd), ENDOR, nuclear quadrupole interaction, zero-point spin deviation 3-75915
- K₂ZnF₄:Mn²⁺, axial anisotropy of Mn²⁺, overlap contribs., e.p.r. obs. 3-50444
- La₂Mg₃(NO₃)₁₂.24H₂O:⁵⁹Co²⁺, e.p.r. and ENDOR studies 3-72515
- LiAl(SiO₃)₂:Fe³⁺, e.p.r. study 3-55461
- MgAl₂O₄, spinel, orthorhombic Cr³⁺ centre, spin Hamiltonian for e.s.r. spectra 3-43788
- MoO₃ cpds., amorphous semicond., localized d¹ electron e.s.r. meas. 3-68847

spin Hamiltonians continued

NH₄Cl:Cu²⁺, optical and e.p.r. spectra, spin Hamiltonian parameters 3-55468
 NaCl, exchange-coupled pairs of Mn²⁺ ions, e.s.r. 3-55470
 NaCl:[Ni(CN)₄]²⁻, X-irrad., e.p.r., paramag. species identification 3-64544
 α-NiSO₄·6H₂O e.p.r. measurements, single crystals, spin Hamiltonian parameters, direction cosines of crystalline field 3-50440
 Pr₂Ti Van Vleck paramagnet, spin-phonon coupling 3-46981
 Rb₂MF₄:Mn²⁺ (M=Mg, Zn, Cd), ENDOR, nuclear quadrupole interaction, zero-point spin deviation 3-75915
 SrTiO₃:Fe³⁺, electric field effect on e.p.r. spectrum 3-72513
 V₂O₃-Cr₂O₃, antiferromag. state, n.m.r., hyperfine field, mag. moment, spin moment 3-55478
 V₂O₃ cpds., amorphous semicond., localized d¹ electron e.s.r. meas. 3-68847
 YIG:Cr, mag. anisotropy of Cr³⁺ calc., rel. to ferromag. resonance obs. 3-41415
 YIG:Yb, ferromagnetic resonance anomalies, transverse relaxation instability 3-68848

spin-lattice relaxation

alkaline single cryst., nuclear spin-lattice relax. anisotropy 3-75907
 alkalooids, large, nols., ¹³C spectral assignments using spin-lattice relax. times 3-67874
 as clathrate deuterate, proton spin-lattice relax. time 3-54727
 p-azoxyanisole nematic liquid crystal, proton spin relaxation of dipolar energy, frequency depend. 3-55491
 borate glasses, ²³Na and ⁷Li n.m.r. studies (German) 3-72544
 t-butylamine, p.m.r. absorption and relaxation study 3-55492
 t-butylamine clathrate deuterate, p.m.r. absorption and relaxation, study, isotropic molecular rotation 3-55492
 t-butylchloride, self-diffusion coeff. and rot. correlation time determ. 3-68872
 camphor, mol. dynamics, ¹³C n.m.r. relax. times 3-68881
 chloroform crystalline, quadrupole relaxation of ³⁵Cl nucleus and effect on CCl₃ group mobility 3-75902
 cross relax. determ. of short quadrupolar spin-lattice relax. rates in solids 3-47164
 crystals with trigonal and tetragonal structure, dipole and quadrupole relax. 3-44311
 cyclohexane: nitroxide free radical, molecular self-diffusion, nuclear spin-lattice relaxation and dynamic polarisation 3-49854
 cyclopropane, solid, and cyclopropane deuterate, molecular rotation determ. 3-44346
 diethylamine, solid, p.m.r. second moment and spin-lattice relax., mol. motion study 3-55497
 diethylamine clathrate deuterate, solid, p.m.r. second moment and spin-lattice relax., mol., motion study 3-55497
 dimethoxybenzene, ortho, meta and para, nuclear spin-lattice relaxation, cross correlation effects 3-55490
 displaced charge sum rule in terms of perturbing force due to defect and phonons 3-43838
 electron, effect of phonon bottleneck on cross-relaxation, Zubarev's method 3-72508
 electronic spin system, cross relax. mechanism 3-47131
 epoxy resin, thermoplastic polymer mixture, mol. mobility 3-64578
 ethylene glycol, with Cr(V) complexes, dynamic proton polarisation and spin-lattice relax. 3-72543
 eucarvone, protonated, n.m.r. study 3-75076
 exponential time constants, computer meas., noise present 3-62191
 fluorene, pyrene-d₁₀ doped, exciton density correl. with triplet spin-lattice relax. 3-64708
 furan, liquid, proton-spin relaxation and molecular motions 3-44344
 glycerine-water solution, Mn²⁺ ion effect 3-53035
 glycine single cryst., nuclear spin-lattice relax. anisotropy 3-75907
 hexamethylenetetramine, proton and ¹⁴N rotational correlation times in chloroform 3-75900
 hexamethylphosphoramide, pulsed ¹⁴N n.q.r., use of multichannel accumulators 3-73829
 holmium ethyl sulphate:Ho³⁺, Van Vleck orbit-lattice interaction 3-50450
 Hubbard model, half filled band, thermodynamic and dynamic high temp. props. 3-41324
 hydrocarbons, liq., proton relax., press. depend., mol. motions 3-41446
 hydrocarbons, long chain viscous, nuclear spin-lattice relaxation, rotational motion mechanism 3-54769
 ice, hexagonal, proton spin dipolar energy, relax. 3-47158
 2',3'-isopropylideneadenosine, mol. interaction in soln., deuterium substitution effect on proton relax. times 3-75899
 lanthanum ethyl sulphate:Pr³⁺, Van Vleck orbit-lattice interaction 3-50450
 liquid, effect of hydrodynamic asymptotics of molecular heat motion (Russian) 3-79941
 liquid, mol. motion effects 3-68883
 liquid metals and alloys, spin relaxation of conduction electrons, theory, review 3-50460
 lithium stearate n.m.r. measurements, polycrystalline samples, room temp., Provotorov theory, Redfield theory 3-58437
 metal, large samples, second derivative detection theory 3-60986
 metal foils, of implanted ⁸Li, Knight shift determ., mag. dipole moments 3-40409
 methane, solid, spin conversion, proton magnetisation, spin-lattice relaxation 3-75903
 methanol, liquid, ¹³C nuclear magnetic relaxation mechanism 3-44345
 methyl iodide, liq., rot. diffusion obs. 3-75976
 methylammonium alum, Ti³⁺ Orbach relax. rate anisotropy, dynamic Jahn-Teller effect 3-75877
 2-methyltetrahydrofuran glass, p-irradiated, ELDOR study of trapped electrons mag. energy transfer between two different spin systems 3-44727
 molecular conformational anal. by ¹³C n.m.r., lanthanide shift reagents, T₁ meas. 3-67855
 molecular crystals, rel. to random molecular reorientation 3-75895
 molecular interaction in soln., deuterium substitution effect on proton relax. times 3-75899
 monosaccharides, amorphous n.m.r., temp. depend. 3-79940
 montmorillonite, adsorption of water, n.m.r. of single and double layer system 3-68867

spin-lattice relaxation continued

nitrogenase active centre, e.s.r. meas. of dimens. 3-67871
 n.m.r., intramolecular dipole-dipole interaction, influence of cross-relaxation on time 3-75071
 n.m.r., pulsed Fourier transform meas. 3-68824
 n.m.r. relaxation studied by Fourier transform methods 3-70334
 nuclear, Lorentzian cross-relaxation curve, mag. impurity induced 3-75905
 nuclear dipole reorientation relaxation, nondiffusional, stochastic theory 3-79244
 nuclear relax. time meas. using repetitive sweep techniques 3-59616
 nuclear spin diffusion phenomenon, new approach 3-75901
 nuclei of paramagnetic ions, calc. 3-55471
 oligomer, temp. depend. of relaxation times, bulk and thin layers (Russian) 3-71669
 optically oriented atoms, modulation technique for determ. 3-56979
 organic ammonium salts, ¹³C and ¹⁴N relax. 3-68882
 organic compounds, of ¹¹⁷Sn and ¹¹⁹Sn, temp. depend., n.m.r. time meas. 3-68884
 organic liquids, ¹³C multiplet spectra, Fourier transform., cross-relax. effects 3-68879
 organic molecular crystals, localised triplet states, anisotropy and temp. depend. 3-75917
 organosilicon compounds, ²⁹Si n.m.r., ²⁹Si-¹H nuclear Overhauser enhancement 3-64574
 paramagnetic spin-lattice relaxation, effect of odd normal vibrs. 3-58102
 phthalocyanine complexes of the platinum metals, dynamics of triplet state in zero field 3-50846
 picryl-N-amino carbazyl, temp. depend., three reservoir model 3-79898
 plastic crystal, p.m.r., mol. self-diffusion and reorientation, press. depend. 3-61005
 plastic crystals, self-diffusion, n.m.r. study 3-68438
 polyalkyl acrylates, spin-lattice and dielectric relaxation, effect of chain length and kinetic flexibility (Russian) 3-50487
 polyalkyl methacrylates, spin-lattice and dielectric relaxation, effect of chain length and kinetic flexibility (Russian) 3-50487
 polyethylene terephthalate, amorphous Zeeman and dipolar relaxation 3-75909
 polyethyleneterephthalate, n.m.r. study of crystallisation, orientation effect, molecular movement (Russian) 3-71691
 polymethylmethacrylate, dynamics, spin lattice relax. study 3-67880
 polypropylene oxide and deuterated derivative, dynamics, spin lattice relax. and neutron scatt. 3-67880
 polystyrene containing paramagnetic impurity, spin-lattice relaxation of protons 3-72540
 polyvinyl esters, spin-lattice and dielectric relaxation, effect of chain length and kinetic flexibility (Russian) 3-50487
 potassium caproate n.m.r. measurements, polycrystalline samples, room temp., Provotorov theory, Redfield theory 3-58437
 pulse method, time meas., nucl., electron 3-66297
 radical, transient effects in time resolved ESR 3-80536
 rare gas:⁵⁷Fe, frozen, Mossbauer obs. 3-41451
 ruby, cross relaxation, negative electron temps., role of Al nucleus (Russian) 3-64547
 semiconductors, cond. electrons, optical pumping technique 3-68845
 silicate glasses, ²³Na and ⁷Li n.m.r. studies (German) 3-72544
 small particles, superconducting fluctuations, pair breaking and nuclear relax. 3-60933
 solute-solute forces obs. by n.m.r. relax. 3-53350
 steroids, ¹³C spectral assignments using spin-lattice relax. times 3-67874
 superconductor, two-band, interband electron scatt. influence on nucl. spin relax. time (Russian) 3-79799
 superconductor with electron transition, nonmag. impurity effects 3-58345
 superconductors, thermodynamic fluctuations, nuclear spin-lattice relaxation time, magnetic field enhancement 3-46930
 TCNQ·NH₄⁺, proton spin-lattice relaxation time, temp. dependence 3-55498
 1, 1, 1, 2-tetrachloro-2-methylpropane, solid, n.m.r. static and rotating frame relaxation 3-72538
 tetrahydrofuran, as clathrate deuterate, proton spin-lattice relax. time 3-54727
 theory at low temp., e.p.r., acoustic e.p.r. and spontaneous spin-lattice relax. (Russian) 3-79889
 three-spin system, nonexponential, spin lattice relaxation, orientation dependence 3-72539
 thulium ethyl sulphate, ¹⁶⁹Tm n.m.r. study 3-64577
 time meas., progressive saturation methods (Rumanian) 3-64537
 transition metal, supercond. calc. 3-55356
 trichloromethyl derivatives of P, CCl₃PCl₄ and (CCl₃)₂PCl₃, n.q.r. spectroscopy and mol. dynamics 3-75912
 triethylene diamine, as clathrate deuterate, proton spin-lattice relax. time 3-54727
 triphenyltin fluoride, chloride, bromide, and hydroxide, mol. motion study from spin-lattice relax. times and second moments meas. 3-46325
 tunnelling centres, Zeeman nuclear relax. 3-72542
 two-phase system, nucl. spin relax. theory (German) 3-68865
 unsymmetric molecule nucl. spin-rot., internal rot., rate eqn. 3-68880
 water, proton spin-lattice relaxation time meas. 3-71577
 yttrium ethyl sulphate: Dy, Yb, proton polarisation and relaxation, pulsed refrigerator optimal conditions 3-47161
 yttrium ethyl sulphate:Pr³⁺, Tb³⁺, Ho³⁺, Van Vleck orbit-lattice interaction 3-50450
 yttrium ethyl-sulphate 9H₂O:Yb³⁺, nuclear spin diffusion barrier obs. 3-75904
 zeolitic germanates, pulsed n.m.r. meas. rel. to diffusion processes 3-55495
 Ag halides, ¹¹⁰Ag depolarization due to temp. depend. spin-lattice relaxation 3-61006
 Ag₂AsS₃, proustite, n.q.r. spectrum and spin-lattice relax. time of ⁷⁵As, 300-4.2K (Russian) 3-79944
 Ag₂H₂O₆, antiferroelec., proton-iodine cross relax. determ., of short quadrupolar spin-lattice relax. 3-47164

spin-lattice relaxation continued

- Ag₂H₃IO₆, nucl. quadrupole interaction of ¹²⁷I, phase transform, behaviour (*German*) 3-53034
- Al, spin relaxation of surface conduction electrons 3-72522
- ¹³C, use of added Cr(III) in solutions in measurements 3-55496
- Caf₂ n.m.r. measurements, polycrystalline samples; room temp., Proctorov theory, Redfield theory 3-58437
- CdWO₄:Co²⁺, monoclinic, conc. and freq. depend. 3-50453
- CeSn_{1-x}In_x alloy, ¹¹⁹Sn n.m.r. Knight shifts and spin lattice relax. time 3-50480
- Co, hexagonal, n.m.r. of ⁵⁹Co at domain wall, spin-lattice relax. 3-47162
- Co complex, [Co(NH₃)₄CO₃]₂SO₄, thermal motion of ammine groups, spin-lattice relax. obs. 3-50484
- CoBe, of ⁹Be and ⁵⁹Co, relax. time meas. (*French*) 3-41443
- Cr-Mn antiferromagnetic alloys, n.m.r. 3-68857
- Cr(III) doping of solutions for obtaining ¹³C relaxation data 3-55496
- CsPF₆, reorientation motions and spin-rotation interaction 3-53033
- CsPF₆ pulsed n.m.r., F spin-lattice relaxation 3-47159
- CuBe, of ⁹Be and ⁶³Cu, relax. time meas. (*French*) 3-41443
- CuBr:⁶³Cu, ⁶⁵Cu, ⁸¹Br, n.m.r. observations, temp. depend. between 78 K and 300 K 3-55493
- Cu_{0.4}Cd_{0.6}Fe₂O₄, ferrite, as u.s. absorpt. mechanism near Curie point 3-75840
- CuCl:⁶³Cu, ⁶⁵Cu, ⁸¹Br, n.m.r. observations, temp. depend. between 78 K and 300 K 3-55493
- CuSO₄(SO₄)₂·6H₂O Tutton salt, direct spin-lattice relaxation meas. 3-47134
- CuI:⁶³Cu, ⁶⁵Cu, ⁸¹Br, n.m.r. observations, temp. depend. between 78 K and 300 K 3-55493
- CuSO₄·5H₂O, modulation method for relaxation time measurement 3-68829
- DyBe₁₃, susceptibility, mag. moment and ⁹Be nuclear mag. relax. (*French*) 3-55427
- Gd, modulation method for relaxation time measurement 3-68829
- GdBe₁₃, susceptibility, mag. moment and ⁹Be nuclear mag. relax. (*French*) 3-55427
- H₂, h.c.p., nuclear-longitudinal relax. time, 5.5 and 29 MHz 3-53036
- H₂, solid, low conc. of orthomolecules, freq. depend. 3-79939
- H₂, solid, n.m.r., 0.2-4.2K 3-68866
- H₂ collisions with He and Ne, spin-lattice relaxation, anisotropic part of intermolecular potential 3-40683
- HD-He mixtures spin-lattice relaxation 3-46326
- H₂SO₄:anthracene, conc. depend. relax. times, spin echo expts. 3-41400
- ³He, nucl. polarisation by optical pumping, apparatus development and relax. time meas. (*French*) 3-46185
- ³He, nucl. polarization by optical pumping, relax. time meas. at surfaces (*French*) 3-46186
- ³He, potential parameters determ. from T₁ meas. 3-46215
- ³He gas, nuclear spin-lattice relax. rel. to O₂ conc., at 23°C 3-54793
- ¹⁹⁹Hg vapour, optically oriented, mag. field depend. of nucl. relax. rate, adsorption energy eval. 3-67676
- Ho, spin spiral state, rel. to longitudinal u.s. attenuation 3-41387
- In, pure and impure, nuclear spin-lattice relax. 3-46933
- KCl:Li⁺, of F₀ centres, cross relax. effects 3-72520
- KCl:Li⁺, Zeeman nuclear relax. of tunnelling centres 3-72542
- KPF₆, pulsed n.m.r., F spin-lattice relaxation 3-47159
- Kr gas, of ⁸³Kr, mechanism (*German*) 3-49395
- LaAl₂, n.m.r., Knight shift, spin lattice relax., rel. to s-electrons hyperfine interactions, 90-300 K 3-41438
- LaSn₃In_{3(1-x)}, meas. rel. to paramag. susceptibility and local electronic props. 3-46803
- MnF₂, antiferromag. linewidth obs., 1.5-40 K 3-41412
- NaPF₆, ¹⁴N and ³⁵Cl relaxation as function of temperature 3-55494
- NH₄ClO₄, proton spin-lattice relax. and exchange splitting of torsional ground state 3-44343
- (NH₄)₂(Cu₂Fe₂Zn_{1-x-y})(SO₄)₂·6H₂O, cross relax. mechanism in electronic spin system 3-47131
- NH₄H₂AsO₄, mol. reorientation, n.m.r. obs., Curie pt. behaviour, high temp. phase transition 3-61004
- (NH₄)₂H₃IO₆, antiferroelec., proton-iodine cross relax. determ., of short quadrupolar spin-lattice relax. 3-47164
- (NH₄)₂PtBr₆, displacive phase transition ⁷⁹Br n.q.r. and spin-lattice relaxation time meas. 3-41449
- Na, liquid, nuclear magnetic relaxation rate of ²³Na spin, temp. depend. 3-47160
- Na-Hg, liquid alloys, nuclear magnetic relaxation rate of ²³Na spin, temp. depend. 3-47160
- Na-Tl, liquid alloys, nuclear magnetic relaxation rate of ²³Na spin, temp. depend. 3-47160
- Na₂Cd(SO₄)₂·2H₂O:Co²⁺, single cryst., one phonon and Raman scatt. processes 3-50455
- Na(D₂H_{1-x})(SeO₃)₂, n.m.r. investigation, ferroelectric transitions 3-79938
- NaPF₆, pulsed n.m.r., F spin-lattice relaxation 3-47159
- NaPF₆, reorientation motions and spin-rotation interaction 3-53033
- Na₂Zn(SO₄)₂·4H₂O:Co²⁺, single cryst., one phonon and Raman scatt. processes 3-50455
- NiBe, of ⁹Be, relax. time meas. (*French*) 3-41443
- NiTi₂(SO₄)₂·6H₂O, cross, spin-lattice relax., a.c. susceptibility meas. 3-79892
- Pd_{1-x}Al_x, (x < 0.03), impurity atom electronic struct. calc., rel. to spin-lattice relax. time 3-44034
- Pd_{1-x}Cu_x, (x < 0.03), impurity atom electronic struct. calc., rel. to spin-lattice relax. time 3-44034
- PtSn n.m.r. measurements, Knight shift, energy band structure, OPW calculation 3-41440
- PuAl₂, of ²⁷Al, spin fluctuation effects 3-41441
- RbPF₆, pulsed n.m.r., F spin-lattice relaxation 3-47159
- Si compounds, ²⁹Si, time meas., n.m.r. 3-68878
- TbBe₁₃, susceptibility, mag. moment and ⁹Be nuclear mag. relax. (*French*) 3-55427
- UAl₂, of ²⁷Al, spin fluctuation effects 3-41441
- V-Ru alloy, near equiatomic, electronic transition, ⁵¹V n.m.r. study 3-53032
- YAsO₄, pair interaction and mag. relax. of Yb³⁺ (*German*) 3-53014

spin-lattice relaxation continued

- YCl₃·6H₂O:Yb, proton polarisation and relaxation, pulsed refrigerator optimal conditions 3-47161
- YPO₄, pair interaction and mag. relax. of Yb³⁺ (*German*) 3-53014
- ZnWO₄:Co²⁺, monoclinic, conc. and freq. depend. 3-50453
- spin-orbit interactions**
- actinide ion electronic spectra, F-level intermediate spin-orbit coupling 3-69011
- alkali metal atoms collisional depolarization of ²P states, weak spin-orbital coupling 3-54586
- amines, non-planar aromatic, spin-forbidden electronic transitions 3-46237
- aminopyridines, phosphoresc. emission and polarization, triplet states 3-65101
- atom, photoioniz. cross sections for states split by spin-orbit coupling 3-67684
- atom + electron scattering, combined effect of spin-orbit interaction and electron exchange 3-71419
- atom and ion, isoelectronic energy levels, interpolation formulae for Z, 1 to 137 3-74791
- benzene in rare gas hosts, triplet lifetimes and emission spectra, external heavy atom effects 3-55675
- carbon tetrachloride matrix, dissolved aromatic molecules, phosphoresc. 3-72743
- coupling operator and CNDO approach in molecular spectroscopy 3-74950
- dilute mag. alloys, spin-orbit interaction rel. to e.s.r. 3-55466
- elastic scattering, spin effects at angles near 180° (*Russian*) 3-40327
- e.m., energy difference of nuclear analogue states 3-67227
- enones, conjugated, spin-orbit coupling effects on the zero field splitting of (π,π*) triplet states, ODMR obs. 3-65103
- heavy atoms, highly ionized, relativistic effects in elec. dipole transitions 3-54564
- magnetic semiconductors, photoconductivity, band structure, Hall effect 3-41214
- many electron systems, matrix elements evaluation of spin-dependent two-body operators 3-63258
- metalloporphyrins, spin-orbit coupling and heavy atom effect on radiationless transitions 3-63498
- metals, magnetic, magneto-optical effect, plasma minimum determ. using Boltzmann's transport and Maxwell's eqns. 3-47237
- methanol, hyperfine struct. in internal rotor molecules, spin rotation interactions 3-78817
- methylene, spin dipole-dipole parameters, ab initio calcs. 3-74939
- molecular integrals of relativistic effects with Gaussian-type orbitals 3-57622
- naphthalene in p-dihalogenated benzene host crystals 3-80106
- noble muonic atoms, electron paramag., spin-orbit interaction effects 3-46217
- non-radiative intercombination transitions, spin-orbital perturbation (*Russian*) 3-68964
- nonspherical cryst. pots., magnetocryst. anisotropy energy rel. to cryst. field, spin-orbit coupling 3-41315
- paramagnetic admixed ions fine structure with anisotropic interactions in intermediate cryst. field 3-44179
- planar mols., dπ orbitals, contrib. 3-54643
- PO valence shell states, spin-orbit coupling consts. variation with internuclear distance 3-71514
- polynuclear many-electron systems, Heisenberg model, ground state splitting 3-58359
- relativistic correction term to spin orbit coupling 3-46801
- relativistic effects in magnetic hyperfine structure of 3dⁿ4s² series 3-74796
- semiconductor, multivalley, Knight shift theory, orbital and dipolar shift effects 3-44341
- spectroscopic transition amplitudes represent. as sum of multipolar interactions with radiation field 3-52346
- superconducting thin films, tunnelling conductance, temp. depend. in high magnetic fields 3-44174
- t_{2g}⁴ electronic configuration, rel. to mag. props. 3-44181
- tetraphenylporphine halogen derivatives, fluorescence spectra, internal heavy atom effect 3-63503
- three-electron model system, correlation effects, natural spin orbital formalism, Hartree-Fock method 3-74955
- transition metal, liq., spin-orbit coupling effect on Hall effect (*German*) 3-52826
- transition metal complexes, radiationless relaxation processes 3-43473
- transition metal magnetism, effect of electron correlation on orbital interactions 3-72442
- trigonal systems, d² and d⁸ energy levels calc. 3-72325
- vibronic and spin-orbit splitting in spectra, Jahn-Teller effect 3-67763
- zero-field splitting of 3d⁵ ions, anisotropic spin-orbit coupling contribution 3-55214
- ²⁰⁸Pb, emission spectrum analysis 3-60446
- ⁴⁰Ca(p,p')⁴⁰Ca*, excitation of t_{1/2}-d_{3/2}-1 states, effect of vector and tensor forces 3-67328
- CdGeAs₂, valence band splitting, photocond. spectra obs. 3-64686
- Cf⁴⁺, electronic spectra, spin-orbit coupling diagram prediction 3-69012
- Cm⁴⁺, electronic spectra, spin-orbit coupling diagram prediction 3-69012
- Co²⁺ low lying electronic levels, Raman spectra 3-68997
- Cu_{0.85}Co_{0.15}Fe_{0.05}O₄ ferrite, mag. anisotropy effect on elec. cond. 3-72358
- DF, photoelectron spectra determ. of spin-orbit coupling consts. and ionisation pot. 3-71609
- Fe²⁺ low lying electronic levels, Raman spectra 3-68997
- FeF₂ Raman spectra, paramag. crystal, parameters, energy levels 3-64645
- Gd₂Th_{1-x}Ru₂, cond. electron scatt., e.p.r., crit. field correl. 3-72418
- Ge, fine structure details in LMM Auger spectra 3-69139
- Ge, high resolution LMM Auger spectra, L-S coupling model 3-69115
- H₂, para, d(3p)³Π_u (ν=0-3) fine struct. via microwave ODMR induced by electrons, spin-orbit coupling consts. determ. 3-40657

spin-orbit interactions continued

- I_2 , ioniz. pots., Koopmans theorem inconsistency, spin-orbit perturbation effect 3-60482
 KCl, R-centre, spin-orbit const., mag. circular dichroism obs. 3-69027
 $KMgF_3$, Fe^{2+} , rel. to far i.r. absorpt. 3-47298
 $MnSiO_3$, optical absorption spectrum of Mn^{2+} , spin-orbit coupling coefficient 3-61056
 Mo, determination from de Haas-van Alphen data 3-58206
 N_2 , triplet states parameters calc. 3-60421
 $(NiC_2H_4)_2ZnLi_2NiLi_2^{2-}$, mag. circular dichroism spectrum, spin-orbit splitting, quenching 3-50601
 NO, a^4I_1 state, spin-forbidden lifetime, cooperative optical phenomena 3-54665
 Ni, precision reflectance 2-3 eV obs. 3-41525
 Ni fine structure, exchange-split energy bands, precision reflectance measurements, 2 to 3 eV 3-52780
 $NiFe_4^{4-}$, $NiCl_4^{4-}$ clusters, mol. orbital calcs., coupling constant 3-68553
 Pd, in e.s.r., numerical calc. 3-41395
 Rh(III) complex, halopentammine, radiative and radiationless decay processes 3-73158
 Si, valence band, spin-orbit effect 3-60857
 $SiC(6H)$, exciton electroabsorption spectra splittings, group anal. 3-72677
 $Te(S^{3+}P_1)$, $Te(S^{3+}P_0)$, spin-orbit quenching by gases, rates, cross-sections 3-71371
 TiO_2 , Cr^{3+} , Zeeman effect of no-phonon $^4\alpha_{2g}-^4T_{2g}$ transition 3-53124
 Ti, $6^2P_{3/2}$, collisional deactivation, temp. depend. 3-78504
 UCL_4 , vapour spectrum interpretation using cryst. field model 3-71541
 $(XeH)^+$, pot. energy curves, LCAO-MO-SCF calcs. 3-74943

spin-phonon interactions

- anisotropic ferromagnets below transition point, diagram techniques 3-60966
 exchange interaction effect on phonon bottleneck effect and phonon avalanche formation 3-55391
 ferromagnet, effect on energy distrib. of one-phonon neutron scatt. (Russian) 3-55437
 Hamiltonian, rel. to mag. anomalies in Mossbauer effect 3-58462
 Heisenberg antiferromagnet, magnon-phonon scatt. rel. to sound absorpt. 3-68751
 Ising model, rel. to renormalization of Curie temp. 3-46963
 methylammonium alum, Ti^{3+} Orbach relax. rate anisotropy, dynamic Jahn-Teller effect 3-75877
 nuclear acoustic resonance obs. 3-75896
 paramagnetic spin interaction with heat pulses 3-55050
 paramagnetic spin-lattice relaxation, effect of odd normal vibrs. 3-58102
 phonon scattering by paramagnetic ions, drone-fermion representation, spin-phonon system lifetimes 3-40990
 Schottky specific heat 3-72205
 symmetrical triad spectrum and spin-phonon interaction 3-79830
 Al_2O_3 , V^{3+} , spin-phonon coupling by quantitative spectroscopy with phonons 3-58104
 CoO, rel. to thermal cond. minimum at Neel temp. 3-58379
 GaAs: Fe^{2+} (Fe^{3+}), meas. from a.p.r. 3-75878
 LiF, nuclear quadrupole spin-phonon coupling, u.s. wave propag. 3-75891
 NaCl(F), nuclear quadrupole spin-phonon coupling, u.s. wave propag. 3-75891
 NiO, rel. to thermal cond. minimum at Neel temp. 3-58379
 Pr_2Ti , Van Vleck paramagnet, spin-phonon coupling 3-46981
 $TmVO_4$, phonon instabilities, near Jahn-Teller phase transition 3-55069

spin-spin nuclear coupling in molecules *see molecular nuclear coupling***spin-spin relaxation**

- Boltzmann equation derivation, temp. change, cross relax. effect 3-72504
 butene-1 on A- and Y-zcolites, mobility, proton spin relax. (German) 3-64245
 N,N' -dideuteroparachloroaniline, mag. dipole interact. in ND_2 group, ^{14}N n.q.r. Zeeman effects 3-75910
 ferric ions in $Fe(NO_3)_3 \cdot 9H_2O$ and frozen aqueous solns., mag. field depend. 3-75924
 gas phase n.m.r., review 3-60521
 hydrates, solid echo expt. for direct meas. of spin-1/2 pair dipolar interactions 3-79934
 liquid, measurement errors 3-79935
 liquid, mol. motion effects 3-68883
 liquid, paramagnetic probe motion from electron spin relaxation 3-64542
 methyl substituted aromatic radical ions, proton spin relax., CH_3 linewidth 3-63517
 molecular crystals, rel. to random molecular reorientation 3-75895
 n.m.r. relaxation studied by Fourier transform methods 3-70334
 n.m.r. spectra, transverse relax. rates, spin echo, Fourier transform 3-64576
 non-exponential decay, analysis 3-44333
 nonmetallic diamagnetic crystal, nuclear spin diffusion and relaxation 3-41444
 organic ammonium salts, ^{13}C and ^{14}N relax. 3-68882
 picryl-N-amino carbazyl, temp. depend., three reservoir model 3-79898
 polysaccharide aqueous solutions, protons, conc. depend. 3-68876
 quinoline in durene host, multiple spin echoes in photo-excited triplet state 3-80564
 ruby, self-induced transparency, temp.-depend phase memory 3-62747
 simulation of n.m.r. measurements 3-56708
 solute-solute forces obs. by n.m.r. relax. 3-53350
 spectral diffusion coefficient, electron-nucl. cross-relax. contrib., calc. 3-68830
 thulium ethyl sulphate, ^{169}Tm n.m.r. study 3-64577
 transition metal complexes, electron relax. time determ. by ^{13}C and ^{14}N n.m.r. 3-75078
 trimethylene oxide, p.m.r. spectra, ring puckering vibr., chem. shifts and spin-spin coupling meas. 3-54726

spin-spin relaxation continued

- trimethylene sulphide, p.m.r. spectra, ring puckering vibr., chem. shifts and spin-spin coupling meas. 3-54726
 yttrium ethyl sulphate: Dy, Yb, proton polarisation and relaxation, pulsed refrigerator optimal conditions 3-47161
 zeolitic germanates, pulsed n.m.r. meas. rel. to diffusion processes 3-55495
 Cr^{3+} aquacomplex in viscous soln., intermediate effect between Overhauser and solid effects 3-75079
 $CuCl_2 \cdot 2H_2O$, spin-spin relaxation, resonance-like dip at Larmor field 3-68839
 Fe_2P , ferromagnetic, n.m.r. obs., ^{31}P and ^{57}Fe spin relaxation times, low temp. spin-spin coupling 3-41442
 Gd_2Co_{17} , spin echo obs., 77 K (French) 3-79933
 MnF_2 , antiferromag. linewidth obs., 1.5-40 K 3-41412
 MnF_2 , low-field resonance and zero-field relaxation 3-60989
 Ni^{3+} aquacomplex in viscous soln., intermediate effect between Overhauser and solid effects 3-75079
 $NiCl_2$, antiferromagnet, crit. e.p.r. spin dynamics, linewidth divergence, spin-spin relax. rate depend. 3-47136
 Sc, electronic struct., Knight shift, nuclear spin relax., mag. susceptibility anisotropy 3-50333
 $YCl_3 \cdot 6H_2O$: Yb, proton polarisation and relaxation, pulsed refrigerator optimal conditions 3-47161
 Y_2Co_{17} , spin echo obs., 77 K (French) 3-79933

spin systems

- see also magnetic properties of substances; magnetism*
 Bloch equations, rel. to possible limitation of n.m.r. thermometers at very low temp. 3-55480
 classical spin, effects on superconductivity, coherent potential approx. to impurity problems 3-58331
 continuous, changeover from crit. line to tricrit. point in large N-limit 3-77929
 correlation functions, time depend., rigorous upper and lower bounds 3-41313
 cross relaxation, nonequidistant energy spectrum, transport eqns. 3-72504
 dipolar coupled, rigid lattice, tetrahedral magic echo generation 3-72531
 dynamics, anisotropy effects study from second moment behaviour 3-44226
 equilibrium states, existence and uniqueness 3-57161
 exchange interaction effect on phonon bottleneck effect and phonon avalanche formation 3-55391
 ferromagnetic relaxation of magnetisation fluctuations, above Curie point, dipole-dipole interactions, spin dynamics 3-50465
 Fixed length spin systems extended to negative spin dimensionality 3-77907
 Heisenberg, two-dimensional, high-temp. susceptibilities 3-52942
 Heisenberg, with uniaxial and exchange anisotropy, freq. moments, short range-order effects 3-55400
 Heisenberg and X-Y magnets, spectral weight function of spin-pair correlation function 3-46965
 Heisenberg spin system on f.c.c. lattice with second neighbour interaction magnetisation process 3-72433
 helical, two-magnon Raman scattering, Green's function method 3-41519
 hierarchical model, Dyson, spherical, simulation of long-range Ising problem, phase transition critical temperature 3-59816
 Ising and Heisenberg models, statistical props., constant coupling approx. 3-44183
 Ising ferromagnet of general spin with degeneracy or symmetric potentials, rigorous results 3-64460
 Ising model, two dimensional, boundary spins + 1, transfer matrix for a pure phase 3-60946
 isotropic, critical behaviour, high temp. series expansion 3-68745
 lattice models, mean field theory validity for infinitely long-range forces 3-74160
 magnetic semiconductors, photoconductivity, band structure, Hall effect 3-41214
 magnetisation, periodic longit., of transverse r.f. wave irrad. spin system at e.s.r. 3-50441
 magnetism theory, spin in a time-depend. mag. field 3-68743
 many electron systems, matrix elements evaluation of spin-dependent two-body operators 3-63258
 metals, next divergent terms for singlet ground state of localised spin 3-64442
 modified F model, treatment as spin system, and comparison with Ising model 3-58480
 molecular crystal, PMDR in exciton states and coherent states of triplet spin ensemble 3-72546
 Mossbauer freq. shift in spin order systems, second order Doppler shift 3-68898
 multilevel spin system, magnetic dipole-dipole interaction (Russian) 3-44310
 multiple scattering theory and magnetic properties 3-44176
 narrow domain wall, analytical derivation of spin configuration and intrinsic coercive field 3-64525
 neutron inelastic scatt. theory on local spin fluctuation systems 3-55420
 n.m.r. spectrometry, student teaching of concepts 3-77356
 one-dimensional, finite range potential, uniqueness of states satisfying Kubo-Martin-Schwinger boundary condition 3-62601
 pair correlation function determ. for isotropic Heisenberg ferromagnet 3-75823
 paramagnetic phase of Heisenberg ferromagnet, temperature dependence of thermodynamic properties 3-64462
 rare earth compounds, Tm_2O_3 , ($T=Nd, Tb, Er$), sinusoidal and helical mag. structs., neutron diff. (French) 3-44223
 rare earth cubic compounds, mag. ordering and phase changes 3-52976
 s-d, magnetic susceptibility, generalised self-consistent field method 3-68758
 s-d system, ground state energy, next singular contrib. binding energy 3-64441
 solutions, coupled spin systems, intermolecular nuclear Overhauser effect 3-50489
 spins canted by external magnetic fields, antiferromag. reson., spin wave theory 3-44327

spin systems continued

- superexchange energy, potential and kinetic, spin orientations, crystal field influence, MO and CT approximations, 3 centre 4 electron model 3-52971
- symmetrical spin system with arbitrary spin I, theory of n.m.r. spectra (*German*) 3-53031
- symmetrical spin systems with $I=Y_2$, theory of n.m.r. spectra (*German*) 3-53030
- three-spin system, nonexponential, spin lattice relaxation, orientation dependence 3-72539
- transition metal tantalates, MeTaO_4 , atomic and mol. ordering, mag. structure from 4.2 to 300K 3-79849
- translation groups, neutron diff. analysis 3-79843
- two spin systems, chemical shift interaction in solids, dipolar echo maximum modulation 3-55488
- two-level system, free induction decay with radiation damping, general treatment 3-55479
- (CoMn) $_{1-x}\text{Fe}_x$, antiferromag. props. and atomic ordering, neutron diff. obs. 3-58387
- Cr_2O_3 , stress induced spin flop, anisotropy and magnetoelasticity origin 3-44227
- CrSe, spin translation groups, neutron diff. analysis, umbrella arrangements 3-79843
- Fe, isomer shift anomaly nr. Curie point, Van Hove singularity effect 3-41322
- Fe:Nd, transverse component, simple continuum model 3-41339
- γ -Fe-Mn alloys, dislocation motion in antiferromagnetic structure 3-53009
- Fe^{3+} high-spin system, magnetic circular dichroism of spin forbidden transitions 3-72663
- FeGe, antiferromag., hexagonal, localised versus itinerant electrons, molecular field model 3-41351
- ^{165}Ho , neutron scatt. amplitude spin depend. part, neutron diff. obs. from 4.2-1.4 K (*French*) 3-50377
- InSb, near reson. spontaneous spin-flip Raman scatt. 3-44415
- KMnF_3 , equilibrium spin configuration and antiferromagnetic resonance for low temp. phase 3-72523
- $\text{MnFe}_{2-x}\text{Cr}_x\text{O}_4$, ferrite mag. moments, exchange interactions and canted spin configs. 3-75844
- $\text{Ni}_{1-x}\text{Zn}_x\text{Fe}_2\text{O}_4$ high field Mossbauer study 3-79963
- RBe_{13} intermetallic compounds, (R=La, Ce, Nd, Gd) magnetic properties, hyperfine interactions, spin dynamics 3-52969
- UP_2 , UBi_2 , uniaxial antiferromagnet, transversal spin disorder resistivity, temp. dependence 3-41219

spin wave resonance *see ferromagnetic resonance***spin waves***see also magnons*

- amorphous Heisenberg ferromagnet, Landau-Lifshitz theory 3-44186
- antiferromagnet, biaxial, temp. depend. of reson. freq., activation energy of spin wave branch 3-72525
- antiferromagnet, Heisenberg model, spin wave spectrum calc. 3-52946
- antiferromagnet, itinerant, multiple band, theory 3-79854
- antiferromagnet, rutile type, photon pumped spin wave instability, Raman scatt. 3-79851
- antiferromagnet, two-dimensional Heisenberg model, zero-point spin deviation 3-46954
- antiferromagnetic substances, nuclear, influence of free surface 3-79856
- antiferromagnets, relaxation processes 3-50472
- antiferromagnets, rutile-type, instability caused by photon beam 3-50383
- exchange interaction, spin and field of vacuum, classical approach 3-70688
- exchange interactions and spin wave theory, review 3-64451
- ferrimagnetic crystal, propag., obs., coherence, geometry depend. (*French*) 3-75847
- ferrimagnetic semiconductors, current carriers and electron impurity centres, weak interaction 3-52987
- ferrimagnets, localized spin wave states caused by antiferromagnetic impurity, two-sublattice model 3-60953
- ferrite, parametric excitation near phase transitions 3-72479
- ferrite, polycryst., rel. to microwave losses, review 3-41393
- ferrite, rel. to magnetoacoustic reson. 3-55454
- ferrites, transthreshold susceptibility for excitation, determ. method 3-73814
- ferromagnet, antisymmetric exchange effect on spin wave dispersion 3-44210
- ferromagnet, compressible, magnetic excitations spectra and magnetisation, explicit expressions 3-50395
- ferromagnet, dispersion relations, magnetisation density of inhomogeneous precession of domain struct. 3-79850
- ferromagnet, effect of electron correl. in narrow band 3-55406
- ferromagnet, Heisenberg model, spin wave spectrum calc. 3-52946
- ferromagnet, mag. moment switching by neutron beam 3-72476
- ferromagnet, magnetostatic wave focusing and defocusing in cylindrically symmetric non-Laplacian mag. field 3-47073
- ferromagnet, parametric magnon excitation, theory, self consistent field method 3-58390
- ferromagnet, switching in constant field, nonlinear response 3-60962
- ferromagnetic alloy, dilute, $T^{1/2}$ specific heat term, impurity scatt. of spin waves 3-72464
- ferromagnetic conducting plates, Maxwell's eqns., coupling with e.m. waves 3-72478
- ferromagnetic critical point, ele. resist. rel. to spin fluctuations, single band model 3-47029
- ferromagnetic cubic insulators, Dyson's theory reconsidered 3-52985
- ferromagnetic insulator, with weak anisotropy, rel. to low temp u.s. absorpt. 3-55451
- ferromagnetic metals with p-type conductivity, spin wave interaction with e.m. waves 3-50550
- ferromagnetic substances, nuclear, influence of free surface 3-79856
- ferromagnetic transition metal alloys, spin wave stiffness constant 3-75846
- ferromagnets, amorphous, spin wave behaviour, theory 3-50388

spin waves continued

- ferromagnets, uniaxial, plate-like domain structure, phenomenological spin wave theory 3-50311
- Heisenberg dilute ferromagnet, nature of percolation channels 3-46967
- Heisenberg ferromagnet, localised spin waves, impurity spin anisotropy effects 3-58389
- Heisenberg ferromagnet, surface, acoustical 3-64466
- Heisenberg ferromagnet, surface, dispersion laws 3-79821
- Heisenberg model, one-dimensional, dynamic properties, spin-wave-like excitations and lattice dimensionality 3-64461
- INVAR, cellular model of magnetism at finite temp. 3-52986
- itinerant ferromagnet, long wavelength spin waves, transverse spin susceptibility, dispersion relation 3-46970
- localized states in two-sublattice ferromagnet, mode in forbidden band 3-41338
- magnetic excitons in single triplet system, temp. depend. 3-58388
- magnetisation reversal mechanism, spin wave activation 3-79915
- metals, Doppler-shifted spin resonance in electron fluid 3-50387
- nuclear and electronic coupled modes in mag. ordered material, dispersion relation 3-47076
- nuclear and electronic spin wave mode coupling with quadrupolar interaction 3-44224
- paramagnetic metal films, e.m. field excitation, pinning, reson. 3-72524
- parametric excitation, strong turbulence and self focusing 3-72480
- semiconductor, magnetic, carrier autolocalised fluctuation states 3-46810
- spins canted by external magnetic fields, antiferromag. reson., spin wave theory 3-44327
- surface modes in ferromag. films and spin wave reson. 3-41426
- TMPD-TCNQ, delocalised triplet state excitations, spin susceptibility, e.s.r. 3-60970
- two-sublattice Heisenberg ferromagnet spin wave renormalisation by Green-function method 3-46959
- CdCr_2Se_4 , amplification through interaction of magnons with drifting carriers 3-41355
- Co-Fe alloy, temp. dependence of mag. excitations below and above the Curie temp. 3-79853
- Dy, magnon-phonon mode mixing, magnetoelastic interaction 3-47112
- $\text{Er}_{0.75}\text{Lu}_{0.25}$, neutron diff. obs., transitions to c-axis longit. spin wave, antiferromag. conical structs. 3-79847
- Fe garnet, rare earth ion effects on linewidths 3-41422
- $\text{FeNH}_4(\text{SO}_4)_2 \cdot 12\text{H}_2\text{O}$, paramagnetic with pure dipole-dipole coupling, Mossbauer spectra, relaxation phenomena, spin wave model (*German*) 3-58463
- $\alpha\text{-Fe}_2\text{O}_3$, hematite, acoustic soft magnon modes, spin wave theory 3-68794
- $\alpha\text{-Fe}_2\text{O}_3$, hematite, easy plane antiferromag., collective oscill., microwave applic. 3-50382
- Gd, exchange coupling parameters, determ. from spin wave dispersion curves 3-47013
- GdYFe garnet: Co^{2+} resonance linewidth rel. to latching phase shifter applic. 3-47097
- K_2MnF_4 , planar antiferromag., spin wave dispersion and mag. ordering 3-50385
- K_2MnF_4 , quadratic layer antiferromag., theory rel. to sublattice magnetisation 3-50384
- K_2NiF_4 , quadratic layer antiferromag., theory rel. to sublattice magnetisation 3-50384
- $\text{Li}(\text{TCNQ})$, spin susceptibility, low temp. sp. ht., e.s.r. linewidths 3-58415
- $(\text{Mn,Zn})\text{F}_2$, dilute antiferromagnet, coherent potential theory 3-47071
- MnCO_3 , parametric excitation of mixed pair of quasiparticles 3-41354
- MnCO_3 , parametric excitation of spin waves 3-41428
- MnF_2 , Frenkel exciton coherence and dynamics 3-64508
- MnO antiferromagnet, low temperature, neutron inelastic scatt. technique, dispersion relations 3-52982
- $(\text{Mn}_{1-x}\text{Zn}_x)\text{F}_2$, dilute antiferromagnet, spin wave theory for disordered systems 3-44225
- NiF_2 , antiferromagnetic, spectra, magnetic field effects 3-47075
- $\text{Ni}_{0.86}\text{Fe}_{0.14}$ alloy, magnetic excitations, inelastic neutron scattering 3-79857
- RbMnF_3 , antiferromag. reson. near Neel temp., u.s. wave coupling to antiferromag. spin waves (*French*) 3-41427
- Rb_3MnF_4 , quadratic layer antiferromag., theory rel. to sublattice magnetisation 3-50384
- RbNiF_3 , spin wave sp. ht., a.c. temp. calorimetry, 1.5-4K 3-50381
- Tb, exchange coupling parameter, determ. from spin wave dispersion curves 3-47013
- Tb, magnon-phonon mode mixing, magnetoelastic interaction 3-47112
- $\text{Y}_3\text{Fe}_{5-x}\text{Ga}_x\text{O}_{12}$, $\text{Y}_3\text{Fe}_{5-x}\text{In}_x\text{O}_{12}$, garnets, instability, parallel pumping 3-79859
- YIG, epitaxial film, identification of magnetostatic surface spin wave modes 3-64557
- YIG, epitaxial film, propag. of surface and volume spin waves, device applications 3-47074
- YIG, Faraday rotation obs. 3-47231
- YIG, film, nonpropagating magnetic surface modes, angle, temp. and freq. depend. 3-41352
- YIG, periodic domain structure, magnetisation 3-75848
- YIG, polycryst. and impurity doped, longitudinal χ'' in strong r.f. fields 3-64554
- YIG, resonance phenomena in parametric spin wave system 3-50470
- YIG film, physical model for excitation 3-41353
- YIG rod, axially magnetised, instabilities 3-44326
- YIG type materials, spin wave exchange, ferromag. resonance obs. 3-50462

spinor groups *see group theory***spirality** *see elementary particle theory***splines (mathematics)***see also function approximation; interpolation*

- cubic spline functions in nuclear data processing 3-57500
- cubic-spline basis functions for solving radial Schrodinger equation 3-40147

splines (mathematics) continued

finite difference function reln. to spline function (*Russian*)
3-70525

sponges see porous materials**sponginess** see porosity**spooling** see winding (process)**sporadic-E layer**

auroral zone, movement, correlation with geomagnetic activity, IGY and IQSY 3-73358
blanketing at mag. equator due to horizontal wind shears 3-42046
blanketing type Es-layer, analysis based on empirical formula 3-51131
chemical releases at sunset, Aladdin II meas. 3-61548
counter-electrojet current belt rel. to Esq disappearance during quiet periods 3-42039
E_s-q sudden disappearance rel. to reversal of equatorial elec. fields 3-61544
equatorial, effect of thunderstorms on multiple reflections 3-65461
equatorial, polar magnetic sub-storms effect 3-61547
equatorial E_s disappearance rel. to geomag. H component changes 3-56214
equatorial E_s-layer during geomagnetic storms 3-59143
equatorial region characts., meas. in Gulf of Guinea 3-42037
formation of middle-latitude Es-layer with wind shear and two kinds of ions 3-56210
metal ion profile redistrib. effects on E_s-layer formation 3-42036
probability of appearance of flat and auroral types, geographical distribution 3-69662
Project Aladdin II, dynamic numerical model of E-region rel. to digi-sonde obs. 3-65468
rocketborne magnetometers measurements validity of B values 3-76810
solar and lunar tidal effects, review 3-42022
spatial structure determ. using spaced soundings 3-56212
vertical movement rel. to internal atmospheric gravity waves 3-53528
wind component exchange and rapid vertical movement 3-80804
wind shear theory of formation, Aladdin II meas. 3-61500
wind shear theory of formation, test 3-56216

sports and entertainment

tinted lens for aviators and skiers, spectral transmission assessment 3-66182

sprays

see also aerosols; drops; jets

air-water interface, evaporation and energy transfer, effect of wind and waves 3-47679
arc plasma for thick films production of Ni-Zn ferrites 3-55731
drop dimensions, degree of dispersion, spray jet 3-48341
droplet system produced by EHD spraying, minimum energy state inaccessibility 3-69391
liquid, in flowing hot gas, rapid cooling processes 3-71806
spray in atmospheric surface layer, laboratory study 3-51029
xylene, spray electrification 3-79759

spurious see elementary particles**sputtering**

see also integrated circuit production; thin films

alkali halides, neutral beam sputtering of positive ion clusters 3-80137
amorphous solid, growth of topography 3-79548
cathode sputtering installations evacuation conditions effects on pressure of active gases 3-51565
controlled thermonuclear reactor first wall sputtering and wall life estimates 3-40548
cylindrical diode continuous vacuum sputtering machine for Ta thin film circuit production 3-39890
d.c., reedblade contacts, modified configuration for improved deposition rates 3-53873
d.c. glow discharge, for tantalum-titanium alloy thin film preparation 3-64416
d.c. sputtering system, probe meas. of cathode dark space shape 3-40815
ferroelectric thin films, reactive 3-41630
glass electrode membranes, Li conc. profile and cation mobilities, determ. by ion sputtering 3-69471
glassy carbon based binary glasses, prep. and characteriz. 3-76246
glow discharge, measurement of cathode sputtering rate 3-54892
glow discharge, sputter cleaning parameters and cathode surface contaminants 3-44507
heavy targets, relative yields, from range, damage calcs., keV energy 3-69116
insulating surface, sputtered ion deflection by surface charges 3-61093
insulator, by ion bombardment, applic. to surface finishing of optical materials 3-72775
ion beams, and ion implantation applications, book 3-44553
ion bombarded surface topography, prediction using Frank's cryst. dissolution theory 3-58575
ion etching, figuration of wedge shaped and parabolic surfaces 3-66917
ion gun attachment to SEM for Auger electron spectroscopy 3-42673
ion implantation profile modification, determ. using penetration distrib. function 3-79400
ion source, cluster obs. 3-61092
ion-bombardment thinning for TEM specimen prep. 3-57977
magnetic electron spectrometer, energy range 0 to 2000 eV, surface study (*French*) 3-80140
metal, in oxidizing atmosphere, model 3-64758
metal, sputtering coeff., sputtering saturation model and trapped amounts for metal ion injection 3-61083
metal ion injection into metals, irradiation system and expt. techniques 3-59635
metal polycrystalline surfaces, sputtering with high energetic inert gas ions, mean velocity of ejected particles 3-47341
metal-ZnS-metal structures, h.f. reactive cathode, dielectric props. (*French*) 3-58474
metallic films, getter sputtering device, static mode, low impurity const. 3-76128
oxides, coeffs., temp. depend., surface binding energy 3-69119

sputtering continued
plasma, at cathode, transverse ion energy component (*Russian*) 3-71969
polycrystalline target, energy distrib. of secondary ions 3-80135
polymer films, fluorocarbon, struct. and props. depend. on sputtering conditions (*French*) 3-80157
selective, glow discharge ion gun, for etching 3-53871
semiconductors, sputtering using Ar ions, surface topography 3-61085
solar wind, darkening of lunar silicate rocks 3-65797
solid targets, ion bombardment, consistent theory using power potential law 3-80126
surface damage and topography changes produced during sputtering 3-61088
surface interactions, 30 keV instrument 3-48587
thin films, light ion bombard., yield calcs. 3-69116
Ag, effective coeff. of cathode sputtering, in noble gases (*Russian*) 3-69128
Ag, polycryst., oblique Ar⁺ bombardment in 1 keV range, sputtering yield, ion incident angle depend. (*German*) 3-47342
Ag, yield with 15 and 45 keV ions 3-80130
Ag-Pd alloy films, prep. and optical props. (*French*) 3-41527
Al, polycryst., oblique Ar⁺ bombardment in 1 keV range, sputtering yield, ion incident angle depend. (*German*) 3-47342
Al, sputtering ion source, cluster obs. 3-61092
Al target, solid and liquid, temp. dependence of emission 3-80136
Al₂O₃, sintered, inert-ion sputtering obs. of impurities role in densification 3-69343
Al₂O₃ deposit prep. and characteriz. 3-76127
AlTa film, r.f. cosputtering, X-ray, resistivity and t.c.r. obs. 3-50096
As₂S₃, thin film growth by laser sputtering, mol. comp. of condensate vapours 3-55176
AsSe, thin film growth by laser sputtering, mol. comp. of condensate vapours 3-55176
As₂Se₃, thin film growth by laser sputtering, mol. comp. of condensate vapours 3-55176
Au, polycryst., oblique Ar⁺ bombardment in 1 keV range, sputtering yield, ion incident angle depend. (*German*) 3-47342
Au sputtering yield variation with ion dose, u.h.v. apparatus 3-61087
Au-Cr alloy, structure and electrical conductivity of cosputtered films 3-43963
Bi₂Te₃, thin films, parameters, effect on composition and resistivity 3-41279
CaO thin film, sputtering rate determination by fluorescence of sputtered atoms 3-44508
CaO:Sm, Tb, r.f., luminescence during sputtering 3-69097
CdS, during Bi ion implantation, rel. to saturated Bi conc. 3-69167
Co, in oxidizing atmosphere, expt. confirmation of model 3-64758
Cu, polycryst., oblique Ar⁺ bombardment in 1 keV range, sputtering yield, ion incident angle depend. (*German*) 3-47342
Cu atoms resputtering effects by measurements of angular distributions 3-58582
Cu films, yield for 33 to 150 keV protons, contribution of backscattered ions 3-80128
Cu sputtering and Ni ion injection, anomalous diffusion at room temp. and 77 K 3-61084
Cu target, 20 keV Ar⁺ and Ne⁺ ion beam, temp. behaviour of sputtering ratio 3-80129
Cu-Ni alloy, surface after Ar ion bombardment, Auger spectroscopy study 3-44514
Er, quantitative determination of surface oxide thickness on deposited films by ion bombardment 3-45555
Fe, in oxidizing atmosphere, expt. confirmation of model 3-64758
Fe₂O₃, on steel asymmetric r.f., corrosion resistance, structure of film, film electrical resistance 3-47436
GaAs thin films, glow discharge optical spectroscopy for chemical analysis 3-42705
Ge, sputtered amorphous film, velocity of propag. in shock crystn. 3-58190
KCl, preferential ejection pattern 3-41603
KNaNbO₃, ferroelectric, sputter machining, rel. to use as acoustic transducer 3-64966
LaO:Sm, Tb, r.f., luminesc. during sputtering 3-69097
MgO:Sm, Tb, r.f., luminescence during sputtering 3-69097
MgO-Au cermet, for high efficiency secondary electron emission 3-53160
Mo, effective coeff. of cathode sputtering, in noble gases (*Russian*) 3-69128
Mo by Cs⁺, ang. dependence of energy spectra of ions 3-50639
Mo-Ti alloy, from Mo target, film structure and lattice parameters (*Japanese*) 3-64777
Nb atoms to form getter internal coating on Cr-Ni steel, reactor fuel cans (*German*) 3-71306
Nb sputtering yields by D in keV range 3-60294
NbN superconducting films deposited by reactive sputtering, upper critical fields (*Japanese*) 3-68710
Ni, effective coeff. of cathode sputtering, in noble gases (*Russian*) 3-69128
Ni, polycryst., oblique Ar⁺ bombardment in 1 keV range, sputtering yield, ion incident angle depend. (*German*) 3-47342
Ni atoms sputtered by Ar ions in pulsed discharge 3-61111
Pd, polycryst., oblique Ar⁺ bombardment in 1 keV range, sputtering yield, ion incident angle depend. (*German*) 3-47342
PrCo₅, permanent mag. material, heat treatment and hysteresis obs. 3-44251
Pt film, sputtered in Ar discharge, optical and mass spectrometric analysis 3-43961
Pt film, sputtered in Ar/N₂ discharge, optical and mass spectrometric analysis 3-43962
Si, pre- and backsputtering as cleaning processes, surface structure and chem. 3-55161
Si, sputtering ion source, cluster obs. 3-61092
Si yield with 15 and 45 keV ions 3-80130
SiO₂ films, plasma oxidized dielectric strength and interface-state density 3-44154
SiO₂ films on Si, ion bombardment effect on electrical props. 3-41268

sputtering continued

- SmCo₅, permanent mag. material, heat treatment and hysteresis obs. 3-44251
 Ta, effective coeff. of cathode sputtering, in noble gases (*Russian*) 3-69128
 Ta, polycryst., oblique Ar⁺ bombardment in 1 keV range, sputtering yield, ion incident angle depend. (*German*) 3-47342
 Ta film, sputtered, factors controlling struct. 3-41111
 Ta film, sputtered in Ar discharge, optical and mass spectrometric analysis 3-43961
 Ta film, sputtered in Ar/N₂ discharge, optical and mass spectrometric analysis 3-43962
 Ta films, resistivity, Ar pressure effects 3-41276
 β -Ta r.f., thin films, resistivity, impurity, residual stresses, structure 3-52766
 Ti, effective coeff. of cathode sputtering, in noble gases (*Russian*) 3-69128
 Ti, polycryst., oblique Ar⁺ bombardment in 1 keV range, sputtering yield, ion incident angle depend. (*German*) 3-47342
 W, polycryst., oblique Ar⁺ bombardment in 1 keV range, sputtering yield, ion incident angle depend. (*German*) 3-47342
 W single cryst. surface, of clusters, angular depend. 3-61091
 W thin films, deposited by r.f. sputtering, microstructure growth, resistivity and stresses 3-43959
 Zn sputtering and Ni ion injection, anomalous diffusion at room temp. and 77 K 3-61084
 ZnO film, prep. by cold plasma condensation, growth kinetics (*French*) 3-52772
 ZnO sputtered films, diagnostic rate monitoring by interference spectroscopy 3-45418
 Zr, polycryst., oblique Ar⁺ bombardment in 1 keV range, sputtering yield, ion incident angle depend. (*German*) 3-47342

stabilisation *see stability***stabilisers** *see controllers***stability**

- see also frequency stability; Lyapunov methods; plasma instability*
 air, differentially heated inclined layers, stability, expt. obs. 3-46395
 analytic continuation in elementary particle calcs. 3-40373
 arc, in vacuum switches 3-57963
 atmosphere dry, inversion-capped, convectively unstable boundary layer 3-65384
 atmospheric two-layer fluid model, stability to nongeostrophic disturbances 3-47770
 axisymmetric shells deformed by fluid pressure, influence of back pressure on point of instability 3-54111
 baroclinic vortex, two-layer fluid, instability, separate circulations 3-46426
 beam, elastoplastic, influence of strain hardening, computation (*Japanese*) 3-62505
 Benard problem, instability mechanism in horizontal convective fluid layer 3-67924
 bridge, combined arch, vibrations for uniform motion of load in semitrip form (*Russian*) 3-66583
 bubble chain stability and breakup 3-43580
 buckling instability in tubes under internal and external axial fluid flow 3-67452
 bulk S-shaped negative differential conductivity media 3-41193
 bunched beams, longitudinal stability criterion 3-57264
 cable in incompressible flow, dynamic instability 3-63724
 Cambridge electron accelerator, USA, dependence of phase instabilities on bunch length 3-56909
 charged fluid, homogeneous spherically symmetric in general relativity 3-74132
 circular restricted three-body problem, global stability 3-69806
 clouds, nonprecipitating Trade cumuli field, stability analysis 3-65352
 composite structure biaxially loaded longitudinally stiffened, elastic stability 3-59764
 compressible boundary layer stability relative to a local disturbance (*Russian*) 3-67925
 compressible fluid flow through parallel elastic plates, stability 3-75235
 continuum mechanics, conference, Los Angeles, USA (August 1971) 3-74018
 convection, finite amplitude sideways diffusive, resonant instability 3-49554
 convective stationary motion in vertical layer caused by internal heat sources (*Russian*) 3-67906
 cosmic rays stations on spacecraft, construction of stabilizing platform using three-stage universal joint, electrohydraulic drives (*Russian*) 3-65979
 Couette flow, circular, with const. finite acceleration, linear stability anal. 3-71758
 Couette flow, dissipative axial and transverse magnetic field with coaxial cylinders 3-79009
 Couette flow, non-dissipative, axial mag. field, stability 3-71798
 Couette flow, viscoelastic, polymeric, stability prediction based on network rupture hypothesis, analysis 3-75277
 cryogen, liquid, thermodynamic instability, contact with warmer host liquid 3-49997
 cyclical accelerators and storage rings with resonant systems, beams longitudinal stability 3-73839
 cylindrical beams, axial flow, dynamical effect, hydroelastic instabilities 3-70653
 cylindrical shell, flexural equilibrium beyond elastic limit (*Russian*) 3-62497
 cylindrical shell, nonlinear, stochastically excited, stability 3-70555
 cylindrical shell, stability to dynamic axial loading (*Russian*) 3-57082
 cylindrical shells, discretely stringer-stiffened, stability 3-70556
 cylindrical shells under axial compression, postbuckling behaviour 3-70595
 damped system, with travelling wave 3-74069
 deformational, incompressible elastic bodies, finite subcritical strains 3-80485
 device, stabilising emission spectrum, reduction of meas. error, spark-arc discharge generator 3-73754
 dialable constant current supply, high stability 3-39973

stability continued

- differential eqns., linear abstract, stability theorems in Beurling spaces for parabolic regularizations (*Italian*) 3-40087
 differential equations, ordinary, asymptotic stability, study using Lyapunov functions (*Italian*) 3-77775
 discs loaded by concentrated force, dynamic stability (*Russian*) 3-62443
 dissipative systems, linear continuous, applic. to fluids and magnetofluids 3-75250
 dynamic, of pipe conveying pulsatile flow 3-67944
 dynamic, supersonic flow of gas part plates of complex form (*Russian*) 3-74076
 Dyuffinga eqn., generalised, stability of almost periodic soln. (*Russian*) 3-62411
 elastic axially loaded column, Galerkin's method, generalised, appl. of variant to eigenvalue problems, boundary problems (*Russian*) 3-73999
 elastic cylinder, deformed, correlation of generalised orthogonality in equilibrium problem (*Russian*) 3-42773
 elastic disc with moving mass system, dynamic response 3-70663
 elastic systems 3-62484
 elastically supported rigid disc with moving massive load, dynamic response 3-62457
 elastoplastic rod, centrally compressed, with cross-like cross-section stability (*Russian*) 3-42795
 electrode-electrolyte interface, multisteady states, reaction path, impedance, local stability conditions (*French*) 3-73139
 electron accelerator, linear, 600 MeV (*French*) 3-59618
 electron rings, negative mass instability in hollow cylinders 3-57277
 equilibrium point of one-degree of freedom system with nonlinear viscoelastic suspension (*Polish*) 3-70680
 excitons, degenerated, absolute instability 3-68582
 fading memory materials with internal variables, equilibrium state 3-66562
 falling liquid films, stability conditions, boiling and non-boiling films, interface conditions, Cu/H₂O/air (*German*) 3-46500
 fibre reinforced infinite body, 3-dimensional problem for large elastic deformation (*Russian*) 3-64984
 fibre with sub-critical deformation (*Russian*) 3-47462
 figures of equilibrium with inner motion 3-67957
 finite linear viscoelastic fluid plane Poiseuille flow stability 3-49541
 flows, inviscid plane parallel, boundary conditions 3-71794
 fluid elliptic cylinder with inner motion 3-67956
 fluid layers, impulsively heated or cooled, global stability of time-dependent flows 3-60536
 Foppl's vortices stability analysis 3-71759
 formation function, stability const. determ., graphical anal., real cross-over point 3-70484
 frame, elastoplastic, computation (*Japanese*) 3-62505
 free shear layer, nonlinear interactions in transition, expt. obs. 3-52478
 frequency, of gas lasers, review 3-62155
 galactic models, uniformly rotating stellar discs 3-53697
 glass reinforced plastic, cylindrical shell with elastic core, torsional stability 3-80449
 gravimeters, reading scale (*Russian*) 3-73962
 gravitating systems with quadratic potential, astrophysical appl. 3-61640
 gravitational, compressible polytropic cylinder surrounded by halo gas 3-65876
 growing sphere from supersaturated solution 3-68180
 gyrodendulum mounted on moving base, combinative parametric resonance, analysis (*Russian*) 3-59546
 gyroscope, astatic gimbals mounted, vibro-shock regimes (*Russian*) 3-74062
 gyrostabilized platform, for cinematography from moving automobile (*Russian*) 3-51645
 half-bubble magnetic domain, in double layer film, stability calc., variational model 3-47087
 Hamiltonian system, autonomous, third and fourth order resonances 3-66515
 helicopter, motion stability in nonlinear resonance conditions (*Russian*) 3-62441
 high current discharge, alternating, self-compression, theory of equilibrium and stability (*Russian*) 3-57966
 holonomic mechanical systems with partial dissipation, equilibrium instability (*Russian*) 3-77847
 hydrodynamic, of liquid flow over simple membranous surface (*Russian*) 3-63690
 hyperbolic eqns., asymptotic properties of solns. to mixed problem (*Polish*) 3-70535
 ideal fluid, stability of three-dimensional flow for unlimited increase in vorticity (*Russian*) 3-67919
 indicating gyrostabiliser with rotation of 3-stage gyroscope (*Russian*) 3-59547
 inverse logarithmic potential problem (*Russian*) 3-77782
 irreversible processes, nonlinear, system motion in thermodynamic theory 3-74174
 jet, elliptic, instability 3-57867
 jets, laminar, viscous, stability, influence of nozzle shape 3-79041
 jets and wakes, laminar axisymmetric, stability 3-75280
 Josephson tunnel junctions, oxide barriers 3-60941
 Kelvin-Helmholtz flow, MHD stability 3-49608
 laser, single-freq. travelling-wave type 3-42996
 laser interferometer for length measurement, output phase stability (*Japanese*) 3-59592
 lateral instability of thin walled beams, effect of spaced loading points (*Italian*) 3-40096
 linear systems, effects of determinant perturbation and random perturbation (*Russian*) 3-62409
 liquid mixture, laminar flow stability with temp. gradient 3-60526
 local, of Einstein-Maxwell-Boltzmann system 3-74163
 long period seismographs, noise suppression and stability 3-76883
 Lyapunov function for analysis of continuously rotating solid body (*Russian*) 3-42755
 Lyapunov method for stability of non-autonomous differential eqns. (*Russian*) 3-62417
 magnetohydrodynamic flow, convection 3-79036
 Maine Yankee reactor, damping of Xe oscillations 3-74699

stability continued

- margarite, upper stability in presence of quartz 3-41885
 matrix equation arising in electromagnetics 3-77932
 mechanical systems complex, bifurcation and stability of stabilising motions (*Russian*) 3-66511
 MHD Couette flow via non-axisymmetric oscillatory critical modes, instability 3-75256
 MHD parallel flow stability of an ideal heterogeneous fluid 3-43600
 MHD stability against axially symmetric perturbations 3-75255
 microlamp radiation stabilisation ccts. 3-39917
 multidimensional system, soln. of aggregation problem, using L-problem of moments theory (*Russian*) 3-77777
 natural convection boundary layer flow over horizontal and slightly inclined surfaces, stability 3-40722
 nearly parallel flows, linear stability (*French*) 3-63732
 neutrons stars, rotating, radial pulsations 3-61770
 n.m.d.r. spectrometer, instability investig. 3-42619
 nonlinear differential equations, third order global asymptotic stability 3-77776
 nonlinear differential systems, stability and asymptotic stability of solutions, equivalent inner products method 3-73990
 nonlinear system, asymptotic stability of solns. determ. using Hartman-Olech theorem (*Polish*) 3-66596
 nuclear reactor with prompt feedback, stability with changes in eigenvalue 3-43280
 nuclear reactors, liquid metal fast breeder, investigation, computer applic. 3-67506
 numerical, for Lagrange solns. of limited problem of three bodies (*Russian*) 3-77795
 oceanographic two-layer fluid model, stability to nongeostrophic disturbances 3-47770
 oceanography, baroclinic instability in western boundary current, numerical model 3-44857
 one dimensional stellar systems, thermodynamic instability criterion 3-73485
 orthotropic cylindrical shells, elastic, critical stress determ., stability, variable pressure 3-70579
 oscillations of body partly filled with viscous fluid, boundary layer method (*Russian*) 3-62536
 particle accelerators with LC tuned circuit, stabilization of particle energy 3-53967
 pendent liquid drops stability in narrow gap 3-57868
 photomultipliers, stabilization of receiving-amplifying path 3-56964
 plagioclase, high pressure stability, spinel gabbro xenoliths, Kerguelen Archipelago 3-44772
 plane shock waves stability 3-43574
 plasma confinement, toroidal, low-pressure axisymmetric stability analysis 3-46546
 plastic rigid struct. at yield-point load 3-51792
 plates, nonlinearly flexible, in presence of random initial stresses (*Russian*) 3-62474
 plumes, stability of wet and dry bent-over elements 3-47754
 Poiseuille flow, stability analysis for two- and three-dimensional disturbances 3-40703
 polycrylamide solutions, viscoelastic liquid, flow patterns upstream of orifices 3-71754
 polymer solution, high viscosity, wedge and channel flow stability 3-54825
 power reactors, subject to stochastic macroscopic parameter variation 3-74652
 proton relativistic beams, coherent longitudinal instability 3-57265
 raindrop falling at terminal velocity in vertical electric field, stresses, hydrodynamic instability 3-47766
 Rayleigh-Taylor instability, expt. obs. 3-71793
 Rayleigh-Taylor instability, Hall effect, finite depth inhomogeneous fluid, vertical magnetic field 3-79010
 reaction kinetics, asymptotic stability, Onsager fluxes, admissible entropy functions 3-65073
 relativistic electron rings, envelope instabilities 3-57276
 restricted 3-body problem, stability of periodic solutions 3-73429
 retinal image, model (*Japanese*) 3-70126
 revolving fluid, variable density, oscillatory instability 3-71789
 ring, bifurcation under concentrated centrally directed loads 3-70591
 rods and plates, rotating, buckling behaviour 3-57070
 rotating fluid layer, convection, buoyancy-surface tension instability 3-71790
 salinity profile, porous medium layer, effect on marginal stability, overstability and thermal convection 3-47710
 scalar nonlinear wave equation for a cubic medium, stability of the fundamental mode (*Russian*) 3-66497
 shaft, whirling, with internal and external damping, stability of motion 3-57047
 shallow rectangular cavities, adjacent to compressible flow, possible excitation frequencies 3-46464
 sheet of fluid, axisymmetric holes behaviour 3-43582
 shell, triple layered cylindrical, numerical soln. to stability problem (*Russian*) 3-62464
 shells, cylindrical, beyond elastic limit, axial compression and external side pressure (*Russian*) 3-72915
 shells, thick many-layered with differing compressibilities nonlinear theory (*Russian*) 3-66544
 shells of revolution, formulation of local stability problems 3-40117
 shells weakened by holes, stability, stress distrib. around holes (*Russian*) 3-45654
 solar, against spherical thermal perturbations 3-76964
 solar, nonspherical thermal instabilities, conditions of existence 3-76965
 solid fuel powder, surface phenomena, linear nonstationary effects, instability (*Russian*) 3-47545
 spherical shells, rigid plastic, rate problem for finite deform. under hydrostatic press. 3-62498
 stratified shear flows, linear inviscid theory, linear initial value problem 3-63678
 stabilisation of a mass in a vibrating body, formulation and preliminary results 3-74058
 stars, supermassive rotating objects 3-69933
 stationary motion of quasi-cyclical coordinate system, mechanical equilibrium under magnetic field (*Russian*) 3-66512

stability continued

- steady state rot. of solid body with cavity containing liquid (*Russian*) 3-57049
 stellar, relativistic, determ. using PPN formalism 3-61760
 stochastic differential eqns., asymptotic reduction (*Russian*) 3-66490
 stratified rotating conducting fluids, universal stability under influence of mag. field and Coriolis force 3-40735
 streamer breakdown, rate calc., stability rel. to streamer front thickness (*Russian*) 3-46568
 superconducting devices, force-cooled, propagating thermal waves rel. to stability characs. 3-62029
 superconducting loop, current persistence, BCS theory 3-72412
 superconductor, internally cooled, steady state temp. profile (*Japanese*) 3-41305
 supermassive stars, non adiabatic perturbation, post-Newtonian approximation 3-61767
 s.w. ionospheric propagation, phase instability distribution parameters (*Russian*) 3-42020
 thermal, in horizontal layers of non-Newtonian fluid (*Russian*) 3-43549
 thermohydraulic, of steam generators for pressurised water reactors (*German*) 3-71231
 three-mirror ring resonator, with Gaussian diaphragm, field and loss properties 3-74255
 trailing vortex pair instability 3-49565
 transversely isotropic shells, elastic filler, stability, mech. loading, temp., effect of shear strength 3-70580
 travelling wave instability in conduction regime of natural convection in vertical slot 3-57730
 two-degree-of-freedom systems, geometrical stability of nonlinear normal modes 3-57101
 unstable system, finite energy states decay rate 3-40146
 vertical cut in plastic media, wall collapse problems 3-74051
 vibrating systems, multiple-degree-of-freedom, stability limit of nonlinear resonances 3-70641
 viscous fluids Taylor stability, film boiling 3-75238
 visual information transmission (*Italian*) 3-56525
 wake, Gaussian, incompressible, two-dimensional, in steady viscous flow, spatial stability 3-71840
 $\text{Ca}_3(\text{PO}_4)_2$, saturation of Black Sea water 3-80709
 HCN laser for i.r. frequency synthesis 3-45832
 He-Ne laser, stabilisation at 3.39μ using sharp resonances in methane 3-62706
 V-V₂O₅-Pb, Josephson tunnel junctions, U-I characteristics, mag. field depend. of critical current 3-58348
- stability criteria**
 multiple reach channel flow, reach friction parameter identification, influence coeff. algorithm 3-54796
 transient two-dimensional heat conduction in solids, stability and oscillation characteristics of finite-element, finite-difference and weighted residual methods 3-62625
- stability of numerical methods** *see convergence of numerical methods*
- stacking faults**
 alloys with A15 structure, superconducting, influence on superconducting critical temp. 3-46931
 alloys with low stacking fault energies, deform. effects at temps. above M_s (*Russian*) 3-69186
 crystal, i.r. microscopy study of defects 3-54955
 f.c.c and h.c.p. stacking sequence energies from asymptotic potential approx. 3-54973
 II-VI semiconductor, cathodoluminescence rel. to SEM obs. 3-72760
 lattice displacements in vicinity, distortion determ. for Al using pair potentials 3-79364
 niobium oxides, stoichiometric variability in block structure and tunnel structures 3-40909
 rare earth-Co, rel. to coercivity 3-47089
 steel, austenitic, containing Nb, neutron irradi. induced swelling, influence of quenching conditions (*French*) 3-40538
 steel, Mn-type, martensitic transform., stacking fault density variation in austenite (*Russian*) 3-72824
 steel, quenched, residual austenite obs. (*Russian*) 3-53216
 steel, X-ray obs. of stacking faults, effect on resistance to plastic deformation (*Russian*) 3-69269
 steel with low stacking fault energies, deform. effects at temps. above M_s (*Russian*) 3-69186
 wollastonite (CaSiO_3), stacking disorder 3-68277
 Ag film, vacuum-deposited, internal friction peak due to stacking faults (*Russian*) 3-72284
 Ag thin films, effect on internal friction, vibr. damping (*Russian*) 3-72859
 β -Ag-Al alloys, splat-quenched, massive phase transform. phenomena 3-58613
 Al, energy, yield point, influence of electron irradiation (*Russian*) 3-55008
 Au-Cd-In alloy, double h.c.p., X-ray obs. 3-58043
 Co-Fe alloys, stacking fault energy, conc. and temp. depend. 3-41706
 Cu, energy, yield point, influence of electron irradiation (*Russian*) 3-55008
 Cu, physical perfection, random density 3-72089
 Cu thin films, effect on internal friction, vibr. damping (*Russian*) 3-72859
 Cu-Al (15.6 at.%Al), low stacking fault energy, dislocation interactions, Shockley dipole locks 3-68256
 Cu-Al alloy, β_1 to β_1' martensitic transform. crystallography (*Japanese*) 3-61128
 Cu-Sn alloy, martensitic transform., phenomenological analysis (*Japanese*) 3-50680
 Cu(Co), stacking fault energy near coherent twin boundary 3-55784
 Fe-Cr-Ni alloys, deform. recovery and recrystn. of austenite 3-69285
 Fe-Ni and Fe-Ni-Cr alloys, stacking fault energy, conc. depend., effect on martensitic transform. (*Russian*) 3-41715
 LiFe_2O_4 , rel. to order-disorder reaction 3-68275
 Mg-In-Cd alloys, long-period layer structure 3-50696
 Mo-C(Ta) alloys, stacking fault form. probability (*Russian*) 3-80275

stacking faults continued

- MoTe₂, stacking fault energy calc. 3-68276
 Nb, rel. to deform. mechanisms, 20-300K (*French*) 3-79409
 Ni, energy, yield point, influence of electron irradiation (*Russian*) 3-55008
 Ni-Co alloys, dispersion-hardened, stacking fault energy effect on stress/strain curves 3-58670
 Ni₃Ga, deformed single cryst., nature of stacking faults, partial dislocations 3-79363
 PbI₂, polytypic crystals, transform. 290-310°C, stacking fault mechanism 3-43874
 Si, bulk cryst., circular and hexagonal faults as possible dislocation dipoles 3-49899
 Si, dislocation free crystals, float-zoned, dislocation generation along swirls, thermal oxidation 3-41648
 Si, line stacking faults generation at coherent twist boundary 3-64058
 Si epitaxial layer, rel. to thickness measurement 3-64799
 Si p-n junction diode, elec. characs., oxidation-induced stacking fault effects 3-41259
 SiC, reaction-sintered, self-bonding characs., TEM obs. 3-76301
 TiCr₂, Laves phase, X-ray diff. study 3-69238
 ZnS, thermal stability, TEM obs. 3-58044
 ZnS-Mn²⁺, excitation and emission spectra, lines due to stacking faults 3-50619

staff *see* **personnel****standard microphones** *see* **microphones****standard voltage generators** *see* **signal generators****standardisation**

- automation engineering in industrial processes, trends and views (*German*) 3-48332
 emulsions, for super-8 optical-sound prints (*German*) 3-53923
 h.v. insulation/metal enclosed switchgear and control equipment (*German*) 3-48333
 Molch tester volumetric standard flow measuring equipment (*German*) 3-59541
 nuclear instrumentation, in Italy (*Italian*) 3-42620
 radiation protection from X-ray apparatus (*French*) 3-70178
 radioactive materials handling and radiation protection, French standards (*French*) 3-66060
 thermophysical meas., metrological problems 3-73686
 β^+ emitter circular disc source, standardization by β^+ annihilation and γ - γ coincidence methods 3-42634

standards

- see also constants; measurement standards; units (measurement)*
 air quality, application of pollutant concentration statistical model 3-59463
 ASTM, for polyester and epoxide resin systems 3-64983
 contact voltage with neutral conductor, standard JUS N.CO.010 (*Slovenian*) 3-66127
 distribution transformers, maintenance 3-59539
 electrical installation 3-61979
 electronic components, in Europe 3-39849
 electrotechnical products (*Slovenian*) 3-61978
 laser safety performance standards in United States 3-66788
 National Standard Reference Data System, critical evaluation of physical sciences data 3-48336
 national standards and quality assurance, dependence 3-66129
 nuclear, education 3-61959
 nuclear, information availability 3-74620
 nuclear applications standards hierarchy and interrelationships 3-67380
 nuclear power plants, standards and operating procedures, personnel, safe and reliable plant operation 3-73642
 nuclear program, status 3-67381
 nuclear reactor design, teaching 3-61971
 nuclear reactors, architectural engineering 3-63160
 nuclear reactors, licensing 3-63159
 nuclear reactors, preparation, ANS role 3-63158
 nuclear reactors, training 3-61958
 nuclear responsibilities of industry and Atomic Energy Commission 3-67382
 nuclear standardization, responsibilities of industry and Atomic Energy Commission 3-67383
 photographic objectives, diaphragm settings (*German*) 3-42591
 quantum efficiency, in GaP and GaAsP light emitting diodes 3-73662
 radiation, U.S. atomic energy program, pollution control 3-43319
 radiation protection, permissible doses (*Dutch*) 3-78392
 radioactive sterilisation of doses of protective and steroid hormones (*Italian*) 3-54050
¹⁶⁶Ho^m, as efficiency calibration standard for Ge(Li) detectors 3-48335

standing wave detectors *see* **standing wave meters****standing wave indicators** *see* **standing wave meters****standing wave meters**

- sound waves, standing, in tube, simple expt. 3-59529

Stark broadening *see* **Stark effect****Stark effect**

- see also atomic spectra*
 absorption spectrum, radiation stochastic props. effects 3-43330
 alkali earth metal atoms, singly ionised, Stark broadening and shift 3-54566
 aromatic hydrocarbons, condensed, static elec. polarizability changes 3-76012
 atom, multiphoton effects, anal. by Keldysh method, and perturbation method 3-74825
 atom, multiphoton processes, expt. results for H and inert gases 3-74826
 atomic state decay, improved Hamiltonian for Bethe-Lamb equations 3-63269
 azulene, benzophenone (naphthalene), impurity change of polarisability and dipole moment, $\pi\pi^*$ state 3-72662
 p-benzoquinone, single crystals, Stark effect on lowest ¹B_{1g}($\pi\pi^*$) state 3-80065
 p-benzoquinone, single crystals, Stark effects on low energy electronic states 3-76468
 carbon difluoride, microwave spectra, centrifugal distortion anal. force field and dipole moments 3-78820

Stark effect continued

- coherence resonances, second kind, elec. field modulation, fluoresc. intensity 3-71372
 cyclopent-3-enone, electric dipole moment determ. 3-60466
 cyclopropenone, molecular, electric dipole moment determ. 3-63482
 3,6-dioxabicyclo[3.1.0]hexane, microwave spectrum, dipole moment, conformation 3-63486
 fluorite series, effect of indirect exchange interaction on crystal field parameters of Er³⁺ centres 3-50139
 p-fluoroaniline, dipole moments determ., orientational Stark splitting obs. 3-63433
 garnet:Er³⁺, Eu³⁺, Nd³⁺, crystal field theory 3-72331
 high-frequency field effect 3-74800
 interstellar H₂O masers, molecular radio line splitting 3-81194
 interstellar OH masers, molecular radio line splitting 3-81194
 ions, helium-like, multicharged, relativistic theory, external elec. field (*Russian*) 3-71366
 methane-stabilised laser, frequency shifts with laser power, temp. and press. of gas 3-78014
 methyl fluoride, Stark effect of transitions of ν_3 band (*French*) 3-46271
 molecular dipole moment determ., environmental effects 3-72600
 molecular dipole moments determ. by Stark spectroscopy, environmental effects 3-63433
 multiphoton effects, appl. perturbation theory 3-74824
 multiphoton ionisation of excited atoms, resonance phenomena, Stark shift 3-46197
 in plasma, overlapping neutral-atom lines, electron broadening, quadrupole contribs. 3-46520
 plasma, thermal and nonthermal, field probability distrib., density and temp. 3-67985
 plasma electron density determ. from H _{α} lines broadened by combined Stark and Zeeman effect 3-43691
 positronium, relativistic contrib. to combined Zeeman and Stark effects 3-71483
 pulse plasma accelerator, spectral line broadening with time (*Russian*) 3-63889
 quasienergy and quasienergetic states, strong monochromatic e.m. wave perturbation of atoms and mols. 3-74219
 rare earth metals, free-ion energy levels, comparison of calc. and exptl. values 3-52795
 singly ionised atoms, comparison of measured and calculated Stark parameters 3-43336
 solar He line in sunspot flare spectra, electron density determ. 3-45021
 symmetric top rotor calc. of polarisability anisotropies and permanent electric dipole moment 3-40155
 p-terphenyl mixed crystals, with tetracene and pentacene, second-order Stark effect on ¹B_{2u} state 3-53128
 tetracene, mol. cryst. film, electron absorpt. band 3-72678
 s-triazine, lower electronic states, 1.8°K optical study 3-64674
 2,8,9-trioxadamanthane, microwave spectrum, dipole moment from second order Stark effect 3-40636
 two state system, non-resonant levels effect, Schrodinger eqn. representation, Stark shift 3-45782
 Al II, meas. of Stark broadened and shifted lines 3-40574
 Be, singly ionised, electron-impact induced, meas. and calc. of broadening 3-67688
 C V and VI $\Delta n=1$ transitions Stark broadening in laser-produced plasma 3-63871
 CN, electric dipole moment of A² Π state meas. by level anticrossing spectroscopy 3-75001
 COS, dipole moment function determ. 3-78768
 CaF₂:Dy³⁺, f⁹-electrons in cubic crystal fields 3-79638
 CaF₂:Eu²⁺, in zero-phonon spectra of local centres, modulation obs. 3-55665
 Ca₃(PO₄)₂:F:Eu³⁺, in zero-phonon spectra of local centres, modulation obs. 3-55665
 CdSe cryst., free and bound excitons, Stark splitting 3-72333
 D, Rydberg const., precision meas. 3-46177
 D, Rydberg const. exptl. Determ. 3-46176
 D discharge, Stark broadening of Paschen lines 3-43334
 D₂O dipole moment determ. from Stark meas. 3-75000
 Eu(NO₃)₃, hydrated and anhydrous, temp. depend. as function of hydration (*Russian*) 3-72720
 F₂CS dipole moment determ. from Stark effect 3-67827
 GdAlO₃:Er³⁺ energy levels of ion in lattice 3-72704
 H, coherent excitation of S and P states of n=2 term, Stark induced beat signal 3-54579
 H, interference of 2p_{1/2} state 3-63272
 H, Lyman- β emission, Stark beats 3-78439
 H, Lyman-series emission, Stark beats 3-67660
 H atom, soln. of eqns. using Bubnov Galerkin method (*Russian*) 3-78398
 H isotopes, Rydberg const., precision meas. 3-46177
 H lines, Stark broadened, structure effect of plasma instability 3-40640
 H plasma, n- α lines, high principal quantum number, Stark broadening 3-40802
 H plasma, partially ionised, dense, Lyman- α asymmetry calc. 3-71851
 H spectral line profiles, boundary determination for electron quasi-stationarity using the asymmetry of the wings 3-43335
 HDO dipole moment determ. from Stark meas. 3-75000
 HNO and DNO, microwave spectra analysis 3-63488
 H₂O dipole moment determ. from Stark meas. 3-75000
 H₂PBH₃, dipole moment, internal rotation barrier, microwave spectra 3-54699
 He I plasma spectral lines, Stark shifts 3-63868
 He II transitions, Stark effect modulations 3-78440
 He⁺, hydrogen-like, nonlinear Stark effect meas. 3-67668
 Hg, atomic electron struct. distortion due to high-intensity laser field 3-74772
 Kr, quadratic Stark effect calcs., Coulomb approx. (*Russian*) 3-79636
 Li, hyperfine Stark shift, many-electron perturbation approach 3-67639
 Li III transitions, Stark effect modulations 3-78440

Stark effect continued

- LiF, in zero-phonon spectra of local N_1 colour centres, modulation obs. 3-55665
 LiF vibrational energy, production from Li + SF₆ mol. beams, electric resonance spectra 3-43522
 Nd³⁺ ion excited state crystals, investigation of elementary cross-relaxation 3-64305
 OD, A²Σ⁺ state, Stark studies and high field level crossing 3-40654
 PbMoO₄:Nd³⁺, cryst. Stark splitting, optical absorpt. and Zeeman spectra obs. 3-47297
 SF radical, microwave spectra, dipole moment calc. from Stark effect 3-40637
 Si, neutral and ionised spectral lines from shock tube plasma 3-67659
 T, Rydberg const., precision meas. 3-46177
 T, Rydberg const. exptl. determ. 3-46176
 TbAlG: Tb³⁺, absorption and fluorescence spectra, 4K, 77K 3-76067
 Xe levels, Stark splitting calcs. (Russian) 3-75710
 YAlO₃:Dy (Ho)(Er)(Tm)(Yb), absorpt., luminesc. spectra, cryst. levels 3-72674
 YVO₄:Eu³⁺, nonthermalization and large variation in multiphonon relax. rate among Stark levels 3-53144

stars

see also stellar
 see also multiple stars; neutron stars; novae; sun; variable stars; white dwarfs

- 5M₊, main sequence evolution, computational techniques 3-77046
 AO Ia supergiants, non-LTE models and influence of He abundance 3-81031
 A5-V class, photosphere model using Mustel's method (Russian) 3-73490
 A-G type stars, 3-dimensional representation (French) 3-81077
 A-type supergiants, line intensities from high dispersion spectrograms 3-81097
 absolute magnitude and temp. of stars, IAU Symposium 54 (Geneva, Switzerland, 12-15 Sept. 1972) 3-81064
 absolute magnitudes and proper motion determ. 3-81066
 Am-type stars, catalogue of 418 objects with known spectral type 3-65885
 Ap type, problems in search for Tc II lines rel. to promethium controversy 3-81049
 Ap-type stars, search in open clusters 3-61771
 51 Aquilae, G dwarf star, metal-rich, u.v. four colour photometry 3-48015
 astrometric obs. from lunar surface using equal-altitude method 3-77034
 B5V-A5V stars in Catalogue of Geneva Observatory, apparent diameters of 172 objects 3-53655
 B supergiants absolute magnitudes and intrinsic colours 3-81080
 B-type supergiants in SMC, spectra weakened lines 3-81055
 α Canis Majoris (Sirius), u.v. spectrophotometry, Gemini XII 3-48048
 21 Capricorni, close approach of Jupiter, 1973 May 3-76990
 catalogue differences, representation using spherical harmonics 3-59240
 catalogues, spectral analysis of right ascension errors 3-53633
 catalogues for star position and proper motion for Washington and Richmond photographic zenith tubes 3-76947
 Chamaeleon 16, nebulous object in Chamaeleon T assoc., i.r. photometry 3-77145
 circumzenith and refraction pairs, International Latitude Station obs. 3-77033
 circumzenith stars, catalogue of 30 precise declinations 3-53635
 classification according to low dispersion spectra, technique and criteria (Russian) 3-61785
 cold and protostars, i.r. emission mechanism and energy sources 3-42219
 comparison stars, multivariate analysis to parallax solns., effect of magnitudes and colours 3-77057
 β Coronae Borealis, identification of actinides 3-65890
 diameter measurements, by speckle interferometry, near-diffraction-limited information in presence of atmospheric turbulence 3-61884
 differential star catalogue compilation by computer input of meridian-circle obs. 3-53634
 double beam photon-counting spectrometer high resolving power (Russian) 3-45242
 E model sequence, multiple solns. of eqns. of stellar structure 3-77039
 early type, interpretation of spectra 3-73508
 early type, surrounded by dirty ice particles, interstellar extinction from i.r. to far u.v. wavelengths 3-61768
 early type southern stars, UVB obs. 3-48020
 early-type, absolute magnitudes and colours rel. to Hβ photometric system 3-81076
 early-type, heavy ion acceleration by radiation pressure 3-81042
 evolved, CN/C₂ and CO/C₂ ratios in cool C stars 3-81023
 FK 4 stars, right ascension determ. south of -42° declination 3-77035
 FKSZ stars, catalogue of R.A. and comparison with other catalogues 3-59239
 flare stars, photoelectric obs. (Italian) 3-61789
 fundamental reference system, extension to radio sources and faint objects 3-59241
 G giants, calibration of luminosity criteria by trigonometric parallaxes 3-77059
 giants and supergiants, i.r. absorption due to SiO 3-81054
 giants in disc population, discontinuity of props. 3-61849
 HD37806, radio emission detection at 10.63 GHz 3-65901
 hot main sequence, UVB system review and effect of interstellar reddening 3-81086
 HR 465, problems in search for Tc II lines rel. to promethium controversy 3-81049
 HR standard star, photometric criteria for choice 3-81087
 image formation, high resolution, through turbulent atm., star maps 3-73564
 interferometric meas. of stellar apparent diameters (French) 3-70065
 i.r. stars from IRC Survey with long wave excesses 3-65912

stars continued

- isolated systems of identical stars random gravit. encounters and evolution 3-53696
 K giants, calibration of luminosity criteria by trigonometric parallaxes 3-77059
 Kapteyn Selected Areas, photoelectric UVB photometry of 128 stars 3-73503
 late M-type dwarfs, absolute magnitudes in red and i.r. 3-81067
 late type, effect of saturation on ¹²C/¹³C ratios from CO first overtone bands 3-73494
 LMC member stars, 2nd list (French) 3-65926
 luminosity discriminant for red giants and supergiants 3-61780
 α Lyrae (Vega), absolute flux meas. for calibration of V-magnitudes of stars 3-81081
 M dwarfs, medium spectral resolution scan photometry, Spinrad-Taylor system 3-69942
 M-type dwarfs, magnitude, TiO absorption bands (Russian) 3-45114
 Maclaurin stellar disc, oscillation spectrum 3-61640
 magnetic, accretion accounting for stellar rotation and magnetic field, forming X-ray source 3-73533
 magnetic, effect of interstellar mag. fields on stellar evolution (German) 3-56372
 magnetic, photoelectric obs. (Italian) 3-61787
 magnetic rotating stars, toroidal and poloidal oscillations, decaying field 3-77074
 mass distribution of eclipsing binaries 3-77070
 α Mensae, G dwarf star, metal-rich, u.v. four colour photometry 3-48015
 metal poor, mass loss in stellar wind for fast rotation 3-77060
 MWC 349, radio star, photoelectric obs. 3-81802
 nearby, revised parallaxes for 10 objects 3-48007
 neutral stellar objects, identification with radio sources 3-53679
 NGC 2129 region, spectral classification of faint stars (Russian) 3-61786
 O and B standards, energy distrib. in u.v. spectra (French) 3-81089
 O- and Of-type stars, temp. and spectra 3-77080
 OB stars in Milky Way system, two-colour diagrams 3-48016
 open cluster stars, escape from cluster 3-61859
 optical appearance of star orbiting black hole 3-65616
 near Orion nebula, non-colour photometry and i.r. excesses 3-69952
 parallax meas. of 35 stars using Yale 26 in. telescope 3-61777
 peculiar, spectral classification 3-77068
 peculiar A stars, elemental abundance anal. 3-65879
 photoelectric UVB of 203 stars by Palomar telescope 3-73504
 photographic zenith tube plate meas. and identification of stars by computer (Japanese) 3-65976
 photospheres, coefficient of absorption of radiation by H⁺ ions (Russian) 3-73491
 Population I, instability strip computation 3-73477
 Population II, evolution of horizontal branch of stars with 0.63 solar mass 3-73486
 Population II, instability strip computation 3-73477
 protostars, cooling mechanisms by volume energy losses (Russian) 3-77041
 red, recognition, colour photography, anomalous images, visual examination 3-81056
 red giants in M15 and M92, interpretation of two colour and colour magnitude diagrams 3-73495
 red giants in M 5, M 10, M 92, spectral anal. 3-53702
 relativistic rotating, review of known properties (Polish) 3-65619
 Royal Greenwich Observatory Time and Latitude Service for 1972 July-September 3-61756
 Sanduleak 160, optical counterpart of 2U 0115-73 (SMC X-1) 3-73535
 Sanduleak 160, proposed optical candidate for SMC X-1, photographic photometry 3-51377
 SAO 76530, 4 August 1972, grazing occultation 3-65897
 δ Scorpis, u.v. spectrum, interstellar H₂ 3-48123
 α Sculptoris, weak-He-line star, chemical abundance 3-48030
 solar-type, secular stability, reaction kinetics of proton-proton chain 3-81021
 speckle pattern star image processing methods 3-59396
 superflares, possible origin of γ-ray burst 3-73506
 supergiants, chemical composition determ. from evolutionary tracks, bolometric calibration and spectral type 3-81051
 supergiants, mass-luminosity relations giving hydrogen and metal abundances 3-73512
 supergiants, type G and K Ib, equivalent width data 3-73501
 supermassive, dynamical evolution of nonrotating H and He burning stars 3-69924
 supermassive, stabilities for non adiabatic perturbation, post-Newtonian approximation 3-61767
 supermassive slowly rotating 7.5 × 10⁵ M_⊙, hydrodynamic model, collapse and explosion 3-77040
 telescope image profiles 3-77066
 time and latitude bulletin of Tokyo Astronomical Observatory (July 1972) 3-47978
 time and latitude bulletin of Tokyo Astronomical Observatory (August 1972) 3-47979
 time and latitude service of RGO for 1972 January to March period 3-51321
 Tokyo Astronomical Obs., Time and Latitude Bulletins (September 1972) 3-47980
 Universal Time determ., effect of right-ascension errors in stellar positions 3-77032
 upper main sequence, ionizing radiation production in galaxies 3-81052
 u.v., ionisation of interstellar gas, model analysis 3-70027
 VY2-2, i.r. object, radio emission detection at 10.63 MHz 3-65900
 WC stars, binary separations rel. to Wolf-Rayet subclasses 3-81063
 Wolf-Rayet, classification and distrib. rel. to WN sequence interpretation 3-81059
 Wolf-Rayet, effective temperatures 3-81060
 Wolf-Rayet, extended atmospheres and non-classical atmospheric models 3-77051
 Wolf-Rayet, nature and physical structure 3-81038
 Wolf-Rayet, u.v. and radiofrequency obs. 3-77078
 Wolf-Rayet and high temp. stars, IAU Symposium (Buenos Aires, 9-14 Aug. 1971) 3-77036

stars continued

- Wolf-Rayet stars rel. to P Cygni-type stars 3-81061
- Ba II type in NGC 2420 open cluster, absolute magnitude and stellar population 3-81085
- Be, emission-ring line profile rel. to long-period V/R variation 3-69953
- C-O core growth phase, stellar model 3-77047
- He-weak, u.v. energy distrib., comparison of OAO-2 obs. with UVB photometry 3-81084
- OH stars, type I, optical props. 3-61781
- OH/IR stars, search in globular clusters at 1665 MHz 3-61840
- δ Pavonis, G dwarf star, metal-rich, u.v. four colour photometry 3-48015

state of the art studies *see reviews*static (atmospherics) *see atmospherics*static electricity *see electrostatics*

static electrification

- see also triboelectricity*
- dielectric materials, meas., soln. (Italian) 3-50262
- metal-polymer contact, surface charge effects 3-46673
- polyethylene film, diffusion of antistatic agents, surface cond. study 3-65004
- polymers, during extrusion 3-47482
- water drops, electrification during condensation and evaporation 3-49985
- xylene, spray electrification 3-79759

statics

- see also hydrostatics*
- alterable systems, analytical statics problems (Russian) 3-54073
- moment stress elasticity, finite-strain force, kinematics and statics 3-70588
- relativistic, covariant asynchronous formulation 3-66712
- thin circular elastic plate resting on a two-parameter Winkler type foundation 3-66521

stations, power *see power stations*

statistical analysis

- see also measurement errors; probability; random processes; statistical theory of nuclear reactions and scattering*
- accelerated tests, statistical anal. of accuracy of Locati method, fatigue damage, rel. to 'stairs' method 3-53296
- aerosol particle size 3-65030
- aerothermodynamic calculations, temp. of mandatory pressures, statistical determ., model atmosphere 3-53495
- Atlantic, tropical, discriminant statistical analysis of oceanological characteristics, probability estimates of formation of water masses (Russian) 3-80694
- of atmospheric, natural signals, computer software system 3-59187
- atomic and molecular orbitals, $X\alpha$ method comparison with ensemble average method 3-67646
- autocorrelation function of certain random process, statistical evaluation (Polish) 3-70538
- bimodal criticality distributions in few group neutron diffusion analysis 3-63108
- β Cephei stars 3-56390
- chemical reactions statistical theories, distributions in the transition region 3-41845
- comets characteristics, statistical connection (Russian) 3-61738
- data smoothing, problem of weighting (Russian) 3-61881
- diatomic and linear polyatomic molecules; rotational structure of spectra analysis by statistical and computer methods 3-63429
- dielectric materials, elec. strength, statistical determ., variation due to defects 3-44371
- digital computer program for fundamental statistical distributions 3-42745
- dog, statistical nature of blood pressure and flow waves in cardiovascular system 3-65980
- dry solids, random and non-random mixtures, stat. props., variance of sample comp. 3-55907
- earthquake-explosion discrimination, statistical capabilities, false alarm probabilities at given deterrence 3-80621
- earthquakes, statistical method of detection and prediction 3-80839
- elasticity, reinforced plastic, internal stress of shrinkage origin 3-64988
- electron transfer reactions theory 3-41842
- electron velocities in crossed magnetic and electric fields, statistics 3-52504
- energy levels repulsion phenomenon, statistical measure 3-57474
- examination results by computer 3-66122
- fluctuations of meas. equipment recordings, applications (German) 3-48337
- Forbush decreases and preceding cosmic-ray intensity increases, statistical analysis 3-42098
- free fall teaching experiment, statistical analysis 3-51490
- galaxies in nearby groups, statistical appl. of virial theorem 3-81162
- Gaussian light, photoelectric counting statistics, spatial coherence effect 3-42987
- geophysical variables, turbulent or wave-like fluctuations, computational technique 3-47803
- heavy particle transport in homogeneous turbulent fluid flow 3-46482
- hydrologic parameter accuracy, streamflow regression simulation 3-59215
- illumination field under wavy surface, correlation function and power spectrum 3-73264
- implementation errors, seismic source and geophone array design 3-76533
- injection lasers, statistical distribution of failure 3-48925
- intersection of cylinder and ellipsoid, stressed by internal pressure, unit load determ., resistive elec. extensometry (Rumanian) 3-73667
- laser, in several axial modes, photoelectron probability distribution, analysis by photo counting method 3-62731
- lifetimes of melt water films 3-63945
- logistic distribution as approx. to normal probability function 3-42747
- lunar disk albedo, statistical distrib. 3-61721
- β Lyrae eclipsing binary stars 3-53656
- mechanics, solid, heterogeneous materials, statistical theory, recent developments, review 3-74017

statistical analysis continued

- medical radiosintigraphy, classification, rejection/acceptance of small fluctuations, likelihood ratio test 3-51464
- molecular collision induced dissociation 3-40661
- molecular rotational constants calc. method 3-63416
- n.m.r. linear spectrum measurements 3-75867
- nuclear reactor, JMTR, application of on-line digital noise analysis to reactor diagnosis 3-71161
- nuclear reactors, engineered safety features, design, probability, statistical risk 3-71179
- operational statistics, manuals of operation and their logics 3-74113
- optimum smoothing parameter for experimental data 3-74007
- peripheral glomerular basement membrane, thickness distrib., statistical anal. 3-56484
- photoelectron counting statistics, quasimonochromatic light, clipped correlation function 3-57217
- photolithographic operations in IC manufacture statistical analysis (Russian) 3-42592
- planetary satellite bodies distrib. according to mean distances 3-59265
- plasma electron cyclotron heating in magnetic mirror field, statistical model 3-43676
- Poisson process, nonstationary, registration with fixed dead-time systems 3-77789
- population explosion, mathematical conditions 3-48704
- probabilistic method for nuclear reactor failed fuel element identification using gas tag technique 3-71170
- quadratic kinetic potentials, continuously perturbed equivalent classes of asymptotically stable kinetic equations 3-47557
- radio aurora, statistical zone of occurrence 3-61493
- radiometric well logging, statistical unification and estimation of compactness and shalyness indices 3-73188
- rainfall, probabilistic study for Charente and Seudre river basins (France) (French) 3-61464
- rainfall from tropical cyclone systems crossing Appalachians 3-47746
- random processes, non Gaussian, nonlinear conversion eqns. (Russian) 3-74005
- scaling models, high energy multiparticle production in hadron hadron collisions 3-62868
- SdB-type rapid variable stars 3-59344
- sea-surface temp., large scale fluctuations 3-59029
- similarity theory, factorial planning of experiment 3-42746
- size distrib., true diameter of synaptic vesicles 3-57005
- small samples, uncertainty in conclusions, sampling procedure 3-62434
- solar activity, test for short periodicities 3-45019
- solar granulation plate, autocorrelation function and power spectrum 3-65972
- sound level meter, statistical anal., motorway noise 3-53793
- spectra automatic peak analysis, using minicomputer 3-48421
- steel, heat resistant, tensile strength 3-80375
- steel, u.s. inspection, flaw detectability study, ASNT Sonics and Aerospace Committees 3-47517
- structural reliability and minimum creep life at elevated temp., stat. eval. method 3-62494
- sunshine, rel. to cloudiness over India, regression anal. 3-80745
- superconductor, pinning on point defects, statistical theory 3-79798
- thermal diffusion coefficients calc. by statistical method 3-46725
- tropical cyclone motion, statistical predictability 3-47747
- underwater sound, CW propagation between Eleuthera and Bermuda 3-42449
- universal correlation failure, intermolecular processes, absorption and luminescence spectra 3-76040
- W Ursae Majoris eclipsing binary stars 3-53656
- vibrating systems, coupled, statistical energy analysis, proportionality constant, prediction and measurement 3-81343
- yield stress, rel. to load and composition of steel 3-55800
- Al alloy, u.s. inspection, flaw detectability study, ASNT Sonics and Aerospace Committees 3-47517
- Cd-Se, thin film spectrophotometric chemical analysis, precision and accuracy 3-51758
- F₂-region, irregularities, application of correlation techniques 3-51123
- GaP-GaAs, GaAs-InAs, X-ray spectra, inhomogeneities, statistical models in local anal. 3-48658
- Hg-Cd-Te, thin film spectrophotometric chemical analysis, precision and accuracy 3-51758
- Ni alloy, heat resistant, tensile strength 3-80375

statistical distributions *see statistical analysis*

statistical mechanics

- see also lattice theory and statistics; quantum statistical mechanics*
- atoms, small face centred cubic cluster, 3 to 87 atoms, configuration free energy, atomistic calc. nucleation rate calc. 3-48824
- binary mixtures, classical, space-time correlation function determ. 3-74152
- Boltzmann's H-theorem, improved presentation 3-53813
- charged particle system, integral eqns. for radial distrib. function, long- and short-range potentials 3-74151
- chemical kinetics, fluctuations around steady states, phase-space and stochastic descriptions 3-65083
- defect concentration in crystals, method of calculation for students 3-56599
- dipole correlation functions for isolated sphere and spherical region in continuous medium 3-77899
- dynamics of gravitational system, solar system applications 3-66675
- Einstein-Maxwell-Boltzmann system, existence, uniqueness and local stability 3-74163
- ergodic properties of sample model system with collisions 3-74149
- ergodic theory, developments and history 3-42883
- Fermi gas, dense, three-body collisions (Japanese) 3-74153
- fluid system processes, statistical thermodynamics (German) 3-48813
- Fokker-Planck eqn. for systems far from equil., Boltzmann distrib. function 3-62605
- functional random-walk model, entropy productivity and maximum-entropy state 3-74177
- functional random-walk model for irreversible processes steady-state 3-40195

statistical mechanics continued

- gas equation of state for medium-density high-temperature conditions 3-52413
- Green-Kubo integrals, kinetic approach to long-time behaviour of dense fluids 3-48796
- Hamiltonian dynamics, generalization to three dimensional phase space 3-42884
- hard sphere fluid approach to liquid-solid phase transitions 3-75605
- hard sphere gas, dense, developments of Enskog and virial theories (*French*) 3-45738
- homogeneous stationary gas, reacting, distrib. function calc., comparison of Boltzmann's law and Enskog's methods 3-71611
- ideal fluid, polytropic hypersonic transform. (*French*) 3-62590
- ideal-gas, pressure fluctuations, statistics and thermodynamics, implicit averaging 3-42882
- interesting walks and equivalence in graphs 3-62592
- ionic fluids, equil. field theory 3-48794
- ionic fluids, onset of short-range order 3-48795
- kinetic eqn. theory for fundamental state variables, appl. to dense gases and liquids 3-57168
- kinetic eqns., normal soln. determ. by boundary conditions 3-54160
- kinetic equation derivation for functional distrib. function, projection operator method 3-48797
- Kirkwood-Salsburg eqn., series soln. and radius of convergence 3-62406
- Krylov-Kolmogorov dynamic entropy minimization in nonequilibrium steady state 3-74180
- Langevin equations, generalised linear and nonlinear 3-62595
- Lennard Jones gas, expansion of second virial coeff. reply to comment 3-59811
- Lennard Jones gas high temp. behaviour, expansion of second virial coeff. using hard-sphere basis functions, comment 3-59810
- Lennard-Jones fluid, surface density and tension, stat. mech. and quasithermodynamic calcs. 3-60790
- Liouville eqn., chemically induced dynamic spin polarisation 3-80537
- Liouville equation, derivation of Markovian kinetic equations 3-74150
- Liouville theorem generalization, particular integrals (*Russian*) 3-45629
- liquid-gas interface, density structure, statistical-mechanical determ. 3-49520
- localized vibrational excitations in system of nonlinear oscillators 3-54174
- Lorentz gas, cluster expansions and autocorrelation functions, self diff. coeffs. 3-77898
- macroscopic observables in classical gas, time-correl. function 3-62591
- many-particle system, evolutionary operator through projection operator 3-51831
- material indifference principle violation 3-62446
- melting curve maxima and solid-solid transitions, high pressure, two species model 3-49976
- microscopic anal. of long-time tail in autocorrelation function and diffusion coefficient 3-70753
- mixture exhibiting phase separation, mean spherical model 3-54183
- molecular fluids, pair correl. functions, integral eqn. derivation 3-74147
- molecules, stereochem. invariance law, combinatorial theory 3-53313
- N-body gravitation problem, integration scheme, near and distant stars 3-70726
- nonuniform classical system, properties of canonical density distrib. in thermodynamic limit 3-62634
- nuclear state, deformed, intrinsic, angular momentum distrib. and average temp. 3-71067
- one dimensional stellar systems, instability criterion 3-73485
- one-dimensional classical systems with slowly decreasing potentials, analyticity of correlation functions 3-59827
- one-dimensional kinetic system, equilibrium props. simulation 3-59809
- one-dimensional system, construction of dynamics 3-54159
- open systems; kinetic analysis, Zubov's construction in the asymptotic stability domain 3-42898
- percolation level in three-dimensional random potential 3-57153
- perfect gas description using coherent states, grand partition function (*French*) 3-51830
- phase changes in many particle systems, macroscopic collective excitations 3-74181
- phase distribution functions, establishment of generalised kinetic eqn. (*Russian*) 3-77897
- phase transitions, partition function in several complex variables, zeros limiting distribution 3-66713
- phase transitions of hard sphere system (*German*) 3-62628
- plasma, three component ionised system, classical kinetic eqns. derivation 3-43653
- radial distrib. function of fluids, new types of integral eqn. for high densities 3-40174
- random sequential filling of intervals on a line 3-42880
- Rayleigh's piston, spectral theory 3-70752
- self-diffusion, Green-Kubo formulas and long tail of velocity autocorrelation function 3-54158
- single component system, reaction in heavy-gas thermostat, disturbance of Maxwellian distrib., effect on reaction rate 3-73131
- stationary random ergodic processes, comparison of Fourier transform method with a correlation method, spectral density estimation (*Russian*) 3-70312
- thermodynamic compensation law and thermal death of unicellular organisms 3-48825
- thermodynamic perturbation theory, second-order, study of short range potential (*Russian*) 3-74172
- thermodynamics and dynamics, unified formulation 3-62629
- thermodynamics partition and approach to equilibrium 3-48823
- transformations relating probability densities and correlation functions 3-74148
- tribology, statistical formulation of friction systems 3-72126
- weighting function for system of variable parameters, detn. of state variable representation 3-42879
- H₂, statistical mechanics at high pressure rel. to planetary models 3-60508

statistical mechanics continued

- He-chlorotrifluoromethane system, binary diffusion coefficients at 300 K, 1 atm., Chapman-Enskog theory test 3-52419
- statistical methods** see *statistical analysis*
- statistical tests** see *statistical analysis*
- statistical theory** see *statistical analysis*
- statistical theory of nuclear reactions and scattering**
- compound model rel. to $^{12}\text{C}(^{12}\text{C}, ^{12}\text{C})^{12}\text{C}$ scattering, analysis of cross sections, direct model comparison 3-67360
- compound nuclear theory rel. to ^{154}Sm level spine and parities 3-67196
- compound-nucleus reactions, conserved isospin quantum number consequences 3-60148
- Ericson fluctuations in presence of direct reactions, Hauser-Feshbach theory 3-74549
- evaporation model, Hagedorn-Macke, corrections (*Spanish*) 3-43228
- evaporation model for compound-nucleus reactions, excitation functions and photon emission 3-63083
- exciton model, emission and formation probability of complex particles 3-60137
- exciton model approach to pre-equil. decay 3-43230
- independence hypothesis and isospin conservation in compound statistical reactions 3-71093
- multigroup neutron cross section adjustment by correlation method 3-43262
- photoneuclear processes involving γ -bremsstrahlung, correlation effects and stability of inverse problem solns. (*Russian*) 3-52169
- pre-equilibrium reactions, fluctuations in excitation function and emitted particle spectra 3-40475
- quantum theory of stationary irreversible processes 3-40476
- screening factors for nuclear reactions, intermediate screening and astrophysical appl. 3-47861
- screening factors for nuclear reactions in dense plasma, general theory 3-47860
- (ν , n) reaction on one neutron deficient nuclei, photoneutron mean energies, level density parameters 3-60080
- (n,p) reactions, activation cross sections and isomer ratios as a function of incident energy, statistical model calc. (*German*) 3-52173
- $^{10}\text{B}(\text{d}, \text{n})^{11}\text{B}$, low energy branching ratios, isobaric analogue states 3-74599
- $^{10}\text{B}(\text{d}, \text{p})^{11}\text{B}$, low energy, branching ratios, isobaric analogue states 3-74599
- $^{12}\text{C}(^3\text{He}, \text{p})^{14}\text{N}$, 3-11 MeV, compound-nucleus statistical model, ρ - ρ angular correlation meas. 3-63074
- $^{198}\text{Hg}(\text{n}, \text{n}')$, cross section near energy threshold, deviations from statistical model (*Russian*) 3-74568
- $^{200}\text{Hg}(\text{n}, \text{n}')$, cross section near energy threshold, deviations from statistical model (*Russian*) 3-74568
- $^{202}\text{Hg}(\text{n}, \text{n}')$, cross section near energy threshold, deviations from statistical model (*Russian*) 3-74568
- $^{175}\text{Lu}(\text{p}, \text{xnp})^{\text{A}}\text{Hf}$, $\text{x}=2, 4, 6$, $\text{A}=174, 172, 170$, compound nucleus reaction de-excitation 3-49191
- ^{60}Ni , neutron elastic and inelastic scatt. from 2 to 8.5 MeV, differential and total cross-sections calc. 3-57531
- $^{206}\text{Pb}(\text{n}, \text{n}')$, cross section near energy threshold, deviations from statistical model (*Russian*) 3-74568
- ^{239}Pu , multilevel effects in unresolved resonance region 3-71114
- ^{240}Pu fission, mass distrib. of fragments, statistical model 3-60235
- $^{31}\text{Si}(\text{d}, \alpha)^{28}\text{Al}$, 4.850-5.825 MeV, reliability of statistical model predictions of relative cross sections 3-49262
- $^{30}\text{Si}(\text{d}, \text{p})^{31}\text{Si}$, low deuteron energies, proton angular distrib. comparison of direct and compound nucleus mechanisms (*Russian*) 3-71119
- $^{181}\text{Ta}(\text{p}, \text{xnp})^{\text{A}}\text{W}$, $\text{x}=2, 4$, $\text{A}=180, 178$, compound nucleus reaction de-excitation 3-49191
- $^{169}\text{Tm}(\text{p}, \text{xnp})^{\text{A}}\text{Yb}$, $\text{x}=2, 4$, $\text{A}=168, 166$, compound nucleus reaction de-excitation 3-49191
- ^{235}U , multilevel analysis of neutron capture and fission cross sections up to 60 eV 3-63094
- ^{235}U , multilevel effects in unresolved resonance region 3-71114
- statistical thermodynamics** see *statistical mechanics*
- statistics**
- see also *error statistics; game theory; Monte Carlo methods; probability; queuing theory*
- climatological, noise level for general circulation model 3-59097
- Earth evolution, dynamics-statistics of gravit. differentiation 3-47608
- Gaussian distribution skewed function, analytical moments 3-70537
- glass transition, confidence limits for the abscissa of intersection of two linear regressions 3-66504
- mass anomalies and gravity disturbances, stationary statistical models 3-58857
- meteorology, maximum/minimum surface temp. automatic prediction, use of model output statistics 3-59194
- meteorology, surface wind automated prediction, use of model output statistics 3-59193
- meteors detection, optimum processing (*Russian*) 3-77021
- micropulsation model as random temporal process 3-56104
- Poisson distribution, teaching note 3-70536
- radiometric information optimum processing (*Russian*) 3-77020
- rainfall, floods and droughts prediction, γ -like transformable normal freq. distrib. 3-56172
- rainfall rates near earth's surface for effect on radiowave propagation 3-69577
- steel wire fatigue, cycles to failure and stress to failure Weibull distributions 3-41833
- vacuum, elec. breakdown, time lag, statistical behaviour (*Czech*) 3-63896
- stators**
- electrically conducting liquid rotation inside stator with a rotating field (*Russian*) 3-57817
- steady-state theory** see *cosmology*
- steam**
- air-steam mixture, laminar film condensation on vertical surface 3-52452
- condensing, flow through Laval nozzle, shock waves 3-71831
- free convection film condensation of vertical surface in presence of non-condensing gases 3-46387

steam continued

- nuclear reactor produced, use in pilot plant for methane reforming (*German*) 3-69495
- oxidation acceleration in high pressure steam of Zircaloy-2 3-71300
- saturated steam, film condensation on a horizontal tube 3-64163
- spontaneous condensation in u.s. nozzles 3-52493
- steam-water-ice phase system, 2 dimensional bonded lattice model, first order approximation, long range and short range order 3-41006
- superheated, in rod fuel bundles, forced convective heat transfer 3-63182
- thermal conductivity in supercritical region 3-52415
- turbulent flow in pipe, radiative transport 3-52436
- Si(111) surface oxidation and reduction Auger electron emission obs. 3-41097

steam plants

- condenser chamber failure in nuclear reactor, cause and counter-measures (*German*) 3-74707
- generators, PWR, dynamic response characteristics, frequency response functions 3-71217

steam power stations

- environmental pollution effects, quantitative analysis (*Italian*) 3-41963

steel

- 21 Mn Mo 55, irradiation response to Pellini and NDT tests, rel. to MZFR pressure vessel evaluation (*German*) 3-73113
- 21 Mn Mo Ni 55, irradiation response to Pellini and NDT tests, rel. to MZFR, pressure vessel evaluation (*German*) 3-73113
- A19 alloy, Be, Ti and Zr additions effect on struct. and mech. props. (*Russian*) 3-72850
- A302(B), irradiation response to Pellini and NDT tests, rel. to MZFR pressure vessel evaluation (*German*) 3-73113
- A-302-B, embrittlement and annealing after neutron irradiation, model based on Davidenkov criterion 3-72914
- acetone deposition of C, inhibition by poisoning with S 3-73168
- acoustic emission, spectrum anal., deformation and crack propagation 3-47509
- activated corrosion product radiation levels, in fast flux test facility 3-63169
- adhesion strength of polyethylene film, heat-treated, metal-catalysed oxidation 3-73057
- adhesive joints, effect of feeble electric fields and surface treatment 3-64963
- AISI 4340 foil, stress corrosion cracking in aqueous acid solns. 3-69257
- analysis, using styluscope SL-12 (*Russian*) 3-62368
- anisothermal stress relax. processes 3-69279
- archive samples, metallographic exam. 3-80258
- armature, thermally hardened, nominal yield stress rel. to load and composition, statistical anal. 3-55800
- ASTM A533-B, fatigue crack propag. behaviour, temp. and neutron irradiation effect 3-44611
- austenite, deformation, recrystallisation kinetics, Nb effect (*French*) 3-72872
- austenite, dissolution kinetics of $M_{23}C_6$ carbides 3-64839
- austenite, effect of heat shocks on transform. kinetics and morphology in lower bainite region 3-64820
- austenite, nucleation of pearlite at grain boundaries 3-58635
- austenite, solid soln. decomp., dislocation effects 3-50710
- austenite, stainless, low cycle fatigue, high temp., fracture surfaces, electron microscopy 3-44637
- austenite, transformation rel. to thermomechanical treatment (*German*) 3-76151
- austenite EI-257, prolonged ageing influence on hardness and sub-struct. (*Russian*) 3-80273
- austenite form. during accelerated heating (*Russian*) 3-41695
- austenite grain refining, deform. effect 3-55825
- austenite stabilisation rel. to heat treatment 3-80219
- austenite thermal stabilization kinetics 3-50728
- austenite transform., Mn dendritic segregation effect 3-50684
- austenitic, analysis of precipitation of σ phase (*Polish*) 3-72843
- austenitic, containing Si on Ti, phase characteriz. 3-69222
- austenitic, corrosion due to Cs at the fuel/cladding interface in a fast breeder reactor (*German*) 3-71307
- austenitic, Cr-Ni, solubility of N, temp. and Cr content depend. (*German*) 3-47367
- austenitic, high-Mn, 110G13L, fine structure after high-speed straining (*Russian*) 3-64836
- austenitic, in pile compatibility with nuclear reactor oxide fuel elements (*German*) 3-71313
- austenitic, intergranular corrosion rel. to deformation degree (*German*) 3-76194
- austenitic, low C, high temp. creep deformation, surface struct. (*Japanese*) 3-76168
- austenitic, magnetiz. variation near martensitic pt., role of positive and negative interactions (*Russian*) 3-75852
- austenitic, micro-yield region behaviour, stress/residual strain curves (*Russian*) 3-58648
- austenitic, N alloyed Cr-Ni intergranular corrosion caused by Cr_2N precipitation, thermodynamic interpretation (*German*) 3-47368
- austenitic, Ni-P, martensite temp. decrease due to incoherent particles (*German*) 3-47357
- austenitic, quenched, reaction kinetics in bainitic region (*French*) 3-41700
- austenitic, stainless, deformed Type 316, microstructural characterization as function of deformation 3-47393
- austenitic, stainless, Type 316, microstruct. stability of thermomechanically pretreated type 3-47392
- austenitic, time temp. precipitation diagram, X-ray and electron microscope obs. (*German*) 3-47364
- austenitic stainless, α -irrad., recrystn. influence on high-temp. embrittlement 3-44614
- austenitic stainless, a.c. electroetching for metallographic differentiation of δ -ferrite (*German, English*) 3-64866
- austenitic stainless, chloride stress corrosion cracking, design of containment spray additive system, nuclear reactor appl. 3-67425
- austenitic stainless, cold working effect on helium embrittlement and creep rupture 3-44612
- austenitic stainless, corrosion by Na and H_2O in nuclear reactor pressure vessels 3-74719
- steel continued
- austenitic stainless, crit. work hardening of nucleation and migration for recrystn. (*French*) 3-61152
- austenitic stainless, cyclic stress/strain curves in M_s - M_d range 3-64829
- austenitic stainless, durability during low-cycle torsion in corrosive solns. (*Russian*) 3-80324
- austenitic stainless, extrinsic grain boundary dislocations, diffraction contrast effects 3-61156
- austenitic stainless, irradi., with Ti and B additions, high-temp. deform. and fracture 3-63188
- austenitic stainless, long-term sodium exposure effects on comp. and microstruct. 3-40555
- austenitic stainless, low temp. deformation, mag. susceptibility, martensitic transformation 3-50720
- austenitic stainless, low-C, corrosion-fatigue failure, elevated temp. (*Russian*) 3-58646
- austenitic stainless, thermal expansion, Young's modulus, magnetostiction, 80-280K (*Russian*) 3-44604
- austenitic stainless steel, mag. and thermal props. at low temp. 3-44609
- austenitic stainless steel, void volume swelling rel. to grain size 3-64864
- austeno-ferritic stainless, struct. development by holding between 600 and 1100°C (*French*) 3-44582
- bainite Fe-C-Si, austenite decomp. kinetics (*French*) 3-47358
- bainite hardenability treatment increase during thermomech. treatment 3-50742
- bainitic ferrite nucleation and growth depend. on austenite pretransform. state (*Czech*) 3-55760
- bainitic ferrite nucleation and growth depend. on pretransform. state of austenite (*Czech*) 3-55758
- balls, rupture testing, ultracentrifuge, rotating mag. field, stress at centre of ball, residual deformation 3-53304
- balls, wear, effect of lubricating oils, universal four-ball machine 3-53307
- Barkhausen effect, crack growth determ., tensile tests 3-69237
- Bauschinger effect, torsional prestrain effect 3-64928
- beam, plastic bending and failure by low cycle fatigue 3-80520
- bimetallic discs, steel/Cu, stressed state characteriz. 3-44633
- boiler tube billets, n.s. inspection, flow detection quality of tubes rel. to macrodefects 3-53303
- borated, residual stress curve predeterm. (*Russian*) 3-80320
- boride layer growth, carbon influence (*Czech*) 3-55803
- borided, B diffusion saturation, mag. powder metallography 3-80281
- boriding in powder mixture, high wear resistance 3-80350
- boro-carburization, B_4C -alkaline carbonate bath dipping (*Japanese*) 3-72908
- boron stainless, uncoupling effects, shell containing ^{235}U spheres, immersion in UO_2 (NO_3) $_2$ solutions 3-63196
- Brinell hardness testing, difficult to reach areas, polystyrene replica 3-5806
- brittle failure and means of prevention 3-47428
- brittle fracture, microscopic crack growth 3-58639
- brittle fracture susceptibility interrelationships (*Russian*) 3-80325
- brittle strength, cladding layer effect 3-76213
- brittleness, strain ageing rel. to drawing temp. 3-76215
- carbon-manganese and as-rolled mild, silicon and nitrogen influence on impact properties 3-68332
- carbonitrided, wear behaviour 3-64956
- carbonitriding, surface hardening, corrosion and wear resistance 3-80351
- carburized, quenching in fluidized bed effects on struct. and props. 3-50735
- case depth and C determ. by electron microprobe 3-73956
- case hardening depth, nondestructive detn. using ultrasonics (*French*) 3-58790
- castings, Cr-Mo-V, strength and deformability under creep rupture stresses (*German*) 3-47400
- castings, low-alloy, solidification behaviour 3-64901
- cementite, dynamic spheroidization, electron microscope obs. 3-50714
- cementite, solubility of alloying elements, Si, Mo and Cr (*German*) 3-76160
- cementite particles, dissolution, in situ obs., h.v. electron microscopy 3-50706
- chemical analysis, H_2 content, rapid determination (*German*) 3-66440
- chemical analysis of H_2 content, carrier gas method (*German*) 3-66442
- cladding- UO_2 composite body heat conduction with simultaneous solidification and melting 3-54548
- cold-rolled, inspection using Lamb waves 3-41832
- cold-rolled strip, rapid cooling under tension during annealing (*German*) 3-80300
- component and small specimen block load fatigue test data comparison 3-65045
- composite, filamentary, prestrain effects on tensile props. 3-64996
- compressive strain hardening rel. to C content 3-80372
- Comsteel En 25, fracture toughness 3-64896
- constrained disc burst tests, elastic-plastic analysis 3-50822
- constructional, crit. opening and cracks and fracture microstruct. (*Russian*) 3-80255
- converter, Nb-microalloyed, precip. processes (*Slovak*) 3-55773
- corrosion cracking stability in hot chloride solns., nitriding effect (*Russian*) 3-80335
- corrosion fatigue inhibitor behaviour (*Russian*) 3-58653
- corrosion fatigue of thermomechanically treated steel, H_2SO_4 soln., cyclic strength (*Russian*) 3-41766
- corrosion fatigue strength in sea water, cathodic polarization influence (*Russian*) 3-80316
- corrosion fatigue testing, environmental and superimposed wave effects (*Japanese*) 3-41830
- corrosion inhibition by chemical composition modification rel. to nuclear reactor fuel element cladding 3-71308
- corrosion protection, sputtered surface of Fe_2O_3 , r.f., structure and electrical props. of film 3-47436
- corrosion resistance improvement by Sn diffusion coating 3-80338

steel continued

- corrosion-resistant, potentiodynamical method for intercryst. corrosion sensitivity estimation (*Czech*) 3-55805
- crack detection, u.s. shear wave techniques, influence of residual stress 3-47514
- crack development resist. and yield stress, temp.-rate relationships (*Russian*) 3-58651
- crack growth law, fatigue failure, statistical analysis 3-80366
- crack propag. resist. of components, surface layer structural state influence (*Russian*) 3-58644
- creep, cyclic rate change, rel. to non-steady-state loading parameters 3-61176
- creep, defect behaviour, stress concentrator effects 3-69319
- creep and tensile props. of Type 304 stainless plates 3-47435
- creep rupture as cause of operational damage (*German, English*) 3-61174
- creep rupture behaviour, 500-700°C, Rajakovich method (*German*) 3-47397
- creep tests, supporting effect of bending specimens, 400-500°C (*German*) 3-69421
- cyclic nonisothermal elastoplastic loading, diagram represent. 3-69431
- cylindrical specimen with ringcrack applic. to strength determ. in material with brittle fracture (*Russian*) 3-41760
- cylindrical steel, dynamic deformation behaviour, compression wave 3-80374
- damping of vibrations, noise producing, vibration absorption by steel-viscoelastic-steel composites 3-70275
- desorption of H₂ from stainless steel surface, spatial distribts. 3-55154
- die, resistance to fracture 3-55817
- diffusion coeff., elec. transport of C in transeutectoid steel (*Russian*) 3-76163
- diffusion Cr plated, corrosion stability in nitric acid medium (*Russian*) 3-80336
- diffusion mobility of hydrogen, temp. and time depend. (*Russian*) 3-41718
- direct-replica prep. technique 3-46581
- disc reinforced polycarbonate, strength improvement 3-80440
- dislocation distrib. at 650°C, stress effect (*Russian*) 3-58628
- dislocation struct. and internal oxidation, cooling rate during solidification effect (*Russian*) 3-53220
- dispersion hardening, time-to-rupture and substruct. under u.s. treatment (*Russian*) 3-53247
- drilling of G₁₃, 45 and R₁₈ F5K, types, effect of liq. Sn-Zn eutectic (*Russian*) 3-76311
- ductile-brittle transition, Mossbauer and X-ray obs. 3-55815
- ductility, fuel cladding, solid loaded irradiated 3-47433
- duplex, heat treatment, aging, precipitate compositions 3-64850
- elastic moduli, neutron irradiation effect 3-69272
- elastoplastic deformation effects at temps. above M_s (*Russian*) 3-69186
- electrochemical dimensioning of steel 45 (*Russian*) 3-72898
- electron bombarded, low-temp. reversible disorder-order phenomena and carbon redistrib. (*Russian*) 3-69187
- electron microscope determ. of ductile component in fracture 3-62282
- electrotechnical, dynamic mag. props. description method (*Russian*) 3-79866
- embrittlement, 500°F, fracture toughness (*Japanese*) 3-76202
- embrittlement by hydrogen, dislocation stability influence (*Russian*) 3-80326
- embrittlement by hydrogen, galvanic chrome plating, technological factors influence (*Russian*) 3-80319
- En352, ion implantation, friction changes 3-47410
- endurance at normal and low temps., effect of surface finish and surface treatment method 3-44634
- eutectoid-composition, finely spheroidized, thermal mech. treatments influence 3-53258
- fast reactor, void formation by ion bombardment 3-71284
- fatigue, size effect, X-ray obs. of machine parts 3-64882
- fatigue bending tests, stress gradient as cause of scale effect in brittle fracture 3-58782
- fatigue crack initiation and propagation from different configuration notches, effect of mean stress 3-41749
- fatigue crack propag., crit. range of stress intensity factor 3-69286
- fatigue crack propag. vel., depend. on degree of rarefaction of air, apparatus design (*Russian*) 3-80510
- fatigue failure, effect of hardening induced by cyclic overloading 3-58683
- fatigue fracture rel. to inelastic deform. in torsion 3-47422
- fatigue props. rel. to inclusion size, shape and distrib. 3-61178
- fatigue strength, corrosion fatigue failure, humidity depend. (*Russian*) 3-41764
- fatigue strength, effect of alloying element C and heat treatment, reln. to static strength 3-41750
- fatigue strength, loading freq. depend. 3-44629
- fatigue strength, lubricating materials influence (*Russian*) 3-58655
- fatigue strength change during explosive strengthening 3-64944
- fatigue strength of Al coated steel 3-55797
- fatigue tests, h.f., energy dissipation 3-58694
- fatigue tests, low cycle fracture resist. in stress conc. zones, high temp. 3-69435
- Fe-C-V, crystal segregations, eutectic carbide precipitations, effect of alloying elements, Cr, Mo, W and V (*German*) 3-72845
- ferrite, vanadium carbide precip. phenomena 3-69225
- ferrite-class, substructure and its effects on mech. behaviour (*Russian*) 3-53225
- ferrite-perlitic network structure, micromechanisms of fracture 3-64905
- ferritic, quenching and tempering effects on stress corrosion cracking 3-64880
- ferritic stainless, 475°C embrittlement phenomena 3-64914
- field-ion atom-probe analysis applics. 3-76170
- fracture, effects of type II MnS inclusions 3-69223
- fracture, quasibrittle, ferritic matrix, stochasticity (*German*) 3-47396
- fracture of notched plates, J-integral use 3-64890
- fracture safe assurance, toughness variations influence 3-50744
- fretting fatigue strength 3-44594

steel continued

- fusion reactor blanket, Na cooling, neutron and gamma heating rates 3-60328
- fusion reactor blanket design features, choice of constructional materials 3-67584
- grain refinement by rapid cyclic heating 3-61169
- graphitic cast, graphitization behaviour 3-50685
- hardened, fatigue limit parameters 3-64939
- hardened, martensite atomic and mag. struct. 3-41742
- hardened, microstruct. of breaks and fracture toughness (*Russian*) 3-41716
- hardened, segregation phenomena and fractography (*Russian*) 3-55781
- hardness of specimens with 15% and 55% carbon, ultrasonic vibro-indentation testing 3-41753
- heat resistance, chem. comp. effect 3-55824
- heat resistant, tensile strength, statistical analysis 3-80375
- heat resistant low-alloy CrMoWV type, Ti and Zr effects on long-term plasticity 3-69323
- heat resistant low-alloyed CrMoV type, probability interpret. of creep (*Czech*) 3-55804
- heat treated, inspection by electromagnetic comparator (*German*) 3-69417
- heat treated, residual stress distrib. (*Japanese*) 3-41777
- heat treated to different strength levels, adsorptional relief of failure (*Russian*) 3-58650
- heat treatment, relaxation strength relations 3-55801
- heat-resistant, deform. and destruction in thermal fatigue and creep 3-64937
- heat-resistant materials, failure at low number of cycles of simultaneous temp. and load fluctuations 3-44625
- high tensile, fatigue crack growth at low stress levels (*Russian*) 3-69305
- high tensile, stress analysis of tubular samples, influence of geometry on load carrying capacity (*Russian*) 3-76221
- high tensile structural and welded joints, fatigue strength 3-44596
- high-alloy, P spectrometric determ. (*Japanese*) 3-70478
- high-alloy Cr and Cr-Mn, metallographic studies as supplement to short-time corrosion tests 3-44623
- high-C, chromium effect on hardenability (*Korean*) 3-53256
- high-C, dynamic elasticity and vib. decrement, 20-1200°C, obs. and mechanism (*Russian*) 3-53249
- high-Ni, martensite decomp. during tempering (*Russian*) 3-72827
- high-Ni, martensitic transform. kinetics of deformed austenite (*Russian*) 3-80206
- high-speed, welded blanks, struct. and props. after annealing 3-55814
- high-speed maraging Fe-Co-W type, strengthening phases nature (*Russian*) 3-80308
- high-strength, brittle fracture resistance 3-44631
- high-strength, corrosion cracking in NaCl soln., electrochem. soln. and hydrogen embrittlement role (*Russian*) 3-80334
- high-strength, creep rupture behaviour, effect of interruption in mechanical stress (*German*) 3-69253
- high-strength, crippling allowables for elevated temp. and creep environments 3-64962
- high-strength, hydrogenated, relax. effect on mech. props. (*Russian*) 3-80315
- high-strength, quenched, short-term testing props. correl. with fatigue limit (*Russian*) 3-80321
- high-strength, test method for transient stress conditions characteriz. at elevated temps. 3-69432
- high-strength 4340M, grain refinement effect on microstruct. and mech. props. 3-64854
- hot deformation cracking, rel. to δ -ferrite content 3-80280
- hot torsion tests for solid and tubular specimens, specimen geometry effect 3-55925
- impact by plane lead plate at 500 m/s, boundary instability (*Russian*) 3-64086
- impact test, repeated tension loading (*German*) 3-76395
- impact toughness, brittle fracture, -160-100°C, nitriding effect 3-80348
- inclusions, nonmetallic, effect of sectioning errors on microscopic determ. 3-69229
- inclusions, nonmetallic, local isolation by electron irradiation method 3-51741
- induction hardened, fatigue strength, tempering temp. influence (*Japanese*) 3-41778
- industrial atmospheric corrosion behaviour prediction 3-69261
- ingot, temp. and internal stress distrib. on cooling 3-69321
- ingots, ShKh15, electron beam effects on melting (*Russian*) 3-72924
- intercrystalline crack formation, heat treatment and creep conditions influence (*German*) 3-80302
- intergrain slip, in molten zone, arc welding, interferometry, statistical anal. (*Russian*) 3-41790
- internal friction rel. to thermomechanical treatment, martensitic transformation 3-80352
- ion bombardment, ³He⁺, He distrib. profiles, ³He(d,p)³He reaction 3-63209
- irradiated reaction products identification by electron probe microanalysis and gamma-ray spectrometry 3-66447
- isothermal internal friction technique applic. to precip., Cu-bearing type steels 3-80268
- joints, high-strength, with low-strength weldment 3-69295
- Knoop microhardness analysis 3-61242
- laser absorption waves, coupling loss mechanism, exptl. obs. with 5 ms 10.6 μ radiation 3-66858
- ledeburitic, carbide distrib. charact. by stereometric analysis (*German, English*) 3-53235
- LMFBR subassembly duct wall, thermal stress analysis for severe thermal loading 3-46161
- low alloy, stress corrosion cracking initiation mechanism 3-64881
- low-alloy, phase anal., microprobe anal., electron microscopy 3-76179
- low-alloy chromium type, charact. struct. rel. to ductile/brittle transition (*Russian*) 3-55780
- low-alloy corrosion by Na and H₂O in nuclear reactor pressure vessels 3-74719

steel continued

- low-C, aging, structural changes electron microscope studies 3-47388
- low-C, corrosion by Na and H₂O in nuclear reactor pressure vessels 3-74719
- low-C, creep delay at room temp. 3-44628
- low-C, cyclic loading effect on subsequent yielding 3-44593
- low-C, delayed yielding and hysteresis phenomenon under tensile fatigue load 3-44595
- low-C, diffusivity of hydrogen, room temp. obs. (*Japanese*) 3-41727
- low-C, durability during low-cycle torsion in corrosive solns. (*Russian*) 3-80324
- low-C, dust particle erosion rates 3-76279
- low-C, effects of melting processes, microstructures, season and annealing on sliding wear behaviour 3-41754
- low-C, embrittlement, micromechanisms of cementite function (*Slovak*) 3-55774
- low-C, fatigue crack propag. under doubly repeated stress, residual stress and plastic strain (*Japanese*) 3-41734
- low-C, form. of δ' -nitride and niobium carbonitride (*Russian*) 3-72856
- low-C, high strain fatigue tests, weld effects 3-69317
- low-C, low cycle fatigue concepts extension 3-69318
- low-C, mechanical properties, effect of interruptions in loading 3-55916
- low-C, plastic deformation, microyield region, dislocations, electron microscopy 3-80287
- low-C, plastic instability phenomena (*French*) 3-69301
- low-C, pressurized, Portevin-Le Chatelier effect 3-80289
- low-C, prestrained, temp. effect on mech. props. anisotropy 3-47427
- low-C, texture form. during deform. (*Russian*) 3-53218
- low-C, use in boiling water reactors, critical concentration of O₂ and Cl (*German*) 3-67594
- low-C, wear characts. rel. to surface temp. (*Japanese*) 3-44620
- low-C austenite, transform. to ferrite after small plastic strains 3-58615
- low-C chromium, M₃C to M₇C₃ transform. 3-80210
- low-C electromelted, comp. and complex deoxidizing effects on mech. props. (*Russian*) 3-58647
- low-C quenchability rel. to alloying additions and cooling rate (*French*) 3-69294
- low-C unalloyed, strengthening by small Nb additions 3-64922
- low-C vanadium, controlled-rolled and continuously cooled, microstruct. obs. by TEM 3-80259
- machine parts, surface work hardening for increase of low cycle fatigue resist. 3-44632
- maraging, Co influence on ageing mechanism (*Russian*) 3-53243
- maraging, fibre reinforced Cu alloys, cold drawing 3-64994
- maraging, low cycle fatigue props., hydrostatic press. effect 3-80519
- maraging, microstruct., strength and toughness 3-44598
- maraging, struct. evolution under high speed cumulative thermal cycling (*French*) 3-80267
- maraging, synergistic Co-Mo age-hardening interaction in Fe-10%Mn martensite 3-69284
- martensite, ferrous, tempered, ion microscopic study, effects of carbon content, lattice strain 3-58630
- martensite, fracture surface charact., quant. evaluation 3-64906
- martensite, loading effect in macroelastic range on X-ray diffr. line-width (*Russian*) 3-61133
- martensite, manganese substitution reaction during tempering, kinetics (*German*) 3-80301
- martensite, residual microstresses, internal friction peak height change at 200°C 3-58672
- martensite fracture surfaces, quantitative characts. (*Russian*) 3-58623
- martensitic, internal friction and isothermal aging, -50 to 25°C (*French*) 3-64931
- martensitic, stress corrosion cracking susceptibility (*Czech*) 3-55806
- martensitic high-strength, stress corrosion cracking resist. (*French*) 3-47415
- martensitic Ni-Cr-Mo-Co, toughness and strength characteriz. 3-64915
- martensitic transformations, crystallographic theory 3-76158
- martensitic transformations of Mn-type, stacking fault density variation in austenite (*Russian*) 3-72824
- martensitically-aged, cracking in H₂S and NH₄CNS solns. (*Russian*) 3-58659
- mechanical characteristics, etching medium comp. influence (*Russian*) 3-61164
- mechanical properties obs. by mag. field induced rot. sphere method (*Russian*) 3-80313
- medium-C, cyclic loading, dynamic deformation aging 3-80364
- melt, precipitation hardening, recrystallisation temp. 3-76214
- melt, reactions with refractory materials, silica and silica-containing materials, calc. O₂ diffusion (*German*) 3-72969
- metallurgical equipment materials, thermal fatigue mechanism 3-69316
- metastable austenite form. during heating (*Russian*) 3-44601
- microalloyed structural, metallographic investigations by phase diagrams (*German*) 3-80202
- microanalysis, laser with controlled excitation delay, in plasma (*Russian*) 3-70490
- microstructure, G.TsK polycrystals, effects of deformation hydrostatic pressure, dislocations, X-ray examination (*Russian*) 3-55787
- mild, cavitation erosion for low cavitation intensity 3-41751
- mild, dislocation loops generated by 1 MeV electron irrad., 550° C 3-76171
- mild, plates, yielding in front of through cracks in pure bending 3-76382
- mild, plotting full fatigue curves problem 3-58673
- mild, recrystallisation, texture, Al passivation effect (*French*) 3-76173
- mild, stress corrosion cracking by nitrate solutions 3-55794
- mild, stress corrosion cracking by phosphate solution 3-55795
- mild, stress wave propagation, obeying the constitutive eqn. of the Johnston-Gilman type 3-64088

steel continued

- mild, tubular specimens, precise meas. of plastic behaviour under combined torsion/axial force 3-76199
- mild, twins influence on fracture 3-69282
- mild, uncoupling effects, shell containing ²³⁵U spheres, immersion in UO₂ (NO₃)₂ solutions 3-63196
- molten, sampling probe evaluation and testing (*German*) 3-76190
- monotonic concentration factor, localised and gross plasticity effects 3-64903
- Mossbauer effect, local mag. struct. of carbides formed during ϵ - χ - θ transforms (*Russian*) 3-79951
- Mossbauer obs. of industrial Fe-C steel, mag. hyperfine field and quadrupole splitting (*Rumanian*) 3-47188
- moving coil magnetometer, for coercive force of soft steel 3-62186
- nichrome, corrosion resistance in Al₂Br₆ and Al₂Cl₆ eutectic (*Russian*) 3-75684
- non-linear material beam, structural behaviour at finite deformation 3-54112
- non-propagating fatigue crack hypothesis 3-55796
- nondestructive testing, u.s. variable angle transducer, welded steel pipe 3-47505
- optimal heat treatment conditions for machinability improvement 3-50738
- oxidized, corrosion and electrochem. characts. 3-50730
- pearlite transform., isothermal, manganese role (*Japanese*) 3-41697
- pearlitic, work hardening rate 3-69298
- permeability of hydrogen, structure influence (*Russian*) 3-80254
- permeation tests, He (*German*) 3-72887
- phase anal. by Faraday method 3-75853
- phase analysis, methodology (*German, English*) 3-69202
- phase transformation characts., low-temp. DTA obs. (*German*) 3-64832
- phosphated, hydrostatic extrusion, nonuniformity of deform., lubricating medium influence (*Russian*) 3-69326
- photometric determ. of Al after separation on a cation-exchanger (*German*) 3-45603
- plasma torch, 100 KW DC for varied steel cutting 3-72928
- plastic, critical stress intensity factor, determ. methods 3-58684
- plastic bending of edge-cracked specimen 3-64897
- plastic deform. of microstruct. below honed surfaces (*German*) 3-41743
- plastic deformation, hardening in NaCl soln., annealing, uniaxial compression diag. (*Russian*) 3-41767
- plastic deformation, wear resistance rel. to additions 3-80347
- plastic deformation, X-ray obs. of effect of stacking faults in 0Kh18N10T steel (*Russian*) 3-69269
- plastic deformation and ageing effects on structure and mech. props. (*Russian*) 3-69265
- plastic deformation investigation using exoelectron emission 3-48585
- plastic flow irregularity, microhardness indentations method, fracture zone 3-76399
- plastic low-alloy, alkaline cracking under steady pot. (*Russian*) 3-41719
- plastic shear props., high strain rates 3-58787
- plate, anisotropic, notched, upper field strength, stress-strain, finite element anal. (*Japanese*) 3-55798
- plate, Charpy-V impact props., stat. analysis 3-50824
- plate, notched, elastic stress distribution rel. to curvature 3-80370
- plate, notched, stressed state, thickness depend. 3-80362
- plates and strips, simple u.s. testing equipment for defect indication efficiency of 100% (*German*) 3-47520
- plates with oblique hole, corner shape effect on elastic stress and strain conc. 3-50823
- polymer coated plate, effect of internal stresses in the coating on vibrations and static bending 3-58671
- potentiostatic structure development for detection of precipitates, etching tests (*German*) 3-47369
- precipitation hardened, heat treated under relative stable conditions, recovery creep props. 3-69313
- precipitation strengthening, heat treatment effect on niobium precipitates 3-72862
- pressure vessel, brittle strength eval. 3-58693
- pressure vessel, low-alloy, correlation between microstructure and electron fractography 3-47389
- pressure vessels, struct. stability characteriz. 3-69322
- pressure vessels, thick-walled, fracture mechanics aspects 3-76409
- pressure vessels for LWR, in-service exam. 3-67456
- quenchability influence on carbide precip. during continuous cooling (*French*) 3-47416
- quenched, residual austenite obs. (*Russian*) 3-53216
- quenched, substruct. changes during heating (*Russian*) 3-53213
- quenched, tempered, fine structure rel. to wear deformation 3-80279
- radiographic examination, equivalent penetrometer sensitivity 3-65050
- with rare earth additions, brittle fracture susceptibility rel. to state of grain boundaries (*Russian*) 3-72894
- rare-earth inoculated, contact microradiography obs. 3-61146
- reactor structure, mechanical properties, strain-rate influence, meas. equipment 3-67537
- recrystallisation, structural inheritance, overheating and tempering temp. depend. 3-80282
- reflector in EBR-II, reactivity feedback analysis 3-46131
- reinforcement bar, deformation, fatigue strength, spot welding effect (*German*) 3-44638
- reinforcing, cyclic load behaviour 3-64935
- residual austenite behaviour during deform. (*Russian*) 3-41756
- resulphurized, solidifying rate and form. of sulphide inclusions 3-61181
- ribbon reinforced Al composite, fatigue strength behaviour 3-41809
- SAE 4340, fatigue life and inelastic strain response under complex history 3-69289
- sampling, H₂ evolution anal., technical steel heats, effect of alloy composition and structure (*German*) 3-66441
- scale effect in fatigue and corrosion fatigue 3-41785
- secondary martensite struct., atomic ordering effect (*Russian*) 3-61134

steel continued

- serrated grain boundaries form. during hot deform. (*Russian*) 3-80252
- sheet, Al-stabilized, directional depend. of integral breadth of diffraction profile and microbeam spots (*Japanese*) 3-41729
- sheet, with 4.5-7.7%Si, mag. and mech. props. (*Japanese*) 3-41787
- shock and rarefaction waves, structure rel. to heat treatment (*Russian*) 3-64110
- shock wave interaction with wedge shaped cavity (*Russian*) 3-80304
- shock-hardening, by laser 3-69291
- short-time stress/strain characteristic, temp. depend., thermally activated models 3-69309
- shot peening, surface stress and strain 3-76196
- sintered, fracture-resistance, Cu and carbon addition effects 3-69307
- sintered R18 steel, structure and props. 3-80396
- slab, solidification simulation, thermohydraulic analog model (*German*) 3-76149
- solidification, calc. interdendritic C, O enrichment (*German*) 3-69251
- solidification rate calc., heat balance integral (*German*) 3-76148
- spring, fatigue phenomena in large plate specimen after shot-peening treatment (*Japanese*) 3-41779
- stainless, 17 wt.% Cr, microsegregation of alloying elements, high temperatures 3-76205
- stainless, 18 Cr-8 Ni, pitting and crevice corrosion, OH⁻, SO₄²⁻ and NO₃⁻ ions effect (*Japanese*) 3-72907
- stainless, 18Cr-8Ni, rapidly deformed, temperature rises meas. (*Japanese*) 3-41781
- stainless, 20% Cr/25% Ni niobium stabilized, acetone heterogeneous decomposition 3-71299
- stainless, 304, thermal cond. and elec. resist. meas. up to 1200K 3-52817
- stainless, adsorption of stearic acid, contact angle rel. to surface coverage 3-43933
- stainless, AISI Type 304, high strain rate tensile props. 3-80386
- stainless, austenitic, neutron irradiated, fracture surfaces, Auger spectroscopy 3-69248
- stainless, austenitic, stress corrosion cracking, electrochemical testing method by separating crack anode from cathode 3-47492
- stainless, austenitic transmission electron microscopy, 2.5 MeV, penetration meas. 3-56982
- stainless, bonded with sodium, compatibility with carbide fuel, carbon transfer kinetics 3-43307
- stainless, carburization-decarburization in Na environment 3-63215
- stainless, cold work meas., nondestructive methods 3-47504
- stainless, cold-worked, neutron irradiated, void formation, effect of irradiation temp. 3-68289
- stainless, corrosion by liquid sodium 3-43310
- stainless, corrosion pit, pot. distrib. 3-64929
- stainless, decontamination of impure specimens and Al/steel couples 3-60283
- stainless, dendritic structure dispersion rel. to solidification rate 3-80278
- stainless, dispersion form. of carbides, nitrides (*French*) 3-53231
- stainless, duct pressure response anal., FFTF fuel assembly, ANSYS computer code 3-71293
- stainless, fast neutron irradiated, fatigue propagation 3-69296
- stainless, fragmentation, molten fuel-coolant interactions, Na coolant 3-74730
- stainless, gas evolution in a high vacuum 3-55155
- stainless, He-implanted, elevated temp. fatigue characteristics in reln. to fusion reactors 3-61183
- stainless, heating surface, effect of thermophys. props. on heat transfer during boiling of water and ethanol 3-52693
- stainless, high-silicon, intercryst. corrosion susceptibility 3-50713
- stainless, implanted He, effect on fatigue life, microstructural effects 3-64947
- stainless, in EBR II, anisotropic scattering calc. 3-46071
- stainless, instantaneous strain, proof stress, creep rupture testing 3-47437
- stainless, intercryst. corrosion causes 3-50711
- stainless, martensite reversion to austenite, strengthening effect 3-80214
- stainless, martensitic cast, phase anal., microprobe anal., electron microscopy 3-76179
- stainless, mech. props. determined in high-speed extension (*Russian*) 3-53250
- stainless, Mossbauer linewidth due to hyperfine interactions 3-47175
- stainless, Mossbauer spectra isomer shift, pressure depend. 3-72554
- stainless, neutron irradi. effect on elastic consts., ultrasonic technique 3-78386
- stainless, nickel ion bombarded, gross swelling direct meas. 3-40540
- stainless, nitrided, phase identification 3-64838
- stainless, nuclear reactor fuel, performance in pressurised water reactor, Indian Point Unit No. 1 3-67569
- stainless, porous, thermal and electrical conductivity prediction 3-76392
- stainless, reflector in EBR-II, loading, startup, and initial operation 3-46130
- stainless, reflector in experimental breeder reactor for use as irradiation facility 3-71196
- stainless, strengthening by deform., martensitic transform. and ageing 3-50731
- stainless, strengthening by direct and reverse martensitic transforms. 3-50732
- stainless, stressed during irradi., microstruct. obs. 3-69245
- stainless, structure sensitive fatigue fracture 3-58663
- stainless, thermal diffusivity meas., rel. to Hf and Zircaloy-2, thickness effect 3-44556
- stainless, Type 304, effect of exposed nonmetallic inclusions on corrosion resistance in simulated, reactor environment 3-53240
- stainless, Type 304, Ni ion bombardment, void swelling behaviour 3-46139
- stainless, type 304L, stress corrosion cracking and hydrogen embrittlement, dislocation density effects 3-53241

steel continued

- stainless, Type 316, cold-worked Frank loop development, irradiation effects 3-44576
- stainless, Type 316, helium re-emission and surface deform. during -170 to 700°C implantation 3-46651
- stainless, Type 316, irradi., stress-biased loop nucleation 3-67553
- stainless, Type 316, mech. and struct. props. for LMFBFR cladding, rupture 3-47394
- stainless, Type 316, proton irradi., void form. and hydrogen effects 3-46138
- stainless, Young's modulus, effect of neutron irradiation-induced void formation 3-68310
- stainless 18-8, embrittlement and phase transformation, H absorption (*Japanese*) 3-76201
- stainless 304, laser-supported absorption waves, 5-ms pulses of 10.6 μ radiation 3-72999
- stainless 304, vacuum degassed, obs. on adsorption of H₂, CO, O₂ 3-60836
- stainless Mossbauer spectroscopy by scattered electrons using proportional counter. 3-66384
- stainless steel surfaces, analysis by secondary ion mass spectroscopy 3-48675
- stainless steel/Al₂O₃ interfacial and adhesion energy meas. by SEM 3-75659
- static and fatigue props., temp. and strain rate influence 3-69312
- stator sheet, mag. induction rel. to annealing temp. and furnace atmos. 3-80354
- steel/Li system, adsorption role in mechanisms of intergranular penetration of metals by molten metals (*French*) 3-47383
- steel/Ti, explosion weld, effect of hot and cold rolling 3-72927
- Strainflex X-ray stress analyzer with Side Inclining method (*Japanese*) 3-39855
- strength, corrosion in caustic soda, heat treatment and H₂ absorption effect 3-80355
- strengthening mechanism, high-temp. thermomech. treatment (*Russian*) 3-80309
- stress distrib., magnetoelastic method 3-76397
- stress meas., X-ray diff. apparatus operating condition effects on line profile and peak position (*Japanese*) 3-40829
- stress meas. from spotty X-ray diff. rings, method (*Japanese*) 3-41731
- stress relaxation tests, bending, tension, time factor effect 3-50803
- stress state around nonmetallic inclusion, microthermal e.m.f. meas. (*Russian*) 3-61137
- stress state at fatigue crack tip obs. by X-ray microbeam technique (*Japanese*) 3-41736
- stress-rupture data, computerized time-temp. parametric analysis 3-50746
- structural, alternately stressed, stress relieving, diffusion of interstitial atoms (*German*) 3-69252
- structural, catalytic poisoning and stress corrosion cracking control 3-64889
- structural, creep tests, rel. to rectangular plates dimensioning 3-69438
- structural, crit. plane-strain stress intensity factor, tensile ductility, microscopic fracture mode 3-64888
- structural, ductility assessment on failure mechanics criteria basis 3-80377
- structural, fatigue resistance in biaxial state of stress 3-80378
- structural, low cycle fatigue effect on brittle fracture characteristics (*German*) 3-47523
- structural, medium-alloyed, transform. induced hardening of austenite (*Russian*) 3-72828
- structural, prefatigue influence on transition temp. (*German*) 3-69420
- structural, quenched and tempered, nitride phase effect on toughness 3-55822
- structural, reversible temper brittleness range, Mo and Ni content effect 3-80349
- structural, test for localized heating effects determ. 3-69436
- structural props. at cryogenic temperatures 3-64887
- structure, mechanical properties, of warm extruded austenitic stainless steels 3-50749
- surface decarburizing, approx. calc. method 3-50729
- surface layers under hydrostatic pressing, MoS₂ lubrication (*Russian*) 3-72896
- surface texture, persistence of asperities in indentation experiments 3-72125
- technical cohesive strength determ. from internal energy 3-44627
- tempering, carbide form. (*Russian*) 3-53242
- tempering and reheating effects 3-55821
- testing equipment, automatic, heat resistance, distortion due to temp. fluctuation 3-42531
- textured electrotechnical, normal induction components (*Russian*) 3-58397
- textured strip, bending influence on saturation magnetostriction (*Russian*) 3-53007
- thermal and mechanical properties, temp. depend., rel. to linear theory of thermoelasticity 3-59753
- thermal contact resistance between metal pairs, heat pulse meas. technique 3-70286
- thermal cycling, effect of chem. heterogeneity on distortion of C steel 3-80383
- thermal fatigue of 1Kh2M, effect of preliminary work hardening 3-80382
- thermal fatigue under complex stress distrib. conditions 3-58688
- thermodynamic activity measurement, radiometric method, ¹⁴C, C + 2H₂ = CH₄, equilibrium and kinetic study 3-54039
- thermoplastic hardening, heat resist. test from fracture toughness (*Russian*) 3-72899
- thermoplastic shear and fracture during high-velocity sliding in rocket-sled testing 3-50748
- through hardened, prediction of rolling-element fatigue lives 3-76226
- transformer type, thermomag. treatment effectiveness, sheet thickness and surface finish depend. (*Russian*) 3-68809
- tube, degree of oxidation influence on glass coating quality (*Russian*) 3-58657
- tuffrided, fatigue crack propag. rel. to substruct. (*Japanese*) 3-41733

steel continued

- UHB stainless 724LN, austenitic, improved creep strength mechanism 3-69324
 upper bainite struct. of silicon steel, morphology and substruct. (*Czech*) 3-55772
 u.s. attenuation rel. to temp. in 1% carbon steel 3-43834
 u.s. inspection, flaw detectability study, ASNT Sonics and Aerospace Committees 3-47517
 viscoelastic prop. effect on strain wave front 3-44597
 weakly textured electrotechnical grain size effects on mag. induction (*Russian*) 3-52993
 wear and friction during boundary lubrication, predeform. effect (*Russian*) 3-40968
 wear resistance, electrospray surface alloying effect 3-50739
 wear resistance increase by diffusional impregnation (*Russian*) 3-58656
 weld metal, low-alloy, thickness effect on fatigue crack propag. above and below general yield 3-47413
 weld metal, Type 316, tensile and creep-rupture props. 3-47434
 welded, crack formation and propagation behaviour under fluctuating stress 3-72911
 welded beams, fatigue crack growth eval. using fracture mechanics 3-64893
 welded joint, Cr-Mo-V high temp. type, creep rupture strength, structure (*German*) 3-47398
 welded joints, fatigue strength at high temp. and low cycle loading 3-44706
 welding, max. heating temp. calc. (*Russian*) 3-41789
 weldment, T-1 type, stress relief annealing (*Japanese*) 3-41774
 white layers formed during treatment, characteriz. (*Russian*) 3-80330
 wire, elec. resist. and tensile strength, effect of hydrogen, alcohols and moisture (*Russian*) 3-80314
 wire reinforced Mg-Li(8%) alloy, deform. and rupture (*Russian*) 3-73011
 wire-wrapped cylinder, fracture resistance 3-50825
 wires, fatigue, cycles to failure and stress to failure Weibull distributions 3-41833
 wires, tensile strength in aqueous-alcoholic and alcoholic HCl solns. with added Sb_2O_3 (*Russian*) 3-80331
 wrought, inclusions, quant. impurity indices 3-50693
 X-ray analysis of phases in austenitic stainless steel 3-47391
 X-ray stress meas. of specimen with steep stress gradient in near surface layer (*Japanese*) 3-41730
 yield stress in compression rel. to mech. props. 3-58681
 Zr/steel rolled joints, hydriding and protection in reactors 3-57572
 n shield, nuclear reactor, 1.5 ft thick, deep penetration cross-sections 3-74633
 B content analysis by activation and absorption method 3-66458
 Cr and Cr-Ni high-alloy steels, metallography, supplement to corrosion tests 3-47387
 13-Cr-Mo44 alloy, permeation rate of tritium, water moderated reactors (*German*) 3-71315
 Cr-Mn type, effect of carbon addition on mech. props. 3-47432
 Cr-Mo, quenched, crack propag. and creep conditions 3-69276
 Cr-Mo-Ni, softening of austenite, effect of deformation to fracture by tensile stress (*German*) 3-72888
 Cr-Mo-V, low-alloy, creep rupture strength, effect of carbide repartition (*German*) 3-69255
 Cr-Mo-V type, creep rupture of tubular specimens under axial loads and internal press. 3-69308
 Cr-Mo-V weld metal, fracture resist. under low cycle loading 3-58682
 Cr-Ni, austenitic corrosion-resistant, in welded sheet construction, grain disintegration (*German, English*) 3-69426
 Cr-Ni austenitic, creep rupture as cause of operational damage (*German, English*) 3-61174
 Cr-Ni austenitic stainless, a.c. electroetching for metallographic differentiation of δ -ferrite (*German, English*) 3-64866
 Cr-Ni type, austenite struct. and strength changes during ageing (*Russian*) 3-80277
 Cr-Ni-Mn type, strength and ductility, carbon and nitrogen conc. depend. 3-64785
 Cr-type, increase of hardness and dislocation density, effect of cathodic charging of H_2 3-80241
 Fe-Cr-C, austenite range, chem. diffusion, diffusion annealing, microprobe anal. (*German*) 3-72886
 Fe-Mn-C type, isothermal transform. induced struct. and props. 3-69224
 Fe-Si, graphite layer containing, wear, antifriction props. 3-80353
 Mn, high-manganese steel, dislocation structure and strain hardening (*Russian*) 3-69218
 Mn, kinetics and morphology of surface layer formation in liquid zinc (*Polish*) 3-72842
 Mn-Mo and Mn-Mo-Ni type, normalizing and austenizing effects on mech. props. 3-50747
 Ni 9%, low temperature notch toughness (*Japanese*) 3-41770
 Ni-Cr-Mo, medium-C type, impact toughness of martensite and bainite 3-61180
 Ni-Mo, post-sintering heat treatment and microstruct. phenomena 3-69306
 Ni-Mo-Cr alloy, for reactor vessel cladding, chemical analysis (*German*) 3-72929
 NiCrMo, mechanical hysteresis loop, Fortran program, low cycle fatigue test data processing (*Japanese*) 3-55799
 Si, grain growth modes by strain anneal 3-76169
 Si, grain orientated, mag. props. 3-50347
 Si-Mn type, comparative evaluation of performance 3-55917
 W-Mo high-speed, carbide phase behaviour 3-55813

steel manufacture

- dust elimination from gases, acoustic coagulation of O_2 aerosol 3-76390
 explosion welding Ti to steel, effect of hot and cold rolling 3-72927
- stellar atmospheres**
 A0Ia supergiants, non-LTE models and influence of He abundance 3-81031
 A-type supergiants, line intensities from high dispersion spectrograms 3-81097
 Algol-type binary secondary component, departures from LTE 3-51326

stellar atmospheres continued

- aligned rotating magnetosphere, general analysis 3-59330
 Aurigae, eclipsing binary, Ca I satellite lines rel. to expanding circumstellar cloud 3-53666
 B type, light ion spectra giving neon abundances 3-73493
 B-type main sequence stars, u.v. flux envelopes, 1100-6000 Å obs. 3-48026
 B-type stars, effective temp. determ. and comparison with model atm. 3-45095
 B-type stars, last Balmer lines and $\text{H}\gamma$ 3-61773
 BCA photospheric model, dissociation equilibrium 3-76970
 Be-type stars, i.r. excesses, low-temp. free-free emission 3-61757
 binaries, temperature distrib. using solns. to eqn. of transfer (*Russian*) 3-73488
 binary stars, evolution of circumstellar matter 3-77056
 close binary system, atm. interaction with X-ray source irradiation 3-73478
 binary X-ray sources, effect on atmosphere of binary companion, optical periodicity 3-51373
 α^2 Canum Venaticorum, spectrum variable, u.v. obs. of line blanketing 3-81039
 ν Capricorni, model-atmosphere abundance analysis of B9-type star 3-56388
 S Carinae, Mira-type variable, Coude spectra through cycle, atmospheric parameters 3-42191
 chromospheric activity of solar type, photoelectric obs. (*Italian*) 3-61788
 classical Cepheids, Q-method for colour excesses 3-45102
 close binaries, spectral type of cool component assuming convective envelope 3-47988
 convection in main-sequence stars and metal-deficient subdwarfs 3-51322
 curvature effects in extended atmospheres with pure absorption 3-51325
 V1016 Cygni, expansion, spectroscopic studies, emission line structure 3-69969
 density gradient inversions in stellar envelopes rel. to mass loss 3-45085
 differential rotation including spatial dependence of meridional circulation 3-81053
 dust formation in cool stars 3-77171
 dynamic process parameterization 3-73322
 early-type stars surrounded by dirty ice particles, interstellar extinction from i.r. to far u.v. wavelengths 3-61768
 early-type supergiants with variable $\text{H}\alpha$ profiles rel. to mass loss and turbulence 3-56375
 eclipsing binary system envelopes 3-53645
 eclipsing binary systems, light curve for objects with extensive atmosphere 3-77064
 electron density determ. using photoelectric spectrometer 3-61889
 envelopes, supercrit. luminosity, power dependence of opacity, effect of convection 3-69925
 ν Eridani, β Cephei variable, non-central H line filling-in 3-56392
 evolved stars, CN/ C_2 and CO/ C_2 ratios in cool C stars 3-81023
 expanding envelopes, structure and interpretations 3-77054
 extended and expanding atmospheres, theory 3-77055
 extended atm. stars., picket fence model 3-45086
 extended atmospheres and circumstellar matter in spectroscopic binary systems, IAU Symposium 51 (Parksville, Canada, 6-12 September, 1972) 3-77052
 F type, microturbulence rel. to temp., luminosity and metal abundance 3-69932
 fission in stellar plasma, of heavy nuclides, shell and surface symmetry effects 3-69940
 flare stars, photoelectric obs. (*Italian*) 3-61789
 flux constant line-blanketed model atmospheres for solar-type stars 3-77044
 Fm stars, incidence and abundance anomalies, curve-of-growth anal. 3-47987
 G type, microturbulence rel. to temp., luminosity and metal abundance 3-69932
 gaseous motion around stars 3-77053
 giants and supergiants, i.r. absorption due to SiO 3-81054
 HD 96446, H-deficient star, fine anal. 3-56393
 105 Her K4 II star, physical parameters, anomalous abundance of lithium (*Russian*) 3-77096
 hydrodynamics, eqns. describing rotating gaseous medium 3-47865
 K type, microturbulence rel. to temp., luminosity and metal abundance 3-69932
 late type stars model atmosphere opacity code for CN red system 3-69923
 late-type stars, effects of Rayleigh scatt. by atoms and negative ion absorpt. 3-51330
 late-type stars, importance of molecular Rayleigh scattering 3-65874
 ϵ Leonis, G-type giant, model atmospheres and high dispersion spectrograms 3-48051
 light scattering, superposition of layers in radiative transfer 3-47994
 LTE atm., effect of absorbers on thermal structure 3-73481
 magnetic null lines for mag. peculiar A-type star atm. studies 3-45115
 MHD stability, finite Larmor radius effects 3-80911
 microturbulence from photoelec. obs. of Fe I 6065 Å line 3-81018
 models, use in temperature-gravity calibration 3-81040
 moving atm., coupling between thermal conduction and radiative transfer 3-73483
 multiple scatt. of resonance radiation in plane layer and sphere 3-69918
 non-LTE line transfer, interpolation method for soln. 3-73484
 nova outburst interpretation rel. to thermal waves in stars 3-53649
 novae, origin of light, luminosity 3-65870
 α Orionis, model compared with scanner obs. 3-61798
 ι Orionis B, ^3He content from coude spectrogram 3-81099
 p-n junctions in pulsar magnetospheres 3-81124
 β Persei type, eclipsing, condition for atmospheric hydrostatic equilibrium. (*Russian*) 3-73489
 photon bubbles, analogy with fluidized bed 3-53651
 plane-parallel, matrix method for determ. of internal radiation field 3-69929

stellar atmospheres continued

- plasma oscillations in magnetic and gravitational fields, dispersion relations (*Russian*) 3-43669
- protostars, radiative energy loss from shock front generated during collapse 3-65877
- pulsar magnetosphere model of Goldreich-Julian 3-77121
- radiation absorption through photoionisation in magnetic field 3-77049
- radiative opacity, accuracy of metal absorpt. coeffs. 3-47982
- radiative transfer, integrated kernels and exact solns. to problems in spherical geometries 3-61758
- radiative transfer, numerical evaluation of formal soln. in spherical geometry 3-69935
- radiative transfer curvature effect, absorpt. and scatt. 3-69928
- radiative transfer H-matrix, existence and uniqueness theorems 3-56373
- radiative transfer in inhomogeneous magnetic field, numerical integration of equations (*Russian*) 3-77043
- radioactive envelopes, meridian circulation with rapid differential rotation 3-53636
- red giants of class III luminosity, convection in model envelopes 3-45084
- reddening law parameters calc. using atmosphere models (*French*) 3-77042
- resonance line formation in atm. filled by three-level atoms 3-71359
- Saha's equation, thermodynamic non-equilibrium 3-76952
- α Sculptoris, spectrum variable, u.v. obs. of line blanketing 3-81039
- self-consistent model computation for solar and stellar chromospheres 3-53612
- SMC stars, uvby obs. compared with LTE and non-LTE model atm. 3-48004
- spectra rel. to extended atmospheres 3-77082
- spectral line broadening, non-coherent scattering study 3-52376
- spectral line formation in extended atm. 3-51331
- spectral line formation in spherical atm. 3-45087
- spherical circumstellar dust shell, radiative transfer eqn. for polarised light scatt. 3-69954
- supergiants, line effects on radiative accel. 3-47981
- T Tauri stars, grain formation in expanding envelopes 3-48001
- T Tauri type, transition radiation from fast electrons in dust envelope 3-81032
- time dependent radiative transfer, development of formalism 3-59333
- transfer of polarised radiation, appl. to gray atm. 3-53637
- W Ursae Majoris systems, convective envelope model, light curve analysis 3-69926
- white dwarfs, dependence of envelope structure on surface gravity and composition 3-81030
- Wolf-Rayet, extended atmospheres and non-classical atmospheric models 3-77051
- Wolf-Rayet binaries and atmospheric stratification 3-81037
- Wolf-Rayet stars, theory of emission spectra, expanding envelope hypothesis 3-81062
- X-ray and radio emission from solar-type stellar coronae, model 3-45078
- X-ray radiation from stellar coronae rel. to soft X-ray background 3-42220
- CO vibration-rotation LTE in late-type star model atmospheres 3-61761
- Fe group elements, forbidden lines transition probabilities, tables 3-74814
- He envelopes of white dwarfs, upper bounds of mass 3-81211
- He I plasma spectral lines, Stark shifts 3-63868
- He I spectra in B stars, analysis 3-65881
- Si Ap stars, theoretical intensity of Si lines 3-53659

stellar binaries see binary stars

stellar clusters

- Basel 10, open cluster, UVB photometric obs. (*German*) 3-73541
- Basel 11 in Taurus, RGU-colour photometry 3-81174
- Berkeley 65, open cluster, UVB photometric obs. (*German*) 3-73541
- bolometric calibration and spectral type rel. to chemical composition 3-81051
- cassiopeiae-A, 26.3 MHz obs., interferometry 3-48047
- ω Centauri, $^{12}\text{C}/^{13}\text{C}$ ratio for two CH-stars 3-45194
- ω Centauri, globular cluster, i.r. photometry and spectral types 3-65928
- ω Centauri globular cluster, UVB photoelectric data for 126 bright stars 3-48110
- Chamaeleon T assoc., i.r. photometry of Chamaeleon 16, nebulous object 3-77145
- Collinder 107, open cluster and stellar ring in Monoceros (*German*) 3-65927
- collision of two 25-member clusters, numerical study 3-48099
- contraction of stellar system, due to dissipation of kinetic energy through direct and gravitational interactions 3-59252
- Cygnus OB2 assoc., stars, diffuse interstellar features 3-56383
- Czernik 10, open cluster, UVB photometric obs. (*German*) 3-73541
- Czernik 11, open cluster, UVB photometric obs. (*German*) 3-73541
- Czernik 13, open cluster, UVB photometric obs. (*German*) 3-73541
- Czernik 8, open cluster, UVB photometric obs. (*German*) 3-73541
- Czernik 9, open cluster, UVB photometric obs. (*German*) 3-73541
- Fornax dwarf galaxy, photometric obs. of integrated light 3-59370
- galactic absorption map, distance and absorpt. of open clusters 3-45213
- globular, black hole obs. 3-44986
- globular cluster stars, chemical comp. and form of horizontal branch 3-61856
- globular clusters, age rel. to horizontal branch stars (*Russian*) 3-45173
- globular clusters, cosmological hypothesis of origin 3-53600
- globular clusters, neutral H obs. in 8 objects 3-45198
- globular clusters, origin in the Galaxy (*Italian*) 3-61850

stellar clusters continued

- globular clusters, photometric information for stars on Palomar Sky Survey prints 3-53700
- globular clusters, search for new planetary nebulae, H α observations 3-45229
- globular clusters, search for OH/IR stars at 1665 MHz 3-61840
- horizontal branch stars, populations rel. to globular clusters 3-56382
- Hyades, chemical comp. and location of main sequence 3-53703
- Hyades, distance determ. using UBVB $_1$ B $_2$ V $_1$ G photometry 3-81256
- Hyades, far u.v. flux difference between stars in Pleiades 3-81186
- Hyades, HR diagrams, calibration of MK types 3-81079
- Hyades, program for accurate trigonometric parallax 3-81185
- IC 2157, open cluster, three colour photometry 3-81175
- IC 2581 open cluster, differential reddening 3-77132
- IC 4756, open cluster, determ. of membership probabilities from proper motions 3-48098
- isolated systems of identical stars random gravit. encounters and evolution 3-53696
- King 4, open cluster, UVB photometric obs. (*German*) 3-73541
- Kron 3, globular cluster, carbon stars, spectroscopic obs. 3-70022
- LMC globular clusters, BV photometry of Cepheid variables 3-65882
- M15, detection of emission at 10.2 μ 3-81180
- M22, globular cluster, metal abundance of RR Lyrae-type stars 3-45196
- M29 (NGC 6913), galactic cluster V photoelectric obs. of 3-61847
- in M31, globular clusters, V magnitudes and colour indices 3-77150
- M31, variables 5 and 9, periods for two RR Lyrae-type stars 3-42202
- M35, UVB photometric obs. 3-73542
- M4, globular cluster, 4-colour obs. of early-type stars 3-56426
- M5, long-term amplitude changes for RR Lyrae stars in globular cluster 3-48010
- M67, metallicity of and spectral types of main-sequence stars in cluster 3-48088
- M67, old open cluster, DDO photometry rel. to cyanogen strength and Fe/H ratio 3-45186
- M92, G-band anomaly of asymptotic-branch stars, CH abundance 3-51381
- M 10, globular, spectral anal. of red giants 3-53702
- M 5, globular, spectral anal. of red giants 3-53702
- M 92, globular, spectral anal. of red giants 3-53702
- in Magellanic Clouds, photometric obs. of integrated light 3-59370
- Markarian 6, open cluster, UVB photometric obs. (*German*) 3-73541
- model for axisymmetric clusters of stars with uniform mass 3-53708
- NGC 121, globular cluster, carbon stars, spectroscopic obs. 3-70022
- NGC 1778, open cluster, UVB obs. and age determ. 3-45184
- NGC 1835, globular in LMC, mass determ. 3-51390
- NGC 1850, globular in LMC, B,V obs. 3-56434
- NGC 1893, photoelectric magnitude and UVB colours for 56 stars 3-48089
- NGC 2210, globular in LMC, mass determ. 3-51390
- NGC 2264, spectroscopic obs. of u.v.-excess stars 3-56419
- NGC 2264, stellar polarisation and nature of circumstellar shells 3-53698
- NGC 2420, colour-magnitude diagram from obs. of Ba II star 3-81085
- NGC 2477, C-star rel. to age of cluster 3-70021
- NGC 2477, open cluster, photometric obs. 3-56429
- NGC 2660, N-type C star member, evolution rel. to UVB study 3-45110
- NGC 2660 (open cluster) and nearby C star, photoelectric and photographic photometry 3-70011
- NGC 362, globular cluster, carbon stars, spectroscopic obs. 3-70022
- NGC 419, globular cluster, carbon stars, spectroscopic obs. 3-70022
- NGC 6352, abnormally metal-rich globular cluster 3-56418
- NGC 6383, proof that G 353.3 + 0.1 is not its counterpart β -77110
- NGC 6522, globular, study of RR Lyrae stars in Baade's field 3-56376
- NGC 6522, globular cluster, periods for RR Lyrae stars in Baade's field 3-59374
- NGC 6752 globular cluster, UVB photoelectric data for bright stars 3-48111
- NGC 6809, Stromgren 4-colour photometry of 10 blue horizontal-branch stars 3-45195
- NGC 6838, photoelectric magnitude and UVB colours for 13 stars 3-48089
- NGC 6934, globular cluster, BV photometric obs. 3-45180
- NGC 7031, open cluster, photometric obs. 3-73544
- open clusters, escape of stars 3-61859
- open clusters, list and maps of suspected Southern Milky Way objects 3-45185
- open clusters, orbital plane distrib. determ. of binaries 3-44983
- open clusters, photographic UVB photometry of 10 clusters (*German*) 3-73541
- open clusters, search for Ap stars 3-61771
- southern open clusters, UVB-H β photometry of 28 objects 3-65925
- Ophiuchus dark-cloud, 2 μ map, discovery of i.r. cluster 3-81209
- Orion cluster, radial rel. determ. 3-45197
- Orion Nebula Cluster, motions of 14 member stars 3-51380
- Orion Nebula cluster, spectroscopic obs. of u.v.-excess stars 3-56419
- α Persei, HR diagrams, calibration of MK types 3-81079
- α Persei cluster, star formation period rel. to age and total mass of stars (*Russian*) 3-45176
- Pleiades, comparison of obs. absolute proper motion with catalogue values 3-47857
- Pleiades, far u.v. flux difference between stars in Hyades 3-81186
- Pleiades, obs. of 2 UV Ceti-type stars behind cluster 3-45138
- Praesepe, distance determ. using UBVB $_1$ B $_2$ V $_1$ G photometry 3-81256
- Praesepe, H.R. diagram, Galactic evolution 3-51238
- Praesepe cluster stars, luminosity functions 3-61793
- Praesepe main sequence rel. to solar neutrino problem 3-61666
- proto-star interaction in collapsing cluster 3-42224

stellar clusters continued

- Sco-Cen association, elimination of 3 SEG stars on radial vel. basis 3-48100
 II Scorpii, HR diagrams, calibration of MK types 3-81079
 Scorpio-Centaurus association, H α and H β photoelectric measurements 3-81187
 Scorpio-Centaurus association rel. to SEG stars, radial velocities and Scorpius X-1 distance 3-45094
 star formation in clusters from condensation of nebulae, T Tauri stars 3-47999
 stellar ring 58, distances of 26 member stars 3-61782
 Tombaugh 4, open cluster, UBV photometric obs. (*German*) 3-73541
 total mass of stars rel. to main sequence lifetimes and formation period (*Russian*) 3-45175
 Trumpler 27, obs. of red star 3-61775
 47 Tucanae, discontinuity in props. of giant stars 3-61849
 47 Tucanae, globular cluster, i.r. photometry and spectral types 3-65928
 47 Tucanae, globular cluster, UBV photoelectric photometry of 60 stars 3-65929
 UBV photometric diagrams for detection of open star clusters 3-45181
 He cosmic abundance rel. to horizontal branch stars in globular clusters 3-69948

stellar colour see stellar spectrophotometry**stellar composition***see also element origin*

- Ap magnetic stars, discussion of chemical composition anomalies 3-65889
 Ap stars, element abundance anomalies 3-81057
 53 Aurigae, course analysis of peculiar A-type star 3-51358
 B type, light ion spectra giving neon abundances 3-73493
 ν Capricorni, model-atmosphere abundance analysis of B9-type star 3-56388
 central stars of planetary nebulae rel. to hot liquefying white dwarfs, cores, masses and luminosity 3-61877
 collapsing dense stars, effect of electron capture on temperature and chemical composition 3-65878
 β Coronae Borealis, identification of actinides 3-65890
 E model sequence, multiple solns. of eqns. of stellar structure 3-77039
 evolved stars, CN/C₂ and CO/C₂ ratios in cool C stars 3-81023
 F- and G-type dwarf stars, metal abundance and age distrib. solar neighbourhood 3-45101
 F-type stars in solar neighbourhood, abundance and age distrib. 3-56384
 Fm stars, incidence and abundance anomalies, curve-of-growth anal. 3-47987
 G-type dwarf stars, metal-rich, u.v. four colour photometry, 31 Aquilae, δ Pavonis, α Mensae 3-48015
 K-giant stars, N₂ enrichment due to meridional circulation, rel. CN-strength 3-69949
 globular cluster stars, chemical comp. and form of horizontal branch 3-61856
 Gmb 1830, subdwarf, Fe, C and N abundances 3-56396
 HD 122563, N abundance of very metal-poor star 3-81091
 HD 184927, He-rich star, spectrophotometric anal. 3-48053
 HD 193722, Si Ap-star, photometric and spectroscopic meas. 3-53663
 HD 96446, H-deficient star, fine anal. 3-56393
 horizontal-branch morphology for metal-poor stars 3-81024
 HR 465, Ap-star, tests and consequences of Pm identification 3-48021
 HR 465, trace element abundance near r-process peaks 3-65891
 Hyades, chemical comp. and location of main sequence 3-53703
 K-type supergiants, Li abundances rel. to evolutionary tracks 3-65887
 RR Lyrae-type stars in globular cluster M22, metal abundance 3-45196
 M67, metallicity of and spectral types of main-sequence stars in cluster 3-48088
 M92, G-band anomaly of asymptotic-branch stars, CH abundance 3-51381
 Magellanic Clouds Cepheids, He abundance determ. 3-53660
 main sequence stars, N₂ enrichment, due to meridional circulation 3-69949
 metal deficient A-type, stellar spectra, four colour photometry 3-77071
 nova outburst characteristics rel. to initial N abundance, hydrodynamic evolution 3-45088
 δ Pavonis, C abundance rel. to UBV and uvby colours and spectrum 3-42201
 peculiar A stars, elemental abundance anal. 3-65879
 r-process abundance, effects of delayed neutron emission 3-80924
 RGO 55, member of ω Centauri cluster, ¹²C/¹³C ratio 3-45194
 RGO 70, member of ω Centauri cluster, ¹²C/¹³C ratio 3-45194
 α Sculptoris, weak-He-line star, chemical abundance 3-48030
 subdwarfs, existence in (M_{bol} , log T_{eff})-plane 3-61776
 sun, C and O abundance corrections based on forbidden transition probabilities 3-45016
 supergiants, chemical composition determ. from evolutionary tracks, bolometric calibration and spectral type 3-81051
 supergiants, mass-luminosity relations giving hydrogen and metal abundances 3-73512
 white dwarfs, dependence of envelope structure on surface gravity and composition 3-81030
 Wolf-Rayet, classification and distrib. rel. to WN sequence interpretation 3-81059
 Wolf-Rayet stars rel. to P Cygni-type stars 3-81061
 C star in NGC 2477 cluster rel. to age 3-70021
 CO vibration-rotation LTE in late-type star model atmospheres 3-61761
 D abundance in protostars 3-73500
 He abundance of Cepheids in the Galaxy, M31 and Magellanic clouds 3-45112
 He binary dwarf supernova evolution, possibility of violent He ignition 3-81029
 He envelopes of white dwarfs, upper bounds of mass 3-81211
 He/H solar abundance, review 3-47894

stellar composition continued

- Hg stars, wavelength shifts and isotopic structure of Pt II 4046 A line 3-61772
- stellar evolution**
- Ap-stars, evolution and classification of magnetic stars (*Russian*) 3-45093
 BD-10°4662, obs. indicating possible post-T Tauri star 3-51350
 binaries, radiative interaction and evolution of medium- and low-mass objects 3-47988
 binary contact systems, models for Case A evolution for 1.8 M \odot system 3-59334
 binary helium dwarf supernova, possibility of violent He ignition 3-81029
 binary stars, evolution of circumstellar matter 3-77056
 binary stars, evolutionary considerations involving internal density concentration parameter 3-53644
 binary stars, reformulation of fission theory 3-53640
 binary systems, comparison of theory and obs. (*Italian*) 3-59338
 blast wave hydrodynamics, cluster of galaxies, supernovae, intergalactic medium 3-47868
 pure C stars, thermal stability rel. to neutrino emission 3-59335
 TX Cancri, W Ursae Majoris type, obs. and evolution 3-65892
 capture by Earth, weak friction approx. and tidal evolution 3-80908
 RS Carum Venaticorum binaries rel. to W Ursae Majoris binaries 3-47998
 Cepheid instability strip, non-pulsating stars, properties and evolution 3-45111
 close binaries, evolution when equipotential surface is reached (*German*) 3-81035
 clusters, total mass of stars rel. to main sequence lifetimes and formation period (*Russian*) 3-45175
 Coalsack, search for flare-star spectra rel. to star formation 3-81208
 collapsing dense stars, effect of electron capture on temperature and chemical composition 3-65878
 convective overshooting, simplified non local mixing-length model 3-73476
 DB white dwarfs relation with DA white dwarfs and planetary nebulae nuclei 3-81028
 double shell source stars, numerical computation of evolution 3-65875
 early evolution 3-59339
 explosive C burning, nucleosynthesis of rare nuclei from seed nuclei 3-53641
 extended atmospheres and circumstellar matter in spectroscopic binary systems, IAU Symposium 51 (Parksville, Canada, 6-12 September, 1972) 3-77052
 F- and G-type dwarf stars, metal abundance and age distrib. solar neighbourhood 3-45101
 F-type stars in solar neighbourhood, abundance and age distrib. 3-56384
 Fermi-Dirac integrals for electron gas, non-interacting, partially relativistic, partially degenerate 3-48002
 fundamental HR-diagram using log g and log T_{eff} 3-81074
 Galactic population and evolution, obs. of high-vel. stars (*Italian*) 3-61850
 Galaxy, Schmidt model, star formation, effect of shock waves and hydrostatic equilibrium 3-61853
 globular cluster stars, chemical comp. and form of horizontal branch 3-61856
 globular clusters, age rel. to horizontal branch stars (*Russian*) 3-45173
 globular clusters, neutral H obs. in 8 objects 3-45198
 globular clusters, search for OH emission from IR stars 3-61840
 halo/old disk cepheids, existence of Hertzsprung progression 3-61790
 HD187399, binary with case B mass-exchange, possible black hole 3-61812
 HZ Herculis, binary star 3-77130
 horizontal branch stars, populations rel. to globular clusters 3-56382
 horizontal branch stars, topology 3-56381
 horizontal-branch morphology for metal-poor stars 3-81024
 hot CNO-Ne cycle hydrogen burning, thermonuclear evolution at const. temp. and density 3-81019
 Hyades, chemical comp. and location of main sequence 3-53703
 interstellar matter condensations, protostar formation 3-48003
 isolated systems of identical stars random gravit. encounters and evolution 3-53696
 Jupiter model, evolution from 0.001 solar mass stellar object 3-42165
 K-type supergiants, Li abundances rel. to evolutionary tracks 3-65887
 L726-8 main seq. visual red dwarf binary, orbit and mass determ. 3-77086
 low-mass main-sequence stars, theory rel. to obs. of nearby stars 3-61765
 RR Lyrae instability strip, non-pulsating stars, properties and evolution 3-45111
 magnetic DC white dwarfs, evolutionary connection with planetary nebulae nuclei 3-81027
 magnetic stars, effect of interstellar mag. fields (*German*) 3-56372
 main sequence, correlation between u.v. excess and deviation from mean 3-77062
 main sequence evolution, computational techniques for star of 5M \odot 3-77046
 main sequences stellar models rel. to ang. momentum 3-59346
 massive close binaries with collapsed component evolution and appl. to Cygnus X-3 3-53650
 massive star explosions, cosmic ray origin and nucleosynthesis 3-80890
 moving clusters HR diagrams, calibration of MK types 3-81079
 multiple star systems, occurrence of trapezia rel. to origin of runaway stars 3-51345
 N-type C star in cluster NGC 2660, evolution rel. to UBV study 3-45110
 neutron emission process 3-80918
 neutron stars, hydrodynamic model for formation in carbon detonation supernova 3-81025
 NGC 2477, C-star rel. to age of cluster 3-70021
 nongeodesic radial accretion in Schwarzschild geometry 3-59250

stellar evolution continued

- nova outburst characteristics rel. to initial N abundance, hydrodynamic evolution 3-45088
- nucleosynthesis, applic. to teaching of nuclear chemistry 3-61964
- nucleosynthesis, role of stars 3-65873
- nucleosynthesis of He^4 , N^{14} and C^{12} , cosmic abundances 3-59337
- α Persei cluster, star formation period rel. to age and total mass of stars (*Russian*) 3-45176
- Population I, instability strip computation 3-73477
- Population II, evolution of horizontal branch of stars with 0.63 solar mass 3-73486
- Population II, instability strip computation 3-73477
- Population II stars of large mass, evolutionary tracks and He production 3-45079
- Praesepe main sequence rel. to solar neutrino problem 3-61666
- proto-star interaction in collapsing cluster 3-42224
- protostars, cooling mechanisms by volume energy losses (*Russian*) 3-77041
- quasars, optically selected, and from radio catalogues, luminosity function comparison 3-69980
- r-process, dynamical calcs. 3-47995
- r-process abundance, effects of delayed neutron emission 3-80924
- red giant evolution rel. to central stellar gravitational field 3-45081
- red giants with H and He shell sources rel. to planetary nebulae formation (*Polish*) 3-45090
- review 3-77038
- rapidly rotating stars, viscous effects with appl. to white dwarf models 3-65871
- S and N stars, hydrodynamic model for plume mixing 3-65868
- secular stability, effect of shell sources on secular spectrum 3-45080
- SMC stars, colour magnitude diagram 3-48004
- spherical systems, gravitational shock heating 3-69920
- star contraction in protogalaxies 3-61641
- subdwarfs, existence in (M_{bol} , $\log T_{\text{eff}}$)-plane 3-61776
- supergiants, chemical composition determ. from evolutionary tracks, bolometric calibration and spectral type 3-81051
- supermassive stars, H and He burning, dynamical evolution 3-69924
- supermassive stars, hydrodynamic model rel. to thermonuclear explosions 3-45082
- supermassive stars, relativistic hydrodynamic model, collapse and explosion 3-77040
- supernova production, teaching approach to gravit. collapse 3-42498
- T Tauri, Orion nebula 3-47999
- T Tauri stars, grain formation in expanding envelopes, nucleation possibility 3-48001
- T Tauri stars, pre-main-sequence evolution 3-61799
- thermal instability of He-burning shell in massive stars 3-51323
- tidal evolution in close binary systems, energy considerations 3-53590
- turn-off luminosity of very faint stars in globular clusters on Palomar Sky Survey prints 3-53700
- URCA process rel. to C core evolution 3-45077
- W Ursae Majoris binaries rel. to RS Canum Venaticorum binaries 3-47998
- viscous Maclaurin spheroids, evolution of secular instability 3-47985
- white dwarfs, cooling time and internal structure for 3 models 3-77048
- white dwarfs, evolution sequence for DA, DB, DC types 3-73482
- white dwarfs stage, masses 3-51335
- Wolf-Rayet stars, evolution rel. to structure and origin 3-81036
- X-ray source member of binaries, differentially rotating degenerate dwarf model 3-69995
- C 0.8 M_{\odot} star, vibrational stability during a C flash (*French*) 3-59336
- C-O core growth phase, stellar model 3-77047
- C-rich stars, evolutionary models for stars with mass 0.75-1.45 M_{\odot} 3-47983
- C-rich stars with He envelopes, evolutionary models compared with planetary nebulae nuclei 3-45075
- CNO abundance variation, effect on, horizontal branch model 3-77045
- D abundance in protostars 3-73500
- H gas, condensation, mol. form., thermal instability, collapse, fragmentation 3-77157
- He burning regions, dependence of structure on molecular weight and burning rates 3-59332
- He central burning, secular stability of static models 3-47990
- He-shell burning stars, convectively driven Urca neutrino losses, thermal consequences in cores 3-69934
- $^{16}\text{O}(p,\alpha)^{13}\text{N}$, total cross section, threshold to 7.7 MeV 3-63043

stellar interiors see stellar internal processes**stellar internal processes**

- see also stellar evolution
- accreting neutron stars nuclear fusion forming X-ray source 3-81026
- Ap magnetic stars, discussion of chemical composition anomalies 3-65889
- blast wave hydrodynamics, evolution, cluster of galaxies, supernovae, intergalactic medium 3-47868
- convection zones, linear convective modes and energy transport 3-81022
- convective overshooting, simplified non local mixing-length model 3-73476
- convectively driven Urca neutrino losses, thermal consequences in cores of He-shell burning stars 3-69934
- critical luminosity in stellar interiors and stellar surface boundary conditions 3-47984
- explosive C burning, nucleosynthesis of rare nuclei from seed nuclei 3-53641
- hot CNO-Ne cycle hydrogen burning, thermonuclear evolution at const. temp. and density 3-81019
- HR 465, trace element abundance near r-process peaks 3-65891
- interstellar abundances of C, N and O isotopes rel. to stellar nuclear reactions 3-81191
- magnetic stars, pinch instabilities 3-51332
- neutron stars, critical parameters rel. to gravitational collapse 3-69922

stellar internal processes continued

- neutron stars, hydrodynamic model for formation in carbon detonation supernova 3-81025
- nucleosynthesis, applic. to teaching of nuclear chemistry 3-61964
- nucleosynthesis, application of fast neutron capture cross section data 3-74566
- nucleosynthesis, carbon burning era, $^{12}\text{C} + ^{12}\text{C}$ nucl. reactions role, low energy 3-40511
- nucleosynthesis, role of stars 3-65873
- nucleosynthesis of He^4 , N^{14} and C^{12} , cosmic abundances 3-59337
- partially degenerate magnetoplasma, thermal conductivity 3-81020
- plume mixing in S and N stars, model 3-65868
- Population II stars of large mass, evolutionary tracks and He production 3-45079
- pressure ionization and opacities based on Thomas-Fermi atom 3-81044
- r-process, dynamical calcs. 3-47995
- r-process in HR 465, evidence 3-65891
- rapidly rotating stars, viscous effects with appl. to white dwarf models 3-65871
- S and N stars, hydrodynamic model for plume mixing 3-65868
- s-process neutron capture time from obs. 3-80910
- screening factors for nuclear reactions, intermediate screening and astrophysical appl. 3-47861
- solar-type stars secular stability, reaction kinetics of proton-proton chain 3-81021
- Sun, stability against spherical thermal perturbations 3-76964
- Sun nonspherical thermal instabilities, conditions of existence 3-76965
- superheavy element synthesis, from r-process calc. with energy-density mass formula 3-65620
- supermassive stars, H and He burning, dynamical evolution 3-69924
- supersonic turbulent stress and structure 3-73479
- T Tauri stars, structure rel. to supersonic convection 3-51334
- temperature dependent nuclear binding energies rel. to nucleosynthesis in stars 3-42112
- thermal instability of He-burning shell in massive stars 3-51323
- thermonuclear detonation in evolved cores, plasma screening theory 3-47996
- URCA process rel. to C core evolution 3-45077
- white dwarf viscous evolutionary sequences 3-65872
- white dwarfs, cooling time and internal structure for 3 models 3-77048
- white dwarfs, gas-liquid phase transitions and critical point 3-53648
- ν processes, Salam-Weinberg weak interaction model, energy loss 3-80919
- C 0.8 M_{\odot} star, vibrational stability during a C flash (*French*) 3-59336
- C ignition in degenerate cores, rel. to supernovae explosions and pulsar origins (*Polish*) 3-45090
- C ignition in strongly coupled Coulomb fluids 3-65869
- C-rich stars, evolutionary models for stars with mass 0.75-1.45 M_{\odot} 3-47983
- C-rich stars with He envelopes, evolutionary models compared with planetary nebulae nuclei 3-45075
- ^{12}C shell-burning stars, radial pulsation stability rel. to pre-white dwarf stars 3-61763
- He burning regions, dependence of structure on molecular weight and burning rates 3-59332
- He central burning, secular stability of static models 3-47990
- He ignition, possibility in binary He dwarf supernova 3-81029
- ^3He equilibrium departures in proton-proton chain, secular stability 3-59331
- $^{16}\text{O}(p,\alpha)^{13}\text{N}$, reaction rate at $4 \times 10^9 \text{K}$, from measurement of total cross sections at 5.4 to 9.9 MeV 3-60178
- ^{187}Re in stars, enhanced β -decay rate rel. to recycling of r-process elements and age of Galaxy 3-42113

stellar magnetism

see also solar magnetism

- aligned rotating magnetosphere, general analysis 3-59330
- Ap magnetic stars, discussion of chemical composition anomalies 3-65889
- Ap stars, abundance anal. for 21 sharp-lined cool objects 3-65879
- Ap stars, evolution and classification of magnetic stars (*Russian*) 3-45093
- DA white dwarfs, interpretation of quadratic Zeeman effect 3-69941
- DC white dwarfs, evolutionary connection with planetary nebulae nuclei 3-81027
- finite-amplitude convection combined effect of rotation and mag. field 3-51258
- Grw + 70°8247, magnetic dwarf, wavelength dependence of polarized radiation 3-51351
- HD 133029, magnetic variable UBV photoelectric photometry obs. 3-77089
- HD 153919 binary, narrow band circular polarization meas. 3-81135
- HD 77581, binary, narrow band circular polarization meas. 3-81135
- HZ Herculis, X-ray binary, magnetic activity and model 3-81132
- interstellar mag. fields, effect on stellar evolution (*German*) 3-56372
- Landau orbital ferromagnetism in white dwarfs and neutron stars 3-61764
- Maclaurin spheroids, stability in toroidal mag. field (*Russian*) 3-51329
- magnetic null lines for mag. peculiar A-type star atm. studies 3-45115
- neutron star, surface superstrong magnetic fields, formation of long molecular chains 3-67723
- oblique rotator model of magnetic stars 3-69936
- partially degenerate magnetoplasma, thermal conductivity 3-81020
- photoelectric obs. of mag. stars (*Italian*) 3-61787
- pinch instabilities in mag. stars, mag. flux destruction 3-51332
- poloidal fields, hydromagnetic instability 3-56386
- polytropes gaseous, equilibrium structure, toroidal mag. fields 3-69927
- pulsar magnetosphere model of Goldreich-Julian 3-77121
- radiation absorption through photoionisation in magnetic field 3-77049
- rapidly rotating stars, photospheric magnetic fields 3-48019

stellar magnetism continued

- rotating stars, radiative equilib., model, multipole mag. fields 3-69946
- spectroscopy, mag. stars, obs. with universal reflecting telescope, Tautenburg 3-48149
- stars, oscillations and stability of rotating masses with magnetic fields 3-47986
- synchrotron radiation model, Stokes parameters, Bessel function routine, effect of mag. field of oblique rotator 3-47867
- white dwarfs, internal magnetic fields 3-59340
- white dwarfs, polarised radiation, exact soln. of Kemp's (1970) model 3-53638
- white dwarfs with large mag. fields, He specera 3-45107
- X-ray source, accretion on compact magnetic stars 3-73533
- X-ray source model, magnetic field twisting in binary star system 3-42223

stellar models

- accretion model investigation of Scorpius X-1 flickering phenomena 3-65919
- accretion model of X-ray sources, circumstellar matter 3-77128
- Algol-type binaries, model for alternate period changes 3-73480
- atmospheres, radiative opacity rel. to metal absorpt. coeff. accuracy 3-47982
- atmospheres, use in temperature-gravity calibration 3-81040
- axisymmetric clusters of stars with uniform mass 3-53708
- axisymmetric oscillations allowing for gravitational radiation 3-45715
- B-type stars, effective temp. determ. and comparison with model atm. 3-45095
- B-type stars, last Balmer lines and H γ 3-61773
- binary contact systems, models for Case A evolution for 1.8 M \odot system 3-59334
- binary stars, eclipsing, reflection model 3-69947
- binary stars, evolutionary considerations involving internal density concentration parameter 3-53644
- pure C stars, thermal stability rel. to neutrino emission 3-59335
- α^2 Canum Venaticorum, u.v. obs. compared with LTE-model calcs. 3-56395
- Cepheids, linear and nonlinear pulsation calculations 3-61762
- classical Cepheids, Q-method for colour excesses 3-45102
- close binary stars, eclipsing, reflection effects, temp. distrib. 3-51327
- compact X-ray sources, models for optically thin bremsstrahlung 3-81149
- DA white dwarfs, interpretation of quadratic Zeeman effect 3-69941
- density gradient inversions in stellar envelopes rel. to mass loss 3-45085
- double shell source stars, numerical computation of evolution 3-65875
- eclipsing binaries, parameter correlation coefficients of spherical model 3-53642
- eclipsing binary system, radiation spectral energy distrib., computation model 3-51328
- extended atm. stars., picket fence model 3-45086
- extended stellar atmospheres with pure absorption, curvature effects 3-51325
- flux constant line-blanketed model atmospheres for solar-type stars 3-77044
- galactic mass distribution models, optimisation by scaling 3-70012
- general-relativistic polytropes, stability and equation of state 3-69921
- Gravitational instability of a cold rotating cylinder 3-77050
- HD 96446, H-deficient star, fine anal. 3-56393
- Hercules X-1, 35-day periodicity rel. to accretion gas flow in binary system 3-48083
- HZ Herculis, eclipsing binary, X-ray beaming and mass transfer 3-48028
- HZ Herculis, X-ray binary, magnetic activity and model 3-81132
- horizontal branch stars, models rel. to He cosmic abundance 3-69948
- horizontal-branch morphology for metal-poor stars 3-81024
- i.r. sources, dust shell models 3-51371
- isolated systems of identical stars random gravit. encounters and evolution 3-53696
- EV Lac flares, explanation of Balmer decrements (*Russian*) 3-77065
- ϵ Leonis, G-type giant, model atmospheres and high dispersion spectrograms 3-48051
- low-mass main-sequence stars, theory rel. to obs. of nearby stars 3-61765
- LTE atm., effect of absorbers on thermal structure 3-73481
- β Lyr, rapid mass exchange model 3-69968
- RR Lyrae models, non-linear pulsations and grey radiative transfer 3-47993
- Maclaurin spheroids, stability in toroidal mag. field (*Russian*) 3-51329
- magnetic stars, oblique rotator model 3-69936
- main sequence models, stellar angular momentum 3-59346
- Me type dwarfs, models for periodic variations, spot model 3-73498
- neutron stars, accretion at magnetic pole 3-81034
- nonspherical eclipsing binary star system modelling, computer program 3-45139
- nova outburst characteristics rel. to initial N abundance, hydrodynamic evolution 3-45088
- novae, origin of light, luminosity 3-65870
- α Orionis, model atm. compared with scanner obs. 3-61798
- oscillations and stability of rotating masses with magnetic fields 3-47986
- oscillatory secular modes rel. to main-sequence stars and He-burning shells 3-51324
- p-n junctions in pulsar magnetospheres 3-81124
- polytropes gaseous, equilibrium structure, toroidal mag. fields 3-69927
- pre-nova model, pulsational instability 3-47992
- pulsational stability of stars in thermal imbalance 3-59329
- radiative transfer, numerical evaluation of formal soln. in spherical geometry 3-69935
- rapidly rotating neutron stars 3-45091
- red giant evolution rel. to central stellar gravitational field 3-45081

stellar models continued

- red giants of class III luminosity, convection in model envelopes 3-45084
 - rotating stars, radiative equilib., model, multipole mag. fields 3-69946
 - S and N stars, hydrodynamic model for plume mixing 3-65868
 - Schwarzschild nonstatic model of expanding or contracting star 3-45092
 - secular stability of uniformly rotating fluid masses, effect of gravitational radiation 3-45076
 - self-consistent model computation for solar and stellar chromospheres 3-53612
 - spherical shell media with complete freq. redistrib., probabilistic models 3-56374
 - stationary outflowing envelopes, 30M \odot stars 3-69931
 - stratified rotating conducting fluids, universal stability under influence of mag. field and Coriolis force 3-40735
 - supermassive stars, hydrodynamic model rel. to thermonuclear explosions 3-45082
 - supermassive stars, relativistic hydrodynamic model, collapse and explosion 3-77040
 - supernova remnants, hydrodynamic considerations of buoyant rise 3-56302
 - synchrotron radiation model, Stokes parameters, Bessel function routine 3-47867
 - Tauri, intrinsic polarization, 0.33-2.2 microns obs. rel. to model 3-48038
 - W Ursae Majoris systems, convective envelope model, light curve analysis 3-69926
 - W Ursae Majoris-type eclipsing binary stars, model for W-type systems 3-47989
 - viscous Maclaurin spheroids, evolution of secular instability 3-47985
 - white dwarf crystalline interior thermodynamic functions, b.c.c. lattice model of heavy-ion plasma 3-73487
 - white dwarf viscous evolutionary sequences 3-65872
 - white dwarfs, cooling time and internal structure for 3 models 3-77048
 - white dwarfs, viscous effects in rapidly rotating stars 3-65871
 - white dwarfs with large mag. fields, He specera 3-45107
 - Wolf-Rayet, extended atmospheres and non-classical atmospheric models 3-77051
 - Wolf-Rayet stars, theory of emission spectra, expanding envelope hypothesis 3-81062
 - X-ray and radio emission from solar-type stellar coronae, model 3-45078
 - X-ray binary sources, expected optical behaviour 3-48082
 - C-O cores, growth phase 3-77047
 - C-rich stars, evolutionary models for stars with mass 0.75-1.45 M \odot 3-47983
 - C-rich stars with He envelopes, evolutionary models compared with planetary nebulae nuclei 3-45075
 - CO vibration-rotation LTE in late-type star model atmospheres 3-61761
 - ^{12}C shell-burning stars, radial pulsation stability rel. to pre-white dwarf stars 3-61763
 - Ca II K-line reversals and simulated stellar chromospheric-photospheric models 3-45104
 - H-He star of 10 M \odot , linear series 3-69930
 - He central burning, secular stability of static models 3-47990
- stellar motion**
see also celestial mechanics
- absolute proper motion rel. to SA 32 galaxies and reference stars 3-77075
 - AC + 65°6955, absolute parallax and analysis of astrometric field 3-48024
 - Aquila, 36 visual binaries, evidence for coplanar system 3-77076
 - axisymmetric clusters of stars with uniform mass, model 3-53708
 - Barnard's Star, planetary system rel. to proper motion obs. 3-59349
 - BD + 66 degrees 34, triple system, astrometric anal. 3-51353
 - BD + 67°552, unresolved astrometric binary, orbital motion and parallax 3-42193
 - BD + 67°552, unresolved binary, orbital motion and parallax determ. 3-48037
 - BD + 69°398, unresolved astrometric binary, orbital motion and parallax 3-42193
 - BD-10°4662, obs. indicating possible post-T Tauri star 3-51350
 - binary stars, general-relativistic periastron advances 3-65880
 - binary stars, orbital parameters determ. 3-51343
 - capture by Earth, weak friction approx. and tidal evolution 3-80908
 - catalogues for star position and proper motion for Washington and Richmond photographic zenith tubes 3-76947
 - common proper motions of three double stars, possible physical binary system 3-53662
 - V453 Cygni, spectroscopic binary, BV obs. showing apsidal motion 3-42199
 - ϵ Eridani, binary, relative parallax and perturbation period determ. 3-48036
 - galactic dynamics, orbits in 2nd Schmidt potential (*French*) 3-73540
 - galactic nucleus, interaction of gas and stars, ablation rel. to gas density 3-48108
 - K-giant stars, N $_2$ enrichment due to meridional circulation, rel. CN-strength 3-69949
 - HD 101799, W Ursae Majoris-type eclipsing binary, UVB obs. and orbit 3-48023
 - Hd 126983, double line spectroscopic binary, orbital obs. from coude spectra 3-77090
 - HD 180553, spectrographic binary, orbital elements determ. 3-65896
 - HD 92740, WR spectroscopic binary, radial vel. meas. 3-48054
 - high-luminosity red stars near Sun, young disc population 3-77067
 - high-vel. stars, population and evolution in the Galaxy (*Italian*) 3-61850
 - IC 4756, open cluster, determ. of membership probabilities from proper motions 3-48098
 - inhomogeneous phase space fluids, stability problems 3-75348
 - kinematics compared with neutral H galactic kinematics 3-45189
 - L726-8, visual red dwarf binary, orbit and mass determ. 3-77086

stellar motion continued

large proper motion stars, subluminoous stars, nearby stars, UVB photometry 3-77072
 LMC member stars, radial vel. (*French*) 3-65926
 M-type giants at South Galactic pole, radial velocities for 30 objects 3-42233
 main sequence stars, N₂ enrichment, due to meridional circulation 3-69949
 N-body gravitation problem, integration scheme, near and distant stars 3-70726
 nearby stars, revised parallaxes for 10 objects 3-48007
 open cluster stars, escape from cluster 3-61859
 Orion Nebula Cluster, motions of 14 member stars 3-51380
 parallax meas. of 35 stars using Yale 26 in. telescope 3-61777
 Pleiades cluster, comparison of obs. absolute proper motion with catalogue values 3-47857
 precession correction from comparison of proper motion 3-77058
 proper motion, anal. of MD and GC catalogues (*Italian*) 3-59242
 proper motion and absolute magnitudes determ. 3-81066
 radial velocity curves for intrinsic variables, nonlinear pulsations iterative theory 3-48009
 radial vels. 10 ms⁻¹ accuracy from spectrograms using telluric absorption lines as comparison 3-48156
 Relaxation time in disk galaxy simulations 3-81164
 rotating stars, radiative equilib., model, multipole mag. fields 3-69946
 rotating stars, struct., J² method, for uniform rotation, Roche approx. 3-69937
 Sco-Cen association, elimination of 3 SEG stars on radial vel. basis 3-48100
 SEG stars, radial velocities and Scorpius X-1 distance 3-45094
 solar secular parallaxes and space velocity from stellar proper motions rel. to galaxies 3-76987
 Southern OB stars, determ. of projected rotational vel. 3-53657
 space velocity, rel. to rotational velocity, field stars earlier than B6, double stars, cluster members 3-61796
 tidal evolution in close binary systems, energy considerations 3-53590
 trigonometric and statistical parallaxes, determ. of stellar absolute magnitudes 3-81065
 variable star, light curve subject to orbital tidal distortion, program description 3-51341
 velocity distrib. due to phase mixing of initial conditions of stellar sub-population in galaxy 3-77144
 velocity field of young stars, Lin's theory of spiral waves 3-73539
 visual binaries, elements and dynamical parallaxes for ten objects 3-42194
 white dwarfs, finite lifetimes and nonzero velocities, effect on interstellar medium 3-59373

stellar origin see stellar evolution

stellar radiation

see also solar radiation; stellar spectrophotometry
 A5-V class, photosphere model, integrated and monochromatic flux determ. (*Russian*) 3-73490
 A- and F-type stars, effect of rotation on photometry for absolute magnitude determ. 3-81069
 absolute magnitude and temp. of stars, IAU Symposium 54 (Geneva, Switzerland, 12-15 Sept. 1972) 3-81064
 absolute magnitude determ. from Balmer H-line photometry 3-81075
 absolute magnitude from 3-dimensional representation of A-G stars (*French*) 3-81077
 absolute magnitudes, calibration of BCD classification, LMC distance modulus (*French*) 3-81073
 absolute magnitudes and colours of early-type stars, calibration of H β system 3-81076
 absolute magnitudes and colours of Mt. Wilson catalogue giant stars 3-81071
 absolute magnitudes and proper motion determ. 3-81066
 absolute magnitudes for A- and F-type stars, effect of rotation on photometry 3-81069
 Absolute magnitudes from trigonometric and statistical parallaxes 3-81065
 absolute magnitudes in red and i.r. of late M-type dwarfs 3-81067
 AC + 39° 12'14-608, flare star, spectral and photoelec. obs., variations in emission (*Russian*) 3-45127
 Ap stars, light variation due to line-blanketing effects 3-61783
 apparent V magnitude determ. on independent basis 3-81088
 UV Aurigae, carbon star, visual primary of binary ADS 3934, spectrophotometry, classification 3-51356
 Aurigae, eclipsing binary, 6-colour obs. of 1963-64 eclipse 3-53665
 B-type main sequence stars, u.v. flux envelopes, 1100-6000 Å obs. 3-48026
 Basel 11 in Taurus, RGU-colour photometry 3-81174
 Be-type stars, i.r. excesses, low-temp. free-free emission 3-61757
 Becklin-Neugebauer i.r. source in Orion Nebula, 3.45 μ circular polarization 3-69993
 Becklin-Neugebauer object in Orion Nebula, 10 μ linear polarization 3-69992
 Becklin-Neugebauer object in Orion Nebula, 2.2 and 3.5 μ polarization meas. 3-69991
 blanketing theory and G-I index for subdwarfs 3-45097
 α Bootis (Arcturus), heterodyne detection at 10.6 μ m 3-77193
 bright stars, spectral classification 3-77068
 Ca II H and k-line absorption features, luminosity effect 3-81045
 δ Canis Majoris, β CMa star, yellow photoelectric obs. rel. to light curve shape 3-42200
 YZ Canis Minoris flare star, 1969 Jan., spectrophotometric investigation (*Russian*) 3-45126
 central stars of planetary nebulae rel. to hot liquefying white dwarfs, cores, masses and luminosity 3-61877
 classical Cepheids, Q-method for colour excesses 3-45102
 contribution functions rel. to spectral line contrast 3-59347
 R Coronae Borealis, polarimetric obs. during light minimum, 0.36 to 1 micron 3-48042
 cosmic background radiation, interstellar absorption line, pressure scanned Fabry-Perot interferometer 3-48013
 V1016 Cygni, peculiar emission object, radio emission interpretation 3-77099

stellar radiation continued

double star images, Fourier transform technique for photoelectric scan analysis 3-53720
 double stars, weak luminosity effects on obs. (*French*) 3-51347
 earth atmospheric turbulence, effect on stellar light waves 3-44898
 eclipsing binaries, relative shifts of minima (*Polish*) 3-65888
 eclipsing binary light curves analysis on computer 3-53654
 eclipsing binary system, radiation spectral energy distrib., computation model 3-51328
 envelopes, supercrit. luminosity, power dependence of opacity, effect of convection 3-69925
 flare stars, continual photoelectric monitoring during 1971 for four objects 3-45140
 G-2 type star, simulator 3-73507
 G-M giants and supergiants, luminosity calibration 3-81072
 galactic Cepheids, intrinsic B-V colour determ. 3-48011
 galaxies, absolute luminosities rel. to magnitude difference of brightest red and blue stars 3-70017
 globular clusters, photometric information for stars on Palomar Sky Survey prints 3-53700
 Grw + 70°8247, magnetic dwarf, wavelength dependence of polarized radiation 3-51351
 HD 221568, Ap-star, light var. rel. to line blanketing 3-45121
 HD 51418, peculiar A-type star, spectrum and light var. 3-69956
 HD 98088, Ap star, photoelec. obs., light variation (*German*) 3-81100
 HDE 226868 (Cygnus X-1), radio variability of spectroscopic binary 3-51359
 heavy ion acceleration by radiation pressure 3-81042
 TX Herculis, eclipsing binary, BV photometry and light curve analysis 3-51357
 AH Herculis, high-speed photometry of dwarf nova, light curve analysis 3-45116
 HZ Herculis, search for optical pulsations at period of Hercules X-1 X-ray pulsations 3-61817
 high-luminosity red stars near Sun, young disc population 3-77067
 Hyades, far u.v. flux difference between stars in Pleiades 3-81186
 IC 2157, open cluster, three colour photometry 3-81175
 image formation, high resolution, through turbulent atm., star maps 3-73564
 interstellar extinction in Southern Milky way 3-42237
 i.r. ground-based obs. at 34 microns 3-69994
 i.r. radiation, comparison of i.r. and stellar luminosity in H II regions 3-45223
 K-line width-absolute magnitude relation 3-80979
 EV Lac, spectrophotometric observation of flares (*Russian*) 3-77095
 CM Lacertae, eclipsing binary light curve, computer study 3-53664
 EV Lacertae polarimetric obs., blue region (*Russian*) 3-45113
 light curves of gravitational lens-like action for binaries with degenerate members 3-59341
 long period Cepheids, radii and fluxes by Wesselink method 3-81083
 luminosity criteria, calibration procedure 3-81070
 luminosity discriminant for red giants and supergiants 3-61780
 RR Lyrae stars, intermediate-band photometry and colours 3-81048
 RR Lyrae stars, mean absolute magnitudes (*French*) 3-81068
 RR Lyrae variables in globular cluster M5, long-term amplitude changes 3-48010
 M-type dwarf stars, magnitude, TiO absorption bands (*Russian*) 3-45114
 l Monocerotis, δ Scuti-type variable, UVB photometry rel. to amplitude var. in light curve 3-48039
 nearby stars, search for narrow band 21-cm signals from other civilizations 3-59353
 neutrino emission rel. to motion in charged matter 3-66981
 neutron stars, nonequilibrium composition of shells and nuclear energy sources 3-61766
 neutron stars, positron-annihilation radiation producing 473 keV feature 3-61759
 new and supernovae stars, sources of relativistic particles (*Russian*) 3-65617
 NGC 1893, photoelectric magnitude and UVB colours for 56 stars in cluster 3-48089
 NGC 6838, photoelectric magnitude and UVB colours for 13 stars in cluster 3-48089
 nightglow stellar component in B wavelength band 3-61794
 Nova Cephei, 1971, photometry, light variations, estimation of photometric distance 3-81101
 Nova Cephei 1971, light curve, early spectral changes 3-77102
 OB stars in Milky Way system, two-colour diagrams 3-48016
 opacity, accuracy of metal absorpt. coeffs. 3-47982
 Ophiuchus, far u.v. photometry of stars rel. to sky background 3-48014
 δ Pavonis, C abundance rel. to UVB and uvby colours and spectrum 3-42201
 EE Pegasi, eclipsing binary light curve, computer study 3-53664
 periodogram Fourier analysis, detection of weak components, frequency meas. and short computation 3-48137
 photon bubbles, analogy with fluidized bed 3-53651
 Pleiades, far u.v. flux difference between stars in Hyades 3-81186
 point light source, detection probability rel. to stellar magnitude and sky brightness 3-51418
 polarisation observations, photon counting polarimeter, non-stable stars, extragalactic objects (*Russian*) 3-42560
 Praesepe cluster stars, luminosity functions 3-61793
 protogalaxies, photoionization by u.v. radiation from massive stars 3-42228
 protostars, radiative energy loss from shock front generated during collapse 3-65877
 radio star binaries rel. to X-ray binaries, possibly two types 3-61823
 radiostars of group 4, observations (*German*) 3-81120
 red stars, recognition, colour photography, anomalous images, visual examination 3-81056
 red variables with very small amplitude and very short period, photometry 3-81046
 reddening law parameters calc. using atmosphere models (*French*) 3-77042
 rotating stars, axisymmetric oscillations allowing for gravitational radiation 3-45715

stellar radiation continued

- FG Sagittae, observational evidence of thermal pulse in old planetary nebula 3-69960
 Scorpius, far u.v. photometry of stars rel. to sky background 3-48014
 Scorpius X-1, accretion model investigation of flickering phenomena 3-65919
 specific luminosity, definition and terminology 3-59342
 stars near Orion nebula, nine-colour photometry and i.r. excesses 3-69952
 supernova remnants, thermal bremsstrahlung in Sedov stage 3-45109
 supernovae, type I, average light curve and properties 3-48008
 synchrotron radiation model, Stokes parameters, Bessel function routine 3-47867
 Tauri, intrinsic polarization, 0.33-2.2 microns obs. rel. to model 3-48038
 IK Tauri, period and spectral range from i.r. obs. over 8 years 3-81093
 HL Tauri, triply-periodic white dwarf, differential blue magnitudes 3-48043
 T Tauri type, transition radiation from fast electrons in dust envelope 3-81032
 temperature calibration by spectrophotometric comparison with standard stars 3-81082
 temperature scales and colour relations, bolometric corrections 3-81086
 Thomas-Fermi atomic model for opacities, accuracy for stellar interiors 3-46191
 ultrashort period variables, intermediate-band photometry and colours 3-81048
 upper main sequence, ionizing radiation production in galaxies 3-81052
 W Ursae Majoris systems, convective envelope model, light curve analysis 3-69926
 W Ursae Majoris type systems, determ. of geometrical elements from contact model light curves 3-73513
 u.v., Telescope Catalogue, magnetic tape version 3-77077
 u.v. colours for main sequence stars, OAO-2 Telescope obs. 3-48005
 u.v. energy meas., Cerenkov radiation as standard source for rocket expt. (French) 3-73557
 variable star, light curve subject to orbital tidal distortion, program description 3-51341
 visibility threshold with unaided eye at different background brightnesses 3-70080
 white dwarfs, ionizing radiation production in galaxies 3-81052
 X-ray and radio emission from solar-type stellar coronae, model 3-45078
 X-ray binary sources, expected optical behaviour 3-48082
 X-ray counterparts of radio stars 3-81147
 X-ray emission region of Sco X-1 type white dwarf with accretion 3-48084
 X-ray radiation from stellar coronae rel. to soft X-ray background 3-42220
 ν processes, Salam-Weinberg weak interaction model, energy loss 3-80919
 Be stars, emission-ring line profile rel. to long-period V/R variation 3-69953
 CO and HCN mm.-wave emission from stars 3-69974
 Ca II H and K line absorption as luminosity indicators for MK classification 3-45103
 H II regions, i.r. nebular luminosity versus stellar luminosity in five regions 3-56449
 Hy-absolute magnitude calibration 3-81078

stellar spectra

see also stellar spectrophotometry

- A- and Ap-type stars, photoelectric obs. of H lines 3-51338
 A-type dwarfs, rotation and shell spectra 3-61774
 A-type stars, anal. of OAO II obs. of u.v. spectra 3-73497
 A-type stars, microturbulence from line profiles of six objects 3-51339
 A-type supergiants, line intensities from high dispersion spectrograms 3-81097
 Am-type double-lined binary stars, equivalent width determ. for 7 objects 3-61791
 Am-type stars, catalogue of 418 objects with known spectral type 3-65885
 Ap stars, element abundance anomalies 3-81057
 Ap type stars problems in search for Tc II lines rel. to promethium controversy 3-81049
 Ap-type stars, search in open clusters 3-61771
 η Aquilae, predicted observability of CO and CO⁺ lines 3-61811
 η Aquilae, prediction for presence of C₂ Swan bands 3-61810
 56 Arietis (HD 19832), He I line spectrum var. 3-81092
 53 Aurigae, course analysis of peculiar A-type star 3-51358
 Aurigae, eclipsing binary, Ca I satellite lines rel. to expanding circumstellar cloud 3-53666
 B type, light ion spectra giving neon abundances 3-73493
 B-star model, last Balmer lines and Hy 3-61773
 B-type main sequence stars, u.v. flux envelopes, 1100-6000 Å obs. 3-48026
 B-type supergiants in SMC, spectra of weakened lines 3-81055
 BD-10°4662, obs. indicating possible post-T Tauri star 3-51350
 Be-type stars, i.r. excesses, low-temp. free-free emission 3-61757
 binary and multiple stars, spectroscopic parameters 3-51346
 blanketing theory and G-I index for subdwarfs 3-45097
 α Bootis (Arcturus), accurate wavelengths of stellar and telluric absorption lines 3-48018
 Ca II H and k-line absorption features, luminosity effect 3-81045
 TX Cancri, W Ursae Majoris type, obs. and evolution 3-65892
 η Canis Majoris, B5 Ia supergiant 3187-6678 Å 3-69957
 VY Canis Majoris, obs. of CO in 5 μ spectra 3-45159
 α Canis Majoris (Sirius), possible discovery of chromosphere from Ca II H-line emission 3-45123
 α Canis Majoris (Sirius), u.v. spectrophotometry, Gemini XII 3-48048
 α Canis Minoris (Procyon), accurate wavelengths of stellar and telluric absorption lines 3-48018
 α^2 Canum Venaticorum, Mg II lines at 2800 Å 3-56395

stellar spectra continued

- α^2 Canum Venaticorum, spectrum variable, u.v. obs. of line blanketing 3-81039
 S Carinae, Mira-type variable, Coude spectra through cycle, atmospheric parameters 3-42191
 SX Cassiopeiae, Algol-type variable, detection of secondary spectrum 3-45135
 γ Cassiopeiae, Be type, i.r. spectra obs. by Fourier spectrometry (French) 3-77094
 β Centauri, energy distrib. and continuous spectrum in 2000-3800 Å range 3-73509
 α Centauri, He I line spectrum var. 3-81092
 α Centauri, He spectrum var., OAO-2 u.v. photometric obs. 3-48049
 α Centauri, spectrum variable, obs. of anomalous Fe I lines 3-53667
 α Centauri (HD 125823), radial rel. variations determ. 3-42198
 ω Centauri cluster, ¹²C/¹³C ratio for two CH-stars using Swan bands 3-45194
 β Cephei, obs. with improved time resolution 3-48035
 ϕ Ceti, speckle interferometry, colour-depend. limb darkening 3-48031
 Chamaeleon 16, nebulous object in Chamaeleon T assoc., spectroscopy 3-77145
 classical Cepheids, Q-method for colour excesses 3-45102
 classification, peculiar and luminous bright stars 3-77068
 classification, technique and criteria (Russian) 3-61785
 close binaries, spectral type of cool component assuming convective envelope 3-47988
 close binary systems, spectral type criterion for envelopes of cool members 3-45096
 Coalsack, search for flare-star spectra rel. to star formation 3-81208
 contribution functions rel. to spectral line contrast 3-59347
 β Coronae Borealis, identification of actinides 3-65890
 CPD -69°2698, H-deficient star, Coude spectrograms and abundance analysis 3-48027
 57 Cygni, apsidal motion and spectral line blending effects 3-73515
 V1016 Cygni, expansion, spectroscopic studies, emission line structure 3-69969
 CI Cygni, symbiotic star, obs. of spectrum during outburst 3-48041
 α Cygni (Deneb), discovery of chromosphere from Ca II K-line emission 3-45123
 DA white dwarfs, interpretation of quadratic Zeeman effect 3-69941
 diatomic molecules, transitions between fine structure in microwave region 3-40604
 diffuse interstellar features in spectra of dust-embedded and field stars 3-56383
 Draconis (HD 155763), high dispersion spectral study of β -type star 3-48025
 dwarfs, strong-line G and K (M_r, R-I) diagram, spectroscopic characteristics 3-69950
 early-type stellar spectra, interpretation 3-73508
 early-type supergiants with variable H α profiles, obs. 3-45106
 early-type supergiants with variable H α profiles rel. to mass loss and turbulence 3-56375
 emission line binaries, search for black holes 3-73431
 ν Eridani, β Cephei variable, behaviour of H lines 3-56392
 α Eridani, interstellar lines, Copernicus u.v. obs. 3-59384
 40 Eridani B, white dwarf, line profiles and rotation meas. 3-45120
 extended atmospheres, obs. of stellar spectra 3-77082
 extinction and scatt. by small planetesimal particles, appl. to T Tauri type stars 3-73496
 F and G stars, continuum photometry 3-56378
 F and G stars, H α line profiles 3-56377
 F-type, peculiar spectra, spectral classification 3-77069
 Fm stars, curve-of-growth anal. 3-47987
 Galactic H II regions H α Fabry-Perot spectrometry 3-77162
 H η 1069, UV Ceti-type star behind Pleiades 3-45138
 H η 230, UV Ceti-type star behind Pleiades 3-45138
 HD173219, periodic Be star, companion possible black hole 3-61813
 HD187399, binary, case B of mass exchange 3-61812
 HD 122563, N abundance of very metal-poor star 3-81091
 HD 126983, double line spectroscopic binary, orbital obs. from coude spectra 3-77090
 HD 144941, H-deficient star, Coude spectrograms and abundance analysis 3-48027
 HD 153919, optical candidate for 2U 1700-37 X-ray source 3-51374
 HD 153919 (=2U 1700-37), spectroscopic obs. 3-61815
 HD 221568, Ap-star, light var. rel. to line blanketing 3-45121
 HD 45677, peculiar Be-star with i.r. excess, spectrographic obs. 3-61804
 HD 51418, peculiar A-type star, spectrum and light var. 3-69956
 HD 77581 (Vela XR-1 optical candidate), Zeeman effect in H β line 3-51352
 α Her A, temperature calc. from spectral bands of TiO γ system (Russian) 3-61805
 105 Her K4 II star, 6870-5800 Å, atmospheric physical parameters, anomalous abundance of lithium (Russian) 3-77096
 88 Herculis, spectrum variability of shell star 3-61809
 88 Herculis, shell star, long time variations (French) 3-77088
 hot supergiants, molecular features around 1720 Å 3-69945
 HR 465, Ap-star, tests and consequences of Pm identification 3-48021
 HR 465, appl. of wavelength coincidence statistics to line production 3-61800
 HR 7575, appl. of wavelength coincidence statistics to line production 3-61800
 HR 7955, spectroscopic binary, high-resolution spectra 3-48029
 interstellar gas abundances from rocket obs. of u.v. absorpt. lines 3-59378
 interstellar lines equivalent widths rel. to colour excesses 3-73555
 interstellar lines in reddened and unreddened stars rel. to interstellar ionization and column densities 3-45212
 ionizing radiation production by UV and OB stars 3-81052
 irregular variable stars, obs. of H α emission profiles 3-73492
 K-line width-absolute magnitude relation 3-80979
 Kapteyn Selected Areas, photoelectric UVB photometry of 128 stars 3-73503

stellar spectra continued

- EV Lac, spectrophotometric observation of flares, energy distribution in spectra (*Russian*) 3-77095
 EV Lac flares, Balmer decrements, proposed model (*Russian*) 3-77065
 10 Lacertae, O-type star, rapid spectral variations 3-45134
 late-type stars, $10\ \mu$ excess emission from interstellar grains 3-53718
 ϵ Leonis, G-type giant, model atmospheres and high dispersion spectrograms 3-48051
 α Leonis, interstellar lines, Copernicus u.v. obs. 3-59384
 α Leonis (HD 87901), high dispersion spectral study of β -type star 3-48025
 line formation in extended atm. 3-51331
 line formation in spherical atm. 3-45087
 long-period variables, period rel. to OH radial-vel. 3-59343
 δ^2 Lyr, temperature calc. from spectral bands of TiO α -system (*Russian*) 3-61805
 α Lyra, energy distrib. and continuous spectrum in 2000-3800 Å range 3-73509
 α Lyrae, uncertainty in Balmer discontinuity 3-45105
 α Lyrae (Vega), discovery of chromosphere from Ca II H-line emission 3-45123
 β Lyrae spectra, variation of H and He lines (*Russian*) 3-45128
 RR Lyrae-type stars in globular cluster M22, metal abundance from equivalent width meas. 3-45196
 M67, metallicity of and spectral types of main-sequence stars in cluster 3-48088
 M-type dwarf stars, magnitude, TiO absorption bands (*Russian*) 3-45114
 M-type giants at South Galactic pole, spectroscopic obs. of 30 objects 3-42233
 M-type supergiants, photospheric and circumstellar H α profiles 3-53661
 magnetic null lines for mag. peculiar A-type star atm. studies 3-45115
 multiplet formation in atoms with split upper level 3-71359
 MWC 645, spectra and energy distrib. rel. to η Carinae 3-42195
 MWC 819, spectra and energy distrib. rel. to η Carinae 3-42195
 nearby, composition of interstellar clouds from Copernicus satellite spectrophotometric results 3-45211
 NGC 2129 region, classification of faint stars (*Russian*) 3-61786
 NGC 2264, spectroscopic obs. of u.v.-excess stars 3-56419
 NGC 2264, stellar polarisation and nature of circumstellar shells 3-53698
 NGC 6809, spectra of three blue horizontal-branch stars 3-45195
 Nova Cephei 1971, light curve 3-77102
 novae, coronal line formation 3-61792
 O and B standards, energy distrib. in u.v. spectra (*French*) 3-81089
 O- and Of-type stars, temp. and spectra 3-77080
 O-type stars, Vega uncertainty in Balmer discontinuity 3-45105
 O-type stars in visual multiple systems, absolute magnitudes and intrinsic colours 3-81080
 OB stars, Mariner 9 meas. of interstellar absorpt. at λ_{α} 3-51337
 OB supergiants, meas. of strength of He I 6678 Å line 3-65883
 Of stars, $\lambda\lambda 4485, 4503$ Å emission lines observed, unidentified 3-81058
 Ophiuchi, detection of interstellar ^7Li 3-73548
 Orion Nebula cluster, spectroscopic obs. of u.v.-excess stars 3-56419
 α Orionis, speckle interferometry, colour-depend. limb darkening 3-48031
 θ^2 Orionis (2U 0525-06 optical candidate), Zeeman effect in H β line 3-51352
 δ Pavonis, C abundance rel. to UVB and uvby colours and spectrum 3-42201
 peculiar A stars, elemental abundance anal. 3-65879
 AG Pegasi symbiotic binary model, M giant absorption spectrum 3-81090
 δ Persei, strong variable 1650 Å emission feature 3-77101
 κ Piscium, spectrovariable, spectral anal. 3-59350
 planetary nebulae nuclei, spectra rel. to massive Population I stars 3-81212
 prediction from atm. turbulence structure 3-65290
 pressure ionization and opacities based on Thomas-Fermi atom 3-81044
 Puppis, eclipsing binary, i.r. spectra 3-45124
 radial vels. $10\ \text{ms}^{-1}$ accuracy from spectrograms using telluric absorption lines as comparison 3-48156
 red giants in M 5, M 10, M 92, spectral anal. 3-53702
 λ Scorpii, interstellar lines, Copernicus u.v. obs. 3-59384
 Σ Sculptoris, long-period Me variable, spectral Tc lines 3-45133
 α Sculptoris, spectrum variable, u.v. obs. of line blanketing 3-81039
 SdB-type rapid variables, statistical anal. 3-59344
 β Sextantis (HD 90994), high dispersion spectral study of β -type star 3-48025
 SMC globular clusters, NGC 121, NGC 419, Kron 3, carbon stars 3-70022
 SN 1972 in NGC 5253, i.r. emission features in spectrum 3-45125
 South Galactic Pole, spectroscopically peculiar stars 3-42190
 Southern OB stars, spectral type of 101 objects 3-53657
 spectral energy distrib. in near i.r. of 6 objects 3-61795
 supergiants, chemical composition determ. from evolutionary tracks, bolometric calibration and spectral type 3-81051
 supergiants, type G and K Ib, equivalent width data 3-73501
 supergiants in h and χ Persei association X-ray observations 3-73510
 supernova remnants, emission-line spectra rel. to properties of galactic nuclei 3-45108
 supernovae spectra, interpretation and atlas 3-51340
 IK Tauri, period and spectral range from i.r. obs. over 8 years 3-81093
 28 Tauri (Pleione), new shell phase in spectrum 3-42192
 RR Telescopii, emission line spectrum during 1968 rel. to nova-like properties 3-42196
 Trumpler 27, open cluster, obs. of red star 3-61775
 two-level source function, dependence on own radiation field 3-48000

stellar spectra continued

- Two-Micron Sky Survey, near i.r. spectroscopy of 235 unidentified sources 3-48072
 W Ursae Majoris mass, radii and luminosity from spectroscopic radial velocity obs. 3-69962
 γ^2 Velorum, eclipsing binary, i.r. spectra 3-45124
 γ^2 Velorum, short period spectral variations at 4660 Å 3-48052
 γ^2 Velorum, spectroscopic binary, C IV emission feature in near-u.v. spectrum of Wolf-Rayet star 3-48022
 α Virginis, β Cephei star, obs. with improved time resolution 3-48035
 CU Virginis silicon Ap-star, H Balmer lines, phase variation (*Russian*) 3-45129
 BW Vulpeculae, β Cephei star, obs. with improved time resolution 3-48035
 white dwarfs, data for 41 southern objects 3-69961
 white dwarfs with large mag. fields, He spectra 3-45107
 Wolf 1346, white dwarf, line profiles and rotation meas. 3-45120
 Wolf-Rayet stars, forbidden transition $2p^2\ ^1\text{SD} - 2s2p\ ^3\text{P}$ in Bel isoelectronic sequence 3-56387
 Wolf-Rayet stars, high dispersion spectra 3-77079
 Wolf-Rayet stars, theory of emission spectra, expanding envelope hypothesis 3-81062
 Wolf-Rayet stars rel. to P Cygni-type stars 3-81061
 CH molecule, i.r. and radio transition probabilities 3-53712
 CO i.r. absorption bands in late-type stars rel. to spectral type 3-81041
 Ca II emission binaries, obs. of variable stars 3-56394
 Ca II H and K line absorption as luminosity indicators for MK classification 3-45103
 Ca II K-line reversals and simulated stellar chromospheric-photospheric models 3-45104
 Ca II resonance linewidth-luminosity relations and chromospheric velocity fields 3-69944
 Eu III resonance line classification 3-81043
 Fe I 6065 Å line rel. to measurements of microturbulence in atmospheres 3-81018
 H $_2$, interstellar detection, u.v. spectrum of δ Scorpii 3-48123
 H $_2$ lines in reddened stars rel. to interstellar gas, Copernicus u.v. obs. 3-59385
 H $_2$ linewidth-luminosity relations and chromospheric velocity fields 3-69944
 H $_2$ O i.r. absorption bands in late-type stars rel. to spectral type 3-81041
 He I spectra in B stars, analysis 3-65881
 Hg stars, wavelength shifts and isotopic structure of Pt II 4046 Å line 3-61772
 Hy-absolute magnitude calibration 3-81078
 Mg II lines near 2800 Å, equivalent widths in spectra of 31 stars 3-45098
 Mg II resonance linewidth-luminosity relations and chromospheric velocity fields 3-69944
 OH molecule, i.r. and radio transition probabilities 3-53712
 Si Ap stars, theoretical intensity of Si lines 3-53659
- stellar spectrophotometry**
see also stellar radiation; stellar spectra
 AOV star, absolute calibration of uvby system of filters 3-81258
 A- and F-type stars, effect of rotation on photometry for absolute magnitude determ. 3-81069
 absolute magnitude determ. from Balmer H-line photometry 3-81075
 AC + 39° 1214-608, flare star, variations in emission (*Russian*) 3-45127
 Algol systems, photometric effects of gas streams 3-53647
 RX Andromedae, Z Cam type variable, photometric obs. during eruption 3-65893
 Ap stars, light variation due to line-blanketing effects 3-61783
 Ap stars with long periods, search 3-45131
 apparent V magnitude determ. on independent basis 3-81088
 ST Aquarii, eclipsing binary, UVB photoelectric photometry obs. 3-77084
 atmosphere electron density determ. using photoelectric spectrometer 3-61889
 UV Aurigae, carbon star, visual primary of binary ADS 3934, spectrophotometry, classification 3-51356
 RT Aurigae, differential UVB photometry of Cepheid 3-77083
 Aurigae, eclipsing binary, 6-colour obs. of 1963-64 eclipse 3-53665
 SS Aurigae, possible Z Camelopardalis type star 3-45130
 B5V-A5V stars in Catalogue of Geneva Observatory, apparent diameters of 172 objects 3-53655
 B-type stars, effective temp. determ. and comparison with model atm. 3-45095
 balloon-borne spectrometer operating in Hartley band, optics/electronics/measurement systems (*French*) 3-73561
 Basel 11 in Taurus, RGU-colour photometry 3-81174
 BD + 10° 2179, hot He-C star, photoelectric spectral scan obs. 3-45117
 BD + 34° 3815 (Cygnus X-1), nature of optical variability 3-61818
 BD + 37° 442, hot He-C star, photoelectric spectral scan obs. 3-45117
 binary star photometry, depend. on component separation 3-51408
 BVRI system, relations between theoretical and observed colours 3-53719
 α Camelopardalis, interstellar grain extinction in u.v., spectrophotometric results from Copernicus satellite 3-51404
 TX Cancri, W Ursae Majoris type, obs. and evolution 3-65892
 SY Cancri, Z Cam type variable, photometric obs. during eruption 3-65893
 α Canis Majoris (Sirius), u.v. spectrophotometry, Gemini XII 3-48048
 YZ Canis Minoris, 1972 photoelectric photometry of flare star 3-73518
 YZ Canis Minoris flare star, 1969 Jan., spectrophotometric investigation (*Russian*) 3-45126
 Case 621, SC star, identification with VX Aquilae 3-45137
 γ Cassiopeiae, Be type, i.r. spectra obs. by Fourier spectrometry (*French*) 3-77094
 AR Cassiopeiae, eclipsing binary, six colour obs. 3-81096

stellar spectrophotometry continued

- ω Centauri, globular cluster, i.r. photometry and spectral types 3-65928
- α Centauri, He spectrum var., OAO-2 u.v. photometric obs. 3-48049
- ω Centauri globular cluster, UVB photoelectric data for 126 bright stars 3-48110
- VV Cephei, eclipsing contact binary, period damages 3-61803
- RZ Cephei, RR Lyrae-type, radial vel., light and colour curves 3-53668
- Cepheid stars, systematic errors in temp. and mass 3-56385
- Cepheid variables in 3 LMC globular clusters, BV obs. 3-65882
- UV Ceti, 1972 photoelectric photometry of flare star 3-73518
- UV Ceti-type flare stars, UVB obs. of 10 objects 3-45099
- chromospheric activity of solar type, photoelectric obs. (Italian) 3-61788
- classical Cepheids, 6-colour photometry rel. to Q-method for colour excesses 3-45102
- Collinder 107, open cluster and stellar ring in Monoceros (German) 3-65927
- colour indices, theoretical and observed comparison of UVB, uvby and Geneva's UBVB₁ B₂ V₁ G systems 3-81257
- comparison stars, multivariate analysis to parallax solns., effect of magnitudes and colours 3-77057
- Copernicus satellite spectrophotometry instrumentation 3-59395
- V1329 Cyg=HBV 475, symbiotic binary, photometric and spectroscopic obs. 3-69965
- 32Cygni, 1971 eclipse, OAO-2 filter photometry 3-51354
- V453 Cygni, spectroscopic binary, BV obs. showing apsidal motion 3-42199
- 31 Cygni, spectroscopic eclipsing binary, 4-colour photometry 3-77106
- double stars, conference (Pennsylvania, USA, 12-15 Apr 1972) 3-51342
- dwarfs, strong-line G and K (M_r, R-I) diagram, spectroscopic characteristics 3-69950
- early type southern stars, UVB obs. 3-48020
- early type stars, u.v. photometry from TD1 satellite obs. 3-56465
- early-type stars, obs. in linearly polarised light of diffuse 6180A band in 49 stars 3-73499
- eclipsing binaries, light curve rectification 3-77073
- exciting stars, UVB and spectral obs. of 45 objects (French) 3-53713
- F- and G-type dwarf stars, uvby colours rel. to metal abundance and age distrib. in solar neighbourhood 3-45101
- Fornax dwarf galaxy, photometric obs. of clusters 3-59370
- G95-59, red dwarf, UVB and PVI obs. 3-45118
- G-type dwarf stars, metal-rich, u.v. four colour photometry, 31 Aquilae, δ Pavonis, and α Mensae 3-48015
- galactic Cepheids, intrinsic B-V colour determ. 3-48011
- Galactic structure by stellar photometry, spectroscopy, colour excess and distance, Cepheus direction (French) 3-77136
- globular clusters in M31 V magnitudes and colour indices 3-77150
- Groningen-Palomar variable star fields, UVB photometry for 170 objects 3-48006
- HD153919 (=2U 1700-37), UVBJHKL photometric obs. 3-61814
- HD 101799, W Ursae Majoris-type eclipsing binary, UVB obs. and orbit 3-48023
- HD 133029, magnetic variable UVB photoelectric photometry obs. 3-77089
- HD 153919, identification as optical counterpart to 2U 1700-37, OAO-2 obs. 3-48032
- HD 153919 (=2U 1700-37), photoelectric UVB obs. of optical variations 3-81133
- HD 184927, He-rich star, spectrophotometric anal. 3-48053
- HD 193722, Si Ap-star, period and radial vel. meas. 3-53663
- HD 217312, spectroscopic binary, B photometry 3-77103
- HD 77581 (2U 0900-40), UVB photoelectric photometry 3-81136
- HD 98088, Ap star, photoelec. obs., light variation (German) 3-81100
- HZ Herculis, B-magnitude light curve 3-45122
- TX Herculis, eclipsing binary, BV photometry and light curve analysis 3-51357
- HZ Herculis, UVB photometry and Hercules X-1 35-day cycle 3-73517
- HZ Herculis (Hercules X-1), nature of optical variability 3-61818
- high-luminosity red stars near Sun, young disc population 3-77067
- HR 1287, δ Scuti type, blue photometric obs. discrepancy in fundamental frequency 3-77087
- HR standard star, photometric criteria for choice 3-81087
- IC 2157, open cluster, three colour photometry 3-81175
- IC 2581 open cluster, differential reddening 3-77132
- interference filters, for broadband photometry in u.v., 1200-1900 Å 3-77175
- interstellar extinction between 1000 and 1200 Å, Copernicus results 3-48136
- interstellar grain extinction in u.v., spectrophotometric results from Copernicus satellite 3-51404
- interstellar lines in reddened and unreddened stars rel. to interstellar ionization and column densities 3-45212
- interstellar lines in unreddened stars, Copernicus u.v. obs. 3-59384
- iris diaphragm meas. reduction to magnitude 3-73559
- Kapteyn Selected Areas, photoelectric UVB photometry of 128 stars 3-73503
- EV Lac, spectrophotometric observation of flares (Russian) 3-77095
- EV Lac flare investigation, Balmer decrements, proposed model (Russian) 3-77065
- BL Lacertae, BV obs. and bibliographic informations (French) 3-73514
- BL Lacertae, photographic and photoelectric obs. of optical variability 3-81095
- EV Lacertae polarimetric obs., blue region (Russian) 3-45113
- AD Leonis, 1972 photoelectric photometry of flare star 3-73518
- LMC H α emission-line stars, photometric obs. 3-48101
- luminosity discriminant for red giants and supergiants 3-61780
- UV Lyncis, W Ursae Majoris star, UVB photometry and photometric orbit 3-65895

stellar spectrophotometry continued

- RZ Lyrae, light gradients and variations with Blazhko effect (Russian) 3-77091
- RZ Lyrae, photometric variations with period of Blazhko effect (Russian) 3-77092
- α Lyrae, uncertainty in Balmer discontinuity 3-45105
- RR Lyrae stars, intermediate-band photometry and colours 3-81048
- RR Lyrae variables near S. Galactic Pole, photometric obs. of 4 objects 3-61778
- M15, interpretation of two colour and colour magnitude diagrams 3-73495
- M29 (NGC 6913), galactic cluster V photoelectric obs. of 3-61847
- M31, dynamics, internal motion of stars and dust, spectrographic obs. 3-65931
- M35, open cluster, UVB photometric obs. 3-73542
- M4, globular cluster, 4-colour obs. of early-type stars 3-56426
- M67, metallicity of and spectral types of main-sequence stars in cluster 3-48088
- M67, old open cluster, DDO photometry rel. to cyanogen strength and Fe/H ratio 3-45186
- M92, interpretation of two colour and colour magnitude diagrams 3-73495
- M dwarfs, medium spectral resolution scan photometry, Spinrad-Taylor system 3-69942
- Magellanic Cloud clusters, photometric obs. of integrated light 3-59370
- magnetic stars, photoelectric obs. (Italian) 3-61787
- main sequence, correlation between u.v. excess and deviation from mean 3-77062
- main sequence stars, u.v. colours from OAO-2 Telescope obs. 3-48005
- Me type dwarfs, models for periodic variations, spot model 3-73498
- metal deficient A-type stars, four-colour photometry 3-77071
- AU Microscopium, VR obs., two-spot model 3-73498
- Milky Way fields, photoelec. UVB photometry, space-density function, distrib. of interstellar matter 3-81177
- Mira variables, near i.r. photometry 3-56380
- 1 Monocerotis, δ Scuti-type variable, UVB photometry rel. to amplitude var. in light curve 3-48039
- ST Monocerotis, Mira-type variable, UVB magnitude sequence 3-45136
- moving clusters HR diagrams, calibration of MK types 3-81079
- MSB 57, N-type star, variability 3-45137
- MWC 349, optical, radio and i.r. obs. 3-73520
- MWC 349, radio star, photoelectric obs. 3-61802
- N-type C star in cluster NGC 2660, evolution rel. to UVB study 3-45110
- N-type stars, temp. and continuum determ. for 20 objects 3-51349
- nearby dwarfs, model calc. rel. to many-colour photometry 3-61765
- nearby stars, composition of interstellar clouds from Copernicus satellite spectrophotometric results 3-45211
- NGC 1778, open cluster, UVB obs. and age determ. 3-45184
- NGC 1850, globular in LMC, B,V obs. 3-56434
- NGC 1893, photoelectric magnitude and UVB colours for 56 stars in cluster 3-48089
- NGC 2477, open cluster, photometric obs. 3-56429
- NGC 2660 (open cluster) and nearby C star, photoelectric and photographic photometry 3-70011
- NGC 6352, metal-rich globular cluster, UVB meas. 3-56418
- NGC 6752 globular cluster, UVB photoelectric data for bright stars 3-48111
- NGC 6809, Stromgren 4-colour photometry of 10 blue horizontal-branch stars 3-45195
- NGC 6838, photoelectric magnitude and UVB colours for 13 stars in cluster 3-48089
- NGC 6934, globular cluster, BV photometric obs. 3-45180
- nightglow stellar component in B wavelength band 3-61794
- Nova Cephei, 1971, photometry, light variations, estimation of photometric distance 3-81101
- Nova Cephei 1971, photoelec. UVB obs. 3-77102
- Nova Doradus 1971a in LMC, UVB obs. 3-56391
- Nova Serpentis 1970, u.v. spectrophotometry 3-48040
- O-type stars, Vega uncertainty in Balmer discontinuity 3-45105
- O-type stars in visual multiple systems, absolute magnitudes and intrinsic colours 3-81080
- OB stars in LMC, UVB photometry 3-81181
- OB stars in Milky Way system, two-colour diagrams 3-48016
- open clusters, list and maps of suspected Southern Milky Way objects 3-45185
- open clusters, photographic UVB photometry of 10 clusters (German) 3-73541
- southern open clusters, UVB-H β photometry of 28 objects 3-65925
- Ophiuchi, interstellar grain extinction in u.v., spectrophotometric results from Copernicus satellite 3-51404
- Ophiuchus, far u.v. photometry of stars rel. to sky background 3-48014
- σ Orionis E, hot He-C star, photoelectric spectral scan 3-45117
- δ Pavonis, C abundance rel. to UVB and uvby colours and spectrum 3-42201
- Persei, interstellar, grain extinction in u.v., spectrophotometric results from Copernicus satellite 3-51404
- ζ Persei, interstellar grain extinction in u.v., spectrophotometric results from Copernicus satellite 3-51404
- δ Persei, OAO-2 and Mariner 9 u.v. obs. rel. to variability 3-77101
- KT Persei, Z Cam type variable, photometric obs. during eruption 3-65893
- photoelectric UVB of 203 stars by Palomar telescope 3-73504
- photograph calibration using brightness profiles of field stars 3-45235
- quartz spectrograph with oscillating plateholder, review of appl. (French) 3-70064
- red variables with very small amplitude and very short period, photometry 3-81046
- ν Sagittarii, hot He-C star, photoelectric spectral scan obs. 3-45117
- Sanduleak 160, optical counterpart of SMC X-1, B photometry 3-81137
- Sanduleak 160, proposed optical candidate for SMC X-1, photographic photometry 3-51377
- Scorpio-Centaurus association, H α and H β photoelectric measurements 3-81187

stellar spectrophotometry continued

- Scorpius, far u.v. photometry of stars rel. to sky background 3-48014
- RZ Scuti, binary, obs. between 3460 and 6800 Å 3-53670
- SMC bright stars, uvbr obs. and comparison with models 3-48004
- SN 1972 in NGC 5253, u.v. photometry 3-48044
- solar diameter determ. at 5000 Å and H α from photoelectric drift scans 3-65653
- stellar radiation temperature calibration by spectrophotometric comparison with standard stars 3-81082
- stellar ring 58, distance determ. of member stars from BV obs. 3-61782
- Stromgren four-colour system, adaptation to photographic photometry 3-59394
- subdwarfs, existence in (M_{bol} , log T_e)-plane 3-61776
- Supernova 1971 I in NGC 5055, light curves from BV photometry 3-77104
- supernovae, absolute magnitude determ. for 43 type I objects 3-48012
- HL Tau-76, triple periodic white dwarf, blue magnitude obs. 3-48034
- 44 Tauri, δ Scuti star, photoelectric obs. in blue light 3-53669
- temperature scales and colour relations, bolometric corrections 3-81086
- ten-colour intermediate band photometry of 148 stars 3-65884
- Trumpler 27, obs. of red star 3-61775
- 47 Tucanae, globular cluster, i.r. photometry and spectral types 3-65928
- 47 Tucanae, globular cluster, UVB photoelectric photometry of 60 stars 3-65929
- 47 Tucanae giant stars, discontinuity in props. 3-61849
- two-beam multi-mode nebular-stellar photometer 3-42251
- UBV, large proper motion stars, subluminal stars, nearby stars 3-77072
- UBV photometric diagrams for detection of open star clusters 3-45181
- UBV photometry of southern stars 3-73505
- UBVB, B_1 , V_1 G photometry rel. to Hyades distance determ. 3-81256
- ultrashort period variables, intermediate-band photometry and colours 3-81048
- W Ursae Majoris, mass-ratio determ. from photometric obs. 3-48050
- v Ursae Majoris, photoelectric light curve determ. 3-45119
- uvby β photoelectric photometric catalogue 3-77063
- uvby photometry of spectroscopically peculiar stars at South Galactic Pole 3-42190
- V-magnitude calibration from absolute flux meas. of Sun and Vega 3-81081
- variable stars small amplitude red disc and halo population, UVRI obs. 3-73502
- visual binaries, Hertzsprung's luminosity colour relation 3-51344
- Wolf 424 AB, flare star, UV Ceti type, flare activity meas., photometric obs. 3-69964
- Ba II type, absolute magnitude and population giving colour magnitude diagram for NGC 2420 3-81085
- H β system, calibration rel. to absolute magnitudes and colours of early-type stars 3-81076
- He-C stars, photoelectric spectral scans of 4 objects 3-45117
- He-weak stars u.v. energy distrib., comparison of OAO-2 obs. with UB-V photometry 3-81084
- OH stars, type I, optical props. 3-61781

stellar structure

- A-type stars, microturbulence from line profiles of six objects 3-51339
- accreting neutron stars nuclear fusion forming X-ray source 3-81026
- Algol systems, photometric effects of gas streams 3-53647
- Algol-type binaries, model for alternate period changes 3-73480
- aligned rotating magnetosphere, general analysis 3-59330
- 53 Aurigae, course analysis of peculiar A-type star 3-51358
- asymmetric oscillations allowing for gravitational radiation 3-45715
- binary star systems, discussion of obs. of flow of matter 3-77081
- binary stars, evolutionary considerations involving internal density concentration parameter 3-53644
- binary stars, reformulation of fission theory 3-53640
- pure C stars, thermal stability rel. to neutrino emission 3-59335
- α Canis Majoris (Sirius), possible discovery of chromosphere from Ca II H-line emission 3-45123
- central stars of planetary nebulae rel. to hot liquefying white dwarfs, cores, masses and luminosity 3-61877
- Cepheid instability strip, non-pulsating stars, properties and evolution 3-45111
- Cepheids, linear and nonlinear pulsation calculations 3-61762
- close binary systems, spectral type criterion for envelopes of cool members 3-45096
- convection in main-sequence stars and metal-deficient subdwarfs 3-51322
- convection zones, linear convective modes and energy transport 3-81022
- convective stars, supersonic turbulent stress and structure 3-73479
- critical luminosity in stellar interiors and stellar surface boundary conditions 3-47984
- α Cygni (Deneb), discovery of chromosphere from Ca II K-line emission 3-45123
- double shell source stars, numerical computation of evolution 3-65875
- E model sequence, multiple solns. of eqns. of stellar structure 3-77039
- eclipsing binary system envelopes 3-53645
- expanding envelopes, structure and interpretations 3-77054
- Fermi-Dirac functions, partially degenerate matter, Chebyshev approximation methods 3-61769
- fundamental HR-diagram using log g and log T 3-81074
- Gravitational instability of a cold rotating cylinder 3-77050
- gravitational instability of compressible polytropic cylinder surrounded by halo gas 3-65876
- HD187399, binary with case B mass-exchange, possible black hole 3-61812
- HD 217312, masses of spectroscopic binary 3-69955

stellar structure continued

- long period Cepheids, radii and fluxes by Wesselink method 3-81083
- α Lyrae (Vega), discovery of chromosphere from Ca II H-line emission 3-45123
- RR Lyrae instability strip, non-pulsating stars, properties and evolution 3-45111
- Maclaurin stellar disc, oscillation spectrum 3-61640
- magnetic stars, pinch instabilities 3-51332
- magnetically distorted polytropes, structure and radial oscill. 3-53639
- main sequence evolution, computational techniques for star of 5 M_{\odot} 3-77046
- mass, max. value 3-51336
- mass loss in stellar wind for fast rotating metal poor stars 3-77060
- massive close binaries with collapsed component evolution and appl. to Cygnus X-3 3-53650
- Me type dwarfs, models for periodic variations, spot model 3-73498
- MHD stability in white dwarfs and neutron stars, rel. to magnetic fields 3-42187
- neutron star cores, possibilities of pion condensation and nucleon crystallization 3-81033
- nova outburst interpretation rel. to thermal waves in stars 3-53649
- oscillations and stability of rotating masses with magnetic fields 3-47986
- oscillatory secular modes rel. to main-sequence stars and He-burning shells 3-51324
- polytropes gaseous, equilibrium structure, toroidal mag. fields 3-69927
- pre-nova model, pulsational instability 3-47992
- pulsational stability of stars in thermal imbalance 3-59329
- r-process, dynamical calcs. 3-47995
- radii of nearby stars, model calc. rel. to obs. 3-61765
- radioactive envelopes, meridian circulation with rapid differential rotation 3-53636
- red giant evolution rel. to central stellar gravitational field 3-45081
- red giants of class III luminosity, convection in model envelopes 3-45084
- relativistic stability determ. using PPN formalism 3-61760
- rotating magnetoelastic stars, variational principle for gravit. field eqns. 3-61632
- rotating stars, struct., J^2 method, for uniform rotation, Roche approx. 3-69937
- rapidly rotating stars, viscous effects with appl. to white dwarf models 3-65871
- S and N stars, hydrodynamic model for plume mixing 3-65868
- secular stability, effect of shell sources on secular spectrum 3-45080
- secular stability of uniformly rotating fluid masses, effect of gravitational radiation 3-45076
- stability of super-massive stars 3-61767
- supergiants, line effects on radiative accel. 3-47981
- supermassive, rotating stars, stability 3-69933
- supernovae remnant buoyancy rise 3-47997
- synchronously rotating close binaries built on polytropic model $\nu=3$, equi-density surfaces 3-53646
- T Tauri stars, structure rel. to supersonic convection 3-51334
- T Tauri type, rotating, mass loss through stellar wind 3-77061
- thermal instability of He-burning shell in massive stars 3-51323
- thermal wave movement in non-uniform media 3-69919
- thermodynamic instability criterion for one dimensional stellar system 3-73485
- Thomas-Fermi atomic model for opacities, accuracy for stellar interiors 3-46191
- vibrationally unstable upper main sequence stars, nonlinear pulsations, perturbation technique 3-42188
- vibrationally unstable upper main sequence stars, nonlinear pulsations, direct numerical integrations 3-42189
- viscous Maclaurin spheroids, evolution of secular instability 3-47985
- white dwarf viscous evolutionary sequences 3-65872
- white dwarf with accretion, X-ray emission region 3-48084
- white dwarfs, cooling time and internal structure for 3 models 3-77048
- white dwarfs, gas-liquid phase transitions and critical point 3-53648
- white dwarfs stage of evolution, masses 3-51335
- Wolf-Rayet stars, evolution rel. to structure and origin 3-81036
- Wolf-Rayet stars, nature and physical structure 3-81038
- Wolf-Rayet stars rel. to P Cygni-type stars 3-81061
- C ignition in strongly coupled Coulomb fluids 3-65869
- C-rich stars, evolutionary models for stars with mass 0.75-1.45 M_{\odot} 3-47983
- C-rich stars with He envelopes, evolutionary models compared with planetary nebulae nuclei 3-45075
- ^{12}C shell-burning stars, radial pulsation stability rel. to pre-white dwarf stars 3-61763
- H model, eqn. of state and phase diagram for dense H 3-42163
- He burning regions, dependence of structure on molecular weight and burning rates 3-59332

stellar variables *see variable stars***stellators**

- British fusion research, history and future prospects 3-49728
- current carrying toroidal plasma filament, dynamic stabilisation in stellator 3-52528
- finite β , $\beta=2$, MHD stability 3-71945
- fusion reactors, feasibility study of cooling schemes for blankets 3-60314
- magnetic configuration perturbation by a longitudinal current in the plasma 3-68079
- plasma density, determ. using open microwave resonator 3-52531
- plasma flow, elec. pot. effect (*Russian*) 3-71878
- steady-state confinement regime in stellators, idealised collisional diffusion model 3-49738

step motors *see stepping motors***step-recovery diodes** *see charge storage diodes***step response**

- see also transient response*
- accelerometer, 2-phase excitation motor type, analysis (*Japanese*) 3-73675

stepped motors *see stepping motors*

stepping motors

- astronomical tracking theodolite, achieved by means of stepping motors (*German*) 3-42265
- particle beam profiles automatic measuring system 3-78074

stereoisomerism *see isomerism***stereoscopy** *see vision***stimulated emission**

see also laser theory

- acetylene-O₂ chemical laser characts. 3-59863
- maser, infinite atom Dicke model, dynamics 3-78003
- methyl fluoride, 496 μ m intense superradiant emission, CO₂ laser pumped 3-53127
- 4-methylumbelliferone, laser action 3-76064
- N two-level molecules system, resonant laser pulses, inversion 3-74214
- organic semiconductors, tetracene impurity-containing anthracene crystals 3-80077
- pulsars, linear acceleration radiation, Einstein coeff. method for electrons 3-73528
- rhodamine 6G, O₂ quenching constant for triplet state from lasing characs. 3-64728
- ruby laser, Q-switched, widening of emission spectrum 3-70822
- semiconductors, band-to-band or band-acceptor transition 3-57237
- superradiance of multiparticle system 3-74218
- two photon process, amplification without inversion 3-70842
- visual detection of stimulated emission or absorption from excited states, sunspot technique 3-45489
- water, stimulated short-wave radiation due to single freq. reson. of third-order nonlinear susceptibility 3-66882
- Ag-H mixture, AgII line pulse excitation, coherent emission (*Russian*) 3-71375
- Ar stimulated emission, multiple photon pumping. 3-66794
- Ar/Xe mixtures at high press. 3-66795
- Cd₅Se_{1-x}, exciton-exciton and exciton-electron interactions, obs. from 10 to 80 K 3-69024
- CdSe, laser emission due to exciton-exciton, exciton-electron interactions 3-64692
- Cu, superradiant emission from pulsed discharges in CuI vapour 3-54217
- Dy³⁺:BaY₂F₈, laser emission at 3 μ 3-54228
- Er³⁺:YAlO₃, obs. 3-72674
- F + H₂ = HF* + H, fast initiation in short high power electric discharge, spectral composition and time dependence of stimulated emission 3-48894
- p-GaAs, high purity, laser emission due to excitonic recomb. processes 3-72683
- GaSe, spectra at 2 K under high optical excitation 3-58550
- H₂, superradiance in vacuum u.v. at atmospheric pressure 3-54221
- H₂ dissociation transition, emission cross section 3-40652
- H₂ i.r. lines, pulsed stimulated emission from cooled gas laser 3-70811
- H₂ maser, H spin-exchange cross section 3-74220
- Ho³⁺:YAlO₃, obs. 3-72674
- KY(WO₄)₂:Nd³⁺ crystal spectroscopic and generation study for laser 3-64691
- Kr gas, high press. stimulated emission 3-66795
- Lu₃Al₅O₁₂:Ho³⁺, Er³⁺, Tm³⁺, spectral characteristics at 77 K, luminescence and absorption spectra 3-61053
- N₂ pulsed u.v. laser 3-48902
- Nd:YAG, stimulated emission cross section at 1061 microns 3-43017
- Nd³⁺ in YAlO₃, Lu₃Al₅O₁₂, CaWO₄ and KY(WO₄)₂ crystals, stimulated emission investigation 3-43018
- Nd³⁺:CaAl₂O₃ spectroscopic and generation characts. 3-72681
- Nd³⁺:CaWO₄-Nd³⁺:LaNa(WO₄)₂, laser luminescence spectra 3-62720
- Nd³⁺:SrF₂-GdF₃ 3-72682
- Nd³⁺:YLAG spectral props. and induced emission 3-53131
- Ne amplified spontaneous emission, high-gain transitions due to electric discharge 3-74805
- O₂ stimulated emission phenomena in high-frequency discharge (*French*) 3-52549
- Pb_{1-x}Sn_xSe and Pb_{1-x}Sn_xTe, stimulated emission of light at 10 μ 3-50600
- Tm³⁺:YAlO₃, obs. 3-72674
- Xe, lowest-bound diatomic state transitions, high pressure, superfluorescent radiation at 1730 Å 3-71569
- Xe, solid, vacuum u.v. emission band obs. 3-55649
- Xe line profile, 3.36 μ m, competition between stimulated emission and absorpt. 3-46175
- Xe stimulated emission, multiple photon pumping 3-66794
- ZnO, and spontaneous, after two-quantum excitation, free, bound exciton form. (*German*) 3-58529

stimulated emission in lasers *see laser theory***stimulation** *see excitation***stochastic processes**

see also random processes

- chemical kinetics, fluctuations around steady states, phase-space and stochastic descriptions 3-65083
- collision models and radiative equilibrium, line shape constraints 3-42888
- crystal ripening, stochastic model, computer simulation 3-63965
- cylindrical shell, nonlinear, stochastically excited, stability 3-70555
- differential eqns., stability, asymptotic reduction (*Russian*) 3-66490
- dynamic system with 3 degrees of freedom, numerical study by dimensional mapping 3-42748
- earthquake swarms, stochastic model 3-61395
- fermions, von Neumann algebra and hypercontractivity 3-45726
- fluid motion, stochastic noise in nonlinear systems (*Russian*) 3-67898
- Galactic magnetic field, stochastic models 3-48113
- irreversible chemical reactions, stochastic formulation of the kinetics 3-47560
- Ising chain kinetics in a class of spin flip models 3-60948
- many-particle system, distribution function, n-time BBGKY hierarchy (*German*) 3-70732
- mathematical models, reversibility 3-40083
- mixed gradient algorithm for optimisation (*Polish*) 3-66505

stochastic processes continued

- neutron noise in boiling reactors evaluation, Langevin analysis of neutron fluctuations 3-67391
- nonlinear perturbed stochastic integral equation, Volterra type, random solution 3-74004
- nonlinear random vibrations of elastic cylindrical shell, iterative soln. (*Polish*) 3-66589
- nonlinear vibration system analysis (*Polish*) 3-66587
- nuclear reactor safety, stochastic decision making procedure 3-46084
- perturbations, derivation of electron anomalous magnetic moment 3-67006
- plasma, mirror trapped, electron cyclotron resonance heating, stochastic theory 3-75407
- plasma in strong e.m. fields, stochastic kinetic theory 3-75288
- plasma stochastic acceleration, survey 3-71936
- plasmas, microwave stochastic reflection, Walsh spectral analysis 3-75301
- plasticity, analysis 3-54108
- polyelectrolytes, dielec. dispersion calc. using stochastic model 3-44370
- population growth problem, Volterra integral eqn. 3-59740
- probability theory rel. to quantum mechanics 3-74097
- propagation, u.s. and seismic in medium with inhomogeneities randomly distributed 3-58828
- quantum, closed formulae for wave function of particle in external e.m. field, Feynman path integral 3-62547
- quantum, Feynman path integral for particles with spin, soln. of Cauchy problems 3-62548
- quantum mechanical system, symmetry breaking of time reversal invariance 3-70729
- quantum mechanics problems, stochastic and deterministic aspects of classical approach 3-62566
- quantum mechanics reformulation, stochastic theory approach 3-62597
- Rayleigh scattering from molecular aggregates, microscopic theory, random-phase-modulation theory and stochastic theory 3-70784
- segmented nonstationary random excitation, structural response 3-45679
- streamflow synthesis technique, transition probability matrices 3-54797
- turbulent flow, particle trajectories 3-46399
- vibrations of one-degree-of-freedom system with nonlinear elastic characteristic, stochastic excitation (*Polish*) 3-70679
- T hot atom reactions with D₂, H₂ and methane, stochastic and analytical investigations 3-65114

stochastic systems

see also random processes

- atomic system, two-state, with stochastic coupling, transition study 3-49387
- biochemical system, nonequilibrium steady states, finite fluctuation effects 3-65082
- chemical reaction, second order, analytical structure of a generalised direct interaction approximation 3-76443
- eye movements during fixation on stationary target, model 3-45304
- inhomogeneous media, nonlinear elastic properties (*Russian*) 3-70583
- nonlinear differential eqns., asymptotic expansion of solns. when parameter $\lambda \rightarrow \infty$ (*Russian*) 3-66493
- population balance, puristic analysis 3-66503
- power reactor stability subject to stochastic macroscopic parameter variation 3-74652
- stochastic-ergodic sigals, measuring techniques (*German*) 3-70258
- streamflow, stochastic methods in hydraulics and hydrology 3-76930

Stokes flow *see flow***Stokes law** *see flow***Stokes lines** *see spectra***Stokes optical law** *see luminescence***stopping of particles** *see energy loss of particles***storage, digital** *see digital storage***storage devices**

see also energy storage devices; optical storage devices; semiconductor storage devices

No entries

storage organisation *see file organisation***storage rings**

- ACO, beam dynamics 3-56812
- beams longitudinal stability in rings with resonant systems 3-73839
- Cambridge electron accelerator, USA, performance at e⁺e⁻ storage ring 3-56824
- CERN proton storage rings (*German*) 3-53961
- colliding beam expts. in electron positron and proton-proton storage rings 3-53965
- DORIS at DESY, pe colliding beam experiment 3-56815
- electron, short bunches production 3-56827
- electron linac improvement, 40 MeV, duty factor, design criteria, tentative designs 3-77600
- electron ring, for ep option at ISABELLE 3-56814
- electron synchrotron, DESY, construction of storage ring (*German*) 3-77599
- EPIC, electron proton intersecting ring complex 3-66305
- intersecting, at CERN, beam-induced gas desorption 3-56811
- intersecting, at CERN, intersection diamonds creation 3-56813
- intersecting, at CERN, layout, physics equipment and use for experiments 3-56823
- intersecting, at CERN, operating results 3-56808
- intersecting, at CERN, space charge induced Q-shifts 3-56820
- intersecting, at CERN, stacking efficiency 3-56818
- intersecting, at CERN 3-42628
- intersecting, beam scrapers for luminosity improvement, background reduction and chamber protection 3-56819
- intersecting, search for quarks and large angle production of stable particles heavier than proton 3-71035
- intersecting, transverse feedback system for Landau damping 3-56822
- intersection, at CERN, extension of energy by acceleration of stacked beams 3-56821
- ISR at CERN, role of small computer system in control 3-66306

storage rings continued

- in Novosibirsk, review of programme 3-56810
- Orsay, proposed synchrotron radiation expts. 3-39993
- PEP design study, review 3-56856
- PEP lattice design, using superconducting rings 3-56816
- relativistic electron bunch, synchrotron instability (*Russian*) 3-70340
- report on usefulness and practicability in high energy physics 3-56858
- SLAC, SPEAR beam transport system 3-56878
- SPEAR, beam-beam interactions, luminosity 3-56829
- SPEAR of SLAC, beam position and intensity monitoring system 3-56788
- SPEAR of SLAC, operating experience 3-56809
- superconducting storage accelerator, controlling nonlinear resonances 3-56826
- synchrotron radiation source, electron, Tantalus I Wisconsin, USA, operation 3-59631
- e⁻e⁺, use for studying weak bosons 3-66966
- en interactions in the context of proposed storage ring systems 3-67048

storage tubes

- see also *image storage tubes*
- No entries

stores (computer) see digital storage**storms**

- see also *magnetic storms; thunderstorms*
- atmosphere and ocean interaction mechanism during a storm 3-76684
- convective, relation of infrasound with ionospheric phase height variations 3-80766
- extratropical cyclone parameters from Nimbus 2 HRIR meas. 3-65359
- forecasting of premonsoon thunderstorm/duststorm activity over Delhi region 3-65523
- hail and hail suppression techniques in USSR 3-61457
- hailstorms, Alberta, structure from radar and photography 3-73331
- hurricane and typhoon effects on upper active ocean layers at OWS Tango in Pacific 3-51001
- hydrograph partial area model for storm flow synthesis 3-59065
- lake effect snowstorms, role in hydrology, Lake Erie 3-47773
- Lake Effect storms, diffusional deposition of ice on AgI, snow crystal struct., Ag content 3-76768
- Martian Great dust storm of 1971, terrestrial hurricane model 3-51291
- Martian sandstorms and eolian erosion, determ. of abrasion rate by particle impact 3-65758
- microseisms, spectral development at Oulu, Finland 3-61341
- motion forecasts and depression track prediction using computer oriented technique 3-80733
- North Pacific, microbaroms azimuth rel. to severe weather systems 3-61485
- ocean wave origin of microbaroms and microseisms during storms 3-65264
- pulsed Doppler weather radar, storm wind velocity isotach displays 3-76911
- satellite pictures of cyclonic disturbances over Bay of Bengal and Arabian Sea 3-80735
- severe storms, environmental wind veer rel. to circulation 3-59117
- snowline mapping with NOAA-2 environmental satellite 3-56174
- snowstorm, 4-5 March 1971, Montreal 3-73330
- tropical cyclone motion, statistical predictability 3-47747
- tropical cyclones of Western North Pacific Ocean, rapid intensification and low-latitude weakening 3-47749
- tropical storms and typhoons, speed after recurvature in N.W. Pacific Ocean 3-65360
- tropical storms/depressions movement forecasting for India, computer technique 3-65326
- typhoon soundings compared with hurricane soundings 3-47748
- typhoons crossing Philippines, changes in characts. 3-47750
- Venezuelan rainstorms, radar obs. 3-47752
- wind, role of press. gradients in form. (*Hungarian*) 3-80723
- Ag distribution, precipitation, seeded Alberta hailstorms 3-76760

strain

- see also *deformation; stress/strain relations*
- aircraft skin panels, acoustically excited, growth rate of edge cracks, effect of bending strains 3-51480
- Aleutian Islands, secular strain meas. before and after CANNIKIN 3-50896
- alkali alloys, dilute, lattice, effect on residual resistivity 3-44055
- Australian Earth strain meas., Cooney Observatory research program 3-47639
- CANNIKIN nuclear explosion, strain and tilt data 3-50898
- CANNIKIN nuclear explosion strain and tilt meas. 3-50897
- cross-anisotropic deposits, settlement using isotropic theory 3-80600
- curved finite elements by the method of initial strains 3-42767
- cycling, biaxial strain, out-of-phase, effects on low cycle fatigue, analysis, results 3-77385
- Earth, monitoring using precise distance meas. 3-58853
- Earth strain meas. for determ. of earthquake source parameters 3-47643
- Earth strain measurements, conference (London 10-11 May, 1972) 3-44757
- Earth tides obs. in California, thermoelastic effects 3-44867
- elastic half-space, linearly nonhomogeneous, plane strain 3-74034
- elasticity virtual power method, the second gradient theory (*French*) 3-62461
- element stiffness matrices, strain energy content, weighted eigenvalue method 3-45638
- isotropic materials, local strains theory, variants for soln. of complex loading problems 3-55005
- magneto-thermo-visco-elasticity, plane strain problems, Kelvin and Maxwell bodies 3-44830
- martensitic transformations triggered by induced elastic instability localised soft mode theory 3-46695
- metal, strain energy function, finite elastic vol. change 3-40949
- New Zealand Earth strain change detection before earthquakes 3-47638

strain continued

- Nimonic 80A, grain boundary cavitation, room temp. pre-strain effects, h.v. electron microscope obs. 3-50701
 - noble metal, de Haas-van Alphen effect, impurity-induced strain influence 3-52782
 - numerical methods of calc., finite element and dynamic relax. methods 3-47808
 - pre-straining in the earth, ray theory 3-76843
 - pressure tube CIRENE prototype reactor, static-elastic conditions of core support 3-67395
 - quantitative strain and stress state criterion, failure in the vicinity of sharp cracks 3-66568
 - random-layer lattice, strain effects on diffr. profiles, Cauchy, Gauss and Laplace distribts. 3-79199
 - rock dilatancy recovery upon unloading 3-58903
 - rock strain patterns and magnitudes in 5 different tectonic regions 3-47644
 - salt-mica, folding and microfabric development in experimentally deformed specimens 3-76605
 - salt-mica, wet, folding at low strain rate 3-76606
 - sandstone, timing, amount and nature of dilatancy 3-61374
 - seismic waves, pre-strained media, Fourier-Laplace transformation 3-44784
 - tectonic, meas. near site of CANNIKIN nuclear explosion 3-50900
 - temperature-strain rate coupling, substances with temperature dependent thermal and mechanical properties 3-59753
 - thin ferromagnetic films, uniaxial strain, attachment for electron microscope (*Russian*) 3-48574
 - tuff (Nevada Test Site), effect of strain rate in loading 3-58904
 - viscoelasticity, linear, stress and strain tensors, unique solns. and approx. methods (*Russian*) 3-66541
 - viscous cylinder, large asymmetric strains due to weight and loading 3-57076
 - wurtzite structure crystals, internal, bond-bending parameter calc. piezoelectric constant 3-47218
 - zincblende structure crystals, internal, bond-bending parameter calc. piezoelectric constant 3-47218
 - Ag-Sb alloys, determ. by method of variance 3-44575
 - β -Co-Cu epitaxial bicrystal, elastic stresses and strains at interface 3-50067
 - GaAs injection laser, strain induced degradation, bonding procedure 3-59869
 - Si, deformed crystals, compressive strain, dislocation structure, surface and bulk layers (*Russian*) 3-40922
- strain gauges**
- see also *strain measurement*
 - aircraft fatigue, strain level counter, magnetic disc autologger, description 3-56621
 - bone-implantable strain transducer 3-57007
 - Earth strainmeters, locations and rock type 3-47810
 - magnetic anisotropy energy constant measurement 3-73671
 - meter for concrete 3-39857
 - microwave instrument for uniaxial strain meas. 3-66147
 - plastic deformation meas. under tension (*German*) 3-65052
 - plastic strain, direct measurement, uniaxial stress condition 3-73100
 - resistors, peculiarities under elastoplastic cyclic loading 3-73099
 - semiconductor strain transducer, description 3-51521
 - speech, lip and jaw motion, strain gauge transduction system, two dimensions, design, calibration 3-73927
 - strainmeter mounts, stability, geophysical application 3-76842
 - Au films, discontinuous gauge factor and temp. coeff. of resistance measurement, aging, humidity effects 3-58248
- strain measurement**
- see also *strain gauges*
 - bone-implantable transducer 3-57007
 - concrete, nine-gauges device, meas. inside elements 3-65055
 - concrete, prestressed, reinforcement position, X-ray obs. (*German*) 3-69418
 - cyclic loading, time monitoring technique 3-41747
 - cyclic strength tests, long-term, methodical features 3-42513
 - diffractographic moire technique 3-39856
 - dilatometers, two capacitance, magnetostrictive strain meas., liquid He temp. 3-51518
 - earth, focal area of underground explosion 3-76548
 - Earth's surface strain meas. instrumentation and technique 3-44939
 - Earth strain meas. in Australia, rod, wire and laser strain meters 3-47639
 - Earth strain meas. using 60m laser strainmeter 3-44943
 - Earth tilt and strain meas., problems 3-44938
 - fibre, continuous measurement of strain, chemical changes (*Russian*) 3-70271
 - gauge reliability, rel. to thin plate bending stress. 3-59548
 - holographic interferometry, evaluation of interference fringes (*German*) 3-66141
 - holographic interferometry for strain analysis of disc under diametral compression 3-61983
 - intersection of cylinder and ellipsoid, stressed by internal pressure, unit load determ., resistive elec. extensometry (*Rumanian*) 3-73667
 - laser interferometer for Earth strain meas. 3-44942
 - lens system, distortion equation derivation using Moire, correction factor eqn. 3-39896
 - Ligtenberg's reflective moire method, mismatches 3-39858
 - magnetostriction fatigue unit, sheet materials, fatigue meas. under plane stress and elevated temp. 3-45417
 - microstrain in compression, compression jig 3-76405
 - microwave frequencies, uniaxial strain, radiation environments 3-66147
 - Moire gauging by projected interference fringes, theory and experiment 3-45494
 - refractories, thermally loaded, deformed state studies 3-44636
 - resistance meas. on thermoplastics, current heating effect 3-50785
 - in seismology, improvements and developments, review 3-44934
 - shear strain meas. for ultrasensitive magnetostriction meas. method 3-39974
 - strain-meter base, nanometre stability of Invar and quartz suspended in catenary 3-44935
 - strain-multiplier, fatigue monitoring, description, operation, fatigue life 3-59554
 - tensometer, with air gap capacitance transducer, for linear meas. 3-53842

strange particles

- see also *hyperons; kaons*
 charmed particles and renormalizable theories of weak interactions 3-66990
 non-Abelian gauge theories with parity and strangeness conservation 3-57393
 production in π^+p interactions to five and six body final states at 8 GeV/c (*Rumanian*) 3-49058
 production in π^-p interactions at 1.69 GeV/c 3-45915
 quark model of interactions, prediction of branching rules between partial cross-sections 3-70944
 π^+p , strange particle production at 3.7 GeV/c 3-54352

strangeness see *strange particles***stratified flow**

- heading is late addition, see also *flow*
 air-oil mixtures, horizontal stratified two-phase flow, pipes, flow patterns 3-71809
 Boussinesq fluid, internal time scales in stratified spin-down 3-80945
 density-stratified fluid with suspension of particles, plane parallel flow 3-71822
 density-stratified spiral flows, hydrodynamic stability 3-57752
 fluid in rotating annulus, upwelling, steady state, numerical soln. 3-52447
 gas-liquid streams, laminar flow in horizontal tube (*Russian*) 3-75262
 horizontal, two-phase, gas-liquid mixtures, pipes 3-71809
 ideal density-stratified liquid, homogeneous region behaviour, numerical investigation (*Russian*) 3-67927
 internal waves around body moving in a density stratified fluid, phase, configuration 3-75243
 laminar free convection, ambient temp. stratification effects 3-63649
 linear spin-up of a strongly stratified fluid of small Prandtl number 3-75204
 oceanic straits and sills, model of two-layer rotating fluid flow 3-59004
 oil-water, immiscible liquids, laminar and turbulent transitional flow, stratified channel flow 3-67963
 rotating fluid layer, effect of shear and stratification on the stability 3-52448
 shear, stability, linear inviscid theory, linear initial value problem 3-63678
 slightly stratified ocean evolution of inertial frequency oscillation 3-69555

stratosphere

- aerosol layers detection at 20 and 50 km 3-51032
 aerosol props. and effects on i.r. radiation 3-51037
 aerosol scatt. optical radar obs. and balloon-borne conc. meas. in lower stratosphere 3-41981
 aerosols, formation of Aitken nuclei and large particles 3-61467
 air mass influx into lower troposphere, after solar flares 3-41969
 annual temp. wave 3-53482
 circulation and thermal structure of stratosphere, lower mesosphere during seasonal transitions 3-59102
 circulation index over Natal, Brazil 3-65378
 cosmic ray intensity, comparison of high latitude station and radio-sonde measurements (*Russian*) 3-65595
 cosmic ray intensity, comparison with altitude, diurnal and latitude dependences of ionic concentrations (*Russian*) 3-65596
 electric fields for fair weather and thunderstorms 3-59090
 emission spectrum in submillimetre range, balloon platform measurements 3-53472
 forcing response in form of white noise freq. distrib. 3-65342
 galactic electrons, energy spectrum measurement by scintillation telescope (*Russian*) 3-65560
 general circulation in Tropics and polar stratosphere meridional interaction 3-65382
 general circulation parameters calculated from SIRS data 3-59106
 glider flight obs. above cumulonimbus clouds 3-47761
 global stratospheric temp. and press. profiles from NIMBUS-5 obs., statistical retrieval techniques 3-59180
 horizontal eddy transports from serial soundings using heat balance method 3-65389
 ion chemistry, extension from D-region, reaction schemes 3-59076
 leewaves and winds over Canterbury, New Zealand during 1970 3-59059
 mesospheric and stratospheric temps. remote sensing by microwave radiometry 3-56260
 methane conc., balloon-borne spectroscopic meas. at 3.3μ 3-73305
 methane mixing ratio, vertical profiles 3-73306
 mixing with lower mesosphere 3-53479
 mobility spectra, tropospheric and stratospheric gas mixtures, drift tube, mass spectrometer, ageing effect 3-59069
 Nimbus 5 meas. of temp., water vapour and cloud 3-76773
 NIMBUS-5, selective chopper radiometer obs. 3-59066
 noctilucent clouds, visibility, effect of dust and ozone content (*German*) 3-76729
 ozone in stratosphere and mesosphere, perturbations 3-59103
 ozone layer, effect of nitrogen oxides from nuclear explosion and jet engines 3-61476
 particle layer, efficiencies of filters and impactors used for collection 3-76905
 periodic atmospheric circulation with 14-16 days cycle 3-59105
 polar, concentration of submicron particles 3-76776
 solar corpuscular radiation, effect of variations on weather 3-80767
 solar mag. sector struct. rel. to stratospheric circulation 3-65401
 spectral features at 8 cm^{-1} of probable solar origin 3-61477
 synergistic baroclinic instability of planetary waves in stratosphere 3-59114
 temp. meas. from changes in satellite radiances 3-51027
 temperature, radiosonde meas. rel. to NOAA-2 satellite meas. 3-56259
 temperature, satellite obs. in $15\mu\text{m}$ CO_2 band 3-80863
 temperature and wind data during 7 March 1970 solar eclipse 3-65341
 temperature structure, effect of water vapour and nitrogen oxides 3-76741
 tropical waves, spectral model of Cisk-barotropic energy sources 3-65385

stratosphere continued

- warming, rel. to OH emission in upper atmosphere 3-65320
 warming rel. to ionospheric absorpt. 3-61522
 water vapour mixing ratio altitude profile, atmospheric emission spectra obs. 3-41951
 wind and temp., total ozone, sea-level press. rel. to sunspot cycle 3-69598
 wind reversals rel. to natural infrasound reception, seasonal variations in polar region 3-59095
 winds, comparison of geostrophic calculations and rocket measurements 3-73317
 zonal harmonic standing waves in troposphere and lower stratosphere 3-65351
 C compounds, photochemical model with vertical transport 3-73316
 CO and methane vertical distrib., model 3-73315
 CO_2 content 3-73327
 N relative concentrations in stratosphere and mesosphere, one-dimensional model 3-69593
 NO abundance, i.r. absorpt. spectra obs. (*French*) 3-61463
 NO detection and comp. determ. (*French*) 3-51012
 NO detection from spectroscopic meas. 3-53490
 NO in situ meas. between 17 and 23 km 3-76775
 NO prod. by N_2O oxidation 3-61450
 NO production from past nuclear explosions, O_3 measurements 3-65348
 NO vertical distrib. from 5.2μ spectral band obs. 3-73318
 O_3 , effect of water vapour and nitrogen oxides 3-76741
 S compounds in aerosols rel. to major volcanic eruptions 3-59058

strays (atmospherics) see *atmospherics***streamer chambers**

- 2m JINR, performance, optimum operational mode 3-77669
 high energy experimental use 3-77663
 hyperon beam use, brief description 3-77666
 Intersecting Storage Rings use 3-77667
 ionisation measurements, search for quarks in high energy air showers 3-77672
 missing mass spectrometer, diffractive dissociation study 3-77671
 multiple firing, conical Blumlein line, fast rise time, low amplitude jitter 3-77670
 technical improvements, SLAC chamber accuracy and resolution 3-77664
 three-electrode $100 \times 60 \times 40\text{ cm}$, design, operation in a magnetic field 3-70396
 μ polarisation measurement 3-77668
 H₂ technical problems, performance evaluation 3-77645

streamers see *discharges (electric)***streaming, acoustic** see *acoustic streaming***strength (mechanical)** see *mechanical strength***stress** see *stresses***stress analysis**

- see also *bending; photoelasticity; strain gauges; torsion*
 adhesive bond, nonlinear shear stress distrib. 3-69410
 Airy stress function, thermal plane stress, governing equations 3-59753
 anisotropic half-space, stresses 3-77803
 anisotropic plate with asymmetrically reinforced edge, stress-state determ. (*Russian*) 3-62481
 anisotropic rigid/plastic materials, plane strain slip line theory 3-47469
 anisotropic semi-infinite plates with arbitrary edge and surface loadings, bending stresses and strains 3-57063
 anisotropic stretched ring, elastic and strength props. analysis 3-80487
 anisotropic two-phase media, interfacial screw disloc., elastic field analysis 3-54964
 anisotropic viscoelastic cylinder, centrifugal stresses analysis, numerical soln. 3-62453
 arch finite elements accuracy and shape functions 3-45639
 axisymmetric concentration, finite element method 3-66536
 axisymmetric loads on elastic half-space containing cylindrical inclusion 3-51787
 bars, naturally uniformly twisted, plastic torsion and tension 3-40132
 beam with trapezoidal cross-section, bending, determ. of stress distrib. (*Russian*) 3-45665
 beams, asymptotic theory (*French*) 3-62460
 Beltrami-Michell type stress equations of motion, uniqueness of solns. 3-51784
 bent plate, transient state on cracking, moment intensity factor 3-77812
 body with large number of cracks, effective characteristics (*Russian*) 3-74026
 bonded anisotropic lap joint, stress distrib. 3-80458
 bonded half planes with crack through interface, stress analysis, numerical soln. 3-48722
 Boussinesq problem, axisymmetric, couple-stress analysis, punch tip penetration 3-77808
 brittle mass weakened by internal flat slit, stress distrib. before collapse (*Russian*) 3-45661
 buckling, cylindrical panels, non-uniform axial compression, load distrib. rel. to crit. stress 3-45675
 buckling under shear, diagonal stiffeners reinforcing clamped infinitely long plate, optimum distribution 3-57088
 circular plate, limiting equilibrium allowing for shear stress (*Russian*) 3-66566
 circular plate, variable-thickness, limit loads accounting for transverse shear 3-57093
 circular stamp on an elastic layer with tangential forces in contact zone (*Russian*) 3-74029
 composite, fibre reinforced, boundary layer phenomena 3-73028
 composite, fibre reinforced, wave propag. in cylindrical cavity 3-53276
 composite, laminated, containing broken layer, stresses and displacements determ. 3-73031
 composite, laminated, continuum theory for dynamical processes 3-73030
 composite bars with oblique boundaries, photoelastic and interferometric obs. 3-44671
 composite cylinder, axially connected, thermal stresses 3-66534

stress analysis continued

- composite orthotropic medium, hot area 3-66526
compressible slabs, hyperbolic equations, from in situ measurements of deformation rate 3-74016
conical shell, oblique, approx. theory of stresses (*Italian*) 3-40115
conical shell inversion, approx. energy analysis 3-48735
conical shell under tension, stress state around elliptic hole 3-48727
contact interaction between spherical shell and rigid stamp, with linkages, non classical eqns. (*Russian*) 3-62470
contact problem for plane with straight line incision (*Russian*) 3-66553
coplanar Griffith cracks in infinitely long elastic strip, stress intensity factors and crack energy 3-48720
couple-stresses, eff. on stress distrib. around elliptic hole (*German*) 3-57061
crack, finite, orthotropy effect on singular stresses 3-70669
crack analysis, collocation and finite elements 3-74036
crack analysis, super-element 3-62459
crack analysis using integral transform methods 3-40124
crack in infinite plane containing circular hole under normal pressure, analysis 3-57060
crack problems, internal, analysis using Laurent series expansion 3-40120
crack problems in elastic strip, Fredholm integral equation 3-70566
crack propagation, shear plane elliptical, dynamic field 3-45648
crack propagation between two dissimilar media, steady state response 3-74043
crack propagation in an elastic solid subjected to stress wave loading 3-45652
crack tip in circular hole, infinite elastic solid, stress distrib., form. energy 3-77810
cracked plates, stress intensity factors, finite element solution 3-40108
cracked plates subjected to biaxial loading, plastic intensity factors 3-68326
cracked structure dynamics with finite elements 3-74040
cracks, field singularities and integral representations 3-40123
cracks, finite element method for calc. of stress intensity factors 3-40126
cracks in plate of finite thickness, slicing procedure for approx. three-dimens. Green's functions 3-68316
creep deformation of solids, stress relaxation and time-dependent boundary conditions, numerical soln. 3-70626
creep relaxation, approximate solns. comparison with exact solns. 3-74021
creeping structures under cyclic loading 3-70634
curved finite elements by the method of initial strains 3-42767
curved two-dimensional finite elements comparison 3-70574
cylinder, infinite elastic, containing rigid disc, stress distrib. force to shift disc. 3-77818
cylinder, stress-deformed, under action of dynamic loads, soln. by series expansion (*Russian*) 3-77825
cylinder subjected to transverse flexure, tangential stresses and testing of strength 3-59760
cylinder with external cylindrical crack, stress field for twisting and tension (*Russian*) 3-42775
cylindrical body, temp. and internal stress distrib. on cooling 3-69321
cylindrical cavity, two strip cracks in infinite elastic solid, intensity, shape energy 3-77817
cylindrical flexure of plate of finite width on elastic halfspace, effective solution (*Russian*) 3-70572
cylindrical shaft with half circular groove, torsion, stress distrib. (*Russian*) 3-45656
cylindrical shell, axial impact against rigid plane (*Russian*) 3-54103
cylindrical shell, optimum conditions for lowering residual stresses by local heating (*Russian*) 3-41761
cylindrical shell, pressurized ribbed, with reinforced hole 3-58781
cylindrical shell, stress conc. produced by internal press. in branch pipe connection region 3-45669
cylindrical shell, thermal fields and stresses during inductive heat treatment (*Russian*) 3-77807
cylindrical shell of finite length, transversally isotropic, contact problem (*Russian*) 3-62479
cylindrical shell of medium thickness, stress conc. near circular holes 3-62482
cylindrical shells, forced oscillations with gas-pressure fluctuations, variable stress analysis (*Russian*) 3-62535
cylindrical shells, transversely-isotropic eqns. including transverse shear and thickness anisotropy (*Russian*) 3-40112
deformation of elastic half-space under random loads (*Russian*) 3-42792
deformation of viscoelastic thick-walled cylinder with elliptic cavity (*Russian*) 3-42791
deformations, finite, of transversely isotropic elastic materials 3-54089
diffraction of stress waves by semi-infinite running crack 3-42808
dilute polymer solutions, thermomechanics, multiple-bead-spring model 3-43530
dipolar stress theory, applic. to torsion in prismatic bar 3-74015
disc, simply-connected, arbitrarily loaded, general soln. (*Polish*) 3-59743
distrib. in vicinity of external crack in infinite elastic thick plate 3-57059
dynamic, spring colliding with rigid body, solid viscosity rel. to nuclear reactor 3-60270
dynamic contact problem for isotropic semi-space, strain of longitudinal shear (*Russian*) 3-62467
dynamic photoelasticity, dual-beam polariscope and framing camera 3-73112
dynamic stresses, spring colliding with rigid body, solid viscosity rel. to nuclear reactor 3-60270
earth, use of microearthquakes, study in Nevada region 3-76546
edge buckling of cylindrical shells with low in-plane shear moduli 3-57087
edge dislocation near partially bonded circular inclusion, stresses and displacements 3-68260
elastic contact surfaces with frictional forces, finite element method 3-66522

stress analysis continued

- elastic cylinder, infinite, bending by rigid rings (*Russian*) 3-66542
elastic cylinder, three-dimensional boundary problems, analysis of stress/strain relations (*Russian*) 3-66539
elastic ellipsoid of resolution, soln. of mixed axisymmetric problem by p-analytic function method (*Russian*) 3-77820
elastic half-space, linearly nonhomogeneous, effect of shear modulus variation with depth 3-74034
elastic medium, anisotropic, with ellipsoidal nonuniformity, stress concentration (*Russian*) 3-42774
elastic plane-parallel system with linear cut, soln. by Miskhelishvili method, mixed boundary conditions (*Russian*) 3-66545
elastic plate, bending formulation 3-54093
elastic plate, circular inclusion effect on stress intensity factors around line crack under concentrated forces 3-74044
elastic plate with circular hole, accuracy of finite element analysis 3-40109
elastic sheet, fibre reinforced, containing circular hole, stresses 3-73001
elastic solid, stress singularity at corners or terminations of crack edges, eigenvalue problem 3-74042
elastic stress intensity factors computation, finite element methods eval. 3-48725
elastic-plastic crack tip, steadily growing, finite element treatment 3-68329
elastic-plastic finite strain, geometrical concept of intermed. config. 3-54087
elastic-plastic material, crack tip small-scale yielding, stress terms and geom. effects 3-74052
elastically constrained conical shells under hydrostatic press., buckling analysis by collocation method 3-59762
elasticity, infinitesimal, classical, second order stresses 3-74025
elasticity, linear, stress eqns. of motion systems, uniqueness theorem 3-51785
elasticity, micropolar theory, second axially symm. problem, stress formulation 3-51783
elastico-plastic stress, heat and mass transfer, net-point method for problems 3-62616
elasto-visco-plastic material, isoclinic parameter expt. 3-43822
elastodynamics, linear asymm., generalised tensorial fields existence 3-51786
elastodynamics, similarity solns. for plane problems 3-45645
elastoplastic plane medium, discretized model 3-40134
elastoplastic solid body weakened by two round openings, plane deformation (*Russian*) 3-42796
electric solid containing inviscid incompressible fluid, finite element method 3-70598
electrovacuum apparatus, thermal fields and stresses in metal-glass joint zone (*Russian*) 3-77418
element stiffness matrices, strain energy content, weighted eigenvalue method 3-45638
elliptic hole, dynamic stress conc. due to plane SH-waves (*German*) 3-57058
elliptic notch and near-by crack interaction 3-49927
failure diagram, calculation from energy criterion (*Russian*) 3-57056
fatigue crack growth theory, stress intensity factor 3-68318
fatigue crack propagation from small holes in linear arrays 3-72122
fibre-reinforced materials, ideal, plane crack problems, stress distrib. 3-76361
fibreglass, rated strength characts. in stress conc. zones 3-80455
field due to Griffith crack at interface of elastic half plane and rigid foundation 3-48719
finite element computer codes development 3-54077
finite element grids based on minimum pot. energy, optimization 3-48726
finite elements for axisymmetric solids under arbitrary loadings with nodes on origin 3-48740
flame forming, transient elastic-plastic thermal stress analysis 3-50745
flexible plates and shells, elastoplastic strain theory applic. to stressed state calc. 3-57095
flow, in pure and doped KCl and KCl:KBr mixed crystals 3-79415
fluid, incompressible, stress fluctuation, Brownian motion 3-70737
generalised hybrid stress finite-element models 3-51781
glass spheres, diametrical compression 3-72960
glass-reinforced plastics, surfaces of equicritical planar stress distribs., fourth degree polynomial description 3-55872
Griffith crack, effect on stress distrib. in semi-infinite two-dimensional medium 3-54097
Griffith crack, partially closed, analysis under polynomial loading function 3-68317
Griffith crack at interface of two bonded dissimilar half-planes, stress and displacement fields 3-66525
Griffith crack opened by parabolic press. distrib., partial closure effect on stress intensity factor 3-68315
grooved shafts in elastic bending, stress conc. factors calc. using point-matching technique 3-54098
half space with periodically constant step characteristics, non-planar deformation (*Russian*) 3-45657
half-plane, heavy with curved boundary under uniform pressure, equilibrium (*Russian*) 3-74030
half-plane problem, non uniformly distributed temp. soln. by functional system (*Russian*) 3-74028
hemisphere with radiating surface, thermal stresses due to internal heat source 3-54096
higher-order cracked finite element 3-74037
hollow shaft subjected to uniform band of external pressure, radial displacements 3-48728
holographic interferometry exptl. results prediction method 3-73783
HTR fuel particle coatings, stress calc., analytical model 3-63190
hydrodynamic simulation method for stress field distrib. around elliptical aperture and streamline orifice (*Russian*) 3-45658
hyperelastic materials, extremum principles 3-57069
ideal plastic material, stress tensor calculation, viscous fluid flow applic. 3-45671
ideally plastic orthotropic material, general plane problem for stress and velocity fields (*Russian*) 3-64087

stress analysis continued

- impact of stamp on elastic medium, determ. of stress distrib. by electrical modelling (*Russian*) 3-45659
- infinite frames, composite characts., stress distrib. 3-62456
- infinite elastic solid, crack forking in anti-plane strain deform. 3-64100
- infinite elastic solid, running penny-shaped crack, exact stress distrib., crack shape and energy 3-68327
- infinite slab isotropic transversely homogeneous elastic material subjected to tension 3-70599
- inhomogeneous semispace, stress-deformation states due to surface loads (*Russian*) 3-66549
- initial strains in multiphase media 3-54081
- isotropic elastic medium, surface stress distrib. due to elliptic crack and thorn (*Russian*) 3-66543
- lamina, inherently aging, on flexible base, bending stresses under transverse forces (*Russian*) 3-45677
- laminated composite with crack normal to and touching interfaces 3-73014
- laminated plate theory, refined 3-70597
- large deflection problems, hybrid stress finite element model for incremental analysis 3-70568
- laser window material, stress and temp. analysis for surface cooling or heating 3-70319
- lateral instability of thin walled beams, effect of spaced loading points (*Italian*) 3-40096
- layer stresses caused by local changes in materials 3-45670
- layered composites, stress distribution 3-55875
- linear elastodynamic analysis, assumed stress hybrid finite element model 3-77799
- LMFBR, potential failure of hexcan wrapper due to thermal stresses from local nonuniform temp. distrib. 3-46108
- material and/or geometrically nonlinear structural analysis, evaluation of solution procedures 3-45673
- material failure by environment-induced cracking, criterion development 3-69273
- metallic plates, yielding in front of through cracks in pure bending 3-76382
- mobile unit for on-site stress analysis (*German*) 3-66139
- model fabrication, epoxy resin-aliphatic resin:polyethylenepolyamine, metal surface finish, dimensional deviations 3-50812
- moving dislocations, stress-fields production 3-49932
- multiwave shell membranes, un-split model forces (*Russian*) 3-42818
- nonlinear properties of stochastically inhomogeneous media (*Russian*) 3-70583
- nonlinear stress equilibrium problem, relaxation method using finite difference eqns. 3-70625
- notched elastic bar, symmetrical, stress distrib. and deformation 3-77809
- oblate spherical cavity, stress conc. factor at equator, approx. soln. 3-64101
- optical polarisation, apparatus for crystal compression 3-73673
- orthotropic cylindrical shell, potential distrib. near surface cut for skew symmetric tensile-deforming state (*Russian*) 3-42786
- orthotropic cylindrical shells, elastic, critical stress determ., stability, variable pressure 3-70579
- panel with special orthotropy, stresses and displacements, analysis (*German*) 3-66529
- Papkovich-Filonenko-Borodich method for construction of stress tensor 3-70604
- paraboloid of resolution loaded at top by axial concentrated force, equilibrium, numerical analysis (*Russian*) 3-62468
- photoelastic, dynamic, incident stress waves, stress concentration, apparatus, techniques (*Japanese*) 3-61991
- photoelasticimetric meas., stress separation by finite element method 3-66559
- photoelasticity, dynamic, resolution of principal stresses 3-58081
- pipe, contoured integrally reinforced branch connection, stress intensification factors 3-48734
- planar problems, stress intensity factors; approx. technique 3-74038
- plane contact problem for frictionless elastic layer 3-51789
- plane elastostatics, generalized plane stress sector problem 3-48721
- plane with arched crack, thermal transmission influence on thermoelastic state (*Russian*) 3-40102
- plastic deformation processes, residual stress distrib. calc. methods 3-48738
- plastic media, vertical cut stability rel. to wall collapse 3-74051
- plastic orthotropic materials, stress and velocity field eqns. for plane flow (*Russian*) 3-66567
- plate, anisotropic, one-dimens. transient waves 3-70668
- plate, anisotropic with elliptical openings, temp. field and stress state for mixed boundary conditions (*Russian*) 3-62480
- plate, axially loaded, with circular hole, three-dimens. photoelastic anal. 3-66137
- plate, infinite, stresses due to diametral forces on circular hole with notch 3-70600
- plate, orthotropic annular, postbuckling behaviour 3-70592
- plate, quadrant shaped, conformal mapping for stress from concentrated forces, any point 3-70563
- plate, stress state at crack tip, concentrated force applic. method influence (*Russian*) 3-40101
- plate, symmetrically-layered, with central crack, stress analysis (*Russian*) 3-42777
- plate, thermoelastic stresses, volumetric cylindrical heat source (*Russian*) 3-40104
- plate, thick, elastic, asymmetric stress distrib., penny-shaped crack 3-77816
- plate containing two circular holes of different sizes under uniform heat flow, thermal stresses 3-42769
- plate of stochastically non-uniform material, tension distrib. around circular hole (*Russian*) 3-45664
- plate under out-of-phase biaxial cyclic loads, strains and stress conc. factors 3-57078
- plate under sudden loading, crack branching phenomena (*Russian*) 3-55014
- plate under tensile loading, crack growth direction (*Russian*) 3-57081
- plate weakened by random contour openings under biaxial tension, stress concentration coeff. (*Russian*) 3-66552

stress analysis continued

- plate with complex periphery, load capacity (*Russian*) 3-54113
- plate with opening filled by rigid core and elastic spacer, control of pressure concentration (*Russian*) 3-42787
- plates, non-linearly flexible, in presence of random initial stresses, stability (*Russian*) 3-62474
- plates with curvilinear apertures with large corner curvatures, concentration of potentials (*Russian*) 3-42784
- PMMA, fatigue crack retardation and closure 3-76381
- polyisobutylene solution, conc., inflow into a flat slot, polarisation-optical study, stress anal. (*Russian*) 3-46366
- polymer fracture mechanics, review 3-76364
- polymer moulding, diametral test, finite element analysis 3-80493
- polymeric plates, yielding in front of through cracks in pure bending 3-76382
- Prandtl Reuss materials, stress analysis on elastoplastic deformation (*German*) 3-65008
- quasi-isotropic composed material, nonisotropic deformation, correlation function of elastic field (*Russian*) 3-42778
- quasi-sudden crack extension, crit. time and length considerations 3-74039
- reactor fuel element stresses at discontinuities and interactions by finite elements in two dimensions 3-63125
- rectangular domain, stresses and displacements, mixed boundary value problem 3-70569
- resilient plate with round compression, influence of friction forces on stress distrib. (*Russian*) 3-45663
- rigid-body motions in curved finite elements, explicit addition 3-45683
- ring method of testing, correl. between high-temp. bending and tension stress relax. 3-69430
- rocks, jointed masses, continuum characterisation, low shear modulus significance 3-76555
- rocks, jointed masses, general constitutive equations 3-76554
- rod, twisted, contact stresses 3-70602
- rods and plates, rotating, buckling behaviour 3-57070
- rotating ellipsoid under concentrated load, stress distrib. (*Russian*) 3-45655
- rotating orthotropic discs of variable thicknesses, elastic stresses and displacements 3-66535
- rubber vulcanizate, Rivlin-Thomas criterion for cut growth, finite element calc. of J integral 3-73045
- screw dislocation near partially bonded circular inclusion, stresses and displacements 3-68261
- semi-infinite body, cylindrical hole, thermal stresses, temp. distrib., linear thermoelasticity 3-70562
- semi-infinite piezoelectric rod, distrib. of temp., displacement, stress, electric field, and entropy density 3-72575
- semi-infinite solid, stress intensity factors for elliptical crack approaching surface 3-64099
- semi-infinite solid, stress intensity factors for elliptical crack approaching surface 3-68325
- semi-transparent rod, elastic, illumination with high-power laser, stresses (*Russian*) 3-62475
- shaft, circular, under torsion, concentration of stresses at base of long circular groove (*Russian*) 3-62477
- shear wave reflection at a half space with periodic constant segment characteristics (*Russian*) 3-70659
- sheet materials, brittle fracture in presence of cracks 3-58690
- shell, anisotropic cylindrical, flexure problem 3-70567
- shell, axisymmetric, load capacity determ. under conditions of piece-wise linear plasticity (*Russian*) 3-57094
- shell, circular cylindrical liquid-filled, contact problem, Fourier series soln. (*Russian*) 3-62469
- shell, finite element stress analysis 3-66537
- shell, thin, elastic deformation, numerical method (*German*) 3-45651
- shell, thin cylindrical, high speed travelling inner pressures, dynamic behaviour 3-45688
- shells, cylindrical with two adjacent circular cut outs, limiting pressure determ. 3-74050
- shells, non-circular cylindrical, initial stresses, vibrations 3-70650
- shells, stiffened slanting rectangular, stress-strain state (*Russian*) 3-62471
- shells of revolution, spherical, pole loaded, stress deformation states, numerical soln. (*Russian*) 3-66550
- shells of rotation, mathematically equivalent problems, statico-geometric analogy (*Russian*) 3-66532
- shells weakened by holes, stability, stress distrib. around holes (*Russian*) 3-45654
- single reinforcing members, parameters governing load transfer 3-41810
- solid solution, elastic gradient energy coeff. concept 3-64810
- sphere, stresses due to uniform heat sources for strain hardening material 3-57077
- sphere subjected to large deform., stress fields 3-57074
- spherical pressure vessel, non-linear viscoelastic material, random loading 3-70564
- spherical shells, shallow, large deflection when subjected to variable normal load 3-45640
- square cylinder with circular hole, thermal stresses and couple-stresses 3-45642
- statics of discrete elastic Cosserat lattice type shells 3-54084
- statics of elastic lattice-type shells 3-54085
- steel, Cr-Mo, quenched, crack propag. and creep conditions 3-69276
- steel, determ. of critical range of stress-intensity factor necessary for fatigue crack propag. 3-69286
- steel, high tensile, tubular, influence of geometric form on load carrying capacity (*Russian*) 3-76221
- steel, in LMFBR subassembly duct wall, thermal stress analysis for severe thermal loading 3-46161
- steel, plastic, critical stress intensity factor, determ. methods 3-58684
- steel plate, notched, distribution rel. to curvature 3-80370
- steel plates with oblique hole, corner shape effect on elastic stress and strain conc. 3-50823
- strain nomogram method 3-80363
- strand, response to axial and torsional displacements 3-72901

stress analysis continued

- strip composite, plane elastostatic soln. for symmetrically loaded crack 3-66524
- structures with buckling constraints, optimal design using iterative finite element method 3-45649
- tectonic folding stress anal. in viscoelastic and elastoplastic media 3-76602
- temperature in a partly clamped orthotropic plate (*Russian*) 3-74031
- tension and flexion in thin plates, finite difference method soln. (*Italian*) 3-40116
- thermoelastic stresses in a long hollow cylinder under local heating of the side surface 3-70573
- thermoelastic stresses in expanding rectangle, appl. of extended source method and new numerical techniques 3-70586
- thermomechanical analysis of structures 3-66558
- thermoplasticity, uncoupled, principles for stress rate, strain rate 3-77828
- thick plates, stress-deformation states in three-dimensional theory by orthogonal projection method (*Russian*) 3-66548
- thick rectangular elastic plate under bending, stress state problem in double trigonometric series (*Russian*) 3-66531
- thin elastic shells, arbitrary edge loads, effect on stress and deformation, asymptotic expansion of tensor eqn. 3-70585
- time and site dependent distribution in BWR fuel can under variable power conditions (*German*) 3-67609
- toroidal shells, geometrically nonlinear deformation, soln. of Meissner eqns. by matrix method (*Russian*) 3-66551
- torsion, finite elastic cylindrical and partially bonded to infinite elastic cylinder 3-77819
- torsion of bodies of revolution, integral eqn. method (*German*) 3-57057
- transient thermal stresses in disc of linearly strain-hardening material 3-54107
- triangular bending elements with derivative smoothing, computer subroutines in FORTRAN 3-40106
- turbulent boundary layer, high order moments of Reynolds shear stress fluctuations calc. 3-46435
- turbulent flow, Reynolds stresses, two-point correlation model and redistribution 3-49555
- twisted angle or channel, Conway's formula for maximum stress 3-70565
- twisted non-homog. circular cylinder 3-48718
- two-dimensional continuum with nonlinear characts., transient response and failure simulation 3-48729
- two-dimensional structures, photoelastic model investigations of optimum shapes (*Polish*) 3-59750
- two-phase material, laminated, opening of finite crack normal to interface 3-70601
- viscoelastic body, transient crack problems, path-independent integral 3-57075
- viscoelasticity, linear, stress and strain tensors, unique solns. and approx. methods (*Russian*) 3-66541
- volume creep, non-conservative, under different stress states, discussion of original paper 3-61171
- Walther's stress model and irradiation expts. on nuclear reactor coated fuel particles (*German*) 3-71318
- welded connections of members with variable cross-sections, stress computation 3-69329
- X-ray examination, apparatus for crystal compression 3-73673
- yielding materials, stress intensity factors at crack tip by method of caustics 3-68328
- C/C composite, fracture toughness 3-55853
- Cu/Mo composite, deformation state, microhardness obs. 3-80369
- Ti alloy, dynamic creep, random stresses, statistical laws 3-80373
- Ti alloy, tubular, influence of geometric form on load carrying capacity (*Russian*) 3-76221

stress birefringence see mechanical birefringence

stress effects

- α -brass water-jet erosion of prestressed material 3-72902
- anthracene crystals, effects on polarized reflection spectrum during cooling 3-69008
- biaxially stressed elastic media, wave propagation dispersion equations 3-42819
- brass, fracture, elevated temp. and volume stressed state obs. 3-58676
- α -brass, prestrained, stress corrosion cracking and dislocation arrays (*Japanese*) 3-44577
- brass, stress corrosion sensitivity investigation, alloy composition depend. (*German*) 3-44640
- buckling, thin walled cylinder with axisymmetric loading, stability 3-54076
- ceramic, quantitative thermal shock test 3-73094
- ceramic specimens, miniature, high temp. tensile test 3-72961
- ceramic spherical shells, load-bearing capacity under external press. 3-64977
- composite, glass reinforced epoxy resin, crit. stress intensity factors 3-55862
- composite, graphite/epoxy laminated fracture specimens, fractographic study 3-55870
- composite spherical shell, radial vibrations due to periodic shearing stress 3-59774
- corrosion crack testing using potentiostatic dynamic strain technique 3-61247
- crack tip stress intensity factor, Mode I, determ. by holographic interferometry 3-73108
- cylindrical specimen with ringcrack applic. to strength determ. in material with brittle fracture (*Russian*) 3-41760
- displacement, measurement, conference, Paris, France, 12-18 April (1973) 3-56619
- ductile alloy, corrosion resistant, crack propagation rate rel. to oxide rupture 3-61167
- effect of transverse shear stresses 3-45676
- elastic constants of stressed crystals, acoustic harmonic generation 3-72115
- elastic layer, cylindrical hole, nonuniform axisymmetric radial displacement, Navier's equations 3-62510
- elastic wave diffraction, and dynamic stress concs., book 3-70683
- embrittlement by liquid metals, review 3-47421
- stress effects continued
- epoxy resin, short-term action of static loading and aggressive liq. media influence on mech. props. (*Russian*) 3-80469
- fatigue crack initiation and propagation from different configuration notches, effect of mean stress 3-41749
- fatigue crack propagation, varying loads 3-64885
- fibreglass, fatigue strength, cyclic strength under shear loading, stress weakening by notches or steps 3-53297
- fluids with couple stresses, secondary flow caused by rotation of sphere 3-54806
- glass, organic, yielding of two-dimens. void assembly 3-58735
- glass fibre ware, orthogonally reinforced, crack form. 3-64993
- glass reinforced polyester, breakdown mechanism in interface region by artificial weathering 3-41808
- glass reinforced polyester, surface microcracking, artificial weathering 3-76359
- graphite, ATJ-S, fracture under multiaxial stresses 3-72964
- graphite, ATJ-S, hydrostatic press. response 3-72963
- graphite, reactor, oxidation reaction rate in damp atmosphere, mech. strength (*German*) 3-71271
- graphite, tension-compression tests, strength in a plane stressed condition 3-53298
- graphite, Young's modulus, annealing and pre-stressing effect 3-41816
- group-IV semiconductors with group II double acceptor impurities, group theoretical treatment of uniaxial stress 3-58228
- hippuric acid, crystal twisting rel. to surface stress, approx. model 3-54931
- ice, polycrystalline, creep under complex stress 3-64096
- ice crystal, dynamical behaviour of dislocations under stress 3-68257
- large and small specimens, linear-elastic fracture mechanics, strain rate effect on characteristic value (*German*) 3-47522
- liquid, non-Newtonian, rotational flow, interaction with stationary surface, stress effects 3-40715
- liquid crystals., instability, strain induced, monodomain smectic A and cholesteric, dislocations 3-49841
- loading at anchorage points rel. to liner design for stressed concrete nuclear reactor (*German*) 3-74713
- materials testing device, volume stressed state, to 300C, effect of pressure, force and bending 3-50813
- metal, polycryst., hydrostatic stress effect on tensile creep at elevated temps., X-ray obs. (*Japanese*) 3-40830
- metal, stress corrosion, quantitative criterion (*Russian*) 3-41095
- metal, structural, catalytic poisoning and stress corrosion cracking control 3-64889
- metal, uniaxial stress effects on Fermi surface (*French*) 3-60852
- metallic single crystals, f.c.c., tensile behaviour, theoretical model (*French*) 3-64089
- microwave ferrite, temp. and stress sensitivities, review 3-41366
- Perspex, water-jet erosion of prestressed materials 3-72902
- plane stress, yield criterion, second order effects, tension-torsion loading 3-62489
- plastic buckling of cylindrical shell subject to external fluid pressure 3-62506
- PMMA, fraction mechanism in methanol at low temp. (*Russian*) 3-58723
- polyacrylonitrile fibres, stress relaxation peculiarities 3-63602
- polycarbonate, craze formation, kinetics, stress intensity factor 3-55887
- polyethylene, crystal twisting rel. to surface stress, approx. model 3-54931
- polyethylene, environmental stress cracking 3-67885
- polyethylene terephthalate fibre, effect of thermal treatment on thermomechanical props. (*Russian*) 3-80496
- polymer, amorphous and crystalline, durability study 3-61222
- polymer chain, absorption band intensity change under loading 3-63580
- polymer crystallization morphology 3-79240
- polymer diffusion of a solvent with small mols., stress-dependent diffusion equation 3-57688
- polymer-impregnated porous brittle materials, stress conc./factors 3-55839
- polymethylmethacrylate, craze formation, kinetics, stress intensity factor 3-55887
- polyurethane, creep under varying temperature for nonlinear uniaxial stress 3-53283
- polyurethane, elevated temp. creep under nonlinear torsional stress with step changes in torque 3-53284
- quartz, deformation lamellae in ion thinned foils 3-69522
- α -quartz, effect on Raman spectrum at liq. He temps. 3-53102
- rock fracture, initiation from compressive stress concentrations around elastic flaws 3-76552
- rock mechanics and crack theory, conditions for finiteness of stresses in elasticity theory 3-47659
- rock strain-durability, samples with loading history (*Russian*) 3-65157
- rocks, h.v. radiography, dual microdensitometry 3-45516
- rocks, magnetisation, press, uniaxial, nonmagnetic, tiltable piston 3-70330
- rods and plates, rotating, buckling behaviour 3-57070
- semi-infinite anisotropic elastic medium, disturbance by impulsive twist on plane surface 3-74032
- silicate glass, nonisothermal stress relaxation (*Russian*) 3-47478
- soda-lime glass, slow fracture characts 3-76268
- soda-lime-silica glasses, org. liq. environment effects on crack propagation 3-72968
- solid under inhomogeneous stress, modulus defect and internal friction 3-55030
- steel, AISI 4340 foil, stress corrosion cracking in aqueous acid solns. 3-69257
- steel, cold-rolled strip, rapid cooling under tension during annealing (*German*) 3-80300
- steel, computerized time-temp. parametric analysis of stress-rupture data 3-50746
- steel, Cr-Mo-Ni, softening of austenite, effect of deformation to fracture by tensile stress (*German*) 3-72888
- steel, dislocation distrib. at 650°C (*Russian*) 3-58628
- steel, ferritic, quenching and tempering effects on stress corrosion cracking 3-64880

stress effects continued

- steel, fracture safe assurance, toughness variations influence 3-50744
- steel, fretting fatigue strength 3-44594
- steel, high-strength, creep rupture behaviour, effect of interruption in mechanical stress (*German*) 3-69253
- steel, low alloy, stress corrosion cracking initiation mechanism 3-64881
- steel, low-C, cyclic loading effect on subsequent yielding 3-44593
- steel, low-C, fatigue crack propag. under doubly repeated stress, residual stress and plastic strain (*Japanese*) 3-41734
- steel, low-C, prestrained, temp. effect on mech. props. anisotropy 3-47427
- steel, martensitic, stress corrosion cracking susceptibility (*Czech*) 3-55806
- steel, martensitic high-strength, stress corrosion cracking resist. (*French*) 3-47415
- steel, mild, cavitation erosion for low cavitation intensity 3-41751
- steel, mild, stress corrosion cracking by phosphate solution 3-55795
- steel, perforated round samples, fatigue tests below limit 3-64884
- steel, SAE 4340, fatigue life and inelastic strain response under complex history 3-69289
- steel, stainless, austenitic, stress corrosion cracking, electrochemical testing method by separating crack anode from cathode 3-47492
- steel, stainless, type 304L, stress corrosion cracking and hydrogen embrittlement, dislocation density effects 3-53241
- steel, stainless, Type 316, irradiat., stress-biased loop nucleation 3-67553
- steel, stainless, Type 316, mech. and struct. props. for LMFBF cladding, rupture 3-47394
- steel, stress relaxation tests, bending, tension, time factor effect 3-50803
- steel, structural, alternately stressed, stress relieving, diffusion of interstitial atoms (*German*) 3-69252
- steel mild, stress corrosion cracking by nitrate solutions 3-55794
- steel plate, notched, thickness depend. 3-80362
- steel weldment, T-I type, stress relief annealing (*Japanese*) 3-41774
- steel X 8 CrNiMoNb 16 16, heat treatment, creep conditions (*German*) 3-80302
- steels, high tensile, fatigue crack growth at low stress levels (*Russian*) 3-69305
- stress corrosion cracking prediction by triboellipsometry 3-47420
- stress corrosion cracking susceptibility test procedure 3-69402
- tensile testing small local deviations, influence in specimen diameter on conventional strain at maximum load in tensile test (*German*) 3-47524
- thermal, in cryogenic winds 3-62023
- thin films thickness measurement using quartz resonator, stress effects (*Czech*) 3-56612
- time-dependent strength and failure, eqn. development 3-65020
- uniaxial creep recovery and stress relax., model based on residual stress distrib. 3-58666
- viscoelastic liquids, normal stresses effect, vel. fields, skin friction coeff. calc. 3-79028
- water-jet impact, transient stress distrib. 3-72903
- Zircaloy, stress corrosion cracking behaviour in iodine vapour 3-43297
- Zircaloy-2, corrosion of oxide layer, subsurface pitting, stress cracks 3-80387
- Zircaloy-2, stress corrosion cracking in neutral aqueous chloride solns., 25°C 3-69260
- Ag film, vacuum-deposited, internal friction peak due to stacking faults (*Russian*) 3-72284
- Al, harmonically deformed, u.s. attenuation coeff., dislocation string model approach (*Russian*) 3-43833
- Al, polycryst., hydrostatic stress effect on tensile creep at elevated temps., X-ray obs. (*Japanese*) 3-40830
- Al alloy, fracture, elevated temp. and volume stressed state obs. 3-58676
- Al alloy 7075-T6511, fatigue crack propag., effect of single and multiple peak overloads 3-64895
- Al alloy sheet, fatigue crack propag., effect of loading conditions 3-64943
- Al alloys, fretting fatigue strength 3-44594
- Al alloys, variable load effect on fatigue properties 3-47402
- Al single cryst., flow stress down to 1.4 K, temp. depend. singularities 3-52663
- Al-Cu(1 wt.%) alloy, stress corrosion cracking, slip characts., grain boundary misorientation (*Japanese*) 3-44578
- Al-Mg (AMg6), quality rating, macroscopic failure diagrams effect of stress on crack length 3-44608
- Al-Mg alloys, morphology of stress corrosion cracks and crack branching 3-80265
- Al-Zn-Mg alloy, grain boundary precipitate effects on stress corrosion cracking (*Japanese*) 3-50725
- Al₃Ga_{1-y}As - Al₃Ga_{1-x}As - Al₃Ga_{1-y}As, double heterostructure lasers 3-78045
- Al₂O₃, alumina ceramics, fracture mirrors 3-55851
- Al₂O₃, polycryst., fracture toughness, crit. stress intensity factor 3-55841
- Al₂O₃ ceramic with compressive surface stresses, surface damage effect on strengthening 3-44653
- BAF₂, Raman spectra rel. to uniaxial stress at 15K 3-53103
- Bi₁₂GeO₂₀, Raman spectra rel. to uniaxial stress at 15K 3-53103
- BiI₃, absorption spectrum, effect of uniaxial deformation, 4.2K, line shifts 3-50595
- CaF₂, Raman spectra rel. to uniaxial stress at 15K 3-53103
- Cr-Ni alloy, stress relaxation resist. rel. to training loading, 850°C 3-80368
- Cr₂O₃, stress induced spin flop, anisotropy and magnetoelasticity origin 3-44227
- Cs halides, derivatives of static and high frequency dielectric constants, two ion polarisable shell model 3-47198
- Cu, effect on fatigue process, cracking 3-64883
- Cu, fretting fatigue strength 3-44594
- Cu and alloys, internal friction temp. depend., reversible motion of block boundaries (*Russian*) 3-69214
- Cu hot water system, T-joint fracture, fatigue vs. stress corrosion, comments 3-69427

stress effects continued

- Cu-Au, stress corrosion sensitivity investigation, alloy composition depend. (*German*) 3-44640
- Fe, cast, high tensile pearlitic, torsional fatigue damage evaluation, changes in fatigue props. and microhardness 3-53252
- Fe, cast, spheroidal graphite, microfractography (*French*) 3-72874
- Fe alloy, AK4-1, creep for complex loading (*Russian*) 3-69304
- Fe plastically deformed and heat treated, corrosion cracking resist. (*Russian*) 3-58645
- Fe-Al(40 at.%) alloy, ordered, slip systems, shear stress induced (*French*) 3-53212
- FeCl₂, Mossbauer effect study under uniaxial stress (*French*) 3-58460
- GaAs, dislocation mobility, temp. and stress depend. 3-49897
- n-GaSb, stress-induced decoupling of valence bands, resist. and Hall effect study 3-46797
- Ge, phonon interaction with stress-split acceptor states 3-55048
- n-Ge plasma frequency shift due to uniaxial stress, free carrier dispersion, polarised radiation, electron transfer model 3-72376
- KCl:CN⁻, vibr. absorpt., broadening, tunnelling 3-69040
- LiF:Mg, dislocation velocity, stress and temp. depend., 773-973K 3-54967
- Li₂O-ZnO-SiO₂, glass-ceramic, creep tested, tension, compression 3-76319
- γ Mn, electrodeposition conditions, rel. to microstructure, effect of microstresses, lattice parameters and hardness 3-47563
- Nb, plastic deform. at 2.17-300 K, yield stresses and dislocation structures (*French*) 3-55004
- β-Nb-Zr, deform. temp. depend., shear stresses for yield and fracture 3-52662
- Ni thin film, with magnetisation, electron microscope obs. (*German*) 3-72291
- Ni-base alloys, thermal and mechanical stress effect 3-64955
- Ni-Fe, supercritical film, external stresses influence on stripe domains 3-72497
- Rb halides, derivatives of static and high frequency dielectric constants, two ion polarisable shell model 3-47198
- Si, phonon interaction with stress-split acceptor states 3-55048
- Sn, gray, zero-gap semiconductor, stress-dependent dielectric constant 3-44365
- Te, cyclotron reson. under uniaxial stress, band structure obs. 3-58217
- α-Ti, cleavage fracture 3-80296
- Ti and alloys, stress relaxation data interpret. 3-64926
- Ti-Al alloys, stress corrosion cracking mechanisms in methanol-ACI solns. 3-47401
- Ti-Al-V-Sn alloy, stress corrosion cracking, influential factors and effect on anodic oxidation 3-47406
- Ti-V-Cr-Al alloy, cold work influence on stress corrosion susceptibility 3-69258
- TiO₂, rutile, compressive creep in vacuum 3-44660
- U-Mo(10 wt.%) alloy, stress corrosion cracking, acoustic emission (*French*) 3-69404
- U-Nb(4.5 wt.%) alloy, aged, stress corrosion cracking 3-69259
- U-Nb(4.5 wt.%) alloy, Al-coated, stress corrosion cracking 3-47411
- W, formation of large-angle grain boundaries under mech. stresses 3-55786
- ZnSe:Mn²⁺ splitting, fine structure of ⁴E level, uniaxial stress method 3-47295
- Zr alloys, neutron irradiat., stress-relax. rel. to creep rates 3-40541
- Zr and alloys, stress relaxation data interpret. 3-64926
- Zr and Zircaloy-2, oxidized, wear in water, characteriz. 3-57573
- stress measurement**
- ceramic, quantitative thermal shock test 3-73094
- earth, focal area of underground explosion 3-76548
- flat structure using optical method (*French*) 3-59551
- fluids, viscoelastic, subjected to spatial stress, relaxation time meas. method (*German*) 3-70269
- forgings, residual stress meas., toroidal core method (*German*) 3-72885
- integrated polariscope response 3-39859
- mechanical design props. of materials test method 3-50817
- metal, magnetoelastic method, stress distrib. across thickness 3-76397
- metal, thermal and structural stresses, electrical heating, const. length 3-73105
- mobile unit for on-site stress analysis (*German*) 3-66139
- perforated tube, star-shaped profiles, stress conc. meas., photoelastic methods, internal and external pressures (*Russian*) 3-74053
- photoelasticimetric meas., stress separation by finite element method 3-66559
- photoelasticity sandwich technique, cement development 3-48351
- plate, axially loaded, with circular hole, three-dimens. photoelastic anal. 3-66137
- polymer solutions, normal stress difference meas., cone and plate rheogoniometer, flush-mounted pressure transducers 3-70503
- residual stress meas. and analysis using u.s. techniques 3-53839
- rocks, Elliot Lake area, techniques 3-76514
- semiconductor thin film and substrates, X-ray determ. using automatic Bragg angle control 3-41669
- steel, from spotty X-ray diffr. rings, method (*Japanese*) 3-41731
- steel, X-ray stress meas. of specimen with steep stress gradient in near surface layer (*Japanese*) 3-41730
- Strainflex X-ray stress analyzer with Side Inclining method (*Japanese*) 3-39855
- tubular specimens, thin-walled, three-dimens. stress, testing device 3-73102
- underground explosions, determination of inelastic region 3-76549
- wall shear stress in three-dimensional boundary layers 3-46432
- X-ray diffr. apparatus operating condition effects on line profile and peak position (*Japanese*) 3-40829
- X-ray technique, thin films and substrates, curvature measurement, automatic Bragg angle control 3-62300
- Ge film transducer, on flexible organic substrate 3-56615
- stress/strain curves** see stress/strain relations
- stress/strain diagrams** see stress/strain relations

stress/strain relations

- see also *elastic limit; yield point*
 alloy, dispersion hardened, work hardening, back-stresses, image stresses and mean strains 3-80290
 alloy, fatigue fracture rel. to inelastic deform. in torsion 3-47422
 alloy, plane strain fracture toughness prediction 3-76227
 anisotropic shells, theory 3-70628
 anisotropic stretched ring, circumferential stress concn. coeff. 3-80487
 Bauschinger effect, yield stress drop rel. to pre-strain 3-69293
 beam, plastic bending and failure by low cycle fatigue 3-80520
 biaxial extension, strain nomograms 3-80363
 butyl acrylate copolymer networks, crosslinks of different lengths, extension, swelling 3-55888
 circular plates, unsymmetric wrinkling, edge thrust and lateral pressure effects, determ. wrinkling loads 3-74054
 column, inelastic buckling, effect of imperfections 3-62495
 composite, directionally solidified yield pt. phenomenon interpret. 3-64992
 composite, fibre reinforced, nonlinear elastic behaviour 3-55858
 composite, filamentary, prestrain effects on tensile props. 3-64996
 composite, laminated, nonlinear behaviour 3-55869
 composite, unidirectional, in-plane shear stress/strain response 3-55924
 composite laminates, post-yielding behaviour, inelastic micromechanics 3-55864
 compression jig, microstrain, macrostrain regions 3-76405
 continuous bond failure due to moving force 3-70589
 copolymer, film of vinylidene chloride (vinyl chloride) (*Russian*) 3-73067
 Coulomb material, rigid plastic, Prandtl stress fields, static extension (*French*) 3-70613
 cracks, arbitrarily disposed in elastic media, soln. of integral eqns. (*Russian*) 3-42776
 creep processes, initial small interval, Dirac δ function, stress-strain diagrams 3-70629
 crystal dislocations, sound absorpt., thermal effect (*Russian*) 3-72085
 cyclic creep and relax. of mean stresses at elevated temps. 3-69434
 cyclic elastic-plastic deformation, methods of anal. kinetic characteristics, fatigue damage, crack development 3-55910
 cylinder, axially symmetric temp. field, shifts, influence of cylinder extremities (*Rumanian*) 3-70618
 cylindrical bar, longit. elastic-plastic final duration pulse propag. 3-70635
 deformation histor, internal parameter descriptions, state of stress 3-74046
 disc, simply-connected, arbitrarily loaded, general soln. (*Polish*) 3-59743
 disclinations, continuous and discrete in anisotropic elasticity 3-64044
 dynamic buckling, finite column resting on a nonlinear elastic foundation, step loaded two-time perturbation expansion 3-70633
 Earth, earthquake foci rel. to stresses and strains 3-44800
 earthquake, structure model, micromorphic continuum, deformation of microstructure, focal point props. 3-44824
 elastic cylinder, deformed, correlation of generalised orthogonality in equilibrium problem (*Russian*) 3-42773
 elastic cylinder, three-dimensional boundary problems, analysis of stress/strain relations (*Russian*) 3-66539
 elastic cylinder and a layer in joint torsion, stress-strain state 3-70558
 elastic viscoplastic beam, transient dynamic behaviour, direct finite element anal. 3-70612
 elastic-plastic continua, finite deformation, minimum principle 3-70559
 elastic-plastic solids 3-54109
 elastic/viscoplastic media, cylindrical plane strain wave propag. 3-57091
 elasto-visco-plastic material, isoclinic parameter expt. 3-43822
 elastoplastic material strain hardening, stress evolution characterisation (*French*) 3-70615
 elastoplastic rod, centrally compressed, with cross-like cross-section stability (*Russian*) 3-42795
 elastoplastic thermal stress, temperature dependence analysis, finite element method 3-70627
 elastostatics, sector problem, curved edge stresses, eigenfunction solution 3-70570
 electron metallography, microstruct. anal., bright field images, struct. factor, strain contrast 3-76181
 emulsions, viscoelastic nonlinear properties of semisolids, Weissenberg rheogoniometer 3-69396
 end-loaded conical frustums, influence coefficients 3-40099
 failure under simple and composite stresses, deform. criteria 3-58686
 fatigue crack growth theory, BCS crack theory with work hardening 3-68324
 fatigue crack propagation, notch geometry effects 3-68322
 fibre reinforced materials, effect of interlaminar stiffness and strength, plane stress 3-73023
 finite-strain beam theory, one-dimensional, large displacement, thin curved beams 3-70587
 finite-strain force, moment stress elasticity kinematics and statics 3-70588
 flexible plates and shells, elastoplastic strain theory applic. to stressed state calc. 3-57095
 forgings, residual stress meas., toroidal core method (*German*) 3-72885
 glass laminates, tensile strength, low temp. and high strain rate, stress conc. coeff. 3-73020
 glass reinforced plastics, elastoplastic anisotropy constns. and creep characts., determ. procedure 3-61206
 granodiorite, holocrystalline igneous rock, eqn. of state under compression to 20 kb 3-76559
 graphite, ATJ-S, hydrostatic press. response 3-72963
 graywacke, elastic finegrained sedimentary rock, eqn. of state under compression to 20 kb 3-76559
 groove formation sheet metal under tension, forming limit diag. 3-76197

stress/strain relations continued

- Hooke's law, geometric generalisation from general relativistic elasticity theory, for prestressed materials 3-74138
 hot torsion tests for solid and tubular specimens, specimen geometry effect 3-55925
 human tissue, mech. behaviour 3-42367
 industrial metals and alloys, micro-yield region behaviour (*Russian*) 3-58648
 intersection of cylinder and ellipsoid, stressed by internal pressure, unit load determ., resistive elec. extensometry (*Rumanian*) 3-73667
 isotropic materials, crippling allowables for elevated temp. and creep environments 3-64962
 laminated materials, prestrained, strain-gradient theory, buckling 3-77829
 Makrolon, prolonged storage effect 3-80488
 materials with different tension, compression and yield strengths, stress-strain relations 3-45674
 mechanical hysteresis loop, Fortran programs for stress-strain relationships (*Japanese*) 3-54090
 metal, short-time stress/strain characteristic, temp. depend., thermally activated models 3-69309
 metals, yield surface shape, offset influence, different loading paths, slip theory model anal. 3-72889
 microyielding in cyclic loading using time monitoring technique 3-41747
 nonlinear viscoelastic materials, modelling, identification and prediction using Volterra integral eqn. 3-45646
 Nylon 6, glass fibre reinforced, compressive creep and recovery 3-47456
 Nylon 6, glass fibre reinforced, tensile creep 3-47455
 orthotropic cylindrical shells, elastic, critical stress determ., stability, variable pressure 3-70579
 orthotropic elastic solids, plane micropolar strain, static theory 3-70560
 orthotropic shells, low shear stiffness, resolvents in theory, force moments and stress functions 3-70630
 perforated tube, star-shaped profiles, stress conc. meas., photoelastic methods, internal and external pressures (*Russian*) 3-74053
 plastic flow in hot rolling, math. predictions, temp. distrib. effects 3-80339
 plastic foam, effect of cellular struct. on mech. props. 3-65014
 plastic isotropic materials, math. model of damage accumulation 3-64936
 plastic media, vertical cut stability rel. to wall collapse 3-74051
 plastic strain meas. by strain-gauge methods under uniaxial stress condition 3-73100
 plastic zone size at tip of crack in plane strain state, finite element approach 3-68321
 plate under out-of-phase biaxial cyclic loads, strains and stress conc. factors 3-57078
 plate with external slits, elastoplastic deform. and failure under concentrated loads (*Russian*) 3-77827
 plates, non-linearly flexible, in presence of random initial stresses, stability (*Russian*) 3-62474
 poly(n-butyl methacrylate) networks, viscoelasticity, stress-strain behaviour, effect of reference chain dimension, thermoelastic meas. 3-55890
 polycarbonate, prolonged storage effect 3-80488
 polycarbonate as model material for three-dimens. photoplasticity 3-73064
 polyester dough moulding materials, fibre reinforced, stiffness and strength 3-73007
 polyethylene, combined tension-torsion creep with abrupt stress changes 3-58740
 polyethylene melt, shear and elongational flow, stress-time data, network theory predictions 3-73062
 polyethylene melt, stresses, periodic deformations, effect of vibration frequency and amplitude variations, Weissenberg rheogoniometer 3-76380
 polymers, crystalline, stress-strain dependence, adiabatic and veritable processes (*Rumanian*) 3-73033
 polystyrene solutions, viscosity, effect of mol. weight, range of shear stresses, structure formation and orientation 3-71687
 porous rocks, fluid-saturated, effective stress laws 3-76558
 quantitative strain and stress state criterion, failure in the vicinity of sharp cracks 3-66568
 quartz-phenolic composite, quasistatic uniaxial strain and Hugoniot tests compared 3-73111
 rectangular beam, elasto-plastic deform. under combined compression and bending stresses (*Italian*) 3-48733
 refractory, fireclay, thermal-expansion-under-load behaviour 3-80407
 refractory, thermal expansion under load, test program 3-80406
 reinforced, unreinforced epoxy resin, effect of strain rate and temperature, deformation behaviour 3-50775
 reinforced polymers, tension normal to the fibres, strength and deformability 3-64989
 rock, brittle, prefailure initiation behaviour 3-76553
 rubber, natural, oriented crystallisation, strain-induced, axial stress changes 3-54929
 shearing crack, half-plane, plane strain conditions 3-70606
 shell theory, linear two-dimensional, classification of integrals of dynamic eqns. (*Russian*) 3-77821
 shells, stiffened slanting rectangular, stress-strain state (*Russian*) 3-62471
 soda-lime glass, polymeric coating effects on bend strength 3-76265
 solid, steady wave profiles, nonequil. eqn. of state, conservation laws 3-75567
 solid medium in complex stress state under cyclic loading conditions, hysteretic behaviour 3-46664
 sphere subjected to large deform., stress fields 3-57074
 steel, austenitic stainless, cyclic stress/strain curves in M_1 - M_2 range 3-64829
 steel, Cr-Mo-V type, creep rupture of tubular specimens under axial loads and internal press. 3-69308
 steel, cyclic nonisothermal elastoplastic loading, diagram represent. 3-69431
 steel, fatigue fracture rel. to inelastic deform. in torsion 3-47422
 steel, hardened high C, hardening in NaCl soln., annealing, uniaxial compression diag. (*Russian*) 3-41767

stress/strain relations continued

- steel, high-strength, test method for transient stress conditions characteriz. at elevated temps. 3-69432
- steel, low-C, delayed yielding and hysteresis phenomenon under tensile fatigue load 3-44595
- steel, low-C, pressurized, Portevin-Le Chatelier effect 3-80289
- steel, mild, tubular specimens, precise meas. of plastic behaviour under combined torsion/axial force 3-76199
- steel, NiCrMo, mechanical hysteresis loop, Fortran program, low cycle fatigue test data processing (*Japanese*) 3-55799
- steel, SAE 4340, fatigue life and inelastic strain response under complex history 3-69289
- steel, stainless, instantaneous strain, proof stress, creep rupture testing 3-47437
- steel, static and fatigue props., temp. and strain rate influence 3-69312
- steel, stress state at fatigue crack tip obs. by X-ray microbeam technique (*Japanese*) 3-41736
- steel, structural, crit. plane-strain stress intensity factor, tensile ductility, microscopic fracture mode 3-64888
- steel, thermoplastic hardening, fracture toughness test (*Russian*) 3-72899
- steel, torsional prestrain effect on Bauschinger effect 3-64928
- steel, viscoelastic prop. effect on strain wave front 3-44597
- steel plates with oblique hole, corner shape effect on elastic stress and strain conc. 3-50823
- steel reinforcing, cyclic load behaviour 3-64935
- steel surface, after shot peening to produce work hardened layer 3-76196
- steel with low C content, effect of interruptions in loading 3-55916
- straight bar, deformation determ., discontinuous transverse loading (*Rumanian*) 3-74047
- superplastic alloys, diffusion-accommodated flow 3-40964
- tensile specimen, necking during creep at const. load and ambient temp. (*German*) 3-65051
- thermoelasticity, thick plate containing penny-shaped crack, asymmetric distrib. of thermal stress, iterative soln. 3-70571
- thermoplasticity, uncoupled, principles for stress rate, strain rate 3-77828
- thin elastic shell, elastic Cosserat surface, stress and strain, linear shell theory 3-70561
- three-layered shells with light fillers, static-geometric analogy and complex transform. 3-45668
- toroidal membrane, nonlinear inflated by const. normal press., axially symmetric deformation 3-70584
- transversely isotropic shells, elastic filler, stability, mech. loading, temp. effect of shear strength 3-70580
- transversely-isotropic materials with memory, constitutive equations, reduced forms 3-70610
- Udimet 700, hodographic prediction of cyclic creep 3-64961
- Udimet 700, inelastic high temp. materials behaviour prediction by strain-rate approach 3-64960
- uniform deformation, neck formation, effect on true strain at max. load, effect on longitudinal stress (*German*) 3-69254
- variable-stress creep predictions, influence of scatter 3-41831
- viscoelastic body, heating due to cyclic pressure 3-66555
- AgCd alloy, anomalous relations at martensitic transition 3-58611
- Al, load relaxation studies of high purity polycrystals. 3-41748
- Al, plastic wave propag., tensile and compressive wave profiles 3-58660
- Al, polygonized, subboundary effects, yield peak in tensile diagram (*Russian*) 3-44569
- Al alloy, creep under variable uniaxial tensile loading, strain accumulation and rupture 3-69405
- Al alloy, tensile prestrain effect on fatigue strength in high cycle fatigue 3-64950
- Al alloy RR58, biaxial cyclic high-strain fatigue 3-73107
- Al alloys, mechanical hysteresis loop, Fortran program for low cycle fatigue test data processing (*Japanese*) 3-55799
- Al single crystals, temp. depend. of strength, high plasticity phenomena, 1.4-300K (*Russian*) 3-55003
- Al-Cu-Mg alloy, high temp. fracture toughness test method 3-69433
- Al-Mg alloy, cold work effect on strain rate sensitivity 3-69300
- Al-Mg alloys, discontinuous flow at high temps., Portevin-Le Chatelier effects 3-69299
- Al₂O₃, sapphire filament, creep mechanism 3-76318
- Au-Cu(14 at.%) alloy, Portevin-Le Chatelier band characts. 3-80293
- BaF₂:La³⁺, Y³⁺, Gd³⁺, impurity effects 3-75534
- Cd-Zn alloy single crystals, crit. resolved shear stress, temp. and conc. depend. 3-58069
- Co-Cr alloys, low-ductility dental casting, elongation meas. and interpret. 3-69403
- Cu, high temp. creep, stress-change expts. 3-76206
- Cu, pure, pressurizing effect 3-50717
- Cu, single crystal hydrostatic pressure effect on stress/strain curve 3-40960
- Cu and Cu-Zn alloy, cyclic stress/strain response and fatigue life, low amplitude region 3-47414
- Cu-Al alloy, internally oxidized, particle size effect on yield stress 3-80294
- Cu-Al alloys, stress-strain characts. and slip band formation 3-47407
- α -Cu-Al(As)(Ga)(Ge)(In) alloys, Portevin-Le Chatelier effect (*German*) 3-41746
- Cu-Ge alloys, stress-strain characts. and slip band formation 3-47407
- Cu-Mg solid solns., dislocation dynamic characts. determ. from internal friction (*Russian*) 3-80251
- Cu-Si alloys, stress-strain characts. and slip band formation 3-47407
- α -Cu-Sn alloys, Portevin-Le Chatelier effect (*German*) 3-64907
- Fe, cast, ductile, transform. superplasticity (*Japanese*) 3-44564
- Fe, high temp. creep, stress-change expts. 3-76206
- Fe, plastic asymmetry phenomena 3-80295
- Fe-Ni-C alloy, martensite burst in deformed and thermally stabilized austenite 3-64826
- LiNbO₃, crystal hypersonic waves at 9.4 GHz, associated power, displacement amplitude, deformation and stress (*Russian*) 3-68341
- MgO, pure crystals, dislocation dynamics and thermally-activated deform. 3-72081

stress/strain relations continued

- MgO, pure single crystals, edge and screw dislocation behaviour 3-72080
- MgO-BOF brick, compressive creep, 1200-1500°C 3-80408
- Mn-Cu alloys, γ -phase, comp. effect on internal friction and Young's modulus 3-76208
- Mo, impure, temp. and strain rate influence on plasticity and stress/strain diagram appearance (*Russian*) 3-80344
- NaCl, simple slip on (110) and (100) planes (*German*) 3-46661
- Ni-Co alloys, dispersion-hardened, stacking fault energy effect on stress/strain curves 3-58670
- Ni-Zn ferrite, creep mechanisms at 1000°C-1350°C (*Japanese*) 3-68314
- Pb bar, exptl. study of plastic wave propagation, meas. of stress and strain histories 3-41752
- Si single crystals, dynamical yielding 3-79416
- Si₃N₄, hot-pressed, creep and tensile strength 3-76286
- Ti alloys, strain curves, 20-400°C 3-58680
- Ti and alloys, stress relaxation data interpret. 3-64926
- WC/Co composite, continuum mechanics approach to elastic-plastic behaviour 3-80444
- Zn, fracture, brittle and quasi-brittle, elec. pulse current influence (*Russian*) 3-80345
- Zn, high temp. creep, stress-change expts. 3-76206
- Zr and alloys, stress relaxation data interpret. 3-64926
- stresses**
- see also internal stresses; stress effects
- ceramics, porosity, dep. of creep rate 3-41805
- curvilinear flow, incompressible simple fluid, between rotating concentric spheres, stress functions 3-43541
- earth, elastic dislocation theory, self gravitating elastic config., energy release 3-44753
- earthquake magnitude, rel. to stress-drop and fault size, seismic energy, characteristic stress 3-80622
- earthquakes, frequency distribution, av. stress drop 3-44782
- earthquakes, longitudinal shear crack propag. and stress conc. 3-61314
- elasticity virtual power method, the second gradient theory (*French*) 3-62461
- explosions, prestressed media, stress wave radiation 3-44783
- fault plane swing assoc. stresses rel. to earthquake aftershocks 3-44760
- granite, Winnsboro, tensile anisotropy at 0.5 kbar 3-76611
- lunar, appl. of virial tensor to determ. 3-61720
- mid-oceanic ridges, compressive stress effects 3-41880
- numerical methods of calc., finite element and dynamic relax. methods 3-47808
- photographic films, shrinkage stresses, formation mechanism effect of drying temp. and humidity use of counterbalancing gelatin layer (*Russian*) 3-46675
- pressure tube CIRENE prototype reactor, static-elastic conditions of core support 3-67395
- quantitative strain and stress state criterion, failure in the vicinity of sharp cracks 3-66568
- residual, causes and evaluation 3-55025
- rocks, global meas. of bedrock 3-47647
- sandstone, Navajo, elasticity, dilatancy and failure in effective tension 3-76612
- seismic zones, determ. of stress-drop from body wave displacement spectra 3-47642
- shear, longitudinal laminar flow in finite bundle of seven equal diameter rods, one displaced 3-60267
- shear, photoelasticity technique, Hertzian contact, asperities 3-76225
- steel, automatic testing device, heat resistance, distortion due to temp. fluctuation 3-42531
- tectonic folds, experimentally prod., stress anal. 3-76610
- tectonic plate boundaries, diffusion of stress through lithosphere 3-44796
- tectonic stick-slip stress drops, effect of quartz fault-gouge 3-76627
- thermal, in elastic layer due to instantaneous plane heat source 3-59758
- thermal, increase of earth's radius by heating, allowing for gravitation 3-65162
- thermoelastic in elastic layer, steady state 3-59757
- thin films, setting up of initial stresses, relaxation testing, corrosive media 3-53299
- viscoelasticity, stress relax. at mech. deformations (*German*) 3-60767
- β -Co-Cu epitaxial bicrystal, elastic stresses and strains at interface 3-50067
- Zr alloys, pressure tubes, creep, effect of neutron flux anisotropy rel. to stress directions 3-67565
- stresses, internal** see internal stresses
- striations** see discharges (electric)
- striking** see impact
- strip line components**
- delay line, multiwire proportional chambers, read-out, design, operation 3-77688
- strip lines**
- curved thin films guiding elastic surface waves 3-41081
- field mapping, using conducting fluids and electrically transparent barrier 3-62175
- impedance and e.m. wave scatt. 3-42833
- stripping reactions**
- deuteron cross-section for stripping and dissociation, 2.7 GeV/c, measurement 3-78344
- diffraction model of deuteron stripping, effect of nuclear boundary spread and Coulomb interaction (*Russian*) 3-74548
- DWBA, finite-range, matrix elements calc. method 3-60139
- model-independent analysis of stripping to unbound levels 3-67296
- radial form factor determ. using Green's function method, reln. to alpha-decay width calc. 3-60133
- reversibility Born and DWBA calculations, one-dimensional model 3-60147
- (d,p) and complementary (p,d) reactions, comparative treatment of spectroscopic factors 3-40502
- (d,p) sub-Coulomb stripping and analog-resonance results near closed shells 3-67342

stripping reactions continued

- (d,p) reactions, compound nucleus contribs. to T_{20} analysing power 3-67343
- ¹⁹⁷Au(d,p), 100 MeV, diffraction model, effect of nuclear boundary spread and Coulomb interaction (*Russian*) 3-74548
- ¹²C(³He,p)¹⁴N, 3-11 MeV, reaction mechanism study by use of p-γ angular-correlation method 3-63074
- ¹²C(d,p), coupling const. determ. in peripheral models including form factor effects (*Russian*) 3-74598
- ¹²C(d,p), rel. to model independent anal. of stripping to unbound levels 3-67296
- ¹²C(d,p) to ¹³C unbound states, comparison with DWBA theory 3-54488
- ¹²C(d,p)¹³C, unbound levels in ¹³C, application of real Weinberg state method 3-57471
- ¹²C(p,d)¹¹C high Q-value reaction, sudden approximation study 3-74581
- ¹⁴C(d,p) stripping form factors, continuum shell model for ¹⁵C 3-54401
- Ca region targets, single-nucleon transfer reactions, isospin centroids 3-63028
- ⁴⁰Ca(³He,d)⁴¹Sc, meas. differential cross section, use DWBA to study $T_{1/2}$ proton in ⁴¹Sc 3-74480
- ¹⁴⁰Ce(¹⁶O, ¹⁵N)¹⁴¹Pr, E=56 to 63 MeV, measure excitation functions, DWBA analysis 3-71127
- ¹⁴⁰Ce(¹⁸O, ¹⁷O)¹⁴¹Ce, E=56 to 61 MeV, measure excitation functions, DWBA analysis 3-71127
- ²H(α,t)³He, 82 MeV, multi-interaction finite-range, two-mode DWBA analysis 3-67297
- ⁶Li(³He,p)⁸Be, 17 MeV multi-interaction, finite-range, two-mode DWBA analysis 3-67297
- ²⁴Mg(³He,n)²⁶Si, 5.0 and 5.8 MeV, meas. of angular distrib. of neutron polarisation, DWBA analysis 3-67352
- ⁹²Mo(³He,d)⁹³Tc, 30.2 MeV, stripping to analogue resons. using complex energy eigenstates 3-63081
- ¹⁵N(d,p)¹⁶N(unbound), off shell behaviour rel to R-matrix theory 3-63065
- ²³Na(³He,d)²⁴Mg, study of particle-hole nature of lowest 3- states in ²⁴Mg 3-49151
- Ni region targets, single-nucleon transfer reactions, isospin centroids 3-63028
- ⁵⁸Ni(d,p), 100 MeV, diffraction model, effect of nuclear boundary spread and Coulomb interaction (*Russian*) 3-74548
- ¹⁶O, α-stripping to ground state rotational bands of ¹²C, shell-model calcs. 3-45980
- ¹⁶O(d,p), coupling const. determ. in peripheral models including form factor effects (*Russian*) 3-74598
- ¹⁶O(d,p) to ¹⁷O unbound states, comparison with DWBA theory 3-54488
- ¹⁶O(p,d)¹⁵O high Q-value reaction, sudden approximation study 3-74581
- ³¹P(d,p)³²P, E=10 MeV, angular distributions, ³²P deduced ln, spectroscopic factors 3-60198
- ²⁰⁸Pb, ¹¹B induced transfer reactions above Coulomb barrier, selective excitation of particle, hole states 3-60219
- ²⁰⁸Pb(d⁺,p), 12.3 MeV, vector analysing power, differential cross section, ²⁰⁸Pb deduced levels, DWBA analysis 3-60199
- ³⁰Si(d,p)³¹Si, low deuteron energies, proton angular distrib. comparison of direct and compound nucleus mechanisms (*Russian*) 3-71119
- ¹⁵⁰Sm(d,p)¹⁵¹Sm, transfer l values ¹⁵¹Sm ground state, wave function 3-74594
- ⁸⁸Sr(¹⁶O, ¹⁵N)⁸⁹Y E=42.5 to 50 MeV, measure excitation functions, DWBA analysis 3-71127
- ¹²⁸Te(d,p)¹²⁹Te and complementary (p,d) reactions, comparative treatment of spectroscopic factors 3-40502
- Yb(³He,d), rot. bands of ¹⁷¹Lu 3-62939
- Yb(α,t), rot. bands of ¹⁷¹Lu 3-62939
- Zr region targets, single-nucleon transfer reactions, isospin centroids 3-63028

stroboscopes

- see also velocity measurement
- holographic interferometry, amplitude of vibrating body 3-66235
- holographic interferometry, severe vibr. meas., recording time reduction 3-61992
- magnetic domain wall motion stroboscopic obs. with light emitting diode 3-73819
- magneto-optical observation system, pulsed magnetic reversal of magnetic films, description 3-77579
- oscillation frequency of inertia balance, rel. to student mass meas. 3-59531
- subsurface wetting measurement, dynamic surface tension meas., bubble method, instrument incorporating stroboscope (*Russian*) 3-50071
- GaAs Gunn device, scanning electron microscope, 9 GHz, beam chopping, signal processing 3-70428

strong interactions, elementary particle see elementary particle strong interactions**strong interactions, quantum field theory of** see quantum field theory of strong interactions**strontium**

- alkali halides: Sr²⁺, ionic conductivity measurements as function of temp. 3-68639
- atmospheric comp. after 9th Chinese atmospheric nuclear test 3-53476
- atom, 5s5p ¹P₁ level, lifetime meas. using Hanle reson. 3-46184
- atom Hanle effect meas. of 5s6p ¹P₁ lifetime 3-63283
- atom spectra, autoionisation in neutral strontium 3-74798
- electrical resist., thermal cond. and thermopower meas. from 40-300 K 3-64318
- f.c.c.-b.c.c. phase transition rel. to s-d hybridisation 3-58128
- isotope abundances in acid and basic rocks in Iceland 3-80626
- lattice dynamics calc., dispersion relations, phonon spectrum, θ_d temp. depend. 3-49952
- ocean, Sr content, spectroscopic determination, Sr-Cl ratio (*Russian*) 3-47696
- phonon frequencies and binding energy calcs. using two parameter model pseudopotential 3-46602

strontium continued

- resonance fluorescence quenching meas. in CO and H₂ flames 3-42707
- self-consistent band calc. under high press., metal-semimetal transition 3-68538
- solar isotopic composition, photospheric and sunspot spectra, atomic line studies 3-61672
- transport in graphite, concentration profiles, importance in helium-cooled HTRs (*German*) 3-71243
- KCl: Sr plastically deformed, slip band internal structure by precipitation 3-52632
- MoS₂ (Eu, Yb, Sr), intercalated layer type cpds., lattice parameters change, mag. ordering, Curie temp., supercond. 3-50371
- Sr⁺ in optically pumped ⁵2P_{3/2} excited state, collisional depolarisation by inert gas atoms 3-46210
- Sr²⁺ in KI, luminesc., elec. field effect (*French*) 3-55693
- ⁸⁷Sr/⁸⁶Sr in basalts from Surtsey and Heimaey volcanic eruptions 3-41884
- ⁸⁷Sr/⁸⁶Sr ratios for volcanic rocks from St. Lucia and St. Vincent 3-53396

strontium compounds

- formate dihydrate, deuterated, struct., by deuteron mag. reson. 3-64569
- scheelite type, SrM^{IV}Li₂F₈, (M^{IV}=Th, U, Ce, Tb, Zr, Hf), lattice consts. (*French*) 3-64004
- SrTiO₃, anharmonic interactions and struct. phase transitions 3-58112
- strontium formate, phase matched second harmonic generation and optical mixing 3-40281
- strontium formate dihydrate, phase matched second harmonic generation and optical mixing 3-40281
- Ba_{1-x}Sr_xFe_{12-x}Al₂O₁₉, substitution of Fe³⁺ by Al³⁺, Mossbauer study 3-58452
- Ba_xSr_{1-x}Nb₂O₆ growth striations, domain structure 3-72019
- Ba_xSr_{1-x}Nb₂O₆-BaNb₂O₆ system, eutectic solidification and characterization 3-76237
- CaF₂-SrF₂ solid soln. single crystals, interdiffusion coeffs., comp. depend., 1100-1320°C 3-61190
- NaCl-CdCl₂-SrCl₂ phase diagram, thermography, X-ray methods, Na₂CdCl₄ binary combination, eutectics, Van Rein point (*Russian*) 3-52692
- Sr-Mo-O system, compound formation, SrMoO₄, SrMoO₃ and Sr₃MoO₄ structures 3-68386
- (Sr_{0.75}Ba_{0.25})Nb₂O₆, hologram recording material, electrical fixation, field and time thresholds 3-53915
- Sr_{1-x}Ba_xNb₂O₆, preparation and props. of ferroelec. single crystal 3-80170
- Sr₂Ba_{1-x}Nb₂O₆, anomalous electrooptic props. and their device appl. 3-41501
- Sr_{1-x}Ba_xTeO₃, Sr_{1-x}Ca_xTeO₃ solid solutions, phase transition temps. 3-68938
- (SrCa)S₂O₆·4H₂O, mixed crystals, dispersion of optical activity 3-76026
- SrCl₂, doped with Na⁺ and Rb⁺, F* centre bleaching 3-40917
- SrCl₂, magneto-optical and stress linear dichroism studies 3-64629
- SrCl₂, phonon dispersion curves, i.r. and Raman spectra obs. 3-49951
- SrCl₂: ²⁴³Cm(²⁴⁷Cm), e.p.r. obs. of nuclear spins and mag. moments 3-68841
- SrCl₂: Cu²⁺ e.p.r. obs. for model of centre 3-50451
- SrCl₂: H⁺, U-centres, i.r. absorpt. study 3-69032
- SrCl₂: Yb³⁺, single crystals, photoluminescence (*Russian*) 3-41552
- SrCu_{1/3}Nb_{2/3}O₃-PbZrO₃ system, X-ray diff. phase anal. and dielec. props. 3-72591
- SrFe₂Fe₂O₇, crystal growth and structure 3-69159
- SrF₂, F and F-aggregate centre production by X-irradiation 3-46641
- SrF₂, Knoop microhardness anisotropy, applic. to slip system identification 3-79410
- SrF₂: Gd³⁺, e.s.r. spectrum, cubic splitting parameter, press.-induced changes 3-60990
- SrF₂: Na, conversion of colour centres by doping 3-53133
- SrF₂: Tm²⁺, high press. optical absorpt. studies 3-41540
- SrFe₁₂O₁₉, thin plate, magnetic domain patterns, temp. depend. (*Japanese*) 3-64515
- SrFe₁₂O₁₉, thin plates honeycomb domain structure, temp. depend. 3-60978
- SrFe₁₈O₂₇, phase relationship for varying O partial pressure and temp. 3-52690
- Sr₂FeO₃F, temp. depend. of susceptibility, Curie-Weiss paramagnetism 3-46978
- SrFe₁₂O₁₉ ferrite, liquid phase sintering of magnetically isotropic and anisotropic compacts 3-58701
- SrFe_{2/3}Re_{1/3}O₃, ordered perovskite, semicond., ferrimag. props. below 475 K, Mossbauer obs. 3-79846
- K₂FeReO₆, ordered perovskite, metallic, ferromag. props. below 475 K, Mossbauer obs. 3-79846
- Sr(Fe_{2/3}U_{1/3})O₃, structural, magnetic and dielectric props. and Mossbauer effect 3-72051
- Sr₂, nearly free electron model for equil. behaviour 3-75497
- SrI, band spectrum in 6500-7200 Å region 3-63438
- SrI, band system in 3350-3560 Å region 3-52362
- SrLaCoNbO₆, ordered perovskites, collapse of mag. sublattices 3-72496
- SrLaCoTaO₆, ordered perovskites, collapse of mag. sublattices 3-72496
- SrMnO_{3-x}Mn₂O₄, phase relations, elevated temps. 3-43864
- SrMoO₄, elastic consts., u.s. velocity data 3-49921
- SrMoO₄: Gd³⁺, elec. field effect on e.s.r. 3-72517
- Sr(NO₃)₂, stress-optical coeffs., temp. depend., 30 to 300°C 3-50539
- Sr(NO₃)₂-Nd(NO₃)₃-Na₂WO₄-H₂O system, aqueous solutions, solid phase 3-76422
- SrNb₂O₆-NaNbO₃, phase equilibrium, dielectric characterisation, DTA, Curie point meas. (*French*) 3-79994
- SrO, deformed, compression depend. of luminesc. 3-69049
- SrO, high temp. reaction with SiC, in air, Ar and vacuum 3-74723
- SrO, lattice dynamics, phonon freq. distrib., Debye temp., variations 3-52676
- SrO, vibronic props. of F⁺ centre 3-55062
- SrO dissociation energy determ. in CO/N₂O flames 3-76425

strontium compounds continued

- SrO:Ag²⁺, e.p.r. spectra, Jahn-Teller effects, static to dynamic transition 3-53016
 SrO-BaO-Al₂O₃ system, solid state phase equilib., X-ray anal. 3-72998
 SrO-HfO₂ system, transition temp., zirconia comparison (*French*) 3-72993
 SrO-K₂O-SiO₂ glasses, i.r. spectra, struct., depolymerizing effect 3-68164
 Sr(OH)₂·8H₂O vacuum dehydration, kinetic parameters 3-76432
 SrO.5Fe₂O₃, sintering behaviour and characteriz. 3-61191
 SrO.(6-x)Fe₂O₃.xAl₂O₃, chemical composition, Al/(Al+Fe) atomic ratio determ. 3-52604
 SrO.6Fe₂O₃, cryst. growth from molten strontium borides (*Japanese*) 3-44667
 SrP₃, production and crystal struct. (*German*) 3-79320
 Sr₃(PO₄)₂:Eu²⁺, radiationless recombinations in surface layers (*Russian*) 3-50612
 SrS phosphors, photolum. characts., effect of Bi and Cu activators 3-69054
 SrS:Cu phosphors, preparation and luminescent props. (*Russian*) 3-76057
 SrSO₄-CaSO₄, metastable mixed cryst. formation 3-63996
 Sr₂Sb, crystal structure, least squares refinement 3-60698
 Sr₂SiO₄-Sr₂GeO₄-Ba₂GeO₄-Ba₂SiO₄, solid solubility, polymorphism, lattice constants 3-41803
 SrTb₂Fe₂O₇, ferrite, cryst. struct., X-ray and neutron diffr. obs. 3-58022
 SrTeO₃, ferroelec., piezoelec., and optical props. 3-68938
 SrTiO₃, crit. opalescence, light scatt. near structural phase transition 3-41535
 SrTiO₃, displacive phase transitions, theory 3-72160
 SrTiO₃, e.p.r. of Fe³⁺-V₀ centre, phase transform. dynamics implications (*German*) 3-53015
 SrTiO₃, e.s.r. of light-induced oxygen centres 3-47144
 SrTiO₃, electroreflectance measurements, Kramers-Kronig analysis 3-55613
 SrTiO₃, heat capacity in vicinity of phase transition at 110 K 3-79490
 SrTiO₃, lattice const., 17-300 K, anomaly at cubic-tetragonal transform. 3-60701
 SrTiO₃, neutron scatt., microscopic theory for central peak 3-55060
 SrTiO₃, perovskite-type crystal, band structure calc., electro-optic and electroreflectance effects 3-55552
 SrTiO₃, struct. transition, optical phonon instability induced, sound propagation effects nr. transition 3-46709
 SrTiO₃, supercond. rel. to structural instability, electron-soft phonon interactions 3-58343
 SrTiO₃, tetragonal, e.p.r. of Fe³⁺-V₀ centre (*German*) 3-50445
 SrTiO₃, thermomodulation experiments at cubic-to-tetragonal phase transition 3-55085
 SrTiO₃, wavelength-modulated spectrum, temp. variation of band gap 3-55569
 SrTiO₃ structural phase transition, Wilson theory of critical phenomena, classical isotropic Heisenberg antiferromagnet 3-41013
 SrTiO₃:Cr³⁺, luminesc. excitation mechanisms obs. 3-64704
 SrTiO₃:Fe, photochromic, valence states rel. to colour changes, Mossbauer obs. 3-58461
 SrTiO₃:Fe colour changes for energetic heavy particle detection 3-49911
 SrTiO₃:Fe³⁺, electric field effect on e.p.r. spectrum 3-72513
 SrTiO₃:Fe³⁺, overlap contribution to isomer shift calc. 3-64586
 Sr₂[Cu(OH)₆], crystal structure determ. by Patterson and Fourier synthesis 3-68205

structure (chemical) see *chemical structure*

structure factors (crystals) see *crystal atomic structure*

structure of alloys, crystal see *crystal atomic structure of alloys*

structure of elements, crystal see *crystal atomic structure of elements*

student laboratory apparatus

- adsorption, gases on to C black, specific surface area, heat of adsorption 3-48327
 Atwood's machine, improved determ. of acceleration 3-56606
 ballistic pendulum struck by arrow, student experiment 3-70244
 beta particle energy range formulae and school laboratory expt. 3-77354
 birefringence experiments for introductory physics course 3-77351
 cell holder, Beckman DK-2A Spectrophotometer, temp.-regulated 3-77368
 clock electronic digital, construction as student project 3-70247
 colorimeter, computer controlled 3-62096
 conformational study, equipment for meas. dihedral angles on models 3-77374
 controllable tendon tapper, design details 3-59682
 diffraction illustrated with laser beam and chalk dust 3-70256
 digital filter, simple 3-66114
 dipole moment meas., gas phase, rel. to dielectric theory, undergraduate teaching 3-45401
 DNA, helix coil transition, u.v. photometer, student experiment 3-51422
 electric field plotter, design 3-42503
 electrolysis experiment for electron charge and mass 3-61973
 force table for students to discover the properties of vectors 3-66118
 fringerator for meas. ang. size of Fabry-Perot fringes 3-70253
 instantaneous velocity demonstration using 'hot wheels' 3-70242
 interferometry, double exposure to demonstrate wave nature of light 3-66115
 Josephson effect expt. with Clarke slugs 3-56596
 laser mirror using common commercial glass 3-73651
 light scattering in the atmosphere simulation with glass tank 3-70250
 linear air track for continuous quantitative meas. 3-39846
 liquid-vapour equilibrium, constant temp. 3-64165
 mass spectrometer, use by undergraduates 3-62276
 mechanical energy conservation experiment 3-66103
 microwave expts. on e.s.r., electron cyclotron resonance and plasma electron density 3-56603
 microwave spectroscopy and molecular structure for the student laboratory 3-66102
 molecular light scatt., polarization, experiment for students 3-70233
 student laboratory apparatus continued
 n.m.r. permanent magnet, chemically induced nuclear dynamic polarisation, nuclear and electron spin coupling 3-48324
 nuclear debris measurement 3-61974
 pendulum, normal modes of vibration, demonstration to students 3-48321
 planetarium for \$50, student construction project 3-73658
 refractive index meas., gas phase, interferometry, undergraduate teaching 3-45401
 rotational motion, friction free force table 3-70254
 Rutherford scatt. apparatus, design and expt. results 3-42504
 spectral analysis using 35 mm camera and projected slides 3-73653
 student demonstration using chirp system to meas. distance 3-56602
 telecommunications, building block set, expt. (*Hungarian*) 3-77366
 thermistor thermometer bridges, linearised, small temp. change meas., calorimetry 3-77400
 wiring device for transitions from binding posts to 110 V devices 3-66120
 LiF type N phosphor + C, thermionic electron emission, dosimeter 3-73654
 O₂, paramagnetism, bonding theory, difference between valence bond and mole. orbital approaches 3-48326

SU₃ theory

- (8,8) symmetry breaking, decay rate $\eta' \rightarrow \eta\pi\pi$ 3-74356
 f_1/f_2 derivation, algebraic structure for chiral charges 3-66945
 alpha-decay widths analysis for molecular viewpoints in light nuclei 3-60133
 baryon relativistic effective mass, for strongly interacting superdense matter 3-66668
 baryon spectroscopy and regularities between SU₆ and SU₃ mass-breaking parameters, quark model study 3-78150
 baryon spectrum and reflection partners, SU(3) Regge scheme 3-45900
 bootstrap model, complete, of quarks, mesons, baryons, Yukawa coupling and SU(3) symmetry 3-70946
 broken SU₃ coupling constants, approximate scale invariance 3-57304
 Cabibbo's weak Hamiltonian, nonrelativistic quark model and octet dominance 3-74355
 canonical basis, unitary scheme density matrix (*Russian*) 3-54400
 chiral SU₃ × SU₃ symmetry breaking 3-74334
 chiral SU(3) × SU(3) symmetry, generalized nonlinear Lagrangian for pseudoscalar and scalar mesons 3-66932
 chiral symmetry breaking, connection with Cabibbo angle, model with SU(3) noninvariant vacuum 3-70883
 Clebsch-Gordan coeff. and orthogonalization problem 3-74330
 deformed nuclei, magnetic moments in pseudo SU(3) model 3-49130
 e.m. decay of neutral meson, simple model 3-59966
 exotic baryon resonance assignments, utility of quark model 3-40318
 geometry of adjoint representation of SU₃, physical quantities rel. to orbit families 3-78101
 harmonic oscillator dynamical group construction 3-77868
 hypercharge exchange reactions, amplitude analysis 3-71008
 hypercharge-exchange reactions, analysis of data, impact parameter representation 3-67134
 hyperon decay, NN π vertices, parity violating, scalar meson pole model 3-62809
 inclusive reactions, exotic SU(3) representation in b fragmentation region 3-57462
 mass formula, supermultiplet splitting, strong and e.m. interactions, sum rules (*Russian*) 3-59936
 matrix representations of Lie algebra and Clebsch-Gordan coeffs. 3-62783
 meson fields, asymptotic, explicit and spontaneous chiral symmetry breaking 3-59935
 meson theoretical model rel. to low energy baryon-baryon interactions 3-74408
 meson-baryon scatt. and baryon resonances, partial wave analysis 3-45907
 meson-baryon system, symmetry breaking and triangular representations of chiral SU(3) 3-60001
 mesons, scalar and pseudoscalar in broken non linear chiral SU(3) × SU(3) dynamics (*Russian*) 3-66944
 n-particles, vector coupling coefficients, analytical formulation, program descrip. 3-48989
 neutral currents $\Delta Y=1$ avoidance mechanism involving SU₃ symmetry breaking 3-66963
 nonet formation from $J^P=1^{++}$ mesons with 1^{--} mesons 3-70954
 nonleptonic weak hyperon decays, models, SU₃ breaking criteria 3-43087
 nonlinear chiral symmetry and PCAC Bogoliubov-Parasiuk-Hepp-Zimmermann renormalization 3-54267
 nuclear shell model calc. of coupling in ¹⁶O negative parity states 3-78253
 parton models, e.m. mass shifts and renormalization of Cottingham formula 3-62827
 pseudoscalar mesons, non-analytic terms in Gell-Mann-Okubo reln., symmetry breaking models 3-40369
 quark field, selfinteracting, gauge invariant model, light cone algebra 3-62786
 Regge pole model for total cross section at high energy 3-67151
 resonance decay and magnetic moment predictions, exact reduced-vertex symmetry 3-51986
 schizon scheme of Lee and Yan, formulations, renormalizable gauge theory, $\Delta I=1,2$ rule 3-66961
 SL_{2,C} unitary irreducible representations, relations among baryon magnetic moments 3-59958
 SL(3, C), principal degenerate series of unitary representations 3-62784
 SL(3, C) UIRs, hadron mass levels in the resonance towers 3-62861
 spontaneous symmetry breaking theory for SU₃ × SU₃, coexistence conditions (*Rumanian*) 3-51987
 SU(3) × SU(3) gauge theory, electron-muon mass ratio 3-78106
 SU(3) × SU(3) of currents, SU_w(6) of constituents, e.m. decays 3-67016
 SU(3) ⊃ SO(3) and asymptotic props. of quantum number Ω 3-54275

SU₃ theory continued

- SU(3)⊗SU(3) symmetry breaking and Regge behaviour reln. to dispersion relns. 3-54287
 symmetry and exchange degeneracy of baryon Regge residues 3-54288
 symmetry breaking of zeroth order mass matrix, Han-Nambu quarks 3-62802
 three-triplet quarks, O(4) gauge theory, e.m. and weak interactions 3-62801
 twenty seven, effects of inclusion in strong interaction Hamiltonian density 3-67071
 U₃ symmetry between baryons and mesons 3-57305
 unified gauge theory for weak and e.m. interactions, SU(3)×SU(3) symmetry and quark structure 3-70894
 vector meson production, Regge-pole exchange-degeneracy SU₃ approach 3-57431
 weak and electromagnetic interactions of leptons and hadrons, symmetry breaking effects 3-62800
 Wigner and Racah coefficients, FORTRAN programs 3-66941
 e⁺e⁻ annihilation, SU(3) symmetry breaking and branching ratios 3-62837
 e⁺e⁻→hadron+X, SU(3) prediction for single particle distribns. 3-57367
 e⁺e⁻→hadrons, SU₃ inclusive sum rules for bounds on K/π production ratio 3-78141
 ep→e+hadron+X, SU(3) prediction for single particle distribns. 3-57367
 η'η sigma term, symmetry-breaking models 3-74333
 K→πμ(e)ν, hard-meson (3, 3*)+(3*, 3) model, potentialities and applicability conditions 3-48998
 K→πμ(e)ν, study using SU₃×SU₃ light-cone algebra, sum rules and form factors 3-57320
 K⁺ photoproduction, Regge model from kaon and exchange degenerate K*(892)-K*(1420) trajectories 3-40348
 K⁺d→K⁰pp, charge exchange cross section values, expt., predictions 3-78207
 KN charge and hypercharge exchange reactions, Regge pole model 3-67072
 K⁺n→K⁰p, charge exchange cross section values, expt., predictions 3-78207
 K⁺N, chiral symmetry breaking, PCAC and the σ commutator 3-57415
 nd scatt., SU(3) basis calc. of three-particle states 3-49037
 pp collisions, multiparticle production cross-section, 50-300 GeV/c, model with SU(3) singlet uncorrelated fireballs 3-62910
 π production in high-energy hadron collisions, reasons for SU₃ violation, quark model 3-54355
 πN, charge and hypercharge exchange reactions, Regge pole model 3-67072

SU_n theory

- see also elementary particle symmetry; SU₃ theory
 baryon spectroscopy and regularities between SU₆ and SU₃ mass-breaking parameters, quark model study 3-78150
 chiral SU(2)×SU(2) invariant field theory for massless pions, mechanical analogue, complete solns. 3-48990
 chiral SU(2)×SU(2) symmetry, η→πππ decay and πη scattering 3-45870
 deep inelastic structure functions from collinear SU(1,1) symmetry 3-78149
 dimensionality formulas for irreducible representations, duality of Young diagram 3-73975
 elementary particles, noncompact Lie group representation, extension formulas for SL(4, C) 3-62782
 e.m. wave scattering in terms of functions over group SU₂ 3-42954
 gauge, three-triplet realisations, and e.m. mass differences 3-59962
 global SU(2,2), gauge symmetry of dual resonance models 3-70952
 hadron Hamiltonian function of Cabibbo angle by station projection 3-74314
 harmonic oscillator, anisotropic, with rationally related frequencies, decomposition, reln. to SU(n) 3-48754
 harmonic oscillator relation, representations occurring on degeneracy spaces 3-57303
 isoscalar factors for U_n semicanonical basis, Clebsch-Gordan coeffs. of SU₂ (Russian) 3-57481
 isospin gauge invariance models rel. to n-p mass difference calc. 3-59961
 lepton model, combining Weinberg's model with Lipmanov classification 3-43079
 lowering operators for the reduction of U(n) spin down SO(n) 3-73986
 non-linear chiral SU(2)×SU(2) dynamics, calc. of ππ scattering lengths 3-40381
 recoupling diagrams for duality, closed form general solutions 3-70951
 Reggeized symmetry model, SU(6)×SU(6), high energy pion-nucleon scattering 3-78195
 SL(3,C), projective representations in Z-operator formalism 3-45624
 SO(5), irred. represent., projected basis in theory of 5-D quasi-spin 3-54413
 SU_{1,1} Lie algebra, associated Hamiltonians 3-66625
 SU₂×U₁ gauge model, consequences 3-74335
 SU₂×U₁ gauge model, renormalised coupling constants 3-57337
 SU₂×U₁ gauge models, determ. of mixing angle by general method 3-51984
 SU₂ symmetric core structure of nucleon 3-54311
 SU₄ bilocal algebra determ. of sum rules for deep inelastic spin-dependent νp scattering 3-62812
 SU₄ symmetry breaking effects on ¹⁶O muon capture rate calcs. 3-74543
 SU₆-breaking pattern implied by transformations from constituent to current quarks 3-74332
 SU₆ broken collinear symmetries and suppression of |ΔS|=1 amplitudes 3-48995
 SU₆ multiplet structure in relativistic model 3-51985
 SU_n×SU_n chiral group, nonlinear realisation of symmetries and localisability 3-74338
 SU_n→SO_n reduction, geometrical induction procedure, soln. derivation 3-70882
 SU_n unitary unimodular groups, structural props. 3-59778

SU_n theory continued

- SU_w(6) of constituents and SU(3)×SU(3) of currents, in reln. to e.m. decays 3-67016
 SU(2,1), construction of factorisable dual amplitudes (Russian) 3-74396
 SU(2)×L spin up-invariant non linear spinor equation construction (Russian) 3-62785
 SU(2)×SU(2) charge algebra, Regge couplings from saturation schemes 3-78162
 SU(2)×U(1) gauge theories of weak and e.m. interactions using Han-Nambu quarks 3-45865
 SU(2)⊗U(1), current-mixing gauge theories of weak and e.m. interactions 3-45866
 SU(2)⊗U(1) gauge theories of generalised σ model for π⁰, η, η'→γγ decay 3-57346
 SU(2) nonelectromagnetic symmetry breaking, contrib. to kaon and pion mass differences 3-66932
 SU(2)-Lie functional equations, finite dimensional solns. 3-78102
 SU(4), universal spurion in mass operator and universal form of semi-leptonic current 3-45856
 SU(4)×SU(4) gauge theory, electron-muon mass ratio 3-78106
 SU(4)×SU(4) invariance of hadrons in gauge theory of weak and e.m. interactions 3-43081
 SU(4)⊗SU(4) lepton-hadron symm., and heavy charmed particle existence 3-45857
 SU(6)_w, modified version for πN→πΔ decay 3-62894
 SU(6)_w, pionic reson. decays, quarks 3-78152
 SU(6)_w on light cone, consequences for structure functions in deep inelastic region 3-40319
 SU(6)_w quark algebra, current and constituent, pionic transitions as tests of connection 3-67058
 SU(6), algebra of strengths generated by bilocal currents acting on constituent states 3-57308
 SU(6), meson-baryon scatt. and baryon resonances, partial wave analysis 3-45907
 SU(6)×O(3) structures, production cross section of πN→πN* 3-62892
 SU(6) or U(6) symmetry of quark model (Russian) 3-74389
 SU(p,q), universal covering group parametrization 3-73983
 Thirring model with U(n) symmetry, scale invariance only for fixed values of coupling constant 3-74341
 unified lepton-hadron symmetry and gauge theory of basic interactions 3-70884
 unified SU(2)×U(1) gauge theory of weak and e.m. interactions with ΔI=1/2 rule 3-57316
 unitary irreducible representations, coupled states of two angular momenta as basis functions 3-57302
 e-N inelastic scatt., comparison with photoabsorption in SU(6)×O(3) model 3-43115
 η, pionic and e.m. production, broken SU₆×O₃ model of higher baryon couplings 3-43107
 η→πππ, SU(2) chiral breaking, calc. of decay rate 3-66975
 πK, low energy, chiral SU(2)×SU(2) symmetry, amplitudes consistent with unitarity and crossing 3-57420
 SU(1,3) for calc. of strong interactions of spin 1/2⁺ baryons 3-54284

sublimation

- see also heat of sublimation
 benzoic acid, sublimation enthalpy and Gibbs energy function, microcalorimetric determ. 3-55079
 ice sublimation, local vapour flux velocities determ. 3-72190
 particle fluid mass transfer, multiparticle system 3-63759
 solid sublimation with varying energy liberation by laser radiation, motion of sublimation products (Russian) 3-68055
 sublimation enthalpy and Gibbs energy function, microcalorimetric determ. 3-55079
³⁶Ar, solid, sublimation and vapour press., 23.752-87.375K 3-41012
 CdTe, vaporiz., mass spectrometric obs. 3-68402
 Kr, radiation energy, partial pressure effects, vapour pressure vs. activation energy (French) 3-55081
 La₂(CrO₃)₃, oxidation-vaporiz. kinetics 3-72955
 NH₄ClO₄, vacuum sublimation 3-55080
 NaCl, solid, kinetics and rate meas. from 530C to m.p. 3-72189
 NaF-AlF₃ system, AlF₃-rich, high press. study (French) 3-68392
 RbReO₄, mass spectrometric investigation 3-49990
 RuO₂, sinterability, 800-1000°C (Japanese) 3-44666
 SiC crystal growth by vapour-liquid-solid mechanism in sublimation method 3-80160
 SiC single crystal, improved sublimation growth method (Japanese) 3-47354
 SmS system 3-64174
 ZnSe, vaporiz., mass spectrometric obs. 3-68402

suboptimal control see optimal control

subroutines

- algorithm for correlation of geological sequences from magnetic obs. 3-59165
 algorithm for the linear combination of readings, right rectangular prism, gravity effect, graphical method 3-44945
 computer-aided kinetic analysis thermal decomposition, condensed substances (Russian) 3-47537
 geology, ray tracing through structures, 3 dimensional model of plane or curved surfaces, general algorithm 3-80844
 hydrophysical data transmission telemetering buoys, computer M-220-M, radiochannel, subprogramme details (Russian) 3-47850
 Love waves, torsional free modes, simple algorithm for computation of attenuation factors 3-80620
 statistics, confidence limits for abscissa of intersection of two linear regressions, in FORTRAN 3-66504
 tracking 3 dimens. microscope specimens, automatic focusing algorithm 3-56990
 triangular bending elements analysis with derivative smoothing, in FORTRAN 3-40106

subsets (mathematics) see set theory

substrates

- see also integrated circuit production; semiconductor device manufacture
 alkali halide substrate surface microrelief change induced by radiation damage causing mechanical instabilities in thin films 3-52770

substrates continued

- alumina, sawing with CO₂ laser 3-74290
 alumina with MgO, electrical props. 3-41797
 ceramic, Ni-B alloy applic. by chem. reductive process 3-76235
 chemical nature, role in formation of sputtered Ta films 3-41111
 cleaning for integrated optical waveguides 3-79576
 e.m. interaction force between metallic grain and elec. image in substrate (*French*) 3-79586
 garnet, Czochralski-grown, perfection and charact. for gems, lasers and substrates 3-76131
 garnet, effect of lattice mismatch on mag. anisotropy of epitaxial IO₁₂ 3-44228
 garnet, for mag. epitaxial films, defects obs. by H₃PO₄ etching 3-44302
 glass, temp. effects on mag. anisotropy of oblique incidence Fe films 3-47083
 glass, thin films optical constants calc. by ellipsometry 3-53158
 heatable, construction and operation 3-39879
 holographic recording substrate, chromatic photosensitization (*French*) 3-73775
 interaction energy calc. for adsorbed monoatomic films (*Russian*) 3-58180
 IV-VI semiconductors, thin Au film formation by vacuum evaporation 3-61109
 magnetic thin films, roughness effect on transverse susceptibility meas. 3-79880
 metal, struct. and flux penetration in sputtered supercond. Nb films 3-79788
 mica, for epitaxial Ti, crystallography and interfacial dislocations 3-55168
 mica, influence of substrate temp. on Cu epitaxy 3-44527
 oxide and metal, obs. on sticking coefficients of Ag 3-60840
 polymer powder, influence of temp. on struct. and transport props. of Bi films 3-50091
 Rayleigh waves, surface-to-bulk mode conversion 3-60833
 stress determ. using automatic Bragg angle control 3-41669
 stress determination, X-ray technique, curvature measurement, automatic Bragg angle control 3-62300
 superfluid flow onset in ⁴He films on a variety of substrates 3-43912
 thick films production of Ni-Zn ferrites using arc plasma deposition process 3-55731
 Al₂O₃, alumina, laser beam sawing, pattern contour following 3-76303
 Al₂O₃, sapphire, effect of temp. and orientation on epitaxial Ta structure 3-52762
 Au, adhesion of Au particles in u.h.v. 3-68519
 BeO with Bi film, resistivity variation with temperature 3-52913
 for Bi thin film vacuum deposition, nucleus shape obs. 3-79595
 GaAs, growth of InP thin film, struct. anal. 3-72286
 GaAs, influence of substrate treatment on electron and impurity distrib. of epitaxial GaAs (*Russian*) 3-50663
 n⁺ GaAs(100), HCl-vapour etched, Auger spectra 3-41629
 GdGa garnet, defects effects on garnet epitaxial films 3-58405
 GdGa garnet, for epitaxial garnet films, lattice mismatch 3-64258
 Gd₃Ga₅O₁₂, dislocations near inclusions, Burgers vectors, interstitial loop form. 3-40919
 Gd₃Ga₅O₁₂, for mag. garnet film, X-ray obs. of structural defects 3-44295
 Ge, growth of InP thin film, struct. anal. 3-72286
 Ge (110) and (100) surfaces, Zn deposition obs. using mass spectrometric molecular beam method 3-61110
 InP, growth of InP thin film, struct. anal. 3-72286
 MgO epitaxial film Co, short-range transport app., chem. transport react. 3-72277
 NaCl (001) recrystallisation of Au films 3-72293
 NaCl (001) recrystallisation of Au films 3-72294
 Ni (001), chemisorption bonding of c(2×2) chalcogen overlayers, LEED study 3-60829
 Si, adhesion of Au particles in u.h.v. 3-68519

sudden commencement see magnetic storms

Suhl effect see Hall effect

sulfur see sulphur

sulphur

- acoustic and acoustooptical props. of α -S at u.s. freq., deflection applications (*French*) 3-43836
 adsorbed, c(2×2) overlayers, on Ni(100), struct., LEED study 3-68493
 adsorption on Pt(110) surface, catalytic CO oxidation 3-73166
 adsorption on Pt(110) surface 3-41869
 atoms and ions, computed lifetimes of 3s3p⁴ lifetimes 3-78435
 beam-foil lifetimes meas. in vacuum u.v. 3-78425
 catalytic inhibition of carbon deposition from acetone on steel 3-73168
 corrosive reaction with W 3-50089
 detection in streams and soil, radioactive thin-walled proportional counter low level background meas. 3-51719
 diffusion, in GaAs, solid-to-solid, n-type layer and p-n junc. prep. 3-41189
 Earth's core, possible S content rel. to shock compressional expts. on pyrrhotite 3-44798
 earth core, compression and temperature gradient using thermodynamic Grüneisen ratio 3-76545
 energy levels of 1s²2s²2p⁴ configurations 3-43332
 film, S film on Be foil, X-ray filters, vacuum deposited 3-40053
 lunar soil sample, Apollo 17, abundance 3-65826
 M20, shock front structure at bright rims using S II lines 6717 Å and 6731 Å 3-77161
 M8, shock front structure at bright rims using S II lines 6717 Å and 6731 Å 3-77161
 molecule, configuration, gas-phase photoelectron spectroscopy at 140°C 3-52307
 molecule, selectively excited, Hanle effect lifetime meas. 3-75062
 negative ion formation by electron impact in dissociative reattachment region (*German*) 3-71403
 neutron beam, 25 keV, 'Apsara' reactor, filter material 3-73855
 orthorhombic, potential function parameters 3-54950
 overlayer on Ni(001), chemisorption bonding, LEED study 3-60829
 tensors, T, L and S, calc. from cryst. forces 3-79262

sulphur continued

- X-ray states, central atom vacancy, photoemission spectra 3-66464
 in CuCl, absorpt. spectrum, e.p.r. of point defects, colour centres 3-68844
 GaSb:S, impurity level scheme 3-75722
 n-GaSb:S, long-period conductivity relaxation phenomena 3-79690
 S I, S II, spontaneous emission transition probabilities, calc. in intermediate coupling (*French*) 3-49401
 S X, transition probability for forbidden line in solar spectra 3-42132
 S₁¹²⁵Te, nucl. quadrupole interactions, Mossbauer spectra 3-50501
 S + Ar collisions in gas targets, L X-ray spectra 3-78525
 S⁺ ion implanted in steel, friction changes 3-47410
 S⁺ ion reaction in ionosphere, prod. and loss rates 3-51126
 S₂, mol. dissoc. energy, H.H. and Lipincott three-parameter potential functions 3-78862
 S₃⁻ alkali halide crystal impurity centres 3-68361
 α -S₈ crystals, Raman scatt. spectra, intermolecular vibratory terms splitting 3-72659
 S₈ K β X-ray emission spectra 3-52345
 S₈ molecule in orthorhombic struct. S, cal. of mol. distortion 3-79279
 SI, forbidden transitions 3-40561
³⁴S/³²S ratios in McArthur Pb-Zn-Ag deposits 3-65176
 S₂₀ synthesis, crystal and molecular structure (*German*) 3-64006
^{99m}Tc-S colloid, lung uptake, heart and lung time-activity curves, reticuloendothelial mechanism 3-51459
- sulphur compounds**
 atmospheric particle formation from NH₃-SO₂-H₂O-air gas phase reactions 3-59060
 electronic structure, role of d orbitals, CNDO/2 calc. (*French*) 3-54640
 hydrogen bonded sulphur systems, potential function model 3-46244
 interstellar SO radiowave emission 9.9 and 138.2 GHz, column density meas. 3-81198
 organic and inorganic, tetra- and hexavalent, additive character of displacements of inner atom levels 3-78684
 SF₂OOSO₂SF₆ in liquid phase, vibrational spectra 3-46295
 stratospheric and tropospheric aerosols, S compounds rel. to major volcanic eruptions 3-59058
 stratospheric particles, efficiencies of filters and impactors used for collection 3-76905
 sulphides, free enthalpy of formation, temp. depend. (*French*) 3-69454
 thioclorides, vibrational spectra (*Russian*) 3-63477
 unstable, matrix isolated vibrational spectra, identification of new species 3-78803
 As-S-Te-I glasses, elec. resist. rel. to inhomogeneous struct. (*Japanese*) 3-64391
 Cr-S system, nonstoichiometry and thermodynamics 3-41019
 H₂SO₄.8H₂O + NaOH(aq.) enthalpies of reaction measurement, calorimetric precision test 3-66162
 In-S system, obs. downcooling and phase diag. determ. (*Russian*) 3-75596
 NSF, rot. analysis of 'A'-'A' band system 3-60447
 SClCl₂ energy transfer reactions with metastable Ar and Xe atoms 3-53310
 SCN⁻ spectroscopic props. of admixture in HCl, HBr, LiCl, LiBr 3-64720
 SCO energy transfer reactions with metastable Ar and Xe atoms 3-53310
 SCS energy transfer reactions with metastable Ar and Xe atoms 3-53310
 S₂Cl₂ and SCl₂, positive ioniz. by electron impact (*French*) 3-46328
 SF radical, microwave spectra 3-40637
 SF₆ reactions with C, mass spectra studies 3-55938
 SF₆, breakdown mechanisms (*German*) 3-54878
 SF₆, coherent pulse transmission, reorientational collisions effects 3-51954
 SF₆, energy loss and range straggling of α -particles from ²³⁸Pu, comparison with Payne-Titeica model (*Russian*) 3-59638
 SF₆, gas/solid dielectric interface, surface flashover in vacuum and SF₆, optical obs. 3-46570
 SF₆, gaseous insulator for d.c. accelerators 3-70354
 SF₆, gliding discharges comparison with air (*German*) 3-54879
 SF₆, H₂ + SF₆, muonic F and S X-ray intensities 3-67718
 SF₆, heavy current stabilised arc column, current density and temperature, radial distrib., calc. 3-68106
 SF₆, in homogeneous field, discharge intensities, calc. (*Russian*) 3-52539
 SF₆, liq., mol. reorient., Raman obs. 3-68993
 SF₆, liquid, stimulated Raman scatt. 3-70847
 SF₆, molecular gas, photon echo effect 3-62752
 SF₆, Raman band contour analyses and Coriolis consts. 3-67816
 SF₆, spectra, absorpt. lines, using CO₂ laser 3-45795
 SF₆, voltage tests in Strasbourg MP generator 3-70352
 SF₆ corona discharge in inhomogeneous field 3-49784
 SF₆ discharge at superhigh voltages 3-49785
 SF₆ gas, discharge effects on cast resins dielectric properties (*German*) 3-54880
 SF₆ resonantly absorbing gas, self-focusing of CO₂ laser radiation 3-51950
 SF₆-CO(NH₃), hexadecapole-dipole (quadrupole) interaction, linewidth broadening 3-67863
 SF₆+CO₂ total cross section meas., chemical accelerator 3-80544
 SF₆+D₂(H₂) elastic scatt., crossed beam expts., central-field pots. 3-54753
 SF₆+Li scatt., absolute total cross sections meas. 3-43362
 SF₆⁻ square pyramidal ions, mean amplitudes of vibration calc. (*German*) 3-67781
 SF₆Cl, K type [R₆] splitting coeff. (*French*) 3-46253
 SF₆Cl, rot. spectrum, K-type splitting (*French*) 3-57659
 SF₆OOSF₆ in liquid phase, vibrational spectra 3-46295
 SH⁻, alkali halide crystal impurity centres 3-68361
 SH⁻, photodetachment spectra, rot. line strengths 3-40659
 SH⁻ impurity in KBr(Cl)I, h.p. effects on Raman scatt. 3-80019
 SH(2I_{1/2}) radical in two lowest rotational levels, gas phase e.p.r. spectra, proton hyperfine interactions 3-43490
 SO, Hund's coupling case 3-67785

sulphur compounds continued

- SO, mol. dissoc. energy, H.H. and Lipincott three-parameter potential functions 3-78862
 SO₂, ³B₁-A₁ band system, rotational analysis of (010), (100), and (110) bands 3-40611
 SO₂, 3400-3000 Å absorpt., vibr. analysis 3-67801
 SO₂, air pollutant, automatic sampling and anal. 3-53783
 SO₂, collision-free time-resolved fluoresc. 3-75056
 SO₂, convergence of reduced Hamiltonian, centrifugal distortion, z-axis choice 3-63425
 SO₂, decay fluoresc. from single vibronic levels 3-54708
 SO₂, detection by laser excited fluorescence 3-81329
 SO₂, effect on glass struct. nucl. spectroscopy 3-68165
 SO₂, electronic structure, two atom differential overlap approx. 3-78685
 SO₂, flash excitation, SO(³Σ⁻) prod. 3-58807
 SO₂, i.r. spectra of air pollutants 3-53471
 SO₂, in air, quantitative determ. by gas chromatography using emissive He plasma detector 3-45611
 SO₂, inelastic photon re-emission, air pollutants detect. 3-78832
 SO₂, linewidth parameters for ΔJ=1, 0 ≤ J ≤ 43 rotational transitions 3-43464
 SO₂, matrix isolated, i.r. spectra, bonding, geometry and thermodynamic functions 3-75044
 SO₂, metastable transitions in SO₂ spectra 3-78877
 SO₂, molecular vibration spectra, influence of intermolecular interactions, i.r. absorpt. intensity 3-63473
 SO₂, photoelectron spectra assignment, third band obs. 3-60439
 SO₂, relative Raman cross-section, short-pulse laser scatt. and photon counting obs. 3-57651
 SO₂, remote detection with heterodyne radiometer 3-45330
 SO₂, SOX₂, (X=halide), photoelectron spectra rel. to bond lengths and angles 3-67784
 SO₂, u.v. spectrum in matrix isolation, vibr. struct. of 2348 Å system 3-63443
 SO₂, X-ray emission and absorption spectra of S, mol. energy levels 3-78682
 SO₂ atmospheric, concentration downwind of Keystone stack 3-69565
 SO₂ isolated mols. excited within first allowed absorpt. band, non-radiative decay processes 3-54709
 SO₂ pollution detection using biological method 3-61928
 SO₂ solns. with tertiary aliphatic amines, e.s.r., optical absorption 3-69477
 SO₂/H₂S ratio, S recovery plants, photometric analyser system 3-61932
 SO₂⁻, metastable transitions, mass spectrum 3-78877
 SO₃²⁻ and SO₃F⁻ ions, sulphur Kβ X-ray emission spectra interpret. 3-52315
 SO₄ ion, vibr. freq., environmental influence 3-75999
 SO₄²⁻, electronic structure, two atom differential overlap approx. 3-78685
 SO₄²⁻ ion effect on 18 Cr-8 Ni stainless steel, pitting and crevice corrosion (*Japanese*) 3-72907
 SO₄²⁻ Raman intensities and force constants 3-67822
 S₂O, centrifugal distortion consts., microwave spectra analysis 3-67828
 SO₂BrF molecule, thermodynamic props., 298.16-1000 K 3-60395
 SO₂Cl₂, solid, Raman and infrared spectra rel. to crystallographic structure 3-61035
 SO₂Cl₂ radical anion struct. determ. by e.s.r. 3-55969
 SO₃³⁵Cl₂, nuclear quadrupole coupling constants 3-78839
 SOF₂, molecular force field 3-57639
 SOF₂, molecular structure, electron diffraction determ. 3-43393
 SO₂F₂, molecular force field 3-57639
 S₂O₃F₂, structure by vapour phase electron diffraction 3-67725
 S₂O₃F₂, structure by vapour phase electron diffraction 3-67725
 SO₂(OH)₂ molecule, thermodynamic props., 100-1000 K 3-60395
³²SiO₂, ν₁+ν₃ combination band obs. 3-63453

sum rules

- Adler, *vp-vn* behaviour 3-43077
 Adler and Gross-Llewellyn Smith, testing in high-energy neutrino reactions 3-66987
 Alder-Fubini, modification, application to lepton-hadron scattering 3-48991
 amplitudes involving space-like reggeons, pairs of helicity singularities 3-59941
 analyticity and finite energy sum rule for reggeon-particle amplitude in a+b→c+d+e 3-70957
 asymptotic energy range, form factors for elastic and inelastic electron scatt. (*Russian*) 3-66952
 average multiplicity calcs. using Harari Pomeron-intercept hypothesis in FESR scheme 3-52032
 Bell-Steinberger, evidence for violation of T invariance in non Hermitian interactions 3-74327
 Cabibbo-Radicati, asymptotic behaviour to 1.7 GeV 3-51988
 charge form factors, self consistent radial density and electron scattering 3-67314
 continuous moment, application to π⁻p→π⁰n (*Russian*) 3-40325
 continuous moment, for πN scattering, determ. of Regge amplitudes 3-40394
 crossing, determ. of high-energy bounds for ππ scattering 3-57432
 deep inelastic phenomena, complementary descriptions using resonances and partons 3-67033
 dispersion, for strong and e.m. interactions, review 3-43078
 doubly constrained self consistent field calculation and RPA 3-54292
 Drell-Hearn-Gerasimov, for forward spin-flip amplitude of nucleon Compton scattering, saturation 3-57311
 E2 multipole differential cross section rel. to deuteron photoeffect 3-67299
 electron scatt. by nuclei 3-49242
 electron-nucleus scattering, effect of exchange forces on sum rule (*Russian*) 3-40483
 electroproduction, examination by example from perturbation theory 3-59940
 equal-time canonical commutation rules, break-down 3-45858
 finite-energy, for νN deep inelastic scattering 3-40335
 finite-energy, for exotic meson resonance production in baryon-anti-baryon system 3-43145

sum rules continued

- finite-energy, optimised, application to πN charge exchange amplitudes 3-45914
 fixed mass, and non-perturbative parton model for struct. functions in inelastic electroproduction 3-40323
 fixed mass, derivation, light-cone commutators 3-59939
 fixed pole, wrong signature, inclusive electro- and photoproduction 3-78137
 fragmentation processes, quark model, possible consequences 3-54324
 gauge invariance, for t-channel cut contrib. in π[±] electroproduction, subtraction constant 3-62833
 Generalized dispersive photonic sum rule 3-67309
 gluon model, chiral symmetry breaking divergent sum rules subtraction and deep-inelastic scatt. 3-43121
 helicity amplitude approach to low energy theorems for Compton scattering 3-52007
 hyperon decay, NNπ vertices, parity violating, scalar meson pole model 3-62809
 I₁=1 ππ absorptive part, t-dependence, sum rule reln. to integrals over total cross section 3-52040
 inclusive, for e⁺e⁻ annihilation and eP deep inelastic scattering 3-49012
 inclusive cross sections and correlation function taking account of multipomeron exchanges (*Russian*) 3-74472
 inclusive finite mass, determ. of new relations for two-body reactions 3-45920
 inclusive neutrino reactions high-energy, scaling function sum rules from three-triplet model 3-43092
 inclusive one-particle distrib. and reaction asymmetries within completely symmetric duality scheme 3-60054
 inelastic functions from unitarization of Veneziano partial-wave amplitudes 3-67069
 inelastic reactions, sum rule derivation from boundary dispersion relations 3-40324
 Kallen-Lehmann, determ. from perturbation theory at infinite momentum 3-67019
 Khuri amplitudes, convolution theorem, light-cone Wilson expansion 3-57310
 light cone expansion, constraints due to asymptotic fall-off of elastic form factors 3-67008
 light-cone commutators and chiral symmetry effects in deep-inelastic processes 3-54269
 light-cone dominance, generalisation of duality to off-mass-shell current matrix elements 3-54291
 limiting charge, for hadronic collisions at very high energies 3-62917
 longitudinal conductivity of pure convection current, Kubo formula proof 3-75730
 massless particle total cross sections, Adler condition and high energy bounds 3-59942
 nonleptonic baryon decays 3-66974
 nuclear electric dipole, enhancement factor calc. using perturbation theory 3-78240
 nuclear muon capture, configuration mixing and total capture rates in Primakoff closure approx. 3-67271
 nuclear photoeffect, electric dipole sum rule, retardation effect and relativistic correction 3-67310
 particle mass in baryon octet, mass formula in SU₃ symmetry (*Russian*) 3-59936
 parton model, derivation in Dashen-Gell-Mann's program 3-40322
 parton-model and positivity 3-54294
 PCAC, inclusive reactions 3-78221
 photoabsorption, derivation in parton model 3-70887
 photonic reactions, momentum fluctuation in theory of nonlocal nuclear forces 3-67220
 polycrystalline Fermi liquids, response functions obtained from monocystals 3-64270
 quark-parton model for deep inelastic inclusive electroproduction 3-74385
 reggeon-particle amplitude in a+b→c+d+e, dual resonance model, finite-energy sum rules 3-78163
 Schwinger terms in current interaction field theoretic formulation of parton model 3-78146
 Schwinger-term, divergence, elastic form factor divergence and Pomereanchuk theorem 3-66951
 softened field theory, vector gluons, fixed q² sum rules 3-78086
 spectral function, chiral SU₃ × SU₃ symmetry breaking 3-74334
 spectral-function vector-meson mixing and broken nonet symmetry 3-57306
 spin-dependent finite energy, reln. of current proton scattering amplitude to light-cone commutators 3-51989
 Thomas Reiche Kuhn rule and Ehrenfest's theorem for variational wavefunctions 3-45699
 Thomas-Reiche-Kuhn type, obtained by decomposition technique for many body Schrodinger Hamiltonian 3-59784
 triple Pomeron vertex and complex Pomeron trajectories 3-60007
 two-Reggeon cut derivation, dual resonance model use 3-74401
 uncorrelated jet model for inclusive spectra 3-57463
 weak interaction gauge theories in deep inelastic region, analogues of Adler rule and Llewellyn-Smith reln. 3-59947
 weak interactions mediated by intermediate boson 3-59949
 d, Compton scattering, energy-independent real part 3-59971
 e⁺e⁻→hadrons, SU₃ inclusive sum rules for bounds on K/π production ratio 3-78141
 γγ→h(hadrons), diffractive excitation 3-45880
 K→πμ(e)ν, study using SU₃ × SU₃ light-cone algebra, sum rules and form factors 3-57320
 K-nuclear scattering lengths, current algebra, real part calc. 3-78183
 KN scattering, <600 MeV/c, amplitudes, scatt. lengths, phase shift anal. 3-78185
 K⁺n→K⁰p, 3.8 GeV/c, total, differential cross sections, comparison with SU₃ sum rule 3-60035
 μ capture rates, excitation energy dependence 3-74540
 νN inelastic scattering, spin sum rules, light cone scaling 3-78116
 νN reactions, high energy, higher-order corrections, phenomenology 3-45868
 νp scattering, deep inelastic spin-dependent, determ. of sum rules in SU₄ bilocal algebra 3-62812

sum rules continued

- p,p, scattering total cross section rise, e.m. structure of proton and partons 3-67057
 pp scatt., inclusive sum rules and growth of total cross sections 3-57459
 π charge radius, from current algebra sum rule and short range correlation model 3-49006
 π e.m. mass splitting, sensitivity to spectral-function sum rules, tensor gravity 3-62822
 $\pi^0 \rightarrow \gamma\gamma$, PCAC sum rule for anomalous vertex functions 3-54293
 πN sigma term, on-shell scattering amplitude, recalculation 3-74420
 πR charge exchange comparison between phase-shift analysis amplitudes and high-energy amplitudes 3-57429
 $\pi\pi$ S and P waves, crossing sum rules applied to inequalities 3-52039
 $\pi\pi$ scattering, crossing-symmetric model, low-energy behaviour 3-43138
 $\pi\pi$ scattering, Weinberg scattering length correction 3-74426
 $\rho\pi\pi$ Regge residue function extraction from $\pi\pi$ interactions 3-74444
 ν scattering, rules for verification of gauge theories, weak interactions 3-74358
 ^6Li , electroexcitation form factors and fixed-polarity sum rules 3-49244

sun

- see also solar
 see also cosmic ray solar modulation
 5-minute oscillation, vertical phase var. and mechanical flux 3-80934
 active region spectrum used to identify solar line emission and assess temperature 3-65645
 atom-molecule collision processes 3-74832
 brightness temp. meas. at 345, 450 and 1000 μ 3-61652
 chemical composition and generation spectrum determ. from composition and spectrum of cosmic rays (Russian) 3-65590
 core temperature calculation, neutrino spectra and optical brightness (Hungarian) 3-76973
 data, solar and geomagnetic 3-50972
 diameter determ. at 5000 Å and H α from photoelectric drift scans 3-65653
 differential rotation, pole-equator temp. difference 3-65695
 differential rotation determ. from optical, radio and interplanetary data 3-65697
 early composition inhomogeneities rel. to solar neutrino problem 3-65641
 e.u.v. obs. by spectrometer aboard OSO-6 3-65944
 faculae, annual variation 3-56319
 interior He abundance compared with solar cosmic ray $^4\text{He}/^1\text{H}$ ratio 3-65637
 internal time scales in stratified spin-down 3-80945
 limb brightening, distribution of radio brightness (Russian) 3-45012
 limb darkening eqn., Phillips-Twomey method in presence of noise 3-80933
 lunisolar perturbations, computational method, effect on satellite motion 3-59247
 model calculations, error sources 3-45006
 nonspherical thermal instabilities, conditions of existence 3-76965
 optical heterodyne radiometry of solar surface 3-61654
 photospheric faculae and solar oblateness, reply to work by R.H. Dicke 3-69824
 plasma irregularities and instabilities, obs. of interplanetary scintillations 3-65714
 Radiative damping of internal gravity waves 3-80946
 rotating interior model to explain low neutrino flux measured by Davis 3-73439
 rotation, meas. in chromospheric and coronal e.u.v. lines 3-65696
 rotation vel., interpretation of obs. (Italian) 3-61665
 secular parallaxes and space velocity from stellar proper motions rel. to galaxies 3-76987
 semi-diameter meas., photographic method 3-59404
 Solar Physics Division of Am. Astron. Soc. meeting (Las Cruces, USA, 8-9 Jan. 1973) 3-80935
 stability against spherical thermal perturbations 3-76964
 temperature difference between pole and equator 3-65691
 ^8B photodisintegration in solar interior 3-65642
 ^7Be destruction in solar interior 3-53601
 C abundance corrections based on forbidden transition probabilities 3-45016
 He/H abundance, review 3-47894
 ^3He equilibrium departures in proton-proton chain, secular stability 3-59331
 O abundance corrections based on forbidden transition probabilities 3-45016

sunlight

- see also atmospheric optics; sky brightness
 Direct fluxes of illumination over India 3-80746
 duration of bright sunlight rel. to atmospheric turbidity 3-61486
 Fraunhofer line depth in daytime sky spectrum, brightness and polarisation 3-45033
 green flash at sunset and sunrise model, observations in Alaska 3-44907
 ocular hazard, viewing unprotected and through windows and filters 3-70174
 photochemical applications for direct energy conversion 3-58808
 RNA, formation of cyclobutane type pyrimidine dimers 3-56550
 spectral composition, Antarctica, reflectivity rel. to sea ice 3-80774
 statistical-dynamical model, insolation, seasonal variation of atmosphere circulation 3-44881
 sunshine, rel. to cloudiness over India, regression anal. 3-80745
 vibrational temp., $^0\text{O}_1$ of N_2 and CO_2 , at $50 < z < 130$ km., radiative transfer calc. 3-69623

sunshine see sunlight**sunspots**

- see also solar activity
 1970, obs. over 268 days (French) 3-61671
 1971, obs. over 303 days 3-59263
 1971, visible observations of solar photosphere in Poland 3-73441
 5250.216 Å line profile determ. 3-65703

sunspots continued

- 6610-6770 Å spectra, line identification 3-45002
 active regions, high-resolution radio meas. and sunspot diameters 3-47889
 annual variation 3-56319
 atmospheric ^{14}C content, heliomag. modulation, sunspot and geomag. effects 3-65402
 cosmic ray 27-day variation rel. to sunspot number period 3-53584
 fine structures, morphological and photographic study of H26 spot group (French) 3-45020
 flare spectral anal., Ca II H and K line anal. 3-45021
 frequency distribution function, according to age and lifetime, astrophysical phenomena 3-76951
 groups, E-W asymmetry in number rel. to classification 3-65680
 harmonic analysis of relative number of sunspots 3-42136
 intensity measurements, stray light correction, computer programs 3-65738
 isotope composition, photospheric and sunspot spectra, atomic line studies 3-61672
 l.f. magnetic field oscillations, l.f. radio emission modulation (Russian) 3-80962
 magnetic classification of sunspot 3-65643
 magnetic sector struct., long term stability, sunspot cycle feature 3-65737
 MHD stability, finite Larmor radius effects 3-80911
 models, current sheet, observational constraints 3-65701
 molecular abundances from Zwaan's sunspot model 3-61662
 molecular line formation levels and rotational temps. 3-80931
 number, determ. of solar differential rotation 3-65697
 numbers, annual mean relative, periodicities 3-65681
 oscillations, multichannel spectrometry 3-80955
 penumbra, bright region, magnetic field vertical distribution (Russian) 3-76976
 penumbral intensity, obs. in 13 wavelength regions 3-65702
 periodicity of large sunspot groups 3-61656
 power spectrum, double solar cycle evidence 3-44998
 preferential longit. due to spatial distrib. of emerging flux regions 3-47893
 radiative model, in magnetohydrostatic equil., possibility of construction 3-65678
 radio sources and local magnetic field connection, study during partial eclipse (Russian) 3-76981
 real-time digital videomagnetograph for sunspot magnetic fields 3-59406
 seasonal variations of relative sunspot number, comment 3-61659
 solar cycle variations, phase differences 3-47880
 speckle interferometry, obs. of spatial freq. 3-59256
 stratospheric wind and temp., total ozone, sea-level press. rel. to sunspot cycle 3-69598
 sunspot flares, mechanisms and phenomena 3-42129
 umbra, physical parameters, echelle grating spectra (Russian) 3-76977
 umbrae, magnetic field intensity rel. to brightness 3-61657
 umbral cores, 7-colour photometry with Bartol Coude telescope 3-47886
 umbral flashes and running penumbral waves, source mechanism 3-45003
 umbral flashes and running penumbral waves 3-65679
 umbral Na D $_2$ -5890 Å line, min. intensity meas. 3-65704
 umbral spectra, determ. of TI abundance 3-65716
 CO isotope bands in i.r. spectrum, solar $^{13}\text{C}/^{12}\text{C}$, $^{18}\text{O}/^{16}\text{O}$ and $^{17}\text{O}/^{16}\text{O}$ abundance ratios 3-61651
 H $_2\text{O}$ vapour line intensity determ. at 263°K and 3500°K 3-65705

superaerodynamics see rarefied fluid dynamics**superconducting devices**

- see also cryotrons
 accelerating resonator, interaction with high-current single bunch of particles (Russian) 3-48492
 accelerator, 55 cell structure, and regenerative beam breakup 3-56718
 aerospace cryogenic suspensions, appl. to two-coil supercond. suspension 3-53860
 applications, review 3-59612
 bolometer, receiver-amplifier system, cryostat, design, operation 3-77412
 bolometer, receiving-amplifying system, i.r. radiation 3-73704
 bolometers, thin film, various film characteristics, methods of use 3-59563
 cavity, for electron synchrotron 3-56720
 electromechanical devices, cryostat design description 3-51557
 electron accelerator, demonstration as high-intensity high-resolution device 3-42626
 electron linear recirculator with multi orbit recirculation system 3-56846
 field shielding tube, for CERN 2 metre bubble chamber 3-77658
 fixed point device, for thermometric reference 3-51511
 flux pump, magnetic, automatic superconducting switch, simple design, results 3-59564
 focussing, permanent multipole mag. fields stored in superconductors 3-42631
 force-cooled, propagating thermal waves rel. to stability characts. 3-62029
 helix resonator, for heavy ion acceleration 3-56715
 levitron, hot-electron plasma confinement 3-52529
 magnetometer, use of portable helium dewar, gas-cooled radiation shield 3-48384
 microwave resonant cavity in linac 3-59627
 particle separator, deflecting cavities, r.f. tests 3-56860
 point contact apparatus, for tunnelling expts. 3-64437
 prototype superconducting linac, heavy ion acceleration 3-56716
 quantum flux detector, noise expression derived 3-62182
 quantum voltmeters and magnetometers, operating mode selection 3-70327
 resonant cavities, linear accelerator, heavy-ion, design, cost, feasibility 3-73834
 r.f. electron accelerators, report on prototypes 3-56712
 superconducting helical resonators, electronic tuning and phase control 3-56725
 superconducting r.f. cavities, resonant freq. control 3-56724

superconducting devices continued

- zero gradient synchrotron, superconducting stretcher ring, resonance injection 3-56763
- Nb, superconducting cavity, electron loading 3-56721
- Nb S-band superconducting cavity, with large beam tubes 3-56861
- Nb superconducting cavities, attaining high fields, at SLAC 3-56722
- Nb superconducting cavity, surface preparation techniques 3-56862
- Nb superconducting cavity beam deflectors 3-56863
- Ta with Nb overlay, thin film quantum galvanometer, design, operation 3-70324

superconducting junctions

- see also *Josephson junctions*
- Ginzburg-Landau theory with non-local correction in zero magnetic field 3-64418
- intercalated layer cpds., long range order rel. to Josephson coupling 3-55378
- photon assisted tunnelling theory in junctions with active barrier impurities 3-46938
- tunnel, alpha particle detection 3-77614
- tunnel, as very fast phonon and photon detectors 3-44175
- tunnel junction, photon assisted tunnelling, current density 3-55379
- tunnel junction, second order tunnelling current density 3-55380
- tunnel junctions, phonon bremsstrahlung isolation for phonon spectroscopy 3-53844
- tunnel junctions as phonon sources and detectors 3-55374
- tunnelling junctions, absolute phonon detection sensitivity 3-55376
- weakly coupled, current rel. to off-diagonal long-range order 3-79807
- weakly supercond., thin-film, Notarys-Mercereau structure, a.c. response 3-52935
- Al-Al₂O₃-Pb, junction paraconductivity effect of nonuniform coupling 3-64438
- Al tunnel diodes, 870 GHz phonon emission 3-55381
- Al tunnelling junctions, h.f. relaxation phonon emission 3-55375
- Cu-Pb-Cu proximity effect sandwiches, crit. mag. fields, acoustic surface wave attenuation obs. 3-55377
- Nb₃Sn-Pb(Sn), sputtered film, tunnel characts., energy gap values 3-75818
- Sn film superimposed with Ni, supercond. bridge, microwave-induced current steps 3-46937

superconducting lenses see magnetic lenses**superconducting magnets**

- asymmetric split-pair superconducting magnet, for nuclear polarization experiments 3-56969
- axisymmetric solenoid, rectangular cross-section, radial magnetic field calc. 3-77938
- bending magnets with Fe yokes and rectangular coils, multipole field distortions 3-56801
- Bevatron, Berkeley USA, beam transport magnets, d.c., dipole bending, quadrupole doublet focusing, description 3-56907
- bumpy torus facility, 12-coil, performance, use in plasma research 3-60639
- controlled thermonuclear, analysis of magnet material constraints 3-60167
- cosmic ray composition analysis, satellite installation (*Russian*) 3-65552
- d.c., C-frame, polarised proton target, Argonne USA, description 3-56926
- dipole bending magnet, 40 kG, 30 GeV protons, Brookhaven AGS, USA, performance, reproducibility 3-56906
- electron lens application, for electron microscopes, review (*Czech*) 3-73904
- electron lens system with high resolution (*German*) 3-66365
- electron lenses 3-66908
- energy storage with irreversible switching, design study 3-60304
- fusion reactor, open-ended, magnet material requirements, technical feasibility and cost estimates 3-60325
- fusion reactor, theta pinch, superconducting energy transfer and storage system 3-60305
- fusion reactors, comparison of warm and cold reinforcement magnet systems 3-60310
- high resolution automatic magnetometer applic. 3-48477
- hysteresis loss, improved measurement technique, XY display of loop 3-56700
- impregnation of windings with epoxy resins, mech. props. 3-58786
- indirect cooling, using supercritical He 3-56651
- for intersecting storage accelerators 3-56795
- lens, quadrupole, for particle beam transport, design and construction (*German*) 3-62199
- n.m.r. spectrometer, high resolution, elimination of sidebands due to sample rotation 3-77586
- objective lens, for electron microscope, design (*Czech*) 3-73905
- objective lens with classical ferromagnetic pole pieces, electron microscopy high resolution test 3-77729
- pulsed, particle accelerator applications, recent progress, trends, review 3-56794
- ramped superconducting dipoles, for NAL doubler 3-56807
- recovery currents, effect of interturn heat flow, cryostatic stabilisation, comparison of calculated and measured values 3-56644
- sample holder, for rotating cryst. in supercond. solenoid, magnet anisotropy meas. 3-77582
- solenoid, compensator for nonuniformity in mag. field, elimination of side bands in n.m.r. spectrometer 3-73820
- solenoid, installation for mag. field prod. 3-77580
- solenoid, installation for mag. field prod. with cryostat 3-77581
- for spark chambers, prospects (*German*) 3-73870
- technological applications, use in fusion devices 3-60290
- for testing and calibrating magnetic induction meters 3-39975
- Nb-Sn superconducting solenoid, 50 kG gas cooled, operated at 13 K 3-73700

superconducting materials

- see also *superconductivity; type I superconducting materials*
- A15 type, transition temp. and density of states (*Russian*) 3-52916
- A15 type cpds., impurities influence on T_c (*Russian*) 3-58326
- A-15 compounds, elastic props., role of linear chains 3-58339
- acoustoelectric and thermoelectric effects, theory 3-79803
- alloy, dirty BCS superconductor, vortex struct. calc. 3-52927

superconducting materials continued

- alloys with A15 structure, critical temp., influence of (1/2)<111> stacking faults 3-46931
- amorphous strong coupling supercond., upper critical field, density of states at Fermi surface 3-41288
- applications 3-58325
- b.c.c., fast particle irradi. 3-79395
- bound states in superconductors containing magnetic impurity 3-79783
- composite, propag. velocity of normal and supercond. regions, calc. 3-64436
- critical bulk and surface current density meas. in mixed state 3-41298
- critical current increase due to periodic distrib. of ferromag. particles 3-50295
- critical currents, a.c. field effects, single explanation 3-41301
- critical Ginzburg-Landau parameter separating type II/1 from type II/2 3-79790
- critical state stability 3-50302
- current density applied in square, rectangular sections, crit. currents 3-55367
- current threshold, in longitudinal mag. field, power cryotron applic. 3-50300
- dirty, effect of elec. fields on excess current of Maki process above transition pt. 3-75814
- dirty, gapless, impurity effect on flux-flow resistivity 3-55372
- dirty, thermodynamic and dynamic props., vortex state, theory 3-68731
- dirty two-band superconductor, flux-flow props., mixed state, near H_{c2} 3-55373
- e.p.r. theory for gapless dirty type II supercond. 3-46935
- Fermi surface, of A15 compounds, neutron scatt. investigation 3-46926
- film, type I, anomalous skin effect, theory 3-44102
- film of intermediate thickness, fluctuation cond. and dimensionality change 3-52931
- films, effective penetration depth angular depend. 3-55352
- flux flow resist. 3-64432
- flux jump prediction, magnetisation, mag. and thermal diffusion equations, computer appl. 3-50294
- flux line properties from non-local theory, magnetic field-temp. curves 3-46913
- Ginsburg-Landau theory, non-local extensions 3-41284
- heat, calibration of hysteresis losses (*Russian*) 3-72422
- hard pipes, bench and thermal vacuum testing 3-51548
- intercalated layer cpds., long range order rel. to Josephson coupling 3-55378
- internally cooled, steady state stability (*Japanese*) 3-41305
- Knight shift, magnetic field and temperature dependence 3-55346
- Knight shift (*Rumanian*) 3-64424
- lanthanum-based alloys with actinide impurities, supercond. temp. behaviour, simple model for magnetism 3-50314
- light fluctuation scatt. above critical temp. 3-55369
- low-κ, calcs. on reversible and irreversible magnetisation 3-46919
- magnetic field asymptotic behaviour and attractive interaction between flux lines 3-79791
- magnetic field distrib., microscopic, of mixed state, neutron diffr. exam. 3-72414
- magnetic field distribution, supercond. with small magnetization 3-44162
- magnetic hysteresis, theoretical models 3-52914
- magnetisation of ellipsoids, pinning 3-68734
- magnets, controlled thermonuclear analysis of material constraints 3-60167
- metal, softening during transitions (*Russian*) 3-72415
- metals and alloys, superconducting phase transition rel. to plastic properties 3-55355
- mixed state, correlation between flux-line lattice and crystal axis 3-75809
- non-transition-metal condensed films, changes in Eliashberg function and T_c due to strong lattice defects 3-55357
- non-transition-metal condensed films, changes in Eliashberg function and T_c due to strong lattice defects (*German*) 3-55358
- non-uniform, axial/azimuthal magnetisation and a.c. loss measurement 3-64439
- one band and two band with impurities, electronic density of states 3-46921
- organic solid, one-dimens., supercond. fluctuations 3-58350
- parallel wires, planar array, current and current density distrib., Meissner effect 3-55359
- pinning forces, direct mech. meas. 3-46929
- pinning of rigid and elastic fluxon lattices, floating magnet model 3-50293
- pinning on point defects, statistical theory 3-79798
- semi-infinite, struct. of mixed state near boundary 3-41292
- semiconductor, intra-band electron pairing in presence of radiation field 3-41307
- small grains, thermodynamic props. 3-52921
- specific heat measurement 3-62033
- spin-lattice relaxation, supercond. with electron transition, nonmag. impurity effects 3-58345
- strong-coupling, quasiparticle phenomenology for thermodynamics 3-72416
- surface superconductivity and pinning sites, expts. on Ta₂Nb₈, Ta₂Nb₅ and Nb 3-55365
- thin films, structure of mixed state in transverse mag. fields, Gibbs potential 3-79796
- thin films, tunnelling conductance, temp. depend. in high magnetic fields 3-44174
- thin wire, crit. current, length depend. 3-44170
- transition metal, dirty, thermomag. effects near upper crit. field 3-46934
- transition metal, Knight shift and nuclear spin relax. calc. 3-55356
- transition metals, amorphous, superconductivity theory 3-72421
- transition-metal impurities, magnetic and nonmagnetic cases, Hartree-Fock theory 3-60926
- transverse voltage characteristics, resistive state, magnetic flux motion 3-50284
- type I, magnetisation of ellipsoids, pinning 3-68734

superconducting materials continued

- type I, pure, surface impedance theory in large static mag. fields 3-46925
 type I, surface excitation spectrum in high mag. fields 3-64426
 u.s. attenuation, Andreev scatt. 3-55370
 vector, pot. and order parameter for isolated vortex, asymptotic behaviour 3-55348
 voltage-current characts. in transverse mag. field 3-55366
 vortex lattice rel. to cryst. lattice, magnetoelastic strain fields 3-55351
 vortices, attractive interaction at arbitrary temp. 3-68732
 zero dimensional, effect of fluctuations on diamag. susceptibility below T_c 3-79805
 Al, granular film, angular depend. of crit. mag. field 3-52920
 Al, superconductive fixed point device, for thermometric reference 3-51511
 Al, transition temp., press. and ionic depend. 3-79784
 Al, volume change in superconduction transition (*German*) 3-52918
 Al and dilute alloys, low temp. specific heat, energy gap anisotropy obs. 3-60929
 Al film, resistive transition, effect of perpendicular mag. fields 3-64429
 Al film, two-dimens., order parameter fluctuations ang. depend. in mag. field 3-50296
 Ba, 4f-band superconductors, electronic structure and high pressure effects, review 3-50291
 Ba, high press. elec. resist., correl. with press.-induced supercond. 3-41306
 Be alloys, critical temperature obs. using induction method 3-58333
 Bi, amorphous, thermodynamic props. 3-46917
 Cd, superconductive fixed point device, for thermometric reference 3-51511
 Cd, temp.-depend. peak in electronic attenuation of u.s. shear waves, rel. to Fermi surface geometry 3-79622
 Cd, transition obs. 3-75805
 Cd and dilute alloys, low temp. specific heat, energy gap anisotropy obs. 3-60929
 Cd hexagonal crystals, u.s. study of supercond. state 3-72425
 Ce, 4f-band, electronic structure and high pressure effects, review 3-50291
 Ce_{1-x}Gd_xRu₂, sp. ht., mag. transition, supercond. transition, 1.8-20K 3-55350
 CeRu₂:Fe, e.s.r. obs. 3-79905
 CeRu₂:Gd, local moment e.s.r. 3-44171
 Ce_{1-x}Tb_xRu₂, sp. ht., mag. transition, supercond. transition, 1.8-20K 3-55350
 Ce_{1-x}Y_xRu₂, sp. ht., mag. transition, supercond. transition, 1.8-20K 3-55350
 Cs, 4f-band superconductors, electronic structure and high pressure effects, review 3-50291
 Cu-Nb alloys, dil., electrical resistivity, superconducting volume fraction, metallographic meas. 3-75804
 CuFeS₂, antiferromag. film, supercond. transition for 88<T<90K, thermal expans. jump 3-75808
 Eu_xLi_{1-x} alloys, Mossbauer meas. of coexistence of superconductivity and magnetism 3-44164
 Ga, amorphous, thermodynamic props. 3-46917
 Gd_xB_{1-x}Ru₂ (B=Th,Ce,La), e.p.r. and supercond. correl. transition temp. Gd conc. depend. 3-72417
 Gd_xTh_{1-x}Ru₂, re-entrant crit. field behaviour, e.p.r. correl. 3-72418
 HfV₂, acoustic wave velocity meas., lattice instabilities 3-79801
 In, magneto-optical investigation of intermediate state 3-50285
 In, pressure depend. of T_c , Fermi surface topology effects 3-60928
 In, pure and impure, nuclear spin-lattice relax. 3-46933
 In, resistance jump in pure type I, superconductors 3-52933
 In, superconductive fixed point device, for thermometric reference 3-51511
 In, transition, electronic dislocation drag, stress, temp. and deform. rate depend. 3-41291
 In, tunnelling under pressure 3-52937
 In film, paracond. resistive depend. 3-55371
 In wire, destruction of type I supercond. by current 3-68730
 In-Cd, In-Pb alloys, pressure depend. of T_c , Fermi surface topology effects 3-60928
 In-Gd alloy, film, electron thermal cond., strong coupling effects 3-41300
 La, 4f-band superconductors, electronic structure and high pressure effects, review 3-50291
 La₉₈Lu_{2-x}Tb_x, supercond. crit. fields with short-range mag. order, transition temp. 3-68716
 LaOs₂, transition temps. of 5.9K, 8.9K for hexagonal, cubic forms 3-52919
 LaRu₂:Gd, local moment e.s.r. 3-44171
 LaSn₃:Gd, Tm, upper critical fields for superconductivity, crystalline field effects 3-52925
 Li, transition temp., press. and ionic mass depend. 3-79784
 Li_{1-x}Ti_{2-x}O₄, high temp. superconductivity 3-60930
 Lu, transition temp. and crit. field 3-58338
 Mo-Re(34 at.%), α -phase precip. and flux pinning, electron microscope obs. and mag. hysteresis 3-50697
 Mo-S based ternary forms, transition temp. increase with impurities 3-68718
 MoBe₂₂, external mag. field depend. of T_c (*Russian*) 3-46927
 MoS₂, band structure 3-50126
 MoS₂, layer type structure, electronic props. of two dimensional solids 3-50133
 Nb, anomalous sp. ht., supercond. energy gap 3-46920
 Nb, attenuation of transverse ultrasonic waves 3-72424
 Nb, calc. of press. dependence of superconducting transition temperature 3-79789
 Nb, defect influence on internal friction near normal-supercond. transition 3-52926
 Nb, dirty, microscopic magnetic field distrib., neutron diffraction expts. 3-46923
 Nb, internal friction, I.f. obs. in normal and superconducting state (*Russian*) 3-46678
 Nb, Meissner effect and stable trapping of fields 3-46940

superconducting materials continued

- Nb, misalignment of flux lines, neutron small-angle diffraction study 3-64435
 Nb, point defect density fluctuations, pinning effect, statistical theory 3-68735
 Nb, superpure, prep. of single crystals. (*Russian*) 3-58349
 Nb, temp. depend. of elastic consts. in normal, supercond. states 3-68715
 Nb, u.s. absorpt., purity depend. in normal, Meissner states, meas. and theory 3-64433
 Nb, use as thermal insulations at low temp. 3-39882
 Nb, vortex monocystal creation and control (*French*) 3-50301
 Nb cylinder, permanent multipole mag. field storage, charged particle focussing 3-42631
 Nb film, sputtered on metallic substrates, struct. and flux penetration 3-79788
 Nb-Al-Ge superconducting ribbon, resistive measurements 3-56696
 Nb-Sn superconducting solenoid, 50 kG gas cooled, operated at 13 K 3-73700
 Nb-Ta(20 at.%) alloy, nitride precipitate morphology and struct. 3-64872
 Nb-Ti, microstructure after cold deform., heat treatment, field ion microscope obs. 3-76182
 Nb-Ti (64 at.%) wires, critical current density anisotropy 3-64428
 Nb-Zr wire to Pb-Sn solder, blob junction, self-field effects on Josephson supercurrent 3-52934
 Nb₃Al_{1-x}Be_x(B_y), critical temp. depend on composition and lattice constant critical current density 3-50286
 Nb₃Al_{1-x}M_x, M=Be, B, Al₅ struct., critical temp. obs. 3-50297
 NbAl₂O₃ mixture type films, crit. current density, mixed state form., flux eddies, second crit. field (*Russian*) 3-68728
 Nb₃Au_{1-x}Pt_xA-15 type phases, superconductivity, structure and magnetic susceptibility 3-58334
 NbN, high transition temp. rel. to lattice instability 3-64421
 NbN film, reactively sputtered, critical current anisotropy 3-50299
 NbS₂, band structure 3-50126
 NbSe₂, Ginzburg-Landau parameter anisotropy, penetration depths and coherent distances 3-55349
 NbSe₂, layer type structure, electronic props. of two dimensional solids 3-50133
 NbSe₂, microwave absorption, critical fluctuations 3-41302
 NbSe₂, supercond. transition temp., effect of 3d impurities 3-52922
 NbSe₂, temp. depend. of critical field ratio, elec. cond. meas. 3-68720
 Nb₃Sn, angular dependence of critical currents in transverse mag. field 3-41296
 Nb₃Sn, chemically deposited, longitudinal and transverse currents from 14.5 to 17.5K 3-44169
 Nb₃Sn, critical current density, temp. depend. 3-50298
 Nb₃Sn, cubic A-15 phase stabilization, a.c. heat capacity meas. 3-64422
 Nb₃Sn, field, angular and defect dependence of critical current for $t \leq 4.2K$ 3-44168
 Nb₃Sn, fluxoid pinning on grain boundaries dependence on the mag. field direction 3-44166
 Nb₃Sn, Meissner effect and stable trapping of fields 3-46940
 Nb₃Sn, phonon damping 3-49946
 Nb₃Sn, shock wave synthesis from powder mixtures 3-69328
 Nb₃Sn cylinder, permanent multipole mag. field storage, charged particle focussing 3-42631
 Nb₃Sn multifilamentary composite wires, heat treatment effects on critical currents 3-60938
 Nb₃Sn superconducting tapes, microprocessing by electron-beam microetching 3-56978
 Nb₃Sn tunnel junctions, effective phonon spectrum by electron tunnelling 3-68737
 Nb_{0.73}Ta_{0.27}, pot. difference, current depend., transverse mag. field (*French*) 3-55360
 (Nb_{1-x}Ta_x)Al_{1-x}Ge_x, A15 struct., critical temp. obs. 3-50297
 (Nb_{1-x}Ta_x)Al_{1-x}Ge_x, critical temp., depend. on composition and lattice constant critical current density 3-50286
 NbTi, 40/60 wt.% alloy, critical current density, temp. depend. 3-50298
 NbTi, filamentary superconducting composite, stability behaviour, flux jumps 3-50292
 Nb₃X A-15 cpds., low temp. paramagnetic susceptibility and supercond. crit. temp. (*French*) 3-68724
 Pb, dynamic intermediate state under influence of heat current 3-44167
 Pb, Meissner effect and stable trapping of fields 3-46940
 Pb, plastic deform. in supercond. transition, temp. depend., due to electronic drag of dislocations 3-41285
 Pb, resistance jump in pure type I, superconductors 3-52933
 Pb, superconductive fixed point device, for thermometric reference 3-51511
 Pb, temp. depend. of elastic consts. in normal, supercond. states 3-68715
 Pb, transition, electronic dislocation drag, stress, temp. and deform. rate depend. 3-41291
 Pb, transition temp., press. and ionic mass depend. 3-79784
 Pb, volume change in superconduction transition (*German*) 3-52918
 Pb and Pb-In alloys, surface impedance meas. (*German*) 3-52929
 Pb cylinder, permanent multipole mag. field storage, charged particle focussing 3-42631
 Pb film, mag. struct. of mixed state 3-52932
 Pb foil, interphase surface energy parameter, shadow electron microscopy 3-68719
 Pb thin foil, coexistence of flux spot and laminar intermediate state 3-79794
 Pb-Bi, high-press. d.h.c.p. phase, T_c obs. 3-46916
 Pb-Bi alloy, negative differential resist. at high current densities 3-44165
 Pb-Bi thin films, strong coupling, transition fields measurement 3-58332
 Pb-Gd alloy, film, electron thermal cond., strong coupling effects 3-41300
 Pb-In, strong-coupling, Ginzburg-Landau parameter and upper crit. field, mag. meas. 3-46924
 Pb-In (50 at.%), force free mag. fields in superconductors 3-79804

superconducting materials continued

- Pb-In alloy, temp. depend. of viscosity coeff., differential resist. 3-72426
- Pb-In alloy, transition, electronic dislocation drag, stress, temp. and deform. rate depend. 3-41291
- Pb-In alloys, hydrostatic press. effects, electron tunnelling study 3-52923
- Pb-In(4 at.%) alloy, flow stress in normal and supercond. states, thermal cond. model approach 3-68727
- Pb-Sb alloy, plasticity increase at supercond. transition 3-55001
- Pb₁₋₂Bi₁Tl₁, strong-coupling, Ginzburg-Landau parameter and upper crit. field, mag. meas. 3-46924
- PbMo₆S₈, supercond. and struct. 3-60706
- PbTe-Pb system, diamagnetic susceptibility, field dependent 3-79795
- Pd-H system on metallic hydrogen, superconducting transition temperature 3-58330
- Pd-Ag-H, Pd-Rh-H, Pd-Pt-H, temp. depend. of relative electrical resistance 3-79793
- Pd-D system, superconductivity theory 3-46928
- Pd-H, transition temp., h.p. effect, isotope effect 3-60931
- Pd-H system, superconducting theory 3-46928
- Pd-M system, compositional dependence of superconducting critical temp. 3-64423
- PdH_x, PdRh_xH_x, hydriding pressure effect on supercond. transition temp. 3-68721
- Pt-W alloys, anomalous mag. susceptibility and conc. depend. of supercond. transition temp. (German) 3-41286
- Sn, Cooper-pair density, relax. time 3-41287
- Sn, intermediate state, size effect rel. to thermal cond. (French) 3-58336
- Sn, resistance jump in pure type I superconductors 3-52933
- Sn film superimposed with Ni, supercond. bridge, microwave-induced current steps 3-46937
- Sn films, multiply connected, mag. field depend. of supercurrent 3-55383
- SnAs, formed in decomp. of CdSnAs₂ and ZnSnAs₂, supercond. transition temp. 3-41022
- SrTiO₃, supercond. rel. to structural instability, electron-soft phonon interactions 3-58343
- Ta, differential paramagnetic effect, temp. depend. 3-46932
- Ta, supercond.-normal transition by rectang. current pulse, flux flow and jump 3-68729
- Ta superconducting thin films, nonlinear microwave props. 3-50304
- Ta₇₀Nb₃₀ single crystal, magnetization and pinning 3-58344
- Ti-Nb(35 at.%) alloy, heat treatment effect on microstruct. and supercond. 3-79800
- Ti, Fermi surface, supercond. transition temp., press. effects, pseudopot. calcs. 3-55190
- Ti wire, destruction of type I supercond. by current 3-68730
- α -U, heat capacity and transforms, 2-70K 3-47041
- α -U, single- and polycryst., transition temp. at pressure up to 24 kbar 3-79787
- U₂Fe, supercond. transition temp., stoichiometry effects and U isotope effect 3-68725
- V, calc. of press. dependence of superconducting transition temperature 3-79789
- V, induced voltage due to flux line lattice dislocation motion 3-60937
- V, mixed supercond. state neutron depolarisation rel. to cryst. anisotropy 3-55353
- V-Mn-Ga alloys, neutron powder diffraction, magnetic and superconducting measurements 3-47065
- V-V₂O₅-Pb, Josephson tunnel junctions, U-I characteristics, mag. field depend. of critical current 3-58348
- (V_{1-x}Cr_x)₂Ge ternary solid solns., cond. electron energy spectrum, conc. depend. (Russian) 3-52917
- V₃Ga, annealing, long range order, and supercond. transition temp. 3-55345
- V₃Ga composite wires, processing and superconducting props. 3-68726
- V₃Ga_{1-x}Sn_x, density of states at Fermi level, supercond. transition temp. rel. to electronic struct., n.m.r. obs. 3-41289
- V₃Si, pressure coeff. of transition temp., elastic constants 3-79792
- V₃Si, superconducting transition temps. and crystal structure, influence of compacting pressure 3-50287
- V₃Si tapes, made by new process 3-64430
- V₃Si tapes, prep. and Si conc. depend. of T_c and crit. current (Japanese) 3-60934
- V₃Si-V₃Ge, low temp. paramag. susceptibility and supercond. crit. temp., comp. depend. (French) 3-68723
- V₃(Si_{1-x}Ge_x) solid solns., mag. props., Knight shift, conc. depend. of T_c and Fermi level (Russian) 3-58327
- (V_{1-x}Ti_x)₂Si, relation between T_c and elastic softening 3-68740
- V₃X A-15 cpds., low temp. paramag. susceptibility and supercond. crit. temp. (French) 3-68724
- W, crit. mag. field for supercond. 3-79785
- WBe₂₂, external mag. field depend. of T_c (Russian) 3-46927
- Y, high press. elec. resist., correl. with press.-induced supercond. 3-41306
- Zn, anisotropy in normal-state mass renormalisation and supercond. energy gap 3-75807
- Zn, calc. of phonon-induced gap anisotropy 3-68713
- Zn, superconductive fixed point device, for thermometric reference 3-51511
- Zn and dilute alloys, low temp. specific heat, energy gap anisotropy obs. 3-60929
- Zn hexagonal crystals, u.s. study of supercond. state 3-72425
- Zn-Cr critical temperature and field, down to 0.037 K 3-41290
- Zn-Mn critical temperature and field, down to 0.037 K 3-41290
- ZrS₂, layer type structure, electronic props. of two dimensional solids 3-50133
- ZrV₂, acoustic wave velocity meas., lattice instabilities 3-79801

superconducting thin films

- bolometers, various film characteristics, methods of use 3-59563
- Dayem bridges, subharmonic energy gap structure and Josephson radiation enhanced gap 3-60940
- fluctuation conductivity and dimensionality change, films of intermediate thickness 3-52931

superconducting thin films continued

- II, effective penetration depth angular depend. 3-55352
- inhomogeneous, theory of vortex motion 3-60932
- internal friction and electrical resistance measurement, cryostat apparatus 3-48385
- Josephson effect, destruction of, by fluctuations in order parameter 3-68738
- multilayer system, superconducting thin films and Josephson barriers, critical current 3-58340
- non-transition-metal condensed films, changes in Eliashberg function and T_c due to strong lattice defects 3-55357
- non-transition-metal condensed films, changes in Eliashberg function and T_c due to strong lattice defects (German) 3-55358
- specific heat, peaking, screening-approximation prediction 3-55354
- superheating and supercooling field measurement 3-60925
- tricritical points 3-44163
- tunnelling conductance, temp. depend. in high magnetic fields 3-44174
- tunnelling new peaks, thickness dependent 3-58347
- type I, anomalous skin effect, theory 3-44102
- type II, structure of mixed state in transverse mag. fields, Gibbs potential 3-79796
- vortices, negative differential cond. due to nonlinear vortex response in strong elec. field 3-68733
- weakly coupled particles in film array, model for crit. supercurrent 3-58342
- weakly supercond., Notarys-Mercereau structure, a.c. response 3-52935
- Al, granular, angular depend. of crit. mag. field 3-52920
- Al, resistive transition, effect of perpendicular mag. fields 3-64429
- Al, two-dimens., order parameter fluctuations ang. depend. in mag. field 3-50296
- Al-insulator-Al(Sn),(Pb), tunnelling in vortex state 3-52936
- Cd, Cd_{0.9}Ga_{0.1}, quench-condensed, energy gap and transition temp. 3-46918
- Cu-Pb, Pb diffusion rel. to supercond. props., Auger spectra obs. 3-52722
- CuFeS₂, antiferromag. film, supercond. transition for 88<T<90K, thermal expanse. jump 3-75808
- films, quench. condensed, superconducting transition temperature (German) 3-58335
- In paracond. resistive depend. 3-55371
- In-Gd alloy, electron thermal cond., strong coupling effects 3-41300
- Nb, sputtered on metallic substrates, struct. and flux penetration 3-79788
- NbAl₂O₃ mixture type, crit. current density, mixed state form., flux eddies, second crit. field (Russian) 3-68728
- NbN, reactively sputtered, critical current anisotropy 3-50299
- NbN films deposited by reactive sputtering, upper critical fields (Japanese) 3-68710
- Nb₃Sn-Pb(Sn), sputtered film junction, tunnel characts., energy gap values 3-75818
- Pb, coexistence of flux spot and laminar intermediate state 3-79794
- Pb, mag. struct. of mixed state 3-52932
- Pb foil, interphase surface energy parameter, shadow electron microscopy 3-68719
- Pb microstrips, voltage steps in current-induced resistive state 3-64434
- Pb-Bi, strong coupling, transition fields measurement 3-58332
- Pb-Gd alloy, electron thermal cond., strong coupling effects 3-41300
- Sn, gapless, critical magnetic fields, temp. depend. 3-68722
- Sn, superconducting transitions, non linearity, low temp. technique 3-48390
- Sn bolometer, fluctuation effects 3-39883
- Sn film superimposed with Ni, supercond. bridge, microwave-induced current steps 3-46937
- Sn films, multiply connected, mag. field depend. of supercurrent 3-55383
- Ta, Nb overlay, quantum galvanometer, design, operation 3-70324
- Ta, nonlinear microwave props. 3-50304
- V, evaporation conditions rel. to electrical properties 3-58348
- Zn, quench-condensed, energy gap and transition temps 3-46918

superconducting transition point

- A15 type, transcendental eqns. soln. and d-electron density of state (Russian) 3-52916
- A15 type cpds., impurities influence (Russian) 3-58326
- alloys with A15 structure, influence of 1/2<111> stacking faults 3-46931
- Eliashberg function changes depend. 3-64427
- impurity state influence in excitonic phase, transition temp. reduction 3-55347
- interphase boundary between normal and superconducting domains, stability of movement 3-64420
- lanthanum alloys with actinide impurities, behaviour rel. to simple model for magnetism 3-50314
- magnetic impurity effect, two-band model 3-79780
- metal, softening during transitions (Russian) 3-72415
- metallic system, one-dimensional, application of renormalization group technique 3-64136
- metals and alloys, phase transition rel. to plastic props. 3-55355
- non-transition-metal condensed film, changes in Eliashberg function and T_c due to strong lattice defects 3-55357
- non-transition-metal condensed film, changes in Eliashberg function and T_c due to strong lattice defects (German) 3-55358
- phase transition investigation technique 3-62033
- plasticity change in N-S transition, mechanism 3-79802
- proximity effect, transition temp. calc. variational principle 3-79786
- semiconductor in high power laser radiation, rel. to exciton exchange 3-50290
- semimetal, supercond.-excitonic dielec. phase transition 3-75811
- temperature effect of metal-dielectric phase transition 3-50289
- transition metal alloys, influence of localized spin fluctuations on superconductivity 3-52930
- transition metal compounds, A15-type structure, superconducting transition temp. prediction 3-41295
- transition metal impurities, effect on transition temperature, magnetic and nonmagnetic cases, Hartree-Fock theory 3-60926

superconducting transition point continued

- transition metals, amorphous, superconductivity theory 3-72421
tricritical points of thin superconducting films 3-44163
Al, pressure and ionic mass depend., pseudopotential calc. 3-79784
Al film, resistive transition, effect of perpendicular mag. fields 3-64429
Be alloys, critical temperature obs. using induction method 3-58333
Cd, mutual inductance meas. 3-75805
Ce_{1-x}Gd_xRu₂, sp. ht., 1.8-20K 3-55350
Ce_{1-x}Tb_xRu₂, sp. ht., 1.8-20K 3-55350
Ce_{1-x}Y_xRu₂, sp. ht., 1.8-20K 3-55350
CuFeS₂, antiferromag. film, resist. vanishing and thermal expans. jump for 88 < T < 90K 3-75808
Eu₂La_{1-x} alloys, Mossbauer meas. of coexistence of superconductivity and magnetism 3-44164
films, quench, condensed, superconducting transition temperature (German) 3-58335
In, pressure depend., Fermi surface topology 3-60928
In, tunnelling meas. under pressure 3-52937
In wire, destruction of type I supercond. by current 3-68730
In-Cd, In-Pb alloys, pressure depend., Fermi surface topology 3-60928
(La,Th):Ce alloys, mag. to nonmagnetic transition, temp. depression 3-52924
La₉Lu₂-Tb_x, comp. depend., supercond. crit. fields with short-range mag. order 3-68716
LaOs₂, transition temps. of 5.9K, 8.9K for hexagonal, cubic forms 3-52919
LaSn₃In_{3(1-x)}, rel. to local electronic props. 3-46803
Li, pressure and ionic mass depend., pseudopotential calc. 3-79784
Li_{1/2}Ti_{2-x}O₄, high temp. superconductivity 3-60930
Lu, resist. study 3-58338
Mo-Pt system, homogeneous domains of superconducting phases (French) 3-58329
Nb, calc. of press. dependence of superconducting transition temperature 3-79789
Nb, defect influence on internal friction near transition 3-52926
Nb, temp. depend. of elastic consts. in normal, supercond. states 3-68715
Nb₃Al_{1-x}Be_x(B_y), composition, lattice constant and heat treatment depend. 3-50286
Nb₃Al_{1-x}M_y, M=Be, B, A15 struct., critical temp. obs. 3-50297
Nb₃Au_{1-x}Pt_{(1-x)/2}A-15 type phases, superconductivity, structure and magnetic susceptibility 3-58334
NbN, correl. with heat of formation 3-43878
NbN, high transition temp. rel. to lattice instability 3-64421
NbSe₂, effect of 3d impurities 3-52922
Nb₃Sn, cubic A-15 phase stabilization, a.c. heat capacity meas. 3-64422
(Nb_{1-x}Ta_x)Al_{1-y}Ge_y, A15 struct., critical temp. obs. 3-50297
(Nb_{1-x}Ta_x)₃Al_{1-y}Ge_y, composition, lattice constant and heat treatment depend. 3-50286
Pb, plastic deform. in supercond. transition, temp. depend. due to electronic drag of dislocations 3-41285
Pb, pressures and ionic mass depend., pseudopotential calc. 3-79784
Pb, temp. depend. of elastic consts. in normal, supercond. states 3-68715
Pb-Bi, high-press. d.h.c.p. phase 3-46916
Pb-Bi thin films, strong coupling, transition fields measurement 3-58332
Pb-Sb alloy, plasticity increase at transition 3-55001
Pd-Ag-H, Pd-Rh-H, Pd-Pt-H, temp. depend. of relative electrical resistance 3-79793
Pd-D system, superconductivity theory 3-46928
Pd-H, h.p. effect, isotope effect 3-60931
Pd-H system, superconductivity theory 3-46928
Pd-M system, compositional dependence of superconducting critical temp. 3-64423
Pt-W alloys, conc. depend. (German) 3-41286
SnAs, formed in decomp. of ZnSnAs₂ and CdSnAs₂ 3-41022
Ta, type II, transition by rectang. current pulse, flux flow and jump 3-68729
Ta₂ metal intercalation compounds, preparation and properties 3-72050
Ti, press. effects, pseudopot. calcs. 3-55190
Ti wire, destruction of type I supercond. by current 3-68730
α-U, single- and polycryst., transition temp. at pressure up to 24 kbar 3-79787
UFe, stoichiometry effects and U isopoe effect 3-68725
V, calc. of press. dependence of superconducting transition temperature 3-79789
V-Mn-Ga alloys, determ. using mutual-inductance method 3-47065
V-Ta, rel. to phonon spectrum change with Ta addition 3-75580
V₃Ga, annealing, long range order, and supercond. transition temp. 3-55345
V₃Ga_{1-x}Sn_x, electronic struct. depend. 3-41289
V₃Si, pressed powder compacts, compacting pressure influence 3-50287
V₃Si, pressure coefficient calc. 3-79792
V₃Si tapes, conc. and prep. conditions depend. (Japanese) 3-60934
V₃Si tapes, made by new process 3-64430
V₃Si-V₃Ge, low temp. paramag. susceptibility and supercond. crit. temp., comp. depend. (French) 3-68723
V₃(Si_{1-x}Ge_x) solid solns., conc. depend. (Russian) 3-58327
(V_{1-x}Ti_x)₃Si, relation between T_c and elastic softening 3-68740
V₃X A-15 cpds., low temp. paramag. susceptibility and supercond. crit. temp. (French) 3-68724
Zn-Cr(Mn) alloys, obs. down to 0.037 K 3-41290

superconductivity

- see also BCS theory; nonequilibrium properties of superconductors; superconducting devices; superconducting materials; superconducting transition point; transport properties of superconductors
adiabatic perturbation theory 3-55237
alloy, nonmagnetic, weak-coupling, coherent pot. approx. 3-75800
alloys with A15 structure, critical temp., influence of (1/2)<111> stacking faults 3-46931
applic. in electrotechnology, prospects (German) 3-73870
BCS theory, general aspects 3-75803
boson characteristic function calc. 3-50283

superconductivity continued

- charged Fermi systems, fluctuations (Russian) 3-72413
critical Ginzburg-Landau parameter separating type II/1 from type II/2 3-79790
cylinder subjected to longit. mag. field, current induced supercond. destruction (French) 3-55361
electron gas, polarization operator, Kohn anomalies and charge screening (Russian) 3-41294
electron phonon interactions development of theory 3-72420
elliptical cylinders, transverse critical field calc. using Ginzburg-Landau theory 3-68717
e.p.r. theory for gapless dirty type II supercond. 3-46935
Ginzburg-Landau theory with non-local correction in zero magnetic field 3-64418
glass:Sn, Ga, Mossbauer effect and second-order Doppler shift, tunnel effect 3-75927
Hubbard model, attractive, strongly correlated pairs rel. to supercond. 3-46974
impurity problems, applic. of coherent potential approximation 3-46922
Josephson a.c. effect, exactly solvable microscopic models 3-46936
linear chain conductor, Peierls soft-mode induced supercond. instability, theory 3-72430
macroscopic quantum phenomena 3-44160
macroscopic quantum phenomena from pairing and review of development of theories 3-72412
magnetic impurity effect, two-band model 3-79780
magnetic nucleation fields for superconductor in contact with normal metal (French) 3-55382
Meissner effect and stable trapping of fields 3-46940
metal, electron-phonon interaction and supercond. behaviour 3-75703
metallic system, one-dimens., renormalisation group technique, invariant couplings 3-75799
metallic system, one-dimens., renormalization group techniques, response functions 3-79781
metallic systems, one-dimensional application of renormalisation group technique to phase transition 3-64136
microscopic quantum interference, theory 3-79782
microscopic quantum interference due to singlet-spin pairing 3-72419
microscopic theory, electron interactions, phonon exchange, bound states, appls. (French) 3-75802
mixed state, correlation between flux-line lattice and crystal axis 3-75809
molecular chain, Little's mechanism, renormalization theory for one-dimensional Fermi system 3-40175
non-equilibrium repulsion between particles 3-52915
nuclei, BCS approximation application (Rumanian) 3-64425
one-dimensional conductor, metal-insulator transition, BCS pairing suppression, Peierls instability 3-64388
one-dimensional metallic systems, phase transition, renormalization group approach 3-60927
organic chain molecules, effective electron-electron interaction 3-75801
organic solid, one-dimens., supercond. fluctuations 3-58350
paraelastic interaction between lattice defects and flux lines 3-46914
phase transitions, analogy with mode locking 3-40233
phenomenon, and applications 3-58325
physical principles, general for non-physicist, technological potentialities (French) 3-64419
practical applic. of theory in engineering, design problems 3-68711
predictions and temperature thresholds, comments (French) 3-44161
proximity effect, between materials with different interaction constants 3-60939
quasi-one-dimensional systems, decay of superconductive state (Russian) 3-68712
rotating superconducting cylinders, London moment 3-41283
semiconductor, degenerate polar, theory 3-41293
semiconductor, intra-band electron pairing in presence of radiation field 3-41307
spin fluctuation effect on transition temp. 3-50288
statistical treatment by generalized master equation 3-70754
TCNQ complex, supercond. fluctuations rel. to structural defects 3-55384
TCNQ salts, supercond. and Peierls instability 3-46941
transition metal beryllides, investig. up to 1.7K (Russian) 3-46927
transition metal compounds, A15-type structure, superconducting transition temperature prediction 3-41295
transition metal energy spectra (Russian) 3-58328
TTF-TCNQ, giant cond. 3-68741
tunnelling, anomalous, into mag. ordered dilute alloys in supercond. state 3-68736
type I and type II superconductors, magnetisation of ellipsoids, pinning 3-68734
type II, dirty superconductors., thermodynamic and dynamic props., vortex state, theory 3-68731
type II superconductors, flux line properties from non-local theory, magnetic field-temp. curves 3-46913
type II superconductors, mag. hysteresis 3-52914
type-II superconductors, Ginsburg-Landau theory, non-local extensions 3-41284
vector pot. and order parameter for isolated vortex in type II supercond. 3-55348
vortex lattice in mag. supercond. 3-72423
(La,Th):Ce alloys, mag. to nonmagnetic transition, superconducting temp. depression 3-52924
Mg film, quench-condensed, absence above 0.35 K 3-46918
Nb, dirty, microscopic magnetic field distrib., neutron diffraction expts. 3-46923
Nb₃Al_{1-x}Be_x(B_y), critical temp. measurement, depend. on composition lattice constant and heat treatment 3-50286
NbN, transition temp., correl. with heat of formation 3-43878
Nb₃Sn, shock wave synthesis, phase form. obs. 3-69328
(Nb_{1-x}Ta_x)₃Al_{1-y}Ge_y, critical temp. measurement, depend. on composition lattice constant and heat treatment 3-50286
Pb-In alloy, type II, temp. depend. of viscosity coeff., differential resist. 3-72426

superconductivity continued

- PbMo₇S₈, supercond. and struct. 3-60706
 PbTe-Pb system, diamagnetic susceptibility, field dependent 3-79795
 Pr binary chalcogenides, mag. props., metal-insulator transition, superconductivity 3-41326
 Sn films, gapless, critical magnetic fields, temp. depend. 3-68722
 SrTiO₃, rel. to structural instability, electron-soft phonon interactions 3-58343
 Ta, differential paramagnetic effect, temp. depend. 3-46932
 Tm binary chalcogenides, mag. props., metal-insulator transition, superconductivity 3-41326
 V-Mn-Ga alloys, transition temp. determ. using mutual-inductance method 3-47065
 V₂Si, pressed powder compacts, transition temp., influence of compacting pressure 3-50287
 YbAl₂ and YbAl₃, ambivalence of Yb 3-68552
 Zn, anisotropy in normal-state mass renormalisation and supercond. energy gap 3-75807

superconductor-insulator-superconductor junctions *see* Josephson junctions**superconductors** *see* superconducting materials**supercooling**

- alloy, binary, solute redistrib. during solidification, constitutional supercooling (*French*) 3-76152
 clouds, spherical ice particle growth, dep. on H₂O drop spectrum, size distrib. 3-76767
 ethanol, glassy liquid and crystal state, supercooling rate 3-75484
 liquid, supercooled, freezing in forced turbulent flow inside circular tubes 3-75191
 saline solutions, aqueous, metastable state rupture, transitions to liquid state phenomena (*French*) 3-79492
 saline solutions, aqueous, spontaneous rupture of supercooling and supersaturation states (*French*) 3-79493
 saline solutions, metastable aqueous, spontaneous rupture of supercooling and supersaturation states (*French*) 3-79491
 superconducting thin films, superheating and supercooling field measurement 3-60925
 water drops, radionuclide nucleation of ice 3-76769
 water emulsions, metastable state rupture, transitions to liquid state phenomena (*French*) 3-79492
 water in rock, internal friction measurement (*Japanese*) 3-56034
 zone melting, impurity elimination due to additive and constitutional supercooling phenomena (*French*) 3-47417
 Ag, liq., spontaneous crystn. (*Russian*) 3-58609
 Cu, liq., spontaneous crystn. (*Russian*) 3-58609
 Cu-Ni alloys, dendritic solidification, initial growth of dendrite struts. 3-69199
 Cu-Ni alloys, dendritic solidification, microsegregation 3-69200
 Ge, liq., spontaneous crystn. (*Russian*) 3-58609
 Na₂O-CaO-SiO₂ glass-forming system, nucleation and crystn. 3-72010

superexchange interactions

- copper propionate monohydrate, Zn-doped single crysts., e.s.r. spectra 3-55465
 energy, potential and kinetic, spin orientations, crystal field influence, MO and CT approximations, 3 centre 4 electron model 3-52971
 ferromagnet, Heisenberg model, with defects 3-41316
 ionic solids, superexchange coupling, review of theory 3-47012
 non-orthogonality of three centres, Yamashita-Kondo, Kramers-Anderson mechanisms 3-72457
 polynuclear complex salts, Cr³⁺ ions, luminescence, 4-77K 3-76065
 rare earth insulator, rel. to Neel and Curie temps. 3-72458
 Bi₂La_{1-x}FeO₃, sublattice magnetisations, Neel temps., superexchange isomer shift, elec. field splitting, Mossbauer obs. 3-50490
 Co₂SiO₄, n.m.r. of ²⁹Si, long range via Co-O-Si-O-Co linkages 3-72530
 Cr-Mn spinels, B-B interaction behaviour 3-68777
 Cr(III) complex, $\mu\mu'$ -dihydroxotetrakisethylenediamine dichromium (III) salts, mag. susceptibility, 1.6-300K 3-79825
 LaCuO₃, mag. susceptibility, Pauli paramag., superexchange enhancement (*French*) 3-60955
 LaNiO₃, mag. susceptibility, Pauli paramag., superexchange enhancement (*French*) 3-60955
 NiO, exchange and superexchange parameters 3-41337

superfluidity

- see also* liquid helium; quantum fluids; vortices
³He liquid, zero sound attenuation, superfluid pairing 3-50047
 Bose gas, ideal, superfluidity in ring 3-46738
 Bose systems, two- and one-dimensions 3-54168
 Bose-Fermi system, spectrum of elementary excitations (*Russian*) 3-72241
 critical first-sound absorption near λ -transition 3-68460
 Fermi liquid, Gor'kov's model, kinetic coeffs. 3-60810
 Ginzburg-Landau eqn., generalized, isotropic solns. 3-42894
 Goldstone mode freq., phase transitions, symmetry breaking and asymptotic props. 3-49956
 gyroscopic based on superleaks of liquid He II 3-39853
 He II liquid/solid interface, h.f. phonon transmission 3-64226
 ideal Bose film, specific heat, scaling functions 3-66689
 isotropic Bose system, helicity modulus, superfluidity, scaling 3-70734
 Kapitza temp. discontinuity at solid body-He II boundary 3-75650
 nuclear matter, phase transition to normal state, schematic two-level model of rotation at high angular momenta 3-57483
 pair theory of Fermi or Bose statistics, conserving approx. of superfluid density 3-52729
 vorticity in non-dissipative processes, dynamics, Landau two-fluid equations 3-50035
 He, isothermal flow through narrow channels 3-68456
 He, Kapitza resistance between Fe, Co, Ni, dislocation effects 3-68458
 He, liquid, flow through bed of large angular particles, critical velocity 3-72248
 He, rotating, damping of transverse waves 3-60816
 He film, two-fluid model, thermodynamic approach 3-43910
 He II, dispersion relation and level density of rotons 3-75648

superfluidity continued

- He II, film transfer rates for solid Ar beakers 3-72249
 He II, gas sheath around hot filament, radius measurement by microwave technique 3-50038
 He II, gas-liquid phase transition in system of ³He surface impurities 3-52741
 He II, inhomogeneous density distrib. near λ point, second sound investigation, theory 3-79538
 He II, quasi-isothermal superfluid film oscills., damping and freq. 3-79540
 He II, sound propag. transport eqn., numerical soln. 3-64229
 He II, standing echo waves, optical obs. (*German*) 3-50037
 He II, stimulated surface scattering of light by ponderomotive effect of radiation 3-55105
 He II, superthermal monochromatic phonon dispersion and attenuation 3-68462
 He II, vortex-ring creation, time depend. 3-52736
 He II film, hydrodynamics, flow props. of superfluid, review 3-68454
 He II film, transport over perspex surface 3-52731
 He II films, superflow and anomalous attenuation of third sound, associated with macroscopic quantum uncertainty principle 3-55106
 He porous media, flow conductivity, Ginzburg-Pitaevskii eqn. 3-75646
 He thin films, onset of superfluidity, Ginzburg Pitaevskii eqn., intrinsic flow conductivity 3-75645
 HeII, few-phonon structure functions 3-68457
³He, anisotropic phonon energy, effect on normal fluid density, second and fourth sound 3-68466
³He, anisotropic superfluid, long range distortions 3-52739
³He, first viscosity of Balian-Werthamer phase (*French*) 3-72250
³He, liquid, anisotropic superfluidity, stability, paramagon effect 3-43917
³He, low temp. first viscosity calc. (*French*) 3-58159
³He, relative viscosity meas. along melting curve 10 to 1 mK 3-41061
³He, vortex-ring, generated level differences 3-68467
³He in superfluid ⁴He, dil. soln., kinetic theory 3-46743
³He in superfluid ⁴He, dil. solns., second-viscosity phenomena 3-50048
³He liquid, crit. temp., condensation in L=2 or L=3 state 3-79542
³He superfluid, collisionless, high frequency sound propagation, phenomenological theory 3-50046
³He-⁴He solution, sound propag. 3-58164
³He-⁴He solutions, phase separations and λ lines relation 3-52743
³He-⁴He solutions, two-rotor Raman scattering 3-43919
⁴He, adiabatic rotation in packed powders, cooling effect 3-60817
⁴He, charge carrier mobilities, press. depend. 3-64227
⁴He, creeping film phenomena, theory 3-52730
⁴He, density correlation function, near T _{λ} , light scatt. obs. 3-60813
⁴He, formation of two branches of energy spectrum, possible mechanism (*Russian*) 3-43908
⁴He, freezing liquid, tables for the P₀T of the λ line, thermophysical properties, 4 to 3000 R, pressures up to 15000 PSIA 3-50043
⁴He, in porous media, superfluid density and sp. ht., size effects 3-55104
⁴He, inelastic neutron scatt. from free surface, ripplon spectrum 3-68463
⁴He, interatomic pot. role in microscopic theory development 3-55108
⁴He, light scatt. near λ phase transition, theoretical anal. 3-43909
⁴He, liquid, hydrodynamical equation derivation, condensate wave function 3-55109
⁴He, liquid, pure and with ³He impurities, rotating superfluid, free surface at vortex 3-55112
⁴He, liquid, superfluid, creation of quantised vortex rings 3-60820
⁴He, potential flow past a sphere tangent to a plane 3-60819
⁴He, reson. absorpt. of e.m. energy by ions on vortex 3-60821
⁴He, superfluid, charged vortex rings dynamics 3-52737
⁴He, superfluid, dissipative coefficients calc., Boltzmann equation solution for phonons and rotons 3-43915
⁴He, superfluid critical heat current velocities as a test of Vinen theory 3-75649
⁴He films on variety of substrates, onset for superfluid flow 3-43912
⁴He II, liquid, electron bubble electrical props. 3-72243
⁴He II, liquid, ion currents in turbulent counterflow 3-43911
⁴He II, liquid, thermal props., hot filament study 3-72244
⁴He II liquid, charge carrier production by spark discharges 3-72242
⁴He II under pressure 3-43913
⁴He superfluid layer, higher waves existence 3-79545
⁴He surface, spectral intensity of scatt. light 3-52734
⁴He temperature stabiliser near λ -point 3-62026
⁴He thin films, superfluid onset frequency response, and connectivity 3-55115
⁴He under press., static scaling and universality 3-64228
⁴He under press. near T _{λ} , second sound vel. and superfluid density meas. 3-46741
⁴He-³He liquid mixtures, variation of λ temperature with ³He concentration 3-55117

superheavy nuclei

- see also* nuclei with A \geq 220
²⁵⁷104, daughter X-ray identification 3-63015
 astrophysical superheavy element synthesis, from r-process calc. with energy-density mass formula 3-65620
 binding energy and stability (*Russian*) 3-52067
 charge and mass distrib. calc. by hyperspheric functions method for ²⁸⁰112 and ⁴⁰⁸168 (*Russian*) 3-74479
 cosmic ray photoemulsion events in stratosphere, E > 5 \times 10¹² eV, formation of superheavy fireballs (*Russian*) 3-69784
 critical charge, non-existence 3-43169
 element 114, boiling point, entropy and heat of vaporisation, extrapolation method calc. (*German*) 3-69483
 element 115 (eka-Bi), prediction of props. from Bi 3-80571
 fission barrier calcs. 3-54520
 formation in stellar plasma, heavy element fissionability effects 3-69940
 inertial mass parameter B, determ. in adiabatic approx., 108 \leq Z \leq 124, 172 \leq N \leq 188 3-62924

superheavy nuclei continued

- in natural and proton-irradiated materials, search 3-60231
- problems of synthesis of macroscopic amounts (*Czech*) 3-62923
- shape and stability calcs., spurious state contribs. 3-45926
- spherical, crit. charge, screening effects, calc. 3-54374
- stability, production, fission review (*Japanese*) 3-71133
- X-ray spectra possibility for element identification, quasimolecule obs. 3-60357
- W targets, secondary reactions prod. superheavy elements and actinides 3-60232

superheterodyne receivers

- automatic tracking (*German*) 3-54251

superionic conducting materials

- anomalously fast ionic conductivity in solids, struct. aspects 3-46729
- selection rules for superionic conductors, by electrostatic calc. in ionic compounds 3-43901
- $\text{Ag}_6\text{I}_4\text{WO}_4$, solid state battery applic. 3-43892
- Cu complex, N-alkyl-hexamethylenetetramine-Cu(I) 3-79521

superlattice structure *see crystal atomic structure***supernovae**

- 1970g in M101, variable radio emission 3-42204
- binary helium dwarf supernova evolution, possibility of violent He ignition 3-81029
- buoyant remnants, hydrodynamic considerations 3-56302
- $\beta\text{C}58$ remnant, high resolution interferometry 3-77093
- 3C 10 (Tycho's supernova remnant), interpretation of radio emission 3-42203
- 3C 391, supernova remnant, 18 and 21 cm recombination-line emission 3-70034
- 3C 391 remnant, high freq. obs. and theoretical interpretation of recombination line emission 3-77153
- 3C 398 (W49B), supernova remnant, 21 cm recombination-line emission 3-70034
- Carina nebula NGC 3372, supernova remnant obs. at 30 MHz 3-61871
- Cassiopeia A (3C 461), young supernova remnant, interpretation of radio emission 3-42203
- cosmic ray origin and nucleosynthesis 3-80890
- γ -Cygni remnant, high resolution interferometry 3-77093
- Cygnus Loop, remnant, interferometric meas. of central compact radio source 3-65906
- element formation in neutron rich ejected matter 3-47869
- envelope ejection by mag. pumping 3-53652
- envelopes, origin of Li, Be and B 3-61624
- explosion into interstellar magnetic field, numerical study 3-81192
- explosions rel. to C ignition in degenerate C cores (*Polish*) 3-45090
- explosive phase characts. (*Italian*) 3-59345
- extragalactic, search for optical pulsars 3-65909
- frequency distribution function, according to age and lifetime, astronomical phenomena 3-76951
- Galactic Supernova remnants, observations of second millennium A.D. objects 3-77105
- Galactic supernova remnants, optical photographic atlas of 23 objects 3-81094
- H I filament, radio mapping, association with supernova shell 3-77158
- HB 21, remnant, assoc. with PSR 2021 + 51 indicated by 21 cm obs. 3-65894
- high energy γ -ray flash detection using liquid and plastic scintillators 3-77192
- IC 443, remnant, radio spectrum 3-77098
- Kepler remnant, high resolution interferometry 3-77093
- NGC 5055 (1971 I), light curves 3-77104
- in NGC 5253, light curve study, type I indications 3-81103
- nuclear reactions induced by fast protons in shell of supernova, diffusion in solar system (*Russian*) 3-65618
- plasma turbulence, effect on spectra of scatt. by Langmuir oscill. 3-60611
- production, teaching approach to gravit. collapse 3-42498
- radiotelescope search, 1.4×10^9 Hz 3-77178
- relativistic shock hydrodynamics, eqns. for perfect fluid 3-60582
- remnant, linear polarisation at 2.8 and 4.5 cm 3-77108
- remnant buoyancy rise phenomena in presence of interstellar mag. fields 3-47997
- remnants, 3 C 10, high resolution 21 cm. obs. 3-53676
- remnants, 3 C 461, high resolution 21 cm. obs. 3-53676
- remnants, 53-318 MHz search for compact radio sources 3-45155
- remnants, Cygnus Loop, X-ray spectrum 3-65940
- remnants, emission-line spectra rel. to properties of galactic nuclei 3-45108
- remnants, genetic relationship with pulsars 3-61831
- remnants, high resolution obs. at 80 MHz 3-56398
- remnants, in Magellanic Clouds 3-61839
- remnants, obs. of galactic sources at 1.7 and 2.7 GHz 3-59348
- remnants, search for 1415 MHz emission from young extragalactic objects 3-56400
- remnants, thermal bremsstrahlung in Sedov stage 3-45109
- remnants, X-radiation rel. to mechanisms and evolution 3-81148
- remnants near galactic plane, 8.8 GHz radio obs., brightness distrib. and flux densities 3-53671
- resonant in W51, kinematic distance estimate 3-48057
- Shajn 147, remnant, high. vel. gas 3-61797
- SN 1970-I, obs. at Asiago (1970-I) 3-73516
- SN 1970j, obs. at Asiago (1970-I) 3-73516
- SN 1971-g, obs. at Asiago (1970-I) 3-73516
- SN 1971-i, obs. at Asiago (1970-I) 3-73516
- SN 1971-l, obs. at Asiago (1970-I) 3-73516
- SN 1972 in NGC 5253, i.r. emission features in spectrum 3-45125
- SN 1972 in NGC 5253, u.v. photometry 3-48044
- SN 1972E, upper limit on X-ray flux 3-56410
- spatial distrib. in Galaxy rel. to pulsars 3-42214
- spectra, interpretation and atlas 3-51340
- stellar evolution, blast wave hydrodynamics, cluster of galaxies, supernovae, intergalactic medium 3-47868
- stellar evolution review 3-77038
- Stephan's Quintet of interacting galaxies, H II region and supernova obs. 3-70004

supernovae continued

- Tycho's supernova remnant (3C 10), interpretation of radio emission 3-42203
- Tycho remnant, high resolution interferometry 3-77093
- type I, absolute magnitude determ. for 43 objects 3-48012
- type I, average light curve and properties 3-48008
- type II, D prod. in envelope shocks 3-47991
- Vela, X-ray structure of PSR 0833-45 from Uhuru obs. 3-73530
- Vela X supernova remnant, emission line spectrum 3-81098
- very long baseline interferometric obs. of radio sources 3-65908
- C detonation supernova, hydrodynamic model for neutron star formation 3-81025
- CO obs. in 6 supernovae remnants 3-45214

superparamagnetism

- magnetic glass, review 3-46977
- magnetite, superparamagnetic and single-domain threshold sizes 3-53400
- magnetite suspension in paraffin oil, magnetisation curves, superparamagnetism (*Russian*) 3-44280
- Co ferrite, superparamag. particles, struct. and mag. props. rel. to milling 3-50425
- Cu-Co alloy, dil., sp.ht., 1.6-4.2K, in mag. field 3-47042
- Fe ferrite, superparamag. particles, struct. and mag. props. rel. to milling 3-50425
- Fe-graphite layered compounds, Mossbauer investigation 3-50503
- Fe-Ni (31 at.%) fine particles, superparamag. behaviour, Mossbauer obs. 3-41378
- Fe_3O_4 Mossbauer spectra, behaviour of ultrafine particles, hyperfine spectrum 3-41465
- Fe_3O_4 particles, magnetite, Mossbauer effect, h.f. splitting obs. (*German*) 3-50494
- Ni fine particles, temp. and mag. field depend. of magnetn. 3-68819
- Ni-Cu alloys, behaviour of localised moment of Ni 3-72475
- Ni-Cu alloys, origin 3-47053
- NiZn ferrite, superparamag. particles, struct. and mag. props. rel. to milling 3-50425

superplasticity

- activation energy for superplastic flow 3-60765
- alloy, diffusion accommodated flow 3-40964
- brass, large grained, high temp. deform. behaviour 3-64933
- brass, large grained, high temp. deform. behaviour 3-64934
- Coronze CDA 638, grain size strengthening and weakening 3-58662
- extrusion, material behaviour influence on force requirements and velocity (*German*) 3-41795
- grain boundary glide, elastic resist. to shear (*Russian*) 3-72853
- metal, superplasticity and surface tension at phase transition, fluctuation model 3-49924
- metals, electron emission during transition to superplastic state 3-60763
- optimum conditions during martensitic transforms (*Russian*) 3-76153
- Al-CuAl₃ eutectic composites, lamellar and particulate, phase size influence on elevated temp. deform. 3-64958
- Al-Zn-Mg alloys, superplastic phenomena and microstruct. (*Japanese*) 3-50700
- Bi_2O_3 - Sm_2O_3 eutectoid, transform. deform., stress and temp. depend. 3-76231
- Cu, high temp. deform. mechanisms 3-76223
- Cu-Al alloys, large grained, high temp. deform. behaviour 3-64933
- Cu-Al alloys, large grained, high temp. deform. behaviour 3-64934
- Fe, cast, ductile, transform. superplasticity (*Japanese*) 3-44564
- Ni-Cr(49 wt. %), relation between superplasticity effects and extent of interphase boundary (*Russian*) 3-72895
- Sn-Bi (1 wt. %) alloy, superplastic deform. enhanced grain growth 3-80230
- Ti alloys, large grained, high temp. deform. behaviour 3-64933
- Ti alloys, large grained, high temp. deform. behaviour 3-64934
- Zn-Al (30 wt. %) alloy, solid soln. decomp. and superplasticity behaviour (*French*) 3-47418
- Zn-Al eutectoid alloy, in situ expts., 1 MV electron microscope 3-50705
- Zn-Al(40 wt. %) alloy, basal plane pole figures 3-69220

superradiance *see stimulated emission***supersaturation measurement** *see chemical variables measurement***supersonic flow**

- see also hypersonic flow; shock waves*
- ablation material anelastic behaviour on crosshatching due to supersonic turbulent boundary layer flow 3-46441
- aeroacoustic environment about a slender cone, expt. determ. 3-63703
- aerodynamic noise and boundary layer transition measurements in supersonic test facilities 3-46442
- aerodynamic noise emission from turbulent shear layers 3-60534
- boundary layer flows, small protuberances effect 3-71762
- boundary layer transition, influence of total temperature 3-57781
- compressible boundary layer stability relative to a local disturbance (*Russian*) 3-67925
- conical-shaped vehicle in wind tunnel, acoustic environment prediction 3-46449
- delta wing expansion side at supersonic speed obs. 3-78980
- entry vehicle dynamics, instability caused by forebody blowing 3-43571
- expanding gas cloud, dynamical evolution 3-81206
- gas dynamic lasers, rapid expansion nozzles 3-45788
- gas dynamical laser cavity, density inhomogeneity due to energy release 3-45789
- gas in finite length nozzle, solns. for mixed subsonic and supersonic flows 3-46447
- gas part plates of complex form, use of R-functions in dynamic stability calc. (*Russian*) 3-74076
- heterogeneous, stoichiometric hydrogen-air mixture with suspended Al and Mg powders (*Russian*) 3-63768
- high-power lasers, supersonic flow aerodynamic windows 3-77540
- high-speed turbulent radiating boundary layers, numerical solns. of integro-differential equations 3-52453
- high-speed viscous flow over cone at incidence, predictor corrector method 3-49586

supersonic flow continued

- hypersonic and supersonic flowfields around slab delta wing, algorithm for three-dimensional method of characteristics 3-49580
- hypersonic flow, nonsteady shock wave propag. (German) 3-54815
- hypersonic rarefied gas flow past convex body, ray reflection model 3-54813
- hypersonic sphere wakes, laminar and turbulent, Mach 13.5, density and temp. distributions 3-40753
- incipient separation pressure rise for a Mach 3.8 turbulent boundary layer 3-63709
- jet, effect of swirl, theory and exptl. obs. 3-78982
- jet, supersonic, escaping from nozzle into off-design modes, apparent mass investigation 3-60587
- jet engines, effect on inlet distortion, high response pressure measurement, steady and time variant 3-57032
- jet flows, noise reduction 3-43637
- jets, flow expansions, base pressures by hydraulic analogy 3-63786
- jets, supersonic, noise reduction 3-52489
- jets, supersonic, underexpanded, impingement upon flat plate 3-75276
- jets, two-dimensional supersonic flow impingement on a normal surface, expt. obs. 3-43636
- laminar, over a wedge, base pressure 3-75222
- laminar compressible boundary layer on a cone near a plane of symmetry 3-46430
- laminar supersonic flow over a two-dimensional compression corner, numerical solutions 3-49593
- laminar wakes, pressure distrib. and velocity profiles, method of integral relations 3-54810
- lasers, electrical gas dynamic, kinetics 3-74238
- linearised, past harmonically vibrating cylindrical body, cylindrical integral transformation application 3-60555
- liquid jet injection across supersonic stream, drop size distribution 3-71830
- Ludwig tubes, high performance, aerodynamics 3-63704
- moon, Silver Spur, cross-hatching, hypersonic and supersonic turbulent gas flow 3-69903
- multishocked three dimensional supersonic flowfields with real gas effects around space shuttle 3-63705
- Navier-Stokes equations, compressible, numerical experiments 3-49585
- Newtonian aerodynamic forces from Poisson's equation 3-57779
- nonequilibrium, chemically reacting, in 3-D rising bicharacteristics method 3-57783
- nonequilibrium nozzle flows entropy of vibrationally relaxing diatomic gases 3-43633
- nonlinear aerodynamics of bodies in coning motion 3-46440
- nonlinear hyperbolic equations, second and third order noncentred difference schemes 3-43568
- nonuniform, construction of contour of minimal wave resistance using variational method (Russian) 3-67930
- nozzle flows calc. using Pade fractions 3-57854
- nozzles, coaxial axisymmetric supersonic, sonic line 3-57855
- panel flutter in supersonic gas flow 3-49583
- panel flutter of finite cylindrical shells, first-order freq. effects 3-70665
- perfect gas unsteady transonic flows with shock waves in two-dimensional channels 3-67929
- plasma high Mach number flows, laminar interactions 3-63826
- plasma supersonic jet, stability investigations in magnetic field (Russian) 3-68009
- plenum, rapidly filling unsteady flow processes 3-46453
- rarefied gas flow, rate meas., drift of marker ion, electron beam produced (Russian) 3-45622
- real gas supersonic flow presence of heat transfer 3-40709
- reference temp. method for predicting skin-friction coefficient in compressible turbulent boundary layer, Mach number range 2-20 3-43557
- relativistic irrotational ideal gas flow, equation for supersonic stream 3-43632
- rotational relaxing gas flows geometry 3-78960
- separated laminar supersonic boundary layers, integral props. meas. 3-57786
- separated shear layer, inviscid reattachment 3-49591
- shock diffraction theory, antisymmetric problems 3-67941
- shock shape around concave and convex bodies 3-63717
- slot injection into a supersonic stream, expt. study 3-63700
- Sound generation by open supersonic rotors 3-81345
- space shuffle flowfields computation using noncentred finite difference schemes 3-43569
- spinning cone, boundary layer distortion 3-52450
- stagnation heat transfer rates effect of surface catalytic activity 3-63785
- stagnation pressure probe, new, high pressure recovery, cylindrical compression surface 3-57033
- starting process in the nozzle of a nonreflected shock tunnel 3-46495
- steady flow at Mach number one past wing airfoil, computational method 3-52463
- strong shock over a sharp leading edge, Navier-Stokes eqns., finite difference treatment 3-49598
- subsonic and sonic flow in heat pipe, spectroscopic obs. 3-40726
- surface flow for predicting crosshatch patterns 3-75216
- T Tauri stars, structure rel. to supersonic convection 3-51334
- thermal sources, in perfect gas 3-75173
- thick axisymmetric boundary layers, turbulent skin friction analysis 3-71776
- thin delta wing, pressure distrib., board finite velocities (Rumanian) 3-75217
- three-dimensional, polytropic gas, precise method for solving problems 3-75224
- three-dimensional, steady, isentropic flow, charact. schemes, comparison 3-46439
- three-dimensional transonic flow about wings, relaxation techniques 3-46443
- transonic, around blunt wedges, numerical soln. (German) 3-54812
- transonic aerodynamic field around airfoils, numerical procedure for a free boundary-value problem in hodograph plane 3-49584

supersonic flow continued

- transonic and subsonic separated flows over airfoils, finite-difference relaxation method 3-52464
 - transonic approximate shock-free solution for a symmetric profile at zero incidence 3-63707
 - transonic flow about lifting configurations 3-63710
 - transonic flow about wing-cylinder combinations and lifting swept wings, relaxation methods 3-49589
 - transonic flow around airfoils, time dependent calc. 3-49592
 - transonic flow around plane and axisymmetrical bodies, numerical approach 3-49590
 - transonic flow past lifting wings 3-63708
 - transonic flow theory involving lift, equivalence rule 3-78981
 - transonic flows over blunt nosed geometries with detached bow shocks, relaxation method 3-52465
 - transonic irrotational flow shock waves and drag, numerical calc. 3-78984
 - transonic laminar boundary layers with surface curvature 3-57769
 - transonic nozzle flow with a parabolic temperature distribution 3-40752
 - transonic nozzle flow with uniform gas properties 3-43634
 - transonic turbulent viscous-inviscid interactions in airfoil trailing edge 3-63702
 - transonic unsteady aerodynamics of oscillating wings with thickness 3-57790
 - turbulent boundary layer flow downstream from 90° corner 3-54811
 - turbulent heat transfer and skin friction calc. 3-78935
 - turbulent heat transfer to a fine leading edge 3-57725
 - turbulent jet mixing 3-54814
 - two-dimensional relaxed flow of gas in convergent-divergent pipe (French) 3-52462
 - two-phase flow meas. with laser-Doppler velocimeter (Russian) 3-77756
 - vibrations, self-excited and forced, of rectangular plate in flow, aerodynamic appl. 3-62534
 - viscous supersonic flow over cone at moderate incidence 3-60553
 - viscous-inviscid interaction, mathematical formulation 3-78974
 - at wavy wall in channel, mixed boundary-value problem (German) 3-57778
 - wing panel behaviour in transitional region in gas flow, numerical analysis (Russian) 3-46446
 - Ar, shock produced ionized, supersonic current interaction with elec. and mag. fields (French) 3-40776
 - H₂ nozzle beam, meas. of cluster distrib. 3-63562
 - HF c.w. diffusion-type chemical laser, H₂ diffusion into supersonic stream 3-43000
 - He, oblique shock-sound interaction at $M_\infty \approx 20$ 3-40727
 - N₂ expanding into CO + N₂ atmosphere, low density supersonic stream, diffusion processes, electron beam techniques (Russian) 3-46462
 - N₂ gas flow interaction with plasma, turbulence, light emission fluctuations 3-68008
 - N₂-N₂O mixture, expanding supersonic jet, rapid cooling, dissociation reactions (Russian) 3-57872
- supersonics** see *supersonic flow*
- supply systems (electric)** see *power systems*
- supports**
see also *poles and towers*
particle track chamber, multiwire, sense wire support, melinex strip compared to nylon cord 3-77682
- surface activity** see *surface energy*
- surface chemistry**
see also *chemisorption; corrosion; oxidation*
acetone in steel vessel, inhibition of carbon deposition by sulphur poisoning 3-73168
alloy systems, binary, surface composition and catalytic activity, new investigative technique 3-44743
Auger electron spectroscopy, technological appls. 3-55706
Auger electron spectroscopy in SEM 3-55707
diffusing particles, absorption rate thermometric meas. 3-65117
glass, surface comp. from photoelectron spectra (French) 3-54037
internal reflection spectroscopy, electrochem. studies 3-66226
i.r. internal reflectance spectrometry appls. 3-73164
Mattauch-Herzog spectrograph, surface chemical analysis, ionic implantation profiles (French) 3-77747
modulation spectroscopy, electrochem. appl. 3-55967
reactions in porous catalysts in molecular transition and Knudsen regimes 3-80572
steel, boro-carburization, B₄C-alkaline carbonate bath dipping (Japanese) 3-72908
ternary liquid mixtures adsorption on solids 3-76486
AgBr, epitaxial attachment of dye aggregates to surface, ligand bonds red shift, benzothiazolocarbocyanine 3-53342
Al, Hg-wetted, reactions with liquid water 3-58812
C black, oxide formation in electrochem. oxidation by H₂PO₄ 3-69461
Cr, thin film, thermochemical interaction of laser radiation 3-58797
Fe, boro-carburization, B₄C-alkaline carbonate bath dipping (Japanese) 3-72908
Pd-Ag alloys, equilib. surface comp., chemisorbed CO 3-79577
Pt single cryst., low- and high-Miller-index planes, H₂ + D₂ exchange, mol.-beam study 3-47599
Pt(110) surface, adsorbate interactions, H₂S, S and CO adsorption 3-41869
Pt(110) surface, S + O₂ adsorption, catalytic CO oxidation 3-73166
Si, pre- and backspitting as cleaning processes, surface structure and chem. 3-55161
Ta chemisorption of CO and O₂, polycrystalline tapes, helium molecular beam reflection study, chemical interactions (French) 3-44742
Te, electrodisolution, reduction and oxidation at graphite electrode, HBr and HCl 3-73137
Ti-Zr alloys, wear resist. in H₂O, increase by oxide surface layer formation 3-58697
W, (100), (110) and (111) cryst. faces, NH₃ catalytic decomposition 3-55987

surface contours

- boundary layers, compressible turbulent, roughness, heat transfer and press. gradient effects 3-49571
- contact profilometer calibration, roughness standard production and evaluation (*Slovak*) 3-66128
- double beam interferometry, electrochem. studies, review 3-66236
- ellipsometry, electrochem. studies, surfaces and surface films, review 3-66197
- flatness, non-optical surfaces, oblique incidence interferometry, transmission diffraction gratings, techniques 3-66234
- holographic surface mapping system, with computer analysis of video signals 3-66241
- human articular surfaces, contour examination, profile recorder, stereomicroscopy, replication 3-59409
- Mars, surface features, comparison with Moon and Earth surfaces (*Hungarian*) 3-76989
- metal, epoxy resin-aliphatic resin:polyethylenepolyamine models, appl. to optical method of stress anal. 3-50812
- nondestructive optical contour mapping method 3-51516
- optical component testing by interferometry, HeNe c.w. laser 3-77521
- photostimulated emission, surveying of deformed metal surface, structural distortions 3-48406
- planoidal aspherical, profile inspection on measuring microscope using contact interferometer 3-66208
- PMMA, fracture surface relief, rel. to kinetics of main crack growth 3-73054
- polycaprolactam, fracture surface relief, rel. to kinetics of main crack growth 3-73054
- roughness measurement, significance of profile length 3-42520
- turbulent boundary layer flow along flat plate with linearly increasing surface roughness, expt. 3-57765

surface diffusion

see also sorption

- butene-1 on A- and Y-zeolites, mobility, proton spin relax. (*German*) 3-64245
- electrocrystallisation, surface diffusion model 3-53322
- field emitter, adsorbate covered, current fluctuations for diffusion coeff. determ. 3-54009
- flow, irreversible thermodynamics, straight and cross-coefficients, diffusion and self diffusion 3-46460
- metal, external surface displacement during diffusional saturation (*Russian*) 3-58177
- metal, oxygen diffusion out under flash desorption 3-72271
- metal surfaces, gas adsorption diffusion and dissolution at low pressures 3-75673
- metals, gas evolution in a high vacuum, diffusion eqn. boundary conditions 3-55155
- segregation kinetics, solute atoms (*French*) 3-79569
- steel, boride layer, carbon influence (*Czech*) 3-55803
- steel, corrosion cracking stability in hot chloride solns., nitriding effect (*Russian*) 3-80335
- steel, Sn diffusion coating, effect on corrosion resist. 3-80338
- thermal transpiration eqns. 3-41085
- zeolite adsorbates, reln. between intracrystalline and self-diffusion, kinetic approach (*German*) 3-64244
- Al₂O₃, sapphire whiskers, stability in Ni matrix, 1100-1400°C 3-76357
- Al₂O₃ sapphire in Ni matrix, morphological change kinetics, 1100-1400°C 3-76358
- C, of O₂, sorption and oxidation kinetics 3-75662
- Cu, of hydrogen, bulk and surface components (*Russian*) 3-79519
- Cu, self-diffusion, facet orientation dependence, scratch levelling method (*Russian*) 3-43929
- Cu oxidation kinetics, Cu₂O layer struct., Cu⁺ diffusion growth mechanism 3-75681
- Cu/silica system, work hardening, diffusional stress relax., surface diffusion coeffs. 3-55827
- Fe, Armco, diffusion coating prod. by isothermal mass transfer in liq. metals (*Russian*) 3-80332
- Fe, of hydrogen, bulk and surface components (*Russian*) 3-79519
- NaCl crystals, H₂, D₂ diffusion and solubility, desorption obs., isotopic effects 3-72233
- Ni, of hydrogen, bulk and surface components (*Russian*) 3-79519
- Ni, pack-aluminizing, boundary conditions for diffusion 3-64964
- Si, B diffusion anisotropy under oxidizing atm. 3-50077
- Si, doping by B diffusion source glass, selective etching 3-79578
- Ta cell, of Ag, coeff. determ. by Knudsen method (*German*) 3-52754
- UO₂, stoichiometric, 1400-1700°C 3-46137
- W, surface self-diffusion, influence of adsorbed Ni layer 3-43940
- W-emitters, K-covered, noise spectral densities, field emission flicker noise theories, diffusion induced 3-76122

surface discharges

see also corona

- dielectric surface, in vacuum and SF₆, optical obs. 3-46570
- steatite ceramic, work function determ. from surface ionization and discharge triggering (*Russian*) 3-44506
- steatite ceramics, surface discharge development, nanosecond region (*Russian*) 3-46567
- BaTiO₃, surface discharge development, nanosecond region (*Russian*) 3-46567
- TiO₂ surface discharge development, nanosecond region (*Russian*) 3-46567
- W, work function determ. from surface ionization and discharge triggering (*Russian*) 3-44506

surface electron states

- absorbing media, plasmon mean free path 3-52885
- alkali halides, refl. meas., surface effects 3-58494
- anthracene crystal, excitons, low temp. refl. spectra study 3-69017
- Bloch's electrons and phonons interaction with a crystal surface, review (*French*) 3-50249
- calculation method within one-electron approx. 3-55329
- density of states in tight-binding approximation 3-55327
- diamond lattices, Heine-Jones model, (111) faces 3-52882
- dielectric-metal interface, electron and exciton states of dielec. 3-72396
- diffraction grating, sinusoidal, light absorpt. and re-emission due to surface plmons 3-74201

surface electron states continued

- electron gas, surface plasmon freq., De Gennes correlation function method, appl. 3-46776
- electron gas, two-dimens., oscillatory quasiparticle g factor, surface electron density and mag. field depend. 3-52886
- electron mean free path, spatial variation near surface 3-41251
- excitons of electron-hole type 3-52883
- field emission, one-dimensional model, tunnelling 3-79755
- field emission energy distribution from cold cathode 3-53171
- heterojunctions, present state of the theory (*Czech*) 3-52891
- heteropolar compounds, energy calcs. using Green's function method, ionicity effects 3-41248
- intercalation compounds, electronic props., ESCA (*German*) 3-72391
- interface states, Aerts model 3-55332
- Kronig-Penney model, existence conditions rel. to Tamm conditions 3-68686
- liquid metals, density distrib. rel. to surface energy and bulk compressibility 3-72261
- local surface plasmon dispersion relation, mag. field effects 3-60910
- localised states in thin layers, due to surface geometrical defects 3-75788
- magnetic surface modes in ferromag. films and spin wave reson. 3-41426
- magnetoplasmon obs. 3-52884
- metal, correlation effects in surface energy 3-58316
- metal, current noise with time-dependent impurity scatt. 3-50250
- metal, plasmon contrib. to surface energy 3-58315
- metal, response to static and moving point charges and polarisable charge distrib. 3-58312
- metal, solid, surface energy calc. from work function and electron config. data 3-64393
- metal, sum rule for electronic scatt. phase shifts 3-50256
- metal, surface-plasmon dispersion relation calc. using variational principle 3-55324
- metal, with voids, vacancies and surfaces, positron behaviour 3-46808
- metal magnetic surface levels, resonance width 3-50260
- metal surface, elec. field screening, tunnelling currents 3-50650
- metal surface energy, surface charge influence 3-55330
- metal-adsorbate system, electronic configuration, screening parameter, image potential energy 3-44129
- metal-metal surface energy, analytical model of electron density 3-55331
- metal-vacuum interface, image charge, surface plasmon contrib. 3-41246
- metallic films on metal substrate, theory of proximity effect for non-superconducting state 3-79670
- m.i.s. structures, density measurement by surface photovoltage method 3-52903
- m.i.s. structures, effect of X-rays from electron beam evaporation (*Japanese*) 3-50273
- molecular crystal, semi-infinite with 2 molecules per cell, exciton states (*Russian*) 3-72335
- m.o.s., current instability rel. to surface barrier instability 3-44157
- m.o.s., effective impurity charge density, surface treatment 3-64410
- M.O.S., structure, interface-state density determination in presence of statistical fluctuations of surface potential 3-68704
- m.o.s. device modelling by computer, surface state density peaks, Gray-Brown studies 3-50270
- m.o.s. structure, CV doping profile obs., correction for interface state errors 3-55338
- m.o.s. structure, d.c. obs. under non steady-state conditions 3-46901
- m.o.s. structure, inversion layer quantisation, exptl. verification, temp. range 25-75 K 3-55339
- m.o.s. structure, near surface impurity density distrib., CV charac. obs. 3-64408
- m.o.s. structure, with p-n junction collector, for diffused layer meas. 3-41202
- m.o.s. structures, inhomogeneity, Hg probe capacitance, cond. meas. 3-72406
- m.o.s.t., rel. to channel conductance in weak inversion 3-50274
- naphthalene crystal, luminescence spectra, surface effects, exciton states 3-44483
- organic mol. cryst., surface guest states, mag. quenching of prompt fluoresc. 3-72724
- perovskites, d-band, surface states and catalysis 3-46885
- photovoltage spectroscopy, role of surface trapping 3-55328
- plasmon, principal mode, nonlocal shift in quantizing mag. field 3-50252
- plasmon dispersion and damping to pot. barrier shape, sensitivity calc. 3-41247
- polariton, virtual excitation type, on anisotropic media 3-41163
- polaritons, study by transition radiation 3-46888
- pseudopotential method applied to surface wave functions (*French*) 3-72395
- quantization effects in semiconductor inversion and accumulation layers 3-64414
- recombination statistics through quasicontinuous spectrum 3-68688
- relativistic theory 3-41250
- semiconductor, adsorption of gases, modified Morrison-Melnick model (*Russian*) 3-68488
- semiconductor, surface galvanomag. recomb. depend. on field electrode pot. (*Russian*) 3-55287
- semiconductors, surface quantisation, review 3-50261
- semiconductors surface structure of electron-hole droplets 3-60911
- surface barrier junction, current instability 3-44157
- surface current noise, i.f., influence of surface recomb. 3-79752
- transition metal, resonant d-level position 3-41245
- transition metal, surface mag. resonance and spin reversal 3-41392
- transition metals, generalized surface states existence 3-64392
- transition metals, relaxation, force constants, interatomic distances (*French*) 3-79757
- transition metals, surface props. 3-50255
- transition metals, surface reconstruction, electronic free energy 3-79758

surface electron states continued

Ag films, (111) and (100) single crystals, photoemission anisotropy obs. 3-64763
AgCl, in different atmospheres, surface luminescence centre origin 3-80087
Al, epitaxial, surface plasmons, LEED obs. 3-50257
Al, surface plasmon dispersion, electron energy loss expts. 3-50253
Al film, surface plasmon dispersion from LEED 3-50258
Al-oxide-Ag tunnel diode, Kondo effect rel. to 3d transition metal atomic layer at interface 3-55343
Al-oxide-Al tunnel diode, Kondo effect rel. to 3d transition metal atomic layer at interface 3-55343
As₂O₃ thin films between alkali halide discs, i.r. and Raman spectra, surface interaction effects 3-64638
Be-Se, barrier heights, surface density of states, Fermi level location (*Rumanian*) 3-64395
C surface, soft X-ray incidence potential spectroscopy (*German*) 3-72763
Cd, reflectivity and surface plasma resonances 3-41538
CdS, modulation spectroscopy, spectral depend. of surface photoconductivity 3-55323
CdS_{1-x}Se_x-electrolyte interface, charging of slow surface states 3-50263
CdS(Se)(Te)-electrolyte interface, charging of slow surface states 3-50263
Cr, reflectivity and surface plasma resonances 3-41538
Cu, monolayer, electronic props., Green's function method calc. 3-50254
Cu thin films, surface plasma oscillations 3-44133
Fe, b.c.c., (110) plane, Shockley surface states 3-46886
Ga, Azbel-Kaner cyclotron resonance at far i.r. frequencies 3-58313
n-GaAs, epitaxial, recomb. processes near surface, photocond. and photomag. effect obs. 3-75756
n-GaAs, epitaxial film, surface sensitive effect at 20K, carrier depletion 3-60912
GaAs, polar (111) and (111) faces, photoelectron spectroscopy obs. 3-72394
GaAs, Schottky surface barriers, high-resolution electroreflectance meas. 3-55630
n-GaAs, with dominant impurity cond., low temp. field effect 3-68640
GaAs film on substrate, props. of surface polaritons 3-58505
GaAs thin film, Raman scatt. from surface polaritons 3-58504
GaAs-metal interface, energy structure, Schottky barrier height, Fermi level 3-60916
n-GaAs-Si₃N₄, energy spectrum of states at boundary (*Russian*) 3-50271
GaAsP m.i.s. struct., prep. by thermal oxidation, density instability 3-64789
Ge, (100) Facet, field emission obs. from electron energy distrib. 3-55728
Ge, atom free single-crystal surfaces obs. using e.p.r., adsorption methods, free radical formation (*Russian*) 3-64394
Ge, caesiated, cond. and field effect meas. 3-79753
Ge, calc. method within one-electron approx. 3-55329
Ge, energy level spectra at (111), (110) and (100) surfaces, ion neutralisation spectroscopy 3-58578
Ge, laser excitation, carrier recomb. in deep and shallow surface centres 3-41253
Ge, modulation spectroscopy, spectral depend. of surface photoconductivity 3-55323
Ge, shallow centres, recombination at power optical excitation photoconductivity, surface photovoltage 3-60899
n-Ge, surface lifetime degradation under low energy electron bombardment 3-44091
Ge, surface slow states, effective parameters from slow relax. in elec. field 3-44131
n-Ge:Ni, rel. to quasisurface cond. in strong elec. fields 3-75751
In, liq., energy gain of fast electrons interacting with surface plasmons 3-69114
InSb, real surface, fast and slow state distrib., photoelec. meas. 3-55326
InSb, surface magnetoplasmon-optic phonon modes, meas. 3-68687
KI, photoemission, electronic structure and scattering props. 3-55721
LaF₃, reflectivity and surface plasma resonances 3-41538
Li, with Na and K impurities, singly and doubly ionized states, Auger transitions 3-69122
Mg, refl., absorpt. and photoelec. meas. in vacuum u.v., surface plasmon excitation 3-44520
Mg, surface plasmon dispersion, electron energy loss expts. 3-50253
Nb, reflectivity and surface plasma resonances 3-41538
Ni, LEED intensity profiles, surface states 3-50259
Ni, surface props. 3-50255
Ni(110)-c(2×2)S surface, electron excited Auger spectrum, correlation with ion neutralization 3-44511
PbS film, physically treated, role of surface complexes in photosensitivity 3-79734
PrF₃, reflectivity and surface plasma resonances 3-41538
Rb, granular thin films, surface plasma oscill., light absorption (*French*) 3-55702
Si, atom free single-crystal surfaces obs. using e.p.r., adsorption methods, free radical formation (*Russian*) 3-64394
Si, calc. method within one-electron approx. 3-55329
Si, energy level spectra at (111), (110) and (100) surfaces, ion neutralisation spectroscopy 3-58578
Si, laser excitation, carrier recomb. in deep and shallow surface centres 3-41253
Si, modulation spectroscopy, spectral depend. of surface photoconductivity 3-55323
Si, real surface, fast and slow state distrib., photoelec. meas. 3-55326
Si, rel. to surface-sensitive photoeffects (*Russian*) 3-79739
Si, rel. to theory of surface-sensitive photoeffects (*Russian*) 3-79738
Si, surface Fermi level position at 1350-1500 K 3-58314
n-Si, surface inversion layers, g-factor determ. for cond. electrons 3-58430

surface electron states continued

n-Si, surface lifetime degradation under low energy electron bombardment 3-44091
Si, surface-state transitions using electron energy-loss spectra 3-52887
Si (111), electronic structure, Slater-Koster parameters 3-72392
Si clean surface physics, review 3-50059
Si inversion layers, g-factors of interaction electrons 3-79754
Si negative electron affinity surfaces using Rb/o dipole layer 3-44128
n-Si surface inversion layers, g-factor for electrons 3-46887
Si surface layer obs. after r.f. glow discharge, surface recombination rate meas. (*Russian*) 3-68685
Si:Ge, oxidised, density function measurement, oxide interface properties 3-60921
Si-electrolyte interface, density of localised states in amorphous Si 3-72397
Si-SiO₂ interface, energy spectrum of surface states, determ. from m.o.s. C-V characts. 3-58321
Si-SiO₂-Au, interface state occupancy, incremental conductance freq. depend. obs. 3-58323
Si-SiO₂-electrolyte system, rel. to electrorefl. spectra in strong surface elec. fields 3-50543
SiO layer on Si, cathodoluminesc. from centres responsible for radiation induced space-charge build up 3-50275
SiO₂ films, plasma oxidized dielectric strength and interface-state density 3-44154
Si(111), surface states and bonds, pot. construction 3-52888
Si(111)7 surface, folding and nonfolding electron distrib. in ion neutralisation spectroscopy and electronic superlattice 3-58579
Sn, surface impedance in strong mag. field, cond. electron scatt. 3-72379
Sr₃(PO₄)₂:Eu²⁺, radiationless recombinations in surface layers (*Russian*) 3-50612
W, directional photoemission obs. normal to (100), (110) 3-55725
Y₂O₃:Eu³⁺, Tb³⁺, radiationless recombinations in surface layers (*Russian*) 3-50612
Zn-Se, barrier heights and surface state density (*Rumanian*) 3-64395
ZnO, modulated photoconductivity measurements 3-55325
ZnO, modulation spectroscopy, spectral depend. of surface photoconductivity 3-55323
ZnO (0001) surfaces, electronic and structural characteristics 3-79756
ZnO(0001) surfaces, negative photoconductivity obs., correlation with LEED expts. 3-68689

surface energy
see also surface electron states
alkyl phenol polyethylene glycol ether, friction props., effect of surface-active agents 3-73056
bimetallic interface, adhesion, binding energy vs. separation, overlap effects 3-55138
contact angle method for substrate free energy determ. 3-46750
electrolyte thin film, Van der Waals forces, effect of wall pressure 3-61258
glass, powder, kinetics of wetting, surface energy and surface tension, modification by siloxanes (*German*) 3-53279
E-glass, surface free energy of wetting by vapours 3-55146
glass/iron substrate systems, interfacial reactions and enhanced wetting 3-55880
graphite, desorption of surface oxide as CO and CO₂, activation energies 3-64247
graphite, work of fracture and fracture toughness 3-55926
liquid, surface excess internal energy determ. by integration of Kirkwood-Buff-Fowler eqns. 3-68482
liquid metals, relation to bulk compressibility and thickness of electron density distrib. 3-72261
liquid/solid and solid/solid systems, interfacial and adhesion energy meas. by SEM 3-75659
lying-drop method, installation for meas., temp. dep. for Cu, Ti, Pt, Sn and Mg 3-73687
metal, correlation effects 3-58316
metal, plasmon contrib. 3-58315
metal, solid, calc. from work function and electron config. data 3-64393
metal, surface charge influence 3-55330
metal electrodes, surface thermodynamics, electrocapillary phenomena, surface stress rel. to charge density 3-55960
metal-metal interface, analytical model of electron density 3-55331
metal/metal interface, differential modulus effects on mech. behaviour 3-40921
oxides, sputtering, surface binding energy 3-69119
PMMA, friction props., effect of surface-active agents 3-73056
polymer crystallisation, surface energy rel. to chain flexibility (*Russian*) 3-79243
polymer fracture surface energy, dependence on mol. wt., entanglement model 3-63595
refractory, thermal shock damage resistance depend. 3-80404
response theory based formalism 3-60834
rubber, wettability and stability in aqueous solns. (*Russian*) 3-41813
solid, free energy components from wetting data 3-68480
water film on quartz surface, isotherm of separating pressure 3-46751
C and carbides, wetting by Cu alloys, model approach 3-41084
C fibre, strength, fracture behaviour (*German*) 3-73041
Fe, cast, liq., Mg and Ce additions effect 3-69221
Fe, solid and molten, surface free energy, temp. dependence, 0 to 2000 K (*German*) 3-72823
Fe-Si alloy, surface free energy anisotropy, thermal etching obs. 3-64845
Fe-Si alloys, effectiveness in brittle fracture (*Russian*) 3-80272
LiF, anisotropy, crystal growth from drop of melt 3-76136
NaCl, anisotropy, crystal growth from drop of melt 3-76136
NaF, anisotropy, crystal growth from drop of melt 3-76136
Pb superconducting thin foil, interphase parameter, shadow electron microscopy 3-68719
Si, rel. to orientation depend. of selective epitaxial growth 3-44546
UO₂, stoichiometric, temp. depend. 3-46137

surface films see films

surface ionisation

see also *thermionic emission; work function*

- halogen atoms, hyperthermal, negative surface ionis. 3-78475
inhomogeneous positive ion emitter with uncompensated patch fields, surface ionisation 3-55717
metal, solid surface photoemission, laser multiphoton phenomena 3-76121
source, alkali ions, high current density, design, properties (*German*) 3-62278
statite ceramic, work function determ. from surface ionization and discharge triggering (*Russian*) 3-44506
Al ionised by Ir, ion source for implantation doping 3-41599
In ionisation by Ir, ion source for implantation doping 3-41599
Ni(100), (110) surface, reson. tunnelling, Auger and autoionization processes with He⁺(2s), He²⁺ ions 3-47339
W, work function determ. from surface ionization and discharge triggering (*Russian*) 3-44506

surface measurement

- Auger and energy loss spectroscopy, surface electron structure 3-48570
colloidal crystalline materials, surface area meas. by N₂ and Kr adsorption 3-48343
contact profilometer calibration, roughness standard production and evaluation (*Slovak*) 3-66128
displacement meas., holographic interferometry methods 3-51532
double beam interferometry, electrochem. studies, review 3-66236
droplet interferometry, for smooth surfaces 3-51620
dynamics of surface processes, field ion microscopy, three colour field ion images 3-73900
electric contacts, laser interference fringe microscopy 3-56671
ellipsometry, electrochem. studies, surfaces and surface films, review 3-66197
ellipsometry, principles of technique, application to electrochem. studies, review 3-66196
fibre, porosity studies, electron microscopic methods, transmission and stereoscaning (*Polish*) 3-73902
field ion microscopy computer modelling of atomic positions on surface of acicular b.c.c. crystals 3-79203
flatness, non-optical surfaces, oblique incidence interferometry, transmission diffraction gratings, techniques 3-66234
holographic surface mapping system, with computer analysis of video signals 3-66241
human articular surfaces, contour examination, profile recorder, stereomicroscopy, replication 3-59409
interdisciplinary nature 3-48356
interferometric grazing incidence examination of non-optical surfaces, report 3-56674
ion surface interactions, 30 keV instrument 3-48587
LEED and RHEED techniques for structure analysis 3-50057
light-sectioning attachment, shop measuring microscope BK 70 × 50, VEB Carl Zeiss JENA, surface and thickness meas. 3-51585
liquid/fluid dynamic adhesion tension meas. 3-48344
low energy in backscattering technique 3-48586
metals, mass spectrometric determination of desorbed ions 3-48558
nondestructive optical contour mapping method 3-51516
optical interference method for solid surface roughness inspection 3-62120
reactor, catalytic vacuum-insulated for surface study 3-42667
roughness analysis, interference microscope method (*German*) 3-66140
roughness measurement, significance of profile length 3-42520
stainless steel surfaces, analysis by secondary ion mass spectroscopy 3-48675
thermionic emitter, work function distribution plotting, technique, apparatus 3-73811
u.h. vac. reflection electron diffraction system 3-50058
vertical section geometry meas. technique, by electron microscope 3-54013
Hg-cyclohexane interfacial tensions from shape of pendant Hg drops, adsorption meas. 3-45420
Si, mechanical props. rel. to planar technology 3-69179

surface phenomena

- see also *acoustic surface waves; capillarity; crystal surface and interface vibrations; emissivity; interface phenomena; liquid surface waves; sorption; surface chemistry; surface diffusion; surface discharges; surface energy; surface ionisation; surface potential; surface tension; surface treatment*
acoustic surface-wave scattering in homogeneous three-quarter space 3-41074
adhesion of disperse particles in electrolyte solutions 3-65027
Atlantic Ocean, isotope formation of surface waters, distrib. of salinity and ¹⁸O (*Russian*) 3-47694
atom-atomic oscillator collisions, unitary transition probabilities 3-74827
atomic scattering, many-phonon scattering, angular distrib. 3-55712
atomic scattering calc., gas-solid interaction model 3-55139
ceramic, composition analysis by scattering of low energy noble gas ions 3-40041
ceramic nuclear materials, applic. of surface anal. to porosity study (*Czech*) 3-61237
differential thermal analysis, attachment for heating microscope, surface observations, specimen shrinkage, 1600 °C 3-53856
dynamical image interactions of charged particles with surface, classical theory 3-75554
dynamics of surface processes, field ion microscopy, three colour field ion images 3-73900
elastic surface wave scattering from point mass defects in solid 3-58173
elastic waves, guided, dispersion relations, integral-equation approach 3-68478
electric field arising from three-dimens. defects 3-50056
ellipsometer, modulated, for study of surface dynamics 3-53885
ellipsometry, electrochem. studies, surfaces and surface films, review 3-66197
ferromagnet-semiconductor structures, e.m. surface wave spectrum, static external electric fields, stability 3-50437
ferromagnetic resonance equations, electron and magnon surface scattering 3-41425
frictionally excited thermoelastic instabilities, role of thermally insulating films 3-55022

surface phenomena continued

- glass, composition analysis by scattering of low energy noble gas ions 3-40041
gradient-sensitive liquids, non-linear theory 3-55137
h.f. vibrations of piezoelectric crystal surfaces plated with electrodes 3-41082
inelastic light scattering, semiclassical study, cross section rel. to dielectric constant 3-50536
ion impact, inelastic energy loss dependence on atomic number 3-80133
ion scattering by atomic chains on single crystal surfaces 3-80131
ion scattering from solids, experimental technique 3-69118
ionic crystals, microhardness, humidity effects 3-58174
laser damage statistics, identification of intrinsic breakdown processes 3-61020
liquid, Newtonian and non-Newtonian, rotational flow, interaction with stationary surface 3-40715
magnet surface props., scaling relations for crit. exponents 3-46943
magnetisation, three-dimensional Ising model, low-temp. series expansion 3-52943
metal, cubic, binding energies 3-60681
metal, He beam scattering, Debye-Waller factor applic. 3-69113
metal powder, milling, specific surface, grain size distrib. rel. to surface active additive 3-80390
metal surfaces, impact boundary instability (*Russian*) 3-64086
molten fuel-coolant interaction, reduction of gas-expansion work, cold liquid, heat flow to liquid surfaces 3-71177
moving steps interaction with dispersed particles 3-50055
nonferrous alloys, blackness, temp. depend., machining effect 3-79496
perfectly cond. surface, interference of transient radiation 3-42962
permeable surface, frictional drag, heat transfer, effect of free convection (*Russian*) 3-57746
piezoelectric cryst. surface, nonlinear interaction of u.s. waves with opposite propag. directions (*French*) 3-41078
piezoelectric crystal, harmonic generation of surface waves (*French*) 3-41079
plane layer, dynamic coupled thermoelastic problem, pressure-time, temp.-time functions, surface appl. (*Russian*) 3-70582
polyethylene terephthalate electret, surface charge obs. 3-68917
Polypropylene film, effects of corona discharge 3-60651
prosthesis, bioceramic vascular, surface props. rel. to blood compatibility etc. 3-64969
quartz, acoustic surface waves, second harmonic generation and parametric amplification, nonlinear, theory and obs. 3-70196
quartz glass, fused, hydrolytic surface defects and high-strength state 3-72274
quartz substrate, gas desorption induced by surface acoustic waves 3-50079
quartz rod, attenuation of e.m. wave in dissipative medium 3-66747
semi-infinite solid, e.m. induction, impulsive motion TEM wave emission from surface 3-40199
semiconductor surface carrier waves, transverse mag. field effect 3-55321
SH-wave source, elastic half-space, non-homogeneous surface layer 3-44827
shadowing, acoustic wave loss at randomly rough surfaces, measurements 3-77311
silicate glasses, surface crystallization, morphology and kinetics 3-75477
solid, during fracture and deformation in adsorption-active media 3-50084
solid fuel powder, linear nonstationary effects, instability, reaction kinetics (*Russian*) 3-47545
solid surface thermodynamics, symbols and nomenclature 3-52711
sphere, surface waves, Legendre functions, Hilbert transform 3-42055
spheroid, surface charge density, boundary value problem, Green's function expansion, spherical coords., numerical soln. 3-70774
spin-wave resonance linewidth, surface spin wave mode identification 3-79916
transparent dielectric, surface damage during short light pulse irradiation 3-48937
u.s. wave, meas. of variations in velocity and absorpt. by buckling method (*French*) 3-39864
u.s. waves, optical probing of nonlinear elastic effects 3-39902
wave propagation, biaxially stressed elastic media, dispersion equations 3-42819
wave propagation, long nonlinear, on free surface 3-54124
X-ray diffr. peak shifts, surface relax. effects, kinematic theory 3-54906
Al, spin relaxation of surface conduction electrons 3-72522
Al, temp. depend. of surface oxide thickness 3-53260
Al electron scattering, inelastic, angular distribution, energy dependence, experiment and theory 3-49810
Au, effective surface Debye-Waller temp., mean-square displacements, LEED obs. 3-58110
Bi, surface impedance at large a.c. e.m. field amplitudes 3-46884
C black, thermal self-ignition, nonuniform surface, critical temp. computer calc., reaction kinetics (*Russian*) 3-50830
CdS, single crystal platelets, photoluminescence, electron bombardment, photoexcitation and gas adsorption effects 3-41573
Co metal, surface state of ferromagnet from Mossbauer spectra 3-72551
Fe liquid alloy, H₂ and N₂ absorption and effusion, material exchange processes (*German*) 3-76150
Gd₂(MoO₄)₃, acoustic wave velocity, Z-cut ferroelastic-ferroelectric polarisation method 3-50064
Ge, conductivity, slow relaxation of charge 3-55320
³He, nucl. polarization by optical pumping, relax. time meas. at surfaces (*French*) 3-46186
In, r.f. surface impedance, propag. helicon waves 3-79619
KCl, V_k centres, self-trapping energy calcs. 3-40918
LiF (001) cleavage plane, atomic O scattering process by fast adsorption-desorption 3-41600
LiNbO₃ acoustic surface wave generation, Al interdigital transducers on piezoelectric substrate, optical spectroscopy 3-50065
LiNbO₃ acoustic surface waves, second harmonic generation and parametric amplification, nonlinear, theory and obs. 3-70196

surface phenomena continued

- Mo (100) crystal face, molecular orbital excitation (*French*) 3-79563
 NaCl, V_k centres, self-trapping energy calcs. 3-40918
 Nb monocrystals, orientation depend. of blister form. by He⁺ implantation 3-72111
 Si, deformed crystals, compressive strain, dislocation structure, surface and bulk layers (*Russian*) 3-40922
 Si covered with Au, low temp. migration obs. by means of e.s.c.a. 3-50028
 SiC, etching by Na₂O₂, SiO₂ film, O₂ diffusion 3-68508
 TiO₂, thin film sandwich, depth composition profile 3-40041
 YIG, partially metallised plate, magnetostatic surface waves 3-64509
 ZnS phosphors, surface energy losses, electron and hole diffusion (*Russian*) 3-44462

surface potential

- colloid, coagulation mechanism 3-61229
 dielectric thin film, determ. by charged particle bombardment, secondary emission 3-69120
 free molecular flow, impulsive tridimensional interaction model with solid surface 3-57802
 graphite, inert gas adsorption, potential energies calc. 3-52751
 high ohmic devices, meas. of potential distrib. using electron gun (*German*) 3-50251
 ice-sodium polystyrene sulphate soln. interface, transient elec. pot. 3-41255
 inhomogeneous positive ion emitter with uncompensated patch fields, surface ionisation 3-55717
 insulating surface, sputtered ion deflection by surface charges 3-61093
 lyophobic sol particles, Stern model, stability 3-61230
 metal, monovalent, work function, and surface double layer potentials, from network model 3-41252
 metal-adsorbate system, electronic configuration, screening parameter, image potential energy 3-44129
 molecular beams interaction with solid surfaces 3-57801
 solid in vacuum, rel. to effect of elastic deformation on the work function 3-47564
 transition metals, relaxation, force constants, interatomic distances (*French*) 3-79757
 X-ray photoelectron spectroscopy, binding energy meas., surface charge errors, external standards 3-72777
 AgI particles, adsorption, dielectric, electrokinetic determ. 3-65028
 CdS crystallographic polarity, etching rate, single crystals bonding 3-41249
 Si(111), surface states and bonds, pot. construction 3-52888

surface structure

- see also interface structure; surface texture
 alkali halide substrate surface microrief change induced by radiation damage causing mechanical instabilities in thin films 3-52770
 alloy, binary, surface long range ordering 3-46747
 amorphous solid, growth of topography during sputtering 3-79548
 ceramic, ion scatt., Auger effect, secondary ion mass anal. 3-80418
 ceramic surface diagnostics, laser specular reflectometer 3-48559
 defect obs. with interferential microscopy, crystal topography at screw dislocation (*Rumanian*) 3-50054
 defects, three-dimens., rel. to elec. field distortion 3-50056
 dihedral angles meas. by SEM 3-60657
 ESCA, X-ray photoelectron spectra, surface sensitivity, angular dependence 3-44522
 FEM tip, microcrater form. on microparticle bombard. at limited field emission currents 3-44523
 glass, 0.1 μ m periodic surface struct. prod. by laser interference on surface photoresists 3-59901
 glass, Ag-containing, cryst. growth under electron bombardment 3-64065
 impurity obs., noble gas ion backscatt. technique 3-60837
 Incoloy 901, glaze oxide layers, structure and mechanism of formation during high temp. wear 3-64254
 ion bombarded surface topography, prediction using Frank's cryst. dissolution theory 3-58575
 Kapron monofilaments, breakdown surface, microdeformation, cracks, scanning electron microscope studies (*Russian*) 3-47480
 LEED and RHEED techniques 3-50057
 LEED as analytical tool, review 3-50060
 LEED perturbation theories, tau and t-matrix approaches 3-55129
 LEED studies, theory and technique 3-46746
 liquid-vapour density transition, BGY eqn. 3-50072
 mica, cleaved, depth analysis by LEED, Auger obs. 3-60830
 mica, electrical relief of matching cleavage structures 3-52889
 microroughness of metal surface determ. using adsorbed layer reflectance 3-47334
 moving steps interaction with dispersed particles 3-50055
 Nimonic 75, C263 and 108, glaze oxide layers, structure and mechanism of formation during high temp. wear 3-64254
 phase transformations, superstruct. disappearance 3-79550
 point mass defect scattering of elastic surface waves 3-58173
 polyethylene single cryst., amorphous surface layers thickness 3-58168
 polytetrafluoroethylene, and Na-treated polytetrafluoroethylene, wettability, roughness and anisotropy effects 3-58739
 porous substances, replica technique for electron microscopy 3-68142
 reconstruction, soft-mode theory 3-41065
 shear stress effect, Hertzian contact, photoelasticity meas. 3-76225
 steel, low C austenitic, high temp. creep deformation (*Japanese*) 3-76168
 Ag, thin film stoichiometry, adsorption of O₂, kinetics, sticking probabilities, slow and fast adsorption 3-46755
 Al, changes on chem. polishing, electron microscope obs. 3-43946
 Al, LEED, t-matrix perturbation method analysis 3-50052
 Al (001) surface, LEED perturbation theories, tau and t-matrix approaches 3-55129
 AlGaAs, epitaxial layers grown from liq. phase, surface irregularities due to spiral growth 3-58185
 Au, Auger spectra of clean polycrystal 3-72255
 Au (100) surface, unit lattices derived from LEED and RHEED, comments 3-43923
 Au(100), LEED investigation 3-72257

surface structure continued

- Au (100) surface, unit lattices derived from LEED and RHEED, reply to comments 3-43924
 β -B, rhombohedral, LEED obs. of (111) 3-64232
 BaTiO₃-BiO₃:La composite ceramic, surface barrier layer, a.c. characts. 3-79696
 CaF₂, electrical relief of matching cleavage structures 3-52889
 CdS crystallographic polarity, potential, etching rate single crystals, bonding 3-41249
 CdS thin films surface morphology, substrate effects (*Korean*) 3-72356
 Cu, high temp. creep deformation (*Japanese*) 3-76168
 Cu, indentations made by cone indenters on cube face, apex-angles influences (*Japanese*) 3-58169
 Cu films (111) grown in ultrahigh vacuum 3-41108
 Cu oxidation kinetics and internal irregular structure of Cu₂O layer 3-75681
 Cu-Ni, alloy Auger electron spectroscopy, surface comp. changes due to Ar ion bombardment 3-44514
 Fe crystal, scratch deformation, electron microscope (*Japanese*) 3-72871
 Fe-Si alloys Auger spectroscopy, surface impurity concentrations, ionisation cross-sections, estimation 3-43925
 α -Fe₂O₃, hematite, interpretation of etch figures (*French*) 3-64252
 GaAs, after polishing with perhydrol-alkaline mixture (*Polish*) 3-76138
 GaAs, epitaxial layers grown from vapour, surface struct. rel. to condition 3-58592
 GaP, reflection X-ray topography, disloc. contrast obs. 3-41070
 GaP (111), Auger, mass spectra and LEED obs., C atom contamination 3-75654
 GaP (111) faces, low energy electron diffr. patterns, rotation and translation symmetry (*French*) 3-79551
 GdGa garnet, epitaxial films, substrate defect effects 3-58405
 Ge, obs. of (111) surface by LEED during O₂ adsorption 3-50078
 Ge/Cs/O (100) surface, struct. analysis rel. to photoemissive props. 3-69134
 Ge-Se glasses, electron microscopy investigation 3-41064
 InGaAsP, epitaxial layers grown from liq. phase, surface irregularities due to spiral growth 3-58185
 InP, reflection X-ray topography, disloc. contrast obs. 3-41070
 Ir, LEED and Auger studies of CO and O₂ adsorption on (110) surfaces 3-60831
 KBr, u.v. irradi., electron microscope and opt. obs. (*Russian*) 3-43921
 (K₂O-P₂O₅)_{1-x}(WO₃)_{1-x}, glass, microphase separation, electron microscope obs. of surface replicas 3-72007
 LiF, electrical relief of matching cleavage structures 3-52889
 MgO, electrical relief of matching cleavage structures 3-52889
 Mo, anisotropic surface struct. change during directional transport processes 3-55130
 NaCl, electrical relief of matching cleavage structures 3-52889
 Nb, (100) surface, LEED investigation of reaction with O and N 3-55124
 Nb alloys, surface blistering by He ions, effect in fusion reactor operation 3-60289
 Ni, high temp. creep deformation (*Japanese*) 3-76168
 Ni, Pd, Au coatings, gas adsorpt. obs., noble gas ion backscatt. technique 3-60837
 Ni (001), chemisorption bonding of c(2x2) chalcogen overlayers, LEED study 3-60829
 Ni alloys, glaze oxide layers, structure and mechanism of formation during wear at high temp. 3-64254
 NiO surface, adsorption theory, structural and chemical defects (*Russian*) 3-79556
 Si, gettering action of phosphosilicate glasses and ion implementation damage layers, MeV ⁴He⁺ backscatt. obs. 3-41644
 Si, microdeform. of surface layers in brittle transition temp. region, surface-volume dislocation interactions (*Russian*) 3-79411
 Si, pre- and backspattering as cleaning processes, surface structure and chem. 3-55161
 Si clean surface physics, review 3-50059
 Si homoepitaxy with ion sputtering, growth mechanism 3-44550
 Si surfaces, Auger electron spectroscopy 3-68472
 Si thin films, homoepitaxial, defects, electron microscopy, formation processes 3-52765
 α -SiC, 6H and 15R polytypes, intensities of X-ray refl. from basal plane 3-55131
 β -SiC, hexagonal pillar shape, surface polarities 3-43922
 Tb thin film, effect on photoelectron spectrum 3-61106
 V alloys, surface blistering by He ions, effect in fusion reactor operation 3-60289
 V-20% Ti alloys, surface blistering by He ions, effect in fusion reactor operation 3-60289
 W, anisotropic surface struct. change during directional transport processes 3-55130
 W, electron spectroscopy (*Hungarian*) 3-72256
 W, surface atomic struct., effects of high hydrostatic press. 3-41069
 W/O₂ system, RHEED intensities, kinematic anal. 3-55126
 ZnO, epitaxial growth on sapphire and spinel, vapour phase deposition 3-80164
 ZnO (0001) faces, electronic properties 3-79756
 ZnO(0001), LEED experiments, correlation with electronic properties 3-68689

surface tension

- alkane derivative polymers, homologous series of liquids 3-50070
 bubbles, equilibrium shapes and quasistatic formation, at submerged orifice 3-64237
 calcium caproate aqueous solns., physical props. meas. 3-58769
 capillary rise, correction terms for calc. 3-50068
 critical point fluid, surface tension and interfacial density profile, coexisting phases 3-75611
 discrete element structural theory and discrete element idealisation of an incompressible fluid, surface tension and sloshing effects 3-62444
 dislocations, heterogeneous nucleation, influence of surface tension 3-54971
 droplets, in shock tube study of condensation kinetics 3-79478
 fluid layer, free boundaries, thermal convection, surface tension instability 3-79555

surface tension continued

- glass, powder, kinetics of wetting, surface energy and surface tension, modification by siloxanes (*German*) 3-53279
- interfacial convection induced by surface tension, rel. to mass transfer 3-78940
- Ising model, two dimensional, transfer matrix for pure phase, pair correlations, two coexisting phases 3-60946
- jets, liquid, cylindrical, capillary breakup, numerical analysis 3-75278
- Lennard-Jones fluid, stat. mech. and quasithermodynamic calcs. 3-60790
- Lifshitz theory of van der Waals forces, diffuse area of fluid interface, surface tension calc. 3-75656
- liquid-vapour density transition, BGY eqn. 3-50072
- liquid/fluid dynamic adhesion tension meas. 3-48344
- liquid/solid system, contact angle interpretations, wetting 3-68479
- metal, superplasticity and surface tension at phase transition, fluctuation model 3-49924
- microemulsions, spontaneous formation and interfacial instability 3-58768
- molecular theory, integration of Kirkwood-Buff-Fowler eqns. 3-68482
- noble and transition metals, interionic pair potentials 3-43746
- nonassociated liquids, surface tension, diamagnetism, dispersion potentials, effective electron numbers (*German*) 3-72262
- opal glass, phase separated, opacity improvement by alterations of interfacial tension 3-76258
- oxide-amine systems, interface adsorption densities in flotation 3-75663
- packed bed, liquid hold-up rel. to liquid distribution 3-63791
- pendent liquid drops stability in narrow gap 3-57868
- polyethylene, environmental stress cracking in presence of liquids 3-67885
- polymer solution, applic. of Prigogine-Marechal theory 3-53346
- refrigerant, liquid on solid, contact angles, optical meas. method 3-70273
- relationship with dielectric constant, Lifshitz macroscopic forces theory 3-43926
- rotating fluid layer, convection, buoyancy-surface tension instability 3-71790
- semiconductors, surface structure of electron-hole droplets, surface tension calc. for electron-hole liquid 3-60911
- solids, low-energy, calc. 3-68481
- surface behaviour of gradient-sensitive liquids, non-linear theory 3-55137
- thermocapillary flow influence on heat transfer in film condensation 3-43567
- thin liquid films creeping laminar flow under influence of surface tension gradients 3-57762
- two-phase meniscus progression during displacement of immiscible fluids (*French*) 3-79552
- two-phase mixtures, surface tension contribs. to viscosity 3-72219
- water, effect on thermal expansion meas. in capillaries 3-61227
- water, role in acoustic cavitation inception 3-71791
- water/oil interface, hydrostatic press. depend. (*French*) 3-79553
- zero, transitory states, multilayer model (*French*) 3-75657
- Ag-Cu alloy, liq., meas. by sessile drop method (*French*) 3-79554
- Cu-Sn liquid alloy, density, temp. and comp. depend. (*Japanese*) 3-72820
- Fe solid surface, wetted by oxide melt, elastic deformation obs. 3-68483
- Fe-C-S, liquid, containing C and S, surface tension meas., 1550C, max. bubble pressure method (*German*) 3-72883
- He, thermophysical properties, HEPROP computer program 3-50042
- ³He-⁴He liq. mixture, lamination boundary surface tension, surface wave meas. 3-52742
- ⁴He, saturated vapour and liquid, thermophysical properties, 4 to 3000 R, pressures up to 15000 PSIA 3-50043
- Hg, liquid, surface tension determ., drop-weight technique application 3-43928
- K, up to 850°C, maximum bubble pressure meas. apparatus 3-70272
- Li-LiCl, interfacial tension up to 850°C, maximum bubble pressure meas. apparatus 3-70272
- Pb, liq., determ. by capillary rise method (*Japanese*) 3-58176
- Sn, liq., determ. by capillary rise method (*Japanese*) 3-58176
- Sn, liquid, sessile drop method, effect of graphite (*Japanese*) 3-53828

surface tension measurement

- bubble maximum pressure meas. apparatus, appl. to K surface and Li-LiCl interface 3-70272
- lipid spherical bilayers, surface tension and contact angle meas. method 3-42693
- optical method, refrigerant, liquid on solid, contact angles 3-70273
- refractory liquids, opaque, wetting angle, capillary rise 3-72260
- removal of ring method, 60 mm diameter nichrome wire ring 3-51524
- subsurface wetting, bubble method, instrument incorporating stroboscope (*Russian*) 3-50071
- Sn, liquid, sessile drop method, effect of graphite (*Japanese*) 3-53828

surface texture

- alumina with MgO, electrical props. 3-41797
- austenite planes, orientation in surface layer of ferric polycrystalline specimen (*Spanish*) 3-72844
- binary alloys, surface struct. due to plane shock wave (*Russian*) 3-80306
- damage-induced surface topography during particle bombardment 3-80134
- glass, strength rel. to microstructure, roughness 3-44674
- graphite, Auger electron emission micrographic study of cleavage surface 3-55705
- Kapton monofilaments, breakdown surface, microdeformation, cracks, scanning electron microscope studies (*Russian*) 3-47480
- magnetic films, substrate roughness effect on transverse susceptibility 3-79880
- mathematical approach, heterogeneous systems 3-64768
- measurement by low-angle laser light scattering 3-40293

surface texture continued

- metal, surface oriented struct. form. under laser beam action 3-41786
- microscopic rough surface, scattering effect on light (*German*) 3-59842
- optical interference method for solid surface roughness inspection 3-62120
- photoemission electron microscopy, surface treatment effects on image brightness and contrast (*German*) 3-50061
- rare earth sesquioxides, surface steps (*French*) 3-60832
- ring wave production in metallic surfaces in laser radiation zone (*Russian*) 3-69111
- roughness, electron diffraction intensity distrib., modification function 3-55125
- roughness generating mechanism, forming process of single asperity 3-43825
- sand grains, depositional histories, surface texture examination 3-69517
- semiconductors, sputtering using Ar ions, surface topography 3-61085
- sputtering, surface damage and topography changes produced during sputtering 3-61088
- steel, extra mild, recrystallisation, Al passivation (*French*) 3-76173
- steel, heat treated to different strength levels, adsorption relief of failure (*Russian*) 3-58650
- steel, persistence of asperities in indentation experiments 3-72125
- steel, phosphated, hydrostatic extrusion, nonuniformity of deform., lubricating medium influence (*Russian*) 3-69326
- steel, spring, fatigue phenomena in large plate specimen after shot-peening treatment (*Japanese*) 3-41779
- steel, stainless, Type 316, helium re-emission and surface deform. during -170 to 700°C implantation 3-46651
- steel, transformer type, thermomag. treatment effectiveness depend. (*Russian*) 3-68809
- steel components, crack propag. resist., surface layer structural state influence (*Russian*) 3-58644
- Ag thin films, effect of residual gas during deposition 3-80001
- Al, etch pit shapes rel. to recrystn., orientation relationships (*French*) 3-44584
- Al, single crystals, scratch-deformed surface layer, electron microscope observation 3-61131
- Al crystal, diamond scratch deformation, cell structure (*Japanese*) 3-72867
- Al₂O₃, environment effect on surface damage penetration, SEM obs. 3-80420
- Al₂O₃, sapphire, hardness and damage resist. depend. on surface finishing 3-69342
- Al₂O₃ ceramic with compressive surface stresses, surface damage effect on strengthening 3-44653
- Be, tensile behaviour under hydrostatic pressure, effect of surface conditions, ductility 3-61182
- Fe, cast, etch pits, effect of dislocations and nonmetallic inclusions, topography, FEM studies 3-50695
- Fe, rolled, annealed twins, orientation, texture angle calc., 3-50694
- Fe-X-O alloy, scale struct., (X=Ni, Cr, Mo) (*German*) 3-76195
- GaP, liquid phase epitaxy, growth characs. and surface morphology 3-41685
- LiNbO₃, surface microtopography arising from 35° domain walls 3-53068
- MgO, defect formation on surface during thermal decomposition, obs. (*French*) 3-72971
- MgO single crystals, TEM obs. of surface deform. 3-72962
- MgO-Al₂O₃ solid state reaction, interface phenomena and spinel orientation 3-68517
- Mo alloy steel, surface layer struct. rel. to recrystallization, X-ray analysis 3-76175
- Ni, etch pit shapes rel. to recrystn., orientation relationships (*French*) 3-44584
- Si, epitaxially grown from SiH₄-H₂ and SiH₄-He mixtures, comparison 3-41626
- Si, wafers, surface defect detection, scattered light meas., He-Ne laser 3-41663
- SiC, surface film etching, chemical and discharge treatment (*Russian*) 3-68509
- Zr and Zircaloy-2, oxidized, wear in water, characteriz. 3-57573

surface treatment

- see also etching; polishing
- cleaning, argon ion gun, low energy, operation 3-66311
- cleaning, ion bombardment, ion gun, surface cleaning in LEED camera, description 3-77605
- n-GaAs, chemical decoration of regions of different electron conc. (*Russian*) 3-58181
- glass, heating, strengthening, stability, SO₂ effect 3-68165
- glass, polished optical, exoelectron emission, rel. to surface structure and stress 3-72784
- glow discharge, sputter cleaning parameters and cathode surface contaminants 3-44507
- glow-discharge cleaning, specimen preparation 3-48562
- metal, external surface displacement during diffusional saturation (*Russian*) 3-58177
- monochromator, cleaning by action of O atoms 3-39909
- m.o.s., effective impurity charge density in surface states 3-64410
- optical material, finishing, applic. of ion bombardment of insulators 3-72775
- photoemission electron microscope specimen, effects on image brightness and contrast (*German*) 3-50061
- silica-reinforced composites, surface ablation 3-80438
- steel, effect on adhesive joints 3-64963
- steel, endurance at normal and low temps., effect of surface finish and surface treatment method 3-44634
- steel components, crack propag. resist., surface layer structural state influence (*Russian*) 3-58644
- Substrate cleaning for integrated optical waveguides 3-79576
- Al₂O₃, effect of surface treatment on the grinding ability of abrasive grains (*Japanese*) 3-80431
- Al₂O₃, environment effect on surface damage penetration, SEM obs. 3-80420
- As₂Se₃, vitreous, influence of surface conditions on photoconductivity 3-79731

surface treatment continued

- Cu, clean surface production by heating, ion bombardment and annealing, photoelectric meas. 3-41616
 Cu, diffusion bonding, surface contamination effect 3-80399
 Cu, effect on Kapitza resistance between Cu and ⁴He, 1.2 to 2.0 K 3-75641
 Cu mirror surfaces, for high power i.r. lasers, polishing and coating techniques 3-62153
 GaAs, surface luminescence at laser excitation, surface treatment and cleavage effects 3-44484
 GaAs-electrolyte interface, non-equilibrium depletion, surface-barrier photoeffect, effect of doping and surface treatment (Russian) 3-73144
 Mo(110) surface, cleaning procedures, low press. high temp. methods (Japanese) 3-50083
 NaCl, (001) face, factors responsible for complex form. of Au decorating particles 3-75671
 Nb, carburizing in glow discharge plasma 3-76217
 Ni sheet and (111), (100) surfaces, effectiveness of cleaning techniques using auger electron spectroscopy 3-60841
 Si, dislocation-free crystals, distribution of point defects Cu decoration, X-ray topography, etching 3-41650
 Si, exoelectron emission, temp. effects, extended and abraded mat., activation energy determ. (Russian) 3-53170
 Si, m.o.s. structure charge density, defects (Slovak) 3-46894
 Si, pre- and backspitting as cleaning processes, surface structure and chem. 3-55161
 Si clean surface physics, review 3-50059
 Si surface, nitridation, LEED and Auger electron spectroscopy 3-43944
 Si surface, passivation mechanism, e.s.r. obs. 3-43943
 SiO₂ films on Si, ion bombardment effect on electrical props. 3-41268
 V₂O₅, thermal and low energy electron bombardment induced O₂ loss, transition into V₆O₁₃ 3-41099
 W, carburizing in glow discharge plasma 3-76217
 W, preparation of atomically clean surfaces, Auger electron spectroscopy 3-76116

surface vibrations see *crystal surface and interface vibrations*

surface wave acoustic devices see *acoustic surface wave devices*

surface waves, liquid see *liquid surface waves*

surgery

- mass spectrometer usage 3-45600
 u.s. welding and cutting, biological tissue 3-66405

surgical operations see *surgery*

surveying

- see also *geophysical equipment*
 aeromagnetic surveying, oceanic crust, structural inhomogeneities 3-69723
 Automatic Geodetic Level, Ni 002, VEB Carl Zeiss JENA 3-53547
 Automatic Precision Zenith Plummet, PZL 100, VEB Carl Zeiss JENA 3-53548
 electronic distance meas. using gravity cable (German) 3-44955
 geophysical prospecting in Gulf of Mexico, three dimensional model giving geological composition 3-65145
 gravity surveying, for ground-water study in Great Basin 3-59167
 magnetic surveying, solution of the inverse two-dimensional problem for small unknown susceptibility 3-65236
 marine exploration, computer control systems for real time data output 3-65494
 Slovakia, Danube Plane, refraction determ. (German) 3-58852
 terrestrial photogrammetric plotting, comparison of Technocart and Stereoaograph 3-65507

susceptance see *electrical impedance*

susceptibility, magnetic see *magnetic susceptibility*

suspensions

- air pollutant automatic sampling and anal. 3-53783
 air with Al₂O₃, heat transfer from a reflected shock wave (Russian) 3-52470
 Baltic Sea, determination of suspended inorganic substance, attenuation spectral method (German) 3-76916
 bentonite suspensions, magnetooptical birefringence 3-47486
 bentonite, in laminar flow, birefringence (French) 3-80500
 bentonite-water suspensions structure in shear flow, mechanical props. 3-50794
 bentonite-water suspensions structure in shear flow, optical properties 3-50795
 boundary layer flow, similarity solution based on constitutive equation 3-63683
 cells and other charged particles, adsorbed polymer effect on diffuse double layer 3-61235
 cells and other charged particles, neutral polymer effect on electrokinetic potential, zeta potential increases 3-61234
 chain polymer solutions, transport of compact particles 3-47487
 charged particles, Brownian motion in mag. field, incorporation of hydrodynamic after effect 3-42899
 coarse particle suspension in high-concentration flow 3-75266
 crystallizer working conditions, MSMRP, sieve anal. 3-72793
 density-stratified fluid with particle suspension, plane parallel flow 3-71822
 dextran-mediated cellular interactions, electrostatic effects 3-61893
 dextran/erythrocyte systems, electrokinetic potential of cells and other charged particles 3-61892
 dilute polymer solution jet, destruction of high C steel 3-72913
 Drag reduction of solid-liquid suspensions in pipe flow 3-80505
 dust-laden gas suspension, entropy losses in the flow in a nozzle 3-63773
 elastic sphere transverse motion in a shear field 3-49614
 energy balance equations, of suspension carrying stream of high concentration (Russian) 3-63769
 ferro-suspension, entrainment by travelling mag. field (Russian) 3-79016
 ferroliquids flowing in a magnetic field, particle interaction effects (Russian) 3-79012
 ferromagnetic fluids thermodynamics, review (Russian) 3-79878
 ferromagnetic liquid, flow in magnetic field (Russian) 3-43609
 fine dispersed particles with cubic crystalline symmetry, viscosity in mag. field (Russian) 3-79879
 fixed and free, settling speed, viscous fluid 3-73091

suspensions continued

- flame, gas and solid particle mixture, radiation front (Russian) 3-69456
 flow, determ. of critical velocity 3-63774
 flow, solid particles in gas, propagation of pressure waves 3-79029
 flowing, particle collection under London and gravity forces 3-40747
 gas with dust particles, turbulent friction drag, reduction mechanism 3-40744
 gas/solid mixtures, acoustic velocity and critical flow state calc. (German) 3-67965
 isothermal and nonisothermal laminar inelastic non-Newtonian tube entrance flow following a contraction 3-43543
 Kakhovka reservoir, suspended sediment flow rate 3-76928
 laminar tube flows, behaviour of falling and suspended sphere, rotation, tubular pinch effect 3-71821
 latex, ordered structure obs. by metallurgical microscope 3-76385
 liquid droplets in a gas flow, deformation and disintegration 3-63775
 low Peclet number mass or heat transfer 3-79024
 metallic oxide dust in gas, shock waves, thermionic emission 3-67935
 metallic particle suspension in crossed electric and magnetic fields, effective conductance determ. (Russian) 3-79015
 Mossbauer effect of Brownian particles suspended in liquid, theory (Russian) 3-72559
 multi-component ionised gas-solid suspension, transport properties 3-71865
 particles in large amplitude acoustic field, hydrodynamic interaction, acoustic aggregation (French) 3-40745
 PMMA in dibutyl phthalate, rheological props. 3-61231
 polyethylene oxide, viscoelastic flow, hole error meas. 3-67966
 polyethyleneimine-polyacrylate, rotation viscometer study of Newtonian flow 3-43630
 polyisobutylene fluids, normal stress data correlation 3-67892
 polymer, rheological equations 3-73083
 polymer dilute soln. non-Newtonian flow, mass transfer with rotating disc 3-71816
 polymer dilute solns., round turbulent jet, laser-Doppler meas. 3-75283
 polymer dilute solns. behaviour in inlet region of pipe 3-75267
 polymer latexes, synthetic, mech. stability 3-50791
 polystyrene dilute theta solns. in cyclohexane, translational diffusion 3-49514
 polystyrene latex colloidal suspensions, size distribution by light scattering 3-47485
 polystyrene particles, aqueous, dielectric properties at microwave frequencies 3-44692
 rigid particle, subjected to const. vel. gradient flow, non-Newtonian viscosity correl. with Maxwell effect (French) 3-80501
 sampler for particle size analysis 3-65040
 seawater, determ. of trace elements, by atomic absorption with arc atomiser 3-80875
 sepiolite, elec. birefringence transients 3-44691
 slow viscous shear flow, particle motion, orientation statistics, laser study 3-40746
 solid, laminar flow with radiating fluid radiative heat transfer, gas-cooled nuclear reactor 3-40529
 solid multiparticle systems, fluidisation, sedimentation, review 3-79030
 solid/liquid dispersions, cohesion versus adhesion 3-50789
 sphere impaction and collection, diffusion effect 3-55905
 sphere motion near wall boundary a Poiseuille flow, pressure drop 3-60574
 Stokes problem for conducting fluid with particle suspension 3-49605
 supersonic flow, heterogeneous, stoichiometric hydrogen-air mixture with suspended Al and Mg powders in detonating wave (Russian) 3-63768
 suspension of ellipsoidal macromolecules, two dimens. laminar flow, orientation distrib. function, Legendre coeffs. 3-40749
 swirling laminar pipe flow 3-71823
 synthetic lattices, rheology, influence of shear rate and temp. 3-69393
 teflon in water, modelling of hydrophobic interactions 3-65026
 thermophoresis in liquids 3-76386
 turbulent flow properties, effect of particles in suspension (French) 3-60572
 two arbitrary sized touching spheres in a linear shear field, creeping motion 3-52486
 viscoelasticity, theory 3-54821
 water density, pycnometric determ., phase dispersion 3-61228
 water flows with polymer additives, hydraulic losses investigation 3-57829
 water streams containing some macromolecular substances, boundary layer turbulence 3-71819
 weak polymer solns., turbulent flow in a pipe, expt. obs. 3-71818
 Al₂O₃ in flames, average particle diameter and spectral characteristics determ. (Russian) 3-62365
 Au, plate like particles, fibrous aggregation, long range attractive forces 3-44689
 Fe₂O₃ dielectric ferromagnetic suspension, flow in a rotating magnetic field (Russian) 3-63776
 SiO₂ suspension, electroviscous nonaqueous, shear flow in transverse electric field 3-73080
 V₂O₅ in laminar flow, birefringence (French) 3-80500
 ZnO aqueous suspensions, reproducible e.s.r. spectra 3-75872

swept-frequency oscillators

- microelectrode impedance testing 3-42687
 microwave frequency lock system, digital, design and performance 3-77578

switches

- see also *relays; semiconductor switches*
 cryogenic systems, spaceborne, gas-gap thermal switch, cooler/component interface 3-56645
 four-stage, for multistage spark gap 3-77572
 high speed, laser beam applic. in spark gap triggering 3-66893
 liquid crystal optical transparency, reduction of switching time 3-45779
 optical, controllable liquid crystal transparency 3-45778

switches continued

- radiometer switch, m.m. band, input, crossed waveguide system, description, operation (*Russian*) 3-80859
- vacuum, arc stability charact. 3-57963

switchgear

- see also switches*
- h.v. insulation/metal enclosed, standardisation problems (*German*) 3-48333
- vacuum arc-quenching chambers using Cu for contact systems 3-52540

switchgear testing

- contact erosion, electric arc motion, by injected plasma, test results (*Russian*) 3-43702
- h.v. standardisation problems (*German*) 3-48333

switching

- see also electrical conductivity transitions; ferroelectric switching; magnetic switching; switches*
- chalcogenide glass thin amorphous films, reversible switching 3-60908
- chalcogenide glass-Si heterojunctions, switching and photoelectric behaviour 3-60913
- laser triggered, high pressure gas filled spark gap, 575 kV, nanosecond delay, subnanosecond jitter 3-63911
- liquid crystal waveguide, low loss, electro-optic switching 3-44393
- m.i.s.i.m. structure, dynamic current switching regime (*Russian*) 3-44153
- PTC-resistor device, thermal behaviour, cooling parameters and conductivity effects 3-60909
- thermal switching and breakdown, rel. to law of electrical conductivity 3-60877
- toll centre room, acoustic noise meas. 3-66089
- vacuum-arc phenomena 3-57962
- Ag-SiO superlattices, switching effect 3-72400
- Al_{0.5}Ga_{0.5}As-GaAs, single heterojunction injection laser, self-switching 3-70829
- As-S-Te-I glasses, inhomogeneous struct. depend. of I-V characts. (*Japanese*) 3-64391

switching circuits

- chopper, magnetically driven using read relays, for potentiometry on thermoelectric samples 3-39970
- discrete sweep circuit for isotopic analysis 3-51760
- electronic HVDC circuit interrupter for inductive energy storage systems 3-60638
- inductive energy storage systems in nuclear fusion research, switching equipment 3-60308
- irreversible, with superconducting magnetic energy storage, design study 3-60304
- thyatron switch for pulsed n.m.r. apparatus 3-66290

switching functions

- see also Boolean functions*
- pseudo random, rel. to continuous chromatographic analysis 3-66432

switching transitions *see electrical conductivity transitions***symbols *see nomenclature and symbols*****synchrocyclotrons**

- 1 GeV, at Leningrad Nuclear Physics Institute, status report 3-56750
- Dubna, medical uses for treatment of malignant tumours 3-59440
- Lawrence Berkeley laboratory 184-in synchrocyclotron proton beam intensity improvements 3-56746
- Nevis, radiation resistant Al magnet coils 3-56797
- Nevis, secondary emission beam monitor 3-56890
- space charge effects in vertical plane during injection 3-56833

synchronisation

- auditory-nerve discharges, effects of stimulus frequency, quantitative model 3-77218
- clocks, requirements for astronomy and geodesy (*Italian*) 3-51419
- heart synchronised by external signal, experiment with rats described 3-61897
- high speed neutron radiography, image quality, scintillator screen, image intensifier, synchronisation features 3-45515
- laser modes, nonpolar synchronization, effect on frequency conversion efficiency (*Russian*) 3-70799
- network, for solid laser with repetition frequency of several Hz 3-51636
- resistance measurement, low-resistance specimens, a.c. synchronous detection 3-48471
- rotating high speed objects, exam. technique, non-stroboscopic system 3-48410
- thermodynamics theory rel. to nonlinear interacting irreversible processes 3-74174

synchronism *see synchronisation***synchroscopes *see cathode-ray oscilloscopes*****synchrotron radiation**

- astronomical radio sources, polarisation variation in self-absorbed synchrotron sources 3-51361
- atomic and mol. spectroscopy 3-39937
- atomic and molecular absorpt. spectroscopy ESRIN-Bonn-Imperial College expt. with synchrotron radiation 3-40060
- C-ray reflectivity meas. 3-40062
- at Cambridge electron accelerator 3-56850
- charged particle bunch emission making multiple passes through a cylindrical cavity 3-48494
- cosmic sources, stimulated amplification of radiation 3-53680
- Crab Nebula, 912-90 Å, Zanstra's method (*Russian*) 3-77097
- Crab Nebula, relativistic particle and magnetic field distributions, synchrotron radiation mechanism 3-77166
- cyclotron radiation from a rarefied inhomogeneous magnetoplasma 3-68048
- Daresbury Facility, recent development 3-39991
- data handling at Deutsches Elektronen Synchrotron 3-39989
- electron beam modulated, e.m. emission 3-48839
- electron moving in weakly focussing magnetic field, radiation (*Russian*) 3-43095
- electron synchrotron emission (*Dutch*) 3-49020
- for electronic and optical properties study of matter 3-56986
- electrons, relativistic, synchrotron radiation field, spatial coherence 3-43098

synchrotron radiation continued

- emissivity variations due to power-law distrib. of ultrarelativistic particles 3-51257
- experimental usage, conference, Lancashire, England, January (1973) 3-39987
- extragalactic X-ray sources generation mechanisms 3-81153
- fluorescence, time-resolved, and lifetime meas. with ACO synchrotron radiation 3-40651
- formaldehyde, production and decay of excited states by photon impact 3-40665
- heterochromatic photometry using calibrated detector 3-39995
- holographic concave grating, use with normal incidence monochromators 3-39934
- induced, for electron in helical trajectory, quantum electrodynamic study (*Russian*) 3-43117
- inert gas photoionisation cross section and photoelectron ang. distribution 3-40579
- integrals evaluation for case of guide fields comprising magnetic segments 3-57184
- Jupiter, electron and proton flux, synchrotron energy loss, radial diffusion model 3-69895
- Jupiter magnetosphere, energetic electron diffusion, synchrotron emission Monte-Carlo computer program 3-65787
- models for pulsars and compact extragalactic objects 3-69971
- molecules and molecular crystal spectroscopy from 5 to 260 eV 3-40061
- monochromator, grazing incidence, focusing radiation 3-39935
- Orsay storage rings, proposed expts. 3-39993
- Physikalisches Institut der Universität Bonn, operation and development 3-39992
- plasma, laser produced, anomalous and inverse synchrotron (*Rumanian*) 3-63856
- plasma, thermonuclear, radiation losses calc. 3-75408
- plasma heating in Tokamak, heat loss processes 3-68057
- plasma wave synchrotron instability 3-40784
- production facilities and experimental uses 3-39988
- pulsar X-ray emission mechanism model 3-45156
- quantum theory of electron motion, autophasing field 3-78123
- radiosources, X-ray emission by Compton-synchrotron or Compton black-body effect, comparison 3-53674
- Schwarzschild metric, rotating searchlight effect, black hole mass 3-80917
- soft photon emission, domination by radiation damping effects 3-70917
- solar corona magnetoplasma, low freq. suppression 3-73444
- solar radio-bursts, coherent emission mechanisms, coherent synchrotron radiation conversion (*Dutch*) 3-51283
- solar self-absorpt. of gyro-synchrotron emission in mag. dipole field 3-65710
- solids and polyatomic gases, absorption spectra 3-40614
- source, storage ring synchrotron, electron, Tantalus I Wisconsin, USA, operation 3-59631
- source theory extension for small pitch angles 3-69970
- spectro-monochromator using two gratings, grazing incidence 3-40056
- spectrometry at Daresbury Facility, CAMAC system for computer control 3-39990
- spectroscopy at grazing incidence, diffraction gratings 3-40057
- storage ring, synchrotron instability of relativistic electron bunch (*Russian*) 3-70340
- tokamak reactor, thermal stability analysis including anomalous diffusion and synchrotron radiation 3-60636
- u.v. spectral light source, 10-1000 Å, applications in atomic, molecular and solid state spectroscopy 3-39930
- v.u.v. mounting design 3-39994
- wavelength modulation spectroscopy in 10-40 eV range using synchrotron radiation 3-39938
- X-ray, scanning microscope for thick specimens 3-42684
- X-ray monochromators, grazing incidence spectrometers and crystal spectrometers 3-40055
- X-ray photoelectron spectroscopy 3-40059
- X-ray reflectors, gratings and spectrometers 3-40058
- He, simultaneous excitation-photoionisation by synchrotron radiation, high resolution optical meas. 3-40580
- KI, photoemission, electronic structure and scattering props., synchrotron radiation meas. of energy distributions 3-55721
- Kr, photoabsorption coeffs. from 48 to 210 Å 3-40566
- LaF₃, reflectivity and surface plasma resonances 3-41538
- N₂, photoabsorption coeffs. from 400 to 650 Å using synchrotron radiation 3-40566
- N₂O, dissociative excitation and ionisation excitation with synchrotron radiation 3-43504
- O₂, photoabsorption coeffs. from 400 to 650 Å using synchrotron radiation 3-40566
- PrF₃, reflectivity and surface plasma resonances 3-41538
- stellar model, Stokes parameters, Bessel function routine 3-47867
- Xe, photoabsorption coeffs. from 48 to 210 Å 3-40566

synchrotrons*see also cosmotrons*

- 1 GeV, nuclear spectrometry (*French*) 3-59620
- AGS, dipole magnets, for closed orbit correction 3-56831
- AGS, magnetic beam position monitor 3-56892
- AGS, multiturn injection system, performance 3-56868
- air-filled ion chambers, for beam loss monitoring at zero gradient synchrotron 3-56934
- alternating-gradient, Brookhaven USA, 30 GeV proton accelerator, operation, performance results 3-56742
- beam transfer, fast shaving ejection from CPS to CERN 300 GeV machine 3-56876
- beam transfer from national accelerator laboratory booster synchrotron to main ring system 3-56870
- Bevatron, Berkeley USA, heavy ion acceleration, first phase 3-56734
- Bevatron, composition of heavy ion beams for medical uses 3-61921
- Bevatron, control technology applications 3-56780
- Bevatron, cryopumping description 3-56719
- Bevatron, dynamic graphic display terminal 3-56957
- Bevatron, radiobiological experiments using heavy ions 3-59441
- Bevatron, r.f. noise effect on bunching 3-56828

synchrotrons continued

- bremstrahlung fluxmeter, linear relative monitor 3-70335
 Cambridge electron accelerator, synchrotron radiation 3-56850
 CERN proton synchrotron, Q measurement with swept RC filter 3-56781
 closed orbit distortion correction 3-56836
 coils, for zero gradient synchrotron, failures analysis 3-56803
 Cornell, Ti vacuum chamber liners 3-56727
 DESY, pe colliding beam experiment 3-56815
 electron, 3 GHz superconducting cavity 3-56720
 electron, DESY, technical development and exptl. results (*German*) 3-77599
 electron, DESY Germany, performance, recent progress, beam intensity studies 3-56743
 electron, r.f. phase control system 3-56785
 electron accelerator, Argonne National Laboratory, booster injector for Zero Gradient Synchrotron, operating results 3-56737
 injection linac, 50 MeV 3-56842
 injector system, for zero gradient synchrotron polarized proton beam program 3-56764
 internal electron beam, collimation using beam scrapers 3-62200
 magnet coil protection, in zero gradient synchrotrons 3-56804
 multi-turn injection, new methods 3-56871
 NAL Batavia, 200 to 400 GeV, operating results, first year of operation, protons 3-56736
 NIMROD, prediction of induced activity levels 3-73841
 NIMROD, quarterly report 3-70341
 NIMROD, r.f. system 3-56769
 Nimrod operation and development, quarterly report (July-Sept. 1972) 3-48497
 NINA, beam variation plot with Q value 3-56889
 orbit warp measurement, equilibrium, zero gradient synchrotron Argonne USA, fast technique at injection 3-56895
 phase motion, effect of random fluctuations 3-56835
 Physikalisches Institut der Universität Bonn, operation and development 3-39992
 pole face winding equipment, for eddy current correction at zero gradient synchrotron 3-56765
 power supply, for national accelerator laboratory main ring system 3-56948
 proton, 76 GeV, operation at high intensities 3-56751
 proton, beam intensity increase in injector 3-51676
 proton, ITEP, Moscow, medical uses for treatment of malignant tumours 3-59440
 proton, national accelerator laboratory, USA, CAMAC for interfacing remote components 3-56956
 proton, vacuum system (*Japanese*) 3-48493
 proton beam, of NAL booster synchrotron, correction for particle loss 3-56911
 proton booster, CERN, 800 MeV, present performance 3-56741
 proton synchrotron, 200 GeV, computer controlled (*Czech*) 3-56710
 proton synchrotron at NAL, monitoring proton losses 3-56933
 proton synchrotron dense critical beam interaction 3-53964
 pulsed beam shutter magnet, for r.f. separated beams at zero gradient synchrotron 3-56806
 quadrupole magnets, parameter study 3-56832
 r.f. modulated electron gun, for NINA injection equipment 3-56766
 r.f. recirculating cavity of high field gradient, for increasing electron energy by 10 MeV per turn 3-56843
 r.f. structure monitor, for zero gradient synchrotron 3-56786
 Serpukhov fast ejection, beam diagnostic system 3-56886
 stopped K-mesons, high intensity beams, Bevatron 3-56771
 zero gradient, Faraday cups, for studying injection parameters 3-56885
 zero gradient, orthogonal automatic beam steering using achromatic magnets 3-56891
 zero gradient, retuning after installation of vacuum chamber and pole-face windings 3-56747
 zero gradient, superconducting stretcher ring, resonance injection 3-56763
 zero gradient, visualization and manipulation of orbit warps 3-56784
 zero gradient synchrotron, external proton beam lines 3-56883
 zero gradient synchrotron booster, fast-spinning stripper 3-56762
 zero gradient synchrotron injection computer program for beam parameters control 3-56887
 zero-gradient, Argonne USA, acceleration of polarised protons, depolarisation problems, corrections, operation 3-56740
 zero-gradient, ion sources, Argonne USA, control philosophy, design concepts, multiplicity 3-56925

synoptic climatology *see climatology*

synthetic rubber *see rubber*

system theory

- see also artificial intelligence; identification; information theory; modelling; pattern recognition; simulation*
 measurement engineering aspects of further education in signal/system/information theory (*German*) 3-59536
 retinal nerve nets, optical illusion interpretation, applic. 3-45308

systems analysis

- see also systems engineering*
 surface runoff system, storm records, determ. of optimal kernels, computational technique 3-56243
 urban planning and air pollution control, systems approach 3-81331

systems design *see systems analysis*

systems engineering

- see also systems analysis*
 ecosystem modelling for Lake George NY 3-47714

systems programming *see systems analysis*

Szilard-Chalmers reactions *see radiochemistry*

T invariance

- angular correlations in pair conversion process in polarised nuclei (*Russian*) 3-52125
 beta-decay, allowed isospin-hindered, test for time-reversal invariance 3-60124
 in classical mechanics time-reversal invariance with 2-body collisions, matrix description, teaching paper 3-77353

T invariance continued

- nuclear electromagnetic transitions, 7.79 to 0.79 MeV cascade accompanying ^{35}Cl capture of slow polarised neutrons (*Russian*) 3-57492
 redefinition of operators for invariance under full Poincare group 3-78100
 review of symmetries in physical laws (*German*) 3-66939
 space-time symmetries for system of particles with electric and magnetic changes 3-51983
 spontaneous T violation theory, complex spin-0 fields 3-70881
 stochastic symmetry breaking 3-70729
 violation, evidence from non-Hermitian interactions 3-74327
 $K^0 \rightarrow \pi^- \mu^+ \nu_\mu$, muon polarisation meas. and time-reversal invariance expt. test 3-40334
 $\Sigma^- p \rightarrow \Lambda n$, determ. of $\Lambda\Sigma\pi$ coupling const., test of charge-independence hypothesis and T invariance 3-70974
 ^{192}Pt , gamma decay, phenomenological T-violating internucleon potential 3-62988

table-top computers *see minicomputers*

tables (data) *see collections of physical data*

tachometers

- see also angular velocity measurement*
 gyrotachometer, determ. of probability distrib. for nonlinear case using Fokker-Planck eqn. (*Polish*) 3-66517

tachyons

- charged, e.m. field, eqns. of motion 3-70710
 experimental searches and hypotheses concerning their nature, review 3-67170
 field model of interacting tachyon (*Korean*) 3-70858
 generalized special-relativity theory, non-emission of Cherenkov radiation in vacuum 3-51818
 mass limits, reln. to stability of protons and electrons 3-43168

tackiness *see adhesion*

tandem accelerators *see particle accelerators*

tantalum

- β -structure, r.f. sputtered, thin film, resistivity, impurity residual stresses, structure 3-52766
 anelastic relax. and internal friction after annealing in ultra high vacuum 3-43829
 anodic oxidation, O migration 3-80553
 atom, photoelectric cross section for 145 keV gamma rays 3-49406
 cathode sputtering coeff., Ar, He and Xe discharges, role of ion capture (*Russian*) 3-69128
 cell, effusion of Ag, surface diffusion, Knudsen determ. (*German*) 3-52754
 chemical analysis, review 3-59695
 chemico-optical spectroscopy, fluorescence, Ta microanal., industrial effluent soln. 3-48657
 crystalline layer on sapphire substrate, orientation relations by X-ray analysis (*German*) 3-52759
 defect superlattice form., elastic interaction theory 3-54957
 diffusion of H and D 3-52725
 diffusion of hydrogen and deuterium, residual resist. meas. of mobility 3-64216
 elastic properties, temp. range 4-300K 3-64080
 energy loss of 2.0-MeV ^4He ions, meas. 3-40944
 FEM tip, microcrater form. on microparticle bombard. at limited field emission currents 3-44523
 film, epitaxial, on sapphire, prep. and struct. 3-52762
 film, lattice consts., X-ray diff. study 3-43966
 film, secondary ion emission, microanalysis 3-62321
 film, sputtered, factors controlling struct. 3-41111
 films, sputtered, Ar pressure effects on resistivity 3-41276
 foil, self-restoring autocathode, pulsed X-ray tube 3-73912
 matrix isolation spectra using triode sputtering source 3-61046
 mechanical properties, effects of interstitial solute additions 3-80340
 metal, b.c.c., lattice distortion due to gas interstitials 3-64029
 in minerals, determ., X-ray fluorescence spectroscopy 3-56253
 nitriding, struct. changes, h.v. electron microscopy, in situ obs. 3-50707
 oxidation investigation by static method of secondary ion mass spectrometry 3-75683
 powder compacts, porous, shrinkage in sintering (*Korean*) 3-53265
 proton irradi., void form. and hydrogen effects 3-46138
 solubility of H_2 at 703K 3-69196
 strain rate cycling, thermally activated flow, mobile dislocation density, 77-403 K (*Japanese*) 3-41741
 substrate, implantation of ^{13}C and ^{19}F ions, range determ. (*German*) 3-49913
 superconducting, differential paramagnetic effect, temp. depend. 3-46932
 superconducting thin film quantum galvanometer, NB overlay 3-70324
 superconducting thin films, nonlinear microwave props. 3-50304
 superconductor, type II, transition by rectang. current pulse, flux flow and jump 3-68729
 surface, anodic film field crystallisation 3-61261
 surface, interaction with O_2 , high temperature (*French*) 3-79574
 surface, polycryst., oblique Ar^+ bombardment in 1 keV range, sputtering yield, ion incident angle depend. (*German*) 3-47342
 surface-carburized, carbide precip. phenomena (*French*) 3-61153
 thin film circuits, cylindrical diode continuous vacuum sputtering machine 3-39890
 thin film resistors, thermal coeff. of resistivity, effect of Ar, O, N ion bombardment 3-58054
 thin film sputtered in Ar discharge, optical and mass spectrometric analysis 3-43961
 thin film sputtered in Ar/N_2 discharge, optical and mass spectrometric analysis 3-43962
 thin films, phase composition and texture analysis by energy dispersive X-ray analysis 3-45566
 thinning using twin-jet electropolishing unit, for transmission electron microscopy 3-50085
 wetting of Ag, hot-filament silver vapour source 3-39892
 work function determ. near melting point using d.c. arc 3-69132
 Nb:W, Ta, impurity redistrib. by electron beam float zone refining 3-44540
 β -Ta, crystal structure 3-46603

tantalum continued

- Ta chemisorption of CO and O₂, polycrystalline tapes, helium molecular beam reflection study, chemical interactions (*French*) 3-44742
 Ta/Li high temp. heat pipes, corrosion mechanism 3-40543
 Ta/Ta₂O₅/electrolyte system, ion current transients, dielec. relax. model 3-80549
 Ta/Ta₂O₅/electrolyte system, Faradaic-current driven polarization processes 3-80550
 Ta-Ta₂O₅-ZnS: Tb³⁺-Au, films, electroluminescent, electron injection via electron tunnelling mechanism 3-50626
 Ta-Ta₂O₅-ZnS: Tb³⁺-SiO₂-Au films, electroluminescent electron injection via electron tunnelling mechanism 3-50626
 α-Ti, electric field grad. at Ta in group IV B metal 3-58458
 α-Zr, electric field grad. at Ta in group IV B metals 3-58457
 ω-Zr, electric field grad. at Ta in group IVB metal 3-58459

tantalum alloys

- see also tantalum compounds*
 (7.9 and 2.3%), Ta-W-Hf neutron irradiation effect on tensile props. 3-79386
 Al-Ta film, r.f. cosputtered, X-ray analysis, resistivity and t.c.r. obs. 3-50096
 Au-Ta film, struct. and thermal stability 3-64837
 Co-Ta intermetallics, orbital susceptibility and ⁵⁹Co Knight shift, d-electron motion (*Russian*) 3-52954
 Fe-Ni-Ta, coherency strains influence on precipitate shape 3-69246
 Mo-Ta, stacking fault form. probability (*Russian*) 3-80275
 Nb-Ta (20 at. %), nitride precipitate morphology and struct. 3-64872
 Nb_{0.73}Ta_{0.27}, supercond., pot. difference, current depend., transverse mag. field (*French*) 3-55360
 (Nb_{1-x}Ta_x)Al_{1-y}Ge_y, Al₁₅ struct., superconducting critical temp. obs. 3-50297
 (Nb_{1-x}Ta_x)Al_{1-y}Ge_y, superconducting critical temp., critical current density 3-50286
 Ni-Ta-Cr-Mn system dendritic duplex crystals, topography 3-41725
 Ta-Al, resistor film, sputtered Seebeck effect, rapid compositional analysis 3-41275
 Ta-W (10wt.%W), elec. resist., specific heat and emittance at 1500-3200K, high-speed simultaneous meas. 3-52705
 Ta₇₀Nb₃₀, supercond. single cryst., magnetization and pinning 3-58344
 Ti, thin film preparation 3-64416
 V-Ta, phonon spectrum change with Ta addition, specific heat meas. 3-75580
 W-Ta-ZrC, recrystallization, deformation depend., microstructure 3-76334
 W-Ta(Fe), local moment formation, and magnetic interactions 3-50345

tantalum compounds

- see also tantalum alloys*
 Ta/Ta₂O₅/electrolyte system, ion current transients, dielec. relax. model 3-80549
 Ta/Ta₂O₅/electrolyte system, Faradaic-current driven polarization processes 3-80550
 Ta-H systems 3-49993
 Ta-O solid solns., thermodynamic props., e.m.f. meas. 3-41030
 Ta-Ta₂O₅-ZnS: Tb³⁺-Au, films, electroluminescent, electron injection via tunnelling mechanism 3-50626
 Ta-Ta₂O₅-ZnS: Tb³⁺-SiO₂-Au, films, electroluminescent, electron injection via tunnelling mechanism 3-50626
 TaBO₄, i.r. spectra, Raman spectra and u.v. excited luminesc. 3-68989
 TaC, stoichiometric, dislocation dissociation using weak-beam technique of electron microscopy 3-60729
 TaC, TaN, TaO, heat of formation calc. 3-43878
 TaC, X-ray determ. of Debye temp., thermal at. vibr. amplitude 3-72156
 TaC, X-ray determination of Debye temperature 3-52686
 TaC_{0.98}, sintered, galvanomag. props., 300 and 20.4 K (*Russian*) 3-50222
 TaC_{1-x}TaN_x-HfN system, hot pressed, annealed, lattice parameters, microhardness rel. to comp. (*German*) 3-80392
 TaF₅³⁻, fund. vibr. modes, normal coord. anal. 3-52335
 TaN, thin films, optical, elec. props., on fused silica surface 3-64755
 Ta₂N thin film, oxidised layer, anodisation, basic properties (*German*) 3-46762
 Ta₉₂Nb₈, Ta₉₅Nb₅ surface superconductivity and pinning sites 3-55365
 Ta₂O₃, anodic, thermal effects during formation and dissolution 3-80548
 Ta₂O₃, anodic, implanted ¹⁹⁸Au⁺, surface effects in range meas. by oxide dissolution 3-68300
 Ta₂O₃ anodic film, elec. cond., rectification, transport processes and electronic struct. 3-46839
 Ta₂O₃ anodic films, ellipsometric investigation of electro-optic and electrostrictive effects 3-80122
 Ta₂O₃ pyrolytic film characterisation 3-58591
 Ta₂O₃ thin films by anodic oxidation with non-aqueous solutions, elect. prep. (*Japanese*) 3-46912
 Ta₂O₃-CaO-SiO₂, new oxide glass, form. by laser spin melting and free fall cooling 3-68168
 TaS₂, 4Hb-type, prep. and props. 3-55084
 1sTaS₂, semiconductor, layer structure, mag. susceptibility, Van Vleck theory 3-41327
 TaS₂ metal intercalation compounds, preparation and properties 3-72050
 TaS_{2-x}Se_x, phase diagram, X-ray analysis, atomic scattering factors 3-41016
 TaX₃ (X=Cl, F, Br) normal coordinate analysis and thermodynamic functions 3-54654

tantalum electrolytic capacitors *see electrolytic capacitors***tape recorders**

- see also magnetic heads; magnetic recording*
 cassette, for data loggers in pollution analysis 3-70190
 cassette recorders, digital, interfacing with analytical instrumentation 3-48600
 earthquakes, recording on mag. tape multiflex f.m. system 3-80837

tape recorders continued

- elementary particle physics data, acquisition by video tape recorder and computer 3-54023
 NRAO tape-recorder interferometer system 3-65960

t.d.m. *see time division multiplexing***teaching**

- see also demonstrations; education; student laboratory apparatus; training*
 acoustics, nonlinear 3-66101
 algebra, problem for students involving average speeds 3-73631
 amorphous semiconductors, conductivity processes, teaching analogy, automobile travel 3-77358
 amplitude transmission coefficients for internal reflection 3-51496
 angular momentum conservation, a simpler derivation for students 3-56594
 animal growth for introductory physics course 3-70239
 astrology in introductory astronomy courses 3-51489
 astronomy, use of closed-circuit television 3-42505
 astronomy, use of computer graphics and animation 3-42506
 astronomy exercise on coordinate systems using computer 3-77363
 atmospheric radioactivity, student experiment 3-56598
 atom, use of antenna theory in teaching 3-70240
 atomic orbitals, method for generating sets of orthonormal hybrid atomic orbitals 3-49379
 Atwood's machine, improved determ. of acceleration 3-56606
 Audiovisual aids for astronomy and space physics at an urban college 3-70255
 ballistic pendulum struck by arrow, student experiment 3-70244
 beta particle energy range formulae and school laboratory expt. 3-77354
 Biot's polariscope, working model 3-59533
 birefringence experiments for introductory physics course 3-77351
 black holes, neutron stars and pulsars semi-quantitative treatment for introductory college physics course 3-77348
 Boltzmann's H-theorem, improved presentation 3-53813
 calculus, crash course 3-66113
 centrifugal force and rot. motion, teaching approach 3-42497
 charge and pole, classical dynamics 3-51495
 charged particle in low magnetic field with finite boundary conditions 3-66609
 chemical physics, student exercises, book 3-60347
 chemistry course for engineering students 3-53811
 chemistry lecturer's role 3-77347
 Chladni figures, coloured under u.v. light 3-59532
 computer program giving numerical soln., for students 3-77361
 conformational study, equipment for meas. dihedral angles on models 3-77374
 conservation principles, integral invariants, linear systems 3-66109
 continuum mechanics, undergraduate 3-61961
 continuum mechanics course, elastic and plastic solids and the formation of cracks, book 3-62485
 controlled fusion at Wisconsin University, education and research 3-63238
 coordination theory applic. to crystallography, Pfeiffer's contrib. 3-53816
 Coriolis deflection of trajectories 3-66100
 course in physics with illustrative material from biology and medicine 3-53810
 deaf, using computer 3-61898
 defect concentration in crystals, method of calculation 3-56599
 dipole moment meas., gas phase rel. to dielectric theory, undergraduate teaching 3-45401
 electrical engineering, instructional experiments, Si in ultrahigh vacuum, elec. properties 3-68684
 electricity and electronics course, nuclear instrument and control, technicians 3-73645
 electrodynamics foundations, graduate textbook 3-62543
 electron pair creation by γ-rays, student expt., comment 3-73630
 electrostatics, images and point charge capacitor problem 3-74187
 element origin, nucleosynthesis theory 3-61963
 elementary particle physics, fundamental, book 3-62762
 environmental physics teaching course 3-51486
 expectation values error limits in quantum mechanical calculations 3-51804
 falling faster than g 3-51498
 fast reactor education, Pb slowing down time neutron spectrometer 3-63161
 Fourier transform n.m.r. spectroscopy 3-53957
 free fall experiment, statistical analysis 3-51490
 frictional forces and accelerated frames of references 3-73637
 frontier molecular orbitals, link between kinetics and bonding theory, elementary university chem. teaching 3-77355
 fusion reactor engineering in the nuclear engineering curriculum at Texas University 3-61956
 fusion technology at Michigan university, educational and research activities 3-61955
 fusion technology first year graduate course at Illinois University 3-61954
 galvanometer for lecture halls of simple design 3-66119
 game, guessing the rules as an illustration of techniques in physics 3-77365
 general relativity, approach to the concepts 3-56600
 geometrical optics problems 3-42502
 graphical display system, phase-plane technique 3-66121
 gravitational collapse and black holes 3-42498
 group theory, chem. applications, overhead projection of character tables 3-77371
 Hamilton's principle, modified, derivation 3-77352
 humanistic and traditional methods of teaching physics 3-66098
 hydrocarbon molecules, graphical model 3-66108
 instantaneous velocity demonstration using 'hot wheels' 3-70242
 interdisciplinary nuclear science at a liberal arts college 3-51487
 interplanetary flight, energy requirements 3-42501
 inverse-square law rigorous elementary derivation from Kepler's laws 3-53588
 Josephson effects, student expt. using Clarke slugs 3-56596
 Kronig-Penny model analogue computer simulation 3-51494
 Lagrangian formalism for a classical particle moving in Riemannian space with dissipative forces 3-77349
 lecture halls, new design 3-70252

teaching continued

- light, colour and photography, teaching course for artists 3-51485
 light scattering in the atmosphere simulation with glass tank 3-70250
 materials science, mathematical framework, solved problems, book 3-56601
 mathematical interpretation of experimental data in schools 3-66110
 mathematics, optimisation as model building theme 3-66112
 mathematics, outlook development, curriculum 3-66111
 mathematics for science in secondary school 3-59515
 mechanics, demonstration of ski turns using a spinning gyroscope wheel 3-70243
 mechanics, work-energy relations 3-61962
 molecular structure prediction, VSEPR rule for teaching, criticism, alternative procedure 3-53815
 music, synthesis, tape studio teaching techniques 3-45403
 negative energy wave functions for the Coulomb field 3-70687
 Newton's laws on photographs for teaching (*Hungarian*) 3-39847
 n.m.r. spectrometry, spin system, set of nuclei, chem. shift and mag. equivalence, virtual coupling 3-77356
 noise measurement in a university, an open-ended student experiment 3-56604
 nonlinear optics on the atomic scale, physical interpretation 3-70235
 nuclear chemistry teaching, applic. of stellar nucleosynthesis 3-61964
 nuclear engineering, industrial and educational needs, role of the university 3-61957
 nuclear reactor design, role of standards 3-61971
 observer in the classroom, interaction with instructor 3-70231
 observers, use for helping teachers 3-70230
 optics, plotting principal-ray diagrams by computer 3-73652
 optics experiment involving 2 mirrors and multiple images 3-70246
 orbital hybridization model limitations: H_2O lone pair orbital energies 3-61966
 orbitals maximum overlap and HF compared 3-70236
 oscillators coupled as student illustration of many body system 3-70234
 pendulum, rubber band, behaviour 3-66513
 periodic potential, one-dimensional, soln. using Laplace transform method 3-77853
 physics course, introductory, using multiple techniques 3-70229
 physics course for pre-medical students 3-70228
 physics examinations, grading system 3-53817
 planetarium appl. in science teaching 3-42507
 planetariums, educational programmes 3-42508
 Poisson distribution, teaching note 3-70536
 potential energy, method of explaining 3-70248
 practical reactor design, teaching at undergraduate level 3-61972
 pre-medical physics course, nerve conductions 3-77350
 quantum chemistry, review of development of subject, suggested introduction into chemistry courses (*German*) 3-67742
 quantum mech. tunnelling, expt. using thin soap films 3-42500
 quantum mechanical measurement problem 3-51501
 quantum mechanical problem of measurement 3-51500
 quantum mechanics in secondary schools, plan (*Hungarian*) 3-61960
 radial momentum operator 3-51493
 rate constant, first-order, rapid calc. in the student laboratory 3-77360
 refractive index meas., gas phase, interferometry, undergraduate teaching 3-45401
 refractive index of liquid, using laser, school expt. 3-59526
 refractive index of liquid, using laser, school expt. 3-59527
 reluctance of a paper gap meas., student experiment 3-70251
 Russell-Saunders symbols, rules for the ground state, student teaching 3-48322
 scattering theory, computer calc. for student 3-77362
 School Telescope TELEMENTOR, VEB Carl Zeiss JENA, teaching of astronomy 3-51503
 Schrodinger equation in orthogonal curvilinear coordinates 3-73632
 science fiction courses, example 3-66099
 science for the nonscience major, a course for adults 3-70227
 singing and whistling range difference 3-51497
 sliding friction, problems, practical applications of pure and sliding rolling (*Hungarian*) 3-73634
 sound waves, standing, in tube, simple expt. 3-59529
 stick-propeller device, why does it rotate 3-59523
 stroboscope and inertia balance, rel. to student mass meas. 3-59531
 student laboratory experiments on e.s.r. cyclotron resonance and electron density of a plasma 3-56603
 student X-ray diffraction experiment 3-51491
 telecommunication, building block sets (*Hungarian*) 3-77366
 textbook on e.m. fields, energy and waves, for undergraduate 3-62641
 thermodynamic derivation of $\epsilon = h\nu$ 3-51499
 time-reversal invariance with 2-body collisions, matrix description 3-77353
 trifilar pendulum, inherent errors in measurement of moment of inertia 3-39845
 velocity without limits for elementary physics courses 3-51492
 visual aids, stereoscopic films of rotating molecular models 3-61976
 wavepacket propagation through square wells and potential barriers, simple calc. method for students 3-66104
 weighing expt. using ruler and coin 3-70245
 WKB energy levels for a class of one-dimensional potentials 3-53814
 zero-point energy in a bounded continuum 3-51803
 Cl_2 bond strength, dissociation, student teaching 3-48320
 H, electron density plots, three dimensional, computer programme for undergraduate teaching 3-48325
 H, operator domain paradox and relativistic correction to energy levels 3-66107
 H energy level relativistic mass correction 3-66105
 H operator domain paradox and relativistic correction to energy levels 3-66106

teaching approaches to particular topics *see teaching*

teaching demonstrations *see demonstrations*

technetium

- Ap type stars problems in search for Tc II lines rel. to promethium controversy 3-81049
 S Sculptoris, long-period Me variable star, spectral Tc lines 3-45133
 $^{99}Tc^{m}$ ferrous hydroxide labelled for lung scanning 3-42369
 $^{99}Tc^{m}$ for myelosclerosis, radiation effects 3-42371

technetium alloys

see also technetium compounds

No entries

technetium compounds

see also technetium alloys

- $H_2TcCl_6 \cdot 9H_2O$, X-ray diffraction, cryst. structure 3-79310

technical information centres *see information services*

technicians *see personnel*

technological forecasting

see also research and development management

- earthquake prediction, anomalous seismic velocity ratio, rock dilatancy model 3-80649
 icebergs, anal. of accompanying circulation features, forecast of 1973 iceberg season, Labrador and Newfoundland 3-80718
 icebergs, anal. of accompanying circulation features, forecast of 1973 iceberg season, Labrador and Newfoundland 3-80719
 nuclear fuel, enriched uranium for Western Europe (*Italian*) 3-63186
 planetary system, physical limitations rel. to technology development (*Hungarian*) 3-76946
 planning of scientific research, USSR, US, Japan, Great Britain, France and East Germany (*German*) 3-73623
 transport phenomena role, national problem areas 3-71695

tectonics

see also earth crust

- Afar depression, misinterpretations of aerial and space photographs 3-65510
 Afghanistan seismotectonic model 3-47645
 Africa, Bouguer gravity anomaly map, anomaly patterns rel. to tectonic patterns 3-80645
 African stationary plate rel. to moving Eurasian plate 3-65193
 Aleutian Trench, mag. anomalies rel. to tectonic processes 3-58973
 Alps in central Europe, plate tectonics model for Alpine-type orogeny 3-50956
 American and European plates collision boundary in New England 3-65196
 S. American continental margin, plate motion and seismology 3-65200
 aseismic ridges rel. to subduction processes 3-76638
 Asia, fault plane solutions of shallow earthquakes and contemporary tectonics 3-56026
 SE Asia and Indonesia rel. to Gondwanaland 3-76580
 Assam, India, gravity anomalies rel. to tectonics 3-50955
 NE Atlantic, fossil triple plate junction from extended aeromagnetic survey 3-53424
 Atlantic fracture zones, geophysical study 3-58872
 Atlantic hot spots, relative and latitudinal motion 3-76571
 Australia, Musgrave Block-Amadeus Basin, plate tectonics model 3-69520
 Australia, sedimentary history rel. to cretaceous transgressions 3-69523
 Australia-Antarctica-New Zealand region plate movements 3-76585
 Baffin Island earthquake, surface wave spectrum analysis, tectonic implications 3-76567
 Bahama platform, plate tectonic evolution 3-65198
 Barbados uplift rates, sea levels 3-76595
 Brazilian African coasts, ancient metamorphic migmatite belts rel. to rifting process 3-65173
 central California, geodetic determ. of relative plate motions 3-50917
 Cambrian Gondwanaland reconstruction rel. to palaeomagnetism of Central India 3-50984
 Canadian Cordillera, gravity anomalies, crustal structure and plate tectonics 3-56023
 Canadian Shield, integrated model for Pb isotopic evolution 3-47616
 CANNIKIN nuclear explosion, fracturing stages 3-50901
 CANNIKIN nuclear explosion, related seismic and tectonic events 3-50893
 CANNIKIN nuclear explosion, strain and ground deform. meas. 3-50900
 CANNIKIN nuclear explosion, strain and tilt meas. 3-50897
 CANNIKIN nuclear explosion, strain-release meas. 3-50894
 CANNIKIN nuclear explosions, strain and tilt data 3-50898
 Cape Ray Fault, possible cryptic suture in S.W. Newfoundland 3-65175
 Carpathian-Balkan region, secular geomagnetic field var. rel. to crustal structure and movements 3-41915
 Chesapeake Bay, elevation change rates determ. by precise levelling 3-76601
 clay outcrop, Rome, paleomorphology, prevolcanic tectonic features (*Italian*) 3-73185
 Cocos plate, Cenozoic motion rel. to asthenospheric flow and low heat flow 3-58859
 continental drift in Arctic, palaeomagnetic evidence in Late Mesozoic basaltic lavas 3-73248
 continental drift rel. to metallic ore deposits 3-41883
 continental drift rel. to resources of oil and natural gas 3-44794
 continental interiors vertical deform., Phanerozoic history and mode 3-69531
 continental rifting in Brazil and Angola rel. to opening of South Atlantic 3-76583
 crust, slow tectonic deformations rel. to earthquakes in USSR 3-44804
 crust-mantle interface, south central Alaska 3-76832
 crustal motion due to subcrustal phase transition 3-65190
 crustal movements, recent, effect on levelling results (*Russian*) 3-65154
 crustal stresses and slow deformation rel. to earthquake mechanism and tectonophysics 3-44805
 crustal stresses due to topographic irregularities 3-58831
 crustal tectonophysical characteristics of stresses, fracture and deformation mechanisms 3-50960

tectonics continued

- deep focus earthquakes as triggered dislocation processes 3-44811
 descending lithosphere, thermal structure, active volcano distribution 3-76556
 dislocation energy rel. to earthquake energy release 3-47640
 Donet's basin, recent vertical crustal movements (*Russian*) 3-65156
 drifting islands, bobbing motion due to depth anomalies caused by bumpy asthenosphere 3-73216
 driving mechanism of plate tectonics rel. to intraplate earthquakes and lithosphere 3-76575
 dunite, Twin Sisters, frictional props. 3-76629
 Earth Resources Technology Satellite, earth imaging, appl. to tectonics, volcanology, mineral resources and landform anal. 3-80852
 Earth strain monitoring using distance meas. 3-58853
 Earth-Moon gravit. couple effect on tectonism 3-47646
 earthquake displacement fields, effect of Earth layering 3-53370
 earthquake location prediction rel. to major plate boundaries in Pacific and Caribbean 3-50939
 earthquake swarms, Volcano Aso, Japan 3-76529
 earthquakes, Archambeau's source theory rel. to slip on fault 3-56010
 east Pacific Ocean, using new earthquake epicentre evaluation 3-73221
 East Pacific Rise at 6° and 11°S, sea-floor spreading rates 3-53385
 eastern N. America, intra-plate earthquakes, contemporary stresses, plate tectonics driving mechanism 3-69534
 Elliot Lake area, history 3-76514
 Emperor Seamount chain formation 3-56038
 ensialic model for Precambrian Africa and South America using palaeomagnetic evidence 3-76573
 Eurasia-American and Pacific American plates rotation rate (*Italian*) 3-58839
 fault creep events, dislocation theory anal. 3-58905
 fault creep kinematics, anal. of San Andreas fault data 3-50948
 fault creep obs. using water level changes in wells 3-61376
 fault displacement meas. by optical parallax and photographs 3-51164
 fault expansion mechanism at earthquake foci, radiation of body waves 3-44812
 fault movement determ., precision of Geodolite meas. 3-76859
 fault plane swing assoc. local stresses rel. to earthquakes aftershocks 3-44760
 fault sliding, quasi-static, model 3-76623
 faults, generation of large earthquakes 3-76633
 faults, stick-slip propag. vel. 3-53369
 Fiji plateau, low vel. zone 3-61315
 folding, rock rheology from wavelength selection 3-76603
 folding stress anal. in viscoelastic and elastoplastic media 3-76602
 folds, comparison of experimental created and natural large-scale drape folds 3-76609
 folds, experimentally prod., stress anal. 3-76610
 fracture, finite element models 3-61368
 gabbro, frictional sliding at high temp. and press., time-depend. 3-76631
 Galapagos hotspot, magnetic record of asymmetrical spreading 3-58863
 Galapagos Islands and adjacent ridges, chemistry and petrology of tholeiites 3-80636
 Galapagos Spreading Centre, E. Pacific, lithospheric cooling 3-56092
 Galapagos spreading centre, faulting rel. to near-bottom soundings 3-65201
 geodynamics, use of VLBI 3-56247
 Gibbs Fracture Zone rel. to projection of Hercynian Front into N. America 3-80634
 global, rel. to Carpathian system (*Russian*) 3-56033
 global plate motion rel. to Earth's obliquity 3-65192
 Godavari Rift Valley, tectonic history of region rel. to mechanism of 1969 April earthquake 3-50912
 granite and granite/serpentine, frictional characts. at high press. 3-76626
 Great Glen fault and timing of granite intrusion on Proto-Atlantic continental margins 3-61339
 SE Greenland, rifting and doming rel. to mantle plumes 3-56041
 Grenville Front, Labrador, Seal and Croteau rocks, polar wander and tectonic implications 3-76657
 Grenville Province, Ontario, posn. of formation from Precambrian palaeomagnetic poles 3-76655
 Grenville Province, palaeopoles rel. to plate convergence in Late Precambrian 3-56137
 ground surface motions, effect on local soil conditions 3-53371
 Gulf of Alaska, seamount ages rel. to Pacific plate motion during Miocene 3-58860
 Hawaiian Islands, origin rel. to plate tectonics and mantle plumes 3-56085
 Hindu Kush region, seismotectonic regime 3-73186
 horizontal plate motions from gravity anomalies and vertical tectonics 3-56081
 Iceland, nature of transform faults 3-65194
 Indian-Pacific rotation pole position determ. from earthquake epicentres 3-47631
 intraplate earthquakes, contemporary stresses, plate tectonics driving mechanism 3-69535
 island arc and underthrust plate geometry 3-76639
 island arcs and intra-arc spreading, induced heat flow 3-76637
 isostatic rebound, fill data and example of South Saskatchewan River 3-47618
 Jan Mayen Ridge, structure rel. to local sea floor spreading 3-58871
 S.W. Japan, southward motion rel. to age provinces in Korea 3-65202
 SW Japan margin, seismic reflection meas. rel. to major tectonics 3-53417
 Jharia coal field, mag. survey, correl. with tectonics 3-44852
 Lesser Antilles subduction zone in Barbados region 3-61336
 lithospheric fault creep processes, models 3-47641
 lithospheric fractionation into separate plates 3-47627
 location of mineral resources rel. to plate tectonics 3-76597
 lunar laser ranging for tectonic motions meas. 3-44936

tectonics continued

- Macquarie Island, mag. props. rel. to seafloor spreading 3-61413
 mantle plume-spreading ridge system, geochemical evidence 3-56088
 mantle plumes, possibility of magnetic telechemistry in oceanic crust 3-76579
 mantle roll, comparison of plume traces with palaeomagnetic data 3-76577
 Mariana island arc, palaeomagnetic evidence for rotation 3-58958
 Mediterranean coast of Israel, downwarping and submergence 3-76574
 Mediterranean plate tectonics rel. to Triassic palaeogeography 3-56037
 Melanesia, heat flow meas. rel. to plate boundaries 3-50938
 metamorphic aureoles beneath ophiolite suites and Alpine peridotites, with West Newfoundland examples 3-65130
 Mexican ridges, Gulf of Mexico sea floor, geology and salt tectonism 3-53416
 mid-Atlantic plate boundary in Iceland, hypocentre and fault plane solns. for microearthquakes 3-73215
 Mid-Atlantic Ridge, asymmetrical bathymetry rel. to fracture zones 3-58861
 Mid-Atlantic Ridge structure and plate motion rel. to Icelandic rift zone 3-65195
 mid-ocean ridges, effects of compressive stress 3-41880
 mid-ocean ridges, numerical model for accretion in axial zone 3-56093
 mid-ocean ridges, temp. and composition of ascending magmas 3-61309
 mid-oceanic rift zones and development of continents 3-56090
 mid-plate tectonics rel. to crustal extension 3-58840
 MILROW nuclear explosion, related seismic and tectonic events 3-50893
 modern arc-trench gap widths rel. to fast duration of igneous activity in magmatic arcs 3-61312
 Moravian Palaeozoic, southern part, synsedimentary tectonics 3-44836
 Motagua Fault, Late Palaeozoic tectonics rel. to subduction-collision model 3-65199
 Nazca oceanic plate subduction in Chile, earthquake focal mechanism solns. and general seismicity 3-73213
 Neogene Carpathian arc, island arc features of a continental arc 3-73212
 New Caledonia, tertiary plate tectonics 3-44835
 Ninety East ridge, origin from seismic, gravity and geomagnetic obs. 3-76565
 northwestern African margin, sea floor spreading from six geophysical profiles 3-73259
 numerical modelling of instantaneous plate tectonics 3-56077
 oceanic crust and thermal aspects of sea-floor spreading 3-50954
 oceanic crust representation by ophiolites 3-76640
 oceanic Rift Valley formation, asymmetry, opening rates and development of walls and uplift 3-80646
 oceanic spreading centres, simple mechanical model 3-61313
 orogenesis, computer model 3-76641
 orogenic deformation data application for plate boundary recognition 3-73211
 S Pacific Ocean, magnetic anomalies and evolution rel. to hot spots 3-56086
 Pacific plate, oceanic lithosphere extension and continental lithosphere compression 3-44821
 Pacific plate motion rel. to hot spots, ages of seamounts and islands 3-56078
 Pacific plate movement rel. to mantle, rigid plate model 3-61397
 E Pacific Rise between 5° and 12° S rel. to faulting 3-56089
 Pailin, Cambodia, fission track age of gem deposit rel. to recent tectonics 3-53421
 Peru-Chile trench, geomorphology 3-80638
 Phanerozoic eugeosynclines development 3-65189
 plate, appl. to pre-Mesozoic time 3-61328
 plate separation by Rayleigh-Benard convection, laboratory experiments 3-56094
 plates, determ. of forces 3-76642
 plume mechanics rel. to plate tectonics 3-56080
 plume-generated triple junctions rel. to rifting 3-56083
 pore fluids rel. to P and S velocity ratio, earthquake aftershocks, fault creep and magnetic precursors 3-76512
 western Pyrenees plate boundary, magnetisation of Permian basaltic flows and dikes 3-73246
 relative motions rel. to observable time scales 3-58858
 Rhine graben rift system, plate tectonics and transform faulting 3-56097
 Rhinegraben rift system, local interference and temporal interaction with Alpine orogenesis 3-73208
 rock strain patterns and magnitudes in 5 different tectonic regions 3-47644
 rock stress, global meas. of bedrock 3-47647
 San Andreas fault, anal. of fault-creep data 3-50948
 San Andreas fault, pore pressure changes during creep events 3-50919
 San Andreas Fault Experiment, simulation 3-56061
 San Fernando earthquake, Feb. 9 1971, faulting process 3-56016
 San Fernando earthquake 1971 focal mechanisms and tectonics 3-80640
 sandstone partial melting during frictional sliding in triaxial expt. 3-76628
 Sardinia, palaeomag. evidence of rotation during Early Miocene 3-44795
 satellite-determined isostatic gravity anomalies rel. to geotectonics 3-56060
 Scandinavia, post-glacial uplift, resolving power of data for upper mantle 3-61399
 schistosity and penetrative mineral lineation giving palaeostain directions 3-76518
 sea floor spreading, fluid dynamic models, review 3-80639
 seismic ground motion, topographic effects 3-56018
 Seldovia, Alaska, significance of mineral ages of blueschists 3-50936
 shallow earthquakes in crust, cause rel. to land deformation, Japanese islands 3-44806

tectonics continued

- sinking slab, seismically dead, west USA, detect. by P-wave delays 3-58892
- sliding friction and stick-slip rel. to foliation, grain size and comp. 3-76624
- sliding mode and stick-slip stress drops, effect of quartz fault-gouge 3-76627
- S. of South Africa, structure and evolution of sea-floor 3-53387
- Southern Caledonides of Great Britain, plate tectonic reconstruction 3-80635
- southern Tyrrhenian Sea, volcanism and its geodynamic implications 3-73222
- stillborn marginal ocean in Caledonian orogenic belt of N.W. Norway 3-76584
- Strait of Gibraltar, regional tectonics 3-50935
- stress diffusion from plate boundaries through lithosphere 3-44796
- strike slip faulting, analysis of dynamics 3-50920
- subduction rel. to deep earthquakes 3-58894
- subduction zones, discontinuities rel. to earthquake magnitude distribution 3-50943
- Sweden, tilt meas. using servo-controlled horizontal pendulum 3-47807
- Tasman Sea, evidence of seafloor spreading 3-50945
- thrust sheet motion, sliding law 3-76616
- tilt meas. using pendulums and accelerometers 3-56233
- triple junctions, evolution and stability 3-58842
- Troodos ophiolitic complex, formation in island arc 3-53384
- underthrust lithosphere rel. to island arc magmas 3-65223
- Upper Cretaceous spreading rates rel. to transgression and regression 3-58087
- upper crust, state of stress in upper crust from mines and tectonophysical and seismological studies 3-44803
- Variscan-Appalachian orogeny, transatlantic correlation 3-69497
- V. Venezuela, seismicity and tectonics 3-53376
- viscous cylinder, large asymmetric strains due to weight and loading 3-57076
- volcanic rock tectonic setting using trace element anal. 3-53545
- Walvis Ridge, structure of marginal termination 3-65197
- Western Brazil earthquake, 1963 November 9, source processes and tectonic implications, comments and reply 3-50953
- western equatorial Pacific Ocean, heat flow measurements at plate boundary 3-73220
- Western USA, intermountain seismic belt, intraplate tectonics, seismicity 3-69536
- Wyoming Province differential uplift and downdrop 3-69533
- Yellowstone convection plume, rifting mechanism 3-41882

tektites see meteorites**telecommunication**

- see also biocommunications; communication channels; communications applications of computers; optical communication; telemetering conference, Washington, D.C., USA, Oct. (1972) 3-42378*
- teaching set, building blocks, assembly (Hungarian) 3-77366

telecommunication systems

- see also data communication systems; digital communication systems*
- acoustic, applic. to programmable automatic analyser for clinical chemical laboratory 3-48633
- e.l.f., biological research 3-42379
- information transmission by gravitational waves (Rumanian) 3-74144

telecommunication theory see information theory**telecontrol**

- see also alarm systems; telemetering*
- meteorology and hydrology, problems in telemetry (French) 3-47828
- radar system for weather data acquisition 3-42059

telecontrol equipment

- RATAN-600, radiotelescope, circular reflector, reading and setting device (Russian) 3-81231
- RATAN-600, radiotelescope, circular reflector, reference reading and setting device (Russian) 3-81232

television

- see also telerecording*
- TV monitoring unit, for motion-picture filming (Russian) 3-51647

telemetering

- air pollution analysis, using remote Raman spectroscopy 3-56563
- airborne and satellite remote sensing of Anacapa Island natural resources 3-51006
- atmospheric temp. field at 20 km altitude using Nimbus III (Italian) 3-61604
- blood flow telemetry, using implanted Doppler effect directional velocity meter (German) 3-62311
- blood pO₂, in vivo radio telemetry 3-73922
- boreholes, electronic measurement of parameters (Rumanian) 3-44944
- cortical evoked potentials using remote digital computer (Italian) 3-56500
- natural resource surveillance, processing techniques (Italian) 3-61594
- oil pollution, detection and monitoring techniques 3-70194
- remote sensing from aircraft 3-51173
- remote sensing from space rel. to man's effect on environment 3-51074
- satellite programmes for continuous remote sensing of land resources 3-51176
- security and policing instrumentation, conference, New York, USA, 20-21 Sept (1972) 3-66277
- Skylab, multispectral scanner, calibration 3-77461
- spectrometric and interferometric devices, earth resources applic. 3-51172

telemetering equipment

- automatic measuring buoy for oceanographic and meteorological meas. (Italian) 3-59198

telemetering systems

- biological temperature meas. system, 3 channel implantable 3-57010
- electric field surrounding trout, non contact sensing 3-57011
- hydrophysical data transmission telemetering buoys, computer M-220-M, radiochannel, subprogramme details (Russian) 3-47850

telemetering systems continued

- living organisms' physiological parameters recording (Russian) 3-73936
- meteorology and hydrology, problems in telemetry (French) 3-47828
- tide level in Lagoon of Venice (Italian) 3-51206
- telemeters see telemetering**
- telemetry see telemetering**
- telephone equipment**
- see also microphones; repeaters*
- six-channel t.d.m., using GaAs laser diode (Japanese) 3-59847

telerecording

- see also telefilming*
- TV monitoring unit, for motion-picture filming (Russian) 3-51647

telescopes

- see also astronomical telescopes*
- acoustic spark camera in telescope for obs. of primary cosmic p-rays, shock wave effects (Russian) 3-65550
- cosmic ray meson, for obs. of ionic short-period variations at Moscow latitudes (Russian) 3-65585
- cosmic ray meson supertelecope for plastic scintillation, coupling coeff. determ. (Russian) 3-65549
- imagery from segmented mirror synthetic aperture telescopes, new processing method 3-77446
- i.r., design and applications 3-39904
- three mirror anastigmatic design 3-77432
- triggering telescope, extra-terrestrial gamma-rays experiment, COS-B satellite, ESRO 3-62223
- visual resolution, effect of vibration, allowable angular oscillations 3-56467

television

- see also colour television; video signals*
- closed-circuit, appl. in astronomy teaching 3-42505
- monitoring unit, for motion-picture filming (Russian) 3-51647

television applications

- blind rehabilitation programme, Veterans Administration USA, experience with CCTV for low vision patients 3-77229
- bubble chamber tracks, automatic scanning and measuring machine 3-77692
- closed-circuit TV appl. in astronomy teaching 3-42505
- comparison bet. remote atomic clocks, by TV signals (Japanese) 3-54008
- daytime lightning flashes, video tape recording 3-65526
- electron microscope display system 3-62287
- gas flow visualization, in hf laser 3-74231
- infrared television microscope studies, resolution, processed semiconductor materials 3-41664
- light propagation study through turbulent atmosphere 3-62080
- mammalian cell clones, number and size distributions 3-45573
- Mariner 9 TV from Mars orbit, digital image processing 3-59275
- metallographic analyser, vol. percentage, specific interface, size distrib. 3-51584
- Northern lights study with aid of TV and computer 3-42004
- physical demonstrations (Russian) 3-48323
- planetary landing site selection system, exptl. and simulation study 3-59402
- remote sensing from space platforms (Italian) 3-61595
- resource surveillance from space (Italian) 3-61593
- security and policing instrumentation, conference, New York, USA, 20-21 Sept (1972) 3-66277

television broadcasting

- ionospheric transmission of v.h.f. signals beyond horizon Central Europe (1962 to 1971) (German) 3-65441

television camera tubes

- see also image storage tubes*
- faint astronomical objects detection, image orthicon system, effective quantum efficiency 3-48145
- image pickup tube, for coherent optics 3-39948
- for low-light-level imaging, review 3-48413
- lunar transient phenomena, three colour blink technique, image orthicon TV system 3-47943
- particle track coordinates recording by vidicon automatic systems in spark chambers 3-51720
- Return Beam Vidicon camera system, Earth Resources Technology Satellite, earth imaging systems 3-80851
- vidicon in polarising-microscope obs. of 'opaque' minerals with transmitted i.r. light 3-42555
- Si dipole array target vidicons, review of technology 3-48373

television cameras

- colorimetric characteristics 3-62095
- Mariner 9 TV cameras, verification of performance 3-65945
- striped encoding filters, colour television, spectral characteristics 3-73749
- vidicon, deflection system, electron trajectories in twisted e.s. deflection yokes 3-74293
- vidicon, slow-scan, for fluctuating illumination patterns analysis 3-62080

television reception

- ionospheric transmission of v.h.f. signals beyond horizon Central Europe (1962 to 1971) (German) 3-65441

television reception quality see television reception**television signals see video signals****television systems**

- i.r., hf chemical laser gas flow visualization 3-74231
- mammalian cell clones, number and size distributions 3-45573
- medical fluoroscopic, blood flow measurement 3-59686
- multichannel TV coupling modulation, wide bandwidth, low power consumption, CO₂ laser 3-40300
- particle-accelerator beam monitoring system, SPEAR Stanford USA, synchrotron light diagnosis 3-56900
- particle-accelerator beam viewer, radial position width and brightness, CCTV system, ZGS Argonne USA, description 3-56893
- sonar display, improvements 3-51205
- stereo, holographic technique (German) 3-59597
- X-ray diagnosis, dose reducing fluoroscopy 3-45329

tellurium

- acceptor action of dislocations, theory and expt. 3-79692

tellurium continued

- adsorption on Ni(001), LEED spectra determ. of atomic location 3-64240
 alkali halide: TI^+ , moments of dichroic spectra of $(s)^2$ impurity ions 3-41541
 anisotropic chemical shift of n.m.r., theoretical analysis 3-41437
 anisotropy of elastic electron scattering in energy loss experiments 3-43815
 atom, spin-orbit quenching by gases, rates, cross-sections 3-71371
 band gap as function of lattice parameters 3-79634
 conduction band structure 3-55197
 cyclotron reson. under uniaxial stress, band structure obs. 3-58217
 electro dissolution, oxidation and reduction at graphite electrode, HB and HCl 3-73137
 energy loss of 2.0-MeV ^4He ions, meas. 3-40944
 enthalpy of solution in liquid Bi, 625K 3-55989
 enthalpy of sublimation, microcalorimetric determ. (French) 3-68403
 epitaxial growth of Se, on Te cryst. planes, non-symm. 3-68516
 film, resist., Hall coeff. and thermoelec. power, 78-450 K 3-41187
 heat capacity, 99.999% pure polycrystalline specimen, 1.5 to 20 K, Debye temperature 3-41024
 impact ionisation, time behaviour of breakdown determ. 3-79703
 influence of acceptor concentration on Hall effect 3-41205
 intervalence band transitions, absorption spectra for polarisation $E \perp c$ 3-79631
 lunar soil, analysis of 5 Apollo 17 samples 3-65831
 multi-photon absorption after laser irradiation, carrier generation 3-55284
 nonohmic behaviour, at intrinsic and near-intrinsic carrier conc. 3-68643
 overlayer on Ni(001), chemisorption bonding, LEED study 3-60829
 p-type, magnetoresistance and time-dependent non-ohmic conductivity at 2K 3-79700
 phonon dispersion relations, simple bond charge model 3-40987
 photoelectric effects in Te thin layers, temp. depend. of elec. resist. 3-64368
 semi-empirical LCAO band structures for different crystalline phases 3-46794
 short-range order effect on energy spectrum in disordered phases 3-68534
 single crystal at high temp., u.s. propagation, elastic parameters calc. 3-79434
 thermal expansion, linear coefficients, 2 to 30 K and 55 to 90 K, Gruneisen parameters, measurements 3-41031
 thin films, optical absorption between 39 and 250 eV 3-58522
 thin films, partial superposition of Bi thin films, microrelief appearance (French) 3-52769
 undoped, cross modulation cyclotron resonance for holes, sharp resonance peaks 3-64288
 vapour-phase epitaxial growth of Se on (1010) cleavage surface 3-80182
 Bi:Te, nuclear quadrupole interactions, calorimetric measurements 3-68559
 Bi₂Se₃:Te, anisotropy of elec. cond., Hall coeff. and thermoelec. power, doping effects 3-41185
 n-GaAs:Te, 0.94, 1.01, 1.29 eV luminescence bands 3-61068
 GaAs:Te, donor impurities, effect on dislocation mobility 3-72094
 GaAs:Te, Ge, radiative recomb. depend. on degree of compensation 3-41579
 GaAs:Te, ion-implanted, photolum. degradation, dose depend. 3-64074
 GaAs_{1-x}P_x:Te, Se, deep levels due to shallow donors, i.r. absorpt. and Hall effect obs. 3-44039
 GaAs_{1-x}P_x:Te,Se, impurity levels, activation energies, Hall effect, carrier mobility, 100-800K 3-44037
 GaP, liquid phase epitaxy, Te and O₂ incorporation 3-50090
 GaSb:Cu, Zn, Te, Zn and Te influence on Cu diffusion and solubility 3-72232
 GaSb:Te, impurity level scheme 3-75722
 GeSe amorphous semicond. film, holographic recording of information 3-74212
 InAs:Te, band struct., impurity conc. effect obs. 3-75708
 In₂Ga_{1-x}As_x:Te, epitaxial growth, effect of substrate orientation on growth rate in (111)-(100) range (Russian) 3-64255
 InP:Te, Zn, carrier density rel. to solubility of donor, acceptor dopants 3-60886
 n-InSb:Te, Shubnikov-de Haas oscills., reversal effect 3-58284
 KCl:Te(In) two photon multistage radiation during interaction of a single electron-vacancy pair with activating centres (Russian) 3-41557
 p-type Te, evaporated films, resistivity meas., strain sensitivity 3-41278
 Te:¹²⁵Te, nucl. quadrupole interactions, Mossbauer spectra 3-50501
 p-Te:Sb, impurity band cond. and negative magnetoresist., low temp. 3-44094
 Te(I) transitions within ground configuration, high dispersion measurements 3-46182
 ZnS:Te, isoelectronic traps, bound states in forbidden energy gap 3-58226

tellurium compounds

- glassy semiconductors based on Te, As, Si, Ge, temp. dependence of conductivity (Russian) 3-60870
 monohalide and monohydride molecules, rotational and hyperfine structure constants tables 3-49446
 monomethyl tellurium radical, u.v. absorptopn spectra 3-46261
 Ag-Se-Te glasses, thermal stability, energies and rates of crystallization 3-75478
 As-S-Te-I glasses, elec. resist. rel. to inhomogeneous struct. (Japanese) 3-64391
 As-Te glasses, glass forming ability and related properties 3-43756
 As-Te glasses, structural model, local order parameters 3-40848
 As-Te-Ge glasses, kinetics of growth of conductive filament during memory process 3-41240
 As-Te-Ge-Si, amorphous, local potential distrib. and I-V characts. 3-64343
 Cu-Te system, phase diagram, Cu_{2-x}Te region, DTA anal. (French) 3-72181
 Ge-Te amorphous alloys, thermally induced structural and electrical effects 3-58259

tellurium compounds continued

- Ge₂₀Te₃₀As₄₀, T-L type switch, design and performance 3-55316
 H₂Te₂O₆, crystal structure of Te(IV,VI) oxyhydroxide 3-43765
 Mn-Bi-Te magnetic film, diffraction efficiency rel. to holographic storage 3-42976
 Se-Te alloys, transition in conducting from extrinsic to intrinsic semiconducting mechanism 3-52881
 SiTeAsGe amorphous glass thin film switch, injection processes and threshold switching characs. 3-55317
 Tb-Te films, simple cubic structure 3-52768
 Te-Ag, amorphous films, condensation, struct. obs. using electron microscope 3-75692
 Te-As-Ge-Si system, amorphous, e.s.r. obs. of Mn²⁺ from 420 to 77K and at 4.2K 3-64550
 Te-Au, amorphous films, condensation, struct. obs. using electron microscope 3-75692
 Te-Cu, amorphous films, condensation, struct. obs. using electron microscope 3-75692
 Te-Se melt, high temp. semicond. to metallic cond. transition 3-72390
 Te₆₀As₂₅Ge₁₅S(Se), glass, physico-chem. props. (French) 3-60666
 Te₄₀As₃₅Ge₂₅Si₁₈, threshold switching in presence of photo-excited charge carriers 3-41244
 TeF₆, Raman band contour analyses and Coriolis const. 3-67816
 TeF₆-square pyramidal ions, mean amplitudes of vibration calc. (German) 3-67781
 TeF₆Cl, microwave spectra of isotopic species 3-46304
 Te₈₁Ge₁₅As₄ amorphous film, laser induced crystallisation, writing-in 3-70839
 TeI, cryst. struct., optical props. 3-72059
 TeO₂, free energy of formation from e.m.f. meas. 3-58138
 α -TeO₂, hydrothermal crystallization 3-80154
 TeO₂, i.r. refl., polar phonon spectrum 3-53106
 TeO₂, matrix isolated, i.r. spectra, bonding, geometry and thermodynamic functions 3-75044
 TeO₂, nonlinear susceptibility dispersion, 0.35-0.53 μm 3-43034
 TeO₂, paratellurite, suppression of constitutional supercooling during Czochralski growth 3-80168
 TeO₂, u.s. attenuation, c.w. acoustooptical and pulse-echo techniques 3-45427
 TeO₂ deflection devices based on light diffraction by u.s. wave 3-56693
 TeO₂ glasses, highly refracting, effect of H₂O on i.r. transmission 3-64620
 TeO₂-Fe₂O₃, phase equilibrium and elec. conductivity 3-60784
 Te_{100-x}Tl_x, (15 $\leq x \leq 50$), obtained by rapid cooling from liq. state, cryst. 3-64814
 TiBO₃, calcite-type borate, structure and props. 3-40871
 TlI, (n²P-n²D₂) resonance lines, collision broadening, cross-sections (Russian) 3-72770
- temper brittleness** see brittleness
- temperature**
 see also atmospheric temperature; boiling point; Curie temperature; Debye temperature; Neel temperature; temperature scales
 fluctuations in small systems, the two level atom 3-74171
 photoluminescent AlO clouds, temps., diffusion coeffs. and densities 3-59136
 solar, from cryst. spectrometry of active regions 3-65645
 Sun, central core, calculation based on moon rock age (Hungarian) 3-76973
- temperature compensation** see compensation
- temperature control**
 see also thermostats
 ammeters, temperature compensation, permanent magnet moving coil type with shunt, design (Japanese) 3-62174
 automatic temperature regulator 3-48368
 constant logarithmic decrement controller, for constant temp. differential 3-66165
 cryostat, for flash photolysis installation 3-53861
 crystal growth by Czochralski method using induction heating 3-53181
 electronic thermostat, with on-off control 3-51540
 fatigue testing machine with programmed load changes at room and elevated temps. 3-61243
 isodromic, heat of solution, elements in metals 3-70281
 neutron irradiation container 3-51706
 stabilization system, high precision, 30 to 100C, ferroelectric crystals study 3-62009
 thermodynamic methods, for low temperatures (German) 3-73691
 thermostat, 8 to 400 K, in n.m.r. at high pressures 3-51551
 thermostat, with electronic temp. stabilization 3-70278
 GaP single crystals, liquid encapsulated Czochralski pulling 3-72811
 ^4He superfluid, temperature stabiliser near λ -point 3-62026
- temperature distribution**
 aerosol particles, thermophoretic force calcs. 3-63767
 air, spark-over, fireball, laser irradiation, cooling of heated region, temp. and density distrib., rel. to degree of ionisation (Russian) 3-57968
 alloys solidification in cylinder with axial and radial-axial heat transfer 3-80217
 anisotropic half space, transient temp. distribution 3-57170
 Arctic Ocean, temp. microstructure anomalies 3-53452
 North Atlantic, 1948-68 water temp. anomalies, long-period var. 3-41937
 E. Atlantic, obs. of variability in thermohaline staircase 3-53460
 atmospheric low-level vertical temp. profiles, meas. instrument 3-51188
 atmospheric vertical profiles of small-scale temp. structure 3-65299
 axially symmetric region convection, temp. field distribution calc. 3-59824
 Bristol channel, circulation rel. to salinity and temp. distribution 3-65261
 close binary stars, eclipsing, model, reflection effects, temp. distrib. 3-51327
 crystal growth, chemical vapour transport method, heat transfer and temp. oscillations 3-64774

temperature distribution continued

- current leads, cooling, thermodynamic optimisation, refrigerator min. power input calc. 3-48382
- cylinder, infinite, appl. of linearized functions to error estimation (*Russian*) 3-70756
- cylindrical body, temp. and internal stress distrib. on cooling 3-69321
- cylindrical crystals, internal stress depend. during growth 3-75490
- earth core-mantle interface, temp. gradients 3-47630
- eddy diffusivities in tube bundles with cross flow (*German*) 3-63663
- in electron beam heated solid body, mathematical analysis (*Russian*) 3-53262
- explicit finite-difference scheme, space and time steps choice 3-59825
- fluid, viscous incompressible, flow in rectangular channel 3-75195
- fluid, viscous incompressible flow, const. heat generation, flow in channel, pipe 3-78950
- freshwater lake temperature structures, temporal changes 3-61610
- fuel element in nuclear reactor, dependence on power gradient (*German*) 3-67486
- geothermal state distribution, ground water system 3-76528
- geothermal systems, temperature inversions 3-76543
- gray medium in rectangular enclosure, radiative equilibrium temp. distributions 3-54180
- half-space, transpiration cooled, temp. distrib. determ. by variational method 3-54178
- half-space under action of thermal shock on bounding surface 3-54095
- heat carrier flow with axial heat conduction and internal sources, temp. field determ. 3-60541
- heat pipe, liquid N₂, thermal cond. meas., effect of power load and angle of inclination 3-53859
- heat transfer by natural convection between vertically eccentric spheres 3-46401
- hollow cylinder, temp. fields in presence of heat source under boundary conditions 3-59826
- hypersonic sphere wakes, laminar and turbulent, Mach 13.5, density and temp. distributions 3-40753
- hypersonic tunnel wall, upstream wall temps. effects, turbulent boundary layer profile meas. 3-57780
- Indian E. Coast, sea temp. variations 3-47667
- infinite plate with rectangular hole, Riemann-Hilbert problem 3-62621
- jet, temperature and velocity distribution, three-dimensional, surface heat loss, gravitational stability 3-46505
- jets in cross flow, turbulence intensity, temp. and vel. distrib. 3-46491
- Jupiter temperature and ammonia profiles from inversion of i.r. spectrum 3-80983
- lakes, deep temperate, seasonal thermal structure 3-65547
- laminar boundary layer flow, porous flat plate, asymptotic suction temp. profile 3-78951
- laser beam machining of thin films, temperature distributions induced by irradiation of Gaussian beam (*Japanese*) 3-59906
- laser rod, optically pumped, transient temp. distrib. for single shot and repetitively pulsed operation 3-59866
- linear heat source in turbulent boundary layer, temp. fluctuation meas. (*French*) 3-78939
- liquid-crystal contact lens for corneal temp. distrib. meas. 3-56995
- lithospheric downgoing slab in deep seismic zones 3-47642
- low-loss materials for waveguides, light-induced temp. rise 3-51949
- neptune adiabatic temp. distrib. determ., comparison with core melting tem. 3-47928
- non-Newtonian flow, ducts, asymptotic Nusselt numbers, heat transfer, temp. profiles 3-40704
- nuclear reactor, EBR-II, thermal mixing in outlet plenum 3-67431
- nuclear reactor, liquid metal fast breeder, heat exchanger components, calc. 3-67506
- ocean, internal wave strain, temp. perturbations, vertical spectra 3-47677
- ocean frontal system in upwell regime, west of Cape Town 3-73275
- ocean mapping, wind and tide effects 3-41944
- oceans, seasonal surface water temp. var. and annual patterns 3-51002
- optimum temp. distrib. at surface of plate, flow stabilisation by preheating (*Russian*) 3-63626
- Pacific Ocean, circulation and temp. distribution, two-level numerical model predictions 3-59005
- plasma, electron temp. gradient stabilising effect on collisionless drift instabilities 3-52513
- plate containing two circular holes of different sizes under uniform heat flow, thermal stresses 3-42769
- polyethylene, non-Newtonian flow under conditions of an inhomogeneous temp. distribution 3-63593
- PWR, exptl. verification of temp. distrib. in primary shield during power operation 3-54536
- quasi-isothermal quasi-isobaric conds., decomp. reactions, Derivatograph 3-73689
- radial heat flow between two concentric spheres 3-66699
- random, rel. to non linear creep buckling in reactor materials 3-74671
- rarefield gas flow, binary gas mixtures, He (*Russian*) 3-46370
- rectangle, expanding, appl. of extended source method and new numerical techniques 3-70586
- rods, two semi-infinite, continuous and discrete moving heat sources 3-70757
- seawater, thermal expansion, adiabatic temp. gradient and potential temp., new polynomials 3-53444
- semi-infinite body, cylindrical hole, thermal stresses, temp. distrib., linear thermoelasticity 3-70562
- semi-infinite piezoelectric rod, distrib. of temp., displacement, stress, electric field, and entropy density 3-72575
- semi-infinite-finite solid having contact resistance, linear heat flow 3-70758
- semiconductor, electron-beam alloying, local temp. fields, calc. method and exptl. obs. (*Russian*) 3-53192
- semitransparent cylindrical medium solidification, heat conduction and radiation 3-46701

temperature distribution continued

- shock wave, spherical, in plastic compressible medium (*Russian*) 3-42826
- solar pole-equator temp. differences, energetics and momentum balance 3-69823
- solids temperature fields under natural heat exchange conditions with the atmosphere 3-77916
- spherical cone, finite, steady state calc. using Naylor transform 3-62640
- spherical thermoacoustic receiver, temperature field calc. 3-59557
- steady temperatures in rectangles with broken boundary conditions, separated variables solution 3-45740
- submerged stream of overheated metal, mathematical model for temp. and kinematic fields (*Russian*) 3-69331
- Sun, temperature difference between pole and equator 3-65691
- superconductor, internally cooled, steady state temp. profile (*Japanese*) 3-41305
- surges, propagation in Na cooled fast reactor following local primary circuit blockage (*German*) 3-67491
- temperature changes in rivers, math. model 3-44969
- terrestrial planets, present thermal state, viscosity-temp. relationship 3-42171
- thermal plume, dynamic surface temp. structure, airborne thermal imagery 3-43649
- thin layers, heated by electron beam, brightness temperature method (*Russian*) 3-55174
- time dependence, in MTR type fuel elements (*German*) 3-74644
- transfer functions for temp. of a body in the presence of generalized thermal effects 3-66702
- transient temps. in a plate from a Gaussian distribution of normal heat flux and current flow, application to arc discharge 3-45735
- transonic nozzle flow with a parabolic temperature distribution 3-40752
- TRIGA nuclear reactor, numerical soln. of Poisson's eqn. by computer using finite difference techniques 3-63150
- turbulent lubrication, thermal effects 3-54804
- Uranus adiabatic temp. distrib. determ., comparison with core melting tem. 3-47928
- vibrational, chemical reactions, exothermic, population inversion 3-65070
- water horizontal layer, turbulent convection 3-60537
- He hollow cathode discharge, temp. distribution of the gas in the negative glow 3-49780
- Mo, electron beam heated, mathematical analysis (*Russian*) 3-53262
- NaK, eutectic mixture, temp. and eddy diffusivity profiles 3-52432
- SF₆, heavy current stabilised arc column, current density and temperature, radial distrib., calc. 3-68106
- temperature measurement**
- see also pyrometers; spectral methods of temperature measurement; temperature scales; thermocouples; thermometers
- airborne temp. data, correction method for sensor response time 3-47837
- atmospheric low-level vertical temp. profiles, meas. instrument 3-51188
- atmospheric temperature difference recorder for 0 to 50°C range 3-47829
- automatic precision titration calorimeter, temp. meas. 3-45594
- bibliography (Jan. 1953 to Dec. 1969) 3-42540
- biological telemetry system, 3 channel implantable 3-57010
- carbon resistor, 0.3 to 4.2K, empirical function between resistance and temp. 3-48387
- cryogenic linear temperature sensor, Micro-Measurements Ltd., magnetoresistance, 4.2 to 300 K 3-59565
- deep tissue, thermometers 3-73923
- ethylene-O₂ flames, 3 torr, double-probe electron temp. meas., current-voltage charact. 3-80523
- ferrite magnetic permeability thermometer, temp. dep. of permeability of ferrites, appl. of thermometer 3-73703
- furnace system, versatile time-temp. programming and elec. meas. capability 3-77406
- gas, Kurlbaum's and Na D-line reversal methods, analysis consideration error 3-56635
- gases, thermoelectric thermometer, cancellation of radiation error (*Japanese*) 3-66166
- gauges, industrial appl. (*Italian*) 3-66159
- glass, hot, errors, thermocouple and spectral methods 3-66169
- in high press., electrical connection for thermocouples 3-45434
- in high-pressure chambers 3-51560
- hydrostatic pressure region, using GaAs diode transducer (*Polish*) 3-39876
- in-reactor monitor, indirect determ. of vapour pressure 3-67403
- instantaneous, using electronic circuit 3-77405
- ionospheric electron temp. meas., effect of isotropic nonequilibrium plasma 3-73351
- Kelvin reciprocal sensor, using Pt resist. thermometer 3-77403
- lakes, Italian, i.r. technique (*Italian*) 3-61613
- lens polishing zone, dynamic conditions 3-62091
- marine and fresh water, remote sensing using airborne differential radiometer 3-73607
- micropyrometers with i.r. microscope and scanning device, small ambient temperature differences (*German*) 3-59561
- mixed-oxide fuel pin centreline temps., meas. to 2700°C 3-45453
- neutron temperature, rel. to temp. of medium, fission track detectors 3-48539
- night min. air temp. forecasts at Wyton using embedded thermometers 3-65531
- Nimbus 5 borne selective chopper radiometer for atmospheric temperature sounding 3-69736
- n.m.r. thermometers below 1 mK, possible limitation 3-55480
- nuclear reactor coolants, frequency shift caused by thermal expansion of microwave resonant cavity 3-70282
- oblique grid shadow graph for meas. of temperature distrib. in transparent fluid 3-39898
- ocean surface, using polarised i.r. radiometer (*French*) 3-65536
- plasma, direct display meter using Langmuir probe 3-68092
- polypropylene melt, temp. meas., i.r. fibre optics 3-45436
- primary acoustic thermometry, systematic errors, range 2-20 K 3-62032
- Pt resistance thermometer, on IPTS-68 scale (*German*) 3-42530

temperature measurement continued

- pyrometers, infra-red, selective absorption, high temperature monitoring of waste gases from industrial furnaces 3-70284
 pyrometry, high temp. optimal utilization of redundant inform. in thermal radiation 3-70290
 rarefied gas flow, binary gas mixtures, He (*Russian*) 3-46370
 sea surface, by S-band radiometer 3-76920
 sea surface temp., improved radiometric meas. using polarizing radiometer (*French*) 3-51207
 sea surface water temp. meas. using airborne dual-channel i.r. radiometer 3-51204
 small temp. variations meas. technique 3-56633
 stratosphere and lower mesosphere temps. from changes in satellite radiances 3-51027
 surface, convex surfaces, thermocouple network 3-39881
 thermal medium, meas. of temp. fluctuations by light intensity modulation 3-73682
 thermal plume, dynamic surface temp. structure, airborne thermal imagery 3-43649
 thermistor thermometer bridges, linearised, small temp. change meas., calorimetry 3-77400
 thermocouple, Cu-Fe alloy electrode, temp. meas. 4 to 273 K 3-73705
 thermodynamic methods, for low temperatures (*German*) 3-73691
 thermometer, ultrasonic, in-reactor fuel rod centreline high-temp. meas. 3-45454
 thermometer screen design rel. to effect on observed temperature 3-48371
 thin films, metallic and semiconducting, laser radiation, steady and transient temp. field calc. (*Russian*) 3-40277
 three-colour pyrometer, for high temps. (*Russian*) 3-51552
 ultralow temperatures, 1.7 mK to 0.5K, nuclear magnetic thermometry, magnetometer measurements of AuIn₂ susceptibility 3-73817
 u.s. thermometry, temp. meas. up to 2400C, inaccessible objects 3-42521
 water, relative threshold nucleation temps. for active nucleation catalysts 3-49971
 welding, steel, Ti alloys, max heating temp. calc. (*Russian*) 3-41789
 Ge melt, apparatus for meas. temp. fluctuations (*Russian*) 3-66160
 H₂ plasma, using Ar laser 3-46550
 Ni resist. element, linear temp. bridge design, math. approach 3-51543
 Pt resist. element, linear temp. bridge design, math. approach 3-51543
 (U,Pu)O₂, thermoelec., resist., and u.s. centreline thermometry 3-45455
 W, neutron irradi., irradi. temp. monitoring, void superlattice const. meas. 3-68291

temperature scales

- 2.2 K to 13.81 K, based on reduced resistance of Pt (*German*) 3-59540
 conversion equation, International Practical Temperature Scale-1968 3-77379
 international, practical, secondary fixed point determ. 3-73661
 paramagnetic salt temperature scale, NBS-acoustic scale, IPTS-68, relationship 3-61980
 pyrometric meas., optimal utilization of redundant inform. in thermal radiation 3-70290
 superconductive fixed point devices, for thermometric reference 3-51511
 Ce₂Mg₃(NO₃)₁₂.24H₂O, magnetothermodynamics, temp. scale between 0.0006 and 4.2K 3-48334

tenacity see tensile strength**tensile strength***see also fracture*

- alloy, b.c.c., neutron irradi. effect on tensile props. 3-79386
 boiler drums, non-steady operating conditions, life testing, varying tension, high temp. and pressure 3-50808
 ceramic specimens, miniature, high temp. tensile test 3-72961
 composite, B/epoxy, off-axis strength test 3-55868
 composite, fibrous, ductility, fibre-matrix interface effect 3-80454
 composite, filamentary, prestrain effects 3-64996
 composite, notched laminated, strength postulates 3-55866
 composite, unidirectional, yielding under external loads and temp. changes 3-55865
 composite laminates, post-yielding behaviour, inelastic micromechanics 3-55864
 construction materials, calc. for different ratios of main stresses 3-58687
 Coranex CDA 638, grain size strengthening and weakening 3-58662
 cryostat, reloading device, tensile testing at 20 K 3-51558
 cyclic strength tests, long-term, methodical features 3-42513
 design props. of materials test method 3-50817
 1,4-diaminopiperazine polymers and metal chelates, dynamic mechanical, thermal electrical and tensile props. 3-80462
 edge-notched tension specimens, elastic-plastic deform. under plane stress conditions 3-64953
 epoxy resin, short-term action of static loading and aggressive liq. media influence on mech. props. (*Russian*) 3-80469
 failure criterion for strengthened materials 3-44626
 failure under simple and composite stresses, deform. criteria 3-58686
 fatigue testing, low-cycle, compression-tension, in gaseous media, elevated temp. apparatus (*Russian*) 3-61240
 fatigue testing machine, operation of inductive dynamometer 3-76403
 f.c.c. crystal, theoretical strength calc. using exponentially attractive and repulsive interatomic interactions 3-68304
 fibre glass, unidirectional, ultimate strength determ. 3-47464
 fibre-glass shells manufactured in vacuum, tensile and deforming characteristics (*Russian*) 3-64990
 fibreglass, rated strength characts. in stress conc. zones 3-80455
 fibreglass-reinforced composite, fracture possibility under transverse tension and shear (*Russian*) 3-64991
 glass, K8, tensile strength and microhardness, and LiF crystal 3-73063
 glass fibre epoxy laminates, orthotropic characts. under plane stress 3-53274
 glass fibre reinforced plastic, flexural strength, optimum volume fraction 3-50765
 glass fibre reinforced plastics, low-cycle fatigue strength and notch factor 3-69373
 glass fibre strands, tensile tests, fibre surface area effect on strength 3-50769
 glass fibre ware, orthogonally reinforced, crack form. 3-64993
 glass laminates, tensile strength, low temp. and high strain rate, stress conc. coeff. 3-73020
 glass reinforced epoxy resin with Vulkador A crosslinking agent, mech. props. enhancement 3-58709
 glass reinforced plastic, effect of composition and porosity on tensile strength and elasticity 3-58713
 glass ribbon composite, fabrication and characteriz. 3-76348
 glass spheres, diametrical compression 3-72960
 glycerol, dynamic tensile failure, technique for liquids 3-39852
 granite, Winsboro, tensile anisotropy at 0.5 kbar 3-76611
 granular materials, effect of moistening and demisting, influence of porosity (*German*) 3-47488
 graphite, reactor, neutron irradiation, tensile stress expansion (*German*) 3-71263
 graphite, reactor, oxidation reaction rate in damp atmosphere, stress effect (*German*) 3-71271
 graphite, tension-compression tests, strength in a plane stressed condition 3-53298
 human tissue, mech. behaviour 3-42367
 Inconel 718 sheet, time-depend. edge-notch sensitivity rel. to mech. and microstruct. characts. 3-64952
 interfacial tension measuring apparatus using DuNouy ring method 3-42518
 isotropic materials, strength criteria representation in two-dimens. invariant space 3-55897
 long term, thermodynamics 3-80367
 long-duration slow-cycle testing, thyristor servo drive, single-phase reversible 3-73106
 Makrolon, prolonged storage effect 3-80488
 metal, b.c.c., neutron irradi. effect on tensile props. 3-79386
 metal, failure process in complex stress state, mechanism 3-58689
 metal, short-time stress/strain characteristic, temp. depend., thermally activated models 3-69309
 metal sheet, groove formation, influence of plastic props. in forming limit diag. 3-76197
 metal/metal interface, differential modulus effects on mech. behaviour 3-40921
 metallic single crystals, f.c.c., tensile behaviour, theoretical model (*French*) 3-64089
 nonmetallic material testing apparatus for -80 to +300°C 3-65058
 n-pentane, by acoustic cavitation 3-46476
 plastic isotropic materials, math. model of damage accumulation 3-64936
 polycaprolactam, glass fibre addition rel. to mech. props. (*Polish*) 3-58710
 polycarbonate, prolonged storage effect 3-80488
 polyester dough moulding materials, fibre reinforced, stiffness and strength 3-73007
 polyethylene terephthalate film, solid-state transitions investigation by temperature tear strength method 3-61221
 polyimides, strength and relaxation props. (*Russian*) 3-80499
 polymer, breakdown under load, i.r. spectral obs. 3-58747
 polyoxymethylene, acicular single crystals, strength props. 3-54779
 polypropylene composites, thermoplastic fibre reinforced, transcrystalline morphology 3-64985
 polypropylene melt, processing, aging, effective viscosity, tensile strength, effect of polymeric antioxidants 3-73058
 powder, temp. effect, coating with liq. films 3-80507
 PVC, long term strength, flat stressed state 3-58751
 quartz-phenolic composite, quasistatic uniaxial strain and Hugoniot tests compared 3-73111
 reinforced polymers, tension normal to the fibres, strength and deformability 3-64989
 ring method of testing, correl. between high-temp. bending and tension stress relax. 3-69430
 rod specimen, light-weight grips 3-44702
 small local deviations influence in specimen diameter on conventional strain at maximum load in tensile test (*German*) 3-74752
 snow, volume strengths rel. to density and type 3-76789
 spring alloy, cold deformation, ageing, relaxation resist., elec. resist. 3-76210
 steel, austenitic stainless, warm extruded, struct. and mech. props. 3-50749
 steel, carburized, quenching in fluidized bed effects on struct. and props. 3-50735
 steel, cold-rolled strip, rapid cooling under tension during annealing (*German*) 3-80300
 steel, constrained disc burst tests, elastic-plastic analysis 3-50822
 steel, corrosion resist., heat treatment and H₂ absorption effect 3-80355
 steel, Cr-Mo type, effect of carbon addition 3-47432
 steel, Cr-Ni-Mn type, carbon and nitrogen conc. depend. 3-64785
 steel, effect of alloying element C and heat treatment on fatigue strength, reln. to static strength 3-41750
 steel, effects of geometric form (*Russian*) 3-76221
 steel, fatigue props. rel. to inclusion size, shape and distrib. 3-61178
 steel, fatigue tests, low cycle fracture resist. in stress conc. zones, high temp. 3-69435
 steel, Fe-Mn-C type, isothermal transform. induced struct. and props. 3-69224
 steel, ferritic, anisothermal stress relax. processes 3-69279
 steel, grain refinement by rapid cyclic heating 3-61169
 steel, heat resistant, statistical analysis 3-80375
 steel, high tensile structural and welded joints, fatigue strength 3-44596
 steel, high-strength, test method for transient stress conditions characteriz. at elevated temps. 3-69432
 steel, high-strength 4340M, grain refinement effect on microstruct. and mech. props. 3-64854

tensile strength continued

- steel, induction hardened, fatigue strength, tempering temp. influence (*Japanese*) 3-41778
- steel, low-C, plastic instability phenomena (*French*) 3-69301
- steel, low-C, prestrained, temp. effect on mech. props. anisotropy 3-47427
- steel, low-C unalloyed, strengthening by small Nb additions 3-64922
- steel, martensite, manganese substitution reaction during tempering, kinetics (*German*) 3-80301
- steel, Mn-Mo and Mn-Mo-Ni type, normalizing and austenizing effects 3-50747
- steel, Ni-Mo, post-sintering heat treatment and microstruct. phenomena 3-69306
- steel, repeated impact tension loading (*German*) 3-76395
- steel, rolled plates, anisotropy 3-69256
- steel, stainless, AISI Type 304, high strain rate tensile props. 3-80386
- steel, stainless, Type 304, shielded metal-arc weldments, props. 3-47435
- steel, stress relaxation tests, bending, tension, time factor effect 3-50803
- steel, temp. and strain rate influence 3-69312
- steel, thermal stress analysis of LMFBR subassembly duct wall for severe thermal loading 3-46161
- steel, thermo-mech. treated, corrosion fatigue in H_2SO_4 soln. cyclic strength (*Russian*) 3-41766
- steel, weld metal, Type 316, struct. and props. 3-47434
- steel, yield stress in compression rel. to mech. props. 3-58681
- steel castings, Cr-Mo-V creep-rupture investigations as function of structure condition, tempering treatment, impurity content (*German*) 3-47400
- steel cylinder, wire-wrapped, fracture resistance 3-50825
- steel, maraging, heat treatment influence 3-44598
- steel welded joint, high temp. Cr-Mo-V type, rel. to struct. (*German*) 3-47398
- steel wire, effect of hydrogen, alcohols and moisture, correl. with elec. resist. (*Russian*) 3-80314
- steel wires, in aqueous-alcoholic and alcoholic HCl soln. with added Sb_2O_3 (*Russian*) 3-80331
- steels, structural, low cycle fatigue effect on brittle fracture characteristics (*German*) 3-47523
- stress corrosion cracking susceptibility test procedure 3-69402
- strip, weakened by array of holes, uniaxial tension, initiation and propagation of plastic zones 3-70611
- testing machine extension for axial load and torque action, low temp. 3-58784
- tubular specimens, thin-walled, three-dimens. stress, testing device 3-73102
- ultimate strength and plasticity of materials in complex stress state, stat. criteria 3-58685
- Zircaloy-2, quenched, strain ageing behaviour 3-58665
- Al, polygonized, subboundary effects, yield peak in tensile diagram (*Russian*) 3-44569
- Al 6061-T651, yield stress, effect of very short time at temperature 3-6290
- Al alloy, 2024-T3, fatigue crack delay and arrest due to single-peak tensile overloads 3-58789
- Al alloy, tensile prestrain effect on fatigue strength in high cycle fatigue 3-64950
- Al alloy castings with as-cast struct., mech. props. estimation method 3-55808
- Al alloys, fatigue resistance, evaluation of endurance limit, rel. to ultimate tensile stress 3-53253
- Al alloys, fracture strength under static and cyclic loads comparison 3-47424
- Al alloys, recrystallized extruded, anisotropy 3-55810
- Al and alloys, yield stress in compression rel. to mech. props. 3-58681
- Al composite, reinforced, short-term, long-term and cyclic strengths (*Russian*) 3-41806
- Al/B composite, heating effect on mech. props. 3-58708
- Al/Cu composite arranged in chequered flag pattern (*Japanese*) 3-50726
- Al/graphite fibre reinforced composite, high temp. props. (*Japanese*) 3-44669
- Al-Al₃Ni aligned eutectic, tensile fracture behaviour at 293, 593, and 743 K 3-47408
- Al-CuAl₂ aligned eutectic, tensile fracture behaviour at 293, 593, and 743 K 3-47408
- Al-Cu(4 wt.%) alloy, substruct. and dispersion hardening 3-69231
- Al-Mg alloy, cold work effect on strain rate sensitivity 3-69300
- Al-Mg alloys, discontinuous flow at high temps., Portevin-Le Chatelier effects 3-69299
- Al-Mg-Zn alloys, soln. softening effect of zinc at high temps. 3-64948
- Al-Zn-Mg alloys, high-strength, tensile deform. and fracture props. 3-76207
- Al-Zn-Mg-Cu alloy 7075, improved fatigue resist. through thermomech. processing 3-64917
- Al₂O₃, sapphire filament, creep mechanism 3-76318
- B fibres, determined by defects at B sheath-core interface 3-80451
- Be, fracture toughness of hot pressed block and metal sheets 3-50814
- Be, fracture toughness props. of S-200 grade specimens 3-50816
- Be, tensile behaviour under hydrostatic pressure, effect of surface conditions, ductility 3-61182
- Be fine wire, prep. conditions characteriz. 3-55811
- Bi₂Te₃-Bi₂Se₃ linear expansion coefficient, mechanical props. 3-75628
- C fibre, crack formation, heat treatment temp. depend. (*German*) 3-76372
- C fibre, fracture behaviour rel. to surface energy (*German*) 3-73041
- C fibre, PAN-based, effect of defect struct. 3-50780
- C fibre, rel. to composite material props. (*German*) 3-76354
- C fibres, influence of ribbon unbending during extension 3-58733
- C/C composites, fibre volume percent depend. 3-55854
- c/c composites, geometric effects 3-76344

tensile strength continued

- Cu, hydrostatically extruded, heavy deform. influence (*Russian*) 3-72892
- Cu and alloys, yield stress in compression rel. to mech. props. 3-58681
- Cu filaments, U.T.S. and ductility (*Russian*) 3-69267
- Cu strengthening curves for thread-like crystals, orientation dependence during deformation by elongation and torsion 3-80360
- Cu/Fe composite arranged in chequered flag pattern (*Japanese*) 3-50726
- Cu-Al alloy, internally oxidized, particle size effect on yield stress 3-80294
- Cu-Al(1 wt.%) with Ag, Pd, As and In additions, internally oxidized, soln. and dispersion strengthening (*Japanese*) 3-44618
- Cu-B eutectic alloy, unidirectional structure 3-76155
- Cu-Cu₂Zr eutectic, tie-line cond. and tensile props. 3-47409
- Cu-CuZrGe pseudobinary eutectic, tie-line cond. and tensile props. 3-47409
- Cu-Ni-Zn alloys, high strength microduplex, characteriz. 3-64911
- (Fe, Cr)-(Cr, Fe)₃C₃ in-situ grown unidirectionally solidified composite primary precipitates influence 3-58664
- Fe, cast, damping capacity correl. with mech. props. and microstruct. 3-50721
- Fe alloys, substitutional, static strain aging 3-69280
- Fe-Al-Cr, alloys, effect of Ti and Mo additions 3-61179
- Fe-Mn alloy, fatigue cracked fracture toughness, sulphur content and grain size effects 3-69292
- Fe-Ni alloy, low temp. mech. props. characteriz. 3-50737
- LiF crystal, tensile strength and microhardness, and K8 glass 3-73063
- Mo, cast, boundary strength increase by V microadditions 3-61177
- Mo alloy, electrothermal treatment, cold deformation 3-76216
- Mo single crystals, electron bombardment effect, cryst. orientation depend. (*Russian*) 3-61163
- Mo/Cu, Mo/Cu-Cr fibre reinforced composite cold rolling deformation (*Japanese*) 3-73017
- Mo-Permalloy/Cu, core mag. composite drawn wire characteriz. for memory applics. (*Japanese*) 3-50394
- Nb, high purity single cryst., plastic deform. at 2.17-300 K (*French*) 3-55004
- Nb, interstitial effects on tensile behaviour, 20 to 1000°C (*French*) 3-80291
- Nb, yield point temp. depend. rel. to dislocation pinning by oxygen interstitials (*Russian*) 3-72854
- β -Nb-Zr, deform. temp. depend., slip, twinning and dislocations rel. to yield and fracture 3-52662
- Ni alloy, heat resistant, statistical analysis 3-80375
- Ni-Fe, alloys polycrystalline, degree of order, dislocations, slip lines, structure 3-53233
- Pb(Zr,Ti)O₃ transducer ring, cold pressed, anisotropy 3-75944
- Sb₂Te₃-Bi₂Te₃ linear expansion coefficient, mechanical props. 3-75628
- Si₃N₄, hot-pressed, depend. on temp., stress, strain rate and impurity content 3-76286
- Si₃N₄, hot-pressed, UTS, room temp. to 2800°F 3-76291
- Ti alloy, ageing 3-80356
- Ti alloy, effects of geometric form (*Russian*) 3-76221
- Ti alloy, high-strength, strengthening and rupture characteriz. 3-47429
- Ti alloy, VT3-1, annealing effect 3-76211
- Ti alloys, and welded seams, 4-700 K 3-61175
- Ti alloys, fatigue resistance under asymmetrical cyclic loading, struct. effect 3-44635
- Ti alloys, fracture strength under static and cyclic loads comparison 3-47424
- Ti sheet, produced by high rate vapour deposition process, condensation temp. influence 3-76481
- Ti/Mo wire reinforced composite characteriz. 3-58719
- Ti-Al-Mn alloy, hydrogen embrittlement, tensile and stress-to-rupture tests 3-69277
- Ti-Al-V-Sn alloys, heat treatment effects 3-50727
- U, warm working effects on mech. and fabrication props. 3-72904
- U-Nb(Ti) alloys, fracture toughness and mode correl. with microstruct. 3-76414
- V-Ti, neutron irradiat. effect on high temp. mech. props. 3-79385
- W wire, effect of hydrogen, alcohols and moisture, correl. with elec. resist. (*Russian*) 3-80314
- W/Cu fibre reinforced composite, cold rolling deformation (*Japanese*) 3-73017
- Zn, coated with liq. metal, failure under brittle fracture to plastic flow transition conditions 3-50741
- Zn-Al (30 wt.%) alloy, solid soln. decomp. and superplasticity behaviour (*French*) 3-47418
- Zr-Cr-Nb, effect of heat treatment on tensile strength and hardness 3-61165
- ZrC creep testing variation in C distrib., laser microanalyser 3-72977
- tensimeters see vapour pressure measurement
- tensors
- asymmetric wave stress tensors and wave spin, Hamiltons variational principle 3-43586
- Bel Robinson, connection to gravitational radiation, based on Einstein canonical pseudo-tensor 3-62588
- canonical operators, structure in unitary groups, boson polynomials 3-74106
- crystal classes without centre of symmetry, equivalent tensor coordinate system 3-72029
- curvature, theorems, almost product and almost decomposable manifolds 3-54060
- cylinder demagnetisation tensor 3-44254
- earthquake, structure model, micromorphic continuum, microanisotropy, tensor of microinertia 3-44824
- elastic shell, isotropic, response function represents. 3-59761
- elastodynamics, linear asymm., generalised tensorial fields existence 3-51786
- electrodynamics of moving media, and symmetrical momentum-energy field tensor 3-42926
- energy-momentum, eigenvectors, Einstein-Maxwell theory 3-66663
- Fierz energy-momentum, for a gravitational field 3-66670
- finite groups, irreducible tensor operators in group algebra 3-73977

tensors continued

- gravitation, general covariant two-tensor theory (*German*) 3-48793
 hydrodynamic tensor wave equation 3-75350
 icosahedral irreducible tensors and mol. applics. 3-57623
 impulse-energy, rel. to determ. of eqns. of motion of interaction of magnetic moment with e.m. field (*French*) 3-66603
 irreducible formalism, Hanle effect of molecules (*French*) 3-71572
 Killing, props. for geodesics and charge particle motion 3-45718
 Killing, role in Einstein-Maxwell theory, geometric form of Einstein equations 3-74133
 Killing, spacetimes 3-57140
 magnetotelluric impedance tensors, Australia, conductive-resistive-conductive layering 3-44840
 magnetotelluric study, western Canadian sedimentary basin, tensor analysis, numerical model 3-44853
 mechanics, fundamental principles, tensoric considerations 3-42759
 metric, derivation of post-Newtonian integrals of motion 3-62575
 molecular spherical tensors, ensemble averages 3-43493
 N interacting particles, Brownian motion, diffusion tensor matrix hydrodynamical evaluation 3-70738
 nuclei in mol., elec. dipole shielding tensors 3-43434
 octahedral spinor group, irreducible tensors 3-62561
 polarization, correlation function, depolarized Rayleigh line 3-78828
 Ricci, trace-free, of spherically symmetric spacetime metrics, Petrov-Plebanski classification 3-40161
 Riemann tensor formulation of gravitational wave eqn. 3-42873
 scalar-tensor theories of gravity, conformal invariance 3-66672
 space-time curvature, classification for restricted form of Einstein field eqns. 3-70720
 statistical, determ. in sequential decays odd L 3-62820
 stress, construction in Papkovitch-Filonenko-Borodich method 3-70604
 symmetry of Petrov-type N spaces 3-73978
 thin elastic shells, arbitrary edge loads, effect on stress and deformation, asymptotic expansion of tensor eqn. 3-70585

terbium

- DMSO: Tb³⁺, Eu³⁺ electronic excitation energy transfer 3-47300
 exchange coupling and macroscopic magnetic properties 3-47013
 ferromagnetic, PAC obs. of mag. hyperfine field 3-64591
 film, magnetostrictive generation of elastic waves 3-47115
 film, photoelectron spectrum, struct. effects 3-61106
 glass activator, differences in photo- and cathodoluminesc. 3-64719
 Heisenberg spin system with uniaxial and exchange anisotropy, freq. moments, short-range-order effects 3-55400
 impurity in La_{0.98}Tb_{0.02}Al₂; anomaly in thermoelectric power due to crystal field split in impurities 3-50187
 magnetic anisotropy, field depend., torque meas. 4.2-300K 3-47081
 magnetic phase transition, sound propagation effects nr. transition 3-46709
 magnetic susceptibility near Neel point, temp. depend. 3-79829
 magnetic transitions, thermal expansion and compressibility meas. 3-79834
 magnon-phonon mode mixing, magnetoelastic interaction 3-47112
 melt growth by crystn. 3-44537
 paramagnetic susceptibility, adaption of translation balance for meas. 3-42609
 phonon dispersion, phenomenological model 3-72149
 X-ray absorption spectrum, ultrasoft X-ray region 3-61081
 X-ray photoemission, 4f and valence bands obs. 3-80144
 CaO: Tb film, r.f. sputtered, luminesc. during sputtering 3-69097
 CeMgAl₁₁O₁₉: Tb³⁺, luminescence 3-76066
 GdFe garnet: Tb, ferromag. resonance, high pressure effects on anisotropy and relax. 3-41421
 LaO: Tb film, r.f. sputtered, luminesc. during sputtering 3-69097
 La₂O₃ single crystals, e.p.r. of Tb³⁺ and Pr³⁺ 3-68835
 MgO: Tb film, r.f. sputtered, luminesc. during sputtering 3-69097
 MgO.B₂O₃: Tb, thermoluminescence relation to composition for radiation dosimetry (*Russian*) 3-44499
 MgO.SiO₂: Tb, thermoluminescence relation to composition for radiation dosimetry (*Russian*) 3-44499
 Tb³⁺, energy transfer to and from dyes in liq. soln., electrostatic interaction 3-76093
 Tb³⁺, in YIG, high pressure effects on anisotropy anomalies, ferro-mag. resonance obs. 3-50468
 Tb³⁺, paramag. relax. in yttrium ethyl sulphate 3-50450
 Tb³⁺ in DMSO, radiative and nonradiative transitions rel. to energy transfer model 3-64732
 YIG: Tb, ferromag. resonance, high pressure effects on anisotropy and relax. 3-41421
 Y₂O₃: Eu³⁺, Tb³⁺, radiationless recombinations in surface layers (*Russian*) 3-50612

terbium compounds

- terbium aromatic dyes, nonradiative energy transfer 3-64714
 TbAl garnet, crystal field splittings in electronic Raman spectra 3-41312
 TbAlG: Tb³⁺, absorption and fluorescence spectra analysis, 4K, 77K 3-76067
 Tb₂Dy_{1-x}Fe₂, magnetocrystalline anisotropy predictions 3-47077
 TbF₃-KF system differential thermal, X-ray, crystalloptical anal., phase diagrams 3-64148
 TbFe₂, magnetocrystalline anisotropy predictions 3-47077
 TbFe₂, magnetostriction, at room temp. and temp. depend. 3-44305
 TbFe₂ film, magnetostrictive generation of elastic waves 3-47115
 TbFe_{1-x}Cr_xO₃, Mossbauer spectra fine struct., hyperfine field distrib. 3-58445
 TbFeO₃, orthoferrite, magnetic bubbles, dynamic behaviour 3-50409
 Tb₂Ge₂O₇, flux growth, mag. transition temps. 3-41638
 TbMn₂O₅, mag. struct., neutron diff. (*French*) 3-44223
 Tb(OH)₃, ferromagnetic, anisotropic exchange effects in optical spectrum of isolated Er³⁺ impurities 3-47010
 Tb₂O₃.S, mag. structure and susceptibility meas., antiferromag. ordering 3-44207
 Tb₂O₃Se, mag. structure and susceptibility meas., antiferromag. ordering 3-44207
 TbSb, elec. resistivity, effect of mag. field 3-41171
 Tb_{1-x}Y_{1-x}Sb, sublattice magnetisation, exchange interaction, Neel temp. 3-68775

terrestrial age see earth age

terrestrial atmosphere

- see also air; clouds; ozonosphere; stratosphere; troposphere; upper atmosphere
 aerosol stratifications by laser sounding (*Russian*) 3-69574
 ancient atmospheres anal. for methane and CO conc. 3-73313
 Atmosphere Explorer, scientific objectives 3-42066
 boundary layer, non-stationarity effects 3-65317
 boundary layer gravity wave generation by shear instability 3-61458
 diurnal and semi-diurnal barometric oscillations global distrib., annual variations 3-44906
 electron density distributions at high altitudes around entry vehicles, theory and expt. comparison 3-44911
 e.m. propagation, effect of waves and turbulence in stable layers, symposium (La Jolla, June 1972) 3-65295
 environmental monitoring from space for European demands 3-51075
 evolution, including role of living organisms (*German*) 3-76777
 First GARP Global Experiment, simulation studies and design 3-42053
 four-dimensional data assimilation, transient suppression in optimal sequential analysis 3-65358
 GARP rel. to numerical modelling and weather prediction 3-51072
 greenhouse effect, critique 3-65370
 ground-based remote sensing, techniques and limitations 3-42082
 optical communication, mean universal curve for optical angle of refraction 3-51077
 origin and evolution, relevance to Mars and Venus 3-65773
 PAET, entry probe experiment in Earth's atmosphere 3-47730
 planetary waves, vertical structure (*German*) 3-65321
 Polar Experiment, review 3-56155
 radiative transfer, multiple scattering theory in inhomogeneous atmospheres 3-48815
 remote sensing from space rel. to man's effect on environment 3-51074
 remote sounding from artificial satellites and space probes 3-47767
 remote sounding methods, comparison of sensitivity and resolution 3-42084
 Rossby number similarity theory, A B (μ) functions, variability of empirical determ. 3-65319
 satellite pictures, synoptic model for evaluation 3-51076
 O. Yu Schmidt's ideas in atm. science review 3-47606
 solar activity, effect on solar terrestrial relationship 3-69496
 solar wind interaction rel. to ionization and mass loss 3-65783
 spherical harmonics series summation, alternative algorithm 3-47758
 statistical study of natural atm. signals, computer software system 3-59187
 two-layer fluid model, stability to nongeostrophic disturbances 3-47770
 water cycle, hydrologic studies, control 3-44909

terrestrial composition see earth composition

terrestrial electricity

- air-earth conduction current, meas. of two components in tropics 3-47721
 anomalous dielectric properties of some terrain materials 3-56136
 auroral particle precipitation rel. to electric field, Injun 5 obs. 3-51105
 Carpathian region, electrical cond. anomalies in crust 3-61408
 clay bedrock, l.f. survey, membrane polarisation, apparent specific resistivity variations (*German*) 3-73256
 conducting vein, e.m. response pattern for transmitter-receiver orientations 3-50968
 conducting infinite horizontal cylinder in e.m. input field, geophysical appl. 3-50967
 conducting overburden, enhancement of e.m. anomalies 3-50969
 conductivity anomalies in Japan, review of recent studies 3-73252
 crustal current induced by tidally influenced ionosphere 3-69547
 deep sounding, Rhine Graben, 1967, interpretation model (*German*) 3-73255
 dipole location in horizontally stratified medium, sparse observation network 3-76853
 dipole sounding resistivity measurements, direct interpretation, layered earth 3-76841
 electro-telluric field, rotation, electrolytic model tank 3-44947
 electrotelluric predecessors of earthquakes, source 3-58918
 e.m. induction, by non-symmetric non-uniform source 3-80673
 e.m. induction in Earth by symmetric non-uniform source 3-58916
 e.m. sounding on step model of reference electric horizons (*Russian*) 3-47813
 equatorial electrojet, Kosmos-321 measurements of magnetic effects rel. to Earth's nonconducting layer 3-41985
 faulted basement, Graben, telluric field computation 3-69538
 field anomalies over faulted basement, analysis 3-76593
 field of inhomogeneous plane e.m. wave at anisotropic half space surface 3-57186
 geoelectric cross-section of crust and mantle of Russian Platform based on magneto-telluric soundings 3-44843
 geoelectric surveys using transient and magnetotelluric sounding in horizontally inhomogeneous media (*Russian*) 3-47814
 geomagnetic coastal effect, E-polarisation case, numerical models 3-80672
 geomagnetic micropulsation measurement, conductivity anomalies, effect of induced mag. fields 3-44928
 geomagnetic variation anomaly, coastal areas of Japan Sea, South-Western Japan 3-76658
 glaciers, radiointerferometry depth sounding 3-80659
 granite, electrical conductivity, high pressures, 300 to 1500°C 3-76659
 groundwater, resistivity surveys, Aurangabad Sub-division, Gaya district, Bihar, India 3-76667
 induced current, Northern Gulf of California, anomalous geomagnetic variation 3-76661
 induced current distribution, conductive two-layer spherical body, interpretation of data over ore deposits 3-80657
 induced currents, Central Gulf of California, anomalous geomagnetic variations 3-76662
 inductive dipole profiling over electrically conducting thin plate 3-44845

terrestrial electricity continued

- interpretation of induced polarisation field prospecting, apparent fictitious resistivity 3-76839
- isolated reefs, Midland Basin, Texas, telluric anomalies, resistivity distrib., post-reef sediments 3-80658
- L/M parameter of time-domain induced polarization meas., computational analysis 3-50965
- lava flow subsurface geoelectric mapping, Laacher See, W. Germany 3-61589
- layered lunar/earth surfaces, measurement of electrical parameters, bibliography 3-45241
- line source, scattered e.m. fields over nonuniform stratified Earth 3-50865
- Lunar tides in earth current at Barrow 3-80664
- magnetoelastic plane waves, cosserat medium 3-44829
- magnetosphere, from movements of NASA MPE barium cloud 3-80827
- magnetosphere balloon borne expts. in NASA MPE barium ion cloud project 3-80824
- magnetospheric electric fields, large scale, semiempirical model 3-51137
- magnetotelluric impedance tensors, Australia, conductive-resistive-conductive layering 3-44840
- magnetotelluric interpretation using geomagnetic storms 3-53432
- magnetotelluric rel. to field penetration depth analyses for electrical conductivity meas. 3-59149
- magnetotelluric response two dimensional sloping contact 3-76865
- magnetotelluric study, western Canadian sedimentary basin, tensor analysis, numerical model 3-44853
- mantle, relations between elec. cond. and fluctuating mag. fields 3-41906
- mantle currents, propagator matrix formulation 3-76866
- mantle electrical conductivity distribution from secular geomagnetic field variation data 3-69541
- multilayer analogs in geoelectrics and hydrology, boundary value problem solution 3-56244
- NASA/MPE barium ion cloud project, geomagnetic and geoelectric expt. 3-80822
- negative charge and unitary variation of electric field, control by cosmic rays (*Russian*) 3-65598
- nonstationary field of electric dipole on horizontally stratified medium 3-76669
- oceanic electric currents induced by fluid convection 3-73249
- outer core, electrical transport properties of liquid metals at high pressures 3-41896
- Paktia, E. Afghanistan, geoelectrical survey 3-50966
- perturbation fields due to conductivity inhomogeneities, frequency dependence 3-76656
- Pi 2 harmonic frequency content, spectral analysis of Earth current records 3-65248
- plasma sphere, penetration of magnetospheric electric fields and plasma convection 3-80833
- potential anomalies, calc. 3-44929
- radiointerferometry depth sounding, theoretical wave nature of electromagnetic fields, appl. to meas. of elec. props. 3-80843
- resistive parallelepiped, homogeneous isotropic media, apparent resistivity profiles effect of dimensions (*Italian*) 3-73241
- resistivity logging, hydraulic cylindrical probe, boreholes (*Russian*) 3-76897
- resistivity sounding, geometrical progression of depths, curve matching by computer programme 3-76838
- sub-Icelandic crust, electrical model 3-50964
- subsurface layer excitation using e.m. probe, range dependence of surface impedance and wave tilt 3-80846
- tidal motion across geomagnetic field, infinitely long model ocean 3-73251
- Ukrainian shield, elec. cond. anomaly in Kirovograd block 3-44844
- upper mantle, electrical conductivity meas. during long period magnetic variations 3-58928

terrestrial heat

- see also volcanology*
- Alps, Bouguer gravity anomaly, thermally caused (*German*) 3-56056
- Calabria, Italy, heat flow meas. 3-56046
- Canada, Atlantic side, heat flow and prod. meas. 3-76621
- climate changes, effect of world energy prod. on heat flow 3-56171
- Cocos plate, Cenozoic motion rel. to asthenospheric flow and low heat flow 3-58859
- convection arrangement by lunar gravity, gravit. couple effect on tectonism 3-47646
- core, physical state rel. to thermal regime 3-47633
- core, thermal regime rel. to heat production and convection 3-50950
- depth of location of sources using quantitative interpretation of gravity anomalies 3-65165
- earth mantle convection, viscosity depend. on temp. 3-76644
- earth mantle convection instability inferred from Frank-Kamenetskii approx. to dissipation 3-76645
- earth-atmosphere system, annual radiation balance, Nimbus 3 1969-70 meas. 3-65335
- East Pacific Rise at 39°S, thermal environment 3-76618
- energy balance and climate rel. to human activities and atmospheric particles 3-41975
- flow anomalies, geological interpretation (*Russian*) 3-65153
- flow measurement, Austria, heat flow maps, Central Europe 3-73239
- geothermal resources in Earth crust 3-56274
- geothermics, O.Yu. Schmidt hypothesis and problems 3-47625
- global energy, time-depend. model eqn. of earth-atm.-ocean 3-47609
- Gulf of California, heat flow meas. rel. to sedimentation 3-53445
- hot spots, Atlantic, relative and latitudinal motion 3-76571
- insolation regimes and chronology rel. to interglacials 3-41974
- island arcs and intra-arc spreading, induced heat flow 3-76637
- land and sea breezes, effects of turbulent transfer processes, numerical method 3-76680
- lithospheric cooling on Galapagos Spreading Centre, E. Pacific 3-56092
- mantle convection in shear flow 3-76646
- Melanesia, heat flow meas. rel. to plate boundaries 3-50938

terrestrial heat continued

- mid-ocean ridges, temp. and composition of ascending magmas 3-61309
- New Mexico, heat flow data 3-76620
- Northern Hemisphere, gravity map comparison with crust and mantle heat flow data 3-56066
- Northern Hemisphere oceans, annual poleward energy transport 3-65270
- Norway, heat flow-heat generation meas. 3-76622
- oceanic crust and thermal aspects of sea-floor spreading 3-50954
- outer core, composition and temperature rel. to pressure-density model 3-50940
- S Rio Grande Rift, heat-flow and Bouguer gravity anomaly map 3-76619
- shear wave attenuation and melting beneath Mid-Atlantic ridges 3-76566
- Southern Colorado, heat flow data 3-76620
- Sovanco fracture zone, heat-flow variations 3-76617
- stationary geothermal perturbation due to deep water rise, numerical study (*French*) 3-42092
- Swiss lakes, heat flow meas. 3-76699
- temperature-depth distribution, crust and upper mantle, model calculations for Alps (*German*) 3-58851
- thermal i.r. images, model for periodic heating of layer on semi-infinite solid 3-76857
- thermal plumes in earth mantle 3-61327
- N Central United States, heat flow determinations 3-50915
- upper earth mantle convection with variable viscosity 3-76643
- S.W. Virginia, flow meas. at Cripple Creek and Grundy 3-50931
- viscous heat prod. in a slab 3-50937
- western equatorial Pacific Ocean, heat flow measurements at plate boundary 3-73220

terrestrial magnetic field *see geomagnetism***terrestrial magnetism *see geomagnetism*****test equipment***see also automatic test equipment*

- atmospheric pressure compensation devices 3-51522
- calliper device to run load programs, probe force on specimen (*German*) 3-80513
- compression jig, microstrain, macrostrain regions 3-76405
- fatigue testing machine, h.p. 3-80519
- four-ball machine, reduced machine time, lengthy friction path, wear of steel balls, effect of lubricating oils 3-53307
- multiposition test machine for high temp. testing in vacuum and gaseous media (*Russian*) 3-80511
- optical component testing by interferometry, HeNe c.w. laser 3-77521
- stands for impact testing, impact loading, intermediate crank and rotating crank 3-53305
- superconducting, for testing magnetic induction meters 3-39975
- vertical compression moulding, casting machine, durability testing, tool materials 3-53306

test facilities*see also aerospace test facilities*

- EBR-II hydraulic test facility, flow-modelling studies for homogeneous core loading 3-46117
- Fast Flux, eddy-current flowmeter for Na flow velocity meas. 3-45621
- force measuring and generating equipment, engineering mechanics section NBS 3-65063
- nuclear reactor hydraulic, study of thermal mixing in EBR-II outlet plenum 3-67431

testers *see test equipment***testing**

- see also automatic testing; computer testing; electron device testing; environmental testing; impulse testing; inspection; materials testing; mechanical testing; nondestructive testing; optical testing; production testing; switchgear testing*
- charcoal filters used for cleaning air in reactor environments 3-71344
- dosimetric instruments, apparatus 3-73605
- electrostatic spray guns, ignition test procedure, safety assessment 3-70778
- Fallout from nuclear weapons testing and interhemispheric transport of nuclear debris 3-69567
- flow measuring equipment, Molch tester-volumetric standard (*German*) 3-59541
- FTR driver fuel assembly, prototypic, test in flowing sodium, final inspection 3-46122
- HTR fuel elements, irradiation dosages, dimensional and density changes (*German*) 3-67592
- nuclear reactor, single pin expulsion and reentry test 3-67417
- portable exposure meter, for X- and γ -rays in radiological protection 3-48538

testing apparatus *see test equipment***testing equipment *see test equipment*****testing machines *see test equipment*****tetraneutrons *see neutrons*****tetrodes**

- two-grid tube with bipotential grid, potential distrib. calc. 3-43051

textile industry

- colour matching system employing computer 3-51605

texture*see also surface texture*

- alloy, recrystn. texture prediction (*Russian*) 3-72848
- Berycolloy, effect of additives on annealing textures 3-61136
- ceramic, unfired, transmission electron microscopy 3-76333
- CZC, effect of additives on annealing textures 3-61136
- grain orientation of polycrystals, determ. using thermal corrosion phenomenon (*French*) 3-61147
- inverse pole figure studies, random samples use 3-47380
- laminates, prestrained, strain gradient theory, buckling 3-77829
- liquid crystals, review 3-79227
- metal, recrystn. texture prediction (*Russian*) 3-72848
- metal lattice research, minicomputer appls. 3-80266
- neutron diffraction method, applic. to cold-rolled Zr sheets 3-64847
- Nibcolloy, effect of additives on annealing textures 3-61136

texture continued

- Permalloy, electroplated thin film, isochronal annealing behaviour 3-79881
- Permalloy, mag. texture influence on resist. to irradi. and temp. variations (*Russian*) 3-50406
- polyethylene, high-density, with single cryst. texture, structure 3-57993
- polyethylene, linear, single-cryst. texture, thermal expansion, 0 to -190°C 3-58734
- quartz, syntectonic recrystallisation and texture development 3-61326
- sheet, rolling and recrystn. textures, three-dimens. represent. (*French*) 3-61151
- steel, austenitic, stainless, Type 316, microstruct. stability of thermally-mechanically pretreated type 3-47392
- steel, borated, residual stress curve predeterm. (*Russian*) 3-80320
- steel, low-C, texture form. during deform. (*Russian*) 3-53218
- steel, textured strip, bending influence on saturation magnetostriction (*Russian*) 3-53007
- steel, weakly textured electrotechnical, grain size effects on mag. induction (*Russian*) 3-52993
- steel, X-ray stress meas. of specimen with steep stress gradient in near surface layer (*Japanese*) 3-41730
- thin films, fibre textures determ. by electron diffraction 3-79585
- X-ray diffraction obs., using variable movement specimen holder 3-71984
- X-ray diffraction technique, rolling texture determ. combination of inverse polar figure and direct figure 3-53227
- Zircaloy, stress corrosion cracking behaviour in iodine vapour 3-43297
- Al, films, phase transform. on ion bombard., electron diffr. obs. 3-72195
- Al, polycryst., single [111] fibre texture development (*Japanese*) 3-61143
- Al, substructural hardening, yield stress, dependence on subgrain size, texture and orientation (*Russian*) 3-41720
- Al plates, textured, rolled and coarse grained, shock wave effects (*Russian*) 3-69264
- Al-Cu (4 wt.%) alloy, substruct. and dispersion hardening 3-69231
- Al-Fe alloys, rapidly solidified, iron precip. behaviour (*German*) 3-41744
- Cr bronze, rolling texture determ., X-ray diffraction technique, combination of inverse polar and direct figures 3-53227
- Cu, drawn, rel. to extinction effect magnitude, X-ray refl. intensities (*Russian*) 3-76162
- Cu plates, textured, rolled and coarse grained, shock wave effects (*Russian*) 3-69264
- Cu-Cr (0.5 wt.%) alloy, grain growth during annealing (*Russian*) 3-72852
- Fe-Ge alloy, deformation, recrystallisation struct. 3-76177
- Fe-Si (3 wt.%) alloy, textured matrix orientations rel. to misaligned grains (*Russian*) 3-69211
- Fe-Si (3 wt.%) single crystals, rolled, deform. texture form. (*Russian*) 3-58622
- KCl, hot worked, strength and deformation rel. to microstruct. 3-76252
- MgO-Al₂O₃ solid state reaction formed spinel, mode of orientation (*Japanese*) 3-58704
- Nb single crystals, deformed in rolling at 77K, defect struct. (*Russian*) 3-58627
- Si film, chem. deposited, effect of deposition conditions on struct. 3-41112
- SmCo₅, powder-based magnets, texture perfection degree, particle orientation angles distrib. (*Russian*) 3-61135
- SrFe₁₂O₁₉, development by hot working 3-76250
- Ta, surface-carburized, carbide precip. phenomena (*French*) 3-61153
- Ti bonded with finely cryst. diamond particles, ω -Ti phase obs. (*Russian*) 3-73010
- β -Ti-Mo-Cr-Fe-Al alloy, recrystallization, microstructure 3-76178
- U-Ti (7 wt.%) alloy, extrusion, shear spinning and heat treatment effects 3-69228
- W sheets, recrystn. texture (*German*) 3-55792
- Zn-Al (40 wt.%) alloy, superplastic, basal plane pole figures 3-69220
- Zr, cold-rolled sheets, neutron diffr. determ. 3-64847
- Zr and alloys, cold work and stress-relieving effect on irradi. growth behaviour 3-41773

texture, surface | see surface texture

thallium

- alkali halide: Tl⁰, ²P_{1/2} to ²P_{3/2} optical transition rel. to Jahn-Teller electron-phonon interaction 3-64698
- alkali halide: Tl, Ag, tunnel luminescence (*Russian*) 3-41560
- alkali iodides, Tl doped γ -scintillations 90 K-300 K (*Russian*) 3-55684
- atom, ⁶P_{3/2}, collisional deactivation, temp. depend. 3-78504
- atom, excitation by electron impact, absolute cross-section meas. (*Russian*) 3-67706
- atom in ⁶P_{3/2} state, fluorescence impact depolarisation 3-52267
- atoms, excitation of ion lines by electron collisions (*Russian*) 3-40585
- electron relax. time, temp. depend., r.f. size effect meas. 3-44064
- Fermi surface, supercond. transition temp., press. effects, pseudopot. calcs. 3-55190
- ions dependence of ³P₁ level on difference between radii of activator and substituted cation (*French*) 3-64712
- laser, superradiant pulse power, dependence on discharge parameters, isotopic and hyperfine line splitting (*Russian*) 3-66823
- melt, free surface energy, contact angle, density, meas. installation, lying-drop method 3-73687
- mineral-groundmass partition coefficients for Tl rel. to Rb. in volcanic rocks 3-56030
- muonic atom, magnetic hyperfine splitting due to magnetization density 3-49209
- muonic atom, test for vacuum polarisation correction to 5-4 transitions (*German*) 3-52302
- optical absorption spectra 3-44425
- quenched thin film, Hall effect, annealing behaviour (*German*) 3-72349
- solar abundance determ. from umbral spectra 3-65716

thallium continued

- superconducting wire, type I, supercond. destruction by current 3-68730
- CaO(S):Tl phosphors, prep., emission and excitation spectra (*Russian*) 3-76052
- β -Ca₃(PO₄)₂:Ga⁺, Ge²⁺, In⁺, Sn²⁺, Sb³⁺, Tl⁺, Pb²⁺, phosphorescence (*Russian*) 3-50613
- CsBr:Tl, enhancement of vacuum u.v. excited luminescence by electric field (*Russian*) 3-50624
- CsI:Na⁺, Tl⁺, V_k centres, e.p.r. and light absorpt. obs., thermolum. study of thermal migration 3-64035
- Ge:Br, Tl, excitation spectra, Zeeman effect 3-50594
- Hg+Tl sensitized fluorescence, excitation processes 3-71414
- KBr:Tl, phonon dispersion relations 3-55596
- KBr:Tl⁺, phonon props. and electron-phonon interaction 3-58098
- KCl:Tl, hole diffusion absorption method, 170 K-177 K (*Russian*) 3-55267
- KCl:Tl, lattice sp. ht., force const. change effects 3-41026
- KCl:Tl, photoluminescence (*Russian*) 3-41556
- KCl:Tl luminescence at excitation in region of fundamental absorption 3-80116
- KCl:Tl⁰, tunnelling transitions (*Russian*) 3-44447
- KCl:Tl⁺, Jahn-Teller effect in 3000 Å emission, time resolved spectroscopy 3-69061
- KCl:Tl⁺, phonon props. and electron-phonon interaction 3-58098
- KCl-In, Tl, ionic crystals containing electron traps, thermally stimulated luminescence peaks 3-76105
- KI:Tl, enhancement of vacuum u.v. excited luminescence by electric field (*Russian*) 3-50624
- KI:Tl, luminesc., hot photoelectron impact excitation processes (*Russian*) 3-44493
- KI:Tl thermoluminescence, electric field effect 3-55694
- KI:Tl⁺, phonon props. and electron-phonon interaction 3-58098
- LaAl₂:Th, conduction electron spin flip scattering obs. 3-41411
- NaCl:Tl, luminescence, influence of channelling under the influence of positive ions (*Russian*) 3-41550
- NaCl:Tl, thermoluminescence glow peaks, intensity as function of Tl concentration 3-47321
- NaCl:Tl, Cd, Cs, impurity precipitates meas. by u.s. velocity changes 3-64060
- PbN₂:Bi, Tl, and pure thin films, i.r. absorption spectra 3-64647
- Tl:KI type phosphor, double luminesc., excited in A band, theory 3-69087
- Tl III spark spectra assignments 3-67656
- Tl⁺, excited electronic states and electron-lattice interac. from optic. abs. meas. 3-55650
- Tl⁺, in alkali halide, luminesc. band position depend. on host lattice cation and anion ionic radii 3-76042
- Tl⁺, in KCl, (KBr), (KI), luminesc., slow electron impact excitation 3-41590
- Tl⁺, luminesc. tracer, polymorphic transition obs. in alkyl ammonium halides 3-72755
- Tl⁺ phosphor, absorpt. and emission spectra in glasses 3-58547
- (Tl⁺)₂ activator centre in alkali halides, mol. orbital calcs. 3-68566

thallium alloys

- see also thallium compounds
- Bi_{0.85}Tl_{0.15}, amorphous strong coupling supercond., upper critical field, density of states at Fermi surface 3-41288
- In-Tl, containing Cd and/or Sn, axial ratio and phase changes 3-79269
- In-Tl, single cryst. prep. by modified Bridgman method 3-44534
- Na-Tl, liquid, nuclear magnetic relaxation rate of ²³Na spin, temp. depend. 3-47160
- Pb₁₋₂:Bi, Tl₁, strong-coupling supercond., mag. meas. of equilib. props. 3-46924
- Sn-In-Tl, molten, effect on mech. props. of Sn-Pb alloy (*Russian*) 3-72897
- Te_{100-x}Tl_x, (15 ≤ x ≤ 50), obtained by rapid cooling from liq. state, cryst. 3-64814
- ThFe₃, non-centrosymmetric structure type for ferromag. Gd₇Pd₃ 3-52601
- Tl-Te, liquid viscosities and densities, composition, temperature, activation energy, volume of mixing, thermal expansion, stoichiometry 3-50023

thallium compounds

- see also thallium alloys
- halides, polar dissociation and reactive ionisation by inert gas collisions 3-76448
- As-Se-Tl glasses, refractive index, density, polarisation, absorption spectra (*Russian*) 3-50584
- Cs(Tl_{0.1}O_{0.9}), preparation and crystallography (*German*) 3-79322
- InTlSe₃ film, struct., electron diffr. obs. 3-75693
- Rb(Tl_{0.1}O_{0.9}), preparation and crystallography (*German*) 3-79322
- Sb₂Se₃/Tl₂Se phase diagram existence of Tl₂SbSe₆ and TlSbSe₂ by DTA (*German*) 3-55073
- Tl-As-Se, semicond. glass, ²⁰⁵Tl n.m.r. meas., chem. shifts rel. to bonding 3-44339
- TlBr, collision induced dissociative ion pair formation by Xe and Kr atoms, absolute cross sections 3-46353
- TlBr, collision induced dissociative ion pair formation by Xe and Kr atoms, threshold behaviour 3-46354
- TlBr, electroabsorpt. of excitons, high field regime 3-55639
- TlBr-KBr single crystal, luminescence centres, characts. 3-64722
- TlBr-TlCl, interdiffusion meas. at 400C 3-79527
- Tl₂CS₃ vibrational spectra of CS₃²⁻ 3-46298
- TlCl, collision induced dissociative ion pair formation by Xe and Kr atoms, absolute cross sections 3-46353
- TlCl, collision induced dissociative ion pair formation by Xe and Kr atoms, threshold behaviour 3-46354
- TlCl, film, electron diff. intensities, elec. recording, electron filter 3-72292
- TlCl-TlBr, interdiffusion meas. at 400C 3-79527
- TlCl₄⁻, orbital valence force field const. and Coriolis coupling const. calc. 3-49449
- TlCl(Br), exciton levels in mag. field 3-41158
- TlCl_{0.6}Br_{0.4}, Raman spectrum near resonance 3-64639
- TlCoF₃, light scatt. from magnons and excitons, 4 K 3-50547
- TlF, molecular beam, electron scattering, total cross section 3-75109

thallium compounds continued

- TlF-NpF₄, solid-liq. equil. diag., phase identification (*French*) 3-60787
 TlF₆³⁻, solid, i.r. and Raman spectra 3-72627
 (TlF)_x, x=1 or 2, photoelectron spectra 3-49495
 TlGaSe₂, cryst. structure obs. 3-72054
 TlI, collision induced dissociative ion pair formation by Xe and Kr atoms, absolute cross sections 3-46353
 TlI, collision induced dissociative ion pair formation by Xe and Kr atoms, threshold behaviour 3-46354
 TlI, cryst. growth in gel, press. effect on cubic modification (*French*) 3-55729
 TlI₂⁻, orbital valence force field consts. and Coriolis coupling consts. calc. 3-49449
 Tl(III) chloro- and bromo-complexes, in benzene soln., far i.r. spectra, 413 to 33 cm⁻¹ 3-47275
 Tl(I)(Tl(III)Cl₂Br₂), electrical conductivity meas. 3-58258
 TlInSe₂, piezophotorestrictive effect in single cryst. 3-68674
 TlNO₃, longit. mode freqs., PSR i.r. spectra 3-75975
 TlNO₃, molten, Ag⁺ interdiffusion, cation association 3-72215
 TlNO₃-M(II)(NO₃)₂ glass, thermodynamic props. 3-72009
 TlNO₃·III, cryst. struct. rel. to vibr. spectrum splitting 3-75997
 TlNb₂O₇F pyrochlores, new cryst. position for Tl⁺ in Fd3m space group (*French*) 3-40885
 Tl₂O-GeO₂-SiO₂ glasses, i.r. detection of depolymerization 3-58500
 Tl₂O₃(c), heat capacity meas., 298-800 K, drop calorimetry and differential scanning calorimetry 3-46717
 Tl₂PbCu(NO₂)₆, phase transitions and Jahn-Teller effect, e.s.r. obs. 3-50136
 TlRF₄·III transformation to TlBF₄·IV high-pressure phase, D.T.A. and volumetric techniques 3-64176
 TlSbS₂ films, structure and some electrophysical props. (*Russian*) 3-79588
 Tl_{1-x/6}(Ta_{1/6}W_{1-x/6})O₆, non stoichiometric pyrochlores, Tl ion distrib. (*French*) 3-40886
 TlTe, low temp. electronic transport props. 3-52844
 TlTe, single crystal growth, electrical props. 3-80176
 Tl₂Te, thermal cond., 300-625 K 3-79535
 TlTh₂(PO₄)₃, prep and cryst. data (*French*) 3-58015
 Tl₃VS₄, switching effect 3-46881

thawing see melting**The Galaxy**

- 327 MHz observation of centre, possible deuterium absorption line 3-77154
 absorption map based on planetary nebulae extinctions 3-45213
 absorption reddening rel. to Galactic latitude and redshift-distance relation 3-70005
 age, r-process path termination in nuclear yield ratios 3-73437
 anticentre, soft X-ray flux rel. to radio continuum features 3-51376
 background radio emission, 3.75 cm-3.5 m 3-77151
 background spectrum 130-2600 kHz, IMP-6 satellite measurements 3-77139
 central i.r. sources, 350 μ obs. 3-65913
 central region, gamma-ray astronomy and cosmic-ray studies 3-45205
 centre, obs. of HI, contour diagrams of antenna temp. 3-81176
 centre, radio pulse search 3-69978
 centre region, neutron star accretion upper limit at X-ray wavelength 3-42231
 Cetus Arc nebulosity around Loop II, Hα radial velocity meas. 3-59391
 cosmic electrons, energy dependent escape from Galaxy 3-51222
 cosmic ray propagation and isotropization, role of plasma effects 3-51218
 diffuse far u.v. background, 1440 to 1620 Å, galactic latitude dependence 3-48104
 diffuse far u.v. background, galactic latitude dependence mirror-geiger tube photometers 3-48103
 diffuse Galactic light polarisation meas. 3-56430
 disc continuum radio structure, model based on density wave theory 3-77140
 distance estimating method for Galactic plane 3-53725
 electromagnetic pulses from centre, searches 3-42232
 evolution rel. to solar luminosity variations 3-51238
 extensive phenomena at high latitudes, H I regions, nebulosity and giant radio loops 3-42230
 fine structure in centre region, 2695 and 8085 MHz obs. 3-45203
 fine structure of next inner spiral arm, u.v. photography and photometry (*German*) 3-48090
 formaldehyde radiation, absence in galactic plane cold region 3-51392
 galactic centre, sensitive search for microwave pulses 3-70024
 gamma-ray sources recent Apollo and satellite expts. 3-81160
 gas-dust ratio, H I column density in direction of known colour excess globular clusters 3-81170
 giant dust complex detection in Perseus arm 3-51403
 gravitational radiation focusing into Galactic plane 3-42875
 Groningen-Palomar variable star fields, UVB photometry for 170 objects 3-48006
 HI regions, large-scale peculiar motions 3-61867
 high velocity neutral H₂ features, spatial and velocity distrib. 3-48109
 high-luminosity red stars near Sun, young disc population 3-77067
 interstellar absorption of soft X-rays, 21 cm obs. of H column density 3-81156
 interstellar extinction in Southern Milky way 3-42237
 interstellar medium structure, effect of hot white dwarfs above Galactic plane 3-59373
 interstellar molecular clouds, evolutionary role 3-65938
 i.r. anomalies assoc. with gravitational events at Galactic Centre 3-42218
 i.r. maps of nucleus 3-81165
 i.r. radiation source in galactic centre, magnetic bremsstrahlung 3-59360
 kinematics of stars and neutral H, comparison 3-45189
 local spiral arm, evidence of assoc. shock 3-45178
 Loop III, effect of galactic spur on H I regions velocity distrib. 3-45182
 Loop III, effect on interstellar neutral hydrogen, velocity distribution analysis 3-77155
 magnetic field, stochastic models 3-48113
 magnetic field models, cosmic ray origin 3-80891
 magnetic fields, generation and dissipation, turbulent diffusion 3-69826
 magneto-gravit. and thermal instability in Galactic disc 3-56425
 Map of the Galactic nucleus at 10 μ 3-70020
 mass determ. using density wave model of spiral arms 3-51385
 Milky Way fields, photoelec. UVB photometry, space-density function, distrib. of interstellar matter 3-81177
 model based on logarithmic density law 3-61846
 nearby classical Cepheids, places of formation rel. to history of spiral structure 3-48091
 neutral H spiral structure outside solar circle, new 21 cm map 3-70014
 night sky radiation, obs. of linearly polarised radiation in anti-solar hemisphere 3-61753
 night sky surface brightness at 1500-4250 Å, rel. to diffuse galactic light 3-53701
 Nonlinear gaseous density waves and Galactic shocks 3-70010
 northern galactic pole, excess γ fluxes, Cosmos-264 obs. 3-48081
 nuclear disc, neutral H obs. 3-61841
 OB stars in Milky Way system, two-colour diagrams 3-48016
 one-armed spiral density waves, props. 3-45191
 optical and radio brightness distributions, correlation with direction of spiral arms and radiospurs 3-61854
 Perseus arm feature of Cassiopeia A, aperture synthesis of interstellar H I absorption 3-81105
 linear polarisation survey of region around l=140°, b=+8° at 240.5 MHz 3-61822
 radioemission, linear polarisation at 210 MHz (*Russian*) 3-81178
 recombination lines toward galactic centre, 1.621 GHz obs. 3-51379
 Sagittarius A and B sources, 350 μ obs. 3-45204
 Sagittarius A West, nonthermal radiosource properties rel. to galactic centre 3-42207
 Schmidt model, shock waves propagating in the spiral arms, hydrostatic equilibrium rel. to star formation 3-61853
 solar neighbourhood, distribution and kinematics of interstellar clouds 3-45210
 solar neighbourhood, H I distribution about local standard of rest 3-48127
 South Galactic Pole, spectroscopic obs. of 30 M-type giant stars 3-42233
 South Galactic Pole, spectroscopically peculiar stars 3-42190
 Southern Milky Way, 100 μ survey 3-45158
 spatial distrib. of supernovae and pulsars 3-42214
 spiral arms, bending of Galactic plane and nature of high vel. clouds 3-77135
 spiral structure, kinematics, azimuthal and radial components of streaming motions 3-45187
 spiral structure density-wave map from 21 cm obs. 3-45190
 spiral structure map from 21 cm obs. 3-45188
 stellar dynamics, orbits in 2nd Schmidt potential (*French*) 3-73540
 stellar population and evolution, obs. of high-vel. stars (*Italian*) 3-61850
 strongly magnetized plasmas, enhanced diffusion 3-80914
 structure, development of theory during 1920-40 period 3-45209
 structure, distrib. of X-ray sources 3-59362
 structure and stellar content 3-45208
 structure by stellar photometry, spectroscopy, colour excess and distance, Cepheus direction (*French*) 3-77136
 transient X-ray sources, Galactic origin 3-59361
 X-ray sources, galactic distribution from sounding rocket obs. 3-45165
 CO distrib. between galactic longit. 10 and 75 degrees 3-48121
 D₂, presence, radioastronomical obs. 3-42236
 H I 21 cm line, spiral structure mapping 3-65930
 H I motion near centre and 3-kpc arm 21 cm line obs. 3-77134
 H I regions, Hα Fabry-Perot spectrometry 3-77162
 HI region, Galactic anticentre, detection against background spatial fluctuations 3-77159
 HNCO detection in Galactic centre at 21.98 GHz 3-53711
 He abundance of galactic Cepheids rel. to theoretical pulsation calculations 3-45112
 He cosmic abundance rel. to horizontal branch stars in globular clusters 3-69948
¹⁸⁷Re in stars, enhanced β-decay rate rel. to recycling of r-process elements and age of Galaxy 3-42113
theorem proving
 meta-DENDRAL and heuristic DENDRAL, use in organic chemistry mass spectrometry 3-45552
theoretical mechanics see mechanics
theory of quantum electrodynamics
 Adler anomalies in pion electrodynamics, reln. to η→πππ puzzle 3-52001
 anomalous dimension of isovector tensor operator, deep inelastic structure functions and p-n mass difference 3-49002
 anomalous origin of masses, vacuum energy density as function of bare parameters 3-57338
 betatron oscillations, nonlinear, Hill's equations, Krylov-Bogoliubov averaging, analysis 3-77869
 charged particle scattering, energy transfer in strong e.m. field 3-66999
 Dirac electron in field of quantised e.m. wave and in homogeneous magnetic field, eigenfunction determ. 3-70911
 Dirac equation, inhomogeneous, manifestly covariant Hamiltonian form, external e.m. field 3-78120
 Dirac particles in constant external vector potential, asymptotic group invariance, determ. of α=e²2π/hc 3-57336
 dual symmetry, magnetic charge anal. and charge quantisation condition 3-74364
 eikonal approximation for three-body generalized ladder graphs in QED 3-51991
 Euclidean, S-matrix element eqns., generating operator and perturbation series 3-54303
 field renormalisation and reduction formula 3-40341
 field theory in infinite momentum limit 3-40312
 finite, inversion-invariant of leading singularity of electron-photon vertex 3-67000

The Galaxy continued

theory of quantum electrodynamics continued

- gauge invariant axial-vector current, short-distance behaviour using Callan-Symanzik eqns. 3-67003
 gravity-modified QED, higher order infinity regularization 3-49001
 gravity-modulated, nonperturbative solution to one-loop correction to tree diagrams 3-66676
 Gupta-Bleuler, renormalisation procedure 3-74313
 Heisenberg-picture, radiation-reaction and vacuum field effects 3-70909
 i.r. divergence problem, electron induced cohesive photon retinue 3-66994
 i.r. divergences and adiabatic switching, radiative corrections to Coulomb scattering 3-45875
 massless, formulation as bootstrap, self-consistent approach to fine structure constant 3-66993
 maximal field strength, nonperturbative techniques 3-67004
 Maxwell field with three polarisation directions, quantisation 3-66992
 mesic atoms, self-consistency of vacuum polarisation (*German*) 3-52304
 microcausality in electrodynamics, determ. of functions $W_i(v, q^2)$ (*Russian*) 3-78125
 model, nonperturbative treatment, determ. of high-energy behaviour of electron and photon propagation 3-40339
 nonlocal, free of ultraviolet infinities 3-48999
 nonrelativistic particle in field of e.m. wave, group-theoretical analysis in dipole approx. 3-52003
 null plane, covariant Feynman rules 3-66997
 operator gauge transformations 3-54301
 photon Green's function, false pole 3-54302
 photon-neutrino weak coupling and self-consistent theory for weak interactions 3-45864
 polarised vacuum quantum theory (*German*) 3-62821
 polarizability contributions to neutron-lepton amplitude at threshold 3-78134
 positivity, implication for dimension of axial vector current 3-70908
 positronium h.f.s., fourth order vacuum polarisation correction 3-40340
 radiation of spinless electrons in homogeneous magnetic field 3-67002
 relativistic convergent quantum mechanics of interacting particles, realistic model, S-matrix elements 3-59920
 relativistic cyclotron motion, degeneracy 3-43100
 relativistic electrons, wave packet construction, light cone 3-78078
 r.f. resonances, validity of semiclassical description 3-45704
 S-matrix, adiabatic definition when i.r. divergences are present 3-54282
 single-photon exchange diagrams in quasi-potential approach, calc. using polarization operator 3-70910
 spin 1/2 particle in e.m. field, free field solns. and magnetic moment electron 3-78124
 spontaneous emission, radiative corrections 3-74363
 synchrotron electron motion, autophasing field, wave functions, energies 3-78123
 ultraviolet infinities, removal using cosmic field 3-49000
 vacuum modes in Van der Waals' attraction 3-40338
 vacuum polarisation, influence of strong interactions 3-49007
 vacuum polarization by external field, Stieltjes summability and convergence of Padé approximants 3-74362
 vacuum polarization for massive gauge field by source theory 3-78119
 vacuum-polarisation potential, finite-size effects and Coulomb propagator 3-67001
 wave packet motion in crossed fields for particle with $e < 0$ (*Russian*) 3-78122
 weakly bound states, of charged particle in finite dipole yield 3-74365
 Yang-Mills-Maxwell system in Weinberg model 3-48981
 e mass, calc. in unified theory of weak and e.m. interactions 3-43101
 π scattering, Compton kernel from invariant 4-vector representation 3-74374
 p polarisability bounds, h hyperfine interval recoil corrections 3-66998

thermal capacity see *specific heat*

thermal conductivity

- see also *Kapitza resistance; thermal conductivity of gases; thermal conductivity of liquids; thermal conductivity of solids; thermal diffusivity; thermal insulating materials*
 biological systems, u.s. attenuation 3-42274
 comminuted aggregates, effective thermal conductivity 3-62623
 computer program for simultaneous analysis of multiproperty data 3-72166
 conference, Atlanta, USA, (Aug 1973) 3-71702
 forced convection with variable thermal conductivity on a flat plate, numerical soln. 3-40707
 gas density balance as calibration technique, applic. to relative response factors for thermal conductivity detectors 3-66422
 hard sphere gas, dense, developments of Enskog and virial theories (*French*) 3-45738
 inhomogeneous, anisotropic medium, phenomenological definition 3-57171
 integral balance method for molar-molecular heat and mass transfer analysis (*Russian*) 3-66697
 ionospheric electron thermal conductivity for weakly ionised gas 3-47785
 Kapitza thermal boundary resistance, theory including phonon scattering within either material 3-60779
 lunar surface radiative transfer, effects of scattering and thermal conduction 3-61684
 Mercury, surface radiative transfer, effects of scattering and thermal conduction 3-61684
 multi-component ionised gas-solid suspension, transport properties 3-71865
 nonlinear least squares determ. technique 3-62627
 organic fluids, HB-40, toluene, dimethylphthalate 3-72236
 packed beds, radiating gas effect on effective thermal conductivity 3-40706
 plasma laser fusion, thermal conduction limitations 3-46517

thermal conductivity continued

- plasma thermal conductivity, longitudinal, effect on ohmic heating in Tuman-1 3-71930
 plasma thermal conductivity calc. 3-75290
 plasma transverse electron thermal conductivity meas. in mag. field 3-54841
 plasmas, laser heated, limitations on electron thermal conduction 3-49734
 pressure gauge using thermal conductivity cell 3-42546
 solar wind, thermal conductivity of quiet plasma and consequences 3-61650
 solar wind heat conduction, effect of fluctuations in interplanetary magnetic field 3-56371
 stellar cores, partially degenerate magnetoplasma 3-81020
 superleak, normal-superfluid separator, conductivity measurement, 0.06 to 1 K 3-56648
 Ar afterglow, electron thermal conductivity along the magnetic field 3-49786
 Au-Gd-³He, improved thermal contact at ultralow temps. 3-52740
 Pd:Fe-³He, improved thermal contact at ultralow temps. 3-52740
 VO₂ coplanar switching devices, heat transport eqn. soln. in pulse response theory 3-79747
- thermal conductivity measurement**
 a.c. heated wire method for liquids 3-72204
 apparatus, heat loss due to radiation calc. 3-42533
 comparative cut-bar apparatus, construction, error analysis, typical data, operation 3-59562
 DTA cell block characts. evaluation using thermal analogue of Ohm's law 3-73690
 dynamic technique, in cylindrical geometry 3-59559
 electrically conducting materials, thermophysical prop. meas. apparatus, measurement errors 3-53855
 fluid heat transfer and dielec. props. determ. method using capacitance meas. 3-62019
 heat pipe, liquid N₂, effect of power load and angle of inclination, axial temp. distrib. 3-53859
 intrinsic thermocouple, numerical soln. for dynamic behaviour, nuclear reactor application 3-45444
 liquid metals, 1100-2100 K, thermal capacity, diffusivity and conductivity, simultaneous meas. 3-42543
 liquid metals, measurement method, sample radiation in vacuo, heat flux, steady-state temp. profile, i.r. microscope 3-48374
 low temperature for large specimens, 4.2 to 5.0 K 3-56650
 manometer, enthalpy of sublimation meas. 3-45460
 metallic short specimens above 1000°C, thermal conductivity, electrical conductivity and emissivity determ. method 3-77563
 particulate samples, transient methods, line source method, differential line source method, comparison 3-62017
 Peltier effect, thermo-e.m.f. and thermal cond., determ., thermocouple method, low reference temp. 3-51656
 plasma cond. coeffs. in Tokamaks expt., possible direct meas. 3-49758
 polymers, -40° to +250°C device 3-48367
 porous materials, foams, high temp., electron bombardment heating (*German*) 3-42542
 refractory materials, sintered, thermal conductivity meas., modified Krishnan and Jain method, 1000-2200°C (*Czech*) 3-70288
 solid, elec. conducting, direct heating methods for temps. above 1500K 3-48375
 solid, rapid meas. using linear regular regime 3-62011
 solids, 300 to 900 K, apparatus, Pt resist. thermometers 3-73695
 thermal insulating materials, using miniature heat flow sensors 3-77396
 thin film, temp. coeff. determ. 3-62018
 thin film techniques 3-73696
 Al, from 1.3 to 2.1 K 3-41297
 Al-Mg, quenched and annealed, age-hardening, lattice heat cond meas., cryostat technique 3-48383
 Cu, from 1.3 to 2.1 K 3-41297
 F₂, analysis in fluorination of U, in-line gas analyzer 3-42532
 Nb, from 1.3 to 2.1 K 3-41297
 UF₆, analysis in fluorination of U, in-line gas analyzer 3-42532
 UO₂, pellets and vipac, in-pile 3-63220
 UO₂-PuO₂, pellets and sol-gel, in-pile 3-63220
- thermal conductivity of gases**
 binary gas mixtures, computation of thermal conductivity 3-63611
 dense gases, transport properties calc. 3-52417
 heat flow birefringence calc. 3-52475
 inert gas mixtures at low and mod. densities 3-71704
 inert gases, dilute, at mod. and high temps. 3-71716
 inert gases, measurement by transient hot wire method 3-71700
 kinetic theory approach, review 3-71655
 methane, Senftleben-Beenakker effect 3-71705
 molecular, mag. field depend. of thermal corrls. 3-40696
 one component fluids, near gas-liq. crit. point 3-72185
 positive column characterization, electric arc in a gas flushed channel (*Russian*) 3-71968
 rarefied polyatomic gases, behaviour in static mag. field 3-52476
 steam, thermal conductivity in supercritical region 3-52415
 thermophysical properties computation and production of self-consistent tables and Mollier charts 3-60510
 transport and equilibrium props., utility of m-6-8 potential function 3-60512
 transport coefficients in the intermediate relativistic regime, special models 3-60516
 Ar, 1000-2500K, column method 3-75172
 Ar, absolute meas. to 200°C and 1600 atmospheres 3-71703
 CO, Senftleben-Beenakker effect 3-71705
 CO₂, 0 to 150 C meas. using hot wire method (*Russian*) 3-75175
 CO₂, measurement by transient hot wire method 3-71700
 CO₂, thermal conductivity in supercritical region 3-52415
 CO₂-N₂O mixture, 0 to 150 C meas. using hot wire method (*Russian*) 3-75175
 H₂, determ. using hot filament and coaxial cylinders, accommodation effect at gas/solid interface 3-49522
 H₂, para, at room temperature, heat conductivity, Senftleben-Beenakker effect, quantum mechanical calc. 3-52418
 H₂ and water vapour binary mixture, thermal conductivity and viscosity calc. 3-63609

thermal conductivity of gases continued

- He, thermophysical properties, HEPROP computer program 3-50042
 He-air mixture, 270-650 K 3-71706
 He-Ar mixtures, least-square calc. of conductivity in range 196-5000 K 3-40699
⁴He, thermophysical properties, 4 to 3000 R, pressures up to 15000 PSIA 3-50043
⁴He, thermophysical props. tables from 2 to 1500 K with pressures to 1000 atmospheres 3-60822
 N₂, 0 to 150 C meas. using hot wire method (*Russian*) 3-71575
 N₂, absolute meas. to 200°C and 1600 atmos. 3-71703
 N₂, measurement by transient hot wire method 3-71700
 N₂, Senffleben-Beenakker effect 3-71705
 N₂-N₂O mixture, 0 to 150C meas. using hot wire method (*Russian*) 3-75175
 NO, Senffleben-Beenakker effect 3-71705
 N₂O, 0 to 150 C meas. using hot wire method (*Russian*) 3-75175
 N₂O₄ = 2NO₂, with diluents, heat cond. at 25°C 3-50834
 Ne, 1000-1500K, column method 3-75172
 O₂ and water vapour binary mixture, thermal conductivity and viscosity calc. 3-63609
 Xe, 1000-1500K, column method 3-75172

thermal conductivity of liquids

- aerosol particle, eqns. for temp. distrib. 3-63767
 alloy, binary, calc. from component props. and conc. 3-50171
 benzoic acid, enthalpy of sublimation meas., thermal cond. manometer 3-45460
 benzophenone, enthalpy of sublimation meas., thermal cond. manometer 3-45460
 cast basalt stone, solid, liq., two-phase states, thermal cond., heat capacity, elec. modelling (*Russian*) 3-41057
 coaxial cylinders method, formula 3-77401
 Dowtherm A and Isopar M, a.c. heated wire method 3-72204
 ferrocene, enthalpy of sublimation meas., thermal cond. manometer 3-45460
 glass, heat penetration number rel. to workability (*German*) 3-55877
 human blood, thermal properties calc. during freezing process 3-70097
 Isopar M, a.c. heated wire method 3-72204
 metal and alloy, conf., Tokyo, Japan (Sept. 1972) 3-49820
 metallic melts, rel. to viscosity (*Russian*) 3-44057
 metals, measurement method, sample radiation in vacuo, heat flux, steady-state temp. profile, i.r. microscope 3-48374
 microscopic processes, review 3-64199
 organic liq., nomogram method 3-72237
 perturbation theory, dense fluid transport properties 3-72221
 sea, Baltic, turbulent thermal conductivity calc. (*German*) 3-65263
 trans-stilbene, enthalpy of sublimation meas., thermal cond. manometer 3-45460
 thermophysical properties computation and production of self-consistent tables and Mollier charts 3-60510
 n-tridecane, 30-400°C, press. up to 500 bar 3-52726
 Bi-Se alloy, ambipolar thermal diffusion, elec. and thermal cond. changes 3-64220
 Ga, Lorenz no. determ. (*German*) 3-50162
 Ga, Lorenz number, Kohlrausch meas. method 3-75737
 Ga Lorenz number, Kohlrausch direct measurement, electrical conductivity, Wiedemann Franz law 3-50181
 H₂O films on mica crystals, conductivity rel. to structure 3-60847
 He, thermophysical properties, HEPROP computer program 3-50042
³He liquid, high-temperature transport properties 3-60824
⁴He, heat flow at 0.1-0.7 K, T³ depend. 3-75644
⁴He, thermophys. props., 4-3000 R, press. to 15000 PSIA 3-50043
⁴He, thermophysical props. tables from 2 to 1500 K with pressures to 1000 atmospheres 3-60822
⁴He II, liquid, thermal props., hot filament study 3-72244
 Hg, Lorenz no., Wiedemann-Franz law (*German*) 3-50170
 Hg, Lorenz number, Kohlrausch meas. method 3-75737
 Hg Lorenz number, Kohlrausch direct measurement, electrical conductivity, Wiedemann Franz law 3-50181
 Hg-In, alloy Lorenz number, Kohlrausch direct measurement, electrical conductivity, Wiedemann Franz law 3-50181
 Hg-In, Lorenz number, Kohlrausch meas. method 3-75737
 Hg-In alloys, Lorenz no., Wiedemann-Franz law (*German*) 3-50170
 N₂O₄, meas. of coeff. of conductivity, temp. up to 400 K, 120 and 160 bar, coaxial cylinder method 3-41872

thermal conductivity of solids

- anharmonic crystals, calc. 3-40999
 anisotropic insulator, three-phonon scatt. processes, variational treatment 3-68374
 austenitic stainless steel, at low temp. 3-44609
 Ba, elec. resist., thermal cond. and thermopower meas. from 40 to 300 K 3-64318
 brittle materials, heat resist. problems and rupture 3-58702
 cast basalt stone, solid, liq., two-phase states, thermal cond., heat capacity, elec. modelling (*Russian*) 3-41057
 ceramics, influence of microstructural characteristics 3-76316
 ceresin-Al composite, thermal cond., effect of composition inhomogeneities 3-50033
 coatings, mixed composition plasma-sprayed, thermal conductivity 3-53267
 composite, effective cond., case of inclusions of arbitrary shape 3-57173
 composite material, radiative heat transfer, photon mean free path depend. 3-55103
 dielectric crystal, complex, theory rel. to anharmonic three phonon interactions 3-43906
 dielectric crystal, reduced thermal cond. rel. to phonon scatt. 3-79534
 garnet, Czochralski-grown, perfection and charact. for gems, lasers and substrates 3-76131
 gaylussite, thermal properties by simultaneous thermal analysis 3-73196
 glass, chalcogenide, temp. depend. above 300K 3-72239
 glass, tunnelling model rel. to temp. laws below 1K, acoustic props. (*French*) 3-40975
 thermal conductivity of solids continued
 glass reinforced plastics, relation with interlaminar shear modulus 3-80445
 glassfibre reinforced plastics, mean thermal cond., elastic modulus, 4-77 K, 4-300 K 3-73702
 graphite, exfoliated foils, thermal and elec. cond., low temp. 3-50032
 graphite, heat resistance, temp. depend. 3-80435
 graphite, lattice dynamics, interatomic forces, thermal props., half-continuum model appl. (*German*) 3-72158
 graphite, neutron irradiated, thermal cond. meas., 50 to 1000 C 3-46648
 graphite, pyrolytic, thermal diffusivity and thermal cond., 300-2700 K 3-46723
 graphite, thermal properties, theoretical exposition with associated experimental data 3-72153
 graphite reactor material from gilsonite coke, radiation behaviour, dimensional stability (*German*) 3-71260
 o-H₂, low temp. libron heat cond. and phonon heat cond. (*Russian*) 3-64138
 heat pipe, liquid N₂, effect of power load and angle of inclination, axial temp. distrib. 3-53859
 II-VI semiconductors, thermal comparator measurement 3-72240
 Inconel 718, and elec. resist. meas. up to 1200K 3-52817
 inert gas, Gruneisen parameter at T=0 K, first-order self-consistent phonon calcs. 3-46691
 isotropic media, relativistic theory of dissipative magnetoelastic interactions 3-79884
 laser pulse heated, soln. to one-dimens. problem for semi-infinite body (*Russian*) 3-53172
 lattice conductivity, high temp., relax. time approx. 3-68375
 lattice conductivity, low temp., relax. time approx. 3-68376
 lattice thermal conductivity, theory 3-68377
 lattice with impurities, nonlinear heat transfer, isotopica and dislocation scatt. 3-64133
 Lorenz number and thermal resistivity in nearly mag. alloys 3-72343
 Lorenz ratios of technically important metals and alloys 3-55246
 lunar granular aggregates, contribution of contact conductivity 3-73458
 lunar regolith, Apollo 15 meas. 3-61713
 measurement technique, linear-regular regime, coefficient 3-62011
 metal, heat resistance estimation method for variable temp. conditions (*Russian*) 3-80425
 metal, two-band, electron conductivity calc. 3-75815
 metal film-quartz, thermal phonon radiation with substrate 3-55043
 metal pairs, thermal contact resist., heat pulse meas. technique 3-70286
 noble metals, electrical and thermal resist., temp. variation 3-55239
 nuclear fuel, porosity depend. 3-40537
 nuclear fuel elements, loose coated particles in packed beds, under irradiation (*German*) 3-67542
 phonon, cubic crystals, with narrow quasilocalized vibr. modes 3-72159
 phonon transport, Monte Carlo simulation 3-68379
 phonon-phonon scatt. rel. to high-temp. lattice cond. 3-50034
 plasma deposited metallic films, thermal conductivity calc. 3-60863
 polyethylene, pressure dependence from 0 to 25 kbar 3-43881
 polyethylene filled with wood flow, dielectric and thermophysical props. meas. 3-65006
 polymer crystal, acoustic phonon effects (*German*) 3-60777
 polystyrene foam, density depend. (*German*) 3-65044
 porous metallic materials, thermal and electrical conductivity prediction 3-76392
 refractory materials, sintered, thermal conductivity meas., modified Krishnan and Jain method, 1000-2200°C (*Czech*) 3-70288
 semiconductor, mag. field depend., theory 3-75759
 solid-solid interface, effect of defect scattering on phonon transmission 3-55134
 steel, heat resistance, chem. comp. effect 3-55824
 steel, stainless 304, and elec. resist. meas. up to 1200K 3-52817
 terrestrial heat flow measurement, Austria, heat flow maps, Central Europe 3-73239
 thermal contact conductance correlations in vacuo 3-47430
 thin film meas. techniques 3-73696
 transition metals, Lorentz function, high temp., band structure effects, electron-electron scattering 3-46823
 transition metals and dil. alloys, phonon-induced interband transitions role (*Russian*) 3-44049
 triglycine sulphate crystals, thermal diffusivity, ferroelectric and paraelectric, effect of growth conditions 3-50031
 vitreous material, temperature maximum appearance under external radiation 3-60798
 Zircaloy-2 oxide film, heat transfer characts. 3-60278
 Ag, heat flux depend., precise obs., 2-5 K 3-55236
 Ag film, temp. coeff., 300-900 K 3-62018
 Al, heat flux depend., precise obs., 2-5 K 3-55236
 Al, single crystal, dynamic obs. using cylindrical geometry 3-59559
 Al film, temp. coeff., 300-900 K 3-62018
 Al-BN-B₄C, and thermal expansion meas. from 20-2000K (*German*) 3-52727
 Al-Mg, quenched and annealed, age-hardening, lattice heat cond meas., cryostat technique 3-48383
 AlN-BN-B₄C, and thermal expansion meas. from 20-2000K (*German*) 3-52727
 B₄C, B/C ratio depend. 3-80403
 BN, pyrolytic, longitudinal, temp. depend. 3-75640
 B₂O₃, thermal conductivity meas. 3-55832
 B₂O₃, suboxide, 38 to 540°C 3-68421
 Ba-mica/Al₂O₃ composites characteriz. 3-76342
 BeO + b₂O₃, thermal conductivity meas. 3-55832
 Bi, 1.3-6K, sample dimensions and quality effects 3-58271
 Bi film, influence of polymer powder substrate temp. 3-50091
 (Bi_{1-x}Sb_x)₂Te₃, Bi₂(Te_{1-x}Se_x)₃, semicond., charge carrier and phonon contrib. 3-68451
 BiSe-group IV telluride solid solutions, effect of carriers 3-64179
 C, low density, high temp. effects 3-72974
 C, pyrolytic, meas. from 25-1100°C after fast neutron irradi., reactor material appl. 3-49367

thermal conductivity of solids continued

- C/C composite, felt, heat treatment 3-69367
 C/C composites, fibre volume percent depend. 3-55854
 Ca, elec. resist., thermal cond. and thermopower meas. from 325-425 K 3-64318
 $\text{Ca}_2\text{La}_8(\text{SiO}_4)_6\text{O}_2$, laser host material 3-43819
 CdAs_2 vitreous alloys, eff. of Ge atoms on $\text{CdAs}_3\text{-CdGeAs}_2$ 3-72238
 Cd_3As_2 film, thermal detect., Nernst coeff. ratio meas. 3-68651
 $\text{CdS}_x\text{Se}_{1-x}$, temp. range 100-300K, role of phonon scatt. obs. 3-64221
 $\text{CdSnAs}_2\text{-CdSe}$ solid solution, electron and phonon components, in mag. field 3-58155
 CeIn_3 , rel. to anomalously large thermoelec. cooling figure of merit 3-50182
 CePd_3 , rel. to anomalously large thermoelec. cooling figure of merit 3-50182
 Co, ferromagnetic metal, transport properties meas. 3-52814
 CoO , at Neel temp. 3-58379
 Cu-Al alloy, temp.-wave method, simultaneous measurement with thermal diffusivity 3-51545
 Cu-B, and elec. resist. meas. up to 1200K 3-52817
 Cu-W, fibre reinforced composite, phys. props. rel. to fibre vol. and prep. technique 3-64986
 Cu-Zn(Ga)(Ge)(As) dilute alloy, low temp. total and lattice cond., impurity and defect effects 3-68591
 Fe, Armcro, cylindrical specimens, thermal conductance at light loads 3-47395
 Fe, cast, malleable, heat resist. and struct. changes during thermal cycling 3-50734
 Fe based superalloy, A286, and elec. resist. meas. up to 1200K 3-52817
 $\text{Fe}_{75}\text{P}_{15}\text{C}_{10}$ amorphous alloy, splat cooled, physical props. 3-60758
 Ga, high purity single crystal, temperature variation of Lorenz ratio 1.4-4.2 K 3-55234
 Ga, Lorenz no. determ. (German) 3-50162
 GaSb, thermal diffusivity meas., Angstrom method, doping effect (French) 3-75639
 GaSb-InSb alloy, lattice thermal cond. from 4 to 10K 3-43905
 Ge, three phonon-umklapp resistivity, variational calc. 3-68378
 ^4He , h.c.p., anisotropic heat conduction obs. 3-52744
 ^4He , h.c.p. cryst., meas. rel. to phonon scatt. by isotopic impurities 3-55122
 $\text{Hg}_{1-x}\text{Cd}_x\text{Te}$, at low temp., phonon spectra and scattering obs. 3-60809
 HgSe, lattice thermal cond., depression due to phonon reson. scatt. between 4 and 30K 3-41058
 InP, phonon polarization effects on thermal conductivity, 300-800K (French) 3-75638
 InSb-MbSb, eutectic alloy, due to lattice component 3-64222
 In thermal props. at high temps. 3-79666
 KBr:Ti^+ , phonon props. and electron-phonon interaction 3-58098
 KCl, three-phonon umklapp resistivity, variational calc. 3-68378
 KCl:Ti^+ , phonon props. and electron-phonon interaction 3-58098
 KI:Ti^+ , phonon props. and electron-phonon interaction 3-58098
 La, meas. in 80 to 750K range, over first phase transition, lattice contrib. 3-75734
 MgAl_2O_4 , transparent shaped mat., fabrication and props. 3-72967
 Mo-Ti, (0.5 at.%Ti), and elec. resist. meas. up to 1200K 3-52817
 N₂ crystal, N-containing flashes and glows at low temp. due to thermal instability 3-72762
 NaCl, three-phonon umklapp resistivity, variational calc. 3-68378
 Nb, cold deformed, short-term heat resist., gaseous medium influence (Russian) 3-80427
 Nd, and Lorenz function 2-45 K, rel. to magnetic transition 3-50165
 Ne, isotopic mixtures, phonon scattering relaxation rates, possibility of second sound propagation 3-55067
 NiO, at Neel temp. 3-58379
 n-PbTe solid solution, separation of lattice and electronic components in strong mag. field 3-58154
 PbTe-SnTe-PbS system, thermal conductivity and structural study 3-79533
 $\text{Pd}_{32}\text{Si}_{18}$ amorphous alloy, splat cooled, physical props. 3-60758
 Pr, high purity, polycrystalline, Lorenz number, 2-40 K 3-55235
 PtSb_2 mobilities and effective masses of electrons and holes calc. 3-68650
 Rh thermal props. at high temps. 3-79666
 Si, boundary scatt. effects at room and dry-ice temps. 3-43904
 Si, single crystal, dynamic obs. using cylindrical geometry 3-59559
 Si, three phonon-umklapp resistivity, variational calc. 3-68378
 SiC, high density, 25-1300°C 3-76293
 $\beta\text{-SiC}$, pyrolytic, neutron irradi. 3-40539
 SmS, region of homogeneity, comp. effect 3-64178
 SmS, temperatures and composition depend. obs. 3-60871
 Sn, intermediate state, size effect (French) 3-58336
 Sr, elec. resist., thermal cond. and thermopower meas. from 40 to 300 K 3-64318
 Ti_2Te , 300-625K 3-79535
 Tm, resistance, magnetic field effect 3-60864
 (U,Pu) O_2 fuel pins, in-pile radial temp. profiles, simulation 3-46142
 UO_2 , porous stoichiometric and hyperstoichiometric 670-1270 K 3-43304
 UO_2 and U_3O_8 , 100 to 300 K, phonon mean free path 3-40542
 W-Mo alloys 3-72972
 Yb, Lorenz function and thermal cond., 90-300K 3-50167
 ZnO:Li doped and undoped crystals, 1.1 to 300 K, anisotropy, Debye-Calloway model analysis 3-43907

thermal convection *see convection***thermal critical constants**

- see also boiling point*
 triple-point cells, water, simple filling method 3-66163
 C black, thermal self-ignition, nonuniform surface, critical temp. computer calc., reaction kinetics (Russian) 3-50830

thermal decomposition *see chemical reactions***thermal diffusion**

- see also thermal diffusion in gases; thermal diffusion in liquids; thermal diffusion in solids*
 nonlinear boundary value problem, variational soln. and error bound 3-48822
 outgassing of solids during tempering 3-62041
 turbulent, parallel to plane wall for $y_1=2\text{-}300$ (French) 3-46384
- thermal diffusion columns** *see isotope separation; thermal diffusion in gases*
- thermal diffusion in gases**
 cloud nuclei counter, Gagin and Terliuc, anal. of wall effects 3-76914
 evaluation, and Onsager coeff. calc. (Hungarian) 3-75178
 isotopes separation plant for oxygen and krypton, automatic control system 3-77743
 methane, binary mixtures with CD_4 , CF_4 , diffusion and thermal diffusion coeffs., mag. field effects, model calcs. 3-54789
 molecular, mag. field depend. of thermal correl. 3-40696
 nonpolar polyatomic gases, mol. shape effect on transport and equil. props. 3-75179
 transport and equilibrium props., utility of m-6-8 potential function 3-60512
 Ar isotopic thermal diffusion meas., 200-900 K, intermolecular potential deduced 3-71713
 Ar thermal diffusion, state potentials 3-75171
 He-Ne, c.w. laser, effects rel. to beam intensity fluctuations 3-66816
 Kr isotopic thermal diffusion meas., 200-900 K, intermolecular potential deduced 3-71713
 Kr thermal diffusion, state potentials 3-75171
 $\text{N}_2 + \text{CO}$, diffusion and thermal diffusion coeffs., mag. field effects, model calcs. 3-54789
 Ne thermal diffusion, state potentials 3-75171
 $^{20}\text{Ne} + ^{22}\text{Ne}$, Clusius Dickel column, effect of column misalignment 3-78928
 Xe thermal diffusion, state potentials 3-75171
- thermal diffusion in liquids**
 Benard cell, oscillatory motion due to the Soret effect 3-67946
 carbon tetrachloride-cyclohexane system, thermogravitational thermal diffusion, end effects 3-41037
 critical binary mixture, liquid-vapour points (French) 3-50014
 gravitational thermal diffusion columns, steady state, application binary organic system (French) 3-41035
 gravitational thermal diffusion columns, steady state, numerical calc. (French) 3-41034
 organic solvents, of amines, diaphragm cell technique 3-72216
 toluene, of polystyrene 3-60500
 water alcohol liquid layers, finite amplitude oscill. motions in two component Benard problem 3-67950
 water and salt solution of dextran 3-60500
 Bi-Se alloy, ambipolar thermal diffusion, elec. and thermal cond. changes 3-64220
 Cu_2Se , Cu_2Te , melt, electron transfer, e.m.f. meas. thermal diffusion 3-44070
 ^3He - ^4He , diffusion and thermodiffusion, theory (French) 3-58163
 ^3He - ^4He mixture, near tricritical point, mode-mode coupling calc. 3-60825
 ^4He - ^3He liq. mixture, conc. grad. due to heat flow, thermodiffusion and convection (French) 3-58162
 Na, thermotransport of Be and Hg 3-64197
 Na melts, of Armcro iron, diffusion acceleration mechanism (Russian) 3-41717
- thermal diffusion in solids**
 coefficients calc. by statistical method 3-46725
 graphite, pyrolytic, thermal diffusivity and thermal cond., 300-2700 K 3-46723
 ice, temperature-gradient migration of liquid droplets 3-79522
 insulator, effect of diffusion on space charge currents 3-79704
 interstitial diffn. in thermal gradient, implicit method with supersaturation 3-46732
 metal, oxygen diffusion out under flash desorption 3-72271
 sintering, heterodiffusion effects 3-69364
 $\text{As}_2\text{S}_3\text{:Ag(Cu)}$, bulk glass, photo and thermal diffusions of Ag(Cu) 3-43903
 Be, isotopic tracer steady-state distrib., thermotransport 3-55100
 CsI:Na^+ , Ti^+ , V_k centres, thermolum. obs. of thermal migration 3-64335
 Fe:Si, Fe:P, Fe:Si:P alloys (German) 3-80240
 n-GaP, of Zn, ternary sources, 850°C, non-ideal kinetics 3-72228
 KCl, stability of droplets migrating in thermal gradient 3-43887
 KCl:Li, single crystals, vacancy mechanism of Li diffusion 3-72231
 Li, of ^{64}Cu , ^{195}Au , ^{110m}Ag , ^{65}Zn , ^{115m}Cd , thermotransport obs. by steady-state technique 3-60803
 NaCl, motion and deform. of cavities in temp. gradient field 3-58152
 NaCl, of Ba^{2+} , isothermal, temp. depend. of diffusion coeff. 3-60804
 (Ti, W)C solid solution form., investigation 3-64975
 Ti alloys, diffusion of hydrogen due to comp., temp. and stress gradients 3-64213
 Ti-Al-V-Sn alloy, of H_2 , meas. using non-reactive technique 3-72235
 TiCl-TiBr, interdiffusion meas. at 400C 3-79527
 (U, Pu)-Co-O system, thermal diffusion mechanisms 3-63232
 (U,Pu) O_2 fuel, conservation eqns. governing porosity and actinide redistrib. 3-46145
 (U,Pu) O_2 fuel pins, plutonium redistrib. considerations 3-46141
 U-C system thermal diffusion mechanisms 3-63232
 U-C-H system, thermal diffusion mechanisms 3-63232
 U-C-O system, thermal diffusion mechanisms 3-63232
 UO_2 , thermal-gradient migration of helium bubbles 3-67552
- thermal diffusivity**
 ceramic electrolytes, review of current research 3-69459
 constant thermal diffusivity flows over in finite plane wall, soln. by Wiener-Hopf technique 3-46400
 electrically conducting materials, thermophysical prop. meas. apparatus, measurement errors 3-53855
 fluid heat transfer and dielec. props. determ. method using capacitance meas. 3-62019

thermal diffusivity continued

liquid metals, 1100-2100 K, thermal capacity, diffusivity and conductivity, simultaneous meas. 3-42543

liquid metals, high temp., laser flash technique 3-45448

lower thermospheric model, variability of neutral winds and vertical eddy diffusivity 3-61514

measurement method for cylindrical specimens at intermediate temps. (French) 3-56632

measurement technique, linear regular regime, coefficient 3-62011

one component fluids, near gas-liq. crit. point 3-72185

polyethylene, pressure dependence from 0 to 25 kbar 3-43881

polyethylene filled with wood flow, dielectric and thermophysical props. meas. 3-65006

polyhexene-1, amorphous, cooling rate influence on heat capacity and thermal transitions 3-50008

polymer, light heat wave irradiated, two layer slab method 3-68448

polymer, two layer slab method, edge effect losses 3-68450

polymer, two layer slab method, temp. carrier sensor transient response 3-68449

specific heat meas., pulsed electron beam method 3-45447

stainless steel, compared to Hf and Zircaloy-2, thickness effect 3-44556

succinonitrile plastic crystal, rel. to Rayleigh scatt. spectrum, interpretation (French) 3-42727

superconductors, type II, flux jump prediction, magnetisation, mag. and thermal diffusion equations 3-50294

tangential eddy diffusivity in a circular tube calc. 3-57736

triglycine sulphate crystals, ferroelectric domain wall thickness, evaluation from thermal diffusivity data 3-50522

triglycine sulphate crystals, thermal conductivity, ferroelectric and paraelectric, effect of growth conditions 3-50031

Zircaloy-2, compared to stainless steel and Hf, thickness effect 3-44556

C, pyrolytic, for thermal cond. meas. after neutron irradi., high-temp. reactor appl. 3-49367

Cu-Al alloy, temp.-wave method, simultaneous measurement with thermal conductivity 3-51545

Fe, liquid, solidification of Fe-C (German) 3-72884

Fe₃P₁₅C₁₀ amorphous alloy, splat cooled, physical props. 3-60758

Ga, liq., 45-512°C 3-68594

GaSb, doping effect on thermal cond., Angstrom method meas. (French) 3-75639

⁴He, determ. near gas-liquid crit. point, Rayleigh spectra obs. 3-50039

⁴He, thermophysical properties, 4 to 3000 R, pressures up to 15000 PSIA 3-50043

⁴He, thermophysical props. tables from 2 to 1500 K with pressures to 1000 atmospheres 3-60822

Hf, compared to stainless steel and Zircaloy-2, thickness effect 3-44556

Ir thermal props. at high temps. 3-79666

NaK, eutectic mixture, temp. and eddy diffusivity profiles 3-52432

Pd₂Si₁₈ amorphous alloy, splat cooled, physical props. 3-60758

Rh thermal props. at high temps. 3-79666

ThO₂, thermal diffusivity meas., 900 to 2550 C, flash method (French) 3-47445

UO₂, thermal diffusivity meas., 750 to 2700 C, flash method (French) 3-47445

UO₂ and U₃O₈, 100 to 300 K, phonon mean free path 3-40542

ZrBr₂, pyrolytic, thermal diffusivity at high temps. 3-61200

thermal effects in magnetism see *magneto-thermal effects*

thermal expansion

see also *Grüneisen coefficient*

alkali halides, 70-570 K, Grüneisen parameter determ. 3-68424

anisotropy in crystal physical props. represented by surfaces of rotation 3-79247

aragonite, stereographic projection of indicative surface 3-72018

ceramics, frame for linear expansion compensation, elec. cond. meas., temp. dependence studies 3-53851

clinopyroxene, lattice deform. depend. on chem. substitution and temp. 3-80592

α-Co solid, lattice temp. dependence determ. using X-ray diffraction methods 3-79508

composite material, fibrous, expt. study 3-50770

concrete beam, flexure testing rig, furnace combination 3-47496

cryogenic window, stresses 3-62023

crystal, semiconductor laser, deformation of emitting face 3-48928

crystals, local lattice impurity centres, struct. spectra 3-68563

diffusely reflecting samples, holographic interferometry measurement 3-39949

electron gas, non-interacting, relation to magnetostriction 3-50339

ferrites, capacitance dilatometer technique, 80 to 273 K, linear coefficients 3-52713

garnet, Czochralski-grown, perfection and charact. for gems, lasers and substrates 3-76131

glass, frame for linear expansion compensation, elec. cond. meas., temp. dependence studies 3-53851

glass, low temperature, tunnelling states model 3-60800

glass, mixed nitrate, M(I)NO₃ + M(II)(NO₃)₂ 3-72009

glass reinforced plastics, thermal expansion coeffs. at low and high temps. 3-47465

glassfibre reinforced Araldite epoxy resin, thermal contraction meas., use in thermal cond. app. 3-7300 K 3-73005

graphite, lattice dynamics, interatomic forces, thermal props., half-continuum model appl. (German) 3-72158

graphite, neutron irradiation, dimensional instability, density changes (German) 3-71256

graphite, neutron irradiation, high temp. (German) 3-71257

graphite, thermal properties, theoretical exposition with associated experimental data 3-72153

graphite, universal expansiometer for high temp. studies 3-73697

Invar alloy, mag. contrib., itinerant electron model 3-50433

Invar alloys, theory based on magnetostriction due to exchange interactions 3-50356

liquid crystals, pretransition phenomena just above clearing point 3-63950

magnesite-asbestos system, comp. depend. 3-64978

mathematical framework, solved problems, book contrib. 3-58133

measurement at high pressure 3-77383

thermal expansion continued

metallic elements, atomistic expression, Grüneisen parameter determ. 3-41033

metallic hexaborides, temp. depend. of lattice consts., X-ray diff. anal. 3-68423

methanol + carbon disulphide liq. sytem, crit. region thermal expansion 3-68384

muscovite, anisotropy, electron diff. obs. (Russian) 3-49877

naphthalene mol. crystals, calc. of temp. dependence of thermal expansion coeff. using quasi-harmonic model (Russian) 3-68368

penton film, molten, morphology, heat treatment effect (Polish) 3-53282

polyethylene, linear, single-cryst. texture, 0 to -190°C 3-58734

polyethylene, negative coeff. of thermal expansion obs., following elongation 3-58140

polyethylene, tensile deformation effect 3-80483

polyethylene/fibrous fillers composites, coeffs. calcs. 3-80450

polymer, glass transition temp. rel. to expansion coeffs. 3-54935

polymer, linear, free vol. rel. to temp., expansion coeff. change, vitreous state (Russian) 3-71689

polymer, vel. coeff. rel. to specific vol., effect of hydrostatic pressure 3-73053

potassium acid phthalate crystals, coefficient perpendicular to cleavage planes, X-ray diffraction application 3-64191

rare earth metals, alloys, heavy, meas. at mag. transitions 3-79834

rare earth-Fe, rel. to Curie temp. pressure depend. 3-58385

reactor fuel element stresses at discontinuities and interactions by finite elements in two dimensions 3-63125

reduction of gas-expansion work, cold liquid, heat flow to liquid surfaces, appl. to molten fuel-coolant interaction 3-71177

refractories, brittle, thermal stress resist. caused by anisotropic behaviour of grains in polycryst. matrix (German) 3-61187

refractory, fireclay, thermal-expansion-under-load behaviour 3-80407

refractory, thermal expansion under load, test program 3-80406

refractory polycrystalline compounds, thermal expansion coefficients, temp. depend. 3-76310

rock, petrofabric anal., holographic interferometry, thermal expansion tensors, preferred orientation determ. 3-80652

seawater, thermal expansion, adiabatic temp. gradient and potential temp., new polynomials 3-53444

shock wave condensed media compression, temp. estimation by thermodynamic method (Russian) 3-79423

solid, and specific heat at high temp., one dimens. anharmonic lattice model 3-50006

solid, cooperative meas. techniques from 1000-2600°C 3-48376

solids absorption of laser energy, optical excitation of acoustic pulse 3-53081

specularly reflecting samples, by moiré interferometry 3-39944

steel, austenitic stainless, γ-α transform. effects, 80-280K (Russian) 3-44604

steel, borated, residual stress curve predeterm. (Russian) 3-80320

stishovite, thermal expansion coeffs. from X-ray diffraction study 3-65210

titania-silica glasses, thermal expansion meas. by photoelastic and u.s. techniques 3-51593

triglycine sulphate, ferroelec., irradi. effects (Polish) 3-50526

u.s. propagation, Rao's constant, ratio to temp. coefficient of u.s. velocity, theoretical study 3-77326

water, discussion of different tables for 0 to 40 deg. C 3-64190

water, in independent cylindrical capillaries 3-61227

Zircaloy cladding, high temp.-testing for use as thermocouple sheath in PWR 3-47431

AgI, polycrystalline, 170-500°C 3-75629

Al, quasi-local vibrs. due to Ag impurity influence (Russian) 3-79506

Al-BN-B₄C, and thermal cond. meas. from 20-2000K (German) 3-52727

Al-Cu system, statistically isotropic heterogeneous medium, coeff. calc. 3-60760

Al_{0.9}Ga_{0.1}As-GaAs heterostructure, interface stresses due to different thermal expansion coeffs. rel. to laser operation 3-59872

AlN-BN-B₄C, and thermal cond. meas. from 20-2000K (German) 3-52727

Al₂O₃, corundum struct. type 3-69340

Ar, coeff. of mol. crystals, calc. of temp. dependence using quasi-harmonic model (Russian) 3-68368

As-Se glass, coeff., glass transition temp. and deform. point (Japanese) 3-79510

B₄C, hot-pressed, high-temp. characteriz. 3-69348

B₄C, B/C ratio depend. 3-80403

B₂O₃-SiO₂-GeO₂ glasses, characteriz. w.r.t. struct 3-76271

B₂O₃, suboxide, -190 to 900°C 3-68421

Ba₂NaNb₃O₁₅, ferroelec., struct. behaviour in Curie pt. region 3-41488

Bi film, quantum temp. size effect, temp. depend. of thermal expansion 3-72212

Bi₂Te₃-Bi₂Se₃ linear expansion coefficient, mechanical props. 3-75628

C, glassy, linear expansion from 23 to 2300°C 3-50012

C, pyrolytic, coating for HTGR fuel particles, fluidised bed deposition, X-ray obs., 300-1100°C (German) 3-71249

C/C composites, felt, heat treatment 3-69367

C/C composites, fibre volume percent depend. 3-55854

Cd₂La₈(SiO₄)₆O₂, laser host material 3-43819

Cd₃As₂, lattice parameter measurement between 23 and 700°C using X-ray diffractometer 3-68426

Co, ferromagnetic metal, transport properties meas. 3-52814

Cr, from X-ray determ. of lattice const. 3-68427

Cr-based ternary alloy, b.c.c. struct., antiferromag., Invar props. 3-50434

Cr₂O₃, corundum struct. type 3-69340

Cs halides, thermal expansion and Grüneisen parameters at low temp. 3-43885

Cu-W, fibre reinforced composite, phys. props. rel. to fibre vol. and prep. technique 3-64986

CuCr₂O₄ 3-72048

CuFeS₂, antiferromag. film, supercond. transition for 88 < T < 90K, thermal expans. jump 3-75808

thermal expansion continued

- CuGaMnO₄, spinel, ionic order and cation valencies, thermal expansion meas. 3-68194
 Dy, dispersion relations and lattice thermal expansion 3-79456
 Er, and phonon dispersion, Keatings method calc. 3-68345
 Fe, liq., 1560-1750°C 3-50013
 Fe-Mn(18 wt.%) alloy, antiferromag. of ϵ -phase, second order transform. (*Russian*) 3-72462
 Fe-Ni alloys, Invar phenomena, plastic deform. and heat treatment effect (*Russian*) 3-58409
 Fe-Ni alloys, Invar type, Ti addition effect on phys. props. (*Russian*) 3-79883
 Fe-Ni-Co alloy, Invar, irreversible high field behaviour at low temps. 3-50435
 Fe₂O₃, corundum struct. type 3-69340
 Fe₇P₁₅C₁₀ amorphous alloy, splat cooled, physical props. 3-60758
 Ga₂O₃, corundum struct. type 3-69340
 α -Ga₂O₃, directional coeffs. 3-61199
 GaSb, Gruneisen coeff., temp. depend. of i.r. dispersion obs. 3-50583
 p-H₂, solid, obs. of, possible phase transition at 14K 3-75623
 p-H₂ solid, 10.5 to 13.8 K, in premelting region 3-79509
 H₂O films on mica crystals, anomalous expansion 3-60847
 He, solid and liquid, pressure-vol.-temp. relations 3-52732
 He superfluid transition under press., static scaling and universality 3-64228
 HfO₂, Y₂O₃ stabilized, mean coeffs. determ. 3-61195
 InBi, single cryst., thermal expansion, lattice const. behaviour, -186 to +100°C 3-55093
 InS(Se)(Te), thermal expansion and isothermal compressibility 3-55094
 KBr, calc. using anharmonic models 3-40997
 KBr, thermal expansion from lattice const. temp. depend. 3-52712
 KCl-RbCl solid solution single crystals, linear expansion coeff., 25-500°C (*Russian*) 3-79507
 KTaO₃, ferroelec. mode freq., thermal expansion and compressibility 3-55071
 Kr, coeff. of mol. crystals, calc. of temp. dependence using quasi-harmonic model (*Russian*) 3-68368
 La_{0.62}Pb_{0.38}MnO₃, possible evidence for coupling between elastic and magnetic exchange forces 3-47014
 LiH, magnitude and isotope effects, Born theory calc. 3-68425
 Li₂O-Al₂O₃-SiO₂ glass ceramic, crystallinity depend., heat treatment 3-76302
 Lu, high purity, physical and metallurgical properties 3-63981
 MgTi₂O₇, hot-pressed, grain size effects 3-69339
 Mn-Cu-Fe alloys, Elinvar props. 3-64533
 Mn-Cu-Mo alloys, Elinvar props. 3-64534
 Mn-Ni-Mo nonmag. Elinvar-type alloy characteriz. (*Japanese*) 3-44617
 MnO, magnetoelastic interaction, Neel temp., thermal expansion, uniaxial stress expts. 3-41390
 Mo, high temp. effects 3-69351
 (NH₄)₂BeF₄, temp. depend., nonlinearity, phase transitions 3-72207
 Na, solid, isobaric, and isothermal compressibility, data 3-79414
 Na, vaporised coolant, simulation of mech. energy release, reactor energy source characterisation 3-74674
 Na halides, thermal expansion and Gruneisen parameters at low temp. 3-43885
 NaF, thermal expansion from lattice const. temp. depend. 3-52712
 Ni-Fe alloys, Invar type, substruct. effects (*Russian*) 3-53224
 Ni₂6H₂O, approx. layer cryst. structure rel. to expansion anisotropy (*French*) 3-52611
 NiS, NiSe, NiTe, linear coeff., temp. depend. in region 85K to 300K 3-46722
 PbMoO₄, thermal expansion, X-ray determination 3-46719
 PbO-GeO₂ glasses characteriz. w.r.t. comp. 3-76270
 Pb₃P₂O₈, phase transition characterisation, temp. depend. 3-72191
 Pd₈₂Si₁₈ amorphous alloy, splat cooled, physical props. 3-60758
 PtGe, linear expansivities from lattice constants, temp. depend. 3-68214
 PtSi, linear expansivities from lattice constants, temp. depend. 3-68214
 Rb halides, thermal expansion and Gruneisen parameters at low temp. 3-43885
 RbBr, thermal expansion from lattice const. temp. depend. 3-52712
 RbCl, thermal expansion using shell model 3-52714
 Rh₂O₃, corundum struct. type 3-69340
 Rh₂O₃, corundum structure, directional thermal expansion coeffs. meas. 3-41032
 Sb₂Te₃-Bi₂Te₃ linear expansion coefficient, mechanical props. 3-75628
 ScBO₃, temp. depend., 30-702°C 3-68422
 SiC refractories, bonded, room temp. to 1200°C, characteriz. 3-76288
 Si₃N₄, shape and thermal shock behaviour 3-76289
 Te linear coefficients, 2 to 30 K and 55 to 90 K, Gruneisen parameters, measurements 3-41031
 TiB₂, 25-1200°C, X-ray diff. obs. 3-44657
 TiO₂, rutile, Gruneisen coeff. for soft mode 3-41027
 Ti₂O₃, corundum struct., X-ray diff. obs. 3-64189
 Ti₂O₃, corundum struct. type 3-69340
 VN_{0.96}, 300 to 1000K 3-69341
 V₂O₃, corundum struct., X-ray diff. obs. 3-64189
 V₂O₃, corundum struct. type 3-69340
 W, 293 to 1800 K, twin microscope method, Fizean interferometry 3-46720
 W, high temp. effects 3-69351
 W-Re, W-Nb alloys, coeff., anomalous conc. depend. 3-72213
 Xe, coeff. of mol. crystals, calc. of temp. dependence using quasi-harmonic model (*Russian*) 3-68368
 Zn silicate glass, alkali, nucleation and crystallisation properties 3-75476
 Zn₃As₂, lattice parameter measurement between 23 and 700°C using X-ray diffractometer 3-68426
 ZrFe₂, rel. to Curie temp. pressure depend. 3-58385
 ZrO₂-MgO system, directional solidification and oriented eutectic composite behaviour 3-76236
 ZrSiO₄, anisotropic thermal expansion and compressibility, high temp. and high pressure X-ray diffraction, neutron diffraction 3-46721

thermal expansion continued

- ZrZn₂ intermetallic phase, very weak itinerant electron ferromagnet 3-68771

thermal insulating materials

- see also thermal conductivity*
 ablative, testing, laser activated model surface recession compensator system 3-59908
 aluminosilicate fibre blanket, use as evacuated thermal insulation 3-76312
 conductivity measurement using miniature heat flow sensors 3-77396
 fibrous, heat transfer modes 3-55891
 mullite fibre, fine diameter, characteriz. for high temp. use 3-76275
 opacified microporous silical aerogel, use as evacuated thermal insulation 3-76312
 refractory oxide fibre eval. for high temp. rigidized insulation applic. 3-76276
 C foams, syntactic, review 3-80443

thermal insulation

- vacuum superinsulation heat transfer mechanism 3-59560

thermal noise

- impedance-field method calc., application to single injection 3-68638
 Josephson junctions, current-biased, phase-modulated quasiparticle current obs. 3-75816
 laser field, effect 3-70796
 nuclear reactor sodium loop, temperature noise measurement 3-67453
 optical p.c.m. repeater, using GaAs laser, rel. to error rate 3-66897
 solids, space charge limited conduction 3-68628
 superconducting quantum flux detector, derivation 3-62182
 Si, space charge limited conduction 3-68628
 Si p⁺-n-n⁺ photoparametric upconverter diode, base parameter effects on signal to noise ratio 3-66885

thermal properties of substances

- see also specific heat; thermal conductivity; thermal diffusivity; thermal expansion; thermal variables measurement*
 No entries

thermal quenching *see heat treatment***thermal radiation** *see heat radiation***thermal resistivity** *see thermal conductivity***thermal spikes** *see crystal defects; radiation effects***thermal transformations** *see phase transformations***thermal variables control**

- see also temperature control*
 crystal growth, Czochralski method, digital automatic adaptive control system 3-69156
 heating rate, automatic recording potentiometer 3-73688

thermal variables measurement

- see also bolometers; calorimeters; calorimetry; temperature measurement; thermal conductivity measurement; thermocouples; thermometers*
 contact resistance between metal pairs, heat pulse technique 3-70286
 Derivatograph, DTA, activation energy, malonic acid 3-76440
 Derivatograph, quasiisothermal quasi-isobaric conds., decomp. reactions 3-73689
 differential analysis device, differential thermograms recording (*Russian*) 3-73684
 diffusivity meas. method for cylindrical specimens at intermediate temps. (*French*) 3-56632
 direct heating methods for solid thermophysical props. above 1500K 3-48375
 emissivity, technique, apparatus, applic. to quartz glass 3-70289
 emittance, total hemispherical, of metal wires as function of temperature 3-62021
 expansion, cooperative meas. techniques for solids from 1000-2600°C 3-48376
 fluid heat transfer and dielec. props. determ. method using capacitance meas. 3-62019
 heat measurement, reactor γ -ray, thermoluminescence dosimeters and calorimeters 3-74753
 heat pulse expts. and h.f. phonons, technique and results 3-53853
 heating microscope, attachment for differential thermal anal., high-temp. technique, 1600 C, course of reaction in furnaces 3-53856
 Joule Thomson effect and enthalpy measurement for N₂, CO₂ ethylene gases 3-71708
 liquid binary alloys, heat of mixture rel. to molar volume changes on formation (*Russian*) 3-45446
 liquid binary alloys, volume changes on formation, meas. method (*Russian*) 3-45445
 lunar samples and minerals, simultaneous X-ray and thermal analysis 3-65805
 melting point of eutectics, use as secondary temp. standard above 2327K (*French*) 3-51550
 metrological problems 3-73686
 microanalysis, differential, apparatus, 25 to 600 C, operational examples (*French*) 3-56629
 phonon study at high freq. by heat pulse technique (*French*) 3-43845
 polymer, light heat wave irradiated, thermal diffusivity by two layer slab method 3-68448
 polymer, thermal diffusivity, two layer slab method, edge effect losses 3-68450
 polymer, thermal diffusivity, two layer slab method, temp. sensor transient response 3-68449
 polymer oxidation study, thermistor based DTA apparatus 3-77397
 pulse method measurement of thermal parameters, disturbing factors influence, complex analysis 3-56631
 radiometry, precision meas. 3-77391
 rocks and crystals, thermal and elastic moduli from holographic interferometric technique 3-61398
 scaling heat resistance meas. method for metallic materials (*Polish*) 3-50719
 solid diffusivity and conductivity rapid meas. using linear regular regime 3-62011

thermal variables measurement continued

- specific heat, apparatus, 1.5 to 310 K, adiabatic method, temperature drift corrected, actinide compounds (*French*) 3-56628
 specific heat, of small samples, heat pulse method 3-52707
 specific heat, pulse method meas. at high pressure 3-77404
 specific heat superconductors in mixed phase 3-62033
 submarine pyranometers, ang. characts. (*Russian*) 3-47825
 temperature, high, fast pulse heating system controlled by digital computer 3-48377
 thermography, for nondestructive testing 3-48364
 thermogravimetric data analysis 3-70287
 thin film, total emissivity, temp. coeff. determ. 3-62018
 thin film windows, alaphaphone for meas. heat absorption by infrasonic method 3-73784
 titania-silica glasses, thermal expansion meas. by photoelastic and u.s. techniques 3-51593
 Ge film thermal energy transducer 3-56615
 Ta-W (10 wt.%W), elec. resist., specific heat and emittance at 1500-3200K, high-speed simultaneous meas. 3-52705

thermionic cathodes

- application in high-resolution scanning transmission electron microscopy 3-42674
 sintered materials for electric vacuum devices 3-80398
 ZrC, with Pt and Ir additions 3-69131

thermionic conversion

- collisionless thermionic converter, oscillations obs. 3-49771
 mirror fusion reactor, electrical design of 1000 megawatt direct converter, engineering study 3-60318

thermionic electron emission

- see also Schottky effect; thermionic cathodes*
 detection and recording, proportional counter coupled to multichannel analyser 3-62225
 electrodes, retarding potential curves shift by two-dimensional condensation 3-69133
 electron gas exchange energy role in current density (*Russian*) 3-80141
 insulators, electron penetration depth determ., thermally stimulated electron emission technique 3-68281
 metal, solid surface photoemission, laser multiphoton phenomena 3-76121
 metal films, electron photoejection and thermionic emission, cyclotron resonance spectra 3-72503
 metallic oxide dust, gas suspension, shock wave effect 3-67935
 refractory metals, work function determ. near melting point using d.c. arc 3-69132
 work function, distribution plotting, technique, apparatus 3-73811
 work function distrib. of emitter from total energy spectrum (*French*) 3-55718
 Al₂O₃ in Cs vapour, work function determ. 3-55719
 BeO, energy spectrum, retarding pot. analyser, photon irradi. 3-69130
 He II, electron bubble production, gas sheath around hot filament 3-50038
 LiF type N phosphor + C, LiF Teflon, dosimeter 3-73654
 MgO crystal, u.v. excitation, deep hole trap, hole-release Auger mechanism 3-72776
 Mo, anisotropic surface struct. change during directional transport processes 3-55130
 NaCl:Ni, X-irradiated, stimulated processes 3-41592
 NaCl:V²⁺ crystals, Z-like centres study 3-52812
 Si, single crystal, in ultrahigh vacuum, instructional experiments for undergraduates 3-68684
 Si single crystals, adsorbed water and oxygen effects in electron exoemission 3-64759
 W, anisotropic surface struct. change during directional transport processes 3-55130
 ZrC, with Pt and Ir additions 3-69131

thermionic emission

- see also thermionic electron emission*
 No entries

thermionic generators *see thermionic conversion***thermionic ion emission**

- electrodes, retarding potential curves shift by two-dimensional condensation 3-69133
 Li⁺, ion gun characteristics, thermionic emission from β -eucryptite 3-62207

thermionic power generation *see thermionic conversion***thermionic tubes**

- see also cathode-ray tubes; electron-wave tubes; gas-discharge tubes; rectifier tubes; vacuum tubes*
 No entries

thermionic valves *see thermionic tubes***thermistors**

- application, in beam position monitor 3-48501
 differential thermal analysis apparatus, polymer oxidation studies 3-77397
 dosimeters, energy measurement, microwave induced, interaction with microwave field 3-70187
 NTC, MnO-NiO, resistivity and energy constant, obs. 3-75744
 simultaneous electrochemical/DTA meas., thermistor bimetal thermocouple hemisphere electrode 3-39878
 thermometer bridges, linearised, small temp. change meas., calorimetry 3-77400

thermo-optical effects

- see also thermoreflexance*
 anthracene, cryst., excitation band structure, thermoabsorpt. obs. 3-55230
 defocusing, transient thermal, intensity limitation and energy spreading in optical field 3-70848
 filter, polarisation, interference-type, thermo-optic compensation of wide-angle controllable stages 3-62135
 liquid, absorpt. loss spectrum, thermo-optical meas. technique 3-62103
 rhodamine 6G with detergent, excitation soln. generation, thermo-optical distortions (*Russian*) 3-70819
 Au film, d-band position and width, low temp. thermomodulation meas. 3-55632

thermo-optical effects continued

- POCl₃.SnCl₄.Nd³⁺ liquid laser, spectral luminescent characts. of thermo-optical coeffs. 3-70817

thermochemistry

- see also chemical reactions*
 binary mixtures, Flory's theory, crit. press. estimation 3-53349
 computer program for simultaneous evaluation and correlation of thermochemical data 3-65127
 metal or metal oxide, oxidation rate const. maximum value w.r.t. temp. 3-65085
 CO₂ and hydrate, photodetachment cross section, reply 3-71605
 CO₂ and hydrate, photodetachment cross sections, comment 3-75091
 Co-Au alloys, liq., activity determ. 3-76490
 Cu(II) complexes, reduction at high pressure 3-61253
 GaAs_{1-x}P_x vapour growth, thermochemical calc. of AsH₃-PH₃-HCl-Ga-H₂ system 3-41676
 UO₂, particles, TRISCO coated, thermochem. stability 3-78384

thermoclines *see temperature distribution***thermocouples**

- see also thermopiles*
 in absolute calorimeter, for CO₂ laser energy output meas. 3-42588
 calibration by modified wire method 3-66168
 dosimeters, energy measurement, microwave induced, interaction with microwave field 3-70187
 glass temperature measurement errors 3-66169
 high press. temp. meas., electrical connection 3-45434
 improved wire calibration method 3-66167
 intrinsic, numerical soln. for dynamic behaviour, nuclear reactor applications 3-45444
 low temperature measurement, 4 to 273 K, Cu-Fe alloy electrode 3-73705
 network, for surface temp. meas. 3-39881
 Peltier effect, thermo-e.m.f. and thermal cond., determ., thermocouple method, low reference temp. 3-51656
 probe, recovery characteristics measurement, low pressure, subsonic speeds 3-77398
 relaxation stress testing device, thermocouple indicator, 300 to 1000C, sheet materials 3-53300
 simultaneous electrochemical/DTA meas., thermistor bimetal thermocouple hemisphere electrode 3-39878
 susceptibility measurement, ferrite transthreshold for spin wave excitation 3-73814
 temperature calibration system for creep testing lab. (*German*) 3-62014
 Au:Fe, dilute alloy thermoelectric power, magnetic field orientation dependence 3-59558
 Cu-constantan, temp. curves, calibration at high temp. 3-62020
 Pt/Pt-10% Rh, e.m.f. rel. to press. (*French*) 3-45450
 Pt/Pt10Rh, drift in single stage piston cylinder apparatus 3-70277
 W3Re/W25Re, drift in single stage piston cylinder apparatus 3-70277

thermodynamic changes of state *see phase transformations***thermodynamic cooling** *see cooling***thermodynamic equations of state** *see equations of state***thermodynamic properties**

- see also enthalpy; entropy; Gruneisen coefficient; latent heat; specific heat*
 ABA block copolymers, statistical thermodynamics microstructure model, free energy change calc. 3-54775
 adiabatic exponent of gases, determination, instrument 3-53849
 alkali halide, rhombic dimer molecules, thermodynamic functions and molecular parameters 3-49428
 alkali halide in mantle, lattice model calc. high press. and temp. 3-41897
 alkali halides, NaCl lattice struct. 3-52685
 alloy, condensed phases, eval. and analysis, model approach (*German*) 3-41702
 alloy, liquid, activity coeffs. of nonmetallic elements, comp. depend. 3-79505
 alloys, thermodynamic activity measurement, radiometric method, ¹⁴C, C + 2H₂ = CH₄ 3-54039
 amorphous solids, photocrystallisation characts. (*French*) 3-75624
 atoms, small face centred cubic cluster, 3 to 87 atoms, configuration free energy, atomistic calc. nucleation rate calc. 3-48824
 bibliography, introductory physical chem. course 3-77357
 ceramic electrolytes, review of current research 3-69459
 cholesteryl valerate, liquid crystal, specific volume obs. up to 1000 atm and temp. range 80-129°C 3-57987
 clay minerals in aqueous solution, thermodynamic stability diagrams 3-41889
 colloids, micellisation, micellar binding and solubilisation, thermodynamic parameters calc. 3-41826
 cryogen, liquid, thermodynamic instability, contact with warmer host liquid 3-49997
 dehydration of hydrated ions in solution, theoretical free energy of activation, thermodynamic formulation 3-73136
 dilute polymer solutions, thermomechanics, multiple-bead-spring model 3-43530
 electrolyte, partial molar volumes, expansibilities, determ. from heats and free energies of dilution 3-80557
 electrolytes, theory and gen. eqns. 3-53319
 ethane-ethylene solutions, molecular thermodynamics in normal and critical regions 3-65121
 ethanol, limit of superheat 3-75612
 α excimer, solvent effect 3-80584
 ferroelectric transitions, appls. (*French*) 3-75949
 ferromagnetic fluids thermodynamics, review (*Russian*) 3-79878
 gas chromatography, stationary phase polarity, methylene group, Gibbs free energy 3-70451
 glass, mixed nitrate, M(I)NO₃ + M(II)(NO₃)₂ 3-72009
 glassy polymers, structure, packing density, free volume concepts, mech. behaviour 3-46592
 glassy polymers 3-46718
 hard sphere system, phase transitions (*German*) 3-62628
 harmonic crystals, dispersion theorem 3-60780
 harmonic solids, modified-moments method 3-58109
 Heisenberg ferromagnetic spin system, two-dimens. 3-79819
 hydrocarbons, critical properties, prediction methods 3-76487

thermodynamic properties continued

- III-V semiconductor, thermodynamics of solns. of n-components 3-79468
- Invar, ferromagnetic, thermodynamic properties calculations 3-52710
- Ising ferromagnets, decay of correlations 3-68754
- Ising model, transverse, free energy calc. 3-58115
- liquid binary alloys, heat of mixture rel. to molar volume changes on formation (*Russian*) 3-45446
- liquid binary alloys, volume changes on formation, meas. method (*Russian*) 3-45445
- liquid metal and alloy, conf., Tokyo, Japan (Sept. 1972) 3-49820
- liquid metals, electron theory 3-50011
- liquid metals and alloys, thermodynamic props. interpretation, review 3-50010
- liquid mixtures theoretical treatment by means of equilibrium models (*German*) 3-44746
- liquid-liquid equilibrium data correlations, properties of NRTL equation 3-46713
- magnetic system, anisotropic layered, Green function approach, extended random phase approximation 3-41310
- maleic acid-styrene, copolymer, conformational transition in NaCl soln., standard free energy, volume change 3-54765
- mathematical framework, solved problems, book contrib. 3-58133
- metal electrodes, surface thermodynamics, electrocapillary phenomena, surface stress rel. to charge density 3-55960
- metal oxides in water-cooled reactor, oxidation-reduction kinetics 3-57582
- metals, alloys, expt. meas. techniques, review (*German*) 3-42539
- metals and alloys, exptl. methods, review (*German*) 3-53200
- methanol, limit of superheat 3-75612
- mixtures, athermal, and nonathermal, equilibrium association constants calc., effect of conc. constant, soln. composition (*Russian*) 3-50863
- mixtures, critical properties prediction methods 3-76488
- molecular complex formation equilibria, solvent effects, nonpolar analog model 3-53358
- N-methylacetamide, solid state transition 3-60796
- nuclear matter, schematic model including effective mass concept 3-67249
- oxides, oxygen partial molar parameters and stoichiometry deviations, model (*French*) 3-68419
- para-halostyrenes, thermodynamic functions calc. 3-52416
- phases with very small dimens., equil. press. 3-40194
- plastic flow activation entropy w.r.t. Gibbs free energy and effective stress 3-64092
- polar liquids, extension of partition function to mixtures using Scott's two fluid theory 3-65123
- polymer, linear, free volume rel. to temp., chain thickness, spectral factor (*Russian*) 3-71689
- polymer dilute solutions, modified Huggins' eqn. of thermodynamic interaction parameter 3-47602
- polymer particle engulfment by solidifying melts, thermodynamics 3-61210
- polymeric liquids, equilibrium model based on cell theory extended to polymeric molecules 3-63940
- polystyrene, stability limits rel. to glass transition (*German*) 3-60675
- propylene-CO₂ solutions, molecular thermodynamics in normal and critical regions 3-65121
- quasi-thermodynamic mass-action systems, complex graphs 3-73129
- quasi-thermodynamic mass-action systems, reaction diagrams 3-73128
- quasi-thermodynamic mass-action systems, three short complexes 3-73130
- random-impurity system, effective energy formulation 3-75716
- rare earth chalcogenides, electronic struct. depend. 3-72322
- rare earth phosphides, cryst. chemistry and phys. props., review 3-64018
- silicates, liq., thermodynamic props. of Masson polymerization models 3-65081
- simple liquid mixtures, Percus-Yevick theory evaluation 3-52708
- solid solution, free energy calc., convergence of cumulant expansion technique 3-41029
- solid solution, multicomponent, clustering and ordering, fluctuations and kinetics 3-55751
- solid solutions, ternary, containing two interstitial solutes, Onsager off diagonal coefficients determ. 3-80235
- solutions in normal and critical regions, molecular thermodynamics 3-65120
- spinodal decomposition kinetics, higher derivative terms 3-41689
- steel, austenite, deformation, recrystallisation kinetics (*French*) 3-72872
- steel, austenitic Cr-Ni, N-alloyed intergranular corrosion caused by Cr₂N precipitation (*German*) 3-47368
- steel, thermodynamic activity measurement, radiometric method, ¹⁴C, C + 2H₂ = CH₄ 3-54039
- superconductor, Gibbs free energy barrier against irreversible mag. flux entry 3-75806
- superconductors, thermodynamic fluctuations, nuclear spin-lattice relaxation time, magnetic field enhancement 3-46930
- ternary aqueous solutions, water activity from binary data 3-65122
- ternary systems, ideally associated vapour composition rel. to soln., thermodynamics (*Russian*) 3-50864
- tetracyanoethylene with mesitylene and benzene, charge transfer complexes, solvent effect, thermodynamic props. and optical absorpt. spectra 3-44429
- thermophysical props. conf., Atlanta, USA, (Aug 1973) 3-71702
- transition metal alloys of extraordinary stability, generalized Lewis-acid-base interactions 3-64823
- unit compressibility line, analysis at intersection with inversion curve at non zero pressure 3-62630
- UWC₂, standard free energy of form. from e.m.f. meas. (*Japanese*) 3-61125
- Van der Waals crystal, stationary distribution function 3-68373
- viscous liquids, glass transition, thermodynamic equations 3-52580
- wustite, oxygen activities and phase boundaries 3-55843
- Ag-Bi(Sb) alloys, liq., activities, enthalpies of mixing, conc. depend. (*German*) 3-55756

thermodynamic properties continued

- Ag-Pb liq. alloys solubility of S, thermodynamics (*German*) 3-72882
- Ag-Sn liq. alloys, solubility of S, thermodynamics of (*German*) 3-72882
- Ag₂MI₃(M = Cs, Rb and K), thermal power of solid electrolytes and molten mixtures 3-50835
- Al-Cu alloys, liq., high temp. mass spectra obs. (*French*) 3-80196
- Al-Si-Fe system, liq., activity meas. by e.m.f. method 3-50673
- Ar, atoms, small clusters, mol. dynamics study 3-43859
- Ar-H plasmas, equil. compositions and thermodynamic props., 10⁻²-10³ atmos., 2000-35000K 3-71855
- Ar-N₂ solutions, molecular thermodynamics in normal and critical regions 3-65121
- As-Te glasses, structural model, explanation of anomalies and discontinuities 3-40848
- Au-Bi alloys, liq., activities, enthalpies of mixing, conc. depend. (*German*) 3-55756
- Au-In and Cu-Au-In α -solid solns., indium activity 3-80199
- CO₂-H₂O gaseous mixtures, 450 to 800°C, 0 to 500 bars 3-69489
- Co₂-B₂O₃(P₂O₅) glasses, characteriz. w.r.t. struct. 3-76273
- Co-Au alloys, liq., activity determ., CoO equilibration, Gibbs-Duhem relation 3-76490
- Cr-S system, nonstoichiometry and thermodynamics 3-41019
- Cr-Si alloys, thermodynamic properties of liquid system at 1900 K 3-72835
- Cu, plastically deformed, discrepancy between sp. ht. and stored energy data 3-64186
- Cu-Bi alloys, liq., activities, enthalpies of mixing, conc. depend. (*German*) 3-55756
- Cu-In and Cu-Au-In α -solid solns., indium activity 3-80199
- Cu-Mg alloys, liq., thermodynamic props. determ. by vapour press. meas. 3-64807
- Cu-Mg alloys, liquid, thermodynamic props. determ. by vapour pressure meas. 3-72822
- Cu-Ni alloys, thermodynamic functions determ. by e.m.f. meas. using solid electrolyte (*Japanese*) 3-61124
- DBF₂, mean square vibr. amplitudes and thermodynamic functions 3-67775
- Fe-Si alloy, surface free energy anisotropy, thermal etching obs. 3-64845
- Fe-Si-C_{sat}, interaction parameters, 0.016-0.37 mol fraction Si, 1773-1973 K (*Polish*) 3-50675
- Fe-V(W) alloys, thermodynamic variables, calcs., from phase diag. 3-64818
- Fe-Zn binary system, distrib. of Zn between ferrite and austenite (*German*) 3-47356
- GaAs, e.m.f. meas., 365 to 468 C, thermodynamic characteristics 3-42600
- 2Ga(l) + 3/2O₂(g) = Ga₂O₃(s) equilibrium, e.m.f. obs. 3-69464
- H-He mixture, high press. characteriz., astron. appl. 3-42161
- H₂, thermodynamic props. calc. using intermolecular potential 3-60508
- HBFe₂, mean square vibr. amplitudes and thermodynamic functions 3-67775
- H₂O and isotopes, thermal behaviour by calorimeter method 3-72210
- He to ~2 K, computer program 3-64225
- ³He in superfluid ⁴He, dil. soln., kinetic theory 3-46743
- In-Sb alloys, liquid, activity of In 3-50838
- InAs, e.m.f. meas., 360 to 510 C, thermodynamic characteristics 3-42600
- InSb/Te, e.m.f. meas., low conc. soln. thermodynamic properties 3-44071
- In₂Se₃, calcs., p-T-x phase diagram 3-64147
- K, liquid, multielectronic theory using perturbation theory (*Russian*) 3-55092
- KNO₃-CsNO₃-NaNO₃ phase diagram, thermodynamic calc., thermography (*Russian*) 3-52692
- Kr, solid, free energy, convergence of anharmonic terms 3-55064
- Li-Se system, e.m.f. obs. 3-43884
- LiSO₄.D₂O, i.r. spectra, thermodynamic props. 3-72618
- LiSO₄.H₂O, i.r. spectra, thermodynamic props. 3-72618
- Lu, high purity, physical and metallurgical properties 3-63981
- Mn-C system, carbide standard free energies of form. by e.m.f. meas. (*Japanese*) 3-61126
- MoS₂, MoSe₂, MoTe₂, lamellar lattice, heat capacity, thermodynamic props. 3-41028
- N₂, Ar, methane ternary and binary systems, liquid-vapour equilibria at 112.00K, Gibbs free energy calc. 3-58120
- N₂, pVT data up to 1000°C and 5000 bar 3-49523
- Na, liquid, multielectronic theory using perturbation theory (*Russian*) 3-55092
- Na, liquid, two-phase and subcooled, thermodynamic props., calc. molten fuel-coolant interactions, potential accidents 3-71288
- NbX₃ (X = Cl, F, Br) normal coordinate analysis and thermodynamic functions 3-54654
- Ne, liquid, from m.p. to b.p., from u.s. velocity measurements 3-68420
- Ne + H₂, liquid mixtures, excess volume from molar volume obs., 25-31K, up to 34 atm. 3-49965
- Ni, pure, carbon solubility and activity (*Czech*) 3-55769
- Ni complex, hexapyridinenickel (II) nitrate, 13-300 K (*French*) 3-49961
- Ni-Cu system, activities of both components at 1400 K 3-64819
- Ni-Mo alloys, thermodynamic functions determ. by e.m.f. meas. using solid electrolyte (*Japanese*) 3-61124
- Pb-Au-Ag system, central atom model applic. (*German*) 3-64811
- PbBr₂-NaBr-CdBr₂, diagram of melting, thermodynamic calc. (*Russian*) 3-49967
- PbSe, free energy of form. 3-64187
- SO₂(OH)₂ molecule, 100-1000 K 3-60395
- SeO₂(OH)₂ molecule, 100-1000 K 3-60395
- Se₂BrF molecule, 298.16-1000 K 3-60395
- TaX₃ (X = Cl, F, Br) normal coordinate analysis and thermodynamic functions 3-54654
- Ti near melting point 3-72211
- TiC_x, activities of Ti (*Japanese*) 3-50761
- (U,Pu)O₂ mixed fuels, hypostoichiometric 3-57569
- U-Nd-O system, oxygen pot. meas. 3-72933

thermodynamic properties continued

- UFeC₂, standard free energy of form. from e.m.f. meas. (*Japanese*) 3-61125
 U₂N₃, nonstoichiometry, statistical model for anal. of thermodynamic props. 3-68190
 UO_{2+x}, FBR fuel, oxygen pressures calc., model 3-40536
 W-halogen-O-H reaction systems, C influence on chem. reactions and transport processes (*German*) 3-53362
 Zn thin film deposition on surfaces of Ge single crystals 3-61110

thermodynamics

- see also *atmospheric thermodynamics; critical phenomena; entropy; equations of state; Joule-Thomson effect; statistical mechanics*
 adiabatic gamma for two-dimensional compression of unstable plasma 3-49637
 adsorption of nonelectrolytes from soln. 3-41086
 alloy, thermodynamic approach to analysis of diffusion controlled processes in interstitial phases 3-80361
 arrows of time, correlation 3-54187
 bibliography, heat (1971) 3-61953
 bibliography, introductory physical chem. course 3-77357
 bibliography of Soviet works 3-62620
 binary mixtures, Flory's theory, crit. press. estimation 3-53349
 classical and relativistic fluid, entropy supply 3-59831
 Coleman-Noll rotational thermodynamics (*Czech*) 3-54182
 compensation law, obs. in elec. cond. of semiconductors 3-45744
 compensation law and thermal death of unicellular organisms 3-48825
 constraint theory of simple materials extended to thermomechanical restrictions 3-62445
 convective phenomena, description by methods of nonequilib. thermodynamics 3-48821
 creep, long term strength 3-80367
 critical binary mixture, possible violation of two-parameter universality 3-51843
 critical exponents, skeleton graph expansion, Wilson model 3-48810
 critical exponents above T_c to $O(1/n)$ 3-45745
 critical points for multicomponent systems, order and scaling classification at tricrit. points 3-48828
 critical points of complex systems, classification scheme by order, notation 3-42907
 critical systems with spatial anisotropy, renormalization group approach 3-51842
 electron gas, non-interacting, partially relativistic, partially degenerate, appl. to stellar evolution 3-48002
 equations of state, determ. for O₂ and N₂, selection of functional form, least squares fitting 3-75593
 equilibrium constant calcs. using programmable calculations 3-54185
 equilibrium problem solving by free energy minimization, iterative procedure 3-54184
 exchange energies and potentials at finite temp., Hartree-Fock-Slater calc. 3-54165
 extremal equilibrium states, representation as limit of Gibbs states in finite volumes 3-57160
 fading memory materials with internal variables, equilibrium state 3-66562
 fading memory materials with internal variables, general theory 3-66561
 f.c.c. and h.c.p. lattices, entropy, comparison of H theorem method with vibrational anal. 3-70768
 ferroelectric dispersion and transitions, theory 3-44379
 ferromagnet, classical n-vector model, rel. to self avoiding walk problem 3-68747
 ferromagnetic domain theory, review 3-75863
 Feynman graph expansion for tricrit. exponents, Wilson classical spin model 3-48827
 fluid system processes, statistical thermodynamics (*German*) 3-48813
 formation function, stability const. determ., graphical anal., real cross-over point 3-70484
 Free energy of non-isothermal systems 3-77928
 freezing water-soil system, heat and mass transfer, multiphase water distrib., irreversible thermodynamics 3-56053
 fundamentals of classical thermodynamics, book 3-51844
 gas equation of state for medium-density high-temperature conditions 3-52413
 gas phase n.m.r., review 3-60521
 heat and mass transfer, bibliography, Soviet works 3-52435
 heat and mass transfer bibliography of Soviet works 3-40190
 homogeneous isotropic continuum stress-strain reln. determ. from Gibbs-Duhem thermodynamic eqn. 3-42922
 homogeneous processes, as variational equality 3-54181
 ideal Boson film, specific heat, scaling functions 3-66689
 ideal-gas, pressure fluctuations, statistics and thermodynamics, implicit averaging 3-42882
 irreversible processes, nonlinear interacting, stability analysis of system motion 3-74174
 Ising chain, random mag. moments, thermodynamic functions 3-70745
 Ising model, two-dimens., anisotropic boundary conditions 3-50324
 isothermal, non-isothermal kinetics, rational approach 3-76433
 isotherms, congruence, thermodynamic and math. consequences, heuristic method for modelling ΔG 3-72267
 isotropic Bose system, helicity modulus, superfluidity, scaling 3-70734
 Krylov-Kolmogorov dynamic entropy minimization in nonequilibrium steady state 3-74180
 Lennard-Jones fluid, surface density and tension, stat. mech. and quasithermodynamic calcs. 3-60790
 liquid general equation of state calc. 3-58117
 Low density form of the free energy for real matter 3-70767
 many-body system, weak self-consistent approx. scheme 3-40181
 materials with memory, thermomech. coupling, history of temp. gradient, deformation gradient and temp. 3-70766
 mathematical introduction, solved problems, book contrib. 3-57176
 metal-water system at elevated temps., computer calcs. 3-44748
 mixture exhibiting phase separation, mean spherical model 3-54183
 multi-component fluids, primary medium effect in electric field 3-73178

thermodynamics continued

- multicomponent stressed solids, linear theory of thermochem. equil. 3-79503
 multicomponent systems, scaling hypothesis at crit. points of arbitrary order 3-54186
 non-equilibrium theory, probability distrib. function for quantum mechanical expectation value at stationary state 3-70771
 non-isothermal elastic-plastic deformations, thermodynamic considerations of phenomenological theory 3-40129
 nonequilibrium steady-state systems, theory of irreversible processes 3-74182
 nonlinear dynamics of fluctuations, renormalization of kinetic coeffs. by projector-operator method 3-42901
 nonlinear irreversible processes, transfer eqns. 3-59829
 nonuniform classical system, properties of canonical density distrib. in thermodynamic limit 3-62634
 nuclear fuel-sodium interaction, kinetic energy and pressure calc. 3-67531
 nuclear polarisation, dynamic, thermodynamics, phonons, electrons and impurities interaction (*German*) 3-79946
 one-dimensional classical systems with slowly decreasing potentials, analyticity of correlation functions 3-59827
 one-dimensional system, construction of dynamics 3-54159
 Onsager coeff. calc. from time-depend. gaseous diffusion eqns. (*Hungarian*) 3-75178
 Onsager thermostatical theory, rel. to variation principle in transport theory based on Boltzmann equations 3-57167
 order parameter fluctuations in external fields near phase transition points (*Russian*) 3-40196
 paramagnetic system, Pauli's master equation, continuum thermodynamic limit 3-57166
 partition and approach to equilibrium 3-48823
 perturbation theory, second-order, study of short range potential (*Russian*) 3-74172
 polarizable, magnetizable medium, Gibbs relation 3-72573
 polymer solution, thermodynamic studies on diffusion (*Japanese*) 3-40692
 pulsatile Newtonian frictional losses in rigid tube 3-49625
 quantum statistical, spatial distrib. function calc., linear partial differential equation, Schrodinger equation 3-70769
 radiating plasma column, numerical soln. of Abel integral equations, piecewise polynomials 3-71849
 rate equations, structure, materials with internal variables 3-62626
 relativistic, covariant asynchronous formulation 3-66712
 relaxation system, linear, vector-valued, theory 3-66709
 rubber elasticity explanation, general review (*Hungarian*) 3-76376
 Second Law, Wilkie's revised statement, validity 3-59828
 second law demonstration using a deck of cards 3-70238
 small cluster of atoms, melting, theory 3-46699
 solid surface thermodynamics, symbols and nomenclature 3-52711
 solidification in porous media, thermodynamic relations, dependence of energy of transformation on curvature of interfaces (*French*) 3-75607
 solute-solute forces obs. by n.m.r. relax. 3-53350
 spheres with dipoles, Monte Carlo free energy with multistage sampling 3-74173
 spin systems, 1-d, finite range potential, uniqueness of states satisfying Kubo-Martin-Schwinger boundary condition 3-62601
 sputtered ion mass spectroscopy, quantitative interpretation 3-70454
 square-well fluid, Percus-Yevick theory and energy equation, van der Waal type phase transition 3-48826
 statistical, mathematical framework, solved problems, book contrib. 3-57177
 statistical equilibrium and relative entropy concept 3-62633
 statistical non-equilibrium, unified formulation with dynamics 3-62629
 steady-state currents in solids, transport and thermodynamic anal. 3-43893
 superconducting films, type II, Gibbs potential calc., transverse mag. field 3-79796
 superfluidity of Bose systems, two- and one-dimensions, thermodynamic functions and phase transition 3-54168
 surface flow, irreversible thermodynamics, straight and cross-coefficients, diffusion and self diffusion 3-46460
 susceptibility extremum points in critical state vicinity, props. of matter 3-74183
 temperature fluctuations of small systems, the two level atom 3-74171
 thermal electric fluctuations, nonlinear theory, model, cubic fluctuation-dissipational thermodynamics (*Russian*) 3-66717
 thermoelectrical processes, Gyarmati's principle 3-77922
 Tokamak equilibria, thermodynamic theory 3-57880
 transversely-isotropic materials with memory, constitutive equations, reduced forms, heat flux of a simple thermodynamic material 3-70610
 triglycine sulphate, phenomenological parameters, mol. field and thermodynamic theories 3-79991
 van der Waals fluid mixtures near critical point, transport coefficients 3-48817
 vapour-liquid equilibrium, overall area tests for thermodynamic consistency, effect of random error 3-58119
 variational principle, Hamiltonian-type, connection of entropy to first law 3-74175
 viscoplasticity, mechanisms affecting strain rate and temperature sensitivity 3-57090
 viscoplasticity, thermodynamic theory of rheological material with internal structure changes 3-57089
 white dwarf crystalline interior thermodynamic functions, b.c.c. lattice model of heavy-ion plasma 3-73487
 Widom-Rowlinson fluid model, soln. of Percus-Yevick eqn. critical density 3-62637
 Wilson ϵ expansion, failure of length scaling 3-66714
 Co-H₂O system, thermodynamics at elevated temps. 3-47605
 CsCl strongly noneideal ion plasma 3-49636
 Cu exploding wire, first phase 3-63901
 Fe-H₂O system, thermodynamics at elevated temps. 3-44749
 He film, two-fluid model, thermodynamic approach 3-43910
 He refrigerator cycle with cascade coupling of expansion engines, optimisation 3-62632

thermodynamics continued

- N_2O_4 chemically reacting system, thermodynamic parameters, use in nuclear power stations (*Czech*) 3-44713
 Na- NH_3 solns., chemical potentials, related thermodynamics 3-73135
 TiO_2 , rutile, analysis of lattice defects, and H and D impurities rel. to band struct. 3-55218
 W-X-O-H systems, X-halogen, gas phase composition and chem. transport reactions (*German*) 3-44747
 W exploding wire, first phase 3-63901

thermoelasticity

- acceleration waves in isotropic elastic bodies, thermal properties 3-42923
 adhesive fibrous nonfabric material with polyurethane binders, thermomechanical props. 3-58715
 anisotropic half space, transient temp. distribution 3-57170
 axisymmetrically heated orthotropic cylinder fastened to a pliable elastic cylinder, stability under shear 3-57084
 beams, coupled thermally induced vibrations 3-77834
 bending of solid elastic circular plate due to concentrated heat nucleus 3-66523
 ceramic, thermal-shock resistance prediction during heating at very high rates 3-61194
 circular cylinder, thermoelastic response, generalised dynamical theory of thermoelasticity 3-42789
 composite cylinder, axially connected, thermal stresses 3-66534
 composite orthotropic medium, hot area 3-66526
 composite plates, thermal bending, Green's function analysis 3-77815
 contact potential for hot circular die on transversely-isotropic semi-space with heat transfer at interface (*Russian*) 3-40191
 coupled, appl. to half-space under action of thermal shock on bounding surface 3-54095
 crystal growth, stress calcs. 3-75490
 cylinder with internal aperture, determ. of non-stationary temperature field by numerical method (*Russian*) 3-45662
 cylindrical shell, inhomogeneous, residual stress removal by varying temp. field (*Russian*) 3-57068
 cylindrical shell, optimum conditions for lowering residual stresses by local heating (*Russian*) 3-41761
 cylindrical shell, thermal fields and stresses during inductive heat treatment (*Russian*) 3-77807
 dilatational wave propagation shock structures, low temp. 3-62509
 Earth strain tides obs. in California, thermoelastic effects 3-44867
 elastic constants of stressed crystals, acoustic harmonic generation 3-72115
 elastic layer, effect of instantaneous plane heat source 3-59758
 elastoplastic thermal stress, temperature dependence analysis, finite element method 3-70627
 ethylene-vinyl acetate copolymer, equilib. stress, temp. depend., 38-42°C 3-69386
 finite body with thermally insulated external circular crack, three-dimens. thermoelastic problem (*Russian*) 3-40103
 flame forming, transient elastic-plastic thermal stress analysis 3-50745
 FORTRAN program CHANTER, thermoelastic deformations, segment of a hollow non-circular cylinder 3-48730
 frictionally excited instabilities, role of insulating surface films 3-55022
 generalized, plane waves soln. of frequency eqn. 3-48742
 half-plane problem, soln. using a functional system (*Russian*) 3-74028
 half-space, dynamical thermoelasticity problem in regions with moving boundaries (*Russian*) 3-57080
 half-space, transpiration cooled, temp. distrib. determ. by variational method 3-54178
 hemisphere with radiating surface, thermal stresses due to internal heat source 3-54096
 indentation, of semi infinite elastic solid by hot sphere 3-74024
 instability in seal-like configuration 3-55021
 linear theory modification to include temperature dependence of thermal and mechanical properties 3-59753
 magneto-thermo-visco-elasticity, plane strain problems, Kelvin and Maxwell bodies 3-44830
 nonlinear thermoelasticplastic and creep analysis by finite element method 3-66570
 nonstationary temperature field in plane bounded by finite noncircular contour (*Russian*) 3-42781
 nonuniform hereditary media, potentials and deformations (*Russian*) 3-42782
 nuclear reactor fuel sheath deformed by cracked fuel pellet, FORT-RAN program CHANTER 3-48730
 plane layer, dynamic coupled thermoelastic problem, pressure-time, temp.-time functions, surface appl. (*Russian*) 3-70582
 plane with arched crack, thermal transmission influence on thermoelastic state (*Russian*) 3-40102
 plate, anisotropic with elliptical openings, temp. field and stress state for mixed boundary conditions (*Russian*) 3-62480
 plate, thermoelastic stresses, volumetric cylindrical heat source (*Russian*) 3-40104
 plate containing two circular holes of different sizes under uniform heat flow, thermal stresses 3-42769
 plates, coupled thermoelastic vibrations 3-70642
 PMMA, heat outputs from plastic zones of fast running cracks 3-65002
 poly(n-butyl methacrylate) networks, viscoelasticity, stress-strain behaviour, effect of reference chain dimension, thermoelastic meas. 3-55890
 polymer, crystalline, uniaxially oriented, thermoelasticity rel. to supermol. structure 3-71683
 polyvinyl alcohol, cross linked networks, solvent effects 3-63601
 prestressed media, damping of stress- and velocity-discontinuities (*German*) 3-66528
 refractories, thermal stability, dispersion of fracture temp. drops 3-47453
 reinforced laminate, temperature stress 3-61205
 relativistic thermo-magneto-viscoelastic waves, propag. in Voigt type material 3-62515
 semi-infinite body, cylindrical hole, thermal stresses, temp. distrib., linear thermoelasticity 3-70562

thermoelasticity continued

- semi-transparent rod, elastic, illumination with high-power laser, stresses (*Russian*) 3-62475
 shock wave prod. in elastic solid by supersonic thermal sources 3-62532
 shock waves in elasto-plastic media, soln. of eqns., thermodynamic functions (*Russian*) 3-42815
 sphere, stresses due to uniform heat sources for strain hardening material 3-57077
 square cylinder with circular hole, thermal stresses and couple-stresses 3-45642
 stability of structures at high temps. 3-66560
 stress in elastic layer, steady state 3-59757
 stresses and temps. in expanding rectangle, appl. of extended source method and new numerical techniques 3-70586
 stresses in a long hollow cylinder under local heating of the side surface 3-70573
 temperature stress calc. in a partly clamped orthotropic plate (*Russian*) 3-74031
 thermal contact resistance for rough surfaces, pressure dependence 3-77915
 thermomechanical analysis of structures 3-66558
 thermoviscoelastic media, steady state wave propagation, dual variational principles 3-70647
 thermoviscoelastic solid, amplitude behaviour of shock waves 3-79426
 thermoviscoelasticity method of elastic solutions 3-62465
 thick plate containing penny-shaped crack, asymmetric distrib. of thermal stress, iterative soln. 3-70571
 transversely isotropic shells, elastic filler, stability, mech. loading, temp. effect of shear strength 3-70580
 unbounded thermoelastic media, one-dimensional wave modes, finite thermal wave propagation vel. 3-54125
 viscoelastic body with cylindrical cavity, cyclic pressure, solutions 3-66555
 wave propagation in isotropic semi-infinite medium (*Italian*) 3-40143
 wave propagation in random media, uncoupled theory, random boundary conditions 3-66574
 wave propagation in transversely isotropic circular cylinder 3-66599
 Al-Cu system, statistically isotropic heterogeneous medium, thermal expansion coeff. and elastic constants determ. 3-60760
 Fe, solid and molten, isotropic compression modulus calc., elasticity coeffs., surface free energy (*German*) 3-72823
 $\text{Fe}_{75}\text{P}_{15}\text{C}_{10}$ amorphous alloy, splat cooled, thermal props. from internal friction obs. 3-60758
 n-Ge, increase of phonon viscosity and thermoelastic absorpt. of u.s. waves with doping 3-40979
 KCN, cubic, anomalous thermoelastic behaviour 3-54998
 NaCl type crystals, calc. of thermoplastic and residual stresses 3-79417
 $\text{Pd}_{82}\text{Si}_{18}$ amorphous alloy, splat cooled, thermal props. from internal friction obs. 3-60758

thermoelectric conversion

- radioisotope thermoelectric generator, fuel capsule vent system, He, Viking mission to Mars 3-67402

thermoelectric effect *see* thermoelectricity**thermoelectric generators** *see* thermoelectric conversion**thermoelectricity**

- see also thermocouples; thermopiles*
 alkali metals, elec. resist. and thermopower, phonon drag effect 3-46681
 alkaline earth metals, liquid, meas. of thermoelectric power 3-79677
 amorphous semiconductors, hopping thermoelectric and thermomagnetic phenomena, heat-current operator 3-79719
 diamond, Sb ion-implanted 3-46846
 dilute magnetic alloy, theory 3-64319
 disordered semiconductors, effect of electric field and temperature gradient 3-64333
 fluid metals, conductivity, volume expansion effects, super- and sub-critical temps., metal-insulator transition 3-50179
 glass, ion conducting, thermoelectric effect in single sample and at junction of dissimilar glasses 3-58289
 glasses, amorphous, Peltier and Seebeck coeffs., temp. depend. and sign 3-46861
 liquid metals and alloys, rare earth or transition, thermoelectric power, virtual bound state model 3-50193
 metal, isotopic scatt. influences on thermoelec. power 3-52829
 metallic thin film, continuous, obs. thermoelectric. power and temp. coeff. of resistance 3-75797
 $n \pm n$ semiconductor junction with near-intrinsic conductivity, charge carrier and heat balance distribution 3-68700
 nitrobenzene, thermo-electret state, form. processes 3-72568
 noble metals, longitudinal piezo-thermoelectric effect in polycrystalline wires 3-72347
 Peltier effect, thermo-e.m.f. and thermal cond., determ., thermocouple method, low reference temp. 3-51656
 rare earth compound, R_2NiO_4 , R_2CuO_4 , resist. and thermoelec. power, structure interpretation 3-41180
 semiconductor, antiferromagnetic, thermoelec. power near Neel temp., calc. 3-68655
 semiconductor, compensated, thermoelec. current instability rel. to spatial charge exchange waves 3-64349
 semiconductor, mag. field depend., theory 3-75759
 semiconductor, size effect theory, review 3-58253
 semiconductor alloys, positive thermoelectric power, principles of electrical behaviour 3-55314
 semiconductors, amorphous, Peltier and Seebeck coeffs., temp. depend. and sign 3-46861
 semiconductors, meas. technique 3-60889
 semiconductors with narrow forbidden gaps, resonance scattering of current carriers by ionised defects 3-46831
 superconductor, theory 3-79803
 temperature measurement of gases, cancellation of radiative error (*Japanese*) 3-66166
 thermogalvanic corrosion elements, irregular thermal loading 3-73104

thermoelectricity continued

- TTF-TCNQ, thermopower, 10-300K, metal-insulator transition 3-64387
- Ag, plastically deformed, thermo-e.m.f. meas. of recovery stages, defects contrib. (*Russian*) 3-79663
- Ag/AgI/Ag thermocell, mechanisms 3-79720
- Ag-Gd, dilute, mag. susceptibility, n.m.r. and thermoelec. power obs. of impurity state 3-68765
- AgI + MI (M=Na, K, Rb, Cs) molten systems, thermoelectric power 3-72375
- AgSbTe₂, liquid, thermoelectric power, activation energy, temp. depend. 3-55264
- Ag₂Te, polymorphism obs. 3-68406
- Al, liquid, pseudopotential calcs., dielectric function effects 3-44058
- Al alloys, dilute, thermopower obs. from 2 to 6K, mag. field depend. 3-68596
- α -AlB₁₂, power meas., temp. depend., polaron mechanism 3-72357
- AsSI, thermally stimulated currents 3-44099
- AsSeI, thermally stimulated currents 3-44099
- AsSe_{1-x}Pb_{0.13}, cond., thermo-e.m.f. study 3-72352
- As₂Se₃Te_{1-x}, thermopower measurements as function of temperature 3-55265
- Au, magnetic impurity effects, student expt. 3-41173
- Au, plastically deformed, thermo-e.m.f. meas. of recovery stages, defects contrib. (*Russian*) 3-79663
- Au-Fe, dilute alloy thermocouple wire, thermoelectric power, magnetic field orientation dependence 3-59558
- Au-Ag system, solid, absolute thermoelectric power obs., composition depend. at high temps. 3-68599
- Au-Fe alloy, dil., theory and expt. 3-64319
- Ba, elec. resist., thermal cond. and thermopower meas. from 40 to 300 K 3-64318
- Bi, magneto-oscillation of thermoelec. power 3-79714
- Bi, semimetal thin films, electrical conductivity, grain boundary theory, grain size, de Broglie wave (*French*) 3-46910
- Bi, thermal waves preceding shock front, oscillographic obs. using thermoelectric effect (*Russian*) 3-64188
- Bi alloys, ternary liquid, thermoelectric powers, absolute, temperature, composition 3-50195
- Bi film, influence of polymer powder substrate temp. 3-50091
- Bi film, on glass substrate 3-64267
- Bi film, thermoelec. power, quantum size effects (*French*) 3-55293
- Bi_{1-x}Sb_x, cooling due Ettingshausen and Peltier effects 3-64362
- Bi_{1-x}Sb_{1-x}, film, thermoelec. power, quantum size effects (*French*) 3-55293
- (BiSb)₂Te₃ film, influence of mech. stresses 3-61123
- n-BiSe₃, magneto-Seebeck coeff. in strong transverse magnetic fields conduction band density of states determ. 3-41216
- Bi₂Se₃:Te(In)(Pb), anisotropy of elec. cond., Hall coeff. and thermoelec. power, doping effects 3-41185
- n-Bi₂Te₃, magneto-Seebeck effect between 20 and 100 K 3-79717
- C fibre, carrier mobility, Seebeck effect (*German*) 3-75739
- C fibre, e.s.r. g-value, resist., thermoelec. power and magnetoresist., correlations 3-80477
- C fibres:K, rayon based, struct. effects (*French*) 3-68607
- CKI(Br)(I), off-centre Cu⁺ ions, ionic thermocurrent study 3-41478
- Ca, elec. resist., thermal cond. and thermopower meas. from 325-425 K 3-64318
- Cd₃As₂ film, thermal detect., seebeck coeff. meas. 3-68651
- CdF₂ ionic thermocurrents, reorientation of Na⁺ vacancy and Y³⁺ interstitial complexes, space charge formation 3-44367
- Cd₃P₂, mag. field power depend., effective electron mass determ. 3-68548
- Cd₃Pb_{1-x}Te, Seebeck coeff., effect of deposition conditions 3-64265
- CeIn₃ cooling figure of merit, large anomaly, Kondo system, Peltier effect, thermopower, low temps. 3-50182
- CePd₃ cooling figure of merit, large anomaly, Kondo system, Peltier effect, thermopower, low temps. 3-50182
- Co, ferromagnetic metal, transport properties meas. 3-52814
- Co_{1-x}Fe_xO₄, CoFe_{2-x}Ti_xO₄, electrical conduction mechanism, temp. range 78K to 300K 3-50206
- Cr_{1-x}V_xSi₃, thermal e.m.f., 78-300K (*Russian*) 3-68611
- Cs liquid, thermoelectric power pressure effects, up to 40 kbar and 220 C, metal and alloys 3-50196
- Cs-Na liquid alloys, electron transport properties, energy levels, thermoelectric power at high pressures 3-50113
- Cu, plastically deformed, thermo-e.m.f. meas. of recovery stages, defects contrib. (*Russian*) 3-79663
- Cu alloys, thermo-e.m.f. generated at junction of coarsely and finely grained specimens (*Russian*) 3-68595
- Cu-Ni alloy, thermopower meas., Nordheim-Gorter plot, Ni clusters 3-68598
- Cu-Sb, liquid alloy, partial interf., pair correlation, thermoelec. power and elec. resist. calcs. 3-52565
- Cu-Sn-Se system, phase diagram study 3-72174
- CuBr-CuI system, surface thermo-emf distrib. curves 3-72164
- CuCr₂Se₂Br, charge transfer mechanism, temp. depend. between 100 and 500K 3-72371
- CuI + MI (M=Na, K, Rb, Cs) molten systems, thermoelectric power 3-72375
- CuNi:Fe, differential thermoelectric power, temp. depend. 3-79678
- Cu₂S(Se)(Te), thermo-e.m.f., temp. depend., 500-1200°C 3-50203
- EuB₆, Seebeck coeff., comparison with EuB₆ (*French*) 3-64332
- Fe thermoelectric power, near magnetic critical points, conduction electron scattering by short range spin fluctuations, Fisher Langer approach 3-50186
- Fe-N(0.1 wt.%) alloy, precipitation, resistivity and thermoelectric power behaviour 3-80297
- Ga, temperature depend. between 4.2 and 1.4K 3-68597
- β -Ga₂O₃, 650-900K 3-68631
- Gd_{3-x}V_xS₄, semiconductor, conductivity activation energy, thermoelectric power, effect of applied mag. field 3-41215
- n-Ge, thermal e.m.f., crystal boundary effects (*Russian*) 3-75758
- Ge film, on flexible organic substrate, rel. to thermal energy transducer 3-56615
- GeTe, annealed, thermo-e.m.f. meas., temp. depend. 3-68654

thermoelectricity continued

- Hg, fluid thermoelectric power, 600 to 1650C, 0 to 2 kbar, metal-dielectric transition, density of states 3-50194
- Hg alloys liquid, electrical resistivity, thermoelectric power, pressure dependence up to 5000 bar 3-50192
- Hg alloys liquid, pseudopotential form factor, resistivity, anomalous thermopower, experimental determination 3-50104
- Hg-Ga alloys, liq., cluster form. role in t.e.p. minimum 3-50191
- Hg_{1-x}Cd_xTe, thermoelectric power at low temp., phonon spectra and scattering obs. 3-60809
- InAs-CdTe solid soln., electron effective mass, thermoelec. power and i.r. refl. meas. 3-41141
- K₂Pt(CN)₄Br_{0.3}·3(H₂O), anisotropic Seebeck effects, temp. dependence, reln. to metal-insulator transition (*German*) 3-50184
- K₂Pt(CN)₄Br_{0.3}·3(H₂O), Pt Mossbauer meas. as test for metal-insulator transition with localisation of conduction electrons (*German*) 3-50492
- La_{0.98}Tb_{0.02}Al₂, anomaly in thermoelectric power due to crystal field split tb impurities 3-50187
- Li-Bi, liquid alloy electronic transport, spin-flip scattering, e.s.r., thermoelectric power, conductivity 3-50180
- Li_{1-x}Zn_xFe₂O₄ mixture, Seebeck voltage, cond. mechanism, comp. depend. 3-52846
- Lu, high purity, physical and metallurgical properties 3-63981
- Mo thin films, laser-induced anisotropic thermoelectric voltages 3-60867
- Nb single crystals, high temp. heating influence on electrophys. props. (*Russian*) 3-41172
- Ni, liq., thermopower, d resonance calc. 3-44059
- Ni-Hf(Re) (W) alloys, thermo-e.m.f., temp. depend., 77-1300K (*Russian*) 3-72346
- Ni-transition metal alloys, thermoelec. power and elec. resist. near Curie point 3-44213
- NiS⁵⁷Fe paramagnetic metal-antiferromagnetic nonmetal transition, Mossbauer study 3-44357
- Ni_{1-x}S_x⁵⁷Fe, metal-nonmetal transition, Mossbauer effect, 4.2 to 300K 3-44030
- Pb, liquid, thermoelec. power calc. using model pseudopot. 3-64279
- PbTe film, prep. by closed volume method 3-60873
- PbTe:Bi, carrier density and temp. depend., 100-400K 3-44038
- Pd, liq., thermopower, d resonance calc. 3-44059
- Pd, temp. depend. over 77 to 750 K range, thermal e.m.f. (*Russian*) 3-75738
- Pt complexes, thermoelectric power 3-50185
- PtSb₂ thermoelectric power, temp. depend. mobilities and effective masses of carriers 3-68650
- Rh, thermo-e.m.f., temp. depend., 77-750K (*Russian*) 3-52825
- Ru, thermo-e.m.f., temp. depend., 77-750 K (*Russian*) 3-52825
- Sb, thermal e.m.f., press. depend. up to 14.5 kbar 3-64338
- Si, epitaxial film, thermal e.m.f. meas. 3-45526
- n-Si, thermal e.m.f., crystal boundary effects (*Russian*) 3-75758
- SmS, comp. depend. 3-64178
- SmS, differential thermopower, temp. and composition depend. 3-60871
- A-Sn, electron beam induced n→p transition, resistance and thermoelec. e.m.f. obs. 3-68614
- Sn_{1-x}In_xTe, Hall coeff., thermoelec. power, elec. cond., rel. to In content 3-44098
- Sr, elec. resist., thermal cond. and thermopower meas. from 40 to 300 K 3-64318
- Ta-Al, resistor film, sputtered, Seebeck effect, rapid compositional analysis 3-41275
- Te film, 78-450 K 3-41187
- Ti₂O₃, pure and V-doped, Seebeck coeff. meas. from 54 to 500 K 3-58290
- TiSbS₂ films, amorphous, polycrystalline and textured (*Russian*) 3-79588
- (V_{0.3}Nb_{0.7})O₂, meas. of Seebeck effect 3-41239
- W thin films, laser-induced anisotropic thermoelectric voltages 3-60867
- WO₃-P₂O₅-Li₂O semiconducting glass, thermoelec. polaris. obs. (*Polish*) 3-41176
- YbB₆, Seebeck coeff., comparison with EuB₆ (*French*) 3-64332
- ZnS:Mn, thermally stimulated e.m.f. with trap-filling gradient 3-64363
- ω -Zr, absolute thermo-e.m.f., temp. depend., 80-280K (*Russian*) 3-79665
- ZrO₂, elec. cond. and thermoelec. force, 1000 to 1700°C, 1 to 10⁻¹⁶ atm. O₂ partial pressure (*German*) 3-68604
- ZrO₂-CaO, elec. cond. and thermoelec. force, 1000 to 1700°C, 1 to 10⁻¹⁶ atm. O₂ partial pressure (*German*) 3-68604

thermography

- ceramic casting, equipment for determ. physical and mechanical props., heat treatment, pouring 3-50809
- dynamon thermal dissociation, computer aided thermographic investigation (*Russian*) 3-65071
- instruments, design, parameters and features of thermographs (*Polish*) 3-45437
- liquid-crystal contact lens for conneal temp. distrib. meas. 3-56995
- medical, convective heat transfer effects 3-77258
- medical applications of technique 3-48629
- refractory metal cooling, thermographic method to study rapid crystn. 3-45452
- thermal diffusivity meas. method for cylindrical specimens at intermediate temps. (*French*) 3-56632
- KCl-LiCl-FeCl₃, KCl-LiCl-AlCl₃, immiscible systems, diagrams of melting, thermography (*Russian*) 3-52691
- KNO₃-CsNO₃-NaNO₃ phase diagram, thermodynamic calc., thermography (*Russian*) 3-52692
- LiCl-NaCl solid solution, thermographic and X-ray study, crystn. temp., peritectical transformation (*Russian*) 3-72196
- NaCl-CdCl₂-SrCl₂ phase diagram, thermography, X-ray methods, Na₂CdCl₄ binary combination, eutectics, Van Rein point (*Russian*) 3-52692

thermoluminescence

- activated, fast neutron dosimetry 3-77276
- alkali halide crystals thermoluminescence of additional molecular ions (*Russian*) 3-44501

thermoluminescence continued

- alkali halides activated, hole recombination luminescence (*Russian*) 3-44498
- alkaline earth fluorides: Sc, Y, La, thermoluminescence, donor-acceptor pairs (*Russian*) 3-44500
- application in thermal analysis, activation energies, frequency factors, order of kinetics 3-70287
- complex glow curves, analysis using kinetics 3-76102
- concrete, γ -ray transmission curve and build-up factors 3-43318
- dating applications in art and archaeology, review 3-53809
- diamonds, semiconducting, thermoluminescence (*Russian*) 3-41593
- dosimeter readout instruments, measurement errors due to light source containing β -emitters 3-48271
- dosimetry, analysis of shielding expts. in fast test reactor 3-71223
- dosimetry, Beagle dog eyes, 20, 35 and 45 MeV proton irradiation 3-48258
- dosimetry, bibliography from 1968 to 1972 3-48273
- ethylene glycol + water glassy mixture, trapped electron excitation mechanism, e.s.r. obs. 3-65099
- gamma-ray exposure, dose estimation by thermoluminescence obs. of wrist watch jewels 3-71332
- heating systems, with and without feedback (*German*) 3-42564
- inorganic luminescent materials, e.p.r. study of $^{25}\text{Si}_{1/2}$ ions comparison with luminescence spectra (*Russian*) 3-44318
- inorganic materials, $^{25}\text{Si}_{1/2}$ state ions, varying ligand ions, 1.6 K to 450 K 3-76041
- lunar fines, trapping parameters of some glow peaks 3-69902
- measurement device for single crystals, appl. to CaO emission (*French*) 3-70308
- nucleic acids, nitrogen bases, storage and migration of u.v. emission energy, mechanisms, effect of Ca^{2+} , Mg^{2+} and Mn^{2+} additions (*Russian*) 3-69102
- nucleotide solutions, storage and migration of u.v. emission energy, mechanisms, effect of Ca^{2+} , Mg^{2+} and Mn^{2+} additions (*Russian*) 3-69102
- polyethylene, due to molecular oxygen and aromatic molecules (*German*) 3-61080
- polyethylene, high temp. thermoluminescence obs. 3-64746
- quartz, effect of radiation from radioactive material 3-76104
- quartz, natural, study of geological differences from glow peaks 3-69499
- tetraalkyl ammonium iodides, self-trapped exciton spectroscopy 3-69034
- N, N, N', N'-tetramethyl-p-phenylenediamine, thermal glow curves, effects of added solutes 3-41571
- tryptophan in ethylene glycol/water glass, recombination luminescence and trapped electron decay 3-55695
- volcanic lava dating, fading effects 3-76572
- AgBr photographic emulsions and crystals, photostimulated thermoluminesc., electron and hole traps 3-53340
- AgBr photographic emulsions and crystals, luminesc. spectra and flash, thermal quenching, electron trapping 3-55983
- AgBr(I) photographic emulsions and crystals, luminesc. spectra and flash, thermal quenching, electron trapping 3-55983
- AgCl, determ. of electron trap depth, reln. to latent-photographic-image formation 3-55696
- Al_2O_3 film, electrochem. obtained, thermolum., emission centres activation energy 3-47320
- BeO ceramic detectors, TSEE dosimetry system 3-77278
- Ca halophosphates, thermoluminescence, dislocation mechanism (*Russian*) 3-50629
- CaI_2 , cryst., pure and doped, X-ray luminesc. and thermoluminesc., 90 to 300 K, scintillation props. 3-44482
- CaO phosphors with Ag centres, trapping centre obs. (*Russian*) 3-76054
- CaS phosphors with Ag centres, trapping centre obs. (*Russian*) 3-76054
- CaS:Cr phosphor, e.s.r. and thermolum. studies (*Russian*) 3-75876
- $\text{CdBr}_2(\text{PbI}_2)$ spectra, delocalisation of activator excitations (*Russian*) 3-55308
- Co complex, chelate, γ -irradiated, decay kinetics of thermoluminescence 3-47319
- $\text{CsI}:\text{Na}^+$, TI^+ , V_k centres, thermolum. obs. of thermal migration 3-64035
- CuS-Bi(In) meas. absolute energy output under alpha and gamma irradiation at 100 to 700 K (*Russian*) 3-76100
- KBr:In , meas. absolute energy output under alpha and gamma irradiation at 100 to 700 K (*Russian*) 3-76100
- KBr:Na , thermal recovery of radiation hardening, thermoluminescence and thermal decay of V_1 band 3-68247
- KCl, activated, monomolecular recombination (*Russian*) 3-44456
- KCl, spectra, decoloration of F-band (*Russian*) 3-54961
- KCl:In , Ag, meas. absolute energy output under alpha and gamma irradiation at 100 to 700 K (*Russian*) 3-76100
- KCl:TI , excitation in region of fundamental absorption 3-80116
- KCl-In , KCl-In , TI , ionic crystals containing electron traps, thermally stimulated luminescence peaks 3-76105
- KI, divalent ion doped, elec. field effect (*French*) 3-55693
- KI:Ag crystals, stimulated, nonisothermal relaxation 3-76036
- KI:TI, low temp. irradiation, static electric field effect on thermoluminescence (*French*) 3-53153
- KI:TI thermoluminescence, electric field effect 3-55694
- LiB_4O_7 thermoluminescent dosimeters, photon induced fading 3-77277
- LiCl-Ni X-ray photolum. and thermolum. (*Russian*) 3-69068
- LiF, chips, thermoluminescence as function of electron energy 3-77283
- LiF, heavily γ -irradiated 3-69100
- MgO crystal, u.v. excitation, deep hole trap, hole-release Auger mechanism 3-72776
- $\text{MgO.B}_2\text{O}_3:\text{Tb}$, thermoluminescence relation to composition for radiation dosimetry (*Russian*) 3-44499
- $\text{MgO.SiO}_2:\text{Tb}$, thermoluminescence relation to composition for radiation dosimetry (*Russian*) 3-44499
- N_2 crystal, N-containing, low temp. flashes and glows 3-72762
- NaCl , X-ray coloured, thermoluminescence, isothermal decay 3-53154
- NaCl whiskers, radiative coloration and recombination luminescence (*Russian*) 3-44497

thermoluminescence continued

- $\text{NaCl}:\text{Cd}^{2+}$ form., growth of F-centres, activation energy meas. 3-72688
- NaCl:Ni , X-irradiated, stimulated processes 3-41592
- NaCl:TI , intensity of glow peaks as function of TI concentration 3-47321
- NaCl:V^{2+} crystals, Z-like centres study 3-52812
- RbCl(Br) , F-centre growth kinetics and thermolum. 3-69101
- SiC , n-type hexagonal, thermoluminescence phosphorescence and cryoluminescence 3-55681
- $\text{SrTiO}_3:\text{Cr}^{3+}$, luminesc. excitation mechanism obs. 3-64704
- $\text{YAlO}_3:\text{TR}^{3+}$ (TR=rare earth), colour centres, absorption and thermoluminescence spectra 3-44441
- ZnS , spectra, optical and thermal depth of shallow traps 3-60860
- ZnS(In, Cu) , energy storage, laminar morphology 3-76103
- ZnS:Cu , cubic and hexagonal, thermoluminescence glow curves (*German*) 3-69103
- ZnS:Cu.Cr.Cl , Cr^+ centres, characteristics 3-76101
- ZnS:Cu(Bi) meas. absolute energy output under alpha and gamma irradiation at 100 to 700 K (*Russian*) 3-76100
- thermomagnetic cooling** see magnetic cooling
- thermomagnetic effects** see magnetothermal effects
- thermometers**
see also pyrometers; resistance thermometers; temperature measurement; thermocouples; thermopiles
- bathothermographs, mechanical, reliability study 3-76921
- for deep tissue temperature measurement 3-73923
- e.p.r., $\text{NiSiF}_6.6\text{H}_2\text{O}$ applic. 3-44317
- ferrite, magnetic permeability, temp. dep. of permeability of ferrites, appl. of thermometer 3-73703
- i.f. scanning, calorimetric measurement of pulsed high current electron beam 3-77399
- n.m.r. millidegree, continuous wave, design, low temp. application 3-48388
- quartz thermometer probe, as fluid stirring agitator 3-42538
- screen design rel. to effect on observed temperature 3-48371
- temperature measurement of gases, cancellation of radiative error (*Japanese*) 3-66166
- thermistor thermometer bridges, linearised, small temp. change meas., calorimetry 3-77400
- ultrasonic, in-reactor fuel rod centreline high-temp. meas. 3-45454
- ultrasonic and refractory, mixed-oxide fuel pin centreline temps., meas. to 2700°C 3-45453
- u.s. thermometry, temp. meas. up to 2400C, inaccessible objects 3-42521
- wet bulb, in large screens 3-73402
- (U,Pu) O_2 , thermoelec., resist., and u.s. centreline thermometry 3-45455
- thermonuclear devices** see plasma devices
- thermonuclear reactions**
see also nuclear fusion
- chain, laser beam applic. (*French*) 3-60291
- controlled, prospects for fusion power, review 3-52232
- controlled thermonuclear fusion expts. and engineering aspects, conference, Austin, Texas, USA (Nov. 1972) 3-60295
- controlled thermonuclear reactor first wall sputtering and wall life estimates 3-40548
- fissioning matter, microcritical mass production by supercompression, ultrastrong magnetic fields and particle acceleration prod. 3-54513
- fusion, laser-induced, review 3-71330
- fusion reactions in plasma control of energy balance 3-57930
- hybrid fission-fusion reactor, energy balance eqn. and particle conservation eqns. 3-67392
- isotope separation methods using lasers 3-60299
- laser ignited fusion reactors, economics 3-49373
- laser implosion with consequent compressions of fissionable material 3-63233
- micro fission-fusion chain reactions, bootstrap mass coupling and critical mass reduction 3-54514
- micro-fission chain reactions, application to controlled release of thermonuclear energy 3-52215
- plasma engineering, monograph 3-49632
- plasma heating, laser concentric cumulation, heat of nuclear fusion consideration 3-63855
- stars, hot CNO-Ne cycle hydrogen burning, thermonuclear evolution at const. temp. and density 3-81019
- stellar evolved cores, plasma screening theory and effects on thermonuclear detonation 3-47996
- tokamak-like CTR plasma, self-consistent energy balance studies 3-60637
- D-T and D plasma heating by short laser pulses, neutron yields calc. 3-54866
- D-T and D-D fusion, neutron energies and spectra 3-40519
- D-T plasma heating, escape of α particles 3-49737
- DT plasma, fast α particle reactions 3-57925
- U-D thermonuclear plasma, controlled fusion, obtained by composite macro-particle collisions 3-49733
- thermopiles**
electrolytic formation, etching sensitivity, plating, coil shape depend. 3-80546
- thermoelectric thermometer for gases, cancellation of radiation error (*Japanese*) 3-66166
- thermoreflectance**
graphite, π bands, 0.5 to 9 eV, optical investigation 3-53123
- graphite, π -band structure (*German*) 3-72315
- semiconductor, II-IV-V₂, for band structure obs., review 3-55205
- Au film, piezo, thermo and electoreflectance spectra, comparative props. 3-55631
- Au-Ni, thin film couple, diffusion studied by optical reflectivity technique 3-79528
- Bi_2Se_3 , spectra, obs. at room temp. and liquid N temp. 3-55611
- Bi_2Te_3 , spectra, obs. at room temp. and liquid N temp. 3-55611
- CdTe, reflectivity peaks in vacuum u.v. spectra 3-55623
- CoO , spectra, interband gap between anion 2p and cation 4s bands determ. 3-55612
- $\alpha\text{-Cr}_2\text{O}_3$, thermoreflectance investigation of antiferromagnetic-to-paramagnetic transition 3-55432
- GaAs, reflectivity peaks in vacuum u.v. spectra 3-55623

thermoreflectance continued

Ge, reflectivity peaks in vacuum u.v. spectra 3-55623
HgTe, band structure, electro-, thermo- and piezoreflectance obs. 3-55635
HgTe, example of i.r. laser modulation spectroscopy 3-55597
InSb, reflectivity peaks in vacuum u.v. spectra 3-55623
Kl, Rydberg series of gamma₁ exciton 3-55623
MnO, spectra, interband gap between anion 2p and cation 4s bands determ. 3-55612
NiO, spectra, interband gap between anion 2p and cation 4s bands determ. 3-55612
PbS(Se)(Te), epitaxial film, spectra from 0.7 to 5.6 eV, fine structures 3-55622
Rbl, Rydberg series of gamma₁ exciton 3-55623
SnTe, epitaxial film, spectra from 0.7 to 5.6 eV, fine structures 3-55622
ZnGeP₂, chalcopyrite crystals, spectra, energy band structure 3-44007

thermosphere

heading is late addition, see also upper atmosphere
arc, stable auroral red, vertical distrib. of mol. N₂ vibr. energy 3-69620
composition, evidence for latitudinal and temporal variations 3-61512
composition, horizontal variations 3-61513
composition, latitudinal/season characts. 3-61508
diurnal var. of total mass density, number density and temperature in upper thermosphere 3-65415
equatorial, H₂ emission interpret., proton precip. (French) 3-59127
equatorward winds and semiturbulent mixing causing ionospheric disturbances 3-76809
global model forOGO-6 mass spectrometer meas. 3-61510
global thermospheric dynamics, theoretical model including diffusion 3-61515
gravity wave-mean flow interactions, heat budget 3-65406
heating due to Joule dissipation of ionospheric electric fields 3-76801
interaction with small meteoroids 3-65854
lower, chemistry and dynamics 3-61499
model, photochemical, including ionospheric processes 3-65412
models, vertical diffusivities for lower boundary 3-61514
quenching of vibrationally excited N₂ by O in lower thermosphere 3-69621
semiannual effect, interpretation 3-61498
temperature and density, analysis of phase difference 3-61517
temperature variations with solar activity and time of day 3-69600
tidal motion excited by electric field transmission 3-76802
wind, causing evening enhancement of electron concentration in ionosphere 3-76798
winds, effect on F2 ionisation, position of mid-latitude crests 3-73355
winds rel. to superrotation of upper atmosphere 3-61516
N₂ density and temp. diurnal and semidiurnal var. from thermosphere probe meas. 3-80784
O₂ photodissociation, solar u.v. flux variations 3-80756

thermostats

see also temperature control; thermistors
8 to 400 K, in n.m.r. at high pressures 3-51551
for diffractometer for lattice parameters 3-53852
electronic, with on-off control 3-51540
with electronic temp. stabilization 3-70278
heavy-gas, reacting single component system, disturbance of Maxwellian distrib., effect on reaction rate 3-73131
liquid, use in installation for research at high press., up to 20 kbar 3-73709
temperature stabilisation system, high precision, 30 to 100C, ferroelectric crystals study 3-62009
TL150 ultrathermostat, contactless heater switch 3-70279
X-ray chamber, thermostatically controlled, for struct. investigation of alloys and solns. 3-73913

theta pinch see pinch effect

thick film circuits

focus control, colour TV 3-66905
production, computer controlled laser trimming, of resistors (German) 3-48956
resistance adjustment methods (Hungarian) 3-66894
resistor trimming, using YAG laser 3-45837

thick film devices

No entries

thick film resistors

laser beam trimming, IC technology 3-45829
laser trimming, material reactions 3-45838
laser trimming, trim quality and resistor damage rel. to beam parameters 3-45837
resistance adjustment methods, integrated cct., insulating substrate (Hungarian) 3-66894

thick films

No entries

thickness control

glasses, on-line technique using mm wavelength transmission 3-77486
MnBi ferromagnetic film production by optical control of vac. deposition and annealing 3-50659

thickness measurement

coatings, X-ray powder diffr. method 3-73676
corneal refractive index rel. to thickness and pachometric meas. errors 3-70123
coulometric, simple device for end-point indication 3-42603
dielectric layer, inductive method, compensation of lift-off effect (German) 3-66282
eddy current heating, megahertz frequencies, O layers on Ti, fatigue crack detection 3-45531
eddy current instruments, nondestructive inspection, performance specification 3-45530
electron probe thin film analysis method 3-46770
electroplated coatings, by fluorescent X-ray methods 3-42517
ellipsometry of fluid interfaces, and membrane-like systems, review 3-77427
epitaxial layers, by laser radiation diffraction 3-51523

thickness measurement continued

f.e.t. devices, electron microprobe determ. of thickness and P conc. of gate oxide phosphosilicate glass 3-42725
film, electron probe microanalysis (Japanese) 3-73951
film on glass substrate, X-ray method 3-73665
films, refr. index and thickness from single angle refl. meas. 3-51594
foil, X-ray transmission, error sources 3-61987
gamma ray backscattering, error minimisation 3-42643
light-sectioning attachment, shop measuring microscope BK 70 x 50, VEB Carl Zeiss JENA, surface and thickness meas. 3-51585
liquid film in two-phase flow, by conductance probe 3-61989
metal foil, meas. using intersecting slip traces 3-47372
metallic foils, monoenergetic electron beam absorption 3-70264
metallisation, during continuous vacuum process, computer data collection and processing (French) 3-51570
monolayers, built-up, thickness meas. by multiple beam interferometry 3-39850
monolayers, built-up, thickness meas. by multiple beam interferometry, comments 3-39851
multiphase particulate materials, scanning electron microscopy 3-70420
narrow band interference filters optical thickness control (French) 3-51603
nondestructive interference method for two-film systems 3-58488
optical fibre radius determ., outer and inner to outer ratio 3-77504
ozone layer thickness variations, stellar spectrophotometer (French) 3-73561
peripheral glomerular basement membrane, thickness distrib., statistical anal. 3-56484
physical quantities meas. from natural vibrations attenuation of oscillator circuit (Czech) 3-56695
using piezoelectric laser beam deflector 3-48358
radioactive isotope method 3-40039
rocket motor case line, laser gauge technique 3-45423
semiconductor epitaxial layer, thickness meas., computer approx., interference pattern 3-41667
surface film thickness determ. by refl. meas. 3-45413
thin film, by ATR i.r. spectroscopy 3-48442
thin film, quartz resonator and multiple interference methods (German) 3-62000
thin film narrow band optical filters, thickness monitoring by turning method, absorpt. effects 3-51531
thin films, epitaxial, dielec., monitoring on i.r. spectrophotometers 3-73759
thin films, from lattice absorption bands 3-56616
thin films, quartz oscillator, theoretical models, relationships with frequency and period (French) 3-45426
thin films of Ag/Ag/Pyrex, comparative study of methods including Tolanski interference (Spanish) 3-73666
thin films thickness measurement using quartz resonator, stress effects (Czech) 3-56612
thin reaction layer, between substrate and overlayer, X-ray fluoresc. method (German) 3-61996
transparent film, on metal substrate, ellipsometric method 3-62049
transparent foils, transmission electron microscope specimens 3-70417
Zircaloy tubing, u.s. inspection, wall thickness and ID meas., multiplexed instrumentation 3-47516
Al cladding, thickness meas., U fuel elements, gamma ray attenuation 3-47500
Al₂O₃ films, ion-induced X-rays and Rutherford backscattering 3-43960
CaO thin film, sputtering rate determination by fluorescence of sputtered atoms 3-44508
Er thin film surface oxide, Auger spectroscopy and ion bombardment 3-45555
Fe, thickness meas., gamma radiation apparatus 3-48591
Si, epitaxial layer thickness meas., Fourier transform method, scanning Michelson interferometer 3-41666
Si detectors, thickness measurement of sensing region 3-53979
Si epitaxial film, down to 0.5 μm 3-44548
Si epitaxial films, error analysis of thickness measurement by interference of i.r. rays 3-61985
Si epitaxial layer, bevel and stain, stacking fault, and i.r. fringe methods 3-64799
Si(Li) detector, Au-layer and dead-layer thickness determ. 3-51713
ZnO sputtered films, diagnostic rate monitoring by interference spectroscopy 3-45418

thin film capacitors
dispersion characteristics, meas. at low freq. 3-45528

thin film circuits
laser micromachining, thermal analysis 3-40298
resistor network, automated laser trimming 3-45836
tantalum-titanium alloy thin film preparation 3-64416
Ag electrodeposition, effect of temp. and metaphosphate, relay timing in electronic circuit 3-50836
Ta, cylindrical diode continuous vacuum sputtering machine 3-39890

thin film devices
see also magnetic thin film devices
bolometers, superconducting, various film characteristics, methods of use 3-59563
cathodes, field emitted electron energy distribution 3-41622
elastic surface wave guide, curved thin film 3-41076
filters, multilayer type, for thermal detectors, fabrication 3-62010
holographic grating coupler, for optical waveguide, perturbation analysis 3-66177
particle detectors, response to passage of accelerated heavy ions, results 3-77625
Permalloy T-bar cct., on orthoferrite, generation and propagation characs. 3-50410
semiconductor coplanar switch, static characts., theory 3-79748
CaWO₄:Nd³⁺ laser, liquid phase epitaxial growth 3-54230
Cr film cathode, pulsed field emission at high current density 3-69143
InSb Hall effect bubble domain detector 3-47110
SiTeAsGe threshold switch, injection process and switching characs. 3-55317
V₂O₅ resistor calorimeter, for low energy laser pulses 3-53918

thin film devices continued

- YAG:Nd³⁺ laser, liquid phase epitaxial growth 3-54230
 ZnS piezoelectric transducer, surface elastic wave motion, computer analysis (*Japanese*) 3-41482
 ZnS:Mn electroluminescent cell, ion implantation fabrication 3-41588
 ZnTe, memory switching device 3-68683

thin film resistors

- laser beam trimming, IC technology 3-45829
 precision trimming, automated laser system 3-45836
 Ta, thermal coeff. of resistivity, effect of Ar, O, N ion bombardment 3-58054
 Ta-Al, sputtered, Seebeck effect, rapid compositional analysis 3-41275
 V₂O₅, low energy laser pulse calorimeter applic. 3-53918

thin film transistors

- m.i.m.s. tunnel triodes, rel. to hot electron attenuation in Al films 3-79777
 CdS on SiO₂, transverse field effect on elec. cond. (*Korean*) 3-72356
 MgF₂-CaF₂ mixtures, evaporated films for PbTe t.f.t.s 3-79779
 p-type Te, evaporated films, resistivity meas., strain sensitivity 3-41278

thin film triodes *see thin film transistors***thin films**

- see also insulating thin films; magnetic thin films; metallic thin films; substrates; superconducting thin films*
 amorphous semiconducting materials, optical and electronic props. 3-41123
 anodic oxide film formation, space charge and conc. gradient effects 3-50651
 anodic oxide film growth on GaP 3-50652
 Auger electron spectroscopy, apparatus, technique (*Hungarian*) 3-80124
 barium stearate thin films, Faucher's ellipsometric formula validity 3-66183
 cellophane and polyethylene films, adhesion, microrheological process effects 3-55893
 celluloid, alpha particle track fading by u.v. heating hot air and liquid circumstances 3-59648
 chalcogen overlayers on Ni(001), chemisorption bonding, LEED study 3-60829
 chalcogenide glass films, reversible hologram recording 3-66257
 chemical analysis methods, review 3-59693
 chromatography, letter copying machines, secondary standards 3-70481
 coalescence of islets, differential equation (*Russian*) 3-68518
 colour contrast layer formation, on metallographic specimens, gas etching technique, microscope obs. (*German, English*) 3-69240
 colour contrast layer formation in gas-ion-reaction chamber under electron irradi., microscope obs. (*German, English*) 3-69239
 crystallographic defects, SEM obs., imaging 3-72075
 curved, guiding elastic surface waves 3-41081
 deposition, thickness comparison for various types of ring vapour source 3-41633
 deposition rate requirements 3-61107
 dielectric, on Si, refr. index and thickness, ellipsometric method, accuracy 3-51591
 diffusion at film-substrate boundary, laser radiation (*Russian*) 3-41042
 diffusion microcouples in ternary alloys, feedback-controlled three-source evaporator system for preparation 3-55732
 electrochemical thinning of metal disc, technique description 3-48568
 electron probe microanalysis, thickness and chemical comp. determ. (*Japanese*) 3-73951
 electron probe thin film analysis method 3-46770
 electron scattering, depth selection and line profiles 3-40001
 electronic density of states of f.c.c. band 3-52776
 electropolishing at low temp. for electron microscopy 3-45562
 ellipsometry, electrochem. studies, surfaces and surface films, review 3-66197
 ellipsometry, principles of technique, application to electrochem. studies, review 3-66196
 epitaxial, dielec., thickness monitoring on i.r. spectrophotometer, device 3-73759
 epitaxial, RHEED study, obtaining and interpretation of diffraction patterns 3-41105
 epitaxial growth, chem. transport reaction, diffusion of gaseous product, establishment of stationary state 3-72282
 falling, stability conditions, boiling and non-boiling films, interface conditions, Cu/H₂O/air (*German*) 3-46500
 ferroelectric, polarisation instability 3-47201
 ferroelectric, reactive sputtering and high-temp. conversion 3-41630
 fluorescence spectrometry, multiple internal reflection 3-66414
 growth, migrating crystallites, coalescence kinetics 3-68520
 growth process, residual gas influence (*Japanese*) 3-64773
 heating and melting, by laser beam, one dimensional heat flow calc. 3-75691
 heterogeneous nucleation theory, application of cluster growth rates 3-43964
 inhomogeneous films, determination of distribution of material 3-45421
 initial stress application, relaxation testing, corrosive media 3-53299
 ion-implanted, giant transmission e.p.r. theory 3-41402
 ionic migration rel. to growth kinetics under electron equil., metal oxidation 3-43950
 ionic transport equation for cryst. solid film, metal oxidation 3-43949
 laser beam machining, temperature distributions induced by irradiation of Gaussian beam (*Japanese*) 3-59906
 laser beam machining, threshold power density requirement 3-54252
 lattice vibrations investigation using Green's function method 3-55175
 liquid, gravitational flow, along vertical channel walls (*Russian*) 3-46382
- thin films continued**
 liquid, role of cavities in initiation and growth of explosives 3-78995
 MBBA liq. cryst. films, microstruct., Williams domains 3-52574
 measurement, Raman spectroscopic method (*German*) 3-45488
 mechanical instabilities caused by substrate surface microrelief change induced by radiation damage 3-52770
 microanalysis, scanning electron microscope, rough samples 3-66469
 nonlinear, sum-frequency e.m. generation (*Russian*) 3-54247
 nucleation kinetics, additional processes 3-79596
 optical characterization, theory 3-50534
 optical constants calc. by ellipsometry 3-53158
 optical properties determ. by reflectance analogue computer 3-45476
 optical props., specimen transfer devices 3-53889
 oxide on Fe-18 Cr sealing alloy, elec. resist. rel. to additions and oxidation atmos. (*Japanese*) 3-72905
 2,4,6,8,10-pentamethylundecane crystalline and glassy films, i.r. spectra and rotational isomerism 3-47268
 penton film, morphology, heat treatment effect (*Polish*) 3-53282
 phase transitions, role of size-effects, bulk sample instability (*German*) 3-46771
 phthalocyanines, emission spectra 3-61074
 plasma deposition, powder heating in plasma stream (*Russian*) 3-53176
 plasma deposition, powder particle acceleration in plasma stream (*Russian*) 3-53175
 plasma slabs, e.m. wave reflection 3-71866
 polyethylene, chain extended crystallisation, lamellar thickening 3-69390
 polyethylene, dynamic light scattering, expt. procedure 3-57694
 polyethylene film, diffusion of antistatic agents, surface cond. study 3-65004
 polyethylene terephthalate film, solid-state transitions investigation by temperature tear strength method 3-61221
 polyethyleneterephthalate, Lawsonite film, liquid hydrogen target production 3-48502
 polymer, fluorocarbon, struct. and props. depend. on sputtering conditions (*French*) 3-80157
 polymer, impact testing technique 3-50807
 polymer, laboratory methods of prep., review 3-48346
 polymer, subject to static and fatigue loading, arterial crack growth 3-55895
 polymer, viscoelastic deform. following extended Voigt model 3-40955
 polymer lubricant films, friction coefficient as function of pressure, reply to comments 3-44676
 polythreepptide, Fermi resonance in i.r. spectra 3-75169
 polyvinyl carbazole, perylene doped, energy transfer 3-76062
 polyvinylidene fluoride film, metal ions injection in an electric field, effect on complex dielectric constant 3-58466
 rupture machine for mechanical tests 3-76404
 scintillation detectors, response to light and heavy ions 3-48512
 scintillation phosphor material on perspex, light pipes for SEM 3-77722
 soap, cond. meas. to illustrate tunnelling 3-42500
 specular reflection spectroscopy, electrode-solution interphase, ultra-thin surface films, kinetics, review 3-66227
 specularly reflected radiation properties of absorbing films, at normal incidence 3-51858
 sputtering yield of light ions, calc. 3-69116
 stress due to vol. change on solification 3-41008
 structure and composition analysis, ion beam techniques for structure and composition analysis 3-57973
 supersonic gain possibility, under conditions of size quantisation (*Russian*) 3-58489
 surface, thermally insulating, frictionally excited thermoelastic instabilities 3-55022
 surface film thickness determ. by refl. meas. 3-45413
 surface geometrical defects, rel. to localised state form. in thin layers 3-75788
 temperature distribution when heated by electron beam (*Russian*) 3-55174
 thermal conductivity meas. techniques 3-73696
 thickness determination, X-ray method 3-73665
 thickness measurement, quartz resonator and multiple interference methods (*German*) 3-62000
 thickness measurement, theoretical models of quartz oscillator, relationships with frequency and period (*French*) 3-45426
 thickness measurement and chemical characterisation, by ATR i.r. spectroscopy 3-48442
 thickness measurement using quartz resonator, stress effects (*Czech*) 3-56612
 thin reaction layer, between substrate and overlayer, thickness meas., X-ray fluoresc. method (*German*) 3-61996
 three dimensional layer growth by diffusion 3-52764
 toluene, photoexcitation, fluorescence of benzyl radicals (*Russian*) 3-72701
 transmission and reflectance monitoring, during deposition, using modulated beam photometer 3-53901
 transparent, on metal substrate, thickness and dispersion meas., ellipsometric method 3-62049
 Ag/Ag/Pyrex, thickness measurement, comparative study of methods including Tolanski interference (*Spanish*) 3-73666
 AgI-Ag photosensitive film, refl. spectra, 370 to 500 nm 3-53121
 AlN, piezoelec., on sapphire, acoustic surface wave props. 3-55135
 Au goniospectrophotometer, reflectance and transmittance measurements, 0.25 to 1 micron polarised light (*French*) 3-39926
 B, amorphous structure, radial atomic distrib., electron diffraction obs. 3-75694
 Ba_{1-x}Ti_{1-x}O_{3-x}, 0 ≤ x ≤ 0.1, amorphous condensates, structure using electron diff. 3-75690
 BkCl₃, thin films, absorption spectrum, crystal field components, energy level scheme 3-41530
 C, amorphous structure, radial atomic distrib., electron diffraction obs. 3-75694
 CsCl, X-ray irradiation effect on phase transition 3-68409
 EuS, h.v. epitaxial growth on mica, structure, X-ray obs. 3-68512
 GaN, piezoelec., on sapphire, acoustic surface wave props. 3-55135

thin films continued

GdO₂, electron microscopy, diffr. study, of form., comp., struct. 3-72290
H₂O solid, sticking coefficient of CO₂, molecular beam obs. 3-41093
⁴He, superfluid, creeping film phenomena, theory 3-52730
KCl, (KBr), (KI):Ti⁴⁺, luminesc., slow electron impact excitation 3-41590
KCl:Al, porous, Al effect on transmitted secondary electron emission 3-50633
Li₂Na_{1-x}I solid solutions, persistence of first absorption peaks 3-72665
MgO-Au cermet, sputtered, for high efficiency secondary electron emission 3-53160
NH₄Cl, electron diffraction intensity investigation 3-72292
NaCl, electron diffraction intensity investigation 3-72292
NaCl, surface optical vibrations obs. 3-50063
Na₂WO₃ phase form. by Na⁺ diffusion in soda glass-WO₃ thin film system (French) 3-55169
Ni₂N, electron state determ. by electron diffraction 3-79297
P on Si substrate, secondary electron characteristic energies 3-41601
PbN₂:Bi, Ti, and pure thin films, i.r. absorption spectra 3-64647
PbO, fibre textures determ. by electron diffraction 3-79585
PbO, vapour deposited, chemisorption of HCl, partial substitution of O in surface layer 3-68506
Pr₂O₃, optical properties meas. by photometry and ellipsometry 3-53159
ReOF₄, vibrational spectra 3-72626
S, on Be foil, X-ray filters, vacuum deposited 3-40053
Sb₂O₃, refractive index, 300-4000 nm, rel. to microstructure 3-76113
SnO₂, sputter etching 3-79580
Te-Ag(Au)(Cu), amorphous, condensation, struct. obs. using electron microscope 3-75692
TiC, crystalline state obs., ESCA spectra 3-80142
TiO₂ goniospectrophotometer, reflectance and transmittance measurements, 0.25 to 1 micron polarised light (French) 3-39926
TiCl₃, electron diffraction intensity investigation 3-72292

Thirring model see quantum field theory

thixotropy

alkaline perbutan latex dispersion as negative-thixotropic fluid 3-69394

Thomas-Fermi method see atomic structure

Thomson effect see thermoelectricity

thorium

HTR cores, design with prismatic fuel elements 3-67457
ion implantation in Nb, surface analysis by secondary emission mass spectrography (French) 3-40946
ionisation energy calc. 3-60376
isolation from ores, history, atomic energy programme 3-67560
isotopes, atomic mass meas. 3-43322
itinerant 5f states observation by reflectivity meas. 3-43992
LWR, potential when fuelled with metallic thorium, advantage over metallic uranium 3-67585
nuclear pure samples Cr traces spectrochemical determ. 3-70493
phonon spectrum, electron-phonon interactions, neutron scatt. meas. 3-58092
solubility in Pb-Li liquid alloys 3-58131
(La,Th):Ce alloys, mag. to nonmagnetic transition, superconducting temp. depression 3-52924
Th-U ores, gamma spectral borehole logging methods of registration (Russian) 3-73394
Th-U ores spectral assay using scintillation counters, influence of resolution (Russian) 3-73390
Th + O(O₂)(N₂O) vapour oxidation, chemi-ioniz. 3-80533
Th⁺, second spectrum, energy levels and classified lines 3-78416
²²⁸Th, ²³⁰Th and ²³²Th abundance in interstitial water from Pacific Ocean sediment 3-65267

thorium compounds

dispersion in Ni, interfacial and adhesion energy meas. by SEM 3-75659
Al₃Th, AlTh, magnetic susceptibility meas., contribution to Knight shift (Russian) 3-47157
ThB₄:Gd³⁺, ThB₆:Gd³⁺, e.s.r., mag. susceptibility meas. influence of U admixture 3-41406
ThB₆ X-ray diffr. anal., thermal props. 3-68423
ThC₂N_{1-x} formation in ThN, graphite carbothermic reaction 3-74724
Th(IV) complex, acetylacetonate, tetrahedral, octahedral and cubic complexes dielectric relaxation 3-55520
ThN carbothermic reaction with graphite, effects of reaction temp. and particle size 3-74724
Th(NO₃)₄, fast neutron meas., ³He spectrometer 3-71157
ThO₂, colloidal sol, particle size distrib., small angle X-ray scatt. anal. 3-73079
ThO₂, light emission during adsorption of CO and O₂ 3-79561
ThO₂, pure and CaO-doped, a.c. total cond., 600-1400°C 3-72364
ThO₂, Raman spectra 3-72610
ThO₂, thermal diffusivity meas., 900 to 2550 C, flash method (French) 3-47445
ThO₂ dispersed NiCr, high temp. stability and coarsening 3-64855
ThO₂ dispersion in Ni, impurity induced recrystn. 3-64849
ThO₂ dispersion in W wire, recrystn. process 3-64857
ThO₂ dispersions in Fe, effect on ductility and fracture 3-64904
ThO₂ powders, phys. props. and influence on sinterability 3-80402
ThO₂:Ca²⁺(Y³⁺), optical absorpt. and fluoresc. 3-55678
ThO₂:Er³⁺, e.p.r. of Er sites, axial g values 3-41405
ThO₂:Gd³⁺, temp. dependence of hyperfine interaction 3-64551
ThO₂-PuO₂ HTGR lattice, temp. dependence of infinite-medium neutron multiplication factor 3-49345
ThO₂-PuO₂ lattice temp. dependence of conversion ratio 3-71171
ThO₂-Y₂O₃(90 mole%)-Nd₂O₃(1 mole%), transparent, powder prep. and processing 3-64968
ThP-UP solid soln., lower temp. antiferro-paramag. transition, susceptibility obs. 3-68782
(U,Th)O₂ fuel particles, pyrolytic-graphite coated, creep deformation, 800-1200°C following irradiation (German) 3-71314
(U,Th)O₂ solid solns., elec. cond., 800-1200°C 3-67549

thorium compounds continued

(U,Th)O₂ industrial production, for use in HTGR (German) 3-67591
UC₂-ThC₂ spherules, pyrolytic C encased, HTGR elements, radiation testing (German) 3-71266
UO₂-ThO₂-(Th,U)O₂ sol-gel-oxide, HTGR fuel element manufacture, neutron irradiation (German) 3-71266

three-phase flow see multiphase flow

throat microphones see microphones

thulium

atom, neutral, spectrum and energy level 3-63273
atom, radiative lifetime measurements by beam-foil method, solar abundance determination 3-78442
electric and thermal resistance, magnetic field effect 3-60864
ferromagnetic, PAC obs. of mag. hyperfine field 3-64591
germanate glass: Tm³⁺, Er³⁺, oscillator strengths, emission and excitation spectra 3-72712
glass: Tm³⁺, Er³⁺, intensity parameters of electronic transitions in visible, i.r. spectra 3-58535
phase transformation, high press. polymorph, X-ray obs. 3-75500
CaF₂:Tm³⁺, high press. optical absorpt. studies 3-41540
EuF₂:Tm²⁺, high press. optical absorpt. studies 3-41540
LaSn₂:Gd, Tm, upper critical fields for superconductivity, crystalline field effects 3-52925
Lu₃Al₅O₁₂:Tm³⁺, stimulated emission, luminescence and absorption spectra 3-61053
SrF₂:Tm²⁺, high press. optical absorpt. studies 3-41540
Tm I, hyperfine struct. of even levels 4f¹²5d6s² + 4f¹²6s6p (French) 3-74794

thulium compounds

binary chalcogenides, mag. props., metal-insulator transition, superconductivity 3-41326
ethyl sulphate, ¹⁶⁹Tm n.m.r. study 3-64577
CaF₂:PrF₃(NdF₃, DyF₃, HoF₃, ErF₃, TmF₃), gamma-luminescence, phosphorescence, photoluminescence 3-53140
Tm orthoferrite, submillimetre intrinsic domain wall reson. 3-75886
TmB₁₂, Mossbauer spectra for ¹⁷⁰Yb Debye-Waller factor (French) 3-72552
TmFeO₃, bubble domain sensing using planar magnetoresistive detector 3-56702
Tm₂Ge₂O₇, flux growth, mag. transition temps. 3-41638
TmVO₄, phonon instabilities, near Jahn-Teller phase transition 3-55069
Y_{3-2x}Eu_xTm_xGa_{1-x}Fe_{5-x}O₁₂ epitaxial film for bubble device appl., characts. 3-60975

thunderstorms

see also lightning

atmospheric water vapour injection by thunderstorms, radiometric obs. 3-61469
centres rel. to two-hop whistler sources 3-56186
charge transfer from highly electrically stressed water surface, thundercloud formation 3-76746
cosmic ray generation of charges (Russian) 3-65597
diurnal variation at Manchester Airport 3-73334
drag on storm by winds, expt. analogy 3-51031
F₂-region, acoustic wave vel. meas. 3-65465
fields for fair weather and thunderstorms 3-59090
S. Florida summer thunderstorms, 500 kHz spherics and radar PPI data 3-65363
forecasting, Delhi State, rel. to meteorological parameters 3-80855
forecasting of premonsoon thunderstorm/duststorm activity over Delhi region 3-65523
formation of severe storms rel. to hydrodynamic instability theories 3-59116
hailstone model, growth and trajectories in simple cloud model 3-47738
infrasonic thunder, electrostatic generation mechanism 3-51038
ionospheric disturbance 3-44920
lightning, duration, cyclic variation in mean, noise monitored, correlation with thundercloud structure and activity 3-73303
lightning as acoustic source to determine near-storm atmospheric parameters 3-59184
ocean sand-scatt. layer depth decrease during thunderstorm 3-65284
Schumann cavity resonances, variation with solar ionizing radiation, zenith angle and storms 3-76747
surface runoff system, storm records, determ. of optimal kernels, computational technique 3-56243
Thumba equatorial station, India, effect of thunderstorms on multiple reflections of r.w. from E_s region 3-65461
thunderclouds and lightning conductors, structure and theory 3-61969
viscous flow, unsteady, between parallel plates in electric field 3-79011

thyristors

switch, for pulsed n.m.r. apparatus 3-66290

thyristor applications

geoelectric generator unit (type 67) thyristor inverter (Russian) 3-47815
servo drive, for slow cycle testing mech. equipment 3-73106

thyristors

Si, epitaxial growth, p-n junctions, thyristor manufacture 3-41256

ticking stars see pulsars

tides

Arctic Seas, dissipation of tidal energy (Russian) 3-73268
atmospheric lunar diurnal tide, classical tidal theory calculations 3-59113
Bay of Biscay, vertical structure of semi-diurnal tidal currents 3-53457
beaches and bays, effect of storm tides on motion and height of water 3-58990
braking torque on earth's rotation, from up-to-date cotidal charts 3-76493
California, Earth strain tides obs. thermoelectric effects 3-44867
Combarjua canal, connecting Mandovi and Zuari estuaries, tidal flow characteristics 3-76687
continental slope, meas. of internal tides 3-59022
Coral Sea, tidal resonance obs. 3-53455
Earth, long-term component effects on geysers 3-76613
Earth, perturbations of Beacon Explorer C spacecraft 3-56073

tides continued

- Earth rotation, deceleration, energy dissipation in the asthenosphere due to tidal retarding couple, force of zonal wind 3-80651
 Earth tidal amplitude and phase from orbital inclination of Beacon Explorer C satellite 3-65172
 Earth tide anal. using spectral summation 3-56245
 eastern Caribbean, tidal harmonic constns. near an amphidrome 3-76686
 electric currents caused by flow across geomagnetic field 3-73251
 English Channel, cause of M_2 geomagnetic variations 3-73250
 equilibrium tide theory, rotational corrections 3-56007
 estuaries, shoaling, influence of density stratification 3-76685
 estuary, obs. of turbulent flow 3-51214
 geophysical aspects of Earth tides 3-44866
 gravimeter calibration, TRG-1 recording meter 3-44941
 Gulf of California, tidal patterns and energy balance 3-41935
 lake Biwa-ko seiche, numerical experiments using nonlinear two dimensional model 3-76925
 level in Lagoon of Venice, telemetry system (*Italian*) 3-51206
 long-period tidal waves determ. by gravity meas. 3-44860
 long-period tides, variations in harmonic characts. 3-65278
 Longman tidal formulae, resolution of horizontal components 3-50941
 Louisiana coast, subsidence rate determ. from tidal meas. 3-53450
 lunar, anal. of methods of determ. 3-65504
 lunar semi monthly tides in horizontal geomagnetic intensity at the Indian equatorial region, equatorial electrojet effect 3-61414
 M_2 tidal currents, structure in N.W. Atlantic 3-65259
 Mandovi estuary, premonsoon tidal flow characteristics 3-76688
 observations near amphidrome in NE Caribbean Sea 3-59045
 ocean, distortion of Earth's gravit. potential field by M_2 tide 3-47707
 ocean mapping of temperature and saltness, effects of winds and tides 3-41944
 oscillation, surface waves, rotating fluid 3-47675
 quartz fibre accelerometer for seismic and tidal meas. 3-47805
 San Francisco Bay region, tidal tilt data evaluation and prediction 3-47806
 satellite motion perturbations, computational method 3-59247
 sea and reservoir surfaces, wind induced tidal oscillations 3-76682
 semi-diurnal tidal effects on photographic zenith tube obs. 3-50952
 solid Earth tides rel. to changes in situ seismic vel. 3-50930
 Texas coast, subsidence rate determ. from tidal meas. 3-53450
 tilt anomalies, obs. and mechanism predictions 3-41878
 tilt meas., instrumentation and techniques 3-47804
 tilt meas. in Europe, amplitude and phase errors 3-41877
 triggering of volcanic eruptions by Earth tides 3-61310
 tsunami in Ust-Kamchatsk (*Russian*) 3-47713
 two-dimensional numerical tidal model with unequal grid-spacing 3-59007
 volcanic eruptions, tidal cycles rel. to frequency, intensity and latitude 3-61311
 Wachapreague tidal inlet, response characts. 3-59042
 Waltair, Indian E. coast, tidal currents rel. to continental shelf shell zone 3-47668

tilting control see attitude control

timber see wood

time conservation see T invariance

time delays see delays

time division multiplexing

- six-channel t.d.m. telephone equipment, using GaAs laser diode (*Japanese*) 3-59847

time interval measurement see time measurement

time measurement

- see also clocks; frequency measurement
 camera shutter effective exposures, digital instrument 3-39961
 comparison bet. remote atomic clocks, by TV signals (*Japanese*) 3-54008
 earth rotation, solar flare effects on length of day 3-61329
 fluorimeter, decay time of luminescence (*French*) 3-66455
 interval between pulses in Rossi- α -experiment, magnetic tape storage 3-66328
 interval deviation measurement, nanosecond 3-73670
 lifetimes, nuclear excited states, scintillation single crystal time spectrometer, description 3-70409
 Mossbauer spectrometer, using multichannel analyzer 3-56987
 physical time scales determ., astron. appl. (*Italian*) 3-61625
 picosecond, using linear accelerator and r.f. separator 3-56851
 radiation intervals distribution meas. for identifying decaying nuclides 3-62257
 reactor period meas., digital instrument 3-60254
 relay operate time, digital millisecond meter, contact var. 3-77564
 time scale clamping, using v.l.f. radiowave propagation 3-51510
 time-interval meters, digital, methods, design principles, comparison, review 3-66281
 Turin Astronomical Observatory regular time service (*Italian*) 3-70062
 Universal Time, UT1, determ. using Cambridge 5 km telescope 3-65952
 Universal Time determ., effect of right-ascension errors in stellar positions 3-77032
 zero-time detector, for heavy ion spectroscopy time-of-flight spectroscopy 3-40037

time of flight spectrometers

- accelerator beam energy meas., accuracy $1.5:10^5$, tested by ^{60}Ni excitation energies 3-73884
 accelerator beam energy measurements 3-51677
 distortions of signals, review 3-42608
 using electrostatic particle guide, for high-resolution charged-particle mass identification 3-48553
 using electrostatic particle guide, transmission and shifts for low energy ions 3-48550
 fission fragment mass distribution meas. utilizing particle channelling 3-62266
 gated ion source 3-62263
 ion lifetimes, organic molecules ionised by electron impact 3-57679
 ion mass analysis, satellite peaks on spectra 3-56973
 mass spectrometer, beam modulation technique 3-54003

time of flight spectrometers continued

- molecular beam velocity analysis using time-of-flight method with PDP-11 multiscaling interface 3-78908
 molecular beams, based on charged particle oscillator 3-77617
 multiparticle atom probe time-of-flight meas., 10 nsec resolution counter 3-40043
 neutron, detection efficiency, tailored source spectra 3-62262
 neutron, Harwell synchrocyclotron, total cross section of iron meas., 24-1000 keV 3-71117
 neutron, resonance energy meas. for calibration 3-60174
 neutron spectrometer facility 3-51731
 zero-time detector, for heavy ion spectroscopy 3-40037
 n, 4 to 7.6 A, spectrometer with three synchronized choppers, 150 m guide tube 3-78333

time varying parameters see time-varying systems

time-varying systems

- linear conceptual catchment models, time variance, rainfall rel. to runoff 3-56242

timing see time measurement

timing circuits

- particle-accelerator system, PRIMET, Batavia USA, control system synchronisation, single line clock transmission, serial encoding 3-56901
 time stretcher, for nuclear physics experiments 3-51730
 time-interval meters, digital, methods, design principles, comparison, review 3-66281
 Ag electrodeposition, effect of temp. and metaphosphate, relay timing in electronic circuit 3-50836

tin

- alloying addition to battery grid alloy, Pb-Ca, effects on grain struct., mech. props., corrosion 3-41724
 atom, photoelec. cross sections, Z-depend. 3-67681
 atom, photoelectric cross section for 145 keV gamma rays 3-49406
 band edge effects on strain modulation electron tunnelling in m.i.m. diode 3-55344
 crystal growth, Bridgman method, reaction of foreign particles with crystn. front 3-75492
 crystal growth from melt, growth orientation rel. to gravity 3-44535
 dendrites, on surface of supercooled melt, cryst. orientation determ. 3-75697
 diffusion coatings on steel, corrosion resist. 3-80338
 diffusion in Cu, pre-exponential factor and activation energy determ. (*Russian*) 3-50025
 electron probe microanalysis, mass absorption coeffs. for CuLa line (*Japanese*) 3-57022
 embrittlement by liq. metals, temp. effect (*Russian*) 3-80333
 film on quartz, thermal phonon radiation into substrate 3-55043
 film superimposed with Ni, supercond. bridge, microwave-induced current steps 3-46937
 foil, absorption of beta particles from ^{32}P , ^{91}Y , ^{89}Sr sources 3-49376
 glass:Sn, Ga, Mossbauer effect and second-order Doppler shift, superconductivity 3-75927
 gray, zero-gap semiconductor, stress-dependent dielectric constant 3-44365
 heat of solution of Eu, calorimetric meas., EuSn_3 enthalpy of form. meas. (*French*) 3-53351
 internal friction, twofold resonance for both flexural and longitudinal vibr. 3-79428
 ions, effect on deposition of Zn powder on steel from alkaline Zn electrolytes 3-80556
 ions in crystals, mol. aspects of interactions 3-68565
 liquid, diffusivity and solubility of oxygen 3-41051
 liquid, electron structure, photoemission meas. 3-50107
 liquid, fragmentation when dropped in water, automatic picture scanner 3-74730
 liquid, Knight shift and mag. susceptibility meas. 3-50483
 liquid, pair interaction pot. calcs. 3-49838
 liquid, structure, by time of flight neutron diffr. 3-68149
 liquid, surface tension, determ. by capillary rise method (*Japanese*) 3-58176
 liquid, surface tension meas., sessile drop method, effect of graphite (*Japanese*) 3-53828
 liquid, wettability on solid Cu alloys, rel. to soldering 3-50754
 liquid, self-diffusion, 665-1746K 3-64195
 low resistance contact, for GaAs, formed by sequential deposition of Ag and Sn (*Russian*) 3-52899
 melt, free surface energy, contact angle, density, meas. installation, lying-drow method 3-73687
 melt, undercooling rel. to additives (*Japanese*) 3-76203
 minerals, precipitation and separation of single phases metallurgical products, Sn production 3-50671
 n-type, grey, interband electronic Raman scatt., threshold characts. 3-50580
 resistance jump in pure type I superconductors 3-52933
 segregation coeff. of Zn in Sn 3-69227
 static friction, effect of a.c. electric current on static surface friction 3-72127
 superconducting bolometer, receiving-amplifying system, i.r. radiation 3-73704
 superconducting film bolometer fluctuation effects 3-39883
 superconducting films, gapless, critical magnetic fields, temp. depend. 3-68722
 superconducting films, multiply connected, mag. field depend. of supercurrent 3-55383
 superconductor, Cooper-pair density, relax. time 3-41287
 superconductor in intermediate state, size effect, rel. to thermal cond. (*French*) 3-58336
 surface impedance in strong mag. field, cond. electron scatt. 3-72379
 thin film, α - and β -Sn, volume plasmon energy, density depend. 3-41221
 thin film, superconducting transitions, non linearity, low temp. technique 3-48390
 white, lattice dynamics, effect of conduction electrons, phonon dispersion relation 3-79448
 X-ray emission spectra, application of chemical effects in analysis 3-62353
 X-rays from superheavy quasi-atoms ($Z=130$) produced by bombardment with 25 MeV I ions 3-78596

- tin** continued
- Al-Sn, Cu, impurity-impurity interaction, pseudopot. calcs. 3-54976
- Al-insulator-Sn, supercond. thin films, tunnelling in vortex state 3-52936
- Al₃Ga_{1-x}As:Sn, liquid phase epitaxial growth, electrical props. 3-46764
- β -Ca₃(PO₄)₂:Ga⁺, Ge²⁺, In⁺, Sn²⁺, Sb³⁺, Tl⁺, Pb²⁺, Bi³⁺, phosphorescence (*Russian*) 3-50613
- Cu:Sn, low temp. lattice sp. ht. enhancement by Sn impurities 3-55087
- α -Fe₂O₃:Sn, hematite, Morin transition temp., Sn⁴⁺ impurity effects 3-72472
- GaAs epitaxial growth from liquid, incorporation of Sn 3-43955
- GaAs:Sn,Ge, epitaxial growth from liquid, electrical props. 3-46765
- GaAs:Sn films, epitaxial growth, effect of substrate orientation on growth rate in (111)-(100) range (*Russian*) 3-64255
- KCl:Sn, impurity centre investigations using Mossbauer effect and polarised luminescence 3-41456
- KI:Sn²⁺, negative mag. circular polarisation of A-band emission 3-44486
- NaCl:Sn, impurity centre investigations using Mossbauer effect and polarised luminescence 3-41456
- Ni:¹¹³Sn, valence effect in electromigration 3-75637
- NiO:Sn⁴⁺, impurity state determ. by Mossbauer spectra 3-72100
- ¹²¹Sb, hyperfine broadening of X-ray lines 3-49391
- Si in solution, etching, solubility, metal impurity effects, rel. to liq. phase epitaxy 3-69165
- α -Sn, electron beam induced n \rightarrow p transition, resistance and thermoelec. e.m.f. obs. 3-68614
- Sn-GaAs, interface, energy structure, Schottky barrier height, Fermi level 3-60916
- Sn-GaAs nonrectifying contact, resist. obs. 3-75793
- Sn-Nb₃Sn, supercond. junction, tunnel charact., energy gap values 3-75818
- Sn + O₂ \rightarrow SnO₂, matrix isolation i.r. study, characterisation of products 3-76427
- Sn⁺ ion implanted in steel, friction changes 3-47410
- tin alloys**
- see also tin compounds
- bell bronze, effect of composition on bell tonal quality 3-61140
- liquid, adiabatic compressibility and concentration fluctuations 3-54991
- Ag-Sn, dilute, dislocation mobility and temp. depend. of yield stress 3-49891
- Ag-Sn, liq., solubility of S, thermodynamics (*German*) 3-72882
- Al-Sn, liq., partial struct. factors and elec. resist. (*Russian*) 3-73444
- Al-Sn, soft structural component effect on damping power 3-58679
- Au-Sn phase prepared by splat cooling, metastability 3-64821
- Bi-Sn binary alloy, effect of ternary addition on positron annihilation, m.p. effects 3-68279
- CeSn₃, d.c. electrical resistivity determ., influence of 4f electrons 3-79674
- CeSn₃In_{3-x}, ¹¹⁹Sn n.m.r. Knight shifts and spin lattice relax. time 3-50480
- Co₂MnSn, Mossbauer determ. of nuclear mag. moment for ¹¹⁹Sn 3-52075
- Cu-Ag-Sn, elastic moduli, effect of Sn 3-64806
- Cu-Pb-Sn, elastic moduli, effect of Sn 3-64806
- Cu-Sn, liq., mag. susceptibility and elec. resist., anomalies 3-50342
- Cu-Sn, liquid, surface tension, density, temp. and comp. depend. (*Japanese*) 3-72820
- Cu-Sn, liquid, viscosity rel. to comp. (*Japanese*) 3-72819
- Cu-Sn, martensitic transform., phenomenological analysis (*Japanese*) 3-50680
- Cu-Sn, martensitic transform., deform. and recovery of form (*Russian*) 3-69189
- α -Cu-Sn, Portevin-Le Chatelier effect (*German*) 3-64907
- Cu-Zn-Sn, elastic moduli, effect of Sn 3-64806
- CuNi-Sn directional solidification, melt vs. cryst. comp., ternary distrib. coeffs. (*German*) 3-55762
- Fe-Sn, cast, hardness as guide to wear characteristics 3-55831
- Fe-Sn system α -solid solns., continuous and discontinuous precip. behaviour 3-64860
- Fe₃Sn, Mossbauer determ. of nuclear mag. moment for ¹¹⁹Sn 3-52075
- Fe₂TiSn, Heusler type alloy, cryst. structure and Curie-Weiss paramag. props. 3-58003
- LaSn₃, d.c. electrical resistivity determ., influence of 4f electrons 3-79674
- LaSn₃In_{3(1-x)}, local electronic props., paramag. susceptibility and n.m.r. meas. 3-46803
- Li-Sn, liq., struct., X-ray determ. 3-49827
- Nb-Sn superconducting solenoid, 50 kG gas cooled, operated at 13 K 3-73700
- Nb₃Sn, angular dependence of critical currents in transverse mag. field, microstruct. analysis 3-41296
- Nb₃Sn, chemically deposited, longitudinal and transverse currents from 14.5 to 17.5 K 3-44169
- Nb₃Sn, field, angular and defect dependence of critical current for $t \leq 4.2$ K 3-44168
- Nb₃Sn, fluxoid pinning on grain boundaries dependence on the mag. field direction 3-44166
- Nb₃Sn, phonon damping 3-49946
- Nb₃Sn, supercond., critical current density, temp. depend. 3-50298
- Nb₃Sn, supercond., cubic A-15 phase stabilization, a.c. heat capacity meas. 3-64422
- Nb₃Sn, supercond., shock wave synthesis from powder mixtures 3-69328
- Nb₃Sn multifilamentary composite wires, heat treatment effects on critical currents 3-60938
- Nb₃Sn supercond. cylinder, permanent multipole mag. field storage, charged particle focussing 3-42631
- Nb₃Sn superconducting tapes, microprocessing by electron-beam microetching 3-56978
- Nb₃Sn superconducting tunnel junctions, effective phonon spectrum by electron tunnelling 3-68737
- tin alloys continued**
- Nb₃Sn-Pb(Sn), sputtered film supercond. junction, tunnel charact., energy gap values 3-75818
- NdSn₃, d.c. electrical resistivity determ., influence of 4f electrons 3-79674
- NpSn₃, hyperfine interactions, ²³⁷Np Mossbauer obs. 3-68905
- Pb-Sn, corrosion-resistant, surface obs. by ESCA 3-76209
- Pb-Sn molten, diffusion of Cd 3-43886
- Pb-Sn solder to Nb-Zr wire, blob junction, self-field effects on Josephson supercurrent 3-52934
- Pb-Sn-Cu, elastic moduli, effect of Cu 3-64806
- Pd₂MnSn, local mag. ordering of ⁵⁷Fe impurities 3-79832
- PrSn₃, d.c. electrical resistivity determ., influence of 4f electrons 3-79674
- PtMnSn, Mossbauer obs. of hyperfine field at ¹¹⁹Sn site 3-68899
- Sn-Bi (1 wt.%), superplastic deform. enhanced grain growth 3-80230
- Sn-Cd, liquid, Knight shift and mag. susceptibility meas. 3-50483
- Sn-Cd, mag. field effect on directional solidification 3-80213
- Sn-Cd alloy system, temp. and conc. effect on mag. susceptibility 3-52959
- Sn-Cd eutectic, coarsening at room temperature 3-64844
- Sn-Cd unidirectionally solidifying binary melt, with natural convection, neutron radiography study 3-72877
- Sn-In unidirectionally solidifying binary melt, with natural convection, neutron radiography study 3-72877
- Sn-In-Tl, molten, effect on mech. props. of Sn-Pb alloy (*Russian*) 3-72897
- Sn-Pb, eutectic solidification front, thermal microanalysis (*French*) 3-59705
- Sn-Pb, mag. field effect on directional solidification 3-80213
- Sn-Pb alloy, brittleness development, molten metal effects (*Russian*) 3-72897
- Sn-Pb liquid, viscosity, temperature dependency, Arrhenius relationship, composition dependency, structural changes 3-50024
- Sn-Zn, liquid eutectic, effect on drilling of refractories (*Russian*) 3-76311
- SnCo, liquid, dil., Knight shift of ⁵⁹Co, importance of orbital magnetism in system 3-64572
- Sn_{0.86}Cu_{0.14}, amorphous strong coupling supercond., upper critical field, density of states at Fermi surface 3-41288
- Sn_{1-x}Mn_xTe, resistivity and Hall effect spin depend., exchange coupling const. 3-46859
- SnPb, interaction with NO₂, alloy composition effect 3-68484
- Ti-Al-Sn, material failure by environment-induced cracking, criterion development 3-69273
- Ti-Al-V-Sn, heat treatment effects on mech. props. 3-50727
- Ti-Al-V-Sn, stress corrosion cracking, influential factors and effect on anodic oxidation 3-47406
- Ti-Mo-Zr-Sn, β_{III} , isothermal transforms. (*French*) 3-80203
- tin compounds**
- see also tin alloys
- IV-VI compounds, matrix isolation studies of i.r. spectra, laser-excited emission bands 3-78804
- photoelectron spectra, binding energy shifts 3-54638
- tetra-allyl tin, vibrational spectra 3-46294
- Au-Se-SnO₂ system, amorphous optical memory obs., depend. on Se film thickness 3-50541
- BaTiO₃-SnO₂ solid solutions, quadratic electro-optical coeffs. (*Russian*) 3-80011
- Br₃SnFe(CO)₄⁻, vibr. spectra, bonding 3-78797
- CdGe, Sn_{1-x}As₂ vitreous alloy, thermal conductivity, comparison with microhardness, density 3-72238
- Cl₃SnFe(CO)₄⁻, vibrational spectra, bonding 3-78797
- Cu-Se-Sn system, DTA, X-ray phase analysis, microhardness, thermo-e.m.f. 3-72174
- Cu-Sn-Se system, DTA, microstructural and X-ray phase analysis, cross sections 3-72175
- Hg/SnI₂ arcs, absorpt., emission and temp. meas. 3-54887
- In₂O₃:Sn thin films, growth, fine struct., annealing effects, resistivity (*French*) 3-79593
- Nd₂O₃-POCl₃-SnCl₄ solutions Nd³⁺ luminescence, self-quenching 3-64713
- Pb_{1-x}Sn_xSe and Pb_{1-x}Sn_xTe, stimulated emission of light at 10 μ 3-50600
- Pb_{1-x}Sn_xTe diode lasers with improved mirror quality, high-power output 3-43024
- PbTe-SnTe-PbS system, thermal conductivity and structural study 3-79533
- SeOCl₂:SnCl₄ solution, Pr³⁺ doped, fluorescence spectra 3-76049
- Sn chalcogenides, radiation defects generated by (n, γ) reaction 3-72556
- Sn chalcogenides, small energy gap semiconductor, bond structure, review (*Polish*) 3-41131
- Sn complex, trimethylsilylmethyltin, HeI photoelectron spectra 3-54642
- SnAs, formed in decomp. of CdSnAs₂ and ZnSnAs₂, supercond. transition temp. 3-41022
- SnAs₃-Pb-SnAs ternary subsystem 3-49966
- SnCl radical, analysis of the α -X system (3400-3900 Å) (*French*) 3-49462
- SnCl radical, rotational anal., excited by Ar high tension discharge, ¹²⁰Sn, B² Σ^+ -X² Π_1 transition (*French*) 3-75006
- Sn(ClO₄)₂.3H₂O, SnBu₄, SnBu₃Cl₂ and SnBu₂SO₄, Mossbauer absorption spectroscopy meas. of after-effects of ^{119m}Sn isomeric transition 3-55985
- SnCl₄(SnBr₄) and tributylphosphate complexes, i.r. and Raman spectra (*French*) 3-46280
- SnF₂, matrix isolated, i.r. spectra 3-40630
- SnH₄, ground state energies and bond distances, stat. OCE calcs. (*German*) 3-67745
- SnI spectral bands between 215 and 250 nm 3-40612
- SnI₄, narrow-band charge transport, temp. depend. of carrier mobility, transient photoconductivity obs. 3-55263
- SnI₄ in soln., reson. Raman effects, stretching vibr. enhancement 3-75013
- Sn(II) complex, bis-(N,N-diethyldithiocarbamate) tin(II), crystal and molecular structure determ. 3-68202
- Sn(IV) complex, (CH₃)_{4-x}SnX_x, effect of donor atom and ligand size on crystal and mol. struct. 3-79330

tin compounds continued

- Sn(IV) complex, bis(2,4-pentanedionato)dimethyltin(IV), oriented single crystals and solns., laser Raman spectra, mol. struct. in soln. 3-47257
- Sn_{1-x}In_xTe, Hall coeff., thermoelec. power, elec. cond., rel. to In content 3-44098
- Sn₂Nb₂(Ta₂O₇), nonstoichiometric, Sn(II) and Sn(IV) valency states, Mossbauer obs. 3-50491
- SnO magnetic susceptibility anisotropy, mol. g_f-factor (*German*) 3-71538
- SnO₂, anal. of exciton absorpt. spectrum at 1.5, 4.2 K 3-41164
- SnO₂, antireflection coatings, moisture resistant vac. evaporation 3-62074
- SnO₂, crystal growth from vapour 3-80161
- SnO₂, film, sputter etching 3-79580
- SnO₂, from Sn + O₂ reaction matrix isolation i.r. study, characterisation 3-76427
- SnO₂, sintering, MnO₂ content effect (*Polish*) 3-44663
- SnO₂, sputtering, surface binding energy, temp. depend. 3-69119
- SnO₂ film, prep. by vapour deposition, elec. props., chemical composition depend. 3-44073
- SnO₂ film cold cathodes, electron emission into vacuum, obs. 3-41621
- SnO₂-CdSe n-n heterojunction, elec. and optical props. (*Korean*) 3-72399
- SnP, dissociation energy from SiP mass spectroscopic meas. 3-75096
- SnS, absorption spectra and valence band spectra 3-41534
- SnS₂, energy band calcs. by pseudopotential methods 3-41138
- Sn₃S₄, Sn₂S₃, identification by Mossbauer effect, X-ray struct. anal. 3-72548
- SnS₂(Se₂), electronic energy bands, local empirical pseudopot. approach 3-43998
- Sn_{1-x}Sb_xO₂ system, Mossbauer spectra, electronic structure 3-68890
- SnSe, absorption spectra and valence band spectra 3-41534
- SnSe₂, energy band calcs. by pseudopotential methods 3-41138
- SnTe, epitaxial film, thermoreflectance spectra from 0.7 to 5.6 eV 3-55622
- SnTe, semiconductor material, electrolytic synthesis 3-69168
- SnTe solid soln. with BiSe, cond., solubility 3-64179
- TiO₂-SnO₂ system, subsolidus equil. 3-76240
- (Zn_{1-x}Sn_x)Mn₃C, solid solns., magnetic, crystallographic properties (*French*) 3-79836
- (Zn_{1-x}Sn_x)Mn₃C solid soln., mag. and crystallographic behaviour, comp. depend. (*French*) 3-47050

titanium

- annealed, irradiation effect on Bauschinger effect 3-64945
- atom, ion induced K X-ray de-excitation spectra 3-54596
- cathode sputtering coeff., Ar, He and Xe discharges, role of ion capture (*Russian*) 3-69128
- chemical analysis methods, review 3-59694
- cleavage fracture in α -Ti 3-80296
- crippling allowances for elevated temp. and creep environments 3-64962
- discharge pump, for evacuation of mixtures containing Cl₂ 3-51563
- eddy current heating, megahertz frequencies, O layers on Ti, fatigue crack detection 3-45531
- electrochemical behaviour, neutral methanolic and ethanolic, NaCl soln., stress corrosion cracking 3-55959
- epitaxial growth on mica, crystallography and interfacial dislocations 3-55168
- e.p.r. in methylammonium alum, Orbach relax. rate anisotropy, dynamic Jahn-Teller effect 3-75877
- fatigue, work hardening, slip band form. and crack initiation 3-64891
- fatigue crack closure meas. 3-69274
- in Fe, cast, effect on spheroidisation of graphite (*Japanese*) 3-80359
- film, O implantation, TiO cermet struct. 3-72112
- high-pressure treated, orientation reln. between α - and ω -phases 3-72876
- impact by plane lead plate at 500 m/s, boundary instability (*Russian*) 3-64086
- low temperature behaviour, Debye temp., energy role (*Russian*) 3-79498
- lunar orange soil, low oxidation states 3-65849
- magnetic anisotropy and microstructure 3-53228
- micro-vial region behaviour, stress/residual strain curves (*Russian*) 3-58648
- neutron irradiation, fast vs thermal neutrons, defect production, elec. cond. monitoring 3-64073
- optical constants and electronic characts. 3-72594
- oxidation, anodic, review 3-41096
- oxidation from 25 to 100°C 3-55167
- oxidation products, diffuse reflectance spectra obs. (*French*) 3-69287
- phase transformation, $\alpha \rightarrow \omega$, hysteresis, T-P diagram (*Russian*) 3-44560
- plastic deform. under static and cyclic loading (*Russian*) 3-41762
- plastic shear props., high strain rates 3-58787
- α -quartz:Ti³⁺, electron spin resonance 3-79904
- saturated vapour pressure determ. by atomic absorption method (*Russian*) 3-48679
- selective etching, GaP, basic ferricyanide soln., Ti masking 3-41642
- sheet, produced by high rate vapour deposition process, condensation temp. influence on tensile props. and microstruct. 3-64851
- slip, orientation dependent, polycrystalline sheet 3-76164
- spectral analysis, fractional distillation for increased sensitivity (*Russian*) 3-77751
- steel/Ti, explosion weld, effect of hot and cold rolling 3-72927
- stress relaxation data interpret. 3-64926
- surface, polycryst., oblique Ar⁺ bombardment in 1 keV range, sputtering yield, ion incident angle depend. (*German*) 3-47342
- thermophysical properties near the melting point, enthalpy, entropy, heat of fusion, emissivity 3-72211
- thin film, Hz diffusion, coefficient, change in resistance meas. 3-51657
- thin film, single and polycryst., volume plasmon energy, density depend. 3-41221

titanium continued

- thin films, work function, Au and Ag substrates, ultra-high vacuum deposition 3-44130
- vacuum arc cathode, erosion and ionisation 3-57957
- vacuum brazing to ferrite ceramic 3-76229
- vacuum chamber liners, Cornell electron synchrotron 3-56727
- X-ray emission, K β , electron excitation, origin 3-71361
- X-ray emission K β , β' spectrum, fine struct. 3-67661
- X-ray emission spectra, electron structure 3-55700
- Al₂O₃ containing Ti, synthesis conditions and optical spectra 3-80171
- Al₂O₃:Ti³⁺, Jahn-Teller pot. energy, covalency effects 3-41149
- CdS:Ti²⁺, CdSe:Ti²⁺, e.p.r. spectra at 27K and 77K 3-47138
- CdSe:Ti, absorpt. spectra, oscill. strength, crystal field splitting and Racah parameters detn. 3-55652
- GaAs:Ti, Co compensated, elec. and optical props. 3-58266
- rel. to Li₂O-Al₂O₃-SiO₂ glass ceramic production 3-54928
- Ti-Ti targets, optimum thickness for production of 14 MeV neutrons by 150 keV deuterons 3-51682
- α -Ti, electric field grad. at Ta in group IV B metal 3-58458
- Ti I, II, III and IV, beam-foil lifetimes, absolute oscillator strengths 3-78426
- Ti I-IV atomic lifetimes and absolute oscillator strengths 3-46190
- Ti II, lifetime, transition moments and energy calcs. HF and perturbation theory 3-71352
- Ti-⁴⁷Sc corrosion of Ti, radiometric study 3-42703
- Ti:Mn(W)(Cu)(Mo)(An), neutron activation anal. 3-42703
- Ti/Mo wire reinforced composite, mech. props. 3-58719
- Ti²⁰⁺, lifetime meas. of ²³S, state 3-60372
- Ti²⁺ impurity in CdS, CdSe, Jahn-Teller struct. of absorpt. spectra 3-69035
- Ti³⁺ activator centres, in quartz glass, symmetry, e.s.r. and optical spectra obs. 3-64296
- Ti⁴⁺ migration in Ni₂TiO₄ solid solutions, spinel struct., distrib. 3-72454
- ZnSe:Ti, autoionisation of ³Ti(³P) state, photoconductivity meas. and absorption spectra 3-64375
- ZrSiO₄:Ti³⁺, 9300 MHz, 77K 3-79904

titanium alloys

- see also titanium compounds
- aged β -phase, long period superlattice 3-72878
- ageing, strength, ductility 3-80356
- b.c.c., with ω -phase, short-range struct., diffraction pattern interpretation 3-79198
- brazing, thermal microanalysis (*French*) 3-59705
- brittle rupture resistance (*Russian*) 3-80323
- commercial, low temp. deform. phenomena (*Japanese*) 3-44616
- commercial α and ($\alpha + \beta$) phase, grain growth kinetics (*Japanese*) 3-61144
- composite, bonded with finely cryst. diamond particles ω -Ti phase obs. (*Russian*) 3-73010
- cracking induced by solid Cd 3-69262
- creep, scale factor effect 3-64941
- creep and fracture, stress-rupture strength energy criterion, 400-550°C 3-58692
- creep dynamics, random stresses, statistical laws 3-80373
- crippling allowances for elevated temp. and creep environments 3-64962
- diffusion of hydrogen due to comp., temp. and stress gradients 3-64213
- ductility of VT3-1 rel. to heat treatment 3-76211
- electrical resistivity, exponential temp. dependence, rel. to Brillouin zone 3-44051
- embrittlement by hydrogen of α - β type alloy 3-64918
- fatigue crack closure meas. 3-69274
- fatigue failure, creep resistance, temp. depend. 3-76212
- fatigue resistance under asymmetrical cyclic loading, struct. effect 3-44635
- fatigue tests, h.f., energy dissipation 3-58695
- fracture, micromechanisms, hydrogen influence (*Russian*) 3-80322
- fracture strength under static and cyclic loads comparison 3-47424
- glass, elastic constants meas. by pulse echo method 3-48347
- high-strength, strengthening and rupture characteriz. 3-47429
- Inconel 718 type alloys, morphology of precipitates and thermal stability 3-69232
- large grained, superplasticity 3-64933
- large grained, superplasticity 3-64934
- machine parts, surface work hardening for increase of low cycle fatigue resist. 3-44632
- magnetic field effects on weld structure (*Russian*) 3-61184
- mechanical properties determined in high-speed extension (*Russian*) 3-53250
- mechanical strength AT-2 and AT-3 and welded seams, 4-700 K 3-61175
- metastable β -phase, hydrogen effect on ageing and precip. (*Japanese*) 3-41726
- oxidation, anodic, review 3-41096
- oxidation products, of TA6V alloy, diffuse reflectance spectra obs. (*French*) 3-69287
- shock-hardening, by laser 3-69291
- solid solution strengthening and phase stability, physical basis 3-64809
- strain curves, 20-400°C 3-58680
- stress analysis of tubular samples, influence of geometry on load carrying capacity (*Russian*) 3-76221
- stress relaxation data interpret. 3-64926
- tantalum, thin film preparation 3-64416
- Ti-Ni reactor component bonding, phase form. and diffusion behaviour 3-57571
- Ticalon, critical temp. of mag. change pt., apparatus development 3-53956
- Ticalon, domain struct. features (*Russian*) 3-72487
- Ticalon alloy, $\alpha \rightarrow \alpha + \gamma$ transformation, rare earth additions effect 3-80220
- two-phase, fatigue failure in vacuum (*Russian*) 3-41759
- two-phase, fatigue fracture topography 3-55816
- two-phase, microstruct. singularities of deform., rel. to ductility (*Russian*) 3-69216
- VT16, α'' -martensite decomp. (*Russian*) 3-72825

titanium alloys continued

- welding, max. heating temp. calc. (*Russian*) 3-41789
 Al-Ti, grain refinement by metastable phases 3-55793
 B-C-Ti indenters, high-temp. hardness meas. on refractories 3-80515
 Co-Ti-based Heusler alloys, mag. and chem. order 3-68791
 CoTi intermetallics, orbital susceptibility and ^{59}Co Knight shift, d-electron motion (*Russian*) 3-52954
 CoTiSb, Heusler type, cryst. structure and Pauli paramag. props. 3-58003
 Cr-Ti, oxidation, comp. depend. 3-58661
 Fe-Cr-Ti, titanium effects on strength 3-69283
 Fe-Cu-Ti-(C), micro- and macro-deform. resist., temp. depend. (*Russian*) 3-64835
 Fe-Mn-Ti-Si, martensitic, precip. hardening mechanism (*French*) 3-80303
 Fe-Ni-Ti, continuous decomp. of γ -solid soln. (*Russian*) 3-58621
 Fe-Ni-Ti, Invar type, Ti addition effect on phys. props. (*Russian*) 3-79883
 Fe-Ti, Fe-rich, sp. ht. 600-1150K, Curie temp. determ. 3-50363
 Fe-Ti (0.16 wt.%) single crystals, orientation, temp. and strain rate effects on deform. 3-64909
 FeTiSb, Heusler type, cryst. structure and Curie-Weiss paramag. props. 3-58003
 Fe₂TiSn, Heusler type alloy, cryst. structure and Curie-Weiss paramag. props. 3-58003
 Mo-Ti, (0.5 at.%Ti), thermal cond. and elec. resist. meas. up to 1200K 3-52817
 Mo-Ti alloy, sputtering from Mo target, film structure and lattice parameters (*Japanese*) 3-64777
 Mo-Ti (0.5%), neutron irradiat. temp. effect on hardness 3-79387
 Nb-Ti, ordered dislocation structure, hydrostatic pressure effects (*Russian*) 3-55788
 Nb-Ti, supercond., microstructure after cold deform., heat treatment 3-76182
 Nb-Ti (64 at.%) superconducting wires, critical current density anisotropy 3-64428
 Nb-W-Mo-Ti-Zr-C, quenching, ageing, carbide precipitation hardening 3-76176
 NbTi, 40/60 wt.%, supercond., critical current density, temp. depend. 3-50298
 NbTi, filamentary superconducting composite, stability behaviour, flux jumps 3-50292
 Ni-Fe-Mo-Ti-Nb, for mag. recording heads, mag. and mech. props. 3-44265
 NiTiSb, Heusler type, cryst. structure and Pauli paramag. props. 3-58003
 Pu-Ti, f.c.c. solid solution, retention at room temp. 3-76154
 Ti-Al, electrical erosion of crystal lattices, depend. on interatomic bond strength (*Russian*) 3-77749
 Ti-Al, strengthening by Al, local order mechanism 3-64919
 Ti-Al alloys, stress corrosion cracking mechanisms in methanol-ACI solns. 3-47401
 Ti-Al-Mn, hydrogen embrittlement, tensile and stress-to-rupture tests 3-69277
 Ti-Al-Sn, material failure by environment-induced cracking, criterion development 3-69273
 Ti-Al-V, crack detection, u.s. shear wave techniques, influence of residual stress 3-47514
 Ti-Al-V-Sn, heat treatment effects on mech. props. 3-50727
 Ti-Al-V-Sn, stress corrosion cracking, influential factors and effect on anodic oxidation 3-47406
 Ti-Al-V-Sn alloy, diffusion of H₂, meas. using non-reactive technique 3-72235
 Ti-C system, grain growth kinetics 3-64877
 Ti-Cr, aged, decomp. processes prior to omega phase detection 3-61148
 Ti-Fe, conc. depend. of constitution and plastic deform. (*Russian*) 3-58640
 Ti-Fe, electrical erosion of crystal lattices, depend. on interatomic bond strength (*Russian*) 3-77749
 Ti-Mo-C-N system, boundary phase stability and crit. phenomena 3-80212
 β -Ti-Mo-Cr-Fe-Al, recrystallization, microstructure, texture 3-76178
 Ti-Mo-Zr-Sn, β_{m} , isothermal transforms. (*French*) 3-80203
 Ti-Nb, superconductors, welding, reduction of current degradation 3-41788
 Ti-Nb-Zr, superconductors, welding, reduction of current degradation 3-41788
 Ti-Nb (35 at.%), heat treatment effect on microstruct. and supercond. 3-79800
 Ti-O system, grain growth kinetics 3-64876
 Ti-V, athermal $\beta \rightarrow \omega$ transform., interstitial oxygen effect 3-64827
 Ti-V-Cr-Al, cold work influence on stress corrosion susceptibility 3-69258
 Ti-V-Cr-Al, metastable, recrystallisation and X-ray diff. invest. of age-hardening (*German*) 3-72880
 Ti-Zr, wear resist. in H₂O, increase by oxide surface layer formation 3-58697
 TiCo, elec. resist. and mag. susceptibility meas. 3-52956
 TiCr₂, X-ray diff. study of Laves phase imperfections 3-69238
 TiFe, densities of states and K X-ray spectra, SCF calcs. 3-75705
 TiFe₂, thermal expansion rel. to Curie temp. pressure depend. 3-58385
 TiFe₂Co_{1-x}, magnetisation, weak itinerant electron ferromag. model 3-55442
 TiNi, twin and antiphase boundary formation, inhomogeneous shear mechanism, elec. resistivity anomaly 3-54972
 TiNi intermetallic, shape memory effect obs. (*Russian*) 3-80310
 U-Ti, fracture toughness and mode correl. with microstruct. 3-76414
 U-Ti (7 wt.%), texture 3-69228
 V-20% Ti, surface blistering by He ions, effect on fusion reactor operation 3-60289
 V-Ti, neutron irradiat., anneal hardening 3-79384
 V-Ti, neutron irradiat. effect on high temp. mech. props. 3-79385
 W-Cu-Ti, micro- and macrodeform. characts., foreign atom binding effects (*Russian*) 3-80271

titanium alloys continued

- Zn-Ti, hypereutectic, struct. controlling by unidirectional solidification (*Japanese*) 3-53206
 (Zr_{1-x-y}Hf_xTi_y)Zn₂ ferromagnets, itinerant weak, magnetic measurements, $0.05 \leq x, y \leq 0.2$, magnetisation, Curie temp. 3-52967
- titanium compounds**
see also titanium alloys
- alkali borate + TiO₂ mixtures, fused, acid-base reactions 3-58818
 basalt, Pacific Ocean, petrology observations, Curie temperature, remanence 3-58967
 c TiO₂, rutile, vacuum reduction 3-41800
 glasses, elemental anal., X-ray energy dispersive system, scanning electron microscope 3-45588
 oxides, TiO, TiO₂, Ti₂O₃, mass spectrometry evaporated by electron beam 3-75097
 silica glasses:TiO₂, small angle neutron scattering for inhomogeneous structure obs. 3-68169
 titania-silica glasses, thermal expansion meas. by photoelastic and u.s. techniques 3-51593
 titanian-chromian spinel series, Ti-poor chromite to Cr-poor titanomagnetite, layer formation, eastern Bushveld Complex 3-44762
 titanomagnetites Kirkland Lake, Ontario, Archean mafic volcanics, palaeomagnetic and petrologic correlations 3-58969
 BaO-CeO₂-TiO₂ system, subsolidus phase relations 3-44650
 CoFe_{2-x}Ti_xO₄, electrical conduction, a.c. resistivity and thermoelectric power measurements 3-50206
 FeTi₂O₅-Ti₃O₅ system, X-ray and Mossbauer obs. 3-58020
 Fe_{3-x}Ti_xO₄ oceanic basalts, low temperature oxidation causing carriers of natural remanence to become superparamagnetic 3-58971
 FeTi₂S₄, magnetic torque and magnetisation measurements 3-72491
 Fe₂TiSi₂, intercalation cpds., cryst. struct. and mag. props. 3-46623
 K₂TiSi₃O₉, crystal structure and hydrothermal synthesis 3-60716
 MgO-Al₂O₃-TiO₂ system, phase relations, 1100-1550°C 3-76339
 PbO-TiO₂-SiO₂ system glass, Al₂O₃ addition effect on glassy phase separation and crystn. (*Japanese*) 3-65023
 SiO₂/TiO₂ antireflection coating on glass, evaluation (*Czech*) 3-66189
 (Ti,V)₂O₃ systems, sp.ht. anomalies, electronic d levels 3-64303
 Ti complex (pyH)₃TiCl₆, Jahn-Teller manifestation in orbital triplet coupled to E_g and T_{2g} modes, magnetic susceptibility 3-46952
 Ti oxides, crystal growth and props., semiconductor-to-metal transitions (*German*) 3-53194
 Ti-S system polytypes characterization (*French*) 3-46633
 Ti-Zr-H system Knight shift obs., temp. depend. 3-79932
 Ti³⁺ fassaite, Allende meteorite, crystal structure and optical props. 3-45052
 TiB₂, sonic fatigue rel. to thermal shock and microstructure 3-69359
 TiB₂, thermal expansion, 25-1200°C, X-ray diff. obs. 3-44657
 TiB₂ crystal, metal bath growth, Knoop hardness (*Japanese*) 3-72130
 TiBr₄(Cl₄)(F₄)(I₄), orbital valence force field consts. 3-67768
 TiC, NaCl structure, band structure calc. 3-41142
 TiC, single cryst., prep. by r.f. floating zone process 3-53186
 TiC, single crystals and thin films, ESCA spectra 3-80142
 TiC in WC, diffusion mechanism during form. 3-64975
 TiC-Cr pseudobinary system, phase equilibrium relation 3-53270
 TiC-Mo-Ni-C cermet, microstructure 3-64833
 TiC-ZrC system, monochromatic emittance, 1800K, comp. depend. 3-52703
 TiCo₉₆, single crystals, microhardness, temp. depend., room temp. through ductile-brittle transition 3-47446
 TiCo₉₉, sintered, galvanomag. props., 300 and 20.4 K (*Russian*) 3-50222
 TiC_x, activities of Ti (*Japanese*) 3-50761
 TiCl₆²⁻, force consts. and mean vibr. amplitudes 3-67771
 TiCrAs, Fe₂P structure, crystallographic data, metal-metal bonding 3-79315
 TiF₃, photoelectron spectra, large satellite separations from core electron emission 3-69136
 TiF₃⁺, limited-structure valence bond wavefunctions 3-67757
 TiF₆³⁻, electronic spectra calc. by multiple scatt. method 3-52340
 TiFeAs, Fe₂P structure, crystallographic data, metal-metal bonding 3-79315
 TiFe₂Se₄, 3d-electron delocalization (*French*) 3-72550
 Ti(III)/Ti(IV) hydroxide, spectroscopic props. and interaction absorption 3-55606
 TiMnAs, Fe₂P structure, crystallographic data, metal-metal bonding 3-79315
 TiMnGe, TiFeSi structure, crystallographic data, metal-metal bonding 3-79315
 TiN, diffusion barrier in Ni based composite materials (*Russian*) 3-73012
 TiN, NaCl structure, band structure calc. 3-41142
 TiNb₂O₇, powder neutron diffraction determ. of cation distribution 3-60713
 ortho-TiNb₁₀O₂₉, powder neutron diffraction determ. of cation distribution 3-60713
 TiO, absorpt. coefficients for CO₂ laser radiation, rel. to interaction at metal surface 3-70837
 TiO, NaCl structure, band structure calc. 3-41142
 TiO effects on equil. among refractory phases of CaO-MgO-iron oxide system 3-44655
 TiO γ -system, rel. to vibrational temperature of stars δ^2 Lyr and α Her A (*Russian*) 3-61805
 TiO₂, amorphous thin film, d.c. and a.c. construction 3-75798
 TiO₂, effect of minor addition to BeO during sintering, upon densification and microstructure 3-69366
 TiO₂, film, in m.i.s. struct., dielec. props. obs. 3-50276
 TiO₂, phonon aided hopping of polarons, dielectric props. meas. 3-79647
 TiO₂, rutile, abrasion, material removal mechanism 3-44658
 TiO₂, rutile, chemical polishing with KOH-NaOH melt mixture 3-55162
 TiO₂, rutile, compressive creep in vacuum 3-44660
 TiO₂, rutile, Gruneisen coeff. for soft mode 3-41027
 TiO₂, rutile, thermodynamic analysis of lattice defects, H and D impurities 3-55218
 TiO₂, static compression, isentropic bulk modulus 3-41876
 TiO₂, trace element spectrochemical analysis (*Polish*) 3-73955

titanium compounds continued

- TiO₂, u.s. attenuation meas., c.w. acoustooptical and pulse-echo techniques 3-45427
 TiO₂ addition to ZrSiO₄, effect on sintering (*Japanese*) 3-80436
 TiO₂ antireflection coatings on fluorite lenses 3-62068
 TiO₂ compacts, sintering flash heating technique, kinetic study of shrinkage (*French*) 3-72996
 TiO₂ pigment, quantitative anal. of transition metal impurities 3-62335
 TiO₂ surface discharge development, nanosecond region (*Russian*) 3-46567
 TiO₂ thin film sandwich, ion scattering spectrometry, depth composition profile 3-40041
 TiO₂ thin films, goniospectrophotometer, reflectance and transmittance measurements, 0.25 to 1 micron polarised light (*French*) 3-39926
 TiO₂:Al, rutile, slightly reduced, paraelec. reson. at liq. helium temp. 3-55514
 TiO₂:Cr³⁺, w. maser 3-42988
 TiO₂:Cr³⁺, dynamic nuclear polarisation meas. of ¹⁷O spectrum, determ. of field gradient tensor (*German*) 3-50488
 TiO₂:Cr³⁺, Zeeman effect of no-phonon ⁴A_{2g}-⁴T_{2g} transition 3-53124
 TiO₂:Fe³⁺, hyperfine struct., e.p.r. obs. 3-58421
 TiO₂:H₂D, rutile, i.r. absorp., impurity conc. detn. 3-58530
 TiO₂-C adsorbents, water vapour adsorption 3-43931
 TiO₂-CdS, three-layer system, propag. of elastic transversal waves, dispersion eqns. (*Russian*) 3-55026
 TiO₂-K₂B₂O₃ system, phase equilibria diagram 3-68387
 TiO₂-Na₂O.B₂O₃ system, phase equilibria diagram 3-68387
 TiO₂-SiO₂ glass, Ne migration, activation energy, strain energy depend. 3-76330
 TiO₂-SiO₂ glasses, e.p.r. study of Ti³⁺-Ti⁴⁺ reaction 3-76418
 TiO₂-SiO₂-Li₂O-K₂O glass, n.m.r. spectra of ⁷Li, ion struct. 3-72528
 TiO₂-SnO₂ system, subsolidus equil. 3-76240
 Ti₂O₃, corundum struct., thermal expansion, X-ray diffr. obs. 3-64189
 Ti₂O₃, corundum struct. type, thermal expansion 3-69340
 Ti₂O₃, elastic const. through elec. transition, u.s. wave meas. 3-43821
 Ti₂O₃, pressure effects on the semiconductor-semimetal transition 3-79750
 Ti₂O₃, pure and V-doped, thermoelectric effects 3-58290
 Ti₂O₃, specific heat meas., anomalies near. elec. transition 3-43882
 Ti₂O₃, sputtering, surface binding energy, temp. depend., conversion to Ti₂O₃ 3-69119
 Ti₄O_{2n-1}, oxid. products of Ti and TA6V alloy, diffuse reflectance spectra obs. (*French*) 3-69287
 TiO₂.7Nb₂O₅, defect struct., high resolution electron microscope obs. 3-43804
 TiS₂, KKR energy band calcs. 3-46793
 Ti_{1.25}S₂, electron microscope structure obs., lattice fringe resolution 3-52610
 Ti_{1.50}S₂, electron microscope structure obs., lattice fringe resolution 3-52610
 Ti_{1.60}S₂, electron microscope structure obs., lattice fringe resolution 3-52610
 TiS₃, preparation, crystal structure determ. 3-40903
 Ti₃Se_{4-x}Te_x twinned cryst. prep. and struct. (*French*) 3-46634
 Ti₃Si₃, TiSi₃ and TiSi₂, electron structure from X-ray emission spectra 3-55700
 TiTaO₄, rutile structure, atomic and mol. ordering, mag. structure from 4.2 to 300K 3-79849
 TiC, TiN, TiO, heat of formation calc. 3-43878

Tokamak devices

- Adiabatic Toroidal Compressor, heating studies 3-68073
 Bootstrap equilibria, neutral injection, energy balance 3-79156
 British fusion research, history and future prospects 3-49728
 CLEO Tokamak neutral injection system 3-49769
 conductivity coeffs., possible direct meas. 3-49758
 construction at Frascati, including toroidal magnet and air core transformer 3-60640
 controlled thermonuclear reaction plasma, self-consistent energy balance studies 3-60637
 design for optimum power 3-63236
 fusion reactor, analysis of material constraints on superconducting CTR magnets 3-60167
 fusion reactor, conceptual design, system aspects 3-60641
 fusion reactors, comparison of warm and cold reinforcement magnet systems 3-60310
 fusion reactors, feasibility study of cooling schemes for blankets 3-60314
 fusion reactors, simplified parametric study 3-60642
 heating in a Tokamak plasma 3-68057
 inductive energy storage requirements 3-60306
 JFT-2 shell-less, leakage magnetic field measurement 3-52527
 low density reactor ignition by fast neutral atom injection, density build up with moving limiter 3-78388
 LT-3, runaway-electron drift surfaces and magnetic surfaces 3-63864
 MHD equilibrium, numerical calc. 3-49745
 MHD wave heating in Tokamak plasmas 3-68060
 multipole Tokamak equilibria 3-63861
 nonlinear heating effects 3-46545
 ohmic and neutral injection heating of Tokamaks 3-71938
 ORMAK neutral injection system 3-68071
 plasma generator, magnetic field analysis by finite element analysis 3-68078
 poloidal rotation decay 3-71861
 preionisation by TM mode 3-75402
 reactors, thermal stability analysis including anomalous diffusion and synchrotron radiation 3-60636
 slightly asymmetric, MHD equilibrium 3-40797
 ST, ion cyclotron heating expts. 3-68064
 ST device, ion cyclotron and fast hydromag. wave generation 3-54863
 tearing mode in cylindrical Tokamak 3-60608

Tokamak devices continued

- TO-1, with automatic control, plasma filament confinement, discharge characts. 3-46547
 Tokamak-6 device, runaway electron discharge regime 3-63834
 toroidal diffuse pinch, plasma processes discussion (*Dutch*) 3-49768
 toroidal effects on MHD modes in tokamaks 3-63827
 turbulent heating, high electric field effect on design 3-60644
 D-T fusion reactor, low-β, Li coolant performance 3-60315

topology

- see also graph theory
 convergence of C_p, p-norms 3-73981
 crystal electro-optics 3-72597
 Earth's topography, spherical harmonic analysis, correction 3-50867
 in general relativity 3-42871
 highly mobile Einstein spaces in the large, composition law and topological structure 3-57137
 Hilbert spaces, generalised operator domains 3-77765
 horizontal branch stars, topology 3-56381
 irregular surfaces, mathematical modelling rel. to fine-structure topography 3-51775
 polyatomic molecules and ions, genealogy in mol. spectroscopy, aromatic π-electron spectroscopy 3-63432
 turbulent gases, topological dissipation and small-scale fields 3-56303

torque

- blocks with transverse sections in form of multiconnected regions, plastic torque 3-42798
 earth core-mantle precessional coupling by inertial and dissipative torques 3-76536
 metal, hot torsion testing for flow stress determ. 3-76416
 polyurethane, elevated temp. creep under nonlinear torsional stress with step changes in torque 3-53284
 rarefield polyatomic gas, thermomag. gas torque, horizontal field effect 3-60522
 relativistic, on freely spinning rotor, application of Hubble's law 3-73438
 rigid strip, bonded to an elastic layer, static response 3-62451
 thermal torque in Scott effect expt. Knudsen effects 3-71701
 torque coefficient functional dependence of coaxial cylinders on gap width and Reynolds numbers 3-63673

torque measurement

- see also dynamometers
 liquid crystals, inertial coeff. determ. in rot. or vibr. e.m. fields 3-68155
 magnetic anisotropy, strain gauge anisometer 3-73671
 rotationally symmetrical e.m. field torque meas. (*Russian*) 3-59660

torque meters see torquemeters**torquemeters**

- capacitance, magnetometer, low field de Haas-van Alphen oscillations, small displacement measurement 3-56701

torsion

- see also elastic constants; stress analysis
 angle meas. using diffraction gratings with strong dispersion 3-48352
 bars, naturally uniformly twisted, plastic torsion and tension 3-40132
 biaxial split Hopkinson bar, for simultaneous torsion and compression of specimens 3-45425
 bodies of revolution, stress analysis by integral eqn. method (*German*) 3-57057
 bounds for torsional rigidity with no end warping 3-42793
 composite, C fibre reinforced plastics, shear damage effects on torsional behaviour 3-55856
 composite, fibre reinforced, dynamic props. in flexure and torsion 3-55855
 Cosserat surfaces of revolution, rotationally symmetric deformations 3-57065
 cylindrical shaft with half circular groove, torsion, stress distrib. (*Russian*) 3-45656
 elastic cylinder and a layer in joint torsion! stress-strain state 3-70558
 glass, torsional strength under hydrostatic pressure 3-65021
 glass reinforced plastic, cylindrical shell with elastic core, torsional stability 3-80449
 high vacuum torsion pendulum with low instrumental decrement 3-61988
 hot torsion tests for solid and tubular specimens, specimen geometry effect 3-55925
 large-deflection torsion of initially curved elastic strips 3-70578
 liquid crystals, smectic, continuum theory 3-40842
 metal, failure process in complex stress state, mechanism 3-58689
 metal, hot torsion testing for flow stress determ. 3-76416
 multi-disc rotor, joint deflectional-torsional oscillations (*Russian*) 3-42817
 plane stress, yield criterion, second order effects, tension-torsion loading 3-62489
 plate, pretwisted, harmonic vibrs. 3-57102
 polyurethane, elevated temp. creep under nonlinear torsional stress with step changes in torque 3-53284
 pretwisted rods, conservative end loading, theory 3-77813
 prismatic bar, dipolar stress theory 3-74015
 of prismatic bars 3-48715
 prismatic shaft of different materials, problem solution (*Russian*) 3-74014
 proper frequencies, critical anal. of Biot's method (*Italian*) 3-77832
 rigid circular body on inhomogeneous elastic stratum, torsional vibr. and shear modulus 3-57108
 rod, finite elastic cylindrical, partially bonded to infinite elastic cylinder 3-77819
 rod, twisted, contact stresses 3-70602
 semi-plate, elastic condition, infinite order algebraic system of eqns., iterative soln. (*Russian*) 3-77824
 shaft, circular, under torsion, concentration of stresses at base of long circular groove (*Russian*) 3-62477
 shells of revolution of variable thickness, torsional vibrations 3-42812

torsion continued

- slow crack growth test method 3-65048
- solid of revolution, nonhomogeneous material 3-59748
- steel, low-C and austenitic stainless, durability during low-cycle torsion in corrosive solns. (*Russian*) 3-80324
- steel, mild, tubular specimens, precise meas. of plastic behaviour under combined torsion/axial force 3-76199
- steel, torsional prestrain effect on Bauschinger effect 3-64928
- strand, response to axial and torsional displacements 3-72901
- testing machine, for programmed simulation of hot working 3-53836
- tests, plotting of flow curves, effect of specimen dimensions on slope (*German*) 3-73098
- vibration, torsional, circular (conical) shaft, two-rotor system, composite structure 3-74064
- vibration frequency measurement, dynamic shear modulus determination, thin ribbons 3-51526
- Al alloys, B/epoxy and glass/epoxy reinforced, torsional instability, elastic buckling strength 3-50778
- Fe, cast, deform. under high hydrostatic press., tests 3-64886
- Fe, cast, high tensile pearlitic, torsional fatigue damage evaluation, changes in fatigue props. and microhardness 3-53252
- Ge, screw type dislocations in threadlike crystals 3-68312
- Ni wire, excitation of torsional vibrs. 3-53008

torsion loading *see torsion***towers** *see poles and towers***town and country planning**

- urban planning and air pollution control, systems approach 3-81331

Townsend coefficient *see Townsend discharge***Townsend discharge**

- gases compressed, electrical strength, effect of electrode roughness 3-75446
- positive ions drift velocities (*Dutch*) 3-49778
- streamer chamber, three electrodes, neon filling <1 atm., ns HV pulse generator rel. to cosmic ray detection (*Russian*) 3-62252
- N₂, electron-molecule collision freq. in crossed elec. and mag. fields 3-71970
- N₂, secondary electron emission by metastable particle impact in ioniz. growth expts. 3-68116
- N₂, secondary electron emission by metastable particle impact in ioniz. growth expts. 3-68117
- O, first ionisation coeff. measurement in time resolved avalanche studies 3-68121

tracers*see also radioactive tracers*

- atmospheric tracer dispersion rel. to horizontal eddy diffusivity and height 3-59122
- biological tracer data analysis, exponential components of response, calc. by numerical technique 3-70177
- flow visualisation, turbulent mixing of liquids, dye tracer (*Russian*) 3-57745
- fluorescent particle atmospheric, containing Cd, health hazards discussion on paper by Dr. L.A. Spomer 3-66072
- hospital air movement study using gas chromatography 3-59699
- rarefied gas flow, rate meas., drift of marker ion, electron beam produced supersonic and nonisotropic currents (*Russian*) 3-45622
- trichlorofluoromethane, atmospheric level, tracer for air and water mass movements 3-65372
- ¹⁵N, isotopic analysis using opt. spectrometry, use for biological research (*Rumanian*) 3-62113

track visualisation, elementary particles *see particle track visualisation***track visualisation, particle** *see particle track visualisation***tracking***see also radar*

- Apollo Lunar Rover tracking using VLBI 3-65958
- Automatic Camera for Astrogeodesy, Czechoslovakia, ISAGEX-programme, satellite geodesy 3-48151
- geopotential determ. using satellite tracking 3-56075
- laser tracking stations, relative position determ. 3-56074
- Lunar Rover, differential radio interferometry appl. 3-45249
- satellite, by lidar 3-51196
- satellite position measurement, laser pulse method 3-48150
- satellite positions, Automatic Camera for Astrogeodesy, photographic obs. 3-48152
- station coordinates of Goddard Earth Model 3-56072
- vision, oculomotor tracking, two dimensional, recognition of component differences 3-77236
- visual tracking simulator 3-48616

tracking (insulation) *see surface discharges***tracking (sonar)** *see sonar***tracking systems***see also radar systems*

- astronomical theodolite using stepping motors (*German*) 3-42265
- laser, detection relationships rel. to return signal fluctuations 3-53919
- photoelectric, error signal storage, light sources (*Russian*) 3-45243
- star, digital, high accuracy, for advanced planetary missions 3-73565

tracks, particle *see particle tracks***trade** *see commerce***trade fairs** *see exhibitions***trade shows** *see exhibitions***training***see also education; teaching*

- Advanced Test Reactor personnel, available operating time improvement 3-74695
- nondestructive testing, video tape training programme 3-45402
- nuclear instrument and control technicians, basic elec. and electronics course 3-73645
- nuclear plant, operators 3-52223
- nuclear plant instructors, selection and development guidelines 3-73647
- nuclear power plant, operators 3-52225
- nuclear power plant operator, Brunswick Nuclear Plant training programme 3-73644

training continued

- nuclear power plant operator, on-site systems training, operator requalification 3-73643
- nuclear power plant operators, candidate selection, training 3-73629
- nuclear power plant operators, cold licence AEC exam., on-site systems training 3-73646
- nuclear power plant operators, selection and training 3-73628
- nuclear power plant operators, training, use of simulators 3-73648
- nuclear power plant personnel, Brunswick, Steam Electric Plant, start-up and operating procedures, emergency and fuel handling procedures 3-73641
- nuclear power plant personnel, operating procedures, manual for plant safety 3-73639
- nuclear power plant personnel, operating procedures, min. risk to health and safety 3-73638
- nuclear power plant personnel, Pilgrim Station, operating procedures, plant safety 3-73640
- nuclear power plant personnel, standards and operating procedures, safe and reliable plant operation 3-73642
- nuclear reactor, personnel 3-52222
- nuclear reactor, simulator, computer controlled 3-52226
- nuclear reactor personnel, operating procedures, standards and experience, conf., Myrtle Beach, South Carolina, USA (Aug 1973) 3-74691
- nuclear reactor plant operators, training, in-plant production of black and white video tapes 3-73649
- nuclear ship, merchant marine officers and engineers 3-52224
- pilot, using helmet mounted camera and display system 3-62168
- reactor operator, present state and future trends 3-52221

tramcars *see road vehicles***transducers***see also accelerometers; acoustic transducers; extensometers; Hall effect transducers; piezoelectric transducers; pressure transducers; strain gauges*

- air gap capacitor, for tensometer linear meas. 3-53842
- arterial dilation measurement, phasic diameter changes of arteries 3-59687
- biological, linear models and impulse train spectra 3-56497
- calorimetric, non catalytic coating, recombination vel. const. of N₂ (*Russian*) 3-63610
- displacement, developments in seismology, review 3-44934
- dual induction-differential translation transducer for creep 3-53833
- electroluminescent transducer for magnetostriction measurement 3-61986
- electromechanical, frequency responses, determination, impulse excitation Fourier spectra (*German*) 3-56624
- ferrite films for shear and surface elastic wave transducer 3-47351
- galvanomagnetic, supercond. test equipment for calibration 3-39975
- heat-flux, high temp. calibration 3-62020
- inductive dynamometer for fatigue testing machine, operation 3-76403
- i.r., for space use 3-45433
- Josephson junction, measurement applications 3-48474
- magnetic ferrite, metallic housing mat. (Ti), vacuum brazing 3-76229
- magnetically anisotropic, stress distrib. determ. in metals 3-76397
- Mossbauer digital spectrometer, multichannel analyser controlled 3-70438
- oceanic internal wave obs. using directional h.f. transducer 3-59038
- screened grid vacuum tube, for magnetic field strength measurement (*Russian*) 3-66285
- semiconductor strain transducer, description 3-51521
- torsional long-period vibration pickup, design and performance 3-61580
- velocity, dynamic calibration, linear air bearing sled system 3-59552
- vibration viscometer calibration 3-73969
- GaAs diode, temp. transducer in hydrostatic pressure region (*Polish*) 3-39876
- Ge film, stress and thermal energy transducer 3-56615

transducers *see saturable core reactors***transfer functions**

- biological transducers, using delta function trains 3-56497
- constant temp. thermoanemometer, for transfer function and dynamic properties study (*Russian*) 3-42737
- digital filter, approx. using Laplace transforms 3-66114
- EBR-II, nuclear reactor, noise anal., time-dependent fluctuations, reactivity transfer function, neutron detector power spectra 3-71215
- electro-optical m.t.f. of form $\exp(-f/f_c)^n$ 3-57208
- electron microscope phase contrast transfer functions, beam aperture influence (*French*) 3-66345
- fault tree analysis, new approach, application to nuclear reactors 3-46068
- fibre-optic components, modulation transfer functions, determ. from edge response curves 3-42974
- geomagnetic depth sounding profile analysis, Central British Columbia 3-76653
- glow discharge, positive column, equivalent circuit determ. (*German*) 3-52551
- image tube m.t.f. meas. by laser interferometer 3-56675
- modulation, degradation, mutual coherence of separated paths through atmosphere 3-77992
- modulation transfer function visualisation by speckle pattern techniques 3-51856
- MTF meas. in visible and i.r., interferometric technique for airborne expts. 3-51616
- MTF of form $\exp(-\omega/\omega_c)^n$, point spread functions, line spread functions, edge response functions 3-40220
- nuclear reactor, zero power transfer function measurement, reactivity oscillation technique (*Portuguese*) 3-46060
- optical, rel. to image evaluation 3-54204
- optical modulation, wide-angle camera lenses, new direct measurement method 3-53940
- optical m.t.f. analyser model FPK-1, description 3-59582
- phase contrast, electron microscopy 3-57001
- seismograph transfer function numerical inversion by recursive filtering (*French*) 3-76511

transfer functions continued

- seismometers, seismic noise, prediction convolving the microbarogram with a transfer function 3-80838
- thin transparent membrane, between phosphor and photosensitive material, modulation transfer function 3-66768
- underground explosions, simulation, generation of longitudinal and transverse waves, expression for transfer function 3-80603
- X-ray systems image quality, two dims. MTF evaluation method 3-51749

transferred electron devices

- see also *Gunn devices*
- LSA-like mode operation, Monte-Carlo simulation 3-55280
- material selection and preparation 3-80185
- GaAs, quasistatic analysis of velocity field characs. rel. to neg. differential mobility (*Polish*) 3-41192
- GaAs $n^+ - n - n^+$ diode, continuous multilayer epitaxial growth 3-41688

transferred electron effects see *high field effects***transfluxors** see *magnetic cores***transformations, phase** see *phase transformations***transformer insulation**

- see also *insulating oils*
- oil gases automatic analysis gas chromatography using automatic analyser 3-51759
- oils, detection of DBPC antioxidant by gas chromatography 3-66443

transformers

- see also *power transformers*
- e.m. analysis, boundary-value solutions (*Russian*) 3-45752
- e.m. field in screening semi-infinite solid, distribution due to currents in parallel conductors (*Polish*) 3-57181

transforms

- see also *Fourier transforms; Laplace transforms*
- $\sigma\pi$ vertex scale transformation of axial current (*Russian*) 3-59938
- Bogolyubov transformation in strong coupling theory 3-54279
- canonical, finite and infinitesimal, linear differential eqns. 3-62407
- complex, in $\pi\pi$ cross section determ. by Chew Low extrapolation 3-70986
- crack analysis using integral transform methods 3-40124
- cylindrical integral, linearised supersonic flow past harmonically vibrating cylindrical body 3-60555
- elastic cylindrical shell, echo-signal of finite spherical impulse, triple integral transformation soln. (*Russian*) 3-45690
- Hankel's integral, for soln. of deformation of semispace under action of surface load (*Russian*) 3-66549
- integral, for hydraulic impact in circular cylindrical shell 3-67955
- Lagrange's implicit function theorem rel. to Lie transform theory 3-66487
- lattice dynamics, Helmholtz free energy, Taylor expansion of potential energy, integral transformation of cubic term 3-40981
- Naylor, use in calculating steady state temperature distribution in spherical cone 3-62640
- nonlinear, effect on computation of weak solns. 3-71731
- orthogonal polynomial kernels, definition and applic. 3-48698
- perturbation eqn. integration procedure based on transformational behaviour 3-66618
- relativistic quasispace group, integration of infinitesimal transformations 3-57312
- statistical mechanics, transformations relating probability densities and correlation functions 3-74148

transient response

- see also *step response*
- acoustic noise, test techniques, steady-state and pulse-train (transient) acoustic meas. 3-51538
- electromagnetic, wire loop in homogeneous conducting sphere 3-76867
- e.m., of spherical conducting shell over conducting half-space 3-42933
- laminated plate, stress wave response to impulse load, mixture theory 3-70652
- small cavities, approximation 3-40205

transient stability see *stability***transient voltages** see *transients***transients**

- fast reactor, energy synthesis method, flux and bilinear flux few-group collapsing schemes 3-63116
- hollow elliptical cylinder transient current distrib. (*German*) 3-40200
- impulse voltages across sphere gaps and crossed cylinder gaps, influence of radiation 3-52548
- LMFBR, application of Pajarito Dynamics Code to power transient study 3-46082
- lumped parameter system, non-dispersive wave propag. by transient excitation technique 3-59476
- nuclear reactor containments, safety margins in pressure-temperature transients calc. 3-46091
- nuclear reactor operation, scram system trip, obs. (*Russian*) 3-67514
- nuclear reactors, liquid metal fast breeder, transient effects, minimisation 3-67506
- propagation in dispersive media, effect of losses 3-77942
- PWR protection system, effects of electrical underfrequency transients 3-46085
- semiconductor, totally depleted, transient photocurrent theory 3-64376
- n-Si, overdepleted, s.c.l.c., light pulse excited 3-64335

transistor-transistor logic

- see also *logic circuits*
- ECL universal counter, for counting speeds up to 110 MHz 3-40026

transistors

- see also *bipolar transistors; field effect transistors; phototransistors; thin film transistors*
- No entries

transit time devices

- see also *IMPATT devices*
- No entries

transit time noise

- e.p.r., computer meas. of experimental time const. 3-62191

transition functions see *transfer functions***transition metal alloys**

- see also *alloys of individual transition metals e.g. nickel alloys*
- see also *transition metal compounds*
- beryllides, supercond. investig. (*Russian*) 3-46927
- binary, electronic density of states, superposition model 3-79602
- dilute, actinide impurities, simple model of magnetism 3-50314
- dilute, electrical and thermal cond., phonon-induced interband transitions role (*Russian*) 3-44049
- electrical conduction, concentrated, disordered, low temperature coefficient of resistance 3-52822
- electron energy distribution, X-ray spectral investigations 3-43993
- electronic configuration, valence bond model, review 3-41309
- electronic heat capacity, alternative to rigid band model 3-79497
- ferromagnetic alloys, spin wave stiffness constant 3-75846
- fourth homologous class, spatial correl. of electrons (*German*) 3-79272
- lattice parameter and magnetic moment, Invar effect origin 3-52965
- liquid, Hall coeff., elec. resist. and susceptibility, rel. to electronic struct. 3-50112
- liquid, mag. susceptibility (*German*) 3-55418
- liquid, magnetic susceptibility, change at melting point, itinerant electron scheme 3-50343
- liquid, magnetic susceptibility, review 3-46982
- liquid, reson. scatt. and Ziman theory approach to resist. (*German*) 3-50169
- order dependence of electrical resistivity 3-64317
- pseudo potential band calculations, review 3-41320
- rare earth metal, hard mag. props. rel. to permanent magnets 3-44266
- rare earth transition metal silicides, structure types, X-ray obs. 3-58010
- rare earth-transition metal compounds, 3d states influence on stability, Fermi level, mag. props. 3-58002
- solid solution strengthening and phase stability, physical basis 3-64809
- superconducting transition point, effect of localised spin fluctuations 3-52930
- thermodynamic stability, generalized Lewis-acid-base interactions 3-64823
- Co-transition metal intermetallics, orbital susceptibility and ^{59}Co Knight shift, d-electron motion (*Russian*) 3-52954
- Ni-transition metal, dil., electronic sp.ht., virtual bound levels model (*French*) 3-46715
- Ni-transition metal alloys, thermoelec. power and elec. resist. near Curie point 3-44213
- Sb-3d-transition metal dilute liquid alloys, electrical resistivity, localised impurity states 3-72345

transition metal compounds

- see also *compounds of individual transition metals e.g. nickel compounds*
- see also *transition metal alloys*
- absorption from 35 to 33000 cm^{-1} of 3d iodates for characterisation 3-53120
- arsenides, structure, equiatomic and metal-rich compositions 3-40902
- arsenophosphides, structural evolution (*French*) 3-46629
- borides, perovskite structure, preparation, X-ray and metallographic studies 3-40907
- bridged metal-metal bonded species, spectra 3-78796
- carbide reinforced composite, directionally solidified, yield pt. phenomenon interpret. 3-64992
- carbide/ Al_2O_3 composites, sintering parameters correl. with mech. props. 3-73002
- carbides, ionicity 3-68186
- carbides, ordered vacancy arrangements, electron diffraction studies 3-40913
- carbides, Ostwald ripening in liq. Ni and Co (*German*) 3-41745
- carbides, perovskite structure, preparation, X-ray and metallographic studies 3-40907
- carbonyls, cyanides, mol. geometry, nodal features of mol. orbital approach 3-78658
- carbonyls in gas and liq. soln., vib.-rot. coupling effects on correlation functions 3-67825
- chalcogenides, cryst. chem. and semiconduction (*French*) 3-46847
- chelates, metal-DL- β -phenylalanine type, i.r. absorpt. spectra, normal coord. analysis 3-78771
- complex, metal pyridine tetracyanonickelate, i.r. and Raman spectra 3-63467
- complex, $[\text{M}(1,8\text{-naphthyridine})_4](\text{ClO}_4)_2$ and $\text{K}_4[\text{M}(\text{oxalate})_4]$, i.f. i.r. obs. 3-78776
- complex of 2,4-pentanedione ligands, 3-substituted, vibr. spectra, cryst. field effects 3-64650
- complexes, 3d, with N_2 , electronic struct. calc., N_2 bonding 3-71518
- complexes, allene ligand geometry, CNDO calc. of ligand excited states 3-60419
- complexes, electron relax. time determ. by ^{13}C and ^{14}N n.m.r. 3-75078
- complexes, linear relationships in ligand field theory rel. to optical spectra interpret. 3-63437
- complexes, radiationless relaxation processes 3-43473
- complexes, stability 3-54642
- complexes with organic ligands, exciton phenomena 3-72338
- crystallographic, mag. and nonlinear optic survey of 3d iodates 3-52609
- diarsine complexes, containing high oxidation state metals, i.r. study 3-78774
- dipnictides, crystal chemistry 3-40899
- Fermi surface, effect of bond formation 3-41143
- fluorides, octahedral, electronic spectra calc. by multiple scatt. method 3-52340
- germanides, structure equiatomic and metal-rich compositions 3-40902
- group IIIB and IVB complexes, cis-1,2-dicyanoethylenedithiolate ion, electronic and vibrational spectra 3-57654
- Group IVA carbides, nitrides, and oxides, superlattice structure 3-60717

transition metal compounds continued

- group Va carbides, nitrides, and oxides, superlattice structure 3-60717
 interstitial compounds, RY, (R=IVa or Va metal, Y=C, N, O), heat of formation calc. 3-43878
 iodides, S-containing complexes, adsorbed iodide, photo-electron spectra 3-41617
 $M^{II}M^{IV}F_6A$ (A=Rb, Cs, Tl; M=3d transition metal), structure mag. props. Mossbauer spectra 3-40880
 mixed valency pair compounds, electronic props. of one-dimensional solids, review 3-50134
 monoxide, band struct., and electronic props., X-ray photoelectron spectra obs. 3-46791
 nitrides, ordered vacancy arrangements, electron diffraction studies 3-40913
 octahedral anions, force consts. and mean vibr. amplitudes 3-67771
 oxides, sputtering, surface binding energy, temp. depend. 3-69119
 paramagnetic metal complexes, with porphyrin, quasiluminesc. and absorpt. spectra 3-72732
 perovskite type compounds, non-stoichiometry investigation (French) 3-64014
 perovskites, d-band, surface states and catalysis 3-46885
 phosphine and arsine complexes, metal localized emission 3-41855
 photoemission, valence-band structure 3-47348
 pnictides, M_2X , ($M_{1-x}M_x$) $_2X$, structure and magnetic interpretation 3-64469
 rare earth chalcogenides, $LnCrSe_3$ group, magnetic properties, resistivity and Hall effect 3-64497
 refractories, carbides, borides, kinetics of recrystn., deform., electron microscopy 3-72976
 solid, conf., Geneva, Switzerland, (Apr. 1973) 3-40897
 superconducting transition temperature prediction, Al $_5$ -type structure 3-41295
 transition metal complexes, $2E_g \rightarrow 4A_{2g}$ transition, vibr. anal. 3-76061
 transition metal complexes, Fermi-contact term calc. from unrestricted Hartree-Fock MO method 3-74934
 tungstates, i.r., Raman spectra assignments, valence force field calc. (French) 3-80020
 ultrafine powder, gas phase synthesis in a plasma, particle size 3-41827
 X-ray $L\beta_{2,15}$, $L\alpha_{1,2}$ and $K\beta_5$ lines shift due to chem. combination 3-55698
 X-ray spectra, interpretation, band structure calc. 3-41594
 ($Ni_{1-x}T_x$) $_2B$, electronic specific heat, transition metal impurities, density of states at Fermi level 3-41118
 Pt metal silicides and germanides, ordered pyrite structure, diamagnetism, semiconducting, valence electron conc. 3-40906

transition metals

- see also the individual transition metals e.g. nickel
 adsorption of O_2 , high temp., interaction model (French) 3-68495
 amorphous, superconductivity theory 3-72421
 cubic, elastic consts., electronic contrib. 3-54996
 elastic moduli meas. under hydrostatic press. by u.s. vel. method (French) 3-54994
 electrical and thermal cond. phonon-induced interband transitions role (Russian) 3-44049
 electron-phonon coupling calc., band structure parameters 3-79441
 electron-phonon mass enhancement factor, wave theory 3-68543
 electronegativity parameter, heat of form. and charge transfer for alloys 3-52594
 Fermi momenta, Compton profile of Cr for 3d electrons 3-52781
 ferromagnetism and photoemission 3-46969
 in InAs, distrib. in melt, under flux, radioactive isotope method 3-75626
 ion, core electron binding energy multiplet hole splitting 3-44021
 liquid, Hall coeff., elec. resist. and susceptibility, rel. to electronic struct. 3-50112
 liquid, Hall effect, spin-orbit coupling effect (German) 3-52826
 liquid, interionic pair potentials using Born-Green eqn. 3-43746
 liquid, magnetic susceptibility, change at melting point, itinerant electron scheme 3-50343
 liquid, magnetic susceptibility, review 3-46982
 liquid, resistivity, electron-ion potential, muffin-tin form. calculations 3-50176
 liquid, reson. scatt. and Ziman theory approach to resist. (German) 3-50169
 Lorentz function, high temp., band structure effects, electron-electron scattering 3-46823
 low symmetry ions, g-matrix of Zeeman spin Hamiltonian, diagonalization 3-64450
 magnetic model, effect of electron correlation on orbital interactions 3-72442
 multiplet hole theory, core electron binding energies, transition metal ions, X-ray photoelectrons spectra 3-52794
 plasma, collective excitation phenomena (Russian) 3-68571
 scattering mechanisms of conduction electrons, electrical resistance 3-41169
 solutes in liquid Cu, electromigration 3-79514
 spark-source mass spectrometry, quantitative anal. in TiO_2 pigment 3-62335
 superconducting, Knight shift and nuclear spin relax. calc. 3-55356
 superconducting state, energy spectra (Russian) 3-58328
 superconductor, type II, dirty, thermomag. effects near upper crit. field 3-46934
 superconductor impurities, magnetic and nonmagnetic cases, Hartree-Fock theory 3-60926
 surface, chemisorption of gases, one-dimens. square well model 3-55156
 surface, interaction with O_2 high temp. (French) 3-79574
 surface, relaxation, force constants, interatomic distances (French) 3-79757
 surface electron states 3-50255
 surface electronic properties, resonant d-level position 3-41245
 surface magnetic properties, resonances and spin reversal 3-41392
 surface reconstruction, electronic free energy 3-79758
 surface states, generalized, existence 3-64392
 X-ray emission spectra, L-series, of 4d group (Russian) 3-53155
 X-ray $L\beta_{2,15}$, $L\alpha_{1,2}$ and $K\beta_5$ lines shift due to chem. combination 3-55698

transition metals continued

- Fe group, shape of X-ray $K\alpha$ lines, fine structure obs. 3-71362
translation (language) see language translation and linguistics
translators (repeaters) see repeaters
transmission
 see also light transmission; power transmission
 Helmholtz eqn. and wave propagation in inhomogeneous media 3-48708
 mm wavelength, glasses, on line technique for thickness control 3-77486
transmission line theory
 e.m. field of line (Hungarian) 3-66722
transmission network calculations
 acoustic four-terminal transmission network, transmission loss by finite-element method 3-48289
transmission networks
 acoustic four-terminal transmission network, transmission loss by finite-element method 3-48289
transmitters
 bisensory stimulation, encoded signal transmitter for vibrotactile and visual stimuli 3-62305
transmitting see transmission
transparency see transparency
transparency
 see also light transmission; optical constants
 Atlantic tropical zone, transparency, attenuation coeff. rel. to density gradient, effect of plankton biomass (Russian) 3-47700
 atmospheric, determ. using limiting stellar magnitudes 3-47717
 cholesteryl nonanoate, effect of bulk impurities 3-55541
 high-molecular organic materials, aq. soln., optical density and refr. index, conc. depend. (Russian) 3-50860
 inhomogeneous waves in transparent isotropic medium, energy trajectories and flux lines 3-42967
 liquid crystals, reduction of switching time 3-45779
 liquid crystals as optical switches for hologram recording 3-45778
 liquids, meas. using scanistor photoelectrocalorimeter 3-73728
 macroscopic theory of self-induced transparency 3-66877
 ocean, attenuation coeff., effect of instrument movement, role of zoo- and phytoplankton (Russian) 3-47691
 ruby, self-induced transparency, temp.-depend phase memory 3-62747
 Sea of Azov, diurnal variations of transparency, light pulse method (Russian) 3-69564
 self-induced, Maxwell-Bloch equations, N soliton solutions 3-62734
 Tropical Atlantic, water transparency rel. to temp., salinity, density and relative turbidity (Russian) 3-47693
 Li-In discharge, high-current, space-time distrib. of plasma optical density 3-49749
 NH_3 gas, self induced with CO_2 laser pulses 3-66866
 $Pb_{1-x}La_x(Zr_{0.65}Ti_{0.35})_{1-x/4}O_3$ transparent electrooptic ceramics, fabrication by atmosphere sintering 3-55838
 Rh, films, mirrors, evaporated, reflectance, transmittance, optical constants, effect of surface dielectric films 3-66203
transport see transportation
transport equation see Boltzmann equation
transport phenomena see transport processes
transport processes
 see also Boltzmann equation; carrier density; carrier lifetime; diffusion; electrical conductivity; high field effects; plasma transport processes; thermal conductivity; thermal diffusivity; transport properties of superconductors; viscosity
 air, transport coeffs., calc. of distrib. functions, collision integrals, elec. cond. 3000 to 25000 K, 0.1 to 100 atm. (Russian) 3-57705
 atmospheric e.m. wave propagation, turbulence, transport velocity dispersion, influence of chaotic component of transport (Russian) 3-69592
 binary gas mixtures, entropy and transport coefficients calc. (German) 3-40694
 Boltzmann's equation, second law of thermodynamics 3-70750
 Boltzmann equation, equilibrium electronic transport, nonequilibrium electronic transport 3-72339
 Boltzmann generalized collision integral, theory, diagrammatic methods (Russian) 3-74164
 calculation procedures, theoretical bases and error characterisation of analytic methods 3-71328
 chemical/thermodynamic approach for electron exchange analysis of materials in contact (French) 3-79760
 classical and quantum systems far from equil., distrib. function 3-62605
 classical lattice system, two-dimensional, time evolution, dynamical theory 3-54173
 coefficients evaluation, analogy between Frisch-Berne and Watts perturbation theories 3-42910
 conductivity sum rule for free particles in cyclic box 3-62612
 conference, Providence, USA (1973) 3-70748
 dechannelling of ions, kinetic Fokker-Planck eqn. (Russian) 3-72107
 dense fluid, Enskog theory 3-72218
 dense fluid, perturbation theory 3-72221
 dense systems, statistical mechanical theory of kinetic equations 3-57168
 electrons, flight time distrib. in scattering medium in electric field, truncation procedure 3-51836
 energy transfer equations, nonlinear irreversible processes 3-59829
 Fokker Planck eqn. for elastic and inelastic scatt. in orbital clustering, solar system appl. 3-65627
 Fokker-Planck eqn., soln. method using chronological time operator (German) 3-66698
 Fokker-Planck eqn. soln. rel. to atomic coherent state representation of superradiance 3-66872
 Fokker-Planck equation, stationary soln. near detailed balance 3-77909
 gas mixture, indeterminacy in heat transfer (Russian) 3-67933
 generalised master eqns., statistical treatment of open systems 3-70754
 insulating materials, charge injection, storage and transport, review 3-46832

transport processes continued

- inverse transport coeffs., resist. formula 3-46822
- liquid, correlation for, laser light and n.m.r. techniques 3-72214
- liquid, fully renormalized kinetic theory of thermal fluctuations 3-64193
- liquid, isotope effects on motions in classical limit 3-64194
- liquid, molecular motion, conf., Orsay, France, Jul.(1973) 3-64192
- magnetic material, equations of motion for electron spin and trajectory 3-44093
- magnetospheric trapped charged particles, relations between transport eqns. 3-69689
- master eqn. for single mode radiation in cavity approach to equilibrium 3-42984
- master equation, Markovization 3-51837
- master equation, strongly interacting systems 3-70794
- matter at high temperature and pressure, rel. to structure of Jupiter and Saturn 3-69884
- molecular chaos assumption, non-Markovian behaviour 3-70749
- molecular gases, collision cross sections, rotational relaxation processes 3-71622
- m.o.s. structure, bulk lifetime detn. from capacitance and current obs. 3-55341
- multigroup eqns., Jacobian polynomials for description of γ -ray angular distrib. 3-40553
- nonlinear, anal. in terms of density expansions, mutual diffusion coefficient, viscosity 3-70753
- nonlinear dynamics of fluctuations, renormalization of kinetic coeffs. by projector-operator method 3-42901
- one component fluids, binary liquids, especially shear viscosity 3-72185
- one-dimensional hard rod system, kinetic theory, origin of divergences 3-74165
- particle transfer equations, nonlinear irreversible processes 3-59829
- Pauli's master equation, continuum thermodynamic limit 3-57166
- phase-space finite elements, two dims. transport calcs. 3-45733
- photon coherent-incoherent scattering by atoms, discrete ordinates transport calcs., computer program 3-74756
- photon transport in two-layered media, analytical determ. of build-up factors 3-74765
- proton transfer reactions, classical time correlation function theory 3-80522
- quarter space, two-dimensional transport, uniform source problem 3-62613
- radiation, class of second order approximate formulations of deep penetration problems 3-63243
- radiative transport, nonlocal variational formulation 3-70751
- Rayleigh's piston, spectral theory 3-70752
- relativistic kinetic theory (German) 3-57169
- semiconductor, in one dimens. superlattice 3-60868
- semiconductor, ionisation coefficients, nonlocalised property 3-58256
- solar corona, large scale drift transport of flare protons 3-65721
- solid, electronic, mathematical introduction, solved problems, book contrib. 3-58241
- systems far from thermal equilb., Fokker-Planck eqn. soln., distrib. function 3-54163
- technological problems, role of transport. props. of fluids and solids 3-71695
- thermoelectrical processes, Gyarmati's principle 3-77922
- two-level atom system, superradiant fluctuations, Brownian motion model, Fokker Planck eqn. soln. 3-54212
- unidirectional energy transfer in nonlin. wave-wave interactions 3-48816
- van der Waals, fluid mixtures near critical point, coeffs. 3-48817
- variation principles in quantum and classical theories 3-57167
- wire immersion heater, ion transport contrib. to enhanced ht. flux in non-uniform electric fields 3-60808
- X-ray transport theory, analytic method 3-74763
- Cs, in coated fuel particles in HTR with heavy burn-up (German) 3-71320
- FeAl, electron transport anomalies rel. to mag. props. 3-44053
- He to ~ 2 K, computer program 3-64225
- ^3He in superfluid ^4He , dil. soln., kinetic theory 3-46743
- ^3He - ^4He mixtures, transport coefficients, multiple-scatt. corrections 3-64230
- NiAl, electron transport anomalies rel. to mag. props. 3-44053
- Si, carrier lifetime, effect of edge dislocations 3-55270
- Si, heavily doped, general transport eqns. 3-55260
- SiO_2 , time depend. of injection currents, homogeneous charge trapping 3-46841

transport properties see transport processes**transport properties of superconductors**

- acoustic surface wave absorpt. 3-50303
- composite conductors, propag. velocity of normal and supercond. regions, calc. 3-64436
- conductivity, negative differential, due to nonlinear vortex response in strong elec. field 3-68733
- critical currents, type II materials, a.c. field effects, single explanation 3-41301
- critical-velocity model 3-79797
- dirty superconductor, Maki process, effect of elec. fields in excess electric current above transition pt. 3-75814
- dirty two-band superconductor, flux-flow props., mixed state, near H_{c2} 3-55373
- electron thermal conductivity of two band with an impurity 3-75815
- film of intermediate thickness, fluctuation cond. and dimensionality change 3-52931
- flux-flow resistivity in gapless superconductors, impurity effect 3-55372
- inhomogeneous film, theory of vortex motion 3-60932
- intrinsic resistive transitions, narrow superconducting channels, current-reducing fluctuations (Russian) 3-50306
- Josephson effect, destruction of, by fluctuations in order parameter 3-68738
- Meissner effect, parallel superconducting wires, planar array, current and current density distrib. 3-55359
- phonon fluorescence in superconductors 3-55362
- s-d scatt. supercond., temp. depend. of normal state resist. 3-58341
- thermal cond. and u.s. attenuation in superconds. with overlapping bands 3-55368

transport properties of superconductors continued

- thermal conductivity of intermediate state of superconductors 3-60936
- thin films, tunnelling conductance, temp. depend. in high magnetic fields 3-44174
- thin wire, crit. current, length depend. 3-44170
- transition metal, type II, dirty, thermomag. effects near upper crit. field 3-46934
- type I, kinetics of destruction of superconductivity for cylindrical wire submitted to longitudinal magnetic field 3-55364
- type II, flux flow resist. 3-64432
- type II, pinning forces, direct mech. meas. 3-46929
- type II materials, critical bulk and surface current density meas. in mixed state 3-41298
- type II superconductor, in longitudinal mag. field, power cryotron appl. 3-50300
- vortex pinning and irreversible processes 3-75812
- weakly coupled, current rel. to off-diagonal long-range order 3-79807
- weakly supercond., thin-film, Notarys-Mercereau structure, a.c. response 3-52935
- Al, electron-phonon interactions 3-55363
- Al film, fluctuation conductivity measurement, effect of perpendicular mag. fields 3-64429
- Al film, two-dimens., order parameter fluctuations ang. depend. in mag. field 3-50296
- Al-insulator-Al₂(Sn),(Pb), supercond. thin films, tunnelling in vortex state 3-52936
- Ge amorphous films, semiconducting to metallic phase transition, pressure induced, low temp. superconductivity 3-50247
- In, resistance jump in pure type I superconductors 3-52933
- In film, paracond. resistive depend. 3-55371
- In-Gd alloy, film, electron thermal cond., strong coupling effects 3-41300
- Lu, resist., 0.03-4.2 K 3-58338
- Nb-Ti (64 at.%) wires, critical current density anisotropy 3-64428
- Nb-Zr wire to Pb-Sn solder, blob junction, self-field effects on Josephson supercurrent 3-52934
- Nb₃Al_{1-x}Be₂(B_y), critical current density, magnetic field depend. 3-50286
- Nb₃Al_{1-x}M_y, M=Be, B, Al5 struct., critical temp. obs. 3-50297
- NbAl₂O₃ mixture type films, crit. current density, mixed state form., flux eddies, second crit. field (Russian) 3-68728
- NbN film, reactively sputtered, critical current anisotropy 3-50299
- NbSe₂, cond. meas. for temp. depend. of critical field ratio of superconductor 3-68720
- Nb₃Sn, chemically deposited, longitudinal and transverse currents from 14.5 to 17.5K 3-44169
- Nb₃Sn, critical current density, temp. depend. 3-50298
- Nb₃Sn, feasibility of nonphonon mechanism of superconductivity 3-41299
- Nb₃Sn, field, angular and defect dependence of critical current for $t \leq 4.2\text{K}$ 3-44168
- Nb₃Sn multifilamentary composite wires, heat treatment effects on critical currents 3-60938
- (Nb_{1-x}Ta_x)Al_{1-y}Ge_y, Al5 struct., critical temp. obs. 3-50297
- (Nb_{1-x}Ta_x)₃Al_{1-y}Ge_y, critical current density, magnetic field depend. 3-50286
- NbTi, 40/60 wt.% alloy, critical current density, temp. depend. 3-50298
- Pb, resistance jump in pure type I superconductors 3-52933
- Pb-Bi alloy, negative differential resist. at high current densities 3-44165
- Pb-Gd alloy, film, electron thermal cond., strong coupling effects 3-41300
- Pd-H system, electrical resistance in mag. field 3-64423
- Sn, intermediate state, size effect rel. to thermal cond. (French) 3-58336
- Sn, resistance jump in pure type I superconductors 3-52933
- Sn, thin film, superconducting transitions, non linearity, low temp. technique 3-48390
- Sn films, multiply connected, mag. field depend. of supercurrent 3-55383
- Ti-Nb(35 at.%) alloy, heat treatment effect, flux pinning 3-79800
- V, induced voltage due to flux line lattice dislocation motion 3-60937
- V-V₂O₅-Pb, Josephson tunnel junctions, mag. field depend. of critical current 3-58348
- V₃Si tapes, crit. current density, conc. and prep. conditions depend. (Japanese) 3-60934
- V₃Si tapes, made by new process 3-64430

transport theory see transport processes**transportation**

see also aircraft; road traffic

- balloons appl. 3-56257
- ceramic composites characteriz. for transportation 3-69338
- conference, Washington, D.C., USA, Oct. (1972) 3-42378
- gas jet recoil transport system, for radioactive products in neutron reactions 3-51671
- magnetic levitation forces, anal., effects of finite conductor size 3-40197
- noise and vibration, human response 3-59435
- nuclear fuel, spent, Yankee Atomic Electric Co. shipping experience 3-67576
- nuclear fuel via sea, licensing, German Atomic Law (German) 3-63185
- radioactive waste disposal, soln. 3-43294

transportation networks see transportation**transportation services see transportation****transportation systems see transportation****trapped free radicals see free radicals****traps, electron see electron traps****travelling-wave-tubes**

see also backward-wave tubes

No entries

treatment, heat see heat treatment**treatment, patient see patient treatment****treatment, surface see surface treatment**

treatment, water *see water treatment*

trees (mathematical)

- fault tree analysis, new approach, application to nuclear reactors 3-46068
- fault tree reliability analysis, totally automated probabilistic approach 3-46069
- minimal, conjecture of Gilbert and Pollak 3-70512

triboelectric emission *see electron emission*

triboelectricity

- see also static electrification*
- polystyrene, triboelec. props., xerographic powder manuf. (Polish) 3-76379
- styrene-methyl, ethyl and butyl methacrylate copolymers, triboelec. props., xerographic powder manuf. (Polish) 3-76379

tribology

- see also friction; lubrication; wear*
- drilling tools, eutectic Sn-Zn alloy effect on steel drilling (Russian) 3-76311
- metal-polymer contact, surface charge effects 3-46673
- stamp impression with friction and adhesion present, Fuchs type soln. 3-40969
- steel, persistence of asperities in indentation experiments 3-72125
- surface roughness generating mechanism, forming process of single asperity 3-43825
- thermoelastic instability in seal-like configuration 3-55021
- work of forces and external couples (French) 3-79421

triboluminescence

- tartrate crystals, triboluminescence and simultaneous charge produced at fracture 3-69045

triodes

No entries

triodes (semiconductor) *see transistors*

triple point *see thermal critical constants*

tritium

- for β sources (French) 3-53972
- N Atlantic, fallout tritium and mixing in main thermocline 3-59034
- battery, theory and performance, for microwatt range 3-53950
- breeding blankets for fusion reactors, expt. on ${}^7\text{Li}(n,n'\text{T})\text{He}$ reaction 3-60327
- concentration in North Pacific, liquid scintillation counting 3-69561
- counting by emulsion scintillators, external standard channel ratio method 3-66317
- D-T plasma, concentric laser cumulation 3-63855
- French production facilities (French) 3-57550
- fusion reactor power plants, environmental contamination 3-60319
- fusion reactor technology studies at ORNL 3-60320
- fusion reactors, inventories and leakage calcs. for conceptual power plant 3-60300
- fusion reactors, problems associated with use, mass transfer, isotopic separation and swamping 3-60301
- gas quantitative analysis (French) 3-57018
- Greenland snow, T and D content determ. 3-53572
- handling, radiation protection (French) 3-59458
- Havero meteorite radioactivity meas. 3-45066
- hot atom reactions with D_2 , H_2 and methane, stochastic and analytical investigation 3-65114
- HTG reactor, tritium release during normal running and fault condition 3-67455
- identification and exact meas. in gas sample (French) 3-57019
- internal contamination by tritiated water, dose equivalent determ. 3-73604
- inventory, fusion reactor, various conditions (German) 3-71331
- isotope separation using laser, use with controlled thermonuclear reactors 3-60299
- leak rate through steel, diffusion process theory (German) 3-71315
- monitor, continuous, for conc. in air 3-77301
- natural gas, radiation dose calcs., hypothetical exposure 3-78395
- neutron generating tube, design with tritium target, hot cathode and ion source 3-42633
- participation in water cycle (French) 3-59047
- plasma, two-temp., general eqns. for laser heating including fusion heat 3-60617
- Rydberg const., precision meas. 3-46177
- Rydberg const. exptl. determ. 3-46176
- sampler, atmospheric, ruggedized ultrasensitive 3-77302
- D-T and D-D fusion, neutron energies and spectra 3-40519
- D-T fuel, for mirror fusion reactor, 200 MWe, design study 3-60311
- D-T fusion, breeding ratio cross-section sensitivity in fusion reactor blanket 3-63098
- D-T fusion reactor, stationary and start up heating with fast neutral beam injection 3-79157
- D-T plasma, concentric laser cumulation, averaged equations numerical analysis 3-57922
- D-T plasma compression by laser beam, averaged equations 3-68040
- D-T plasma compression by laser beam, averaged description 3-68041
- D-T plasma heating, escape of α particles 3-49737
- D-T plasma heating by short laser pulses 3-54866
- D-T plasma in pulsed high-beta fusion reactor based on θ pinch 3-60303
- D-T pulsed reactor, calc. of Lawson criteria for exponentially decaying ion density and temp. 3-60623
- D-T small mirror fusion device, 14 MeV neutron flux capabilities 3-63857
- D-T theta pinch thermonuclear reactor, plasma energy direct conversion by high magnetic compression and expansion 3-63234
- D-T Tokamak reactor, low- β , Li coolant performance 3-60315
- DT plasma, fast α particle reactions 3-57925
- D-T inhomogeneous plasma, numerical analysis of thermal stability rel. to fuel injection 3-60619
- D-T tokamak, thermal stability analysis including anomalous diffusion and synchrotron radiation 3-60636
- LiF, growth of V_k -centres by beta-rays from irradiation produced tritium, e.p.r. 3-72519
- T-Ti targets, optimum thickness for production of 14 MeV neutrons by 150 keV deuterons 3-51682

tritium continued

- T + H_2 , T + D_2 , and R + HD exchange collisions in 10 eV range, prediction of spectator stripping dynamics 3-76453
- T + methane hot atom reactions, energy-dependent cross sections 3-44737
- T + methyl fluoride hot atom reactions, substitution processes 3-44738

tritium compounds

- T_2O , ruggedized ultrasensitive field air sampler 3-77302

triton interactions

see also nuclear reactions and scattering due to tritons
No entries

triton scattering

see also nuclear reactions and scattering due to tritons
No entries

tritons

- cluster exchange in reaction ${}^7\text{Li}(\alpha, \alpha)$, 8.6-12.5 MeV and 17-22.5 MeV 3-63071
- production spectra in 30 to 60 MeV proton bombardment of nuclei with A = 12 to 209 3-74588

trolleybuses *see road vehicles*

troposphere

- see also tropospheric electromagnetic wave propagation*
- aerosols, summer background level over Greenland and N. Atlantic Ocean 3-47756
- Australia, monthly mean wind patterns at 40000 feet 3-59055
- detection using forward scatter c.w. radar 3-59188
- dynamics of upper troposphere rel. to Nimbus 4 THIR 6.7 μ water vapour data 3-59107
- equatorial rainfall, effect of disturbances in subtropical westerlies upon jet stream 3-80761
- general circulation in Tropics and polar stratosphere meridional interaction 3-65382
- general circulation model, mathematical eqns. 3-69590
- general circulation parameters calculated from SIRS data 3-59106
- heating, gravity waves 3-76906
- hemisphere heating, parameterisation temperature variance fields 3-76779
- ion chemistry, extension from D-region, reaction schemes 3-59076
- i.r. absorption, separation of absorbers in 8-13 μ region 3-76719
- Japan, Southwest Islands, wind and thermal structures (Jan 1968) 3-76717
- kinetic energy budgets of mid-latitude synoptic scale systems rel. to general circulation 3-59108
- leewaves and winds over Canterbury, New Zealand during 1970 3-59059
- methane budget, photochemical model 3-73311
- methane mixing ratio, vertical profiles 3-73306
- microthermal turbulence, balloon-borne temp. sensors, wind speed profile, wind shear calc. 3-44884
- mid and upper troposphere, anomalous warmth during 19-21 Feb 1964 period 3-47742
- mobility spectra, tropospheric and stratospheric gas mixtures, drift tube, mass spectrometer, ageing effect 3-59069
- noctilucent clouds, effect of tropospheric turbidity on visibility (German) 3-76729
- Patna City area, 1967 September 19-20, exceptional rainfall rel. to mid-tropospheric easterly and westerly waves interaction 3-51016
- periodic atmospheric circulation with 14-16 days cycle 3-59105
- remote sensing of wind velocity in lower troposphere using acoustic sounder 3-65518
- scanning f.m.-c.w. radar sounder for tropospheric sensing 3-42083
- seasonal changes, pressure gradient, wind circulation and rainfall, India 3-80747
- small scale structure, variations of temperature, humidity and refractive index, effect on radiowave propagation 3-65313
- solar corpuscular radiation, effect of variations on weather 3-80767
- stratified layers, trans-horizon propagation techniques for examining disturbances 3-65522
- stratified turbulent layers, forward scatter radio techniques 3-65521
- stratospheric air masses, influx into lower troposphere, after solar flares 3-41969
- trace element, global distribution (Russian) 3-73296
- trace gas concentration fluctuations, model 3-51030
- tropical waves, spectral model of Cisk-barotropic energy sources 3-65385
- turbulent diffusion, appl. to pollution 3-59087
- turbulent waves on tropospheric inversion producing sudden changes in temperature and wind 3-65383
- vertical velocities, from serial soundings using heat balance method 3-65389
- wet zenith range correction of refraction, surface meas. method 3-59191
- wind and static stability rel. to lee waves and convective cell patterns 3-53487
- zonal harmonic standing pressure waves, slope with height in troposphere 3-59109
- zonal harmonic standing waves in troposphere and lower stratosphere 3-65351
- ${}^{37}\text{Ar}$ activity variation (German) 3-51013
- C-H chemistry, temporal model 3-73310
- CO budget, photochemical model 3-73311
- CO₂ concentration 3-73328
- CO₂ content 3-73327
- S compounds in aerosols rel. to major volcanic eruptions 3-59058

tropospheric electromagnetic wave propagation

- long distance, above 1000 MHz (German) 3-76785
- randomly inhomogeneous troposphere, propagation of laser radiation and diagnostics (Russian) 3-69732
- range meas. effects at oblique angles 3-56249
- refractivity var., use of radiosonde data in range correction 3-76786
- wet zenith range correction of refraction, surface meas. method 3-59191

truth tables *see formal logic*

TTL *see transistor-transistor logic*

tubes (electronic) *see electron tubes*

tuners *see tuning*

- tungsten**
- abundance in oceanic and continental basalts 3-65221
- adhesion coefficients of O₂, (100) and (110) planes, 78-950K (*Russian*) 3-79558
- adsorbed Ge, field emission study 3-64764
- adsorption and desorption kinetics of CO, N₂ 3-79568
- adsorption of Ba on W(112) face 3-72770
- adsorption of Cs, H₂, LEED and workfunction investigation of C(2×2) structure 3-55145
- adsorption of O₂, oxidation, secondary ion mass spectrometry and electron-induced desorption investigation 3-75669
- adsorption of O₂ coverage at 78 and 973K, field ion investigation 3-46752
- adsorption of oxygen, 1800-2750 K, Auger spectroscopy meas. (*German*) 3-52749
- adsorption of Pb on single crystal faces, energy meas. (*French*) 3-79565
- adsorption of transition atoms, binding energy determ. 3-75668
- atomic oscillator, He atom collisions, unitary transition probabilities 3-74827
- bicrystal, misalignment angle influence on brittleness (*Russian*) 3-69215
- carburizing in glow discharge plasma 3-76217
- cathode, electron emission processes 3-54885
- chemical analysis, review 3-59695
- chemical vapour deposition kinetics, 6-60 Torr, 500-870°C 3-41628
- chemisorption, concept of surface molecule 3-75677
- chemisorption, of α -CO, i.r. spectra, reflection-adsorption, ultra-high vacuum 3-44417
- chemisorption of CO, desorption kinetics, lateral interaction model 3-46759
- chemisorption of CO, desorption spectra, electron stimulated desorption 3-46758
- chemisorption of CO using combined flash desorption and electron stimulated desorption techniques 3-55158
- co-adsorption of NaI and Hg, field emission obs., work function determ. 3-80145
- coadsorption of Cs and H₂, LEED and work function measurements 3-75665
- coadsorption of Cs and O₂, work function 3-75666
- composite, filamentary, prestrain effects on tensile props. 3-64996
- condensation on its own surface 3-52752
- conductor, cylindrical, thermodynamics of explosion, first phase 3-63901
- dechannelling of H⁺, ³He and ⁴He ions, expt. obs. 3-49916
- desorption, electric field, of Yb and Nd ions (*Russian*) 3-68504
- desorption of K, mol. beam meas. of residence time 3-60839
- desorption of La and Nd, determination of kinetic characts. by temp. modulation method 3-50080
- diffusion of He atoms, vacancy mechanism, migration activation energy 3-68443
- ductile/brittle transition phenomena, struct. factor changes (*Russian*) 3-55753
- dust particle erosion rates 3-76279
- electrode erosion in H₂ arc discharge, effects of electrode temp. (*Russian*) 3-52542
- electron emission, gun for microscope, parallel plate 3-66378
- electron field emission, long time current stability at 2×10⁻⁷Pa, residual gas and heating effects (*German*) 3-69141
- electron field emitter, lifetime, noise levels, pressure, current 3-66374
- electron impact desorption of H₂, D₂ isotope effect 3-79572
- electron impact desorption of hydrogen, deuterium isotope effect 3-64246
- emitters, K-covered, noise spectral densities, field emission flicker noise theories, diffusion induced 3-76122
- energy loss of 2.0-MeV ⁴He ions, meas. 3-40944
- enthalpy meas., calorimeter calibration 3-72208
- exploding wires with high energy input 3-68128
- FEM tip, microcrater form. on microparticle bombard. at limited field emission currents 3-44523
- fibre reinforced Cu composite, phys. props. rel. to fibre vol. and prep. technique 3-64986
- fibre reinforced fused SiO₂ composite, hot pressing, mech. strength 3-76360
- fibre reinforced Si₃N₄, strength characteriz. for high temp. applics. 3-76352
- fibre reinforced zirconia, thermal shock resist. 3-76353
- fibre-reinforced UO₂ composite, melt-grown, selective chem. etching for electron emitter applics. 3-75680
- field emission energy distribution, 78-950K, electron-phonon interactions 3-69145
- field emission of hot electrons, expt. and barrier penetration theory explanation of results 3-44524
- field emitter, field induced oxidation 3-64767
- field ion microscope images, bright spot contrast interpreted as (011) ledge W atoms 3-54894
- film growth, phase composition and structure, mol. beam deposition 3-79592
- fracture surface energy rel. to thickness, 77K 3-55015
- grain boundaries, large-angle, formation under mech. stresses 3-55786
- hemispherical total emittance from hot wires as function of temperature 3-62021
- high angle grain boundaries, regular defect structs. 3-40920
- high temp. thermophysical props. 3-72975
- impurity analysis, separation methods (*Hungarian*) 3-70480
- interstitial plasticity of microcrystals, FIM study 3-60766
- ion irradiated, field ion microscope study of point defect struct. 3-79392
- low temperature behaviour, Debye temp., energy role (*Russian*) 3-79498
- low-impedance W microelectrode for recording from sensory ganglia 3-56993
- matrix isolation spectra using triode sputtering source 3-61046
- microdeformation and macrodeformation characts., foreign atom binding effects (*Russian*) 3-80271
- monochromatic emissivity at high temp. 3-69352
- needles, drawing out by elec. field, 10⁷ V/cm, 2300-2700K 3-45563
- tungsten continued**
- neutron irradiated, irr. temp. monitoring, void superlattice const. meas. 3-68291
- neutron irradiated, void formation, lower threshold temp. 3-68290
- permeability of hydrogen, in mono- and polycrystals. (*Russian*) 3-58144
- photoelectric L-shell cross section of 32.88 keV photons 3-50641
- photoemission, directional, normal to (100), (110) faces, surface states and band structure 3-55725
- plasma, laser induced, energetic ion origin 3-75392
- plasma coatings on Armco iron, form. kinetics and physico-mech. props. (*Russian*) 3-80318
- plastic deformation and annealing of single crystals, struct. changes (*Russian*) 3-58624
- powder, swaged, diffusion of ⁵⁹Fe and ¹⁸⁵W, autoradiography, 1300-1900°C (*Hungarian*) 3-72987
- powder compacts, low temp. sintering (*Korean*) 3-53264
- powder metal after hydroextrusion, physico-mech. props. (*Russian*) 3-72922
- quenched, defects behaviour, superfluid He quench 3-79344
- recrystallization texture of rolled sheets (*German*) 3-55792
- ribbon lamps, self calibration by relative meas. of spectral, integral radiant energy 3-73751
- secondary electron emission, anisotropy, 300 K 3-55715
- self-diffusion, surface, influence of adsorbed Ni layer, field electron microscope study 3-43940
- single crystal, temp. dependence of Hall effect, Nerista-Ettinghausen effect, elec. resistivity and thermo-e.m.f. (*Russian*) 3-68600
- sputtering of clusters from W single cryst. surface, angular depend. 3-61091
- sulphurization 3-50089
- superconductivity, crit. field, normal state heat capacity 0.35-25 K 3-79785
- surface, (100), (110) and (111) cryst. faces, NH₃ catalytic decomposition 3-55987
- surface, (100) single crystal O₂ adsorption 3-79564
- surface, (211) H₂ chemisorption 3-72272
- surface, atomically clean, Auger electron spectroscopy 3-76116
- surface, condensation of metal vapours 3-79562
- surface, electron induced O⁺ desorption cross section, temp. depend. 3-75675
- surface, polycryst., oblique Ar⁺ bombardment in 1 keV range, sputtering yield, ion incident angle depend. (*German*) 3-47342
- surface atomic struct., effects of high hydrostatic press. 3-41069
- surface structure, anisotropic change during directional transport processes 3-55130
- surface structure, electron spectroscopy (*Hungarian*) 3-72256
- surfaces, (100) and (110), heat of adsorption of Ba 3-55151
- surfaces, adsorbed CO, field-emitted electrons, total energy distrib., appl. to binding models 3-41618
- thermal expansion at high temp. 3-69351
- thermal expansion meas., 293 to 1800 K, twin microscope method, Fizean interferometry 3-46720
- thermal expansion of sintered W, cooperative meas. techniques from 1000-2600°C 3-48376
- thermographic method to study rapid crystn. of molten W on cooling 3-45452
- thin films, deposited by r.f. sputtering, microstructure growth, resistivity and stresses 3-43959
- thin films, laser-induced anisotropic thermoelectric voltages 3-60867
- vacancy generation by rapid rate deform. at elevated temps. 3-80234
- vacuum deposited, dislocation struct. changes due to thermal cycling (*Russian*) 3-53245
- vapour pressure and heat of sublimation measurement 3-64172
- wetting of Ag, hot-filament silver vapour source 3-39892
- wire, high temp. creep, grain boundary cavity formation rel. to filament lifetime (*Hungarian*) 3-72988
- wire, Ni-based composite material penetration, TiN barrier (*Russian*) 3-73012
- wire, recrystallization, impurities, creep, research review (*Hungarian*) 3-72989
- wire fibre, reinforcement for sintered W-Ni-Fe composite 3-69370
- wire reinforcement of Ni, diffusion, carbide layer formation, recrystallization rel. to weakening (*Russian*) 3-53272
- work function, determ. from surface ionisation and discharge triggering (*Russian*) 3-44506
- work function determ. by field emission, effect of adsorbed gases (*German*) 3-47350
- work function determ. near melting point using d.c. arc 3-69132
- HfO₂/W composites, Y₂O₃ stabilized, unidirectional solidification behaviour 3-61203
- Nb:W, Ta, impurity redistrib. by electron beam float zone refining 3-44540
- Si:W, negative differential cond. in carrier capture by repulsive centres, double injection conditions 3-50216
- W and Mo bearing seam, X-radiometric logging of boreholes (*Russian*) 3-73395
- W:Be doped filament, strength, secondary β -W formation (*Hungarian*) 3-72986
- W:Si(C), work function depend. on adsorbed layer thickness, electron field emission obs. 3-43930
- w:Th, sensor, u.s. thermometry, temp. meas. up to 2400C, inaccessible objects 3-42521
- W/Au-SiO₂-Si, low temp. treatment at 300 to 400 C, H₂ ambient, change of threshold voltage meas. 3-55337
- W/O₂ system, surface structure, RHEED intensities, kinematic anal. 3-55126
- W-Ge-Ni, point contacts, submm. wave detector (*Russian*) 3-73805
- W-X-O-H systems, X-halogen, gas phase composition and chem. transport reactions (*German*) 3-44747
- W(112)-O₂ system, adsorbed layer models, LEED and optical diffraction pattern comparison 3-68500
- tungsten alloys**
- see also tungsten compounds
- (7.9 and 2.3%), Ta-W-Hf neutron irr. effect on tensile props. 3-79386

tungsten alloys continued

- Al-W, Al-rich, liquid-quenched, metastable phase behaviour 3-41696
 Co-W-P, electrolytically deposited, mag. props. (*Russian*) 3-64531
 Cu-W composite, diffusion of Ni (*Russian*) 3-53222
 Fe-Ni-W, struct. changes during ageing of martensite (*Russian*) 3-80247
 Fe-W, redistrib. of atoms, Mossbauer obs. (*Russian*) 3-53223
 Fe-W alloys, thermodynamic variables, calcs. from phase diag. 3-64818
 Fe-W binary system, tungsten solubility in α and γ phases (*Czech*) 3-55771
 Fe-W melt, N_2 diffusion, addition effect (*German*) 3-47363
 Mo-Ti (0.5%), fast reactor neutron irradi., effect on tensile props. 3-79386
 N-W solid soln., interdiffusion coeffs., conc. depend., correl., with solidus line shape (*Russian*) 3-41712
 Nb-W-Mo-Ti-Zr-C, quenching, ageing, carbide precipitation hardening 3-76176
 Ni-Co-W, struct. changes during ageing of martensite (*Russian*) 3-80247
 Ni-W, thermo-e.m.f., temp. depend., 77-1300K (*Russian*) 3-72346
 Ni₃(Al,W) single crystals, yield stress, dislocation rearrangements 3-80298
 Pd-W solid soln., interdiffusion coeffs., conc. depend., correl. with solidus line shape (*Russian*) 3-41712
 Pt-W, anomalous mag. susceptibility and conc. depend. of supercond. transition temp. (*German*) 3-41286
 Ta-W (10wt.%W), elec. resist., specific heat and emittance at 1500-3200K, high-speed simultaneous meas. 3-52705
 UC₂-W alloys, high temp. creep 3-72948
 UWC₂, standard free energy of form. by e.m.f. meas. (*Japanese*) 3-61125
 W-Cu-Ti, micro- and macrodeform. characts., foreign atom binding effects (*Russian*) 3-80271
 W-Mo, electrical resistivity and thermal conductivity 3-72972
 W-Mo alloy structure using field electron and field ion microscopes (*German*) 3-57972
 W-Nb, thermal expansion coeff., anomalous conc. depend. 3-72213
 W-Ni-Fe, ductility, fracture resistance rel. to microstructure (*German*) 3-80391
 W-Ni-Fe sintered composite, reinforcement with W wire fibres 3-69370
 W-Re, micro- and macrodeform. characts., foreign atom binding effects (*Russian*) 3-80271
 W-Re, thermal expansion coeff., anomalous conc. depend. 3-72213
 W-Re b.c.c. solid solns., electronic struct. anomalies (*Russian*) 3-79621
 W-Ta-ZrC, recrystallization, deformation depend., microstructure 3-76334
 W-Ta(Fe), local moment formation and magnetic interactions 3-50345
 W-ThO₂ (1 wt.%) wire, recrystn. process 3-64857
 WBe₂₂, supercond. investig. (*Russian*) 3-46927
 WC-Co sintered compacts, precip. effect on mag. props. from expts. on Co-W alloys 3-64527
 W(Fe), local moment formation and magnetic interactions 3-50345
 WN₃, atomic struct. and microstruct., X-ray obs. (*Russian*) 3-79271
 WSi₂, formation kinetics in W/PtSi/Si film system, rel. to IC metal-lithiation 3-64787

tungsten compounds

- see also tungsten alloys*
 peroxo tungstates, i.r. spectra and structure 3-57656
 rare earth tungstates, of Ln₂WO₆ type where Ln=Ce to Lu 3-64001
 wolframite, laser spectral analysis in plasma with controlled excitation delay (*Russian*) 3-70490
 [W(CO₅L)]- (L=iodide, phthalimide, succinimide, saccharide), resonance Raman effect (*German*) 3-78775
 Bi₂O₃-WO₃ system, phase relations 3-76242
 U_{0.8}Pu_{0.2}C-W system, phase diagram obs. 3-47451
 W-H₂, H₂ solubility, partial molar enthalpy, excess entropy 3-80236
 W-halogen-O-H reaction systems, C influence on chem. reactions and transport processes (*German*) 3-53362
 WC, partial dislocations, by weak-beam electron microscope technique 3-60730
 WC in TiC, diffusion mechanism during form. 3-64975
 WC/Al₂O₃ composite ceramics, prep. and characteriz. for cutting tools 3-69344
 WC/Co (15 wt.%), fracture toughness (*French*) 3-72990
 WC/Co composite, continuum mechanics approach to elastic-plastic behaviour 3-80444
 WC/Co powder, sintering, shrinkage rel. to milling 3-80393
 WC-Co composite materials, precipitation and magnetic hardening, coercivity and saturation magnetisation obs. 3-60973
 WC-Co compound powder, plasma spraying on hard metals (*German*) 3-50752
 WC-Co sintered compacts, precip. effect on mag. props. from expts. on Co-W alloys 3-64527
 WC-ZrC system, phase equil. and microstruct. 3-72939
 WC, cermet, press. dependence of elastic moduli 3-44646
 W(CO)₆, in gas and liq. soln., vib.-rot. coupling effects on correlation functions 3-67825
 WCl₆, force constants and mean amplitudes of vibration calc. 3-60436
 WF₆, negative ion formation by electron impact 3-43497
 WF₆, Raman band contour analyses and Coriolis splits. 3-67816
 WN film, elec. and optical props., conducting neutral density filter applic. 3-64753
 WO₃, Fermi surface obs., quantum Landau oscils. 3-75709
 WO₂:Be doped powder, W filament production, secondary β -W formation (*Hungarian*) 3-72986
 WO₃, powdered and sintered, positron annihilation 3-79372
 WO₃ with Si or Ge, tungsten bronze preparation by chemical transport process, X-ray study 3-53178
 WO₃-P₂O₅-Li₂O, semiconducting glass, resistivity and thermoelectric polarisation obs. (*Polish*) 3-41176
 (WO₃)_{1-x}(K₂O-P₂O₅)_x 3-72007

tungsten compounds continued

- WO_{3-x}F_x (0.03 \leq x \leq 0.09), crystal structure and electrical props. 3-40879
 WS₄²⁻, mag. circular dichroism assignment of longest wavelength band 3-54663
 WS₂(Se₂), lubricating action mechanism (*Russian*) 3-41798
tuning
see also oscillators; receivers; resonance
 crystal oscillator, automatic phase tuning cct., with controlled phase inverter 3-54250
 dye laser, range extension using third harmonic Nd:YAG pump 3-66829
 dye laser, rapid tuning using electrooptic Lyot filter 3-51928
 dye laser, using pellicles, nitrocellulose membrane intracavity elements 3-54227
 far i.r. generation, by difference freq. mixing in InSb 3-54239
 optical waveguides, phase matching 3-48848
 oscillator-amplifier dye laser with tunable high powers 3-48905
 polymethine dye lasers, flashlamp excited, i.r. emission, mode locking, tuning 3-45801
 semiconductor laser compound cavity, electrooptic and piezoelectric 3-62723
 Nd:glass laser, CW, freq. tuning, mode locking 3-51930
 PbSe injection laser, tuning by hydrostatic press. 3-43025
 Pb_{1-x}Sn_xTe diode laser, tuning characts. in 8-12 μ m region 3-70828
 YIG filter, tunable, using meander-line spin wave transducer 3-47074

tuning forks *see vibrating bodies***tunnel diode oscillators**

No entries

tunnel diode storage devices *see semiconductor storage devices; tunnel diodes***tunnel diodes***see also tunnelling*

No entries

tunnel effect *see tunnelling***tunnel triodes** *see thin film transistors***tunnelling**

- alkali halide:Ti, Ag, tunnel luminescence (*Russian*) 3-41560
 alkali halides, librational and tunnelling levels of OH⁻ impurity 3-79453
 asymmetric complexes, proton tunnelling effect on internal vibr. 3-60427
 current oscillations in normal metal-metal, or semicond.-semicond. tunnel structures 3-64396
 dielectric, absorption current, dielectric constant and dielectric loss 3-44369
 dislocations, quantum and classical motion in Peierls potential relief 3-60737
 disordered dielectric film between metal electrodes, electron tunnelling probability 3-46903
 disordered one-dimens. structure, anisotropic elec. cond. interchain tunnelling 3-46838
 ferroelectric, hydrogen bonded, coherent neutron scatt. at low temps., theory, tunnelling quasipin model 3-55535
 ferromagnetic thin films, tunnelling mechanism for viscous wall motion 3-41376
 field emission tails and tunnelling lifetimes 3-41619
 finite superlattice, I-V charact. 3-44134
 formic acid, proton barrier, i.r. spectra, theory 3-63390
 frozen aqueous solutions at 77 K, electron tunnelling 3-47576
 glass:Sn, Ga, Mossbauer effect and second-order Doppler shift, superconductivity 3-75927
 glass, low temp. thermal expansion model 3-60800
 glass, tunnelling model for acoustic and thermal props. at low temp. (*French*) 3-40975
 into impurity band across junction, theory 3-68690
 ionic transport theory in cryst. tunnels 3-43899
 Jahn-Teller theory, new type of adiabatic pot. minima and inversion (tunnelling) splitting 3-68551
 Josephson a.c. effect, exactly soluble microscopic models 3-46936
 Josephson effect, destruction of, by fluctuations in order parameter 3-68738
 Josephson tunnelling current in supercond., quantum Markovian process 3-44172
 junctions, calibrated current-voltage characteristics meas. 3-53952
 libration in Devonshire O_h potential, ground state tunnel levels 3-52803
 metal, solid surface photoemission, laser multiphoton phenomena 3-76121
 metal surface, elec. field screening, tunnelling currents 3-50650
 metal-dielectric contact, rel. to I-V characts. (*Russian*) 3-44145
 metal-insulator boundaries, effect of lattice oscill. 3-50280
 metal-semicond. contact, quantum and electronic theory accounting for free electron tunnelling 3-44148
 methyl group, weakly hindered, tunnelling rotation rate, e.p.r. and ENDOR meas. 3-47125
 m.i.m. diode, strain modulation electron tunnelling, metal band edge effects 3-55344
 m.i.m. structure, dispersion relation, effects of barrier shape and WKB approx. 3-46905
 m.i.m. tunnel structure, potential barrier parameters, two temp. method of determ. (*Russian*) 3-50279
 m.i.s. Schottky barrier diode, VI characs. allowing for tunnelling through space charge region (*Russian*) 3-52908
 m.i.s. Schottky barrier structure, potential barrier transparency coefficient (*Russian*) 3-52907
 m.n.o.s. memory capacitors, back tunnelling, direct obs. method 3-60917
 m.n.o.s. structure, discharge mechanisms at applied voltages and elevated temps. 3-55342
 non-radiative tunnel transitions, in strong e.m. field 3-76046
 oxide layer with metallic inclusions, tunnel junction, zero anomalies in resist. 3-75789
 point contact apparatus, for supercond. device expts. 3-64437
 point junctions, nonlinearity mechanism of volt-ampere characts. 3-75794
 polaron tunnelling, small, at high temp., transport mechanism 3-64312

tunnelling continued

- polyimide film, thermally assisted tunnelling in elec. cond. 3-46851
- proton transfer in hydrogen bond, damped harmonic vibr. model 3-63384
- proton transfer reactions in soln., tunnelling 3-55956
- rare earth metals and compounds Bloch wall, probability calcs. 3-41375
- ribbon-filament tunnel superconducting contacts, matching with free space 3-68739
- Schottky barrier, I-V characs., image force and tunnelling effects (*Russian*) 3-41266
- Schottky-barrier diode, through space charge region, shot noise (*Russian*) 3-72402
- semiconductor with superlattice, elec. props., theory 3-75750
- semiconductor-metal contact, tunnel effect phonon contrib., pot. fluctuations (*French*) 3-44150
- semiconductors, surface quantisation meas. technique, review 3-50261
- superconducting junctions, alpha particle detection 3-77614
- superconducting junctions with active barrier impurities, photon assisted tunnelling theory 3-46938
- into superconducting state mag. ordered dilute alloys, anomalous props. 3-68736
- superconducting thin films, conductance, temp. depend. in high magnetic fields 3-44174
- superconducting tunnel junction, as very fast phonon and photon detectors 3-44175
- superconducting tunnel junction, photon assisted tunnelling, current density 3-55379
- superconducting tunnel junction, second order tunnelling current density 3-55380
- superconducting tunnel junctions as phonon sources and detectors 3-55374
- superconducting tunnelling junctions, absolute phonon detection sensitivity 3-55376
- surface states, one-dimensional model for field emission 3-79755
- teaching project, thin soap films cond. meas. 3-42500
- thin films, thickness dependence of new peak structure 3-58347
- tryptophan in ethylene glycol/water glass, recombination luminescence and trapped electron decay 3-55695
- two-proton system with hindered rot., methyl group tunnelling, n.m.r. lineshapes 3-64562
- Zeeman nuclear relax. of tunnelling centres 3-72542
- Al film, hot carrier attenuation obs. using m.i.m.s. struct. 3-79777
- Al superconducting tunnelling junctions, h.f. relaxation phonon emission 3-55375
- Al-insulator-Al,(SN),(Pb), supercond. thin films, tunnelling in vortex state 3-52936
- Au-NaCl-TiO₂-Ti, m.i.m. struct., stable tunnelling 3-79776
- CdS-Al barriers, junction tunnelling 3-44147
- H₂ through barrier of double-well pot. 3-57594
- H₂ + CL → H + HCl, force field and tunnelling effects, kinetic-isotope effects 3-50833
- H₂O₂*, tunnelling in proton transfer between water mols. 3-78867
- He, liquid, tunnelling from electronic bubble states through liquid-vapour interface 3-46740
- In, tunnelling in superconductor under pressure 3-52937
- KCl, F-centres luminescence, electron tunnel transfer (*Russian*) 3-41551
- KCl:CN⁻, orientational, vibr. absorpt. of mol. defects 3-69040
- KCl:In, tunnel ionization of excited In⁺ centres, 7-300 K 3-55688
- KCl:Li⁺, Zeeman nuclear relax. of tunnelling centres 3-72542
- KCl:OH⁻, tunnel levels for librator in Devonshire O_h potential 3-52803
- K₂V₂Mo_{1-x}O₃, new tunnel cryst. struct. (*French*) 3-79302
- NH₄Br, proton magnetic resonance study of tunnelling of NH₄⁺ ions 3-44332
- (NH₄)₂CrO₄, proton magnetic resonance study of tunnelling of NH₄⁺ ions 3-44332
- NH₄l, proton magnetic resonance study of tunnelling of NH₄⁺ ions 3-44332
- NH₄NO₃, proton magnetic resonance study of tunnelling of NH₄⁺ ions 3-44332
- NH₄SCN, proton magnetic resonance study of tunnelling of NH₄⁺ ions 3-44332
- NaCl:OH⁻, tunnel levels for librator in Devonshire O_h potential 3-52803
- Nb₃Sn superconducting junctions, effective phonon spectrum by electron tunnelling 3-68737
- Nb₃Sn-Pb(Sn), sputtered film supercond. junction, tunnel characs., energy gap values 3-75818
- Ni(100), (110) surface, reson. tunnelling, Auger and autoionization processes with He⁺(2s), He²⁺ ions 3-47339
- Pb based alloys, electron, order and annealing studies by phonon spectrum and resistance measurements 3-41110
- Pb-In alloy, supercond., hydrostatic press. effects, electron tunnelling study 3-52923
- RbBr(I), unstressed crystal, one phonon and activated tunnelling as relax. mechanisms 3-44325

tunnels, wind *see* wind tunnels**turbidimeters** *see* turbidimetry**turbidimetry**

- polymers, molecular wt. distribution determ. by temperature drop turbidimetry 3-57682
- river and lake monitoring, Earth Resources Technology Satellite 3-80716

turbidity

- see also* turbidimetry
- atmosphere, effect on radiance of terrestrial infrared radiation 3-76721
- atmosphere, extinction of solar radiation, discussion on paper by D. Randerson 3-65293
- atmospheric, spectral optical thickness over sea and continent (*Russian*) 3-80751
- currents, parameters, methods of computing 3-80713
- interstellar silicate grains, ice-coated, opacity calc. interstellar extinction curve 3-48124

turbidity continued

- noctilucent clouds, effect of tropospheric turbidity on visibility (*German*) 3-76729
- opal glass, phase separated, opacity improvement by alterations of interfacial tension 3-76258
- Sahara, radiometric obs. (Spring 1967) (*German*) 3-69584
- spectrophotometry, optimum reference wavelength selection 3-62101
- stellar envelopes, supercrit. luminosity, power dependence of opacity, effect of convection 3-69925
- Strait of Gibraltar, scatt. at 1100m depth 3-59035
- Tropical Atlantic, water transparency rel. to temp., salinity, density and relative turbidity (*Russian*) 3-47693
- AgBr photographic sol conversion to AgI, reaction kinetics, turbidimetric studies effect on gelatin protection and unsubstituted polyethylene oxides 3-53338

turbines

- see also* compressors; gas turbines
- vibration measurement of moving turbine blades, laser Doppler instrument 3-66144

turbulence

- see also* cavitation; plasma turbulence; turbulent flow; vortices
- acoustic, shock wave generation 3-63655
- acoustic echo-sounding techniques and appl. to gravity-wave, turbulence and stability studies 3-65517
- acoustic wave multiple scattering in inhomogeneous atmosphere 3-51468
- acoustic wave scattering, correction 3-73610
- advection fogs, effect of turbulent mixing on dynamical model 3-59120
- aerodynamic noise emission from turbulent shear layers 3-60534
- Aerodynamic sound and the low-wavenumber wall-pressure spectrum of nearly incompressible boundary-layer turbulence 3-70207
- air, angle-of-arrival difference spectrum of interferometer 3-42575
- air, boundary-layer wall pressure spectrum, low-wavenumber region study 3-42466
- air, rel. to intense laser beam instability 3-62729
- airborne noise generation, shock structure 3-40730
- astronomical turbulence limited telescopes, image degradation 3-45251
- astrophysical gases, topological dissipation and small-scale fields 3-56303
- atmosphere, gravity centre shift, focused light beam, time correlation fn. (*Russian*) 3-44875
- atmosphere, investigation of laser light intensity fluctuation (*Russian*) 3-65334
- atmosphere, quasi-geostrophic, numerical simulation 3-73324
- atmosphere, radar and sodar probing of waves and turbulence in statically stable clear-air layers 3-65516
- atmospheric, appl. of meteor trails 3-65347
- atmospheric, building response to 3-59482
- atmospheric, effect on astronomical image quality 3-61888
- atmospheric, effect on oscillatory flow dispersion in soils 3-46487
- atmospheric, Eole experiment, results and objectives 3-61456
- atmospheric, intermittency of small-scale structure 3-65302
- atmospheric, refractive index calc. 3-76749
- atmospheric, role in optical image degradation 3-80754
- atmospheric, turbulence, behaviour of focused laser beams 3-51023
- atmospheric, two-dimensional, enstrophy cascading inertial range 3-76742
- atmospheric buoyancy driven boundary flow in stably stratified medium, instabilities 3-61460
- atmospheric fluctuations, spectral attenuation meas. using space filter (*Russian*) 3-73289
- atmospheric turbulence breakdown coeff. determ. 3-73297
- atmospheric turbulence measurement sensors, international intercomparison, Tsimslyansk field experiment 3-51180
- atmospheric turbulent diffusion near ground, Rn 220 study (*French*) 3-65395
- atmospheric turbulent transfer processes near surface 3-65304
- boundary layer, Reynolds stress, statistical characs., comments 3-49576
- boundary layer, temp. fluctuation meas. behind linear heat source (*French*) 3-78939
- boundary-layer turbulence and noise, wave mechanical treatment 3-46437
- bow shock crossings, struct. of turbulence, effect of cold and heated solar wind, satellite obs. 3-80836
- buoyant thermal motion in calm stably stratified atmosphere 3-51067
- Burger's turbulence, an exact 2-point distribution 3-43550
- clear air, effect on line-of-sight e.m. wave propagation, refractive index fluctuations 3-65310
- clear air, probability, from satellite recorded radiance gradients 3-65309
- clear air turbulence, India, effect of upper air flow patterns 3-80744
- clear air turbulence, radar detection 3-44962
- closed vessel, turbulence intensity decay 3-43542
- compressible boundary layers, roughness, heat transfer and press. gradient effects 3-49571
- cosmic, sound generation, origin of galaxies 3-65625
- Cramer's theorem appl. to axisymmetric incompressible turbulence, comments and reply 3-52426
- cyclone, reverse flow, two-dimensional turbulent diffusion model 3-71820
- diffusion, re-derivation of Saffman's result 3-57744
- diffusion downstream from linear source in plane parietal jet (*French*) 3-49549
- direct-interaction approximation by modal-interaction perturbation technique 3-63654
- electrojet type I and II irregularities, unified theory 3-51116
- entrainment model, vortex ring, fluid interface 3-75203
- flame-turbulence interaction, shear wave passage through plane flame front 3-63630
- flames, mean turbulence visualization, optical spatial filtering method 3-56665
- flow noise, steam piping in nuclear power plants, prediction and control 3-42482
- fluid system processes, statistical thermodynamics (*German*) 3-48813

turbulence continued

- galaxy formation from primeval universal turbulence 3-61643
 galaxy formation rel. to dissipation of strong cosmic turbulence 3-47871
 gas absorption into a turbulent liquid 3-49623
 general oceanic turbulence equations study (*French*) 3-65268
 geophysical variables, statistical anal., turbulent or wave-like fluctuations 3-47803
 gravity waves in continuous density field, traumatic effect on continuous stratification 3-60557
 grid-generated turbulence coherence 3-71751
 Gulf Stream, obs. of cyclonic eddy 3-59013
 high altitude clear air turbulence variations 3-76748
 horizontal turbulent diffusion coeffs. in littoral zone of Black Sea using aerial survey data 3-51004
 hydrodynamic tensor wave equation 3-75350
 hypersonic boundary layer, turbulent props. 3-46429
 inertial range spectrum 3-67905
 interfacial, rel. to mass transfer and drag coefficients 3-78940
 interfacial mixing in atmospheric, dry, inversion-capped, convectively unstable boundary layer 3-65384
 ionospheric electrostatic turbulence, seasonal and geomagnetic dependence 3-61541
 ionospheric irregularities, turbulence, power spectra, total ion conc. meas., Retarding Potential analyser 3-80802
 irradiance functions in uniformly turbulent air, calc. and comparison with data 3-80755
 isotropic turbulent energy spectrum, multipoint distribution 3-60542
 jet, double concentric, nozzle conditions influence on main region characts. 3-54828
 jet, turbulent liquid, breakup in a gaseous atmosphere 3-75281
 jets in cross flow, turbulence intensity, temp. and vel. distrib. 3-46491
 Kelvin-Helmholtz billows, finite amplitude 3-61459
 kinematic dynamo theory, appl. of Kraichnan's direct interaction approx. for incompressible isotropic turbulence 3-75252
 kinematic dynamo theory, comments on criticisms including isotropic turbulence 3-61634
 laser beam spread in turbulent atmosphere (*Japanese*) 3-41970
 liquid, power dissipation, stationary value (*Italian*) 3-43646
 liquid surface wave interaction, wave attenuation calc. (*Russian*) 3-46474
 magneto-, in liquid core of Moon, magnetic field generation 3-47956
 magnetospheric micropulsations rel. to h.f. turbulence during substorms 3-61557
 measurement, yawed hot wires, static calibration procedure 3-54056
 MHD conducting fluid turbulence (*Russian*) 3-79013
 microthermal, balloon-borne temp. sensors, wind speed profile, wind shear calc. 3-44884
 nonlinear expansion theory, diagram approach (*Japanese*) 3-57743
 ocean, turbulent fields of velocity and temp., great depths, bottom currents, surface active layer (*Russian*) 3-47701
 ocean capillary waves, moving gust patterns, 'Cat's paws' 3-47680
 ocean currents, the regularity of reconstruction of a mesoscale turbulent structure (*Russian*) 3-80696
 oceanic, energy containing eddies, theoretical model 3-65254
 optical beam, finite, in turbulent medium, mutual coherence function 3-74204
 optical beam analysis, folded-path weighting function, h.f. spherical wave, optical filter function, theory 3-66767
 parallel high β shocks, collisionless, relaxation phenomena, shock structure, turbulence 3-69670
 phase-space fluid, stochasticity limit and turbulent motion 3-57266
 pipe flow, sound attenuation 3-42402
 planetary atmosphere, remote sensing by radio spectrum analysis 3-42176
 planetary boundary layer, Richardson number profiles through instability wave regions 3-61599
 planetary boundary layer, turbulence structure 3-65300
 primordial, in expanding universe, generation of sound 3-76959
 pseudospectral (collocation) approximation for two-dimensional incompressible system 3-46398
 shear flow, stratified, internal wave generation in tank expt. 3-63726
 shear layer between 2 streams of different salinities and speeds, lab. expt. 3-60531
 shock waves, weak, turbulent thickening possibility 3-46458
 short-term average optical beam spread, in turbulent medium 3-41968
 simple universal equilibrium spectrum 3-49556
 solar and galactic magnetic fields, generation and dissipation, turbulent diffusion 3-69826
 solar atmosphere, macroturbulent velocity field, one-dimensional approx. 3-80937
 solar photosphere, Fe I lines, effect of LTE departures and microturbulence 3-65673
 sound transmission through pipe walls, transmission loss as fn. of flow within pipe 3-42483
 spectra, using solid state hot wire anemometer feedback controller 3-47830
 stars, supersonic turbulent stress and structure 3-73479
 stellar atmospheres, microturbulence from photoelec. obs. of Fe I 6065 A line 3-81018
 stellar light waves perturbation by atmospheric turbulence, mutual coherence function determ. 3-44898
 stratified fluid, turbulent mixing, away from boundary layer influence, review 3-60532
 stratified shearing flow 3-60533
 streams, lifetime of inhomogeneities, definition (*Russian*) 3-67909
 Strouhal number and flat plate oscillation in air stream 3-71753
 structure of turbulent flow, modelling and analysis 3-57738
 theory, Navier-Stokes eqns. closure problems, review 3-78956
 thermal diffusion parallel to plane wall for $y_2=2-300$ (*French*) 3-46384
 troposphere stratified turbulent layers, forward scatter radio techniques 3-65521
 two-stream mixing layer, turbulent correlation measurements 3-78936

turbulence continued

- uncollimated beam wave in turbulent medium, mean square depolarisation, analysis 3-40207
 upper atm. turbulence spectra of dissipation rates and diffusion coeff., Aladdin II meas. 3-61501
 upper atmosphere composition and thermal structure, effects of eddy turbulence 3-61518
 water jet, submerged, large scale characteristics 3-71749
 weak homogeneous turbulence, theory (*Japanese*) 3-54801
 whistler turbulence and vel. space diffusion, in magnetospheric, simulation 3-56228
 wind convection, similarity model of turbulent regime 3-51009
 ^4He , superfluid critical heat current velocities as a test of Vinen theory 3-75649
- turbulent flow**
 ablation material anelastic behaviour on crosshatching due to supersonic turbulent boundary layer flow 3-46441
 aeroacoustic environment about a slender cone, expt. determ. 3-63703
 aerosol, through tube or channel, deposition, particle charge and re-entrainment effects 3-40748
 air, convective, transition to turbulence, low Rayleigh number 3-75197
 air, in channel with elastic walls, mean velocity profile (*Russian*) 3-63627
 air, induced noise, panel vibrations, viscoelastic damping materials 3-70274
 airflow above natural waves, turbulence wave-related fluctuations 3-47740
 anisotropic turbulence decay 3-57722
 astrophysical bodies, new Reynolds stress tensor 3-47864
 atmospheric internal intermittency, structure at large Reynolds number, scale similarity expts. 3-59054
 atmospheric sound scattering, by jets and wind 3-42407
 barotropic instability and predictability difference energy spectra 3-44890
 boundary layer, aircraft cockpit noise 3-77341
 boundary layer, at partially moving lamina, theoretical analysis (*Russian*) 3-63689
 boundary layer, compressible, ratio of Reynolds shear stress to turbulence kinetic energy 3-49575
 boundary layer, generalised correlation of roughness density effects 3-43559
 boundary layer, high order moments of Reynolds shear stress fluctuations calc. 3-46435
 boundary layer, plate, quadrupole radiation intensity 3-75198
 boundary layer, probability distributions and correlations 3-49574
 boundary layer, turbulent with injection through porous flat plate and small pressure increase (*German*) 3-63694
 boundary layer, two and three dimensional, velocity profiles, wall shear stress inference 3-63695
 boundary layer along flat plate with linearly increasing surface roughness, expt. 3-57765
 boundary layer flow above a change in surface roughness, mixing lengths and energy eqn. models comparison 3-52461
 boundary layer flow from stationary to moving surfaces 3-78937
 boundary layer flow over flat plates calc. with different turbulence theories and variable Prandtl number 3-52451
 boundary layer on a porous plate, velocity pulsation energy spectra (*Russian*) 3-67926
 boundary layer on flat plate, incompressible fluid, pulsating energy balance eqn. (*Russian*) 3-63691
 boundary layer shape after corner expansion, numerical calculation 3-57856
 boundary layer turbulence, small scale props. 3-71771
 boundary layer turbulent, three-dimensional, calc., using streamline coordinates 3-52455
 boundary layer with pressure gradient, heat transfer prediction 3-57723
 boundary layers, convex curvature effects obs. 3-57774
 boundary layers, effect of disturbances by vibrating vane (*Russian*) 3-63686
 boundary layers, effective viscosity model 3-43560
 boundary layers, separation zones, subsonic jet blown into flow (*Russian*) 3-63692
 boundary layers, turbulent, Reynolds stress, structure meas. 3-75212
 Burgers' model equations 3-52438
 channel flow, two dimens., diffusion of passive scalar for laminar and turbulent cases 3-52449
 channel flow for mean turbulent energy closures, asymptotic analysis 3-71747
 channel inlets, development charact. 3-71734
 characteristics, principal and pulsation, calc., structural equil. (*Russian*) 3-46418
 chemical reactant in turbulent flow, one-point concentration moments relation to Lagrangian probability density 3-63803
 chemical reactions, consecutive, in tubular reactor, kinetics 3-49619
 circular cylinder, wake determ. 3-67922
 coastal upwelling, turbulent diffusion horizontal and vertical Prandtl numbers 3-47682
 coaxial cylinders with outer rot. cylinder, frictional moment and press. drop of flow 3-54805
 coexistence of laminar and turbulent flow in a narrow triangular duct 3-60535
 coflowing axisymmetric streams, shear stress and turbulent intensity models 3-78938
 compressible three dimensional turbulent boundary layers on adiabatic walls, small cross flow theory 3-78975
 compressible two-dimensional boundary layers, laminar-turbulent transition, finite-difference procedure 3-60548
 condensed systems turbulent burning, gas dynamic parameters calc., analytical method 3-57861
 conical-shaped vehicle in wind tunnel, acoustic environment prediction 3-46449
 convective flow, turbulence transitions 3-49563
 convective heat transfer coefficient in a turbulent thermal entrance region, Prandtl number dependence 3-60529
 coolant crossflow induction in a flat channel by wall fins 3-74669

turbulent flow continued

- cooled surfaces, full-coverage film, experimental results 3-75215
 Couette turbulent flow, wall shear flow 3-60543
 Cross flows in bounded three-dimensional turbulent boundary layers 3-71769
 diffusion in channels, longitudinal pressure gradient effect (*Russian*) 3-52429
 drop formation, liquids, wall-effect, theory isotropic flow (*Japanese*) 3-63764
 drops and bubbles splitting by turbulent fluid flow 3-63737
 eddy conductivity and turbulent Prandtl number model 3-63661
 eddy diffusivities in tube bundles with cross flow (*German*) 3-63663
 electrically conducting liquid rotation with a free surface in a rotating field (*Russian*) 3-57817
 electrolytes in capillary porous systems under MHD pressure 3-75271
 elliptical ducts, fully developed turbulent flow and heat transfer 3-63664
 falling turbulent and laminar liquid rippling films down vertical wall, heat transfer, numerical soln. (*German*) 3-57731
 fan noise, isolated rotor, inflow turbulence 3-81344
 fan noise, reduction, annulus boundary layer removal 3-81346
 film cooling of flat plate downstream of a tangential slot with turbulent boundary layer 3-63799
 finite-dimensional probability distributions of pulsating variables 3-63656
 flame-turbulence interaction, applic. to flame propag. in turbulent flow 3-63630
 flow structure in inlet sections of smooth and rough pipes, expt. obs. 3-57726
 flow turbulence characteristics determ. by flow visualisation meth, estimation of the accuracy 3-54053
 fluid in hydrodynamic laminar or turbulent regime, mass transport study using rotating ring electrodes (*French*) 3-60585
 fluidised beds, fixed and homogeneous, momentum, heat and mass transfer 3-57823
 free stream, stagnation flow enhancement, heat and mass transfer 3-78933
 free turbulent jet with constant amplitude transverse pressure gradients near nozzle exit, sinusoidal excitation 3-60590
 free turbulent mixing flows without a net momentum defect, analysis 3-46494
 friction factors, tube rotating around its own axis 3-67912
 fuel rods, unbaffled, heat transfer 3-60268
 fully developed, in vertical tubes, with various stream entry conditions, expt. obs. 3-57727
 fully developed isotropic turbulence, helicity cascades 3-71748
 fully developed turbulence intermittency, as a consequence of the Navier-Stokes equations 3-43548
 gas, interacting with liquid laminar flow, motion of two component system (*Russian*) 3-75262
 gas fluctuations, simultaneous comparisons of laser Doppler and hot wire methods 3-62375
 gas mixing meas. using a laser Schlieren technique 3-48689
 gas quenching velocity, detn. from heat transfer criterial relations (*Russian*) 3-52441
 gas with dust particles, turbulent friction drag, reduction mechanism 3-40744
 gaseous suspension flow of solid and liq. particles with internal heating, radiative heat transfer 3-60576
 heat diffusion from a line source downstream of a turbulence grid 3-57724
 heat transfer and drag, for fluid with variable viscosity and heat cond., calc. (*Russian*) 3-52440
 heat transfer and periodic viscous sublayer 3-46389
 heat transfer during flow from centre to periphery between two rotating discs 3-63637
 heat transfer to a fin leading edge 3-57725
 heavy particle transport in homogeneous turbulent fluid flow 3-46482
 helical turbulence and absolute equilibrium 3-57742
 high-speed turbulent flow, recovery factor, theoretical analysis 3-67907
 high-speed turbulent radiating boundary layers, numerical solns. of integro-differential equations 3-52453
 hypersonic boundary layer on flat plate, heat transfer 3-67902
 hypersonic boundary layer with press. gradients and cross flow, expt. and theoretical investigation 3-46428
 hypersonic sphere wakes, laminar and turbulent, Mach 13.5, density and temp. distributions 3-40753
 hypersonic tunnel wall, upstream wall temps. effects, turbulent boundary layer profile meas. 3-57780
 hypersonic turbulent boundary layer interactions, plateau pressure 3-49548
 incipient separation pressure rise for a Mach 3.8 turbulent boundary layer 3-63709
 incompressible fluid gradientless turbulent flow over flat plate, turbulent boundary layer (*Russian*) 3-63681
 inert turbulent boundary layer swirl flows prediction 3-78958
 inflation of automotive safety in air bag, noise sources 3-46420
 interaction of a mag. field with a turbulent conducting liquid (*Russian*) 3-43612
 jet, cylindrical, initial core velocity distribution (*French*) 3-75275
 jet, elliptic, turbulent, instability 3-57867
 jet, free turbulent mixing in axial press. gradients 3-75201
 jet, plane, impinging normally on flat smooth wall, behaviour and characts. 3-67974
 jet, two-dimensional turbulent, propagation from a linear source placed at the vertex of a wedge 3-71835
 jet, two-phase, turbulent axisymmetric, dispersion of heavy admixture 3-60588
 jet flows, application of energy equation of turbulence (*Russian*) 3-52491
 jets, conducting liquid laminar and turbulent, in a transverse magnetic field (*Russian*) 3-57819
 jets, plane, turbulent, impinging on smooth wall 3-54834
 jets, reattaching shear layer heat transfer 3-52488
 jets, vapour, submerged, penetration in subcooled liquids 3-75273
 jets hot, effect of temp. on mixing noise 3-79053

turbulent flow continued

- laminar film condensation with vapour drag on flat surface 3-63648
 land and sea breezes, effects of turbulent transfer processes, numerical method 3-76680
 laser, chemical, turbulent, performance calc. 3-78010
 laser cross-beam intensity-correlation spectrum 3-73964
 laser Doppler velocimeter, optical design (*Russian*) 3-45508
 laser-Doppler velocimeter, application to turbulence meas. 3-66475
 liquid, mixing, flow visualisation, dye tracer, laser i.r. radiation (*Russian*) 3-57745
 liquid, turbulent mixing region, flow visualisation, dye tracer, laser i.r. radiation (*Russian*) 3-57745
 liquid crystal, in stationary elec. field 3-72003
 liquid drop breakup in turbulent flow, residence time and flow velocity depend. 3-49615
 liquid in rectangular channel, velocity distributions (*Russian*) 3-63633
 liquid in round tube, heat transfer and adiabatic wall temp. 3-49550
 liquid metal MHD rotating flow, expt. obs. 3-75254
 local mass transfer sensor to estimate the turbulence characteristics of the near-water layer of an air flow 3-57024
 low turbulence hydrodynamic test rig, laminar boundary layer stability (*Russian*) 3-62376
 lubricant films, bulk-flow theory for turbulence 3-54803
 lubricant films, thermal effects 3-54804
 Ludwig tubes, high performance, aerodynamics 3-63704
 magnetic field effect on turbulence behind a grid (*Russian*) 3-43604
 mass transfer from a single bubble, turbulent counter current liquid flow 3-71737
 mean turbulent field closure models, survey 3-63624
 measurement using laser velocimeter, frequency domain analysis of laser Doppler signals 3-62159
 MHD channel flow under alternating pressure gradient 3-75251
 MHD flow in channels and tubes, pulsed energy balance equation (*Russian*) 3-43605
 MHD rotating Couette flow in a coplanar field, expt. obs. (*Russian*) 3-60562
 mixtures, concentration probabilities distribution and alternation (*Russian*) 3-54800
 mixtures two-phase, friction during turbulent flow in smooth tubes and channels 3-43627
 model optimization using logical search algorithm 3-49547
 molecular diffusion influence on mass transfer between turbulent liquids 3-40705
 moon, Silver Spur, cross-hatching, hypersonic and supersonic turbulent gas flow 3-69903
 multicomponent mass transfer in turbulent flow 3-60530
 non-Newtonian pipe flow heat transfer 3-57719
 ocean, with rectangular boundary, β -effect (*Russian*) 3-47712
 oil-water, immiscible liquids, laminar and turbulent transitional flow, stratified channel flow 3-67963
 ordinary and confluent boundary layer flows, parametric relations 3-63784
 particle eddy diffusivity, particle size effect, turbulent Schmidt numbers 3-79032
 particles in suspension, effect on turbulent flow properties (*French*) 3-60572
 phase-space fluid, stochasticity limit 3-57266
 pipe and channel flows, moderately large Reynolds number 3-78954
 pipe flow, heat and mass transfer in electrochemical reactions 3-57848
 pipe flow, momentum transfer, spectral meas. 3-78955
 in pipes with artificially roughened walls 3-49560
 plane channel, incompressible fluid, pulsating energy balance eqn. (*Russian*) 3-63691
 plane parallel unstable flow, numerical study of mildly non-linear partial differential equation 3-49545
 plane wall, self-preserving pressure gradient 3-79048
 plasma jet, turbulent, heterogeneous electron behaviour 3-46527
 polymer concentrated solns., heterogeneous drag, reduction system, turbulent pipe flow, heat transfer 3-52434
 polymer dilute solns., round turbulent jet, laser-Doppler meas. 3-75283
 polymer soln., dilute, turbulent flow, spectral characts. of press. fluctuations 3-49559
 polymer solution turbulent submerged jets, long-range nature 3-57860
 polymer solutions, reduced drag in turbulent and transient laminar flows near a flat plate 3-63778
 polymer solutions, turbulent drag reduction in external rotational flows 3-60571
 polymer solutions, turbulent flow, influence of high-molecular weight additives 3-57832
 polymer soln., dil., frictional resist. of rotating disc 3-43628
 polymer threads, drag reduction in turbulent flow 3-40739
 reference temp. method for predicting skin-friction coefficient in compressible turbulent boundary layer, Mach number range 2-20 3-43557
 Reynolds stresses, two-point correlation model and redistribution 3-49555
 rotating neutrally buoyant fluid, angular momentum mixing 3-78957
 round tube, incompressible fluid, pulsating energy balance eqn. (*Russian*) 3-63691
 shear, generation and maintenance mechanisms 3-75194
 shear flow, mag. field influence (*Russian*) 3-43603
 shock wave-turbulent boundary layer interactions in rectangular channels 3-43572
 skin friction on a rotating disc, integral calc. 3-57721
 slip flow past infinite porous plate, Rayleigh problem 3-46433
 solar and galactic magnetic fields, generation and dissipation, turbulent diffusion 3-69826
 solar wind interaction with Earth's magnetosphere 3-53611
 solution along semipermeable barrier, hyperfiltration (*Russian*) 3-63636
 Sound generation by open supersonic rotors 3-81345

turbulent flow continued

- standardisation of turbulence characteristics in boundary layer simulation 3-67901
- steam, turbulent flow in pipe, radiative transport 3-52436
- stellar envelopes, meridian circulation with rapid differential rotation 3-53636
- stochastic particle trajectories 3-46399
- streams, lifetime of inhomogeneities, definition (*Russian*) 3-67909
- structure, modelling and analysis 3-57738
- structure parameters in inhomogeneous strain field 3-46383
- submerged heated effluents in a waterway, flow props. 3-43635
- subsonic diffuser with moving walls for boundary layer control 3-43558
- supercooled liquid freezing in forced turbulent flow inside circular tubes 3-75191
- supersonic boundary layer flow downstream from 90° corner 3-54811
- supersonic jet, shock associated noise 3-75229
- supersonic jet mixing 3-54814
- surface entrainment by high velocity water jets, turbulent and laminar boundary layers 3-49622
- surface waves, wind energy transfer to waves, turbulence, asymptotic joint expansions (*Russian*) 3-47686
- swirling turbulent pipe flows expt. 3-75205
- tangential eddy diffusivity in a circular tube calc. 3-57736
- test rig for meas. flow near elastic walls (*Russian*) 3-62377
- theory, Navier-Stokes eqns. closure problems, review 3-78956
- thermally stratified air-flow layer near a water surface under wind gust conditions, turbulence struct. meas. 3-59048
- thick axisymmetric boundary layers, turbulent skin friction analysis 3-71776
- thick turbulent boundary layer along a circular cylinder, mean velocity profile 3-71764
- three dimensional film cooling slots effectiveness predictions 3-57729
- three-dimensional boundary layers, wall shear stress meas. using surface fences 3-46432
- three-dimensional flow, at input of compressor with varying inlet radius (*Russian*) 3-63632
- three-dimensional incompressible turbulent boundary layers, mean velocity profiles 3-46431
- tidal estuary flow, tidal current vel. meas. 3-51214
- torque coefficient functional dependence of coaxial cylinders on gap width and Reynolds numbers 3-63673
- trail behind cylinder, energy of pulsation (*Russian*) 3-63714
- transition from laminar, single and two-phase flow 3-78946
- transition in a pipe, puffs and slugs origin and flow in a turbulent slug 3-52439
- transition to turbulent convection 3-67904
- transonic turbulent viscous-inviscid interactions in airfoil trailing edge 3-63702
- tropical Atlantic, large scale anti cyclonic eddy velocity disturbance, detection by anchored buoy stations 3-73257
- turbulent boundary layers, Van Driest damping parameter with mass transfer 3-43555
- turbulent flow in channel inlets, boundary layer flow 3-71734
- turbulent heat transfer and skin friction calc. 3-78935
- turbulent wall jet, parametric analysis 3-79045
- two-dimensional free mixing flows, numerical solution 3-63662
- two-dimensional turbulence in a magnetic field (*Russian*) 3-43613
- two-phase mixing for annular flow in simulated rod bundle geometries 3-43281
- unsteady heat exchange for gas cooling in duct, depend. of temp. and wall thickness 3-40714
- unsteady turbulent flow, r.m.s. vel. fluctuations meas. method (*Russian*) 3-62378
- unsteady turbulent streams, radial structure and hydraulic resistance, expt. obs. (*Russian*) 3-52428
- vapour-liquid mixture flow, pressure fluctuations meas. 3-71810
- variable property turbulent flow in a horizontal smooth tube during uniform heating and constant surface-temperature cooling 3-46414
- velocity distribution, in rough channel, cinematographic method, obs. 3-54802
- velocity distribution expression for turbulent flow in smooth pipes 3-57718
- vessel discharge, heat transfer, mean and fluctuating gas temperatures 3-46409
- viscous fluid, boundary layer heat transfer and drag calc. (*Russian*) 3-52457
- viscous fluid flow rel. to relax. time, nature of turbulent flow (*Russian*) 3-63618
- viscous liquid, flow equation considering relaxation properties (*Russian*) 3-63634
- viscous non-Newtonian fluids flowing through tubes, heat and momentum transfer 3-75200
- vortices, line turbulent, structure 3-71756
- wake, axisymmetric final period turbulent, scalar, asymptotic behaviour 3-57864
- wake, free turbulent mixing in axial press. gradients 3-75201
- wake, turbulent, rel. to body shape 3-49629
- wake, turbulent flow behind plate, kinematic and dynamic characteristics 3-57862
- wakes, hypersonic, at high Reynolds numbers, turbulent boundary layers 3-79044
- wakes, interacting, turbulence meas. 3-52492
- wall jets and turbulent boundary layers over curved surfaces, calc. 3-57852
- water, 90° bend, Goertler vortices, laminar flow transforms to turbulent flow 3-63667
- water, swirling cavity flow, through straight circular pipe 3-57754
- water, turbulent Prandtl number determ. near smooth wall (*French*) 3-63647
- water horizontal layer, turbulent convection 3-60537
- water in 50 mm dia. flexible tubes, obs. (*Russian*) 3-63635
- water in flat rough tubes, effect of polyacrylamide admixture (*Russian*) 3-63770
- water jet, coanda effect, for case of adding control flow (*Japanese*) 3-46502

turbulent flow continued

- water streams containing some macromolecular substances, boundary layer turbulence 3-71819
- water surface waves, growth rates due to turbulent channel airflow 3-46467
- weak polymer solns., turbulent flow in a pipe, expt. obs. 3-71818
- wind fluctuations near surface of drifting snow (*Japanese*) 3-56159
- wind scoop, snow drifting, autocorrelation function, power spectrum (*Japanese*) 3-56160
- wind tunnels, model noise expts., basic acoustic considerations 3-75223
- wind turbulence associated with basin cooling (*Japanese*) 3-56161
- H₂O, measurement of intensity 3-59724
- He, liquid, flow through bed of large angular particles, critical velocity 3-72248
- ⁴He II, liquid, ion currents in turbulent counterflow 3-43911
- Hg flow in rotating mag. field, onset of turbulence (*Russian*) 3-79021
- N₂O₄ → 2NO₂ → 2NO + O₂ reversible reaction, heat and mass transfer determ. (*Russian*) 3-76447
- Na, in LMFBF 19-rod fuel assembly, edge-channel swirl flow, analysis using ORRIBLE code 3-46110
- Na, transport properties for thermal design of LMFBF cores 3-46112
- Na turbulent channel flow, incipient-boiling superheats, temperature rise rate effect 3-64168

TV see television**twilight**

- see also night sky
- enhancement of 6300 Å, 5577 Å oxygen emission lines 3-65424
- green flash at sunset and sunrise model, observations in Alaska 3-44907
- luminance due to primary scatt. (*French*) 3-61491
- post-dusk effects, obs. 3-61448
- Na airglow data, comparison of 2 methods 3-61597
- O I 5577 Å radiation and differential photoelectron flux spectrum in twilight airglow 3-53508
- O I 6300 Å airglow, morning twilight enhancement 3-59132

twinning

- crystal, GaP, defects rel. to growth from non-stoichiometric melts 3-44555
- crystal, i.r. microscopy study of defects 3-54955
- diamond, synthetic ballas, metallographic and electron microscope obs. 3-64059
- dislocation theory of dynamic behaviour of twins, rel. to transition emission of sound 3-58040
- electrical resist. due to twin boundaries, pseudopotential calcs. 3-44056
- lithium formate monohydrate, defect struct., X-ray topographic investigation (*German*) 3-43803
- quartz, Dauphine twins, direct obs. using second harmonic light 3-52637
- quartz, synthetic, ion damage, fluence depend. 3-60748
- rare earth sesquioxides, thin crystals interpenetration of mechanical twins, role of microtwins electron microscope obs. of mechanical twins (*French*) 3-68278
- steel, austenitic, high-Mn, 110G13L, fine structure after high-speed straining (*Russian*) 3-64836
- steel, low-C vanadium, controlled-rolled and continuously cooled, microstruct. obs. by TEM 3-80259
- steel, mild, twins influence on fracture 3-69282
- steel, stainless, structure sensitive fatigue fracture 3-58663
- tourmaline minerals, n.m.r. studies, crystal structure 3-44768
- triglycine sulphate, equilibrium domain structure near Curie point, electrical twinning 3-79997
- X-ray diffraction, from crystal with deform. twins 3-75456
- Ag, twin boundary elec. resist., pseudopotential calcs. 3-44056
- β-Ag-Al alloys, splat-quenched, massive phase transform. phenomena 3-58613
- Al₂O₃, sapphire, hardness and damage resist. depend. on surface finishing 3-69342
- BaSO₄, barite, plastic deform. rel. to twin orientation 3-46663
- Be single cryst., deformation under laser action, defect obs. (*Russian*) 3-52661
- Cd u.s. irradiation effects, 20 kHz, deformation localization zone, incoherent twin-matrix interface 3-49901
- Co-Fe (8 wt.%) alloy single crystals., twin-slip, twin-twin and slip-twin interactions 3-40930
- Cu, annealing-twin formation and annihilation study 3-47371
- Cu, deformation in high speed cutting, microstructure and hardness obs. (*Russian*) 3-80257
- Cu-Al alloys, annealing-twin formation and annihilation study 3-47371
- Cu-Cr (0.5 wt.%) alloy, grain growth during annealing (*Russian*) 3-72852
- Cu-Sn alloy, martensitic transform., phenomenological analysis (*Japanese*) 3-50680
- Cu(Co), stacking fault energy near coherent twin boundary 3-55784
- Fe, rolled, annealed twins, orientation, texture angle calc. 3-50694
- Fe alloys containing V, twin morphology 3-41708
- Fe single crystals., ZrH₂ refined, with C and N in soln., low temp. mech. props. 3-58696
- Fe-Ti (0.16 wt.%) single crystals., orientation, temp. and strain rate effects on deform. 3-64909
- GaAs, thin film, vapour deposition on sapphire 3-80184
- GaAs epitaxial layers, effect of growth rate and crystallisation conditions on defect formation 3-80192
- GaP epitaxial layers, effect of growth rate and crystallisation conditions on defect formation 3-80192
- In single crystals, rel. to spasmodic creep, 78 and 180K (*Russian*) 3-64954
- K₄(Ni₂CN)₆, symmetry, polytypism, twinning (*German*) 3-40893
- α-LiIO₃ polar crystal, obs. of electro-optical twinning 3-72028
- Mg, compressed along c-axis, twinning deform. 3-80263
- Mg, tensile deformation at 293K, 77K (*German*) 3-52665
- Mg-Cd (10 at.%) tensile deformation at 293K, 77K (*German*) 3-52665

twinning continued

- Mn-Cu alloys, γ -phase, comp. effect on internal friction and Young's modulus 3-76208
 Mo-Re(35 at.%) alloy, interaction of twins with grain boundaries, substructures 3-41707
 NH_4NO_3 , twinning accompanying transform., Mediangesetz 3-40931
 β -Nb-Zr, deform. temp. depend., slip, twinning and dislocations rel. to yield and fracture 3-52662
 Ni, deformation in high speed cutting, microstructure and hardness obs. (Russian) 3-80257
 Ni, electrodeposited dispersion-hardened, electron micrographic obs. 3-61142
 Ni 270 work hardened in tension, annealing twins role in primary recrystn. (French) 3-44585
 Ni-Al(36 at.%) alloy, martensite struct. and behaviour (Russian) 3-80250
 Ni-Al(36.8 at.%) martensite, cryst. struct. and internal twins 3-50718
 Ni_3Mo alloy, plastic deform., twinning for ordered phase, slip in disordered phase 3-79408
 Si, line stacking faults generation at coherent twist boundary 3-64058
 SiC, reaction-sintered, β -SiC growth during sintering, microstruct. characteriz. 3-76300
 SiC, reaction-sintered, self-bonding characts., TEM obs. 3-76301
 β -SiC, X-ray topography, optical probe exam. 3-72097
 Ti-Fe alloys, conc. depend. of constitution and plastic deform. (Russian) 3-58640
 TiNi, twin boundary formation, inhomogeneous shear mechanism, elec. resistivity anomaly 3-54972
 V_3N , precipitate in α -V, structure, morphology and orientation relationships 3-50698
 VO_2 :Cr, by reticular pseudo-merohedry, twin laws 3-79362
 Y, h.c.p., deform. modes, 77-497K 3-64912
 YAlO_3 :Nd, Czochralski growth 3-69158
 $\text{Y}_2(\text{Ta}_{1-x}\text{W}_x)\text{O}_3$, non-stoichiometric perovskite, elec. microscope obs. (French) 3-58018
 Zr single crysts., compression parallel to c-axis, 78-1100 K 3-46659
 ZrO_2 , monoclinic-tetragonal transition, high temp. obs., twin form. 3-72931

two-phase flow

- aerosol, flow through polydisperse model filter, press. drop, flow field, diffusional deposition 3-40751
 aerosol, through tube or channel, deposition, particle charge and re-entrainment effects 3-40748
 aerosol diffusophoresis of large particles, accounting for inertial terms in Navier-Stokes eqn. 3-49616
 aerosol particle-gas, vel. of gas, eqns. 3-63767
 aerosol particles, deposition, flow round sphere capture coeff., jet method 3-63766
 air suspension with Al_2O_3 , heat transfer from a reflected shock wave (Russian) 3-52470
 air-oil mixtures, horizontal stratified two-phase flow, pipes, flow patterns 3-71809
 air-solid in segmental bends (German) 3-60577
 air-water medium, effect of flow on pressure wave propagation, expt. 3-43622
 Air-water tests on a venturi for entraining liquid films 3-66473
 annular flow, interchange and entrainment from tracer meas. 3-63750
 annular two-phase flow, entrainment, heat and mass transport, droplet formation 3-40741
 body motion in ideal incompressible fluid (Russian) 3-79027
 bubble transport theory with application to the upper ocean 3-49612
 bubbles in viscous fluids and whole blood, acoustic effects 3-45320
 bubbles in water, terminal velocity meas. 3-63765
 bubbling fluidised bed, solids circulation rate estimation 3-40742
 charged aerosol particles in unidimensional electrostatic dynamic flow (Russian) 3-57833
 cloud droplets, collision efficiencies, two spherical drops falling into a viscous fluid 3-44888
 coarse particle suspension in high-concentration flow 3-75266
 colloids viscosity meas., mag. method for ferromag. systems 3-73071
 deformed bubble motion in sparging layer (Russian) 3-63754
 density-stratified fluid with particle suspension, plane parallel flow 3-71822
 diffusing flow in a self-controlled heat pipe, condensation, approximate analysis 3-46408
 diphasic boiling fluids, thermics and heat exchanges (French) 3-43624
 diphasic fluid flow, qualitative description (French) 3-43625
 Drag reduction of solid-liquid suspensions in pipe flow 3-80505
 dust-laden gas suspension, entropy losses in the flow in a nozzle 3-63773
 dusty fluid, laminar flow through elliptical annulus 3-79034
 dusty gas flow through annular space between two concentric circular cylinders 3-79031
 dusty viscous liquid, unsteady flow in a circular tube, change in velocity profile 3-71815
 elastic sphere transverse motion in a shear field 3-49614
 emulsions, moving, influence of particle orientation on its conductivity (Russian) 3-43617
 film boiling of saturated binary mixtures 3-64161
 flow through circular cylinder, press. drop due to spherical droplet 3-43623
 fluidisation, sedimentation, Reynolds number and drag coeff. definitions, review 3-79030
 fluidised beds bubbles variation in shape and size 3-40743
 Freon-114 diabatic local void fraction meas. using hot-wire anemometer 3-46128
 gas with dust particles, turbulent friction drag, reduction mechanism 3-40744
 gas-liquid, statistical characts. of slug lengths, upward flow, analysis (Japanese) 3-63763
 gas-liquid mixed medium, structure of weak shock wave front 3-43577
 gas-liquid mixture, horizontal two-phase flow, local frictional drag meas., electrodiffusional method (Russian) 3-57028

two-phase flow continued

- gas-liquid mixtures, swirl flow heat transfer in a vertical tube fitted with twisted-tapes 3-52437
 gas-liquid system, separated, wave propagation 3-71813
 gas-liquid systems, motion in porous medium, heat and mass transfer 3-71824
 gas-solid mixture, downflow in standpipes 3-63777
 gas/liquid reactive propeller with ballast-boosted traction (Russian) 3-63794
 gas/solid mixtures, acoustic velocity and critical flow state calc. (German) 3-67965
 heat pipe analysis, two-phase Mach numbers 3-71808
 heat transfer bibliography, Japanese works 3-57735
 heat transfer in two phase flows, exp. study 3-40708
 heated gas, atomised liquid, vertical pipes, pressure loss induced by evaporation 3-63757
 heavy particle transport in homogeneous turbulent fluid flow 3-46482
 high temp. dust gas transverse flow past cylinder, heat transfer 3-60538
 horizontal stratified, gas-liquid mixtures, pipes 3-71809
 jet, two-phase, turbulent axisymmetric, dispersion of heavy admixture 3-60588
 jets, vapour, submerged, penetration in subcooled liquids 3-75273
 Kakhovka reservoir, suspended sediment flow rate 3-76928
 laminar, along plane barrier, hyperfiltration (Russian) 3-63753
 laminar, in MHD, flow rates 3-71800
 laminar to turbulent flow, transition, Hanks stability criterion 3-78946
 laminar tube flows, behaviour of falling and suspended sphere, rotation, tubular pinch effect 3-71821
 light scatt. photometer for kinetic studies of flowing aerosols, particle size distrib. 3-40082
 liquid drop breakup in turbulent flow, residence time and flow velocity depend. 3-49615
 liquid droplets in a gas flow, deformation and disintegration 3-63775
 liquid film flow over cylindrical surface, evaporation, heat and mass transfer 3-79026
 liquid films, wavy, in horizontal shear flow, convective diffusion 3-57714
 liquid mixing by large gas bubbles in bubble column 3-63748
 liquid with polymer admixture, applicability of viscoelastic hypothesis (Russian) 3-63771
 liquid-gas media, low velocity detonation, approximate model (Russian) 3-78988
 liquid-gas mixture, flow through porous beds, gravity conditions effect 3-59210
 lung, inertial deposition of aerosol particles 3-73593
 Mass transfer in upwards co-current gas-liquid annular flow 3-63752
 Maxwell fluid, dusty, flow from oscillating infinite flat plate 3-79033
 melt film motion in a cyclone chamber, effect of gas flow and separating particles 3-57825
 MHD elastico-viscous flow past plane porous plate, velocity field soln. 3-40736
 mixing for annular flow in simulated rod bundle geometries 3-43281
 mixture, two-phase, annular flow, hydraulic resistance meas. 3-60575
 mixtures two-phase, friction during turbulent flow in smooth tubes and channels 3-43627
 non-Brownian particles flow past disc collectors, deposition under colloidal forces 3-43629
 nozzle, analysis, equilib. flow with solidification (Russian) 3-63758
 nozzle processes, effect of initial parameters 3-49624
 oil-water, immiscible liquids, laminar and turbulent transitional flow, stratified channel flow 3-67963
 one component fluid, two-phase interface, continuum model 3-43561
 packed columns liquid distribution 3-49611
 particle eddy diffusivity, particle size effect in turbulent flow 3-79032
 particles, negatively charged, space charge flow in air, charge depletion mechanism 3-54819
 particles in suspension, effect on turbulent flow properties (French) 3-60572
 particulate systems, low Peclet number mass or heat transfer 3-79024
 Poiseuille flow, aspherical particle rotation obs., resistance pulse technique 3-54826
 polyacrylamide admixture effect on turbulent flow of water in flat rough tubes (Russian) 3-63770
 polyethyleneimine-polycrylate, rotation viscometer study of Newtonian flow 3-43630
 polyisobutylene solutions, dynamic viscosity and elasticity, effect of steady-state flow 3-71686
 polymer aqueous solutions, hydrodynamic influence of polymer additives in external flow around a sphere 3-57830
 polymer dilute solns. behaviour in inlet region of pipe 3-75267
 polymer solution, high viscosity, wedge and channel flow stability 3-54825
 polymer solutions, turbulent flow, influence of high-molecular weight additives 3-57832
 polymer threads, drag reduction in turbulent flow 3-40739
 polystyrene, elastomers, mol. wt. effect on viscosity 3-71676
 in porous media 3-57835
 powder particle acceleration in plasma stream for deposition of coatings (Russian) 3-53175
 power law gas-liquid two phase annular flow, liquid film thickness 3-40738
 pressure losses in flow along pipe calc, reln. to nuclear reactor cooling 3-74668
 propagation velocities of pressure and void by cross correlation of fluctuations in $\text{N}_2\text{H}_2\text{O}$ flow 3-70499
 radiation interrogation dynamic-bias 3-46394
 shock solutions existence in 2 fluid system, limitations 3-63762
 similarity and equivalent transport properties concept 3-79022

two-phase flow continued

- solid suspension laminar flow with radiating fluid, radiative heat transfer, gas-cooled nuclear reactor 3-40529
- sphere motion near wall boundary a Poiseuille flow, pressure drop 3-60574
- spouting bed of polymeric material, effect of gas flow fluctuations 3-63756
- sprays, liquid, in flowing hot gas, rapid cooling processes 3-71806
- Stokes problem for conducting fluid with particle suspension 3-49605
- supersonic two-phase flow meas. with laser-Doppler velocimeter (*Russian*) 3-77756
- surfactant molecules adsorption at the surface of growing bubble, time depend. of conc. at surface 3-63755
- suspension, particle collection under London and gravity forces 3-40747
- suspension, slow viscous shear flow, particle motion, orientation statistics, laser study 3-40746
- suspension, swirling laminar pipe flow 3-71823
- suspension flow, determ. of critical velocity 3-63774
- suspension of ellipsoidal macromolecules, two dims. laminar flow, orientation distrib. function, Legendre coeffs. 3-40749
- suspension of solid particles in gas, propagation of pressure waves 3-79029
- two arbitrary sized touching spheres in a linear shear field, creeping motion 3-52486
- two component stratified gas liquid stream in horizontal tube, motion determ. (*Russian*) 3-75262
- vapour-liquid mixture flow, pressure fluctuations meas. 3-71810
- velocity ratio equation, friction rel. to void fraction 3-49613
- vertical film flow, surfactant effect on evaporative heat transfer 3-64162
- viscoplastic disperse system, steady-state isothermal flow in elbow pipe of circular cross section 3-71817
- viscous, effect of fluid circulation in drop on drag force (*Russian*) 3-43626
- void fraction during two-phase flow 3-67964
- void fraction meas. by gamma-ray attenuation technique, channelling corrections, reactor application 3-46127
- water cooling systems, instabilities 3-60569
- water flows with polymer additives, hydraulic losses investigation 3-57829
- water streams containing some macromolecular substances, boundary layer turbulence 3-71819
- Fe_2O_3 dielectric ferromagnetic suspension, flow in a rotating magnetic field (*Russian*) 3-63776
- Na boiling simulation using a water model, voiding and re-entry processes 3-46703
- NaK-N_2 flow in rectangular cross section channel with large aspect ratio, frictional pressure drop 3-71811
- SiO_2 sol, ultramicroscopy, coagulation mechanism 3-65029

TWT see travelling-wave-tubes

type I superconducting materials

No entries

typesetting, computer-controlled see computer controlled typesetting

u.h.f. tubes see ultra-high-frequency tubes

ultimate tensile strength see tensile strength

ultra-high-frequency tubes

see also microwave tubes

No entries

ultracentrifuges see centrifuges

ultrasonic absorption

see also acoustic paramagnetic resonance; nuclear acoustic resonance

- acrylic monomers, hypersonic attenuation temp. depend., Brillouin spectra, thermal relax. effect 3-55990
- alloys, dilute, magnetic, u.s. attenuation, s-d interaction model 3-79823
- antiferromagnet, in strong mag. field 3-41391
- antiferromagnetism, itinerant, u.s. absorpt. above Neel temp. 3-72441
- attenuation meas. by spectrum analysis of pulses in buffer rods 3-42523
- backscatter and absorption, by pulse echo method (*German*) 3-51471
- benzene single crystal, pulse method meas. 3-43837
- benzol emulsion, u.s. wave absorption and scattering, impulsion method (*Russian*) 3-50796
- biological systems, u.s. attenuation and thermal conduction 3-42274
- brominebenzene emulsion, u.s. wave absorption and scattering, impulsion method (*Russian*) 3-50796
- capillary porous substances, effect of porous struct. and absorbed moisture on u.s. propagation 3-61238
- carbon tetrachloride, press. depend., 1-4000 kg/cm² 3-71995
- carbon tetrachloride, separation of various contributions as function of pressure 3-49942
- conference, Paris, France, Sep. 1972 3-42408
- crystal absorption, transducer, bond energy losses 3-75573
- crystal with off-centre impurity ions, paraelec. acoustic reson. absorpt. (*French*) 3-40977
- cupric formate tetrahydrate single crystals, for elastic const. determ. 3-79403
- electron excitation energy migration via phonon field, u.s. stimulation 3-68347
- energy cooperation, coherent and u.s.-stimulated via elementary excitations 3-75969
- erythrocytes, fixed, macromolecular interaction 3-45255
- ethylene and vinyl acetate copolymers, partly crystalline, molecular mobility, dynamic meas. (*German*) 3-63589
- eugenol, press. depend., 1-4000 kg/cm² 3-71995
- ferromagnetic insulator, with weak anisotropy, low temp. u.s. absorpt. 3-55451
- glass, tunnelling model for temp. and freq. depend., thermal props. (*French*) 3-40975
- ice, fresh water and sea, attenuation, 200-1100 kHz 3-77327
- interaction of u.s. waves, phonons, with crit. fluctuations (*French*) 3-40978
- kidney tissue, v.h.f. u.s. attenuation 3-59455

ultrasonic absorption continued

- liquid, u.s. interferometer, wide-band piezosemiconductor unit 3-42522
- liquid crystal, nematic-isotropic transition region, anomalous u.s. absorpt. and dispersion 3-79229
- liquid crystal, shear mech. impedance of nematic and cholesteric mesophases (*French*) 3-40844
- liquid crystals, pretransition phenomena just above clearing point 3-63950
- low temperature attenuation by phonons, calc., effect of approx. 3-79436
- measurement, millilitre liquid samples, 0.5 to 100 MHz, resonator and pulse method 3-62006
- measurement, pulse-echo technique 3-45429
- metal, ultrasonic backward scattering of conduction electrons, Umklapp scattering processes 3-72141
- metal hexagonal crystals, Mg, Zn, Cd, u.s. studies, electronic struct. 3-72312
- metal hexagonal crystals, u.s. study of supercond. state 3-72425
- nitrobenzene emulsion, u.s. wave absorption and scattering, impulsion method (*Russian*) 3-50796
- nitrobenzene-n-nonane system, u.s. absorption near critical region 3-49941
- nonlinear effects, interaction in solids (*French*) 3-42422
- in organic liquids, absorpt. and dispersion, depend. on bulk viscosity coeff. 3-49940
- organic liquids, amplitude coefficient of absorption, 10 MHz to 3 GHz, vibrational relaxation mechanism 3-58084
- partial melting during tempering, determ. by u.s. methods 3-53251
- polyelectrolytes in aqueous soln., u.s. obs. rel. to chemical equilibria kinetics (*French*) 3-43835
- polyisobutylene in transformer oil, inf. of press. and temp. 3-75572
- n-propanol, adiabatic volume viscosity and structure by ultrasonics 3-68431
- semiconductors, nondegenerate, influence of linear and point defects on hypersonic attenuation by free carriers 3-55310
- silica, vitreous, anomalous absorpt. of longit. waves down to 0.4K 3-79437
- solid-liquid interface, anomalous reflection with attenuation 3-41077
- steel, 1% C, attenuation rel. to temp. 3-43834
- superconductor, two-zone type, pure, dislocation retardation and weakening effect due to transition (*Russian*) 3-52928
- superconductor with overlapping bands, u.s. absorpt. and thermal cond. 3-55368
- surface, meas. of variations in velocity and absorpt. by buckling method (*French*) 3-39864
- t-butyl alcohol-water system, frequency dependence, relaxation processes, model 3-59478
- toluene, rel. to pressure, explanation using concept of holes in liquid lattice 3-43831
- vinyl acetate and ethylene copolymers, partly crystalline, molecular mobility, dynamic meas. (*German*) 3-63589
- water and heavy water mixture, volume viscosity and struct. u.s. study 3-50020
- water-benzene-ethyl alcohol ternary system, shear viscosity and u.s. absorpt. near plait pt. 3-64204
- Al, dislocation movement, u.s. wave velocity and absorpt. meas. (*French*) 3-43796
- Al, harmonically deformed, attenuation coeff., dislocation string model approach (*Russian*) 3-43833
- Al alloy, type D16, partial melting during tempering, determ. by u.s. methods 3-53251
- Al-Cu(Zn) alloys, single crystals, alloying effects (*Russian*) 3-72138
- As₂Se₃, glassy semicond., temp. depend. (*French*) 3-40976
- Bi, excitonic phase transition under strong mag. fields down to 1.06 K, u.s. attenuation 3-72327
- Bi, hypersonic attenuation, Bragg light scatt. by sound obs. (*Russian*) 3-79435
- Bi₁₂GeO₂₀, Bi₁₂SiO₂₀, Bi₁₂(Ge_{0.5}Si_{0.5})O₂₀, selection rule existence for interaction mechanism, anomalous attenuation 3-58085
- Cd, temp.-depend. peak in electronic attenuation of u.s. shear waves, rel. to Fermi surface geometry 3-79622
- CdGeAs₂, glassy semicond., temp. depend. (*French*) 3-40976
- CdS, lattice u.s. absorpt. deduced from optoacoustic scatt. 3-58086
- Cu, u.s. pulse method obs. of dislocation struct. (*Russian*) 3-41713
- Cu-Pb-Cu proximity effect sandwichs, crit. mag. fields, acoustic surface wave attenuation obs. 3-55377
- Cu_{0.4}Cd_{0.6}Fe₂O₄, crit. props. near Curie point, spin-lattice relax. as absorpt. mechanism 3-75840
- D₂O, pressure dependent, lattice model calculations 3-46680
- n-Ge, pure and doped, determ. from third order elastic moduli meas. 3-40979
- Ho, spin spiral state, longitudinal u.s. attenuation 3-41387
- n-InSb, conduction electron absorpt., effect of microinhomogeneities 3-49943
- InSb, lattice u.s. absorpt., 77K, 0.25-6.0 GHz 3-58087
- n-InSb, rel. to phonon study by heat pulse technique, deform. pot. coupling (*French*) 3-43845
- K₂O-B₂O₃ melts viscosity behaviour investigations, relaxation time 3-41040
- LiNbO₃, surface acoustic wave attenuation, effect of 80 keV ion implantation 3-52746
- NH₄Br(Cl), lambda order-disorder transition, u.s. obs., mode-mode coupling theory 3-41000
- NH₄Cl, temp. depend. anal. results rel. to critical relaxation of order-disorder lambda transition 3-72139
- NH₄H₂PO₄ crystal, u.s. attenuation and velocity temp. dependence 3-40980
- Na₂O-B₂O₃-SiO₂, glass, absorpt. in immiscibility region, structural relax. 3-72140
- Nb, purity depend. in normal, Meissner states, meas. and theory 3-64433
- Nb, superconducting, attenuation of transverse waves, real metal parameters 3-72424
- Nb₃Sn, phonon damping 3-49946
- Pb, dislocation pinning by point defects, u.s. detection, migration energies 3-54979

ultrasonic absorption continued

- Pb, dislocation pinning by point defects, u.s. detection, model 3-54980
 RbMnF₃, antiferromag. reson. near Neel temp., u.s. wave coupling to antiferromag. spin waves (*French*) 3-41427
 Re, high purity, transverse and longitudinal attenuation measurements of superconducting energy gap 3-58337
 α -S, acoustic and acoustooptical props., modulation and deflection applications (*French*) 3-43836
 Se-Ge, glassy semicond., temp. depend. (*French*) 3-40976
 Si, u.s. attenuation due to acceptor holes, internal stresses effects 3-50145
 TeO₂, attenuation, c.w. acoustooptical and pulse-echo techniques 3-45427
 TiO₂, attenuation, c.w. acoustooptical and pulse-echo techniques 3-45427

ultrasonic applications

- alkali halides, strain-optical constant ratios, u.s. determ. 3-80007
 anisotropy measurements and mechanical properties of polymers 3-53308
 atomic absorption spectrometry, pulse u.s. nebulizer system 3-45581
 blood flow telemetry, using implanted Doppler effect directional velocity meter (*German*) 3-62311
 blood flowmeter 3-42690
 brittle materials, apparatus for recording acoustic signals from cracks 3-42519
 canning tubes testing 3-40544
 coil and cold-rolled steel, using Lamb waves 3-41832
 convolver, enhanced Rayleigh surface wave, using piezoelec. CdS 3-42421
 cylinder, thick-walled, fatigue crack growth meas. and anal. technique 3-76413
 diagnosis, by u.s. imaging 3-48631
 diagnostic and therapeutic, effects and side effects in medicine (*German*) 3-77249
 electron microscope disc specimen preparation, by u.s. impact grinding 3-40049
 flaw size estimation study by u.s. scanning method with relative threshold 3-47521
 gas-liberation, evacuation of vacuum electronic equipment, theory, conditions 3-56657
 graphite, pressure depend. of C-axis elastic parameters, by pulse echo technique 3-79404
 heat exchanger tubing, base line end in-service inspection u.s. testing 3-47506
 hologram, acoustic, prod. by 256 x 256 matrix of electrostatic transducers (*French*) 3-42413
 holography, acoustic, use of Pohlman cell 3-42415
 holography, acoustic 3-42412
 human female breast, composition determ. 3-59678
 image prod., digital enhancement 3-42418
 imaging of eye structure, intensity in focus, possible damage 3-65998
 imaging system, quasi monochromatic partially coherent, resolution 3-42416
 imaging systems, high resolution, high contrast 3-42414
 imaging with u.s. camera system, comparison with other methods (*French*) 3-42417
 ionospheric obs. using u.s. image forming technique 3-47843
 Lamb wave u.s. bond inspection, airframe struct. 3-47512
 laser beam deflection devices based on light diffraction by u.s. wave 3-56693
 light guided in thin layer, diffr. by u.s. surface waves (*French*) 3-40215
 light interaction with u.s. surface waves, for fast printers, document reading, memories (*French*) 3-42423
 light modulator, half-wave plate behaviour 3-70211
 liver scanning, automated A-scan analysis 3-61917
 material testing, unconventional generation, reception and coupling of u.s. waves 3-53294
 materials testing, solids, hidden defects, shape and size determination, analytical method 3-73677
 NDT, cylindrical work pieces with central bore-hole, u.s. wave attenuation (*French*) 3-69414
 NDT, spectral analysis applics. 3-76411
 NDT, u.s. generation, detection and coupling, unconventional methods (*German*) 3-50820
 NDT, use of nearfield and farfield terms (*German*) 3-69413
 NDT of nucl. fuel 3-57553
 nondestructive testing, computer use for anal. routines, r.f. waveform, Fourier anal. 3-47515
 nondestructive testing, conf., Los Angeles, USA, (Mar. 1973) 3-47497
 nondestructive testing, elastic wave analysis 3-50819
 nondestructive testing, u.s. interaction with defects 3-56571
 nondestructive testing, u.s. variable angle transducer, welded steel pipe 3-47505
 nonlinear effects in air, study using powerful u.s. source (*French*) 3-42425
 nuclear fuel cladding tube, standard defect machining for test applic. (*Japanese*) 3-63132
 nuclear reactor pressure vessel testing compensation from base material, surface and group differentials (*German*) 3-70276
 nuclear reactors, light water systems, automated u.s. in-service inspection 3-47503
 optical modulation, circular dichroism study 3-73726
 piezoelectric devices, for industrial, communication and medical uses 3-42410
 porcelain enamel adherence to steel, u.s. determ., nondestructive eval. 3-73097
 pulse-echo testing, DONAR computer processing system 3-61997
 signal processing using surface elastic waves, past, present and future 3-45370
 simple u.s. testing equipment for defect indication efficiency of 100% for steel plates and strips (*German*) 3-47520
 small u.s. bubble chambers 3-77650
 speech, tongue displacements, on-line pulsed through-transmission ultrasonic monitoring system 3-73925
 stainless steel, cold work meas., nondestructive methods 3-47504

ultrasonic applications continued

- steel, boiler tube billets, n.s. inspection, flow detection quality of tubes rel. to macrodefects 3-53303
 steel, carbon, ultrasonic vibro-indentation hardness, resistance to plastic deformation 3-41753
 steel, case hardening depth, detn. (*French*) 3-58790
 steel, crack detection, u.s. shear wave techniques, influence of residual stress 3-47514
 steel, stainless, meas. of neutron irradi. effect on elastic consts. 3-78386
 steel, u.s. inspection, flaw detectability study, ASNT Sonics and Aerospace Committees 3-47517
 striscopy, linear, of u.s. fields in air (*French*) 3-42420
 Substrate cleaning for integrated optical waveguides 3-79576
 surface wave, solid-state, for scanning optical patterns 3-39865
 testing methods, information transfer approach 3-44701
 thermometer, in-reactor fuel rod centreline temp. meas. 3-45454
 thermometry, temp. meas. up to 2400C, inaccessible objects 3-42521
 titania-silica glasses, thermal expansion meas. by photoelastic and u.s. techniques 3-51593
 transducer, linear array, directivity pattern, flaw detect. and diagnostics 3-42436
 u.s. holography, u.s. hologram, real image (*Czech*) 3-51877
 welding biological tissue 3-66405
 Zircaloy tubing, u.s. inspection, wall thickness and ID meas., multiplexed instrumentation 3-47516
 Al, crack detection, u.s. shear wave techniques, influence of residual stress 3-47514
 Al alloy, fatigue crack detection, u.s., X-radiographic and eddy current techniques 3-47511
 Al alloy, u.s. inspection, flaw detectability study, ASNT Sonics and Aerospace Committees 3-47517
 liquid H₂ u.s. bubble chamber at Dubna 3-77651
 LiNbO₃, piezoelec. transducer, nuclear reactors, u.s. inspection 3-65061
 α -S, as deflector in visible region, acoustic and acoustooptical props. (*French*) 3-43836
 SiC tubes testing 3-43314
 Ti-Al-V, crack detection, u.s., shear wave techniques, influence of residual stress 3-47514

ultrasonic delay lines

No entries

ultrasonic devices

- see also *ultrasonic delay lines*; *ultrasonic transducers*
 acoustic contact, investigation of polymers, organosilicon oil-talc mixture 3-73678
 convolver, enhanced Rayleigh surface wave, using piezoelec. CdS 3-42421
 Doppler velocity meter, M-sequence modulation method (*Japanese*) 3-70265
 Langevin, attempts to produce and receive u.s. waves, first devices (*French*) 3-42409
 light guided in thin layer, diffr. by u.s. surface waves (*French*) 3-40215
 light interaction with u.s. surface waves, applications (*French*) 3-42423
 light modulator, half-wave plate behaviour 3-70211
 signal processing using surface elastic waves, past, present and future 3-45370
 unconventional generation, reception and coupling for u.s. testing 3-53294
 α -S, as deflector in visible region, acoustic and acoustooptical props. (*French*) 3-43836

ultrasonic diffraction

- striscopic linear images for u.s. diffraction and reflection problems (*French*) 3-42420

ultrasonic dispersion

- liquid crystal, nematic-isotropic transition region, anomalous u.s. absorpt. and dispersion 3-79229
 in organic liquids, absorpt. and dispersion, depend. on bulk viscosity coeff. 3-49940
 vinyl, substituted compound, u.s. relax. of conformational equilibria 3-54615
 Ca₂SiO₄, effect on polymorphic transitions, anal. 3-72192
 NO, temp. depend., 423-500 K 3-40670

ultrasonic effects

- biological tissue destruction, thermal factors 3-42376
 brain tissue, mammalian, thermal lesion production, thresholds, frequency dependence 3-77267
 bubble, vapour, in liquid H₂, dynamics 3-73875
 cavitation, in biological tissue 3-42375
 damage in crystals 3-43832
 hardening of electrodeposits by ultrasound, scanning electron microscope study 3-61172
 high power impulse discharge channel, structural and spectroscopic studies (*Russian*) 3-49787
 light diffraction, by successive u.s. waves, beat freq. spectra obs. 3-70783
 light diffraction by ultrasound, spectral intensities for Bragg incidence, Brillouin theory (*French*) 3-42965
 light guided in thin layer, diffr. by u.s. surface waves (*French*) 3-40215
 liquid, u.s. light diffr. for laser beam generating third harmonic 3-41500
 medical, side effects and safety margins in diagnostic and therapeutical applications (*German*) 3-77249
 mitotic activity reduction in rat liver 3-42377
 noncritical optical heterodyning using two successive ultrasonic light modulators 3-51611
 nonlinear effects, dimensionless Mach and Reynolds numbers (*French*) 3-42422
 nonresonance intermolecular energy transfer, u.s. pumping effects 3-72602
 photomixing, light beat by a.m. u.s. wave, application to speed of sound measurements 3-66154
 steel, dispersion hardening, time-to-rupture and substruct. under u.s. treatment (*Russian*) 3-53247

ultrasonic effects continued

- Ag halide microcrystals, effect of u.s. waves on growth mode during emulsification, electron microscopy (*Russian*) 3-47595
- Al alloys, wetting by low melting solders, u.s. tinning, joint formation (*Russian*) 3-41791
- Al-Mg alloys, u.s. vibr. effects on mech. props. and fine struct. (*Russian*) 3-72849
- Cd, twinning, u.s. irradiation effects, 20 kHz, deformation localisation zone, incoherent twin-matrix interface 3-49901
- Cu-Ni multilayer system, u.s. vibrs. effect on pore form. and Kirken-dall effect (*Russian*) 3-79518
- GaAs, etching (*German*) 3-52756
- n-InSb acoustoelectric energy conversion, e.m. radiation at 77K, externally injected u.s. wave, conversion efficiency, electric and magnetic field effects 3-50245
- Mg alloy MA2-1, u.s. treatment during solidification effects 3-55812
- Mo, vibr. effects on dislocation struct. and mech. props. (*Russian*) 3-69207
- NaCl-type ionic crystals, effective valences and repulsive parameters using Born model on ultrasonic data for Ca_4 3-64082
- Ni, treatment effects on vacancy and dislocation conc. (*Russian*) 3-41714
- Ni alloy, u.s. treatment during vacuum arc melting, ingot struct. refinement, plasticity, corrosion-resistance (*Russian*) 3-53263
- Ni-Al(1.18 wt.%) alloy, substruct. misorientation changes during u.s. treatment and creep tests (*Russian*) 3-69212
- Pb glass, cavitation failure, leaching under u.s. action (*Czech*) 3-56570

ultrasonic equipment

- absorption measurement apparatus, millilitre liquid samples, 0.5 to 100 MHz, resonator and pulse method 3-62006
- flowmeter, Doppler, pulsed, velocity profiles in man 3-73928
- imaging with u.s. camera system, comparison with other methods (*French*) 3-42417
- Pohlman cell, use in acoustic holography 3-42415

ultrasonic measurement

- absorption, millilitre liquid samples, 0.5 to 100 MHz, resonator and pulse method 3-62006
- adhesive bond strength, metal-to-metal joint, prediction 3-69410
- attenuation by spectrum analysis of pulses in buffer rods 3-42523
- attenuation meas., pulse-echo technique 3-45429
- lattice dynamics problems, elastic const. determ. and Szigeti's relations (*French*) 3-43844
- liquid, u.s. interferometer, wide-band piezosemiconductor unit 3-42522
- liquid helium film on CaF_2 surface, acoustic interferometry for standing wave detect. 3-39863
- phonon study at high freq. by heat pulse technique (*French*) 3-43845
- piezoelectric effect for u.s. wave generation and detect. beyond 100 GHz 3-42411
- polyelectrolytes in aqueous soln., u.s. absorpt. rel. to chem. equilibria kinetics (*French*) 3-43835
- polymers, acoustic contact, 2.1 to 240 K, organosilicon oil-talc mixture 3-73678
- primary acoustic thermometry systematic errors analysis, range 2-20 K 3-62032
- surface waves, variations in velocity and absorpt. by buckling method (*French*) 3-39864
- testing methods, information transfer approach 3-44701
- Al, dislocation movement, u.s. wave velocity and absorpt. meas. (*French*) 3-43796
- TeO_2 , attenuation, c.w. acoustooptical and pulse-echo techniques 3-45427
- TiO_2 , attenuation, c.w. acoustooptical and pulse-echo techniques 3-45427
- Ti_2O_3 , elastic const. through elec. transition, u.s. wave transit time 3-43821

ultrasonic propagation

- see also *ultrasonic diffraction; ultrasonic dispersion; ultrasonic reflection; ultrasonic refraction; ultrasonic scattering; ultrasonic transmission*
- backscatter and absorption, by pulse echo method (*German*) 3-51471
- capillary porous substances, effect of porous struct. and absorbed moisture on u.s. propagation 3-61238
- conference, Paris, France, Sep. 1972 3-42408
- defects interaction, Schlieren and computer studies 3-56571
- diffuse sound field, cavitation meas. (*German*) 3-51470
- ferroelectric ceramics, periodically polarised 3-55035
- ferromagnetic dielec. with multidomains, Mossbauer study of u.s. generation by r.f. field 3-44307
- gas, hypersound propag. const. using macroscopic theory of fast processes in translation-invariant systems 3-59822
- impulsive wave, directivity and reflectivity (*French*) 3-42419
- with inhomogeneities randomly distributed 3-58828
- kerosene beam edge effect 3-46679
- light diffraction analysis of u.s. fields 3-53787
- liquid, laser beam induced sound wave, time and freq. behaviour 3-64116
- liquid, mol. motion from viscoelastic and u.s. relax. obs. 3-64205
- piezoelectric cryst. surface, nonlinear interaction of u.s. waves with opposite propag. directions (*French*) 3-41078
- piezoelectric effect for u.s. wave generation and detect. beyond 100 GHz 3-42411
- piezoelectric semiconducting crystal, inhomogeneous, acoustoelectric interaction, nonuniformities 3-58310
- piezoelectric substrate, acoustic surface wave correlation by space charge nonlinearity 3-52747
- rocks under uniaxial compression, u.s. travel-times 3-76635
- schlieren system, using pulsed gas laser 3-45428
- second harmonic, resonance generation in elastic solids 3-59477
- surface waves, optical probing of nonlinear elastic effects 3-39902
- AIN epitaxial film, on sapphire, acoustic surface wave props. 3-55135
- BaSO_4 , barite, plastic deform. rel. to longit. u.s. propag. vel. 3-46663
- $\text{Bi}_{12}\text{GeO}_{20}$, minimal diffraction cuts for acoustic surface wave propagation 3-58172

ultrasonic propagation continued

- CdS , acoustoelec. amplification rel. to current saturation, Brillouin diff. obs. (*French*) 3-44118
- CdS , photocond., acoustoelec. amplification of Bleustein-Gulyaev waves (*French*) 3-44121
- CdS phonon maser structures, u.s. wave propagation 3-53788
- GaN epitaxial film, on sapphire, acoustic surface wave props. 3-55135
- InSb, hypersonic wave propag., suppression of nonlinear effects in strong elec. field 3-58311
- LiF , nuclear quadrupole spin-phonon coupling, u.s. wave propag. 3-75891
- LiNbO_3 , acoustic radiation from a high-coupling cut 3-55136
- LiNbO_3 , third order elastic constants, u.s. wave obs. 3-68929
- LiNbO_3 -Si layered structure, acoustoelectric effects 3-58308
- NaCl(F) , nuclear quadrupole spin-phonon coupling 3-75891
- Ni, e.m. excitation of u.s. waves, 5 and 10 MHz 3-55452
- PbMoO_4 , acoustic anharmonic effects, acousto-optical obs. 3-68339
- Te, single crystal at high temp., u.s. propagation, elastic parameters calc. 3-79434
- Ti_2O_3 , elastic const. through elec. transition 3-43821
- V_2Si , harmonic-phonon generation by shear waves in region 5 to 10 MHz 3-52673
- ZnS , wurtzite, single cryst. elastic const., u.s. pulse superposition meas. 3-58063

ultrasonic radiation see *ultrasonic waves***ultrasonic reflection**

- backscatter and absorption, by pulse echo method (*German*) 3-51471
- impulsive wave, directivity and reflectivity (*French*) 3-42419
- liquid-liquid interface, critical-angle phenomena by Bragg diffraction of laser light 3-42426
- liquid-solid interface, study using cylindrical transducer and pulsed schlieren system 3-48291
- pulsed reactor fuel, NDT, dye penetrant, u.s. reflection, X-radiography, immersion density methods 3-67559
- solid-liquid interface, anomalous reflection with attenuation 3-41077
- strioscopic linear images for u.s. diffraction and reflection problems (*French*) 3-42420

ultrasonic refraction

No entries

ultrasonic scattering

- backscatter and absorption, by pulse echo method (*German*) 3-51471
- backscattering from ensemble of scatterers excited by sine wave bursts 3-45368
- benzol emulsion, u.s. wave absorption and scattering, impulsion method (*Russian*) 3-50796
- brominebenzole emulsion, u.s. wave absorption and scattering, impulsion method (*Russian*) 3-50796
- chlorobenzene, nonlinear phenomena 3-68336
- cyclohexane, nonlinear phenomena 3-68336
- heptane, nonlinear phenomena 3-68336
- metal backward scattering of conduction electrons, Umklapp scattering processes 3-72141
- nitrobenzene emulsion, u.s. wave absorption and scattering, impulsion method (*Russian*) 3-50796
- octane, nonlinear phenomena 3-68336
- ^4He liquid, structure and excitations, review 3-58158

ultrasonic transducers

- blood flow meas. 3-42690
- conference, Paris, France, Sep. 1972 3-42408
- hologram, acoustic, prod. by 256×256 matrix of electrostatic transducers (*French*) 3-42413
- interdigital, on piezoelec. substrate, Rayleigh wave prod. and detect. (*French*) 3-45369
- linear array, for 500 to 1000 kHz. freq. range, directivity pattern 3-42436
- novel, for u.s. testing 3-53294
- piezoelectric, for depletion and diffusion layer transducers 3-42410
- piezoelectric and ferroelec. materials, props. rel. to transducer limitations 3-41484
- piezoelectric effect for u.s. wave generation and detect. beyond 100 GHz 3-42411
- probe, sound field measurement by automatic installations (*German*) 3-69416
- radiator, bending vibrations in beam 3-48290
- surface wave excitation above 1000 MHz with transducer obtained by electron beam masking (*French*) 3-42424
- variable angle, nondestructive testing, welded steel pipe 3-47505
- welded steel pipe, nondestructive testing, u.s. variable angle transducer 3-47505
- LiNbO_3 , interdigital, high coupling cut 3-55136
- ZnO thin layer prep. for use in GHz. band (*German*) 3-53193

ultrasonic transmission

- imaging systems, standing wave pattern modulated by object transmiss. props. 3-42414

ultrasonic velocitysee also *ultrasonic dispersion*

- acrylic monomers, hypersonic vel. temp. depend., Brillouin spectra, thermal relax. effect 3-55990
- araldite-hardener mixtures, hardener effect on transition temps., rot. plate method 3-69381
- binary, third metal addition effect on elastic moduli 3-64806
- composite, C fibre reinforced resins, unidirectional, longit. shear characts. 3-64997
- cupric formate tetrahydrate single crystals, for elastic const. determ. 3-79403
- 1,3-dioxolane-water mixtures, rel. to water shell stabilization hypothesis 3-65125
- elastic constants meas. by pulse echo method 3-48347
- glass, elastic constant, u.s. velocity meas. as a function of pressure 3-80650
- glass reinforced plastics, interlaminar shear modulus, relation with thermal conductivity 3-80445
- human female breast 3-59678
- igneous rocks with water saturation under high pressure (*Russian*) 3-65158

ultrasonic velocity continued

- liquid crystal, nematic, vel. minimum at transition, molar sound vel. 3-68338
- liquid crystal, smectic-A, anisotropic vel., elastic const. determ. 3-79432
- lithium salicylate and citrate aqueous and nonaqueous solns., temp. depend. 3-69491
- methane, solid, mol. orientation and lambda anomaly 3-55031
- polymers, at liq. He temp. 3-43532
- Rao's constant, temperature coefficient, ratio to expansion coefficient, theoretical study 3-77326
- refractory spinels, elastic moduli, porosity depend. 3-72942
- residual stress meas. and analysis using u.s. techniques 3-53839
- steel, elastic moduli, neutron irradiation effect 3-69272
- water, LiOH effect on vel. maximum 3-68337
- Al, for meas. of third-order elastic const. at 80K, nonlocal pseudopot. model 3-60759
- Al-Cu(Zn) alloys, single crystals., alloying effects (*Russian*) 3-72138
- As-Se system glasses, elastic props. determ. (*Japanese*) 3-64084
- Au polycrystalline disc, elastic properties at high pressure, u.s. velocity meas. 3-64085
- CO₂-methane, gas mixture vibrational relaxation, u.s. velocity measurements 3-57680
- CsCl, aq. soln., hypersonic vel., molar conc. depend., Brillouin scatt. meas. 3-49934
- Cu pressure dependence, {001} plane, nonlinear acoustic theory, results 3-49938
- In-Hg liquid alloy, sound velocity, anomalies 3-49936
- KCN, cubic, elastic const., temp. depend. determ. 3-54998
- KCl, aq. soln., hypersonic vel., molar conc. depend., Brillouin scatt. meas. 3-49934
- KCl single crystal, shear elastic constant C₄₄ meas. 3-43876
- LiBr(Cl)(I) aqueous and nonaqueous solns., temp. depend. 3-69491
- LiCl, aq. soln., hypersonic vel., molar conc. depend., Brillouin scatt. meas. 3-49934
- LiNO₃ aqueous and nonaqueous solns., temp. depend. 3-69491
- LiSO₄·H₂O aqueous and nonaqueous solns., temp. depend. 3-69491
- methane-CO₂ gas mixture, vibrational relaxation, u.s. velocity measurements 3-57680
- Mo, elastic moduli meas. under hydrostatic press. (*French*) 3-54994
- NH₄H₂PO₄ crystal, u.s. attenuation and velocity temp. dependence 3-40980
- NaCl, aq. soln., hypersonic vel., molar conc. depend., Brillouin scatt. meas. 3-49934
- NaCl-Tl, Cd, Cs, impurity precipitates meas. by u.s. velocity changes 3-64060
- Nb, elastic moduli meas. under hydrostatic press. (*French*) 3-54994
- Ne, liquid, measurements of thermodynamic parameters from m.p. to b.p. 3-68420
- Ni, elastic const. meas. by u.s. pulse echo method (*Japanese*) 3-50723
- O₂, liquid, hypersonic velocity meas. by Brillouin scattering 3-75570
- Pd, elastic moduli meas. under hydrostatic press. (*French*) 3-54994
- RbCl, aq. soln., hypersonic vel., molar conc. depend., Brillouin scatt. meas. 3-49934
- SiC, hot-pressed, shear modulus meas., 350-1000°C 3-72944
- Si₃N₄, hot-pressed, shear modulus meas., 350-1000°C 3-72944
- SrMoO₄, for elastic const. determ. 3-49921
- Zr, elastic parameters of single crystals., oxygen effects 3-76204

ultrasonic velocity measurement

- echo-pulse installation, phase comparison and time delay methods, apparatus, techniques 3-77388
- frozen ottawa sand, dilatational and shear velocities, variation with water content 3-47660
- liquid, pulse method for vel. variations with temp. and comp. meas. 3-66152
- liquid, u.s. interferometer, wide-band piezosemiconductor unit 3-42522
- pulse transmission technique, high resolution, dispersive media, attenuating media 3-62007

ultrasonic wave propagation *see ultrasonic propagation***ultrasonic waves***see also ultrasonic propagation*

- convolver, enhanced Rayleigh surface wave, using piezoelec. CdS 3-42421
- diffraction of light by waves travelling in opposite directions 3-48846
- dilatational and shear velocities, variation with water content, frozen ottawa sand 3-47660
- metal, excitation by charged particle beams 3-55034
- piezoelectric crystal, harmonic generation of surface waves (*French*) 3-41079
- second harmonic, resonance generation in elastic solids 3-59477
- semiconductor, amplification by transverse elec. current prod. hot electrons 3-58309
- signal processing using surface elastic waves, past, present and future 3-45370
- surface, diffraction of light guided in thin layer (*French*) 3-40215
- surface wave excitation above 1000 MHz with transducer obtained by electron beam masking (*French*) 3-42424
- surface waves, applications for interactions with light (*French*) 3-42423
- transducer, interdigital, on piezoelec. substrate, Rayleigh wave prod. and detect. (*French*) 3-45369
- Ba₂NaNb₅O₁₅, ferroelectric, polarised microwave echo obs. 3-75951
- CdS, photocond., acoustoelec. amplification of Bleustein-Gulyaev waves (*French*) 3-44121
- LiNbO₃-Si(CdSe), layered structure, acoustoelec. effect due to elec. fields of u.s. surface waves 3-44120
- ultrasonics**
- see also acousto-optical effects; ultrasonic applications; ultrasonic devices; ultrasonic equipment; ultrasonic waves*
- amplitude on phase modulation of light (*Russian*) 3-66758
- conference, Paris, France, Sep. 1972 3-42408
- ultrasonics continued**
- Langevin, attempts to produce and receive u.s. waves, first devices (*French*) 3-42409
- piezoelectricity and growth of ultrasonics 3-42410
- signal processing using surface elastic waves, past, present and future 3-45370
- ultraviolet astronomical observations**
- A-type stars, anal. of OAO II obs. of u.v. spectra 3-73497
- absolute solar intensities and constant, accuracy of aircraft and ground based obs. 3-80980
- Apollo 17 for u.v. spectrometer expt. 3-48157
- B6-type stars, high dispersion spectrograms and scans in 1100-6700 Angstroms range 3-48025
- B-type main sequence stars, u.v. flux envelopes, 1100-6000 Å obs. 3-48026
- α Canis Majoris (Sirius), u.v. spectrophotometry, Gemini XII 3-48048
- α² Canum Venaticorum, Mg II lines at 2800 Å 3-56395
- α² Canum Venaticorum, spectrum variable, u.v. obs. of line blanketing 3-81039
- Celestec Catalogue, magnetic tape version 3-77077
- β Centauri, energy distrib. and continuous spectrum in 2000-3800 Å range 3-73509
- α Centauri, He spectrum var., OAO-2 u.v. photometric obs. 3-48049
- chromosphere-corona transition region structure obs. from limb/disc e.u.v. intensity ratios 3-69831
- chromospheric-coronal transition layer model from e.u.v. obs. 3-65629
- cluster of galaxies, Mariner 9 meas. of upper limits of Lα flux 3-51378
- clusters of galaxies, Mariner 9 u.v. spectrophotometric obs. 3-45199
- X Comae Berenicens, optical variability, UVB colours 3-81171
- comet Bennett (1969 i), spectropolarimetric obs. of head (*Russian*) 3-77012
- comet Bennett (1969 i), H production rates, 1970 April 1-19, Lyman-α obs. 3-69910
- Comet Tago-Sato-Kosaka (1969g), Lα image 3-56358
- CPD - 69°26'9", H-deficient star, Coude spectrograms and abundance analysis 3-48027
- EUV absorption, and thermospheric heating by Joule dissipation of ionospheric electric fields 3-76801
- e.u.v. broad band solar radiation absorption in Earth's upper atmosphere, OSO 5 obs. 3-53511
- G-type dwarf stars, metal-rich, u.v. four colour photometry, 31 Aquilae, δ Pavonis, and α Mensae 3-48015
- galactic latitude dependence, diffuse far u.v. background, mirror-geiger tube photometers 3-48103
- galactic latitude dependence, diffuse far u.v. background 1440 to 1620 Å 3-48104
- Galaxy, fine structure of next inner spiral arm, u.v. photography and photometry (*German*) 3-48090
- H II regions, dust extinction props. in u.v. 3-48130
- HD 144941, H-deficient star, Coude spectrograms and abundance analysis 3-48027
- HD 153919, identification as optical counterpart to 2U 1700-37, OAO-2 obs. 3-48032
- Hyades, far u.v. flux difference between stars in Pleiades 3-81186
- interstellar absorption lines in γ² Vel spectrum 3-70030
- interstellar CH spectra, predissociation in C²Σ⁺ state 3-81189
- interstellar cloud comp., Copernicus obs. 3-59383
- interstellar clouds, molecule abundances, Copernicus obs. 3-59386
- interstellar clouds, u.v. absorption lines, ionisation of C, N and O, effect of X-ray flux 3-48129
- interstellar gas abundances from rocket obs. of u.v. absorpt. lines 3-59378
- interstellar grain extinction in u.v., spectrophotometric results from Copernicus satellite 3-51404
- interstellar lines in unreddened stars, Copernicus u.v. obs. 3-59384
- interstellar medium, opacity to u.v. radiation, effective cross section per H atom 3-48126
- interstellar molecular H, Copernicus u.v. obs. 3-59385
- interstellar radiation density between 1250 and 4250 Å 3-48114
- Jupiter, far u.v. spectrum from sounding rocket obs. 3-80986
- lunar atmosphere, Apollo 17 far u.v. meas. 3-69905
- lunar dust from Apollo 11, 12 and 14 sites, for u.v. reflectivity meas. 3-45041
- α Lyra, energy distrib. and continuous spectrum in 2000-3800 Å range 3-73509
- main sequence, correlation between u.v. excess and deviation from mean 3-77062
- main sequence stars, u.v. colours from OAO-2 Telescope obs. 3-48005
- Mars, 1971 dust storm, Mariner 9 u.v. spectrometer experiment obs. 3-42145
- Mars, atm. scatt. props., Mariner 9 u.v. spectrometer data 3-65763
- Mars, atmospheric temp., Mariner 9 OI 1304-A emission 3-69875
- Mars, obs. by Mars 2 and 3 satellites 3-56337
- Mars, polar region, ozone, seasonal variation, Mariner 9 u.v. spectra obs. 3-45038
- Mars, u.v. albedo in 2000-3600 Angstroms region, OAO-2 observations 3-42146
- NGC 1300 barred spiral, UVB photoelectric drift scan 3-77133
- NGC 7027, planetary nebula, relative line intensities in spectral range 3000-5000 Angstroms 3-45228
- night sky radiation in u.v. and visible, Kosmos 51 and 213 obs. in space (*Russian*) 3-44878
- night sky radiation in u.v. and visible kosmos 51 and 213 observations in space (*Russian*) 3-44877
- night sky surface brightness meas. in 1500-4250 Å region 3-53701
- northern sky, EUV rocket survey 3-48144
- Nova Serpentis 1970, u.v. spectrophotometry 3-48040
- O and B standards, energy distrib. in u.v. spectra (*French*) 3-81089
- OB stars, Mariner 9 meas. of interstellar absorpt. at Lα 3-51337
- Opilichus, far u.v. photometry of stars rel. to sky background 3-48014
- δ Persei, OAO-2 and Mariner 9 u.v. obs. rel. to variability 3-77101
- PHL957, system A absorption spectra in H I cloud 3-81203
- Pleiades, far u.v. flux difference between stars in Hyades 3-81186

ultraviolet astronomical observations continued

- QSOs, search in direction of Abell clusters of galaxies 3-69983
 satellite-borne X-ray and ultraviolet techniques and observations, Copernicus 3-65953
 Saturn, 0.62 μ methane band absorpt. and near-u.v. charact. 3-61695
 Scorpius, far u.v. photometry of stars rel. to sky background 3-48014
 α Sculptoris, spectrum variable, u.v. obs. of line blanketing 3-81039
 SN 1972 in NGC 5253, u.v. photometry 3-48044
 solar 5-minute oscillations, near u.v. obs. of phase lags 3-80943
 solar chromosphere, spectrum and details in 1190 to 1320 Å range 3-51267
 solar chromospheric and coronal e.u.v. lines, rotation determ. 3-65696
 solar corona, K-coronometric and photographic meas. during 1972 July 10 eclipse, comparison study (French) 3-61653
 solar coronal identifications below 400 Å 3-80974
 solar e.u.v. spectrum of active region 3-51266
 solar flare, 1967, March 27, impulsive e.u.v. spectra 3-80950
 solar flare e.u.v. emission, comparison of OSO-6 obs. and SFD data 3-45023
 solar high resolution spectra from rocket-borne spectrography in 1200-1320 Å region 3-80942
 solar inner coronal continuum obs. below 2220 Å 3-45018
 solar obs. by OSO-6 Harvard e.u.v. expt. 3-65944
 solar photosphere, search for continuous u.v. opacity sources 3-65649
 solar spectra, forbidden lines below 2200 Å, chromosphere and corona 3-80975
 solar transition region and corona, temp., conductive flux, electron density variations with line intensity 3-80952
 solar u.v. irradiance variability, Nimbus 3 and 4 obs. 3-56323
 solar u.v. obs. with 3840 Å interference filter 3-80944
 solar x.u.v. flash spectrum, anal. and comparison with model 3-65650
 sun, e.u.v. rocket spectrometer obs. of spectrum in 50-300 Å range 3-61648
 Sun, temp. determ. using CN mol. band system 3-61669
 Titan, toroidal ring, u.v. photography 3-80998
 UVB photometry of southern stars 3-73505
 variable stars small amplitude red disc and halo population, UVBRI obs. 3-73502
 γ^2 Velorum, spectroscopic binary, C IV emission feature in near-u.v. spectrum of Wolf-Rayet star 3-48022
 Venus, CO₂ absorpt. strength variations 3-45034
 Wolf-Rayet stars 3-77078
 B, interstellar abundance from u.v. lines 3-81195
 H₂, interstellar detection, u.v. spectrum of δ Scorpii 3-48123
 He I 584 Å diffuse radiation, evidence and model of interplanetary source 3-47977
 He I 584 Å interstellar or interplanetary u.v. source, evidence 3-65857
 He-weak stars u.v. energy distrib., comparison of OAO-2 obs. with UVB photometry 3-81084
 Mg II lines near 2800 Å, equivalent widths in spectra of 31 stars 3-45098

ultraviolet astronomy

- A-type stars, anal. of OAO II obs. of u.v. spectra 3-73497
 broadband u.v. refl. filters 3-48139
 Copernicus satellite, instrumentation and performance 3-45238
 Copernicus satellite spectrophotometry instrumentation 3-59395
 early type stars, u.v. photometry from TD1 satellite obs. 3-56465
 Eu III resonance line classification 3-81043
 e.u.v. photometer for solar obs. from Atmosphere Explorer 3-42262
 e.u.v. spectroheliograph on rocket or satellite, evaluation of pinholes in metal film filters 3-65946
 e.u.v. spectrophotometer on Atmosphere Explorer for solar radiation meas. 3-42261
 galaxies with u.v. continuum, 46 objects with broad emission lines (Russian) 3-45166
 Harvard Smithsonian Reference Atmosphere, near u.v. flux 3-65668
 interference filters, for broadband photometry in u.v., 1200-1900 Å 3-77175
 interstellar gas ionisation by u.v. stars, model analysis 3-70027
 Mars, He abundance determ. method and estimate of x.u.v. dayglow 3-69883
 northern sky, EUV rocket survey 3-48144
 solar Lyman- α radiation transfer through plane-parallel atm. 3-53615
 solar obs. by OSO-6 Harvard e.u.v. expt. 3-65944
 stellar energy mass., Cerenkov radiation as standard source for rocket expts. (French) 3-73557
 TD-1A satellite u.v. sky-survey telescope 3-65951
 Al reflectance coatings, LiF-protected, use in u.v. space optics 3-81252

ultraviolet communication *see optical communication***ultraviolet detectors**

- biologically weighted hazard monitor 3-77281
 channel secondary electron multiplier, construction 3-77569
 hygrometer for field meas., meteorological appl. (Russian) 3-73399
 radiation hazard meas., optical spectrophotometer 3-73753
 secondary electron multiplier, in high vac., construction 3-77568
 v.u.v. radiometry 3-39936
 He⁺ + rare gas atom collisions, vacuum u.v. emissions, optical excitation apparatus 3-71467

ultraviolet lamps *see mercury vapour lamps***ultraviolet sources** *see light sources***umklapp process** *see electron-phonon interactions; lattice dynamics***uncertainty principle** *see indeterminacy***underwater acoustics** *see underwater sound***underwater sound**

- see also hydrophones; oceanography; sonar*
 acoustic transducers, calibration, in reverberant water tank 3-42528
 attenuation by scholled anchovies, 1 to 20 kHz, laboratory measurements 3-70216

underwater sound continued

- attenuation of low frequency sound in ocean 3-42437
 axially symmetric directivity patterns meas., near rough surface 3-39872
 backscattering, ocean volume between Vancouver Island and Hawaii, spectral characteristics, depth ranging 3-77330
 backscattering, volume, Tasman Sea, Coral Sea, Indian Ocean, 2.5 to 16 kHz, characteristics, effects of fish 3-81340
 cavitation threshold models, verification by pulsed sound cavitation in gas saturated water 3-75232
 channel, normal mode expansion of field 3-45372
 circular lenses, for longitudinal acoustical viewing systems for ocean bottom 3-48294
 coastal divergent channel, point source representation, comments and reply 3-77334
 coherence, vertical, two deep hydrophones, near surface source, additive vertical array, effect on gain 3-70215
 coherent component of specularly scattered sound, dependence on probability density function of rough surface 3-59485
 CW propagation between Eleuthera and Bermuda, statistical analysis 3-42449
 cylindrical receiving arrays with non-uniform hydrophone response and optimum weighting, directional characteristics 3-45376
 deep ocean channels, response to wide band pulses 3-42440
 Epstein-type under-ocean duct, normal-mode approach 3-41948
 explosions, loading of a submerged structure, shockwave propagation, numerical solution 3-75228
 fish tracking 3-42446
 function of temperature salinity and pressure, ocean soundings correction using computer 3-65543
 generators, hydropneumatic, l.f., operating principles, fundamental parameters, developments, applications 3-59493
 h.f. sound reflection at normal incidence from ocean bottom 3-61942
 human hearing and underwater sound localisation 3-45277
 hydroacoustic transduction, review 3-42456
 hydrophones, array, vertical, maximum likelihood signal processing, technique 3-77389
 ice, fresh water and sea, attenuation, 200-1100 kHz 3-77327
 inland seas, ocean coast, underwater ambient noise distrib. 3-77331
 l.f. absorption 3-59488
 long-range propagation, influence of subsurface sound channel 3-42439
 magnetostrictive transducer 3-53792
 Mediterranean, shallow water sound transmission data, decay laws 3-41950
 moving fluid, upstream and downstream radiation from stationary source 3-42457
 multi-path interference of refracted-refracted propagation about deep sound channel axis 3-42448
 noise signature of aircraft, lateral wave contribution 3-59490
 North-east Pacific, seasonal variation of underwater noise 3-41933
 ocean, acoustic pulse propagation, amplitude spectra 3-81339
 ocean, ambient noise, meas., free diving buoy 3-53569
 ocean stratified in depth and range, applic. of normal mode theory 3-42441
 ocean surface-generated noise, envelope structure 3-42465
 ocean-bottom acoustic-transponder-array survey, nonclassical determ. of spatial coords. 3-44965
 parametric waveform generation from spherical primary fields 3-45374
 pressure due to source in air 3-59489
 projectors directivity index meas. 3-61941
 propagation, wave speed time variation slower than wave frequency, two-time perturbation methods 3-70214
 reflection and scattering, from ocean bottom 3-45373
 reflection from ocean bottom, spatial correlation of sound signal envelopes, frequency correlation 3-59492
 reverberation, diurnal variation in California current, 3 to 30 kHz, frequency dependence 3-77329
 scattering from waves, amplitude characteristics 3-77332
 sea noise, energy spectral characteristics 3-77333
 sea/air interface, rough, sound transmission, spectral characteristics 3-70213
 seaquakes study 3-42447
 seawater equation of state from sound velocity data 3-58987
 sonar l.f. transmission loss, nomograms 3-42442
 sonar echoes from fish and rocks, discrimination 3-51472
 sound localization in noisy environment 3-45288
 source near surface, vertical coherence and effect on gain of additive vertical array 3-42444
 South Pacific, long range sound propagation, effect of bottom topology 3-41946
 steel cylinders implsions, acoustic signatures generation 3-45375
 surface as random filter 3-42451
 surface backscattering strength at low frequency, relationship with gravity wave spectrum 3-42450
 surface channel, rough boundary, sound field, scattering decay, experimental determination 3-59494
 surface duct propagation loss measurements, using explosive source 3-41947
 T-phase radiation from CANNIKIN underground nuclear explosion, sonar hydrophone recordings 3-53401
 through tidal bore, thermal fluctuations effects 3-41949
 transducer, linear array, directivity pattern, flaw detect. and diagnostics 3-42436
 transmission, channel, bilinear sound speed and environmental variations, ray characteristics 3-70212
 transmission loss, interference structure due to bottom-refracted energy 3-59487
 velocity, in-situ meas. aboard DEEPSTAR-4000 3-42455
 velocity calculation for sound in seawater from hydrologic data 3-51473
 velocity depth profile, ray theory, series expansions 3-70217
 velocity increase with oceanic depth, $v(z)$ functions (German) 3-66090
 velocity profile, ray theory, modified ray theory and normal mode theory comparison 3-42443
 velocity variations in Sargasso Sea, eddy patterns 3-80681
 velocity when source in air 3-59491

underwater sound continued

- vertical velocity distrib. at great depths in Pacific Ocean 3-42438
- volume scattering, net-haul data prediction 3-42452
- wave equation in medium with time-dependent boundary 3-59486
- B concentration dependence of low frequency relaxation 3-42454
- MgSO₄ relaxation frequency, pressure dependence 3-42453

unified field theories

- Belinfante-Swihart, analysis 3-59807
- charged particle model 3-66661
- Einstein's, cylindrically symm. electrostatic field 3-77883
- Einstein's cylindrically symm. magnetostatic field 3-77882
- Einstein's equations of motion of charged particle in cylindrically symm. field 3-77894
- Einstein-Straus non-symmetric theory only 4-dimens. extension of general relativity 3-77893
- gauge invariant structures, quantizable dynamical systems, charge and spin structures 3-54154
- gravitational collapse, scalar-tensor theory of gravity, hydrodynamic calcs. 3-47870
- for massive spin-1 fields 3-54153
- nonsymmetric, variational technique for derivation of transposition invariant equations 3-66674
- Poincare gauge invariant spinor theory and the gravitational field 3-40172
- spinor fields interaction with gravitation, massless Dirac eqn. rel. to Heisenberg's Unified Field Theory 3-59806
- Weyl's gauge-invariant geometry exptl. test using Mossbauer effect 3-42877

units (measurement)

see also constants; dimensions; measurement; nomenclature and symbols

- absolute atom masses and number, use instead of molar quantities (*German*) 3-45408
- ambiguities in the use of unit names 3-42510
- atomic and molecular physics, natural units 3-42509
- rel. to energy levels, in masers and lasers (*Spanish*) 3-59542
- high vacuum, logarithmic 3-51506
- intensity of magnetisation 3-39848
- logarithmic quantities and units 3-66125
- materials testing, quantities employed and relationship to basic SI units (*Hungarian*) 3-44703
- metre, in terms of light velocity (*Norwegian*) 3-70261
- nuclear reactivity unit conversion, dep. on reactor operating conditions, effective delayed neutron fraction 3-74640
- palaeomagnetic stratigraphy scale (*Russian*) 3-65232
- radiation and radiology measurement, SI rationalisation, problems, recommendations of ICRU 3-77245
- rontgen absolute determination, magnetic field pressure ionization chamber construction (*German*) 3-48274
- rontgen absolute determination, X-ray source construction and testing (*German*) 3-45326
- SI, definitions and symbols, book 3-77377
- SI system development (*Danish*) 3-77376
- SI units in radiology and radiation measurement 3-53773
- steradian, remarks on significance of solid angle (*German*) 3-59538
- X-ray lines, wavelength relative to visible standards 3-73660

universe see cosmology**universe models see cosmology****untuned power amplifiers see power amplifiers****unwinding see winding (process)****upper atmosphere**

see also exosphere; magnetosphere; mesosphere; radiation belts; thermosphere

- acoustic-gravity waves, nonlinear effects 3-47780
- acoustic/gravity waves, coupling to ionosphere, generation mechanism 3-42002
- aerosol layers, laser radar obs. 3-56190
- aircraft propulsion effluents, climatic impact assessment 3-41979
- airglow, i.r., correl. of fluctuations, vibration-rotation bands of OH molecule 3-80789
- Aladdin II, results and achievements for mesosphere and lower thermosphere 3-69608
- alkali element conc., determ. using Earth's shadow on Li trail 3-53513
- arc, stable auroral red, vertical distrib. of mol. N₂ vibr. energy in thermosphere 3-69620
- aspects of conference, Norwegian Physical Society, Tromsø, Norway, (June 1972) 3-39842
- astrometric meas. of artificial clouds in upper atmosphere (*French*) 3-53553
- Atmosphere Explorer, low-energy electron analyzers for flux measurements 3-42079
- Atmosphere Explorer, magnetometer for field measurements in auroral region 3-42080
- Atmosphere Explorer, photoelectron spectrometer for flux measurements 3-42078
- atomic and molecular scattering of electrons in reln. to space travel, upper atmosphere, sun (*Dutch*) 3-63317
- atomic reactions, photochem. air pollution, O and O₃ concs., discharge flow method 3-69605
- auroral Birkeland currents and energetic particle fluxes 3-51081
- auroral electrojet arcs, transverse velocities from induction model 3-69614
- auroral electrons, interaction with atm. at 95-268 km. height 3-65430
- auroral oval, reevaluation rel. to particle precipitation, all-sky photographs 3-47777
- auroral radar scattering parameter measurement, ideal antenna configuration determ. 3-80788
- comet dust influxes into earth's atm., times and location 3-59125
- composition and thermal structure, effects of eddy turbulence 3-61518
- eddy diffusion from internal atmospheric gravity waves 3-59135
- equatorial aeronomy, symposium (Ibadan, Nigeria, 4-9 September 1972) 3-42021
- equatorial electrojet, development of model inc. neutral-air winds and two-stream instability 3-42024
- e.u.v. broad band solar radiation absorption, OSO 5 obs. 3-53511

upper atmosphere continued

- F₂-layer thickness and height of maximum, global distrib. rel. to neutral atmosphere 3-42034
- foil cloud sensor meas. in height range 80 to 95 km 3-53491
- geocorona and magnetosphere obs. from Moon with Apollo 16 for u.v. camera/spectrograph 3-81216
- global thermosphere dynamics, theoretical model including diffusion 3-61515
- gravity wave-mean flow interactions, energy and momentum transport 3-65406
- heating of low-latitude atm. by decaying mag. storm ring current 3-65474
- infrasonic fluctuation spectra, nonlinear theory 3-47781
- instabilities meas. by Aladdin II 3-61502
- ion cloud diffusion rel. to model and electric fields 3-51102
- ion composition meas. from ISIS-II satellite at 1400 km 3-69646
- i.r. airglow, photographic studies, detailed struct. determ. 3-80787
- i.r. airglow, photographic studies, detailed struct. determ. 3-80790
- lower thermosphere, chemistry and dynamics 3-61499
- lower thermosphere, interaction with small meteoroids 3-65854
- lower thermosphere, meridian model of density and comp. 3-51087
- lower thermosphere neutral comp., O loss in sounding rocket mass spectrometer ion sources 3-51184
- lower thermospheric model, variability of neutral winds and vertical eddy diffusivity 3-61514
- luminous optically dense gas layer, temperature measurement by homodyne detection method 3-69731
- magnetic fluctuations at auroral latitudes, three axis meas. 3-61437
- marine weather extremes, temp., rel. humidity, wind speed, visibility, salinity and upper air temp. 3-53496
- meridional neutral wind at mid-latitudes 3-76792
- midlatitude thermospheric winds from ionospheric plasma vertical drift meas. 3-69611
- multiflash whistlers at low latitudes, propagation characteristics 3-65408
- multiple mid-latitude 6300 Å (O I) arc obs. during geomag. storm recovery 3-61494
- near-equatorial neutral thermosphere, density anomalies at mag. equator 3-51090
- neutral atmospheric species, mass and momentum modelling, Aladdin II experiment 3-69607
- neutral particle mass spectrometer data, gas surface interactions on walls of instrument 3-69603
- neutral thermosphere temp. from Explorer 32 density scale height meas. 3-51084
- neutron flux obs. 3-69606
- nightglow of HeII 304 Å, HeI 584 Å, obs. at 180 km, altitude from rocket telescope system 3-65533
- particle and auroral obs. from ESO I/AURORAE polar orbiting satellite 3-76790
- physics and chemistry of terrestrial and planetary upper atmospheres 3-41982
- plasma sphere, airglow in 150-1500 Å range, He⁺ reson. scatt. of solar 304 Å line 3-69739
- polar cap absorption, ground and satellite obs. of 2 Nov 1969 event 3-59140
- Project Aladdin II, dynamic numerical model of E-region rel. to digi-sonde obs. 3-65468
- rocket meas. rel. to OPTIR code results 3-65422
- sequential neutral wind profiles, using D₁ method 3-76793
- spacecraft microthrusters vapour jets, emission due to light scatt. 3-59128
- temp. rel. to solar and geomag. activity 3-69602
- temperature var. during solar activity min. from topside ionosphere sounding data 3-80780
- thermosphere, equatorial, H₂ emission interpret, proton precip. (*French*) 3-59127
- thermosphere, global empirical model for gaseous distribution 3-61508
- thermosphere, global model for magnetically quiet conditions using gas density data from OGO-6 3-61510
- thermosphere, horizontal variations in atomic oxygen and helium concentrations 3-61513
- thermosphere, latitudinal and temporal variations in O, O₂ and O₃ abundance 3-61512
- thermosphere, lower, quenching of vibrationally excited N₂ by O, temp. depend. 3-69621
- thermosphere, mag. storm characts. 3-51096
- thermosphere, phase difference between temp. and density 3-61517
- thermosphere, semiannual effect 3-61498
- thermosphere, static model for O, O₂ and N₂ 3-56179
- thermosphere, transient movement and Joule heating due to geomagnetic disturbances 3-69612
- thermospheric atomic O comp. meas. using quadrupole mass spectrometer with strongly focusing ion source 3-51185
- thermospheric composition, characteristics of diurnal maxima of constituents 3-61509
- thermospheric density variations rel. to auroral electrojet activity 3-65409
- thermospheric ion composition results, OGO 4 and 6, parametric description 3-51080
- thermospheric Li vapour trails, growth, motion and brightness of day-time releases 3-65418
- thermospheric neutral composition, equatorial phenomena rel. to ionospheric variations 3-41987
- thermospheric neutral temperature rel. to Ca plage and 2800 MHz intensities, obs. analysis 3-51079
- thermospheric obs., ionospheric drifts and Sq current system determ. 3-53532
- thermospheric structure, correl. of mass spectrometry and incoherent scatter sounding 3-53502
- thermospheric temperature, global mean, rel. to solar extreme u.v. radiation 3-53500
- thermospheric temperature variations with solar activity and time of day 3-69600
- thermospheric wind effects on He and Ar distrib. 3-56180
- thermospheric winds and gravity waves generated by auroral zone heating 3-69613
- thermospheric winds rel. to superrotation of upper atmosphere 3-61516

upper atmosphere continued

- tracer dispersion in atmosphere rel. to horizontal eddy diffusivity and height 3-59122
 tropical red arc north boundary motion 3-61489
 turbulence spectra of dissipation rates and diffusion coefft., Aladdin II meas. 3-61501
 twilight enhancement of 6300 Å, 5577 Å oxygen emission lines at 200 km. 3-65424
 upper thermosphere, diurnal var. of total mass density, number density and temperature 3-65415
 vibrational temp., 001, of N₂ and CO₂, at 50 < z < 130 km., radiative transfer calc. 3-69623
 whistler propagation characteristics at low latitudes, electron density horizontal gradients effect 3-65407
 whistlers, low-latitude ducted propag. 3-59131
 winds and shear, Aladdin II meas. 3-61500
 zonal winds, determ. using orbit anal. of 1965-11D 3-53591
 CO₂, fluoresc. at 4.3 μm rel. to 2.7 μm, solar radiation absorpt. 3-69622
 He atom loss mechanism 3-76450
 N density meas. optical method 3-40582
 N₂ photodissoc. continuum determ. 3-49497
 N₂ vibrational temp. in lower thermosphere, effect of O quenching 3-53512
 NO concentrations from eclipse var. of ion concentrations 3-69610
 NO density meas. during sunrise at Kauai, Hawaii 3-53503
 Na concentration enhancement rel. to sporadic extraterrestrial dust influxes 3-44912
 O, comparison of concentration with that of impurity CO₂ 3-61506
 O, in upper atmosphere concentration above 85 km measured by rocket-borne mass spectrometer 3-61505
 O column density variations, u.v. photometry from OGO-6 satellite 3-61511
 O I 6300 Å emission, average nighttime vertical profile 3-80778
 O transport in lower thermosphere rel. to hemispheric imbalance 3-51100
 O₂, vibrationally excited, production and decay in 50-100 km layer 3-69601
 O₂ photodissoc. continuum determ. 3-49497
 O₂ quenching profile between 75 and 115 km 3-76796
 O₃ concentration decrease with decreasing ionization during PCA event 3-69594
 O₃ concentrations in mesosphere and lower thermosphere at sunset, rocket obs. 3-51099
 OH emission, infrasonic variations 3-61490
 OH emission rel. to stratospheric warming 3-65320
 OH profiles and concentrations, ICECAP '72 rocket-borne i.r. radiometric obs. 3-65421
 OH vibrational excitation, possible mechanisms rel. to radiation 3-80779

uranium

see also nuclear fission of uranium

- accumulations, diffusion plant equipment, radiation monitoring nuclear criticality 3-63250
 admixture, periodicity of equil. coeffs. of distribution (Russian) 3-60282
 adsorption and desorption in soils, effect of CO₃²⁻ conc. 3-69516
 alpha type, tear formation and growth, effect of internal stresses 3-63205
 coupled cores, kinetics meas., ZED-2 reactor 3-71210
 criticality studies, Dow Rocky Flats Nuclear Safety Laboratory 3-63229
 cylindrical array, fast neutron meas., ³He spectrometer 3-71157
 depleted, fast neutron spectra, anal. and interpretation, ENDF/B-III data 3-71154
 electrochemical behaviour in acid media, influence of V, Cr and C additions (French) 3-47561
 electron microscope obs., imaging of U atoms in mellitic acid by phase contrast 3-54912
 enriched, for Western Europe, forecasts (Italian) 3-63186
 enriched, supply to European countries, future trends (French) 3-60288
 fission track technique, U content in minerals, geochronology appl. 3-44831
 fuel, enrichment processes, review 3-71286
 fuel, isotope (233) separation from thorium and thorium oxide, pilot plant at Trombay 3-71301
 fuel, recovery by fluorination process using BrF₃ 3-43289
 fuel element, analysis of effects of stat. fluctuations on structure (Czech) 3-43312
 fuel elements, buckling meas. from cooling-channel temp. coeffs. (German) 3-67588
 heat capacity and transformations, in α-U, 2-70K 3-47041
 HTR cores, design with prismatic fuel elements 3-67457
 ionisation energy calc. 3-60376
 isolation from ores, history, atomic energy programme 3-67560
 isotopes, atomic mass meas. 3-43322
 lunar soil, analysis of 5 Apollo 17 samples 3-65831
 LWR, potential when fuelled with metallic thorium, advantage over metallic uranium 3-67585
 M-shell ionisation cross sections by collisions of simple heavy charged particles 3-43377
 mass spectroscopic determ. by isotope dilution method (Czech) 3-42708
 mechanical and fabrication props., warm working effects 3-72904
 mining, miner exposure, dosimetry, ²¹⁰Pb blood concentration, evaluation 3-70182
 muonic, quadrupole splitting in X-ray spectra, determ. of nuclear quadrupole moment 3-49133
 natural, irradi. fuel, Pu recovery using tertiary amine extractants, anal. methods 3-57583
 nuclear fuel elements, Al cladding thickness meas., gamma ray attenuation 3-47500
 nuclear fuel rods, CP-3, methods of fabrication, history 3-67561
 nuclear power growth and uranium demand, overview 3-43291
 nuclear reactor fuel, Japanese activities 3-63143
 ore processing, techniques and prospects (French) 3-49366
 photoelectric L-shell cross section of 32.88 keV photons 3-50641
 pile, neutron spectrum meas., inelastic and capture cross-sections of ²³⁸U, LMFBR assemblies 3-71155

uranium continued

- plasma, d.c. arc, burning in air, transport of U free particles 3-73959
 plasma, emission coeff. meas., theory comparison for design calcs. 3-78385
 plastic flow, high temp., in α, β and γ phases 3-41772
 pure samples, spectrophotometric determ. of Ag 3-70472
 reactor grade, adjusted, void nucleation behaviour 3-63192
 resources and production in United States, review 3-74722
 superconducting transition temp. at pressure up to 24 kbar, single and polycryst. α-U 3-79787
 thin foils, meas. of Doppler effect in thermal reactor up to 729°C 3-74679
 X-ray absorption analyser for U content determ. in ion-exchange plants 3-70495
 Eu⁶⁺, in alkaline earth tellurate, fluoresc. props. 3-44478
 LaAl₂U, conduction electron spin flip scattering obs. 3-41411
 Pu-U mixtures, criticality safety, effect of Gd, B-containing Raschig rings 3-63228
 U II line identification in spectrum of β Coronae Borealis 3-65890
 U/graphite system, neutron wave interference phenomena 3-60276
 U-D thermonuclear plasma, controlled fusion, obtained by composite macro-particle collisions 3-49733
 U-metal spherical assemblies, neutron importance and fission density 3-49302
 U-Th ores, gamma spectral borehole logging methods of registration (Russian) 3-73394
 U-Th ores, spectral assay using scintillation counters, influence of resolution (Russian) 3-73390
 U + 3/2H₂ ⇌ UH₃, kinetics study 3-61255
 U + O(O₂) vapour oxidation, chemi-ioniz. 3-80533
²³⁴U and ²³⁸U abundance in interstitial water from Pacific Ocean sediment 3-65267
²³⁵U, replacement of natural U as fuel in heavy water reactors (German) 3-71317
²³⁵U, with improved performance 3-52231
²³⁵U content in U slab, determ. by source-sample fission coincidence and random driver 3-62232
²³⁵U enriched, spheres, immersed in UO₂ (NO₃)₂ solutions, mild or boron stainless steel shells, uncoupling effects 3-63196
²³⁵U enrichment, gaseous diffusion plant, operation 3-74720
²³⁵U enrichment in separation nozzle process, added light gases H₂, He and D₂ comparison (German) 3-69493
²³⁵U enrichment in separation nozzle process, entropy production mechanisms (German) 3-69494
²³⁵U/²³⁸U isotope ratio in UF₆, computer controlled mass spectrometry system, U enrichment plant 3-70479

uranium compounds

- alloys, thermomechanical testing under conditions of rapid fission heating 3-47531
 carbides equilibria in molten fluoride solns. of UF₃ and UF₄ in graphite at 850K 3-43290
 dichalcogenides, magnetic properties with composition close to UY₂, rel. to crystal structure 3-64485
 glasses, calibration and thermal neutron fluence measurements 3-51726
 magnetism theory, modified free electron model, extended mol. field approx. 3-58353
 oxides, macrodetermination of O₂ by graphite reduction method 3-66411
 refractory fuels, factors affecting swelling at high temperatures 3-63198
 UO₂²⁺ complexes, circular dichroism and interpretation of electronic spectra 3-76029
 uranates, hydrated, of form mXO.2UO₃.(4-2m)H₂O, X=Ca, Sr, Pb, Ba, NH₄, X-ray patterns, bivalent cations (French) 3-43776
 uranyl compounds, luminescence props. (Russian) 3-44471
 uranyl compounds, spectra of optically active mol. crystals, vibr., symm. 3-72603
 uranyl diformate, anhydrous and monohydrate, luminescence spectra, 77K (French) 3-69065
 X-ray photoelectron spectra obs. of 4f binding energies 3-76119
 Pu-U nitrate solns., computer calcs. of criticality factors based on exptl. data 3-46152
 PuO₂-UO₂, nuclear reactor fuel, performance and design, GE BWR, Oyster Creek 3-67567
 PuO₂-UO₂-polystyrene mixtures, LWR, 7.6 wt% Pu, criticality expts., computer calcs. 3-46154
 Rb-U complex fluorides, far i.r. absorption spectra 3-58499
 (U, Pu)C pellets manufacture by reactive sintering (German) 3-43302
 (U, Pu)O₂ mixtures, exptl. examination after irradiation in HWR (German) 3-67614
 (U, Pu)O_{2-x}, oxygen redistrib. behaviour 3-43308
 (U,Ce)O₂ mixed oxide fuels, chem. anal. by redox method 3-66459
 (U,Pu)O₂ pellets, sintering variable effects on chem. and phys. characterization. 3-78379
 (U,Pu)O₂, early-in-life failures, release of fuel and fission products 3-63223
 (U,Pu)O₂, fuel, cladding attack causes and control 3-78383
 (U,Pu)O₂, fuel fabrication, chem. process characterization. 3-78380
 (U,Pu)O₂, fuel rods, failed, effect of O₂ availability on expansion 3-63224
 (U,Pu)O₂, LMFBR fuel rods, thermal and mech. eval. of oxide microstruct. 3-78381
 (U,Pu)O₂, thermoelec., resist., and u.s. centreline thermometry 3-45455
 (U,Pu)O₂ fuel, brittle fracture behaviour 3-43309
 (U,Pu)O₂ fuel, conservation eqns. governing porosity and actinide redistrib. 3-46145
 (U,Pu)O₂ fuel, irradi., O/M ratio effect on Pu redistrib. 3-46147
 (U,Pu)O₂ fuel pins, in-pile radial temp. profiles, simulation 3-46142
 (U,Pu)O₂ fuel pins, plutonium redistrib. considerations 3-46141
 (U,Pu)O₂ fuel rods, irradi., Pu and U diffusion 3-46143
 (U,Pu)O₂ mixed fuels, thermodynamic behaviour 3-57569
 (U,Pu)O₂ pellets, parametrically designed, atmospheric stability obs. 3-78382
 (U,Pu)O₂ pellets, quantification of processing parameter effects on chem. and phys. chars. 3-78378

uranium compounds continued

- (U,Pu)₂O₃ solid solns., oxidation props., model interpret. 3-54542
 (U,Pu)O_{2-x} fuel pellets, creep at high stress 3-72950
 (U,Pu)O_{2-x} fuel pellets, compressive creep, comp. depend. 3-74728
 (U,Th)O₂ fuel particles, pyrolytic-graphite coated, creep deformation, 800-1200°C following irradiation (*German*) 3-71314
 (U,Th)O₂ solid solns., elec. cond., 800-1200°C 3-67549
 U alloys, nuclear fuel, fission gas release, effect of vol. swelling, probabilistic model 3-63208
 U-B system, temp.-comp. diagram 3-72940
 U-C system, thermal diffusion mechanisms 3-63232
 U-C-H system, thermal diffusion mechanisms 3-63232
 U-C-O system, thermal diffusion mechanisms 3-63232
 γ-U-Mo, fast burst reactor fuel, deformation and fracture behaviour 3-63207
 γ-U-Mo, pulsed reactor fuel, mechanical props. 3-63206
 U-Nb, niobium segregation phenomena 3-61149
 U-Nd-O system, oxygen pot. meas. 3-72933
 U-Pu, nuclear fuel, fission gas release, effect of vol. swelling, probabilistic model 3-63208
 U-Pu carbide nuclear reactor fuels, summary of development, properties and uses 3-63211
 U-Pu-N ternary system, equil. assessments 3-46136
 U-Se and U-Se-C systems, solid-state relationships 3-43299
 (U/Th)O₂ industrial production, for use in HTGR (*German*) 3-67591
 UAl₃, nuclear spin-lattice relax. of ²⁷Al, spin fluctuation effects 3-41441
 UAl₃ fuel, in research reactors, advantages, disadvantages and operating experience 3-71296
 U(BH₄)₄ in Hf(BH₄)₄ host, electronic absorpt., optical and e.p.r. spectra assignments 3-76033
 U(BH₄)₄/Hf(BH₄)₄, optical and e.p.r. spectra of mol. crystals, exciton theory 3-68973
 UB₂, uniaxial antiferromagnet, transversal spin disorder resistivity, temp. dependence 3-41219
 UC, fission-enhanced self-diffusion of uranium 3-71281
 UC, irradi., microprobe obs., precipitate distrib. (*German*) 3-57567
 UC-graphite compacted neutron target (*German*) 3-71258
 UC-US system UC-rich solid soln., prep. procedure 3-63193
 UC+N₂ reaction, graphitization of precipitating free carbon 3-47553
 UC₂, production by oxalate method, in particle form, as fuel for FBR (*German*) 3-67608
 UC₂ kernels in coated fuel particles, amoeba effect, high temp. failure (*German*) 3-67550
 UC₂-ThC₂ spherules, pyrolytic C encased, HTGR elements, radiation testing (*German*) 3-71266
 UC_x, actinide diffusion, phase boundary behaviour, high temp. 3-43298
 UC_x, bainitic transforms., carbide phase nomenclature 3-55836
 UC_x, compatibility with stainless steel bonded with sodium, carbon transfer kinetics 3-43307
 UC_x-W alloys, high temp. creep 3-72948
 UCl₄, anhydrous, crystal structure, neutron diffraction study 3-68207
 UCl₄, vapour spectrum interpretation using cryst. field model 3-71541
 UF₃, UF₄ molten fluoride solutions in graphite at 850K equilibria of uranium carbides 3-43290
 UF₄, production by UO₃ electrolyte reduction, pilot plant test runs (*Spanish*) 3-76460
 UF₆, ²³⁵U/²³⁸U isotope ratio, computer controlled mass spectrometry system, U enrichment plant 3-70479
 UF₆, partial pressure determ. from meas. on U radioactivity (*German*) 3-66462
 UF₆, Raman band contour analyses and Coriolis consts. 3-67816
 UF₆ analysis in fluorination of U, in-line gas analyzer diff. thermal conductivity measurements 3-42532
 UF₆ conversion to ceramic grade UO₂ powder 3-57580
 UF₆ gas, isotope separation by nozzle-separation technique (*German*) 3-71302
 UF₆·2.5H₂O, position and mobility of H₂O, n.m.r. 3-79925
 UFeC₂, standard free energy of form. by e.m.f. meas. (*Japanese*) 3-61125
 UN_x (x>1.75), preparation and X-ray investigation (*German*) 3-50759
 U₂N₃, nonstoichiometry, statistical model for anal. of thermodynamic props. 3-68190
 U₃N₄ production by oxalate method, in particle form, as fuel for FBR (*German*) 3-67608
 UO, UO₂, UO₃, i.r. spectra, 700 to 900 cm⁻¹, stretching modes study 3-40625
 UO₂, criticality safety in LWR fuel fabrication 3-57577
 UO₂, diffusional creep, limitation by interfacial processes 3-80400
 UO₂, elec. resist., grain boundary effects 3-44648
 UO₂, entrapment of low energy inert gas ions, thermal evolution spectrometry 3-60756
 UO₂, fission gas swelling, long range migration, low temp. 3-63174
 UO₂, fission-enhanced self-diffusion of uranium 3-71281
 UO₂, fragmentation, molten fuel-coolant interactions, Na coolant 3-74730
 UO₂, high temp. oxidation, effect of compaction, exposed area and initial composition 3-60275
 UO₂, hyperstoichiometric single crystals., deform. model 3-55849
 UO₂, in-reactor radiation induced creep behaviour 3-54543
 UO₂, insulator pellets, effect on axial ²³⁵U fission rate distrib., EBR-II 3-63167
 UO₂, irradi., morphology and growth rate of interlinked porosity 3-43306
 UO₂, manufacture in continuous vortex sheet reactor, development of in-line monitoring instruments (*German*) 3-67606
 UO₂, melted in air, He, rate of fission product release (*Japanese*) 3-74726
 UO₂, microsphere compressibility determ., microscopy, porosity depend. 3-80424
 UO₂, molten, thermal interaction with liquid sodium, obs. 3-67527
 UO₂, particles, TRISCO coated, thermochem. stability 3-78384

uranium compounds continued

- UO₂, porous stoichiometric and hyperstoichiometric, thermal cond., 670-1270 K 3-43304
 UO₂, Raman spectra 3-72610
 UO₂, re-solution effects and fission gas swelling 3-43301
 UO₂, slightly enriched, H.B. Robinson Unit No.2, Cycle 1 fuel performance 3-74733
 UO₂, sputtering, surface binding energy, temp. depend. 3-69119
 UO₂, stoichiometric, primary creep 3-72949
 UO₂, stoichiometric, surface and interfacial props. 3-46137
 UO₂, surface fission tracks, replica electron microscopy obs. 3-63187
 UO₂, thermal cond., 100 to 300 K, phonon mean free path 3-40542
 UO₂, thermal diffusivity meas., 750 to 2700 C, flash method (*French*) 3-47445
 UO₂, thermal-gradient migration of helium bubbles 3-67552
 UO₂, Zircaloy-4 clad, fuel performance, C-E, KWU pressurised water reactors 3-67571
 UO₂ (NO₃)₂ solution, immersion of ²³⁵U spheres with mild or boron stainless steel shells, uncoupling effects 3-63196
 UO₂ bars, thermally shocked, crack healing, isothermal annealing effect 3-74727
 UO₂ coated particles, exptl. determ. of effective resonance integral and Doppler effect in I/E neutron spectrum 3-43273
 UO₂ complex, uranyl β-diketonates, luminesc. spectra, relax. mechanism 3-72753
 UO₂ DTA curves, heat of reaction UO₂-U₃O₇ 3-73690
 UO₂ fuel, Pu-enriched in ZED-2 expt., booster effect on neutron density and reactivity 3-71226
 UO₂ fuel rods, Zircaloy clad, fuel performance 3-67570
 UO₂ helices, γ-radiation effect on creep 3-57570
 UO₂ microsphere fabrication by hydrolysis from uranyl nitrate soln., controlled porosity 3-46146
 UO₂ particles in water, heat removal, simulation expt. for fast reactor fuel debris 3-46093
 UO₂ pellets, crack sintering rates meas. 3-46144
 UO₂ powder, conversion from UF₆ 3-57580
 UO₂ powders, microstruct. evolution during press. sintering 3-78377
 UO₂ powders, thermal precip. from sols 3-67555
 UO₂ single crystals., CVD growth 3-72797
 UO₂ solid layer, penetration by liq. Na jet, theory 3-80342
 UO₂ surface film thickness determ. by refl. meas. 3-45413
 UO₂/PuO₂ fuel elements, electron micro-probe analysis of radiation induced changes (*German*) 3-71311
 UO₂-cladding composite body, heat conduction with simultaneous solidification and melting 3-54548
 UO₂-Na interactions, pressure pulses, estimates 3-67617
 UO₂-Na vapours, mechanism of explosive interactions 3-60284
 UO₂-PuO₂, creepage under neutron irradiation up to 1000°C (*German*) 3-71324
 UO₂-PuO₂ fuel use in thermal reactors 3-57579
 UO₂-PuO₂ fuel pins, irradi., oxygen pot. gradient 3-63189
 UO₂-PuO₂ nuclear reactor fuel elements, irradiated, data evaluation (*German*) 3-71310
 UO₂-SiO₂ system melts, spinodal decomp. and primary crystn. 3-72984
 UO₂-SiO₂ vitroc ceramic rods, Cu admission and distribution 3-57581
 UO₂-ThO₂-(Th,U)O₂ sol-gel-oxide, HTGR fuel element manufacture, neutron irradiation (*German*) 3-71266
 UO₂-W, melt-grown composite, selective chem. etching for electron emitter applics. 3-75680
 UO₂⁺ in glasses, excited, non-radiative relax. 3-72749
 UO₂⁺, high temp. specific heat, Debye approx. and anharmonicity terms 3-52704
 UO₂-MgO system, phase equilibrium using X-ray diffraction methods 3-74725
 UO₂+x, FBR fuel, oxygen pressures calc., model 3-40536
 UO₂²⁺-Yb³⁺ activated glass, cooperative sensitisation 3-76095
 UO₃, electrolytic reduction to form UF₄, pilot plant tests (*Spanish*) 3-76460
 UO₃ supply in West Germany, overview (*German*) 3-63184
 UO₃, high-temp. phase transition, 300-800°C 3-64972
 UO₃, thermal cond., 100 to 300 K, phonon mean free path 3-40542
 (UO₂Br₄)²⁻, force field, progressive rigidity calc. 3-74985
 UO₂Cl₂, exciton-phonon interactions, luminesc., absorpt. 3-72751
 UO₂Cl₂, structure from powder neutron diffraction 3-43768
 (UO₂Cl₂)²⁻, force field, progressive rigidity calc. 3-74985
 UO₂Cl₂·3H₂O, Raman spectra and cryst. struct. (*French*) 3-68221
 (UO₂F₃)³⁻, force field, progressive rigidity calc. 3-74985
 UO₂MoO₄ crystal structure 3-79325
 UO₂(NO₃)₂, exciton-phonon interaction, luminesc., absorpt. 3-72751
 UO₂(NO₃)₂·6H₂O 3-67407
 U₃O₅P₂O₇, X-ray powder diffraction data 3-43774
 UO₂SO₄, electron-vibr. spectra, fine struct. 3-72752
 UO₂ZrO₂CaO, fuel element for TREAT convertor 3-63219
 UO₂·2H₂O, thermal decomposition (*Czech*) 3-69449
 UP, model for magnetic phase transitions 3-47035
 UP-ThP solid soln., lower temp. antiferro-paramag. transition, susceptibility obs. 3-68782
 UP₂, uniaxial antiferromagnet, transversal spin disorder resistivity, temp. dependence 3-41219
 UP₄, neutron diff. study of mag. struct. 3-68793
 UPTE, magnetic properties investigation in temp. range 4.2 to 1000 K 3-68813
 U_{0.79}Pu_{0.21}C_{1.02}, compressive creep and hot hardness 3-61188
 U_{0.8}Pu_{0.2}C-W system, phase diagram obs. 3-47451
 U_{0.75}Pu_{0.25}O_{2-x} fuels, equil. oxygen pot., conc. depend. 3-54541
 U₃Si, polycryst., lattice parameters, counter-diffractometer parameter determ. 3-41802
 UTe hyperfine field by Mossbauer spectroscopy, magnetic moment by neutron diffraction, temp. depend., magnetic ordering 3-44356
 UTeO₅, synthetic schmitterite, space group, cell consts. (*French*) 3-46610
 U(VI) azide complex, reson. Raman effect (*German*) 3-78775
 UWC₂, standard free energy of form. by e.m.f. meas. (*Japanese*) 3-61125
²³⁸U-²³⁹Pu oxide-fuelled LMFBR, calcs. of fission product poisoning 3-49356

Uranus

- 21-cm. line obs. by new method of radio interferometry of faint moving sources 3-61674
 adiabatic temp. distrib. determ., comparison with core melting tem. 3-47928
 albedo, wavelength dependence from 0.3 to 1.1 μ photoelectric photometry 3-80982
 atmosphere, review 3-65780
 atmosphere dynamics rel. to planetary dynamics 3-47936
 gravitational field constraints on model of interior 3-47933
 interferometer obs. of 11.1 and 3.7 cm 3-56333
 interior processes model testing using atm. meas. 3-47934
 ionospheric physical and chemical processes 3-47937
 nonthermal radio emission 3-42154
 spectrum, molecular H₂, 3-0 band obs. 3-47905
 survey of present knowledge 3-45039
 H planet, high-pressure phenomena 3-42152
 H quadrupole lines in (3-0) and (4-0) bands 3-80984
 H₂ 3-0 quadrupole band i.r. obs., equivalent widths and temp. determ. 3-61673

urban planning *see town and country planning*u.v. detectors *see ultraviolet detectors*V-centres *see colour centres*

vacancies (crystal)

- see also Frenkel defects; Schottky defects*
 adamantane, self-diffusion in rotator cryst. phase, temp. depend. 3-64206
 agglomeration of vacancies and point defects 3-48383
 alkali halide:Ti, Ag, tunnel luminescence, vacancy and electron centres dispersion (Russian) 3-41560
 alkali halides, entropy of formation, effect of anharmonicity 3-49889
 alkali metal, atomic relax. and elec. resist. due to vacancies 3-46639
 alkali metal halides, phosphors, ionisation of luminescence centres by unrelaxed vacancies (Russian) 3-41559
 alloy, Kirkendall effect and noncompensated vacancy flow (Russian) 3-43889
 alloys, long-lived vacancies, relaxation technique, elec. resistivity, kinetics of adjustment to temp. jump 3-48466
 cladding materials, void nucleation suppression by vacancy trapping mechanism 3-63200
 clustering process analysis, temp. and aging depend. 3-49886
 defect superlattice form., elastic interaction theory 3-54957
 diamond, ordering of energy levels using defect molecule method 3-72077
 diffusional creep inhibition by second phase particles 3-46668
 electromigration and IC metallisation lifetime 3-43891
 entropy of formation, rel. to preexponential term in diffusion coeff. 3-68007
 f.c.c. lattice, isothermal annealing of vacancies and impurities, chem. reaction scheme 3-52619
 formation and motion, activation volumes 3-41049
 formation energy, concentrated random alloys, liquid state, heat of fusion, quasi-chemical approach 3-49978
 p-Ge, annealing of thermal defects 3-52620
 grain boundaries as vacancy sources or sinks, dislocation nonconservative motion 3-49896
 graphite, calc. of expansion for low concentration of vacancies (Spanish) 3-64070
 graphite reactor material, radiation damage, X-ray obs. (German) 3-71255
 hexagonal compounds, A₂B_nC₂X₁₄ with n=1/2, 2/3, 1, 4/3 and 2 (French) 3-64016
 III-V compounds, impurity distribution coefficients, ionic radius-lattice defect model, solubility 3-52639
 insulators, surface impurity effect on tracer diffusion 3-58149
 ionic crystal, vacancy subsystem behaviour in temp. gradient field (Russian) 3-40911
 metal, driving forces for electromigration, pseudopotential based theory 3-41047
 metal, failure process in complex stress state, mechanism 3-58689
 metal, formation entropy of single vacancy, evaluation from positron annihilation data 3-46640
 metal, obs. by quenching method under pressure up to 100 kbar 3-77417
 metal, theory of vacancy-impurity interactions, pseudopot. method 3-64030
 metal, with voids, vacancies and surfaces, positron behaviour 3-46808
 metals, high-temp. void formation under fast neutron irradiation, dislocation vibration as cure 3-40941
 migrating monovacancy, relaxation region vol. around defect 3-68248
 neutron irradiation softening and effect of interstitials 3-79343
 positron annihilation obs. 3-68245
 positron capture, A-centre model for exciton states 3-68578
 quench hardening, isothermal recovery 3-64920
 reactor graphite, radiation damage, 600-1400°C (German) 3-71254
 rigid disk hexagonal lattices, determ. of interactions between vacancies 3-40188
 semiconductor, defect zinc-blende struct. type 3-72621
 silver halide, mechanism of ion movement, vacancy migration 3-79525
 sputtering, surface damage and topography changes produced during sputtering 3-61088
 transition metal carbides and nitrides, ordered vacancy arrangements, electron diffraction studies 3-40913
 unstable vacancy-atom pairs in interstices, thermodynamics 3-58031
 voids, gas-filled, equil. shape 3-68241
 X-ray photon emission spectroscopy, ligand characterisation 3-66464
 Zircaloy-2, quenched and aged, vacancy precip. phenomena 3-80231
 Ag, plastically deformed, contrib. to elec. resist. and thermo-e.m.f. (Russian) 3-79663
 Ag, recrystn., point defects influence, internal friction obs. (French) 3-64111
 Ag formation energy, positron annihilation gamma rays, trapping model 3-49888

vacancies (crystal) continued

- Ag₂₋₃Au₃Se, solid solution, semiconductor electronic cond., electron mobility 3-41190
 AgBr:CdBr₂, ionic cond., rel. contrib. of vacancies and interstitials 3-73636
 AgCl, rel. to Zn²⁺ tracer diffusion, 209-441°C 3-68441
 AgCl:CdCl₂, physical cluster theory, cation vacancies interaction with impurity cations 3-75524
 Al, Al₂O₃ inclusions, high-temp. vacancies slow quenching as secondary defects 3-55765
 Al, dislocation configs., vacancy sources and sinks during thermal treatment 3-52627
 Al, dislocation loop size distrib., annealing behaviour, vacancy condensation 3-41704
 Al, electrical resistivity of voids, calc. using phase shift and pseudo-potential methods 3-44054
 Al, impurity-vacancy binding energy, core radius, Debye and melting temps., relations 3-52622
 Al, migration, relaxation method, simulation using pair potential 3-79529
 Al, plastic deform. effect on diffusivity, vacancy prod. by thermal jogs (German) 3-64218
 Al, point defect cluster formation and annihilation by 3 MeV electrons 3-54981
 Al, thin sample, quenching dislocation loop enlargement mechanism, annealing 3-72092
 Al alloy, point defect cluster formation and annihilation by 3 MeV electrons 3-54981
 Al-Ge, alloys precipitation of Ge nuclei, supersaturated alloy, below 140°C, X-ray and resistivity analysis, vacancies 3-53234
 Al₂O₃ systems, defects ordering phenomena X-ray anal. (French) 3-76335
 Al₂O₃-SiO₂, on Si, interface charge, traps due to oxygen vacancies 3-68705
 Al₁₀V, Einstein solid, resistivity, specific heat, localised phonon mode domination 3-40865
 Au, 2.0 to 2.5 MeV electron irradi., point defect cluster form. 3-79339
 Au, plastically deformed, contrib. to elec. resist. and thermo-e.m.f. (Russian) 3-79663
 Au, point defect cluster formation and annihilation by 3 MeV electrons 3-54981
 Au, positron trapping by vacancies, temp. independ. 3-60741
 C fibre, acrylic polymer oxidation, tempering, small angle X-ray scatt. (German) 3-76371
 CaO-MO-V₂O₅, (M=Mg, Co, Ni, Zn, Mn, Cd), defect garnet structure, cation vacancies 3-75525
 CaWO₄, e.p.r. of divacancy centres 3-55475
 Cd, supersaturation during oxidation, rel. to climb of superjogs (French) 3-64047
 CdF₂:Na⁺-anion complex, dielectric polarisation, ionic thermocurrents, reorientation space charge formation 3-44367
 Ce, self-diffusion mechanism (French) 3-46730
 CeO₂, defect equilibria for extended point defects, effect of O₂ pressure 3-79340
 CeO₂, nonstoichiometric, defect struct. above 700°C 3-68244
 (Co,Ni)O, cation diffusion, semiconductivity and nonstoichiometry 3-41050
 Co, quenched vacancy behaviour, resist. obs. (Korean) 3-53232
 (Co₂Mg_{1-x})O, (Co₂Mg_{1-x})₂SiO₄, solid solns., point defect thermodynamics (German) 3-64028
 (Co₃P)₂O₈, vacancies ordering, struct. 3-40912
 CrAsi-x, crystal structure, mag. susceptibility meas. 3-44209
 Cr₂N, interacting defect model 3-64031
 Cs halides, intrinsic and extrinsic defect pairs 3-52621
 Cu, Frenkel pair creation, computer simulation of atomic dynamics at energies near displacement threshold 3-79341
 Cu, mechanism for He atom diffusion 3-68443
 Cu, plastic deform. effect on diffusivity, vacancy prod. by thermal jogs (German) 3-64218
 Cu, plastically deformed, contrib. to elec. resist. and thermo-e.m.f. (Russian) 3-79663
 Cu, proton, neutron and fission neutron damage comparison 3-72105
 Cu formation energy, positron annihilation gamma rays, trapping model 3-49888
 α -Cu-Al alloys, local atomic arrangements and anomalous behaviour 3-50715
 α -Cu-Al(As)(Ga)(Ge)(In) alloys, Portevin-Le Chatelier effect (German) 3-41746
 Cu-Ni alloys, void form. resist. 3-67547
 α -Cu-Sn alloys, Portevin-Le Chatelier effect (German) 3-64907
 α -Fe, Mossbauer obs. of low temp. radiation damage 3-64587
 Fe, point defect cluster formation and annihilation by 3 MeV electrons 3-54981
 Fe, steady-state creep, substruct. parameters (Russian) 3-53217
 Fe-C alloy, effect of electron irradiation on quench aging 3-80260
 Fe-Co-V atomic order recovery, influence of vacancies, X-ray diffraction study (French) 3-58638
 Fe-Zn diffusion couple, intermetallic compound formation kinetics, annealing, 240-320°C (Japanese) 3-76167
 Fe_{1-x}O, structure examination, X-ray and electron diffraction (Russian) 3-49885
 Fe₂P, Mossbauer spectroscopy, vacancy distribution, mag. transition 3-41469
 Fe₃Se₄, ferrimag. moments, mechanism for pressure effect on Curie temp. 3-72469
 Fe₂S₃ electron diff. obs. 3-40867
 FeTi₂S₄, order-disorder transition of vacancies mag. props. 3-60721
 Fe_{2-x}n, powder, mag. susceptibility meas. 3-41336
 Ga₂Te₃, unstable equilibrium and radiation defects 3-52645
 Gd_{3-x}V₂S₄, semiconductor, conductivity activation energy, thermoelectric power, effect of applied mag. field 3-42125
 Ge, dislocation-free growth from melt, prevention of cluster formation 3-72810
 Ge, i.r. absorpt. meas. rel. to divacancy centres 3-43783
 Ge impurity distribution coefficients, ionic radius-lattice defect model, solubility 3-52639
 He, positive ion mobility, vacancy ion mechanism 3-41063

vacancies (crystal) continued

- HgSe (Te), solid solutions, diffusion, irradiation effect on electrical props. 3-64071
 Ho₂O₃, quasi-stoichiometric, electronic cond. mechanism (*French*) 3-79746
 In₂Te₃, unstable equilibrium and radiation defects 3-52645
 K(Cl, Br, I) whisker crystals, ionic conductivity determ. 40 to 300°C (*Russian*) 3-79598
 KCl, hardening, conc. effect on flow stress, interaction with dislocations 3-60723
 KCl, reactor irradiation damage recombination anal. 3-79378
 KCl:K₂SO₄ single crystals, interaction of mol. impurities and vacancies 3-72102
 KCl:Li, single crystals, vacancy mechanism of Li diffusion 3-72231
 KCl:Te(In), two-photon multistage radiation during interaction of a single electron-vacancy pair with activating centres (*Russian*) 3-41557
 KCl + KBr:Ca⁺⁺ mixed crystals, dielectric relaxation by vacancy dipole mechanism 3-64599
 KH₂PO₄, direct current conduction, proton vacancies migration 3-41198
 KN₃, rel. to self-diffusion of K, 85-254°C 3-43898
 LiF, Debye-Huckel cloud form. at dislocations, cation vacancy mobility, conc. 3-72234
 Mg, electrical resistivity of voids, calc. using phase shift and pseudo-potential methods 3-44054
 Mg ferrite, non-stoichiometric, ionic distrib., oxygen parameter, vacancies 3-54944
 MgMn ferrite, non-stoichiometric, ionic distrib., oxygen parameter, vacancies 3-54944
 MgO, deformation effect on optical absorption 3-64697
 (Mg₂□)P₂O₈, vacancies ordering, struct. 3-40912
 Mn₂Mg_{1-x}Y₂S₄, polycryst. solid soln., mag. susceptibility, Curie-Weiss behaviour 3-41328
 Mo, migration, electrical resistivity recovery stages III and IV 3-60722
 Mo, reactor irradi., 650°C, damage struct. 3-46649
 NH₄H₂PO₄, direct current conduction, proton vacancies migration 3-41198
 Na, electrical resistivity of voids, calc. using phase shift and pseudo-potential methods 3-44054
 NaCl, press. dependence of self-diffusion of ²²Na 3-58150
 NaCl, whisker crystals, ionic conductivity determ. 40 to 300°C (*Russian*) 3-79598
 NaCl: Cd, soln. of impurity-vacancy complexes, ionic thermocond. study 3-41020
 NaCl:Sb²⁺, Sb³⁺, defect centres, optical absorpt., elec. cond., dielec. loss and e.p.r. obs. 3-60739
 Nb, quenched, H-vacancy complex behaviour, internal friction obs. (*Russian*) 3-52671
 Ni, u.s. treatment influence on conc. (*Russian*) 3-41714
 Ni alloy, heat-resistant, deformability changes kinetics (*Russian*) 3-44602
 NiO:Sn⁴⁺, complex form., Mossbauer study for Sn⁴⁺ site determ. 3-72100
 NiO-Al₂O₃ system, interdiffusion coeffs., vacancy conc. depend. 3-72222
 NiO-CoO solid solns., defect struct. characteriz. 3-61192
 NiS₂, (Ni_{1-x}Cu_x)S₂, (Ni_{1-x}Co_x)S₂, band structure, insulator-metal transition, weak ferromagnetism 3-41144
 Ni_{1-x}S_x:⁵⁷Fe, metal-nonmetal transition, Mossbauer effect, 4.2 to 300K 3-44030
 PbBr₂, pure and NaBr-doped, rel. to ionic cond., 60-320°C 3-46728
 PbCl₂(Br₂)₂(I₂), anion vacancy migration, role in photolysis 3-72229
 PbO-MO-V₂O₅, (M=Mg, Co, Ni, Zn, Mn, Cd), defect garnet structure, cation vacancies 3-75525
 Pt wires, quenched, field ion microscopy and elec. resist. obs. 3-43780
 Pt wires, quenched, field ion microscopy and elec. resist. obs. 3-43781
 RbCl, migration energy of Sr²⁺ impurity-vacancy dipoles 3-43902
 Si, dislocation free crystals, float-zoned, dislocation generation along swirls, thermal oxidation 3-41648
 Si, dislocation-free growth from melt, prevention of cluster formation 3-72810
 Si, divacancy-oxygen complex and A-centre form. on electron irradi. 3-41166
 Si, float-zoned crystals, growth striations and swirls, electron microscopy 3-41649
 Si, high-purity crystal, investigation by Li decoration 3-43782
 Si, ordering of energy levels using defect molecule method 3-72077
 Si, rel. to diffusion of group III and group V elements (*Russian*) 3-43890
 Si amorphisation during different mass ion implantation 3-60754
 Si impurity distribution coefficients, ionic radius-lattice defect model, solubility 3-52639
 Si swirls, interaction with dislocations, comparison to striations 3-41647
 Si:B, rel. to negative creep during bending 3-55012
 Si:B, vacancy diffraction length at 1000°C, rel. to impurity profile 3-64788
 Si:Li, electron irradi. effects, Li impurity vacancy interaction 3-64069
 Si:Li, irradiated, spectra of Li-defect complexes 3-44434
 Si:Sb(P), (Au), zone refined, distribution of impurity elements, quantitative autoradiography 3-41651
 TaS_{2-x}, Se_x, phase diagram, X-ray analysis, atomic scattering factors 3-41016
 TiO₂, amorphous thin film, d.c. and a.c. construction 3-75798
 (U,Pu)O₂ mixed fuels, thermodynamic behaviour 3-57569
 VC_{0.75}, short-range ordered, diffuse scattering, neutron diffraction studies 3-40914
 V₆C₅, ordering, long period structure 3-54959
 V₆C₅, V₆C₇, ordering effect on thermodynamic props. 3-72973
 W, mechanism for He atom diffusion 3-68443
 W, quenched, defects behaviour, superfluid He quench 3-79344
 W, vacancy generation by rapid rate deform. at elevated temps. 3-80234
 ZnS, S-vacancies, thermal stability determ. using e.s.r. absorption of F-centres (*Russian*) 3-75881

vacancies (crystal) continued

- Zr-Al alloys, quenched and aged, vacancy precip. phenomena 3-80231
 ZrO₂ systems, defects ordering phenomena X-ray anal. (*French*) 3-76335
 ZrO₂:Ca²⁺, Raman scatt., massive point defect behaviour 3-68975
vacancy breakdown *see* diffusion in solids
vacuum apparatus
see also vacuum gauges; vacuum pumps; vacuum techniques
 alkali halides, cleavage device 3-76126
 casting device for use with Ar arc furnace 3-73699
 cathode sputtering installations evacuation conditions effects on pressure of active gases 3-51565
 chamber for cyclotron isotope production 3-39999
 continuous vacuum furnace for brazing Al (*Japanese*) 3-56642
 deposition of oxide films, h.f. glow discharge, polycrystalline oriented films, technique, apparatus 3-80158
 electrovacuum, thermal fields and stresses in metal-glass joint zone (*Russian*) 3-77418
 ellipsometer, for interface optical const. meas., construction 3-73727
 freeze dryer, centrifugal, for small-volume multiple fractions of solvents 3-66453
 friction properties of polymers, vacuum apparatus and method (*Russian*) 3-80470
 harmonic drive, as rotary feedthrough for u.r. vacuum 3-53869
 holder for spark cutting specimen blanks for electron microscopy 3-62283
 leak testing apparatus, selective membrane for mass spectrometric monitoring 3-73716
 lock, tab-type, high speed, rapid cut-off, 0.5 sec operating time, description 3-73715
 manipulator for use in high vacuum 3-39891
 mechanical pumps, devices for prevention of diffusion of oil vapours 3-51568
 multiposition test machine for high temp. testing in vacuum and gaseous media (*Russian*) 3-80511
 oven, 400°C, uniform temp. bake-out 3-70297
 perfluoropolyether vacuum fluid, effect of ion and electron bombardment, comparison with other vacuum fluids 3-77421
 probe holder, having rotating and rectilinear motion within cone angle of 34° 3-62038
 rotatable target holder for LEED diffractometer 3-42672
 sample machining device in u.h. vacuum 3-56655
 self-excited triggered arc gap 3-56654
 silicides, application as anti-emission materials (*French*) 3-59573
 for surface studies by ion scattering 3-42547
 synchrotron, K_K proton, vacuum system for (*Japanese*) 3-48493
 torsion pendulum with low instrumental decrement 3-61988
 valve, poppet, modified for quasisteady gas injection into vacuum, quasisteady arcjet, design and construction 3-73718
 vaporiser, finely dispersive substances, description, operating characteristics 3-77419
 versatile system for study of molecular beam scattering 3-39893
 zero gradient synchrotron, retuning after installation of vacuum chamber and pole-face windings 3-56747
 H, triatomic ions, gas analysers, formation in ion source 3-39894
 Ta thin film circuits, cylindrical diode continuous sputtering machine 3-39890
vacuum control
 leaks, calibrated, for high and ultrahigh vacuum systems (*Rumanian*) 3-45464
vacuum gauges
see also barometers; manometers; vacuum measurement
 Atmosphere Explorer, ion gauge and capacitance manometer for pressure measurements 3-42071
 Bayard-Alpert, modulation of the desorbed ion current following exposure to O₂ 3-59568
 cold cathode gauge, physical dimensions reduction 3-51569
 McLeod, improved cleaning technique 3-53875
 thin-plate, thermal conductivity type, 5 × 10⁻⁴ to 10² Torr (*Japanese*) 3-45465
 valve unit for calibration of very small quantities of gas by isotopic dilution (*French*) 3-59572
 viscosity type, theory 3-77423
vacuum measurement
see also vacuum gauges
 gauges, indication and calibration, medium/high/ultra-high vacuum range 3-48398
 gauges, indication and calibration 3-48398
 hydrocarbon partial pressure, ¹⁴C-labelled, meas. using CaF₂:Eu scintillation counter (*French*) 3-62039
 ionisation gauges utilisation in leak detection in vacuum systems (*French*) 3-56658
 manometer, ionisation, noise immune, 10⁻⁹ to 10⁻³ torr, design, construction, operation 3-73714
 McLeod pressure gauge, automatic 3-48395
 new logarithmic unit 3-51506
 partial pressure, mass spectrometer-ion current amplifier system, calibration extension to ultrahigh vacuum range 3-70296
 thin plate vacuum gauge, thermal conductivity type, 5 × 10⁻⁴ to 10² Torr (*Japanese*) 3-45465
 ultra high, below 10⁻¹⁰ torr 3-45466
 O₂ partial pressure gauge, use of stabilized ZrO₂ solid electrolyte 3-73713
vacuum polarisation *see* quantum electrodynamics
vacuum pumps
see also cryopumping; diffusion pumps; ion pumps
 electron microscope pumping system, outgassing (*Japanese*) 3-73901
 mechanical pumps, devices for prevention of diffusion of oil vapours 3-51568
 performance characteristics, review 3-56653
 rotary mechanical pump to reduce organic contamination in electron microscope 3-77724
 H pumping, new catalytic, factors determining pumping speed 3-39888
 Tj discharge pump, for evacuation of mixtures containing Cl₂ 3-51563

vacuum sintering *see sintering*

vacuum techniques

see also cryopumping; getters
beam chopper, piezoelectric, high vacuum use 3-77571
Bevatron, rectangular vacuum windows 3-56864
brazing Ti to ferrite ceramic 3-76229
condensed hydrogen jet, target production, in vacuo 3-48503
continuous metallisation, computer data collection and processing (*French*) 3-51570
continuous vacuum furnace for brazing Al (*Japanese*) 3-56642
cryogenic surface, capture and accommodation coeffs., high sensitivity gas ionisation detector 3-48402
electron microscope pumping system, outgassing (*Japanese*) 3-73901
etching, glow discharge ion gun, selective sputtering 3-53871
evacuation of vacuum electronic equipment, gas liberation by u.s. irradiation, theory, conditions 3-56657
evaporated metal films for polarising coatings 3-77460
evaporation, formation of thin Au film on metallic chalcogenides 3-61109
fibre-glass shells manufactured in vacuum, tensile and deforming characteristics (*Russian*) 3-64990
film deposition rate determ. device description 3-53868
film deposition, electron evaporated 3-62074
friction properties of polymers, vacuum apparatus and method (*Russian*) 3-80470
furnace for heat treatment and quenching in laboratory (*French*) 3-70291
gas leakages by diffusion through materials 3-51566
HBS system, for STEM 3-73910
heat pipes, bench and thermal vacuum testing 3-51548
high vacuum, pre-breakdown cond., gas-press. depend., comments 3-48400
high vacuum, pre-breakdown cond., gas-press. depend., reply to comments 3-48401
h.v. electrodes assembly, alignment device 3-53870
intermetallic composite, for vacuum evaporation (*Japanese*) 3-69371
ion source vacuum system, pressure differential gate valve 3-56919
leaks, calibrated, for high and ultrahigh vacuum systems (*Rumanian*) 3-45464
mechanically operated air admittance valve, to protect u.h.v. system after power cutoff 3-39895
molecular beam scattered by surface, veloc. distrib. (*French*) 3-56656
optical thin films, specimen transfer devices 3-53889
outgassing of Cu pinchoffs, character of gases released 3-59569
outgassing of metals 3-53874
outgassing of solids during tempering 3-62041
permeation and outgassing 3-59570
pneumatic micrometer for use in vacuum 3-59567
resonance-impulse method, determ. of elastic const., internal friction, resonant frequency meas. room temp. to 2200 C 3-51527
seal, slide type, metal gasketing, ultrahigh vacuum systems 3-48399
sealants, gas-evolution kinetics, optomechanical appls. 3-62040
soldering of Zircaloy-4 spacers for nuclear power station (*German*) 3-72930
solenoid latching valve, protection of vacuum systems 3-77422
synchrotron, KEK proton, vacuum system for (*Japanese*) 3-48493
telescope mirror aluminizers, description 3-77188
u.h. vac. reflection electron diffraction system, surface meas. 3-50058
ultra high vac. production below 10^{-10} torr, limiting factors 3-45467
ultra high vacuum production below 10^{-10} torr 3-45466
water vapour outgassing, improved heat treatment technique 3-77424
GaSb, deposition of nonrectifying contacts 3-51567
H⁺ multipulse source, rapid cycling vacuum system valve 3-56918
He leak detection, mass spectrometric, vacuum tightness, probe method, sensitivity increase, technique 3-73887
He mass spectrometer leak detection systems 3-66172
85Kr leak testing technique 3-51562
Mo(110) surface, cleaning procedures, low press. high temp. methods (*Japanese*) 3-50083
Si, solid-solid vac. diffusion doping process 3-58600
Si in ultrahigh vacuum, elec. properties, instructional experiments for undergraduates 3-68684
Ti chamber liners, Cornell electron synchrotron 3-56727

vacuum tubes

see also diodes; pentodes; tetrodes; triodes
evacuation of vacuum electronic equipment, gas liberation by u.s. irradiation, theory, conditions 3-56657
screened-grid, transducer for magnetic field strength measurement (*Russian*) 3-66285
SnO₂ film cold cathodes, electron emission obs. 3-41621

valence bands

diamond, X-ray photoemission cross-section modulation 3-44012
holes, integrated scattering probability for two-band valence band structure 3-64324
homopolynucleotides, CNDO/2 and MINDO/2 energy band structs. 3-60498
polyethylene, band calcs., density of electron states 3-79629
quartz, SCF X α calcs. of X-ray photoelectron, X-ray emission and u.v. spectra, valence orbitals 3-52793
rare earth-transition metal compounds, 3d-band, rel. to Fermi level using mag. props. 3-58002
refractory metal compounds, X-ray spectra interpretation, rel. to density of states of valence electrons 3-41594
semiconductor, p-type with chalcopyrite lattice, rel. to mag. susceptibility anal. (*Russian*) 3-44000
transition metal compounds, photoemission, valence-band structure 3-47348
transition metal monoxide, photoelectron spectra obs. 3-46791
and X-ray photoelectron spectroscopy, review 3-57646
p-ZnTe, free holes, spin-flip scattering, g-values 3-76018
Ag, valence band Auger electron spectra 3-50638
Ag₃AsS₃, proustite, valence band splitting, light absorpt. obs. 3-44017
AgGaS₂, valence band, X-ray photoemission obs. 3-55720

valence bands continued

Al, valence band Auger electron spectra 3-50638
Al-noble metal alloy, X-ray photoelectron obs. 3-64287
Al₂O₃, positron annihilation investigation of valence electrons 3-72317
Au foil, spectra studies using monochromatised X-rays 3-50119
Au-Ag alloys, X-ray photoelectron spectra, binding energy with respect to Fermi level 3-64284
Bi₂Sb₃, valence band struct. from magnetoplasma wave dispersion 3-44020
Bi₂Te₃, arbitrary-field theory developed from galvanomagnetic measurements 3-64291
p-Bi₂Te₃, galvanomag. effects, two valence subband model 3-72373
p-CdGeAs₂, electroreflectance spectra investigations 3-44427
CdGeAs₂, photocond. spectra obs. 3-64686
CdSe, photoemission and density of valence states 3-69138
CdTe, photoemission and density of valence states 3-69138
CoSi, electron struct. determ. by X-ray electron and X-ray spectra (*Russian*) 3-58568
Cu X-ray spectroscopic structure analyses, comparison of emission and photoemission spectra 3-46790
Cu-Au alloy, density of states from X-ray photoelectron spectra 3-79601
CuBr, cond. and valence bands, combined TB and OPW calcs. (*French*) 3-58209
CuBr, X-ray photoelectron study of valence bands 3-52789
CuCl, calcs. using Slater exchange potentials 3-41137
CuCl, electronic struct., rel. to X-ray emission and absorpt. spectra 3-50129
CuCl, valence band to 2p level transition, Cl-L_{2,3} emission spectrum 3-47325
CuCl, X-ray photoelectron study of valence bands 3-52789
CuI, X-ray photoelectron study of valence bands 3-52789
FeSi, electron struct. determ. by X-ray electron and X-ray spectra (*Russian*) 3-58568
p-GaSb, Hall effect in acoustoelec. domain, carrier trapping by pot. wave in valence band 3-44095
n-GaSb, stress-induced decoupling of valence bands, resist. and Hall effect study 3-46797
Ge, (100) surface state field emission, energy distrib. rel. to bands 3-55728
Ge, X-ray photoemission cross-section modulation 3-44012
GeTe, amorphous and crystalline, X-ray and u.v. photoemission spectroscopy measurements 3-41121
H₂, solid, ortho, degeneracy at Brillouin zone cube edges, Davydov splittings 3-44005
HgSe, photoemission and density of valence states 3-69138
HgTe, photoemission and density of valence states 3-69138
p-InSb:Cu, film, negative magnetoresist. meas., quantum size effect influence 3-41209
LiF, X-ray photoelectron obs. rel. to Hartree-Fock calcs. 3-79628
Mo, X-ray emission, M_V, M_{IV,III}-bands, wave functions of valence band electrons (*Russian*) 3-80117
NaBr, photoemission obs., comparison with densities of state calcs. for valence and cond. bands 3-44015
Nb, X-ray emission, M_V, M_{IV,III}-bands, wave functions of valence band electrons (*Russian*) 3-80117
Ni-Au alloy, density of states from X-ray photoelectron spectra 3-79601
NiAl-based ternary β Hume-Rothery phases, optical const., rel. to valence electron conc. and defect struct. 3-68965
NiS, X-ray photoelectron obs. of density of states 3-50124
NiSi, electron struct. determ. by X-ray electron and X-ray spectra (*Russian*) 3-58568
PbS(Se)(Te), high resolution X-ray photoemission spectra obs. 3-44011
Pt-Au alloy, density of states from X-ray photoelectron spectra 3-79601
RbCl, X-ray photoemission meas. 3-50125
SO₃²⁻ and SO₃F⁻ ions, sulphur K β X-ray emission spectra interpret. 3-52315
p-Sb₂Te₃, Shubnikov-de Haas obs., two valence band model 3-64357
Se, amorphous and trigonal, density of states, x-ray, u.v. photoemission obs. 3-50117
Si, surface-state transitions using electron energy-loss spectra 3-52887
Si, valence band, spin-orbit effect 3-60857
Si, valence electron momentum distrib. by Compton effect measurements 3-79633
Si, X-ray photoemission cross-section modulation 3-44012
SiC(6H), indirect transitions to exciton states, spectrum, selection rules 3-72677
SnS, absorption spectra and valence band spectra 3-41534
SnSe, absorption spectra and valence band spectra 3-41534
Te, absorption spectra for polarisation E \perp c, intervalence band transitions 3-79631
V₃X type compounds, structure, X-ray emission and absorption spectra (*Russian*) 3-55207
ZnGeP₂, chalcopyrite crystals, crystal-field and spin-orbit splittings, thermorefectance spectra 3-44007
ZnTe, photoemission and density of valence states 3-69138

valency
molecular orbital admixture coeffs. rel. to Raman scatt. 3-57624
moments development methods for covalency in elementary structures and AB compounds (*French*) 3-49867
YbAl₃ and YbAl₂, ambivalence of Yb, lattice const., sp.ht., and elec. props. study 3-68552

valve voltmeters *see voltmeters*

valves
see also diaphragms
ion source vacuum system, pressure differential gate valve 3-56919
leak-free gas-switching valve for isotope-ratio mass spectrometry 3-77716
mass spectrometer leak admission valve, continuous monitoring 3-73717
mechanically operated air admittance valve, to protect u.h.v. system after power cutoff 3-39895
outlet, malfunction and failure obs. in Wurgassen BWR circulating system (*German*) 3-67460

valves continued

- poppet, modified for quasisteady gas injection into vacuum, quasisteady arcjet, design and construction 3-73718
 relief, blow off rel. to condensation meas. in nuclear reactor (*German*) 3-74710
 safety and relief, opening characteristics in a BWR, and half opening time (*German*) 3-74708
 solenoid, latching valve, protection of vacuum systems 3-77422
 Teflon, mass spectrometer, quick introduction of gases 3-48557
 H⁻ multipulse source, rapid cycling vacuum system valve 3-56918

valves (electronic) see electron tubes**Van Allen radiation see radiation belts****Van Allen radiation belts see radiation belts****van de Graaff accelerators see linear accelerators****Van de Graaff generators**

- 14 UD Pelletron, Australian Nat. Univ. nuclear structure facility 3-70349
 accelerator, e.m. modes 3-70357
 accelerator tube, inclined field, 5 MV Van de Graaff KFKI Budapest, design, manufacture, operational experience 3-73850
 beam scanner for 1 MeV Van de Graaff 3-73851
 chain generator, electrostatic Right type, oil-immersed, viability of liquid insulator 3-73845
 charging, induction, Reading U.K., high current systems, conducting pulleys, systems studies 3-70360
 charging system, pellet chains, Kyushu Japan, development for tandem use 3-70359
 Cyclo-Graaff system, Australian Nat. Univ. nuclear structure facility 3-70349
 high gradient FN tandem, Florida State Univ. 3-70348
 High gradient stack investigations at AWRE 3-70353
 MP, Strasbourg, voltage tests in SF₆ 3-70352
 MP tandem, Chalk River, upgrading to 13 MV operation 3-70346
 MP tandem, Univ. Rochester, upgrading programme 3-70345
 rontgen absolute determination, X-ray source using Van de Graaff generator (*German*) 3-45326
 strippers, foil, Erlangen EN tandem Germany, development, operational experience, designs 3-73847
 T11/25 tandem facility, Democritos Greece 3-70347
 tandem, NSF, h.v. test programme 3-70355
 tandem, nuclear spectroscopy study (*French*) 3-59619
 tandem Van de Graaff, Minnesota Univ., operating experience 3-70351
 tandem Van de Graaff accelerator, validation of e.s. design of NSF 20/30 MV 3-70358
 three-stage tandem, Kyushu Univ., construction 3-70350

Van der pol oscillators see relaxation oscillators**Van der Waals forces**

- aerosol particle, spherical, rel. to near-wall motion 3-65037
 amino group, two-component solns., spectroscopic study of intermolecular interactions (*Russian*) 3-80050
 anisotropic, bodies (*Russian*) 3-66724
 carbonyl group, two-component solns., spectroscopic study of intermolecular interactions (*Russian*) 3-80050
 classical mechanical model of Van der Waals cryst., stationary distrib. function 3-68373
 colloid of metal spheres, dispersion forces, London-Van der Waal attraction 3-50793
 cylinders, thin anisotropic dielectric, appl. to chain molecule polarisation 3-70773
 between dielectric cylinders, nonretarded limit 3-57053
 between dielectric cylinders, retarded interaction 3-54075
 dielectric layer, single structure, theory 3-60827
 dielectric layer, triple layer structure, theory 3-60828
 electrolyte, non-uniform, interaction of like colloidal particles 3-71659
 electrolyte thin film, screening by walls 3-61258
 emulsion, spherical particles, Van der Waals interaction rel. to adsorpt. 3-41820
 equation of state of fluids, intermolecular repulsions 3-57700
 fluid mixtures near critical point, transport coefficients 3-48817
 fluid near critical point, Yang-Lee distrib. 3-57175
 gas-phase e.p.r. linewidths and intermolecular potentials, exper. results F-He-F₂ system 3-71368
 gas-phase e.p.r. linewidths and intermolecular potentials, theory, 2nd order dipole-dipole potential model 3-71367
 graphite crystal, non-bonded C atom interaction, anisotropic potential laws 3-63974
 graphite crystal, non-bonded C atom interaction, Lennard-Jones and Buckingham potentials 3-63973
 inert gas complexes with atoms and molecules, review of molecular beam studies 3-78912
 Lifshitz theory, stability of diffuse interface, surface tension, interface width calc. 3-75656
 limiting dispersion formulae, upper and lower limits 3-60361
 many-body interaction free energy to infinite order, collective behavior 3-46357
 many-body interaction free energy to infinite order, general susceptibility formulation 3-46356
 methane-propane gaseous mixtures, Van der Waals type eqn. for enthalpy departure 3-63608
 N-methyl acetamide crystal, molecular packing 3-43762
 multimolecular adsorption on cell surfaces under influence of van der Waals forces 3-61894
 nematic liquid crystals response to Van der Waals forces 3-46588
 nonlocal conductivity systems, external polarisation, calc. 3-70772
 retarded, at all distances derived from classical electrodynamics with classic electromagnetic zero-point radiation 3-42831
 scattering at thermal energies, atom-diatom mol. system 3-60496
 solids, in and between layers 3-49869
 suspension, flowing, particle collection under London and gravity forces 3-40747
 symmetric array of macroscopic bodies, average quantum energy of electromagnetic modes 3-57121
 theory rel. to states of matter 3-59514
 vacuum modes in Van der Waals' attraction 3-40338
 Ar multipole polarisability, Van der Waals consts. 3-71365
 Ar-HCl, struct. determ. from microwave and r.f. spectra 3-75049

Van der Waals forces continued

- ArHCl complex, structure determ. by mol. beam electric resonance spectroscopy 3-78824
 Au particle, adhesion to Si and Au substrates in u.h.v. 3-68519
 Be atoms, ground state, long-range interaction 3-46183
 C atoms, ground state, long-range interaction 3-46183
 C-H Van der Waals dipole-dipole interaction 3-63350
 H₂, exchange polarization energy, multipole struct. 3-75154
 H₂O, influence on vibrational spectra, i.r. absorp. intensity 3-63473
 He, polarizability of interacting atoms rel. to CIS light and dielectric model 3-67696
 He films on variety of substrates, onset for superfluid flow, Van der Waals constants for substrates 3-43912
 Kr multipole polarisability, Van der Waals consts. 3-71365
 N₂-Ar Van der Waals complex, i.r. absorption spectra, internal rotation 3-78805
 Ne multipole polarisability, Van der Waals consts. 3-71365
 Ne polarisability and C(6) coefficient calc. from oscillator strength distribution 3-71363
 O-H Van der Waals dipole-dipole interaction 3-63350
 O₂-Ar Van der Waals complex, i.r. absorption spectra, internal rotation 3-78805
 (O₂)₂, van der Waals molecule, i.r. and visible spectra 3-43447
 SO₂, influence on vibrational spectra, i.r. absorp. intensity 3-63473
 Xe multipole polarisability, Van der Waals consts. 3-71365

vanadium

- atomic forbidden lines transition probabilities, tables 3-74814
 Auger electron emission spectroscopy, characteristic ionisation losses 3-55710
 chemical analysis, review 3-59695
 Compton profile, determ. of anisotropy of electron momentum distrib. 3-72103
 Compton profile, Fermi surfaces, KKR method calcs. 3-79617
 defect superlattice form., elastic interaction theory 3-54957
 diffusion of H and D 3-52725
 dislocation motion, interstitial oxygen effect 3-58631
 Fermi surface, band structure, state-depend. potentials calcs. 3-79615
 film, vacuum-deposited, constitution and struct. (*Russian*) 3-72283
 interstitial nitrogen conc. depend of lattice parameter and mech. props. (*French*) 3-46656
 ion implantation and re-emission of He, temp. depend. 3-79394
 ion irradiation by ⁴He⁺, bubble and blister formation 3-79393
 magnetization and total energy, as function of lattice const. 3-68757
 metal, b.c.c., lattice distortion due to gas interstitials 3-64029
 mixed supercond. state, neutron depolarisation rel. to cryst. anisotropy 3-55353
 oxidation investigation by static method of secondary ion mass spectrometry 3-75683
 point defects in highly deformed V 3-44587
 polygonization singularities in polycryst. (*Russian*) 3-53215
 recovery after fast neutron irradiation at low temp. 3-68287
 saturated vapour pressure determ. by atomic absorption method (*Russian*) 3-48679
 solubility and diffusivity of H isotopes at high temps., reln. to CTR components 3-61161
 solubility of O₂, temp. dependence from 200 to 750°C 3-49998
 superconducting, fast particle irradiation effects 3-79395
 superconducting, induced voltage due to flux line lattice dislocation motion 3-60937
 superconducting, Knight shift and nuclear spin relax. calc. 3-55356
 superconducting transition temperature, calc. of press. dependence 3-79789
 thermodynamic props., effusion mass-spectrometric study 3-44662
 Al₂O₃:V³⁺, phonon spectroscopy using bremspectrum of superconducting tunnel junctions 3-53844
 Al₂O₃:V³⁺, spin-phonon coupling by quantitative spectroscopy with phonons 3-58104
 Au:V, lattice specific heat reduction due to V impurities 3-55065
 BaF₂, e.p.r. of V²⁺ at 77K 3-50456
 BaO-P₂O₅ glass:V⁴⁺, Cu²⁺, Co²⁺, e.p.r. ultrafine structure, interaction of V⁴⁺ with Cu²⁺ and Co²⁺ 3-58424
 CdF₂:V, charge conversion, optical absorption and e.p.r. spectra 3-55659
 CdSe:V, absorpt. spectra, oscill. strength, crystal field splitting and Racah parameters detn. 3-55652
 KZnF₃:V²⁺, Cr³⁺, fluorine hyperfine interactions, ENDOR obs. 3-79947
 MgO:V, charge transfer band, mag. circular dichroism and optical absorpt. obs. 3-52804
 NaCl:V²⁺ crystals, Z-like centres study 3-52812
 SiO₂-V system, chem. reactions, C-V characs., thermal instability 3-72404
 Ti₂O₃, pure and V-doped, thermoelectric effects 3-58290
 V I, oscillator strengths determ. by atomic beam absorpt. 3-46173
 V I-III atomic lifetimes and absolute oscillator strengths 3-43352
 V V, spectrum, 480-800 Å and energy levels 3-78419
 V:O neutron irradiation, and radiation anneal hardening, recovery and temp. depend. 3-79383
 V-SiO₂ system, heterogeneous reactions, deposition conditions, heat treatment 3-72405
 V-V₂O₅-Pb, Josephson tunnel junctions, U-I characteristics, mag. field depend. of critical current 3-58348

vanadium alloys**see also vanadium compounds**

- surface blistering by He ions, effect on fusion reactor operation 3-60289
 Al₁₀V, Einstein solid, crystal struct., resistivity, specific heat 3-40865
 Al₁₀V, Einstein solid, low temp. specific heat and electrical resistivity meas. 3-43855
 CoV intermetallics, orbital susceptibility and ⁵⁹Co Knight shift, d-electron motion (*Russian*) 3-52954
 Co₃V-Ni₃V quasi-binary alloy, long range ordered structs. 3-55767
 Cr-V, oxidation, comp. depend. 3-58661
 Fe-Co(49 wt.%)-(V(2 wt.%) workhardened, tempered, for high flux density apparatus (*French*) 3-68810

vanadium alloys continued

- Fe-Cr-V, correl. between exper. and theoretical diagram based on binary comp. systems 3-72841
 Fe-Cr-V-C system, carbide equil. with α and γ solid solns., chem. comp. (Czech) 3-55759
 Fe-V, low temp. ductility recovery heat treatments influence 3-53257
 Fe-V, sigma phase, Mossbauer obs., internal mag. field determ. 3-58444
 Fe-V, sp. ht., 600-1200K 3-72468
 Fe-V, spin echo spectra of ^{51}V at 4.2K 3-58435
 Fe-V alloys, thermodynamic variables, calcs. from phase diag. 3-64818
 Fe-V binary system, vanadium solubility in α and γ phases (Czech) 3-55771
 Fe-V system, thermodynamic props. and equil. diagram 3-69191
 Fe-V-N system, abnormal Snoek peak obs. 3-80229
 HfV₂, supercond., acoustic wave velocity meas., lattice instabilities 3-79801
 (Mn,V)₁₁Sb, with B8-type struct., ferrimag. props. 3-60960
 Mo-V, vanadium microalloying effect on boundary strength of cast Mo 3-61177
 Ni-V, dil., ^{51}V n.m.r. line, environment effects near mag. transition critical conc. 3-64566
 Pd-V, dil., incremental resist., 1.4-300K, high spin-fluctuation and Kondo models 3-55245
 Ti-Al-V, crack detection, u.s. shear wave techniques, influence of residual stress 3-47514
 Ti-Al-V-Sn, heat treatment effects on mech. props. 3-50727
 Ti-Al-V-Sn, stress corrosion cracking, influential factors and effect on anodic oxidation 3-47406
 Ti-V, athermal $\beta \rightarrow \omega$ transform., interstitial oxygen effect 3-64827
 Ti-V-Cr-Al, cold work influence on stress corrosion susceptibility 3-69258
 Ti-V-Cr-Al, metastable, recrystallisation and X-ray diff. invest. of age-hardening (German) 3-72880
 V-20% Ti, surface blistering by He ions, effect on fusion reactor operation 3-60289
 V-Cr(10%), neutron irradi. effect on tensile props. 3-79386
 V-Fe-Al powder, milling, specific surface, grain size distrib., additive effect 3-80390
 V-Fe-Co, atomic order recovery, influence of vacancies, X-ray diffraction study (French) 3-58638
 V-Mn-Ga, neutron powder diffraction, magnetic and superconducting measurements 3-47065
 V-N, dil., metastable phase behaviour 3-64976
 V-Ru, near-equiaxial, electronic transition, ^{51}V n.m.r. study 3-53032
 V-Ta, phonon spectrum change with Ta addition, specific heat meas. 3-75580
 V-Ti, and V interstitial alloys, neutron irradi., anneal hardening 3-79384
 V-Ti, neutron irradi. effect on high temp. mech. props. 3-79385
 V₃Al, formation between 20 and 70 kbar and 1000-2000°C 3-58005
 (V_{1-x}Cr_x)Be₂, high temp. elec. resist., comp. depend. (French) 3-79662
 (V_{1-x}Cr_x)₃Ge ternary solid solns., cond. electron energy spectrum, conc. depend. (Russian) 3-52917
 V₃Ga, acoustic plasmons in metal with overlapping d-, s-bands 3-58234
 V₃Ga, annealing, long range order, and supercond. transition temp. 3-55345
 V₃Ga composite wires, processing and superconducting props. 3-68726
 V₃Ga_{1-x}Sn_x, density of states at Fermi level, supercond. transition temp. rel. to electronic struct., n.m.r. obs. 3-41289
 V₁₁Sb, with B8-type struct., paramag. props. 3-60960
 V₃Si tapes, made by new process, supercond. props. 3-64430
 V₃Si tapes, supercond., prep. and Si conc. depend. of T_c and crit. current (Japanese) 3-60934
 V₃Si-V₃Ge, low temp. paramag. susceptibility and supercond. crit. temp., comp. depend. (French) 3-68723
 V₃(Si_{1-x}Ge_x) solid solns., mag. props., Knight shift, conc. depend. of T_c and Fermi level (Russian) 3-58327
 V₃X A-15 cpds., low temp. paramag. susceptibility and supercond. crit. temp. (French) 3-68724
 ZrV₂, supercond., acoustic wave velocity meas., lattice instabilities 3-79801

vanadium compounds

- carbide precip. in steel during continuous cooling (French) 3-47416
 vanadates, analysis of mean bond lengths 3-40875
 vanadyl complex of porphyrins, quasiline phosphorescence spectra, vibrational analysis at 77 K 3-53138
 X-ray photoelectron spectra, binding energy 3-50642
 CaO-MgO-SiO₂-V₂O₅ system, phase equilib. diagram, 1500°C 3-76337
 CaO-MgO-SiO₂-V₂O₅ system, phase equilib. diagrams, 1450°C 3-76338
 Mo₂V_{1-x}O₂ whiskers, metal-semicond. transition phenomena, comp. depend. 3-60907
 (Ti,V)₂O₃ systems, sp.ht. anomalies, electronic d levels 3-64303
 V complex, (quin H₂)VOCl₄, Jahn-Teller manifestation in orbital triplet coupled to Eg and T_{2g} modes, magnetic susceptibility 3-46952
 V complexes, trisacetylacetonate, CF₃ substituents, charge density distrib., n.m.r. 3-75064
 V oxides, crystal growth and props., semiconductor-to-metal transitions (German) 3-53194
 V-base cladding materials with ceramic fuels, reactivity and compatibility studies 3-43288
 V-H systems, nonclassical phase transformation 3-49993
 V-V₂O₅-Pb, Josephson tunnel junctions, I-I characteristics, mag. field depend. of critical current 3-58348
 VC, NaCl structure, band structure calc. 3-41142
 VC, VN, VO, heat of formation calc. 3-43878
 VC_{0.75}, short-range ordered, diffuse scattering, neutron diffraction studies 3-40914
 VC_{1-x}, electronic struct., APW calcs., virtual cryst. approx. 3-50127
 V₆C₅, elec. resist. meas., order-disorder transform. influence 3-44075

vanadium compounds continued

- V₆C₅, single crystals, microhardness, temp. depend., room temp. through order-disorder transition 3-47446
 V₆C₅, V₆C₇, vacancy ordering effects on thermodynamic props. 3-72973
 V₆C₅, vacancy ordering, long period structure 3-54959
 V₆C₇, elec. resist. meas., order-disorder transform. influence 3-44075
 VC₂H₂, L α emission bands, electron struct. determ. 3-72764
 VCl₄ in soln., reson. Raman effects, stretching vibrs. enhancement 3-75013
 V₃Co, valence and conduction band structures, X-ray spectra (Russian) 3-55207
 VCoAs, Co₂P structure, crystallographic data, metal-metal bonding, magn. props. 3-79315
 V_{1-x}Cr_xO₂, (0 \leq x \leq 0.15), phase diagram, magnetic susceptibility, DTA, X-ray diff. meas. (French) 3-79472
 V_{1-x}Cr_xO₂, disordered bond model of M₃ phase 3-46619
 V₂D₃, V₄D₃, crystal structure and structural transitions at low temps., X-ray and neutron diffraction studies 3-46710
 V₃Ga, electronic structure from X-ray spectral obs. (Russian) 3-47329
 V₃Ga, valence band and conduction band structures, X-ray spectra (Russian) 3-55207
 V₃Ge, valence and conduction band structures, X-ray spectra (Russian) 3-55207
 VH₂, L α emission bands, electron struct. determ. 3-72764
 VN, dispersion form. in stainless steel (French) 3-53231
 VN, NaCl structure, band structure calc. 3-41142
 VN, thin films, optical, elec. props., on fused silica surface 3-64755
 VN thermodynamic props., effusion mass-spectrometric study 3-44662
 VN-CrN mixed cpds., mag. props., conc. depend. (French) 3-47047
 VN_{0.96}, thermal expansion, 300 to 1000K 3-69341
 VN_(1-x), precipitation hardening of austenitic stainless steel 3-69324
 V₃N, precipitate in α -V, structure, morphology and orientation relationships 3-50698
 (V_{0.3}Nb_{0.7})O₂, electrical transport props. 3-41239
 V_{1-x}Nb_xO₂, (0 \leq x \leq 0.33), vapour phase prep. and characteriz. of single crystals (French) 3-72802
 VNiAs, Co₂P structure, crystallographic data, metal-metal bonding 3-79315
 VO, NaCl structure, band structure calc. 3-41142
 VO₂, passage of current across semicond.-metallic phase boundary 3-44149
 VO₂ coplanar switching devices, pulse response theory 3-79747
 VO₂ single crystal, heat capacity meas. above and below metal-semicond. transition 3-41025
 VO₂Cr, twinning by reticular pseudo-merohedry, twin laws 3-79362
 VO₂⁺ in dimethylformamide and dimethylacetamide solns., n.m.r., e.p.r. study of coordination 3-41433
 VO₄³⁻, mag. circular dichroism assignment of longest wavelength band 3-54663
 VO₄³⁻, valence electron levels study by X-ray photoelectron spectroscopy 3-63388
 V₂O₃, ^{51}V n.m.r., temp. depend. up to 1000K 3-68861
 V₂O₃, corundum struct., thermal expansion, X-ray diff. obs. 3-64189
 V₂O₃, corundum struct. type, thermal expansion 3-69340
 V₂O₃, metal-insulator transition, current carriers density discontinuous change 3-72326
 V₂O₃, rhombohedral, empirical band scheme, optical and soft X-ray data 3-41130
 V₂O₃, single cryst. prep. by chem. transport reaction 3-72801
 V₂O₃Cr, impurity effects on strongly correlated electrons in narrow band 3-55195
 V₂O₃-Cr₂O₃, antiferromag. state, n.m.r., hyperfine field, mag. moment, spin moment 3-55478
 V₂O₃-Sc₂O₃ system, elec. cond. transition 3-72388
 V₂O₃x, nonstoichiometry detection (Japanese) 3-64979
 V₂O₄, new monoclinic phases, semiconductor to metal transition temperatures 3-63979
 V₂O₅, Auger electron emission spectroscopy, characteristic ionisation losses 3-55710
 V₂O₅, electric field effect on electronic struct., electroreflection spectra 3-76021
 V₂O₅, liquid semicond.-metal interface, nonlinearity of current-voltage characts. 3-41265
 V₂O₅, single cryst., electroreflectance, resonance due to conduction band fine struct. 3-50598
 V₂O₅, thermal and low energy electron bombardment induced O₂ loss, transition into V₆O₁₃ 3-41099
 V₂O₅ suspensions in laminar flow, birefringence (French) 3-80500
 V₂O₅ thin film, low energy laser pulse calorimeter applic. 3-53918
 V₂O₅:MoO₃ solid solutions, magnetic characteristics, 4.6-300K using Faraday-Curie balance 3-72459
 V₂O₅-MoO₃, physico-chemical props. 3-80582
 V₂O₅-Na₂O-Fe₂O₃(Cr₂O₃)(MgO), ternary, solid-liq. phase diagrams 3-46696
 V₂O₅, structure type of intergrowth in Cr₂O₃-Fe₂O₃-TiO₂-ZrO₂ system 3-68389
 V₆O₁₃, phase transform., cryst. structure obs. at room and liquid nitrogen temps. 3-52698
 V_nO_{2n-1}, Magneli phases, mag. and metal-insulator transitions, review 3-46805
 V_nO_{2n-1}, metal-insulator transition and magnetic props. 3-44028
 V₂O₅ cpds., amorphous semicond., localized d¹ electron e.s.r. meas. 3-68847
 VS₄²⁻, mag. circular dichroism assignment of longest wavelength band 3-54663
 VS₂, NiAs-MnP type structure change 3-64571
 V₃Si, elastic properties and superconductivity at high pressure 3-79792
 V₃Si, harmonic-phonon generation by shear waves in region 5 to 10 MHz 3-52673
 V₃Si, mag. field induced structural phase transform. prediction 3-46711

vanadium compounds continued

- V₃Si, superconducting transition temps. and crystal structure, influence of compacting pressure 3-50287
 V₃Si, valence band and conduction band structures, X-ray spectra (*Russian*) 3-55207
 V₃Sn, valence and conduction band structures, X-ray spectra (*Russian*) 3-55207
 VTaO₄, rutile structure, atomic and mol. ordering, mag. structure from 4.2 to 300K 3-79849
 (V_{1-x}Ti_x)₂Si, supercond., relation between T_c and elastic softening 3-68740
 Va₂O₅ reaction with Eu₂O₃, X-ray anal., lattice consts. determ. 3-75598

vaporisation

- see also boiling; evaporation; heat of vaporisation
 alloy, ordered, volatilisation, statistical theory (*Russian*) 3-69185
 spectral line intensity rel. to weight of sample vaporised with laser microprobe 3-45556
 sprays, liquid, in flowing hot gas, droplets vaporisation 3-71806
 vapouriser, finely dispersive substances, description, operating characteristics 3-77419
 vapour explosions, mechanism 3-69455
 variable composition mixtures, homogeneity region determ. 3-75625
 volatilisation rate of free particles in d.c. arc plasma in air at atmospheric pressure 3-63914
 water, transient heat fluxes and vapour generation rate meas. 3-52431
 Fe-Cr melt, dissolved elements, rate coeffs. (*German*) 3-76191
 La₂(CrO₃)₃, oxidation-vaporiz. kinetics 3-72955
 MgAl₂O₄ spinels, vaporiz. rates of MgO in vacuum (*Japanese*) 3-60791
 Na, coolant, LMFBR fuel-coolant interaction, noncoherence and heat transfer cutoff 3-71289
 Na, expanding coolant, simulation of mech. energy release, reactor energy source characterisation 3-74674
 NaF-AlF₃ system, AlF₃-rich, high press. study (*French*) 3-68392
 Ti vapour laser, superradiant pulse power, dependence on discharge parameters, isotopic and hyperfine line splitting (*Russian*) 3-66823
 U-Pu-N ternary system, equil. assessments 3-46136

vaporising see vaporisation**vapour density** see density of gases**vapour-liquid transformations** see liquid-vapour transformations**vapour pressure**

- see also humidity; vaporisation
⁴He-nD₂ and ³He-nH₂ binary systems, liquid vapour equilibrium 3-50041
 boiling refrigerants, pressure drop and convective heat transfer, three flow regions (*German*) 3-46385
 curve for pure substance, critical slope 3-72169
 evaporation, enthalpy and entropy calc., from vapour pressure, programmable desk calculator 3-49986
 LMFBA, use of saturated liquid Na properties in fuel-coolant interaction analysis 3-46157
 LMFBR, local molten fuel-coolant interaction, pressure pulse on subassembly wall 3-46073
 LMFBR, voided-core disassembly, fuel-coolant interactions 3-46075
 LMFBR disassembly calcs. fuel-coolant interaction and differential motion effects 3-46074
 O₂ transfer to fermentations, effect of pressure 3-66696
 reactor molten fuel-coolant interactions, role of nucleation in vapor explosions 3-46077
 thermal transpiration eqns. 3-41085
 thermophysical properties computation and production of self-consistent tables and Mollier charts 3-60510
 variable composition mixtures, homogeneity region determ. 3-75625
 water, normal and heavy, 273.15-298.15 K 3-49988
 Ar formulae, comparison, new rational method 3-79480
³⁶Ar, solid, sublimation and vapour press., 23.752-87.375K 3-41012
 As, effect on deep-level impurity conc. depth profile in epitaxial GaAs (*Japanese*) 3-55736
 As-Bi(Pb) alloys, liq., thermodynamics props. partial vapour press. meas. (*German*) 3-72839
 Cs, saturated vapour press., 755-1600°C, 2.14-80.5 atm. 3-49981
 Cu-Mg alloys, liq., thermodynamic props. determ. by vapour press. meas. 3-64807
 Cu-Mg alloys, liquid, thermodynamic props. determ. by vapour pressure meas. 3-72822
 GaAs, evaporation under equil. and non-equilib. conditions using modulated beam technique 3-68395
 H₂-D₂ liquid solutions, below 20.4K 3-64166
³He-⁴He mixture, in 0.7 to 1.3K temp. range 3-75652
³He-nD₂ and ³He-nH₂ binary systems, liquid vapour equilibrium 3-50041
⁴He, thermophysical props. tables from 2 to 1500 K with pressures to 1000 atmospheres 3-60822
 K, 2100 F up to critical temp., pressure tube meas. method 3-75616
 Kr, sublimation, rel. to activation energy (*French*) 3-55081
 Li-Zn-Ca halide soln., liquid-vapour phase behaviour, air conditioning appl. 3-75615
 N₂ formulae, comparison, new rational method 3-79480
 Rb, 1400 F up to critical temp., pressure tube meas. method 3-75617
 Rb, saturated vapour press., 683-1649°C, 0.97-101.5 atm. 3-49981
 U-Pu-N ternary system, equil. assessments 3-46136
 UO_{2+x}, FBR fuel, oxygen pressures calc., model 3-40536
 W, and heat of sublimation 3-64172

vapour pressure measurement

- device description 3-62035
 hydrocarbon partial pressure, ¹⁴C-labelled, meas. using CaF₂:Eu scintillation counter (*French*) 3-62039
 in-reactor temperature monitor, indirect determ. of vapour pressure 3-67403
 metals, alloys, thermodynamic props. expt. meas. techniques, review (*German*) 3-42539

vapour pressure measurement continued

- torsion effusion, bifilar suspension 3-53865
 Ar, new technique, state of the art assessment, formulae, comparison, new rational method 3-79480
 Cu, saturated vapour pressure determ. by atomic absorption method (*Russian*) 3-48679
 N₂ new technique, state of the art assessment, formulae, comparison, new rational method 3-79480
 Rb, by optical absorption, at 330 K 3-48396
 Ti, saturated vapour pressure determ. by atomic absorption method (*Russian*) 3-48679
 V, saturated vapour pressure determ. by atomic absorption method (*Russian*) 3-48679

vapour-solid transformations see solid-vapour transformations**varactors**

- material selection and preparation 3-80185
 GaAs microwave diodes, abrupt junction, liquid phase epitaxy 3-50662

variable stars

- 1633+38, identification with visible object 3-77111
 AC+39° 1214-608, flare star, spectral and photoelec. obs. (*Russian*) 3-45127
 Algol systems, photometric effects of gas streams 3-53647
 Algol-type binaries, model for alternate period changes 3-73480
 Algol-type binary secondary component, departures from LTE 3-51326
 RX Andromedae, Z Camelopardalis type star, high-speed photometric obs. 3-65893
 Ap stars, light variation due to line-blanking effects 3-61783
 Ap stars with long periods, search 3-45131
 V 433 Aql, photographic obs. (*Russian*) 3-61807
 ST Aquarii, eclipsing binary, UBV photoelectric photometry obs. 3-77084
 CY Aquarii dwarf Cepheid, beat period and characts. 3-69959
 η Aquilae, predicted observability of CO and CO+ lines 3-61811
 η Aquilae, prediction for presence of C₂ Swan bands 3-61810
 RT Aurigae, differential UBV photometry of Cepheid 3-77083
 Aurigae, eclipsing binary, 6-colour obs. of 1963-64 eclipse 3-53665
 Aurigae, eclipsing binary, Ca I satellite lines rel. to expanding circumstellar cloud 3-53666
 SS Aurigae, possible Z Camelopardalis type star 3-45130
 BD+34°3815 (Cygnus X-1), nature of optical variability 3-61818
 BD-10°4662, possible post-T Tauri star 3-51350
 4C 38.41, identification with visible object 3-77111
 TX Cancr., W Ursae Majoris type, obs. and evolution 3-65892
 SY Cancr., Z Camelopardalis type star, high-speed photometric obs. 3-65893
 ζ Canis Majoris, β CMA star, yellow photoelectric obs. rel. to light curve shape 3-42200
 VY Canis Majoris, obs. of CO in 5μ spectra 3-45159
 YZ Canis Minoris, 1972 photoelectric photometry of flare star 3-73518
 YZ Canis Minoris, flare star, 1971 photoelectric monitoring 3-45140
 YZ Canis Minoris flare star, 1969 Jan., spectrophotometric investigation (*Russian*) 3-45126
 α² Canum Venaticorum, u.v. obs. compared with LTE-model calcs. 3-56395
 S Carinae, Mira-type variable, Coude spectra through cycle, atmospheric parameters 3-42191
 η Carinae rel. to MWC 645 and 819, spectra and energy distrib. similarities 3-42195
 RS Carum Venaticorum binaries rel. to W Ursae Majoris binaries 3-47998
 Case 621, identification with VX Aquilae, possible Mira-type 3-45137
 SX Cassiopeiae, Algol-type variable, detection of secondary spectrum 3-45135
 AR Cassiopeiae, eclipsing binary, six colour obs. 3-81096
 cataclysmic variables, masses of white dwarf primaries 3-48017
 CD-42° 14462, oscillations 29 sec. 3-69963
 α Centauri, spectrum variable, obs. of anomalous Fe I lines 3-53667
 α Centauri (HD 125823), radial rel. variations determ. 3-42198
 VW Cephei, eclipsing contact binary, period damages 3-61803
 VV Cephei, high-dispersion spectrum, Hα structure, radial velocities 3-51355
 β Cephei, obs. with improved time resolution 3-48035
 RZ Cephei, RR Lyrae-type, radial vel., light and colour curves 3-53668
 β Cephei stars, statistical anal. 3-56390
 Cepheid F and G stars, Hα line profiles 3-56377
 Cepheid instability strip, non-pulsating stars, properties and evolution 3-45111
 Cepheid stars, systematic errors in temp. and mass 3-56385
 Cepheid variables in 3 LMC globular clusters, BV obs. 3-65882
 Cepheids, continuum photometry of F and G stars 3-56378
 Cepheids, double mode, mass determ. from period ratios of 8 examples 3-69958
 Cepheids, He abundance of objects in Galaxy and local group galaxies 3-45112
 Cepheids, linear and nonlinear pulsation calculations 3-61762
 Cepheids, period-radius relation 3-51348
 UV Ceti, 1972 photoelectric photometry of flare star 3-73518
 UV Ceti, flare star, 1971 photoelectric monitoring 3-45140
 o Ceti, speckle interferometry, colour-depend. limb darkening 3-48031
 UV Ceti stars, stimulated amplification of synchrotron radiation 3-53680
 UV Ceti-type flare stars, UBV obs. of 10 objects 3-45099
 classical Cepheids, Q-method for colour excesses 3-45102
 close-binary light curve synthesis, appl. to eclipsing binaries TX Ursae Majoris and MR Cygni 3-42197
 Coalsack, search for flare-star spectra rel. to star formation 3-81208
 RZ Comae Berenices, contact eclipsing binary, differential correction analysis rel. to gravity darkening 3-56389
 γ Comae field, 4 new obs. with Schmidt telescope 3-69966
 R Coronae Borealis, polarimetric obs. during light minimum, 0.36 to 1 micron 3-48042

variable stars continued

V1329 Cyg=HBV 475, symbiotic binary, photometric and spectroscopic obs. 3-69965
32Cygni, 1971 eclipse, OAO-2 filter photometry 3-51354
V1016 Cygni, detection of radio emission 3-65899
P Cygni, detection of radio emission at 5 and 10.68 GHz 3-81119
MR Cygni, eclipsing binary, close-binary light curve synthesis 3-42197
V1016 Cygni, expansion, spectroscopic studies, emission line structure 3-69969
χ Cygni, Mira-type, 4000-6700 cm⁻¹ spectra 3-45132
V1016 Cygni, peculiar emission object, radio emission interpretation 3-77099
V1057 Cygni, photometric outburst rel. to pre-main-sequence evolution 3-61799
V453 Cygni, spectroscopic binary, BV obs. showing apsidal motion 3-42199
31 Cygni, spectroscopic eclipsing binary, 4-colour photometry 3-77106
CI Cygni, symbiotic star, obs. of spectrum during outburst 3-48041
Cygni-A, radioastronomical obs., scanning the diagram of the variable profile antenna (*Russian*) 3-81248
PCygni-type stars rel. to Wolf-Rayet stars 3-81061
eclipsing, natural motion of 122 stars (*Russian*) 3-61808
eclipsing binaries, light curve rectification 3-77073
eclipsing binaries, mass distribution 3-77070
eclipsing binaries, parameter correlation coefficients of spherical model 3-53642
eclipsing binaries, reflection model 3-69947
eclipsing binaries, relative shifts of minima (*Polish*) 3-65888
eclipsing binary light curves analysis on computer 3-53654
eclipsing binary system, radiation spectral energy distrib., computation model 3-51328
eclipsing binary system envelopes 3-53645
eclipsing binary systems, light curve for objects with extensive atmosphere 3-77064
ι Eridani, β Cephei variable, behaviour of H lines 3-56392
faint variable objects in M31 region 3-48064
flare stars, absence of associated cosmic γ-ray bursts 3-77127
galactic Cepheids, intrinsic B-V colour determ. 3-48011
General Catalogue of Variable Stars, search for extragalactic objects 3-48093
GR-29, magnitude and brightness distribution functions from photographic plate (*Russian*) 3-61806
Groningen-Palomar variable star fields, UVB photometry for 170 objects 3-48006
RS Gruis, photometric obs. 3-65898
GX 339-4 X-ray variable, OSO-7 obs. of intensity 3-81134
H₁ 1069, UV Ceti-type star behind Pleiades, spectral obs. 3-45138
H₁ 230, UV Ceti-type star behind Pleiades, spectral obs. 3-45138
halo/old disk cepheids, existence of Hertzsprung progression 3-61790
HD153919 (=2U 1700-37), UVBJHKL photometric obs. 3-61814
HD173219, periodic Be star, companion possible black hole 3-61813
HD 101799, W Ursae Majoris-type eclipsing binary, UVB obs. and orbit 3-48023
HD 133029, magnetic variable UVB photoelectric photometry obs. 3-77089
HD 153919, identification as optical counterpart to 2U 1700-37, OAO-2 obs. 3-48032
HD 153919, optical candidate for 2U 1700-37 X-ray source 3-51374
HD 153919 (=2U 1700-37), spectroscopic obs. 3-61815
HD 153919 (=2U 1700-37), photoelectric UVB obs. of optical variations 3-81133
HD 21339, Ca II emission binary 3-56394
HD 217312, spectroscopic binary, B photometry 3-77103
HD 221568, Ap-star, light var. rel. to line blanketing 3-45121
HD 51418, peculiar A-type star, spectrum and light var. 3-69956
HD 77581, optical counterpart to 2U 0900-40, X-ray source 3-56415
HD 77581 (2U 0900-40), UVB photoelectric photometry 3-81136
HD 98088, Ap star, photoelec. obs., light variation (*German*) 3-81100
Hercules X-1, 35-day periodicity rel. to accretion gas flow in binary system HZ Herculis 3-48083
HZ Herculis, B-magnitude light curve 3-45122
HZ Herculis, binary star, evolution 3-77130
TX Herculis, eclipsing binary, BV photometry and light curve analysis 3-51357
HZHerculis, eclipsing binary, X-ray beaming and mass transfer 3-48028
HZ Herculis, Hercules X-1, X-ray source, neutron star, mass meas. 3-45164
AH Herculis, high-speed photometry of dwarf nova, light curve analysis 3-45116
HZ Herculis, optical pulsations 3-61801
HZ Herculis, reflection effect due to energy transfer 3-48033
HZ Herculis, search for optical pulsations at period of Hercules X-1 X-ray pulsations 3-61817
HZ Herculis, UVB photometry and Hercules X-1 35-day cycle 3-73517
HZ Herculis (Hercules X-1), optical obs. 3-59365
HZ Herculis (Hercules X-1) nature of optical variability 3-61818
BD Herculis visible observations at Kazan observatory (*Russian*) 3-73519
88 Herculis, shell star, long time variations (*French*) 3-77088
HR 1287, δ Scuti type, blue photometric obs. discrepancy in fundamental frequency 3-77087
HR 7275, Ca II emission binary 3-56394
HR 8703, Ca II emission binary 3-56394
IRC stars, identification 3-61779
irregular variable stars, obs. of Hα emission profiles 3-73492
EV Lac, spectrocolorimetric observation of flares (*Russian*) 3-77095
AR Lacertae, Algol-type eclipsing and spectroscopic binary, obs. of radio emission 3-45148
BL Lacertae, BV obs. and bibliographic informations (*French*) 3-73514

variable stars continued

CM Lacertae, eclipsing binary light curve, computer study 3-53664
EV Lacertae, flare star, 1971 photoelectric monitoring 3-45140
10 Lacertae, O-type star, rapid spectral variations 3-45134
BL Lacertae, photographic and photoelectric obs. of optical variability 3-81095
BL Lacertae, radio structure variations 3-56405
EV Lacertae polarimetric obs., blue region (*Russian*) 3-45113
AD Leonis, 1972 photoelectric photometry of flare star 3-73518
R Leonis, angular diameter from obs. during lunar occultations 3-77085
AD Leonis, flare star, 1971 photoelectric monitoring 3-45140
light curve, subject to orbital tidal distortion, calc. program description 3-51341
long period Cepheids, radii and fluxes by Weselink method 3-81083
long-period variables, period rel. to OH radial-vel. 3-59343
UV Lyncis, W Ursae Majoris star, UVB photometry and photometric orbit 3-65895
β Lyr, rapid mass exchange between components 3-69968
RZ Lyrae, light gradients and variations with Blazhko effect (*Russian*) 3-77091
RZ Lyrae, photometric variations with period of Blazhko effect (*Russian*) 3-77092
β Lyrae eclipsing binaries, statistical anal. 3-53656
RR Lyrae instability strip, non-pulsating stars, properties and evolution 3-45111
RR Lyrae models, non-linear pulsations and grey radiative transfer 3-47993
β Lyrae spectra, variation of H and He lines (*Russian*) 3-45128
RR Lyrae stars, intermediate-band photometry and colours 3-81048
RR Lyrae stars, mean absolute magnitudes (*French*) 3-81068
RR Lyrae stars in Baade's field near NGC 6522 globular cluster 3-59374
RR Lyrae type, erratic period variations in globular clusters 3-73486
RR Lyrae variables in globular cluster M5, long-term amplitude changes 3-48010
RR Lyrae variables near S. Galactic Pole, photometric obs. of 4 objects 3-61778
RR Lyrae-type stars in globular cluster M22, metal abundance 3-45196
M29 (NGC 6913), galactic cluster V photoelectric obs. of 3-61847
M31, variables 5 and 9, periods for two RR Lyrae-type stars 3-42202
Magellanic Clouds Cepheids, He abundance determ. 3-53660
Me type dwarfs, models for periodic variations, spot model 3-73498
Mira variables, near i.r. photometry 3-56380
Mira-type, obs. of type I OH stars 3-61781
1 Monocerotis, δ Scuti-type variable, UVB photometry rel. to amplitude var. in light curve 3-48039
ST Monocerotis, Mira-type variable, UVB magnitude sequence 3-45136
MSB 57, C-star, photometric study 3-45137
nearby classical Cepheids, places of formation rel. to history of spiral structure 3-48091
in NGC 6934, globular cluster, BV photometric obs. 3-45180
nonspherical eclipsing binary star system modelling, computer program 3-45139
Nova Cephei, 1971, photometry, light variations, estimation of photometric distance 3-81101
ρ Ophiuchi, dark clouds, extinction and polarisation, wavelength dependence 3-48046
α Orionis, model atm. compared with scanner obs. 3-61798
α Orionis, speckle interferometry, colour-depend. limb darkening 3-48031
Orionis-A, radioastronomical obs., scanning the diagram of the variable profile antenna (*Russian*) 3-81248
EE Pegasi, eclipsing binary light curve, computer study 3-53664
AG Pegasi symbiotic binary model, M giant absorption spectrum 3-81090
periodogram Fourier analysis, detection of weak components, frequency meas. and short computation 3-48137
β Persei, 5GHz obs. 3-61816
δ Persei, OAO-2 and Mariner 9 u.v. obs. rel. to variability 3-77101
KT Persei, Z Camelopardalis type star, high-speed photometric obs. 3-65893
β Persei (Algol), optical and radio determ. of position 3-81102
β Persei type, eclipsing, condition for atmospheric hydrostatic equilibrium. (*Russian*) 3-73489
κ Piscium, spectral anal. 3-59350
Puppis, eclipsing binary, i.r. spectra 3-45124
radial velocity curves for intrinsic variables, nonlinear pulsations iterative theory 3-48009
rapidly fluctuating stars, early visual detection 3-53658
red variables with very small amplitude and very short period, photometry 3-81046
RR Lyrae stars in Baade's field near NGC 6522 (globular cluster) 3-56376
RZ Cancri unstable eclipsing giant system 3-69967
FG Sagittae, observational evidence of thermal pulse in old planetary nebula 3-69960
FG Sagittae, symmetrical emission nebula expansion 3-70044
Sanduleak 160, optical counterpart of SMC X-1, B photometry 3-81137
S Sculptoris, long-period Me variable, spectral Tc lines 3-45133
RZ Scuti, spectrophotometric obs. 3-53670
δ Scuti stars, search among nearby A and F-type stars 3-65886
SdB-type rapid variables, statistical anal. 3-59344
small amplitude red disc and halo population, UVRI obs. 3-73502
spectroscopic binaries, 12th complementary catalogue (*French*) 3-45100
HL Tau-76, triple periodic white dwarf, blue magnitude obs. 3-48034
44 Tauri, δ Scuti star, photoelectric obs. in blue light 3-53669
RZ Tauri, contact eclipsing binary, differential correction analysis rel. to gravity darkening 3-56389
Tauri, dark clouds, extinction and polarisation, wavelength dependence 3-48046
T Tauri, evolution Orion nebula 3-47999

variable stars continued

- Tauri, optical and infrared obs., model for wavelength dependence of polarisation 3-73511
 IK Tauri, period and spectral range from i.r. obs. over 8 years 3-81093
 HL Tauri, triply-periodic white dwarf, differential blue magnitudes 3-48043
 28 Tauri (Pleione), new shell phase in spectrum 3-42192
 T Tauri stars, extinction and scatt. by small planetesimal particles 3-73496
 T Tauri stars, grain formation in expanding envelopes 3-48001
 T Tauri stars, pre-main-sequence evolution 3-61799
 T Tauri stars, supersonic turbulent stress and structure 3-73479
 T Tauri type, rotating, mass loss through stellar wind 3-77061
 T Tauri type, transition radiation from fast electrons in dust envelope 3-81032
 T Tauri-type stars in OH clouds 3-45219
 RR Telescopii, emission line spectrum during 1968 rel. to nova-like properties 3-42196
 Two-Micron Sky Survey stars, identification 3-61779
 2U 1543-47, late-type irregular variable as optical candidate of X-ray source 3-69997
 ultrashort-period, intermediate-band photometry and colours 3-81048
 W Ursae Majoris, binary, mass-ratio determ. from photometric obs. 3-48050
 AW Ursae Majoris, contact eclipsing binary, differential correction analysis rel. to gravity darkening 3-56389
 TX Ursae Majoris, eclipsing binary, close-binary light curve synthesis 3-42197
 v Ursae Majoris, photoelectric light curve determ. 3-45119
 W Ursae Majoris binaries rel. to RS Canum Venaticorum binaries 3-47998
 W Ursae Majoris eclipsing binaries, statistical anal. 3-53656
 W Ursae Majoris systems, convective envelope model, light curve analysis 3-69926
 W Ursae Majoris-type eclipsing binary stars, model for W-type systems 3-47989
 γ^2 Velorum, eclipsing binary, i.r. spectra 3-45124
 α Virginis, β Cephei star, obs. with improved time resolution 3-48035
 CU Virginis silicon Ap-star, H Balmer lines, phase variation (*Russian*) 3-45129
 W Virginis stars in globular clusters, relation He abundance and richness 3-61856
 Virginis-A, radioastronomical obs., scanning the diagram of the variable profile antenna (*Russian*) 3-81248
 BW Vulpeculae, β Cephei star, obs. with improved time resolution 3-48035
 Wolf 424 AB, flare star, UV Ceti type, flare activity meas., photometric obs. 3-69964
 WR-96 and WR-96(2) magnitude and brightness distribution functions from photographic plate (*Russian*) 3-61806
 V1057 Cygni, light outburst, 1970 rel. to T Tauri star properties 3-47999

variational calculus see variational techniques**variational techniques**

- advanced elastic postbuckling analysis by a perturbation procedure 3-62492
 asymmetric wave stress tensors and wave spin, Hamiltons variational principle 3-43586
 atom + electron scattering, inelastic, variational method applic. 3-71436
 atom + electron scattering, multichannel, variational calcs. 3-71435
 atomic and mol. calcs., bivariational solns., transcorrelated method 3-49383
 atomic dynamic polarisabilities, dipole-dipole and dipole-quadrupole contributions to dispersion energy calc. 3-43386
 atoms photoionisation probability, variational method 3-43356
 averaged lagrangians containing higher derivatives 3-57043
 averaged variational principles including Lagrangians containing higher-order derivatives 3-54066
 axially symmetric region convection, temp. field distribution calc. 3-59824
 biharmonic boundary value problems for plate bending 3-66540
 boundary value problem, nonlinear, theory of laminar boundary layers 3-71770
 boundary-value problems of hermitian differential eqns. with elliptical type derivatives (*Russian*) 3-62410
 chemical reaction rates calc. 3-73120
 continuum corrections to overlap, variational calc. 3-54563
 controlled thermonuclear reactor blanket studies 3-60330
 Coulomb pot. generalized screened, critical screening parameters 3-70694
 critical reactors, variational estimates for integral parameters 3-74688
 cross-section sensitivity studies for ZPR-6 assembly 7 using VARI-1D variational program 3-74680
 cylindrical shell, three-layer, rigid-plastic direct design, Mises and Tresca yield conditions, variational problem (*Russian*) 3-70631
 dense system energy calc. method 3-40178
 Dirichlet boundary condition 3-62647
 earth mantle, transmission of elastic waves through a soft layer, variational method 3-44930
 elastic scattering, electrons from semi-infinite lattices 3-68143
 elastic-plastic continua, finite deformation, minimum principle 3-70559
 electrodynamics, boundary-value problems solved by stationary functionals 3-66605
 electron gas correlation energy, variational calc. 3-70733
 electrostatics, boundary-value problem soln. improvement 3-74191
 exciton levels in magnetic field, calc. 3-41158
 extrusion, axial symmetric, determ. of geometry and force, variation calc. (*German*) 3-69325
 finite element calculations, partial differential equations, variational principle, math. aspects 3-63111
 generalized mechanics, extension to higher-order negative and positive derivatives 3-57046
 Gurtin type theorem of porous materials, isotropic, homogeneous, quasi-static case 3-65043
 half-space, transpiration cooled, temp. distrib. determ. by variational method 3-54178
 Hartree-Fock approx., single-particle expectation values, determ. 3-67645
 heat carrier flow with axial heat conduction and internal sources, temp. field determ. 3-60541
 heat conduction in ablating solid with variable thermal properties 3-54179
 heat transfer, chain system and moment Lagrangian methods 3-78944
 Hiemenz flow, local potential variational method 3-71763
 high-frequency induction discharge, variational approach to design, approx. channel model (*Russian*) 3-57967
 inelastic and rearrangement scatt. processes, variation-perturbation treatment 3-62569
 integro-differential eqns., scattering problems, applic. to elastic electron scatt. from H 3-71434
 ions, isoelectronic series of He, Hartree-Fock orbitals, variational method 3-74787
 Kato's lemma on Schwinger's variational principle for scattering phase, new proof 3-45706
 Lagrange principle for dissipative systems, sea-air interactions appl. 3-69554
 Lagrangians, equivalent, in generalized mechanics 3-48763
 Laplace's eqn., mixed problem with free boundary, soln. existence and uniqueness 3-74002
 length and velocity formulas, comment, approx. oscillator-strength calcs. 3-71354
 linear elastodynamic analysis, assumed stress hybrid finite element model 3-77799
 linear elastodynamics, variational formulation for boundary-initial value problem using convolution bilinear form 3-40114
 LMFB dynamics, improved reactivity table model using variational estimates 3-49339
 Love waves, modulation, travel times, variational method, nonhorizontally layered struct. 3-80616
 MHD system, uniformly rot., variational principle and virial theorem 3-57821
 microwave electrodynamics, boundary-value problems 3-66742
 minimum variance method applied to atom + electron scatt. 3-71437
 mixtures, fluid dynamics, conservation laws, theory and numerical methods 3-49531
 multichannel scattering, variational formulation of R matrix method 3-63325
 neutron transport theory, higher-order scattering anisotropy effects, variational calc. 3-54522
 nonlinear boundary value problem in heat diffusion, variational soln. and error bound 3-48822
 nuclear collective motion for shell model with R(5) symmetry 3-62961
 nuclei, Jastrow corrls., variational approach 3-54414
 orbital variational trial functions, optimisation 3-40556
 orthogonal projection method in three-dimensional elasticity theory, appl. to thick plates (*Russian*) 3-66548
 orthotropic cylindrical shell, potential distrib. near surface cut for skew symmetric tensely-deforming state (*Russian*) 3-42786
 orthotropic plate, clamped, estimation of natural numbers of differential problem (*Russian*) 3-40141
 Pade approximant theory, appl. to time-dependent Schrodinger eqn. 3-62426
 Palatini method extension, derivation of transposition invariant field equations 3-66674
 perturbation improvement of SCF orbitals 3-40555
 piezoelectricity, linear, variational principles for complete set of governing equations 3-55526
 plasma, composite, dynamic stability, finite resistivity effect 3-43666
 plates, constructionally anisotropic, variational eqns., full functional determ. (*Russian*) 3-62473
 positron-helium bound state, variational calc. 3-43388
 potential scattering, equivalent variational functions from differential and integral eqns. 3-62557
 potential scattering problems 3-66623
 quantum fluid-solid transition, short range, square well repulsive potential 3-57155
 radiation transport, deep penetration, class of second-order approx. formulations 3-63243
 radiative transport equations, nonlocal variational formulation 3-70751
 rarefied gas flow, variational principle 3-71785
 Ritz method for integration of eqn. for oscillations of nonhomogeneous elastic bodies 3-42802
 scalar wave and diffusion eqns., variational formulation 3-40088
 scattering theory, relationship between variational methods 3-57122
 scattering theory electron-atom, asymptotic soln. 3-71405
 Schrodinger eqn., variation-of-parameters method of soln. for scatt. problem, improved method 3-42843
 shell, quasi-shallow, variational principle for finite deformations 3-57072
 shell, shallow spherical, inelastic buckling under external pressure 3-48736
 singular integral eqns. with bounded soln., variational principle, appl. to elasticity problems 3-51788
 stratified rotating conducting fluids, universal stability under influence of mag. field and Coriolis force 3-40735
 structures, optimum design through variational principles 3-74045
 superconductor, proximity effect, transition temp. calc. 3-79786
 supersonic flow, nonuniform, construction of contour of minimal wave resistance using variational method (*Russian*) 3-67930
 ternary homonuclear systems, dipole moment 3-78664
 thermal convection, effect of combined rotation and magnetic field 3-78934
 thermodynamics, Hamiltonian type principle to determ. transformations 3-74175
 thermoplasticity, uncoupled, principles for stress rate, strain rate 3-77828
 thermoviscoelastic media, steady state wave propagation, dual variational principles 3-70647

variational techniques continued

- three-particle system, Gilbert Schmidt eigenvalues, resonance wave function (*Russian*) 3-60093
- time-dependent variational principle derivation from Hamilton's expression 3-74098
- topological classification of phase transforms., critical exponents 3-77930
- transport processes, quantum and classical theories 3-57167
- two-level systems, variational principle for weak stimulated absorpt. with energy minimizing fields 3-52341
- unified variational approach to class of integral inequalities 3-59736
- variational estimation of a wide class of functionals $F(\varphi, \varphi)$ 3-66635
- wavefunctions, Ehrenfest's theorem and generalised TRK sum rule 3-45699
- He, perturbation-variational calc. for $1s^2\ ^1S$ 3-60351
- He₂, bound state existence, variational calc. 3-63566
- ⁴He, ground state, pseudometric approach, separation of centre-of-mass contributions 3-60074
- Li, electron elastic scattering, variational calc. 3-43365
- Li, lowest ²P state, variational calc. 3-67644
- Li⁺ ¹S state, Delves variational principle using numerical excited Hartree-Fock basis 3-52242
- Si:P, calc. of quadratic Zeeman effect 3-58515

varistors

No entries

varnish

see also coating techniques

No entries

Vavilov-Cherenkov radiation see Cherenkov radiation**vector diagrams** see vectors**vector mesons** see meson resonances**vectors**

- current vector fields in classical field theories, rel. to generalized Euler eqn. 3-59776
- elastic shell, isotropic, response function represents. 3-59761
- energy-momentum tensor, eigenvectors, Einstein-Maxwell theory 3-66663
- force table for students to discover the properties of vectors 3-66118
- Hilbert spaces, generalised operator domains 3-77765
- Lie algebras and diffeomorphism groups (*French*) 3-62389
- Riemann-Hilbert problem for holomorphic vector in totally-differentiable boundary conditions (*Russian*) 3-70527

velocity

- see also acoustic wave velocity; ion mobility; light velocity
- instantaneous velocity demonstration using 'hot wheels' 3-70242
- monochromatic wave, of a liquid 3-79006
- NGC 7332, galaxy, vel. dispersion determ. 3-56428
- oceanic velocity shear fluctuations meas. 3-59033
- projected rotational vel. of 101 Southern OB stars 3-53657
- rigid body general motion, velocities by plane axial vector coordinate method (*French*) 3-62437
- seismic propag. vel. in anisotropic stratified-fractured media (*Russian*) 3-47648
- solar fields, different levels in quiet regions (*Russian*) 3-76974
- solar photosphere fields, from radial velocities (*Russian*) 3-76975
- solar wind velocity fine structure detection test 3-45007
- stellar space velocity, rel. to rotational velocity, field stars earlier than B₆, double stars, cluster members 3-61796
- stick-slip propag. vel. and seismic source mechanism 3-53369
- thermoelastic media, prestressed, damping of stress- and velocity-discontinuities (*German*) 3-66528
- velocity without limits for elementary physics courses 3-51492

velocity control

- filter, separated fields, improved stigmatic focusing (*German*) 3-70410
- molecular beam, slotted disc velocity selector, stabilized motor speed control system 3-54007

velocity measurement

- see also acoustic wave velocity measurement; angular velocity measurement; laser velocimeters; light velocity measurement; stroboscopes
- acoustic Doppler wind measuring system, profile at up to 1 km 3-42081
- acoustic plane waves, error analysis of velocity and direction measurements using thick large-aperture arrays 3-48285
- air flow, const. temp. hot wires for velocity fluctuations due to temp. fluctuations 3-62382
- VV Cephei, eclipsing, high-dispersion spectrum, H α structure, radial velocities 3-51355
- compressional velocity distribution, upper mantle, lower crust, Early Rise explosions, North America 3-80612
- compressor rotor passage gas velocity, using laser Doppler velocimeter 3-59602
- current measurements, Lake Superior, 1971, aerial photography and photogrammetry 3-47683
- diffracted wave time-travel curves (*Russian*) 3-76886
- Doppler-radar laser applic. (*German*) 3-45833
- elasticity variation, water saturated rocks, at melting point of ice 3-76530
- electrolyte diffusion in presence of mag. induction, applic. to local velocity meas. (*French*) 3-65086
- electron beams, transverse velocity 3-54254
- electron velocity analyser, Mollenstedt type, high efficiency and adjustable resolution 3-62259
- flow meter, laser Doppler system, reversing velocities, optical design 3-57027
- flowmeter, pulsed ultrasonic Doppler, velocity profiles in man 3-73928
- fluid, laser Doppler anemometry, theory, application 3-57031
- fluid, particle timing laser velocity meter 3-57026
- galactic centre, high velocity neutral H₂ features, spatial and velocity distrib. 3-48109
- holographic interferometry, evaluation of interference fringes (*German*) 3-66141
- laser Doppler velocimeter, flow field measurements, dual-scatter, no artificial seeding, wind tunnel application 3-56685
- laser Doppler velocimeter, turbulent flow obs. (*Russian*) 3-45508

velocity measurement continued

- molecular beam velocity analysis using time-of-flight method with PDP-11 multiscaling interface 3-78908
- molecular beams, space modulation of radiofrequency field, shift of Zeeman pattern, devices (*French*) 3-49507
- non-contact, comparison of coherent/incoherent optical systems 3-73795
- by optical Doppler effect, using Cd vapour laser 3-73674
- partially molten rock analogues, extensional wave velocity meas. technique 3-65204
- phase velocity, H₂O surface waves monochromatic of small and large steepness (*Russian*) 3-63740
- using piezoelectric laser beam deflector 3-48358
- propagation velocities of pressure and void by cross correlation of fluctuations in N-H₂O flow 3-70499
- pulsatile blood flow, in transilluminated microvessels 3-42691
- pulsating fluid flow, ionised particle injection method (*French*) 3-62384
- seismic in upper mantle, travel-time tables, deep earthquakes 3-80606
- seismic waves, Kamchatka focal zone 3-76547
- stellar radial vels. 10 ms⁻¹ accuracy from spectrograms using telluric absorption lines as comparison 3-48156
- surf swash, western Kamchatka 3-80711
- transducers, dynamic calibration, linear air bearing sled system 3-59552
- transient velocity and pressure meas. by gaseous ionisation 3-49528
- turbulent flow, in rough channel, cinematographic method 3-54802
- u.s. Doppler velocity meter, M-sequence modulation method (*Japanese*) 3-70265

velocity meters see velocity measurement**velocity microphones** see microphones**velocity-modulation tubes**

No entries

velocity spectrometers see particle spectrometers**Veneziano model**

- crossing-symmetric representations with finite-width resonances and Regge asymptotic behaviour 3-57375
- exchange degenerate Regge pole model for np and pp charge exchange scattering 3-60033
- factorizing dual amplitude with Mandelstam analyticity 3-59995
- generalized potential in partial-wave dispersion relation, failure of p meson bootstrap 3-43122
- Nakanishi amplitude, origin of unitarity and duality, continuous Veneziano term expansion 3-40366
- pseudoscalar scattering, consistency with partial conservation of octet and singlet axial-vector currents 3-62855
- Regge eikonal representation for scattering amplitude containing virtual Veneziano blocks 3-62860
- two-body scattering, high-mass exotic resonances and plane consistency 3-78175
- unitarization of partial-wave amplitudes by truncated N/D method, sum rules for inelastic functions 3-67069
- unitarized, approximation to nature below 800 MeV 3-74444
- vector mesons, heavy, Veneziano-type representations of form factors and couplings 3-67007
- $\Delta(1236)$, magnetic transition form factor 3-67013
- $K^- d \rightarrow K^0 n^- p$, 5.5 GeV/c, discussion of final state 3-57447

πN scattering, Veneziano-type amplitudes, charge-exchange polarisations, differential cross sections 3-62876

ventilating see ventilation**ventilation**

see also air conditioning

- hospital air movement study using gas chromatography 3-59699
- nuclear reactor buildings, of stressed concrete (*German*) 3-74716
- radioisotope thermoelectric generator, fuel capsule vent system, He, Viking mission to Mars 3-67402

ventilators see ventilation**Venus**

- atmosphere, determ. of characts. of light-scatt. particles 3-59267
- atmosphere, helium content estimation from radioactive progenitors and ionization profiles 3-61704
- atmosphere, microwave meas., absence of water vapour 3-51296
- atmosphere, remote sounding from artificial satellites and space probes 3-47767
- atmosphere, stability of CO₂, removal of photodecomposition products 3-61705
- atmospheric circulation model driven by polar and diurnal surface temp. variations 3-47924
- atmospheric evolution and origin 3-65773
- brightness temp. meas. at 8.6 mm and 3.1 mm 3-47922
- brightness temperature and absolute flux density scale at 608 MHz 3-69851
- cloud tops rel. to radiative instability of cloudy planetary atmosphere 3-61679
- core composition of terrestrial planets, Fe₂O occurrence 3-42149
- dayside upper ionosphere, model for ion and electron gases 3-65785
- high altitude retrograde horizontal winds rel. to cloud layers 3-69886
- interior physical properties 3-42169
- internal convection evidence from first-order topography 3-47930
- ionosphere, estimation of He content 3-69876
- ionospheric heating on simple one-dimensional model 3-65784
- i.r. radiative heating and cooling of mesosphere, day-to-night var. 3-51292
- limb radiance, 600 to 700 cm⁻¹, calculations, application to spacecraft navigation 3-73452
- lower ionosphere, ionization rates and ion chemistry model 3-69887
- microwave brightness temps. at 430 MHz 3-73449
- natural radioactive elements in Venusian rock, γ -ray spectra 3-61698
- planetary patrol programme, international 3-65967
- satellite loss, effect of solar tidal friction 3-69837
- silicate mineral stability, under approach. Venusian surface conditions 3-45037
- specific effective scatt. area in r.f. range 3-56312
- stratosphere, gravity wave-mean flow interactions, 4-day circulation 3-65406

Venus continued

- transits, obs. from Japan, Dec. 9, 1874 event, reviews 3-61700
- upper atmosphere, 4-day rotation from u.v. photographs analysis 3-65776
- upper atmospheric 4 day circulation, dynamical aspects 3-65777
- Venera 8 results 3-45040
- weather, probe obs. comparison with Earth 3-65767
- winds, differential radio interferometry appl. 3-45249
- xenoliths in Maar-type volcanoes and diatremes rel. to Moon, Mars and Venus 3-53403
- CO₂ absorpt. strength variations 3-45034
- CO₂ production kinetics rel. to inferred surface temp. 3-61683
- CO₂+ 2890 Å band, photoionization excitation rel. to column excitation rates for planetary atmospheres 3-54732
- H₂SO₄ in clouds, chemical processes and spectrum 3-69857
- H₂SO₄ solution in water rel. to composition, structure, characteristics and spectra of clouds 3-47909
- O I 1304 and 1356 Å emissions from atmosphere rel. to rocket and Venera data 3-56346

Verdet constant see Faraday effect

Verneuil process see crystal growth from melt

vertex functions see elementary particle theory; functions

vibrating bodies

- see also elastic waves; pendulums; piezoelectric oscillations
- acoustic radiator, directionality determ. from scatt. of coherent light from vibrating surface 3-62005
- bar of variable cross section torsional vibrations 3-54119
- bar with circular plates, flexural vibrs. 3-42803
- beam, axially creeping with random material parameters, damped lateral vibration 3-42806
- beam, floating on ideal fluid 3-81349
- beam, stepped cantilever, transverse vibr. caused by elastic load impact 3-70644
- beam, two-span, random vibrations, noise excited, theoretical solution 3-74059
- beam, undamped statically loaded, vibr. freqs. 3-66577
- beam under axial compression, optimum design 3-40135
- beams, continuous curved, freq. determ. for in-plane vibrations 3-74068
- beams, multiple layer damping treatments, dynamic response, parametric study 3-74067
- beams, non-uniform non-homogeneous, transient response, finite element analysis 3-54121
- beams, plates, rings, shells, modal equations, Lagrange method 3-74057
- beams, uniform elastic, time dependent boundary conditions 3-74056
- beams in forced oscillation, determ. of two frequency transients (Russian) 3-62528
- Chladni figures, coloured under u.v. light 3-59532
- circular conical shells, natural unsymmetric oscillations (Russian) 3-57052
- circular cylinder, thermoelastic response, generalised dynamical theory of thermoelasticity 3-42789
- circular plate, loaded periphery, frequencies 3-62518
- circular plates of linearly varying thickness, axisymmetric vibrations 3-42829
- composite spherical shell, radial vibrations 3-59774
- coupled vibrating systems, statistical energy analysis, proportionality constant, prediction and measurement 3-81343
- cylinder, composite, torsional vibrations 3-62519
- cylinder, in linearised supersonic flow cylindrical integral transformation application 3-60555
- cylinder on liquid surface, forced transverse vibration, soln. of wave problem (Russian) 3-46473
- cylinders, circular, analysis by holography, techniques 3-73616
- cylindrical shell, nonlinear random vibration, iterative soln. (Polish) 3-66589
- distributed systems, strongly coupled at discrete points, random vibration, analysis 3-81342
- elastic disc with moving mass system, dynamic response 3-70663
- elastic shell, asymptotic distrib. of eigenfrequencies 3-62540
- flexible cables, about static equilib. position, numerical soln. (Italian) 3-40142
- flexural vibration, beams and plates, large amplitude, modal equation, general conclusions 3-74060
- four plate structure, natural frequencies and normal modes 3-56583
- granular material, friction characteristics on horizontally vibrating plane 3-65042
- gyroscope, vibro shock damping of forced vibrations (Russian) 3-74062
- gyroscopic pendulum subjected to random vibrations, analysis of motion (Russian) 3-66578
- gyrotachometer, determ. of probability distrib. for nonlinear case using Fokker-Planck eqn. (Polish) 3-66517
- internal, perturbations on motion of rigid body, transmitted moment determ. (Russian) 3-74010
- mechanical impulse sound source 3-39870
- mechanical signature analysis, ball bearings 3-56590
- mechanical system, n degrees of freedom, parametric vibrations under e.m. force 3-74072
- multiple-degree-of-freedom, stability limit of nonlinear resonances 3-70641
- non-symmetrical hard, in process of orientation, angular movements dynamics (Russian) 3-45634
- nonlinear system, asymptotic stability of solns. determ. using Hartman-Olech theorem (Polish) 3-66596
- nonlinearity, large deflections, frequency response from impulse response 3-70649
- nuclear reactor subassembly, correlation of mechanical noise with neutron noise 3-67450
- orthotropic plate, finite difference method 3-81348
- plate, elliptical, free edge, free-flexural vibrations, Mathieu function analysis 3-77339
- plate, isosceles right angled triangle of anisotropic material on elastic foundation 3-54118
- plate with point clamped constraints, deflection characts. 3-70671
- plates, coupled thermoelastic vibrations 3-70642
- plates, forced extensional vibrations 3-54122

vibrating bodies continued

- polymer-coated square plates, bending vibrs., damping 3-44683
- quartz plate, thickness-shear vibrations, e.m. radiation 3-41483
- rectangular plates, parabolically varying thickness, free transverse vibr. 3-77843
- resonance frequency (damping), vector response loci, numerical analysis 3-70651
- rigid circular body, vertical vibration, harmonic rocking of rigid rectangular body on elastic stratum 3-42807
- rigid circular body, vertical vibration, harmonic rocking of rigid rectangular body on elastic stratum 3-45687
- ring, damped, discontinuously constrained, forced response, experimental and theoretical 3-70220
- rings, tapered, oval, in-plane free vibrations, theoretical analysis 3-77338
- satellite coupled vibration-rotation motion, Lie transform perturbation theory 3-69808
- shell, aeolotropic cylindrical, varying density, radial vibr., mag. field 3-70645
- shells, fluid filled spherical, characteristic freq. 3-54127
- shells, layered, cylindrical, symmetric general orthotropic, non-symmetric cross-ply, frequencies 3-59768
- shells, non-circular cylindrical, initial stresses 3-70650
- shells of revolution of variable thickness, torsional vibrations 3-42812
- skew stiffened plates, parametric reson. problems 3-70662
- square plate, on-diagonal supports, upper bound for lowest freq., finite element approach 3-74065
- stabilisation of a mass in a vibrating body, formulation and preliminary results 3-74058
- string, dissipative ends, bounded, or nearly periodic solns. to nonlinear eqns. (French) 3-77837
- string, dissipative ends, bounded or nearly periodic solns. to nonlinear eqns. (French) 3-77838
- surface, pressure and gradient relationship 3-42822
- thin circular elastic plate resting on a two-parameter Winkler type foundation 3-66521
- torsional vibration, circular (conical) shaft, two-rotor system, composite structure 3-74064
- transverse, of elastic bar, determ. of difference eqns. using collocation method (German) 3-42828
- tuning fork, for electronic watch, vibration analysis by speckling 3-51535
- tuning fork element in watch, energy relationships (Russian) 3-59767
- tuning forks, plain, piezoelectric ceramic modified, measurement of constants, differential type filter 3-61950
- two-degree of freedom system, vibro-impact, boundedness of solns. to eqn. of motion (Polish) 3-66597
- unsymmetrical sandwich plates, theory of vibratory bending 3-54115
- vibrating panel, radiation resistance, direct derivation 3-56580

vibration control

- see also damping
- damping, acoustic noise absorption by steel-viscoelastic-steel composites 3-70275
- damping, panel vibration, turbulent air flow induced, acoustic noise, viscoelastic damping materials 3-70274
- fatigue testing machine with program control of specimen vibr. amplitude 3-61244
- machinery vibration, isolation and absorption 3-48295
- system, digital test instrumentation, minicomputer based, high performance control and analysis 3-70270

vibration excitation

- acoustic propagation distributions, single, multi-modes 3-61936
- aircraft skin panels, acoustically excited, growth rate of edge cracks, effect of bending strains 3-51480
- beam, uniform, subjected to displacement excitation, reaction parameters 3-48743
- cylindrical shell, nonlinear, stochastically excited, stability 3-70555
- cylindrical shell, simply supported, large amplitude forced vibrs. 3-70666
- harmonic force, non linear systems dynamic interaction of oscillatory mechanism (Russian) 3-74061
- nonstationary nonlinear multidegree-of-freedom systems, resonances 3-77833
- parallel plates, connecting plate member influence on flexural vibrs. excitation and propag. (Russian) 3-57107
- parametrical non linear systems dynamic interaction of oscillatory mechanism (Russian) 3-74061
- segmented nonstationary random excitation, structural response 3-45679
- shallow rectangular cavities, adjacent to compressible flow, possible excitation frequencies 3-46464
- shock pulse non linear systems dynamic interaction of oscillatory mechanism (Russian) 3-74061
- thin metallic targets, mech. vibrs. excited by relativistic charged particles 3-52641

vibration measurement

- see also seismometers
- adhesive bond strength, nondestructive vibrational meas., honeycomb sandwich panels 3-47513
- amplitude meas., time average holography, interf. fringes interpretation 3-66143
- cat ear basilar membrane, Mossbauer method (German) 3-51426
- concrete, resonant vibration freq. determ. method 3-73664
- concrete, resonant vibration frequency, acoustic impact technique 3-69408
- cylinders, circular, analysis by holography, techniques 3-73616
- displacement, noisy gramophone pick-up 3-59549
- fringe method using incoherent light 3-59550
- holographic interferometry, amplitude of vibrating body 3-66235
- holographic recording, repetitively pulsed lasers 3-51632
- holography, time-average, of objects vibrating sinusoidally and moving with const. accel. 3-66249
- infrasonic meas. of elastic consts. and damping in flexure using Balanced Resonator 3-48348
- laser interferometer, for ultra-small vibration measurement, 2.5 to 150 kHz 3-70267

vibration measurement continued

- laser methods, conference, Teddington, Middx., England (1973) 3-51534
- laser photography application 3-48361
- long-period torsional vibration pickup, design and performance 3-61580
- loudspeaker cones, scanning holographic investigation 3-51880
- loudspeaker membranes, holographic vibration analysis 3-51881
- mechanical design props. of materials test method 3-50817
- mode visualization, by holography 3-51536
- modified interferometer, for amplitude obs. 3-48360
- Moiré gauging by projected interference fringes, theory and experiment 3-45494
- moving turbine blades, laser Doppler instrument for 3-66144
- natural, hollow cylinder surface vibration, photographic recording using time-average holography (*German*) 3-48446
- piezoelectric transducer electronics, vibration and pressure applications, comparison with charge amplifiers 3-56623
- resonance in forced vibr., coupled pendulum meas. system (*Russian*) 3-66133
- Rhine inland ships, 2 to 1000 Hz 3-73619
- road vehicles, source diagnosis, synchronous integration technique, problems, feasibility 3-56622
- shifted reference holographic interferometry 3-51517
- speckle pattern techniques 3-51856
- stroboscopic holographic interferometry, severe vibr. meas. 3-61992
- system, digital test instrumentation, minicomputer based, high performance control and analysis 3-70270
- torsional, l.f. installation for meas. internal friction 3-73669
- torsional vibration frequency measurement, dynamic shear modulus determination, thin ribbons 3-51526
- tuning fork, for electronic watch, vibration analysis by speckling 3-51535
- violin, acoustic vibrations, laser speckle interferometry, effects of clamping, formal model, main wood resonance 3-59497
- visualization, speckle reference beam holography 3-51537

vibrational states in disordered systems

- anharmonic chain with symmetric potential, modulated waves 3-43856
- binary alloy, optical modes 3-40996
- noncrystalline solids, theory of phonon-like excitations 3-79454
- NH₄⁺ halides, Raman spectra, phonon modes, polarisation chars. 3-72651
- Ni-Pt, mass-defect disordered alloy, phonon modes 3-64127

vibrations

- see also *molecular vibration*
- Acoustical Society of America, 85th Meeting, Boston, Mass., USA (1973) 3-39866
- amplitude meas., modified interferometer 3-48360
- amplitude measurement, by interference method when greater than wavelength of radiation source 3-51519
- asymmetrical cycle, generalization of eqns. of outline of hysteresis loop 3-42823
- axisymmetric plate with stabilised rotation, centre of mass motion (*Russian*) 3-62525
- beam, flexible, small transverse vibrations under action of acid force (*Russian*) 3-77845
- beam, two-span, random vibrations, noise excited, theoretical solution 3-74059
- beams, coupled thermally induced vibrations 3-77834
- beams translating between fixed end supports, transverse modes and frequencies 3-62522
- Bernoulli-Euler plate in contact with elastic half-space, steady motion 3-70667
- bifurcation and stability of stabilising motions of complex mechanical systems (*Russian*) 3-66511
- bridge, combined arch, for uniform motion of load in semistrip form (*Russian*) 3-66583
- buildings, finite element programs and response to turbulence and sonic boom 3-59482
- cantilever, freq., damping, lateral vibrs. 3-62516
- ceramic, dynamic modulus technique 3-70262
- ceramic, elastic moduli and mech. Q of small specimens, resonant beam technique 3-70263
- Chladni's figures, circular metal plates, normal mode frequency determination, empirical equations 3-59496
- circular cylinder, vibrating, heat transfer, acoustic streaming flow field 3-57732
- circular cylinders, first-order shell theory application 3-59769
- circulatory systems, multiple parameter, divergence instability 3-70547
- composite spherical shell, radial vibrations 3-59774
- constrained layer damping equation, evaluation by high-damping meas. 3-51796
- Constrained shell vibrations 3-77836
- cracked structure dynamics with finite elements 3-74040
- cross-ply rectangular plates, unsymmetrically laminated 3-64998
- crystal resonator, vibration patterns of thickness modes 3-62003
- crystal surfaces plated with electrodes, two-dimensional dynamic theory of h.f. vibrations 3-41082
- curved tubes conveying fluid, out-of-plane vibr. and stability 3-71795
- cylinder, thin flexible, towed in viscous fluid 3-42811
- cylindrical gravitational wave detectors, flexural frequencies 3-45692
- cylindrical shell, forced axially symmetric vibrs. induced by periodic shock waves (*Russian*) 3-57106
- cylindrical shell behaviour under influence of moving pulsating press. jumps 3-57109
- damped three-layered sandwich rings, mechanical impedance 3-45682
- double curvature shells, travelling-wave soln. 3-77343
- dynamic analysis of structures, shock spectra eval. 3-70661
- dynamical processes, developments in damping systems (*Polish*) 3-66586
- Einstein's theory of gravitation for particle at centre of inertia of terrestrial spherical satellite 3-70715
- elastic natural and forced oscillations, calculated from boundary problem for integro-differential eqns. (*Russian*) 3-62521

vibrations continued

- elastic plate resting on Winkler foundation, natural freqs. of transverse vibrs. 3-70670
- elastic rod with dry friction, random excited vibrations (*Polish*) 3-66592
- elastic shell, thin, arbitrary shape, asymptotic formula for distrib. of natural frequencies (*Russian*) 3-77846
- elastic solid, penny shaped crack, torsional vibration, compression and shear wave scattering, analysis 3-70221
- elastically supported rigid disc with moving massive load, dynamic response 3-62457
- elastoplastic strains under forced vibrs. in complex medium 3-57110
- endurance limit, accelerated determ. method 3-58785
- flat strip in liquid surface, acoustically excited vibrations 3-42459
- flexibly mounted gyroscopes, vibrations 3-66136
- flexural vibration, beams and plates, large amplitude, modal equation, general conclusions 3-74060
- flexural wave fields, infinite beam reinforced plates, point excitation, integral transform analysis 3-59506
- flexural wave mechanics, periodic structures 3-56582
- fluid-structure interaction problems, l.f., perturbation method 3-74081
- forced, liquid jet, production of monodispersed drops, water, glycerol, human serum albumin 3-71833
- forced, of mechanical elastic-friction system with periodic excitation (*Polish*) 3-70681
- frames with axially loaded Timoshenko members, natural frequencies 3-40137
- fuel rods, slender, in cylindrical duct, acoustically induced vibrs. 3-71174
- Galerkin finite element method applied to vibration problems 3-57098
- glass Textolites, damping props. under bending vibrs., 213-363K 3-58763
- graphite fibre honeycomb panels, resonant frequencies and modal damping 3-59508
- heated cylinders, vibrating vertical array, heat transfer rate 3-71736
- high amplitude system with random excitations, synthesis of parameters (*Polish*) 3-66591
- holonomic mechanical systems with partial dissipation, equilibrium instability (*Russian*) 3-77847
- Hooke's law for stereomechanical multiple systems, multi-index generalization as large systems (*Polish*) 3-66595
- human performance, interactive effects of noise and vibration 3-48233
- human visual vibrational analyser, hybrid computer investigation of model (*Russian*) 3-48243
- indicator electrode, vibrating, polarography, amperometric titration, polarometry 3-48652
- laminated rectangular plate, anisotropic, nonlinear vibr. 3-70664
- linear and nonlinear struct. models, dynamic parameters identification from exptl. data 3-59772
- linear dynamical systems, with stationary excitations 3-56581
- loudspeaker design, mathematical theory of high fidelity 3-42484
- mechanical system, n degrees of freedom, parametric vibrations under e.m. force 3-74072
- mechanical systems, optimisation of damping of transient processes (*Polish*) 3-66518
- mechanical vibrator, principles and engineering details (*Rumanian*) 3-42511
- mechanical-stereomechanical analogy in class of Lagrange's single-index eqns. of second kind (*Polish*) 3-66594
- membrane, n-dimensional problem, eigenfunctions, solns. of Helmholtz eqn. 3-70677
- membranes, analysis by optical spatial filtering method 3-42478
- modal response to transient acceleration 3-48744
- multilayered composite plates, free vibrations 3-77835
- multispan curved beams, coupled twist-bending waves and natural frequencies 3-48298
- n-degree-of-freedom systems, determ. of probability characteristics using Fokker-Planck eqn. (*Polish*) 3-66593
- nonlinear wave propagation, perturbation method treatment 3-45632
- nonlinear distributed systems, multi-wave interactions, mathematical methods (*Russian*) 3-70656
- nonlinear driving system with cardan shafts, torsional vibrations 3-40139
- nonlinear system subject to harmonic forcing, small transient motions 3-54120
- nonlinear systems, stochastic processes (*Polish*) 3-66587
- nonlinear systems with many degrees of freedom, normal coords. in principal resons. anal. (*Polish*) 3-59771
- oblate spherical shell with losses, curvature influence on vibrations 3-42821
- one-degree of freedom system with nonlinear viscoelastic suspension, stability of equilibrium point (*Polish*) 3-70680
- one-degree-of-freedom mechanical system with jump-like variable mass, probabilistic problems (*Polish*) 3-66590
- one-degree-of-freedom system with nonlinear elastic characteristic, stochastic excitation (*Polish*) 3-70679
- optimal active vibration suppression, optimal control problem solution (*Russian*) 3-66575
- orthotropic plate, clamped, estimation of natural numbers of differential problem (*Russian*) 3-40141
- orthotropic triangular plates, nonlinear vibration 3-62512
- oscillogyro, dynamics 3-66135
- panels, spherically curved, natural frequency analogy with flat plates, similitude analysis 3-73615
- parametric, of system with two degrees of freedom 3-62533
- pendulum, normal modes of vibration, demonstration to students 3-48321
- piezoelectric, semi-infinite, coated with conducting thin film, effect of time-dependent heat flow on disturbances 3-74073
- plate, isosceles right angled triangle of anisotropic material on elastic foundation 3-54118
- plate, isotropic elastic rectangular, resting on elastic foundation, flexural vibrs. 3-57103
- plate, large amplitude vibrs., assumed-time-mode soln. 3-70673
- plate, pretwisted, harmonic vibrs. 3-57102
- plate, random wideband vibr. due to point forces (*Russian*) 3-54123

vibrations continued

- plate, rectangular, carrying concentrated mass, nonlinear vibrs. 3-74082
- plate, rectangular, self-excited and forced vibrs. in supersonic flow, aerodynamic appl. 3-62534
- plates, coupled thermoelastic vibrations 3-70642
- plates, orthotropic, flexural natural freq. calc. 3-42809
- plates, polar orthotropic annular, natural frequencies 3-40138
- plates, rectangular, lateral vibrations, buckling, inplane loads, Ritz analysis 3-73617
- plates, trapezoidal, free vibration characteristics by finite element study 3-42814
- polyethylene melt, stresses, periodic deformations, effect of vibration frequency and amplitude variations, Weissenberg rheogoniometer 3-76380
- polymer coated plate, effect of internal stresses in the coating on vibrations and static bending 3-58671
- polymer-coated square plates, bending vibrs., damping 3-44683
- polymethane, rigid, porous, vibrocreep, recovery 3-73052
- polyurethane, vibrocreep, biaxial loading, small vibrations 3-80480
- polyurethane, vibrocreep, under composite loading 3-58746
- pressurized shells of revolution partially filled with liquid, breathing vibrs. 3-62542
- prismatic shells filled with fluid, transverse vibrations 3-75236
- random nonlinear, of one-degree-of-freedom system, Fokker-Planck eqn. (Polish) 3-66588
- random response probabilistic and deterministic approaches 3-74066
- real time visualization, hologram interferometer 3-48363
- rectangular plate, flexible, approx. method for determ. of proper frequencies (Russian) 3-62539
- resiliently supported railway track slabs 3-42470
- rigid circular body on inhomogeneous elastic stratum, torsional vibr. and shear modulus 3-57108
- rigid-body motions in curved finite elements, explicit addition 3-45683
- ring, discontinuously constrained and damped, forced resonance 3-40145
- ring stiffened circular plates, axisymmetric vibrations 3-62523
- rings, thin circular, shear effects and rotary inertia influence 3-40144
- rod, flexural vibrs., viscoelastic coating, axial force 3-62517
- rotating beam, random vibrations, in-core finite difference method, separable boundary value problems 3-70548
- rotating slender beam under aerodynamic couplings, stiffening effect of centrifugal force on fund. coupling 3-57104
- sandwich beams of unsymmetrical structure, free transverse vibrations, natural frequencies calc. 3-70639
- shaft, rotating, nonautonomous bending vibrations 3-62529
- shear walls, asymmetrical and coupled, finite element displacement model study 3-51477
- shell, vibration and eigenfrequency calcs. 3-48741
- shells of revolution of variable thickness, torsional vibrations 3-42812
- sinusoidal low amplitude acoustic sources, intrinsic nonlinear effect on flow field 3-77309
- spherical shell, shallow, dynamic buckling 3-70660
- spheroidal shell, oblate and inflated, free vibrations 3-51476
- spinning aeolotropic disc, transverse vibration 3-42804
- stability theory for general dynamical systems 3-74084
- stick slip cycle, static friction 3-64107
- string, random wideband vibr. due to point forces (Russian) 3-54123
- structural dynamic analysis, condensation of finite element eigenproblems 3-45680
- structural frequency eqns. reduction 3-70640
- structural response to noise 3-59509
- supersonic panel flutter of finite cylindrical shells, first-order freq. effects 3-70665
- surface, pressure and gradient relationship 3-42822
- suspended flexible line, small oscillations, power series solns. 3-70672
- system with two degrees of freedom, in mixed resonance, parametric 3-74070
- telescopes, visual resolution, effect of vibration, allowable angular oscillations 3-56467
- theory, including selection of physical models, methods of analysis and solns. 3-70678
- thin rings, equations of motion governing small elastic displacements 3-40136
- torsional, in bar of variable cross section 3-54119
- torsional, in branched systems, calc. of frequencies and modes by impedance method, computer calcs. (Polish) 3-70682
- torsional of composite cylinder 3-62519
- transient interaction of a flexible ring-reinforced shell and a fluid medium 3-45681
- transportation, human response 3-59435
- transverse, of beam on elastic support under section of perturbing force at near self-resonance frequencies (Russian) 3-70657
- two discrete vibrating systems synthesis using eigenvalue modification 3-42753
- two-degree-of-freedom systems, geometrical stability of nonlinear normal modes 3-57101
- unidimensional system of masses, aperiodic irregular motion resulting from collisions (Russian) 3-62520
- variable mass system excited by impact forces, boundedness of solns. (Polish) 3-66598
- viscoelastic beam on supports, forced vibrations 3-42824
- viscously damped nonlinear beam, ultraharmonic motion 3-62513
- Vocal tract damping and cavity wall vibrations 3-77211
- wakes, bevelled trailing edge effect on vortex shedding and vibration 3-43650
- Ag thin films, damping (Russian) 3-72859
- Cu thin films, damping (Russian) 3-72859

vibrations, crystal lattice see lattice dynamics**vibrations, molecular see molecular vibration****vibrations of crystal lattices see lattice dynamics****vibrometers see vibration measurement****vibronic states of molecules see molecular vibration****video recording**

- colour TV laser-recorded microtrack records (Polish) 3-43043
- daytime lightning flashes, video tape recording 3-65526
- electrical signals with one-dimensional holograms 3-56683
- elementary particle physics data, by video tape recorder and computer 3-54023
- geodetic meas. using radio interferometers 3-44937
- monitoring unit, for motion-picture filming (Russian) 3-51647
- nondestructive testing, video tape training programme 3-45402
- nuclear reactor plant operators, training, in-plant production of black and white video tapes 3-73649
- particle tracks recorded on video-tape, device and program for data processing of event in FORTRAN 3-56946
- prerecorded video, replication of relief-phase holograms 3-77524
- vesicular film applic. in electro-optical scanning system 3-42597
- video-to-film colour image recorder, laser applic. 3-73800

video signals

- sea ice probing with video pulse sequence 3-73406
- video-densitometric vascular flowrate measurement 3-59686

vidicons see television camera tubes**viewing screens see screens (display)****virial coefficients see equations of state****viscoelasticity**

- see also plasticity
- acceleration waves in isotropic simple materials 3-57099
- acoustic dry coupling materials, design concepts interfacial bonding, spatial attenuation, impedance matching 3-48300
- adhesive bond strength, nondestructive vibrational meas., viscoelasticity rel. to elastic moduli and damping capacity 3-47513
- anisotropic stretched ring, elastic and strength props. analysis 3-80487
- anisotropic viscoelastic cylinder, centrifugal stresses analysis, numerical soln. 3-62453
- arterial wall, dilation measurement recorded simultaneously with blood pressure, used to estimate viscosity 3-59687
- axisymmetric shells under impulsive loadings, viscoelastoplastic response 3-57086
- axisymmetrically heated orthotropic cylinder fastened to a pliable elastic cylinder, stability under shear 3-57084
- beam on supports, forced vibrations 3-42824
- bentonite-water suspensions structure in shear flow, mechanical props. 3-50794
- bentonite-water suspensions structure in shear flow, optical properties 3-50795
- biaxial extensional flow, material functions 3-67888
- Bingham fluid, conducting, non-steady flow in annulus in presence of time-varying toroidal pressure gradient 3-46423
- Bingham fluid, steady motion in curved annulus, streamlines 3-75279
- Bingham plastic, dissipative non-Newtonian flow through ducts, asymptotic Nusselt numbers 3-40704
- biopolymers oriented by hydrodynamic flow, dichroic spectra 3-43529
- Boltzmann-Volterra constitutive law for linear viscoelastic materials (French) 3-54091
- bone, analysis as three component system with mineral phase, organic phase and pores 3-50771
- cellophane and polyethylene films, adhesion, microrheological process effects 3-55893
- cellulose, viscoelastic props. depend. on water content 3-52411
- combined steady and oscillatory flows, motions with superposed proportional stretch histories 3-71832
- contact between a curved viscoelastic beam and a rigid plane, bending deflections theory 3-40110
- copolymer, film of vinylidene chloride (vinyl chloride), strain mechanisms, electron microscope (Russian) 3-73067
- copolymer, three-block, structure, rheological properties and pouring index (Russian) 3-71690
- Couette flow, polymeric, stability prediction based on network rupture hypothesis, analysis 3-75277
- creeping flow, completely incompressible, high order finite element method 3-40105
- crossover effect, experimental demonstration 3-56614
- cylindrical cavity, heating due to cyclic pressure, solutions 3-66555
- damped three-layered sandwich rings, mechanical impedance 3-45682
- damping materials, panel vibrations, turbulent air flow induced acoustic noise 3-70274
- damping of vibrations, noise producing, vibration absorption by steel-viscoelastic-steel composites 3-70275
- deformation of viscoelastic thick-walled cylinder with elliptic cavity (Russian) 3-42791
- disclinations, circular twist, in viscoelastic materials 3-64041
- disperse systems, mechanical parameters under cyclic deformation with various amplitudes 3-73081
- drag reducing solutions, in presence of high-phase velocity disturbances, laminar pipe flows stability 3-60570
- dynamic contact problem for semi-space with adhesion under rigid punch (Russian) 3-77848
- dynamic contact problem integro-differential eqn. (Russian) 3-42779
- dynamic problems, averaging method soln. 3-54104
- Earth, four parameter viscoelastic model for long period geodynamics 3-65191
- elastico-viscous liquids, rectilinear flow, numerical solutions 3-71841
- elastomer, chain rigidity from i.r. spectra (Russian) 3-71670
- elastoviscoplastic constitutive relns., finite element formulation for soln. of viscoplasticity 3-40098
- elastoviscoplastic medium, flow theory 3-71836
- electrohydrodynamic flow of a visco-plastic fluid (Russian) 3-43608
- emulsions, semisolid, nonlinear props. Weissenberg rheogoniometer 3-69396
- energy and plane waves in linear viscoelastic media 3-53411
- environmental response of systems with differing behaviour, calc. method (French) 3-77797
- epoxide, thick walled tubes, nonlinear creep under internal pressure rel. to nonlinear generalized Maxwell equations 3-58754

viscoelasticity continued

- equations of motion, derived from conservation laws, phenomenological theory of nonequilibrium processes 3-71684
- Euler stability of viscoelastic rod, asymptotic bending 3-45667
- fibreglass, creep due to interlaminar shift under sustained external pressure, based on Volterra's principle 3-58716
- finite linear viscoelastic fluid plane Poiseuille flow stability 3-49541
- flow in square cavity, comparison with Newtonian fluid (*French*) 3-79055
- flow instability, nonisothermal, of viscoelastic media 3-43592
- flow of liquids with polymer admixture, applicability of viscoelastic hypothesis (*Russian*) 3-63771
- flow of materials, biaxial extensional, bubble inflation technique 3-67890
- flow of viscoelastic material, finite element analysis (*Russian*) 3-45660
- flow past flat plate, heat and mass transfer 3-78945
- fluid, critical test for nonlinear constitutive eqns. 3-66556
- fluid, flow between infinite parallel plates, hole error meas. 3-67966
- fluid, incompressible, stress fluctuation, Brownian motion 3-70737
- fluid, relax.-type, stability, comments 3-49542
- fluid flow, pressure meas., hole errors 3-67887
- fluid flow rel. to relax. time, Navier-Stokes eqns. generalisation (*Russian*) 3-63618
- fluids, applic. to dilute suspensions and incompress. Newtonian fluids 3-54821
- fluids, viscoelastic, subjected to spatial stress, relaxation time meas. method (*German*) 3-70269
- glass reinforced plastic, creep and recovery, in uniaxial tension 3-58711
- glass reinforced plastics, solution of boundary value problems using experimental and theoretical values of relaxation properties and pliability 3-58717
- glassy polymers, relaxation processes 3-46676
- glassy polymers, use of Rheoribron for meas. of dynamic moduli 3-42515
- glycerol, 10 to 10^7 poises, u.s. frequencies, relaxation range 3-61993
- half space deformation by shear dislocations 3-58896
- half-space, linear, propagation of one-dimensional thermal shock wave (*Russian*) 3-42827
- hereditary media, temp.-time analogy, conditions for existence 3-54778
- hydrocarbons, supercooled liquids and derivatives, viscoelastic behaviour 3-46364
- jets, liquid, cylindrical, capillary breakup, numerical analysis 3-75278
- linear, stress and strain tensors, unique solns. and approx. methods (*Russian*) 3-66541
- linearly viscoelastic materials, governing eqn. for quasi-static crack growth 3-74041
- liquid, decay of vortices 3-67917
- liquid, heat transfer by fluctuating flow, past infinite plate with time varying suction 3-52442
- liquid, laminar flow 3-79028
- liquid, mol. motion from viscoelastic and u.s. relax. obs. 3-64205
- liquid crystal cholesteric polymer solutions, shear induced structural changes mechanism, reflectance spectra, rheological props. 3-49843
- liquids, asymmetrical, sound propagation, dissipative processes, viscoelastic properties 3-59475
- liquids, intermediate rheological models, damped oscillations (*Italian*) 3-78999
- liquids, wedge and cone flows 3-60547
- locust, adult female, rheological props. of extensible intersegmental membrane 3-42272
- magnetic and viscoelastic field interaction in hereditary layer 3-59755
- magnetically induced deformation in Fener type substance 3-59756
- magneto-thermo-visco-elasticity, plane strain problems, Kelvin and Maxwell bodies 3-44830
- Maxwell fluid, dusty, flow from oscillating infinite flat plate 3-79033
- Maxwellian fluid, generalised Couette flow, convection 3-71744
- melts, temperature-invariant rheological dependences obtained using Leonov-Vinogradov model 3-57699
- MHD flow past plane porous plate, velocity field soln. 3-40736
- muscle tissue, continuous mechanical and chemical model (*Russian*) 3-70094
- Newtonian fluid, filling a rectangular channel, theoretical analysis, application to injection moulding 3-76377
- Newtonian liquid, die swell 3-58760
- non-linear viscoelastic material for spherical pressure vessel, random loading 3-70564
- non-Newtonian fluids, entrance flows 3-52485
- non-Newtonian fluids, horizontal layers, onset of convection, stability (*Russian*) 3-43549
- nonhomogeneous isotropic viscoelastic media, cylindrical and spherical shear wave propag. 3-45684
- nonlinear suspension of one-degree-of-freedom system, stability of equilibrium point (*Polish*) 3-70680
- nonlinear systems, dynamic loading, method of successive approximations 3-70603
- nonlinear theory, stress pots. 3-62466
- nonlinear viscoelastic fluid, dynamics theory 3-71837
- nonlinear viscoelastic materials, modelling, identification and prediction using Volterra integral eqn. 3-45646
- nonlinear wave propagation, review 3-70646
- nonuniform hereditary media, potentials and deformations (*Russian*) 3-42782
- oils, elastic behaviour during impact 3-60761
- plane, high-elastic incompressible material, surface instability 3-80485
- plastic board, nonlinear viscoelastic, cubical approximation method of calc. (*German*) 3-65009
- PMMA, dynamic compliance, creep 3-80492

viscoelasticity continued

- PMMA, max. Newtonian viscosity and dipole relaxation polarisation (*Russian*) 3-80495
- polyethylene, non-Newtonian flow under conditions of an inhomogeneous temp. distribution 3-63593
- poly(amide carboxylic acid) solution, flow birefringence, 30°C, molecular dimensions, triethylamine addition effect 3-54781
- poly(n-butyl methacrylate) networks, viscoelasticity, stress-strain behaviour, effect of reference chain dimension, thermoelastic meas. 3-55890
- poly-1-butene, effect of allotropic form on static mech. props. (*French*) 3-63592
- polyacrylamide solutions, viscoelastic liquid, flow patterns upstream of orifices 3-71754
- polyacrylonitrile fibres, stress relaxation peculiarities 3-63602
- polyethylene terephthalate, molecular mobility and structure 3-60502
- polyethylene, low density, effect of filling melt on the first difference of the normal stresses and on tangential stresses 3-58758
- polyethylene, molten, steady flow and dynamic props. 3-67886
- polyethylene glycol dilute soln. elastico-viscous liquid, oscillatory laminar flow, velocity profiles in tubes of circular section 3-54822
- polyethylene melt, shear and elongational flow, stress-time data, network theory predictions 3-73062
- polyethylene melt, stresses, periodic deformations, effect of vibration frequency and amplitude variations, Weissenberg rheogoniometer 3-67880
- polyethylene melt, viscoelastic flow through converging ducts, wall normal stresses, die swell behaviour 3-80459
- polyethylene terephthalate, molten, departure from Newtonian behaviour 3-53285
- polyethyleneimine-polyacrylate, rotation viscometer study of Newtonian flow 3-43630
- polyimides, strength and relaxation props. (*Russian*) 3-80499
- polyisobutylene, equal biaxial extensional flow, bubble inflation technique 3-67890
- polyisobutylene fluids, normal stress data correlation 3-67892
- polyisobutylene solutions, dynamic viscosity and elasticity, effect of steady-state flow 3-71686
- polymer, branched, solutions, viscoelastic props. calc. based on Zimm-Kilb theory 3-54776
- polymer, high-pressure, torsion pendulum for viscoelastic studies 3-51529
- polymer, hydrostatic press. effect on mech. props., review 3-80475
- polymer, long term creep, phenomenological prediction, in time dependent systems 3-58745
- polymer, multiphase mixtures, pair additivity principle 3-73042
- polymer aqueous solutions, hydrodynamic influence of polymer additives in external flow around a sphere 3-57830
- polymer concentrated solns., heterogeneous drag, reduction system, turbulent pipe flow, heat transfer 3-52434
- polymer dilute soln. non-Newtonian flow, mass transfer with rotating disc 3-71816
- polymer dilute solns., round turbulent jet, laser-Doppler meas. 3-75283
- polymer dilute solns. behaviour in inlet region of pipe 3-75267
- polymer dilute solutions flow over a rough surface, wall pressure fluctuations 3-54823
- polymer flow between calender roll, force and energy parameters 3-61218
- polymer flow between two rotating cylinders 3-40725
- polymer fluid behaviour in elongational flow (*Polish*) 3-60501
- polymer liquids, teaching demonstrations 3-42499
- polymer melt extrusion, instability theory 3-67889
- polymer melt rheology, recent publications, review 3-50784
- polymer melts, effect of pressure, shear rates 3-63599
- polymer melts, flow between coaxial cylinders under complex shear conditions 3-73048
- polymer melts, shearing flow, anisotropy, second normal stress difference meas. 3-71842
- polymer melts and solns., effect of mol. wt. and mol. wt. distrib. on viscoelastic props. 3-69384
- polymer soln., dilute, turbulent flow, spectral characts. of press. fluctuations 3-49559
- polymer solution, dilute, torsional quartz crystal method 3-77381
- polymer solution, high viscosity, wedge and channel flow stability 3-54825
- polymer solution, zero shear viscosity, conc. depend. 3-71679
- polymer solutions, capillary viscosimeter flow meas. 3-57831
- polymer solutions, internal viscosity models evaluation 3-53288
- polymer solutions, normal stress difference meas., cone and plate rheogoniometer, flush-mounted pressure transducers 3-70503
- polymer solutions, reduced drag in turbulent and transient laminar flows near a flat plate 3-63778
- polymer solutions, turbulent drag reduction in external rotational flows 3-60571
- polymer solutions, turbulent flow, influence of high-molecular weight additives 3-57832
- polymer solutions, viscoelasticity, hole size and soln. concentration effects 3-53290
- polymer solutions and melts, periodic deformation, viscous flow, under stepwise vibrations 3-58755
- polymer solutions and melts, periodic deformation and viscous flow 3-54780
- polymer suspensions, rheological equations 3-73083
- polymer thin films, deform. following extended Voigt model 3-40955
- polymer threads, drag reduction in turbulent flow 3-40739
- polymer-particle disperse systems, dynamic viscoelasticity (*Japanese*) 3-40693
- polymeric streaming fluid, flow birefringence obs. (*German*) 3-60592
- polymeric systems, high-elastic deform. phenomena 3-67881
- polymers, amorphous, in rubberlike elastic state, viscoelastic props. as function of nature and length of chain 3-73047
- polymers, molten, helical flow in a cylindrical annulus 3-73061
- polymers, percolation expts. 3-71677
- polymers, regular networks with stable points linking four chains, viscoelastic behaviour, theory 3-54777

viscoelasticity continued

- polymers, unstable, Il'yushin approx. 3-57083
 polymers, u.s. velocity, at liq. He temp. 3-43532
 polypropylene melt, effect of micro-additions on viscoelasticity (*Russian*) 3-80497
 polypropylene melt, processing, aging, effective viscosity, tensile strength, effect of polymeric antioxidants 3-73058
 polypropylene melt, viscoelastic flow through converging ducts, wall normal stresses, die swell behaviour 3-80459
 polystyrene mixtures with elastomers, mol. wt. effect 3-71676
 polystyrene solutions, viscoelastic props. 3-53291
 polystyrene solutions, viscosity, effect of mol. weight, range of shear stresses, structure formation and orientation 3-71687
 polyurethane, creep under varying temperature for nonlinear uniaxial stress 3-53283
 polyvinyl acetate, self healing of cracks, molecular weight, and environment effects 3-58749
 porous flat vertical plate, natural convection flow of liquid 3-78952
 PVC board, nonlinear viscoelastic, cubical approximation method of calc. (*German*) 3-65009
 relativistic thermo-magneto-viscoelastic waves, propag. in Voigt type material 3-62515
 relaxation, retardation spectra, numerical method 3-66557
 resin, 10 to 10⁷ poises, u.s. frequencies, relaxation range 3-61993
 rheogoniometer, for viscoelastic properties of polymeric systems 3-53831
 rheological model of solids and liquids, variable order derivative (*Italian*) 3-70557
 rod, coated, flexural vibrs., axial force, damping 3-62517
 rubber, creep and stress relax., stress history and temp. changes 3-58731
 rubber, elasticity in high temperature subregion, above glass transition temperature 3-58757
 rubber, natural, cross-linked by dicumyl peroxide, shear modulus, exptl. obs. 3-65003
 rubber, stress-relaxation, effect of infrasonic vibration (*German*) 3-65011
 rubber reinforced plastics, transition magnitudes and impact improvement 3-50783
 second-order fluid flow over flat plate with suction and const. heat sources, heat transfer 3-75187
 slide bearing performance under fluctuating speed using non-Newtonian viscoelasticity fluid lubricant 3-75565
 solutions, nonlinear viscoelastic functions, analysis and temp. dependence 3-53289
 solvent effect in rotation of dipole molecules in applied field 3-47604
 spiral motion of a cylinder in a non-Newtonian fluid 3-63672
 spring colliding with rigid body, viscoelastic model, rel. to nuclear reactor 3-60270
 steel, effect on strain wave front 3-44597
 stress pulse propagation, plane, semi-infinite viscoelastic Maxwell solid, analysis 3-70654
 stress relaxation, at mechanical deformation, in glass transition temp. range (*German*) 3-60767
 stretched viscoelastic tube, filled with viscous fluid, phase velocity and damping of torsional waves 3-59415
 suspension of ellipsoidal macromolecules, two dimensional laminar flow, orientation distribution function, Legendre coeffs. 3-40749
 synthetic lattices, rheology, influence of shear rate and temp. 3-69393
 tectonic folding stress anal. in viscoelastic and elastoplastic media 3-76602
 thermoviscoelastic media, steady state wave propagation, dual variational principles 3-70647
 thermoviscoelastic solid, amplitude behaviour of shock waves 3-79426
 thermoviscoelasticity method of elastic solutions 3-62465
 thick walled, slowly rotating cylinder, deformation undergravitational load 3-59754
 transient crack problems, path-independent integral 3-57075
 transient cylindrical shear waves, propagation, reflection and transmission 3-40100
 unsteady flow past infinite flat plate with variable suction 3-71760
 unvulcanized rubbers, unstable flow, in open and closed channels 3-58756
 viscoelastic media, plane waves propagated by transient shock load (*Russian*) 3-69508
 viscoplastic disperse system, steady-state isothermal flow in elbow pipe of circular cross section 3-71817
 viscoplastic fluid axial laminar flow in annular tube 3-71838
 viscoplastic media hydrodynamics, time-dependent problems, Monte Carlo soln. method 3-71839
 wave propagation, finite amplitude, soln. of Kortweg-de Vries-Burgers eqns. (*Russian*) 3-45691
 weak polymer solns., turbulent flow in a pipe, exptl. obs. 3-71818
 Weissenberg effect, observation methods 3-67891
 welded components, weak joint, viscous strength, effect of mech. inhomogeneity (*Russian*) 3-41792

viscometers

- see also viscosity measurement*
 air, series capillary transpiration viscometer, for absolute viscosity of air at high press. and low temp. 3-71715
 capillary, Pinkevich type, to measure dynamical viscosity 3-51769
 capillary, slip correction 3-77761
 capillary, theory 3-40080
 coiled-capillary, curved pipe flow effects, correction method 3-73972
 falling-sphere, precision, wide range, photographic sphere velocity measurement, description 3-66474
 Ostwald, modified, time of flow measurement for liquids 3-48693
 piezoelectric vibration viscometer, bimorphous plates, gas viscosity 3-70498
 polymer melts, viscometer, frictional heat meas., capillary rheometry, calorimetric method, appl. to extrusion 3-70502
 process viscometer (*German*) 3-54052
 radioisotope vibroviscometer, γ radiation shift detection 3-73968

viscometers continued

- rheogoniometer, for viscoelastic properties of polymeric systems 3-53831
 rolling ball, power law fluids, flow curve meas., shear rate variation, carboxymethylcellulose, polyacrylamide 3-71688
 rotating cylinder, automatic, glass viscosity determ. (*Japanese*) 3-77384
 rotation, RV-8, bell-type coaxial cylinders, reduction of edge effects, rheological characteristics, highly viscous liquids 3-54054
 rotation rheometer, voltage meas., during shear flow (*German*) 3-70504
 slags, simultaneous viscosity and elec. cond. meas. vibration viscosity meter 3-48467
 vibration, calibration, liquid density effect 3-73969
 vibration, fixed frequency, error anal., simple measuring circuit 3-48691
 VIR-70 micro-viscometer meas. of blood viscosities 3-59414
- viscoplasticity** *see plasticity*
viscosimeters *see viscometers*
viscosity
see also electroviscous effect; viscosity of gases; viscosity of liquids
 aerosol particles, spherical, diffusiophoresis and drag in gas mixture 3-73084
 artificial, improved form from second Rankine-Hugoniot equation 3-46457
 artificial, Lagrangian hydrodynamics code, R-H relations 3-74063
 atmospheric planetary boundary layer, height-dependent model of eddy viscosity 3-51058
 cantilever, effect on lateral vibrs. 3-62516
 dense gases, transport properties calc. 3-52417
 Earth core, viscosity rel. to rel. to viscosity of core 3-41902
 Earth mantle, shallow convection model rel. to viscous stratification 3-41901
 earth mantle convection, viscosity depend. on temp. 3-76644
 earth upper mantle, determ. using Stokes's law 3-41891
 e.m. wave propagation, electroconductive media, compressible viscous media (*Russian*) 3-45763
 epoxy resin systems of reduced viscosity, gamma-irradiated, mechanical properties 3-50786
 Euler equations, manifolds diffeomorphic to two dim. sphere, initial problem 3-63617
 Euler equations on two dim. sphere, proof of existence and uniqueness of initial value problem 3-63616
 ferromagnetic thin films, tunnelling mechanism for viscous wall motion 3-41376
 fine dispersed particles with cubic crystalline symmetry, viscosity in mag. field (*Russian*) 3-79879
 flow past a thin oblate spheroid, infinite viscous fluid, streamfunction and vorticity calc. appl. to cloud physics 3-43552
 fluid circulation in drop, effect on drag force in viscous flow and rate of evaporation (*Russian*) 3-43626
 glass fibre, mech. props., comp. (*Polish*) 3-44681
 glycerol, laminar pipe flow, non-isothermal, velocity profiles, pressure drops and heat transfer 3-63629
 glycidyl amine resin systems of reduced viscosity, gamma-irradiated, mechanical properties 3-50786
 hypersonic turbulent boundary layer, eddy-viscosity calc. 3-46429
 imperfect fluid Friedmann cosmology, role of bulk viscosity 3-42117
 incompressible fluid, convective flow generation (*Russian*) 3-63645
 incompressible fluid, external motions caused by jet suction (*Russian*) 3-43564
 isotropic media, stresses, relativistic theory of dissipative magnetoelastic interactions 3-79884
 laminar pipe flow, non-isothermal, heat transfer and hydrodynamics for variable viscosity fluid 3-63628
 low Reynolds number fall of slender cylinders near boundaries 3-43562
 lunar interior viscosity during mare formation 3-42180
 microscopic anal. of long-time tail in autocorrelation function and diffusion coefficient 3-70753
 monosaccharides, amorphous, activation energy, temp. depend. 3-79940
 multi-component ionised gas-solid suspension, transport properties 3-71865
 Newtonian fluid, non-isothermal laminar pipe flow, velocity profiles, pressure drops and heat transfer 3-63629
 non-Newtonian fluids, viscous flow prediction, conduits, packed beds, porous media fluid models 3-71730
 ocean circulation, two-layer model 3-73265
 plasma, composite, hydromagnetic stability determination 3-68007
 plasma, inhomogeneous, dynamic viscosity coefficient determ. 3-54846
 plasma, nonequilibrium, in mag. field, influence of viscosity on motion of nonuniformities 3-49673
 poly(caproamide), salted, rel. to melting behaviour 3-52410
 polyphenyl ether, high-press. viscosity meas. 3-62386
 quartzite, nonlinear model for folds 3-76604
 semiconductors, piezoelectric, renormalised viscosity for high acoustic flux 3-60904
 solid, dynamic behaviour of spring colliding with rigid bod. rel. to nuclear reactor 3-60270
 stars, rapidly rotating, viscous effects with appl. to white dwarf models 3-65871
 surface wave development, viscous fluid, finite depth flat Koshi-Poisson problem (*Russian*) 3-46472
 suspension, rigid particle, subjected to const. vel. gradient flow, non-Newtonian viscosity correl. with Maxwell effect (*French*) 3-80501
 suspensions, fixed and free, settling speed, viscous fluid 3-73091
 terrestrial planets, present thermal state, viscosity-temp. relationship 3-42171
 thermophysical props. conf., Atlanta, USA, (Aug 1973) 3-71702
 unsteady boundary layer, on flat plate, effects of viscosity-temp. law 3-71767
 upper earth mantle convection with variable viscosity 3-76643
 viscoelastic media, temp. depend. rel. to nonisothermal flow instability 3-43592

viscosity continued

- viscous flow, incompressible fluid, rectangular cavities, finite-difference equations, behaviour of vortices 3-71755
 wave velocity in parallel flows of a viscous fluid 3-43584
 white dwarf viscous evolutionary sequences 3-65872
 Al_2O_3 colloidal dispersions, rheological props. 3-53287
 ^4He , thermophysical props. tables from 2 to 1500 K with pressures to 1000 atmospheres 3-60822
 $\text{K}_2\text{O}-\text{BaO}-\text{B}_2\text{O}_3$ glasses, rheological properties, activation energy 3-58070
 $\text{Li}_2\text{O} \cdot 2\text{SiO}_2$ glass, apparent viscosity during crystallisation (Japanese) 3-68428
 $\text{Pb}-\text{In}$, type II supercond., temp. depend. of viscosity coeff., differential resist. 3-72426
 Se , stress and temperature depend. 3-55000
 Zn silicate glass, alkali, nucleation and crystallisation properties 3-75476

viscosity measurement

- see also viscometers
 air, series capillary transpiration viscometer, for absolute viscosity of air at high press. and low temp. 3-71715
 capillary viscometer, theory 3-40080
 Couette viscometer, for meas. of high-press. viscosity of polyphenyl ether 3-62386
 p -dichlorobenzene melt, viscosity meas., modified Ostwald viscometer 3-48693
 ferromagnetic system, mag. method 3-73071
 fibre-elongation method applied to vitreous systems (Japanese) 3-68428
 glass, using automatic rotating cylinder viscometer (Japanese) 3-77384
 nematic liquid cryst. shear viscosity coeffs. determ. method, mag. susceptibility anisotropy 3-51771
 rheometers, eccentric cylinder and displaced hemisphere, Weissenberg rheogoniometer, anomalous results, highly viscous fluids, cavitation 3-39854
 slags, simultaneous viscosity and elec. cond. meas. vibration viscosity meter 3-48467
 viscometer, coiled-capillary, curved pipe flow effects, correction method 3-73972

viscosity of gases

- air, determination of the absolute viscosity of air at high press. and low temp. 3-71715
 air resistance, work by Benjamin Robins (1707-51) 3-59512
 atmospheric mesoscale cellular convection, model including eddy viscosity effects 3-47731
 inert gases, dil., temp. depend. 3-71716
 kinetic theory approach, review 3-71655
 multicomponent mixtures, Sutherland coeff. 3-71717
 nonpolar polyatomic gases, mol. shape effect on transport and equil. props. 3-75179
 piezoelectric vibration viscometer, bimorphous plates, gas viscosity 3-70498
 planar correlation, Lennard-Jones potential, mol. struct. 3-71718
 shear viscosity, near gas-liq. crit. point 3-72185
 transport and equilibrium props., utility of $m-6-8$ potential function 3-60512
 transport coefficients in the intermediate relativistic regime, special models 3-60516
 vacuum gauge theory 3-77423
 viscomagnetic effect, temp. depend. 3-52420
 volume viscosity in a model consisting of particles with excited states 3-60517
 Ar , coeff. meas. at h.p. (French) 3-78925
 Ar , dilute/dense viscosity ratio, press. depend. (French) 3-78927
 Ar , hard sphere fluid approach, press. depend. (French) 3-78926
 Ar , liquid and gas, viscosity meas. 3-67896
 Ar -methyl chloride gas mixtures, viscosity and polar-nonpolar molecular interactions 3-60515
 H_2 , ortho and para, multipole interactions and macroscopic differences 3-71661
 H_2 and water vapour binary mixture, thermal conductivity and viscosity calc. 3-63609
 H_2 thermodynamic and transport props. calc. using Tabcode-II computer programs 3-60511
 HD -inert gas mixtures, viscomagnetic effect 3-52421
 He , thermophysical properties, HEPROP computer program 3-50042
 ^4He , thermophysical properties, 4 to 3000 R, pressures up to 15000 PSIA 3-50043
 Kr -methyl chloride gas mixtures, viscosity and polar-nonpolar molecular interactions 3-60515
 N_2 -inert gas mixtures, viscomagnetic effect 3-52421
 Ne -methane, gas mixtures, viscosity and polar-nonpolar molecular interactions 3-60515
 Ne -methyl chloride gas mixtures, viscosity and polar-nonpolar molecular interactions 3-60515
 O_2 and water vapour binary mixture, thermal conductivity and viscosity calc. 3-63609
 Xe -methyl chloride gas mixtures, viscosity and polar-nonpolar molecular interactions 3-60515

viscosity of liquids

- see also lubrication
 aerosol particles, hydrodynamic tensor for stresses, motion rate 3-63767
 anorthite, meas. in $1450^\circ\text{--}1620^\circ\text{C}$ and $820^\circ\text{--}950^\circ\text{C}$ ranges 3-69511
 asymmetric cavitation bubble collapse, liquid viscosity effect 3-63736
 binary liquids, near crit. point 3-72185
 blood flow 3-56492
 blood viscosity meas. with VIR-70 micro-viscometer 3-59414
 calcium caproate aqueous solns., physical props. meas. 3-58769
 cellulose tributylate molecules, sedimentation constant, diffusion coeff., intrinsic viscosity, optical anisotropy effect of different solvents (Russian) 3-46368
 copolymer, three-block, structure, rheological properties and pouring index (Russian) 3-71690
 damping of motion of two plates, stability, effect on critical parameters 3-74069

viscosity of liquids continued

- p -dichlorobenzene melt, viscosity meas., modified Ostwald viscometer 3-48693
 electrolyte, effect of viscosity on ion diffusion coeff. (French) 3-65087
 film on inner side of horizontal capillary, instability of phenomena 3-72259
 flow, non-stationary uniform, in deforming tube (Russian) 3-46380
 flowing thin film, travelling and rolling waves, calc. of perturbations in film thickness (Russian) 3-57810
 fluidity and liquid structure 3-72220
 fluidity-temp. relationship 3-54832
 glass transition, thermodynamic equations 3-52580
 gravity waves produced by oscillating vertical plate in viscous liquid, amplitude and mechanism 3-75246
 internal wave dissipation, variable depth basin, effect of viscosity (Russian) 3-50997
 laminar condensation heat transfer, temperature-dependent viscosity effect 3-68398
 lubricant flow in circular tube pressure induced viscosity changes effects 3-79042
 maleic acid-styrene copolymer, conformational transition in NaCl soln., effect of intrinsic viscosity 3-54765
 MBBA, nematic, mag. susceptibility anisotropy and twist viscosity (German) 3-52577
 metallic melts, rel. to thermal cond. (Russian) 3-44057
 metals, atomic transport properties, viscosity self-diffusion results, techniques, theories, models, correlations, review 3-50015
 metals, rare earth and actinide, viscous flow models, f -orbital electronic contribution 3-50021
 microscopic processes, review 3-64199
 mixture, binary, internal relaxation, light scattering 3-80013
 molecular motion, computer simulation 3-68432
 molecular motions and mutual viscosities of polar molecules in solutions 3-47604
 molten multiphase slag, influence of viscosity on MHD separation process (Russian) 3-61168
 nematic liquid cryst. shear viscosity coeffs. determ. method, mag. susceptibility anisotropy 3-51771
 nitrothane-3-methylpentane mixture, shear dependence of the viscosity in the critical region 3-41039
 noble and transition metals, interionic pair potentials 3-43746
 non-Newtonian, non-linear viscous response, rotational flow, interaction with stationary surface 3-40715
 non-Newtonian fluids, jet instability 3-67967
 organic liquids, u.s. wave absorpt. and dispersion, depend. on bulk viscosity coeff. 3-49940
 Ostwald viscometer, modified time of flow measurement for liquids 3-48693
 perturbation theory, dense fluid transport properties 3-72221
 plastic melt, non-Newtonian flow, temp. depend. (German) 3-65010
 PMMA, max. Newtonian viscosity and dipole relaxation polarisation (Russian) 3-80495
 PMMA suspension in dibutyl phthalate, shear rate effect 3-61231
 polyethylene melt, effect of pressure 3-65019
 polyethylene solutions, Mark-Houwink relations 3-71680
 polyisobutylene solutions, dynamic viscosity and elasticity, effect of steady-state flow 3-71686
 polymer, molecular weight determination, gel permeation chromatography (German) 3-71662
 polymer melt, effect of entanglements 3-57687
 polymer melt, effect of pressure on viscosity 3-65019
 polymer solution, rigid ellipsoid type, shear rate depend. 3-80478
 polymer solution, zero shear, conc. depend. 3-71679
 polymer solutions, capillary viscosimeter flow meas. 3-57831
 polymer solutions, structure formation, viscosity obs. (Russian) 3-49518
 polymer unperturbed chain dimensions from intrinsic viscosities, determ. in good solvents 3-52407
 polymers, molten, helical flow, non-Newtonian fluid, cylindrical annulus, shear dependence of viscosity 3-73061
 polymers, monodisperse, depend. of zero-shear viscosity on mol. wt. distrib. 3-57696
 polysiloxanes, liquid, viscous flow at high pressures, free energy, enthalpy, entropy, vol. of activation calc. (Russian) 3-46367
 polystyrene elastomer mixture, mol. wt. effect 3-71676
 polystyrene solutions, viscosity, effect of mol. weight, range of shear stresses, structure formation and orientation 3-71687
 polystyrene-cyclohexane, mixture shear dependence of the viscosity in the critical region 3-41039
 power dissipation during motion, theorem for minimum (Italian) 3-43646
 n -propanol, adiabatic volume viscosities determ. using ultrasonic absorption data 3-68431
 saturated nonpolar liquids, viscosities at elevated pressures 3-60801
 solution viscosity and temp. effects on the concentration depolarisation of fluorescence 3-49486
 stability of oscillations of body partly filled with viscous fluid, boundary layer method (Russian) 3-62536
 temperature dependence, nonexponential formulation 3-79513
 tetracyanoethylene-toluene charge transfer complex, in glassy soln. effect on fluoresc. spectra 3-69076
 turbulent wall boundary layers using effective viscosity model 3-43560
 two-phase mixtures, surface tension contribs. 3-72219
 viscometer, rotation, bell-type coaxial cylinders, reduction of edge effects, rheological characteristics, highly viscous liquids 3-54054
 viscosity/temperature relationship, exponential and 'fracture' formulae (German) 3-64203
 viscous conducting liquid, flow between porous concentric circular cylinders, effect of radial mag. field 3-40734
 water and heavy water mixture, volume viscosity and struct. u.s. study 3-50020
 water-benzene-ethyl alcohol ternary system, shear viscosity and u.s. absorpt. near plait pt. 3-64204
 Ar , liquid, correlation between bulk viscosity and electron mobility 3-64202
 Ar , liquid and gas, viscosity meas. 3-67896

viscosity of liquids continued

- Ar, shear viscosity via Lennard-Jones potential with equilibrium and nonequilibrium molecular dynamics 3-55096
 Cu-Sn alloy, rel. to comp. (*Japanese*) 3-72819
 D₂O, pressure dependent volume viscosity, lattice model calculations 3-46680
 Fe-Ni, alloys structure sensitivity, oscillating crucible method, liquidus to 1700 °C, viscosity coefficient, activation energy 3-50022
 He, thermophysical properties, HEPROP computer program 3-50042
³He, relative viscosity meas. along melting curve, 10 to 1 mK, superfluidity evidence 3-41061
³He, superfluid, first viscosity of Balian-Werthamer phase (*French*) 3-72250
³He, superfluid, low temp. first viscosity calc. (*French*) 3-58159
³He liquid, high-temperature transport properties 3-60824
³He-⁴He mixture, third viscosity, near tricritical point, mode-mode coupling calc. 3-60825
⁴He, superfluid, dissipative coefficients calc., Boltzmann equation solution for phonons and rotons 3-43915
⁴He, thermophysical properties, 4 to 3000 R, pressures up to 15000 PSIA 3-50043
⁴He, thermophysical props. tables from 2 to 1500 K with pressures to 1000 atmospheres 3-60822
 K₂O-B₂O₃ melts isothermal, ultrasonic relaxation studies 3-41040
 Ni-Cr alloy, 1300-1800°C, 0.90 wt.%Cr (*Russian*) 3-50172
 Ni-Fe, alloys, structure sensitivity, oscillating crucible method, liquidus to 1700 °C, viscosity coefficient, activation energy 3-50022
 Pb-Sn, alloys temperature dependency, Arrhenius relationship, composition dependency structural changes 3-50024
 Sn-Pb, alloys temperature dependency, Arrhenius relationship, composition dependency, structural changes 3-50024
 Ti-Te, alloys densities, composition, temperature, activation energy, volume of mixing, thermal expansion, stoichiometry 3-50023

visibility

- see also *atmospheric optics; brightness; light transmission*
 afterimage visibility of horizontal-vertical illusion as a function of figure orientation and angular separation 3-81297
 astrolimate, image vibration in Mongolia by track's method (*Russian*) 3-73281
 highway objects, nighttime driving situations 3-53469
 light attenuation measurement, transmissometer, automatic recording, 0.9 microns, mists and fogs 3-59178
 marine weather extremes, temp., rel. humidity, wind speed, visibility, salinity and upper air temp. 3-53496
 Mauna Kea, Hawaii, evaluation as an observatory site 3-77194
 Mt. Lemmon, optical seeing tests at astronomical observatory site 3-69566
 point source, effect of spectral content of background 3-73507
 point source, visibility, effect of spectral content of background 3-73507
 rain drop size distrib. effect (*German*) 3-47764
 stars, visibility threshold with unaided eye at different background brightnesses 3-70080
 stellar image formation, high resolution, through turbulent atm., star maps 3-73564
 vision difficulties, surroundings conditioned, eye sequence investigation method, elucidation (*German*) 3-70116
 White Sands Missile Range, apparent 7-day period 3-51041

visible astronomical observations

- 1633 + 38, identification of radio source with blue object 3-77111
 A- and Ap-type stars, photoelectric obs. of H lines 3-51338
 A-type dwarfs, rotation and shell spectra 3-61774
 A-type stars, microturbulence from line profiles of six objects 3-51339
 absolute solar intensities and constant, accuracy of aircraft and ground based obs. 3-80980
 AC + 65°6955, absolute parallax and analysis of astrometric field 3-48024
 Am-type double-lined binary stars, equivalent width determ. for 7 objects 3-61791
 Andromeda III, dwarf spheroidal companion galaxy to Andromeda Nebula 3-48097
 Ap star spectra, element abundance anomalies 3-81057
 Ap stars, abundance anal. for 21 sharp-lined cool objects 3-65879
 Ap-type stars, search in open clusters 3-61771
 η Aquarid meteor shower, magnitudes, trail lengths, directions 3-81010
 CY Aquarii dwarf Cepheid, beat period and characts. 3-69959
 Aquilus variables, photographic obs. (*Russian*) 3-61807
 artificial night-sky illumination and seeing at astronomical observatories 3-65374
 asteroid positions in 1971, Turin Observatory photographs 3-69912
 asteroids, polarimetric obs. of 6 objects 3-47969
 asteroids, position determ. of 19 objects (*French*) 3-73465
 asteroids, position meas. of 5 objects 3-73466
 asteroids, spectral reflectivities of 36 objects rel. to 22 ordinary chondritic meteorites. 3-61740
 astrolimate, image vibration in Mongolia by track's method (*Russian*) 3-73281
 atmospheric extinction, determ. using limiting stellar magnitudes 3-47717
 UV Aurigae, carbon star, visual primary of binary ADS 3934, spectrophotometry, classification 3-51356
 53 Aurigae, course analysis of peculiar A-type star 3-51358
 Aurigae, eclipsing binary, Ca I satellite lines rel. to expanding circumstellar cloud 3-53666
 Automatic Camera for Astrogeodesy, Czechoslovakia, ISAGEX-programme, satellite geodesy 3-48151
 B6-type stars, high dispersion spectrograms and scans in 1100-6700 Angstroms range 3-48025
 B-type main sequence stars, u.v. flux envelopes, 1100-6000 Å obs. 3-48026
 Barnard's Star, planetary system rel. to proper motion obs. 3-59349
 BD + 30°3639, planetary nebula H β meas. rel. to scattered continuum, optical depth 3-51402
 BD + 66 degrees 34, triple system, astrometric anal. 3-51353
 BD + 67°552, unresolved astrometric binary, orbital motion and parallax 3-42193

visible astronomical observations continued

- BD + 67°552, unresolved binary, orbital motion and parallax determ. 3-48037
 BD + 60°398, unresolved astrometric binary, orbital motion and parallax 3-42193
 Bennett (1969 i), photometry by equidensity method (*Russian*) 3-77014
 5C3 radio sources, M 31 region, optical identifications of quasars and galaxies 3-42212
 4C 05.34, absorption spectra, search for high ionisation redshift systems 3-77116
 4C 31.63, quasar, spectroscopic and photometric obs. 3-51364
 4C 38.41, identification of radio source with blue object 3-77111
 3C 390.3, deep integration prints of compact galaxy 3-42235
 TX Cancr, W Ursae Majoris type, obs. and evolution 3-65892
 β Canis Majoris stars 15 and ζ^1 CMA, yellow photoelectric observations 3-42200
 YZ Canis Minoris flare star, 1969 Jan., spectrophotometric investigation (*Russian*) 3-45126
 SX Cassiopeiae, Algol-type variable, detection of secondary spectrum 3-45135
 catalogues for star position and proper motion for Washington and Richmond photographic zenith tubes 3-76947
 CD-42° 14462, oscillations 29 sec. 3-69963
 4C Centauri, energy distrib. and continuous spectrum in 2000-3800 Å range 3-73509
 α Centauri, spectrum variable, obs. of anomalous Fe I lines 3-53667
 α Centauri (HD 125823), radial rel. variations determ. 3-42198
 ω Centauri cluster, ¹²C/¹³C ratio for two CH-stars using Swan bands 3-45194
 VV Cephei, eclipsing, high-dispersion spectrum, H α structure, radial velocities 3-51355
 β Cephei, spectral obs. with improved time resolution 3-48035
 Cepheid F and G stars, H α line profiles 3-56377
 Cepheid variables in 3 LMC globular clusters, BV obs. 3-65882
 Cepheids, double mode, mass determ. from period ratios of 8 examples 3-69958
 Ceres, astrophysical position determ. 3-45051
 o Ceti, speckle interferometry, colour-depend. limb darkening 3-48031
 Cetus Arc nebulosity around Loop II, H α radial velocity meas. 3-59391
 circumzenith stars, catalogue of 30 precise declinations 3-53635
 clusters of galaxies, possible systematic red shifts 3-56420
 X Comae Berenices, optical variability, UVB colours 3-81171
 comet Abe (1970g), photography at Poznan Observatory (1970) 3-69909
 Comet Bennet (1970 II), brightness profile of C₂ and CN in neutral coma spectra 3-81004
 comet Bennet (1969 i), spectropolarimetric obs. of head (*Russian*) 3-77012
 comet Bennet (1970 II), interpretation of Lyman α obs. 3-53627
 comet Bennet (1970 II), photometric scans through head and tail 3-59319
 Comet Bennet (1970 II), solar wind interaction and kink in ion tail 3-65855
 Comet Heck-Sause (1973a), photographs and spectra 3-47975
 comet Ikeya-Seki (1968 I), photoelectric magnitude estimates 3-47974
 comet P/Encke (1971 II) interpretation of Lyman α obs. 3-53627
 comet photography at Poznan Observatory (1970) 3-69909
 comet photography at Wroclaw Observatory (1970) 3-69908
 Comet Tago-Sato-Kosaka (1969 g), equidensity method (*Russian*) 3-77013
 comet Tago-Sato-Kosaka (1969g), photography at Wroclaw Observatory (1970) 3-69908
 Comet Tuttle-Giacobini-Kresak (1973b), violent changes in magnitude 3-81011
 comets, brightness law dependence on distance, implication of photometer diaphragm size 3-61737
 comets, position meas. of 5 objects 3-73466
 common proper motions of three double stars, possible physical binary system 3-53662
 CPD - 69°2698, H-deficient star, Coude spectrograms and abundance analysis 3-48027
 Crab Nebula, H and He atoms, ionisation and relative abundance (*Russian*) 3-45226
 Crab pulsar, PSR 0531 + 21, optical obs. of steady and discontinuous changes and period of rotation (*German*) 3-81125
 V1329 Cyg = HBV 475, symbiotic binary, photometric and spectroscopic obs. 3-69965
 32Cygni, 1971 eclipse, OAO-2 filter photometry 3-51354
 57 Cygni, apsidal motion and spectral line blending effects 3-73515
 V1016 Cygni, expansion, spectroscopic studies, emission line structure 3-69969
 CI Cygni, symbiotic star, obs. of spectrum during outburst 3-48041
 Cygnus X-1, optical obs. and model from He II emission line 3-56411
 Cygnus X-1 (BD + 34°3815), nature of optical variability 3-61818
 Demos, Mariner 9 TV obs. 3-69866
 diffuse Galactic light polarisation meas. 3-56430
 diffuse interstellar bands, proof that preionisation of H⁻ is not the source 3-73546
 diffuse interstellar features in spectra of dust-embedded and field stars 3-56383
 30 Doradus, giant H II region, nature of luminous central object 3-51399
 double stars discovered at Nice (9th series) (*French*) 3-61784
 early-type stars, obs. in linearly polarised light of diffuse 6180 Å band in 49 stars 3-73499
 early-type supergiants with variable H α profiles 3-45106
 early-type supergiants with variable H α profiles rel. to mass loss and turbulence 3-56375
 eclipsing variable stars, natural motion of 122 stars (*Russian*) 3-61808
 elliptical galaxies, (U-B) colour indices, hydrogen line strengths 3-71148
 ϵ Eridani, binary, relative parallax and perturbation period determ. 3-48036
 Europa, occultation by IO, indication of polar cap 3-61690

visible astronomical observations continued

- extra-solar-planets, detection by wavelength optimisation of signal/noise 3-81253
 extragalactic X-ray sources, properties from visible obs. 3-81152
 F and G stars, continuum photometry 3-56378
 faint astronomical objects detection, image orthicon system, effective quantum efficiency 3-48145
 faint variable objects in M31 region 3-48064
 FK 4 stars, right ascension determ. south of -42° declination 3-77035
 FKSZ stars, catalogue of R.A. and comparison with other catalogues 3-59239
 flare stars, continual photoelectric monitoring during 1971 for four objects 3-45140
 flare stars, photoelectric obs. (*Italian*) 3-61789
 Fm stars, curve-of-growth anal. 3-47987
 Fornax dwarf galaxy, photometric obs. of clusters 3-59370
 Fraunhofer lines, central intensity oscillations, effect of progressive sound wave (*Russian*) 3-76966
 G and K giants calibration of luminosity criteria by trigonometric parallaxes 3-77059
 galactic centre, high velocity neutral H₂ features, spatial and velocity distrib. 3-48109
 Galactic H II regions H α Fabry-Perot spectrometry 3-77162
 galactic nebulae at $|b| > 20^\circ$, H β photometry 3-56452
 Galactic supernova remnants, optical photographic atlas of 23 objects 3-81094
 galactic X-ray sources, X-ray absorption and optical extinction in interstellar space 3-59363
 galaxies, absolute luminosities rel. to magnitude difference of brightest red and blue stars 3-70017
 galaxies, BVR photometry and Galactic reddening rel. to latitude 3-70005
 galaxies, BVR photometry of rich clusters and sparse groups 3-70006
 galaxies, Byurakan classification 5 for central parts of 87 bright objects (*Russian*) 3-45170
 galaxies, central condensations in E and SO-type objects, classifications (*Russian*) 3-45169
 galaxies, distant clusters, red shifts of H and K lines 3-77146
 galaxies, emission-line, spectrophotometric obs. of 3 objects 3-59369
 galaxies, radius parameter and surface brightness as function of total magnitude for clusters 3-77131
 galaxies, spectral energy distrib. in 3500-5530 Å range 3-48102
 galaxies, surface photometry, comparison of parameters of southern galaxies measured at Cordoba and Mt. Stromlo 3-48112
 galaxies identified with 4C radio sources, redshifts for 51 objects 3-51382
 galaxies redshifts for nine objects below declination 60° S 3-48087
 galaxies with bright nuclei, optical obs. of M81 and NGC 4594 rel. to stellar content and metal abundance 3-42225
 gegenschein obs. from Pioneer 10 imaging photopolarimeter 3-45074
 geodesic direction azimuth from obs. of stars at the first vertical (*Russian*) 3-73568
 Giacobinids 1972, crepuscular meas. (*French*) 3-81007
 globular clusters, search for new planetary nebulae, H α observations 3-45229
 RS Gruis, photometric obs. 3-65898
 H_{II} 1069, UV Ceti-type star behind Pleiades, spectral obs. 3-45138
 H_{II} 230, UV Ceti-type star behind Pleiades, spectral obs. 3-45138
 HD153919 (=2U 1700-37), spectroscopic obs. 3-61815
 HD173219, periodic Be star, spectroscopic obs. 3-61813
 HD187399, binary, spectroscopic obs. 3-61812
 HD 122563, N abundance of very metal-poor star 3-81091
 HD 126983, double line spectroscopic binary, orbital obs. from coude spectra 3-77090
 HD 144941, H-deficient star, Coude spectrograms and abundance analysis 3-48027
 HD 153919 (=2U 1700-37), photoelectric UVB obs. of optical variations 3-81133
 HD 213389 variable Ca II emission binary 3-56394
 HD 217312, spectroscopic binary, B photometry 3-77103
 HD 51418, peculiar A-type star, spectrum and light var. 3-69956
 HD 77581, optical counterpart to 2U 0900-40, X-ray source 3-56415
 HD 92740, WR spectroscopic binary, radial vel. meas. 3-48054
 HD 96446, H-deficient star, fine anal. 3-56393
 HD 98088, Ap star, photoelec. obs., light variation (*German*) 3-81100
 105 Her K4 II star, physical parameters, anomalous abundance of lithium (*Russian*) 3-77096
 Hercules X-1 (HZ Hercules), nature of optical variability 3-61818
 HZ Herculis, 'on' and 'off' eclipse phenomena, photographs, 1890 to 1972 3-48075
 AH Herculis, high-speed photometry of dwarf nova, light curve analysis 3-45116
 HZ Herculis, optical pulsations 3-61801
 HZ Herculis, search for optical pulsations at period of Hercules X-1 X-ray pulsations 3-61817
 88 Herculis, shell star, fading of spectral lines (*French*) 3-77088
 88 Herculis, spectrum variability of shell star 3-61809
 HZ Herculis (Hercules X-1), optical obs. 3-59365
 BD Herculis using 162 mm Merz comet telescope at Kazan observatory (*Russian*) 3-73519
 HR 1287, δ Scuti type, blue photometric obs. discrepancy in fundamental frequency 3-77087
 HR 7275, possible variable Ca II emission binary 3-56394
 HR 7955, spectroscopic binary, high-resolution spectra 3-48029
 HR 8703, variable Ca II emission binary 3-56394
 IC429A, most extreme Seyfert galaxy, line profiles 3-48095
 IC 4756, open cluster, determ. of membership probabilities from proper motions 3-48098
 image quality, effect of atmospheric temp. and vel. fields 3-61888
 interstellar ⁷Li detection in spectrum of Ophiuchi 3-73548
 interstellar clouds, Copernicus' spectrophotometric obs. of molecular lines 3-48117
 interstellar clouds, determ. of CaI absorpt. and electron densities 3-65933

visible astronomical observations continued

- interstellar clouds, search for H α emission 3-48115
 interstellar CO+/CO abundance ratio determ. 3-59380
 interstellar matter, visual opacity from gas-dust ratio 3-81170
 interstellar medium, faint optical emission line obs. 3-45216
 interstellar molecular H, Copernicus satellite obs. 3-48116
 Io, post eclipse brightening, review 3-69859
 Io, post eclipse brightening (June 25 1971) 3-69860
 Iris, astrophysical position determ. 3-45051
 irregular variable stars, obs. of H α emission profiles 3-73492
 Juno, astrophysical position determ. 3-45051
 Jupiter, occultation of β_1 Scorpii, photometric obs. 3-45035
 Jupiter, polarimetric obs. between 0.37 and 0.80 μ 3-61694
 Jupiter, positional obs. for 1965-1967 period (*French*) 3-80985
 Jupiter, south equatorial belt disturbance, June 1971 initial development 3-65744
 Jupiter, spectroscopic obs. at 8000-3000 cm⁻¹, search for minor atm. constituents 3-69891
 Jupiter's Galilean satellites, narrow-band photometry in 0.3-1.1 microns range 3-69855
 Jupiter's Galilean satellites, spectral albedos from 0.36-3.4 micron photometry 3-69856
 Klemola 30, interconnected group of galaxies, slit spectra obs. 3-65922
 L726-8 main seq. visual red dwarf binary, orbit and mass determ. 3-77086
 EV Lac, spectrophotometric observation of flares, energy distribution in spectra (*Russian*) 3-77095
 BL Lacertae, BV obs. and bibliographic informations (*French*) 3-73514
 BL Lacertae, deep integration prints of compact galaxy 3-42235
 10 Lacertae, O-type star, rapid spectral variations 3-45134
 BL Lacertae, photographic and photoelectric obs. of optical variability 3-81095
 EV Lacertae polarimetric obs., blue region (*Russian*) 3-45113
 ϵ Leonis, G-type giant, model atmospheres and high dispersion spectrograms 3-48051
 light pollution, high pressure Na lamps, concern to astronomers 3-76778
 LMC, photographic photometry of H α emission-line stars 3-48101
 lunar disk albedo, statistical distrib. 3-61721
 lunar eclipse, 1972 January 30, photoelectric obs. 3-45043
 lunar eclipses 1971, 6 August, photoelectric and visual obs. 3-69897
 lunar occultations, photoelectric meas. of timings 3-61710
 lunar range meas. using laser system 3-42177
 lunar transient phenomena, three colour blink technique, image orthicon TV system 3-47943
 UV Lyncis, W Ursae Majoris star, UVB photometry and photometric orbit 3-65895
 α Lyra, energy distrib. and continuous spectrum in 2000-3800 Å range 3-73509
 β Lyrae spectra, variation of H and He lines (*Russian*) 3-45128
 RR Lyrae stars in Baade's field near NGC 6522 globular cluster 3-59374
 RR Lyrae variables in globular cluster M5, long-term amplitude changes 3-48010
 RR Lyrae variables near S. Galactic Pole, photometric obs. of 4 objects 3-61778
 RR Lyrae-type stars in globular cluster M22, metal abundance from equivalent width meas. 3-45196
 M20, kinematics from H α , N II 6583 Å, and O III 5007 Å line profiles 3-70039
 M20, shock front structure and interaction of ionised gas with absorption lanes from S II lines 3-77161
 M29 (NGC 6913), galactic cluster V photoelectric obs. of 3-61847
 M2-9, planetary nebula, spectral obs. 3-56456
 M31, spectrophotometric obs. of central region 3-56432
 M31, variables 5 and 9, periods for two RR Lyrae-type stars 3-42202
 M33, radial vel. field of neutral H 3-61848
 M35, open cluster, UVB photometric obs. 3-73542
 M87, energy distribution of jet ejected from nucleus, using optical and i.r. emission 3-61852
 M8, kinematics from H α , N II 6583 Å, and O III 5007 Å line profiles 3-70339
 M8, shock front structure and interaction of ionised gas with absorption lanes from S II lines 3-77161
 M92, G-band anomaly of asymptotic-branch stars, CH abundance 3-51381
 M 42, photography with naturally-cooled emulsion at -35° C 3-65949
 M-type giants at South Galactic pole, radial velocities and spectra of 30 objects 3-42233
 M-type supergiants, photospheric and circumstellar H α profiles 3-53661
 Maffei 1 and 2, interstellar observation 3-51370
 Magellanic Cloud clusters, photometric obs. of integrated light 3-59370
 Magellanic Clouds, supernova remnant discovery 3-61839
 magnetic stars, obs. with universal reflecting, telescope, Tautenburg 3-48149
 Markarian 132, absorption lines in coude spectra using integrating television scanner 3-77117
 Markarian 132, QSO, absorpt.-line spectrum 3-59356
 Markarian 6, peculiarities of spectra and physical properties of nucleus of galaxy (*Russian*) 3-45174
 Markarian 6, spectroscopic obs. of galaxy with UAGS spectrograph and new image-tube (*Russian*) 3-45168
 Markarian galaxies, spectral obs. of 16 objects 3-73538
 Markarian galaxies, UVB obs. 3-65923
 Mars, analysis of Mariner 9 occultation data 3-61708
 Mars, charts based on Mariner 9 TV photos 3-80994
 Mars, eolian deposits and dunes, Mariner 9 obs. 3-65757
 Mars, geologic map from Mariner 9 photographs 3-65748
 Mars, Mariner 9 obs. of cratering 3-65754
 Mars, Mariner 9 obs. of north polar region 3-65760
 Mars, Mariner 9 observations, volcanic structure, CO₂ and water ice crystal clouds 3-47903
 Mars, Mariners 6 and 7 obs. 3-56338

visible astronomical observations continued

- Mars, O I day airglow emissions of 5577 and 6300 Å lines 3-65742
 Mars, obs. by Mars 2 and 3 satellites 3-56337
 Mars, photographic obs. (1963 to 1967) (*Russian*) 3-61678
 Mars, polar regions, Mariner 9 evidence of wind erosion 3-61687
 Mars, regional contrasts, time variations, blue light obs. 3-69861
 Mars, surface albedo features rel. to topography 3-59268
 Mars, traditional albedo features rel. to Mariner geologic map 3-65746
 Mars, yellow cloud prod. mechanism and nature (*French*) 3-80989
 Mars' volcanic features, Mariner 9 obs. 3-65750
 Mars south polar cap seasonal variations (1971 July 18 to Sept. 5) 3-69882
 Mars south polar region, Mariner 9 albedo map 3-69874
 Martian atmosphere, Mariner 9 Extended Mission TV results 3-69865
 Martian cartographic products from Mariner 9 mission 3-69873
 Martian maria in equatorial zone of southern hemisphere, spectral values of contrast (*Russian*) 3-73450
 Martian polar regions, Mariner 9 obs. of layered deposits 3-65761
 Martian south polar pits and etched terrain, Mariner 9 obs. 3-69863
 Martian surface, Mariner 9 evidence of wind erosion 3-65756
 Martian surface, Mariner 9 obs. of debris mantle distrib. 3-65755
 Martian surface coordinates, methods and Mariner 9 results 3-69870
 Martian topography, Mariner 9 analytic photogrammetry 3-69872
 Martian variable features, Mariner 9 global results 3-65759
 Me type dwarfs, models for periodic variations, spot model 3-73498
 Medusa Nebula (A21), interferometric obs. 3-53715
 meridian-circle star obs., differential star catalogue compilation by computer input 3-53634
 Method of Dependences, accuracy of plate reductions (*French*) 3-65947
 Milky Way fields, photoelec. UVB photometry, space-density function, distrib. of interstellar matter 3-81177
 ST Monocerotis, Mira-type variable, UVB magnitude sequence 3-45136
 moon, black spots, reflectivity and radio backscatter, comparison with surface structure and composition 3-77005
 Moon, meridian obs. of orbital elements, corrections to Watt's charts (*Russian*) 3-77002
 moon, monochromatic phase waves and albedos determ. 3-45042
 Moon, occultation of 139 Tauri, position of centre determ. 3-65790
 Moon, surface composition, remote optical analysis 3-65802
 Moon megalithic lunar observatory, Ring of Brogar 3-65613
 Mt. Lemmon, optical seeing tests at astronomical observatory site 3-69566
 MWC 349, optical, radio and i.r. obs. 3-73520
 MWC 349, radio star, photoelectric obs. 3-61802
 MWC 645, spectra and energy distrib. rel. to η Carinae 3-42195
 MWC 819, spectra and energy distrib. rel. to η Carinae 3-42195
 nearby stars, revised parallaxes for 10 objects 3-48007
 NGC 1068, Seyfert galaxy, obs. of emission lines 3-56422
 NGC 1265 (3C 83.1 B), peculiar morphology of outer regions from deep photographs 3-42226
 NGC 1300 barred spiral, UVB photoelectric drift scan 3-77133
 NGC 1566, Seyfert galaxy, luminosity distribution, long and short-exposure photographs 3-48105
 NGC 1850, globular in LMC, B,V obs. 3-56434
 NGC 185-1, planetary nebula in elliptical galaxy, chemical abundances 3-45231
 NGC 205, galaxy, structure determ. from UVB obs. 3-61838
 NGC 2237-2246 (Rosette), obs. of gas motions in central cavity 3-51398
 NGC 2264, spectroscopic obs. of u.v.-excess stars 3-56419
 NGC 2477, open cluster, photometric obs. 3-56429
 NGC 2782, galaxy with hot spot nucleus, comparison with Seyfert galaxies 3-61851
 NGC 3516, Seyfert galaxy, H α line profile 3-56427
 NGC 3603, giant H II region, nature of luminous central object 3-51399
 NGC 4151, Seyfert, upper limit to ang. diameter 3-56421
 NGC 4254, spiral arm patches, dimensions, absolute magnitudes, colour characteristics (*Russian*) 3-77142
 NGC 4314, galaxy, photometric obs. of bar 3-61837
 NGC 5194, galaxy, spectral characts. of red and blue spiral arms 3-45192
 NGC 5194, spiral arm patches, dimensions, absolute magnitudes, colour characteristics (*Russian*) 3-77142
 NGC 5195, Sc spiral, stellar content determ. by spectroscopy 3-56424
 NGC 520, irregular galaxy, spectroscopic obs. 3-73537
 NGC 5548, Seyfert galaxy, H α line profile 3-56427
 NGC 628, spiral arm patches, dimensions, absolute magnitudes, colour characteristics (*Russian*) 3-77142
 NGC 6352, metal-rich globular cluster, UVB meas. 3-56418
 NGC 6445 (p-k 008 + 03¹), irregular ring nebula, spectrophotometric study 3-56451
 NGC 6778, planetary nebulae, line identifications 3-61874
 NGC 7027, obs. of high-n Balmer transitions 3-53714
 NGC 7027, planetary nebula, relative line intensities in spectral range 3000-5000 Å 3-45228
 NGC 7031, open cluster, photometric obs. 3-73544
 NGC 7293, planetary nebula, meas. of ang. expansion rate 3-45233
 NGC 7293, planetary nebulae, trigonometric parallax determ. for central star 3-45234
 NGC 7332, galaxy, vel. dispersion determ. 3-56428
 NGC 7469, Seyfert galaxy, internal motions and nuclear mass 3-56423
 NGC 7720 (3C 465), peculiar morphology of outer regions from deep photographs 3-42226
 night sky radiation, obs. of linearly polarised radiation in anti-solar hemisphere 3-61753
 night sky radiation in u.v. and visible, Kosmos 51 and 213 obs. in space (*Russian*) 3-44878
 night sky radiation in u.v. and visible kosmos 51 and 213 observations in space (*Russian*) 3-44877
 night sky surface brightness meas. in 1500-4250 3-53701
 nightglow stellar component in B wavelength band 3-61794
 non-stationary galaxies, obs. with universal reflecting telescope, Tautenburg 3-48149

visible astronomical observations continued

- North American Nebula, variations in ratio of H α abd [N II] lines 3-56453
 Nova Cephei, 1971, photometry, light variations, estimation of photometric distance 3-81101
 novae and supernovae explosive phase characts., Asiago obs. (*Italian*) 3-59345
 NP 0532, optical pulsations rel. to detection of pulsed high energy gamma rays from Crab Nebula 3-48074
 NP 0532, optical timing obs. 3-53686
 nuclei of bright galaxies, UBVKHKL obs. 3-51387
 OB supergiants, meas. of strength of He I 6678 Å line 3-65883
 southern open clusters, UVB-H β photometry of 28 objects 3-65925
 ρ Ophiuchi dark cloud, obs. of interstellar dust in cloud 3-51400
 OQ172, second QSO with $z > 3$, Lick obs. 3-45207
 Orion cluster, radial rel. determ. 3-45197
 Orion Nebula, O underabundance meas. 3-56454
 Orion Nebula, obs. of high-n Balmer transitions 3-53714
 Orion Nebula, obs. of linear polarisation 3-73552
 Orion Nebula, OII brightness and HCHO radio emission rel. to globules 3-61865
 Orion Nebula Cluster, motions of 14 member stars 3-51380
 Orion Nebula cluster, spectroscopic obs. of u.v.-excess stars 3-56419
 α Orionis, speckle interferometry, colour-depend. limb darkening 3-48031
 γ Orionis B, ^3He content in atmosphere from coude spectrogram 3-81099
 outer planets and satellites, imaging techniques 3-48160
 Padova and Asiago Observatories, astrometric programs (*Italian*) 3-61886
 peculiar and luminous bright stars, spectral classification 3-77068
 AG Pegasi symbiotic binary model, M giant absorption spectrum 3-81090
 Pelican Nebula, variations in ratio of H α and [N II] lines 3-56453
 penumbral intensities, scattered light, correction method 3-61891
 β Persei (Algol), optical and radio determ. of position 3-81102
 Perseid meteors, variations in distribution and physical properties 3-81002
 PHL957, system A absorption spectra in H I cloud 3-81203
 PHL 938, absorption spectra, search for high ionisation redshift systems 3-77116
 PHL 957, absorption spectra, search for high ionisation redshift systems 3-77116
 Phobos, Mariner 9 TV obs. 3-69866
 using photoelectric scanning photometer (*German*) 3-77190
 photographic zenith tube obs., semi-diurnal tidal effects 3-50952
 photographs using Kitt Peak 158 inch reflector 3-70025
 photography with naturally-cooled emulsion at -35°C 3-65949
 phosphore, C₂, CH, CN, MgH, NH and OH molecular lines and oscillator strengths 3-69829
 κ Piscium, spectrovariable, spectral anal. 3-59350
 PKS 0237-23, absorption spectra, search for high ionisation redshift systems 3-77116
 planetary nebula formerly designated as Wray 1876, Be' star 3-53716
 planetary nebulae, expansion velocities in six old objects, O III 5007 Å line profiles 3-45232
 planetary nebulae, identification of 20 objects within elliptical galaxies 3-45230
 planetary nebulae, optical positions for 153 objects 3-45227
 planetary nebulae, radial velocities 3-77167
 planetary nebulae, recognition, colour photography, anomalous images, visual examination 3-81056
 planetary nebulae, search in globular clusters for new objects, H α observations 3-45229
 planetary nebulae in Local Group galaxies NGC 185, NGC 205 and NGC 221, identifications 3-70045
 Pluto, polarization curve 3-80981
 point light source, detection probability rel. to stellar magnitude and sky brightness 3-51418
 Praesepe cluster stars, luminosity functions 3-61793
 pulsars, optical, search in extragalactic supernovae 3-65909
 QSO 1331 + 170, absorption line spectrum in visible and near i.r. 3-69982
 QSO historical light curves rel. to optical variability of 20 objects 3-48063
 QSOs, search in direction of Abell clusters of galaxies 3-69983
 radioresources, optical identification by coincidence of radio and optical positions 3-77107
 radioresources, optical identification problems 3-81108
 rapidly fluctuating variable stars, early visual detection 3-53658
 red giants in M 5, M 10, M 92, spectral anal. 3-53702
 red stars, recognition, colour photography, anomalous images, visual examination 3-81056
 Rosette Nebula, obs. of gas motions in central cavity 3-51398
 Royal Greenwich Observatory Time and Latitude Service for 1972 July-September 3-61756
 RZ Cancri unstable eclipsing giant system 3-69967
 FG Sagittae, observational evidence of thermal pulse in old planetary nebula 3-69960
 FG Sagittae, symmetrical emission nebulosity expansion 3-70044
 SAO 76530, 4 August 1972, grazing occultation 3-65897
 Saturn, 0.62 μ methane band absorpt. and near-u.v. characts. 3-61695
 Saturn, astrolabe obs. during 1971-72 winter (*French*) 3-56336
 Saturn, cloud layer and overcloud atmosphere by photographic obs. between 3620 and 6250 Å (*Russian*) 3-76988
 Saturn, H quadrupole lines in (3-0) and (4-0) 3-80984
 Saturn's rings, effective optical thickness and dark-side illumination 3-42139
 Saturn's rings, photographic obs. (*French*) 3-56340
 SBC galaxies, multicolour photometry (*Russian*) 3-45206
 SCL galaxies, radial velocity distrib. of 74 objects 3-70016
 S Sculptoris, long-period Me variable star, spectral Tc lines 3-45133
 δ Scuti stars, search among nearby A and F-type stars 3-65886
 SEG stars, radial velocities and Scorpius X-1 distance 3-45094
 setting errors in obs. of disc-shape objects 3-59397
 Seyfert galaxies, photoelectric UVB obs. beyond nucleus 3-77149

visible astronomical observations continued

- Seyfert or Seyfert-like galaxies, historical light curves rel. to optical variability of 3 objects 3-48063
 Shajn 147, supernovae remnant, radial vel. meas. 3-61797
 sky illumination at Blue Mesa Observatory 3-47718
 SN 1970-1 obs. at Asiago (1970-1) 3-73516
 SN 1970j, obs. at Asiago (1970-1) 3-73516
 SN 1971-g, obs. at Asiago (1970-1) 3-73516
 SN 1971-i, obs. at Asiago (1970-1) 3-73516
 SN 1971-l, obs. at Asiago (1970-1) 3-73516
 solar arch filament systems, H α structure, mag. structure 3-65709
 solar chromosphere, mottles near limb, H α contrast profiles 3-65652
 solar chromospheric H α features—type III bursts assoc. 3-45027
 solar chromospheric H α mottles, high-resolution photography 3-65651
 solar corona, fast transient events in green coronal emission line 3-80949
 solar corona photography, early daylight attempts 3-65634
 solar coronal emission line at 5303 Å, height gradient 3-61658
 solar coronal Fe XIV 5303 Å line, linear polarisation meas. 3-45001
 solar coronal helmets, evolution during solar cycle 20 ascending phase 3-65713
 solar diameter determ. at 5000 Å and H α from photoelectric drift scans 3-65653
 solar differential rotation determ. from optical, radio and interplanetary data 3-65697
 solar eclipse, 1973, June 30, obs. 3-73447
 solar eclipse, June 30 1973 3-80977
 solar eclipse of 1972, July 10, report of observation from arctic circle 3-76983
 solar eclipse of 1972 July 10, F corona and inner zodiacal light obs. 3-47881
 solar eclipses, total, obs. from fixed station on Earth 3-65718
 solar flare, 1972, August 7, 3643-8542 Å spectrograph obs. 3-80956
 solar flare 1972 Aug. 11 event 3-65684
 solar flare of 1961, July 12, metal lines and emission region properties 3-76985
 solar granulation, cinematography using red continuum filtergrams 3-80951
 solar isotopic composition, photospheric and sunspot spectra, atomic line studies 3-61672
 solar loop prominences of August 1972, magnetic field obs. 3-80939
 solar loop structures, coronal graded height spectra and filtergrams 3-80959
 solar Mg I 4571 Å line, one-dimensional approx. to macroturbulent velocity field 3-80937
 solar moustaches, H α filtergrams and H α spectra 3-65706
 solar Na D₂ line profile inversion 3-73442
 solar photosphere, sunspots for 1971, Polish observations 3-73441
 solar photosphere filament feet positions determ. rel. to supergranular Ca network 3-65669
 solar secular parallaxes and space velocity from stellar proper motions rel. to galaxies 3-76987
 solar speckle interferometry, sunspot spatial freq. 3-59256
 solar spicules, morphological study 3-65676
 solar supergranular cells, H α line profile 3-65677
 solar surface, optical heterodyne radiometry 3-61654
 Southern OB stars, determ. of projected rotational vel. 3-53657
 spectral reflectivity difference detection, isoluminous additive colour method, lunar orbital multispectral photography 3-45517
 spherical lenses, obs., information and optical synthetic aperture 3-66907
 spiral galaxy nuclei, optical properties and ionisation mechanism 3-77137
 star catalogues, spectral analysis of right ascension errors 3-53633
 stars, circumzenith and refraction pairs, International Latitude Station obs. 3-77033
 stars, double beam photon-counting spectrometer, high resolving power (Russian) 3-45242
 stars, ten-colour intermediate band photometry of 148 stars 3-65884
 stars near Orion nebula, nine-colour photometry and i.r. excesses 3-69952
 stellar absolute proper motion rel. to SA 32 galaxies and reference stars 3-77075
 stellar and telluric absorption lines, accurate wavelengths near 7000 Ångströms 3-48018
 stellar apparent diameters, interferometric meas. (French) 3-70065
 Stephan's Quintet of interacting galaxies, H II region and supernova obs. 3-70004
 Sun, airborne white light photometry of outer corona during 1972, July 10 eclipse 3-47882
 Sun, Ca XV 5694 Å line obs. of active regions 3-76968
 sun, H β line obs. of active limb prominence 3-65659
 Sun, limb darkening at extreme solar limb during 1972, July 10 eclipse 3-47883
 Sun, photospheric quasiperiodic wavelike motions, direct spectroscopic meas. 3-53613
 sun, umbral spectra, determ. of Ti abundance 3-65716
 sunspot 6610-6770 Å spectra, line identification 3-45002
 sunspot fine structures, morphological and photographic study of H26 spot group (French) 3-45020
 sunspot penumbral intensity obs. 3-65702
 sunspot umbra physical parameters, 5600 to 6300 Å (Russian) 3-76977
 sunspot umbrae, magnetic field intensity rel. to brightness 3-61657
 sunspot umbral cores, 7-colour photometry with Bartol Coude telescope 3-47886
 sunspot umbral Na D₂-5890 Å line, min. intensity meas. 3-65704
 sunspots in 1970, obs. over 268 days (French) 3-61671
 supernova in NGC 5253, light curve, type I indications 3-81103
 supernovae, absolute magnitude determ. for 43 type I objects 3-48012
 tables, azimuth determ. from transits of stars at the first vertical (Russian) 3-73569
 Tago-Sato-Kosaka (1969g), ¹²C/¹³C isotope ratio from spectrogram 3-77010
 Tauri, model for wavelength dependence of polarisation 3-73511

visible astronomical observations continued

- 139 Tauri, occultation by Moon, position determ. 3-65790
 HL Tauri, triply-periodic white dwarf, differential blue magnitudes 3-48043
 28 Tauri (Plejone), new shell phase in spectrum 3-42192
 RR Telescopii, emission line spectrum during 1968 rel. to nova-like properties 3-42196
 threshold brightness as function of location of source in instrument field of view 3-62062
 time and latitude bulletin of Tokyo Astronomical Observatory (July 1972) 3-47978
 time and latitude bulletin of Tokyo Astronomical Observatory (August 1972) 3-47979
 time and latitude service of RGO for 1972 January to March period 3-51321
 Tokyo Astronomical Obs., Time and Latitude Bulletins (September 1972) 3-47980
 Tokyo Astronomical Obs. Time and Latitude Bulletins, 1972, December 3-73428
 Tokyo meridian circle, reduction of observational data (Japanese) 3-70085
 Tom 256, galaxy/quasar-like object, spectrum of extra-nuclear regions 3-45183
 TON 1530, absorption spectra, search for high ionisation redshift systems 3-77116
 (1685) Toro, 0.4-0.8 μ spectrophotometric obs. 3-61734
 (1685) Toro, asteroid, visible and near i.r. spectral reflectivity curve derivation 3-61733
 (1685) Toro, photometric and polarimetric obs. 3-61732
 Trumpler 27, open cluster, obs. of red star 3-61775
 type II cometary tails, particle size distribution and tail orientation at 5-15 AU 3-81003
 2U 0115-73 (=SMC X-1), Sanduleak 160 as optical counterpart 3-73535
 2U 1543-47, late-type irregular variable as optical candidate of X-ray source 3-69997
 UBV photometry of southern stars 3-73505
 UBV-system for a 12 inch telescope, Oslo solar observatory 3-59405
 Uranus, H quadrupole lines in (3-0) and (4-0) 3-80984
 uranus spectrum, molecular H₂, 3-0 band obs. 3-47905
 ν Ursae Majoris, photoelectric light curve determ. 3-45119
 ν Ursae Majoris mass, radii and luminosity from spectroscopic radial velocity obs. 3-69962
 variable stars in γ Comae field, 4 new obs. with Schmidt telescope 3-69966
 variable stars small amplitude red disc and halo population, UBVRI obs. 3-73502
 variable stars WR-96, WR-96(2) and GR-29, photographic obs. (Russian) 3-61806
 Vela X supernova remnant, emission line spectrum 3-81098
 velocity field meas., double magnetograph obs. of active regions (Russian) 3-45009
 velocity fields, mag. fields, brightness meas. (Russian) 3-45008
 γ 2 Velorum, short period spectral variations at 4660 Å 3-48052
 Venus' transits, obs. from Japan, Dec. 9, 1874 event, reviews 3-61700
 α Virginis, β Cephei star, spectral obs. with improved time resolution 3-48035
 CU Virginis silicon Ap-star, H Balmer lines, phase variation (Russian) 3-45129
 Virgo cluster of galaxies, four-colour photoelec. photometry 3-77147
 visual binaries, elements and dynamical parallaxes for ten objects 3-42194
 BW Vulpeculae, β Cephei star, spectral obs. with improved time resolution 3-48035
 white dwarf stars, line profiles and rotation meas. 3-45120
 white dwarfs, spectroscopic data for 41 southern objects 3-69961
 X-ray star optical candidates, Zeeman effect in H β line 3-51352
 zodiacal light, OSO-6 photometric obs. 3-53630
 zodiacal light obs. from ecliptic to poles 3-56369
 zodiacal light perturbation in Earth-Moon system 3-53631
 zodiacal light reinforcement at 100 R₀ from sun, photometric obs. and deductions (French) 3-69913
 Be stars, emission-ring line profile rel. to long-period V/R variation 3-69953
 Ca flocculae on solar surface, structural changes and regularities during Cycle 19 period 3-51268
 Ca II k₁-line obs. of solar 5-minute oscillation, vertical phase var. and mechanical flux 3-80934
 Ca II resonance linewidth-luminosity relations and chromospheric velocity fields 3-69944
 Ca II solar resonance and subordinate lines, correlation analysis from high resolution spectra 3-80941
 Fe I 6065 Å line from stellar atmospheres rel. to meas. of macroturbulence 3-81018
 H II regions, radial velocities from Fabry-Perot interferometry of regions in Cygnus 3-42247
 H α stellar linewidth-luminosity relations and chromospheric velocity fields 3-69944
 Mg II resonance linewidth-luminosity relations and chromospheric velocity fields 3-69944
- vision**
 see also colour vision; eye
 accommodation, accommodative vergence and disparity vergence, freq. analysis 3-65994
 achromatic human, mathematical models of edge-contrast phenomena, review (Russian) 3-48235
 acuity, optimal classification and presentation of optotypes, testing, absolute determinations (German) 3-73582
 adaptation to bifocals 3-51434
 after image, test of Brindley's hypothesis 3-81279
 aftereffect of linear motion, spatial determinants 3-66013
 aftereffect of movement, temporal factors (French) 3-56508
 afterimage visibility of horizontal-vertical illusion as a function of figure orientation and angular separation 3-81297
 afterimages, binocular rivalry and fusion 3-42353
 alert monkey, accommodative vergence, motor unit analysis 3-66008

vision continued

- amblyopic system, visual evoked potential and spatial transfer function 3-51439
- anomalies at low illumination 3-51442
- apparent movement, with subjective contours 3-56514
- Asian 'clawless' otter, underwater vision and visual acuity 3-65991
- astigmatic subjects, nervous alteration study by evoked potential technique 3-66016
- bee ommatidium image detection 3-81290
- Benedetto Castelli's 17th century discourse on vision, translation and comments 3-59510
- binary classification of patterns by humans, experiments (*German*) 3-45305
- binocular, assessment utilising Pulfrich and Venetian blind effects 3-77228
- binocular, fused, refractive error correction method 3-77230
- binocular fusion of moving stimuli, Mach-Dvorak phenomenon 3-51446
- binocular rivalry, frequency analysis 3-51451
- Binocular-masking-level differences in sinusoidal-grating detection 3-81286
- blind rehabilitation programme, Veterans Administration USA, experience with CCTV for low vision patients 3-77229
- brightness contrast, evoked potentials 3-42347
- brightness function, effect of area and duration 3-61901
- Broca-Sulzer phenomenon, spatial factors 3-51435
- cat, on-center retinal ganglion cells, center-surround interactions 3-66006
- cat, on-centre retinal ganglion cells, peripheral responses 3-66004
- cat, retinal ganglion cell, response to moving stimuli 3-66001
- cat, visual cortex, complex and hypercomplex receptive fields, spatial frequency filters 3-77235
- cat, visual cortex, integration of auditory information 3-65992
- characteristics pertinent to displays 3-70131
- children in hypnotic sleep, electroretinographic investigations 3-61907
- cognitive, visual recognition/detection, symposium, USA 1973 3-70121
- complex stimuli, production technique 3-65989
- contrast modulation, h.f. grating detected against l.f. background grating 3-81280
- contrast using evoked potentials (*Italian*) 3-56522
- Contrast-modulation threshold as a function of spatial frequency 3-81283
- corrective saccades and visual inflow during prior saccade 3-81295
- crustacean visual system, spatial integration, peripheral and central sources of nonlinear summation 3-77232
- crustaceans, long term adaptation by monochromatic light 3-66000
- dark-adapted retina, broad- versus narrow-band filters at absolute threshold 3-51437
- dazzle of one eye, influence on state of adaptation of other eye in normal subjects (*French*) 3-51445
- de-Lange characteristics, freshwater turtle and pigeon, temporal modulation transfer functions, comparison 3-77233
- diagnosis, ophthalmological, electric stimulation of retina, excitability, method (*German*) 3-65997
- difficulties, surroundings conditioned, eye sequence investigation method, elucidation (*German*) 3-70116
- disability glare factor estimate, influence of depth-of-field of eye 3-51440
- distribution coding in visual pathway 3-48248
- double Purkinje image eyetracker, electronic image stabilisation 3-81299
- early dark adaptation, area effects and rapid threshold decrease 3-45311
- early receptor potentials, summary of parameters 3-51436
- e.e.g. peak-to-peak amplitude variability compared to visual performance variability 3-51438
- electroretinogram of white mice, effect of parathion (*French*) 3-42357
- extended border enhancement during intermittent illumination 3-56507
- eye movements during fixation on stationary target, stochastic model 3-45304
- figure and ground, neurophysiological basis 3-81296
- flies, head movement during visually guided flight 3-45310
- flies, visual nervous system, development and applic. of white-noise modelling techniques 3-45307
- foveal increment thresholds, multiple flashes, TEpee effect 3-51433
- frog's visual analyser, information processing principles, model of novelty neurons (*Russian*) 3-48241
- frog rods, dark adaptation, isolated retina 3-77243
- goat retinal ganglion cells, receptive fields and topographical organization 3-51448
- grating and line detectors, orientational selectivity 3-66003
- grating pattern, detection of spatial changes of contrast 3-81281
- human, stimulus specificity, test gratings of variable contrast, orientation, spatial frequency, results 3-77237
- human and animal visual analysers, neural network model (*Russian*) 3-48237
- human brain, abnormal early visual experience effect on visual pathways 3-59421
- human central fovea, sensitivity variations, eigenvectors, measurements 3-77234
- human foveal cone, Stiles-Crawford effect explanation 3-51449
- human monocular field of view during motion of visual axis, analysis (*Russian*) 3-48236
- human monocular perception, mathematical models (*Russian*) 3-48239
- human scotopic luminosity fns., determ. with optokinetic systagmus 3-42354
- human visual perception mechanisms, mathematical model of image-edge intensification (*Russian*) 3-70120
- human visual receptive field, optic-electronic model of local detectors of visual analyser (*Russian*) 3-70129
- human visual vibrational analyser, hybrid computer investigation of model (*Russian*) 3-48243
- image intensifier aided, effect of noise on visual detection threshold 3-61900

vision continued

- increment thresholds, for striped and uniform test fields 3-42346
- increment thresholds for multiple identical flashes in peripheral retina 3-81289
- insect visual system, fundamental mechanism of motion detection 3-45306
- kitten visual cortex, short-term stimulus-induced changes in connectivity 3-73585
- laser speckle, to determine ametropia and accommodative response of eye, comment 3-77240
- line, edge and grating detectors, spatial arrangement 3-66002
- linear summation of spatial harmonics 3-66011
- living systems, visual information model (*Italian*) 3-56524
- low spatial freq. sine wave targets, visibility 3-81285
- luminance-duration threshold relationship under monocular and binocular viewing conditions 3-61904
- Mach bands, physiological, in Limulus eye 3-81293
- man, contrast evoked responses 3-65995
- model relating stabilised retinal image (*Japanese*) 3-70126
- monkey's cone receptor potential, slowed decay by intense stimuli and protection by light adaptation 3-61905
- monkeys, deficits in visual acuity and spectral sensitivity rel. to laser irradiation 3-42360
- monkeys rod receptor potential, photopic suppression by cone-initiated lateral inhibition 3-66012
- monocular field-of-view physical space/subjective transformation, mathematical model (*Russian*) 3-70119
- monocular versus binocular, design of instruments for visual task evaluation 3-70115
- movement detectors sensitive to direction of contrast 3-61909
- movement perception, during voluntary saccadic movements 3-56510
- moving objects in peripheral visual field, apparent contraction and disappearance 3-42352
- mudpuppy, retina, rod and cone sensitivity, intracellular recordings 3-73589
- neural inhibition, contrast effects, visual sensitivity 3-42351
- nonlinear response process, thresholds of spatial beat freqs. 3-56506
- normal fixation of eccentric targets 3-42348
- numerical system, monocular perception, metrical properties of field of vision (*Russian*) 3-48242
- oculomotor system, human, movements for stationary and moving targets, characteristics, signal and noise 3-77239
- oculomotor tracking, two dimensional, recognition of component differences 3-77236
- optical illusions, interpretation of psychophysical experiment by systems theory methods 3-45308
- Optical Soc. America meeting, Rochester, N.Y., USA(1973) 3-77430
- Optical Society of America, conference, Rochester, USA (1973) 3-77431
- optical-aids, interaction, image evaluation methods 3-70117
- parafoveal recognition of single words, visual interference 3-42356
- perceived spatial frequency, temporal determinants 3-81284
- perceptual structure of Necker cube 3-53742
- peripheral visual response, effect of passive 70° head-up tilt 3-73583
- photoreceptors, absorption in conical optical fibres 3-48246
- plane images, normalisation of rotation, interference effects (*Russian*) 3-48240
- primate cones, temporal response characteristics 3-81294
- rabbit, development of visual cortex, late appearance of a class of receptive fields 3-73590
- rabbit, receptive-field characteristics of superior colliculus neurons after cortical lesions 3-77238
- Raman, spatial frequency channels and threshold for adaptation 3-61906
- random visual textures, production technique 3-65990
- receptive field size and acuity, invariance with viewing distance 3-61903
- recognition, masking, effects of two dimensional filtered noise, experiments 3-73584
- redundancy reduction of visual information, image preprocessing unit for computer input (*Russian*) 3-70130
- residual visual function after brain wounds involving central visual pathways 3-45309
- response to flash of light, mechanism characteristics 3-70122
- responsiveness, intra-day variations 3-77231
- retina, isolated, frog, recovery of cone receptor activity, gross potential measurements 3-77242
- retinal units of teleost fish, intracellularly recorded responses 3-66017
- saccadic eye movements, generations of muscle force, model 3-53744
- scotopic threshold, rhodopsin bleaching 3-42358
- shape-sensitive adaptation responses, nonlinearity of visual signals 3-66015
- spatial freq. channels, lateral inhibition 3-81291
- Spatio-temporal contrast sensitivities for moving and flickering stimuli 3-81282
- spherical error determ. by laser refraction 3-48244
- square wave gratings, adaptation, third harmonic 3-56509
- stabilized target visibility, fn. of flicker freq. 3-56511
- stars, visibility threshold with unaided eye at different background brightnesses 3-70080
- stereoscopic, cortical eye limitation, disparity scaling 3-73592
- stereoscopic cues, rivalry 3-81287
- stereoscopic depth effects, random dot patterns 3-56519
- stereoscopic effect in films of rotating molecular models 3-61976
- stereoscopic perception of random-dot patterns, figure-in-depth study 3-51450
- stereoscopy, generalised theory for vertical scale exaggeration in contour mapping 3-53884
- Stiles-Crawford effect, additivity for Fraunhofer image 3-81292
- striate cortex, orientation specificity and response variability of cells 3-61908
- subjective patterns in flickering field, binocular versus monocular obser. 3-48245
- temporal facilitation, perceived motion 3-81298

vision continued

- texture density effects, lateral interaction between neural channels 3-73587
- threshold illumination, depend on light distrib. at object 3-65999
- tilt illusion, spatial frequency selectivity 3-70128
- total retinal area, substantial accommodation 3-51444
- tracking tasks, interaction between horizontal and vertical eye-rotations 3-66014
- visual information transmission, stability (*Italian*) 3-56525
- visual MTF meas. 3-81288
- visual stimulation generator (*French*) 3-56512
- visual stimulus generator, for periodic stimuli 3-56513
- visually evoked responses to pattern stimuli, binocular summation 3-65993
- young children, visual acuity testing 3-70118

visual auroras see aurora

visualisation, particle track see particle track visualisation

vitreous state

- see also glass
- alkali borate + TiO₂ mixtures, fused, acid-based reactions 3-58818
- ardite-hardener mixtures, hardener effect on transition temps., rot. plate method 3-69381
- aromatic hydrocarbons in vitreous media, identification of autoassociated species by absorption spectra (*French*) 3-50590
- binary silicate and borate glass melts, relation of vitron theory to 2 layer-liquid immiscibility 3-63957
- borate glasses, structure theory 3-43757
- di-n-butyl phthalate, in o-terphenyl, supercooled liquid, dielectric relaxation 3-49850
- 9,10-dibromo- and dichloro-anthracene in vitreous solutions, autoassociation study by absorption spectra (*French*) 3-50591
- ethanol, glassy liquid and crystal state, supercooling rate 3-75484
- 6Fe₂O₃ glasses, ultra-fast quenching, binary mixtures 3-72982
- fluorenone, in o-terphenyl and mixed solvents, supercooled liquid, dielectric relaxation 3-49850
- glass-crystalline materials, cast, rupture character 3-47475
- glassy carbon based binary glasses, prep. and characteriz. 3-76246
- ice hydrogen bond spectral shifts temp. depend., vitreous to cubic I phase transformation 3-47262
- insulating oil, polymeric nature, secondary relax. obs. in supercooled state 3-46595
- metallic glasses, bending deform., brittleness 3-41783
- 2,4,6,8,10-pentamethylundecane crystalline and glassy films, i.r. spectra and rotational isomerism 3-47268
- plastic fibres, determ. of strength limit for shearing, anal. method 3-53281
- plastics, glassy, longevity of structures 3-55901
- PMMA, glassy state, cyclically changing temps. effect during subsequent loading 3-55900
- polyethylene, kinetics of high-elastic deform. 3-67881
- polyethylene, multiple transitions, glass temp., low-temp. toughness 3-63962
- polymer, linear, free vol. rel. to temp., expansion coeff. change, vitreous state (*Russian*) 3-71689
- polymeric glasses, residual entropies calc. 3-58137
- polymers, cracking and crazing 3-46672
- polymers, creep 3-46669
- polymers, diffusion and sorption of gases, mechanism 3-46734
- polymers, physics, book 3-46591
- polymers, post-yield behaviour 3-46666
- polymers, relaxation processes 3-46676
- polymers, semi-crystalline, multiple transitions esp. double glass 3-63962
- polymers, structure, packing density, free volume concepts, mech. behaviour 3-46592
- polymers, thermodynamics 3-46718
- polymers, toughening by rubber reinforcement, review 3-47481
- polymers, yield behaviour 3-46665
- random copolyamides, thermal behaviour and H-bonding effects 3-67882
- Rayleigh, Brillouin and Raman scatt. from viscous liquids and glasses 3-80026
- silica, anomalous u.s. absorpt. down to 0.4K, glass tunnelling model 3-79437
- temperature maximum appearance under external radiation 3-60798
- 1,3,5-trinitrobenzene-aromatic hydrocarbon charge-transfer complexes in glassy solns., temperature effects on absorption and fluorescence spectra (*French*) 3-50847
- viscous liquids, glass transition, thermodynamic equations 3-52580
- As-Se-Pb. glass formation (*Russian*) 3-73069
- As₂S₃, glassy, structure obs., γ -irrad. effects (*Russian*) 3-46647
- C, 1800°C processed, lattice struct. 3-60664
- C, glassy, submicroscopic void obs. 3-58737
- C, interatomic bonds thermal transformation 3-40849
- C, static fatigue characts. 3-76365
- C, struct. anal., profile matching 3-68161
- C fibre, manufacture (*German*) 3-76370
- CdAs₂ alloys, thermal conductivity 3-72238
- CdGeP₂, semiconductor, glass-crystal phase transition, NMR of P³¹ (*Russian*) 3-72197
- Fe(ClO₄)₃·6H₂O aqueous soln., frozen, Mossbauer effect, thermal analysis, phase separation 3-41453
- Fe(ClO₄)₃·6H₂O aqueous soln., frozen, Mossbauer effect, thermal analysis, phase separation 3-41452
- Ge-Se semiconductor glasses, mag. susceptibility, temp. dependence, glass-fusion transition (*Russian*) 3-72456
- Li₂O-Fe₂O₃-SiO₂ compositions, magnetic, elec. and physical props. 3-64967
- Li₂O·2SiO₂ glass, apparent viscosity during crystallisation (*Japanese*) 3-68428
- Na bisilicate, packing density calc., relaxation properties (*Russian*) 3-47478
- Ni-glass-ceramic composite material, heat treatment, crystn. of dispersed glassy phase (*Russian*) 3-41799
- P₂Se₃, semiconductor, glass-crystal phase transition, NMR of P³¹ (*Russian*) 3-72197
- Pb₂SiO₄, enthalpy of fusion 3-44659
- Se, sputtered vitreous film, Monte Carlo model of atomic arrangement 3-64264
- SiO₂, diffusion of O₂ 3-76331

Vlasov equation

- continuum eigenfunctions and dispersion function relation of Vlasov operator 3-66481
- geomagnetic tail neutral sheet, prediction of ion plasma oscills. 3-53535
- inhomogeneous phase space fluids, stability problems 3-75348
- initial value problem solution using contraction mapping theorem, rel. to e.m. fields in hot dilute plasmas 3-57949
- Langmuir waves, nonlinear Schrodinger eqn., Vlasov formulation 3-43675
- liquid, collective motion, mol.-kinetic theory 3-68147
- magnetotail current sheet structure model 3-69701
- nonlinear, comparison of Fourier-Hermite and power transform solutions 3-46534
- nonlinear, for weakly turbulent plasma, renormalization of wave-particle interaction 3-43656
- ordinary mode instability, electrons' negative press. effect, using linearized Vlasov-Maxwell eqns. 3-49700
- plasma, relativistic, e.m. wave theory, large amplitude, thermal effects 3-68104
- plasma, three component ionised system, classical kinetic eqns. derivation 3-43653
- plasma, Vlasov-Maxwell operators in self-adjoint form 3-52496
- plasma exact nonlinear waves, family of solns. to Vlasov's equations 3-79072
- plasma fluctuations and nonlinear susceptibilities 3-49641
- plasma high Mach number flows, laminar interactions 3-63826
- plasma in collisionless Q-machine, step-like density perturbations 3-75421
- plasma in constant mag. field, correlation functions calc. 3-79131
- plasma inhomogeneous beams eigenmodes 3-79122
- plasma ion acoustic waves study 3-79142
- plasma nonlinear quasi-monochromatic waves amplitude modulation theory 3-79091
- plasma nonlinear wave interaction and fluctuations 3-49706
- plasmas, two-dimensional collision-free, stability 3-75412
- slanting shell theory, soln. (*Russian*) 3-62472
- two-fluid eqns. numerical integration calc. for mag. pulse anomalous penetration 3-46536
- weakly turbulent plasmas, oscillation centre quasilinear theory 3-63839

voice see speech

voids (solid)

- alloy, neutron irrad. creep during void form. 3-40939
- anthracene crystal strained during cooling submicroscopic voids 3-69008
- brass, free-machining, hydrostatic press. depend. of tensile fracture, void development 3-80292
- BWR core, varying hydrogen-to-metal ratio, criticality study, various temps. and void conditions 3-49335
- cladding materials, void nucleation suppression by vacancy trapping mechanism 3-63200
- defect superlattice form., elastic interaction theory 3-54957
- fast reactor core composition, systematic optimisation, integral reactor parameters, void reactivity 3-63226
- films, amorphous, growth instabilities in deposition 3-55173
- flux synthesis calculations, fast reactors, control rod and sodium voiding worths 3-63115
- gas-filled, equil. shape 3-68241
- glass, organic, yielding of two-dimens. void assembly 3-58735
- irradiated materials, growth, swelling and termination of voids with high temp. high dosage 3-79336
- metal, irrad., void nucleation kinetics, impurity effects 3-64072
- metal, neutron irrad. creep during void form. 3-40939
- metal, with voids, vacancies and surfaces, positron behaviour 3-46808
- metal formation during wear, delamination theory 3-72129
- metallic thin films, defect effects 3-75633
- metals, lower and upper irradiation temp. limits 3-68242
- oxide nuclear fuel, vacant space distribution analysis during irradiation (*German*) 3-71322
- point defects, diffusion towards voids, grain boundary, screw dislocation, computer code, DEPORT 3-64032
- polystyrene, craze morphology rel. to shear-band morphology 3-58732
- silica-reinforced composites, surface ablation void fraction effect 3-80438
- stainless steel, cold-worked, neutron irradiated, effect of irradiation temp. 3-68289
- stainless steel, Young's modulus, effect of neutron irradiation-induced void formation 3-68310
- steel, fast reactor, formation by ion bombardment 3-71284
- steel, sintered, microvoid coalescence rel. to fracture-resistance 3-69307
- steel, stabilised, voiding ratio meas. following irradiation by neutrons and C⁺ ions (*German*) 3-71303
- steel, stainless, nickel ion bombardment, gross swelling direct meas. 3-40540
- steel, stainless, Type 304, Ni ion bombardment, void swelling behaviour 3-46139
- steel, stainless, Type 316, cold-worked, neutron irrad. effects 3-44576
- steel, stainless, Type 316, proton irrad., hydrogen effects 3-46138
- steel, stainless austenitic, void volume swelling rel. to grain size 3-64864
- Al, electrical resistivity calcs. using phase shift and pseudopotential methods 3-44054
- Al, ion irrad., partially-ordered void lattice obs. 3-46650
- Al, neutron irrad. void form., deform. influence (*French*) 3-40940
- Al₂O₃, fracture process and crack struct. 3-72957
- Au film, dislocation loop and void damage after He ion irrad., TEM obs. 3-60733
- B₁₃C₂, void morphologies 3-71282
- C, glassy, submicroscopic void obs. 3-58737
- Cu, irrad. with 500 keV Cu⁺ ions, void form. phenomena (*French*) 3-54986
- Cu-Ni alloys, void form. resist. 3-67547
- Fe-Cr-Ni, electron irrad., solute segreg. to voids, transmission electron microscopy 3-64874

voids (solid) continued

- LiF, macroprobe production due to thermal neutron and electron irradiation (*Russian*) 3-68288
 LiF film, electron irradiated, separation of metallic Li 3-75547
 Mg, electrical resistivity calcs. using phase shift and pseudopotential methods 3-44054
 Mo, irradi., electron diffr. patterns of void and bubble arrays 3-52564
 Mo, neutron irradiated, irradi. temp. monitoring, void superlattice const. meas. 3-68291
 Mo, neutron irradiated, void formation, lower threshold temp. 3-68290
 Mo, reactor irradi., 650°C, damage struct. 3-46649
 Na, electrical resistivity calcs. using phase shift and pseudopotential methods 3-44054
 Nb₂O₅, N⁺ irradi. effect of O impurity on void formation 3-79335
 Ni, irradi. with Ni⁺ ions, swelling phenomena (*French*) 3-58053
 Ni, void form. due to bombardment with 100 keV Ni²⁺ ions (*French*) 3-40942
 Pu, self-irradiation damage obs. by positron annihilation 3-63194
 Si film, amorphous, optical and elec. props., model for effect of voids 3-68629
 β -SiC, pyrolytic, irradi. induced void behaviour 3-63191
 Ta, proton irradi., hydrogen effects 3-46138
 U adjusted, void nucleation behaviour 3-63192
 UO₂ powders, microstruct. evolution during press. sintering 3-78377
 W, neutron irradiated, irradi. temp. monitoring, void superlattice const. meas. 3-68291
 W, neutron irradiated, void formation, lower threshold temp. 3-68290
 Zr and alloys, void formation under irradiation in high-voltage electron microscope 3-78387

Voigt effect *see* **Magneto-optical effects****volatilisation** *see* **vaporisation****volcanology**

- alkaline rocks from Vermont, petrology, Mesozoic alkaline magmatism 3-76522
 Archean rocks near Sioux Lookout, Ontario, granodiorite intrusion period 3-65132
 Atlantic hot spots, relative and latitudinal motion 3-76571
 basaltic magmas, analysis of possible source rocks 3-50914
 Cane Valley diatreme, Utah, carbonate-kimberlite relations 3-53404
 Columbia plateau basalt production rate, K/Ar age data 3-76596
 conical volcanoes, heights and volumes of land volcanoes 3-53423
 cordierite lava, St. Helena, S. Atlantic 3-80586
 Darfur province, W. Sudan, Tertiary to Recent volcanism 3-41888
 descending lithosphere, thermal structure, active volcano distribution 3-76556
 Earth Resources Technology Satellite, earth imaging, appl. to volcano monitoring 3-80852
 earthquake swarms, Volcano Aso, Japan 3-76529
 geothermal state distribution, ground water system 3-76528
 geysers, effects of long-term Earth tidal forces 3-76613
 Great Bear batholith, calc-alkaline volcanism and plutonism 3-76525
 Great Glen fault and timing of granite intrusion on Proto-Atlantic continental margins 3-61339
 Grenville Province, petrology of metavolcanic rocks 3-56022
 Hawaiian linear volcanic chain, seismic array evidence of core boundary source 3-50934
 Heimaey eruptive fissure, distance measurements across shear zone 3-65171
 Iceland, non-primary magmas and mantle plumes 3-53422
 igneous activity rel. to metallic ore deposits and continental drift 3-41883
 igneous rocks near Hedley B.C., K-Ar ages constraints on petrological model for Similkameen batholith 3-76521
 island arc magmas from underthrust lithosphere 3-65223
 island drains, theory of magmatic provinces 3-61332
 late and postglacial volcanics, acid and basic rocks 3-80626
 lava dating, thermoluminescence fading effects 3-76572
 lava flow, geomagnetic polarity changes and duration of volcanism 3-76671
 lava flows in Laacher See, W. Germany geomagnetic and geoelectric mapping of subsurface 3-61589
 lava-water dynamic mixing effects 3-61331
 lavas, palaeomagnetism, palaeosecular variation, Norfolk and Philip Islands 3-76664
 lunar glass, Apollo 15 and 17, orange and green 3-65840
 lunar glass and cinder formation 3-65819
 lunar glasses, orange and green, props. rel. to mare basalts, model 3-65839
 magmas ascending along mid-ocean ridges, temp. and composition 3-61309
 mantle plumes, present population rel. to volcanic records 3-56079
 Mt. Edziza, British Columbia, fission track dating of volcanic glass 3-76515
 nonexplosive submarine volcanism, sofar obs. 3-76569
 Oregon Cascade lava flows study of NRM 3-76672
 palaeomagnetism of volcanogene formations of Carpathian region (*Russian*) 3-65231
 Permian igneous dikes, in Baerum cauldron, petrographical data 3-80641
 pillow lavas, magnetic properties and submarine weathering 3-58862
 popping rocks and lava tubes from Mid-Atlantic rift valley 3-76578
 seismic tremors at S. Italian volcanoes, analysis 3-61363
 E. Sidlaw Hills, Perth., melting relations of calc. alkaline lavas 3-53386
 Soufriere volcano (St. Vincent Island), 1971-72 eruption 3-73234
 South Sandwich Islands volcanic rocks, ⁸⁷Sr/⁸⁶Sr ratios 3-61293
 southern Tyrrhenian Sea, volcanism and its geodynamic implications 3-73222
 southernmost Africa, possible linear plume 3-76581
 St. Lucia volcanic rocks, Sr isotopic ratios 3-53396
 St. Vincent volcanic rocks, Sr isotopic ratios 3-53396
 submarine eruptions rel. to fuel-coolant interactions 3-76576

volcanology continued

- Surtsey and Heimaey eruptions, comparison of Sr isotopes comp. in basalts 3-41884
 surveillance system for 15 volcanoes with data collection using ERTS-A satellite 3-65511
 tectonic setting of basalt rocks using trace element anal. 3-53545
 Temiscaming, Quebec, stratigraphical relations between Pontiac group and metavolcanic Baby Rift (*French*) 3-76526
 tidal cycles of volcanic eruptions rel. to frequency, intensity and latitude 3-61311
 tidal triggering of volcanic eruptions 3-61310
 Troodos Massif, aeromagnetic survey 3-53426
 Troodos ophiolitic complex, formation in island arc 3-53384
 tuffaceous rocks, shock wave response, porosity and saturation effects 3-58876
 volcanic clouds, Iceland, produced by lava in contact with seawater, lightning 3-80773
 Water solubility in basic and ultrabasic magmas 3-80637
 Wedowee Group, Piedmont, USA, stratigraphy, metamorphism 3-80602
 xenoliths in Maar-type volcanoes and diatremes rel. to Moon, Mars and Venus 3-53403
 S compounds in stratospheric and tropospheric aerosols rel. to major volcanic eruptions 3-59058

volt-ampere meters

see also **power measurement; wattmeters**

No entries

Volta effect *see* **contact potential****voltage** *see* **electric potential****voltage controllers** *see* **voltage regulators****voltage distribution**

see also **electric breakdown; surface discharges; transients**

- Penning's discharge cell, negative space charge and potential distribution 3-68125
 two-grid tube with bipotential grid, potential distrib. calc. 3-43051

voltage dividers

see also **potentiometers**
 high precision, calibration 3-51662

voltage drop *see* **electric potential****voltage measurement**

- see also* **potentiometers; voltmeters**
 bioelectric, c.r.o. adaptation 3-77206
 bioelectric, equipment, preamplifier (*German*) 3-66399
 digital instrument for d.c. circuits, specification 3-73808
 electrode, potential of zero charge, meas. by time-of-contact method 3-58798
 flat band voltage, automatic measurement 3-48465
 Hall effect, double a.c. method 3-77574
 h.t., using Pockels effect 3-73803
 h.v. measurement applied to X-ray tubes on plants in operation (*French*) 3-54021
 Kelvin-Varley potentiometer and voltage dividers, high precision calibration 3-51662
 metals, alloys, thermodynamic props. expt. meas. techniques, review (*German*) 3-42539
 photoconductivity, electrometric amplifier construction 3-77565
 potentiometry, on thermoelec. samples, magnetically driven chopper cct. 3-39970
 sphere gaps and crossed cylinder gaps stressed with impulse voltages, influence of radiation 3-52548
 standard, volt, methods for absolute determination (*Hungarian*) 3-73663
 surface potential distrib. at high ohmic devices, electron gun meas. (*German*) 3-50251
 tunnel junctions, calibrated current voltage characteristics 3-53952
 X-ray tubes, diagnostic filtration and kilovoltage checking method 3-66383

voltage reference diodes *see* **avalanche diodes****voltage regulator diodes** *see* **avalanche diodes****voltage regulators**

potentiostat, maintains working electrode potential, electrochem. cell, phase struct. anal. 3-48472

voltage stabilizers *see* **voltage regulators****voltage transients** *see* **transients****voltmeters**

see also **digital voltmeters; potentiometers**
 superconducting quantum, operating mode selection 3-70327

volume control

antidiuretic-hormone bioassay body-fluid, control system 3-73932

volume control (gain) *see* **gain control****volume measurement**

- automatic gas burette without liquid, instrument description 3-54055
 Burnett cell, design description 3-48350
 gases, by liquid displacement method 3-66337
 gases, small changes, isobaric conditions 3-77380
 pneumotachograph used to measure dV/dt, V is volume displaced in breathing, hence V obtained using variometer 3-59681
 porous and granular materials, device developed 3-70266

vortex flow *see* **vortices****vortexes** *see* **vortices****vortices**

see also **cavitation; turbulence**

- ablate spheroidal particle assemblages, viscous flow at intermediate Reynolds numbers 3-63751
 acoustic pulse reflection by plane vortex sheet 3-70210
 aircraft wake vortex sensing, acoustic pulse deflection and velocity field measurements 3-57759
 airfoil, two-dimensional, unsteady aerodynamic response obs., vortex shedding 3-57788
 alloy, dirty BCS superconductor, vortex struct. calc. 3-52927
 artificially excited vortex trail behind a jet flap aerofoil, thrust coefficient 3-46493
 atmosphere, two layer model rel. to eddies and waves 3-58999
 atmospheric, barotropic, non-divergent vorticity equation, spectral form, approximate analytical solutions 3-76728

vortices continued

- atmospheric vortex street features, simulation in wind tunnel 3-59118
- baroclinic, two-layer fluid, instability, separate circulations, appl. to oceanic vortices 3-46426
- barotropic instability, Rossby wave motion β effect, vorticity equation 3-44892
- barotropic instability and predictability difference energy spectra 3-44890
- barotropic vorticity equation, lateral boundary conditions 3-44891
- boundary layer flow around sphere rel. to vortices in flow separation 3-78965
- boundary layer flows small protuberances effects, review 3-71762
- boundary layer separation at a free streamline, bathtub vortex paradox 3-57866
- breakdown in swirling flows in streamtubes of variable cross section 3-78959
- coaxial cylinders with outer rot. cylinder, frictional moment and press. drop of flow 3-54805
- compressible flow through vortex swirl cup injector, analytical model 3-71779
- compressible perfectly conducting fluid, MHD stability of vortex sheet 3-75260
- conservation of vorticity transport 3-57758
- convective flow in ellipsoidal cavity, oceanographic appl. 3-71741
- Couette circular flow, equilib. vortex motion 3-67913
- Couette flow, circular, with const. finite acceleration, linear stability anal. 3-71758
- on delta wings at hypersonic speeds, lee-side vortices, fluid dynamical investigation 3-46421
- density-stratified fluid with particle suspension, plane parallel flow 3-71822
- entrance region flow at low Reynolds numbers, axial transport of vorticity 3-63697
- equation derivation, rate of change of angular momentum 3-67918
- extratropical cyclone parameters from Nimbus 2 HRIR meas. 3-65359
- falling body, natural mode of oscillation of vortex (Russian) 3-62440
- flow in tube with circumferential wall cavity, numerical soln. 3-71774
- flow past a thin oblate spheroid, infinite viscous fluid, streamfunction and vorticity calc. appl. to cloud physics 3-43552
- flow past circular cylinder, shedding freq. 3-67922
- flow past inclined flat plate, two dimensional vortex shedding simulation 3-78967
- Foppl's vortices stability analysis 3-71759
- force on a slender fish-like body, vortex sheet 3-43641
- fully developed viscous flow in coiled circular pipes 3-57750
- galaxies, origin of rotation rel. to shock wave generated vorticity 3-42227
- Goertler, water, 90° bend, laminar flow transforms to turbulent flow 3-63667
- helical filament, nonlinear fluctuations, solns. to wave eqns. higher harmonics (Russian) 3-63670
- helicopter rotor blade loads and noise 3-43547
- hydrofoil theory, unsteady supercavitating, at non-zero cavitation numbers, vortex flow models 3-43594
- ideal fluid, stability of three-dimensional flow for unlimited increase in vorticity (Russian) 3-67919
- infinite viscous fluid, streamfunction and vorticity calc. appl. to cloud physics 3-43552
- insect wing, lift generation, Weis-Fogh mechanism vortices shedding 3-60554
- interaction with a flat surface (Russian) 3-67921
- jet, submerged laminar round, initial development, spherical vortex 3-57869
- jet flaps, two-dimensional, discrete vortex method 3-79043
- jet induced flow, distrib. 3-63668
- jets, confined heterogeneous, laminar mixing, expt. obs. and theory 3-46497
- jets, supersonic, noise reduction, periodic vortex shedding 3-52489
- jets, supersonic, underexpanded, impingement upon flat plate 3-75276
- Karman vortex-street modes, flow around obstacle 3-78961
- laminar trailing vortices behind wing, axial flow 3-57756
- Martian Great dust storm of 1971, terrestrial hurricane model 3-51291
- multicomponent airfoils, two-dimensional incompressible potential flow 3-46424
- non-Newtonian fluids, entrance flows 3-52485
- numerical soln. of vorticity transport eqn. 3-49568
- obstacle on and near wall, effects on wake pattern 3-67975
- ocean, two layer model rel. to eddies and waves 3-58999
- oceanic quasi-geostrophic waves in tropical Atlantic rel. to observed eddies 3-59000
- oceanography, vortex formation over rippled beds by progressive waves 3-58992
- piles in water, vortex excitation 3-60545
- plasma, moving in quickly changing mag. field, current vortices development (Russian) 3-79078
- plasma MHD generalised flux-vorticity theorem 3-40812
- polymer dilute solutions, Taylor vortices and evaluation of material constants 3-60573
- potential vortex stability, rotating, non-rotating jet core 3-75202
- Rankine vortex, heat transfer 3-46415
- rapid flow, vortex method, numerical soln. 3-49567
- relativistic motion, general relativity eqn., astron. appl. 3-60584
- ring, behind sphere in aerosol jet flow 3-63766
- ring, in incompressible potential flow, past axisymmetric bodies in cylindrical pipes 3-78963
- ring, nonlinear fluctuations, solns. to wave eqns. higher harmonics (Russian) 3-63670
- rings, sharp density interface, turbulent entrainment model 3-75203
- rotating circular cylinder, flow field survey and aerodynamic force meas. 3-43551
- secondary vorticity, generalised expressions using intrinsic coordinates 3-52446
- shedding from bluff bodies in a shear flow 3-67915
- shedding in main branch of arterial junction 3-65983

vortices continued

- sheet, interaction with sound 3-79054
- shock wave, vortex discontinuity in thermodynamic variables (French) 3-78986
- sphere in infinite fluid, hydrodynamic field calc. by smoothing method (French) 3-46422
- spin-up, linearized 3-63674
- spinning bodies of revolution, Magnus effect 3-57751
- spinning ogive nose cylinder, Magnus characteristics meas., lee-side vortices 3-78973
- spiral flows in channels of simple shape (Russian) 3-52445
- spiral sheets, in flow round rolling slender wing with leading edge separation 3-75218
- stable vortex path in vertical tubes with various stream entry conditions, expt. obs. 3-57727
- statistical lattice description of vortex system props, (French) 3-54170
- steady separated flow over finite flat plate in linearly decelerated free stream 3-57770
- steady supercritical Taylor vortex flow 3-46425
- stratified shear flow, stability 3-63678
- streamwise vorticity decay in three dimensional boundary layer flow, exact solutions 3-60546
- Strouhal number and flat plate oscillation in air stream 3-71753
- supercavitating flow at non-zero cavitation numbers, lifting line theory 3-43593
- superconducting film, inhomogeneous, theory of vortex motion 3-60932
- superconductor, magnetic, vortex lattice 3-72423
- superconductor, nonlinear response due to strong elec. field 3-68733
- superconductor, type II, attractive interaction between vortices at arbitrary temp. 3-68732
- superconductor, type II, dirty, theory 3-68731
- superconductor, type II, vector pot. and order parameter for isolated vortex 3-55348
- superconductor, vortex interaction with boundary between two superconductors 3-60935
- superfluid vorticity in non-dissipative processes, dynamics, Landau two-fluid equations 3-50035
- supersonic jet flows, noise reduction, vortex shedding phenomenon 3-43637
- suspension, swirling laminar pipe flow 3-71823
- Taylor's toroidal vortices instability between rotating coaxial cylinders (Russian) 3-67916
- Taylor vortices growth between rotating eccentric cylinders (Russian) 3-67920
- Taylor vortices in time-dependent rotational Couette flow, numerical study 3-49564
- thermal entrance region of a horizontal parallel plate channel heated from below, convective instability, vortex rolls 3-46405
- thunderstorm cell flow, drag expt. 3-51031
- tornado at Diamond Harbour, India on 21 March 1969, general description 3-80727
- trailing vortex pair instability 3-49565
- trapped wave model of vortex breakdown in critical flows 3-46469
- trough development, 300-mb, rel. to geomag. storms 3-44846
- tube flow, steady and developing, of vanishing Reynolds number, field descriptions 3-71733
- turbulence, Burgers' model equations, vorticity 3-52438
- turbulent flow structure, modelling and analysis 3-57738
- turbulent line vortices structure 3-71756
- two-dimensional guiding centre plasma, negative temperature states, vortex structures 3-57875
- unsteady starting flows past spheres and elliptic cylinders 3-71757
- unsteady thin airfoil theory for subsonic flow, vortex wake strength 3-43570
- viscoelastic liquids, decay of vortices 3-67917
- viscous flow, incompressible fluid, rectangular cavities, finite-difference equations, behaviour of vortices 3-71755
- viscous supersonic flow over cone at moderate incidence, swirling pairwise symmetric vortices 3-60553
- vortex flow adjacent to stationary surface 3-71752
- wake, axisymmetric final period turbulent, scalar, asymptotic behaviour 3-57864
- wake splitter plates, effect on flow past circular cylinder, $10^4 < R < 5 \times 10^4$ 3-79051
- wake vortices, aerodynamics 3-57853
- wakes, bevelled trailing edge effect on vortex shedding and vibration 3-43650
- wakes two-dimensional, smoke visualization of three-dimensional flow patterns, Foppl vortices 3-63802
- water vapour condensation in swirling wake following longitudinal flow along a plate 3-57859
- Al-insulator-Al,(Sn),(Pb), supercond. thin films, tunnelling in vortex state 3-52936
- He, liquid, rel. to nonuniform states, theory 3-60815
- He II, Effect of axial heat current on negative ion trapping by vortex lines 3-58157
- He II, vortex-ring creation, time depend. 3-52736
- ³He, vortex-ring, generated level differences 3-68467
- ⁴He, liquid, pure and with ³He impurities, rotating superfluid, free surface at vortex 3-55112
- ⁴He, liquid, superfluid, creation of quantised vortex rings 3-60820
- ⁴He, superfluid, charged vortex rings dynamics 3-52737
- ⁴He II, liquid, roton effects on electron bubble mobility 3-72243

waiting line theory see queuing theory

wakes

- aircraft wake vortex sensing, acoustic pulse deflection and velocity field measurements 3-57759
- airfoil trailing edge, transonic turbulent viscous-inviscid interactions 3-63702
- artificial satellites, sheath and wake structures 3-60591
- artificially excited vortex trail in jet flap aerofoil wake, thrust coefficient 3-46493
- axisymmetric final period turbulent, asymptotic behaviour of scalar 3-57864
- bevelled trailing edge effect on vortex shedding and vibration 3-43650

wakes continued

- entry vehicle dynamics, instability caused by forebody blowing 3-43571
- flow around symmetrical profiles (*French*) 3-49621
- flow past an impulsively started circular cylinder, length of separated wake 3-57775
- fluid flow around and through screen, mathematical model 3-75213
- free turbulent mixing flows without a net momentum defect, analysis 3-46494
- free turbulent mixing in axial press. gradients 3-75201
- Gaussian, incompressible, two-dimensional, in steady viscous flow, spatial stability 3-71840
- hypersonic, at high Reynolds numbers, turbulent boundary layers 3-79044
- hypersonic sphere wakes, laminar and turbulent, Mach 13.5, density and temp. distributions 3-40753
- interacting wakes, turbulence meas. 3-52492
- ionospheric plasma surrounding satellite, wake struct., laboratory simulation 3-44915
- ionospheric satellite, electron temperatures 3-61529
- ionospheric satellite and rocket wakes, electron depletion, Langmuir probe and antenna obs. 3-51120
- ionospheric satellites, electron temperatures 3-61529
- jet, double concentric, nozzle conditions influence on main region characts. 3-54828
- laminar axisymmetric, stability, critical Reynolds number 3-75280
- laminar trailing vortices behind wing, axial flow 3-57756
- large fixed roof oil storage tanks, angle of wake variation 3-63711
- mass transfer between the attached wake of a bluff body and the free stream 3-40756
- MHD, uniform flow past bodies in a longitudinal magnetic field (*Russian*) 3-60564
- MHD steady flow past oblique flat plate, wide wake flow field 3-43598
- near wake, spiral vortices, boundary layer flows, review 3-71762
- obstacle on and near wall, effects on wake pattern 3-67975
- ordinary and confluent boundary layer flows, parametric relations 3-63784
- Pacific Equatorial Undercurrent, wake phenomenon, 1967, Spring 3-47681
- plasma magnetised flow past an obstacle, wake formation 3-40774
- precipitation-size waterdrops, wake effect interactions rel. to cloud physics 3-51028
- projectile Mach 16 wakes, electron density fluctuations, turbulent scattering spectra 3-79169
- pulse energy, analytic representation 3-67973
- radial flow passage, wakes and eddies, flow model 3-75208
- radial-flow passage, wakes and eddies, experimental observations 3-75207
- rotating circular cylinder, flow field survey and aerodynamic force meas. 3-43551
- satellites, interaction with ionospheric plasma 3-61528
- sharp trailing edge with attached free streamline, boundary layer separation 3-57866
- sounding rocket, effect of wake boundaries on boom mounted probes 3-75284
- sounding rocket wakes, effect on ionospheric electron density probe performance 3-51192
- sounding rockets, split and double probe measurements 3-61603
- splitter plates, effect on flow past circular cylinder, $10^4 < R < 5 \times 10^4$ 3-79051
- supersonic laminar, pressure distrib. and velocity profiles, method of integral relations 3-54810
- time-mean wake of row of circular cylinders 3-79046
- turbulent, rel. to body shape 3-49629
- turbulent boundary layer shape after corner expansion 3-57856
- turbulent flow behind plate, kinematic and dynamic characteristics 3-57862
- turbulent of a circular cylinder placed normal to the plane surface in a uniform stream 3-67922
- two-dimensional, smoke visualization of three-dimensional flow patterns 3-63802
- two-dimensional flat plate, shear flows, stability, non-parallel flow corrections 3-60586
- unsteady thin airfoil theory for subsonic flow, vortex wake strength 3-43570
- viscoelastic liquids, decay of vortices 3-67917
- viscous, wave height and resistance 3-49627
- viscous flow past thin oblate spheroid, streamfunction and vorticity calc., appl. to cloud physics 3-43552
- vortices in wake of circular cylinder, numerical soln. 3-49567
- water towing tank, DFVLR Freiburg, applic. 3-51772
- water vapour condensation in swirling wake following longitudinal flow along a plate 3-57859
- water wave scattering, generated by a moving pressure point 3-63731
- wing trailing vortices, aerodynamics 3-57853

Walsh functions

- see also *encoding; filtering and prediction theory*
- elasticity variation, water saturated rocks, at melting point of ice 3-76530
- neutron transport equation, approx. 3-63117

warning systems see *alarm systems***waste disposal**

- chemisorbentgenospectral fluorescence, Ta microanal., industrial effluent soln. 3-48657
- deep-sea disposal of radioactive waste, safety evaluation models 3-70192
- E Florida coast, unusual plume behaviour from ocean outfall 3-61444
- ground disposal site for radioactive wastes, internal dose estimation by sensitivity analysis 3-40550
- heated discharge, coastal zones, effluent dynamics modelling 3-53462
- hydrodynamic dispersion of injected contaminant in fractured rock aquifer, model 3-51212
- Long Island Sound, dredge spoil disposal, biological, chem. and phys. studies 3-53782

waste disposal continued

- nuclear, nondestructive assay, criticality problems and solutions 3-63248
- pollutant dispersion and seepage, beneath open channels, porous media 3-56562
- radioactive, alternative storage areas 3-71338
- radioactive, deep self burial utilising decay heat to melt rock 3-67415
- radioactive, light water reactors up to 800 MW(e) 3-43294
- radioactive, LWR type, storage, design (*French*) 3-46133
- radioactive, quartz matrix isolation 3-71334
- radioactive waste, monitoring information system 3-74751
- radioactive waste, selection of ground disposal site using computer (*Japanese*) 3-43317
- radioactive waste, site for ground disposal, migration of multiple nuclides 3-78393
- radioactive wastes in ground, point-rating chart for safety evaluation 3-70191
- rivers, time variable waste input, dynamic water quality response, effect of longitudinal dispersion 3-56272
- salt mines, behaviour of rock salt under particle irradiation from high level nuclear waste (*German*) 3-53420

water

- see also *heavy water; ice; moisture; seawater; steam*
- acoustic cavitation inception, surface tension role 3-71791
- adsorbed layer on SiO_2 , N.M.R. 3-61000
- adsorption by clay minerals, review (*Polish*) 3-44832
- adsorption on Au, surface sensitivity of HeI photoelectron spectroscopy 3-55148
- adsorption on montmorillonite, n.m.r. of single and double layer system 3-68867
- aerosol, charged, electrical discharges, oil tanker washing operation, electrical and atmospheric conditions 3-40817
- aerosol, influence of microstructure on phase function, asymmetry and polarisation of scattered light (*Russian*) 3-70785
- air-water interface, lateral waves produced by laser beam 3-59882
- air-water interface, transfer of O_2 , CO_2 and water vapour 3-44855
- air-water medium, effect of flow on pressure wave propagation, expt. 3-43622
- amide-water systems, deviations from ideal behaviour of mixtures 3-53356
- Apollo 12 lunar fines, alteration by H_2O vapour absorpt. 3-47946
- aquifers beneath Venice, isotopes and circulations (*French*) 3-53571
- astronomical water masers in protostellar gas cloud rel. to multi-level line transfer cocoon stars 3-59382
- atmosphere, saturation pseudoadiabats and equivalent potential temp. 3-76765
- atmospheric and terrestrial cycle, hydrologic studies, control 3-44909
- atmospheric particle formation from NH_3 - SO_2 - H_2O -air gas phase reactions 3-59060
- atmospheric water vapour content above Mt. Kobau and Calgary rel. to i.r. astronomical meas. 3-65345
- boiling, heat transfer, effect of thermophys. props. of heating surface material 3-52693
- boiling, transient heat transfer at vertical plate of reactor pressure vessel 3-63127
- bond orbital analysis of hydrogen bond 3-54618
- Bragg diffraction of light by two orthogonal u.s. waves 3-44392
- broadband picosecond continuum and light gate, time resolution and characteristics 3-45820
- bubble dynamics 3-43621
- bubbles in water, terminal velocity meas. 3-63765
- cavitation thresholds at 14 kHz 3-45431
- centrifugal and rot. consts. calcs., appl. of energy moments method (*Russian*) 3-78701
- combined natural and forced convection from horizontal cylinders to water 3-40710
- condensation, optical determ. of droplet size in expansion cloud chamber 3-68394
- connate, flow of immiscible liquids through porous medium 3-79037
- convective storm clouds, water content 3-76787
- countercurrent flow with Hg in packed columns, holdup flooding and pressure drop 3-60567
- cyclic polymers stability, LCAO-SCF-MO calc. 3-46584
- dams, water pressure during earthquakes, calc. (*Japanese*) 3-61361
- density in suspension, pycnometric determ. compaction, eqns. 3-61228
- depolarization of negative muons, temp. depend. 3-41853
- dielectric properties of aqueous suspension of polystyrene particles at microwave frequencies 3-44692
- diffusion in moist materials, drying effects 3-79039
- dipole moment determ. from Stark meas. 3-75000
- discharges, approx. calc. of spark energy (*German*) 3-54881
- dissociative attachment of H_2O , HDO, D_2O for H^- , D^- form., isotope effects (*French*) 3-49496
- drop rest times and films shapes for oil/water deformable drops 3-47484
- droplet growth meas. by laser scattering in Ar and He 3-73077
- droplets, charging in corona discharge region 3-68119
- droplets migrating in thermal gradient in solids, stability 3-43887
- drops, evaporation rate determ. (*Russian*) 3-73291
- drops collision vel. rel. to delay time before coalescence 3-53477
- drops splashing on water surface, corona produced by strong electric field 3-57958
- electrification of condensing and evaporating water drops 3-49985
- e.m. pulse reflection from multilayered medium, geophysical applications 3-61582
- emulsion, metastable state rupture, transitions to liquid state phenomena (*French*) 3-79492
- emulsion, with dispersed conducting phases (*French*) 3-80502
- enthalpy of ionisation from 298 to 418K, calorimetric determination 3-69452
- film, evaporation from rotating disc, heat transfer 3-63641
- film condensation augmentation on outside of horizontal tubes 3-79477
- film drainage mechanism for oil/water deformable drops 3-50788
- film on quartz surface, isotherm of separating pressure 3-46751

water continued

- films entrainment, venturi device, air-water tests 3-66473
 finite amplitude oscill. motions in two component Benard problem, water alcohol liquid layers 3-67950
 flooding, effect on microearthquakes, Los Angeles, Newport-Inglewood Fault 3-80610
 flow, laminar boundary layer hydrodynamic stability at elasticity damping surface (*Russian*) 3-63679
 flow, vertical component of velocity in along-shore currents (*Russian*) 3-63621
 flow, vortex excitation of piles 3-60545
 flow distrib. of environmental tracers, finite state mixing cell models 3-56275
 flow in capillaries, films, relax. phenomena 3-60579
 flow measurement facilities at N.E.L., 1 May 1973 3-70506
 flows with polymer additives, hydraulic losses investigation 3-57829
 freezing and supercooling in porous rocks, internal friction measurement (*Japanese*) 3-56034
 freezing water-soil system, heat and mass transfer, multiphase water distrib., irreversible thermodynamics 3-56053
 fresh, escaping into seawater, lens formation, shape for linear evaporation law (*Russian*) 3-67977
 gamma-radiolysis under N₂ gas bubbling, reln. to reactor cooling 3-71277
 gas bubble shape, size and movement (*German*) 3-75261
 gas phase, H₂O-trimethylamine complex, Raman spectra 3-78800
 geothermal state distribution, ground water system 3-76528
 glassy mixture with ethylene glycol, trapped electron excitation mechanism, e.s.r., thermoluminescence 3-65099
 glow and microwave discharges comparison 3-75436
 ground state calc., field form of perturbation theory 3-71521
 groundwater, resistivity surveys, Aurangabad Sub-division, Gaya district, Bihar, India 3-76667
 groundwater flow subject to time-varying recharge 3-73414
 groundwater-levels, tidal influence and seasonal stream effects 3-59741
 heat transfer by natural convection between vertically eccentric spheres 3-46401
 heated horizontal cylinder immersed in water, mass flow rate in natural convection plume 3-63658
 heavy water reactors, light water infiltration reactivity effects, Ames Laboratory Research Reactor, safety considerations 3-74736
 high velocity water jets, surface entrainment of air 3-49622
 horizontal layer, turbulent convection 3-60537
 hydrated electron structure modified CNDO/2 method for water and ice 3-73174
 hydrometeorological phenomena, periodicity, Furhich's autocorrelation method (*German*) 3-76845
 interaction with molten lead, obs. 3-67528
 interface with paraffin oil, hydrostatic press. depend. of interface tension (*French*) 3-79553
 intermolecular energy transfer, vib. to rot. 3-52402
 intermolecular potential as effective cross section 3-71654
 interstellar molecule masering, line radiation transfer calcs. 3-45215
 interstellar sources assoc. with H II regions OH emission 3-51394
 ion extraction from layer of air flowing around electrometer electrode (*Polish*) 3-73278
 ion-molecule reaction with methane, resonant cyclotron ejection 3-73118
 ionic partition between surface and bulk water in silica gel, biological model 3-56491
 ionisation and dissociation by electron impact 3-43495
 i.r. spectra, aqueous solutions, internal reflection spectroscopy 3-75042
 i.r. spectra, Lambert absorpt. coeff., refr. index determ. 3-61039
 isobaric specific heat, specific enthalpy at zero pressure, water and isotopes 3-71709
 jet, penetration of solid Al layer, theory 3-80342
 jet, submerged, large scale turbulence characteristics 3-71749
 jet erosion of prestressed materials 3-72902
 jet impact, transient stress distrib. 3-72903
 jets, high-speed from vertically accelerated rotating cones 3-75282
 laser, vapour, correlation of output power and discharge products comp. 3-70812
 lava-water dynamic mixing effects 3-61331
 Leidenfrost temp. calc. 3-64169
 light, neutron field slowing down and up-scattering problems, theory 3-60246
 liquid, near i.r. spectra, further anal. concerning vibr. assignments 3-43450
 liquid and vapour two phase flow, heat transfer, expt. study 3-40708
 liquid struct. from H₂O + organic base i.r. study, vibr. assignments 3-46275
 LMFBFR, sodium cooled, water leaks into sodium, monitoring 3-63148
 lone pair orbital energies 3-61966
 long nonlinear shallow-water waves, amplification and decay 3-46468
 lunar water, possible sources and degassing from lunar interior 3-53623
 Mars, i.r. spectroscopic evidence for bound water 3-42144
 Martian atmosphere, H₂O content, Mars 3 spacecraft obs. 3-65781
 mechanically generated surface waves, wind-induced growth 3-46467
 melt films, lifetimes, meas., theory 3-63945
 moisture content determ. by microwave absorption in capillary-porous materials 3-73093
 moisture diffusion dynamics through a partially filled porous matrix 3-57837
 molecular motions, mol. dynamics calcs. 3-79222
 molecular orbital calcs. density localisation 3-71501
 molecular vibration spectra, influence of intermolecular interactions, i.r. absorpt. intensity 3-63473
 molecule, $3p_2$ band study, rotational levels 3-67823
 molecule, bending potential calc. 3-74971
 molecule, collisional deactivation of HBr in (V=1) state 3-71624
 molecule, electron impact, dissociative excitation, cross section meas. 3-75119

water continued

- molecule, electron impact, dissociative excitation processes, spectroscopic investigations 3-75114
 molecule, electron impact, dissociative excitations, emission cross sections, absolute meas. 3-75120
 molecule, electron impact ionization, energy loss and momentum transfer 3-40584
 molecule, electronic excitation energies, ab initio calc., CI method and RPA applies. 3-74940
 molecule, excited state force consts. calc. from bond charge model 3-52334
 molecule, F⁻ and Cl⁻ interaction, Hartree Fock approx. calc. 3-49819
 molecule, Fourier transform spectrum, between 2930 and 4255 cm⁻¹ 3-78767
 molecule, H₂¹⁶O, (000) and (020) states study, 2930 to 4255 cm⁻¹ region 3-78766
 molecule, high resolution i.r. spectra of $\nu_1 + \nu_2$ and $\nu_2 + \nu_3$ bands (*French*) 3-75025
 molecule, ionisation by electron impact at low energies 3-75129
 molecule, ioniz. pots. determ. from photoelectron spectra 3-63536
 molecule, IR vacuum spectra of vapour 3-78762
 molecule, natural orbitals calc. by perturbation theory, diagonalization of one-electron density matrix 3-74942
 molecule, new basis set for molecular wavefunctions 3-71506
 molecule, position and mobility in UF₄.2.5H₂O, n.m.r. 3-79925
 molecule, rot. mag. moments calc. 3-60443
 molecule, structure, quadratic force field, spectral analysis calcs. 3-78715
 molecule coupled Hartree-Fock method calcs. of one-electron properties 3-71515
 molecule in solid hydrates, correlations between free and H-bonded mols., ab initio calcs. 3-74991
 monitoring of geothermal spring water by neutron capture gamma rays using ²⁵²Cf 3-62360
 monomolecular film covered, low amplitude capillary waves, dispersion relation, light scatt. obs. 3-46748
 muscle water, proton mobilities by n.m.r. 3-56486
 natural convection flow patterns in spherical annuli 3-57734
 neutron activation analysis, determination of Cu in parts per 10⁹ 3-40074
 neutron moderator temp. discontinuity, effective thermal neutron temp., spatial variation, weighted residuals method 3-40527
 neutron slowing down spectrum, calc. using Green's function 3-54521
 neutron slowing-down times, effect of anisotropy 3-74634
 nonflowing air-water system, propagation of pressure and density 3-71812
 one-dimensional model, bulk and boundary effects 3-79220
 optical dispersion eval. using two-state theory 3-68951
 optical strength, effect of Cu²⁺ salt additives 3-57252
 optimum temp. distrib. at surface of plate, flow stabilisation by preheating (*Russian*) 3-63626
 pH, effect of various gases 3-53359
 photography, for water quality research 3-65542
 p.m.r., obs. of change in nuclear susceptibility and angular momentum transfer 3-41435
 polar molecule slow electron scattering 3-46342
 polymers, molecular interactions, studies comparison using different MO basis sets 3-40679
 polywater, anal. of anomalous condensates 3-61286
 polywater, anal. of explanations and experimental data, review (*German*) 3-40841
 power reactor steam generators, safety against sodium-water reaction 3-67615
 precipitation-size waterdrops, wake effect interactions rel. to cloud physics 3-51028
 preconcentration of metals using electrodeposition, X-ray fluorescence analysis 3-66423
 proton affinity from D₂O + D₂ reaction 3-61254
 proton affinity prediction 3-74909
 Proton energy degradation in water vapor 3-71637
 proton spin-lattice relaxation time meas. 3-71577
 pulsatile laminar flow in distensible tubes, friction factors determ. 3-57805
 pulse discharges, approximate calc. (*Russian*) 3-68109
 pure rotation spectrum, approximate mean absorption coefficient 3-67833
 Raman band shapes, depolarization ratio spectra 3-75020
 Raman spectra, effect of hydrogen bonding on intramolecular vibrations 3-80022
 Raman spectra, quasi-Fermi resonance effects 3-75046
 Rayleigh-wing scatt., depolarized 3-72607
 refraction spectrum at submillimetre wavelengths, direct meas. 3-47331
 refractive index meas., between 250 and 700 nm. 3-66190
 refractive index meas. up to dynamic press. of 10 kbar 3-41495
 relative threshold nucleation temps. for active nucleation catalysts 3-49971
 resources, Rayleigh-Ritz and Galerkin elements in diffusion-convection problems 3-73413
 rotational levels, rigid and nonrigid top models 3-60433
 Rydberg states, ionisation and excitation energies calc. 3-46268
 salt composition of rain and river water in USSR, role of sea salts 3-51066
 saturated rocks, elasticity rel. to temp. and pressure 3-61306
 self diffusion in temp. range 1-45°C 3-52715
 self-diffusion meas. 3-68430
 self-diffusivity, neutron diff., n.m.r. spin echo, mol. dynamics methods 3-72217
 shallow, long wave motion, N-soliton soln. 3-48807
 shallow water waves, solitons and synacetics 3-45633
 shock waves, spherical, in water 3-40728
 shock-compression freezing 3-43865
 skeleton-liquid-vapour-air-ice, transpiration, heat, mass transfer eqns. unsteady conditions 3-63642
 smooth air-water interface, thermal radiative propt. 3-45736
 solid thin film, sticking coeff. of CO₂ 3-41093
 solidification in porous media, calorimetric method, latent heat determ., effect of pore radius, hysteresis (*French*) 3-75606

water continued

- solubility in basic and ultrabasic magmas 3-80637
 sonic-boom overpressures investigation, ballistic range investigation for various Mach numbers 3-57792
 spectral line strengths and widths in 2950-3400 cm^{-1} region 3-71568
 standing waves in canal of arbitrary shape, determ. of natural freqs. 3-43596
 steam, effect of rainfall on free surface on velocity (*German*) 3-40733
 steam-water-ice phase system, 2 dimensional bonded lattice model, first order approximation, long range and short range order 3-41006
 stimulated short-wave radiation due to single freq. reson. of third-order nonlinear susceptibility 3-66882
 stratospheric water vapour mixing ratio altitude profile, atmospheric emission spectra obs. 3-41951
 streamflow, stochastic methods in hydraulics and hydrology 3-56280
 streams containing some macromolecular substances, boundary layer turbulence 3-71819
 structure, effect of ions, i.r. spectra of water and aqueous solutions, 1.15 microns band, experiment 3-72605
 structure at 20°C and 1 atm, cluster theory, two-dimensional model 3-57980
 subcooled, at low Reynolds numbers, transient and forced convective film boiling 3-52695
 subcooled boiling, in top-generated swirl flow 3-68401
 submillimetre wave dielectric dispersion in liquid H_2O and D_2O 3-47205
 supercooled, freezing in electric field, laboratory expt. 3-65380
 supercooled drops ice particles, freezing during free fall in wind tunnel 3-65390
 supercritical, forced convection, wall-temp. oscillations (*Japanese*) 3-40713
 surfactant-induced cooperative stabilization of water structure at vapour-water interface 3-79481
 swirling cavity flow, through straight circular pipe 3-57754
 t-butyl alcohol-water system, u.s. absorption, frequency dependence, relaxation processes, model 3-59478
 telluride glasses, highly refracting, effect of H_2O on i.r. transmission 3-64620
 thermal diffusion of dextran 3-60500
 thermal expansion in independent cylindrical capillaries 3-61227
 thermal expansion tables, discussion of different tables for 0 to 40 deg. C 3-64190
 thermal interaction with molten aluminium thermal interaction under impact conditions for pressures calc. 3-67530
 thermally stratified air-flow layer near a water surface under wind gust conditions, turbulence struct. meas. 3-59048
 thermodynamic properties from 50°C to critical point for H_2O and isotopes 3-72210
 thin films on mica crystals, structure and props. 3-60847
 trace element analysis by proton activation 3-66415
 transient heat fluxes and vapour generation rates meas. 3-52431
 transport of cohesionless, fine graded, flaked sediment by water 3-80705
 triple-point cells, simple filling method 3-66163
 turbulent flow in 50 mm dia. flexible tubes, obs. (*Russian*) 3-63635
 turbulent flow in flat rough tubes, effect of polyacrylamide admix-ture (*Russian*) 3-63770
 turbulent Prandtl number determ. near smooth wall (*French*) 3-63647
 unconfined groundwater, Boussinesq eqn. modified to accept recharge 3-73235
 underground water, simulation of flow (*Russian*) 3-63620
 underwater spark, resistance, energy balance equation 3-49782
 underwater spark discharges, electromechanical efficiency (*German*) 3-54882
 u.s. velocity maximum, LiOH effect 3-68337
 vapour, atm. meas. up to 35 km altitude (*French*) 3-61449
 vapour, atmospheric, radiothermal obs. (*Russian*) 3-80749
 vapour, atomic resonance radiation quenching of $\text{O}(2^1\text{D}_2)$ in vacuum ultraviolet 3-71370
 vapour, CW laser, low-signal gain at 28 μm 3-51909
 vapour, effect on output power of CO_2 gas-dynamic laser 3-66813
 vapour, energy distrib. of secondary electrons released by fast electrons 3-80561
 vapour, fugacity control in solid media high-pressure apparatus 3-73896
 vapour, homogeneous nucleation using diffusion cloud chamber 3-64164
 vapour, in sunspot spectra, line intensity determ. 3-65705
 vapour, production from lunar breccia by exposure to hydrogen and outgassing, implications 3-73462
 vapour, solar radiation absorption 3-44895
 vapour, sparking potentials between concentric sphere-hemisphere electrodes 3-63908
 vapour, weak absorption line detection, using glass:Nd laser 3-39933
 vapour adsorption on sulphopolystyrene during heat treatment 3-61250
 vapour attenuation correction, sea surface temp. meas. at 12 μm 3-59124
 vapour condensation in swirling wake following longitudinal flow along a plate 3-57859
 vapour in stratosphere, effect on ozone and temperature structure 3-76741
 vapour pressure, 273.15-298.15K 3-49988
 vapour transitions, tunable laser meas., 5 μm region 3-40622
 vibrational spectra isolated in D_2 matrices 3-43443
 water and heavy water mixture, volume viscosity and struct. u.s. study 3-50020
 water-benzene-ethyl alcohol ternary system, shear viscosity and u.s. absorpt. near plait pt. 3-64204
 water-beryllium square lattice, pulsed neutron expts., one-group diffusion model 3-71144
 water/polymer emulsions, medium and high internal phase ratio 3-50792

water continued

- wave scattering, generated by a moving pressure point 3-63731
 waves, Korteweg-de Vries equation solutions 3-60560
 well hydraulics, potential theory, flow of ground water (*German*) 3-76929
 wetting of polyethylene 3-43927
 CO_2 gasdynamic laser with water vapour content, operation characts. 3-45797
 $\text{CO}_2\text{-H}_2\text{O}$ gaseous mixtures, thermodynamic properties 450 to 800°C, 0 to 500 bar 3-69489
 Co- H_2O system, thermodynamics at elevated temps. 3-47605
 Cu electrode, alternatively polarised, moisture effects (*Polish*) 3-58802
 Cu- H_2O systems, thermodynamics, at elevated temps. 3-44748
 D_2O dipole moment determ. from Stark meas. 3-75000
 Fe- H_2O system, thermodynamics at elevated temps. 3-44749
 H_2 and water vapour binary mixture, thermal conductivity and viscosity calc. 3-63609
 HDO, liquid Raman intensities of uncoupled OD oscillators 3-75979
 HDO dipole moment determ. from Stark meas. 3-75000
 HDO in rare earth chloride soln., Raman spectra 3-75980
 H_2O dimer, config. computed, Monte Carlo simulation of liquid state 3-71488
 H_2O molecule, NDDO calculations 3-52312
 H_2O -acetic acid-carbon tetrachloride, coexistence curve shape near plait point 3-75600
 H_2O -argon, mixture atmospheric ion mobilities, positive ions 3-59071
 H_2O -He system, intermol. forces, ab initio calcs. 3-54755
 H_2O - NH_3 , electron correlation, basis effects, H bond theory (*French*) 3-71502
 (H_2O)₂, microwave and r.f. transitions obs. by mol. beam electric resonance method 3-78825
 H_3O^+ , minimum energy struct. and inversion barrier 3-74909
 H_2O_2^+ , tunnelling in proton transfer between water mols. 3-78867
 $\text{H}_2\text{O}_2\text{Cl}_2$ complex, i.r. and CNDO/2 study 3-54686
 H_2O -HCl complex in solid N_2 , i.r. spectrum 3-52369
 ^3H participation in water cycle (*French*) 3-59047
 O_2 and water vapour binary mixture, thermal conductivity and viscosity calc. 3-63609
- water conditioning** see water treatment
- water pollution**
 see also pollution detection and control; waste disposal; water treatment
 α -detector for monitoring waste water 3-53765
 bio-oxygen stabilisation in wastewater, using hydrogen peroxide 3-45333
 chemicoresonantgenospectral fluorescence, Ta microanal., industrial effluent soln. 3-48657
 coastline water, diffusion dispersive calc. 3-65269
 ecosystem modelling for Lake George NY 3-47714
 environmental testing and control, conf., Anaheim, Calif., USA (April 1973) 3-53551
 E Florida coast, unusual plume behaviour from ocean outfall 3-61444
 fuel oil hydrocarbons and mineral particles in seawater and marine sediments 3-53456
 groundwater, flowing, mass transport, appl. to prediction and control of contaminants 3-47853
 heated discharge, coastal zones, effluent dynamics modelling 3-53462
 kinetic modelling of aeration basins for wastewater treatment 3-45334
 lidar polarimeter, remote water quality meas. 3-42384
 Long Island Sound, dredge spoil disposal, biological, chem. and phys. studies 3-53782
 marine and fresh water, remote sensing of chlorophyll and temp. 3-73607
 neutron activation analyzer for continuous monitoring 3-62358
 ocean and coastal zone, pollution monitoring, Earth Resources Technology Satellite 3-80717
 oil, remote sensing techniques for detection and monitoring 3-70194
 oil slick, viscous-gravity spreading 3-58979
 oil slick on sea surface, microwave meas. of effects at 2.66 GHz 3-50991
 oil slicks, i.r. characs., comparison with natural slicks 3-69744
 oil spill detection using 13.3 GHz radar scatterometer 3-51213
 oil spills, cleanup using waste paper, technique 3-81330
 photography, for water quality research 3-65542
 pollutant dispersion and seepage, beneath open channels, porous media 3-56562
 porous media, longit. dispersion with nonlinear adsorpt. 3-56276
 radiation, dose from nuclear plants 3-74748
 radioactive, γ -spectrometer probe 3-56261
 radioactive, dosimetric implications for man 3-77300
 radioactive, sources and inventory 3-77298
 radioisotopes, medical diagnostics, control of release to environment through excreta 3-77296
 radionuclides, sampling and meas. 3-77299
 remote sensing from aircraft 3-51173
 river, biochemical oxygen demand, three dimens. analytical soln. 3-59209
 river effluent, monitoring system (*Japanese*) 3-66076
 rivers, time variable waste input, dynamic water quality response, effect of longitudinal dispersion 3-56272
 sea surface pollution meas. by satellite (*Italian*) 3-61609
 seawater, chemical properties, effect of oil 3-80710
 temperature changes in rivers, math. model 3-44969
 trace element analysis by proton activation 3-66415
 turbidity meas., technique review 3-61930
 Upper Colorado River, economic-hydrologic-air pollution model 3-59216
 Vellar estuary, distribution of dissolved silicon 3-77304
 Vembanad lake, distribution of phosphorus in sediments 3-77305
 Br concentration, rapid determ. by neutron activation 3-62357
 CN, electrode measurement for waste waters 3-53781

water purification see water treatment

water supply

- see also *dams*
 artesian well, unsteady drawout finite element method 3-56273
 bio-oxygen stabilisation in wastewater, using hydrogen peroxide 3-45333
 groundwater, flowing, mass transport, appl. to prediction and control of contaminants 3-47853
 hydrologic decision strategies, minimax vs. expected value criteria 3-59062
 intracoastal waterway, quality management model 3-58983
 lake effect snowstorms, role in hydrology, Lake Erie 3-47773
 linear conceptual catchment models, time variance, rainfall rel. to runoff 3-56242
 multireservoir system, water storage and transfer, hydrologic simulation model 3-59217
 pumped well, unconfined aquifer, unsteady radial flow, model 3-46489
 pumped well, water table drawdown, unconfined aquifer, unsteady radial flow 3-46490
 stochastic snow model for water supply prediction and flood forecasting 3-59063
 surface runoff system, storm records, determ. of optimal kernels, computational technique 3-56243
 Upper Colorado River, economic-hydrologic-air pollution model 3-59216

water treatment

- alum-floc radiation treatment plants, efficiency 3-74748
 bio-oxygen stabilisation in wastewater, using hydrogen peroxide 3-45333
 filtering flow, imperfect tanks, seepage, silting, capillarity, eqns. (Russian) 3-63800
 kinetic modelling of aeration basins 3-45334
 nuclear power reactors, water treatment problems 3-74768
 reverse osmosis, for semiconductor processing 3-50668
 sewage, magnetic filtration 3-77306

watthour meters

- see also *power measurement*
 electronic standard meter, for precision measurements (French) 3-51512

wattmeters

- see also *power measurement; volt-ampere meters*
 No entries

wave analysers

- see also *spectral analysers*
 polarography, multiparameters curve filtering, minicomputer programming 3-70447

wave equations

- see also *Dirac equation; Schrodinger equation*
 atomic orbitals of Na and Mg ground states, analytical functions 3-49380
 averaged variational principles including Lagrangians containing higher-order derivatives 3-54066
 Bloch, n.m.r. simulation 3-56708
 cylindrically symmetric potential, s-waves, semiclassical approximation 3-70692
 fluid-structure interaction problems, i.f., perturbation method 3-74081
 general Moshinsky bracket 3-66624
 Hartree-Fock equations, derivation 3-67734
 hydrodynamic tensor wave equation 3-75350
 infinite component, quantisation, causal ghost-free covariant harmonic oscillator model 3-48984
 infinite-component, with linear mass spectrum, completeness of solns. 3-51977
 Klein Gordon eqn. in Riemannian space 3-62778
 Klein-Gordon eqn., two-particle, for e.m. scattering amplitude of equal mass spinless particles 3-62878
 Klein-Gordon operator, iterated, causal elementary solns. 3-62766
 Korteweg-de Vries eqn., decay of continuous spectrum for solutions 3-73993
 Lagrangians for particles of spins 3/2, 2 and 5/2 in Gel'fand-Naimark formalism 3-62771
 LCAO molecular orbital calculations, solution of secular eqns., interactive computer program, min. input effort 3-77370
 light propagation in inhomogeneously absorbing medium 3-66765
 Lippmann-Schwinger equation, moment methods for numerical solutions 3-62563
 long, limits of time stepping for numerical solutions 3-40701
 Majorana equation, infinite component, internal coordinates introduction 3-42852
 Mathieu equation, two-timing solution to second order, perturbation technique 3-74120
 N-soliton solutions for long waves in shallow-water and nonlinear lattices 3-48807
 Newman-Penrose, e.m. radiation from unmoving charge 3-74128
 nonlinear, envelope-soliton solutions, exact 3-48806
 nonlinear, in cubic medium, stability of lowest-order mode 3-66627
 nonlinear c-number field, $\lambda\phi^4$ model, plane wave modes, energy density 3-57286
 numerical integration of one-dim equation 3-70705
 one-body problem, motion of deformable medium having charge and magnetic polarisation 3-74094
 quantum mechanical, two particles of arbitrary spin with instantaneous interaction 3-78076
 quasilinear, zeroth approx. soln., appl. to deformation of elastic semi-space (Russian) 3-66495
 radial, in Schwarzschild metric, behaviour of solns. near singular points 3-62582
 relativistic, for zero-mass particles with invariant helicities, quantisation 3-45843
 relativistic, multi mass, theory 3-78091
 relativistic nonlinear classical integration by Lie series method 3-62765
 relativistic partonlike eqns., difficulty in formulation 3-54257
 resonant scatt. from inhomogeneous nonspherical targets 3-45631
 scalar, mixmaster universe, solution of Helmholtz equation 3-69821
 scalar, variational formulation in bilinear convolution form 3-40088
 scalar eqn. of spin corpuscle in nonrelativistic mechanics (French) 3-42838

wave equations continued

- scalar nonlinear wave equation for a cubic medium, stability of the fundamental mode (Russian) 3-66497
 scattering and diffraction, random media 3-66510
 sine-Gordon eqn., initial value problem, inverse scatt. method soln. 3-45708
 spin 1/2 particle in e.m. field, free field solns. and magnetic moment electron 3-78124
 spin $1/2$, explicit representations for matrices for algebraic hierarchy 3-78090
 spin corpuscles, nonrelativistic approach, fluid interpret. (French) 3-42839
 surface impedance given, numerical solution 3-64235
 variable phase equation generalisation 3-42836
 weak reflection by slowly varying plane layered media, solns. near zeros of parameters, WKB method 3-74111
 zero-mass spin 1/2 particles, C.P.T. properties and equivalence of eqns. 3-54258
 H atom, as relativistic elem. particle, scatt. and photo-effect problems 3-67634
 H atom as relativistic elem. particle, wave eqn. and mass formulae 3-67652

wave functions

- see also *orbital calculation methods*
 alkali ion-atom collisions, excitation and electron capture cross-section, small impact parameter 3-71447
 amplitudes, initial state and relative probability densities 3-77857
 atom, 2p-series, orbit-depend., h.f.s., 2p-series atoms, Hartree-Fock wave functions 3-67648
 atom, electron ionisation, Born approx. 3-74876
 atomic, density matrix elements, first order, direct analytical calc. through third order 3-74779
 atomic and molecular excited-state wavefunctions, constrained variation method 3-71511
 atomic nonrelativistic wavefunctions correlation effects on isotope shifts 3-67642
 atoms with single valence electron, construction of analytic wave functions (Rumanian) 3-49381
 Born-Oppenheimer approx. for wave functions and spectra, validity 3-63385
 bound state, of multiparticle systems, exponential decay 3-59779
 Brillouin's theorem, restriction on usage in orthogonal HF approx. 3-74781
 Brueckner (maximum overlap) soln. stability conditions in independent particle wave functions 3-67743
 central potentials, l-wave reduction to s-wave 3-60087
 centre-of-mass motion and angular momentum projection, rotational energies calc. 3-67247
 charged particle in low magnetic field with finite boundary conditions 3-66609
 CNDO, deuteron quadrupole coupling consts. calc. using core model approach 3-74937
 configuration interaction wavefunctions, Coulomb holes and expectation values 3-71357
 constrained particle wave functions in guide potentials, collective nuclear motion 3-43200
 Coulomb pot. generalized screened, critical screening parameters 3-70694
 crystal, symmetry projection, computer programs 3-75495
 cubic crystals, LCAO wave-functions and energies, convergence of solns. for different lattice consts. 3-79599
 cyclic molecules, quadrupole moments and diamag. susceptibilities calc. 3-63377
 deformed-harmonic oscillator, method of generating functions for matrix element calc. 3-74508
 density matrix, irreducible decomp. for tensorial wave functions (Russian) 3-54399
 deuteron, neutral pion photoproduction cross-sections 3-70918
 diatomic molecular wave functions and rotational line strengths calc. by RAM method including nuclear spin effect (French) 3-52339
 dimers, strong coupling and spectral consequences 3-78699
 discrete ambiguities and equivalent potentials 3-66634
 DWBA and Born calculations, (d,p) stripping reaction reversibility, one-dimensional model 3-60147
 effective interaction in nuclei, non-perturbative calc. using Pade approximants 3-67221
 electron + atom (molecule) inelastic scattering, adiabatic limit and nonadiabatic effects in second order transition pot. 3-74850
 electron gas correlation energy, variational calc. 3-70733
 electron motion in synchrotron, autophasing field 3-78123
 electron pair production by photons, exact calc. for unscreened atomic field 3-67654
 excited state CI studies, reduced partitioning procedure 3-74953
 Gartenhaus-Schwartz transform, rel. to centre-of-mass motion in many-particle systems 3-40179
 Gaussian wave packet, time-evolution by information theory 3-77862
 group-function expansions of correlated wave functions 3-57627
 Hamiltonian eigenvalue derivatives to fifth order, rel. to mol. characters. 3-59786
 harmonic oscillator, semi-coherent wave packets, $\Delta x \cdot \Delta p > 1/2$ 3-77867
 Hartree-Bogoliubov states, number and ang. momentum projection 3-71071
 Hartree-Fock, converging closed shell, level-shifting method 3-74776
 Hartree-Fock, unrestricted and spin extended, spin-correlation problems 3-74956
 Hartree-Fock approx., single-particle expectation values, variational determ. 3-67645
 hydrogenic radial r^4 matrix elements, closed form, factorisation method 3-67647
 hydrogenic wavefunctions and perturbation theory 3-63266
 hypervirial relations, simultaneous, for approx. wave functions 3-77859
 inelastic scatt. elements from approx. wavefunctions in L^2 basis 3-45695
 inert gases, at. quadrupole moments of excited states 3-71364
 intrinsic hyperspherical coordinate, rel. to evaluation of nuclear charge form factor 3-67182

wave functions continued

- inverse problem with constraints, reln. to method of completely orthogonalized plane waves 3-66638
 Jastrow, extended, for many-boson system such as liquid ^4He 3-68453
 Kronig-Penny model analogue computer simulation 3-51494
 length and velocity formulas, comment, approx. oscillator-strength calcs. 3-71354
 localization, Schrodinger eqn. with random potential, functional integral approach 3-77863
 many-electron theory, electronic quadrupole moments of excited states and charge distrib. wavefunction 3-74802
 metal IIB, meas. $^2D_{5/2} : ^2D_{3/2}$ branching ratios relativistic version Hartree-Slater method 3-71393
 methylene, spin dipole-dipole parameters, ab initio calcs. 3-74939
 molecular, density matrix elements, first order, direct analytical calc. through third order 3-74779
 molecular geometries and force constants calc. from CNDO wavefunctions by the force method 3-43396
 molecular vibrational transition integrals, r-centroid approx. implications 3-46245
 molecule, diatomic bound states, model calc. of avoided-crossing problem 3-78723
 mononuclear systems, diamag. susceptibility calc. using Brandus method 3-67640
 multichannel scattering, variational formulation of R matrix method 3-63325
 multiconfigurational zeroth-order wavefunctions iterative perturbation calculations of ground and excited state energies 3-49436
 multiple scattering by two hard spheres 3-66614
 negative energy wave functions for the Coulomb field 3-70687
 nuclear force, new theory 3-74504
 nuclear quadrupole deformation, microscopic treatment of collective motion 3-49173
 optical, interpretation of Mitra three-body model 3-57126
 optimal separation of centre-of-mass motion, determ. of best internal wave function 3-74512
 orbital variational trial functions, optimisation 3-40556
 particle in external e.m. field, using quantum stochastic processes theory, Feynman path integral 3-62547
 perturbation energy variational formula 3-66608
 polar molecules, symmetry of negative ions 3-60422
 quantised systems with G_2 symmetry, construction of wave functions 3-40157
 quasienergy and quasienergetic states, strong monochromatic e.m. wave perturbation of atoms and mols. 3-74219
 relativistic h.f.s. correction factors for d and f electrons from hydrogenic wave functions 3-63271
 Saxon-Woods potential, computer program for s-state binding energy and wave functions 3-67289
 scattering, time dependent theory, algebraic, wave operators (*French*) 3-77854
 scattering and diffraction, random media 3-66510
 scattering by spherically symmetric potentials, existence and completeness of wave operators 3-42849
 scattering theory for abstract differential eqns. of second order, existence of wave operators 3-40151
 Schrodinger eqn., unbound solns., expansion in terms of harmonic oscillator wave functions multiplied by Gauss one 3-57128
 single determinant function, correlation component estimation 3-74790
 single-configuration, recursive construction of irreducible tensor spaces of unitary groups and fractional parentage expansion 3-62571
 solvable electron network model development for mols. and crystals. 3-50101
 sphere, surface waves, Legendre functions, Hilbert transform, wave form changes 3-42055
 three-particle resonance, variational expression for Gilbert Schmidt eigenvalues (*Russian*) 3-60093
 time-dependent variational principle derivation from Hamilton's expression 3-74098
 two-nucleon T matrix off energy shell, wave function models 3-78258
 valence-bond wavefunctions and population analyses 3-78665
 variable phase equation generalisation, wave function decomposition 3-42836
 variational, Ehrenfest's theorem and generalised TRK sum rule 3-45699
 variational scattering theory of electron-atom scattering asymptotic soln. 3-71405
 Woods-Saxon and others, description of $^9\text{Be}(p,p\alpha)^8\text{He}$, 35 to 160 MeV, α -clusters for ^9Be 3-60179
 Ar, atom, atomic wave functions from the (e,2e) reaction 3-74875
 B, ground state, single excitations in multiconfig. wavefunctions 3-71351
 Be, ground state, single excitations in multiconfig. wavefunctions 3-71351
 BeH₂, ground state, nonorthogonal configuration interaction, vibration frequencies calc. from wave functions 3-40591
 C, ground state, single excitations in multiconfig. wavefunctions 3-71351
 C, SCF wavefunctions and energies for valence and excited states 3-74773
 F, ground state, single excitations in multiconfig. wavefunctions 3-71351
 Ge, magnetic field effects, field dependent central cell correction 3-79642
 H, single-particle bound-state radial wavefunction, Rayleigh-Ritz-Galerkin with cubic splines 3-74780
 H₂, Davidson-Jones, diff. cross section for elastic electron scatt. 3-75103
 H₂, intermediate states, calc. of cross-sections for dissociative recomb. and associative ionisation 3-75098
 H₂, long-range interatomic force, appl. of electrostatic Hellmann-Feynman theorem 3-74905
 H₂ autoionisation, energy depend. of $^1\Pi_u$ states on internuclear separation stabilization method 3-75099
 H₂⁺, exchange polarization energy, multipole struct. 3-75154
 H₂O₂⁺, STO double zeta SCF, solvation process 3-71504

wave functions continued

- He, 1P first excited state, He-like ions, floating orbitals, rot. projections 3-71355
 He, autoioniz. and electronic correl. 3-63301
 He, autoionization, $2s^2(^1S)$ resonance, by protons, coupling anal. by diagonalization method 3-74903
 He, autoionizational decay of highly excited states, solns. of Schrodinger eqn. 3-71391
 He, direct and reson. by fast electrons and protons, diagonalization approach 3-71445
 He, ground-state wavefunctions, continuum corrections to overlap, variational calc. 3-54563
 He, polarizability of interacting atoms rel. to CIS light and dielectric model 3-67696
 He atoms, radiative transitions involving autoionising in S-nsn 1P transitions 3-74820
 He perturbation-variational calc. for $1s^2\ ^1S$ 3-60351
 He-like ions, first-order Hartree-Fock eqns. for nsms 1S states 3-60352
 Hez⁺ mol., LC wave function of Slater type AO, one electron model (*Russian*) 3-54620
 Hg, atomic electron struct. distortion due to high-intensity laser field 3-74772
 Li, lowest 2P state, variational calc. 3-67644
 Li⁺ + Li(2s), excitation and electron capture cross-sections, calc. 3-71446
 Mn²⁺, relativistic effects in the ground-state splitting parameters 3-79637
 N, ground state, single excitations in multiconfig. wavefunctions 3-71351
 N, SCF wavefunctions and energies for valence and excited states 3-74773
 N₂, generalised oscillator strength 3-74949
 NF and NF⁺, wave functions and potential energy curves calc. 3-40593
 NH₃, floating one-centre Slater, potential constants det. 3-74963
 Ne, Auger transition energies, fluorescence yield nonrelativistic HFS atomic model 3-71385
 Ne I, LS-term depend. of Slater integrals, single-config. approx. deviations 3-67641
 Ne I, parametric study of isotope shifts 3-67643
 ^{20}Ne , generator coordinate method, rel. to low lying nuclear states 3-60094
 O, electron scatt., total cross sections, multi-config. expansion 3-67699
 O, ground state, single excitations in multiconfig. wavefunctions 3-71351
 Sb, odd-A isotopes, two-particle-one-hole states 3-54406
 Sc II, semiempirical calculation of gf values, LS transition arrays, transition integrals, eigenvectors 3-74786
 (XeH)⁺, pot. energy curves, LCAO-MO-SCF calcs. 3-74943

wave mechanics

- see also *wave equations; wave functions*
 boundary-layer turbulence and noise 3-46437
 correlation functions, orthogonal operator expansion, zero-freq. anomaly 3-77856
 electron optics, geometrical, rel. to wave mechanics (*German*) 3-78070
 electrons in matter, their nature and function, theoretical and experimental techniques book 3-77871
 ocean engineering wave mechanics, book 3-56264
 physical world as system of self-regulated signals (*French*) 3-51483
 review of developments by de Broglie (*French*) 3-66615
 wavepacket propagation through square wells and potential barriers, simple calc. method for students 3-66104

wave propagation

- see also *acoustic wave propagation; electromagnetic wave propagation*
 abstract theory of scattering on Hilbert, space 3-51778
 acceleration waves, inhomogeneous elastic nonconductors of heat, amplitude behaviour 3-62508
 acceleration waves in isotropic elastic bodies, thermal properties 3-42923
 anharmonic diatomic lattices, time evolution of nonlinearly modulated waves 3-46687
 anisotropic elastic half-space propag. of seismic waves 3-47611
 complex gamma function, approx. use in wave propagation problems 3-48755
 composite, fibre reinforced, longit. shear wave propag. 3-58707
 composite, fibre reinforced, wave propag. in cylindrical cavity 3-53276
 composite, laminated, continuum theory for wave propag. 3-73026
 composite material, dynamic equivalence and eigenstrain problems 3-73025
 cubic crystal with random mass defects, dispersion eqn. analysis 3-75578
 cylindrical shell, layered, elastic wave propag. phenomena (*Russian*) 3-57105
 demonstration of group velocity for students using oscilloscope 3-70237
 diffraction, finite bodies of revolution, stationary diffraction, method of perturbation of boundary forms (*Russian*) 3-70545
 dipolar fluid, oscillatory flow due to infinite plate 3-79001
 earth mantle, transmission of elastic waves through a soft layer, variational method 3-44930
 elastic, in porous laminated composite with spherical voids 3-51797
 elastic-plastic wave propag., one-dimens., hodograph method extension 3-54117
 elastic/viscoplastic media, cylindrical plane strain wave propag. 3-57091
 electrostatic plasma waves, frequency exceeding gyrofrequency in the magnetosphere, propagation, instability 3-69671
 equatorial electrojets type I irregularities, convective amplification 3-73350
 exothermic two-state reaction, steady-state propagation of the front, asymptotic anal. (*Russian*) 3-47559
 flame-turbulence interaction, shear wave passage through plane flame front 3-63630
 flexural, infinite thin elastic plate with circular holes 3-77841

wave propagation continued

- fluid dynamics, propagation velocity of wave front (*Italian*) 3-43588
 gas-liquid system, separated, propagation of disturbance 3-71813
 heat conduction, generalized theory, wave propagation aspects 3-42918
 Helmholtz eqn. and reflection and transmission coeffs. in inhomogeneous media 3-48708
 hydraulic impact in coaxial cylindrical tubes, parameters of wave motion 3-67954
 liquid crystals, smectic, continuum theory 3-40842
 long nonlinear, on free surface 3-54124
 lumped parameter system, non-dispersive waves, transient excitation technique 3-59476
 magneto-thermo-visco-elasticity, plane strain problems, Kelvin and Maxwell bodies 3-44830
 medium with randomly rough boundary, reflection coeff. 3-42750
 nonflowing air-water system, propagation of pressure and density 3-71812
 nonhomogeneous elastic media, plane-disturbance propagation 3-77842
 nonlinear, perturbation method treatment 3-45632
 nonlinear modulation, perturbation method, integro-partial differential eqns. 3-77864
 nonlinear periodic waves in inhomogeneous medium, scatt. and transform. 3-40158
 nonlinear radial wave propagation in low density flows, application to free jet 3-49628
 Poiseuille flow in circular pipe least damped disturbances 3-79004
 in polymorphic rocks, wave vel. and attenuation 3-53395
 potential barrier system, exact and approx. methods 3-59787
 pressure wave propagation, anal., buffer reservoir tapped on a pipe system 3-75233
 pure helical velocity waves interaction, turbulence and absolute equilibrium 3-57742
 radiative magnetogasdynamics, growth of pressure shocks 3-44925
 random media, kinetic theory, rel. to geometrical optics scatt. theory, half-space scatt. 3-66506
 relativistic thermo-magneto-viscoelastic waves, propag. in Voigt type material 3-62515
 rotating elastic media, two dimensional waves 3-70637
 scalar wave, reflection from plane with random impedance 3-77790
 scalar wave diffr. on nonclosed surface with Dirichlet boundary conduction, Enskog method 3-40093
 scattering and diffraction, random media 3-66510
 scattering problems 2-dimensional, convergent long wavelength expansion method 3-54069
 SH-wave source, elastic half-space, non-homogeneous surface layer 3-44827
 shock, radiation-driven, study of self-similar flows behind shock 3-63719
 shock wave, in gravitational field, self-generated flows, energy dependence on Mach number (*Russian*) 3-67937
 shock wave one-dimensional thermal, in linear viscoelastic half-space (*Russian*) 3-42827
 shock wave propag. vel. of shocks assoc. with solar flares 3-56322
 slightly stratified shear flow, wave induced distortions, nonlinear critical layer effect 3-43585
 snow, wave propagation 3-53363
 solid, steady wave profiles, nonequil. eqn. of state, conservation laws 3-75567
 in solids, compression waves due to explosion in air cavity (*Russian*) 3-66572
 solitons and synacetics 3-45633
 spatially growing wave trails of an inviscid fluid discontinuity, eigenvalue equation 3-43583
 sphere, surface waves, Legendre functions, Hilbert transform 3-42055
 stress wave propag. in bar of variable cross-section 3-54116
 thermoelastic, in random media, uncoupled theory, random boundary conditions 3-66574
 thermoelastic wave propag. in transversely isotropic circular cylinder 3-66599
 thermoelasticity, dilatational wave propagation, shock structures, low temp. 3-62509
 thermoviscoelastic media, steady state wave propagation, dual variational principles 3-70647
 thermoviscoelastic solid, amplitude behaviour of shock waves 3-79426
 Tollmien-Schlichting waves in nearly parallel flows (*French*) 3-63732
 transient cylindrical shear waves, propagation, reflection and transmission 3-40100
 trapped wave model of vortex breakdown in critical flows 3-46469
 travelling sources, induction of two-dimensional field 3-75259
 travelling wave instability in conduction regime of natural convection in vertical slot 3-57730
 viscoelastic, nonlinear propagation, review 3-70646
 viscoelastic, of finite amplitude, soln. of Kortweg-de Vries-Burgers eqns. (*Russian*) 3-45691
 viscoelastic propag. is nonhomogeneous isotropic media 3-45684
 viscous fluid parallel flow, wave velocity 3-43584
 viscous wake wave height and wave resistance 3-49627
 weak discontinuities in quasi-linear hyperbolic systems with discontinuous coeffs. 3-51779
 Pb bar, exptl. study of plastic wave propagation, meas. of stress and strain histories 3-41752

wave scattering see scattering**waveform analysis**

- acoustic speech, vocal tract shape estimation 3-61943
 anharmonic lattices, dispersion relation, wave solution, Kortweg de Vries continua 3-60778
 normal resting electrocardiogram, spectral analysis 3-61896
 oceanic quasi-geostrophic waves in tropical Atlantic rel. to observed eddies 3-59000
 respiratory waveforms, programmable digital desk calculator 3-59684
 spectra, absorption line frequencies, least square convolution, curve fitting 3-73750

waveform analysis continued

- transient wave analysis by space-time cross spectra, Fourier analysis 3-48702

wavefront-reconstruction imaging see holography**waveguide antennas**

- array of planar waveguides with projecting dielectric plates, diffraction 3-42960
 sectorial horn radiation calc., superiority of self-consistent field method 3-70782

waveguide attenuators

- circular waveguide dielectric-lined, approximation method for attenuation charact. calc. 3-54131

waveguide components

- see also ferrite applications; ferrite devices; microwave filters*
 microwave passage through laser flash evaporated metallized film 3-70852
 radiometer switch, m.m. band, input, crossed waveguide system, description, operation (*Russian*) 3-80859
 reflectometers analysis, power equation concepts 3-57115

waveguide connectors see waveguide couplers**waveguide couplers**

- dielectric filled, e.m. wave propagation 3-42832
 holographic thin film coupler, for optical waveguide, perturbation analysis 3-66177
 holographic thin film coupling resonances 3-77536
 optical, grating prod. by SEM 3-70298
 GaAs diode laser, stripe geometry, light coupling into optical fibre with spherical end 3-43022

waveguide joints see waveguide couplers**waveguide junctions see waveguide couplers****waveguide theory**

- see also guided electromagnetic wave propagation*
 acoustic wave propagation 3-61935
 circularly symmetric waves in nonlinear medium, phase-plane analysis 3-54196
 dielectric rod, uniformly corrugated, E_0 mode, surface wave and radiation characts. 3-77939
 electric field intensity in cylindrical waveguide employing analogue computer 3-74190
 energy transport velocity, soln. using eddy power flow concept 3-42951
 ionosphere, spherical surface waveguide, field amplitude and phase velocity of low frequency waves 3-69632
 isotropic dielectrics, guided waves nonreciprocal propagation in sliding luminae 3-52503
 mode conversion, imperfections, bends 3-77851
 piezoelectric crystals, thin semiconducting guiding layer, amplification of surface waves 3-64605
 reflection diagnostic method for plasma column in waveguide, analysis 3-43684
 relativistic electron beam interaction with plasma in waveguide (*Russian*) 3-43661
 scattering by obstacles, in inhomogeneously filled waveguide 3-66753
 self-focusing waveguides, struct. of three-component vector fields 3-59897
 surface wave, numerical solutions, general wave equation given surface impedance, inviscid liquid in gravity field 3-64235
 surface waves across equally spaced metallic discs, e.m. interaction 3-66746
 transition radiation in a rectangular waveguide (*Russian*) 3-57192
 transition radiation in waveguide piecewise homogeneous dielectric filling 3-42942

waveguides

- see also circular waveguides; optical waveguides; rectangular waveguides*
 acoustic, corrugated surface, directionality from point source 3-77317
 acoustic, having negative sound veloc. gradient, propagation effects 3-45348
 acoustic field theory develop. 3-72137
 dielectric line feeder for millimetric-wave radiotelescope 3-42267
 earth-ionosphere, field representation in ELF range 3-59139
 Earth-ionosphere, low latitude whistler propag. 3-59141
 Earth-ionosphere, under nighttime ionospheres, v.l.f. propagation 3-51122
 Earth-ionosphere wave-guide, VLF propag. meas. 3-53531
 elastic surface waves, curved thin film 3-41076
 hollow dielectric He-Xe waveguide laser, 3.5 μm , self stabilised 3-51903
 ionospheric, numerical soln. of differential eqns. for Pc1 micropulsation propagation 3-73349
 microsound surface waveguides, analysis and behaviour 3-48278
 oceanic, microseism propag. 3-61342
 piezoelectric elastic waveguides, finite element analysis 3-70199
 Schumann earth-ionosphere e.l.f. cavity reson. line splitting rel. to solar activity 3-65456

wavemeters

- see also frequency meters*
 heterodyne, frequency changes, liquid systems, capacitance meas. 3-48470

waves

- see also elastic waves; electromagnetic waves; gravitational waves; gravity waves; liquid waves; magnetohydrodynamic waves; magnetostatic waves; plasma waves; spin waves; wave propagation*
 atmosphere, energetics of planetary scale wave fluctuations 3-59104
 atmosphere Kelvin waves, white noise freq. distrib. 3-65342
 atmospheric zonal and harmonic standing pressure waves, slope with height in troposphere 3-59109
 density waves in spiral galaxies 3-61857
 equatorial, over S.E. Asia during summer monsoon 3-51049
 fluid/membrane/fluid, Brillouin scattering from thermally excited wave 3-48171
 in galactic disks, wave patterns 3-59372
 galactic one-armed spiral waves, props. 3-45191
 generation in rotating fluids by travelling forcing effects 3-79005

waves continued

- high amplitude annulus waves in differentially heated rotating fluid, heat transfer and boundary layers 3-43544
- instructional use of computer for superposition of sine waves 3-53818
- internal, around body moving in a density stratified fluid, phase configuration 3-75243
- isentropic and isopycnic waves, superpressure balloons as tracers 3-53559
- lee, stratospheric obs. during glider flight 3-47761
- leewaves and winds over Canterbury, New Zealand during 1970 3-59059
- nonlinear, dispersive, derivative-expansion method 3-77791
- nova outburst interpretation rel. to thermal waves in stars 3-53649
- oscillatory chemical reactions, phase waves, diffusion equation 3-50826
- sand ridges and waves on tidal sea shelves 3-47706
- Stokes waves, standing, maximum height, analytic expression 3-75239
- stratospheric annual temp. wave 3-53482
- stratospheric planetary waves, synergistic baroclinic instability 3-59114
- thermal, in stellar atmospheres 3-69919
- thermal wave interaction with acoustic waves, generation of short heat pulses 3-55042
- thermal wave propag. through sea floor sediment 3-50993
- topographic Rossby waves over shallow topographies 3-57811
- unidirectional energy transfer in nonlin. wave-wave interactions 3-48816
- westerly winds, energetics of developing wave 3-47771

waxes

- microcrystalline, structure and props., X-ray and i.r. obs. 3-54952
- thin transparent coatings on particulates, eval. by focal plane screening technique 3-55098

waxes (electrets) see electrets**waxing see polishing****weak interactions, elementary particle see elementary particle weak interactions****weak interactions, quantum field theory of see quantum field theory of weak interactions****weapons**

- Fallout from nuclear weapons testing and interhemispheric transport of nuclear debris 3-69567

wear**see also abrasion; hardness**

- α -brass water-jet erosion of prestressed material 3-72902
- abrasive wear specimen testing apparatus (Russian) 3-61239
- Auger electron spectroscopy, technological applics. 3-55706
- high C steel, destruction by jet of dilute polymer solution 3-72913
- ceramic, dust particle erosion rates 3-76279
- composite material, self-lubricating, friction 3-50764
- diamond, wear studies 3-58080
- ductile materials, erosion prediction, statistically derived model 3-40971
- fibre reinforced polymeric cage materials characteriz. for roller bearings 3-50772
- fretting fatigue damage, characterization by SEM analysis 3-49930
- friable materials, vibration stand for weight wear 3-55923
- fuel-rod grid-spacer wear and fretting in gas-cooled fast breeder reactor 3-67444
- gears, local fatigue failure 3-64902
- graphite antifriction materials, wear and friction properties, influence of adsorption 3-50810
- grey cast iron, effect of P 3-64957
- Incoloy 901, glaze oxide layers, structure and mechanism of formation during high temp. wear 3-64254
- metal coatings, wear resistance from electrical resistance 3-73103
- metal delamination theory 3-72129
- metal surface, water-jet impact, transient stress distrib. 3-72903
- metallic materials, dust particle erosion rates 3-76279
- Nimonic 75, C263, Nimonic 108, Incoloy 901, in air at room temp. 3-64955
- Nimonic 75, C263 and 108, glaze oxide layers, structure and mechanism of formation during high temp. wear 3-64254
- Perspex, water-jet erosion of prestressed material 3-72902
- polycapromide, diffusion-stabilized, wear resist. (Russian) 3-58725
- polymer, amorphous and crystalline, durability study 3-61222
- polymer sliding on metals, chem. change obs. (Russian) 3-80466
- porous circular discs, squeeze film behaviour, design of clutch plates 3-40970
- radionuclide measurement techniques (German) 3-72919
- resistance determining instrument based on artificial base method 3-55922
- roughness measurement, significance of profile length 3-42520
- solid layer, penetration by liq. jet, theory, appl. to Al/H₂O and UO₂/Na systems 3-80342
- static loading effects on surface parameters 3-55020
- steel, balls, effect of lubricating oils, universal four-ball machine 3-53307
- steel, boriding in powder mixture 3-80350
- steel, carbonitrided 3-64956
- steel, carbonitriding, surface hardening 3-80351
- steel, die, resistance to fracture 3-55817
- steel, during boundary lubrication, predeform. effect (Russian) 3-40968
- steel, fretting fatigue strength 3-44594
- steel, low-C, effects of melting processes, microstructures, season and annealing on sliding wear behaviour 3-41754
- steel, low-C, wear characts. rel. to surface temp. (Japanese) 3-44620
- steel, plastic deformation, additions effect 3-80347
- steel, quenched, tempered, fine structure rel. to contact zone deformation 3-80279
- steel, Si, graphite layer containing 3-80353
- steel, thermoplastic, shear and fracture during high-velocity sliding in rocket-sled testing 3-50748
- steel, wear resistance, electrospray surface alloying effect 3-50739
- steel, wear resistance increase by diffusional impregnation (Russian) 3-58656
- Wankel motor sealing strips, lubricating oil monitoring, γ -ray scintillation technique (German) 3-56980
- Al, during boundary lubrication, predeform. effect (Russian) 3-40968
- Al alloys, fretting fatigue strength 3-44594
- Au, tribological behaviour, SEM obs. (German) 3-64109
- Cu, fretting fatigue strength 3-44594
- Fe, cast, abrasion, Holm's law, hardness depend. (Japanese) 3-72909
- Fe, cast, wear characts. rel. to surface temp. (Japanese) 3-44619
- Fe alloys, hard facing materials characteriz. 3-55823
- Fe-B-C hard facing alloy characteriz. 3-50740
- Fe-Sn, cast, hardness as guide to wear characteristics 3-55831
- HfN-ZrB₂ ceramics, cutting tool material, densification, microstructure, wear resistance 3-50758
- MgAl₂O₄, transparent shaped mat., fabrication and props. 3-72967
- MgO, bombardment damage due to Al₂O₃ microspheres 3-72128
- MgO single crystals, TEM obs. of surface deform. 3-72962
- Ni alloys, abrasion resistance during friction, hot H₂SO₄ and HCl soln., wear, effect of hardness 3-55914
- Ni alloys, glaze oxide layers, structure and mechanism of formation during wear at high temp. 3-64254
- Ti-Zr alloys, wear resist. in H₂O, increase by oxide surface layer formation 3-58697
- Zr and Zircaloy-2, oxidized, wear in water, characteriz. 3-57573

weather see meteorology**webs (membranes) see membranes****weighers see balances****weighing**

- electronic systems 3-61998
- student experiment using ruler and coin 3-70245
- thermal gravimetric apparatus, high-temperature, 50 to 1700C, weight determ. 3-77407
- weighing system analysis (Japanese) 3-40079

weighing machines see balances**weight, atomic see atomic mass****weight, molecular see molecular weight****weight control**

- crystal growth from melt, automated crystal puller 3-41639

weight indicators see balances**weight measurement see weighing****Weissenberg cameras see cameras; X-ray crystallography apparatus****welding****see also electric welding; electron beam welding**

- crystal orientation in joints, corrosion resistance inside reactor pressure vessels, three types of weld (German) 3-72929
- delayed weld cracking test with C-type variable restraint jig 3-61246
- fatigue of welded structures, crack growth rate 3-69310
- reactor control rod guide tube repair, remote controlled operation (German) 3-71236
- room-temperature non indium metallic bond, tested by welding acoustic shear wave transducers to paratellurite 3-76230
- solid phase, struct. form. in joints (Russian) 3-72925
- steel, Cr-Mo-V weld metal, fracture resist. under low cycle loading 3-58682
- steel, high-speed, welded blanks, struct. and props. after annealing 3-55814
- steel, low-C, high strain fatigue tests, weld effects 3-69317
- steel, max. heating temp. calc. (Russian) 3-41789
- steel, structural, tests for localized heating effects determ. 3-69436
- steel, welded joints, fatigue strength at high temp. and low cycle loading 3-44706
- steel bar reinforcement, deformation, fatigue strength, spot welding effect (German) 3-44638
- steel joints, high-strength, with low-strength weldment 3-69295
- steel pipe, nondestructive testing, u.s. variable angle transducer 3-47505
- steel under fluctuating stress, crack formation and propagation behaviour 3-72911
- steel weldment, T-1 type, stress relief annealing (Japanese) 3-41774
- steel/Ti explosion welding Ti to steel, effect of hot and cold rolling 3-72927
- u.s., biological tissue 3-66405
- welded components, weak joint, viscous strength, effect of mech. inhomogeneity (Russian) 3-41792
- welded connections of members with variable cross-sections, stress computation 3-69329
- Zircaloy cladding, high temp. -testing for use as thermocouple sheath in PWR 3-47431
- Cu, diffusion bonding, surface contamination effect 3-80399
- Nb alloys, superconducting wires, reduction of current degradation 3-41788
- Ti alloys, max. heating temp. calc. (Russian) 3-41789
- Ti alloys magnetic field effects on weld structure (Russian) 3-61184

welding equipment

- hot wire anemometer, welding assembly for laboratory repairs 3-57030

Wentzel-Kramers-Brillouin method see quantum theory**Wertheim effect see magnetomechanical effects****wetting**

- cellulose, gamma-irradiated, changes in strength, heat of wetting, during storage 3-73059
- glass, powder, kinetics of wetting, surface energy and surface tension, modification by siloxanes (German) 3-53279
- E-glass, surface free energy of wetting by vapours 3-55146
- glass/iron substrate systems, interfacial reactions and enhanced wetting 3-55880
- glass/metal substrate systems, interfacial reactions and adherence 3-55882
- liquid/solid system, contact angle interpretations, critical surface tension 3-68479
- metal composite, fibre reinforced, bonding and compatibility at dividing boundary (Russian) 3-53273

wetting continued

- nuclear reactor surface rewetting in emergency core cooling, expts. 3-74667
 polyethylene, by water, methylene iodide and methyl iodide-decalin mixtures 3-43927
 polytetrafluoroethylene, and Na-treated polytetrafluoroethylene, wettability, roughness and anisotropy effects 3-58739
 refractory liquids, surface tension, wetting angle determ. 3-72260
 rubber, wettability and stability in aqueous solns. (*Russian*) 3-41813
 salol single crystal, wetting by its own melt 3-75660
 solid, surface free energy components estimation 3-68480
 subsurface, dynamic surface tension meas., bubble method, instrument incorporating stroboscope (*Russian*) 3-50071
 Al alloys, wetting by low melting solders, u.s. tinning, joint formation (*Russian*) 3-41791
 Al_2O_3 , by liq. Al, contact angle temp. and time depend. (*Slovak*) 3-55850
 C, by silicon and alloys, contact angle meas., rel. to reaction sintering 3-76298
 C and carbides, by Cu alloys, model approach 3-41084
 Cu alloys, wettability of liq. Sn, rel. to soldering 3-50754
 Fe surface, by oxide melt, elastic deformation obs. 3-68483
 Mo, of Ag, hot-filament silver vapour source 3-39892
 Pt, of glass sessile drops, contact phenomena 3-58175
 SiC, by silicon and alloys, contact angle meas., rel. to reaction sintering 3-76298
 Si_3N_4 , by silicon and alloys, contact angle meas., rel. to reaction sintering 3-76298
 Ta, of Ag, hot-filament silver vapour source 3-39892
 W, of Ag, hot-filament silver vapour source 3-39892

whiskers (crystal)

- diamond crystals, growth in needle and plate form. 3-75698
 ice, densities on basal faces rel. to domain densities 3-51036
 NaCl, growth rate, kinetics 3-72298
 polyoxymethylene, acicular single crystals, strength props. 3-54779
 spinel based ceramic/ceramic composites, plastically deformed, microstruct. features 3-76343
 Ag, mass production by reduction, effect of halide impurities 3-64269
 Al_2O_3 , growth by vapour-liquid-solid phase mechanism (*Russian*) 3-72297
 Al_2O_3 , sapphire in Ni matrix, morphological and chemical stability 3-76357
 $\alpha-Al_2O_3$, whisker crystal growth, Al_2O_3 reduction, condensation of Al nucleation centres (*Russian*) 3-41624
 Al_2O_3 sapphire in Ni matrix, morphological change kinetics, 1100-1400°C 3-76358
 Al_2O_3 whisker/Ni composite, compatibility limits 3-80441
 C, pyrolytic, growth, methane pyrolysis, reduced press., 1500-1700°C (*German*) 3-76369
 CdS layers, growth structure junctions, bridge-like systems 3-75696
 Co, mass production by reduction, effect of halide impurities 3-64269
 Cu, fibrous bundle growth process 3-76125
 Cu, higher order elastic consts., deviations from Hooke's law 3-50097
 Fe, domain config., Bloch walls, magnetisation process, susceptibility, 0.200 kHz 3-50399
 Fe, fibrous bundle growth process 3-76125
 GaAs, vapour-liquid-crystal growth mechanism 3-72300
 p-Ge, microplasticity due to dislocations 3-72299
 Ge, vapour-liquid-crystal growth mechanism 3-72300
 InSb, breaking pt. and strength (*Russian*) 3-41113
 K(Cl, Br, I) ionic conductivity, 40 to 300C, effects of X-ray irradiation (*Russian*) 3-79598
 $Mo_xV_{1-x}O_2$, metal-semicond. transition phenomena, comp. depend. 3-60907
 NaCl, internal friction and reversible creep (*Russian*) 3-43828
 NaCl, ionic conductivity, 40 to 300C, effects of X-ray irradiation (*Russian*) 3-79598
 NaCl whiskers, radiative coloration and recombination luminescence (*Russian*) 3-44497
 $Na_2Mo_3O_{10}$, growth in aq. soln., continuous conc. meas. apparatus 3-72792
 Ni, higher order elastic consts., deviations from Hooke's law 3-50097
 Ni, mass production by reduction, effect of halide impurities 3-64269
 Si, filamentary growth from soln., mechanism 3-69164
 Si, vapour-liquid-crystal growth mechanism 3-72300
 SiC, growth by vapour-liquid-solid phase mechanism (*Russian*) 3-72297
 ZnO, antiphase boundaries, transmission electron microscope obs. 3-79597
 ZrO_2 -MgO system, directional solidification and oriented eutectic composite behaviour 3-76236

whistlers

- see also *ionospheric electromagnetic wave propagation*
 absolute whistler instabilities, nonlinear theory 3-79146
 collisionless electron cyclotron damping, expt. obs. 3-75299
 dayside-cusp ionosphere Whistler mode hiss and soft electron fluxes 3-69638
 decay instability in three dimensions 3-79106
 electron, upward propag. into ionosphere 3-65448
 electron and ion, 10-1500 Hz, satellite obs. of densities geomagnetic field and temp. versus altitude 3-42028
 induced amplitude perturbation in subionospheric VLF transmissions 3-69667
 instability enhancement in magnetosphere by cold plasma injection 3-69696
 interplanetary, cyclotron damping 3-65735
 ionospheric, low latitude propag. 3-59141
 low-latitude, ducted propag., simultaneous obs. 3-59131
 low-latitude, effect mag. storms on ducted propag. 3-56185
 magnetosphere, monochromatic wave propagation 3-49663
 magnetosphere balloon borne expts. in NASA MPE barium ion cloud project 3-80824
 in magnetospheric plasma, propag. of large amplitude whistlers 3-69690

whistlers continued

- magnetospheric structure from v.l.f. whistler obs. at Halley Bay 3-51156
 magnetospheric whistler dispersion characts. rel. to local plasma 3-51147
 microwave propagation in large waveguide containing magnetoplasma, boundary effects 3-68000
 mode instability, nonlinear development and Fourier analysis 3-46522
 mode propagation in ionosphere, in longitudinal electrostatic field 3-73343
 modulational instability, cold and hot plasmas 3-49679
 multiflash whistlers at low latitudes, propagation characteristics 3-65408
 nonlinear wave-particle interaction in a nonuniform mag. field 3-75364
 nonlinear whistler instability in computer experiment, magnetospheric implications 3-73368
 nose frequencies and delay, obs. at Sofia 3-61495
 nose frequency and min. group delay 3-76816
 Ogo 6 experiment, results of electric and e.m. fields in 20 Hz to 540 kHz range 3-56200
 plasma, finite anisotropic with hot electrons, e.m. instabilities 3-40779
 plasmasphere, nonducted, pseudo-noise (*Japanese*) 3-56206
 plasmasphere depletion, whistler obs. during magnetic substorm 3-51144
 plasmasphere recovery following magnetic storm from whistler obs. 3-61569
 plasmasphere structure during mag. recovery, whistler ground based data (*French*) 3-61555
 plasmaspheric ELF hiss, whistler mode freq. meas. 3-51146
 polar cap phase anomalies of v.l.f. waves, August 1972, proton flare associated PCD's 3-56128
 propagation characteristics at low latitudes, electron density horizontal gradients effect 3-65407
 propagation depends on pulse length 3-69629
 propagation mode, determ. of plasma bulk flow in magnetosphere 3-44949
 outer radiation belts, simulation of gyroresonant electron-whistler interactions 3-61559
 ray paths, effects of collisions, lower ionosphere 3-80801
 Sofia, nose frequencies and delay obs. 3-61495
 solitary waves parametric instability 3-79107
 storm time characteristics at low latitudes 3-76822
 trans-equatorial v.l.f. whistler mode propagation, OGO-4 plasmopause obs. 3-61570
 triggering of correlated X-rays and VLF riser bursts 3-69655
 turbulence and vel. space diffusion in magnetospheric plasma, simulation 3-56228
 two-hop, localisation of sources over Europe, Interkosmos 3 obs. 3-56186
 v.l.f. and e.l.f. waves absorption during night 3-76751
 v.l.f. and e.l.f. waves absorption rel. to sunrise and sunset effects 3-76750
 v.l.f. emission during geomag. storm, August 9, 1972, ISIS-2 obs. 3-56129
 v.l.f. ionometer obs. at Halley Bay, equipment and meas. of signal bearing 3-51190
 VLF input impedance of loop antenna in magnetosphere 3-76823
 v.l.f. wave propagation in upper ionosphere and magnetosphere, parameter determ. 3-42063

white dwarfs

- RX Andromedae, Z Cam type variable, photometric obs. during eruption 3-65893
 SY Cancri, Z Cam type variable, photometric obs. during eruption 3-65893
 cataclysmic variables, masses of white dwarf primaries 3-48017
 central stars of planetary nebulae rel. to hot liquefying white dwarfs, cores, masses and luminosity 3-61877
 cooling time and internal structure for 3 models 3-77048
 critical point existence and gas-liquid phase transitions 3-53648
 crystalline interior thermodynamic functions, b.c.c. lattice model of heavy-ion plasma 3-73487
 DA type, relation with DB white dwarfs and planetary nebulae nuclei 3-81028
 DA white dwarfs, interpretation of quadratic Zeeman effect 3-69941
 DB type, relation with DA white dwarfs and planetary nebulae nuclei 3-81028
 electron gas ferromag. state to maintain strong mag. fields, density of states calc. 3-51256
 envelope structure, dependence of surface gravity and composition 3-81030
 40 Eridani B, line profiles and rotation meas. 3-45120
 evolution sequence for DA, DB, DC type dwarfs 3-73482
 evolutionary stage, masses involved 3-51335
 gravitational layering and convection, appl. to Jupiter 3-47901
 Grw + 70°8247, magnetic dwarf, wavelength dependence of polarized radiation 3-51351
 AH Herculis, high-speed photometry of dwarf nova, light curve analysis 3-45116
 internal magnetic fields 3-59340
 interstellar medium structure, effect of hot white dwarfs above Galactic plane 3-59373
 ionizing radiation production in galaxies 3-81052
 i.r. radiation source in galactic centre, magnetic bremsstrahlung 3-59360
 Landau orbital ferromagnetism, temp. aspects 3-61764
 light curves of gravitational lens-like action for binaries with degenerate members 3-59341
 magnetic, polarised radiation, exact soln. of Kemp's (1970) model 3-53638
 magnetic DC type evolutionary connection with planetary nebulae nuclei 3-81027
 MHD stability in white dwarfs and neutron stars, rel. to magnetic fields 3-42187
 nova outburst, nebulosity, non-spherical struct., influence of white dwarf 3-69938
 KT Persei, Z Cam type variable, photometric obs. during eruption 3-65893

white dwarfs continued

- quasiradial pulsation freq. determ. using general relativity theory 3-53653
- rapidly rotating stars, viscous effects 3-65871
- rapidly rotating stars, viscous evolutionary sequences 3-65872
- spectroscopic data for 41 southern white dwarfs 3-69961
- HL Tau-76, triply periodic white dwarf, blue magnitude obs. 3-48034
- HL Tauri, triply-periodic white dwarf, differential blue magnitudes 3-48043
- Wolf 1346, line profiles and rotation meas. 3-45120
- X-ray astronomical observation, binary system component identification 3-61835
- X-ray emission in close binary systems 3-45163
- X-ray emission region of Sco X-1 type objects with accretion 3-48084
- ¹²C shell-burning stars, radial pulsation stability rel. to pre-white dwarf stars 3-61763
- He envelopes, upper bounds of mass 3-81211
- He spectra in stars with large mag. fields, Zeeman effect calcs. 3-45107

white noise

- atmosphere Kelvin waves, white noise freq. distrib. 3-65342
- audibility of harmonics 3-48218
- microwave stochastic reflection, Walsh spectral analysis 3-75301
- modelling techniques for insect visual nervous system studies 3-45307
- nerve afferent responses to pseudorandom binary white noise, real-time cross-correlation analysis 3-42278
- sound transmission, 'A' weighting curve, noise meas. 3-53795

wideband amplifiers

- h.f. plasma properties (*Russian*) 3-43694

Wiedemann effect *see* magnetostriction**Wiedemann-Franz law** *see* electrical conductivity of solids; thermal conductivity of solids**Wien effect** *see* electrical conductivity of electrolytic liquids**Wigner coefficients** *see* Clebsch-Gordan coefficients**Wigner effect** *see* radiation effects**Wilson cloud chambers** *see* cloud chambers**Wimshurst machines** *see* electrostatic generators**wind**

- acoustic Doppler wind measuring system, profile at up to 1 km 3-42081
- acoustic wave scattering 3-42388
- air flow obs. in pine forest 3-73336
- air-water interface, evaporation and energy transfer, effect of wind and waves 3-47679
- Aladdin II meas. at 90-160 kms. 3-61500
- Aladdin II meas. in 36 to 110 km range 3-59126
- Athens Observatory, sea breeze diurnal variation and duration 3-76770
- eastern south Atlantic, wind field and derivatives 3-65376
- atmosphere and ocean interaction mechanism during a storm 3-76684
- atmospheric diffusion, numerical model accounting for increase of wind speed with height 3-76708
- atmospheric wave instabilities, effect of wind shear, FM/CW radar obs. 3-65298
- Australia, monthly mean wind patterns at 40000 feet 3-59055
- Brookhaven, N.Y., wind direction effect on CO₂ comp. 3-51033
- clear air turbulence, India, effect of upper air flow patterns 3-80744
- clear air turbulence, radar detection 3-44962
- cloud shadow effects on navifac 3-59020
- coastal upwelling, β effect, wind-driven model, longshore and offshore flow 3-47671
- coastal upwelling, ocean circulation model, time-dependent winds 3-47672
- coastal upwelling, wind-driven, effect of bathymetry subsurface motion, induced jet 3-47673
- currents, calc., South Pacific Ocean, fields of density, wind, level surface equation (*Russian*) 3-47690
- currents induced in shallow lake or sea 3-76692
- direction persistence as a function of speed, averaging time or sector width 3-61455
- disturbed airflow over mountains, aircraft measurements 3-44910
- Eole experiment, results and objectives 3-61456
- equatorial electrojet, development of model inc. neutral-air winds and two-stream instability 3-42024
- evaporation, rel. to meteorological factors, correl. techniques 3-80739
- extreme wind speeds in gusts over India 3-65330
- F-region, meridional neutral wind at mid-latitudes 3-76792
- F-region perturb. at mid-latitudes during mag. storms 3-53530
- F-region theoretical profile 3-61545
- fluctuations in low-freq. range in presence of convection 3-69575
- geostrophic drag coefficients, relation to surface wind 3-76711
- geostrophic wind rel. to radiation fog and stratus formation, Belmont mast wind data 3-59056
- Gill UVW anemometer response error corrections 3-76913
- global zonal wind circulation, seasonal variations, biennial term, earth's rotation 3-41966
- gust factors over open water and built-up country 3-51010
- Harmattan season rel. to seasonal variation in atm. radioactivity at Ibadan 3-47772
- h.f. wind fluctuations in atmospheric boundary layer, obs. at Cardington 3-41958
- horizontal coherence of fluctuations in turbulence 3-76713
- horizontal wind motion and vertical electric field at magnetic equator 3-53429
- hurricane and typhoon effects on upper active ocean layers at OWS Tango in Pacific 3-51001
- hydrodynamics, forces, pressure gradients, storms (*Hungarian*) 3-80723
- instabilities meas. by Aladdin II 3-61502
- instability of 2 level quasi-geostrophic waves in horizontal shear, seasonal var. and latitudinal distribution 3-73325
- ionosphere sequential neutral wind profiles, using D₁ method 3-76793
- ionospheric sporadic-E layer, wind component exchange and rapid vertical movement 3-80804
- Japan, Southwest Islands, thermal structures (Jan 1968) 3-76717
- Kelvin wave period oscillations, zonal and meridional winds, climatological analysis, (1959-1971) 3-44880
- Labrador and Newfoundland coast, effect on icebergs, forecast of 1973 iceberg season 3-80718
- Labrador and Newfoundland coast, effect on icebergs, forecast of 1973 iceberg season 3-80719
- lake levels, response to unsteady wind stress 3-42091
- laser vector velocimeter meas., signal conditioning electronics 3-77762
- leewaves and winds over Canterbury, New Zealand during 1970 3-59059
- logarithmic wind profile in planetary boundary layers rel. to micrometeorology 3-47735
- mapping North Atlantic winds applying h.f. radar 3-59174
- marine air, Aitken and giant nuclei, salt conc., wind speed 3-47741
- marine weather extremes, temp., rel. humidity, wind speed, visibility, salinity and upper air temp. 3-53496
- Mars, wind erosion in polar regions 3-61687
- maximum wind pressure in gusts in India 3-47727
- microseisms generation, hydrometeorological conditions 3-61345
- microthermal turbulence, balloon-borne temp. sensors, wind speed profile, wind shear calc. 3-44884
- midlatitude thermospheric winds from ionospheric plasma vertical drift meas. 3-69611
- moving gust patterns, 'Cat's paws', surface capillary waves 3-47680
- New Zealand Earth strain meas., wind and rain effects 3-47638
- Nimbus 4 THIR 6.7 μ obs. rel. to regional and global wind field analysis 3-51057
- numerical analysis of stream distributions around buildings (*Japanese*) 3-49544
- objective analysis scheme, atmospheric wind field, spectral analyses 3-76860
- ocean, rotating, long wave generation 3-65285
- ocean circulation, induced by continental slopes, wind stress 3-47670
- ocean currents, surge and ebb, role of non uniformity of wind, inertial effects, bottom topography (*Russian*) 3-80691
- ocean currents, wind driven, Washington continental shelf, effect of surface current and wind direction 3-80721
- ocean currents calc., wind stress, variable ocean depth (*Russian*) 3-47687
- ocean dynamics, mean wind behaviour in open ocean 3-50995
- ocean h.f. waves rel. to aerodynamic roughness and wind speed 3-61440
- ocean mapping of temperature and salinity, effects of winds and tides 3-41944
- ocean waves, horizontal orbital velocity and acceleration spectra determ. (*Polish*) 3-44868
- ocean wind-mixed layer, deepening rel. to model of mixing process 3-44858
- Oklahoma, diurnal wind variation in lowest 1500 ft. during June 1966-May 1967 period 3-47753
- orographic effect on wind and rain distribution around mountain gap 3-65327
- Pacific Ocean, current calc., wind and density nonuniformities, bottom topography discharge of Antarctic circular current (*Russian*) 3-47697
- Passighat, India, local wind rel. to geography and temp. 3-80729
- Pleistocene wind strength and temp. correl. in Saharan coast deep-sea core 3-80763
- profile near ground 3-65318
- pulsed Doppler weather radar, storm wind velocity isotach displays 3-76911
- rain showers, wind gradients and Doppler spectra variance from radar obs. 3-76762
- remote sensing of wind velocity in lower troposphere using acoustic sounder 3-65518
- sea and reservoir surfaces, wind induced tidal oscillations 3-76682
- sea waves and drift current, wind maintained, energy expended 3-76683
- sea-air interface dynamic roughness rel. to wind-wave interactions 3-59019
- sea-level wind speeds, remote sensing 3-51046
- severe storms, environmental wind veer rel. to circulation 3-59117
- shallow sea, nonlinear nonstationary wind circulation problem (*Russian*) 3-80687
- shear convection, similarity model of turbulent regime 3-51009
- sound propagation over barriers, wind effect 3-45366
- sound scattering by turbulent flows 3-42407
- Southeast Asia, weather and equatorial waves during summer monsoon 3-51049
- spectrum analysis of correlation with pollution data 3-76703
- sporadic E-layer blanketing at mag. equator due to horizontal wind shears 3-42046
- sporadic-E formation, test of wind shear theory 3-56216
- sporadic-E layer, wind-shear theory, validity of rocketborne magnetometer measurements 3-76810
- St-Santin, neutral wind and temp. oscill. meas. in F-region 3-53529
- stratospheric comparison of geostrophic calculations and rocket measurements 3-73317
- stratospheric wind and temp., total ozone, sea-level press. rel. to sun-spot cycle 3-69598
- stratospheric wind during 7 March 1970 solar eclipse 3-65341
- stratospheric wind reversals rel. to natural infrasound reception 3-59095
- surface divergence field, computation for wind over Oklahoma 3-65367
- surface waves, wind energy transfer to waves, turbulence, asymptotic joint expansions (*Russian*) 3-47686
- surface wind, effect of geostrophic shear on cross-isobar angle 3-41961
- surface wind automated prediction, use of model output statistics 3-59193
- surface wind over upwelling area off coast near Pisco, Peru 3-41962

wind continued

- thermally stratified air-flow layer near a water surface under wind gust conditions, turbulence struct. meas. 3-59048
- thermospheric Li vapour trails, motion of daytime releases rel. to winds 3-65418
- thermospheric neutral air, effect on F2 ionisation and crest positions 3-73355
- thermospheric wind effects on He and Ar distrib. 3-56180
- thermospheric wind system rel. to geomagnetic S_q variations 3-76666
- thermospheric winds and gravity waves generated by auroral zone heating 3-69613
- thermospheric winds rel. to superrotation of upper atmosphere 3-61516
- thunderstorm, wind and temp. profiles using lightning as acoustic source 3-59184
- thunderstorm cell flow, drag expt. 3-51031
- tornado at Diamond Harbour, India on 21 March 1969, general description 3-80727
- tropopause, source of high-level (stratospheric) waves 3-47761
- tropopause, turbulent waves producing sudden changes in temperature and wind 3-65383
- troposphere over India, seasonal changes in pressure gradient, wind circulation and rainfall 3-80747
- tropospheric wind and static stability rel. to lee waves and convective cell patterns 3-53487
- turbulence associated with basin cooling (*Japanese*) 3-56161
- turbulence near surface of drifting snow (*Japanese*) 3-56159
- turbulence round obstacle, snow drifting (*Japanese*) 3-56160
- upper atm. zonal winds determ. using orbit anal. of 1965-11D 3-53591
- upper-air flow, zonal and meridional winds, Southern Hemisphere temp. latitudes, GHOST balloon flights 3-44879
- urban, wind tunnel simulation of lower third 3-63676
- urban boundary layer, wind derived flow fields and aerosol concs. 3-59091
- urban boundary layer simulation in wind tunnel 3-63675
- velocity determ. from billow clouds, satellite obs. 3-59093
- velocity fields above sea surface (*Russian*) 3-73267
- vertical profiles, rawinsonde obs. 3-76752
- vertical wind shear in lowest layers of atmosphere over Thumba 3-65333
- waves in a sea, two-dimensional energy spectrum, calc. of direction of propagation of spectral components and angular width (*Russian*) 3-80699
- westerlies, energetics of developing wave 3-47771
- zonal, terrestrial deceleration, internal dissipation of energy, force of zonal wind 3-80651
- zonal stratospheric over Natal (Brazil), Thumba (India) and Sonmiani (Arabian Sea islands) 3-65378

wind tunnels

- atmospheric surface layer, volumetric flow control, wind tunnel studies 3-53561
- diffusion in stably stratified flow in wind tunnel rel. to atmospheric boundary layer 3-40720
- hailstone aerodynamic testing 3-76740
- high Reynolds number tunnel, exhaust noise environment 3-46419
- hypersonic, high pressure air-heating plasma torch (*German*) 3-46559
- hypersonic gun tunnel, two-stage, Kobe University 3-70500
- internal waves in stratified flow 3-61462
- large-scale, NASA Ames 40 × 80-foot, acoustic research on short take off and landing concepts 3-62002
- model noise expts., basic acoustic considerations 3-75223
- noise sources diagnosis, by cross-correlation techniques 3-46448
- plasma, model of magnetosphere 3-43651
- rectangular block, static and aeroelastic characteristics, wind tunnel expt. 3-71778
- simulation of atmospheric vortex street features 3-59118
- sonic booms, wind-tunnel investigation method 3-46451
- supersonic, short duration, shock tube with Laval nozzle applic. 3-51773
- urban boundary layer flow, lower third, simulation 3-63676
- urban boundary layer flow simulation 3-63675

winding (process)

- filament winding method for model epoxy composites 3-50773
- filament-wound shells, glass reinforced plastic, geodesic winding characteristics 3-80446
- glass ribbon composite, fabrication and characteriz. 3-76348
- $\text{Li}_2\text{O} \cdot \text{Al}_2\text{O}_3 \cdot n\text{SiO}_2$ graphite fibre reinforced composite, fabrication and low temp. props. 3-76350

windings

- see also coils*
- glass-reinforced plastics, winding, change in degree of anisotropy, elastic and strength props. 3-73024
- poleface winding system, for independent multipole fields in AGS magnets 3-56796
- zero gradient synchrotron, retuning after installation of vacuum chamber and pole-face windings 3-56747

wires (electric)

- see also conductors (electric); insulated wires*
- current leads, thermodynamic optimisation, refrigerator min. power input calc. 3-48382
- electric leads, sealed, helium cryostat 3-48386
- elliptical cross-section, magnetic field produced by current (*German*) 3-48834
- Cu, cylindrical, thermodynamics of explosion, first phase 3-63901
- Fe, in toroidal geom., fluxconduction for reversible mag. processes (*German*) 3-59833
- Nb alloys, superconducting, welding, reduction of current degradation 3-41788
- W, cylindrical, thermodynamics of explosion, first phase 3-63901

wiring

- see also building wiring; printed circuits*
- device for transitions from binding posts to 110 V devices in the student laboratory 3-66120

wiring diagrams *see circuit diagrams***WKB method** *see quantum theory***wolfram** *see tungsten***wood**

- coniferous wood tissues molecular rheology 3-52412
- floor-ceiling assemblies, wood framed, trowelled floor toppings, sound attenuation 3-77328
- opalized fossil wood, structure comparison with high-tridymite 3-73194

work function

- see also electron emission; Schottky effect*
- elastic deformation effect, rel. to change in surface potential of solid in vacuum 3-47564
- electrodes, retarding potential curves shift by two-dimensional condensation 3-69133
- exoelectron current, electron work function depend., theory 3-58587
- FEM, probe hole measurements, rapid changes in work function in adsorption, technique 3-62290
- field emission energy distribution from cold cathode 3-53171
- graphite, variation during Ar adsorption, polarisation phenomena (*French*) 3-79567
- Kelvin measurement method, analysis and improvement 3-62178
- metal, as electronegativity meas., for alloy form. 3-63975
- metal, electron potential emission yield function 3-69117
- metal, monovalent, and surface double layer potentials, from network model 3-41252
- metal, solid, surface energy calc. from work function and electron config. data 3-64393
- negative electron affinity photoemitter, physical model 3-47343
- refractory metals, thermionic emission, direct-current arc 3-69132
- steatite ceramic, determ. from surface ionization and discharge triggering (*Russian*) 3-44506
- thermionic emitter, distribution plotting, technique, apparatus 3-73811
- thermoelectronic emitter, work function distrib. from total energy spectrum (*French*) 3-55718
- Ag adsorption of oxygen effect, single crystals, (111) face, electron and argon ion bombardment cleaned under ultra high vacuum 3-43938
- Al, work function meas. on (100), (110) and (111) surfaces. 3-72393
- Al_2O_3 in Cs vapour, thermionic electron emission obs. 3-55719
- Ca, film, elec. field effect on photoelec. efficiency, work function 3-64760
- Cu, photoelectric work function for clean surfaces, meas. by Fowler method 3-41616
- EuO:Gd, photoemission, excited energy states, absorpt. edge behaviour (*German*) 3-50646
- Fe-Si alloy (100) single crystals, photoelectric, Auger electron spectroscopy 3-61082
- GaAs, photoemission, escape probability elec. field enhancement of negative electron affinity surfaces 3-61103
- GaAs-metal interface, Fermi level shift by metal work function 3-60916
- Hg, melting pt. behaviour, photoemission obs. (*German*) 3-50647
- Mo/adsorbed Ge system, coverage effects, field emission study 3-64764
- Ni(100), (110) surface, Auger and autoionization processes with $\text{He}^+(2s)$, He^{2+} ions, work function changes 3-47339
- Pb, rel. to exoelectron under recrystallisation conditions during plastic deformation 3-69146
- Pt, (111) and (100) surfaces, benzene, naphthalene and pyridine adsorbed layer characterization 3-55127
- SbS₃-metal electrical contacts, photoconducting film, contact types 3-46893
- Si, photoemission, escape probability elec. field enhancement of negative electron affinity surfaces 3-61103
- Ti thin films on Au and Ag substrates, ultra-high vacuum deposition 3-44130
- W, determ. from surface ionization and discharge triggering (*Russian*) 3-44506
- W, field emission determ., effects of adsorbed gases (*German*) 3-47350
- W:Si(C), depend. on adsorbed layer thickness electron field emission obs. depend. on adsorbed layer thickness 3-43930
- W/adsorbed Ge system, coverage effects, field emission study 3-64764
- W/Hg/NaI, W/NaI systems, co-adsorption, field emission obs. 3-80145
- W(100), of Cs, H₂, LEED and workfunction investigation of C(2 × 2) structure 3-55145
- W(100) surface, coadsorption of Cs and H₂ 3-75665
- W(100) surface, coadsorption of Cs and O₂ 3-75666
- W(211) H₂ chemisorption, adsorption, desorption, work function data 3-72272

work hardening

- see also cold working*
- acoustic emission monitoring, nondestructive evaluation, strain hardening transitions 3-47508
- alloy, B2-type, thermal and nonthermal cross-slip effect 3-47374
- alloy, dispersion hardened, back-stresses, image stresses and mean strains 3-80290
- alloy, machine parts, surface work hardening for increase of low cycle fatigue resist. 3-44632
- alloy, plane strain fracture toughness prediction 3-76227
- anisotropic metal, bulge test and simple tension test data 3-68311
- anisotropic metals, bulge caused by rolling 3-69271
- Bauschinger effect, yield stress drop rel. to pre-strain 3-69293
- beam, effect on elastoplastic stability (*Japanese*) 3-62505
- composite, plastic deform. anisotropy and work hardening rate 3-76356
- cylindrical bar, longit. elastic-plastic final duration pulse propag. 3-70635
- deformational hardening, uniaxial creep, metals and alloys (*Russian*) 3-41765
- elastic/viscoplastic media, cylindrical plane strain wave propag. 3-57091
- elastoplastic material strain hardening, stress evolution characterisation (*French*) 3-70615
- fatigue crack growth theory, BCS crack theory with work hardening 3-68324
- f.c.c. structures, influence on microhardness anisotropy 3-53259

work hardening continued

- halide laser windows, press forged, mech. props., grain size and alloying depend. 3-73786
 internal energy dissipation simulation in elastoplastic connections using analogue computers 3-57096
 i.r. transmitting mat., hot pressing 3-76253
 machined carbon steel, surface layer, fatigue 3-64882
 metal, delay of yield and hardening in high-speed deform., model 3-76222
 metal, group IV to VIII, friction-hardened surfaces, microhardness obs. (Russian) 3-80329
 metal, rel. to stored energy of cold work, book 3-44642
 metal/metal interface, differential modulus effects on mech. behaviour 3-40921
 metallic single crystals, f.c.c., tensile behaviour, theoretical model (French) 3-64089
 metals, load-elongation curves of pure b.c.c. structure at low temp. 3-72118
 microyielding in cyclic loading using time monitoring technique 3-41747
 plastic deformation hardening of G31, Cu and Ni by shock waves (Russian) 3-64898
 polymer, creeping deformation, irreversible, under stepwise stressing rel. to theory of hardening 3-58743
 powder compaction, strain hardening effects 3-69336
 shells of revolution, transient creep 3-42794
 spherical shells, rigid plastic, rate problem for finite deform. under hydrostatic press. 3-62498
 steel, 1Kh2M, effect of preliminary work hardening on thermal fatigue 3-80382
 steel, austenitic, high-Mn, fine struct. after high-speed straining (Russian) 3-64836
 steel, austenitic stainless, crit. work hardening of nucleation and migration for recrystn. (French) 3-61152
 steel, bainite hardenability treatment increase during thermomech. treatment 3-50742
 steel, brittleness, strain ageing rel. to drawing temp. 3-76215
 steel, carbonitrided, effect on wear 3-64956
 steel, compressive strain hardening rel. to C content 3-80372
 steel, fatigue failure, effect of hardening induced by cyclic overload-ing 3-58683
 steel, hardened high C, hardening in NaCl soln., annealing, uniaxial compression diag. (Russian) 3-41767
 steel, high-Mn, dislocation structure and strain hardening (Russian) 3-69218
 steel, internal friction rel. to heat treatment, martensitic transformation 3-80352
 steel, low-C, cyclic loading effect on subsequent yielding 3-44593
 steel, low-C, low cycle fatigue concepts extension 3-69318
 steel, medium-C, cyclic loading, dynamic deformation aging 3-80364
 steel, pearlitic, internal stress approach 3-69298
 steel, shot peening to produce surface layer, depth and residual surface stress meas. 3-76196
 steel, stainless, strengthening by direct and reverse martensitic transformations. 3-50732
 steel, thermoplastic hardening, heat resist. test from fracture toughness (Russian) 3-72899
 steel, white layers formed during treatment, characteriz. (Russian) 3-80330
 steel, X-ray obs. of stacking faults, effect on resistance to plastic deformation (Russian) 3-69269
 strain-gauge resistors, var. under cyclic loading 3-73099
 wire, residual stress recovery, temp. and holding time depend. (French) 3-61170
 yielding materials, stress intensity factors at crack tip by method of caustics 3-68328
 Al, polycryst., grain size effect 3-80225
 Al, substructural hardening, yield stress, dependence on subgrain size, texture and orientation (Russian) 3-41720
 Al alloy, cyclic concentration factor, localised and gross plasticity effects 3-64903
 Al-Al₂O₃ alloys, ball-milled, room and elevated temp. props. 3-44613
 Cu, crit. work hardening of nucleation and migration for recrystn. (French) 3-61152
 Cu, cubic centred, axes of anisotropy and work hardening rates 3-68311
 Cu, fatigue, dislocation struct. 3-80288
 Cu, polycryst., grain size effect 3-80225
 Cu, pure, pressurizing effect 3-50717
 Cu strengthening curves for thread-like crystals, orientation dependence during deformation by elongation and torsion 3-80360
 Cu/silica system, work hardening, diffusional stress relax., surface diffusion coeffs. 3-55827
 Cu-Be (1.83 wt.%) alloy, dynamic strain-ageing 3-80341
 Cu-Fe alloy single crystals, containing γ -Fe precipitates work hardening phenomena 3-80226
 Cu-Pt alloys, short-range order in hardened alloys (Russian) 3-69270
 Fe, Armcio, by diffusion from media at high temp. and press. (Russian) 3-72858
 Fe, technical, deform. and fracture mechanisms in complex stress state, low temp. 3-44624
 Fe-Ni-Mo and Fe-Ni-Co-Mo martensites, hardening by tempering, comp. depend. (French) 3-44622
 Fe-Ti (0.16 wt.%) single crystals., orientation, temp. and strain rate effects on deform. 3-64909
 KCl, hot worked, strength and deformation behaviour 3-76252
 LiF:Mg, deform. hardening under simple slip conditions 3-58075
 Mg, single cryst., crit. shear stress temp. and rate depend. for basal slip, obs. and mechanism 3-80381
 MgAl₂O₄, transparent shaped mat., fabrication and props. 3-72967
 Mo, impure, temp. and strain rate influence on plasticity and stress/strain diagram appearance (Russian) 3-80344
 Nb, interstitial effects on tensile behaviour, 20 to 1000°C (French) 3-80291
 Nb single crystals., deformed in rolling at 77K, defect struct. (Russian) 3-58627

work hardening continued

- Nb-W-Mo-Zr, aged carbide phase distrib., mech. strength, hardening (Russian) 3-41721
 Ni 270 work hardened in tension, annealing twins role in primary recrystn. (French) 3-44585
 Ni-Al alloys with large vol. contents of γ' -phase, plastic deform. mechanism (Russian) 3-61162
 Ni-base alloys, thermal and mechanical stress effect 3-64955
 Ni₃(Al,W) single crystals, yield stress, exhaustion hardening 3-80298
 Ni₃Fe and Ni₃FeCr alloys, dislocation struct. at various strain hardening stages (Russian) 3-58626
 SrFe₁₂O₁₉, texture development by hot working 3-76250
 Ti, fatigue tests with const. strain amplitude 3-64891
 Zr, compression of single crystals. parallel to c-axis, 78-1100 K 3-46659

workers see personnel**wrapping see packaging****Wratten filters see optical filters****X-ray absorption**

- see also X-ray absorption spectra
 binary X-ray sources, effect on atmosphere of binary companion, optical periodicity 3-51373
 composite materials, effect of photoelectron migration on energy deposition 3-74759
 foil thickness measurement, transmission obs., error sources 3-61987
 high-energy attenuation obs., rel. to shielding, betatron expts. (Japanese) 3-42630
 imperfect crystals, anomalous absorption with X-ray diffraction (German) 3-43729
 interaction cross-section review, reln. to X-ray energy deposition in materials 3-74758
 materials response to X-ray loadings, review 3-74757
 phosphor, noise equivalent absorption, rel. to integrated scintillation obs. 3-77733
 plasmon excitation by X-rays, review 3-44047
 Scorpius X-1, rocket obs. of X-ray absorpt. measure 3-53693
 stellar sources, role of circumstellar matter in accretion model 3-77128
 GaAs, K-edges, Laue diffr., intensity jumps, processes 3-71986
 Ge, normal and anomalous absorpt. 3-43724
 Ge, six-beam Borrmann diffr., linear absorpt. coeffs. calc. 3-43725
 Si, normal and anomalous absorpt. 3-43724

X-ray absorption spectra

- fluoromethane molecules, C and F X-ray emission and F K absorption spectra 3-43430
 methylchlorosilanes, L_{II-III} X-rays, electronic structure calcs. 3-78671
 solid, atomic one-electron vs. band calcs. 3-47323
 transition elements, X-ray L $\beta_{2,15}$, L $\alpha_{1,2}$ and K β_3 lines shift due to chem. combination 3-55698
 Al, correlation with X-ray emission, appearance pot. spectroscopy 3-55699
 BN, hexagonal, selective maxima rel. to band structure 3-50631
 Be, correlation with X-ray emission, appearance pot. spectroscopy 3-55699
 CS₂, electronic structure investigation 3-78683
 CdMn₂O₄, spinel structure, K-absorpt. edges of cations 3-44502
 Ce, M_{4,5} spectrum, γ - α phase transition 3-76106
 Co and compounds, K absorpt. edge, chem. shift 3-47326
 Co cpds., chemical shifts and fine struct. of K-absorption edge 3-72765
 Cr, Cr₂N and CrN, L_{III} and K absorpt. 3-80118
 CrCl₃ Cl K-X-ray absorption spectra, metal ionisation energies relationship 3-47324
 Cu, L_{III} absorption, rel. to L α emission spectra 3-72767
 Cu compounds, L_{III} absorption, reln. to L α emission spectra 3-72767
 CuCl, electronic struct., rel. to X-ray emission and absorpt. spectra 3-50129
 CuCl₂ Cl K-X-ray absorption spectra, metal ionisation energies relationship 3-47324
 CuMn₂O₄, spinel structure, K-absorpt. edges of cations 3-44502
 GaSe(Te), effective ionic charge and bonding, from chem. shift of K-absorpt. discontinuities 3-54940
⁶⁴Gd, forbidden transition L_{III}N_{II} in X-ray spectrum 3-47322
 HgI, 20 to 120 Å, excitation of 4f and 5s subshells 3-78448
 KI:Ag crystals, stimulated, 85 K 3-76036
 La, L subshell X-ray yield 3-54567
 Li alloys, many electron effects 3-72766
 Li Mahan soft X-ray anomaly, relationship to Knight shift 3-69105
 LiF, absorption of soft X-rays with a forbidden excitonic transition 3-69104
 Mg, correlation with X-ray emission, appearance pot. spectroscopy 3-55699
 Mg_{1-x}Mn_xFe₂O₄, spinel structure, K-absorpt. edges of cations 3-44502
 MgMn₂O₄, spinel structure, K-absorpt. edges of cations 3-44502
 Mn-M solid solution, M=Cu, Ni, Co, Fe, K absorpt. edge obs. 3-64747
 MnP, K absorpt., electronic band struct. obs. 3-64748
 N, excitation of K shell, saturation 3-63278
 Nb, K-absorption edge investigation for various Nb compounds 3-55697
 NiMn₂O₄, spinel structure, K-absorpt. edges of cations 3-44502
 Re, L_{III} absorption discontinuity, fine struct. 3-47327
 SO₂, electronic structure investigation 3-78682
 Si crystals, Borrmann effect, Compton scattering 3-69107
 Tb, ultrasoft X-ray region 3-61081
 TiFe, K spectra, SCF calcs., densities of states 3-75705
 V₂O₃, rhombohedral, empirical band scheme, optical and soft X-ray data 3-41130
 V₂X type compounds, valence band and conduction band structures (Russian) 3-55207
 ZnCl₂ Cl K-X-ray absorption spectra, metal ionisation energies relationship 3-47324
 ZnMn₂O₄, spinel structure, K-absorpt. edges of cations 3-44502

X-ray absorption spectra continued

Zr cpds. with group II element, K-absorpt. edges, band electrons mean free path (*Russian*) 3-80119

X-ray analysis

see also *X-ray chemical analysis; X-ray crystallography; X-ray diffraction examination of materials; X-ray spectroscopy*
data processing, computer control, conf. Bournemouth, England (Nov. 1972) 3-73906

larynx, soft tissue intensification in frontal roentgenography 3-56544

roentgenmicrography of human neonatal lung 3-56543

X-ray apparatus

see also *biomedical equipment; X-ray crystallography apparatus; X-ray monochromators; X-ray spectrometers; X-ray tubes*
capacitor discharge unit, mobile, radiographic examination of chest, practical experience 3-66390

diagnostic, test system for performance 3-66029

diffraction equipment in New Zealand, safety features 3-48268

for electronic image processing 3-48628

filters, spatially inhomogeneous, ultra-soft region, 50-2000 Å 3-45568

fluorescence single element analyzer, design description 3-48595

fluorescent screen, calc. of modulation transfer function 3-62294

generation and application apparatus, standardisation of radiation protection (*French*) 3-70178

hard-ray therapy apparatus, RT 255, RT 305, operation method, practical experience 3-66389

image intensifier, large input field, improved image quality 3-66393

image intensifier, using external CsI(Na) input oscillator 3-40050

image intensifiers, for radiology 3-48627

image quality, two dims. MTF evaluation method 3-51749

microscope, scanning, using synchrotron radiation 3-42684

Polytome, image intensifier fluoroscopy and tomography 3-66388

portable generator for pulse response meas. of p-i-n-Si rectifiers 3-73918

radiometric logging of boreholes for Mo and W bearing seam (*Russian*) 3-73395

soft X-ray source, for photoelectron spectroscopy 3-45570

stress determination, thin films and substrates, curvature measurement, automatic Bragg angle control 3-62300

synchrotron radiation, gratings and reflectors 3-40058

telescope, grazing incidence, design 3-53723

transmission gratings for soft X-rays, electrooptic prod. method (*German*) 3-56988

S film filters, on Be foil, vacuum deposited 3-40053

X-ray applications

see also *radiography*

autoradiography, high resolution electron microscopy, radioactive tracers, metal structural defects (*French*) 3-48561

binary and quasibinary mixture, composition checking, accuracy 3-69428

chest diagnosis with monoenergetic beam, Monte Carlo appl. 3-73600

densitometry, for bone mineral measurement 3-66408

diagnosis, incorporating TV camera, dose reduction 3-45329

disease diagnosis, in maxillofacial region 3-53747

film thickness determination, glass substrate 3-73665

foil thickness measurement, transmission obs., error sources 3-61987

hypotonic duodenography 3-56540

lymphography and supplementary procedures 3-56541

motion tomography, general theory 3-70159

nondispersive techniques, for nondestructive elemental analysis 3-59676

particle accelerator tubes, inclined field, conditioning X-ray survey, technique, Orsay MP tube, France 3-70363

patient diagnosis, ferrite powder applications 3-42372

polymers, time of flight determ. of carrier mobility 3-60876

radiation protection, standardisation (*French*) 3-70178

radiology, densitometry, development, trends 3-70139

renal arteriography 3-56542

speech, vocal tract X-ray films, computer assisted measurement system 3-77210

tomography, transverse axial, computerized 3-70166

TaC, X-ray determination of Debye temperature 3-52686

X-ray astronomical observations

see also *X-ray sources (astronomical)*

2U0900-40 eclipsing binary, X-ray spectra, position rel. to HD77581, Uhuru obs. 3-48045

Aquila XR-1, hard X-rays 3-69999

3C 273, X-ray spectrum rel. to intergalactic He abundance 3-56412

Cassiopeia A, X-ray spectrum, Fe line emission evidence 3-73534

Centaurus region sources, long-term variations in hard X-ray flux 3-56414

Centaurus X-3, soft X-ray emission below 2 keV 3-65915

Circinus X-1, Copernicus satellite obs. of off state 3-61833

clusters of galaxies, thermal gas flow solns. compared with obs. 3-45200

Coma cluster, 7-40 keV flux determ. 3-65921

Coma cluster of galaxies, soft X-ray flux obs. and ang. diameter 3-65917

Crab, synchrotron radiation, 912-90 Å, Zanstra's method (*Russian*) 3-77097

Cygnus Loop, 0.2 to 2.5 keV obs. 3-65940

Cygnus X-1 and X-3, OSO-7 obs. above 7 keV 3-73536

Cygnus X-3, i.r. and X-ray variability 3-77126

energetic background X-rays, review of experimental obs. 3-81159

experimental methods and obs. (in book) 3-65920

Explorer 42, 116 sources (*Italian*) 3-59366

extragalactic Uhuru X-ray sources, radio structure 3-81129

flare-time temp. in soft X-ray sources 3-53690

galactic distribution of X-ray sources, sounding-rocket obs. 3-45165

Galactic sources, UHURU results 3-81141

galactic southern sky sources, spectra of 10 objects 3-56413

galactic X-ray sources, X-ray absorption and optical extinction in interstellar space 3-59363

GX5-1, accurate position from lunar occultations, Copernicus satellite obs. 3-59367

X-ray astronomical observations continued

GX 1+4, high energy X-ray spectra by balloon borne obs. 3-73532

GX 301-2, high energy X-ray spectra by balloon borne obs. 3-73532

GX 304-1, high energy X-ray spectra by balloon borne obs. 3-73532

GX 339-4 X-ray variable, OSO-7 obs. of intensity 3-81134

GX 3+1, high energy X-ray spectra by balloon borne obs. 3-73532

GX 5-1, high energy X-ray spectra by balloon borne obs. 3-73532

hard cosmic X-ray sources, review of obs. status 3-81144

HD 153919 binary, narrow band circular polarization meas. 3-81135

HD 77581, binary, narrow band circular polarization meas. 3-81135

Hercules X-1, hard X-ray spectrum, balloon obs. in 20 to 100 keV range 3-56417

Hercules X-1, intensity meas. in 4 to 12 keV range 3-56416

Hercules X-1, neutron star, mass meas. 3-45164

Hercules X-1, OSO-7 obs. of spectrum and variability 3-45162

Hercules X-1, upper limit for pulsed emission above 100 keV 3-81138

Hercules X-1, X-ray pulse profile and celestial position 3-51372

lunar composition, spectroscopy, Apollo orbital measurements 3-56355

MP0736-40, upper limit to X-ray flux 3-61830

MP0835-40, upper limit to X-ray flux 3-61830

NP0532, arrival times of 100-400 keV pulses 3-53689

NP 0525, 7 to 18 keV meas. 3-61829

NP 0532, 7 to 18 keV meas. 3-61829

OSO-7 obs. in 1-60 keV range 3-81142

β Persei, X-ray emission during radio flares, upper limits 3-65903

Perseus cluster, 7-40 keV flux determ. 3-65921

PSR0835-45, upper limit to X-ray flux 3-61830

pulsars, UHURU satellite obs. 3-51368

Scorpius X-1, Bragg spectroscopy in search of Fe XXV emission lines 3-69996

Scorpius X-1, balloon borne obs. in 17 to 106 keV range 3-53691

Scorpius X-1, rocket obs. of X-ray absorpt. meas. 3-53693

soft X-ray absorption, 21 cm obs. of H column density in the Galaxy 3-81156

soft X-ray background, contribution from extragalactic sources 3-81155

solar corona, identification of coronal hole 3-65667

solar Fe XVII and XVIII lines during flares, soft X-ray spectrum 3-61667

solar flare spectra from 8.5 to 16 angstroms 3-45024

solar flare X-ray spectra, Intercosmos-4 and Vertical-2 obs. 3-65663

solar flares of 2 August 1972, OSO-7 5-300 keV obs. 3-80948

solar hard X-ray bursts, obs. by OSO-6 satellite 3-45000

solar spectra, active region spectrum obtained by rocket borne X-ray spectrometer 3-65645

solar X-ray emitting spots, pinhole camera image (*German*) 3-80973

solar X-ray flares, continuous energy injection at bright points 3-65662

solar X-ray thin-target emission from 26 February 1972 flare 3-80947

source identification, white dwarfs, neutron stars, black hole, satellite obs. 3-61835

sun, coronal survey of O VII and Ne IX 3-65712

sun, X-ray spectroheliograms in Mg XI, Mg XII 3-65654

supergiants in h and γ Persei association 3-73510

supernova remnants, X-radiation, rel. to mechanisms and evolution 3-81148

2 U 0832-45, at pulsar PSR 0833-45 X-ray structure observed from Uhuru 3-73530

2U 0900-40, binary source, Uhuru obs. 3-59364

2U 1700-37, possible binary companion to HD 153919, Of star 3-48073

UHURU results on extragalactic X-ray sources 3-81151

XN 1972E, upper limit on X-ray flux 3-56410

X-ray astronomy

2 U 1700-37, identification of HD 153919 as optical counterpart 3-48032

accreting magnetic neutron star, radiation beaming rel. to X-ray pulsars 3-45083

atomic physics and astrophysics, book 3-65614

binary X-ray sources, effect on atmosphere of binary companion, optical periodicity 3-51373

binary X-ray sources, expected optical behaviour 3-48082

black holes with accretion discs, X-ray variability 3-53596

clusters of galaxies, flow solns. for thermal gas compared with obs. 3-45200

Compton models of isotropic X-ray background 3-45161

Copernicus satellite, instrumentation and performance 3-45238

cosmic X-ray prod. by transition radiation 3-51217

Cygnus X-1, low mass primary for HDE 226868 rel. to existence of black hole 3-42222

distance determ. of variable sources 3-53724

experimental methods and obs. (in book) 3-65920

Explorer 42, 116 sources (*Italian*) 3-59366

focusing collector, cosmic X-rays, rocket borne equipment 3-42260

galactic anticentre, soft X-ray flux rel. to radio continuum features 3-51376

galactic distribution of X-ray sources, sounding-rocket obs. 3-45165

Galactic X-ray polarimetry and high-resolution X-ray spectroscopy 3-81259

galactic X-ray sources, luminosity accretion models, He II ion determining flow of gas 3-48080

Her X-1, hard X-ray dip, balloon obs. 3-48076

Hercules X-1, 35-day periodicity rel. to accretion gas flow in binary system 3-48083

Hercules X-1, spectrum and variability, OSO-7 obs. 3-45162

Hercules X-1, X-ray pulse profile and celestial position 3-51372

Hercules X-1, X-ray source, neutron star, mass meas. 3-45164

HZ Herculis, 'on' and 'off' eclipse phenomena, photographs, 1890 to 1972 3-48075

HZ Herculis, eclipsing binary, X-ray beaming and mass transfer 3-48028

HZ Herculis, optical counterpart of Hercules X-1, B-magnitude light curve 3-45122

HZ Herculis, reflection effect due to energy transfer 3-48033

X-ray astronomy continued

- IAU Symposium on X and γ -ray astronomy (Madrid, 11-13 May, 1972) 3-81140
- interstellar gas thermal structure and evolution, soft X-ray effects 3-56437
- Jovian magnetospheric diffusion rates, expected X-ray flux at Earth 3-47898
- LMC X-1 proximity of radiosources MC76 and MC77 rel. to optical candidate 3-53694
- loops as fossil, Stromgren spheres, radio and X-ray emission 3-56450
- massive close binaries with collapsed component evolution and appl. to Cygnus X-3 3-53650
- model X-ray sources, magnetic field twisting in binary star system 3-42223
- neutron star accretion at the Galactic centre, upper limit of X-ray wavelength 3-42231
- NGC 5128 (Centaurus A), size and nature of X-ray source 3-53692
- proportional counter, gas density control system 3-65950
- pulsar emission mechanism, model 3-45156
- pulsating X-ray sources, speed-up and evolution 3-51375
- radiosources, X-ray emission by Compton-synchrotron or Compton black-body effect, comparison 3-53674
- satellite-borne X-ray and ultraviolet techniques and observations, Copernicus 3-65953
- Scorpius X-1, balloon borne obs. in 17 to 106 keV range 3-53691
- Scorpius X-1, distance determ. 3-48100
- Scorpius X-1, rocket obs. of X-ray absorpt. measure 3-53693
- Scorpius X-1 flares, UVB obs. 3-48085
- search for black holes rel. to X-ray sources 3-44980
- soft X-ray background rel. to stellar coronae X-ray radiation 3-42220
- solar flare non-thermal ionisation and recombination processes 3-45022
- solar flare spectra from 8.5 to 16 angstroms 3-45024
- solar hard X-ray bursts, obs. by OSO-6 satellite 3-45000
- solar X-ray flares, albedo determ. up to 300 keV 3-45025
- stellar coronae, X-ray and radio emission rel. to soft X-ray background 3-45078
- Sun, K α line emission during solar flares rel. to X-ray bursts 3-47887
- telescope, grazing incidence, design 3-53723
- thermal X-ray sources with strong magnetic field, luminosity 3-42221
- transition radiation as source of X-rays 3-59248
- transition radiation from interstellar dust grains, suppression at X-ray freq. 3-56457
- 2U 1700-37, possible binary system, HD 153919 suggested companion 3-48073
- 2U 1700-37, obs. of HD 153919, optical candidate 3-51374
- universal x-ray background origin, comments on theory and further arguments 3-42095
- Wolter-Schwarzschild X-ray telescope 3-42252
- X-ray pulsars, UHURU satellite obs. 3-51368
- X-ray source at M87, X-ray spectra, thermal bremsstrahlung function 3-48077
- X-ray sources, high energy, Southern sky, balloon obs. 3-48078

X-ray characteristic temperature *see specific heat***X-ray chemical analysis**

- see also X-ray diffraction examination of materials*
- air particulates, multielement analysis, X-ray emission spectrometry 3-59718
- air pollution particles 3-61447
- AUREOL analyser for U content determ. 3-70495
- calculation of element content, intensity of anal. line, mass coeff. of absorption, surface density 3-48661
- clinical chemistry, pharmacology, automation, quality control (*Italian*) 3-66409
- computer program, Elliott 803B, for quantitative corrections of X-ray microanalysis (*Polish*) 3-70467
- electrocast materials, physical methods of chem. analysis (*French*) 3-70468
- electron microprobe, primary X-ray analysis depth determ. method 3-45596
- element fingerprinting in semiconductor and field emission components 3-42711
- elemental, characteristic X-rays, proton and X-ray induced 3-59719
- elemental analysis, X-ray energy dispersive system, scanning electron microscope computer multichannel analyser 3-45588
- elements fluorine to boron 3-45605
- emission spectroscopy for chemical analysis, survey 3-70469
- emission spectroscopy for chemical analysis methods, survey 3-70470
- filter paper used in air pollution control, analysis by X-ray fluorescence 3-45610
- fluorescence spectroscopy, determ. of Nb and Ta in minerals 3-56253
- geological samples, chelating ion exchange resins for trace element analysis using X-ray fluorescence 3-62329
- glass, ion exchanged, conc. profiles determ. using electron microprobe 3-76263
- high-resolution emission, application of chemical effects in analysis 3-62353
- metal powders, fluorescence anal., sample preparation 3-62336
- metals, in water, preconcentration using electrodeposition 3-66423
- minerals, VD-1 vacuum transducer for X-radiometric analyser (*Russian*) 3-73393
- muonic X-rays, fissionable material assay 3-63201
- polymer X-ray filters for dispersionless analysis for light elements (*Russian*) 3-70492
- radioisotopes in X-ray fluorescence analysis, review 3-62372
- reagent, ultrapure, quality monitoring, neutron activation, X-ray fluorescence 3-70459
- refractory, X-ray fluorescent and atomic absorpt. anal. methods and characteriz. 3-80410
- scanning electron microscope 3-66466
- SEM rough specimens, stereoscopic techniques 3-66467
- silicon organic esters of phosphoric acids, crystalline roentgenofluorescent anal., Si and P determ. 3-48662

X-ray chemical analysis continued

- spectral analyzer for high-speed analysis of chemical composition 3-54017
- thin biological specimens, X-ray fluorescence microanalysis 3-54025
- thin films and fine structure, Monte Carlo techniques in SEM 3-71989
- trace element, using semiconductor detector spectrometer 3-66412
- X-ray fluorescence, Fe ores and mixtures, determ. Si and Al, rel. error calc. 3-48655
- X-ray fluorescence, rocks, rock-forming elements, conc. determ., error anal. 3-48654
- X-ray fluorescence, weight fractions, linear regression equations, consistent solution 3-73937
- X-ray fluorescence analysis, of heavy elements using electrodeposit technique (*Japanese*) 3-62355
- X-ray fluorescence analysis, Z=47(Ag) to 92(U), L spectra, primary radiation 3-48653
- Al₂O₃ films, compositional information from ion-induced X-rays and Rutherford backscattering 3-43960
- As impurities, H₂SO₄ catalyst, AsK α line intensity rel. to composition 3-48656
- Cu-Ni ores Pt, Rh and Pd determ., X-ray spectrometry, segregation 3-48659
- Fe oxidation, kinetics of thin film formation using proton impact excited X-ray analysis 3-50087
- GaP-GaAs, GaAs-InAs, inhomogeneities, statistical models in local anal. 3-48658
- Pb-Ba minerals, X-ray radiometric fluorescence anal., ¹⁰⁹Cd radioisotope source 3-48660
- Ta, industrial effluent, chemico-roentgenospectral fluorescence 3-48657
- X-ray crystallography**
- For results of structure analysis see crystal atomic structure*
see also X-ray crystallography apparatus; X-ray crystallography calculation methods; X-ray crystallography technique
- biographical review (*German*) 3-77346
- Debye-Waller parameters depend. on atomic form factors, appl. to diamond 3-79278
- diffraction from crystal with deform. twins 3-75456
- diffuse scattering, influence of matrix distortions during phase transformations. (*Russian*) 3-52557
- distorted crystals, dynamical diffraction theory 3-40835
- double-crystal diffractometry using white X-rays 3-52559
- dynamic theory, X-ray diffraction by cryst. cylindrical cavity 3-75454
- isotropic crystal containing random defect distrib., elastic X-ray and neutron scatt., static correl. functions (*German*) 3-52561
- Laue-Bragg diffraction in case of strong X-ray waves disperse surface eqn. for Ge (*Russian*) 3-57975
- mathematical framework, solved problems, book contrib. 3-57976
- non-crystallographic symmetry used to determine X-ray phases for tobacco mosaic virus protein 3-63925
- polycrystalline materials, magnification in diffraction patterns 3-76855
- powder patterns, standard 3-49801
- screw dislocations core structs., direct determ. method, struct. factor 3-54905
- screw dislocations square grid in twist boundary, struct. factor 3-54904
- surface relax. effects on X-ray diffraction peak shifts, kinematic theory 3-54906
- thermal gradient effects on diffracted ray intensity, obs. using TGS (*French*) 3-63924
- thin crystals, charact. X-ray production 3-40833
- three beam diffraction of CuK α radiation by (111) and (111) in a Ge crystal (*German*) 3-60656
- X-ray crystallography apparatus**
- see also goniometers*
- aberrations of fixed-angle energy-dispersive powder diffractometer 3-43717
- automation data acquisition and control 3-48596
- automation of crystallographic meas. (*Czech*) 3-56985
- camera, Berg-Barrett, design improvements, total enclosure, scanning attachment 3-62299
- camera, disorientation within grains, oscillating specimen 3-51754
- camera, for obs. at liquid nitrogen temp. (*German*) 3-71983
- camera, liquid He cryostat, for structure studies 3-48590
- cassette powder camera, with interchangeable specimen mounts 3-63927
- chamber, thermostatically controlled, for struct. investigation of alloys and solns. 3-73913
- cryostat for topography appl. 3-71985
- diffractometer, energy dispersive, for rapid determ. of GaP polarity sense 3-72053
- diffractometer attachment, sample rot., Berg-Barrett-Weissman method 3-75451
- diffractometer information extraction, digital, on punched tape for computer 3-73915
- divergence slit assembly shield 3-63928
- energy dispersive diffractometer, escape peaks due to Ge(Li) detector 3-54899
- furnace for data collection, single crystals 3-77734
- high precision combined X-ray spectrometer (*German*) 3-48589
- Kossel diffraction camera, design requirements 3-46575
- laboratory notes 3-68137
- low temperature high pressure cell, 0 to -60C, 30 bar 3-43712
- manipulator, inexpensive, in x, y, z directions, for mounting single crystals 3-71979
- microscope, high-temp., internal structure, metallurgy 3-48592
- powder diffractometry, low temp., 65 to 320 K (*French*) 3-49800
- sample holder, in glasslike carbon, for high temp. Guinier camera 3-43713
- simple spectrometer for measuring X-ray integrated intensities 3-45567
- simple topographic Lang-type camera 3-43720
- single crystal diffractometer, Philips PW 1100, automatic with built-in computer control 3-52560
- single crystal heater for precession camera and 4 circle diffractometer 3-70436
- specimen cell for studying oriented liq. crystals 3-57974

X-ray crystallography apparatus continued

- specimen holder, variable movement, for texture studies 3-71984
- thermostat for diffractometer for lattice parameters 3-53852
- three-crystal X-ray polarimeter, collimator and spectrometer 3-66385
- URS-50IM attachment, X-ray diffraction, material content, continuous monitoring 3-48593
- Weissenberg goniometer, low temp. attachment 3-68136

X-ray crystallography calculation methods

- accuracy of camera powder data, geometrical and statistical aspects 3-43715
 - atomic scattering factors, isoelectronic sequence of first row atoms, calc. from analytical SCF functions 3-79201
 - atomic scattering factors, neutral first row atoms, aspherical charge distrib., anal. s.c.f. functions 3-79202
 - Bijvoet ratio cumulative function for noncentrosymmetric crystals. 3-52554
 - Bragg case, dynamic scatt. theory, spherical wave approximation 3-79204
 - Bragg reflection intensity, for powder diffr., computer program description 3-49797
 - calculator for solving Bragg equation, design, operation 3-73920
 - Cohen's method of least squares and systematic indexing of powder data, accuracy of cell dimensions 3-43714
 - complex structures, phase relationships, E maps, Cooley-Tukey fast Fourier transform technique, computer analysis 3-40825
 - computer analysis of results 3-73657
 - computer control, powder diffr. file, search-match retrieval program 3-75458
 - computer program, Miller indices calculation direct from Laue diffraction spots 3-63929
 - computer simulation of cryst. struct., appl. to superstruct. of cubic SiP_2O_7 3-46626
 - crystal structure analysis, Fourier program using Cooley-Tukey algorithm 3-43719
 - diffraction profile separation method, computer program 3-46576
 - diffractometer information extraction, digital, on punched tape for computer 3-73915
 - Fourier transforms fast computing via external storage 3-52555
 - heavy atom moduli isolation, noncentrosymmetric crystals. 3-71988
 - heavy atom Patterson functions, automated deconvolution by modified vector-verification 3-49796
 - integral diffraction data separation method for metal melts (Russian) 3-43709
 - interatomic vectors, cross section through generalised function 3-79208
 - kinematic intensity evaluation of diffr. patterns, computational techniques, appl. to Ti, Zr alloys 3-79198
 - least squares refinement of structure, allowing for anisotropy of thermal vibr. of atoms 3-71980
 - least-squares calcs. for weak reflections 3-63923
 - metals, equation selection for correction of primary extinction 3-79209
 - methods of variance, particle size and strain determ. for Ag-Sb alloys 3-44575
 - noncentrosymmetric structs. soln. by symbolic tangent refinement 3-49795
 - ORTEP program, graphic display version 3-54900
 - P1 and related space groups, symbolic addition procedure 3-49794
 - Patterson diagram, vector subsystem soln. method for triclinic system with 195 parameters 3-46628
 - Patterson function, criterion for transition to point vector system 3-54901
 - Patterson function, duplicated, structure-localizing sections 3-75455
 - Patterson function analysis, vector subsystems rel. to several multiple peaks 3-75453
 - Patterson function as a vector segment system, Fedorov group P1 3-49865
 - Patterson synthesis, lower system crystals, rhombus extraction 3-71987
 - peak profile functions, diffractometer performance 3-73919
 - pole figure generation, computer program for contour plotting 3-75457
 - powder diagram automatic indexing routine 3-68134
 - powder mixtures, quantitative phase analysis method (German) 3-43718
 - precession photography, extrapolation method for more accurate cell dimensions 3-63926
 - programs for phase determ. by direct methods 3-63921
 - radial distrib. functions, computation of glass diffraction data 3-79237
 - real structures in $\text{P}2_1/\text{c}$, reliability of Σ_2 reln. 3-63920
 - screenless precession photographs, prediction of partially recorded reflections 3-52556
 - single cryst. diffr. intensities from max. peak height meas. (French) 3-54897
 - small angle X-ray scattering, collimation corrections, weighting functions calc. 3-49793
 - spherical wave theory of Moire fringes produced under conditions of Borrmann transmission by two crystals separated by a gap 3-43730
 - three-dimensional represent. of rolling and recrystn. textures, computer program (French) 3-61151
 - three-wave diffraction, system of oblique coordinates (Russian) 3-40832
 - Warren-Averbach analysis, effect of non-linearity error 3-43716
 - Co(III) complex, cryst. struct., three dims. Patterson function anal. 3-75512
- X-ray crystallography technique**
- alloys, coarse-grained, X-ray studies, effect of turning, reciprocating and swinging motion 3-52558
 - automatic plotting of reciprocal lattice zones 3-80270
 - automation data acquisition and control 3-48596
 - Bragg angles misalignment effect in zero-layer Weissenberg X-ray photographs 3-49798
 - counter-diffractometer step-scan determ. of U_3Si parameters 3-41802
 - diffracting particles volume determ., influence of divergence 3-43711
 - energy-scanning diffraction, appl. to liq. struct. anal. 3-40831
 - Guinier-Lenne camera, good high temp. patterns, method 3-54898

X-ray crystallography technique continued

- $2\text{HBr} \cdot 2\text{H}_2\text{O}$, calycanthine, absolute config. determ. by X-ray Bijvoet and circular dichroism methods 3-54903
 - ice, crystal axis determination, Laue photographs (Japanese) 3-54902
 - inverse pole figure studies, random samples use 3-47380
 - laboratory notes 3-68137
 - lattice parameters, determ. of small variations by least squares fitted method 3-71982
 - limited topographs, modified method 3-43722
 - local structure anal. with pencil of X-rays convergence in solid angle 3-46577
 - multiple-crystal arrangements, $(n_1, + n_2)$ setting, use of asymm. dynamical diffr. 3-43728
 - polymer, partially cryst., lamellar structure determ. from small angle X-ray scatt. 3-72011
 - powder pattern indexing 3-79207
 - powder patterns, automatic peak determ. technique 3-54896
 - rolling texture determination, X-ray diffraction technique, combination of inverse polar and direct figures 3-53227
 - shock compressed materials, flash X-ray diffraction studies, film system 3-40052
 - signal averaging techniques for X-ray diffraction measurements 3-79205
 - small angle X-ray scattering, collimation corrections, weighting functions calc. 3-49793
 - spinel cation distribution, effective temp. factor 3-68135
 - student X-ray diffraction experiment 3-51491
 - uniaxial crystals, mosaic and block structure, axis directions, method 3-53013
 - GaP, polarity sense, rapid determ. by energy dispersive diffractometer 3-72053
 - Zn, characterisation of dislocation loops by X-ray topography 3-43802
- X-ray detection and measurement**
- see also dosimetry; X-ray spectrometers
 - colour TV radiation monitors, calibration 3-73911
 - curved-crystal spectrometer, K-shell autoionization probability, ^{143}Pr β -decay 3-78294
 - dosimeter calibration against primary ^{241}Am beams, connection methods (French) 3-56556
 - electron probe analysis, energy dispersive, escape peaks in Si(Li) detector 3-42730
 - electron-capture radioactivity, total cross-sections 3-48531
 - monitoring instruments and test methods (French) 3-66315
 - multiple pinhole images, direct method of decoding 3-62295
 - non-dispersive X-ray data analysis by computer 3-42726
 - portable exposure meter, requirements and test procedures 3-48538
 - proportional counter, gas flow, soft X-ray detection, compact design, construction 3-73867
 - proportional counter unlimited operating service life, construction, parameters 3-70380
 - protection equipment, principles, design, construction and operation (Spanish) 3-61924
 - scintillation counters, proportional, gas, peak shifts under high X-ray fluxes 3-77619
 - Ge(Li) detector efficiency curve near Ge K-edge, method of determination 3-77624
 - $^{103}\text{Rh}(n,n')^{103\text{m}}\text{Rh}$, thick foils, absolute counting of K X-rays 3-66316
 - Si dosimeter, adiabatic calorimeter, doses $> 10^2$ rad., pulses 1 sec. or less, description 3-66386
 - Si(Li) detectors, for proton-induced $\text{C(K}_\alpha)$ X-rays 3-51707
- X-ray diffraction**
- see also X-ray crystallography; X-ray scattering
 - asymmetric case, anomalous absorpt. total internal refl. 3-68138
 - Borrmann effect, determ. of atomic scatt. factors imaginary parts in Si 3-43775
 - chamber, new, with high resolution, for examination of molecular structure (Czech) 3-62296
 - diffractometer attachment, sample rot., Berg-Barret-Weissman method 3-75451
 - distorted crystals, dynamical diffr. theory 3-40835
 - Fresnel zone plates, scaled, for coded aperture imaging of X-rays 3-66391
 - imperfect crystals, anomalous absorption with X-ray diffraction (German) 3-43729
 - KRM-1 small angle diffraction installation 3-54018
 - mathematical framework, solved problems, book contrib. 3-57976
 - momentum transfer condition from beam to crystal 3-77956
 - multiple-crystal arrangements, $(n_1, + n_2)$ setting, use of asymm. dynamical diffr. 3-43728
 - at NPL, instrumentation 3-66392
 - plane reflection grating hologram, soft X-ray diffraction performance 3-62145
 - polymer, lamellar structure, small angle scatt. analysis (German) 3-60671
 - reference lines, X-ray to visible wavelength ratios 3-73660
 - shock compressed materials, flash X-ray diffraction studies, film system 3-40052
 - single crystal diffractometer, Philips PW 1100, automatic with built-in computer control 3-52560
 - spherical wave theory of Moire fringes produced under conditions of Borrmann transmission by two crystals separated by a gap 3-43730
 - surface relax. effects on X-ray diffr. peak shifts, kinematic theory 3-54906
 - synchrotron spectroscopy at grazing incidence, diffraction gratings 3-40057
 - three-wave diffraction, system of oblique coordinates (Russian) 3-40832
 - transition radiation, diffr. theory approach 3-75549
 - uniformly bent crystal, X-ray wavefield beam propag. 3-43723
 - vibrating crystal, transition from dynamical to kinematical refl. power 3-43726
 - Weissenberg goniometer, low temp. attachment 3-68136
 - Ge, normal and anomalous absorpt. 3-43724
 - Ge, single crystal, X-ray wave fields, energy flow 3-40834
 - Ge, six-beam Borrmann diffr., linear absorpt. coeffs. calc. 3-43725
 - Si, normal and anomalous absorpt. 3-43724
 - Si crystals, Borrmann effect, Compton scattering 3-69107

X-ray diffraction examination of liquids

- acetonitrile, structure determ. (*German*) 3-63944
 alkali metal, struct. factor, press. effects 3-49823
 cholesteryl nonanoate, cholesteric-isotropic (solid) transitions, X-ray halo scatt. obs. 3-79230
 computer programs for data processing 3-79216
 energy-scanning diffraction, appl. to liq. struct. anal. 3-40831
 lamellar liquid-crystalline phase in Aerosol OT-water system struct. obs. 3-75467
 MBBA, nematic-isotropic (solid) transitions, X-ray halo scatt. obs. 3-79230
 metal, monovalent, elec. cond. behaviour at melting pt., rel. to struct. factor (*Russian*) 3-79664
 metal, paracrystalline distortions, cause 3-49830
 metal, struct. and pair potentials, relation 3-49824
 metal and alloy, struct., review 3-49821
 metal melts, struct. heterogeneity determ. by diff. methods (*Russian*) 3-43709
 GeTe-PbTe alloys, solubility, one phase prod. 3-64146
⁴He liquid, structure and excitations, review 3-58158
 Hg, energy-scanning X-ray diff. study 3-40831
 Li-Ag(Sn)(Pb) alloys, struct. determ. 3-49827
 LiBr(Cl), aqueous soln., structure obs. 3-71996
 LiCl, aq. soln., neutron and X-ray diff. struct. examination 3-43745
 NaBr(Cl), aqueous soln., structure obs. 3-71996
 Ni-Si alloys, short-range order (*Russian*) 3-41690
 PbTe-GeTe alloys, solubility, one phase prod. 3-64146

X-ray diffraction examination of materials

- for results of crystal structural analysis see crystal atomic structure
 see also X-ray chemical analysis
 alkali borate + TiO₂ mixtures, fused, acid-based reactions 3-58818
 alloy, binary, evidence for clustering, X-ray small-angle scatt. 3-49829
 ammonium hydrogen oxalate hemihydrate, dislocation lines direction obs. 3-64037
 amorphous polymers struct. 3-46593
 asymmetrical transmission of X-rays, direction of energy flux (*Russian*) 3-49799
 bilayer with protein outside 3-48176
 biphenyl orthosubstituted derivatives, hydrogen bridges role in crystn. (*French*) 3-79475
 cellulose nitrate, track-etch radiography, alpha particles, protons, fast and thermal neutrons 3-67627
 ceramic, corundum struct. type, thermal expansion 3-69340
 ceramic, for high temp. e.m. windows, thermal cycling effects on struct. and props. 3-76280
 ceramic materials, cordierite Mg₂Al₄Si₅O₁₈, infrared and X-ray diffraction studies 3-53271
 chalcophyllite, simulated X-ray powder pattern data 3-73198
 α -CO, structure and thermal expansion determ. 3-79508
 coatings, thickness determ. 3-73676
 computer evaluation, high energy X-radiography, detectability of cracks prediction 3-45572
 concrete, prestressed, reinforcement position, strain meas. (*German*) 3-69418
 copper phthalocyanine polymorph, dimeric struct., i.r., X-ray, electronic, e.p.r. spectra 3-52599
 cosmic dust trace element distribution in deep sea core 3-51005
 crystals under static uniaxial compression, investigation apparatus 3-73673
 diamond, charge density study 3-40826
 diamond, growth, struct. anal. (*Japanese*) 3-72069
 diamond, X-ray Debye-Waller parameters depend. on atomic form factors 3-79278
 3,4-dihydro-2H-1,5-benzodioxepin-2,4-dicarboxylic acid, conformation 3-74921
 2,4-dinitrobenzenesulphonyl chloride, single cryst. struct. data 3-68240
 diphenylsulphone-2-sulphonyl chloride, single cryst. struct. data 3-68240
 dislocation morphology, review 3-61139
 β eucryptite, atomic structure rel. to temperature 3-73192
 Fortisan, variance range anal. of line broadening of profiles 3-79241
 garnet film, and substrate, structural defects obs. 3-44295
 Ge Debye temp. determ. by means of Borrmann effect (*German*) 3-60781
 glass, small-angle scatt. from supercrit. comp. fluctuations 3-75482
 glass-plastic, ageing and media effects on struct., shadow microscopy obs. (*Russian*) 3-41814
 glassy carbon based binary glasses, prep. and characteriz. 3-76246
 grain boundary and vol. diffusion 3-41043
 graphite analysis after electrolytic disgregation, HTG reactor fuel reprocessing 3-71283
 heptyloxyazobenzene, smectic-phase order-parameter fluctuations in nematic phase 3-63952
 high cristobalite, Bragg intensities determ. 3-61338
 high energy X-radiography, precision meas., dimensional change monitoring 3-45569
 ice, crystal axis determination, Laue photographs (*Japanese*) 3-54902
 imperfect crystals, anomalous absorption with X-ray diffraction (*German*) 3-43729
 KH₂PO₄, topography, dislocations, cryst. growth 3-68177
 lipid-cytochrome c membrane, structure 3-48177
 lunar samples and minerals, simultaneous X-ray and thermal analysis 3-65805
 lysozyme, refinement of X-ray data to relieve atomic overlaps 3-58025
 magnesium diethyl phosphate, structure, diffraction method 3-54951
 mammalian tissue, ultrathin frozen dried sections, elemental composition, transmission electron microscopy, X-ray microanal. 3-56476
 melt, monovalent, elec. cond. behaviour at melting pt., rel. to struct. factor (*Russian*) 3-79664
 metal, plastic flow, direct study by X-ray motion picture filming 3-76402
 metal powders, fluorescence anal., sample preparation 3-62336
 metallic hexaborides, thermal props., lattice const. 3-68423
 minerals, braggite, Patterson methods, crystal structure 3-56008
 natrolite single crystal, structure at high temperature 3-73191
 nuclear fuel elements, automatic testing system, scanning (*German*) 3-80512
 oriented clay mineral specimen preparation for X-ray diff. anal. by filter-membrane peel technique 3-51159
 paraffin, X-ray excitation of thermal spikes 3-43731
 PLZT, polymorphism and piezoelectricity 3-50524
 polyamide-6 fibres, effect of drawing, X-ray diffraction patterns, intensity distrib. along layer lines (*Russian*) 3-47476
 polyauroclactam, effect of N-substitution on crystallinity 3-63961
 polycarbonate, bisphenol-A, short range intermol. ordering obs. by radial distrib. functions 3-80473
 polycarbonate plastics, track-etch radiography, alpha particles, protons, fast and thermal neutrons 3-67627
 polyethylene, biaxially oriented linear, mech. α -relax. anisotropy 3-58727
 polyethylene, crystallite size distrib. and lattice distortion, Debye-Scherrer line profiles 3-40850
 polyethylene, paracrystalline lattice, small angle X-ray scatt. 3-72012
 polyethylene, semiequil. crystn. state, branching obs. 3-54930
 polyethylene, small angle X-ray scatt. curve evaluation, two phase model validity 3-72013
 polyethylene fibres, effect of drawing, X-ray diffraction patterns, intensity distrib. along layer lines (*Russian*) 3-47476
 polyethylene terephthalate fibre, effect of thermal treatment on thermomechanical props. (*Russian*) 3-80496
 polyethylene terephthalate, crystallinity determ., comparison with density measurements 3-43758
 polymeric insulation, chemical treeing, X-ray microprobe analysis 3-50516
 polyoxymethylene, paracrystalline lattice, small angle X-ray scatt. 3-72012
 polyoxymethylene, radial streaking 3-75485
 polyvinyl alcohol fibres, effect of drawing, X-ray diffraction patterns, intensity distrib. along layer lines (*Russian*) 3-47476
 powder, compressed, Poisson's ratio determ. (*Czech*) 3-54993
 powder, hexagonal close-packed, correction of integrated intensities for preferred orientation 3-75452
 powder diffractometry, low temp., 65 to 320 K (*French*) 3-49800
 quartz, thin layers, diff. analysis precision rel. to particle analysis 3-59674
 quartz-stishovite shock induced transition, X-ray and optical obs. 3-76560
 rare earth metal perovskite carbides and borides, preparation, X-ray and metallographic studies 3-40907
 rare earth transition metal silicides, structure types 3-58010
 residual stress determination, metals, X-ray method, elastic constant 3-47501
 retinal rod photoreceptor membranes and cornea examination 3-42362
 Roentgen photographs, influence of object motion using modulation transfer functions 3-66021
 semiconductor thin film and substrates, stress determ. using automatic Bragg angle control 3-41669
 silicate glass, semiconducting glaze, for porcelain insulator, phase changes, growth rate 3-47442
 silicate glasses, obs. of surface crystallization 3-75477
 sil wax, dipole orientation, X-ray diff. investigation 3-53058
 steel, ductile-brittle transition obs. 3-55815
 steel, electron bombarded, low-temp. reversible disorder-order phenomena and carbon redistrib. (*Russian*) 3-69187
 steel, heat treated, residual stress distrib. (*Japanese*) 3-41777
 steel, low-c, form. of δ' -nitride and niobium carbonitride (*Russian*) 3-72856
 steel, secondary martensite struct., atomic ordering effect (*Russian*) 3-61134
 steel, stress meas. from spotty X-ray diff. rings, method (*Japanese*) 3-41731
 steel, stress meas. of specimen with steep stress gradient in near surface layer (*Japanese*) 3-41730
 stress analyzer, Strainflex, with Side Inclining method (*Japanese*) 3-39855
 stress meas., diff. apparatus operating condition effects on line profile and peak position (*Japanese*) 3-40829
 tanane, ferroelastic-ferroelectric compound, paraferroelectric transition meas. 3-55536
 ternary zincblende substitutional solid solutions, SRO parameters 3-52596
 track-etch radiography, alpha particles, protons, fast and thermal neutrons, polycarbonate plastics, cellulose nitrate 3-67627
 transition metal perovskite carbides and borides, preparation, X-ray and metallographic studies 3-40907
 1,3,5-trinitrobenzene, crystals grown by precipitant infusion 3-80153
 2,4,6-trinitrotoluene, crystals grown by precipitant infusion 3-80153
 trioctahedral mica, fluorophlogopite and annite, crystal struct. 3-80596
 1,3,5-triphenylbenzene, thermal diffuse scattering, elastic-vibration amplitudes 3-64118
 wax, microcrystalline, structure obs. 3-54952
 zeolites, sedimentary, Mexico, X-ray diffraction and electron microscope studies 3-44774
 Ag single crystals, dislocation free, growth by Czochralski method 3-44539
 Ag-Cr thin film mixtures, charact. determination 3-80002
 Ag-Sb alloys, particle size and strain determ. by method of variance 3-44575
 β -AgI, formed from reaction of I vapour on Ag film 3-55171
 Ag(I) complex, bis(2-methyl benzothiazole) Ag(I) perchlorate, cryst. struct., X-ray obs. 3-72046
 Ag₃In, order-disorder transition behaviour 3-64831
 Ag₂Te, polymorphism obs. 3-68406
 Al, dislocation configs., vacancy sources and sinks during thermal treatment 3-52627

X-ray diffraction examination of materials continued

- Al, stressed single crystal, Lang topography technique for obs. of dislocation behaviour 3-68268
- Al, thermal diffuse scattering investigation 3-54895
- Al alloy, fatigue crack detection, u.s., X-radiographic and eddy current techniques 3-47511
- Al-Ge, alloys precipitation of Ge nuclei, supersaturated alloy, below 140C, X-ray and resistivity analysis, vacancies 3-53234
- Al-Zn (22 at %) alloy, liq.-quenched, spinodal decomp. 3-64868
- Al₂O₃, oxinitride form., cationic vacancy ordering (French) 3-76335
- Al₂O₃ films, compositional information from ion-induced X-rays and Rutherford backscattering 3-43960
- Al₂O₃ sputtered deposit prep. and characteriz. 3-76127
- Al₂O₃-Cr₂O₃ powders, condensed from plasma, struct. exam. 3-47448
- Al₂O₃-Na₂O system, range of existence and stability of β and β'' alumina (French) 3-69365
- AlTa film, r.f. sputtered, structure obs. 3-50096
- β -Al₂TiO₅, calculated powder diff. data 3-60700
- As-Se glasses, atomic radial distribution functions 3-57990
- As-Se-Te glasses, thermal stability toward crystallization 3-75478
- As-Te glasses, local order parameters and structural model 3-40848
- As-Te-Ge glasses, memory phenomena investigations 3-41240
- As₂S₃, As₂Se₃, structure change due to ⁶⁰Co γ -radiation (Russian) 3-57991
- Au films on NaCl (001) substrate, recrystallisation, thermal annealing, strains calc. 3-72294
- Au-Ta film, struct. and thermal stability obs. 3-64837
- Ba₂CdS(Se)₃, BaCu₂S(Se)₂, preparation, crystal structure, X-ray diffraction studies 3-40905
- BaFeO_{3-x}, struct. of two phases, X-ray study 3-46608
- BaFe₂O₉, substituted, solid solns., intrinsic coercivity meas. 3-41357
- BaLa₂Fe₂O₇, ferrite, cryst. struct. detn. 3-58022
- Ba₂MReO₆, M=Mn, Fe, Ni, Co, solid-state synthesis and mag. props. 3-75829
- Ba₂NaNb₂O₁₅, ferroelec., struct. behaviour in Curie pt. region 3-41488
- BaO-CeO₂-TiO₂ system, subsolidus phase relations 3-44650
- BaO.5.5 Fe₂O₃, mag. phase analysis 3-58381
- BaSnS₂ crystal structure, NaCl type variant 3-60684
- Be single crystal, X-ray plasmon scattering 3-55227
- Bi film, struct. determ. 3-64267
- Bi V, h.p. struct. by a Bragg-Brentano X-ray reflection technique 3-72045
- C, pyrolytic, coating for HTGR fuel particles, fluidised bed deposition, thermal expansion, 300-1100°C (German) 3-71249
- C, soft, partially graphitised, atomic layers mutual arrangement (French) 3-46620
- C glassy, struct. analysis by X-ray Fourier transform technique 3-46590
- CaB₂O₄.5H₂O, pentahydroborate, crystal structure 3-64020
- CaF₂-NdF₃(YF₃) system phase relations and characteriz. (German) 3-47443
- Ca(NO₃)₂.4H₂O crystal structure analysis 3-60688
- CaO-MgO-SiO₂ glass system, crystallisation obs. (Russian) 3-52582
- CaSiO₃ (wollastonite), polytypism and stacking disorder 3-68277
- CaSiO₃-Gd₂SiO₅ system, variable phase comp. 3-68385
- Cd₃As₂, lattice parameter measurement between 23 and 700°C using X-ray diffractometer 3-68426
- CdO-GeO-LiCl-H₂O system, crystn., product identification 3-72027
- CdS vibr. cryst., diff. behaviour, dynamical to kinematical refl. power transition 3-43726
- CeO₂-B₂O₃(P₂O₅) glasses, characteriz. w.r.t. struct. 3-76273
- CeO₂-ZrO₂-CoO system, fluorite type phase obs. (French) 3-64183
- Co-Si eutectic alloy, struct. and mag. props. of phases 3-80201
- Co-Sm magnet, after quenching, oxides identified 3-47100
- Co-Sm permanent magnet alloy, lattice parameter variation with composition and temp. 3-43763
- Co-Ti-based Heusler alloys, mag. and chem. order 3-68791
- Cr, lattice const. meas., thermal expansion coeff. determ. 3-68427
- Cr-B, solid soln. unit cell dimensions, powder diffractometry 3-41023
- Cr-Rh alloy, system, constitution diagram obs. 3-69193
- CrAs_{1-x}, crystal structure, mag. susceptibility meas. 3-44209
- CrO₂ conversion into CrOOH, crystallographic axial relation 3-61256
- Δ -Cr₂O₃, new high temp. form, X-ray powder diffraction and i.r. spectrum meas. 3-75509
- CsBi(MoO₄)₂, identification, dimens., heating effect 3-72047
- CsCrBr₃, complex crystal structure, optical spectra, effect of exchange coupling 3-61043
- Cu, elec. cond. behaviour at melting pt., rel. to struct. factor (Russian) 3-79664
- Cu-As alloy, deformed, recovery during heating, mechanism (Russian) 3-58643
- Cu-B, solid soln. unit cell dimensions, powder diffractometry 3-41023
- Cu-Be (0.25 wt.%) alloy, oxide particle size and distrib. (French) 3-44586
- Cu-Ni, nondestructive atomic studies, X-ray diffraction techniques 3-42681
- Cu-Pt alloys, short-range order in hardened alloys (Russian) 3-69270
- Cu-Sb, liquid alloy, structure combined neutron and X-ray diffraction obs. 3-52566
- CuCr₂O₄ Jahn-Teller effect 3-72048
- CuInS₅ (Se₂,Te₂), uniformity meas., synthesis, struct. 3-69447
- Cu₂Mn_{1-x}O₄ system, stability range of cubic spinel struct. 3-60786
- CuPt alloy, crystallographic ordering mechanism and modified microstruct. 3-80215
- α -Cu₂Se, crystal, Laue pattern, phase transitions 3-68405
- Cu₂Se, structural transform. studied by high temp. roentgenography 3-52700
- Eu₂O₃ reactions with Nb₂O₅, V₂O₅, lattice consts. 3-75598

X-ray diffraction examination of materials continued

- EuS film, epitaxial, h.v. evaporation on mica, structure obs. 3-68512
- (Fe, Ni)₉S₁₁, eclogite nodules, kimberlite pipe, South Africa, phase equilib. 3-44764
- Fe-Al alloy films, lattice parameters (Russian) 3-60844
- Fe-Al-Ge alloy, lattice constant, hardness, conc. depend. 3-76159
- Fe-Al(16.3 at %) alloy, short-range order (Russian) 3-72893
- Fe-B, solid soln. unit cell dimensions, powder diffractometry 3-41023
- Fe-C system, pseudohexagonal Fe₇C₃ and Fe₃C-Fe₇C₃ eutectic studies 3-41692
- Fe-Cr solid solns., disordered, lattice parameters, temp. and conc. depend. (Russian) 3-53199
- Fe-Mn-Cr sealing alloy, high temp. oxidation and sealability, effects of Al, Mn and Si additions (Japanese) 3-44615
- Fe-Ni alloy films, annealing effect on constitution (Russian) 3-60984
- Fe-Pt alloy, ordered equiatomic, mag. and atomic struct. (Russian) 3-68787
- Fe_{1-x}O, structure examination, X-ray and electron diffraction (Russian) 3-49885
- Fe_{1-x}S epitaxial growth on Fe single crystals in H₂S-H₂ mixture (Japanese) 3-58187
- FeTi₂O₅-Ti₂O₅ system, crystal struct. 3-58020
- Ga_{0.16}Al_{0.84}As solid solution, short range order parameters 3-52596
- Ga_{1-x}Al_xAs heteroepitaxial layer, on GaP, soln. grown, characterisation 3-41682
- GaAs, Laue diffraction near absorpt. K-edges 3-71986
- GaAs heteroepitaxial layer, on GaP, soln. grown, characterisation 3-41682
- GaAs₂Sb_{1-y} alloy variation of lattice parameter 3-75602
- GaP, polarity sense, rapid determ. by energy dispersive diffractometer 3-72053
- Gd-Ga garnet substrate, cryst. perfection and residual defects 3-40926
- Ge, effect of neutron irradiation and B doping on X-ray diffraction 3-68286
- Ge, single crystal, X-ray wave fields, energy flow 3-40834
- Ge, six-beam Borrmann diff., linear absorpt. coeffs. calc. 3-43725
- Ge crystal, three beam diffraction of CuK α radiation by (111) and (111) planes (German) 3-60656
- Ge-Te, amorphous alloys, structure investigation, non crystalline to crystalline state transformation 3-58259
- H₂TcCl₉H₂O, oscillating crystal method 3-79310
- HfO₂-CaO, HfO₂-Y₂O₃ systems, phase investigation, stabilisation and destabilisation of solid solns. 3-75599
- HfO₂-Y₂O₃ solid soln., phase diagram boundaries detn., X-ray analysis 3-64153
- HfMn₂Fe_{1-x}O₃, ferrite, reorientation range, transition type 3-60964
- In₂O₃-Sn thin films, growth, fine struct., annealing effects, resistivity (French) 3-79593
- InP thin films on GaAs, Ge, InP substrates, struct. anal. 3-72286
- InSb, liquid phase epitaxial layer on CdTe, rel. to metallurgical aspects (French) 3-64794
- KAl₂Br₇ crystal structure, diffraction study 3-54943
- KD₂PO₄, crystal structure investigation at 20°C 3-49879
- KH₂PO₄, diffraction intensity contrast and Pendellosung fringes due to lattice distortions 3-68267
- KH₂PO₄, intensity var. with changing temp. gradient, meas. 3-79295
- KH₂PO₄, obs. of domain structure by low-temp. X-ray photography 3-50527
- KMnP and KMnAs powders, synthesis, crystal structure, X-ray studies 3-40900
- K₂(Ni₂CN)₆, struct. from X-ray diff. (German) 3-40894
- KNiF₃, lattice constants measurement, double-crystal diffractometry using white X-rays 3-52559
- K₂PtCl₆ structure, single crystal and powder, diffraction refinement 3-58013
- K₂SO₄, neutron irradiation effects on single crystals 3-79379
- K₂(UO₂)₂F₇.2H₂O, Patterson, electron density syntheses 3-79311
- K₂[Pt(CN)₄]ClO₃.xH₂O, stability in wet and dry atmospheres, obs. 3-46627
- K₄[Zr₂(SO₄)₆4H₂O], complete X-ray structure, heavy-atom method determ. 3-79309
- Kf-TbF₃ system, phase diagram, struct. 3-64148
- LaCrO₃, hexagonal-cubic transform, high temp., lattice parameter changes (French) 3-52697
- LaFe(CN)₆.5H₂O structure, single crystal, diffraction study, least squares analysis 3-58012
- LaMg_{1-x}Ni_xFeO₄ system, phase analysis rel. to mag. props. (German) 3-52968
- LiCl-NaCl solid solution, thermographic and X-ray study, crystn. temp., peritectical transformation (Russian) 3-72196
- Li(Fe, Zn)[PO₄], crystal struct. 3-64021
- LiNbO₃, neutron irradiation effects on single crystals 3-79379
- LiNbO₃-KNbO₃ system, phase diagram, Curie temp. 3-72590
- Li₂O-Al₂O₃-SiO₂, glass, nucleation and crystn. phenomena 3-54928
- Li₂O-SiO₂ glasses crystallized after ion exchange below T_g, characteriz. 3-76266
- LiOH reaction layer on LiH, structure 3-43952
- Li(Ta, Sb_{1-x})O₃, phase diagram, ferroelec. props. 3-72589
- Li₂Ga₂(BO₃)₄, Patterson, electron density syntheses 3-79312
- Mg ferrite, non-stoichiometric, ionic distrib., oxygen parameter, vacancies 3-54944
- MgMn ferrite, non-stoichiometric, ionic distrib., oxygen parameter, vacancies 3-54944
- MgO, defect formation on surface during thermal decomposition (French) 3-72971
- MgO-Al₂O₃||I₂ high-quartz solid solns., ordering by substitutions affecting superlattice refs. 3-44656
- Mn-Al, δ -phase, one dimens. disordered cryst., intensity equations for diffracted X-rays 3-58004
- Mn-B, solid soln. unit cell dimensions, powder diffractometry 3-41023
- MnBi film, formation process, Bi and Mn layer deposition and annealing 3-44298
- Mn_{1-x}Fe_xAs phase, crystal structure, mag. props. 3-40901
- MnS, synthesized, and solubility in PbS 3-72200

X-ray diffraction examination of materials continued

- MoO₂Cl₂·H₂O, polytype struct. from non-space group extinctions 3-49873
- NH₄H₂PO₄, diffraction intensity contrast and Pendellosung fringes due to lattice distortions 3-68267
- γ-Na₂BeF₄, X-ray diff., precession photography 3-40892
- NaCl, Berg-Barett and Fujiwara methods, polygonisation under sign-varying deformation 3-75560
- NaCl, lattice parameter, at high pressure and low temp. 3-63998
- NaCl-CdCl₂-SrCl₂ phase diagram, thermography, X-ray methods, Na₂CdCl₄ binary combination, eutectics, Van Rein point (*Russian*) 3-52692
- Na₃(Mn, Na)₃ Mn[Si₆O₁₈], synthetic metasilicate, cryst. struct. 3-64019
- NaNO₃, neutron irradiation effects on single crystals 3-79379
- Na₂O-SiO₂ glasses, diff. study 3-72008
- Na₂O·2Al₂O₃, lattice dimensions, powder diff. data 3-72932
- 2Na₂O·2Al₂O₃·3SiO₂ based glasses, crystn. 3-73032
- Na₃(P₂O₆N₃H₃) reactions with aq. solns. of MCl₃, M=Al, Ga, In, product props. 3-73114
- Na₂PrGeO₄(OH), struct., X-ray analysis 3-40887
- Na₂Si crystal structure, linear diffractometer method 3-60683
- Nb-Ru system, martensitic transitions, temp. and conc. depend. (*French*) 3-58126
- NbC, Bragg intensity meas., Debye temp. determ. 3-72156
- Nb₃Sn, supercond., shock wave synthesis, phase form. obs. 3-69328
- Nb₂Zr₆O₁₇, crystal structure 3-58019
- Nd(OH)₂Cl, cryst. struct. 3-49884
- A-Nd₂O₃-A-La₂O₃ and A-Nd₂O₃-C-Y₂O₃, investigation of the binary systems (*French*) 3-64152
- NdSBr crystal structure, diffraction study, rare earth sulfobromide iso-types (*French*) 3-60687
- Ni sulphides in Ni-base superalloys, crystal structure and morphology 3-40864
- Ni-P films, annealing effect on struct. (*Russian*) 3-60843
- Ni-Ta-Cr-Mn system dendritic duplex crysts., topography 3-41725
- NiAl₂O₄:CaO, sintered spinel, struct. rel. to CaO content (*Polish*) 3-44664
- Ni₃Cu_{1-x}MnSb atomic and magnetic structure, X-ray and neutron diffraction, magnetometry, 0.05 ≤ x ≤ 0.4 3-49870
- Pb, f.c.c.-h.c.p. transformation, pressure induced, based on the NaCl internal standard 3-72834
- PbMoO₄, thermal expansion, X-ray determination 3-46719
- PbO-TiO₂-SiO₂ system glass, Al₂O₃ addition effect on glassy phase separation and crystn. (*Japanese*) 3-65023
- 5PbO·3GeO₂, ferroelec., struct. obs. 3-68226
- PbS, synthesized, and solubility of MnS 3-72200
- PbTe-SnTe-PbS system, thermal conductivity and structural study 3-79533
- PbZrO₃-SrCu_{1/3}Nb_{2/3}O₃ system, X-ray diff. phase anal. dielec. props., Curie point determ. 3-72591
- PrCo₅, Pr₂Co₁₇, Al substituted, struct. and phase relations obs. 3-69194
- PrO₂-O system, pseudophase behaviour in epilón and iota regions 3-64180
- PuWC_{1.75} ternary phase, cryst. struct. and comp. 3-44649
- Rh-Mn-Sb alloys, Cl₂ type, lattice parameters 3-64490
- α-Sb₂O₃, oriented crystallisation during heating of Sb₂O₃ (*Russian*) 3-40854
- ScBO₃, thermal expansion, temp. depend., 30-702°C 3-68422
- Si, C⁺ implantation, X-ray interferometry of volume changes 3-43817
- Si, dislocation-free crystals, distribution of point defects Cu decoration, X-ray topography, etching 3-41650
- Si, effect of neutron irradiation and B doping on X-ray diffraction 3-68286
- Si, nearly perfect crystal, imaginary parts of atomic scatt. factors using Borrmann effect 3-43775
- Si, screw dislocations, intensity distrib. in Bragg case 3-58037
- Si, uniformly bent cryst., X-ray wavefield beam propag. 3-43723
- Si single crystals, nearly perfect, lattice curvature, dislocation loops 3-60738
- Si swirls, interaction with dislocations, comparison to striations 3-41647
- Si wafers, of O, X-ray double crystal method, lattice strain meas. 3-41662
- Si: Au wafers, EIDP deposited, Si₂W crystallite growth on surface 3-72813
- α-SiC, 6H and 15R polytypes, intensities of X-ray refl. from basal plane 3-55131
- SiC, 6H polytype, diffusion-doped, struct. imperfections 3-55741
- SiC, reaction-sintered, growth characts., polytype distrib., 6H₂ struct. absence 3-76299
- SiC, solution growth from liquid Si, polytypes obs. 3-64771
- SiC films, liquid-phase epitaxy 3-72278
- SiC polytype 189R, structure and growth, X-ray diffraction analysis 3-60689
- SiO₂ support, NaOH addition effects on morphology and struct. 3-58773
- SmCo₅, Sm₂Co₁₇, Al substituted, struct. and phase relations obs. 3-69194
- Sn-S system, identification of SnS, Sn₂S₃, SnS₂, Sn₃S₄ 3-72548
- Sr(NO₃)₂-Nd(NO₃)₃-Na₂WO₄·H₂O system, solid phase, X-ray phase analysis 3-76422
- SrO-BaO-Al₂O₃ system, solid state phase equilib., struct. 3-72998
- Si₂SiO₄-Sr₂GeO₄-Ba₂GeO₄-Ba₂SiO₄, solid solubility, polymorphism, lattice constants 3-41803
- SrTi₂Fe₂O₇, ferrite, cryst. struct. detn. 3-58022
- SrTiO₃, lattice const., 17-300 K, anomaly at cubic-tetragonal trans-form. 3-60701
- Su, diffuse scatt. by radiation prod. defects, meas. in anomalous transmission and near Bragg refl., comparison 3-43727
- β-Ta, film, lattice constants determ., structural model 3-43966
- Ta films, phase composition and texture analysis by energy dispersive X-ray analysis 3-45566
- TaC, Bragg intensity meas., Debye temp. determ. 3-72156
- Ta₂S_{2-x}, Se_x, phase diagram, X-ray analysis, atomic scattering factors 3-41016
- Tel, cell parameters, space groups 3-72059

X-ray diffraction examination of materials continued

- Ti, α → ω transform, hysteresis, T-P diagram (*Russian*) 3-44560
- Ti alloy, VT16, α'-martensite decomp. (*Russian*) 3-72825
- TiB₂, thermal expansion, 25-1200°C 3-44657
- Ti₂O₃, corundum struct., thermal expansion obs. 3-64189
- TiBr-KBr single crystal, lattice const., luminescence centres 3-64722
- Tm, high press. polymorph 3-75500
- UN₃ (x > 1.75), preparation and X-ray investigation (*German*) 3-50759
- U₄O₉, high-temp. phase transition, 300-800°C 3-64972
- UO₂·xMgO system, phase equilibrium and transformation determ. 3-74725
- U₁₀Pu_{0.7}C-W system, phase diagram obs. 3-47451
- U₃Si, polycryst., lattice parameters, counter-diffractometer parameter determ. 3-41802
- V-N dil. alloys, metastable phase behaviour 3-64976
- V_{1-x}Cr_xO₂, (0 ≤ x ≤ 0.15), powder spectra, phase diagram determination (*French*) 3-79472
- V₂D, V₄D₃, crystal structure determ. between 5K and 425K structural transitions 3-46710
- VN_{0.96}, thermal expansion, 300 to 1000K 3-69341
- V₂O₃, corundum struct., thermal expansion obs. 3-64189
- W/PtSi/Si film system, kinetics of WSi₂ formation, rel. to IC metal-lisation 3-64787
- Y₂Al(Co_{1-x}Fe_x)_{17-2x} intermetallic compound, magnetocryst. anisotropy obs. 3-44230
- Y₂O₃-CaO system, phase diagram characteriz. 3-76241
- Yb-Pd system, phase diagram determ. 3-64151
- Zn, characterisation of dislocation loops by X-ray topography 3-43802
- Zn silicate glass, alkali, nucleation and crystallisation properties 3-75476
- Zn₃As₂, lattice parameter measurement between 23 and 700°C using X-ray diffractometer 3-68426
- Zn₃As₂(Zn₃P₂ solid solutions, struct. determ., semicond. 3-79712
- α-Zn(H₂O)₆SeO₄:Co, laevorotatory, cryst. struct. and absolute config. 3-40866
- Zr, α → ω transform, hysteresis, T-P diagram (*Russian*) 3-44560
- Zr, phases and compressibility up to 120 kbars 3-72833
- ZrC, solubility of O₂, X-ray diffraction 3-41804
- α-Zr(HPO₄)₂·H₂O, crystalline, prep. and characterisation 3-55730
- ZrO₂, anionic vacancy ordering (*French*) 3-76335
- ZrO₂, calcia-stabilized, fluorite type solid soln., ordering (*French*) 3-72991
- ZrO₂, crystallisation, X-ray diffraction and electron microscope studies (*Japanese*) 3-80432
- ZrO₂, monoclinic-tetragonal transition, high temp. obs., twin form. 3-72931
- ZrSiO₄, anisotropic thermal expansion and compressibility, high temp. and high pressure X-ray diffraction, neutron diffraction 3-46721

X-ray diffraction examination of microstructure

- alloys, coarse-grained, X-ray studies, effect of turning, reciprocating and swinging motion 3-52558
- binary alloys, surface struct. due to plane shock wave (*Russian*) 3-80306
- calcite, crystal defects formed during hydrothermal growth (*French*) 3-64024
- camera, disorientation within grains, oscillating specimen 3-51754
- capron, submicrocrack formation and concentration, in loading and unloading 3-58742
- cellulose acetate fibres, heat-treated, peak resolution and crystallinity determ. 3-72016
- cellulose fibres, crystallinity and crystallite size meas. in Ramie and Fortisan 3-72017
- cellulose triacetate fibres, heat-treated, correl. crystallinity, lattice perfection 3-72015
- clinopyroxene, lattice deform. depend. on chem. substitution and temp. 3-80592
- coal, heat treatment, linear profile analysis, graphite crystallites (*German*) 3-73035
- ethylene-phosphonic acid copolymers, X-ray study of structure 3-54934
- fatigue crack, total misorientation, excess dislocation density, lattice strain, subgrain size 3-69242
- graphite matrix material and pyrocarbon in HTR fuel elements, micro-porosity exam. (*German*) 3-71319
- graphite reactor materials, radiation damage, interstitials, vacancies (*German*) 3-71255
- III-V semiconductors, thermal decomp. by laser beam 3-73152
- lithium formate monohydrate, defect struct., X-ray topographic investigation (*German*) 3-43803
- metal, polycryst., hydrostatic stress effect on tensile creep at elevated temps. (*Japanese*) 3-40830
- orthoferrite, magnetic domain config. obs. 3-64518
- pigeonite from lunar rock 12053, anti-phase domains from X-ray dif-fraction 3-65816
- polycrystalline materials, magnification in diffraction patterns 3-76855
- polyethylene, fibre and row struct., X-ray pole diag. obs. (*German*) 3-61224
- polyethylene, high density, electron microscope, X-ray analysis of crystal distortion (*Russian*) 3-71692
- polyethylene, high-density, with single cryst. texture, structure 3-57993
- polyethylene, submicrocrack formation and concentration, in loading and unloading 3-58742
- polyethyleneterephthalate, meander model (*German*) 3-60669
- polymer, crystallisation, isotropic small angle scatt. models for lamellar struct. (*German*) 3-60670
- polymer, lamellar struct., small angle scatt. analysis (*German*) 3-60671
- polymer, partially cryst., lamellar structure determ. from small angle X-ray scatt. 3-72011
- polymer, semi-crystalline, small angle scatt. obs. 3-69388
- polymers, semicrystalline, small angle X-ray scattering, theoretical models 3-57994
- polystyrene-polybutadiene-polystyrene copolymer, macrolattice based on lamellar morphology 3-63960
- quartz, deform. dislocations obs. 3-75539

X-ray diffraction examination of microstructure continued

- reactor matrix material, microporosity, neutron irradiation effect (*German*) 3-71252
- reyerite, hydrated Ca-silicate, anal. 3-50885
- rolling texture determination, X-ray diffraction technique, combination of inverse polar and direct figures 3-53227
- steel, austenite EI-257, prolonged ageing influence (*Russian*) 3-80273
- steel, austenitic, high-Mn, fine struct. after high-speed straining (*Russian*) 3-64836
- steel, austenitic, stainless, phase analysis 3-47391
- steel, austenitic, time-temp. precipitation diagram (*German*) 3-47364
- steel, Cr-Ni type, austenite struct. and strength changes during ageing (*Russian*) 3-80277
- steel, G.TsK polycrystals, effects of deformation, hydrostatic pressure, dislocations (*Russian*) 3-55787
- steel, heat resistant low-alloy CrMoWV type, Ti and Zr effects on long-term plasticity 3-69323
- steel, low-C, fatigue crack propag. under doubly repeated stress, residual stress and plastic strain (*Japanese*) 3-41734
- steel, low-C, texture form. during deform. (*Russian*) 3-53218
- steel, machined, size effect on fatigue strength 3-64882
- steel, martensite, loading effect in macroelastic range on X-ray diff. linewidth (*Russian*) 3-61133
- steel, mild, stress corrosion cracking by phosphate solution 3-55795
- steel, Mn-type, martensitic transform., stacking fault density variation in austenite (*Russian*) 3-72824
- steel, obs. of stacking faults, effect on resistance to plastic deformation (*Russian*) 3-69269
- steel, plastic deform. of microstruct. below honed surfaces (*German*) 3-41743
- steel, quenched, residual austenite obs. (*Russian*) 3-53216
- steel, stress state at fatigue crack tip obs. by X-ray microbeam technique (*Japanese*) 3-41736
- steel sheet, Al-stabilized, directional depend. of integral breadth of diff. profile and microbeam spots (*Japanese*) 3-41729
- styrene-butadiene-styrene block copolymer, domain struct., hexagonal convection cell, anisotropy, X-ray diffraction studies 3-54933
- Ag alloys, cold-worked, Voigt profile analysis for particle size and strain determ. 3-61141
- Al, coarse crystals, fatigue damage mechanism (*Japanese*) 3-41732
- Al, creep, X-radiographical study, mosaic block fragmentation (*Russian*) 3-58629
- Al, electromigration of polygonization substructures 3-79523
- Al, imperfect structure after low-temp. rolling and annealing (*Russian*) 3-69208
- Al, polycryst., hydrostatic stress effect on tensile creep at elevated temps. (*Japanese*) 3-40830
- Al, polycryst., single [111] fibre texture development (*Japanese*) 3-61143
- Al shock wave effects on plates, textured, rolled, coarse grained (*Russian*) 3-69264
- Al-Ag alloy, liquid quenching effects and precip. 3-80261
- Al-Cu-Li alloy, microstruct. after isothermal heat treatment, precipitation behaviour (*German*) 3-44590
- Al-Cu(4 wt.%) alloy, substruct. and dispersion hardening 3-69231
- Al-Ge(4 wt.%) solid soln. decomp. phenomena (*Russian*) 3-58619
- Al-Zn (28 at.%) alloy, liquid-quenched, phase decomp. 3-41740
- Al-Zn(9 at.%) - Ag(1 at.%), Al(90 at.%) - Zn(10 at.%) , Guinier-Preston zone, structural features of decomposition process (*Russian*) 3-41723
- Al₂O₃, abrasion, plastic deformation, debris, microstrain 3-69357
- Al₂O₃, high integrity body design using chem.-mineralogical phase anal. 3-76274
- Al₂O₃ refractories, phase changes during service in high temp. kiln 3-80411
- Au-Cd-In alloy, double h.c.p., X-ray powder pattern obs. 3-58043
- BaTiO₃:LiF-MgO, small tetragonal distortion 3-80415
- C, glassy, submicroscopic void obs. 3-58737
- C fibre, acrylic polymer oxidation, vacancy tempering out (*German*) 3-76371
- Ca₂SiO₄, anal. of phase comp. on heating 3-72192
- Cd, climb of super-jogs and dislocation configs. during oxidation (*French*) 3-64047
- CdSb, dislocation struct. obs. (*Russian*) 3-75541
- CoO-ZnO-Al₂O₃-Cr₂O₃-Fe₂O₃ spinel solid soln., formation and colour variations (*Japanese*) 3-50763
- Cr bronze, rolling texture determ., X-ray diffraction technique, combination of inverse polar figure and direct figure 3-53227
- Cu, deformed in wide range of loading rates, substructure (*Russian*) 3-44568
- Cu, drawn, texture rel. to extinction effect magnitude, X-ray refl. intensities (*Russian*) 3-76162
- Cu alloys, cold-worked, Voigt profile analysis for particle size and strain determ. 3-61141
- Cu shock wave effects on plates, textured, rolled, coarse grained (*Russian*) 3-69264
- Cu-Ni alloys, mag. permeability correl. with microstruct. 3-75856
- Cu-Ni ores, Pt, Rh and Pd determ., X-ray spectrometry, segregation 3-48659
- Cu-Se-Sn system, DTA, X-ray phase analysis, microhardness, thermo-e.m.f. 3-72174
- Cu-Sn-Se system, DTA, microstructural and X-ray phase analysis, cross sections 3-72175
- Fe, steady-state creep, substruct. parameters (*Russian*) 3-53217
- Fe-Co-V atomic order recovery, influence of vacancies, X-ray diffraction study (*French*) 3-58638
- Fe-N(1.5 wt.%) alloy, tempering of martensite, precip. processes 3-64859
- Fe-Si, shock loaded, struct. changes during heating (*Russian*) 3-80248
- Fe-Si (3 wt.%), 90° Bloch walls, effect of anomalous absorption on diffraction contrast 3-44273
- Fe-Si(3 wt.%) single cryst., rolled, deform. texture form. (*Russian*) 3-58622
- Fe-Sn system α -solid solns., continuous and discontinuous precip. behaviour 3-64860
- α -Fe-Zn, precipitation behaviour, effect of Si, Ge, Sn and Cu, morphology and kinetics of precipitation (*German*) 3-72847

X-ray diffraction examination of microstructure continued

- FeCl₃ graphite intercalation compound, disordered layer struct. (*German*) 3-73036
- GaAs, shallow surface layer, disloc. contrast, refl. X-ray topography obs. 3-41070
- GaP, shallow surface layer, disloc. contrast, refl. X-ray topography obs. 3-41070
- Ge, dislocation structure, two beam tilt lattice image obs. 3-68263
- InP, shallow surface layer, disloc. contrast, refl. X-ray topography obs. 3-41070
- KCl, dislocation struct. determ., appl. of methods of X-ray scatt. dynamic theory (*Russian*) 3-68274
- KCl, hot worked, strength and deformation rel. to microstruct. 3-76252
- LiO₂-Al₂O₃-SiO₂ glass dependence on composition 3-55902
- Mn₅₋₈Fe₂Si₃, at. and mag. struct. determ. 3-68792
- Mo alloy sheet, surface layers, recrystallisation 3-76175
- Mo alloys, grain boundary precipitate constitution and conc., annealing influence (*Russian*) 3-44572
- Mo-C(Ta) alloys, stacking fault form. probability (*Russian*) 3-80275
- Mo-Re-C alloy, ageing, heat treatment, 1400-1800°C 3-76174
- MoNi₃, α -f.c.c. phase (*Russian*) 3-79271
- Nb-Zr, interdiffusion, prolonged heating, X-ray microanal. (*Russian*) 3-69250
- Nb₃Au₂Pt_(1-x)A-15 type phases, superconductivity, structure and magnetic susceptibility 3-58334
- Ni, annealed, recrystallisation centre growth rate, X-ray diffraction study 3-72861
- Ni-Al cast superalloys, constitution and microstructure 3-50709
- Ni-glass-ceramic composite material, heat treatment, crystn. of dispersed glassy phase (*Russian*) 3-41799
- Ni₃Fe, alloys structural state, mechanical properties, polycrystalline, degree of order, dislocations, slip lines 3-53233
- NiO-CaO solid soln., exsoln. kinetics and microstruct. development 3-72941
- NiO-CoO solid solns., defect struct. characteriz. 3-61192
- PbZr_{0.5}Ti_{0.5}O₃ synthesis, microstruct. development, effect of ZrO₂ particle size and struct. 3-61201
- Re-ZrC system, high temp. phase equilib. determ. 3-72978
- Sb₂Se₃-GeSe₂, Sb₂-Se₃-GeSe systems, condition state diagrams, thermal, X-ray and microstructure anal. (*Russian*) 3-49968
- Si, anomalous transmission and topography, oxygen precip. and heat treatment 3-68413
- Si, fracture, Pendellosung fringe and double-cryst. diffractometry obs. 3-64102
- Si dislocations, diffusion induced, simple planar structures, X-ray diff. contrast study, Burgers vectors 3-43798
- Si homoepitaxial layer, misfit disloc. on (110), (112), and (113) 3-64256
- SiC, powder diffraction, to determ. reaction products from SiC, SrO high temp. reaction 3-74723
- β -SiC, topographic exam., struct. defects rel. to photoelec. props. 3-72097
- SiO₂-PbO-P₂O₅ system glasses, heat treatment effects 3-76261
- SmCo₅, powder-based magnets, texture perfection degree, particle orientation angles distrib. (*Russian*) 3-61135
- Ta, surface-carburized, carbide precip. phenomena (*French*) 3-61153
- ThO₂, colloidal sol, particle size distrib., small angle X-ray scatt. anal. 3-73079
- (Ti, W)C, solid solution, diffusion mechanism during form. 3-64975
- Ti alloys, metastable β -phase, hydrogen effect on ageing and precip. (*Japanese*) 3-41726
- Ti-V-Cr-Al metastable alloy, recrystallisation and X-ray diff. invest. of age-hardening (*German*) 3-72880
- TiCr₂, Laves phase imperfections, double hexagonal refl. 3-69238
- U-Nb alloys, niobium segregation phenomena 3-61149
- WC-Co compound powder, plasma spraying on hard metals, phases study (*German*) 3-50752
- WNi₃, α -f.c.c. and γ -b.c.c. phases (*Russian*) 3-79271
- Zn, melt grown single crystals, dislocation struct., seed cryst. perfection and seeding method effects (*Russian*) 3-69153
- Zn-Al (30 wt.%) alloy, solid soln. decomp. and superplasticity behaviour (*French*) 3-47418
- Zn-Al(40 wt.%) alloy, superplastic, basal plane pole figures 3-69220
- ZnO-Bi₂O₃ nonohmic ceramics, phase morphology 3-80416
- Zr-H, γ - and δ -phase hydride form. on cooling from α -phase field, powder diff. obs. 3-72864
- ZrO₂, mixtures of crystal forms, X-ray phase anal., URS-501M diffractometer 3-53269

X-ray diffraction examination of molecular structure

see also molecular configurations and dimensions

- adenosyl-3', 5'-uridine phosphate, X-ray structure anal. 3-40688
- catalase, struct. model from small angle X-ray scatt. data 3-49509
- cellulose, paracrystalline lattice disorders, powder X-ray diffraction, anal., two phase hypothesis 3-54932
- diffraction chamber, new, with high resolution (*Czech*) 3-62296
- γ -globulin molecule in suspension characteristic function determ. from small angle X-ray scattering data 3-67866
- hexamine, thermal diffuse scattering, lattice dynamical models, theoretical maps, results comparison 3-40828
- hexamine, thermal diffuse scattering, Laue method and interfilm correlation 3-40827
- random copolyamides in glassy state, H-bonding effects 3-67882
- X-ray diffractometers** see diffractometers; X-ray crystallography apparatus; X-ray diffraction
- X-ray effects**
- absorbed dose, Monte Carlo calculations 3-61927
- N-acetylglycine, single crystals, X-ray damage, e.s.r. meas. 3-73146
- N-acetylglycine X-irradiated crystal, ENDOR under intense r.f. field 3-55504
- β -alanine, X-irrad., recrystn. effect on e.s.r. spectra 3-55970
- alkali halides plastic deformation polarity, indenter penetration, X-ray irrad. (*Russian*) 3-40959
- aminoethyldithioacetic acid formation, X-radiation of cystamine and dithiodiglycolic acid, chain reaction 3-47566

X-ray effects continued

- blood flow changes, mouse tissues, ^{86}Rb extraction, appl. to clinical radiation therapy 3-48263
 cell division delay in synchronized tetrahymena pyriformis 3-45324
 cells of Chinese hamster, polyploidy 3-45322
 Chinese hamster, X-ray induced delay in cell-cycle 3-66044
 Chinese hamster, X-ray irradiation of mitotic cells, damage expression and recovery in surviving daughter cells 3-66045
 chloroform dosimeter, obs. on dose-effect curve 3-63240
 chromosome aberration dosimetry using human lymphocytes, in simulated partial body irradiation 3-53771
 clinical linear electron accelerators, X-ray beams produced neutron dose measurements 3-53769
 cystamine and dithiodiglycolic acid, X-radiation, formation of mixed disulphide aminoethyldithioacetic acid, chain reaction 3-47566
 cytidine, X-irradiated, ENDOR and e.s.r. studies 3-44726
 dithiodiglycolic acid and cystamine, X-radiation, formation of mixed disulphide aminoethyldithioacetic acid, chain reaction 3-47566
 fluorescein, chemiluminescence of aqueous solutions, effect of pH 3-47568
 frozen aqueous solutions at 77 K, electron tunnelling 3-47576
 genetic dose, exposure from man made sources, review (*German*) 3-74744
 glycine, X-ray radical yield 3-66047
 hamsters, Chinese, effect of 2450 MHz microwaves on x-ray radiation response 3-66058
 heating, blowoff impulse technology 3-74760
 HeLaS_3 u.v. sensitive cells, sensitivity to carcinogen 4-nitroquinoline 1-oxide, X-radiation repair of DNA damage 3-48168
 honeybee prepupa and waxmoth larva, hemolymph free amino acid pool 3-66056
 interstellar clouds, u.v. absorption lines, ionisation of C, N and O, effect of X-ray flux 3-48129
 mammalian cell transform., dose-response curve 3-51465
 mammalian cells, hypoxia, X-radiation survival curves, rel. to partial pressure of O_2 3-48259
 materials response to X-ray loadings, review 3-74757
 omnice, life shortening rel. to body area exposure 3-66048
 m.i.s. structures, X-rays from electron beam evaporation (*Japanese*) 3-50273
 mouse jejunum, intestinal radiosensitization by actinomycin D 3-42270
 mouse lung, exposure-response curve of X-ray induced tumors 3-66055
 naphthalene, e.p.r. and optical absorpt. obs. of radiation-induced radicals 3-55473
 Neurospora crassa, X-ray induced ad-3B mutants, genetic alterations, revertibility 3-48262
 plasma-protein synthesis, role of adrenals 3-59451
 quartz, X-irrad., e.p.r. and paraelec. reson. study 3-64552
 radioresistance, protective effect of Rauscher leukemia virus, SJL/J mouse, X-radiation 3-48269
 rat glial tumor cells, morphological modifications after X-irradiation 3-66054
 renal tumours, X-radiation, parabiosed rats 3-48266
 simulation of high dose rate heating effect, rel. to nuclear weapon and missile design 3-74762
 solids, X-irradiated, apparatus for luminescence properties meas. (*Russian*) 3-48560
 thermal gas, electron, proton and X-ray ionization, secondary electrons and energy per ion-pair 3-43354
 transport theory, analytic method 3-74763
 triglycine sulphate, X-ray struct. damage 3-49903
 $\text{BaF}_2:\text{Gd}^{3+}$, X-irrad., V_k centre emission 3-47302
 CaF_2 , F and F-aggregate centre production, efficiency as function of temp. 3-46641
 $\text{CdF}_2:\text{Gd}^{3+}$, X-irrad., V_k centre emission 3-47302
 CdS , frozen-in X-ray cond. 3-44117
 CsCl thin films, radiation damage, effect on phase transition 3-68409
 Ge , X-ray photoemission and electronic structure 3-64762
 HfO_3 single crystals, X and γ irradiated, 10 atom e.s.r. obs. 3-72518
 p-InSb , neutral acceptor donor complex form. and impurity migration 3-41165
 $\text{KBr}:\text{OH}^-$, X-irrad., photocond. and optical bleaching of F-centres 3-60902
 $\text{K}(\text{Cl}, \text{Br}, \text{I})$ whisker crystals, ionic conductivity determ. (*Russian*) 3-79598
 KCl , mutual transformation of $V_3 \approx V$ centres, thermoluminescence and e.p.r. spectra (*Russian*) 3-54961
 $\text{KCl}:\text{OH}^-$, X-irrad., photocond. and optical bleaching of F-centres 3-60902
 $\text{KCl} + \text{LiCl}$, additive coloured, roentgenised, transformation processes of $\text{F} = \text{F}_a$ centres, electron-hole recomb. (*Russian*) 3-54962
 $\text{KI}:\text{Ti}$ thermoluminescence, electric field effect 3-55694
 LiF , effect of point defects on dislocation mobilities (*Spanish*) 3-75528
 NaBrO_3 , Raman spectra of irradiated crystals, internal oscill. 3-55654
 NaCl , dislocation density, interstitials 3-52631
 NaCl , scratching method for damage evaluation 3-76398
 NaCl , whisker crystals, ionic conductivity determ. (*Russian*) 3-79598
 NaCl , X-irradiated, point defect distrib. of crystals aged after quenching 3-58028
 NaCl , X-ray coloured, thermoluminescence, isothermal decay 3-53154
 NaCl whiskers, radiative coloration and recombination luminescence (*Russian*) 3-44497
 $\text{NaCl}:[\text{Ni}(\text{CN})_4]^{2-}$, irrad., e.p.r., paramag. species identification 3-64544
 $\text{NaCl}:\text{Ni}$, X-irradiated, stimulated processes 3-41592
 $\text{RbCl}(\text{Br})$, X-irrad., F-centre growth kinetics and thermolum. 3-69101
 RbI , F-centres, optical density, 80-160 K (*German*) 3-52626
 Si , X-ray photoemission and electronic structure 3-64762
 SrF_2 , F and F-aggregate centre production, efficiency as function of temp. 3-46641

X-ray emission spectra

- see also X-ray fluorescence
 β -ray excited, β -rays from radioisotopes (*Rumanian*) 3-62301

X-ray emission spectra continued

- atom and molecule K-shell emission and ioniz. cross sections by proton and He^+ impact 3-46334
 beam-foil technique and solid targets, various ion beams and targets 3-78446
 chemical analysis methods, survey 3-70470
 chlorides, Cl^- $\text{L}_{2,3}$ emission spectra (*Russian*) 3-44504
 continuous, line structure, coherent electron scattering 3-43721
 detection and production for chemical analysis, survey 3-70469
 diamond, X-ray spectroscopic investigation of electronic structure 3-64294
 dibenzyl sulphide, $\text{K}\beta$ X-ray emission spectra 3-52345
 electron probe analysis, energy dispersive, background subtraction 3-42727
 electron probe analysis, energy dispersive, computer method for peak location and identification 3-42731
 electron probe analysis, energy dispersive, escape peaks in $\text{Si}(\text{Li})$ detector 3-42730
 electron probe analysis, energy dispersive, smoothing technique 3-42728
 element, low at. no., electron probe analysis, X-ray intensity, depth distrib., rel. to accelerating voltage (*Japanese*) 3-73952
 enhancement of projectile $\text{K}\alpha$ X-ray cross-sections 3-78597
 fixed-charge fragments, stopped and moving, meas. emission times for various charges (*Russian*) 3-67173
 fluoromethane molecules, C and F X-ray emission and F K absorption spectra 3-43430
 graphite, C K-band, anisotropic emission 3-53156
 heavy elements, electron probe analysis, mass absorption coeffs., O $\text{K}\alpha$ line, voltage depend. (*Japanese*) 3-73953
 heavy elements, X-ray two photon emission 3-43341
 heavy ion induced K-shell X-rays, anomalous low-energy satellites 3-78599
 heavy ion-atom collisions, production of inner shell vacancies 3-46192
 high-Z heavy ion impact, K-vacancy creation 3-52299
 intergalactic gas clouds, nonuniform model based on galaxy group and cluster obs. 3-70003
 ion-atom collisions, high-energy, target Z-depend. of $\text{K}\alpha$ X-ray prod. cross sections 3-67714
 methane, H^+ and He^+ impact, K emission cross-sections 3-78606
 plasma, laser produced, electron temp. and ioniz. state 3-68047
 plasma gun, coaxial, in deuterium, soft X-ray emission 3-68101
 plasmon excitations, O bombardment 3-72768
 quartz, SCF $\text{X}\alpha$ scattered wave method calcs. of valence orbitals 3-52793
 refractory metal compounds, X-ray spectra interpretation, band structure calc. 3-41594
 ScO X-1, Bragg spectroscopy in search of Fe XXV emission lines 3-69996
 semiconductors and insulators, soft X-ray appearance potential spectroscopy 3-64749
 superheavy $^{257}\text{104}$, daughter X-ray identification 3-63015
 superheavy quasi-atoms ($Z=130$) produced by bombardment of Au and Sn by 25 MeV I ions 3-78596
 transition metal, 4D, L-series spectra, linewidths (*Russian*) 3-53155
 transition metal alloys, electron energy distribution, K, L and M emission bands 3-43993
 X-ray source at M87, thermal bremsstrahlung function 3-48077
 Ag, differential cross section for K-shell ionization 3-71411
 Al, 30 MeV O^+ bombarded, anomalous low energy $\text{K}\alpha$ lines 3-44503
 Al, appearance pot. spectroscopy, correlation with X-ray absorpt., density of states 3-55699
 Al, $\text{K}\alpha$ satellite structure, dependence on energy of bombarding N ion beam 3-78598
 Al, X-ray band $\text{K}\beta$ emission band spectrum, selfabsorpt. effects in fluoresce. 3-50630
 Ar, theoretical Auger and radiative rates for K-shell of multiply ionised atom 3-78499
 Ar + Ar^+ differential scattering, coincidence meas. of LM X-ray yield versus final ion charge 3-78594
 Ar + Cl_2 , caramboles (double collision processes) 3-78595
 Ar + heavy ion collisions, Hartree-Fock-Slater calculations 3-71452
 Ar + Ne, K X-ray prod. exponential projectile charge depend. 3-49422
 $\text{Ar}^+ + \text{Ar}$ collisions, calculation of fluorescence yields 3-78559
 BN, hexagonal, selective maxima rel. to band structure 3-50631
 Be, appearance pot. spectroscopy, correlation with X-ray absorpt., density of states 3-55699
 Br, ion beam $\text{K}\alpha$ X-ray cross-sections, enhancement dependence on Z-number of target 3-78597
 $^{35}\text{Br} + ^{35}\text{Br}$, 30 and 60 MeV collisions, $Z=70$ quasiautomic K X-ray obs. 3-49416
 C, fluoresc. yield, K-shell X-ray prod. absolute cross sections 3-52271
 C, proton impact induced K-shell X-rays, anomalous low-energy satellites 3-78599
 C surface, soft X-ray incidence potential spectroscopy (*German*) 3-72763
 CS_2 , electronic structure investigation 3-78683
 Ca, K X-ray spectra produced by ion beam bombardment 3-63344
 Ce, (Niv, v) emission spectra 3-64750
 Cl, K production in Cl^+ ion collisions with gas targets 3-78607
 Cl ions, foil excited, lifetimes of metastable states 3-78445
 Cl VII to XIII beam-foil spectra, tandem Van der Graaf energies 3-78447
 Cl-beam X-rays, double to single K-shell vacancy prod., anomalous target Z depend. 3-52282
 Cl-K, production in violent collisions with Al, Ti, Cu targets, impact parameter dependence 3-78524
 CoSi, electron struct. determ. (*Russian*) 3-58568
 Cr, Cr_2N and CrN , $\text{L}_{1,2,3}$ and $\text{K}\beta_5$ emission 3-80118
 Cr, in cpds., electronic structure 3-55700
 Cr cpds., rel. to chem. bonding (*Japanese*) 3-69106
 Cr $\text{K}\beta$, application of chemical effects in analysis 3-62353
 CrSi, Cr $_3$ Si, Cr $_5$ Si $_3$ and CrSi $_2$, electron structure from X-ray emission spectra 3-55700
 Cu, differential cross section for K-shell ionization 3-71411

X-ray emission spectra continued

- Cu, $L\alpha$ emission, reln. to L_{III} absorption spectra 3-72767
 Cu compounds, $L\alpha$ emission, rel. to L_{III} absorption spectra 3-72767
 Cu valence band structure, comparison with photoemission spectroscopy 3-46790
 CuCl, Cl- $L_{2,3}$ emission spectrum 3-47325
 CuCl, electronic struct., rel. to X-ray emission and absorpt. spectra 3-50129
 Dy isotopes, isotope shifts and variations of nuclear charge radii 3-67662
 ^{151}Eu , hyperfine broadening of X-ray line-ray lines 3-49391
 F, highly ionised, X-ray decay energies beam-foil technique 3-74801
 F, metastable emitters, high resolution study 3-40568
 F ion collisions in Ar gas, 34.8 MeV, one- and two-electron excited states prod. 3-63338
 Fe foil, anomalous structure in appearance potential spectra 3-55703
 Fe transition metals, shape of $K\alpha$ lines, fine structure obs. 3-71362
 FeSi, electron struct. determ. (*Russian*) 3-58568
 Ge ion-excited L-series X-ray spectra 3-43342
 H+H⁺ collisions, Doppler shift α identification of H(2p) and H(2s) collision induced states 3-74885
 K, p, α and O ion beam bombardment, K X-ray de-excitation spectra 3-54596
 KHSO₄, HSO₄⁻ SK β emission spectra 3-47328
 K₂S₂O₈, S₂O₈²⁻ SK β emission spectra 3-47328
 Kr, X-ray emission spectrum, $M_{2,3}$ region 3-71360
 La, ($N_{IV,V}$) emission spectra 3-64750
 ^{175}Lu , muonic quadrupole splitting in X-ray spectra, determ. of nuclear quadrupole moment 3-49133
 ^{175}Lu pionic atom, search for strong interaction quadrupole effect 3-49134
 Mg, appearance pot. spectroscopy, correlation with X-ray absorpt., density of states 3-55699
 Mg, K β hypersatellite obs. 3-54569
 Mn cpds., rel. to chem. bonding (*Japanese*) 3-69106
 Mn K α and K β , application of chemical effects in analysis 3-62353
 MnP, K β emission, electronic band struct. obs. 3-64748
 Mo, Fermi edge isochromat spectroscopic localisation in conduction band 3-79624
 Mo, M ν , $M_{II,III}$ -bands, wave functions of valence band electrons (*Russian*) 3-80117
 Mo and MoGe₂, M ν , $V_{O_{II,III}}$, L_{β_2} and L_{γ_1} bands 3-58569
 N ion beam, highly stripped, Lyman X-rays 3-63279
 N₂+H⁺, (He⁺), K emission cross-sections 3-78606
 Nb, M ν , $M_{II,III}$ -bands, wave functions of valence band electrons (*Russian*) 3-80117
 Nd isotopes, isotope shifts and variations of nuclear charge radii 3-67662
 ^{141}Nd → ^{141}Pr , obs. of γ -ray, X-ray, $\gamma\gamma$ -coincidence, conversion electron and positron spectra (*Russian*) 3-52092
 Ne, K α X-ray transitions, oxygen-projectile charge state depend. 3-63308
 Ne+Ar¹²⁻¹⁷⁺ fast collisions, exponential projectile charge dependence of Ar K and Ne K X-ray production 3-78601
 Ne+H⁺, (He⁺), K emission cross-sections 3-78606
 Ne+H⁺ collisions at 100-600 keV, simultaneous meas. of X-rays and Auger electrons 3-78602
 Ni, ion beam K α X-ray cross-sections, enhancement dependence on Z-number of target 3-78597
 NiSi, electron struct. determ. (*Russian*) 3-58568
 O cpds., rel. to chem. bonding (*Japanese*) 3-69106
 O V to VIII beam-foil spectra, tandem Van der Graaf energies 3-78447
 ^{235}Pa → ^{235}U , gamma- and X-ray spectra obs. using semiconductor detectors and coincidence techniques 3-74535
 Pb isotopes, isotope shifts and variations of nuclear charge radii 3-67662
 Pd, Fermi edge isochromat spectroscopic localisation in conduction band 3-79624
 S+Ar collisions in gas targets, L X-ray spectra 3-78525
 S α K β X-ray emission spectra 3-52345
 SO₂, electronic structure investigation 3-78682
 SO₃²⁻ and SO₃F⁻ ions, sulphur K β spectra interpret. 3-52315
 ^{121}Sb , hyperfine broadening of X-ray lines 3-49391
 Si, 30 MeV O⁺ bombarded, anomalous low energy K α lines 3-44503
 Si, in cpds., electronic structure 3-55700
 Sm isotopes, isotope shifts and variations of nuclear charge radii 3-67662
 Sn L β , application of chemical effects in analysis 3-62353
 Ti, in cpds. electronic structure 3-55700
 Ti, K $\beta_1\beta_2$ spectrum, fine struct. 3-67661
 Ti, p, α and O ion beam bombardment, K X-ray de-excitation spectra 3-54596
 Ti, primary K η emission, electron excitation, origin 3-71361
 TiFe, K spectra, SCF calcs., densities of states 3-75705
 Ti₃Si₃, TiSi and TiSi₂, electron structure from X-ray emission spectra 3-55700
 ^{235}U , muonic quadrupole splitting in X-ray spectra, determ. of nuclear quadrupole moment 3-49133
 V₂O₅, electronic structure (*Russian*) 3-47329
 V H_x , VC H_x , L α emission bands, electron struct. determ. 3-72764
 V₂X type compounds, valence band and conduction band structures (*Russian*) 3-55207
 Yb isotopes, isotope shifts and variations of nuclear charge radii 3-67662

X-ray fluorescence

- analysis, weight fractions, linear regression equations, consistent solution 3-73937
 astronomical ultraminiature fluorescence spectrometer for Mars' geochemical anal. 3-61883
 coordination compounds, pseudo-central atom probe for nonidentical ligand differentiation 3-52381
 electrocast materials, physical methods of chem. analysis (*French*) 3-70468
 electrodeposit method, analysis of heavy elements (*Japanese*) 3-62355
 electroplated coating thickness meas. by fluorescent X-ray methods 3-42517

X-ray fluorescence continued

- geological samples, chelating ion exchange resins for trace element analysis using X-ray fluorescence 3-62329
 graphite, C K-band, anisotropic emission 3-53156
 L spectra, primary radiation, analysis, Z=47(Ag) to 92(U) 3-48653
 lunar surface mapping 3-65804
 metal powders, sample preparation, melting 3-62336
 metals, in water, preconcentration using electrodeposition 3-66423
 modulation transfer function of X-ray fluoresc. screen, calc. 3-62294
 nuclear target backings, for charged particle induced X-ray fluorescence analysis of biomedical specimens 3-51681
 Oka carbonate complex, X-ray fluorescence anal. of Sc abundance 3-80587
 radioisotope, chemical analysis (*Afrikaans*) 3-62198
 radioisotope in X-ray chemical analysis, review 3-62372
 rare earth trace metals detection by X-ray excited optical fluorescence in YPO₄ and YVO₄ 3-48635
 reagent, ultrapure, chemical analysis 3-70459
 refractory, X-ray fluorescent and atomic absorpt. anal. methods and characteriz. 3-80410
 rocks, rock-forming elements, conc. determ., error anal. 3-48654
 silicon organic esters of phosphoric acids, crystalline roentgenofluorescent anal., Si and P determ. 3-48662
 spectroscopy, determ. of Nb and Ta in minerals 3-56253
 thin biological specimens, X-ray fluorescence microanalysis 3-54025
 thin reaction layer, between substrate and overlayer, thickness meas., X-ray fluoresc. method (*German*) 3-61996
 Al, X-ray band K β emission band spectrum, selfabsorpt. effects in fluoresc. 3-50630
 Ar, K-shell fluorescence field transition energies and intensities, multiple ionisation effects 3-67673
 Ar collisions with H⁺, H₂⁺ and He⁺, charge state depend. of Ar fluorescence yield 3-78600
 cl⁽¹⁶⁾, heliumlike, decay of 2S_{1/2} state 3-60373
 Cu₂SO₄.gelatin, X-ray laser emission 3-66835
 Fe ores and mixtures, determ. Si and Al, rel. error calc. 3-48655
 GaAs, Sb_{1-x}, variation of lattice parameter with composition 3-75602
 Ne, Auger transition energies, fluorescence yield nonrelativistic HFS atomic model 3-71385
 Ne, K X-ray fluoresc. spectrum 3-43351
 Ne, K α X-ray transitions, oxygen-projectile charge state depend. 3-63308
 Ne, vacuum u.v. radiation, lifetime, pressure depend. 3-71373
 Ne+H⁺ collisions at 100-600 keV, simultaneous meas. of X-rays and Auger electrons 3-78602
 Ni complex, bis(O,O'-diethyldithiophosphato)nickel(ii) and related cpds., P atom-ligand bonding probe 3-52381
 Pb-Ba minerals, X-ray radiometric fluorescence anal., ^{109}Cd radioisotope source 3-48660
 Sr fluorescence yield from ^{88}Y β -decay 3-74544
 Ta microanalysis, chemicoerenigenospectral fluorescence, industrial effluent soln. 3-48657
 Zn-Mn ferrites, estimation of Ca by X-ray fluorescence method 3-62340

X-ray monochromators

- calibration of diffracting gratings, crystals, specifications 3-77732
 diffraction profile separation method, computer program 3-46576
 polymer X-ray filters for dispersionless analysis for light elements (*Russian*) 3-70492
 synchrotron radiation, grazing incidence spectrometers and crystal spectrometers 3-40055
 synchrotron radiation, spectro-monochromator using two gratings, grazing incidence 3-40056

X-ray photoeffect see photoemission**X-ray production**

- see also X-ray tubes
 130-280 Å region 3-51750
 emission spectroscopy for chemical analysis, survey 3-70469
 laser produced plasma, numerical calc. of characs. 3-63893
 plasma, rarefied, inconsistency of classical theory with cut-off for X-ray power density 3-67984
 radiation protection, standardisation (*French*) 3-70178
 rontgen absolute determination, X-ray source construction and testing (*German*) 3-45326
 targets, window-type, for X-ray tubes (*Russian*) 3-42682
 thin crystals, charact. X-ray production 3-40833

X-ray protection see radiation protection**X-ray reflection**

- at NPL, instrumentation 3-66392
 synchrotron radiation, X-ray reflectivity meas. 3-40062

X-ray scattering

- see also Compton effect; X-ray diffraction
 atom, electronic correls. role 3-52248
 Bragg case, spherical wave approximation, crystal wave fields 3-79204
 continuous spectra, line structure, coherent electron scattering 3-43721
 cross-section review, reln. to X-ray energy deposition in materials 3-74758
 ferromagnetic colloid, X-ray and optical scatt. factors, assoc. phenomena 3-44279
 hexamine, thermal diffuse scattering, lattice dynamical models, theoretical maps, results comparison 3-40828
 hexamine, thermal diffuse scattering, Laue method and interfilm correlation 3-40827
 interstellar dust, distance determ. of variable X-ray sources 3-53724
 isotropic crystal containing random defect distrib., elastic X-ray and neutron scatt., static correl. functions (*German*) 3-52561
 plasmon excitation by X-rays, review 3-44047
 poly-o-bromostyrene in benzene soln., high-resolution small-angle X-ray and light scatt. for mol. wt. determ. 3-67868
 Al, anharmonic contributions to elastic and inelastic X-ray scattering at Bragg reflections 3-58091
 GaAs_{0.5}P_{0.5}, effect of atomic radius on diffuse X-ray scattering (*German*) 3-79206
 Ga_{0.5}In_{0.5}As, effect of atomic radius on diffuse X-ray scattering (*German*) 3-79206

X-ray scattering continued

$K_2Pt(CN)_4Br_{0.30} \cdot xH_2O$, low temp. phase transition, condensation of soft modes by Kohn anomaly 3-64177

X-ray sources (astronomical)

see also *X-ray astronomical observations*

accreting magnetic neutron star, radiation beaming rel. to X-ray pulsars 3-45083
accreting neutron stars nuclear fusion forming X-ray source 3-81026
accretion onto compact stars accounting for stellar rotation and magnetic field 3-73533
Aquila XR-1, hard X-rays 3-69999
background, Compton models compared with obs. 3-45161
background radiation, intensity fluctuations due to evolutionary effects 3-81157
background radiation, review of local theories 3-81158
binary member, differentially rotating degenerate dwarf model 3-69995
binary star systems as X-ray sources, review 3-81143
binary star X-ray sources rel. to two types of radio star binaries 3-61823
binary stars, accuracy of mass determination 3-77100
binary X-ray sources, expected optical behaviour 3-48082
binary X-ray stars, self excited mass flow 3-81127
black hole search among X-ray sources and emission line binaries 3-73431
black holes search rel. to X-ray sources 3-44980
bremsstrahlung spectrum, effect of Compton scattering 3-81047
3C 273, X-ray spectrum rel. to intergalactic He abundance 3-56412
Cassiopeia A, X-ray spectrum, Fe line emission evidence 3-73534
Centaurus region, meas. of diffuse X-ray background 3-56410
Centaurus region sources, long-term variations in hard X-ray flux 3-56414
Centaurus X-3, binary orbital period decrease rel. to mass loss 3-81139
Centaurus X-3, conditions for self sustained mass flow 3-81050
Centaurus X-3, interpretation of X-ray spectrum 3-65916
Centaurus X-3, soft X-ray emission below 2 keV 3-65915
Circinus X-1, Copernicus satellite obs. of off state 3-61833
Coma cluster, viability of thermal intergalactic medium from analysis of X-ray spectra 3-81161
Coma cluster of galaxies, soft X-ray flux obs. and ang. diameter 3-65917
compact sources, models for optically thin bremsstrahlung 3-81149
Cygnus X-1, low mass primary for HDE 226868 rel. to existence of black hole 3-42222
Cygnus X-1, optical obs. and model from He II emission line 3-56411
Cygnus X-1 (BD +34°3815), nature of optical variability 3-61818
Cygnus X-1 and X-3, OSO-7 obs. above 7 keV 3-73536
Cygnus X-2, peculiar blue star counterpart, obs. of radio emission 3-45148
Cygnus X-3, 8 GHz obs. during September 1972 outburst 3-70001
Cygnus X-3, appl. of theory of massive dose binaries with collapsed component 3-53650
Cygnus X-3, i.r. and X-ray variability 3-77126
Cygnus X-3, model for second radio outburst rel. to source structure 3-61834
Cygnus X-3, obs. and interpretations 3-61832
Cygnus X-3 bursts, possible response of terrestrial low ionosphere to very hard X-rays 3-53517
diffuse background, small-scale fluctuations 3-56409
discrete and background, progress report 3-77129
distance determ. of variable sources 3-53724
energetic background X-rays, review of experimental obs. 3-81159
extragalactic, contribution to soft X-ray background 3-81155
extragalactic, integrated contribution to diffuse background 3-81154
extragalactic sources, properties from visible obs. 3-81152
extragalactic sources, UHURU results 3-81151
extragalactic Uhuru sources, radio structure 3-81129
extragalactic, X-ray generation mechanisms 3-81153
flare-time temp. in soft X-ray sources 3-53690
galactic, luminosity, accretion models, He II ion determining flow of gas 3-48080
galactic anticentre, soft X-ray flux rel. to radio continuum features 3-51376
Galactic centre (GCX), upper limit for neutron star accretion 3-42231
galactic distribution of X-ray sources, sounding-rocket obs. 3-45165
Galactic sources, luminosity function for Uhuru sources 3-81131
Galactic sources, radio obs., review 3-81146
Galactic sources, UHURU results 3-81141
galactic sources, X-ray absorption and optical extinction in interstellar space 3-59363
galactic southern sky sources, spectra of 10 objects 3-56413
GX3 + 1, correction to position from timing error 3-59368
GX5 - 1, accurate position from lunar occultations, Copernicus satellite obs. 3-59367
GX 1 + 4, high energy X-ray spectra by balloon borne obs. 3-73532
GX 301-2, high energy X-ray spectra by balloon borne obs. 3-73532
GX 304-1, high energy X-ray spectra by balloon borne obs. 3-73532
GX 339-4 variable, OSO-7 obs. of intensity variations 3-81134
GX 3 + 1, detection of gamma-ray spectral line by balloon borne FWHM instruments 3-77125
GX 3 + 1, high energy X-ray spectra by balloon borne obs. 3-73532
GX 5-1, high energy X-ray spectra by balloon borne obs. 3-73532
H I regions ionization and heating by soft X-rays and subcosmic rays 3-61866
hard cosmic X-ray sources, review of obs. status 3-81144
HD 153919 (=2U 1700-37), photoelectric UVB obs. of optical variations 3-81133
HD 153919 binary, narrow band circular polarization meas. 3-81135
HD 77581, binary, narrow band circular polarization meas. 3-81135
Her X-1, hard X-ray dip, balloon obs. 3-48076
Hercules X-1, 35-day periodicity rel. to accretion gas flow in binary system 3-48083
Hercules X-1, binary component, neutron star theory 3-77130
Hercules X-1, hard X-ray spectrum, balloon obs. in 20 to 100 keV range 3-56417
Hercules X-1, intensity meas. in 4 to 12 keV range 3-56416

X-ray sources (astronomical) continued

Hercules X-1, neutron star, mass meas. 3-45164
Hercules X-1, optical obs. 3-59365
Hercules X-1, OSO-7 obs. of spectrum and variability 3-45162
Hercules X-1, search for optical pulsations from HZ Herculis at period of X-ray pulsations 3-61817
Hercules X-1, UVB photometry of HZ Herculis rel. to 35-day cycle 3-73517
Hercules X-1, upper limit for pulsed emission above 100 keV 3-81138
Hercules X-1, X-ray pulse profile and celestial position 3-51372
Hercules X-1 (HZ Herculis), nature of optical variability 3-61818
Hercules X-1 (HZ Herculis), obs. of optical pulsations 3-61801
Hercules X-1 magnetic activity and model for HZ Herculis 3-81132
Hercules X-3, conditions for self sustained mass flow 3-81050
HZ Herculis, 'on' and 'off' eclipse phenomena, photographs, 1890 to 1972 3-48075
HZ Herculis, eclipsing binary, X-ray beaming and mass transfer 3-48028
HZ Herculis, reflection effect due to energy transfer 3-48033
Herculis X-1, effect on atm. of binary companion, optical periodicity 3-51373
Herculis X-1, variability and pulse shape from Uhuru obs. 3-73531
high energy, Southern sky, balloon obs. 3-48078
interstellar hydrogen absorption of soft X-rays 21 cm obs. of H column density in the Galaxy 3-81156
LMC X-1, proximity of MC76 and MC77 rel. to optical candidate 3-53694
M87, X-ray spectra, thermal bremsstrahlung function 3-48077
massive dose binaries with collapsed component, appl. to Cygnus X-3 3-53650
model X-ray sources, magnetic field twisting in binary star system 3-42223
Models for compact pulsing X-ray sources 3-81150
in NGC 5128 (Centaurus A), size determ. 3-53692
number-intensity distrib. of sources in Uhuru catalogue 3-59362
OSO-7 obs. in 1-60 keV range 3-81142
 β Persei, X-ray emission during radio flares, upper limits 3-65903
pulsars, UHURU satellite obs. 3-51368
Pulsars and X-ray sources 3-81126
pulsating sources, speed-up and evolution 3-51375
radio counterparts of X-ray sources 3-81147
radio halos around double radio sources, source of hard X-rays 3-61824
radiosources, X-ray emission by Compton-synchrotron or Compton black-body effect, comparison 3-53674
satellite observation, white dwarfs, neutron stars and black hole identification 3-61835
Sco X-1, Bragg spectroscopy in search of Fe XXV emission lines 3-69996
SCO X-1, emission mechanism, white dwarf model 3-45163
Scorpius X-1, accretion model investigation of flickering phenomena 3-65919
Scorpius X-1, balloon borne obs. in 17 to 106 keV range 3-53691
Scorpius X-1, black hole with UV Ceti type optical component 3-77130
Scorpius X-1, distance determ. 3-48100
Scorpius X-1, rocket obs. of X-ray absorpt. meas. 3-53693
Scorpius X-1, simultaneous X-ray, optical and radio obs. 3-81145
Scorpius X-1, UVB obs. of flares 3-48085
Scorpius X-1 distance rel. to radial velocities of nearby SEG stars 3-45094
SMC X-1, B photometry of Sanduleak 160, optical counterpart 3-81137
SMC X-1, photographic photometry of star Sanduleak 160, proposed optical candidate 3-51377
SMC X-1 (=2U 0115-73), Sanduleak 160 as optical counterpart 3-73535
solar flares, continuous energy injection at bright points 3-65662
solar hard X-ray bursts, self-absorpt. of gyro-synchrotron emission 3-65710
solar X-ray emitting spots, pinhole camera image (German) 3-80973
stellar, circumstellar matter in accretion model of X-ray emission 3-77128
stellar atmosphere interaction with X-ray source irradiation in close binary systems 3-73478
stellar coronae, X-ray and radio emission rel. to soft X-ray background 3-45078
stellar coronae, X-ray radiation rel. to soft X-ray background 3-42220
supernova remnants, X-radiation rel. to mechanisms and evolution 3-81148
thermal sources with strong magnetic field, luminosity 3-42221
transient, distances indicating Galactic origin 3-59361
transition radiation as source of X-rays 3-59248
2U 0115-73 (=SMC X-1), Sanduleak 160 as optical counterpart 3-73535
2U 0115-73 in SMC, optical periodicity 3-51373
2U 0832-45, at pulsar PSR 0833-45 X-ray structure observed from Uhuru 3-73530
2U 0900-40, binary source, Uhuru obs. 3-59364
2U 0900-40, HD 77581 as optical counterpart 3-56415
2U 0900-40 (HD 77581), UVB photoelectric photometry 3-81136
2U 1543-47, late-type irregular variable as optical candidate of X-ray source 3-69997
2U 1700-37, identification of HD 153919 as optical counterpart 3-48032
2U 1700-37, possible binary companion to HD 153919, Of star 3-48073
2U 1700-37 (=HD153919), spectroscopic obs. 3-61815
2U 1700-37 (=HD153919), UVJHKL photometric obs. 3-61814
2U 1700-37, obs. of HD 153919, optical candidate 3-51374
universal X-ray background origin, comments on theory and further arguments 3-42095
white dwarf with accretion, X-ray emission region 3-48084
white dwarfs in close binary system 3-45163
XN 1972E, upper limit on X-ray flux 3-56410

X-ray spectra

- see also *X-ray absorption spectra*; *X-ray chemical analysis*; *X-ray emission spectra*
 2U0900-40 eclipsing binary, X-ray spectra position rel. to HD77581, Uhuru obs. 3-48045
 appearance potential spectra, d.c. soft X-rays, computer differentiation 3-77737
 blood vessel phantom, X-ray pattern, X-ray spectrum and screen-film unshortness effect 3-66033
 discontinuous Compton scatt. by K- and L-electrons, intensity, chem. shift, fine shift angular depend. 3-55701
 field theoretical relativistic corrections 3-60354
 fission fragments, light, at different kinetic energies (*Russian*) 3-40522
 galactic X-ray sources, luminosity accretion models, He II ion determining flow of gas 3-48080
 metals, scattering theory of X-ray edge 3-72769
 multiply ionized atoms, new rule for X-ray spin doublets 3-40576
 plasmon observation using high-energy photons 3-41595
 superheavy and quasi-superheavy element identification possibility 3-60357
 Al alloys, potential model 3-76107
 Co complexes, use of Co K β_2 lines to determ. electronic and geometric structures 3-57633
 Cr complexes, use of Cr K β_2 line to determ. electronic and geometric structures 3-57633
¹⁷⁵Lu μ , quadrupole splitting of X-ray transitions, determ. of nuclear quadrupole moment 3-49096
 Ne, Compton profiles, incident X-ray energy dependence 3-54568
 Ni-Rh alloys, electronic density of states determ. 3-79603
¹⁹²Os, effects on ν -instability on muonic X-rays 3-60112
 Pb isotopes, muonic spectrum, nucl. polarization effects 3-63351
²³⁵U μ , quadrupole splitting of X-ray transitions, determ. of nuclear quadrupole moment 3-49096

X-ray spectrometers

- see also *X-ray crystallography apparatus*
 analyzer for high-speed analysis of chemical composition 3-54017
 appearance potential spectrometer 3-48597
 astronomical ultraminiature fluorescence spectrometer for Mars' geochemical anal. 3-61883
 beam-foil spectroscopy, Doppler-tuned 3-77735
 calibration, from grating diffraction efficiency and plate response factors 3-62297
 calibration for absolute intensity, from branching ratios to visible and near u.v. 3-62298
 crystal diffraction, X-ray anal. with scanning electron microscope 3-66466
 high precision combined X-ray spectrometer (*German*) 3-48589
 monochromator conversion, detector calibration, specifications 3-77732
 at NPL, instrumentation 3-66392
 polar co-ordinate X-ray grating spectrometer, synchrotron radiation 3-40058
 rocket borne crystal spectrometer, for solar observation of soft X-ray emission 3-65645
 SEM system, ultramicroscopic particle characts. 3-70421
 simple spectrometer for measuring X-ray integrated intensities 3-45567
 synchrotron radiation, grazing incidence spectrometers and crystal spectrometers 3-40055
 three-crystal X-ray polarimeter, collimator and spectrometer 3-66385
 trace element, determ., fluorescence analysis using semiconductor detector spectrometer 3-66412
 HgI₂ high resolution spectrometers 3-66382

X-ray spectroscopy

- see also *X-ray crystallography*; *X-ray diffraction*; *X-ray spectra*
 β -rays from radioisotopes (*Rumanian*) 3-62301
 appearance potential spectra, d.c. soft X-rays, computer differentiation 3-77737
 atomic and molecular absorpt. spectroscopy ESRIN-Bonn-Imperial College expt. with synchrotron radiation 3-40060
 chemical effects in high-resolution spectrometry applied to chemical analysis 3-62353
 electroplated coating thickness meas. by fluorescent X-ray methods 3-42517
 emission, pseudo-central atom probe for nonidentical ligand differentiation in coordination compounds 3-52381
 emission spectroscopy for chemical analysis, survey 3-70469
 emission spectroscopy for chemical analysis methods, survey 3-70470
 energy dispersive data, time-shared computer treatment 3-66468
 fluorescence, determ. of Nb and Ta in minerals 3-56253
 Galactic X-ray polarimetry and high-resolution X-ray spectroscopy 3-81259
 ligand characterisation, high resolution photon emission 3-66464
 photoelectron spectroscopy using synchrotron radiation 3-40059
 Sco X-1, Bragg spectroscopy in search of Fe XXV emission lines 3-69996
 synchrotron, at grazing incidence, diffraction gratings 3-40057
 synchrotron radiation, spectro-monochromator using two gratings, grazing incidence 3-40056
 wavelength modulation spectroscopy in 10-40 eV range using synchrotron radiation 3-39938
 Cu emission and photoemission, valence band structures, comparison 3-46790
 Cu-Pb ores, determ. of Pb content by standard single channel spectrometer (*Russian*) 3-73392

X-ray tubes

- with controllable focus producing soft and ultrasoft radiation 3-51752
 diagnostic, filtration and kilovoltage checking method 3-66383
 focal spots, pinhole camera method investigation 3-59675
 h.v. measurement on plants in operation (*French*) 3-54021
 pulsed, self-restoring Ta foil autocathode 3-73912
 targets, window type, investigation (*Russian*) 3-42682

X-rays

- see also *nuclear reactions and scattering due to photons*; *photons*
 auroral bursts, rocket obs. (2 November 1972) 3-65437

X-rays continued

- filtering to improve signal-to-noise input in soft X-ray appearance potential spectroscopy 3-73917
 shadow casting holography, techniques 3-70318
 whistler triggering of correlated X-rays and VLF riser bursts 3-69655

X-Y model

- heading is late addition, see also *lattice theory*; *statistics*; *ferromagnetism*
 algebraic approach, subalgebra of spin operators 3-79812
 Baxter states, diagonalization 3-48805
 correlation inequalities and phase transition 3-50323
 cubic lattice, susceptibility and fluctuation near crit. temp. 3-55401
 partition function, high temp. expansions, for spin 1/2 X-Y model 3-79817
 spectrum and eigenfunctions in inhomog. fields 3-44190
 spin chain, energy spectrum with impurity 3-52950
 spin-pair correlation, singular behaviour of spectral weight function 3-46965
 susceptibility, in transverse mag. field 3-75825
 thermal critical quantities for spin 1/2 mag. model, estimates 3-79816
 CsNiF₃, ferromag. chains with X-Y like anisotropy 3-58392

xenon

- arc column, super high pressure, thermal characteristics (*Russian*) 3-75964
 arc lamp, spectroscopic study of plasma (*Russian*) 3-77499
 atom, electron impact excitation, elastic scattering, cross section meas. 3-74866
 atom, line profile, 3.36 μ m, competition between stimulated emission and absorpt. 3-46175
 atom., Penning ionisation cross-sections for He(2'S) impact, temperature dependence 3-78535
 atom, photoproduction of Xe⁺ in vicinity of outer d-subshell threshold 3-78486
 atom, resonant structure in excitation functions of first four states 3-78551
 atom collision with CO, fluoresc. excitation 3-46308
 atom elastic scattering with He⁺ 3-43378
 atom electron scattering, free-free absorption coefficients calc. 3-43371
 atomic quadrupole moments of excited states 3-71364
 autoionisation, u.v. absorption spectra 3-43355
 azimuthal oscillations, effect of temp. coupling in high temp. reactors (*German*) 3-67494
 carbonaceous chondrite meteorites, Xe isotope composition rel. to solar wind 3-61743
 collisional broadening of HCl vibration-rotation lines 3-43467
 collisions with H atoms in energy range 80-2000 eV, H⁻ production 3-46211
 collisions with NO, anisotropy of total cross section, glory struct. 3-78868
 collisions with NO, orientational anisotropy in total collision cross section 3-46355
 collisions with TlCl, TlI, TlBr, dissociative ion pair formation, absolute cross section 3-46353
 collisions with TlCl, TlI, TlBr, dissociative ion pair formation, threshold behaviour 3-46354
 condensation on graphite (0001) face, growth of layers, ellipsometry (*French*) 3-79560
 crystal surface relaxation effects on adsorption of Ne 3-46753
 damping of oscillations, Maine-Yankee reactor 3-74699
 discharge, cathode sputtering coeff., Ag, Mo, Ta, Ti and Ni, role of ion capture (*Russian*) 3-69128
 discharge, Faraday effect 3-62702
 equation of state, reduced, for saturated liquid (*Spanish*) 3-43862
 excitation by electron impact, cross sections meas. 3-60386
 excitation cross-sections of lines of multicharged ions during electron collisions (*Russian*) 3-63331
 fission gas, produced by β -decay of precursor ¹³³I in graphite at 1000°C, release procedure 3-71278
 fission product release in ZrU and ZrH₂U fuel elements 3-63122
 gas, high pressure, vacuum u.v. emission excited by relativistic electron beams 3-52378
 gas, stimulated emission, multiple photon pumping 3-66794
 gas, transport and equilibrium props., utility of m-6-8 potential function 3-60512
 gas mixtures with H₂, He, D₂ and N₂, trace interdiffusion coefficients, temp. depend. 3-75181
 harmonic power generation using nonlinear optical polarisabilities 3-57260
 hyperfine struct., GaAs laser absorpt. spectroscopy 3-49386
 instabilities, optimal control in large power reactors (*German*) 3-67493
 intermolecular pot. energy function using semi-inversion techniques 3-54758
 ion implanted, in Al, behaviour during anodic oxid., He backscatt. obs. 3-68511
 i.r. emitting laser levels, decay rates 3-54220
 isotopic gas tag compositions for locating failed fuel elements in fast reactors 3-49361
 laser, high average power, transversely excited, pulsed, characts. 3-40246
 laser, high press., optical gain at 1730 Å 3-48878
 laser, plasma, dynamically compressed, parameters 3-40241
 laser, pulsed and CW, new laser lines 3-40248
 laser plasma, high press., stimulated vacuum u.v. emission, kinetic mode 3-59855
 liquid, ionisation by α -particles 3-65095
 liquid multiwire proportional chambers, study of parameters 3-48525
 metastable atoms energy transfer reactions with SCS, SCO and SCCL₂ 3-53310
 molecular laser, vacuum u.v. emission, electron beam excited 3-66808
 multiply charged ion source based on electron cyclotron heating 3-62209
 multipole polarisabilities, Van der Waals consts. 3-71365
 nuclear reactor fission product, spatial oscillations, control procedures, simulations and tests 3-46132

xenon continued

- photoabsorpt. cross-section at He 584A line 3-49407
 photoabsorption coefficients from 48 to 210 Å using synchrotron radiation 3-40566
 photoelectron angular distributions in autoionisation resonances 3-43360
 plasma, electrical conductivity calc. 3-79063
 plasma, hard excitation of feedback controlled instabilities 3-79124
 plasma, mag. field effect on rot. (*Russian*) 3-71872
 plasma, non Maxwellian electronic longitudinal modes propagation obs. 3-79139
 plasma produced by shock waves, thermodynamic variables, interferometric meas. (*German*) 3-68099
 plasma shock adiabats calc. (*Russian*) 3-68032
 pulsed discharge, density meas. 3-75440
 reactivity effects following power reductions in WWR-SM type reactors 3-67394
 resonances in electron impact, energies and width 3-52288
 shock ionised, radiative energy loss, struct. determ. 3-68090
 solid, adsorption of Ar, two dimensional second and third virial coefficients 3-68499
 solid, Debye-Waller factor, mean-square nuclear displacements calc. 3-72154
 solid, LEED of single cryst., energy and temp. depend. 3-50053
 solid, phonon frequency measurement by inelastic neutron scattering dispersion curves 3-64120
 solid, plastic deform. 3-58076
 solid, potential function for exchange interaction, logarithmic form 3-49949
 solid, surface vibr. props., surface Debye temp., LEED 3-50062
 solid, u.v. absorption spectra, deposition temp. depend. 3-69018
 solid, vacuum u.v. emission band obs. 3-55649
 solid, vacuum u.v. emission spectrum, temp. depend. 3-69066
 solid and liq., band struct. from refl. spectra 3-50130
 sound vel., low freq. meas. in crit. region, compressibility and sp. ht. calc. 3-43533
 spatial control in reln. to load changes, assessment of overload operation in reactors 3-49313
 spatial oscillations in power reactor, control 3-57556
 spectroscopic constants calcs., ground state potentials 3-63400
 spin-orbit quenching of Te(⁵P₁) and Te(⁵P₀) 3-71371
 Stark splitting calcs. of Xe levels (*Russian*) 3-75710
 superfluorescent radiation, at 1730 Å, due to stimulated emission in high pressure gas 3-71569
 thermal conductivity, column method, 1000-1500K 3-75172
 thermal diffusion, state potentials 3-75171
 thermal expansion coeff. of mol. crystals, calc. of temp. dependence using quasi-harmonic model (*Russian*) 3-68368
 transient, in Pu recycle fuelled reaction 3-49340
 Ar/Xe mixtures at high press., stimulated emission 3-66795
 Ar-Xe rainbow struct. for Kihara core potential by using the uniform approximation 3-52301
 CsI + Xe → Cs* + I⁻ + Xe, reaction dynamics 3-76449
 H⁺ + Xe → H⁺ + Xe²⁺, double charge transfer meas. using monoenergetic H⁺ beam 3-78612
 H₂-Xe mixtures, collision induced i.r. absorpt. quadrupole-induced transitions, diffusional narrowing 3-78882
 He-Xe, self-stabilised 3.5 μm waveguide laser 3-51903
 Kr-Xe radioactive mixtures, stack monitor for γ-ray exposure from power station 3-78394
 Ne-Xe-Hg mixture, d.c. discharge, cataphoretic segregation effects 3-57959
 Xe I(II) lines, absolute transition probabilities 3-63275
 Xe vacuum u.v. spectra in solid Ne 3-71546
 Xe-methyl chloride gas mixtures, viscosity and nonpolar-polar molecular interactions 3-60515
 Xe-Xe, (He), (Ne), (Kr), (Ar), ground state pot. energy curves, model 3-40589
 Xe + Li⁺ collisions, elastic and inelastic scatt. comparison with Fano-Lichten model 3-74884
 Xe⁺, excitation by electron impact, cross sections meas. 3-60386
 Xe⁺ + Xe, differential elastic scattering cross-section, 20-200 eV 3-71457
 Xe⁺ + Xe rainbow scatt. meas. 3-57611
 Xe₂, deexcitation rates meas. 3-71631
 Xe²⁺, excitation by electron impact, cross sections meas. 3-60386
 Xe_m(²P_{0,2}) + He_m(²1²S) → (Xe⁺)^{*} + He₀ + e, metastable atom collision, excitation, ionisation, cross section 3-46209
¹²⁷Xe, appl. to biomedical imaging with Anger camera 3-42373

xenon compounds

- XeCl⁻ form. in gas phase from ion-mol. reaction 3-52396
 (XeH)⁺, pot. energy curves, LCAO-MO-SCF calcs. 3-74943
 XeOF₂, XeO₂F₂, and XeOF₄, Wolfsberg-Helmholz MO calc. of electronic and geometric structures 3-43414
 XeO₂F₂, cryst. struct. and symmetry determ. by neutron diffraction 3-54946

xerography see electrophotography; reproduction (copying)**yield point**

- alloy, two-phase, dynamic model, dislocation motion 3-80371
 anisotropic rigid/plastic materials, plane strain slip line theory 3-47469
 bars, naturally uniformly twisted, plastic torsion and tension 3-40132
 Bauschinger effect, yield stress drop rel. to pre-strain 3-69293
 circular plate, limiting equilibrium allowing for shear stress (*Russian*) 3-66566
 circular plate, variable-thickness, limit loads accounting for transverse shear 3-57093
 composite, directionally solidified, yield pt. phenomenon interpret. 3-64992
 composite, unidirectional, yielding under external loads and temp. changes 3-55865
 cylindrical shell, three-layer, rigid-plastic direct design, Mises and Tresca yield conditions, variational problem (*Russian*) 3-70631
 dislocation forest density depend. 3-79418
 eccentrically compressed wall, strain limit determ. by column-curvature curve method 3-70622
 elastic-plastic material, crack tip small-scale yielding, stress terms and geom. effects 3-74052

yield point continued

- Inconel 718 sheet, time-depend. edge-notch sensitivity rel. to mech. and microstruct. characts. 3-64952
 industrial metals and alloys, micro-yield region behaviour (*Russian*) 3-58648
 isotropic elastic material, fracture, yield conditions, stress-strain relation 3-62452
 isotropic materials, crippling allowables for elevated temp. and creep environments 3-64962
 Johnston-Gilman's theory, inhomogeneous deformation 3-49922
 laminated media, anisotropic, yield criterion 3-53275
 large and small specimens, linear-elastic fracture mechanics, strain rate effect on characteristic value (*German*) 3-47522
 lower yield stress rel. to dislocation mobility 3-68313
 Makrolon, prolonged storage effect 3-80488
 metal, f.c.c. and b.c.c. lattices, rate relationships of dynamic yield pt. 3-43824
 metals, yield surface shape, offset influence, different loading paths, slip theory model anal. 3-72889
 microyielding in cyclic loading using time monitoring technique 3-41747
 plane stress, yield criterion, second order effects, tension-torsion loading 3-62489
 plastic constrained bodies 3-70616
 plastic rigid struct. at yield-point load, stability 3-51792
 plate, impulsively loaded, nonoccurrence of von Mises yielding 3-70636
 PMMA, compression yield behaviour, temp. and strain rate depend. 3-58728
 polycarbonate, Charpy notched impact strength, A and B forms comparison 3-80474
 polycarbonate, prolonged storage effect 3-80488
 polycarbonate as model material for three-dimens. photoplasticity 3-73064
 polymer, hydrostatic press. effect on mech. props., review 3-80475
 polypropylene composites, thermoplastic fibre reinforced, transcrystalline morphology 3-64985
 shallow shells, compression-bent, rigid-plastic collapse, limit analysis solns. 3-70620
 shells, thin, yield surface, effect of transverse shear stresses 3-45676
 steel, anisothermal stress relax. processes 3-69279
 steel, armature, thermally hardened, nominal yield stress rel. to load and composition, statistical anal. 3-55800
 steel, cold-rolled strip, rapid cooling under tension during annealing (*German*) 3-80300
 steel, crack development resist. and yield stress, temp.-rate relationships (*Russian*) 3-58651
 steel, creep rupture behaviour, 500-700°C, Rajakovic's method (*German*) 3-47397
 steel, eutectoid-composition, finely spheroidized, thermal mech. treatments influence on mech. props. 3-53258
 steel, low-C, cyclic loading effect on subsequent yielding 3-44593
 steel, low-C, delayed yielding and hysteresis phenomenon under tensile fatigue load 3-44595
 steel, low-C, plastic deformation, microyield region, dislocations, electron microscopy 3-80287
 steel, low-C, pressurized, Portevin-Le Chatelier effect 3-80289
 steel, martensitic Ni-Cr-Mo-Co, toughness and strength characteriz. 3-64915
 steel, plastic bending of edge-cracked specimen 3-64897
 steel, residual austenite behaviour during deform. (*Russian*) 3-41756
 steel, torsional prestrain effect on Bauschinger effect 3-64928
 steel, yield stress in compression rel. to mech. props. 3-58681
 steel plate, anisotropic, notched, upper yield strength, stress-strain, finite element anal. (*Japanese*) 3-55798
 steel weld metal, low-alloy, thickness effect on fatigue crack propag. above and below general yield 3-47413
 strength gradient depend. of crack propag. rates 3-76228
 tensile specimen, necking during creep at const. load and ambient temp. (*German*) 3-65051
 thin shells, Ilyushin-Shapiro yield surfaces accounting for transverse shear 3-70614
 viscoplasticity, thin circular plate, dynamic yield surface, uniformly distributed transverse pressure 3-62488
 Zircaloy-2, quenched, strain ageing behaviour 3-58665
 Ag, Ag-Sn dilute alloy, temp. depend. of yield stress, dislocation mobility 3-49891
 Al, electron irradiation influence on programme loading effect, depend. on stacking fault energy (*Russian*) 3-55008
 Al, polygonized, subboundary effects, yield peak in tensile diagram (*Russian*) 3-44569
 Al, substructural hardening, yield stress, dependence on subgrain size, texture and orientation (*Russian*) 3-41720
 Al 6061-T651 alloy, effect of very short time at temperature 3-69290
 Al alloy, yield and fracture in presence of plane stress pattern, low temp. effects 3-47425
 Al and alloys, yield stress in compression rel. to mech. props. 3-58681
 Al single crystal, deform. rate depend. of yield limit (*Russian*) 3-72916
 Al-Mg-Si 6061 alloy, mechanical props. after very rapid heating 3-47405
 Al₂O₃, sapphire, dislocation-multiplication mechanism 3-55846
 Be, textured sheet, temp. depend. (*Russian*) 3-53246
 Cu, electron irradiation influence on programme loading effect, depend. on stacking fault energy (*Russian*) 3-55008
 Cu and alloys, yield stress in compression rel. to mech. props. 3-58681
 Cu single crystal, deform. rate depend. of yield limit (*Russian*) 3-72916
 Cu-Al alloy, internally oxidized, particle size effect on yield stress 3-80294
 Fe, high-purity, temp. depend. between 23C and -125C (*German*) 3-47399
 Fe alloys, substitutional, yield stress-grain size relation 3-64853
 Fe-Cu-Ti(-C) alloys, micro- and macro-deform. resist., temp. depend. (*Russian*) 3-64835

yield point continued

- Fe-Mo solid solns., low temp. strength, alloy softening, scavenging of interstitials 3-64921
 Fe-Ti (0.16 wt.%) single crystals, orientation, temp. and strain rate effects on deform. 3-64909
 Mg-In solid soln. single crystals, conc. depend. (*Japanese*) 3-41776
 MgO, pure crystals, dislocation dynamics and thermally-activated deform. 3-72081
 Nb, plastic deform. at 2.17-300 K, yield stresses and dislocation structures (*French*) 3-55004
 Nb, temp. depend. rel. to dislocation pinning by oxygen interstitials (*Russian*) 3-72854
 β -Nb-Zr, deform. temp. depend., slip, twinning and dislocations rel. to yield and fracture 3-52662
 Ni, electron irradiation influence on programme loading effect, depend. on stacking fault energy (*Russian*) 3-55008
 Ni₃(Al,W) single crystals, yield stress, dislocation rearrangement 3-80298
 Si₃N₄, hot-pressed, low cycle fatigue 3-76287
 Ti, annealed, neutron irradiation effect on Bauschinger effect 3-64945
 Ti sheet, produced by high rate vapour deposition process, condensation temp. influence 3-64851
 Ti/Mo wire reinforced composite characteriz. 3-58719
 Zn-Cd (0.01 wt.%) alloy sheets, dislocation damping and yielding phenomena 3-64927

Young's modulus

- axially symmetric theory of elasticity, differential eqn. soln. when Young's modulus changes exponentially (*Russian*) 3-66538
 cellulose triacetate fibres, heat-treated, temp. depend., 180-220°C 3-72015
 composite, fibre reinforced, dynamic props. in flexure and torsion 3-55855
 ebonite, dynamic Young's modulus determ. 3-79402
 glass, calc. from chemical compositions 3-40951
 glass, mixed alkali silicate, electric field relaxation, mech. relaxation rel. to ionic diffusion 3-76327
 glass-fibre-reinforced polyester resin, Young's modulus, shear modulus, damping, fibre diam. effects 3-47460
 graphite, annealing and pre-stressing effect 3-41816
 graphite, neutron irradiation, thermal annealing effect 3-67554
 infilled frames, composite characters, stress distrib. 3-62456
 infinite slab isotropic transversely homogeneous elastic material subjected to tension 3-70599
 infrasonic meas. in flexure using Balanced Resonator 3-48348
 isotropic materials, crippling allowables for elevated temp. and creep environments 3-64962
 polymeric coating on metal, radius of contact of stressing sphere meas. 3-73672
 red blood cell membranes, strain energy function 3-48175
 reinforced materials, directionally fibre reinforced, Young's ratio, microstress field 3-73018
 sarcolemma of frog 3-48173
 silicate ceramic, theoret. and exptl. mech. props. comparison 3-72956
 slender curved rod, linear and nonlinear theories 3-70605
 stainless steel, effect of neutron irradiation-induced void formation 3-68310
 steel, austenitic stainless, γ - α transform. effects, 80-280K (*Russian*) 3-44604
 steel, neutron irradiation effect 3-69272
 steel, stainless, neutron irradiation effect, ultrasonic technique 3-78386
 Al, dynamic Young's modulus determ. 3-79402
 Al alloy, tensile prestrain effect on fatigue strength in high cycle fatigue 3-64950
 As-Se system glasses, u.s. vel. obs., temp. and comp. depend. (*Japanese*) 3-64084
 B₂O₃, suboxide, porosity depend. 3-72943
 Ba-mica/Al₂O₃ composites characteriz. 3-76342
 C fibres, influence of ribbon unbending during extension 3-58733
 C fibres, rel. to three-dimens. struct. models 3-76346
 Fe, sintered, elastic modulus and ductility 3-50753
 Fe₇₃P₁₃C₁₀ amorphous alloy, splat cooled, physical props. 3-60758
 Gd₂O₃, polycrystalline monoclinic, shear modulus, rel. to porosity 3-76326
 Li₂O-Al₂O₃-4SiO₂ graphite fibre reinforced composite, elevated temp. props. 3-76351
 Li₂O-Al₂O₃-nSiO₂ graphite fibre reinforced composite, fabrication and low temp. props. 3-76350
 Mn-Cu alloys, γ -phase, comp. effect 3-76208
 Mn-Cu-Fe alloys, Elinvar props. 3-64533
 Mn-Cu-Mo alloys, Elinvar props. 3-64534
 Mn-Ni-Mo nonmag. Elinvar-type alloy characteriz. (*Japanese*) 3-44617
 Nb alloys with small alloying additions, resist. to light plastic deform. (*Russian*) 3-72890
 Ni, meas. by u.s. pulse echo method (*Japanese*) 3-50723
 Pd₈₂Si₁₈ amorphous alloy, splat cooled, physical props. 3-60758
 SiC refractories, bonded, room temp. to 1200°C, characteriz. 3-76288
 Si₃N₄, hot-pressed, UTS, room temp. to 2800°F 3-76291
 Si₃N₄-SiC composite system, microstruct. effect on strength 3-76296
 U alloys, testing under conditions of rapid fission heating 3-47531
 V, interstitial nitrogen conc. depend. (*French*) 3-46656
 ω -Zr, temp. depend., 80-280K (*Russian*) 3-79665

ytterbium

- glass:Nd³⁺, Yb³⁺, segregation and energy transfer from Nd³⁺ to Yb³⁺ (*Russian*) 3-64735
 Hall effect and magnetoresist. through f.c.c.-h.c.p. transform., 1.8-420K 3-50183
 ions, electric field, desorption from W (*Russian*) 3-68504
 Lorentz function and thermal cond., 90-300K 3-50167
 thin film, elec. resistivity thickness depend., 200-850Å 3-75796
 X-ray isotope shifts and variations of nuclear charge radii 3-67662
 ytterbium ethyl sulphate: Dy, Yb, proton polarisation and relaxation, pulsed refrigerator optimal conditions 3-47161
 ytterbium ethyl-sulphate 9H₂O:Yb³⁺, nuclear spin diffusion barrier obs. 3-75904
 Ag:Er, Dy, Yb, γ -ray angular correlation by implanted ions, crystal field effects 3-41460

ytterbium continued

- Al:Er, Dy, Yb, γ -ray angular correlation by implanted ions, crystal field effects 3-41460
 Au-Yb dilute alloy, Mossbauer spectra, obs. on Kondo anomaly on relaxation rate 3-53050
 BaY₂F₈:Yb,Er, efficient i.r.-to-visible conversion by confinement of excitation energy 3-59887
 CaF₂:Eu²⁺ (Yb²⁺), luminescence excitation by ruby and Nd lasers (*Russian*) 3-64739
 CaF₂:Yb²⁺ crystal, polarised luminescence 3-76071
 CaF₂:Yb³⁺, near nuclei magnetic resonance 3-44334
 Cs₂HfCl₆:Yb³⁺, e.s.r. and fluoresc. obs. rel. to octahedral symm. 3-68840
 Cu:Er, Dy, Yb, γ -ray angular correlation by implanted ions, crystal field effects 3-41460
 Fe, Yb implanted, lattice location, hyperfine field and radiation damage 3-52649
 MoS₂ (Eu, Yb, Sr), intercalated layer type cpds., lattice parameters change, mag. ordering, Curie temp., supercond. 3-50371
 Rh:Er, Dy, Yb, γ -ray angular correlation by implanted ions, crystal field effects 3-41460
 SrCl₂:Yb²⁺, single crystals, photoluminescence (*Russian*) 3-41552
 YAsO₄:Yb³⁺ and YPO₄:Yb³⁺, pair interaction and mag. relax. (*German*) 3-53014
 YCl₃.6H₂O:Yb, proton polarisation and relaxation, pulsed refrigerator optimal conditions 3-47161
 YIG:Yb, ferromagnetic resonance anomalies, transverse relaxation instability 3-68848
 Yb II atomic spectrum, one-electron, singly ionised, hollow cathode discharge, hyperfine structure 3-71380
 Yb³⁺, in silicate glass:Cr³⁺, energy transfer and fluoresc. sensitisation 3-72705
 Yb³⁺-Er³⁺ doped matrices, radiative transfer between Yb³⁺ in anti-Stokes fluoresc. mechanism (*French*) 3-80088
 Yb³⁺-UO₂²⁺ activated glass, cooperative sensitisation 3-76095

ytterbium compounds

- Eu_{0.9}Yb_{0.1}Fe₃O₁₂ and Eu_{1.7}Yb_{0.3}Fe₃O₁₂, epitaxial film development 3-79583
 Sm_{0.75}Yb_{0.25}Fe₃O₁₂ and Sm_{1.5}Yb_{0.5}Fe₃O₁₂, epitaxial film development 3-79583
 Yb complexes, chemical shift, effect of complexes on mol. struct. 3-67852
 YbAl garnets, elec. field gradients at Al³⁺ nucleus 3-79635
 YbB₆, elec. cond. and Seebeck coeff., comparison with EuB₆ (*French*) 3-64332
 YbB₆, Mossbauer spectra for ¹⁷⁰Yb Debye-Waller factor (*French*) 3-72552
 YbB₆, X-ray diffraction, anal., thermal props. 3-68423
 Yb_{2.9}-₃Bi_{0.1}Ca₂Fe_{3-x}Si₃O₁₂, Curie temp., mag. susceptibility and anisotropy, mol. field statistical model 3-50365
 Yb_{2.9}-₃Bi_{0.1}Ca₂Fe_{3-x}Si₃O₁₂, diamag. substituted garnet, spontaneous magnetisation, mol. field statistical model 3-50421
 YbD, Hund's coupling case 3-67785
 Yb_{1-x}Eu_xGa_{0.5}Fe_{4.5}O₁₂, ferrimagnetic damping of epitaxial garnet film 3-53024
 Yb₃Ga₅Fe_{3-x}O₁₂, diamag. substituted garnet, spontaneous magnetisation, mol. field statistical model 3-50422
 Yb₃Ga₅Fe_{3-x}O₁₂, Curie temp., mag. susceptibility and anisotropy, mol. field statistical model 3-50365
 YbH, Hund's coupling case 3-67785

yttrium

- alkaline earth fluorides: Sc, Y, La, thermoluminescence, donor-acceptor pairs (*Russian*) 3-44500
 conduction electron m.f.p. and concentration 3-79679
 electrical resistivity, high press., correl. with press.-induced supercond. 3-41306
 h.c.p., deform. modes, 77-497K 3-64912
 magnetic susceptibility of high purity samples, 1.5-300 K, impurity effects 3-75827
 melt growth by crystal. 3-44537
 phonon dispersion, phenomenological model 3-72149
 BaF₂:Y³⁺, dislocation mobility, stress-strain curves, microhardness 3-75534
 CdF₂:Y³⁺-fluorine complex dielectric polarisation, ionic thermocurrents, reorientation space charge formation 3-44367
 ThO₂:Y³⁺, optical absorpt. and fluoresc. 3-55678
 Y:Gd, single crystal, e.p.r. and antiferromagnetic reson. study 3-47143
⁹¹Y, trapping in Indian Ocean sediment 3-65281

yttrium alloys

- see also yttrium compounds
 Al-Y alloys, electro production from molten fluorides 3-65091
 Al₃Y, AlY, magnetic susceptibility meas., contribution to Knight shift (*Russian*) 3-47157
 Er₂Y_{1-x}Al₂, crystalline electric field levels, determ. by neutron spectroscopy 3-50312
 Er₂Y_{1-x}Fe₂, Mossbauer effect, dipolar contributions to mag. hyperfine fields 3-79959
 Gd-Y alloys, magnetocrystalline anisotropy, susceptibility, saturation magnetisation, temp. depend. 3-50390
 Mg-Y, electroproduction from molten fluorides 3-65091
 Pr₂Y_{1-x}Al₂, crystalline electric field levels, determ. by neutron spectroscopy 3-50312
 Tb₂Y_{1-x}Fe₂, Mossbauer effect, dipolar contributions to mag. hyperfine fields 3-79959
 Tm₂Y_{1-x}Al₂, crystalline electric field levels, determ. by neutron spectroscopy 3-50312
 Tm_{0.25}Y_{0.75}Al₂, neutron crystal field spectroscopy, paramagnetic phase, energy distribution, field parameters 3-52955
 YCo₂, paramag. susceptibility, press. depend., correl. with Curie temp. of LnCo₂ alloys 3-55419
 YFe₂, n.m.r. spin echo spectra of Y hyperfine fields 3-79922
 YFe₂, thermal expansion rel. to Curie temp. pressure depend. 3-58385
 YFe₃, n.m.r. spin echo spectra of Y hyperfine fields 3-79922
 Y₂Fe₁₇, n.m.r. spin echo spectra of Y hyperfine fields 3-79922
 Y_{1-x}Th_xFe₃, magnetisation vs. temp. behaviour hybrid local moment-band model 3-47094

yttrium compounds

- see also yttrium alloys
- ethyl sulphate, hyperfine interaction of ^{166}Er , γ - γ directional correl. obs. (French) 3-47179
- ethyl sulphate, hyperfine interactions of $^{166}\text{Ho}^{3+}$, influence of directional correl. of γ - γ cascade (French) 3-53039
- ethyl sulphate paramagnetic relaxation rates of Pr^{3+} , Tb^{3+} , Ho^{3+} 3-50450
- ethyl-sulphate $9\text{H}_2\text{O}:\text{Yb}^{3+}$, nuclear spin diffusion barrier obs. 3-75904
- ethylsulphate, Raman spectra 3-50564
- rare earth yttrium iron garnet, $\text{R}_{0.3}\text{Y}_{2.7}\text{Fe}_3\text{O}_{12}$, ^{57}Fe n.m.r. by spin echo method 3-50475
- sulphides, containing two III_a elements, comparison of crystal struct. (French) 3-58021
- yttrium ethyl sulphate: Dy, Yb, proton polarisation and relaxation, pulsed refrigerator optimal conditions 3-47161
- yttrium ethyl sulphate: Er, c.w. n.m.r. spectrometer for H_1 field meas. 3-45538
- $[\text{Y}_{3-x}\text{La}_x\text{Na}_x]\text{Fe}_{5-x}\text{Ge}_2\text{O}_{12}$, $x=0, 0.5, 1.5, 2$ and 2.5 , sublattice magnetocaloric effects (Russian) 3-47107
- $\text{Al}_2\text{O}_3\text{-Y}_2\text{O}_3$ eutectic, directionally solidified, fracture surface energies 3-72937
- $\text{CaF}_2\text{-YF}_3$ system phase relations and characteriz. (German) 3-47443
- $\text{CeO}_2\text{-Y}_2\text{O}_3$ system, solid solution formation, equilib. structure absence, X-ray obs. 3-69361
- $(\text{Eu}, \text{Y})_3(\text{Fe}, \text{Ga})_2\text{O}_{12}$, mag. bubble films, rotation effects on isothermal growth by LPE 3-76133
- $\text{Eu}_{0.7}\text{Y}_{2.3}\text{Fe}_{3.84}\text{Ga}_{1.16}\text{O}_{12}$ film, suppression of hard bubbles by thin Permalloy layer 3-47086
- $\text{Eu}_{0.65}\text{Y}_{2.35}\text{Fe}_{3.8}\text{Ga}_{2.2}\text{O}_{12}$ epitaxial films, on garnet substrates, mag. anisotropy, effect of lattice mismatch 3-44228
- $\text{EuYbGaFe}_4\text{O}_{12}$ film, suppression of hard bubbles by thin Permalloy layer 3-47086
- $\text{HfO}_2\text{-Y}_2\text{O}_3$ solid soln., phase diagram boundaries detn., X-ray analysis 3-64153
- $\text{Mn}_x\text{Mg}_{1-x}\text{Y}_2\text{S}_4$, polycryst. solid soln., mag. susceptibility, Curie-Weiss behaviour 3-41328
- Nd:YAG laser, pumping by miniature diode 3-66836
- Nd:YAG laser action on $^4\text{F}_{3/2} \rightarrow ^4\text{I}_{13/2}$ transition manifold, lasing at $1.35\text{ }\mu\text{m}$ 3-45804
- Nd:YAlO₃ laser action on $^4\text{F}_{3/2} \rightarrow ^4\text{I}_{13/2}$ transition manifold, lasing at $1.35\text{ }\mu\text{m}$ 3-45804
- Nd³⁺:YAG burst mode freq. doubled laser for high speed photography and holography application 3-43015
- Nd³⁺:YAG cryst., meas. of relax. time of laser transition 3-70821
- Nd³⁺:YAG laser, cavity dumped, instability due to time varying reflections 3-40263
- A-Nd₂O₃-A-La₂O₃ and A-Nd₂O₃-C-Y₂O₃, investigation of the binary systems (French) 3-64152
- (Y,Gd)₃(Fe,Ga,Al)₂O₁₂, heat treatment effects on dislocation density (Russian) 3-52629
- YAG, elec. field gradients at Al^{3+} nucleus 3-79635
- YAG, Nd doped, fluorescence quenching rel. to use as laser material 3-48907
- YAG, Nd³⁺:YAG, Czochralski-grown, perfection and characts. for gems, lasers and substrates 3-76131
- YAG:Cr, population determ. of metastable level (Russian) 3-50149
- YAG:Cr³⁺, laser generation at $6874\text{ }\text{\AA}$ 3-74244
- YAG:Nd, Lu, repetitively pulsed flashlamp-pumped laser material, thermal transient effects 3-62716
- YAG:Nd, stimulated emission cross section at $1061\text{ }\mu\text{m}$ 3-43017
- YAG:Nd c.w. laser with vortex stabilised lamp 3-45806
- YAG:Nd³⁺, energy level temp. shift, absorp. and luminesc. spectra obs. 3-64727
- YAG:Nd³⁺, Ho^{3+} epitaxial film, laser oscillations obs. 3-51929
- YAG:Nd³⁺ single crystals, absorption bands (Russian) 3-69025
- YAG:Nd³⁺ thin film laser, liquid phase epitaxial growth 3-54230
- YAG:Sc³⁺, Nd³⁺, solubility enhancement of Nd³⁺ by lattice expansion with Sc^{3+} 3-68415
- YAlO₃, biaxial cryst., refr. indices 3-41492
- YAlO₃, Czochralski-grown single crystals, cracking, effects and minimisation procedures 3-46670
- YAlO₃:Ce³⁺, optical spectra and sensitised fluorescence 3-58531
- YAlO₃:Dy (Ho)(Er)(Tm)(Yb), absorpt., luminesc. spectra, Stark levels, stimulated emission 3-72674
- YAlO₃:Nd, Czochralski growth 3-69158
- YAlO₃:Nd³⁺ stimulated emission in $^4\text{F}_{3/2} \rightarrow ^4\text{I}_{13/2}$ transition 3-43018
- YAlO₃:rare earth, absorpt. and emission intensities for trivalent rare earth ions 3-47296
- YAlO₃:rare earth, nonradiative relax. by multiphonon emission 3-47309
- YAlO₃:rare earth ion, fluoresc. sensitisation using Cr ions 3-69057
- YAlO₃:TR³⁺ (TR=rare earth), colour centres, absorption and thermoluminescence spectra 3-44441
- YAlO₃:Yb³⁺, Er³⁺, radiative transfer between Yb³⁺ ions in anti-Stokes fluoresc. mechanism (French) 3-80088
- Y₃Al₅O₁₂:Ce³⁺, firing and excitation conditions rel. to exponential luminesc. decay curves 3-50625
- Y₃Al₅O₁₂:Cr³⁺, 300K, 77K, absorption and luminescence spectra 3-50605
- YAsO₄, multiphonon relax. of excited states of rare earth ions 3-53143
- YAsO₄, pair interaction and mag. relax. of Yb³⁺ (German) 3-53014
- Yb₃ X-ray diffr. anal., thermal props. 3-68423
- Y_{2.7}Bi_{0.3}Fe_{3.8}Ga_{1.2}O₁₂ film, liq. phase epitaxial, Faraday rotation and domain wall velocity effect of Bi 3-47102
- Y_{3-x}Bi_xFe₃O₁₂ garnet film, Faraday rotation and optical absorpt. 3-53085
- YBr₃.6H₂O, ^{79}Br and ^{81}Br n.q.r. 3-75913
- Y_{2.8-2.2x}Ca_{0.2Hx}Fe_{4.8-3x}Sn_{0.2Vx}O₁₂, mag. fields on Sn^{4+} nuclei, Mossbauer study (Russian) 3-41467
- Y(ClO₄)₃, aqueous solutions, density, compressibility, expansibility, sound velocity (Russian) 3-72114
- YCl₃.6H₂O:Yb, proton polarisation and relaxation, pulsed refrigerator optimal conditions 3-47161

yttrium compounds continued

- YCo₅, liquid phase sintered, mag. props. 3-44268
- YCo₁₇, permanent mag. material, modified Czochralski growth 3-44529
- Y₂₄(Co_{1-y}Fe_y)_{17-2x} intermetallic compound, magnetocryst. anisotropy, X-ray diffr. obs. 3-44230
- YCo₅Ge₂, lattice parameters, diffr. pattern 3-58016
- YCrS₃, cryst. growth, struct., and optical absorpt. 3-40869
- YEu garnet, epitaxial film, uniaxial mag. anisotropy obs. 3-44283
- YEu garnet, liquid phase epitaxy, saturation temp. and empirical binary phase diagram 3-44287
- Y_{3-2x}Eu_xTm_{2x}Ga_{1-2x}Fe_{3-2x}O₁₂ epitaxial film for bubble device appl., characts. 3-60975
- YEuYb garnet film, ion implanted, annealing of mag. props. 3-44288
- YF₂, YF₃, matrix isolated compounds, i.r. spectra, 40 to 800 cm^{-1} , freq. assignments 3-52370
- YF₃ in CaF_2 , colour centre obs. following γ and p irradiation and annealing 3-72694
- Y₃Fe_{4.81}Al_{0.19}O₁₂, garnet, magnetoelastic coupling of Fe^{3+} ions, single ion model 3-53011
- YFe_{1-x}Co_xO₃, floating zone grown crystal, Co effect on spin reorientation 3-47080
- YFe_{1-x}Co_{x/2}Ti_{1/2}O₃, floating zone grown crystal, Co effect on spin reorientation 3-47080
- Y₃Fe_{5-x}Ga_xO₁₂, garnet, parallel pumping of spin wave instability 3-79859
- Y₃Fe_{5-x}Ga_xO₁₂, magnetic, compensation bubble obs. 3-64520
- Y₃Fe_{5-x}Ga_xO₁₂, nonlinear susceptibility and three-magnon confluence, magnetization effects (Russian) 3-72455
- Y₃Fe_{5-x}In_xO₁₂, garnet, parallel pumping of spin wave instability 3-79859
- Y₃Fe_{5-x}In_xO₁₂, nonlinear susceptibility and three-magnon confluence, magnetization effects (Russian) 3-72455
- Y₃Fe_{5-x}Mn_xO_{12-xF_x}, M=3d transition element, ion site occupation determ. (French) 3-79305
- YFeO₃Mn₂O₃, spin reorientation, Mossbauer and neutron diffr. obs. 3-55434
- YFeO₃, antiferromag. reson. 3-41429
- YFeO₃, covalency parameters for Fe^{3+} , comparison with LaFeO₃ and K₂FeF₆ 3-40860
- YFeO₃, hysteresis of magnetization reversal 3-58401
- YFeO₃, orthoferrite, magnetic bubbles, dynamic behaviour 3-50409
- YFeO₃:Co, Cr, spin reorientation rel. to Co and Cr substitution 3-64503
- Y₃Fe₅O₁₂, heat treatment effects on dislocation density (Russian) 3-52629
- Y₃Fe_{5-x}Ru_xO₁₂, magnetostriction, single-ion model calc. 3-47122
- Y₃Fe_{5-x}Sc_xO₁₂, garnet, magnetoelastic coupling of Fe^{3+} ions, single ion model 3-53011
- YGa garnet, nuclear quadrupole moment of ^{53}Cr , ENDOR measurements 3-64582
- YGaG:Re³⁺ garnet, strain variation of Ru ion energy levels, magnetostriction calcs., e.p.r. obs. (French) 3-58420
- Y₃Ga₂O₁₂:Pb³⁺ diamag. garnet cryst., e.s.r. anal. of Pb^{3+} ions in dodecahedral sites 3-47141
- Y_{3-x}Gd_xFe_{5-y}Ga_yO₁₂ epitaxial films, garnets, magnetic anisotropy, temp. depend., optical memory applications 3-44303
- Y_{3-x}Gd_xGa₂Fe_{5-x/2}O₁₂, electron microprobe analysis of composition and corresponding mag. props. 3-44296
- YGd₂Tm garnet, epitaxial film, uniaxial mag. anisotropy obs. 3-44283
- YGd₂Tm garnet film, ion implanted, annealing of mag. props. 3-44288
- (YGdYbEu)₃(Al,Ga)₂Fe_{5-x}O₁₂, bubble domain mobility, optical obs. 3-44292
- YH_{1.95}, positron annihilation, proton model 3-50131
- YIG, anisotropy of attenuation of hypersound 3-72502
- YIG, critical exponents β and δ 3-72465
- YIG, critical props., reduced total magnetisation, Faraday rot. obs. 3-47030
- YIG, Curie point existence in presence of static mag. field 3-72470
- YIG, damping of magnetoelastic waves, melt growth conditions influence (Russian) 3-75864
- YIG, domain wall energy determ. from hysteresis loops 3-79873
- YIG, effect of 60 kbar pressure on Curie point (French) 3-72463
- YIG, effect of dipolar forces on response functions, and light scatt. spectra 3-68795
- YIG, epitaxial film, identification of magnetostatic surface spin wave modes 3-64557
- YIG, epitaxial film, spin-wave propag., device applications 3-47074
- YIG, exchange-free magnetoelastic plane wave propagation 3-44306
- YIG, Faraday rotation obs. of spin waves 3-47231
- YIG, ferrimagnetic resonance absorption and second harmonic generation measurement 3-53022
- YIG, film, nonpropagating magnetic surface modes, angle, temp. and freq. depend. 3-41352
- YIG, Ga-substituted, growth from melt under isothermal conditions (German) 3-69157
- YIG, Ga-substituted, high homogeneity specification by Mossbauer spectra 3-41463
- YIG, gyromagnetic ratio anisotropy, ferromag. resonance obs. 3-41423
- YIG, laminar domain structure, magnetisation processes 3-75859
- YIG, magnetoelastic coupling, ferromag. resonance and e.p.r. obs. 3-47119
- YIG, magnetostatic wave convolution at microwave freqs. 3-41386
- YIG, Mossbauer study of u.s. generation by r.f. field 3-44307
- YIG, n-type, inhomogeneous polycryst., non-Ohmic current behaviour 3-72363
- YIG, nonlinear magnetic susceptibility in high frequency magnetic field near Curie temp. 3-50350
- YIG, optical absorption and Faraday rotation in range 1 to $0.35\text{ }\mu\text{m}$ at 300, 20 and 6K 3-64684
- YIG, partially metallised plate, magnetostatic surface waves 3-64509
- YIG, periodic domain structure, spin wave measurements using laser light 3-75848

yttrium compounds continued

- YIG, polycryst. and impurity doped, longitudinal χ'' in strong r.f. fields 3-64554
 YIG, Raman-Nath scatt. of light by magnetostatic waves 3-55439
 YIG, reflection spectra in range 9000 to 200000 cm^{-1} 3-76023
 YIG, resonance phenomena in parametric spin wave system 3-50470
 YIG, Sn-substituted, quadrupole splitting and stretching vibrations 3-41464
 YIG, wavelength modulated reflectivity, crystal field transitions obs. 3-47281
 YIG discs, secondary magnetoacoustic resonance, 3-44308
 YIG epitaxial films, optical transmission and magneto-optical props. 3-44505
 YIG film, spin wave excitation, physical model 3-41353
 YIG films on Gd-Ga-garnet substrates, ferromagnetic resonance linewidth at 2 to 8 GHz 3-79917
 YIG rod, axially magnetised, spin wave instabilities 3-44326
 YIG slab, magnetostatic surface waves, magnetisation perpendicular to direction of propagation 3-75845
 YIG:Ce, mag. anisotropy, ferromag. reson. obs. 3-72482
 YIG:Cr, mag. anisotropy of Cr^{3+} , ferromag. resonance obs. 3-41415
 YIG:Ga, wavelength modulated reflectivity, crystal field transitions obs. 3-47281
 YIG:Ga substituted, 180 degree compensation wall obs. 3-44240
 YIG:Ga substituted film, epitaxial growth using coaxially arranged c.v.d. reactor 3-44286
 YIG:Gd, Ga substituted, l.p.e. grown, uniaxial mag. anisotropy dependence on misfit strain 3-44284
 YIG:Si, low temp. magnetostriction 3-58407
 YIG:Si, photoinduced linear dichroism, temp. depend. calc. 3-47226
 YIG:Tb, Pr, ferromag. resonance, high pressure effects on anisotropy and relaxation 3-41421
 YIG:Tb $^{3+}$, anisotropy anomalies, high pressure effects, ferromag. resonance obs. 3-50468
 YIG:Yb, ferromagnetic resonance anomalies, transverse relaxation instability 3-68848
 YIG-n-InSb, adjacent films, magnetostatic wave amplif. due to carrier drift current 3-72372
 YIO $_5$.4H $_2$ O, X-ray diffr., isostructurality, unit cell dimensions 3-72067
 YIn $_2$ Ga $_3$ O $_{12}$, cryst. structure, X-ray powder data 3-72056
 YLAG:Nd $^{3+}$, spectral props. and induced emission 3-53131
 YNbO $_4$, internal vibration modes of NbO $_4^{3-}$ tetrahedra, i.r. and Raman spectra obs. 3-53095
 Y $_2$ O $_3$, shrinkage, dependence on heating rate 3-72980
 Y $_2$ O $_3$, zirconia-stabilized, fast neutron damage effects 3-78373
 Y $_2$ O $_3$ films, luminesc. during oxidation of Y 3-64741
 Y $_2$ O $_3$ part per giga level determination of rare earth impurities 3-48635
 Y $_2$ O $_3$ stabilised zirconia, current blackening, optical absorpt. study 3-47449
 Y $_2$ O $_3$ stabilized HfO $_2$, thermal expansion 3-61195
 Y $_2$ O $_3$ stabilized HfO $_2$ /W composites, unidirectional solidification behaviour 3-61203
 Y $_2$ O $_3$ stabilized ZrO $_2$, current-blackened single crystals, dielec. consts. and loss tangent 3-79972
 Y $_2$ O $_3$ stabilized ZrO $_2$, high temp. creep parameters 3-72951
 Y $_2$ O $_3$:Bi phosphor, luminescence centres (Russian) 3-44458
 Y $_2$ O $_3$:Eu $^{3+}$, energy transfer interaction between Eu $^{3+}$ ions situated in different lattice positions (Russian) 3-41565
 Y $_2$ O $_3$:Eu $^{3+}$, luminescence (French) 3-64731
 Y $_2$ O $_3$:Eu $^{3+}$, Tb $^{3+}$, radiationless recombinations in surface layers (Russian) 3-50612
 Y $_2$ O $_3$ -CaO system, phase diagram characteriz. 3-76241
 Y $_2$ O $_3$ -stabilised ZrO $_2$:Er $^{3+}$, absorpt. spectrum, O $_2^{2-}$ coordination, crystal structure 3-41539
 Y $_2$ O $_3$ -ThO $_2$ (10 mole%)-Nd $_2$ O $_3$ (1 mole%), transparent powder prep. and processing 3-64968
 Y(OH) $_3$:Er $^{3+}$, Ho $^{3+}$, crystal field studies, mag. susceptibility and Schottky sp. ht. 3-79840
 Y $_2$ O $_3$:S:Eu phosphor, emission colour detn. 3-44494
 YPO $_4$, multiphonon relax. of excited states of rare earth ions 3-53143
 YPO $_4$, pair interaction and mag. relax. of Yb $^{3+}$ (German) 3-53014
 YPO $_4$ host for rare earth trace metals detection by X-ray excited optical fluorescence 3-48635
 β -YSF crystalline structure, least squares refinement (French) 3-60693
 Y $_3$ Sc $_2$ Ga $_3$ O $_{12}$, cryst. structure, X-ray powder data 3-72056
 YSeF, crystal struct. (French) 3-79283
 YSeF polytypes, cryst. struct. (French) 3-46632
 Y $_{3-x}$ Sm $_x$ Fe $_2$ O $_{12}$, flux grown, cubic and uniaxial anisotropy, composition depend. 3-79861
 Y $_2$ S $_2$ Mo $_4$ Ga $_2$ Fe $_3$ O $_{12}$ epitaxial film, controlled adjustment of bubble domain collapse field by annealing 3-72488
 YTaO $_4$, internal vibration modes of NbO $_4^{3-}$ tetrahedra, i.r. and Raman spectra obs. 3-53095
 Y $_x$ (Ta $_{1-x}$ W $_{1-3x}$)O $_3$, non stoichiometric perovskite, structural evolution, elec. microscope obs. (French) 3-58018
 YVO $_4$, host for rare earth trace metals detection by X-ray excited optical fluorescence 3-48635
 YVO $_4$, multiphonon relax. of excited states of rare earth ions 3-53143
 YVO $_4$:Eu $^{3+}$, luminescence (French) 3-64731
 YVO $_4$:Eu $^{3+}$, nonthermalization and large variation in multiphonon relax. rate among Stark levels 3-53144
 ZrO $_2$ -Y $_2$ O $_3$ cubic solid soln. stability below 1500°C (French) 3-76309
 ZrO $_2$ -Y $_2$ O $_3$ solid soln. chem. vapour deposition and characteriz. 3-76234

Yukawa potential see meson field theory; nuclear forces

Z pinch see pinch effect

Zeeman effect

see also atomic spectra; Hanle effect; spectral line breadth
 alkali metal atoms, optically pumped, spin-exchange shift and narrowing of magnetic resonance lines 3-54580

Zeeman effect continued

- anthracene, adsorbed Rhodamine B, charge transfer state, hyperfine modulation 3-69089
 atomic g-factor beam-foil meas. techniques 3-78458
 1-chloro-2,4-dinitrobenzene, n.q.r. study 3-43480
 cyclopropenone, molecular, g values and magnetic susceptibility anisotropies 3-63482
 DA white dwarfs, interpretation of quadratic Zeeman effect 3-69941
 N,N'-dideuteroparachloroaniline, mag. dipole interact. in ND $_2$ group, ^{14}N n.q.r. Zeeman effects 3-75910
 e.s.r. spectra, non-collinear Zeeman, hyperfine and fine structure tensors effect 3-47127
 flip-flop sequence for restoring Zeeman order in laboratory reference frame 3-53029
 Hanle effect applic. to small mag. field meas. 3-78457
 Hanle effect of molecules, irreducible tensor operators applic. (French) 3-71572
 Hanle effect on levels deexciting by elec. quadrupole transitions (French) 3-52265
 Hanle experiments with accelerated ion beams in gaseous targets 3-78462
 interstellar masers, trapped i.r. lines and cross-relaxation 3-51393
 master oscillator, Zeeman mol. beam, nonlinear effects 3-78005
 metastable atomic states, hyperfine and Zeeman studies by atomic-beam magnetic resonance, review 3-49393
 3-methylene oxetane, μ -wave spectrum, mol. Zeeman effect, mag. susceptibility anisotropy, quadrupole moment meas. 3-52372
 molecular beams, velocity distrib., space modulation of radiofrequency field, shift of Zeeman pattern, devices (French) 3-49507
 multiplet interpretation and spectral analysis, role of spectroscopic instrumentation (French) 3-39927
 nitromethane, rotational Zeeman effect (German) 3-43432
 organic compounds, polycryst., Zeeman ^{35}Cl n.q.r. spectra 3-75911
 3-oxetanone, μ -wave spectrum, mol. Zeeman effect, mag. susceptibility anisotropy, quadrupole moments meas. 3-52372
 plasma, homogeneous magnetoactive, Zeeman sublevel transitions (Russian) 3-43652
 plasma electron density determ. from H $_2$ lines broadened by combined Stark and Zeeman effect 3-43691
 polyethylene terephthalate, amorphous, spin-lattice relaxation 3-75909
 positronium, relativistic contrib. to combined Zeeman and Stark effects 3-71483
 pyrone, molecular, high field, g value and mag. susceptibility anisotropies 3-63481
 Shpol'ski hosts, absorpt. and emission spectra of Zn porphyrin 3-72737
 spin-gravitational interaction analogue calc. (Russian) 3-77879
 symmetric top molecules, vibrational Zeeman effect 3-43427
 s-triazine, lower electronic states, 1.8°K optical study 3-64674
 tropone, molecular, high field, g value, mag. susceptibility anisotropies 3-63481
 tunnelling centres, Zeeman nuclear relax. 3-72542
 white dwarfs with large mag. fields, He spectra 3-45107
 X-ray star optical candidates, Zeeman effect in H β line 3-51352
 Ba lifetimes and g-factors of 6s 2 p and 5d6p levels, Hanle effect meas. 3-78468
 COS, dipole moment function determ. 3-78768
 CaF $_2$:Dy $^{3+}$, crystalline field study 3-52799
 CaF $_2$:Er $^{3+}$, optical absorption spectrum, energy level identification of type I crystal 3-55605
 Cd, Hanle effect in the case of impulse excitation of 6 $^1\text{D}_2$ level 3-63293
 Cs atom, 6 ^2P , depolarization by collisions with inert gases in variable mag. field 3-78515
 Cs $_3$ CoBr $_3$ tetragonal crystals, anisotropy of Zeeman effect in optical absorption spectra 3-72670
 Cs $_3$ CoBr $_3$ tetragonal crystals, anisotropy of Zeeman effect in optical absorpt. spectra, selection rules 3-72671
 Cs $_3$ CoCl $_3$ tetragonal crystals, anisotropy of Zeeman effect in optical absorption spectra 3-72670
 Cs $_3$ CoCl $_3$ tetragonal crystals, anisotropy of Zeeman effect in optical absorpt. spectra, selection rules 3-72671
 EuI 4f 7 (^8S)6s 2 level, hyperfine struct. of y ^8P -multiplet by determ. by level crossing method 3-46315
 ^{19}F , nuclear Zeeman splitting by anal. linear polarization 3-71081
 Fe I, mean lifetimes and f-values for 4 excited states, Hanle effect obs. 3-63282
 GaAs, Zeeman spectroscopy of shallow donor states 3-41543
 GaP:N, Zeeman splitting of B-line at low mag. fields 3-50615
 Ge:B, TI, excitation spectra, Zeeman effect 3-50594
 H, n=3 level behaviour produced by electron impact induced dissociation of H $_2$ 3-60363
 H atom, quadratic Zeeman effect, sturmian functions applic. 3-63259
 HCO nonlinear free radical, Zeeman effect, microwave spectra theory and analysis 3-46306
 Hf(BH $_4$) $_4$:U(BH $_4$) $_4$, electronic absorpt., optical and e.p.r. spectra assignments 3-76033
 HgCl $_2$, ^{35}Cl n.q.r., Zeeman effect 3-44349
 ^{198}Hg + ^{199}Hg collisional transfer of orientation, double reson. obs. 3-52281
 InP, Zeeman spectroscopy of shallow donor states 3-41543
 KCl:Li $^+$, Zeeman nuclear relax. of tunnelling centres 3-72542
 Li $^+$ isotopes, beam-foil excited, Larmor precessions in 2^2P and 4^2P terms 3-78459
 ^{17}Li , hyperfine struct. meas. by atomic beam magnetic resonance method 3-71374
 MnK $_4$ H $_2$ (SO $_4$) $_4$.2H $_2$ O, absorption spectra and Zeeman effect of Mn $^{2+}$ at low temp. 3-44423
 NCO, Renner-Teller effect and vibronically induced bands in electronic spectrum 3-75048
 NO, CO laser Q-switching applic. 3-66812
 Na Hanle effect, inert gas influence 3-74807
 Ne, 2p 5 3p level lifetimes, Hanle effect meas. 3-78460
 Ne, Hanle effect meas. of g-factors and polarizations of excited states 3-78461
 OH, OD, optical r.f. double reson. studies and zero-field level crossing 3-40653

Zeeman effect continued

- PbMoO₄:Nd³⁺, cryst. Stark splitting, optical absorpt. and Zeeman spectra obs. 3-47297
 Rb, rot. frame coherent resons. on fund. level of ⁸⁵Rb (*French*) 3-54574
 Rb II analysis, atomic spectrum in discharges, hyperfine structure, experimental 3-71379
 S₂, selectively excited, Hanle effect lifetime meas. 3-75062
 Sb, 541.5 and 609.8 nm lines 3-78453
 SbCl₃, polycrystalline, Zeeman n.q.r. 3-61008
 Si:P, variational calc. of quadratic effect 3-58515
 Sr, 5s5p ¹P₁ level, lifetime meas. using Hanle reson. 3-46184
 Sr atom, Hanle effect meas. of 5s6p ¹P₁ lifetime 3-63283
 TiO₂:Cr³⁺, n-phonon ⁴A_{2g}-⁴T_{2g} transition 3-53124
 Tm spectra 3-63273

Zener breakdown see *Zener effect***Zener diodes**

No entries

Zener effectsee also *Zener diodes*

No entries

zero soundsee also *liquid helium sound propagation*

- ³He liquid, zero sound attenuation, superfluid pairing 3-50047
 Fermi liquid, Kapitza resistance, single-particle versus zero-sound coupling 3-50044
 quantum crystals, phonon modes, dispersion laws, stability 3-72253
³He, liquid, dispersion relation for transverse zero sound 3-46742
⁴He, Feynman phonon as zero sound quantum 3-50040
⁴He, liquid, theory accurate for collective oscill. at infinitely long wavelength 3-68455

zeta-potential see *electrokinetic effects***zinc**

- adsorption on (100), (111), (111) GaAs surfaces 3-55150
 atom, branching ratios, ²D_{5/2}; ²D_{3/2} ratios meas. by photoelectron spectroscopy 3-71393
 atom, electron impact excitation, effective cross section determ. 3-74869
 atom, electron impact ioniz., effective cross sections 3-63318
 atom, photoioniz. cross sections for states split by spin-orbit coupling 3-67684
 atomic absorption spectroscopy, trace metals, human body fluids and tissues, sampling techniques 3-48643
 Azbel'-Kaner cyclotron resonance between 1.5 K and 4.2 K 3-43991
 basal dislocation motion, influence of thermal jogs 3-60736
 brittle fracture, current pulses influence 3-55819
 chemical diffusion into Co, 858 to 1198°C 3-46733
 coated with liq. metal, failure under brittle fracture to plastic flow transition conditions 3-50741
 creep, high temp., stress-change expts. 3-76206
 critical shear stress, metal purity and temp. depend., single crystals. (*Russian*) 3-52660
 crystal growth, Bridgman method, reaction of foreign particles with crystn. front 3-75492
 crystal growth on C substrate, high perfection (*German*) 3-61115
 cyclic deformation, dissipated energy and fatigue fracture 3-40962
 diffusion, in Li, impurities, force transport, electro- and thermo-transport, steady-state technique 3-52724
 diffusion in Al, intergranular mechanism (*French*) 3-41052
 diffusion in GaAs, precipitation studied by transmission electron microscopy 3-80188
 diffusion in GaP ternary sources, 850°C, non-ideal kinetics 3-72228
 diffusion of Zn²⁺ tracer in AgCl, 209-441°C, substitutional mechanism 3-68441
 dislocation block boundaries, double-layer, in single crystals. (*Russian*) 3-43792
 dislocation loop characterisation by X-ray topography 3-43802
 dislocation motion initiation stress and internal stress meas. (*Russian*) 3-58620
 dislocation networks in basal plane of Zn single crystals., form. during growth, annealing 3-75540
 dislocation structure of melt grown single crystals., seed cryst. perfection and seeding method effects (*Russian*) 3-69153
 droplets quenched from liq. state, cryst. struct. (*Russian*) 3-69268
 elastic wave reflection from free boundary 3-46677
 electron probe microanalysis, mass absorption coeffs. for CuL_α line (*Japanese*) 3-57022
 electronic structure, u.s. attenuation studies 3-72312
 enthalpy of sublimation, microcalorimetric determ. (*French*) 3-68403
 Fermi surface, uniaxial stress depend. 3-41127
 Fermi surface, uniaxial stress effect, de Haas-van Alphen and oscillatory magnetostriiction obs. (*French*) 3-60852
 forest dislocations, interaction with primary dislocations at 1.5K 3-75533
 fracture, brittle and quasi-brittle, elec. pulse current influence (*Russian*) 3-80345
 in InAs, distrib. in melt, under flux, radioactive isotope method 3-75626
 internal friction, amplitude depend., temp. effects, 100-300K (*Russian*) 3-72132
 ion implantation of ZnS 3-72817
 ionic level population, role of electron deexcitation in He-Zn discharge 3-63319
 liquid, fragmentation when dropped in water, automatic picture scanner 3-74730
 liquid metal, resistivity calculation, neutron scattering data, band structure, role of d states 3-50177
 low temperature behaviour, Debye temp., energy role (*Russian*) 3-79498
 low-temperature electron irradiation effects 3-60744
 macroscopic crack propag. during extension in presence of Hg (*Russian*) 3-58649
 magnetic breakdown between second and third zones, de Haas-van Alphen effect 3-68540
 photoelectron emission, d band location 3-58585
 plastic deform. during friction in food-industry media (*Russian*) 3-40967

zinc continued

- plastic deformation effects on acoustic and elec. emission (*Russian*) 3-79413
 quadrupole interaction of implanted polarised ¹⁹F, sign determ. from γ-ray angular correlation 3-49081
 quenched thin film, Hall effect, annealing behaviour (*German*) 3-72349
 secondary electron emission, ion bombardment of (0001) surface, 3 keV He⁺ and Ne⁺ ions, energy distribution 3-44512
 segregation coeff. in Sn 3-69227
 shear modulus change, depend. on amplitude of oscillating stress 3-75557
 n-Si, Zn-compensated, very high resistivity, photocurrent decay, temp. depend. 3-79725
 single crystals, critical resolved shear stress, biaxial loading effect 3-46658
 sputtering and Ni ion injection anomalous diffusion at room temp. and 77 K 3-61084
 steel (4% Mn), kinetics and morphology of surface layer formation in liquid zinc (*Polish*) 3-72842
 superconducting, calc. of phonon-induced gap anisotropy 3-68713
 superconducting, specific heat, energy gap anisotropy obs. 3-60929
 superconducting energy gap anisotropy rel. to normal-state mass renormalisation 3-75807
 superconducting film, quency-condensed, energy gap and transition temp. 3-46918
 superconducting state, u.s. studies of electronic struct. 3-72425
 superconductive fixed point device, for thermometric reference 3-51511
 thermally activated glide of single crystals., 4.2 to 373 K 3-40957
 vacuum arc cathode, erosion and ionisation 3-57957
 Al₃Ga_{1-x}P_x:Zn, green light emission 3-50608
 CaS:Ag, Zn, spectral characteristics, formation of [AgVs]⁺e⁻ traps (*Russian*) 3-76060
 Cd-Zn vapour laser, isotopic splitting, increased amplification factor (*Russian*) 3-40240
 films, quench. condensed, superconducting transition temperature (*German*) 3-58335
 GaAs:Zn, acceptor impurities, effect on dislocation mobility 3-72094
 GaP:Zn, deep level centres and Zn-O pairs rel. to l.e.d. efficiency 3-72757
 GaSb:Cu, Zn, Te, Zn and Te influence on Cu diffusion and solubility 3-72232
 GaSb:Zn, impurity level scheme 3-75722
 Ge:Zn, group theoretical treatment of uniaxial stress 3-58228
 Ge:Zn⁺ energy state symmetries and deform. pot. consts., spectra obs. 3-44439
 InP:Te, Zn, carrier density rel. to solubility of donor, acceptor dopants 3-60886
 InP:Zn, acceptor impurity, elec. and photoluminesc. props. 3-41581
 Pb_{1-x}Sn_xTe:Zn, carrier conc. reduction 3-69173
 Si:Zn, induced impurity photocond. 3-41233
 Si:Zn, short wavelength quenching of photocond. 3-50240
 Si:Zn, thermal capture of electronic and holes at Zn centres, p-n junction obs. 3-68562
 in SiO₂ films, i.r. spectra, struct., stability 3-64646
 Zn-Se, barrier heights and surface electron density of states (*Rumanian*) 3-64395
 Zn²⁺, electronic polarisability in fluorides 3-72567
 Zn²⁺/Zn(Hg), electrode kinetics, potentiostatic method 3-76463
⁶⁵Zn, diffusion in Li, thermotransport obs. 3-60803
- zinc alloys**
 see also *zinc compounds*
 die casting, ageing, kinetic analysis (*Japanese*) 3-72910
 dilute nonmagnetic superconducting, energy gap anisotropy, specific heat obs. 3-60929
 rare earth zinc intermetallic, RE(Zn), type, RE=Ce, Pr, Nd, Sm, Gd, Gy and Er, lattice parameter for CaCu₂ (D_{2d}) struct 3-68198
 Ag-Zn, α-phase, rigidity modulus, temp. depend. 3-69183
 Ag-Zn solid solns., interdiffusion coeffs., conc. depend. (*Russian*) 3-72225
 β'-AgZn, band structure and Fermi surface, APW calcs. 3-64281
 AgZn₃, formation in Al-Zn-Ag alloy (*Russian*) 3-41723
 Al-Ag-Zn, (5 at.% Ag, Zn), liquidus quenched, precipitation, GP zone form. 3-72865
 Al-Mg-Zn, Al-Mg-Zn-Cu, precipitation, Guinier-Preston zone, ageing, 130-225°C, elec. resist. obs. (*Japanese*) 3-72868
 Al-Mg-Zn, soln. softening effect of zinc at high temps. 3-64948
 Al-Zn, axisymm. extrusion, activation enthalpy and material consts. depend., relation to recrystn., substruct., mech. props. 3-47403
 Al-Zn, eutectoid transformation, phase boundary diffusion as rate-determining step (*German*) 3-80218
 Al-Zn, single cryst. growth by Bridgman method (*Czech*) 3-55734
 Al-Zn, single crystals., alloying effect on acoustic props. (*Russian*) 3-72138
 Al-Zn, soft structural component effect on damping power 3-58679
 Al-Zn (22 at.%), liq.-quenched, spinodal decomp. 3-64868
 Al-Zn (28 at.%), liquid-quenched, phase decomp. 3-41740
 Al-Zn (28at%), discontinuous precip., h.v. electron microscope in situ obs. 3-50708
 Al-Zn channelling of protons, atomic displacement effects in Guinier-Preston zone 3-49914
 Al-Zn-Ag, changes in structure during recovery, metastable phase AgZn₃ characteristics (*Russian*) 3-80256
 Al-Zn-Mg, axisymm. extrusion, activation enthalpy and material consts. depend., relation to recrystn., substruct., mech. props. 3-47403
 Al-Zn-Mg, extrusion-limit diagrams, construction and struct. information 3-47404
 Al-Zn-Mg, grain boundary precipitate effects on stress corrosion cracking (*Japanese*) 3-50725
 Al-Zn-Mg, high-strength, tensile deform. and fracture props. 3-76207
 Al-Zn-Mg, superplastic phenomena and microstruct. (*Japanese*) 3-50700
 Al-Zn-Mg-Cu 7075, improved fatigue resist. through thermomech. processing 3-64917

zinc alloys continued

- Al-Zn-Mg-Cu-Cr, as-cast, ingot processing effects on subgrain struct. 3-80264
 Al-Zn(10 at.%), structural features of decomposition process, X-ray diffraction (*Russian*) 3-41723
 Al-Zn(50 wt.%), supersaturated, precip. process, plastic deformation effects (*Polish*) 3-50690
 Al-Zn(9 at.%)-Ag(1 at.%), structural features of decomposition process, X-ray diffraction (*Russian*) 3-41723
 CaZn₅ type cryst. structure for Sm₂Co₁₇ high temp. phase 3-52600
 Cd-Zn, h.c.p., ordering, pseudopotential study 3-69195
 Cd-Zn, single crystals, crit. resolved shear stress, temp. and conc. depend. 3-58069
 Cd₂Zn_{1-x}Te semiconductor, cation interdiffusion, conc. and temp. depend. (*German*) 3-79532
 CeCu₂ type structure 3-58009
 Cu-Ni-Zn, high strength microduplex, characteriz. 3-64911
 Cu-Zn, α -phase, rigidity modulus, temp. depend. 3-69183
 Cu-Zn, bainitic $\beta \rightarrow \alpha$ transform, cryst. geom. obs. (*Russian*) 3-80205
 Cu-Zn, compositional modulation, absorpt. peaks rel. to band structure 3-55633
 Cu-Zn, dil., thermal cond., low temp., impurity and defect effects 3-68591
 CuZn, dilute, charge density oscillation parameters calc. at impurity 3-64302
 ErZn₂, antiferromagnetic, low temp. props. 3-79835
 Fe-Zn, diffusion of Zn into γ and α -iron 3-72840
 Fe-Zn, ferritic, cellular precipitation, kinetics (*German*) 3-44591
 α -Fe-Zn, precipitation behaviour, effect of Si, Ge, Sn and Cu, morphology and kinetics of precipitation (*German*) 3-72847
 Fe-Zn, thermodynamic props., distrib. of Zn between ferrite and austenite (*German*) 3-47356
 Fe-Zn diffusion couple, intermetallic compound formation kinetics, annealing, 240-320°C (*Japanese*) 3-76167
 Fe-Zn-Al system, phase constitution at 450°C 3-53208
 HoZn, mag. anisotropy 3-68801
 HoZn₂, magnetocrystalline anisotropy, applied field effect on sinusoidal mag. structure 3-60972
 SmZn₁₂, paramagnetic susceptibility, Curie-Weiss law 3-44198
 Sn-Zn, liquid eutectic, effect on drilling of refractories (*Russian*) 3-76311
 TbZn, mag. anisotropy 3-68801
 TbZn₂, magnetocrystalline anisotropy, applied field effect on sinusoidal mag. structure 3-60972
 Zn:transition metal alloys, Hartree-Fock theory of transition metal impurities in a semiconductor, comparison with expt. 3-60926
 Zn-Al, acoustic investigation of intercrystalline corrosion 3-69249
 Zn-Al (30 wt.%), solid soln. decomp. and superplasticity behaviour (*French*) 3-47418
 Zn-Al(40 wt.%), superplastic, basal plane pole figures 3-69220
 Zn-Cd (0.01 wt.%) sheets, dislocation damping and yielding phenomena 3-64927
 Zn-Cr, superconducting properties, critical temperatures and field, down to 0.037 K 3-41290
 Zn-Mn, cryst. field splitting and Kondo effect 3-52939
 Zn-Mn alloys, dil., low-temp. susceptibility 3-46991
 Zn-Mn superconducting properties, critical temperature and field, down to 0.037 K 3-41290
 Zn-Ti, hypereutectic, struct. controlling by unidirectional solidification (*Japanese*) 3-53206
 ZnAg phonon resistivity 3-79669
 ZnAl eutectoid alloy, in situ superplasticity expts., 1 MV electron microscope 3-50705
 ZnAl phonon resistivity 3-79669
 Zn₁₃Co, zeta phase, mag. susceptibility and transport props. 3-64477
 Zn₁₃Fe, zeta phase, mag. susceptibility and transport props. 3-64477
 ZnMn, dilute, film, Kondo resist. down to 0.35 K, lattice defect influence 3-52820
 Zn₁₃Mn, zeta phase, mag. susceptibility and transport props. 3-64477
 (Zn_{1-x-y}Hf_xTi_y)Zn₂ ferromagnets, itinerant weak, magnetic measurements, $0.05 \leq x, y \leq 0.2$, magnetisation, Curie temp. 3-52967
 ZrZn₂, itinerant ferromagnet, measurement of hyperfine field by s-d hybridization, detection by n.m.r. 3-64449
 ZrZn₂ intermetallic compound, very weak itinerant electron ferromagnet, theory and exptl. 3-68771

zinc compounds

- see also zinc alloys
 (35-x)NiO.8ZnO.xCoO.57Fe₂O₃, induced anisotropy in magnetic spectra, variation with amount of Co ions 3-47104
 acetate, irradiated single crystals ELDOR study, nuclear spin exchange influence 3-53326
 alkaline zinc electrolytes, deposition of Zn powder on steel, effect of foreign atoms 3-80556
 chalcogenides, structural transformation at high pressures (*German*) 3-52699
 dialkyl zinc, magneto-optical conformational analysis (*French*) 3-54609
 formate, Mossbauer investigation of cation position in mixture with iron formate (*German*) 3-79967
 metal-ZnS-metal structures, h.f. sputtered, capacity and loss tangent obs. (*French*) 3-58474
 monomethyl zinc radical, u.v. absorption spectra 3-46261
 phosphate glass, optical absorpt., molecular coordination struct. (*German*) 3-68163
 phthalocyanine, in n-decane matrix, multiplet struct. of quasiline spectra 3-72734
 porphyrin, in Shpol'ski hosts, optical and Zeeman studies 3-72737
 silicate glass, alkali, nucleation and crystallization properties 3-75476
 triphenylene:Zn porphyrin, low temp. optical absorption spectra 3-55653
 zinc phthalocyanine, photoconductivity induced by ruby and glass lasers, thermally stimulated current, drift mobility 3-50237
 p-ZnTe, free holes, spin-flip scattering, g-values 3-76018
 Ba₂ZnFe₁₂O₂₂, hexagonal ferrite, three-magnon linewidth in ferro-mag. reson. absorpt., effective exchange const. 3-55476

zinc compounds continued

- Cd_{3-x}Zn_xAs₂ solid solns. influence of pressure on electrical props. 3-79718
 CoO-ZnO-Al₂O₃-Cr₂O₃-Fe₂O₃ spinel solid soln., formation and colour variations (*Japanese*) 3-50763
 Cu-Zn ferrites, dielectric behaviour from -130° to +120°C 3-53055
 K(Ni, Zn)F₃, Heisenberg antiferromagnetic alloys, insulating, coherent potential approximation 3-55395
 Li_{1-x}Zn_xFe₂O₄ mixture, physical properties, comp. depend. 3-52846
 (Mn,Zn)F₂, dilute antiferromag., spin waves, coherent potential theory 3-47071
 Mn-Zn, ferrites nonstoichiometric, magnetic sublattices, nuclear gamma ray resonance study 3-52981
 MnZn ferrite, prep. conditions, effect on mag. props. 3-50760
 Mn₂Zn_{1-x}Fe₂O₄, low freq. mag. reson. observed in thermal change of permeability 3-64556
 Na₂ZnGeO₄, Franz-Keldysh effect in impurity absorpt. region 3-55553
 Ni-Zn ferrite, hot pressed, prep. and props. for mag. head applic. 3-44264
 Ni_{1-x}Zn_xFe₂O₄, high field Mossbauer study 3-79963
 Ta-Ta₂O₅-ZnS:Tb³⁺-Au, films 3-50626
 Ta-Ta₂O₅-ZnS:Tb³⁺-SiO₂-Au, films, electroluminescent, electron injection via tunnelling mechanism 3-50626
 Zn blende structure materials, third order elastic moduli, lattice interaction model 3-72117
 Zn complex, 2,2'-iminobis(acetamidoxime) zinc (II), n.m.r. study of barrier to rotation 3-52331
 Zn complex, metal pyridine tetracyanonickelate, i.r. and Raman spectra 3-63467
 Zn-Cl trigonal boracites, dielectric and thermal anomalies 3-79998
 Zn-Mn ferrites, estimation of Ca by X-ray fluorescence method 3-62340
 ZnAl₂O₄, Mossbauer study of magnetic hyperfine fields in Fe³⁺ ions 3-50498
 ZnAl₂O₄ spinel, equil. cation distrib., temp. depend. 3-55840
 Zn₃As₂, thermal expansion and phase transitions 3-68426
 Zn₃As₂-Cd₃As₂ interface, comp. profile, electron probe microanalysis 3-79549
 Zn₃As₂-Zn₃P₂ solid solutions, prep., semicond. props., X-ray anal., dilatometric meas. 3-79712
 Zn₂Cd_{1-x}S:Cu,Cl solid soln., peculiarities of recombination processes 3-52875
 Zn₂Cd_{1-x}Te mixed crystals, $0 \leq x \leq 1$, optical absorption measurements, 81K, 183K and 300K 3-53116
 Zn₂Cd_{1-x}Te, grown from melt, optical props. in lowest band gap region 3-69154
 Zn₂Cd_{1-x}Te, multiphonon resonance combination scattering spectrum at 77K 3-76022
 ZnCl₂ Cl K-X-ray absorption spectra, metal ionisation energies relationship 3-47324
 Zn(ClO₄)₂ aqueous solution, mag. moment of ⁶⁷Zn and shielding of Zn ions by water, n.m.r. obs. 3-79926
 ZnCr₂Se₄, Neel temp., hydrostatic press. effects 3-58377
 ZnF₂:Mn²⁺, zero-field splitting if 3d⁵ ions, anisotropic spin-orbit coupling contribution 3-55214
 ZnFe₂O₄, elastic constants from i.r. spectrum 3-64083
 ZnGa₂O₄, exchange interactions of nearest neighbour Cr³⁺ pairs, spectra obs. 3-53142
 ZnGeN₂, ordering of Zn, Ge atoms, neutron diffraction (*French*) 3-79314
 ZnGeP₂, calc. band struct. and reflectivity spectra 3-41135
 ZnGeP₂, chalcopyrite crystals, thermoreflectance spectra and energy band structure 3-44007
 ZnGeP₂, electrical props. of high resistance single crystals 3-44077
 ZnGeP₂, Hall effect, conductivity, hole mobility, temp. depend. 3-68625
 ZnGeP₂, wavelength modulation spectrum rel. to band structure 3-55625
 ZnGeP₂ phase relations of ZnP₂-Ge join, large crystal growth, directional solidification 3-72180
 ZnGeP₂ with pseudodirect energy gaps, band struct. 3-41136
 ZnGeP₂(As₂), band structure and modulation spectra, review 3-55205
 α -Zn(H₂O)₆SeO₄:Co, laevorotatory, cryst. struct. and absolute config. 3-40866
 Zn(II) complex, chelate of anthranilic acid, i.r. spectra, metal-ligand stretching frequencies 3-54688
 Zn(II) complex, ZnX₂ (X=Cl, Br, I) in tri-n-butylphosphate soln., vibrational spectra 3-75034
 Zn(II) complexes, organophosphoric anions, unit cell dimensions, chemical bonding (*French*) 3-75504
 Zn(II) complexes, organophosphoric anions, halogen, pseudohalogen perturbations i.r. and n.m.r. spectra (*French*) 3-75505
 ZnIn₂S₄ layer compound, switching and memory properties 3-64389
 ZnKAsO₄, crystal structure, isotopic with ZnKPO₄, hexagonal system (*French*) 3-40884
 ZnKPO₄, crystal structure, isotopic with ZnKAsO₄, hexagonal system (*French*) 3-40884
 ZnMn₂C, n.m.r. and neutron diff., mag. struct. changes (*French*) 3-79924
 ZnMn₂O₄, spinel structure, X-ray K-absorpt. edges of cations 3-44502
 Zn₂Ni_{1-x}Fe₂O₄, Yafet-Kittel canting angles, low-temp. Mossbauer obs. 3-47185
 ZnO, adsorption of H₂, temperature programmed desorption study 3-68503
 ZnO, adsorption of NO 3-41091
 ZnO, diffusion of O, by proton activation analysis of ¹⁸O 3-64208
 ZnO, dispersion of nonlinear refractive index 3-75959
 ZnO, e.p.r. of chemisorbed O₂ 3-43942
 ZnO, elec. cond. in atomic N, recombination-adsorpt. model (*Russian*) 3-75740
 ZnO, epitaxial growth on sapphire and spinel, vapour phase deposition 3-80164
 ZnO, extended defects rel. to nonstoichiometry, transmission electron microscope obs. 3-79333
 ZnO, i.r. absorption by acoustoelectric domains 3-72617

zinc compounds continued

- ZnO, modulation spectroscopy, surface electron states photoconductivity 3-55323
- ZnO, phosphor, kinetics of radical recomb. luminesc. with N excitation (*Russian*) 3-80091
- ZnO, photoproduced holes in oxidation of organic compounds 3-41100
- ZnO, pseudopotential method of computing band structure, density of states and reflectivity 3-64292
- ZnO, reson. second harmonic generation in exciton region, freq. depend. 3-51956
- ZnO, spontaneous and stimulated emission, free, bound exciton form. (*German*) 3-58529
- ZnO, surface state spectroscopy, modulated photoconductivity measurements 3-55325
- ZnO, thermal conductivity, thermal comparator measurement 3-72240
- ZnO (0001) surfaces, electronic and structural characteristics 3-79756
- ZnO aqueous suspensions, reproducible e.s.r. spectra 3-75872
- ZnO film, epitaxially grown, electro-optic and acousto-optic interactions 3-47228
- ZnO film, prep. by cold plasma condensation, growth kinetics (*French*) 3-52772
- ZnO powder, logarithmic time law for adsorption of O₂ (*German*) 3-64239
- ZnO powder, photosorption capacity, rel. to O₂, apparatus (*Russian*) 3-48572
- ZnO sputtered films, diagnostic rate monitoring by interference spectroscopy 3-45418
- ZnO thin films, dye sensitised, photoresponse, self-quenching effect 3-46871
- ZnO thin layers as u.s. transducers, prep. (*German*) 3-53193
- ZnO whiskers, antiphase boundaries, transmission electron microscope obs. 3-79597
- ZnO:Ag,Cl phosphors, photolum. emission characts. 3-69056
- ZnO:Ga scintillation screen, for detection of fission fragments 3-48527
- ZnO:Li, photo-induced persistent internal quadrupole moment 3-46876
- ZnO:Li thermal conductivity, doped and undoped crystals, 1.1 to 300 K, anisotropy, Debye-Calloway model analysis 3-43907
- ZnO-Bi₂O₃ ceramics, nonohmic, microstructure, phases, elec. props. 3-80416
- ZnO-Li₂O-SiO₂, glass-ceramic, high temp. creep, tension, compression 3-76319
- ZnO-Li₂O-SiO₂, glass-ceramic, compression creep and recovery, 590-750°C 3-76320
- (Zn-MgO):Fe(O), photoconductor, thermally stimulated current curves for different cooling schedules 3-46883
- 2Zn(OH)₂.Zn(NO₃)₂, crystal structure, least squares refinement (*French*) 3-60697
- Zn(OH)₂.Zn(NO₃)₂.2H₂O, structural investigation (*French*) 3-63990
- xZn(OH)₂.yZn(NO₃)₂.zH₂O, structural classification (*French*) 3-60696
- ZnO(0001) surfaces, electronic and structural characteristics, photoconductivity 3-68689
- ZnO(0001), polar surfaces, contaminated, LEED, AES and X-ray photoelectron spectroscopy obs. 3-75653
- ZnO(c), heat capacity meas., 298-1800 K, drop calorimetry and differential scanning calorimetry 3-46717
- ZnP₂, edge absorpt. spectrum at 4.2K 3-44424
- Zn₃P₂-Cd₃As₂ solid-solution, semiconducting, preparation, physical and electrical properties 3-53188
- Zn₃P₂-Zn₃As₂ solid solutions, prep., semicond. props., X-ray anal., dilatometric meas. 3-79712
- Zn(S, Se):I annealed in liquid Zn, resistivity and photoluminescence 3-58544
- ZnS, anomalous photovoltaic effect 3-44111
- ZnS, crystal growth, thermal treatment in H₂S, scanning electron microscopy 3-80166
- ZnS, dispersion of nonlinear refractive index 3-75959
- ZnS, effect of firing atm. on rate of cubic-hexagonal transformations 3-43873
- ZnS, effective charges and lattice dynamics, zone-boundary phonon freq. calcs. 3-40994
- ZnS, growth by chemical transport in I₂ 3-44526
- ZnS, ion implantation, annealing, luminesc., cond. change 3-72817
- ZnS, optical and thermal depth of shallow traps 3-60860
- ZnS, photolum., visible region, electron irradi. effects 3-47318
- ZnS, polytype form., layer transposition mechanism inapplicability 3-54947
- ZnS, polytypes and stacking faults, TEM obs. 3-58044
- ZnS, spontaneous and stimulated luminescence excited by multiphoton optical pumping 3-58557
- ZnS, structure of stimulation spectra and trap processes (*Russian*) 3-76059
- ZnS, thermal conductivity, thermal comparator measurement 3-72240
- ZnS, thermal stability of S vacancies, determ. using e.s.r. absorption of F-centres (*Russian*) 3-75881
- ZnS, two-photon photocond., spectral and intensity-depend. meas. 3-41229
- ZnS, undamaged and ion implanted, depth resolved cathodoluminesc. obs. 3-58567
- ZnS, wurtzite, single cryst. elastic const. and anharmonic props., pressure depend. 3-58063
- ZnS and cryolite contrast dielec. narrow-band interference filters, half-width 1 to 3 nm, optical props. 3-42577
- ZnS film, dielec. props., temp. and freq. depend., 78-380 K and 10²-10⁵ Hz 3-41474
- ZnS film, on Sb, thickness and dispersion meas., ellipsometric method 3-62049
- ZnS film, piezoelec., surface elastic wave motion computer analysis (*Japanese*) 3-41482
- ZnS phosphors, surface energy losses, electron and hole diffusion (*Russian*) 3-44462
- ZnS thin films, 1.08μ laser radiation damage 3-59881

zinc compounds continued

- ZnS wurtzite and zincblende structures, electronic charge density, empirical pseudopotential method 3-41117
- ZnS:(In, Cu), energy storage, thermoluminescence 3-76103
- ZnS:Ag, Cu phosphor, spectral response to fast ions 3-50628
- ZnS:Ag/ZnS.CdS:Ag/Bi₂S₃ luminescent screens, spectral characteristics (*Russian*) 3-50623
- ZnS:Cu, blue luminescent centre, emission mechanism 3-44436
- ZnS:Cu, cubic and hexagonal, thermoluminescence glow curves (*German*) 3-69103
- ZnS:Cu, electrolum. spectra, effect of exciting frequency and temperature 3-80112
- ZnS:Cu, electroluminescence comets, scanning with needle electrode 3-76096
- ZnS:Cu, gamma ray and u.v. irradiation, electron-hole pair production (*Russian*) 3-76056
- ZnS:Cu, photoelectrolum., u.v. flux and appl. voltage amplitude and freq. depend. 3-58565
- ZnS:Cu, polycryst., memory of Gudden-Pohl effect of three kinds (*Russian*) 3-72759
- ZnS:Cu, relations between luminesc. centres and electron traps (*Polish*) 3-58552
- ZnS:Cu,Cl films, Franz-Keldysh effect in electroluminescence 3-80114
- ZnS:Cu,Co phosphor, phosphoresc. decay obs. of trap distrib. (*French*) 3-80089
- ZnS:Cu,Cr,Cl, Cr⁺ centres, luminescence 3-76101
- ZnS:Cu,Fe(Co,Ni)O, rise, decay and temp. depend. of photocurrents 3-46867
- ZnS:Cu,H phosphors, double band electrolum., synthesis and emission characts. 3-69095
- ZnS:Cu double band electroluminescence, emission, freq. depend. 3-72756
- ZnS:Cu electroluminescence, effect of applied-field frequency on comet length, Fischer model 3-50627
- ZnS:Cu monocrystals, shift in band maxima with temp. (*Russian*) 3-72722
- ZnS:Cu(Bi), thermoluminescence energy meas., alpha and gamma irradiation at 100 to 700 K (*Russian*) 3-76100
- ZnS:Cu(Mn), radical-recomb. luminesc., temp. depend. of stationary intensity (*Russian*) 3-44448
- ZnS:Er³⁺ film, electrolum., impact excitation by hot electrons 3-80111
- ZnS:I, single cryst., mass spectrometry and luminescent props. 3-64745
- ZnS:Mn, Cu, Cl electroluminescent films, electron diffraction study of Cu-rich layer 3-47315
- ZnS:Mn, Cu, phosphor, d.c. electroluminescence, brightness, efficiency 3-58563
- ZnS:Mn film, ion implanted for electroluminescent cell fabrication 3-41588
- ZnS:Mn powdered phosphor, d.c. electroluminescence, pulse response 3-61075
- ZnS:Mn, thermally stimulated e.m.f. with trap-filling gradient 3-64363
- ZnS:Te, isoelectronic traps, bound states in forbidden energy gap 3-58226
- ZnS/MgF₂ laser mirrors, periodic multilayer dielectric systems, normal incidence, reflectivity, design formulae and graphs 3-45505
- ZnS-CdS:Cu, effect on protons on radical recombination luminescence, radiation defects 3-53152
- ZnS-Cu, ZnS-Mn, photoluminescence, depth and frequency factor of traps determ. by u.v. amplitude modulated excitation 3-41570
- ZnS-Cu electroluminescence, brightness wave properties (*Russian*) 3-41583
- ZnS-Cu luminophore, photoluminescence, effect of milling 3-80086
- ZnS-Cu phosphors, relaxation of space charge during electroluminescence (*Russian*) 3-80109
- ZnS-MgF₂ optical coating of variable refr. index, prep. and props. 3-62093
- ZnS-Mn²⁺, excitation and emission spectra, lines due to stacking faults 3-50619
- n-ZnS-p-GaAs, heterojunctions, negative resistance at 77 to 293 K (*Russian*) 3-79761
- ZnSO₄.7H₂O, isomorphism, M²⁺.SO₄.7H₂O series, M=Mg, Zn, Ni, Fe, Co (*German*) 3-52613
- ZnSO₄.7H₂O:Cu²⁺ e.p.r. spectra as function of orientation of mag. field 3-64549
- ZnS(Se)(Te), isothermal bulk modulus, calc. 3-72116
- ZnSe, critical binding of exciton to donor-acceptor pair, Coulomb interaction 3-79652
- ZnSe, donor-acceptor pair recomb. obs. of electro-luminescence edge emission 3-80110
- ZnSe, electro-optical effects (*French*) 3-58492
- ZnSe, electroluminescence in reverse-biased Schottky diodes 3-58564
- p-ZnSe, Hall and drift mobility 3-79716
- n-ZnSe, light emission from hot electrons, band structure 3-72758
- ZnSe, optical material, chemical vapour deposition production techniques 3-77470
- ZnSe, pair spectra and shallow acceptors 3-58555
- ZnSe, plastic deformation, electric field effects, temp. depend. 3-58071
- ZnSe, thermal conductivity, thermal comparator measurement 3-72240
- ZnSe, vaporiz., mass spectrometric obs. 3-68402
- ZnSe:Mn, luminescence, excitation and emission spectra obs. at 85K 3-61064
- ZnSe:Mn, luminescence origin 3-53147
- ZnSe:Mn⁺⁺ splitting, fine structure of 4E level, uniaxial stress method 3-47295
- ZnSe:Ti, autoionisation of ³Ti(P) state, photoconductivity meas. and absorption spectra 3-64375
- ZnSe-GaAs solid solutions, prep., props of epitaxial layers 3-75685
- ZnSe-ZnTe n-p heterojunction, blue electrolum. 3-64740
- p-ZnSiAs₂, growth by vapour transport 3-61112
- p-ZnSiAs₂ crystals, conductivity in high temp. region 3-52842
- ZnSiF₆.6H₂O, cryst. field splitting of Fe²⁺ ion, Mossbauer obs. 3-55506

zinc compounds continued

- ZnSiO₄:Mn, radical-recomb. luminesc., temp. depend. of stationary intensity (*Russian*) 3-44448
 p-ZnSiP₂, conductivity, Hall effect, mobility, temp. depend. 3-68624
 ZnSiP₂ with pseudodirect energy gaps, band struct. 3-41136
 ZnSiP₂-ZnSiAs₂ range of semiconductors, optical absorption edges at 300 K and 80 K 3-55604
 ZnSiP₂(As₂), band structure and modulation spectra, review 3-55205
 ZnSnAs₂, decomp. under high press., SnAs₂ supercond. transition temp. 3-41022
 (Zn_{1-x}Sn_x)Mn₂C, solid solns., magnetic, crystallographic properties (*French*) 3-79836
 (Zn_{1-x}Sn_x)Mn₂C solid soln., mag. and crystallographic behaviour, comp. depend. (*French*) 3-47050
 p-ZnSnP₂, electrorefl. spectra, 1.5-4.5 eV, 77 and 295 K 3-44430
 ZnSnP₂(As₂), band structure and modulation spectra, review 3-55205
 ZnTe, band structure, fundamental reflectivity spectra (*Polish*) 3-41132
 ZnTe, deep traps, elec. and photoelec. obs. 3-68673
 ZnTe, exciton effect in electrorefl. spectra 3-64678
 ZnTe, exciton spectrum, reflectivity phase determ. by modulated piezoreflectance 3-53887
 ZnTe, film, non-polarised memory switching characs. 3-68683
 ZnTe, frequency dependence of electrical conductivity 3-64364
 p-ZnTe, Hall and drift mobility 3-79716
 ZnTe, photoemission and density of valence states 3-69138
 ZnTe, photolum. at 77-295K, obs. of seven bands from green to i.r. 3-61073
 ZnTe, thermal conductivity, thermal comparator measurement 3-72240
 ZnTe, vibr. normal modes, freq. wave vector dispersion relations 3-52680
 ZnTe photoluminescent excitation intensity, direct meas. of nonlinear dependence 3-51613
 ZnTe thin films, electron irradiation effect on crystalline struct. 3-52771
 ZnTe thin films on GaAs, InAs and GaP, epitaxially grown heterodiodes 3-44138
 ZnTe vacuum evaporated film conductivity rel. to substrate temp. (20 to 440°C) and ambient atmosphere 3-58324
 ZnTe:Cu, impurity and native defect levels determ. 3-41153
 ZnTe-CdSe heterojunction, growth, elec. props., interface parameters 3-68698
 ZnTe-CdSe heterojunction, photoelec. and luminesc. props. 3-79767
 ZnTe-CdTe solid solutions, negative photocond., field depend. (*Russian*) 3-72383
 ZnTe-Ge heterojunction, irreversible switching of conductivity states 3-68702
 ZnTe-ZnSe heterojunction, electrolumines., red and green emission (*French*) 3-53151
 ZnV₂O₄, spinel, reciprocal mag. susceptibility, mag. structure, neutron diffraction patterns 3-60969
 α-Zn₂V₂O₇, crystal structure and refinement 3-49875
 ZnWO₄, e.s.r. spectrum of Fe³⁺ at low concentrations, superhyperfine structure 3-41404
 ZnWO₄:Co²⁺, monoclinic, spin-lattice relax., conc. and freq. depend. 3-50453
 ZnWO₄:Cr³⁺ single crystal, optical absorption, luminescence spectra 3-76070

zirconium

- allotropic α-β transform. kinetics (*Russian*) 3-53201
 atom, photoelectric cross section for 145 keV gamma rays 3-49406
 chemical analysis, review 3-59695
 compression of single crystals, parallel to c-axis, 78-1100 K 3-46659
 diffusion of oxygen, using ¹⁸O(p,α)¹⁵N reaction (*Russian*) 3-58142
 elastic parameters of single crystals, oxygen effects 3-76204
 electron probe microanalysis, mass absorption coeffs. for CuLa_x line (*Japanese*) 3-57022
 high-pressure treated, orientation reln. between α- and ω-phases 3-72876
 neutron irradi., resist. changes, recovery changes 3-69288
 neutron irradi. at 24K, point defect creation and elimination (*French*) 3-52643
 neutron irradi. growth behaviour, cold work and stress-relieving effect 3-41773
 nuclear reactor material, void formation under irradiation in high-voltage electron microscope 3-78387
 oxidized, wear in water, characteriz. 3-57573
 phase transformation, α→ω, hysteresis, T-P diagram (*Russian*) 3-44560
 phases and compressibility up to 120 kbars 3-72833
 physical properties of ω-phase (*Russian*) 3-79665
 pre-exponential factor in rate eqn. for plastic flow 3-46662
 precipitation of hydrogen, resistometric obs. 3-64875
 sorption of O₂, kinetics, at very low press. 3-55140
 stress relaxation data interpret. 3-64926
 surface, polycryst., oblique Ar⁺ bombardment in 1 keV range, sputtering yield, ion incident angle depend. (*German*) 3-47342
 texture in cold-rolled sheets, neutron diff. determ. 3-64847
 α-Zr, electric field grad. at Ta in group IV B metals 3-58457
 ω-Zr, electric field grad. at Ta in group IVB metal 3-58459
 α-Zr, h.c.p., electron diffraction patterns 3-49872
 Zr-O₂ system, quasi-equilibrium approach to combustion 3-58793
 Zr(IV) complex, acetylacetonate, tetrahedral, octahedral and cubic complexes, dielectric relaxation 3-55520

zirconium alloys

- see also zirconium compounds
 b.c.c., with ω-phase, short-range struct., diffraction pattern interpretation 3-79198
 corrosion films, thinning for transmission electron microscopy exam (*German, English*) 3-61157
 electrical resistivity, exponential temp. dependence, rel. to Brillouin zone 3-44051
 electrochemical properties and oxidation, in molten salts at 300-500°C 3-72918

zirconium alloys continued

- Nb-Zr(1%), fast reactor neutron irradi., effect on tensile props. 3-79386
 neutron irradi., stress-relax. rel. to creep rates 3-40541
 nuclear reactor material, void formation under irradiation in high-voltage electron microscope 3-78387
 pressure tubes, creep, effect of neutron flux anisotropy rel. to stress directions 3-67565
 stress relaxation data interpret. 3-64926
 Zircaloy, hydrogen supercharging during corrosion 3-44610
 Zircaloy, stress corrosion cracking behaviour in iodine vapour 3-43297
 Zircaloy clad UO₂ fuel rods, fuel performance, hydride attack 3-67570
 Zircaloy cladding, high temp.-testing for use as thermocouple sheath in PWR 3-47431
 Zircaloy tubing, u.s. inspection, wall thickness and ID meas., multiplexed instrumentation 3-47516
 Zircaloy-2, accelerated oxidation in steam at high pressure following heat treatment 3-71300
 Zircaloy-2, corrosion of oxide layer, subsurface pitting, stress cracks 3-80387
 Zircaloy-2, meas. of total neutron cross section, 0.4 to 2.4 MeV 3-60285
 Zircaloy-2, morphology of thick oxide films 3-43951
 Zircaloy-2, neutron irradi. growth behaviour, cold work and stress-relieving effect 3-41773
 Zircaloy-2, oxidized, wear in water, characteriz. 3-57573
 Zircaloy-2, quenched, strain ageing behaviour 3-58665
 Zircaloy-2, quenched and aged, vacancy precip. phenomena 3-80231
 Zircaloy-2, stress corrosion cracking in neutral aqueous chloride solns., 25°C 3-69260
 Zircaloy-2, thermal diffusivity meas., rel. to stainless steel and Hf, thickness effect 3-44556
 Zircaloy-2 corrosion in flowing water and steam, 310-320°C (*Japanese*) 3-71280
 Zircaloy-2 oxide film, heat transfer characs. 3-60278
 Zircaloy-2 pressure tubes, Hanford N reactor, monitoring, changes in material props., H content 3-67564
 Zircaloy-4, β-α phase transform. 3-47361
 Zircaloy-4 clad UO₂, fuel performance, C-E, KWU pressurised water reactors 3-67571
 Zircaloy-4 spacers, vacuum soldering process (*German*) 3-72930
 Zircaloy-H system, hydride precip., resistometric obs. 3-64875
 Zr/steel rolled joints, hydriding and protection in reactors 3-57572
 ZrH₂U fuel elements, release of fission product Xe 3-63122
 Al-Mg-Li 01420 alloy with Zr, microstruct. 3-55783
 Al-Zr, grain refinement by metastable phases 3-55793
 Cu/Zr-Nb and Cu/Zr-Cu diffusion couple behaviour, intermediate phase props. (*Japanese*) 3-58612
 Cu-Cu₂Zr eutectic, microhardness, depend. on indenter/lamellar relative orientation 3-47459
 Cu-Cu₂Zr eutectic, tie-line cond. and tensile props. 3-47409
 Cu-Cu₂Zr pseudobinary eutectic, tie-line cond. and tensile props. 3-47409
 Cu-CuZrSi eutectic, microhardness, depend. on indenter/lamellar relative orientation 3-47459
 Cu-Zr, interactions of impurity atoms with dislocations in dilute copper solutions (*Russian*) 3-72131
 Mo-Zr, grain coarsening during high temp. creep 3-64940
 Nb-W-Mo-Ti-Zr-C, quenching, ageing, carbide precipitation hardening 3-76176
 β-Nb-Zr, deform. temp. depend., slip, twinning and dislocations rel. to yield and fracture 3-52662
 Nb-Zr, interdiffusion, prolonged heating, X-ray microanal. (*Russian*) 3-69250
 Nb-Zr, solubility and diffusivity of H isotopes at high temps., reln. to CTR components 3-61161
 Nb-Zr, steady-state creep, Zr conc. depend. (*Russian*) 3-58642
 Nb-Zr (1 wt.%) alloy, sp. heat, electrical resistivity and hemispherical total emittance determination 3-64971
 Nb-Zr wire to Pb-Sn solder, blob junction, self-field effects on Josephson supercurrent 3-52934
 Nb-Zr(1%), neutron irradi. temp. effect on hardness 3-79387
 Ti-Mo-Zr-Sn, β_{III}, isothermal transforms. (*French*) 3-80203
 Ti-Zr, wear resist. in H₂O, increase by oxide surface layer formation 3-58697
 UO₂ fuel rods with Zr alloy cladding, manuf., present state in Germany (*German*) 3-43285
 UO₂-in-Zircaloy fuel assemblies, performance in CANDU reactors, Canada 3-67568
 Zr-Al, quenched and aged, vacancy precip. phenomena 3-80231
 Zr-Cr-Nb, effect of heat treatment on tensile strength and hardness 3-61165
 Zr-H, γ- and δ-phase hydride form. on cooling from α-phase field 3-72864
 Zr-H system, γ-phase formation by peritectoid reaction 3-58617
 Zr-Nb, carbide-oxide reaction prep. 3-72821
 Zr-Nb (19 wt.%), transform. and age hardening behaviour 3-47412
 Zr-Nb (20 at wt.%), Mossbauer scatt. study of solid state phase transformations 3-55068
 Zr-Nb alloy preparation by carbide-oxide reaction, nuclear reactor use 3-60279
 Zr-Nb(2.5 wt.%), neutron irradi. growth behaviour, cold work and stress-relieving effect 3-41773
 Zr-O(8.5 at.%), fracture surface behaviour 3-47375
 Zr-Ti-Nb, superconductor, welding, reduction of current degradation 3-41788
 Zr₂Al₃, fast neutron irradi., disordering 3-49909
 ZrFe₂, thermal expansion rel. to Curie temp. pressure depend. 3-58385
 (Zr_{1-x-y}Hf_xTi_y)Zn₂ ferromagnets, itinerant weak, magnetic measurements, 0.05 ≤ x, y ≤ 0.2, magnetisation, Curie temp. 3-52967
 ZrU fuel elements, release of fission product Xe 3-63122
 ZrV₂, supercond., acoustic wave velocity meas., lattice instabilities 3-79801
 ZrZn₂, itinerant ferromagnet, measurement of hyperfine field by s-d hybridization, detection by n.m.r. 3-64449

zirconium alloys continued

ZrZn₂ intermetallic compound, very weak itinerant electron ferromagnet, theory and exptl. 3-68771

zirconium compounds

see also zirconium alloys

- group II element cpds., X-ray K-absorpt. edges, band electrons mean free path (Russian) 3-80119
- zircon morphology, crystallographic indicator 3-52592
- Al₂O₃-ZrO₂ eutectic, directionally solidified, fracture surface energies 3-72937
- CeO₂-ZrO₂-CoO system, fluorite type phase obs. (French) 3-64183
- Cs₂ZrBr₆·Os⁴⁺, absorpt. and mag. circular dichroism spectra, 17000 to 31000 cm⁻¹ 3-44437
- Ti-Zr-H system Knight shift obs., temp. depend. 3-79932
- TiC-ZrC system, monochromatic emittance, 1800K, comp. depend. 3-52703
- W-Ta-ZrC alloy, recrystallization, deformation depend., microstructure 3-76334
- WC-ZrC system, phase equil. and microstruct. 3-72939
- Zr alkali borosilicates, crystallochemical features, stereometrically mixed framework 3-72063
- Zr-As-S(Se)(Te) system ternary cpds., cryst. chem. (French) 3-46630
- Zr₂.₀₀As₂.₈₆Te_{0.92}, quadrat. cryst. structure obs. (French) 3-52605
- ZrB₂/metal and ZrB₂/SiC/C composites, hot-pressed, fracture surface energies 3-76232
- ZrB₂-HfN ceramics, cutting tool material, densification, microstructure, wear resistance 3-50758
- ZrBr₃, pyrolytic, thermal diffusivity at high temps. 3-61200
- ZrBr₄(Cl₄)(F₄)(I₄), orbital valence force field consts. 3-67768
- ZrC, nonstoichiometric, C distrib. change during creep tests, laser microanalyser 3-72977
- ZrC, reaction with Re, phase equil., high temp. 3-72978
- ZrC, solubility of O₂, X-ray diffraction 3-41804
- ZrC, with Pt and Ir additives, thermionic emission 3-69131
- ZrC, ZrN, ZrO, heat of formation calc. 3-43878
- ZrC and ZrC-B alloys, arc melting and homogenization 3-80430
- ZrC neutron irradiation effects on structure, properties 3-73016
- ZrC-C pseudobinary system, phase equilibrium relation 3-53270
- ZrC_{0.94}, single crystals, microhardness, temp. depend., room temp. through ductile-brittle transition 3-47446
- ZrC_{0.98}, sintered, galvanomag. props., 300 and 20.4 K (Russian) 3-50222
- ZrCl₆²⁻, force consts. and mean vibr. amplitudes 3-67771
- ZrF₄-alkali fluoride systems, melts and polycryst. solids, Zr(IV) fluoride complex ions, Raman spectra 3-72614
- ZrH_{1.97}, positron annihilation, proton model 3-50131
- ZrH₂ modified Fe single crystals with C and N in soln., low temp. mech. props. 3-58696
- ZrH₄, heavy formations, rel. to damage to BWR fuel elements (German) 3-67610
- α-Zr(HPO₄)₂·H₂O, crystalline, prep. and characterisation 3-55730
- ZrMnGe, Co₂P structure, crystallographic data, metal-metal bonding 3-79315
- Zr(MoO₄)₂, crystn. from soln. in Li₂O-MoO₃ melt, form., struct. 3-75486
- ZrO₂, antireflection coatings, moisture resistant, vac. evaporation 3-62074
- ZrO₂, calcia-stabilized, fluorite type solid soln., ordering (French) 3-72991
- ZrO₂, castable, elec. resist. from 900-1700K, calcia stabilisation rel. to furnace appl. 3-52832
- ZrO₂, comparison with HfO₂ systems, transition temps. (French) 3-72993
- ZrO₂, crystallisation, X-ray diffraction and electron microscope studies (Japanese) 3-80432
- ZrO₂, elec. cond. and thermoelec. force, 1000 to 1700°C, 1 to 10⁻¹⁶ atm. O₂ partial pressure (German) 3-68604
- ZrO₂, form., decomp. of rare earth oxide solid solns. 3-76314
- ZrO₂, mixtures of crystal forms, X-ray phase anal., URS-50IM diffractometer 3-53269
- ZrO₂, monoclinic, e.s.r. experiments of Gd³⁺ ions 3-47139
- ZrO₂, monoclinic-tetragonal transition, high temp. obs., twin form. 3-72931
- ZrO₂, partially stabilized with calcia, SiO₂ role in sintering 3-69346
- ZrO₂, photoluminescence spectra of powder (Russian) 3-64737
- ZrO₂, porous powder compact specific surface area, pore struct. rel. to compaction, adsorpt. obs. 3-41801
- ZrO₂, resistance to crack propagation, thermal shock 3-76322
- ZrO₂, Sc₂O₃-stabilized, high temperature neutron diffraction, phase equilibrium studies 3-64150
- ZrO₂, stabilized solid electrolyte, use as O₂ source and sensor in ultrahigh vacuum 3-73713
- ZrO₂, trace element spectrochemical analysis (Polish) 3-73955
- ZrO₂, X-ray fluorescence determ., rel. to physical methods of chem. analysis (French) 3-70468
- ZrO₂, Y₂O₃ stabilized, current-blackened single crystals, dielec. consts. and loss tangent 3-79972
- ZrO₂, yttria stabilised, current blackening, optical absorpt. study 3-47449
- ZrO₂, yttria stabilized, high temp. creep parameters 3-72951
- ZrO₂, yttria-stabilized, fast neutron damage effects 3-78373
- ZrO₂ coatings, thickness meas. by X-ray diffr. 3-73676
- ZrO₂ crystal growth by localized cooling method using Na₂B₄O₇-KF flux 3-44538
- ZrO₂ in Mo alloy, form. on grain-, sub-boundaries and within grains during annealing (Russian) 3-76161
- ZrO₂ microspheres preparation, CaO stabilization, sol-gel process 3-72992
- ZrO₂ oxygen-pump die for hot pressing 3-76256
- ZrO₂ systems, defects ordering phenomena, vacancies, X-ray study (French) 3-76335
- ZrO₂:Ca²⁺, Raman scatt., massive point defect behaviour 3-68975
- ZrO₂:Ce⁴⁺, Pr⁴⁺ and Tb⁴⁺, electron transfer spectra 3-55655
- ZrO₂:Er³⁺, Y₂O₃-stabilised, absorpt. spectrum, O²⁻ coordination, crystal structure 3-41539
- ZrO₂/Mo, sintered cermet, elec. cond., 20-1700°C (German) 3-76308

zirconium compounds continued

- ZrO₂/W and ZrO₂/ZrO₂ fibre composites, thermal shock resist. 3-76353
- ZrO₂-Al₂O₃-BaO subsolidus structure, fusibility 3-72177
- ZrO₂-CaO, elec. cond. and thermoelec. force, 1000 to 1700°C, 1 to 10⁻¹⁶ atm. O₂ partial pressure (German) 3-68604
- ZrO₂-CaO-SiO₂, new oxide glass, form. by laser spin melting and free fall cooling 3-68168
- ZrO₂-CeO₂-CoO system, elec. cond., rel. to cryst. struct., meas. 3-72997
- ZrO₂-Er₂O₃(La₂O₃)(Y₂O₃) cubic solid soln. stability below 1500°C (French) 3-76309
- ZrO₂-MgO system, directional solidification and oriented eutectic composite behaviour 3-76236
- ZrO₂-Y₂O₃ solid soln. chem. vapour deposition and characteriz. 3-76234
- ZrO₂-Zr₂La₂O₇, eutectics melting point, use as secondary temp. standard above 2327K (French) 3-51550
- ZrO₂-CaO₂UO₂, fuel element for TREAT convertor 3-63219
- Zr(OH)₄, granulated, sorption of B and Si from Black Sea (Russian) 3-80698
- β-ZrO₂.12Nb₂O₅, cryst. struct., high resolution electron microscope obs. 3-43777
- ZrS₂, layer type structure, electronic props. of two dimensional solids 3-50133
- ZrS₂ with alkali metal insertions, cryst. chem. (French) 3-46635
- ZrS₂, layer trichalcogenide semiconductor single crystals, growth, optical absorption, simple model 3-44428
- Zr₃Se_{2-x}, growth conditions and crystal structure parameters 3-68235
- ZrSi₂, application as anti-emission materials (French) 3-59573
- ZrSiO₄, anharmonicity in silicate crystals, temp. depend. of A_u vibr. modes 3-79449
- ZrSiO₄, anisotropic thermal expansion and compressibility, high temp. and high pressure X-ray diffraction, neutron diffraction 3-46721
- ZrSiO₄, e.p.r., defect anion radical traps struct. 3-68843
- ZrSiO₄, plasma sprayed, reheating, pore contraction 3-76332
- ZrSiO₄, sintering, TiO₂ addition effects (Japanese) 3-80436
- ZrSiO₄:Ti³⁺, electron spin resonance 3-79904

zodiacal light

see also sky brightness

- Apollos 11-16 results, review 3-45046
- brightness and polarisation meas. from ecliptic to poles 3-56369
- circular polarisation by single scatt. of unpolarised light from lossless nonspherical particles 3-51318
- diffuse Galactic light polarisation meas. 3-56430
- gegenschein obs. from Pioneer 10 imaging photopolarimeter 3-45074
- inner, brightness and linear polarisation meas. during 1972 July 10 solar eclipse 3-47881
- i.r. spectrum 3-81017
- night sky radiation, obs. of linearly polarised radiation in anti-solar hemisphere 3-61753
- photometric obs. from space, OSO-6 meas. 3-53630
- photometric perturbation in Earth-Moon system 3-53631
- reinforcement at 100 R_e from sun, photometric obs. and deductions (French) 3-69913
- surface brightness meas. from 2.4 microns balloon-borne obs. 3-51319
- temporal constancy obs. 3-76984

zonal heating see atmospheric thermodynamics

zone melting and refining

see also crystal growth

- Alnico-8 magnet alloy, zone melting conditions influence on mag. props. (Japanese) 3-50724
- aromatic hydrocarbon, efficiency of method 3-41641
- chromatography apparatus, metal chelate separation 3-64786
- impurity elimination due to additive and constitutional supercooling phenomena (French) 3-47417
- irregular eutectics, effect of zone refining on structure 3-80175
- optical zone melting, growth of single oxide crystals, light oven design, techniques (German) 3-64784
- rare earth oxide/metal composites, unidirectional solidification 3-76347
- refractory metals, preparation of bicrystals, controllable orientations, zonal melting technique 3-80174
- solid-phase impurity diffusion and influence of separating impure end 3-41640
- stability of zone melting with temp. gradient 3-80177
- temperature distribution in thin films (Russian) 3-55174
- Cu alloy rods, binary, crystn. characts. determ. by temp. meas. during zone melting (German) 3-55763
- CuNi-Sn alloys, directional solidification melt vs. cryst. comp., ternary distrib. coeffs. (German) 3-55762
- GaP crucible-free zonal melting, installation, description 3-80173
- Ge, motion of Ge-Au alloy droplet along surface under temp. gradient 3-76137
- Ge epitaxial layer on Si substrate (Russian) 3-55735
- Nb bicrystals, using Y-shaped seed from partially split single crystal 3-69160
- Nb-W, Ta, impurity redistrib. by electron beam float zone refining 3-44540
- Sb₂Se₃, high-resistivity, prep. by two-step refining process 3-61116
- Si, characts. of [115] dislocation-free float zoned crystals 3-50664
- Si, dislocation free crystals, float-zoned, dislocation generation along swirls, thermal oxidation 3-41648
- Si, dislocation-free crystals, distribution of point defects Cu decoration, X-ray topography, etching 3-41650
- Si, float zone crystals, gas doping 3-58601
- Si, float-zone growth, resistivity topography rel. facet growth 3-41646
- Si, float-zoned crystals, growth striations and swirls, electron microscopy 3-41649
- Si, growth by internal work coil float zoner 3-64796
- Si:Sb(P), (Au), zone refined, distribution of impurity elements, quantitative autoradiography 3-41651
- Si-Al-Au alloy, conc. depend. of motion, crystn. rate, temp. gradient 3-68176
- TiC, single cryst., prep. by r.f. floating zone process 3-53186

zone melting and refining continued

TlTe, horizontal zone melting, single crystal 3-80176

zone plates *see light diffraction***zone refining** *see zone melting and refining***zoology**

alert monkey, accommodative vergence, motor unit analysis 3-66008

animal coats, thermal radiation and structure 3-53734

Asian 'clawless' otter, underwater vision and visual acuity 3-65991

bats, auditory systems, f.m. signal producing, coding and processing 3-70111

bats, echolocating, neural processing mechanisms, differences in emitted sounds 3-70109

bats, echolocating, sonar ranging, acuity of resolution, species comparison 3-70110

bats, echolocation behaviour, survey 3-70108

beetle shell struct. and mech. props. 3-41807

carp, optic tectum, localized unit responses 3-66007

cat, isolated perfused eye, S-potentials 3-66009

cat, on-center retinal ganglion cells, center-surround interactions 3-66006

cat, on-centre retinal ganglion cells, peripheral responses 3-66004

cat, retinal ganglion cell, response to moving stimuli 3-66001

cat, visual cortex, complex and hypercomplex receptive fields 3-77235

cat, visual cortex, integration of auditory information 3-65992

cat retina, on-center neurons, receptive field periphery 3-66005

crab Cancer pagurus, tension receptor reflexes in walking legs 3-42276

crustacean visual system, spatial integration, peripheral and central sources of nonlinear summation 3-77232

crustaceans, long term adaptation by monochromatic light 3-66000

zoology continued

delphinid sonar, echolocation, measurement, acquisition, storage, analysis, problems 3-66153

electric fish Eigenmannia, 'electromotor responses' 3-45264

excised dog larynx, vibration patterns 3-48193

flies, head movement during visually guided flight 3-45310

flies, visual nervous system, development and applic. of white-noise modelling techniques 3-45307

freshwater turtle and pigeon, de-Lange charac. 3-77233

frog isolated retina, recovery of cone receptor activity 3-77242

frog neuromuscular transmission, presynaptic and postsynaptic effects of Pb 3-45265

frog rods, dark adaptation, isolated retina 3-77243

insect visual system, fundamental mechanism of motion detection 3-45306

locust, adult female, rheological props. of extensible intersegmental membrane 3-42272

mammals, isolated perfused eye, intercellular recording 3-66010

marine animals, conc. of radionuclides, monitoring sensitivity, San

Onofre Nuclear Generating Station 3-74767

marine delphinids, fresh water dolphin, echolocation, review 3-70112

mongoose, vocal repertoire 3-48198

pigeon, thalamus, opponent-colour units 3-66019

rabbit, thermoregulatory reactions 3-56496

rabbit, visual receptive-field characteristics of superior colliculus neurons after cortical lesions 3-77238

rat, blood pressure meas. apparatus 3-54024

stick insects, neuromuscular transmission, effect of glutamic acid 3-56495

Tursiops truncatus, sound localization expts. 3-45287

zoosemiotics *see biocommunications***Zr** *see zirconium*

ABSTRACTS AND CURRENT PAPERS JOURNALS

Three main subject areas are covered by INSPEC abstracts and current papers journals: physics, electrical and electronics engineering, and computer and control engineering. For each field an abstracts journal and a companion titles journal are published. The abstracts journals are intended as library tools for retrospective information retrieval, whereas the companion titles journals, which omit the abstracts and associated indexes, are intended as low-cost current-awareness tools for the individual.

SUBSCRIPTION PRICES

ABSTRACTS JOURNALS

PHYSICS ABSTRACTS

Paper or Microfiche
Paper and Microfiche

ELECTRICAL & ELECTRONICS ABSTRACTS

Paper or Microfiche
Paper and Microfiche

COMPUTER & CONTROL ABSTRACTS

Paper or Microfiche
Paper and Microfiche

EEA/CCA COMBINED SUB.

Paper or Microfiche
Paper and Microfiche

CURRENT PAPERS IN PHYSICS

CURRENT PAPERS IN ELECTRICAL & ELECTRONICS

CURRENT PAPERS ON COMPUTERS & CONTROL

ISMEC BULLETIN INDEXES

METRON

USA		JAPAN, via AIR DELIVERY		REST OF WORLD	
\$		£		£	
380		157		145	
570		229		217	
290		120		115	
435		177		172	
150		68		65	
225		100		97	
375		160		150	
562		235		225	
40 (NM)	20 (M)	22.50 (NM)	10 (M)	20 (NM)	10 (M)
40 (NM)	20 (M)	22.50 (NM)	10 (M)	20 (NM)	10 (M)
40 (NM)	20 (M)	18 (NM)	8.50 (M)	17 (NM)	8.50 (M)
140		55		50	
50		22		20	
75		30		30	

NOTE: (NM) represents non-member subscription rates.
(M) represents subscription rates for members of IEE, AIP, IEEE, IOP, IERE.

CUMULATIVE INDEXES

Cumulative indexes are available for *Physics Abstracts*, *Electrical & Electronics Abstracts* and *Computer & Control Abstracts*, for both authors and subjects. These cumulations generally cover a period of four years, with the exception of *Computer & Control Abstracts* where the initial volume covered the period 1966-68. The table below shows the prices and periods for the two types of cumulative index.

	PHYSICS ABSTRACTS				ELECTRICAL & ELECTRONICS ABSTRACTS				• COMPUTER & CONTROL ABSTRACTS			
	AMERICAS		REST OF WORLD		AMERICAS		REST OF WORLD		AMERICAS		REST OF WORLD	
	Subject	Author	Subject	Author	Subject	Author	Subject	Author	Subject	Author	Subject	Author
	\$	\$	£	£	\$	\$	£	£	\$	\$	£	£
1955-59	50	50	20	20	38	50	15	20	—	—	—	—
1960-64	100	43	40	17	50	30	20	12	—	—	—	—
1965-68	150	75	63	25	88	50	35	20	—	—	—	—
1969-72	545	343	222	140	180	160	72	64	123	78	48	30
1966-68	—	—	—	—	—	—	—	—	38		15	

ORDERING PROCEDURE

THE AMERICAS

North (including Canada), Central and South

All orders from the above areas, and orders from members of Institute of Electrical and

Electronics Engineers Inc. anywhere in the world, should be sent to Fulfillment Manager, Institute of Electrical & Electronics Engineers Inc., 345 East 47th Street, New York, NY 10017, USA.

REMAINDER OF THE WORLD

All remaining subscriptions should be sent to INSPEC Marketing Department, IEE, Savoy Place, London WC2R 0BL, England. Telephone 01-240 1871, Telex 261176, Telegrams Voltampere London, WC2.

OTHER INSPEC SERVICES

SDI

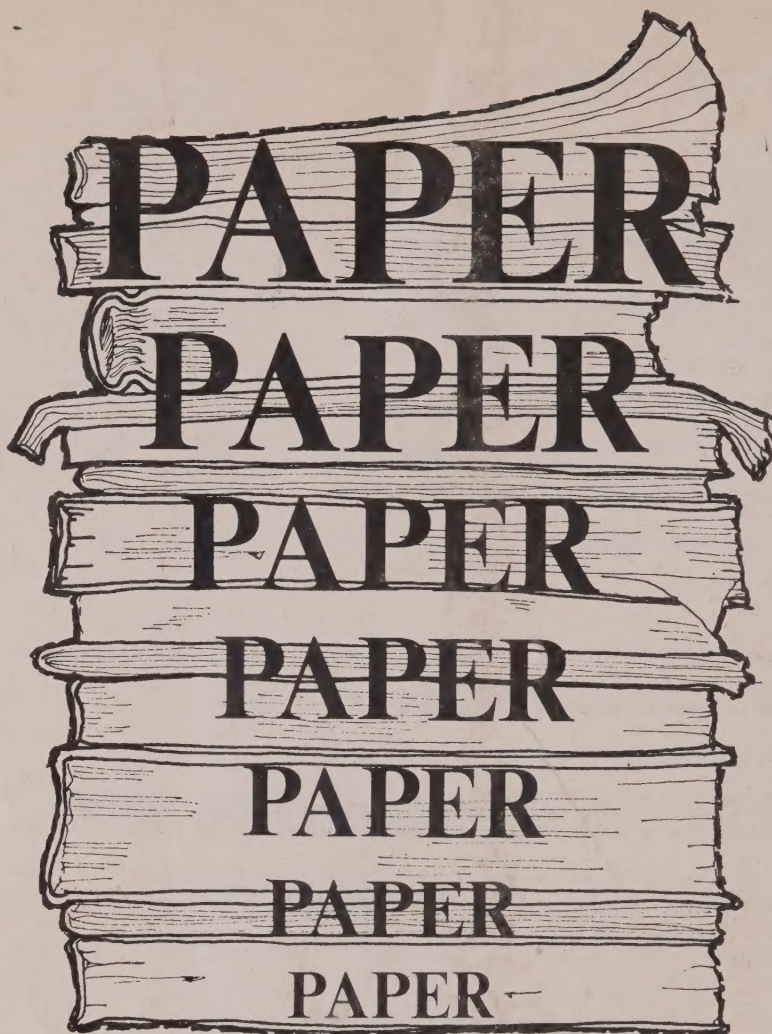
(Selective Dissemination of Information.) This is a service individually tailored to the requirements and interests of the engineer or research worker. Details of information relevant to the interest profile of the individual subscriber are selected from the data being processed for the INSPEC database. Information is dispatched weekly on 150 mm x 100 mm (6" x 4") cards.

TOPICS

This is an SDI service based on standard profiles. There are 73 subjects covering high-activity areas of research and development. This is an inexpensive card service designed to alert engineers and researchers to the availability of literature within their subject area.

MAGNETIC TAPES

These are produced, containing all the information included in the INSPEC publications. They enable the larger research and development organisations to produce their own internal information and current-awareness services.



MICROFILM

SAVE YOURSELF THE TROUBLE

ALL BACK ISSUES OF INSPEC JOURNALS
ARE AVAILABLE ON **MICROFILM**

WRITE, TELEPHONE OR TELEX FOR FULL DETAILS TO



inspec
The Institution of Electrical Engineers

INSPEC Marketing Department
IEE, Savoy Place,
LONDON WC2R 0BL

Telephone: 01-240 1871

Telex: 261176